

AERONAUTICAL ENGINEERING

(NASA-SP-7037(300)) AERONAUTICAL
ENGINEERING: A CUMULATIVE INDEX TO
A CONTINUING BIBLIOGRAPHY
(SUPPLEMENT 300) (NASA) 673 p

N94-28537

Unclass

00/01 0001785

1993 CUMULATIVE INDEX

The NASA STI Program ... in Profile

Since its founding, NASA has been dedicated to the advancement of aeronautics and space science. The NASA Scientific and Technical Information (STI) Program plays a key part in helping NASA maintain this important role.

The NASA STI Program provides access to the NASA STI Database, the largest collection of aeronautical and space science STI in the world. The Program is also NASA's institutional mechanism for disseminating the results of its research and development activities.

Specialized services that help round out the Program's diverse offerings include creating custom thesauri, translating material to or from 34 foreign languages, building customized databases, organizing and publishing research results ... even providing videos.

For more information about the NASA STI Program, you can:

- **Phone** the NASA Access Help Desk at (301) 621-0390
- **Fax** your question to the NASA Access Help Desk at (301) 621-0134
- **E-mail** your question via the **Internet** to help@sti.nasa.gov
- **Write** to:

NASA Access Help Desk
NASA Center for AeroSpace Information
800 Elkridge Landing Road
Linthicum Heights, MD 21090-2934

NASA SP-7037 (300)

February 1994

AERONAUTICAL ENGINEERING

1993 CUMULATIVE INDEX



National Aeronautics and Space Administration
Scientific and Technical Information Program
Washington, DC

1994

SUPPLEMENTS COVERED IN THIS ISSUE

<i>Document</i>	<i>Page Range</i>	<i>Date</i>	<i>Coverage</i>
NASA SP-7037(288)	1-106	February 1993	January 1993
NASA SP-7037(289)	107-236	March 1993	February 1993
NASA SP-7037(290)	237-456	April 1993	March 1993
NASA SP-7037(291)	457-572	May 1993	April 1993
NASA SP-7037(292)	573-676	June 1993	May 1993
NASA SP-7037(293)	677-762	July 1993	June 1993
NASA SP-7037(294)	763-854	August 1993	July 1993
NASA SP-7037(295)	855-946	September 1993	August 1993
NASA SP-7037(296)	947-1042	October 1993	September 1993
NASA SP-7037(297)	1043-1174	November 1993	October 1993
NASA SP-7037(298)	1175-1228	December 1993	November 1993
NASA SP-7037(299)	1229-1266	January 1994	December 1993

INTRODUCTION

WHAT THIS CUMULATIVE INDEX IS

This publication is a cumulative index to the abstracts contained in NASA SP-7037 (288) through NASA SP-7037 (299) of *Aeronautical Engineering: A Continuing Bibliography*. NASA SP-7037, and its supplements have been compiled by the Center for AeroSpace Information of the National Aeronautics and Space Administration (NASA). Entries are identified as follows:

1. NASA entries by *STAR* accession numbers N93-10000.
2. Open literature entries by accession numbers A93-10000.

HOW THIS CUMULATIVE INDEX IS ORGANIZED

This Cumulative Index includes a subject, personal author, corporate source, foreign technology, contract number, report number, and accession number index.

HOW TO USE THE SUBJECT INDEX

Two types of cross-references appear in the subject index:

1. Use (U) references indicate that the subject term is not "postable," i.e., not a valid term, and that the following term or terms are used instead. For example:

AIRCRAFT PROTUBERANCES

U PROTUBERANCES

FLIGHT PERFORMANCE

U FLIGHT CHARACTERISTICS

2. Narrower Term (NT) references refer the user to more specific headings in the same subject area, under which additional material on the subject may be found. For example:

FLOW RESISTANCE

NT AERODYNAMIC DRAG

NT FRICTION DRAG

NT SUPERSONIC DRAG

In addition, a searcher may use the title or title and title extension in the index to narrow further his quest for particular items; this is because subject terms may include documents on different aspects of the same subject term. For example:

AIRLINE OPERATIONS

All-weather operations, including pilot role, instrument landing systems and guidance aids.

Airport congestion as constraint on air travel, considering runway capacity and adjusted demand.

HOW TO USE THE PERSONAL AUTHOR INDEX

All personal authors used in the abstract section citations in the individual supplements appear in the index. Differences in translation schemes may require multiple searching on the index for variants of an author's name. For example:

EMELIANOV, M. D.

and

YEMELYANOV, M. D.

HOW TO USE THE CORPORATE SOURCE INDEX

The corporate source index entries are abridged versions of the corporate sources used in the abstract section citations in the individual supplements. The corporate source supplementary (organizational component) does not appear in the index. For example:

BOEING CO., SEATTLE, WASH. MILITARY AIRCRAFT SYSTEMS DIV.

(Source citation entry)

BOEING CO., SEATTLE, WASH.

(Source index entry)

HOW TO USE THE FOREIGN TECHNOLOGY INDEX

The foreign technology index identifies research performed outside of the United States. Listings in this index are arranged alphabetically by country of intellectual origin. For example:

CHINA, PEOPLE'S REPUBLIC OF

HOW TO USE THE CONTRACT NUMBER INDEX

All contract numbers that are identified in the abstract section citations in the individual supplements appear in this index. Changes by agencies in the style in which contract numbers are presented may require multiple searching for variants. For example:

AF 33(615)-71-C-1758

F33615-71-C-1758

HOW TO USE THE REPORT NUMBER INDEX

All report numbers that have been assigned by the corporate source, monitoring agency or cataloging activity appear in this index. Variations in cataloging may result in different report number series. For example:

TP-924

ONERA-TP-924

HOW TO USE THE ACCESSION NUMBER INDEX

All documents that were acquired, indexed, and announced in *STAR* during the year which have been assigned a unique identification number appear in this index. For example:

N93-10001

N93-10002

IDENTIFICATION OF DESIRED SUPPLEMENT

The abstract and descriptive cataloging for any accession number selected from the indexes may be found in the appropriate supplement. The page number range of each supplement appears on page ii of this index. Once the range of page numbers containing the selected accession number is located in the second column, the desired supplement number will be found in the first column. For example:

Page 500 will be found in Supplement 291

AVAILABILITY OF DOCUMENTS

Information concerning the availability of documents announced in *Aeronautical Engineering* is found in the Introduction to the most currently issued supplement.

FEDERAL DEPOSITORY LIBRARY PROGRAM

In order to provide the general public with greater access to U.S. Government publications, Congress established the Federal Depository Library Program under the Government Printing Office (GPO), with 53 regional depositories responsible for permanent retention of material, inter-library loan, and reference services. At least one copy of nearly every NASA and NASA-sponsored publication, either in printed or microfiche format, is received and retained by the 53 regional depositories. A list of the regional GPO libraries, arranged alphabetically by state, appears on the inside back cover. These libraries are *not* sales outlets. A local library can contact a Regional Depository to help locate specific reports, or direct contact may be made by an individual.

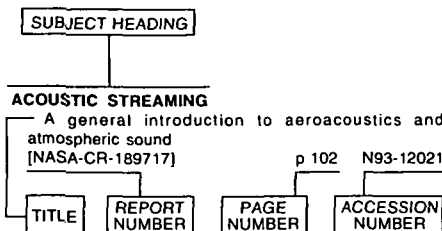
PUBLIC COLLECTIONS OF NASA DOCUMENTS

An extensive collection of NASA and NASA-sponsored publications is maintained by the British Library Lending Division, Boston Spa, Wetherby, Yorkshire, England for public access. The British Library Lending Division also has available many of the non-NASA publications cited in *STAR*. European requesters may purchase facsimile copy or microfiche of NASA and NASA-sponsored documents, those identified by both the symbols # and * from ESA-Information Retrieval Service European Space Agency, 8-10 rue Mario-Nikis, 75738 CEDEX 15, France.

TABLE OF CONTENTS

Subject Index	A-1
Personal Author Index.....	B-1
Corporate Source Index	C-1
Foreign Technology Index	D-1
Contract Number Index	E-1
Report Number Index.....	F-1
Accession Number Index	G-1

Typical Subject Index Listing



The subject heading is a key to the subject content of the document. The title is used to provide a description of the subject matter. When the title is insufficiently descriptive of document content, a title extension is added, separated from the title by three hyphens. The accession number and the page number are included in each entry to assist the user in locating the abstract in the abstract section. If applicable, a report number is also included as an aid in identifying the document. Under any one subject heading, the accession numbers are arranged in sequence.

A

- A-3 AIRCRAFT**
The whale with a tail p 803 A93-38837
- A-320 AIRCRAFT**
Cost control of the A320 software - The aircraft manufacturer's point of view p 227 A93-15044
- A-6 AIRCRAFT**
Trends in air power - New systems, old platforms? p 856 A93-43650
Study of statistical variations of load spectra and material properties on aircraft fatigue life [AD-A257961] p 339 N93-18451
- A-7 AIRCRAFT**
Evaluation of alternatives for increasing A-7D rearward visibility [AD-A255071] p 50 N93-12488
Software requirements for the A-7E aircraft [AD-A255746] p 229 N93-15052
- ABILITIES**
Identifying ability requirements for operators of future automated air traffic control systems [AD-A256615] p 152 N93-14276
- ABLATION**
Low-to-high altitude predictions of three-dimensional ablative re-entry flowfields p 1027 A93-46407
Simulation of ablation in Earth atmospheric entry [AIAA PAPER 93-2789] p 1027 A93-46531
Thermal response and ablation characteristics of light weight ceramic ablaters [AIAA PAPER 93-2790] p 1018 A93-46532
Evaluation of decomposition kinetic coefficients for a fiber-reinforced intumescent-epoxy [AIAA PAPER 93-1856] p 1144 A93-49734
Aerothermal ablative characterization of selected external insulator candidates [AIAA PAPER 93-1857] p 1145 A93-49735
Preparation and characterization of continuous fiber reinforced zirconium diboride matrix composites for a leading edge material p 1211 A93-53445

- Ablation problems using a finite control volume technique [DE93-009861] p 942 N93-29187
- ABLATIVE MATERIALS**
Thermal response and ablation characteristics of light weight ceramic ablaters [AIAA PAPER 93-2790] p 1018 A93-46532
- ABRASION RESISTANCE**
F-14 wing lug coating investigation [AD-A257384] p 328 N93-15858
- ABRASIVES**
Ultrasonic polishing p 750 N93-25580
- ABSORBERS (MATERIALS)**
Evaluation of acoustic impedance models for a perforated plate [NAL-TR-1133] p 102 N93-12375
- ABSORPTION SPECTRA**
Remote sensing of O₂ in a supersonic combustor using diode lasers and fiber optics [AIAA PAPER 92-5090] p 414 A93-22360
- ABSTRACTS**
AFOSR Contractors Meeting in Propulsion [AD-A254484] p 195 N93-12575
Summaries of the 1991 publications of DLR research reports and DLR communications [ETN-93-92588] p 572 N93-21022
NASA SBIR abstracts of 1990 phase 1 projects [NASA-TM-108145] p 572 N93-21794
Bibliography on propulsion airframe integration technologies for high-speed civil transport applications, 1980-1991 [NASA-TM-105602] p 678 N93-26136
NASA SBIR abstracts of 1991 phase 1 projects [NASA-TM-108240] p 945 N93-29323
- ACCELERATED LIFE TESTS**
Accelerated corrosion fatigue test methods for aging aircraft p 198 A93-16623
Life assessment of gas turbine bucket coating based on degradation analysis p 533 A93-24464
Environmental definition of a multi-platform avionics system p 896 A93-42855
Reanalysis of multiple-wheel landing gear traffic tests [AD-A256593] p 194 N93-14238
Liquid flow reactor and method of using [AD-D015392] p 222 N93-15232
Brush seal bristle flexure and hard-rub characteristics [NASA-TM-105864] p 421 N93-18321
Efficient fault diagnosis of helicopter gearboxes [NASA-TM-106253] p 1032 N93-31846
- ACCELERATION (PHYSICS)**
Determination of balloon gas mass and revised estimates of drag and virtual mass coefficients p 7 A93-11362
The improvement of the static launch method in Japan p 26 A93-11364
A minimum-time acceleration control strategy for a two-rotor aeroengine p 172 A93-14499
Initial acceleration effects on the flow field development around rapidly pitching airfoils [AIAA PAPER 93-0438] p 286 A93-23352
Initial acceleration effects on flow evolution around airfoils pitching to high angles of attack p 961 A93-45750
Supersonic flow past a rectangular wing of finite thickness p 1086 A93-50972
Evaluation of CKU-5/A ejection seat catapults under varied acceleration levels [AD-A248021] p 29 N93-12489
- ACCELERATORS**
An estimate of the 'doomed propellant fraction' for a Superdetonative Ram Accelerator [AIAA PAPER 93-0359] p 385 A93-23042
Research and development of a turbo-accelerator for super/hypersonic transport [ISABE 93-7066] p 1200 A93-54042
- ACCELEROMETERS**
An overview of the evolution of vibrating beam accelerometer technology p 412 A93-21934
Integration of a course and position reference system with GPS p 499 A93-27911

- A study of the influence of the data acquisition system sampling rate on the accuracy of measured acceleration loads for transport aircraft p 1000 A93-46808
The LN-200 fiber gyro based tactical grade IMU [AIAA PAPER 93-3798] p 1106 A93-51391
Design, test, and evaluation of three active flutter suppression controllers [NASA-TM-4338] p 63 N93-10070
Accuracy improvement of linear estimated motion using differential type sensors [NAL-TR-1135] p 91 N93-12365
Rarefied-flow Shuttle aerodynamics model [NASA-TM-107698] p 458 N93-19976
- ACCIDENT INVESTIGATION**
The probable cause --- aircraft accidents p 1240 A93-56417
Aircraft Accidents: Trends in Aerospace Medical Investigation Techniques [AGARD-CP-532] p 490 N93-19653
Reportable accidents to UK registered aircraft, and to foreign registered aircraft in UK airspace, 1990 [CAP-600] p 991 N93-31730
- ACCIDENT PREVENTION**
Graph-theory studies of the possibility of occurrence of flight accidents and incidents during the take-off under special operating conditions p 306 A93-18365
Sensing a change in the wind p 307 A93-21627
First moves towards an 'intelligent' GPWS p 896 A93-43624
Unusual attitudes - Helicopters and instrument flight p 1240 A93-54550
Aircraft Accidents: Trends in Aerospace Medical Investigation Techniques [AGARD-CP-532] p 490 N93-19653
How do we investigate the human factor in aircraft accidents? p 491 N93-19655
The human factor problem in the Canadian Forces aviation p 491 N93-19657
Underlying causes of accidents: Casual networks p 491 N93-19658
Aid in investigation by figure animation p 491 N93-19659
Combat and training aircraft class A mishaps in the Belgian Air Force 1970-1990 p 492 N93-19677
Royal Naval helicopter ditching experience p 492 N93-19684
Towards an integrated approach to proactive monitoring and accident prevention p 495 N93-19700
- ACCIDENTS**
A review of civil aviation propeller-to-person accidents: 1980-1989 [AD-A260695] p 705 N93-25896
- ACCUMULATORS**
Nozzle diffuser for use with an open test section of a wind tunnel [NASA-CASE-LAR-14424-1-SB] p 731 N93-25996
- ACCURACY**
Measurement technique for Loran-C pulse wave distortion measures and performance in an environment of noise p 29 A93-10988
Statistical quality control for kinematic GPS positioning p 314 A93-21162
Accuracy of GPS-derived acceleration from moving platform tests p 1240 A93-55973
The effect of clock, media, and station location errors on Doppler measurement accuracy p 885 N93-29588
Ground- and satellite-derived flight-path measurements as demonstrated in the AFES Avionics Flight Evaluation System (AFES) p 993 N93-31281
The application of phase tracking GPS for flight test trajectory determination [NLR-TP-91349-U] p 994 N93-32337
- ACETYLENE**
Theoretical study of the bond dissociation energies of propyne (C₃H₄) p 230 A93-14099
- ACOUSTIC ATTENUATION**
On sound attenuation in boundary layers p 446 A93-19164
Inter-noise '91; Proceedings of the 20th International Conference on Noise Control Engineering, Sydney, Australia, Dec. 2-4, 1991. Vols. 1 & 2 [ISBN 0-909882-12-6] p 557 A93-28476

- An aeroacoustic stand for evaluating the efficiency of sound-absorbing structures under conditions of acoustic wave propagation in a moving medium p 1140 A93-51762
- Evaluation of acoustic impedance models for a perforated plate [NAL-TR-1133] p 102 N93-12375
- Consecutive plate acoustic suppressor apparatus and methods [NASA-CASE-LEW-15430-1] p 453 N93-17051
- In-flight evaluation of noise levels and assessment of active noise reduction systems in the Seahawk S-70B-2 helicopter [AD-A260689] p 759 N93-25649
- Detection performance of digital polarity sampled phase reversal code pulse compressors [AD-A262930] p 842 N93-28289
- ACOUSTIC COUPLING**
- Experimental and analytical investigations of fuselage modal characteristics and structural-acoustic coupling p 451 A93-19229
- Structural-acoustic coupling in aircraft fuselage structures p 1243 A93-55856
- Nozzle installation effects on the noise from supersonic exhaust plumes p 100 N93-10681
- Combustion noise and combustion instabilities in propulsion systems p 100 N93-10682
- Active control of aeroacoustic couplings by means of adaptive systems [ECL-91-18] p 64 N93-11576
- ACOUSTIC DUCTS**
- Researches on sonic fatigue of the air-inlet duct of XX aircraft p 154 A93-14256
- Measured acoustic characteristics of ducted supersonic jets at different model scales [AIAA PAPER 93-0731] p 563 A93-24821
- ACOUSTIC EMISSION**
- Acoustic emission monitoring of aging aircraft structures p 407 A93-19697
- Predicting rotorcraft transmission noise p 850 A93-35968
- Detection and classification of acoustic signals from fixed-wing aircraft p 850 A93-37032
- An experimental system for studying the vibrations and acoustic emission of cylindrical shells and panels in a field of turbulent pressure pulsations p 1140 A93-51754
- An approach to the calculation of the far acoustic field of a propeller p 1124 A93-51760
- An Acoustic Emission Pre-failure Warning System for composite structural tests p 1161 A93-52560
- Acoustic emission technology for smart structures p 1263 A93-55331
- ACOUSTIC EXCITATION**
- Separation control and lift enhancement on airfoil using unsteady excitations p 118 A93-14305
- Flow past a finite-span wing in the presence of external acoustic loading p 127 A93-16707
- Excitation of velocity fluctuations and noise in a wind tunnel p 444 A93-18242
- Improvement of high-AOA airfoil stalling performance by internal acoustic excitation p 243 A93-19134
- Nonlinear vibration and radiation from a panel with transition to chaos induced by acoustic waves p 398 A93-19173
- Experimental measurement of structural intensity on an aircraft fuselage p 544 A93-26999
- Finite element nonlinear random response of beams to acoustic and thermal loads applied simultaneously [AIAA PAPER 93-1427] p 740 A93-33978
- Correction of the frequency characteristic of the waveguide circuit of an acoustic-jet temperature transducer p 832 A93-39036
- Investigation of helicopter air resonance in hover by complex coordinates and mutual excitation analysis p 893 A93-43777
- Transonic flutter suppression using active acoustic excitations [AIAA PAPER 93-3285] p 969 A93-46841
- The effect of temperature on the natural frequencies and acoustically induced strains in CFRP plates p 1260 A93-56331
- Initial streamwise vorticity formation in a two-stream mixing layer p 698 N93-25752
- Quiet by design: Numerical acousto-elastic analysis of aircraft structures [ISBN-90-386-0042-9] p 893 N93-29268
- Modal measurements and propeller field excitation on acoustic full scale mockup of SAAB 340 aircraft [FFA-TN-1992-08] p 1039 N93-31051
- Enhanced mixing of a rectangular supersonic jet by natural and induced screech [NASA-TM-106245] p 989 N93-31672
- ACOUSTIC FATIGUE**
- Researches on sonic fatigue of the air-inlet duct of XX aircraft p 154 A93-14256
- Nonlinear response of a clamped beam and plate to high levels of excitation p 397 A93-19141
- A review of crack propagation under unsteady loading p 399 A93-19207
- Sonic fatigue analysis of an aircraft wing flap by the matrix difference equation method p 399 A93-19208
- Nonlinear response and sonic fatigue of high speed aircraft p 399 A93-19211
- Unsteady pressures on exhaust nozzle interior surfaces - Empirical correlations for prediction p 244 A93-19219
- Fatigue effects of noise among airplane mechanics p 558 A93-28495
- Tiltrotor interior noise characteristics p 509 A93-29421
- Effect of a combination of design and process-related factors on the fatigue strength of bolted joints in acoustically loaded aircraft structures p 745 A93-35278
- Review of crack propagation under unsteady loading p 837 A93-39416
- Recent advances of time domain approach for nonlinear response and sonic fatigue p 1022 A93-45106
- Nonlinear analyses of composite aerospace structures in sonic fatigue [NASA-CR-193124] p 930 N93-29154
- ACOUSTIC FREQUENCIES**
- Scale-up of the spectra of aerodynamic pressure pulsations with narrowband maxima p 1088 A93-51756
- High-frequency acoustic radiation from a curved duct of circular cross section [ONERA, TP NO. 1993-55] p 1173 A93-51937
- Comparison of methodologies for describing relaxation in nonequilibrium gaseous systems p 419 N93-16786
- ACOUSTIC IMPEDANCE**
- Evaluation of acoustic impedance models for a perforated plate [NAL-TR-1133] p 102 N93-12375
- ACOUSTIC INSTABILITY**
- Comparison of confined, compressible, spatially developing mixing layers with temporal mixing layers p 1234 A93-55352
- The prediction of noise radiation from supersonic elliptic jets p 100 N93-10684
- Numerical simulation of the acoustic instability in the spatially developing, confined, supersonic mixing layer p 132 N93-13521
- ACOUSTIC MEASUREMENT**
- Optical microphone for the detection of hidden helicopters p 205 A93-14542
- Acoustic mode measurements in the inlet of a model turbofan using a continuously rotating rake - Data collection/analysis techniques [AIAA PAPER 93-0599] p 361 A93-23324
- Acoustic mode measurements in the inlet of a model turbofan using a continuously rotating rake [AIAA PAPER 93-0598] p 563 A93-24783
- Signal processing of jet noise from flyover test data [AIAA PAPER 93-0736] p 563 A93-24826
- Role of leading-edge vortex flows in prop-fan interaction noise p 565 A93-28614
- Human response to helicopter noise - A test of A-weighting p 567 A93-29424
- Acoustic mode measurements in the inlet of a model turbofan using a continuously rotating rake: Data collection/analysis techniques [NASA-TM-105936] p 179 N93-15403
- Acoustic mode measurements in the inlet of a model turbofan using a continuously rotating rake [NASA-TM-105989] p 362 N93-16705
- Rotating rake design for unique measurement of fan-generated spinning acoustic modes [NASA-TM-105946] p 724 N93-26161
- Loudness and annoyance response to simulated outdoor and indoor sonic booms [NASA-TM-107756] p 852 N93-27271
- A laboratory study of subjective response to sonic booms measured at White Sands Missile Range [NASA-TM-107746] p 852 N93-27272
- External acoustical noise measurements for aviation systems [AD-A263138] p 943 N93-29480
- Instrumentation for in-flight acoustic measurements in an engine inlet duct of a Fokker 100 aircraft [NLR-TP-91200-U] p 1001 N93-32332
- ACOUSTIC PROPAGATION**
- The numerical calculation for the coupling of multiple propeller discrete noise and its interaction with the fuselage boundary p 231 A93-14268
- Radiated noise of ducted fans p 450 A93-19215
- A novel algorithm for the solution of compressible Euler equations in wave/particle split (WPS) form p 957 A93-45093

- High-frequency acoustic radiation from a curved duct of circular cross section [ONERA, TP NO. 1993-55] p 1173 A93-51937
- The acoustics of axial compressors [ONERA, TP NO. 1993-102] p 1226 A93-53615
- Acoustic-wave propagation in ducts and free-field radiation [ONERA, TP NO. 1993-103] p 1226 A93-53616
- Developing numerical techniques for solving low Mach number fluid-acoustic problems p 1235 A93-55353
- Sonic boom minimization - Myth or reality? p 1264 A93-55859
- Sonic boom problem for future highspeed aircraft [ONERA-NT-1990-3] p 876 N93-30020
- ACOUSTIC PROPERTIES**
- Acoustic performance of low pressure axial fan rotors with different blade chord length and radial load distribution p 449 A93-19212
- Experimental determination of the main noise sources in a profan model by analysis of the acoustic spinning modes in the exit plane p 449 A93-19214
- Experimental and analytical investigations of fuselage modal characteristics and structural-acoustic coupling p 451 A93-19229
- Vibro-acoustic analysis of propeller aircraft, integrating advanced experimental modeling with in-flight data analysis p 451 A93-19230
- Takeoff/approach noise for a model counterrotation propeller with a forward-swept upstream rotor [AIAA PAPER 93-0596] p 519 A93-24782
- Acoustic mode measurements in the inlet of a model turbofan using a continuously rotating rake [AIAA PAPER 93-0598] p 563 A93-24783
- Measured acoustic characteristics of ducted supersonic jets at different model scales [AIAA PAPER 93-0731] p 563 A93-24821
- Far-field hover acoustic characteristics of the XV-15 tiltrotor aircraft with Advanced Technology Blades p 566 A93-29412
- Acoustic characteristics of advanced model rotor systems p 567 A93-29419
- Euler solutions to nonlinear acoustics of non-lifting rotor blades p 568 A93-29433
- Effects of ingested atmospheric turbulence on measured tail rotor acoustics p 849 A93-35964
- Acoustical properties of sound absorbing structures at high temperature p 1172 A93-48522
- Acoustic noise generation at the air/ocean boundary [DREA-CR-90-445] p 99 N93-10642
- Combustion noise and combustion instabilities in propulsion systems p 100 N93-10682
- Acoustic mode measurements in the inlet of a model turbofan using a continuously rotating rake [NASA-TM-105989] p 362 N93-16705
- Takeoff/approach noise for a model counterrotation propeller with a forward-swept upstream rotor [NASA-TM-105979] p 362 N93-16715
- Multidisciplinary tailoring of hot composite structures [NASA-TM-106027] p 550 N93-19971
- Development of a flight instrument package [AD-A260830] p 719 N93-25783
- Rotating rake design for unique measurement of fan-generated spinning acoustic modes [NASA-TM-105946] p 724 N93-26161
- An integrated optimum design approach for high speed prop-rotors including acoustic constraints [NASA-CR-193222] p 893 N93-29153
- Unsteady vortex loop/dipole theory applied to the work and acoustics of an ideal low speed propeller [AD-A264057] p 876 N93-29891
- ACOUSTIC RETROFITTING**
- Noise reduction programs for in-service jet transports p 521 A93-28479
- ACOUSTIC SCATTERING**
- Interaction of the sonic boom with atmospheric turbulence [AIAA PAPER 93-2943] p 1171 A93-48140
- ACOUSTIC STREAMING**
- A general introduction to aeroacoustics and atmospheric sound p 1264 A93-55852
- A general introduction to aeroacoustics and atmospheric sound [NASA-CR-189717] p 102 N93-12021
- ACOUSTIC VELOCITY**
- Introduction of small velocity and pressure variation into a stationary compressible fluid p 473 A93-25060
- ACOUSTICS**
- Recent advances in integrated multidisciplinary optimization of rotorcraft [AIAA PAPER 92-4777] p 325 A93-20369
- AHS, Annual Forum, 48th, Washington, June 3-5, 1992, Proceedings, Vols. 1 & 2 p 763 A93-35901
- Recent advances in multidisciplinary optimization of rotorcraft [NASA-TM-107665] p 47 N93-10968

- Publications on acoustics research at the Langley Research Center, January 1987 - September 1992
[NASA-TM-107674] p 102 N93-12080
- An experimental examination of the thermal and acoustic environments on runway joint seals
[AD-A257965] p 382 N93-17734
- Development of a flight instrument package
[AD-A260830] p 719 N93-25783
- Cumulative reports and publications
[NASA-CR-191440] p 847 N93-27063
- Unsteady vortex loop/dipole theory applied to the work and acoustics of an ideal low speed propeller
[AD-A264057] p 676 N93-29891
- ACTIVE CONTROL**
- Finite memory approximations for a singular neutral system arising in aeroelasticity p 97 A93-13246
- Research and applications in structural dynamics and aeroelasticity p 153 A93-14223
- Feasibility study of an active aeroelastic control system for the F-16 aircraft p 181 A93-14224
- Recent progress in the implementation of active combustion control p 171 A93-14272
- Dynamic stability, coupling and active control of elastic vehicles with unsteady aerodynamic forces modeling p 182 A93-14282
- Analytic continuation of Pade approximations to the unsteady kernel functions to obtain a better understanding of the analytic continuation of Pade approximations to unsteady parameters in general p 117 A93-14283
- Extending the useful frequency of 'rigid' wind tunnel models with active control p 190 A93-14299
- Parametric aeroelastic analysis of composite wing-boxes with active strain-energy tuning p 156 A93-14361
- Active control of interior noise in model aircraft fuselages using piezoceramic actuators p 231 A93-14540
- Experiments on the active control of boundary layer transition p 243 A93-19133
- Active aerodynamic control of wake-airfoil interaction noise - Experiment p 445 A93-19153
- Active aerodynamic control of wake-airfoil interaction noise - Theory p 445 A93-19154
- Active control of sound transmission through stiff lightweight composite fuselage constructions p 447 A93-19187
- Experimental results on propeller noise attenuation using an 'active noise control' technique p 450 A93-19223
- Reduction of propeller noise by active noise control p 450 A93-19224
- Active stabilization of compressor instability and surge in a working engine p 348 A93-19335
- [ASME PAPER 92-GT-88] p 348 A93-19335
- Evaluation of approaches to active compressor surge stabilization p 352 A93-19407
- [ASME PAPER 92-GT-182] p 352 A93-19407
- Active control of wing rock of a delta wing at post-stall using tangential leading edge blowing p 367 A93-20169
- [AIAA PAPER 93-0056] p 367 A93-20169
- Some issues concerning active control of combustion instability in a ramjet p 360 A93-22566
- [AIAA PAPER 93-0116] p 360 A93-22566
- Prediction of active control of subsonic centrifugal compressor rotating stall p 274 A93-22591
- [AIAA PAPER 93-0153] p 274 A93-22591
- Active control of fan noise from a turbofan engine p 452 A93-23323
- [AIAA PAPER 93-0597] p 452 A93-23323
- Active control of the shear layer on a static airfoil p 286 A93-23353
- [AIAA PAPER 93-0442] p 286 A93-23353
- Approximation methods for control of structural acoustics models with piezoceramic actuators p 452 A93-23744
- Active control of interior noise in a large scale cylinder using piezoelectric actuators p 568 A93-29425
- Active control of helicopter transmission noise p 568 A93-29428
- An overview of possible and not-so-possible tasks for active control of sound and vibration p 568 A93-29429
- Active control of vibratory airloads induced by helicopter rotor-fuselage interactions p 726 A93-33930
- [AIAA PAPER 93-1363] p 726 A93-33930
- Modal sensors and actuators for individual blade control p 712 A93-34225
- [AIAA PAPER 93-1703] p 712 A93-34225
- Preliminary experiments on active control of fan noise from a turbofan engine p 759 A93-34957
- Integrated structure/control/aerodynamic synthesis of actively controlled composite wings p 818 A93-37392
- Electrorheologically controlled landing gear p 1021 A93-44851
- Theoretical studies of the active control of propeller induced cabin noise using secondary force inputs p 995 A93-45124
- Active control of aerothermoelastic effects for a conceptual hypersonic aircraft p 1007 A93-45137
- Active boundary-layer control in diffusers p 966 A93-46798
- [AIAA PAPER 93-3255] p 966 A93-46798
- Control of the dynamic-stall vortex over a pitching airfoil by leading-edge suction p 969 A93-46832
- [AIAA PAPER 93-3267] p 969 A93-46832
- Active flow control with neural networks p 1037 A93-46834
- [AIAA PAPER 93-3273] p 1037 A93-46834
- The prediction and the active control of surge in multi-stage axial-flow compressors p 1002 A93-46945
- On the aerodynamics and performance of active vortex generators p 979 A93-47234
- [AIAA PAPER 93-3447] p 979 A93-47234
- Active control of asymmetric conical flow using spinning and rotary oscillations p 1048 A93-48152
- [AIAA PAPER 93-2958] p 1048 A93-48152
- Side force augmentation at high angle of attack from pneumatic vortex flow control p 1124 A93-48153
- [AIAA PAPER 93-2959] p 1124 A93-48153
- Local nonlinear control of stall inception in axial flow compressors p 1080 A93-50036
- [AIAA PAPER 93-2230] p 1080 A93-50036
- Active control for fin buffet alleviation p 1133 A93-51408
- [AIAA PAPER 93-3817] p 1133 A93-51408
- Linear quadratic tracking problems in Hilbert space - Application to optimal active noise suppression p 1224 A93-52763
- Active aerodynamic control of wake-airfoil interaction noise - Experiment p 1225 A93-53206
- Review of stall, surge and active control in axial compressors p 1184 A93-53987
- [ISABE 93-7011] p 1184 A93-53987
- Periodic chemical energy release for active combustion control p 1198 A93-54019
- [ISABE 93-7043] p 1198 A93-54019
- Active control of vortex breakdown by a spinning wave generator p 1219 A93-54021
- [ISABE 93-7045] p 1219 A93-54021
- Reduction of propeller noise by active noise control p 101 N93-10692
- Active flutter suppression using dipole filters p 186 N93-13367
- [NASA-TM-107594] p 186 N93-13367
- An investigation of dynamic stress reduction of multi-body aircraft using active gust control p 187 N93-13916
- Active control of combustion instability in a ramjet using large-eddy simulations p 175 N93-14111
- [AD-A255226] p 175 N93-14111
- Vibration isolation technology: An executive summary of systems development and demonstration p 110 N93-15573
- [NASA-TM-105937] p 110 N93-15573
- Active control of stall and surge p 423 N93-18725
- Applications of active adaptive noise control to jet engines p 522 N93-21210
- [NASA-CR-192277] p 522 N93-21210
- In-flight evaluation of noise levels and assessment of active noise reduction systems in the Seahawk S-70B-2 helicopter p 759 N93-25649
- [AD-A260689] p 759 N93-25649
- Active stabilization of aeromechanical systems p 725 N93-26335
- [AD-A261366] p 725 N93-26335
- Noise transmission properties and control strategies for composite structures p 919 N93-30436
- A theoretical and computational study on active wake control p 878 N93-30892
- Control of jet noise p 1040 N93-32221
- [NASA-CR-193552] p 1040 N93-32221
- ACTUATORS**
- Active control of interior noise in model aircraft fuselages using piezoceramic actuators p 231 A93-14540
- The integrated actuation package approach to primary flight control p 185 A93-14630
- [SAE PAPER 920968] p 185 A93-14630
- Advanced cooling for high power electric actuators p 158 A93-14649
- [SAE PAPER 921022] p 158 A93-14649
- A thermal analysis of an F/A-18 wing section for actuator thermal management p 158 A93-14650
- [SAE PAPER 921023] p 158 A93-14650
- Actuation strain decoupling through enhanced directional attachment in plates and aerodynamic surfaces p 394 A93-17727
- Adaptive/conformal wing design for future aircraft p 320 A93-17728
- Evaluation of piezoceramic actuators for control of aircraft interior noise p 447 A93-19186
- Control of a high performance aircraft with unacceptable zero-dynamics p 369 A93-22905
- Approximation methods for control of structural acoustics models with piezoceramic actuators p 452 A93-23744
- Active control of interior noise in a large scale cylinder using piezoelectric actuators p 568 A93-29425
- Modal sensors and actuators for individual blade control p 712 A93-34225
- [AIAA PAPER 93-1703] p 712 A93-34225
- Fail safety aspects of the V-22 pylon conversion actuator p 798 A93-35984
- Spoiler actuator - A problem investigation p 801 A93-37175
- Actuator and aerodynamic modeling for high-angle-of-attack aeroservoelasticity p 818 A93-37433
- [AIAA PAPER 93-1419] p 818 A93-37433
- V-22 nacelle conversion actuator p 889 A93-40438
- Stiffness enhancement of flight control actuator p 1006 A93-44151
- Optical actuators for fly-by-light applications p 1172 A93-49475
- A comparison of two multi-variable integrator windup protection schemes p 1123 A93-51404
- [AIAA PAPER 93-3812] p 1123 A93-51404
- Analysis of unstated supersonic flutter in cascade by semiactuator disk theory p 1181 A93-53841
- Harmonic oscillation in FBW system p 1206 A93-53877
- Periodic chemical energy release for active combustion control p 1198 A93-54019
- [ISABE 93-7043] p 1198 A93-54019
- A study upon structural optimization of elastic rotors for mechanical systems p 83 N93-10310
- [INPE-5376-TDI/471] p 83 N93-10310
- Control of panel flutter at high supersonic speed p 47 N93-10900
- Electro-optic architecture for servicing sensors and actuators in advanced aircraft propulsion systems p 232 N93-13762
- [NASA-CR-182269] p 232 N93-13762
- Multiple model adaptive estimation applied to the VISTA F-16 with actuator and sensor failures, volume 2 p 371 N93-16165
- [AD-A256569] p 371 N93-16165
- Active stabilization to prevent surge in centrifugal compression systems p 424 N93-18862
- [NASA-CR-191625] p 424 N93-18862
- In-flight structural mode excitation system for flutter testing p 526 N93-19915
- An improved method of structural dynamic test design for ground flying and its application to the SH-2F and SH-2G helicopters p 512 N93-19928
- Analytical and experimental investigation of flutter suppression by piezoelectric actuation p 513 N93-20584
- [NASA-TP-3241] p 513 N93-20584
- Applications of active adaptive noise control to jet engines p 522 N93-21210
- [NASA-CR-192277] p 522 N93-21210
- Strategic avionics technology definition studies. Subtask 3-1A: Electrical Actuation (ELA) systems p 914 N93-29215
- [NASA-CR-193237] p 914 N93-29215
- Articulated fin/wing control system p 909 N93-29278
- [AD-D015712] p 909 N93-29278
- Development and flight testing of a fault-tolerant fly-by-light yaw control system p 1010 N93-31280
- Electropneumatic actuator, phase 1 p 1033 N93-31876
- [PB93-174951] p 1033 N93-31876
- Design and application of Active Magnetic Bearings (AMB) for vibration control p 1033 N93-32279
- ADA (PROGRAMMING LANGUAGE)**
- Pave Pillar in-house research final report p 927 A93-42781
- Expert system for redundancy and reconfiguration management p 938 A93-42785
- Complexity metrics for avionics software p 939 A93-42829
- Design of an Ada expert system shell for the VHSIC avionics modular flight processor p 98 N93-11947
- Software Engineering Laboratory Ada performance study: Results and implications p 441 N93-17172
- A model for determining task set schedulability in the presence of system effects p 443 N93-19338
- [AD-A258915] p 443 N93-19338
- Software design document for the generic avionics data bus tool kit p 519 N93-21259
- [AD-A259329] p 519 N93-21259
- Toward reusable graphics components in Ada p 849 N93-28577
- [AD-A262568] p 849 N93-28577
- ADAPTATION**
- Specification of adaptive aiding systems p 159 N93-12602
- [AD-A254537] p 159 N93-12602
- Theory and design of adaptive automation in aviation systems p 160 N93-12613
- [AD-A254595] p 160 N93-12613
- ADAPTIVE CONTROL**
- Design of an adaptive flight control system with uncertainties p 95 A93-12322
- Stabilization of the dynamic characteristics of the automatic control systems of a flight vehicle p 62 A93-12802
- Adaptive control of aircraft in windshear p 62 A93-13126
- Variable structure controller design and its real-time analysis for microprocessor-based flight control systems p 181 A93-14229
- An adaptive algorithm for estimation of a state vector in the system of remotely-piloted aircraft control using Kalman filter p 181 A93-14232
- Stochastic modeling and adaptive control algorithm of brake bending p 227 A93-14417

- Adaptive aeroelastic composite wings - Control and optimization issues p 185 A93-14818
- Adaptive/conformal wing design for future aircraft p 320 A93-17728
- 3-D adaptive grid-embedding Euler technique [AIAA PAPER 93-0330] p 415 A93-23021
- Failure-accommodating neural network flight control [AIAA PAPER 92-4394] p 523 A93-24495
- Direct multivariable adaptive controller with application to wing flutter p 524 A93-26946
- Integrated structural tailoring and adaptive control of advanced flight vehicle structural vibration [AIAA PAPER 93-1697] p 757 A93-34219
- Active rib experiment for shape control of an adaptive wing [AIAA PAPER 93-1700] p 712 A93-34222
- Sensor-adaptive control for aircraft paint stripping [SME PAPER AD92-200] p 855 A93-40663
- Multiple model adaptive estimation applied to the VISTA F-16 flight control system with actuator and sensor failures p 907 A93-42806
- Real-time parameter identification applied to flight simulation p 1006 A93-44142
- Adaptive engine stall margin control p 1108 A93-49200
- On the estimation algorithm for adaptive performance optimization of turbofan engines [AIAA PAPER 93-1823] p 1111 A93-49710
- A U-D factorization-based adaptive extended Kalman filter and its application to flight state estimation p 1169 A93-51198
- A Hopfield neural network for adaptive control [AIAA PAPER 93-3729] p 1130 A93-51329
- Space marching calculations about hypersonic configurations using a solution-adaptive mesh algorithm p 1177 A93-53212
- Active control of aeroacoustic couplings by means of adaptive systems [ECL-91-18] p 64 A93-11576
- Specification of adaptive aiding systems [AD-A254537] p 159 A93-12602
- Theory and design of adaptive automation in aviation systems [AD-A254595] p 160 A93-12613
- Subsonic flight test evaluation of a propulsion system parameter estimation process for the F100 engine [NASA-TM-4426] p 175 A93-13155
- Adaptive control of nonlinear nonminimum phase systems p 229 A93-14470
- Multiple model adaptive estimation applied to the VISTA F-16 with actuator and sensor failures [AD-A256444] p 188 A93-14608
- Applications of active adaptive noise control to jet engines [NASA-CR-192277] p 522 A93-21210
- Control of complex dynamic systems by neural networks p 758 A93-25611
- ADAPTIVE FILTERS**
- A new aircraft integrated positioning and communication system based on satellite p 150 A93-14236
- Some limitations on the effectiveness of airborne adaptive radar p 501 A93-29596
- Preliminary experiments on active control of fan noise from a turbofan engine p 759 A93-34957
- Adaptive clutter suppression for airborne array radars using clutter subspace approximation p 883 A93-43411
- Adaptive array processing for airborne radar p 883 A93-43412
- Adaptive Cartesian grid methods for representing geometry in inviscid compressible flow [AIAA PAPER 93-3385] p 955 A93-45076
- Adaptive filtering of Doppler velocimeter errors due to the characteristics of the reflecting surface p 992 A93-45650
- ADDITIVES**
- Effect of a metal deactivator fuel additive on fuel deposition in fuel atomizers at high temperature [AD-A260915] p 736 A93-25914
- Process optimization of Hexoloy SX-SiC towards improved mechanical properties [DE93-007913] p 826 A93-28564
- ADHESIVE BONDING**
- Fundamentals of composite repair [SME PAPER EM92-100] p 196 A93-14101
- PAA-core aluminum honeycomb - An end user's evaluation p 209 A93-15738
- Development of polyimide adhesives for 371 C (700 F) structural performance for aerospace bonding applications - FM 680 system p 198 A93-15757
- Ultrasonic NDE of adhesive and sealant bonded aluminum lap-splices p 407 A93-19595
- Automation of disbond detection in aircraft fuselage through thermal image processing p 407 A93-19598
- 'No VOC' water-borne corrosion resistant primers for aerospace bonding applications p 1211 A93-53419

- Evaluation of water-borne adhesive bonding primers for use on the advanced aircraft material aluminum-lithium p 1211 A93-53420
- Durability properties for adhesively bonded structural aerospace applications p 1217 A93-53515
- ADHESIVES**
- Performance of thermal adhesives in forced convection p 924 A93-30974
- ADJUSTING**
- Variable speed rotary compressor and adjustable speed drive efficiencies measured in the laboratory [DE92-040026] p 222 A93-15278
- ADVANCED VERY HIGH RESOLUTION RADIOMETER**
- Calibration results for NOAA-11 AVHRR channels 1 and 2 from congruent path aircraft observations p 1143 A93-51237
- Identification of icing water clouds by NOAA AVHRR satellite data [DLR-FB-92-11] p 434 A93-16477
- ADVECTION**
- A solution scheme for the Euler equations based on a multi-dimensional wave model [AIAA PAPER 93-0065] p 261 A93-20178
- A multi-dimensional upwind scheme for the Euler equations on structured grids p 862 A93-42430
- AERATION**
- In-situ bioventing: Two US EPA and Air Force sponsored field studies [PB93-194231] p 1035 A93-32089
- AERIAL EXPLOSIONS**
- Experimental and theoretical investigation of a research atomizer/comustion chamber configuration [ASME PAPER 92-GT-137] p 401 A93-19369
- Dual-spray airblast fuel nozzle for advanced small gas turbine combustors [AIAA PAPER 93-2336] p 1116 A93-50113
- AERIAL PHOTOGRAPHY**
- Using ultralight flight vehicles for large-scale aerial photography p 92 A93-10098
- AERIAL RECONNAISSANCE**
- Wind tunnel test techniques for UAV separation investigations [AIAA PAPER 93-0626] p 524 A93-24743
- An unmanned aircraft for dropwindsonde deployment and hurricane reconnaissance p 677 A93-34587
- Contributions to the American Meteorological Society's 26th International Conference on Radar Meteorology [AD-A263385] p 936 A93-29257
- Development of nose structure of a reconnaissance container for a supersonic jet aircraft [MBB-LME-242-S-PUB-0451] p 998 A93-31046
- AEROACOUSTICS**
- ONERA makes progress in rotor aerodynamics, aeroelasticity, and acoustics p 2 A93-11621
- Aeroacoustic environment of an advanced short takeoff and vertical landing aircraft in hover p 231 A93-14539
- Acoustic control of flow separation on a straight and a yawed wing p 125 A93-15256
- DGLR/AIAA Aeroacoustics Conference, 14th, Aachen, Germany, May 11-14, 1992, Proceedings. Vols. 1 & 2 [DGLR BERICHT 92-03] p 444 A93-19126
- Toward an integration of aerodynamics and aeroacoustics of rotors p 243 A93-19127
- Improvement of high-AOA airfoil stalling performance by internal acoustic excitation p 243 A93-19134
- Sound transmission through stiffened double-panel structures lined with elastic porous materials p 444 A93-19139
- Acoustic flight test experience with the XV-15 Tiltrotor aircraft with the Advanced Technology Blade (ATB) p 445 A93-19143
- Effects of a trailing edge flap on the aerodynamics and acoustics of rotor blade-vortex interactions p 244 A93-19144
- New design concepts for silencing aerodynamic wind tunnels p 445 A93-19147
- Development of the Boeing Low Speed Aeroacoustic Facility (LSAF) p 374 A93-19148
- The design of test-section inserts for higher speed aeroacoustic testing in the Ames 80- by 120-Foot Wind Tunnel p 374 A93-19149
- Technical prospects for computational aeroacoustics p 244 A93-19150
- Dispersion-relation-preserving schemes for computational aeroacoustics p 244 A93-19151
- Experimental investigation of tip clearance noise in axial flow machines p 445 A93-19155
- The noise from supersonic elliptic jets p 445 A93-19156
- Acoustic properties of supersonic helium/air jets at low Reynolds numbers p 446 A93-19160
- On the acoustic radiation nature of a turbulent vortex ring p 446 A93-19167
- A new technique for aerodynamic noise calculation p 447 A93-19177

- Lynx: High performance - Low noise p 322 A93-19185
- Active control of sound transmission through stiff lightweight composite fuselage constructions p 447 A93-19187
- The critical role of turbulence modeling in the prediction of supersonic jet structure for acoustic applications p 398 A93-19193
- On the scaling of small-scale jet noise to large scale p 448 A93-19195
- Control of coherent structures and aero-acoustic characteristics of subsonic and supersonic turbulent jets p 448 A93-19196
- A numerical method for the prediction of quadrupole shock wave noise p 448 A93-19201
- Helicopter noise prediction - The current status and future direction p 448 A93-19202
- Effect of nozzle design on near acoustic field of supersonic circular and rectangular jets p 448 A93-19203
- Combined noise and flow control of supersonic jets using swirl p 398 A93-19204
- A review of crack propagation under unsteady loading p 399 A93-19207
- Aeroacoustic wind tunnel testing of a counterrotating shrouded propfan-model p 449 A93-19213
- Prediction of jet mixing noise in high-speed flight p 450 A93-19216
- Unsteady pressures on exhaust nozzle interior surfaces - Empirical correlations for prediction p 244 A93-19219
- Forward rotor vortex effects on counter rotating propeller noise p 245 A93-19221
- An assessment of wake structure behind forward swept and aft swept propfans at high loading p 245 A93-19222
- Reduction of propeller noise by active noise control p 450 A93-19224
- Experimental and analytical investigations of fuselage modal characteristics and structural-acoustic coupling p 451 A93-19229
- Accuracy considerations in the computational analysis of jet noise [AIAA PAPER 93-0146] p 451 A93-19804
- Experimental study on the characteristics of the near wake of a rotating flat plate. III - Influence of the shape near the trailing edge on periodic-velocity-fluctuation phenomena p 451 A93-21727
- Takeoff/approach noise for a model counterrotation propeller with a forward-swept upstream rotor [AIAA PAPER 93-0596] p 519 A93-24782
- A third order upwind scheme for aero-acoustic applications [AIAA PAPER 93-0149] p 564 A93-25504
- AHS and Royal Aeronautical Society, Technical Specialists' Meeting on Rotorcraft Acoustics/Fluid Dynamics, Philadelphia, PA, Oct. 15-17, 1991, Proceedings p 565 A93-29401
- Sensitivity of acoustic predictions to variation of input parameters p 565 A93-29404
- Theoretical modelling of rotor noise radiation p 566 A93-29407
- A comparative analysis of XV-15 tiltrotor hover test data and WOPWOP predictions incorporating the fountain effect p 509 A93-29414
- Validation of high frequency airload calculations using full scale flight test acoustic data p 567 A93-29417
- Data acquisition and analysis on a Macintosh p 562 A93-29422
- ADDRAS - An integrated systems approach p 562 A93-29423
- Acoustics due to flow-structural interaction and its transmission through a double-panel in high-speed cruising flight [AIAA PAPER 93-1431] p 710 A93-33981
- Laser velocimetry around helicopter blades in the DNW wind tunnel of the NLR [ONERA, TP NO. 1992-143] p 831 A93-38613
- Two-dimensional laser velocimetry for the study of dual-flow jets with flight effect in the CEPRA 19 anechoic wind tunnel [ONERA, TP NO. 1992-144] p 831 A93-38614
- Identification of noise sources based on experimental amplitude-frequency noise characteristics of aircraft p 851 A93-39040
- Review of crack propagation under unsteady loading p 837 A93-39416
- Helicopter external noise prediction and reduction [ONERA, TP NO. 1993-48] p 1039 A93-47450
- An acoustic suppressor for the jet noise of a turbojet engine p 1003 A93-47510
- Acoustic experiments of two scaled-model propellers on the ground p 1172 A93-48507
- Secondary instability mechanisms in compressible axisymmetric boundary layers p 1070 A93-49009

SUBJECT INDEX

AERODYNAMIC CHARACTERISTICS

The effect of unsteady blade loading on the aerodynamics of a pusher propeller
[AIAA PAPER 93-1805] p 1173 A93-49694

An aeroacoustic stand for evaluating the efficiency of sound-absorbing structures under conditions of acoustic wave propagation in a moving medium
p 1140 A93-51762

Experimental investigation into the mechanism of discrete frequency noise (DFN) generation from a NACA 0012 blade
p 1225 A93-53194

The low frequency aerodynamics of buried nozzle systems
p 1205 A93-54244

The quiet helicopter; Proceedings of the Conference, London, United Kingdom, Mar. 17, 1992
[ISBN 1-85768-020-0] p 1262 A93-54718

Noise characteristics of helicopters with the NOTAR anti-torque system
p 1262 A93-54722

Review of helicopter noise research in Europe
p 1263 A93-54725

International Congress on Recent Developments in Air- and Structure-Borne Sound and Vibration, 2nd, Auburn Univ., AL, Mar. 4-6, 1992, Proceedings. Vols. 1-3
p 1259 A93-55851

A general introduction to aeroacoustics and atmospheric sound
p 1264 A93-55852

Response variability observed in reverberant acoustic test of a model aerospace structure
p 1264 A93-55857

Sonic boom minimization - Myth or reality?
p 1264 A93-55859

Tilt rotor hover aeroacoustics
[NASA-CR-177598] p 99 N93-10458

Comparison of flyover noise data from aircraft at high subsonic speeds with prediction
p 100 N93-10674

Nozzle installation effects on the noise from supersonic exhaust plumes
p 100 N93-10681

Prediction of jet mixing noise for high subsonic flight speeds
p 100 N93-10685

Mechanisms of sound generation in subsonic jets
p 101 N93-10688

Active control of aeroacoustic couplings by means of adaptive systems
[ECL-91-18] p 64 N93-11576

A general introduction to aeroacoustics and atmospheric sound
[NASA-CR-189717] p 102 N93-12021

Report on the final panel discussion on computational aeroacoustics
[NASA-CR-189718] p 231 N93-12986

Investigations of detail design issues for the high speed acoustic wind tunnel using a 60th scale model tunnel. Part 1: Tests with open circuits
[NASA-CR-191671] p 137 N93-14737

Investigations of detail design issues for the high speed acoustic wind tunnel using a 60th scale model tunnel. Part 2: Tests with the closed circuit
[NASA-CR-191672] p 137 N93-14738

Tiltrotor aircraft noise: A summary of the presentations and discussions at the 1991 FAA/Georgia Tech Workshop
[DOT/FAA/RD-91/23] p 232 N93-14912

Takeoff/approach noise for a model counterrotation propeller with a forward-swept upstream rotor
[NASA-TM-105979] p 362 N93-16715

Experimental analysis of the aeroacoustics of cascaded airfoils
[AD-A257945] p 420 N93-18121

Numerical simulation of a high Mach number jet flow
[NASA-TM-105985] p 551 N93-20057

Rotating rake design for unique measurement of fan-generated spinning acoustic modes
[NASA-TM-105946] p 724 N93-26161

A large hemi-anechoic enclosure for community-compatible aeroacoustic testing of aircraft propulsion systems
[NASA-TM-106015] p 760 N93-26551

In-flight near- and far-field acoustic data measured on the Propfan Test Assessment (PTA) testbed and with an adjacent aircraft
[NASA-TM-103719] p 852 N93-27058

Numerical simulation of free shear flows: Towards a predictive computational aeroacoustics capability
[NASA-CR-191015] p 781 N93-27097

User's manual for UCAP: Unified Counter-Rotation Aero-Acoustics Program
[NASA-CR-191034] p 852 N93-27148

Some aspects of the aeroacoustics of high-speed jets
[NASA-CR-191458] p 843 N93-28975

Contribution to the study of the interaction between acoustic waves and coherent structures induced by a prismatic cylinder in a rectangular cavity
[ONERA-NT-1990-10] p 918 N93-30203

Control of jet noise
[NASA-CR-193552] p 1040 N93-32221

AEROASSIST

Near wake structure for a generic ASTV configuration
[AIAA PAPER 93-0271] p 268 A93-21103

Computational flow predictions for hypersonic drag devices
p 777 A93-39257

Matched asymptotic expansion of the Hamilton-Jacobi-Bellman equation for aeroassisted plane-change maneuvers
[AIAA PAPER 93-3752] p 1143 A93-51348

Self-tuning guidance applied to aeroassisted plane change problems
[AIAA PAPER 93-3791] p 1143 A93-51386

Hypersonic lateral and directional stability characteristics of aeroassist flight experiment configuration in air and CF4
[NASA-TM-4435] p 875 N93-29166

AEROBRAKING

A convective and radiative heat transfer analysis for the FIRE II forebody
[AIAA PAPER 93-3194] p 1021 A93-44231

Comparisons between DSMC and the Navier-Stokes equations for reentry flows
[AIAA PAPER 93-2810] p 964 A93-46549

Recent advances in computational analysis of hypersonic vehicles
p 1179 A93-53364

Determination of heat transfer to flow in a duct with a pseudodiscontinuity
p 1179 A93-53365

AERODYNAMIC BALANCE

Comprehensive analysis of bearingless rotors - Model development and experimental correlation of modes, response, trim and stability
[AIAA PAPER 93-0624] p 504 A93-24741

Experimental analysis of rotary derivatives on a modern aircraft configuration
[AIAA PAPER 93-3514] p 985 A93-47278

Determination of the aerodynamic balance efficiency of aircraft
p 1130 A93-48903

A new and working automatic calibration machine for wind tunnel internal force balances
[AIAA PAPER 93-2467] p 1138 A93-50214

Pitch control trimming system for canard design aircraft
[CA-PATENT-APPL-SN-2013236] p 63 N93-10374

Arguments concerning wind tunnel test studies of the trim characteristics of objects with small asymmetries
[AD-A254111] p 19 N93-10858

Trim analysis by shooting and finite elements and Floquet eigenanalysis by QR and subspace iterations in helicopter dynamics
p 163 N93-13914

An integrated finite-state model for rotor deformation, nonlinear airloads, inflow, and trim
p 715 N93-25538

AERODYNAMIC BRAKES

Computational flow predictions for hypersonic drag devices
p 777 A93-39257

AERODYNAMIC CHARACTERISTICS

A study of the possibility of the parallel execution of a program for calculating the aerodynamic characteristics of flight vehicles using an improved panel method
p 95 A93-10045

Regimes of supersonic flow past the windward side of V-shaped wings
p 5 A93-10144

Subsonic high-lift flight research on the NASA Transport System Research Vehicle (TSRV)
[AIAA PAPER 92-4103] p 38 A93-11275

Research on the stability and control of soaring birds
[AIAA PAPER 92-4122] p 61 A93-11284

Transport processes in hypersonic flows
p 7 A93-11302

A low-speed aerodynamic model for harmonically oscillating aircraft configurations
p 8 A93-11500

Weighted average method for evaluating the aerodynamic properties of transition flow
p 8 A93-11872

Dynamic characteristics of an airfoil at high speed change of pitch angle
p 10 A93-12324

Numerical solution of the integral equations of the aerodynamics of porous surfaces
p 13 A93-12768

A method for calculating flow past an arbitrary airfoil profile in the presence of flow separation
p 13 A93-12807

Shock wave interference on a wing with a partition at hypersonic velocities
p 13 A93-12839

Increasing the lift-drag ratio of wings of small aspect ratio at hypersonic velocities
p 13 A93-12933

Effect of canard position on the longitudinal aerodynamic characteristics of a close-coupled canard-wing-body configuration
[AIAA PAPER 92-4632] p 14 A93-13304

Nonlinear aerodynamic parameter estimation and model structure identification
[AIAA PAPER 92-4502] p 15 A93-13308

Numerical simulation of STOL operations using thrust-vectoring
[AIAA PAPER 92-4254] p 15 A93-13342

HSCT high-lift aerodynamic technology requirements
[AIAA PAPER 92-4228] p 44 A93-13355

Aerodynamic characteristics of a next generation high-speed civil transport
[AIAA PAPER 92-4229] p 15 A93-13356

Taking the measure of aerodynamic testing
p 16 A93-13434

Navier-Stokes analysis of turbine blade heat transfer and performance
p 201 A93-13978

Aerodynamic characteristics of transport airplanes in low speed configuration
p 113 A93-14172

Accelerated method of the Euler equation solution in transonic airfoil flow problem
p 113 A93-14193

The value of a computational/experimental partnership in aerodynamic design
p 114 A93-14215

A prediction of the stalling for wings with rear separation
p 116 A93-14264

The aerodynamic and structural design of a variable camber wing (VCW)
p 117 A93-14291

Lateral aerodynamics characteristics of forebodies at high angle of attack in subsonic and transonic flows
p 118 A93-14302

Drag/thrust estimation via aircraft performance flight testing
p 156 A93-14322

A low speed wind-tunnel with extreme flow quality - Design and tests
p 190 A93-14352

A low-speed wind tunnel study of vortex interaction control techniques on a chine-forebody/delta-wing configuration
p 122 A93-14409

Concurrent processing adaptation of aeroelastic analysis of propfans
p 173 A93-14624

Subsonic separated flow past slender delta wings
p 124 A93-15109

Flow past a finite-span wing in the presence of external acoustic loading
p 127 A93-16707

Toulouse - Flight tests of the Airbus A340
p 159 A93-16859

Estimation of aerodynamic characteristics from flight test data. II - Analysis methods under in-flight wind tunnel test concept
p 191 A93-16934

Effect of real air properties on integral aerodynamic characteristics
p 242 A93-18241

Method and results of studies of flow past supersonic flight vehicles at moderate and large angles of attack
p 242 A93-18377

The use of the Polhamus and discrete vortex methods for calculating the nonlinear characteristics of delta wings and wings with a strake
p 242 A93-18379

Estimation of the external loading of airships in flight
p 366 A93-18383

Effect of the Reynolds number on the aerodynamic characteristics of a body of revolution over a wide range of angles of attack
p 242 A93-18384

Experience with boundary element methods to calculate the aerodynamic characteristics of aircraft
p 243 A93-19130

Improvement of high-AOA airfoil stalling performance by internal acoustic excitation
p 243 A93-19134

Profile losses of an annular turbine cascade in unsteady periodic flow
[ASME PAPER 92-GT-153] p 249 A93-19380

Navier-Stokes computation on a pivoting doors thrust reverser and comparison with tests
[ASME PAPER 92-GT-254] p 353 A93-19463

Investigation of the characteristics of 3-dimensional separated flow in an annular compressor blade row with large angles of attack
p 259 A93-20116

A fool-proof aerodynamic design code for turbine cascades
p 259 A93-20117

Investigation of leading edge ice accretion with cyclical pneumatic boot inflation
[AIAA PAPER 93-0007] p 306 A93-20130

An overview of the system identification procedure with applications to the X-31 drop model
[AIAA PAPER 93-0010] p 366 A93-20132

Effects of icing on the aerodynamic performance of high lift airfoils
[AIAA PAPER 93-0026] p 259 A93-20144

The aerodynamic effects of sideslip on double delta wings
[AIAA PAPER 93-0053] p 261 A93-20166

An efficient approach to optimal aerodynamic design. I - Analytic geometry and aerodynamic sensitivities
[AIAA PAPER 93-0099] p 264 A93-20204

Unsteady effects of camber on the aerodynamic characteristics of a thin aerofoil moving near the ground
p 270 A93-21719

Overview of Japanese aerospace plane
[AIAA PAPER 92-5005] p 384 A93-22282

3-D LDV measurements over a delta wing in pitch-up motion
[AIAA PAPER 93-0185] p 275 A93-22610

Expanding the waverider design space using general supersonic and hypersonic generating flows
[AIAA PAPER 93-0505] p 283 A93-23253

Stability and control of hypersonic waveriders
[AIAA PAPER 93-0508] p 370 A93-23255

- The design of optimized airfoils in subcritical flow
[AIAA PAPER 93-0532] p 285 A93-23273
- An application of artificial neural networks to experimental data approximation
[AIAA PAPER 93-0408] p 440 A93-23330
- Aerodynamic analysis of flapping wing propulsion
[AIAA PAPER 93-0484] p 286 A93-23386
- Aircraft take-off laboratory simulation for de/anti-icing study
p 528 A93-23840
- Optically smart surfaces for aerodynamic measurements
[AIAA PAPER 92-3895] p 539 A93-24484
- Some effects of wing and body geometry on the aerodynamic characteristics of configurations designed for high supersonic Mach numbers
[AIAA PAPER 92-4246] p 463 A93-24493
- A study of aerodynamic performance of a contra-rotating axial compressor stage
p 463 A93-24524
- Corrections to fringe distortion due to flow density gradients in optical interferometry
[AIAA PAPER 93-0631] p 539 A93-24748
- Aerodynamic performance of scramjet inlet models with a single strut
[AIAA PAPER 93-0741] p 466 A93-24831
- Experiments on a 60 deg delta wing with vortex flaps and vortex plates
p 477 A93-27482
- Helicopters - Handbook --- Russian book
[ISBN 5-203-00804-3] p 458 A93-28874
- Aerodynamic applications of pressure sensitive paint
p 549 A93-29301
- Progress in laser spectroscopic techniques for aerodynamic measurements - An overview
p 549 A93-29308
- A numerical study of advanced rotor blades
p 481 A93-29436
- Prandtl theory applied to paraglider aerodynamics
[AIAA PAPER 93-1220] p 690 A93-35169
- Computation of aeroelastic characteristics and stress-strained state of parachutes
[AIAA PAPER 93-1237] p 744 A93-35178
- AHS, Annual Forum, 48th, Washington, June 3-5, 1992, Proceedings. Vols. 1 & 2
p 763 A93-35901
- Design of the variable pitch fan for the McDonnell Douglas MD 520N helicopter equipped with the NOTAR system
p 794 A93-35908
- Effects of blowing on delta wing vortices during dynamic pitching
p 768 A93-37384
- Comment on 'Equation decoupling - A new approach to the aerodynamic identification of unstable aircraft'
p 818 A93-37406
- The strake - A simple means for directional control improvement
p 802 A93-37997
- F-16 Digital Flight Control System improvements
p 818 A93-38843
- X-29 vortex flow control tests
p 804 A93-38846
- Aerodynamic resistance of three-dimensional bodies with a starlike cross section at supersonic velocities, and problems of its calculation
p 774 A93-39116
- Aerodynamic questions related to the safety and cost-effective utilization of airships --- Russian book
p 818 A93-39125
- Hypersonic limiting flows of a relaxing gas with pressure changes in the main approximation
p 776 A93-39135
- Effect of the thermodynamic air model on the aerodynamic characteristics of profiles with bends
p 776 A93-39136
- Calculation of the effect of flow concavity in a hypersonic nozzle on the aerodynamics of a flight vehicle model
p 776 A93-39142
- An aerodynamic model for flapping-wing flight
p 858 A93-40470
- Toward the second-generation supersonic transport
[ONERA, TP NO. 1993-26] p 890 A93-41038
- Aerodynamic investigation with focusing schlieren in a cryogenic wind tunnel
[AIAA PAPER 93-3485] p 910 A93-41059
- Inverse simulation of large-amplitude aircraft maneuvers
p 906 A93-41893
- Current methods of selecting the configurations and parameters of flight vehicles
p 891 A93-42369
- Comparison of numerical methods in transonic aerodynamics
p 864 A93-42446
- Three-dimensional vortex method for parachutes
p 872 A93-42874
- The development of an efficient ornithopter wing
p 873 A93-43685
- Efficient free wake calculations using analytical/numerical matching
p 874 A93-43780
- Air dissociation effects on aerodynamic characteristics of an aerospace plane
p 959 A93-45149
- Leading-edge transition and relaminarization phenomena on a subsonic high-lift system
[AIAA PAPER 93-3140] p 959 A93-45154
- Effects of nozzle contour on the aerodynamic characteristics of underexpanded annular impinging jets
p 1024 A93-45563
- Problems in the aerodynamics, strength, and flight operations of aircraft
p 947 A93-45659
- Determination of the takeoff and landing characteristics of aircraft by using a conditional polar
p 1007 A93-45662
- Optimization of the blade angle of the AV-2 propeller for improving the flight performance characteristics of An-2 aircraft
p 996 A93-45663
- A strategy for the optimal design of nozzle contours
[AIAA PAPER 93-2720] p 962 A93-46476
- Navier-Stokes simulations of the Shuttle Orbiter aerodynamic characteristics with emphasis on pitch trim and bodyflap
[AIAA PAPER 93-2814] p 965 A93-46552
- High speed propeller acoustics and aerodynamics - A boundary element approach
p 967 A93-46804
- Comparative wind tunnel tests at high Reynolds numbers of NACA 64 621 airfoils with two alleron configurations
p 967 A93-46823
- Low-speed wind tunnel test results of the Canard Rotor/Wing concept
[AIAA PAPER 93-3412] p 975 A93-47209
- The effect of a high thrust pusher propeller on the flow over a straight wing
[AIAA PAPER 93-3436] p 978 A93-47228
- Aerodynamic characteristics of a delta wing with a body-hinged leading-edge extension
[AIAA PAPER 93-3446] p 978 A93-47233
- Wind-tunnel tests of an inclined cylinder having helical grooves
[AIAA PAPER 93-3456] p 979 A93-47239
- Free-spin damping measurement techniques
[AIAA PAPER 93-3457] p 1014 A93-47240
- Development of an innovative natural laminar flow wing concept for high-speed civil transports
[AIAA PAPER 93-3466] p 980 A93-47247
- On the modelling of separated flows about airfoils
[AIAA PAPER 93-3479] p 981 A93-47257
- Curvature and leading edge sweep back effects on grid fin aerodynamic characteristics
[AIAA PAPER 93-3480] p 981 A93-47258
- Application of computational fluid dynamics in transonic aerodynamic design
[AIAA PAPER 93-3481] p 982 A93-47259
- Aerodynamic characteristics of the MMPT ATD vehicle at high angles of attack
[AIAA PAPER 93-3493] p 982 A93-47265
- A 3D Navier-Stokes analysis of a generic ground vehicle shape
[AIAA PAPER 93-3521] p 985 A93-47283
- Aerodynamic flow simulation using a pressure-based method and a two-equation turbulence model
[AIAA PAPER 93-2902] p 1147 A93-48111
- A viscous flow based membrane wing model
[AIAA PAPER 93-2955] p 1047 A93-48149
- Behaviour of the Johnson-King turbulence model in axisymmetric supersonic flows
[AIAA PAPER 93-3032] p 1056 A93-48214
- Design efficiency evaluation for transonic airfoil optimization - A case for Navier-Stokes design
[AIAA PAPER 93-3112] p 1062 A93-48282
- Shape optimization for aerodynamic efficiency and low observability
[AIAA PAPER 93-3115] p 1062 A93-48285
- Identification of a full subsonic envelope nonlinear aerodynamic model of the F-14 aircraft
[AIAA PAPER 93-3634] p 1065 A93-48319
- On the use of back propagation with feed-forward neural networks for the aerodynamic estimation problem
[AIAA PAPER 93-3638] p 1165 A93-48323
- Acoustic experiments of two scaled-model propellers on the ground
p 1172 A93-48507
- Numerical analysis of aerodynamic losses in film-cooled vane cascade
p 1066 A93-48517
- Aerodynamic phenomena in high pulse repetition rate XeCl laser
p 1150 A93-48806
- An experimental study of the thrust and aerodynamic characteristics of an operating ramjet engine in a blowdown wind tunnel
p 1107 A93-48828
- Determination of the shape of a wing profile in boundary layer flow with a given velocity diagram
p 1067 A93-48844
- Aerodynamic characteristics and static stability margin of conical star-shaped bodies at supersonic velocities
p 1067 A93-48848
- Problems in the aerodynamics of flight vehicles and their parts
p 1068 A93-48901
- Aerodynamic characteristics of a sweptforward-wing aircraft model in unsteady motion at large angles of attack in subsonic flow
p 1068 A93-48902
- A study of the effect of the shape of a parasail on its lift-drag ratio
p 1069 A93-48913
- Approximate method for the aerodynamic design of flight vehicles for high supersonic flight speeds
p 1069 A93-48966
- A method for calculating the aerodynamic and mass characteristics of coaxial rotors with rigid blade fastening (the ABC system)
p 1071 A93-49323
- Hypersonic aerodynamic characteristics for Langley Test Technique Demonstrator
[AIAA PAPER 93-3443] p 1072 A93-49516
- Introduction to the physical aspects of hypersonic aerodynamics
p 1072 A93-49522
- Experimental evaluation of a cooled radial-inflow turbine
[AIAA PAPER 93-1795] p 1110 A93-49685
- Unsteady aerodynamic flow phenomena in a transonic compressor stage
[AIAA PAPER 93-1868] p 1075 A93-49743
- Integrated CFD modeling of gas turbine combustors
[AIAA PAPER 93-2196] p 1115 A93-50008
- High Reynolds number and turbulence effects on aerodynamics and heat transfer in a turbine cascade
[AIAA PAPER 93-2252] p 1155 A93-50050
- High speed test results of subsonic, turbobfan scarf inlets
[AIAA PAPER 93-2302] p 1082 A93-50087
- Experimental studies of aerodynamic performances of hypersonic scramjet in impulse hot-shot tunnel
[AIAA PAPER 93-2446] p 1120 A93-50198
- IHPET exhaust nozzle technology demonstrator --- integrated high performance turbine energy technology
[AIAA PAPER 93-2569] p 1121 A93-50287
- Aerodynamics design of convergent-divergent nozzles
[AIAA PAPER 93-2574] p 1085 A93-50290
- Numerical simulations of flows in centrifugal turbomachinery
[AIAA PAPER 93-2578] p 1085 A93-50293
- X-29 high-angle-of-attack flight testing
p 1101 A93-50487
- New derivation of relationship between Mach angle and Mach number
p 1086 A93-51190
- The influence of swirl generator characteristics on flow and combustion in turbulent diffusion flames
p 1159 A93-51632
- Optimal wing shapes in a hypersonic nonequilibrium flow
p 1088 A93-51770
- Numerical optimization methods for variational inverse boundary value problems of aerodynamics
p 1088 A93-51771
- Modeling the flow around a body via the solution of the relaxation kinetic equation
p 1089 A93-51868
- Approximate calculation of the aerodynamic characteristics of simple bodies in hypersonic rarefied-gas flow
p 1090 A93-51869
- Calculation of the aerodynamic characteristics of bodies with meshlike surfaces in hypersonic rarefied-gas flow
p 1090 A93-51870
- Certain improved algorithms for calculating the aerodynamic characteristics of flight vehicles in free-molecular flow
p 1090 A93-51872
- Effect of Reynolds number on the aerodynamic characteristics of a semicone with a wing in the case of hypersonic flow velocities
p 1090 A93-51878
- Problems in the aerodynamics of flight vehicles and their components
p 1091 A93-51901
- A finite difference study of the aerodynamic characteristics of wing profiles at transonic velocities
p 1091 A93-51903
- A study of the aerodynamics of a wing with end slots
p 1092 A93-51907
- A study of air intake parameters on the aerodynamic characteristics of a parasail
p 1092 A93-51908
- Aerodynamic characteristics of airship models of different shapes
p 1092 A93-51909
- Determination of the aerodynamic characteristics of thin bodies of revolution with an arbitrary number of cantilever surfaces in inhomogeneous flow
p 1092 A93-51911
- Numerical simulation of unsteady flow induced by a flat plate moving near ground
p 1094 A93-52432
- Experimental study on the aerodynamic effects of a forward-sweep angle
p 1094 A93-52434
- Flight update of aerodynamic math model
[AIAA PAPER 93-3596] p 1224 A93-52687
- Stabilization of the dynamic characteristics of the two-channel automatic control system of aircraft
p 1205 A93-52941
- Identification of the phase characteristics and wind-induced perturbations of an aircraft from flight test results
p 1206 A93-52943
- Effect of boundary layer suction on the thrust and aerodynamic efficiency of a hypersonic flight vehicle
p 1176 A93-52959
- Aerodynamic characteristics of conical triangular-planform wings of low aspect ratio in subsonic stalled flow
p 1180 A93-53574
- Unsteady aerodynamic characteristics of three rectangular wings of different aspect ratios
p 1180 A93-53575
- Aerodynamic characteristics of the HL-20
p 1181 A93-53736

SUBJECT INDEX

AERODYNAMIC CHARACTERISTICS

- Some measurements of stall in an axial impeller
[ISABE 93-7008] p 1183 A93-53984
- Design of high-load aviation turbomachines using modern 3D computational methods
[ISABE 93-7032] p 1196 A93-54008
- Starting characteristics of scramjet inlets
[ISABE 93-7105] p 1203 A93-54081
- Off-design performance of scramjet nozzles
[ISABE 93-7108] p 1203 A93-54084
- Aerodynamics of turbine blades with trailing-edge damage - Measurements and computations
[ISABE 93-7130] p 1189 A93-54105
- Avionic systems in support of covert helicopter operations
p 1193 A93-54294
- Estimation of aerodynamic characteristics from flight-test data. IV - Principal component analysis and perpendicular error method
p 1241 A93-54551
- Estimation of aerodynamic characteristics from flight-test data. V - Effects of gust and its time lag
p 1230 A93-54560
- The effect of outboard leading-edge bluntness of double-delta wing on its aerodynamic characteristics
p 1230 A93-54589
- Vectoring jet effects on the flow and aerodynamic behaviors of fighter model
p 1241 A93-54590
- AIAA Lighter-Than-Air Systems Technology Conference, 10th, Scottsdale, AZ, Sept. 14-16, 1993, Technical Papers
p 1229 A93-54601
- Airship applications of modern flight test techniques
[AIAA PAPER 93-4035] p 1242 A93-54606
- Aerodynamics of the TCOM 71M aerostat
[AIAA PAPER 93-4036] p 1231 A93-54607
- Aerodynamic characteristics of a semibuoyant station in the shape of a torus
[AIAA PAPER 93-4034] p 1231 A93-54615
- Worst-case wind modeling and its influence on capturing of aircraft penetration trajectory
p 1248 A93-54857
- Equations of the steady motion of aircraft in spin and spiral dive
p 1248 A93-54969
- Steady-state supersonic flow of a vibrationally excited gas past a slender body of revolution at a small angle of attack
p 1233 A93-55014
- Effect of blade leaning on the development of passage vortices and losses in the passage of turbine cascade with a great turning angle
p 1236 A93-55397
- Vibration isolation of aviation power plants taking into account real dynamic characteristics of engine and aircraft
p 1244 A93-55863
- Thermodynamic aspects of model testing in cryogenic wind tunnels
p 1251 A93-56222
- The integration of geometric modeling into an inverse design method and application of a PC-based inverse design method and comparison with test results
p 81 N93-10058
- Forced unsteady separated flows on a 45 degree delta wing
p 82 N93-10305
- Wind tunnel spin data reduction to obtain aerodynamic spin damping coefficients by using nonlinear equation of motion
[AD-A253880] p 19 N93-10811
- Effect of planform and body on supersonic aerodynamics of multibody configurations
[NASA-TP-3212] p 19 N93-10824
- Development of nonlinear aerodynamic models for unsteady responses
p 19 N93-10845
- Flight test results from a supercritical mission adaptive wing with smooth variable camber
[NASA-TM-4415] p 49 N93-11863
- Numerical study of advanced rotor blades
p 23 N93-11899
- Measured data for the Sandia 34-meter vertical axis wind turbine
[DE92-019807] p 94 N93-12075
- An experimental investigation of the flow in a diffusing S-duct
[NASA-TM-105809] p 60 N93-12077
- Modeling and model simplification of aeroelastic vehicles: An overview
[NASA-TM-107691] p 64 N93-12216
- An approach to constrained aerodynamic design with application to airfoils
p 24 N93-12321
- A summary of the forebody high-angle-of-attack aerodynamics research on the F-18 and the X-29A aircraft
[NASA-TM-104261] p 25 N93-12353
- Wind tunnel investigation of a twin-engine jet transport semi-span model with upper surface blown jet flap
[NAL-TR-1134] p 26 N93-12503
- X-29 linear aerodynamic perturbation model
[AD-A254810] p 160 N93-12752
- Determination of the stability and control derivatives of the F/A-18 HARV from flight data using the maximum likelihood method
[NASA-CR-191216] p 186 N93-12903
- Test techniques for engine/airframe integration
p 213 N93-13200
- Aerodynamic analysis of slipstream/wing/nacelle interference for preliminary design of aircraft configurations
p 130 N93-13205
- The jet behaviour of an actual high-bypass engine as determined by LDA-measurements in ground tests
p 175 N93-13218
- AGARD WG13 aerodynamics of high speed air intakes: Assessment of CFD results
p 215 N93-13220
- Survey on techniques used in aerodynamic nozzle/airframe integration
p 161 N93-13224
- Effects of forebody strakes and Mach number on overall aerodynamic characteristics of configuration with 55 deg cropped delta wing
[NASA-TP-3253] p 131 N93-13353
- High-speed aerodynamics of upper surface blowing aircraft configurations
p 132 N93-13729
- A laboratory investigation of raindrop oscillations
p 224 N93-13790
- The Application of CFD to rotary wing flow problems
[NASA-TM-102803] p 139 N93-15483
- Special publication of National Aerospace Laboratory [DE93-716195] p 239 N93-15949
- Modeling and control study of the NASA 0.3-meter transonic cryogenic tunnel for use with sulfur hexafluoride medium
[NASA-CR-189737] p 418 N93-16379
- Drag due to gaps round undeflected trailing-edge controls and flaps at subsonic speeds
[ESDU-92039] p 290 N93-16634
- Interferometric reconstruction of three-dimensional high-speed aerodynamic flows
p 291 N93-16765
- Prediction of the performances in combustion of ramjets and stato-rockets by isothermal experiments and modeling
p 363 N93-17622
- Flowfield computations over the Space Shuttle orbiter with a proposed canard at a Mach number of 5.8 and 50 deg angle of attack
[AD-A258058] p 293 N93-17756
- Aerodynamic design and analysis of fans using 3D computational codes
[DS-2140] p 294 N93-17880
- Beyond the frequency limits of time-linearized methods
[NLR-TP-91216-U] p 295 N93-17929
- Operational and research aspects of a radio-controlled model flight test program
[NASA-TM-104266] p 339 N93-18616
- Investigation of advanced counterrotation blade configuration concepts for high speed turboprop systems. Task 4: Advanced fan section aerodynamic analysis computer program user's manual
[NASA-CR-187127] p 364 N93-18702
- Stall in axial flow aero engine compressors
p 422 N93-18723
- A study of stall in a low hub/tip ratio fan
p 423 N93-18729
- Numerical investigation of performance degradation of wings and rotors due to icing
[NASA-CR-192233] p 339 N93-18783
- System identification for X-31A project support: Lessons learned so far
p 512 N93-19914
- Rarefied-flow Shuttle aerodynamics model
[NASA-TM-107698] p 458 N93-19976
- Application of a flush airdata sensing system to a wing leading edge (LE-FADS)
[NASA-TM-104267] p 518 N93-20163
- Advanced adaptive computational methods for Navier-Stokes simulations in rotorcraft aerodynamics
[NASA-CR-192282] p 483 N93-20256
- Methodology for sensitivity analysis, approximate analysis, and design optimization in CFD for multidisciplinary applications
[NASA-CR-192172] p 552 N93-20297
- Investigation of advanced counterrotation blade configuration concepts for high speed turboprop systems. Task 5: Unsteady counterrotation ducted propfan analysis. Computer program user's manual
[NASA-CR-187125] p 521 N93-20583
- Experimental and analytical investigation of dynamic characteristics of extension-twist-coupled composite tubular spars
[NASA-TP-3225] p 553 N93-20585
- Investigation of advanced counterrotation blade configuration concepts for high speed turboprop systems. Task 5: Unsteady counterrotation ducted propfan analysis
[NASA-CR-187126] p 521 N93-20773
- The aerodynamic performance of laser drilled sheets
[AERO-REPT-9204] p 484 N93-20806
- Program of research in flight dynamics in the JIAFS at NASA-Langley Research Center
[NASA-CR-191885] p 484 N93-21562
- Structural Tailoring of Advanced Turboprops (STAT). Theoretical manual
[NASA-CR-191017] p 556 N93-22005
- Aerodynamic design and synthesis of the oblique flying wing supersonic transport
p 713 N93-24768
- Computational study of the aerodynamics and control by blowing of asymmetric vortical flows over delta wings
p 693 N93-24772
- Grid sensitivity for aerodynamic optimization and flow analysis
[NASA-CR-192980] p 694 N93-25117
- Integrated aerodynamic-structural wing design optimization
p 714 N93-25279
- Computation of transonic flow over a porous surface projectile
p 696 N93-25409
- Structural and aerodynamic optimization of joined-wing aircraft
p 715 N93-25526
- Tangential fuselage blowing on an ogive cylinder
p 697 N93-25545
- Structural dynamic analysis of bearingless rotor blade
p 717 N93-25719
- Experimental study of the effect of helical grooves on an infinite cylinder
[AD-A260890] p 751 N93-25912
- Jet-induced ground effects on a parametric flat-plate model in hover
[NASA-TM-104001] p 700 N93-26099
- Aerodynamic analysis of hypersonic waverider aircraft
[NASA-CR-192981] p 780 N93-27093
- Experimental investigation of turbine disk cavity aerodynamics and heat transfer
[NASA-CR-193831] p 812 N93-27115
- An aerodynamic model for one and two degree of freedom wing rock of slender delta wings
[NASA-CR-193130] p 781 N93-27150
- Analysis of wind-tunnel data for elliptic cross-sectioned forebodies at Mach numbers 0.4 to 5.0
p 782 N93-27221
- Aerodynamic forces on maglev vehicles
[PB93-154813] p 782 N93-27413
- Recent progress in the analysis of iced airfoils and wings
p 784 N93-27441
- Some recent applications of Navier-Stokes codes to rotorcraft
p 786 N93-27452
- Dynamic System Coupler Program (DYSCO 4.1). Volume 1: Theoretical manual
[AD-B131156L] p 848 N93-27531
- Dynamic System Coupler Program (DYSCO 4.1). Volume 2: User's manual
[AD-B131157L] p 848 N93-27589
- Dynamic System Coupler Program (DYSCO 4.1). Volume 3: User's manual supplement
[AD-B131158L] p 848 N93-27590
- Effect of canard wing positions on aerodynamic characteristics of swept-forward wing
[AD-A262373] p 789 N93-28493
- International aviation (Selected articles)
[AD-A262566] p 765 N93-28576
- Experimental evaluation of a cooled radial-inflow turbine
[NASA-TM-106230] p 816 N93-28697
- An integrated optimum design approach for high speed prop-rotors including acoustic constraints
[NASA-CR-193222] p 893 N93-29153
- High Reynolds number and turbulence effects on aerodynamics and heat transfer in a turbine cascade
[NASA-TM-106187] p 930 N93-29157
- The application of concentric vortex simulation to calculating the aerodynamic characteristics of bodies of revolution at high angles of attack
[AD-A263879] p 876 N93-29919
- Heat transfer and aerodynamics of a 3D design nozzle guide vane tested in the Pyestock Isentropic Light Piston Facility
p 901 N93-29928
- Experimental study of heat transfer close to a plane wall heated in the presence of multiple injections (subsonic flow)
p 901 N93-29931
- The aerodynamic effect of coolant ejection in the leading edge region of a film-cooled turbine blade
p 904 N93-29958
- A computational model that couples aerodynamic and structural dynamic behavior of parachutes during the opening process
[AD-A264115] p 877 N93-30119
- Low-speed wind tunnel study of the direct side-force characteristics of a joined-wing airplane with an upper fin
[DE93-767966] p 988 N93-31189
- Definition of an airfoil family for the EUROFAR rotor
[DLR-FB-92-04] p 998 N93-31197
- Three-dimensional flow calculations inside SSME GGGT first stage blade rows
p 1017 N93-31585
- Localization of aeroelastic modes in mistuned high-energy turbines
p 1032 N93-31586
- Reynolds number influences in aeronautics
[NASA-TM-107730] p 989 N93-31732

Supersonic aerodynamic characteristics of an advanced F-16 derivative aircraft configuration [NASA-TP-3355] p 989 N93-31733

Development of a method to predict transonic limit cycle oscillation characteristics of fighter aircraft [NLR-TP-91359-U] p 999 N93-32338

Panel methods for aerodynamic analysis and design [NLR-TP-91404-U] p 990 N93-32357

AERODYNAMIC COEFFICIENTS

A method for determining the aerodynamic coefficients of asymmetric bodies with allowance for nonlinear influence factors of the body shape p 5 A93-10142

Probing questions for aerodynamic testing p 80 A93-13437

Flutter of grouped turbine blades [ASME PAPER 92-GT-227] p 404 A93-19444

Flow around two circular cylinders by the random-vortex method p 271 A93-21925

Application of structured singular value synthesis to a fighter aircraft p 368 A93-22865

Experimental and nonlinear vortex lattice method results for various wing-canard configurations p 479 A93-28607

Nonplanar Doublet-Point method for supersonic unsteady aerodynamics [AIAA PAPER 93-1588] p 682 A93-34120

Parafoil steady turn response to control input [AIAA PAPER 93-1241] p 728 A93-35180

Study of soft-in-torsion blades - ROSOH operation [ONERA, TP NO. 1992-124] p 803 A93-38598

Milisecond aerodynamic force measurement with side-jet model in the ISL shock tunnel p 822 A93-39414

Experiments on the heat transfer and on the aerodynamic coefficients of a delta wing in rarefied hypersonic flows p 870 A93-42638

Aerodynamics of Shuttle Orbiter at high altitudes [AIAA PAPER 93-2815] p 965 A93-46553

Unsteady ground effects on aerodynamic coefficients of finite wings with camber [AIAA PAPER 93-3423] p 976 A93-47218

Grid and aerodynamic sensitivity analyses of airplane components [AIAA PAPER 93-3475] p 981 A93-47254

Flowfield measurements about a multi-element airfoil at high Reynolds numbers [AIAA PAPER 93-3137] p 1064 A93-48300

Nonlinear aerodynamic modeling using multivariate orthogonal functions [AIAA PAPER 93-3636] p 1065 A93-48321

Estimation of aerodynamic coefficients using neural networks [AIAA PAPER 93-3639] p 1165 A93-48324

Determination of the aerodynamic balance efficiency of aircraft p 1130 A93-48903

Application of structured singular value synthesis to a fighter aircraft p 1130 A93-49594

Investigation of supersonic shaped nozzles in a low-pressure wind tunnel p 1091 A93-51881

Flight update of aerodynamic math model [AIAA PAPER 93-3596] p 1224 A93-52687

Calculation of real-gas effects on airfoil aerodynamic characteristics p 1229 A93-54477

Numerical minimization of the moment coefficient of a supercritical airfoil section p 1238 A93-56214

Determination of the transonic flow field around an airfoil section for a given lift force coefficient p 1239 A93-56215

Interaction of compressible vortices with a rigid plate p 1239 A93-56219

A method of testing two-dimensional airfoils [AD-A253210] p 17 N93-10375

Harmonic analysis of the aerodynamic forces on a Darnieus rotor p 18 N93-10551

Wind tunnel spin data reduction to obtain aerodynamic spin damping coefficients by using nonlinear equation of motion [AD-A253880] p 19 N93-10811

Development of nonlinear aerodynamic models for unsteady responses p 19 N93-10845

Arguments concerning wind tunnel test studies of the trim characteristics of objects with small asymmetries [AD-A254111] p 19 N93-10858

Lift coefficient of a randomly oscillating hydroplane [DRA/MAR-TM(MTH)-91320] p 21 N93-11377

A wall interference assessment/correction system [NASA-CR-190617] p 68 N93-11910

An experimental study of the relationship between forces and moments and vortex breakdown on a pitching delta wing p 49 N93-12206

Program for calculation of aileron rolling moment and yawing moment coefficients at subsonic speeds [ESDU-88040] p 136 N93-14514

Maximum lift of wings with leading-edge devices and trailing-edge flaps deployed [ESDU-92031] p 290 N93-16522

An experimental investigation of a finite circulation control wing [AD-A259044] p 340 N93-18896

Shock-dependent, optimum thrust wings in supersonic flow p 483 N93-20169

Aerodynamic foundations for use of unsteady aerodynamic effects in flight control p 695 N93-25274

Experimental and computational ice shapes and resulting drag increase for a NACA 0012 airfoil p 784 N93-27440

Hypersonic lateral and directional stability characteristics of aerassist flight experiment configuration in air and CF4 [NASA-TM-4435] p 875 N93-29166

AERODYNAMIC CONFIGURATIONS

Numerical simulations of high-speed flows about waveriders with sharp leading edges p 9 A93-12007

Integrated aerodynamics and control system design for tailless aircraft [AIAA PAPER 92-4604] p 42 A93-13284

Nonlinear aerodynamic parameter estimation and model structure identification [AIAA PAPER 92-4502] p 15 A93-13308

Structural and aerodynamic considerations for an oblique all-wing aircraft [AIAA PAPER 92-4220] p 43 A93-13336

Using aerodynamic analysis codes to assist in structural design and optimization of ducted rotor/wing blades [AIAA PAPER 92-4280] p 44 A93-13353

Improving the lift to drag characteristics of low boom configuration [AIAA PAPER 92-4218] p 16 A93-13380

Multi-point design of transonic airfoils using optimization [AIAA PAPER 92-4225] p 16 A93-13382

The influence of the fuselage on high alpha vortical flows and the subsequent effect on fin buffeting p 116 A93-14263

On the configuration buffet of a transport aircraft p 117 A93-14298

A conformal-integral method for solving the direct problem in turbomachine cascade aerodynamics p 125 A93-15217

Aerodynamic optimization of an HSCT configuration using variable-complexity modeling [AIAA PAPER 93-0101] p 322 A93-19806

Aerodynamic degradation due to distributed roughness on high lift configuration [AIAA PAPER 93-0028] p 260 A93-20146

Integrated aerodynamic-structural-control wing design [AIAA PAPER 92-4694] p 324 A93-20307

Improving the efficiency of aerodynamic shape optimization procedures [AIAA PAPER 92-4697] p 264 A93-20309

Aerodynamic shape optimization via sensitivity analysis on decomposed computational domains [AIAA PAPER 92-4698] p 265 A93-20310

Exact solution sensitivities for boundary element aerodynamics codes [AIAA PAPER 92-4745] p 436 A93-20343

Massively parallel aerodynamic shape optimization p 266 A93-20729

Supersonic dynamic stability characteristics of the test technique demonstrator NASP configuration [AIAA PAPER 92-5009] p 367 A93-22285

The design of optimized airfoils in subcritical flow [AIAA PAPER 93-0532] p 285 A93-23273

Waverider design for generalized shock geometries [AIAA PAPER 93-0774] p 467 A93-24858

Interaction strength and model geometry effects on the structure of crossing-shock wave/turbulent boundary-layer interactions [AIAA PAPER 93-0780] p 467 A93-24862

Aerodynamic analyses for design and education [AIAA PAPER 92-2664] p 473 A93-24988

Progress in high-lift aerodynamic calculations [AIAA PAPER 93-0194] p 474 A93-25512

A hypersonic waverider research vehicle [AIAA PAPER 93-0402] p 505 A93-25522

Propulsion/airframe integration issues for waverider aircraft [AIAA PAPER 93-0506] p 505 A93-25533

Measurements of aerodynamic rotary stability derivatives using a whirling arm facility p 525 A93-28603

Tiltrotor ground noise reduction from rotor parametric changes as predicted by ROTONET p 567 A93-29415

Flutter calculations for fixed and rotating wings with state-space inflow dynamics [AIAA PAPER 93-1300] p 709 A93-33877

Aeroelastic character of a National Aerospace Plane demonstrator concept [AIAA PAPER 93-1314] p 782 A93-33890

A method of predicting quasi-steady aerodynamics for flutter analysis of high speed vehicles using steady CFD calculations [AIAA PAPER 93-1364] p 682 A93-33931

Commercial turbofan engine exhaust nozzle flow analyses p 689 A93-34489

Numerical calculation of helicopter rotor equations and comparison with experiment [ONERA, TP NO. 1992-128] p 772 A93-38602

The application of an adaptive unstructured grid method to the solution of hypersonic flows past double ellipse and double ellipsoid configurations p 868 A93-42609

Hypersonic flows over a double or simple ellipse p 868 A93-42614

Unstructured grids on NURBS surfaces — NonUniform Rational B-Splines [AIAA PAPER 93-3454] p 949 A93-44232

Mesh generation for the computation of flowfields over complex aerodynamic shapes p 995 A93-44888

The status of CFD - An Air Force perspective [AIAA PAPER 93-3293] p 1021 A93-44997

Aerodynamic shape optimization using preconditioned conjugate gradient methods [AIAA PAPER 93-3322] p 952 A93-45016

A novel development of the Ludwig tube, for extended test duration p 1011 A93-45529

Supersonic/hypersonic aerodynamic methods for aircraft design and analysis p 967 A93-46816

The determination of hybrid analytical-numerical solutions for the three-dimensional compressible boundary layer p 1029 A93-46979

Side-force control on a forebody of diamond cross-section at high angles of attack [AIAA PAPER 93-3407] p 1008 A93-47206

Unstructured grid generation using interactive three-dimensional boundary and efficient three-dimensional volume methods [AIAA PAPER 93-3452] p 1037 A93-47237

Secondary flow control on slender, sharp-edged configurations [AIAA PAPER 93-3470] p 980 A93-47250

Calculation of AGARD Wing 445.6 flutter using Navier-Stokes aerodynamics [AIAA PAPER 93-3476] p 981 A93-47255

Preliminary design estimates of high-speed streamlines on arbitrary shaped vehicles defined by quadrilateral elements [AIAA PAPER 93-3491] p 982 A93-47263

Aerodynamic characteristics of the MMPT ATD vehicle at high angles of attack [AIAA PAPER 93-3493] p 982 A93-47265

Numerical solution of the Euler equations for complex aerodynamic configurations using an edge-based finite element scheme [AIAA PAPER 93-2933] p 1046 A93-48131

The prediction of viscous nonequilibrium hypersonic flows about ablating configurations using an upwind parabolized Navier-Stokes code [AIAA PAPER 93-2998] p 1053 A93-48188

Design of axisymmetric channels with rotational flow [AIAA PAPER 93-3117] p 1062 A93-48287

Analysis of stability characteristics of a high performance aircraft [AIAA PAPER 93-3616] p 1125 A93-48303

A qualitative assessment of control effects on an advanced fighter configuration [AIAA PAPER 93-3627] p 1127 A93-48312

Base drag prediction on missile configurations [AIAA PAPER 93-3629] p 1064 A93-48314

Aircraft with single axis aerodynamically deployed wings [AIAA PAPER 93-3673] p 1129 A93-48350

Dynamic model testing of the X-31 configuration for high-angle-of-attack flight dynamics research [AIAA PAPER 93-3674] p 1129 A93-48351

Calculation of subsonic flow of a gas past an airfoil p 1068 A93-48908

Design and test of a small two stage counter-rotating turbine for rocket engine application [AIAA PAPER 93-2136] p 1142 A93-49954

Experimental studies of supersonic flow past wedges with longitudinal slots on the windward side p 1089 A93-51786

Steady state supersonic flows of a vibrationally excited gas past thin bodies p 1089 A93-51818

Three-dimensional Navier-Stokes/full-potential coupled analysis for viscous transonic flow p 1178 A93-53218

Analysis of spatial motion dynamics of a helicopter for various models of the induced velocity field p 1191 A93-53721

Experimental studies in the Aachen hypersonic shock tunnel p 1251 A93-56032

Low-speed aerodynamics of the hypersonic research configuration ELAC I p 1237 A93-56035

- Flow computation for the hypersonic configuration ELAC
I at low speeds and large incidence p 1238 A93-56036
- A European collaborative NLF nacelle flight
demonstrator [PNR-90992] p 20 N93-11113
- Artificial intelligence and CFD: Expert systems for the
design of airfoils and for grid generation [DIGE-EST-TN-016] p 48 N93-11161
- Low-speed longitudinal and lateral-directional
aerodynamic characteristics of the X-31 configuration [NASA-TM-4351] p 22 N93-11622
- A preliminary study associated with the experimental
measurement of the aero-optic characteristics of
hypersonic configurations [AD-A253792] p 24 N93-12063
- Water tunnel studies of inlet/airframe interference
phenomena p 215 N93-13216
- Application of subsonic first-order panel methods for
prediction of inlet and nozzle aerodynamic interactions with
airframe p 130 N93-13223
- Computational analysis of hypersonic flows past
elliptic-cone waveriders p 138 N93-14767
- Chemical kinetic and aerodynamic structures of
flames [AD-A256015] p 391 N93-15931
- An advanced graphics-interactive system for a
multi-block structured grid generation within an industrial
environment [ETN-92-92885] p 440 N93-16288
- Development of a computer assisted toolbox for
aerodynamic design of aircraft at subcritical conditions with
application to three-surface and canard aircraft [ISBN-90-6275-768-5] p 441 N93-16567
- The F-92 RELIANT: Air transport system design
simulation [NASA-CR-192050] p 339 N93-18386
- A simple grid generation technique for hypersonic flow
around complex configuration p 299 N93-19275
- Aerodynamic surface tip vortex attenuation system
[AD-D015606] p 483 N93-20017
- Computational analysis of hypersonic flows past
generalized cone-derived waveriders p 483 N93-20288
- A computational aerodynamic design optimization
method using sensitivity analysis p 716 N93-25552
- Computational methods for aerodynamic design of
aircraft components [NLR-TP-92072-4] p 987 N93-31148
- Review of aerodynamic design in the Netherlands
[NLR-TP-91260-U] p 999 N93-31840
- AERODYNAMIC DRAG**
- Effect of longitudinal microribbing on the drag of a body
of revolution p 5 A93-10147
- Drag and drag partition on rough surfaces p 79 A93-12460
- Effect of the drag of the front body on the restructuring
of flow between two bodies in the path of supersonic flow,
with one body located in the wake of the other p 14 A93-12973
- Hypersonic design p 156 A93-14346
- Application of laminar flow to aero engine nacelles p 128 A93-17256
- Lord Rayleigh and hydrodynamic similarity p 211 A93-17408
- Performance degradation due to hoar frost on lifting
surfaces p 305 A93-17798
- A comparison of the drag-reducing benefits of riblets
in internal and external flows p 395 A93-18054
- Constrained optimization of three-dimensional
hypersonic vehicle configurations [AIAA PAPER 93-0039] p 260 A93-20152
- The legal status of ekranoplanes p 453 A93-20900
- The effect of shock motion on entropy production [AIAA PAPER 93-0665] p 465 A93-24777
- Computational analysis of methods for reduction of
induced drag [AIAA PAPER 93-0524] p 474 A93-25536
- Application of Oswatitsch's theorem to supercritical
airfoil drag calculation p 768 A93-37399
- Aerodynamic resistance of three-dimensional bodies
with a starlike cross section at supersonic velocities, and
problems of its calculation p 774 A93-39116
- Reduction of aerodynamic skin-friction drag p 871 A93-42656
- Computation of induced drag for elliptical and
crescent-shaped wings p 958 A93-45136
- Zero-thrust glide testing for drag and propulsive
efficiency of propeller aircraft p 995 A93-45143
- Some measurements on dependence of rectangular
cylinder drag on elevation p 1025 A93-45745
- Computations of aerodynamic drag for turbulent
transonic projectiles with and without spin [AIAA PAPER 93-3416] p 975 A93-47212
- An improved far field drag calculation method for
nonlinear CFD codes [AIAA PAPER 93-3417] p 975 A93-47213
- A method for the prediction of induced drag for planar
and nonplanar wings [AIAA PAPER 93-3420] p 976 A93-47216
- Drag measurements on blunted cones and a scramjet
vehicle in hypervelocity flow [AIAA PAPER 93-2979] p 1050 A93-48172
- An experimental study of the effects of deformable tip
on the performance of fins and finite wings [AIAA PAPER 93-3000] p 1053 A93-48190
- Base drag prediction on missile configurations [AIAA PAPER 93-3629] p 1064 A93-48314
- Effects of a rear stagnation jet on the wake behind a
cylinder p 1151 A93-49026
- Surface drag instabilities in the atmospheric boundary
layer p 1163 A93-49069
- Drag characteristics of extra-thin-fin-riblets in an air flow
conduit p 1151 A93-49240
- Identification of integrated airframe-propulsion effects
on an F-15 aircraft for application to drag minimization [AIAA PAPER 93-3764] p 1101 A93-51359
- Reentry control to a drag vs. energy profile [AIAA PAPER 93-3790] p 1143 A93-51385
- The reduction of skin friction by riblets under the
influence of an adverse pressure gradient p 1218 A93-53810
- Reynolds number dependence of the drag coefficient
for laminar flow through fine-scale photoetched screens p 1218 A93-53815
- Control of lift and drag in unsteady flows [AD-A253146] p 17 N93-10340
- A method of testing two-dimensional airfoils [AD-A253210] p 17 N93-10375
- Experimental investigation of flows behind different
Large-Eddy Breakup (LEBU) devices in thick boundary
layers p 18 N93-10550
- Development of nonlinear aerodynamic models for
unsteady responses p 19 N93-10845
- Characteristics of separated flows including cavitation
effects p 84 N93-10874
- Application of laminar flow to aero engine nacelles
[PNR-90916] p 20 N93-11020
- Numerical investigations into the base drag of various
wedges using the base flow model developed by Mauri
Tanner [REPT-B-36] p 26 N93-12414
- Dynamic stall effects on hingeless rotor stability with
experimental correlation p 129 N93-13010
- Hypersonic propulsion system force accounting p 175 N93-13229
- High-speed aerodynamics of upper surface blowing
aircraft configurations p 132 N93-13729
- Quantitative-force measurements of pneumatic control
on a wing/stroke model [AD-A257343] p 289 N93-16157
- Lift and drag forces on droplets and particles in
wall-bounded shear flows [DE93-002678] p 419 N93-17761
- An experimental investigation of a finite circulation
control wing [AD-A259044] p 340 N93-18896
- Professor Wittenberg: His speciality and versatility [ISBN-90-6275-670-0] p 240 N93-19002
- Propelling force and resistance p 298 N93-19003
- Computation of H₂/air reacting flowfields in
drag-reduction external combustion [NASA-CR-191071] p 536 N93-20237
- Analysis and evaluation of an integrated laminar flow
control propulsion system [NASA-CR-192162] p 551 N93-20268
- Aerodynamic design and synthesis of the oblique flying
wing supersonic transport p 713 N93-24768
- Fundamental studies of droplet interactions in dense
sprays [AD-A261165] p 737 N93-25948
- Uniform roughness studies [WL-TR-92-3041] p 751 N93-25951
- The generation of side force by distributed suction [NASA-CR-193129] p 839 N93-27151
- Aerodynamic forces on maglev vehicles [PB93-154813] p 782 N93-27413
- Experimental and computational ice shapes and
resulting drag increase for a NACA 0012 airfoil p 784 N93-27440
- Efficient simulation of incompressible viscous flow over
multi-element airfoils p 784 N93-27443
- Reynolds and Mach number effects on multielement
airfoils p 785 N93-27446
- Quantitative three-dimensional low-speed wake
surveys p 785 N93-27447
- Modeling the effects of drop drag and breakup on fuel
sprays [AD-A263650] p 931 N93-29388
- Construction, wind tunnel testing and data analysis for
a 1/5 scale ultra-light wing model p 876 N93-29778
- Vortex shedding by blunt/bluff bodies at high Reynolds
numbers. Volume 4: Rectangles [AD-A264154] p 877 N93-30151
- AERODYNAMIC FORCES**
- Collection of works on measuring and computing
systems for research on the aerodynamics, dynamics, and
strength of flight vehicles p 75 A93-10026
- Measurement of aerodynamic forces at high
temperatures p 75 A93-10030
- An analysis of helicopter dynamic response to turbulence
using fuselage and blade element atmospheric sampling
techniques [AIAA PAPER 92-4148] p 43 A93-13314
- Taking the measure of aerodynamic testing p 16 A93-13434
- Shedding new light on gas dynamics p 80 A93-13435
- A proposal concerning the dynamic analysis method of
continuous gust design rules p 181 A93-14197
- Aeroservoelastic analysis of an aircraft model
incorporating the minimum state method for approximating
unsteady aerodynamics p 154 A93-14258
- Dynamic stability, coupling and active control of elastic
vehicles with unsteady aerodynamic forces modeling p 182 A93-14282
- Analytic continuation of Pade approximations to the
unsteady kernel functions to obtain a better understanding
of the analytic continuation of Pade approximations to
unsteady parameters in general p 117 A93-14283
- Experimental study of dynamic fluid forces and moments
for a long annular seal p 209 A93-15684
- Experimental study on the unsteady aerodynamic
response of a three dimensional cascade with oscillating
blades p 242 A93-18499
- Aeroservoelasticity in HiSAIR — High Speed Airframe
Integration Research [AIAA PAPER 92-4719] p 324 A93-20322
- On some recent advances in multidisciplinary analysis
of hypersonic vehicles [AIAA PAPER 92-5026] p 438 A93-22302
- Control of a high performance aircraft with unacceptable
zero dynamics p 369 A93-22905
- Shock-dependent, thrust wings for supersonic flow
[AIAA PAPER 93-0321] p 280 A93-23013
- Incompressible flow computation of forces and moments
on bodies of revolution at incidence [AIAA PAPER 93-0787] p 541 A93-24867
- Aerodynamic forces and moments on a dihedral swept
wing in a translation with attack and side-slip angle p 476 A93-26903
- Flowfield measurements of a two-element airfoil with
large separation p 480 A93-29307
- A method of predicting quasi-steady aerodynamics for
flutter analysis of high speed vehicles using steady CFD
calculations [AIAA PAPER 93-1364] p 682 A93-33931
- ISAC — A tool for aeroservoelastic modeling and analysis
— Interaction of Structures, Aerodynamics, and Control [AIAA PAPER 93-1421] p 726 A93-33974
- An analysis of the post-instability behaviour of a
two-dimensional airfoil with a structural nonlinearity [AIAA PAPER 93-1474] p 726 A93-34020
- Application of differential quadrature to the analysis of
static aeroelastic phenomena [AIAA PAPER 93-1505] p 711 A93-34044
- Comparison of electrostatic and aerodynamic forces
during parachute opening [AIAA PAPER 93-1210] p 689 A93-35160
- Radii effect on the translation spring constant of force
transducer beams p 829 A93-37867
- Millisecond aerodynamic force measurement with
side-jet model in the ISL shock tunnel p 822 A93-39414
- A study of the interaction between a wake vortex and
an encountering airplane [AIAA PAPER 93-3642] p 858 A93-40714
- Validation of engineering methods for predicting
hypersonic vehicle control forces and moments p 906 A93-41897
- On model for predicting blade force defect in end wall
boundary layer inside axial compressor cascade p 862 A93-42271
- Experimental density flowfields over a delta wing located
in rarefied hypersonic flows p 870 A93-42637
- Numerical experiment of the flight trajectory simulation
by fluid dynamics and flight dynamics coupling [AIAA PAPER 93-3324] p 952 A93-45018
- Static aeroelastic control of an adaptive lifting surface p 995 A93-45147
- Behavior of precipitating water drops under the influence
of electrical and aerodynamic forces p 1034 A93-45176

- The effect of Reynolds number on control of forebody asymmetry by suction and bleed
[AIAA PAPER 93-3265] p 968 A93-46831
- Two dimensional incompressible flow through a vibrating bladed disc - Theoretical model p 973 A93-46991
- Computational analysis of off-design waveriders
[AIAA PAPER 93-3488] p 982 A93-47262
- Effects of aft geometry on vortex behavior and force production by a tangential jet on a body at high alpha
[AIAA PAPER 93-2961] p 1048 A93-48155
- Effect of geometry, static stability, and mass distribution on the tumbling characteristics of generic flying-wing models
[AIAA PAPER 93-3615] p 1125 A93-48302
- Kinematics and aerodynamics of the velocity vector roll
[AIAA PAPER 93-3625] p 1126 A93-48310
- Nonlinear aerodynamic modeling using multivariate orthogonal functions
[AIAA PAPER 93-3636] p 1065 A93-48321
- Analysis on space shape and tension distribution of towed flexible cables p 1043 A93-48554
- The representation of the aerodynamic torque in simulations of a spacecraft rotary motion
p 1141 A93-48835
- Use of neural networks in control of high-alpha maneuvers p 1130 A93-49593
- Shock tunnel experiments and approximative methods on hypervelocity side-jet control effectiveness
[AIAA PAPER 93-1929] p 1077 A93-49794
- A new and working automatic calibration machine for wind tunnel internal force balances
[AIAA PAPER 93-2467] p 1138 A93-50214
- Supersonic flow past a rectangular wing of finite thickness p 1086 A93-50972
- Dynamics of hypersonic flight vehicles exhibiting significant aeroelastic and aeropropulsive interactions
[AIAA PAPER 93-3763] p 1131 A93-51358
- An aerodynamic model for the longitudinal motion of flight training devices p 1207 A93-54278
- An improved method for determining force balance calibration accuracy p 1254 A93-54369
- Consideration of mass elements of the control system in a flutter analysis p 1249 A93-56217
- Transonic aeroelastic analysis of systems with structural nonlinearities p 217 A93-13769
- Navier-Stokes calculation of transonic flow past the NTF 65-deg delta wing p 292 A93-16797
- Propelling force and resistance p 298 A93-19003
- Calculations of aerodynamic forces on a wing with thrust using BEM p 300 A93-19286
- Experimental investigation of the aerodynamics of independently rotating cylindrical shells
[AD-A258917] p 305 A93-19340
- Rarefied-flow Shuttle aerodynamics model
[NASA-TM-107698] p 458 A93-19976
- Fluid/structures interactions. Aircraft considerations p 527 A93-20628
- Development of a non-linear simulation for generic hypersonic vehicles - ASUHS1
[NASA-CR-192710] p 516 A93-22003
- Prediction of forces and moments for hypersonic flight vehicle control effectors
[NASA-CR-193033] p 728 A93-24762
- Optimal finite-thrust time-bounded direct-ascent interception p 734 A93-25272
- Aerodynamic foundations for use of unsteady aerodynamic effects in flight control p 695 A93-25274
- Helicopter forced response vibration analysis method RTVIB20
[AD-A261809] p 730 A93-26260
- Analysis of wind-tunnel data for elliptic cross-sectioned forebodies at Mach numbers 0.4 to 5.0
p 782 A93-27221
- Aerodynamic forces on maglev vehicles
[PB93-154813] p 782 A93-27413
- Vortex shedding by blunt/bluff bodies at high Reynolds numbers. Volume 4: Rectangles
[AD-A264154] p 877 A93-30151
- ### AERODYNAMIC HEAT TRANSFER
- Extreme value heat transfer problems for three-dimensional bodies moving at hypersonic velocities p 4 A93-10079
- Approximate methods for heat flows toward the surface of three-dimensional bodies p 4 A93-10080
- A study of heat transfer from a disk in a rotating cavity with axial and radial-axial flow of a liquid
p 54 A93-12812
- Hot streaks and phantom cooling in a turbine rotor passage. I - Separate effects
[ASME PAPER 92-GT-75] p 401 A93-19325
- Nonequilibrium excitation of internal molecular degrees of freedom in the shock layer during hypersonic flight
p 412 A93-21922
- On the coupled thermomechanical analysis of hypersonic flight vehicle structures
[AIAA PAPER 92-5018] p 413 A93-22294
- Computation of nonequilibrium radiating shock layers
[AIAA PAPER 93-0144] p 414 A93-22588
- Quasi-one-dimensional modelling of free-piston shock tunnels
[AIAA PAPER 93-0352] p 377 A93-23037
- Real gas effects for compressible nozzle flows
p 682 A93-33757
- Probabilistic turbine blade tip durability analysis
[AIAA PAPER 93-1383] p 719 A93-33946
- A study of the temperature of bodies in the flow-around regime in the case of surface gas injection
p 691 A93-35344
- Digital image processing applied to heat transfer measurement in hypersonic wind tunnel
[ONERA, TP NO. 1992-118] p 831 A93-38593
- Nonequilibrium heat transfer near the critical point of blunt bodies p 777 A93-39145
- Some recommendations concerning the prevention of fuel boiling in the igniters of the combustion chambers of gas turbine engines p 812 A93-39200
- Engineering method for calculating surface pressures and heating rates on vehicles with embedded shocks
p 777 A93-39255
- Experimental study of the longitudinal hypersonic corner flow field - HERMES-R&D research program, problem no. 5
p 867 A93-42602
- Leeside flow over delta wing at $M = 7.15$. Experimental results for test case 7.1.2
p 870 A93-42632
- Experiments on the heat transfer and on the aerodynamic coefficients of a delta wing in rarefied hypersonic flows p 870 A93-42638
- An investigation of aerodynamic heating to spherically blunted cones at angle of attack
[AIAA PAPER 93-2764] p 963 A93-46510
- Survey of nonequilibrium re-entry heating for entry flight conditions
[AIAA PAPER 93-3230] p 1039 A93-46682
- Heat transfer on blunt cones in nonuniform supersonic flow in the presence of gas injection from the surface
p 972 A93-46975
- Abnormal peaks of increased heat-transfer on the blunted delta wing in the hypersonic flow
[AIAA PAPER 93-3129] p 1063 A93-48294
- A study of the interaction of a nonstationary shock wave with a boundary layer on a plate in the transition regime
p 1150 A93-48850
- Numerical calculation of polars and heat transfer for supersonic three-dimensional flow past wings with allowance for radiation p 1068 A93-48905
- Supersonic flow past energy release regions
p 1069 A93-48973
- Effect of the formation of excited oxygen molecules on the kinetics of exchange reactions and the heat flux during braking in the upper layers of the atmosphere
p 1070 A93-48975
- Flow and heat transfer in a turbulent boundary layer through skewed and pitched jets p 1151 A93-49007
- Heat transfer on tip fins in hypersonic flow
p 1088 A93-51775
- Supersonic flow past a cone with heat transfer near its tip p 1089 A93-51780
- A study of turbulent flow in a viscous shock layer in the case of gas flow past oblong blunt bodies
p 1089 A93-51820
- Experimental simulation of the aerodynamic heating of bodies in a molecular region p 1090 A93-51871
- Investigation of the effect of physical processes on heat transfer to blunt bodies at low Reynolds numbers
p 1090 A93-51877
- Determination of heat transfer to flow in a duct with a pseudodiscontinuity p 1179 A93-53365
- Pressure field and drag of a single cavity with rounded and sharp edges p 1258 A93-55018
- Conjugate modeling of high-temperature nosecap and wing leading edge heat pipes p 1259 A93-55465
- Leading edge film cooling heat transfer including the effect of mainstream turbulence p 23 A93-11886
- Fluid flow and heat convection studies for actively cooled airframes
[NASA-CR-190956] p 216 A93-13406
- Increased heat transfer to elliptical leading edges due to spanwise variations in the freestream momentum: Numerical and experimental results
[NASA-TM-106150] p 838 A93-27020
- Experimental investigation of turbine disk cavity aerodynamics and heat transfer
[NASA-CR-193831] p 812 A93-27115
- The effect of orthogonal-mode rotation on forced convection in a circular-sectioned tube fitted with full circumferential transverse ribs p 932 A93-29937
- ### AERODYNAMIC HEATING
- A very efficient tool for the structural analysis of hypersonic vehicles under high temperature aspects
p 203 A93-14194
- Experimental investigation of aerothermal problems associated with hypersonic flight of HST
p 120 A93-14380
- Heat flux microsensor measurements
[AIAA PAPER 92-5038] p 413 A93-22312
- The X-15 airplane - Lessons learned
[AIAA PAPER 93-0309] p 456 A93-23005
- Overview of technical challenges of reentry analysis of radioisotope heat sources
[AIAA PAPER 93-0379] p 386 A93-23059
- Aerothermoelastic analysis of a NASP demonstrator model
[AIAA PAPER 93-1366] p 733 A93-33933
- Bending-torsion flutter of linear viscoelastic wings including structural damping
[AIAA PAPER 93-1475] p 711 A93-34021
- Methods and results of theoretical investigations for high-speed parachute systems
[AIAA PAPER 93-1227] p 690 A93-35173
- Hypersonic flutter of a curved shallow panel with aerodynamic heating
[AIAA PAPER 93-1318] p 829 A93-37428
- Digital image processing applied to heat transfer measurement in hypersonic wind tunnel
[ONERA, TP NO. 1992-118] p 831 A93-38593
- Hypersonic propulsion - Breaking the thermal barrier
p 897 A93-40437
- Infrared thermography characterization of Goertler vortex type patterns in hypersonic flows
[ONERA, TP NO. 1993-13] p 925 A93-41029
- Toward the second-generation supersonic transport
[ONERA, TP NO. 1993-26] p 890 A93-41038
- Active control of aerothermoelastic effects for a conceptual hypersonic aircraft p 1007 A93-45137
- Aerodynamic heating phenomenon in three dimensional shock wave/turbulent boundary layer interaction induced by sweptback fins in hypersonic flows
p 960 A93-45507
- Nonlinear flutter of orthotropic composite panel under aerodynamic heating p 1025 A93-45740
- A preliminary investigation of the Helmholtz resonator concept for heat flux reduction
[AIAA PAPER 93-2742] p 963 A93-46493
- An investigation of aerodynamic heating to spherically blunted cones at angle of attack
[AIAA PAPER 93-2764] p 963 A93-46510
- Aerodynamic heating in the vicinity of hypersonic, axisymmetric, shock-wave boundary-layer interactions
[AIAA PAPER 93-2766] p 963 A93-46512
- Aerodynamic heating with boundary layer transition and heat protection with mass addition on blunt body in hypersonic flows
[AIAA PAPER 93-2984] p 1051 A93-48177
- Aerothermodynamic heating due to shock wave/laminar boundary-layer interactions in high-enthalpy hypersonic flow
[AIAA PAPER 93-3135] p 1064 A93-48299
- Effect of anomalous aerodynamic heating during the descent of a parachute along a trajectory
p 1069 A93-48924
- Evaluation of decomposition kinetic coefficients for a fiber-reinforced intumescent-epoxy
[AIAA PAPER 93-1856] p 1144 A93-49734
- Experimental simulation of the aerodynamic heating of bodies in a molecular region p 1090 A93-51871
- A procedure for the thermal and strength testing of radiotransparent shells p 1209 A93-52976
- Evaluation of 2D ceramic matrix composites in aeroconvective environments p 1212 A93-53459
- Aerodynamic heating environment definition/thermal protection system selection for the HL-20
p 1181 A93-53739
- Hypersonic flow of a gas past wing with heat transfer
p 1234 A93-55030
- One type of automatically adjusted difference scheme with artificial viscosity to calculate ablated exterior shapes
[AD-A254108] p 19 A93-10856
- Active cooling from the sixties to NASP
p 49 A93-12458
- Time dependent heat transfer rates in high Reynolds number hypersonic flowfields p 216 A93-13664
- A finite element model for analysis of thermoviscoplastic behavior of hypersonic leading edge structures subject to intense aerothermal heating p 137 A93-14631
- Aerodynamic heating analysis for axisymmetric bodies in supersonic flow p 303 A93-19312
- The infrared measurement for the reentry-body-translation
[AD-A263100] p 914 A93-29134

- Ablation problems using a finite control volume technique
[DE93-008861] p 942 A93-29187
- AERODYNAMIC INTERFERENCE**
- Assessment and correction of tunnel wall interference by Navier-Stokes solutions p 116 A93-14275
- The influence of rotor and fuselage wakes on rotorcraft stability and control p 183 A93-14373
- Experimental study on the mechanism of favourable interferences of body strakes p 121 A93-14405
- Preliminary assessment of tunnel wall interference in the NDA cryogenic wind tunnel
[AIAA PAPER 93-0421] p 285 A93-23340
- Aerodynamic analysis of flapping wing propulsion
[AIAA PAPER 93-0484] p 286 A93-23386
- Numerical investigations on airfoil performance subjected to aerodynamic interference from an upstream airfoil
[AIAA PAPER 93-0639] p 463 A93-24754
- On the favorable interference in the supersonic flow p 679 A93-33713
- Adaptive wall wind tunnel with two measured interfaces - Theory and experiment p 679 A93-33717
- The influence of wall friction on sidewall interference p 680 A93-33723
- On the principle of sidewall effects on airfoil testing p 730 A93-33732
- Asymptotic methods for the prediction of transonic wind-tunnel wall interference p 730 A93-35625
- A new adaptive test section at ONERA Chalais-Meudon
[ONERA, TP NO. 1992-117] p 822 A93-38592
- Effect of the aerodynamic interference of the rotor and the fuselage on the power requirements for the horizontal flight of a helicopter p 819 A93-39179
- The adaptive wall test section for the NASA Langley 0.3-m Transonic Cryogenic Tunnel p 1013 A93-46825
- Numerical simulation of linear interference wave development in three-dimensional boundary layers p 1029 A93-46993
- Dynamic-overlapped-grid simulation of aerodynamically determined relative motion
[AIAA PAPER 93-3018] p 1055 A93-48205
- Development of an accuracy criteria for body-on-fin carryover interference
[AIAA PAPER 93-3633] p 1065 A93-48318
- Identification of actuation system and aerodynamic effects of direct-lift-control flaps p 1103 A93-52435
- Ground facility interference on aircraft configurations with separated flow p 1140 A93-52441
- Lateral aerodynamic interference between tanker and receiver in air-to-air refueling p 1136 A93-52444
- Characteristics of separated flows including cavitation effects p 84 A93-10874
- A wall interference assessment/correction system
[NASA-CR-190617] p 68 A93-11910
- Investigation of interference phenomena of modern wing-mounted high-bypass-ratio engines by the solution of the Euler-equations p 213 A93-13204
- Aerodynamic analysis of slipstream/wing/nacelle interference for preliminary design of aircraft configurations p 130 A93-13205
- Recent developments in low-speed TPS-testing for engine integration drag and installed thrust reverser simulation p 160 A93-13207
- Hypersonic propulsion system force accounting p 175 A93-13229
- Pitching moment of low aspect ratio wing-body combinations up to high angles of attack at supersonic speeds
[ESDU-92043] p 333 A93-17958
- A wall interference assessment/correction system
[NASA-CR-191889] p 296 A93-18384
- Wind tunnel wall interference correction at subsonic speeds p 304 A93-19320
- Effect of pylon cross-sectional geometries on propulsion integration for a low-wing transport
[NASA-TP-3333] p 788 A93-28070
- A break-down of sting interference effects
[NLR-TP-91220-U] p 1014 A93-31042
- AERODYNAMIC LOADS**
- Wing pressure loads in canard configurations - A comparison between numerical results and experimental data p 7 A93-11499
- An adaptive region method for computation of vortex sheet behind wing in compressible flow p 116 A93-14262
- In-flight tailload measurements p 155 A93-14285
- Unsteady transonic aerodynamic loadings on the airfoil caused by heaving, pitching oscillations and control surface p 126 A93-15627
- Acoustic performance of low pressure axial fan rotors with different blade chord length and radial load distribution p 449 A93-19212
- An assessment of wake structure behind forward swept and aft swept propfans at high loading p 245 A93-19222
- Investigation of compressor rotor wake structure at peak pressure rise coefficient and effects of loading
[ASME PAPER 92-GT-32] p 246 A93-19292
- Blade loading and shock wave in a transonic circular cascade diffuser
[ASME PAPER 92-GT-34] p 246 A93-19294
- Aeroloids and secondary flows in a transonic mixed flow turbine stage
[ASME PAPER 92-GT-72] p 248 A93-19322
- Surface-curvature-distribution turbine-cascade performance
[ASME PAPER 92-GT-84] p 248 A93-19333
- Influence of blade aerodynamic loading on efficiency of radial-inflow turbines
[ASME PAPER 92-GT-91] p 249 A93-19337
- Investigations on a radial compressor tandem-rotor stage with adjustable geometry
[ASME PAPER 92-GT-218] p 404 A93-19440
- On aerodynamic loading of linear compressor cascades
[ASME PAPER 92-GT-275] p 253 A93-19468
- Unsteady aerodynamics and gust response in compressors and turbines
[ASME PAPER 92-GT-422] p 258 A93-19570
- Experimental investigation of vortex-fin interaction
[AIAA PAPER 93-0050] p 260 A93-20163
- The suppression of single-fin buffeting using tangential leading edge blowing on a delta wing p 270 A93-21677
- A wideband, embedded/conformal, antenna subsystem concept p 327 A93-22002
- Development of highly loaded root end attachments for composite material high speed flying surfaces p 539 A93-24122
- Determination of nonstationary aerodynamic loading on cascade blades in the case of dynamic changes of the angle of attack p 544 A93-26817
- The aerodynamic loads on aircraft components in violent longitudinal manoeuvres p 476 A93-26898
- Linearized Euler predictions of unsteady aerodynamic loads in cascades p 480 A93-29318
- Sensitivity of acoustic predictions to variation of input parameters p 565 A93-29404
- The development of a prediction method for the calculation of blade-vortex interaction noise based on measured airloads p 566 A93-29409
- Blade-vortex interaction data obtained from a pressure-instrumented model rotor at the DNW p 568 A93-29430
- Correlation of airloads on a two-bladed helicopter rotor p 481 A93-29438
- Unsteady wake effect on rotor vibratory airloadings p 509 A93-29439
- A numerical method of unsteady separating flow over delta wings p 681 A93-33746
- Prediction of helicopter component loads using neural networks
[AIAA PAPER 93-1301] p 756 A93-33878
- Recent advances in the numerical analysis of ram air wings - The three dimensional simulation code 'PARA3D'
[AIAA PAPER 93-1203] p 702 A93-35154
- Turns - A free-wake Euler/Navier-Stokes numerical method for helicopter rotors p 692 A93-35634
- Aerodynamic and wake methodology evaluation using model UH-60A experimental data p 767 A93-35997
- Hypersonic flutter of a curved shallow panel with aerodynamic heating
[AIAA PAPER 93-1318] p 829 A93-37428
- Aerodynamic rotor loads prediction method with free wake for low speed descent flights
[ONERA, TP NO. 1992-122] p 772 A93-38596
- Effect of temperature on nonlinear two-dimensional panel flutter using finite elements p 1022 A93-45133
- Time domain panel method for wings p 958 A93-45135
- Sensitivity analysis of a wing aeroelastic response p 958 A93-45142
- Turbine blade forces due to partial admission p 1029 A93-46928
- Direct and inverse problems of calculating the axisymmetric and 3D flow in axial compressor blade rows p 972 A93-46938
- Synchronous X-ray Sinography for nondestructive imaging of turbine engines under load
[AIAA PAPER 93-1819] p 1153 A93-49707
- An iterative multidisciplinary analysis for rotor blade shape determination
[AIAA PAPER 93-2085] p 1114 A93-49912
- Active control for fin buffet alleviation
[AIAA PAPER 93-3817] p 1133 A93-51408
- Calculation of aerodynamic loads on the wing of rigid and elastic aircraft with allowance for load correction from experimental data p 1103 A93-51905
- Methodology for integration of digital control loaders in aircraft simulators
[AIAA PAPER 93-3551] p 1207 A93-52655
- The fluid physics of parachute inflation p 1189 A93-54347
- Damped advanced composite parts p 1253 A93-55871
- ONERA calculation model of dynamic flow separation on an airfoil section p 1238 A93-56212
- Numerical minimization of the moment coefficient of a supercritical airfoil section p 1238 A93-56214
- Performance parameters and assessment p 81 A93-10052
- Measurement of aerodynamic shear stress using side chain liquid crystal polymers
[AD-A254312] p 72 A93-10770
- Design of a high-temperature experiment for evaluating advanced structural materials
[NASA-TM-105833] p 88 A93-11624
- User's Guide for the NREL Force and Loads Analysis Program
[DE92-010579] p 216 A93-13524
- User's Guide for the NREL Teetering Rotor Analysis Program (STRAP)
[DE92-010580] p 216 A93-13525
- An investigation of dynamic stress reduction of multi-body aircraft using active gust control p 187 A93-13916
- Hypersonic panel flutter in a rarefied atmosphere p 188 A93-13928
- The unsteady aerodynamics of a delta wing undergoing large-amplitude pitching motions p 134 A93-13929
- Multi-disciplinary optimization of aeroservoelastic systems
[NASA-CR-191255] p 220 A93-14766
- Wind load design methods for ground-based heliostats and parabolic dish collectors
[DE93-002737] p 433 A93-15839
- Transition induced normal forces and their effects on the aerodynamic characteristics of slender sharp cones
[AD-A256802] p 288 A93-15889
- Fatigue propagation behaviour of short cracks in aluminum alloys
[ESDU-92030] p 392 A93-16641
- Statistical fatigue analysis of the SH-60B servo beam rail component
[AD-A257474] p 332 A93-17660
- Beyond the frequency limits of time-linearized methods
[NLR-TP-91216-U] p 295 A93-17929
- Study of statistical variations of load spectra and material properties on aircraft fatigue life
[AD-A257961] p 339 A93-18451
- A discussion of the results of the rainflow counting of a wide range of dynamics associated with the simultaneous operation of adjacent wind turbines
[DE93-000016] p 434 A93-18705
- The effect of aircraft inlets on the behaviour of aero engine axial flow compressors p 422 A93-18722
- Assessment of helicopter component statistical reliability computations
[AD-A258931] p 510 A93-19447
- Experiments on smooth cantilevered circular cylinders in a low-turbulence uniform flow. Part 2: Fluctuating loads on a cantilever of aspect ratio 30
[PB93-110500] p 555 A93-21382
- Combined experiment, phase 1
[DE93-000012] p 485 A93-21766
- Stress calculation for the Sandia 34-meter wind turbine using the local circulation method and turbulent wind
[DE93-004480] p 560 A93-22045
- General aviation aircraft: Normal acceleration data analysis and collection project
[DOT/FAA/CT-91/20] p 713 A93-24739
- A feasibility study of using Langley 0.3-m transonic cryogenic tunnel sidewall boundary-layer removal system for heavy gas testing
[NASA-CR-191438] p 747 A93-25087
- An integrated finite-state model for rotor deformation, nonlinear airloads, inflow, and trim p 715 A93-25538
- Hypersonic panel flutter in a rarefied atmosphere
[NASA-CR-4514] p 780 A93-27084
- Evaluation of four advanced nozzle concepts for short takeoff and landing performance
[NASA-TP-3314] p 875 A93-29165
- Report on the test set-up for the structural testing of the Airmass Sunburst Ultralight Aircraft p 895 A93-29775
- NASTRAN analysis for the Airmass Sunburst model 'C' Ultralight Aircraft p 931 A93-29777
- Construction, wind tunnel testing and data analysis for a 1/5 scale ultra-light wing model p 876 A93-29778

- Selection and static calibration of the Marsh J1678 pressure gauge p 931 N93-29779
 Overview of aerothermodynamic loads definition study p 1016 N93-31583
 Three-dimensional analysis of the Pratt and Whitney alternate design SSME fuel turbine p 1031 N93-31584

AERODYNAMIC NOISE

- The effects of temperature on supersonic jet noise emission p 446 A93-19159
 Acoustic properties of supersonic helium/air jets at low Reynolds numbers p 446 A93-19160
 On the acoustic radiation nature of a turbulent vortex ring p 446 A93-19167
 Boundary conditions for direct computation of aerodynamic sound generation p 447 A93-19176
 A new technique for aerodynamic noise calculation p 447 A93-19177
 Numerical analysis of acoustic effect of rotor wakes in rotor-stator interaction p 447 A93-19182
 Control of coherent structures and aero-acoustic characteristics of subsonic and supersonic turbulent jets p 448 A93-19196
 Combined noise and flow control of supersonic jets using swirl p 398 A93-19204
 Experimental investigations and efficiency prediction of jet noise reduction techniques p 449 A93-19206
 Prediction of jet mixing noise in high-speed flight p 450 A93-19216
 Accuracy considerations in the computational analysis of jet noise p 451 A93-19804
 [AIAA PAPER 93-0146] p 451 A93-19804
 The role of noise in two-dimensional vortex merging p 408 A93-19967
 Experimental study on the characteristics of the near wake of a rotating flat plate. III - Influence of the shape near the trailing edge on periodic-velocity-fluctuation phenomena p 451 A93-21727
 Radiation mechanism for the aerodynamic sound of gears - An explanation for the radiation process by air flow observation p 451 A93-21859
 Numerical prediction of aerodynamic noise radiated from low Mach number turbulent wake p 452 A93-22589
 [AIAA PAPER 93-0145] p 452 A93-22589
 Effect of leading-edge porosity on blade-vortex interaction noise p 563 A93-24727
 [AIAA PAPER 93-0601] p 563 A93-24727
 The analysis of viscous wakes noise in axial flow compressor p 759 A93-33710
 Numerical prediction of aerodynamic sound using large eddy simulation p 850 A93-38150
 Numerical computation of aerodynamic noise radiation by the large eddy simulation p 850 A93-38151
 Analytical study on plate edge noise (Noise generation from tandemly situated trailing and leading edges) p 1038 A93-45561
 On the possibility of singularities in the acoustic field of supersonic sources when BEM is applied to a wave equation p 1039 A93-46805
 Boundary conditions for direct computation of aerodynamic sound generation p 1172 A93-49005
 Some acoustic features of perforated test section walls with splitter plates p 1226 A93-53222
 A dynamic stiffness/boundary element method for the prediction of interior noise levels p 1226 A93-53817
 The quiet helicopter; Proceedings of the Conference, London, United Kingdom, Mar. 17, 1992 (ISBN 1-85768-020-0) p 1262 A93-54718
 Non-propulsive aerodynamic noise p 99 N93-10673
 Comparison of flyover noise data from aircraft at high subsonic speeds with prediction p 100 N93-10674
 The prediction of noise radiation from supersonic elliptic jets p 100 N93-10684
 Prediction of jet mixing noise for high subsonic flight speeds p 100 N93-10685
 Mechanisms of sound generation in subsonic jets p 101 N93-10688
 Reduction of propeller noise by active noise control p 101 N93-10692
 A concept for a counterrotating fan with reduced tone noise p 101 N93-11370
 [NASA-TM-105736] p 101 N93-11370
 Report on the final panel discussion on computational aeroacoustics p 231 N93-12986
 [NASA-CR-189718] p 231 N93-12986
 Far field rotor noise p 759 N93-25651
 [AD-A260703] p 759 N93-25651
 User's manual for UCAP: Unified Counter-Rotation Aero-Acoustics Program p 852 N93-27148
 [NASA-CR-191034] p 852 N93-27148
 Subjective response to simulated sonic booms with ground reflections p 852 N93-28692
 [NASA-TM-107764] p 852 N93-28692
 Computation of far-field helicopter rotor tone noise [ONERA-P-1990-5] p 943 N93-30110

AERODYNAMIC STABILITY

- Research on the stability and control of soaring birds [AIAA PAPER 92-4122] p 61 A93-11284
 High Mach number dynamic stability of blunt slender cones at angle of attack p 271 A93-21721
 Stability of the vertical autorotation of a single-winged samara p 274 A93-22443
 Experimental and numerical analysis of the wing rock characteristics of a 'wing-body-tail' configuration [AIAA PAPER 93-0187] p 368 A93-22612
 Stability and control of hypersonic waveriders [AIAA PAPER 93-0508] p 370 A93-23255
 Unsteady aerodynamics in airplane stall-spin departure p 523 A93-24739
 [AIAA PAPER 93-0622] p 523 A93-24739
 Microchannel plate modal gain variations with temperature p 477 A93-27445
 Current status of computational methods for transonic unsteady aerodynamics and aeroelastic applications p 480 A93-29175
 Aeromechanical stability of rotorcraft with advanced geometry blades p 725 A93-33880
 [AIAA PAPER 93-1304] p 725 A93-33880
 Aeromechanical stability of a bearingless composite rotor in forward flight p 726 A93-33881
 [AIAA PAPER 93-1305] p 726 A93-33881
 An efficient procedure for cascade aeroelastic stability determination using nonlinear, time-marching aerodynamic solvers p 719 A93-34159
 [AIAA PAPER 93-1631] p 719 A93-34159
 Smart structures stabilized unstable control surfaces [AIAA PAPER 93-1701] p 712 A93-34223
 [AIAA PAPER 93-1701] p 712 A93-34223
 The rebirth of the tiltrotor - The 1992 Alexander A. Nikolsky Lecture p 712 A93-34256
 The stability and aerodynamic performances of clusters of small cruciform parachutes p 690 A93-35181
 [AIAA PAPER 93-1242] p 690 A93-35181
 Effects of dynamic stall and structural modeling on aeroelastic stability of elastic bending and torsion of hingeless rotor blades with experimental correlation p 794 A93-35902
 Aeromechanical stability of helicopters with composite rotor blades in forward flight p 794 A93-35904
 Transonic panel flutter [AIAA PAPER 93-1476] p 829 A93-37438
 The SAAB 2000 initial flight test - Status report p 804 A93-38847
 A numerical study of the flutter of conical shells p 927 A93-42405
 Active algorithms for controlling the rotational motion of flight vehicles p 908 A93-43079
 Mathematical model for the effect of turbulent velocity pulsations on the stability of a powerplant p 1003 A93-47508
 Solution of the Euler equations for airfoils using asymptotic methods p 1045 A93-48130
 [AIAA PAPER 93-2931] p 1045 A93-48130
 A simplified approach for control of rotating stall. I - Theoretical development p 1080 A93-50035
 [AIAA PAPER 93-2229] p 1080 A93-50035
 Non-linear flight dynamics [ONERA, TP NO. 1993-109] p 1206 A93-53621
 A study of the stability of vortical structures in supersonic inlets p 1187 A93-54079
 [ISABE 93-7103] p 1187 A93-54079
 Effect of the atmosphere density gradient on aerodynamic stabilization p 1252 A93-55034
 Recent advances in steady compressible aerodynamic sensitivity analysis p 1236 A93-55400
 Active control of aeroacoustic couplings by means of adaptive systems p 64 N93-11576
 [ECL-91-18] p 64 N93-11576
 Low-speed longitudinal and lateral-directional aerodynamic characteristics of the X-31 configuration [NASA-TM-4351] p 22 N93-11622
 X-29 linear aerodynamic perturbation model [AD-A254810] p 160 N93-12752
 Program for calculation of aileron rolling moment and yawing moment coefficients at subsonic speeds (ESDU-88040) p 136 N93-14514
 Design of robust suboptimal controllers for a generalized quadratic criterion p 372 N93-17670
 [AD-A257746] p 372 N93-17670
 The effect of aircraft inlets on the behaviour of aero engine axial flow compressors p 422 N93-18722
 Stall and surge in axial flow compressors p 423 N93-18724
 AEW aircraft design [AD-A261800] p 718 N93-26444
 Airfoil stability in turbulent flow p 781 N93-27212
 AERODYNAMIC STALLING
 A prediction of the stalling for wings with rear separation p 116 A93-14264
 Flow structures around a constant-rate pitching airfoil and mechanism of dynamic stall p 118 A93-14332
 Breaking the stall barrier p 159 A93-17502

- Improvement of high- α airfoil stalling performance by internal acoustic excitation p 243 A93-19134
 A wide-range axial-flow compressor stage performance model p 348 A93-19308
 [ASME PAPER 92-GT-58] p 348 A93-19308
 An inviscid-viscous interaction approach to the calculation of dynamic stall initiation on airfoils [ASME PAPER 92-GT-128] p 249 A93-19362
 Separated flow in a low speed two-dimensional cascade. I - Flow visualization and time-mean velocity measurements p 257 A93-19521
 [ASME PAPER 92-GT-356] p 257 A93-19521
 The problem of dynamic stall simulation revisited [AIAA PAPER 93-0091] p 264 A93-20197
 Experimental study of dynamic stall on an oscillating airfoil p 266 A93-20804
 The computation of the post-stall behavior of a circulation controlled airfoil p 277 A93-22625
 [AIAA PAPER 93-0207] p 277 A93-22625
 Interferometric investigations of compressible dynamic stall over a transiently pitching airfoil [AIAA PAPER 93-0211] p 278 A93-22628
 Estimation of unsteady lift on a pitching airfoil from wake velocity surveys p 286 A93-23351
 [AIAA PAPER 93-0437] p 286 A93-23351
 Initial acceleration effects on the flow field development around rapidly pitching airfoils p 286 A93-23352
 [AIAA PAPER 93-0438] p 286 A93-23352
 Unsteady aerodynamics in airplane stall-spin departure p 523 A93-24739
 [AIAA PAPER 93-0622] p 523 A93-24739
 Corrections to fringe distortion due to flow density gradients in optical interferometry [AIAA PAPER 93-0631] p 539 A93-24748
 Dynamic stall on a three-dimensional rectangular wing [AIAA PAPER 93-0637] p 463 A93-24753
 Pressure-based high-order TVD methodology for dynamic stall simulation p 466 A93-24788
 [AIAA PAPER 93-0680] p 466 A93-24788
 Elementary stall flutter of an aircraft wing p 545 A93-27289
 Investigation of the aircraft spin via sensitivity analysis p 524 A93-27300
 Schlieren studies of compressibility effects on dynamic stall of transiently pitching airfoils p 480 A93-28608
 Studies of the dynamic stall problem on airfoils p 681 A93-33747
 Turbulence and stall in plane diffusers - Computational study p 744 A93-34311
 Vortex initiation during dynamic stall of an airfoil p 684 A93-34335
 Effects of dynamic stall and structural modeling on aeroelastic stability of elastic bending and torsion of hingeless rotor blades with experimental correlation p 794 A93-35902
 Dynamic stall of sinusoidally oscillating three-dimensional swept and unswept wings in compressible flow p 766 A93-35995
 Influence of coupling incidence and velocity variations on the airfoil dynamic stall p 767 A93-35999
 Nonequilibrium turbulence modeling study on light dynamic stall of a NACA0012 airfoil p 768 A93-37379
 Permeable airfoils in incompressible flow p 768 A93-37401
 Numerical calculation of separated flows around wing section in unsteady motion by using incompressible Navier-Stokes equations p 770 A93-38158
 Navier-Stokes stall predictions using an algebraic Reynolds-stress model p 778 A93-39260
 Velocity and vorticity distributions over an oscillating airfoil under compressible dynamic stall p 778 A93-39403
 Low-frequency flow oscillation over airfoils near stall p 861 A93-41931
 Nonlinear large amplitude aeroelastic behavior of composite rotor blades p 997 A93-45741
 Initial acceleration effects on flow evolution around airfoils pitching to high angles of attack p 961 A93-45750
 Sound generation by rotating stall in centrifugal turbomachines p 1039 A93-46701
 Two leading-edge droop modifications for tailoring stall characteristics of a general aviation trainer configuration p 1008 A93-46807
 Control of the dynamic-stall vortex over a pitching airfoil by leading-edge suction p 969 A93-46832
 [AIAA PAPER 93-3267] p 969 A93-46832
 The moving wall effect vis-a-vis other dynamic stall flow mechanisms p 1008 A93-47219
 [AIAA PAPER 93-3424] p 1008 A93-47219
 On the modelling of separated flows about airfoils [AIAA PAPER 93-3479] p 981 A93-47257
 A flowfield study of a close-coupled canard configuration [AIAA PAPER 93-3499] p 983 A93-47269

- Prediction of stall and post-stall behavior of airfoils at low and high Reynolds numbers p 983 A93-47270
[AIAA PAPER 93-3502]
- Tip vortex, stall vortex, and separation observations on pitching three-dimensional wings p 1049 A93-48166
[AIAA PAPER 93-2972]
- Transition effects on compressible dynamic stall of transiently pitching airfoils p 1050 A93-48171
[AIAA PAPER 93-2978]
- Results and lessons learned from two Wright Laboratory flight research programs p 1099 A93-48341
[AIAA PAPER 93-3661]
- A wake singularity potential flow model for airfoils experiencing trailing-edge stall p 1067 A93-48544
- Adaptive engine stall margin control p 1108 A93-49200
- Tip shock structures in transonic compressor rotors [AIAA PAPER 93-1869] p 1075 A93-49744
- Stall inception in single stage, high-speed compressors with straight and swept leading edges p 1076 A93-49745
[AIAA PAPER 93-1870]
- Application of a dynamic compression system model to a low aspect ratio fan - Casing treatment and distortion p 1111 A93-49746
[AIAA PAPER 93-1871]
- An approach to the stall monitoring in a single stage axial compressor p 1112 A93-49747
[AIAA PAPER 93-1872]
- Computational analysis of nonlinear aeroelastic phenomena during stall flutter of cascaded airfoils [AIAA PAPER 93-2082] p 1079 A93-49909
- Compressor unsteady aerodynamic response to rotating stall and surge excitations p 1079 A93-49914
[AIAA PAPER 93-2087]
- A simplified approach for control of rotating stall. I - Theoretical development p 1080 A93-50035
[AIAA PAPER 93-2229]
- Local nonlinear control of stall inception in axial flow compressors p 1080 A93-50036
[AIAA PAPER 93-2230]
- Spatial domain characterization of abrupt rotating stall initiation in an axial flow compressor p 1081 A93-50040
[AIAA PAPER 93-2238]
- Stall inception in a multi-stage high speed axial compressor p 1117 A93-50153
[AIAA PAPER 93-2386]
- Multielement airfoil performance due to Reynolds and Mach number variations p 1095 A93-52442
- Aerodynamic characteristics of conical triangular-planform wings of low aspect ratio in subsonic stalled flow p 1180 A93-53574
- A comparative study of semi-empirical dynamic stall models p 18 N93-10544
- Harmonic analysis of the aerodynamic forces on a Darrieus rotor p 18 N93-10551
- The convection speed of the dynamic stall vortex [AD-A247258] p 21 N93-11464
- Nonlinear stall flutter of wings with bending-torsion coupling [AD-A254323] p 186 N93-12959
- Dynamic stall effects on hingeless rotor stability with experimental correlation p 129 N93-13010
- Estimation of unsteady lift on a pitching airfoil from wake velocity surveys p 138 N93-14791
[NASA-TM-105947]
- The Application of CFD to rotary wing flow problems [NASA-TM-102803] p 139 N93-15483
- Quantitative-force measurements of pneumatic control on a wing/stroke model p 289 N93-16157
[AD-A257343]
- Lift enhancement using a close-coupled oscillating canard p 296 N93-18336
[AD-A257877]
- Axial Flow Compressors, volume 1 p 422 N93-18721
[VKI-LS-1992-02-VOL-1]
- Stall in axial flow aero engine compressors p 422 N93-18723
- Stall and surge in axial flow compressors p 423 N93-18724
- Active control of stall and surge p 423 N93-18725
- Stall transients including effects of inlet distortion and intake geometry p 423 N93-18726
- Experimental investigation of rotating stall in a mismatched three stage axial flow compressor p 423 N93-18727
- Application of recess vaned casing treatment to axial flow fans p 423 N93-18728
- A study of stall in a low hub/tip ratio fan p 423 N93-18729
- Axial Flow Compressors, volume 2 p 423 N93-18731
[VKI-LS-1992-02-VOL-2]
- Determination of the zone of the stall cell by means of the baroclinic wave theory p 424 N93-18733
- Rotating stall cell and Von Karman vortex street: A meteorological theory p 424 N93-18734
- Stall departure resistance enhancer [NASA-CASE-LAR-14221-1] p 344 N93-19023
- Characterization of stall inception in high-speed single-stage compressors [AD-A258973] p 365 N93-19093
- Numerical calculations of separating flows around oscillating airfoil p 300 N93-19284
- Numerical simulation of unsteady large scale separated flow around oscillating airfoil p 300 N93-19285
- X-31A high angle of attack and initial post stall flight testing p 511 N93-19911
- Combined experiment, phase 1 [DE93-000012] p 485 N93-21766
- Effect of underwing frost on transport aircraft takeoff performance [DOT/FAA/CT-TN93/9] p 791 N93-2752
- Investigation of forced unsteady separated flows using velocity-vorticity form of Navier-Stokes equations p 840 N93-27451
- Dynamic airfoil stall investigations p 786 N93-27453
- Prediction of airfoil stall using Navier-Stokes equations in streamline coordinates p 787 N93-27456
- Simulation, characterization and control of forced unsteady viscous flows using Navier-Stokes equations [AD-A264333] p 934 N93-30369
- ### AERODYNAMICS
- Boundary integral equation methods for aerodynamics p 9 A93-12158
- A flow calculation and aerodynamic design method for turbomachine cascades p 12 A93-12764
- Nonstationary flow of a viscous incompressible fluid past an airfoil p 79 A93-12922
- ICAS, Congress, 18th, Beijing, China, Sept. 20-25, 1992, Proceedings. Vols. 1 & 2 [ISBN 1-56347-046-2] p 107 A93-14151
- Computational methods applied to the aerodynamics of spaceplanes and launchers [ONERA, TP NO. 1992-140] p 114 A93-14216
- Development of a system for aerodynamic fast-response probe measurements p 203 A93-14325
- Advanced technology constant challenge and evolutionary process p 109 A93-15054
- The science of flight - Pilot-oriented aerodynamics --- Book [ISBN 0-8138-0398-5] p 240 A93-17526
- Problems in the aerodynamics and dynamics of flight vehicles in the light of K.E. Tsiolkovsky's ideas; Lectures Devoted to K.E. Tsiolkovsky's Ideas, 25th, Kaluga, Russia, Sept. 11-14, 1990, Transactions --- Russian book p 237 A93-18376
- Technical prospects for computational aeroacoustics p 244 A93-19150
- Experimental investigation of tip clearance noise in axial flow machines p 445 A93-19155
- Heat transfer and aerodynamics of a high rim speed turbine nozzle guide vane with profiled end walls [ASME PAPER 92-GT-243] p 253 A93-19452
- Accuracy and efficiency assessments for a weak statement CFD algorithm for high-speed aerodynamics [ASME PAPER 92-GT-433] p 435 A93-19576
- Flight vehicle aerodynamics calculated by a Galerkin finite element/finite difference method p 266 A93-20738
- The modelling of aerodynamic flows by solution of the Euler equations on mixed polyhedral grids p 269 A93-21218
- Measured thrust losses associated with secondary air injection through nozzle walls p 270 A93-21656
- On the structure and response of aerodynamically-strained planar premixed flames [AIAA PAPER 93-0246] p 390 A93-22657
- 3D Euler flow solutions using unstructured Cartesian and prismatic grids [AIAA PAPER 93-0331] p 281 A93-23022
- F-14A aircraft low-speed maneuvering aerodynamics [AIAA PAPER 93-0523] p 283 A93-23265
- Application of a Navier-Stokes aeroelastic method to improve fighter wing performance at maneuver flight conditions [AIAA PAPER 93-0529] p 284 A93-23270
- Investigation on bi-flat jet separated flow in a rectangular combustor p 459 A93-23778
- National Conference on Aerodynamics, 6th, Bangalore, India, Sept. 1992, Proceedings p 460 A93-24076
- Aerodynamically efficient wing design with structural considerations p 460 A93-24081
- Exact-gradient shape optimization of a 2-D Euler flow p 462 A93-24308
- Fundamental issues in subsonic/transonic expansion corner aerodynamics [AIAA PAPER 93-0649] p 465 A93-24764
- Solution-adaptive and quality-enhancing grid generation p 480 A93-28610
- Calculation of the flow around a high-lift airfoil using an explicit code and an algebraic Reynolds stress model p 685 A93-34344
- Dynamics of the behavior of nematic films in gasdynamic flows p 746 A93-35345
- A numerical procedure for aerodynamic optimization of helicopter rotor blades [ONERA, TP NO. 1992-121] p 771 A93-38595
- The problem of two Coulomb centers and its applications in physical aerodynamics p 776 A93-39132
- Rarefied-flow shuttle aerodynamics flight model [AIAA PAPER 93-3441] p 859 A93-41057
- Societe Francaise des Mecaniciens, SNECMA, and ONERA, Symposium on Recent Advances in Compressor and Turbine Aerothermodynamics, Courbevoie, France, Nov. 24, 25, 1992, Reports p 1001 A93-46926
- Some Fuchs-type equations in fluid mechanics p 1165 A93-48967
- Computational methods in hypersonic aerodynamics [ISBN 0-7923-1673-8] p 1072 A93-49521
- The development of a large annular facility for testing gas turbine combustor diffuser systems [AIAA PAPER 93-2546] p 1139 A93-50269
- Vector unsymmetric eigenequation solver for nonlinear flutter analysis on high-performance computers p 1160 A93-52449
- Aerodynamic inverse design and analysis for a full engine [ISABE 93-7086] p 1186 A93-54062
- Advanced aerodynamic airframe/nozzle integration [ISABE 93-7099] p 1187 A93-54075
- Aerodynamic investigation of radial turbines using computational methods p 81 N93-10056
- Aeronautical technologies for the twenty-first century [NASA-CR-190918] p 4 N93-10647
- The engine design engine. A clustered computer platform for the aerodynamic inverse design and analysis of a full engine [NASA-TM-105838] p 21 N93-11223
- Formulation and validation of high-order mathematical models of helicopter flight dynamics p 162 N93-13821
- An investigation of jet engine test cell aerodynamics by means of scale model test studies with comparisons to full-scale test results p 193 N93-14060
- Flight testing: Past, present, and future p 164 N93-14615
- Subsonic aerodynamic research laboratory [AD-A256060] p 137 N93-14661
- L.D.V. measurements of unsteady flow fields in radial turbine [AD-A255728] p 221 N93-15065
- Analysis of in-flight structural failures of P-3C wing leading edge segments [AD-A256212] p 165 N93-15238
- Flight dynamics system software development environment (FDS/SDE) tutorial [NASA-TM-108580] p 230 N93-15502
- Technology benefits and ground test facilities for high-speed civil transport development [NASA-TM-107670] p 378 N93-15790
- Lanchester: The man p 456 N93-16464
- The Goldstein Aeronautical Engineering Research Laboratory [AERO-REPT-9111] p 240 N93-16465
- 1991 research and technology [NASA-TM-103924] p 456 N93-16652
- National Aeronautics and Space Administration p 454 N93-17097
- Current European rotorcraft research activities on development of advanced CFD methods for the design of rotor blades (BRITE/EURAM DACRO project) [MBB-UD-0601-91-PUB] p 293 N93-17568
- Turbomachinery and potential computations [DS-2026] p 363 N93-17740
- Hypersonic reconnaissance aircraft [NASA-CR-192049] p 333 N93-17804
- Heat transfer and aerodynamics of a high rim speed turbine nozzle guide vane with profiled end walls [AD-A258346] p 295 N93-17991
- Experimental Investigation of Nozzle/Plume Aerodynamics at Hypersonic Speeds [NASA-CR-191368] p 386 N93-18085
- SR-SCARLET 1: Peregrin [NASA-CR-192048] p 337 N93-18155
- High speed civil transport [NASA-CR-192041] p 337 N93-18161
- Identification of system dynamics of a high incidence research model [RR-407] p 339 N93-18507
- Experimental investigation of the aerodynamics of independently rotating cylindrical shells [AD-A258917] p 305 N93-19340

- Guidance and flight control law development for hypersonic vehicles
[NASA-CR-192102] p 526 N93-19960
- Adaptivity-fluids-localization. The challenge to computational mechanics p 553 N93-20618
- Applied aerodynamics: Challenges and expectations [NASA-TM-103963] p 694 N93-25091
- Optimal thrust magnitude on a singular arc in atmospheric flight p 758 N93-25410
- A computational aerodynamic design optimization method using sensitivity analysis p 716 N93-25552
- Numerical simulation of hypersonic aerodynamics and the computational needs for the design of an aerospace plane p 699 N93-25894
- Radial inflow turbine study [AD-A260767] p 724 N93-25917
- Cumulative reports and publications [NASA-CR-191440] p 847 N93-27063
- Collection of papers of the 31st Israel Annual Conference on Aviation and Astronautics [ITN-93-85187] p 764 N93-27166
- Hypersonics revisited p 781 N93-27167
- Center for Aeronautics and Space Information Sciences [NASA-CR-193140] p 848 N93-27289
- The Fifth Symposium on Numerical and Physical Aspects of Aerodynamic Flows [NASA-CR-193000] p 783 N93-27427
- Aerodynamics of a finite wing with simulated ice p 784 N93-27437
- High-lift aerodynamics: Prospects and plans p 784 N93-27442
- Quantitative three-dimensional low-speed wake surveys p 785 N93-27447
- Unsteady transition measurements on a pitching three-dimensional wing p 820 N93-27450
- International aviation (Selected articles) [AD-A262566] p 765 N93-28576
- Construction, wind tunnel testing and data analysis for a 1/5 scale ultra-light wing model p 876 N93-29778
- Reynolds number influences in aeronautics [NASA-TM-107730] p 989 N93-31732
- AEROELASTIC RESEARCH WINGS**
- Influence of sweep on structural optimization of a fighter wing [AIAA PAPER 92-4794] p 323 A93-20290
- Structural modeling of low-aspect ratio composite wings [AIAA PAPER 93-1371] p 739 A93-33937
- Estimation of wing stability in flow from the characteristics of the transient process p 836 A93-39177
- A viscous flow based membrane wing model [AIAA PAPER 93-2955] p 1047 A93-48149
- The unified method of aeroelasticity p 372 N93-18143
- AEROELASTICITY**
- ONERA makes progress in rotor aerodynamics, aeroelasticity, and acoustics p 2 A93-11621
- Nonlinear problems of aeroelasticity p 78 A93-12153
- Nonlinear aeroelasticity and chaos p 79 A93-12165
- Transonic flutter/divergence characteristics of aeroelastically tailored and non-tailored high-aspect-ratio forward-swept wings p 10 A93-12273
- Numerical simulation for aeroelasticity in turbomachines with vortex method. I - Theory and method p 53 A93-12452
- Robust control of an aeroelastic system modeled by a singular integro-differential equation p 97 A93-13197
- Finite memory approximations for a singular neutral system arising in aeroelasticity p 97 A93-13246
- Research and applications in structural dynamics and aeroelasticity p 153 A93-14223
- Feasibility study of an active aeroelastic control system for the F-16 aircraft p 181 A93-14224
- Engineering optimization of aeronautical structures p 154 A93-14227
- Aeroservoelastic analysis of an aircraft model incorporating the minimum state method for approximating unsteady aerodynamics p 154 A93-14258
- Study of aeroservoelastic stability of an aircraft p 182 A93-14259
- Aeroelastic investigations as applied to Airbus airplanes p 155 A93-14280
- Aeroelastic stability characteristics of composite cylindrical shells by the finite element method p 203 A93-14312
- An interactive numerical procedure for rotor aeroelastic stability analysis using elastic lifting surface p 155 A93-14313
- Parametric aeroelastic analysis of composite wing-boxes with active strain-energy tuning p 156 A93-14361
- Aeroelastic analysis of composite wing with control surface p 157 A93-14386
- Modified sparse time domain technique for rotor stability testing p 157 A93-14593
- Concurrent processing adaptation of aeroelastic analysis of propfans p 173 A93-14624
- The rotor blade flap bending problem - An analytical test case p 158 A93-14783
- Adaptive aeroelastic composite wings - Control and optimization issues p 185 A93-14818
- On the static aeroelastic tailoring of composite aircraft swept wings modelled as thin-walled beam structures p 158 A93-14820
- Instability of the periodic deflection of a panel surface in a turbulent boundary layer p 208 A93-15188
- On orthogonal search method of flutter analysis p 208 A93-15402
- Strong coupling between inviscid fluid and boundary layer for airfoils with a sharp edge. II - 2D unsteady case for isolated airfoil and straight blade cascade p 126 A93-16473
- Improving the service characteristics of an aircraft through the gyroscopic damping of its structure p 366 A93-18363
- Structural analysis of a nonlinear problem of aeroelasticity for CFC structures p 397 A93-18989
- Boundary-layer induced noise in aircraft p 444 A93-19137
- Advances in the numerical integration of the 3-D Euler equations in vibrating cascades [ASME PAPER 92-GT-170] p 351 A93-19396
- Coupled 3-D aeroelastic stability analysis of bladed disks [ASME PAPER 92-GT-171] p 351 A93-19397
- Aeroelastic optimization of a composite helicopter rotor [AIAA PAPER 92-4780] p 323 A93-20287
- Structural optimization with frequency constraints - A review [AIAA PAPER 92-4813] p 408 A93-20293
- Multidisciplinary design integration system for a supersonic transport aircraft [AIAA PAPER 92-4841] p 324 A93-20296
- Coupled finite-difference/finite-element approach for wing-body aeroelasticity [AIAA PAPER 92-4680] p 409 A93-20302
- Flutter calculations for a system with interacting nonlinearities [AIAA PAPER 92-4682] p 409 A93-20304
- Integrated aerodynamic-structural-control wing design [AIAA PAPER 92-4694] p 324 A93-20307
- APPLE - An aeroelastic analysis system for turbomachines and propfans [AIAA PAPER 92-4712] p 358 A93-20320
- Aeroservoelasticity in HISAIR - High Speed Airframe Integration Research [AIAA PAPER 92-4719] p 324 A93-20322
- Aeroelastic model design using structural optimization [AIAA PAPER 92-4730] p 409 A93-20329
- Exact solution sensitivities for boundary element aerodynamics codes [AIAA PAPER 92-4745] p 436 A93-20343
- On alternative problem formulations for multidisciplinary design optimization [AIAA PAPER 92-4752] p 436 A93-20350
- Observations on computational methodologies for use in large-scale, gradient-based, multidisciplinary design [AIAA PAPER 92-4753] p 436 A93-20351
- Static aeroelastic analysis of a maneuvering aircraft with damaged wing [AIAA PAPER 92-4765] p 325 A93-20360
- Development of a structural optimization capability for the aeroelastic tailoring of composite rotor blades with straight and swept tips [AIAA PAPER 92-4779] p 326 A93-20370
- An approach to tiltrotor wing aeroservoelastic optimization through increased productivity [AIAA PAPER 92-4781] p 326 A93-20371
- Flutter optimization of large transport aircraft [AIAA PAPER 92-4795] p 326 A93-20381
- Examples of dynamic response optimization using MSC/NASTRAN [AIAA PAPER 92-4814] p 436 A93-20394
- Structural non-linearity effects on flutter of a swept wing in transonic flows p 410 A93-20714
- Dynamic analysis of pretwisted elastically-coupled rotor blades p 326 A93-21125
- On some recent advances in multidisciplinary analysis of hypersonic vehicles [AIAA PAPER 92-5026] p 438 A93-22302
- Application of a Navier-Stokes aeroelastic method to improve fighter wing performance at maneuver flight conditions [AIAA PAPER 93-0529] p 284 A93-23270
- Optimal control law synthesis for flutter suppression using active acoustic excitations p 370 A93-23516
- Modeling, analysis, and prediction of flutter at transonic speeds p 416 A93-23553
- Direct solution of two-dimensional Navier-Stokes equations for static aeroelasticity problems p 417 A93-23554
- Elementary stall flutter of an aircraft wing p 545 A93-27289
- Structural analysis of box beams using symbolic manipulation technique p 548 A93-28615
- Simultaneous structure/control design optimization of a wing structure with a gust load alleviation system p 525 A93-28616
- Current status of computational methods for transonic unsteady aerodynamics and aeroelastic applications p 480 A93-29175
- Structure-attached corotational fluid grid for transient aeroelastic computations p 480 A93-29326
- HHC study in the DNW to reduce BVI noise - An analysis p 565 A93-29405
- The role of blade elasticity in the prediction of blade-vortex interaction noise p 566 A93-29406
- Unsteady wake effect on rotor vibratory loadings p 509 A93-29439
- An overview of aeroelasticity studies for the National Aero-Space Plane [AIAA PAPER 93-1313] p 732 A93-33889
- Aeroelastic character of a National Aerospace Plane demonstrator concept [AIAA PAPER 93-1314] p 732 A93-33890
- A unified hypersonic/supersonic method for aeroelastic applications including shock-unsteady wave interaction [AIAA PAPER 93-1317] p 738 A93-33892
- Impact of aeroelasticity on propulsion and longitudinal flight dynamics of an air-breathing hypersonic vehicle [AIAA PAPER 93-1367] p 733 A93-33934
- Supersonic aeroelastic instability results for a NASP-like wing model [AIAA PAPER 93-1369] p 682 A93-33935
- On the order reduction of LQG designed controllers [AIAA PAPER 93-1420] p 756 A93-33973
- ISAC - A tool for aeroservoelastic modeling and analysis - Interaction of Structures, Aerodynamics, and Control [AIAA PAPER 93-1421] p 726 A93-33974
- Wing flutter boundary prediction using unsteady Euler aerodynamic method [AIAA PAPER 93-1422] p 739 A93-33975
- Finite element nonlinear random response of beams to acoustic and thermal loads applied simultaneously [AIAA PAPER 93-1427] p 740 A93-33978
- Acoustics due to flow-structural interaction and its transmission through a double-panel in high-speed cruising flight [AIAA PAPER 93-1431] p 710 A93-33981
- Dynamic analysis of multiple row fuselage stiffened structures [AIAA PAPER 93-1438] p 710 A93-33987
- Hammerhead aeroelastic stability revisited [AIAA PAPER 93-1477] p 740 A93-34022
- Application of differential quadrature to the analysis of static aeroelastic phenomena [AIAA PAPER 93-1505] p 711 A93-34044
- A refined structural model of composite aircraft wings for the enhancement of vibrational and aeroelastic response characteristics [AIAA PAPER 93-1536] p 740 A93-34073
- Calculation of numerical boundary measure for wavelet-Galerkin approximations in aeroelasticity [AIAA PAPER 93-1539] p 741 A93-34076
- An inverse method for computation of structural stiffness distributions of aeroelastically optimized wings [AIAA PAPER 93-1540] p 741 A93-34077
- Extension of a nonlinear systems theory to general-frequency unsteady transonic aerodynamic responses [AIAA PAPER 93-1590] p 683 A93-34122
- Experimental unsteady pressures at flutter on the Supercritical Wing Benchmark Model [AIAA PAPER 93-1592] p 683 A93-34123
- Unsteady transonic potential flow over a flexible fuselage [AIAA PAPER 93-1593] p 683 A93-34124
- Nonlinear aeroelastic response of panels [AIAA PAPER 93-1599] p 741 A93-34130
- An efficient procedure for cascade aeroelastic stability determination using nonlinear, time-marching aerodynamic solvers [AIAA PAPER 93-1631] p 719 A93-34159
- Unsteady aerodynamics and flutter of propfans using a three-dimensional Full-Potential Solver [AIAA PAPER 93-1633] p 720 A93-34161
- A new sensitivity analysis for structural optimization of composite rotor blades [AIAA PAPER 93-1644] p 742 A93-34169
- Sensitivity analysis of aeroelastic response of a wing using piecewise pressure representation [AIAA PAPER 93-1645] p 742 A93-34170

- Sensitivity analysis of flutter response of a typical section and a wing in transonic flow
[AIAA PAPER 93-1646] p 742 A93-34171
- Efficient sensitivity analysis for rotary-wing aeromechanical problems
[AIAA PAPER 93-1648] p 711 A93-34173
- Aeroelastic challenges for a High Speed Civil Transport
[AIAA PAPER 93-1478] p 712 A93-34240
- Effect of an unsteady three-dimensional wake on elastic blade-flapping eigenvalues in hover
p 683 A93-34260
- Efficient hybrid scheme for the analysis of counter-rotating propellers
p 688 A93-34483
- Computation of aeroelastic characteristics and stress-strained state of parachutes
[AIAA PAPER 93-1237] p 744 A93-35178
- Effects of dynamic stall and structural modeling on aeroelastic stability of elastic bending and torsion of hingeless rotor blades with experimental correlation
p 794 A93-35902
- Aeroelastic behavior of composite rotor blades with swept tips
p 827 A93-35978
- Investigation of subharmonic response of limit cycle flutter of wing-store system
p 800 A93-36339
- A study of the effect of the static aeroelasticity of a swept wing on its weight response
p 801 A93-36798
- Robust stabilization of an aero-elastic system
p 817 A93-37044
- Evaluation and extension of the flutter-margin method for flight flutter prediction
p 828 A93-37393
- Multiple pole rational-function approximations for unsteady aerodynamics
p 769 A93-37404
- Comment on 'In-flight measurement of static pressures'
p 807 A93-37407
- Actuator and aerodynamic modeling for high-angle-of-attack aeroservoelasticity
[AIAA PAPER 93-1419] p 818 A93-37433
- Transonic panel flutter
[AIAA PAPER 93-1476] p 829 A93-37438
- Nonclassical aileron buzz in transonic flow
[AIAA PAPER 93-1479] p 829 A93-37439
- Nonlinear flutter of composite plates with damage evolution
[AIAA PAPER 93-1546] p 829 A93-37441
- Aeroelastic dynamics of mistuned blade assemblies with closely spaced blade modes
[AIAA PAPER 93-1628] p 810 A93-37446
- The minimal multiplier method in calculations of the stability, limiting vibration cycles, and limiting states of nonlinearly deformed structures
p 836 A93-39176
- Alternative approximations for integrated control/structure aeroservoelastic synthesis
p 819 A93-39418
- Supersonic flutter analysis of composite plates and shells
p 837 A93-39419
- Experimental and theoretical study for nonlinear aeroelastic behavior of a flexible rotor blade
p 837 A93-39422
- Research in unsteady aerodynamics and computational aeroelasticity at the NASA Langley Research Center
p 804 A93-39498
- Effect of structural uncertainties on flutter analysis
p 924 A93-40445
- Aeroelastic response, loads, and stability of a composite rotor in forward flight
p 906 A93-41919
- Stability analysis of dynamic meshes for transient aeroelastic computations
[AIAA PAPER 93-3325] p 1022 A93-45019
- Time-accurate simulation of a self-excited oscillatory supersonic external flow with a multi-block solution-adaptive mesh algorithm
[AIAA PAPER 93-3387] p 956 A93-45078
- Active control of aerothermoelastic effects for a conceptual hypersonic aircraft
p 1007 A93-45137
- Sensitivity analysis of a wing aeroelastic response
p 958 A93-45142
- Static aeroelastic control of an adaptive lifting surface
p 995 A93-45147
- Use of eigenvectors in the solution of the flutter equation
p 1022 A93-45151
- Nonlinear large amplitude aeroelastic behavior of composite rotor blades
p 997 A93-45741
- Unsteady aerodynamic response of two-dimensional subsonic and supersonic oscillating cascades with chordwise displacement and flexible deformation
p 971 A93-46922
- Analysis of aeroelastic and resonance responses of a wind tunnel model support system
p 1013 A93-47022
- Optimization of an aeroelastic system using the dynamic stability condition
p 1029 A93-47085
- Dynamic analysis of a compound elastic surface
p 1030 A93-47086
- Aeroelastic computation for a flexible airfoil using the small perturbation method comparison with wind-tunnel results
[ONERA, TP NO. 1993-43] p 987 A93-47448
- Parameter estimates of an aeroelastic aircraft as affected by model simplifications
[AIAA PAPER 93-3640] p 1127 A93-48325
- Aeroelastic effects on the B-2 maneuver response
[AIAA PAPER 93-3664] p 1128 A93-48344
- Numerical simulation of unsteady flow in a transonic cascade
p 1066 A93-48502
- Three-dimensional time-marching aeroelastic analyses using an unstructured-grid Euler method
p 1100 A93-49012
- Computational analysis of nonlinear aeroelastic phenomena during stall flutter of cascaded airfoils
[AIAA PAPER 93-2082] p 1079 A93-49909
- An iterative multidisciplinary analysis for rotor blade shape determination
[AIAA PAPER 93-2085] p 1114 A93-49912
- Unsteady aerodynamics and flutter based on the potential equation
[AIAA PAPER 93-2086] p 1079 A93-49913
- Optimization of blade arrangement in a randomly mistuned cascade using simulated annealing
[AIAA PAPER 93-2254] p 1115 A93-50052
- Aeroelastic stability of supersonic nozzles with separated flow
[AIAA PAPER 93-2588] p 1142 A93-50300
- Coupling characteristics analysis of elastic vehicle --- design of modern flight control systems
p 1169 A93-51189
- Robust control of hypersonic vehicles considering propulsive and aeroelastic effects
[AIAA PAPER 93-3762] p 1131 A93-51357
- Dynamics of hypersonic flight vehicles exhibiting significant aeroelastic and aeropropulsive interactions
[AIAA PAPER 93-3763] p 1131 A93-51358
- Order reduction of aeroelastic models through LK transformation and Riccati iteration
[AIAA PAPER 93-3795] p 1159 A93-51388
- Calculation of aerodynamic loads on the wing of rigid and elastic aircraft with allowance for load correction from experimental data
p 1103 A93-51905
- Implicit schemes for unsteady Euler equations on unstructured meshes
[ONERA, TP NO. 1993-64] p 1171 A93-51944
- Application of nonlinear systems theory to transonic unsteady aerodynamic responses
p 1095 A93-52438
- Finite state aeroelastic model for use in rotor design optimization
p 1104 A93-52454
- Envelope function - A tool for analyzing flutter data
p 1136 A93-52455
- Nonlinear aspects of transonic aeroelasticity
p 1096 A93-52642
- Flutter analysis of stiffened laminated composite plates and shells in supersonic flow
p 1216 A93-53224
- Finite element analysis of natural vibrations of an aeroplane with asymmetric variable wing geometry
p 1218 A93-53776
- Data acquisition for aeroelastic testing at the NASA Langley Transonic Dynamics Facility
p 1250 A93-54397
- Damped advanced composite parts
p 1253 A93-55871
- The whirl-flutter problem in aircraft construction
p 1249 A93-56218
- Navier-Stokes dynamics and aeroelastic computations for vortical flows, buffet and aeroelastic applications
[NASA-CR-190692] p 17 N93-10098
- Nonlinear aeroelasticity of composite structures
[AD-A254285] p 47 N93-10842
- Modeling and model simplification of aeroelastic vehicles: An overview
[NASA-TM-107691] p 64 N93-12216
- Stochastic sensitivity measure for mistuned high-performance turbines
[NASA-TM-105821] p 90 N93-12277
- The Fourth Workshop on Dynamics and Aeroelastic Stability Modeling of Rotorcraft Systems
[AD-A255065] p 50 N93-12485
- Nonlinear stall flutter of wings with bending-torsion coupling
[AD-A254323] p 186 N93-12959
- Dynamic stall effects on hingeless rotor stability with experimental correlation
p 129 N93-13010
- Active flutter suppression using dipole filters
[NASA-TM-107594] p 186 N93-13367
- Transonic aeroelastic analysis of systems with structural nonlinearities
p 217 N93-13769
- Hypersonic panel flutter in a rarefied atmosphere
p 188 N93-13928
- A compilation of the mathematics leading to the doublet lattice method
[AD-A256304] p 136 N93-14441
- The effect of wake dynamics on rotor eigenvalues in forward flight
p 137 N93-14595
- Multi-disciplinary optimization of aeroservoelastic systems
[NASA-CR-191255] p 220 N93-14766
- Finite-state inflow applied to aeroelastic flutter of fixed and rotating wings
p 188 N93-14830
- Aeroelastic stability and response of rotating structures
[NASA-CR-191803] p 371 N93-16560
- Developing a control system for ARES 2
p 371 N93-16769
- Introduction to Flutter of Winged Aircraft, volume 1
[VKI-LS-1992-01] p 372 N93-18142
- The unified method of aeroelasticity
p 372 N93-18143
- Computational Fluid Dynamics, volume 2
[VKI-LS-1992-04-VOL-2] p 421 N93-18563
- Algorithm development with applications to aerodynamics and aeroelasticity
p 422 N93-18566
- Structural dynamics branch research and accomplishments to FY 1992
[NASA-TM-105824] p 552 N93-20368
- The influence of structural optimization on the aeroelastic properties of a vertical tail
[AD-A259140] p 513 N93-20575
- Analytical and experimental investigation of flutter suppression by piezoelectric actuation
[NASA-TP-3241] p 513 N93-20584
- Fluid/structures interactions. Aircraft considerations
p 527 N93-20628
- Structural Tailoring of Advanced Turboprops (STAT). Theoretical manual
[NASA-CR-191017] p 556 N93-22005
- An aeroelastic model structure investigation for a manned real-time rotorcraft simulation
p 693 N93-24756
- Application of finite-state inflow to flap-lag-torsion damping in hover
p 714 N93-25486
- Aeroelastic response and aeromechanical stability of helicopters with elastically coupled composite rotor blades
p 715 N93-25530
- An integrated finite-state model for rotor deformation, nonlinear airloads, inflow, and trim
p 715 N93-25538
- Supersonic aeroelastic instability results for a NASP-like wing model
[NASA-TM-107739] p 718 N93-26553
- A transfer matrix approach to vibration localization in mistuned blade assemblies
[NASA-TM-106112] p 838 N93-27088
- Towards an analytical treatment of the aerostatic problem of a circular wing
p 781 N93-27214
- The natural excitation technique (NEXT) for modal parameter extraction from operating wind turbines
[DE93-010611] p 845 N93-28603
- Transonic flows on an oscillating airfoil and their effect on the flutter-boundary
[DLR-FB-92-08] p 790 N93-29006
- An integrated optimum design approach for high speed prop-rotors including acoustic constraints
[NASA-CR-193222] p 893 N93-29153
- Integrated structural design, vibration control, and aeroelastic tailoring by multiobjective optimization
p 1030 N93-31137
- Localization of aeroelastic modes in mistuned high-energy turbines
p 1032 N93-31586
- On the dynamics of aeroelastic oscillators with one degree of freedom
[REPT-92-96] p 1040 N93-31653
- AERONAUTICAL ENGINEERING**
- Specific educational aspects of airport engineering in Spain and the Hispanic world
p 103 A93-12560
- Aeronautical fatigue: Key to safety and structural integrity: Proceedings of the 16th ICAF Symposium, Tokyo, Japan, May 22-24, 1991
[ISBN 4-9900181-1-7] p 80 A93-13626
- Structural integrity challenges
p 3 A93-13627
- Aircraft tracking optimization of parameters selection
p 3 A93-13628
- Annual Paul E. Hemke Lecture in aerospace engineering
p 107 A93-14067
- Looking and seeing - A practical problem --- aircraft maintenance and inspection
p 238 A93-18758
- Aeronautical engineering education for the armed forces
p 453 A93-21681
- AIAA's role in aerospace education
[AIAA PAPER 93-0324] p 454 A93-23016
- Reform of the aeronautics and astronautics curriculum at MIT
[AIAA PAPER 93-0325] p 454 A93-23017
- The development of a mature external Master's degree program in aeronautical engineering - A university/industry partnership
[AIAA PAPER 92-4256] p 570 A93-24296
- Being an engineer - A risky occupation? Proceedings of the Conference, London, United Kingdom, June 8, 1993
[ISBN 1-85768-120-7] p 945 A93-43869
- Design of aircraft, helicopters, and aviation engines --- Russian book
[ISBN 5-277-01192-7] p 947 A93-44508

- Aeronautical technologies for the twenty-first century
[NASA-CR-190918] p 4 N93-10647
- Review of aeronautical fatigue investigation activities developed in Alenia-GAT during the period May 1990 - March 1991
[ETN-92-92884] p 329 N93-16287
- The Goldstein Aeronautical Engineering Research Laboratory
[AERO-REPT-9109] p 240 N93-16465
- Aeronautical Engineering Group publications: 1950 - present
[AERO-REPT-9108] p 454 N93-16563
- Industry survey of space system cost benefits from New Ways Of Doing Business
p 454 N93-17325
- Dr. Alexander H. Flax: Technologist of aeronautics
[AD-A258441] p 456 N93-17890
- Proceedings of the Ninth NAL Symposium on Aircraft Computational Aerodynamics
[NAL-SP-16] p 299 N93-19273
- LES turbulence modeling using DNS data base
p 299 N93-19274
- A simple grid generation technique for hypersonic flow around complex configuration
p 299 N93-19275
- Computation of internal flows using unstructured triangular meshes
p 299 N93-19276
- Numerical computations using multi-domain technique
p 299 N93-19277
- Numerical simulations of hypersonic rarefied transition regime flows: DSMC method and Navier-Stokes computation
p 299 N93-19278
- Monte Carlo simulation of normal shock wave. Part 1: Lennard-Jones potential
p 300 N93-19279
- Satisfying the customer's requirements
[PNR-90988] p 521 N93-20735
- Modelisation and computation of composite materials
p 537 N93-21518
- JPRS report: Central Eurasia. Aviation and cosmonautics, no. 9, September 1992
[JPRS-UAC-93-003] p 678 N93-26325
- Aeronautics and space report of the President: Fiscal year 1992 activities
p 854 N93-27041
- Aviation production engineering: Selected articles
[AD-A261231] p 764 N93-27056
- JPRS report: Science and technology. Central Eurasia: Engineering and equipment
[JPRS-UEQ-92-007] p 842 N93-28635
- JPRS report: Science and technology. Central Eurasia: Engineering and equipment
[JPRS-UEQ-92-006] p 842 N93-28636
- JPRS report: Science and technology. Central Eurasia: Engineering and equipment
[JPRS-UEQ-92-010] p 842 N93-28674
- JPRS report: Science and technology. Central Eurasia: Engineering and equipment
[JPRS-UEQ-92-008] p 842 N93-28675
- JPRS report: Science and technology. Central Eurasia: Engineering and equipment
[JPRS-UEQ-93-003] p 842 N93-28691
- Preliminary design studies of an advanced general aviation aircraft
p 894 N93-29717
- AERONAUTICAL SATELLITES**
The use of satellites for aeronautical communications, navigation and surveillance
p 881 A93-40436
- AERONAUTICS**
The aeronautical volcanic ash problem
p 309 A93-22156
- Evolutionary NASA - Inventors to bureaucrats
p 1174 A93-50330
- AGARD index of publications, 1989-1991
[AGARD-INDEX-89-91] p 104 N93-10610
- Index to NASA news releases and speeches, 1991
[NASA-TM-108004] p 104 N93-10815
- Index to NASA news releases and speeches, 1990
[NASA-TM-108003] p 104 N93-10872
- Winds of change: Expanding the frontiers of flight. Langley Research Center's 75 years of accomplishment, 1917-1992
[NASA-NP-130] p 104 N93-11100
- Directory of factual and numeric databases of relevance to aerospace and defence R and D
[AGARD-R-777] p 104 N93-11710
- Coordinating Council. Fourth Meeting: NACA Documents Database Project
[NASA-TM-108017] p 234 N93-12671
- Coordinating Council. Sixth Meeting: Who Are Our Key Users?
[NASA-TM-108021] p 234 N93-12672
- NASA aeronautics: Research and technology program highlights
[NASA-NP-159] p 109 N93-13110
- The 1992 Research/Technology report
[NASA-TM-105924] p 459 N93-20902
- JPRS report: Central Eurasia. Aviation and cosmonautics, no. 9, September 1992
[JPRS-UAC-93-003] p 678 N93-26325

- Research and technology objectives and plans: Summary fiscal year 1991
[NASA-TM-103086] p 946 N93-29452
- Reynolds number influences in aeronautics
[NASA-TM-107730] p 989 N93-31732
- AERONOMY**
Aeronomy coexperiments on drag-free satellites with proportional thrusters: GP-B and STEP
p 195 N93-13922
- AEROSERVOELASTICITY**
Aeroservoelastic analysis of an aircraft model incorporating the minimum state method for approximating unsteady aerodynamics
p 154 A93-14258
- Study of aeroservoelastic stability of an aircraft
p 182 A93-14259
- Aeroservoelasticity in HiSAIR --- High Speed Airframe Integration Research
[AIAA PAPER 92-4719] p 324 A93-20322
- An approach to tiltrotor wing aeroservoelastic optimization through increased productivity
[AIAA PAPER 92-4781] p 326 A93-20371
- ISAC - A tool for aeroservoelastic modeling and analysis --- Interaction of Structures, Aerodynamics, and Control
[AIAA PAPER 93-1421] p 726 A93-33974
- Actuator and aerodynamic modeling for high-angle-of-attack aeroservoelasticity
[AIAA PAPER 93-1419] p 818 A93-37433
- Alternative approximations for integrated control/structure aeroservoelastic synthesis
p 819 A93-39418
- Multi-disciplinary optimization of aeroservoelastic systems
[NASA-CR-191255] p 220 N93-14766
- AEROSOLS**
Wind lifting of aerosol particles
p 223 A93-15079
- Measurements of jet aircraft emissions at cruise altitude. I - The odd-nitrogen gases NO, NO₂ and HNO₃
p 556 A93-24391
- Potential impact of combined NO(x) and SO(x) emissions from future High Speed Civil Transport aircraft on stratospheric aerosols and ozone
p 753 A93-35372
- Atmospheric aerosols due to aircraft and ecological problems
p 1162 A93-48846
- NO(x) scavenging on carbonaceous aerosol surfaces in aircraft exhaust plumes. I
[AIAA PAPER 93-2343] p 1164 A93-50117
- Particulates and aerosols characterized in real time for harsh environments using the UMR mobile aerosol sampling system (MASS)
[AIAA PAPER 93-2344] p 1156 A93-50118
- Lift and drag forces on droplets and particles in wall-bounded shear flows
[DE93-002678] p 419 N93-17761
- An analysis of lift forces on aerosols in a wall bounded turbulent shear flow
[DE93-003362] p 747 N93-24963
- Natural and augmented snowfall growth processes and their interactions with the natural and modified aerosol
[PB93-153096] p 755 N93-25874
- AEROSPACE ENGINEERING**
Computational nonlinear mechanics in aerospace engineering
[ISBN 1-56347-044-6] p 78 A93-12151
- Stochastic computational mechanics for aerospace structures
p 78 A93-12157
- Aerospace - Collected translations of selected papers, 1992
p 2 A93-12726
- DLR, Annual report 1991/92
p 383 A93-18717
- AIAA/USAF/NASA/OAI Symposium on Multidisciplinary Analysis and Optimization, 4th, Cleveland, OH, Sept. 21-23, 1992, Technical Papers. Pts. 1 & 2
p 435 A93-20301
- Advanced aerospace hydraulic systems and components
[SAE SP-885] p 412 A93-21840
- The design of a senior-level CAD course with emphasis on fluid/thermal systems
[AIAA PAPER 93-0426] p 454 A93-23344
- Construction of a one-third scale model of the NASP
[AIAA PAPER 93-0427] p 386 A93-23345
- Trends in international aerospace ground test facilities
[AIAA PAPER 93-0348] p 528 A93-25518
- The importance of configuration management - An overview with test program sets
p 853 A93-35926
- An application of knowledge-based engineering to composite tooling design
p 846 A93-36010
- Applications to fixed-wing aircraft and spacecraft
p 996 A93-45432
- Development of computational solid mechanics and its application in aerospace engineering
p 1255 A93-54419
- NDT for corrosion in aerospace structures; Proceedings of the Conference, London, United Kingdom, Feb. 12, 1992
[ISBN 0-903409-99-2] p 1257 A93-54894

- NDT for corrosion in aerospace structures - A review of NDT techniques
p 1258 A93-54897
- AGARD index of publications, 1989-1991
[AGARD-INDEX-89-91] p 104 N93-10610
- Index to NASA news releases and speeches, 1991
[NASA-TM-108004] p 104 N93-10815
- Index to NASA news releases and speeches, 1990
[NASA-TM-108003] p 104 N93-10872
- Neutron diffraction residual stress studies for aero-engine component applications
[PNR-90908] p 85 N93-11014
- Rotational CARS measurements in a rotating cavity with axial throughflow of cooling air: Oxygen concentration measurements
[PNR-90935] p 72 N93-11035
- Innovation in engineering
[PNR-90889] p 59 N93-11207
- Simultaneous engineering in aero gas turbine design and manufacture
[PNR-90890] p 59 N93-11208
- The changing nature of design
[PNR-91011] p 48 N93-11334
- Directory of factual and numeric databases of relevance to aerospace and defence R and D
[AGARD-R-777] p 104 N93-11710
- Development of a menu driven materials data base for use on personal computers: Aircraft structures technical memorandum
[AD-A256317] p 392 N93-16403
- 1991 research and technology
[NASA-TM-103924] p 456 N93-16652
- The F-18 systems research aircraft facility
[NASA-TM-4433] p 381 N93-16753
- National Aeronautics and Space Administration
p 454 N93-17091
- The 1992 Research/Technology report
[NASA-TM-105924] p 459 N93-20902
- Scientific visualization using the Flow Analysis Software Toolkit (FAST)
p 758 N93-25600
- Aeronautics in NACA and NASA
[NASA-NP-156] p 678 N93-26422
- Aeronautics and space report of the President: Fiscal year 1992 activities
p 854 N93-27041
- Collection of papers of the 31st Israel Annual Conference on Aviation and Astronautics
[ITN-93-85187] p 764 N93-27166
- Center for Aeronautics and Space Information Sciences
[NASA-CR-193140] p 848 N93-27289
- International aviation (Selected articles)
[AD-A262566] p 765 N93-28576
- JPRS report: Science and technology. Central Eurasia: Engineering and equipment
[JPRS-UEQ-92-007] p 842 N93-28635
- JPRS report: Science and technology. Central Eurasia: Engineering and equipment
[JPRS-UEQ-92-006] p 842 N93-28636
- JPRS report: Science and technology. Central Eurasia: Engineering and equipment
[JPRS-UEQ-92-010] p 842 N93-28674
- JPRS report: Science and technology. Central Eurasia: Engineering and equipment
[JPRS-UEQ-92-008] p 842 N93-28675
- JPRS report: Science and technology. Central Eurasia: Engineering and equipment
[JPRS-UEQ-93-003] p 842 N93-28691
- Research and technology objectives and plans: Summary fiscal year 1991
[NASA-TM-103086] p 946 N93-29452
- Design study to simulate the development of a commercial transportation system
p 894 N93-29718
- NASA-UVA light aerospace alloy and structure technology program supplement: Aluminum-based materials for high speed aircraft
[NASA-CR-4517] p 1019 N93-31643
- European aerospace science and technology, 1992: A bibliography with indexes
[NASA-SP-7105] p 949 N93-32404
- AEROSPACE INDUSTRY**
Practical considerations in waverider applications
[AIAA PAPER 92-4247] p 43 A93-13326
- Accuracy of a simple hole damage analysis method in composite structures
p 197 A93-15748
- The development of a mature external Master's degree program in aeronautical engineering - A university/industry partnership
[AIAA PAPER 92-4256] p 570 A93-24296
- CST gives aircraft industry a lift --- computational structures technology
p 560 A93-25086
- Europe adapts CST to its needs --- computational structures technology for aerospace industry
p 560 A93-25088
- Computed tomography of advanced materials and processes
p 832 A93-38975
- Airbus or the revival of European civil aviation
p 856 A93-42655

SUBJECT INDEX

- International aerospace STI p 1227 A93-53826
Status of R&D of high-performance materials for severe environments (Composite materials) p 1253 A93-54728
Damping in aerospace composite materials p 1260 A93-55869
Special publication of National Aerospace Laboratory [DE93-716195] p 239 N93-15949
Professor Wittenberg: His speciality and versatility [ISBN-90-6275-670-0] p 240 N93-19002
Applied aerodynamics: Challenges and expectations [NASA-TM-103963] p 694 N93-25091
French aerospace equipment p 1041 N93-31734
Applications of structural optimization methods to fixed-wing aircraft and spacecraft in the 1980s [NASA-TM-103939] p 1033 N93-32212
- AEROSPACE MEDICINE**
Postmortem alcohol production in fatal aircraft accidents [AD-A255766] p 143 N93-14026
Aircraft Accidents: Trends in Aerospace Medical Investigation Techniques [AGARD-CP-532] p 490 N93-19653
US Army's aviation life support equipment retrieval program real world design successes from proactive investigation p 494 N93-19690
- AEROSPACE PLANES**
Integrated air separation and propulsion system for aerospace plane with atmospheric oxygen collection [SAE PAPER 920974] p 195 A93-14633
Subsonic static and dynamic stability characteristics of the test technique demonstrator NASP configuration [AIAA PAPER 93-0519] p 268 A93-21111
Overview of Japanese aerospace plane [AIAA PAPER 92-5005] p 384 A93-22282
Closed form solutions of constrained trajectories - Application in optimal ascent of aerospace plane [AIAA PAPER 92-5012] p 385 A93-22288
An aerospace plane as a detonation wave ramjet/airframe integrated waverider [AIAA PAPER 92-5022] p 272 A93-22298
Test results on air turbo ramjet for a futurespace plane [AIAA PAPER 92-5054] p 359 A93-22325
Stratospheric turbulence measurements and models for aerospace plane design [AIAA PAPER 92-5072] p 433 A93-22342
Numerical simulation of supersonic flow around space plane for airframe-engine integration [AIAA PAPER 93-0886] p 471 A93-24946
Spaceplanes - Back to the future p 733 A93-34265
MAKS - Eastern promise? --- multi-purpose aerospace system p 733 A93-34266
Aerospace plane design challenge - Credible computations p 1015 A93-45145
Air dissociation effects on aerodynamic characteristics of an aerospace plane p 959 A93-45149
Near-term two-stage-to-orbit, fully reusable, horizontal take-off/landing launch vehicle p 1015 A93-45441
Simulation of hypersonic flight - A concerted European effort p 1136 A93-49301
Will aerospace plane development go international? p 1043 A93-49331
Analytical solutions to constrained hypersonic flight trajectories p 1141 A93-49596
Fusion-electric propulsion for hypersonic flight [AIAA PAPER 93-2611] p 1142 A93-50318
Analysis of a turning point problem in flight trajectory optimization p 1210 A93-52885
HL-20 operations and support requirements for the Personnel Launch System mission p 1210 A93-53745
Development study on Air Turbo Ramjet engine for a future space plane [ISABE 93-7016] p 1195 A93-53992
Complementary role of ground testing, flight testing, and computations in aerospace plane propulsion development [ISABE 93-7034] p 1197 A93-54010
Effect of film cooling/regenerative cooling on scramjet engine performances p 1197 A93-54012
Performance analysis of a turbofan as a part of an airbreathing propulsion system for space shuttles p 1252 A93-56039
A configuration development strategy for the NASP p 46 N93-10011
Simulation analysis of a cable-mount system used for dynamic wind tunnel tests [NAL-TR-1127] p 68 N93-12359
On stability and control of SSTO spaceplane in super- and hypersonic ascending phase [NAL-TR-1128T] p 65 N93-12361
Current Technology for Thermal Protection Systems [NASA-CP-3157] p 69 N93-12447

- Current research in oxidation-resistant carbon-carbon composites at NASA, Langley Research Center p 74 N93-12456
Thermal control/oxidation resistant coatings for titanium-based alloys p 74 N93-12457
Active cooling from the sixties to NASP p 49 N93-12458
NASA aeronautics: Research and technology program highlights [NASA-NP-159] p 109 N93-13110
National Aero-Space Plane: Key issues facing the program. Testimony before the Subcommittee on Technology and Competitiveness, Committee on Science, Space, and Technology, House of Representatives [GAO/T-NSIAD-92-26] p 161 N93-13253
Stratospheric turbulence measurements and models for aerospace plane design [NASA-TM-104262] p 223 N93-13288
Performance and control of ascending trajectories to minimize heat load for transatmospheric aero-space planes p 133 N93-13745
Robust nonlinear feedback guidance for an aerospace plane: A geometric approach p 189 N93-14835
National Aeronautics and Space Administration p 454 N93-17091
Increase of stagnation pressure and enthalpy in shock tunnels p 295 N93-18086
Hypersonic flows as related to the national aerospace plane [NASA-CR-191980] p 296 N93-18378
Analytical solutions to constrained hypersonic flight trajectories [NASA-CR-191987] p 297 N93-18602
National aero-space plane: Restructuring future research and development efforts [AD-A258799] p 340 N93-18981
Nozzle/cowl optimization for a hypersonic vehicle on a typical trajectory [AD-A258827] p 341 N93-19089
Flight simulator for hypersonic vehicle and a study of NASP handling qualities p 530 N93-19456
The National Aero-Space Plane program: A revolutionary concept p 511 N93-19908
Turbulence modeling for hypersonic flight [NASA-CR-192288] p 483 N93-20235
Research on combined HOPE navigation technology p 533 N93-20428
Trajectory optimization for the National aerospace plane [NASA-CR-192954] p 716 N93-25670
Numerical simulation of hypersonic aerodynamics and the computational needs for the design of an aerospace plane [AD-A260681] p 699 N93-25894
Supersonic aeroelastic instability results for a NASP-like wing model [NASA-TM-107739] p 718 N93-26553
Hypersonics revisited p 781 N93-27167
Technology transfer: Potential of BMFT concept for hypersonics [MBB-LME-202-S-PUB-0505] p 1041 N93-31045
- AEROSPACE SAFETY**
A review of civil aviation propeller-to-person accidents: 1980-1989 [AD-A260695] p 705 N93-25896
PROAV Cable Warning System (CWS) - U.S. Army aircraft Integration assessment and OCONUS field evaluation [AD-A261233] p 705 N93-26263
Airborne derivation of microburst alerts from ground-based Terminal Doppler Weather Radar information: A flight evaluation [NASA-TM-108990] p 1000 N93-32223
- AEROSPACE SCIENCES**
Aerospace '92 - The year in review p 455 A93-19976
Multidisciplinary computational aerosciences p 437 A93-20711
AGARD index of publications, 1989-1991 [AGARD-INDEX-89-91] p 104 N93-10610
Index to NASA news releases and speeches, 1991 [NASA-TM-108004] p 104 N93-10815
Index to NASA news releases and speeches, 1990 [NASA-TM-108003] p 104 N93-10872
Winds of change: Expanding the frontiers of flight, Langley Research Center's 75 years of accomplishment, 1917-1992 [NASA-NP-130] p 104 N93-11100
Coordinating Council. Sixth Meeting: Who Are Our Key Users? [NASA-TM-108021] p 234 N93-12672
1991 research and technology [NASA-TM-103924] p 456 N93-16652
JPRS report: Science and technology. Japan. 30th National Aerospace Laboratory Conference [JPRS-JST-93-009] p 761 N93-25418

AEROTHERMOCHEMISTRY

- Aeronautics in NACA and NASA [NASA-NP-156] p 678 N93-26422
Center for Aeronautics and Space Information Sciences [NASA-CR-193140] p 848 N93-27289
Research and technology objectives and plans: Summary fiscal year 1991 [NASA-TM-103086] p 946 N93-29452
European aerospace science and technology, 1992: A bibliography with indexes [NASA-SP-7105] p 949 N93-32404
- AEROSPACE SYSTEMS**
Electro-optic architecture (EOA) for sensors and actuators in aircraft propulsion systems [NASA-CR-182270] p 233 N93-15116
Technical needs and research opportunities provided by projected aeronautical and space systems [NASA-CR-192124] p 386 N93-16629
The National Aero-Space Plane program: A revolutionary concept p 511 N93-19908
Application of artificial neural networks to the design optimization of aerospace structural components [NASA-TM-4389] p 555 N93-21831
Game theoretic synthesis for robust aerospace controllers p 819 N93-27171
Parameter identification for nonlinear aerodynamic systems [NASA-CR-193072] p 782 N93-27282
Center for Aeronautics and Space Information Sciences [NASA-CR-193140] p 848 N93-27289
- AEROSPACE TECHNOLOGY TRANSFER**
CST gives aircraft industry a lift --- computational structures technology p 560 A93-25086
MIDAS technology transfer p 845 A93-35920
Improved Airframe Manufacturing Technology p 763 A93-35971
What can Japan teach the U.S. about composites? p 1144 A93-49336
AGARD index of publications, 1989-1991 [AGARD-INDEX-89-91] p 104 N93-10610
JPRS report: Science and technology. Japan. 30th National Aerospace Laboratory Conference [JPRS-JST-93-009] p 761 N93-25418
Technology transfer: Potential of BMFT concept for hypersonics [MBB-LME-202-S-PUB-0505] p 1041 N93-31045
- AEROSPACE VEHICLES**
Aerospace '92 - The year in review p 455 A93-19976
Near wake structure for a generic ASTV configuration [AIAA PAPER 93-0271] p 268 A93-21103
Trends in international aerospace ground test facilities [AIAA PAPER 93-0348] p 528 A93-25518
Application of advanced guidance and navigation systems to flight control of aircraft and future space vehicles p 500 A93-28153
Analytical solutions to constrained hypersonic flight trajectories p 1141 A93-49596
Thermostructural applications of heat pipes for cooling leading edges of high-speed aerospace vehicles p 91 N93-12460
Experiments and analysis concerning the use of external burning to reduce aerospace vehicle transonic drag p 70 N93-12537
Multidisciplinary design optimization using response surface analysis p 330 N93-16796
Increase of stagnation pressure and enthalpy in shock tunnels p 295 N93-18086
Analytical solutions to constrained hypersonic flight trajectories [NASA-CR-191987] p 297 N93-18602
Dynamic System Coupler Program (DYSCO 4.1). Volume 2: User's manual [AD-B131157L] p 848 N93-27589
Advanced electromagnetic methods for aerospace vehicles [NASA-CR-193468] p 936 N93-31036
NASA-Uva light aerospace alloy and structure technology program supplement: Aluminum-based materials for high speed aircraft [NASA-CR-4517] p 1019 N93-31643
- AEROTHERMOCHEMISTRY**
COF2 radiation from an air-TEFON wake p 12 A93-12659
Fluid/chemistry modeling for hypersonic flight analysis p 111 A93-14120
Role of hydrogen/air chemistry in nozzle performance for a hypersonic propulsion system p 359 A93-21668
An upwind, kinetic flux-vector splitting method for flows in chemical and thermal non-equilibrium [AIAA PAPER 93-0894] p 472 A93-24954
Reacting gas and surface coupling in high temperature air flows p 686 A93-34353
Simulation of ablation in Earth atmospheric entry [AIAA PAPER 93-2789] p 1027 A93-46531

Aerothermal ablative characterization of selected external insulator candidates p 1145 A93-49735
 [AIAA PAPER 93-1857]
 Numerical model for predictions of reverse flow combustor aerothermal characteristics p 1123 A93-51645
 Chemical nonequilibrium effects of Mach reflection p 1233 A93-54816
 Chemical kinetic and aerodynamic structures of flames [AD-A256015] p 391 A93-15931
 Computational study of real gas effects in high speed high temperature flow, volume 2 [AERO-REPT-9203-VOL-2] p 289 A93-16470

AEROTHERMODYNAMICS
 Extreme value heat transfer problems for three-dimensional bodies moving at hypersonic velocities p 4 A93-10079
 Thermal shock capabilities of infrared dome materials p 70 A93-11454
 Viscous equilibrium computations using program LAURA p 8 A93-12002
 Payload vehicle aerodynamic re-entry analysis p 69 A93-12004
 Shuttle Orbiter computation p 9 A93-12020
 Flow problems posed by reentry in planetary atmospheres p 11 A93-12432
 Fluid/chemistry modeling for hypersonic flight analysis p 111 A93-14120
 Calculation of radiant energy transfer in hypersonic flow past blunt bodies using the P1 and P2 approximations of the spherical harmonic method p 124 A93-15209
 Hot streaks and phantom cooling in a turbine rotor passage. II - Combined effects and analytical modelling [ASME PAPER 92-GT-76] p 401 A93-19326
 Heat transfer and turbulence in a turbulated blade cooling circuit [ASME PAPER 92-GT-187] p 402 A93-19412
 Life cycle assessment of an impingement-cooled gas turbine blade [AIAA PAPER 92-4716] p 358 A93-20321
 Aerothermodynamic analysis of combined-cycle propulsion systems p 359 A93-21671
 German university research in hypersonics [AIAA PAPER 92-5033] p 239 A93-22307
 Validation of aerodynamic simulation methods for Hermes spaceplane and future hypersonic vehicles [AIAA PAPER 92-5065] p 273 A93-22335
 A comparison of hypersonic flight and prediction results [AIAA PAPER 93-0311] p 280 A93-23006
 Isolator-combustor interaction in a dual-mode scramjet engine [AIAA PAPER 93-0358] p 360 A93-23041
 An estimate of the 'doomed propellant fraction' for a Superdetonative Ram Accelerator [AIAA PAPER 93-0359] p 385 A93-23042
 Overview of technical challenges of reentry analysis of radioisotope heat sources [AIAA PAPER 93-0379] p 386 A93-23059
 Development of Polytechnic University's supersonic wind tunnel facility [AIAA PAPER 93-0798] p 528 A93-24876
 Hypersonic inviscid and viscous flow computations with a new optimized thermodynamic equilibrium model [AIAA PAPER 93-0893] p 471 A93-24953
 Consideration of the completeness of combustion and dissociation and recombination processes in mathematical models of jet engines for high supersonic flight velocities p 520 A93-27627
 Effect of the thermodynamic air model on the aerodynamic characteristics of profiles with bends p 776 A93-39136
 Numerical modeling of ionization in nonequilibrium nitrogen flows in hypersonic nozzles p 836 A93-39137
 Flow density distribution in a two-phase submerged jet p 836 A93-39144
 Energetics of gas-surface interactions in transitional flows at entry velocities p 778 A93-39259
 Application of the multigrid solution technique to hypersonic entry vehicles [AIAA PAPER 93-2721] p 858 A93-41049
 Gas-kinetic and Navier-Stokes simulations of reentry flows p 865 A93-42582
 Intrusive and nonintrusive measurements of flow properties in arc jets p 943 A93-42584
 Application of program LAURA to thermochemical nonequilibrium flow through a nozzle p 871 A93-42644
 Microsensors for high heat flux measurements p 928 A93-42920
 An approximate method for calculating heating rates on three-dimensional vehicles [AIAA PAPER 93-2881] p 949 A93-44228

An overview of Ames experimental aerothermodynamics p 1011 A93-45496
 Solution strategy for three-dimensional configurations at hypersonic speeds p 962 A93-46406
 Simulation of ablation in Earth atmospheric entry [AIAA PAPER 93-2789] p 1027 A93-46531
 Measurement and analysis of nitric oxide radiation in an arc-jet flow [AIAA PAPER 93-2800] p 1016 A93-46540
 Numerical simulation of aerothermodynamics processes in gas turbine engine components p 1002 A93-46939
 Three dimensional aero-thermal characteristics of a high pressure turbine nozzle guide vane p 1002 A93-46942
 Langley proposed advanced hypervelocity aerophysics facility - A status report p 1013 A93-47015
 A family of multiblock codes for computational aerothermodynamics - Application to complete vehicle hypersonic flows [AIAA PAPER 93-3042] p 1056 A93-48223
 The European Data Base - A new CFD validation tool for the design of space vehicles [AIAA PAPER 93-3045] p 1057 A93-48225
 Aerothermodynamic heating due to shock wave/laminar boundary-layer interactions in high-enthalpy hypersonic flow [AIAA PAPER 93-3135] p 1064 A93-48299
 Simplified mathematical model and digital simulation of aerodynamic p 1106 A93-48511
 Computational aerothermodynamics for 2D and 3D space vehicles p 1073 A93-49533
 Harnessing nitrous oxide for elevation of temperature and pressure in piston facilities [AIAA PAPER 93-2016] p 1137 A93-49854
 Aerothermodynamics in combustors: IUTAM Symposium, National Taiwan Univ., Taipei, June 3-5, 1991, Selected Papers [ISBN 0-387-55404-1] p 1146 A93-51626
 New calculation methods contribution on turbomachinery design and development [ONERA, TP NO. 1993-60] p 1092 A93-51940
 An extended insight into hypersonic flow phenomena using numerical methods p 1093 A93-51999
 Aerodynamic heating environment definition/thermal protection system selection for the HL-20 p 1181 A93-53739
 HL-20 computational fluid dynamics analysis p 1181 A93-53740
 Studies on coolant problems in aeronautical turbine cascades [ISABE 93-7074] p 1220 A93-54050
 Static and dynamic errors in heat flux measurements p 1254 A93-54366
 Spectral measurements of shock layer radiation in an arc-jet wind tunnel p 1251 A93-54409
 Hypersonic vehicle research by using a large shock tunnel [AAS PAPER 91-607] p 1250 A93-55841
 Design of a high-temperature experiment for evaluating advanced structural materials [NASA-TM-105833] p 88 A93-11624
 Leading edge film cooling heat transfer including the effect of mainstream turbulence p 23 A93-11886
 Thermostructural applications of heat pipes for cooling leading edges of high-speed aerospace vehicles p 91 A93-12460
 A finite element model for analysis of thermoviscoplastic behavior of hypersonic leading edge structures subject to intense aerothermal heating p 137 A93-14631
 Aerothermodynamic flow phenomena of the airframe-integrated supersonic combustion ramjet [NASA-TM-4376] p 196 A93-15528
 Investigation of the aerothermodynamics of hypervelocity reacting flows in the ram accelerator [NASA-CR-191715] p 140 A93-15588
 Hot experimental technique: A new requirement of aerothermodynamics [MBB-FE-202-S-PUB-480] p 293 A93-17543
 H-P adaptive methods for finite element analysis of aerothermal loads in high-speed flows [NASA-CR-189739] p 420 A93-18093
 Issues and approach to develop validated analysis tools for hypersonic flows: One perspective [NASA-TM-103937] p 305 A93-19379
 Heat loads as key problem of hypersonic flight [MBB-FE-202-S-PUB-0486] p 484 A93-21054
 Numerical methods for aerothermodynamic design of hypersonic space transport vehicles [MBB-FE-211-S-PUB-0481] p 514 A93-21056
 Aerothermodynamic properties of hypersonic flows over radiation-adiabatic surfaces [DLR-FB-91-42] p 485 A93-21761
 Development and application of computational aerothermodynamics flowfield computer codes [NASA-CR-192940] p 692 A93-24736

Fuel Injector: Air swirl characterization aerothermal modeling, phase 2, volume 2 [NASA-CR-189193-VOL-2] p 721 A93-25106
 Increased heat transfer to elliptical leading edges due to spanwise variations in the freestream momentum: Numerical and experimental results [NASA-TM-106150] p 838 A93-27020
 The addition of algebraic turbulence modeling to program LAURA [NASA-TM-107758] p 840 A93-27250
 Heat transfer in high turbulence flows: A 2-D planar wall jet p 932 A93-29935
 Aerothermic calculations of flows in interdisc cavities of turbines p 903 A93-29947
 Aero-thermal design of a cooled transonic NGV and comparison with experimental results p 904 A93-29957
 Overview of aerothermodynamic loads definition study p 1016 A93-31583

AEROTHERMOELASTICITY
 Aerothermoelastic analysis of a NASP demonstrator model [AIAA PAPER 93-1366] p 733 A93-33933
 Nonlinear flutter of orthotropic composite panel under aerodynamic heating p 1025 A93-45740

AFTERBODIES
 Comparison of algebraic turbulence models for afterbody flows with jet exhaust p 123 A93-14554
 PNS predictions of axisymmetric hypersonic blunt-body and afterbody flowfields [AIAA PAPER 93-2725] p 962 A93-46479
 A visualizing method of streamlines around hypersonic vehicles [AIAA PAPER 93-3440] p 1014 A93-47230
 Supersonic base flow experiments in the near-wake of a cylindrical afterbody [AIAA PAPER 93-2924] p 1045 A93-48125
 An adaptive grid/Navier-Stokes methodology for the calculation of nozzle afterbody base flows with a supersonic freestream [AIAA PAPER 93-1922] p 1076 A93-49788
 A numerical analysis of supersonic flow over an axisymmetric afterbody [AIAA PAPER 93-2347] p 1083 A93-50121
 Optimization of afterbodies and engine nozzle by using CFD methods [ISABE 93-7098] p 1187 A93-54074
 Survey on techniques used in aerodynamic nozzle/airframe integration p 161 A93-13224
 CFD calibration for three-dimensional nozzle/afterbody configurations p 215 A93-13226
 Fabrication of the V-22 composite AFT fuselage using automated fiber placement p 920 A93-30443

AFTERBURNING
 Design verification of ground run-up noise suppressors for afterburning engines p 910 A93-42892
 The turbulence and mixing characteristics of the complex flow in a simulated augmentor p 1123 A93-51642
 Low-frequency combustion oscillations in a model afterburner p 1193 A93-53702
 A study on 3-D velocity distribution of isothermal flows behind an afterburner flame stabilizer [ISABE 93-7039] p 1197 A93-54015
 The design and development of an afterburner [ISABE 93-7041] p 1198 A93-54017
 Thrust augmentation system for low-cost-expendable turbojet engine [AD-A263727] p 905 A93-30877

AGE FACTOR
 Increase in mortality rates due to aircraft noise p 1163 A93-49551

AGING
 The civil scene - The authorities re-appraisal of ageing aircraft p 1229 A93-54895

AGING (MATERIALS)
 Aging review of the YS-11 aircraft p 46 A93-13635
 Analysis of multiple crack propagation in stiffened sheet p 81 A93-13638
 Acoustic emission monitoring of aging aircraft structures p 407 A93-19697
 Emerging technology for large-area scanning of aging aircraft [SME PAPER AD92-205] p 925 A93-40666
 Structural integrity of aging airplanes [ISBN 0-540-53461-X] p 947 A93-45772
 Towards quantitative non-destructive evaluation of aging aircraft p 1025 A93-45773
 Computational schemes for integrity analyses of fuselage panels in aging airplanes p 1025 A93-45774
 Risk analysis for aging aircraft fleets p 1025 A93-45775
 Aspects of aging aircraft - A transatlantic view p 1026 A93-45776
 The civil Damage Tolerance Requirements in theory and practice p 1026 A93-45777

- A damage tolerance approach for management of aging gas turbine engines p 1001 A93-45779
- Aging jet transport structural evaluation programs p 947 A93-45781
- NASA airframe structural integrity program p 1026 A93-45782
- The Aloha Airlines accident - A new era for aging aircraft p 991 A93-45783
- Structural integrity of aging airplanes - A perspective p 948 A93-45789
- How likely is multiple site damage? p 1027 A93-45791
- Results of review of Fokker F '28 'Fellowship' maintenance program p 948 A93-45793
- Estimation of requirements of inspection intervals for panels susceptible to Multiple Site Damage p 948 A93-45795
- Case study and simulation of fatigue damages and DTE of aging aircraft - A review of researches in Japan p 948 A93-45800
- The degradation of parachutes: Age and mechanical wear [AD-A252243] p 24 N93-12179
- AGING (METALLURGY)**
- Ageing aircraft research in the Netherlands [NLR-TP-91443-U] p 999 N93-32203
- AGREEMENTS**
- No rescue in sight for Warsaw plaintiffs from either courts or legislature - Montreal Protocol 3 drowns in committee p 945 A93-42999
- Sales, not subsidies, are the sticking point p 945 A93-43677
- Implications of European legislation post 1992: Proceedings of the Conference, London, United Kingdom, Mar. 12, 1992 [ISBN 1-85768-015-4] p 1043 A93-50353
- AH-64 HELICOPTER**
- AH-64A rotating load usage monitoring from fixed system information p 507 A93-27953
- Investigation of the flight mechanics simulation of a hovering helicopter p 798 A93-35990
- Development and validation of a comprehensive real time AH-64 Apache simulation model p 799 A93-35992
- Hydrogen-induced stress corrosion cracking susceptibility analysis of pitch links from the AH-64 Apache helicopter [AD-A260692] p 736 N93-25895
- AILERONS**
- Design of a full time wing leveler system using tab driven aileron controls [AIAA PAPER 92-4193] p 63 A93-13345
- Modelling for aileron induced unsteady aerodynamic effects for parameter estimation p 118 A93-14323
- A thermal analysis of an F/A-18 wing section for actuator thermal management [SAE PAPER 921023] p 158 A93-14650
- Nonclassical aileron buzz in transonic flow [AIAA PAPER 93-1479] p 829 A93-37439
- Spanwise aileron oscillations p 819 A93-39190
- Aileron and sideslip-induced unsteady aerodynamic modeling for lateral parameter estimation p 1007 A93-45144
- Comparative wind tunnel tests at high Reynolds numbers of NACA 64 621 airfoils with two aileron configurations p 967 A93-46823
- Cost effective process selection for composite structure [SME PAPER EM93-100] p 1043 A93-51727
- Program for calculation of aileron rolling moment and yawing moment coefficients at subsonic speeds [ESDU-88040] p 136 N93-14514
- AIR**
- Brush seal leakage performance with gaseous working fluids at static and low rotor speed conditions [ASME PAPER 92-GT-304] p 405 A93-19494
- Development and use of hydrogen-air torches in an altitude facility [AIAA PAPER 93-2176] p 1137 A93-49988
- Parameters influencing the hot-spot ignition of aviation fuel/air and ethylene/air mixtures p 704 N93-24886
- AIR BAG RESTRAINT DEVICES**
- US Army helicopter inertia reel locking failures p 493 N93-19689
- The effectiveness of airbags in reducing the severity of head injury from gunshot strikes in attack helicopters p 494 N93-19691
- AIR BREATHING BOOSTERS**
- Takeoff and landing analysis methodology for an airbreathing space booster p 914 A93-42927
- AIR BREATHING ENGINES**
- Hyperonic design p 156 A93-14346
- Integrated air separation and propulsion system for aerospace plane with atmospheric oxygen collection [SAE PAPER 920974] p 195 A93-14633
- The United States in the conquest of the hypersonic p 109 A93-15056
- Some topics of research on hypersonic airbreathing engines at National Aerospace Laboratory [ASME PAPER 92-GT-256] p 353 A93-19465
- Air-breathing hypersonic cruise - Prospects for Mach 4-7 waverider aircraft [ASME PAPER 92-GT-437] p 384 A93-19579
- Evaluation of some significant issues affecting trajectory and control management for air-breathing hypersonic vehicles [AIAA PAPER 92-5011] p 384 A93-22287
- Study of flow phenomena in high speed intakes [AIAA PAPER 92-5029] p 272 A93-22304
- Numerical simulation of supersonic flow around space plane for airframe-engine integration [AIAA PAPER 93-0886] p 471 A93-24946
- Propulsion/airframe integration issues for waverider aircraft [AIAA PAPER 93-0506] p 505 A93-25533
- Impact of aeroelasticity on propulsion and longitudinal flight dynamics of an air-breathing hypersonic vehicle [AIAA PAPER 93-1367] p 733 A93-33934
- Computational fluid dynamics for hypersonic airbreathing aircraft p 865 A93-42581
- CFD for hypersonic propulsion p 865 A93-42585
- Langley 8-foot high-temperature tunnel oxygen measurement system p 1010 A93-44892
- A propulsion device driven by reflected shock waves p 1001 A93-45550
- AEDC H2 Facility - New test capabilities for hypersonic air-breathing vehicles [AIAA PAPER 93-2781] p 1012 A93-46525
- Screening studies of advanced control concepts for airbreathing engines [AIAA PAPER 92-3320] p 1108 A93-49329
- Aerothermal ablative characterization of selected external insulator candidates [AIAA PAPER 93-1857] p 1145 A93-49735
- CFD applications in an aeropropulsion test environment [AIAA PAPER 93-1924] p 1112 A93-49790
- Numerical simulations of a pulsed detonation wave augmentation device [AIAA PAPER 93-1985] p 1112 A93-49832
- Advancing the state of the art hypersonic testing - HYTEST/MTMI [AIAA PAPER 93-2023] p 1113 A93-49860
- Thrust loss due to supersonic mixing [AIAA PAPER 93-2140] p 1114 A93-49958
- Boron particle ignition in high-speed flow [AIAA PAPER 93-2202] p 1145 A93-50014
- An experimental study of supersonic air-intake with 5-shock system at Mach 3 [AIAA PAPER 93-2305] p 1082 A93-50089
- The application of intelligent search strategies to robust flight control for hypersonic vehicles [AIAA PAPER 93-3732] p 1143 A93-51331
- Robust control of hypersonic vehicles considering propulsive and aeroelastic effects [AIAA PAPER 93-3762] p 1131 A93-51357
- High temperature heat exchangers for gas turbines and future hypersonic air breathing propulsion [ONERA, TP NO. 1993-75] p 1218 A93-53596
- ISABE - International Symposium on Air Breathing Engines, 11th, Tokyo, Japan, Sept. 20-24, 1993, Proceedings, Vols. 1 & 2 [ISBN 1-56347-071-3] p 1194 A93-53976
- Japan's research and development program for airbreathing engine technologies [ISABE 93-7005] p 1194 A93-53981
- Development study on Air Turbo Ramjet engine for a future space plane [ISABE 93-7016] p 1195 A93-53992
- Design and testing methods of high performance combustors for airbreathing engines [ISABE 93-7024] p 1196 A93-54000
- Thermal design and analysis of an exhaust diffuser unit in a ceramic composite [ISABE 93-7060] p 1220 A93-54036
- High density strained hydrocarbon fuels for air breathing propulsion [ISABE 93-7081] p 1213 A93-54057
- Performance analysis of a turbofan as a part of an airbreathing propulsion system for space shuttles p 1252 A93-56039
- Predicted aircraft effects on stratospheric ozone p 93 N93-11096
- Air-breathing hypersonic vehicle guidance and control studies: An integrated trajectory/control analysis methodology, phase 2 [NASA-CR-189703] p 65 N93-12413
- Experiments and analysis concerning the use of external burning to reduce aerospace vehicle transonic drag p 70 N93-12537
- Performance and control of ascending trajectories to minimize heat load for transatmospheric aero-space planes p 133 N93-13745
- Advanced hypersonic aircraft design [NASA-CR-192046] p 334 N93-18037
- Screening studies of advanced control concepts for airbreathing engines [NASA-TM-106042] p 721 N93-25079
- Turbulence interacting with chemical kinetics in airbreathing combustion of ducted rockets p 734 N93-26012
- AIR CARGO**
- Terrorism and air-specific perils and the liability of air freight carriers under Article 17 of the Warsaw Agreement p 570 A93-24252
- The development of a parachute system for aerial delivery from high speed cargo aircraft [DE93-008339] p 790 N93-29035
- Longitudinal acceleration test of overhead luggage bins in a transport airframe section [DOT/FAA/CT-92/9] p 991 N93-31652
- AIR CONDITIONING**
- Study on dynamic characteristics of heat exchanger p 924 A93-40492
- Engine driven chiller and thermal storage integration (Large tonnage engine driven chiller development) [PB92-227891] p 555 N93-21465
- AIR COOLING**
- Rotor cavity flow and heat transfer with inlet swirl and radial outflow of cooling air [ASME PAPER 92-GT-378] p 406 A93-19536
- Effective sealing of a disk cavity using a double-toothed rim seal [ASME PAPER 92-GT-379] p 406 A93-19537
- A compact, intercooled and regenerated gas turbine for HALE applications [ASME PAPER 92-GT-401] p 355 A93-19550
- Heat pipe turbine vane cooling p 519 A93-26114
- An experimental study of the air drying process in air coolers p 834 A93-39059
- Experimental evaluation of a cooled radial-inflow turbine [AIAA PAPER 93-1795] p 1110 A93-49685
- The study of experimental turboramjets - Heat state and cooling problems [AIAA PAPER 93-1989] p 1112 A93-49834
- Measurements and computational analysis of heat transfer and flow in a simulated turbine blade internal cooling passage [AIAA PAPER 93-1797] p 1218 A93-53585
- Rotational CARS measurements in a rotating cavity with axial throughflow of cooling air: Oxygen concentration measurements [PNR-90935] p 72 N93-11035
- Mach 4 testing of scramjet inlet models [NAL-TR-1137] p 26 N93-12369
- An evaluation of thermal energy storage options for precooled gas turbine inlet air [DE93-005980] p 754 N93-24975
- Experimental evaluation of a cooled radial-inflow turbine [NASA-TM-106230] p 816 N93-28697
- Transient thermal behaviour of a compressor rotor with axial cooling air flow and co-rotating or contra-rotating shaft p 903 N93-29946
- Impingement/effusion cooling p 932 N93-29954
- Measurements and computational analysis of heat transfer and flow in a simulated turbine blade internal cooling passage [NASA-TM-106189] p 1032 N93-31647
- AIR CURRENTS**
- Dynamic compensator design in nonlinear aerospace systems p 1036 A93-44150
- AIR CUSHION LANDING SYSTEMS**
- Some aspects of the design of combination landing gear --- for stable aircraft motion on runways p 891 A93-42374
- AIR DATA SYSTEMS**
- Recent flight-test results of optical airdata techniques [AIAA PAPER 92-4086] p 51 A93-13265
- Application of a flush airdata sensing system to a wing leading edge (LE-FADS) [AIAA PAPER 93-0634] p 516 A93-24750
- A fault-tolerant Air Data/Inertial Reference Unit p 807 A93-37074
- Discussion for the ideal AIMS p 167 N93-15153
- Software flexibility and configuration control for the A340/A330 Aircraft Condition Monitoring System (ACMS) p 167 N93-15154
- FDAMS: An extendable and reconfigurable solution for avionics data management systems p 168 N93-15157
- AIR DEFENSE**
- A database approach to aircraft carrier airplan production [AD-A257737] p 240 N93-17666

AIR DROP OPERATIONS

AIR DROP OPERATIONS

- Development testing of large ram air inflated wings [AIAA PAPER 93-1204] p 702 A93-35155
- Radial reefing method for accelerated and controlled parachute opening [AIAA PAPER 93-1209] p 702 A93-35159
- The development of a parachute system for aerial delivery from high speed cargo aircraft [AIAA PAPER 93-1232] p 703 A93-35174

AIR DUCTS

- Determination of fan noise in a lined duct with flow using the Green function method p 1124 A93-51761

AIR FILTERS

- Development and demonstration of a new filter system to control emissions during jet engine testing [AD-A261203] p 755 N93-26243

AIR FLOW

- A transfer standard of an air flow rate unit VET 150-2-87 p 66 A93-10049
- Viscous equilibrium computations using program LAURA p 8 A93-12002
- COF2 radiation from an air-tenon wake p 12 A93-12659
- Effect of the powerplant configuration on the air flow rate of the jet shield p 54 A93-12820
- An experimental study of dc discharges in supersonic and subsonic air flows p 14 A93-12980
- Wind lifting of aerosol particles p 223 A93-15079
- Effect of real air properties on integral aerodynamic characteristics p 242 A93-18241
- Design features of the GTD 8000 and GTD 15000 marine gas turbine engines [ASME PAPER 92-GT-15] p 400 A93-19287
- Simulation of the secondary air system of aero engines [ASME PAPER 92-GT-68] p 348 A93-19318
- Emissions reduction by varying the swirler airflow split in advanced gas turbine combustors [ASME PAPER 92-GT-110] p 349 A93-19347
- Air flow dynamics around an aerofoil by the stabilized finite difference method p 266 A93-20741
- Radiation mechanism for the aerodynamic sound of gears - An explanation for the radiation process by air flow observation p 451 A93-21859
- Development of an engineering level prediction method for high angle of attack aerodynamics [AIAA PAPER 93-0208] p 278 A93-22626
- Comparison of experimental ground testing and computational fluid dynamics for the re-engined 727-100 center engine inlet [AIAA PAPER 92-3920] p 462 A93-24294
- Reacting gas and surface coupling in high temperature air flows p 686 A93-34353
- AEDC expanded flow arc facility (HEAT-H2) description and calibration p 821 A93-37872
- A data system for the observation of flow conditions on an aircraft wing p 808 A93-37882
- The numerical model of supersonic air flow field with hydrogen transverse injection p 859 A93-41736
- Shock tunnel studies of external combustion in high supersonic air flows p 1017 A93-45517
- A preliminary investigation of the Helmholtz resonator concept for heat flux reduction [AIAA PAPER 93-2742] p 963 A93-46493
- Experimental and numerical investigation of supersonic turbulent flow in an annular duct [AIAA PAPER 93-3123] p 1063 A93-48291
- 3-D viscous flow CFD analysis of the propeller effect on an advanced ducted propeller subsonic inlet [AIAA PAPER 93-1847] p 1075 A93-49728
- Application of a dynamic compression system model to a low aspect ratio fan - Casing treatment and distortion [AIAA PAPER 93-1871] p 1111 A93-49746
- Real gas simulation of air Blow-Down Facilities [AIAA PAPER 93-2022] p 1137 A93-49859
- Tandem transverse hydrogen gas injection into a supersonic airflow [ISABE 93-7069] p 1201 A93-54045
- A general introduction to aeroacoustics and atmospheric sound p 1264 A93-55852
- Rotational CARS measurements in a rotating cavity with axial throughflow of cooling air: Oxygen concentration measurements [PNR-90935] p 72 N93-11035
- A general introduction to aeroacoustics and atmospheric sound [NASA-CR-189717] p 102 N93-12021
- ASTOVL model engine simulators for wind tunnel research p 192 N93-13213
- A preliminary study of the effect of equivalence ratio on a low emissions gas turbine combustor using KIVA-2 [DE92-018616] p 215 N93-13321
- A numerical investigation of 3D transverse injection into the supersonic flow behind rearward facing step p 303 N93-19316

- Uniform roughness studies [WL-TR-92-3041] p 751 N93-25951
- Method of measuring cross-flow vortices by use of an array of hot-film sensors [NASA-CASE-LAR-14824-1-SB] p 751 N93-26000
- Visualization of a Mach 2 reacting flow using Planar Laser-Induced Fluorescence (PLIF) p 731 N93-26006
- Efficient simulation of incompressible viscous flow over multi-element airfoils p 784 N93-27443
- Computational method in optimal bending-twisting comprehensive design of wings of subsonic and supersonic aircraft [AD-A262374] p 806 N93-27694
- Ventilation effects on smoke and temperature in an aircraft cabin quarter-scale model [DOT/FAA/CT-89/25] p 791 N93-28055
- Modification and calibration of the Naval Postgraduate School Academic Wind Tunnel [AD-A262092] p 823 N93-28189
- Jet mixer noise suppressor using acoustic feedback [NASA-CASE-LEW-15170-1] p 853 N93-28953
- The 3-D viscous flow CFD analysis of the propeller effect on an advanced ducted propeller subsonic inlet [NASA-TM-106240] p 900 N93-29162
- Aero-thermic calculations of flows in interdisc cavities of turbines p 903 N93-29947

AIR INTAKES

- Effect of the powerplant configuration on the air flow rate of the jet shield p 54 A93-12820
- Passive boundary-layer bleed for supersonic intakes p 114 A93-14212
- Researches on sonic fatigue of the air-inlet duct of XX aircraft p 154 A93-14256
- A digital simulation and its experimental investigation for the response of gas-turbine engines to intake flow distortion p 120 A93-14366
- Experimental and numerical study on the basic performance of a two-dimensional right-angled intake flow p 208 A93-15486
- Numerical simulation of the flow field around supersonic air-intakes [ASME PAPER 92-GT-206] p 251 A93-19430
- Experimental study of mixed compression air-intake for hypersonic airbreathing engines [ASME PAPER 92-GT-349] p 355 A93-19519
- Aircraft engine integration for the M88-Rafale couple [ASME PAPER 92-GT-403] p 322 A93-19552
- Interference of an oblique shock with a shock layer on a blunt edge for small Reynolds numbers p 775 A93-39120
- Mathematical model for the effect of turbulent velocity pulsations on the stability of a powerplant p 1003 A93-47508
- Intake flow modeling in a four stroke diesel using KIVA3 [AIAA PAPER 93-2952] p 1148 A93-48146
- Advanced SST auxiliary air intakes design and analysis [AIAA PAPER 93-2304] p 1082 A93-50088
- An experimental study of supersonic air-intake with 5-shock system at Mach 3 [AIAA PAPER 93-2305] p 1082 A93-50089
- Two-dimensional numerical simulation for Mach-3 multishock air-intake with bleed systems [AIAA PAPER 93-2306] p 1082 A93-50090
- A study of air intake parameters on the aerodynamic characteristics of a parasail p 1092 A93-51908
- Effect of boundary layer suction on the thrust and aerodynamic efficiency of a hypersonic flight vehicle p 1176 A93-52959
- On the numerical simulation of the two-dimensional flow field around a hypersonic air-intake-compressibility effects [ISABE 93-7100] p 1187 A93-54076
- Wind tunnel tests of the model of intake-airframe integration [ISABE 93-7101] p 1192 A93-54077
- Design of air intakes and nozzles for transonic rotational flows [ISABE 93-7102] p 1187 A93-54078
- A study on Mach 3 two-dimensional mixed compression air-intakes [ISABE 93-7106] p 1188 A93-54082
- A Eulerian/Lagrangian modelling to calculate the evolution of a water droplets spray [ISABE 93-7121] p 1221 A93-54096
- The combustion time lag and its role in ramjet combustion instability p 73 N93-11137
- Wind tunnel investigation of a twin-engine jet transport semi-span model with upper surface blown jet flap [NAL-TR-1134] p 26 N93-12503
- A novel-high-performance system for recording and analysing instantaneous total pressure distortion in air intakes p 214 N93-13215
- AGARD WG13 aerodynamics of high speed air intakes: Assessment of CFD results p 215 N93-13220

SUBJECT INDEX

- The effect of aircraft inlets on the behaviour of aero engine axial flow compressors p 422 N93-18722
 - Stall transients including effects of inlet distortion and intake geometry p 423 N93-18726
 - Numerical simulation of flows in a supersonic air intake p 303 N93-19314
 - A numerical simulations of inner flow of scramjet p 304 N93-19318
 - An evaluation of thermal energy storage options for precooled gas turbine inlet air [DE93-005980] p 754 N93-24975
- ### AIR JETS
- Experimental study of condensation vapor-air jets p 76 A93-10180
 - Acoustic properties of supersonic helium/air jets at low Reynolds numbers p 446 A93-19160
 - Optimization of circular orifice jets mixing into a heated crossflow in a cylindrical duct [AIAA PAPER 93-0249] p 361 A93-23246
 - Control of separation by dynamic air jets p 1066 A93-48504
 - Swirling flows in a contoured-wall combustion chamber [AIAA PAPER 93-1765] p 1073 A93-49661
 - Optimization of circular orifice jets mixing into a heated cross flow in a cylindrical duct [NASA-TM-105984] p 179 N93-15359
 - Fuel injector: Air swirl characterization aerothermal modeling, phase 2, volume 1 [NASA-CR-189193-VOL-1] p 721 N93-24754
 - Fuel injector: Air swirl characterization aerothermal modeling, phase 2, volume 2 [NASA-CR-189193-VOL-2] p 721 N93-25106
 - Control of jet noise [NASA-CR-193552] p 1040 N93-32221
- ### AIR LAND INTERACTIONS
- Drag and drag partition on rough surfaces p 79 A93-12460
 - Wind lifting of aerosol particles p 223 A93-15079
 - Spatial and temporal variations of the fluxes of carbon dioxide and sensible and latent heat over the FIFE site p 425 A93-20586
 - FIFE atmospheric boundary layer budget methods p 426 A93-20591
 - Assessing spatial and seasonal variations in grasslands with spectral reflectances from a helicopter platform p 426 A93-20621
 - Variability of geophysical parameters from aircraft radiance measurements for FIFE p 426 A93-20622
 - Remote sensing cloud properties from high spectral resolution infrared observations p 1034 A93-46780
- ### AIR LAUNCHING
- Wind tunnel test techniques for UAV separation investigations [AIAA PAPER 93-0626] p 524 A93-24743
- ### AIR LAW
- South American latest developments in the air law and air policy fields p 103 A93-12719
 - The creation of a Community cabotage area in the European Community and its implications for the US bilateral aviation system p 104 A93-13423
 - Air transport within the European single market - How will it look after 1992? A suggested view on the future p 104 A93-13424
 - Introduction to regulatory problems for supersonic transports p 234 A93-15032
 - Recent developments in aviation case law p 569 A93-23870
 - Obstacles to increasing airspace - Jumping through environmental law hoops p 569 A93-23872
 - Responsibility and assignment of roles on overlong flights p 570 A93-24253
 - Airlines, airports and antitrust - A proposed strategy for enhanced competition p 760 A93-34821
 - Tobacco smoking in aircraft - A fog of legal rhetoric? p 944 A93-40474
 - Federal preemption in commercial aviation - Tort litigation under 49 U.S.C. section 1305 p 944 A93-42997
 - The Foreign Sovereign Immunities Act of 1976 - Misjoinder, nonjoinder, and collusive joinder p 944 A93-42998
 - No rescue in sight for Warsaw plaintiffs from either courts or legislature - Montreal Protocol 3 draws in committee p 945 A93-42999
 - Bilateral transfers of safety oversight will prove beneficial to all states p 1174 A93-49279
 - Air carriers' liability for passenger injury or death - The Japanese Initiative and Response to the recent EC Consultation Paper p 1226 A93-52930
 - Air transport and the environment - Regulating aircraft noise p 1226 A93-52931
 - Flight safety in Europe p 1227 A93-53726
 - A general framework for analyzing choice-of-law problems in air crash litigation p 1265 A93-56537

- Promoting general aviation safety - A revision of pilot negligence law p 1265 A93-56540
- AIR NAVIGATION**
- Civil standardization of the Global Positioning System for the aviation community p 29 A93-10981
- A fault-tolerant air data/inertial reference system p 50 A93-10982
- Automatic dependant surveillance focus of civil avionics integration p 30 A93-10998
- Integrating TCAS into the airspace management system p 30 A93-11005
- Capacity as a consideration for providing aeronautical mobile satellite air traffic services in the U.S. domestic airspace p 30 A93-11007
- Integration of full scale development aircraft GPS user equipment (AN/ARN-151) with Doppler radar systems p 31 A93-11012
- Design, capabilities, and performance of the miniaturized airborne GPS receiver p 32 A93-11014
- Differential GPS/inertial navigation approach/landing flight test results p 32 A93-11019
- Jeppesen worldwide electronic NOTAM service --- Notice to Airmen p 1 A93-11020
- Magnetic variation - A primitive concept and its hold on contemporary navigation p 32 A93-11021
- The Microwave Landing System - A precision approach for the future p 32 A93-11023
- Maintaining high accuracy GPS positioning 'on the fly' --- using traverse closures, residual analysis, inertial navigation in aircraft p 92 A93-11028
- GPS integrity monitoring and system improvement with ground station and multistationary satellite support p 33 A93-11044
- History of aerial polar navigation p 104 A93-11300
- The 21st century navigation station p 34 A93-12123
- Options for control and navigation of unmanned aircraft p 34 A93-12124
- Optimization of time saving in navigation through an area of variable flow p 34 A93-12125
- The Tenth Conference on Air Navigation - A landmark in the history of civil aviation p 34 A93-12559
- ICAS, Congress, 18th, Beijing, China, Sept. 20-25, 1992, Proceedings. Vols. 1 & 2 p 107 A93-14151
- Precision increasing and integrity monitoring of navigation data for GPS/inertial hybrid solution p 149 A93-14157
- A new aircraft integrated positioning and communication system based on satellite p 150 A93-14236
- The employment of artificial intelligence for analyzing air accidents p 226 A93-14375
- European navigation into the 21st century - Frequency considerations p 311 A93-17754
- Model of a map indicator p 341 A93-18532
- The SSR mode-S data-link p 312 A93-18553
- Applications of space techniques to civil aviation operations p 312 A93-20007
- Integrated use of GPS and GLONASS in civil aviation navigation. II - Experience with GLONASS p 313 A93-21142
- GPS/GLONASS flight test, lab test and coverage analysis tests p 313 A93-21143
- A distributed, message-based, airspace environment p 313 A93-21144
- Airport navigation and surveillance using GPS and ADS p 313 A93-21145
- Update on GPS integrity requirements of the RTCA MOPS p 314 A93-21155
- GPS continuity - Initial findings p 314 A93-21167
- Planning for complementary MLS/GPS operations p 315 A93-21180
- MIAS, the integration of MLS with DGPS/DLoran-C p 315 A93-21181
- GPS availability and reliability for aircraft precision approach p 315 A93-21182
- Analysis of DGPS/INS and MLS/INS final approach navigation errors and control performance data p 315 A93-21183
- The applications, benefits, and issues of employing GPS and Glonass with Automatic Dependent Surveillance p 316 A93-21188
- Terminal area surveillance using GPS p 316 A93-21190
- Automatic Dependent Surveillance capacity of a geostationary satellite system in the U.S. domestic airspace p 316 A93-21192
- False alarm probability determination for the Honeywell Hexad Fault-Tolerant INS p 342 A93-21193
- Integrated Soviet VLF/Omega Receiver design p 316 A93-21198
- Maps and charts for visual air navigation p 498 A93-25170
- A history of visual approach guidance indicator systems in Australia p 498 A93-25171
- Position reporting using GPS/OMEGA and INS p 498 A93-25173
- Sensors and sensor systems for guidance and navigation II; Proceedings of the Meeting, Orlando, FL, Apr. 22, 23, 1992 p 547 A93-28151
- [SPICE-1694] p 547 A93-28151
- Application of advanced guidance and navigation systems to flight control of aircraft and future space vehicles p 500 A93-28153
- GNSS - A global system of satellite-aided navigation p 500 A93-28194
- Differential GPS and its applications in the aeronautical realm p 500 A93-28195
- Can one do without the magnetic reference? p 501 A93-28197
- Satcom Pacific Ocean trials p 501 A93-28198
- Transition to a seamless communications system requires much experimentation p 792 A93-38564
- The navigation and flying equipment of the Yak-42 aircraft --- Russian book p 792 A93-39204
- The use of satellites for aeronautical communications, navigation and surveillance p 881 A93-40436
- Half-scale modeling experience in the testing of radio navigation and landing systems p 882 A93-43112
- Evolution of European air space toward precision navigation (P/RNAV) p 882 A93-43369
- British Airways ETOPS flight planning system p 990 A93-45164
- The use of digital map data to provide enhanced navigation and displays for poor weather penetration and recovery p 992 A93-45165
- Adaptive filtering of Doppler velocimeter errors due to the characteristics of the reflecting surface p 992 A93-45650
- Receiver Autonomous Integrity Monitoring (RAIM) of GPS and GLONASS p 993 A93-46891
- Exact closed-form solution of generalized proportional navigation p 1130 A93-49598
- Automatic navigation in the air and at sea p 1099 A93-52593
- A primary flight display for four-dimensional guidance and navigation influence of tunnel size and level of additional information on pilot performance and control behaviour p 1208 A93-52668
- [AIAA PAPER 93-3570] p 1208 A93-52668
- The development of SIMONA - A simulator facility for advanced research into simulation techniques, motion system control and navigation systems technologies p 1208 A93-52670
- [AIAA PAPER 93-3574] p 1208 A93-52670
- Rotorcraft en route ATC route standards p 35 A93-10323
- [AD-A249129] p 35 A93-10323
- Future FAA telecommunications plan p 89 A93-11760
- [AD-A249133] p 89 A93-11760
- Detection of spoofing, jamming, or failure of a Global Positioning System (GPS) p 319 A93-18951
- [AD-A259023] p 319 A93-18951
- Effect of personal and situational variables on noise annoyance: With special reference to implications for en route noise p 569 A93-21317
- [NASA-CR-189676] p 569 A93-21317
- Satellite communications for aeronautical and navigation service p 838 A93-26648
- Advanced Transport Operating System (ATOPS) Flight Management/Flight Controls (FM/FC) software description p 808 A93-28621
- [NASA-CR-191457] p 808 A93-28621
- Engineering management consideration for an integrated aeronautical mobile satellite service p 933 A93-30337
- Adapting system engineering principles to the Canadian Airspace System p 887 A93-30338
- AIR PIRACY**
- Tomorrow's security p 141 A93-15058
- Terrorism and air-specific perils and the liability of air freight carriers under Article 17 of the Warsaw Agreement p 570 A93-24252
- Air piracy and terrorism directed against U.S. Air carriers p 880 A93-30194
- [AD-A264120] p 880 A93-30194
- AIR POLLUTION**
- Evolving noise issue could persist into the next century p 99 A93-10731
- Turbine engine developers explore ways to lower NO(x) emission levels p 52 A93-10732
- DNW test highlights related to aircraft environment p 190 A93-14274
- Real-time optical measurement of alkali species in air for jet engine corrosion testing p 541 A93-24870
- [AIAA PAPER 93-0791] p 541 A93-24870
- Potential impact of combined NO(x) and SO(x) emissions from future High Speed Civil Transport aircraft on stratospheric aerosols and ozone p 753 A93-35372
- The impact of air traffic on the atmospheric environment p 936 A93-42659
- Plume and wake dynamics, mixing, and chemistry behind a high speed civil transport aircraft p 1034 A93-45139
- Atmospheric aerosols due to aircraft and ecological problems p 1162 A93-48846
- NO(x) reduction additives for aircraft gas turbine engines p 1122 A93-50306
- [AIAA PAPER 93-2594] p 1122 A93-50306
- Stratospheric aircraft: Impact on the stratosphere? [DE92-016997] p 94 A93-12104
- Stratospheric aircraft exhaust plume and wake chemistry studies p 94 A93-12299
- [NASA-CR-189688] p 94 A93-12299
- Impact of supersonic and subsonic aircraft on ozone: Including heterogeneous chemical reaction mechanisms [DE92-019619] p 224 A93-13655
- The 1990 high-speed civil transport studies p 330 A93-16947
- [NASA-CR-189618] p 330 A93-16947
- The 1990 high-speed civil transport studies. Summary report p 330 A93-16999
- [NASA-CR-189619] p 330 A93-16999
- AQUIS: A PC-based air quality and permit information system p 434 A93-18587
- [DE92-040092] p 434 A93-18587
- Particulate emissions from gas turbine engines p 725 A93-26339
- [AD-A261374] p 725 A93-26339
- Improved selective catalytic NOx control technology for compressor station reciprocating engines p 755 A93-26529
- [PB93-158566] p 755 A93-26529
- Oxides of nitrogen emissions from turbulent hydrocarbon/air jet diffusion flames, phase 2 [PB93-152478] p 756 A93-26533
- Air Traffic and Environment p 1034 A93-31925
- [GSF-BAND-8] p 1034 A93-31925
- Climatic effects of turbofan emissions in the stratosphere and the higher troposphere p 1035 A93-31927
- Effects of commercial flight pollution on human health p 1035 A93-31931
- Making clean gasoline: The effect on jet fuels [AD-A264302] p 1019 A93-32085
- AIR QUALITY**
- Test results of the effects of air ionization on cigarette smoke particulate levels within a commercial airplane [SAE PAPER 921183] p 855 A93-41362
- AQUIS: A PC-based air quality and permit information system p 434 A93-18587
- [DE92-040092] p 434 A93-18587
- Making clean gasoline: The effect on jet fuels [AD-A264302] p 1019 A93-32085
- AIR SAMPLING**
- Particulates and aerosols characterized in real time for harsh environments using the UMR mobile aerosol sampling system (MASS) p 1156 A93-50118
- [AIAA PAPER 93-2344] p 1156 A93-50118
- Parametric study of air sampling cyclones p 135 A93-14173
- AIR START**
- Experimental investigation on starting of a turbojet engine in flight p 898 A93-41740
- Ground test simulation fidelity of turbine engine airstarts p 1137 A93-49986
- [AIAA PAPER 93-2173] p 1137 A93-49986
- AIR TO AIR MISSILES**
- New analytical solutions for proportional navigation p 728 A93-34545
- Development of an accuracy criteria for body-on-fin carryover interference p 1065 A93-48318
- [AIAA PAPER 93-3633] p 1065 A93-48318
- AIR TO AIR REFUELING**
- Investigation on air refueling scheduling p 108 A93-14315
- Lateral aerodynamic interference between tanker and receiver in air-to-air refueling p 1136 A93-52444
- The testing of fixed wing tanker and receiver aircraft: to establish their air-to-air refuelling capabilities, volume 11 p 514 A93-21305
- [AGARD-AG-300-VOL-11] p 514 A93-21305
- AIR TRAFFIC**
- The legal status of ekranoplanes p 453 A93-20900
- Ice prediction systems for runways p 376 A93-22174
- Air traffic noise monitoring in and around Lisbon Airport p 564 A93-28494
- The impact of air traffic on the atmospheric environment p 936 A93-42659
- Flight safety in Europe p 1227 A93-53726
- Upgrade Precision Runway Monitor (PRM) Operational Test and Evaluation (OT/E) test plan p 67 A93-11616
- [DOT/FAA/CT-TN92/13] p 67 A93-11616
- A NASPAC-based analysis of the delay and cost effects of the Dallas/Fort Worth metroplex plan p 193 A93-13447
- [DOT/FAA/CT-TN92/21] p 193 A93-13447
- Terminal area forecasts FY 1992 - 2005 p 149 A93-15390
- [AD-A255797] p 149 A93-15390
- Results of DATAS investigation of illegal mode S ID's at JFK Airport p 318 A93-16841
- [DOT/FAA/CT-92/26] p 318 A93-16841

- Proceedings of the AIAA/FAA Joint Symposium on General Aviation Systems p 240 N93-17732
 [AD-A257780]
 Report to Congress: Long-term availability of adequate airport system capacity p 319 N93-18202
 [AD-A258209]
 Domain engineering validation case study: Synthesis for the air traffic display/collision warning monitor domain version 01.00.03 p 503 N93-21671
 [AD-A259407]
 The ATC evaluation of the prototype Airport Surveillance Radar Wind Shear Processor (ASR-WSP) at Orlando International Airport p 748 N93-25210
 [DOT/FAA/CT-TN92/48]
 Design of an air traffic computer simulation system to support investigation of civil tiltrotor aircraft operations [NASA-CR-192920] p 707 N93-26052
 Two simulation studies of precision runway monitoring of independent approaches to closely spaced parallel runways p 911 N93-29815
 [AD-A263433]
 Air Traffic and Environment p 1034 N93-31925
 [GSF-BAND-8]
AIR TRAFFIC CONTROL
 Automatic dependent surveillance focus of civil avionics integration p 30 A93-10998
 Integrating TCAS into the airspace management system p 30 A93-11005
 A minimum rate of position reporting in the future oceanic air traffic control system p 30 A93-11006
 Capacity as a consideration for providing aeronautical mobile satellite air traffic services in the U.S. domestic airspace p 30 A93-11007
 Requirements for integrated flight and traffic management during final approach p 31 A93-11009
 The Microwave Landing System - A precision approach for the future p 32 A93-11023
 The Tenth Conference on Air Navigation - A landmark in the history of civil aviation p 34 A93-12559
 Specification of a class of discrete event processes and their controllers p 96 A93-13078
 TCAS display issues p 51 A93-13351
 [AIAA PAPER 92-4242]
 ICAS, Congress, 18th, Beijing, China, Sept. 20-25, 1992, Proceedings, Vols. 1 & 2 p 107 A93-14151
 [ISBN 1-56347-046-2]
 TCAS II testing conflicts and resolutions p 165 A93-14158
 Interrelationships between commercial airplane design and operational requirements and procedures p 153 A93-14219
 Experimental working position simulator to analyse, develop and optimize concepts for computer-aided Air Traffic Management p 191 A93-14412
 Airports, air traffic control, and their clients - Reflections on system optimization p 234 A93-15035
 Future systems for air traffic control p 150 A93-15052
 In the pursuit of a single European air traffic control system p 150 A93-15053
 Wind identification along a flight trajectory. I - 3D-kinematic approach p 223 A93-16324
 Fixed and rotary wing all weather operations; Proceedings of the Conference, London, United Kingdom, Apr. 23, 24, 1991 p 142 A93-17301
 [ISBN 0-903409-90-9]
 Autoland, the developing need p 142 A93-17302
 Air Traffic Control ground movement control in low visibility p 151 A93-17308
 Flight management systems p 311 A93-17757
 A distributed, message-based, airspace environment p 313 A93-21144
 The applications, benefits, and issues of employing GPS and Glonass with Automatic Dependent Surveillance p 316 A93-21188
 Terminal area surveillance using GPS p 316 A93-21190
 Automatic Dependent Surveillance capacity of a geostationary satellite system in the U.S. domestic airspace p 316 A93-21192
 The Federal Aviation Administration (FAA) and the National Weather Service (NWS) modernization programs - Catalysts for change in weather services p 427 A93-22114
 The Meteorologist Weather Processor for U.S. National Weather Service units at Federal Aviation Administration sites p 428 A93-22130
 FAA weather processor programs - Real-time dissemination of weather information to aviation end-users p 428 A93-22131
 MIST - A remote briefing system p 437 A93-22132
 Automated Weather Distribution System (AWDS) for support of global aviation p 428 A93-22134
 Impact of weather on aviation - A global view p 308 A93-22143
 Operational aviation weather service requirements p 429 A93-22145
 Weather information requirements for Terminal Air Traffic Control Automation p 429 A93-22146
 A summary of investigations of severe turbulence incidents using airline flight records p 308 A93-22153
 Validation of aviation weather products for the Advanced Traffic Management System p 430 A93-22161
 Short range forecasts for air traffic control using high resolution aircraft data p 431 A93-22164
 An improved gust front detection algorithm for the TDWR p 432 A93-22191
 Performance prediction of the interacting multiple model algorithm p 439 A93-22926
 Maneuver option manager - Automated simplification of complex air traffic control problems p 498 A93-25480
 Using TRACON as a teaching tool p 571 A93-27166
 The analysis of expert performance in the redesign of the en route air traffic control curriculum p 571 A93-27189
 The role of flight management in future air traffic control p 499 A93-27909
 Ground Movement and Control System (GMCS) p 499 A93-27913
 SIPORT DEPCOS and SIPORT ARRCOS - More than an electronic airstrip replacement p 499 A93-27914
 Satcom Pacific Ocean trials p 501 A93-28198
 Managing the world's air traffic p 501 A93-28392
 Three-dimensional cellular systems for aeronautical mobile radio communications p 502 A93-29639
 The application of automatic surface lights to improve airport safety p 821 A93-37069
 Multiple function sensors for Enhanced Vision application p 807 A93-37071
 Transition to a seamless communications system requires much experimentation p 792 A93-38564
 The use of satellites for aeronautical communications, navigation and surveillance p 881 A93-40436
 A constrained flight route monitor system in terminal control area for air traffic control p 882 A93-42816
 Increasing the reliability of an air traffic control radio system p 882 A93-43110
 Evolution of European air space toward precision navigation (P/RNAV) p 882 A93-43369
 Radar 92; Proceedings of the International Conference, Brighton, United Kingdom, Oct. 12, 13, 1992 p 929 A93-43376
 [ISBN 0-85296-533-2]
 Ground clutter measurements using an aerostat surveillance radar p 929 A93-43381
 Dual band tuned radomes for radar applications p 929 A93-43405
 An SSR/IFF Environment Model --- Secondary Surveillance Radar p 883 A93-43406
 Measurements of SSR bearing errors due to site obstructions --- Secondary Surveillance Radar p 883 A93-43407
 Airport surveillance radar design for increased air traffic p 883 A93-43410
 NODE-air traffic management systems p 884 A93-43428
 The development of a prototype aircraft height monitoring unit utilising an SSR-based difference in time of arrival technique p 884 A93-43432
 An integrated weather channel designed for an up-to-date ATC radar system p 929 A93-43434
 Bistatic radar using satellite-borne illuminators of opportunity p 914 A93-43437
 Radar signals analysis oriented to target characterization applied to civilian ATC radar p 885 A93-43475
 The Aloha Airlines accident - A new era for aging aircraft p 991 A93-45783
 The challenges of simulating wake vortex encounters and assessing separation criteria p 1096 A93-49518
 [AIAA PAPER 93-3568]
 Performance prediction of the interacting multiple model algorithm p 1167 A93-50638
 Control theoretic approach to air traffic conflict resolution p 1097 A93-51421
 [AIAA PAPER 93-3832]
 Statistical techniques for traffic flow management p 1098 A93-51423
 [AIAA PAPER 93-3834]
 The dependent converging instrument approach procedure p 1098 A93-51424
 [AIAA PAPER 93-3835]
 Pseudo Aircraft Systems - A multi-aircraft simulation system for air traffic control research p 1209 A93-52679
 [AIAA PAPER 93-3585]
 A reactive approach for distributed air traffic control [ONERA, TP NO. 1993-83] p 1190 A93-53603
 CAAASH - A coordinated collision avoidance system [ONERA, TP NO. 1993-84] p 1191 A93-53604
 Advanced terrain displays to transport category aircraft p 35 N93-10065
 [PB92-197136]
 Rotorcraft en route ATC route standards p 35 N93-10323
 [AD-A249129]
 Air traffic control visual scanning p 35 N93-10459
 [DOT/FAA/CT-TN92/16]
 Defence electronics industry profile, 1993-1991 p 84 N93-10653
 [CTN-92-60515]
 A description of the Mode Select beacon system (Mode S) and its associated benefits to the National Airspace System (NAS) p 35 N93-10738
 [DOT/FAA/SE-92/6]
 Methods and principles for determining task dependent interface content p 36 N93-10961
 [NASA-CR-190837]
 Design of an air traffic computer simulation system to support investigation of civil tiltrotor aircraft operations [NASA-CR-190811] p 36 N93-11139
 Activities report of the German Institute for Flight Safety p 28 N93-11375
 [ETN-92-92272]
 High Capacity Voice Recorder (HCVR) Operational Test and Evaluation (OT/E) integration test report p 88 N93-11460
 [DOT/FAA/CT-TN92/30]
 Upgrade Precision Runway Monitor (PRM) Operational Test and Evaluation (OT/E) test plan p 67 N93-11616
 [DOT/FAA/CT-TN92/13]
 Controller evaluation of initial data link terminal air traffic control services: Mini study 2, volume 1 p 36 N93-11704
 [DOT/FAA/CT-92/2-VOL-1]
 Controller evaluation of initial data link terminal air traffic control services: Mini study 2, volume 2 p 36 N93-11705
 [DOT/FAA/CT-92/2-VOL-2]
 Implementing system simulation of C3 systems using autonomous objects p 89 N93-11716
 [NASA-CR-190845]
 Airport stand assignment model p 67 N93-11728
 [TT-9104]
 Future FAA telecommunications plan p 89 N93-11760
 [AD-A249133]
 Limited production Precision Runway Monitor (PRM) master test plan p 192 N93-12899
 [DOT/FAA/CT-TN92/23]
 Prototype stop bar system evaluation at John F. Kennedy International Airport p 192 N93-12902
 [AD-A258667]
 Identifying ability requirements for operators of future automated air traffic control systems p 152 N93-14276
 [AD-A256615]
 Information systems for airport operations p 152 N93-14729
 [TT-9202]
 Terminal area forecasts FY 1992 - 2005 p 149 N93-15390
 [AD-A255797]
 FAA Technical Center Aeronautical Data Link Research Plan p 417 N93-15698
 [DOT/FAA/CT-92/23]
 Terminal area traffic management p 317 N93-16213
 [LR-684]
 DME-derived positions compared with MLS- and ILS-derived positions p 318 N93-16343
 [NLR-TP-90119-U]
 The effect of TCAS interrogations on the Chicago O'Hare ATCRBS system p 318 N93-16498
 [DOT/FAA/CT-92/22]
 Proceedings of the AIAA/FAA Joint Symposium on General Aviation Systems p 240 N93-17732
 [AD-A257780]
 NARSIM and EFMS: Tools for research on integrated ATM p 319 N93-17954
 [NLR-TP-89336-U]
 National Airspace System flight planning operational concept NAS-SR-131 p 310 N93-18031
 [PB93-124659]
 En route air traffic controllers use of flight progress strips: A graph-theoretic analysis p 319 N93-18927
 [AD-A259062]
 A simulation study of the effects of communication delay on air traffic control p 502 N93-19966
 [AD-A258593]
 National Airspace System: Air traffic control and airspace management operational concept NAS-SR-132 p 502 N93-20164
 [DOT/FAA/SE-92/5]
 Comparison of performance on the Shipley Institute of Living Scale, Air Traffic Control Specialist Selection Test, and FAA Academy Screen p 502 N93-20582
 [AD-A259249]
 Data Multiplexing Network (DMN), Phase 3: Equipment Operational Test and Evaluation (OT/E) integration test report p 503 N93-20612
 [DOT/FAA/CT-TN92/49]
 Fundamentals of adaptive anticipation techniques for the detection of threatening air traffic conflicts: Investigation of the horizontal proximity situation in the case of expected heading changes p 503 N93-21004
 [DLR-MITT-91-21]
 Poland civil aviation master plan and investment program p 459 N93-21343
 [PB92-213693]

- Definitional mission for civil aviation master plan for Poland
[PB92-213974] p 459 N93-21713
- Preliminary studies of planning and flight strip use as air traffic controller memory aids
[DOT/FAA/CT-TN92/22] p 503 N93-21759
- The ATC evaluation of the prototype Airport Surveillance Radar Wind Shear Processor (ASR-WSP) at Orlando International Airport
[DOT/FAA/CT-TN92/48] p 748 N93-25210
- Runway Visual Range (RVR) Operational Test and Evaluation (OT&E) integration and OT&E operational test report
[DOT/FAA/CT-TN92/37] p 706 N93-25243
- Design of a cooperative problem-solving system for enroute flight planning: An empirical study of its use by airline dispatchers
[NASA-CR-192709] p 707 N93-25330
- Design of an air traffic computer simulation system to support investigation of civil tiltrotor aircraft operations
[NASA-CR-192920] p 707 N93-26052
- Piloted simulation of an air-ground profile negotiation process in a time-based Air Traffic Control environment
[NASA-TM-107748] p 707 N93-26087
- The Data Multiplexing Network (DMN) phase 3 Extended Distance Data Cable (EDDC) test and evaluation
[DOT/FAA/CT-TN93/11] p 752 N93-26160
- Satellite communications for aeronautical and navigation service
p 838 N93-26648
- Next Generation Weather Radar (NEXRAD) Principal User Processor (PUP) Operational Test and Evaluation (OT&E) operational test plan
[DOT/FAA/CT-TN93/22] p 841 N93-28054
- Results of DATAS investigation of ATCFBS environment at the Los Angeles International Airport
[DOT/FAA/CT-93/6] p 793 N93-28625
- Data Multiplexing Network (DMN) equipment Operational Test and Evaluation (OT&E) integration test report
[AD-A263172] p 942 N93-29490
- The 1991-1992 aviation system capacity plan
[AD-A263436] p 911 N93-29788
- Two simulation studies of precision runway monitoring of independent approaches to closely spaced parallel runways
[AD-A263433] p 911 N93-29815
- Classification of radar clutter in an air traffic control environment
p 886 N93-30299
- Evolution of radar data processing in the French air traffic control system
p 886 N93-30325
- Engineering management consideration for an integrated aeronautical mobile satellite service
p 933 N93-30337
- Adapting system engineering principles to the Canadian Airspace System
p 887 N93-30338
- Issues of ATC conflict resolution under real-time constraints
p 887 N93-30350
- National Airspace System Performance Analysis Capability (NASPAC) simulation model
p 887 N93-30351
- Enhancing availability, performance, and flexibility of air traffic control air-ground services
p 887 N93-30353
- Changing role of telecommunications management in air traffic control in the FAA
p 888 N93-30354
- Airspace Design Expert System (ADES), a 2D/3D mapping and modelling tool incorporating an expert system for use in instrument approach design
p 888 N93-30357
- An analysis of en route controller-pilot voice communications
[AD-A264784] p 935 N93-30611
- Flight test of avionics and air-traffic control systems
[ESA-TT-1279] p 993 N93-31271
- ATTAS experimental-cockpit and ATMOS for component and system investigations in flight guidance
p 1014 N93-31276
- Testing of an experimental FMS
p 998 N93-31277
- Testing concept of a taxiing control system, summary
p 1010 N93-31278
- UK airmasses involving commercial air transport, September - December 1991
[ETN-93-93930] p 992 N93-32409
- Evaluation of the flyability of MLS curved approaches for wide-body aircraft
[NLR-TP-91396-U] p 999 N93-32416
- AIR TRAFFIC CONTROLLERS (PERSONNEL)**
- Developing the Aviation Gridded Forecast System
p 427 N93-22124
- The development of an Altitude Awareness Program - An integrated approach
p 486 N93-27136
- The analysis of expert performance in the redesign of the en route air traffic control curriculum
p 571 N93-27189
- Aircraft collision avoidance using statistical decision theory
p 500 N93-28155
- Air traffic control visual scanning
[DOT/FAA/CT-TN92/16] p 35 N93-10459
- Performance of color-dependent tasks of air traffic control specialists as a function of type and degree of color vision deficiency
[AD-A256614] p 151 N93-14275
- Identifying ability requirements for operators of future automated air traffic control systems
[AD-A256615] p 152 N93-14276
- En route air traffic controllers use of flight progress strips: A graph-theoretic analysis
[AD-A259062] p 319 N93-18927
- Preliminary studies of planning and flight strip use as air traffic controller memory aids
[DOT/FAA/CT-TN92/22] p 503 N93-21759
- Conversion of the CTA, Inc., en route operations concepts database into a formal sentence outline job task taxonomy
[AD-A261410] p 708 N93-26447
- Two simulation studies of precision runway monitoring of independent approaches to closely spaced parallel runways
[AD-A263433] p 911 N93-29815
- An analysis of en route controller-pilot voice communications
[AD-A264784] p 935 N93-30611
- AIR TRANSPORTATION**
- European merger control in the air transport industry - Comments on the Delta Air Lines/Pan Am decision of the European Commission
[ISBN 3-452-22293-4] p 103 A93-11412
- Evolution of helicopters and the status of technology in India
p 2 A93-12234
- Critical considerations on European air transport politics
p 103 A93-12718
- South American latest developments in the air law and air policy fields
p 103 A93-12719
- Air transport within the European single market - How will it look after 1992? A suggested view on the future
p 104 A93-13424
- Advanced technologies airships
p 108 A93-14183
- The value of a computational/experimental partnership in aerodynamic design
p 114 A93-14215
- Jet streams and associated turbulence and their effects on air transport flight operations
p 154 A93-14231
- Progress and taboos in air safety orientations of research in human factors in air transport
p 141 A93-14374
- Experimental investigation of aerothermal problems associated with hypersonic flight of HST
p 120 A93-14380
- Air transportation system for shipping outsized cargoes
p 141 A93-14394
- High capacity aircraft
p 157 A93-14395
- 1992 - The year of the radome?
p 209 A93-15525
- The user friendly airliner (The 37th Roy Chadwick Lecture)
p 307 A93-21718
- Weather-related accidents in the Canadian aviation industry - An analysis of the chief contributory factors
p 307 A93-22106
- New initiatives for aviation meteorology training - 1989 through 1991
p 307 A93-22109
- Improving weather questions on Federal Aviation Administration exams
p 308 A93-22110
- Improved efficiency of air transportation through aviation weather system modernization
p 308 A93-22144
- Validation of aviation weather products for the Advanced Traffic Management System
p 430 A93-22161
- Volcanic ash and aircraft operations
p 309 A93-22181
- Preliminary results from a study of community response to noise from military aircraft exercise
p 558 A93-28484
- Competition in a single European air transport market; Proceedings of the Conference, London, United Kingdom, Dec. 1, 1992
[ISBN 1-85768-080-4] p 458 A93-29473
- Air transport growth - How will airports manage? Proceedings of the Conference, London, United Kingdom, Oct. 21, 1992
[ISBN 1-85768-065-0] p 458 A93-29475
- A French look at the future supersonic transport
[ONERA, TP NO. 1992-209] p 803 A93-38763
- It's time to go supersonic
p 949 A93-44099
- Advanced cargo aircraft may offer a potential renaissance in freight transportation
p 991 A93-47023
- Application of a parabolized Navier-Stokes code to an HST configuration and comparison to wind tunnel test data
[AIAA PAPER 93-3537] p 986 A93-47288
- Matching engine and aircraft lapse rates for the HST
[AIAA PAPER 93-1809] p 1100 A93-49698
- Propfan engines
[AIAA PAPER 93-1981] p 1112 A93-49828
- Implications of European legislation post 1992; Proceedings of the Conference, London, United Kingdom, Mar. 12, 1992
[ISBN 1-85768-015-4] p 1043 A93-50353
- Air transport and the environment - Regulating aircraft noise
p 1226 A93-52931
- On definition and use of systems engineering processes, methods and tools
p 1225 A93-53642
- Report to Congress: State Block Grant Program
[AD-A254569] p 193 N93-13882
- Terminal area forecasts FY 1992 - 2005
[AD-A255797] p 149 N93-15390
- Hermes CX-7: Air transport system design simulation
[NASA-CR-192082] p 335 N93-18056
- Arrow 227: Air transport system design simulation
[NASA-CR-192053] p 336 N93-18063
- Report to Congress: Long-term availability of adequate airport system capacity
[AD-A258209] p 319 N93-18202
- The S.T.o.R.M. (tm): Air transport system design simulation
[NASA-CR-192070] p 338 N93-18349
- JEFF: Air transport system design simulation
[NASA-CR-192069] p 338 N93-18350
- The F-92 RELIANT: Air transport system design simulation
[NASA-CR-192050] p 339 N93-18386
- Consumer interest in the air safety data of the airline quality rating. Testimony to the US House of Representatives, Committee on Government Operations, Government Activities and Transportation Subcommittee
[NIAR-92-4] p 495 N93-19941
- Summaries of the 1991 publications of DLR research reports and DLR communications
[ETN-93-92588] p 572 N93-21022
- Definitional mission for civil aviation master plan for Poland
[PB92-213974] p 459 N93-21713
- Design study to simulate the development of a commercial transportation system
p 894 N93-29718
- The 1991-1992 aviation system capacity plan
[AD-A263436] p 911 N93-29788
- Air piracy and terrorism directed against U.S. Air carriers
[AD-A264120] p 880 N93-30194
- AIR WATER INTERACTIONS**
- Acoustic noise generation at the air/ocean boundary
[DREA-CR-90-445] p 99 N93-10642
- AIRBORNE EQUIPMENT**
- Design, capabilities, and performance of the miniaturized airborne GPS receiver
p 32 A93-11014
- Fast-response aircraft temperature sensors
p 167 A93-17095
- Airborne trials of Loran-C
p 311 A93-17756
- Data communication for airborne differential GPS/GLONASS application
p 499 A93-27910
- Advanced airborne 3D computer image generation systems technologies for the year 2000
p 518 A93-28176
- Utilization of CAD/CAE for concurrent design of structural aircraft components
[AIAA PAPER 93-1466] p 710 A93-34014
- The Airborne Collision Avoidance System (ACAS)
p 883 A93-43370
- Thermal control of a lidar laser system using a non-conventional ram air heat exchanger
p 1028 A93-46821
- An introduction to the onboard LAN (OLAN)
p 1166 A93-49480
- Electro-optical navigation for aircraft
p 1097 A93-50643
- A technique for the measurement of cloud structure on centimeter scales
p 1158 A93-51243
- Airborne gravimetry from a light aircraft
p 1245 A93-55972
- Accuracy of GPS-derived acceleration from moving platform tests
p 1240 A93-55973
- Multiple receiver, zero-length baseline kinematic GPS positioning techniques for airborne gravity measurement
p 1240 A93-55974
- Airborne gravimetry, altimetry, and GPS navigation errors
p 1240 A93-55975
- Requirements for airborne vector gravimetry
p 1241 A93-55976
- Airborne vector gravimetry with an aided inertial survey system
p 1241 A93-55977
- Controlling common mode stabilization errors in airborne gravity gradiometry
p 1245 A93-55978
- Embedded training capabilities for the LAMPS MK 3 system
[AD-A250697] p 49 N93-11838
- Airborne Wind Shear Detection and Warning Systems. Fourth Combined Manufacturers' and Technologists' Conference, part 2
[NASA-CR-10105-PT-2] p 144 N93-14844

- NASA/LMSC coherent LIDAR airborne shear sensor: System capabilities and flight test plans p 144 N93-14847
- Development of the Advance Warning Airborne System (AWAS) p 144 N93-14849
- Systems issues in airborne Doppler radar/LIDAR certification p 145 N93-14855
- Example of statistical techniques applied to analysis of measurements of the landing airborne manoeuvre. (Multiple linear regression with two independent variables and one dependent variable.) p 330 N93-16636 [ESDU-92022]
- Airborne Wind Shear Detection and Warning Systems: Fourth Combined Manufacturers' and Technologists' Conference, part 1 p 488 N93-19590 [NASA-CP-10105-PT-1]
- Program overview: 1991 flight test objectives p 488 N93-19591
- Air/ground wind shear information integration: Flight test results p 488 N93-19594
- Airborne doppler radar research at Rockwell International p 489 N93-19602
- Acquisition and use of Orlando, Florida and Continental Airbus radar flight test data p 489 N93-19603
- Ground clutter measurements using the NASA airborne doppler radar: Description of clutter at the Denver and Philadelphia airports p 490 N93-19608
- Signal processing for airborne doppler radar detection of hazardous wind shear as applied to NASA 1991 radar flight experiment data p 490 N93-19612
- Comparison of the electrical charging and discharging environments of multiple aircraft-borne electric-field measurement systems p 704 N93-24887
- A concluding study of the altitude determination deficiencies of the Service Aircraft Instrumentation Package (SAIP) p 897 N93-29971 [AD-A263515]
- AIRBORNE LASERS**
- Misalignments of airborne laser beams due to mechanical vibrations p 394 A93-17762
- Autonomous mobile laser complex p 395 A93-17767
- A high resolution airborne multisensor system p 343 A93-21966
- AIRBORNE RADAR**
- Integration of full scale development aircraft GPS user equipment (AN/ARN-151) with Doppler radar systems p 31 A93-11012
- Electronic Counter Countermeasures/Advanced Radar Test Bed (ECCM/ARTB) [AIAA PAPER 92-4098] p 34 A93-13267
- The SSR mode-S data-link p 312 A93-18553
- Volume-imaging lidar observations of the convective structure surrounding the flight path of a flux-measuring aircraft p 425 A93-20579
- Superresolution radar imaging with linear prediction data extrapolation p 342 A93-20851
- A comparison of several airborne measures of turbulence p 308 A93-22121
- Microbursts detection with airborne Doppler lidar p 433 A93-22201
- Results from a VHF impulse synthetic-aperture radar p 501 A93-28219
- Some limitations on the effectiveness of airborne adaptive radar p 501 A93-29596
- Comparison of three methods to deduce three-dimensional wind fields in a hurricane with airborne Doppler radar p 844 A93-37691
- Comparison of airborne dual-Doppler and airborne/ground-based dual-Doppler analyses of North Dakota thunderstorms p 844 A93-37694
- A technique to correct airborne Doppler data for coordinate transformation errors using surface clutter p 807 A93-37699
- Update on the NASA ER-2 Doppler radar system (EDOP) p 807 A93-37737
- The whale with a tail p 803 A93-38837
- A dual polarised active phased array antenna with low cross polarisation for a polarimetric airborne SAR p 883 A93-43401
- Adaptive clutter suppression for airborne array radars using clutter subspace approximation p 883 A93-43411
- Antenna design for adaptive airborne MTI p 884 A93-43440
- Space-time processing for AEW radar p 884 A93-43444
- The PHARUS project, first results of the realization phase --- Phased Array Universal SAR p 884 A93-43454
- A refined procedure to generate calibrated imagery from airborne synthetic aperture radar data p 1162 A93-47657
- The realization phase of the PHARUS project --- Phased ARay Universal SAR p 1162 A93-47658
- JPL AIRSAR processing activities and developments p 1162 A93-47865
- Technical operating report on the Data Integration and Collection Environment (DICE) instrumentation system design [AD-A258444] p 455 N93-17891
- Airborne Wind Shear Detection and Warning Systems: Fourth Combined Manufacturers' and Technologists' Conference, part 1 p 488 N93-19590 [NASA-CP-10105-PT-1]
- Doppler radar results p 488 N93-19595
- Airborne doppler radar research at Rockwell International p 489 N93-19602
- Ground clutter measurements using the NASA airborne doppler radar: Description of clutter at the Denver and Philadelphia airports p 490 N93-19608
- NASA airborne radar wind shear detection algorithm and the detection of wet microbursts in the vicinity of Orlando, Florida p 490 N93-19611
- Signal processing for airborne doppler radar detection of hazardous wind shear as applied to NASA 1991 radar flight experiment data p 490 N93-19612
- AIRBORNE SURVEILLANCE RADAR**
- Ground clutter measurements using an aerostat surveillance radar p 929 A93-43381
- Adaptive array processing for airborne radar p 883 A93-43412
- AIRBORNE/SPACEBORNE COMPUTERS**
- Advanced real time integrated processors --- for Lockheed F-22 advanced tactical fighter p 50 A93-11000
- Development of a TRN/INS/GPS integrated navigation system p 30 A93-11004
- Rapid prototyping via automatic software code generation from formal specifications - A case study p 227 A93-14685
- Increased safety through knowledge-based pilot assistance p 518 A93-27499
- A design concept for a flight vehicle computer system with artificial intelligence elements p 757 A93-35663
- A performance assessment of a byzantine resilient fault-tolerant computer p 938 A93-41296
- [AIAA PAPER 89-3064] p 938 A93-41296
- JIAWG compatible development boards for the i960 [SAE PAPER 931596] p 1104 A93-49345
- Neutron-induced single event upsets in static RAMs observed at 10 KM flight altitude p 1158 A93-50561
- Requirements analysis notebook for the flight data systems definition in the Real-Time Systems Engineering Laboratory (RSEL) p 69 N93-10960
- [NASA-CR-185698] p 69 N93-10960
- A brief overview of NASA Langley's research program in formal methods p 228 N93-12958
- Rewritable optical disk: Application to flight recording p 221 N93-15160
- DAR-2: On-board data acquisition system for aircraft engines p 169 N93-15166
- Monitoring of powerplants in advanced commercial aircraft p 178 N93-15171
- Mission planning systems for tactical aircraft (pre-flight and in-flight) p 496 N93-21187
- [AGARD-AR-313] p 496 N93-21187
- Avionics systems architectures p 808 N93-27169
- A real-time, hardware-in-the-loop simulation of an unmanned aerial research vehicle p 893 N93-29409
- [AD-A262477] p 893 N93-29409
- Advanced Transport Operating System (ATOPS) utility library software description p 1000 N93-32218
- [NASA-CR-191469] p 1000 N93-32218
- AIRCRAFT**
- Winds of change: Expanding the frontiers of flight. Langley Research Center's 75 years of accomplishment, 1917-1992 p 104 N93-11100
- [NASA-NP-130] p 104 N93-11100
- International aircraft operator information system [DOT/FAA/CT-93/4] p 949 N93-32232
- AIRCRAFT ACCIDENT INVESTIGATION**
- The development of an efficient take-off performance monitor (TOPM) p 180 A93-14186
- The hazard and alarm of windshear p 141 A93-14317
- Progress and taboos in air safety orientations of research in human factors in air transport p 141 A93-14374
- The employment of artificial intelligence for analyzing air accidents p 226 A93-14375
- Wind identification along a flight trajectory. I - 3D-kinematic approach p 223 A93-16324
- Flight safety and human errors p 141 A93-16860
- Weather-related accidents in the Canadian aviation industry - An analysis of the chief contributory factors p 307 A93-22106
- Improving weather questions on Federal Aviation Administration exams p 308 A93-22110
- The importance of proper aviation weather dissemination to pilots - An airline captain's perspective p 308 A93-22115
- Potential aircraft hazards in the vicinity of convective clouds - A review from the perspective of a scale-model study p 427 A93-22116
- The aeronautical volcanic ash problem p 309 A93-22156
- A quantitative method to estimate the microburst wind shear hazard to aircraft p 309 A93-22172
- SAAW - Italy's answer to the windshear challenge p 431 A93-22175
- Anemometer siting criteria for low level wind shear alert system p 413 A93-22178
- The redesigned Low Level Wind Shear Alert System p 431 A93-22179
- Towards quantitative non-destructive evaluation of aging aircraft p 1025 A93-45773
- The Aloha Airlines accident - A new era for aging aircraft p 991 A93-45783
- Structural integrity of aging airplanes - A perspective p 948 A93-45789
- How likely is multiple site damage? p 1027 A93-45791
- Efforts to reduce CFIT accidents should address failures of the aviation system itself p 1096 A93-49280
- Operating helicopters in a demanding environment - Mountain flying/high evaluations p 1190 A93-54289
- Aircraft accident report: Atlantic Southeast Airlines, Inc. Flight 2311, uncontrolled collision with terrain, an Embraer EMB-120, N270AS, Brunswick, Georgia, 5 April 1991 [PB92-910403] p 28 N93-11471
- Aircraft accident report: Explosive decompression-loss of cargo door in flight, United Airlines Flight 811, Boeing 747-122, N4713U, Honolulu, HI, 24 February 1989 [PB92-910402] p 28 N93-12193
- Evaluation of CKU-5/A ejection seat catapults under varied acceleration levels p 29 N93-12489
- [AD-A248021] p 29 N93-12489
- Aircraft accident report: Britt Airways, Inc., d/b/a, Continental Express Flight 2574, in-flight structural breakup, EMB-120RT, N33701, Eagle Lake, Texas, September 11, 1991 [PB92-910405] p 143 N93-13426
- Postmortem alcohol production in fatal aircraft accidents p 143 N93-14026
- [AD-A255766] p 143 N93-14026
- Special investigation report: Piper Aircraft Corporation PA-46 Malibu/Mirage Accidents/Incident, 31 May 1989 - 17 March 1991 [PB92-917007] p 149 N93-15577
- A method for investigating human factor aspects of military aircraft accidents p 491 N93-19656
- The human factor problem in the Canadian Forces aviation p 491 N93-19657
- Underlying causes of accidents: Casual networks p 491 N93-19658
- 737-400 at Kegworth, 8 January 1989: The AAIB investigation p 491 N93-19661
- F-16 accidents: The Norwegian experience p 492 N93-19674
- Category A F-16 accidents in the Belgian Air Force p 492 N93-19675
- Air accidents in the French Air Force p 492 N93-19676
- Combat and training aircraft class A mishaps in the Belgian Air Force 1970-1990 p 492 N93-19677
- Underlying causes of human error in US Army rotary wind accidents p 492 N93-19678
- Royal Naval helicopter ditching experience p 492 N93-19684
- Canadian Forces helicopter ditchings: 1952-1990 p 493 N93-19685
- Helicopter accidents over water in the national navy: Epidemiological study over the period 1980-1991 p 493 N93-19686
- Helicopter crash survival at sea: United States Navy/Marine Corps experience 1977-1990 p 493 N93-19687
- Crash experience of the US Army Black Hawk helicopter p 493 N93-19688
- The effectiveness of airbags in reducing the severity of head injury from gunshot strikes in attack helicopters p 494 N93-19691
- Correlations between engineering, medical and behavioural aspects in fire-related aircraft accidents p 494 N93-19693
- Towards an integrated approach to proactive monitoring and accident prevention p 495 N93-19700
- Accidents and errors: A review of recent UK Army Air Corps accidents p 495 N93-19701
- Prediction of success from training p 495 N93-19702
- Aircraft accident report: Tomy International, Inc., d/b/a Scenic Air Tours flight 22, Beech Model E18S, N342E in-flight collision with terrain, Mount Haleakala, Maui, Hawaii, 22 April 1992 [PB93-910401] p 705 N93-25827

- The use of multiple models in case-based diagnosis p 759 N93-25969
- Aircraft accident report: Takeoff stall in icing conditions. USAIR Flight 405 FOKKER F-28, N485US, LaGuardia Airport, Flushing, New York, 22 March 1992 [PB93-910402] p 790 N93-27034
- Aircraft accident report: Controlled collision with terrain GP Express Airlines, Inc., Flight 861, A Beechcraft C99, N118GP, Anniston, Alabama, 8 June 1992 [PB93-910403] p 790 N93-27035
- ### AIRCRAFT ACCIDENTS
- Handling the legal consequences of aviation disasters - Passenger compensation [ISBN 3-452-22293-4] p 103 A93-11411
- Breaking through the 10 exp 6 barrier --- decreasing aircraft accident fatality rate per million flight hours p 27 A93-11498
- Review of human error accidents in civil aviation p 27 A93-12367
- Development of laser conducting landing system p 150 A93-14320
- Graph-theory studies of the possibility of occurrence of flight accidents and incidents during the take-off under special operating conditions p 306 A93-18365
- Effective 406-MHz ELT demonstrates the potential to save more lives p 311 A93-18543
- Recent aircraft accidents p 307 A93-20819
- Development of an expert system for cockpit emergency procedures p 845 A93-35915
- The role of the radiologist in the medicolegal procedure after an aviation accident p 853 A93-39701
- Progress and taboos in flight safety - Human-factors research in air transportation p 879 A93-42654
- First moves towards an 'intelligent' GPWS p 896 A93-43624
- Air carriers' liability for passenger injury or death - The Japanese Initiative and Response to the recent EC Consultation Paper p 1226 A93-52930
- Instrumentation and data acquisition for full-scale aircraft crash testing p 1250 A93-54399
- Unusual attitudes - Helicopters and instrument flight p 1240 A93-54550
- The probable cause --- aircraft accidents p 1240 A93-56417
- A general framework for analyzing choice-of-law problems in air crash litigation p 1265 A93-56537
- Promoting general aviation safety - A revision of pilot negligence law p 1265 A93-56540
- UK airmisses involving commercial air transport, May-August 1991 [ETN-92-92260] p 28 N93-11357
- UK airmisses involving commercial air transport, January-April 1991 [ETN-92-92261] p 87 N93-11358
- Aircraft accident report: Atlantic Southeast Airlines, Inc. Flight 2311, uncontrolled collision with terrain, an Embraer EMB-120, N270AS, Brunswick, Georgia, 5 April 1991 [PB92-910403] p 28 N93-11471
- Aircraft accident report: Explosive decompression-loss of cargo door in flight, United Airlines Flight 811, Boeing 747-122, N4713U, Honolulu, HI, 24 February 1989 [PB92-910402] p 28 N93-12193
- Aircraft accident report: Britt Airways, Inc., d/b/a. Continental Express Flight 2574, in-flight structural breakup, EMB-120RT, N33701, Eagle Lake, Texas, September 11, 1991 [PB92-910405] p 143 N93-13426
- Aircraft accident/incident summary report: Controlled flight into terrain, Bruno's Inc., Beechjet, N25BR, Rome, Georgia, December 11, 1991 [PB92-910404] p 143 N93-13470
- Postmortem alcohol production in fatal aircraft accidents [AD-A255766] p 143 N93-14026
- Aviation accidents, incidents, and violations: Psychological predictors among US pilots p 144 N93-14693
- Trans-cockpit authority gradient in Navy/Marine aircraft mishaps p 146 N93-15016
- Taxonomy of flight variables p 147 N93-15022
- Embedded ADM reduces helicopter human error accidents p 147 N93-15024
- Special investigation report: Piper Aircraft Corporation PA-46 Malibu/Mirage Accidents/Incident, 31 May 1989 - 17 March 1991 [PB92-917007] p 149 N93-15577
- Special investigation report: Flight attendant training and performance during emergency situations [PB92-917008] p 310 N93-16834
- Aircraft Accidents: Trends in Aerospace Medical Investigation Techniques [AGARD-CP-532] p 490 N93-19653
- How do we investigate the human factor in aircraft accidents? p 491 N93-19655
- A method for investigating human factor aspects of military aircraft accidents p 491 N93-19656
- The human factor problem in the Canadian Forces aviation p 491 N93-19657
- Aid in investigation by figure animation p 491 N93-19659
- 737-400 at Kegworth, 8 January 1989: The AAIIB investigation p 491 N93-19661
- F-16 accidents: The Norwegian experience p 492 N93-19674
- Category A F-16 accidents in the Belgian Air Force p 492 N93-19675
- Air accidents in the French Air Force p 492 N93-19676
- Combat and training aircraft class A mishaps in the Belgian Air Force 1970-1990 p 492 N93-19677
- Underlying causes of human error in US Army rotary wind accidents p 492 N93-19678
- Royal Naval helicopter ditching experience p 492 N93-19684
- Canadian Forces helicopter ditchings: 1952-1990 p 493 N93-19685
- Helicopter accidents over water in the national navy: Epidemiological study over the period 1980-1991 p 493 N93-19686
- Helicopter crash survival at sea: United States Navy/Marine Corps experience 1977-1990 p 493 N93-19687
- Crash experience of the US Army Black Hawk helicopter p 493 N93-19688
- US Army's aviation life support equipment retrieval program real world design successes from proactive investigation p 494 N93-19690
- The effectiveness of airbags in reducing the severity of head injury from gunsight strikes in attack helicopters p 494 N93-19691
- Correlations between engineering, medical and behavioural aspects in fire-related aircraft accidents p 494 N93-19693
- Accidents and errors: A review of recent UK Army Air Corps accidents p 495 N93-19701
- T-38 forward windshield development and performance demonstration report [AD-A259240] p 513 N93-20579
- The effectiveness of hand-held fire extinguishers on cargo container fires [DOT/FAA/CT-TN92/42] p 496 N93-21821
- Aircraft accident report: Tomy International, Inc., d/b/a Scenic Air Tours flight 22, Beech Model E18S, N342E in-flight collision with terrain, Mount Haleakala, Maui, Hawaii, 22 April 1992 [PB93-910401] p 705 N93-25827
- A review of civil aviation propeller-to-person accidents: 1980-1989 [AD-A260695] p 705 N93-25896
- The use of multiple models in case-based diagnosis p 759 N93-25969
- Annual review of aircraft accident data: US general aviation calendar year 1989 [PB93-160687] p 790 N93-27033
- Aircraft accident report: Takeoff stall in icing conditions. USAIR Flight 405 FOKKER F-28, N485US, LaGuardia Airport, Flushing, New York, 22 March 1992 [PB93-910402] p 790 N93-27034
- Aircraft accident report: Controlled collision with terrain GP Express Airlines, Inc., Flight 861, A Beechcraft C99, N118GP, Anniston, Alabama, 8 June 1992 [PB93-910403] p 790 N93-27035
- Autogenic-feedback training improves pilot performance during emergency flying conditions [NASA-TM-104005] p 790 N93-27076
- World commercial aircraft accidents [DE93-010892] p 791 N93-28571
- Reportable accidents to UK registered aircraft, and to foreign registered aircraft in UK airspace, 1990 [CAP-600] p 991 N93-31730
- ### AIRCRAFT ANTENNAS
- A wideband, embedded/conformal, antenna subsystem concept p 327 A93-22002
- Propagation results of aeronautical satellite communication experiments using INMARSAT satellite p 533 A93-29607
- A self-steering array for the SHARP microwave-powered aircraft p 792 A93-37090
- Antennas now and future p 764 A93-39540
- Corroboration of a moment-method calculation of the maximum mutual coupling between two HF antennas mounted on a helicopter p 881 A93-40332
- ELF, VLF and LF radiation from a very large loop antenna with a mountain core p 924 A93-40334
- Selecting locations for avionics antennas - A structured approach p 892 A93-42794
- Calculation of the passive noise power for onboard single-pulse automatic direction tracking systems p 882 A93-43111
- Wind-tunnel tests of an inclined cylinder having helical grooves [AIAA PAPER 93-3456] p 979 A93-47239
- Inflight antenna diagram determination of spaceborne and airborne SAR-systems p 1161 A93-47583
- Fuzzy logic control algorithm for suppressing E-6A Long Trailing Wire Antenna wind shear induced oscillations [AIAA PAPER 93-3868] p 1171 A93-51454
- Modeling and control of a trailing wire antenna towed by an orbiting aircraft [AD-A256450] p 219 N93-14610
- Experimental study of the effect of helical grooves on an infinite cylinder [AD-A260890] p 751 N93-25912
- Models for performance assessment of HF antennas on the CH-135/Twin Huey helicopter p 933 N93-30291
- Coupling gain computation between antennas on circular cylinders at SHF/EHF frequencies p 933 N93-30309
- Installations and methods for measurement of aircraft radio components and systems p 1031 N93-31284
- ### AIRCRAFT APPROACH SPACING
- Requirements for integrated flight and traffic management during final approach p 31 A93-11009
- The role of simulation in determining safe aircraft landing separation criteria p 306 A93-18712
- Analysis of approach paths of a single aircraft p 367 A93-20823
- A constrained flight route monitor system in terminal control area for air traffic control p 882 A93-42816
- A wind shear hazard window useful in studying the effect of wind shear on the airplane during the landing approach [AIAA PAPER 93-3643] p 1127 A93-48327
- Control theoretic approach to air traffic conflict resolution [AIAA PAPER 93-3832] p 1097 A93-51421
- Visual approach data collection at St. Louis Lambert Field (STL) [DOT/FAA/CT-TN93/2] p 706 N93-24948
- The dependent converging instrument approach procedure: An analysis of its safety and applicability [DOE/FAA/RD-93/6] p 707 N93-25456
- Developing automation for terminal air traffic control: Case study of the imaging aid p 888 N93-30356
- ### AIRCRAFT BRAKES
- Aircraft braking systems p 995 A93-44850
- Wheel and brake design and test requirements for military aircraft [SAE ARP 1493] p 1103 A93-52165
- Analysis of aircraft noise levels in the vicinity of start-of-takeoff roll at Baltimore-Washington International Airport [PB92-221605] p 559 N93-21501
- ### AIRCRAFT CARRIERS
- Integration of flight control and carrier landing aid system [ONERA, TP NO. 1993-6] p 181 A93-14187
- EH 101 ship interface trials p 796 A93-35954
- Automatic carrier landing system utilizing aircraft sensors p 1097 A93-49590
- A database approach to aircraft carrier airplan production [AD-A257737] p 240 N93-17666
- Follow-on operational test and evaluation of the NAVSTAR global positioning system air integration/installation program [AD-A263067] p 793 N93-27925
- ### AIRCRAFT COMMUNICATION
- Flight management systems information exchange with AERA to support future air traffic control concepts --- Automated En Route ATC p 31 A93-11008
- A new aircraft integrated positioning and communication system based on satellite p 150 A93-14236
- Design considerations for air-to-air laser communications p 312 A93-18932
- Applications of space techniques to civil aviation operations p 312 A93-20007
- A distributed, message-based, airspace environment p 313 A93-21144
- A baseline GPS RAIM scheme and a note on the equivalence of three RAIM methods p 317 A93-21823
- The Meteorological Data Collection and Reporting System - Status and future directions p 428 A93-22133
- A context-based introduction to aircraft radio communications p 570 A93-27164
- Propagation results of aeronautical satellite communication experiments using INMARSAT satellite p 533 A93-29607
- Transition to a seamless communications system requires much experimentation p 792 A93-38564
- The use of satellites for aeronautical communications, navigation and surveillance p 881 A93-40436
- An internetworking router for avionics applications --- Bridge/Router unit in fiber optics aircraft communication p 1097 A93-49479

- An introduction to the onboard LAN (OLAN) p 1166 A93-49480
- The development of the speaker independent ARM continuous speech recognition system p 87 N93-11383 [RSRE-MEMO-4473]
- Controller evaluation of initial data link terminal air traffic control services: Mini study 2, volume 1 p 36 N93-11704 [DOT/FAA/CT-92/2-VOL-1]
- Controller evaluation of initial data link terminal air traffic control services: Mini study 2, volume 2 p 36 N93-11705 [DOT/FAA/CT-92/2-VOL-2]
- Advances in speech processing p 550 N93-19771
- Satellite communications for aeronautical and navigation service p 838 N93-26648
- Design issues and initial performance of an adaptive air/ground/air HF communication system p 934 N93-30342
- Enhancing availability, performance, and flexibility of air traffic control air-ground services p 887 N93-30353
- AIRCRAFT COMPARTMENTS**
- Comparison of toxicity rankings of six aircraft cabin polymers by lethality and by incapacitation in rats p 26 A93-10328
- Human factors of aircraft cabin safety p 140 A93-14218
- Active control of interior noise in model aircraft fuselages using piezoceramic actuators p 231 A93-14540
- Comparison of advanced turboprop interior noise control ground and flight test data p 444 A93-19136
- Cabin noise source-path identification for AD-200 ultralight aircraft p 444 A93-19138
- On sound attenuation in boundary layers p 446 A93-19164
- Matrix difference equation analysis of coupled structural-acoustic models for aircraft fuselage vibration and interior noise reduction p 446 A93-19172
- Evaluation of piezoceramic actuators for control of aircraft interior noise p 447 A93-19186
- Vibro-acoustic analysis of propeller aircraft, integrating advanced experimental modeling with in-flight data analysis p 451 A93-19230
- Study of the method for determining residual stress induced by machining in airplane canopies made of PMMA p 534 A93-27366
- New cabin electronics p 804 A93-39542
- Cabin accommodations for passengers with ambulatory disabilities - Transport category aircraft [SAE ARP 4387] p 1103 A93-52166
- Interconversion of two kinds of methods for cabin leakage test p 1192 A93-53874
- A new methodology for helicopter internal noise reduction application to the AS332 L2 p 1243 A93-54723
- European research into helicopter internal noise p 1243 A93-54724
- Effects of seating configuration and number of type 3 exits on emergency aircraft evacuation [AD-A256616] p 143 N93-14277
- A model study of the aircraft cabin environment resulting from in-flight fires [DOT/FAA/CT-90/22] p 496 N93-21557
- The effectiveness of hand-held fire extinguishers on cargo container fires [DOT/FAA/CT-TN92/42] p 496 N93-21821
- In-flight evaluation of noise levels and assessment of active noise reduction systems in the Seahawk S-70B-2 helicopter [AD-A260689] p 759 N93-25649
- Ventilation effects on smoke and temperature in an aircraft cabin quarter-scale model [DOT/FAA/CT-89/25] p 791 N93-28055
- Longitudinal acceleration test of overhead luggage bins in a transport airframe section [DOT/FAA/CT-92/9] p 991 N93-31652
- AIRCRAFT CONFIGURATIONS**
- A low-speed aerodynamic model for harmonically oscillating aircraft configurations p 8 A93-11500
- Transport resurrection p 41 A93-12434
- Test pilot's notes on flying the Low Altitude/Airspeed Unmanned Research Aircraft (LAURA) [AIAA PAPER 92-4078] p 42 A93-13269
- The F-18 High Alpha Research Vehicle - A high-angle-of-attack testbed aircraft [AIAA PAPER 92-4121] p 42 A93-13273
- Aircraft concept optimization using the global sensitivity approach and parametric multiobjective figures of merit [AIAA PAPER 92-4221] p 45 A93-13381
- Aerodynamic characteristics of transport airplanes in low speed configuration p 113 A93-14172
- A parametric approach to preliminary design for aircraft and spacecraft configuration p 225 A93-14201
- Human factors of aircraft cabin safety p 140 A93-14218
- Research and applications in structural dynamics and aeroelasticity p 153 A93-14223
- Assessment and design of low boom configurations for supersonic transport aircraft p 446 A93-19163
- Aerodynamic optimization of an HSCT configuration using variable-complexity modeling [AIAA PAPER 93-0101] p 322 A93-19806
- Development of the quasi-procedural method for use in aircraft configuration optimization [AIAA PAPER 92-4693] p 322 A93-20278
- Survey - Applications of structural optimization methods to fixed wing aircraft and spacecraft [AIAA PAPER 92-4726] p 325 A93-20328
- Structural optimization for joined-wing synthesis [AIAA PAPER 92-4761] p 325 A93-20356
- A gridless Euler/Navier-Stokes solution algorithm for complex-aircraft applications [AIAA PAPER 93-0333] p 268 A93-21107
- Subsonic static and dynamic stability characteristics of the test technique demonstrator NASP configuration [AIAA PAPER 93-0519] p 268 A93-21111
- Development of a flexible and efficient multigrid-based multiblock flow solver [AIAA PAPER 93-0677] p 269 A93-21117
- Development and application of GASP 2.0 [AIAA PAPER 92-5067] p 438 A93-22337
- Aerodynamic foundations for use of unsteady aerodynamic effects in flight control [AIAA PAPER 93-0188] p 276 A93-22613
- Turbulence model evaluation for the prediction of flows over a supercritical airfoil with deflected aileron at high Reynolds number [AIAA PAPER 93-0191] p 276 A93-22615
- Development of an engineering level prediction method for high angle of attack aerodynamics [AIAA PAPER 93-0208] p 278 A93-22626
- An installed nacelle design method using multiblock Euler solver [AIAA PAPER 93-0528] p 284 A93-23269
- Aerodynamic analysis of flapping wing propulsion [AIAA PAPER 93-0484] p 286 A93-23386
- Multi-block grid generation for complete aircraft configurations p 460 A93-23838
- A multi-functional computer-aided aircraft exterior shape modelling prototype system p 504 A93-24032
- Some effects of wing and body geometry on the aerodynamic characteristics of configurations designed for high supersonic Mach numbers [AIAA PAPER 92-4246] p 463 A93-24493
- Hybrid prismatic/tetrahedral grid generation for complex 3-D geometries [AIAA PAPER 93-0669] p 465 A93-24778
- A study of CFD algorithms applied to complete aircraft configurations [AIAA PAPER 93-0784] p 468 A93-24864
- Vortex/surface interaction [AIAA PAPER 93-0863] p 468 A93-24925
- Investigation of three-dimensional separation at wing/body junctions in supersonic flows using TVD MacCormack's scheme [AIAA PAPER 93-0884] p 471 A93-24945
- Regional fanjet aircraft optimization studies p 508 A93-28602
- Aeroelastic system identification of advanced technology aircraft through higher order signal processing p 525 A93-29297
- The rebirth of the tiltrotor - The 1992 Alexander A. Nikolsky Lecture p 712 A93-34256
- The criticalness of spares effectivity checks for aircraft configuration control p 763 A93-35923
- Logistic Support Analysis - An integrated approach to configuration management p 763 A93-35924
- Controlling hazardous configurations in helicopter systems p 763 A93-35927
- Introduction of the M-85 high-speed rotorcraft concept p 797 A93-35980
- The Cabri two-seat helicopter - Design and first flights p 799 A93-36019
- The V-22 for SOF p 800 A93-36026
- Detection and classification of acoustic signals from fixed-wing aircraft p 850 A93-37032
- The whale with a tail p 803 A93-38837
- Using current numerical methods in a mathematical model of flight vehicle synthesis p 804 A93-39188
- Engineering method for calculating surface pressures and heating rates on vehicles with embedded shocks p 777 A93-39255
- Development of a transonic Euler method for complete aircraft configurations p 779 A93-39721
- Design development for advanced general aviation aircraft, II p 897 A93-40475
- Validation of engineering methods for predicting hypersonic vehicle control forces and moments p 906 A93-41897
- Current methods of selecting the configurations and parameters of flight vehicles p 891 A93-42369
- Formalization of the problem of preliminary aircraft design p 891 A93-42375
- Comparison of numerical methods in transonic aerodynamics p 864 A93-42446
- Actuated forebody strake controls for the F-18 high alpha research vehicle [AIAA PAPER 93-3675] p 1006 A93-44233
- Two leading-edge droop modifications for tailoring stall characteristics of a general aviation trainer configuration p 1008 A93-46807
- The adaptive wall test section for the NASA Langley 0.3-m Transonic Cryogenic Tunnel p 1013 A93-46825
- AIAA Applied Aerodynamics Conference, 11th, Monterey, CA, Aug. 9-11, 1993, Technical Papers, Pts. 1 & 2 p 974 A93-47201
- CFD drag predictions for a wide body transport fuselage with flight test verification [AIAA PAPER 93-3418] p 976 A93-47214
- A visualization study of the vortical flow over a double-delta wing in dynamic motion [AIAA PAPER 93-3425] p 976 A93-47220
- A zonal CFD method for three-dimensional wing simulations [AIAA PAPER 93-3433] p 977 A93-47225
- Wavenders with finlets [AIAA PAPER 93-3442] p 978 A93-47231
- Computation of wake roll-up for complete aircraft configurations [AIAA PAPER 93-3509] p 984 A93-47275
- Experimental analysis of rotary derivatives on a modern aircraft configuration [AIAA PAPER 93-3514] p 985 A93-47278
- Flow visualization of mast-mounted-sight/main rotor aerodynamic interactions [AIAA PAPER 93-3517] p 1009 A93-47280
- Application of a parabolized Navier-Stokes code to an HSCT configuration and comparison to wind tunnel test data [AIAA PAPER 93-3537] p 986 A93-47288
- Interpretation of waverider performance data using computational fluid dynamics [AIAA PAPER 93-2921] p 1044 A93-48122
- Computations of transonic wind tunnel flows about a fully configured model of aircraft by using multi-domain technique [AIAA PAPER 93-3022] p 1055 A93-48207
- Transonic mutual interference of wing-pylon-multiple body configurations using an overlapping grid scheme [AIAA PAPER 93-3023] p 1055 A93-48208
- Aircraft control requirements and achievable dynamics prediction [AIAA PAPER 93-3648] p 1128 A93-48331
- The use of triangular elements in panel methods for calculating flow past flight vehicles p 1068 A93-48904
- Three-dimensional time-marching aeroelastic analyses using an unstructured-grid Euler method p 1100 A93-49012
- Wind tunnel results for an advanced fighter configuration employing transverse thrust for enhanced STOL capability [AIAA PAPER 93-1933] p 1100 A93-49796
- Development of the F/A-18 E/F air induction system [AIAA PAPER 93-2152] p 1101 A93-49969
- X-29 high-angle-of-attack flight testing p 1101 A93-50487
- Certain improved algorithms for calculating the aerodynamic characteristics of flight vehicles in free-molecular flow p 1090 A93-51872
- Aerodynamic characteristics of airship models of different shapes p 1092 A93-51909
- Aerodynamic calculation of complex three-dimensional configurations p 1094 A93-52426
- Ground facility interference on aircraft configurations with separated flow p 1140 A93-52441
- Low aspect ratio wing code validation experiment p 1176 A93-53202
- Space marching calculations about hypersonic configurations using a solution-adaptive mesh algorithm p 1177 A93-53212
- Vectoring jet effects on the flow and aerodynamic behaviors of fighter model p 1241 A93-54590
- AIAA Lighter-Than-Air Systems Technology Conference, 10th, Scottsdale, AZ, Sept. 14-16, 1993, Technical Papers p 1229 A93-54601
- Advanced technologies for enhancement of airships [AIAA PAPER 93-4040] p 1242 A93-54610
- The largest freight airship that can fit in Moffett hangar no. 1 [AIAA PAPER 93-4046] p 1242 A93-54613
- Aerodynamic characteristics of a semibuoyant station in the shape of a torus [AIAA PAPER 93-4034] p 1231 A93-54615
- Fighting for air p 1243 A93-54650
- Bear facts --- Soviet Tu-95 aircraft p 1229 A93-55175
- A configuration development strategy for the NASP p 46 N93-10011

- Water tunnel studies of inlet/airframe interference phenomena p 215 N93-13216
- Some aspects of intake design, performance and integration with the airframe p 161 N93-13219
- High-speed aerodynamics of upper surface blowing aircraft configurations p 132 N93-13729
- DESAID (the development of an expert system for aircraft initial design) p 163 N93-14448
- The 3D Navier-Stokes flow analysis for shared and distributed memory MIMD computers [AD-A256038] p 221 N93-15187
- The design of a long range megatransport aircraft [NASA-CR-192077] p 332 N93-17711
- Open aircrew VTOL concepts [NASA-CR-177603] p 240 N93-17883
- The S.T.O.R.M. (tm): Air transport system design simulation [NASA-CR-192070] p 338 N93-18349
- Identification of system dynamics of a high incidence research model [RR-407] p 339 N93-18507
- Apparatus and method for improving spin recovery on aircraft [NASA-CASE-LAR-14747-1] p 526 N93-20039
- Application of the Euler method EULFLEX to a fighter-type airplane configuration at transonic speed [MBB-FE-211-S-PUB-0489-A] p 484 N93-21059
- Structural and aerodynamic optimization of joined-wing aircraft p 715 N93-25526
- An approach to configuration design synthesis of subsonic transport aircraft using artificial intelligence techniques p 716 N93-25692
- High-altitude reconnaissance aircraft p 894 N93-29713
- Supersonic aerodynamic characteristics of an advanced F-16 derivative aircraft configuration [NASA-TP-3355] p 989 N93-31733
- ### AIRCRAFT CONSTRUCTION MATERIALS
- Multidisciplinary design of composite aircraft structures by Lagrange p 76 A93-10273
- Comparison of toxicity rankings of six aircraft cabin polymers by lethality and by incapacitation in rats p 26 A93-10328
- Current developments in structural technology p 77 A93-10780
- Getting it together p 78 A93-11682
- The approach to airworthiness clearance with the introduction of advanced materials and manufacturing technologies into the design of aerospace structures p 2 A93-12235
- The conceptual study of supersonic transport structure [AIAA PAPER 92-4219] p 43 A93-13348
- Out with the mechanical fasteners — design of aircraft using composite materials [AIAA PAPER 92-4210] p 44 A93-13378
- Composites roll sevens — aircraft structures p 3 A93-13448
- Flight simulation and constant amplitude fatigue crack growth in aluminum-lithium sheet and plate p 71 A93-13644
- ICAS, Congress, 18th, Beijing, China, Sept. 20-25, 1992, Proceedings, Vols. 1 & 2 [ISBN 1-56347-046-2] p 107 A93-14151
- Mechanical testing analyses of new aluminum alloy SPF typical-parts in aircraft p 196 A93-14174
- Cost - The challenge for advanced materials and structures p 233 A93-14338
- Choice of materials for military helicopters p 158 A93-15028
- Thermoplastic and thermosetting matrix composite structures - Comparison of mechanical properties p 197 A93-15029
- Sandwich construction in the Starship p 159 A93-15737
- The design development of the monolithic CFRP centre fuselage skin of the European fighter aircraft p 159 A93-15782
- Technological challenges with smart structures in German aircraft industry p 320 A93-17714
- Ultrasonic NDE of adhesive and sealant bonded aluminum lap-splices p 407 A93-19595
- Potential aerospace applications for metal matrix composites p 389 A93-21678
- The structure and material testing facility needed for future SST/HST development [AIAA PAPER 92-3887] p 528 A93-24481
- AHS National Technical Specialists' Meeting on Rotorcraft Structures, Williamsburg, VA, Oct. 29-31, 1991, Proceedings p 506 A93-27951
- A retrospective of 3600 composite blades p 507 A93-27963
- The effects of composite material on the configuration and design of the V-22 wing p 507 A93-27964
- Repair of a severely damaged composite fuel pod p 508 A93-27966
- An accurate nonlinear finite element analysis and test correlation of a stiffened composite wing panel p 546 A93-27968
- Coupled composite rotor blades under bending and torsional loads p 546 A93-27970
- Advanced composite helicopter MISERS GOLD test/analysis p 508 A93-27974
- Rapid detection and quantification of impact damage in composite structures p 547 A93-27978
- High-temperature materials warm up for debut p 535 A93-28393
- Quantification of uncertainties in composites [AIAA PAPER 93-1440] p 734 A93-33989
- Tapered geometries for improved crashworthiness under side loads p 743 A93-34259
- AHS, Annual Forum, 48th, Washington, June 3-5, 1992, Proceedings, Vols. 1 & 2 p 763 A93-35901
- The Cabri two-seat helicopter - Design and first flights p 799 A93-36019
- Birth of the betas p 824 A93-38200
- Materials problems connected with the propulsion of supersonic air carriers [ONERA, TP NO. 1992-157] p 824 A93-38736
- High-efficiency machining methods for aviation materials [ISBN 5-230-16902-8] p 835 A93-39084
- The effect of exfoliation corrosion on the fatigue behavior of structural aluminum alloys p 1017 A93-45778
- Boeing 777 gets a boost from titanium p 1018 A93-45987
- What can Japan teach the U.S. about composites? p 1144 A93-49336
- An aeroacoustic stand for evaluating the efficiency of sound-absorbing structures under conditions of acoustic wave propagation in a moving medium p 1140 A93-51762
- Overview of NASA's advanced high temperature engine materials technology program p 1212 A93-53453
- Case studies - Applications of laser systems for cutting and welding aerospace parts p 1217 A93-53498
- Material requirements for the High Speed Civil Transport [ISABE 93-7067] p 1200 A93-54043
- Advanced technologies for enhancement of airships [AIAA PAPER 93-4040] p 1242 A93-54610
- Nondestructive evaluation of ceramic and metal matrix composites for NASA's HITEMP and enabling propulsion materials programs [NASA-TM-105807] p 85 N93-10963
- Materials: Toward the non-metallic engine [PNR-90915] p 56 N93-11019
- Surface protection in the aircraft industry [MBB-Z-0432-92-PUB] p 72 N93-11027
- Aero engine ceramics: The vision, the reality, and the progress [PNR-90983] p 72 N93-11066
- Advanced materials in gas turbine engines: An assessment [PNR-90946] p 58 N93-11105
- Fatigue in single crystal nickel superalloys [AD-A254603] p 74 N93-12237
- Stress corrosion susceptibility of ultra-high strength steels for Naval aircraft applications [AD-A256126] p 199 N93-15189
- Fiber reinforced composites: A new class of glass and glass ceramic materials for thermomechanical applications [REPT-921-430-104] p 200 N93-15490
- Development of a menu driven materials data base for use on personal computers: Aircraft structures technical memorandum [AD-A256317] p 392 N93-16403
- Fatigue in single crystal nickel superalloys [AD-A258038] p 393 N93-17704
- Supersonic transport: Which material for the engine [DS-2023] p 522 N93-21459
- Selection criteria for metallic high temperature structural materials in hypersonic flying equipment [MBB-LME-221-HYPAC-PUB-2-A] p 515 N93-21479
- Numerical modelling of induced effects of lightning strike on an all composite helicopter p 703 N93-24879
- Comparison of the damage for various types of fibre reinforced composites due to different lightning test standards (MIL-STD-1757A, German military VG-standard 96903) p 736 N93-24891
- Fatigue in single crystal nickel superalloys [AD-A261742] p 737 N93-26282
- Structural tailoring of aircraft engine blade subject to ice impact constraints [NASA-TM-106033] p 838 N93-26999
- A demonstration of simple airfoils: Structural design and materials choices [DE93-007882] p 789 N93-28662
- Nonlinear analyses of composite aerospace structures in sonic fatigue [NASA-CR-193124] p 930 N93-29154
- Advanced technology composite aircraft structures [NASA-CR-190420] p 894 N93-29498
- Static and dynamic large deflection flexural response of graphite-epoxy beams [NASA-CR-4118] p 934 N93-30374
- Composites: A viable option p 918 N93-30429
- Advanced composite structural concepts and material technologies for primary aircraft structures p 918 N93-30430
- Structural evaluation of curved stiffened composite panels fabricated using a THERM-Xsm process p 919 N93-30435
- Lessons learned for composite structures p 920 N93-30444
- First NASA Advanced Composites Technology Conference, part 2 [NASA-CP-3104-PT-2] p 921 N93-30841
- Development of resins for composites by resin transfer molding p 921 N93-30853
- Advanced fiber/matrix material systems p 921 N93-30854
- Mechanical and analytical screening of braided composites for transport fuselage applications p 922 N93-30855
- Construction and testing of simple airfoils to demonstrate structural design, materials choice, and composite concepts p 879 N93-30979
- Aircraft structures in 2000: A technological challenge? [MBB-LME-202-S-PUB-0485] p 998 N93-31058
- NASA-UVA light aerospace alloy and structure technology program supplement: Aluminum-based materials for high speed aircraft [NASA-CR-4517] p 1019 N93-31643
- Fatigue in single crystal nickel superalloys [AD-A265451] p 1019 N93-31795
- ### AIRCRAFT CONTROL
- Precision navigation with an integrated navigation system p 29 A93-10782
- Adaptive control of aircraft in windshear p 62 A93-13126
- Nonlinear time-series-based adaptive control applications p 97 A93-13230
- H(infinity) optimal controllers for a distributed model of an unstable aircraft p 62 A93-13247
- Integrated aerodynamics and control system design for tailless aircraft [AIAA PAPER 92-4604] p 42 A93-13284
- Optimization-based linear and nonlinear design methodologies for aircraft control. II - Final simulations [AIAA PAPER 92-4627] p 62 A93-13285
- Linear and nonlinear aircraft flight control for the AIAA Controls Design Challenge [AIAA PAPER 92-4628] p 62 A93-13286
- Piloted simulation study of two tilt-wing control concepts [AIAA PAPER 92-4236] p 63 A93-13338
- ICAS, Congress, 18th, Beijing, China, Sept. 20-25, 1992, Proceedings, Vols. 1 & 2 [ISBN 1-56347-046-2] p 107 A93-14151
- Vortex control technology p 111 A93-14152
- Optimality-based control laws for real-time aircraft control via parameter optimization p 180 A93-14161
- Automatic guidance and control for recovery of remotely piloted vehicles p 181 A93-14188
- An adaptive algorithm for estimation of a state vector in the system of remotely-piloted aircraft control using Kalman filter p 181 A93-14232
- Aeroelastic investigations as applied to Airbus airplanes p 155 A93-14280
- Stochastic measures of performance robustness in aircraft control systems p 185 A93-14595
- Phase II simulation evaluation of the flying qualities of two tilt-wing flap control concepts [SAE PAPER 920988] p 185 A93-14635
- Advanced cooling for high power electric actuators [SAE PAPER 921022] p 158 A93-14649
- Limit cycle in the longitudinal motion of the USB STOL ASKA - Control system functional mockup and actual aircraft [SAE PAPER 921040] p 185 A93-14660
- Synthesis of robust motion stabilization laws for flight vehicles p 227 A93-16777
- Selection of methods and equipment for monitoring the technical condition of booster system components — of aircraft hydraulic systems p 395 A93-18329
- Analysis of random components during measurements in the computerized diagnostic system Analiz-86 p 321 A93-18344
- Developing control strategies for ASTOVL aircraft p 366 A93-18777
- Static roll moment characteristics of asymmetric tangential leading edge blowing on a delta wing at high angles of attack [AIAA PAPER 93-0052] p 261 A93-20165

Active control of wing rock of a delta wing at post-stall using tangential leading edge blowing
[AIAA PAPER 93-0056] p 367 A93-20169

Application of structured singular value synthesis to a fighter aircraft p 368 A93-22865

A dynamic inversion control approach for high-Mach trajectory tracking p 385 A93-22870

Control of a high performance aircraft with unacceptable aerodynamics p 369 A93-22905

Output tracking control of nonlinear systems with weakly non-minimum phase p 439 A93-22968

Design of insensitive multirate aircraft control using optimized eigenstructure assignment p 370 A93-23515

Optimal control law synthesis for flutter suppression using active acoustic excitations p 370 A93-23516

Pilot control identification using Minimum Model Error estimation
[AIAA PAPER 92-4421] p 523 A93-24497

Development of circulation control technology for application to advanced subsonic transport aircraft
[AIAA PAPER 93-0644] p 464 A93-24759

A nonsearch adaptive control system with a reference model and derivative measurement p 561 A93-26838

Controls and displays for Douglas Aircraft for the 1990s p 545 A93-27241

Active aircraft recovery from a spin p 524 A93-27295

A data processing and control system for counteracting wind shear p 524 A93-27604

Application of new GPS aircraft control/display system to topographic mapping of the Greenland ice cap p 499 A93-28152

Mathematical phenomenology for thrust-vectoring-induced agility comparisons p 525 A93-28613

Selection of transducer measuring ranges in flight vehicle control systems p 526 A93-29691

Controller design using fuzzy logic - A case study p 756 A93-33793

X-31A flight flutter test excitation by control surfaces
[AIAA PAPER 93-1538] p 727 A93-34075

Smart structures stabilized unstable control surfaces
[AIAA PAPER 93-1701] p 712 A93-34223

Generalized guidance law for collision courses p 727 A93-34533

Optimal discrete-time dynamic output-feedback design - A w-domain approach p 757 A93-34536

Robustness evaluation of a flexible aircraft control system p 727 A93-34540

Zero-gravity atmospheric flight by robust nonlinear inverse dynamics p 728 A93-34550

The criticalness of spares effectivity checks for aircraft configuration control p 763 A93-35923

Design and evaluation of a robust dynamic neurocontroller for a multivariable aircraft control problem p 817 A93-37004

Neural network controllers for the X29 aircraft p 817 A93-37005

Spoiler actuator - A problem investigation p 801 A93-37175

Optimal takeoff procedures for a transport category tiltrotor p 802 A93-37377

Computational investigation of a pneumatic forebody flow control concept p 768 A93-37383

Comment on 'Equation decoupling - A new approach to the aerodynamic identification of unstable aircraft' p 818 A93-37406

Nonlinear analysis and flight dynamics
[ONERA, TP NO. 1992-83] p 818 A93-38568

F/A-18 controls released departure recovery - Flight test evaluation p 803 A93-38839

The problem of avoiding aircraft collisions during group flights p 819 A93-39191

Experimental investigation on aircraft dynamic stability parameters p 905 A93-40328

Robust sampled data eigenstructure assignment using the delta operator --- in relation to autopilot design p 906 A93-41889

Neurocontrol design and analysis for a multivariable aircraft control problem p 906 A93-41894

Validation of engineering methods for predicting hypersonic vehicle control forces and moments p 906 A93-41897

A nonlinear control strategy for robust sliding mode performance in the presence of unmatched uncertainty p 938 A93-42556

Integrating controls and avionics on commercial aircraft p 892 A93-42778

Reliability assessment for self-repairing flight control systems p 907 A93-42804

The UTA autonomous aerial vehicle - Automatic control and navigation p 908 A93-42813

Real-time parameter identification applied to flight simulation p 1006 A93-44142

Dynamic compensator design in nonlinear aerospace systems p 1036 A93-44150

Stiffness enhancement of flight control actuator p 1006 A93-44151

Artificial transition - A tool for high Reynolds number simulation?
[AIAA PAPER 93-3258] p 967 A93-46799

Side-force control on a forebody of diamond cross-section at high angles of attack
[AIAA PAPER 93-3407] p 1008 A93-47206

Forebody vortex control on an F/A-18 using small, rotatable 'tip-strakes'
[AIAA PAPER 93-3450] p 1009 A93-47236

Forebody vortex control - A progress review
[AIAA PAPER 93-3540] p 986 A93-47292

AIAA Atmospheric Flight Mechanics Conference, Monterey, CA, Aug. 9-11, 1993, Technical Papers p 1125 A93-48301

Status of the validation of high-angle-of-attack nose-down pitch control margin design guidelines
[AIAA PAPER 93-3623] p 1126 A93-48308

Aircraft control requirements and achievable dynamics prediction
[AIAA PAPER 93-3648] p 1128 A93-48331

Development of lateral-directional departure criteria
[AIAA PAPER 93-3650] p 1128 A93-48333

Nonsmooth trajectory optimization - An approach using continuous simulated annealing
[AIAA PAPER 93-3657] p 1099 A93-48337

Aeroelastic effects on the B-2 maneuver response
[AIAA PAPER 93-3664] p 1128 A93-48344

A new flying qualities criterion for flying wings
[AIAA PAPER 93-3668] p 1128 A93-48346

Pilots' control behavior including feedback structures identified by an improved method
[AIAA PAPER 93-3669] p 1129 A93-48347

F/A-18 departure recovery improvement evaluation
[AIAA PAPER 93-3671] p 1129 A93-48349

Efforts to reduce CFIT accidents should address failures of the aviation system itself p 1096 A93-49280

Development methodology for contemporary avionics systems
[SAE PAPER 931591] p 1104 A93-49340

Compact high reliability fiber coupled laser diodes for avionics and related applications p 1152 A93-49470

Optical actuators for fly-by-light applications p 1172 A93-49475

Onboard Connectivity Network for command and control aircraft p 1166 A93-49481

Investigation of high-alpha lateral-directional control power requirements for high-performance aircraft
[AIAA PAPER 93-3647] p 1130 A93-49519

Use of neural networks in control of high-alpha maneuvers p 1130 A93-49593

Application of structured singular value synthesis to a fighter aircraft p 1130 A93-49594

Full envelope multivariable control law synthesis for a high-performance test aircraft p 1130 A93-49595

Reduced order proportional integral observer with application p 1166 A93-49605

Dual Engine application of the Performance Seeking Control algorithm
[AIAA PAPER 93-1822] p 1110 A93-49709

A new approach to robust fault detection and identification p 1166 A93-50631

Control of takeoff of a hypersonic aircraft using neural networks p 1167 A93-50744

Definition of the structure of expert preferences for the multicriterial analysis of control systems p 1168 A93-50953

Multilevel control systems and optimization of their structures p 1168 A93-50954

An information-search system in cybernetics p 1168 A93-50957

Prediction and planning of a flight vehicle route in the presence of motion inhibiting factors p 1130 A93-50961

Control augmentation system (CAS) synthesis via adaptation and learning
[AIAA PAPER 93-3728] p 1170 A93-51328

Multiple radial basis function networks in modeling and control
[AIAA PAPER 93-3731] p 1170 A93-51330

Hodograph analysis in aircraft trajectory optimization
[AIAA PAPER 93-3742] p 1101 A93-51338

The Generalized Legendre-Clebsch Condition on state/control constrained arcs
[AIAA PAPER 93-3746] p 1170 A93-51342

Near-optimal, asymptotic tracking in control problems involving state-variable inequality constraints
[AIAA PAPER 93-3748] p 1170 A93-51344

Identification of integrated airframe-propulsion effects on an F-15 aircraft for application to drag minimization
[AIAA PAPER 93-3764] p 1101 A93-51359

Nonlinear command augmentation system for a high performance aircraft
[AIAA PAPER 93-3777] p 1132 A93-51372

A pseudo-loop design strategy for the longitudinal control of hypersonic aircraft
[AIAA PAPER 93-3814] p 1132 A93-51405

Automated control of aircraft in formation flight
[AIAA PAPER 93-3852] p 1134 A93-51439

Decentralized autonomous attitude determination using an inertially stabilized payload
[AIAA PAPER 93-3857] p 1134 A93-51444

Fault detection, isolation, and reconfiguration for aircraft using neural networks
[AIAA PAPER 93-3870] p 1135 A93-51456

A new technique for nonlinear control of aircraft
[AIAA PAPER 93-3881] p 1135 A93-51466

Optimal performance of airplanes flying through windshear
[AIAA PAPER 93-3846] p 1102 A93-51480

The application of scheduled H-infinity controllers to a VSTOL aircraft p 1135 A93-52249

Computation of maximized gust loads for nonlinear aircraft using matched-filter-based schemes p 1136 A93-52452

Envelope function - A tool for analyzing flutter data p 1136 A93-52455

Methodology for integration of digital control loaders in aircraft simulators
[AIAA PAPER 93-3551] p 1207 A93-52655

Hybrid complex of the aircraft intellectualized control systems simulation at the stage of their research projecting
[AIAA PAPER 93-3559] p 1222 A93-52660

Stabilization of the dynamic characteristics of the two-channel automatic control system of aircraft p 1205 A93-52941

Solution of the boundary value problem in flight dynamics by the opposite motion method p 1206 A93-52944

A vision-based method for autonomous landing p 1190 A93-53172

A reactive approach for distributed air traffic control
[ONERA, TP NO. 1993-83] p 1190 A93-53603

Estimation of aerodynamic characteristics from flight-test data. IV - Principal component analysis and perpendicular error method p 1241 A93-54551

Boeing 777 high lift control system p 1249 A93-55753

Estimation of aircraft inertia characteristics from bifilar pendulum test data p 1249 A93-56029

Pitch control trimming system for canard design aircraft
[CA-PATENT-APPL-SN-2013236] p 63 A93-10374

Initial piloted simulation study of geared flap control for tilt-wing V/STOL aircraft
[NASA-TM-103872] p 64 A93-10741

Application of eigenstructure assignment to the control of powered lift combat aircraft p 64 A93-11871

Modeling and model simplification of aeroelastic vehicles: An overview
[NASA-TM-107691] p 64 A93-12216

Computational nonlinear control
[AD-A253547] p 98 A93-12258

A monitor for the laboratory evaluation of control integrity in digital control systems operating in harsh electromagnetic environments
[NASA-TM-4402] p 65 A93-12304

Analysis of fault-tolerant neurocontrol architectures
[NASA-TM-105898] p 65 A93-12305

DYNAC: A computer program for analyzing the dynamical stability of aircraft
[REPT-8-31] p 66 A93-12415

Application of concurrent engineering methods to the design of an autonomous aerial robot
[AD-A254968] p 212 A93-12555

Determination of the stability and control derivatives of the F/A-18 HARV from flight data using the maximum likelihood method
[NASA-CR-191216] p 186 A93-12903

A stochastic optimal feedforward and feedback control methodology for superagility
[NASA-CR-4471] p 229 A93-13370

Ideal aircraft handling quality models: Longitudinal axis
[NAL-PD-FC-9203] p 187 A93-13566

Multiplexing electro-optic architectures for advanced aircraft integrated flight control systems
[NASA-CR-182268] p 187 A93-13735

An examination of wing rock for the F-15
[AD-A256613] p 188 A93-14252

Adaptive control of nonlinear nonminimum phase systems p 229 A93-14470

Multiple model adaptive estimation applied to the VISTA F-16 with actuator and sensor failures
[AD-A256444] p 188 A93-14608

Multi-disciplinary optimization of aeroservoelastic systems
[NASA-CR-191255] p 220 A93-14766

- F/A-18 controls released departure recovery flight test evaluation p 189 N93-15396
[AD-A256522]
- Propulsion system performance resulting from an integrated flight/propulsion control design p 180 N93-15525
[NASA-TM-105874]
- Maximum lift of wings with leading-edge devices and trailing-edge flaps deployed p 290 N93-16522
[ESDU-92031]
- Design of robust suboptimal controllers for a generalized quadratic criterion p 372 N93-17670
[AD-A257746]
- Design of the advanced regional aircraft, the DART-75 p 333 N93-17972
[NASA-CR-192044]
- MM-122: High speed civil transport p 334 N93-17974
[NASA-CR-192011]
- Identification of system dynamics of a high incidence research model p 339 N93-18507
[RR-407]
- Longitudinal-control design approach for high-angle-of-attack aircraft p 373 N93-19108
[NASA-TP-3302]
- A simulation study on take-off and landing dynamics of the aircraft of a fly-by-wire control system p 510 N93-19849
[AD-A259286]
- Controller partitioning for integrated flight/propulsion control implementation p 527 N93-21197
[NASA-TM-105804]
- Prediction of forces and moments for hypersonic flight vehicle control effectors p 728 N93-24762
[NASA-CR-193033]
- Robust nonlinear control of vectored thrust aircraft p 728 N93-25199
[NASA-CR-192727]
- Control and optimization of aircraft trajectories p 729 N93-25543
- Robustness enhancement of neurocontroller and state estimator p 819 N93-26907
[NASA-TM-106028]
- An aerodynamic model for one and two degree of freedom wing rock of slender delta wings p 781 N93-27150
[NASA-CR-193130]
- Low bandwidth robust controllers for flight p 819 N93-27156
[NASA-CR-193085]
- New adaptive controllers for aircraft p 847 N93-27180
- Robust crossfeed design for hovering rotorcraft p 805 N93-27241
[NASA-CR-193107]
- Design, analysis, and control of large transport aircraft utilizing engine thrust as a backup system for the primary flight controls p 820 N93-27308
[NASA-CR-192938]
- Status of the Fiber Optic Control System Integration (FOCSI) program p 841 N93-28053
[NASA-TM-106151]
- Artificial intelligence methodologies in flight related differential game, control and optimization problems p 848 N93-28498
[AD-A262405]
- Low-speed wind tunnel study of the direct side-force characteristics of a joined-wing airplane with an upper fin p 988 N93-31189
[DE93-767966]
- Testing concept of a taxiing control system, summary p 1010 N93-31278
- Design and implementation of fuzzy logic controllers p 1038 N93-31649
[NASA-CR-193268]
- AIRCRAFT DESIGN**
- MPC75 as the forerunner of a new regional aircraft family p 37 N93-10776
- Transonic profile design in curvilinear coordinates using an approximate factorization algorithm p 7 N93-10778
- Current developments in structural technology p 77 N93-10780
- Unorthodoxy rising --- VTOL p 1 N93-11250
- A330 - Completing the family p 40 N93-11418
- The smart truck --- structure, systems, avionics of C-17 airlifter p 40 N93-11420
- Wheel shimmy analysis for main landing gear of aircraft p 41 N93-11809
- The investigation on vibration characteristics of all-movable stabilizer of an aircraft p 41 N93-11821
- A civil aircraft industry for India p 2 N93-12233
- Aerospace - Collected translations of selected papers, 1992 p 2 N93-12726
- Structural and aerodynamic considerations for an oblique all-wing aircraft p 43 N93-13336
[AIAA PAPER 92-4220]
- Oblique wing supersonic transport concepts p 43 N93-13337
[AIAA PAPER 92-4230]
- Extracting dimensional geometric parameters from B-spline surface models of aircraft p 43 N93-13340
[AIAA PAPER 92-4283]
- The conceptual study of supersonic transport structure p 43 N93-13348
[AIAA PAPER 92-4219]
- RDS - A PC-based aircraft design, sizing, and performance system p 97 N93-13354
[AIAA PAPER 92-4226]
- HSCT high-lift aerodynamic technology requirements p 44 N93-13355
[AIAA PAPER 92-4228]
- Teaching aircraft preliminary design - The first three years p 103 N93-13363
[AIAA PAPER 92-4257]
- Design for global competition - The Boeing 777 p 2 N93-13368
[AIAA PAPER 92-4190]
- Aircraft model for multicriterial analysis in decision making p 44 N93-13370
[AIAA PAPER 92-4192]
- An ultralight freewheeling aircraft design study p 44 N93-13371
[AIAA PAPER 92-4194]
- Out with the mechanical fasteners --- design of aircraft using composite materials p 44 N93-13378
[AIAA PAPER 92-4210]
- Aircraft designer's viewpoint of reliability and maintainability p 45 N93-13404
- Aircraft tracking optimization of parameters selection p 3 N93-13628
- The role of fatigue testing in the design, development and certification of the ATR 42/72 p 46 N93-13637
- Maintainable A330 p 107 N93-13957
- Annual Paul E. Hemke Lecture in aerospace engineering p 107 N93-14067
- ICAS, Congress, 18th, Beijing, China, Sept. 20-25, 1992, Proceedings, Vols. 1 & 2 p 107 N93-14151
[ISBN 1-56347-046-2]
- Prospects for a second generation supersonic transport p 108 N93-14154
- Spanish-Indonesian cooperation in the development, production, certification and marketing of CN-235 commuter aircraft p 108 N93-14156
- The new challenge of computational aeroscience p 112 N93-14169
- A proposal concerning the dynamic analysis method of continuous gust design rules p 181 N93-14197
- A parametric approach to preliminary design for aircraft and spacecraft configuration p 225 N93-14201
- Integration of aircraft design and manufacture using artificial intelligence paradigms p 225 N93-14202
- Designing to aircraft system effectiveness/cost/time with VERT - The system analysis method for aircraft p 153 N93-14204
- Aircraft optimization by a system approach - Achievements and trends p 153 N93-14205
- The value of a computational/experimental partnership in aerodynamic design p 114 N93-14215
- Interrelationships between commercial airplane design and operational requirements and procedures p 153 N93-14219
- Study of aeroservoelastic stability of an aircraft p 182 N93-14259
- Aeroelastic investigations as applied to Airbus airplanes p 155 N93-14280
- A synthesized method in durability analysis p 203 N93-14286
- MPC75 - The evolution of a new regional airliner for the late nineties p 155 N93-14289
- The aerodynamic and structural design of a variable camber wing (VCW) p 117 N93-14291
- Design of manoeuvrable simple and complex planform transonic wings with attained thrust, panel- and Euler-methods p 117 N93-14301
- The simulation of aircraft landing gear dynamics p 155 N93-14318
- Cost - The challenge for advanced materials and structures p 233 N93-14338
- Structural optimization in preliminary aircraft design - A finite-element approach p 226 N93-14340
- High capacity aircraft p 157 N93-14395
- The Aircraft/Propulsion Integrated Assessment System p 226 N93-14396
- A control technology of integrated system of engineering supported by software engineering environments p 226 N93-14415
- Hybrid laminar flow control applied to advanced turbofan engine nacelles p 123 N93-14628
[SAE PAPER 920962]
- Low-cost approaches to proving of high-risk fast VTOL designs p 157 N93-14636
[SAE PAPER 920989]
- SAE Aero Design '92 p 157 N93-14641
[SAE PAPER 921009]
- A short range passenger/freighter canard - Some problems of a preliminary aerodynamic concept p 157 N93-14642
[SAE PAPER 921012]
- Study of a Mach 2 supersonic transport aircraft p 124 N93-15034
- Improving anti-fatigue optimum design through AI-search strategy p 208 N93-15342
- The Concorde wing - A useful model p 126 N93-16400
- Technological challenges with smart structures in German aircraft industry p 320 N93-17714
- Adaptive/conformal wing design for future aircraft p 320 N93-17728
- Refinement of algorithms for calculating the remaining life from magnetic recording instrument data --- for IL-86 aircraft wing p 320 N93-18330
- Analysis of the pump station of an aircraft hydraulic system as a subject of diagnosis p 321 N93-18374
- The designs for safety --- considering human factors in aircraft maintenance p 321 N93-18755
- The human factors aspects of aircraft ground handling p 237 N93-18756
- Civil aircraft challenges in engine/airframe integration p 322 N93-19299
[ASME PAPER 92-GT-45]
- Aerodynamic optimization of an HSCT configuration using variable-complexity modeling p 322 N93-19806
[AIAA PAPER 93-0101]
- Development of the quasi-procedural method for use in aircraft configuration optimization p 322 N93-20278
[AIAA PAPER 92-4693]
- Variable-complexity aerodynamic-structural design of a high-speed civil transport wing p 323 N93-20279
[AIAA PAPER 92-4695]
- Concurrent optimization of airframe and engine design parameters p 323 N93-20281
[AIAA PAPER 92-4713]
- Influence of sweep on structural optimization of a fighter wing p 323 N93-20290
[AIAA PAPER 92-4794]
- Multidisciplinary design integration system for a supersonic transport aircraft p 324 N93-20296
[AIAA PAPER 92-4841]
- A multi-point optimization for transonic airfoil design p 264 N93-20303
[AIAA PAPER 92-4681]
- Integrated aerodynamic-structural-control wing design p 324 N93-20307
[AIAA PAPER 92-4694]
- Preliminary wing design of a high speed civil transport aircraft by multilevel decomposition techniques p 325 N93-20323
[AIAA PAPER 92-4721]
- Structural Tailoring/Analysis for Hypersonic Components - A computational simulation p 325 N93-20324
[AIAA PAPER 92-4722]
- Survey - Applications of structural optimization methods to fixed wing aircraft and spacecraft p 325 N93-20328
[AIAA PAPER 92-4726]
- Structural optimization for joined-wing synthesis p 325 N93-20356
[AIAA PAPER 92-4761]
- Geometric requirements for multidisciplinary analysis of aerospace-vehicle design p 436 N93-20366
[AIAA PAPER 92-4773]
- Flutter optimization of large transport aircraft p 326 N93-20381
[AIAA PAPER 92-4795]
- Thermal/structural analysis and aircraft design p 409 N93-20420
- Design of a wing shape for study of hypersonic crossflow transition in flight p 265 N93-20713
- The legal status of ekranoplanes p 453 N93-20900
- Design of a hypersonic waverider-derived airplane p 384 N93-21108
[AIAA PAPER 93-0401]
- Simulation in aeronautics p 437 N93-21868
- Some aspects of the aerodynamic methodology in hypersonic vehicle concept studies p 272 N93-22303
[AIAA PAPER 92-5027]
- Grid and design variables sensitivity analyses for NACA four-digit wing-sections p 276 N93-22616
[AIAA PAPER 93-0195]
- Engine/airframe integration for waverider cruise vehicles p 283 N93-23254
[AIAA PAPER 93-0507]
- The effects of hypersonic flight test requirements on research vehicle design p 386 N93-23258
[AIAA PAPER 93-0511]
- A re-evaluation of the waverider design process p 440 N93-23326
[AIAA PAPER 93-0404]
- Aerodynamically efficient wing design with structural considerations p 460 N93-24081
- Measurement of diffusion in supercritical fluid systems - A review p 534 N93-24884
[AIAA PAPER 93-0809]
- Natural environment application for NASP-X-30 design and mission planning p 531 N93-24915
[AIAA PAPER 93-0851]
- CST and rotorcraft - Expanding the view p 560 N93-25085
- Europe adapts CST to its needs --- computational structures technology for aerospace industry p 560 N93-25088
- Zen and the art of airplane sizing p 504 N93-25174
- Future supersonic transport studies at Aerospatiale p 505 N93-25491
- Eurofan rotor aerodynamic tests p 475 N93-26880
[ONERA, TP NO. 1992-173]
- Designed for work --- British Aerospace Jetstream 41 regional aircraft p 506 N93-27276
- Integration of high bypass ratio engines on modern transonic wings for regional aircraft p 506 N93-27479
- Problems in the optimum design of a wing profile for nonseparated flow over a range of angles of attack p 477 N93-27614

AHS National Technical Specialists' Meeting on Rotorcraft Structures, Williamsburg, VA, Oct. 29-31, 1991, Proceedings p 506 A93-27951

Application of a two-point exponential approximation method in optimizing rotorcraft airframe structures p 507 A93-27956

The effects of composite material on the configuration and design of the V-22 wing p 507 A93-27964

Regional fanjet aircraft optimization studies p 508 A93-28602

Conceptual assessment of two high-speed rotorcraft p 508 A93-28612

Mathematical phenomenology for thrust-vectoring-induced agility comparisons p 525 A93-28613

Quiet operations key to MD-90 success p 708 A93-33700

Energy-absorbing-beam design for composite aircraft subfloors [AIAA PAPER 93-1339] p 709 A93-33909

Advanced transparency development for USAF aircraft [AIAA PAPER 93-1391] p 710 A93-33954

Lessons from application of equivalent plate structural modeling to an HSCT wing [AIAA PAPER 93-1413] p 739 A93-33969

The use of artificial intelligence for buffet environments [AIAA PAPER 93-1534] p 727 A93-34071

In-flight investigation of a rotating cylinder-based structural excitation system for flutter testing [AIAA PAPER 93-1537] p 711 A93-34074

Foreign object impact assessment of a high-Mach engine inlet [AIAA PAPER 93-1630] p 711 A93-34158

Active rib experiment for shape control of an adaptive wing [AIAA PAPER 93-1700] p 712 A93-34222

Smart structures stabilized unstable control surfaces [AIAA PAPER 93-1701] p 712 A93-34223

Active constrained layer viscoelastic damping [AIAA PAPER 93-1702] p 743 A93-34224

Aeroelastic challenges for a High Speed Civil Transport [AIAA PAPER 93-1478] p 712 A93-34240

The rebirth of the tiltrotor - The 1992 Alexander A. Nikolsky Lecture p 712 A93-34256

C-17 - High-tech 'lifter from Long Beach' p 713 A93-34519

Some contributions to propulsion theory - Fuel consumption formulae and general range equation p 713 A93-34850

Management miscues, delays snarl C-17 program p 760 A93-34944

Ensuring the reliability and service life of flight vehicle structures by engineering methods p 745 A93-35276

Mathematical statement of the problem of optimizing the design of an airframe for ease of manufacture p 745 A93-35286

AHS, Annual Forum, 48th, Washington, June 3-5, 1992, Proceedings. Vols. 1 & 2 p 763 A93-35901

The criticalness of spares effectivity checks for aircraft configuration control p 763 A93-35923

Handling qualities testing using the mission oriented requirements of ADS-33C p 817 A93-35961

Cost/weight savings for the V-22 wing stow p 797 A93-35981

Advancing tiltrotor state-of-the-art with variable diameter rotors p 797 A93-35982

Design and manufacturing concepts of Eurofar Model No. 2 blades p 798 A93-35983

Evaluation of tilt rotor aircraft design utilizing a realtime interactive simulation p 798 A93-35989

The development of a crashworthy composite fuselage and landing gear p 799 A93-36001

Design developments for advanced general aviation aircraft. I p 801 A93-37174

Fundamentals of low radar cross-sectional aircraft design p 802 A93-37376

Integrated structure/control/aerodynamic synthesis of actively controlled composite wings p 818 A93-37392

A data system for the observation of flow conditions on an aircraft wing p 808 A93-37882

Flight Deflection Measurement System p 808 A93-37885

Russians completing new ground-effect vehicle p 853 A93-38535

The whale with a tail p 803 A93-38837

B-2 flight test update p 803 A93-38844

Using current numerical methods in a mathematical model of flight vehicle synthesis p 804 A93-39188

Optimization of the parameters of the lift-augmentation devices of the wing of a maneuverable aircraft equipped with an active load-reduction system p 804 A93-39189

Avionic systems/design and maintenance; Proceedings of the Conference, Hounslow, United Kingdom, Apr. 22, 1993 [ISBN 1-85768-095-2] p 764 A93-39535

HIRF and lightning --- EMC of aircraft systems and installations for safe operation p 764 A93-39539

C-17 should fulfill USAF airlift mission p 805 A93-39599

Development of a transonic Euler method for complete aircraft configurations p 779 A93-39721

Hypersonic propulsion - Breaking the thermal barrier p 897 A93-40437

V-22 nacelle conversion actuator p 889 A93-40438

Optimization of constant altitude-constant airspeed flight for piston-prop aircraft p 889 A93-40473

Design development for advanced general aviation aircraft. II p 897 A93-40475

A software for optimum design of an aircraft structure p 938 A93-40495

Machining cost comparison of silicon carbide discontinuously reinforced aluminum, unreinforced aluminum, and titanium [SME PAPER EM92-252] p 925 A93-40656

The effects of high-pressure water on the material integrity of selected aircraft coatings and substrates [SME PAPER AD92-207] p 855 A93-40688

Toward the second-generation supersonic transport [ONERA, TP NO. 1993-26] p 890 A93-41038

A thermal/structural analysis process incorporating concurrent engineering [SAE PAPER 921185] p 938 A93-41364

Testing of an energy efficient environmental control system for a patrol-type aircraft [SAE PAPER 921225] p 890 A93-41399

Current methods of selecting the configurations and parameters of flight vehicles p 891 A93-42369

Optimization of equipment layout in the fuselage of maneuverable aircraft p 891 A93-42370

Selection of the primary aircraft structure at the preliminary design stage p 891 A93-42371

Structure of a knowledge base used in the computerized synthesis of aircraft layout p 891 A93-42373

Some aspects of the design of combination landing gear --- for stable aircraft motion on runways p 891 A93-42374

Formalization of the problem of preliminary aircraft design p 891 A93-42375

Computerized synthesis of three-dimensional kinematic landing gear schemes with a single turning axis p 891 A93-42376

Determination of the takeoff characteristics of jet engines during the preliminary design of aircraft p 892 A93-42378

Characteristics of data processing during the development of a data base for a CAD system for aircraft design p 892 A93-42381

Big time doorstep delivery p 892 A93-42995

The development of a prototype aircraft height monitoring unit utilizing an SSR-based difference in time of arrival technique p 884 A93-43432

Ilyushin takes on the market p 945 A93-43623

ARPA starts push for joint-service ASTOVL p 856 A93-43625

The development of an efficient ornithopter wing p 873 A93-43685

Fundamentals of flight vehicle design --- Russian book [ISBN 5-217-01299-4] p 893 A93-43831

Design of aircraft, helicopters, and aviation engines --- Russian book [ISBN 5-277-01192-7] p 947 A93-44508

Static aeroelastic control of an adaptive lifting surface p 995 A93-45147

Elements of NASA's high-speed research program [AIAA PAPER 93-2942] p 947 A93-45155

Calculation of the position of aircraft center of gravity on an IBM PC p 996 A93-45671

Fuselage longitudinal splice design p 997 A93-45784

Experience in specifying/prolonging the airframe time limits p 948 A93-45797

Backfire unveiled p 997 A93-46024

Effects of floor location on response of composite fuselage frames p 997 A93-46809

Supersonic/hypersonic aerodynamic methods for aircraft design and analysis p 967 A93-46816

The all-electric aircraft - In your future? p 997 A93-46824

Advanced cargo aircraft may offer a potential renaissance in freight transportation p 991 A93-47023

Requirements for facilities and measurement techniques to support CFD development for hypersonic aircraft p 1014 A93-47024

Aerodynamic design of a hypersonic body with a constant favorable pressure gradient [AIAA PAPER 93-3444] p 978 A93-47232

Computational study of a conical wing having unit aspect ratio at supersonic speeds [AIAA PAPER 93-3505] p 984 A93-47272

A CFD-based design strategy for advanced transonic wing concepts with practical ramifications for subsonic transports [AIAA PAPER 93-2946] p 1047 A93-48143

Application of parabolized Navier-Stokes technique for high-L/D, hypersonic vehicle design [AIAA PAPER 93-2948] p 1047 A93-48144

Design efficiency evaluation for transonic airfoil optimization - A case for Navier-Stokes design [AIAA PAPER 93-3112] p 1062 A93-48282

Demonstration of multipoint design procedures for transonic airfoils [AIAA PAPER 93-3114] p 1062 A93-48284

Design of axisymmetric channels with rotational flow [AIAA PAPER 93-3117] p 1062 A93-48287

Development of flying qualities and agility evaluation maneuvers [AIAA PAPER 93-3645] p 1127 A93-48329

Investigation of roll requirements for carrier approach [AIAA PAPER 93-3649] p 1128 A93-48332

A method of wind shear detection for powered-lift STOL aircraft [AIAA PAPER 93-3667] p 1104 A93-48345

An aerodynamic design program for contra-rotating turbine cascades p 1067 A93-48521

Determination of the aerodynamic balance efficiency of aircraft p 1130 A93-48903

Screening studies of advanced control concepts for airbreathing engines [AIAA PAPER 92-3320] p 1108 A93-49329

Aircraft cryogenic fuel system design issues [AIAA PAPER 93-2567] p 1121 A93-50285

Wheel and brake design and test requirements for military aircraft [SAE ARP 1493] p 1103 A93-52165

Cabin accommodations for passengers with ambulatory disabilities - Transport category aircraft [SAE ARP 4387] p 1103 A93-52166

Aspects of fatigue affecting the design and maintenance of modern military aircraft p 1043 A93-52548

Flight research simulation takes off p 1192 A93-53769

Engineering simulators enhance 777 development p 1192 A93-53771

Optimization of afterbodies and engine nozzle by using CFD methods [ISABE 93-7098] p 1187 A93-54074

AIAA Lighter-Than-Air Systems Technology Conference, 10th, Scottsdale, AZ, Sept. 14-16, 1993, Technical Papers p 1229 A93-54601

National airborne surveillance system - An engineering student study [AIAA PAPER 93-4031] p 1242 A93-54603

Aerodynamics of the TCOM 71M aerostat [AIAA PAPER 93-4036] p 1231 A93-54607

Structural analysis of the light weight hard nose of the 71M aerostat [AIAA PAPER 93-4037] p 1255 A93-54608

Advanced technologies for enhancement of airships [AIAA PAPER 93-4040] p 1242 A93-54610

Zeppelin NT - A new concept in airship technology, based on rigid airship principles [AIAA PAPER 93-4045] p 1242 A93-54612

The largest freight airship that can fit in Moffett hangar no. 1 [AIAA PAPER 93-4046] p 1242 A93-54613

The development progress of the U.S. Army's SASS LITE, unmanned robot airship [AIAA PAPER 93-4047] p 1243 A93-54614

Aerodynamic characteristics of a semibuoyant station in the shape of a torus [AIAA PAPER 93-4034] p 1231 A93-54615

Fighting for air p 1243 A93-54650

Future aero engine design trade offs p 1246 A93-54836

Potential use of alternative fuels in aviation p 1243 A93-54838

Russian survivor --- Tu-334 aircraft p 1243 A93-54867

A numerical study of aerodynamic wing design for supercritical conditions of an advanced training and military aircraft p 1238 A93-56213

West powers East p 1244 A93-56349

Overview of supersonic laminar flow control research on the F-16XL ships 1 and 2 [NASA-TM-104257] p 20 N93-11221

The changing nature of design [PNR-91011] p 48 N93-11334

An approach to constrained aerodynamic design with application to airfoils [NASA-TP-3260] p 24 N93-12321

- Concurrent optimization of airframe and engine design parameters
[NASA-TM-105908] p 60 N93-12402
- Aerodynamic Engine/Airframe Integration for High Performance Aircraft and Missiles
[AGARD-CP-498] p 213 N93-13199
- Test techniques for engine/airframe integration
p 213 N93-13200
- Aerodynamic analysis of slipstream/wing/nacelle interference for preliminary design of aircraft configurations
p 130 N93-13205
- Euler analysis of turbofan/superfan integration for a transport aircraft
p 214 N93-13206
- Aerodynamic integration of thrust reversers on the Fokker 100
p 160 N93-13208
- Some aspects of intake design, performance and integration with the airframe
p 161 N93-13219
- AGARD WG13 aerodynamics of high speed air intakes: Assessment of CFD results
p 215 N93-13220
- Survey on techniques used in aerodynamic nozzle/airframe integration
p 161 N93-13224
- CFD calibration for three-dimensional nozzle/afterbody configurations
p 215 N93-13226
- Optimum design of aircraft structures with manufacturing and buckling constraints
p 162 N93-13815
- An examination of wing rock for the F-15
[AD-A256613] p 188 N93-14252
- DESAID (the development of an expert system for aircraft initial design)
p 163 N93-14448
- A90 project: Design of a composite fin
[ETN-92-92773] p 329 N93-16562
- Development of a computer assisted toolbox for aerodynamic design of aircraft at subcritical conditions with application to three-surface and canard aircraft
[ISBN-90-6275-768-5] p 441 N93-16567
- 1991 research and technology
[NASA-TM-103924] p 456 N93-16652
- Definition of the 2005 flight deck environment
[NASA-CR-4479] p 343 N93-16693
- The F-18 systems research aircraft facility
[NASA-TM-4433] p 381 N93-16753
- The NASA High-Speed Research Program
p 330 N93-16761
- Design optimization of natural laminar flow bodies in compressible flow
[NASA-CR-4478] p 292 N93-16940
- A domain-specific design architecture for composite material design and aircraft part redesign
p 442 N93-17522
- Mathematical optimization: A powerful tool for aircraft design
[MBB-FE-2-S-PUB-478] p 331 N93-17564
- Practical architecture of design optimisation software for aircraft structures taking the MBB-LAGRANGE code as an example
[MBB-FE-251-S-PUB-479] p 331 N93-17565
- The design of a long range megatransport aircraft
[NASA-CR-192077] p 332 N93-17711
- Exodus: Prime Mover
[NASA-CR-192051] p 332 N93-17803
- Hypersonic reconnaissance aircraft
[NASA-CR-192049] p 333 N93-17804
- A manned hypersonic reconnaissance vehicle which does not require airborne fueling
p 333 N93-17888
- CFD-based approximation concepts for aerodynamic design optimization with application to a 2-D scramjet vehicle
[AD-A258084] p 333 N93-17893
- Design of the advanced regional aircraft, the DART-75
[NASA-CR-192044] p 333 N93-17972
- MM-122: High speed civil transport
[NASA-CR-192011] p 334 N93-17974
- Phoenix: Preliminary design of a high speed civil transport
[NASA-CR-192024] p 334 N93-17976
- Tesseract: Supersonic business transport
[NASA-CR-192072] p 334 N93-17977
- Eagle RTS: A design for a regional transport aircraft
[NASA-CR-192032] p 334 N93-18017
- Advanced hypersonic aircraft design
[NASA-CR-192046] p 334 N93-18037
- Proposal and preliminary design for a high speed civil transport aircraft. Swift: A high speed civil transport for the year 2000
[NASA-CR-192023] p 335 N93-18049
- The Edge supersonic transport
[NASA-CR-192074] p 335 N93-18055
- Hermes CX-7: Air transport system design simulation
[NASA-CR-192082] p 335 N93-18056
- A second-generation high speed civil transport: Stingray
[NASA-CR-192022] p 336 N93-18059
- The Trojan --- supersonic transport
[NASA-CR-192013] p 336 N93-18060
- Preliminary design of a high speed civil transport: The Opus 0-001
[NASA-CR-192018] p 336 N93-18061
- Arrow 227: Air transport system design simulation
[NASA-CR-192053] p 336 N93-18063
- High speed civil transport
[NASA-CR-192041] p 337 N93-18161
- RTJ-303: Variable geometry, oblique wing supersonic aircraft
[NASA-CR-192054] p 337 N93-18166
- Add-on damping treatment for the F-15 upper-outer wing skin
[AD-A258470] p 337 N93-18248
- JEFF: Air transport system design simulation
[NASA-CR-192069] p 338 N93-18350
- The F-92 RELIANT: Air transport system design simulation
[NASA-CR-192050] p 339 N93-18386
- Study of statistical variations of load spectra and material properties on aircraft fatigue life
[AD-A257961] p 339 N93-18451
- Aircraft performance in practice
p 340 N93-19004
- Formulation of a structural model for flutter analysis of low aspect ratio composite aircraft wings
p 372 N93-19019
- Improvements to LQGI/LTR methodology for plants with lightly damped or low frequency poles
[AD-A258841] p 443 N93-19112
- On the roles of wind tunnel testing and computational fluid dynamics in the aircraft development
p 341 N93-19322
- X-31A high angle of attack and initial post stall flight testing
p 511 N93-19911
- On-line aircraft state and parameter estimation
p 512 N93-19929
- Apparatus and method for improving spin recovery on aircraft
[NASA-CASE-LAR-14747-1] p 526 N93-20039
- YIDOUY and its application to aircraft design
[AD-A259262] p 513 N93-20605
- Fluid/structures interactions. Aircraft considerations
p 527 N93-20628
- Heat loads as key problem of hypersonic flight
[MBB-FE-202-S-PUB-0486] p 484 N93-21054
- The integrated design and manufacturing of composite structures for aircraft using an advanced tape layering technology
[MBB-LME-251-S-PUB-0491-A] p 515 N93-21401
- Application of artificial neural networks to the design optimization of aerospace structural components
[NASA-TM-4389] p 555 N93-21831
- Aerodynamic design and synthesis of the oblique flying wing supersonic transport
p 713 N93-24768
- A procedure for defining lightning risk to air vehicles
p 703 N93-24885
- Screening studies of advanced control concepts for airbreathing engines
[NASA-TM-106042] p 721 N93-25079
- Grid sensitivity for aerodynamic optimization and flow analysis
[NASA-CR-192980] p 694 N93-25117
- Integrated aerodynamic-structural wing design optimization
p 714 N93-25279
- Structural and aerodynamic optimization of joined-wing aircraft
p 715 N93-25526
- An approach to configuration design synthesis of subsonic transport aircraft using artificial intelligence techniques
p 716 N93-25692
- ASTOVL combat aircraft design synthesis and optimization
p 717 N93-25704
- Techniques for designing rotorcraft control systems
[NASA-CR-192960] p 729 N93-26046
- AEW aircraft design
[AD-A261800] p 718 N93-26444
- Adjoint methods for aerodynamic wing design
[NASA-CR-193086] p 805 N93-27089
- Collection of papers of the 31st Israel Annual Conference on Aviation and Astronautics
[ITN-93-85187] p 764 N93-27166
- The development of aircraft in the Lockheed Skunk Works from 1954 to 1991
p 805 N93-27168
- Reynolds and Mach number effects on multielement airfoils
p 785 N93-27446
- Computational method in optimal bending-twisting comprehensive design of wings of subsonic and supersonic aircraft
[AD-A262374] p 806 N93-27694
- International aviation (Selected articles)
[AD-A262566] p 765 N93-28576
- Reliability assessment at airline inspection facilities. Volume 2: Protocol for an eddy current inspection reliability experiment
[DOT/FAA/CT-92/12-VOL-2] p 842 N93-28685
- An integrated optimum design approach for high speed prop-rotors including acoustic constraints
[NASA-CR-193222] p 893 N93-29153
- Quiet by design: Numerical acousto-elastic analysis of aircraft structures
[ISBN-90-386-0042-9] p 893 N93-29268
- High-altitude reconnaissance aircraft
p 894 N93-29713
- Project ARES 2: High-altitude battery-powered aircraft
p 894 N93-29715
- Preliminary design studies of an advanced general aviation aircraft
p 894 N93-29717
- Design study to simulate the development of a commercial transportation system
p 894 N93-29718
- Design of a turbofan powered regional transport aircraft
p 894 N93-29721
- Solar powered multipurpose remotely powered aircraft
p 895 N93-29722
- Preliminary development of a VTOL unmanned air vehicle for the close-range mission
[AD-A263514] p 933 N93-29969
- Sonic boom problem for future highspeed aircraft
[ONERA-NT-1990-3] p 876 N93-30020
- Cost studies for commercial fuselage crown designs
p 920 N93-30440
- A unified approach for composite cost reporting and prediction in the ACT program
p 920 N93-30441
- Lessons learned for composite structures
p 920 N93-30444
- First NASA Advanced Composites Technology Conference, part 2--
[NASA-CP-3104-PT-2] p 921 N93-30841
- Multi-parameter optimization tool for low-cost commercial fuselage crown designs
p 922 N93-30858
- Design and analysis of grid stiffened concepts for aircraft composite primary structural applications
p 922 N93-30861
- A comparison of classical mechanics models and finite element simulation of elastically tailored wing boxes
p 922 N93-30863
- Tailored composite wings with elastically produced chordwise camber
p 923 N93-30876
- Aircraft structures in 2000: A technological challenge?
[MBB-LME-202-S-PUB-0485] p 998 N93-31058
- Computational methods for aerodynamic design of aircraft components
[NLR-TP-92072-4] p 987 N93-31148
- Definition of an airfoil family for the EUROFAIR rotor
[DLR-FB-92-04] p 998 N93-31197
- Review of aerodynamic design in the Netherlands
[NLR-TP-91260-U] p 999 N93-31840
- Applications of structural optimization methods to fixed-wing aircraft and spacecraft in the 1980s
[NASA-TM-103939] p 1033 N93-32212
- Selected experiments in laminar flow: An annotated bibliography
[NASA-TM-103989] p 990 N93-32226
- Civil tiltrotor transport point design: Model 940A
[NASA-CR-191446] p 1019 N93-32234
- Panel methods for aerodynamic analysis and design
[NLR-TP-91404-U] p 990 N93-32357
- Analytical and experimental investigations of the oblique detonation wave engine concept
[NASA-TM-102839] p 1006 N93-32374
- ### AIRCRAFT DETECTION
- FIFE atmospheric boundary layer budget methods
p 426 A93-20591
- Assessing spatial and seasonal variations in grasslands with spectral reflectances from a helicopter platform
p 426 A93-20621
- Variability of geophysical parameters from aircraft radiance measurements for FIFE
p 426 A93-20622
- A high resolution airborne multisensor system
p 343 A93-21966
- Track moving emitters with Kalman processing
p 317 A93-22275
- Calculation of the passive noise power for onboard single-pulse automatic direction tracking systems
p 882 A93-43111
- A Mode S implementation - Experiments about data-link and interconnected Mode S sensors
p 883 A93-43409
- An integrated weather channel designed for an up-to-date ATC radar system
p 929 A93-43434
- Exact closed-form solution of generalized proportional navigation
p 1130 A93-49598
- Correlation filters for aircraft identification from radar range profiles
p 1097 A93-50636
- Calibration results for NOAA-11 AVHRR channels 1 and 2 from congruent path aircraft observations
p 1143 A93-51237
- Ultra wide band 3-D cross section (RCS) holography
[DE92-019133] p 89 N93-11802
- Aircraft trajectory tracking and prediction
[AD-A259039] p 340 N93-18999
- The development of aircraft in the Lockheed Skunk Works from 1954 to 1991
p 805 N93-27168

AIRCRAFT ENGINES

- A study of a pulsed electrical field near the jet of a turbojet engine p 52 A93-10179
ICAO analyses trends in fuel consumption by world's airlines p 1 A93-10733
Flight testing of an electric powered vehicle [AIAA PAPER 92-4077] p 37 A93-11262
Potent Trent p 53 A93-11419
Advanced three-shaft engines - Configured for reliability, efficiency and growth p 53 A93-12236
Numerical solution of dynamic equations arising in a jet engine simulation p 53 A93-12237
A mathematical model to determine the health of components based on SOAP data --- spectrometric oil analysis program p 53 A93-12238
Midhani alloys in aeronautical service p 70 A93-12368
Microstructural study of aluminide surface coatings on single crystal nickel base superalloy substrates p 70 A93-12771
An experimental study of a method for reducing the jet noise of bypass engines using mechanical flow mixers p 53 A93-12810
Parametric diagnostics of the steady states of gas turbine engines p 54 A93-12815
Evaluation of the efficiency of the direct search method in solving the problem of numerical calculation of the complex hydraulic cooling systems of aviation gas turbine engines p 54 A93-12818
Effect of the powerplant configuration on the air flow rate of the jet shield p 54 A93-12820
A nomographic model for multicriterial optimization during the design of a flight vehicle powerplant p 95 A93-12821
A method for estimating the technico-economic efficiency of measures increasing the reliability of gas turbine engines in service p 54 A93-12822
Higher velocity thermal spray processes produce better aircraft engine coatings [SAE PAPER 920947] p 202 A93-14090
Advancements in aircraft gas turbine engines - Past and future p 170 A93-14153
The optimum design of air cycle refrigeration system with high pressure water separation p 202 A93-14180
Integrated utilities management system for aircraft p 153 A93-14208
Combined engines for hypersonic flight p 171 A93-14244
Application of flight data for diagnostic purposes p 166 A93-14295
Flight-determined benefits of integrated flight-propulsion control systems p 183 A93-14370
Hybrid real-time simulation of a two-rotor engine p 172 A93-14497
Application of model reference adaptive control to speed control system in an aeroengine p 172 A93-14498
A minimum-time acceleration control strategy for a two-rotor aeroengine p 172 A93-14499
Experimental techniques for the assessment of fuel thermal stability p 197 A93-14504
Generic developmental turbojet fuel control p 172 A93-14519
Prediction of engine casing temperature of fighter aircraft for infrared signature studies [SAE PAPER 920961] p 206 A93-14627
The integral starter/generator development progress [SAE PAPER 920967] p 173 A93-14629
The application of human factors engineering at General Electric Aircraft Engines [SAE PAPER 921039] p 108 A93-14659
The modeling of forging and precision-casting forming processes p 207 A93-15030
The control of aircraft engines in the 1990's p 173 A93-15042
Optimization of pneumatic subsystems for transport aircraft p 159 A93-15049
Advanced technology constant challenge and evolutionary process p 109 A93-15054
Welding wire selection critical to jet engine repair work p 208 A93-15375
Application of laminar flow to aero engine nacelles p 128 A93-17256
Probability analysis of a method for diagnosing gas turbine engines on the basis of thermogasdynamic parameters p 345 A93-18337
Effect of design and service-related factors on the formation of combustion residues in the fuel nozzles of gas turbine engines p 345 A93-18342
Calculation of fuel economy for the Tu-154 aircraft in relation to the washing of the NK-8-2U engine at civil aviation maintenance facilities p 345 A93-18356
A system for washing the combustion chamber nozzles and flow path components of the NK-8-2U engine during service p 373 A93-18357
Assessment of flight data in real time p 341 A93-18364
A unified approach to the construction of the throttle characteristics of postrepair turbojet engines, with the NK-8-2U engine used as an example p 345 A93-18372
Aero engine reliability, integrity and safety; Proceedings of the Conference, Bristol, United Kingdom, Oct. 17, 18, 1991 [ISBN 0-903409-70-4] p 345 A93-18778
ETOPS across the Atlantic --- extended range operation of twin-engined transport aircraft p 306 A93-18780
Aero-engine reliability - A GE view p 345 A93-18782
Lifting philosophies for aero engine fracture critical parts p 345 A93-18783
Aspects of turbine blade design for integrity p 345 A93-18784
Reliability and safety considerations in engine management systems design p 346 A93-18786
Engine Health Monitoring p 346 A93-18787
Engine reliability from an independent overhaul shops perspective p 239 A93-18788
Very high reliability - Cost and consequences p 397 A93-18789
Using advanced technology to achieve reliability as well as high performance p 346 A93-18790
Instability of rectangular jets p 398 A93-19157
Unsteady pressures on exhaust nozzle interior surfaces - Empirical correlations for prediction p 244 A93-19219
Coupled multi-disciplinary simulation of composite engine structures in propulsion environment [ASME PAPER 92-GT-6] p 346 A93-19279
Extending the fatigue life of aircraft engine components by hole cold expansion technology [ASME PAPER 92-GT-77] p 401 A93-19327
The design and evaluation of a high pressure ratio radial turbine [ASME PAPER 92-GT-93] p 349 A93-19339
Markov fatigue in single crystal airfoils [ASME PAPER 92-GT-95] p 387 A93-19341
Modification of combustor stoichiometry distribution for reduced NO(x) emission from aircraft engines [ASME PAPER 92-GT-108] p 349 A93-19346
Innovative high temperature aircraft engine fuel nozzle design [ASME PAPER 92-GT-132] p 350 A93-19365
Aerodesign and performance analysis of a radial transonic impeller for a 9:1 pressure ratio compressor [ASME PAPER 92-GT-183] p 352 A93-19408
Low aspect ratio transonic rotors. I - Baseline design and performance [ASME PAPER 92-GT-185] p 352 A93-19410
Influence of surface heating condition on local heat transfer in a rotating square channel with smooth walls and radial outward flow [ASME PAPER 92-GT-188] p 402 A93-19413
Flexible manufacturing of aircraft engine parts [ASME PAPER 92-GT-229] p 404 A93-19446
Aircraft engine integration for the M88-Rafale couple [ASME PAPER 92-GT-403] p 322 A93-19552
Fuel cell powered electric propulsion for HALE aircraft [ASME PAPER 92-GT-404] p 356 A93-19553
Aircraft turbine engine NOx emission limits - Status and trends [ASME PAPER 92-GT-415] p 357 A93-19563
On-board condition management for aircraft gas turbines [ASME PAPER 92-GT-416] p 357 A93-19564
High speed flight effects on transmission of sound through a nonflexible vibrating panel due to flow structural interaction in the ambience [AIAA PAPER 92-4708] p 451 A93-20316
Multidisciplinary propulsion simulation using NPSS [AIAA PAPER 92-4709] p 435 A93-20318
Structural tailoring of aircraft engine blade subject to ice impact constraints [AIAA PAPER 92-4710] p 358 A93-20319
APPLE - An aeroelastic analysis system for turbomachines and propfans [AIAA PAPER 92-4712] p 358 A93-20320
Life cycle assessment of an impingement-cooled gas turbine blade [AIAA PAPER 92-4716] p 358 A93-20321
Measured thrust losses associated with secondary air injection through nozzle walls p 270 A93-21656
Maximum hail concentration that can be met by an aircraft in stormy precipitations p 430 A93-22152
Time-dependent 3-component laser-Doppler-anemometer and simultaneous position measurements in the flow of an aircraft engine p 538 A93-23809
On closed-loop identification of a certain aeroengine under flight conditions p 519 A93-24026
Implicit Euler calculation of supersonic vortex wake/engine plume interaction [AIAA PAPER 93-0656] p 540 A93-24769
Advances in the design of jet engine test facilities for military aircraft in Australia p 529 A93-28491
Quiet operations key to MD-90 success p 708 A93-33700
Probabilistic turbine blade tip durability analysis [AIAA PAPER 93-1383] p 719 A93-33946
Thrust vectoring nozzles give pilots an edge p 720 A93-34375
Approach of modeling continuous turbine engine operation from startup to shutdown p 721 A93-34495
Protective properties of aviation oils p 735 A93-35299
T55 engine - The challenge of torque measurement p 809 A93-35929
Aeroelastic dynamics of mistuned blade assemblies with closely spaced blade modes [AIAA PAPER 93-1628] p 810 A93-37446
Dynamic processes in the powerplants and power-generating equipment of flight vehicles p 832 A93-39027
A study of the stability of the acceleration circuit of the hydromechanical automatic control system of an aviation gas turbine engine p 810 A93-39028
Absolute stability of an automatic control system for gas turbine engines p 810 A93-39033
Correction of the frequency characteristic of the waveguide circuit of an acoustic-jet temperature transducer p 832 A93-39036
A study of the effect of the working medium on the start-up characteristic of an aviation gas turbine engine p 811 A93-39037
Heat exchangers of gas turbine engines p 833 A93-39044
The use of aviation gas-liquid heat exchangers employing heat pipes p 833 A93-39050
Development of a process for fabricating a plate heat exchanger for the heat recovery system of gas turbine engines p 834 A93-39053
A method for calculating the dynamic characteristics of heat exchangers with single-phase cryogenic coolants p 851 A93-39057
An experimental study of the air drying process in air coolers p 834 A93-39059
Quality of the surface layer and operating properties of aircraft engine components p 834 A93-39061
Prediction and control of the service-related properties of parts at the technological preparation stage and during the manufacture process --- of aircraft engine components p 834 A93-39062
Enhancing the performance of aircraft engine blades by surface hardening p 811 A93-39072
Effect of ion treatments on the fatigue strength of blades p 811 A93-39073
Characteristics of friction and wear in flight vehicle engine components p 811 A93-39075
Automated measurement of residual stresses in the surface layer of parts p 834 A93-39081
Selection of the scheme and optimal parameters of the turbine of a high-temperature bypass engine with a low bypass ratio p 811 A93-39180
Expert evaluation of the technological level of aviation gas turbine engine designs p 811 A93-39187
An experimental study of thrust reverser models --- of axisymmetric exhaust systems of aerjet engines p 812 A93-39195
The possibility of reducing the emission of benzo(a)pyrene with the exhaust gases of aviation gas turbine engines by water injection into the combustion chamber p 812 A93-39201
Experimental investigation on starting of a turbojet engine in flight p 898 A93-41740
Effect of gasdynamic parameters on the specific weight of gas-turbine aircraft engines p 899 A93-42372
Selection of the turbofan engine size p 899 A93-42379
Selection of the powerplant for a thermoplane p 899 A93-42380
Design verification of ground run-up noise suppressors for afterburning engines p 910 A93-42892
Analysis of the effects of blade pitch on the radar return signal from rotating aircraft blades p 885 A93-43476
Ilyushin takes on the market p 945 A93-43623
Design of aircraft, helicopters, and aviation engines --- Russian book [ISBN 5-277-01192-7] p 947 A93-44508
Optimization of a highly-loaded axial splitters rotor design p 1002 A93-46931
Mathematical model for the effect of turbulent velocity pulsations on the stability of a powerplant p 1003 A93-47508
Simplified mathematical model and digital simulation of aeroengine p 1106 A93-48511
Dynamic analysis of a gear drive system in aeroengine p 1149 A93-48514
On engine parameter estimation with flight test data p 1107 A93-48520

- Exhaust system model test and research p 1107 A93-48525
- An experimental study of the thrust and aerodynamic characteristics of an operating ramjet engine in a blowdown wind tunnel p 1107 A93-48828
- Atmospheric aerosols due to aircraft and ecological problems p 1162 A93-48846
- Screening studies of advanced control concepts for airbreathing engines [AIAA PAPER 92-3320] p 1108 A93-49329
- Optical temperature compensation schemes of spectral modulation sensors for aircraft engine control p 1105 A93-49471
- Optical sensors and multiplexing for aircraft engine control p 1105 A93-49474
- Flight testing of a fiber optic temperature sensor p 1105 A93-49476
- A review of chemically reactive turbulent flow mixing mechanisms and a new design for a low NO(x) combustor p 1109 A93-49508
- Analysis of a high bypass ratio engine installation using the chimera domain decomposition technique [AIAA PAPER 93-1808] p 1100 A93-49697
- Matching engine and aircraft lapse rates for the HSC [AIAA PAPER 93-1809] p 1100 A93-49698
- Lightweight aircraft turbine protection [AIAA PAPER 93-1815] p 1110 A93-49703
- Synchronous X-ray Sinography for nondestructive imaging of turbine engines under load [AIAA PAPER 93-1819] p 1153 A93-49707
- On the estimation algorithm for adaptive performance optimization of turbofan engines [AIAA PAPER 93-1823] p 1111 A93-49710
- Real-time simulation of maneuverable aircraft flight conditions on altitude test cell [AIAA PAPER 93-1845] p 1137 A93-49726
- Modern propeller systems for advanced turboprop aircraft [AIAA PAPER 93-1846] p 1111 A93-49727
- Aero-engine component damping estimation from full-scale aeromechanical test data [AIAA PAPER 93-1873] p 1112 A93-49748
- Propfan engines [AIAA PAPER 93-1981] p 1112 A93-49828
- Evaluation of a nonlinear PSC algorithm on a variable cycle engine [AIAA PAPER 93-2077] p 1114 A93-49904
- High speed, heavily loaded and precision aircraft type epicyclic gear system dynamic analysis overview and special considerations [AIAA PAPER 93-2151] p 1154 A93-49968
- Studies into the hail ingestion characteristics of turbofan engines [AIAA PAPER 93-2174] p 1115 A93-49987
- Review of NASA's Hypersonic Research Engine Project [AIAA PAPER 93-2323] p 1116 A93-50103
- Study of a circular cross section thrust augmenting ejector [AIAA PAPER 93-2439] p 1118 A93-50191
- Unique development testing at Allison Gas Turbine [AIAA PAPER 93-2450] p 1138 A93-50200
- On the stability of the process of formation of combustion generated particles by coagulation and simultaneous shrinkage due to particle oxidation [AIAA PAPER 93-2478] p 1146 A93-50220
- Flight-determined engine exhaust characteristics of an F404 engine in an F-18 airplane [AIAA PAPER 93-2543] p 1121 A93-50267
- F405 engine in-flight thrust methodology development [AIAA PAPER 93-2544] p 1121 A93-50268
- Developments in silicon carbide for aircraft propulsion system applications [AIAA PAPER 93-2581] p 1157 A93-50295
- The well made engine p 1122 A93-50352
- A transfer matrix method for calculation of support stiffness of aeroengine stator p 1122 A93-51193
- The turbulence and mixing characteristics of the complex flow in a simulated augmentor p 1123 A93-51642
- Calculation of a plane supersonic jet simulating the exhaust jet of a hypersonic flight vehicle engine p 1103 A93-51912
- Estimation of the parameters of the electrodynamic system engine-exhaust jet p 1193 A93-52965
- Clean melting and the removal of defects from aero-engine materials p 1217 A93-53503
- Ongoing challenges for titanium alloy cleanliness improvement in aircraft engine disk materials p 1212 A93-53506
- The application of diffusion bonding in the manufacture of aeroengine components p 1217 A93-53514
- Selection of a method for protecting aircraft gas turbine engines against damage by foreign objects (Mathematical models) p 1193 A93-53554
- ISABE - International Symposium on Air Breathing Engines, 11th, Tokyo, Japan, Sept. 20-24, 1993, Proceedings. Vols. 1 & 2 [ISBN 1-56347-071-3] p 1194 A93-53976
- Research and development of aircraft engine in Japan - Historical review [ISABE 93-7000] p 1227 A93-53977
- The challenge of IHPTET - Integrated High Performance Turbine Engine Technology [ISABE 93-7001] p 1194 A93-53978
- Design and technology for engine manufacture - for Rolls-Royce aerospace business [ISABE 93-7002] p 1194 A93-53979
- Propulsion technology challenges for turn-of-the-century commercial aircraft [ISABE 93-7003] p 1194 A93-53980
- Japan's research and development program for airbreathing engine technologies [ISABE 93-7005] p 1194 A93-53981
- Mach 5 turbofanjet requirements and design approach [ISABE 93-7015] p 1194 A93-53991
- Conceptual design study on combined-cycle engine for hypersonic transport [ISABE 93-7018] p 1195 A93-53994
- Energy management - aircraft propulsion system performance [ISABE 93-7019] p 1195 A93-53995
- An ultra low NO(x) pilot combustor for staged low NO(x) combustion [ISABE 93-7020] p 1195 A93-53996
- Low NO(x) combustor development using aerodynamic staging [ISABE 93-7021] p 1195 A93-53997
- The prediction of thermal NO(x) in gas turbine exhausts [ISABE 93-7022] p 1195 A93-53998
- Emission characteristics of a model gas turbine combustor at practical conditions [ISABE 93-7023] p 1196 A93-53999
- Two and three-dimensional prediffuser combustor studies with air-water mixture [ISABE 93-7025] p 1213 A93-54001
- Blowout of turbulent disc/pilot stabilized jet diffusion flames [ISABE 93-7026] p 1213 A93-54002
- Design of high-load aviation turbomachines using modern 3D computational methods [ISABE 93-7032] p 1196 A93-54008
- Study of a pulse ramjet based on twin valveless combustors coupled to operate in antiphase [ISABE 93-7038] p 1197 A93-54014
- Thermal fatigue life assessment of a convection-cooled gas turbine blade [ISABE 93-7062] p 1199 A93-54038
- Variable cycle engine concept [ISABE 93-7065] p 1200 A93-54041
- Research and development of high pressure compressor for SST and HST engine [ISABE 93-7068] p 1186 A93-54044
- Test results of the hydrogen fueled model combustor for the air turbo ramjet engine [ISABE 93-7082] p 1201 A93-54058
- New developments with the V2500 engine [ISABE 93-7085] p 1202 A93-54061
- Performance and configuration analysis of jet-engine off-design behavior [ISABE 93-7087] p 1202 A93-54063
- Developments towards versatility in digital engine control units [ISABE 93-7088] p 1202 A93-54064
- Effect of nozzle design on the performance of a highly loaded turbine stage [ISABE 93-7096] p 1203 A93-54072
- Measurement and prediction of flow in a gas turbine engine exhaust plume [ISABE 93-7113] p 1204 A93-54088
- Various applications of robots in aircraft engine overhaul [ISABE 93-7129] p 1175 A93-54104
- Aerodynamics of turbine blades with trailing-edge damage - Measurements and computations [ISABE 93-7130] p 1189 A93-54105
- Development of a real time dynamic engine simulation model of a turbo fan engine [ISABE 93-7132] p 1205 A93-54107
- The low frequency aeroacoustics of buried nozzle systems p 1205 A93-54244
- Development of MIL-H-53119, -54 C to 175 C high-temperature nonflammable hydraulic fluid for Air Force systems p 1214 A93-54250
- Novel nozzle p 1245 A93-54450
- A study of military aircraft and engine tactical/technical performance evaluation p 1242 A93-54596
- A diesel powerplant development program for airships [AIAA PAPER 93-4038] p 1246 A93-54609
- Future aero engine design trade offs p 1246 A93-54836
- All-composite fan blade for advanced ducted engines p 1246 A93-54837
- ADP - Engine concept of the future p 1246 A93-54842
- Laser and skill enhance results p 1257 A93-54843
- An experimental investigation of the effects of swirling flow on the performance of nozzles p 1247 A93-54859
- Turbofan propulsion simulator p 1247 A93-55493
- Small gas turbines in the 21st century p 1247 A93-55494
- Control of supersonic throughflow turbomachines discrete frequency noise generation by aerodynamic detuning p 1248 A93-55860
- Vibration isolation of aviation power plants taking into account real dynamic characteristics of engine and aircraft p 1244 A93-55863
- West powers East p 1244 A93-56349
- Engine for change p 1248 A93-56350
- LV software for supersonic flow analysis [NASA-CR-190911] p 16 N93-10069
- SAPNEW: Parallel finite element code for thin shell structures on the Alliant FX/80 [NASA-CR-190663] p 84 N93-10372
- Nondestructive evaluation of ceramic and metal matrix composites for NASA's HITEMP and enabling propulsion materials programs [NASA-TM-105807] p 85 N93-10963
- Materials: Toward the non-metallic engine [PNR-90915] p 56 N93-11019
- Application of laminar flow to aero engine nacelles [PNR-90916] p 20 N93-11020
- An experimental evaluation of prediction methods for contrafans [PNR-90924] p 56 N93-11023
- On the basis of experience: Built in product reliability [PNR-90932] p 85 N93-11034
- Rolls-Royce civil engine technology [PNR-90936] p 56 N93-11036
- The Trent: Towards greater thrust [PNR-90937] p 56 N93-11037
- From RB211 to Trent: An ongoing development strategy [PNR-90938] p 56 N93-11038
- Introduction to the Rolls-Royce design process [PNR-90939] p 57 N93-11039
- The application of manufacturing systems engineering for aero engine gears [PNR-90944] p 86 N93-11054
- Simultaneous engineering in the design of aero engines [PNR-90973] p 57 N93-11062
- Aero engine ceramics: The vision, the reality, and the progress [PNR-90983] p 72 N93-11066
- Advanced three-shaft engines: Configured for reliability, efficiency, and growth [PNR-90986] p 58 N93-11068
- Maintainability of large gas turbine aero engines [PNR-90987] p 58 N93-11069
- A combined experimental and theoretical study of laminar flow control with particular relevance to aero engine nacelles [PNR-90991] p 20 N93-11070
- Civil aircraft engines: The next generation [PNR-90962] p 58 N93-11085
- The development of the Rolls-Royce Trent aero gas turbine [PNR-90949] p 58 N93-11108
- Overview of high performance aircraft propulsion research [NASA-TM-105839] p 59 N93-11530
- Evaluation of acoustic impedance models for a perforated plate [NAL-TR-1133] p 102 N93-12375
- Overview on test cases for computation of internal flows in turbomachines p 214 N93-13209
- Electro-optic architecture for servicing sensors and actuators in advanced aircraft propulsion systems [NASA-CR-182269] p 232 N93-13762
- SAPNEW: Parallel finite element code for thin shell structures on the Alliant FX-80 [NASA-CR-189212] p 220 N93-14799
- Electro-optic architecture (EOA) for sensors and actuators in aircraft propulsion systems [NASA-CR-182270] p 233 N93-15116
- Integrated engine control and monitoring with experiences derived from OLMOS p 178 N93-15168
- Monitoring of powerplants in advanced commercial aircraft p 178 N93-15171
- EJ 200 engine monitoring system: On- and off-board data capture, analysis, and management system p 178 N93-15172

RB199 engine oil system failure diagnostics by comparison of measured and calculated oil consumption using the OLMOSS on-board monitoring system p 178 N93-15173

A philosophy for integrated monitoring system design p 178 N93-15174

Modelling the engine temperature distribution between shut down and restart for life usage monitoring p 169 N93-15177

Deformation mechanisms of NIAI cyclically deformed near the brittle-to-ductile transformation temperature [NASA-CR-191649] p 391 N93-15830

Preliminary analysis of the J-52 aircraft engine component improvement program [AD-A257640] p 363 N93-17686

Turbomachinery and potential computations [DS-2026] p 363 N93-17740

Direct numerical simulation of combustion in turbulent supersonic flow [DS-2138] p 393 N93-17746

The beta-CEZ, a new high performance titanium alloy for aerospace engines [DS-2022] p 393 N93-17852

The technological evolution of high thrust turbine engines [DS-1881] p 364 N93-17882

Control of in-service damage: Application to aircraft engines [DS-2027] p 364 N93-18151

The effect of aircraft inlets on the behaviour of aero engine axial flow compressors p 422 N93-18722

Stall in axial flow aero engine compressors p 422 N93-18723

Stall and surge in axial flow compressors p 423 N93-18724

Stall transients including effects of inlet distortion and intake geometry p 423 N93-18726

Experimental investigation of rotating stall in a mismatched three stage axial flow compressor p 423 N93-18727

Development of an engine/airframe performance matching scheme for jet engine retrofit [AD-A258822] p 365 N93-18997

Professor Wittenberg: His speciality and versatility [ISBN-90-6275-670-0] p 240 N93-19002

Propelling force and resistance p 298 N93-19003

What is the progress in propulsion? p 298 N93-19006

Role of wind tunnel tests and CFD analysis for the development of aero-engines in IHI p 365 N93-19326

Handling and using information systems with new technology [PNR-90910] p 572 N93-20734

Satisfying the customer's requirements [PNR-90988] p 521 N93-20735

Optimization and sensitivity computations for the conception of internal ventilation system in the aircraft engine [ETN-93-93375] p 521 N93-20913

Supersonic transport: Which material for the engine [DS-2023] p 522 N93-21459

Aerodynamic design and synthesis of the oblique flying wing supersonic transport p 713 N93-24768

Screening studies of advanced control concepts for airbreathing engines [NASA-TM-106042] p 721 N93-25079

Simulation of aircraft gas turbine engine p 723 N93-25751

Development and demonstration of a new filter system to control emissions during jet engine testing [AD-A261203] p 755 N93-26243

Particulate emissions from gas turbine engines [AD-A261374] p 725 N93-26339

A large hemi-anechoic enclosure for community-compatible aeroacoustic testing of aircraft propulsion systems [NASA-TM-106015] p 760 N93-26551

Structural tailoring of aircraft engine blade subject to ice impact constraints [NASA-TM-106033] p 838 N93-26999

Collection of papers of the 31st Israel Annual Conference on Aviation and Astronautics [ITN-93-85187] p 764 N93-27166

Design, analysis, and control of large transport aircraft utilizing engine thrust as a backup system for the primary flight controls [NASA-CR-192938] p 820 N93-27308

Effect of pylon cross-sectional geometries on propulsion integration for a low-wing transport [NASA-TP-3333] p 788 N93-28070

Estimating characteristic life and reliability of an aircraft engine component improvement in the early stages of the implementation process [AD-A262118] p 815 N93-28184

An analysis of the correlation between the J52 engine component improvement program and improved maintenance parameters [AD-A262062] p 816 N93-28984

Blasim: A computational tool to assess ice impact damage on engine blades [NASA-TM-106225] p 1031 N93-31193

Propulsion technology challenges for turn-of-the-century commercial aircraft [NASA-TM-106192] p 1005 N93-32351

Analytical and experimental investigations of the oblique detonation wave engine concept [NASA-TM-102839] p 1006 N93-32374

AIRCRAFT EQUIPMENT

A proposed multi-modal FM/CW aircraft radar for use during ground operations p 206 A93-14678

Analysis of random components during measurements in the computerized diagnostic system Analiz-86 p 321 A93-18344

Laboratory for modelling of prospective board equipment systems for aircraft p 374 A93-18529

Airborne MLS equipment p 312 A93-18555

Knowledge based systems and avionics equipment failure diagnosis p 238 A93-18765

Instrument systems of flight vehicles and their design --- Russian book [ISBN 5-217-00793-1] p 718 A93-35678

Algorithms for constructing models of the interaction of diagnostic systems with reserved aviation equipment p 847 A93-39043

The navigation and flying equipment of the Yak-42 aircraft --- Russian book p 792 A93-39204

Installation of electrical cable looms p 764 A93-39536

Critical dispatch - A pilot's view p 790 A93-39541

Versatility, automation key to C-17 cargo operations p 805 A93-39600

Study on dynamic characteristics of heat exchanger p 924 A93-40492

Microburst avoidance crew procedures for forward-look sensor equipped aircraft [AIAA PAPER 93-3942] p 1007 A93-44234

Algorithmic method for optimizing the precision characteristics of a fuel metering system p 999 A93-45681

Repair and maintenance of fiber optic data links on Navy aircraft p 1172 A93-48538

Fiber optics for aircraft entertainment systems p 1172 A93-49478

Automatic navigation in the air and at sea p 1099 A93-52593

Definition study PHARUS [AD-A256560] p 221 N93-14805

Test and integration concept for complex helicopter avionics systems [MBB-UD-0605-91-PUB] p 343 N93-17547

Ground clutter measurements using the NASA airborne doppler radar: Description of clutter at the Denver and Philadelphia airports p 490 N93-19608

Aviation safety: Users differ in views of collision avoidance system and cite problems. Report to the Chairman, Subcommittee on Investigations and Oversight, Committee on Science, Space, and Technology, House of Representatives [GAO/RCED-92-113] p 502 N93-19843

The effectiveness of hand-held fire extinguishers on cargo container fires [DOT/FAA/CT-TN92/42] p 496 N93-21821

Alternative equipment test procedures for simultaneous current injection on multiple cable bundles p 747 N93-24903

Special tooling disposition for aircraft entering post production support [AD-A261614] p 678 N93-26168

Aircraft ice detectors and related technologies for onground and inflight applications [DOT/FAA/CT-92/27] p 791 N93-27269

Standardization of automatic test equipment in the US Air force [AD-A262076] p 809 N93-29004

The NASA SBIR product catalog [NASA-TM-108242] p 945 N93-29322

High reliability, maintenance-free INS battery development [AD-A264521] p 934 N93-30406

The DLR test aircraft in the FZ-BS, -VFW 614/ATTAS, Dornier DO 228-101, MBB BO105 S-3 p 1018 N93-31272

French aerospace equipment p 1041 N93-31734

AIRCRAFT FUEL SYSTEMS

Experimental techniques for the assessment of fuel thermal stability p 197 A93-14504

Computational models of dampers for computer-aided design p 832 A93-39032

The required damping and control process quality in a fuel pressure regulator p 810 A93-39034

Maintenance of the liquid and gas systems of the IL-76 aircraft p 804 A93-39203

Surge recovery and compressor working line control using compressor exit Mach number measurement p 897 A93-40435

Aircraft cryogenic fuel system design issues [AIAA PAPER 93-2567] p 1121 A93-50285

AIRCRAFT FUELS

Evaporation and specific heats of motor fuels p 71 A93-12823

Viscosity of aviation fuel components (n-alkanes) p 71 A93-12824

Optimizing the cruising fuel efficiency of commercial aircraft on the basis of flight manual data p 321 A93-18351

Static tests of jet fuel thermal and oxidative stability p 389 A93-21651

Low area ratio aircraft fuel jet-pump performances with and without cavitation p 272 A93-22264

Measurement of diffusion in supercritical fluid systems - A review [AIAA PAPER 93-0809] p 534 A93-24884

Taking to the skies under hydrogen power - Deutsche Aerospace Airbus studies the use of alternative fuels for civil aviation p 677 A93-34947

Protective properties of aviation oils p 735 A93-35299

Fuel film formation in the fuel-air premixer of the combustion chamber p 812 A93-39193

Classification of the principal fuel saving methods in flight operations p 996 A93-45660

Effect of aqueous solutions of water-crystallization inhibiting fluids on Thiokol-based sealants p 1017 A93-45689

Investigation of flame stabilizers in the form of perforated grids p 1003 A93-47513

Experimental research on a semiwater-gas-fired gas-turbine p 1107 A93-48524

A new type of fuel control model p 1108 A93-49204

Viscosity of aviation fuel components - Aromatic hydrocarbons (alkyl benzenes) p 1211 A93-52961

A study of surge control by using pulse cut-off for dual spool turbo-jet engine p 1194 A93-53862

Potential use of alternative fuels in aviation p 1243 A93-54838

Advanced thermally-stable, coal-derived, jet fuels program: Experiment system and model development [AD-A262747] p 917 N93-29402

AIRCRAFT GUIDANCE

The Texas Instruments/Honeywell GPS Guidance Package p 32 A93-11015

Adaptive control of aircraft in windshear p 62 A93-13126

A guidance display system for single pilot operation [AIAA PAPER 92-4196] p 51 A93-13373

Investigation of precise approach and landing of civil aircraft using integrated system based on GPS p 180 A93-14159

Automatic guidance and control for recovery of remotely piloted vehicles p 181 A93-14188

HUD Guidance for the ASKA Experimental STOL Aircraft using Radar Position Information [SAE PAPER 921041] p 150 A93-14661

Guidance accuracy considerations for realtime GPS interferometry p 342 A93-21146

An MLS for the twenty-first century p 316 A93-21197

Sensors and sensor systems for guidance and navigation II; Proceedings of the Meeting, Orlando, FL, Apr. 22, 23, 1992 p 547 A93-28151

Application of advanced guidance and navigation systems to flight control of aircraft and future space vehicles p 500 A93-28153

AFTI/F-16 night close air support system testing p 808 A93-38841

Passive range estimation for rotorcraft low-altitude flight p 948 A93-46608

Electro-optical navigation for aircraft p 1097 A93-50643

Guidance law based on piecewise constant control for hypersonic gliders [AIAA PAPER 93-3888] p 1144 A93-51472

A primary flight display for four-dimensional guidance and navigation influence of tunnel size and level of additional information on pilot performance and control behaviour [AIAA PAPER 93-3570] p 1208 A93-52668

Passive range estimation for rotorcraft low-altitude flight p 1190 A93-52681

Multirate and event-driven Kalman filters for helicopter flight p 1245 A93-55760

Hybrid guidance for maneuvering flight vehicles [AD-A254110] p 69 N93-11798

- Estimation of rate of climb
[ESDU-92019] p 164 N93-14541
- Discrete range clustering using Monte Carlo methods
[NASA-TM-104004] p 706 N93-24914
- Control and optimization of aircraft trajectories
p 729 N93-25543
- Image-based ranging and guidance for rotorcraft
[NASA-CR-177608] p 708 N93-26549
- Advanced Transport Operating System (ATOPS) Flight Management/Flight Controls (FM/FC) software description
[NASA-CR-191457] p 809 N93-28621
- Evaluation of category 3 MLS designs
p 888 N93-30358
- Aircraft guidance for wind shear avoidance:
Decision-making under uncertainty p 889 N93-31005
- Aerial cartography using SICAD NAV-AIR
p 1034 N93-31258
- Flight evaluation of a computer aided low-altitude helicopter flight guidance system
[NASA-TM-103998] p 994 N93-32225
- A high-fidelity, six-degree-of-freedom batch simulation environment for tactical guidance research and evaluation
[NASA-TM-4440] p 1010 N93-32380
- AIRCRAFT HAZARDS**
- Effects of thrust line offset on neutral point determination in stability flight testing
[AIAA PAPER 92-4082] p 61 A93-11265
- Slicing model for foreign soft-body objects impacting on blade rows
p 28 A93-12372
- An impact dynamics investigation on some problems in bird strike on windshields of high speed aircraft
p 197 A93-15346
- Hazard assessment and cockpit presentation issues for microburst alerting systems
p 308 A93-22112
- Potential aircraft hazards in the vicinity of convective clouds - A review from the perspective of a scale-model study
p 427 A93-22116
- Sea fog and stratus - A major aviation hazard in the northern Gulf of Mexico
p 429 A93-22141
- Diagnostic studies of clear air turbulence in isentropic coordinates
p 430 A93-22154
- A fine structure of the gust front observed with sonic anemometer
p 430 A93-22158
- The role of national meteorological services in aviation servicing under the final phase of the World Area Forecast System
p 431 A93-22162
- A quantitative method to estimate the microburst wind shear hazard to aircraft
p 309 A93-22172
- Elevated array detection and measurement of microbursts using Theta(E)
p 412 A93-22173
- The redesigned Low Level Wind Shear Alert System
p 431 A93-22179
- Seasonal weather hazards
p 431 A93-22180
- Volcanic ash and aircraft operations
p 309 A93-22181
- Status of the Terminal Doppler Weather Radar one year before deployment
p 431 A93-22184
- Reliability considerations for weather hazard warning radar
p 431 A93-22187
- Terminal Doppler Weather Radar program at Denver's Stapleton International Airport during 1989 and 1990
p 432 A93-22188
- Microburst observations in tropical Australia
p 432 A93-22198
- Structure of downbursts associated with heavy rainfall observed in Tokyo
p 433 A93-22200
- Evaluation of clear-air radar PROUST and Doppler radar RONSARD for airport low level-wind shear detection
p 433 A93-22202
- Remote sensing of volcanic ash hazards to aircraft
p 556 A93-24213
- Volcanic clouds --- aircraft hazards
p 487 A93-28196
- Controlling hazardous configurations in helicopter systems
p 763 A93-35927
- Mechanical damage to aircraft structures from lightning strikes
p 879 A93-40432
- Engineering a visual system for seeing through fog
[SAE PAPER 921130] p 895 A93-41318
- Aircraft wing compartment liner concept to reduce fuel spillage
[DOT/FAA/CT-TN92/34] p 331 N93-17219
- The 1992 International Aerospace and Ground Conference on Lightning and Static Electricity: Addendum
[DOT/FAA/CT-92/20-ADD-1] p 753 N93-24875
- Lightning phenomenology bases for full threat return stroke occurrence following extended leader sweep at flight altitudes
p 754 N93-24895
- Applications of stress envelope concepts to aircraft EMP and lightning survivability
p 704 N93-24898
- PROAV Cable Warning System (CWS) - U.S. Army aircraft integration assessment and OCONUS field evaluation
[AD-A261233] p 705 N93-26263
- Annual review of aircraft accident data: US general aviation calendar year 1989
[PB93-160687] p 790 N93-27033
- Aircraft ice detectors and related technologies for onground and inflight applications
[DOT/FAA/CT-92/27] p 791 N93-27269
- AIRCRAFT HYDRAULIC SYSTEMS**
- Improvement of aircraft maintenance methods
p 395 A93-18326
- Selection of methods and equipment for monitoring the technical condition of booster system components --- of aircraft hydraulic systems
p 395 A93-18329
- Design characteristics of the functional systems of aircraft and prediction of their technical condition
p 320 A93-18334
- A method for evaluating the technical condition of hydraulic control boosters without their disassembly --- repair of aircraft systems
p 395 A93-18335
- Diagnostics of the hydraulic system of Tu-204 aircraft
p 396 A93-18360
- Characteristics of the diagnostics of booster system components
p 321 A93-18361
- Monitoring the purity of the working fluids of aircraft hydraulic systems during service
p 321 A93-18367
- Analysis of the pump station of an aircraft hydraulic system as a subject of diagnosis
p 321 A93-18374
- Dynamic processes in the powerplants and power-generating equipment of flight vehicles
p 832 A93-39027
- Control of the quality of dynamic processes in the valves of power-generating equipment
p 832 A93-39030
- Computational models of dampers for computer-aided design
p 832 A93-39032
- AIRCRAFT ICING**
- Investigation of leading edge ice accretion with cyclical pneumatic boot inflation
[AIAA PAPER 93-0007] p 306 A93-20130
- Micro-physical models for simulating realistic ice accretions
[AIAA PAPER 93-0025] p 307 A93-20143
- Effects of icing on the aerodynamic performance of high lift airfoils
[AIAA PAPER 93-0026] p 259 A93-20144
- Prediction of the ice accretion with viscous effects on aircraft wings
[AIAA PAPER 93-0027] p 307 A93-20145
- Aerodynamic degradation due to distributed roughness on high lift configuration
[AIAA PAPER 93-0028] p 260 A93-20146
- Impact ice interface shear stresses caused by blade bending and twisting
[AIAA PAPER 93-0030] p 307 A93-20147
- Structural tailoring of aircraft engine blade subject to ice impact constraints
[AIAA PAPER 92-4710] p 358 A93-20319
- A proposed icing severity index based upon meteorology
p 429 A93-22136
- Numerical forecasting of liquid water content to assess airframe icing risk
p 429 A93-22147
- An evaluation of aircraft icing forecasts for the continental United States
p 429 A93-22149
- Liquid water profiling using remote sensor observations
p 429 A93-22150
- Results of Low Power Deicer tests on a swept inlet component in the NASA Lewis Icing Research Tunnel
[AIAA PAPER 93-0032] p 327 A93-22551
- CFD zonal modeling of leading-edge ice effects for a complete aircraft
[AIAA PAPER 93-0167] p 275 A93-22601
- Improvement of the ONERA 3D icing code, comparison with 3D experimental shapes
[AIAA PAPER 93-0169] p 275 A93-22603
- The Air Force Flight Test Center artificial icing and rain testing capability upgrade program
[AIAA PAPER 93-0295] p 376 A93-22695
- Modeling and strain gauging of eddy current repulsion deicing systems
[AIAA PAPER 93-0296] p 327 A93-22696
- Icing testing of a large full-scale inlet at the Arnold Engineering Development Center
[AIAA PAPER 93-0299] p 376 A93-22697
- LDV flowfield measurements on a straight and swept wing with a simulated ice accretion
[AIAA PAPER 93-0300] p 280 A93-23001
- The FAA aircraft icing Forecasting Improvement Program - Validation of aircraft icing forecasts in the Denver area
[AIAA PAPER 93-0393] p 309 A93-23069
- Investigation of an electrothermal de-icer pad using a three-dimensional finite element simulation
[AIAA PAPER 93-0397] p 327 A93-23072
- Close-up analysis of aircraft ice accretion
[AIAA PAPER 93-0029] p 309 A93-23239
- Surface roughness due to residual ice in the use of low power deicing systems
[AIAA PAPER 93-0031] p 282 A93-23240
- Numerical modeling of anti-icing systems and comparison to test results on a NACA 0012 airfoil
[AIAA PAPER 93-0170] p 327 A93-23242
- Advancements in the LEWICE Ice Accretion Model
[AIAA PAPER 93-0171] p 309 A93-23243
- Ice accretion and performance degradation calculations with LEWICE/NS
[AIAA PAPER 93-0173] p 310 A93-23244
- Ice accretion prediction for a typical commercial transport aircraft
[AIAA PAPER 93-0174] p 310 A93-23245
- An overview of shed ice impact studies in the NASA Lewis Icing Research Tunnel
[AIAA PAPER 93-0301] p 283 A93-23247
- Aircraft icing problems - After 50 years
[AIAA PAPER 93-0392] p 486 A93-24239
- CWAS - Clean wing advisory system: A new approach to ice detection
[AIAA PAPER 93-0747] p 516 A93-24835
- Anti-icing failure detection instrumentation using realtime optical measurement of anti-icing fluid properties
[AIAA PAPER 93-0748] p 540 A93-24836
- Field studies of hold-over-times for type II anti-icing fluids - Results and insights
[AIAA PAPER 93-0749] p 486 A93-24837
- Experimental assessment of airframe damage due to impacting ice
[AIAA PAPER 93-0751] p 504 A93-24838
- Parameter selection of electro-impulse de-icing systems
p 889 A93-40493
- Developments in icing test techniques for aerospace applications in the RAE Pyestock (England) altitude test facility
[RAE-TM-P-1214] p 48 N93-11485
- Icing prevention by ultrasonic nucleation of supercooled water droplets in front of subsonic aircraft
[AD-A258212] p 142 N93-12816
- Results of low power deicer tests on a swept inlet component in the NASA Lewis icing research tunnel
[NASA-TM-105968] p 138 N93-14911
- Surface roughness due to residual ice in the use of low power deicing systems
[NASA-TM-105971] p 139 N93-15338
- Numerical modeling of anti-icing systems and comparison to test results on a NACA 0012 airfoil
[NASA-TM-105975] p 148 N93-15345
- Ice accretion and performance degradation calculations with LEWICE/NS
[NASA-TM-105972] p 148 N93-15354
- Close-up analysis of aircraft ice accretion
[NASA-TM-105952] p 148 N93-15360
- An overview of shed ice impact in the NASA Lewis Icing Research Tunnel
[NASA-TM-105969] p 139 N93-15404
- Ice accretion prediction for a typical commercial transport aircraft
[NASA-TM-105976] p 149 N93-15522
- Numerical investigation of performance degradation of wings and rotors due to icing
[NASA-CR-192233] p 339 N93-18783
- Aircraft ice detectors and related technologies for onground and inflight applications
[DOT/FAA/CT-92/27] p 791 N93-27269
- A passive infrared ice detection technique for helicopter applications
[NASA-CR-193187] p 880 N93-29152
- FAA international conference on airplane ground deicing
[AD-A263617] p 880 N93-29286
- AIRCRAFT INDUSTRY**
- A civil aircraft industry for India
p 2 A93-12233
- General aviation turbine markets - An economic overview
[AIAA PAPER 92-4191] p 103 A93-13369
- Stochastic modeling and adaptive control algorithm of brake bending
p 227 A93-14417
- PAA-core aluminum honeycomb - An end user's evaluation
p 209 A93-15738
- Improvement of aircraft maintenance methods
p 237 A93-18352
- Large-area aircraft scanner
p 407 A93-19693
- Methods of economic evaluation - Forecasting critique
[AIAA PAPER 92-4285] p 570 A93-24300
- Improved Airframe Manufacturing Technology
p 783 A93-35971
- Design developments for advanced general aviation aircraft. I
p 801 A93-37174
- Ilyushin takes on the market
p 945 A93-43623
- Sales, not subsidies, are the sticking point
p 945 A93-43677

- Propulsion technology challenges for turn-of-the-century commercial aircraft
[ISABE 93-7003] p 1194 A93-53980
- Future development and application of general structural analysis softwares in the aviation industry in China
p 1262 A93-54420
- The economic effectiveness analysis of technological progress in aviation industry
p 1265 A93-54854
- The civil scene - The authorities re-appraisal of ageing aircraft
p 1229 A93-54895
- Assessment of NDT reliability
p 1258 A93-54900
- Surface protection in the aircraft industry
[MBB-Z-0432-92-PUB] p 72 N93-11027
- The application of manufacturing systems engineering for aero engine gears
[PNR-90944] p 86 N93-11054
- Activities report of Lufthansa
[ETN-92-92100] p 28 N93-11319
- French aerospace equipment
p 1041 N93-31734
- Propulsion technology challenges for turn-of-the-century commercial aircraft
[NASA-TM-106192] p 1005 N93-32351
- AIRCRAFT INSTRUMENTS**
- Integration of full scale development aircraft GPS user equipment (AN/ARN-151) with Doppler radar systems
p 31 A93-11012
- Design, capabilities, and performance of the miniaturized airborne GPS receiver
p 32 A93-11014
- The derivation of path following error and control motion noise filters for the reduction of Global Positioning System flight test data
p 32 A93-11022
- Maintaining high accuracy GPS positioning 'on the fly' - using traverse closures, residual analysis, inertial navigation in aircraft
p 92 A93-11028
- Phase I flight test of MIAG advanced development model
[AIAA PAPER 92-4076] p 95 A93-11261
- Design and conduct of a windshear detection flight experiment
[AIAA PAPER 92-4092] p 38 A93-11268
- Flight experience with lightweight, low-power miniaturized instrumentation systems
[AIAA PAPER 92-4111] p 39 A93-11280
- Study on aircraft microwave remote sensing of sea-water surface salinity
p 92 A93-12407
- In-flight detection of flow separation, stagnation, and transition
p 166 A93-14326
- Onboard maintenance monitoring systems in modern aircraft
p 167 A93-15047
- The static-memory crash recorders
p 167 A93-15048
- The start of the laboratory - The beginnings of the MIT Instrumentation Laboratory
p 235 A93-17326
- USCG HU-25A/GPS integration
p 313 A93-21130
- Performance analysis of a miniaturized airborne GPS receiver
p 313 A93-21147
- Advancing helicopters
p 327 A93-21836
- Measurements of jet aircraft emissions at cruise altitude.
I - The odd-nitrogen gases NO, NO₂, HNO₂ and HNO₃
p 556 A93-24391
- Increased safety through knowledge-based pilot assistance
p 518 A93-27499
- New cathode-ray tube (CRT) gun interconnection assembly
p 547 A93-28175
- Aircraft measurement of electric field - Self-calibration
p 753 A93-34694
- Instrument systems of flight vehicles and their design
--- Russian book
[ISBN 5-217-00793-1] p 718 A93-35678
- IR window damage measured by reflective scatter
p 851 A93-39544
- A novel aircraft-based tandem mass spectrometer for atmospheric ion and trace gas measurements
p 925 A93-40672
- Engineering a visual system for seeing through fog
[SAE PAPER 921130] p 895 A93-41318
- Topographic mapping using a Ku-band airborne elevation interferometer
p 896 A93-42786
- Preliminary results of the ISM campaign - The Landes, South West France
p 1161 A93-47553
- PBMR observations of surface soil moisture in Monsoon 90
p 1162 A93-47676
- Development methodology for contemporary avionics systems
[SAE PAPER 931591] p 1104 A93-49340
- STANAG 3910 - The data bus for the next generation of European avionics systems
[SAE PAPER 931595] p 1104 A93-49344
- Changing the utility subsystem paradigm
[SAE PAPER 931598] p 1165 A93-49347
- Specialty fiber optic systems for mobile platforms and plastic optical fibers; Proceedings of the Meeting, Boston, MA, Sept. 9-11, 1992
[SPIE-1799] p 1105 A93-49462
- Fiber optic position sensors --- in aircraft flight control systems
p 1105 A93-49465

- Ladar fiber optic sensor system for aircraft applications
p 1105 A93-49467
- Implementation of fiber optic technology in flight controls
p 1105 A93-49473
- New concepts for fiber optic position sensors
p 1106 A93-49477
- The Airborne Ocean Color Imager - System description and image processing
p 1157 A93-50369
- An aircraft instrument design for in situ tropospheric OH measurements by laser induced fluorescence at low pressures
p 1159 A93-51528
- Development of a microcomputer-based magnetic heading sensor
p 1160 A93-52152
- Aureole lidar - Instrument design, data analysis, and comparison with aircraft spectrometer measurements
p 1160 A93-52419
- Instrumentation and telemetry systems for free-flight drop model testing
p 1209 A93-52754
- CRAASH - A coordinated collision avoidance system
[ONERA, TP NO. 1993-84] p 1191 A93-53604
- Instrumentation and data acquisition for full-scale aircraft crash testing
p 1250 A93-54399
- Passive IR surveillance for helicopter systems - The Sea Owl equipment
p 1244 A93-55299
- Flight simulator evaluation of D-size liquid crystal flat panel displays
[NAL-TR-1136] p 52 N93-12367
- Liquid crystal flat panel display evaluation tests using a flight simulator
[NAL-TR-1122] p 52 N93-12383
- Measurement of the dynamic undercarriage response of a Sikorsky S-70B-2 helicopter: Instrumentation and test methods: Flight mechanics technical memorandum
[AD-A256319] p 329 N93-16404
- A multi-faceted engineering study of aerodynamic errors of the Service Aircraft Instrumentation Package (SAIP)
[AD-A258059] p 293 N93-17677
- Realization of real time graphics in vehicles with high dynamic motion
[ETN-93-92739] p 443 N93-18630
- Airborne Wind Shear Detection and Warning Systems: Fourth Combined Manufacturers' and Technologists' Conference, part 1
[NASA-CP-10105-PT-1] p 488 N93-19590
- Flight test operations
p 488 N93-19592
- NASA wind shear flight test in situ results
p 488 N93-19593
- Airborne doppler radar research at Rockwell International
p 489 N93-19602
- Topological approach for the study of electromagnetic coupling
[ONERA-P-1992-2] p 551 N93-20230
- Comparison of the electrical charging and discharging environments of multiple aircraft-borne electric-field measurement systems
p 704 N93-24887
- Avionics systems architectures
p 808 N93-27169
- Aircraft ice detectors and related technologies for onground and inflight applications
[DOT/FAA/CT-92/27] p 791 N93-27269
- A concluding study of the altitude determination deficiencies of the Service Aircraft Instrumentation Package (SAIP)
[AD-A263515] p 897 N93-29971
- Pallet for helicopter test instrumentation
p 1000 N93-31279
- AIRCRAFT LANDING**
- Differential GPS/inertial navigation approach/landing flight test results
p 32 A93-11019
- Flight testing and simulation of an F-15 airplane using throttles for flight control
[AIAA PAPER 92-4109] p 39 A93-11278
- Wheel shimmy analysis for main landing gear of aircraft
p 41 A93-11809
- Investigation of precise approach and landing of civil aircraft using integrated system based on GPS
p 180 A93-14159
- Integration of flight control and carrier landing aid system
[ONERA, TP NO. 1993-6] p 181 A93-14187
- Flight simulator research into advanced MLS approach and departure procedures
p 149 A93-14234
- The simulation of aircraft landing gear dynamics
p 155 A93-14318
- Development of laser conducting landing system
p 150 A93-14320
- Expanding the operation scope of aircraft through the use of air-cushion landing gear
p 321 A93-18354
- The role of simulation in determining safe aircraft landing separation criteria
p 306 A93-18712
- Unsteady effects of camber on the aerodynamic characteristics of a thin aerofoil moving near the ground
p 270 A93-21719
- Weather forecasts for aviation in Canada (FACN and FICN) - The way they are taught and how they can be made more suitable to the needs of pilots
p 454 A93-22108

- Integrated Terminal Weather System (ITWS)
p 428 A93-22127
- Laser Centerline Localizer and Laser Glideslope Indicator for visual guidance on approach to landing
p 500 A93-28156
- Scanning Laser Aircraft Surveillance System for carrier flight operations
p 500 A93-28157
- Alternative approach routes to runway 24 at Oslo Airport, Fornebu
p 487 A93-28481
- MI-26 autorotational landings
p 816 A93-35955
- Half-scale modeling experience in the testing of radio navigation and landing systems
p 882 A93-43112
- Aircraft braking systems
p 995 A93-44850
- The evolution of a nose-wheel steering system
p 995 A93-44852
- Determination of the takeoff and landing characteristics of aircraft by using a conditional polar
p 1007 A93-45662
- Characteristics of the detection of overloads in the center of mass of Ii-76 and An-12 aircraft due to runway irregularities by a standard on-board recorder
p 1008 A93-45666
- Operating an aircraft during the landing on an airfield with a substantial longitudinal macroslope of the runway
p 1008 A93-45667
- Backfire unveiled
p 997 A93-46024
- A wind shear hazard window useful in studying the effect of wind shear on the airplane during the landing approach
[AIAA PAPER 93-3643] p 1127 A93-48327
- Investigation of roll requirements for carrier approach
[AIAA PAPER 93-3649] p 1128 A93-48332
- Automatic carrier landing system utilizing aircraft sensors
p 1097 A93-49590
- Initial results of an in-flight investigation of longitudinal flying qualities for augmented, large transports in approach and landing
[AIAA PAPER 93-3816] p 1133 A93-51407
- Fault tolerant navigation for aircraft landing
p 1191 A93-53866
- Longitudinal closed-loop pilot/vehicle analysis of DFBW aircraft during approach and landing
p 1206 A93-54277
- NASA Langley's Aircraft Landing Dynamics Facility
p 1250 A93-54400
- Optimization of oleo-pneumatic shock absorber of aircraft
p 1243 A93-55415
- A simulation study on take-off and landing dynamics of fly-by-wire control system aircraft
p 1249 A93-55590
- Integrated DGPS/IMU systems for airborne navigation in Poland
p 1241 A93-56049
- Summary of findings from the PIREP-based analyses conducted during the 1988 to 1990 evaluations of TDWR-based and TDWR/LLWAS-based alert services provided to landing/departing pilots
[AD-A253859] p 93 N93-11144
- A problem formulation for glideslope tracking in wind shear using advanced robust control techniques
[NASA-TM-104164] p 64 N93-11176
- DME-derived positions compared with MLS- and ILS-derived positions
[NLR-TP-90119-U] p 318 N93-16343
- Energy method for analysis of measured airspeed change in landing airborne manoeuvre
[ESDU-92020] p 335 N93-18042
- Aircraft landing gear shimmy
p 340 N93-19029
- A simulation study on take-off and landing dynamics of the aircraft of a fly-by-wire control system
[AD-A259286] p 510 N93-19849
- Visual approach data collection at St. Louis Lambert Field (STL)
[DOT/FAA/CT-TN93/2] p 706 N93-24948
- Development of a large-scale, outdoor, ground-based test capability for evaluating the effect of rain on airfoil lift
[NASA-TM-4420] p 779 N93-26899
- Low bandwidth robust controllers for flight
[NASA-CR-193085] p 819 N93-27156
- Coherent systems in the terahertz frequency range: Elements, operation, and examples
p 841 N93-27727
- A model-based approach for detection of objects in low resolution passive millimeter wave images
[NASA-CR-193161] p 808 N93-28418
- Helicopter approach capability using the differential global positioning system
[NASA-CR-193183] p 793 N93-28936
- Evaluation of four advanced nozzle concepts for short takeoff and landing performance
[NASA-TP-3314] p 875 N93-29165
- Land subsidence and problems affecting land use at Edwards Air Force Base and vicinity, California, 1990
[PB93-182236] p 1036 N93-32191
- AIRCRAFT MAINTENANCE**
- Electronics show their age
p 80 A93-13447

- Aircraft tracking optimization of parameters selection p 3 A93-13628
- Reassessment of the C-141 structural life p 46 A93-13631
- Maintaining the safety of an aging fleet of aircraft p 3 A93-13632
- Fleet fatigue cracking threshold prediction p 3 A93-13633
- A review of aging aircraft technology - An I.A.I. perspective p 3 A93-13634
- Aging review of the YS-11 aircraft p 46 A93-13635
- Analysis of multiple crack propagation in stiffened sheet p 81 A93-13638
- Damage tolerance assessment on the multisite cracks for the YS-11 aircraft p 46 A93-13642
- Maintainable A330 p 107 A93-13957
- Fundamentals of composite repair [SME PAPER EM92-100] p 196 A93-14101
- In-service inspection of commercial aircraft composite structure [SME PAPER EM92-124] p 107 A93-14116
- ICAS, Congress, 18th, Beijing, China, Sept. 20-25, 1992, Proceedings, Vols. 1 & 2 [ISBN 1-56347-046-2] p 107 A93-14151
- A fuzzy dynamic analysis method for aeromaintenance system p 225 A93-14177
- The application of human factors engineering at General Electric Aircraft Engines [SAE PAPER 921039] p 108 A93-14659
- Onboard maintenance monitoring systems in modern aircraft p 167 A93-15047
- Welding wire selection critical to jet engine repair work p 208 A93-15375
- Accuracy of a simple hole damage analysis method in composite structures p 197 A93-15748
- Managing mistakes --- quality assurance in aircraft maintenance p 109 A93-17100
- Improvement of aircraft maintenance methods p 395 A93-18326
- A model of the maintenance of a fleet of TU-204 aircraft at a maintenance and repair center p 237 A93-18327
- Selection of methods and equipment for monitoring the technical condition of booster system components --- of aircraft hydraulic systems p 395 A93-18329
- A method for evaluating the technical condition of hydraulic control boosters without their disassembly --- repair of aircraft systems p 395 A93-18335
- Improvement of aircraft maintenance methods p 237 A93-18352
- Vibrational monitoring and diagnostics of the technical condition of gas turbine engines at civil aviation repair facilities p 374 A93-18362
- A unified approach to the construction of the throttle characteristics of postrepair turbojet engines, with the NK8-2U engine used as an example p 345 A93-18372
- Key trends in human factors of aircraft maintenance; Proceedings of the Conference, London, United Kingdom, Oct. 31, 1991 [ISBN 1-85768-0057] p 237 A93-18754
- The designs for safety --- considering human factors in aircraft maintenance p 321 A93-18755
- Looking and seeing - A practical problem --- aircraft maintenance and inspection p 238 A93-18758
- BITE vs human judgement - The aircraft side --- Built In Test Equipment p 238 A93-18759
- Integrating the maintenance requirement maintenance ground based data systems - The missing link? p 238 A93-18760
- Artificial intelligence techniques for improving aircraft maintenance efficiency; Proceedings of the Conference, London, United Kingdom, Feb. 21, 1991 [ISBN 0-903409-84-4] p 238 A93-18761
- Expert systems for maintenance engineering p 434 A93-18762
- Calling the right shots in aircraft maintenance with artificial intelligence p 238 A93-18763
- The Royal Air Force experience of artificial intelligence aircraft maintenance p 435 A93-18764
- Knowledge based systems and avionics equipment failure diagnosis p 238 A93-18765
- Advanced expert systems increase aircraft maintenance efficiency - An overview p 238 A93-18767
- Very high reliability - Cost and consequences p 397 A93-18789
- Using advanced technology to achieve reliability as well as high performance p 346 A93-18790
- TEMPER - A gas-path analysis tool for commercial jet engines [ASME PAPER 92-GT-315] p 354 A93-19501
- An automated flow line for gas turbine blade repair [ASME PAPER 92-GT-367] p 375 A93-19531
- Water instead of chemical corrosives against aircraft paint - Environment-friendly paint-stripping methods could mean drastic cost reductions for the aircraft industry p 239 A93-21850
- Battle damage repairs p 239 A93-22698
- Repair of delaminations and impact damage in composite aircraft structures p 457 A93-24107
- The National Plan for Aviation Human Factors - Maintenance research issues p 457 A93-27132
- Future availability of aircraft maintenance personnel p 570 A93-27133
- Ongoing and planned R&D efforts in airway facilities maintenance p 458 A93-27134
- A damage tolerance/life processor for structural integrity and force management p 507 A93-27962
- Repair of a severely damaged composite fuel pod p 508 A93-27966
- Evolution of permanent composite repair designs p 508 A93-27967
- Fatigue effects of noise among airplane mechanics p 558 A93-28495
- RACE pulls for shared control --- tolerances and automation technology for aircraft maintenance and inspection p 458 A93-29130
- Robotic aircraft refueling - A concept demonstration p 846 A93-37041
- A practical course in aircraft maintenance. I - The powerplant --- Russian book p 811 A93-39175
- Maintenance of the liquid and gas systems of the Il-76 aircraft p 804 A93-39203
- Avionic systems/design and maintenance; Proceedings of the Conference, Hounslow, United Kingdom, Apr. 22, 1993 [ISBN 1-85768-095-2] p 764 A93-39535
- Installation of electrical cable looms p 764 A93-39536
- Software - Design for maintenance p 847 A93-39537
- On-board maintenance aids p 764 A93-39538
- HIRF and lightning --- EMC of aircraft systems and installations for safe operation p 764 A93-39539
- Ultra-high pressure water jet technology - An overview of a new process for aerospace paint stripping [SME PAPER AD92-196] p 855 A93-40661
- Robotic aircraft painting with SAFARI [SME PAPER AD92-198] p 855 A93-40662
- Sensor-adaptive control for aircraft paint stripping [SME PAPER AD92-200] p 855 A93-40663
- Robotic inspection and refurbishment of aircraft canopy transparencies [SME PAPER AD92-203] p 855 A93-40665
- Emerging technology for large-area scanning of aging aircraft [SME PAPER AD92-205] p 925 A93-40666
- Automated Laser Paint Stripping (ALPS) [SME PAPER AD92-206] p 855 A93-40667
- R&M 2000 field data requirements for a SPO operation p 856 A93-42853
- TEAMS - Technical expert aircraft maintenance system p 941 A93-42865
- The Aloha Airlines accident - A new era for aging aircraft p 991 A93-45783
- Bonded repair of multi-site damage p 947 A93-45786
- Results of review of Fokker F 28 'Fellowship' maintenance program p 948 A93-45793
- Repairs to damage tolerant aircraft p 948 A93-45799
- Repair and maintenance of fiber optic data links on Navy aircraft p 1172 A93-48538
- Carbon composite repairs of helicopter metallic primary structures p 1101 A93-50429
- Eddy current inspection of open fastener holes in aluminum aircraft structure [SAE ARP 4402] p 1160 A93-52167
- Aspects of fatigue affecting the design and maintenance of modern military aircraft p 1043 A93-52548
- Wet layup materials for repair of bismaleimide composites p 1212 A93-53451
- Repair materials and processes for the MD-11 Composite Tailcone p 1216 A93-53452
- Neural network fault diagnosis of a turbofan engine [ISABE 93-7091] p 1203 A93-54067
- Various applications of robots in aircraft engine overhaul [ISABE 93-7129] p 1175 A93-54104
- Aerodynamics of turbine blades with trailing-edge damage - Measurements and computations [ISABE 93-7130] p 1189 A93-54105
- The use of non-destructive testing to detect and monitor aircraft corrosion in service p 1258 A93-54896
- Maintainability of large gas turbine aero engines [PNR-90987] p 58 A93-11069
- Rotorcraft health and usage monitoring systems: A literature survey [DOT/FAA/RD-91/6] p 48 A93-11461
- Using NDT techniques in the maintenance of aeronautical products [REPT-921-430-102] p 88 A93-11587
- Action composition for the animation of natural language instructions p 228 A93-12554
- [AD-A254963] p 228 A93-12554
- Aircraft accident report: Britt Airways, Inc., d/b/a, Continental Express Flight 2574, in-flight structural breakup, EMB-120RT, N33701, Eagle Lake, Texas, September 11, 1991 [PB92-910405] p 143 A93-13426
- Bearing servicing tool [NASA-CASE-MSC-21881-1] p 221 A93-14871
- Proceedings of the 16th Symposium on Aircraft Integrated Monitoring Systems [DLR-MITT-92-01] p 167 A93-15152
- The Teledyne controls aircraft condition monitoring system p 168 A93-15155
- Ground Support Equipment (GSE) for Aircraft Condition Monitoring System (ACMS) p 110 A93-15158
- Detection of technical states with aircraft p 168 A93-15159
- Monitoring of powerplants in advanced commercial aircraft p 178 A93-15171
- Failure diagnostic with MAINTEx based on AIMS at Swissair p 110 A93-15181
- Onboard System Evaluation of Rotors Vibration, Engines (OBSEVE) monitoring system [AD-A255386] p 165 A93-15227
- Conditioned based machinery maintenance (helicopter fault detection) [AD-A255796] p 329 A93-16396
- Dual-band infrared imaging applications: Locating buried minefields, mapping sea ice, and inspecting aging aircraft [DE93-000516] p 453 A93-17225
- Analysis of consolidation of intermediate level maintenance for Atlantic Fleet T700-GE-401 engines [AD-A257754] p 363 A93-17695
- Turbomachinery and potential computations [DS-2026] p 363 A93-17740
- An investigation of the influence of advanced aircraft diagnostics on the technological sophistication of maintenance personnel [AD-A258988] p 240 A93-18887
- Nondestructive inspection of in-service aircraft [ETN-93-93059] p 496 A93-20928
- Reliability assessment at airline inspection facilities. Volume 1: A generic protocol for inspection reliability experiments [DOT/FAA/CT-92/12-VOL-1] p 704 A93-25110
- Investigation of corrosion in aluminum/adhesive lap-splices using pulse-echo ultrasonic techniques [DE93-008074] p 749 A93-25518
- An analysis of the reliability and maintainability of the Jian 6 and Jian 7 aircraft and ways to improve them [AD-A261060] p 678 A93-26238
- Reliability assessment at airline inspection facilities. Volume 2: Protocol for an eddy current inspection reliability experiment [DOT/FAA/CT-92/12-VOL-2] p 842 A93-28685
- Aircraft and refueler bonding and grounding study [AD-A262027] p 911 A93-29398
- Performance of gas turbine compressor cleaners [NLR-TP-91237-U] p 1003 A93-31111
- Aging aircraft research in the Netherlands [NLR-TP-91443-U] p 999 A93-32203
- Damage severity of monitored fatigue load spectra [NLR-TP-92009-U] p 999 A93-32205
- AIRCRAFT MANEUVERS**
- A robust direct-integration method for rotorcraft maneuver and periodic response p 61 A93-10919
- The F-18 High Alpha Research Vehicle - A high-angle-of-attack testbed aircraft [AIAA PAPER 92-4121] p 42 A93-13273
- The method for developing F-by-F load spectra of fighter aircraft based on maneuvers p 154 A93-14254
- Aeroservoelastic analysis of an aircraft model incorporating the minimum state method for approximating unsteady aerodynamics p 154 A93-14258
- Design of manoeuvrable simple and complex planform transonic wings with attained thrust-, panel- and Euler-methods p 117 A93-14301
- Cobra maneuver considerations p 182 A93-14306
- Investigation on air refueling scheduling p 108 A93-14315
- Design of digital multiple model-following integrated flight propulsion control systems p 183 A93-14371
- Stability considerations for enhanced manoeuvrability - An overview p 184 A93-14397
- A new method for calculation of helicopter maneuvering flight p 184 A93-14401
- Agility potential --- flight qualities and maneuverability of rotorcraft and V/STOL aircraft [SAE PAPER 921016] p 185 A93-14645
- Static aeroelastic analysis of a maneuvering aircraft with damaged wing [AIAA PAPER 92-4765] p 325 A93-20360

Aircraft experiments on microgravity pool boiling - Vapor-liquid behaviour and heat transfer characteristics in boiling of n-pentane, CFC-113 and water p 410 A93-20920

Turbulence avoidance p 309 A93-22160

What makes the Cobra maneuver possible? [AIAA PAPER 93-0183] p 367 A93-22609

F-14A aircraft low-speed maneuvering aerodynamics [AIAA PAPER 93-0523] p 283 A93-23265

Numerical simulation of delta-wing roll [AIAA PAPER 93-0554] p 285 A93-23293

Flight simulator fidelity assessment in a rotorcraft lateral translation maneuver p 378 A93-23510

Flight performance of hypersonic minor circle turning maneuvers [AIAA PAPER 93-0627] p 531 A93-24744

Fundamental issues in subsonic/transonic expansion corner aerodynamics [AIAA PAPER 93-0649] p 465 A93-24764

Maneuver option manager - Automated simplification of complex air traffic control problems p 498 A93-25480

The aerodynamic loads on aircraft components in violent longitudinal manoeuvres p 476 A93-26898

Active aircraft recovery from a spin p 524 A93-27295

Investigation of the aircraft spin via sensitivity analysis p 524 A93-27300

High-performance aircraft propulsion research p 529 A93-27904

Load variability of a two-bladed helicopter p 507 A93-27954

Aircraft collision avoidance using statistical decision theory p 500 A93-28155

Measurements of aerodynamic rotary stability derivatives using a whirling arm facility p 525 A93-28603

Mathematical phenomenology for thrust-vectoring-induced agility comparisons p 525 A93-28613

A Taguchi analysis of helicopter maneuverability and agility p 763 A93-35944

X-29 vortex flow control tests p 804 A93-38846

The problem of avoiding aircraft collisions during group flights p 819 A93-39191

Kinematics of aeroinertial aircraft rotation p 819 A93-39192

Inverse simulation of large-amplitude aircraft maneuvers p 906 A93-41893

Optimization of equipment layout in the fuselage of maneuverable aircraft p 891 A93-42370

Operating an aircraft during the landing on an airfield with a substantial longitudinal macroslope of the runway p 1008 A93-45667

Initial acceleration effects on flow evolution around airfoils pitching to high angles of attack p 961 A93-45750

The moving wall effect vis-a-vis other dynamic stall flow mechanisms [AIAA PAPER 93-3424] p 1008 A93-47219

Effect of forebody tangential slot blowing on flow about a full aircraft geometry [AIAA PAPER 93-2962] p 1048 A93-48156

Computation of delta-wing roll maneuvers [AIAA PAPER 93-2975] p 1050 A93-48169

Estimation of neutral and maneuver points of aircraft by dynamic maneuvers [AIAA PAPER 93-3620] p 1126 A93-48307

Status of the validation of high-angle-of-attack nose-down pitch control margin design guidelines [AIAA PAPER 93-3623] p 1126 A93-48308

Unsteady aerodynamic models for maneuvering aircraft [AIAA PAPER 93-3626] p 1126 A93-48311

On computing vortex asymmetries about cones at angle of attack using the conical Navier-Stokes equations [AIAA PAPER 93-3628] p 1064 A93-48313

Development of flying qualities and agility evaluation maneuvers [AIAA PAPER 93-3645] p 1127 A93-48329

Aircraft control requirements and achievable dynamics prediction [AIAA PAPER 93-3648] p 1128 A93-48331

Development of lateral-directional departure criteria [AIAA PAPER 93-3650] p 1128 A93-48333

Optimum poststall turning and supersonic turning [AIAA PAPER 93-3659] p 1128 A93-48339

Results and lessons learned from two Wright Laboratory flight research programs [AIAA PAPER 93-3661] p 1099 A93-48341

Aeroelastic effects on the B-2 maneuver response [AIAA PAPER 93-3664] p 1128 A93-48344

Analysis on space shape and tension distribution of towed flexible cables p 1043 A93-48554

Use of neural networks in control of high-alpha maneuvers p 1130 A93-49593

Cancellation control law for lateral-directional dynamics of a supermaneuverable aircraft [AIAA PAPER 93-3775] p 1131 A93-51370

Quasi-optimal steady state and transient maneuvers with and without thrust vectoring [AIAA PAPER 93-3778] p 1132 A93-51373

Design of a controller for a high performance fighter aircraft using Robust Inverse Dynamics Estimation (RIDE) [AIAA PAPER 93-3779] p 1132 A93-51374

Fuzzy logic control algorithm for suppressing E-6A Long Trailing Wire Antenna wind shear induced oscillations [AIAA PAPER 93-3868] p 1171 A93-51454

Monitoring load experience of individual aircraft p 1103 A93-52450

A dual-Euler method for solving all-attitude angles of the aircraft [AIAA PAPER 93-3589] p 1223 A93-52682

Non-linear flight dynamics [ONERA, TP NO. 1993-109] p 1206 A93-53621

Analysis of spatial motion dynamics of a helicopter for various models of the induced velocity field p 1191 A93-53721

A study of aircraft global dynamic stability in rapid rolling maneuver p 1206 A93-53869

Minimum time turn of a helicopter p 1248 A93-54554

Worst-case wind modeling and its influence on capturing of aircraft penetration trajectory p 1248 A93-54857

Equations of the steady motion of aircraft in spin and spiral dive p 1248 A93-54969

A study on low level windshear hazard index p 1240 A93-55414

Inverse simulation: A tool for the validation of simulation programs - First results --- for helicopter flight tests and control p 1249 A93-56046

Forced unsteady separated flows on a 45 degree delta wing p 82 N93-10305

Flight test and analysis procedures for new handling criteria [RAE-TM-FM-26] p 47 N93-10803

Hybrid guidance for maneuvering flight vehicles [AD-A254110] p 69 N93-11798

Propulsion integration results of the STOL and Maneuver Technology Demonstrator p 161 N93-13228

Statistical fatigue analysis of the SH-60B servo beam rail component [AD-A257474] p 332 N93-17660

Aircraft turns into and down wind [AERO-REPT-9201] p 337 N93-18131

On automated analysis of flight test data p 512 N93-19913

Dynamic airfoil stall investigations p 786 N93-27453

Computation of a delta-wing roll-and-hold maneuver [AD-A264704] p 909 N93-30498

Advanced aircraft with thrust vector control [MBB-FE-1-S-PUB-0504] p 998 N93-31043

A high-fidelity, six-degree-of-freedom batch simulation environment for tactical guidance research and evaluation [NASA-TM-4440] p 1010 N93-32380

AIRCRAFT MODELS

Flight test and wind-tunnel study of a scaled unmanned air vehicle [AIAA PAPER 92-4075] p 37 A93-11260

Nonlinear multi-point modelling and parameter estimation of the DO 28 research aircraft p 41 A93-12727

H(infinity) optimal controllers for a distributed model of an unstable aircraft p 62 A93-13247

An analysis of helicopter dynamic response to turbulence using fuselage and blade element atmospheric sampling techniques [AIAA PAPER 92-4148] p 43 A93-13314

Extracting dimensional geometric parameters from B-spline surface models of aircraft [AIAA PAPER 92-4283] p 43 A93-13340

Aircraft model for multicriterial analysis in decision making [AIAA PAPER 92-4192] p 44 A93-13370

Application of SPEED in aviation industry p 225 A93-14178

Aeroservoelastic analysis of an aircraft model incorporating the minimum state method for approximating unsteady aerodynamics p 154 A93-14258

Results of testing of models of joint-wing utility class aircraft [SAE PAPER 921013] p 157 A93-14643

A model of the maintenance of a fleet of TU-204 aircraft at a maintenance and repair center p 237 A93-18327

An overview of the system identification procedure with applications to the X-31 drop model [AIAA PAPER 93-0010] p 366 A93-20132

Flight simulator fidelity assessment in a rotorcraft lateral translation maneuver p 378 A93-23510

Operational and research aspects of a radio-controlled model flight test program [AIAA PAPER 93-0625] p 504 A93-24742

Problems in the modeling of helicopter flight p 506 A93-27293

Modeling and control design of a wind tunnel model support p 529 A93-29281

Lessons from application of equivalent plate structural modeling to an HSCT wing [AIAA PAPER 93-1413] p 739 A93-33969

Development and validation of a comprehensive real time AH-64 Apache simulation model p 799 A93-35992

Numerical computation and approximations of H(infinity) optimal controllers for a 2-parameter distributed model of an unstable aircraft p 817 A93-37040

Recent experiences with implementing a video based six degree of freedom measurement system for airplane models in a 20 foot diameter vertical spin tunnel p 821 A93-37763

Design philosophy for wind tunnel model positioning control systems p 822 A93-37877

Output feedback eigenstructure assignment using two Sylvester equations p 847 A93-38214

Calculation of the effect of flow conicity in a hypersonic nozzle on the aerodynamics of a flight vehicle model p 776 A93-39142

Analytical development of an equivalent system mismatch function --- for longitudinal axis of fighter aircraft in nonterminal flight phase p 906 A93-41890

Applying variations of the quantitative feedback technique (QFT) to unstable, non-minimum phase aircraft dynamics models p 939 A93-42797

Determination of the takeoff and landing characteristics of aircraft by using a conditional polar p 1007 A93-45662

Investigation of the radiance from the leading edge of a wing [AIAA PAPER 93-2728] p 1039 A93-46482

Computations of transonic wind tunnel flows about a fully configured model of aircraft by using multi-domain technique [AIAA PAPER 93-3022] p 1055 A93-48207

An advanced parallel rotorcraft flight simulation model - Stability characteristics and handling qualities [AIAA PAPER 93-3618] p 1125 A93-48305

Unsteady aerodynamic models for maneuvering aircraft [AIAA PAPER 93-3626] p 1126 A93-48311

Identification of a full subsonic envelope nonlinear aerodynamic model of the F-14 aircraft [AIAA PAPER 93-3634] p 1065 A93-48319

On the use of back propagation with feed-forward neural networks for the aerodynamic estimation problem [AIAA PAPER 93-3638] p 1165 A93-48323

Parameter estimates of an aeroelastic aircraft as affected by model simplifications [AIAA PAPER 93-3640] p 1127 A93-48325

Development of lateral-directional departure criteria [AIAA PAPER 93-3650] p 1128 A93-48333

A simplified wing rock prediction method [AIAA PAPER 93-3662] p 1128 A93-48342

Aerodynamic characteristics of a sweptforward-wing aircraft model in unsteady motion at large angles of attack in subsonic flow p 1068 A93-48902

Use of neural networks in control of high-alpha maneuvers p 1130 A93-49593

Multiple radial basis function networks in modeling and control [AIAA PAPER 93-3731] p 1170 A93-51330

Order reduction of aeroelastic models through LK transformation and Riccati iteration [AIAA PAPER 93-3795] p 1159 A93-51388

Aerodynamic characteristics of airship models of different shapes p 1092 A93-51909

A method for the spectral-time identification of the longitudinal and lateral motions of an aircraft p 1205 A93-52942

Analysis of spatial motion dynamics of a helicopter for various models of the induced velocity field p 1191 A93-53721

Finite element analysis of natural vibrations of an aeroplane with asymmetric variable wing geometry p 1218 A93-53776

Data acquisition for aeroelastic testing at the NASA Langley Transonic Dynamics Facility p 1250 A93-54397

Application of eigenstructure assignment to the control of powered lift combat aircraft p 64 A93-11871

Introduction of electronic pressure scanning at the Royal Aerospace Establishment [RAE-TM-AERO-2222] p 23 A93-11882

Study of optical techniques for the Ames unitary wind tunnels. Part 4: Model deformation [NASA-CR-190980] p 68 A93-12349

- Simulation analysis of a cable-mount system used for dynamic wind tunnel tests
[NAL-TR-1127] p 68 N93-12359
- Design philosophy for wind tunnel model positioning systems
[AD-A254958] p 192 N93-12552
- ASTOVL model engine simulators for wind tunnel research
p 192 N93-13213
- Sensor fault detection using nonlinear observer and polynomial classifier
p 170 N93-15182
- Conditioned based machinery maintenance (helicopter fault detection)
[AD-A255796] p 329 N93-16396
- Hermes CX-7: Air transport system design simulation
[NASA-CR-192082] p 335 N93-18056
- Arrow 227: Air transport system design simulation
[NASA-CR-192053] p 336 N93-18063
- Operational and research aspects of a radio-controlled model flight test program
[NASA-TM-104266] p 339 N93-18616
- Rarefied-flow Shuttle aerodynamics model
[NASA-TM-107698] p 458 N93-19976
- Improved ceramic slip casting technique — application to aircraft model fabrication
[NASA-CASE-LAR-14471-1] p 536 N93-20041
- A computational approach to predicting the extent of arc root damage in CFC panels
p 735 N93-24890
- Fabrication of composite propfan blades for a cruise missile wind tunnel model
[NASA-TM-105270] p 752 N93-26202
- Adjoint methods for aerodynamic wing design
[NASA-CR-193086] p 805 N93-27089
- A demonstration of simple airfoils: Structural design and materials choices
[DE93-007882] p 789 N93-28662
- Modal survey of a full-scale F-18 wind tunnel model
[AD-A262482] p 875 N93-29410
- Solution of Euler equations for forebody-inlet ensemble of aircraft at high angle of attack
[AD-A263905] p 876 N93-29862
- RCS of fundamental scatterers in the HF band by wire-grid modelling
p 933 N93-30320
- Supersonic aerodynamic characteristics of an advanced F-16 derivative aircraft configuration
[NASA-TP-3355] p 989 N93-31733
- AIRCRAFT NOISE**
- European environmental studies focus on impact of engine emissions
p 92 A93-10730
- Evolving noise issue could persist into the next century
p 99 A93-10731
- Effect of flight conditions on the sound insulation of the aircraft passenger compartment
p 42 A93-12978
- DNW test highlights related to aircraft environment
p 190 A93-14274
- Active control of interior noise in model aircraft fuselages using piezoceramic actuators
p 231 A93-14540
- Optical microphone for the detection of hidden helicopters
p 205 A93-14542
- Comparison of advanced turboprop interior noise control ground and flight test data
p 444 A93-19136
- Boundary-layer induced noise in aircraft
p 444 A93-19137
- New design concepts for silencing aeroacoustic wind tunnels
p 445 A93-19147
- Development of the Boeing Low Speed Aeroacoustic Facility (LSAF)
p 374 A93-19148
- Active aerodynamic control of wake-airfoil interaction noise - Experiment
p 445 A93-19153
- Matrix difference equation analysis of coupled structural-acoustic models for aircraft fuselage vibration and interior noise reduction
p 446 A93-19172
- Advances in tilt rotor noise prediction
p 447 A93-19184
- Lynx: High performance - Low noise
p 322 A93-19185
- Evaluation of piezoceramic actuators for control of aircraft interior noise
p 447 A93-19186
- Active control of sound transmission through stiff lightweight composite fuselage constructions
p 447 A93-19187
- Noise evaluation of light propeller-driven aircraft
p 398 A93-19189
- A contribution to noise improvements for aircraft by noise measurement evaluation
p 448 A93-19190
- Control measures used to reduce community noise from civil aviation in Denmark
p 425 A93-19191
- Final results from a study of community response to aircraft noise around Oslo Airport Fornebu
p 425 A93-19192
- The critical role of turbulence modeling in the prediction of supersonic jet structure for acoustic applications
p 398 A93-19193
- On the scaling of small-scale jet noise to large scale
p 448 A93-19195
- A numerical method for the prediction of quadrupole shock wave noise
p 448 A93-19201
- Helicopter noise prediction - The current status and future direction
p 448 A93-19202
- Combined noise and flow control of supersonic jets using swirl
p 398 A93-19204
- Experimental determination of the main noise sources in a propfan model by analysis of the acoustic spinning modes in the exit plane
p 449 A93-19214
- Radiated noise of ducted fans
p 450 A93-19215
- The noise of jet aircraft flying with high speeds at low altitudes
p 450 A93-19218
- Experimental results on propeller noise attenuation using an 'active noise control' technique
p 450 A93-19223
- Reduction of propeller noise by active noise control
p 450 A93-19224
- Wing vortex refraction effects from BAC 1-11 flight tests
p 450 A93-19226
- Experimental and analytical investigations of fuselage modal characteristics and structural-acoustic coupling
p 451 A93-19229
- Numerical simulation of jet noise
p 265 A93-20716
- An interaction noise between vortex and airfoil
[AIAA PAPER 93-0600] p 562 A93-24726
- Takeoff/approach noise for a model counterrotation propeller with a forward-swept upstream rotor
[AIAA PAPER 93-0596] p 519 A93-24782
- Loudness versus level of aircraft noise
p 557 A93-28477
- Alternative approach routes to rwy 24 at Oslo Airport, Fornebu
p 487 A93-28481
- The airnoise boundary concept for airport noise management
p 564 A93-28482
- Influence of aircraft noise on speech intelligibility
p 558 A93-28483
- Preliminary results from a study of community response to noise from military aircraft exercise
p 558 A93-28484
- Night aircraft noise index and sleep research results
p 558 A93-28485
- Final results from a study of community response to aircraft noise around Oslo Airport Fornebu
p 558 A93-28486
- Technical solutions to reduce and to control the noise load in the Netherlands — generated by aircraft engines
p 564 A93-28492
- The costs of noise at the new Munich airport
p 558 A93-28493
- Air traffic noise monitoring in and around Lisbon Airport
p 564 A93-28494
- Fatigue effects of noise among airplane mechanics
p 558 A93-28495
- Noise-induced reaction in a work community adjacent to aircraft runways - The Royal Australian Airforce
p 559 A93-28496
- Computer-based modelling of aircraft noise impact
p 559 A93-28497
- Role of leading-edge vortex flows in prop-fan interaction noise
p 565 A93-28614
- A study of blade-vortex interaction sound generation and directionality
p 565 A93-29402
- Shock waves and the Ffowcs Williams-Hawkings equation
p 480 A93-29411
- Far-field hover acoustic characteristics of the XV-15 tiltrotor aircraft with Advanced Technology Blades
p 566 A93-29412
- NOTAR system - A quiet character
p 567 A93-29418
- Tiltrotor interior noise characteristics
p 509 A93-29421
- Human response to helicopter noise - A test of A-weighting
p 567 A93-29424
- Active control of interior noise in a large scale cylinder using piezoelectric actuators
p 568 A93-29425
- Transmission error and load distribution analysis of spur and double helical gear pairs used in a split path helicopter transmission design
p 549 A93-29426
- Active control of helicopter transmission noise
p 568 A93-29428
- An overview on practical application of helicopter noise certification rules
p 487 A93-29442
- Helicopter noise standards - Requirements, compliance, and improvements
p 569 A93-29443
- Control of land use near airports is best means of reducing impact of aircraft noise
p 571 A93-29575
- A closed loop controller for BVI impulsive noise reduction by Higher Harmonic Control
p 849 A93-35963
- Effects of ingested atmospheric turbulence on measured tail rotor acoustics
p 849 A93-35964
- An analysis on high speed impulsive noise of transonic helicopter rotor
p 849 A93-35965
- Prediction of BVI noise patterns and correlation with wake interaction locations
p 849 A93-35966
- Blade-vortex interaction noise - Prediction and comparison with flight and wind tunnel tests
[ONERA, TP NO. 1992-126] p 851 A93-38600
- Toward the silent helicopter
[ONERA, TP NO. 1992-229] p 851 A93-38774
- Identification of noise sources based on experimental amplitude-frequency noise characteristics of aircraft
p 851 A93-39040
- Helicopter external noise prediction and reduction
[ONERA, TP NO. 1993-48] p 1039 A93-47450
- Increase in mortality rates due to aircraft noise
p 1163 A93-49551
- A comparison between the impact of noise from aircraft, road traffic and trains on long-term recall and recognition of a text in children aged 12-14 years
p 1163 A93-49552
- The influence of nocturnal aircraft noise on sleep and on catecholamine secretion
p 1163 A93-49554
- Results of a low-altitude flight noise study in Germany - Acute extraaural effects
p 1163 A93-49557
- Specific features of military low-altitude flight noise - Criteria for risk of damage and physiological effects
p 1164 A93-49558
- Review - Extraaural health effects of aircraft noise
p 1164 A93-49559
- Determination of the natural vibrations of an acoustic medium in the cabin of a passenger aircraft by the finite element method
p 1102 A93-51752
- Correction of a method for calculating the noise levels of aircraft at control points during acoustic flight testing
p 1102 A93-51758
- Acoustic intensity of nonisothermal coaxial jets with an inverted velocity profile
p 1124 A93-51759
- An approach to the calculation of the far acoustic field of a propeller
p 1124 A93-51760
- Determination of fan noise in a lined duct with flow using the Green function method
p 1124 A93-51761
- Air transport and the environment - Regulating aircraft noise
p 1226 A93-52931
- Experimental investigation into the mechanism of discrete frequency noise (DFN) generation from a NACA 0012 blade
p 1225 A93-53194
- Active aerodynamic control of wake-airfoil interaction noise - Experiment
p 1225 A93-53206
- Engine technology challenges for a 21st Century High-Speed Civil Transport
[ISABE 93-7064] p 1200 A93-54040
- Helicopter noise - Public perspective
p 1261 A93-54719
- Helicopter noise certification
p 1262 A93-54720
- Noise characteristics of helicopters with the NOTAR anti-torque system
p 1262 A93-54722
- European research into helicopter internal noise
p 1243 A93-54724
- The community response to aircraft noise around six Spanish airports
p 1264 A93-55845
- Tilt rotor hover aeroacoustics
[NASA-CR-177598] p 99 N93-10458
- Non-propulsive aerodynamic noise
p 99 N93-10673
- Comparison of flyover noise data from aircraft at high subsonic speeds with prediction
p 100 N93-10674
- Reduction of propeller noise by active noise control
p 101 N93-10692
- Publications on acoustics research at the Langley Research Center, January 1987 - September 1992
[NASA-TM-107674] p 102 N93-12080
- Report on the final panel discussion on computational aeroacoustics
[NASA-CR-189718] p 231 N93-12986
- Evaluation of three models used for predicting noise propagated long distances overground
[AD-A255963] p 232 N93-14406
- Air Force procedure for predicting noise around airbases: Noise exposure model (Noisemap)
[AD-A255769] p 224 N93-14655
- Tiltrotor aircraft noise: A summary of the presentations and discussions at the 1991 FAA/Georgia Tech Workshop
[DOT/FAA/RD-91/23] p 232 N93-14912
- Experimental investigation of an ejector-powered free-jet facility
[NASA-TM-105868] p 291 N93-16704
- Takeoff/approach noise for a model counterrotation propeller with a forward-swept upstream rotor
[NASA-TM-105979] p 362 N93-16715
- Effect of personal and situational variables on noise annoyance: With special reference to implications for en route noise
[NASA-CR-189676] p 569 N93-21317
- Calculation of noise emission caused by jet aircraft during takeoff, approach and horizontal flyover
[DLR-MITT-91-15] p 569 N93-21368
- Analysis of aircraft noise levels in the vicinity of start-of-takeoff roll at Baltimore-Washington International Airport
[PB92-221605] p 559 N93-21501
- Rotating rake design for unique measurement of fan-generated spinning acoustic modes
[NASA-TM-105946] p 724 N93-26161

- User's manual for UCAP: Unified Counter-Rotation Aero-Acoustics Program
[NASA-CR-191034] p 852 N93-27148
- A laboratory study of subjective response to sonic booms measured at White Sands Missile Range
[NASA-TM-107746] p 852 N93-27272
- A prediction model for noise from low-altitude military aircraft
[AD-A262494] p 852 N93-27662
- External acoustical noise measurements for aviation systems
[AD-A263138] p 943 N93-29480
- Engine technology challenges for a 21st Century High-Speed Civil Transport
[NASA-TM-106216] p 1004 N93-31671
- Effects on health of noise disturbances due to air traffic
p 1035 N93-31929
- Reaction to aircraft noise near general aviation airfields
[DORA-8203] p 1040 N93-32377
- Transmission of sound through a rotor
[NLR-TP-92014-U] p 1006 N93-32386
- ### AIRCRAFT PARTS
- Mixed mode stress intensity-factors in transversely loaded plates
p 200 A93-13943
- Integrated utilities management system for aircraft
p 153 A93-14208
- Rapid fabrication of flight worthy composite parts
p 209 A93-15792
- Photoelastic stress analysis of skewed cutout in a sandwich skew plate subjected to inplane and transverse eccentric load
p 210 A93-16604
- Accelerated corrosion fatigue test methods for aging aircraft
p 198 A93-16623
- LEWICE droplet trajectory calculations on a parallel computer
[AIAA PAPER 93-0172] p 438 A93-22604
- Some characteristics of the design of heads for the cutting of bevel gears with negative curvature of the circular-arc tooth line
p 835 A93-39093
- A mathematical model of the vibrational impact hardening of parts
p 837 A93-39185
- Comparison measurements of currents induced by radiation and injection
p 926 A93-41575
- MOI - Magneto-optic eddy current imaging
p 927 A93-41751
- Optical methods of stress analysis applied to cracked components
p 1027 A93-45798
- Problems of the strength and fatigue of the elements of aircraft structures
p 1029 A93-47076
- Grid and aerodynamic sensitivity analyses of airplane components
[AIAA PAPER 93-3475] p 981 A93-47254
- Thermoplastic composite parts manufacture at Du Pont
[SME PAPER EM93-106] p 1159 A93-51728
- Advantages of a one-part resin system for processing aerospace parts by Resin Transfer Molding (RTM)
[SME PAPER EM93-112] p 1159 A93-51729
- Ongoing challenges for titanium alloy cleanliness improvement in aircraft engine disk materials
p 1212 A93-53506
- Durability properties for adhesively bonded structural aerospace applications
p 1217 A93-53515
- ### AIRCRAFT PERFORMANCE
- 757 fly-by-wire demonstrator flight test
[AIAA PAPER 92-4099] p 38 A93-11271
- Flight experience with lightweight, low-power miniaturized instrumentation systems
[AIAA PAPER 92-4111] p 39 A93-11280
- Design of an adaptive flight control system with uncertainties
p 95 A93-12322
- Test pilot's notes on flying the Low Altitude/Airspeed Unmanned Research Aircraft (LAURA)
[AIAA PAPER 92-4078] p 42 A93-13269
- Practical considerations in waverider applications
[AIAA PAPER 92-4247] p 43 A93-13326
- ICAS, Congress, 18th, Beijing, China, Sept. 20-25, 1992, Proceedings. Vols. 1 & 2
[ISBN 1-56347-046-2] p 107 A93-14151
- Development of generic helicopter performance methodology for real time mission analyses
p 152 A93-14185
- Drag/thrust estimation via aircraft performance flight testing
p 156 A93-14322
- Agility potential --- flight qualities and maneuverability of rotorcraft and V/STOL aircraft
[SAE PAPER 921016] p 185 A93-14645
- Using advanced technology to achieve reliability as well as high performance
p 346 A93-18790
- Concurrent optimization of airframe and engine design parameters
[AIAA PAPER 92-4713] p 323 A93-20281
- The user friendly airliner (The 37th Roy Chadwick Lecture)
p 307 A93-21718
- Turbulence model evaluation for the prediction of flows over a supercritical airfoil with deflected aileron at high Reynolds number
[AIAA PAPER 93-0191] p 276 A93-22615
- Operational and research aspects of a radio-controlled model flight test program
[AIAA PAPER 93-0625] p 504 A93-24742
- Speed, range boost Saab 2000's appeal
p 505 A93-25495
- Current technologies for waverider aircraft
[AIAA PAPER 93-0400] p 505 A93-25521
- East Europe's aircraft builders look West
p 458 A93-28396
- Optimization of endurance performance --- of aircraft
p 713 A93-34400
- Optimal cruise performance
p 802 A93-37394
- Nonlinear analysis and flight dynamics
[ONERA, TP NO. 1992-83] p 818 A93-38568
- The SAAB 2000 initial flight test - Status report
p 804 A93-38847
- Periodic maximum range cruise with singular control
p 890 A93-41903
- Big time doorstep delivery
p 892 A93-42995
- Problems in the aerodynamics, strength, and flight operations of aircraft
p 947 A93-45659
- General concepts related to the determination of the individual flight performance characteristics of aircraft for establishing fuel consumption standards and optimal flight regimes
p 996 A93-45673
- Analysis of stability characteristics of a high performance aircraft
[AIAA PAPER 93-3616] p 1125 A93-48303
- Nonsmooth trajectory optimization - An approach using continuous simulated annealing
[AIAA PAPER 93-3657] p 1099 A93-48337
- Dual Engine application of the Performance Seeking Control algorithm
[AIAA PAPER 93-1822] p 1110 A93-49709
- Experimental studies of aerodynamic performances of hypersonic scramjet in impulse hot-shot tunnel
[AIAA PAPER 93-2446] p 1120 A93-50198
- X-29 high-angle-of-attack flight testing
p 1101 A93-50487
- Performance-seeking control - Program overview and future directions
[AIAA PAPER 93-3765] p 1102 A93-51360
- Robust, nonlinear, high angle-of-attack control design for a supermaneuverable vehicle
[AIAA PAPER 93-3774] p 1131 A93-51369
- Design of a flight control system for a highly maneuverable aircraft using mu synthesis
[AIAA PAPER 93-3776] p 1132 A93-51371
- Quasi-optimal steady state and transient maneuvers with and without thrust vectoring
[AIAA PAPER 93-3778] p 1132 A93-51373
- TVC control for the AIAA design challenge airplane
[AIAA PAPER 93-3810] p 1122 A93-51402
- Antiwindup analysis and design approaches for MIMO systems
[AIAA PAPER 93-3811] p 1123 A93-51403
- Initial results of an in-flight investigation of longitudinal flying qualities for augmented, large transports in approach and landing
[AIAA PAPER 93-3816] p 1133 A93-51407
- Aircraft failure detection and identification using neural networks
[AIAA PAPER 93-3869] p 1171 A93-51455
- Fault detection, isolation, and reconfiguration for aircraft using neural networks
[AIAA PAPER 93-3870] p 1135 A93-51456
- Optimal performance of airplanes flying through windshear
[AIAA PAPER 93-3846] p 1102 A93-51480
- Instrumentation and telemetry systems for free-flight drop model testing
p 1209 A93-52754
- A study of military aircraft and engine tactical/technical performance evaluation
p 1242 A93-54596
- Airship applications of modern flight test techniques
[AIAA PAPER 93-4035] p 1242 A93-54606
- Concurrent optimization of airframe and engine design parameters
[NASA-TM-105908] p 60 N93-12402
- Subsonic flight test evaluation of a propulsion system parameter estimation process for the F100 engine
[NASA-TM-4426] p 175 N93-13155
- A stochastic optimal feedforward and feedback control methodology for superagility
[NASA-CR-4471] p 229 N93-13370
- Czechoslovak development and experience in flight data recorder readout and analysis
p 168 N93-15162
- Real-time in-flight engine performance and health monitoring techniques for flight research application
p 169 N93-15169
- Example of statistical techniques applied to analysis of measurements of the landing airborne manoeuvre. (Multiple linear regression with two independent variables and one dependent variable.)
[ESDU-92022] p 330 N93-16636
- The role of under-determined approximations in engineering and science application
p 441 N93-16763
- An investigation of two-propeller tilt wing V/STOL aircraft flight characteristics
[AD-A257751] p 332 N93-17694
- Open airscrew VTOL concepts
[NASA-CR-177603] p 240 N93-17883
- MM-122: High speed civil transport
[NASA-CR-192011] p 334 N93-17974
- Operational and research aspects of a radio-controlled model flight test program
[NASA-TM-104266] p 339 N93-18616
- Stall in axial flow aero engine compressors
p 422 N93-18723
- Stall and surge in axial flow compressors
p 423 N93-18724
- Adverse weather test site selection study
[AD-A259012] p 339 N93-18895
- An experimental investigation of a finite circulation control wing
[AD-A259044] p 340 N93-18896
- Professor Wittenberg: His speciality and versatility
[ISBN-90-6275-670-0] p 240 N93-19002
- Aircraft performance in practice
p 340 N93-19004
- Wind shear hazard determination
p 488 N93-19597
- AM-X high angle of attack flight test experience (single and two seat versions)
p 511 N93-19910
- In-flight structural mode excitation system for flutter testing
p 526 N93-19915
- Apparatus and method for improving spin recovery on aircraft
[NASA-CASE-LAR-14747-1] p 526 N93-20039
- Failure identification using multiple model adaptive estimation for the LAMBDA flight vehicle
[AD-A259137] p 527 N93-20596
- Applications of stress envelope concepts to aircraft EMP and lightning survivability
p 704 N93-24898
- Experimental performance of a ventral nozzle with pitch and yaw vectoring capability for SSTOVL aircraft
[NASA-TM-106054] p 722 N93-25129
- Generic hypersonic vehicle performance model
[NASA-CR-192953] p 714 N93-25162
- Jet-induced ground effects on a parametric flat-plate model in hover
[NASA-TM-104001] p 700 N93-26099
- Development of a large-scale, outdoor, ground-based test capability for evaluating the effect of rain on airfoil lift
[NASA-TM-4420] p 779 N93-26899
- Effect of underwing frost on transport aircraft takeoff performance
[DOT/FAA/CT-TN93/9] p 791 N93-27252
- Evaluation of four advanced nozzle concepts for short takeoff and landing performance
[NASA-TP-3314] p 875 N93-29165
- Flight mechanical model for performance calculations and interactions between flight vehicle and ramjet in regard to the flight orbit
[ESA-T1-1267] p 893 N93-29464
- A high-fidelity, six-degree-of-freedom batch simulation environment for tactical guidance research and evaluation
[NASA-TM-4440] p 1010 N93-32380
- ### AIRCRAFT PILOTS
- The hazard and alarm of windshear
p 141 A93-14317
- The user friendly airliner (The 37th Roy Chadwick Lecture)
p 307 A93-21718
- New initiatives for aviation meteorology training - 1989 through 1991
p 307 A93-22109
- The importance of proper aviation weather dissemination to pilots - An airline captain's perspective
p 308 A93-22115
- Detection of microburst-related gust fronts using Doppler radar
p 427 A93-22118
- MIST - A remote briefing system
p 437 A93-22132
- A proposed icing severity index based upon meteorology
p 429 A93-22136
- An evaluation of aircraft icing forecasts for the continental United States
p 429 A93-22149
- Responsibility and assignment of roles on overlong flights
p 570 A93-24253
- Aircraft collision avoidance using statistical decision theory
p 500 A93-28155
- System Status - The diagnostic edge of the pilot's associate
p 808 A93-37853
- Pilots' control behavior including feedback structures identified by an improved method
[AIAA PAPER 93-3669] p 1129 A93-48347

- Nonlinear command augmentation system for a high performance aircraft
[AIAA PAPER 93-3777] p 1132 A93-51372
- Longitudinal closed-loop pilot/vehicle analysis of DFBW aircraft during approach and landing
p 1206 A93-54277
- Adaptive automation and human performance: Multi-task performance characteristics
[AD-A254596] p 186 A93-12578
- Cockpit decision making p 146 A93-15015
- Trans-cockpit authority gradient in Navy/Marine aircraft mishaps p 146 A93-15016
- Performance-based testing and success in Naval advanced flight training
[AD-A260838] p 717 A93-25933
- ### AIRCRAFT POWER SUPPLIES
- Evolution of the Boeing 777 electrical power system
p 519 A93-25998
- Computational and experimental investigation of a solar energy system for an atmospheric flight vehicle
p 521 A93-29655
- Flight-vehicle drives (2nd revised and enlarged edition) --- Russian book
[ISBN 5-217-00802-4] p 713 A93-35676
- A new resonant link aircraft power generating system
p 809 A93-36268
- A self-steering array for the SHARP microwave-powered aircraft
p 792 A93-37090
- Method for assessing the electric power system reliability of multiple-engined aircraft
p 810 A93-37398
- Dynamic processes in the powerplants and power-generating equipment of flight vehicles
p 832 A93-39027
- The all-electric aircraft - In your future?
p 997 A93-46824
- Document for 270 Voltage Direct Current (270 V dc) System
[SAE ARP 4729] p 1160 A93-52170
- Air cell --- model aircraft power supplies
[CA-PATENT-APPL-SN-2001346] p 83 A93-10368
- ### AIRCRAFT PRODUCTION
- Current developments in structural technology
p 77 A93-10780
- Integration of aircraft design and manufacture using artificial intelligence paradigms
p 225 A93-14202
- Aeroelastic investigations as applied to Airbus airplanes
p 155 A93-14280
- Engine reliability from an independent overhaul shops perspective
p 239 A93-18788
- Ensuring the reliability and service life of flight vehicle structures by engineering methods
p 745 A93-35276
- Mathematical statement of the problem of optimizing the design of an airframe for ease of manufacture
p 745 A93-35286
- Modeling and optimization of aircraft assembly --- Russian book
[ISBN 5-217-00808-3] p 677 A93-35677
- B-2 flight test update
p 803 A93-38844
- Thermoplastic composite parts manufacture at Du Pont
[SME PAPER EM93-106] p 1159 A93-51728
- Optimum design of aircraft structures with manufacturing and buckling constraints
p 162 A93-13815
- Special tooling disposition for aircraft entering post production support
[AD-A261614] p 678 A93-26168
- Aviation production engineering: Selected articles
[AD-A261231] p 764 A93-27056
- ### AIRCRAFT PRODUCTION COSTS
- Bilateral transfers of safety oversight will prove beneficial to all states
p 1174 A93-49279
- Cost effective process selection for composite structure
[SME PAPER EM93-100] p 1043 A93-51727
- ### AIRCRAFT RELIABILITY
- Handling qualities flight test techniques and analyses used with the proposed MIL-H-8501B
[AIAA PAPER 92-4081] p 61 A93-11264
- The approach to airworthiness clearance with the introduction of advanced materials and manufacturing technologies into the design of aerospace structures
p 2 A93-12235
- New lamps for old - Safety regulation through structural airworthiness standards
p 28 A93-13630
- Reassessment of the C-141 structural life
p 46 A93-13631
- A review of aging aircraft technology - An I.A.I. perspective
p 3 A93-13634
- MPC75 - The evolution of a new regional airliner for the late nineties
p 155 A93-14289
- The certification of head up displays for category 3 operation
p 142 A93-17304
- Improvement of aircraft maintenance methods
p 395 A93-18326
- Advanced expert systems increase aircraft maintenance efficiency - An overview
p 238 A93-18767
- Aero engine reliability, integrity and safety; Proceedings of the Conference, Bristol, United Kingdom, Oct. 17, 18, 1991
[ISBN 0-903409-70-4] p 345 A93-18778
- Safety through integrity and reliability --- for passenger and military aircraft
p 239 A93-18779
- ETOPS across the Atlantic --- extended range operation of twin-engined transport aircraft
p 306 A93-18780
- Aero-engine reliability - A GE view
p 345 A93-18782
- Reliability and safety considerations in engine management systems design
p 346 A93-18786
- Engine reliability from an independent overhaul shops perspective
p 239 A93-18788
- Very high reliability - Cost and consequences
p 397 A93-18789
- Using advanced technology to achieve reliability as well as high performance
p 346 A93-18790
- Human factors in crashes of commuter airplanes
p 486 A93-24048
- Ongoing and planned R&D efforts in airway facilities maintenance
p 458 A93-27134
- A structural reliability evaluation of fail-safe helicopter dynamic components
p 506 A93-27952
- A damage tolerance/life processor for structural integrity and force management
p 507 A93-27962
- Modal analysis in the certification of a commercial aircraft
p 509 A93-29241
- Ensuring the reliability and service life of flight vehicle structures by engineering methods
p 745 A93-35276
- Extended range operations of two and three turbofan engined airplanes
p 802 A93-37391
- Method for assessing the electric power system reliability of multiple-engined aircraft
p 810 A93-37398
- Advanced Tupolev twinjet combines Russian and Western technologies
p 802 A93-38565
- Installation of electrical cable looms
p 764 A93-39536
- HIRF and lightning --- EMC of aircraft systems and installations for safe operation
p 764 A93-39539
- Emerging technology for large-area scanning of aging aircraft
[SME PAPER AD92-205] p 925 A93-40666
- R&M 2000 field data requirements for a SPO operation
p 856 A93-42853
- TEAMS - Technical expert aircraft maintenance system
p 941 A93-42865
- Structural integrity of aging airplanes
[ISBN 0-540-53461-X] p 947 A93-45772
- Towards quantitative non-destructive evaluation of aging aircraft
p 1025 A93-45773
- Computational schemes for integrity analyses of fuselage panels in aging airplanes
p 1025 A93-45774
- Risk analysis for aging aircraft fleets
p 1025 A93-45775
- Aspects of aging aircraft - A transatlantic view
p 1026 A93-45776
- The civil Damage Tolerance Requirements in theory and practice
p 1026 A93-45777
- Aging jet transport structural evaluation programs
p 947 A93-45781
- NASA airframe structural integrity program
p 1026 A93-45782
- The Aloha Airlines accident - A new era for aging aircraft
p 991 A93-45783
- Fuselage longitudinal splice design
p 997 A93-45784
- Applications of advanced fracture mechanics to fuselage
p 1026 A93-45787
- Structural integrity of aging airplanes - A perspective
p 948 A93-45789
- How likely is multiple site damage?
p 1027 A93-45791
- Results of review of Fokker F 28, 'Fellowship' maintenance program
p 948 A93-45793
- Estimation of requirements of inspection intervals for panels susceptible to Multiple Site Damage
p 948 A93-45795
- Experience in specifying/prolonging the airframe time limits
p 948 A93-45797
- Case study and simulation of fatigue damages and DTE of aging aircraft - A review of researches in Japan
p 948 A93-45800
- The well made engine
p 1122 A93-50352
- Advanced three-shaft engines: Configured for reliability, efficiency, and growth
[PNR-90986] p 58 A93-11068
- Rotorcraft health and usage monitoring systems: A literature survey
[DOT/FAA/RD-91/6] p 48 A93-11461
- Aircraft accident report: Explosive decompression-loss of cargo door in flight, United Airlines Flight 811, Boeing 747-122, N4713U, Honolulu, HI, 24 February 1989
[PB92-910402] p 28 A93-12193
- Structural fatigue aspects of the P-3 Orion
[ARL-STRUC-TM-558] p 161 A93-13256
- Embedded ADM reduces helicopter human error accidents
p 147 A93-15024
- Helicopter flight data recorder and health and usage monitoring system
p 169 A93-15178
- Helicopter health monitoring: Current practice and future trends
p 169 A93-15179
- Airbus Industrie TCAS experience
p 152 A93-15186
- Nondestructive inspection of in-service aircraft
[ETN-93-93059] p 496 A93-20928
- An analysis of the reliability and maintainability of the Jian 6 and Jian 7 aircraft and ways to improve them
[AD-A261060] p 678 A93-26238
- Damage tolerance assessment and usage variation analysis for C-130 aircraft in the Israeli Air Force
p 839 A93-27210
- Estimating characteristic life and reliability of an aircraft engine component improvement in the early stages of the implementation process
[AD-A262118] p 815 A93-28184
- Ageing aircraft research in the Netherlands
[NLR-TP-91443-U] p 999 A93-32203
- ### AIRCRAFT SAFETY
- Breaking through the 10 exp 6 barrier --- decreasing aircraft accident fatality rate per million flight hours
p 27 A93-11498
- Nonlinear multi-point modelling and parameter estimation of the DO 28 research aircraft
p 41 A93-12727
- Joint NASA/USAF Airborne Field Mill Program - Operation and safety considerations during flights of a Lear 28 airplane in adverse weather
[AIAA PAPER 92-4093] p 93 A93-13262
- Aeronautical fatigue: Key to safety and structural integrity; Proceedings of the 16th ICAF Symposium, Tokyo, Japan, May 22-24, 1991
[ISBN 4-9900181-1-7] p 80 A93-13626
- New lamps for old - Safety regulation through structural airworthiness standards
p 28 A93-13630
- Maintaining the safety of an aging fleet of aircraft
p 3 A93-13632
- Effects of prior fatigue damage on crack propagation rates in 2024-T351 aluminum alloy
p 71 A93-13640
- ICAS, Congress, 18th, Beijing, China, Sept. 20-25, 1992, Proceedings, Vols. 1 & 2
[ISBN 1-56347-046-2] p 107 A93-14151
- Human factors of aircraft cabin safety
p 140 A93-14218
- Tomorrow's security
p 141 A93-15058
- Autoland, the developing need
p 142 A93-17302
- The designs for safety --- considering human factors in aircraft maintenance
p 321 A93-18755
- Recent aircraft accidents
p 307 A93-20819
- The legal status of ekranoplanes
p 453 A93-20900
- Advancing helicopters
p 327 A93-21836
- Ice prediction systems for runways
p 376 A93-22174
- New results in optimal missile avoidance analysis
p 369 A93-22937
- The National Plan for Aviation Human Factors - Maintenance research issues
p 457 A93-27132
- The tilt wing advantage - for high-speed VSTOL aircraft
p 506 A93-27903
- New European regulations for rotorcraft; Proceedings of the Conference, London, United Kingdom, Mar. 16, 1993
[ISBN 1-85768-085-5] p 701 A93-34616
- Controlling hazardous configurations in helicopter systems
p 763 A93-35927
- Fail safety aspects of the V-22 pylon conversion actuator
p 798 A93-35984
- The development of a crashworthy composite fuselage and landing gear
p 799 A93-36001
- Damage tolerance assessment of the fighter aircraft 37 Viggen main wing attachment
p 802 A93-37390
- Aerodynamic questions related to the safety and cost-effective utilization of airships --- Russian book
p 818 A93-39125
- HIRF and lightning --- EMC of aircraft systems and installations for safe operation
p 764 A93-39539
- A study of the interaction between a wake vortex and an encountering airplane
[AIAA PAPER 93-3642] p 858 A93-40714
- Increasing airport safety and capacity using automated maneuvering area control
p 885 A93-43550
- Experience in specifying/prolonging the airframe time limits
p 948 A93-45797
- Two leading-edge droop modifications for tailoring stall characteristics of a general aviation trainer configuration
p 1008 A93-46807
- Bilateral transfers of safety oversight will prove beneficial to all states
p 1174 A93-49279
- Aircraft safety evaluation
p 1043 A93-50486
- Aspects of fatigue affecting the design and maintenance of modern military aircraft
p 1043 A93-52548

- Promoting general aviation safety - A revision of pilot negligence law p 1265 A93-56540
- Activities report of the German Institute for Flight Safety [ETN-92-92272] p 28 N93-11375
- Aircraft accident report: Atlantic Southeast Airlines, Inc. Flight 2311, uncontrolled collision with terrain, an Embraer EMB-120, N270AS, Brunswick, Georgia, 5 April 1991 [PB92-910403] p 28 N93-11471
- Aircraft accident report: Explosive decompression-loss of cargo door in flight, United Airlines Flight 811, Boeing 747-122, N4713U, Honolulu, HI, 24 February 1989 [PB92-910402] p 28 N93-12193
- Public-sector aviation issues: Graduate research award papers, 1990 - 1991 [PB92-22629] p 143 N93-13787
- Effects of seating configuration and number of type 3 exits on emergency aircraft evacuation [AD-A256616] p 143 N93-14277
- Measuring risk in single-engine and twin-engine helicopters p 148 N93-15025
- The FAIR (Flight Animated and Interactive Reconstruction) tool p 148 N93-15164
- Special investigation report: Piper Aircraft Corporation PA-46 Malibu/Mirage Accidents/Incident, 31 May 1989 - 17 March 1991 [PB92-917007] p 149 N93-15577
- Aviation safety research at the National Institute for Aviation Research Wichita State University: A report to the FAA Technical Center [NIAR-92-2] p 310 N93-16455
- Special investigation report: Flight attendant training and performance during emergency situations [PB92-917006] p 310 N93-16834
- Preliminary analysis of the J-52 aircraft engine component improvement program [AD-A257640] p 363 N93-17686
- The human factor problem in the Canadian Forces aviation p 491 N93-19657
- Correlations between engineering, medical and behavioural aspects in fire-related aircraft accidents p 494 N93-19693
- Aviation safety: Problems persist in FAA's inspection program. Report to the Chairman, Subcommittee on Aviation, Committee on Public Works and Transportation, House of Representatives [GAO/RCED-92-14] p 495 N93-19841
- Aviation safety: Users differ in views of collision avoidance system and cite problems. Report to the Chairman, Subcommittee on Investigations and Oversight, Committee on Science, Space, and Technology, House of Representatives [GAO/RCED-92-113] p 502 N93-19843
- Consumer interest in the air safety data of the airline quality rating. Testimony to the US House of Representatives, Committee on Government Operations, Government Activities and Transportation Subcommittee [NIAR-92-4] p 495 N93-19941
- T-38 forward windshield development and performance demonstration report [AD-A259240] p 513 N93-20579
- Nondestructive inspection of in-service aircraft [ETN-93-93059] p 496 N93-20928
- Proceedings of the First International Symposium on Explosive Detection Technology [DOT/FAA/CT-92/11] p 496 N93-21856
- The UK perspective on aviation security p 496 N93-21858
- Principles of nuclear-based explosive detection systems p 497 N93-21861
- A review of the development of a luggage explosive detection system p 497 N93-21862
- The 1992 International Aerospace and Ground Conference on Lightning and Static Electricity: Addendum [DOT/FAA/CT-92/20-ADD-1] p 753 N93-24875
- Zoning of aircraft: A review of the definitions p 703 N93-24880
- A procedure for defining lightning risk to air vehicles p 703 N93-24885
- Parameters influencing the hot-spot ignition of aviation fuel/air and ethylene/air mixtures p 704 N93-24886
- Lightning phenomenology bases for full threat return stroke occurrence following extended leader sweep at flight altitudes p 754 N93-24895
- Narrow-body aircraft water spray optimization study [DOT/FAA/CT-TN93/3] p 705 N93-25224
- A review of civil aviation propeller-to-person accidents: 1980-1989 [AD-A260695] p 705 N93-25896
- Aircraft accident report: Takeoff stall in icing conditions. USAir Flight 405 FOKKER F-28, N485US, LaGuardia Airport, Flushing, New York, 22 March 1992 [PB93-910402] p 790 N93-27034
- Aircraft accident report: Controlled collision with terrain GP Express Airlines, Inc., Flight 861, A Beechcraft C99, N118GP, Anniston, Alabama, 8 June 1992 [PB93-910403] p 790 N93-27035
- Protection of taxiing traffic in airports through mode S secondary radar technology [ETN-93-93455] p 791 N93-28206
- FAA international conference on airplane ground deicing [AD-A263617] p 880 N93-29286
- Progress through precedent: Going where no helicopter simulator has gone before p 913 N93-30686
- Aircraft guidance for wind shear avoidance: Decision-making under uncertainty p 889 N93-31005
- Longitudinal acceleration test of overhead luggage bins in a transport airframe section [DOT/FAA/CT-92/9] p 991 N93-31652
- International aircraft operator information system [DOT/FAA/CT-93/4] p 949 N93-32232
- UK airmisses involving commercial air transport, September - December 1991 [ETN-93-93930] p 992 N93-32409
- ### AIRCRAFT SPECIFICATIONS
- Russians completing new ground-effect vehicle p 853 A93-38535
- The whale with a tail p 803 A93-38837
- ### AIRCRAFT SPIN
- Rudder and elevator effects on the incipient spin characteristics of a typical general aviation training aircraft [AIAA PAPER 93-0016] p 367 A93-20138
- Active aircraft recovery from a spin p 524 A93-27295
- Equations of the steady motion of aircraft in spin and spiral dive p 1248 A93-54969
- Apparatus and method for improving spin recovery on aircraft [NASA-CASE-LAR-14747-1] p 526 N93-20039
- ### AIRCRAFT STABILITY
- Sensor alignment Kalman filters for inertial stabilization systems p 50 A93-11018
- Effects of thrust line offset on neutral point determination in stability flight testing [AIAA PAPER 92-4082] p 61 A93-11265
- Correlation of forebody pressures and aircraft yawing moments on the X-29A aircraft at high angles of attack [AIAA PAPER 92-4105] p 38 A93-11273
- Piloted simulation evaluation of pitch control designs for highly augmented STOV aircraft [AIAA PAPER 92-4234] p 63 A93-13328
- Study of aeroservoelastic stability of an aircraft p 182 A93-14259
- Cobra maneuver considerations p 182 A93-14306
- The influence of rotor and fuselage wakes on rotorcraft stability and control p 183 A93-14373
- Stability considerations for enhanced manoeuvrability - An overview p 184 A93-14397
- A sensitivity analysis of the stability of a tug-rope-sailplane system p 184 A93-14400
- Static roll moment characteristics of asymmetric tangential leading edge blowing on a delta wing at high angles of attack [AIAA PAPER 93-0052] p 261 A93-20165
- Subsonic static and dynamic stability characteristics of the test technique demonstrator NASP configuration [AIAA PAPER 93-0519] p 268 A93-21111
- Icing effects on aircraft stability and control determined from flight data - Preliminary results [AIAA PAPER 93-0398] p 370 A93-23073
- Measurements of aerodynamic rotary stability derivatives using a whirling arm facility p 525 A93-28603
- Aeroelastic system identification of advanced technology aircraft through higher order signal processing p 525 A93-29297
- Aeromechanical stability of rotorcraft with advanced geometry blades [AIAA PAPER 93-1304] p 725 A93-33880
- ISAC - A tool for aeroservoelastic modeling and analysis --- Interaction of Structures, Aerodynamics, and Control [AIAA PAPER 93-1421] p 726 A93-33974
- An algorithm with prediction in a control problem with functional constraints p 757 A93-35307
- Frequency-domain identification of coupled rotor/body models of an advanced attack helicopter p 816 A93-35960
- Numerical computation and approximations of H(infinity) optimal controllers for a 2-parameter distributed model of an unstable aircraft p 817 A93-37040
- Spoiler actuator - A problem investigation p 801 A93-37175
- Comment on 'Equation decoupling - A new approach to the aerodynamic identification of unstable aircraft' p 818 A93-37406
- F-16 Digital Flight Control System improvements p 818 A93-38843
- X-29 vortex flow control tests p 804 A93-38846
- Experimental investigation on aircraft dynamic stability parameters p 905 A93-40328
- Multiple model adaptive estimation applied to the VISTA F-16 flight control system with actuator and sensor failures p 907 A93-42806
- Pilot-in-the-loop analysis of propulsive-only flight control systems p 908 A93-42812
- Using numerical control algorithms in stabilization systems with digital correction p 941 A93-43113
- Real-time parameter identification applied to flight simulation p 1006 A93-44142
- Problems in the aerodynamics, strength, and flight operations of aircraft p 947 A93-45659
- Transonic flutter suppression using active acoustic excitations [AIAA PAPER 93-3285] p 969 A93-46841
- Attenuation of airplane wake vortices by excitation of far-field instability [AIAA PAPER 93-3511] p 984 A93-47277
- Experimental analysis of rotary derivatives on a modern aircraft configuration [AIAA PAPER 93-3514] p 985 A93-47278
- The cusp catastrophe and the stability problem of helicopter ground resonance p 1099 A93-48059
- AIAA Atmospheric Flight Mechanics Conference, Monterey, CA, Aug. 9-11, 1993, Technical Papers p 1125 A93-48301
- Effect of geometry, static stability, and mass distribution on the tumbling characteristics of generic flying-wing models [AIAA PAPER 93-3615] p 1125 A93-48302
- Analysis of stability characteristics of a high performance aircraft [AIAA PAPER 93-3616] p 1125 A93-48303
- Calculation of transonic longitudinal and lateral-directional characteristics of aircraft by the small disturbance theory [AIAA PAPER 93-3617] p 1125 A93-48304
- An advanced parallel rotorcraft flight simulation model - Stability characteristics and handling qualities [AIAA PAPER 93-3618] p 1125 A93-48305
- Estimation of neutral and maneuver points of aircraft by dynamic maneuvers [AIAA PAPER 93-3620] p 1126 A93-48307
- Status of the validation of high-angle-of-attack nose-down pitch control margin design guidelines [AIAA PAPER 93-3623] p 1126 A93-48308
- Kinematics and aerodynamics of the velocity vector roll [AIAA PAPER 93-3625] p 1126 A93-48310
- A simplified wing rock prediction method [AIAA PAPER 93-3662] p 1128 A93-48342
- Aircraft with single axis aerodynamically deployed wings [AIAA PAPER 93-3673] p 1129 A93-48350
- Antiwindup analysis and design approaches for MIMO systems [AIAA PAPER 93-3811] p 1123 A93-51403
- A pseudo-loop design strategy for the longitudinal control of hypersonic aircraft [AIAA PAPER 93-3814] p 1132 A93-51405
- Initial development of a research flight simulator software [AIAA PAPER 93-3590] p 1223 A93-52683
- Stabilization of the dynamic characteristics of the two-channel automatic control system of aircraft p 1205 A93-52941
- Identification of the phase characteristics and wind-induced perturbations of an aircraft from flight test results p 1206 A93-52943
- A study of aircraft global dynamic stability in rapid rolling maneuver p 1206 A93-53869
- Estimation of aerodynamic characteristics from flight-test data. V - Effects of gust and its time lag p 1230 A93-54560
- Aerodynamics of the TCOM 71M aerostat [AIAA PAPER 93-4036] p 1231 A93-54607
- Equations of the steady motion of aircraft in spin and spiral dive p 1248 A93-54969
- The whirl-flutter problem in aircraft construction p 1249 A93-56218
- Correlation of forebody pressures and aircraft yawing moments on the X-29A aircraft at high angles of attack [NASA-TM-4417] p 22 N93-11532
- Rigid body mode identification of the PAH-2 helicopter using the eigensystem realization algorithm [NASA-TM-107690] p 88 N93-11544
- The 13 ft by 9 ft low speed wind tunnel facility at DRA (Aerospace Division) Bedford (England) [RAE-TM-AERO-2228] p 23 N93-11883
- DYNAC: A computer program for analyzing the dynamical stability of aircraft [REPT-B-31] p 66 N93-12415

- Program for calculation of aileron rolling moment and yawing moment coefficients at subsonic speeds [ESDU-88040] p 136 A93-14514
- Ice effects on aircraft stability and control determined from flight data: Preliminary results [NASA-TM-105977] p 188 A93-14831
- Design of robust suboptimal controllers for a generalized quadratic criterion [AD-A257746] p 372 A93-17670
- An investigation of two-propeller tilt wing V/STOL aircraft flight characteristics [AD-A257751] p 332 A93-17694
- Design of the advanced regional aircraft, the DART-75 [NASA-CR-192044] p 333 A93-17972
- Introduction to Flutter of Winged Aircraft, volume 1 [VKI-LS-1992-01] p 372 A93-18142
- The unified method of aeroelasticity p 372 A93-18143
- The testing of fixed wing tanker and receiver aircraft to establish their air-to-air refuelling capabilities, volume 11 [AGARD-AG-300-VOL-11] p 514 A93-21305
- ### AIRCRAFT STRUCTURES
- Collection of works on measuring and computing systems for research on the aerodynamics, dynamics, and strength of flight vehicles p 75 A93-10026
- Multidisciplinary design of composite aircraft structures by Lagrange p 76 A93-10273
- The smart truck — structure, systems, avionics of C-17 airlifter p 40 A93-11420
- Analysis of structural dynamic response for aircraft operating in the environment of nuclear explosion shock waves p 78 A93-11810
- Investigation of cabin noise reduction in the Y12 p 41 A93-11816
- The approach to airworthiness clearance with the introduction of advanced materials and manufacturing technologies into the design of aerospace structures p 2 A93-12235
- Nonlinear deformation mechanics of multilayer transparency elements - General theory relations p 79 A93-12800
- Structural and aerodynamic considerations for an oblique all-wing aircraft [AIAA PAPER 92-4220] p 43 A93-13336
- The conceptual study of supersonic transport structure [AIAA PAPER 92-4219] p 43 A93-13348
- Maintaining the safety of an aging fleet of aircraft p 3 A93-13632
- Support of composite fuel cells [SME PAPER EM92-101] p 152 A93-14102
- Economical view on composite structures maintenance [SME PAPER EM92-102] p 233 A93-14103
- Commercial airplane primary structure [SME PAPER EM92-115] p 107 A93-14112
- A tooling trend at BCA - What and why [SME PAPER EM92-111] p 202 A93-14114
- In-service inspection of commercial aircraft composite structure [SME PAPER EM92-124] p 107 A93-14116
- Mechanical testing analyses of new aluminum alloy SPF typical-parts in aircraft p 196 A93-14174
- A new production technology for complex-shaped structural elements 'creep forming' p 202 A93-14175
- The fretting damage and effect of temperature in typical joint of aircraft construction p 203 A93-14196
- Researches on sonic fatigue of the air-inlet duct of XX aircraft p 154 A93-14256
- In-flight tailload measurements p 155 A93-14285
- A new method to study the forming process of complicated sheetmetal aero-parts p 204 A93-14363
- Nonlinear vibration and radiation from a panel with transition to chaos p 205 A93-14543
- Fourier analysis of clamped moderately thick arbitrarily laminated plates p 206 A93-14571
- Common failure modes for composite aircraft structures due to secondary loads p 207 A93-14812
- Sandwich construction in the Starship p 159 A93-15737
- Development of polyimide adhesives for 371 C (700 F) structural performance for aerospace bonding applications - FM 680 system p 198 A93-15757
- Computer-aided cure optimization p 209 A93-15804
- Aircraft fatigue failures and tasks of structural reliability analysis p 210 A93-16246
- Video holography and laser vibrometry...The dynamic duo p 210 A93-16611
- Actuation strain decoupling through enhanced directional attachment in plates and aerodynamic surfaces p 394 A93-17727
- Justification for the linear recording of fatigue damage summation for aircraft structures under operating conditions p 320 A93-18331
- Improving the service characteristics of an aircraft through the gyroscopic damping of its structure p 366 A93-18363
- Crack growth under conditions of service loading p 396 A93-18370
- Improvement of rotating brushes for surface cleaning p 396 A93-18371
- Selection of the time scale for preventive measures under service conditions p 237 A93-18375
- Coherent X-ray imaging for corrosion evaluation - A preliminary assessment p 396 A93-18611
- Comparison of heating protocols for detection of disbonds in lap joints p 396 A93-18627
- Elastic constants for unidirectional boron-epoxy composites p 387 A93-18636
- Nonlinear response of a clamped beam and plate to high levels of excitation p 397 A93-19141
- Nonlinear vibration and radiation from a panel with transition to chaos induced by acoustic waves p 398 A93-19173
- Sonic fatigue analysis of an aircraft wing flap by the matrix difference equation method p 399 A93-19208
- Nonlinear response and sonic fatigue of high speed aircraft p 399 A93-19211
- Assessment of aircraft structural integrity by detecting disbonds through ultrasonic scanning p 406 A93-19587
- Acoustic emission monitoring of aging aircraft structures p 407 A93-19697
- p-version finite element modeling for NDE p 407 A93-19699
- A method of finite element dynamic model optimization p 367 A93-20812
- Embedded fiber optic sensors in large structures p 410 A93-21085
- Application issues of fiber optic sensors in aircraft structures p 410 A93-21094
- Damage detection in smart structures using neural networks and finite-element analyses p 438 A93-22540
- Data analysis techniques for pressure- and temperature-sensitive paint [AIAA PAPER 93-0176] p 414 A93-22605
- Two-directional skin friction measurement utilizing a compact internally mounted thin-liquid-film skin friction meter [AIAA PAPER 93-0180] p 414 A93-22608
- Construction of a one-third scale model of the NASP [AIAA PAPER 93-0427] p 386 A93-23345
- Repair of delaminations and impact damage in composite aircraft structures p 457 A93-24107
- The structure and material testing facility needed for future SST/HST development [AIAA PAPER 92-3887] p 528 A93-24481
- CST and rotorcraft - Expanding the view p 560 A93-25085
- Ultrasonic thickness measurement using the angle technique p 542 A93-25353
- The aerodynamic loads on aircraft components in violent longitudinal manoeuvres p 476 A93-26898
- Design of advanced beams considering elasto-plastic behaviour of material p 544 A93-26904
- Investigation of cabin noise reduction in the Y12 p 506 A93-27371
- A method and a software for constructing F-by-F random load spectrum p 506 A93-27375
- Estimation of the life of aircraft structures under stochastic steady state loading p 545 A93-27620
- AHS National Technical Specialists' Meeting on Rotorcraft Structures, Williamsburg, VA, Oct. 29-31, 1991, Proceedings p 506 A93-27951
- The development and evaluation of advanced Kevlar sandwich structure for application to rotorcraft airframes p 546 A93-27965
- Repair of a severely damaged composite fuel pod p 508 A93-27966
- Novel approaches to complex geometry structure p 546 A93-27969
- An experimental and analytical investigation on the response of GR/EP composite I-frames p 546 A93-27975
- Rapid detection and quantification of impact damage in composite structures p 547 A93-27978
- Thermoelastic vibration test techniques p 549 A93-29293
- Probabilistically configured adaptive composite structures [AIAA PAPER 93-1679] p 743 A93-34191
- Integrated structural tailoring and adaptive control of advanced flight vehicle structural vibration [AIAA PAPER 93-1697] p 757 A93-34219
- Active rib experiment for shape control of an adaptive wing [AIAA PAPER 93-1700] p 712 A93-34222
- Single-impact calibrated electromagnetic tightening of long-life bolted joints in aviation structures p 745 A93-35277
- Effect of a combination of design and process-related factors on the fatigue strength of bolted joints in acoustically loaded aircraft structures p 745 A93-35278
- High-strength combination fasteners for joint assembly in aircraft structures p 745 A93-35283
- A method for estimating the survivability of bodies of revolution p 745 A93-35287
- Stress-strain state of the elements of a single-stringer riveted panel p 746 A93-35288
- Effect of overloads on the service life of the structural elements of aircraft p 746 A93-35289
- Thermoplastic applications in helicopter components p 796 A93-35952
- New developments in organized wire systems p 764 A93-35973
- Nonlinear analysis of composite thin-walled helicopter blades p 827 A93-36006
- Stress-strain analysis and optimal design of aircraft structures p 827 A93-36782
- Methodology for studying the fracture of aircraft structures in static tests p 801 A93-36785
- Problems of the organization of the mass testing of large structural elements of aircraft using testing machines p 821 A93-36791
- Load-bearing capacity of an aircraft wing based on the condition of compressed surface fracture p 801 A93-36794
- Optimal design of honeycomb sandwich shell aircraft structures of composite materials p 828 A93-36800
- Flight Deflection Measurement System p 808 A93-37885
- Modal identification of aircraft structures - ONERA methods [ONERA, TP NO. 1992-86] p 802 A93-38570
- Activities of the GARTEUR high lift research program [ONERA, TP NO. 1992-152] p 803 A93-38731
- The limit model of a thin strip exhibiting two delaminations [ONERA, TP NO. 1992-212] p 832 A93-38764
- Theory of the machining of polyhedral holes by plunge cutting p 835 A93-39091
- Hardening/finishing treatment of compressor blades using a machine with planetary container motion p 835 A93-39102
- The minimal multiplier method in calculations of the stability, limiting vibration cycles, and limiting states of nonlinearly deformed structures p 836 A93-39176
- Alternative approximations for integrated control/structure aeroservoelastic synthesis p 819 A93-39418
- Mechanical damage to aircraft structures from lightning strikes p 879 A93-40432
- A software for optimum design of an aircraft structure p 938 A93-40495
- Creep crack growth and tail part behavior of low alloy steels and Ni based super alloy p 916 A93-40808
- Selection of the primary aircraft structure at the preliminary design stage p 891 A93-42371
- Comparison of some direct multi-point force appropriation methods p 928 A93-43338
- Design of aircraft, helicopters, and aviation engines — Russian book [ISBN 5-277-01192-7] p 947 A93-44508
- Structural integrity of aging airplanes [ISBN 0-540-53461-X] p 947 A93-45772
- Structural integrity of aging airplanes - A perspective p 948 A93-45783
- Test facility for evaluation of structural integrity of stiffened and jointed aircraft curved panels p 1012 A93-45794
- Problems of the strength and fatigue of the elements of aircraft structures p 1029 A93-47076
- Coupling conditions for substructures with varying idealization p 1029 A93-47078
- A study of the effect of the support fastening compliance on the stress-strain state of aircraft transparencies p 997 A93-47079
- An analytical-experimental method for studying the strength and stability of thin-walled structures p 1029 A93-47084
- Aircraft with single axis aerodynamically deployed wings [AIAA PAPER 93-3673] p 1129 A93-48350
- Problems in the aerodynamics of flight vehicles and their parts p 1068 A93-48901
- Composite airframe structures. Practical design information and data — Book [ISBN 962-7128-06-6] p 1100 A93-49105
- Advanced composite fiber/metal pressure vessels for aircraft applications [AIAA PAPER 93-2248] p 1155 A93-50047

- Carbon composite repairs of helicopter metallic primary structures p 1101 A93-50429
- On design methods for bolted joints in composite aircraft structures p 1158 A93-50430
- Main directions of improving the quality of aluminum-lithium alloys for welded aircraft structures p 1146 A93-51104
- Calculation of aerodynamic loads on the wing of rigid and elastic aircraft with allowance for load correction from experimental data p 1103 A93-51905
- Eddy current inspection of open fastener holes in aluminum aircraft structure p 1160 A93-52167
- [SAE ARP 4402] Stringer peeling effects at stiffened composite panels in the postbuckling range p 1160 A93-52453
- Nonlinear deformation mechanics of multilayer transparency elements - Some calculation results - for aircraft portholes p 1191 A93-52937
- A nonlinear finite element of an arbitrary beam p 1215 A93-52939
- A study of optical distortions arising in radiation transmission through cavities with gas flow around them p 1225 A93-52945
- Design and fabrication of panels with cutouts p 1215 A93-52973
- A procedure for the thermal and strength testing of radiotransparent shells p 1209 A93-52976
- A finite element for modeling skins of composite materials p 1215 A93-52979
- Evaluation of water-borne adhesive bonding primers for use on the advanced aircraft material aluminum-lithium p 1211 A93-53420
- 3-D braided preforms; cost to manufacture: Magnawave. I - Identifying cost factors p 1226 A93-53423
- Structural applications of Avimid K3B LDF thermoplastic composites - for advanced aircraft p 1216 A93-53429
- Development of computational solid mechanics and its application in aerospace engineering p 1255 A93-54419
- Optimization of sandwich structures with respect to local instabilities with MBB-LAGRANGE p 1255 A93-54540
- AIAA Lighter-Than-Air Systems Technology Conference, 10th, Scottsdale, AZ, Sept. 14-16, 1993, Technical Papers p 1229 A93-54601
- Zeppelin NT - A new concept in airship technology, based on rigid airship principles [AIAA PAPER 93-4045] p 1242 A93-54612
- NDT for corrosion in aerospace structures - A review of NDT techniques p 1258 A93-54897
- The inspection of aeronautical structures using transient thermography p 1258 A93-54899
- International Congress on Recent Developments in Air- and Structure-Borne Sound and Vibration, 2nd, Auburn Univ., AL, Mar. 4-6, 1992, Proceedings, Vols. 1-3 p 1259 A93-55851
- Structural-acoustic coupling in aircraft fuselage structures p 1243 A93-55856
- Response variability observed in reverberant acoustic test of a model aerospace structure p 1264 A93-55857
- Noise and vibration analysis in propeller aircraft by advanced experimental modeling techniques p 1264 A93-55862
- Passive damping technology p 1259 A93-55866
- An evaluation of a method of reconstituting fatigue loading from Rainflow counting [RAE-TR-89057] p 82 A93-10198
- Magneto-optic imaging inspection of selected corrosion specimens [DOT/FAA/CT-TN92/20] p 88 A93-11617
- DYNAC: A computer program for analyzing the dynamical stability of aircraft [REPT-B-31] p 66 A93-12415
- Probabilistic evaluation of fuselage-type composite structures [NASA-TM-105881] p 212 A93-12735
- Structural fatigue aspects of the P-3 Orion [ARL-STRUC-TM-558] p 161 A93-13256
- Hermetic sealing and EMI shielding gasket [AD-D015359] p 199 A93-13414
- Optimum design of aircraft structures with manufacturing and buckling constraints p 162 A93-13815
- Hypersonic panel flutter in a rarefied atmosphere p 188 A93-13928
- Stress corrosion susceptibility of ultra-high strength steels for Naval aircraft applications [AD-A256126] p 199 A93-15189
- Development of a menu driven materials data base for use on personal computers: Aircraft structures technical memorandum [AD-A256317] p 392 A93-16403
- Dual-band infrared imaging applications: Locating buried minefields, mapping sea ice, and inspecting aging aircraft [DE93-000516] p 453 A93-17225
- Practical architecture of design optimization software for aircraft structures taking the MBB-LAGRANGE code as an example [MBB-FE-251-S-PUB-479] p 331 A93-17565
- Statistical fatigue analysis of the SH-60B servo beam rail component [AD-A257474] p 332 A93-17660
- Design of the advanced regional aircraft, the DART-75 [NASA-CR-192044] p 333 A93-17972
- Study of statistical variations of load spectra and material properties on aircraft fatigue life [AD-A257961] p 339 A93-18451
- Formulation of a structural model for flutter analysis of low aspect ratio composite aircraft wings p 372 A93-19019
- Lumped mass modelling for the dynamic analysis of aircraft structures p 510 A93-19460
- Topological approach for the study of electromagnetic coupling [ONERA-P-1992-2] p 551 A93-20230
- YIDOUY and its application to aircraft design [AD-A259262] p 513 A93-20605
- MSC/NASTRAN structure optimization test module version 67 (preliminary) p 554 A93-20907
- REPT-5-191025 p 554 A93-20907
- Selection criteria for metallic high temperature structural materials in hypersonic flying equipment [MBB-LME-221-HYPAC-PUB-2-A] p 515 A93-21479
- Damage detection by Acousto-Ultrasonic Location (AUL) p 555 A93-21529
- Crashworthiness of composite seats for civil aircraft p 703 A93-24773
- Numerical modelling of induced effects of lightning strike on an all composite helicopter p 703 A93-24879
- A procedure for defining lightning risk to air vehicles p 703 A93-24885
- Comparison of the damage for various types of fibre reinforced composites due to different lightning test standards (MIL-STD-1757A, German military VG-standard 96903) p 736 A93-24891
- Grid sensitivity for aerodynamic optimization and flow analysis [NASA-CR-192980] p 694 A93-25117
- Design and analysis of curved composite components for rotorcraft fuselage frames p 716 A93-25701
- Hydrogen-induced stress corrosion cracking susceptibility analysis of pitch links from the AH-64 Apache helicopter [AD-A260692] p 736 A93-25895
- Thermally induced stresses in a composite exposed to fire [AD-A261714] p 737 A93-26371
- Probabilistic assessment of composite structures [NASA-TM-106024] p 825 A93-27092
- Numerical modeling of runback water on ice protected aircraft surfaces p 840 A93-27438
- Reliability assessment at airline inspection facilities. Volume 2: Protocol for an eddy current inspection reliability experiment [DOT/FAA/CT-92/12-VOL-2] p 842 A93-28685
- Nonlinear analyses of composite aerospace structures in sonic fatigue [NASA-CR-193124] p 930 A93-29154
- Advanced technology composite aircraft structures [NASA-CR-190420] p 894 A93-29498
- The Ultra Light Aircraft Testing [NASA-CR-193043] p 895 A93-29774
- Report on the test set-up for the structural testing of the Airmass Sunburst Ultralight Aircraft p 895 A93-29775
- Static and dynamic large deflection flexural response of graphite-epoxy beams [NASA-CR-4118] p 934 A93-30374
- Composites: A viable option p 918 A93-30429
- Advanced composite structural concepts and material technologies for primary aircraft structures p 918 A93-30430
- Composites technology for transport primary structure p 918 A93-30431
- Design, analysis, and fabrication of the technology integration box beam p 919 A93-30433
- Structural evaluation of curved stiffened composite panels fabricated using a THERM-Xsm process p 919 A93-30435
- Resin transfer molding for advanced composite primary aircraft structures p 919 A93-30438
- Consolidation of graphite thermoplastic textile preforms for primary aircraft structure p 919 A93-30439
- F-15 composite engine access door p 920 A93-30442
- First NASA Advanced Composites Technology Conference, part 2 [NASA-CP-3104-PT-2] p 921 A93-30841
- Advanced fiber/matrix material systems p 921 A93-30854
- Multi-parameter optimization tool for low-cost commercial fuselage crown designs p 922 A93-30858
- Design and analysis of grid stiffened concepts for aircraft composite primary structural applications p 922 A93-30861
- Optimization of composite sandwich cover panels subjected to compressive loadings p 922 A93-30862
- Advanced fiber placement of composite fuselage structures p 923 A93-30864
- Structural response of bead-stiffened thermoplastic shear webs p 923 A93-30873
- An overview of the crash dynamics failure behavior of metal and composite aircraft structures p 923 A93-30875
- Construction and testing of simple airfoils to demonstrate structural design, materials choice, and composite concepts p 879 A93-30979
- Consideration of impact damages by dimensioning CFC (Carbon Fiber Reinforced Composites) components [MBB-FE-221-S-PUB-0501] p 1018 A93-31044
- Aircraft structures in 2000: A technological challenge? [MBB-LME-202-S-PUB-0485] p 998 A93-31058
- Computational methods for aerodynamic design of aircraft components [NLR-TP-92072-4] p 987 A93-31148
- NASA-JVA Light Aerospace Alloy and Structures Technology Program (LA2ST) [NASA-CR-193412] p 1019 A93-31739
- AIRCRAFT SURVIVABILITY**
- Battle damage repairs p 239 A93-22698
- Advanced composite helicopter MISERS GOLD test/analysis p 508 A93-27974
- Applications of stress envelope concepts to aircraft EMP and lightning survivability p 704 A93-24898
- AIRCRAFT TIRES**
- Braking, steering, and wear performance of radial-belted and bias-ply aircraft tires [SAE PAPER 921036] p 158 A93-14656
- High speed aircraft tire dynamics/issues [SAE PAPER 921037] p 158 A93-14657
- Determination of tire-wheel interface pressure distribution for aircraft wheels [AIAA PAPER 93-1343] p 709 A93-33913
- Wheel and brake design and test requirements for military aircraft [SAE ARP 1493] p 1103 A93-52165
- AIRCRAFT WAKES**
- An aerodynamic model of multiple lifting surfaces including wake deformation and tip effect p 10 A93-12366
- Active aerodynamic control of wake-airfoil interaction noise - Experiment p 445 A93-19153
- Active aerodynamic control of wake-airfoil interaction noise - Theory p 445 A93-19154
- Numerical analysis of acoustic effect of rotor wakes in rotor-stator interaction p 447 A93-19182
- Wake ingestion propulsion benefit p 411 A93-21660
- Doppler global velocimetry measurements of the vortical flow above an F/A-18 [AIAA PAPER 93-0414] p 415 A93-23333
- Estimation of unsteady lift on a pitching airfoil from wake velocity surveys [AIAA PAPER 93-0437] p 286 A93-23351
- Experimental investigation of rotor/lifting surface interactions [AIAA PAPER 93-0871] p 469 A93-24932
- A new method for improved rotor free-wake convergence [AIAA PAPER 93-0872] p 469 A93-24933
- Potential hazard of aircraft wake vortices in ground effect with crosswind p 479 A93-28606
- The influence of quadrupole sources in the boundary layer and wake of a blade on helicopter rotor noise p 566 A93-29410
- Decay of aircraft vortices near the ground p 961 A93-45751
- An investigation of the effects of a rear stagnation jet on the wake behind a cylinder [AIAA PAPER 93-3274] p 969 A93-46835
- Computation of wake roll-up for complete aircraft configurations [AIAA PAPER 93-3509] p 984 A93-47275
- Attenuation of airplane wake vortices by excitation of far-field instability [AIAA PAPER 93-3511] p 984 A93-47277
- Measurements in 80- by 120-foot wind tunnel of hazard posed by lift-generated wakes [AIAA PAPER 93-3518] p 1014 A93-47281

Computation of wake/exhaust mixing downstream of advanced transport aircraft
[AIAA PAPER 93-2944] p 1162 A93-48141

Elliptic cross section tip effects on the vortex wake of an axisymmetric body at angle of attack
[AIAA PAPER 93-2960] p 1124 A93-48154

Simulation of DD-963 ship airwake by Navier-Stokes method
[AIAA PAPER 93-3002] p 1053 A93-48192

Wake-vortex structure from lift and torque induced on a following wing
[AIAA PAPER 93-3013] p 1054 A93-48202

The challenges of simulating wake vortex encounters and assessing separation criteria
[AIAA PAPER 93-3568] p 1096 A93-49518

Active aerodynamic control of wake-airfoil interaction noise - Experiment p 1225 A93-53206

Construction of wakes in the discrete vortex method p 1179 A93-53333

Estimation of unsteady lift on a pitching airfoil from wake velocity surveys
[NASA-TM-105947] p 138 A93-14791

Proceedings of the Aircraft Wake Vortices conference, volume 1
[PB93-126449] p 485 A93-21796

Proceedings of the Aircraft Wake Vortices conference, volume 2
[PB93-127728] p 559 A93-21799

Determination of surface heat transfer and film cooling effectiveness in unsteady wake flow conditions p 902 A93-29933

Vortex wake characteristics of B757-200 and B767-200 aircraft using the tower fly-by technique
[PB93-180255] p 878 A93-30387

Vortex wake characteristics of B757-200 and B767-200 aircraft using the tower fly-by technique
[PB93-180263] p 878 A93-30388

AIRFIELD SURFACE MOVEMENTS

Alternative approach routes to runway 24 at Oslo Airport, Fornebu p 487 A93-28481

Spanwise aileron oscillations p 819 A93-39190

The evolution of a nose-wheel steering system p 995 A93-44852

Using spectral analysis for estimating the effect of runway irregularities on the loading of transport aircraft structures p 996 A93-45669

Protection of taxiing traffic in airports through mode S secondary radar technology
[ETN-93-93455] p 791 A93-28206

Testing concept of a taxiing control system, summary p 1010 A93-31278

AIRFOIL OSCILLATIONS

The effect of wind tunnel constraint on unsteady aerodynamics experiments p 190 A93-14300

Separation control and lift enhancement on airfoil using unsteady excitations p 118 A93-14305

Prediction and control of slender-wing rock p 182 A93-14331

Flow structures around a constant-rate pitching airfoil and mechanism of dynamic stall p 118 A93-14332

Leading edge vortices in a chordwise periodic flow p 119 A93-14333

Unsteady transonic aerodynamic loadings on the airfoil caused by heaving, pitching oscillations and control surface p 126 A93-15627

A finite element study of incompressible flows past oscillating cylinders and aerofoils p 241 A93-17750

Some asymptotic aspects of the nonstationary airfoil theory p 259 A93-19966

A unified model for rotating stall and surge p 259 A93-20119

Air flow dynamics around an aerofoil by the stabilized finite difference method p 266 A93-20741

Experimental study of dynamic stall on an oscillating airfoil p 266 A93-20804

Transitional characteristics of vortices issued from a body which creates asymmetric flow field - In a case of thin symmetrical airfoil with angle of attack under rotational oscillation of small amplitude p 267 A93-20923

Single passage Euler analysis of oscillating cascade unsteady aerodynamics for arbitrary interblade phase angle
[AIAA PAPER 93-0389] p 282 A93-23067

A study of flow separation on an oscillating flap at Mach number 2.4
[AIAA PAPER 93-0436] p 286 A93-23350

Estimation of unsteady lift on a pitching airfoil from wake velocity surveys
[AIAA PAPER 93-0437] p 286 A93-23351

Active control of the shear layer on a static airfoil
[AIAA PAPER 93-0442] p 286 A93-23353

Corrections to fringe distortion due to flow density gradients in optical interferometry
[AIAA PAPER 93-0631] p 539 A93-24748

Comparison of PMARC and analytic results for two-dimensional unsteady airfoils p 463 A93-24752

[AIAA PAPER 93-0636] p 463 A93-24752

Structure-attached corotational fluid grid for transient aeroelastic computations p 480 A93-29326

Studies of the dynamic stall problem on airfoils p 681 A93-33747

Nonplanar Doublet-Point method for supersonic unsteady aerodynamics
[AIAA PAPER 93-1588] p 682 A93-34120

The role of Kutta waves on oscillatory shock motion on an airfoil experiencing heavy buffeting
[AIAA PAPER 93-1589] p 682 A93-34121

Effect of an unsteady three-dimensional wake on elastic blade-flapping eigenvalues in hover p 683 A93-34260

Vortex initiation during dynamic stall of an airfoil p 684 A93-34335

Influence of coupling incidence and velocity variations on the airfoil dynamic stall p 767 A93-35999

Velocity and vorticity distributions over an oscillating airfoil under compressible dynamic stall p 778 A93-39403

Unsteady transonic two-dimensional Euler solutions using finite elements p 778 A93-39412

Low-frequency flow oscillation over airfoils near stall p 861 A93-41931

Subsonic/transonic cascade flutter using a full-potential solver p 861 A93-41934

Newtonian and hypersonic flows over oscillating bodies of revolution. II - Parabolic bodies p 872 A93-42931

Virtual zone Navier-Stokes computations for oscillating control surfaces
[AIAA PAPER 93-3363] p 955 A93-45056

Time-accurate simulation of a self-excited oscillatory supersonic external flow with a multi-block solution-adaptive mesh algorithm
[AIAA PAPER 93-3387] p 956 A93-45078

An acceleration technique for time accurate calculations --- of unsteady flow around pitching delta wings p 957 A93-45092

The effects of forced oscillations on the performance of airfoils
[AIAA PAPER 93-3264] p 968 A93-46829

Vortex capture by a two-dimensional airfoil with a small oscillating leading-edge flap
[AIAA PAPER 93-3266] p 968 A93-46830

Control of the dynamic-stall vortex over a pitching airfoil by leading-edge suction
[AIAA PAPER 93-3267] p 969 A93-46832

Unsteady aerodynamic response of two-dimensional subsonic and supersonic oscillating cascades with chordwise displacement and flexible deformation p 971 A93-46922

Numerical simulation of wing-wall juncture flow for a pitching wing
[AIAA PAPER 93-3401] p 974 A93-47203

Separated flowfield and lift on an airfoil with an oscillating leading-edge flap
[AIAA PAPER 93-3422] p 976 A93-47217

The moving wall effect vis-a-vis other dynamic stall flow mechanisms
[AIAA PAPER 93-3424] p 1008 A93-47219

Effect of canard oscillations on the vortical flowfield of a X-31A-like fighter model in dynamic motion
[AIAA PAPER 93-3427] p 1008 A93-47222

Precise pitching airfoil computations by use of dynamic unstructured meshes
[AIAA PAPER 93-2971] p 1049 A93-48165

Transition effects on compressible dynamic stall of transiently pitching airfoils
[AIAA PAPER 93-2978] p 1050 A93-48171

Order reduction of aeroelastic models through LK transformation and Riccati iteration
[AIAA PAPER 93-3795] p 1159 A93-51388

Implicit schemes for unsteady Euler equations on unstructured meshes
[ONERA, TP NO. 1993-64] p 1171 A93-51944

A summary of further measurements of steady and oscillatory pressures on a rectangular wing p 1096 A93-52594

A preliminary investigation of the control of separated flow by means of excitation p 1182 A93-53859

Forcing function modeling for flow induced vibration
[ISABE 93-7027] p 1196 A93-54003

The unsteady flow past a supersonic splitter plate
[ISABE 93-7047] p 1185 A93-54023

Reynolds stress profiles in the near wake of an oscillating airfoil p 1236 A93-55380

Interaction of compressible vortices with a rigid plate p 1239 A93-56219

A comparative study of semi-empirical dynamic stall models p 18 A93-10544

New acceleration potential method for supersonic unsteady aerodynamics of lifting surfaces, further extension of the nonplanar supersonic doublet point method, and nonlinear, nongradient optimized rational function approximations for supersonic, transient response unsteady aerodynamics p 25 A93-12344

Estimation of unsteady lift on a pitching airfoil from wake velocity surveys
[NASA-TM-105947] p 138 A93-14791

A computational and experimental investigation of the propulsive and lifting characteristics of oscillating airfoils and airfoil combinations in incompressible flow
[AD-A258019] p 294 A93-17819

Spurious frequencies as a result of numerical boundary treatments p 839 A93-27170

Airfoil stability in turbulent flow p 781 A93-27212

AIRFOIL PROFILES

Review of the normal force fluctuations of aerofoils with separated flow p 10 A93-12317

Dynamic characteristics of an airfoil at high speed change of pitch angle p 10 A93-12324

Use of NASA LS (1) general aviation airfoil for a small wind turbine - An experience in Denmark p 92 A93-12364

A method for calculating flow past an arbitrary airfoil profile in the presence of flow separation p 13 A93-12807

Multi-point design of transonic airfoils using optimization
[AIAA PAPER 92-4225] p 16 A93-13382

Computer aided aerodynamic design of high pressure axial flow fan blade element p 16 A93-13649

Accelerated method of the Euler equation solution in transonic airfoil flow problem p 113 A93-14193

Generalized multipoint inverse airfoil design p 122 A93-14541

Hybrid grid approach to study dynamic stall p 122 A93-14548

Integral equations in the problem of flow past an airfoil p 395 A93-18243

Improvement of high-AOA airfoil stalling performance by internal acoustic excitation p 243 A93-19134

Active aerodynamic control of wake-airfoil interaction noise - Experiment p 445 A93-19153

A statistical approach to the experimental evaluation of transonic turbine airfoils in a linear cascade
[ASME PAPER 92-GT-5] p 245 A93-19278

Aerodynamic design of pivotable nozzle vanes for radial-inflow turbines
[ASME PAPER 92-GT-94] p 349 A93-19340

Forcing function effects on unsteady aerodynamic gust response. II - Low solidity airfoil row response
[ASME PAPER 92-GT-175] p 251 A93-19401

Incidence angle and pitch-chord effects on secondary flows downstream of a turbine cascade
[ASME PAPER 92-GT-184] p 251 A93-19409

An experimental study of heat transfer in a large-scale turbine rotor passage
[ASME PAPER 92-GT-195] p 403 A93-19420

Prescribed-curvature-distribution airfoils for the preliminary geometric design of axial-turbomachinery cascades
[ASME PAPER 92-GT-366] p 257 A93-19530

Erosion resistant titanium nitride coating for turbine compressor applications
[ASME PAPER 92-GT-417] p 388 A93-19565

Investigation of leading edge ice accretion with cyclical pneumatic boot inflation
[AIAA PAPER 93-0007] p 306 A93-20130

The problem of dynamic stall simulation revisited
[AIAA PAPER 93-0091] p 264 A93-20197

An efficient approach to optimal aerodynamic design. I - Analytic geometry and aerodynamic sensitivities
[AIAA PAPER 93-0099] p 264 A93-20204

A multi-point optimization for transonic airfoil design
[AIAA PAPER 92-4681] p 264 A93-20303

A new technique for analysis of unsteady aerodynamic responses of cascade airfoils with blunt leading edge. I - Theory p 267 A93-20909

A gridless Euler/Navier-Stokes solution algorithm for complex-aircraft applications
[AIAA PAPER 93-0333] p 268 A93-21107

Tracking of raindrops in flow over an airfoil
[AIAA PAPER 93-0168] p 275 A93-22602

The effect of Reynolds number and turbulence on airfoil aerodynamics at -90 degrees incidence
[AIAA PAPER 93-0206] p 277 A93-22624

Shock-dependent, thrust wings for supersonic flow
[AIAA PAPER 93-0321] p 280 A93-23013

Unsteady compressible airfoil aerodynamics using an adaptive time-discontinuous GLS finite element method
[AIAA PAPER 93-0339] p 281 A93-23027

Preliminary assessment of tunnel wall interference in the NDA cryogenic wind tunnel
[AIAA PAPER 93-0421] p 285 A93-23340

- Experimental investigation of a 2D parallel vortex/airfoil interaction p 538 A93-23808
- Effect of leading-edge porosity on blade-vortex interaction noise [AIAA PAPER 93-0601] p 563 A93-24727
- Numerical investigations on airfoil performance subjected to aerodynamic interference from an upstream airfoil [AIAA PAPER 93-0639] p 463 A93-24754
- Development of circulation control technology for application to advanced subsonic transport aircraft [AIAA PAPER 93-0644] p 464 A93-24759
- Navier-Stokes computations and experimental comparisons for multielement airfoil configurations [AIAA PAPER 93-0645] p 464 A93-24760
- Hysteresis effects on wind tunnel measurements of a two-element airfoil [AIAA PAPER 93-0646] p 464 A93-24761
- A physically guided zonal approach for two-dimensional airfoil flows [AIAA PAPER 93-0790] p 468 A93-24869
- Numerical simulation of vortex generation and capture above an airfoil [AIAA PAPER 93-0864] p 468 A93-24926
- Euler study on porous transonic airfoils with a view toward multipoint design p 479 A93-28604
- Backward bifurcation for structural divergence of a wing section p 526 A93-29351
- Experimental study of a single strong vortex-airfoil interaction p 481 A93-29432
- Airfoil shape optimization using sensitivity analysis on viscous flow equations p 682 A93-33755
- An analysis of the post-instability behaviour of a two-dimensional airfoil with a structural nonlinearity [AIAA PAPER 93-1474] p 726 A93-34020
- Experimental unsteady pressures at flutter on the Supercritical Wing Benchmark Model [AIAA PAPER 93-1592] p 683 A93-34123
- Computation of viscous transonic airfoil flows using eddy-viscosity based turbulence models p 687 A93-34360
- Transonic flow around the leading edge of a thin airfoil with a parabolic nose p 688 A93-34405
- Calculation of compressible boundary layers by a hybrid finite element method p 692 A93-35613
- Nonequilibrium turbulence modeling study on light dynamic stall of a NACA0012 airfoil p 768 A93-37379
- Effect of the thermodynamic air model on the aerodynamic characteristics of profiles with bends p 776 A93-39136
- Subsonic natural-laminar-flow airfoils p 860 A93-41780
- Calculation of optimum airfoils using direct solutions of the Navier-Stokes equations [AIAA PAPER 93-3323] p 952 A93-45017
- Numerical experiment of the flight trajectory simulation by fluid dynamics and flight dynamics coupling [AIAA PAPER 93-3324] p 952 A93-45018
- Initial acceleration effects on flow evolution around airfoils pitching to high angles of attack p 961 A93-45750
- Comment on "Flow near the trailing edge of an airfoil" p 961 A93-45754
- Kinematic domain decomposition for boundary-motion-induced flow simulations p 1028 A93-46811
- A multiblock, multigrid solution procedure for multielement airfoils p 967 A93-46812
- Comparative wind tunnel tests at high Reynolds numbers of NACA 64 621 airfoils with two aileron configurations p 967 A93-46823
- On the construction and calculation of optimal nonlifting critical airfoils p 969 A93-46857
- Numerical analysis of airfoil cascades subjected to unsteady flow p 972 A93-46944
- High lift multiple element airfoil analysis with unstructured grids [AIAA PAPER 93-3478] p 981 A93-47256
- A computational method for inverse design of transonic airfoil and wing [AIAA PAPER 93-3482] p 982 A93-47260
- Multiple solutions of the transonic perturbation equation p 987 A93-47331
- Solution of the Euler equations for airfoils using asymptotic methods [AIAA PAPER 93-2931] p 1045 A93-48130
- Vortex developments over steady and accelerated airfoils incorporating a trailing edge jet [AIAA PAPER 93-3008] p 1054 A93-48198
- Design efficiency evaluation for transonic airfoil optimization - A case for Navier-Stokes design [AIAA PAPER 93-3112] p 1062 A93-48282
- Demonstration of multipoint design procedures for transonic airfoils [AIAA PAPER 93-3114] p 1062 A93-48284
- Shape optimization for aerodynamic efficiency and low observability [AIAA PAPER 93-3115] p 1062 A93-48285
- Flowfield measurements about a multi-element airfoil at high Reynolds numbers [AIAA PAPER 93-3137] p 1064 A93-48300
- A wake singularity potential flow model for airfoils experiencing trailing-edge stall p 1067 A93-48544
- Upwind finite-volume Navier-Stokes computations on unstructured triangular meshes p 1070 A93-49011
- Verification of the TOTLOS method for calculating aerodynamic loss in film-cooled turbine cascade p 1087 A93-51191
- Spline-collocation solution of a Fredholm equation of the second kind in the problem of flow past an airfoil p 1092 A93-51904
- Unsteady aerodynamic behavior of an airfoil with and without a slat p 1093 A93-52007
- Computation of subsonic viscous and transonic viscous-inviscid unsteady flow p 1094 A93-52012
- Efficient simulation of incompressible viscous flow over single and multielement airfoils p 1095 A93-52448
- Active aerodynamic control of wake-airfoil interaction noise - Experiment p 1225 A93-53206
- Effects of turn region treatments on pressure loss through sharp 180-degree bends p 1256 A93-54636
- An airfoil in transonic flow in the presence of wind gusts and weak shock waves p 1233 A93-55015
- A numerical study of aerodynamic wing design for supercritical conditions of an advanced training and military aircraft p 1238 A93-56213
- Determination of the transonic flow field around an airfoil section for a given lift force coefficient p 1239 A93-56215
- The convection speed of the dynamic stall vortex [AD-A247258] p 21 N93-11464
- Further buffering tests in a cryogenic wind tunnel [NASA-TM-107621] p 22 N93-11610
- Overall effects of separation on thin airfoils [ISBN-0-315-67464-4] p 135 N93-13930
- Computational investigations of a NACA 0012 airfoil in low Reynolds number flows [AD-A257300] p 288 N93-15920
- The aerodynamic characteristics of the Gottingen 797 and Wortmann FX63-137 airfoil sections at very low Reynolds numbers [ETN-93-92999] p 295 N93-18128
- Numerical investigation of swirl-airfoil interactions in transonic area [MPIS-8/1991] p 297 N93-18627
- Aerodynamics of a finite wing with simulated ice p 784 N93-27437
- Computational methods for aerodynamic design of aircraft components [NLR-TP-92072-4] p 987 N93-31148
- ### AIRFOILS
- Finite memory approximations for a singular neutral system arising in aeroelasticity p 97 A93-13246
- Turbulence modelling requirements for the prediction of viscous transonic airfoil flows p 115 A93-14249
- Performance degradation due to hoar frost on lifting surfaces p 305 A93-17798
- Periodic Euler and Navier-Stokes solutions about oscillating airfoils p 241 A93-17799
- Effect of airfoil porosity on the shock wave position and intensity at transonic velocities p 241 A93-18222
- Hot streaks and phantom cooling in a turbine rotor passage. I - Separate effects [ASME PAPER 92-GT-75] p 401 A93-19325
- An inviscid-viscous interaction approach to the calculation of dynamic stall initiation on airfoils [ASME PAPER 92-GT-128] p 249 A93-19362
- Numerical solutions for unsteady subsonic vortical flows around loaded cascades [ASME PAPER 92-GT-173] p 250 A93-19399
- Effects of icing on the aerodynamic performance of high lift airfoils [AIAA PAPER 93-0026] p 259 A93-20144
- Flow visualization studies on sidewall effects in two dimensional transonic airfoil testing [AIAA PAPER 93-0090] p 263 A93-20196
- An efficient approach to optimal aerodynamic design. II - Implementation and evaluation [AIAA PAPER 93-0100] p 264 A93-20205
- Development of a Shape-controlled airfoil by use of SMA --- Shape Memory Alloys p 411 A93-21739
- Unsteady laminar separation on low-Reynolds-number airfoils [AIAA PAPER 93-0209] p 278 A93-22627
- Numerical modeling of anti-icing systems and comparison to test results on a NACA 0012 airfoil [AIAA PAPER 93-0170] p 327 A93-23242
- The design of optimized airfoils in subcritical flow [AIAA PAPER 93-0532] p 285 A93-23273
- Estimation of unsteady lift on a pitching airfoil from wake velocity surveys [AIAA PAPER 93-0437] p 286 A93-23351
- Initial acceleration effects on the flow field development around rapidly pitching airfoils [AIAA PAPER 93-0438] p 286 A93-23352
- Effect of sidewall suction on flow in two-dimensional wind tunnels p 287 A93-23538
- Modeling, analysis, and prediction of flutter at transonic speeds The effect of Reynold's number on a natural low frequency flow oscillation over an airfoil near stall [AIAA PAPER 92-4040] p 463 A93-24489
- Lift enhancement of an airfoil using a Gurney flap and vortex generators [AIAA PAPER 93-0647] p 464 A93-24762
- Airfoil design using the Navier-Stokes equations [AIAA PAPER 93-0648] p 464 A93-24763
- Two-dimensional Navier-Stokes analysis of high-lift multi-element airfoils using the q-omega turbulence model [AIAA PAPER 93-0679] p 466 A93-24787
- Pressure measurements on a pitching airfoil in a water channel [AIAA PAPER 93-0184] p 473 A93-25510
- Oscillatory blowing, a tool to delay boundary layer separation [AIAA PAPER 93-0440] p 474 A93-25529
- Physics of forced unsteady flow for a NACA 0015 airfoil undergoing constant-rate pitch-up motion p 478 A93-27922
- Karman vortex street-airfoil interaction p 678 A93-33703
- An experimental study on location of transitional separation bubble on a low Reynolds numbers airfoil p 680 A93-33725
- On the principle of sidewall effects on airfoil testing p 730 A93-33732
- Calculation of the flow around a high-lift airfoil using an explicit code and an algebraic Reynolds stress model p 685 A93-34344
- Results of a low power ice protection system test and a new method of imaging data analysis p 795 A93-35932
- Rotor blade airfoil design by numerical optimization and unsteady calculations [ONERA, TP NO. 1992-65] p 766 A93-35993
- Initial lift approximations for two-dimensional subsonic flow as obtained from oscillatory measurements p 768 A93-37385
- Integrated structure/control/aerodynamic synthesis of actively controlled composite wings p 818 A93-37392
- Permeable airfoils in incompressible flow p 768 A93-37401
- Turbulent flow simulation around the airfoil with pseudo-compressibility p 830 A93-38155
- Navier-Stokes stall predictions using an algebraic Reynolds-stress model p 778 A93-39260
- Comparison of numerical methods in transonic aerodynamics p 864 A93-42446
- On the construction and calculation of optimal nonlifting critical airfoils p 969 A93-46857
- A Laplace interaction law for the computation of viscous airfoil flow in low and high speed aerodynamics [AIAA PAPER 93-3462] p 979 A93-47244
- Prediction of stall and post-stall behavior of airfoils at low and high Reynolds numbers [AIAA PAPER 93-3502] p 983 A93-47270
- Investigation of flows in a controlled diffusion airfoil cascade passage p 1071 A93-49188
- Computational analysis of nonlinear aeroelastic phenomena during stall flutter of cascaded airfoils [AIAA PAPER 93-2082] p 1079 A93-49909
- A new technique for analysis of unsteady aerodynamic responses of cascade airfoils with blunt leading edge - Unsteady aerodynamic responses of the cascade in incompressible flow p 1086 A93-51122
- Navier-Stokes investigation of blunt trailing-edge airfoils using O grids p 1095 A93-52459
- Zonal-local solution method for the turbulent Navier-Stokes equations p 1177 A93-53205
- Impingement cooling with film coolant extraction in the airfoil leading edge regions [ISABE 93-7078] p 1220 A93-54054
- Calculation of real-gas effects on airfoil aerodynamic characteristics p 1229 A93-54477
- An inverse method with regularity condition for transonic airfoil design p 1230 A93-54583
- A method for aerodynamic calculation by placing linear vari-strength vortex panels on airfoil contour p 1231 A93-54597
- The body-fitted coordinates generation for multi-element airfoils p 1231 A93-54598
- Oscillatory blowing - A tool to delay boundary-layer separation p 1235 A93-55362

A prediction model for the vortex shedding noise from the wake of an airfoil or axial flow fan blades p 1265 A93-55995

Free streamline-boundary layer analysis for separated flow over an airfoil p 1239 A93-56327

Effect of passive flow-control devices on turbulent low-speed base flow p 82 N93-10304

A method of testing two-dimensional airfoils [AD-A253210] p 17 N93-10375

Nonlinear aeroelasticity of composite structures [AD-A254285] p 47 N93-10842

Boundary layer relaminarization device [NASA-CASE-LAR-14470-1] p 23 N93-11876

Dynamic analysis of a pre-and-post ice impacted blade [NASA-TM-105829] p 90 N93-12197

Fatigue in single crystal nickel superalloys [AD-A254603] p 74 N93-12237

An approach to constrained aerodynamic design with application to airfoils p 24 N93-12321

[NASA-TP-3260] p 24 N93-12321

Fatigue in single crystal nickel superalloys [AD-A254704] p 198 N93-12746

Airfoil-vortex interaction and the wake of an oscillating airfoil p 134 N93-13803

Solution of compressible Navier-Stokes equations using spectral methods on arbitrary two-dimensional domains p 218 N93-14041

Multi-point inverse design of isolated airfoils and airfoils in cascade in incompressible flow p 163 N93-14462

Direct prediction of a separation boundary for airfoils using a viscous-coupled calculation method [ESDU-92008] p 136 N93-14516

Estimation of unsteady lift on a pitching airfoil from wake velocity surveys p 138 N93-14791

[NASA-TM-105947] p 138 N93-14791

Numerical modeling of anti-icing systems and comparison to test results on a NASA 0012 airfoil [NASA-TM-105975] p 148 N93-15345

Maximum lift of wings with leading-edge devices and trailing-edge flaps deployed [ESDU-92031] p 290 N93-16522

Wind tunnel seeding particles for laser velocimeter p 292 N93-16770

Two- and three-dimensional blade vortex interactions [NASA-CR-177567] p 293 N93-16942

Fatigue in single crystal nickel superalloys [AD-A258038] p 393 N93-17704

A computational and experimental investigation of the propulsive and lifting characteristics of oscillating airfoils and airfoil combinations in incompressible flow [AD-A258019] p 294 N93-17819

Numerical calculations of separating flows around oscillating airfoil p 300 N93-19284

Numerical simulation of unsteady large scale separated flow around oscillating airfoil p 300 N93-19285

Application of the program profile for the design of low-speed, low-observable configuration airfoils [AD-A258842] p 305 N93-19364

The semi-discrete Galerkin finite element modelling of compressible viscous flow past an airfoil [NASA-CR-192161] p 483 N93-20018

Fatigue in single crystal nickel superalloys [AD-A259191] p 536 N93-20275

Unsteady Navier-Stokes method for accelerated moving airfoils with separation [DLR-FB-92-03] p 485 N93-21763

Combined experiment, phase 1 [DE93-000012] p 485 N93-21766

Swept wing attachment line contamination fence [NASA-CASE-LAR-13400-1] p 485 N93-22015

Aerodynamic foundations for use of unsteady aerodynamic effects in flight control p 695 N93-25274

Flow control of low heat load turbine airfoils [AD-A260941] p 724 N93-26219

Fatigue in single crystal nickel superalloys [AD-A261742] p 737 N93-26282

Stability investigations of airfoil flow by global analysis p 783 N93-27436

A composite structured/unstructured-mesh Euler method for complex airfoil shapes p 784 N93-27439

Experimental and computational ice shapes and resulting drag increase for a NACA 0012 airfoil p 784 N93-27440

Efficient simulation of incompressible viscous flow over multi-element airfoils p 784 N93-27443

An interactive boundary-layer approach to multielement airfoils at high lift p 785 N93-27445

Reynolds and Mach number effects on multielement airfoils p 785 N93-27446

Flow prediction over a transport multi-element high-lift system and comparison with flight measurements p 785 N93-27448

Investigation of forced unsteady separated flows using velocity-vorticity form of Navier-Stokes equations p 840 N93-27451

Dynamic airfoil stall investigations p 786 N93-27453

Prediction of airfoil stall using Navier-Stokes equations in streamline coordinates p 787 N93-27456

Development and testing of the Perseus proof-of-concept aircraft [DE93-010121] p 806 N93-28586

A demonstration of simple airfoils: Structural design and materials choices [DE93-007882] p 789 N93-28662

Development of an unstructured solution adaptive method for the quasi-three-dimensional Euler and Navier-Stokes equations [NASA-CR-193241] p 930 N93-29213

A parallel implicit incompressible flow solver using unstructured meshes [AD-A263395] p 931 N93-29851

Keynote address: Unsteady, multimode transition in gas turbine engines p 901 N93-29927

Determination of surface heat transfer and film cooling effectiveness in unsteady wake flow conditions p 902 N93-29933

Prediction of jet impingement cooling scheme characteristics (airfoil leading edge application) p 932 N93-29941

Construction and testing of simple airfoils to demonstrate structural design, materials choice, and composite concepts p 879 N93-30979

Definition of an airfoil family for the EUROFAR rotor [DLR-FB-92-04] p 998 N93-31197

The influence of variable flow velocity on unsteady airfoil behavior [DLR-FB-92-22] p 988 N93-31320

Fatigue in single crystal nickel superalloys [AD-A265451] p 1019 N93-31795

Review of aerodynamic design in the Netherlands [NLR-TP-91260-U] p 999 N93-31840

AIRFRAME MATERIALS

The development and evaluation of advanced Kevlar sandwich structure for application to rotorcraft airframes p 546 A93-27965

Evolution of permanent composite repair designs p 508 A93-27967

Novel approaches to complex geometry structure p 546 A93-27969

An experimental and analytical investigation on the response of GR/EP composite I-frames p 546 A93-27975

Composite airframe structures. Practical design information and data --- Book [ISBN 962-7128-06-6] p 1100 A93-49105

Fiber reinforced composites: A new class of glass and glass ceramic materials for thermomechanical applications [REPT-921-430-104] p 200 N93-15490

Review of aeronautical fatigue investigations in the Netherlands during the period March 1989 - March 1991 [NLR-TP-91092-U] p 331 N93-17535

Damage tolerance behaviour of aluminium-lithium sheet alloys [NLR-TP-91244-U] p 392 N93-17540

AIRFRAMES

Lockheed adopts media blast dry stripping for the C-130 [SAE PAPER 920949] p 107 A93-14092

RISK - Interactive multidisciplinary system for designing airframes p 226 A93-14337

Imaging flaws in thin metal plates using a magneto-optic device p 397 A93-18670

Concurrent optimization of airframe and engine design parameters [AIAA PAPER 92-4713] p 323 A93-20281

Analysis of the NASA Hypersonic Wing Test Structure [AIAA PAPER 92-4724] p 409 A93-20326

Recent advances in integrated multidisciplinary optimization of rotorcraft [AIAA PAPER 92-4777] p 325 A93-20369

Numerical forecasting of liquid water content to assess airframe icing risk p 429 A93-22147

Icing effects on aircraft stability and control determined from flight data - Preliminary results [AIAA PAPER 93-0398] p 370 A93-23073

An overview of shed ice impact studies in the NASA Lewis Icing Research Tunnel [AIAA PAPER 93-0301] p 283 A93-23247

The structure and material testing facility needed for future SST/HST development [AIAA PAPER 92-3887] p 528 A93-24481

Experimental assessment of airframe damage due to impacting ice [AIAA PAPER 93-0751] p 504 A93-24838

Application of a two-point exponential approximation method in optimizing rotorcraft airframe structures p 507 A93-27956

Progress in the application of a non-linear programming methodology to the design of a low-vibration airframe p 507 A93-27959

The NASA/industry design analysis methods for vibrations (DAMVIBS) program - Accomplishments and contributions p 508 A93-27971

Experiences at Langley Research Center in the application of optimization techniques to helicopter airframes for vibration reduction p 508 A93-27972

Effect of modeling techniques in the coupled rotor-body vibration analysis [AIAA PAPER 93-1360] p 710 A93-33928

Response of laminated composite plates to low-speed impact by airgun-propelled and dropped-weight impactors [AIAA PAPER 93-1402] p 739 A93-33962

Mathematical statement of the problem of optimizing the design of an airframe for ease of manufacture p 745 A93-35286

PDT approach for developing RAH-66 Comanche airframe systems p 795 A93-35909

Three-dimensional calculations of rotor-airframe interaction in forward flight p 795 A93-35940

Improved Airframe Manufacturing Technology p 763 A93-35971

Evaluation of thermoplastic stiffened panels for application to rotorcraft airframes p 827 A93-36000

CFD for hypersonic propulsion p 865 A93-42585

Simplified finite element representation of fuselage frames with flexible castellations p 892 A93-43570

A frequency domain theory for structural identification p 930 A93-43778

NASA airframe structural integrity program p 1026 A93-45782

Experience in specifying/prolonging the airframe time limits p 948 A93-45797

Actively cooled panel testing perils, problems, and pitfalls --- for aerospace vehicles p 1028 A93-46802

Effects of floor location on response of composite fuselage frames p 997 A93-46809

Transonic mutual interference of wing-pylon-multiple body configurations using an overlapping grid scheme [AIAA PAPER 93-3023] p 1055 A93-48208

Non-propulsive aerodynamic noise p 99 N93-10673

Contributions to the experimental investigation of rotor/body aerodynamic interactions p 20 N93-10877

Recent advances in multidisciplinary optimization of rotorcraft [NASA-TM-107665] p 47 N93-10968

Concurrent optimization of airframe and engine design parameters [NASA-TM-105908] p 60 N93-12402

Water tunnel studies of inlet/airframe interference phenomena p 215 N93-13216

Some aspects of intake design, performance and integration with the airframe p 161 N93-13219

Structural fatigue aspects of the P-3 Orion [ARL-STRUC-TM-558] p 161 N93-13256

Experimental and analytical investigation of the vibration characteristics of a remotely piloted helicopter [AD-A256131] p 163 N93-14248

Proceedings of the USAF Structural Integrity Program [AD-A255379] p 110 N93-14549

Icing effects on aircraft stability and control determined from flight data: Preliminary results [NASA-TM-105977] p 188 N93-14831

A neural network prototype for predicting F-14B strains at the B.L. 10 longeron [AD-A255272] p 165 N93-15004

Aeroplane crashes on the runway: Validation and final evaluation of the method of modeling an airframe structure [IMFL-91-32] p 165 N93-15126

An overview of shed ice impact in the NASA Lewis Icing Research Tunnel [NASA-TM-105969] p 139 N93-15404

Basic research on design analysis methods for rotorcraft vibrations [NASA-CR-191917] p 422 N93-18576

Development of an engine/airframe performance matching scheme for jet engine retrofit [AD-A258822] p 365 N93-18997

Heat loads as key problem of hypersonic flight [MBB-FE-202-S-PUB-0486] p 484 N93-21054

The NASA/industry Design Analysis Methods for Vibrations (DAMVIBS) program: A government overview p 514 N93-21311

The NASA/industry Design Analysis Methods for Vibrations (DAMVIBS) program: Bell Helicopter Textron accomplishments p 514 N93-21312

The NASA/industry Design Analysis Methods for Vibrations (DAMVIBS) program: Boeing Helicopters airframe finite element modeling p 515 N93-21313

The NASA/industry Design Analysis Methods for Vibrations (DAMVIBS) program: McDonnell-Douglas Helicopter Company achievements p 515 N93-21314

The NASA/industry Design Analysis Methods for Vibrations (DAMVIBS) program: Sikorsky Aircraft: Advances toward interacting with the airframe design process p 515 N93-21315
A computational approach to predicting the extent of arc root damage in CFC panels p 735 N93-24890
Zoning of aircraft by electric field modelling p 704 N93-24894
Helicopter forced response vibration analysis method RTVIB20 [AD-A261809] p 730 N93-26260
AEW aircraft design [AD-A261800] p 718 N93-26444
Development and testing of the Perseus proof-of-concept aircraft [DE93-010121] p 806 N93-28586
A unified approach for composite cost reporting and prediction in the ACT program p 920 N93-30441
Fabrication of the V-22 composite AFT fuselage using automated fiber placement p 920 N93-30443

AIRLINE OPERATIONS
European merger control in the air transport industry - Comments on the Delta Air Lines/Pan Am decision of the European Commission [ISBN 3-452-22293-4] p 103 A93-11412
Managing mistakes --- quality assurance in aircraft maintenance p 109 A93-17100
Autoland, the developing need p 142 A93-17302
Low-level wind-shear terminology p 426 A93-22104
Distribution of aviation weather graphics via airline communications networks p 426 A93-22113
Responsibility and assignment of roles on overlong flights p 570 A93-24253
An industry held hostage p 486 A93-26423
Spatial orientation and wayfinding in airport passenger terminals - Implications for environmental design p 487 A93-27168
A study on the marginal analysis method for the airline yield management p 487 A93-27370
Recent experiment focuses on operational impact of jet stream forecast errors p 487 A93-27394
Aeronautical technologies and communications - Toward advanced technology passenger terminals p 529 A93-27477
Air transport growth - How will airports manage?; Proceedings of the Conference, London, United Kingdom, Oct. 21, 1992 [ISBN 1-85768-065-0] p 458 A93-29475
Airlines, airports and antitrust - A proposed strategy for enhanced competition p 760 A93-34821
Extended range operations of two and three turbofan engine airplanes p 802 A93-37391
British Airways ETOPs flight planning system p 990 A93-45164
Problems in the aerodynamics, strength, and flight operations of aircraft p 947 A93-45659
Bilateral transfers of safety oversight will prove beneficial to all states p 1174 A93-49279
Desert store --- of mothballed commercial jet aircraft p 1229 A93-54866
An investigation of ground access mode choice for departing passengers [TT-9201] p 67 N93-11224
Aircraft accident report: Atlantic Southeast Airlines, Inc. Flight 2311, uncontrolled collision with terrain, an Embraer EMB-120, N270AS, Brunswick, Georgia, 5 April 1991 [PB92-910403] p 28 N93-11471
Airport stand assignment model [TT-9104] p 67 N93-11728
Future regional transport aircraft market, constraints, and technology stimuli [NASA-TM-107669] p 109 N93-13025
A NASPAC-based analysis of the delay and cost effects of the Dallas/Fort Worth metroplex plan [DOT/FAA/CT-TN92/21] p 193 N93-13447
Public-sector aviation issues: Graduate research award papers, 1990 - 1991 [PB92-222629] p 143 N93-13787
In-service evaluation of wind shear systems p 146 N93-14857
The airline quality report, 1992 [NIAR-92-11] p 310 N93-18036
TBD(exp 3) [NASA-CR-192075] p 335 N93-18054
Scheduling of an aircraft fleet p 443 N93-18665
IOPS advisor: Research in progress on knowledge-intensive methods for irregular operations airline scheduling p 443 N93-18686
Principles of nuclear-based explosive detection systems p 497 N93-21861
PFNA technique for the detection of explosives p 497 N93-21865
A pulsed fast-thermal neutron interrogation system p 497 N93-21866
Explosive detection system based on Electronic Neutron Generator (ENG) p 497 N93-21870

Design concepts for the development of cooperative problem-solving systems [NASA-CR-192708] p 707 N93-25261
The 1991-1992 aviation system capacity plan [AD-A263436] p 911 N93-29788

AIRPORT LIGHTS
Prototype stop bar system evaluation at John F. Kennedy International Airport [AD-A258667] p 192 N93-12902

AIRPORT PLANNING
Specific educational aspects of airport engineering in Spain and the Hispanic world p 103 A93-12560
Spatial orientation and wayfinding in airport passenger terminals - Implications for environmental design p 487 A93-27168
Aeronautical technologies and communications - Toward advanced technology passenger terminals p 529 A93-27477
Comparison of airport noise calculation models p 564 A93-28480
The airnoise boundary concept for airport noise management p 564 A93-28482
The costs of noise at the new Munich airport p 558 A93-28493
Air transport growth - How will airports manage?; Proceedings of the Conference, London, United Kingdom, Oct. 21, 1992 [ISBN 1-85768-065-0] p 458 A93-29475
Control of land use near airports is best means of reducing impact of aircraft noise p 571 A93-29575
Aircraft monitoring of the planeness of the existing and new runways p 991 A93-45668
Stumbling blocks for airport construction in the new German federal states p 1227 A93-53727
Airport stand assignment model [TT-9104] p 67 N93-11728
Report to Congress: State Block Grant Program [AD-A254569] p 193 N93-13882
Report to Congress: Long-term availability of adequate airport system capacity [AD-A258209] p 319 N93-18202
Airport landside planning and operations [PB93-167880] p 822 N93-26636

AIRPORT SECURITY
Tomorrow's security p 141 A93-15058
An industry held hostage p 486 A93-26423
Criminal acts against civil aviation [AD-A258760] p 495 N93-19867
Insights into US domestic aviation p 496 N93-21859
A review of the development of a luggage explosive detection system p 497 N93-21862
Experience with explosive detection systems in airports p 498 N93-21895
Future directions in aviation security p 880 N93-30274

AIRPORT SURFACE DETECTION EQUIPMENT
DLR research program overview on airport surface movement guidance and control p 499 A93-27912
Ground Movement and Control System (GMCS) p 499 A93-27913
Airport surveillance radar design for increased air traffic p 883 A93-43410

AIRPORT TOWERS
DLR research program overview on airport surface movement guidance and control p 499 A93-27912
Terminal area forecasts FY 1992 - 2005 [AD-A255797] p 149 N93-15390

AIRPORTS
Airports, air traffic control, and their clients - Reflections on system optimization p 234 A93-15035
Future systems for air traffic control p 150 A93-15052
Airport navigation and surveillance using GPS and ADS p 313 A93-21145
Terminal area surveillance using GPS p 316 A93-21190
Integrated runway meteorological observation system (IRMOS/SIOMA) p 428 A93-22128
Identification and conversion of foundation parameters for airport pavement p 538 A93-24035
Airport technology international 1993 p 532 A93-26920
New slant visual range measuring device promises improved airport operations p 529 A93-27395
Wind shear alert system brings safety improvements to major U.S. airports p 529 A93-27396
SIPORT DEPCOS and SIPORT ARRCOS - More than an electronic airstrip replacement p 499 A93-27914
Fracture of highway and airport pavements p 547 A93-28290
Airlines, airports and antitrust - A proposed strategy for enhanced competition p 760 A93-34821
Increasing airport safety and capacity using automated maneuvering area control p 885 A93-43550

Airport radar systems (2nd revised and enlarged edition) --- Russian book [ISBN 5-277-00610-9] p 992 A93-44505
Calculation of safe altitudes p 991 A93-45675
Increase in mortality rates due to aircraft noise p 1163 A93-49551
The dependent converging instrument approach procedure [AIAA PAPER 93-3835] p 1098 A93-51424
Red-hot simulation p 1209 A93-53774
The community response to aircraft noise around six Spanish airports p 1264 A93-55845
An investigation of ground access mode choice for departing passengers [TT-9201] p 67 N93-11224
In situ material characterization for pavement evaluation by the Spectral-Analysis-of-Surface-Waves (SASW) method [AD-A255660] p 194 N93-14128
Terminal Doppler weather radar/low-level wind shear alert system integration algorithm specification, version 1.1 [AD-A255319] p 224 N93-14547
Information systems for airport operations [TT-9202] p 152 N93-14729
Terminal area forecasts FY 1992 - 2005 [AD-A255797] p 149 N93-15390
Development of a unified airport pavement analysis and design system p 380 N93-16317
Unified airport pavement design procedure p 380 N93-16318
Three-dimensional stress analysis of multilayered airport pavements: Integral transform approach p 381 N93-16319
Results of DATAS investigation of illegal mode S ID's at JFK Airport [DOT/FAA/CT-92/26] p 318 N93-16841
Estimating the regional economic significance of airports [AD-A257658] p 382 N93-17793
Scheduling of an aircraft fleet p 443 N93-18665
Adverse weather test site selection study [AD-A259012] p 339 N93-18895
Poland civil aviation master plan and investment program: Executive summary [PB92-213665] p 459 N93-21342
Poland civil aviation master plan and investment program [PB92-213693] p 459 N93-21343
Calculation of noise emission caused by jet aircraft during takeoff, approach and horizontal flyover [DLR-MITT-91-15] p 569 N93-21368
Analysis of aircraft noise levels in the vicinity of start-of-takeoff roll at Baltimore-Washington International Airport [PB92-221605] p 559 N93-21501
Proceedings of the Aircraft Wake Vortices conference, volume 1 [PB93-126449] p 485 N93-21796
Proceedings of the Aircraft Wake Vortices conference, volume 2 [PB93-127728] p 559 N93-21799
Insights into US domestic aviation p 496 N93-21859
A transportable luggage examination system based on neutron interrogation p 497 N93-21863
Visual approach data collection at St. Louis Lambert Field (STL) [DOT/FAA/CT-TN93/2] p 706 N93-24948
The dependent converging instrument approach procedure: An analysis of its safety and applicability [DOE/FAA/RD-93/6] p 707 N93-25456
Expedient repair of structural facilities [AD-A260727] p 731 N93-25656
Airport landside planning and operations [PB93-167880] p 822 N93-26636
The 1991-1992 aviation system capacity plan [AD-A263436] p 911 N93-29788
Effects of commercial flight pollution on human health p 1035 N93-31931
Effects of air traffic on nature and environment in the neighborhood of airports by example of the Munich 2 Airport (Germany) p 1035 N93-31932

AIRSHIPS
ICAS, Congress, 18th, Beijing, China, Sept. 20-25, 1992, Proceedings, Vols. 1 & 2 [ISBN 1-56347-046-2] p 107 A93-14151
Advanced technologies airships p 108 A93-14183
Steady state model for the thermal regimes of shells of airships and hot air balloons p 207 A93-15072
Selection of the powerplant for a thermoplane p 899 A93-42380
Prediction of fatigue crack growth kinetics in the plane structural elements of aircraft in the biaxial stress state p 1025 A93-45670

- The fuel/timing problem in a computer-aided flight preparation system for civil aircraft p 996 A93-45672
- Aerodynamic characteristics of airship models of different shapes p 1092 A93-51909
- AIAA Lighter-Than-Air Systems Technology Conference, 10th, Scottsdale, AZ, Sept. 14-16, 1993, Technical Papers p 1229 A93-54601
- National airborne surveillance system - An engineering student study [AIAA PAPER 93-4031] p 1242 A93-54603
- Airship/U.S. naval vessels UHF communications relay demonstration [AIAA PAPER 93-4032] p 1240 A93-54604
- Airship: The 'Look Out' - A versatile surveillance platform [AIAA PAPER 93-4033] p 1229 A93-54605
- Airship applications of modern flight test techniques [AIAA PAPER 93-4035] p 1242 A93-54606
- Aerodynamics of the TCOM 71M aerostat [AIAA PAPER 93-4036] p 1231 A93-54607
- Structural analysis of the light weight hard nose of the 71M aerostat [AIAA PAPER 93-4037] p 1255 A93-54608
- A diesel powerplant development program for airships [AIAA PAPER 93-4038] p 1246 A93-54609
- Advanced technologies for enhancement of airships [AIAA PAPER 93-4040] p 1242 A93-54610
- Airship insurance in London [AIAA PAPER 93-4043] p 1265 A93-54611
- Zeppelin NT - A new concept in airship technology, based on rigid airship principles [AIAA PAPER 93-4045] p 1242 A93-54612
- The largest freight airship that can fit in Moffett hangar no. 1 [AIAA PAPER 93-4046] p 1242 A93-54613
- The development progress of the U.S. Army's SASS LITE, unmanned robot airship [AIAA PAPER 93-4047] p 1243 A93-54614
- Aerodynamic characteristics of a semi-buoyant station in the shape of a torus [AIAA PAPER 93-4034] p 1231 A93-54615
- AIRSPACE**
- Automatic dependent surveillance (ADS) Pacific engineering trials (PET) p 30 A93-10999
- Integrating TCAS into the airspace management system p 30 A93-11005
- In the pursuit of a single European air traffic control system p 150 A93-15053
- The value of GNSS to aircraft operators p 498 A93-25172
- Rotorcraft en route ATC route standards [AD-A249129] p 35 N93-10323
- A simplified numerical procedure to compute the optimal trajectory of an aircraft p 48 N93-11719
- National Airspace System: Air traffic control and airspace management operational concept NAS-SR-132 [DOT/FAA/SE-92/5] p 502 N93-20164
- Poland civil aviation master plan and investment program: Executive summary [PB92-213685] p 459 N93-21342
- Poland civil aviation master plan and investment program [PB92-213693] p 459 N93-21343
- The 1991-1992 aviation system capacity plan [AD-A263436] p 911 N93-29788
- Airspace Design Expert System (ADES), a 2D/3D mapping and modelling tool incorporating an expert system for use in instrument approach design p 888 N93-30357
- AIRSPED**
- Airspeed calibration using GPS [AIAA PAPER 92-4090] p 51 A93-13272
- The noise of jet aircraft flying with high speeds at low altitudes p 450 A93-19218
- Optimal cruise performance p 802 A93-37394
- Optimisation of constant altitude-constant airspeed flight for piston-prop aircraft p 889 A93-40473
- Results of operational testing of a system for computing optimal flight regimes - of aircraft flight p 996 A93-45665
- Alternative solution to optimum gliding velocity in a steady head wind or tail wind p 1136 A93-52458
- Analysis of spatial motion dynamics of a helicopter for various models of the induced velocity field p 1191 A93-53721
- An investigation of the dynamic response of lifting surfaces with concentrated structural nonlinearities p 162 N93-13807
- Development of the Advance Warning Airborne System(AWAS) p 144 N93-14849
- Energy method for analysis of measured airspeed change in landing airborne manoeuvre [ESOU-92020] p 335 N93-18042
- Aircraft turns into and down wind [AERO-REPT-9201] p 337 N93-18131
- General aviation aircraft: Normal acceleration data analysis and collection project [DOT/FAA/CT-91/20] p 713 N93-24739
- ALBEDO**
- Small satellites and RPA's in global-change research [AD-A260762] p 755 N93-25837
- ALGEBRA**
- A three-dimensional algebraic grid generation scheme for gas turbine combustors with inclined slots [NASA-CR-191095] p 746 N93-24759
- The addition of algebraic turbulence modeling to program LAURA [NASA-TM-107758] p 840 N93-27250
- ALGORITHMS**
- Tranconic profile design in curvilinear coordinates using an approximate factorization algorithm p 7 A93-10778
- A comparative analysis of algorithms for solving systems of high-order linear algebraic equations p 96 A93-12977
- Periodic Euler and Navier-Stokes solutions about oscillating airfoils p 241 A93-17799
- A new procedure for dynamic adaption of three-dimensional unstructured grids [AIAA PAPER 93-0672] p 560 A93-24780
- A fast algorithm for image-based ranging p 544 A93-27045
- Implicit upwind solution algorithms for three-dimensional unstructured meshes p 691 A93-35607
- Analysis of implicit treatments for a centred Euler solver p 864 A93-42449
- Inviscid calculations by an upwind finite element method of hypersonic flows over a double (single) ellipse p 869 A93-42626
- Improvements in code validation algorithms for secondary surveillance radar p 883 A93-43408
- Solution of the Euler and Navier Stokes equations on parallel processors using a transposed/Thomas ADI Algorithm [AIAA PAPER 93-3310] p 1036 A93-45006
- Adaptive refinement-coarsening scheme for three-dimensional unstructured meshes p 961 A93-45735
- Statistical methods in flight vehicle control theory p 1165 A93-49306
- Dual Engine application of the Performance Seeking Control algorithm [AIAA PAPER 93-1822] p 1110 A93-49709
- Using a diagonal implicit algorithm to calculate transonic nozzle flow [AIAA PAPER 93-2345] p 1082 A93-50119
- Minimizing the wall effects in wind tunnels with a sectional pressure chamber p 1085 A93-50965
- A collocated finite volume method for predicting flows at all speeds p 1087 A93-51736
- A parameter optimization approach to controller partitioning for integrated flight/propulsion control application p 1206 A93-54268
- Sweeping algorithm for unstructured-grid generation on two-dimensional non-convex domains p 1262 A93-56413
- Improved numerical simulation of Euler equations p 83 N93-10309
- Rigid body mode identification of the PAH-2 helicopter using the eigensystem realization algorithm [NASA-TM-107690] p 88 N93-11544
- Automated extraction of aircraft runway patterns from radar imagery [AD-A254258] p 68 N93-11751
- Computational nonlinear control [AD-A253547] p 98 N93-12258
- Simulation of two-dimensional icing, de-icing and anti-icing phenomena p 142 N93-13364
- Ideal aircraft handling quality models: Longitudinal axis [NAL-PD-FC-9203] p 187 N93-13566
- Terminal Doppler weather radar/low-level wind shear alert system integration algorithm specification, version 1.1 [AD-A255319] p 224 N93-14547
- Modelling the engine temperature distribution between shut down and restart for life usage monitoring p 169 N93-15177
- Sensor fault detection using nonlinear observer and polynomial classifier p 170 N93-15182
- Multiple model adaptive estimation applied to the VISTA F-16 with actuator and sensor failures, volume 2 [AD-A256569] p 371 N93-16165
- Volume 2: Explicit, multistage upwind schemes for Euler and Navier-Stokes equations [NASA-CR-191647] p 418 N93-16558
- The role of under-determined approximations in engineering and science application p 441 N93-16763
- Identification of system dynamics of a high incidence research model [RR-407] p 339 N93-18507
- Computational Fluid Dynamics, volume 2 [VKI-LS-1992-04-VOL-2] p 421 N93-18563
- Algorithm development with applications to aerodynamics and aeroelasticity p 422 N93-18566
- Scheduling of an aircraft fleet p 443 N93-18665
- NASA wind shear flight test in situ results p 488 N93-19593
- NASA airborne radar wind shear detection algorithm and the detection of wet microbursts in the vicinity of Orlando, Florida p 490 N93-19611
- Signal processing for airborne doppler radar detection of hazardous wind shear as applied to NASA 1991 radar flight experiment data p 490 N93-19612
- Methodology for sensitivity analysis, approximate analysis, and design optimization in CFD for multidisciplinary applications [NASA-CR-192172] p 552 N93-20297
- Unsteady Navier-Stokes method for accelerated moving airfoils with separation [DLR-FB-92-03] p 485 N93-21763
- An experimental health monitoring unit for GPS and GLONASS p 706 N93-25018
- A contribution to the great Riemann solver debate [NASA-CR-191409] p 694 N93-25083
- Control of complex dynamic systems by neural networks p 758 N93-25611
- Setting values for TDWR/LLWAS 3 integration parameters [AD-A260740] p 755 N93-25645
- Practical input optimization for aircraft parameter estimation experiments [NASA-CR-191462] p 820 N93-27264
- Unstructured mesh algorithms for aerodynamic calculations p 785 N93-27444
- Implementation of a multidomain Navier-Stokes code on the Intel iPSC2 hypercube [FFA-TN-1992-37] p 843 N93-28994
- Reference equations of motion for automatic rendezvous and capture [NASA-CR-185676] p 914 N93-29652
- Computation of a delta-wing roll-and-hold maneuver [AD-A264704] p 909 N93-30498
- ALIGNMENT**
- Sensor alignment Kalman filters for inertial stabilization systems p 50 A93-11018
- ALKALI METAL COMPOUNDS**
- Real-time optical measurement of alkali species in air for jet engine corrosion testing [AIAA PAPER 93-0791] p 541 A93-24870
- ALKANES**
- Viscosity of aviation fuel components (n-alkanes) p 71 A93-12824
- Application of a sulphur-doped alkane system to the study of thermal oxidation of jet fuels [ASME PAPER 92-GT-122] p 387 A93-19356
- ALKYL COMPOUNDS**
- Viscosity of aviation fuel components - Aromatic hydrocarbons (alkyl benzenes) p 1211 A93-52961
- ALL-WEATHER AIR NAVIGATION**
- Fixed and rotary wing all weather operations system requirements p 142 A93-17303
- ALL-WEATHER LANDING SYSTEMS**
- Fixed and rotary wing all weather operations; Proceedings of the Conference, London, United Kingdom, Apr. 23, 24, 1991 [ISBN 0-903409-90-9] p 142 A93-17301
- Landing guidance systems for CAT III operations p 151 A93-17307
- Air Traffic Control ground movement control in low visibility p 151 A93-17308
- Coherent systems in the terahertz frequency range: Elements, operation, and examples p 841 N93-27727
- ALLOCATIONS**
- National Aeronautics and Space Administration Authorization Act, fiscal year 1993 [S-REPT-102-364] p 234 N93-13798
- NASA authorization, 1993, volume 2 [GPO-56-943-VOL-2] p 234 N93-13799
- NASA's fiscal year 1993 budget [S-HRG-102-707] p 234 N93-13800
- ALLOYING**
- Fatigue in single crystal nickel superalloys [AD-A265451] p 1019 N93-31795
- ALOUPETTE HELICOPTERS**
- The development of a new air filtration system for the Alouette III helicopter [ISABE 93-7048] p 1199 A93-54024
- ALPS MOUNTAINS (EUROPE)**
- Operating helicopters in a demanding environment - Mountain flying/high evaluations p 1190 A93-54289
- ALTERNATING CURRENT**
- An ac thin film electroluminescent (TFEL) display unit for cockpit control display unit application p 518 A93-28179

- Modeling limits of the EMV analysis program CONCEPT by example of the influence of a helicopter structure on a frame antenna
[MBB-UD-0614-92-PUB] p 223 A93-15487
- ALTERNATING DIRECTION IMPLICIT METHODS**
Improving the efficiency of aerodynamic shape optimization procedures
[AIAA PAPER 92-4697] p 264 A93-20309
Solution of the Euler and Navier Stokes equations on parallel processors using a transposed/Thomas ADI Algorithm
[AIAA PAPER 93-3310] p 1036 A93-45006
Navier-Stokes simulation of external/internal transonic flow on the forebody/inlet of the AV-8B Harrier II
[AIAA PAPER 93-3057] p 1058 A93-48234
Aerodynamic heating analysis for axisymmetric bodies in supersonic flow p 303 A93-19312
- ALTERNATIVES**
Evaluation of alternatives for increasing A-7D rearward visibility
[AD-A255071] p 50 A93-12488
Enhanced Aeronautical Resource Management training alternatives p 147 A93-15019
- ALTIMETERS**
The development of an Altitude Awareness Program - An integrated approach p 486 A93-27136
- ALTIMETRY**
European studies to investigate the feasibility of using 1000 ft vertical separation minima above FL(290). III - Further results and overall conclusions p 992 A93-45166
Mapping new and old worlds with laser altimetry p 1034 A93-45699
- ALTITUDE CONTROL**
The development of an Altitude Awareness Program - An integrated approach p 486 A93-27136
Use of PCs in controlling simulated altitude environmental test conditions in support of turbine engine testing p 846 A93-37856
The development of a prototype aircraft height monitoring unit utilising an SSR-based difference in time of arrival technique p 884 A93-43432
- ALTITUDE SIMULATION**
Research of starting test of the small turbojet in simulated altitude condition p 53 A93-11870
Use of PCs in controlling simulated altitude environmental test conditions in support of turbine engine testing p 846 A93-37856
Ground test simulation fidelity of turbine engine airtests
[AIAA PAPER 93-2173] p 1137 A93-49986
Engine testing at simulated altitude conditions
[AIAA PAPER 93-2452] p 1120 A93-50201
- ALTITUDE TESTS**
The acoustic response of altitude test facility exhaust systems to axisymmetric and two-dimensional turbine engine exhaust plumes p 449 A93-19209
- ALUMINIDES**
Microstructural study of aluminide surface coatings on single crystal nickel base superalloy substrates p 70 A93-12771
Evaluation of simple aluminide and platinum modified aluminide coatings on high pressure turbine blades after factory engine testing - Round II
[ASME PAPER 92-GT-140] p 388 A93-19372
Isothermal oxidation behavior of alpha-2 titanium aluminide alloys p 535 A93-29563
Chemical stability of titanium diboride reinforcement in nickel aluminide matrices p 1147 A93-52473
Friction surfacing and linear friction welding p 1217 A93-53499
Thermal barrier design of gamma-TiAl Functionally Graded Materials (FGMs) for scramjet engine applications p 1246 A93-54556
HIP consolidation of aluminum-rich intermetallic alloys and their composites
[NAWCADWAR-92003-60] p 199 A93-14726
Compatibility of potential reinforcing ceramics with Ni and Fe aluminides
[NASA-CR-192232] p 394 A93-18784
Platinum-modified diffusion aluminide coatings on nickel-base superalloys
[AD-A263597] p 917 A93-29981
- ALUMINUM**
PAA-core aluminum honeycomb - An end user's evaluation p 209 A93-15738
Thermoelastic vibration test techniques p 549 A93-29293
Investigation of corrosion in aluminum/adhesive lap-splices using pulse-echo ultrasonic techniques
[DE93-008074] p 749 A93-25518
- ALUMINUM ALLOYS**
Effects of prior fatigue damage on crack propagation rates in 2024-T351 aluminum alloy p 71 A93-13640
Economical view on composite structures maintenance
[SME PAPER EM92-102] p 233 A93-14103
Mechanical testing analyses of new aluminum alloy SPF typical-parts in aircraft p 196 A93-14174
Accelerated corrosion fatigue test methods for aging aircraft p 198 A93-16623
Effect of stress level of gust cycles on fatigue crack propagation behavior (Acceleration and retardation of crack propagation under simplified flight simulation loading) p 198 A93-17033
Selection of the time scale for preventive measures under service conditions p 237 A93-18375
Ultrasonic thickness measurement using the angle technique p 542 A93-25353
Selecting a method for sealing riveted joints in fuel compartments p 746 A93-35295
Machining cost comparison of silicon carbide discontinuously reinforced aluminum, unreinforced aluminum, and titanium
[SME PAPER EM92-252] p 925 A93-40656
The effect of exfoliation corrosion on the fatigue behavior of structural aluminum alloys p 1017 A93-45778
An evaluation of the pressure proof test concept for 2024-T3 aluminum alloy sheet p 1026 A93-45780
Advanced composite fiber/metal pressure vessels for aircraft applications
[AIAA PAPER 93-2246] p 1155 A93-50047
Eddy current inspection of open fastener holes in aluminum aircraft structure
[SAE ARP 4402] p 1160 A93-52167
Fatigue life under random load history derived from exceedance curves using different algorithms p 1260 A93-56544
FNAS modify matrix and transparent experiments
[NASA-CR-184442] p 198 A93-13311
Deformation mechanisms of NiAl cyclicly deformed near the brittle-to-ductile transformation temperature
[NASA-CR-191649] p 391 A93-15830
Fatigue propagation behaviour of short cracks in aluminum alloys
[ESDU-92030] p 392 A93-16641
Damage tolerance behaviour of aluminium-lithium sheet alloys
[NLR-TP-91244-U] p 392 A93-17540
Flight simulation and constant amplitude fatigue crack growth in aluminum-lithium sheet and plate
[NLR-TP-91104-U] p 331 A93-17562
Application of the cyclic J-integral to fatigue crack propagation p 839 A93-27182
NASA-UVa light aerospace alloy and structure technology program supplement: Aluminum-based materials for high speed aircraft
[NASA-CR-4517] p 1019 A93-31843
Crack growth prediction models p 1004 A93-31747
Accelerated and real-time corrosion testing of aluminum-lithium alloys
[NLR-TP-91203-U] p 1020 A93-32385
- ALUMINUM BORON COMPOSITES**
Inelasticity effect in a unidirectional boron/aluminum composite under uniaxial tension p 825 A93-39024
- ALUMINUM COMPOUNDS**
Process optimization of Hexoloy SX-SiC towards improved mechanical properties
[DE93-007913] p 826 A93-28564
- ALUMINUM-LITHIUM ALLOYS**
Flight simulation and constant amplitude fatigue crack growth in aluminum-lithium sheet and plate p 71 A93-13644
Main directions of improving the quality of aluminum-lithium alloys for welded aircraft structures p 1146 A93-51104
Evaluation of water-borne adhesive bonding primers for use on the advanced aircraft material aluminum-lithium p 1211 A93-53420
Friction surfacing and linear friction welding p 1217 A93-53499
- AMBIENT TEMPERATURE**
An evaluation of thermal energy storage options for precooled gas turbine inlet air
[DE93-005980] p 754 A93-24975
- AMINO RADICAL**
Theoretical characterization of the reaction $\text{NH}_2 + \text{O}$ yields products p 1263 A93-55666
- AMORPHOUS MATERIALS**
Research support for the Laboratory for Lightwave Technology
[AD-A261488] p 760 A93-26343
- AMPHIBIOUS VEHICLES**
Canadian experience with air cushion vehicle skirts p 837 A93-39722
- AMPLIFICATION**
Three-dimensional compressible stability-transition calculations using the spatial theory p 783 A93-27431
- AMPLITUDE MODULATION**
Analysis of the effects of blade pitch on the radar return signal from rotating aircraft blades p 885 A93-43476
- AMPLITUDES**
The start of the laboratory - The beginnings of the MIT Instrumentation Laboratory p 235 A93-17326
- AN-2 AIRCRAFT**
Optimization of the blade angle of the AV-2 propeller for improving the flight performance characteristics of An-2 aircraft p 996 A93-45663
- ANALOG CIRCUITS**
Analysis of fault-tolerant neurocontrol architectures
[NASA-TM-105898] p 65 A93-12305
- ANALOG DATA**
Digitization of analog data from in-flight lightning strikes p 753 A93-24884
- ANALOG SIMULATION**
Analog simulation as part of a power supply design analysis universal platform p 543 A93-25962
Calculation of the position of the flow separation line in an analog model of flow past a body p 1176 A93-52958
- ANALOG TO DIGITAL CONVERTERS**
Data acquisition and analysis on a Macintosh p 562 A93-29422
Silicon differential pressure transducer line pressure effects and compensation p 830 A93-37890
A novel-high-performance system for recording and analysing instantaneous total pressure distortion in air intakes p 214 A93-13215
Digital data acquisition and preliminary instrumentation study for the F-16 laminar flow control vehicle p 292 A93-16784
Digitization of analog data from in-flight lightning strikes p 753 A93-24884
- ANALOGIES**
The use of multiple models in case-based diagnosis p 759 A93-25969
- ANALYSIS (MATHEMATICS)**
Acoustic noise generation at the air/ocean boundary
[DREA-CR-90-445] p 99 A93-10642
- ANALYTIC GEOMETRY**
An efficient approach to optimal aerodynamic design. I - Analytic geometry and aerodynamic sensitivities
[AIAA PAPER 93-0099] p 264 A93-20204
- ANECHOIC CHAMBERS**
Development of the Boeing Low Speed Aeroacoustic Facility (LSAF) p 374 A93-19148
Two-dimensional laser velocimetry for the study of dual-flow jets with flight effect in the CEPRA 19 anechoic wind tunnel
[ONERA, TP NO. 1992-144] p 831 A93-38614
A large hemi-anechoic enclosure for community-compatible aeroacoustic testing of aircraft propulsion systems
[NASA-TM-106015] p 760 A93-26551
Modal measurements and propeller field excitation on acoustic full scale mockup of SAAB 340 aircraft
[FFA-TN-1992-08] p 1039 A93-31051
- ANEMOMETERS**
Anemometer siting criteria for low level wind shear alert system p 413 A93-22178
Effect of Reynolds number on the standards of a simplified anemocinometric probe
[IMFL-91-31] p 293 A93-17542
- ANGLE OF ATTACK**
Numerical modeling of supersonic flows past wings of different aspect ratios over a wide range of angles of attack within the framework of the plane section law p 5 A93-10141
A method for determining the aerodynamic coefficients of asymmetric bodies with allowance for nonlinear influence factors of the body shape p 5 A93-10142
In-flight flow visualization results from the X-29A aircraft at high angles of attack
[AIAA PAPER 92-4102] p 38 A93-11272
Pitch control margin at high angle of attack - Quantitative requirements (flight test correlation with simulation predictions)
[AIAA PAPER 92-4107] p 39 A93-11277
High angle-of-attack inviscid Shuttle Orbiter computation p 9 A93-12020
Three-dimensional boundary-layer transition on a cone at Mach 3.5 p 9 A93-12177
Viscous shock-layer numerical calculations of three dimensional nonequilibrium flows over hypersonic blunt bodies at high angle of attack p 12 A93-12651
Application of multigrid and adaptive grid embedding to the two-dimensional flux-split Euler equations p 202 A93-13990
Calculation of transonic flow over bodies of varying complexity using Singular Perturbation Method p 116 A93-14265
Lateral aerodynamics characteristics of forebodies at high angle of attack in subsonic and transonic flows p 118 A93-14302

- Wing rock of lifting systems p 118 A93-14330
- Analytical solutions for hypersonic flow past slender power-law bodies at small angle of attack p 122 A93-14550
- The Concorde wing - A useful model p 126 A93-16400
- Experimental study of controlled tip disturbance effect on flow asymmetry p 211 A93-17417
- Breaking the stall barrier p 159 A93-17502
- Method and results of studies of flow past supersonic flight vehicles at moderate and large angles of attack p 242 A93-18377
- Effect of the Reynolds number on the aerodynamic characteristics of a body of revolution over a wide range of angles of attack p 242 A93-18384
- Separated flow in a low speed two-dimensional cascade. II - Cascade performance [ASME PAPER 92-GT-357] p 257 A93-19522
- A new semiempirical method for computing nonlinear angle-of-attack aerodynamics on wing-body-tail configurations [AIAA PAPER 93-0034] p 260 A93-20148
- Numerical analysis of a chined forebody with asymmetric strakes [AIAA PAPER 93-0051] p 260 A93-20164
- High Mach number dynamic stability of blunt slender cones at angle of attack p 271 A93-21721
- Development of an engineering level prediction method for high angle of attack aerodynamics [AIAA PAPER 93-0208] p 278 A93-22626
- Flowfield computations over the Space Shuttle Orbiter with a proposed canard at a Mach number of 5.8 and 50 degrees angle of attack [AIAA PAPER 93-0322] p 281 A93-23014
- Icing effects on aircraft stability and control determined from flight data - Preliminary results [AIAA PAPER 93-0398] p 370 A93-23073
- Three-dimensional flow structure on delta wings at high angle-of-attack - Experimental concepts and issues [AIAA PAPER 93-0550] p 285 A93-23289
- Doppler global velocimetry measurements of the vortical flow above an F/A-18 [AIAA PAPER 93-0414] p 415 A93-23333
- Numerical computation of viscous hypersonic flow around spherically blunted cones at angle of attack p 460 A93-24082
- The effect of Reynold's number on a natural low frequency flow oscillation over an airfoil near stall [AIAA PAPER 92-0400] p 463 A93-24489
- Body-axis rolling motion critical states of a 65-degree delta wing [AIAA PAPER 93-0621] p 523 A93-24738
- Incompressible flow computation of forces and moments on bodies of revolution at incidence [AIAA PAPER 93-0787] p 541 A93-24867
- Effect of a rotating propeller on the separation angle of attack [AIAA PAPER 93-0017] p 472 A93-24978
- Structure of vortex breakdown on a pitching delta wing [AIAA PAPER 93-0434] p 474 A93-25528
- Determination of nonstationary aerodynamic loading on cascade blades in the case of dynamic changes of the angle of attack p 544 A93-26817
- Measurements of aerodynamic rotary stability derivatives using a whirling arm facility p 525 A93-28603
- Experimental and nonlinear vortex lattice method results for various wing-canard configurations p 479 A93-28607
- Flowfield measurements of a two-element airfoil with large separation p 480 A93-29307
- Analysis of slender bodies of revolution with an angle of attack in extreme ground effect p 679 A93-33716
- A numerical method of unsteady separating flow over delta wings p 681 A93-33746
- Composite 'Exoskin' doubler extends F-15 Vertical Tail fatigue life [AIAA PAPER 93-1341] p 709 A93-33911
- Effects of blowing on delta wing vortices during dynamic pitching p 768 A93-37384
- Slender wing rock revisited p 768 A93-37386
- Comparison of two Navier-Stokes codes for simulating high-incidence vortical flow p 768 A93-37387
- Actuator and aerodynamic modeling for high-angle-of-attack aeroservoelasticity [AIAA PAPER 93-1419] p 818 A93-37433
- Subsonic natural-laminar-flow airfoils p 860 A93-41780
- Inverse simulation of large-amplitude aircraft maneuvers p 906 A93-41893
- Problem 6.4.1 - Rarefied flow around a double ellipse p 869 A93-42630
- Leeside flow over delta wing at $M = 7.15$ - Experimental results for test case 7.1.2 p 870 A93-42632
- Appraisal of the rarefied flow computations (problems 6.4.1 and 7.2.1) p 871 A93-42640
- An approximate method for calculating heating rates on three-dimensional vehicles [AIAA PAPER 93-2881] p 949 A93-44228
- CFD analysis of the X-29 inlet at high angle of attack p 958 A93-45140
- Reynolds number effects on supersonic asymmetrical flows over a cone p 958 A93-45141
- Computational fluid dynamics code validation using a free piston hypervelocity shock tunnel p 960 A93-45545
- Numerical investigation of subsonic and supersonic asymmetric vortical flow p 961 A93-45727
- Initial acceleration effects on flow evolution around airfoils pitching to high angles of attack p 961 A93-45750
- An investigation of aerodynamic heating to spherically blunted cones at angle of attack [AIAA PAPER 93-2764] p 963 A93-46510
- Tangential Forebody Blowing-yaw control at high alpha [AIAA PAPER 93-3406] p 1008 A93-47205
- Side-force control on a forebody of diamond cross-section at high angles of attack [AIAA PAPER 93-3407] p 1008 A93-47206
- Secondary flow control on slender, sharp-edged configurations [AIAA PAPER 93-3470] p 980 A93-47250
- Preliminary design estimates of high-speed streamlines on arbitrary shaped vehicles defined by quadrilateral elements [AIAA PAPER 93-3491] p 982 A93-47263
- Effect of leeward flow dividers on the wing rock of a delta wing [AIAA PAPER 93-3492] p 982 A93-47264
- Aerodynamic characteristics of the MMPT ATD vehicle at high angles of attack [AIAA PAPER 93-3493] p 982 A93-47265
- Flow control over delta wings at high angles of attack [AIAA PAPER 93-3494] p 983 A93-47266
- An experimental study of droop leading edge modifications on high and low aspect ratio wings up to 50 deg angle of attack [AIAA PAPER 93-3496] p 983 A93-47268
- Forebody vortex control - A progress review [AIAA PAPER 93-3540] p 986 A93-47292
- Side force augmentation at high angle of attack from pneumatic vortex flow control [AIAA PAPER 93-2959] p 1124 A93-48153
- Elliptic cross section tip effects on the vortex wake of an axisymmetric body at angle of attack [AIAA PAPER 93-2960] p 1124 A93-48154
- Effects of aft geometry on vortex behavior and force production by a tangential jet on a body at high alpha [AIAA PAPER 93-2961] p 1048 A93-48155
- Effect of forebody tangential slot blowing on flow about a full aircraft geometry [AIAA PAPER 93-2962] p 1048 A93-48156
- The hemisphere-cylinder in dynamic pitch-up motions [AIAA PAPER 93-2963] p 1048 A93-48157
- Flow field characteristics of a complex blade tip at high angles of attack [AIAA PAPER 93-3083] p 1060 A93-48257
- Status of the validation of high-angle-of-attack nose-down pitch control margin design guidelines [AIAA PAPER 93-3623] p 1126 A93-48308
- Lateral control at high angles of attack using pneumatic blowing through a chined forebody [AIAA PAPER 93-3624] p 1126 A93-48309
- Kinematics and aerodynamics of the velocity vector roll [AIAA PAPER 93-3625] p 1126 A93-48310
- Unsteady aerodynamic models for maneuvering aircraft [AIAA PAPER 93-3626] p 1126 A93-48311
- On computing vortex asymmetries about cones at angle of attack using the conical Navier-Stokes equations [AIAA PAPER 93-3628] p 1064 A93-48313
- Analysis of missile configurations with wrap-around fins using computational fluid dynamics [AIAA PAPER 93-3631] p 1064 A93-48316
- Nonlinear aerodynamic modeling using multivariate orthogonal functions [AIAA PAPER 93-3636] p 1065 A93-48321
- Development of flying qualities and agility evaluation maneuvers [AIAA PAPER 93-3645] p 1127 A93-48329
- Investigation of roll requirements for carrier approach [AIAA PAPER 93-3649] p 1128 A93-48332
- Development of lateral-directional departure criteria [AIAA PAPER 93-3650] p 1128 A93-48333
- Optimum poststall turning and supersonic turning [AIAA PAPER 93-3659] p 1128 A93-48339
- Results and lessons learned from two Wright Laboratory flight research programs [AIAA PAPER 93-3661] p 1099 A93-48341
- Dynamic model testing of the X-31 configuration for high-angle-of-attack flight dynamics research [AIAA PAPER 93-3674] p 1129 A93-48351
- Effect of flexural and rotational wing oscillations on the prevention of flow separation p 1150 A93-48911
- Hypersonic flow past a low-aspect-ratio triangular plate at large angles of attack p 1069 A93-48974
- Periodic vortex shedding over delta wings p 1070 A93-49002
- Thoughts on conical flow asymmetry p 1070 A93-49003
- Installed F/A-18 inlet flow calculations at 60 deg angle-of-attack and 10 deg side slip [AIAA PAPER 93-1806] p 1074 A93-49695
- Robust, nonlinear, high angle-of-attack control design for a supermaneuverable vehicle [AIAA PAPER 93-3774] p 1131 A93-51369
- Unsteady pressure and load measurements on an F/A-18 vertical fin p 1095 A93-52451
- An improved calibration technique for wind tunnel model attitude sensors p 1253 A93-54356
- Experimental investigation of effect of particles on blade pressure distribution in impulse cascade flow p 1236 A93-55398
- Local heat transfer distribution in a rotating serpentine rib-roughened flow passage p 1259 A93-55459
- Arguments concerning wind tunnel test studies of the trim characteristics of objects with small asymmetries [AD-A254111] p 19 A93-10858
- The hemisphere-cylinder at an angle of attack p 21 N93-11250
- The convection speed of the dynamic stall vortex [AD-A247258] p 21 N93-11464
- Correlation of forebody pressures and aircraft yawing moments on the X-29A aircraft at high angles of attack [NASA-TM-4417] p 22 N93-11532
- An experimental study of the relationship between forces and moments and vortex breakdown on a pitching delta wing p 49 N93-12206
- The influence of intake swirl distortion on the steady-state performance of a low bypass, twin-spool engine p 214 N93-13211
- Comparative performance tests of a pilot-inlet in several European wind-tunnels at subsonic and supersonic speeds p 130 N93-13221
- In-flight flow visualization results from the X-29A aircraft at high angles of attack [NASA-TM-4430] p 131 N93-13322
- Airfoil-vortex interaction and the wake of an oscillating airfoil p 134 N93-13803
- The unsteady aerodynamics of a delta wing undergoing large-amplitude pitching motions p 134 N93-13929
- Pressure drag and lift contributions for blunted forebodies of fineness ratio 2.0 in transonic flow (M infinity less than or equal to 1.4) [ESDU-89033] p 136 N93-14515
- Icing effects on aircraft stability and control determined from flight data: Preliminary results [NASA-TM-105977] p 188 N93-14831
- Flowfield study of a close-coupled canard configuration [AD-A256311] p 139 N93-15245
- Effect of a rotating propeller on the separation angle of attack and distortion in ducted propeller inlets [NASA-TM-105935] p 290 N93-16625
- Contribution of ventral fins to sideslip and yawing moment derivatives due to sideslip at low angle of attack [ESDU-92029] p 291 N93-16638
- Lift enhancement using a close-coupled oscillating canard [AD-A257877] p 296 N93-18336
- Identification of system dynamics of a high incidence research model [RR-407] p 339 N93-18507
- Stall departure resistance enhancer [NASA-CASE-LAR-14221-1] p 344 N93-19023
- Longitudinal-control design approach for high-angle-of-attack aircraft [NASA-TP-3302] p 373 N93-19108
- Flight and wind-tunnel calibrations of a flush airdata sensor at high angles of attack and sideslip and at supersonic Mach numbers [NASA-TM-104265] p 344 N93-19110
- AM-X high angle of attack flight test experience (single and two seat versions) p 511 N93-19910
- X-31A high angle of attack and initial post stall flight testing p 511 N93-19911
- Application of a flush airdata sensing system to a wing leading edge (LE-FADS) [NASA-TM-104267] p 518 N93-20163
- Research in robust control for hypersonic vehicles [NASA-CR-192127] p 527 N93-20296
- The transient development of vortices over delta wings p 695 N93-25269

- Computation of transonic flow over a porous surface
projectile p 696 N93-25409
- Conical Euler analysis and active roll suppression for
unsteady vortical flows about rolling delta wings
[NASA-TP-3259] p 701 N93-26134
- Assessment of a flow-through balance for hypersonic
wind tunnel models with scramjet exhaust flow
simulation [NASA-TM-4441] p 779 N93-27005
- Effect of vortex behavior on loads acting on a 65 deg
delta wing oscillating in roll at high incidence
p 782 N93-27220
- Analysis of wind-tunnel data for elliptic cross-sectioned
forebodies at Mach numbers 0.4 to 5.0
p 782 N93-27221
- Efficient simulation of incompressible viscous flow over
multi-element airfoils p 784 N93-27443
- Prediction of vortex breakdown on a delta wing
p 787 N93-27459
- An experimental study of flow over a 6 to 1 prolate
spheroid at incidence p 874 N93-29124
- NASTRAN analysis for the Airmass Sunburst model 'C'
Ultralight Aircraft p 931 N93-29777
- Solution of Euler equations for forebody-inlet ensemble
of aircraft at high angle of attack
[AD-A263905] p 876 N93-29862
- The application of concentric vortex simulation to
calculating the aerodynamic characteristics of bodies of
revolution at high angles of attack
[AD-A263879] p 876 N93-29919
- Flight control system design factors for applying
automated testing techniques p 910 N93-30764
- Experiments in the control of wing rock at high angle
of attack using tangential leading edge blowing
p 1009 N93-31068
- ANGULAR VELOCITY**
- Selection of transducer measuring ranges in flight
vehicle control systems p 526 A93-29691
- Kinematics of aeroinertial aircraft rotation
p 819 A93-39192
- Active algorithms for controlling the rotational motion
of flight vehicles p 908 A93-43079
- Optimization of the blade angle of the AV-2 propeller
for improving the flight performance characteristics of An-2
aircraft p 996 A93-45663
- Exact closed-form solution of generalized proportional
navigation p 1130 A93-49598
- Development of the wake behind a circular cylinder
impulsively started into rotatory and rectilinear motion
p 1236 A93-55736
- ANIMATION**
- Aid in investigation by figure animation
p 491 N93-19659
- ANISOTROPIC MEDIA**
- Optimization of anisotropic structures considering
strength, stiffness and aeroelastic constraints
[AIAA PAPER 92-4796] p 408 A93-20291
- Exact flutter solution of advanced anisotropic composite
cantilevered wing structures [AIAA PAPER 93-1535] p 727 A93-34072
- ANISOTROPIC SHELLS**
- Dynamic analysis of rotor flexbeams based on nonlinear
anisotropic shell models p 743 A93-34261
- ANISOTROPY**
- Effects of substrate anisotropy on coupled bilateral
finlines p 208 A93-15409
- Mechanical anisotropy in directionally solidified turbine
blade p 1018 A93-47356
- ANNEALING**
- An effective Mixed Annealing/Heuristic Algorithm for
problems in kinematic mechanical design
[AIAA PAPER 93-1581] p 741 A93-34113
- Use of titanium castings without a casting factor
[AD-A264414] p 1018 N93-31192
- ANNUAL VARIATIONS**
- Assessing spatial and seasonal variations in grasslands
with spectral reflectances from a helicopter platform
p 426 A93-20621
- ANNULAR DUCTS**
- Experimental and numerical investigation of supersonic
turbulent flow in an annular duct [AIAA PAPER 93-3123] p 1063 A93-48291
- ANNULAR FLOW**
- Estimation of maximal local temperature at exit of
annular combustor p 172 A93-14496
- Profile losses of an annular turbine cascade in unsteady
periodic flow [ASME PAPER 92-GT-153] p 249 A93-19380
- Three-dimensional unstructured grid Euler method
applied to turbine blades [AIAA PAPER 93-0196] p 461 A93-24233
- Effects of nozzle contour on the aerodynamic
characteristics of underexpanded annular impinging jets
p 1024 A93-45563
- A numerical investigation of supersonic strut/endwall
interactions in annular flow with varying strut thickness
[AIAA PAPER 93-2927] p 1045 A93-48128
- Experimental and numerical investigation of supersonic
turbulent flow in an annular duct [AIAA PAPER 93-3123] p 1063 A93-48291
- Combustion characteristics and passive control of an
annular dump combustor [AIAA PAPER 93-1772] p 1110 A93-49668
- Investigation of a strut/endwall interaction in supersonic
annular flow [AIAA PAPER 93-1925] p 1076 A93-49791
- Computation of the flow field in an annular gas turbine
combustor [AIAA PAPER 93-2074] p 1113 A93-49903
- The low frequency aeroacoustics of buried nozzle
systems p 1205 A93-54244
- Experimental study of the flow field inside a whirling
annular seal p 85 N93-10892
- Time-dependent predictions and analysis of turbine
cascade data in the transonic flow region
[PNR-90957] p 139 N93-15489
- Prediction of turbine cascade flows with a
quasi-three-dimensional rotor viscous code and the
extension of the algebraic turbulence model
[AD-A256831] p 223 N93-15635
- ANNULAR NOZZLES**
- Enhancement of mixing in high-speed heated jets using
a counterflowing nozzle p 1235 A93-55359
- Heat transfer and aerodynamics of a high rim speed
turbine nozzle guide vane with profiled end walls
[AD-A258346] p 295 N93-17991
- Analytical and experimental investigation of annular
propulsive nozzles [AD-A262685] p 815 N93-28391
- ANNULAR PLATES**
- Calculation of a collector-type annular plate heat
exchanger p 833 A93-39045
- ANNULAR SUSPENSION AND POINTING SYSTEM**
- Large angle magnetic suspension test fixture
[NASA-CR-193123] p 1015 N93-31836
- ANTARCTIC REGIONS**
- Status of the NASA Balloon Program p 1 A93-11365
- The GRAD Supernova Observer - First Flight of a very
large balloon over Antarctica p 27 A93-11367
- Polar Patrol Balloon Experiment in Antarctica
p 27 A93-11373
- ANTENNA ARRAYS**
- A self-steering array for the SHARP microwave-powered
aircraft p 792 A93-37090
- Experimental results on RIAS digital beamforming
radar p 929 A93-43392
- A dual polarised active phased array antenna with low
cross polarisation for a polarimetric airborne SAR
p 883 A93-43401
- Antenna design for adaptive airborne MTI
p 884 A93-43440
- The PHARUS project, first results of the realization phase
--- Phased Array Universal SAR p 884 A93-43454
- Design optimization study for F-15 propulsion/toward
fairing compatibility [AIAA PAPER 93-3484] p 1003 A93-47291
- The ILS mathematical modeling study of the Runway
10 ILS Localizer at Luis Munoz Marin International Airport,
San Juan, Puerto Rico [DOT/FAA/CT-TN93/10] p 792 N93-27017
- ANTENNA DESIGN**
- Selecting locations for avionics antennas - A structured
approach p 892 A93-42794
- Antenna design for adaptive airborne MTI
p 884 A93-43440
- ILS mathematical modeling study of the effects of an
ASR-9 structure at the Long Island MacArthur Airport, Islip,
NY [DOT/FAA/CT-TN92/25] p 192 N93-12668
- The real aperture antenna of SAR, a key element for
performance p 213 N93-13053
- The ILS mathematical modeling study of the Runway
10 ILS Localizer at Luis Munoz Marin International Airport,
San Juan, Puerto Rico [DOT/FAA/CT-TN93/10] p 792 N93-27017
- ANTENNA RADIATION PATTERNS**
- A wideband, embedded/conformal, antenna subsystem
concept p 327 A93-22002
- ELF, VLF and LF radiation from a very large loop antenna
with a mountain core p 924 A93-40334
- Selecting locations for avionics antennas - A structured
approach p 892 A93-42794
- Calculation of the passive noise power for onboard
single-pulse automatic direction tracking systems
p 882 A93-43111
- Dual band tuned radomes for radar applications
p 929 A93-43405
- Inflight antenna diagram determination of spaceborne
and airborne SAR-systems p 1161 A93-47583
- Receiving and scattering characteristics of an imaged
monopole beneath a lossy sheet p 1158 A93-50543
- Models for performance assessment of HF antennas
on the CH-135/Twin Huey helicopter p 933 N93-30291
- Advanced electromagnetic methods for aerospace
vehicles [NASA-CR-193468] p 936 N93-31036
- Operation of the helicopter antenna radiation prediction
code [NASA-CR-193259] p 1030 N93-31110
- ANTENNAS**
- Modeling limits of the EMV analysis program CONCEPT
by example of the influence of a helicopter structure on
a frame antenna [MBB-UD-0614-92-PUB] p 223 N93-15487
- ANTICING ADDITIVES**
- Anti-icing failure detection instrumentation using realtime
optical measurement of anti-icing fluid properties
[AIAA PAPER 93-0748] p 540 A93-24836
- Field studies of hold-over-times for type II anti-icing fluids
- Results and insights [AIAA PAPER 93-0749] p 486 A93-24837
- Experimental evaluation of flat plate boundary layer
growth over an anti-icing fluid film p 1140 A93-52645
- ANTIOXIDANTS**
- Development of a method to determine the autoxidation
of turbine fuels [AD-A260578] p 736 N93-25902
- ANTIREFLECTION COATINGS**
- The history and development of coated Contrast
Enhancement Filters for cockpit displays p 564 A93-28180
- ANTONOV AIRCRAFT**
- The whirl-flutter problem in aircraft construction
p 1249 A93-56218
- APPLICATIONS OF MATHEMATICS**
- Current research activities: Applied and numerical
mathematics, fluid mechanics, experiments in transition
and turbulence and aerodynamics, and computer
science [NASA-CR-191408] p 758 N93-25084
- Cumulative reports and publications [NASA-CR-191440] p 847 N93-27063
- APPLICATIONS PROGRAMS (COMPUTERS)**
- RISK - Interactive multidisciplinary system for designing
airframes p 226 A93-14337
- A set of application programs for the smoothing of curves
and surfaces by the method of monoidal transformations
in the geometric module of a CAD system for the design
of flight vehicles p 561 A93-27629
- A set of IBM PC software for processing helicopter flight
tests data to determine the flight performance
characteristics p 1037 A93-45661
- Interactive grid generation program for CAP-TSD
[NASA-TM-102705] p 17 N93-10349
- An interactive preprocessor for the NASA engine
performance program [NASA-TM-105786] p 56 N93-10983
- Numerical analysis of the flow fields in a RQL gas turbine
combustor [DE92-017509] p 89 N93-11767
- Computer program for calculating and fitting
thermodynamic functions [NASA-RP-1271] p 231 N93-12967
- User's Guide for the NREL Force and Loads Analysis
Program [DE92-010579] p 216 N93-13524
- User's Guide for the NREL Teetering Rotor Analysis
Program (STRAP) [DE92-010580] p 216 N93-13525
- Ideal aircraft handling quality models: Longitudinal axis
[NAL-PD-FC-9203] p 187 N93-13566
- Program for calculation of aileron rolling moment and
yawing moment coefficients at subsonic speeds
[ESDU-88040] p 136 N93-14514
- Air Force procedure for predicting noise around airbases:
Noise exposure model (Noisemap) [AD-A255769] p 224 N93-14655
- BLSTA: A boundary layer code for stability analysis
[NASA-CR-4481] p 220 N93-14797
- SAPNEW: Parallel finite element code for thin shell
structures on the Alliant FX-80 [NASA-CR-189212] p 220 N93-14799
- A critical analysis of the accuracy of several numerical
techniques for combustion kinetic rate equations
[NASA-TP-3315] p 362 N93-16941
- Software Engineering Laboratory Ada performance
study: Results and implications p 441 N93-17172
- A database approach to aircraft carrier airplan
production [AD-A257737] p 240 N93-17666
- An improved method of structural dynamic test design
for ground flying and its application to the SH-2F and SH-2G
helicopters p 512 N93-19928

- Projectile base bleed technology. Part 2: User's guide
CMINT computer code, version 5.04-BRL
[AD-A258630] p 551 N93-19999
- Further development of the CANAERO computer code
to include a time-stepping capability
[DREA-CR-91-478] p 562 N93-21820
- Development of a non-linear simulation for generic
hypersonic vehicles - ASUHS1
[NASA-CR-192710] p 516 N93-22003
- A computational approach to predicting the extent of
arc root damage in CFC panels p 735 N93-24890
- Techniques for designing rotorcraft control systems
[NASA-CR-192960] p 729 N93-26046
- Probabilistic assessment of composite structures
[NASA-TM-106024] p 825 N93-27092
- Aerodynamic analysis of hypersonic waverider aircraft
[NASA-CR-192981] p 780 N93-27093
- Adaptive EAGLE dynamic solution adaptation and grid
quality enhancement p 788 N93-27464
- Summer research program (1992). High School
Apprenticeship Program (HSAP) reports. Volume 16:
Arnold Engineering Development Center Civil Engineering
Laboratory
[AD-A262024] p 945 N93-29396
- APPROACH**
- GPS continuity - Initial findings p 314 A93-21167
- Takeoff/approach noise for a model counterrotation
propeller with a forward-swept upstream rotor
[AIAA PAPER 93-0596] p 519 A93-24782
- Initial results of an in-flight investigation of longitudinal
flying qualities for augmented, large transports in approach
and landing
[AIAA PAPER 93-3816] p 1133 A93-51407
- Development of advanced approach and departure
procedures
[AIAA PAPER 93-3833] p 1098 A93-51422
- Overview of the FAA's differential GPS CAT III technical
feasibility demonstration program
[AIAA PAPER 93-3836] p 1098 A93-51425
- Takeoff/approach noise for a model counterrotation
propeller with a forward-swept upstream rotor
[NASA-TM-105979] p 362 N93-16715
- Flight simulation evaluation of the flyability of curved
MLS approaches with wide-body aircraft
[NLR-TP-90238-U] p 382 N93-17875
- Visual approach data collection at St. Louis Lambert
Field (STL)
[DOT/FAA/CT-TN93/2] p 706 N93-24948
- APPROACH CONTROL**
- The Microwave Landing System - A precision approach
for the future p 32 A93-11023
- Analysis of approach paths of a single aircraft
p 367 A93-20823
- A constrained flight route monitor system in terminal
control area for air traffic control p 882 A93-42816
- NODE-air traffic management systems
p 884 A93-43428
- Statistical techniques for traffic flow management
[AIAA PAPER 93-3834] p 1098 A93-51423
- The dependent converging instrument approach
procedure
[AIAA PAPER 93-3835] p 1098 A93-51424
- DME-derived positions compared with MLS- and
ILS-derived positions
[NLR-TP-90119-U] p 318 N93-16343
- The effect of TCAS interrogations on the Chicago O'Hare
ATCRBS system
[DOT/FAA/CT-92/22] p 318 N93-16498
- Controller partitioning for integrated flight/propulsion
control implementation
[NASA-TM-105804] p 527 N93-21197
- The dependent converging instrument approach
procedure: An analysis of its safety and applicability
[DOE/FAA/RD-93/6] p 707 N93-25456
- Control of complex dynamic systems by neural
networks p 758 N93-25611
- Developing automation for terminal air traffic control:
Case study of the imaging aid p 888 N93-30356
- Evaluation of the flyability of MLS curved approaches
for wide-body aircraft
[NLR-TP-91396-U] p 999 N93-32416
- APPROACH INDICATORS**
- Developing automation for terminal air traffic control:
Case study of the imaging aid p 888 N93-30356
- APPROPRIATIONS**
- National Aeronautics and Space Administration
Authorization Act, fiscal year 1993
[S-REPT-102-364] p 234 N93-13798
- NASA authorization, 1993, volume 2
[GPO-56-943-VOL-2] p 234 N93-13799
- NASA's fiscal year 1993 budget
[S-HRG-102-707] p 234 N93-13800
- National Aeronautics and Space Administration
p 454 N93-17091
- APPROXIMATION**
- Approximation methods for control of structural
acoustics models with piezoceramic actuators
p 452 A93-23744
- Application of a two-point exponential approximation
method in optimizing rotorcraft airframe structures
p 507 A93-27956
- Numerical computation and approximations of H(infinity)
optimal controllers for a 2-parameter distributed model of
an unstable aircraft p 817 A93-37040
- Indicial lift approximations for two-dimensional subsonic
flow as obtained from oscillatory measurements
p 768 A93-37385
- An integral equation solution for multistage
turbomachinery design calculations
[NASA-TM-105970] p 179 N93-15521
- The role of under-determined
approximations in
engineering and science application
p 441 N93-16763
- CFD-based approximation concepts for aerodynamic
design optimization with application to a 2-D scramjet
vehicle
[AD-A258084] p 333 N93-17893
- Effect of design selection on response surface
performance
[NASA-CR-4520] p 895 N93-29885
- AQUEOUS SOLUTIONS**
- Field studies of hold-over-times for type II anti-icing fluids
- Results and insights
[AIAA PAPER 93-0749] p 486 A93-24837
- ARC HEATING**
- An experimental investigation of hydrogen-fueled
supersonic combustor p 53 A93-12733
- Suggestions for development of three-phase 60 Hz arc
heated wind tunnels
[AIAA PAPER 93-0795] p 528 A93-24874
- AEDC expanded flow arc facility (HEAT-H2) description
and calibration p 821 A93-37872
- Non-equilibrium flow in an arc heated wind tunnel
p 910 A93-42642
- Flow calibration of two hypersonic nozzles in the AEDC
HEAT-H2 high-enthalpy arc-heated wind tunnel
[AIAA PAPER 93-2782] p 1012 A93-46526
- Development and operation of new arc heater
technology for a large-scale scramjet propulsion test
facility
[AIAA PAPER 93-2786] p 1016 A93-46528
- Thermal response and ablation characteristics of light
weight ceramic ablators
[AIAA PAPER 93-2790] p 1018 A93-46532
- Thermal analysis of an arc heater electrode with a
rotating arc foot
[AIAA PAPER 93-2855] p 1028 A93-46590
- ARC JET ENGINES**
- Arc jet testing in NASA Ames Research Center
thermophysics facilities
[AIAA PAPER 92-5041] p 385 A93-22315
- Measurement and analysis of nitric oxide radiation in
an arc-jet flow
[AIAA PAPER 93-2800] p 1016 A93-46540
- AFOSSR Contractors Meeting in Propulsion
[AD-A254484] p 195 N93-12575
- ARCHITECTURE (COMPUTERS)**
- The development of an airborne information
management system for flight test
[AIAA PAPER 92-4113] p 51 A93-11281
- Hetero-redundant architecture with Kalman filter for input
processing in flight control system p 182 A93-14293
- An application of artificial neural networks to
experimental data approximation
[AIAA PAPER 93-0408] p 440 A93-23330
- The Pave Pace integrated core processor
p 941 A93-42856
- JIAWG compatible development boards for the i960
[SAE PAPER 931596] p 1104 A93-49345
- High speed databus evaluation - Further work
[SAE PAPER 931597] p 1151 A93-49346
- Implementation of fiber optic technology in flight
controls p 1105 A93-49473
- An introduction to the onboard LAN (OLAN)
p 1166 A93-49480
- Onboard Connectivity Network for command and control
aircraft p 1166 A93-49481
- WNN 92: Proceedings of the 3rd Workshop on Neural
Networks: Academic/Industrial/NASA/Defense, Auburn
Univ., AL, Feb. 10-12, 1992 and South Shore Harbour,
TX, Nov. 4-6, 1992
[SPIE-1721] p 1167 A93-50726
- Architecture of multiprocessor data processing
machines and dispatching of the knowledge acquisition
process in flight control p 1168 A93-50958
- Requirements analysis notebook for the flight data
systems definition in the Real-Time Systems Engineering
Laboratory (RSEL)
[NASA-CR-185698] p 69 N93-10960
- Analysis of fault-tolerant neurocontrol architectures
[NASA-TM-105898] p 65 N93-12305
- Personal computer based test- and emulation equipment
for maintenance and ground support
p 110 N93-15185
- Design for tactical situation awareness display
[AD-A256194] p 170 N93-15235
- Numerical Wind Tunnel: Requirements and the outline
p 383 N93-19288
- The operating system for Numerical Wind Tunnel
p 383 N93-19290
- Mission planning systems for tactical aircraft (pre-flight
and in-flight)
[AGARD-AR-313] p 496 N93-21187
- A comparison using APPL and PVM for a parallel
implementation of an unstructured grid generation
program
[NASA-CR-191425] p 757 N93-25073
- Information requirements analyses for transatmospheric
vehicles
[AD-A261189] p 718 N93-25949
- Center for Aeronautics and Space Information
Sciences
[NASA-CR-193140] p 848 N93-27289
- ARCS**
- Optimal thrust magnitude on a singular arc in
atmospheric flight p 758 N93-25410
- ARCTIC REGIONS**
- Arctic environment - Helicopter operations in cold
climates p 1189 A93-54288
- Airground issues and initial performance of an adaptive
air/ground/air HF communication system
p 934 N93-30342
- AREA NAVIGATION**
- The future of area navigation in Western Europe
p 311 A93-17752
- Design and implementation of a Global Positioning
System (GPS) supported area navigation system with
electronic aircraft
[ILR-MITT-275(1992)] p 889 N93-30671
- ARGON**
- Hypervelocity flows of argon produced in a free piston
driven expansion tube p 1012 A93-45530
- ARIANE LAUNCH VEHICLE**
- Computational methods applied to the aerodynamics of
spaceplanes and launchers
[ONERA, TP NO. 1992-140] p 114 A93-14216
- ARMED FORCES (FOREIGN)**
- Battle damage repairs p 239 A93-22698
- ARMED FORCES (UNITED STATES)**
- Aeronautical engineering education for the armed
forces p 453 A93-21681
- USAF supercritical hydrocarbon fuels interests
[AIAA PAPER 93-0807] p 533 A93-24883
- The status of CFD - An Air Force perspective
[AIAA PAPER 93-3293] p 1021 A93-44997
- Dr. Alexander H. Flax: Technologist of aeronautics
[AD-A258441] p 456 N93-17890
- Technical operating report on the Data Integration and
Collection Environment (DICE) instrumentation system
design
[AD-A258444] p 455 N93-17891
- Aircraft electrical and environmental systems, AFSCs
452x5, 454x5, and 454x6
[AD-A261213] p 717 N93-25733
- ARMOR**
- Lightweight aircraft turbine protection
[AIAA PAPER 93-1815] p 1110 A93-49703
- AROMATIC COMPOUNDS**
- Viscosity of aviation fuel components - Aromatic
hydrocarbons (alkyl benzenes) p 1211 A93-52961
- ARRAYS**
- Adaptive array processing for airborne radar
p 883 A93-43412
- Method of measuring cross-flow vortices by use of an
array of hot-film sensors
[NASA-CASE-LAR-14824-1-SB] p 751 N93-26000
- ARTIFICIAL INTELLIGENCE**
- Merger and acquisition - Enhancing Loran propagation
technology with artificial intelligence p 29 A93-10987
- Integration of aircraft design and manufacture using
artificial intelligence paradigms p 225 A93-14202
- An engineering method with artificial intelligence
characteristics used for structural layout of wings
p 225 A93-14290
- The employment of artificial intelligence for analyzing
air accidents p 226 A93-14375
- Improving anti-fatigue optimum design through AI-search
strategy p 208 A93-15342
- Calling the right shots in aircraft maintenance with
artificial intelligence p 238 A93-18763
- The Royal Air Force experience of artificial intelligence
aircraft maintenance p 435 A93-18764
- The use of artificial intelligence for buffet
environments
[AIAA PAPER 93-1534] p 727 A93-34071

- A design concept for a flight vehicle computer system with artificial intelligence elements p 757 A93-35663
- System Status - The diagnostic edge of the pilot's associate p 808 A93-37853
- Intelligent robotics; Proceedings of the International Symposium, Bangalore, India, Jan. 2-5, 1991 [SPIE-1571] p 1166 A93-49350
- Multilevel intelligent control systems for flight vehicles p 1168 A93-50955
- An information-search system in cybernetics p 1168 A93-50957
- Intelligent diagnostics systems p 98 A93-11931
- A domain-specific design architecture for composite material design and aircraft part redesign p 442 A93-17522
- An investigation of discovery-based learning in the route planning domain [AD-A259141] p 513 A93-20560
- Mission planning systems for tactical aircraft (pre-flight and in-flight) [AGARD-AR-313] p 496 A93-21187
- An approach to configuration design synthesis of subsonic transport aircraft using artificial intelligence techniques p 716 A93-25692
- Artificial intelligence methodologies in flight related differential game, control and optimization problems [AD-A262405] p 848 A93-28498
- Optimal trajectories for aircraft terrain following and terrain avoidance: A literature review update [AD-A264075] p 910 A93-30604

ARTIFICIAL SATELLITES

- Small satellites and RPA's in global-change research [AD-A260762] p 755 A93-25837

ASCENT

- Autonomous guidance, navigation and control bridging program plan p 532 A93-27046

ASCENT TRAJECTORIES

- Analytical solutions to constrained hypersonic flight trajectories p 1141 A93-49596
- On stability and control of SSTO spaceplane in super- and hypersonic ascending phase [NAL-TR-1128T] p 65 A93-12361
- Performance and control of ascending trajectories to minimize heat load for transatmospheric aero-space planes p 133 A93-13745
- Analytical solutions to constrained hypersonic flight trajectories [NASA-CR-191987] p 297 A93-18602
- Optimal finite-thrust time-bounded direct-ascent interception p 734 A93-25272

ASHES

- Volcanic clouds --- aircraft hazards p 487 A93-28196

ASPECT RATIO

- On the use of the method of matched asymptotic expansions in propeller aerodynamics and acoustics p 8 A93-11553
- Low aspect ratio transonic rotors. I - Baseline design and performance [ASME PAPER 92-GT-185] p 352 A93-19410
- The three-dimensional separated flow structure in a variable aspect ratio sudden expansion duct [AIAA PAPER 93-0213] p 278 A93-22630
- Computational study of a conical wing having unit aspect ratio at supersonic speeds [AIAA PAPER 93-3505] p 984 A93-47272
- Application of a dynamic compression system model to a low aspect ratio fan - Casing treatment and distortion [AIAA PAPER 93-1871] p 1111 A93-49746
- Unsteady aerodynamic characteristics of three rectangular wings of different aspect ratios p 1180 A93-53575
- An experimental investigation of a finite circulation control wing [AD-A259044] p 340 A93-18896
- Experiments on smooth cantilevered circular cylinders in low-turbulence uniform flow. Part 1: Mean loading with aspect ratios in the range 4 to 30 [PB93-111763] p 555 A93-21383

ASPHALT

- Thermoviscoelastic analysis of pavements p 379 A93-16313
- State of the art review of rutting and cracking in pavements p 380 A93-16316
- State-of-the-art survey of flexible pavement crack sealing procedures in the United States [AD-A258050] p 382 A93-17708

ASSEMBLING

- High-strength combination fasteners for joint assembly in aircraft structures p 745 A93-35283

ASSEMBLY

- Stress-strain state of the elements of a single-stringer riveted panel p 746 A93-35288

ASSESSMENTS

- Advanced materials in gas turbine engines: An assessment [PNR-90946] p 58 A93-11105
- Pre-flight risk assessment in Emergency Medical Service (EMS) helicopters p 494 A93-19692

ASTRONOMICS

- Requirements analysis notebook for the flight data systems definition in the Real-Time Systems Engineering Laboratory (RSEL) [NASA-CR-185698] p 69 A93-10960

ASTRONAUTICS

- Astronautics and society p 383 A93-18391
- AGARD index of publications, 1989-1991 [AGARD-INDEX-89-91] p 104 A93-10610
- JPRS report: Central Eurasia. Aviation and cosmonautics, no. 9, September 1992 [JPRS-UAC-93-003] p 678 A93-26325
- European aerospace science and technology, 1992: A bibliography with indexes [NASA-SP-7105] p 949 A93-32404

ASYMMETRY

- Control of asymmetric jet [AD-A255967] p 219 A93-14400
- Passive control of supersonic asymmetric vortical flows around cones p 220 A93-14692
- Effect of sonic boom asymmetry on subjective loudness [NASA-TM-107708] p 453 A93-16755
- Axisymmetric vortex sheet roll-up p 788 A93-28078

ASYMPTOTIC METHODS

- An asymptotic model of a closed separation region in supersonic flow p 4 A93-10139
- On the use of the method of matched asymptotic expansions in propeller aerodynamics and acoustics p 8 A93-11553
- An approach for multi-stage calculations incorporating unsteadiness [ASME PAPER 92-GT-282] p 253 A93-19474
- Some asymptotic aspects of the nonstationary aerofoil theory p 259 A93-19966
- The asymptotic theory of hypersonic boundary-layer stability p 462 A93-24409
- The long-wave limit in the asymptotic theory of hypersonic boundary-layer stability p 462 A93-24410
- Asymptotic methods for the prediction of transonic wind-tunnel wall interference p 730 A93-35625
- Problems in physical gas dynamics p 775 A93-39126
- Asymptotic structure of a limiting hypersonic flow in a shock wave p 776 A93-39131
- A numerical solution of the asymptotic problem of boundary layer separation in an incompressible liquid upstream of the corner point of a body p 965 A93-46699

- Three-dimensional hypersonic flow of a gas past wings p 1069 A93-48971
- Near-optimal, asymptotic tracking in control problems involving state-variable inequality constraints [AIAA PAPER 93-3748] p 1170 A93-51344
- Analysis of a turning point problem in flight trajectory optimization p 1210 A93-52885
- Stability analysis through bifurcation theory. I, II [ONERA, TP NO. 1993-108] p 1225 A93-53620
- Lift and drag forces on droplets and particles in wall-bounded shear flows p 419 A93-17761
- [DE93-002678] p 419 A93-17761
- The stability of a trailing-line vortex in compressible flow [NASA-CR-189738] p 298 A93-18771

- Three-dimensional hypersonic flow of a gas past wings p 1069 A93-48971
- Near-optimal, asymptotic tracking in control problems involving state-variable inequality constraints [AIAA PAPER 93-3748] p 1170 A93-51344

- Analysis of a turning point problem in flight trajectory optimization p 1210 A93-52885
- Stability analysis through bifurcation theory. I, II [ONERA, TP NO. 1993-108] p 1225 A93-53620
- Lift and drag forces on droplets and particles in wall-bounded shear flows p 419 A93-17761
- [DE93-002678] p 419 A93-17761
- The stability of a trailing-line vortex in compressible flow [NASA-CR-189738] p 298 A93-18771

ASYMPTOTIC PROPERTIES

- Model reference control of a linear plant with feedthrough element p 846 A93-37034
- Control of nonlinear systems under input constraints with applications to flight control p 729 A93-25353

ASYMPTOTIC SERIES

- Matched asymptotic expansion of the Hamilton-Jacobi-Bellman equation for aeroassisted plane-change maneuvers [AIAA PAPER 93-3752] p 1143 A93-51348

ATMOSPHERIC ATTENUATION

- Evaluation of three models used for predicting noise propagated long distances overground [AD-A255963] p 232 A93-14406

ATMOSPHERIC BOUNDARY LAYER

- The composite shape and structure of coherent eddies in the convective boundary layer p 93 A93-12643
- Motion and decay of trailing vortices within the atmospheric surface layer p 425 A93-18548
- FIFE atmospheric boundary layer budget methods p 426 A93-20591
- Surface drag instabilities in the atmospheric boundary layer p 1163 A93-49069
- Study of artificial and natural turbulence in atmospheric boundary layer with a CW Doppler CO2 lidar p 1257 A93-54799

- Surface shear stress estimates from geostrophic winds for use in sensible and latent heat flux formulations p 936 A93-30044

ATMOSPHERIC CHEMISTRY

- Short-term atmospheric effects of high-altitude aircraft emissions p 559 A93-28865
- Potential impact of combined NO(x) and SO(x) emissions from future High Speed Civil Transport aircraft on stratospheric aerosols and ozone p 753 A93-35372
- Computation of wake/exhaust mixing downstream of advanced transport aircraft [AIAA PAPER 93-2944] p 1162 A93-48141
- Atmospheric aerosols due to aircraft and ecological problems p 1162 A93-48846
- Effect of the formation of excited oxygen molecules on the kinetics of exchange reactions and the heat flux during braking in the upper layers of the atmosphere p 1070 A93-48975
- Kinetic scheme selection in describing detonation in an H₂-air mixture behind shock waves p 1253 A93-55032

- Stratospheric aircraft: Impact on the stratosphere? [DE92-016997] p 94 A93-12104
- Stratospheric aircraft exhaust plume and wake chemistry studies [NASA-CR-189688] p 94 A93-12299
- Meeting review: Third NCAR Research Aircraft Fleet Workshop [PB92-222710] p 223 A93-12818
- Impact of supersonic and subsonic aircraft on ozone: Including heterogeneous chemical reaction mechanisms [DE92-019619] p 224 A93-13655
- Climatic effects of turbofan emissions in the stratosphere and the higher troposphere p 1035 A93-31927

ATMOSPHERIC CIRCULATION

- Motion and decay of trailing vortices within the atmospheric surface layer p 425 A93-18548
- Studies of atmospheric eddy dynamics and energetics and climate problems [ISBN 5-286-00610-8] p 753 A93-35689
- Meeting review: Third NCAR Research Aircraft Fleet Workshop [PB92-222710] p 223 A93-12818

ATMOSPHERIC COMPOSITION

- A novel aircraft-based tandem mass spectrometer for atmospheric ion and trace gas measurements p 925 A93-40672
- NO(y) from sub-sonic aircraft emissions - A global three-dimensional model study p 1261 A93-56236
- Predicted aircraft effects on stratospheric ozone p 93 A93-11096

ATMOSPHERIC CORRECTION

- The effects of ionospheric errors on single-frequency GPS users p 313 A93-21141

ATMOSPHERIC DENSITY

- Higher-order viscous shock-layer solutions for high altitude flows [AIAA PAPER 93-2724] p 858 A93-41050
- Effect of the atmosphere density gradient on aerodynamic stabilization p 1252 A93-55034
- Aeronomy coexperiments on drag-free satellites with proportional thrusters: GP-B and STEP p 195 A93-13922

ATMOSPHERIC EFFECTS

- SAAW - Italy's answer to the windshear challenge p 431 A93-22175
- AIAA Atmospheric Flight Mechanics Conference, Monterey, CA, Aug. 9-11, 1993, Technical Papers p 1125 A93-48301
- Effect of rotary atmospheric gusts on fighter airplane [AIAA PAPER 93-3644] p 1127 A93-48328
- Effect of the atmosphere density gradient on aerodynamic stabilization p 1252 A93-55034
- The atmospheric effects of stratospheric aircraft. Report of the 1992 Models and Measurements Workshop. Volume 1: Workshop objectives and summary [NASA-RP-1292-VOL-1] p 754 A93-25157
- The atmospheric effects of stratospheric aircraft. Report of the 1992 Models and Measurements Workshop. Volume 2: Comparisons with global atmospheric measurements [NASA-RP-1292-VOL-2] p 754 A93-25158
- The atmospheric effects of stratospheric aircraft. Report of the 1992 Models and Measurements Workshop. Volume 3: Special diagnostic studies [NASA-RP-1292-VOL-3] p 754 A93-25159

ATMOSPHERIC ELECTRICITY

- Volcanic clouds --- aircraft hazards p 487 A93-28196
- Aircraft measurement of electric field - Self-calibration p 753 A93-34894
- The onset of disintegration and corona in water drops falling at terminal velocity in horizontal electric fields p 1163 A93-49130

- The 1992 International Aerospace and Ground Conference on Lightning and Static Electricity: Addendum
[DOT/FAA/CT-92/20-ADD-1] p 753 N93-24875
- Zoning of aircraft: A review of the definitions p 703 N93-24880
- Zoning of aircraft by electric field modelling p 704 N93-24894
- Lightning phenomenology bases for full threat return stroke occurrence following extended leader sweep at flight altitudes p 754 N93-24895
- Development of models for predicting the triggering of lightning by launch vehicles p 734 N93-24899
- A single-point warning system for thunderstorms and electric fields p 747 N93-24900
- ATMOSPHERIC ENTRY**
- Extreme value heat transfer problems for three-dimensional bodies moving at hypersonic velocities p 4 A93-10079
- Flow problems posed by reentry in planetary atmospheres p 11 A93-12432
- Atmospheric reentry flight test of winged space vehicle p 385 A93-22324
- [AIAA PAPER 92-5053] p 385 A93-22324
- Nuclear thermal rocket entry heating and thermal response preliminary analysis p 385 A93-23058
- [AIAA PAPER 93-0378] p 385 A93-23058
- Shock/boundary layer interaction in a hypersonic flow in the presence of an entropy layer p 773 A93-38743
- [ONERA, TP NO. 1992-181] p 773 A93-38743
- Application of the multigrid solution technique to hypersonic entry vehicles p 858 A93-41049
- [AIAA PAPER 93-2721] p 858 A93-41049
- Hypersonic flows over a double or simple ellipse p 868 A93-42614
- Review of chemical-kinetic problems of future NASA missions. I - Earth entries p 872 A93-42899
- Simulation of ablation in Earth atmospheric entry p 1027 A93-46531
- [AIAA PAPER 93-2789] p 1027 A93-46531
- Survey of nonequilibrium re-entry heating for entry flight conditions p 1039 A93-46682
- [AIAA PAPER 93-3230] p 1039 A93-46682
- AIAA Atmospheric Flight Mechanics Conference, Monterey, CA, Aug. 9-11, 1993, Technical Papers p 1125 A93-48301
- Effect of the formation of excited oxygen molecules on the kinetics of exchange reactions and the heat flux during braking in the upper layers of the atmosphere p 1070 A93-48975
- Investigation of the structure of a multicomponent viscous shock layer p 1090 A93-51879
- Six-degree-of-freedom guidance and control-entry analysis of the HL-20 p 1210 A93-53737
- The infrared measurement for the reentry-body-translation p 914 N93-29134
- [AD-A263100] p 914 N93-29134
- ATMOSPHERIC IONIZATION**
- A computer simulation of the production of an artificially ionized layer using the Arecibo facility p 937 N93-30487
- [DE92-010817] p 937 N93-30487
- ATMOSPHERIC MODELS**
- Stratospheric turbulence measurements and models for aerospace plane design p 433 A93-22342
- [AIAA PAPER 92-5072] p 433 A93-22342
- Digital simulation of atmospheric turbulence for Dryden and von Karman models p 416 A93-23517
- Atmospheric turbulence aloft - A review of possible methods for detection, warning, and validation of prediction models p 557 A93-24914
- [AIAA PAPER 93-0847] p 557 A93-24914
- Studies of atmospheric eddy dynamics and energetics and climate problems p 753 A93-35689
- [ISBN 5-286-00610-8] p 753 A93-35689
- A comparison of wind speed measured by the Special Sensor Microwave Imager (SSM/I) and the Geosat altimeter p 1033 A93-44862
- Nonequilibrium shock layer radiation in a simulated Titan atmosphere p 1233 A93-54805
- A problem formulation for glideslope tracking in wind shear using advanced robust control techniques p 64 N93-11176
- [NASA-TM-104164] p 64 N93-11176
- Stratospheric turbulence measurements and models for aerospace plane design p 223 N93-13288
- [NASA-TM-104262] p 223 N93-13288
- Impact of supersonic and subsonic aircraft on ozone: Including heterogeneous chemical reaction mechanisms [DE92-019619] p 224 N93-13655
- Three-dimensional numerical simulation of the 20 June 1991, Orlando microburst p 488 N93-19598
- Comparison of simulated and actual wind shear radar data products p 490 N93-19610
- The atmospheric effects of stratospheric aircraft. Report of the 1992 Models and Measurements Workshop. Volume 1: Workshop objectives and summary p 754 N93-25157
- [NASA-RP-1292-VOL-1] p 754 N93-25157
- The atmospheric effects of stratospheric aircraft. Report of the 1992 Models and Measurements Workshop. Volume 2: Comparisons with global atmospheric measurements [NASA-RP-1292-VOL-2] p 754 N93-25158
- The atmospheric effects of stratospheric aircraft. Report of the 1992 Models and Measurements Workshop. Volume 3: Special diagnostic studies [NASA-RP-1292-VOL-3] p 754 N93-25159
- ATMOSPHERIC MOISTURE**
- An observational study of the dryline p 844 A93-36034
- ATMOSPHERIC OPTICS**
- Detection and parameter estimation of atmospheric turbulence by ground-based and airborne CO2 Doppler lidars p 395 A93-17862
- A study of optical distortions arising in radiation transmission through cavities with gas flow around them p 1225 A93-52945
- ATMOSPHERIC PHYSICS**
- Langley proposed advanced hypervelocity aerophysics facility - A status report p 1013 A93-47015
- Summaries of the 1991 publications of DLR research reports and DLR communications [ETN-93-92588] p 572 N93-21022
- ATMOSPHERIC PRESSURE**
- Extremely low level jet in the evening in Kanto Plain p 430 A93-22159
- Calculation of safe altitudes p 991 A93-45675
- Surface drag instabilities in the atmospheric boundary layer p 1163 A93-49069
- SAC contrail formation study [AD-A254410] p 159 N93-12605
- Surface shear stress estimates from geostrophic winds for use in sensible and latent heat flux formulations p 936 N93-30044
- ATMOSPHERIC REFRACTION**
- Evaluation of three models used for predicting noise propagated long distances overground p 232 N93-14406
- [AD-A255963] p 232 N93-14406
- ATMOSPHERIC SOUNDING**
- Calibration results for NOAA-11 AVHRR channels 1 and 2 from congruent path aircraft observations p 1143 A93-51237
- Coherent systems in the terahertz frequency range: Elements, operation, and examples p 841 N93-27727
- ATMOSPHERIC TEMPERATURE**
- The composite shape and structure of coherent eddies in the convective boundary layer p 93 A93-12643
- Short range forecasts for air traffic control using high resolution aircraft data p 431 A93-22164
- An observational study of the dryline p 844 A93-36034
- Testing of an energy efficient environmental control system for a patrol-type aircraft [SAE PAPER 921225] p 890 A93-41399
- A horizontal atmospheric temperature sounder - Applications to remote sensing of atmospheric hazards p 929 A93-43502
- Arctic environment - Helicopter operations in cold climates p 1189 A93-54288
- SAC contrail formation study [AD-A254410] p 159 N93-12605
- ATMOSPHERIC TURBULENCE**
- An analysis of helicopter dynamic response to turbulence using fuselage and blade element atmospheric sampling techniques p 43 A93-13314
- [AIAA PAPER 92-4148] p 43 A93-13314
- Equivalent deterministic inputs for atmospheric turbulence p 183 A93-14351
- Wind lifting of aerosol particles p 223 A93-15079
- Detection and parameter estimation of atmospheric turbulence by ground-based and airborne CO2 Doppler lidars p 395 A93-17862
- A comparison of several airborne measures of turbulence p 308 A93-22121
- A summary of investigations of severe turbulence incidents using airline flight records p 308 A93-22153
- A microcomputer program for estimating low altitude wind and turbulence fields p 438 A93-22163
- Stratospheric turbulence measurements and models for aerospace plane design p 433 A93-22342
- [AIAA PAPER 92-5072] p 433 A93-22342
- Turbulence/gust alleviation using spoiler control p 369 A93-22886
- Digital simulation of atmospheric turbulence for Dryden and von Karman models p 416 A93-23517
- Flight safety in a perturbed atmosphere --- Russian book p 487 A93-29431
- [ISBN 5-277-00815-2] p 487 A93-29431
- Atmospheric turbulence simulation for rotorcraft applications p 757 A93-34264
- Studies of atmospheric eddy dynamics and energetics and climate problems p 753 A93-35689
- [ISBN 5-286-00610-8] p 753 A93-35689
- Effects of ingested atmospheric turbulence on measured tail rotor acoustics p 849 A93-35964
- Helicopter response to atmospheric turbulence p 817 A93-35987
- A horizontal atmospheric temperature sounder - Applications to remote sensing of atmospheric hazards p 929 A93-43502
- Decay of aircraft vortices near the ground p 961 A93-45751
- Interaction of the sonic boom with atmospheric turbulence p 1171 A93-48140
- [AIAA PAPER 93-2943] p 1171 A93-48140
- A new flying qualities criterion for flying wings p 1128 A93-48346
- [AIAA PAPER 93-3668] p 1128 A93-48346
- Surface drag instabilities in the atmospheric boundary layer p 1163 A93-49069
- Atmospheric disturbances over mountains and the flight safety p 1164 A93-51856
- Response of B-2 aircraft to nonuniform spanwise turbulence p 1135 A93-52437
- Identification of the phase characteristics and wind-induced perturbations of an aircraft from flight test results p 1206 A93-52943
- Study of artificial and natural turbulence in atmospheric boundary layer with a CW Doppler CO2 lidar p 1257 A93-54799
- Reynolds stress profiles in the near wake of an oscillating airfoil p 1236 A93-55380
- Estimation of aircraft inertia characteristics from bifilar pendulum test data p 1249 A93-56029
- A problem formulation for glideslope tracking in wind shear using advanced robust control techniques p 64 N93-11176
- [NASA-TM-104164] p 64 N93-11176
- A theory for the analysis of rotorcraft operating in atmospheric turbulence p 48 N93-11725
- Stratospheric turbulence measurements and models for aerospace plane design p 223 N93-13288
- [NASA-TM-104262] p 223 N93-13288
- A simulation model of atmospheric turbulence for rotorcraft applications p 224 N93-14588
- Stress calculation for the Sandia 34-meter wind turbine using the local circulation method and turbulent wind [DE93-004480] p 560 N93-22045
- ATOMIC EXCITATIONS**
- Nonequilibrium excitation of internal molecular degrees of freedom in the shock layer during hypersonic flight p 412 A93-21922
- ATOMIZERS**
- Effect of a metal deactivator fuel additive on fuel deposition in fuel atomizers at high temperature p 736 N93-25914
- [AD-A260915] p 736 N93-25914
- Velocity and drop size measurements in a swirl-stabilized, combustor spray p 813 N93-27130
- [NASA-TM-106130] p 813 N93-27130
- ATOMIZING**
- Characteristics of liquid jet atomization across a high-speed airstream. I - Experiment on shape of spray, spatial distribution of injected liquid and Sauter mean diameter p 411 A93-21743
- Characteristics of liquid jet atomization across a high-speed airstream. II - Calculation of spatial distribution of liquid, variation of drop diameter and drop trajectory p 412 A93-21744
- Atomization of JP-10/B4C gelled slurry fuel [AD-A256827] p 391 N93-15686
- Fuel injector: Air swirl characterization aerothermal modeling, phase 2, volume 1 p 721 N93-24754
- [NASA-CR-189193-VOL-1] p 721 N93-24754
- Fuel injector: Air swirl characterization aerothermal modeling, phase 2, volume 2 p 721 N93-25106
- [NASA-CR-189193-VOL-2] p 721 N93-25106
- ATTACK AIRCRAFT**
- Investigation of high-alpha lateral-directional control power requirements for high-performance aircraft p 1130 A93-49519
- [AIAA PAPER 93-3647] p 1130 A93-49519
- The effectiveness of airbags in reducing the severity of head injury from gunsight strikes in attack helicopters p 494 N93-19691
- ATTENUATION**
- Attenuation of airplane wake vortices by excitation of far-field instability p 984 A93-47277
- [AIAA PAPER 93-3511] p 984 A93-47277
- ATTITUDE (INCLINATION)**
- Optimal symmetric trajectories over a fixed-time domain p 1133 A93-51435
- [AIAA PAPER 93-3848] p 1133 A93-51435
- A dual-Euler method for solving all-attitude angles of the aircraft p 1223 A93-52682
- [AIAA PAPER 93-3589] p 1223 A93-52682
- Attitude determination using GPS: Development of an all solid-state guidance, navigation, and control sensor for air and space vehicles based on the global positioning system p 888 N93-30605
- ATTITUDE CONTROL**
- Dynamical variable structure control of a helicopter in vertical flight p 369 A93-22887
- Pilot-in-the-loop analysis of propulsive-only flight control systems p 908 A93-42812

- Robust, nonlinear, high angle-of-attack control design for a supermaneuverable vehicle
[AIAA PAPER 93-3774] p 1131 A93-51369
- Dynamic attitude measurement system
[AIAA PAPER 93-3801] p 1139 A93-51393
- Decentralized autonomous attitude determination using an inertially stabilized payload
[AIAA PAPER 93-3857] p 1134 A93-51444
- An improved calibration technique for wind tunnel model attitude sensors
p 1253 A93-54356
- A study upon structural optimization of elastic rotors for mechanical systems
[INPE-5376-TDI/471] p 83 N93-10310
- Reference equations of motion for automatic rendezvous and capture
[NASA-CR-185676] p 914 N93-29652
- ATTITUDE STABILITY**
- Hypersonic aerodynamic characteristics for Langley Test Technique Demonstrator
[AIAA PAPER 93-3443] p 1072 A93-49516
- AUDIO DATA**
- Design, fabrication, and testing of a three-dimensional acoustic orientation instrument (3-D AOI): Drawings, engineering and associated lists (conceptual and development design)
[AD-A260934] p 760 N93-25915
- AUDIO EQUIPMENT**
- High Capacity Voice Recorder (HCVR) Operational Test and Evaluation (OT/E) integration test report
[DOT/FAA/CT-TN92/30] p 88 N93-11460
- Inflight evaluation of an acoustic orientation instrument
[AD-A260752] p 719 N93-25909
- AUDIO SIGNALS**
- Fly-by voice, a technology demonstration
p 526 N93-19918
- Design, fabrication, and testing of a three-dimensional acoustic orientation instrument (3-D AOI): Drawings, engineering and associated lists (conceptual and development design)
[AD-A260934] p 760 N93-25915
- AUDITORY DEFECTS**
- Fatigue effects of noise among airplane mechanics
p 558 A93-28495
- AUDITORY PERCEPTION**
- Human response to helicopter noise - A test of A-weighting
p 587 A93-29424
- AUDITORY SIGNALS**
- Inflight evaluation of an acoustic orientation instrument
[AD-A260752] p 719 N93-25909
- Design, fabrication, and testing of a three-dimensional acoustic orientation instrument (3-D AOI): Drawings, engineering and associated lists (conceptual and development design)
[AD-A260934] p 760 N93-25915
- AUGMENTATION**
- Side force augmentation at high angle of attack from pneumatic vortex flow control
[AIAA PAPER 93-2959] p 1124 A93-48153
- The turbulence and mixing characteristics of the complex flow in a simulated augmentor
p 1123 A93-51642
- AUSTENITIC STAINLESS STEELS**
- Friction surfacing and linear friction welding
p 1217 A93-53499
- AUTOClaves**
- Development and fabrication of an autoclave molded PES/Quartz sandwich radome
p 547 A93-28279
- AUTOMATED EN ROUTE ATC**
- Flight management systems information exchange with AERA to support future air traffic control concepts --- Automated En Route ATC
p 31 A93-11008
- Rotorcraft en route ATC route standards
[AD-A249129] p 35 N93-10323
- The Canadian Automated Air Traffic System
p 886 N93-30323
- Procedural development prototype in Automated En Route Air Traffic Control
p 887 N93-30352
- AUTOMATED TRANSIT VEHICLES**
- The use of digital road data by a navigation system
p 993 N93-31269
- AUTOMATIC CONTROL**
- Automatic guidance and control for recovery of remotely piloted vehicles
p 181 A93-14188
- Rapid prototyping via automatic software code generation from formal specifications - A case study
p 227 A93-14685
- Automation of aircraft service testing tasks using the automatic control system Bezopasnost'-3
p 306 A93-18345
- Search strategies for a sequence of baseline indices for building sections of a flight-safety automatic control system in the interactive mode
p 306 A93-18346
- A methodological approach to the development of service and technical specifications for an actively controlled multistrut landing gear
p 321 A93-18349
- Automatic guidance and control laws for helicopter obstacle avoidance
p 728 A93-35518

- Flight-vehicle drives (2nd revised and enlarged edition) --- Russian book
[ISBN 5-217-00802-4] p 713 A93-35676
- Design philosophy for wind tunnel model positioning control systems
p 822 A93-37877
- A study of the stability of the acceleration circuit of the hydromechanical automatic control system of an aviation gas turbine engine
p 810 A93-39028
- Absolute stability of an automatic control system for gas turbine engines
p 810 A93-39033
- Optimization of the parameters of the lift-augmentation devices of the wing of a maneuverable aircraft equipped with an active load-reduction system
p 804 A93-39189
- The UTA autonomous aerial vehicle - Automatic control and navigation
p 908 A93-42813
- Increasing airport safety and capacity using automated maneuvering area control
p 885 A93-43550
- DeAs - A programming system for data processing and system control: New software developments for wind tunnel operation
p 1036 A93-44452
- Statistical techniques for traffic flow management
[AIAA PAPER 93-3834] p 1098 A93-51423
- Automated control of aircraft in formation flight
[AIAA PAPER 93-3852] p 1134 A93-51439
- Design philosophy for wind tunnel model positioning systems
[AD-A254958] p 192 N93-12552
- Application of concurrent engineering methods to the design of an autonomous aerial robot
[AD-A254968] p 212 N93-12555
- Theory and design of adaptive automation in aviation systems
[AD-A254595] p 160 N93-12613
- Automatic pulse shaping with the AN/FPN-42 and AN/FPN-44A Loran-C transmitters
[AD-A257860] p 319 N93-18309
- En route air traffic controllers use of flight progress strips: A graph-theoretic analysis
[AD-A259062] p 319 N93-18927
- HELITRAK: A helicopter-tracking receiver system for television outside broadcast links
[BBC-RD-1992/5] p 552 N93-20573
- Mission planning systems for tactical aircraft (pre-flight and in-flight)
[AGARD-AR-313] p 496 N93-21187
- Current projects in Fuzzy Control
p 1038 N93-31442
- AUTOMATIC CONTROL VALVES**
- A pressure distribution measuring system with pneumatic switches and automatic band selection
p 75 A93-10029
- Control of the quality of dynamic processes in the valves of power-generating equipment
p 832 A93-39030
- AUTOMATIC FLIGHT CONTROL**
- Stabilization of the dynamic characteristics of the automatic control systems of a flight vehicle
p 62 A93-12802
- Helicopter automatic flight control systems for all weather operations - EH101 and beyond
p 186 A93-17310
- Flight management systems
p 311 A93-17757
- Selection of transducer measuring ranges in flight vehicle control systems
p 526 A93-29691
- Piloted simulator investigations of a civil tilt-rotor aircraft on steep instrument approaches
p 800 A93-36023
- MD-11 Automatic Flight System
p 818 A93-37075
- An information-search system in cybernetics
p 1168 A93-50957
- Guidance and control law for automatic landing flight experiment of reentry space vehicle
[AIAA PAPER 93-3818] p 1143 A93-51409
- Stabilization of the dynamic characteristics of the two-channel automatic control system of aircraft
p 1205 A93-52941
- Research on combined HOPE navigation technology
p 533 N93-20428
- Discrete range clustering using Monte Carlo methods
[NASA-TM-104004] p 706 N93-24914
- Development and flight testing of a fault-tolerant fly-by-light yaw control system
p 1010 N93-31280
- AUTOMATIC LANDING CONTROL**
- Automatic guidance and control for recovery of remotely piloted vehicles
p 181 A93-14188
- Fixed and rotary wing all weather operations; Proceedings of the Conference, London, United Kingdom, Apr. 23, 24, 1991
[ISBN 0-903409-90-9] p 142 A93-17301
- Autoland, the developing need
p 142 A93-17302
- Fixed and rotary wing all weather operations system requirements
p 142 A93-17303
- The certification of head up displays for category 3 operation
p 142 A93-17304
- A review of alternative philosophies --- methods for operating in ICAO category 3 weather conditions
p 142 A93-17305

- The development and implementation of a head-up guidance system (HGS) for manual CAT III landings
p 151 A93-17306
- Weather information requirements for Terminal Air Traffic Control Automation
p 429 A93-22146
- GPS autoland considerations
p 792 A93-38203
- A control algorithm for a navigation-landing system in the case of a priori indeterminacy of failure data
p 882 A93-43108
- Automatic carrier landing system utilizing aircraft sensors
p 1097 A93-49590
- Guidance and control law for automatic landing flight experiment of reentry space vehicle
[AIAA PAPER 93-3818] p 1143 A93-51409
- Advanced Transport Operating System (ATOPS) Flight Management/Flight Controls (FM/FC) software description
[NASA-CR-191457] p 808 N93-28621
- AUTOMATIC PILOTS**
- Stabilization of the dynamic characteristics of the automatic control systems of a flight vehicle
p 62 A93-12802
- Control design for robust eigenstructure assignment in linear uncertain systems
p 97 A93-13241
- Linear and nonlinear aircraft flight control for the AIAA Controls Design Challenge
[AIAA PAPER 92-4628] p 62 A93-13286
- Vertical guidance for a Lockheed L1011-100 using optimal dynamic interpolation
p 369 A93-22884
- Automated control of aircraft in formation flight
[AIAA PAPER 93-3852] p 1134 A93-51439
- Stabilization of the dynamic characteristics of the two-channel automatic control system of aircraft
p 1205 A93-52941
- The design of a robust autopilot for the Archytas prototype via linear quadratic synthesis
[AD-A262151] p 820 N93-27546
- Analytical foundations of gain scheduling
[AD-A264682] p 909 N93-30550
- A high-fidelity, six-degree-of-freedom batch simulation environment for tactical guidance research and evaluation
[NASA-TM-4440] p 1010 N93-32380
- AUTOMATIC TEST EQUIPMENT**
- Automation of aircraft service testing tasks using the automatic control system Bezopasnost'-3
p 306 A93-18345
- BITE vs human judgement - The aircraft side --- Built In Test Equipment
p 238 A93-18759
- Problems of the organization of the mass testing of large structural elements of aircraft using testing machines
p 821 A93-36791
- A new and working automatic calibration machine for wind tunnel internal force balances
[AIAA PAPER 93-2467] p 1138 A93-50214
- An investigation of the influence of advanced aircraft diagnostics on the technological sophistication of maintenance personnel
[AD-A258988] p 240 N93-18887
- Standardization of automatic test equipment in the US Air force
[AD-A262076] p 809 N93-29004
- Flight control system design factors for applying automated testing techniques
[NASA-TM-4242] p 910 N93-30764
- AUTOMATIC WEATHER STATIONS**
- The Federal Aviation Administration (FAA) and the National Weather Service (NWS) modernization programs - Catalysts for change in weather services
p 427 A93-22114
- Automated Weather Distribution System (AWDS) for support of global aviation
p 428 A93-22134
- AUTOMATION**
- Advanced technology and the pilot
p 45 A93-13412
- An automated flow line for gas turbine blade repair
[ASME PAPER 92-GT-367] p 375 A93-19531
- Automation of disbond detection in aircraft fuselage through thermal image processing
p 407 A93-19598
- Maneuver option manager - Automated simplification of complex air traffic control problems
p 498 A93-25480
- Identifying ability requirements for operators of future automated air traffic control systems
[AD-A256615] p 152 N93-14276
- Developing automation for terminal air traffic control: Case study of the imaging aid
p 888 N93-30356
- AUTOMOBILE ENGINES**
- Performance simulation of a combustion engine charged by a variable geometry turbocharger. I - Prerequisites, boundary conditions and model development. II - Simulation algorithm, computed results
p 1256 A93-54648
- Advanced Turbine Technology Applications Project (ATTAP)
[NASA-CR-189228] p 455 N93-18762

AUTOMOBILES

- Differential GPS control of Starcar 2 p 317 A93-21201
- A comparison between the impact of noise from aircraft, road traffic and trains on long-term recall and recognition of a text in children aged 12-14 years p 1163 A93-49552
- Lanchester: The man [AERO-REPT-9111] p 456 N93-16464
- Advanced Turbine Technology Applications Project (ATTAP) [NASA-CR-189228] p 455 N93-18762
- AUTONOMOUS NAVIGATION**
 - A fast algorithm for obtaining dense depth maps for high speed navigation p 435 A93-19080
 - A formalization and implementation of topological visual navigation in two dimensions p 435 A93-19101
 - Autonomous guidance, navigation and control bridging program plan p 532 A93-27046
 - The UTA autonomous aerial vehicle - Automatic control and navigation p 908 A93-42813
 - Decentralized autonomous attitude determination using an inertially stabilized payload [AIAA PAPER 93-3857] p 1134 A93-51444
 - A parallel implementation of a multisensor feature-based range-estimation method p 1099 A93-51967
 - A vision-based method for autonomous landing p 1190 A93-53172
 - Application of concurrent engineering methods to the design of an autonomous aerial robot [AD-A254968] p 212 N93-12555
 - The use of digital road data by a navigation system p 993 N93-31269

AUTONOMY

- A parallel implementation of a multisensor feature-based range-estimation method p 1099 A93-51967
- Implementing system simulation of C3 systems using autonomous objects [NASA-CR-190845] p 89 N93-11716

AUTOROTATION

- Stability of the vertical autorotation of a single-winged samara p 274 A93-22443
- MI-26 autorotational landings p 816 A93-35955

AUXILIARY POWER SOURCES

- Comparison of all-electric secondary power systems for civil transport p 519 A93-25997
- Comparison of all-electric secondary power systems for civil subsonic transports [NASA-TM-105852] p 55 N93-10456

AVAILABILITY

- Work performed in the United Kingdom to establish the feasibility of RAIM in a GPS receiver in flight p 314 A93-21157
- Decision making for a public differential GPS service p 314 A93-21165
- Future availability of aircraft maintenance personnel p 570 A93-27133

AVIATION METEOROLOGY

- Optimization of time saving in navigation through an area of variable flow p 34 A93-12125
- Joint NASA/USAF Airborne Field Mill Program - Operation and safety considerations during flights of a Lear 28 airplane in adverse weather [AIAA PAPER 92-4093] p 93 A93-13262
- Aircraft lightning initiation and interception from in situ electric measurements and fast video observations p 140 A93-14064
- Jet streams and associated turbulence and their effects on air transport flight operations p 154 A93-14231
- Principles of the design of automated meteorological support systems for aviation [ISBN 5-286-00342-7] p 151 A93-15224
- Motion and decay of trailing vortices within the atmospheric surface layer p 425 A93-18548
- International Conference on Aviation Weather Systems, 4th, Paris, France, June 24-28, 1991, Preprints p 426 A93-22101
- An index of resource materials for aviation meteorology education and training p 453 A93-22105
- Weather-related accidents in the Canadian aviation industry - An analysis of the chief contributory factors p 307 A93-22106
- Weather forecasts for aviation in Canada (FACN and FTGN) - The way they are taught and how they can be made more suitable to the needs of pilots p 454 A93-22108
- New initiatives for aviation meteorology training - 1989 through 1991 p 307 A93-22109
- Improving weather questions on Federal Aviation Administration exams p 308 A93-22110
- An experimental cockpit display for TDWR wind shear alerts p 343 A93-22111
- Hazard assessment and cockpit presentation issues for microburst alerting systems p 308 A93-22112
- Distribution of aviation weather graphics via airline communications networks p 426 A93-22113

- The Federal Aviation Administration (FAA) and the National Weather Service (NWS) modernization programs - Catalysts for change in weather services p 427 A93-22114
- The importance of proper aviation weather dissemination to pilots - An airline captain's perspective p 308 A93-22115
- Detection of microburst-related gust fronts using Doppler radar p 427 A93-22118
- Preliminary results of the detection of clear air turbulence by the Wind Profiler Demonstration Network p 427 A93-22119
- Improvement in gust front algorithm detection capability using reflectivity thin lines versus azimuthal shears p 427 A93-22120
- A comparison of several airborne measures of turbulence p 308 A93-22121
- A 'new age' in aviation weather forecasting p 427 A93-22123
- Developing the Aviation Gridded Forecast System p 427 A93-22124
- The Aviation Weather Products Generator p 428 A93-22125
- Integrated Terminal Weather System (ITWS) p 428 A93-22127
- Integrated runway meteorological observation system (IRMOS/SIOMA) p 428 A93-22128
- The Meteorologist Weather Processor for U.S. National Weather Service units at Federal Aviation Administration sites p 428 A93-22130
- FAA weather processor programs - Real-time dissemination of weather information to aviation end-users p 428 A93-22131
- MIST - A remote briefing system p 437 A93-22132
- The Meteorological Data Collection and Reporting System - Status and future directions p 428 A93-22133
- Automated Weather Distribution System (AWDS) for support of global aviation p 428 A93-22134
- A proposed icing severity index based upon meteorology p 429 A93-22136
- Sea fog and stratus - A major aviation hazard in the northern Gulf of Mexico p 429 A93-22141
- Impact of weather on aviation - A global view p 308 A93-22143
- Improved efficiency of air transportation through aviation weather system modernization p 308 A93-22144
- Operational aviation weather service requirements p 429 A93-22145
- Weather information requirements for Terminal Air Traffic Control Automation p 429 A93-22146
- Numerical forecasting of liquid water content to assess airframe icing risk p 429 A93-22147
- An evaluation of aircraft icing forecasts for the continental United States p 429 A93-22149
- Liquid water profiling using remote sensor observations p 429 A93-22150
- Buoyancy wave hazards to aviation p 430 A93-22151
- Maximum hail concentration that can be met by an aircraft in stormy precipitations p 430 A93-22152
- A summary of investigations of severe turbulence incidents using airline flight records p 308 A93-22153
- Diagnostic studies of clear air turbulence in isentropic coordinates p 430 A93-22154
- A fine structure of the gust front observed with sonic anemometer p 430 A93-22158
- Extremely low level jet in the evening in Kanto Plain p 430 A93-22159
- Turbulence avoidance p 309 A93-22160
- Validation of aviation weather products for the Advanced Traffic Management System p 430 A93-22161
- The role of national meteorological services in aviation servicing under the final phase of the World Area Forecast System p 431 A93-22162
- A microcomputer program for estimating low altitude wind and turbulence fields p 438 A93-22163
- Short range forecasts for air traffic control using high resolution aircraft data p 431 A93-22164
- Terminal forecast amendments - A 'cloudy' issue - valid for up to 24 hours for airport areas p 431 A93-22167
- A quantitative method to estimate the microburst wind shear hazard to aircraft p 309 A93-22172
- Elevated array detection and measurement of microbursts using Theta(E) p 412 A93-22173
- Ice prediction systems for runways p 376 A93-22174
- SAAW - Italy's answer to the windshear challenge p 431 A93-22175
- An automated system for the measurement of slant visual range p 413 A93-22176
- The redesigned Low Level Wind Shear Alert System p 431 A93-22179
- Seasonal weather hazards p 431 A93-22180
- Volcanic ash and aircraft operations p 309 A93-22181

- Status of the Terminal Doppler Weather Radar one year before deployment p 431 A93-22184
- Reliability considerations for weather hazard warning radar p 431 A93-22187
- Terminal Doppler Weather Radar program at Denver's Stapleton International Airport during 1989 and 1990 p 432 A93-22188
- Performance results and potential operational uses for the prototype TDWR microburst prediction product p 432 A93-22190
- An improved gust front detection algorithm for the TDWR p 432 A93-22191
- The detection and warning of low-level wind shear based on terminal single Doppler radar p 432 A93-22195
- The dynamics of microbursts as revealed by Doppler radar observations and numerical simulations p 432 A93-22196
- Microburst observations in tropical Australia p 432 A93-22198
- Doppler radar observation of tornado and microburst around Chitose Airport p 432 A93-22199
- Structure of downbursts associated with heavy rainfall observed in Tokyo p 433 A93-22200
- Microbursts detection with airborne Doppler lidar p 433 A93-22201
- Evaluation of clear-air radar PROUST and Doppler radar RONSARD for airport low level-wind shear detection p 433 A93-22202
- Two and three-dimensional prediffuser combustor studies with air-water mixture [AIAA PAPER 93-0240] p 390 A93-22652
- Atmospheric turbulence aloft - A review of possible methods for detection, warning, and validation of prediction models p 557 A93-24914
- [AIAA PAPER 93-0847] p 557 A93-24914
- Flight safety in a perturbed atmosphere --- Russian book [ISBN 5-277-00815-2] p 487 A93-29431
- Nowcasts of thunderstorm initiation and evolution p 752 A93-33773
- Electrostatic discharges [ONERA, TP NO. 1992-82] p 844 A93-38567
- Atmospheric disturbances over mountains and the flight safety p 1164 A93-51856
- Visual weather simulation using meteorological databases [AIAA PAPER 93-3566] p 1207 A93-52665
- Proceedings of the National Weather Service Aviation Workshop: Postprint volume [PB92-176148] p 94 N93-11803
- Adverse weather test site selection study [AD-A259012] p 339 N93-18895
- Airborne Wind Shear Detection and Warning Systems: Fourth Combined Manufacturers' and Technologists' Conference, part 1 [NASA-CP-10105-PT-1] p 488 N93-19590
- Program overview: 1991 flight test objectives p 488 N93-19591
- NASA airborne radar wind shear detection algorithm and the detection of wet microbursts in the vicinity of Orlando, Florida p 490 N93-19611
- Signal processing for airborne doppler radar detection of hazardous wind shear as applied to NASA 1991 radar flight experiment data p 490 N93-19612
- The 1992 International Aerospace and Ground Conference on Lightning and Static Electricity: Addendum [DOT/FAA/CT-92/20-ADD-1] p 753 N93-24875
- A procedure for defining lightning risk to air vehicles p 703 N93-24885
- A statistical characterization of Denver-area microbursts [AD-A262127] p 845 N93-27675
- Meteorological information for aviation: A systems approach p 937 N93-30298
- Preliminary evaluation of aviation-impact variables derived from numerical models [PB93-190197] p 1034 N93-31202
- AVIATION PSYCHOLOGY**
 - Specification of adaptive aiding systems [AD-A254537] p 159 N93-12602
 - Theory and design of adaptive automation in aviation systems [AD-A254595] p 160 N93-12613
 - The human factor problem in the Canadian Forces aviation p 491 N93-19657
 - Underlying causes of accidents: Casual networks p 491 N93-19658
 - Human factors causes and management strategies in US Air Force F-16 mishaps 1984-present p 492 N93-19673
- AVIONICS**
 - Optical interconnection and packaging technologies for advanced avionics systems p 77 A93-10960
 - A large flat panel multifunction display for military and space applications p 77 A93-10963

A fault-tolerant air data/inertial reference system p 50 A93-10982

Automatic dependant surveillance focus of civil avionics integration p 30 A93-10998

Sensor alignment Kalman filters for inertial stabilization systems p 50 A93-11018

Trends of the airborne cockpit display format p 50 A93-11203

Real-time capture, archiving, retrieval, processing, and presentation of large quantities of flight test/research information p 95 A93-11258

[AIAA PAPER 92-4073] Phase I flight test of MIAG advanced development model p 95 A93-11261

[AIAA PAPER 92-4076] TCAS display issues p 51 A93-13351

[AIAA PAPER 92-4242] Electronics show their age p 80 A93-13447

TCAS II testing conflicts and resolutions p 165 A93-14158

Control of the pilot-system interface p 166 A93-15040

Methodology in the development of avionics p 166 A93-15043

Cost control of the A320 software - The aircraft manufacturer's point of view p 227 A93-15044

Radiated electric field measurements in U.S. Army helicopters p 209 A93-16163

Trends in advanced avionics --- Book [ISBN 0-8138-0749-2] p 341 A93-17574

ARINC 629 DATABUS; Proceedings of the Conference, London, United Kingdom, Sept. 24, 1991 [ISBN 0-903409-95-X] p 311 A93-17835

BITE vs human judgement - The aircraft side --- Built In Test Equipment p 238 A93-18759

Digital avionics systems - Principles and practices (2nd revised and enlarged edition) --- Book [ISBN 0-07-060333-2] p 342 A93-19801

Finding fault with avionics p 410 A93-21629

Advancing helicopters p 327 A93-21836

Fully automatic FEM data pre-processing for aeronautical electrical machine p 538 A93-24030

Analog simulation as part of a power supply design analysis universal platform p 543 A93-25962

Digital map databases in support of avionic display systems p 544 A93-26888

Neural network controllers for the X29 aircraft p 817 A93-37005

SAFEbus p 828 A93-37072

A fault-tolerant Air Data/Inertial Reference Unit p 807 A93-37074

Avionic systems/design and maintenance; Proceedings of the Conference, Hounslow, United Kingdom, Apr. 22, 1993 [ISBN 1-85768-095-2] p 764 A93-39535

Software - Design for maintenance p 847 A93-39537

Antennas now and future p 764 A93-39540

Enhanced heat transport in environmental systems using microencapsulated phase change materials [SAE PAPER 921224] p 926 A93-41398

Integrated modular avionics p 896 A93-42777

Integrating controls and avionics on commercial aircraft p 892 A93-42778

Application of modular avionics to the EF-111A systems improvement program p 896 A93-42780

Pave Pillar in-house research final report p 927 A93-42781

Cross channel dependency requirements of the multi-path redundant avionics suite p 928 A93-42782

Reconfigurable photonic data networks for military aircraft p 928 A93-42783

The PAVE PACE integrated RF architecture for next generation avionics p 896 A93-42784

Selecting locations for avionics antennas - A structured approach p 892 A93-42794

Direct optical control - A lightweight backup consideration p 907 A93-42808

Avionics software performability p 939 A93-42822

Complexity metrics for avionics software p 939 A93-42829

Database management for integrated avionics system p 939 A93-42831

Functionally Integrated Resource Manager for real-time avionics data p 940 A93-42832

Additional developments in embedded computer performance measurement p 940 A93-42833

Evaluating the IOBIDS specification using gate-level system simulation p 940 A93-42851

New developments in a PI-Bus specification by the JIAWG and SAE p 940 A93-42852

Environmental definition of a multi-platform avionics system p 896 A93-42855

The Pave Pace integrated core processor p 941 A93-42856

Getting a handle on designing for avionics software supportability and maintainability p 941 A93-42862

Computer-aided design of avionic diagnostics algorithms p 941 A93-42863

Optical correlator field test results p 1038 A93-44458

Use of Convex supercomputers for flight simulation at NASA Langley p 1013 A93-46806

Development methodology for contemporary avionics systems [SAE PAPER 931591] p 1104 A93-49340

STANAG 3910 - The data bus for the next generation of European avionics systems [SAE PAPER 931595] p 1104 A93-49344

JIAWG compatible development boards for the i960 [SAE PAPER 931596] p 1104 A93-49345

High speed databus evaluation - Further work [SAE PAPER 931597] p 1151 A93-49346

Changing the utility subsystem paradigm [SAE PAPER 931598] p 1165 A93-49347

Compact high reliability fiber coupled laser diodes for avionics and related applications p 1152 A93-49470

An interworking router for avionics applications --- Bridge/Router unit in fiber optics aircraft communication p 1097 A93-49479

Single event upset in avionics p 1158 A93-50566

On definition and use of systems engineering processes, methods and tools p 1225 A93-53642

Integrated fire control simulation systems p 1192 A93-53876

Avionic systems in support of covert helicopter operations p 1193 A93-54294

Fighting for air p 1243 A93-54650

Future trends in IR sensors p 1258 A93-55295

Aeronautical technologies for the twenty-first century [NASA-CR-190918] p 4 N93-10647

Requirements analysis notebook for the flight data systems definition in the Real-Time Systems Engineering Laboratory (RSEL) [NASA-CR-185698] p 69 N93-10960

Integration of radar altimeter, precision navigation, and digital terrain data for low-altitude flight [NASA-TM-103958] p 36 N93-12320

A brief overview of NASA Langley's research program in formal methods p 228 N93-12958

FDAMS: An extendable and reconfigurable solution for avionics data management systems p 168 N93-15157

Personal computer based test- and emulation equipment for maintenance and ground support p 110 N93-15185

Using software metrics and software reliability models to attain acceptable quality software for flight and ground support software for avionic systems p 442 N93-17305

Test and integration concept for complex helicopter avionic systems [MBB-UD-0605-91-PUB] p 343 N93-17547

Technical operating report on the Data Integration and Collection Environment (DICE) instrumentation system design [AD-A258444] p 455 N93-17891

Joint Integrated Avionics Working Group (JIAWG) object-oriented domain analysis method (JODA), version 3.1 [AD-A258468] p 344 N93-18270

Detection of spoofing, jamming, or failure of a Global Positioning System (GPS) [AD-A259023] p 319 N93-18951

YF-22A prototype advanced tactical fighter demonstration/validation flight test program overview p 511 N93-19906

USA aviation digest index, 1989, volume 11 [AD-A258673] p 571 N93-20388

Index to USA aviation digest, 1990 [AD-A258678] p 572 N93-20389

Index to USA aviation digest, 1991 [AD-A258679] p 572 N93-20390

Software design document for the generic avionics data bus tool kit [AD-A259329] p 519 N93-21259

Alternative equipment test procedures for simultaneous current injection on multiple cable bundles p 747 N93-24903

Aircraft electrical and environmental systems, AFSCs 452x5, 454x5, and 454x6 [AD-A261213] p 717 N93-25733

Avionics systems architectures p 808 N93-27169

YF-22A prototype advanced tactical fighter demonstration/validation flight test program overview p 805 N93-27173

Standardization of automatic test equipment in the US Air force [AD-A262076] p 809 N93-29004

Strategic avionics technology definition studies. Subtask 3-1A: Electrical Actuation (ELA) systems [NASA-CR-193237] p 914 N93-29215

Flight test of avionic and air-traffic control systems [ESA-TT-1279] p 993 N93-31271

Instigation and processing of flight tests in DLR p 998 N93-31275

AVOIDANCE

Airbus Industrie TCAS experience p 152 N93-15186

AXES OF ROTATION

A study of heat transfer from a disk in a rotating cavity with axial and radial-axial flow of a liquid p 54 A93-12812

Computerized synthesis of three-dimensional kinematic landing gear schemes with a single turning axis p 891 A93-42376

AXIAL COMPRESSION LOADS

Effect of stiffness characteristics on the response of composite grid-stiffened structures p 1022 A93-45148

AXIAL FLOW

On the use of the method of matched asymptotic expansions in propeller aerodynamics and acoustics p 8 A93-11553

Analytical method for subsonic cascade profile p 12 A93-12730

Prediction of the inception of rotating stall for multistage axial flow compressors p 12 A93-12731

Effect of hub treatment on performance of an axial flow compressor p 53 A93-12736

A study of heat transfer from a disk in a rotating cavity with axial and radial-axial flow of a liquid p 54 A93-12812

Computer aided aerodynamic design of high pressure axial flow fan blade element p 16 A93-13649

Recess vane passive stall control [ASME PAPER 92-GT-36] p 246 A93-19296

Flow studies in ducted twin-rotor contra-rotating axial flow fans [ASME PAPER 92-GT-390] p 258 A93-19545

An optical comparison of wall and axial injection for high enthalpy reacting scramjet flows [AIAA PAPER 93-0357] p 377 A93-23040

Some measurements of stall in an axial impeller [ISABE 93-7008] p 1183 A93-53984

Application of recess vane casing treatment to axial flow fans p 423 N93-18728

The WINCOF-I code: Detailed description [NASA-CR-190779] p 677 N93-24760

AXIAL FLOW TURBINES

One-dimensional methods for accurate prediction of off-design performance behavior of axial turbines [ASME PAPER 92-GT-54] p 347 A93-19304

Turbulence evaluation within the secondary flow region of a turbine cascade [ASME PAPER 92-GT-60] p 247 A93-19310

Three dimensional transonic flow measurements in an axial turbine with conical walls [ASME PAPER 92-GT-61] p 247 A93-19311

Tip clearance effect on heat transfer and leakage flows on the shroud-wall surface in an axial flow turbine [ASME PAPER 92-GT-200] p 403 A93-19425

The measurement and prediction of the tip clearance flow in linear turbine cascades [ASME PAPER 92-GT-214] p 252 A93-19437

A simple method for estimating secondary losses in turbines at the preliminary design stage [ASME PAPER 92-GT-294] p 254 A93-19484

Ingestion into the upstream wheel-space of an axial turbine stage [ASME PAPER 92-GT-303] p 354 A93-19493

Multipassage three-dimensional Navier-Stokes simulation of turbine rotor-stator interaction p 688 A93-34484

Optimization of a highly-loaded axial splitters rotor design p 1002 A93-46931

3D viscous flow analysis in axial turbine including tip leakage phenomena p 972 A93-46940

Intensive industrial use of 3D Euler numerical methods for axial flow turbine analysis and design p 1002 A93-46943

3-dimensional interactions in the rotor of an axial turbine [AIAA PAPER 93-2255] p 1081 A93-50053

Three-dimensional flow field in a turbine nozzle passage [AIAA PAPER 93-2556] p 1084 A93-50278

3D and 2.5D viscous flow computations for axial flow turbine blades [ISABE 93-7093] p 1186 A93-54069

Stall in axial flow aero engine compressors p 422 N93-18723

Stall and surge in axial flow compressors p 423 N93-18724

Aero-thermal design of a cooled transonic NGV and comparison with experimental results p 904 N93-29957

SUBJECT INDEX

BALLOON-BORNE INSTRUMENTS

The ViB-code to simulate 3-D stator/rotor flow in axial turbines
[DLR-FB-92-19] p 1003 N93-31170
Penn State axial flow turbine facility: Performance and nozzle flow field p 1032 N93-31588

AXIAL LOADS

Design of advanced beams considering elasto-plastic behaviour of material p 544 A93-26904
An evaluation of the pressure proof test concept for 2024-T3 aluminium alloy sheet p 1026 A93-45780
Testing experience with unheated strain-gage balances in the NTF - National Transonic Facility p 1013 A93-47021

AXIAL STRESS

Prediction of fatigue crack growth kinetics in the plane structural elements of aircraft in the biaxial stress state p 1025 A93-45670

AXISYMMETRIC BODIES

Dynamic stability of bodies of revolution in compressible flow p 12 A93-12558
Near-field behavior of a tip vortex p 288 A93-23549
Three-dimensional flow simulation over axisymmetric bodies using Navier-Stokes equations at hypersonic Mach numbers p 461 A93-24090
Hypersonic nonequilibrium flow computations using the Roe flux-difference split scheme p 692 A93-35609
Hypersonic chemically reacting flow of a reentry body p 769 A93-38147
Enhancements to viscous-shock-layer technique p 962 A93-46408
Aerodynamic heating in the vicinity of hypersonic, axisymmetric, shock-wave boundary-layer interactions [AIAA PAPER 93-2766] p 963 A93-46512
Observations of large-scale structures in wakes behind axisymmetric bodies p 965 A93-46748
Active forcing of an axisymmetric leading-edge turbulent separation bubble [AIAA PAPER 93-3245] p 966 A93-46790
Transition in supersonic flow past axisymmetric bodies p 967 A93-46817
Elliptic cross section tip effects on the vortex wake of an axisymmetric body at angle of attack [AIAA PAPER 93-2960] p 1124 A93-48154
A numerical analysis of supersonic flow over an axisymmetric afterbody [AIAA PAPER 93-2347] p 1083 A93-50121
A study upon structural optimization of elastic rotors for mechanical systems [INPE-5376-TD/471] p 83 N93-10310
Design optimization of natural laminar flow bodies in compressible flow [NASA-CR-4478] p 292 N93-16940
Aerodynamic heating analysis for axisymmetric bodies in supersonic flow p 303 N93-19312
Analysis of wind-tunnel data for elliptic cross-sectioned forebodies at Mach numbers 0.4 to 5.0 p 782 N93-27221
Investigations on entropy layer along hypersonic hyperboloids using a defect boundary layer p 787 N93-27462

AXISYMMETRIC FLOW

Direct numerical simulation of laminar breakdown in high-speed, axisymmetric boundary layers p 8 A93-11527
Calculation of separated axisymmetric flow past bodies by solving Euler equations in the inner vortex region p 14 A93-12975
Viscous flow field prediction in axisymmetric passages p 204 A93-14478
Experimental study of controlled tip disturbance effect on flow asymmetry p 211 A93-17417
Breakdown of steady state axisymmetric flow in a shock layer formed as a result of the impingement of a supersonic underexpanded jet on a perpendicular plane obstacle p 241 A93-18230
A viscous axisymmetric throughflow prediction method for multi-stage compressors [ASME PAPER 92-GT-293] p 254 A93-19483
Numerical study of an axisymmetric turbulent jet-impingement flow [AIAA PAPER 93-0652] p 543 A93-25545
Convenient method to convert two-dimensional CFD codes into axisymmetric ones p 689 A93-34499
Experimental validation of a discrete vortex method for inviscid axisymmetric flow around parachute canopies [AIAA PAPER 93-1216] p 689 A93-35165
Hydrodynamics and heat transfer near the stagnation point in an arbitrary axisymmetric nonswirling flow incident on a rotating obstacle p 691 A93-35270
Experimental investigations of asymmetric vortex flows behind elliptic cones at incidence p 757 A93-35637
An implicit finite-difference algorithm for the numerical simulation of supersonic flow over blunt bodies p 770 A93-38325

Numerical study of spontaneous nitrogen condensation in the axisymmetric hypersonic nozzles of wind tunnels p 777 A93-39143
Analysis of hypersonic nozzles including vibrational nonequilibrium and intermolecular force effects p 861 A93-41916
Mach disk of dual coaxial axisymmetric jets p 861 A93-41932
Numerical simulation of two-dimensional and axisymmetric compressible flows p 960 A93-45546
A viscous shock-layer analysis of 2-D and axisymmetric flows [AIAA PAPER 93-2751] p 963 A93-46500
Direct and inverse problems of calculating the axisymmetric and 3D flow in axial compressor blade rows p 972 A93-46938
Behaviour of the Johnson-King turbulence model in axisymmetric supersonic flows [AIAA PAPER 93-3032] p 1056 A93-48214
Design of axisymmetric channels with rotational flow [AIAA PAPER 93-3117] p 1062 A93-48287
Experimental study of transitional axisymmetric shock-boundary layer interactions at Mach 5 [AIAA PAPER 93-3131] p 1063 A93-48296
The numerical calculation on the flowfields of transverse jet interaction in the base of vehicle at supersonic speeds [AIAA PAPER 93-1931] p 1077 A93-49795
A simplified approach for control of rotating stall. I - Theoretical development [AIAA PAPER 93-2229] p 1080 A93-50035
Design of shockless supersonic region in the axisymmetric transonic flow p 1230 A93-54587
Two problems applied to the rheographical transformation of axisymmetric flow p 1231 A93-54599
Algebraic determination of the shock wave shape in axisymmetric flow over a circular cylinder p 1237 A93-56030
BLSTA: A boundary layer code for stability analysis [NASA-CR-4481] p 220 N93-14797
Numerical simulation of a high Mach number jet flow [NASA-TM-105985] p 551 N93-20057
Simulation of vortex bursting p 699 N93-25881
The addition of algebraic turbulence modeling to program LAURA [NASA-TM-107758] p 840 N93-27250
Turbulence characteristics of an axisymmetric reacting flow [NASA-CR-4110] p 877 N93-30373
Numerical simulation of the flow in a 1:57-scale axisymmetric model of a large blast simulator [AD-A265551] p 1015 N93-31916

AZIMUTH

Improvement in gust front algorithm detection capability using reflectivity thin lines versus azimuthal shears p 427 A93-22120
The real aperture antenna of SAR, a key element for performance p 213 N93-13053

B

B-2 AIRCRAFT

B-2 flight test program - An update [AIAA PAPER 92-4118] p 42 A93-13266
B-2 flight test update p 803 A93-38844
Aeroelastic effects on the B-2 maneuver response [AIAA PAPER 93-3664] p 1128 A93-48344
Response of B-2 aircraft to nonuniform spanwise turbulence p 1135 A93-52437

BACKGROUND RADIATION

Stray radiation in optical systems II; Proceedings of the Meeting, San Diego, CA, July 20-22, 1992 [SPIE-1753] p 1263 A93-55176

BACKSCATTERING

Fundamentals of low radar cross-sectional aircraft design p 802 A93-37376

BACKUPS

Direct optical control - A lightweight backup consideration p 907 A93-42808

BACKWARD FACING STEPS

Correlation of mean velocity measurements downstream of a swept backward-facing step p 123 A93-14552
Effects of injector geometry on scramjet combustor performance p 359 A93-21670
The three-dimensional separated flow structure in a variable aspect ratio sudden expansion duct [AIAA PAPER 93-0213] p 278 A93-22630
A coupled multi-block solution procedure for spray combustion in complex geometries [AIAA PAPER 93-0108] p 539 A93-24230
Experimental supersonic hydrogen combustion employing staged injection behind a rearward-facing step p 744 A93-34496

Computation of hypersonic turbulent flow over a rearward facing step p 865 A93-42587
Laser holographic interferometric measurements of the flow behind a rearward facing step [AIAA PAPER 93-3515] p 985 A93-47279
Numerical study of supersonic flow over a backward step with transverse injection p 1182 A93-53853
An experimental investigation on laminar boundary layer separation over a backward-facing step p 1230 A93-54588
Effect of passive flow-control devices on turbulent low-speed base flow p 82 N93-10304
Characteristics of separated flows including cavitation effects p 84 N93-10874
Velocity and temperature measurements in a non-premixed reacting flow behind a backward facing step p 132 N93-13632
A realizable Reynolds stress algebraic equation model [NASA-TM-105993] p 290 N93-16596
An experimental investigation of the separating/reattaching flow over a backstep [NASA-CR-192105] p 298 N93-18781

BAGGAGE

A review of the development of a luggage explosive detection system p 497 N93-21862
Longitudinal acceleration test of overhead luggage bins in a transport airframe section [DOT/FAA/CT-92/9] p 991 N93-31652

BALANCING

Optimum balancing of flexible rotor p 205 A93-14489
A data acquisition system for high-speed rotor balancing p 1261 A93-54396

BALLAST (MASS)

Recent refinements and increased capabilities in balloon vertical performance analysis p 40 A93-11361
Determination of balloon gas mass and revised estimates of drag and virtual mass coefficients p 7 A93-11362

BALLISTIC RANGES

Upgrade of ballistic range facilities at AEDC - Two-thirds complete [AIAA PAPER 93-0349] p 377 A93-23034
A combined facility of ballistic range and shock tunnel using a fast action valve p 1012 A93-45532

BALLOON FLIGHT

Recent refinements and increased capabilities in balloon vertical performance analysis p 40 A93-11361
Determination of balloon gas mass and revised estimates of drag and virtual mass coefficients p 7 A93-11362
NASA balloon design and flight - Philosophy and criteria p 40 A93-11363
The improvement of the static launch method in Japan p 26 A93-11364
Trans-oceanic, polar patrol balloons and future prospects p 26 A93-11366
The GRAD Supernova Observer - First Flight of a very large balloon over Antarctica p 27 A93-11367
Review and prospect of Chinese scientific balloon activities p 1 A93-11368
Long-duration balloon flights in the middle stratosphere p 40 A93-11369
NASA Long Duration Balloon capability development project p 2 A93-11370
Concept for an open-neck stratospheric balloon with long-duration flight capability p 40 A93-11371
Trans-oceanic balloon flight over east China sea p 27 A93-11372
Polar Patrol Balloon Experiment in Antarctica p 27 A93-11373
A joint Soviet-Bulgarian scientific program for free-flight and tethered aerostat observations p 2 A93-11374
Scientific ballooning payload termination loads p 27 A93-11383
Estimation of the external loading of airships in flight p 366 A93-18383
Effect of the Reynolds number on the aerodynamic characteristics of a body of revolution over a wide range of angles of attack p 242 A93-18384

BALLOON-BORNE INSTRUMENTS

The unrealized potential for heavy balloon payloads p 39 A93-11359
Determination of balloon gas mass and revised estimates of drag and virtual mass coefficients p 7 A93-11362
The improvement of the static launch method in Japan p 26 A93-11364
The GRAD Supernova Observer - First Flight of a very large balloon over Antarctica p 27 A93-11367
Review and prospect of Chinese scientific balloon activities p 1 A93-11368
Long-duration balloon flights in the middle stratosphere p 40 A93-11369
NASA Long Duration Balloon capability development project p 2 A93-11370

- Trans-oceanic balloon flight over east China sea p 27 A93-11372
- Scientific ballooning payload termination loads p 27 A93-11383
- Resonance frequencies of a gondola submitted to a forced rotation under a stratospheric balloon p 27 A93-11384

BALLOONS

- NASA balloon design and flight - Philosophy and criteria p 40 A93-11363
- Status of the NASA Balloon Program p 1 A93-11365

- Review and prospect of Chinese scientific balloon activities p 1 A93-11368
- NASA Long Duration Balloon capability development project p 2 A93-11370
- Steady state model for the thermal regimes of shells of airships and hot air balloons p 207 A93-15072

BANDPASS FILTERS

- The history and development of coated Contrast Enhancement Filters for cockpit displays p 564 A93-28180
- Design and implementation of digital filters for analysis of F/A-18 flight test data p 17 A93-10342
- IR imaging for combustion characteristics and optical properties of boron/boron oxide p 393 A93-17693

BANDWIDTH

- The real aperture antenna of SAR, a key element for performance p 213 A93-13053
- Low bandwidth robust controllers for flight [NASA-CR-191774] p 372 A93-17800
- Robo-line storage: Low latency, high capacity storage systems over geographically distributed networks [NASA-CR-192910] p 758 A93-25130
- Bandwidth and SIMDUCE as simulator fidelity criteria p 913 A93-30690

BAROCLINIC WAVES

- Determination of the zone of the stall cell by means of the baroclinic wave theory p 424 A93-18733
- Rotating stall cell and Von Karman vortex street: A meteorological theory p 424 A93-18734

BARRIERS

- Experiments on shock-wave/boundary-layer interactions produced by two-dimensional ramps and three-dimensional obstacles p 865 A93-42589
- A synthesis of results on the calculation of flow over a 2D ramp and a 3D obstacle - Antibes test cases 3 and 4 p 867 A93-42601

BASE FLOW

- An adaptive grid/Navier-Stokes methodology for the calculation of nozzle afterbody base flows with a supersonic freestream [AIAA PAPER 93-1922] p 1076 A93-49788
- A numerical analysis of supersonic flow over an axisymmetric afterbody [AIAA PAPER 93-2347] p 1083 A93-50121
- Effect of passive flow-control devices on turbulent low-speed base flow p 82 A93-10304
- Numerical investigations into the base drag of various wedges using the base flow model developed by Mauri Tanner [REPT-B-36] p 26 A93-12414
- Computation of H₂/air reacting flowfields in drag-reduction external combustion [NASA-CR-191071] p 536 A93-20237

BEAM SPLITTERS

- The HYDICE instrument design and its application to planetary instruments p 842 A93-28766

BEAMFORMING

- Experimental results on RIAS digital beamforming radar p 929 A93-43392

BEAMS (SUPPORTS)

- On the static aeroelastic tailoring of composite aircraft swept wings modelled as thin-walled beam structures p 158 A93-14820
- Nonlinear response of a clamped beam and plate to high levels of excitation p 397 A93-19141
- Design of advanced beams considering elasto-plastic behaviour of material p 544 A93-26904
- Energy-absorbing-beam design for composite aircraft subfloors [AIAA PAPER 93-1339] p 709 A93-33909
- Finite element nonlinear random response of beams to acoustic and thermal loads applied simultaneously [AIAA PAPER 93-1427] p 740 A93-33978
- Nonlinear large amplitude vibration of composite helicopter blade at large static deflection p 713 A93-35630
- On design and optimization of curved composite beams p 826 A93-35953
- Optimization of the stiffness and mass characteristics of lifting surface structures modeled by an elastic beam p 827 A93-36789

- Radii effect on the translation spring constant of force transducer beams p 829 A93-37867

- The Airbus floor beam: Towards a cost-effective composite design and manufacture research project sponsored by Airbus industry [LR-677] p 329 A93-16283

- Dynamic simulation of flexible body systems by the vector solution method p 553 A93-20666

BEARING (DIRECTION)

- Bearings-only and Doppler-bearing tracking using instrumental variables p 501 A93-29600

BEARING ALLOYS

- On the fatigue life of M50 NiL rolling bearings p 78 A93-11346

BEARINGLESS ROTORS

- Comprehensive analysis of bearingless rotors - Model development and experimental correlation of modes, response, trim and stability [AIAA PAPER 93-0624] p 504 A93-24741
- Aeromechanical stability of a bearingless composite rotor in forward flight [AIAA PAPER 93-1305] p 726 A93-33881
- Developing the MD Explorer p 744 A93-34472
- Application of component mode synthesis to modeling the dynamic response of Bearingless Main Rotors p 796 A93-35976
- Structural dynamic analysis of bearingless rotor blade p 717 A93-25719

BEARINGS

- Improved lubricating greases for aircraft wheel bearings [SAE PAPER 921038] p 197 A93-14658
- High temperature corrosion resistant bearing steel development [AIAA PAPER 93-2000] p 1145 A93-49842
- Optimal output feedback vibration control of rotor-bearing systems p 86 A93-11220
- Bearing servicing tool [NASA-CASE-MSC-21881-1] p 221 A93-14871

BEECHCRAFT AIRCRAFT

- Aircraft accident/incident summary report: Controlled flight into terrain, Bruno's Inc., Beechjet, N25BR, Rome, Georgia, December 11, 1991 [PB92-910404] p 143 A93-13470

- Development of a flight instrument package [AD-A260830] p 719 A93-25783

BELL AIRCRAFT

- Models for performance assessment of HF antennas on the CH-135/Twin Huey helicopter p 933 A93-30291

BELLMAN THEORY

- Behavior of the particular quality characteristics of an intelligent flight vehicle control system in a multicriterial formulation p 1168 A93-50952

- Matched asymptotic expansion of the Hamilton-Jacobi-Bellman equation for aeroassisted plane-change maneuvers [AIAA PAPER 93-3752] p 1143 A93-51348

BEND TESTS

- The measurement of blade deflections - A new implementation of the strain pattern analysis [ONERA, TP NO. 1992-127] p 831 A93-38601

BENDING

- Stochastic modeling and adaptive control algorithm of brake bending p 227 A93-14417
- Impact ice interface shear stresses caused by blade bending and twisting [AIAA PAPER 93-0030] p 307 A93-20147
- Coupled composite rotor blades under bending and torsional loads p 546 A93-27970
- Stiffness, thermal expansion, and thermal bending formulation of stiffened, fiber-reinforced composite panels [AIAA PAPER 93-1569] p 741 A93-34102
- Relationship between mechanical-property and energy-absorption trends for composite tubes [NASA-TP-3284] p 392 A93-16537
- Allowable compression strength for CFRP-components of fighter aircraft determined by CAI-test p 537 A93-21531
- Computational method in optimal bending-twisting comprehensive design of wings of subsonic and supersonic aircraft [AD-A262374] p 806 A93-27694

BENDING FATIGUE

- Low-noise, high-strength, spiral-bevel gears for helicopter transmissions [AIAA PAPER 93-2149] p 1154 A93-49966
- NDE of PWA 1480 single crystal turbine blade material [NASA-TM-106140] p 815 A93-27640

BENDING MOMENTS

- Determination of the membrane and flexural shell deformations from the readings of a two-sided rosette-type strain gage p 75 A93-10047

- Estimation of the external loading of airships in flight p 366 A93-18383

- Nonlinear large amplitude vibration of composite helicopter blade at large static deflection p 713 A93-35630

- Dependence of the service life of a wing on its strength uniformity and landing gear location p 891 A93-42377

- Active control for fin buffet alleviation [AIAA PAPER 93-3817] p 1133 A93-51408

- A nonlinear finite element of an arbitrary beam p 1215 A93-52939

- The effects of end-bend regulations of compressor blade on the outlet flow field [ISABE 93-7033] p 1185 A93-54009

- A discussion of the results of the rainfall counting of a wide range of dynamics associated with the simultaneous operation of adjacent wind turbines [DE93-000016] p 434 A93-18705

- Influence of cross section variations on the structural behaviour of composite rotor blades [MBB-UD-0602-91-PUB] p 332 A93-17569

- Instability of the periodic deflection of a panel surface in a turbulent boundary layer p 208 A93-15188

- Dynamic analysis of pretwisted elastically-coupled rotor blades p 326 A93-21125

- Effect of flexural and rotational wing oscillations on the prevention of flow separation p 1150 A93-48911

- AGARD index of publications, 1989-1991 [AGARD-INDEX-89-91] p 104 A93-10610

- Publications on acoustics research at the Langley Research Center, January 1987 - September 1992 [NASA-TM-107674] p 102 A93-12080

- Composites: A catalogue of books and conference proceedings available in the NAL library [NAL-SP-IC-9201] p 234 A93-13368

- Lanchester: The man [AERO-REPT-9111] p 456 A93-16464

- The Goldstein Aeronautical Engineering Research Laboratory [AERO-REPT-9109] p 240 A93-16465

- Aeronautical Engineering Group publications: 1950 - present [AERO-REPT-9108] p 454 A93-16563

- Bibliography on propulsion airframe integration technologies for high-speed civil transport applications, 1980-1991 [NASA-TM-105602] p 678 A93-26136

- Selected experiments in laminar flow: An annotated bibliography [NASA-TM-103989] p 990 A93-32226

- European aerospace science and technology, 1992: A bibliography with indexes [NASA-SP-7105] p 949 A93-32404

- Canonical correlation relationships among spectral and phytometric variables for twenty winter wheat fields p 433 A93-22992

- Two and three-dimensional prediffuser combustor studies with air-water mixture [ISABE 93-7025] p 1213 A93-54001

- Waterborne polyurethane binder resins for compliant aircraft coatings [AD-A256246] p 199 A93-14573

- Trade-offs arising from mixture of color cueing and monocular, binocular, and stereoscopic cueing information for simulated rotorcraft flight [NASA-TP-3268] p 338 A93-18333

- The influence of nocturnal aircraft noise on sleep and on catecholamine secretion p 1163 A93-49554

- In-situ bioventing: Two US EPA and Air Force sponsored field studies [PB93-194231] p 1035 A93-32089

- Autogenic-feedback training improves pilot performance during emergency flying conditions [NASA-TM-104005] p 790 A93-27076

- Dr. Alexander H. Flax: Technologist of aeronautics [AD-A258441] p 456 A93-17890

- Modeling of human operator actions in the stochastic trajectory tracking problem for a dynamic plant p 228 A93-16783

- The development of the Boeing Human Model p 561 A93-27150

BIOT METHOD

Development of the wake behind a circular cylinder impulsively started into rotatory and rectilinear motion p 1236 A93-55736

BIRD-AIRCRAFT COLLISIONS

Bird impact dynamic response analysis for aircraft arc windshield p 41 A93-11815
Slicing model for foreign soft-body objects impacting on blade rows p 28 A93-12372
New model of bird impact response analysis and its engineering solution p 156 A93-14336
An impact dynamics investigation on some problems in bird strike on windshields of high speed aircraft p 197 A93-15346
Effect of bird impact load types on blade response p 174 A93-16846
Advanced transparency development for USAF aircraft [AIAA PAPER 93-1391] p 710 A93-33954
Foreign object impact assessment of a high-Mach engine inlet [AIAA PAPER 93-1630] p 711 A93-34158
Numerical modeling of the impact of a bird against aircraft transparencies p 801 A93-36797
The 'Rolls-Royce' way of validating fan integrity [AIAA PAPER 93-2602] p 1122 A93-50311
T-38 forward windshield development and performance demonstration report [AD-A259240] p 513 N93-20579
Effects of air traffic on nature and environment in the neighborhood of airports by example of the Munich 2 Airport (Germany) p 1035 N93-31932

BIRDS

Research on the stability and control of soaring birds [AIAA PAPER 92-4122] p 61 A93-11284
Birds mimicking microbursts on 2 June 1990 in Orlando, Florida [AD-A255703] p 143 N93-14024
Effects of air traffic on nature and environment in the neighborhood of airports by example of the Munich 2 Airport (Germany) p 1035 N93-31932

BIREFRINGENCE

An optical fiber based position sensor with immunity to temperature variation p 743 A93-34287

BIREFRINGENT COATINGS

Measurement of aerodynamic shear stress using side chain liquid crystal polymers [AD-A254312] p 72 N93-10770

BISMALEIMIDE

The properties of newly developed highly damage tolerant and easy handleable carbon fiber/modified bismaleimide prepreg system p 1212 A93-53448
Wet layup materials for repair of bismaleimide composites p 1212 A93-53451

BIT ERROR RATE

Optical interconnection and packaging technologies for advanced avionics systems p 77 A93-10960

BLADE SLAP NOISE

Unsteady transonic flow past a quarter-plane p 127 A93-16664
Continuous judgment of helicopter noise - On the validity of Leq and Zwicker's method (ISO 532B) p 558 A93-28478
High-speed helicopter rotor noise - Shock waves as a potent source of sound p 565 A93-29403
The influence of quadrupole sources in the boundary layer and wake of a blade on helicopter rotor noise p 566 A93-29410
Development and validation of 'quiet tail rotor' technology p 567 A93-29416
Acoustic characteristics of advanced model rotor systems p 567 A93-29419
Blade-vortex interaction data obtained from a pressure-instrumented model rotor at the DNW p 568 A93-29430
The quiet helicopter; Proceedings of the Conference, London, United Kingdom, Mar. 17, 1992 [ISBN 1-85768-020-0] p 1262 A93-54718
Helicopter noise reduction programme - AGUSTA achievements p 1262 A93-54721
Review of helicopter noise research in Europe p 1263 A93-54725
Strong parallel blade-vortex interaction and noise propagation in helicopter flight p 944 N93-30980

BLADE TIPS

Tiltrotor Research Aircraft composite blade repairs - Lessons learned p 108 A93-14819
Experimental investigation of tip clearance noise in axial flow machines p 445 A93-19155
Shock formation in overexpanded tip leakage flow [ASME PAPER 92-GT-1] p 245 A93-19276
Electromechanical measurement of turbomachinery blade tip-to-casing running clearance [ASME PAPER 92-GT-50] p 400 A93-19303
The effect of compressor rotor tip crops on turboshaft engine performance [ASME PAPER 92-GT-83] p 348 A93-19332

A study of stall in a low hub/tip ratio fan [ASME PAPER 92-GT-85] p 248 A93-19334
Low aspect ratio transonic rotors. II - Influence of location of maximum thickness on transonic compressor performance [ASME PAPER 92-GT-186] p 352 A93-19411
Measurement of the three-dimensional tip region flowfield in an axial compressor [ASME PAPER 92-GT-211] p 252 A93-19434
Experimental study on the three dimensional flow within a compressor cascade with tip clearance. I - Velocity and pressure fields [ASME PAPER 92-GT-215] p 258 A93-19574
Experimental study on the three dimensional flow within a compressor cascade with tip clearance. II - The tip leakage vortex [ASME PAPER 92-GT-432] p 258 A93-19575
Three-dimensional Navier-Stokes analysis of the tip clearance flow in linear turbine cascades [AIAA PAPER 93-0391] p 282 A93-23068
Euler solutions to nonlinear acoustics of non-lifting rotor blades p 568 A93-29433
A numerical study of advanced rotor blades p 481 A93-29436
Probabilistic turbine blade tip durability analysis [AIAA PAPER 93-1383] p 719 A93-33946
Experimental investigation of counter-rotating propfan flutter at cruise conditions [AIAA PAPER 93-1632] p 720 A93-34160
The interaction between a steady jet flow and a supersonic blade tip p 688 A93-34415
Definition and evaluation of new helicopter rotor blade tips [ONERA, TP NO. 1992-179] p 773 A93-38741
Direct and inverse problems of calculating the axisymmetric and 3D flow in axial compressor blade rows p 972 A93-46938
3D viscous flow analysis in axial turbine including tip leakage phenomena p 972 A93-46940
The three-dimensional boundary layer flow due to a rotor-tip vortex [AIAA PAPER 93-3081] p 1060 A93-48255
Flow field characteristics of a complex blade tip at high angles of attack [AIAA PAPER 93-3083] p 1060 A93-48257
Tip shock structures in transonic compressor rotors [AIAA PAPER 93-1869] p 1075 A93-49744
Numerical and experimental investigation of turbine tip gap flow [AIAA PAPER 93-2253] p 1081 A93-50051
Stator relative, rotor blade-to-blade near wall flow in a multistage axial compressor with tip clearance variation [AIAA PAPER 93-2389] p 1083 A93-50154
Numerical analysis of flow within cascade with tip clearance p 1176 A93-53192
Tip clearance effects on the flow field of an axial turbine rotor blade cascade [ISABE 93-7057] p 1185 A93-54033
Effects of wake interaction of two turbine cascades on secondary/tip-leakage flows and losses [ISABE 93-7058] p 1185 A93-54034
New digital capacitive measurement system for blade clearances p 1254 A93-54376
Three-dimensional Navier-Stokes analysis of tip clearance flow in linear turbine cascades p 1235 A93-55364
A concept for a counterrotating fan with reduced tone noise [NASA-TM-105736] p 101 N93-11370
An experimental and analytical study of TIP clearance effects in axial flow compressors [AD-A256434] p 179 N93-15337
Aerodynamic characteristics of a rotorcraft airfoil designed for the tip region of a main rotor blade [NASA-TM-4264] p 876 N93-29450

BLADE-VORTEX INTERACTION

ONERA makes progress in rotor aerodynamics, aeroelasticity, and acoustics p 2 A93-11621
Unsteady transonic flow past a quarter-plane p 127 A93-16664
Helicopter main rotor/tail rotor noise radiation characteristics from scaled model rotor experiments in the DNW p 445 A93-19142
Effects of a trailing edge flap on the aerodynamics and acoustics of rotor blade-vortex interactions p 244 A93-19144
Advances in tilt rotor noise prediction p 447 A93-19184
Lynx: High performance - Low noise p 322 A93-19185
Forward rotor vortex effects on counter rotating propeller noise p 245 A93-19221
An analysis system for blade forced response [ASME PAPER 92-GT-172] p 352 A93-19398

Experimental study on the three dimensional flow within a compressor cascade with tip clearance. I - Velocity and pressure fields [ASME PAPER 92-GT-215] p 258 A93-19574
Experimental study on the three dimensional flow within a compressor cascade with tip clearance. II - The tip leakage vortex [ASME PAPER 92-GT-432] p 258 A93-19575
The use of interferometry in the study of rotorcraft aerodynamics p 407 A93-19914
Experimental investigation of vortex-fin interaction [AIAA PAPER 93-0050] p 260 A93-20163
Effect of leading-edge porosity on blade-vortex interaction noise [AIAA PAPER 93-0601] p 563 A93-24727
An examination of vortex convection effects during blade-vortex interaction p 473 A93-25360
A study of blade-vortex interaction sound generation and directionality p 565 A93-29402
HHC study in the DNW to reduce BVI noise - An analysis p 565 A93-29405
The role of blade elasticity in the prediction of blade-vortex interaction noise p 566 A93-29406
Noise reduction for transonic blade-vortex interactions p 566 A93-29408
The development of a prediction method for the calculation of blade-vortex interaction noise based on measured airloads p 566 A93-29409
Acoustic characteristics of advanced model rotor systems p 567 A93-29419
Blade-vortex interaction data obtained from a pressure-instrumented model rotor at the DNW p 568 A93-29430
Experimental study of a single strong vortex-airfoil interaction p 481 A93-29432
Recent developments in rotor wake modeling for helicopter noise prediction p 481 A93-29437
Correlation of airloads on a two-bladed helicopter rotor p 481 A93-29438
Full-scale wind tunnel investigation of a helicopter individual blade control system [AIAA PAPER 93-1361] p 726 A93-33929
The use of artificial intelligence for buffet environments [AIAA PAPER 93-1534] p 727 A93-34071
Effect of an unsteady three-dimensional wake on elastic blade-flapping eigenvalues in hover p 663 A93-34260
A closed loop controller for BVI impulsive noise reduction by Higher Harmonic Control p 849 A93-35963
Prediction of BVI noise patterns and correlation with wake interaction locations p 849 A93-35966
Transonic blade-vortex interactions - Noise reduction p 850 A93-37396
Blade-vortex interaction noise - Prediction and comparison with flight and wind tunnel tests [ONERA, TP NO. 1992-126] p 651 A93-38600
Results from a set of low speed blade-vortex interaction experiments p 872 A93-43540
Numerical vorticity capturing for vortex-solid body interaction problems [AIAA PAPER 93-3343] p 954 A93-45037
Two dimensional incompressible flow through a vibrating bladed disc - Theoretical model p 973 A93-46991
The three-dimensional boundary layer flow due to a rotor-tip vortex [AIAA PAPER 93-3081] p 1060 A93-48255
Numerical study of slightly compressible Navier-Stokes simulation of blade-vortex interaction p 1239 A93-56216
Unsteady propeller/wing aerodynamic interactions p 24 N93-12190
The Application of CFD to rotary wing flow problems [NASA-TM-102803] p 139 N93-15483
Two- and three-dimensional blade vortex interactions [NASA-CR-177567] p 293 N93-16942
Numerical investigation of swirl-airfoil interactions in transonic area [MPIS-8/1991] p 297 N93-18627
Flow visualizations of perpendicular blade vortex interactions [NASA-CR-192725] p 748 N93-25208
Computation of far-field helicopter rotor tone noise [ONERA-P-1990-5] p 943 N93-30110
Strong parallel blade-vortex interaction and noise propagation in helicopter flight p 944 N93-30980

BLADES

Flow visualizations of perpendicular blade vortex interactions [NASA-CR-192725] p 748 N93-25208
BLASIUS FLOW
Boundary layer separation in a corner formed by two planes p 6 A93-10188
Instability of flow in a streamwise corner [NASA-CR-191410] p 694 N93-25153

BLAST LOADS

- Advanced composite helicopter MISERS GOLD test/analysis p 508 A93-27974
Numerical simulation of a blast inside a Boeing 747 [AIAA PAPER 93-3091] p 1099 A93-48265

BLEEDING

- An experimental investigation of base bleed effect on the wake turbulent structure behind a two-dimensional blunt model [MPIS-9/1991] p 139 N93-15131

BLOCKING

- An experimental study of flow patterns and endwall heat transfer upstream of a surface-mounted rectangular obstruction in a turbulent boundary layer p 89 N93-11698

BLOWDOWN WIND TUNNELS

- Photoluminescent thermography - Feasibility study with pointwise measurements p 211 A93-16861
Flow quality improvement in a high speed blowdown wind tunnel [AIAA PAPER 93-0353] p 377 A93-23038
Measurements in a pressure-driven three-dimensional turbulent boundary layer during development and decay [AIAA PAPER 93-0543] p 415 A93-23283
Development of Polytechnic University's supersonic wind tunnel facility [AIAA PAPER 93-0798] p 528 A93-24876
Experiments on shock wave-boundary layer interaction at high Mach number with entropy layer effect [ONERA, TP NO. 1992-101] p 771 A93-38581
Measurements in a pressure-driven three-dimensional turbulent boundary layer during development and decay p 927 A93-41911
A novel development of the Ludwig tube, for extended test duration p 1011 A93-45529
CARS studies in hypersonic flows [AIAA PAPER 93-3047] p 1144 A93-48227
Simulation of shock-boundary layer interaction in a fan blade passage [AIAA PAPER 93-1980] p 1078 A93-49827
Real gas simulation of air Blow-Down Facilities [AIAA PAPER 93-2022] p 1137 A93-49859
Observations of liquid jets injected into a highly accelerated supersonic boundary layer p 1177 A93-53214
Photoluminescent thermography in hypersonic blowdown wind tunnel: Feasibility study with pinpoint measurement [ONERA-NT-1992-8] p 297 N93-18617
- BLOWING**
A sensitivity study for pneumatic vortex control on a chined forebody [AIAA PAPER 93-0049] p 260 A93-20162
Active control of wing rock of a delta wing at post-stall using tangential leading edge blowing [AIAA PAPER 93-0056] p 367 A93-20169
Oscillatory blowing, a tool to delay boundary layer separation [AIAA PAPER 93-0440] p 474 A93-25529
Effects of blowing on delta wing vortices during dynamic pitching p 768 A93-37384
The effects of forced oscillations on the performance of airfoils [AIAA PAPER 93-3264] p 968 A93-46829
Heat transfer on blunt cones in nonuniform supersonic flow in the presence of gas injection from the surface p 972 A93-46975
Effect of forebody tangential slot blowing on flow about a full aircraft geometry [AIAA PAPER 93-2962] p 1048 A93-48156
Investigation of the effect of physical processes on heat transfer to blunt bodies at low Reynolds numbers p 1090 A93-51877
Boundary layer and pressure measurements on a cylinder with unsteady circulation control p 1177 A93-53207
Oscillatory blowing - A tool to delay boundary-layer separation p 1235 A93-55362
Experimental investigation of the effects of aft blowing with various nozzle exit geometries on a 3.0 caliber tangent ogive at high angles of attack: Forebody pressure distributions [NASA-CR-190935] p 22 N93-11605
Leading edge film cooling heat transfer including the effect of mainstream turbulence p 23 N93-11886
An investigation of the effects of aft blowing on a 3.0 caliber tangent ogive body at high angles of attack [NASA-CR-190934] p 24 N93-12004
A numerical study of hypersonic flow with strong surface blowing p 129 N93-13128
Modeling variable blowing on a slender cone in hypersonic flow p 138 N93-14836
Quantitative-force measurements of pneumatic control on a wing/strake model [AD-A257343] p 289 N93-16157

- An experimental investigation of a finite circulation control wing [AD-A259044] p 340 N93-18896
Computational study of the aerodynamics and control by blowing of asymmetric vortical flows over delta wings p 693 N93-24772
Tangential fuselage blowing on an ogive cylinder p 697 N93-25545

BLUFF BODIES

- The influence of the boundary layer on the subsonic near-wake of a family of bluff bodies [AIAA PAPER 93-0525] p 284 A93-23266
A 3D Navier-Stokes analysis of a generic ground vehicle shape [AIAA PAPER 93-3521] p 985 A93-47283
Effects of a rear stagnation jet on the wake behind a cylinder p 1151 A93-49026
Quantitative Knudsen-number dependences of density disturbances in front of obstructions in supersonic divergent flows p 1239 A93-56220
Characteristics of separated flows including cavitation effects p 84 N93-10874
Wake similarity and vortex formation for two-dimensional bluff bodies p 138 N93-15101
Experimental analysis of combustion oscillations with reference to ramjet propulsion p 392 N93-17614
Vortex shedding by blunt/bluff bodies at high Reynolds numbers. Volume 1: Data analysis [AD-A264151] p 877 N93-30171
Vortex shedding by Blunt/Bluff bodies at high Reynolds numbers. Volume 2: Cylinders, octagon, hexagon [AD-A264152] p 877 N93-30172
Vortex shedding by blunt/bluff bodies at high Reynolds numbers. Volume 3: Cubes [AD-A264153] p 877 N93-30173
- BLUNT BODIES**
Viscous shock-layer numerical calculations of three dimensional nonequilibrium flows over hypersonic blunt bodies at high angle of attack p 12 A93-12651
Numerical solution of radiative flowfield on the nose region of blunt bodies p 120 A93-14359
Calculation of radiant energy transfer in hypersonic flow past blunt bodies using the P1 and P2 approximations of the spherical harmonic method p 124 A93-15209
Effect of the body shape on head shock attenuation at a large distance from the axis p 127 A93-16708
Two-phase injection from the front surface of a blunt body in hypersonic flow p 241 A93-18233
Influence of second-order boundary layer effects in hypersonic flow past blunt cones of large aspect ratio p 241 A93-18238
Comparison of limiters in flux-split algorithms for Euler equations [AIAA PAPER 93-0068] p 262 A93-20181
High Mach number dynamic stability of blunt slender cones at angle of attack p 271 A93-21721
Computation of nonequilibrium radiating shock layers [AIAA PAPER 93-0144] p 414 A93-22588
Numerical computation of viscous hypersonic flow around spherically blunted cones at angle of attack p 460 A93-24082
Numerical investigation of supersonic flows around a spiked blunt-body [AIAA PAPER 93-0887] p 471 A93-24947
Calculation of optical and electric characteristics from hypersonic blunt-body wakes p 680 A93-33729
Numerical simulation of hypersonic rarefied gas flow over blunt bodies p 687 A93-34356
Unsteady supersonic flow around a blunt body in thermal inhomogeneities in turbulent shock layer flows p 691 A93-35266
A study of the temperature of bodies in the flow-around regime in the case of surface gas injection p 691 A93-35344
An implicit finite-difference algorithm for the numerical simulation of supersonic flow over blunted bodies p 770 A93-38325
Numerical study on atom-molecule radiation flowfield around a hypersonic blunt body p 770 A93-38434
Interference of an oblique shock with a shock layer on a blunt edge for small Reynolds numbers p 775 A93-39120
A numerical investigation of supersonic flow of a viscous gas over long blunt cones, taking into account equilibrium physicochemical transformations p 775 A93-39124
An approximate method for calculating nonequilibrium flows near blunt bodies p 776 A93-39134
Effect of the thermodynamic air model on the aerodynamic characteristics of profiles with bends p 776 A93-39136
Nonequilibrium heat transfer near the critical point of blunt bodies p 777 A93-39145
Spectral solution of the viscous blunt-body problem p 860 A93-41915

- Zonally-decoupled DSMC solutions of hypersonic blunt body wake flows [AIAA PAPER 93-2808] p 949 A93-44227
Singular arcs for blunt endoatmospheric vehicles p 1015 A93-44380
Euler solutions for blunt bodies using triangular meshes - Artificial viscosity forms and numerical boundary conditions [AIAA PAPER 93-3333] p 953 A93-45027
Radiative heat transfer from non-equilibrium high-enthalpy shock layers p 1024 A93-45515
Viscous hypersonic shock-shock interaction on a blunt body at high altitude [AIAA PAPER 93-2722] p 962 A93-46477
Hypersonic stagnation line merged layer flow on blunt axisymmetric bodies of arbitrary shape [AIAA PAPER 93-2723] p 962 A93-46478
PNS predictions of axisymmetric hypersonic blunt-body and afterbody flowfields [AIAA PAPER 93-2725] p 962 A93-46479
A preliminary investigation of the Helmholtz resonator concept for heat flux reduction [AIAA PAPER 93-2742] p 963 A93-46493
Two-layer convective heating prediction procedures and sensitivities for blunt body reentry vehicles [AIAA PAPER 93-2763] p 963 A93-46509
An investigation of aerodynamic heating to spherically blunted cones at angle of attack [AIAA PAPER 93-2764] p 963 A93-46510
Convective heat-transfer rate distributions over a 140 deg blunt cone at hypersonic speeds in different gas environments [AIAA PAPER 93-2787] p 1027 A93-46529
Flow resolution and domain of influence in rarefied hypersonic blunt-body flows [AIAA PAPER 93-2806] p 964 A93-46546
Hypersonic blunt body wake computations using DSMC and Navier-Stokes solvers [AIAA PAPER 93-2807] p 964 A93-46547
Monte Carlo simulation of radiating reentry flows [AIAA PAPER 93-2809] p 964 A93-46548
Control of unsteady shock-induced turbulent boundary layer separation upstream of blunt fins [AIAA PAPER 93-3281] p 969 A93-46839
Heat transfer on blunt cones in nonuniform supersonic flow in the presence of gas injection from the surface p 972 A93-46975
Drag measurements on blunted cones and a scramjet vehicle in hypervelocity flow [AIAA PAPER 93-2979] p 1050 A93-48172
Instability of hypersonic flow past blunt cones - Effects of mean flow variations [AIAA PAPER 93-2983] p 1051 A93-48176
Aerodynamic heating with boundary layer transition and heat protection with mass addition on blunt body in hypersonic flows [AIAA PAPER 93-2984] p 1051 A93-48177
Computation of hypersonic flow past blunt body for nonequilibrium weakly ionized air [AIAA PAPER 93-2995] p 1053 A93-48185
On numerical solutions of Burnett equations for hypersonic flow past 2-D circular blunt leading edges in continuum transition regime [AIAA PAPER 93-3092] p 1060 A93-48266
Abnormal peaks of increased heat-transfer on the blunted delta wing in the hypersonic flow [AIAA PAPER 93-3129] p 1063 A93-48294
Flowfield dynamics in blunt fin-induced shock wave/turbulent boundary layer interactions [AIAA PAPER 93-3133] p 1063 A93-48298
Analysis of the stability characteristics of hypersonic flow of a detonable gas mixture in the stagnation region of a blunt body [AIAA PAPER 93-1918] p 1076 A93-49784
The problem of viscous hypersonic flow past blunt bodies in the spreading plane p 1086 A93-50969
A new technique for analysis of unsteady aerodynamic responses of cascade airfoils with blunt leading edge - Unsteady aerodynamic responses of the cascade in incompressible flow p 1086 A93-51122
A study of turbulent flow in a viscous shock layer in the case of gas flow past oblong blunt bodies p 1089 A93-51820
Investigation of the effect of physical processes on heat transfer to blunt bodies at low Reynolds numbers p 1090 A93-51877
Investigation of the structure of a multicomponent viscous shock layer p 1090 A93-51879
Stagnation point computations of nonequilibrium inviscid blunt body flow p 1093 A93-52005
Effective treatment of the singular line boundary problem for three-dimensional grids p 1177 A93-53204
Application of the small parameter method to the problem of three-dimensional flow of a viscous gas past bodies p 1178 A93-53314

- Comparison of gasdynamic models in hypersonic flow p 1179 A93-53315
- Spectral measurements of shock layer radiation in an arc-jet wind tunnel p 1251 A93-54409
- The effects of reaction rate constants and catalytic wall on the hypersonic flow field over blunt bodies p 1230 A93-54586
- The effect of outboard leading-edge bluntness of double-delta wing on its aerodynamic characteristics p 1230 A93-54589
- Computation of viscous hypersonic non-equilibrium blunt body flow p 1238 A93-56038
- Effect of passive flow-control devices on turbulent low-speed base flow p 82 A93-10304
- Improved numerical simulation of Euler equations p 83 A93-10309
- Investigations on entropy layer along hypersonic hyperboloids using a defect boundary layer p 787 A93-27462
- Hypersonic lateral and directional stability characteristics of aerossist flight experiment configuration in air and CF4 [NASA-TM-4435] p 875 A93-29166
- Vortex shedding by blunt/bluff bodies at high Reynolds numbers. Volume 1: Data analysis [AD-A264151] p 877 A93-30171
- Vortex shedding by Blunt/Bluff bodies at high Reynolds numbers. Volume 2: Cylinders, octagon, hexagon [AD-A264152] p 877 A93-30172
- Vortex shedding by blunt/bluff bodies at high Reynolds numbers. Volume 3: Cubes [AD-A264153] p 877 A93-30173
- BLUNT LEADING EDGES**
- A new technique for analysis of unsteady aerodynamic responses of cascade airfoils with blunt leading edge. I - Theory p 267 A93-20909
- Inviscid hypersonic flow over a delta wing p 870 A93-42634
- Hypersonic leeside delta-wing-flow computations using centered schemes p 870 A93-42635
- Evaluation of contributions for test case 7.1.1 and 7.1.2 p 870 A93-42636
- Active forcing of an axisymmetric leading-edge turbulent separation bubble [AIAA PAPER 93-3245] p 966 A93-46790
- Leading edge film cooling heat transfer including the effect of mainstream turbulence p 23 A93-11886
- BLUNT TRAILING EDGES**
- An experimental investigation of base bleed effect on the wake turbulent structure behind a two-dimensional blunt model [MPIS-9/1991] p 139 A93-15131
- BO-105 HELICOPTER**
- Comprehensive analysis of bearingless rotors - Model development and experimental correlation of modes, response, trim and stability [AIAA PAPER 93-0624] p 504 A93-24741
- Frequency-domain identification of BO 105 derivative models with rotor degrees of freedom p 712 A93-34263
- A contribution to the dynamic feedforward open loop control of multivariable systems and to the optimal design of command functions [DLR-FB-92-05] p 441 A93-16515
- BOATS**
- Modelling of interfacial and thermocline waves [AERO-REPT-9209] p 420 A93-18103
- BOATTAILS**
- Computation of transonic flow over a porous surface projectile p 696 A93-25409
- BODIES OF REVOLUTION**
- Effect of longitudinal microribbing on the drag of a body of revolution p 5 A93-10147
- Dynamic stability of bodies of revolution in compressible flow p 12 A93-12558
- Calculation of separated axisymmetric flow past bodies by solving Euler equations in the inner vortex region p 14 A93-12975
- Near-field behavior of a tip vortex p 288 A93-23549
- Incompressible flow computation of forces and moments on bodies of revolution at incidence [AIAA PAPER 93-0787] p 541 A93-24867
- Analysis of slender bodies of revolution with an angle of attack in extreme ground effect p 679 A93-33716
- A method for estimating the survivability of bodies of revolution p 745 A93-35287
- Newtonian and hypersonic flows over oscillating bodies of revolution. II - Parabolic bodies p 872 A93-42931
- Unstructured grids for sonic-boom analysis [AIAA PAPER 93-2929] p 949 A93-44229
- On the steady subsonic shear flow past a slender body of revolution p 970 A93-46907
- Thoughts on conical flow asymmetry p 1070 A93-49003
- Calculation of supersonic flow past a body of revolution with a piecewise linear distribution of singularities at its axis p 1092 A93-51910
- Determination of the aerodynamic characteristics of thin bodies of revolution with an arbitrary number of cantilever surfaces in inhomogeneous flow p 1092 A93-51911
- Design of shockless supersonic region in the axisymmetric transonic flow p 1230 A93-54587
- Experimental investigations on wing-body combinations and their components at high angles of attack in the subsonic and transonic speed range [DLR-FB-91-43] p 516 A93-21762
- The application of concentric vortex simulation to calculating the aerodynamic characteristics of bodies of revolution at high angles of attack [AD-A263879] p 876 A93-29919
- Navier-Stokes computations for kinetic energy projectiles in steady coning motion: A predictive capability for pitch damping [AD-A264111] p 1033 A93-32028
- BODY CENTERED CUBIC LATTICES**
- Birth of the betas p 824 A93-38200
- Structural stability of 'beta-CEZ' alloy [ONERA, TP NO. 1992-106] p 824 A93-38586
- BODY KINEMATICS**
- An effective Mixed Annealing/Heuristic Algorithm for problems in kinematic mechanical design [AIAA PAPER 93-1581] p 741 A93-34113
- BODY-WING AND TAIL CONFIGURATIONS**
- SAE Aero Design '92 [SAE PAPER 921009] p 157 A93-14641
- A new semiempirical method for computing nonlinear angle-of-attack aerodynamics on wing-body-tail configurations [AIAA PAPER 93-0034] p 260 A93-20148
- Experimental and numerical analysis of the wing rock characteristics of a 'wing-body-tail' configuration [AIAA PAPER 93-0187] p 368 A93-22612
- A study of CFD algorithms applied to complete aircraft configurations [AIAA PAPER 93-0784] p 468 A93-24864
- Simulation of tail buffet using delta wing-vertical tail configuration [AIAA PAPER 93-3688] p 1065 A93-48357
- Low-speed wind tunnel study of the direct side-force characteristics of a joined-wing airplane with an upper fin [DE93-767966] p 988 A93-31189
- NLR inviscid transonic unsteady loads prediction methods in aerolasticity [NLR-TP-91410-U] p 990 A93-32358
- BODY-WING CONFIGURATIONS**
- Unstructured grid solutions to a wing/pylon/store configuration using VGRID3D/USM3D [AIAA PAPER 92-4572] p 14 A93-13303
- Effect of canard position on the longitudinal aerodynamic characteristics of a close-coupled canard-wing-body configuration [AIAA PAPER 92-4632] p 14 A93-13304
- Advanced technology Tilt Wing study [AIAA PAPER 92-4237] p 44 A93-13359
- Supersonic wing/body interference p 121 A93-14391
- An AF3 algorithm for the calculation of transonic nonconservative full potential flows over wings or wing/body combinations p 125 A93-15341
- Coupled finite-difference/finite-element approach for wing-body aerolasticity [AIAA PAPER 92-4680] p 409 A93-20302
- Some effects of wing and body geometry on the aerodynamic characteristics of configurations designed for high supersonic Mach numbers [AIAA PAPER 92-4246] p 463 A93-24493
- Investigation of three-dimensional separation at wing/body junctions in supersonic flows using TVD McCormack's scheme [AIAA PAPER 93-0884] p 471 A93-24945
- Euler solution for wing-body combination at supersonic speeds p 680 A93-33722
- Multiblock Navier-Stokes solutions about the F/A-18 wing-LEX-fuselage configuration p 767 A93-37378
- An experimental study of a turbulent wing-body junction and wake flow p 873 A93-43541
- Mesh generation for the computation of flowfields over complex aerodynamic shapes p 995 A93-44888
- Computation of induced drag for elliptical and crescent-shaped wings p 958 A93-45136
- Aerodynamic heating phenomenon in three dimensional shock wave/turbulent boundary layer interaction induced by sweptback fins in hypersonic flows p 960 A93-45507
- Numerical simulation of wing-wall junction flow for a pitching wing [AIAA PAPER 93-3401] p 974 A93-47203
- Tangential Forebody Blowing-yaw control at high alpha [AIAA PAPER 93-3406] p 1008 A93-47205
- Low-speed wind tunnel test results of the Canard Rotor/Wing concept [AIAA PAPER 93-3412] p 975 A93-47209
- Aerodynamic characteristics of a delta wing with a body-hinged leading-edge extension [AIAA PAPER 93-3446] p 978 A93-47233
- Navier-Stokes calculations for transport wing-body configurations with nacelles and struts [AIAA PAPER 93-2945] p 1047 A93-48142
- A fast robust viscous-inviscid interaction solver for transonic flow about wing/body configurations on the basis of full potential theory [AIAA PAPER 93-3026] p 1056 A93-48211
- Unsteady Navier-Stokes simulation of the canard-wing-body ramp motion [AIAA PAPER 93-3058] p 1058 A93-48235
- Navier-Stokes computations on full-span wing-body configuration with oscillating control surfaces [AIAA PAPER 93-3687] p 1065 A93-48356
- Transonic Navier-Stokes flow computations over wing-fuselage geometries p 1095 A93-52456
- Effect of leading-edge geometry on delta wing unsteady aerodynamics p 1095 A93-52457
- Analysis of wing-body junction flowfields using the incompressible Navier-Stokes equations, volumes 1 and 2 p 17 A93-10320
- Effect of planform and body on supersonic aerodynamics of multibody configurations [NASA-TP-3212] p 19 A93-10824
- Low-speed longitudinal and lateral-directional aerodynamic characteristics of the X-31 configuration [NASA-TM-4351] p 22 A93-11622
- Application of an Euler-equation method to a sharp-edged delta wing configuration with vortex flow [NLR-TP-91306] p 294 A93-17809
- Pitching moment of low aspect ratio wing-body combinations up to high angles of attack at supersonic speeds [ESDU-92043] p 333 A93-17958
- Experimental effects of wing location on wing-body pressures at supersonic speeds [NASA-TM-4434] p 700 A93-26085
- BOEING AIRCRAFT**
- Design for global competition - The Boeing 777 [AIAA PAPER 92-4190] p 2 A93-13368
- Composites roll sevens --- aircraft structures p 3 A93-13448
- A tooling trend at BCA - What and why [SME PAPER EM92-111] p 202 A93-14114
- Development of the Boeing Low Speed Aerocraft Facility (LSAF) p 374 A93-19148
- Evolution of the Boeing 777 electrical power system p 519 A93-25998
- Lessons from application of equivalent plate structural modeling to an HSCT wing [AIAA PAPER 93-1413] p 739 A93-33969
- Valisys - A new quality assurance tool p 845 A93-36007
- Boeing 777 gets a boost from titanium p 1018 A93-45987
- Engineering simulators enhance 777 development p 1192 A93-53771
- 737-400 at Kegworth, 8 January 1989: The AAIB investigation p 491 A93-19661
- BOEING 720 AIRCRAFT**
- Low bandwidth robust controllers for flight [NASA-CR-191774] p 372 A93-17800
- BOEING 727 AIRCRAFT**
- The ISAR image-formation results of Boeing-727 p 342 A93-20857
- ISAR motion compensation and superresolution imaging of aircraft p 928 A93-42793
- BOEING 737 AIRCRAFT**
- Subsonic high-lift flight research on the NASA Transport System Research Vehicle (TSRV) [AIAA PAPER 92-4103] p 38 A93-11275
- Research requirements for a real-time flight measurements and data analysis system for subsonic transport high-lift research p 1244 A93-54391
- BOEING 747 AIRCRAFT**
- Rapid prototyping via automatic software code generation from formal specifications - A case study p 227 A93-14685
- The Boeing 747-400 upper rudder control system with triple tandem valve [SAE PAPER 912133] p 327 A93-21843
- Implicit upwind solution algorithms for three-dimensional unstructured meshes p 691 A93-35607
- Numerical simulation of a blast inside a Boeing 747 [AIAA PAPER 93-3091] p 1099 A93-48265
- The effectiveness of hand-held fire extinguishers on cargo container fires [DOT/FAA/CT-TN92/42] p 496 A93-21821
- Evaluation of the flyability of MLS curved approaches for wide-body aircraft [NLR-TP-91396-U] p 999 A93-32416

BOEING 757 AIRCRAFT

- 757 fly-by-wire demonstrator flight test
[AIAA PAPER 92-4099] p 38 A93-11271
Spoiler actuator - A problem investigation
p 801 A93-37175

- Vortex wake characteristics of B757-200 and B767-200
aircraft using the tower fly-by technique
[PB93-180255] p 878 N93-30387
Vortex wake characteristics of B757-200 and B767-200
aircraft using the tower fly-by technique
[PB93-180263] p 878 N93-30388

BOEING 767 AIRCRAFT

- Vortex wake characteristics of B757-200 and B767-200
aircraft using the tower fly-by technique
[PB93-180255] p 878 N93-30387
Vortex wake characteristics of B757-200 and B767-200
aircraft using the tower fly-by technique
[PB93-180263] p 878 N93-30388

BOILING

- Aircraft experiments on microgravity pool boiling -
Vapor-liquid behaviour and heat transfer characteristics
in boiling of n-pentane, CFC-113 and water
p 410 A93-20920

BOLTED JOINTS

- The fretting damage and effect of temperature in typical
joint of aircraft construction p 203 A93-14196
Contact analysis for riveted and bolted joints of
composite laminates p 204 A93-14384
Single-impact calibrated electromagnetic tightening of
long-life bolted joints in aviation structures
p 745 A93-35277
Effect of a combination of design and process-related
factors on the fatigue strength of bolted joints in
acoustically loaded aircraft structures
p 745 A93-35278

- Ways of increasing the service life and reliability of bolted
joints p 745 A93-35281
On design methods for bolted joints in composite aircraft
structures p 1158 A93-50430

BOLTS

- Single-impact calibrated electromagnetic tightening of
long-life bolted joints in aviation structures
p 745 A93-35277
The technical background to standards for eyebolts
[NPL-DMM(A)-52] p 87 N93-11327
RB 199 high pressure compressor stage 3 spin pit
tests p 176 N93-14893
RB211-524B disc and drive cones hot cyclic spinning
test p 177 N93-14895
F100 second stage fan disk bolthole crack propagation
ferris wheel test p 177 N93-14897

BOLTZMANN DISTRIBUTION

- Development and application of the Monte Carlo method
for solving the Boltzmann equation and its models
p 1173 A93-51867

BOLTZMANN TRANSPORT EQUATION

- Aerothermodynamics of the high-altitude flight
p 1089 A93-51783

BOMBER AIRCRAFT

- Reanalysis of multiple-wheel landing gear traffic tests
[AD-A256593] p 194 N93-14238

BOMBS (ORDNANCE)

- Dual-band infrared imaging applications: Locating buried
minifields, mapping sea ice, and inspecting aging
aircraft
[DE93-000516] p 453 N93-17225

BONDED JOINTS

- Bonded repair of multi-site damage
p 947 A93-45786
A study of the effect of the support fastening compliance
on the stress-strain state of aircraft transparencies
p 997 A93-47079

BONDING

- An experimental examination of the thermal and acoustic
environments on runway joint seals
[AD-A257965] p 382 N93-17734

BOOSTER ROCKET ENGINES

- Rocket engine versus jet engine comparison
[AIAA PAPER 92-3686] p 531 A93-24479
Numerical computations using multi-domain technique
p 299 N93-19277

BOOSTERS

- Characteristics of the diagnostics of booster system
components p 321 A93-18361

BORDERS

- National airborne surveillance system - An engineering
student study
[AIAA PAPER 93-4031] p 1242 A93-54603

BORIDES

- Preparation and characterization of continuous fiber
reinforced zirconium diboride matrix composites for a
leading edge material p 1211 A93-53445

BORON

- Ignition of boron particles coated by a thin titanium
film
[AIAA PAPER 93-2201] p 1145 A93-50013

- Boron particle ignition in high-speed flow
[AIAA PAPER 93-2202] p 1145 A93-50014
IR imaging for combustion characteristics and optical
properties of boron/boron oxide
[AD-A257747] p 393 N93-17693

BORON CARBIDES

- Atomization of JP-10/B4C gelled slurry fuel
[AD-A256827] p 391 N93-15686

BORON OXIDES

- IR imaging for combustion characteristics and optical
properties of boron/boron oxide
[AD-A257747] p 393 N93-17693

BORON-EPOXY COMPOSITES

- Elastic constants for unidirectional boron-epoxy
composites p 387 A93-18636
Reinforcement of the F-111 wing pivot fitting with a
boron/epoxy doubler system - Materials engineering
aspects p 1214 A93-54241
Damage tolerance assessment of boron/epoxy repairs
to fuselage lap joints
[AD-A258383] p 338 N93-18257

BOUNDARY CONDITIONS

- The numerical calculation for the coupling of multiple
propeller discrete noise and its interaction with the fuselage
boundary p 231 A93-14268
Boundary conditions for direct computation of
aerodynamic sound generation p 447 A93-19176
Development of a flexible and efficient multigrid-based
multiblock flow solver
[AIAA PAPER 93-0677] p 269 A93-21117
A hybrid structured-unstructured grid method for
unsteady turbomachinery flow computations
[AIAA PAPER 93-0387] p 282 A93-23066
Nonreflecting boundary conditions for linearized
unsteady aerodynamic calculations
[AIAA PAPER 93-0882] p 475 A93-25553
Nonreflecting boundary conditions of three-dimensional
Euler equation calculations for strut cascades
p 689 A93-34491

- Euler solutions for blunt bodies using triangular meshes
- Artificial viscosity forms and numerical boundary
conditions

- [AIAA PAPER 93-3333] p 953 A93-45027
Surface boundary conditions for the numerical solution
of the Euler equations
[AIAA PAPER 93-3334] p 953 A93-45028
Boundary conditions for direct computation of
aerodynamic sound generation p 1172 A93-49005
Boundary condition procedures for CFD analyses of
propulsion systems - The multi-zone problem
[AIAA PAPER 93-1971] p 1077 A93-49819

- Boundary conditions for unsteady supersonic inlet
analyses
[ISABE 93-7104] p 1187 A93-54080
Recent advances in steady compressible aerodynamic
sensitivity analysis p 1236 A93-55400
Fluid flow and heat convection studies for actively cooled
airframes
[NASA-CR-190956] p 216 N93-13406

- Validation of central and upwind 3D compressible flow
solvers p 421 N93-18564
Parabolized Navier-Stokes methods for hypersonic
flows p 421 N93-18565
The 3D Navier-Stokes calculation of flow about scramjet
inlet with strut p 301 N93-19298
Role of wind tunnel tests and CFD analysis for the
development of aero-engines in IHI p 365 N93-19326

- High-order cyclo-difference techniques: An alternative
to finite differences
[NASA-TM-107745] p 693 N93-25074
Spurious frequencies as a result of numerical boundary
treatments p 839 N93-27170

BOUNDARY ELEMENT METHOD

- Effect of wing planforms on induced drag reduction
p 127 A93-16932
Experience with boundary element methods to calculate
the aerodynamic characteristics of aircraft
p 243 A93-19130

- Exact solution sensitivities for boundary element
aerodynamics codes
[AIAA PAPER 92-4745] p 436 A93-20343

- Study on the numerical problem of the boundary element
method in analysis of flow around a three-dimensional
wing-body p 268 A93-20934
Acoustical analysis of gear housing vibration
p 567 A93-29420

- Crack analysis using discontinuous boundary elements
p 925 A93-40775

- High speed propeller acoustics and aerodynamics - A
boundary element approach p 967 A93-46804
Unstructured grid generation using interactive
three-dimensional boundary and efficient
three-dimensional volume methods
[AIAA PAPER 93-3452] p 1037 A93-47237

- 2-D theoretical analysis of circumferential grooved
casing treatment p 1066 A93-48501

- A dynamic stiffness/boundary element method for the
prediction of interior noise levels p 1226 A93-53817
Numerical analysis of the flow through a centrifugal
impeller by vortex distribution model of a boundary layer
I - Theoretical analysis p 1182 A93-53843

- Numerical study for the study of medium speed internal
noise problems
[DILC-EST-TN-200] p 101 N93-11156

- Development of a boundary element method program
for numerical analysis of supersonic unsteady flow
p 300 N93-19283

- Calculations of aerodynamic forces on a wing with thrust
using BEM p 300 N93-19286

- Nonlinear analyses of composite aerospace structures
in sonic fatigue
[NASA-CR-193124] p 930 N93-29154

BOUNDARY INTEGRAL METHOD

- Boundary integral equation methods for aerodynamics
p 9 A93-12158

- Toward an integration of aerodynamics and
aeroacoustics of rotors p 243 A93-19127

- Computation of subsonic viscous and transonic
viscous-inviscid unsteady flow p 1094 A93-52012

BOUNDARY LAYER COMBUSTION

- Ignition and spread of combustion within a supersonic
boundary layer p 535 A93-27732

BOUNDARY LAYER CONTROL

- Passive boundary-layer bleed for supersonic intakes
p 114 A93-14212

- Hybrid laminar flow control applied to advanced turbofan
engine nacelles
[SAE PAPER 920962] p 123 A93-14628

- Example of the Couette iceform design model - Flat
plate iceformation p 207 A93-15070

- Acoustic control of flow separation on a straight and a
yawed wing p 125 A93-15256

- Boundary layer transition and control; Proceedings of
the Conference, Univ. of Cambridge, United Kingdom, Apr.
8-12, 1991

- [ISBN 0-903409-86-0] p 211 A93-17251

- Engineering aspects of laminar flow research at Handley
Page p 235 A93-17275

- Passive control of pre-entry shock in supersonic
intakes

- [AIAA PAPER 93-0291] p 279 A93-22691

- Oscillatory blowing, a tool to delay boundary layer
separation

- [AIAA PAPER 93-0440] p 474 A93-25529

- Numerical simulation of passive control of
shock-boundary layer interaction for transonic airfoil
p 680 A93-33719

- Passive control of a shock wave/turbulent boundary
layer interaction in a transonic flow p 858 A93-40444

- Natural laminar flow and laminar flow control
[ISBN 0-387-97737-6] p 859 A93-41776

- Laminar flow control - Introduction and overview
p 859 A93-41777

- Laminar flow flight experiments - A review
p 890 A93-41778

- Wave interaction theory and LFC p 860 A93-41781

- Supersonic laminar flow control p 860 A93-41782

- The Langley 8-ft transonic pressure tunnel
laminar-flow-control experiment p 910 A93-41783

- Free shear layer control and its application to fan
noise

- [AIAA PAPER 93-3242] p 965 A93-46787

- Control of a supersonic reattaching shear layer
[AIAA PAPER 93-3248] p 966 A93-46793

- Passive control of shock wave/boundary layer
interaction at hypersonic speed p 966 A93-46794

- [AIAA PAPER 93-3249] p 966 A93-46794

- Active boundary-layer control in diffusers
[AIAA PAPER 93-3255] p 966 A93-46798

- Artificial transition - A tool for high Reynolds number
simulation?

- [AIAA PAPER 93-3258] p 967 A93-46799

- Computational analysis of drag reduction and buffet
alleviation in viscous transonic flow over porous airfoils
[AIAA PAPER 93-3419] p 976 A93-47215

- On the aerodynamics and performance of active vortex
generators

- [AIAA PAPER 93-3447] p 979 A93-47234

- Forebody vortex control with jet and slot blowing on
an F/A-18

- [AIAA PAPER 93-3449] p 1009 A93-47235

- Boundary conditions for unsteady supersonic inlet
analyses

- [ISABE 93-7104] p 1187 A93-54080

- Oscillatory blowing - A tool to delay boundary-layer
separation p 1235 A93-55362

- Experimental investigation of flows behind different
Large-Eddy Breakup (LEBU) devices in thick boundary
layers p 18 N93-10550

- Overview of supersonic laminar flow control research
on the F-16XL ships 1 and 2
[NASA-TM-104257] p 20 N93-11221

SUBJECT INDEX

A wind tunnel investigation to determine buffet countermeasures for STOL aircraft alpha-sweep flight testing [NAL-TR-1129] p 65 N93-12362

A numerical study of hypersonic flow with strong surface blowing p 129 N93-13128

Bypass transition in compressible boundary layers p 417 N93-15801

Digital data acquisition and preliminary instrumentation study for the F-16 laminar flow control vehicle p 292 N93-16784

Three dimensional boundary-layer transition on a swept wing p 419 N93-16818

Analysis and evaluation of an integrated laminar flow control propulsion system [NASA-CR-192162] p 551 N93-20268

Swept wing attachment line contamination fence [NASA-CASE-LAR-13400-1] p 485 N93-22015

Stationary crossflow instability on an infinite swept wing p 699 N93-25865

High-lift aerodynamics: Prospects and plans p 784 N93-27442

The numerical simulation of circulation controlled airfoil flowfields p 879 N93-30947

Selected experiments in laminar flow: An annotated bibliography [NASA-TM-103989] p 990 N93-32226

BOUNDARY LAYER EQUATIONS

Generalized multipoint inverse airfoil design p 122 N93-14541

Numerical simulation of three-dimensional supersonic flows using Euler and boundary layer solvers [AIAA PAPER 93-0531] p 284 N93-23272

A calculation method for the three-dimensional boundary-layer equations in integral form [AIAA PAPER 93-0786] p 541 N93-24868

On the accurate prediction of the wall-normal velocity in compressible boundary-layer flow p 284 N93-27474

The determination of hybrid analytical-numerical solutions for the three-dimensional compressible boundary layer p 1029 N93-46979

Analysis of the effect of surface heating on boundary layer development over an NLS-0215 airfoil [AIAA PAPER 93-3437] p 978 N93-47229

Calculating crossflow separation using boundary layer computations coupled with an inviscid method [AIAA PAPER 93-3459] p 979 N93-47242

A Laplace interaction law for the computation of viscous airfoil flow in low and high speed aerodynamics [AIAA PAPER 93-3462] p 979 N93-47244

Semi-discrete Galerkin solution of the compressible boundary-layer equations with viscous-inviscid interaction [AIAA PAPER 93-3520] p 985 N93-47282

Numerical analysis of aerodynamic losses in film-cooled vane cascade p 1066 N93-48517

Computation of subsonic viscous and transonic viscous-inviscid unsteady flow p 1094 N93-52012

Calculation of a compressible three-dimensional boundary layer on a swept wing p 1179 N93-53551

Vibration excitation in laminar hypersonic boundary layers p 1237 N93-56028

Free streamline-boundary layer analysis for separated flow over an airfoil p 1239 N93-56327

Combustion in supersonic flows p 199 N93-14627

The semi-discrete Galerkin finite element modelling of compressible viscous flow past an airfoil [NASA-CR-192161] p 483 N93-20018

Numerical methods for aerothermodynamic design of hypersonic space transport vehicles [MBB-FE-211-S-PUB-0481] p 514 N93-21056

BOUNDARY LAYER FLOW

Effect of a large-scale inhomogeneity of the incoming flow on flow in a plane turbine cascade p 6 N93-10189

Direct numerical simulation of laminar breakdown in high-speed, axisymmetric boundary layers p 8 N93-11527

Numerical dissipation in F3D thin-layer Navier-Stokes solution for flows with wall transpiration p 9 N93-12010

An algebraic turbulence model with memory for the computation of three dimensional turbulent boundary layers p 115 N93-14248

In-flight surface-flow measurements on a subsonic transport high-lift flap system p 166 N93-14327

Detection of Goertler vortices in hypersonic flow p 120 N93-14382

Coriolis effects on Goertler vortices in the boundary-layer flow on concave wall p 123 N93-14564

Performance degradation due to hoar frost on lifting surfaces p 305 N93-17798

Influence of second-order boundary layer effects in hypersonic flow past blunt cones of large aspect ratio p 241 N93-18238

Partially exposed polymer dispersed liquid crystals for boundary layer investigations p 399 A93-19250

A theoretical approach for describing secondary instability features in three-dimensional boundary-layer flows [AIAA PAPER 93-0080] p 263 A93-20192

The prediction of riblet behaviour with a low-Reynolds number k-epsilon model p 270 A93-21720

Comparison of predictions with measurements for a quiet supersonic tunnel [AIAA PAPER 93-0344] p 376 A93-23031

The influence of the boundary layer on the subsonic near-wake of a family of bluff bodies [AIAA PAPER 93-0525] p 284 A93-23266

An upwind formulation for the solution of thin-layer Navier-Stokes equations p 461 A93-24088

On high speed turbulence modelling of shock-wave boundary-layer interaction [AIAA PAPER 93-0778] p 541 A93-24860

Experimental study of three-dimensional separation on a large-size model [ONERA, TP NO. 1992-174] p 473 A93-25348

On the accurate prediction of the wall-normal velocity in compressible boundary-layer flow p 477 A93-27474

Numerical experiments on the stability of leading edge boundary layer flow - A two-dimensional linear study p 477 A93-27475

Viscous-inviscid interaction coupled calculation of three-dimensional turbulent separated flow over dents p 681 A93-33748

Numerical methods in laminar and turbulent flow; Proceedings of the 7th International Conference, Stanford Univ., CA, July 15-19, 1991. Vol. 7, pts. 1 & 2 [ISBN 0-906674-77-8] p 743 A93-34301

Numerical analysis of the three-dimensional boundary layer on a turbomachinery rotor blade p 685 A93-34341

Hydrodynamics and heat transfer near the stagnation point in an arbitrary axisymmetric nonswirling flow incident on a rotating obstacle p 691 A93-35270

Calculation of compressible boundary layers by a hybrid finite element method p 692 A93-35613

Shock wave/boundary layer interaction in a two-dimensional laminar hypersonic flow [ONERA, TP NO. 1992-182] p 773 A93-38744

High-speed turbulence modelling of shock-wave/boundary-layer interaction p 927 A93-41910

On model for predicting blade force defect in end wall boundary layer inside axial compressor cascade p 862 A93-42271

Two-layer convective heating prediction procedures and sensitivities for blunt body reentry vehicles [AIAA PAPER 93-2763] p 963 A93-46509

Enhanced mixing via geometric manipulation of a splitter plate [AIAA PAPER 93-3244] p 966 A93-46789

Effects of bleed-hole geometry and plenum pressure on three-dimensional shock-wave/boundary-layer/bleed interactions [AIAA PAPER 93-3259] p 967 A93-46800

Transition in supersonic flow past axisymmetric bodies p 967 A93-46817

The moving wall effect vis-a-vis other dynamic stall flow mechanisms [AIAA PAPER 93-3424] p 1008 A93-47219

Analysis of the effect of surface heating on boundary layer development over an NLS-0215 airfoil [AIAA PAPER 93-3437] p 978 A93-47229

A Laplace interaction law for the computation of viscous airfoil flow in low and high speed aerodynamics [AIAA PAPER 93-3462] p 979 A93-47244

Boundary layer effects on the flow of a leading edge vortex [AIAA PAPER 93-3463] p 980 A93-47245

Development of an innovative natural laminar flow wing concept for high-speed civil transports [AIAA PAPER 93-3466] p 980 A93-47247

Preliminary design estimates of high-speed streamlines on arbitrary shaped vehicles defined by quadrilateral elements [AIAA PAPER 93-3491] p 982 A93-47263

Shock-wave/boundary layer interactions at hypersonic speeds by an implicit Navier-Stokes solver [AIAA PAPER 93-2938] p 1046 A93-48136

Improvement of conical similarity rule in swept shock wave/boundary layer interaction [AIAA PAPER 93-2941] p 1046 A93-48139

An analytical description of hypersonic boundary layer stability [AIAA PAPER 93-2981] p 1051 A93-48174

The three-dimensional boundary layer flow due to a rotor-tip vortex [AIAA PAPER 93-3081] p 1060 A93-48255

BOUNDARY LAYER SEPARATION

Hypersonic configuration optimization with an Euler/boundary layer coupling technique [AIAA PAPER 93-3116] p 1062 A93-48286

A blade element method for predicting the off-design performance of compressors p 1107 A93-49187

A laminar flow rotor for a radial inflow turbine [AIAA PAPER 93-1796] p 1074 A93-49686

Simulation of shock-boundary layer interaction in a fan blade passage [AIAA PAPER 93-1980] p 1078 A93-49827

Nontraditional methods of controlling the stability of a laminar subsonic boundary layer p 1085 A93-50962

Stagnation point computations of nonequilibrium inviscid blunt body flow p 1093 A93-52005

A time-accurate high-resolution TVD scheme for solving the Navier-Stokes equations p 1093 A93-52006

Unsteady aerodynamic behavior of an airfoil with and without a slat p 1093 A93-52007

Non-self-similarity of a boundary layer flow of a high-temperature gas in a Laval nozzle p 1176 A93-52946

Effect of boundary layer suction on the thrust and aerodynamic efficiency of a hypersonic flight vehicle p 1176 A93-52959

Boundary layer and pressure measurements on a cylinder with unsteady circulation control p 1177 A93-53207

Numerical analysis of the flow through a centrifugal impeller by vortex distribution model of a boundary layer. I - Theoretical analysis p 1182 A93-53843

Study on unstart and its propagation along modules due to compound choking and/or fluctuations in combustor of scramjet engines [ISABE 93-7052] p 1199 A93-54028

A new method for predicting the end wall boundary layers and the blade force defects inside the passage of axial compressor cascades p 1236 A93-55589

Flow computation for the hypersonic configuration ELAC I at low speeds and large incidence p 1238 A93-56036

Boundary layer relaminarization device [NASA-CASE-LAR-14470-1] p 23 N93-11876

Multi-point inverse design of isolated airfoils and airfoils in cascade in incompressible flow p 163 N93-14462

BLSTA: A boundary layer code for stability analysis [NASA-CR-4481] p 220 N93-14787

Boundary-layer measurements on a high Reynolds number three-element airfoil p 292 N93-16787

Numerical simulations of hypersonic rarefied transition regime flows: DSMC method and Navier-Stokes computation p 299 N93-19278

Application of the program profile for the design of low-speed, low-observable configuration airfoils [AD-A258842] p 305 N93-19364

Crossflow stability and transition experiments in a swept-wing flow [NASA-TM-108650] p 555 N93-21819

Surface and flow field measurements in a symmetric crossing shock wave/turbulent boundary-layer interaction [NASA-TM-106086] p 693 N93-24911

A feasibility study of using Langley 0.3-m transonic cryogenic tunnel sidewall boundary-layer removal system for heavy gas testing [NASA-CR-191438] p 747 N93-25087

Large-eddy simulation of temporally developing boundary layers with embedded streamwise vortices p 750 N93-25753

Model fan passage flow simulation [AD-A261613] p 752 N93-26167

Flow prediction over a transport multi-element high-lift system and comparison with flight measurements p 785 N93-27448

Navier-Stokes simulation of viscous, separated, supersonic flow over a projectile rotating band [AD-A263073] p 788 N93-27955

Flow visualization on helicopter blades using acenaphthen [ESA-TT-1255] p 931 N93-29273

Experimental study of heat transfer close to a plane wall heated in the presence of multiple injections (subsonic flow) p 901 N93-29931

Measurement of turbulent spots and intermittency modelling at gas-turbine conditions p 902 N93-29934

Heat transfer in high turbulence flows: A 2-D planar wall jet p 932 N93-29935

BOUNDARY LAYER SEPARATION

Three-dimensional flow of viscous gas in the blade passage of a straight compressor cascade p 5 A93-10187

Boundary layer separation in a corner formed by two planes p 6 A93-10188

A study of the laminar-turbulent transition in a boundary layer and separation on cones at supersonic velocities p 14 A93-12974

- In-flight detection of flow separation, stagnation, and transition p 166 A93-14326
- Instability of local separated flows with respect to small-amplitude perturbations p 125 A93-15254
- Hypersonic flow separation in shock wave boundary layer interactions
- [ASME PAPER 92-GT-205] p 251 A93-19429
- Transition prediction in attached and separated shear layers using an integral method
- [ASME PAPER 92-GT-281] p 253 A93-19473
- Study of flow phenomena in high speed intakes
- [AIAA PAPER 92-5029] p 272 A93-22304
- Juncture flow improvement for wing/pylon configurations by using CFD methodology
- [AIAA PAPER 93-0522] p 283 A93-23264
- The analysis of unsteady, three-dimensional flow separation
- [AIAA PAPER 93-0642] p 540 A93-24757
- Multigrid techniques for hypersonic viscous flows
- [AIAA PAPER 93-0771] p 467 A93-24855
- Experimental study of three-dimensional separation on a large-size model
- [ONERA, TP NO. 1992-174] p 473 A93-25348
- Oscillatory blowing, a tool to delay boundary layer separation
- [AIAA PAPER 93-0440] p 474 A93-25529
- Flowfield measurements of a two-element airfoil with large separation
- p 480 A93-29307
- An experimental study on location of transitional separation bubble on a low Reynolds numbers airfoil
- p 680 A93-33725
- A numerical method of unsteady separating flow over delta wings
- p 681 A93-33746
- Aerodynamics of maneuvering slender wings with leading-edge separation
- p 778 A93-39401
- Vortex features of F-106B aircraft at subsonic speeds
- [AIAA PAPER 93-3471] p 859 A93-41058
- Computation of hypersonic turbulent flow over a rearward facing step
- p 865 A93-42587
- A numerical solution of the asymptotic problem of boundary layer separation in an incompressible liquid upstream of the corner point of a body
- p 965 A93-46699
- Control of unsteady shock-induced turbulent boundary layer separation upstream of blunt fins
- [AIAA PAPER 93-3281] p 969 A93-46839
- Experiments on shock wave/boundary layer interaction in hypersonic flow
- p 970 A93-46888
- Scaling of incipient separation in high speed laminar flows
- [AIAA PAPER 93-3435] p 978 A93-47227
- Calculating crossflow separation using boundary layer computations coupled with an inviscid method
- [AIAA PAPER 93-3459] p 979 A93-47242
- Experimental study of 3-D separation on a large scale model
- [AIAA PAPER 93-3007] p 1053 A93-48197
- Improvement of transonic wing buffet by geometric modifications
- [AIAA PAPER 93-3024] p 1055 A93-48209
- Effect of flexural and rotational wing oscillations on the prevention of flow separation
- p 1150 A93-48911
- An experimental study of a compound supersonic jet
- p 1069 A93-48914
- Multigrid techniques for hypersonic viscous flows
- p 1071 A93-49027
- 3-D viscous flow CFD analysis of the propeller effect on an advanced ducted propeller subsonic inlet
- [AIAA PAPER 93-1847] p 1075 A93-49728
- A study of incipient separation limits for shock-induced boundary layer separation for Mach 6 high Reynolds flow
- [AIAA PAPER 93-2481] p 1084 A93-50222
- Skin-friction topology over a surface mounted semi-ellipsoidal wing at incidence
- p 1178 A93-53216
- Separation phenomenon in a hypersonic flow with strong wall cooling - Subcritical regime
- p 1189 A93-54266
- An experimental investigation on laminar boundary layer separation over a backward-facing step
- p 1230 A93-54588
- Oscillatory blowing - A tool to delay boundary-layer separation
- p 1235 A93-55362
- The hemisphere-cylinder at an angle of attack
- p 21 N93-11250
- Effects of sweep on the physics of unsteady shock-induced turbulent separated flows
- [AD-A247035] p 22 N93-11742
- Time dependent heat transfer rates in high Reynolds number hypersonic flowfields
- p 216 N93-13664
- Direct prediction of a separation boundary for aerofoils using a viscous-coupled calculation method
- [ESDU-92008] p 136 N93-14516
- A plume-induced boundary layer separation experiment
- [AD-A255397] p 220 N93-14677
- Investigations of detail design issues for the high speed acoustic wind tunnel using a 60th scale model tunnel. Part 1: Tests with open circuits
- [NASA-CR-191671] p 137 N93-14737
- Study of optical techniques for the Ames unitary wind tunnel. Part 5: Infrared imagery
- [NASA-CR-191385] p 194 N93-14809
- Detailed near surface flow about yawed, stranded cables
- [AD-A257382] p 418 N93-15857
- Computational investigations of a NACA 0012 airfoil in low Reynolds number flows
- [AD-A257300] p 288 N93-15920
- Static pressure measurements of the shock-boundary layer interaction in a simulated fan passage
- [AD-A256724] p 361 N93-15979
- Hypersonic flows as related to the national aerospace plane
- [NASA-CR-191980] p 296 N93-18378
- Stall departure resistance enhancer
- [NASA-CASE-LAR-14221-1] p 344 N93-19023
- Two problems reducing the data accuracy in Transonic Wind Tunnel testing
- p 304 N93-19321
- Model fan passage flow simulation
- [AD-A261613] p 752 N93-26167
- Calculation of fully three-dimensional separated flow with an unsteady viscous-inviscid interaction method
- p 786 N93-27455
- Modification and calibration of the Naval Postgraduate School Academic Wind Tunnel
- [AD-A262092] p 823 N93-28189
- An experimental study of flow over a 6 to 1 prolate spheroid at incidence
- p 874 N93-29124
- The 3-D viscous flow CFD analysis of the propeller effect on an advanced ducted propeller subsonic inlet
- [NASA-TM-106240] p 900 N93-29162
- High-Reynolds-number test of a 5-percent-thick low-aspect-ratio semispan wing in the Langley 0.3-meter transonic cryogenic tunnel: Wing pressure distributions
- [NASA-TM-4227] p 875 N93-29449
- Vortex structure and mass transfer near the base of a cylinder and a turbine blade
- p 901 N93-29929
- BOUNDARY LAYER STABILITY**
- Flight evaluation of a stagnation detection hot-film sensor
- [AIAA PAPER 92-4085] p 51 A93-13263
- Oblique wave evolution in a plane subsonic boundary layer
- p 124 A93-15178
- Recent supersonic transition studies with emphasis on the swept cylinder case
- p 127 A93-17252
- A high-frequency, secondary instability of crossflow vortices that leads to transition
- p 128 A93-17253
- Unstable branches of a hypersonic, chemically reacting boundary layer
- p 128 A93-17262
- On the coupling between a supersonic boundary layer and a flexible surface
- p 243 A93-19132
- Unsteady boundary-layer transition in flow periodically disturbed by wakes
- [ASME PAPER 92-GT-283] p 254 A93-19475
- Spatial simulation of boundary layer instability - Effects of surface roughness
- [AIAA PAPER 93-0075] p 262 A93-20187
- Transition studies for swept wing flows using PSE --- parabolized stability equations
- [AIAA PAPER 93-0077] p 263 A93-20189
- Stability and transition on swept wings
- [AIAA PAPER 93-0078] p 263 A93-20190
- Linear stability of three-dimensional boundary layers - Effects of curvature and non-parallelism
- [AIAA PAPER 93-0079] p 263 A93-20191
- A theoretical approach for describing secondary instability features in three-dimensional boundary-layer flows
- [AIAA PAPER 93-0080] p 263 A93-20192
- Instability and transition in three-dimensional supersonic boundary layers
- [AIAA PAPER 92-5049] p 273 A93-22321
- The asymptotic theory of hypersonic boundary-layer stability
- p 462 A93-24409
- The long-wave limit in the asymptotic theory of hypersonic boundary-layer stability
- p 462 A93-24410
- On the breakdown of a hypersonic laminar boundary layer
- [AIAA PAPER 93-0896] p 472 A93-24956
- Stability theory and transition prediction applied to a general aviation fuselage
- p 479 A93-28601
- Intermode exchange in a supersonic boundary layer
- p 691 A93-35346
- Inviscid instability of a skewed compressible mixing layer
- p 769 A93-37941
- Laminar flow control - Introduction and overview
- p 859 A93-41777
- The Langley 8-ft transonic pressure tunnel laminar-flow-control experiment
- p 910 A93-41783
- Numerical simulation of transition in two- and three-dimensional boundary layers
- p 973 A93-46980
- Instability of three-dimensional supersonic boundary layer
- p 973 A93-46987
- Numerical simulation of linear interference wave development in three-dimensional boundary layers
- p 1029 A93-46993
- Aerodynamic design of a hypersonic body with a constant favorable pressure gradient
- [AIAA PAPER 93-3444] p 978 A93-47232
- An analytical description of hypersonic boundary layer stability
- [AIAA PAPER 93-2981] p 1051 A93-48174
- Some stability characteristics of the boundary layer on a yawed cone
- [AIAA PAPER 93-3048] p 1057 A93-48228
- Bypass transition in two- and three-dimensional boundary layers
- [AIAA PAPER 93-3050] p 1057 A93-48230
- Calculation of the parameters of instability waves in the preseparation region
- p 1067 A93-48826
- Effect of curvature on stationary crossflow instability of a three-dimensional boundary layer
- p 1070 A93-49010
- Nontraditional methods of controlling the stability of a laminar subsonic boundary layer
- p 1085 A93-50962
- Laminar boundary-layer breakdown
- [AD-A254489] p 90 N93-12162
- BLSTA: A boundary layer code for stability analysis
- [NASA-CR-4481] p 220 N93-14797
- Three dimensional boundary-layer transition on a swept wing
- p 419 N93-16818
- Experiments on swept-wing boundary-layer transition
- p 419 N93-16829
- Swept wing attachment line contamination fence
- [NASA-CASE-LAR-13400-1] p 485 N93-22015
- Instability of flow in a streamwise corner
- [NASA-CR-191410] p 694 N93-25153
- Large-eddy simulation of temporally developing boundary layers with embedded streamwise vortices
- p 750 N93-25753
- The experimental study of transition and leading edge contamination of swept wings
- [LIB-TRANS-2197] p 782 N93-27274
- BOUNDARY LAYER TRANSITION**
- Direct numerical simulation of laminar breakdown in high-speed, axisymmetric boundary layers
- p 8 A93-11527
- Three-dimensional boundary-layer transition on a cone at Mach 3.5
- p 9 A93-12177
- A study of the laminar-turbulent transition in a boundary layer and separation on cones at supersonic velocities
- p 14 A93-12974
- Cobra maneuver considerations
- p 182 A93-14306
- In-flight detection of flow separation, stagnation, and transition
- p 166 A93-14326
- Boundary layer transition and control; Proceedings of the Conference, Univ. of Cambridge, United Kingdom, Apr. 8-12, 1991
- [ISBN 0-903409-86-0] p 211 A93-17251
- Recent supersonic transition studies with emphasis on the swept cylinder case
- p 127 A93-17252
- A high-frequency, secondary instability of crossflow vortices that leads to transition
- p 128 A93-17253
- Numerical simulation of a three-dimensional wave packet in a growing flat plate boundary layer
- p 128 A93-17265
- Experimental investigation of laminar to turbulent boundary layer transition with separation bubbles at low Reynolds number
- p 128 A93-17277
- Experiments on the active control of boundary layer transition
- p 243 A93-19133
- Boundary layer effects on the transonic flow in a straight turbine cascade
- [ASME PAPER 92-GT-155] p 249 A93-19382
- Transition prediction in attached and separated shear layers using an integral method
- [ASME PAPER 92-GT-281] p 253 A93-19473
- Unsteady boundary-layer transition in flow periodically disturbed by wakes
- [ASME PAPER 92-GT-283] p 254 A93-19475
- Effect of micron-sized roughness on transition in swept-wing flows
- [AIAA PAPER 93-0076] p 262 A93-20188
- Instability and transition in three-dimensional supersonic boundary layers
- [AIAA PAPER 92-5049] p 273 A93-22321
- What makes the Cobra maneuver possible?
- [AIAA PAPER 93-0183] p 367 A93-22609
- A comparison of hypersonic flight and prediction results
- [AIAA PAPER 93-0311] p 280 A93-23006
- Application of CFD to a generic hypersonic flight research study
- [AIAA PAPER 93-0312] p 280 A93-23007
- Transition on a sharp cone at high enthalpy - New measurements in the shock tunnel T5 at GALCIT
- [AIAA PAPER 93-0343] p 281 A93-23030

- The influence of the boundary layer on the subsonic near-wake of a family of bluff bodies
[AIAA PAPER 93-0525] p 284 A93-23266
- Effects of free-stream turbulence on boundary-layer transition
[AIAA PAPER 93-0488] p 416 A93-23390
- Unit-Reynolds-number effects on boundary-layer transition
p 288 A93-23560
- Development of the NASA-Ames low disturbance supersonic wind tunnel for transition research up to Mach 2.5
[AIAA PAPER 92-3909] p 462 A93-24488
- Boundary-layer transition extent measurements on a cone and flat plate at Mach 3.5
[AIAA PAPER 93-0342] p 474 A93-25517
- An experimental study on location of transitional separation bubble on a low Reynolds numbers airfoil
p 680 A93-33725
- Intermode exchange in a supersonic boundary layer
p 691 A93-35346
- Laminar flow flight experiments - A review
p 890 A93-41778
- Artificial transition - A tool for high Reynolds number simulation?
[AIAA PAPER 93-3258] p 967 A93-46799
- Numerical simulation of transition in two- and three-dimensional boundary layers
p 973 A93-46980
- Development of a system for transition characterization for aerodynamic simulations
[AIAA PAPER 93-3465] p 1030 A93-47246
- Experimental study of the effect of external turbulence and the shape of the surface on the characteristics of laminar and transition boundary layers
p 987 A93-47522
- Transition effects on compressible dynamic stall of transiently pitching airfoils
[AIAA PAPER 93-2978] p 1050 A93-48171
- Instability of hypersonic flow past blunt cones - Effects of mean flow variations
[AIAA PAPER 93-2983] p 1051 A93-48176
- Aerodynamic heating with boundary layer transition and heat protection with mass addition on blunt body in hypersonic flows
[AIAA PAPER 93-2984] p 1051 A93-48177
- Developing a data base for the calibration and validation of hypersonic CFD codes - Sharp cones
[AIAA PAPER 93-3044] p 1057 A93-48224
- Some stability characteristics of the boundary layer on a yawed cone
[AIAA PAPER 93-3048] p 1057 A93-48228
- Transition for three-dimensional boundary layers on wings in the transonic regime
[AIAA PAPER 93-3049] p 1057 A93-48229
- Bypass transition in two- and three-dimensional boundary layers
[AIAA PAPER 93-3050] p 1057 A93-48230
- Use of shear-stress-sensitive, temperature-insensitive liquid crystals for boundary layer transition detection in hypersonic flows
[AIAA PAPER 93-3070] p 1059 A93-48245
- Experimental study of transitional axisymmetric shock-boundary layer interactions at Mach 5
[AIAA PAPER 93-3131] p 1063 A93-48296
- A study of the effect of surface riblets on the evolution of a solitary wave packet (lambda vortex) in a laminar boundary layer
p 1067 A93-48827
- A study of the interaction of a nonstationary shock wave with a boundary layer on a plate in the transition regime
p 1150 A93-48850
- Future technology aim of the National Aerospace Plane Program
[AIAA PAPER 93-1988] p 1141 A93-49833
- Nontraditional methods of controlling the stability of a laminar subsonic boundary layer
p 1085 A93-50962
- On boundary-layer transition in transonic flow
p 1087 A93-51280
- Spectra of pressure pulsations on the surface of a cone in the transition region at supersonic flow velocities
p 1088 A93-51755
- Moving wall effects in transverse subsonic flow past a rotating cylinder
p 1179 A93-53573
- Experimental investigation of boundary layer transition on a flat plate with C4 leading edge
[ISABE 93-7123] p 1222 A93-54098
- Flow over a leading edge with distributed roughness
p 18 A93-10549
- Study of optical techniques for the Ames unitary wind tunnel. Part 5: Infrared imagery
[NASA-CR-191385] p 194 A93-14809
- Transition induced normal forces and their effects on the aerodynamic characteristics of slender sharp cones
[AD-A256802] p 288 A93-15889
- Special publication of National Aerospace Laboratory
[DE93-716176] p 239 A93-15946
- Three dimensional boundary-layer transition on a swept wing
p 419 A93-16818
- Experiments on swept-wing boundary-layer transition
p 419 A93-16829
- Modeling the transition region
[NASA-CR-4492] p 298 A93-19015
- The effect of surface suction near the leading edge of a swept-back wing
[AERO-REPT-9205] p 484 A93-20807
- The experimental study of transition and leading edge contamination of swept wings
[LIB-TRANS-2197] p 782 A93-27274
- Keynote address: Unsteady, multimode transition in gas turbine engines
p 901 A93-28927
- Determination of surface heat transfer and film cooling effectiveness in unsteady wake flow conditions
p 902 A93-29933
- Measurement of turbulent spots and intermittency modelling at gas-turbine conditions
p 902 A93-29934
- Selected experiments in laminar flow: An annotated bibliography
[NASA-TM-103989] p 990 A93-32226
- BOUNDARY LAYERS**
- A flat plate wing standing on a wall covered with a thick boundary layer. II - Wing characteristics under the effects of side wall boundary layer and wing tip vortex
p 125 A93-15446
- On sound attenuation in boundary layers
p 446 A93-19164
- Influence of blade aerodynamic loading on efficiency of radial-inflow turbines
[ASME PAPER 92-GT-91] p 249 A93-19337
- Hypersonic flow separation in shock wave boundary layer interactions
[ASME PAPER 92-GT-205] p 251 A93-19429
- Artificial viscosity models for the Navier-Stokes equations and their effect in drag prediction
[AIAA PAPER 93-0193] p 473 A93-25511
- Application of an engineering inviscid-boundary layer method to slender three-dimensional vehicle forebodies
[AIAA PAPER 93-2793] p 963 A93-46534
- Experiments on shock wave/boundary layer interaction in hypersonic flow
p 970 A93-46888
- Experimental evaluation of flat plate boundary layer growth over an anti-icing fluid film
p 1140 A93-52645
- Flight test results from a supercritical mission adaptive wing with smooth variable camber
[NASA-TM-4415] p 49 A93-11863
- Boundary layer relaminarization device
[NASA-CASE-LAR-14470-1] p 23 A93-11876
- Report on the final panel discussion on computational aerodynamics
[NASA-CR-189718] p 231 A93-12986
- AGARD WG13 aerodynamics of high speed air intakes: Assessment of CFD results
p 215 A93-13220
- An experimental/computational study of heat transfer in sharp fin induced shock wave/turbulent boundary layer interactions at low hypersonic Mach numbers
p 217 A93-13826
- Special publication of National Aerospace Laboratory
[DE93-716176] p 239 A93-15946
- Lanchester: The man
[AERO-REPT-9111] p 456 A93-16464
- The effects of viscosity on a conically derived waverider
[AD-A259019] p 424 A93-19101
- Aerodynamic heating analysis for axisymmetric bodies in supersonic flow
p 303 A93-19312
- An analysis of lift forces on aerosols in a wall bounded turbulent shear flow
[DE93-003362] p 747 A93-24963
- A feasibility study of using Langley 0.3-m transonic cryogenic tunnel sidewall boundary-layer removal system for heavy gas testing
[NASA-CR-191438] p 747 A93-25087
- Numerical simulation of leading-edge receptivity to freestream vorticity
p 696 A93-25388
- The addition of algebraic turbulence modeling to program LAURA
[NASA-TM-107758] p 840 A93-27250
- Recent progress in the analysis of iced airfoils and wings
p 784 A93-27441
- An interactive boundary-layer approach to multielement airfoils at high lift
p 785 A93-27445
- Investigation of forced unsteady separated flows using velocity-vorticity form of Navier-Stokes equations
p 840 A93-27451
- Plume effects on the flow around a blunted cone at hypersonic speeds
p 787 A93-27460
- Investigations on entropy layer along hypersonic hyperboloids using a defect boundary layer
p 787 A93-27462
- Ship viscous flow: A report on the 1990 SSPA-IIHR Workshop
p 840 A93-27466
- Development of an unstructured solution adaptive method for the quasi-three-dimensional Euler and Navier-Stokes equations
[NASA-CR-193241] p 930 A93-29213
- Heat transfer with moderate free stream turbulence
p 932 A93-29936
- BOUNDARY LUBRICATION**
- Measurements of wear and acoustic emission from fuel-wetted surfaces
p 744 A93-34925
- BOUNDARY VALUE PROBLEMS**
- Extreme value heat transfer problems for three-dimensional bodies moving at hypersonic velocities
p 4 A93-10079
- Numerical solution of a free-boundary problem in hypersonic flow theory - Nonequilibrium viscous shock layers
p 8 A93-11920
- Finite memory approximations for a singular neutral system arising in aeroelasticity
p 97 A93-13246
- Solving problems with singularities using conformal mappings
p 397 A93-18978
- Direct boundary value solution of wave rotor flow fields
[AIAA PAPER 93-0483] p 415 A93-23385
- Calculation of numerical boundary measure for wavelet-Galerkin approximations in aeroelasticity
[AIAA PAPER 93-1539] p 741 A93-34076
- Determination of the shape of a wing profile in boundary layer flow with a given velocity diagram
p 1067 A93-48844
- Numerical optimization methods for variational inverse boundary value problems of aerodynamics
p 1088 A93-51771
- Solution of the boundary value problem in flight dynamics by the opposite motion method
p 1206 A93-52944
- Effective treatment of the singular line boundary problem for three-dimensional grids
p 1177 A93-53204
- Combining direct and indirect methods in optimal control: Range maximization of a hang glider
[REPT-313] p 371 A93-16618
- BOW WAVES**
- Limitations of linear theory for sonic boom calculations
p 850 A93-37380
- Computational analysis of hypersonic flows past elliptic-cone waveriders
[NASA-CR-191304] p 138 A93-14767
- Kinetics and energy transfer in nonequilibrium fluid flows
[AD-A263612] p 875 A93-29284
- Calculations on unsteady type 4 interaction at Mach 8
[AD-A265214] p 990 A93-32004
- BOX BEAMS**
- Dynamic analysis of pretwisted elastically-coupled rotor blades
p 326 A93-21125
- Structural analysis of box beams using symbolic manipulation technique
p 548 A93-28615
- An analytically designed subcomponent test to reproduce the failure of a composite wing box beam
[AIAA PAPER 93-1344] p 709 A93-33914
- Design, analysis, and fabrication of the technology integration box beam
p 919 A93-30433
- BRAIDED COMPOSITES**
- Automatic Through-the-Thickness braiding
p 209 A93-15789
- Damage tolerance evaluation of new manufacturing techniques for composite helicopter drive shafts
[AIAA PAPER 93-1400] p 739 A93-33960
- 3-D braided preforms; cost to manufacture: Magnawave. I - Identifying cost factors
p 1226 A93-53423
- BRAIN DAMAGE**
- The effectiveness of airbags in reducing the severity of head injury from gunshot strikes in attack helicopters
p 494 A93-19691
- BRAKES (FOR ARRESTING MOTION)**
- Impulse guided Samara decelerator
[AIAA PAPER 93-1234] p 690 A93-35175
- BRAKING**
- Braking, steering, and wear performance of radial-belted and bias-ply aircraft tires
[SAE PAPER 921036] p 158 A93-14656
- BRANCHING (MATHEMATICS)**
- Subharmonic bifurcation analysis of wing with store flutter
p 78 A93-12098
- Local nonlinear control of stall inception in axial flow compressors
[AIAA PAPER 93-2230] p 1080 A93-50036
- Stability analysis through bifurcation theory. I, II
[ONERA, TP NO. 1993-108] p 1225 A93-53620
- An examination of wing rock for the F-15
[AD-A256613] p 188 A93-14252
- BRANCHING (PHYSICS)**
- Backward bifurcation for structural divergence of a wing section
p 526 A93-29351
- BRAYTON CYCLE**
- Models for predicting the performance of Brayton-cycle engines
[ASME PAPER 92-GT-361] p 355 A93-19525
- BIPS Turboalternator-Compressor characteristics and application to the NASA Solar Dynamic Ground Demonstration Program
p 532 A93-25965

BRAZING

Joining carbon composite fins to metal heat pipes using ion beam techniques p 543 A93-25979

BREAKDOWN

Breakdown of steady state axisymmetric flow in a shock layer formed as a result of the impingement of a supersonic underexpanded jet on a perpendicular plane obstacle p 241 A93-18230

BREATHING APPARATUS

Inward contaminant leakage tests of the S-Tron Corporation emergency escape breathing device. Phase 1: Tests of the original design. Phase 2: Tests with the redesigned neck seal [DOT/FAA/AM-92/18] p 704 N93-25205

BRITTLENESS

Deformation mechanisms of NiAl cyclically deformed near the brittle-to-ductile transformation temperature [NASA-CR-191649] p 391 N93-15830

BROADBAND

Results from a VHF impulse synthetic-aperture radar p 501 A93-28219

BROADCASTING

HELITRAK: A helicopter-tracking receiver system for television outside broadcast links [BBC-RD-1992/5] p 552 N93-20573

BROKEN SYMMETRY

Symmetry breaking in vortical flows over cones - Theory and numerical experiments [AIAA PAPER 93-3408] p 859 A93-41056

BRUSH SEALS

Brush seal leakage performance with gaseous working fluids at static and low rotor speed conditions [ASME PAPER 92-GT-304] p 405 A93-19494
Brush seal low surface speed hard-rub characteristics [AIAA PAPER 93-2534] p 1156 A93-50261
Brush seal bristle flexure and hard-rub characteristics [NASA-TM-105864] p 421 N93-18321
Integrity testing of brush seal in shroud ring of T-700 engine [NASA-TM-105863] p 421 N93-18380
Brush seal low surface speed hard-rub characteristics [NASA-TM-106169] p 838 N93-27132

BRUSHES

Integrity testing of brush seal in shroud ring of T-700 engine [NASA-TM-105863] p 421 N93-18380

BUBBLES

Calculation of 3-D unsteady subsonic flow with separation bubble using singularity method p 115 A93-14251

A numerical study of slit V-gutter flows p 171 A93-14273

Vortex generators used to control laminar separation bubbles p 768 A93-37381

Stability of the vapour phase in a rotating two-phase fluid system subjected to different gravitational intensities p 926 A93-41714

Active forcing of an axisymmetric leading-edge turbulent separation bubble [AIAA PAPER 93-3245] p 966 A93-46790

Overall effects of separation on thin aerofoils [ISBN-0-315-67464-4] p 135 N93-13930

Computational investigations of a NACA 0012 airfoil in low Reynolds number flows [AD-A257300] p 288 N93-15920

Simulation of vortex bursting p 699 N93-25881

BUCKLING

Post buckling of laminated composite stiffened curved panels subjected to cyclic shear and compression p 204 A93-14334

Buckling of open-section bead-stiffened composite panels p 1157 A93-50420

Stringer peeling effects at stiffened composite panels in the postbuckling range p 1160 A93-52453

Optimum design of aircraft structures with manufacturing and buckling constraints p 162 N93-13815

Reliability of stiffened structural panels: Two examples [NASA-TM-107687] p 219 N93-14483

Design and analysis of grid stiffened concepts for aircraft composite primary structural applications p 922 N93-30861

BUFFETING

On the configuration buffet of a transport aircraft p 117 A93-14298

A vortex control technique for the attenuation of fin buffet p 121 A93-14408

An experimental investigation of twin fin buffeting and suppression [AIAA PAPER 93-0054] p 261 A93-20167

The suppression of single-fin buffeting using tangential leading edge blowing on a delta wing p 270 A93-21677

The use of artificial intelligence for buffet environments [AIAA PAPER 93-1534] p 727 A93-34071

Comment on 'In-flight measurement of static pressures' p 807 A93-37407

Computational analysis of drag reduction and buffet alleviation in viscous transonic flow over porous airfoils [AIAA PAPER 93-3419] p 976 A93-47215

Improvement of transonic wing buffet by geometric modifications [AIAA PAPER 93-3024] p 1055 A93-48209

Simulation of tail buffet using delta wing-vertical tail configuration [AIAA PAPER 93-3688] p 1065 A93-48357

Active control for fin buffet alleviation [AIAA PAPER 93-3817] p 1133 A93-51408

Unsteady pressure and load measurements on an F/A-18 vertical fin p 1095 A93-52451

Navier-Stokes dynamics and aeroelastic computations for vortical flows, buffet and aeroelastic applications [NASA-CR-190692] p 17 N93-10098

Further buffeting tests in a cryogenic wind tunnel [NASA-TM-107621] p 22 N93-11610

Flight test results from a supercritical mission adaptive wing with smooth variable camber [NASA-TM-4415] p 49 N93-11863

A wind tunnel investigation to determine buffet countermeasures for STOL aircraft alpha-sweep flight testing [NAL-TR-1129] p 65 N93-12362

Fluid/structures interactions. Aircraft considerations p 527 N93-20628

BULGING

Bulging of fatigue cracks in a pressurized aircraft fuselage p 81 A93-13639

BUOYANCY

Heat transfer in rotating serpentine passages with trips skewed to the flow [ASME PAPER 92-GT-191] p 403 A93-19416

Buoyancy wave hazards to aviation p 430 A93-22151

Numerical study of mixed convection between two corotating symmetrically heated disks p 416 A93-23491

Turbulent flow and heat transfer in idealized blade cooling passages p 902 N93-29938

Effects of buoyancy on gas jet diffusion flames [NASA-CR-191109] p 935 N93-31031

BURAN SPACE SHUTTLE

Comparison of gasdynamic models in hypersonic flow p 1179 A93-53315

BURGER EQUATION

Uniform high-order spectral methods for one- and two-dimensional Euler equations p 476 A93-27068

BURNERS

The multi-heat addition turbine engine [AIAA PAPER 92-4272] p 54 A93-13334

Thermal analysis of a shower-head burner [SAE PAPER 921226] p 898 A93-41400

BURNING RATE

Experimental investigation of hydrogen burning and heat transfer in annular duct at supersonic velocity p 171 A93-14247

Gas analysis system for the Eight Foot High Temperature Tunnel p 822 A93-37875

Chemical kinetic and aerodynamic structures of flames [AD-A256015] p 391 N93-15931

BURNING TIME

Development of a hydrogen external burning flight test experiment on the NASA Dryden SR-71A aircraft [SAE PAPER 920997] p 157 A93-14638

BURSTS

The coherent structure in a corner turbulent boundary layer p 548 A93-28575

BUS CONDUCTORS

An optical fiber multi-terminal data bus system for aircraft [NAL-TR-1125] p 52 N93-12370

Software design document for the generic avionics data bus tool kit [AD-A259329] p 519 N93-21259

BYPASS RATIO

Advanced three-shaft engines - Configured for reliability, efficiency and growth p 53 A93-12236

Feasibility study on single bypass variable cycle engine with ejector [AIAA PAPER 92-4268] p 55 A93-13366

Combined engines for hypersonic flight p 171 A93-14244

A numerical investigation into the nozzle flow of high by-pass turbofans [ASME PAPER 92-GT-10] p 346 A93-19283

Design of an advanced nacelle for a very high bypass ratio engine p 505 A93-25362

Integration of high bypass ratio engines on modern transonic wings for regional aircraft p 506 A93-27479

Analysis of a high bypass ratio engine installation using the chimera domain decomposition technique [AIAA PAPER 93-1808] p 1100 A93-49697

Initial test results of 40,000 horsepower fan drive gear system for advanced ducted propulsion systems [AIAA PAPER 93-2146] p 1154 A93-49963

Development of an advanced exhaust mixer for a high bypass ratio turbofan engine [AIAA PAPER 93-2435] p 1118 A93-50188

Japan's research and development program for airbreathing engine technologies [ISABE 93-7005] p 1194 A93-53981

Engine for change p 1248 A93-56350

Investigation of the flowfield around an isolated bypass engine with fan and core jet p 215 N93-13227

Improving military transport aircraft through highly integrated engine-wing design [DS-1607] p 333 N93-17850

Aerodynamic design and analysis of fans using 3D computational codes [DS-2140] p 294 N93-17880

Transient performance of fan engine with water ingestion [NASA-CR-190778] p 677 N93-25134

By-passing of heat exchangers in gas turbines p 814 N93-27189

BYPASSES

A comparison of the measured and predicted flowfield in a modern fan-bypass configuration [ASME PAPER 92-GT-298] p 254 A93-19488

C

C-130 AIRCRAFT

Lockheed adopts media blast dry stripping for the C-130 [SAE PAPER 920949] p 107 A93-14092

Damage tolerance assessment and usage variation analysis for C-130 aircraft in the Israeli Air Force p 839 N93-27210

C-135 AIRCRAFT

Experimental investigation of the management of large-sized drops and the onset of Marangoni-convection p 926 A93-41700

C-141 AIRCRAFT

Why simulators don't fly like the airplane: Data - An update with examples from the C-141B program [AIAA PAPER 92-4161] p 66 A93-13312

Reassessment of the C-141 structural life p 46 A93-13631

C-160 AIRCRAFT

RAMSES: Multi-spectral experimental radar station installed on board the Transall p 550 N93-19925

CABIN ATMOSPHERES

Testing of an energy efficient environmental control system for a patrol-type aircraft [SAE PAPER 921225] p 890 A93-41399

A model study of the aircraft cabin environment resulting from in-flight fires [DOT/FAA/CT-90/22] p 496 N93-21557

CABLES

Analysis on space shape and tension distribution of towed flexible cables p 1043 A93-48554

Alternative equipment test procedures for simultaneous current injection on multiple cable bundles p 747 N93-24903

CABLES (ROPES)

Detailed near surface flow about yawed, stranded cables [AD-A257382] p 418 N93-15857

CALIBRATING

Airspeed calibration using GPS [AIAA PAPER 92-4090] p 51 A93-13272

Measurement of a one-dimensional mobility using a laser-Doppler velocimeter p 210 A93-16647

A preliminary investigation of a method to calibrate strain gauge balances by means of a reference balance p 210 A93-16845

Application of a flush airdata sensing system to a wing leading edge (LE-FADS) [AIAA PAPER 93-0634] p 516 A93-24750

Development of a six component flexured two shell internal strain gage balance [AIAA PAPER 93-0793] p 541 A93-24872

Aircraft measurement of electric field - Self-calibration p 753 A93-34694

Recent experiences with implementing a video based six degree of freedom measurement system for airplane models in a 20 foot diameter vertical spin tunnel p 821 A93-37763

Effects of equipment calibration, test flight procedures and analysing methods on the accuracy of ILS glide path measurements - Book p 881 A93-41600

Calibration of thermal anemometer at very low Reynolds numbers under microgravity p 926 A93-41729

SUBJECT INDEX

Flow calibration of two hypersonic nozzles in the AEDC HEAT-H2 high-enthalpy arc-heated wind tunnel
[AIAA PAPER 93-2782] p 1012 A93-46526

Calibration of a transonic S-hole probe for a multi-element airfoil cascade facility
[AIAA PAPER 93-2471] p 1138 A93-50216

An improved calibration technique for wind tunnel model attitude sensors p 1253 A93-54356

Development of a dynamic pressure response calibrator p 1254 A93-54362

An improved method for determining force balance calibration accuracy p 1254 A93-54369

Icing Research Tunnel rotating bar calibration measurement system p 1255 A93-54398

A method of testing two-dimensional airfoils [AD-A253210] p 17 N93-10375

CFD calibration for three-dimensional nozzle/afterbody configurations p 215 N93-13226

A multi-faceted engineering study of aerodynamic errors of the Service Aircraft Instrumentation Package (SAIP) [AD-A258059] p 293 N93-17677

An improved method of structural dynamic test design for ground flying and its application to the SH-2F and SH-2G helicopters p 512 N93-19928

System for calibrating a gyro navigator [AD-D015668] p 708 N93-26093

The HYDICE instrument design and its application to planetary instruments p 842 N93-28766

Selection and static calibration of the Marsh J1678 pressure gauge p 931 N93-29779

ERS-1 directional wave spectra validation with the airborne SAR PHARS [BCRS-92-18] p 937 N93-31010

CALIFORNIUM ISOTOPES

A transportable luggage examination system based on neutron interrogation p 497 N93-21863

Explosive detection system based on Electronic Neutron Generator (ENG) p 497 N93-21870

CALORIMETERS

Operating experience using venturi flow meters at liquid helium temperature [DE92-014693] p 90 N93-12140

CAMBER

Enhancement of endurance performance by periodic optimal camber control p 727 A93-34541

Aerodynamic foundations for use of unsteady aerodynamic effects in flight control p 695 N93-25274

A comparison of classical mechanics models and finite element simulation of elastically tailored wing boxes p 922 N93-30863

CAMBERED WINGS

Flight test results from a supercritical mission adaptive wing with smooth variable camber [AIAA PAPER 92-4101] p 38 A93-11274

Unsteady effects of camber on the aerodynamic characteristics of a thin aerofoil moving near the ground p 270 A93-21719

Unsteady ground effects on aerodynamic coefficients of finite wings with camber [AIAA PAPER 93-3423] p 976 A93-47218

CAMERAS

Optical design of a wide-angle simulator probe p 211 A93-17140

Visual field information in Nap-of-the-Earth flight by teleoperated Helmet-Mounted displays p 517 A93-26884

Study of optical techniques for the Ames unitary wind tunnel: Digital image processing, part 6 [NASA-CR-192164] p 382 N93-18766

Development of nose structure of a reconnaissance container for a supersonic jet aircraft [MBB-LME-242-S-PUB-0451] p 998 N93-31046

CANADA

Defence electronics industry profile, 1990-1991 [CTN-92-60515] p 84 N93-10653

CANARD CONFIGURATIONS

Wing pressure loads in canard configurations - A comparison between numerical results and experimental data p 7 A93-11499

Effect of canard position on the longitudinal aerodynamic characteristics of a close-coupled canard-wing-body configuration [AIAA PAPER 92-4632] p 14 A93-13304

A short range passenger/freighter canard - Some problems of a preliminary aerodynamic concept [SAE PAPER 921012] p 157 A93-14642

Flowfield computations over the Space Shuttle Orbiter with a proposed canard at a Mach number of 5.8 and 50 degrees angle of attack [AIAA PAPER 93-0322] p 281 A93-23014

Experimental and nonlinear vortex lattice method results for various wing-canard configurations p 479 A93-28607

Low-speed wind tunnel test results of the Canard Rotor/Wing concept [AIAA PAPER 93-3412] p 975 A93-47209

Effect of canard oscillations on the vortical flowfield of a X-31A-like fighter model in dynamic motion [AIAA PAPER 93-3427] p 1008 A93-47222

A flowfield study of a close-coupled canard configuration [AIAA PAPER 93-3499] p 983 A93-47269

Unsteady Navier-Stokes simulation of the canard-wing-body ramp motion [AIAA PAPER 93-3058] p 1058 A93-48235

Interference between a high-lift sweptforward wing and the horizontal nose plane at subsonic velocities p 1135 A93-51906

Pitch control trimming system for canard design aircraft [CA-PATENT-APPL-SN-2013236] p 63 N93-10374

Flowfield study of a close-coupled canard configuration [AD-A256311] p 139 N93-15245

Development of a computer assisted toolbox for aerodynamic design of aircraft at subcritical conditions with application to three-surface and canard aircraft [ISBN-90-6275-768-5] p 441 N93-16567

Flowfield computations over the Space Shuttle orbiter with a proposed canard at a Mach number of 5.8 and 50 deg angle of attack [AD-A258058] p 293 N93-17756

Lift enhancement using a close-coupled oscillating canard [AD-A257877] p 296 N93-18336

Effect of canard wing positions on aerodynamic characteristics of swept-forward wing [AD-A262373] p 789 N93-28493

CANCELLATION

System and method for cancelling expansion waves in a wave rotor [NASA-CASE-LEW-15218-1] p 86 N93-11172

CANONICAL FORMS

Solution of the terminal guidance problem for a flight vehicle using analytical mechanics methods p 228 A93-16778

Canonical correlation relationships among spectral and phytometric variables for twenty winter wheat fields p 433 A93-22992

CANOPIES

Study of the method for determining residual stress induced by machining in airplane canopies made of PMMA p 534 A93-27366

Stable cross type parachute with inflation aid [AIAA PAPER 93-1201] p 702 A93-35152

A simple, approximate model of parachute inflation [AIAA PAPER 93-1206] p 702 A93-35157

The effect of extreme altitude on parachute filling distance [AIAA PAPER 93-1207] p 702 A93-35158

Radial reefing method for accelerated and controlled parachute opening [AIAA PAPER 93-1209] p 702 A93-35159

Experimental validation of a discrete vortex method for inviscid axisymmetric flow around parachute canopies [AIAA PAPER 93-1216] p 689 A93-35165

The development of a parachute system for aerial delivery from high speed cargo aircraft [AIAA PAPER 93-1232] p 703 A93-35174

The stability and aerodynamic performances of clusters of small cruciform parachutes [AIAA PAPER 93-1242] p 690 A93-35181

Influence of the canopy-payload coupling on the dynamic stability in pitch of a parachute system [AIAA PAPER 93-1248] p 690 A93-35185

Parachute canopy control and guidance training requirements and methodology [AIAA PAPER 93-1255] p 703 A93-35188

Robotic inspection and refurbishment of aircraft canopy transparencies [SME PAPER AD92-203] p 855 A93-40665

The fluid physics of parachute inflation p 1189 A93-54347

Evaluation of alternatives for increasing A-7D rearward visibility [AD-A255071] p 50 N93-12488

CANTILEVER BEAMS

PAA-core aluminum honeycomb - An end user's evaluation p 209 A93-15738

Structural optimization of a cantilevered rotating beam p 210 A93-16248

Flexure-torsion behavior of prismatic beams. I - Section properties via power series p 417 A93-23557

Exact flutter solution of advanced anisotropic composite cantilevered wing structures [AIAA PAPER 93-1535] p 727 A93-34072

CANTILEVER MEMBERS

Post-critical behaviour of a tapered cantilever column subjected to a uniformly distributed tangential follower force p 831 A93-38431

CARBON FIBER REINFORCED PLASTICS

CAP CLOUDS

Natural and augmented snowfall growth processes and their interactions with the natural and modified aerosol [PB93-153096] p 755 N93-25874

CAPACITANCE

New digital capacitive measurement system for blade clearances p 1254 A93-54376

On machine capacitance dimensional and surface profile measurement system p 750 N93-25579

CAPTIVE TESTS

Development of a hydrogen external burning flight test experiment on the NASA Dryden SR-71A aircraft [SAE PAPER 920997] p 157 A93-14638

CARBIDES

Effects of grain size and carbides on the creep resistance and rupture properties of a conventionally cast nickel-base superalloy p 389 A93-21699

CARBON

Carbon/silicon carbide composite materials in advanced unmanned gas turbine engine combustors [AIAA PAPER 93-1761] p 1144 A93-49658

CARBON COMPOUNDS

NO(x) scavenging on carbonaceous aerosol surfaces in aircraft exhaust plumes. I [AIAA PAPER 93-2343] p 1164 A93-50117

CARBON DIOXIDE

Brush seal leakage performance with gaseous working fluids at static and low rotor speed conditions [ASME PAPER 92-GT-304] p 405 A93-19494

CARBON DIOXIDE CONCENTRATION

Spatial and temporal variations of the fluxes of carbon dioxide and sensible and latent heat over the FIFE site p 425 A93-20586

CARBON DIOXIDE LASERS

Detection and parameter estimation of atmospheric turbulence by ground-based and airborne CO2 Doppler lidars p 395 A93-17862

A high resolution airborne multisensor system p 343 A93-21966

Automated Laser Paint Stripping (ALPS) [SME PAPER AD92-206] p 855 A93-40667

Study of artificial and natural turbulence in atmospheric boundary layer with a CW Doppler CO2 lidar p 1257 A93-54799

CARBON FIBER REINFORCED PLASTICS

Fundamentals of composite repair [SME PAPER EM92-100] p 196 A93-14101

Economical view on composite structures maintenance [SME PAPER EM92-102] p 233 A93-14103

Commercial airplane primary structure [SME PAPER EM92-115] p 107 A93-14112

Compression after impact (CAI) properties of CF/PEEK (APC-2) and conventional CF/epoxy stiffened panels p 196 A93-14307

The design development of the monolithic CFRP centre fuselage skin of the European fighter aircraft p 159 A93-15782

Lightning protection of composite structure p 141 A93-15801

The production of a monolithic CFRP fuselage skin for the European Fighter Aircraft p 109 A93-15810

Delaminations of barely visible impact damage in CFRP laminates p 737 A93-33798

Low velocity impact in a graphite/PEEK [AIAA PAPER 93-1403] p 734 A93-33963

Thermoplastic applications in helicopter components p 796 A93-35952

Processing of high temperature carbon fiber reinforced polymers [SME PAPER EM92-215] p 925 A93-40654

Characterization of delamination and fiber fractures in carbon fiber reinforced plastics induced from impact p 915 A93-40787

Advanced composite fiber/metal pressure vessels for aircraft applications [AIAA PAPER 93-2246] p 1155 A93-50047

Carbon composite repairs of helicopter metallic primary structures p 1101 A93-50429

Design and manufacture for producibility of carbon fiber/epoxy composite aircraft skins [SME PAPER EM93-104] p 1043 A93-51732

The properties of newly developed highly damage tolerant and easy handleable carbon fiber/modified bismaleimide prepreg system p 1212 A93-53448

Repair materials and processes for the MD-11 Composite Tailcone p 1216 A93-53452

Damping in aerospace composite materials p 1260 A93-55869

The effect of temperature on the natural frequencies and acoustically induced strains in CFRP plates p 1260 A93-56331

Allowable compression strength for CFRP-components of fighter aircraft determined by CAI-test [MBB-FE-221-S-PUB-0483] p 537 N93-21462

- GARTEUR damage mechanics for composite materials: Analytical/experimental research on delaminations p 537 N93-21513
- Allowable compression strength for CFRP-components of fighter aircraft determined by CAI-test p 537 N93-21531
- Consideration of impact damages by dimensioning CFC (Carbon Fiber Reinforced Composites) components [MBB-FE-221-S-PUB-0501] p 1018 N93-31044
- CARBON FIBERS**
- Development of highly loaded root end attachments for composite material high speed flying surfaces p 539 A93-24122
- Polymer infiltration studies [NASA-CR-191652] p 200 N93-15431
- NASA advanced design program: Analysis, design, and construction of a solar powered aircraft [NASA-CR-192040] p 332 N93-17802
- The integrated design and manufacturing of composite structures for aircraft using an advanced tape layering technology [MBB-LME-251-S-PUB-0491-A] p 515 N93-21401
- Numerical modelling of induced effects of lightning strike on an all composite helicopter p 703 N93-24879
- A computational approach to predicting the extent of arc root damage in CFC panels p 735 N93-24890
- Zoning of aircraft by electric field modelling p 704 N93-24894
- CARBON MONOXIDE**
- Carbon monoxide emissions in lean premixed combustion p 197 A93-14503
- Three-dimensional gas turbine combustor emissions modeling [ASME PAPER 92-GT-129] p 350 A93-19363
- Oxides of nitrogen emissions from turbulent hydrocarbon/air jet diffusion flames, phase 2 [PB93-152478] p 756 N93-26533
- Generation of carbon monoxide in compartment fires [PB93-146702] p 880 N93-29211
- Making clean gasoline: The effect on jet fuels [AD-A264302] p 1019 N93-32085
- CARBON-CARBON COMPOSITES**
- Joining carbon composite fins to metal heat pipes using ion beam techniques p 543 A93-25979
- Oxidation-resistant high-temperature materials p 915 A93-40362
- HOPE and its thermal protection systems p 1252 A93-54711
- Status of R&D of high-performance materials for severe environments (Composite materials) p 1253 A93-54728
- Development of advanced carbon-carbon annular flameholders for gas turbines [PNR-90947] p 58 N93-11106
- Small particle impact damage in carbon-carbon composites [PNR-90948] p 73 N93-11107
- Current research in oxidation-resistant carbon-carbon composites at NASA Langley Research Center p 74 N93-12456
- Joining carbon composite fins to titanium heat pipes [AD-A261970] p 825 N93-27667
- CARBURIZING**
- High temperature corrosion resistant bearing steel development [AIAA PAPER 93-2000] p 1145 A93-49842
- CARET WINGS**
- Stability and control of hypersonic waveriders [AIAA PAPER 93-0508] p 370 A93-23255
- CARGO**
- Aircraft accident report: Explosive decompression-loss of cargo door in flight, United Airlines Flight 811, Boeing 747-122, N4713U, Honolulu, HI, 24 February 1989 [PB92-910402] p 28 N93-12193
- CARGO AIRCRAFT**
- The smart truck — structure, systems, avionics of C-17 airlifter p 40 A93-11420
- Air transportation system for shipping outsized cargoes p 141 A93-14394
- The development of a parachute system for aerial delivery from high speed cargo aircraft [AIAA PAPER 93-1232] p 703 A93-35174
- C-17 should fulfill USAF airlift mission p 805 A93-39599
- Versatility, automation key to C-17 cargo operations p 805 A93-39600
- Advanced cargo aircraft may offer a potential renaissance in freight transportation p 991 A93-47023
- The largest freight airship that can fit in Moffett hangar no. 1 [AIAA PAPER 93-4046] p 1242 A93-54613
- Hermes CX-7: Air transport system design simulation [NASA-CR-192082] p 335 N93-18056
- Arrow 227: Air transport system design simulation [NASA-CR-192053] p 336 N93-18063

- JEFF: Air transport system design simulation [NASA-CR-192069] p 338 N93-18350
- Sikorsky Aircraft Advanced Rotorcraft Transmission (ART) program [NASA-CR-191079] p 840 N93-27268
- The development of a parachute system for aerial delivery from high speed cargo aircraft [DE93-008339] p 790 N93-29035
- CARRIER INJECTION**
- Alternative equipment test procedures for simultaneous current injection on multiple cable bundles p 747 N93-24903
- CARRIER WAVES**
- Carrier wave signals interfering with Loran-C [ETN-92-92528] p 318 N93-17584
- CARTESIAN COORDINATES**
- Adaptive Cartesian grid methods for representing geometry in inviscid compressible flow [AIAA PAPER 93-3385] p 955 A93-45076
- 3D automatic Cartesian grid generation for Euler flows [AIAA PAPER 93-3386] p 956 A93-45077
- CASCADE FLOW**
- Three-dimensional flow of viscous gas in the blade passage of a straight compressor cascade p 5 A93-10187
- Effect of a large-scale inhomogeneity of the incoming flow on flow in a plane turbine cascade p 6 A93-10189
- Turbine blade cascade flows p 10 A93-12361
- Analytical method for subsonic cascade profile p 12 A93-12730
- A flow calculation and aerodynamic design method for turbomachine cascades p 12 A93-12764
- Computational studies of the characteristics of axial compressor cascades and stages in unsteady incoming flow p 13 A93-12805
- Heat transfer, adiabatic effectiveness, and injectant distributions downstream of a single row and two staggered rows of compound angle film-cooling holes p 201 A93-13976
- Influence of trailing-edge grid structure on Navier-Stokes computation of turbomachinery cascade flow p 111 A93-14078
- Numerical computations of turbomachinery cascade turbulent flows with shocks by using multigrid scheme p 112 A93-14167
- Calculation of sound field radiated by oscillating cascade p 231 A93-14269
- A fast method for calculating three-dimensional transonic potential flows in turbomachine blade rows p 125 A93-15215
- A conformal-integral method for solving the direct problem in turbomachine cascade aerodynamics p 125 A93-15217
- Numerical analysis of two-dimensional turbulent flows through an oscillating cascade p 126 A93-15494
- Modal analysis of unsteady aerodynamic response of subsonic annular cascade with steady loading under elastic vibration p 126 A93-15495
- Strong coupling between inviscid fluid and boundary layer for airfoils with a sharp edge. II - 2D unsteady case for isolated airfoil and straight blade cascade p 126 A93-16473
- Experimental study on the unsteady aerodynamic response of a three dimensional cascade with oscillating blades p 242 A93-18499
- Recent advances in simulating unsteady flow phenomena brought about by passage of shock waves in a linear turbine cascade [ASME PAPER 92-GT-4] p 245 A93-19277
- A statistical approach to the experimental evaluation of transonic turbine airfoils in a linear cascade [ASME PAPER 92-GT-5] p 245 A93-19278
- Aerodynamic performance of a transonic low aspect ratio turbine nozzle [ASME PAPER 92-GT-31] p 245 A93-19291
- Pressure fluctuation on casing wall of isolated axial compressor rotors at low flow rate [ASME PAPER 92-GT-33] p 246 A93-19293
- Blade loading and shock wave in a transonic circular cascade diffuser [ASME PAPER 92-GT-34] p 246 A93-19294
- Turbulence evaluation within the secondary flow region of a turbine cascade [ASME PAPER 92-GT-60] p 247 A93-19310
- Secondary flows in a transonic cascade - Validation of a 3-D Navier-Stokes code [ASME PAPER 92-GT-62] p 247 A93-19312
- Assessment of a 3-D Euler code for subsonic turbine vane flows and study of the non radial blade stacking [ASME PAPER 92-GT-63] p 247 A93-19313
- Surface-curvature-distribution effects on turbine-cascade performance [ASME PAPER 92-GT-84] p 248 A93-19333

- Aerodynamic design of pivotable nozzle vanes for radial-inflow turbines [ASME PAPER 92-GT-94] p 349 A93-19340
- Analysis of steady and unsteady turbine cascade flows by a locally implicit hybrid algorithm [ASME PAPER 92-GT-127] p 249 A93-19361
- Profile losses of an annular turbine cascade in unsteady periodic flow [ASME PAPER 92-GT-153] p 249 A93-19380
- Boundary layer effects on the transonic flow in a straight turbine cascade [ASME PAPER 92-GT-155] p 249 A93-19382
- Techniques for aerodynamic loss measurement of transonic turbine cascades with trailing-edge region coolant ejection [ASME PAPER 92-GT-157] p 250 A93-19384
- Transonic flow through turbine cascades with nonuniform pitch [ASME PAPER 92-GT-158] p 250 A93-19385
- Viscous interaction upstream and downstream of a turbine stator cascade with a periodic wake field [ASME PAPER 92-GT-162] p 250 A93-19388
- Advances in the numerical integration of the 3-D Euler equations in vibrating cascades [ASME PAPER 92-GT-170] p 351 A93-19396
- Coupled 3-D aeroelastic stability analysis of bladed disks [ASME PAPER 92-GT-171] p 351 A93-19397
- Numerical solutions for unsteady subsonic vortical flows around loaded cascades [ASME PAPER 92-GT-173] p 250 A93-19399
- Forcing function effects on unsteady aerodynamic gust response. II - Low solidity airfoil row response [ASME PAPER 92-GT-175] p 251 A93-19401
- Incidence angle and pitch-chord effects on secondary flows downstream of a turbine cascade [ASME PAPER 92-GT-184] p 251 A93-19409
- The measurement and prediction of the tip clearance flow in linear turbine cascades [ASME PAPER 92-GT-214] p 252 A93-19437
- The optimum value of the nozzle outlet angle of turbine stages [ASME PAPER 92-GT-224] p 404 A93-19442
- On aerodynamic loading of linear compressor cascades [ASME PAPER 92-GT-275] p 253 A93-19468
- Numerical research on flows in nonuniform cascades [ASME PAPER 92-GT-276] p 253 A93-19469
- Investigation of tip clearance phenomena in an axial compressor cascade using Euler and Navier-Stokes procedures [ASME PAPER 92-GT-299] p 255 A93-19489
- Calculation of wake-induced unsteady flow in a turbine cascade [ASME PAPER 92-GT-306] p 255 A93-19496
- The VKI compression tube annular cascade facility CT3 [ASME PAPER 92-GT-336] p 375 A93-19511
- Separated flow in a low speed two-dimensional cascade. I - Flow visualization and time-mean velocity measurements [ASME PAPER 92-GT-356] p 257 A93-19521
- Separated flow in a low speed two-dimensional cascade. II - Cascade performance [ASME PAPER 92-GT-357] p 257 A93-19522
- Prescribed-curvature-distribution airfoils for the preliminary geometric design of axial-turbomachinery cascades [ASME PAPER 92-GT-366] p 257 A93-19530
- A novel approach to high resolution compressible cascade flow analysis using the Navier-Stokes equations [ASME PAPER 92-GT-419] p 258 A93-19567
- Experimental study on the three dimensional flow within a compressor cascade with tip clearance. I - Velocity and pressure fields [ASME PAPER 92-GT-215] p 258 A93-19574
- Experimental study on the three dimensional flow within a compressor cascade with tip clearance. II - The tip leakage vortex [ASME PAPER 92-GT-432] p 258 A93-19575
- A fool-proof aerodynamic design code for turbine cascades p 259 A93-20117
- Unsteady two- and three-dimensional Navier-Stokes simulations of multistage turbomachinery flows p 266 A93-20721
- A new technique for analysis of unsteady aerodynamic responses of cascade airfoils with blunt leading edge. I - Theory p 267 A93-20909
- Blade loading of transonic circular cascade diffuser p 267 A93-20919
- Performance analysis of supersonic through-flow fan by the lifting surface theory. I - Disturbance flow field and determination of blade loadings p 267 A93-20929

- Two-dimensional cascade tests of MCA blades in the high transonic Mach number region. V - Effect of space/chord ratio on the parameters of cascade performance p 267 A93-20930
- Cascade flow calculations by a multigrid Euler method p 270 A93-21662
- An algebraic turbulence model for three-dimensional viscous flows [AIAA PAPER 93-0083] p 274 A93-22552
- Three-dimensional Navier-Stokes analysis of the tip clearance flow in linear turbine cascades [AIAA PAPER 93-0391] p 282 A93-23068
- High accuracy computation of fluid-structure interaction in transonic cascades [AIAA PAPER 93-0485] p 287 A93-23387
- Three-dimensional unstructured grid Euler method applied to turbine blades [AIAA PAPER 93-0196] p 461 A93-24233
- The numerical simulation of the hydrodynamic field from the pump impellers zone by means of the finite element method p 476 A93-26905
- A method for calculating the characteristics of plane compressor cascades for different values of the Reynolds criterion p 545 A93-27616
- Fluid flows around cascades p 479 A93-28518
- Numerical solution of non-isentropic transonic cascade flow by time-marching method p 679 A93-33715
- A comparison between numerical models and measurements in a Kaplan turbine guide vanes p 685 A93-34339
- Inlet turbulence distortion and viscous flow development in a controlled-diffusion compressor cascade at very high incidence p 688 A93-34485
- Nonreflecting boundary conditions of three-dimensional Euler equation calculations for strut cascades p 689 A93-34491
- Deforming grid variational principle for unsteady small disturbance flows in cascades p 692 A93-35623
- Experience in the design of supercritical cascades for the flow straightener of a transonic fan p 777 A93-39196
- Hierarchical development of three direct-design methods for two-dimensional axial-turbomachinery cascades p 812 A93-39271
- Subsonic/transonic cascade flutter using a full-potential solver p 861 A93-41934
- On model for predicting blade force defect in end wall boundary layer inside axial compressor cascade p 862 A93-42271
- Multigrid calculation of three-dimensional viscous cascade flows p 872 A93-42889
- A simple multigrid procedure for explicit time-marching on unstructured grids p 956 A93-45087
- Unsteady aerodynamic response of two-dimensional subsonic and supersonic oscillating cascades with chordwise displacement and flexible deformation p 971 A93-46922
- The three dimensional flow in a compressor cascade at design and off-design conditions p 971 A93-46927
- 3D/quasi-3D trans- and supersonic flow calculation in advanced centrifugal/axial compressor stages p 972 A93-46936
- Numerical simulation of aerothermodynamics processes in gas turbine engine components p 1002 A93-46939
- Navier-Stokes flow simulation in a 2D high pressure turbine cascade with a cooled slot trailing edge p 972 A93-46941
- Numerical analysis of airfoil cascades subjected to unsteady flow p 972 A93-46944
- Experimental and numerical study of transonic turbine cascade flow [AIAA PAPER 93-3064] p 1059 A93-48240
- Averaging techniques for steady and unsteady calculations of a transonic fan stage [AIAA PAPER 93-3065] p 1059 A93-48241
- 2-D theoretical analysis of circumferential grooved casing treatment p 1066 A93-48501
- Numerical simulation of unsteady flow in a transonic cascade p 1066 A93-48502
- Experimental investigation on effect of solid particles on blade pressure distribution in compressor cascade flow p 1066 A93-48513
- Experimental investigation on patterned blades of compressor p 1066 A93-48515
- Numerical analysis of aerodynamic losses in film-cooled vane cascade p 1066 A93-48517
- An aerodynamic design program for contra-rotating turbine cascades p 1067 A93-48521
- An experimental study on blade negative curving in a turbine cascade with a large turning angle p 1071 A93-49185
- A blade element method for predicting the off-design performance of compressors p 1107 A93-49187
- Investigation of flows in a controlled diffusion airfoil cascade passage p 1071 A93-49188
- A nonperiodic boundary approach for computation of compressible viscous flows in advanced turbine cascades [AIAA PAPER 93-1799] p 1074 A93-49688
- A staggered finite volume scheme for solving cascade flow with a two-equation model of turbulence [AIAA PAPER 93-1912] p 1076 A93-49779
- Simulation of shock-boundary layer interaction in a fan blade passage [AIAA PAPER 93-1980] p 1078 A93-49827
- Computational analysis of nonlinear aeroelastic phenomena during stall flutter of cascaded airfoils [AIAA PAPER 93-2082] p 1079 A93-49909
- Blade row interaction effects on flutter and forced response [AIAA PAPER 93-2084] p 1114 A93-49911
- Flow investigation of a low-speed-operated centrifugal compressor over a flow range including zero flow [AIAA PAPER 93-2240] p 1155 A93-50042
- Establishing two-dimensional flow in a large-scale cascade of controlled-diffusion compressor blades [AIAA PAPER 93-2383] p 1083 A93-50151
- Chimera grids in the simulation of three-dimensional flowfields in turbine-blade-coolant passages [AIAA PAPER 93-2559] p 1157 A93-50280
- A new technique for analysis of unsteady aerodynamic responses of cascade airfoils with blunt leading edge - Unsteady aerodynamic responses of the cascade in incompressible flow p 1086 A93-51122
- Verification of the TOTLOS method for calculating aerodynamic loss in film-cooled turbine cascade p 1087 A93-51191
- Estimation of the change of axial-flow compressor characteristics during long-term service p 1193 A93-52949
- Numerical analysis of flow within cascade with tip clearance p 1176 A93-53192
- Multigrid Navier-Stokes calculations for three-dimensional cascades p 1177 A93-53209
- Three-dimensional viscous flow analysis of compressor cascade channels p 1181 A93-53837
- Analysis of unstated supersonic flutter in cascade by semiactuator disk theory p 1181 A93-53841
- Numerical analysis of the flow through a centrifugal impeller by vortex distribution model of a boundary layer. I - Theoretical analysis p 1182 A93-53843
- A 2-D compressible N-S simulation of starting- and stalling-flows in a compressor cascades system [ISABE 93-7006] p 1183 A93-53982
- Numerical study on inception of stall cells in rotating stall [ISABE 93-7007] p 1183 A93-53983
- Some measurements of stall in an axial impeller [ISABE 93-7008] p 1183 A93-53984
- Review of stall, surge and active control in axial compressors [ISABE 93-7011] p 1184 A93-53987
- Forcing function modeling for flow induced vibration [ISABE 93-7027] p 1196 A93-54003
- Performance improvement by forward-skewed blading of axial fan moving blades [ISABE 93-7055] p 1185 A93-54031
- Tip clearance effects on the flow field of an axial turbine rotor blade cascade [ISABE 93-7057] p 1185 A93-54033
- Effects of wake interaction of two turbine cascades on secondary/tip-leakage flows and losses [ISABE 93-7058] p 1185 A93-54034
- Studies on coolant problems in aeronautical turbine cascades [ISABE 93-7074] p 1220 A93-54050
- Navier-Stokes analysis of turbine flowfield and external heat transfer [ISABE 93-7075] p 1186 A93-54051
- A comparative assessment of two present generation turbine analysis codes [ISABE 93-7097] p 1203 A93-54073
- Two-dimensional transonic flow around VKI turbine cascade p 1232 A93-54640
- Analysis of high Reynolds number inviscid/viscid interactions in cascades p 1234 A93-55351
- Three-dimensional Navier-Stokes analysis of tip clearance flow in linear turbine cascades p 1235 A93-55364
- Effect of blade leaning on the development of passage vortices and losses in the passage of turbine cascade with a great turning angle p 1236 A93-55397
- Experimental investigation of effect of particles on blade pressure distribution in impulse cascade flow p 1236 A93-55398
- A new method for predicting the end wall boundary layers and the blade force defects inside the passage of axial compressor cascades p 1236 A93-55589
- Analytical and experimental investigation of flow through a turbine vane cascade p 1248 A93-56348
- Explicit Navier-Stokes computation of turbomachinery flows p 83 N93-10370
- Overview on test cases for computation of internal flows in turbomachines p 214 N93-13209
- An algebraic turbulence model for three-dimensional viscous flows [NASA-TM-105931] p 110 N93-14102
- Multi-point inverse design of isolated airfoils and airfoils in cascade in incompressible flow p 163 N93-14462
- Time-dependent predictions and analysis of turbine cascade data in the transonic flow region [PNR-90957] p 139 N93-15489
- Prediction of turbine cascade flows with a quasi-three-dimensional rotor viscous code and the extension of the algebraic turbulence model [AD-A256831] p 223 N93-15635
- On flutter behavior of a 2-D compressor cascade in incompressible flow [DLR-FB-91-26] p 418 N93-16543
- Three-dimensional fiber-optic LDV measurements in the endwall region of a linear cascade of controlled-diffusion stator blades [AD-A263513] p 933 N93-29968
- CASCADE WIND TUNNELS**
- Testing techniques for straight transonic and supersonic cascades [ONERA, TP NO. 1992-155] p 773 A93-38734
- An experimental investigation of endwall flow control in a compressor plane cascade wind tunnel p 1066 A93-48512
- Calibration of a transonic 5-hole probe for a multi-element airfoil cascade facility [AIAA PAPER 93-2471] p 1138 A93-50216
- CASES (CONTAINERS)**
- Prediction of engine casing temperature of fighter aircraft for infrared signature studies [SAE PAPER 920961] p 206 A93-14627
- CASING**
- Numerical simulation of compressor endwall and casing treatment flow phenomena [ASME PAPER 92-GT-300] p 255 A93-19490
- Design and performance of nozzle-less volute casings for inward flow radial turbines p 722 N93-25471
- CAST ALLOYS**
- Effects of grain size and carbides on the creep resistance and rupture properties of a conventionally cast nickel-base superalloy p 389 A93-21699
- CASTING**
- Development of stitching reinforcement for transport wing panels p 921 N93-30852
- Development of resins for composites by resin transfer molding p 921 N93-30853
- Mechanical and analytical screening of braided composites for transport fuselage applications p 922 N93-30855
- CASTINGS**
- X-ray computed tomography for casting development [AD-A261786] p 752 N93-26526
- Use of titanium castings without a casting factor [AD-A264414] p 1018 N93-31192
- CATALOGS (PUBLICATIONS)**
- Composites: A catalogue of books and conference proceedings available in the NAL library [NAL-SP-IC-9201] p 234 N93-13368
- Facilities and capabilities catalog for landing and escape systems [NASA-RP-1282] p 196 N93-14495
- The NASA SBIR product catalog [NASA-TM-108242] p 945 N93-29322
- CATALYSIS**
- Improved selective catalytic NOx control technology for compressor station reciprocating engines [PB93-158566] p 755 N93-26529
- CATASTROPHE THEORY**
- The cusp catastrophe and the stability problem of helicopter ground resonance p 1099 A93-48059
- CATECHOLAMINE**
- The influence of nocturnal aircraft noise on sleep and on catecholamine secretion p 1163 A93-49554
- CATHODE RAY TUBES**
- New cathode-ray tube (CRT) gun interconnection assembly p 547 A93-28175
- CAUCHY INTEGRAL FORMULA**
- Numerical solution of the integral equations of the aerodynamics of porous surfaces p 13 A93-12768
- CAUCHY PROBLEM**
- Flux limiters in a rotated upwind scheme for the Euler equations [AIAA PAPER 93-0067] p 262 A93-20180
- A second-order upwind finite-volume method for the Euler solution on unstructured triangular meshes p 1087 A93-51738
- Godunov-type schemes applied to detonation flows [NASA-CR-191447] p 780 N93-27090

CAVITATION FLOW

- Rotation and cavitation of a marginal vortex
p 11 A93-12433
- Experimental investigation of laminar to turbulent boundary layer transition with separation bubbles at low Reynolds number
p 128 A93-17277
- Characteristics of separated flows including cavitation effects
p 84 A93-10874
- CAVITIES**
- Hypersonic flow past open cavities
[AIAA PAPER 93-2969] p 1049 A93-48163
- Non-propulsive aerodynamic noise
p 99 A93-10673
- Navier-Stokes simulations of unsteady transonic flow phenomena
[NASA-TM-103962] p 129 A93-12721
- Ultrasonic polishing
p 750 A93-25580
- Aerothermic calculations of flows in interdisc cavities of turbines
p 903 A93-29947
- CAVITY FLOW**
- Calculation of turbulent flow for an enclosed rotating cone
[ASME PAPER 92-GT-70] p 400 A93-19320
- Rotor cavity flow and heat transfer with inlet swirl and radial outflow of cooling air
[ASME PAPER 92-GT-378] p 406 A93-19536
- Effective sealing of a disk cavity using a double-toothed rim seal
[ASME PAPER 92-GT-379] p 406 A93-19537
- Low area ratio aircraft fuel jet-pump performances with and without cavitation
p 272 A93-22264
- Shock/boundary-layer interaction control with vortex generators and passive cavity
p 287 A93-23546
- Driven cavity simulation of turbomachine blade flows with vortex control
[AIAA PAPER 93-0390] p 461 A93-24238
- Unsteady flow computations for a three-dimensional cavity with and without an acoustic suppression device
[AIAA PAPER 93-3402] p 974 A93-47204
- Study of the near-wake structure of a subsonic base cavity flowfield using PIV
[AIAA PAPER 93-3040] p 1056 A93-48221
- Flowfield simulation about the stratospheric observatory for infrared astronomy
p 1095 A93-52446
- Pressure field and drag of a single cavity with rounded and sharp edges
p 1258 A93-55018
- Navier-Stokes simulations of unsteady transonic flow phenomena
[NASA-TM-103962] p 129 A93-12721
- Application of a solution adaptive grid to flow over an embedded cavity
p 130 A93-13141
- Numerical study of cavity natural convection flow with augmenting and counteracting effects by projection finite element method
p 749 A93-25540
- Navier-Stokes simulations of unsteady transonic flow phenomena
p 697 A93-25542
- Experimental investigation of turbine disk cavity aerodynamics and heat transfer
[NASA-CR-193831] p 812 A93-27115
- CENSORED DATA (MATHEMATICS)**
- Accuracy of nonparametric reliability estimates under varying operation conditions
p 396 A93-18343
- CENTER OF GRAVITY**
- An investigation of mode shift flutter suppression scheme for empennages
p 182 A93-14288
- Measurement of the center-of-gravity using X-ray computed tomography
p 396 A93-18619
- Estimation of aircraft inertia characteristics from bifilar pendulum test data
p 1249 A93-56029
- Experimental performance of a ventral nozzle with pitch and yaw vectoring capability for SSTOVL aircraft
[NASA-TM-106054] p 722 A93-25129
- CENTER OF MASS**
- Kinematics of aeroinertial aircraft rotation
p 819 A93-39192
- CENTRAL PROCESSING UNITS**
- Advanced real time integrated processors --- for Lockheed F-22 advanced tactical fighter
p 50 A93-11000
- Concurrent processing adaptation of aeroelastic analysis of propfans
p 173 A93-14624
- A performance assessment of a byzantine resilient fault-tolerant computer
[AIAA PAPER 89-3064] p 938 A93-41296
- The Pave Pace integrated core processor
p 941 A93-42856
- CENTRIFUGAL COMPRESSORS**
- Experimental research for the discharge flow of a centrifugal impeller and the flowfield in the vaneless diffuser
p 11 A93-12454
- A method for optimizing the meridional passage of the rotor in centrifugal compressors
p 119 A93-14344
- A method for optimizing the meridional passage in a centrifugal compressor
p 204 A93-14483
- Experimental and theoretical analysis of the flow in a centrifugal compressor volute
[ASME PAPER 92-GT-30] p 400 A93-19290
- Viscous flows in centrifugal compressor diffusers at transonic Mach numbers
[ASME PAPER 92-GT-48] p 246 A93-19301
- The vortex behaviour of the rotating-stall cell of a centrifugal compressor with vaneless diffuser
[ASME PAPER 92-GT-66] p 400 A93-19316
- The effect of compressor rotor tip crops on turboshaft engine performance
[ASME PAPER 92-GT-83] p 348 A93-19332
- Active stabilization of compressor instability and surge in a working engine
[ASME PAPER 92-GT-88] p 348 A93-19335
- The effects of blade loading in radial and mixed flow turbines
[ASME PAPER 92-GT-92] p 349 A93-19338
- Blade excitation by circumferentially asymmetric rotating stall in centrifugal compressors
[ASME PAPER 92-GT-148] p 351 A93-19376
- Excitation of blade vibration due to surge of centrifugal compressors
[ASME PAPER 92-GT-149] p 351 A93-19377
- Unsteady pressure measurements in a rotating centrifugal impeller
[ASME PAPER 92-GT-152] p 402 A93-19379
- Aerodynamic and performance analysis of a radial transonic impeller for a 9:1 pressure ratio compressor
[ASME PAPER 92-GT-183] p 352 A93-19408
- Experimental and computational investigation of the NASA Low-Speed Centrifugal Compressor flow field
[ASME PAPER 92-GT-213] p 252 A93-19436
- Development and industrial application of the 'all-over-controlled vortex distribution method' for designing radial and mixed flow impellers
[ASME PAPER 92-GT-262] p 405 A93-19466
- Design of multi-stage turbomachinery blading by the circulation method - Actuator duct limit
[ASME PAPER 92-GT-286] p 254 A93-19477
- A CAD computer system for centrifugal compressor impeller with transonic inflow
p 259 A93-20118
- The computation of internal flow fields in centrifugal compressor impellers
p 259 A93-20120
- Advanced direct-design procedure for centrifugal impellers
p 411 A93-21659
- Prediction of active control of subsonic centrifugal compressor rotating stall
[AIAA PAPER 93-0153] p 274 A93-22591
- Dynamics of a high speed impeller - Analysis and experimental verification
[AIAA PAPER 93-1362] p 743 A93-34239
- Effect of radial distortion on the performance of a centrifugal compressor
p 861 A93-42256
- 3D/quasi-3D trans- and supersonic flow calculation in advanced centrifugal/axial compressor stages
p 972 A93-46936
- A model for the selective amplification of spatially coherent waves in a centrifugal compressor on the verge of rotating stall
[AIAA PAPER 93-2236] p 1080 A93-50039
- Flow investigation of a low-speed-operated centrifugal compressor over a flow range including zero flow
[AIAA PAPER 93-2240] p 1155 A93-50042
- Numerical simulations of flows in centrifugal turbomachinery
[AIAA PAPER 93-2578] p 1085 A93-50293
- The flow lag angle in the rotor of a centrifugal compressor with allowance for viscosity effects
p 1179 A93-53555
- Velocity fluctuation based on the difference in the flow pattern in the channels of a centrifugal impeller
p 1182 A93-53842
- Numerical analysis of the flow through a centrifugal impeller by vortex distribution model of a boundary layer. I - Theoretical analysis
p 1182 A93-53843
- Transonic discharge flows around diffuser vanes from a centrifugal impeller
[ISABE 93-7053] p 1185 A93-54029
- Correlations for flow property variation at outlet of a centrifugal impeller
[ISABE 93-7054] p 1185 A93-54030
- Alternative systems for fuel gas boosters for small gas turbine engines
[PB92-223049] p 212 A93-12977
- Active control of stall and surge
p 423 A93-18725
- Active stabilization to prevent surge in centrifugal compression systems
[NASA-CR-191625] p 424 A93-18862
- Numerical modelling of viscous turbomachinery flows with a pressure correction method
p 723 A93-25702
- Active magnetic bearings applied to industrial compressors
p 841 A93-27570
- CENTRIFUGAL FORCE**
- Structural optimization of a cantilevered rotating beam
p 210 A93-16248
- Extending the fatigue life of aircraft engine components by hole cold expansion technology
[ASME PAPER 92-GT-77] p 401 A93-19327

- Some unsteady fluid forces on pump impellers
p 413 A93-22265
- Stability of the vapour phase in a rotating two-phase fluid system subjected to different gravitational intensities
p 926 A93-41714
- Three-dimensional numerical simulation of gradual opening in a wave rotor passage
[AIAA PAPER 93-2526] p 1156 A93-50254
- A numerical and experimental studies of flow characteristics in centrifugal fans
p 695 A93-25339
- CENTRIFUGAL PUMPS**
- Sound generation by rotating stall in centrifugal turbomachines
p 1039 A93-46701
- Application of a neural network as a potential aid in predicting NTF pump failure
[NASA-TM-107667] p 442 A93-18332
- CENTRIFUGES**
- Semi-full-scale dynamic simulation complex on the basis of centrifuge
[AIAA PAPER 93-3577] p 1208 A93-52673
- Parametric study of air sampling cyclones
p 135 A93-14173
- CENTRIPETAL FORCE**
- Three-dimensional numerical simulation of gradual opening in a wave rotor passage
[NASA-CR-191167] p 900 A93-29072
- CERAMIC COATINGS**
- Ceramic coatings enhance material performance
p 71 A93-13648
- Technical note - Plasma-sprayed ceramic thermal barrier coatings for smooth intermetallic alloys
p 209 A93-15702
- The evolution of thermal barrier coatings in gas turbine engine applications
[ASME PAPER 92-GT-203] p 388 A93-19427
- Erosion resistant titanium nitride coating for turbine compressor applications
[ASME PAPER 92-GT-417] p 388 A93-19565
- Ceramics for aero-engine applications
[ASME PAPER 92-GT-439] p 388 A93-19581
- Analysis of the friction and wear mechanisms of multilayered plasma-sprayed ceramic coatings
p 548 A93-28567
- Ceramic Technology Project
[DE92-018748] p 73 A93-11442
- Thermal barrier coating life prediction model development, phase 2
[NASA-CR-189111] p 198 A93-12589
- X ray diffraction and electron microscope studies of Yttria Stabilized Zirconia (YSZ) ceramic coatings exposed to vanadia
[AD-A258055] p 392 A93-17676
- CERAMIC FIBERS**
- Materials: Toward the non-metallic engine
[PNR-90915] p 56 A93-11019
- CERAMIC MATRIX COMPOSITES**
- Ceramic matrix composites for rocket engine turbine applications
[ASME PAPER 92-GT-394] p 388 A93-19547
- Ceramics for aero-engine applications
[ASME PAPER 92-GT-439] p 388 A93-19581
- High-temperature materials warm up for debut
p 535 A93-28393
- Carbon/silicon carbide composite materials in advanced unmanned gas turbine engine combustors
[AIAA PAPER 93-1761] p 1144 A93-49658
- Preparation and characterization of continuous fiber reinforced zirconium diboride matrix composites for a leading edge material
p 1211 A93-53445
- Evaluation of 2D ceramic matrix composites in aeroconvective environments
p 1212 A93-53459
- Corrosion of ceramic matrix composites
[ONERA, TP NO. 1993-82] p 1213 A93-53602
- Thermal design and analysis of an exhaust diffuser unit in a ceramic composite
[ISABE 93-7060] p 1220 A93-54036
- Material requirements for the High Speed Civil Transport
[ISABE 93-7067] p 1200 A93-54043
- Nondestructive evaluation of ceramic and metal matrix composites for NASA's HITEMP and enabling propulsion materials programs
[NASA-TM-105807] p 85 A93-10963
- Aero engine ceramics: The vision, the reality, and the progress
[PNR-90983] p 72 A93-11066
- Ceramic Technology Project
[DE92-018748] p 73 A93-11442
- Fiber reinforced composites: A new class of glass and glass ceramic materials for thermomechanical applications
[REPT-921-430-104] p 200 A93-15490
- Ultrahigh temperature assessment study: Ceramic matrix composites
[AD-A262740] p 826 A93-28592

Characterization of ceramic composite materials for gas turbine applications
[DE93-009719] p 905 N93-30168

CERAMICS

An evaluation system for impact damage and erosion of ceramic gas turbine components p 79 A93-12229
Research and development of ceramic turbine wheels [ASME PAPER 92-GT-295] p 354 A93-19485
Overview of NASA's advanced high temperature engine materials technology program p 1212 A93-53453
Ceramic Technology Project [DE92-018748] p 73 N93-11442
X ray diffraction and electron microscope studies of Yttria Stabilized Zirconia (YSZ) ceramic coatings exposed to vanadia [AD-A258055] p 392 N93-17676
Materials development program, ceramic technology project addendum to program plan: Cost effective ceramics for heat engines [DE93-003663] p 394 N93-18537
Advanced Turbine Technology Applications Project (ATTAP) [NASA-CR-189228] p 455 N93-18762
Compatibility of potential reinforcing ceramics with Ni and Fe aluminides [NASA-CR-192232] p 394 N93-18784
Improved ceramic slip casting technique --- application to aircraft model fabrication [NASA-CASE-LAR-14471-1] p 536 N93-20041
Research support for the Laboratory for Lightwave Technology [AD-A261488] p 760 N93-26343
Ultrahigh temperature assessment study: Ceramic matrix composites [AD-A262740] p 826 N93-28592
Use of local x ray computerized tomography for high-resolution, region-of-interest inspection of large ceramic components for engines [DE93-005564] p 843 N93-28943
Characterization of ceramic composite materials for gas turbine applications [DE93-009719] p 905 N93-30168

CERTIFICATION

The role of fatigue testing in the design, development and certification of the ATR 42/72 p 46 A93-13637
GE90 program moves into high gear p 810 A93-38701
Helicopter noise certification p 1262 A93-54720
Aircraft accident report: Atlantic Southeast Airlines, Inc. Flight 2311, uncontrolled collision with terrain, an Embraer EMB-120, N270AS, Brunswick, Georgia, 5 April 1991 [PB92-910403] p 28 N93-11471
Aircraft accident report: Explosive decompression-loss of cargo door in flight, United Airlines Flight 811, Boeing 747-122, N4713U, Honolulu, HI, 24 February 1989 [PB92-910402] p 28 N93-12193
Review of aeronautical fatigue investigations in the Netherlands during the period March 1989 - March 1991 [NLR-TP-91092-U] p 331 N93-17535
General aviation aircraft: Normal acceleration data analysis and collection project [DOT/FAA/CT-91/20] p 713 N93-24739
Zoning of aircraft: A review of the definitions p 703 N93-24880
Report on the test set-up for the structural testing of the Airmass Sunburst Ultralight Aircraft p 895 N93-29775
Helicopter simulator standards p 912 N93-30675

CESSNA AIRCRAFT

Stability theory and transition prediction applied to a general aviation fuselage p 479 A93-28601

CH-47 HELICOPTER

Onboard System Evaluation of Rotors Vibration, Engines (OBSERVE) monitoring system [AD-A255366] p 165 N93-15227

CHANNEL FLOW

Heat transfer performance comparisons of five different rectangular channels with parallel angled ribs p 397 A93-18752
Experimental and computational investigation of flow in catalytic monolith channels [ASME PAPER 92-GT-118] p 387 A93-19354
Heat transfer in serpentine flow passages with rotation [ASME PAPER 92-GT-190] p 403 A93-19415
Shock oscillation in two-dimensional, inviscid, unsteady channel flow p 288 A93-23563
Effects of longitudinal vortex generators on heat transfer and flow loss in turbulent channel flows p 1021 A93-44222
Design of axisymmetric channels with rotational flow [AIAA PAPER 93-3117] p 1062 A93-48287
Secondary flow computation by means of an inviscid multigrad Finite Volume Lambda Formulation [AIAA PAPER 93-1974] p 1077 A93-49821

Effect of rotation on heat transfer and hydraulic resistance in the radial cooling channels of turbine rotor blades p 1215 A93-52950
Velocity fluctuation based on the difference in the flow pattern in the channels of a centrifugal impeller p 1182 A93-53842
Heat transfer in a five-pass irregular channel with and without pin-fins p 1256 A93-54633
Effects of turn region treatments on pressure loss through sharp 180-degree bends p 1256 A93-54636
LES turbulence modeling using DNS data base p 299 N93-19274
The remarkable ability of turbulence model equations to describe transition p 783 N93-27432
Analysis of unsteady wave processes in a rotating channel [NASA-CR-191154] p 816 N93-28617

CHANNELS (DATA TRANSMISSION)

ARINC 629 DATABUS; Proceedings of the Conference, London, United Kingdom, Sept. 24, 1991 [ISBN 0-903409-95-X] p 311 A93-17835
SAFEbus p 828 A93-37072
New developments in a PI-Bus specification by the JIAWG and SAE p 940 A93-42852
STANAG 3910 - The data bus for the next generation of European avionics systems [SAE PAPER 931595] p 1104 A93-49344
High speed databus evaluation - Further work [SAE PAPER 931597] p 1151 A93-49346
Formal design specification of a Processor Interface Unit [NASA-CR-189698] p 99 N93-12538
Software design document for the generic avionics data bus tool kit [AD-A259329] p 519 N93-21259

CHAOS

Nonlinear aeroelasticity and chaos p 79 A93-12165
Nonlinear vibration and radiation from a panel with transition to chaos p 205 A93-14543
Nonlinear vibration and radiation from a panel with transition to chaos induced by acoustic waves p 398 A93-19173
Application of two chaos methods to Higher Harmonic Control data --- for suppression of helicopter vibration p 909 A93-43783
Laminar boundary-layer breakdown [AD-A254489] p 90 N93-12162
Chaotic vortical motion in the near region of a plane jet p 131 N93-13493
Turbulence and chaos in classical and quantum systems p 232 N93-14144
Chaos in mechanical systems with special reference to rotorcraft and missiles [AD-A263703] p 943 N93-29384

CHAPLYGIN EQUATION

Maximizing the critical Mach number for lifting wing profiles p 13 A93-12841

CHARACTERIZATION

In situ material characterization for pavement evaluation by the Spectral-Analysis-of-Surface-Waves (SASW) method [AD-A255660] p 194 N93-14128

CHARGED PARTICLES

Comparison of the electrical charging and discharging environments of multiple aircraft-borne electric-field measurement systems p 704 N93-24887

CHARTS

Maps and charts for visual air navigation p 498 A93-25170
Design of instrument approach procedure charts: Comprehension speed of missed approach instructions coded in text or icons [PB92-205673] p 36 N93-11252

CHECKOUT

On the typography of flight-deck documentation [NASA-CR-177605] p 571 N93-19970
The NASA/industry Design Analysis Methods for Vibrations (DAMVIBS) program: McDonnell-Douglas Helicopter Company achievements p 515 N93-21314

CHEMICAL ANALYSIS

Compatibility of potential reinforcing ceramics with Ni and Fe aluminides [NASA-CR-192232] p 394 N93-18784
Natural and augmented snowfall growth processes and their interactions with the natural and modified aerosol [PB93-153096] p 755 N93-25874

CHEMICAL ATTACK

Effect of aqueous solutions of water-crystallization inhibiting fluids on Thiocol-based sealants p 1017 A93-45689

CHEMICAL BONDS

Theoretical study of the bond dissociation energies of propyne (C3H4) p 230 A93-14099

CHEMICAL COMPOSITION

The chemistry of Saudi Arabian sand - A deposition problem on helicopter turbine airfoils p 1216 A93-53468
PFNA technique for the detection of explosives p 497 N93-21865

CHEMICAL ELEMENTS

Principles of nuclear-based explosive detection systems p 497 N93-21861

CHEMICAL ENERGY

Kinetics and energy transfer in nonequilibrium fluid flows [AD-A263612] p 875 N93-29284

CHEMICAL EQUILIBRIUM

Viscous equilibrium computations using program LAURA p 8 A93-12002
An upwind, kinetic flux-vector splitting method for flows in chemical and thermal non-equilibrium [AIAA PAPER 93-0894] p 472 A93-24954
Computation of hypersonic flow over a sphere using kinetic flux vector splitting scheme with equilibrium chemistry p 861 A93-42260
Equilibrium and nonequilibrium modeling of hypersonic inviscid flows p 864 A93-42448
Application of program LAURA to thermochemical nonequilibrium flow through a nozzle p 871 A93-42644
Radiative heat transfer from non-equilibrium high-enthalpy shock layers p 1024 A93-45515
Effects of wall conditions on chemically nonequilibrium shock-layer flow over hypersonic reentry bodies p 970 A93-46908
Multi-block calculations for flows in local chemical equilibrium [AIAA PAPER 93-2999] p 1053 A93-48189

CHEMICAL FUELS

Choice of the heating system for high-temperature generators using chemical fuel p 559 A93-29660

CHEMICAL REACTIONS

Simplified jet fuel reaction mechanism for lean burn combustion application [AIAA PAPER 93-0021] p 390 A93-23238
VSL analysis of nonequilibrium flows around a hypersonic body p 769 A93-38146
Hypersonic chemically reacting flow of a reentry body p 769 A93-38147
Computation of thermochemical nonequilibrium flows around a simple and a double ellipse p 869 A93-42629
Chemical nonequilibrium effects of Mach reflection p 1233 A93-54816
Effects of reacting flows with turbulence and shock waves on efficiency of scramjet combustors p 69 N93-11133
Simplified jet-A kinetic mechanism for combustor application [NASA-TM-105940] p 200 N93-15504
A numerical investigation of 3D transverse injection into the supersonic flow behind rearward facing step p 303 N93-19316

CHEMILUMINESCENCE

Calculation of optical and electric characteristics from hypersonic blunt-body wakes p 680 A93-33729
Shock enhancement and control of hypersonic combustion [AD-A254295] p 72 N93-10843

CHILDREN

A comparison between the impact of noise from aircraft, road traffic and trains on long-term recall and recognition of a text in children aged 12-14 years p 1163 A93-49552

CHINA

International aviation (Selected articles) [AD-A262566] p 765 N93-28576

CHINESE AIRCRAFT

An analysis of the reliability and maintainability of the Jian 6 and Jian 7 aircraft and ways to improve them [AD-A261060] p 678 N93-26238

CHIPS (ELECTRONICS)

Reconfigurable photonic data networks for military aircraft p 928 A93-42783
The Pave Pace integrated core processor p 941 A93-42856
Analysis of fault-tolerant neurocontrol architectures [NASA-TM-105898] p 65 N93-12305
Considerations for space and naval aviation applications of ferroelectric memory [AD-A261300] p 759 N93-26294

CHIPS (MEMORY DEVICES)

Formal design specification of a Processor Interface Unit [NASA-CR-189698] p 99 N93-12538

CHIRP

Robust method for estimating the parameters of a linear FM waveform p 1147 A93-47650

CHLOROETHYLENE

Development of MIL-H-53119, -54 C to 175 C high-temperature nonflammable hydraulic fluid for Air Force systems p 1214 A93-54250

CHOKED FLOW

Study on steady and unsteady unstart phenomena due to compound choking and/or fluctuations in combustor of scramjet engines

[AIAA PAPER 92-5102] p 359 A93-22372

Initiation of combustion in the thermally choked ram accelerator p 1016 A93-45501

Study on unstart and its propagation along modules due to compound choking and/or fluctuations in combustor of scramjet engines

[ISABE 93-7052] p 1199 A93-54028

CHOKES (RESTRICTIONS)

Low-frequency combustion oscillations in a model afterburner p 1193 A93-53702

CHORDS (GEOMETRY)

Experiments on swept-wing boundary-layer transition p 419 A93-16829

CIRCUIT BOARDS

JIAWG compatible development boards for the i960 [SAE PAPER 931596] p 1104 A93-49345

CIRCUIT RELIABILITY

Requirements for soldered electrical connections [NHB-5300.4(3A-2)] p 212 N93-12674

CIRCULAR CONES

Experimental investigations of asymmetric vortex flows behind elliptic cones at incidence p 757 A93-35637

Newtonian and hypersonic flows over oscillating bodies of revolution. I - Circular cones p 857 A93-39942

Active control of asymmetric conical flow using spinning and rotatory oscillations

[AIAA PAPER 93-2958] p 1048 A93-48152

Elliptic cross section tip effects on the vortex wake of an axisymmetric body at angle of attack

[AIAA PAPER 93-2960] p 1124 A93-48154

Spectra of pressure pulsations on the surface of a cone in the transition region at supersonic flow velocities

p 1088 A93-51755

Passive control of supersonic asymmetric vortical flows around cones p 220 A93-14692

CIRCULAR CYLINDERS

Turbulent structure in a vortex wake shed from an inclined circular cylinder p 125 A93-15443

The frequency of incipient vortex-shedding from a circular cylinder in a laminar boundary layer (The effect of the gap ratio on the vortex shedding frequency)

p 126 A93-15488

Flow around two circular cylinders by the random-vortex method p 271 A93-21925

Subharmonic and harmonic forced response of the wake of a circular cylinder p 288 A93-23565

Subsonic potential flow and the transonic controversy p 479 A93-28544

Pressure fluctuations on the surface of two circular cylinders in tandem arrangements at high Reynolds numbers p 679 A93-33718

Numerical computation of aerodynamic noise radiation by the large eddy simulation p 850 A93-38151

Supersonic base flow experiments in the near-wake of a cylindrical afterbody

[AIAA PAPER 93-2924] p 1045 A93-48125

Summary of the interaction of a rotor wake with a circular cylinder

[AIAA PAPER 93-3084] p 1060 A93-48258

Boundary layer and pressure measurements on a cylinder with unsteady circulation control

p 1177 A93-53207

Development of the wake behind a circular cylinder impulsively started into rotatory and rectilinear motion

p 1236 A93-55736

Algebraic determination of the shock wave shape in axisymmetric flow over a circular cylinder

p 1237 A93-56030

Solution of compressible Navier-Stokes equations using spectral methods on arbitrary two-dimensional domains

p 218 A93-14041

Computation of re-entry flows with two-temperature model p 301 A93-19295

Experiments on smooth cantilevered circular cylinders in a low-turbulence uniform flow. Part 2: Fluctuating loads on a cantilever of aspect ratio 30

[PB93-110500] p 555 A93-21382

Experiments on smooth cantilevered circular cylinders in low-turbulence uniform flow. Part 1: Mean loading with aspect ratios in the range 4 to 30

[PB93-111763] p 555 A93-21383

Experimental study of the effect of helical grooves on an infinite cylinder

[AD-A260890] p 751 A93-25912

CIRCULAR ORBITS

Modeling and control of a trailing wire antenna towed by an orbiting aircraft

[AD-A256450] p 219 A93-14610

Optimal finite-thrust time-bounded direct-ascent interception p 734 A93-25272

CIRCULAR TUBES

The effect of orthogonal-mode rotation on forced convection in a circular-sectioned tube fitted with full circumferential transverse ribs p 932 A93-29937

CIRCULATION

Measurements of circulation and vorticity in the leading-edge vortex of a delta wing p 288 A93-23548

CIRCULATION CONTROL AIRFOILS

Circulation control wing model study [AIAA PAPER 93-0094] p 264 A93-20200

The computation of the post-stall behavior of a circulation controlled airfoil

[AIAA PAPER 93-0207] p 277 A93-22625

Boundary layer and pressure measurements on a cylinder with unsteady circulation control

p 1177 A93-53207

ONERA calculation model of dynamic flow separation on an airfoil section p 1238 A93-56212

Consideration of mass elements of the control system in a flutter analysis p 1249 A93-56217

Navier-Stokes flowfield computation of wing/rotor interaction for a tilt rotor aircraft in hover

p 135 A93-14035

An experimental study of a turbulent boundary layer in the trailing edge region of a circulation-control airfoil

[NASA-CR-191262] p 295 A93-17934

The numerical simulation of circulation controlled airfoil flowfields p 879 A93-30947

CIRCULATION DISTRIBUTION

Effect of the wing planform on the optimal deformation of the middle surface p 1150 A93-48909

Nonplanar wings with a minimum induced drag

p 1089 A93-51779

Supersonic shock wave/vortex interaction [NASA-CR-192917] p 695 A93-25249

CIRCUMFERENCES

Efficiency of using longitudinal and circumferential bands in the structures of an airtight fuselage

p 801 A93-36795

CITIES

Proceedings of the First International Symposium on Explosive Detection Technology

[DOT/FAA/CT-92/11] p 496 A93-21856

CIVIL AVIATION

ICAO analyses trends in fuel consumption by world's airlines p 1 A93-10733

Automatic dependant surveillance focus of civil avionics integration p 30 A93-10998

A minimum rate of position reporting in the future oceanic air traffic control system p 30 A93-11006

Jeppesen worldwide electronic NOTAM service --- Notice to Airmen p 1 A93-11020

GPS integrity monitoring and system improvement with ground station and multistationary satellite support

p 33 A93-11044

A civil aircraft industry for India p 2 A93-12233

Review of human error accidents in civil aviation

p 27 A93-12367

The Tenth Conference on Air Navigation - A landmark in the history of civil aviation p 34 A93-12559

Critical considerations on European air transport politics p 103 A93-12718

South American latest developments in the air law and air policy fields p 103 A93-12719

HSCT high-lift aerodynamic technology requirements [AIAA PAPER 92-4228] p 44 A93-13355

Aerodynamic characteristics of a next generation high-speed civil transport

[AIAA PAPER 92-4229] p 15 A93-13356

General aviation turbine markets - An economic overview

[AIAA PAPER 92-4191] p 103 A93-13369

Civil spin-off from military aircraft cockpit research

p 45 A93-13415

The creation of a Community cabotage area in the European Community and its implications for the US bilateral aviation system p 104 A93-13423

The methods of reducing impact loads on occupants in the civil aircraft crash condition p 140 A93-14220

Use of alternative fuels for aviation

p 196 A93-14292

Airports, air traffic control, and their clients - Reflections on system optimization p 234 A93-15035

The future of area navigation in Western Europe

p 311 A93-17752

Flight management systems p 311 A93-17757

Vibrational monitoring and diagnostics of the technical condition of gas turbine engines at civil aviation repair facilities p 374 A93-18362

Development of a prototype of an expert system for the design of comprehensive scientific-technical development programs for civil aviation

p 434 A93-18373

Concept of closed-circuit TV system for transport aircraft under examination p 306 A93-18542

Effective 406-MHz ELT demonstrates the potential to save more lives p 311 A93-18543

Control measures used to reduce community noise from civil aviation in Denmark p 425 A93-19191

Civil aircraft challenges in engine/airframe integration [ASME PAPER 92-GT-45] p 322 A93-19299

Conceptual design of turbo-accelerator for HST combined cycle engine

[ASME PAPER 92-GT-253] p 353 A93-19462

Applications of space techniques to civil aviation operations p 312 A93-20007

Variable-complexity aerodynamic-structural design of a high-speed civil transport wing

[AIAA PAPER 92-4695] p 323 A93-20279

Integrated use of GPS and GLONASS in civil aviation navigation. II - Experience with GLONASS

p 313 A93-21142

The user friendly airliner (The 37th Roy Chadwick Lecture) p 307 A93-21718

Airport technology international 1993 p 532 A93-26920

Utilizing a microcomputer based flight simulation in teaching human factors in aviation p 570 A93-27165

A study on the marginal analysis method for the airline yield management p 487 A93-27370

Can one do without the magnetic reference? p 501 A93-28197

Datalinks - Civil aircraft; Proceedings of the Conference, London, United Kingdom, Nov. 24, 1992

[ISBN 1-85768-075-8] p 501 A93-29474

Aeroelastic challenges for a High Speed Civil Transport

[AIAA PAPER 93-1478] p 712 A93-34240

Taking to the skies under hydrogen power - Deutsche Aerospace Airbus studies the use of alternative fuels for civil aviation

p 677 A93-34947

Civil tiltrotor noise impact prediction methodology p 850 A93-35967

Design and manufacturing concepts of Eurofar Model No. 2 blades p 798 A93-35983

Limitations of linear theory for sonic boom calculations p 850 A93-37380

New cabin electronics p 804 A93-39542

Progress and taboos in flight safety - Human-factors research in air transportation p 879 A93-42654

Airbus or the revival of European civil aviation p 856 A93-42655

Federal preemption in commercial aviation - Tort litigation under 49 U.S.C. section 1305

p 944 A93-42997

The Foreign Sovereign Immunities Act of 1976 - Misjoinder, nonjoinder, and collusive joinder

p 944 A93-42998

Airport radar systems (2nd revised and enlarged edition) --- Russian book

[ISBN 5-277-00610-9] p 992 A93-44505

The NASA Computational Fluid Dynamics (CFD) program - Building technology to solve future challenges

[AIAA PAPER 93-3292] p 1041 A93-44996

Problems in the aerodynamics, strength, and flight operations of aircraft p 947 A93-45659

Implications of European legislation post 1992; Proceedings of the Conference, London, United Kingdom, Mar. 12, 1992

[ISBN 1-85768-015-4] p 1043 A93-50353

Overview of NASA's advanced high temperature engine materials technology program p 1212 A93-53453

Propulsion technology challenges for turn-of-the-century commercial aircraft

[ISABE 93-7003] p 1194 A93-53980

Engine technology challenges for a 21st Century High-Speed Civil Transport

[ISABE 93-7064] p 1200 A93-54040

Material requirements for the High Speed Civil Transport

[ISABE 93-7067] p 1200 A93-54043

Predevelopment of a flight control system for a small civil aircraft p 1249 A93-56031

The probable cause --- aircraft accidents

p 1240 A93-56417

Design of an air traffic computer simulation system to support investigation of civil tiltrotor aircraft operations

[NASA-CR-190811] p 36 A93-11139

Activities report of Lufthansa

[ETN-92-92100] p 28 A93-11319

UK airmissses involving commercial air transport, May-August 1991

[ETN-92-92260] p 28 A93-11357

UK airmissses involving commercial air transport, January-April 1991

[ETN-92-92261] p 87 A93-11358

- Formal representation of the requirements for an Advanced Subsonic Civil Transport (ASCT) flight control system
[NASA-CR-189699] p 98 N93-12346
- Public-sector aviation issues: Graduate research award papers, 1990 - 1991
[PB92-222629] p 143 N93-13787
- Report to Congress: State Block Grant Program
[AD-A254569] p 193 N93-13882
- Postmortem alcohol production in fatal aircraft accidents
[AD-A255766] p 143 N93-14026
- Aviation accidents, incidents, and violations: Psychological predictors among US pilots
p 144 N93-14693
- Technology benefits and ground test facilities for high-speed civil transport development
[NASA-TM-107670] p 378 N93-15790
- Unified Airport Design and Analysis Concepts Workshop
[DOT/FAA/RD-92/17] p 378 N93-16309
- State of the art of airport pavement analysis and design
p 378 N93-16310
- Aviation safety research at the National Institute for Aviation Research Wichita State University: A report to the FAA Technical Center
[NIAR-92-2] p 310 N93-16455
- The NASA High-Speed Research Program
p 330 N93-16761
- The 1990 high-speed civil transport studies
[NASA-CR-189618] p 330 N93-16947
- The 1990 high-speed civil transport studies. Summary report
[NASA-CR-189619] p 330 N93-16999
- MM-122: High speed civil transport
[NASA-CR-192011] p 334 N93-17974
- Phoenix: Preliminary design of a high speed civil transport
[NASA-CR-192024] p 334 N93-17976
- The airline quality report, 1992
[NIAR-92-11] p 310 N93-18036
- Proposal and preliminary design for a high speed civil transport aircraft. Swift: A high speed civil transport for the year 2000
[NASA-CR-192023] p 335 N93-18049
- TBD(exp 3)
[NASA-CR-192075] p 335 N93-18054
- High speed civil transport
[NASA-CR-192041] p 337 N93-18161
- Aviation safety: Problems persist in FAA's inspection program. Report to the Chairman, Subcommittee on Aviation, Committee on Public Works and Transportation, House of Representatives
[GAO/RCED-92-14] p 495 N93-19841
- Criminal acts against civil aviation
[AD-A258760] p 495 N93-19867
- Poland civil aviation master plan and investment program: Executive summary
[PB92-213685] p 459 N93-21342
- Poland civil aviation master plan and investment program
[PB92-213693] p 459 N93-21343
- Definitional mission for civil aviation master plan for Poland
[PB92-213974] p 459 N93-21713
- Proceedings of the First International Symposium on Explosive Detection Technology
[DOT/FAA/CT-92/11] p 496 N93-21856
- The UK perspective on aviation security
p 496 N93-21858
- Insights into US domestic aviation
p 496 N93-21859
- Design concepts for the development of cooperative problem-solving systems
[NASA-CR-192708] p 707 N93-25261
- A review of civil aviation propeller-to-person accidents: 1980-1989
[AD-A260695] p 705 N93-25896
- Design of an air traffic computer simulation system to support investigation of civil tiltrotor aircraft operations
[NASA-CR-192920] p 707 N93-26052
- Bibliography on propulsion airframe integration technologies for high-speed civil transport applications, 1980-1991
[NASA-TM-105602] p 678 N93-26136
- Satellite communications for aeronautical and navigation service
p 838 N93-26648
- Aircraft accident report: Controlled collision with terrain GP Express Airlines, Inc., Flight 861, A Beechcraft C99, N118GP, Anniston, Alabama, 8 June 1992
[PB93-910403] p 790 N93-27035
- Helicopter approach capability using the differential global positioning system
[NASA-CR-193183] p 793 N93-28936
- The 1991-1992 aviation system capacity plan
[AD-A263436] p 911 N93-29788
- Rotorcraft master plan
p 857 N93-30677
- The HSCT mission analysis of waverider designs
[NASA-CR-193467] p 879 N93-31037
- Engine technology challenges for a 21st Century High-Speed Civil Transport
[NASA-TM-106216] p 1004 N93-31671
- Reportable accidents to UK registered aircraft, and to foreign registered aircraft in UK airspace, 1990
[CAP-600] p 991 N93-31730
- Civil tiltrotor transport point design: Model 940A
[NASA-CR-191446] p 1019 N93-32234
- Propulsion technology challenges for turn-of-the-century commercial aircraft
[NASA-TM-106192] p 1005 N93-32351
- CL-84 AIRCRAFT**
An investigation of two-propeller tilt wing V/STOL aircraft flight characteristics
[AD-A257751] p 332 N93-17694
- CLASSICAL MECHANICS**
A comparison of classical mechanics models and finite element simulation of elastically tailored wing boxes
p 922 N93-30863
- CLASSIFICATIONS**
Detection and classification of acoustic signals from fixed-wing aircraft
p 850 N93-37032
- CLEANERS**
Performance of gas turbine compressor cleaners
[ASME PAPER 92-GT-360] p 355 A93-19524
- Performance of gas turbine compressor cleaners
[NLR-TP-91237-U] p 1003 N93-31111
- CLEANING**
Hot end cleaning - Corrosion pitting of turbine discs
[SAE PAPER 920930] p 202 A93-14081
- CLEANLINESS**
Ongoing challenges for titanium alloy cleanliness improvement in aircraft engine disk materials
p 1212 A93-53506
- CLEAR AIR TURBULENCE**
Preliminary results of the detection of clear air turbulence by the Wind Profiler Demonstration Network
p 427 A93-22119
- Diagnostic studies of clear air turbulence in isentropic coordinates
p 430 A93-22154
- Turbulence avoidance
p 309 A93-22160
- Atmospheric turbulence aloft - A review of possible methods for detection, warning, and validation of prediction models
[AIAA PAPER 93-0847] p 557 A93-24914
- Infrared detection of high altitude clear air turbulence
[AIAA PAPER 93-0852] p 557 A93-24916
- Effect of rotary atmospheric gusts on fighter airplane
[AIAA PAPER 93-3644] p 1127 A93-48328
- Study of artificial and natural turbulence in atmospheric boundary layer with a CW Doppler CO2 lidar
p 1257 A93-54799
- Research support for the Laboratory for Lightwave Technology
[AD-A261488] p 760 N93-26343
- CLEARANCES**
The effect of compressor rotor tip crops on turboshaft engine performance
[ASME PAPER 92-GT-83] p 348 A93-19332
- Tip clearance effect on heat transfer and leakage flows on the shroud-wall surface in an axial flow turbine
[ASME PAPER 92-GT-200] p 403 A93-19425
- The measurement and prediction of the tip clearance flow in linear turbine cascades
[ASME PAPER 92-GT-214] p 252 A93-19437
- Investigation of tip clearance phenomena in an axial compressor cascade using Euler and Navier-Stokes procedures
[ASME PAPER 92-GT-299] p 255 A93-19489
- Adaptation of a 3-D pressure correction Navier-Stokes solver for the accurate modelling of tip clearance flows
p 971 A93-46932
- New digital capacitive measurement system for blade clearances
p 1254 A93-54376
- An experimental and analytical study of TIP clearance effects in axial flow compressors
[AD-A256434] p 179 N93-15337
- An analysis of en route controller-pilot voice communications
[AD-A264784] p 935 N93-30611
- CLIMATE CHANGE**
Development and testing of the Perseus proof-of-concept aircraft
[DE93-010121] p 806 N93-28586
- Climatic effects of turbofan emissions in the stratosphere and the higher troposphere
p 1035 N93-31927
- CLIMATOLOGY**
Studies of atmospheric eddy dynamics and energetics and climate problems
[ISBN 5-286-00610-8] p 753 A93-35689
- Adverse weather test site selection study
[AD-A259012] p 339 N93-18895
- Development and testing of the Perseus proof-of-concept aircraft
[DE93-010121] p 806 N93-28586
- Air Traffic and Environment
[GSF-BAND-8] p 1034 N93-31925
- CLIMBING FLIGHT**
Adaptive control of aircraft in windshear
p 62 A93-13126
- The development of an efficient take-off performance monitor (TOPM)
p 180 A93-14186
- Wind-shear endurance capability for powered-lift aircraft
[AIAA PAPER 93-3670] p 1129 A93-48348
- Optimal performance of airplanes flying through windshear
[AIAA PAPER 93-3846] p 1102 A93-51480
- An experimental and a theoretical investigation of rotor pitch damping using a model rotor
p 47 N93-10322
- Estimation of rate of climb
[ESDU-92019] p 164 A93-14541
- Effect of underwing frost on transport aircraft takeoff performance
[DOT/FAA/CT-TN93/9] p 791 N93-27252
- CLOCKS**
The effect of clock, media, and station location errors on Doppler measurement accuracy
p 885 A93-29588
- CLOSED CIRCUIT TELEVISION**
Concept of closed-circuit TV system for transport aircraft under examination
p 306 A93-18542
- CLOUD COVER**
Volcanic clouds --- aircraft hazards
p 487 A93-28196
- Preliminary evaluation of aviation-impact variables derived from numerical models
[PB93-190197] p 1034 N93-31202
- CLOUD HEIGHT INDICATORS**
The FAA aircraft icing Forecasting Improvement Program - Validation of aircraft icing forecasts in the Denver area
[AIAA PAPER 93-0393] p 309 A93-23069
- CLOUD PHYSICS**
Remote sensing cloud properties from high spectral resolution infrared observations
p 1034 A93-46780
- CLOUD SEEDING**
Natural and augmented snowfall growth processes and their interactions with the natural and modified aerosol
[PB93-153096] p 755 N93-25874
- CLOUDS (METEOROLOGY)**
Behavior of precipitating water drops under the influence of electrical and aerodynamical forces
p 1034 A93-45176
- A technique for the measurement of cloud structure on centimeter scales
p 1158 A93-51243
- Identification of icing water clouds by NOAA AVHRR satellite data
[DLR-FB-92-11] p 434 N93-16477
- Uplink laser propagation measurements through the sea surface, haze and clouds
[AD-A264687] p 935 N93-30553
- CLUSTER ANALYSIS**
Clustering methods for removing outliers from vision-based range estimates
p 1171 A93-51648
- Discrete range clustering using Monte Carlo methods
[NASA-TM-104004] p 706 N93-24914
- CLUSTERS**
The stability and aerodynamic performances of clusters of small cruciform parachutes
[AIAA PAPER 93-1242] p 690 A93-35181
- CLUTTER**
Some limitations on the effectiveness of airborne adaptive radar
p 501 A93-29596
- A technique to correct airborne Doppler data for coordinate transformation errors using surface clutter
p 807 A93-37699
- Ground clutter measurements using the NASA airborne doppler radar: Description of clutter at the Denver and Philadelphia airports
p 490 N93-19608
- Comparison of simulated and actual wind shear radar data products
p 490 N93-19610
- Signal processing for airborne doppler radar detection of hazardous wind shear as applied to NASA 1991 radar flight experiment data
p 490 N93-19612
- Classification of radar clutter in an air traffic control environment
p 886 N93-30299
- CMOS**
Neutron-induced single event upsets in static RAMs observed at 10 KM flight altitude
p 1158 A93-50561
- COAL**
Effects of external control circuit on coal-fired supersonic diagonal-type MHD generator
p 1173 A93-49619
- COAL DERIVED LIQUIDS**
Advanced thermally-stable, coal-derived, jet fuels program: Experiment system and model development
[AD-A262747] p 917 N93-29402

COANDA EFFECT

The computation of the post-stall behavior of a circulation controlled airfoil
[AIAA PAPER 93-0207] p 277 A93-22625
Boundary layer and pressure measurements on a cylinder with unsteady circulation control p 1177 A93-53207

Aerodynamic surface tip vortex attenuation system [AD-D015606] p 483 N93-20017

COASTAL ZONE COLOR SCANNER

The Airborne Ocean Color Imager - System description and image processing p 1157 A93-50369

COASTS

Physical effects of vegetation on wind-blown sand in the coastal environments of Florida [PB92-188424] p 93 N93-11702

COATING

Robotic aircraft painting with SAFARI [SME PAPER AD92-198] p 855 A93-40662

COATINGS

Starch media blasting for aerospace finishing applications [SAE PAPER 920948] p 107 A93-14091
Experimental investigations of the time and flow-direction responses of shear-stress-sensitive liquid crystal coatings [AIAA PAPER 93-0181] p 542 A93-25508
Optically smart surfaces survivability testing at Mach 3 [AD-A261785] p 760 N93-26566

COAXIAL FLOW

Acoustic intensity of nonisothermal coaxial jets with an inverted velocity profile p 1124 A93-51759

COBALT ALLOYS

Life assessment of gas turbine bucket coating based on degradation analysis p 533 A93-24464
Gas phase hydrogen permeation in a Ni-Fe-Co superalloy p 735 A93-34510
Crack simulation and life assessment of gas turbine nozzles p 915 A93-40805
Erosion predictions and measurements of high-temperature coatings and superalloys used in turbomachines p 74 N93-12189

COCKPIT SIMULATORS

Piloted simulator investigations of a civil tilt-rotor aircraft on steep instrument approaches p 800 A93-36023
An evaluation of software tools for the design and development of cockpit displays [AIAA PAPER 93-3593] p 1224 A93-52685
Advanced terrain displays to transport category aircraft [PB92-197136] p 35 N93-10065
A synthetic environment flight simulator: The AFIT virtual cockpit [AD-A259220] p 530 N93-20576
NASA/FAA helicopter simulator workshop [NASA-CP-3156] p 857 N93-30673
Part 1: Executive summary p 857 N93-30674
Helicopter simulator standards p 912 N93-30675
ATTAS experimental-cockpit and ATMOS for component and system investigations in flight guidance p 1014 N93-31276

COCKPITS

Requirements for integrated flight and traffic management during final approach p 31 A93-11009
Investigation of cabin noise reduction in the Y12 p 41 A93-11816
Advanced cockpit technology in the real world p 2 A93-13409
Civil spin-off from military aircraft cockpit research p 45 A93-13415
Flight simulator research into advanced MLS approach and departure procedures p 149 A93-14234
Control of the pilot-system interface p 166 A93-15040
An experimental cockpit display for TDWR wind shear alerts p 343 A93-22111
Hazard assessment and cockpit presentation issues for microburst alerting systems p 308 A93-22112
Tactical cockpits - The coming revolution p 505 A93-27238
A survey of display technologies for military aircraft cockpit applications p 517 A93-27239
Controls and displays for Douglas Aircraft for the 1990s p 545 A93-27241
Investigation of cabin noise reduction in the Y12 p 506 A93-27371
An ac thin film electroluminescent (TFEL) display unit for cockpit control display unit application p 518 A93-28179
The history and development of coated Contrast Enhancement Filters for cockpit displays p 564 A93-28180
Development of an expert system for cockpit emergency procedures p 845 A93-35915
Concept feasibility demonstration for the Army Cockpit Delethalization Program p 795 A93-35916

The ring laser gyro and its applications

p 927 A93-42657
Theory and design of adaptive automation in aviation systems [AD-A254595] p 160 N93-12613
Does cockpit management training reduce aircrew error? p 146 N93-15014
Cockpit decision making p 146 N93-15015
Trans-cockpit authority gradient in Navy/Marine aircraft mishaps p 146 N93-15016
Simulator evaluation of displays for a revised takeoff performance monitoring system [NASA-TP-3270] p 189 N93-15366
Cockpit resource management proficiency as a factor of primary flight training [AD-A256995] p 328 N93-16262
Definition of the 2005 flight deck environment [NASA-CR-4479] p 343 N93-16693
On the typography of flight-deck documentation [NASA-CR-177605] p 571 N93-19970
A synthetic environment flight simulator: The AFIT virtual cockpit [AD-A259220] p 530 N93-20576
ATTAS experimental-cockpit and ATMOS for component and system investigations in flight guidance p 1014 N93-31276

CODES

Improvements in code validation algorithms for secondary surveillance radar p 883 A93-43408

CODING

Prediction of success from training p 495 N93-19702
Detection performance of digital polarity sampled phase reversal code pulse compressors [AD-A262930] p 842 N93-28289
Internation aircraft operator information system [DOT/FAA/CT-93/4] p 949 N93-32232

COEFFICIENT OF FRICTION

Direct measurements of skin friction in supersonic combustion flow fields [AD-A262878] p 825 N93-28226

COGNITION

Enhanced Aeronautical Resource Management training alternatives p 147 N93-15019
A cognitive model for training decision making in aircrews p 147 N93-15020
Elements of a theory of natural decision making p 147 N93-15021

COGNITIVE PSYCHOLOGY

How expert pilots think p 147 N93-15017
Accidents and errors: A review of recent UK Army Air Corps accidents p 495 N93-19701

COHERENT LIGHT

Position sensor with two wavelength time domain multiplexing for civil aircraft application p 1104 A93-49432

COHERENT RADAR

Solid-state coherent laser radar wind shear measuring systems p 144 N93-14848

COHERENT RADIATION

Undulator Spectromicroscopy Facility at the Advanced Light Source [DE93-007964] p 823 N93-28490

COHERENT SCATTERING

Coherent anti-Stokes Raman scattering (CARS) thermometry in a model gas turbine can combustor [ASME PAPER 92-GT-134] p 387 A93-19366

COLD FLOW TESTS

Investigation of combustion structure inside low NO(x) combustors for a 1500 C-class gas turbine [ASME PAPER 92-GT-123] p 350 A93-19357
Measured acoustic characteristics of ducted supersonic jets at different model scales [AIAA PAPER 93-0731] p 563 A93-24821

Static internal performance tests of single expansion ramp nozzle concepts designed with LO considerations [AIAA PAPER 93-2429] p 1117 A93-50185
Aerodynamics design of convergent-divergent nozzles [AIAA PAPER 93-2574] p 1085 A93-50290
Planar measurement of flow field parameters in nonreacting supersonic flows with laser-induced iodine fluorescence p 133 N93-13801
Analytical and experimental investigation of annular propulsive nozzles [AD-A262685] p 815 N93-28391

COLD PRESSING

Effects of thermal history and jet fuel absorption on the properties of APC-2 p 534 A93-25252

COLD SURFACES

Flow past three-dimensional irregularities in a hypersonic boundary layer on a cooled body p 775 A93-39119

COLLISION AVOIDANCE

Integrating TCAS into the airspace management system p 30 A93-11005
TCAS display issues [AIAA PAPER 92-4242] p 51 A93-13351

TCAS II testing conflicts and resolutions

p 165 A93-14158
Interrelationships between commercial airplane design and operational requirements and procedures p 153 A93-14219

New results in optimal missile avoidance analysis

p 369 A93-22937
Aircraft collision avoidance using statistical decision theory p 500 A93-28155

The problem of avoiding aircraft collisions during group flights p 819 A93-39191
The Airborne Collision Avoidance System (ACAS) p 883 A93-43370

A reactive approach for distributed air traffic control [ONERA, TP NO. 1993-83] p 1190 A93-53603
CRAASH - A coordinated collision avoidance system [ONERA, TP NO. 1993-84] p 1191 A93-53604

The effect of TCAS interrogations on the Chicago O'Hare ATCRBS system [DOT/FAA/CT-92/22] p 318 N93-16498

Results of DATAS investigation of illegal mode S ID's at JFK Airport [DOT/FAA/CT-92/26] p 318 N93-16841

Aviation safety: Users differ in views of collision avoidance system and cite problems. Report to the Chairman, Subcommittee on Investigations and Oversight, Committee on Science, Space, and Technology, House of Representatives [GAO/RCED-92-113] p 502 N93-19843

Testing of an automatic, low altitude, all terrain ground collision avoidance system p 502 N93-19924

Fundamentals of adaptive anticipation techniques for the detection of threatening air traffic conflicts: Investigation of the horizontal proximity situation in the case of expected heading changes [DLR-MITT-91-21] p 503 N93-21004

Domain engineering validation case study: Synthesis for the air traffic display/collision warning monitor domain version 01.00.03 [AD-A259407] p 503 N93-21671

Results of DATAS investigation of ATCRBS environment at the Los Angeles International Airport [DOT/FAA/CT-93/6] p 793 N93-28625

Issues of ATC conflict resolution under real-time constraints p 887 N93-30350

UK airmisses involving commercial air transport, September - December 1991 [ETN-93-93930] p 992 N93-32409

COLLISIONS

Airbus Industrie TCAS experience p 152 N93-15186

Aircraft accident report: Tomy International, Inc., d/b/a Scenic Air Tours flight 22, Beech Model E18S, N342E in-flight collision with terrain, Mount Haleakala, Maui, Hawaii, 22 April 1992 [PB93-910401] p 705 N93-25827

COLOR

Trade-offs arising from mixture of color cueing and monocular, binocular, and stereoscopic cueing information for simulated rotorcraft flight [NASA-TP-3268] p 338 N93-18333

COLOR PHOTOGRAPHY

The Airborne Ocean Color Imager - System description and image processing p 1157 A93-50369

COLOR VISION

Performance of color-dependent tasks of air traffic control specialists as a function of type and degree of color vision deficiency [AD-A256614] p 151 N93-14275

COMBAT

The influence of fighter agility on air combat effectiveness p 184 A93-14398

A database approach to aircraft carrier airplan production [AD-A257737] p 240 N93-17666

Air accidents in the French Air Force p 492 N93-19676

A high-fidelity, six-degree-of-freedom batch simulation environment for tactical guidance research and evaluation [NASA-TM-4440] p 1010 N93-32380

COMBINATORIAL ANALYSIS

Method for assessing the electric power system reliability of multiple-engined aircraft p 810 A93-37398

COMBINED CYCLE POWER GENERATION

Aerothermodynamic analysis of combined-cycle propulsion systems p 359 A93-21671

Studies on methane-fuel ram combustor for HST combined cycle engine [ISABE 93-7080] p 1201 A93-54056

Stall transients including effects of inlet distortion and intake geometry p 423 N93-18726

COMBINED STRESS

Structural optimization of a cantilevered rotating beam p 210 A93-16248

SUBJECT INDEX

Analysis of interlaminar stresses in symmetric and unsymmetric laminates under various loadings
[AIAA PAPER 93-1511] p 740 A93-34050

COMBUSTIBLE FLOW

Theoretical investigation of combustion characteristics in ram-jet dump combustor with side-inlet
p 346 A93-19121

Numerical analysis of reacting flow using finite rate chemistry models
p 389 A93-21666

PdI prediction of supersonic hydrogen flames
[AIAA PAPER 93-0448] p 391 A93-23358

Stability of oblique detonations in RAM accelerators
[AIAA PAPER 92-0089] p 541 A93-24979

Analysis of thermal ignition in supersonic flat-plate boundary layers
p 769 A93-37933

Shock tunnel studies of external combustion in high supersonic air flows
p 1017 A93-45517

Effects of side-inlet angle in a three-dimensional side-dump combustor
p 1109 A93-49610

Nonintrusive, multipoint velocity measurements in high-pressure combustion flows
[AIAA PAPER 93-2032] p 1145 A93-49867

A finite element code for gas turbine combustor flow with Stretched Laminar Flamelet modelling
[ISABE 93-7127] p 1204 A93-54102

Velocity and temperature measurements in a non-premixed reacting flow behind a backward facing step
p 132 A93-13632

Combustion in supersonic flows
p 199 A93-14627

Numerical calculation of flow field in supersonic combustion chamber
p 304 A93-19317

Projectile base bleed technology. Part 2: User's guide CMINT computer code, version 5.04-BRL
[AD-A258630] p 551 A93-19999

Influence of supercritical conditions on pre-combustion chemistry and transport behavior of jet fuels
[AD-A261813] p 737 A93-26268

Comparison of reacting and non-reacting shear layers at a high subsonic Mach number
[NASA-TM-106198] p 814 A93-27610

Direct measurements of skin friction in supersonic combustion flow fields
[AD-A262878] p 825 A93-28226

Turbulence characteristics of an axisymmetric reacting flow
[NASA-CR-4110] p 877 A93-30373

COMBUSTION

Combustion and reaction kinetics; Proceedings of the 22nd International Annual Conference of ICT, Karlsruhe, Germany, July 2-5, 1991
p 535 A93-27726

Shock tube validation experiments for the simulation of ram-accelerator-related combustion and gasdynamic problems
p 1016 A93-45499

Initiation of combustion in the thermally choked ram accelerator
p 1016 A93-45501

Direct numerical simulation of combustion in turbulent supersonic flow
[DS-2138] p 393 A93-17746

Fundamental studies of droplet interactions in dense sprays
[AD-A261165] p 737 A93-25948

Cumulative reports and publications
[NASA-CR-191440] p 847 A93-27063

COMBUSTION CHAMBERS

Numerical solution of dynamic equations arising in a jet engine simulation
p 53 A93-12237

Vaporizer performance
p 79 A93-12784

Numerical simulation of a low-emission gas turbine combustor using KIVA-II
p 170 A93-14077

Supersonic combustion and gasdynamic of scramjet
p 170 A93-14242

Scramjet combustor and nozzle computations
p 171 A93-14243

Experimental investigation of hydrogen burning and heat transfer in annular duct at supersonic velocity
p 171 A93-14247

Numerical simulation of turbulent reacting flows in combustion chambers
p 171 A93-14271

Estimation of maximal local temperature at exit of annular combustor
p 172 A93-14496

Effects of vitiated air on the results of ground tests of scramjet combustor
p 173 A93-16234

A system for washing the combustion chamber nozzles and flow path components of the NK-8-2U engine during service
p 373 A93-18357

A systems dynamics approach to modeling gas turbine combustor wear
[ASME PAPER 92-GT-47] p 347 A93-19300

Effects of back-pressure in a lean blowout research combustor
[ASME PAPER 92-GT-81] p 387 A93-19330

Modification of combustor stoichiometry distribution for reduced NO(x) emission from aircraft engines
[ASME PAPER 92-GT-108] p 349 A93-19346

Emissions reduction by varying the swirler airflow split in advanced gas turbine combustors
[ASME PAPER 92-GT-110] p 349 A93-19347

Engine testing of a prototype low NO(x) gas turbine combustor
[ASME PAPER 92-GT-116] p 401 A93-19352

Experimental and computational investigation of flow in catalytic monolith channels
[ASME PAPER 92-GT-118] p 387 A93-19354

Ignition and exhaust emission characteristics of spray combustion in a pre-chamber type vortex combustor
[ASME PAPER 92-GT-119] p 350 A93-19355

Investigation of combustion structure inside low NO(x) combustors for a 1500 C-class gas turbine
[ASME PAPER 92-GT-123] p 350 A93-19357

Three-dimensional gas turbine combustor emissions modeling
[ASME PAPER 92-GT-129] p 350 A93-19363

Coherent anti-Stokes Raman scattering (CARS) thermometry in a model gas turbine can combustor
[ASME PAPER 92-GT-134] p 387 A93-19366

The combustion of droplets within gas turbine combustors - Some recent observations on combustor efficiency
[ASME PAPER 92-GT-135] p 388 A93-19367

Experimental and theoretical investigation of a research atomizer/combustion chamber configuration
[ASME PAPER 92-GT-137] p 401 A93-19369

Three component LDV velocity measurements in a can type research combustor for CFD validation. I - Isothermal
[ASME PAPER 92-GT-138] p 350 A93-19370

The evolution of thermal barrier coatings in gas turbine engine applications
[ASME PAPER 92-GT-203] p 388 A93-19427

Scaling of the two-phase flow downstream of a gas turbine combustor swirl cup - Mean quantities
[ASME PAPER 92-GT-207] p 404 A93-19431

Ramjet NOx emission - Use of a 3D CFD method for the combustor design of a super/hyper-sonic transport propulsion system
[ASME PAPER 92-GT-255] p 353 A93-19464

The comparison of different simplified mathematical models of the gas turbine combustion chamber as an object of temperature and pressure control
[ASME PAPER 92-GT-347] p 354 A93-19518

Combustion study on methane-fuel Laboratory Scaled Ram Combustor
[ASME PAPER 92-GT-413] p 356 A93-19561

Aircraft turbine engine NOx emission limits - Status and trends
[ASME PAPER 92-GT-415] p 357 A93-19563

Flow measurements behind V-gutter under non-combusting condition
[AIAA PAPER 93-0020] p 408 A93-20139

Computational analysis of hypersonic shock wave/wall jet interaction
[AIAA PAPER 93-0604] p 269 A93-21113

Effects of compression and expansion ramp fuel injector configuration on scramjet combustion and heat transfer
[AIAA PAPER 93-0609] p 358 A93-21114

Influences on the sprays formed by high-shear fuel nozzle/swirler assemblies
p 411 A93-21653

Numerical analysis of reacting flow using finite rate chemistry models
p 389 A93-21666

Effects of injector geometry on scramjet combustor performance
p 359 A93-21670

Combustion performance of a hydrogen-fueled small combustor for a micro gas turbine
p 389 A93-21731

Numerical and experimental investigation of mixing enhancement in scramjets
[AIAA PAPER 92-5063] p 414 A93-22333

Data analysis of the parametric scramjet combustor experiments conducted in the Calspan 96 inch shock tunnel - 4th entry
[AIAA PAPER 92-5098] p 359 A93-22368

Study on steady and unsteady unstart phenomena due to compound choking and/or fluctuations in combustor of scramjet engines
[AIAA PAPER 92-5102] p 359 A93-22372

The effect of entrance radius and film injection on wall heating in scramjet nozzles
p 360 A93-22505

Development of an optical sensor for active control of a gas turbine combustor
[AIAA PAPER 93-0118] p 360 A93-22568

Two and three-dimensional prediffuser combustor studies with air-water mixture
[AIAA PAPER 93-0240] p 390 A93-22652

Three-dimensional NOx modeling for rich/lean combustor
[AIAA PAPER 93-0251] p 360 A93-22660

Isolator-combustor interaction in a dual-mode scramjet engine
[AIAA PAPER 93-0358] p 360 A93-23041

CARS thermometry in a liquid fueled model combustor
[AIAA PAPER 93-0366] p 390 A93-23047

COMBUSTION CHAMBERS

Simplified jet fuel reaction mechanism for lean burn combustion application
[AIAA PAPER 93-0021] p 390 A93-23238

Investigation on bi-flat jet separated flow in a rectangular combustor
p 459 A93-23778

Control of contaminants in gas turbines with variable-flow combustion chambers and hydrogen addition
p 520 A93-27478

Consideration of the completeness of combustion and dissociation and recombination processes in mathematical models of jet engines for high supersonic flight velocities
p 520 A93-27627

Studies of fuel-rich magnesium propellants in a small solid fuel ramjet combustor
p 535 A93-27759

A numerical study of mixing in supersonic combustors with hypermixing injectors
[AIAA PAPER 93-0215] p 520 A93-27801

Numerical simulation of turbine 'hot spot' alleviation using film cooling
p 744 A93-34476

Issues associated with long-duration high-enthalpy scramjet combustor testing
p 721 A93-34497

A numerical simulation of a scram jet combustor flow
p 810 A93-38181

Fuel film formation in the fuel-air premixer of the combustion chamber
p 812 A93-39193

Some recommendations concerning the prevention of fuel boiling in the igniters of the combustion chambers of gas turbine engines
p 812 A93-39200

Thermal analysis of a shower-head burner
[SAE PAPER 921226] p 898 A93-41400

Investigation of flame stabilizers in the form of perforated grids
p 1003 A93-47513

Modelling three-dimensional gas-turbine-combustor model flow using second-moment closure
[AIAA PAPER 93-3104] p 1149 A93-48277

An optimization method for statistical ascertainment of the most probable peak temperature at combustor exit
p 1108 A93-49195

A review of chemically reactive turbulent flow mixing mechanisms and a new design for a low NO(x) combustor
p 1109 A93-49508

Mixing in the dome region of a staged gas turbine combustor
p 1109 A93-49612

Carbon/silicon carbide composite materials in advanced unmanned gas turbine engine combustors
[AIAA PAPER 93-1761] p 1144 A93-49658

Effect of geometry, bleed rates and flow splits on pressure recovery of a canted hybrid vortex-controlled diffuser
[AIAA PAPER 93-1762] p 1109 A93-49659

An efficient liner cooling scheme for advanced small gas turbine combustors
[AIAA PAPER 93-1763] p 1109 A93-49660

Swirling flows in a contoured-wall combustion chamber
[AIAA PAPER 93-1765] p 1073 A93-49661

Correlation of droplet behavior with gas-phase structures in a gas turbine combustor
[AIAA PAPER 93-1767] p 1152 A93-49663

Subscale hot-fire testing of a formed platelet liner
[AIAA PAPER 93-1827] p 1141 A93-49713

The effects of turbulence modeling on the numerical simulation of confined swirling flows
[AIAA PAPER 93-1976] p 1078 A93-49823

The study of experimental turboramjets - Heat state and cooling problems
[AIAA PAPER 93-1989] p 1112 A93-49834

Real gas simulation of air Blow-Down Facilities
[AIAA PAPER 93-2022] p 1137 A93-49859

An analytical study of dilution jet mixing in a cylindrical duct
[AIAA PAPER 93-2043] p 1113 A93-49876

Smoke measurements inside a gas turbine combustor
[AIAA PAPER 93-2070] p 1113 A93-49902

Mixing enhancement and combustion of gaseous fuel in a supersonic combustor
[AIAA PAPER 93-2143] p 1114 A93-49960

Gasdynamics of hydrogen-fueled scramjet combustors
[AIAA PAPER 93-2145] p 1115 A93-49962

Integrated CFD modeling of gas turbine combustors
[AIAA PAPER 93-2196] p 1115 A93-50008

Standing normal detonations and oblique detonations for propulsion
[AIAA PAPER 93-2325] p 1116 A93-50105

An approach to in-situ analysis of scramjet combustor behavior
[AIAA PAPER 93-2328] p 1116 A93-50108

Dual-spray airblast fuel nozzle for advanced small gas turbine combustors
[AIAA PAPER 93-2336] p 1116 A93-50113

Three-dimensional emission modeling for diffusion flame, rich/lean, and lean gas turbine combustors
[AIAA PAPER 93-2338] p 1117 A93-50115

Direct measurements of skin friction in a scramjet combustor
[AIAA PAPER 93-2443] p 1119 A93-50195

- Three-dimensional prediffuser combustor studies with air-water mixture
[AIAA PAPER 93-2474] p 1120 A93-50217
- The development of a large annular facility for testing gas turbine combustor diffuser systems
[AIAA PAPER 93-2546] p 1139 A93-50269
- Aerothermodynamics in combustors; IUTAM Symposium, National Taiwan Univ., Taipei, June 3-5, 1991, Selected Papers
[ISBN 0-387-55404-1] p 1146 A93-51626
- Scalar characteristics in a liquid-fuelled combustor with curved exit nozzle
p 1123 A93-51643
- Measurements of gas composition and temperature inside a can type model combustor
p 1123 A93-51644
- Numerical model for predictions of reverse flow combustor aerothermal characteristics
p 1123 A93-51645
- An ultra low NO(x) pilot combustor for staged low NO(x) combustion
[ISABE 93-7020] p 1195 A93-53996
- Low NO(x) combustor development using aerodynamic staging
[ISABE 93-7021] p 1195 A93-53997
- Emission characteristics of a model gas turbine combustor at practical conditions
[ISABE 93-7023] p 1196 A93-53999
- Design and testing methods of high performance combustors for airbreathing engines
[ISABE 93-7024] p 1196 A93-54000
- Two and three-dimensional prediffuser combustor studies with air-water mixture
[ISABE 93-7025] p 1213 A93-54001
- Study of a pulse ramjet based on twin valveless combustors coupled to operate in antiphase
[ISABE 93-7038] p 1197 A93-54014
- Nozzle effects on linear stability behaviour of combustors
[ISABE 93-7044] p 1198 A93-54020
- Ignition and combustion performance of a scramjet combustor with a fuel injection strut
[ISABE 93-7050] p 1199 A93-54026
- Study on unstart and its propagation along modules due to compound choking and/or fluctuations in combustor of scramjet engines
[ISABE 93-7052] p 1199 A93-54028
- The combustion performance of methane-fueled ram combustor
[ISABE 93-7079] p 1201 A93-54055
- Studies on methane-fuel ram combustor for HST combined cycle engine
[ISABE 93-7080] p 1201 A93-54056
- Test results of the hydrogen fueled model combustor for the air turbo ramjet engine
[ISABE 93-7082] p 1201 A93-54058
- Finite-rate H₂/air combustion effects in CRJ for hypersonic launchers
[ISABE 93-7084] p 1202 A93-54060
- Combustor development for advanced helicopter engines
p 1246 A93-54841
- Laser and skill enhance results
p 1257 A93-54843
- Combustion noise and combustion instabilities in propulsion systems
p 100 N93-10682
- Shock enhancement and control of hypersonic combustion
[AD-A254295] p 72 N93-10843
- Effects of reacting flows with turbulence and shock waves on efficiency of scramjet combustors
p 69 N93-11133
- The combustion time lag and its role in ramjet combustion instability
p 73 N93-11137
- Numerical analysis of the flow fields in a RQL gas turbine combustor
[DE92-017509] p 89 N93-11767
- Hypervelocity scramjet combustor-nozzle analysis and design
[NASA-CR-190965] p 60 N93-12214
- Investigation of hot streak migration and film cooling effects on heat transfer in rotor/stator interacting flows, report 1
[AD-A250688] p 102 N93-12490
- A preliminary study of the effect of equivalence ratio on a low emissions gas turbine combustor using KIVA-2
[DE92-018616] p 215 N93-13321
- Simplified jet-A kinetic mechanism for combustor application
[NASA-TM-105940] p 200 N93-15504
- Atomization of JP-10/B4C gelled slurry fuel
[AD-A256827] p 391 N93-15686
- Combustion instabilities in a side-dump model ramjet combustor
p 362 N93-17613
- Experimental analysis of combustion oscillations with reference to ramjet propulsion
p 392 N93-17614
- Prediction of the performances in combustion of ramjets and stato-rockets by isothermal experiments and modeling
p 363 N93-17622
- Transient/structural analysis of a combustor under explosive loads
[NASA-TM-107660] p 420 N93-17779
- Turbine engine combustor design at SNECMA
[DS-2129] p 363 N93-17851
- A numerical study of mixing in supersonic combustors with hypermixing injectors
[NASA-CR-191027] p 294 N93-17884
- Experimental Investigation of Nozzle/Plume Aerodynamics at Hypersonic Speeds
[NASA-CR-191368] p 386 N93-18085
- Fuel injector: Air swirl characterization aerothermal modeling, phase 2, volume 1
[NASA-CR-189193-VOL-1] p 721 N93-24754
- A three-dimensional algebraic grid generation scheme for gas turbine combustors with inclined slots
[NASA-CR-191095] p 746 N93-24759
- Turbulence interacting with chemical kinetics in airbreathing combustion of ducted rockets
p 734 N93-26012
- Nitric oxide formation in a lean, premixed-prevaporized jet A/air flame tube: An experimental and analytical study
[NASA-TM-105722] p 844 N93-27012
- Experimental investigation of crossflow jet mixing in a rectangular duct
[NASA-TM-106152] p 812 N93-27026
- An analytical study of dilution jet mixing in a cylindrical duct
[NASA-TM-106181] p 814 N93-27160
- Development of a pulse ramjet based on twin valveless pulse combustors coupled to operate in antiphase
p 814 N93-27186
- Experimental study of cross flow mixing in cylindrical and rectangular ducts
[NASA-CR-187141] p 815 N93-27680
- Direct measurements of skin friction in supersonic combustion flow fields
[AD-A262878] p 825 N93-28226
- Heat Transfer and Cooling in Gas Turbines
[AGARD-CP-527] p 901 N93-29926
- The effect of main stream flow angle on flame tube film cooling
p 932 N93-29953
- Impingement/effusion cooling
p 932 N93-29954
- Thrust augmentation system for low-cost-expendable turbojet engine
[AD-A263727] p 905 N93-30877
- Analytical and experimental investigations of the oblique detonation wave engine concept
[NASA-TM-102839] p 1006 N93-32374
- COMBUSTION CHEMISTRY**
- Three-dimensional NO_x modeling for rich/lean combustor
[AIAA PAPER 93-0251] p 360 A93-22660
- Ignition and spread of combustion within a supersonic boundary layer
p 535 A93-27732
- Polyethylene pyrolysis model for combustion calculations in solid fuel ramjets
p 520 A93-27739
- Ignition analysis of unpremixed reactants with chain mechanism in a supersonic mixing layer
p 735 A93-35619
- Shock waves; Proceedings of the 18th International Symposium, Sendai, Japan, July 21-26, 1991. Vols. 1 & 2
[ISBN 0-387-55686-9] p 1023 A93-45451
- High density strained hydrocarbon fuels for air breathing propulsion
[ISABE 93-7081] p 1213 A93-54057
- Modeling of turbulent supersonic H₂-air combustion with an improved joint beta PDF
[NASA-CR-191929] p 391 N93-16389
- Turbulence interacting with chemical kinetics in airbreathing combustion of ducted rockets
p 734 N93-26012
- Generation of carbon monoxide in compartment fires
[PB93-146702] p 880 N93-29211
- COMBUSTION CONTROL**
- Recent progress in the implementation of active combustion control
p 171 A93-14272
- Some issues concerning active control of combustion instability in a ramjet
[AIAA PAPER 93-0116] p 360 A93-22566
- Combustion characteristics and passive control of an annular dump combustor
[AIAA PAPER 93-1772] p 1110 A93-49668
- Periodic chemical energy release for active combustion control
[ISABE 93-7043] p 1198 A93-54019
- Numerical analysis of the flow fields in a RQL gas turbine combustor
[DE92-017509] p 89 N93-11767
- Active control of combustion instability in a ramjet using large-eddy simulations
[AD-A255226] p 175 N93-14111
- Velocity and drop size measurements in a swirl-stabilized, combustor spray
[NASA-TM-106130] p 813 N93-27130
- COMBUSTION EFFICIENCY**
- Mixing and combustion studies using discrete orifice injection at hypervelocity flight conditions
p 205 A93-14523
- Theoretical investigation of combustion characteristics in ram-jet dump combustor with side-inlet
p 346 A93-19121
- The combustion of droplets within gas turbine combustors - Some recent observations on combustor efficiency
[ASME PAPER 92-GT-135] p 388 A93-19367
- Combustion study on methane-fuel Laboratory Scaled Ram Combustor
[ASME PAPER 92-GT-413] p 356 A93-19561
- Data analysis of the parametric scramjet combustor experiments conducted in the Calspan 96 inch shock tunnel - 4th entry
[AIAA PAPER 92-5098] p 359 A93-22368
- A study of aerodynamic performance of a contra-rotating axial compressor stage
p 463 A93-24524
- Development and use of hydrogen-air torches in an altitude facility
[AIAA PAPER 93-2176] p 1137 A93-49988
- The design and development of an afterburner
[ISABE 93-7041] p 1198 A93-54017
- Ignition and combustion performance of a scramjet combustor with a fuel injection strut
[ISABE 93-7050] p 1199 A93-54026
- The combustion performance of methane-fueled ram combustor
[ISABE 93-7079] p 1201 A93-54055
- Employment of radicals and excited state species for supersonic combustion photochemical ignition of premixed hydrogen/oxygen mixtures with ArF laser
p 73 N93-11135
- Atomization of JP-10/B4C gelled slurry fuel
[AD-A256827] p 391 N93-15686
- COMBUSTION PHYSICS**
- Emissions reduction by varying the swirler airflow split in advanced gas turbine combustors
[ASME PAPER 92-GT-110] p 349 A93-19347
- Combustion performance of a hydrogen-fueled small combustor for a micro gas turbine
p 389 A93-21731
- Canadian low-gravity research using parabolic aircraft
p 384 A93-21908
- Induced Mach wave-flame interactions in laminar supersonic fuel jets
p 475 A93-26183
- Effect of combustion on the interaction of an underexpanded wall hydrogen jet with supersonic flow in a plane duct
p 534 A93-27658
- Ignition and spread of combustion within a supersonic boundary layer
p 535 A93-27732
- Progress in laser spectroscopic techniques for aerodynamic measurements - An overview
p 549 A93-29308
- Computations of spray, fuel-air mixing, and combustion in a lean-premixed-prevaporized combustor
[AIAA PAPER 93-2069] p 1153 A93-49901
- Investigation of a combustion zone behind a wedge
p 1146 A93-51631
- High density strained hydrocarbon fuels for air breathing propulsion
[ISABE 93-7081] p 1213 A93-54057
- Employment of radicals and excited state species for supersonic combustion photochemical ignition of premixed hydrogen/oxygen mixtures with ArF laser
p 73 N93-11135
- The combustion time lag and its role in ramjet combustion instability
p 73 N93-11137
- Combustion in supersonic flows
p 199 N93-14627
- Investigation of the aerothermodynamics of hypervelocity reacting flows in the ram accelerator
[NASA-CR-191715] p 140 N93-15588
- Chemical kinetic and aerodynamic structures of flames
[AD-A256015] p 391 N93-15931
- IR imaging for combustion characteristics and optical properties of boron/boron oxide
[AD-A257747] p 393 N93-17693
- Computation of H₂/air reacting flowfields in drag-reduction external combustion
[NASA-CR-191071] p 536 N93-20237
- Visualization of a Mach 2 reacting flow using Planar Laser-Induced Fluorescence (PLIF)
p 731 N93-26006
- Velocity and drop size measurements in a swirl-stabilized, combustor spray
[NASA-TM-106130] p 813 N93-27130
- Thrust augmentation system for low-cost-expendable turbojet engine
[AD-A263727] p 905 N93-30877

SUBJECT INDEX

COMBUSTION PRODUCTS

Comparison of toxicity rankings of six aircraft cabin polymers by lethality and by incapacitation in rats p 26 A93-10328

Use of alternative fuels for aviation p 196 A93-14292

Effect of design and service-related factors on the formation of combustion residues in the fuel nozzles of gas turbine engines p 345 A93-18342

Consideration of the completeness of combustion and dissociation and recombination processes in mathematical models of jet engines for high supersonic flight velocities p 520 A93-27627

Gas analysis system for the Eight Foot High Temperature Tunnel p 822 A93-37875

On the stability of the process of formation of combustion generated particles by coagulation and simultaneous shrinkage due to particle oxidation [AIAA PAPER 93-2478] p 1146 A93-50220

Characteristics of the flame air heater of a hypersonic wind tunnel p 1140 A93-51884

Kinetic scheme selection in describing detonation in an H₂-air mixture behind shock waves p 1253 A93-55032

Development and demonstration of a new filter system to control emissions during jet engine testing [AD-A261203] p 755 N93-26243

Particulate emissions from gas turbine engines [AD-A261374] p 725 N93-26339

Improved selective catalytic NO_x control technology for compressor station reciprocating engines [PB93-158566] p 755 N93-26529

Oxides of nitrogen emissions from turbulent hydrocarbon/air jet diffusion flames, phase 2 [PB93-152478] p 756 N93-26533

Generation of carbon monoxide in compartment fires [PB93-146702] p 880 N93-29211

COMBUSTION STABILITY

An experimental investigation on the combustor with bypass flow in integral liquid fuel ramjet p 174 A93-16235

Investigation of combustion structure inside low NO(x) combustors for a 1500 C-class gas turbine [ASME PAPER 92-GT-123] p 350 A93-19357

Some issues concerning active control of combustion instability in a ramjet [AIAA PAPER 93-0116] p 360 A93-22566

Development update for the NASA Ames 16-Inch Shock Tunnel Facility p 822 A93-37873

Experimental research on a semiwater-gas-fired gas-turbine p 1107 A93-48524

Combustion characteristics and passive control of an annular dump combustor [AIAA PAPER 93-1772] p 1110 A93-49668

On the stability of the process of formation of combustion generated particles by coagulation and simultaneous shrinkage due to particle oxidation [AIAA PAPER 93-2478] p 1146 A93-50220

Investigation of a combustion zone behind a wedge p 1146 A93-51631

Low-frequency combustion oscillations in a model afterburner p 1193 A93-53702

Blowout of turbulent disc/pilot stabilized jet diffusion flames [ISABE 93-7026] p 1213 A93-54002

Study of a pulse ramjet based on twin valveless combustors coupled to operate in antiphase [ISABE 93-7038] p 1197 A93-54014

Nozzle effects on linear stability behaviour of combustors [ISABE 93-7044] p 1198 A93-54020

Low-frequency combustion instability mechanisms in a side-dump combustor p 1247 A93-55220

Combustion noise and combustion instabilities in propulsion systems p 100 N93-10682

The combustion time lag and its role in ramjet combustion instability p 73 N93-11137

Active control of combustion instability in a ramjet using large-eddy simulations p 175 N93-14111

Combustion instabilities in a side-dump model ramjet combustor p 362 N93-17613

Experimental analysis of combustion oscillations with reference to ramjet propulsion p 392 N93-17614

Prediction of the performances in combustion of ramjets and stato-rockets by isothermal experiments and modeling p 363 N93-17622

Contribution to the study of the interaction between acoustic waves and coherent structures induced by a prismatic cylinder in a rectangular cavity [ONERA-NT-1990-10] p 918 N93-30203

COMBUSTION TEMPERATURE

Initial results from the NASA Lewis wave rotor experiment [AIAA PAPER 93-2521] p 1193 A93-53589

CARS temperature measurements in combustion [ONERA, TP NO. 1993-78] p 1212 A93-53599

Initial results from the NASA-Lewis wave rotor experiment [NASA-TM-106148] p 1005 N93-32368

COMBUSTION VIBRATION
Low-frequency combustion oscillations in a model afterburner p 1193 A93-53702

COMBUSTION WIND TUNNELS
Evaluation of candidate working fluid formulations for the electrothermal-chemical wind tunnel [NASA-CR-193366] p 1015 N93-31848

COMMAND AND CONTROL
Ongoing GPS experiments demonstrate potential of satellite navigation technology p 1097 A93-49278

Implementing system simulation of C3 systems using autonomous objects [NASA-CR-190845] p 89 N93-11716

Mission planning systems for tactical aircraft (pre-flight and in-flight) [AGARD-AR-313] p 496 N93-21187

Advanced Unmanned Search System (AUSS) supervisory command, control and navigation [AD-A263171] p 793 N93-28990

COMMAND GUIDANCE
Nonlinear command augmentation system for a high performance aircraft [AIAA PAPER 93-3777] p 1132 A93-51372

A contribution to the dynamic feedforward open loop control of multivariable systems and to the optimal design of command functions [DLR-FB-92-05] p 441 N93-16515

COMMERCE
Activities report of Lufthansa [ETN-92-92100] p 28 N93-11319

Industry survey of space system cost benefits from New Ways Of Doing Business p 454 N93-17325

National aero-space plane: Restructuring future research and development efforts [AD-A258799] p 340 N93-18981

Aircraft performance in practice p 340 N93-19004

COMMERCIAL AIRCRAFT
Breaking through the 10 exp 6 barrier --- decreasing aircraft accident fatality rate per million flight hours p 27 A93-11498

Design for global competition - The Boeing 777 [AIAA PAPER 92-4190] p 2 A93-13368

Effects of turbine cooling assumptions on performance and sizing of high-speed civil transport [AIAA PAPER 92-4217] p 55 A93-13383

Fleet fatigue cracking threshold prediction p 3 A93-13633

Commercial airplane primary structure [SME PAPER EM92-115] p 107 A93-14112

Interrelationships between commercial airplane design and operational requirements and procedures p 153 A93-14219

MPC75 - The evolution of a new regional airliner for the late nineties p 155 A93-14289

Cost - The challenge for advanced materials and structures p 233 A93-14338

Improved lubricating greases for aircraft wheel bearings [SAE PAPER 921038] p 197 A93-14658

The opportunities and risks of the supersonic transport market - The Lufthansa point of view p 234 A93-15033

Study of a Mach 2 supersonic transport aircraft p 124 A93-15034

Optimizing the cruising fuel efficiency of commercial aircraft on the basis of flight manual data p 321 A93-18351

TEMPER - A gas-path analysis tool for commercial jet engines [ASME PAPER 92-GT-315] p 354 A93-19501

Ice accretion prediction for a typical commercial transport aircraft [AIAA PAPER 93-0174] p 310 A93-23245

Methods of economic evaluation - Forecasting critique [AIAA PAPER 92-4285] p 570 A93-24300

The FAA/NASA flight loads monitoring program - The prototype system and its benefits for the aviation community p 486 A93-25125

Communication satellites for commercial aircraft operations p 499 A93-25493

Comparison of all-electric secondary power systems for civil transport p 519 A93-25997

The development of the Boeing Human Model p 561 A93-27150

Modal analysis in the certification of a commercial aircraft p 509 A93-29241

SAFEbus p 828 A93-37072

Design and cost viability of composites in commercial aircraft p 915 A93-39963

Airbus or the revival of European civil aviation p 856 A93-42655

Integrated modular avionics p 896 A93-42777

Integrating controls and avionics on commercial aircraft p 892 A93-42778

Federal preemption in commercial aviation - Tort litigation under 49 U.S.C. section 1305 p 944 A93-42997

The Foreign Sovereign Immunities Act of 1976 - Misjoinder, nonjoinder, and collusive joinder p 944 A93-42998

Sales, not subsidies, are the sticking point p 945 A93-43677

A localizer design to improve missed approach guidance p 992 A93-44143

Methodology for commercial engine/aircraft optimization [AIAA PAPER 93-1807] p 1166 A93-49696

Propulsion technology challenges for turn-of-the-century commercial aircraft [ISABE 93-7003] p 1194 A93-53980

Europe's new windtunnel p 1210 A93-54275

An updated data acquisition and processing system for turbine engine testing p 1250 A93-54389

Airship insurance in London [AIAA PAPER 93-4043] p 1265 A93-54611

A study on low level windshear hazard index p 1240 A93-55414

Comparison of all-electric secondary power systems for civil subsonic transports [NASA-TM-105852] p 55 N93-10456

Civil aircraft engines: The next generation [PNR-90962] p 58 N93-11085

Predicted aircraft effects on stratospheric ozone p 93 N93-11096

Activities report of Lufthansa [ETN-92-92100] p 28 N93-11319

UK airmisses involving commercial air transport, May-August 1991 [ETN-92-92260] p 28 N93-11357

UK airmisses involving commercial air transport, January-April 1991 [ETN-92-92261] p 87 N93-11358

Aircraft accident report: Atlantic Southeast Airlines, Inc. Flight 2311, uncontrolled collision with terrain, an Embraer EMB-120, N270AS, Brunswick, Georgia, 5 April 1991 [PB92-910403] p 28 N93-11471

Aircraft accident report: Explosive decompression-loss of cargo door in flight, United Airlines Flight 811, Boeing 747-122, N4713U, Honolulu, HI, 24 February 1989 [PB92-910402] p 28 N93-12193

Flight simulator evaluation of D-size liquid crystal flat panel displays [NAL-TR-1136] p 52 N93-12367

Liquid crystal flat panel display evaluation tests using a flight simulator [NAL-TR-1122] p 52 N93-12383

Future regional transport aircraft market, constraints, and technology stimuli [NASA-TM-107669] p 109 N93-13025

Detailed analysis of wing-nacelle interaction for commercial transport aircraft p 213 N93-13203

Development of the Advance Warning Airborne System(AWAS) p 144 N93-14849

Monitoring of powerplants in advanced commercial aircraft p 178 N93-15171

Ice accretion prediction for a typical commercial transport aircraft [NASA-TM-105976] p 149 N93-15522

The NASA High-Speed Research Program MM-122: High speed civil transport [NASA-CR-192011] p 334 N93-17974

Phoenix: Preliminary design of a high speed civil transport [NASA-CR-192024] p 334 N93-17976

Tesseract: Supersonic business transport [NASA-CR-192072] p 334 N93-17977

The airline quality report, 1992 [NIAR-92-11] p 310 N93-18036

TBD(exp 3) [NASA-CR-192075] p 335 N93-18054

The Edge supersonic transport [NASA-CR-192074] p 335 N93-18055

A second-generation high speed civil transport: Stingray [NASA-CR-192022] p 336 N93-18059

Applying commercial style acquisition practices to the procurement of commercially available aircraft [AD-A258143] p 455 N93-18087

Scheduling of an aircraft fleet p 443 N93-18665

IOPS advisor: Research in progress on knowledge-intensive methods for irregular operations airline scheduling p 443 N93-18686

- Aviation safety: Problems persist in FAA's inspection program. Report to the Chairman, Subcommittee on Aviation, Committee on Public Works and Transportation, House of Representatives
[GAO/RCED-92-14] p 495 N93-19841
- Evaluation of advanced displays for engine monitoring and control
[NASA-CR-191418] p 718 N93-24764
- Lightning data acquisition p 753 N93-24883
- Applied aerodynamics: Challenges and expectations
[NASA-TM-103963] p 694 N93-25091
- World jet airplane inventory at year-end 1992
[PB93-174324] p 765 N93-27405
- World commercial aircraft accidents
[DE93-010892] p 791 N93-28571
- Effects of intra- and inter-laminar resin content on the mechanical properties of toughened composite materials p 921 N93-30845
- Process and assembly plans for low cost commercial fuselage structure p 923 N93-30865
- Radiation exposure in aircraft p 1035 N93-31928
- Propulsion technology challenges for turn-of-the-century commercial aircraft
[NASA-TM-106192] p 1005 N93-32351
- UK airmisses involving commercial air transport, September - December 1991
[ETN-93-93930] p 992 N93-32409
- COMMUNICATION EQUIPMENT**
- Defence electronics industry profile, 1990-1991
[CTN-92-60515] p 84 N93-10653
- Time delay measurements of current primary FAA air/ground transmitters and receivers
[DOT/FAA/CT-TN93/14] p 842 N93-28555
- The NASA SBIR product catalog
[NASA-TM-108242] p 945 N93-29322
- COMMUNICATION NETWORKS**
- ARINC 629 DATABUS: Proceedings of the Conference, London, United Kingdom, Sept. 24, 1991
[ISBN 0-903409-95-X] p 311 N93-17835
- Distribution of aviation weather graphics via airline communications networks p 426 N93-22113
- The Meteorological Data Collection and Reporting System - Status and future directions p 428 N93-22133
- Transition to a seamless communications system requires much experimentation p 792 N93-38564
- An interworking router for avionics applications --- Bridge/Router unit in fiber optics aircraft communication p 1097 N93-49479
- Controller evaluation of initial data link terminal air traffic control services: Mini study 2, volume 1
[DOT/FAA/CT-92/2-VOL-1] p 36 N93-11704
- Controller evaluation of initial data link terminal air traffic control services: Mini study 2, volume 2
[DOT/FAA/CT-92/2-VOL-2] p 36 N93-11705
- FAA Technical Center Aeronautical Data Link Research Plan
[DOT/FAA/CT-92/23] p 417 N93-15698
- Robo-line storage: Low latency, high capacity storage systems over geographically distributed networks
[NASA-CR-192910] p 758 N93-25130
- The Data Multiplexing Network (DMN) phase 3 Extended Distance Data Cable (EDDC) test and evaluation
[DOT/FAA/CT-TN93/11] p 752 N93-2616C
- Center for Aeronautics and Space Information Sciences
[NASA-CR-193140] p 848 N93-27289
- Changing role of telecommunications management in air traffic control in the FAA p 888 N93-30354
- COMMUNICATION SATELLITES**
- Communication satellites for commercial aircraft operations p 499 N93-25493
- COMMUNITIES**
- Final results from a study of community response to aircraft noise around Oslo Airport Fornebu p 558 N93-28486
- The community response to aircraft noise around six Spanish airports p 1264 N93-55845
- COMMUTER AIRCRAFT**
- The role of fatigue testing in the design, development and certification of the ATR 42/72 p 46 N93-13637
- Spanish-Indonesian cooperation in the development, production, certification and marketing of CN-235 commuter aircraft p 108 N93-14156
- Five years operational experiences with Indonesian Low Speed Tunnel (ILST) p 191 N93-14403
- Designed for work --- British Aerospace Jetstream 41 regional aircraft p 506 N93-27276
- Ground vibration test on Piaggio P. 180 aircraft - Comparison between two modal test methods p 509 N93-29246
- General aviation aircraft: Normal acceleration data analysis and collection project
[DOT/FAA/CT-91/20] p 713 N93-24739

COMPARISON

- Rocket engine versus jet engine comparison
[AIAA PAPER 92-3686] p 531 A93-24479
- ERS-1 directional wave spectra validation with the airborne SAR PHARS
[BCRS-92-18] p 937 N93-31010

COMPARTMENTS

- Generation of carbon monoxide in compartment fires
[PB93-146702] p 880 N93-29211

COMPATIBILITY

- Designing new multi-phase intermetallic materials based on phase compatibility considerations
[ONERA, TP NO. 1992-131] p 772 A93-38605
- Flight analysis of air intake/engine compatibility p 161 N93-13212

COMPENSATORS

- H(infinity) optimal controllers for a distributed model of an unstable aircraft p 62 A93-13247
- A treatment to flight controller nonlinearity effects - An adaptive compensator approach p 524 A93-26948
- Dynamic compensator design in nonlinear aerospace systems p 1036 A93-44150
- Computational nonlinear control
[AD-A253547] p 98 N93-12258
- Approaches to control of the large angle magnetic suspension test fixture p 381 N93-16695
- [NASA-CR-191890] p 819 N93-27171
- Game theoretic synthesis for robust aerospace controllers

COMPENSATORY TRACKING

- Simulation motion effect on single axis compensatory tracking
[AIAA PAPER 93-3579] p 1208 A93-52675

COMPETITION

- Competition in a single European air transport market; Proceedings of the Conference, London, United Kingdom, Dec. 1, 1992
[ISBN 1-85768-080-4] p 458 A93-29473

COMPIERS

- Numerical Wind Tunnel: Requirements and the outline p 383 N93-19288
- A model for determining task set schedulability in the presence of system effects
[AD-A258915] p 443 N93-19338

COMPLEX SYSTEMS

- Multilevel intelligent control systems for flight vehicles p 1168 A93-50955
- Control of complex dynamic systems by neural networks p 758 N93-25611

COMPONENT RELIABILITY

- Ways of increasing the service life and reliability of bolted joints p 745 A93-35281
- Estimation of the service periods for complex systems in the case of a priori indeterminacy of system reliability data --- for radio electronic equipment of onboard navigation and landing p 856 A93-43109
- Load rating for a delta wing box based on a reliability criterion p 1030 A93-47093
- Component and Engine Structural Assessment Research (CAESAR)
[AIAA PAPER 93-2609] p 1122 A93-50316
- Thermodynamic and neutral network computer modelling of implanted component faults in a gas turbine engine
[ISABE 93-7089] p 1202 A93-54065
- Assessment of helicopter component statistical reliability computations
[AD-A258931] p 510 N93-19447

COMPOSITE MATERIALS

- Getting it together p 78 A93-11682
- Out with the mechanical fasteners --- design of aircraft using composite materials
[AIAA PAPER 92-4210] p 44 A93-13378
- Composites roll sevens --- aircraft structures p 3 A93-13448
- Fatigue qualification of high thickness composite rotor components p 81 A93-13646
- Case studies in composite material structural design, manufacture and testing p 157 A93-14385
- Aeroelastic optimization of a composite helicopter rotor
[AIAA PAPER 92-4780] p 323 A93-20287
- Optimization of anisotropic structures considering strength, stiffness and aeroelastic constraints
[AIAA PAPER 92-4796] p 408 A93-20291
- A retrospective of 3600 composite blades p 507 A93-27963
- The effects of composite material on the configuration and design of the V-22 wing p 507 A93-27964
- Repair of a severely damaged composite fuel pod p 508 A93-27966
- Evolution of permanent composite repair designs p 508 A93-27967
- An accurate nonlinear finite element analysis and test correlation of a stiffened composite wing panel p 546 A93-27968

- Advanced composite helicopter MISERS GOLD test/analysis p 508 A93-27974
- Structural modeling of low-aspect ratio composite wings
[AIAA PAPER 93-1371] p 739 A93-33937
- Dynamic analysis of rotor flexbeams based on nonlinear anisotropic shell models p 743 A93-34261
- Optimal design of honeycomb sandwich shell aircraft structures of composite materials p 828 A93-36800
- Computed tomography of advanced materials and processes p 832 A93-38975
- Large-amplitude finite element flutter analysis of composite panels in hypersonic flow p 837 A93-39417
- Supersonic flutter analysis of composite plates and shells p 837 A93-39419
- Nonlinear flutter of orthotropic composite panel under aerodynamic heating p 1025 A93-45740
- What can Japan teach the U.S. about composites? p 1144 A93-49336
- An Acoustic Emission Pre-failure Warning System for composite structural tests p 1161 A93-52560
- Design and fabrication of panels with cutouts p 1215 A93-52973
- An experimental study of reinforced panels of composite materials p 1215 A93-52975
- A finite element for modeling skins of composite materials p 1215 A93-52979
- Advanced materials in gas turbine engines: An assessment
[PNR-90946] p 58 N93-11105
- Design of a high-temperature experiment for evaluating advanced structural materials
[NASA-TM-105833] p 88 N93-11624
- Current Technology for Thermal Protection Systems
[NASA-CP-3157] p 69 N93-12447
- Thermomechanical applications of heat pipes for cooling leading edges of high-speed aerospace vehicles p 91 N93-12460
- Composites: A catalogue of books and conference proceedings available in the NAL library p 234 N93-13368
- Proceedings of the USAF Structural Integrity Program
[AD-A255379] p 110 N93-14549
- Development of a menu driven materials data base for use on personal computers: Aircraft structures technical memorandum
[AD-A256317] p 392 N93-16403
- A domain-specific design architecture for composite material design and aircraft part redesign p 442 N93-17522
- Smart materials p 536 N93-20624
- Supersonic transport: Which material for the engine
[DS-2023] p 522 N93-21459
- Modelisation and computation of composite materials p 537 N93-21518
- Damage detection by Acousto-Ultrasonic Location (AUL) p 555 N93-21529
- Advanced technology composite aircraft structures
[NASA-CR-190420] p 894 N93-29498
- Composites: A viable option p 918 N93-30429
- Advanced composite structural concepts and material technologies for primary aircraft structures p 918 N93-30430
- Composites technology for transport primary structure p 918 N93-30431
- Advanced technology commercial fuselage structure p 918 N93-30432
- Design and manufacturing concepts for thermoplastic structures p 919 N93-30434
- Resin transfer molding for advanced composite primary aircraft structures p 919 N93-30438
- Lessons learned for composite structures p 920 N93-30444
- Development of resins for composites by resin transfer molding p 921 N93-30853
- An overview of the crash dynamics failure behavior of metal and composite aircraft structures p 923 N93-30875
- Construction and testing of simple airfoils to demonstrate structural design, materials choice, and composite concepts p 879 N93-30979
- Advanced electromagnetic methods for aerospace vehicles
[NASA-CR-193468] p 936 N93-31036
- COMPOSITE STRUCTURES**
- Multidisciplinary design of composite aircraft structures by Lagrange p 76 A93-10273
- Current developments in structural technology p 77 A93-10780
- The effects of crushing surface roughness on the crushing characteristics of composite tubes p 77 A93-10918
- Getting it together p 78 A93-11682

The approach to airworthiness clearance with the introduction of advanced materials and manufacturing technologies into the design of aerospace structures p 2 A93-12235

Design sensitivity and optimization of composite cylinders p 71 A93-12781

Fundamentals of composite repair [SME PAPER EM92-100] p 196 A93-14101

Economical view on composite structures maintenance [SME PAPER EM92-102] p 233 A93-14103

Commercial airplane primary structure [SME PAPER EM92-115] p 107 A93-14112

A tooling trend at BCA - What and why [SME PAPER EM92-111] p 202 A93-14114

In-service inspection of commercial aircraft composite structure [SME PAPER EM92-124] p 107 A93-14116

Counting the cost of composites p 107 A93-14117

Aeroelastic stability characteristics of composite cylindrical shells by the finite element method p 203 A93-14312

Post buckling of laminated composite stiffened curved panels subjected to cyclic shear and compression p 204 A93-14334

Parametric aeroelastic analysis of composite wing-boxes with active strain-energy tuning p 156 A93-14361

Contact analysis for riveted and bolted joints of composite laminates p 204 A93-14384

Aeroelastic analysis of composite wing with control surface p 157 A93-14386

Common failure modes for composite aircraft structures due to secondary loads p 207 A93-14812

Adaptive aeroelastic composite wings - Control and optimization issues p 185 A93-14818

Tiltrotor Research Aircraft composite blade repairs - Lessons learned p 108 A93-14819

On the static aeroelastic tailoring of composite aircraft swept wings modelled as thin-walled beam structures p 158 A93-14820

Choice of materials for military helicopters p 158 A93-15028

Thermoplastic and thermosetting matrix composite structures - Comparison of mechanical properties p 197 A93-15029

Accuracy of a simple hole damage analysis method in composite structures p 197 A93-15748

Development of polyimide adhesives for 371 C (700 F) structural performance for aerospace bonding applications - FM 680 system p 198 A93-15757

Automatic Through-the-Thickness braiding p 209 A93-15789

Rapid fabrication of flight worthy composite parts p 209 A93-15792

Lightning protection of composite structure p 141 A93-15801

Composite wing results of Deutsche Airbus technology program p 109 A93-15808

Experimental investigations into composite fuselage impact damage resistance and post-impact compression behavior p 159 A93-15812

Structural analysis of a nonlinear problem of aeroelasticity for CFC structures p 397 A93-18989

Active control of sound transmission through stiff lightweight composite fuselage constructions p 447 A93-19187

Coupled multi-disciplinary simulation of composite engine structures in propulsion environment [ASME PAPER 92-GT-6] p 346 A93-19279

p-version finite element modeling for NDE p 407 A93-19699

Repair of delaminations and impact damage in composite aircraft structures p 457 A93-24107

Model multilayer structured composites p 533 A93-24509

Rapid detection and quantification of impact damage in composite structures p 547 A93-27978

Global/local interlaminar stress analysis of a grid-stiffened composite panel p 548 A93-28543

Vibration and flutter of stiff-inplane elastically tailored composite rotor blades [AIAA PAPER 93-1302] p 725 A93-33879

Aeromechanical stability of a bearingless composite rotor in forward flight [AIAA PAPER 93-1305] p 726 A93-33881

Thermomechanical postbuckling analysis of laminated composite shells [AIAA PAPER 93-1337] p 738 A93-33907

Energy-absorbing-beam design for composite aircraft subfloors [AIAA PAPER 93-1339] p 709 A93-33909

Composite 'Exoskin' doubler extends F-15 Vertical Tail fatigue life [AIAA PAPER 93-1341] p 709 A93-33911

An analytically designed subcomponent test to reproduce the failure of a composite wing box beam [AIAA PAPER 93-1344] p 709 A93-33914

Damage progression in stiffened composite panels [AIAA PAPER 93-1345] p 738 A93-33915

Analysis of interlaminar stresses in symmetric and unsymmetric laminates under various loadings [AIAA PAPER 93-1511] p 740 A93-34050

Exact flutter solution of advanced anisotropic composite cantilevered wing structures [AIAA PAPER 93-1535] p 727 A93-34072

Optimization of composite engine structures for mechanical and thermal loads [AIAA PAPER 93-1583] p 719 A93-34115

A new sensitivity analysis for structural optimization of composite rotor blades [AIAA PAPER 93-1644] p 742 A93-34169

Probabilistically configured adaptive composite structures [AIAA PAPER 93-1679] p 743 A93-34191

On design and optimization of curved composite beams p 826 A93-35953

The development of a crashworthy composite fuselage and landing gear p 799 A93-36001

Environmental conditions for certification testing of helicopter advanced composite main rotor components p 824 A93-36003

Embedded Bragg grating fiber optic sensor for composite flexbeams p 828 A93-37350

Nonlinear flutter of composite plates with damage evolution [AIAA PAPER 93-1546] p 829 A93-37441

The limit model of a thin strip exhibiting two delaminations [ONERA, TP NO. 1992-212] p 832 A93-38764

Design and cost viability of composites in commercial aircraft p 915 A93-39963

Aeroelastic response, loads, and stability of a composite rotor in forward flight p 906 A93-41919

Evaluation by holographic interferometry of impact damage in composite aeronautical structures p 1020 A93-44193

Flutter analysis of composite panels on many supports p 1022 A93-45119

Static aeroelastic control of an adaptive lifting surface p 995 A93-45147

Effect of stiffness characteristics on the response of composite grid-stiffened structures p 1022 A93-45148

Vibration analysis of composite wing with tip mass using finite elements p 1023 A93-45175

Nonlinear large amplitude aeroelastic behavior of composite rotor blades p 997 A93-45741

Effects of floor location on response of composite fuselage frames p 997 A93-46809

Composite airframe structures. Practical design information and data --- Book [ISBN 962-7128-06-6] p 1100 A93-49105

The 'Rolls-Royce' way of validating fan integrity [AIAA PAPER 93-2602] p 1122 A93-50311

Buckling of open-section bead-stiffened composite panels p 1157 A93-50420

On design methods for bolted joints in composite aircraft structures p 1158 A93-50430

Cost effective process selection for composite structure [SME PAPER EM93-100] p 1043 A93-51727

Design for manufacture by resin transfer molding of composite parts for rotorcraft [SME PAPER EM93-103] p 1159 A93-51733

Vector unsymmetric eigenvalue solver for nonlinear flutter analysis on high-performance computers p 1160 A93-52449

Design for cyclic loading endurance of composites p 1216 A93-53395

Innovative bagging techniques on a composite P-51 Mustang replica p 1191 A93-53405

Structural applications of Avimid K3B LDF thermoplastic composites --- for advanced aircraft p 1216 A93-53429

All-composite fan blade for advanced ducted engines p 1246 A93-54837

Damped advanced composite parts p 1253 A93-55871

Nonlinear aeroelasticity of composite structures [AD-A254285] p 47 A93-10842

Current Technology for Thermal Protection Systems [NASA-CP-3157] p 69 A93-12447

Evaluation of alternatives for increasing A-7D rearward visibility [AD-A255071] p 50 A93-12488

Probabilistic evaluation of fuselage-type composite structures [NASA-TM-105881] p 212 A93-12735

Optimum design of aircraft structures with manufacturing and buckling constraints p 162 A93-13815

Reliability of stiffened structural panels: Two examples [NASA-TM-107687] p 219 A93-14483

Stress calculations on the window section of an all-composite aircraft fuselage [LR-688] p 328 A93-16215

Relationship between mechanical-property and energy-absorption trends for composite tubes [NASA-TP-3284] p 392 A93-16537

Mode interaction in stiffened composite shells under combined mechanical and thermal loadings p 419 A93-16793

A domain-specific design architecture for composite material design and aircraft part redesign p 442 A93-17522

Influence of cross section variations on the structural behaviour of composite rotor blades [MBB-UD-0602-91-PUB] p 332 A93-17569

Interlaminar stress analysis at the skin/stiffener interface of a grid-stiffened composite panel [NASA-CR-192177] p 393 A93-17920

Formulation of a structural model for flutter analysis of low aspect ratio composite aircraft wings p 372 A93-19019

Multidisciplinary tailoring of hot composite structures [NASA-TM-106027] p 550 A93-19971

Development of cure cycles: From laboratory analysis and testing to production of large scale composites [MBB-Z-0442-92-PUB] p 536 A93-20845

The integrated design and manufacturing of composite structures for aircraft using an advanced tape layering technology [MBB-LME-251-S-PUB-0491-A] p 515 A93-21401

Modellisation and computation of composite materials p 537 A93-21518

Numerical modelling of induced effects of lightning strike on an all composite helicopter p 703 A93-24879

A procedure for defining lightning risk to air vehicles p 703 A93-24885

A computational approach to predicting the extent of arc root damage in CFC panels p 735 A93-24890

Design and analysis of curved composite components for rotorcraft fuselage frames p 716 A93-25701

Thermally induced stresses in a composite exposed to fire [AD-A261714] p 737 A93-26371

A composite structured/unstructured-mesh Euler method for complex airfoil shapes p 784 A93-27439

Nonlinear analyses of composite aerospace structures in sonic fatigue [NASA-CR-193124] p 930 A93-29154

Advanced technology composite aircraft structures [NASA-CR-190420] p 894 A93-29498

Static and dynamic large deflection flexural response of graphite-epoxy beams [NASA-CR-4118] p 934 A93-30374

Composites: A viable option p 918 A93-30429

Advanced composite structural concepts and material technologies for primary aircraft structures p 918 A93-30430

Composites technology for transport primary structure p 918 A93-30431

Advanced technology commercial fuselage structure p 918 A93-30432

Design, analysis, and fabrication of the technology integration box beam p 919 A93-30433

Design and manufacturing concepts for thermoplastic structures p 919 A93-30434

Structural evaluation of curved stiffened composite panels fabricated using a THERM-Xsm process p 919 A93-30435

Noise transmission properties and control strategies for composite structures p 919 A93-30436

Resin transfer molding for advanced composite primary aircraft structures p 919 A93-30438

Consolidation of graphite thermoplastic textile preforms for primary aircraft structure p 919 A93-30439

Cost studies for commercial fuselage crown designs p 920 A93-30440

A unified approach for composite cost reporting and prediction in the ACT program p 920 A93-30441

F-15 composite engine access door p 920 A93-30442

Fabrication of the V-22 composite AFT fuselage using automated fiber placement p 920 A93-30443

Lessons learned for composite structures p 920 A93-30444

Development of stitching reinforcement for transport wing panels p 921 A93-30852

Advanced fiber/matrix material systems p 921 A93-30854

Mechanical and analytical screening of braided composites for transport fuselage applications p 922 A93-30855

Multi-parameter optimization tool for low-cost commercial fuselage crown designs p 922 A93-30858

- Optimization of composite sandwich cover panels subjected to compressive loadings p 922 N93-30862
 Process and assembly plans for low cost commercial fuselage structure p 923 N93-30865
 A Rayleigh-Ritz analysis methodology for cutouts in composite structures p 923 N93-30869
 An overview of the crash dynamics failure behavior of metal and composite aircraft structures p 923 N93-30875

COMPRESSED AIR

- Autonomous mobile laser complex p 395 A93-17767
 An externally pressurized air bearing system, journals and thrust, for application to small turbomachinery [ASME PAPER 92-GT-382] p 406 A93-19539
 ASTOVL model engine simulators for wind tunnel research p 192 N93-13213

COMPRESSED GAS

- On the compression process in a free-piston shock-tunnel p 1136 A93-48041

COMPRESSIBILITY

- Turbulence modeling for hypersonic flight [NASA-CR-192288] p 483 N93-20235
 Numerical determination of the residual strength of battle damaged composite plates p 537 N93-21533

COMPRESSIBILITY EFFECTS

- Interferometric investigations of compressible dynamic stall over a transiently pitching airfoil [AIAA PAPER 93-0211] p 278 A93-22628
 A study of compressible turbulence [AIAA PAPER 93-0659] p 465 A93-24772
 A new model for super/hypersonic turbulent boundary layers [AIAA PAPER 93-0897] p 472 A93-24957
 An experimental study of the effects of bodyside compression on forward swept sidewall compression inlets ingesting a turbulent boundary layer [AIAA PAPER 93-3125] p 1072 A93-49515
 Three-dimensional simulations of compressible mixing layers - Visualizations and statistical analysis p 1235 A93-55360
 Studies of hydrogen-air diffusion flames and of compressibility effects related to high-speed propulsion p 917 N93-29125

COMPRESSIBLE BOUNDARY LAYER

- Compressible laminar and turbulent boundary layer computation for the three-dimensional wing p 12 A93-12735
 Evaluation and application of the Baldwin-Lomax turbulence model in two-dimensional, unsteady, compressible boundary layers with and without separation in engine inlets [AIAA PAPER 92-3676] p 111 A93-14118
 Flight vehicle aerodynamics calculated by a Galerkin finite element/finite difference method p 266 A93-20738
 Evaluation and application of the Baldwin-Lomax turbulence model in two-dimensional, unsteady, compressible boundary layers with and without separation in engine inlets [AIAA PAPER 92-3676] p 414 A93-22509
 On the accurate prediction of the wall-normal velocity in compressible boundary-layer flow p 477 A93-27474
 The numerical calculation and application of compressible boundary layers on laminar-flow-control and natural-laminar-flow wings p 680 A93-33727
 Calculation of compressible boundary layers by a hybrid finite element method p 692 A93-35613
 Control of a supersonic reattaching shear layer [AIAA PAPER 93-3248] p 966 A93-46793
 The determination of hybrid analytical-numerical solutions for the three-dimensional compressible boundary layer p 1029 A93-46979
 Semi-discrete Galerkin solution of the compressible boundary-layer equations with viscous-inviscid interaction [AIAA PAPER 93-3520] p 985 A93-47282
 Skin friction and velocity profile family for compressible turbulent boundary layers p 1070 A93-49008
 Secondary instability mechanisms in compressible axisymmetric boundary layers p 1070 A93-49009
 Calculation of a compressible three-dimensional boundary layer on a swept wing p 1179 A93-53551
 Evaluation and application of the Baldwin-Lomax turbulence model in two-dimensional, unsteady, compressible boundary layers with and without separation in engine inlets [NASA-TM-105810] p 82 N93-10087
 Effects of sweep on the physics of unsteady shock-induced turbulent separated flows [AD-A247035] p 22 N93-11742
 Bypass transition in compressible boundary layers p 417 N93-15801
 Parametric studies of shock wave/boundary layer interactions over 2D compression corners at Mach 6 [VKI-TN-181] p 988 N93-31538

COMPRESSIBLE FLOW

- On the use of the method of matched asymptotic expansions in propeller aerodynamics and acoustics p 8 A93-11553
 Boundary integral equation methods for aerodynamics p 9 A93-12158
 Computation of viscous compressible flows using an upwind algorithm and unstructured meshes p 9 A93-12163
 Comparison of nonlinear tracking controllers for a compressible flow process p 66 A93-12224
 Numerical simulation of compressible mixing zones p 10 A93-12427
 Dynamic stability of bodies of revolution in compressible flow p 12 A93-12558
 An adaptive region method for computation of vortex sheet behind wing in compressible flow p 116 A93-14262
 A multi-zonal local solution methodology for the accelerated solution of the turbulent Navier-Stokes equations p 117 A93-14279
 Implicit Navier-Stokes solver for three-dimensional compressible flows p 122 A93-14546
 Study on unsymmetrical supersonic nozzle flows p 127 A93-16933
 Adaptive remeshing for three-dimensional compressible flow computations p 242 A93-18851
 A new technique for aerodynamic noise calculation p 447 A93-19177
 Compressible flow pressure losses in wye-junctions [ASME PAPER 92-GT-71] p 248 A93-19321
 A novel approach to high resolution compressible cascade flow analysis using the Navier-Stokes equations [ASME PAPER 92-GT-419] p 258 A93-19567
 The computation of internal flow fields in centrifugal compressor impellers p 259 A93-20120
 Air flow dynamics around an aerofoil by the stabilized finite difference method p 266 A93-20741
 The Burnett shock structures in low density hypersonic flows [AIAA PAPER 92-5048] p 273 A93-22320
 Prediction of fluctuating pressure in attached and separated compressible flow [AIAA PAPER 93-0286] p 279 A93-22667
 Unsteady compressible airfoil aerodynamics using an adaptive time-discontinuous GLS finite element method [AIAA PAPER 93-0339] p 281 A93-23027
 Calculation of the flowfield around an airfoil with spoiler [AIAA PAPER 93-0527] p 284 A93-23268
 Performance of compressible flow codes at low Mach numbers p 287 A93-23540
 Nonlinear relaxation/quasi-Newton algorithm for the compressible Navier-Stokes equations p 287 A93-23541
 A numerical method for solving Navier-Stokes equations for low Mach number compressible flows p 463 A93-24672
 A moving mesh system for the calculation of unsteady flows [AIAA PAPER 93-0641] p 464 A93-24756
 Compressible turbulence measurements in a high-speed high Reynolds number mixing layer [AIAA PAPER 93-0660] p 465 A93-24773
 Numerical simulation of vortex generation and capture above an airfoil [AIAA PAPER 93-0864] p 468 A93-24926
 A comparison of 'new' and 'old' flux-splitting schemes for the Euler equations [AIAA PAPER 93-0876] p 470 A93-24937
 A new model for super/hypersonic turbulent boundary layers [AIAA PAPER 93-0897] p 472 A93-24957
 Characteristic multigrid method application to solve the Euler equations with unstructured and unsteady grids p 476 A93-27065
 On the accurate prediction of the wall-normal velocity in compressible boundary-layer flow p 477 A93-27474
 Schlieren studies of compressibility effects on dynamic stall of transiently pitching airfoils p 480 A93-28608
 Nonsteady, one-dimensional, internal, compressible flows - Theory and applications --- Book [ISBN 0-19-507358-4] p 548 A93-28749
 Compressible flow in a hovercraft air cushion p 480 A93-29316
 Finite element computation of compressible flows with the SUPG formulation p 482 A93-29774
 Real gas effects for compressible nozzle flows p 682 A93-33757
 Spreadsheet microcomputer numerical method for the compressible laminar wake flow p 684 A93-34308
 Compressible flow calculations using a two-equation turbulence model and unstructured grids p 686 A93-34351
 Numerical simulation of two-dimensional compressible flows p 687 A93-34357

- Computation of turbulent compressible flows on a DLR wing and a blade to blade passage using an upwind scheme p 687 A93-34359
 Dynamic stall of sinusoidally oscillating three-dimensional swept and unswept wings in compressible flow p 766 A93-35995
 Modeling of linear isentropic flow systems p 828 A93-37046
 Indicial lift approximations for two-dimensional subsonic flow as obtained from oscillatory measurements p 768 A93-37385
 Numerical solution of viscous compressible flows using algebraic turbulence models p 770 A93-38162
 Viscous-inviscid calculation of high-lift separated compressible flows over airfoils and wings [ONERA, TP NO. 1992-184] p 774 A93-38746
 Velocity and vorticity distributions over an oscillating airfoil under compressible dynamic stall p 778 A93-39403
 Implicit multigrid techniques for compressible flows p 862 A93-42429
 Viscous, 2-D, laminar hypersonic flows over compression ramps p 866 A93-42591
 The application of an adaptive upwind unstructured grid solution algorithm to the simulation of compressible laminar viscous flows over compression corners p 866 A93-42594
 Hypersonic viscous flow over two-dimensional ramps p 866 A93-42596
 Computational results for flows over compression ramps p 866 A93-42599
 Inviscid finite-volume lambda formulation p 872 A93-42888
 Vortex-induced disturbance field in a compressible shear layer p 873 A93-43628
 A perspective on a quarter century of CFD research [AIAA PAPER 93-3291] p 1021 A93-44995
 Computations of inviscid compressible flows using fluctuation-splitting on triangular meshes [AIAA PAPER 93-3301] p 950 A93-44999
 Variant bi-conjugate gradient methods for the compressible Navier-Stokes solver with a two-equation model of turbulence [AIAA PAPER 93-3316] p 951 A93-45012
 A coarse-grid correction/nonlinear relaxation algorithm for the three-dimensional, compressible Navier-Stokes equations [AIAA PAPER 93-3317] p 951 A93-45013
 Multigrid convergence of an implicit symmetric relaxation scheme [AIAA PAPER 93-3357] p 954 A93-45051
 Implicit multigrid Euler solutions with symmetric Total-Variation-Diminishing dissipation [AIAA PAPER 93-3358] p 955 A93-45052
 Line relaxation methods for the solution of 2D and 3D compressible flows [AIAA PAPER 93-3366] p 955 A93-45059
 Adaptive Cartesian grid methods for representing geometry in inviscid compressible flow [AIAA PAPER 93-3385] p 955 A93-45076
 A novel algorithm for the solution of compressible Euler equations in wave/particle split (WPS) form p 957 A93-45093
 Navier-Stokes analysis of three-dimensional S-ducts p 959 A93-45146
 A singularities tracking conservation law scheme for compressible duct flows p 960 A93-45542
 Numerical simulation of two-dimensional and axisymmetric compressible flows p 960 A93-45546
 Organized structure in a compressible turbulent shear layer p 961 A93-45730
 Visual observations of supersonic transverse jets p 965 A93-46750
 Transition in supersonic flow past axisymmetric bodies p 967 A93-46817
 Passive control of coherent vortices in compressible mixing layers [AIAA PAPER 93-3262] p 968 A93-46828
 Adaptation of a 3-D pressure correction Navier-Stokes solver for the accurate modelling of tip clearance flows p 971 A93-46932
 Finite element solution of the 3D compressible Navier-Stokes equations by a velocity-vorticity method p 974 A93-47196
 Numerical solution of the Euler equations for complex aerodynamic configurations using an edge-based finite element scheme [AIAA PAPER 93-2933] p 1046 A93-48131
 Multi-zonal Navier-Stokes code with the LU-SGS scheme [AIAA PAPER 93-2965] p 1148 A93-48159
 Hypersonic flow past open cavities [AIAA PAPER 93-2969] p 1049 A93-48163
 Transition effects on compressible dynamic stall of transiently pitching airfoils [AIAA PAPER 93-2978] p 1050 A93-48171

- Nonlocal vs. local instability of compressible flows including body metric, flow divergence and 3D-wave propagation
[AIAA PAPER 93-2982] p 1051 A93-48175
- A viscous-inviscid interaction method for 2-D unsteady, compressible flows
[AIAA PAPER 93-3019] p 1055 A93-48206
- Application of a two-equation turbulence model for high speed compressible flows using unstructured grids
[AIAA PAPER 93-3029] p 1056 A93-48213
- Behaviour of the Johnson-King turbulence model in axis-symmetric supersonic flows
[AIAA PAPER 93-3032] p 1056 A93-48214
- Audio post-processing for shear layer calculations
[AIAA PAPER 93-3075] p 1059 A93-48250
- DSMC numerical investigation of rarefied compression corner flow
[AIAA PAPER 93-3096] p 1061 A93-48270
- A nonperiodic boundary approach for computation of compressible viscous flows in advanced turbine cascades
[AIAA PAPER 93-1799] p 1074 A93-49688
- Numerical study of the performance of swept, curved compression surface scramjet inlets
[AIAA PAPER 93-1837] p 1074 A93-49721
- An unstructured grid flow solver for turbomachinery flows
[AIAA PAPER 93-1913] p 1076 A93-49780
- Particle dynamics simulations in inlet separator with an experimentally based bounce model
[AIAA PAPER 93-2156] p 1115 A93-49972
- Numerical and experimental investigation of turbine tip gap flow
[AIAA PAPER 93-2253] p 1081 A93-50051
- A comparison between centered and upwind schemes for two-phase compressible flows
[AIAA PAPER 93-2346] p 1083 A93-50120
- Multistage turbomachinery flow solutions using three-dimensional implicit Euler method
[AIAA PAPER 93-2382] p 1083 A93-50150
- Numerical aspects of a block structured compressible flow solver
p 1169 A93-51279
- A collocated finite volume method for predicting flows at all speeds
p 1087 A93-51736
- Calculation of compressible gas flow on optimal difference grids
p 1091 A93-51902
- Flux-vector splitting for compressible low Mach number flow
p 1093 A93-52001
- Numerical simulation and physical aspects of supersonic vortex breakdown
p 1093 A93-52011
- Zonal-local solution method for the turbulent Navier-Stokes equations
p 1177 A93-53205
- Study on surge and rotating stall in axial compressors. III - Numerical model for multiblade-row compressors
p 1181 A93-53799
- Kelvin-Helmholtz wave generation beneath hovercraft skirts
p 1219 A93-53820
- The construction of nearly orthogonal multiblock grids for compressible flow simulation
p 1219 A93-53847
- The streamline throughflow method of axial turbomachinery flow analysis
[ISABE 93-7031] p 1184 A93-54007
- On the numerical simulation of the two-dimensional flow field around a hypersonic air-intake-compressibility effects
[ISABE 93-7100] p 1187 A93-54076
- Recent advances in steady compressible aerodynamic sensitivity analysis
p 1236 A93-55400
- Numerical study of slightly compressible Navier-Stokes simulation of blade-vortex interaction
p 1239 A93-56216
- Interaction of compressible vortices with a rigid plate
p 1239 A93-56219
- An experimental investigation of the flow in a diffusing S-duct
[NASA-TM-105809] p 60 N93-12077
- Application of a solution adaptive grid to flow over an embedded cavity
p 130 N93-13141
- Development and computation of continuum higher order constitutive relations for high-altitude hypersonic flow
p 132 N93-13578
- Solution of compressible Navier-Stokes equations using spectral methods on arbitrary two-dimensional domains
p 218 N93-14041
- An integral equation solution for multistage turbomachinery design calculations
[NASA-TM-105970] p 179 N93-15521
- Design optimization of natural laminar flow bodies in compressible flow
[NASA-CR-4478] p 292 N93-16940
- Validation of central and upwind 3D compressible flow solvers
p 421 N93-18564
- The stability of a trailing-line vortex in compressible flow
[NASA-CR-189738] p 298 N93-18771
- A numerical simulations of inner flow of scramjet
p 304 N93-19318
- The semi-discrete Galerkin finite element modelling of compressible viscous flow past an airfoil
[NASA-CR-192161] p 483 N93-20018
- Unsteady airfoil flow solutions on moving zonal grids
[AD-A261925] p 701 N93-26198
- Turbulence: The chief outstanding difficulty of our subject
p 783 N93-27428
- The transition prediction toolkit: LST, SIT, PSE, DNS, and LES
p 783 N93-27429
- Analysis of unsteady wave processes in a rotating channel
[NASA-CR-191154] p 816 N93-28617
- Heat transfer and leakage in high-speed rotating stepped labyrinth seals
p 903 N93-29951
- Compressible turbulence in a high-speed high Reynolds number mixing layer
p 878 N93-30583
- WBNFLOW: Multi-grid/multi-block potential solver for compressible flow. User's guide
[FFA-TN-1992-43] p 1031 N93-31146
- COMPRESSIBLE FLUIDS**
- On the conservation of rothalpy in turbomachines
[ASME PAPER 92-GT-217] p 252 A93-19439
- Introduction of small velocity and pressure variation into a stationary compressible fluid
p 473 A93-25060
- Comparison of confined, compressible, spatially developing mixing layers with temporal mixing layers
p 1234 A93-55352
- Developing numerical techniques for solving low Mach number fluid-acoustic problems
p 1235 A93-55353
- Three-dimensional simulations of compressible mixing layers - Visualizations and statistical analysis
p 1235 A93-55360
- Compressible and incompressible fluid seals: Influence on rotordynamic response and stability
[NASA-CR-190746] p 85 N93-10891
- COMPRESSION LOADS**
- Tapered geometries for improved crashworthiness under side loads
p 743 A93-34259
- Load-bearing capacity of an aircraft wing based on the condition of compressed surface fracture
p 801 A93-36794
- Optimization of composite sandwich cover panels subjected to compressive loadings
p 922 N93-30862
- Consideration of impact damages by dimensioning CFC (Carbon Fiber Reinforced Composites) components
[MBB-FE-221-S-PUB-0501] p 1018 N93-31044
- COMPRESSION TESTS**
- Allowable compression strength for CFRP-components of fighter aircraft determined by CAI-test
[MBB-FE-221-S-PUB-0483] p 537 N93-21462
- COMPRESSION WAVES**
- Interaction of compression waves with an elastic spherical dome
p 550 A93-29718
- Three-dimensional numerical simulation of gradual opening in a wave rotor passage
[AIAA PAPER 93-2526] p 1156 A93-50254
- Three-dimensional numerical simulation of gradual opening in a wave rotor passage
[NASA-CR-191157] p 900 N93-29072
- COMPRESSIVE STRENGTH**
- Compression after impact (CAI) properties of CF/PEEK (APC-2) and conventional CF/epoxy stiffened panels
p 196 A93-14307
- Experimental investigations into composite fuselage impact damage resistance and post-impact compression behavior
p 159 A93-15812
- Low velocity impact in a graphite/PEEK
[AIAA PAPER 93-1403] p 734 A93-33963
- Reanalysis of multiple-wheel landing gear traffic tests
[AD-A256593] p 194 N93-14238
- Allowable compression strength for CFRP-components of fighter aircraft determined by CAI-test
[MBB-FE-221-S-PUB-0483] p 537 N93-21462
- Allowable compression strength for CFRP-components of fighter aircraft determined by CAI-test
p 537 N93-21531
- Numerical determination of the residual strength of battle damaged composite plates
p 537 N93-21533
- Consideration of impact damages by dimensioning CFC (Carbon Fiber Reinforced Composites) components
[MBB-FE-221-S-PUB-0501] p 1018 N93-31044
- COMPRESSOR BLADES**
- Three-dimensional flow of viscous gas in the blade passage of a straight compressor cascade
p 5 A93-10187
- Analytical method for subsonic cascade profile
p 12 A93-12730
- Computational studies of the characteristics of axial compressor cascades and stages in unsteady incoming flow
p 13 A93-12805
- Calculation of sound field radiated by oscillating cascade
p 231 A93-14269
- The vortex behaviour of the rotating-stall cell of a centrifugal compressor with vaned diffuser
[ASME PAPER 92-GT-66] p 400 A93-19316
- Blade excitation by circumferentially asymmetric rotating stall in centrifugal compressors
[ASME PAPER 92-GT-148] p 351 A93-19376
- Excitation of blade vibration due to surge of centrifugal compressors
[ASME PAPER 92-GT-149] p 351 A93-19377
- On aerodynamic loading of linear compressor cascades
[ASME PAPER 92-GT-275] p 253 A93-19468
- Prediction of secondary losses in axial compressors
[ASME PAPER 92-GT-288] p 254 A93-19479
- Investigation of tip clearance phenomena in an axial compressor cascade using Euler and Navier-Stokes procedures
[ASME PAPER 92-GT-299] p 255 A93-19489
- Numerical simulation of compressor endwall and casing treatment flow phenomena
[ASME PAPER 92-GT-300] p 255 A93-19490
- Effect of manufacturing deviations on performance of axial flow compressor blading
[ASME PAPER 92-GT-326] p 257 A93-19510
- Performance of gas turbine compressor cleaners
[ASME PAPER 92-GT-360] p 355 A93-19524
- Unsteady aerodynamics and gust response in compressors and turbines
[ASME PAPER 92-GT-422] p 258 A93-19570
- Optimization of a multistage axial compressor in a gas turbine engine system
[ASME PAPER 92-GT-424] p 357 A93-19572
- Inverse design of compressor and turbine blades at transonic flow conditions
[ASME PAPER 92-GT-430] p 357 A93-19573
- Experimental study on the three dimensional flow within a compressor cascade with tip clearance. I - Velocity and pressure fields
[ASME PAPER 92-GT-215] p 258 A93-19574
- Experimental study on the three dimensional flow within a compressor cascade with tip clearance. II - The tip leakage vortex
[ASME PAPER 92-GT-432] p 258 A93-19575
- Investigation of the characteristics of 3-dimensional separated flow in an annular compressor blade row with large angles of attack
p 259 A93-20116
- A unified model for rotating stall and surge
p 259 A93-20119
- The computation of internal flow fields in centrifugal compressor impellers
p 259 A93-20120
- Two-dimensional cascade tests of MCA blades in the high transonic Mach number region. V - Effect of space/chord ratio on the parameters of cascade performance
p 267 A93-20930
- Forcing function generator fluid dynamic effects on compressor blade gust response
[AIAA PAPER 93-0157] p 275 A93-22594
- Determination of nonstationary aerodynamic loading on cascade blades in the case of dynamic changes of the angle of attack
p 544 A93-26817
- A method for calculating the characteristics of plane compressor cascades for different values of the Reynolds criterion
p 545 A93-27616
- Computation of turbulent compressible flows on a DLR wing and a blade to blade passage using an upwind scheme
p 687 A93-34359
- Inlet turbulence distortion and viscous flow development in a controlled-diffusion compressor cascade at very high incidence
p 688 A93-34485
- Increasing the durability of gas turbine engine compressor blades by using a combined hardening/finishing treatment to control the stressed state of the surface layer
p 835 A93-39099
- Hardening/finishing treatment of compressor blades using a machine with planetary container motion
p 835 A93-39102
- Effect of the technological process structure on residual stress distribution in the blade foil of gas turbine engines
p 836 A93-39106
- Experience in the design of supercritical cascades for the flow straightener of a transonic fan
p 777 A93-39196
- On model for predicting blade force defect in end wall boundary layer inside axial compressor cascade
p 862 A93-42271
- 2-D theoretical analysis of circumferential grooved casing treatment
p 1066 A93-48501
- An experimental investigation of endwall flow control in a compressor plane cascade wind tunnel
p 1066 A93-48512
- Experimental investigation on effect of solid particles on blade pressure distribution in compressor cascade flow
p 1066 A93-48513
- Experimental investigation on patterned blades of compressor
p 1066 A93-48515

- A blade element method for predicting the off-design performance of compressors p 1107 A93-49187
- Establishing two-dimensional flow in a large-scale cascade of controlled-diffusion compressor blades [AIAA PAPER 93-2383] p 1083 A93-50151
- Estimation of the change of axial-flow compressor characteristics during long-term service p 1193 A93-52949
- Three-dimensional viscous flow analysis of compressor cascade channels p 1181 A93-53837
- Velocity fluctuation based on the difference in the flow pattern in the channels of a centrifugal impeller p 1182 A93-53842
- A 2-D compressible N-S simulation of starting- and stalling-flows in a compressor cascades system [ISABE 93-7006] p 1183 A93-53982
- The leading edge vortex of a rotating stall cell [ISABE 93-7009] p 1183 A93-53985
- The effects of end-bend regulations of compressor blade on the outlet flow field p 1185 A93-54009
- Transonic discharge flows around diffuser vanes from a centrifugal impeller [ISABE 93-7053] p 1185 A93-54029
- Correlations for flow property variation at outlet of a centrifugal impeller [ISABE 93-7054] p 1185 A93-54030
- Integrated Blade Inspection System (IBIS) upgrade study [AD-A258912] p 365 N93-19356
- The effects of reaction on axial compressor performance p 724 N93-25882
- Model fan passage flow simulation [AD-A261613] p 752 N93-26167
- Three-dimensional fiber-optic LDV measurements in the endwall region of a linear cascade of controlled-diffusion stator blades [AD-A263513] p 933 N93-29968
- Performance of gas turbine compressor cleaners [NLR-TP-91237-U] p 1003 N93-31111
- COMPRESSOR EFFICIENCY**
- Effect of steady-state circumferential pressure and temperature distortions on compressor stability p 1106 A93-48503
- Performance improvement by forward-skewed blading of axial fan moving blades [ISABE 93-7055] p 1185 A93-54031
- Research and development of high pressure compressor for SST and HST engine [ISABE 93-7068] p 1186 A93-54044
- Flight analysis of air intake/engine compatibility p 161 N93-13212
- Variable speed rotary compressor and adjustable speed drive efficiencies measured in the laboratory [DE92-040026] p 222 N93-15278
- COMPRESSOR ROTORS**
- Investigation of compressor rotor wake structure at peak pressure rise coefficient and effects of loading [ASME PAPER 92-GT-32] p 246 A93-19292
- Design and rotor performance of a 5:1 mixed-flow supersonic compressor [ASME PAPER 92-GT-73] p 348 A93-19323
- The effect of compressor rotor tip crops on turbohaft engine performance [ASME PAPER 92-GT-83] p 348 A93-19332
- Low aspect ratio transonic rotors. II - Influence of location of maximum thickness on transonic compressor performance [ASME PAPER 92-GT-186] p 352 A93-19411
- Calculation of three-dimensional boundary layers on rotor blades using integral methods [ASME PAPER 92-GT-210] p 252 A93-19433
- Investigations on a radial compressor tandem-rotor stage with adjustable geometry p 404 A93-19440
- The extension of a solution-adaptive 3D Navier-Stokes solver towards geometries of arbitrary complexity [ASME PAPER 92-GT-363] p 257 A93-19527
- Theoretical and experimental investigations concerning the structural integrity of aeroengine compressor discs p 56 N93-10539
- Propulsion and Energetics Panel Working Group 20 on Test Cases for Engine Life Assessment Technology [AGARD-AR-308] p 176 N93-14890
- Introduction to test cases for engine life assessment technology p 176 N93-14891
- CF6-6 high pressure compressor stage 5 locking slot crack propagation spin pit test p 176 N93-14894
- F100 second stage fan disk bolt hole crack propagation ferris wheel test p 177 N93-14897
- Single screw interrupted thread positive displacement mechanism [AD-D015596] p 554 N93-20790
- Transient thermal behaviour of a compressor rotor with axial cooling air flow and co-rotating or contra-rotating shaft p 903 N93-29946

- Flow and heat transfer between gas-turbine discs p 903 N93-29950

COMPRESSORS

- Dynamics of a high-rpm compressor p 75 A93-10009
- Axial length influence on the performance of centrifugal impellers p 205 A93-14517
- Solution schemes for stage-by-stage dynamic compression system modeling [AIAA PAPER 93-0154] p 275 A93-22592
- Compressor surge and stall --- Book [ISBN 0-933283-05-9] p 482 A93-29780
- Surge recovery and compressor working line control using compressor exit Mach number measurement p 897 A93-40435
- Societe Francaise des Mecaniciens, SNECMA, and ONERA, Symposium on Recent Advances in Compressor and Turbine Aerothermodynamics, Courbevoie, France, Nov. 24, 25, 1992, Reports p 1001 A93-46926
- The three dimensional flow in a compressor cascade at design and off-design conditions p 971 A93-46927
- Application of vanadium hydride compressors for Joule-Thomson cryocoolers p 1149 A93-48616
- Theoretical and experimental investigations concerning the structural integrity of aeroengine compressor discs p 56 N93-10539
- Development of the neutron diffraction technique for the determination of near surface residual stresses in critical gas turbine components [PNR-90984] p 58 N93-11112
- The influence of intake swirl distortion on the steady-state performance of a low bypass, twin-spool engine p 214 N93-13211
- A novel-high-performance system for recording and analysing instantaneous total pressure distortion in air intakes p 214 N93-13215
- RB 199 high pressure compressor stage 3 spin pit tests p 176 N93-14893
- Engine life assessment test case TF41 LP compressor shaft torsional fatigue p 177 N93-14896
- Variable speed rotary compressor and adjustable speed drive efficiencies measured in the laboratory [DE92-040026] p 222 N93-15278
- On flutter behavior of a 2-D compressor cascade in incompressible flow [DLR-FB-91-26] p 418 N93-16543
- Experimental and numerical examinations of the influence of inlet distortion perturbations on the working behavior of turbofan compressors [ETN-93-92733] p 364 N93-18628
- Apparatus for reduction of vibration in liquid-injected gas compressor system [AD-D015607] p 554 N93-20772
- Single screw interrupted thread positive displacement mechanism [AD-D015596] p 554 N93-20790
- The WINCOF-1 code: Detailed description [NASA-CR-190779] p 677 N93-24760
- Improved selective catalytic NOx control technology for compressor station reciprocating engines [PB93-158566] p 755 N93-26529
- An assessment of inlet total-pressure distortion requirements for the Compressor Research Facility (CFR) [AD-A262299] p 815 N93-27679
- Detection performance of digital polarity sampled phase reversal code pulse compressors [AD-A262930] p 842 N93-28289
- Thrust augmentation system for low-cost-expendable turbojet engine [AD-A263727] p 905 N93-30877
- Electropneumatic actuator, phase 1 [PB93-174951] p 1033 N93-31876
- COMPUTATION**
- Turbomachinery and potential computations [DS-2026] p 363 N93-17740
- Overview of the NASA Dryden Flight Research Facility aeronautical flight projects testing p 512 N93-19916
- COMPUTATIONAL CHEMISTRY**
- A critical analysis of the accuracy of several numerical techniques for combustion kinetic rate equations [NASA-TP-3315] p 362 N93-16941
- Issues and approach to develop validated analysis tools for hypersonic flows: One perspective [NASA-TM-103937] p 305 N93-19379
- COMPUTATIONAL FLUID DYNAMICS**
- Calculation of a three-dimensional boundary layer at the lee side of a finite-span delta wing in the case of viscous interaction with hypersonic flow p 5 A93-10143
- Calculation of a gas-dispersion laminar boundary layer on a plate with allowance for liquid film formation p 76 A93-10148
- Wing pressure loads in canard configurations - A comparison between numerical results and experimental data p 7 A93-11499

- Weighted average method for evaluating the aerodynamic properties of transition flow p 8 A93-11872
- Computational nonlinear mechanics in aerospace engineering [ISBN 1-56347-044-6] p 78 A93-12151
- Control of numerical diffusion in computational modeling of vortex flows p 9 A93-12156
- Computation of viscous compressible flows using an upwind algorithm and unstructured meshes p 9 A93-12163
- Turbine blade cascade flows p 10 A93-12361
- Numerical simulation for aeroelasticity in turbomachines with vortex method. I - Theory and method p 53 A93-12452
- Three-dimensional flow calculations in turbomachinery using the stream function formulation p 11 A93-12453
- Viscous shock-layer numerical calculations of three dimensional nonequilibrium flows over hypersonic blunt bodies at high angle of attack p 12 A93-12651
- Compressible laminar and turbulent boundary layer computation for the three-dimensional wing p 12 A93-12735
- A flow calculation and aerodynamic design method for turbomachine cascades p 12 A93-12764
- Calculation of the three-dimensional interaction of a shock wave with a boundary layer on a cylinder p 12 A93-12766
- Nonstationary flow of a viscous incompressible fluid past an airfoil p 79 A93-12922
- Calculation of separated axisymmetric flow past bodies by solving Euler equations in the inner vortex region p 14 A93-12975
- A comparative analysis of algorithms for solving systems of high-order linear algebraic equations p 96 A93-12977
- Effect of canard position on the longitudinal aerodynamic characteristics of a close-coupled canard-wing-body configuration [AIAA PAPER 92-4632] p 14 A93-13304
- The numerical study of 3-D flow past control surfaces [AIAA PAPER 92-4650] p 14 A93-13305
- A comparison of upwind schemes for computation of three-dimensional hypersonic real-gas flows [AIAA PAPER 92-4350] p 15 A93-13306
- Geometry based Delaunay tetrahedralization and mesh movement strategies for multi-body CFD [AIAA PAPER 92-4575] p 15 A93-13309
- 'Wingwake' - A computational model for preliminary assessment of wake vortex attenuation schemes [AIAA PAPER 92-4209] p 15 A93-13377
- Numerical solution of transonic full-potential-equivalent equations in von Mises co-ordinates p 111 A93-14080
- Fluid/chemistry modeling for hypersonic flight analysis p 111 A93-14120
- ICAS, Congress, 18th, Beijing, China, Sept. 20-25, 1992, Proceedings, Vols. 1 & 2 [ISBN 1-56347-046-2] p 107 A93-14151
- Numerical investigation of the unsteady flow through a counter-rotating fan p 112 A93-14166
- The new challenge of computational aeroscience p 112 A93-14169
- Nozzle flow computations using the Euler equations p 112 A93-14170
- Navier-Stokes calculations of the flow about wing-flap combinations p 112 A93-14171
- Calculation of transonic viscous flow around a delta wing p 113 A93-14191
- Multizone Navier-Stokes computations for a transonic projectile using MacCormack finite difference method p 113 A93-14192
- Accelerated method of the Euler equation solution in transonic airfoil flow problem p 113 A93-14193
- Numerical solution of 3-D turbulent flows inside of new concept nozzles p 114 A93-14211
- The value of a computational/experimental partnership in aerodynamic design p 114 A93-14215
- Computational methods applied to the aerodynamics of spaceplanes and launchers [ONERA, TP NO. 1992-140] p 114 A93-14216
- Nonintrusive spectroscopic techniques for supersonic/hypersonic aerodynamics and combustion diagnostics p 203 A93-14245
- Numerical simulations of high speed inlet flows p 115 A93-14246
- An algebraic turbulence model with memory for the computation of three dimensional turbulent boundary layers p 115 A93-14248
- Numerical analysis of the 3-D turbulent flow in an S-shaped diffuser p 116 A93-14252
- An adaptive region method for computation of vortex sheet behind wing in compressible flow p 116 A93-14262

Calculation of transonic flow over bodies of varying complexity using Singular Perturbation Method p 116 A93-14265

A numerical study of slit V-gutter flows p 171 A93-14273

Assessment and correction of tunnel wall interference by Navier-Stokes solutions p 116 A93-14275

Parallel implementation of the feature associated mesh embedding method for the 2D-Euler equations (FAME2D) p 225 A93-14278

A multi-zonal local solution methodology for the accelerated solution of the turbulent Navier-Stokes equations p 117 A93-14279

Numerical solution of radiative flowfield on the nose region of blunt bodies p 120 A93-14359

Simulation of a hypersonic flow over vehicles at low Reynolds numbers p 120 A93-14381

Viscous flow field prediction in axisymmetric passages p 204 A93-14478

Digital simulation of transonic flow fields in a planar nozzle p 122 A93-14479

Study on vortex flow control of inlet distortion p 122 A93-14520

The accuracy of cell vertex finite volume methods on quadrilateral meshes p 227 A93-14526

Hybrid grid approach to study dynamic stall p 122 A93-14548

Analytical solutions for hypersonic flow past slender power-law bodies at small angle of attack p 122 A93-14550

Comparison of algebraic turbulence models for afterbody flows with jet exhaust p 123 A93-14554

Generalized vortex lattice method for oscillating lifting surfaces in subsonic flow p 123 A93-14555

Calculation of radiant energy transfer in hypersonic flow past blunt bodies using the P1 and P2 approximations of the spherical harmonic method p 124 A93-15209

A fast method for calculating three-dimensional transonic potential flows in turbomachine blade rows p 125 A93-15215

An AF3 algorithm for the calculation of transonic nonconservative full potential flows over wings or wing/body combinations p 125 A93-15341

Turbulent structure in a vortex wake shed from an inclined circular cylinder p 125 A93-15443

Experimental and numerical study on the basic performance of a two-dimensional right-angled intake flow p 208 A93-15486

Numerical analysis of two-dimensional turbulent flows through an oscillating cascade p 126 A93-15494

A numerical study on the radiation characteristic of an elliptical exhaust jet p 174 A93-16236

Unsteady transonic flow past a quarter-plane p 127 A93-16664

A study of singularity formation in vortex-sheet motion by a spectrally accurate vortex method p 127 A93-16666

Effect of the body shape on head shock attenuation at a large distance from the axis p 127 A93-16708

A finite element study of incompressible flows past oscillating cylinders and aerofoils p 241 A93-17750

Periodic Euler and Navier-Stokes solutions about oscillating airfoils p 241 A93-17799

Longitudinal vortex control - Techniques and applications (The 32nd Lanchester Lecture) p 242 A93-18526

Adaptive remeshing for three-dimensional compressible flow computations p 242 A93-18851

A new Lagrangian method for steady supersonic flow computation. II - Slip-line resolution. III - Strong shocks p 243 A93-18855

A statistical approach to the experimental evaluation of transonic turbine airfoils in a linear cascade [ASME PAPER 92-GT-5] p 245 A93-19278

A numerical investigation into the nozzle flow of high by-pass turbofans p 346 A93-19283

An investigation on the artificial viscosity in the transonic stream function formulation [ASME PAPER 92-GT-49] p 246 A93-19302

An investigation of post stall transients and recoverability of axial compression systems. I - A simplified method [ASME PAPER 92-GT-55] p 347 A93-19305

Secondary flows in a transonic cascade - Validation of a 3-D Navier-Stokes code [ASME PAPER 92-GT-62] p 247 A93-19312

Simulation of the secondary air system of aero engines [ASME PAPER 92-GT-68] p 348 A93-19318

Calculation of turbulent flow for an enclosed rotating cone [ASME PAPER 92-GT-70] p 400 A93-19320

Experimental and computational investigation of flow in catalytic monolith channels [ASME PAPER 92-GT-118] p 387 A93-19354

Analysis of steady and unsteady turbine cascade flows by a locally implicit hybrid algorithm [ASME PAPER 92-GT-127] p 249 A93-19361

An inviscid-viscous interaction approach to the calculation of dynamic stall initiation on airfoils [ASME PAPER 92-GT-128] p 249 A93-19362

Three component LDV velocity measurements in a can type research combustor for CFD validation. I - Isothermal [ASME PAPER 92-GT-138] p 350 A93-19370

Numerical simulation of the flow field around supersonic air-intakes [ASME PAPER 92-GT-206] p 251 A93-19430

A fully three-dimensional inverse method for turbomachinery blading in transonic flows [ASME PAPER 92-GT-209] p 251 A93-19432

Calculation of three-dimensional boundary layers on rotor blades using integral methods [ASME PAPER 92-GT-210] p 252 A93-19433

Experimental and computational investigation of the NASA Low-Speed Centrifugal Compressor flow field [ASME PAPER 92-GT-213] p 252 A93-19436

Overview of the Japanese National Project for Super/Hyper-Sonic Transport propulsion system [ASME PAPER 92-GT-252] p 239 A93-19461

Navier-Stokes computation on a pivoting doors thrust reverser and comparison with tests [ASME PAPER 92-GT-254] p 353 A93-19463

Numerical research on flows in nonuniform cascades [ASME PAPER 92-GT-276] p 253 A93-19469

Transition prediction in attached and separated shear layers using an integral method [ASME PAPER 92-GT-281] p 253 A93-19473

An approach for multi-stage calculations incorporating unsteadiness [ASME PAPER 92-GT-282] p 253 A93-19474

A three-dimensional numerical method for turbomachinery blading [ASME PAPER 92-GT-291] p 254 A93-19482

A viscous axisymmetric throughflow prediction method for multi-stage compressors [ASME PAPER 92-GT-293] p 254 A93-19483

A comparison of the measured and predicted flowfield in a modern fan-bypass configuration [ASME PAPER 92-GT-298] p 254 A93-19488

Investigation of tip clearance phenomena in an axial compressor cascade using Euler and Navier-Stokes procedures [ASME PAPER 92-GT-299] p 255 A93-19489

Numerical simulation of compressor endwall and casing treatment flow phenomena [ASME PAPER 92-GT-300] p 255 A93-19490

The role of laminar-turbulent transition in gas turbine engines - A discussion [ASME PAPER 92-GT-301] p 255 A93-19491

Viscous throughflow modelling for multi-stage compressor design [ASME PAPER 92-GT-302] p 255 A93-19492

Calculation of wake-induced unsteady flow in a turbine cascade [ASME PAPER 92-GT-306] p 255 A93-19496

Three-dimensional Navier-Stokes computations of transonic fan flow using an explicit flow solver and an implicit k-epsilon solver [ASME PAPER 92-GT-309] p 256 A93-19499

Use of advanced CFD codes in the turbomachinery design process [ASME PAPER 92-GT-324] p 256 A93-19508

Meridional flow calculation using advanced CFD techniques [ASME PAPER 92-GT-325] p 256 A93-19509

Accuracy issues in the prediction of supersonic inlet flows [ASME PAPER 92-GT-400] p 258 A93-19549

A novel approach to high resolution compressible cascade flow analysis using the Navier-Stokes equations [ASME PAPER 92-GT-419] p 258 A93-19567

Accuracy and efficiency assessments for a weak statement CFD algorithm for high-speed aerodynamics [ASME PAPER 92-GT-433] p 435 A93-19576

Accuracy considerations in the computational analysis of jet noise [AIAA PAPER 93-0146] p 451 A93-19804

A performance comparison of massively parallel Parabolized Navier-Stokes solutions [AIAA PAPER 93-0059] p 435 A93-20172

Parallel computation of 3-D Navier-Stokes flowfields for supersonic vehicles [AIAA PAPER 93-0064] p 261 A93-20177

A solution scheme for the Euler equations based on a multi-dimensional wave model [AIAA PAPER 93-0065] p 261 A93-20178

Spatial simulation of boundary layer instability - Effects of surface roughness [AIAA PAPER 93-0075] p 262 A93-20187

Quantitative laser velocimetry measurements in the hypersonic regime by the integration of experimental and computational analysis [AIAA PAPER 93-0089] p 263 A93-20195

An efficient approach to optimal aerodynamic design. II - Implementation and evaluation [AIAA PAPER 93-0100] p 264 A93-20205

A multi-point optimization for transonic airfoil design [AIAA PAPER 92-4681] p 264 A93-20303

An approximately factored incremental strategy for calculating consistent discrete aerodynamic sensitivity derivatives [AIAA PAPER 92-4746] p 265 A93-20344

Observations on computational methodologies for use in large-scale, gradient-based, multidisciplinary design [AIAA PAPER 92-4753] p 436 A93-20351

Multidisciplinary computational aerosciences p 437 A93-20711

Design of a wing shape for study of hypersonic crossflow transition in flight p 265 A93-20713

Large-scale simulation of the three-dimensional Navier-Stokes equations p 437 A93-20739

Numerical analysis of two-dimensional flows around elliptic wings above a flat plate p 267 A93-20924

A gridless Euler/Navier-Stokes solution algorithm for complex-aircraft applications [AIAA PAPER 93-0333] p 268 A93-21107

Computational analysis of hypersonic shock wave/wall jet interaction [AIAA PAPER 93-0604] p 269 A93-21113

Spatial adaptation procedures on tetrahedral meshes for unsteady aerodynamic flow calculations [AIAA PAPER 93-0670] p 269 A93-21116

Development of a flexible and efficient multigrid-based multiblock flow solver [AIAA PAPER 93-0677] p 269 A93-21117

Transonic shock oscillations calculated with a new interactive boundary layer coupling method [AIAA PAPER 93-0777] p 269 A93-21119

The modelling of aerodynamic flows by solution of the Euler equations on mixed polyhedral grids p 269 A93-21218

Workshop report - A validation study of Navier-Stokes codes for transverse injection into a Mach 2 flow p 270 A93-21330

Cascade flow calculations by a multigrid Euler method p 270 A93-21662

On some recent advances in multidisciplinary analysis of hypersonic vehicles [AIAA PAPER 92-5026] p 438 A93-22302

Some aspects of the aerodynamic methodology in hypersonic vehicle concept studies [AIAA PAPER 92-5027] p 272 A93-22303

Application of space-marching methods to hypersonic forebody flow fields [AIAA PAPER 92-5030] p 272 A93-22305

CFD comparisons with wind tunnel and flight data for the X-15 [AIAA PAPER 92-5047] p 273 A93-22319

The Burnett shock structures in low density hypersonic flows [AIAA PAPER 92-5048] p 273 A93-22320

A study of hypersonic swept shock wave/turbulent boundary layer interactions using a conical Navier-Stokes code [AIAA PAPER 92-5050] p 273 A93-22322

Numerical and experimental investigation of mixing enhancement in scramjets [AIAA PAPER 92-5063] p 414 A93-22333

Validation of aerodynamic simulation methods for Hermes spaceplane and future hypersonic vehicles [AIAA PAPER 92-5065] p 273 A93-22335

Development and application of GASP 2.0 [AIAA PAPER 92-5067] p 438 A93-22337

An algebraic turbulence model for three-dimensional viscous flows [AIAA PAPER 93-0083] p 274 A93-22552

Computation of nonequilibrium radiating shock layers [AIAA PAPER 93-0144] p 414 A93-22588

Solution schemes for stage-by-stage dynamic compression system modeling [AIAA PAPER 93-0154] p 275 A93-22592

CFD zonal modeling of leading-edge ice effects for a complete aircraft [AIAA PAPER 93-0167] p 275 A93-22601

Tracking of raindrops in flow over an airfoil [AIAA PAPER 93-0168] p 275 A93-22602

Numerical simulation of dynamic lift enhancement using oscillatory leading edge flaps [AIAA PAPER 93-0186] p 276 A93-22611

A three-dimensional inviscid flow solver in Chimera flow simulation [AIAA PAPER 93-0190] p 276 A93-22614

Tracking flow features using overset grids [AIAA PAPER 93-0197] p 276 A93-22617

- Visualization of vortical flows with yet another post-processor
[AIAA PAPER 93-0222] p 415 A93-22638
- Aircraft grid generation using interactive environment
[AIAA PAPER 93-0224] p 438 A93-22639
- Experimental and numerical investigation of Mach 2.5 supersonic mixed compression inlet
[AIAA PAPER 93-0289] p 279 A93-22689
- Evaluation of a CFD code for analysis of normal-shock trains
[AIAA PAPER 93-0292] p 279 A93-22692
- Application of CFD to a generic hypersonic flight research study
[AIAA PAPER 93-0312] p 280 A93-23007
- Numerical solution of inviscid hypersonic flow around a conically-derived waverider
[AIAA PAPER 93-0320] p 280 A93-23012
- CFD analysis of hypersonic chemically reacting flowfields around a generic shape
[AIAA PAPER 93-0323] p 281 A93-23015
- 3-D adaptive grid-embedding Euler technique
[AIAA PAPER 93-0330] p 415 A93-23021
- Upgrade of ballistic range facilities at AEDC - Two-thirds complete
[AIAA PAPER 93-0349] p 377 A93-23034
- An estimate of the 'doomed propellant fraction' for a Superdetonative Ram Accelerator
[AIAA PAPER 93-0359] p 385 A93-23042
- Euler computations of rotor-stator interaction in turbomachinery cascades using adaptive triangular meshes
[AIAA PAPER 93-0386] p 282 A93-23065
- A hybrid structured-unstructured grid method for unsteady turbomachinery flow computations
[AIAA PAPER 93-0387] p 282 A93-23066
- Juncture flow improvement for wing/pylon configurations by using CFD methodology
[AIAA PAPER 93-0522] p 283 A93-23264
- Calculation of the flowfield around an airfoil with spoiler
[AIAA PAPER 93-0527] p 284 A93-23268
- Three-dimensional flow structure on delta wings at high angle-of-attack - Experimental concepts and issues
[AIAA PAPER 93-0550] p 285 A93-23289
- An application of artificial neural networks to experimental data approximation
[AIAA PAPER 93-0408] p 440 A93-23330
- The design of a senior-level CAD course with emphasis on fluid/thermal systems
[AIAA PAPER 93-0426] p 454 A93-23344
- An improved numerical model for wave rotor design and analysis
[AIAA PAPER 93-0482] p 361 A93-23384
- Direct boundary value solution of wave rotor flow fields
[AIAA PAPER 93-0483] p 415 A93-23385
- Analytical comparison of convective heat transfer correlations in supercritical hydrogen
p 416 A93-23477
- Numerical study of mixed convection between two corotating symmetrically heated disks
p 416 A93-23491
- Effect of sidewall suction on flow in two-dimensional wind tunnels
p 287 A93-23538
- Performance of compressible flow codes at low Mach numbers
p 287 A93-23540
- Adaptive finite volume upwind approach on mixed quadrilateral-triangular meshes
p 287 A93-23542
- Engineering approach to the prediction of shock patterns in bounded high-speed flows
p 287 A93-23545
- Numerical prediction of flap losses in a transonic wind tunnel
p 288 A93-23552
- Direct solution of two-dimensional Navier-Stokes equations for static aeroelasticity problems
p 417 A93-23554
- Shock oscillation in two-dimensional, inviscid, unsteady channel flow
p 288 A93-23563
- National Conference on Aerodynamics, 6th, Bangalore, India, Sept. 1992, Proceedings
p 460 A93-24076
- Acoustic flux vector splitting scheme for Euler equations
p 460 A93-24078
- Numerical modeling of leading edge separated flow at incompressible speeds
p 460 A93-24079
- Numerical computation of viscous hypersonic flow around spherically blunted cones at angle of attack
p 460 A93-24082
- A two-dimensional elliptic grid generator for a wing-body section involving grid control functions
p 460 A93-24083
- A Navier-Stokes simulation of vortex shedding from square cylinder in unconfined domain
p 538 A93-24084
- An implicit finite difference algorithm for two dimensional Euler equation
p 461 A93-24085
- An upwind formulation for the solution of thin-layer Navier-Stokes equations
p 461 A93-24088
- Incompressible potential flow calculation about harmonically oscillating three-dimensional configurations
p 461 A93-24089
- Three-dimensional flow simulation over axisymmetric bodies using Navier-Stokes equations at hypersonic Mach numbers
p 461 A93-24090
- Driven cavity simulation of turbomachine blade flows with vortex control
[AIAA PAPER 93-0390] p 461 A93-24238
- Three-dimensional Navier-Stokes calculations using solution-adapted grids
[AIAA PAPER 93-0431] p 462 A93-24240
- Comparison of experimental ground testing and computational fluid dynamics for the re-engined 727-100 center engine inlet
[AIAA PAPER 92-3920] p 462 A93-24294
- Exact-gradient shape optimization of a 2-D Euler flow
p 462 A93-24308
- The asymptotic theory of hypersonic boundary-layer stability
p 462 A93-24409
- The long-wave limit in the asymptotic theory of hypersonic boundary-layer stability
p 462 A93-24410
- Three-dimensional flow over two spheres placed side by side
p 539 A93-24412
- A numerical method for solving Navier-Stokes equations for low Mach number compressible flows
p 463 A93-24672
- Numerical investigations on airfoil performance subjected to aerodynamic interference from an upstream airfoil
[AIAA PAPER 93-0639] p 463 A93-24754
- A moving mesh system for the calculation of unsteady flows
[AIAA PAPER 93-0641] p 464 A93-24756
- Navier-Stokes computations and experimental comparisons for multielement airfoil configurations
[AIAA PAPER 93-0645] p 464 A93-24760
- Numerical simulations of a high Mach number jet flow
[AIAA PAPER 93-0653] p 540 A93-24766
- Implicit Euler calculation of supersonic vortex wake/engine plume interaction
[AIAA PAPER 93-0656] p 540 A93-24769
- Hybrid prismatic/tetrahedral grid generation for complex 3-D geometries
[AIAA PAPER 93-0669] p 465 A93-24778
- A new procedure for dynamic adaption of three-dimensional unstructured grids
[AIAA PAPER 93-0672] p 560 A93-24780
- Two-dimensional Navier-Stokes analysis of high-lift multi-element airfoils using the q-omega turbulence model
[AIAA PAPER 93-0679] p 466 A93-24787
- Pressure-based high-order TVD methodology for dynamic stall simulation
[AIAA PAPER 93-0680] p 466 A93-24788
- Finite element analysis of the Scramaccelerator with finite rate chemistry
[AIAA PAPER 93-0745] p 540 A93-24833
- A multilevel composite grid method for fluid flow computations
[AIAA PAPER 93-0768] p 541 A93-24852
- A study of CFD algorithms applied to complete aircraft configurations
[AIAA PAPER 93-0784] p 468 A93-24864
- A concurrent hybrid Navier-Stokes/Euler approach to fluid dynamic computations
[AIAA PAPER 93-0789] p 468 A93-24865
- Incompressible flow computation of forces and moments on bodies of revolution at incidence
[AIAA PAPER 93-0787] p 541 A93-24867
- A physically guided zonal approach for two-dimensional aeroflow flows
[AIAA PAPER 93-0790] p 468 A93-24869
- Vortex/surface interaction
[AIAA PAPER 93-0863] p 468 A93-24925
- A study of single jet impingement ground effect lift loss
[AIAA PAPER 93-0869] p 469 A93-24930
- A numerical investigation of a subsonic jet in a crossflow
[AIAA PAPER 93-0870] p 469 A93-24931
- Viscous flow computations of flow field around an advanced propeller
[AIAA PAPER 93-0873] p 469 A93-24934
- Investigation of methods for modeling propeller-induced flow fields
[AIAA PAPER 93-0874] p 469 A93-24935
- A fully implicit Navier-Stokes algorithm using an unstructured grid and flux difference splitting
[AIAA PAPER 93-0875] p 470 A93-24936
- A comparison of 'new' and 'old' flux-splitting schemes for the Euler equations
[AIAA PAPER 93-0876] p 470 A93-24937
- Jacobian update strategies for quadratic and near-quadratic convergence of Newton and Newton-like implicit schemes
[AIAA PAPER 93-0878] p 470 A93-24939
- Computation of inviscid flowfield around 3-D aerospace vehicles and comparison with experimental and flight data
[AIAA PAPER 93-0885] p 470 A93-24944
- Numerical simulation of supersonic flow around space plane for airframe-engine integration
[AIAA PAPER 93-0886] p 471 A93-24946
- Numerical investigation of supersonic flows around a spiked blunt-body
[AIAA PAPER 93-0887] p 471 A93-24947
- TGV tunnel entry simulations using a finite element code with automatic remeshing
[AIAA PAPER 93-0890] p 471 A93-24950
- Computing 3-D steady supersonic flow via a new Lagrangian approach
[AIAA PAPER 93-0891] p 471 A93-24951
- Hypersonic inviscid and viscous flow computations with a new optimized thermodynamic equilibrium model
[AIAA PAPER 93-0893] p 471 A93-24953
- An upwind, kinetic flux-vector splitting method for flows in chemical and thermal non-equilibrium
[AIAA PAPER 93-0894] p 472 A93-24954
- Aerodynamic analyses for design and education
[AIAA PAPER 92-2664] p 473 A93-24988
- Experimental and numerical delta wing study at high angles of attack and sideslip
[AIAA PAPER 92-2713] p 473 A93-24990
- Numerical investigation of flow field in a turbine volute
[AIAA PAPER 93-0155] p 542 A93-25505
- Artificial viscosity models for the Navier-Stokes equations and their effect in drag prediction
[AIAA PAPER 93-0193] p 473 A93-25511
- Structure of vortex breakdown on a pitching delta wing
[AIAA PAPER 93-0434] p 474 A93-25528
- Computational analysis of methods for reduction of induced drag
[AIAA PAPER 93-0524] p 474 A93-25536
- Numerical study of an axisymmetric turbulent jet-impinging flow
[AIAA PAPER 93-0652] p 543 A93-25545
- Nonreflecting boundary conditions for linearized unsteady aerodynamic calculations
[AIAA PAPER 93-0882] p 475 A93-25553
- Parameter effects on turbulent swirling flames in combustors
p 534 A93-25911
- Modelling of the flow in the blade-ring design process of turbomachinery
p 520 A93-27291
- A time dependent method in finite volume for transonic diffuser turbulent flows
p 476 A93-27368
- On the accurate prediction of the wall-normal velocity in compressible boundary-layer flow
p 477 A93-27474
- Numerical experiments on the stability of leading edge boundary layer flow - A two-dimensional linear study
p 477 A93-27475
- A numerical study of mixing in supersonic combustors with hypermixing injectors
[AIAA PAPER 93-0215] p 520 A93-27801
- High-performance aircraft propulsion research
p 529 A93-27904
- Physics of forced unsteady flow for a NACA 0015 airfoil undergoing constant-rate pitch-up motion
p 478 A93-27922
- Investigation of vortex breakdown on delta wings using Navier-Stokes equations
p 478 A93-27924
- Prediction of asymmetric vortical flows around slender bodies using Navier-Stokes equations
p 478 A93-27925
- Hypersonic viscous flow simulations
p 478 A93-27926
- Fluid flows around cascades
p 479 A93-28518
- Solution-adaptive and quality-enhancing grid generation
p 480 A93-28610
- Numerical study of the flow establishment time in hypersonic shock tunnels
p 480 A93-29153
- Compressible flow in a hovercraft air cushion
p 480 A93-29316
- Structure-attached corotational fluid grid for transient aeroelastic computations
p 480 A93-29326
- Euler solutions to nonlinear acoustics of non-lifting rotor blades
p 568 A93-29433
- The development of a CFD potential method for the analysis of tilt-rotors
p 481 A93-29434
- Karman vortex street-airfoil interaction
p 678 A93-33703
- Finite-volume-TVD scheme for 3-D Euler transonic flow computations in rotating curvilinear coordinates
p 679 A93-33709
- On the favorable interference in the supersonic flow
p 679 A93-33713
- Numerical solution of non-isentropic transonic cascade flow by time-marching method
p 679 A93-33715

- The numerical calculation and application of compressible boundary layers on laminar-flow-control and natural-laminar-flow wings p 680 A93-33727
- Solution of Euler equations for complex forebody-inlet combinations p 680 A93-33730
- Numerical simulation of the turbulent drag reduction by plate manipulators p 681 A93-33736
- The analysis and computation of viscous-inviscid interactive problem for three dimensional transonic flow p 681 A93-33741
- A method of predicting quasi-steady aerodynamics for flutter analysis of high speed vehicles using steady CFD calculations [AIAA PAPER 93-1364] p 682 A93-33931
- Numerical simulation of starting process in a hypersonic nozzle p 684 A93-34275
- Numerical methods in laminar and turbulent flow; Proceedings of the 7th International Conference, Stanford Univ., CA, July 15-19, 1991. Vol. 7, pts. 1 & 2 [ISBN 0-906674-77-8] p 743 A93-34301
- Spreadsheet microcomputer numerical method for the compressible laminar wake flow p 684 A93-34308
- Turbulence and stall in plane diffusers - Computational study p 744 A93-34311
- Numerical analysis of the three-dimensional boundary layer on a turbomachinery rotor blade p 685 A93-34341
- Calculation of the flow around a high-lift airfoil using an explicit code and an algebraic Reynolds stress model p 685 A93-34344
- Comparison of several convection discretization schemes for all Mach number arbitrary 2D flows p 685 A93-34345
- A cell-vertex TVD scheme for transonic viscous flow p 685 A93-34346
- A technique for accelerated convergence in transonic flow p 685 A93-34347
- Numerical simulation of inviscid transonic flow over two-dimensional slender bodies p 686 A93-34348
- Implicit numerical solution of transonic flows using adaptive triangular grids p 686 A93-34349
- An implicit treatment of two equations turbulence models for high speed flow computations p 686 A93-34350
- Compressible flow calculations using a two-equation turbulence model and unstructured grids p 686 A93-34351
- An Euler code with new energy equation and new enthalpy damping approach p 686 A93-34352
- Reacting gas and surface coupling in high temperature air flows p 686 A93-34353
- Taking into account surface roughness in computing hypersonic re-entry body p 686 A93-34354
- Computation of supersonic crossflow separation using a new parabolized Navier-Stokes code p 687 A93-34355
- Numerical simulation of hypersonic rarefied gas flow over blunt bodies p 687 A93-34356
- Numerical simulation of two-dimensional compressible flows p 687 A93-34357
- Reactive and dissipative hypersonic flow in a wind tunnel nozzle p 687 A93-34358
- Computation of turbulent compressible flows on a DLR wing and a blade to blade passage using an upwind scheme p 687 A93-34359
- Computation of viscous transonic aeroflow flows using eddy-viscosity based turbulence models p 687 A93-34360
- Dynamically adaptive grid and its applications to flow problems p 688 A93-34362
- An integrated flow simulation system on a parallel computer. I - Basic concept. II - The flow solver p 688 A93-34370
- Multipassage three-dimensional Navier-Stokes simulation of turbine rotor-stator interaction p 688 A93-34484
- Computations and experiments for a multiple normal shock/boundary-layer interaction p 688 A93-34486
- Using a full potential solver for propulsion system exhaust simulation p 689 A93-34487
- Study on vortex generator flow control for the management of inlet distortion p 689 A93-34488
- Computational study of advanced exhaust system transition ducts with experimental validation p 689 A93-34490
- Nonreflecting boundary conditions of three-dimensional Euler equation calculations for strut cascades p 689 A93-34491
- Convenient method to convert two-dimensional CFD codes into axisymmetric ones p 689 A93-34499
- Experimental validation of a discrete vortex method for inviscid axisymmetric flow around parachute canopies [AIAA PAPER 93-1216] p 689 A93-35165
- Temperature and suction effects on the instability of an infinite swept attachment line p 691 A93-35486
- Implicit upwind solution algorithms for three-dimensional unstructured meshes p 691 A93-35607
- Hypersonic nonequilibrium flow computations using the Roe flux-difference split scheme p 692 A93-35609
- Study of supersonic intersection flowfield at modified wing-body junctions p 692 A93-35621
- URNS - A free-wake Euler/Navier-Stokes numerical method for helicopter rotors p 692 A93-35634
- Numerical simulation of a hovering rotor using embedded grids p 765 A93-35936
- Navier-Stokes correlations to fuselage wind tunnel test data p 765 A93-35937
- Vortex methods for the computational analysis of rotor/body interaction p 765 A93-35939
- Three-dimensional calculations of rotor-airframe interaction in forward flight p 795 A93-35940
- Computational investigation of a pneumatic forebody flow control concept p 768 A93-37383
- Application of Oswatitsch's theorem to supercritical airfoil drag calculation p 768 A93-37399
- CFD development and a future high speed computer p 847 A93-38128
- The application of CFD to turbomachine design - Past and future p 769 A93-38130
- Turbulent flow simulation around the aeroflow with pseudo-compressibility p 830 A93-38155
- Numerical calculation of separated flows around wing section in unsteady motion by using incompressible Navier-Stokes equations p 770 A93-38158
- Numerical solution of viscous compressible flows using algebraic turbulence models p 770 A93-38162
- Viscous nonequilibrium flow calculations [ONERA, TP NO. 1992-89] p 771 A93-38573
- Calculations of viscous nonequilibrium flows in nozzles [ONERA, TP NO. 1992-91] p 771 A93-38574
- Supersonic vortical flows around an ogive-cylinder - Laminar and turbulent computations [ONERA, TP NO. 1992-111] p 771 A93-38588
- Structured grid variational adaption - Reaching the limit? [ONERA, TP NO. 1992-114] p 771 A93-38590
- Aerodynamic rotor loads prediction method with free wake for low speed descent flights [ONERA, TP NO. 1992-122] p 772 A93-38596
- Application of European CFD methods for helicopter rotors in forward flight [ONERA, TP NO. 1992-125] p 772 A93-38599
- Numerical calculation of helicopter rotor equations and comparison with experiment [ONERA, TP NO. 1992-128] p 772 A93-38602
- Transonic and supersonic flow calculations around aircrafts using a multidomain Euler code [ONERA, TP NO. 1992-137] p 772 A93-38610
- Some special purpose preconditioners for conjugate gradient-like methods applied to CFD p 772 A93-38638
- Characteristics of three-dimensional turbulent jets in crossflow p 772 A93-38695
- Viscous-inviscid calculation of high-lift separated compressible flows over airfoils and wings [ONERA, TP NO. 1992-184] p 774 A93-38746
- Supersonic flow of a gas over a semiinfinite plate with small-scale harmonic spanwise oscillations p 775 A93-39118
- Computational flow predictions for hypersonic drag devices p 777 A93-39257
- Navier-Stokes stall predictions using an algebraic Reynolds-stress model p 778 A93-39260
- Lifting line theory for supersonic flow applications p 778 A93-39402
- Stabilization of the Burnett equations and application to hypersonic flows p 778 A93-39410
- Newtonian and hypersonic flows over oscillating bodies of revolution. I - Circular cones p 857 A93-39942
- Some contributions to propulsion theory - The Stream Force Theorem and applications to propulsion p 924 A93-40472
- Application of the multigrid solution technique to hypersonic entry vehicles [AIAA PAPER 93-2721] p 858 A93-41049
- Comparison of coordinate-invariant and coordinate-aligned upwinding for the Euler equations [AIAA PAPER 93-3306] p 858 A93-41053
- The numerical model of supersonic air flow field with hydrogen transverse injection p 859 A93-41736
- Accuracy of flux-split algorithms in high-speed viscous flows p 860 A93-41912
- Spectral solution of the viscous blunt-body problem p 860 A93-41915
- Analysis of hypersonic nozzles including vibrational nonequilibrium and intermolecular force effects p 861 A93-41916
- On model for predicting blade force defect in end wall boundary layer inside axial compressor cascade p 862 A93-42271
- International Symposium on Computational Fluid Dynamics, 4th, Univ. of California, Davis, Sept. 9-12, 1991, Selected Papers p 862 A93-42426
- A multidimensional generalization of Roe's flux difference splitter for the Euler equations p 863 A93-42437
- Enhanced numerical inviscid and viscous fluxes for cell centered finite volume schemes p 864 A93-42444
- Analysis of implicit treatments for a centered Euler solver p 864 A93-42449
- Comments on experiments for computational validation for fluid dynamic predictions p 927 A93-42578
- Computational fluid dynamics for hypersonic airbreathing aircraft p 865 A93-42581
- CFD for hypersonic propulsion p 865 A93-42585
- Computation of hypersonic turbulent flow over a rearward facing step p 865 A93-42587
- Computational results for 2-D and 3-D ramp flows with an upwind Navier-Stokes solver p 866 A93-42592
- Computation of flows over 2D ramps p 866 A93-42595
- Computational results for flows over compression ramps p 866 A93-42599
- A synthesis of results on the calculation of flow over a 2D ramp and a 3D obstacle - Antibes test cases 3 and 4 p 867 A93-42601
- Solution of the Euler equations around a double ellipsoidal shape using unstructured meshes and including real gas effects p 867 A93-42604
- Navier-Stokes calculations over a double ellipse and a double ellipsoid by an implicit non-centered method p 867 A93-42607
- Computation of the hypersonic flow over a double ellipsoid p 868 A93-42610
- Hypersonic viscous flow past double ellipse and past double ellipsoid - Numerical results p 868 A93-42618
- Attempt to evaluate the computations for test case 6.1 - Cold hypersonic flow past ellipsoidal shapes p 869 A93-42620
- A contribution to the prediction of hypersonic non-equilibrium flows p 869 A93-42624
- Hypersonic leeside delta-wing-flow computations using centered schemes p 870 A93-42635
- Appraisal of the rarefied flow computations (problems 6.4.1 and 7.2.1) p 871 A93-42640
- Quasi monodimensional inviscid non equilibrium nozzle flow computation p 927 A93-42646
- On the accuracy and efficiency of CFD methods in real gas hypersonics p 871 A93-42869
- Treatment of vortex sheets for the transonic full-potential equation p 871 A93-42870
- Blade row interaction effects on compressor measurements p 900 A93-42885
- Inviscid finite-volume lambda formulation p 872 A93-42888
- Multigrid calculation of three-dimensional viscous cascade flows p 872 A93-42889
- Numerical solution of axisymmetric heat conduction problems using finite control volume technique p 928 A93-42909
- A numerical study of wave propagation in a confined mixing layer by eigenfunction expansions p 873 A93-43629
- Efficient free wake calculations using analytical/numerical matching p 874 A93-43780
- An approximate method for calculating heating rates on three-dimensional vehicles [AIAA PAPER 93-2881] p 949 A93-44228
- Unstructured grids on NURBS surfaces - NonUniform Rational B-Splines [AIAA PAPER 93-3454] p 949 A93-44232
- Mesh generation for the computation of flowfields over complex aerodynamic shapes p 995 A93-44888
- A perspective on a quarter century of CFD research [AIAA PAPER 93-3291] p 1021 A93-44995
- The NASA Computational Fluid Dynamics (CFD) program - Building technology to solve future challenges [AIAA PAPER 93-3292] p 1041 A93-44996
- The status of CFD - An Air Force perspective [AIAA PAPER 93-3293] p 1021 A93-44997
- Computations of inviscid compressible flows using fluctuation-splitting on triangular meshes [AIAA PAPER 93-3301] p 950 A93-44999
- Field by field hybrid upwind splitting methods [AIAA PAPER 93-3302] p 950 A93-45000
- A multi-dimensional kinetic-based upwind solver for the Euler equations [AIAA PAPER 93-3303] p 950 A93-45001
- New upwind dissipation models with a multidimensional approach [AIAA PAPER 93-3304] p 950 A93-45002
- An extended Lagrangian method [AIAA PAPER 93-3305] p 951 A93-45003
- Solution of the Euler and Navier Stokes equations on parallel processors using a transposed/Thomas ADI Algorithm [AIAA PAPER 93-3310] p 1036 A93-45006

- Adaptive-prismatic-grid method for external viscous flow computations
[AIAA PAPER 93-3314] p 951 A93-45010
- An implicit time-marching procedure for high speed flow
[AIAA PAPER 93-3315] p 951 A93-45011
- Variant bi-conjugate gradient methods for the compressible Navier-Stokes solver with a two-equation model of turbulence
[AIAA PAPER 93-3316] p 951 A93-45012
- A coarse-grid correction/nonlinear relaxation algorithm for the three-dimensional, compressible Navier-Stokes equations
[AIAA PAPER 93-3317] p 951 A93-45013
- Two-dimensional CFD modeling of wave rotor flow dynamics
[AIAA PAPER 93-3318] p 952 A93-45014
- Aerodynamic shape optimization using preconditioned conjugate gradient methods
[AIAA PAPER 93-3322] p 952 A93-45016
- Calculation of optimum airfoils using direct solutions of the Navier-Stokes equations
[AIAA PAPER 93-3323] p 952 A93-45017
- Numerical experiment of the flight trajectory simulation by fluid dynamics and flight dynamics coupling
[AIAA PAPER 93-3324] p 952 A93-45018
- Progress in local preconditioning of the Euler and Navier-Stokes equations
[AIAA PAPER 93-3328] p 952 A93-45022
- Pseudo-compressibility methods for the incompressible flow equations
[AIAA PAPER 93-3329] p 952 A93-45023
- Numerical wave propagation and steady state solutions. II - Bulk Viscosity Damping
[AIAA PAPER 93-3331] p 953 A93-45025
- Euler solutions for blunt bodies using triangular meshes - Artificial viscosity forms and numerical boundary conditions
[AIAA PAPER 93-3333] p 953 A93-45027
- Surface boundary conditions for the numerical solution of the Euler equations
[AIAA PAPER 93-3334] p 953 A93-45028
- An accuracy assessment of Cartesian-mesh approaches for the Euler equations
[AIAA PAPER 93-3335] p 953 A93-45029
- An efficient method to calculate rotor flow in hover and forward flight
[AIAA PAPER 93-3336] p 953 A93-45030
- Three-dimensional unstructured grid Euler computations using a fully-implicit, upwind method
[AIAA PAPER 93-3337] p 953 A93-45031
- A 3D unstructured adaptive multigrid scheme for the Euler equations
[AIAA PAPER 93-3339] p 954 A93-45033
- Numerical vorticity capturing for vortex-solid body interaction problems
[AIAA PAPER 93-3343] p 954 A93-45037
- A three-dimensional Delaunay unstructured grid generator and flow solver for bodies in relative motion
[AIAA PAPER 93-3349] p 954 A93-45043
- A graphically interactive approach to structured and unstructured surface grid quality analysis
[AIAA PAPER 93-3351] p 954 A93-45045
- Effects of spatial order of accuracy on the computation of vortical flowfields
[AIAA PAPER 93-3371] p 955 A93-45064
- Adaptive inviscid flow solutions for aerospace geometries on efficiently generated unstructured tetrahedral meshes
[AIAA PAPER 93-3390] p 956 A93-45081
- A simulation technique for 2-D unsteady inviscid flows around arbitrarily moving and deforming bodies of arbitrary geometry
[AIAA PAPER 93-3391] p 956 A93-45082
- Unsteady flow simulation on a parallel computer
p 1022 A93-45089
- An acceleration technique for time accurate calculations of unsteady flow around pitching delta wings
p 957 A93-45092
- Simulation of flow past complex geometries using a parallel implicit incompressible flow solver
p 957 A93-45095
- Preconditioned domain decomposition scheme for three-dimensional aerodynamic sensitivity analysis
p 957 A93-45096
- Single block three-dimensional volume grids about complex aerodynamic vehicles
p 957 A93-45099
- CFD analysis of the X-29 inlet at high angle of attack
p 958 A93-45140
- Aerospace plane design challenge - Credible computations
p 1015 A93-45145
- Navier-Stokes analysis of three-dimensional S-ducts
p 959 A93-45146
- Air dissociation effects on aerodynamic characteristics of an aerospace plane
p 959 A93-45149
- Shock waves; Proceedings of the 18th International Symposium, Sendai, Japan, July 21-26, 1991. Vols. 1 & 2
[ISBN 0-387-55686-9] p 1023 A93-45451
- Computation of shock diffraction in external and internal flows
p 1024 A93-45537
- Computation of unsteady nozzle flows
p 960 A93-45543
- Computational fluid dynamics code validation using a free piston hypervelocity shock tunnel
p 960 A93-45545
- Numerical simulation of two-dimensional and axis-symmetric compressible flows
p 960 A93-45546
- Hypersonic flow calculations using a multidomain MUSCL Euler solver
p 960 A93-45547
- Computation of crossing shock/turbulent boundary layer interaction at Mach 8.3
p 961 A93-45726
- Adaptive refinement-coarsening scheme for three-dimensional unstructured meshes
p 961 A93-45735
- Solution strategy for three-dimensional configurations at hypersonic speeds
p 962 A93-46406
- Low-to-high altitude predictions of three-dimensional ablative re-entry flowfields
p 1027 A93-46407
- Enhancements to viscous-shock-layer technique
p 962 A93-46408
- Hypersonic blunt body wake computations using DSMC and Navier-Stokes solvers
[AIAA PAPER 93-2807] p 964 A93-46547
- Navier-Stokes simulations of the Shuttle Orbiter aerodynamic characteristics with emphasis on pitch trim and bodyflap
[AIAA PAPER 93-2814] p 965 A93-46552
- A numerical solution of the asymptotic problem of boundary layer separation in an incompressible liquid upstream of the corner point of a body
p 965 A93-46699
- Artificial transition - A tool for high Reynolds number simulation?
[AIAA PAPER 93-3258] p 967 A93-46799
- Kinematic domain decomposition for boundary-motion-induced flow simulations
p 1028 A93-46811
- Supersonic/hypersonic aerodynamic methods for aircraft design and analysis
p 967 A93-46816
- A three dimensional view of velocity using lasers
p 1028 A93-46822
- The practical application of solution-adaption to the numerical simulation of complex turbomachinery problems
p 970 A93-46916
- Direct and inverse problems of calculating the axisymmetric and 3D flow in axial compressor blade rows
p 972 A93-46938
- Multigrid methods for calculating 3D flows in complex geometries
p 973 A93-46984
- Numerical solution of steady and unsteady Euler equations
p 973 A93-46988
- Requirements for facilities and measurement techniques to support CFD development for hypersonic aircraft
p 1014 A93-47024
- Finite element solution of the 3D compressible Navier-Stokes equations by a velocity-vorticity method
p 974 A93-47196
- AIAA Applied Aerodynamics Conference, 11th, Monterey, CA, Aug. 9-11, 1993, Technical Papers. Pts. 1 & 2
p 974 A93-47201
- Adaptive computations of flow around a delta wing with vortex breakdown
[AIAA PAPER 93-3400] p 974 A93-47202
- Numerical simulation of wing-wall juncture flow for a pitching wing
[AIAA PAPER 93-3401] p 974 A93-47203
- Unsteady flow computations for a three-dimensional cavity with and without an acoustic suppression device
[AIAA PAPER 93-3402] p 974 A93-47204
- Computations of aerodynamic drag for turbulent transonic projectiles with and without spin
[AIAA PAPER 93-3416] p 975 A93-47212
- An improved far field drag calculation method for nonlinear CFD codes
[AIAA PAPER 93-3417] p 975 A93-47213
- CFD drag predictions for a wide body transport fuselage with flight test verification
[AIAA PAPER 93-3418] p 976 A93-47214
- Computational analysis of drag reduction and buffet alleviation in viscous transonic flow over porous airfoils
[AIAA PAPER 93-3419] p 976 A93-47215
- A zonal CFD method for three-dimensional wing simulations
[AIAA PAPER 93-3433] p 977 A93-47225
- Unstructured viscous grid generation by advancing-layers method
[AIAA PAPER 93-3453] p 979 A93-47238
- Computation of passively controlled transonic wing
[AIAA PAPER 93-3474] p 981 A93-47253
- Grid and aerodynamic sensitivity analyses of airplane components
[AIAA PAPER 93-3475] p 981 A93-47254
- Calculation of AGARD Wing 445.6 flutter using Navier-Stokes aerodynamics
[AIAA PAPER 93-3476] p 981 A93-47255
- High lift multiple element airfoil analysis with unstructured grids
[AIAA PAPER 93-3478] p 981 A93-47256
- On the modelling of separated flows about airfoils
[AIAA PAPER 93-3479] p 981 A93-47257
- Application of computational fluid dynamics in transonic aerodynamic design
[AIAA PAPER 93-3481] p 982 A93-47259
- A computational method for inverse design of transonic airfoil and wing
[AIAA PAPER 93-3482] p 982 A93-47260
- Computational analysis of off-design waveriders
[AIAA PAPER 93-3488] p 982 A93-47262
- Numerical simulation of incompressible viscous flow around a propeller
[AIAA PAPER 93-3503] p 984 A93-47271
- Computational study of a conical wing having unit aspect ratio at supersonic speeds
[AIAA PAPER 93-3505] p 984 A93-47272
- Experimental and computational investigations of the flowfield around the F117A
[AIAA PAPER 93-3508] p 984 A93-47274
- Computation of wake roll-up for complete aircraft configurations
[AIAA PAPER 93-3509] p 984 A93-47275
- Semi-discrete Galerkin solution of the compressible boundary-layer equations with viscous-inviscid interaction
[AIAA PAPER 93-3520] p 985 A93-47282
- A pointwise version of the Baldwin-Barth turbulence model
[AIAA PAPER 93-3523] p 985 A93-47284
- Navier-Stokes calculations of rotating BERP platform blade flowfields
[AIAA PAPER 93-3527] p 986 A93-47286
- Calculation of V/STOL aircraft aerodynamics with deflected jets in ground effect
[AIAA PAPER 93-3530] p 986 A93-47287
- Application of a parabolized Navier-Stokes code to an HSCT configuration and comparison to wind tunnel test data
[AIAA PAPER 93-3537] p 986 A93-47288
- Multiple solutions of the transonic perturbation equation
p 987 A93-47331
- Aerodynamic flow simulation using a pressure-based method and a two-equation turbulence model
[AIAA PAPER 93-2902] p 1147 A93-48111
- Trajectory mapping of quasi-periodic structures in a vortex flow
[AIAA PAPER 93-2914] p 1044 A93-48116
- Interpretation of waverider performance data using computational fluid dynamics
[AIAA PAPER 93-2921] p 1044 A93-48122
- CFD study of the flowfield due to a supersonic jet exiting into a hypersonic stream from a conical surface. II
[AIAA PAPER 93-2926] p 1045 A93-48127
- Numerical solution of the Euler equations for complex aerodynamic configurations using an edge-based finite element scheme
[AIAA PAPER 93-2933] p 1046 A93-48131
- High resolution numerical simulation of the linearized Euler equations in conservation law form
[AIAA PAPER 93-2934] p 1148 A93-48132
- A CFD-based design strategy for advanced transonic wing concepts with practical ramifications for subsonic transports
[AIAA PAPER 93-2946] p 1047 A93-48143
- Asymmetric vortical solutions in supersonic corners - Steady 3D space-marching versus time-dependent conical results
[AIAA PAPER 93-2957] p 1047 A93-48151
- Some practical turbulence modeling options for Reynolds-averaged full Navier-Stokes calculations of three-dimensional flows
[AIAA PAPER 93-2964] p 1048 A93-48158
- Numerical solution of Navier-Stokes equations and k-omega turbulence model equations using a staggered upwind method
[AIAA PAPER 93-2968] p 1049 A93-48162
- Precise pitching airfoil computations by use of dynamic unstructured meshes
[AIAA PAPER 93-2971] p 1049 A93-48165
- Computational study of vortex breakdown on a pitching delta wing
[AIAA PAPER 93-2974] p 1050 A93-48168
- Computation of delta-wing roll maneuvers
[AIAA PAPER 93-2975] p 1050 A93-48169
- A high-order streamline Godunov scheme for steady hypersonic equilibrium flows
[AIAA PAPER 93-2997] p 1053 A93-48187

SUBJECT INDEX

COMPUTATIONAL FLUID DYNAMICS

Multi-block calculations for flows in local chemical equilibrium p 1053 A93-48189
 A computational and experimental investigation of a delta wing with vertical tails p 1054 A93-48199
 Transonic mutual interference of wing-pylon-multiple body configurations using an overlapping grid scheme [AIAA PAPER 93-3023] p 1055 A93-48208
 CFD code calibration and inlet-fairing effects on a 3D hypersonic powered-simulation model p 1056 A93-48222
 The European Data Base - A new CFD validation tool for the design of space vehicles p 1057 A93-48225
 Code validation for high speed flow simulation over the VLS launcher fairing - Brazilian satellite launch vehicles [AIAA PAPER 93-3046] p 1057 A93-48226
 An initial comparison of CFD with experiment for a geometrically simplified STOVL model p 1058 A93-48236
 Experimental and numerical study of transonic turbine cascade flow p 1059 A93-48240
 Free-wake computation of helicopter rotor flowfields in forward flight p 1059 A93-48253
 DSMC numerical investigation of rarefied compression corner flow p 1061 A93-48270
 A two layer k-epsilon computation of transonic viscous flow including separation over the DLR-F5 wing [AIAA PAPER 93-3110] p 1061 A93-48281
 Shape optimization for aerodynamic efficiency and low observability p 1062 A93-48285
 Hypersonic configuration optimization with an Euler/boundary layer coupling technique p 1062 A93-48286
 AIAA Atmospheric Flight Mechanics Conference, Monterey, CA, Aug. 9-11, 1993, Technical Papers p 1125 A93-48301
 On computing vortex asymmetries about cones at angle of attack using the conical Navier-Stokes equations [AIAA PAPER 93-3628] p 1064 A93-48313
 Analysis of missile configurations with wrap-around fins using computational fluid dynamics p 1064 A93-48316
 Navier-Stokes computations on full-span wing-body configuration with oscillating control surfaces [AIAA PAPER 93-3687] p 1065 A93-48356
 A calculation of secondary flows and deviation angles in multistage axial-flow compressors p 1066 A93-48509
 Slush hydrogen quantity gaging and mixing for the National Aerospace Plane p 1150 A93-48635
 Approximate method for the aerodynamic design of flight vehicles for high supersonic flight speeds p 1069 A93-48966
 Some Fuchs-type equations in fluid mechanics p 1165 A93-48967
 Three-dimensional time-marching aerodynamic analyses using an unstructured-grid Euler method p 1100 A93-49012
 Model for entropy production and pressure variation in confined turbulent mixing p 1071 A93-49014
 A computer program for meridional flows in multistage axial flow compressors with turbulence and multi-effects of 3-D flows p 1165 A93-49186
 A method for calculating the aerodynamic and mass characteristics of coaxial rotors with rigid blade fastening (the ABC system) p 1071 A93-49323
 Heat Transfer and Fluid Mechanics Institute, 33rd, California State Univ., Sacramento, June 3, 4, 1993, Proceedings p 1152 A93-49505
 Computational methods in hypersonic aerodynamics [ISBN 0-7923-1673-8] p 1072 A93-49521
 Introduction to the physical aspects of hypersonic aerodynamics p 1072 A93-49522
 Computational methods for viscous hypersonic flows p 1152 A93-49523
 Efficient multigrid computation of steady hypersonic flows p 1152 A93-49527
 Second-order effects in hypersonic laminar boundary layers p 1073 A93-49529
 Real gas effects in two- and three-dimensional hypersonic, laminar boundary layers p 1073 A93-49530
 Flow analysis and design optimization methods for nozzle-afterbody of a hypersonic vehicle p 1073 A93-49531
 The computation over unstructured grids of inviscid hypersonic reactive flow by upwind finite-volume schemes p 1073 A93-49532
 Computational aerothermodynamics for 2D and 3D space vehicles p 1073 A93-49533

A nonperiodic boundary approach for computation of compressible viscous flows in advanced turbine cascades p 1074 A93-49688
 Analysis of a high bypass ratio engine installation using the chimera domain decomposition technique [AIAA PAPER 93-1808] p 1100 A93-49697
 Calculation of scramjet inlet with thick boundary-layer ingestion p 1074 A93-49720
 CFD analysis and testing on a twin inlet ramjet [AIAA PAPER 93-1839] p 1075 A93-49723
 CFD validation for scramjet combustor and nozzle flows. I p 1111 A93-49724
 3-D viscous flow CFD analysis of the propeller effect on an advanced ducted propeller subsonic inlet [AIAA PAPER 93-1847] p 1075 A93-49728
 A staggered finite volume scheme for solving cascade flow with a two-equation model of turbulence [AIAA PAPER 93-1912] p 1076 A93-49779
 An unstructured grid flow solver for turbomachinery flows p 1076 A93-49780
 An adaptive grid/Navier-Stokes methodology for the calculation of nozzle afterbody base flows with a supersonic freestream [AIAA PAPER 93-1922] p 1076 A93-49788
 CFD applications in an aeropropulsion test environment p 1112 A93-49790
 The numerical calculation on the flowfields of transverse jet interaction in the base of vehicle at supersonic speeds p 1077 A93-49795
 Boundary condition procedures for CFD analyses of propulsion systems - The multi-zone problem [AIAA PAPER 93-1971] p 1077 A93-49819
 Summary of the GASP code application and evaluation effort for scramjet combustor flowfields [AIAA PAPER 93-1973] p 1077 A93-49820
 Secondary flow computation by means of an inviscid multigrid Finite Volume Lambda Formulation [AIAA PAPER 93-1974] p 1077 A93-49821
 An unstructured adaptive quadrilateral mesh-based scheme for viscous turbomachinery flow calculations [AIAA PAPER 93-1975] p 1077 A93-49822
 Computation of the flow field in an annular gas turbine combustor p 1113 A93-49903
 An iterative multidisciplinary analysis for rotor blade shape determination p 1114 A93-49912
 Mixing enhancement and combustion of gaseous fuel in a supersonic combustor p 1114 A93-49960
 An investigation of shock wave turbulent boundary layer interaction with bleed through normal and slanted slots [AIAA PAPER 93-2155] p 1079 A93-49971
 Applying and validating the RANS-3D flow-solver for evaluating a subsonic serpentine diffuser geometry [AIAA PAPER 93-2157] p 1079 A93-49973
 Integrated CFD modeling of gas turbine combustors [AIAA PAPER 93-2196] p 1115 A93-50008
 Advanced SST auxiliary air intakes design and analysis p 1082 A93-50088
 Using a diagonal implicit algorithm to calculate transonic nozzle flow p 1082 A93-50119
 A comparison between centered and upwind schemes for two-phase compressible flows p 1083 A93-50120
 A numerical analysis of supersonic flow over an axisymmetric afterbody p 1083 A93-50121
 Multistage turbomachinery flow solutions using three-dimensional implicit Euler method [AIAA PAPER 93-2382] p 1083 A93-50150
 Experimental and numerical study of swept ramp injection into a supersonic flowfield [AIAA PAPER 93-2445] p 1119 A93-50197
 A comparison between numerically modelled and experimentally measured loss mechanisms in wave rotors p 1120 A93-50252
 Navier-Stokes analysis of radial turbine rotor performance [AIAA PAPER 93-2555] p 1121 A93-50277
 Decreasing F-16 nozzle drag using computational fluid dynamics p 1084 A93-50289
 3-D turbomachinery Euler and Navier-Stokes calculations with a multidomain cell-centered approach [AIAA PAPER 93-2576] p 1085 A93-50292

Substitution of oriented differences for central differences in a program for calculating smooth supersonic flows p 1085 A93-50966
 Calculation of perturbation propagation upstream in a hypersonic laminar boundary layer p 1086 A93-50968
 A fourth-order MUSCL finite-difference scheme for solving the unsteady compressible Euler equations p 1086 A93-51121
 A new technique for analysis of unsteady aerodynamic responses of cascade airfoils with blunt leading edge - Unsteady aerodynamic responses of the cascade in incompressible flow p 1086 A93-51122
 Analysis of wake-induced unsteady flow in axial compressors - Radial variations of wake excitation forces estimated by strip theory p 1086 A93-51123
 Numerical aspects of a block structured compressible flow solver p 1169 A93-51279
 A collocated finite volume method for predicting flows at all speeds p 1087 A93-51736
 A second-order upwind finite-volume method for the Euler solution on unstructured triangular meshes p 1087 A93-51738
 Numerical solutions of Euler equations by using a new flux vector splitting scheme p 1087 A93-51740
 New calculation methods contribution on turbomachinery design and development [ONERA, TP NO. 1993-60] p 1092 A93-51940
 Implicit schemes for unsteady Euler equations on unstructured meshes [ONERA, TP NO. 1993-64] p 1171 A93-51944
 A time-accurate high-resolution TVD scheme for solving the Navier-Stokes equations p 1093 A93-52006
 Computational effects of inlet representation on powered hypersonic, airbreathing models p 1094 A93-52427
 Numerical simulation of unsteady flow induced by a flat plate moving near ground p 1094 A93-52432
 Euler/experiment correlations of sonic boom pressure signatures p 1095 A93-52439
 Investigation of vortex development on a pitching slender body of revolution p 1095 A93-52445
 Efficient simulation of incompressible viscous flow over single and multiple airfoils p 1095 A93-52448
 Transonic Navier-Stokes flow computations over wing-fuselage geometries p 1095 A93-52456
 Streaming vorticity flux from oscillating walls with finite amplitude p 1160 A93-52517
 Nonlinear aspects of transonic aerodynamicity p 1096 A93-52642
 Progress towards understanding and predicting heat transfer in the turbine gas path p 1215 A93-52751
 Upwind-biased, point-implicit relaxation strategies for hypersonic flowfield simulations on supercomputers p 1175 A93-52770
 Zonal-local solution method for the turbulent Navier-Stokes equations p 1177 A93-53205
 Low-Reynolds-number k-epsilon model for unsteady turbulent boundary-layer flows p 1177 A93-53208
 Multigrid Navier-Stokes calculations for three-dimensional cascades p 1177 A93-53209
 Space marching calculations about hypersonic configurations using a solution-adaptive mesh algorithm p 1177 A93-53212
 Prismatic grid generation for three-dimensional complex geometries p 1178 A93-53217
 Recent advances in computational analysis of hypersonic vehicles p 1179 A93-53364
 HL-20 computational fluid dynamics analysis p 1181 A93-53740
 Numerical analysis of a flat plate in a pitching motion. II - Effect on the flow of the position of the pivot, etc p 1181 A93-53798
 Study on surge and rotating stall in axial compressors. III - Numerical model for multiblade-row compressors p 1181 A93-53799
 The construction of nearly orthogonal multiblock grids for compressible flow simulation p 1219 A93-53847
 CFD for ramjet and scramjet powered vehicles [ISABE 93-7035] p 1197 A93-54011
 Finite-rate H₂/air combustion effects in CRJ for hypersonic launchers [ISABE 93-7084] p 1202 A93-54060
 Aerodynamic inverse design and analysis for a full engine p 1186 A93-54062
 3D and 2.5D viscous flow computations for axial flow turbine blades p 1186 A93-54069
 A comparative assessment of two present generation turbine analysis codes [ISABE 93-7097] p 1203 A93-54073
 Optimization of afterbodies and engine nozzle by using CFD methods [ISABE 93-7098] p 1187 A93-54074

- Characteristics of heat exchanger in supersonic/subsonic flows
[ISABE 93-7119] p 1221 A93-54094
- Numerical method for simulating fluid-dynamic and heat-transfer changes in jet-engine injector feed-arm due to fouling p 1245 A93-54467
- Computation of nonequilibrium hypersonic flowfields around hemisphere cylinders p 1229 A93-54469
- A new method for resolving transonic nozzle flows using orthogonal stream-lines coordinate system p 1230 A93-54584
- Second generation low order panel method and its application for a case of nacelle p 1231 A93-54595
- A method for aerodynamic calculation by placing linear vari-strength vortex panels on airfoil contour p 1231 A93-54597
- Two problems applied to the rheographical transformation of axisymmetric flow p 1231 A93-54599
- Prediction of viscous flows in rotating machinery using Navier-Stokes techniques p 1232 A93-54639
- Two-dimensional transonic flow around VKI turbine cascade p 1232 A93-54640
- Three-dimensional flow analysis of a four-stage transonic axial compressor with inlet guide vanes p 1232 A93-54643
- Numerical studies of Mach reflection with air chemistry p 1233 A93-54815
- Comparison of confined, compressible, spatially developing mixing layers with temporal mixing layers p 1234 A93-55352
- Developing numerical techniques for solving low Mach number fluid-acoustic problems p 1235 A93-55353
- Locally implicit total variation diminishing schemes on mixed quadrilateral-triangular meshes p 1235 A93-55356
- A new method for predicting the end wall boundary layers and the blade force defects inside the passage of axial compressor cascades p 1236 A93-55589
- Preliminary design of experimental sub-scale scramjet engine [AAS PAPER 91-639] p 1247 A93-55816
- Supersonic and hypersonic flow computations for the research configuration ELAC I and comparison to experimental data p 1237 A93-56034
- Flow computation for the hypersonic configuration ELAC I at low speeds and large incidence p 1238 A93-56036
- Computation of viscous hypersonic non-equilibrium blunt body flow p 1238 A93-56038
- Computation of hypersonic high-temperature nozzle flow p 1238 A93-56040
- On the analysis of an impinging jet on ground effects p 1260 A93-56339
- Aerodynamic investigation of radial turbines using computational methods p 81 N93-10056
- LV software for supersonic flow analysis [NASA-CR-190911] p 16 N93-10069
- Navier-Stokes dynamics and aeroelastic computations for vortical flows, buffet and aeroelastic applications [NASA-CR-190692] p 17 N93-10098
- Improved numerical simulation of Euler equations p 83 N93-10309
- Analysis of wing-body junction flowfields using the incompressible Navier-Stokes equations, volumes 1 and 2 p 17 N93-10320
- Interactive grid generation program for CAP-TSD [NASA-TM-102705] p 17 N93-10349
- Explicit Navier-Stokes computation of turbomachinery flows p 83 N93-10370
- A field panel method for transonic flows p 18 N93-10547
- Artificial intelligence and CFD: Expert systems for the design of airfoils and for grid generation [DIGE-EST-TN-016] p 48 N93-11161
- Overview of high performance aircraft propulsion research [NASA-TM-105839] p 59 N93-11530
- Numerical analysis of the flow fields in a RQL gas turbine combustor [DE92-017509] p 89 N93-11767
- Numerical study of advanced rotor blades p 23 N93-11899
- A wall interference assessment/correction system [NASA-CR-190617] p 68 N93-11910
- Hypervelocity scramjet combustor-nozzle analysis and design [NASA-CR-190965] p 60 N93-12214
- An improved numerical model for wave rotor design and analysis [NASA-TM-105915] p 60 N93-12418
- Report on the final panel discussion on computational aeroacoustics [NASA-CR-189718] p 231 N93-12986
- NASA aeronautics: Research and technology program highlights [NASA-NP-159] p 109 N93-13110
- A numerical study of hypersonic flow with strong surface blowing p 129 N93-13128
- Application of a solution adaptive grid to flow over an embedded cavity p 130 N93-13141
- Turbomachinery CFD on parallel computers [NASA-TM-105932] p 228 N93-13154
- Investigation of interference phenomena of modern wing-mounted high-bypass-ratio engines by the solution of the Euler-equations p 213 N93-13204
- Aerodynamic analysis of slipstream/wing/nacelle interference for preliminary design of aircraft configurations p 130 N93-13205
- Euler analysis of turbofan/superfan integration for a transport aircraft p 214 N93-13206
- The PEP Symposium on CFD Techniques for Propulsion Applications p 214 N93-13210
- AGARD WG13 aerodynamics of high speed air intakes: Assessment of CFD results p 215 N93-13220
- CFD calibration for three-dimensional nozzle/afterbody configurations p 215 N93-13226
- Fluid flow and heat convection studies for actively cooled airframes [NASA-CR-190956] p 216 N93-13406
- Numerical simulation of the acoustic instability in the spatially developing, confined, supersonic mixing layer p 132 N93-13521
- Development and computation of continuum higher order constitutive relations for high-altitude hypersonic flow p 132 N93-13578
- Flow prediction for three-dimensional intakes and ducts using viscous-inviscid interaction methods p 218 N93-13953
- Unsteady three-dimensional thin-layer Navier-Stokes solutions for turbomachinery in transonic flow p 218 N93-14025
- Navier-Stokes flowfield computation of wing/rotor interaction for a tilt rotor aircraft in hover p 135 N93-14035
- Solution of compressible Navier-Stokes equations using spectral methods on arbitrary two-dimensional domains p 218 N93-14041
- An algebraic turbulence model for three-dimensional viscous flows [NASA-TM-105931] p 110 N93-14102
- Active control of combustion instability in a ramjet using large-eddy simulations [AD-A255226] p 175 N93-14111
- A study of viscous interaction effects on hypersonic waveriders p 135 N93-14160
- Pressure drag and lift contributions for blunted forebodies of fineness ratio 2.0 in transonic flow (M infinity less than or equal to 1.4) [ESDU-89033] p 136 N93-14515
- Direct prediction of a separation boundary for aerofoils using a viscous-coupled calculation method [ESDU-92008] p 136 N93-14516
- Passive control of supersonic asymmetric vortical flows around cones p 220 N93-14692
- The 3D Navier-Stokes flow analysis for shared and distributed memory MIMD computers [AD-A256038] p 221 N93-15187
- The Application of CFD to rotary wing flow problems [NASA-TM-102803] p 139 N93-15483
- Special publication of National Aerospace Laboratory [DE93-716195] p 239 N93-15949
- An advanced graphics-interactive system for a multi-block structured grid generation within an industrial environment [ETN-92-92885] p 440 N93-16288
- Hypersonic flows including real gas effects [AERO-REPT-9112] p 289 N93-16467
- Computational study of real gas effects in high speed high temperature flow, volume 2 [AERO-REPT-9203-VOL-2] p 289 N93-16470
- Volume 2: Explicit, multistage upwind schemes for Euler and Navier-Stokes equations [NASA-CR-191647] p 418 N93-16558
- Preliminary efforts toward development of data handling and analysis software for unsteady flow measurements: An application for aeroelastic transonic flow configurations p 291 N93-16768
- Current European rotorcraft research activities on development of advanced CFD methods for the design of rotor blades (BRITE/EURAM DACRO project) [MBB-UD-0601-91-PUB] p 293 N93-17568
- A multi-faceted engineering study of aerodynamic errors of the Service Aircraft Instrumentation Package (SAIP) [AD-A258059] p 293 N93-17677
- Direct numerical simulation of combustion in turbulent supersonic flow [DS-2138] p 393 N93-17746
- Flowfield computations over the Space Shuttle orbiter with a proposed canard at a Mach number of 5.8 and 50 deg angle of attack [AD-A258058] p 293 N93-17756
- Aerodynamic design and analysis of fans using 3D computational codes [DS-2140] p 294 N93-17880
- A numerical study of mixing in supersonic combustors with hypermixing injectors [NASA-CR-191027] p 294 N93-17884
- CFD-based approximation concepts for aerodynamic design optimization with application to a 2-D scramjet vehicle [AD-A258084] p 333 N93-17893
- Experimental Investigation of Nozzle/Plume Aerodynamics at Hypersonic Speeds [NASA-CR-191368] p 386 N93-18085
- H-P adaptive methods for finite element analysis of aerothermal loads in high-speed flows [NASA-CR-189739] p 420 N93-18093
- Modelling of interfacial and thermocline waves [AERO-REPT-9209] p 420 N93-18103
- Introduction to Flutter of Winged Aircraft, volume 1 [VKI-LS-1992-01] p 372 N93-18142
- The unified method of aeroelasticity p 372 N93-18143
- Numerical analysis of the flow in a tubulated rectangular duct simulating the cooling passages in a turbine blade [AD-A257855] p 420 N93-18305
- Computational Fluid Dynamics, volume 2 [VKI-LS-1992-04-VOL-2] p 421 N93-18563
- Parabolized Navier-Stokes methods for hypersonic flows p 421 N93-18565
- Algorithm development with applications to aerodynamics and aeroelasticity p 422 N93-18566
- Simulation of unsteady rotational flow over propfan configuration [NASA-CR-192234] p 296 N93-18585
- Exact-gradient shape optimization of a 2D Euler flow [INRIA-RR-1540] p 422 N93-18623
- Numerical investigation of swirl-airfoil interactions in transonic area [MPIS-8/1991] p 297 N93-18627
- Axial Flow Compressors, volume 1 [VKI-LS-1992-02-VOL-1] p 422 N93-18721
- Numerical investigation of performance degradation of wings and rotors due to icing [NASA-CR-192233] p 339 N93-18783
- The effects of viscosity on a conically derived waverider [AD-A259019] p 424 N93-19101
- Proceedings of the Ninth NAL Symposium on Aircraft Computational Aerodynamics [NAL-SP-16] p 299 N93-19273
- LES turbulence modeling using DNS data base p 299 N93-19274
- A simple grid generation technique for hypersonic flow around complex configuration p 299 N93-19275
- Computation of internal flows using unstructured triangular meshes p 299 N93-19276
- Numerical computations using multi-domain technique p 299 N93-19277
- Numerical simulations of hypersonic rarefied transition regime flows: DSMC method and Navier-Stokes computation p 299 N93-19278
- Monte Carlo simulation of normal shock wave. Part 1: Lennard-Jones potential p 300 N93-19279
- Rarefied gas numerical wind tunnel. Part 7: OREX p 382 N93-19280
- Analysis of a 2-D airfoil motion flying in-proximity-to a wavy-wall surface: Lifting-surface-method p 300 N93-19281
- Analysis of a 2-D airfoil motion flying in-proximity-to a wavy-wall surface: Finite difference method p 300 N93-19282
- Development of a boundary element method program for numerical analysis of supersonic unsteady flow p 300 N93-19283
- Numerical calculations of separating flows around oscillating airfoil p 300 N93-19284
- Numerical simulation of unsteady large scale separated flow around oscillating airfoil p 300 N93-19285
- Calculations of aerodynamic forces on a wing with thrust using BEM p 300 N93-19286
- Numerical Wind Tunnel: Requirements and the outline p 383 N93-19288
- Numerical Wind Tunnel hardware p 383 N93-19289
- The operating system for Numerical Wind Tunnel p 383 N93-19290
- The language processor system for the Numerical Wind Tunnel p 383 N93-19291
- Generation of longitudinal vortices in supersonic flow p 301 N93-19292
- The role of computational fluid dynamics in aeronautical engineering. 9: Analysis of hypersonic equilibrium air flow p 301 N93-19294

Computation of re-entry flows with two-temperature model p 301 N93-19295
 Numerical calculation of hypersonic non-equilibrium flow around OREX p 301 N93-19296
 Numerical simulation of hypersonic flow around H-2 Orbiting Plane (HOPE), part 3 p 301 N93-19297
 The 3D Navier-Stokes calculation of flow about scramjet inlet with strut p 301 N93-19298
 Numerical simulation of flow for a scramjet nozzle p 302 N93-19299
 Transonic flow calculation around NACA-0012 p 302 N93-19301
 Numerical simulations of supersonic flow by a fourth-order compact MUSCL TVD scheme p 302 N93-19308
 Analytical and numerical study on steady Mach reflection p 302 N93-19309
 Numerical simulation of the flow through non-uniform airfoil cascade p 302 N93-19310
 Numerical study on transverse hydrogen injection into a supersonic flowfield p 302 N93-19311
 Aerodynamic heating analysis for axisymmetric bodies in supersonic flow p 303 N93-19312
 Three dimensional calculation of flow inside supersonic inlet p 303 N93-19313
 Numerical simulation of flows in a supersonic air intake p 303 N93-19314
 A numerical investigation for supersonic inlet p 303 N93-19315
 A numerical investigation of 3D transverse injection into the supersonic flow behind rearward facing step p 303 N93-19316
 Numerical calculation of flow field in supersonic combustion chamber p 304 N93-19317
 A numerical simulations of inner flow of scramjet p 304 N93-19318
 Wind tunnel wall interference correction at subsonic speeds p 304 N93-19320
 Two problems reducing the data accuracy in Transonic Wind Tunnel testing p 304 N93-19321
 On the roles of wind tunnel testing and computational fluid dynamics in the aircraft development p 341 N93-19322
 Wind tunnel tests and CFD in Fuji Heavy Industries p 304 N93-19323
 Wind tunnel test and CFD in Kawasaki Heavy Industries, Gifu p 304 N93-19324
 Wind tunnel testing and CFD simulation in Mitsubishi Heavy Industries p 305 N93-19325
 Role of wind tunnel tests and CFD analysis for the development of aero-engines in IHI p 365 N93-19326
 Application of the program profile for the design of low-speed, low-observable configuration airfoils [AD-A258842] p 305 N93-19364
 Issues and approach to develop validated analysis tools for hypersonic flows: One perspective [NASA-TM-103937] p 305 N93-19379
 Projectile base bleed technology. Part 2: User's guide CMINT computer code, version 5.04-BRL [AD-A258630] p 551 N93-19999
 Advanced adaptive computational methods for Navier-Stokes simulations in rotorcraft aerodynamics [NASA-CR-192282] p 483 N93-20256
 Computational analysis of hypersonic flows past generalized cone-derived waveriders p 483 N93-20288
 Methodology for sensitivity analysis, approximate analysis, and design optimization in CFD for multidisciplinary applications [NASA-CR-192172] p 552 N93-20297
 Computational parametric study of sidewall-compression scramjet inlet performance at Mach 10 [NASA-TM-4411] p 552 N93-20299
 Adaptivity-fluids-localization. The challenge to computational mechanics p 553 N93-20618
 On the disturbances development in the supersonic boundary layer p 484 N93-20686
 HSCCT mission analysis of waverider designs [NASA-CR-192193] p 515 N93-21646
 Further development of the CANAERO computer code to include a time-stepping capability [DREA-CR-91-478] p 562 N93-21820
 Prediction of forces and moments for hypersonic flight vehicle control effectors [NASA-CR-193033] p 728 N93-24762
 Computational study of the aerodynamics and control by blowing of asymmetric vortical flows over delta wings p 693 N93-24772
 A contribution to the great Riemann solver debate [NASA-CR-191409] p 694 N93-25083
 Prediction of unsteady flows in turbomachinery using the linearized Euler equations on deforming grids [NASA-CR-192919] p 747 N93-25109

Transient performance of fan engine with water ingestion [NASA-CR-190778] p 677 N93-25134
 Instability of flow in a streamwise corner [NASA-CR-191410] p 694 N93-25153
 Direct solutions of the Navier-Stokes equations with application to static aeroelasticity p 748 N93-25259
 Numerical simulation of leading-edge receptivity to freestream vorticity p 696 N93-25388
 Numerical study of cavity natural convection flow with augmenting and counteracting effects by projection finite element method p 749 N93-25540
 Navier-Stokes simulations of unsteady transonic flow phenomena p 697 N93-25542
 A computational aerodynamic design optimization method using sensitivity analysis p 716 N93-25552
 Analysis of wing wake roll-up using a vortex-in-cell method p 697 N93-25706
 Large-eddy simulation of temporally developing boundary layers with embedded streamwise vortices p 750 N93-25753
 A new LU-SGS flow solver for calculating reentry flows p 698 N93-25759
 Stationary crossflow instability on an infinite swept wing p 699 N93-25865
 Simulation of vortex bursting p 699 N93-25881
 Numerical simulation of hypersonic aerodynamics and the computational needs for the design of an aerospace plane [AD-A260681] p 699 N93-25894
 Workshop Report: A validation study of Navier-Stokes codes for transverse injection into a Mach 2 flow p 751 N93-26008
 Influence of supercritical conditions on pre-combustion chemistry and transport behavior of jet fuels [AD-A261813] p 737 N93-26268
 Sensitivity calculations for a 2D, inviscid, supersonic forebody problem [NASA-CR-191444] p 779 N93-27004
 Transition aerodynamics for 20-percent-scale VTOL unmanned aerial vehicle [NASA-TM-4419] p 779 N93-27032
 Unstructured viscous grid generation by advancing-front method [NASA-CR-191449] p 780 N93-27067
 The Center of Excellence for Hypersonics Training and Research at the University of Texas at Austin [NASA-CR-193070] p 781 N93-27126
 CFD mixing analysis of axially opposed rows of jets injected into confined crossflow [NASA-TM-106179] p 813 N93-27128
 Spurious frequencies as a result of numerical boundary treatments p 839 N93-27170
 The Fifth Symposium on Numerical and Physical Aspects of Aerodynamic Flows [NASA-CR-193000] p 783 N93-27427
 The transition prediction toolkit: LST, SIT, PSE, DNS, and LES p 783 N93-27429
 Three-dimensional compressible stability-transition calculations using the spatial theory p 783 N93-27431
 The remarkable ability of turbulence model equations to describe transition p 783 N93-27432
 Stability investigations of airfoil flow by global analysis p 783 N93-27436
 A composite structured/unstructured-mesh Euler method for complex airfoil shapes p 784 N93-27439
 Ship viscous flow: A report on the 1990 SSPA-IIHR Workshop p 840 N93-27466
 Navier-Stokes analysis of radial turbine rotor performance [NASA-CR-191153] p 815 N93-28609
 Analysis of unsteady wave processes in a rotating channel [NASA-CR-191154] p 816 N93-28617
 Implementation of a multidomain Navier-Stokes code on the Intel iPSC2 hypercube [FFA-TN-1992-37] p 843 N93-28994
 The numerical solution of low Mach number flow in confined regions by Richardson extrapolation [TRITA-NA-9207] p 789 N93-29005
 Stabilized space-time finite element formulations for unsteady incompressible flows involving fluid-body interactions p 843 N93-29040
 Studies of hydrogen-air diffusion flames and of compressibility effects related to high-speed propulsion p 917 N93-29125
 The 3-D viscous flow CFD analysis of the propeller effect on an advanced ducted propeller subsonic inlet [NASA-TM-106240] p 900 N93-29162
 A parallel implicit incompressible flow solver using unstructured meshes [AD-A263395] p 931 N93-29851
 Solution of Euler equations for forebody-inlet ensemble of aircraft at high angle of attack [AD-A263905] p 876 N93-29862

The application of concentric vortex simulation to calculating the aerodynamic characteristics of bodies of revolution at high angles of attack [AD-A263879] p 876 N93-29919
 Aerothermic calculations of flows in interdisc cavities of turbines p 903 N93-29947
 Modelling thermal behaviour of turbomachinery discs and casings p 903 N93-29949
 Flow and heat transfer between gas-turbine discs p 903 N93-29950
 Aero-thermal design of a cooled transonic NGV and comparison with experimental results p 904 N93-29957
 The aerodynamic effect of coolant ejection in the leading edge region of a film-cooled turbine blade p 904 N93-29958
 Coupling of 3D-Navier-Stokes external flow calculations and internal 3D-heat conduction calculations for cooled turbine blades p 904 N93-29961
 A Navier-Stokes solver with different turbulence models applied to film-cooled turbine cascades p 904 N93-29962
 Navier-Stokes analysis of three-dimensional flow and heat transfer inside turbine blade rows p 905 N93-29963
 A computational model that couples aerodynamic and structural dynamic behavior of parachutes during the opening process [AD-A264115] p 877 N93-30119
 Simulation, characterization and control of forced unsteady viscous flows using Navier-Stokes equations [AD-A264333] p 934 N93-30369
 Topology and grid adaption for high-speed flow computations [NASA-CR-4216] p 934 N93-30375
 Turbulent drag reduction: Studies of feedback control and flow over riblets p 878 N93-30645
 The numerical simulation of circulation controlled airfoil flowfields p 879 N93-30947
 The HSCCT mission analysis of waverider designs [NASA-CR-193467] p 879 N93-31037
 WBNFLOW: Multi-grid/multi-block potential solver for compressible flow. User's guide [FFA-TN-1992-43] p 1031 N93-31146
 Computational methods for aerodynamic design of aircraft components [NLR-TP-92072-4] p 987 N93-31148
 Three-dimensional flow calculations inside SSME GGGT first stage blade rows p 1017 N93-31585
 Numerical simulation of the flow in a 1:57-scale axisymmetric model of a large blast simulator [AD-A265551] p 1015 N93-31916
 Panel methods for aerodynamic analysis and design [NLR-TP-91404-U] p 990 N93-32357
 NLR inviscid transonic unsteady loads prediction methods in aerelasticity [NLR-TP-91410-U] p 990 N93-32358
 Analytical and experimental investigations of the oblique detonation wave engine concept [NASA-TM-102839] p 1006 N93-32374
COMPUTATIONAL GEOMETRY
 Application of CAD system in geometric modeling for helicopter preliminary design p 153 A93-14203
 Hybrid prismatic/tetrahedral grid generation for complex 3-D geometries [AIAA PAPER 93-0669] p 465 A93-27439
 Improvement of transonic wing buffet by geometric modifications [AIAA PAPER 93-3024] p 1055 A93-48209
COMPUTATIONAL GRIDS
 An effective multigrid method for high-speed flows p 6 A93-10533
 Two modified versions of Hsu-Lee's elliptic solver of grid generation p 95 A93-11085
 Computation of viscous compressible flows using an upwind algorithm and unstructured meshes p 9 A93-12163
 Unstructured grid solutions to a wing/pylon/store configuration using VGRID3D/USM3D [AIAA PAPER 92-4572] p 14 A93-13303
 Navier-Stokes analysis of turbine blade heat transfer and performance p 201 A93-13978
 Adaptive multigrid for the steady Euler equations p 201 A93-13988
 Influence of trailing-edge grid structure on Navier-Stokes computation of turbomachinery cascade flow p 111 A93-14078
 MELINA - A multi-block, multi-grid 3D Euler code with sub block technique for local mesh refinement p 115 A93-14217
 A flux-difference finite volume method for steady Euler equations on adaptive unstructured grids p 116 A93-14277
 Parallel implementation of the feature associated mesh embedding method for the 2D-Euler equations (FAME2D) p 225 A93-14278

The accuracy of cell vertex finite volume methods on quadrilateral meshes p 227 A93-14526

Marching grid generation for external viscous flow problems p 228 A93-16979

Periodic Euler and Navier-Stokes solutions about oscillating airfoils p 241 A93-17799

Adaptive remeshing for three-dimensional compressible flow computations p 242 A93-18851

Secondary flows in a transonic cascade - Validation of a 3-D Navier-Stokes code [ASME PAPER 92-GT-62] p 247 A93-19312

The extension of a solution-adaptive 3D Navier-Stokes solver towards geometries of arbitrary complexity [ASME PAPER 92-GT-363] p 257 A93-19527

A solution scheme for the Euler equations based on a multi-dimensional wave model p 261 A93-20178

Improving the efficiency of aerodynamic shape optimization procedures [AIAA PAPER 92-4697] p 264 A93-20309

Aerodynamic shape optimization via sensitivity analysis on decomposed computational domains p 265 A93-20310

Geometric requirements for multidisciplinary analysis of aerospace-vehicle design [AIAA PAPER 92-4773] p 436 A93-20366

A gridless Euler/Navier-Stokes solution algorithm for complex-aircraft applications [AIAA PAPER 93-0333] p 268 A93-21107

Spatial adaptation procedures on tetrahedral meshes for unsteady aerodynamic flow calculations [AIAA PAPER 93-0670] p 269 A93-21116

The modelling of aerodynamic flows by solution of the Euler equations on mixed polyhedral grids p 269 A93-21218

Grid generation for three-dimensional turbomachinery geometries including tip clearance p 270 A93-21658

Cascade flow calculations by a multigrid Euler method p 270 A93-21662

Flow around two circular cylinders by the random-vortex method p 271 A93-21925

Tracking flow features using overset grids [AIAA PAPER 93-0197] p 276 A93-22617

The effect of Reynolds number and turbulence on airfoil aerodynamics at -90 degrees incidence [AIAA PAPER 93-0206] p 277 A93-22624

3-D adaptive grid-embedding Euler technique [AIAA PAPER 93-0330] p 415 A93-23021

Euler computations of rotor-stator interaction in turbomachinery cascades using adaptive triangular meshes [AIAA PAPER 93-0386] p 282 A93-23065

A hybrid structured-unstructured grid method for unsteady turbomachinery flow computations [AIAA PAPER 93-0387] p 282 A93-23066

Adaptive finite volume upwind approach on mixed quadrilateral-triangular meshes p 287 A93-23542

Three-dimensional unstructured grid Euler method applied to turbine blades [AIAA PAPER 93-0196] p 461 A93-24233

Three-dimensional Navier-Stokes calculations using solution-adapted grids [AIAA PAPER 93-0431] p 462 A93-24240

Numerical investigations on airfoil performance subjected to aerodynamic interference from an upstream airfoil [AIAA PAPER 93-0639] p 463 A93-24754

A moving mesh system for the calculation of unsteady flows [AIAA PAPER 93-0641] p 464 A93-24756

A new procedure for dynamic adaption of three-dimensional unstructured grids [AIAA PAPER 93-0672] p 560 A93-24780

Unstructured 3D Delaunay mesh generation applied to planes, trains and automobiles [AIAA PAPER 93-0673] p 560 A93-24781

A multilevel composite grid method for fluid flow computations [AIAA PAPER 93-0768] p 541 A93-24852

A study of CFD algorithms applied to complete aircraft configurations [AIAA PAPER 93-0784] p 468 A93-24864

A fully implicit Navier-Stokes algorithm using an unstructured grid and flux difference splitting [AIAA PAPER 93-0875] p 470 A93-24936

A numerical study of unsteady supersonic compression ramp flows [AIAA PAPER 93-0883] p 470 A93-24943

MESH3D - A tool for the construction of three-dimensional meshes [ONERA, TP NO. 1992-164] p 561 A93-25339

Progress in high-lift aerodynamic calculations [AIAA PAPER 93-0194] p 474 A93-25512

Recent developments in high order K-exact reconstruction on unstructured meshes [AIAA PAPER 93-0668] p 475 A93-25546

Comparison of airport noise calculation models p 564 A93-28480

Implicit numerical solution of transonic flows using adaptive triangular grids p 686 A93-34349

Compressible flow calculations using a two-equation turbulence model and unstructured grids p 686 A93-34351

Dynamically adaptive grid and its applications to flow problems p 688 A93-34362

Commercial turbofan engine exhaust nozzle flow analyses p 689 A93-34489

Implicit upwind solution algorithms for three-dimensional unstructured meshes p 691 A93-35607

A finite-volume Euler solver for computing rotary-wing aerodynamics on unstructured meshes p 765 A93-35935

Numerical simulation of a hovering rotor using embedded grids p 765 A93-35936

Multiblock Navier-Stokes solutions about the F/A-18 wing-LEX-fuselage configuration p 767 A93-37378

Structured grid variational adaption - Reaching the limit? [ONERA, TP NO. 1992-114] p 771 A93-38590

Research in unsteady aerodynamics and computational aeroelasticity at the NASA Langley Research Center p 804 A93-39498

Implicit multigrid techniques for compressible flows p 862 A93-42429

A multi-dimensional upwind scheme for the Euler equations on structured grids p 862 A93-42430

Solution of three-dimensional supersonic flowfields via adapting unstructured meshes p 863 A93-42442

The application of an adaptive upwind unstructured grid solution algorithm to the simulation of compressible laminar viscous flows over compression corners p 866 A93-42594

Grid-refinement study of hypersonic laminar flow over a 2-D ramp p 866 A93-42597

Solution of the Euler equations around a double ellipsoidal shape using unstructured meshes and including real gas effects p 867 A93-42604

The application of an adaptive unstructured grid method to the solution of hypersonic flows past double ellipse and double ellipsoid configurations p 868 A93-42609

Numerical simulation of hypersonic flow over a double ellipse using a Taylor-Galerkin finite element formulation with adaptive grids p 868 A93-42617

Adaptive mesh embedding for reentry flow problems p 869 A93-42619

Contribution to Problem 6 using an upwind Euler solver with unstructured meshes p 869 A93-42627

A finite-volume Euler solver for computing rotary-wing aerodynamics on unstructured meshes p 874 A93-43782

Generation of unstructured tetrahedral meshes by advancing front technique p 1021 A93-44206

Unstructured grids for sonic-boom analysis [AIAA PAPER 93-2929] p 949 A93-44229

Unstructured grids on NURBS surfaces --- NonUniform Rational B-Splines [AIAA PAPER 93-3454] p 949 A93-44232

Computations of inviscid compressible flows using fluctuation-splitting on triangular meshes [AIAA PAPER 93-3301] p 950 A93-44999

Field by field hybrid upwind splitting methods [AIAA PAPER 93-3302] p 950 A93-45000

A multi-dimensional kinetic-based upwind solver for the Euler equations [AIAA PAPER 93-3303] p 950 A93-45001

Dynamic overset grid communication on distributed memory parallel processors [AIAA PAPER 93-3311] p 1036 A93-45007

Adaptive-prismatic-grid method for external viscous flow computations [AIAA PAPER 93-3314] p 951 A93-45010

A coarse-grid correction/nonlinear relaxation algorithm for the three-dimensional, compressible Navier-Stokes equations [AIAA PAPER 93-3317] p 951 A93-45013

Stability analysis of dynamic meshes for transient aeroelastic computations [AIAA PAPER 93-3325] p 1022 A93-45019

Euler solutions for blunt bodies using triangular meshes - Artificial viscosity forms and numerical boundary conditions [AIAA PAPER 93-3333] p 953 A93-45027

An accuracy assessment of Cartesian-mesh approaches for the Euler equations [AIAA PAPER 93-3335] p 953 A93-45029

Three-dimensional unstructured grid Euler computations using a fully-implicit, upwind method [AIAA PAPER 93-3337] p 953 A93-45031

A 3D unstructured adaptive multigrid scheme for the Euler equations [AIAA PAPER 93-3339] p 954 A93-45033

A three-dimensional Delaunay unstructured grid generator and flow solver for bodies in relative motion [AIAA PAPER 93-3349] p 954 A93-45043

Moving body overset grid methods for complete aircraft tiltrotor simulations [AIAA PAPER 93-3350] p 954 A93-45044

A graphically interactive approach to structured and unstructured surface grid quality analysis [AIAA PAPER 93-3351] p 954 A93-45045

Visual grid quality assessment for 3D unstructured meshes [AIAA PAPER 93-3352] p 1036 A93-45046

Techniques for the visual evaluation of computational grids [AIAA PAPER 93-3353] p 1037 A93-45047

Adaptive Cartesian grid methods for representing geometry in inviscid compressible flow [AIAA PAPER 93-3385] p 955 A93-45076

Time-accurate simulation of a self-excited oscillatory supersonic external flow with a multi-block solution-adaptive mesh algorithm [AIAA PAPER 93-3387] p 956 A93-45078

An adaptive finite element method for turbulent free shear flow past a propeller [AIAA PAPER 93-3388] p 956 A93-45079

Adaptive inviscid flow solutions for aerospace geometries on efficiently generated unstructured tetrahedral meshes [AIAA PAPER 93-3390] p 956 A93-45081

A 3-D finite-volume scheme for the Euler equations on adaptive tetrahedral grids p 956 A93-45083

A simple multigrid procedure for explicit time-marching on unstructured grids p 956 A93-45087

An upwind multigrid algorithm for calculating flows on unstructured grids p 957 A93-45088

Single block three-dimensional volume grids about complex aerodynamic vehicles p 957 A93-45099

Advancing-layers method for generation of unstructured viscous grids p 957 A93-45101

Hypersonic flow calculations using a multidomain MUSCL Euler solver p 960 A93-45547

Kinematic domain decomposition for boundary-motion-induced flow simulations p 1028 A93-46811

A new flux splitting scheme p 973 A93-47189

Adaptive computations of flow around a delta wing with vortex breakdown [AIAA PAPER 93-3400] p 974 A93-47202

Near-field supersonic flow predictions by an adaptive unstructured tetrahedral grid solver [AIAA PAPER 93-3430] p 977 A93-47223

Unstructured grid generation using interactive three-dimensional boundary and efficient three-dimensional volume methods [AIAA PAPER 93-3452] p 1037 A93-47237

Unstructured viscous grid generation by advancing-layers method [AIAA PAPER 93-3453] p 979 A93-47238

High lift multiple element airfoil analysis with unstructured grids [AIAA PAPER 93-3478] p 981 A93-47256

A pointwise version of the Baldwin-Barth turbulence model [AIAA PAPER 93-3523] p 985 A93-47284

Numerical solution of the Euler equations for complex aerodynamic configurations using an edge-based finite element scheme [AIAA PAPER 93-2933] p 1046 A93-48131

Precise pitching airfoil computations by use of dynamic unstructured meshes [AIAA PAPER 93-2971] p 1049 A93-48165

A solution-adaptive hybrid-grid method for the unsteady analysis of turbomachinery [AIAA PAPER 93-3015] p 1148 A93-48204

Dynamic-overlapped-grid simulation of aerodynamically determined relative motion [AIAA PAPER 93-3018] p 1055 A93-48205

Application of a two-equation turbulence model for high speed compressible flows using unstructured grids [AIAA PAPER 93-3029] p 1056 A93-48213

Upwind finite-volume Navier-Stokes computations on unstructured triangular meshes p 1070 A93-49011

Three-dimensional time-marching aeroelastic analyses using an unstructured-grid Euler method p 1100 A93-49012

Efficient multigrid computation of steady hypersonic flows p 1152 A93-49527

The computation over unstructured grids of inviscid hypersonic reactive flow by upwind finite-volume schemes p 1073 A93-49532

An unstructured grid flow solver for turbomachinery flows [AIAA PAPER 93-1913] p 1076 A93-49780

- An adaptive grid/Navier-Stokes methodology for the calculation of nozzle afterbody base flows with a supersonic freestream
[AIAA PAPER 93-1922] p 1076 A93-49788
- Boundary condition procedures for CFD analyses of propulsion systems - The multi-zone problem
[AIAA PAPER 93-1971] p 1077 A93-49819
- An unstructured adaptive quadrilateral mesh-based scheme for viscous turbomachinery flow calculations
[AIAA PAPER 93-1975] p 1077 A93-49822
- Numerical simulations of the unstart phenomenon in a supersonic inlet/diffuser
[AIAA PAPER 93-2239] p 1081 A93-50041
- Numerical aspects of a block structured compressible flow solver
p 1169 A93-51279
- A second-order upwind finite-volume method for the Euler solution on unstructured triangular meshes
p 1087 A93-51738
- Implicit schemes for unsteady Euler equations on unstructured meshes
[ONERA, TP NO. 1993-64] p 1171 A93-51944
- Aerodynamic calculation of complex three-dimensional configurations
p 1094 A93-52426
- Navier-Stokes investigation of blunt trailing-edge airfoils using O grids
p 1095 A93-52459
- Effective treatment of the singular line boundary problem for three-dimensional grids
p 1177 A93-53204
- Space marching calculations about hypersonic configurations using a solution-adaptive mesh algorithm
p 1177 A93-53212
- The construction of nearly orthogonal multiblock grids for compressible flow simulation
p 1219 A93-53847
- Studies on coolant problems in aeronautical turbine cascades
[ISABE 93-7074] p 1220 A93-54050
- Locally implicit total variation diminishing schemes on mixed quadrilateral-triangular meshes
p 1235 A93-55356
- Three-dimensional mesh embedding for the Navier-Stokes equations using upwind control volumes
p 1239 A93-56402
- A frontal approach for internal node generation in Delaunay triangulations
p 1262 A93-56403
- Special publication of National Aerospace Laboratory [DE93-716195] p 239 A93-15949
- Hypersonic flows including real gas effects
[AERO-REPT-9112] p 289 A93-16467
- CFD-based approximation concepts for aerodynamic design optimization with application to a 2-D scramjet vehicle
[AD-A258084] p 333 A93-17893
- H-P adaptive methods for finite element analysis of aerothermal loads in high-speed flows
[NASA-CR-189739] p 420 A93-18093
- A Blottner type numerical model for nonequilibrium viscous hypersonic flows in upwind finite elements
[INRIA-RR-1476] p 297 A93-18648
- Proceedings of the Ninth NAL Symposium on Aircraft Computational Aerodynamics
[NAL-SP-16] p 299 A93-19273
- A simple grid generation technique for hypersonic flow around complex configuration
p 299 A93-19275
- Numerical calculations of separating flows around oscillating airfoil
p 300 A93-19284
- Numerical simulation of the flow through non-uniform airfoil cascade
p 302 A93-19310
- Three dimensional calculation of flow inside supersonic inlet
p 303 A93-19313
- Numerical simulation of flows in a supersonic air intake
p 303 A93-19314
- Advanced adaptive computational methods for Navier-Stokes simulations in rotorcraft aerodynamics
[NASA-CR-192282] p 483 A93-20256
- Adaptivity-fluids-localization. The challenge to computational mechanics
p 553 A93-20618
- A three-dimensional algebraic grid generation scheme for gas turbine combustors with inclined slots
[NASA-CR-191095] p 746 A93-24759
- A contribution to the great Riemann solver debate
[NASA-CR-191409] p 694 A93-25083
- Prediction of unsteady flows in turbomachinery using the linearized Euler equations on deforming grids
[NASA-CR-192919] p 747 A93-25109
- Grid sensitivity for aerodynamic optimization and flow analysis
[NASA-CR-192980] p 694 A93-25117
- Analysis of wing wake roll-up using a vortex-in-cell method
p 697 A93-25706
- Unsteady airfoil flow solutions on moving zonal grids
[AD-A261925] p 701 A93-26198
- Unstructured viscous grid generation by advancing-front method
[NASA-CR-191449] p 780 A93-27067
- Unstructured mesh algorithms for aerodynamic calculations
p 785 A93-27444
- Prediction of vortex breakdown on a delta wing
p 787 A93-27459
- Adaptive EAGLE dynamic solution adaptation and grid quality enhancement
p 788 A93-27464
- Ablation problems using a finite control volume technique
[DE93-009861] p 942 A93-29187
- Simulation, characterization and control of forced unsteady viscous flows using Navier-Stokes equations
[AD-A264333] p 934 A93-30369
- Topology and grid adaption for high-speed flow computations
[NASA-CR-4216] p 934 A93-30375
- The ViB-code to simulate 3-D stator/rotor flow in axial turbines
[DLR-FB-92-19] p 1003 A93-31170
- Blasim: A computational tool to assess ice impact damage on engine blades
[NASA-TM-106225] p 1031 A93-31193
- Numerical simulation of the flow in a 1:57-scale axisymmetric model of a large blast simulator
[AD-A265551] p 1015 A93-31916
- ### COMPUTER AIDED DESIGN
- Extracting dimensional geometric parameters from B-spline surface models of aircraft
[AIAA PAPER 92-4283] p 43 A93-13340
- RDS - A PC-based aircraft design, sizing, and performance system
[AIAA PAPER 92-4226] p 97 A93-13354
- Adaptive optimization of general aviation aircraft
[AIAA PAPER 92-4195] p 44 A93-13372
- Computer aided aerodynamic design of high pressure axial flow fan blade element
p 16 A93-13649
- The new challenge of computational aeroscience
p 112 A93-14169
- Application of SPEED in aviation industry
p 225 A93-14178
- Application of CAD system in geometric modeling for helicopter preliminary design
p 153 A93-14203
- Aircraft optimization by a system approach - Achievements and trends
p 153 A93-14205
- An engineering method with artificial intelligence characteristics used for structural layout of wings
p 225 A93-14290
- RISK - Interactive multidisciplinary system for designing airframes
p 226 A93-14337
- Structural optimization in preliminary aircraft design - A finite-element approach
p 226 A93-14340
- A low speed wind-tunnel with extreme flow quality - Design and tests
p 190 A93-14352
- Rapid wind tunnel prototype using stereolithography and equivalent technologies
p 191 A93-14365
- Flight simulator development in China
p 191 A93-14410
- Experimental working position simulator to analyse, develop and optimize concepts for computer-aided Air Traffic Management
p 191 A93-14412
- Principles of the design of automated meteorological support systems for aviation
[ISBN 5-286-00342-7] p 151 A93-15224
- Use of advanced CFD codes in the turbomachinery design process
[ASME PAPER 92-GT-324] p 256 A93-19508
- A fool-proof aerodynamic design code for turbine cascades
p 259 A93-20117
- A CAD computer system for centrifugal compressor impeller with transonic inflow
p 259 A93-20118
- Aerodynamic performance optimization of a rotor blade using a neural network as the analysis
[AIAA PAPER 92-4837] p 324 A93-20295
- Multidisciplinary design integration system for a supersonic transport aircraft
[AIAA PAPER 92-4841] p 324 A93-20296
- Preliminary wing design of a high speed civil transport aircraft by multilevel decomposition techniques
[AIAA PAPER 92-4721] p 325 A93-20323
- On alternative problem formulations for multidisciplinary design optimization
[AIAA PAPER 92-4752] p 436 A93-20350
- Geometric requirements for multidisciplinary analysis of aerospace-vehicle design
[AIAA PAPER 92-4773] p 436 A93-20366
- Thermal/structural analysis and aircraft design
p 409 A93-20420
- Airspace redesign - Making the GRADE
p 317 A93-21630
- Simulation in aeronautics
p 437 A93-21868
- Validation of aerodynamic simulation methods for Hermes spaceplane and future hypersonic vehicles
[AIAA PAPER 92-5065] p 273 A93-22335
- Experiences in fabrication of a waverider model for wind tunnel testing
[AIAA PAPER 93-0510] p 328 A93-23257
- A re-evaluation of the waverider design process
[AIAA PAPER 93-0404] p 440 A93-23326
- The design of a senior-level CAD course with emphasis on fluid/thermal systems
[AIAA PAPER 93-0426] p 454 A93-23344
- Construction of a one-third scale model of the NASP
[AIAA PAPER 93-0427] p 386 A93-23345
- Fully automatic FEM data pre-processing for aeronautical electrical machine
p 538 A93-24030
- A multi-functional computer-aided aircraft exterior shape modelling prototype system
p 504 A93-24032
- Airfoil design using the Navier-Stokes equations
[AIAA PAPER 93-0648] p 464 A93-24763
- Aerodynamic analyses for design and education
[AIAA PAPER 92-2664] p 473 A93-24988
- CST and rotorcraft - Expanding the view
p 560 A93-25085
- CST gives aircraft industry a lift --- computational structures technology
p 560 A93-25086
- Europe adapts CST to its needs --- computational structures technology for aerospace industry
p 560 A93-25088
- Zen and the art of airplane sizing
p 504 A93-25174
- The development of the Boeing Human Model
p 561 A93-27150
- A set of application programs for the smoothing of curves and surfaces by the method of monoidal transformations in the geometric module of a CAD system for the design of flight vehicles
p 561 A93-27629
- Regional fanjet aircraft optimization studies
p 508 A93-28602
- Utilization of CAD/CAE for concurrent design of structural aircraft components
[AIAA PAPER 93-1466] p 710 A93-34014
- Developing the MD Explorer
p 744 A93-34472
- Selection of protective coatings for parts in a computer-aided design system
p 746 A93-35290
- A method for the optimum design of a large-aspect-ratio wing
p 828 A93-36793
- A numerical procedure for aerodynamic optimization of helicopter rotor blades
[ONERA, TP NO. 1992-121] p 771 A93-38595
- Control of the quality of dynamic processes in the valves of power-generating equipment
p 832 A93-39030
- Computational models of dampers for computer-aided design
p 832 A93-39032
- Expert evaluation of the technological level of aviation gas turbine engine designs
p 811 A93-39187
- A thermal/structural analysis process incorporating concurrent engineering
[SAE PAPER 92-1185] p 938 A93-41364
- Selection of the primary aircraft structure at the preliminary design stage
p 891 A93-42371
- Structure of a knowledge base used in the computerized synthesis of aircraft layout
p 891 A93-42373
- Formalization of the problem of preliminary aircraft design
p 891 A93-42375
- Computerized synthesis of three-dimensional kinematic landing gear schemes with a single turning axis
p 891 A93-42376
- Characteristics of data processing during the development of a data base for a CAD system for aircraft design
p 892 A93-42381
- Inviscid calculations by an upwind finite element method of hypersonic flows over a double (single) ellipse
p 869 A93-42626
- Selecting locations for avionics antennas - A structured approach
p 892 A93-42794
- Computer-aided design of avionic diagnostics algorithms
p 941 A93-42863
- Estimation of the service periods for complex systems in the case of a priori indeterminacy of system reliability data --- for radio electronic equipment of onboard navigation and landing
p 856 A93-43109
- Fundamentals of flight vehicle design --- Russian book
[ISBN 5-217-01299-4] p 893 A93-43831
- Applications to fixed-wing aircraft and spacecraft
p 996 A93-45432
- Calculation of the position of aircraft center of gravity on an IBM PC
p 996 A93-45671
- Application of computational fluid dynamics in transonic aerodynamic design
[AIAA PAPER 93-3481] p 982 A93-47259
- A computational method for inverse design of transonic airfoil and wing
[AIAA PAPER 93-3482] p 982 A93-47260
- Computational analysis of off-design waveriders
[AIAA PAPER 93-3488] p 982 A93-47262
- Design optimization study for F-15 propulsion/forward fairing compatibility
[AIAA PAPER 93-3484] p 1003 A93-47291
- Automated design and fabrication of radio-electronic circuits
p 1151 A93-49000
- Computer aided design of turbo-machinery components
p 1166 A93-50489
- An aircraft instrument design for in situ tropospheric OH measurements by laser induced fluorescence at low pressures
p 1159 A93-51528

- Flight research simulation takes off p 1192 A93-53769
- Design and technology for engine manufacture --- for Rolls-Royce aerospace business p 1194 A93-53979 [ISABE 93-7002]
- Aerodynamic inverse design and analysis for a full engine [ISABE 93-7086] p 1186 A93-54062
- A parameter optimization approach to controller partitioning for integrated flight/propulsion control application p 1206 A93-54268
- Future development and application of general structural analysis softwares in the aviation industry in China p 1262 A93-54420
- SAPNEW: Parallel finite element code for thin shell structures on the Alliant FX/80 [NASA-CR-190663] p 84 N93-10372
- Requirements analysis notebook for the flight data systems definition in the Real-Time Systems Engineering Laboratory (RSEL) [NASA-CR-185698] p 69 N93-10960
- An interactive preprocessor for the NASA engine performance program [NASA-TM-105786] p 56 N93-10983
- Simultaneous engineering in aero gas turbine design and manufacture [PNR-90890] p 59 N93-11208
- The engine design engine. A clustered computer platform for the aerodynamic inverse design and analysis of a full engine [NASA-TM-105838] p 21 N93-11223
- Analysis and design of planar and non-planar wings for induced drag minimization [NASA-CR-191274] p 131 N93-13463
- Optimum design of aircraft structures with manufacturing and buckling constraints p 162 N93-13815
- DESAID (the development of an expert system for aircraft initial design) p 163 N93-14448
- Functional requirements of an advanced instructional design advisor: Simulation authoring, Volume 3 [AD-A256650] p 440 N93-16500
- Development of a computer assisted toolbox for aerodynamic design of aircraft at subcritical conditions with application to three-surface and canard aircraft [ISBN-90-6275-768-5] p 441 N93-16567
- Mathematical optimization: A powerful tool for aircraft design [MBB-FE-2-S-PUB-478] p 331 N93-17564
- Practical architecture of design optimisation software for aircraft structures taking the MBB-LAGRANGE code as an example [MBB-FE-251-S-PUB-479] p 331 N93-17565
- Realization of real time graphics in vehicles with high dynamic motion [ETN-93-92739] p 443 N93-18630
- An investigation of discovery-based learning in the route planning domain [AD-A259141] p 513 N93-20560
- Application of artificial neural networks to the design optimization of aerospace structural components [NASA-TM-4389] p 555 N93-21831
- An approach to configuration design synthesis of subsonic transport aircraft using artificial intelligence techniques p 716 N93-25692
- ASTOVL combat aircraft design synthesis and optimization p 717 N93-25704
- X-ray computed tomography for casting development [AD-A261786] p 752 N93-26526
- Effect of design selection on response surface performance [NASA-CR-4520] p 895 N93-29885
- Robust control of intelligent rotor [AD-A263707] p 909 N93-29985
- Airspace Design Expert System (ADES), a 2D/3D mapping and modelling tool incorporating an expert system for use in instrument approach design p 888 N93-30357
- A unified approach for composite cost reporting and prediction in the ACT program p 920 N93-30441
- Multi-parameter optimization tool for low-cost commercial fuselage crown designs p 922 N93-30858
- Computational methods for aerodynamic design of aircraft components [NLR-TP-92072-4] p 987 N93-31148
- Applications of structural optimization methods to fixed-wing aircraft and spacecraft in the 1980s [NASA-TM-103939] p 1033 N93-32212
- COMPUTER AIDED MANUFACTURING**
- The approach to airworthiness clearance with the introduction of advanced materials and manufacturing technologies into the design of aerospace structures p 2 A93-12235
- Application of SPEED in aviation industry p 225 A93-14178
- Integration of aircraft design and manufacture using artificial intelligence paradigms p 225 A93-14202
- Case studies in composite material structural design, manufacture and testing p 157 A93-14385
- A control technology of integrated system of engineering supported by software engineering environments p 226 A93-14415
- The modeling of forging and precision-casting forming processes p 207 A93-15030
- Rapid fabrication of flight worthy composite parts p 209 A93-15792
- Computer-aided cure optimization p 209 A93-15804
- Flexible manufacturing of aircraft engine parts [ASME PAPER 92-GT-229] p 404 A93-19446
- Calculating the cutting depth during the milling of large gas turbine engine blades p 545 A93-27628
- Mathematical statement of the problem of optimizing the design of an airframe for ease of manufacture p 745 A93-35286
- Modeling and optimization of aircraft assembly --- Russian book [ISBN 5-217-00808-3] p 677 A93-35677
- Modeling of the multiparameter assembly of engineering products for a specified priority of output geometrical parameters p 836 A93-39109
- The well made engine p 1122 A93-50352
- The integrated design and manufacturing of composite structures for aircraft using an advanced tape layering technology [MBB-LME-251-S-PUB-0491-A] p 515 N93-21401
- X-ray computed tomography for casting development [AD-A261786] p 752 N93-26526
- COMPUTER AIDED MAPPING**
- Model of a map indicator p 341 A93-18532
- Digital map databases in support of avionic display systems p 544 A93-26888
- Application of new GPS aircraft control/display system to topographic mapping of the Greenland ice cap p 499 A93-28152
- Aerial cartography using SICAD NAV-AIR p 1034 N93-31258
- COMPUTER AIDED TOMOGRAPHY**
- Correlation of X-ray CT measurements to shear strength in pultruded composite materials p 396 A93-18618
- Measurement of the center-of-gravity using X-ray computed tomography p 396 A93-18619
- Computed tomography of advanced materials and processes p 832 A93-38975
- Computer-aided light sheet flow visualization [AIAA PAPER 93-2915] p 1147 A93-48117
- Interferometric reconstruction of three-dimensional high-speed aerodynamic flows p 291 N93-16765
- X-ray computed tomography for casting development [AD-A261786] p 752 N93-26526
- Use of local x ray computerized tomography for high-resolution, region-of-interest inspection of large ceramic components for engines [DE93-005564] p 843 N93-28943
- COMPUTER ANIMATION**
- Software for flight recorder data evaluation developed by Lufthansa p 230 N93-15163
- The FAIR (Flight Animated and Interactive Reconstruction) tool p 148 N93-15164
- COMPUTER ASSISTED INSTRUCTION**
- Functional requirements of an advanced instructional design advisor: Simulation authoring, Volume 3 [AD-A256650] p 440 N93-16500
- Allowable compression strength for CFRP-components of fighter aircraft determined by CAI-test p 537 N93-21531
- Development of a concept formulation process aid for analyzing training requirements and developing training devices [AD-A263579] p 912 N93-29972
- COMPUTER COMPONENTS**
- New developments in a PI-Bus specification by the JIAWG and SAE p 940 A93-42852
- COMPUTER DESIGN**
- JIAWG compatible development boards for the i960 [SAE PAPER 931596] p 1104 A93-49345
- An examination of wing rock for the F-15 [AD-A256613] p 188 N93-14252
- COMPUTER GRAPHICS**
- RDS - A PC-based aircraft design, sizing, and performance system [AIAA PAPER 92-4226] p 97 A93-13354
- Airspace redesign - Making the GRADE p 317 A93-21630
- Visualization of vortical flows with yet another post-processor [AIAA PAPER 93-0222] p 415 A93-22638
- Aircraft grid generation using interactive environment [AIAA PAPER 93-0224] p 438 A93-22639
- A graphical user-interface for propulsion system analysis [AIAA PAPER 93-0223] p 440 A93-23699
- Advanced airborne 3D computer image generation systems technologies for the year 2000 p 518 A93-28176
- Aero-optical phase measurements using Fourier transform holographic interferometry p 549 A93-29302
- Visualization and view simulation based on transputers p 1037 A93-45150
- Transport delay compensation - An inexpensive alternative to increasing image generator update rate [AIAA PAPER 93-3563] p 1223 A93-52663
- A radar altitude and line of sight attachment [AIAA PAPER 93-3587] p 1223 A93-52680
- Texture as a visual cueing element in computer image generation. I - Representation of the sea surface [AIAA PAPER 93-3560] p 1214 A93-52695
- Simulator evaluation of displays for a revised takeoff performance monitoring system [NASA-TP-3270] p 189 N93-15366
- User's manual for Interactive Data Display System (IDDS) [NASA-TM-105572] p 441 N93-16613
- Realization of real time graphics in vehicles with high dynamic motion [ETN-93-92739] p 443 N93-18630
- Mission planning systems for tactical aircraft (pre-flight and in-flight) [AGARD-AR-313] p 496 N93-21187
- Measurement of modulation transfer functions of simulator displays [AD-A259401] p 530 N93-21268
- Scientific visualization using the Flow Analysis Software Toolkit (FAST) p 758 N93-25600
- Rendering the out-the-window view for the AFIT virtual cockpit [AD-A262599] p 823 N93-28467
- Toward reusable graphics components in Ada [AD-A262568] p 849 N93-28577
- Summer research program (1992). High School Apprenticeship Program (HSAP) reports. Volume 16: Arnold Engineering Development Center Civil Engineering Laboratory [AD-A262024] p 945 N93-29396
- Three-dimensional graphical representation of objects according to movement data in real time [ESA-TT-1258] p 942 N93-30104
- COMPUTER INFORMATION SECURITY**
- Mission planning systems for tactical aircraft (pre-flight and in-flight) [AGARD-AR-313] p 496 N93-21187
- COMPUTER NETWORKS**
- High speed databus evaluation - Further work [SAE PAPER 931597] p 1151 A93-49346
- Representation of vehicle location in networked simulations [AIAA PAPER 93-3582] p 1214 A93-52677
- Networks extend simulation's reach p 1225 A93-53770
- Design of an Ada expert system shell for the VHSIC avionic modular flight processor p 98 N93-11947
- Numerical Wind Tunnel hardware p 383 N93-19289
- Data Multiplexing Network (DMN). Phase 3: Equipment Operational Test and Evaluation (OT/E) integration test report [DOT/FAA/CT-TN92/49] p 503 N93-20612
- Robo-line storage: Low latency, high capacity storage systems over geographically distributed networks [NASA-CR-192910] p 758 N93-25130
- The Data Multiplexing Network (DMN) phase 3 Extended Distance Data Cable (EDDC) test and evaluation [DOT/FAA/CT-TN93/11] p 752 N93-26160
- Center for Aeronautics and Space Information Sciences [NASA-CR-193140] p 848 N93-27289
- Data Multiplexing Network (DMN) equipment Operational Test and Evaluation (OT/E) integration test report [AD-A263172] p 942 N93-29490
- COMPUTER PROGRAMMING**
- An automated mode tracking strategy --- dynamic structural analysis of helicopter structures [AIAA PAPER 93-1414] p 739 A93-33970
- Real-time monitoring for software development and testing p 939 A93-42824
- Complexity metrics for avionics software p 939 A93-42829
- Initial development of a research flight simulator software [AIAA PAPER 93-3590] p 1223 A93-52683
- Reusable code for helicopter simulation [AIAA PAPER 93-3594] p 1224 A93-52686
- Computational nonlinear control [AD-A253547] p 98 N93-12258
- Software requirements for the A-7E aircraft [AD-A255746] p 229 N93-15052

SUBJECT INDEX

Flight dynamics system software development environment (FDS/SDE) tutorial
[NASA-TM-108580] p 230 N93-15502

Software Management Environment (SME) installation guide
[NASA-TM-108578] p 230 N93-15578

Data collection procedures for the Software Engineering Laboratory (SEL) database
[NASA-TM-108579] p 230 N93-15579

A model for determining task set schedulability in the presence of system effects
[AD-A258915] p 443 N93-19338

Design recovery for software library population
[AD-A259292] p 572 N93-20611

Cumulative reports and publications
[NASA-CR-191440] p 847 N93-27063

COMPUTER PROGRAMS

RDS - A PC-based aircraft design, sizing, and performance system
[AIAA PAPER 92-4226] p 97 A93-13354

MELINA - A multi-block, multi-grid 3D Euler code with sub block technique for local mesh refinement
p 115 A93-14217

Nonlinear rotor-fuselage coupled response to generic periodic control modes using advanced computation techniques
p 153 A93-14226

Implicit Navier-Stokes solver for three-dimensional compressible flows
p 122 A93-14546

An AF3 algorithm for the calculation of transonic nonconservative full potential flows over wings or wing/body combinations
p 125 A93-15341

Laboratory for modelling of prospective board equipment systems for aircraft
p 374 A93-18529

TEMPER - A gas-path analysis tool for commercial jet engines
[ASME PAPER 92-GT-315] p 354 A93-19501

Models for predicting the performance of Brayton-cycle engines
[ASME PAPER 92-GT-361] p 355 A93-19525

A comparison of the predictive capabilities of several turbulence models using upwind and central-difference computer codes
[AIAA PAPER 93-0192] p 268 A93-21102

A microcomputer program for estimating low altitude wind and turbulence fields
p 438 A93-22163

Numerical modeling of anti-icing systems and comparison to test results on a NACA 0012 airfoil
[AIAA PAPER 93-0170] p 327 A93-23242

Advancements in the LEWICE Ice Accretion Model
[AIAA PAPER 93-0171] p 309 A93-23243

Ice accretion and performance degradation calculations with LEWICE/NS
[AIAA PAPER 93-0173] p 310 A93-23244

Ice accretion prediction for a typical commercial transport aircraft
[AIAA PAPER 93-0174] p 310 A93-23245

A multi-functional computer-aided aircraft exterior shape modelling prototype system
p 504 A93-24032

ADDRAS - An integrated systems approach
p 562 A93-29423

A new parallel-vector finite element analysis software on distributed-memory computers
[AIAA PAPER 93-1307] p 756 A93-33883

An overview of aeroelasticity studies for the National Aero-Space Plane
[AIAA PAPER 93-1313] p 732 A93-33889

Application of a p-version finite element code to analysis of cracks
[AIAA PAPER 93-1450] p 740 A93-33999

BLASIM - A computational tool to assess ice impact damage on engine blades
[AIAA PAPER 93-1638] p 720 A93-34165

Selection of protective coatings for parts in a computer-aided design system
p 746 A93-35290

Methodology for studying the fracture of aircraft structures in static tests
p 801 A93-36785

Application of European CFD methods for helicopter rotors in forward flight
[ONERA, TP NO. 1992-125] p 772 A93-38599

Algorithms for constructing models of the interaction of diagnostic systems with reserved aviation equipment
p 847 A93-39043

A software for optimum design of an aircraft structure
p 938 A93-40495

Avionics software performability
p 939 A93-42822

Blade row interaction effects on compressor measurements
p 900 A93-42885

DeAs - A programming system for data processing and system control: New software developments for wind tunnel operation
p 1036 A93-44452

Techniques for the visual evaluation of computational grids
[AIAA PAPER 93-3353] p 1037 A93-45047

Calculation of the position of aircraft center of gravity on an IBM PC
p 996 A93-45671

Computer-aided study of flight regimes and fuel consumption for helicopter flight operations
p 897 A93-45674

A family of multiblock codes for computational aerothermodynamics - Application to complete vehicle hypersonic flows
[AIAA PAPER 93-3042] p 1056 A93-48223

Developing a data base for the calibration and validation of hypersonic CFD codes - Sharp cones
[AIAA PAPER 93-3044] p 1057 A93-48224

The European Data Base - A new CFD validation tool for the design of space vehicles
[AIAA PAPER 93-3045] p 1057 A93-48225

A computer program for meridional flows in multistage axial flow compressors with turbulence and multi-effects of 3-D flows
p 1165 A93-49186

Enhancing real-time flight simulation execution by intercepting Run-Time Library calls
[AIAA PAPER 93-3591] p 1224 A93-52684

Reusable code for helicopter simulation
[AIAA PAPER 93-3594] p 1224 A93-52686

Design for cyclic loading endurance of composites
p 1216 A93-53395

LV software for supersonic flow analysis
[NASA-CR-190911] p 16 N93-10069

Design and implementation of digital filters for analysis of F/A-18 flight test data
[AD-A253447] p 17 N93-10342

The engine design engine. A clustered computer platform for the aerodynamic inverse design and analysis of a full engine
[NASA-TM-105838] p 21 N93-11223

Physical effects of vegetation on wind-blown sand in the coastal environments of Florida
[PB92-188424] p 93 N93-11702

A preliminary study associated with the experimental measurement of the aero-optic characteristics of hypersonic configurations
[AD-A253792] p 24 N93-12063

Dynamic analysis of a pre-and-post ice impacted blade
[NASA-TM-105829] p 90 N93-12197

Solution of nonlinear flow equations for complex aerodynamic shapes
[NASA-CR-190979] p 90 N93-12329

Studies of a flat wake rotor theory
[NASA-CR-190936] p 25 N93-12343

DYNAC: A computer program for analyzing the dynamical stability of aircraft
[REPT-B-31] p 66 N93-12415

Probabilistic evaluation of fuselage-type composite structures
[NASA-TM-105881] p 212 N93-12735

Multiple-function multi-input/multi-output digital control and on-line analysis
[NASA-TM-107697] p 162 N93-13565

Extended surface heat sinks for electronic components: A computer optimization
[AD-A256134] p 218 N93-14254

Information systems for airport operations
[TT-9202] p 152 N93-14729

Software requirements for the A-7E aircraft
[AD-A255746] p 229 N93-15052

Software flexibility and configuration control for the A340/A330 Aircraft Condition Monitoring System (ACMS)
p 167 N93-15154

Software for flight recorder data evaluation developed by Lufthansa
p 230 N93-15163

Root damage analysis of aircraft engine blade subject to ice impact
[NASA-TM-105779] p 222 N93-15343

Numerical modeling of anti-icing systems and comparison to test results on a NACA 0012 airfoil
[NASA-TM-105975] p 148 N93-15345

Ice accretion and performance degradation calculations with LEWICE/NS
[NASA-TM-105972] p 148 N93-15354

Finite-difference solution for laminar or turbulent boundary layer flow over axisymmetric bodies with ideal gas, CF₄, or equilibrium air chemistry
[NASA-TP-3271] p 222 N93-15434

Modeling limits of the EMV analysis program CONCEPT by example of the influence of a helicopter structure on a frame antenna
[MBB-UD-0614-92-PUB] p 223 N93-15487

Ice accretion prediction for a typical commercial transport aircraft
[NASA-TM-105976] p 149 N93-15522

Development of a menu driven materials data base for use on personal computers: Aircraft structures technical memorandum
[AD-A256317] p 392 N93-16403

Modifications to Langley 0.3-m TCT adaptive wall software for heavy gas test medium, phase 1 studies
[NASA-CR-189736] p 291 N93-16710

COMPUTER SYSTEMS DESIGN

CFD analysis on control of secondary losses in STME LOX turbines with endwall fences
p 419 N93-17289

Using software metrics and software reliability models to attain acceptable quality software for flight and ground support software for avionic systems
p 442 N93-17305

Technical operating report on the Data Integration and Collection Environment (DICE) instrumentation system design
[AD-A258444] p 455 N93-17891

Investigation of advanced counterrotation blade configuration concepts for high speed turboprop systems. Task 4: Advanced fan section aerodynamic analysis computer program user's manual
[NASA-CR-187127] p 364 N93-18702

737-400 at Kegworth, 8 January 1989: The AAB investigation
p 491 N93-19661

The flight test and data analysis program for the development of a Boeing/De Havilland Dash 8 simulator model
p 512 N93-19930

Investigation of advanced counterrotation blade configuration concepts for high speed turboprop systems. Task 5: Unsteady counterrotation ducted propfan analysis. Computer program user's manual
[NASA-CR-187125] p 521 N93-20583

Design recovery for software library population
[AD-A259292] p 572 N93-20611

MSC/NASTRAN structure optimization test module version 67 (preliminary)
[REPT-5-191025] p 554 N93-20907

Review of initial experiments using the Hawk model, dynamic rig facility, and the CED 1401 digital data acquisition equipment
[CRANFIELD-AERO-9017] p 531 N93-21406

Structural Tailoring of Advanced Turboprops (STAT). Theoretical manual
[NASA-CR-191017] p 556 N93-22005

Development and application of computational aerothermodynamics flowfield computer codes
[NASA-CR-192940] p 692 N93-24736

Use of high performance networks and supercomputers for real-time flight simulation
p 731 N93-25574

Scientific visualization using the Flow Analysis Software Toolkit (FAST)
p 758 N93-25600

Simulation of aircraft gas turbine engine
p 723 N93-25751

Development of a flight instrument package
[AD-A260830] p 719 N93-25783

Design of an air traffic computer simulation system to support investigation of civil tiltrotor aircraft operations
[NASA-CR-192920] p 707 N93-26052

Damage tolerance assessment and usage variation analysis for C-130 aircraft in the Israeli Air Force
p 839 N93-27210

High-lift aerodynamics: Prospects and plans
p 784 N93-27442

Toward reusable graphics components in Ada
[AD-A262568] p 849 N93-28577

Implementation of a multidomain Navier-Stokes code on the Intel iPSC2 hypercube
[FFA-TN-1992-37] p 843 N93-28994

Operation of the helicopter antenna radiation prediction code
[NASA-CR-193259] p 1030 N93-31110

Advanced Transport Operating System (ATOPS) utility library software description
[NASA-CR-191469] p 1000 N93-32218

COMPUTER STORAGE DEVICES

Robo-line storage: Low latency, high capacity storage systems over geographically distributed networks
[NASA-CR-192910] p 758 N93-25130

Considerations for space and naval aviation applications of ferroelectric memory
[AD-A261300] p 759 N93-26294

COMPUTER SYSTEMS DESIGN

Advanced real time integrated processors --- for Lockheed F-22 advanced tactical fighter
p 50 A93-11000

Implementation of BMLS computer model on hypercube systems --- Baseline Microwave Landing System
p 32 A93-11024

The development of an airborne information management system for flight test
[AIAA PAPER 92-4113] p 51 A93-11281

A design concept for a flight vehicle computer system with artificial intelligence elements
p 757 A93-35663

A performance assessment of a byzantine resilient fault-tolerant computer
[AIAA PAPER 89-3064] p 938 A93-41296

Real-time monitoring for software development and testing
p 939 A93-42824

Database management for integrated avionics system
p 939 A93-42831

New developments in a PI-Bus specification by the JIAWG and SAE
p 940 A93-42852

- The Pave Pace integrated core processor
p 941 A93-42856
- JIAWG compatible development boards for the i960
[SAE PAPER 931596] p 1104 A93-49345
- An advanced graphics-interactive system for a multi-block structured grid generation within an industrial environment
[ETN-92-2885] p 440 N93-16288
- NARSIM and EFMS: Tools for research on integrated ATM
[NLR-TP-89336-U] p 319 N93-17954
- Optimal trajectories for aircraft terrain following and terrain avoidance: A literature review update
[AD-A264075] p 910 N93-30604
- COMPUTER SYSTEMS PERFORMANCE**
- A performance assessment of a byzantine resilient fault-tolerant computer
[AIAA PAPER 89-3064] p 938 A93-41296
- Additional developments in embedded computer performance measurement
p 940 A93-42833
- A model for determining task set schedulability in the presence of system effects
[AD-A258915] p 443 N93-19338
- Robo-line storage: Low latency, high capacity storage systems over geographically distributed networks
[NASA-CR-192910] p 758 N93-25130
- Numerical simulation of free shear flows: Towards a predictive computational aeroacoustics capability
[NASA-CR-191015] p 781 N93-27097
- COMPUTER SYSTEMS PROGRAMS**
- Avionics software performance
p 939 A93-42822
- The language processor system for the Numerical Wind Tunnel
p 383 N93-19291
- Advanced Transport Operating System (ATOPS) utility library software description
[NASA-CR-191469] p 1000 N93-32218
- COMPUTER SYSTEMS SIMULATION**
- Summary: Experimental validation of real-time fault-tolerant systems
[NASA-CR-190985] p 175 N93-13697
- FAA Technical Center Aeronautical Data Link Research Plan
[DOT/FAA/CT-92/23] p 417 N93-15698
- COMPUTER TECHNIQUES**
- Inlet design using a blend of experimental and computational techniques
p 114 A93-14210
- BITE vs human judgement - The aircraft side --- Built In Test Equipment
p 238 A93-18759
- High-performance computing for flight vehicles; Proceedings of the Symposium, Washington, Dec. 7-9, 1992
p 437 A93-20701
- Computer-based modelling of aircraft noise impact
p 559 A93-28497
- CFD development and a future high speed computer
p 847 A93-38128
- Computation of induced drag for elliptical and crescent-shaped wings
p 958 A93-45136
- Computational schemes for integrity analyses of fuselage panels in aging airplanes
p 1025 A93-45774
- Generation of a plant description dictionary based on expert survey data
p 1168 A93-50956
- Vector unsymmetric eigenequation solver for nonlinear flutter analysis on high-performance computers
p 1160 A93-52449
- Prismatic grid generation for three-dimensional complex geometries
p 1178 A93-53217
- An investigation of the influence of advanced aircraft diagnostics on the technological sophistication of maintenance personnel
[AD-A258988] p 240 N93-18887
- Design recovery for software library population
[AD-A259292] p 572 N93-20611
- Current research activities: Applied and numerical mathematics, fluid mechanics, experiments in transition and turbulence and aerodynamics, and computer science
[NASA-CR-191408] p 758 N93-25084
- Robo-line storage: Low latency, high capacity storage systems over geographically distributed networks
[NASA-CR-192910] p 758 N93-25130
- Design concepts for the development of cooperative problem-solving systems
[NASA-CR-192708] p 707 N93-25261
- Computational gearing mechanics
[NASA-CR-191127] p 751 N93-25884
- Numerical simulation of free shear flows: Towards a predictive computational aeroacoustics capability
[NASA-CR-191015] p 781 N93-27097
- Flight evaluation of a computer aided low-altitude helicopter flight guidance system
p 820 N93-28869
- Computer-controlled alignment for a 2000-line color monitor
p 886 N93-30324
- Multiparticle imaging technique for two-phase fluid flows using pulsed laser speckle velocimetry
[DE93-011734] p 935 N93-30489

COMPUTER VISION

- Vision-based range estimation using helicopter flight data
p 151 A93-17501
- Validation of vision-based obstacle detection algorithms for low-altitude helicopter flight
p 374 A93-19077
- A fast algorithm for obtaining dense depth maps for high speed navigation
p 435 A93-19080
- A formalization and implementation of topological visual navigation in two dimensions
p 435 A93-19101
- Vision-based range estimation using helicopter flight data
p 317 A93-21525
- RACE pulls for shared control --- telerobotics and automation technology for aircraft maintenance and inspection
p 458 A93-29130
- Passive range estimation for rotorcraft low-altitude flight
p 948 A93-46608
- Vision based techniques for rotorcraft low altitude flight
p 1097 A93-49351
- Vision based obstacle detection and grouping for helicopter guidance
[AIAA PAPER 93-3871] p 1098 A93-51457
- Clustering methods for removing outliers from vision-based range estimates
p 1171 A93-51648
- A parallel implementation of a multisensor feature-based range-estimation method
p 1099 A93-51967
- Passive range estimation for rotorcraft low-altitude flight
p 1190 A93-52881
- A vision-based method for autonomous landing
p 1190 A93-53172
- Automated extraction of aircraft runway patterns from radar imagery
[AD-A254258] p 68 N93-11751
- COMPUTERIZED SIMULATION**
- Design and implementation of a flight simulation system --- Book
p 66 A93-12216
- Numerical solution of dynamic equations arising in a jet engine simulation
p 53 A93-12237
- Dynamic analysis of a pre-and-post ice impacted blade
[AIAA PAPER 92-4273] p 54 A93-13333
- Numerical simulation of a low-emission gas turbine combustor using KIVA-II
p 170 A93-14077
- A new aircraft integrated positioning and communication system based on satellite
p 150 A93-14236
- New model of bird impact response analysis and its engineering solution
p 156 A93-14336
- Simulation of a hypersonic flow over vehicles at low Reynolds numbers
p 120 A93-14381
- Euler solutions simulating strong shock waves and vortex phenomena over 3D wings
p 121 A93-14392
- Flight simulator development in China
p 191 A93-14410
- Hybrid real-time simulation of a two-rotor engine
p 172 A93-14497
- An investigation of real-time diagnostic technique on aeroengine
p 174 A93-16844
- Coupled multi-disciplinary simulation of composite engine structures in propulsion environment
[ASME PAPER 92-GT-6] p 346 A93-19279
- An investigation of post stall transients and recoverability of axial compression systems. II - Numerical simulations
[ASME PAPER 92-GT-56] p 347 A93-19306
- Simulation of the secondary air system of aero engines
[ASME PAPER 92-GT-68] p 348 A93-19318
- Computational techniques for probabilistic analysis of turbomachinery
[ASME PAPER 92-GT-167] p 351 A93-19393
- Improving dynamic response of a single-spool gas turbine engine using a nonlinear controller
[ASME PAPER 92-GT-392] p 355 A93-19546
- Expert systems for the simulation of gas turbine engines
[ASME PAPER 92-GT-408] p 435 A93-19557
- Large-scale simulation of the three-dimensional Navier-Stokes equations
p 437 A93-20739
- Newton-like methods for fast high resolution simulation of hypersonic viscous flows
p 437 A93-20740
- Simulation in aeronautics
p 437 A93-21868
- CFD zonal modeling of leading-edge ice effects for a complete aircraft
[AIAA PAPER 93-0167] p 275 A93-22601
- Nonlinear aircraft flight control using dynamic inversion
p 368 A93-22868
- Control of a high performance aircraft with unacceptable aerodynamics
p 369 A93-22905
- Numerical simulation of flow past the X24C reentry vehicle
[AIAA PAPER 93-0319] p 280 A93-23011
- Simplified jet fuel reaction mechanism for lean burn combustion application
[AIAA PAPER 93-0021] p 390 A93-23238
- Numerical simulations of a high Mach number jet flow
[AIAA PAPER 93-0653] p 540 A93-24766
- CST and rotorcraft - Expanding the view
p 560 A93-25085

- CST gives aircraft industry a lift --- computational structures technology
p 560 A93-25086
- Hypersonic viscous flow simulations
p 478 A93-27926
- Numerical simulation of passive control of shock-boundary layer interaction for transonic airflow
p 680 A93-33719
- Studies of the dynamic stall problem on airfoils
p 681 A93-33747
- Simulation for hot jet by cryogenic wind tunnels
p 730 A93-33750
- Further studies using matched filter theory and stochastic simulation for gust loads prediction
[AIAA PAPER 93-1365] p 726 A93-33932
- Atmospheric turbulence simulation for rotorcraft applications
p 757 A93-34264
- Multipassage three-dimensional Navier-Stokes simulation of turbine rotor-stator interaction
p 688 A93-34484
- Application of parafoils to microwave landing system siting
[AIAA PAPER 93-1213] p 702 A93-35162
- Numerical modeling of the impact of a bird against aircraft transparencies
p 801 A93-36797
- Modeling of linear isentropic flow systems
p 828 A93-37046
- Domain splitting explicit time marching scheme for simulation of unsteady high Reynolds number flow
p 830 A93-38140
- Numerical prediction of aerodynamic sound using large eddy simulation
p 850 A93-38150
- Numerical computation of aerodynamic noise radiation by the large eddy simulation
p 850 A93-38151
- Turbulent flow simulation around the aerofoil with pseudo-compressibility
p 830 A93-38155
- Shock interference prediction using direct simulation Monte Carlo
p 778 A93-39258
- Analysis of hypersonic nozzles including vibrational nonequilibrium and intermolecular force effects
p 861 A93-41916
- Helicopter control law based on sliding mode with model following
p 907 A93-42559
- Pave Pillar in-house research final report
p 927 A93-42781
- Some questions of scale in simulation, and a few answers
p 939 A93-42830
- Evaluating the IOBIDS specification using gate-level system simulation
p 940 A93-42851
- Half-scale modeling experience in the testing of radio navigation and landing systems
p 882 A93-43112
- Stiffness enhancement of flight control actuator
p 1006 A93-44151
- Moving body overset grid methods for complete aircraft tiltrotor simulations
[AIAA PAPER 93-3350] p 954 A93-45044
- Unsteady flow simulation on a parallel computer
p 1022 A93-45089
- Simulation of flow past complex geometries using a parallel implicit incompressible flow solver
p 957 A93-45095
- Numerical simulation of supersonic flows with chemical reactions
p 959 A93-45325
- Representation and probability issues in the simulation of multi-site damage
p 1026 A93-45785
- Case study and simulation of fatigue damages and DTE of aging aircraft - A review of researches in Japan
p 948 A93-45800
- Non-equilibrium thermal radiation from air shock layers modelled with the Direct Simulation Monte Carlo method
[AIAA PAPER 93-2805] p 1028 A93-46544
- Flow resolution and domain of influence in rarefied hypersonic blunt-body flows
[AIAA PAPER 93-2806] p 964 A93-46546
- Hypersonic blunt body wake computations using DSMC and Navier-Stokes solvers
[AIAA PAPER 93-2807] p 964 A93-46547
- Monte Carlo simulation of radiating reentry flows
[AIAA PAPER 93-2809] p 964 A93-46548
- Comparisons between DSMC and the Navier-Stokes equations for reentry flows
[AIAA PAPER 93-2810] p 964 A93-46549
- Navier-Stokes simulations of the Shuttle Orbiter aerodynamic characteristics with emphasis on pitch trim and bodyflap
[AIAA PAPER 93-2814] p 965 A93-46552
- Navier-Stokes flow simulation in a 2D high pressure turbine cascade with a cooled slot trailing edge
p 972 A93-46941
- Analysis of the effect of surface heating on boundary layer development over an NLS-0215 airfoil
[AIAA PAPER 93-3437] p 978 A93-47229
- Development of a system for transition characterization --- for aerodynamic simulations
[AIAA PAPER 93-3485] p 1030 A93-47246

Dynamic-overlapped-grid simulation of aerodynamically determined relative motion
[AIAA PAPER 93-3018] p 1055 A93-48205

Simulation of tail buffet using delta wing-vertical tail configuration
[AIAA PAPER 93-3688] p 1065 A93-48357

Use of full flight simulator technology enhances classroom training sessions
p 1136 A93-49277

Two-dimensional computational analysis of a transport high-lift system and a comparison with flight-test results
[AIAA PAPER 93-3533] p 1072 A93-49517

The challenges of simulating wake vortex encounters and assessing separation criteria
[AIAA PAPER 93-3568] p 1096 A93-49518

An approach to the stall monitoring in a single stage axial compressor
[AIAA PAPER 93-1872] p 1112 A93-49747

The effects of turbulence modeling on the numerical simulation of confined swirling flows
[AIAA PAPER 93-1976] p 1078 A93-49823

Turbulent flowfield simulation using Euler equations with body forces
[AIAA PAPER 93-1978] p 1078 A93-49825

Unsteady, three-dimensional, Navier-Stokes simulations of multistage turbomachinery flows
[AIAA PAPER 93-1979] p 1153 A93-49826

Numerical simulations of a pulsed detonation wave augmentation device
[AIAA PAPER 93-1985] p 1112 A93-49832

Real gas simulation of air Blow-Down Facilities
[AIAA PAPER 93-2022] p 1137 A93-49859

Rapid computer simulation of ramjet performance
[AIAA PAPER 93-2049] p 1113 A93-49882

User-friendly codes for the training on gas turbine engines
[AIAA PAPER 93-2051] p 1166 A93-49884

An investigation of shock wave turbulent boundary layer interaction with bleed through normal and slanted slots
[AIAA PAPER 93-2155] p 1079 A93-49971

Two-dimensional numerical simulation for Mach-3 multishock air-intake with bleed systems
[AIAA PAPER 93-2306] p 1082 A93-50090

Simulation of propulsion system's transient response to planar wave inlet distortion and the effect of compressor wear
[AIAA PAPER 93-2384] p 1117 A93-50152

Three-dimensional numerical simulation of gradual opening in a wave rotor passage
[AIAA PAPER 93-2526] p 1156 A93-50254

Nonlinear dynamic simulation of single- and multi-spool core engines
[AIAA PAPER 93-2580] p 1122 A93-50294

Three-dimensional simulation of the Denver 11 July 1988 microburst-producing storm
p 1164 A93-50373

WNN 92: Proceedings of the 3rd Workshop on Neural Networks: Academic/Industrial/NASA/Defense, Auburn Univ., AL, Feb. 10-12, 1992 and South Shore Harbour, TX, Nov. 4-6, 1992
[SPIE-1721] p 1167 A93-50726

Numerical simulation of unsteady flow induced by a flat plate moving near ground
p 1094 A93-52432

Flowfield simulation about the stratospheric observatory for infrared astronomy
p 1095 A93-52446

Transonic Navier-Stokes flow computations over wing-fuselage geometries
p 1095 A93-52456

A dual-Euler method for solving all-attitude angles of the aircraft
[AIAA PAPER 93-3589] p 1223 A93-52682

Identification of nonlinear mechanical systems using combined state and parameter evaluation
p 1224 A93-52732

Case study of a low-reflectivity pulsating microburst - Numerical simulation of the Denver, 8 July 1989, storm
p 1222 A93-52898

Fast three-dimensional vortex method for unsteady wake calculations
p 1178 A93-53233

Total quality management of forged products through finite element simulation
p 1217 A93-53493

A reactive approach for distributed air traffic control
[ONERA, TP NO. 1993-83] p 1190 A93-53603

Flight research simulation takes off
p 1192 A93-53769

Numerical simulation of ramjet and scramjet combustion using two-dimensional Euler equations with finite rate chemistry
[ISABE 93-7083] p 1202 A93-54059

Thermodynamic and neural network computer modelling of implanted component faults in a gas turbine engine
[ISABE 93-7089] p 1202 A93-54065

Recent developments performed at ONERA for the simulation of 3D inviscid and viscous flows in turbomachinery by the solution of Euler and Navier-Stokes equations
[ISABE 93-7094] p 1186 A93-54070

On the numerical simulation of the two-dimensional flow field around a hypersonic air-intake-compressibility effects
[ISABE 93-7100] p 1187 A93-54076

Numerical simulation of a two-dimensional supersonic mixed-compression inlet
[ISABE 93-7107] p 1188 A93-54083

A finite element code for gas turbine combustor flow with Stretched Laminar Flamelet modelling
[ISABE 93-7127] p 1204 A93-54102

Numerical simulation of gas turbine combustors with complex geometries
[ISABE 93-7128] p 1204 A93-54103

Development of a real time dynamic engine simulation model of a turbo fan engine
[ISABE 93-7132] p 1205 A93-54107

Expert Systems for the simulation of turbofan engines
[ISABE 93-7133] p 1225 A93-54108

Performance simulation of a combustion engine charged by a variable geometry turbocharger. I - Prerequisites, boundary conditions and model development. II - Simulation algorithm, computed results
p 1256 A93-54648

Design of an air traffic computer simulation system to support investigation of civil titrotor aircraft operations
[NASA-CR-190811] p 36 N93-11139

Implementing system simulation of C3 systems using autonomous objects
[NASA-CR-190845] p 89 N93-11716

Airport stand assignment model
[TT-9104] p 67 N93-11728

A preliminary study associated with the experimental measurement of the aero-optic characteristics of hypersonic configurations
[AD-A253792] p 24 N93-12063

Action composition for the animation of natural language instructions
[AD-A254963] p 228 N93-12554

Navier-Stokes simulations of unsteady transonic flow phenomena
[NASA-TM-103962] p 129 N93-12721

Probabilistic evaluation of fuselage-type composite structures
[NASA-TM-105881] p 212 N93-12735

X-29 linear aerodynamic perturbation model
[AD-A254810] p 160 N93-12752

NASA aeronautics: Research and technology program highlights
[NASA-NP-159] p 109 N93-13110

Turbomachinery CFD on parallel computers
[NASA-TM-105932] p 228 N93-13154

Simulation of two-dimensional icing, de-icing and anti-icing phenomena
p 142 N93-13364

Application of a vectorized particle simulation to the study of plates and wedges in high-speed rarefied flow
p 133 N93-13746

An examination of wing rock for the F-15
[AD-A256613] p 188 N93-14252

Modeling and control of a trailing wire antenna towed by an orbiting aircraft
[AD-A256450] p 219 N93-14610

Propulsion and Energetics Panel Working Group 20 on Test Cases for Engine Life Assessment Technology
[AGARD-AR-308] p 176 N93-14890

Introduction to test cases for engine life assessment technology
p 176 N93-14891

Modeling limits of the EMV analysis program CONCEPT by example of the influence of a helicopter structure on a frame antenna
[MBB-UD-0614-92-PUB] p 223 N93-15487

Simplified jet-A kinetic mechanism for combustor application
[NASA-TM-105940] p 200 N93-15504

Special publication of National Aerospace Laboratory
[DE93-716195] p 239 N93-15949

Correction of inertial measurements using GPS updates for underwater navigation
[AD-A257329] p 317 N93-15988

Functional requirements of an advanced instructional design advisor: Simulation authoring, Volume 3
[AD-A256650] p 440 N93-16500

User's manual for Interactive Data Display System (IDDS)
[NASA-TM-105572] p 441 N93-16613

Multidisciplinary design optimization using response surface analysis
p 330 N93-16796

Mission oriented investigation of handling qualities through simulation
[MBB-UD-0600-91-PUB] p 332 N93-17567

An investigation of two-propeller tilt wing V/STOL aircraft flight characteristics
[AD-A257751] p 332 N93-17694

Motion simulation of underwater vehicles
[VTT-PUBS-97] p 443 N93-18698

A model of Global Positioning System (GPS) Master Control Station (MCS) operations
[AD-A258846] p 320 N93-19067

Three-dimensional numerical simulation of the 20 June 1991, Orlando microburst
p 488 N93-19598

Use of microprocessor-based simulator technology and MEG/EEG measurement techniques in pilot emergency-maneuver training
p 530 N93-19706

Method for developing the RAFALE flight control system
p 512 N93-19912

Multidisciplinary tailoring of hot composite structures
[NASA-TM-106027] p 550 N93-19971

Analytic formulation of unsteady profile aerodynamics and its application to simulation of rotors
[ESA-TT-1244] p 485 N93-21659

Crashworthiness of composite seats for civil aircraft
p 703 N93-24773

High-order cyclo-difference techniques: An alternative to finite differences
[NASA-TM-107745] p 693 N93-25074

Rotor design optimization using a free wake analysis
[NASA-CR-177612] p 693 N93-25075

A contribution to the great Riemann solver debate
[NASA-CR-191409] p 694 N93-25083

Computation of transonic flow over a porous surface projectile
p 696 N93-25409

Use of high performance networks and supercomputers for real-time flight simulation
p 731 N93-25574

Gas turbine system simulation: An object-oriented approach
[NASA-TM-106044] p 723 N93-25673

Simulation of aircraft gas turbine engine
p 723 N93-25751

Design of an air traffic computer simulation system to support investigation of civil titrotor aircraft operations
[NASA-CR-192920] p 707 N93-26052

A transfer matrix approach to vibration localization in mistuned blade assemblies
[NASA-TM-106112] p 838 N93-27088

Numerical simulation of free shear flows: Towards a predictive computational aeroacoustics capability
[NASA-CR-191015] p 781 N93-27097

Numerical modeling of runback water on ice protected aircraft surfaces
p 840 N93-27438

Recent progress in the analysis of iced airfoils and wings
p 784 N93-27441

Rendering the out-the-window view for the AFIT virtual cockpit
[AD-A262599] p 823 N93-28467

Three-dimensional numerical simulation of gradual opening in a wave rotor passage
[NASA-CR-191157] p 900 N93-29072

A real-time, hardware-in-the-loop simulation of an unmanned aerial research vehicle
[AD-A262477] p 893 N93-29409

Two simulation studies of precision runway monitoring of independent approaches to closely spaced parallel runways
[AD-A263433] p 911 N93-29815

Three-dimensional graphical representation of objects according to movement data in realtime
[ESA-TT-1258] p 942 N93-30104

Coupling gain computation between antennas on circular cylinders at SHF/EHF frequencies
p 933 N93-30309

National Airspace System Performance Analysis Capability (NASPAC) simulation model
p 887 N93-30351

Procedural development prototype in Automated En Route Air Traffic Control
p 887 N93-30352

A computer simulation of the production of an artificially ionized layer using the Arecibo facility
[DE93-010817] p 937 N93-30487

Validation and upgrading of physically based mathematical models
p 942 N93-30688

The VIB-code to simulate 3-D stator/rotor flow in axial turbines
[DLR-FB-92-19] p 1003 N93-31170

Evaluation of candidate working fluid formulations for the electrothermal-chemical wind tunnel
[NASA-CR-193366] p 1015 N93-31848

Numerical simulation of the flow in a 1:57-scale axisymmetric model of a large blast simulator
[AD-A265551] p 1015 N93-31916

A PC-based simulation of the National Transonic Facility's safety microprocessor
[NASA-TM-109003] p 1038 N93-32224

Investigation of advanced technology for airway facilities maintenance training
[DOT/FAA/CT-TN92/24] p 994 N93-32336

CONCENTRATION (COMPOSITION)

Langley 8-foot high-temperature tunnel oxygen measurement system
p 1010 A93-44892

Rotational CARS measurements in a rotating cavity with axial throughflow of cooling air: Oxygen concentration measurements
[PNR-90935] p 72 N93-11035

- Predicted aircraft effects on stratospheric ozone p 93 N93-11096
- CONCORDE AIRCRAFT**
- Introduction to regulatory problems for supersonic transports p 234 A93-15032
- The Concorde wing - A useful model p 126 A93-16400
- Future supersonic transport studies at Aerospatiale p 505 A93-25491
- Advanced SST auxiliary air intakes design and analysis [AIAA PAPER 93-2304] p 1082 A93-50088
- Concorde propulsion: Did we get it right? The Rolls-Royce/SNECMA Olympus 593 engine reviewed [PNR-90970] p 57 N93-11061
- Supersonic transport: Which material for the engine [DS-2023] p 522 N93-21459
- CONCRETE STRUCTURES**
- State of the art of airport pavement analysis and design p 378 N93-16310
- CONCRETES**
- State of the art review of rutting and cracking in pavements p 380 N93-16316
- State-of-the-art survey of flexible pavement crack sealing procedures in the United States [AD-A258050] p 382 N93-17708
- CONCURRENT PROCESSING**
- Concurrent processing adaptation of aeroelastic analysis of propfans p 173 A93-14624
- Concurrent field service and laboratory testing as a means of improving reliability in creep-rupture applications p 916 A93-40814
- CONDENSATION**
- Numerical study of spontaneous nitrogen condensation in the axisymmetric hypersonic nozzles of wind tunnels p 777 A93-39143
- CONDENSATION NUCLEI**
- Transonic aerodynamics including strong effects from heat addition p 862 A93-42428
- A technique for the measurement of cloud structure on centimeter scales p 1158 A93-51243
- CONDENSED MATTER PHYSICS**
- Turbulent jet flows with condensation and electrophysical effects --- Russian book p 76 A93-10176
- Experimental study of condensation vapor-air jets p 76 A93-10180
- Shock waves; Proceedings of the 18th International Symposium, Sendai, Japan, July 21-26, 1991. Vols. 1 & 2 [ISBN 0-387-55686-9] p 1023 A93-45451
- CONDENSING**
- Condensation of nitrogen in hypersonic flows - Measurements confirm a theoretical model p 111 A93-13945
- The optimum design of air cycle refrigeration system with high pressure water separation p 202 A93-14180
- CONDUCTIVE HEAT TRANSFER**
- A thermal analysis of an F/A-18 wing section for actuator thermal management [SAE PAPER 92-1023] p 158 A93-14650
- Investigation of an electrothermal de-icer pad using a three-dimensional finite element simulation [AIAA PAPER 93-0397] p 327 A93-23072
- A numerical investigation of supersonic flow of a viscous gas over long blunt cones, taking into account equilibrium physicochemical transformations p 775 A93-39124
- Numerical solution of axisymmetric heat conduction problems using finite control volume technique p 928 A93-42909
- Efficient finite element method for aircraft deicing problems p 1103 A93-52443
- Optimization of an internally finned rotating heat pipe [AD-A256725] p 453 N93-15980
- Modelling thermal behaviour of turbomachinery discs and casings p 903 N93-29949
- CONDUCTORS**
- Modeling limits of the EMV analysis program CONCEPT by example of the influence of a helicopter structure on a frame antenna [MBB-UD-0614-92-PUB] p 223 N93-15487
- CONES**
- Influence of second-order boundary layer effects in hypersonic flow past blunt cones of large aspect ratio p 241 A93-18238
- Boundary-layer transition extent measurements on a cone and flat plate at Mach 3.5 [AIAA PAPER 93-0342] p 474 A93-25517
- Hypersonic cone flow predictions using an implicit upwind space-marching code p 865 A93-42588
- Study on flow field around slender diamond cone traveling at hypersonic speed p 1189 A93-54314
- CONFERENCES**
- IEEE PLANS '92 - Position Location and Navigation Symposium, Monterey, CA, Mar. 24-27, 1992, Record [ISBN 0-7803-0469-1] p 29 A93-10976
- AIAA Biennial Flight Test Conference, 6th, Hilton Head Island, SC, Aug. 24-26, 1992, Selected Papers p 37 A93-11251
- Rotorcraft reliability and maintainability: Future design requirements; Proceedings of the Conference, London, United Kingdom, Mar. 20, 1991 [ISBN 0-903409-88-7] p 45 A93-13401
- Aeronautical fatigue: Key to safety and structural integrity; Proceedings of the 16th ICAF Symposium, Tokyo, Japan, May 22-24, 1991 [ISBN 4-9900181-1-7] p 80 A93-13626
- ICAS, Congress, 18th, Beijing, China, Sept. 20-25, 1992, Proceedings. Vols. 1 & 2 [ISBN 1-56347-046-2] p 107 A93-14151
- Boundary layer transition and control; Proceedings of the Conference, Univ. of Cambridge, United Kingdom, Apr. 8-12, 1991 [ISBN 0-903409-86-0] p 211 A93-17251
- Fixed and rotary wing all weather operations; Proceedings of the Conference, London, United Kingdom, Apr. 23, 24, 1991 [ISBN 0-903409-90-9] p 142 A93-17301
- European navigation into the 21st century; Proceedings of the Conference, London, United Kingdom, Feb. 12, 1991 [ISBN 0-903409-82-8] p 311 A93-17751
- ARINC 629 DATABUS; Proceedings of the Conference, London, United Kingdom, Sept. 24, 1991 [ISBN 0-903409-95-X] p 311 A93-17835
- Problems in the aerodynamics and dynamics of flight vehicles in the light of K.E. Tsiolkovsky's ideas; Lectures devoted to K.E. Tsiolkovsky's ideas, 25th, Kaluga, Russia, Sept. 11-14, 1990, Transactions --- Russian book p 237 A93-18376
- Key trends in human factors of aircraft maintenance; Proceedings of the Conference, London, United Kingdom, Oct. 31, 1991 [ISBN 1-85768-005-7] p 237 A93-18754
- Artificial intelligence techniques for improving aircraft maintenance efficiency; Proceedings of the Conference, London, United Kingdom, Feb. 21, 1991 [ISBN 0-903409-84-4] p 238 A93-18761
- Aero engine reliability, integrity and safety; Proceedings of the Conference, Bristol, United Kingdom, Oct. 17, 18, 1991 [ISBN 0-903409-70-4] p 345 A93-18778
- DGLR/AIAA Aeroacoustics Conference, 14th, Aachen, Germany, May 11-14, 1992, Proceedings. Vols. 1 & 2 [DGLR BERICHT 92-03] p 444 A93-19126
- Review of progress in quantitative nondestructive evaluation. Vol. 11B; Proceedings of the 18th Annual Review, Brunswick, ME, July 28-Aug. 2, 1991 Vol. 11B [ISBN 0-306-44206-X] p 406 A93-19582
- AIAA/USAF/NASA/OAI Symposium on Multidisciplinary Analysis and Optimization, 4th, Cleveland, OH, Sept. 21-23, 1992, Technical Papers. Pts. 1 & 2 p 435 A93-20301
- High-performance computing for flight vehicles; Proceedings of the Symposium, Washington, Dec. 7-9, 1992 p 437 A93-20701
- Institute of Navigation, National Technical Meeting, San Diego, CA, Jan. 27-29, 1992, Proceedings p 315 A93-21176
- Advanced aerospace hydraulic systems and components [SAE SP-885] p 412 A93-21840
- International Conference on Aviation Weather Systems, 4th, Paris, France, June 24-28, 1991, Preprints p 426 A93-22101
- National Conference on Aerodynamics, 6th, Bangalore, India, Sept. 1992, Proceedings p 460 A93-24076
- Sensors and sensor systems for guidance and navigation; Proceedings of the Meeting, Orlando, FL, Apr. 2, 3, 1991 [SPIE-1478] p 532 A93-27043
- High-resolution displays and projection systems; Proceedings of the Meeting, San Jose, CA, Feb. 11, 12, 1992 [SPIE-1664] p 544 A93-27237
- Combustion and reaction kinetics; Proceedings of the 22nd International Annual Conference of ICT, Karlsruhe, Germany, July 2-5, 1991 p 535 A93-27726
- AHS National Technical Specialists' Meeting on Rotorcraft Structures, Williamsburg, VA, Oct. 29-31, 1991, Proceedings p 506 A93-27951
- Sensors and sensor systems for guidance and navigation II; Proceedings of the Meeting, Orlando, FL, Apr. 22, 23, 1992 [SPIE-1694] p 547 A93-28151
- Inter-noise '91; Proceedings of the 20th International Conference on Noise Control Engineering, Sydney, Australia, Dec. 2-4, 1991. Vols. 1 & 2 [ISBN 0-909882-12-6] p 557 A93-28476
- AHS and Royal Aeronautical Society, Technical Specialists' Meeting on Rotorcraft Acoustics/Fluid Dynamics, Philadelphia, PA, Oct. 15-17, 1991, Proceedings p 565 A93-29401
- Competition in a single European air transport market; Proceedings of the Conference, London, United Kingdom, Dec. 1, 1992 [ISBN 1-85768-080-4] p 458 A93-29473
- Datalinks - Civil aircraft; Proceedings of the Conference, London, United Kingdom, Nov. 24, 1992 [ISBN 1-85768-075-8] p 501 A93-29474
- Air transport growth - How will airports manage?; Proceedings of the Conference, London, United Kingdom, Oct. 21, 1992 [ISBN 1-85768-065-0] p 458 A93-29475
- AIAA/ASME/ASCE/AHS/ASC Structures, Structural Dynamics, and Materials Conference, 34th and AIAA/ASME Adaptive Structures Forum, La Jolla, CA, Apr. 19-22, 1993, Technical Papers. Pts. 1-6 p 738 A93-33876
- Numerical methods in laminar and turbulent flow; Proceedings of the 7th International Conference, Stanford Univ., CA, July 15-19, 1991. Vol. 7, pts. 1 & 2 [ISBN 0-906674-77-8] p 743 A93-34301
- New European regulations for rotorcraft; Proceedings of the Conference, London, United Kingdom, Mar. 16, 1993 [ISBN 1-85768-085-5] p 701 A93-34616
- AHS, Annual Forum, 48th, Washington, June 3-5, 1992, Proceedings. Vols. 1 & 2 p 763 A93-35901
- Numerical Fluid Dynamics Symposium, 5th, Tokyo, Japan, Dec. 19-21, 1991, Proceedings p 630 A93-38126
- Avionic systems/design and maintenance; Proceedings of the Conference, Hounslow, United Kingdom, Apr. 22, 1993 [ISBN 1-85768-095-2] p 764 A93-39535
- International Symposium on Computational Fluid Dynamics, 4th, Univ. of California, Davis, Sept. 9-12, 1991, Selected Papers p 862 A93-42426
- Hypersonic flows for reentry problems. Vols. 1 & 2 [ISBN 0-387-54428-3] p 864 A93-42576
- Radar 92; Proceedings of the International Conference, Brighton, United Kingdom, Oct. 12, 13, 1992 [ISBN 0-85296-533-2] p 929 A93-43376
- Being an engineer - A risky occupation? Proceedings of the Conference, London, United Kingdom, June 8, 1993 [ISBN 1-85768-120-7] p 945 A93-43869
- Shock waves; Proceedings of the 18th International Symposium, Sendai, Japan, July 21-26, 1991. Vols. 1 & 2 [ISBN 0-387-55686-9] p 1023 A93-45451
- Structural integrity of aging airplanes [ISBN 0-540-53461-X] p 947 A93-45772
- Societe Francaise des Mecaniciens, SNECMA, and ONERA, Symposium on Recent Advances in Compressor and Turbine Aerothermodynamics, Courbevoie, France, Nov. 24, 25, 1992, Reports p 1001 A93-46926
- AIAA Applied Aerodynamics Conference, 11th, Monterey, CA, Aug. 9-11, 1993, Technical Papers. Pts. 1 & 2 p 974 A93-47201
- AIAA Atmospheric Flight Mechanics Conference, Monterey, CA, Aug. 9-11, 1993, Technical Papers p 1125 A93-48301
- Intelligent robotics; Proceedings of the International Symposium, Bangalore, India, Jan. 2-5, 1991 [SPIE-1571] p 1166 A93-49350
- Sources and detectors for fiber communications; Proceedings of the Meeting, Boston, MA, Sept. 8, 9, 1992 [SPIE-1788] p 1151 A93-49455
- Specialty fiber optic systems for mobile platforms and plastic optical fibers; Proceedings of the Meeting, Boston, MA, Sept. 9-11, 1992 [SPIE-1799] p 1105 A93-49462
- Heat Transfer and Fluid Mechanics Institute, 33rd, California State Univ., Sacramento, June 3, 4, 1993, Proceedings p 1152 A93-49505
- Implications of European legislation post 1992; Proceedings of the Conference, London, United Kingdom, Mar. 12, 1992 [ISBN 1-85768-015-4] p 1043 A93-50353
- WNN 92; Proceedings of the 3rd Workshop on Neural Networks: Academic/Industrial/NASA/Defense, Auburn Univ., AL, Feb. 10-12, 1992 and South Shore Harbour, TX, Nov. 4-6, 1992 [SPIE-1721] p 1167 A93-50726
- Integrated optoelectronics for communication and processing; Proceedings of the Meeting, Boston, MA, Sept. 3, 4, 1991 [SPIE-1582] p 1158 A93-51250
- Aerothermodynamics in combustors; IUTAM Symposium, National Taiwan Univ., Taipei, June 3-5, 1991, Selected Papers [ISBN 0-387-55404-1] p 1146 A93-51626

- AIAA Flight Simulation Technologies Conference, Monterey, CA, Aug. 9-11, 1993, Technical Papers
p 1207 A93-52651
- ISABE - International Symposium on Air Breathing Engines, 11th, Tokyo, Japan, Sept. 20-24, 1993, Proceedings, Vols. 1 & 2
[ISBN 1-56347-071-3] p 1194 A93-53976
- Helicopter operations in severe environments; Proceedings of the Conference, London, United Kingdom, June 4, 1992
[ISBN 1-85768-045-6] p 1175 A93-54287
- AIAA Lighter-Than-Air Systems Technology Conference, 10th, Scottsdale, AZ, Sept. 14-16, 1993, Technical Papers
p 1229 A93-54601
- Rotating machinery - Transport phenomena; Proceedings of the 3rd International Symposium on Transport Phenomena and Dynamics of Rotating Machinery (ISROMAC-3), Honolulu, HI, Apr. 1-4, 1990
[ISBN 1-56032-147-4] p 1256 A93-54626
- International Symposium on Ultra-High Temperature Materials, Tajimi, Japan, Dec. 5, 6, 1991, Proceedings
p 1252 A93-54708
- The quiet helicopter; Proceedings of the Conference, London, United Kingdom, Mar. 17, 1992
[ISBN 1-85768-020-0] p 1262 A93-54718
- Stray radiation in optical systems II; Proceedings of the Meeting, San Diego, CA, July 20-22, 1992
[SPIE-1753] p 1263 A93-55176
- IR sensors; Proceedings of the Conference, London, United Kingdom, Feb. 18, 1992
[ISBN 1-85768-010-3] p 1244 A93-55294
- International Congress on Recent Developments in Air- and Structure-Borne Sound and Vibration, 2nd, Auburn Univ., AL, Mar. 4-6, 1992, Proceedings, Vols. 1-3
p 1259 A93-55851
- Proceedings of the National Weather Service Aviation Workshop: Postprint volume
[PB92-176148] p 94 A93-11803
- Aerodynamic Engine/Airframe Integration for High Performance Aircraft and Missiles
[AGARD-CP-498] p 213 A93-13199
- Symposium proceedings on Quantitative Feedback Theory
[AD-A255527] p 187 A93-13872
- Tiltrotor aircraft noise: A summary of the presentations and discussions at the 1991 FAA/Georgia Tech Workshop
[DOT/FAA/RD-91/23] p 232 A93-14912
- Special publication of National Aerospace Laboratory [DE93-716195] p 239 A93-15949
- Airborne Wind Shear Detection and Warning Systems: Fourth Combined Manufacturers' and Technologists' Conference, part 1
[NASA-CP-10105-PT-1] p 488 A93-19590
- Proceedings of the Aircraft Wake Vortices conference, volume 1
[PB93-126449] p 485 A93-21796
- Proceedings of the Aircraft Wake Vortices conference, volume 2
[PB93-127728] p 559 A93-21799
- Proceedings of the First International Symposium on Explosive Detection Technology
[DOT/FAA/CT-92/111] p 496 A93-21856
- The 1992 International Aerospace and Ground Conference on Lightning and Static Electricity: Addendum
[DOT/FAA/CT-92/20-ADD-1] p 753 A93-24875
- JPRS report: Science and technology. Japan. 30th National Aerospace Laboratory Conference
[JPRS-JST-93-009] p 761 A93-25418
- Collection of papers of the 31st Israel Annual Conference on Aviation and Astronautics
[ITN-93-85187] p 764 A93-27166
- Contributions to the American Meteorological Society's 26th International Conference on Radar Meteorology
[AD-A263385] p 936 A93-29257
- FAA international conference on airplane ground deicing
[AD-A263617] p 880 A93-29286
- Heat Transfer and Cooling in Gas Turbines
[AGARD-CP-527] p 901 A93-29926
- First NASA Advanced Composites Technology Conference, part 2
[NASA-CP-3104-PT-2] p 921 A93-30841
- Advanced electromagnetic methods for aerospace vehicles
[NASA-CR-193468] p 936 A93-31036
- Flight test of avionics and air-traffic control systems
[ESA-TT-1279] p 993 A93-31271
- Air Traffic and Environment
[GSF-BAND-8] p 1034 A93-31925
- CONFIGURATION INTERACTION**
Theoretical characterization of the reaction $\text{NH}_2 + \text{O}$ yields products p 1263 A93-55666
- CONFIGURATION MANAGEMENT**
Expert system for redundancy and reconfiguration management p 938 A93-42785
- Software flexibility and configuration control for the A340/A330 Aircraft Condition Monitoring System (ACMS) p 167 A93-15154
- CONFINEMENT**
Model for entropy production and pressure variation in confined turbulent mixing p 1071 A93-49014
- CONFORMAL MAPPING**
A conformal-integral method for solving the direct problem in turbomachine cascade aerodynamics p 125 A93-15217
- Solving problems with singularities using conformal mappings p 397 A93-18978
- Karman vortex street-airfoil interaction p 678 A93-33703
- CONGRESSIONAL REPORTS**
National Aeronautics and Space Administration Authorization Act, fiscal year 1993
[S-REPT-102-364] p 234 A93-13798
- NASA authorization, 1993, volume 2
[GPO-56-943-VOL-2] p 234 A93-13799
- NASA's fiscal year 1993 budget
[S-HRG-102-707] p 234 A93-13800
- National Aeronautics and Space Administration Report to Congress: Long-term availability of adequate airport system capacity
[AD-A258209] p 319 A93-18202
- Aviation safety: Problems persist in FAA's inspection program. Report to the Chairman, Subcommittee on Aviation, Committee on Public Works and Transportation, House of Representatives
[GAO/RCED-92-14] p 495 A93-19841
- Aviation safety: Users differ in views of collision avoidance system and cite problems. Report to the Chairman, Subcommittee on Investigations and Oversight, Committee on Science, Space, and Technology, House of Representatives
[GAO/RCED-92-113] p 502 A93-19843
- Report to the Chairman, Legislation, and National Security Subcommittee, Committee on Government Operations, House of Representatives. Unmanned aerial vehicles: More testing needed before production of short-range system
[AD-A259473] p 513 A93-20245
- CONICAL BODIES**
Tapered geometries for improved crashworthiness under side loads p 743 A93-34259
- Correlation of conical interactions induced by sharp fins and semicones p 692 A93-35635
- Symmetry breaking in vortical flows over cones - Theory and numerical experiments
[AIAA PAPER 93-3408] p 859 A93-41056
- Computational study of a conical wing having unit aspect ratio at supersonic speeds
[AIAA PAPER 93-3505] p 984 A93-47272
- CFD study of the flowfield due to a supersonic jet exiting into a hypersonic stream from a conical surface. II
[AIAA PAPER 93-2926] p 1045 A93-48127
- Aerodynamic characteristics and static stability margin of conical star-shaped bodies at supersonic velocities p 1067 A93-48848
- Supersonic flow past a cone with heat transfer near its tip p 1089 A93-51780
- Correlative behaviours of shock/boundary layer interaction induced by sharp fin and semicone p 1230 A93-54581
- Navier-Stokes computations for kinetic energy projectiles in steady coning motion: A predictive capability for pitch damping
[AD-A264111] p 1033 A93-32028
- CONICAL FLOW**
A study of the laminar-turbulent transition in a boundary layer and separation on cones at supersonic velocities p 14 A93-12974
- Three dimensional transonic flow measurements in an axial turbine with conical walls
[ASME PAPER 92-GT-61] p 247 A93-19311
- Calculation of the effect of flow conicity in a hypersonic nozzle on the aerodynamics of a flight vehicle model p 776 A93-39142
- Reynolds number effects on supersonic asymmetrical flows over a cone p 958 A93-45141
- An investigation of aerodynamic heating to spherically blunted cones at angle of attack
[AIAA PAPER 93-2764] p 963 A93-46510
- Improvement of conical similarity rule in swept shock wave/boundary layer interaction
[AIAA PAPER 93-2941] p 1046 A93-48139
- Active control of asymmetric conical flow using spinning and rotatory oscillations
[AIAA PAPER 93-2958] p 1048 A93-48152
- Developing a data base for the calibration and validation of hypersonic CFD codes - Sharp cones
[AIAA PAPER 93-3044] p 1057 A93-48224
- Some stability characteristics of the boundary layer on a yawed cone
[AIAA PAPER 93-3048] p 1057 A93-48228
- Hypersonic flow past a low-aspect-ratio triangular plate at large angles of attack p 1069 A93-48974
- Thoughts on conical flow asymmetry p 1070 A93-49003
- BLSTA: A boundary layer code for stability analysis
[NASA-CR-4481] p 220 A93-14797
- Development of a boundary element method program for numerical analysis of supersonic unsteady flow p 300 A93-19283
- CONICAL NOZZLES**
An experimental study of under-expanded jets p 696 A93-25467
- CONICAL SHELLS**
A numerical study of the flutter of conical shells p 927 A93-42405
- CONIFERS**
Generation of carbon monoxide in compartment fires
[PB93-146702] p 880 A93-29211
- CONJUGATE GRADIENT METHOD**
Variant bi-conjugate gradient methods for the compressible Navier-Stokes solver with a two-equation model of turbulence
[AIAA PAPER 93-3316] p 951 A93-45012
- Aerodynamic shape optimization using preconditioned conjugate gradient methods
[AIAA PAPER 93-3322] p 952 A93-45016
- CONSERVATION EQUATIONS**
Simulation of nonequilibrium hypersonic flows p 863 A93-42443
- Determination of heat transfer to flow in a duct with a pseudodiscontinuity p 1179 A93-53365
- Developing numerical techniques for solving low Mach number fluid-acoustic problems p 1235 A93-55353
- Improved numerical simulation of Euler equations p 83 A93-10309
- A critical analysis of the accuracy of several numerical techniques for combustion kinetic rate equations
[NASA-TP-3315] p 362 A93-16941
- CONSERVATION LAWS**
Discontinuous Galerkin finite element method for two dimensional conservation laws
[AIAA PAPER 93-0337] p 281 A93-23026
- Characteristic multigrid method application to solve the Euler equations with unstructured and unsteady grids p 476 A93-27065
- A singularities tracking conservation law scheme for compressible duct flows p 960 A93-45542
- High resolution numerical simulation of the linearized Euler equations in conservation law form
[AIAA PAPER 93-2934] p 1148 A93-48132
- A fourth-order MUSCL finite-difference scheme for solving the unsteady compressible Euler equations p 1086 A93-51121
- Discontinuous Galerkin finite element method for Euler and Navier-Stokes equations p 1235 A93-55357
- Improved numerical simulation of Euler equations p 83 A93-10309
- Volume 2: Explicit, multistage upwind schemes for Euler and Navier-Stokes equations
[NASA-CR-191647] p 418 A93-16558
- CONSOLIDATION**
HIP consolidation of aluminum-rich intermetallic alloys and their composites
[NAWCADWAR-92003-60] p 199 A93-14726
- Analysis of consolidation of intermediate level maintenance for Atlantic Fleet T700-GE-401 engines
[AD-A257754] p 363 A93-17695
- Consolidation of graphite thermoplastic textile preforms for primary aircraft structure p 919 A93-30439
- CONSTRAINTS**
Constrained control allocation p 938 A93-41891
- Optimum design of aircraft structures with manufacturing and buckling constraints p 162 A93-13815
- Scheduling of an aircraft fleet p 443 A93-18665
- CONSTRUCTION**
Stumbling blocks for airport construction in the new German federal states p 1227 A93-53727
- Scientific and engineering research facilities at universities and colleges: 1992 p 192 A93-13407
- Subsonic aerodynamic research laboratory
[AD-A256060] p 137 A93-14661
- Estimating the regional economic significance of airports
[AD-A257658] p 382 A93-17793
- NASA advanced design program: Analysis, design, and construction of a solar powered aircraft
[NASA-CR-192040] p 332 A93-17802

Construction and testing of simple airfoils to demonstrate structural design, materials choice, and composite concepts p 879 N93-30979

CONSUMERS

Consumer interest in the air safety data of the airline quality rating. Testimony to the US House of Representatives, Committee on Government Operations, Government Activities and Transportation Subcommittee [NIAR-92-4] p 495 N93-19941

CONTAMINANT

Fiber reinforced structures for turbine engine fragment containment [AIAA PAPER 93-1816] p 1110 A93-49704
Analysis of turbine engine rotor containment and shielding structures [AIAA PAPER 93-1817] p 1110 A93-49705
Aircraft wing compartment liner concept to reduce fuel spillage [DOT/FAA/CT-TN92/34] p 331 N93-17219

CONTAMINANTS

Liquid flow reactor and method of using [AD-D015392] p 222 N93-15232
Particulate emissions from gas turbine engines [AD-A261374] p 725 N93-26339

CONTAMINATION

Monitoring the purity of the working fluids of aircraft hydraulic systems during service p 321 A93-18367
Swept wing attachment line contamination fence [NASA-CASE-LAR-13400-1] p 485 N93-22015
The experimental study of transition and leading edge contamination of swept wings [LIB-TRANS-2197] p 782 N93-27274
In-situ bioventing: Two US EPA and Air Force sponsored field studies [PB93-194231] p 1035 N93-32089

CONTINUOUS WAVE LASERS

Study of artificial and natural turbulence in atmospheric boundary layer with a CW Doppler CO2 lidar p 1257 A93-54799

CONTINUUM FLOW

Numerical simulations of hypersonic rarefied transition regime flows: DSMC method and Navier-Stokes computation p 299 N93-19278

CONTINUUM MECHANICS

Development and application of computational aerothermodynamics flowfield computer codes [NASA-CR-192940] p 692 N93-24736

CONTINUUM MODELING

A viscous flow based membrane wing model [AIAA PAPER 93-2955] p 1047 A93-48149
A study of turbulence in rarefied gases [AIAA PAPER 93-3097] p 1061 A93-48271

CONTINUUMS

Development and computation of continuum higher order constitutive relations for high-altitude hypersonic flow p 132 N93-13578

CONTOURS

Numerical modeling of the impact of a bird against aircraft transparencies p 801 A93-36797
Effects of nozzle contour on the aerodynamic characteristics of underexpanded annular impinging jets p 1024 A93-45563
Numerical study of the performance of swept, curved compression surface scramjet inlets [AIAA PAPER 93-1837] p 1074 A93-49721
Separation phenomenon in a hypersonic flow with strong wall cooling - Subcritical regime p 1189 A93-54266
Effects of turn region treatments on pressure loss through sharp 180-degree bends p 1256 A93-54636

CONTRACTION

Design problems of three-dimensional contractions — in incompressible flow p 1236 A93-55584
Mach 4 testing of scramjet inlet models [NAL-TR-1137] p 26 N93-12369

CONTRACTORS

AFOSR Contractors Meeting in Propulsion [AD-A254484] p 195 N93-12575

CONTRAILS

SAC contrail formation study [AD-A254410] p 159 N93-12605

CONTRAROTATING PROPELLERS

Numerical analysis of three-dimensional viscous flows around an advanced counterrotating propeller p 112 A93-14165
Aeroacoustic wind tunnel testing of a counterrotating shrouded propfan-model p 449 A93-19213
Forward rotor vortex effects on counter rotating propeller noise p 245 A93-19221
Takeoff/approach noise for a model counterrotation propeller with a forward-swept upstream rotor [AIAA PAPER 93-0596] p 519 A93-24782
An experimental evaluation of prediction methods for contrails [PNR-90924] p 56 N93-11023

Takeoff/approach noise for a model counterrotation propeller with a forward-swept upstream rotor [NASA-TM-105979] p 362 N93-16715
Mean flow interactions of a counter-rotating propeller p 552 N93-20289

CONTROL EQUIPMENT

Search strategies for a sequence of baseline indices for building sections of a flight-safety automatic control system in the interactive mode p 306 A93-18346
Increasing the reliability of an air traffic control radio system p 882 A93-43110
Active flow control with neural networks [AIAA PAPER 93-3273] p 1037 A93-46834
Effect of passive flow-control devices on turbulent low-speed base flow p 82 N93-10304
Steering system of a vehicle, such as a snow removing machine for airfields [CA-PATENT-APPL-SN-1293201] p 83 N93-10367
Pitch control trimming system for canard design aircraft [CA-PATENT-APPL-SN-2013236] p 63 N93-10374
Strategic avionics technology definition studies. Subtask 3-1A: Electrical Actuation (ELA) systems [NASA-CR-193237] p 914 N93-29215
Articulated fin/wing control system [AD-D015712] p 909 N93-29278

CONTROL RODS

F/A-18 departure recovery improvement evaluation [AIAA PAPER 93-3671] p 1129 A93-48349

CONTROL SIMULATION

757 fly-by-wire demonstrator flight test [AIAA PAPER 92-4099] p 38 A93-11271
Optimization-based linear and nonlinear design methodologies for aircraft control. II - Final simulations [AIAA PAPER 92-4627] p 62 A93-13285
Phase II simulation evaluation of the flying qualities of two tilt-wing flap control concepts [SAE PAPER 920988] p 185 A93-14635
Nonlinear aircraft flight control using dynamic inversion p 368 A93-22868
Using TRACON as a teaching tool p 571 A93-27166
A new approach to robust fault detection and identification p 1166 A93-50631
Performance prediction of the interacting multiple model algorithm p 1167 A93-50638
System identification of unstable manipulators using ERA methods — Eigensystem Realization Algorithm [AIAA PAPER 93-3842] p 1170 A93-51431
Hybrid complex of the aircraft intellectualized control systems simulation at the stage of their research projecting [AIAA PAPER 93-3559] p 1222 A93-52660
The numerical errors in inverse simulation [AIAA PAPER 93-3588] p 1223 A93-52681
Optimal output feedback vibration control of rotor-bearing systems p 86 N93-11220
Multiple model adaptive estimation applied to the VISTA F-16 with actuator and sensor failures [AD-A256444] p 188 N93-14608
Approaches to control of the large angle magnetic suspension test fixture [NASA-CR-191890] p 381 N93-16695
Use of high performance networks and supercomputers for real-time flight simulation p 731 N93-25574

CONTROL STABILITY

Control design for robust eigenstructure assignment in linear uncertain systems p 97 A93-13241
Design and robustness issues for highly augmented helicopter controls p 185 A93-14594
Robust stabilization based on topological connectedness p 438 A93-22830
Robustness evaluation of a flexible aircraft control system p 727 A93-34540
Design and evaluation of a robust dynamic neurocontroller for a multivariable aircraft control problem p 817 A93-37004
A study of the stability of the acceleration circuit of the hydromechanical automatic control system of an aviation gas turbine engine p 810 A93-39028
Absolute stability of an automatic control system for gas turbine engines p 810 A93-39033
The required damping and control process quality in a fuel pressure regulator p 810 A93-39034
Synthesis of the optimal control of flight vehicle braking with allowance for the discrete nature of control action generation p 1169 A93-51063
Robust, nonlinear, high angle-of-attack control design for a supermaneuverable vehicle [AIAA PAPER 93-3774] p 1131 A93-51369
Cancellation control law for lateral-directional dynamics of a supermaneuverable aircraft [AIAA PAPER 93-3775] p 1131 A93-51370

Design of a controller for a high performance fighter aircraft using Robust Inverse Dynamics Estimation (RIDE)

[AIAA PAPER 93-3779] p 1132 A93-51374
System identification of unstable manipulators using ERA methods — Eigensystem Realization Algorithm [AIAA PAPER 93-3842] p 1170 A93-51431
Adaptive quadratic stabilization control with application to flight controller design [AIAA PAPER 93-3847] p 1133 A93-51434
Automated control of aircraft in formation flight [AIAA PAPER 93-3852] p 1134 A93-51439
The application of scheduled H-infinity controllers to a VSTOL aircraft p 1135 A93-52249
A monitor for the laboratory evaluation of control integrity in digital control systems operating in harsh electromagnetic environments [NASA-TM-4402] p 65 N93-12304
An examination of wing rock for the F-15 [AD-A256613] p 188 N93-14252
Robust nonlinear control of vectored thrust aircraft [NASA-CR-192727] p 728 N93-25199
Control of nonlinear systems under input constraints with applications to flight control p 729 N93-25353
Game theoretic synthesis for robust aerospace controllers p 819 N93-27171

CONTROL STICKS

F/A-18 controls released departure recovery - Flight test evaluation p 803 A93-38839
F/A-18 controls released departure recovery flight test evaluation [AD-A256522] p 189 N93-15396

CONTROL SURFACES

The numerical study of 3-D flow past control surfaces [AIAA PAPER 92-4650] p 14 A93-13305
Vortex control technology p 111 A93-14152
Aeroelastic analysis of composite wing with control surface p 157 A93-14386
Unsteady transonic aerodynamic loadings on the airfoil caused by heaving, pitching oscillations and control surface p 126 A93-15627
Development and application of a nonlinear fin mixer p 368 A93-22869
Backward bifurcation for structural divergence of a wing section p 526 A93-29351
X-31A flight flutter test excitation by control surfaces [AIAA PAPER 93-1538] p 727 A93-34075
Smart structures stabilized unstable control surfaces [AIAA PAPER 93-1701] p 712 A93-34223
Stiffness enhancement of flight control actuator p 1006 A93-44151
Virtual zone Navier-Stokes computations for oscillating control surfaces [AIAA PAPER 93-3363] p 955 A93-45056
Flow control over delta wings at high angles of attack [AIAA PAPER 93-3494] p 983 A93-47266
Forebody vortex control - A progress review [AIAA PAPER 93-3540] p 986 A93-47292
Side force augmentation at high angle of attack from pneumatic vortex flow control [AIAA PAPER 93-2959] p 1124 A93-48153
A numerical study of the effect of geometry variation, turbulence models, and dissipation on the flow past control surfaces [AIAA PAPER 93-2967] p 1048 A93-48161
A qualitative assessment of control effectors on an advanced fighter configuration [AIAA PAPER 93-3627] p 1127 A93-48312
Navier-Stokes computations on full-span wing-body configuration with oscillating control surfaces [AIAA PAPER 93-3687] p 1065 A93-48356
A Hopfield neural network for adaptive control [AIAA PAPER 93-3729] p 1130 A93-51329
Transition correlation in subsonic flow over a flat plate p 1178 A93-53231
Design, test, and evaluation of three active flutter suppression controllers [NASA-TM-4338] p 63 N93-10070
Articulated control surface [AD-D015464] p 371 N93-16463
Aerodynamic surface tip vortex attenuation system [AD-D015606] p 483 N93-20017
Failure identification using multiple model adaptive estimation for the LAMBDA flight vehicle [AD-A259137] p 527 N93-20596
Review of initial experiments using the Hawk model, dynamic rig facility, and the CED 1401 digital data acquisition equipment [CRANFIELD-AERO-9017] p 531 N93-21406
Development of a non-linear simulation for generic hypersonic vehicles - ASUHS1 [NASA-CR-192710] p 516 N93-22003
Swept wing attachment line contamination fence [NASA-CASE-LAR-13400-1] p 485 N93-22015

- Development and testing of the digital control system for the Archytas unmanned air vehicle
[AD-A261656] p 729 A93-26196
- Articulated fin/wing control system
[AD-D015712] p 909 A93-29278
- Experiments in the control of wing rock at high angle of attack using tangential leading edge blowing
p 1009 A93-31068
- Parametric studies of shock wave/boundary layer interactions over 2D compression corners at Mach 6
[VKI-TN-181] p 988 A93-31538

CONTROL SYSTEMS DESIGN

- Vibration control algorithms for flexible rotors
p 95 A93-10741
- Aspects of multivariable flight control law design for helicopters using eigenstructure assignment
p 60 A93-10916
- Limit of sampling periods for nonlinear flight trajectory controller of aircraft
p 61 A93-11207
- Integrated flight propulsion control research results using the NASA F-15 HIDEF Flight Research Facility
[AIAA PAPER 92-4106] p 38 A93-11276
- Nonlinear feedback control of highly manoeuvrable aircraft
p 40 A93-11654
- The application of optimal robust control in control system design of flying vehicles
p 95 A93-11791
- Design of an adaptive flight control system with uncertainties
p 95 A93-12322
- Discrete time $H(\infty)$ control laws for a high performance helicopter
p 96 A93-13007
- Multilevel control of dynamical systems using neural networks
p 96 A93-13011
- Output feedback control for output tracking of nonlinear uncertain systems
p 96 A93-13177
- Robust control of an aeroelastic system modeled by a singular integro-differential equation
p 97 A93-13197
- Nonlinear time-series-based adaptive control applications
p 97 A93-13230
- Neural-network-based catastrophe avoidance control systems
p 97 A93-13233
- Control design for robust eigenstructure assignment in linear uncertain systems
p 97 A93-13241
- $H(\infty)$ optimal controllers for a distributed model of an unstable aircraft
p 62 A93-13247
- Synthesis of a helicopter nonlinear flight controller using approximate model inversion
[AIAA PAPER 92-4668] p 62 A93-13280
- Integrated aerodynamics and control system design for tailless aircraft
[AIAA PAPER 92-4604] p 42 A93-13284
- Optimization-based linear and nonlinear design methodologies for aircraft control. II - Final simulations
[AIAA PAPER 92-4627] p 62 A93-13285
- Linear and nonlinear aircraft flight control for the AIAA Controls Design Challenge
[AIAA PAPER 92-4628] p 62 A93-13286
- Determination of YAV-8B Reaction Control System bleed flow usage
[AIAA PAPER 92-4232] p 54 A93-13330
- Piloted simulation study of two tilt-wing control concepts
[AIAA PAPER 92-4236] p 63 A93-13338
- Design of a full time wing leveler system using tab driven aileron controls
[AIAA PAPER 92-4193] p 63 A93-13345
- A stability augmentation system for student designed remotely-piloted vehicles
[AIAA PAPER 92-4261] p 63 A93-13365
- Optimal vibration control for a flexible rotor with gyroscopic effects
p 98 A93-13420
- Systems integration test laboratory - Application and experiences
p 190 A93-13910
- Variable structure controller design and its real-time analysis for microprocessor-based flight control systems
p 181 A93-14229
- Study of aeroservoelastic stability of an aircraft
p 182 A93-14259
- Hetero-redundant architecture with Kalman filter for input processing in flight control system
p 182 A93-14293
- Design of reduced-order observers with precise loop transfer recovery
p 184 A93-14587
- Design and robustness issues for highly augmented helicopter controls
p 185 A93-14594
- Analysis of airframe and engine control interactions and integrated flight/propulsion control
p 185 A93-14596
- Improvement in application of eigenstructure assignment to flight control system design
p 227 A93-15406
- Synthesis of robust motion stabilization laws for flight vehicles
p 227 A93-16777
- Solution of the terminal guidance problem for a flight vehicle using analytical mechanics methods
p 228 A93-16778
- The smart structures technology in the vibration control of helicopter blades in forward flight
p 366 A93-17721

- A methodological approach to the development of service and technical specifications for an actively controlled multistrut landing gear
p 321 A93-18349
- Developing control strategies for ASTOVL aircraft
p 366 A93-18777
- Reliability and safety considerations in engine management systems design
p 346 A93-18786
- Comparison of advanced turboprop interior noise control ground and flight test data
p 444 A93-19136
- Evaluation of piezoceramic actuators for control of aircraft interior noise
p 447 A93-19186
- Improving dynamic response of a single-spool gas turbine engine using a nonlinear controller
[ASME PAPER 92-GT-392] p 355 A93-19546
- Integrated aerodynamic-structural-control wing design
[AIAA PAPER 92-4694] p 324 A93-20307
- Robust digital control of a high-performance engine --- F-100 turbofan
p 359 A93-21792
- Discrete-time LTR synthesis of delayed control systems
p 439 A93-22855
- Application of structured singular value synthesis to a fighter aircraft
p 368 A93-22865
- Nonlinear aircraft flight control using dynamic inversion
p 368 A93-22868
- Refined $H(\infty)$ controller design for rotorcraft flight control
p 368 A93-22882
- A new flight control design scheme using optimal dynamic output feedback
p 368 A93-22883
- Control of a high performance aircraft with unacceptable aerodynamics
p 369 A93-22905
- Parameter optimization for an H_2 problem with multivariable gain and phase margin constraints
p 439 A93-22971
- Design of flight control systems to meet rotorcraft handling qualities specifications
p 370 A93-23509
- Three-dimensional modeling and control of a twin-lift helicopter system
p 370 A93-23511
- Application of feedback linearization method in a digital restructurable flight control system
p 370 A93-23514
- Design of insensitive multirate aircraft control using optimized eigenstructure assignment
p 370 A93-23515
- Optimal control law synthesis for flutter suppression using active acoustic excitations
p 370 A93-23516
- Failure-accommodating neural network flight control
[AIAA PAPER 92-4394] p 523 A93-24495
- Pilot control identification using Minimum Model Error estimation
[AIAA PAPER 92-4421] p 523 A93-24497
- Development of circulation control technology for application to advanced subsonic transport aircraft
[AIAA PAPER 93-0644] p 464 A93-24759
- Robust integrated flight/propulsion control design for a STOVL aircraft using $H(\infty)$ control design techniques
p 524 A93-26432
- A study of the problem of developing a weakly invariant flight vehicle control system
p 561 A93-27688
- DLR research program overview on airport surface movement guidance and control
p 499 A93-27912
- Ground Movement and Control System (GMCS)
p 499 A93-27913
- Simultaneous structure/control design optimization of a wing structure with a gust load alleviation system
p 525 A93-28616
- Algorithms and automated techniques for the design of control systems for moving objects
p 562 A93-29690
- Controller design using fuzzy logic - A case study
p 756 A93-33793
- On the order reduction of LQG designed controllers
[AIAA PAPER 93-1420] p 756 A93-33973
- Generalized guidance law for collision courses
p 727 A93-34533
- Optimal discrete-time dynamic output-feedback design - A w-domain approach
p 757 A93-34536
- Optimal open multistep discretization formulas for real-time simulation
p 757 A93-34539
- Robustness evaluation of a flexible aircraft control system
p 727 A93-34540
- Synthesis and evaluation of an H_2 control law for a hovering helicopter
p 728 A93-34542
- Preliminary experiments on active control of fan noise from a turbofan engine
p 759 A93-34957
- Effects of higher order dynamics on helicopter flight control law design
p 816 A93-35959
- Design and evaluation of a robust dynamic neurocontroller for a multivariable aircraft control problem
p 817 A93-37004
- Model reference control of a linear plant with feedthrough element
p 846 A93-37034
- Numerical computation and approximations of $H(\infty)$ optimal controllers for a 2-parameter distributed model of an unstable aircraft
p 817 A93-37040
- Robust stabilization of an aero-elastic system
p 817 A93-37044

- Actuator and aerodynamic modeling for high-angle-of-attack aeroservoelasticity
[AIAA PAPER 93-1419] p 818 A93-37433
- Nonlinear flutter of composite plates with damage evolution
[AIAA PAPER 93-1546] p 829 A93-37441
- Design philosophy for wind tunnel model positioning control systems
p 822 A93-37877
- Alternative approximations for integrated control/structure aeroservoelastic synthesis
p 819 A93-39418
- Sensor-adaptive control for aircraft paint stripping
[SME PAPER AD92-200] p 855 A93-40663
- Constrained control allocation
p 938 A93-41891
- Quantitative feedback theory applied to the design of a rotorcraft flight control system
p 906 A93-41895
- Linear quadratic Gaussian/loop transfer recovery design for a helicopter in low-speed flight
p 906 A93-41896
- A nonlinear control strategy for robust sliding mode performance in the presence of unmatched uncertainty
p 938 A93-42556
- Helicopter control law based on sliding mode with model following
p 907 A93-42559
- Reliability assessment for self-repairing flight control systems
p 907 A93-42804
- Design of robust digital model-following flight control systems
p 907 A93-42810
- Design of reconfigurable digital multiple model-following flight control systems
p 908 A93-42811
- Pilot-in-the-loop analysis of propulsive-only flight control systems
p 908 A93-42812
- Flight management system on the F-117A
p 908 A93-42815
- Synthesis of a data processing and measuring system for flight vehicle control systems
p 908 A93-43102
- A control algorithm for a navigation-landing system in the case of a priori indeterminacy of failure data
p 882 A93-43108
- Estimation of the service periods for complex systems in the case of a priori indeterminacy of system reliability data --- for radio electronic equipment of onboard navigation and landing
p 856 A93-43109
- Using numerical control algorithms in stabilization systems with digital correction
p 941 A93-43113
- Dynamic compensator design in nonlinear aerospace systems
p 1036 A93-44150
- Computation of passively controlled transonic wing
[AIAA PAPER 93-3474] p 981 A93-47253
- A new type of fuel control model
p 1108 A93-49204
- Statistical methods in flight vehicle control theory
p 1165 A93-49306
- Problems in the optimization of complex engineering systems
p 1165 A93-49307
- Screening studies of advanced control concepts for airbreathing engines
[AIAA PAPER 92-3320] p 1108 A93-49329
- Implementation of fiber optic technology in flight controls
p 1105 A93-49473
- Trajectory control for a low-lift re-entry vehicle
p 1141 A93-49592
- Application of structured singular value synthesis to a fighter aircraft
p 1130 A93-49594
- Full envelope multivariable control law synthesis for a high-performance test aircraft
p 1130 A93-49595
- Dual Engine application of the Performance Seeking Control algorithm
[AIAA PAPER 93-1822] p 1110 A93-49709
- On the estimation algorithm for adaptive performance optimization of turbofan engines
[AIAA PAPER 93-1823] p 1111 A93-49710
- Advanced instrumentation for next-generation aerospace propulsion control systems
[AIAA PAPER 93-2079] p 1154 A93-49906
- Local nonlinear control of stall inception in axial flow compressors
[AIAA PAPER 93-2230] p 1080 A93-50036
- Application of analog computing to real-time simulation of stall and surge dynamics
[AIAA PAPER 93-2231] p 1080 A93-50037
- A simplified approach for control of rotating stall. II - Experimental results
[AIAA PAPER 93-2234] p 1080 A93-50038
- WNN 92: Proceedings of the 3rd Workshop on Neural Networks: Academic/Industrial/NASA/Defense, Auburn Univ., AL, Feb. 10-12, 1992 and South Shore Harbour, TX, Nov. 4-6, 1992
[SPIE-1721] p 1167 A93-50726
- The use of genetic algorithms in the design of fuzzy logic controllers
p 1167 A93-50779
- An information-search system in cybernetics
p 1168 A93-50957
- Coupling characteristics analysis of elastic vehicle --- design of modern flight control systems
p 1169 A93-51189

- A magnetic suspension system with a large angular range p 1139 A93-51295
- Application of controller partitioning optimization procedure to integrated flight/propulsion control design for a STOVL aircraft p 1131 A93-51361
- [AIAA PAPER 93-3766] p 1131 A93-51361
- Robust, nonlinear, high angle-of-attack control design for a supermaneuverable vehicle p 1131 A93-51369
- [AIAA PAPER 93-3774] p 1131 A93-51369
- Design of a flight control system for a highly maneuverable aircraft using mu synthesis p 1132 A93-51371
- [AIAA PAPER 93-3776] p 1132 A93-51371
- Design of a controller for a high performance fighter aircraft using Robust Inverse Dynamics Estimation (RIDE) p 1132 A93-51374
- [AIAA PAPER 93-3779] p 1132 A93-51374
- Design of a low sensitivity and norm multivariable controller using eigenstructure assignment and the method of inequalities p 1170 A93-51394
- [AIAA PAPER 93-3802] p 1170 A93-51394
- Integrated flight/propulsion control - Subsystem specifications for performance p 1132 A93-51400
- [AIAA PAPER 93-3808] p 1132 A93-51400
- Antiwindup analysis and design approaches for MIMO systems p 1123 A93-51403
- [AIAA PAPER 93-3811] p 1123 A93-51403
- A new way of pole placement in LQR and its application to flight control p 1133 A93-51433
- [AIAA PAPER 93-3845] p 1133 A93-51433
- H(infinity) helicopter flight control law design with and without rotor state feedback p 1134 A93-51436
- [AIAA PAPER 93-3849] p 1134 A93-51436
- Design of a helicopter control system to meet handling quality specifications using H(infinity) techniques p 1134 A93-51437
- [AIAA PAPER 93-3850] p 1134 A93-51437
- Automated control of aircraft in formation flight p 1134 A93-51439
- [AIAA PAPER 93-3852] p 1134 A93-51439
- A test bench for rotorcraft hover control p 1140 A93-51440
- [AIAA PAPER 93-3853] p 1140 A93-51440
- Fuzzy logic control algorithm for suppressing E-6A Long Trailing Wire Antenna wind shear induced oscillations p 1171 A93-51454
- [AIAA PAPER 93-3868] p 1171 A93-51454
- Approximate decoupling flight control system design with output feedback for nonlinear systems p 1135 A93-51465
- [AIAA PAPER 93-3880] p 1135 A93-51465
- A new technique for nonlinear control of aircraft p 1135 A93-51466
- [AIAA PAPER 93-3881] p 1135 A93-51466
- Genetic design of digital model-following flight-control systems p 1135 A93-51468
- [AIAA PAPER 93-3883] p 1135 A93-51468
- The application of scheduled H-infinity controllers to a VSTOL aircraft p 1135 A93-52249
- [AIAA PAPER 93-3884] p 1135 A93-52249
- Methodology for integration of digital control loaders in aircraft simulators p 1207 A93-52655
- [AIAA PAPER 93-3551] p 1207 A93-52655
- Hybrid complex of the aircraft intellectualized control systems simulation at the stage of their research projecting p 1222 A93-52660
- [AIAA PAPER 93-3559] p 1222 A93-52660
- Transport delay compensation - An inexpensive alternative to increasing image generator update rate p 1223 A93-52663
- [AIAA PAPER 93-3563] p 1223 A93-52663
- Solution of the boundary value problem in flight dynamics by the opposite motion method p 1206 A93-52944
- [AIAA PAPER 93-3564] p 1206 A93-52944
- A vision-based method for autonomous landing p 1190 A93-53172
- [AIAA PAPER 93-3559] p 1190 A93-53172
- Developments towards versatility in digital engine control units p 1202 A93-54064
- [ISABE 93-7088] p 1202 A93-54064
- Design of limit-tracking systems incorporating a turbofan engine with constant disturbances p 1203 A93-54066
- [ISABE 93-7090] p 1203 A93-54066
- A parameter optimization approach to controller partitioning for integrated flight/propulsion control application p 1206 A93-54268
- [AIAA PAPER 93-3559] p 1206 A93-54268
- A simulation study on take-off and landing dynamics of fly-by-wire control system aircraft p 1249 A93-55590
- [AIAA PAPER 93-3559] p 1249 A93-55590
- Boeing 777 high lift control system p 1249 A93-55753
- [AIAA PAPER 93-3559] p 1249 A93-55753
- Estimation of aircraft inertia characteristics from bifilar pendulum test data p 1249 A93-56029
- [AIAA PAPER 93-3559] p 1249 A93-56029
- Predevelopment of a flight control system for a small civil aircraft p 1249 A93-56031
- [AIAA PAPER 93-3559] p 1249 A93-56031
- Concorde propulsion: Did we get it right? The Rolls-Royce/SNECMA Olympus 593 engine reviewed [PNR-90970] p 57 N93-11061
- A problem formulation for glideslope tracking in wind shear using advanced robust control techniques [NASA-TM-104164] p 64 N93-11176
- Optimal output feedback vibration control of rotor-bearing systems p 86 N93-11220
- Modeling and model simplification of aeroelastic vehicles: An overview p 64 N93-12216
- [NASA-TM-107691] p 64 N93-12216
- Formal representation of the requirements for an Advanced Subsonic Civil Transport (ASCT) flight control system [NASA-CR-189699] p 98 N93-12346
- Air-breathing hypersonic vehicle guidance and control studies: An integrated trajectory/control analysis methodology, phase 2 [NASA-CR-189703] p 65 N93-12413
- Design philosophy for wind tunnel model positioning systems p 192 N93-12552
- [AD-A254958] p 192 N93-12552
- Application of concurrent engineering methods to the design of an autonomous aerial robot p 212 N93-12555
- [AD-A254968] p 212 N93-12555
- Limited production Precision Runway Monitor (PRM) master test plan p 192 N93-12899
- [DOT/FAA/CT-TN92/23] p 192 N93-12899
- A brief overview of NASA Langley's research program in formal methods p 228 N93-12958
- Active flutter suppression using dipole filters [NASA-TM-107594] p 186 N93-13367
- A stochastic optimal feedforward and feedback control methodology for supergravity p 229 N93-13370
- [NASA-CR-4471] p 229 N93-13370
- Robust controller and estimator design using minimax methods p 229 N93-13925
- Online vibration control of a flexible rotor/bearing system p 219 N93-14468
- Helicopter installations: From motor to rotor [LR-675] p 329 N93-16345
- A contribution to the dynamic feedforward open loop control of multivariable systems and to the optimal design of command functions p 441 N93-16515
- [DLR-FB-92-05] p 441 N93-16515
- Approaches to control of the large angle magnetic suspension test fixture p 381 N93-16695
- [NASA-CR-191890] p 381 N93-16695
- Developing a control system for ARES 2 p 371 N93-16769
- Design of robust suboptimal controllers for a generalized quadratic criterion p 372 N93-17670
- [AD-A257746] p 372 N93-17670
- Low bandwidth robust controllers for flight [NASA-CR-191774] p 372 N93-17800
- MM-122: High speed civil transport [NASA-CR-192011] p 334 N93-17974
- Theoretical constraints in the design of multivariable control systems p 442 N93-18372
- [NASA-CR-191900] p 442 N93-18372
- Active stabilization to prevent surge in centrifugal compression systems p 424 N93-18862
- [NASA-CR-191625] p 424 N93-18862
- Strategies for optimal control design of normal acceleration command following on the F-16 p 373 N93-19095
- [AD-A258975] p 373 N93-19095
- Longitudinal-control design approach for high-angle-of-attack aircraft p 373 N93-19108
- [NASA-TP-3302] p 373 N93-19108
- Improvements to LOGI/LTR methodology for plants with lightly damped or low frequency poles p 443 N93-19112
- [AD-A258841] p 443 N93-19112
- Helicopter flight control system design using the linear quadratic regulator for robust eigenstructure assignment [AD-A258904] p 373 N93-19351
- URV flight test of an Ada implemented self-repairing flight control system p 527 N93-20551
- [AD-A259205] p 527 N93-20551
- Controller partitioning for integrated flight/propulsion control implementation p 527 N93-21197
- [NASA-TM-105804] p 527 N93-21197
- Applications of active adaptive noise control to jet engines p 522 N93-21210
- [NASA-CR-192277] p 522 N93-21210
- Screening studies of advanced control concepts for airbreathing engines p 721 N93-25079
- [NASA-TM-106042] p 721 N93-25079
- Robust nonlinear control of vectored thrust aircraft [NASA-CR-192727] p 728 N93-25199
- Techniques for designing rotorcraft control systems [NASA-CR-192960] p 729 N93-26046
- Game theoretic synthesis for robust aerospace controllers p 819 N93-27171
- The design of a robust autopilot for the Archytas prototype via linear quadratic synthesis [AD-A262151] p 820 N93-27546
- A modified approach to controller partitioning [NASA-TM-106167] p 848 N93-28051
- Noise transmission properties and control strategies for composite structures p 919 N93-30436
- Flight control system design factors for applying automated testing techniques p 910 N93-30764
- [NASA-TM-4242] p 910 N93-30764
- Fight test of avionic and air-traffic control systems [ESA-TT-1279] p 993 N93-31271
- Testing concept of a taxiing control system, summary p 1010 N93-31278
- Development and flight testing of a fault-tolerant fly-by-light yaw control system p 1010 N93-31280
- Design and implementation of fuzzy logic controllers [NASA-CR-193268] p 1038 N93-31649
- CONTROL THEORY**
- Aspects of multivariable flight control law design for helicopters using eigenstructure assignment p 60 A93-10916
- Limit of sampling periods for nonlinear flight trajectory controller of aircraft p 61 A93-11207
- Effects of thrust line offset on neutral point determination in stability flight testing [AIAA PAPER 92-4082] p 61 A93-11265
- Research on the stability and control of soaring birds [AIAA PAPER 92-4122] p 61 A93-11284
- Discrete time H(infinity) control laws for a high performance helicopter p 96 A93-13007
- Optimization-based linear and nonlinear design methodologies for aircraft control. II - Final simulations [AIAA PAPER 92-4627] p 62 A93-13285
- Flight path optimization and suboptimal control laws synthesis for transport mission of maneuverable aircraft p 180 A93-14160
- Optimality-based control laws for real-time aircraft control via parameter optimization p 180 A93-14161
- Integrated control law synthesis of gust load alleviation and flutter margin augmentation for a transport aircraft p 182 A93-14281
- A longitudinal control law integrating flight controls and engine controls p 186 A93-15046
- Evaluation of approaches to active compressor surge stabilization [ASME PAPER 92-GT-182] p 352 A93-19407
- Robust stabilization based on topological connectedness p 438 A93-22830
- Output tracking control of nonlinear systems with weakly non-minimum phase p 439 A93-22968
- Pilot control identification using Minimum Model Error estimation p 523 A93-24497
- [AIAA PAPER 92-4421] p 523 A93-24497
- Algorithms and automated techniques for the design of control systems for moving objects p 562 A93-29690
- An algorithm with prediction in a control problem with functional constraints p 757 A93-35307
- Automatic guidance and control laws for helicopter obstacle avoidance p 728 A93-35518
- Adaptive grid generation using optimal control theory p 770 A93-38187
- Quantitative feedback theory applied to the design of a rotorcraft flight control system p 906 A93-41895
- Pilot-in-the-loop analysis of propulsive-only flight control systems p 908 A93-42812
- Flight management system on the F-117A p 908 A93-42815
- Real-time parameter identification applied to flight simulation p 1006 A93-44142
- Nonsmooth trajectory optimization - An approach using continuous simulated annealing [AIAA PAPER 93-3657] p 1099 A93-48337
- Statistical methods in flight vehicle control theory p 1165 A93-49306
- Problems in the optimization of complex engineering systems p 1165 A93-49307
- Trajectory control for a low-lift re-entry vehicle p 1141 A93-49592
- Control problem for a plant with artificial intelligence p 1168 A93-50960
- Hodograph analysis in aircraft trajectory optimization [AIAA PAPER 93-3742] p 1101 A93-51338
- The Generalized Legendre-Clebsch Condition on state/control constrained arcs [AIAA PAPER 93-3746] p 1170 A93-51342
- Guidance and control law for automatic landing flight experiment of reentry space vehicle [AIAA PAPER 93-3818] p 1143 A93-51409
- Control theoretic approach to air traffic conflict resolution [AIAA PAPER 93-3832] p 1097 A93-51421
- System identification of unstable manipulators using ERA methods - Eigensystem Realization Algorithm [AIAA PAPER 93-3842] p 1170 A93-51431
- H(infinity) helicopter flight control law design with and without rotor state feedback [AIAA PAPER 93-3849] p 1134 A93-51436
- Decentralized autonomous attitude determination using an inertially stabilized payload [AIAA PAPER 93-3857] p 1134 A93-51444
- Fuzzy logic control algorithm for suppressing E-6A Long Trailing Wire Antenna wind shear induced oscillations [AIAA PAPER 93-3868] p 1171 A93-51454
- Guidance law based on piecewise constant control for hypersonic gliders [AIAA PAPER 93-3888] p 1144 A93-51472
- Application of nonlinear systems theory to transonic unsteady aerodynamic responses p 1095 A93-52438

- Integrated fire control simulation systems
p 1192 A93-53876
- Design, test, and evaluation of three active flutter suppression controllers
[NASA-TM-4338] p 63 N93-10070
- Application of eigenstructure assignment to the control of powered lift combat aircraft p 64 N93-11871
- Symposium proceedings on Quantitative Feedback Theory
[AD-A255527] p 187 N93-13872
- A contribution to the dynamic feedforward open loop control of multivariable systems and to the optimal design of command functions
[DLR-FB-92-05] p 441 N93-16515
- Improvements to LQGI/LTR methodology for plants with lightly damped or low frequency poles
[AD-A258841] p 443 N93-19112
- Method for developing the RAFALE flight control system
p 512 N93-19912
- Guidance and flight control law development for hypersonic vehicles
[NASA-CR-192102] p 526 N93-19960
- Analytical and experimental investigation of flutter suppression by piezoelectric actuation
[NASA-TP-3241] p 513 N93-20584
- Optimal thrust magnitude on a singular arc in atmospheric flight p 758 N93-25410
- Control of complex dynamic systems by neural networks p 758 N93-25611
- A modified approach to controller partitioning
[NASA-TM-106167] p 848 N93-28051
- Artificial intelligence methodologies in flight related differential game, control and optimization problems
[AD-A262405] p 848 N93-28498
- Mathematical modeling and control law development for the atmospheric monitoring and control system of the Controlled Environment Research Chamber (CERC) at NASA Ames Research Center
[AD-A261978] p 911 N93-29436
- Turbulent drag reduction*Studies of feedback control and flow over riblets p 878 N93-30645
- CONTROL VALVES**
Action composition for the animation of natural language instructions
[AD-A254963] p 228 N93-12554
- CONTROLLABILITY**
Handling qualities flight test techniques and analyses used with the proposed MIL-H-8501B
[AIAA PAPER 92-4081] p 61 A93-11264
- Flying qualities of a remotely piloted vehicle
[AIAA PAPER 92-4083] p 61 A93-11266
- 757 fly-by-wire demonstrator flight test
[AIAA PAPER 92-4099] p 38 A93-11271
- Piloted simulation evaluation of pitch control designs for highly augmented STOVLC aircraft
[AIAA PAPER 92-4234] p 63 A93-13328
- Piloted simulation study of two tilt-wing control concepts
[AIAA PAPER 92-4236] p 63 A93-13338
- Limit cycle in the longitudinal motion of the USB STOL ASKA - Control system functional mockup and actual aircraft
[SAE PAPER 921040] p 185 A93-14660
- Design of flight control systems to meet rotorcraft handling qualities specifications p 370 A93-23509
- Design of reconfigurable digital multiple model-following flight control systems p 908 A93-42811
- Forebody vortex control on an F/A-18 using small, rotatable 'tip-strakes'
[AIAA PAPER 93-3450] p 1009 A93-47236
- Design of a helicopter control system to meet handling quality specifications using H(infinity) techniques
[AIAA PAPER 93-3850] p 1134 A93-51437
- Envelope function - A tool for analyzing flutter data
p 1136 A93-52455
- Effect of lift-to-drag ratio in pilot rating of the HL-20 landing task p 1210 A93-53738
- Flight test and analysis procedures for new handling criteria
[RAE-TM-FM-26] p 47 N93-10803
- On automated analysis of flight test data p 512 N93-19913
- CONTROLLED ATMOSPHERES**
Mathematical modeling and control law development for the atmospheric monitoring and control system of the Controlled Environment Research Chamber (CERC) at NASA Ames Research Center
[AD-A261978] p 911 N93-29436
- CONTROLLERS**
Limit of sampling periods for nonlinear flight trajectory controller of aircraft p 61 A93-11207
- Comparison of nonlinear tracking controllers for a compressible flow process p 66 A93-12224
- Evaluation of piezoceramic actuators for control of aircraft interior noise p 447 A93-19186
- Output tracking control of nonlinear systems with weakly non-minimum phase p 439 A93-22968
- Direct multivariable adaptive controller with application to wing flutter p 524 A93-26946
- A treatment to flight controller nonlinearity effects - An adaptive compensator approach p 524 A93-26948
- Controller design using fuzzy logic - A case study p 756 A93-33793
- A closed loop controller for BVI impulsive noise reduction by Higher Harmonic Control p 849 A93-35963
- Design and evaluation of a robust dynamic neurocontroller for a multivariable aircraft control problem p 817 A93-37004
- Design philosophy for wind tunnel model positioning control systems p 822 A93-37877
- Constrained control allocation p 938 A93-41891
- Design of a rule-based fuzzy controller for the pitch axis of an unmanned research vehicle p 907 A93-42807
- Reduced order proportional integral observer with application p 1166 A93-49605
- A simplified approach for control of rotating stall. II - Experimental results
[AIAA PAPER 93-2234] p 1080 A93-50038
- Control of takeoff of a hypersonic aircraft using neural networks p 1167 A93-50744
- The use of genetic algorithms in the design of fuzzy logic controllers p 1167 A93-50779
- A magnetic suspension system with a large angular range p 1139 A93-51295
- A comparison of two multi-variable integrator windup protection schemes
[AIAA PAPER 93-3812] p 1123 A93-51404
- Adaptive quadratic stabilization control with application to flight controller design
[AIAA PAPER 93-3847] p 1133 A93-51434
- A test bench for rotorcraft hover control
[AIAA PAPER 93-3853] p 1140 A93-51440
- Approximate decoupling flight control system design with output feedback for nonlinear systems
[AIAA PAPER 93-3880] p 1135 A93-51465
- A new technique for nonlinear control of aircraft
[AIAA PAPER 93-3881] p 1135 A93-51466
- The application of scheduled H-infinity controllers to a VSTOL aircraft p 1135 A93-52249
- A parameter optimization approach to controller partitioning for integrated flight/propulsion control application p 1206 A93-54268
- Design philosophy for wind tunnel model positioning systems
[AD-A254958] p 192 N93-12552
- Multiple-function multi-input/multi-output digital control and on-line analysis
[NASA-TM-107697] p 162 N93-13565
- Robust controller and estimator design using minimax methods p 229 N93-13925
- Online vibration control of a flexible rotor/bearing system p 219 N93-14468
- Propulsion system performance resulting from an integrated flight/propulsion control design
[NASA-TM-105874] p 180 N93-15525
- Upgrade and extension of the data acquisition system for propulsion and gas dynamic laboratories
[AD-A256836] p 235 N93-15637
- Approaches to control of the large angle magnetic suspension test fixture
[NASA-CR-191890] p 381 N93-16695
- Design of robust suboptimal controllers for a generalized quadratic criterion
[AD-A257746] p 372 N93-17670
- Strategies for optimal control design of normal acceleration command following on the F-16
[AD-A258975] p 373 N93-19095
- Guidance and flight control law development for hypersonic vehicles
[NASA-CR-192102] p 526 N93-19960
- A simulation study of the effects of communication delay on air traffic control
[AD-A258593] p 502 N93-19966
- Controller partitioning for integrated flight/propulsion control implementation
[NASA-TM-105804] p 527 N93-21197
- Applications of active adaptive noise control to jet engines
[NASA-CR-192277] p 522 N93-21210
- Techniques for designing rotorcraft control systems
[NASA-CR-192960] p 729 N93-26046
- Development and testing of the digital control system for the Archytas unmanned air vehicle
[AD-A261656] p 729 N93-26196
- Low bandwidth robust controllers for flight
[NASA-CR-193085] p 819 N93-27156
- A modified approach to controller partitioning
[NASA-TM-106167] p 848 N93-28051
- Robust control of intelligent rotor
[AD-A263707] p 909 N93-29985
- Design and implementation of fuzzy logic controllers
[NASA-CR-193268] p 1038 N93-31649
- CONVECTION**
Comparison of several convection discretization schemes for all Mach number arbitrary 2D flows
p 685 A93-34345
- A new flux splitting scheme p 973 A93-47189
- The convection speed of the dynamic stall vortex
[AD-A247258] p 21 N93-11464
- Extended surface heat sinks for electronic components: A computer optimization
[AD-A256134] p 218 N93-14254
- Two-dimensional fin analysis p 750 N93-25737
- CONVECTION CLOUDS**
Potential aircraft hazards in the vicinity of convective clouds - A review from the perspective of a scale-model study p 427 A93-22116
- Structure of downbursts associated with heavy rainfall observed in Tokyo p 433 A93-22200
- Hydrometeor identification using cross polar radar measurements and aircraft verification p 844 A93-37719
- CONVECTIVE FLOW**
Numerical study of mixed convection between two corotating symmetrically heated disks p 416 A93-23491
- Further analysis of high-rate rolling experiments of a 65 deg delta wing
[AIAA PAPER 93-0620] p 523 A93-24737
- Numerical methods in laminar and turbulent flow; Proceedings of the 7th International Conference, Stanford Univ., CA, July 15-19, 1991. Vol. 7, pts. 1 & 2
[ISBN 0-906674-77-8] p 743 A93-34301
- Some special purpose preconditioners for conjugate gradient-like methods applied to CFD p 772 A93-38638
- A novel algorithm for the solution of compressible Euler equations in wave/particle split (WPS) form p 957 A93-45093
- Numerical study of cavity natural convection flow with augmenting and counteracting effects by projection finite element method p 749 N93-25540
- CONVECTIVE HEAT TRANSFER**
Computation of laminar flow and heat transfer over an enclosed rotating disk with and without jet impingement p 201 A93-13982
- Prediction of engine casing temperature of fighter aircraft for infrared signature studies
[SAE PAPER 920961] p 206 A93-14627
- An experimental investigation of convective heat transfer at the leading edge of a gas turbine airfoil
[ASME PAPER 92-GT-248] p 405 A93-19457
- Analytical comparison of convective heat transfer correlations in supercritical hydrogen p 416 A93-23477
- Numerical study of mixed convection between two corotating symmetrically heated disks p 416 A93-23491
- A study of flow structure and heat transfer intensity in the vicinity of an expanding step on a plate p 691 A93-35268
- Hydrodynamics and heat transfer near the stagnation point in an arbitrary axisymmetric nonswirling flow incident on a rotating obstacle p 691 A93-35270
- Experimental density flowfields over a delta wing located in rarefied hypersonic flows p 870 A93-42637
- A convective and radiative heat transfer analysis for the FIRE II forebody
[AIAA PAPER 93-3194] p 1021 A93-44231
- Two-layer convective heating prediction procedures and sensitivities for blunt body reentry vehicles
[AIAA PAPER 93-2763] p 963 A93-46509
- Convective heat-transfer rate distributions over a 140 deg blunt cone at hypersonic speeds in different gas environments
[AIAA PAPER 93-2787] p 1027 A93-46529
- Actively cooled panel testing perils, problems, and pitfalls --- for aerospace vehicles p 1028 A93-46802
- Progress towards understanding and predicting heat transfer in the turbine gas path p 1215 A93-52751
- Mathematical modeling of the three-dimensional temperature fields of turbine blades p 1216 A93-53329
- Evaluation of 2D ceramic matrix composites in aeroconvective environments p 1212 A93-53459
- Thermal fatigue life assessment of a convection-cooled gas turbine blade
[ISABE 93-7062] p 1199 A93-54038
- Fluid dynamics and convective heat transfer in impinging jets through implementation of a high resolution liquid crystal technique
[ISABE 93-7077] p 1220 A93-54053
- The prediction of convective heat transfer in rotating square ducts
[PNR-90929] p 85 N93-11025

CONVENTIONS

- Active cooling from the sixties to NASP p 49 N93-12458
- Extended surface heat sinks for electronic components: A computer optimization p 218 N93-14254 [AD-A256134]
- Two-dimensional fin analysis p 750 N93-25737
- Thermal effects of a coolant film along the suction side of a high pressure turbine nozzle guide vane p 901 N93-29930
- Modelling thermal behaviour of turbomachinery discs and casings p 903 N93-29949
- Performance of thermal adhesives in forced convection p 924 N93-30974
- CONVENTIONS**
- Bilateral transfers of safety oversight will prove beneficial to all states p 1174 A93-49279
- CONVERGENCE**
- A multilevel composite grid method for fluid flow computations [AIAA PAPER 93-0768] p 541 A93-24852
- A new method for improved rotor free-wake convergence [AIAA PAPER 93-0872] p 469 A93-24933
- A technique for accelerated convergence in transonic flow p 685 A93-34347
- Analysis of implicit treatments for a centred Euler solver p 864 A93-42449
- Unstructured mesh algorithms for aerodynamic calculations p 785 N93-27444
- Axisymmetric vortex sheet roll-up p 788 N93-28078
- CONVERGENT NOZZLES**
- Wall jets created by single and twin high pressure jet impingement p 744 A93-34847
- Nozzle effects on linear stability behaviour of combustors [ISABE 93-7044] p 1198 A93-54020
- Performance characteristics of two multiaxis thrust-vectoring nozzles at Mach numbers up to 1.28 [NASA-TP-3313] p 874 N93-29160
- CONVERGENT-DIVERGENT NOZZLES**
- Nozzle flow computations using the Euler equations p 112 A93-14170
- Calculation of pressure ratio at nozzle exit with shock p 122 A93-14480
- Streamline curvature in supersonic shear layers p 244 A93-19194
- Unsteady pressures on exhaust nozzle interior surfaces - Empirical correlations for prediction p 244 A93-19219
- Measured thrust losses associated with secondary air injection through nozzle walls p 270 A93-21656
- NOZZD - A two dimensional explicit inviscid upwind code for convergent divergent nozzles p 460 A93-24080
- Computation of supersonic jet noise under imperfectly expanded conditions [AIAA PAPER 93-0735] p 563 A93-24825
- Internal performance characteristics of vectored axisymmetric ejector nozzles [AIAA PAPER 93-2432] p 898 A93-41046
- Computation of unsteady nozzle flows p 960 A93-45543
- Scale model test results for several spherical/two-dimensional nozzle concepts [AIAA PAPER 93-2430] p 1117 A93-50186
- Aerodynamics design of convergent-divergent nozzles [AIAA PAPER 93-2574] p 1085 A93-50290
- Non-self-similarity of a boundary layer flow of a high-temperature gas in a Laval nozzle p 1176 A93-52946
- Computation of supersonic jet noise under imperfectly expanded conditions [NASA-TM-105961] p 233 N93-15430
- Direct solutions of the Navier-Stokes equations with application to static aeroelasticity p 748 N93-25259
- Cooling predictions in turbofan engine components p 905 N93-29964
- CONVERSION**
- A review of aging aircraft technology - An I.A.I. perspective p 3 A93-13634
- COOLANTS**
- Advanced cooling for high power electric actuators [SAE PAPER 921022] p 158 A93-14649
- Studies on coolant problems in aeronautical turbine cascades [ISABE 93-7074] p 1220 A93-54050
- Thermal effects of a coolant film along the suction side of a high pressure turbine nozzle guide vane p 901 N93-29930
- COOLING**
- Effects of turbine cooling assumptions on performance and sizing of high-speed civil transport [AIAA PAPER 92-4217] p 55 A93-13383
- Advanced cooling for high power electric actuators [SAE PAPER 921022] p 158 A93-14649

- Navier-Stokes flow simulation in a 2D high pressure turbine cascade with a cooled slot trailing edge p 972 A93-46941
- Separation phenomenon in a hypersonic flow with strong wall cooling - Subcritical regime p 1189 A93-54266
- Radial turbine cooling p 82 N93-10061
- Active cooling from the sixties to NASP p 49 N93-12458
- Radial turbine cooling [NASA-TM-105658] p 130 N93-13292
- Two-dimensional fin analysis p 750 N93-25737
- Heat Transfer and Cooling in Gas Turbines [AGARD-CP-527] p 901 N93-29926
- Turbulent flow and heat transfer in idealized blade cooling passages p 902 N93-29938
- Cooling geometry optimization using liquid crystal technique p 902 N93-29939
- Prediction of jet impingement cooling scheme characteristics (airfoil leading edge application) p 932 N93-29941
- Local heat transfer measurement with liquid crystals on rotating surfaces including non-axisymmetric cases p 902 N93-29943
- Performance of thermal adhesives in forced convection p 924 N93-30974
- COOLING FINNS**
- Effect of trailing-edge ejection on local heat (mass) transfer in pin fin cooling channels in turbine blades [ASME PAPER 92-GT-178] p 352 A93-19404
- Heat transfer in a five-pass irregular channel with and without pin-fins p 1256 A93-54633
- COOLING SYSTEMS**
- Evaluation of the efficiency of the direct search method in solving the problem of numerical calculation of the complex hydraulic cooling systems of aviation gas turbine engines p 54 A93-12818
- Hot streaks and phantom cooling in a turbine rotor passage. I - Separate effects [ASME PAPER 92-GT-75] p 401 A93-19325
- Heat transfer and turbulence in a turbulated blade cooling circuit [ASME PAPER 92-GT-187] p 402 A93-19412
- Heat transfer in rotating serpentine passages with trips skewed to the flow [ASME PAPER 92-GT-191] p 403 A93-19416
- Analytical comparison of convective heat transfer correlations in supercritical hydrogen p 416 A93-23477
- Foreign object impact assessment of a high-Mach engine inlet [AIAA PAPER 93-1630] p 711 A93-34158
- Enhanced heat transport in environmental systems using microencapsulated phase change materials [SAE PAPER 921224] p 926 A93-41398
- Actively cooled panel testing perils, problems, and pitfalls --- for aerospace vehicles p 1028 A93-46802
- An efficient liner cooling scheme for advanced small gas turbine combustors [AIAA PAPER 93-1763] p 1109 A93-49660
- Effect of rotation on heat transfer and hydraulic resistance in the radial cooling channels of turbine rotor blades p 1215 A93-52950
- Measurements and computational analysis of heat transfer and flow in a simulated turbine blade internal cooling passage [AIAA PAPER 93-1797] p 1218 A93-53585
- Application of functionally gradient materials to scramjet engines [ISABE 93-7063] p 1200 A93-54039
- A new cooling system for ultra high temperature turbines [ISABE 93-7073] p 1201 A93-54049
- Thermostructural applications of heat pipes for cooling leading edges of high-speed aerospace vehicles p 91 N93-12460
- Turbine engine combustor design at SNECMA [DS-2129] p 363 N93-17851
- Numerical analysis of the flow in a turbulated rectangular duct simulating the cooling passages in a turbine blade [AD-A257855] p 420 N93-18305
- Engine driven chiller and thermal storage integration (Large tonnage engine driven chiller development) [PB92-227891] p 555 N93-21465
- The effect of orthogonal-mode rotation on forced convection in a circular-sectioned tube fitted with full circumferential transverse ribs p 932 N93-29937
- The effect of main stream flow angle on flame tube film cooling p 932 N93-29953
- Impingement/effusion cooling p 932 N93-29954
- Measurements and computational analysis of heat transfer and flow in a simulated turbine blade internal cooling passage [NASA-TM-106189] p 1032 N93-31647
- COORDINATE TRANSFORMATIONS**
- Numerical simulation of the turbulent flow in round jets [AIAA PAPER 93-0199] p 277 A93-22619

SUBJECT INDEX

- A technique to correct airborne Doppler data for coordinate transformation errors using surface clutter p 807 A93-37699
- Representation of vehicle location in networked simulations [AIAA PAPER 93-3582] p 1214 A93-52677
- Adjoint methods for aerodynamic wing design [NASA-CR-193086] p 805 N93-27089
- COORDINATES**
- A preliminary investigation of a method to calibrate strain gauge balances by means of a reference balance p 210 A93-16845
- Visual grid quality assessment for 3D unstructured meshes [AIAA PAPER 93-3352] p 1036 A93-45046
- A new method for resolving transonic nozzle flows using orthogonal stream-lines coordinate system p 1230 A93-54584
- The body-fitted coordinates generation for multi-element airfoils p 1231 A93-54598
- Prediction of airfoil stall using Navier-Stokes equations in streamline coordinates p 787 N93-27456
- COPOLYMERS**
- Waterborne polyurethane binder resins for compliant aircraft coatings [AD-A256246] p 199 N93-14573
- COPPER ALLOYS**
- Fatigue life under random load history derived from exceedance curves using different algorithms p 1260 A93-56544
- CORES**
- Nonlinear dynamic simulation of single- and multi-spool core engines [AIAA PAPER 93-2580] p 1122 A93-50294
- Vortex breakdown incipience: Theoretical considerations [NASA-CR-189734] p 290 N93-16627
- CORIOLIS EFFECT**
- Coriolis effects on Goertler vortices in the boundary-layer flow on concave wall p 123 A93-14564
- Heat transfer in rotating serpentine passages with trips skewed to the flow [ASME PAPER 92-GT-191] p 403 A93-19416
- Sources of helicopter rotor hub inplane shears [AIAA PAPER 93-1358] p 709 A93-33927
- Three-dimensional numerical simulation of gradual opening in a wave rotor passage [AIAA PAPER 93-2526] p 1156 A93-50254
- Three-dimensional numerical simulation of gradual opening in a wave rotor passage [NASA-CR-191157] p 900 N93-29072
- The effect of orthogonal-mode rotation on forced convection in a circular-sectioned tube fitted with full circumferential transverse ribs p 932 N93-29937
- Turbulent flow and heat transfer in idealized blade cooling passages p 902 N93-29938
- Some implications of a differential turbomachinery equation with viscous correction [AD-A264693] p 935 N93-30571
- CORNER FLOW**
- Boundary layer separation in a corner formed by two planes p 6 A93-10188
- Vortical solutions in supersonic corner flows [AIAA PAPER 93-0760] p 466 A93-24845
- The coherent structure in a corner turbulent boundary layer p 548 A93-28575
- Damping of surface pressure fluctuations in hypersonic turbulent flow past expansion corners p 860 A93-41914
- The application of an adaptive upwind unstructured grid solution algorithm to the simulation of compressible laminar viscous flows over compression corners p 866 A93-42594
- Hypersonic viscous flow over two-dimensional ramps p 866 A93-42596
- Experimental study of the longitudinal hypersonic corner flow field - HERMES-R&D research program, problem no. 5 p 867 A93-42602
- A systems approach to a DSMC calculation of a control jet interaction experiment [AIAA PAPER 93-2798] p 964 A93-46538
- A numerical solution of the asymptotic problem of boundary layer separation in an incompressible liquid upstream of the corner point of a body p 965 A93-46699
- Asymmetric vortical solutions in supersonic corners - Steady 3D space-marching versus time-dependent conical results [AIAA PAPER 93-2957] p 1047 A93-48151
- Comparison of ENO and TVD schemes for the parabolized Navier-Stokes equations [AIAA PAPER 93-2970] p 1049 A93-48164
- Experimental study of shock wave and hypersonic boundary layer interactions near a convex corner [AIAA PAPER 93-2980] p 1051 A93-48173

Hypersonic, turbulent viscous interaction past an expansion corner
[AIAA PAPER 93-2985] p 1051 A93-48178

DSMC numerical investigation of rarefied compression corner flow
[AIAA PAPER 93-3096] p 1061 A93-48270

Vortical solutions in supersonic corner flows
p 1071 A93-49015

Effect of rounding side corners on vortices shedding and downwash from square cylinder of finite length placed on a ground plane
p 1160 A93-51893

A study of the stability of vortical structures in supersonic inlets
[ISABE 93-7103] p 1187 A93-54079

Instability of flow in a streamwise corner
[NASA-CR-191410] p 694 A93-25153

CORNERS
Fractographic investigation of IMI 685 crack propagation specimens for SMP SC33 p 1004 A93-31743

COROTATION
Numerical study of mixed convection between two corotating symmetrically heated disks
p 416 A93-23491

Transient thermal behaviour of a compressor rotor with axial cooling air flow and co-rotating or contra-rotating shaft
p 903 A93-29946

CORRECTION
Development of a realtime DGPS system
[DLR-MITT-92-06] p 503 A93-20749

CORRELATION
Correlations between engineering, medical and behavioural aspects in fire-related aircraft accidents
p 494 A93-19693

Comparison of performance on the Shipley Institute of Living Scale, Air Traffic Control Specialist Selection Test, and FAA Academy Screen
[AD-A259249] p 502 A93-20582

CORRELATION COEFFICIENTS
Example of statistical techniques applied to analysis of landing ground roll distance measurements (linear regression, correlation coefficient and F-test)
[ESDU-92021] p 330 A93-16635

CORRELATION DETECTION
Correlation filters for aircraft identification from radar range profiles
p 1097 A93-50636

CORROSION
Electronics show their age
p 80 A93-13447

Corrosion of ceramic matrix composites
[ONERA, TP NO. 1993-82] p 1213 A93-53602

NDT for corrosion in aerospace structures; Proceedings of the Conference, London, United Kingdom, Feb. 12, 1992
[ISBN 0-903409-99-2] p 1257 A93-54894

The use of non-destructive testing to detect and monitor aircraft corrosion in service
p 1258 A93-54896

NDT for corrosion in aerospace structures - A review of NDT techniques
p 1258 A93-54897

Enhancement of conventional NDT methods for corrosion detection in layered skins
p 1258 A93-54898

Magneto-optic imaging inspection of selected corrosion specimens
[DOT/FAA/CT-TN92/20] p 88 A93-11617

CORROSION PREVENTION
A review of aging aircraft technology - An I.A.I. perspective
p 3 A93-13634

Development of MIL-H-53119, -54 C to 175 C high-temperature nonflammable hydraulic fluid for Air Force systems
p 1214 A93-54250

Hermetic sealing and EMI shielding gasket
[AD-D015359] p 199 A93-13414

Performance of gas turbine compressor cleaners
[NLR-TP-91237-U] p 1003 A93-31111

CORROSION RESISTANCE
Ceramic coatings enhance material performance
p 71 A93-13648

Corrosion resistance of Inconel Alloy 617 in simulated gas turbine environments
[ASME PAPER 92-GT-142] p 388 A93-19374

New corrosion resistant nickel-base super-alloys and technological processes of casting gas turbines parts with directional single crystal and regulable equiaxial minimized microporosity structure
p 916 A93-40811

High temperature corrosion resistant bearing steel development
[AIAA PAPER 93-2000] p 1145 A93-49842

'No VOC' water-borne corrosion resistant primers for aerospace bonding applications
p 1211 A93-53419

Advanced turbine design for coal-fueled engines
[DE93-000224] p 554 A93-21254

Field evaluation of six protective coatings applied to T-56 turbine blades after 2000 hours of engine use
[AD-A261112] p 522 A93-21316

CORROSION TESTS
Niobium alloy heat pipes for use in oxidizing environments
p 200 A93-13791

Accelerated corrosion fatigue test methods for aging aircraft
p 198 A93-16623

Coherent X-ray imaging for corrosion evaluation - A preliminary assessment
p 396 A93-18611

Real-time optical measurement of alkali species in air for jet engine corrosion testing
[AIAA PAPER 93-0791] p 541 A93-24870

The chemistry of Saudi Arabian sand - A deposition problem on helicopter turbine airfoils
p 1216 A93-53468

Magneto-optic imaging inspection of selected corrosion specimens
[DOT/FAA/CT-TN92/20] p 88 A93-11617

Stress corrosion susceptibility of ultra-high strength steels for Naval aircraft applications
[AD-A256126] p 199 A93-15189

Hydrogen-induced stress corrosion cracking susceptibility analysis of pitch links from the AH-64 Apache helicopter
[AD-A260692] p 736 A93-25895

Accelerated and real-time corrosion testing of aluminum-lithium alloys
[NLR-TP-91203-U] p 1020 A93-32385

COSMIC RAYS
Single event upset in avionics
p 1158 A93-50566

COST ANALYSIS
Measuring flight test progress on large scale development programs
[AIAA PAPER 92-4070] p 37 A93-11257

Counting the cost of composites
p 107 A93-14117

Cost - The challenge for advanced materials and structures
p 233 A93-14338

Reducing helicopter operating costs
p 486 A93-25249

The costs of noise at the new Munich airport
p 558 A93-28493

CFD development and a future high speed computer
p 847 A93-38128

Design and cost viability of composites in commercial aircraft
p 915 A93-39963

Machining cost comparison of silicon carbide discontinuously reinforced aluminum, unreinforced aluminum, and titanium
[SME PAPER EM92-252] p 925 A93-40656

Advanced cargo aircraft may offer a potential renaissance in freight transportation
p 991 A93-47023

Advanced generating technologies - Motivation and selection process in electric utilities
p 1164 A93-50950

3-D braided preforms; cost to manufacture: Magnawave. I - Identifying cost factors
p 1226 A93-53423

The economic effectiveness analysis of technological progress in aviation industry
p 1265 A93-54854

Industry survey of space system cost benefits from New Ways Of Doing Business
p 454 A93-17325

Analysis of consolidation of intermediate level maintenance for Atlantic Fleet T700-GE-401 engines
[AD-A257754] p 363 A93-17695

Airport landside planning and operations
[PB93-167880] p 822 A93-26636

Cost studies for commercial fuselage crown designs
p 920 A93-30440

A unified approach for composite cost reporting and prediction in the ACT program
p 920 A93-30441

Process and assembly plans for low cost commercial fuselage structure
p 923 A93-30865

COST EFFECTIVENESS
Designing to aircraft system effectiveness/cost/time with VERT - The system analysis method for aircraft
p 153 A93-14204

Ground visual aids - Recent research at RAE Bedford
p 191 A93-17311

Advanced expert systems increase aircraft maintenance efficiency - An overview
p 238 A93-18767

The tilt wing advantage - for high-speed VTOL aircraft
p 506 A93-27903

Configuration management impacts on customer support and satisfaction
p 853 A93-35922

Aerodynamic questions related to the safety and cost-effective utilization of airships --- Russian book
p 818 A93-39125

Hover testing a demonstrated and cost-effective risk reduction tool
[AIAA PAPER 93-2677] p 913 A93-42234

Integrated modular avionics
p 896 A93-42777

A graphically interactive approach to structured and unstructured surface grid quality analysis
[AIAA PAPER 93-3351] p 954 A93-45045

Cost effective process selection for composite structure
[SME PAPER EM93-100] p 1043 A93-51727

USAF in-flight simulation - A cost-effective operating approach
[AIAA PAPER 93-3604] p 1175 A93-52690

The economic effectiveness analysis of technological progress in aviation industry
p 1265 A93-54854

Industry survey of space system cost benefits from New Ways Of Doing Business
p 454 A93-17325

Exodus: Prime Mover
[NASA-CR-192051] p 332 A93-17803

High speed civil transport
[NASA-CR-192041] p 337 A93-18161

Materials development program, ceramic technology project addendum to program plan: Cost effective ceramics for heat engines
[DE93-003663] p 394 A93-18537

Variable-speed generators with flux weakening
p 750 A93-25599

X-ray computed tomography for casting development
[AD-A261786] p 752 A93-26526

COST ESTIMATES
Helicopter noise standards - Requirements, compliance, and improvements
p 569 A93-29443

Space policy 2000
p 1174 A93-50333

National Aero-Space Plane: Key issues facing the program. Testimony before the Subcommittee on Technology and Competitiveness, Committee on Science, Space, and Technology, House of Representatives
[GAO/T-NSIAD-92-26] p 161 A93-13253

COST REDUCTION
Counting the cost of composites
p 107 A93-14117

Cost - The challenge for advanced materials and structures
p 233 A93-14338

Cost control of the A320 software - The aircraft manufacturer's point of view
p 227 A93-15044

Very high reliability - Cost and consequences
p 397 A93-18789

Water instead of chemical corrosives against aircraft paint - Environment-friendly paint-stripping methods could mean drastic cost reductions for the aircraft industry
p 239 A93-21850

Reducing helicopter operating costs
p 486 A93-25249

Cost/weight savings for the V-22 wing stow
p 797 A93-35981

National Aero-Space Plane: Key issues facing the program. Testimony before the Subcommittee on Technology and Competitiveness, Committee on Science, Space, and Technology, House of Representatives
[GAO/T-NSIAD-92-26] p 161 A93-13253

A NASPAC-based analysis of the delay and cost effects of the Dallas/Fort Worth metroplex plan
[DOT/FAA/CT-TN92/21] p 193 A93-13447

Software requirements for the A-7E aircraft
[AD-A255746] p 229 A93-15052

Industry survey of space system cost benefits from New Ways Of Doing Business
p 454 A93-17325

Hot film wall shear instrumentation for compressible boundary layer transition research
[NASA-CR-191360] p 294 A93-17855

Advanced composite structural concepts and material technologies for primary aircraft structures
p 918 A93-30430

Composites technology for transport primary structure
p 918 A93-30431

Advanced technology commercial fuselage structure
p 918 A93-30432

Design and manufacturing concepts for thermoplastic structures
p 919 A93-30434

Resin transfer molding for advanced composite primary aircraft structures
p 919 A93-30438

Consolidation of graphite thermoplastic textile preforms for primary aircraft structure
p 919 A93-30439

COSTS
National Aero-Space Plane: Key issues facing the program. Testimony before the Subcommittee on Technology and Competitiveness, Committee on Science, Space, and Technology, House of Representatives
[GAO/T-NSIAD-92-26] p 161 A93-13253

Technical operating report on the Data Integration and Collection Environment (DICE) instrumentation system design
[AD-A258444] p 455 A93-17891

JEFF: Air transport system design simulation
[NASA-CR-192069] p 338 A93-18350

National aero-space plane: Restructuring future research and development efforts
[AD-A258799] p 340 A93-18981

Prediction of success from training
p 495 A93-19702

Instigation and processing of flight tests in DLR
p 998 A93-31275

COUETTE FLOW
Example of the Couette iceform design model - Flat plate iceformation
p 207 A93-15070

Navier-Stokes simulations of unsteady transonic flow phenomena
[NASA-TM-103962] p 129 A93-12721

Navier-Stokes simulations of unsteady transonic flow phenomena
p 697 A93-25542

Stabilized space-time finite element formulations for unsteady incompressible flows involving fluid-body interactions p 843 N93-29040

COULOMB COLLISIONS

The problem of two Coulomb centers and its applications in physical aerodynamics p 776 A93-39132

COUNTER ROTATION

Numerical investigation of the unsteady flow through a counter-rotating fan p 112 A93-14166

Lifting surface theory for steady aerodynamic analysis of ducted counter rotation propfan [ASME PAPER 92-GT-14] p 347 A93-19286

Flow studies in ducted twin-rotor contra-rotating axial flow fans p 258 A93-19545

[ASME PAPER 92-GT-390] p 258 A93-19545

Using contra-rotating rotors for decreasing sizes and component number in small GTE p 356 A93-19562

[ASME PAPER 92-GT-414] p 356 A93-19562

Takeoff/approach noise for a model counterrotation propeller with a forward-swept upstream rotor p 519 A93-24782

[AIAA PAPER 93-0596] p 519 A93-24782

Experimental investigation of counter-rotating propfan flutter at cruise conditions p 720 A93-34160

[AIAA PAPER 93-1632] p 720 A93-34160

Efficient hybrid scheme for the analysis of counter-rotating propellers p 688 A93-34483

A concept for a counterrotating fan with reduced tone noise p 101 N93-11370

[NASA-TM-105736] p 101 N93-11370

Investigation of advanced counterrotation blade configuration concepts for high speed turboprop systems. Task 4: Advanced fan section aerodynamic analysis p 174 N93-12695

[NASA-CR-187128] p 174 N93-12695

Takeoff/approach noise for a model counterrotation propeller with a forward-swept upstream rotor p 362 N93-16715

[NASA-TM-105979] p 362 N93-16715

Investigation of advanced counterrotation blade configuration concepts for high speed turboprop systems. Task 5: Unsteady counterrotation ducted propfan analysis. Computer program user's manual p 521 N93-20583

[NASA-CR-187125] p 521 N93-20583

Investigation of advanced counterrotation blade configuration concepts for high speed turboprop systems. Task 5: Unsteady counterrotation ducted propfan analysis p 521 N93-20773

[NASA-CR-187126] p 521 N93-20773

User's manual for UCAP: Unified Counter-Rotation Aero-Acoustics Program p 852 N93-27148

[NASA-CR-191034] p 852 N93-27148

Transient thermal behaviour of a compressor rotor with axial cooling air flow and co-rotating or contra-rotating shaft p 903 N93-29946

[NASA-CR-187126] p 903 N93-29946

Flow and heat transfer between gas-turbine discs p 903 N93-29950

[NASA-CR-187126] p 903 N93-29950

Flow and heat transfer between gas-turbine discs p 903 N93-29950

[NASA-CR-187126] p 903 N93-29950

Flow and heat transfer between gas-turbine discs p 903 N93-29950

[NASA-CR-187126] p 903 N93-29950

Flow and heat transfer between gas-turbine discs p 903 N93-29950

[NASA-CR-187126] p 903 N93-29950

Flow and heat transfer between gas-turbine discs p 903 N93-29950

[NASA-CR-187126] p 903 N93-29950

Flow and heat transfer between gas-turbine discs p 903 N93-29950

[NASA-CR-187126] p 903 N93-29950

Flow and heat transfer between gas-turbine discs p 903 N93-29950

[NASA-CR-187126] p 903 N93-29950

Flow and heat transfer between gas-turbine discs p 903 N93-29950

[NASA-CR-187126] p 903 N93-29950

Flow and heat transfer between gas-turbine discs p 903 N93-29950

[NASA-CR-187126] p 903 N93-29950

Flow and heat transfer between gas-turbine discs p 903 N93-29950

[NASA-CR-187126] p 903 N93-29950

Flow and heat transfer between gas-turbine discs p 903 N93-29950

[NASA-CR-187126] p 903 N93-29950

CRACK GEOMETRY

Crack models for a transversely isotropic medium p 557 A93-24566

Application of a p-version finite element code to analysis of cracks [AIAA PAPER 93-1450] p 740 A93-33999

Applications of advanced fracture mechanics to fuselage p 1026 A93-45787

The crack initiation approach for durability analysis p 1259 A93-55585

[AIAA PAPER 93-1450] p 740 A93-33999

Applications of advanced fracture mechanics to fuselage p 1026 A93-45787

The crack initiation approach for durability analysis p 1259 A93-55585

[AIAA PAPER 93-1450] p 740 A93-33999

Applications of advanced fracture mechanics to fuselage p 1026 A93-45787

The crack initiation approach for durability analysis p 1259 A93-55585

[AIAA PAPER 93-1450] p 740 A93-33999

Applications of advanced fracture mechanics to fuselage p 1026 A93-45787

The crack initiation approach for durability analysis p 1259 A93-55585

[AIAA PAPER 93-1450] p 740 A93-33999

Applications of advanced fracture mechanics to fuselage p 1026 A93-45787

The crack initiation approach for durability analysis p 1259 A93-55585

[AIAA PAPER 93-1450] p 740 A93-33999

Applications of advanced fracture mechanics to fuselage p 1026 A93-45787

The crack initiation approach for durability analysis p 1259 A93-55585

[AIAA PAPER 93-1450] p 740 A93-33999

Applications of advanced fracture mechanics to fuselage p 1026 A93-45787

The crack initiation approach for durability analysis p 1259 A93-55585

[AIAA PAPER 93-1450] p 740 A93-33999

Applications of advanced fracture mechanics to fuselage p 1026 A93-45787

The crack initiation approach for durability analysis p 1259 A93-55585

[AIAA PAPER 93-1450] p 740 A93-33999

Applications of advanced fracture mechanics to fuselage p 1026 A93-45787

The crack initiation approach for durability analysis p 1259 A93-55585

[AIAA PAPER 93-1450] p 740 A93-33999

Applications of advanced fracture mechanics to fuselage p 1026 A93-45787

The crack initiation approach for durability analysis p 1259 A93-55585

[AIAA PAPER 93-1450] p 740 A93-33999

Applications of advanced fracture mechanics to fuselage p 1026 A93-45787

The crack initiation approach for durability analysis p 1259 A93-55585

[AIAA PAPER 93-1450] p 740 A93-33999

Applications of advanced fracture mechanics to fuselage p 1026 A93-45787

The crack initiation approach for durability analysis p 1259 A93-55585

[AIAA PAPER 93-1450] p 740 A93-33999

Applications of advanced fracture mechanics to fuselage p 1026 A93-45787

The crack initiation approach for durability analysis p 1259 A93-55585

[AIAA PAPER 93-1450] p 740 A93-33999

Applications of advanced fracture mechanics to fuselage p 1026 A93-45787

The crack initiation approach for durability analysis p 1259 A93-55585

[AIAA PAPER 93-1450] p 740 A93-33999

Applications of advanced fracture mechanics to fuselage p 1026 A93-45787

The crack initiation approach for durability analysis p 1259 A93-55585

[AIAA PAPER 93-1450] p 740 A93-33999

Applications of advanced fracture mechanics to fuselage p 1026 A93-45787

The crack initiation approach for durability analysis p 1259 A93-55585

[AIAA PAPER 93-1450] p 740 A93-33999

The effect of exfoliation corrosion on the fatigue behavior of structural aluminium alloys p 1017 A93-45778

An evaluation of the pressure proof test concept for 2024-T3 aluminium alloy sheet p 1026 A93-45780

NASA airframe structural integrity program p 1026 A93-45782

Representation and probability issues in the simulation of multi-site damage p 1026 A93-45785

Axial crack propagation and arrest in pressurized fuselage p 1026 A93-45788

An evaluation of a method of reconstituting fatigue loading from Rainflow counting [RAE-TR-89057] p 82 N93-10198

Mechanisms and modelling of environment-dependent fatigue crack growth in a nickel based superalloy [AD-A253967] p 71 N93-10717

Short fatigue crack growth in a nickel-base superalloy at room and elevated temperature [PNR-90892] p 72 N93-11031

Fatigue crack growth in AerMet 100 steel [AD-A249068] p 74 N93-12248

Propulsion and Energetics Panel Working Group 20 on Test Cases for Engine Life Assessment Technology [AGARD-AR-308] p 176 N93-14890

Introduction to test cases for engine life assessment technology p 176 N93-14891

LARZAC HP turbine disk crack initiation and propagation spin pit test p 176 N93-14892

CF6-6 high pressure compressor stage 5 locking slot crack propagation spin pit test p 176 N93-14894

Engine life assessment test case TF41 LP compressor shaft torsional fatigue p 177 N93-14896

F100 second stage fan disk bolthole crack propagation ferris wheel test p 177 N93-14897

In-service considerations affecting component life p 177 N93-14898

[NASA-TM-105736] p 101 N93-11370

Investigation of advanced counterrotation blade configuration concepts for high speed turboprop systems. Task 4: Advanced fan section aerodynamic analysis p 174 N93-12695

[NASA-CR-187128] p 174 N93-12695

Takeoff/approach noise for a model counterrotation propeller with a forward-swept upstream rotor p 362 N93-16715

[NASA-TM-105979] p 362 N93-16715

Investigation of advanced counterrotation blade configuration concepts for high speed turboprop systems. Task 5: Unsteady counterrotation ducted propfan analysis. Computer program user's manual p 521 N93-20583

[NASA-CR-187125] p 521 N93-20583

Investigation of advanced counterrotation blade configuration concepts for high speed turboprop systems. Task 5: Unsteady counterrotation ducted propfan analysis p 521 N93-20773

[NASA-CR-187126] p 521 N93-20773

User's manual for UCAP: Unified Counter-Rotation Aero-Acoustics Program p 852 N93-27148

[NASA-CR-191034] p 852 N93-27148

Transient thermal behaviour of a compressor rotor with axial cooling air flow and co-rotating or contra-rotating shaft p 903 N93-29946

[NASA-CR-187126] p 903 N93-29946

Flow and heat transfer between gas-turbine discs p 903 N93-29950

[NASA-CR-187126] p 903 N93-29950

Flow and heat transfer between gas-turbine discs p 903 N93-29950

[NASA-CR-187126] p 903 N93-29950

Flow and heat transfer between gas-turbine discs p 903 N93-29950

[NASA-CR-187126] p 903 N93-29950

Flow and heat transfer between gas-turbine discs p 903 N93-29950

[NASA-CR-187126] p 903 N93-29950

Flow and heat transfer between gas-turbine discs p 903 N93-29950

[NASA-CR-187126] p 903 N93-29950

Flow and heat transfer between gas-turbine discs p 903 N93-29950

[NASA-CR-187126] p 903 N93-29950

Flow and heat transfer between gas-turbine discs p 903 N93-29950

[NASA-CR-187126] p 903 N93-29950

Flow and heat transfer between gas-turbine discs p 903 N93-29950

[NASA-CR-187126] p 903 N93-29950

Flow and heat transfer between gas-turbine discs p 903 N93-29950

[NASA-CR-187126] p 903 N93-29950

Flow and heat transfer between gas-turbine discs p 903 N93-29950

[NASA-CR-187126] p 903 N93-29950

Flow and heat transfer between gas-turbine discs p 903 N93-29950

[NASA-CR-187126] p 903 N93-29950

- Flight simulation and constant amplitude fatigue crack growth in aluminum-lithium sheet and plate [NLR-TP-91104-U] p 331 N93-17562
- An overview of elevated temperature damage mechanisms and fatigue behavior of a unidirectional SCS-6/Ti-15-3 composite [NASA-TM-106131] p 825 N93-26702
- CRACKS**
- A review of aging aircraft technology - An I.A.I. perspective p 3 A93-13634
- On dynamic behavior of cracked rotors p 208 A93-15401
- Nondestructive evaluation of ceramic and metal matrix composites for NASA's HITEMP and enabling propulsion materials programs [NASA-TM-105807] p 85 N93-10963
- State-of-the-art survey of flexible pavement crack sealing procedures in the United States [AD-A258050] p 382 N93-17708
- External stress-corrosion cracking of a 1.22-m-diameter type 316 stainless steel air valve [NASA-TP-3190] p 737 N93-26201
- NDE of PWA 1480 single crystal turbine blade material [NASA-TM-106140] p 815 N93-27640
- CRANES**
- Calculation of the parameters of a crane helicopter with one disabled engine p 366 A93-18381
- CRANK-NICHOLSON METHOD**
- Technical prospects for computational aeroacoustics p 244 A93-19150
- Bypass transition in two- and three-dimensional boundary layers [AIAA PAPER 93-3050] p 1057 A93-48230
- CRASH INJURIES**
- Handling the legal consequences of aviation disasters - Passenger compensation [ISBN 3-452-22293-4] p 103 A93-11411
- Concept feasibility demonstration for the Army Cockpit Delethalization Program p 795 A93-35916
- The effectiveness of airbags in reducing the severity of head injury from gunsight strikes in attack helicopters p 494 N93-19691
- CRASH LANDING**
- Instrumentation and data acquisition for full-scale aircraft crash testing p 1250 A93-54399
- Aeroplane crashes on the runway: Validation and final evaluation of the method of modeling an airframe structure [IMFL-91-32] p 165 N93-15126
- Aircraft accident report: Takeoff stall in icing conditions. USAIR Flight 405 FOKKER F-28, N485US, LaGuardia Airport, Flushing, New York, 22 March 1992 [PB93-910402] p 790 N93-27034
- CRASHES**
- The methods of reducing impact loads on occupants in the civil aircraft crash condition p 140 A93-14220
- Human factors in crashes of commuter airplanes p 486 A93-24048
- Aircraft accident/incident summary report: Controlled flight into terrain, Bruno's Inc., Beechjet, N25BR, Rome, Georgia, December 11, 1991 [PB92-910404] p 143 N93-13470
- Helicopter crash survival at sea: United States Navy/Marine Corps experience 1977-1990 p 493 N93-19687
- Crash experience of the US Army Black Hawk helicopter p 493 N93-19688
- The effectiveness of airbags in reducing the severity of head injury from gunsight strikes in attack helicopters p 494 N93-19691
- CRASHWORTHINESS**
- Test and analysis of an advanced technology landing gear p 37 A93-10917
- The development of a crashworthy composite fuselage and landing gear p 799 A93-36001
- Crashworthy landing gear design [SAE AIR 4566] p 1103 A93-52175
- Aviation safety research at the National Institute for Aviation Research Wichita State University: A report to the FAA Technical Center [NIAR-92-2] p 310 N93-16455
- 737-400 at Kegworth, 8 January 1989: The AIB investigation p 491 N93-19661
- Crash experience of the US Army Black Hawk helicopter p 493 N93-19688
- US Army's aviation life support equipment retrieval program real world design successes from proactive investigation p 494 N93-19690
- Crashworthiness of composite seats for civil aircraft p 703 N93-24773
- Static and dynamic large deflection flexural response of graphite-epoxy beams [NASA-CR-4118] p 934 N93-30374
- CREEP PROPERTIES**
- A new production technology for complex-shaped structural elements 'creep forming' p 202 A93-14175
- Recent evolution of gas turbine materials and the development of models for life prediction p 915 A93-40802
- Effect of environment on creep-fatigue crack propagation in turbine disc superalloys [ONERA, TP NO. 1993-5] p 916 A93-41023
- In-service considerations affecting component life p 177 N93-14898
- Creep fatigue life prediction for engine hot section materials (isotropic) [NASA-CR-189221] p 364 N93-18578
- Ultrahigh temperature assessment study: Ceramic matrix composites [AD-A262740] p 826 N93-28592
- CREEP RUPTURE STRENGTH**
- Effects of grain size and carbides on the creep resistance and rupture properties of a conventionally cast nickel-base superalloy p 389 A93-21699
- Evaluation of metallurgical degradation on gas turbine components p 915 A93-40804
- Concurrent field service and laboratory testing as a means of improving reliability in creep-rupture applications p 916 A93-40814
- CREEP STRENGTH**
- Structure of martensite in titanium alloy Ti-6Al-1.6Zr-3.3Mo-0.3Si p 916 A93-43616
- CREEP TESTS**
- Creep crack growth and tail part behavior of low alloy steels and Ni based super alloy p 916 A93-40808
- CREW PROCEDURES (INFLIGHT)**
- Microburst avoidance crew procedures for forward-look sensor equipped aircraft [AIAA PAPER 93-3942] p 1007 A93-44234
- Cockpit resource management proficiency as a factor of primary flight training [AD-A256995] p 328 N93-16262
- CREW PROCEDURES (PREFLIGHT)**
- Cockpit resource management proficiency as a factor of primary flight training [AD-A256995] p 328 N93-16262
- CREW WORKSTATIONS**
- Civil spin-off from military aircraft cockpit research p 45 A93-13415
- AHS, Annual Forum, 48th, Washington, June 3-5, 1992, Proceedings, Vols. 1 & 2 p 763 A93-35901
- Concept feasibility demonstration for the Army Cockpit Delethalization Program p 795 A93-35916
- CRIME**
- Criminal acts against civil aviation [AD-A258760] p 495 N93-19867
- CRITERIA**
- Design of robust suboptimal controllers for a generalized quadratic criterion [AD-A257746] p 372 N93-17670
- CRITICAL FLOW**
- Flow physics of critical states for rolling delta wings [AIAA PAPER 93-3683] p 1129 A93-48355
- Numerical simulation of flows in a supersonic air intake p 303 N93-19314
- CRITICAL LOADING**
- Air transportation system for shipping outsized cargoes p 141 A93-14394
- Damage progression in stiffened composite panels [AIAA PAPER 93-1345] p 738 A93-33915
- Measurements of wear and acoustic emission from fuel-wetted surfaces p 744 A93-34925
- Effect of overloads on the service life of the structural elements of aircraft p 746 A93-35289
- Mode interaction in stiffened composite shells under combined mechanical and thermal loadings p 419 N93-16793
- Transient/structural analysis of a combustor under explosive loads [NASA-TM-107660] p 420 N93-17779
- Estimating turbine limit load [NASA-CR-191105] p 699 N93-25883
- CRITICAL POINT**
- Nonequilibrium heat transfer near the critical point of blunt bodies p 777 A93-39145
- CRITICAL PRESSURE**
- A one-dimensional theory for supersonic gas jets above the critical pressure p 774 A93-39115
- CRITICAL TEMPERATURE**
- Mechanisms and modelling of environment-dependent fatigue crack growth in a nickel based superalloy [AD-A253967] p 71 N93-10717
- CRITICAL VELOCITY**
- Dynamics of a high-rpm compressor p 75 A93-10009
- CROSS CORRELATION**
- An investigation on planar velocimetry by spatial cross-correlation p 697 N93-25664
- CROSS COUPLING**
- Analysis of airframe and engine control interactions and integrated flight/propulsion control p 185 A93-14596
- CROSS FLOW**
- A study of the effect of a moving ground belt on the vortex created by a jet impinging on the ground in a cross flow [AIAA PAPER 92-4250] p 15 A93-13361
- Ground vortex formation for uniform and nonuniform jets impinging on a ground plane [AIAA PAPER 92-4251] p 80 A93-13362
- Experimental study of crossflow instability and laminar-turbulent transition on a swept wing p 115 A93-14250
- A high-frequency, secondary instability of crossflow vortices that leads to transition p 128 A93-17253
- On the cross-flow instability near a rotating disk p 128 A93-17264
- Unsteady pressures under impinging jets in crossflows p 399 A93-19220
- Two-, three-, and four-poster jets in cross flow [AIAA PAPER 93-0023] p 408 A93-20141
- Receptivity of three-dimensional boundary layers [AIAA PAPER 93-0074] p 262 A93-20186
- Effect of micron-sized roughness on transition in swept-wing flows [AIAA PAPER 93-0076] p 262 A93-20188
- Transition studies for swept wing flows using PSE --- parabolized stability equations [AIAA PAPER 93-0077] p 263 A93-20189
- Linear stability of three-dimensional boundary layers - Effects of curvature and non-parallelism [AIAA PAPER 93-0079] p 263 A93-20191
- Design of a wing shape for study of hypersonic crossflow transition in flight p 265 A93-20713
- Optimization of circular orifice jets mixing into a heated crossflow in a cylindrical duct [AIAA PAPER 93-0249] p 361 A93-23246
- A Laser Doppler Anemometry study of a supersonic jet in a low speed cross-flow p 459 A93-23807
- A calculation method for the three-dimensional boundary-layer equations in integral form [AIAA PAPER 93-0786] p 541 A93-24868
- A numerical investigation of a subsonic jet in a crossflow [AIAA PAPER 93-0870] p 469 A93-24931
- Shock wave ahead of a liquid jet in supersonic cross flow p 477 A93-27605
- Stability theory and transition prediction applied to a general aviation fuselage p 479 A93-28601
- Potential hazard of aircraft wake vortices in ground effect with crosswind p 479 A93-28606
- Computation of supersonic crossflow separation using a new parabolized Navier-Stokes code p 687 A93-34355
- Temperature and suction effects on the instability of an infinite swept attachment line p 691 A93-35486
- Characteristics of three-dimensional turbulent jets in crossflow p 772 A93-38695
- Solution of the problem of determining the dynamic characteristics of the cross-flow heat exchanger of the heat recovery system of gas turbine engines p 834 A93-39055
- Study of mixing flow field of a jet in a supersonic cross flow. I - Experimental facilities and preliminary experiments p 857 A93-40430
- Visual observations of supersonic transverse jets p 965 A93-46750
- Numerical simulation of linear interference wave development in three-dimensional boundary layers p 1029 A93-46993
- Calculating crossflow separation using boundary layer computations coupled with an inviscid method [AIAA PAPER 93-3459] p 979 A93-47242
- Effect of curvature on stationary crossflow instability of a three-dimensional boundary layer p 1070 A93-49010
- Shock tunnel experiments and approximate methods on hypervelocity side-jet control effectiveness [AIAA PAPER 93-1929] p 1077 A93-49794
- Observations of liquid jets injected into a highly accelerated supersonic boundary layer p 1177 A93-53214
- Mixing of multiple jets with a confined subsonic crossflow p 1189 A93-54324
- Dynamics of vortex rings in cross-flow p 134 N93-13917
- Wake similarity and vortex formation for two-dimensional bluff bodies p 138 N93-15101
- Optimization of circular orifice jets mixing into a heated cross flow in a cylindrical duct [NASA-TM-105984] p 179 N93-15359
- Experiments on swept-wing boundary-layer transition p 419 N93-16829

- Experimental investigation of the aerodynamics of independently rotating cylindrical shells
[AD-A258917] p 305 N93-19340
- An experimental investigation of a round turbulent jet in a cross-flow p 553 N93-20689
- The effect of surface suction near the leading edge of a swept-back wing
[AERO-REPT-9205] p 484 N93-20807
- Crossflow stability and transition experiments in a swept-wing flow
[NASA-TM-108650] p 555 N93-21819
- Stationary crossflow instability on an infinite swept wing p 699 N93-25865
- Method of measuring cross-flow vortices by use of an array of hot-film sensors
[NASA-CASE-LAR-14824-1-SB] p 751 N93-26000
- Reduction in size and unsteadiness of a VTOL ground vortex by ground fences
[NASA-CR-192997] p 700 N93-26049
- Experimental investigation of crossflow jet mixing in a rectangular duct p 812 N93-27026
- CFD mixing analysis of axially opposed rows of jets injected into confined crossflow
[NASA-TM-106179] p 813 N93-27128
- Experimental study of cross flow mixing in cylindrical and rectangular ducts p 815 N93-27680
- The ground vortex flow field associated with a jet in a cross flow impinging on a ground plane for uniform and annular turbulent axisymmetric jets
[NASA-CR-4513] p 789 N93-28449
- Experimental study of heat transfer close to a plane wall heated in the presence of multiple injections (subsonic flow) p 901 N93-29931
- On the dynamics of aeroelastic oscillators with one degree of freedom
[REPT-92-96] p 1040 N93-31653
- CROSS POLARIZATION**
- Hydrometeor identification using cross polar radar measurements and aircraft verification p 844 A93-37719
- A dual polarised active phased array antenna with low cross polarisation for a polarimetric airborne SAR p 883 A93-43401
- The PHARUS project, first results of the realization phase --- Phased Array Universal SAR p 884 A93-43454
- CRUISE MISSILES**
- Development of an accuracy criteria for body-on-fin carryover interference p 1065 A93-48318
- Fabrication of composite propfan blades for a cruise missile wind tunnel model
[NASA-TM-105270] p 752 N93-26202
- CRUISING FLIGHT**
- Aerodynamic characteristics of a next generation high-speed civil transport p 15 A93-13356
- Study of a Mach 2 supersonic transport aircraft p 124 A93-15034
- Air-breathing hypersonic cruise - Prospects for Mach 4-7 waverider aircraft
[ASME PAPER 92-GT-437] p 384 A93-19579
- Engine/airframe integration for waverider cruise vehicles p 283 A93-23254
- Measurements of jet aircraft emissions at cruise altitude. I - The odd-nitrogen gases NO, NO₂, HNO₂ and HNO₃ p 556 A93-24391
- Cruise noise of an advanced propeller with swirl recovery vanes p 564 A93-28609
- Acoustics due to flow-structural interaction and its transmission through a double-panel in high-speed cruising flight
[AIAA PAPER 93-1431] p 710 A93-33981
- Enhancement of endurance performance by periodic optimal camber control p 727 A93-34541
- Optimal cruise performance p 802 A93-37394
- A French look at the future supersonic transport
[ONERA, TP NO. 1992-209] p 803 A93-38763
- Periodic maximum range cruise with singular control p 890 A93-41903
- Application of natural laminar flow to a supersonic transport concept
[AIAA PAPER 93-3467] p 997 A93-47248
- High lift multiple element airfoil analysis with unstructured grids p 981 A93-47256
- Effect of rotary atmospheric gusts on fighter airplane
[AIAA PAPER 93-3644] p 1127 A93-48328
- Analytical solutions to constrained hypersonic flight trajectories p 1141 A93-49596
- An investigation of the fuel-optimal periodic trajectories of a hypersonic vehicle p 1101 A93-51349
- Analytical solutions to constrained hypersonic flight trajectories
[NASA-CR-191987] p 297 N93-18602
- Optimized scramjet engine integration on a waverider airframe p 722 N93-25480
- CRYOGENIC COOLING**
- Free-piston Stirling coolers for intermediate lift temperatures p 543 A93-26062
- Linear motor driven Stirling coolers for military and commercial applications p 543 A93-26064
- Recent developments in compressor-based Joule-Thomson cooling --- of thermal imaging equipment in ground and helicopter-borne applications p 547 A93-28244
- Test results of an orifice pulse tube refrigerator p 1149 A93-48612
- Application of vanadium hydride compressors for Joule-Thomson cryocoolers p 1149 A93-48616
- Compact heat exchanger fitted to engines of the inverted type
[ISABE 93-7120] p 1221 A93-54095
- Operating experience using venturi flow meters at liquid helium temperature
[DE92-014693] p 90 N93-12140
- Thermostructural applications of heat pipes for cooling leading edges of high-speed aerospace vehicles p 91 N93-12460
- Three-stage sorption type cryogenic refrigeration systems and methods employing heat regeneration
[NASA-CASE-NPO-18366-1-CU] p 216 N93-13422
- CRYOGENIC EQUIPMENT**
- Linear motor driven Stirling coolers for military and commercial applications p 543 A93-26064
- Testing experience with unheated strain-gage balances in the NTF --- National Transonic Facility p 1013 A93-47021
- Magnetic bearings for cryogenic turbomachines p 1149 A93-48601
- Potential use of alternative fuels in aviation p 1243 A93-54838
- Operating experience using venturi flow meters at liquid helium temperature
[DE92-014693] p 90 N93-12140
- CRYOGENIC FLUID STORAGE**
- National Aerospace Plane Integrated Fuselage/Cryotank Risk Reduction program
[AIAA PAPER 93-2564] p 1142 A93-50284
- Aircraft cryogenic fuel system design issues
[AIAA PAPER 93-2567] p 1121 A93-50285
- CRYOGENIC FLUIDS**
- Taking to the skies under hydrogen power - Deutsche Aerospace Airbus studies the use of alternative fuels for civil aviation p 677 A93-34947
- A method for calculating the dynamic characteristics of heat exchangers with single-phase cryogenic coolants p 851 A93-39057
- CRYOGENIC ROCKET PROPELLANTS**
- Potential use of alternative fuels in aviation p 1243 A93-54838
- CRYOGENIC TEMPERATURE**
- INCOLOY 908, a low coefficient of expansion alloy for high-strength cryogenic applications. I - Physical metallurgy p 534 A93-25686
- Design of a hydrogen test facility p 532 A93-25993
- Cryogenic wind tunnels p 1010 A93-44886
- Flight data for the Cryogenic Heat Pipe (CRYOHP) Experiment
[AIAA PAPER 93-2735] p 1027 A93-46488
- CRYOGENIC WIND TUNNELS**
- The cryogenic approach to simulating hot jet in transonic wind-tunnel testing p 117 A93-14297
- Preliminary assessment of tunnel wall interference in the NDA cryogenic wind tunnel
[AIAA PAPER 93-0421] p 285 A93-23340
- Simulation for hot jet by cryogenic wind tunnels p 730 A93-33750
- Aerodynamic investigation with focusing schlieren in a cryogenic wind tunnel
[AIAA PAPER 93-3485] p 910 A93-41059
- The cryogenic wind tunnel p 1013 A93-46915
- Analysis of aeroelastic and resonance responses of a wind tunnel model support system p 1013 A93-47022
- A new and working automatic calibration machine for wind tunnel internal force balances
[AIAA PAPER 93-2467] p 1138 A93-50214
- Wind of change p 1209 A93-53625
- Europe's new windtunnel p 1210 A93-54275
- Thermodynamic aspects of model testing in cryogenic wind tunnels p 1251 A93-56222
- Further noise measurements in a slotted cryogenic wind tunnel
[RAE-TM-AERO-2201] p 101 N93-10805
- Further buffeting tests in a cryogenic wind tunnel
[NASA-TM-107621] p 22 N93-11610
- Strain-gauge balance performance and internal temperature gradients measured in a cryogenic environment
[RAE-TM-AERO-2232] p 68 N93-11906
- Modeling and control study of the NASA 0.3-meter transonic cryogenic tunnel for use with sulfur hexafluoride medium
[NASA-CR-189737] p 418 N93-16379
- Modifications to Langley 0.3-m TCT adaptive wall software for heavy gas test medium, phase 1 studies
[NASA-CR-189736] p 291 N93-16710
- A feasibility study of using Langley 0.3-m transonic cryogenic tunnel sidewall boundary-layer removal system for heavy gas testing
[NASA-CR-191438] p 747 N93-25087
- A PC-based simulation of the National Transonic Facility's safety microprocessor
[NASA-TM-109003] p 1038 N93-32224
- CRYSTAL OSCILLATORS**
- An overview of the evolution of vibrating beam accelerometer technology p 412 A93-21934
- CRYSTAL STRUCTURE**
- Structural stability of 'beta-CEZ' alloy
[ONERA, TP NO. 1992-106] p 824 A93-38586
- CUES**
- Simulator motion
[AD-A257683] p 381 N93-17687
- Trade-offs arising from mixture of color cueing and monocular, binoptic, and stereoscopic cueing information for simulated rotorcraft flight
[NASA-TP-3268] p 338 N93-18333
- CUMULATIVE DAMAGE**
- Justification for the linear recording of fatigue damage summation for aircraft structures under operating conditions p 320 A93-18331
- Estimation of the life of aircraft structures under stochastic steady state loading p 545 A93-27620
- Damage progression in stiffened composite panels
[AIAA PAPER 93-1345] p 738 A93-33915
- Recent evolution of gas turbine materials and the development of models for life prediction p 915 A93-40802
- An evaluation of a method of reconstituting fatigue loading from Rainflow counting
[RAE-TR-89057] p 82 N93-10198
- CURING**
- Computer-aided cure optimization p 209 A93-15804
- Model multilayer structured composites p 533 A93-24509
- Cost effective process selection for composite structure
[SME PAPER EM93-100] p 1043 A93-51727
- Development of cure cycles: From laboratory analysis and testing to production of large scale composites
[MBB-Z-0442-92-PUB] p 536 N93-20845
- CURVATURE**
- Streamline curvature in supersonic shear layers p 244 A93-19194
- Surface-curvature-distribution effects on turbine-cascade performance
[ASME PAPER 92-GT-84] p 248 A93-19333
- Linear stability of three-dimensional boundary layers - Effects of curvature and non-parallelism
[AIAA PAPER 93-0079] p 263 A93-20191
- An experimental study on blade negative curving in a turbine cascade with a large turning angle p 1071 A93-49185
- An approach to constrained aerodynamic design with application to airfoils
[NASA-TP-3260] p 24 N93-12321
- CURVE FITTING**
- An approach to constrained aerodynamic design with application to airfoils
[NASA-TP-3260] p 24 N93-12321
- CURVED BEAMS**
- A nonlinear finite element of an arbitrary beam p 1215 A93-52939
- Design and analysis of curved composite components for rotorcraft fuselage frames p 716 N93-25701
- Chaos in mechanical systems with especial reference to rotorcraft and missiles
[AD-A263703] p 943 N93-29384
- CURVED PANELS**
- Post buckling of laminated composite stiffened curved panels subjected to cyclic shear and compression p 204 A93-14334
- Hypersonic flutter of a curved shallow panel with aerodynamic heating
[AIAA PAPER 93-1318] p 829 A93-37428
- The free vibration of cylindrically-curved rectangular panels p 1022 A93-45113
- Computational schemes for integrity analyses of fuselage panels in aging airplanes p 1025 A93-45774
- Test facility for evaluation of structural integrity of stiffened and jointed aircraft curved panels p 1012 A93-45794

Buckling of open-section bead-stiffened composite panels p 1157 A93-50420
Structural evaluation of curved stiffened composite panels fabricated using a THERM-Xsm process p 919 N93-30435

CURVES (GEOMETRY)

The integration of geometric modeling into an inverse design method and application of a PC-based inverse design method and comparison with test results p 81 N93-10058

CUTTERS

Some characteristics of the design of heads for the cutting of bevel gears with negative curvature of the circular-arc tooth line p 835 A93-39093

CYCLIC HYDROCARBONS

The possibility of reducing the emission of benzo(a)pyrene with the exhaust gases of aviation gas turbine engines by water injection into the combustion chamber p 812 A93-39201

CYCLIC LOADS

Post buckling of laminated composite stiffened curved panels subjected to cyclic shear and compression p 204 A93-14334
Justification for the linear recording of fatigue damage summation for aircraft structures under operating conditions p 320 A93-18331
Application of generalized force determination to a full scale low cycle fatigue test of the SH-2G helicopter p 795 A93-35949
Design for cyclic loading endurance of composites p 1216 A93-53395

An evaluation of a method of reconstituting fatigue loading from Rainflow counting [RAE-TR-89057] p 82 N93-10198
Verification of rain-flow reconstructions of a variable amplitude load history p 91 N93-12411
Determination of stresses on laminated aircraft transparencies by the strain gage-hole drilling and sectioning method [AD-A255548] p 164 N93-14571
RB211-524B disc and drive cones hot cyclic spinning test p 177 N93-14895
Load experience variability of fighter aircraft [NLR-TP-89172-U] p 514 N93-20742
Low cycle fatigue behaviour of titanium disc alloys p 1004 N93-31745

CYLINDERS

Supersonic vortical flows around an ogive-cylinder - Laminar and turbulent computations [ONERA, TP NO. 1992-111] p 771 A93-38588
Numerical simulation of vortex shedding past triangular cylinders at high Reynolds number using a k-epsilon turbulence model p 871 A93-42873
The generation of side force by distributed suction [NASA-CR-193129] p 839 N93-27151
Vortex structure and mass transfer near the base of a cylinder and a turbine blade p 901 N93-29929

CYLINDRICAL BODIES

Calculation of the three-dimensional interaction of a shock wave with a boundary layer on a cylinder p 12 A93-12766
Design sensitivity and optimization of composite cylinders p 71 A93-12781
Further studies on the asymmetrical flow past yawed cylinders p 118 A93-14304
Hypersonic flow separation in shock wave boundary layer interactions [ASME PAPER 92-GT-205] p 251 A93-19429
A Navier-Stokes simulation of vortex shedding from square cylinder in unconfined domain p 538 A93-24084
Three-dimensional flow past an ogival-cylindrical body in combination with a delta wing p 478 A93-27636
The free vibration of cylindrically-curved rectangular panels p 1022 A93-45113
Plume effects at hypersonic speeds p 959 A93-45494
Some measurements on dependence of rectangular cylinder drag on elevation p 1025 A93-45745
An investigation of the effects of a rear stagnation jet on the wake behind a cylinder [AIAA PAPER 93-3274] p 969 A93-46835
Wind-tunnel tests of an inclined cylinder having helical grooves [AIAA PAPER 93-3456] p 979 A93-47239
Effects of a rear stagnation jet on the wake behind a cylinder p 1151 A93-49026
Effect of rounding side corners on vortices shedding and downwash from square cylinder of finite length placed on a ground plane p 1160 A93-51893
Wake similarity and vortex formation for two-dimensional bluff bodies p 138 N93-15101
The role of computational fluid dynamics in aeronautical engineering. 9: Analysis of hypersonic equilibrium air flow p 301 N93-19294

Tangential fuselage blowing on an ogive cylinder p 697 N93-25545

CYLINDRICAL COORDINATES

Burnett solutions along the stagnation line of a cooled cylinder in low-density hypersonic flows [AIAA PAPER 93-2726] p 962 A93-46480

CYLINDRICAL SHELLS

Aeroelastic stability characteristics of composite cylindrical shells by the finite element method p 203 A93-14312
Efficiency of using longitudinal and circumferential bands in the structures of an airtight fuselage p 801 A93-36795
An experimental system for studying the vibrations and acoustic emission of cylindrical shells and panels in a field of turbulent pressure pulsations p 1140 A93-51754
A dynamic stiffness/boundary element method for the prediction of interior noise levels p 1226 A93-53817
A study upon structural optimization of elastic rotors for mechanical systems [INPE-5376-TDI/471] p 83 N93-10310
Experimental investigation of the aerodynamics of independently rotating cylindrical shells [AD-A258917] p 305 N93-19340

D

DAMAGE

Crack growth/damage tolerance analysis methods as applied to V-22 fuselage and empennage p 795 A93-35948
IR window damage measured by reflective scatter p 851 A93-39544
Mechanical damage to aircraft structures from lightning strikes p 879 A93-40432
The properties of newly developed highly damage tolerant and easy handleable carbon fiber/modified bismaleimide prepreg system p 1212 A93-53448
A study of damage tolerance of the landing gear structure p 1219 A93-53881
Federal Aviation Administration pavement modeling p 379 N93-16315
Control of in-service damage: Application to aircraft engines [DS-2027] p 364 N93-18151
Damage detection by Acousto-Ultrasonic Location (AUL) p 555 N93-21529
Numerical determination of the residual strength of battle damaged composite plates p 537 N93-21533
A computational approach to predicting the extent of arc root damage in CFC panels p 735 N93-24890
Comparison of the damage for various types of fibre reinforced composites due to different lightning test standards (MIL-STD-1757A, German military VG-standard 96903) p 736 N93-24891
Lightning phenomenology bases for full threat return stroke occurrence following extended leader sweep at flight altitudes p 754 N93-24895
Expedient repair of structural facilities [AD-A260727] p 731 N93-25656

DAMAGE ASSESSMENT

The fretting damage and effect of temperature in typical joint of aircraft construction p 203 A93-14196
Damage severity of monitored fatigue load spectra p 154 A93-14253
Researches on sonic fatigue of the air-inlet duct of XX aircraft p 154 A93-14256
Accuracy of a simple hole damage analysis method in composite structures p 197 A93-15748
Video holography and laser vibrometry...The dynamic duo p 210 A93-16611
Elastic constants for unidirectional boron-epoxy composites p 387 A93-18636
Static aeroelastic analysis of a maneuvering aircraft with damaged wing [AIAA PAPER 92-4765] p 325 A93-20360
Damage detection in smart structures using neural networks and finite-element analyses p 438 A93-22540
Battle damage repairs p 239 A93-22698
Experimental assessment of airframe damage due to impacting ice [AIAA PAPER 93-0751] p 504 A93-24838
Application of a p-version finite element code to analysis of cracks [AIAA PAPER 93-1450] p 740 A93-33999
Foreign object impact assessment of a high-Mach engine inlet [AIAA PAPER 93-1630] p 711 A93-34158
BLASIM - A computational tool to assess ice impact damage on engine blades [AIAA PAPER 93-1638] p 720 A93-34165
Damage tolerance assessment of the fighter aircraft 37 Viggen main wing attachment p 802 A93-37390

Nonlinear flutter of composite plates with damage evolution [AIAA PAPER 93-1546] p 829 A93-37441

A practical course in aircraft maintenance. I - The powerplant --- Russian book p 811 A93-39175
Evaluation by holographic interferometry of impact damage in composite aeronautical structures p 1020 A93-44193
Towards quantitative non-destructive evaluation of aging aircraft p 1025 A93-45773
Risk analysis for aging aircraft fleets p 1025 A93-45775
The civil Damage Tolerance Requirements in theory and practice p 1026 A93-45777
A damage tolerance approach for management of aging gas turbine engines p 1001 A93-45779
Representation and probability issues in the simulation of multi-site damage p 1026 A93-45785
Bonded repair of multi-site damage p 947 A93-45786
Applications of advanced fracture mechanics to fuselage p 1026 A93-45787
A laboratory study of fracture in the presence of lap splice multiple site damage p 1027 A93-45790
How likely is multiple site damage? p 1027 A93-45791

Estimation of requirements of inspection intervals for panels susceptible to Multiple Site Damage p 948 A93-45795

Evaluation methodologies applied for pressurized fuselages of Airbus A/C p 948 A93-45796
Repairs to damage tolerant aircraft p 948 A93-45799

Case study and simulation of fatigue damages and DTE of aging aircraft - A review of researches in Japan p 948 A93-45800

A two-dimensional analysis of multiple matrix cracking in a laminated composite close to its characteristic damage state p 1157 A93-50405
Aircraft failure detection and identification using neural networks [AIAA PAPER 93-3869] p 1171 A93-51455

Selection of a method for protecting aircraft gas turbine engines against damage by foreign objects (Mathematical models) p 1193 A93-53554
Aerodynamics of turbine blades with trailing-edge damage - Measurements and computations [ISABE 93-7130] p 1189 A93-54105

An evaluation of a method of reconstituting fatigue loading from Rainflow counting [RAE-TR-89057] p 82 N93-10198
Using NDT techniques in the maintenance of aeronautical products [REPT-921-430-102] p 88 N93-11587

Damage tolerance assessment of boron/epoxy repairs to fuselage lap joints [AD-A258383] p 338 N93-18257
Damage tolerance of a helicopter rotor high-strength steel p 555 N93-21322
Comparison of the damage for various types of fibre reinforced composites due to different lightning test standards (MIL-STD-1757A, German military VG-standard 96903) p 736 N93-24891

Lightning phenomenology bases for full threat return stroke occurrence following extended leader sweep at flight altitudes p 754 N93-24895
An overview of elevated temperature damage mechanisms and fatigue behavior of a unidirectional SCS-6/Ti-15-3 composite [NASA-TM-106131] p 825 N93-26702

Damage tolerance assessment and usage variation analysis for C-130 aircraft in the Israeli Air Force p 839 N93-27210
Reportable accidents to UK registered aircraft, and to foreign registered aircraft in UK airspace, 1990 [CAP-600] p 991 N93-31730

Damage severity of monitored fatigue load spectra [NLR-TP-92009-U] p 999 N93-32205

DAMPERS

Computational models of dampers for computer-aided design p 832 A93-39032

DAMPING

Influence of pitch-lag coupling on damping requirements to stabilize 'ground/air resonance' p 158 A93-14784
Flap-lag damping in hover and forward flight with a three-dimensional wake p 797 A93-35979
Damping of surface pressure fluctuations in hypersonic turbulent flow past expansion corners p 860 A93-41914
Free-spin damping measurement techniques [AIAA PAPER 93-3457] p 1014 A93-47240

A study of the rotary balance technique for predicting pitch damping [AIAA PAPER 93-3619] p 1125 A93-48306

DAMPING TESTS

- Wind tunnel spin data reduction to obtain aerodynamic spin damping coefficients by using nonlinear equation of motion
[AD-A253880] p 19 N93-10811
- Optimum design of high speed prop rotors including the coupling of performance, aeroelastic stability and structures p 337 N93-18066
- Application of finite-state inflow to flap-lag-torsion damping in hover p 714 N93-25486
- Navier-Stokes computations for kinetic energy projectiles in steady coning motion: A predictive capability for pitch damping
[AD-A264111] p 1033 N93-32028

DAMPING TESTS

- Damping in aerospace composite materials p 1260 A93-55869

DATA ACQUISITION

- Software for the control of measurement data acquisition, processing, and monitoring during strength testings p 94 A93-10042
- Merger and acquisition - Enhancing Loran propagation technology with artificial intelligence p 29 A93-10987
- Real-time capture, archiving, retrieval, processing, and presentation of large quantities of flight test/research information
[AIAA PAPER 92-4073] p 95 A93-11258
- The development of an airborne information management system for flight test
[AIAA PAPER 92-4113] p 51 A93-11281
- New concepts in remote sensing and geolocation p 556 A93-24173
- Data acquisition and analysis on a Macintosh p 562 A93-29422
- System Status - The diagnostic edge of the pilot's associate p 808 A93-37853
- Wind tunnel operator aimed comparison between two electronic pressure scanner systems p 830 A93-37876
- Methods and equipment for data processing and acquisition in information management systems p 856 A93-43101
- A study of the influence of the data acquisition system sampling rate on the accuracy of measured acceleration loads for transport aircraft p 1000 A93-46808
- Compound curvature laser window development
[AIAA PAPER 93-2177] p 1173 A93-49989
- An upgraded data acquisition and processing system for the Aeropropulsion Systems Test Facility at Arnold Engineering Development Center
[AIAA PAPER 93-2466] p 1138 A93-50213
- Rotor fatigue monitoring data acquisition system p 1261 A93-54353
- An updated data acquisition and processing system for turbine engine testing p 1250 A93-54389
- Instrumentation and data acquisition system for the C.I.R.A. Transonic Pilot Tunnel p 1250 A93-54395
- A data acquisition system for high-speed rotor balancing p 1261 A93-54396
- Data acquisition for aeroelastic testing at the NASA Langley Transonic Dynamics Facility p 1250 A93-54397
- Icing Research Tunnel rotating bar calibration measurement system p 1255 A93-54398
- Instrumentation and data acquisition for full-scale aircraft crash testing p 1250 A93-54399
- NASA Langley's Aircraft Landing Dynamics Facility p 1250 A93-54400
- Experimental heat transfer results in turbine stators and rotors and a comparison with theory
[PNR-90945] p 57 N93-11055
- Wind tunnel operator aimed comparison between two electronic pressure scanner systems
[DLAS-EST-TR-040] p 67 N93-11225
- Results of in-service evaluation of wind shear systems p 146 N93-14856
- FDAMS: An extendable and reconfigurable solution for avionics data management systems p 168 N93-15157
- DAR-2: On-board data acquisition system for aircraft engines p 169 N93-15166
- Data collection procedures for the Software Engineering Laboratory (SEL) database
[NASA-TM-108579] p 230 N93-15579
- Upgrade and extension of the data acquisition system for propulsion and gas dynamic laboratories
[AD-A256836] p 235 N93-15637
- Identification of icing water clouds by NOAA AVHRR satellite data
[DLR-FB-92-11] p 434 N93-16477
- Preliminary efforts toward development of data handling and analysis software for unsteady flow measurements: An application for aeroelastic transonic flow configurations p 291 N93-16768
- Digital data acquisition and preliminary instrumentation study for the F-16 laminar flow control vehicle p 292 N93-16784

- Acquisition and use of Orlando, Florida and Continental Airbus radar flight test data p 489 N93-19603
- Review of initial experiments using the Hawk model, dynamic rig facility, and the CED 1401 digital data acquisition equipment
[CRANFIELD-AERO-9017] p 531 N93-21406
- Lightning data acquisition p 753 N93-24883
- Visual approach data collection at St. Louis Lambert Field (STL)
[DOT/FAA/CT-TN93/2] p 706 N93-24948
- Advanced thermally-stable, coal-derived, jet fuels program: Experiment system and model development
[AD-A262747] p 917 N93-29402
- The basic measurement equipment of the DLR test aircraft p 1000 N93-31273

DATA BASE MANAGEMENT SYSTEMS

- Design and utilization of a Flight Test Engineering Database Management System at the NASA Dryden Flight Research Facility
[AIAA PAPER 92-4072] p 97 A93-13264
- Airspace redesign - Making the GRADE p 317 A93-21630
- Reusable Ada avionics software packages library system p 944 A93-42828
- Database management for integrated avionics system p 939 A93-42831
- Functionally Integrated Resource Manager for real-time avionics data p 940 A93-42832
- AQUIS: A PC-based air quality and permit information system
[DE92-040092] p 434 N93-18587
- Dynamic System Coupler Program (DYSCO 4.1). Volume 2: User's manual
[AD-B131157L] p 848 N93-27589

DATA BASES

- Model of a map indicator p 341 A93-18532
- An application of artificial neural networks to experimental data approximation
[AIAA PAPER 93-0408] p 440 A93-23330
- Digital map databases in support of avionic display systems p 544 A93-26888
- Characteristics of data processing during the development of a data base for a CAD system for aircraft design p 892 A93-42381
- Developing a data base for the calibration and validation of hypersonic CFD codes - Sharp cones
[AIAA PAPER 93-3044] p 1057 A93-48224
- The European Data Base - A new CFD validation tool for the design of space vehicles
[AIAA PAPER 93-3045] p 1057 A93-48225
- Estimation of aerodynamic coefficients using neural networks
[AIAA PAPER 93-3639] p 1165 A93-48324
- International aerospace STI p 1227 A93-53826
- Appraisal of digital terrain elevation data for low-altitude flight
[NASA-TM-103896] p 35 N93-10745
- Directory of factual and numeric databases of relevance to aerospace and defence R and D
[AGARD-R-777] p 104 N93-11710
- Coordinating Council. Fourth Meeting: NACA Documents Database Project
[NASA-TM-108017] p 234 N93-12671
- Data collection procedures for the Software Engineering Laboratory (SEL) database
[NASA-TM-108579] p 230 N93-15579
- Development of a menu driven materials data base for use on personal computers: Aircraft structures technical memorandum
[AD-A256317] p 392 N93-16403
- A database approach to aircraft carrier airplan production
[AD-A257737] p 240 N93-17666
- AQUIS: A PC-based air quality and permit information system
[DE92-040092] p 434 N93-18587
- The human factor problem in the Canadian Forces aviation p 491 N93-19657
- Analysis of aircraft noise levels in the vicinity of start-of-takeoff roll at Baltimore-Washington International Airport
[PB92-221605] p 559 N93-21501
- Lightning data acquisition p 753 N93-24883
- Digitization of analog data from in-flight lightning strikes p 753 N93-24884
- Bibliography on propulsion airframe integration technologies for high-speed civil transport applications, 1980-1991
[NASA-TM-105602] p 678 N93-26136
- Oxides of nitrogen emissions from turbulent hydrocarbon/air jet diffusion flames, phase 2
[PB93-152478] p 756 N93-26533
- Estimating characteristic life and reliability of an aircraft engine component improvement in the early stages of the implementation process
[AD-A262118] p 815 N93-28184

SUBJECT INDEX

- Crack growth prediction models p 1004 N93-31747
- International aircraft operator information system
[DOT/FAA/CT-93/4] p 949 N93-32232
- DATA COMPRESSION**
- The development of an airborne information management system for flight test
[AIAA PAPER 92-4113] p 51 A93-11281
- DATA FLOW ANALYSIS**
- SIPORT DEPCOS and SIPORT ARRCOS - More than an electronic airstrip replacement p 499 A93-27914
- Data Multiplexing Network (DMN) equipment Operational Test and Evaluation (OT&E) integration test report
[AD-A263172] p 942 N93-29490
- DATA INTEGRATION**
- Technical operating report on the Data Integration and Collection Environment (DICE) instrumentation system design
[AD-A258444] p 455 N93-17891
- DATA LINKS**
- Automatic dependent surveillance (ADS) Pacific engineering trials (PET) p 30 A93-10999
- Capacity as a consideration for providing aeronautical mobile satellite air traffic services in the U.S. domestic airspace p 30 A93-11007
- Requirements for integrated flight and traffic management during final approach p 31 A93-11009
- LOCSTAR - A satellite radiodetermination system for Europe p 150 A93-15037
- Helicopter approaches in low visibility using RGPS and EFIS - EFIS - Electronic Flight Instrumentation System p 142 A93-17309
- The SSR mode-S data-link p 312 A93-18553
- Datalinks - Civil aircraft: Proceedings of the Conference, London, United Kingdom, Nov. 24, 1992
[ISBN 1-85768-075-8] p 501 A93-29474
- Cross channel dependency requirements of the multi-path redundant avionics suite p 928 A93-42782
- A Mode S implementation - Experiments about data-link and interconnected Mode S sensors p 883 A93-43409
- Repair and maintenance of fiber optic data links on Navy aircraft p 1172 A93-48538
- A description of the Mode Select beacon system (Mode S) and its associated benefits to the National Airspace System (NAS)
[DOT/FAA/SE-92/6] p 35 N93-10738
- Controller evaluation of initial data link terminal air traffic control services: Mini study 2, volume 1
[DOT/FAA/CT-92/2-VOL-1] p 36 N93-11704
- Controller evaluation of initial data link terminal air traffic control services: Mini study 2, volume 2
[DOT/FAA/CT-92/2-VOL-2] p 36 N93-11705
- FAA Technical Center Aeronautical Data Link Research Plan
[DOT/FAA/CT-92/23] p 417 N93-15698
- The effect of TCAS interrogations on the Chicago O'Hare ATCRBS system
[DOT/FAA/CT-92/22] p 318 N93-16498
- Results of DATAS investigation of illegal mode S ID's at JFK Airport
[DOT/FAA/CT-92/26] p 318 N93-16841
- Development of a realtime DGPS system
[DLR-MITT-92-06] p 503 N93-20749
- Piloted simulation of an air-ground profile negotiation process in a time-based Air Traffic Control environment
[NASA-TM-107748] p 707 N93-26087
- Status of the Fiber Optic Control System Integration (FOCSI) program
[NASA-TM-106151] p 841 N93-28053
- Results of DATAS investigation of ATCRBS environment at the Los Angeles International Airport
[DOT/FAA/CT-93/6] p 793 N93-28625
- DATA MANAGEMENT**
- Functionally Integrated Resource Manager for real-time avionics data p 940 A93-42832
- The Teledyne controls aircraft condition monitoring system p 168 N93-15155
- Flight data and flight safety in SAS p 168 N93-15156
- FDAMS: An extendable and reconfigurable solution for avionics data management systems p 168 N93-15157
- Ground Support Equipment (GSE) for Aircraft Condition Monitoring System (ACMS) p 110 N93-15158
- Monitoring of powerplants in advanced commercial aircraft p 178 N93-15171
- EJ 200 engine monitoring system: On- and off-board data capture, analysis, and management system p 178 N93-15172
- En route air traffic controllers use of flight progress strips: A graph-theoretic analysis
[AD-A259062] p 319 N93-18927
- DATA PROCESSING**
- Software for the control of measurement data acquisition, processing, and monitoring during strength testings p 94 A93-10042

Real-time capture, archiving, retrieval, processing, and presentation of large quantities of flight test/research information
[AIAA PAPER 92-4073] p 95 A93-11258
Application of flight data for diagnostic purposes p 166 A93-14295
A multisensor-multitarget data association algorithm for heterogeneous sensors p 439 A93-22899
Fully automatic FEM data pre-processing for aeronautical electrical machine p 538 A93-24030
Signal processing and system identification techniques for flutter test data analysis p 529 A93-29282
A data system for the observation of flow conditions on an aircraft wing p 808 A93-37882
Characteristics of data processing during the development of a data base for a CAD system for aircraft design p 892 A93-42381
Application of modular avionics to the EF-111A systems improvement program p 896 A93-42780
Synthesis of a data processing and measuring system for flight vehicle control systems p 908 A93-43102
NODE-air traffic management systems p 884 A93-43428
Motion compensation in a time domain SAR processor p 885 A93-43466
DeAs - A programming system for data processing and system control: New software developments for wind tunnel operation p 1036 A93-44452
Estimation of aerodynamic coefficients using neural networks
[AIAA PAPER 93-3639] p 1165 A93-48324
Parameter estimates of an aeroelastic aircraft as affected by model simplifications p 1127 A93-48325
[AIAA PAPER 93-3640] p 1127 A93-48325
An upgraded data acquisition and processing system for the Aeropropulsion Systems Test Facility at Arnold Engineering Development Center
[AIAA PAPER 93-2466] p 1138 A93-50213
Indian experience in flight data readout and analysis p 168 A93-15161
Czechoslovak development and experience in flight data recorder readout and analysis p 168 A93-15162
Software for flight recorder data evaluation developed by Lufthansa p 230 A93-15163
The FAIR (Flight Animated and Interactive Reconstruction) tool p 148 A93-15164
The SIROM flight data recorder and evaluation system p 168 A93-15165
Design for tactical situation awareness display [AD-A256194] p 170 A93-15235
Preliminary efforts toward development of data handling and analysis software for unsteady flow measurements: An application for aeroelastic transonic flow configurations p 291 A93-16768
On automated analysis of flight test data p 512 A93-19913
Management of Automatic Data Processing (ADP) system documentation in the Department of Defense [AD-A258507] p 571 A93-20048
Program of research in flight dynamics in the JIAFS at NASA-Langley Research Center [NASA-CR-191885] p 484 A93-21562
The basic measurement equipment of the DLR test aircraft p 1000 A93-31273
Instigation and processing of flight tests in DLR p 998 A93-31275

DATA PROCESSING EQUIPMENT
Methods and equipment for data processing and acquisition in information management systems p 856 A93-43101

DATA RECORDERS
Solid state flight data recorders and their application in the flight operation analysis p 166 A93-14200
Application of flight data for diagnostic purposes p 166 A93-14295
High Capacity Voice Recorder (HCVR) Operational Test and Evaluation (OT/E) integration test report [DOT/FAA/CT-TN92/30] p 88 A93-11460
The SIROM flight data recorder and evaluation system p 168 A93-15165
Solid state flight data recorder with rapid data access p 221 A93-15167
Integrated engine control and monitoring with experiences derived from OLMOS p 178 A93-15168

DATA RECORDING
Digital flight recorded data - A method of estimating down draft from digital flight recorded data p 1241 A93-54559
A novel-high-performance system for recording and analysing instantaneous total pressure distortion in air intakes p 214 A93-13215
Design, fabrication, and testing of a three-dimensional acoustic orientation instrument (3-D AOI): Drawings, engineering and associated lists (conceptual and development design) [AD-A260934] p 760 A93-25915

DATA REDUCTION
A data reduction system for processing instrumented flight test data p 847 A93-37866
Wind tunnel spin data reduction to obtain aerodynamic spin damping coefficients by using nonlinear equation of motion [AD-A253880] p 19 A93-10811
Preliminary efforts toward development of data handling and analysis software for unsteady flow measurements: An application for aeroelastic transonic flow configurations p 291 A93-16768
A method for investigating human factor aspects of military aircraft accidents p 491 A93-19656
On automated analysis of flight test data p 512 A93-19913
System identification for X-31A project support: Lessons learned so far p 512 A93-19914
Program of research in flight dynamics in the JIAFS at NASA-Langley Research Center [NASA-CR-191885] p 484 A93-21562
Testing of an experimental system for image reconnaissance p 1040 A93-31283

DATA RETRIEVAL
Flight data and flight safety in SAS p 168 A93-15166
Solid state flight data recorder with rapid data access p 221 A93-15167
Royal Air Force experience of the Harrier information management system p 234 A93-15170
EJ 200 engine monitoring system: On- and off-board data capture, analysis, and management system p 178 A93-15172
Development of a menu driven materials data base for use on personal computers: Aircraft structures technical memorandum [AD-A256317] p 392 A93-16403

DATA SAMPLING
A study of the influence of the data acquisition system sampling rate on the accuracy of measured acceleration loads for transport aircraft p 1000 A93-46808
The HYDICE instrument design and its application to planetary instruments p 842 A93-28766

DATA SIMULATION
Recent improvements on the Dynamic Flight Simulator p 1011 A93-45167
Chimera grids in the simulation of three-dimensional flowfields in turbine-blade-coolant passages [AIAA PAPER 93-2559] p 1157 A93-50280
A study of surge control by using pulse cut-off for dual spool turbo-jet engine p 1194 A93-53862
Inverse simulation: A tool for the validation of simulation programs - First results --- for helicopter flight tests and control p 1249 A93-56046

DATA SMOOTHING
Sequential smoothing and filtering for maneuvering target tracking p 440 A93-22978
Adaptive grid generation using optimal control theory p 770 A93-38187
Beyond the frequency limits of time-linearized methods [NLR-TP-91216-U] p 295 A93-17929

DATA STORAGE
Preconditioned domain decomposition scheme for three-dimensional aerodynamic sensitivity analysis p 957 A93-45096
Estimation of aerodynamic coefficients using neural networks [AIAA PAPER 93-3639] p 1165 A93-48324
Rewritable optical disk: Application to flight recording p 221 A93-15160
Solid state flight data recorder with rapid data access p 221 A93-15167
Preliminary efforts toward development of data handling and analysis software for unsteady flow measurements: An application for aeroelastic transonic flow configurations p 291 A93-16768
Handling and using information systems with new technology [PNR-90910] p 572 A93-20734
Testing of an experimental system for image reconnaissance p 1040 A93-31283

DATA SYSTEMS
Requirements analysis notebook for the flight data systems definition in the Real-Time Systems Engineering Laboratory (RSEL) [NASA-CR-185698] p 69 A93-10960
The SIROM flight data recorder and evaluation system p 168 A93-15165
Results of DATAS investigation of illegal mode S ID's at JFK Airport [DOT/FAA/CT-92/26] p 318 A93-16841
Crack growth prediction models p 1004 A93-31747

DATA TRANSFER (COMPUTERS)
Indian experience in flight data readout and analysis p 168 A93-15161

DATA TRANSMISSION
The SSR mode-S data-link p 312 A93-18553
Data communication for airborne differential GPS/GLONASS application p 499 A93-27910
Software support for a computerized air situation documentation system p 941 A93-43115
A Mode S implementation - Experiments about data-link and interconnected Mode S sensors p 883 A93-43409
Fiber-optic technology for transport aircraft p 1173 A93-50488
Controller evaluation of initial data link terminal air traffic control services: Mini study 2, volume 1 [DOT/FAA/CT-92/2-VOL-1] p 36 A93-11704
Controller evaluation of initial data link terminal air traffic control services: Mini study 2, volume 2 [DOT/FAA/CT-92/2-VOL-2] p 36 A93-11705
An optical fiber multi-terminal data bus system for aircraft [NAL-TR-1125] p 52 A93-12370
Software design document for the generic avionics data bus tool kit [AD-A259329] p 519 A93-21259
Data Multiplexing Network (DMN) equipment Operational Test and Evaluation (OT&E) integration test report [AD-A263172] p 942 A93-29490
The basic measurement equipment of the DLR test aircraft p 1000 A93-31273
Testing of an experimental system for image reconnaissance p 1040 A93-31283

DC 9 AIRCRAFT
Maintaining the safety of an aging fleet of aircraft p 3 A93-13632

DEACTIVATION
Effect of a metal deactivator fuel additive on fuel deposition in fuel atomizers at high temperature [AD-A260915] p 736 A93-25914

DEAD RECKONING
Advanced Unmanned Search System (AUSS) supervisory command, control and navigation [AD-A263171] p 793 A93-28990

DEATH
World commercial aircraft accidents [DE93-010892] p 791 A93-28571

DEBONDING (MATERIALS)
Assessment of aircraft structural integrity by detecting disbands through ultrasonic scanning p 406 A93-19587
Ultrasonic NDE of adhesive and sealant bonded aluminum lap-splices p 407 A93-19595
Automation of disbond detection in aircraft fuselage through thermal image processing p 407 A93-19598
A study of the flexural properties of carbon-epoxy composites in certain environments p 390 A93-21999
Durability properties for adhesively bonded structural aerospace applications p 1217 A93-53515

DECAY
Noise transmission of skin-stringer panels using a decaying wave method p 943 A93-41929

DECCA NAVIGATION
New algorithms for hyperbolic radionavigation p 881 A93-40359

DECISION MAKING
Aircraft model for multicriterial analysis in decision making [AIAA PAPER 92-4192] p 44 A93-13370
Calling the right shots in aircraft maintenance with artificial intelligence p 238 A93-18763
Decision making for a public differential GPS service p 314 A93-21165
Aircraft collision avoidance using statistical decision theory p 500 A93-28155
Optimization using fuzzy set theory p 1037 A93-45431
Behavior of the particular quality characteristics of an intelligent flight vehicle control system in a multicriterial formulation p 1168 A93-50952
Implementing system simulation of C3 systems using autonomous objects [NASA-CR-190845] p 89 A93-11716
Specification of adaptive aiding systems [AD-A254537] p 159 A93-12602
Workshop on Aeronautical Decision Making (ADM). Volume 2: Plenary Session With Presentations and Proposed Action Plan [DOT/FAA/RD-92/14-VOL-2] p 146 A93-15013
Does cockpit management training reduce aircrew error? p 146 A93-15014
Cockpit decision making p 146 A93-15015
How expert pilots think p 147 A93-15017
Methodology for studying and training expertise p 147 A93-15018
A cognitive model for training decision making in aircrews p 147 A93-15020

- Elements of a theory of natural decision making p 147 N93-15021
- Shared mental models and crew decision making p 147 N93-15023
- Measuring risk in single-engine and twin-engine helicopters p 148 N93-15025
- Proposed action plan to improve ADM effectiveness, part 3: Developing a new ADM paradigm on which to build advanced or expert decision making training p 148 N93-15026
- Domain specific software design for decision aiding p 442 N93-17517
- Underlying causes of accidents: Casual networks p 491 N93-19658
- Design of a cooperative problem-solving system for enroute flight planning: An empirical study of its use by airline dispatchers [NASA-CR-192709] p 707 N93-25330
- Aircraft guidance for wind shear avoidance: Decision-making under uncertainty p 889 N93-31005
- DECOMMUTATORS**
- Ground installations for preparation and evaluation of flight tests p 1014 N93-31274
- DECOUPLING**
- Application of eigenstructure assignment to the control of powered lift combat aircraft p 64 N93-11871
- A contribution to the dynamic feedforward open loop control of multivariable systems and to the optimal design of command functions [DLR-FB-92-05] p 441 N93-18515
- Theoretical constraints in the design of multivariable control systems [NASA-CR-191900] p 442 N93-18372
- DEEP SPACE NETWORK**
- The effect of clock, media, and station location errors on Doppler measurement accuracy p 885 N93-29588
- DEEP WATER**
- On hovercraft overwater heave stability p 1219 A93-53819
- DEFECTS**
- Clean melting and the removal of defects from aero-engine materials p 1217 A93-53503
- Nondestructive evaluation of ceramic and metal matrix composites for NASA's HITEMP and enabling propulsion materials programs [NASA-TM-105807] p 85 N93-10963
- Damage detection by Acousto-Ultrasonic Location (AUL) p 555 N93-21529
- Investigation of corrosion in aluminum/adhesive lap-splices using pulse-echo ultrasonic techniques [DE93-008074] p 749 N93-25518
- NDE of PWA 1480 single crystal turbine blade material [NASA-TM-106140] p 815 N93-27640
- Use of local x ray computerized tomography for high-resolution, region-of-interest inspection of large ceramic components for engines [DE93-005564] p 843 N93-28943
- Optimal design and imperfection sensitivity of nonlinear shell structures [FFA-TN-1992-30] p 1030 N93-31123
- DEFENSE INDUSTRY**
- Defence electronics industry profile, 1990-1991 [CTN-92-60515] p 84 N93-10653
- DEFENSE PROGRAM**
- Aeronautical engineering education for the armed forces p 453 A93-21681
- V-22 program overview p 457 A93-24299
- Applying commercial style acquisition practices to the procurement of commercially available aircraft [AD-A258143] p 455 N93-18087
- Special tooling disposition for aircraft entering post production support [AD-A261614] p 678 N93-26168
- International aviation (Selected articles) [AD-A262566] p 765 N93-28576
- First NASA Advanced Composites Technology Conference, part 2 [NASA-CP-3104-PT-2] p 921 N93-30841
- DEFLAGRATION**
- Stability of oblique detonations in RAM accelerators [AIAA PAPER 92-0089] p 541 A93-24979
- DEFLECTION**
- Stress-strain state of the elements of a single-stringer riveted panel p 746 A93-35288
- A High Deflection Diaphragm concept (HDD) for power transmission shafting p 826 A93-35931
- Flight Deflection Measurement System p 808 A93-37885
- The measurement of blade deflections - A new implementation of the strain pattern analysis [ONERA, TP NO. 1992-127] p 831 A93-38601
- Fluid-film foil bearings control engine heat p 924 A93-39949
- Calculation of V/STOL aircraft aerodynamics with deflected jets in ground effect [AIAA PAPER 93-3530] p 986 A93-47287
- FAA unified pavement analysis 3-D finite element method p 379 N93-16314
- Monte Carlo simulation of normal shock wave, Part 1: Lennard-Jones potential p 300 N93-19279
- Static and dynamic large deflection flexural response of graphite-epoxy beams [NASA-CR-41118] p 934 N93-30374
- Advanced aircraft with thrust vector control [MBB-FE-1-S-PUB-0504] p 998 N93-31043
- DEFORMATION**
- Study of optical techniques for the Ames unitary wind tunnels. Part 4: Model deformation [NASA-CR-190980] p 68 N93-12349
- Micro mechanical behavior of pavements p 379 N93-16312
- State of the art review of rutting and cracking in pavements p 380 N93-16316
- Experimental and analytical investigation of dynamic characteristics of extension-twist-coupled composite tubular spars [NASA-TP-3225] p 553 N93-20585
- An integrated finite-state model for rotor deformation, nonlinear airloads, inflow, and trim p 715 N93-25538
- Repair, evaluation, maintenance, and rehabilitation research program. Continuous Deformation Monitoring System (CDMS) [AD-A261833] p 708 N93-26274
- Land subsidence and problems affecting land use at Edwards Air Force Base and vicinity, California, 1990 [PB93-182236] p 1036 N93-32191
- DEGRADATION**
- The degradation of parachutes: Age and mechanical wear [AD-A252243] p 24 N93-12179
- X ray diffraction and electron microscope studies of Yttria Stabilized Zirconia (YSZ) ceramic coatings exposed to vanadia [AD-A258055] p 392 N93-17676
- DEGREES OF FREEDOM**
- Nonequilibrium excitation of internal molecular degrees of freedom in the shock layer during hypersonic flight p 412 A93-21922
- A magnetic suspension system with a large angular range p 1139 A93-51295
- Control augmentation system (CAS) synthesis via adaptation and learning [AIAA PAPER 93-3728] p 1170 A93-51328
- An aerodynamic model for one and two degree of freedom wing rock of slender delta wings [NASA-CR-193130] p 781 N93-27150
- DEICERS**
- Results of Low Power Deicer tests on a swept inlet component in the NASA Lewis Icing Research Tunnel [AIAA PAPER 93-0032] p 327 A93-22551
- Modeling and strain gauging of eddy current repulsion deicing systems [AIAA PAPER 93-0296] p 327 A93-22696
- Surface roughness due to residual ice in the use of low power deicing systems [AIAA PAPER 93-0031] p 282 A93-23240
- Numerical modeling of anti-icing systems and comparison to test results on a NACA 0012 airfoil [AIAA PAPER 93-0170] p 327 A93-23242
- Aircraft take-off laboratory simulation for de/anti-icing study p 528 A93-23840
- Results of a low power ice protection system test and a new method of imaging data analysis p 795 A93-35932
- Maintenance of the liquid and gas systems of the IL-76 aircraft p 804 A93-39203
- Parameter selection of electro-impulse de-icing systems p 889 A93-40493
- Efficient finite element method for aircraft deicing problems p 1103 A93-52443
- Results of low power deicer tests on a swept inlet component in the NASA Lewis icing research tunnel [NASA-TM-105968] p 138 N93-14911
- Surface roughness due to residual ice in the use of low power deicing systems [NASA-TM-105971] p 139 N93-15338
- Numerical modeling of anti-icing systems and comparison to test results on a NACA 0012 airfoil [NASA-TM-105975] p 148 N93-15345
- FAA international conference on airplane ground deicing [AD-A263617] p 880 N93-29286
- DEICING**
- Investigation of leading edge ice accretion with cyclical pneumatic boot inflation [AIAA PAPER 93-0007] p 306 A93-20130
- Results of Low Power Deicer tests on a swept inlet component in the NASA Lewis Icing Research Tunnel [AIAA PAPER 93-0032] p 327 A93-22551
- Investigation of an electrothermal de-icer pad using a three-dimensional finite element simulation [AIAA PAPER 93-0397] p 327 A93-23072
- CWAS - Clean wing advisory system: A new approach to ice detection [AIAA PAPER 93-0747] p 516 A93-24835
- Anti-icing failure detection instrumentation using realtime optical measurement of anti-icing fluid properties [AIAA PAPER 93-0748] p 540 A93-24836
- Field studies of hold-over-times for type II anti-icing fluids - Results and insights [AIAA PAPER 93-0749] p 486 A93-24837
- Results of a low power ice protection system test and a new method of imaging data analysis p 795 A93-35932
- Efficient finite element method for aircraft deicing problems p 1103 A93-52443
- Icing prevention by ultrasonic nucleation of supercooled water droplets in front of subsonic aircraft [AD-A258212] p 142 N93-12816
- Simulation of two-dimensional icing, de-icing and anti-icing phenomena p 142 N93-13364
- Results of low power deicer tests on a swept inlet component in the NASA Lewis icing research tunnel [NASA-TM-105968] p 138 N93-14911
- Aircraft accident report: Takeoff stall in icing conditions. USAIR Flight 405 FOKKER F-28, N485US, LaGuardia Airport, Flushing, New York, 22 March 1992 [PB93-910402] p 790 N93-27034
- FAA international conference on airplane ground deicing [AD-A263617] p 880 N93-29286
- DELAMINATING**
- Tailoring concepts for improved structural performance of rotorcraft flexbeams p 207 A93-14811
- Automatic Through-the-Thickness braiding p 209 A93-15789
- Repair of delaminations and impact damage in composite aircraft structures p 457 A93-24107
- Delaminations of barely visible impact damage in CFRP laminates p 737 A93-33798
- The limit model of a thin strip exhibiting two delaminations [ONERA, TP NO. 1992-212] p 832 A93-38764
- Characterization of delamination and fiber fractures in carbon fiber reinforced plastics induced from impact p 915 A93-40787
- Stringer peeling effects at stiffened composite panels in the postbuckling range p 1180 A93-52453
- GARTEUR damage mechanics for composite materials: Analytical/experimental research on delaminations p 537 N93-21513
- Numerical determination of the residual strength of battle damaged composite plates p 537 N93-21533
- DELAY**
- Transport delay compensation - An inexpensive alternative to increasing image generator update rate [AIAA PAPER 93-3563] p 1223 A93-52663
- A NASPAC-based analysis of the delay and cost effects of the Dallas/Fort Worth metroplex plan [DOT/FAA/CT-TN92/21] p 193 N93-13447
- DELIVERY**
- The development of a parachute system for aerial delivery from high speed cargo aircraft [DE93-008339] p 790 N93-29035
- DELTA FUNCTION**
- Robust sampled data eigenstructure assignment using the delta operator --- in relation to autopilot design p 906 A93-41889
- DELTA WINGS**
- Calculation of a three-dimensional boundary layer at the lee side of a finite-span delta wing in the case of viscous interaction with hypersonic flow p 5 A93-10143
- Breakdown analysis on delta wing vortices p 7 A93-10779
- Shock wave interference on a wing with a partition at hypersonic velocities p 13 A93-12839
- Numerical simulation of STOL operations using thrust-vectoring [AIAA PAPER 92-4254] p 15 A93-13342
- Calculation of transonic viscous flow around a delta wing p 113 A93-14191
- The influence of the fuselage on high alpha vortical flows and the subsequent effect on fin buffeting p 116 A93-14263
- Wing rock of lifting systems p 118 A93-14330
- Leading edge vortices in a chordwise periodic flow p 119 A93-14333
- Vortex breakdown study on a 65-deg delta wing tested in static and dynamic conditions p 121 A93-14407
- A vortex control technique for the attenuation of fin buffet p 121 A93-14408
- A low-speed wind tunnel study of vortex interaction control techniques on a chine-forebody/delta-wing configuration p 122 A93-14409

- Determination of vortex burst location on delta wings from surface pressure measurements p 123 A93-14557
- Subsonic separated flow past slender delta wings p 124 A93-15109
- The use of the Polhamus and discrete vortex methods for calculating the nonlinear characteristics of delta wings and wings with a strake p 242 A93-18379
- Experimental investigation of vortex-fin interaction [AIAA PAPER 93-0050] p 260 A93-20163
- Static roll moment characteristics of asymmetric tangential leading edge blowing on a delta wing at high angles of attack p 261 A93-20165
- [AIAA PAPER 93-0052] p 261 A93-20165
- The aerodynamic effects of sideslip on double delta wings [AIAA PAPER 93-0053] p 261 A93-20166
- Active control of wing rock of a delta wing at post-stall using tangential leading edge blowing [AIAA PAPER 93-0056] p 367 A93-20169
- A performance comparison of massively parallel Parabolized Navier-Stokes solutions [AIAA PAPER 93-0059] p 435 A93-20172
- Calculations of separated vortex flows at low speed for low-aspect-ratio wings p 264 A93-20300
- The suppression of single-fin buffeting using tangential leading edge blowing on a delta wing p 270 A93-21677
- Augmentation of turbulent heat transfer with a vortex generator attached to a LEBU plate p 411 A93-21729
- 3-D LDV measurements over a delta wing in pitch-up motion [AIAA PAPER 93-0185] p 275 A93-22610
- Three-dimensional flow structure on delta wings at high angle-of-attack - Experimental concepts and issues [AIAA PAPER 93-0550] p 285 A93-23289
- Numerical simulation of delta-wing roll [AIAA PAPER 93-0554] p 285 A93-23293
- Vortex breakdown over delta wings in unsteady free stream [AIAA PAPER 93-0555] p 285 A93-23294
- Eduction of swirling structure using the velocity gradient tensor p 416 A93-23547
- Measurements of circulation and vorticity in the leading-edge vortex of a delta wing p 288 A93-23548
- Numerical modeling of leading edge separated flow at incompressible speeds p 460 A93-24079
- Doppler global velocimetry - The next generation? [AIAA PAPER 92-3897] p 539 A93-24486
- Further analysis of high-rate rolling experiments of a 65 deg delta wing [AIAA PAPER 93-0620] p 523 A93-24737
- Body-axis rolling motion critical states of a 65-degree delta wing [AIAA PAPER 93-0621] p 523 A93-24738
- Experimental and numerical delta wing study at high angles of attack and sideslip [AIAA PAPER 92-2713] p 473 A93-24990
- Structure of vortex breakdown on a pitching delta wing [AIAA PAPER 93-0434] p 474 A93-25528
- Experiments on a 60 deg delta wing with vortex flaps and vortex plates p 477 A93-27482
- Three-dimensional flow past an ogival-cylindrical body in combination with a delta wing p 478 A93-27636
- Investigation of vortex breakdown on delta wings using Navier-Stokes equations p 478 A93-27924
- A numerical method of unsteady separating flow over delta wings p 681 A93-33746
- Results from a conical Euler methodology developed for unsteady vortical flows p 692 A93-35612
- Experimental investigations of asymmetric vortex flows behind elliptic cones at incidence p 757 A93-35637
- Effects of pylon yaw and lateral stiffness on the flutter of a delta wing with external store p 800 A93-36330
- Effects of blowing on delta wing vortices during dynamic pitching p 768 A93-37384
- Slender wing rock revisited p 768 A93-37386
- A flutter investigation of all-moveable NASP-like wings at hypersonic speeds [AIAA PAPER 93-1315] p 769 A93-37427
- Extraction of inherent aerodynamic lag poles for the time domain representation of modal unsteady airloads [AIAA PAPER 93-1591] p 829 A93-37443
- Domain splitting explicit time marching scheme for simulation of unsteady high Reynolds number flow p 830 A93-38140
- Laser-velocimeter study of vortex breakdown on a 70-deg swept delta wing in incompressible flow [ONERA, TP NO. 1992-147] p 773 A93-38728
- Calculation of the effect of the shock wave of a delta wing on a second wing at supersonic velocities p 776 A93-39141
- Instantaneous structure of vortex breakdown on a delta wing via particle image velocimetry p 779 A93-39428
- Control of vortices on a delta wing by leading-edge injection p 860 A93-41906
- Leeside flow over delta wing at $M = 7.15$ - Experimental results for test case 7.1.2 p 870 A93-42632
- Finite volume 3DNS and PNS solutions of hypersonic viscous flow around a delta wing using Osher's flux difference splitting p 870 A93-42633
- Inviscid hypersonic flow over a delta wing p 870 A93-42634
- Hypersonic leeside delta-wing-flow computations using centered schemes p 870 A93-42635
- Evaluation of contributions for test case 7.1.1 and 7.1.2 p 870 A93-42636
- Experimental density flowfields over a delta wing located in rarefied hypersonic flows p 870 A93-42637
- Experiments on the heat transfer and on the aerodynamic coefficients of a delta wing in rarefied hypersonic flows p 870 A93-42638
- Rarefied gas flow around a 3D-deltawing p 870 A93-42639
- An acceleration technique for time accurate calculations --- of unsteady flow around pitching delta wings p 957 A93-45092
- Application of leading-edge vortex manipulations to reduce wing rock amplitudes p 1007 A93-45152
- Instantaneous topology of the unsteady leading-edge vortex at high angle of attack p 961 A93-45728
- Strong vortex/boundary layer interactions. II - Vortices low p 965 A93-46744
- A visual study of recessed angled spanwise blowing method on a delta wing [AIAA PAPER 93-3246] p 966 A93-46791
- A three dimensional view of velocity using lasers p 1028 A93-46822
- The three-dimensional representation of the pressure distribution on wedged delta wings with supersonic leading edges in supersonic-hypersonic flow p 973 A93-46989
- Adaptive computations of flow around a delta wing with vortex breakdown [AIAA PAPER 93-3400] p 974 A93-47202
- A visualization study of the vortical flow over a double-delta wing in dynamic motion [AIAA PAPER 93-3425] p 976 A93-47220
- Aerodynamic characteristics of a delta wing with a body-hinged leading-edge extension [AIAA PAPER 93-3446] p 978 A93-47233
- Boundary layer effects on the flow of a leading edge vortex [AIAA PAPER 93-3463] p 980 A93-47245
- Development of an innovative natural laminar flow wing concept for high-speed civil transports [AIAA PAPER 93-3466] p 980 A93-47247
- Secondary flow control on slender, sharp-edged configurations [AIAA PAPER 93-3470] p 980 A93-47250
- Supersonic vortex breakdown over a delta wing in transonic flow [AIAA PAPER 93-3472] p 980 A93-47251
- Effect of leeward flow dividers on the wing rock of a delta wing [AIAA PAPER 93-3492] p 982 A93-47264
- Flow control over delta wings at high angles of attack [AIAA PAPER 93-3494] p 983 A93-47266
- Navier-Stokes prediction of a delta wing in roll with vortex breakdown [AIAA PAPER 93-3495] p 983 A93-47267
- The application of an Euler method and a Navier-Stokes method to the vortical flow about a delta wing [AIAA PAPER 93-3510] p 984 A93-47276
- Shock-vortex interaction over a 65-degree delta wing in transonic flow p 1049 A93-48167
- Computational study of vortex breakdown on a pitching delta wing [AIAA PAPER 93-2974] p 1050 A93-48168
- Computation of delta-wing roll maneuvers [AIAA PAPER 93-2975] p 1050 A93-48169
- A computational and experimental investigation of a delta wing with vertical tails [AIAA PAPER 93-3009] p 1054 A93-48199
- Abnormal peaks of increased heat-transfer on the blunt delta wing in the hypersonic flow [AIAA PAPER 93-3129] p 1063 A93-48294
- Flow physics of critical states for rolling delta wings [AIAA PAPER 93-3683] p 1129 A93-48355
- Simulation of tail buffet using delta wing-vertical tail configuration [AIAA PAPER 93-3688] p 1065 A93-48357
- Numerical calculation of polars and heat transfer for supersonic three-dimensional flow past wings with allowance for radiation p 1068 A93-48905
- Pressure pulsations on a delta wing in incompressible flow p 1069 A93-48912
- Hypersonic flow past a low-aspect-ratio triangular plate at large angles of attack p 1069 A93-48974
- Periodic vortex shedding over delta wings p 1070 A93-49002
- A study of pressure fluctuations on the surface of a delta wing near the sharp leading edge p 1091 A93-51882
- Effect of leading-edge geometry on delta wing unsteady aerodynamics p 1095 A93-52457
- Pressure distribution measurement around hypersonic delta winged semicone - Measurement by means of magnet tape p 1176 A93-53193
- Numerical study of a delta planform with multiple jets in ground effect [SAE PAPER 892283] p 1176 A93-53200
- Active control of vortex breakdown by a spinning wave generator [ISABE 93-7045] p 1219 A93-54021
- The effect of outboard leading-edge bluntness of double-delta wing on its aerodynamic characteristics p 1230 A93-54589
- The forms of unsteady concentrated vortex-breakdown and its reactions to disturbance p 1231 A93-54594
- Pressure measurements at supersonic speeds on the research configuration ELAC I p 1237 A93-56033
- Forced unsteady separated flows on a 45 degree delta wing p 82 N93-10305
- Control of lift and drag in unsteady flows [AD-A253146] p 17 N93-10340
- Development of nonlinear aerodynamic models for unsteady responses p 19 N93-10845
- Further buffeting tests in a cryogenic wind tunnel [NASA-TM-107621] p 22 N93-11610
- An experimental study of the relationship between forces and moments and vortex breakdown on a pitching delta wing p 49 N93-12206
- The influence of intake swirl distortion on the steady-state performance of a low bypass, twin-spool engine p 214 N93-13211
- Effects of forebody strakes and Mach number on overall aerodynamic characteristics of configuration with 55 deg cropped delta wing [NASA-TP-3253] p 131 N93-13353
- An experimental and computational investigation of slender wings undergoing wing rock p 187 N93-13915
- The unsteady aerodynamics of a delta wing undergoing large-amplitude pitching motions p 134 N93-13929
- Flowfield study of a close-coupled canard configuration [AD-A256311] p 139 N93-15245
- Experimental and numerical investigation of vortex flow over a 76/60-deg double-delta wing [LR-680] p 289 N93-16210
- Comparison of solution of various Euler solvers and one Navier-Stokes solver for the flow about a sharp-edged cropped delta wing [NLR-TP-90340-U] p 418 N93-16411
- Navier-Stokes calculation of transonic flow past the NTF 65-deg delta wing p 292 N93-16797
- Application of an Euler-equation method to a sharp-edged delta wing configuration with vortex flow [NLR-TP-91306] p 294 N93-17809
- Advanced hypersonic aircraft design [NASA-CR-192046] p 334 N93-18037
- Algorithm development with applications to aerodynamics and aeroelasticity p 422 N93-18566
- Experimental investigations on wing-body combinations and their components at high angles of attack in the subsonic and transonic speed range [DLR-FB-91-43] p 516 N93-21762
- Computational study of the aerodynamics and control by blowing of asymmetric vortical flows over delta wings p 693 N93-24772
- The transient development of vortices over delta wings p 695 N93-25269
- Experimental effects of wing location on wing-body pressures at supersonic speeds [NASA-TM-4434] p 700 N93-26085
- Conical Euler analysis and active roll suppression for unsteady vortical flows about rolling delta wings [NASA-TP-3259] p 701 N93-26134
- An aerodynamic model for one and two degree of freedom wing rock of slender delta wings [NASA-CR-193130] p 781 N93-27150
- Leading edge vortices in a chordwise periodic flow p 782 N93-27218
- Effect of vortex behavior on loads acting on a 65 deg delta wing oscillating in roll at high incidence p 782 N93-27220
- Prediction of vortex breakdown on a delta wing p 787 N93-27459
- Computation of a delta-wing roll-and-hold maneuver [AD-A264704] p 909 N93-30498
- Supersonic aerodynamic characteristics of an advanced F-16 derivative aircraft configuration [NASA-TP-3355] p 989 N93-31733

DEMOGRAPHY

Aviation accidents, incidents, and violations:
Psychological predictors among US pilots

p 144 N93-14693

Effect of personal and situational variables on noise annoyance: With special reference to implications for en route noise

[NASA-CR-189676] p 569 N93-21317

DENSITY DISTRIBUTION

Planar imaging of OH density distributions in a supersonic combustion tunnel

[AIAA PAPER 93-0042] p 389 A93-20155

Quantitative Knudsen-number dependences of density disturbances in front of obstructions in supersonic divergent flows

p 1239 A93-56220

Analytical and numerical study on steady Mach reflection

p 302 N93-19309

DENSITY MEASUREMENT

Laser selection criteria for OH fluorescence measurements in supersonic combustion test facilities

p 549 A93-29315

DEPLOYMENT

Analytical study on the separation dynamics of LUNAR-A/penetrator

p 1265 A93-56272

DEPOLARIZATION

Hydrometeor identification using cross polar radar measurements and aircraft verification

p 844 A93-37719

DEPOSITION

Joining carbon composite fins to titanium heat pipes

[AD-A261970] p 825 N93-27667

DEPOSITS

Analysis of jet fuel thermal oxidation deposits by spectral fluorometric technique

p 1253 A93-55697

Interferometric JFTOT tube deposit measuring device

[AD-D015599] p 536 N93-20247

DESERTS

Environmental effects of operations during Desert Shield/Desert Storm

p 1190 A93-54291

DESIGN ANALYSIS

NASA balloon design and flight - Philosophy and criteria

p 40 A93-11363

Status of the NASA Balloon Program

p 1 A93-11365

Out with the mechanical fasteners --- design of aircraft using composite materials

[AIAA PAPER 92-4210] p 44 A93-13378

Stirling engine - Available tools for long-life assessment --- for space propulsion

p 195 A93-13824

The influence of main design parameters on helicopter air resonance and its source of instability

p 154 A93-14261

Some dynamic problems in design of aircraft landing gear

p 155 A93-14321

Design philosophies of the Basic Research Simulator

p 191 A93-14414

Low-cost approaches to proving of high-risk fast VTOL designs

[SAE PAPER 920989] p 157 A93-14636

A design study on the effect of support and system parameters on the natural frequencies of rotor systems

p 210 A93-16374

New design concepts for silencing aeroacoustic wind tunnels

p 445 A93-19147

Development of the Boeing Low Speed Aeroacoustic Facility (LSAF)

p 374 A93-19148

An efficient approach to optimal aerodynamic design. I - Analytic geometry and aerodynamic sensitivities

[AIAA PAPER 93-0099] p 264 A93-20204

Development of the quasi-procedural method for use in aircraft configuration optimization

[AIAA PAPER 92-4693] p 322 A93-20278

Integrated Soviet VLF/Omega Receiver design

p 316 A93-21198

Advanced direct-design procedure for centrifugal impellers

p 411 A93-21659

Analysis of a hypersonic waverider research vehicle with a hydrocarbon scramjet engine

[AIAA PAPER 93-0509] p 386 A93-23256

An improved numerical model for wave rotor design and analysis

[AIAA PAPER 93-0482] p 361 A93-23384

Analog simulation as part of a power supply design analysis universal platform

p 543 A93-25962

Evolution of the Boeing 777 electrical power system

p 519 A93-25998

Modelling of the flow in the blade-ring design process of turbomachinery

p 520 A93-27291

The NASA/industry design analysis methods for vibrations (DAMVIBS) program - Accomplishments and contributions

p 508 A93-27971

Experiences at Langley Research Center in the application of optimization techniques to helicopter airframes for vibration reduction

p 508 A93-27972

Global/local interlaminar stress analysis of a grid-stiffened composite panel

p 548 A93-28543

A design concept for a flight vehicle computer system with artificial intelligence elements

p 757 A93-35663

Instrument systems of flight vehicles and their design --- Russian book

[ISBN 5-217-00793-1] p 718 A93-35678

PDT approach for developing RAH-66 Comanche airframe systems

p 795 A93-35909

MIDAS technology transfer

p 845 A93-35920

An application of knowledge-based engineering to composite tooling design

p 846 A93-36010

Integrated structure/control/aerodynamic synthesis of actively controlled composite wings

p 818 A93-37392

Method for assessing the electric power system reliability of multiple-engined aircraft

p 810 A93-37398

Optimal design of centered squeeze film dampers

p 831 A93-38629

Experience in the design of supercritical cascades for the flow straightener of a transonic fan

p 777 A93-39196

Selection of the principal initial parameters for an axial-flow birotary turbine

p 837 A93-39198

Canadian experience with air cushion vehicle skirts

p 837 A93-39722

Design and cost viability of composites in commercial aircraft

p 915 A93-39963

Comments on experiments for computational validation for fluid dynamic predictions

p 927 A93-42578

Design verification of ground run-up noise suppressors for afterburning engines

p 910 A93-42892

Recent improvements on the Dynamic Flight Simulator

p 1011 A93-45167

Optimization of a highly-loaded axial splittler rotor design

p 1002 A93-46931

Application of computational fluid dynamics in transonic aerodynamic design

[AIAA PAPER 93-3481] p 982 A93-47259

The benefits of Maglev technology

[AIAA PAPER 93-2949] p 1174 A93-48145

Desirable characteristics for rotorcraft optical components

p 1172 A93-49466

Flow analysis and design optimization methods for nozzle-afterbody of a hypersonic vehicle

p 1073 A93-49531

Vane optimization for maximum efficiency using design of experiments

[AIAA PAPER 93-1867] p 1111 A93-49742

Structural design and analysis of a Mach zero to five turbo-ramjet system

[AIAA PAPER 93-1983] p 1112 A93-49830

Some key problems in the design of the NPU open-circuit low-turbulence wind tunnel

p 1139 A93-51188

Design for manufacture by resin transfer molding of composite parts for rotorcraft

[SME PAPER EM93-103] p 1159 A93-51733

Crashworthy landing gear design

[SAE AIR 4566] p 1103 A93-52175

Design problems of three-dimensional contractions --- in incompressible flow

p 1236 A93-55584

Performance parameters and assessment

p 81 N93-10052

Aerodynamic investigation of radial turbines using computational methods

p 81 N93-10056

The integration of geometric modeling into an inverse design method and application of a PC-based inverse design method and comparison with test results

p 81 N93-10058

SAPNEW: Parallel finite element code for thin shell structures on the Alliant FX/80

[NASA-CR-190663] p 84 N93-10372

On the basis of experience: Built in product reliability

[PNR-90932] p 85 N93-11034

Rolls-Royce civil engine technology

[PNR-90936] p 56 N93-11036

The Trent: Towards greater thrust

[PNR-90937] p 56 N93-11037

Introduction to the Rolls-Royce design process

[PNR-90939] p 57 N93-11039

The design and commissioning of an acoustic liner for propeller noise testing in the ARA transonic wind tunnel

[PNR-90880] p 101 N93-11204

The use of simultaneous engineering for the design and manufacture of the low pressure turbine for the Rolls-Royce Trent engine

[PNR-90887] p 59 N93-11206

The technical background to standards for shackles

[NPL-DMM(A)-51] p 86 N93-11325

Hypervelocity scramjet combustor-nozzle analysis and design

[NASA-CR-190965] p 60 N93-12214

An improved numerical model for wave rotor design and analysis

[NASA-TM-105915] p 60 N93-12418

The Fourth Workshop on Dynamics and Aeroelastic Stability Modeling of Rotorcraft Systems

[AD-A255065] p 50 N93-12485

Reanalysis of multiple-wheel landing gear traffic tests

[AD-A256593] p 194 N93-14238

Multi-point inverse design of isolated airfoils and airfoils in cascade in incompressible flow

p 163 N93-14462

Experimental evaluation of candidate graphical microburst alert displays

p 145 N93-14853

Analysis of in-flight structural failures of P-3C wing leading edge segments

[AD-A256212] p 165 N93-15238

A90 project: Design of a composite fin

[ETN-92-92773] p 329 N93-16562

Multidisciplinary design optimization using response surface analysis

p 330 N93-16796

Design optimization of natural laminar flow bodies in compressible flow

[NASA-CR-4478] p 292 N93-16940

Domain specific software design for decision aiding

p 442 N93-17517

Design of robust suboptimal controllers for a generalized quadratic criterion

[AD-A257746] p 372 N93-17670

NASA advanced design program: Analysis, design, and construction of a solar powered aircraft

[NASA-CR-192040] p 332 N93-17802

Design of the advanced regional aircraft, the DART-75

[NASA-CR-192044] p 333 N93-17972

MM-122: High speed civil transport

[NASA-CR-192011] p 334 N93-17974

TBD(exp 3)

[NASA-CR-192075] p 335 N93-18054

RPH preliminary design, trend analysis and initial analysis of the NPS hummingbird

[AD-A257854] p 338 N93-18304

The S.T.O.R.M. (tm): Air transport system design simulation

[NASA-CR-192070] p 338 N93-18349

The F-92 RELIANT: Air transport system design simulation

[NASA-CR-192050] p 339 N93-18386

Basic research on design analysis methods for rotorcraft vibrations

[NASA-CR-191917] p 422 N93-18576

Axial Flow Compressors, volume 1

[VKI-LS-1992-02-VOL-1] p 422 N93-18721

Endwall flows and blading design for axial flow compressors

p 423 N93-18730

Performance of controlled diffusion blades

p 424 N93-18735

Active stabilization to prevent surge in centrifugal compression systems

[NASA-CR-191625] p 424 N93-18862

Development of an engine/airframe performance matching scheme for jet engine retrofit

[AD-A258822] p 365 N93-18997

Crash experience of the US Army Black Hawk helicopter

p 493 N93-19688

Shock-dependent, optimum thrust wings in supersonic flow

p 483 N93-20169

HELITRACK: A helicopter-tracking receiver system for television outside broadcast links

[BBC-RD-1992/5] p 552 N93-20573

YIDOUY and its application to aircraft design

[AD-A259262] p 513 N93-20605

Optimization and sensitivity computations for the conception of internal ventilation system in the aircraft engine

[ETN-93-93375] p 521 N93-20913

Numerical methods for aerothermodynamic design of hypersonic space transport vehicles

[MBB-FE-211-S-PUB-0481] p 514 N93-21056

A Government/Industry Summary of the Design Analysis Methods for Vibrations (DAMVIBS) Program

[NASA-CP-10114] p 514 N93-21310

The NASA/industry Design Analysis Methods for Vibrations (DAMVIBS) program: A government overview

p 514 N93-21311

The NASA/industry Design Analysis Methods for Vibrations (DAMVIBS) program: Bell Helicopter Textron accomplishments

p 514 N93-21312

The NASA/industry Design Analysis Methods for Vibrations (DAMVIBS) program: Boeing Helicopters airframe finite element modeling

p 515 N93-21313

The NASA/industry Design Analysis Methods for Vibrations (DAMVIBS) program: McDonnell-Douglas Helicopter Company achievements

p 515 N93-21314

The NASA/industry Design Analysis Methods for Vibrations (DAMVIBS) program: Sikorsky Aircraft: Advances toward interacting with the airframe design process

p 515 N93-21315

The integrated design and manufacturing of composite structures for aircraft using an advanced tape layering technology

[MBB-LME-251-S-PUB-0491-A] p 515 N93-21401

Application of artificial neural networks to the design optimization of aerospace structural components

[NASA-TM-4389] p 555 N93-21831

- Structural Tailoring of Advanced Turboprops (STAT).
Theoretical manual [NASA-CR-191017] p 556 N93-22005
A procedure for defining lightning risk to air vehicles p 703 N93-24885
Rotor design optimization using a free wake analysis [NASA-CR-177612] p 693 N93-25075
Design concepts for the development of cooperative problem-solving systems [NASA-CR-192708] p 707 N93-25261
A numerical and experimental studies of flow characteristics in centrifugal fans p 695 N93-25339
A computational aerodynamic design optimization method using sensitivity analysis p 716 N93-25552
Variable-speed generators with flux weakening p 750 N93-25599
The effects of reaction on axial compressor performance p 724 N93-25882
Techniques for designing rotorcraft control systems [NASA-CR-192960] p 729 N93-26046
Adjoint methods for aerodynamic wing design [NASA-CR-193086] p 805 N93-27089
Aerodynamic analysis of hypersonic waverider aircraft [NASA-CR-192981] p 780 N93-27093
Multidisciplinary design optimization: An emerging new engineering discipline [NASA-TM-107761] p 806 N93-27258
Practical input optimization for aircraft parameter estimation experiments [NASA-CR-191462] p 820 N93-27264
Design, analysis, and control of large transport aircraft utilizing engine thrust as a backup system for the primary flight controls [NASA-CR-192938] p 820 N93-27308
Stability investigations of airfoil flow by global analysis p 783 N93-27436
An interactive boundary-layer approach to multielement airfoils at high lift p 785 N93-27445
Aerodynamic characteristics of a rotorcraft airfoil designed for the tip region of a main rotor blade [NASA-TM-4264] p 876 N93-29450
Effect of design selection on response surface performance [NASA-CR-4520] p 895 N93-29885
Mathematical model of frost heave and thaw settlement in pavements [CIREL-REPT-93-2] p 912 N93-30103
Multi-parameter optimization tool for low-cost commercial fuselage crown designs p 922 N93-30858
Process and assembly plans for low cost commercial fuselage structure p 923 N93-30865
Multiple methods integration for structural mechanics analysis and design p 923 N93-30867
Structural design using neural networks p 942 N93-31029
- DESIGN TO COST**
Economical view on composite structures maintenance [SME PAPER EM92-102] p 233 A93-14103
Designing to aircraft system effectiveness/cost/time with VERT - The system analysis method for aircraft p 153 A93-14204
Composite wing results of Deutsche Airbus technology program p 109 A93-15808
Advanced composite fiber/metal pressure vessels for aircraft applications [AIAA PAPER 93-2246] p 1155 A93-50047
Axial flow compressors - Mechanical design trends [ISABE 93-7061] p 1199 A93-54037
Variable cycle engine concept [ISABE 93-7065] p 1200 A93-54041
Exodus: Prime Mover [NASA-CR-192051] p 332 N93-17803
Process and assembly plans for low cost commercial fuselage structure p 923 N93-30865
- DESTRUCTIVE TESTS**
The effects of crushing surface roughness on the crushing characteristics of composite tubes p 77 A93-10918
Inelasticity effect in a unidirectional boron/aluminum composite under uniaxial tension p 825 A93-39024
Case study and simulation of fatigue damages and DTE of aging aircraft - A review of researches in Japan p 948 A93-45800
Report on the test set-up for the structural testing of the Airmass Sunburst Ultralight Aircraft p 895 N93-29775
Load test set-up for the Airmass Sunburst Ultra-Light Aircraft p 895 N93-29776
- DETECTION**
Conditioned based machinery maintenance (helicopter fault detection) [AD-A255796] p 329 N93-16396
RDR-4B doppler weather radar with forward looking wind shear detection capability p 489 N93-19601
- Fundamentals of adaptive anticipation techniques for the detection of threatening air traffic conflicts: Investigation of the horizontal proximity situation in the case of expected heading changes [DLR-MITT-91-21] p 503 N93-21004
Damage detection by Acousto-Ultrasonic Location (AUL) p 555 N93-21529
The UK perspective on aviation security p 496 N93-21858
Insights into US domestic aviation p 496 N93-21859
Principles of nuclear-based explosive detection systems p 497 N93-21861
A review of the development of a luggage explosive detection system p 497 N93-21862
A transportable luggage examination system based on neutron interrogation p 497 N93-21863
PFNA technique for the detection of explosives p 497 N93-21865
A pulsed fast-thermal neutron interrogation system p 497 N93-21866
Explosive detection system based on Electronic Neutron Generator (ENG) p 497 N93-21870
Experience with explosive detection systems in airports p 498 N93-21895
Aircraft ice detectors and related technologies for onground and inflight applications [DOT/FAA/CT-92/27] p 791 N93-27269
Detection performance of digital polarity sampled phase reversal code pulse compressors [AD-A262930] p 842 N93-28289
- DETECTORS**
Principles of nuclear-based explosive detection systems p 497 N93-21861
A review of the development of a luggage explosive detection system p 497 N93-21862
Explosive detection system based on Electronic Neutron Generator (ENG) p 497 N93-21870
Aircraft ice detectors and related technologies for onground and inflight applications [DOT/FAA/CT-92/27] p 791 N93-27269
- DETERIORATION**
Implementation of an infrared thermal imaging system to measure temperature in a gas turbine engine [AIAA PAPER 93-2469] p 1120 A93-50215
- DETERMINANTS**
A primer on polynomial resultants [AD-A246883] p 98 N93-11463
- DETONABLE GAS MIXTURES**
Development update for the NASA Ames 16-Inch Shock Tunnel Facility p 822 A93-37873
Gas analysis system for the Eight Foot High Temperature Tunnel p 822 A93-37875
Analysis of thermal ignition in supersonic flat-plate boundary layers p 769 A93-37933
Shock tube validation experiments for the simulation of ram-accelerator-related combustion and gasdynamic problems p 1016 A93-45499
Analysis of the stability characteristics of hypersonic flow of a detonable gas mixture in the stagnation region of a blunt body [AIAA PAPER 93-1918] p 1076 A93-49784
Parameters influencing the hot-spot ignition of aviation fuel/air and ethylene/air mixtures p 704 N93-24886
- DETONATION**
Pulsed detonation engine experimental and theoretical review [AIAA PAPER 92-3168] p 531 A93-24478
Godunov-type schemes applied to detonation flows [NASA-CR-191447] p 780 N93-27090
- DETONATION WAVES**
Numerical simulation of shock-induced combustion/detonation p 410 A93-20719
An aerospace plane as a detonation wave ramjet/airframe integrated waverider [AIAA PAPER 92-5022] p 272 A93-22298
Stability of oblique detonations in RAM accelerators [AIAA PAPER 92-0089] p 541 A93-24979
Uniform high-order spectral methods for one- and two-dimensional Euler equations p 476 A93-27068
Reaction zone structure for strong, weak overdriven, and weak underdriven oblique detonations p 746 A93-35492
Shock waves; Proceedings of the 18th International Symposium, Sendai, Japan, July 21-26, 1991. Vols. 1 & 2 [ISBN 0-387-55686-9] p 1023 A93-45451
A propulsion device driven by reflected shock waves p 1001 A93-45550
Analysis of the stability characteristics of hypersonic flow of a detonable gas mixture in the stagnation region of a blunt body [AIAA PAPER 93-1918] p 1076 A93-49784
Numerical simulations of a pulsed detonation wave augmentation device [AIAA PAPER 93-1985] p 1112 A93-49832
- Standing normal detonations and oblique detonations for propulsion [AIAA PAPER 93-2325] p 1116 A93-50105
Experimental Investigation of Nozzle/Plume Aerodynamics at Hypersonic Speeds [NASA-CR-191368] p 386 N93-18085
Analytical and experimental investigations of the oblique detonation wave engine concept [NASA-TM-102839] p 1006 N93-32374
- DEUTERIDES**
Application of vanadium hydride compressors for Joule-Thomson cryocoolers p 1149 A93-48616
- DIAGNOSIS**
An investigation of the influence of advanced aircraft diagnostics on the technological sophistication of maintenance personnel [AD-A258988] p 240 N93-18887
The use of multiple models in case-based diagnosis p 759 N93-25969
- DIAMAGNETISM**
Lifting forces acting on magnets placed above a superconducting plane p 79 A93-12332
- DIAMETERS**
Recess vane passive stall control [ASME PAPER 92-GT-36] p 246 A93-19296
- DIAPHRAGMS (MECHANICS)**
A High Deflection Diaphragm concept (HDD) for power transmission shafting p 826 A93-35931
Double diaphragm driven free piston expansion tube p 1016 A93-45533
- DIATOMIC GASES**
Subsonic potential flow and the transonic controversy p 479 A93-28544
- DIATOMIC MOLECULES**
Computer program for calculating and fitting thermodynamic functions [NASA-RP-1271] p 231 N93-12967
- DIELECTRICS**
Advanced electromagnetic methods for aerospace vehicles [NASA-CR-193468] p 936 N93-31036
- DIESEL ENGINES**
Intake flow modeling in a four stroke diesel using KIVA3 [AIAA PAPER 93-2952] p 1148 A93-48146
A diesel powerplant development program for airships [AIAA PAPER 93-4038] p 1246 A93-54609
Compound cycle engine for helicopter application [NASA-CR-180824] p 55 N93-10348
- DIESEL FUELS**
Making clean gasoline: The effect on jet fuels [AD-A264302] p 1019 N93-32085
- DIFFERENCE EQUATIONS**
An implicit difference scheme of Euler equation for unsteady transonic flow p 1182 A93-53852
One type of automatically adjusted difference scheme with artificial viscosity to calculate ablated exterior shapes [AD-A254108] p 19 N93-10856
- DIFFERENTIAL EQUATIONS**
Robust control of an aeroelastic system modeled by a singular integro-differential equation p 97 A93-13197
One-dimensional methods for accurate prediction of off-design performance behavior of axial turbines [ASME PAPER 92-GT-54] p 347 A93-19304
Uniform high-order spectral methods for one- and two-dimensional Euler equations p 476 A93-27068
Some Fuchs-type equations in fluid mechanics p 1165 A93-48967
Non-linear flight dynamics [ONERA, TP NO. 1993-109] p 1206 A93-53621
Volume 2: Explicit, multistage upwind schemes for Euler and Navier-Stokes equations [NASA-CR-191647] p 418 N93-16558
A critical analysis of the accuracy of several numerical techniques for combustion kinetic rate equations [NASA-TP-3315] p 362 N93-16941
A hybrid multigrid technique for computing steady-state solutions to supersonic flows p 700 N93-26078
Development of an unstructured solution adaptive method for the quasi-three-dimensional Euler and Navier-Stokes equations [NASA-CR-193241] p 930 N93-29213
Some implications of a differential turbomachinery equation with viscous correction [AD-A264693] p 935 N93-30571
- DIFFERENTIAL GEOMETRY**
Robust nonlinear feedback guidance for an aerospace plane: A geometric approach p 189 N93-14835
- DIFFRACTION LIMITED CAMERAS**
Diffraction limited collimating optics for high aspect ratio laser diode arrays p 1172 A93-48411
- DIFFRACTION PATTERNS**
Computation of shock diffraction in external and internal flows p 1024 A93-45537

DIFFUSERS

- Numerical analysis of the 3-D turbulent flow in an S-shaped diffuser p 116 A93-14252
- A semi-empirical theory of the noise in slotted tunnels caused by diffuser suction p 231 A93-14353
- Blade loading and shock wave in a transonic circular cascade diffuser
- [ASME PAPER 92-GT-34] p 246 A93-19294
- Viscous flows in centrifugal compressor diffusers at transonic Mach numbers
- [ASME PAPER 92-GT-48] p 246 A93-19301
- The vortex behaviour of the rotating-stall cell of a centrifugal compressor with vaned diffuser
- [ASME PAPER 92-GT-66] p 400 A93-19316
- Blade loading of transonic circular cascade diffuser
- p 267 A93-20919
- Turbulence and stall in plane diffusers - Computational study
- p 744 A93-34311
- Active boundary-layer control in diffusers
- [AIAA PAPER 93-3255] p 966 A93-46798
- Effect of geometry, bleed rates and flow splits on pressure recovery of a canted hybrid vortex-controlled diffuser
- [AIAA PAPER 93-1762] p 1109 A93-49659
- Applying and validating the RANS-3D flow-solver for evaluating a subsonic serpentine diffuser geometry
- [AIAA PAPER 93-2157] p 1079 A93-49973
- Numerical solutions of Euler equations by using a new flux vector splitting scheme
- p 1087 A93-51740
- Two and three-dimensional prediffuser combustor studies with air-water mixture
- [ISABE 93-7025] p 1213 A93-54001
- Air ejector experiments using the two-dimensional supersonic cascade tunnel: Relationship between ejector performance and throat area ratio, part 1
- [NAL-TM-642-PT-1] p 25 N93-12352
- Investigations of detail design issues for the high speed acoustic wind tunnel using a 60th scale model tunnel. Part 1: Tests with open circuits
- [NASA-CR-191671] p 137 N93-14737

DIFFUSION

- Diffusion controlled evaporation of a multicomponent droplet - Theoretical studies on the importance of variable liquid properties
- p 1021 A93-44224
- The experimental evaluation of annular ejector system under concurrent mixing and diffusion
- p 1250 A93-54593

DIFFUSION COEFFICIENT

- Measurement of diffusion in supercritical fluid systems - A review
- [AIAA PAPER 93-0809] p 534 A93-24884

DIFFUSION FLAMES

- NO(x) sensitivities for gas turbine engines operated on lean-premixed combustion and conventional diffusion flames
- [ASME PAPER 92-GT-115] p 349 A93-19351
- Experimental and numerical investigations of the vortex-flame interactions in a driven jet diffusion flame
- [AIAA PAPER 93-0455] p 534 A93-25532
- Three-dimensional emission modeling for diffusion flame, rich/lean, and lean gas turbine combustors
- [AIAA PAPER 93-2338] p 1117 A93-50115
- The influence of swirl generator characteristics on flow and combustion in turbulent diffusion flames
- p 1159 A93-51632
- Thermometry inside a swirling turbulent flame - CARs advantages and limitations
- p 1146 A93-51634
- Blowout of turbulent disc/pilot stabilized jet diffusion flames
- [ISABE 93-7026] p 1213 A93-54002
- Chemical kinetic and aerodynamic structures of flames
- [AD-A256015] p 391 N93-15931
- Oxides of nitrogen emissions from turbulent hydrocarbon/air jet diffusion flames, phase 2
- [PB93-152478] p 756 N93-26533
- Studies of hydrogen-air diffusion flames and of compressibility effects related to high-speed propulsion
- p 917 N93-29125
- Effects of buoyancy on gas jet diffusion flames
- [NASA-CR-191109] p 935 N93-31031

DIFFUSION WELDING

- The application of diffusion bonding in the manufacture of aeroengine components
- p 1217 A93-53514
- Joining carbon composite fins to titanium heat pipes
- [AD-A261970] p 825 N93-27667

DIGITAL COMPUTERS

- Application of feedback linearization method in a digital restructurable flight control system
- p 370 A93-23514
- Formal verification of algorithms for critical systems
- p 846 A93-37623
- Characterization of the faulted behavior of digital computers and fault tolerant systems
- p 1224 A93-52762

DIGITAL DATA

- Model of a map indicator
- p 341 A93-18532

- A summary of investigations of severe turbulence incidents using airline flight records
- p 308 A93-22153
- Digital map databases in support of avionic display systems
- p 544 A93-26888
- Digital image processing applied to heat transfer measurement in hypersonic wind tunnel
- [ONERA, TP NO. 1992-118] p 831 A93-38593
- Appraisal of digital terrain elevation data for low-altitude flight
- [NASA-TM-103896] p 35 N93-10745
- Integration of radar altimeter, precision navigation, and digital terrain data for low-altitude flight
- [NASA-TM-103958] p 36 N93-12320
- A novel-high-performance system for recording and analysing instantaneous total pressure distortion in air intakes
- p 214 N93-13215
- Digital data acquisition and preliminary instrumentation study for the F-16 laminar flow control vehicle
- p 292 N93-16784
- The use of digital road data by a navigation system
- p 993 N93-31269

DIGITAL ELECTRONICS

- An investigation of real-time diagnostic technique on aeroengine
- p 174 A93-16844
- Digital avionics systems - Principles and practices (2nd revised and enlarged edition) - Book
- [ISBN 0-07-060333-2] p 342 A93-19801
- Digital flight recorded data - A method of estimating down draft from digital flight recorded data
- p 1241 A93-54559
- Avionics systems architectures
- p 808 N93-27169

DIGITAL FILTERS

- The development of an airborne information management system for flight test
- [AIAA PAPER 92-4113] p 51 A93-11281
- Design and implementation of digital filters for analysis of F/A-18 flight test data
- [AD-A253447] p 17 N93-10342

DIGITAL NAVIGATION

- The use of digital map data to provide enhanced navigation and displays for poor weather penetration and recovery
- p 992 A93-45165
- Information-based criteria of terrain navigability. Part 1: Data-base analysis
- p 793 N93-27178

DIGITAL RADAR SYSTEMS

- Digital pulse compression with low range sidelobes
- p 929 A93-43463

DIGITAL SIMULATION

- Direct numerical simulation of laminar breakdown in high-speed, axisymmetric boundary layers
- p 8 A93-11527
- Numerical simulations of high-speed flows about waveriders with sharp leading edges
- p 9 A93-12007
- Numerical simulations of high speed inlet flows
- p 115 A93-14246
- Numerical simulation of turbulent reacting flows in combustion chambers
- p 171 A93-14271
- A digital simulation and its experimental investigation for the response of gas-turbine engines to intake flow distortion
- p 120 A93-14366
- Design of digital multiple model-following integrated flight/proposition control systems
- p 183 A93-14371
- Digital simulation of transonic flow fields in a planar nozzle
- p 122 A93-14479
- Numerical simulation of the flow field around supersonic air-intakes
- [ASME PAPER 92-GT-206] p 251 A93-19430
- Direct numerical simulation of nitric oxide evolution in underexpanded jets
- [ASME PAPER 92-GT-372] p 355 A93-19534
- Structural Tailoring/Analysis for Hypersonic Components - A computational simulation
- [AIAA PAPER 92-4722] p 325 A93-20324
- Numerical simulation of jet noise
- p 265 A93-20716
- Numerical simulation of shock-induced combustion/detonation
- p 410 A93-20719
- Scramjet fuel-air mixing establishment in a pulse facility
- p 359 A93-21667
- The dynamics of microbursts as revealed by Doppler radar observations and numerical simulations
- p 432 A93-22196
- Direct numerical simulation of turbulent flow in a square duct
- [AIAA PAPER 93-0198] p 277 A93-22618
- Quasi-one-dimensional modelling of free-piston shock tunnels
- [AIAA PAPER 93-0352] p 377 A93-23037
- Investigation of an electrothermal de-icer pad using a three-dimensional finite element simulation
- [AIAA PAPER 93-0397] p 327 A93-23072
- Numerical simulation of delta-wing roll
- [AIAA PAPER 93-0554] p 285 A93-23293
- Digital simulation of atmospheric turbulence for Dryden and von Karman models
- p 416 A93-23517

- Numerical simulation of crossing/turbulent boundary layer interaction at Mach 8.3 comparison of zero and two-equation turbulence models
- [AIAA PAPER 93-0779] p 467 A93-24861
- Numerical simulation of vortex generation and capture above an airfoil
- [AIAA PAPER 93-0864] p 468 A93-24926
- Numerical simulation of homogeneous non-Gaussian random vector fields
- p 561 A93-27584
- Numerical simulation of starting process in a hypersonic nozzle
- p 684 A93-34275
- Numerical simulation of turbine 'hot spot' alleviation using film cooling
- p 744 A93-34476
- Numerical simulation of a hovering rotor using embedded grids
- p 765 A93-35936
- A numerical simulation of a scram jet combustor flow
- p 810 A93-38181
- An implicit finite-difference algorithm for the numerical simulation of supersonic flow over blunt bodies
- p 770 A93-38325
- Numerical simulation of laminar hypersonic flow past a double-ellipsoid
- p 868 A93-42612
- Numerical simulation of hypersonic flow over a double ellipse using a Taylor-Galerkin finite element formulation with adaptive grids
- p 888 A93-42617
- Numerical simulation of vortex shedding past triangular cylinders at high Reynolds number using a k-epsilon turbulence model
- p 871 A93-42873
- Numerical simulation of two-dimensional and axisymmetric compressible flows
- p 960 A93-45546
- A systems approach to a DSMC calculation of a control jet interaction experiment
- [AIAA PAPER 93-2798] p 964 A93-46538
- Numerical simulation of aerothermodynamics processes in gas turbine engine components
- p 1002 A93-46939
- Numerical simulation of transition in two- and three-dimensional boundary layers
- p 973 A93-46980
- Numerical simulation of linear interference wave development in three-dimensional boundary layers
- p 1029 A93-46993
- Requirements for facilities and measurement techniques to support CFD development for hypersonic aircraft
- p 1014 A93-47024
- Numerical simulation of incompressible viscous flow around a propeller
- [AIAA PAPER 93-3503] p 984 A93-47271
- High resolution numerical simulation of the linearized Euler equations in conservation law form
- [AIAA PAPER 93-2934] p 1148 A93-48132
- Numerical simulation of upstream disturbance on flows around a slender body
- [AIAA PAPER 93-2956] p 1047 A93-48150
- Audio post-processing for shear layer calculations
- [AIAA PAPER 93-3075] p 1059 A93-48250
- Numerical simulation of a blast inside a Boeing 747
- [AIAA PAPER 93-3091] p 1099 A93-48265
- A study of turbulence in rarefied gases
- [AIAA PAPER 93-3097] p 1061 A93-48271
- Numerical simulation of a shock wave/turbulent boundary layer interaction in a duct
- [AIAA PAPER 93-3127] p 1063 A93-48293
- Simplified mathematical model and digital simulation of aeroengine
- p 1106 A93-48511
- Application of analog computing to real-time simulation of stall and surge dynamics
- [AIAA PAPER 93-2231] p 1080 A93-50037
- Numerical simulation and physical aspects of supersonic vortex breakdown
- p 1093 A93-52011
- Static and dynamic errors in heat flux measurements
- p 1254 A93-54366
- Hybrid guidance for maneuvering flight vehicles
- [AD-A254110] p 69 N93-11798
- Three dimensional boundary-layer transition on a swept wing
- p 419 N93-16818
- Experiments on swept-wing boundary-layer transition
- p 419 N93-16829
- Aerodynamic design and analysis of fans using 3D computational codes
- [DS-2140] p 294 N93-17880
- Proceedings of the Ninth NAL Symposium on Aircraft Computational Aerodynamics
- [NAL-SP-16] p 299 N93-19273
- LES turbulence modeling using DNS data base
- p 299 N93-19274
- A simple grid generation technique for hypersonic flow around complex configuration
- p 299 N93-19275
- Computation of internal flows using unstructured triangular meshes
- p 299 N93-19276
- Numerical computations using multi-domain technique
- p 299 N93-19277
- Numerical simulations of hypersonic rarefied transition regime flows: DSMC method and Navier-Stokes computation
- p 299 N93-19278
- Monte Carlo simulation of normal shock wave. Part 1: Lennard-Jones potential
- p 300 N93-19279

- Rarefied gas numerical wind tunnel. Part 7: OREX p 382 N93-19280
- Analysis of a 2-D airfoil motion flying in-proximity to a wavy-wall surface: Lifting-surface-method p 300 N93-19281
- Analysis of a 2-D airfoil motion flying in-proximity to a wavy-wall surface: Finite difference method p 300 N93-19282
- Development of a boundary element method program for numerical analysis of supersonic unsteady flow p 300 N93-19283
- Numerical calculations of separating flows around oscillating airfoil p 300 N93-19284
- Numerical simulation of unsteady large scale separated flow around oscillating airfoil p 300 N93-19285
- Calculations of aerodynamic forces on a wing with thrust using BEM p 300 N93-19286
- Numerical Wind Tunnel: Requirements and the outline p 383 N93-19288
- Numerical Wind Tunnel hardware p 383 N93-19289
- The operating system for Numerical Wind Tunnel p 383 N93-19290
- The language processor system for the Numerical Wind Tunnel p 383 N93-19291
- Generation of longitudinal vortices in supersonic flow p 301 N93-19292
- The role of computational fluid dynamics in aeronautical engineering. 9: Analysis of hypersonic equilibrium air flow p 301 N93-19294
- Computation of re-entry flows with two-temperature model p 301 N93-19295
- Numerical calculation of hypersonic non-equilibrium flow around OREX p 301 N93-19296
- Numerical simulation of hypersonic flow around H-2 Orbiting Plane (HOPE), part 3 p 301 N93-19297
- The 3D Navier-Stokes calculation of flow about scramjet inlet with strut p 301 N93-19298
- Numerical simulation of flow for a scramjet nozzle p 302 N93-19299
- Transonic flow calculation around NACA-0012 p 302 N93-19301
- Numerical simulations of supersonic flow by a fourth-order compact MUSCL TVD scheme p 302 N93-19308
- Analytical and numerical study on steady Mach reflection p 302 N93-19309
- Numerical simulation of the flow through non-uniform airfoil cascade p 302 N93-19310
- Numerical study on transverse hydrogen injection into a supersonic flowfield p 302 N93-19311
- Three dimensional calculation of flow inside supersonic inlet p 303 N93-19313
- Numerical simulation of flows in a supersonic air intake p 303 N93-19314
- A numerical investigation for supersonic inlet p 303 N93-19315
- A numerical investigation of 3D transverse injection into the supersonic flow behind rearward facing step p 303 N93-19316
- Numerical calculation of flow field in supersonic combustion chamber p 304 N93-19317
- A numerical simulations of inner flow of scramjet p 304 N93-19318
- Wind tunnel wall interference correction at subsonic speeds p 304 N93-19320
- Two problems reducing the data accuracy in Transonic Wind Tunnel testing p 304 N93-19321
- Wind tunnel tests and CFD in Fuji Heavy Industries p 304 N93-19323
- Wind tunnel test and CFD in Kawasaki Heavy Industries, Gifu p 304 N93-19324
- Wind tunnel testing and CFD simulation in Mitsubishi Heavy Industries p 305 N93-19325
- Role of wind tunnel tests and CFD analysis for the development of aero-engines in IHI p 365 N93-19326
- Aerothermodynamic properties of hypersonic flows over radiation-adiabatic surfaces p 485 N93-21761
- DIGITAL SYSTEMS**
- Digital map display technology p 77 A93-11206
- Digital avionics systems - Principles and practices (2nd revised and enlarged edition) --- Book [ISBN 0-07-060333-2] p 342 A93-19801
- Robust digital control of a high-performance engine --- F-100 turbofan p 359 A93-21792
- Using numerical control algorithms in stabilization systems with digital correction p 941 A93-43113
- Genetic design of digital model-following flight-control systems [AIAA PAPER 93-3883] p 1135 A93-51468
- Developments towards versatility in digital engine control units [ISABE 93-7088] p 1202 A93-54064
- A monitor for the laboratory evaluation of control integrity in digital control systems operating in harsh electromagnetic environments [NASA-TM-4402] p 65 N93-12304
- Multiple-function multi-input/multi-output digital control and on-line analysis [NASA-TM-107697] p 162 N93-13565
- Approaches to control of the large angle magnetic suspension test fixture [NASA-CR-191890] p 381 N93-16695
- Development and testing of the digital control system for the Archytas unmanned air vehicle [AD-A261656] p 729 N93-26196
- DIGITAL TECHNIQUES**
- Digital fly-by-wire system for BK117 FBW research helicopter p 181 A93-14209
- Adaptive grid generation using optimal control theory p 770 A93-38187
- Experimental results on RIAS digital beamforming radar p 929 A93-43392
- New digital capacitive measurement system for blade clearances p 1254 A93-54376
- Digitization of analog data from in-flight lightning strikes p 753 N93-24884
- DIGITAL TO ANALOG CONVERTERS**
- Silicon differential pressure transducer line pressure effects and compensation p 830 A93-37890
- DILUTION**
- An analytical study of dilution jet mixing in a cylindrical duct [AIAA PAPER 93-2043] p 1113 A93-49876
- An analytical study of dilution jet mixing in a cylindrical duct [NASA-TM-106181] p 814 N93-27160
- DIMENSIONAL MEASUREMENT**
- On machine capacitance dimensional and surface profile measurement system p 750 N93-25579
- X-ray computed tomography for casting development [AD-A261786] p 752 N93-26526
- DIPHENYL COMPOUNDS**
- Application of a sulphur-doped alkane system to the study of thermal oxidation of jet fuels [ASME PAPER 92-GT-122] p 387 A93-19356
- DIPLOLE ANTENNAS**
- ILS mathematical modeling study of the effects of an ASR-9 structure at the Long Island MacArthur Airport, Islip, NY [DOT/FAA/CT-TN92/25] p 192 N93-12668
- The ILS mathematical modeling study of the Runway 10 ILS Localizer at Luis Munoz Marin International Airport, San Juan, Puerto Rico [DOT/FAA/CT-TN93/10] p 792 N93-27017
- Coupling gain computation between antennas on circular cylinders at SHF/EHF frequencies p 933 N93-30309
- DIPLOLES**
- Computation of far-field helicopter rotor tone noise [ONERA-P-1990-5] p 943 N93-30110
- DIRECT CURRENT**
- An experimental study of dc discharges in supersonic and subsonic air flows p 14 A93-12980
- Document for 270 Voltage Direct Current (270 V dc) System [SAE ARP 4729] p 1160 A93-52170
- DIRECTION FINDING**
- The use of digital road data by a navigation system p 993 N93-31269
- DIRECTIONAL CONTROL**
- Correlation of forebody pressures and aircraft yawing moments on the X-29A aircraft at high angles of attack [AIAA PAPER 92-4105] p 38 A93-11273
- The strake - A simple means for directional control improvement p 802 A93-37997
- Lateral control at high angles of attack using pneumatic blowing through a chined forebody [AIAA PAPER 93-3624] p 1126 A93-48309
- Development of lateral-directional departure criteria [AIAA PAPER 93-3650] p 1128 A93-48333
- Investigation of high-alpha lateral-directional control power requirements for high-performance aircraft [AIAA PAPER 93-3647] p 1130 A93-49519
- Cancellation control law for lateral-directional dynamics of a supermaneuverable aircraft [AIAA PAPER 93-3775] p 1131 A93-51370
- A comparison of two multi-variable integrator windup protection schemes [AIAA PAPER 93-3812] p 1123 A93-51404
- Longitudinal and lateral-directional flying qualities investigation of high-order characteristics for advanced-technology transports [AIAA PAPER 93-3815] p 1133 A93-51406
- DIRECTIONAL SOLIDIFICATION (CRYSTALS)**
- New corrosion resistant nickel-base super-alloys and technological processes of casting gas turbines parts with directional single crystal and regulable equiaxed minimized microporosity structure p 916 A93-40811
- Mechanical anisotropy in directionally solidified turbine blade p 1018 A93-47356
- DIRECTIONAL STABILITY**
- Calculation of transonic longitudinal and lateral-directional characteristics of aircraft by the small disturbance theory [AIAA PAPER 93-3617] p 1125 A93-48304
- Correlation of forebody pressures and aircraft yawing moments on the X-29A aircraft at high angles of attack [NASA-TM-4417] p 22 N93-11532
- Aerodynamic integration of thrust reversers on the Fokker 100 p 160 N93-13208
- Hypersonic lateral and directional stability characteristics of aerobassist flight experiment configuration in air and CF4 [NASA-TM-4435] p 875 N93-29166
- DIRECTORIES**
- Directory of factual and numeric databases of relevance to aerospace and defence R and D [AGARD-R-777] p 104 N93-11710
- DISCHARGE COEFFICIENT**
- Effect of the proximity of the machined surface on the discharge coefficients of laser cutter nozzles p 79 A93-12809
- DISCRETE ADDRESS BEACON SYSTEM**
- The effect of TCAS interrogations on the Chicago O'Hare ATCRBS system [DOT/FAA/CT-92/22] p 318 N93-16498
- DISCRIMINANT ANALYSIS (STATISTICS)**
- Preliminary results on the use of linear discriminant analysis in the ARM continuous speech recognition system [RSRE-MEMO-4511] p 87 N93-11384
- The use of linear discriminant analysis in the ARM continuous speech recognition system [RSRE-MEMO-4512] p 87 N93-11385
- SAC contrail formation study [AD-A254410] p 159 N93-12605
- DISKS (SHAPES)**
- Observations of large-scale structures in wakes behind axisymmetric bodies p 965 A93-46748
- Ongoing challenges for titanium alloy cleanliness improvement in aircraft engine disk materials p 1212 A93-53506
- DISORIENTATION**
- Royal Naval helicopter ditching experience p 492 N93-19684
- DISPLACEMENT**
- Modeling and strain gauging of eddy current repulsion deicing systems [AIAA PAPER 93-0296] p 327 A93-22696
- DISPLAY DEVICES**
- A large flat panel multifunction display for military and space applications p 77 A93-10963
- Trends of the airborne cockpit display format p 50 A93-11203
- Digital map display technology p 77 A93-11206
- Pilot/Vehicle display development from simulation to flight [AIAA PAPER 92-4174] p 51 A93-13310
- TCAS display issues [AIAA PAPER 92-4242] p 51 A93-13351
- A guidance display system for single pilot operation [AIAA PAPER 92-4196] p 51 A93-13373
- Optical design of a wide-angle simulator probe p 211 A93-17140
- Helmet Mounted Sight and display testing p 517 A93-26883
- High-resolution displays and projection systems; Proceedings of the Meeting, San Jose, CA, Feb. 11, 12, 1992 [SPIE-1664] p 544 A93-27237
- Tactical cockpits - The coming revolution p 505 A93-27238
- A survey of display technologies for military aircraft cockpit applications p 517 A93-27239
- Controls and displays for Douglas Aircraft for the 1990s p 545 A93-27241
- SIPORT DEPCOS and SIPORT ARRCOS - More than an electronic airstrip replacement p 499 A93-27914
- Application of new GPS aircraft control/display system to topographic mapping of the Greenland ice cap p 499 A93-28152
- An ac thin film electroluminescent (TFEL) display unit for cockpit control display unit application p 518 A93-28179
- The history and development of coated Contrast Enhancement Filters for cockpit displays p 564 A93-28180
- Data acquisition and analysis on a Macintosh p 562 A93-29422
- Improvements in hover display dynamics for a combat helicopter p 727 A93-34257
- Development methodology for contemporary avionics systems [SAE PAPER 931591] p 1104 A93-49340

- Dynamic simulation fidelity improvement using transfer function state extrapolation
[AIAA PAPER 93-3552] p 1222 A93-52656
- Transport delay compensation - An inexpensive alternative to increasing image generator update rate
[AIAA PAPER 93-3563] p 1223 A93-52663
- A primary flight display for four-dimensional guidance and navigation influence of tunnel size and level of additional information on pilot performance and control behaviour
[AIAA PAPER 93-3570] p 1208 A93-52668
- Pilot evaluations of augmented flight simulator motion
[AIAA PAPER 93-3580] p 1208 A93-52676
- An evaluation of software tools for the design and development of cockpit displays
[AIAA PAPER 93-3593] p 1224 A93-52685
- Advanced terrain displays to transport category aircraft
[PB92-197136] p 35 A93-10065
- Air traffic control visual scanning
[DOT/FAA/CT-TN92/16] p 35 A93-10459
- Methods and principles for determining task dependent interface content
[NASA-CR-190837] p 36 A93-10961
- Advantages of using a projected head-up display in a flight simulator
[AD-A255332] p 194 A93-14559
- Experimental evaluation of candidate graphical microburst alert displays
p 145 A93-14853
- Design for tactical situation awareness display
[AD-A256194] p 170 A93-15235
- Simulator evaluation of displays for a revised takeoff performance monitoring system
[NASA-TP-3270] p 189 A93-15366
- Realization of real time graphics in vehicles with high dynamic motion
[ETN-93-92739] p 443 A93-18630
- Liquid crystal displays replacing the CRT and CLE of future cockpits
p 518 A93-19783
- On the typography of flight-deck documentation
[NASA-CR-177605] p 571 A93-19970
- Measurement of modulation transfer functions of simulator displays
[AD-A259401] p 530 A93-21268
- Evaluation of advanced displays for engine monitoring and control
[NASA-CR-191418] p 718 A93-24764
- Inflight evaluation of an acoustic orientation instrument
[AD-A260752] p 719 A93-25909
- Virtual reality flight control display with six-degree-of-freedom controller and spherical orientation overlay
[NASA-CASE-NPO-18733-1-CU] p 897 A93-30416
- DISRUPTING**
A simulation study of the effects of communication delay on air traffic control
[AD-A258593] p 502 A93-19966
- DISSIPATION**
Reactive and dissipative hypersonic flow in a wind tunnel nozzle
p 687 A93-34358
- Consecutive plate acoustic suppressor apparatus and methods
[NASA-CASE-LEW-15430-1] p 453 A93-17051
- DISSOCIATION**
Air dissociation effects on aerodynamic characteristics of an aerospace plane
p 959 A93-45149
- DISTANCE**
Example of statistical techniques applied to analysis of landing ground roll distance measurements (linear regression, correlation coefficient and F-test)
[ESDU-92021] p 330 A93-16635
- DISTANCE MEASURING EQUIPMENT**
DME/P critical area determination on message passing processors
p 31 A93-11010
- Airborne MLS equipment
p 312 A93-18555
- DME-derived positions compared with MLS- and ILS-derived positions
[NLR-TP-90119-U] p 318 A93-16343
- DISTORTION**
Study on vortex flow control of inlet distortion
p 122 A93-14520
- Corrections to fringe distortion due to flow density gradients in optical interferometry
[AIAA PAPER 93-0631] p 539 A93-24748
- Effect of radial distortion on the performance of a centrifugal compressor
p 861 A93-42256
- Evaluation of alternatives for increasing A-7D rearward visibility
[AD-A255071] p 50 A93-12488
- DISTRIBUTED PROCESSING**
Implementation of an explicit Navier-Stokes algorithm on a distributed memory parallel computer
[AIAA PAPER 93-0063] p 261 A93-20176
- CFD development and a future high speed computer
p 847 A93-38128
- Expert system for redundancy and reconfiguration management
p 838 A93-42785
- A reactive approach for distributed air traffic control
[ONERA, TP NO. 1993-83] p 1190 A93-53603
- Identification and control of non-linear time-varying dynamical systems using artificial neural networks
[AD-A257595] p 372 A93-18193
- The operating system for Numerical Wind Tunnel
p 383 A93-19290
- A comparison using APPL and PVM for a parallel implementation of an unstructured grid generation program
[NASA-CR-191425] p 757 A93-25073
- DISTRIBUTION (PROPERTY)**
Design features influencing the distribution of fuel within the spray from an air blast fuel injector
[ASME PAPER 92-GT-235] p 353 A93-19448
- DISTRIBUTION FUNCTIONS**
Accuracy of nonparametric reliability estimates under varying operation conditions
p 396 A93-18343
- DISTURBANCES**
Supersonic jet control via point disturbances inside the nozzle
p 861 A93-41930
- Vortex-induced disturbance field in a compressible shear layer
p 873 A93-43628
- The forms of unsteady concentrated vortex-breakdown and its reactions to disturbance
p 1231 A93-54594
- DITCHING (LANDING)**
Royal Naval helicopter ditching experience
p 492 A93-19684
- Canadian Forces helicopter ditchings: 1952-1990
p 493 A93-19685
- Helicopter accidents over water in the national navy: Epidemiological study over the period 1980-1991
p 493 A93-19686
- DIVERGENCE**
Backward bifurcation for structural divergence of a wing section
p 526 A93-29351
- DIVERTERS**
Apparatus for reduction of vibration in liquid-injected gas compressor system
[AD-D015607] p 554 A93-20772
- DOCUMENTATION**
The importance of configuration management - An overview with test program sets
p 853 A93-35926
- Software support for a computerized air situation documentation system
p 941 A93-43115
- On the typography of flight-deck documentation
[NASA-CR-177605] p 571 A93-19970
- DOMAINS**
Motion compensation in a time domain SAR processor
p 885 A93-43466
- Domain specific software design for decision aiding
p 442 A93-17517
- A domain-specific design architecture for composite material design and aircraft part redesign
p 442 A93-17522
- An investigation of discovery-based learning in the route planning domain
[AD-A259141] p 513 A93-20560
- DOMES (STRUCTURAL FORMS)**
Thermal shock capabilities of infrared dome materials
p 70 A93-11454
- Interaction of compression waves with an elastic spherical dome
p 550 A93-29718
- Mixing in the dome region of a staged gas turbine combustor
p 1109 A93-49612
- DOORS**
Aircraft accident report: Explosive decompression-loss of cargo door in flight, United Airlines Flight 811, Boeing 747-122, N4713U, Honolulu, HI, 24 February 1989
[PB92-910402] p 28 A93-12193
- Effects of seating configuration and number of type 3 exits on emergency aircraft evacuation
[AD-A256616] p 143 A93-14277
- F-15 composite engine access door
p 920 A93-30442
- DOPPLER EFFECT**
Liquid water content measurements using the Phase Doppler Particle Analyzer in the NASA Lewis Icing Research Tunnel
[AIAA PAPER 93-0298] p 378 A93-23698
- De-Dopplerization of aircraft acoustic signals
[AIAA PAPER 93-0737] p 563 A93-24827
- Helicopter plume detection by using an ultranarrow-band noncoherent laser Doppler velocimeter
p 542 A93-25198
- Studies of superresolution range-Doppler imaging
p 928 A93-43344
- Adaptive clutter suppression for airborne array radars using clutter subspace approximation
p 883 A93-43411
- Nonintrusive, multipoint velocity measurements in high-pressure combustion flows
[AIAA PAPER 93-2032] p 1145 A93-49867
- Vertical wind estimation from horizontal wind measurements
p 489 A93-19604
- Trailing vortex/free-surface interaction
[AD-A261654] p 701 A93-26195
- Some aspects of the aeroacoustics of high-speed jets
[NASA-CR-191458] p 843 A93-28975
- DOPPLER NAVIGATION**
Adaptive filtering of Doppler velocimeter errors due to the characteristics of the reflecting surface
p 992 A93-45650
- Advanced Unmanned Search System (AUSS) supervisory command, control and navigation
[AD-A263171] p 793 A93-28990
- DOPPLER RADAR**
Integration of full scale development aircraft GPS user equipment (AN/ARN-151) with Doppler radar systems
p 31 A93-11012
- Prospective application of neural networks in superresolution radars
p 211 A93-16849
- Superresolution radar imaging with linear prediction data extrapolation
p 342 A93-20851
- An experimental cockpit display for TDWR wind shear alerts
p 343 A93-22111
- Detection of microburst-related gust fronts using Doppler radar
p 427 A93-22118
- Improvement in gust front algorithm detection capability using reflectivity thin lines versus azimuthal shears
p 427 A93-22120
- A comparison of several airborne measures of turbulence
p 308 A93-22121
- The Aviation Weather Products Generator
p 428 A93-22125
- Integrated Terminal Weather System (ITWS)
p 428 A93-22127
- Improved efficiency of air transportation through aviation weather system modernization
p 308 A93-22144
- Extremely low level jet in the evening in Kanto Plain
p 430 A93-22159
- SAAW - Italy's answer to the windshear challenge
p 431 A93-22175
- Anemometer siting criteria for low level wind shear alert system
p 413 A93-22178
- Status of the Terminal Doppler Weather Radar one year before deployment
p 431 A93-22184
- Reliability considerations for weather hazard warning radar
p 431 A93-22187
- Terminal Doppler Weather Radar program at Denver's Stapleton International Airport during 1989 and 1990
p 432 A93-22188
- Performance results and potential operational uses for the prototype TDWR microburst prediction product
p 432 A93-22190
- An improved gust front detection algorithm for the TDWR
p 432 A93-22191
- The detection and warning of low-level wind shear based on terminal single Doppler radar
p 432 A93-22195
- The dynamics of microbursts as revealed by Doppler radar observations and numerical simulations
p 432 A93-22196
- Doppler radar observation of tornado and microburst around Chitose Airport
p 432 A93-22199
- Microbursts detection with airborne Doppler lidar
p 433 A93-22201
- Evaluation of clear-air radar PROUST and Doppler radar RONSARD for airport low level-wind shear detection
p 433 A93-22202
- Comparison of three methods to deduce three-dimensional wind fields in a hurricane with airborne Doppler radar
p 844 A93-37691
- Comparison of airborne dual-Doppler and airborne/ground-based dual-Doppler analyses of North Dakota thunderstorms
p 844 A93-37694
- A technique to correct airborne Doppler data for coordinate transformation errors using surface clutter
p 807 A93-37699
- Update on the NASA ER-2 Doppler radar system (EDOP)
p 807 A93-37737
- Microburst avoidance crew procedures for forward-looking sensor equipped aircraft
[AIAA PAPER 93-3942] p 1007 A93-44234
- Three-dimensional simulation of the Denver 11 July 1988 microburst-producing storm
p 1164 A93-50373
- Study of artificial and natural turbulence in atmospheric boundary layer with a CW Doppler CO2 lidar
p 1257 A93-54799
- Summary of findings from the PIREP-based analyses conducted during the 1988 to 1990 evaluations of TDWR-based and TDWR/LLWAS-based alert services provided to landing/departing pilots
[AD-A253859] p 93 A93-11144
- Terminal Doppler Weather Radar (TDWR) Operational Test and Evaluation (OT/E) integration test plan
[DOT/FAA/CT-TN92/6] p 151 A93-13377
- Birds mimicking microbursts on 2 June 1990 in Orlando, Florida
[AD-A255703] p 143 A93-14024

- Terminal Doppler weather radar/low-level wind shear alert system integration algorithm specification, version 1.1
[AD-A255319] p 224 N93-14547
- NASA/LMSC coherent LIDAR airborne shear sensor: System capabilities and flight test plans
p 144 N93-14847
- The Orlando TDWR testbed and airborne wind shear data comparison results
p 145 N93-14851
- TDWR 1991 Program Review
p 145 N93-14852
- Systems issues in airborne Doppler radar/LIDAR certification
p 145 N93-14855
- Airborne Wind Shear Detection and Warning Systems: Fourth Combined Manufacturers' and Technologists' Conference, part 1
[NASA-CP-10105-PT-1] p 488 N93-19590
- Program overview: 1991 flight test objectives
p 488 N93-19591
- Air/ground wind shear information integration: Flight test results
p 488 N93-19594
- Doppler radar results
p 488 N93-19595
- Three-dimensional numerical simulation of the 20 June 1991, Orlando microburst
p 488 N93-19598
- RDR-4B doppler weather radar with forward looking wind shear detection capability
p 489 N93-19601
- Airborne doppler radar research at Rockwell International
p 489 N93-19602
- Acquisition and use of Orlando, Florida and Continental Airbus radar flight test data
p 489 N93-19603
- Microburst characteristics determined from 1988-1991 TDWR testbed measurements
p 490 N93-19605
- Ground clutter measurements using the NASA airborne doppler radar: Description of clutter at the Denver and Philadelphia airports
p 490 N93-19608
- Signal processing for airborne doppler radar detection of hazardous wind shear as applied to NASA 1991 radar flight experiment data
p 490 N93-19612
- Setting values for TDWR/LLWAS 3 integration parameters
[AD-A260740] p 755 N93-25645
- Contributions to the American Meteorological Society's 26th International Conference on Radar Meteorology [AD-A263385] p 936 N93-29257
- The effect of clock, media, and station location errors on Doppler measurement accuracy
p 885 N93-29588
- Airborne derivation of microburst alerts from ground-based Terminal Doppler Weather Radar information: A flight evaluation
[NASA-TM-108990] p 1000 N93-32223
- DORNIER AIRCRAFT**
- Nonlinear multi-point modelling and parameter estimation of the DO 28 research aircraft
p 41 A93-12727
- Dornier 228 experimental with laminar wing
p 506 A93-27500
- DOUGLAS AIRCRAFT**
- Controls and displays for Douglas Aircraft for the 1990s
p 545 A93-27241
- The 1990 high-speed civil transport studies
[NASA-CR-189618] p 330 N93-16947
- DOWNBURSTS**
- Structure of downbursts associated with heavy rainfall observed in Tokyo
p 433 A93-22200
- The modelling of turbulence and downbursts for flight simulators
p 193 N93-13542
- DOWNWASH**
- Effect of rounding side corners on vortices shedding and downwash from square cylinder of finite length placed on a ground plane
p 1160 A93-51893
- Acoustic noise generation at the air/ocean boundary [DREA-CR-90-445] p 99 N93-10642
- Navier-Stokes flowfield computation of wing/rotor interaction for a tilt rotor aircraft in hover
p 135 N93-14035
- DRAG**
- Determination of balloon gas mass and revised estimates of drag and virtual mass coefficients
p 7 A93-11362
- AIAA Applied Aerodynamics Conference, 11th, Monterey, CA, Aug. 9-11, 1993, Technical Papers. Pts. 1 & 2
p 974 A93-47201
- A method of testing two-dimensional airfoils
[AD-A253210] p 17 N93-10375
- Recent developments in low-speed TPS-testing for engine integration drag and installed thrust reverser simulation
p 160 N93-13207
- Drag due to gaps round undeflected trailing-edge controls and flaps at subsonic speeds
[ESDU-92039] p 290 N93-16634
- Modelling of interfacial and thermocline waves
[AERO-REPT-9209] p 420 N93-18103
- DRAG CHUTES**
- The effect of extreme altitude on parachute filling distance
[AIAA PAPER 93-1207] p 702 A93-35158
- Design of a recovery system for a reentry vehicle
[AIAA PAPER 93-1224] p 733 A93-35171
- DRAG COEFFICIENTS**
- A method for calculating flow past an arbitrary airfoil profile in the presence of flow separation
p 13 A93-12807
- Calculation of flow of a rarefied gas past a sphere for an arbitrary Knudsen number
p 124 A93-15146
- Laminar flow research in the 1940-1950s - A personal recollection
p 235 A93-17271
- Passive drag reduction of a helicopter airfoil in an unsteady transonic flow
p 482 A93-29440
- Aerodynamic resistance of three-dimensional bodies with a starlike cross section at supersonic velocities, and problems of its calculation
p 774 A93-39116
- An improved far field drag calculation method for nonlinear CFD codes
[AIAA PAPER 93-3417] p 975 A93-47213
- Effect of anomalous aerodynamic heating during the descent of a parachute along a trajectory
p 1069 A93-48924
- Approximate calculation of the aerodynamic characteristics of simple bodies in hypersonic rarefied-gas flow
p 1090 A93-51869
- Certain improved algorithms for calculating the aerodynamic characteristics of flight vehicles in free-molecular flow
p 1090 A93-51872
- A method of testing two-dimensional airfoils
[AD-A253210] p 17 N93-10375
- DRAG DEVICES**
- Lanchester: The man
[AERO-REPT-9111] p 456 N93-16464
- DRAG MEASUREMENT**
- Drag measurements on blunted cones and a scramjet vehicle in hypervelocity flow
[AIAA PAPER 93-2979] p 1050 A93-48172
- Aeronomy coexperiments on drag-free satellites with proportional thrusters: GP-B and STEP
p 195 N93-13922
- DRAG REDUCTION**
- DNW test highlights related to aircraft environment
p 190 A93-14274
- Development of a hydrogen external burning flight test experiment on the NASA Dryden SR-71A aircraft
[SAE PAPER 920997] p 157 A93-14638
- Effect of wing planforms on induced drag reduction
p 127 A93-16932
- A comparison of the drag-reducing benefits of riblets in internal and external flows
p 395 A93-18054
- The prediction of riblet behaviour with a low-Reynolds number k-epsilon model
p 270 A93-21720
- The effect of Reynolds number and turbulence on airfoil aerodynamics at -90 degrees incidence
[AIAA PAPER 93-0206] p 277 A93-22624
- Shock-dependent, thrust wings for supersonic flow
[AIAA PAPER 93-0321] p 280 A93-23013
- Airfoil design using the Navier-Stokes equations
[AIAA PAPER 93-0648] p 464 A93-24763
- Computational analysis of methods for reduction of induced drag
[AIAA PAPER 93-0524] p 474 A93-25536
- Recent developments in international laminar flow research programs for transport aircraft
[ONERA, TP NO. 1992-163] p 457 A93-26878
- Problems in the optimum design of a wing profile for nonseparated flow over a range of angles of attack
p 477 A93-27614
- Passive drag reduction of a helicopter airfoil in an unsteady transonic flow
p 482 A93-29440
- Numerical simulation of the turbulent drag reduction by plate manipulators
p 681 A93-33736
- Flight research on natural laminar flow applications
p 890 A93-41779
- Supersonic laminar flow control
p 860 A93-41782
- Reduction of aerodynamic skin-friction drag
p 871 A93-42656
- CFD drag predictions for a wide body transport fuselage with flight test verification
[AIAA PAPER 93-3418] p 976 A93-47214
- Computational analysis of drag reduction and buffet alleviation in viscous transonic flow over porous airfoils
[AIAA PAPER 93-3419] p 976 A93-47215
- A method for the prediction of induced drag for planar and nonplanar wings
[AIAA PAPER 93-3420] p 976 A93-47216
- An overview of recent subsonic laminar flow control flight experiments
[AIAA PAPER 93-2987] p 1052 A93-48180
- Transition for three-dimensional boundary layers on wings in the transonic regime
[AIAA PAPER 93-3049] p 1057 A93-48229
- Demonstration of multipoint design procedures for transonic airfoils
[AIAA PAPER 93-3114] p 1062 A93-48284
- Effect of the wing planform on the optimal deformation of the middle surface
p 1150 A93-48909
- Minimization of the induced drag of nonplanar lifting systems
p 1068 A93-48910
- Drag characteristics of extra-thin-fin-riblets in an air flow conduit
p 1151 A93-49240
- Decreasing F-16 nozzle drag using computational fluid dynamics
[AIAA PAPER 93-2572] p 1084 A93-50289
- Identification of integrated airframe-propulsion effects on an F-15 aircraft for application to drag minimization
[AIAA PAPER 93-3764] p 1101 A93-51359
- Nonplanar wings with a minimum induced drag
p 1089 A93-51779
- Induced drag of a crescent wing planform
p 1094 A93-52430
- Experimental study of pylon cross sections for a subsonic transport airplane
p 1103 A93-52440
- The reduction of skin friction by riblets under the influence of an adverse pressure gradient
p 1218 A93-53810
- A preliminary investigation of the control of separated flow by means of excitation
p 1182 A93-53859
- Experimental investigation of flows behind different Large-Eddy Breakup (LEBU) devices in thick boundary layers
p 18 N93-10550
- Experiments and analysis concerning the use of external burning to reduce aerospace vehicle transonic drag
p 70 N93-12537
- Analysis and design of planar and non-planar wings for induced drag minimization
[NASA-CR-191274] p 131 N93-13463
- An experimental investigation of base bleed effect on the wake turbulent structure behind a two-dimensional blunt model
[MPIS-9/1991] p 139 N93-15131
- Stall departure resistance enhancer
[NASA-CASE-LAR-14221-1] p 344 N93-19023
- Computation of H2/air reacting flowfields in drag-reduction external combustion
[NASA-CR-191071] p 536 N93-20237
- Analysis and evaluation of an integrated laminar flow control propulsion system
[NASA-CR-192162] p 551 N93-20268
- Computation of transonic flow over a porous surface projectile
p 696 N93-25409
- Structural and aerodynamic optimization of joined-wing aircraft
p 715 N93-25526
- The generation of side force by distributed suction
[NASA-CR-193129] p 839 N93-27151
- Flow visualization on helicopter blades using acenaphthen
[ESA-TT-1255] p 931 N93-29273
- Turbulent drag reduction: Studies of feedback control and flow over riblets
p 878 N93-30645
- Selected experiments in laminar flow: An annotated bibliography
[NASA-TM-103989] p 990 N93-32226
- DREDGING**
- System analysis for a kinematic positioning system based on the global positioning system
[AD-A262830] p 885 N93-29468
- DRILLING**
- Theory of the machining of polyhedral holes by plunge cutting
p 835 A93-39091
- Presence and future of the electro-chemical processes in aero-engine production
p 1257 A93-54840
- Determination of stresses on laminated aircraft transparencies by the strain gage-hole drilling and sectioning method
[AD-A255548] p 164 N93-14571
- DRONE AIRCRAFT**
- Application of concurrent engineering methods to the design of an autonomous aerial robot
[AD-A254968] p 212 N93-12555
- Report to the Chairman, Legislation, and National Security Subcommittee, Committee on Government Operations, House of Representatives. Unmanned aerial vehicles: More testing needed before production of short-range system
[AD-A259473] p 513 N93-20245
- DROOPED AIRFOILS**
- An experimental study of droop leading edge modifications on high and low aspect ratio wings up to 50 deg angle of attack
[AIAA PAPER 93-3496] p 983 A93-47268
- DROP SIZE**
- The combustion of droplets within gas turbine combustors - Some recent observations on combustor efficiency
[ASME PAPER 92-GT-135] p 388 A93-19367
- Characteristics of liquid jet atomization across a high-speed airstream. II - Calculation of spatial distribution of liquid, variation of drop diameter and drop trajectory
p 412 A93-21744
- LEWIS droplet trajectory calculations on a parallel computer
[AIAA PAPER 93-0172] p 438 A93-22604

DROP TESTS

- Experimental investigation of the management of large-sized drops and the onset of Marangoni-convection p 926 A93-41700
The combustion time lag and its role in ramjet combustion instability p 73 N93-11137
A laboratory investigation of raindrop oscillations p 224 N93-13790
Atomization of JP-10/B4C gelled slurry fuel [AD-A256827] p 391 N93-15686
Velocity and drop size measurements in a swirl-stabilized, combustor spray [NASA-TM-106130] p 813 N93-27130
Modeling the effects of drop drag and breakup on fuel sprays [AD-A263650] p 931 N93-29388

DROP TESTS

- Response of laminated composite plates to low-speed impact by air-gun-propelled and dropped-weight impactors [AIAA PAPER 93-1402] p 739 A93-33962
Stable cross type parachute with inflation aid [AIAA PAPER 93-1201] p 702 A93-35152
Development testing of large ram air inflated wings [AIAA PAPER 93-1204] p 702 A93-35155
Impulse guided Samara decelerator [AIAA PAPER 93-1234] p 690 A93-35175
Materials processing in low gravity [NASA-CR-184421] p 91 N93-12401

DROPS (LIQUIDS)

- Ignition process of fuel droplet arrays in a supersonic flowfield p 535 A93-27786
Diffusion controlled evaporation of a multicomponent droplet - Theoretical studies on the importance of variable liquid properties p 1021 A93-44224
Behavior of precipitating water drops under the influence of electrical and aerodynamic forces p 1034 A93-45176
The onset of disintegration and corona in water drops falling at terminal velocity in horizontal electric fields p 1163 A93-49130
Correlation of droplet behavior with gas-phase structures in a gas turbine combustor [AIAA PAPER 93-1767] p 1152 A93-49663
A technique for the measurement of cloud structure on centimeter scales p 1158 A93-51243
Lift and drag forces on droplets and particles in wall-bounded shear flows [DE93-002678] p 419 N93-17761
The WINCOF-I code: Detailed description [NASA-CR-190779] p 677 N93-24760
Fundamental studies of droplet interactions in dense sprays [AD-A261165] p 737 N93-25948
Three-dimensional water droplet trajectory code validation using an ECS inlet geometry [NASA-CR-191097] p 791 N93-27267

DROPS ONDES

- An unmanned aircraft for dropwindsonde deployment and hurricane reconnaissance p 677 A93-34587

DRYING APPARATUS

- An experimental study of the air drying process in air coolers p 834 A93-39059

DUCT GEOMETRY

- Experimental results of shock trains in rectangular ducts [AIAA PAPER 92-5103] p 274 A93-22373
Computational study of advanced exhaust system transition ducts with experimental validation p 689 A93-34490
Design of axisymmetric channels with rotational flow [AIAA PAPER 93-3117] p 1062 A93-48287
Applying and validating the RANS-3D flow-solver for evaluating a subsonic serpentine diffuser geometry [AIAA PAPER 93-2157] p 1079 A93-49973
High-frequency acoustic radiation from a curved duct of circular cross section [ONERA, TP NO. 1993-55] p 1173 A93-51937

DUCTED FAN ENGINES

- Advanced Ducted Engines - Impact of unsteady aerodynamics on fan vibration properties [ASME PAPER 92-GT-228] p 252 A93-19445
Flow studies in ducted twin-rotor contra-rotating axial flow fans [ASME PAPER 92-GT-390] p 258 A93-19545
Acoustic mode measurements in the inlet of a model turbofan using a continuously rotating rake [AIAA PAPER 93-0598] p 563 A93-24783
All-composite fan blade for advanced ducted engines p 1246 A93-54837
ADP - Engine concept of the future p 1246 A93-54842
Acoustic mode measurements in the inlet of a model turbofan using a continuously rotating rake [NASA-TM-105989] p 362 N93-16705

DUCTED FANS

- Radiated noise of ducted fans p 450 A93-19215

- Lifting surface theory for steady aerodynamic analysis of ducted counter rotation propfan [ASME PAPER 92-GT-14] p 347 A93-19286
Determination of fan noise in a lined duct with flow using the Green function method p 1124 A93-51761
Comparison of radiated noise from shrouded and unshrouded propellers p 1264 A93-55861
Investigation of advanced counterrotation blade configuration concepts for high speed turbofan systems. Task 5: Unsteady counterrotation ducted propfan analysis [NASA-CR-187126] p 521 N93-20773

DUCTED FLOW

- Noncoaxial mixing in a rectangular duct p 205 A93-14518
Study on vortex flow control of inlet distortion p 122 A93-14520
Flowfield measurements for a supersonic mixer ejector in forward flight p 399 A93-19217
Scramjet fuel-air mixing establishment in a pulse facility p 359 A93-21667
Direct numerical simulation of turbulent flow in a square duct [AIAA PAPER 93-0198] p 277 A93-22618
Optimization of circular orifice jets mixing into a heated crossflow in a cylindrical duct [AIAA PAPER 93-0249] p 361 A93-23246
Determination of gas flow rate in a duct from measured static pressures p 520 A93-27625
Effect of combustion on the interaction of an underexpanded wall hydrogen jet with supersonic flow in a plane duct p 534 A93-27658
Some contributions to propulsion theory - The Stream Force Theorem and applications to propulsion p 924 A93-40472
Stability conditions for a transonic decelerating flow in a duct p 872 A93-43027
Some contributions to propulsion theory - Non-isentropic duct flow and the general drag wake traverse p 874 A93-43688

- Navier-Stokes analysis of three-dimensional S-ducts p 959 A93-45146
A singularities tracking conservation law scheme for compressible duct flows p 960 A93-45542
A three-dimensional pressure flux-split RNS application to sub/supersonic flow in inlets and ducts [AIAA PAPER 93-3063] p 1058 A93-48239
Experimental and numerical investigation of supersonic turbulent flow in an annular duct [AIAA PAPER 93-3123] p 1063 A93-48291
Numerical simulation of a shock wave/turbulent boundary layer interaction in a duct [AIAA PAPER 93-3127] p 1063 A93-48293
Investigation of a strut/endwall interaction in supersonic annular flow [AIAA PAPER 93-1925] p 1076 A93-49791
Initial test results of 40,000 horsepower fan drive gear system for advanced ducted propulsion systems [AIAA PAPER 93-2146] p 1154 A93-49963
A comparative study of Full Navier-Stokes and Reduced Navier-Stokes analyses for separating flows within a diffusing inlet S-duct [AIAA PAPER 93-2154] p 1079 A93-49970
Determination of heat transfer to flow in a duct with a pseudodiscontinuity p 1179 A93-53365
The low frequency aeroacoustics of buried nozzle systems p 1205 A93-54244
Instability of a supersonic vortex sheet inside a circular duct p 1234 A93-55142
An experimental investigation of the flow in a diffusing S-duct [NASA-TM-105809] p 60 N93-12077
Optimization of circular orifice jets mixing into a heated cross flow in a cylindrical duct [NASA-TM-105984] p 179 N93-15359
Numerical simulation of the flow through non-uniform airfoil cascade p 302 N93-19310
Experimental investigation of crossflow jet mixing in a rectangular duct [NASA-TM-106152] p 812 N93-27026
CFD mixing analysis of axially opposed rows of jets injected into confined crossflow [NASA-TM-106179] p 813 N93-27128
Experimental study of cross flow mixing in cylindrical and rectangular ducts [NASA-CR-197141] p 815 N93-27680

DUCTED ROCKET ENGINES

- Turbulence interacting with chemical kinetics in airbreathing combustion of ducted rockets p 734 N93-26012
Analysis of thrust modulation of ram-rockets by a vortex valve p 814 N93-27187

DUCTILITY

- Deformation mechanisms of NiAl cyclicly deformed near the brittle-to-ductile transformation temperature [NASA-CR-191649] p 391 N93-15830

DUCTS

- Study on vortex flow control of inlet distortion p 122 A93-14520
High-frequency acoustic radiation from a curved duct of circular cross section [ONERA, TP NO. 1993-55] p 1173 A93-51937
The prediction of convective heat transfer in rotating square ducts [PNR-90929] p 85 N93-11025
The combustion time lag and its role in ramjet combustion instability p 73 N93-11137
Evaluation of acoustic impedance models for a perforated plate [NAL-TR-1133] p 102 N93-12375
CFD analysis on control of secondary losses in STME LOX turbines with endwall fences p 419 N93-17289
Numerical analysis of the flow in a turbulent rectangular duct simulating the cooling passages in a turbine blade [AD-A257855] p 420 N93-18305
Investigation of advanced counterrotation blade configuration concepts for high speed turbofan systems. Task 5: Unsteady counterrotation ducted propfan analysis. Computer program user's manual [NASA-CR-187125] p 521 N93-20583
Turbulent flow and heat transfer in idealized blade cooling passages p 902 N93-29938

DUMP COMBUSTORS

- Recent progress in the implementation of active combustion control p 171 A93-14272
Noncoaxial mixing in a rectangular duct p 205 A93-14518
An experimental investigation on the combustor with bypass flow in integral liquid fuel ramjet p 174 A93-16235
Theoretical investigation of combustion characteristics in ram-jet dump combustor with side-inlet p 346 A93-19121
Flow field characteristics of an axisymmetric sudden-expansion pipe flow with different initial swirl distribution p 411 A93-21688
Experimental study on turbulent two-phase flow in a dual-inlet side dump combustor p 1106 A93-48506
Effects of side-inlet angle in a three-dimensional side-dump combustor p 1109 A93-49610
Combustion characteristics and passive control of an annular dump combustor [AIAA PAPER 93-1772] p 1110 A93-49668
Periodic chemical energy release for active combustion control [ISABE 93-7043] p 1198 A93-54019
Low-frequency combustion instability mechanisms in a side-dump combustor p 1247 A93-55220
Control of asymmetric jet [AD-A255967] p 219 N93-14400
Thrust augmentation system for low-cost-expendable turbojet engine [AD-A263727] p 905 N93-30877

DURABILITY

- A synthesized method in durability analysis p 203 A93-14286
'No VOC' water-borne corrosion resistant primers for aerospace bonding applications p 1211 A93-53419
Advanced Turbine Technology Applications Project (ATTAP) [NASA-CR-189228] p 455 N93-18762

DUST

- Two-phase injection from the front surface of a blunt body in hypersonic flow p 241 A93-18233
Environmental effects of operations during Desert Shield/Desert Storm p 1190 A93-54291

DYES

- Simultaneous mapping of the unsteady flow fields by Particle Displacement Velocimetry (PDV) p 786 N93-27454

DYNAMIC CHARACTERISTICS

- Dynamic analysis of a pre-and-post ice impacted blade [AIAA PAPER 92-4273] p 54 A93-13333
A study of dynamic characteristics of axial compression systems by heat addition p 202 A93-14168
The simulation of aircraft landing gear dynamics p 155 A93-14318
Dynamic characteristics of two new vibration modes of the disk-shell shaped gear p 204 A93-14484
High speed aircraft tire dynamics/issues [SAE PAPER 921037] p 158 A93-14657
On dynamic behavior of cracked rotors p 208 A93-15401
The problem of dynamic stall simulation revisited [AIAA PAPER 93-0091] p 264 A93-20197
Impact of aeroelasticity on propulsion and longitudinal flight dynamics of an air-breathing hypersonic vehicle [AIAA PAPER 93-1367] p 733 A93-33934
Improved static and dynamic performance of helicopter powerplant p 809 A93-35928

SUBJECT INDEX

Determination of the dynamic characteristics of heat exchangers for the heat recovery system of gas turbine engines p 834 A93-39054

A method for calculating the dynamic characteristics of heat exchangers with single-phase cryogenic coolants p 851 A93-39057

Study on dynamic characteristics of heat exchanger p 924 A93-40492

Experimental and algorithmic means of identifying mathematical models of flight vehicle p 909 A93-43103

On dynamics of the juncture vortex [AIAA PAPER 93-3473] p 980 A93-47252

Longitudinal dynamics of a towed sailplane p 1130 A93-49577

Application of analog computing to real-time simulation of stall and surge dynamics [AIAA PAPER 93-2231] p 1080 A93-50037

Nonlinear dynamic simulation of single- and multi-spool core engines [AIAA PAPER 93-2580] p 1122 A93-50294

Experiments on low aspect ratio hydroplanes to measure lift under static and dynamic conditions [ARE-TM(UHR)-90306] p 21 N93-11365

Wind shear related research at Princeton University p 145 N93-14854

Lumped mass modelling for the dynamic analysis of aircraft structures p 510 N93-19460

Experimental and analytical investigation of dynamic characteristics of extension-twist-coupled composite tubular spars [NASA-TP-3225] p 553 N93-20585

Computational gearing mechanics [NASA-CR-191127] p 751 N93-25884

A computational model that couples aerodynamic and structural dynamic behavior of parachutes during the opening process [AD-A264115] p 877 N93-30119

DYNAMIC CONTROL

Output feedback control for output tracking of nonlinear uncertain systems p 96 A93-13177

Dynamical variable structure control of a helicopter in vertical flight p 369 A93-22887

Multiple radial basis function networks in modeling and control [AIAA PAPER 93-3731] p 1170 A93-51330

Online vibration control of a flexible rotor/bearing system p 219 N93-14468

A contribution to the dynamic feedforward open loop control of multivariable systems and to the optimal design of command functions [DLR-FB-92-05] p 441 N93-16515

Articulated fin/wing control system [AD-D015712] p 909 N93-29278

Design and application of Active Magnetic Bearings (AMB) for vibration control p 1033 N93-32279

DYNAMIC LOADS

The prediction of nonlinear dynamic loads on helicopters from flight variables using artificial neural networks p 322 A93-19231

Unsteady loads measurements in a generic high speed engine model by means of recessed transducers [AIAA PAPER 93-0287] p 342 A93-21104

Optimization of composite engine structures for mechanical and thermal loads [AIAA PAPER 93-1583] p 719 A93-34115

Validation of R85/METAR on the Puma RAE flight tests [ONERA, TP NO. 1992-123] p 802 A93-38597

Spanwise aileron oscillations p 819 A93-39190

Aeroelastic stability of supersonic nozzles with separated flow [AIAA PAPER 93-2588] p 1142 A93-50300

Monitoring load experience of individual aircraft p 1103 A93-52450

An experimental study of the relationship between forces and moments and vortex breakdown on a pitching delta wing p 49 N93-12206

An investigation of dynamic stress reduction of multi-body aircraft using active gust control p 187 N93-13916

Root damage analysis of aircraft engine blade subject to ice impact [NASA-TM-105779] p 222 N93-15343

Wind load design methods for ground-based heliostats and parabolic dish collectors p 433 N93-15839

Statistical fatigue analysis of the SH-60B servo beam rail component [AD-A257474] p 332 N93-17660

Development of nose structure of a reconnaissance container for a supersonic jet aircraft [MBB-LME-242-S-PUB-0451] p 998 N93-31046

Localization of aeroelastic modes in mistuned high-energy turbines p 1032 N93-31586

DYNAMIC MODELS

Synthesis of a helicopter nonlinear flight controller using approximate model inversion [AIAA PAPER 92-4468] p 62 A93-13280

A fuzzy dynamic analysis method for aeromaintenance system p 225 A93-14177

A systems dynamics approach to modeling gas turbine combustor wear [ASME PAPER 92-GT-47] p 347 A93-19300

A method of finite element dynamic model optimization p 367 A93-20812

Using system identification to improve the performance of a low-cost flight simulator p 369 A93-22885

A simple, approximate model of parachute inflation [AIAA PAPER 93-1206] p 702 A93-35157

Reaction zone structure for strong, weak overdriven, and weak underdriven oblique detonations p 746 A93-35492

Effects of dynamic stall and structural modeling on aeroelastic stability of elastic bending and torsion of hingeless rotor blades with experimental correlation p 794 A93-35902

Identification of the open loop dynamics of the T700 turboshaft engine p 809 A93-35934

Applying variations of the quantitative feedback technique (QFT) to unstable, non-minimum phase aircraft dynamics models p 939 A93-42797

Aileron and sideslip-induced unsteady aerodynamic modeling for lateral parameter estimation p 1007 A93-45144

Recent improvements on the Dynamic Flight Simulator p 1011 A93-45167

Dynamic model testing of the X-31 configuration for high-angle-of-attack flight dynamics research [AIAA PAPER 93-3674] p 1129 A93-48351

Semi-full-scale dynamic simulation complex on the basis of centrifuge [AIAA PAPER 93-3577] p 1208 A93-52673

Finite element analysis of natural vibrations of an aeroplane with asymmetric variable wing geometry p 1218 A93-53776

A simulation study on take-off and landing dynamics of fly-by-wire control system aircraft p 1249 A93-55590

A comparative study of semi-empirical dynamic stall models p 18 N93-10544

Modeling and model simplification of aeroelastic vehicles: An overview [NASA-TM-107691] p 64 N93-12216

Formulation and validation of high-order mathematical models of helicopter flight dynamics p 162 N93-13821

Modeling and control of a trailing wire antenna towed by an orbiting aircraft [AD-A256450] p 219 N93-14610

Design of high speed propellers using multiobjective optimization techniques p 336 N93-18065

Theoretical constraints in the design of multivariable control systems [NASA-CR-191900] p 442 N93-18372

Research in robust control for hypersonic vehicles [NASA-CR-192127] p 527 N93-20296

An aeroelastic model structure investigation for a manned real-time rotorcraft simulation p 693 N93-24756

A simple, approximate model of parachute inflation [DE93-002465] p 694 N93-25121

Dynamic System Coupler Program (DYSCO 4.1). Volume 1: Theoretical manual [AD-B131156L] p 848 N93-27531

Dynamic System Coupler Program (DYSCO 4.1). Volume 2: User's manual [AD-B131157L] p 848 N93-27589

Experiments in the control of wing rock at high angle of attack using tangential leading edge blowing p 1009 N93-31068

DYNAMIC PRESSURE

Excitation of blade vibration due to surge of centrifugal compressors [ASME PAPER 92-GT-149] p 351 A93-19377

Estimation of the maximum values of instantaneous distortion index DC sub theta --- of fluid flow p 266 A93-20806

Aeroelastic character of a National Aerospace Plane demonstrator concept [AIAA PAPER 93-1314] p 732 A93-33890

The development of swirl five-hole probe p 987 A93-47341

Near-optimal, asymptotic tracking in control problems involving state-variable inequality constraints [AIAA PAPER 93-3748] p 1170 A93-51344

On stability and control of SSTO spaceplane in super- and hypersonic ascending phase [NAL-TR-1128T] p 65 N93-12361

Performance and control of ascending trajectories to minimize heat load for transatmospheric aero-space planes p 133 N93-13745

User manual for NASA Lewis 10 by 10 foot supersonic wind tunnel [NASA-TM-105626] p 194 N93-15498

Application of a flush airdata sensing system to a wing leading edge (LE-FADS) [NASA-TM-104267] p 518 N93-20163

DYNAMIC PROGRAMMING

Practical input optimization for aircraft parameter estimation experiments [NASA-CR-191462] p 820 N93-27264

DYNAMIC RESPONSE

Analysis of structural dynamic response for aircraft operating in the environment of nuclear explosion shock waves p 78 A93-11810

Bird impact dynamic response analysis for aircraft arc windshield p 41 A93-11815

Effect of bird impact load types on blade response p 174 A93-16846

The combined closed form-perturbation approach to the analysis of mistuned bladed disks [ASME PAPER 92-GT-125] p 350 A93-19359

The dynamic characteristics of a high pressure turbine stage in a transient wind tunnel [ASME PAPER 92-GT-166] p 375 A93-19392

Improving dynamic response of a single-spool gas turbine engine using a nonlinear controller [ASME PAPER 92-GT-392] p 355 A93-19546

Examples of dynamic response optimization using MSC/NASTRAN [AIAA PAPER 92-4814] p 436 A93-20394

Sensitivity-based scaling for approximating structural response p 548 A93-28618

Finite element nonlinear random response of beams to acoustic and thermal loads applied simultaneously [AIAA PAPER 93-1427] p 740 A93-33978

A refined structural model of composite aircraft wings for the enhancement of vibrational and aeroelastic response characteristics [AIAA PAPER 93-1536] p 740 A93-34073

Dynamics of rotating multicomponent turbomachinery systems [AIAA PAPER 93-1629] p 742 A93-34157

Application of component mode synthesis to modeling the dynamic response of Bearingless Main Rotors p 796 A93-35976

Helicopter response to atmospheric turbulence p 817 A93-35987

Alternative approximations for integrated control/structure aeroservoelastic synthesis p 819 A93-39418

Recent advances of time domain approach for nonlinear response and sonic fatigue p 1022 A93-45106

Aircraft control requirements and achievable dynamics prediction [AIAA PAPER 93-3648] p 1128 A93-48331

Response of B-2 aircraft to nonuniform spanwise turbulence p 1135 A93-52437

Optimization of oleo-pneumatic shock absorber of aircraft p 1243 A93-55415

Compressible and incompressible fluid seals: Influence on rotordynamic response and stability [NASA-CR-190746] p 85 N93-10891

Stochastic sensitivity measure for mistuned high-performance turbines [NASA-TM-105821] p 90 N93-12277

Transonic aeroelastic analysis of systems with structural nonlinearities p 217 N93-13769

An investigation of the dynamic response of lifting surfaces with concentrated structural nonlinearities p 162 N93-13807

Formulation and validation of high-order mathematical models of helicopter flight dynamics p 162 N93-13821

Multi-disciplinary optimization of aeroservoelastic systems [NASA-CR-191255] p 220 N93-14766

Development of a unified airport pavement analysis and design system p 380 N93-16317

Measurement of the dynamic undercarriage response of a Sikorsky S-70B-2 helicopter: Instrumentation and test methods: Flight mechanics technical memorandum [AD-A256319] p 329 N93-16404

Dynamics of rotating multi-component turbomachinery systems [NASA-TM-105997] p 421 N93-18426

A discussion of the results of the rainfall counting of a wide range of dynamics associated with the simultaneous operation of adjacent wind turbines [DE93-000016] p 434 N93-18705

A Government/Industry Summary of the Design Analysis Methods for Vibrations (DAMVIBS) Program [NASA-CP-10114] p 514 N93-21310

- Aeroelastic response and aeromechanical stability of helicopters with elastically coupled composite rotor blades p 715 N93-25530
- Dynamic System Coupler Program (DYSCO 4.1). Volume 1: Theoretical manual p 848 N93-27531
- Dynamic System Coupler Program (DYSCO 4.1). Volume 3: User's manual supplement p 848 N93-27590
- Analysis of the static and dynamic response of a T-38 wing and comparison with experimental data [AD-A262363] p 806 N93-27692
- A computational model that couples aerodynamic and structural dynamic behavior of parachutes during the opening process [AD-A264115] p 877 N93-30119
- Static and dynamic large deflection flexural response of graphite-epoxy beams [NASA-CR-4118] p 934 N93-30374

DYNAMIC STABILITY

- Dynamic stability of bodies of revolution in compressible flow p 12 A93-12558
- Stabilization of the dynamic characteristics of the automatic control systems of a flight vehicle p 62 A93-12802
- The influence of main design parameters on helicopter air resonance and its source of instability p 154 A93-14261
- Dynamic stability, coupling and active control of elastic vehicles with unsteady aerodynamic forces modeling p 182 A93-14282
- Supersonic dynamic stability characteristics of the test technique demonstrator NASP configuration [AIAA PAPER 92-5009] p 367 A93-22285
- Selection of transducer measuring ranges in flight vehicle control systems p 526 A93-29691
- An experimental and analytical study of a lifting-body wind-tunnel model exhibiting body-freedom flutter [AIAA PAPER 93-1316] p 732 A93-33891
- Dynamic stability derivatives evaluation in a low-speed wind tunnel p 821 A93-37402
- Optimization of an aeroelastic system using the dynamic stability condition p 1029 A93-47085
- Estimation of neutral and maneuver points of aircraft by dynamic maneuvers [AIAA PAPER 93-3620] p 1126 A93-48307
- On hovercraft overwater heave stability p 1219 A93-53819
- A study of aircraft global dynamic stability in rapid rolling maneuver p 1206 A93-53869
- Compressible and incompressible fluid seals: Influence on rotordynamic response and stability [NASA-CR-190746] p 85 N93-10891
- On stability and control of SSTD spaceplane in super- and hypersonic ascending phase [NAL-TR-11287] p 65 N93-12361
- DYNAC: A computer program for analyzing the dynamical stability of aircraft [REPT-B-31] p 66 N93-12415
- Stability of elastically tailored rotor blades p 164 N93-14828
- Active stabilization to prevent surge in centrifugal compression systems [NASA-CR-191625] p 424 N93-18862
- Aircraft landing gear shimmy p 340 N93-19029
- Structural dynamic analysis of bearingless rotor blade p 717 N93-25719
- Supersonic aeroelastic instability results for a NASP-like wing model [NASA-TM-107739] p 718 N93-26553
- Active magnetic bearings applied to industrial compressors p 841 N93-27570
- Vibration analysis in turbomachines p 1005 N93-32274

DYNAMIC STRUCTURAL ANALYSIS

- Analysis of structural dynamic response for aircraft operating in the environment of nuclear explosion shock waves p 78 A93-11810
- A proposal concerning the dynamic analysis method of continuous gust design rules p 181 A93-14197
- Some dynamic problems in design of aircraft landing gear p 155 A93-14321
- RISK - Interactive multidisciplinary system for designing airframes p 226 A93-14337
- Nonlinear vibration and radiation from a panel with transition to chaos p 205 A93-14543
- Dynamics of skin-stringer panels using modified wave methods p 206 A93-14561
- Turbomachine blade vibration --- Book [ISBN 0-470-21764-2] p 344 A93-17899
- Structural analysis of a nonlinear problem of aeroelasticity for CFC structures p 397 A93-18989
- The combined closed form-perturbation approach to the analysis of mistuned bladed disks [ASME PAPER 92-GT-125] p 350 A93-19359

- An analysis system for blade forced response [ASME PAPER 92-GT-172] p 352 A93-19398
- High speed flight effects on transmission of sound through a nonflexible vibrating panel due to flow structural interaction in the ambience [AIAA PAPER 92-4708] p 451 A93-20316
- Exact solution sensitivities for boundary element aerodynamics codes [AIAA PAPER 92-4745] p 436 A93-20343
- Dynamic analysis of pretwisted elastically-coupled rotor blades p 326 A93-21125
- The NASA/industry design analysis methods for vibrations (DAMVIBS) program - Accomplishments and contributions p 508 A93-27971
- Experiences at Langley Research Center in the application of optimization techniques to helicopter airframes for vibration reduction p 508 A93-27972
- Structural analysis of box beams using symbolic manipulation technique p 548 A93-28615
- AIAA/ASME/ASCE/AHS/ASC Structures, Structural Dynamics, and Materials Conference, 34th and AIAA/ASME Adaptive Structures Forum, La Jolla, CA, Apr. 19-22, 1993, Technical Papers. Pts. 1-6 p 738 A93-33876
- An automated mode tracking strategy --- dynamic structural analysis of helicopter structures [AIAA PAPER 93-1414] p 739 A93-33970
- Acoustics due to flow-structural interaction and its transmission through a double-panel in high-speed cruising flight [AIAA PAPER 93-1431] p 710 A93-33981
- Dynamic analysis of multiple row fuselage stiffened structures [AIAA PAPER 93-1438] p 710 A93-33987
- Exact flutter solution of advanced anisotropic composite cantilevered wing structures [AIAA PAPER 93-1535] p 727 A93-34072
- Dynamics of rotating multicomponent turbomachinery systems [AIAA PAPER 93-1629] p 742 A93-34157
- Unsteady aerodynamics and flutter of proplains using a three-dimensional Full-Potential Solver [AIAA PAPER 93-1633] p 720 A93-34161
- On the static stability of forward swept proplains [AIAA PAPER 93-1634] p 720 A93-34162
- Sensitivity analysis of aeroelastic response of a wing using piecewise pressure representation [AIAA PAPER 93-1645] p 742 A93-34170
- Sensitivity analysis of flutter response of a typical section and a wing in transonic flow [AIAA PAPER 93-1646] p 742 A93-34171
- Dynamics of a high speed impeller - Analysis and experimental verification [AIAA PAPER 93-1362] p 743 A93-34239
- Dynamic analysis of rotor flexbeams based on nonlinear anisotropic shell models p 743 A93-34261
- AHS, Annual Forum, 48th, Washington, June 3-5, 1992, Proceedings. Vols. 1 & 2 p 763 A93-35901
- Post-critical behaviour of a tapered cantilever column subjected to a uniformly distributed tangential follower force p 831 A93-38431
- Modal identification of aircraft structures - ONERA methods [ONERA, TP NO. 1992-86] p 802 A93-38570
- Dynamic processes in the powerplants and power-generating equipment of flight vehicles p 832 A93-39027
- Experimental and theoretical study for nonlinear aeroelastic behavior of a flexible rotor blade p 837 A93-39422
- Effect of structural uncertainties on flutter analysis p 924 A93-40445
- Supersonic panel flutter analysis of shallow shells p 827 A93-41935
- A multibody formulation for helicopter structural dynamic analysis p 892 A93-43776
- Investigation of helicopter air resonance in hover by complex coordinates and mutual excitation analysis p 893 A93-43777
- A frequency domain theory for structural identification p 930 A93-43778
- Stability analysis of dynamic meshes for transient aeroelastic computations [AIAA PAPER 93-3325] p 1022 A93-45019
- Recent advances of time domain approach for nonlinear response and sonic fatigue p 1022 A93-45106
- Vibration analysis of composite wing with tip mass using finite elements p 1023 A93-45175
- Dynamic analysis of a compound elastic surface p 1030 A93-47086
- Dynamic analysis of a gear drive system in aeroengine p 1149 A93-48514
- Improving the design of the main fuel pump of Turbo-Jet p 1107 A93-48555
- Stability of fluttered panels subjected to in-plane harmonic forces p 1151 A93-49017

- Unsteady aerodynamics and flutter based on the potential equation [AIAA PAPER 93-2086] p 1079 A93-49913
- High speed, heavily loaded and precision aircraft type epicyclic gear system dynamic analysis overview and special considerations [AIAA PAPER 93-2151] p 1154 A93-49968
- Structural analysis of the light weight hard nose of the 71M aerostat [AIAA PAPER 93-4037] p 1255 A93-54608
- Rotating machinery - Transport phenomena; Proceedings of the 3rd International Symposium on Transport Phenomena and Dynamics of Rotating Machinery (ISROMAC-3), Honolulu, HI, Apr. 1-4, 1990 [ISBN 1-56032-147-4] p 1256 A93-54626
- All-composite fan blade for advanced ducted engines p 1246 A93-54837
- Dynamic analysis of annular cascade structures p 1259 A93-55586
- SAPNEW: Parallel finite element code for thin shell structures on the Alliant FX/80 [NASA-CR-190663] p 84 N93-10372
- Measured data for the Sandia 34-meter vertical axis wind turbine [DE92-019807] p 94 N93-12075
- Modeling and model simplification of aeroelastic vehicles: An overview [NASA-TM-107691] p 64 N93-12216
- DYNAC: A computer program for analyzing the dynamical stability of aircraft [REPT-B-31] p 66 N93-12415
- NASA aeronautics: Research and technology program highlights [NASA-NP-159] p 109 N93-13110
- A domain decomposition method for parallel transient response calculations p 187 N93-13827
- An investigation of dynamic stress reduction of multi-body aircraft using active gust control p 187 N93-13916
- Experimental and analytical investigation of the vibration characteristics of a remotely piloted helicopter [AD-A256131] p 163 N93-14248
- Transient/structural analysis of a combustor under explosive loads [NASA-TM-107660] p 420 N93-17779
- RPH preliminary design, trend analysis and initial analysis of the NPS hummingbird [AD-A257854] p 338 N93-18304
- Dynamics of rotating multi-component turbomachinery systems [NASA-TM-105997] p 421 N93-18426
- Lumped mass modelling for the dynamic analysis of aircraft structures p 510 N93-19460
- Structural dynamics branch research and accomplishments to FY 1992 [NASA-TM-105824] p 552 N93-20368
- Resonant response analysis of a high speed gear p 553 N93-20662
- Dynamic simulation of flexible body systems by the vector solution method p 553 N93-20666
- Stochastic finite element analysis for high speed rotors p 554 N93-20696
- A Government/Industry Summary of the Design Analysis Methods for Vibrations (DAMVIBS) Program [NASA-CP-10114] p 514 N93-21310
- The NASA/industry Design Analysis Methods for Vibrations (DAMVIBS) program: Boeing Helicopters airframe finite element modeling p 515 N93-21313
- The NASA/industry Design Analysis Methods for Vibrations (DAMVIBS) program: McDonnell-Douglas Helicopter Company achievements p 515 N93-21314
- The NASA/industry Design Analysis Methods for Vibrations (DAMVIBS) program: Sikorsky Aircraft: Advances toward interacting with the airframe design process p 515 N93-21315
- Structural Tailoring of Advanced Turboprops (STAT). Theoretical manual [NASA-CR-191017] p 556 N93-22005
- Structural dynamic analysis of bearingless rotor blade p 717 N93-25719
- Computational gearing mechanics [NASA-CR-191127] p 751 N93-25884
- Helicopter forced response vibration analysis method RTVIB20 [AD-A261809] p 730 N93-26260
- A transfer matrix approach to vibration localization in mistuned blade assemblies [NASA-TM-106112] p 838 N93-27088
- Analysis of the static and dynamic response of a T-38 wing and comparison with experimental data [AD-A262363] p 806 N93-27692
- An integrated optimum design approach for high speed prop-rotors including acoustic constraints [NASA-CR-193222] p 893 N93-29153
- Modal survey of a full-scale F-18 wind tunnel model [AD-A262482] p 875 N93-29410

- Static and dynamic large deflection flexural response of graphite-epoxy beams
[NASA-CR-4118] p 934 N93-30374
- Structural dynamic characteristics of individual blades
p 1005 N93-32272
- Structural dynamic characteristics of bladed assemblies
p 1005 N93-32273
- Vibration analysis in turbomachines
p 1005 N93-32274

DYNAMIC TESTS

- Vortex breakdown study on a 65-deg delta wing tested in static and dynamic conditions p 121 A93-14407
- The use of subscale models to predict self-induced oscillations of flight vehicles
[AIAA PAPER 93-0093] p 264 A93-20199
- Dynamic model testing of the X-31 configuration for high-angle-of-attack flight dynamics research
[AIAA PAPER 93-3674] p 1129 A93-48351
- Hysteresis and bristle stiffening effects of conventional brush seals
[AIAA PAPER 93-1996] p 1153 A93-49839
- US Army helicopter inertia reel locking failures
p 493 N93-19689
- An improved method of structural dynamic test design for ground flying and its application to the SH-2F and SH-2G helicopters
p 512 N93-19928
- The NASA/industry Design Analysis Methods for Vibrations (DAMVIBS) program: McDonnell-Douglas Helicopter Company achievements p 515 N93-21314
- Analysis of the static and dynamic response of a T-38 wing and comparison with experimental data
[AD-A262363] p 806 N93-27692

DYNAMIC SYSTEMS

- Multilevel control of dynamical systems using neural networks p 96 A93-13011
- Identification of weakly nonlinear dynamic systems by means of random excitations p 227 A93-16472
- Numerical simulation of homogeneous non-Gaussian random vector fields p 561 A93-27584
- An identification method for dynamic systems with delay p 562 A93-27689
- Influence of the canopy-payload coupling on the dynamic stability in pitch of a parachute system
[AIAA PAPER 93-1248] p 690 A93-35185
- An algorithm with prediction in a control problem with functional constraints p 757 A93-35307
- Effects of higher order dynamics on helicopter flight control law design p 816 A93-35959
- A nonlinear control strategy for robust sliding mode performance in the presence of unmatched uncertainty
p 938 A93-42556
- Statistical methods in flight vehicle control theory
p 1165 A93-49306
- Optimal control of the rocking and damping of swings
p 1263 A93-54998
- Laminar boundary-layer breakdown
[AD-A254489] p 90 N93-12162
- Identification and control of non-linear time-varying dynamical systems using artificial neural networks
[AD-A257595] p 372 N93-18193

E**E GLASS**

- Fiber pulling apparatus modification
[NASA-CR-184498] p 220 N93-14763

E-2 AIRCRAFT

- AEW aircraft design
[AD-A261800] p 718 N93-26444

EARLY WARNING SYSTEMS

- Space-time processing for AEW radar
p 884 A93-43444
- Domain engineering validation case study: Synthesis for the air traffic display/collision warning monitor domain version 01.00.03
[AD-A259407] p 503 N93-21671

EARPHONES

- Inflight evaluation of an acoustic orientation instrument
[AD-A260752] p 719 N93-25909

EARTH ORBITAL ENVIRONMENTS

- MAKS - Eastern promise? --- multi-purpose aerospace system p 733 A93-34266
- Two-layer convective heating prediction procedures and sensitivities for blunt body reentry vehicles
[AIAA PAPER 93-2763] p 963 A93-46509
- Aerodynamics of Shuttle Orbiter at high altitudes
[AIAA PAPER 93-2815] p 965 A93-46553
- DSMC simulation of ionized rarefied flows
[AIAA PAPER 93-3095] p 1061 A93-48269

EARTH RADIATION BUDGET

- FIFE atmospheric boundary layer budget methods
p 426 A93-20591
- Remote sensing cloud properties from high spectral resolution infrared observations p 1034 A93-46780

EARTH SCIENCES

- Scientific visualization using the Flow Analysis Software Toolkit (FAST) p 758 N93-25600

EARTH SURFACE

- Adaptive filtering of Doppler velocimeter errors due to the characteristics of the reflecting surface
p 992 A93-45650
- Land subsidence and problems affecting land use at Edwards Air Force Base and vicinity, California, 1990
[PB93-182236] p 1036 N93-32191

EARTHQUAKE DAMAGE

- Expedient repair of structural facilities
[AD-A260727] p 731 N93-25656

ECOLOGICAL

- The ecological balance of Swissair: An example of waste management p 1035 N93-31930

ECONOMIC ANALYSIS

- General aviation turbine markets - An economic overview
[AIAA PAPER 92-4191] p 103 A93-13369
- Economical view on composite structures maintenance
[SME PAPER EM92-102] p 233 A93-14103
- The opportunities and risks of the supersonic transport market - The Lufthansa point of view
p 234 A93-15033
- Methods of economic evaluation - Forecasting critique
[AIAA PAPER 92-4285] p 570 A93-24300
- Airlines, airports and antitrust - A proposed strategy for enhanced competition p 760 A93-34821
- Internally coherent system of innovation - The case of flight simulation
[AIAA PAPER 93-3548] p 1226 A93-52653
- Future regional transport aircraft market, constraints, and technology stimuli
[NASA-TM-107669] p 109 N93-13025
- The 1990 high-speed civil transport studies
[NASA-CR-189618] p 330 N93-16947
- Aerodynamic design and synthesis of the oblique flying wing supersonic transport p 713 N93-24768
- AEW aircraft design
[AD-A261800] p 718 N93-26444

ECONOMIC DEVELOPMENT

- The 1990 high-speed civil transport studies. Summary report
[NASA-CR-189619] p 330 N93-16999

ECONOMIC FACTORS

- Prospects for a second generation supersonic transport p 108 A93-14154
- Keynote address - Advanced Technology demonstrators, prototypes and hypersonic flight
[AIAA PAPER 92-4999] p 456 A93-22276
- Spaceplanes - Back to the future p 733 A93-34265
- Protective properties of aviation oils
p 735 A93-35299
- Classification of the principal fuel saving methods in flight operations p 996 A93-45660
- Engine technology challenges for a 21st Century High-Speed Civil Transport
[ISABE 93-7064] p 1200 A93-54040
- Applied aerodynamics: Challenges and expectations
[NASA-TM-103963] p 694 N93-25091
- Engine technology challenges for a 21st Century High-Speed Civil Transport
[NASA-TM-106216] p 1004 N93-31671

ECONOMIC IMPACT

- Sales, not subsidies, are the sticking point
p 945 A93-43677
- Estimating the regional economic significance of airports
[AD-A257658] p 382 N93-17793

ECONOMICS

- Airports, air traffic control, and their clients - Reflections on system optimization p 234 A93-15035
- Estimating the regional economic significance of airports
[AD-A257658] p 382 N93-17793

EDDY CURRENTS

- Imaging flaws in thin metal plates using a magneto-optic device p 397 A93-18670
- Modeling and strain gauging of eddy current repulsion deicing systems
[AIAA PAPER 93-0296] p 327 A93-22696
- MOI - Magneto-optic/eddy current imaging
p 927 A93-41751
- Experimental investigation of flows behind different Large-Eddy Breakup (LEBU) devices in thick boundary layers p 18 N93-10550
- Active control of combustion instability in a ramjet using large-eddy simulations
[AD-A255226] p 175 N93-14111
- Reliability assessment at airline inspection facilities. Volume 2: Protocol for an eddy current inspection reliability experiment
[DOT/FAA/CT-92/12-VOL-2] p 842 N93-28685

EDDY VISCOSITY

- Computation of viscous transonic aerofoil flows using eddy-viscosity based turbulence models p 687 A93-34360

- The addition of algebraic turbulence modeling to program LAURA
[NASA-TM-107758] p 840 N93-27250
- Prediction of airfoil stall using Navier-Stokes equations in streamline coordinates p 787 N93-27456

EDGE DETECTION

- Automated extraction of aircraft runway patterns from radar imagery
[AD-A254258] p 68 N93-11751
- Merging sparse optical flow and edge connectivity between image features: A representation scheme for 2-D display of scene depth p 845 N93-27179

EDGE LOADING

- Secondary flow control on slender, sharp-edged configurations
[AIAA PAPER 93-3470] p 980 A93-47250
- A study on aerodynamic sound generated by interaction of jet and plate
[AIAA PAPER 93-3118] p 1171 A93-48288

EDUCATION

- Specific educational aspects of airport engineering in Spain and the Hispanic world p 103 A93-12560
- Teaching aircraft preliminary design - The first three years
[AIAA PAPER 92-4257] p 103 A93-13363
- Aeronautical engineering education for the armed forces p 453 A93-21681
- An index of resource materials for aviation meteorology education and training p 453 A93-22105
- Improving weather questions on Federal Aviation Administration exams p 308 A93-22110
- AIAA's role in aerospace education
[AIAA PAPER 93-0324] p 454 A93-23016
- Reform of the aeronautics and astronautics curriculum at MIT
[AIAA PAPER 93-0325] p 454 A93-23017
- Total Quality Management in curriculum development
[AIAA PAPER 93-0326] p 454 A93-23018
- Aerodynamic analyses for design and education
[AIAA PAPER 92-2664] p 473 A93-24988
- Utilizing a microcomputer based flight simulation in teaching human factors in aviation p 570 A93-27165
- Using TRACON as a teaching tool p 571 A93-27166
- The analysis of expert performance in the redesign of the en route air traffic control curriculum
p 571 A93-27189
- Embedded training capabilities for the LAMPS MK 3 system
[AD-A250697] p 49 N93-11838
- The modelling of turbulence and downbursts for flight simulators p 193 N93-13542
- NSF Science and Technology Centers
[NSF-92-104] p 193 N93-13712
- Proposed action plan to improve ADM effectiveness, part 3: Developing a new ADM paradigm on which to build advanced or expert decision making training
p 148 N93-15026
- Lessons learned from an historical look at flight testing p 511 N93-19904
- T-38 forward windshield development and performance demonstration report
[AD-A259240] p 513 N93-20579
- Aircraft electrical and environmental systems, AFSCs 452x5, 454x5, and 454x6
[AD-A261213] p 717 N93-25733
- Performance-based testing and success in Naval advanced flight training
[AD-A260838] p 717 N93-25933
- The Center of Excellence for Hypersonics Training and Research at the University of Texas at Austin
[NASA-CR-193070] p 781 N93-27126
- A demonstration of simple airfoils: Structural design and materials choices
[DE93-007882] p 789 N93-28662
- Construction and testing of simple airfoils to demonstrate structural design, materials choice, and composite concepts p 879 N93-30979
- Efficient fault diagnosis of helicopter gearboxes
[NASA-TM-106253] p 1032 N93-31846

EFFECTIVE PERCEIVED NOISE LEVELS

- Final results from a study of community response to aircraft noise around Oslo Airport Fornebu p 425 A93-19192
- Loudness versus level of aircraft noise
p 557 A93-28477
- Human response to helicopter noise - A test of A-weighting p 567 A93-29424
- Helicopter noise certification p 1262 A93-54720

EFFECTIVENESS

- The influence of fighter agility on air combat effectiveness p 184 A93-14398

EFFICIENCY

- Variable speed rotary compressor and adjustable speed drive efficiencies measured in the laboratory
[DE92-040026] p 222 N93-15278
- Adaptivity-fluids-localization. The challenge to computational mechanics p 553 N93-20618
- Variable-speed generators with flux weakening p 750 N93-25599

EFFUSIVES

- Remote sensing of volcanic ash hazards to aircraft p 556 A93-24213

EGRESS

- Effects of seating configuration and number of type 3 exits on emergency aircraft evacuation
[AD-A256616] p 143 N93-14277

EIGENVALUES

- Design of reduced-order observers with precise loop transfer recovery p 184 A93-14587
- Improvement in application of eigenstructure assignment to flight control system design p 227 A93-15406
- Optimum design of rotor-bearing systems with eigenvalue constraints
[ASME PAPER 92-GT-307] p 405 A93-19497
- Design of insensitive multirate aircraft control using optimized eigenstructure assignment p 370 A93-23515

- An efficient procedure for cascade aeroelastic stability determination using nonlinear, time-marching aerodynamic solvers
[AIAA PAPER 93-1631] p 719 A93-34159

- Output feedback eigenstructure assignment using two Sylvester equations p 847 A93-38214
- A numerical study of wave propagation in a confined mixing layer by eigenfunction expansions p 873 A93-43629

- Vector unsymmetric eigenequation solver for nonlinear flutter analysis on high-performance computers p 1160 A93-52449

- Trim analysis by shooting and finite elements and Floquet eigenanalysis by QR and subspace iterations in helicopter dynamics p 163 N93-13914
- The effect of wake dynamics on rotor eigenvalues in forward flight p 137 N93-14595

- Airfoil stability in turbulent flow p 781 N93-27212

EIGENVECTORS

- Improvement in application of eigenstructure assignment to flight control system design p 227 A93-15406
- Robust sampled data eigenstructure assignment using the delta operator --- in relation to autopilot design p 906 A93-41889

- Use of eigenvectors in the solution of the flutter equation p 1022 A93-45151
- Design of a low sensitivity and norm multivariable controller using eigenstructure assignment and the method of inequalities p 1170 A93-51394

- Application of eigenstructure assignment to the control of powered lift combat aircraft p 64 N93-11871

EJECTION INJURIES

- Evaluation of CKU-5/A ejection seat catapults under varied acceleration levels
[AD-A248021] p 29 N93-12489

EJECTION SEATS

- Zvezda - The Russian pioneer in the field of life-support and escape systems for aeronautics and space p 195 A93-16878
- Evolution of the SIIIS-3 Ejection Seat into a Reduced Weight (RW) ejection seat p 1239 A93-54549
- Evaluation of CKU-5/A ejection seat catapults under varied acceleration levels
[AD-A248021] p 29 N93-12489

EJECTORS

- Flowfield measurements for a supersonic mixer ejector in forward flight p 399 A93-19217
- Optimization aspects of an ejector type hypersonic thrust nozzle
[ASME PAPER 92-GT-402] p 355 A93-19551

- An advanced method for predicting the performance of helicopter propulsion system ejectors p 809 A93-35933

- Internal performance characteristics of vectored axisymmetric ejector nozzles
[AIAA PAPER 93-2432] p 898 A93-41046

- The use of streamwise vorticity to enhance ejector performance
[AIAA PAPER 93-3247] p 966 A93-46792

- Study of a circular cross section thrust augmenting ejector
[AIAA PAPER 93-2439] p 1118 A93-50191

- Initial development of the two-dimensional ejector shear layer - Experimental results
[AIAA PAPER 93-2440] p 1118 A93-50192

- Comparison of the initial development of shear layers in two-dimensional and axisymmetric ejector configurations
[AIAA PAPER 93-2441] p 1119 A93-50193

- The experimental evaluation of annular ejector system under concurrent mixing and diffusion p 1250 A93-54593

- Air ejector experiments using the two-dimensional supersonic cascade tunnel: Relationship between ejector performance and throat area ratio, part 1
[NAL-TM-642-PT-1] p 25 N93-12352

- Experimental investigation of an ejector-powered free-jet facility
[NASA-TM-105868] p 291 N93-16704

ELASTIC BENDING

- The rotor blade flap bending problem - An analytical test case p 158 A93-14783

- Flutter calculations for fixed and rotating wings with state-space inflow dynamics
[AIAA PAPER 93-1300] p 709 A93-33877

- Bending-torsion flutter of linear viscoelastic wings including structural damping
[AIAA PAPER 93-1475] p 711 A93-34021

- Effects of dynamic stall and structural modeling on aeroelastic stability of elastic bending and torsion of hingeless rotor blades with experimental correlation p 794 A93-35902

- Nonlinear stall flutter of wings with bending-torsion coupling
[AD-A254323] p 186 N93-12959

ELASTIC BODIES

- Dynamics of a high-rpm compressor p 75 A93-10009
- Dynamic stability, coupling and active control of elastic vehicles with unsteady aerodynamic forces modeling p 182 A93-14282

- Nonlinear aeroelastic response of panels
[AIAA PAPER 93-1599] p 741 A93-34130
- A parametric study of real time mathematical modeling incorporating dynamic wake and elastic blades p 798 A93-35986

- Optimization of the stiffness and mass characteristics of lifting surface structures modeled by an elastic beam p 827 A93-36789

- Dynamic analysis of a compound elastic surface p 1030 A93-47086

- Coupling characteristics analysis of elastic vehicle --- design of modern flight control systems p 1169 A93-51189

- Optimization of large scale systems in elasticity p 1255 A93-54544

ELASTIC BUCKLING

- Effect of stiffness characteristics on the response of composite grid-stiffened structures p 1022 A93-45148

ELASTIC DAMPING

- Measurements of dynamic Young's modulus and damping in single crystals of a nickel-based superalloy as a function of temperature p 1147 A93-52513

ELASTIC DEFORMATION

- Determination of the membrane and flexural shell deformations from the readings of a two-sided rosette-type strain gage p 75 A93-10047

- A study of the effect of the static aeroelasticity of a swept wing on its weight response p 801 A93-36798
- A multibody formulation for helicopter structural dynamic analysis p 892 A93-43776

- Characteristics of deformable leading edge for high performance helicopter rotor
[AIAA PAPER 93-3526] p 986 A93-47285

- Aeroplane crashes on the runway: Validation and final evaluation of the method of modeling an airframe structure
[IMFL-91-32] p 165 N93-15126

ELASTIC MEDIA

- Sound transmission through stiffened double-panel structures lined with elastic porous materials p 444 A93-19139

ELASTIC PLATES

- Nonlinear aeroelasticity and chaos p 79 A93-12165

ELASTIC PROPERTIES

- Vibration and flutter of stiff-inplane elastically tailored composite rotor blades
[AIAA PAPER 93-1302] p 725 A93-33879

- Waterborne polyurethane binder resins for compliant aircraft coatings
[AD-A256246] p 199 N93-14573

- Quiet by design: Numerical acousto-elastic analysis of aircraft structures
[ISBN-90-388-0042-9] p 893 N93-29268

ELASTIC SCATTERING

- Scattering kernels for gas-surface interaction p 943 A93-42580

ELASTIC SHELLS

- Interaction of compression waves with an elastic spherical dome p 550 A93-29718

ELASTIC SYSTEMS

- Micro mechanical behavior of pavements p 379 N93-16312

ELASTIC WAVES

- A novel development of the Ludwig tube, for extended test duration p 1011 A93-45529

- Development of separation due to interaction between a shock wave and a turbulent boundary layer perturbed by rarefaction waves p 1233 A93-55019

- System and method for cancelling expansion waves in a wave rotor
[NASA-CASE-LW-15218-1] p 86 N93-11172

ELASTODYNAMICS

- High speed, heavily loaded and precision aircraft type epicyclic gear system dynamic analysis overview and special considerations
[AIAA PAPER 93-2151] p 1154 A93-49968

ELASTOHYDRODYNAMICS

- Multilevel solution of the elasto-hydrodynamic lubrication of concentrated contacts in spiroid gears p 1161 A93-52606

ELASTOMERS

- Oxidation-resistant high-temperature materials p 915 A93-40362
- Innovative bagging techniques on a composite P-51 Mustang replica p 1191 A93-53405

ELASTOPLASTICITY

- Design of advanced beams considering elasto-plastic behaviour of material p 544 A93-26904

ELECTRIC BATTERIES

- Evolution of the Boeing 777 electrical power system p 519 A93-25998
- Development of a model to predict electric vehicle performance over a variety of driving conditions p 570 A93-26011

ELECTRIC CHARGE

- Behavior of precipitating water drops under the influence of electrical and aerodynamical forces p 1034 A93-45176

ELECTRIC CONNECTORS

- High voltage quick-disconnect harness system for helmet-mounted displays p 516 A93-25922
- New cathode-ray tube (CRT) gun interconnection assembly p 547 A93-28175

- Requirements for soldered electrical connections
[NHB-5300.4(3A-2)] p 212 N93-12674

ELECTRIC CONTROL

- Effects of external control circuit on coal-fired supersonic diagonal-type MHD generator p 1173 A93-49619
- The Trent family of engines
[PNR-90974] p 58 N93-11063

ELECTRIC CURRENT

- Comparison measurements of currents induced by radiation and injection p 926 A93-41575

ELECTRIC DISCHARGES

- An experimental study of dc discharges in supersonic and subsonic air flows p 14 A93-12980
- Electrostatic discharges
[ONERA, TP NO. 1992-82] p 844 A93-38567

- A visualizing method of streamlines around hypersonic vehicles
[AIAA PAPER 93-3440] p 1014 A93-47230

- Comparison of the electrical charging and discharging environments of multiple aircraft-borne electric-field measurement systems p 704 N93-24887

- Aircraft and refueler bonding and grounding study
[AD-A262027] p 911 N93-29398

ELECTRIC FIELDS

- A study of a pulsed electrical field near the jet of a turbojet engine p 52 A93-10179
- Joint NASA/USAF Airborne Field Mill Program - Operation and safety considerations during flights of a Lear 28 airplane in adverse weather
[AIAA PAPER 92-4093] p 93 A93-13262

- Aircraft measurement of electric field - Self-calibration p 753 A93-34694
- Effect of a deformed electric field on the precision of the electrochemical machining of gas turbine engine components p 835 A93-39094

- The onset of disintegration and corona in water drops falling at terminal velocity in horizontal electric fields p 1163 A93-49130

- A monitor for the laboratory evaluation of control integrity in digital control systems operating in harsh electromagnetic environments
[NASA-TM-4402] p 65 N93-12304

- Comparison of the electrical charging and discharging environments of multiple aircraft-borne electric-field measurement systems p 704 N93-24887

- Zoning of aircraft by electric field modelling p 704 N93-24894
- Development of models for predicting the triggering of lightning by launch vehicles p 734 N93-24899

- A single-point warning system for thunderstorms and electric fields p 747 N93-24900

ELECTRIC GENERATORS

- Power generation source for an electrothermal hypersonic wind tunnel
[AIAA PAPER 92-5045] p 376 A93-22317

SUBJECT INDEX

- Comparison of all-electric secondary power systems for civil transport p 519 A93-25997
- Choice of the heating system for high-temperature generators using chemical fuel p 559 A93-29660
- Comparison of all-electric secondary power systems for civil subsonic transports [NASA-TM-105852] p 55 N93-10456
- Engine driven chiller and thermal storage integration (Large tonnage engine driven chiller development) [PB92-227891] p 555 N93-21465
- ELECTRIC IGNITION**
- A procedure for defining lightning risk to air vehicles p 703 N93-24885
- Parameters influencing the hot-spot ignition of aviation fuel/air and ethylene/air mixtures p 704 N93-24886
- ELECTRIC MOTOR VEHICLES**
- Development of a model to predict electric vehicle performance over a variety of driving conditions p 570 A93-26011
- ELECTRIC MOTORS**
- Flight-vehicle drives (2nd revised and enlarged edition) --- Russian book [ISBN 5-217-00802-4] p 713 A93-35676
- ELECTRIC POTENTIAL**
- Alternative equipment test procedures for simultaneous current injection on multiple cable bundles p 747 N93-24903
- ELECTRIC POWER**
- The all-electric aircraft - In your future? p 997 A93-46824
- ELECTRIC POWER PLANTS**
- Advanced generating technologies - Motivation and selection process in electric utilities p 1164 A93-50950
- An evaluation of thermal energy storage options for precooled gas turbine inlet air [DE93-005980] p 754 N93-24975
- ELECTRIC POWER SUPPLIES**
- Analog simulation as part of a power supply design analysis universal platform p 543 A93-25962
- Comparison of all-electric secondary power systems for civil transport p 519 A93-25997
- Comparison of all-electric secondary power systems for civil subsonic transports [NASA-TM-105852] p 55 N93-10456
- ELECTRIC POWER TRANSMISSION**
- Installation of electrical cable looms p 764 A93-39536
- ELECTRIC PROPULSION**
- Flight testing of an electric powered vehicle [AIAA PAPER 92-4077] p 37 A93-11262
- Fuel cell powered electric propulsion for HALE aircraft [ASME PAPER 92-GT-404] p 356 A93-19553
- ELECTRIC PULSES**
- A study of a pulsed electrical field near the jet of a turbojet engine p 52 A93-10179
- Parameter selection of electro-impulse de-icing systems p 889 A93-40493
- ELECTRIC ROCKET ENGINES**
- AFOSS Contractors Meeting in Propulsion [AD-A254484] p 195 N93-12575
- ELECTRIC WIRE**
- Installation of electrical cable looms p 764 A93-39536
- Aircraft and refueler bonding and grounding study [AD-A262027] p 911 N93-29398
- ELECTRICAL ENGINEERING**
- Finding fault with avionics p 410 A93-21629
- ELECTRICAL GROUNDING**
- Aircraft and refueler bonding and grounding study [AD-A262027] p 911 N93-29398
- ELECTRICAL INSULATION**
- Installation of electrical cable looms p 764 A93-39536
- ELECTRICAL MEASUREMENT**
- New digital capacitive measurement system for blade clearances p 1254 A93-54376
- Comparison of the electrical charging and discharging environments of multiple aircraft-borne electric-field measurement systems p 704 N93-24887
- A single-point warning system for thunderstorms and electric fields p 747 N93-24900
- ELECTRO-OPTICS**
- Electro-optical navigation for aircraft p 1097 A93-50643
- Integrated optoelectronics for communication and processing: Proceedings of the Meeting, Boston, MA, Sept. 3, 4, 1991 [SPIE-1582] p 1158 A93-51250
- Sensors with centroid based common sensing scheme and their multiplexing --- fiber optic sensors in aircraft and aircraft engine applications p 1192 A93-52994
- Multiplexing electro-optic architectures for advanced aircraft integrated flight control systems [NASA-CR-182268] p 187 N93-13735

- Electro-optic architecture for servicing sensors and actuators in advanced aircraft propulsion systems [NASA-CR-182269] p 232 N93-13762
- Electro-optic architecture (EOA) for sensors and actuators in aircraft propulsion systems [NASA-CR-182270] p 233 N93-15116
- Status of the Fiber Optic Control System Integration (FOCSI) program [NASA-TM-106151] p 841 N93-28053
- ELECTROCHEMICAL CORROSION**
- Investigation of corrosion in aluminum/adhesive lap-splices using pulse-echo ultrasonic techniques [DE93-008074] p 749 N93-25518
- ELECTROCHEMICAL MACHINING**
- Effect of a deformed electric field on the precision of the electrochemical machining of gas turbine engine components p 835 A93-39094
- Increasing the efficiency of the electrochemical dimensional machining of gas turbine engine blades of EP718VD alloy p 835 A93-39095
- Presence and future of the electro-chemical processes in aero-engine production p 1257 A93-54840
- ELECTRODES**
- Thermal analysis of an arc heater electrode with a rotating arc foot [AIAA PAPER 93-2855] p 1028 A93-46590
- ELECTRODYNAMICS**
- Estimation of the parameters of the electrodynamic system engine-exhaust jet p 1193 A93-52965
- ELECTROHYDRODYNAMICS**
- Turbulent jet flows with condensation and electrophysical effects --- Russian book p 76 A93-10176
- ELECTROLUMINESCENCE**
- An arc thin film electroluminescent (TFEL) display unit for cockpit control display unit application p 518 A93-28179
- Miniature display technologies for integrated helmet systems p 718 A93-34819
- ELECTROMAGNETIC COMPATIBILITY**
- HIRF and lightning --- EMC of aircraft systems and installations for safe operation p 764 A93-39539
- Comparison measurements of currents induced by radiation and injection p 926 A93-41575
- Modeling limits of the EMV analysis program CONCEPT by example of the influence of a helicopter structure on a frame antenna [MBB-UD-0614-92-PUB] p 223 N93-15487
- Coupling gain computation between antennas on circular cylinders at SHF/EHF frequencies p 933 N93-30309
- ELECTROMAGNETIC COUPLING**
- Validation of electromagnetic-topology concepts on a complex structure [ONERA, TP NO. 1992-63] p 542 A93-25327
- Corroboration of a moment-method calculation of the maximum mutual coupling between two HF antennas mounted on a helicopter p 881 A93-40332
- Topological approach for the study of electromagnetic coupling [ONERA-P-1992-2] p 551 N93-20230
- ELECTROMAGNETIC FIELDS**
- Validation of electromagnetic-topology concepts on a complex structure [ONERA, TP NO. 1992-63] p 542 A93-25327
- PROAV Cable Warning System (CWS) - U.S. Army aircraft integration assessment and OCONUS field evaluation [AD-A261233] p 705 N93-26263
- ELECTROMAGNETIC INTERFERENCE**
- Optical interconnection and packaging technologies for advanced avionics systems p 77 A93-10960
- Radiated electric field measurements in U.S. Army helicopters p 209 A93-16163
- A new resonant link aircraft power generating system p 809 A93-36268
- Dual band tuned radomes for radar applications p 929 A93-43405
- An SSR/IFF Environment Model --- Secondary Surveillance Radar p 883 A93-43406
- Adaptive array processing for airborne radar p 883 A93-43412
- Hermetic sealing and EMI shielding gasket [AD-D015359] p 199 N93-13414
- Topological approach for the study of electromagnetic coupling [ONERA-P-1992-2] p 551 N93-20230
- ELECTROMAGNETIC PULSES**
- Comparison measurements of currents induced by radiation and injection p 926 A93-41575
- A monitor for the laboratory evaluation of control integrity in digital control systems operating in harsh electromagnetic environments [NASA-TM-4402] p 65 N93-12304
- Applications of stress envelope concepts to aircraft EMP and lightning survivability p 704 N93-24898

ELECTRONIC COUNTERMEASURES

- A computer simulation of the production of an artificially ionized layer using the Arecibo facility [DE93-010817] p 937 N93-30487
- ELECTROMAGNETIC RADIATION**
- Operation of the helicopter antenna radiation prediction code [NASA-CR-193259] p 1030 N93-31110
- ELECTROMAGNETIC SCATTERING**
- Research on ISAR motion compensation and imaging by modeling electromagnetic data p 342 A93-20852
- ELECTROMAGNETIC SHIELDING**
- Hermetic sealing and EMI shielding gasket [AD-D015359] p 199 N93-13414
- ELECTROMAGNETIC WAVE FILTERS**
- Adaptive clutter suppression for airborne array radars using clutter subspace approximation p 883 A93-43411
- ELECTROMAGNETIC WAVE TRANSMISSION**
- A computer simulation of the production of an artificially ionized layer using the Arecibo facility [DE93-010817] p 937 N93-30487
- ELECTROMAGNETISM**
- Advanced electromagnetic methods for aerospace vehicles [NASA-CR-193468] p 936 N93-31036
- ELECTROMECHANICAL DEVICES**
- Advanced cooling for high power electric actuators [SAE PAPER 92-1022] p 158 A93-14649
- Electromechanical measurement of turbomachinery blade tip-to-casing running clearance [ASME PAPER 92-GT-50] p 400 A93-19303
- The NASA SBIR product catalog [NASA-TM-108242] p 945 N93-29322
- Electropneumatic actuator, phase 1 [PB93-174951] p 1033 N93-31876
- ELECTRON BEAMS**
- Nonintrusive spectroscopic techniques for supersonic/hypersonic aerodynamics and combustion diagnostics p 203 A93-14245
- Characterization of electron beam propagation for hypersonic flight research applications [AIAA PAPER 92-5087] p 452 A93-22357
- Electron beam probing of blow-down hypersonic flows [ONERA-NT-1992-7] p 298 N93-18701
- ELECTRON DENSITY (CONCENTRATION)**
- Determination of the N2(+) + e recombination rate constant from ballistic experiments p 1234 A93-55026
- ELECTRON DISTRIBUTION**
- Characterization of electron beam propagation for hypersonic flight research applications [AIAA PAPER 92-5087] p 452 A93-22357
- ELECTRON GUNS**
- New cathode-ray tube (CRT) gun interconnection assembly p 547 A93-28175
- ELECTRON IMPACT**
- Non-equilibrium thermal radiation from air shock layers modelled with the Direct Simulation Monte Carlo method [AIAA PAPER 93-2805] p 1028 A93-46544
- ELECTRON MICROSCOPES**
- X ray diffraction and electron microscope studies of Yttria Stabilized Zirconia (YSZ) ceramic coatings exposed to vanadia [AD-A258055] p 392 N93-17676
- ELECTRON MICROSCOPY**
- Undulator Spectromicroscopy Facility at the Advanced Light Source [DE93-007964] p 823 N93-28490
- ELECTRON PRESSURE**
- Introduction of electronic pressure scanning at the Royal Aerospace Establishment [RAE-TM-AERO-2222] p 23 N93-11882
- ELECTRON SCATTERING**
- Characterization of electron beam propagation for hypersonic flight research applications [AIAA PAPER 92-5087] p 452 A93-22357
- ELECTRONIC AIRCRAFT**
- AEW aircraft design [AD-A261800] p 718 N93-26444
- ELECTRONIC CONTROL**
- Electromechanical measurement of turbomachinery blade tip-to-casing running clearance [ASME PAPER 92-GT-50] p 400 A93-19303
- Electro-optic architecture (EOA) for sensors and actuators in aircraft propulsion systems [NASA-CR-182270] p 233 N93-15116
- Strategic avionics technology definition studies. Subtask 3-1A: Electrical Actuation (ELA) systems [NASA-CR-193237] p 914 N93-29215
- ELECTRONIC COUNTERMEASURES**
- Electronic Counter Countermeasures/Advanced Radar Test Bed (ECCM/ARTB) [AIAA PAPER 92-4098] p 34 A93-13267
- The PAVE PACE integrated RF architecture for next generation avionics p 896 A93-42784

ELECTRONIC EQUIPMENT

- Finding fault with avionics p 410 A93-21629
Wind tunnel operator aimed comparison between two electronic pressure scanner systems p 830 A93-37876
New cabin electronics p 804 A93-39542
STANAG 3910 - The data bus for the next generation of European avionics systems [SAE PAPER 931595] p 1104 A93-49344
Defence electronics industry profile, 1990-1991 [CTN-92-60515] p 84 N93-10653
Wind tunnel operator aimed comparison between two electronic pressure scanner systems [DLAS-EST-TR-040] p 67 N93-11225
Extended surface heat sinks for electronic components: A computer optimization p 218 N93-14254
Performance of thermal adhesives in forced convection p 924 N93-30974

ELECTRONIC EQUIPMENT TESTS

- Algorithms for constructing models of the interaction of diagnostic systems with reserved aviation equipment p 847 A93-39043
Alternative equipment test procedures for simultaneous current injection on multiple cable bundles p 747 N93-24903
Standardization of automatic test equipment in the US Air force [AD-A262076] p 809 N93-29004
- ELECTRONIC MODULES**
Integrated modular avionics p 896 A93-42777
Integrating controls and avionics on commercial aircraft p 892 A93-42778
Application of modular avionics to the EF-111A systems improvement program p 896 A93-42780
Pave Pillar in-house research final report p 927 A93-42781

ELECTRONIC TRANSDUCERS

- Radii effect on the translation spring constant of force transducer beams p 829 A93-37867
Effect of Reynolds number on the standards of a simplified anemoclinometric probe [IMFL-91-31] p 293 N93-17542

ELECTROPLATING

- Surface protection in the aircraft industry [MBB-Z-0432-92-PUB] p 72 N93-11027

ELECTORHEOLOGICAL FLUIDS

- Electrorheologically controlled landing gear p 1021 A93-44851

ELECTROSTATIC CHARGE

- Comparison of electrostatic and aerodynamic forces during parachute opening [AIAA PAPER 93-1210] p 689 A93-35160
Electrostatic discharges [ONERA, TP NO. 1992-82] p 844 A93-38567
Aircraft and refueler bonding and grounding study [AD-A262027] p 911 N93-29398

ELECTROSTATIC PROBES

- An electrostatic probe for determining particle characteristics in disperse flow p 76 A93-10178
Intrusive and nonintrusive measurements of flow properties in arc jets p 943 A93-42584

ELECTROSTATIC SHIELDING

- An electrostatic probe for determining particle characteristics in disperse flow p 76 A93-10178

ELECTROTHERMAL ENGINES

- Power generation source for an electrothermal hypersonic wind tunnel [AIAA PAPER 92-5045] p 376 A93-22317

ELEVATION ANGLE

- Topographic mapping using a Ku-band airborne elevation interferometer p 896 A93-42786

ELEVATORS (CONTROL SURFACES)

- Rudder and elevator effects on the incipient spin characteristics of a typical general aviation training aircraft [AIAA PAPER 93-0016] p 367 A93-20138

ELLIPSES

- Application of the Galerkin/least-squares formulation to the analysis of hypersonic flows. II - Flow past a double ellipse p 868 A93-42608
2D hypersonic viscous flow past a double ellipse geometry p 868 A93-42613
Hypersonic flows over a double or simple ellipse p 868 A93-42614
Numerical simulation of hypersonic flow over a double ellipse using a Taylor-Galerkin finite element formulation with adaptive grids p 868 A93-42617
Adaptive mesh embedding for reentry flow problems p 869 A93-42619
A contribution to the prediction of hypersonic non-equilibrium flows p 869 A93-42624
Reactive and inert inviscid flow solutions by quasi-linear formulations and shock fitting p 927 A93-42625
Contribution to Problem 6 using an upwind Euler solver with unstructured meshes p 869 A93-42627

- Computation of thermochemical nonequilibrium flows around a simple and a double ellipse p 869 A93-42629

Problem 6.4.1 - Rarefied flow around a double ellipse

- p 869 A93-42630

The hypersonic double ellipse in rarefied flow

- p 869 A93-42631
Appraisal of the rarefied flow computations (problems 6.4.1 and 7.2.1) p 871 A93-42640
Calculation of real-gas effects on airfoil aerodynamic characteristics p 1229 A93-54477

ELLIPSOIDS

- Effect of real air properties on integral aerodynamic characteristics p 242 A93-18241
Experimental study of the flow around a double ellipsoid configuration p 867 A93-42603
Solution of the Euler equations around a double ellipsoidal shape using unstructured meshes and including real gas effects p 867 A93-42604
An upwind relaxation method for hypersonic viscous flows over a double-ellipsoidal body p 867 A93-42606
Navier-Stokes calculations over a double ellipse and a double ellipsoid by an implicit non-centered method p 867 A93-42607
The application of an adaptive unstructured grid method to the solution of hypersonic flows past double ellipse and double ellipsoid configurations p 868 A93-42609
Computation of the hypersonic flow over a double ellipsoid p 868 A93-42610
Numerical simulation of laminar hypersonic flow past a double-ellipsoid p 868 A93-42612
Viscous and inviscid hypersonic flow about a double ellipsoid p 868 A93-42616
Hypersonic viscous flow past double ellipse and past double ellipsoid - Numerical results p 868 A93-42618
Attempt to evaluate the computations for test case 6.1 - Cold hypersonic flow past ellipsoidal shapes p 869 A93-42620

- Skin-friction topology over a surface mounted semi-ellipsoidal wing at incidence p 1178 A93-53216
Hypersonic lateral and directional stability characteristics of an aerostatic flight experiment configuration in air and CF4 [NASA-TM-4435] p 875 N93-29166

ELLIPTIC FUNCTIONS

- Two modified versions of Hsu-Lee's elliptic solver of grid generation p 95 A93-11085

EMBEDDED COMPUTER SYSTEMS

- Parallel implementation of the feature associated mesh embedding method for the 2D-Euler equations (FAME2D) p 225 A93-14278
Real-time monitoring for software development and testing p 939 A93-42824
Additional developments in embedded computer performance measurement p 940 A93-42833
Design of an Ada expert system shell for the VHSIC avionic modular flight processor p 98 N93-11947
Formal design specification of a Processor Interface Unit [NASA-CR-189698] p 99 N93-12538
Technical operating report on the Data Integration and Collection Environment (DICE) instrumentation system design [AD-A258444] p 455 N93-17891

EMBEDDING

- Application of multigrid and adaptive grid embedding to the two-dimensional flux-split Euler equations p 202 A93-13990
Guidelines for NAVSTAR GPS embedded receiver applications p 315 A93-21184

EMERGENCIES

- Development of an expert system for cockpit emergency procedures p 845 A93-35915
Effects of seating configuration and number of type 3 exits on emergency aircraft evacuation [AD-A256616] p 143 N93-14277
Special investigation report: Flight attendant training and performance during emergency situations [PB92-917006] p 310 N93-16834
Pre-flight risk assessment in Emergency Medical Service (EMS) helicopters p 494 N93-19692
Correlations between engineering, medical and behavioural aspects in fire-related aircraft accidents p 494 N93-19693
Low bandwidth robust controllers for flight [NASA-CR-193085] p 819 N93-27156

EMERGENCY BREATHING TECHNIQUES

- Inward contaminant leakage tests of the S-Tron Corporation emergency escape breathing device. Phase 1: Tests of the original design. Phase 2: Tests with the redesigned neck seal [DOT/FAA/AM-92/18] p 704 N93-25205

EMERGENCY LIFE SUSTAINING SYSTEMS

- Helicopter accidents over water in the national navy: Epidemiological study over the period 1980-1991 p 493 N93-19686

EMERGENCY LOCATOR TRANSMITTERS

- Effective 406-MHz ELT demonstrates the potential to save more lives p 311 A93-18543

EMISSION SPECTRA

- Numerical study on atom-molecule radiation flowfield around a hypersonic blunt body p 770 A93-38434

EMISSIONS

- IR imaging for combustion characteristics and optical properties of boron/boron oxide [AD-A257747] p 393 N93-17693

EMULSIONS

- Combustion of microemulsion sprays [AIAA PAPER 93-0131] p 390 A93-22578

ENERGETIC PARTICLES

- Single event upset in avionics p 1158 A93-50566

ENERGY ABSORPTION

- Test and analysis of an advanced technology landing gear p 37 A93-10917
The effects of crushing surface roughness on the crushing characteristics of composite tubes p 77 A93-10918

- Energy-absorbing-beam design for composite aircraft subfloors [AIAA PAPER 93-1339] p 709 A93-33909

- Electrorheologically controlled landing gear p 1021 A93-44851

- Relationship between mechanical-property and energy-absorption trends for composite tubes [NASA-TP-3284] p 392 N93-16537

ENERGY ABSORPTION FILMS

- Fundamentals of low radar cross-sectional aircraft design p 802 A93-37376

ENERGY CONSERVATION

- On the conservation of rothalpy in turbomachines [ASME PAPER 92-GT-217] p 252 A93-19439
Aircraft braking systems p 995 A93-44850

ENERGY CONSUMPTION

- Summer research program (1992). High School Apprenticeship Program (HSAP) reports. Volume 16: Arnold Engineering Development Center Civil Engineering Laboratory [AD-A262024] p 945 N93-29396

ENERGY CONVERSION EFFICIENCY

- Computational and experimental investigation of a solar energy system for an atmospheric flight vehicle p 521 A93-29655

ENERGY DISSIPATION

- Implicit Navier-Stokes solver for three-dimensional compressible flows p 122 A93-14546
Prediction of secondary losses in axial compressors [ASME PAPER 92-GT-288] p 254 A93-19479
A simple method for estimating secondary losses in turbines at the preliminary design stage [ASME PAPER 92-GT-294] p 254 A93-19484
Experimental measurement of structural intensity on an aircraft fuselage p 544 A93-26999
Electrorheologically controlled landing gear p 1021 A93-44851
The energy dissipation in a rotating stall cell [ISABE 93-7010] p 1183 A93-53986
Effect of blade leaning on the development of passage vortices and losses in the passage of turbine cascade with a great turning angle p 1236 A93-55397

ENERGY DISTRIBUTION

- Analysis and development of a total energy control system for a large transport aircraft p 183 A93-14372
Vortex-induced energy separation in shear flows p 837 A93-39427

- Supersonic flow past energy release regions p 1069 A93-48973

- Relaxation of discrete rotational energy distributions using a Monte Carlo method p 1234 A93-55146

ENERGY METHODS

- Numerical study for the study of medium speed internal noise problems [DILC-EST-TN-200] p 101 N93-11156
Energy method for analysis of measured airspeed change in landing airborne manoeuvre [ESDU-92020] p 335 N93-18042

ENERGY REQUIREMENTS

- Parameter selection of electro-impulse de-icing systems p 889 A93-40493
Testing of an energy efficient environmental control system for a patrol-type aircraft [SAE PAPER 921225] p 890 A93-41399
Investigation of high-alpha lateral-directional control power requirements for high-performance aircraft [AIAA PAPER 93-3647] p 1130 A93-49519
Strategic avionics technology definition studies. Subtask 3-1A: Electrical Actuation (ELA) systems [NASA-CR-193237] p 914 N93-29215

ENERGY TECHNOLOGY

- JPRS report: Science and technology. Central Eurasia: Engineering and equipment [JPRS-UEQ-93-003] p 842 N93-28691

ENERGY TRANSFER

- Energy management --- aircraft propulsion system performance
[ISABE 93-7019] p 1195 A93-53995
- Modelling the engine temperature distribution between shut down and restart for life usage monitoring
p 169 N93-15177
- Multi-heat addition turbine engine
[NASA-CASE-LEW-15094-1] p 522 N93-22034
- Kinetics and energy transfer in nonequilibrium fluid flows
[AD-A263612] p 875 N93-29284
- Some implications of a differential turbomachinery equation with viscous correction
[AD-A264693] p 935 N93-30571
- ENGINE AIRFRAME INTEGRATION**
- ICAS, Congress, 18th, Beijing, China, Sept. 20-25, 1992, Proceedings, Vols. 1 & 2
[ISBN 1-56347-046-2] p 107 A93-14151
- Analysis of airframe and engine control interactions and integrated flight/propulsion control p 185 A93-14596
- Civil aircraft challenges in engine/airframe integration
[ASME PAPER 92-GT-45] p 322 A93-19299
- Aircraft engine integration for the M88-Rafale couple
[ASME PAPER 92-GT-403] p 322 A93-19552
- Concurrent optimization of airframe and engine design parameters
[AIAA PAPER 92-4713] p 323 A93-20281
- Aeroservoelasticity in HISAIR --- High Speed Airframe Integration Research
[AIAA PAPER 92-4719] p 324 A93-20322
- An aerospace plane as a detonation wave ramjet/airframe integrated waverider
[AIAA PAPER 92-5022] p 272 A93-22298
- Engine/airframe integration for waverider cruise vehicles
[AIAA PAPER 93-0507] p 283 A93-23254
- Analysis of a hypersonic waverider research vehicle with a hydrocarbon scramjet engine
[AIAA PAPER 93-0509] p 386 A93-23256
- Numerical simulation of supersonic flow around space plane for airframe-engine integration
[AIAA PAPER 93-0886] p 471 A93-24946
- Propulsion/airframe integration issues for waverider aircraft
[AIAA PAPER 93-0506] p 505 A93-25533
- Integration of high bypass ratio engines on modern transonic wings for regional aircraft p 506 A93-27479
- Solution of Euler equations for complex forebody-inlet combinations p 680 A93-33730
- Design development for advanced general aviation aircraft, II p 897 A93-40475
- Computational fluid dynamics for hypersonic airbreathing aircraft p 865 A93-42581
- The effect of a high thrust pusher propeller on the flow over a straight wing
[AIAA PAPER 93-3436] p 978 A93-47228
- Methodology for commercial engine/aircraft optimization
[AIAA PAPER 93-1807] p 1166 A93-49696
- Matching engine and aircraft lapse rates for the HSCT
[AIAA PAPER 93-1809] p 1100 A93-49698
- Structural design and analysis of a Mach zero to five turbo-ramjet system
[AIAA PAPER 93-1983] p 1112 A93-49830
- Identification of integrated airframe-propulsion effects on an F-15 aircraft for application to drag minimization
[AIAA PAPER 93-3764] p 1101 A93-51359
- A comparative study of multivariable robustness analysis methods as applied to integrated flight and propulsion control
[AIAA PAPER 93-3809] p 1102 A93-51401
- Study on unstart and its propagation along modules due to compound choking and/or fluctuations in combustor of scramjet engines
[ISABE 93-7052] p 1199 A93-54028
- Variable cycle engine concept
[ISABE 93-7065] p 1200 A93-54041
- Advanced aerodynamic airframe/nozzle integration
[ISABE 93-7099] p 1187 A93-54075
- Wind tunnel tests of the model of intake-airframe integration
[ISABE 93-7101] p 1192 A93-54077
- Vibration isolation of aviation power plants taking into account real dynamic characteristics of engine and aircraft p 1244 A93-55863
- A configuration development strategy for the NASP
p 46 N93-10011
- Concurrent optimization of airframe and engine design parameters
[NASA-TM-105908] p 60 N93-12402
- Aerodynamic Engine/Airframe Integration for High Performance Aircraft and Missiles
[AGARD-CP-498] p 213 N93-13199
- Test techniques for engine/airframe integration p 213 N93-13200

- Investigation of interference phenomena of modern wing-mounted high-bypass-ratio engines by the solution of the Euler-equations p 213 N93-13204
- Aerodynamic analysis of slipstream/wing/nacelle interference for preliminary design of aircraft configurations p 130 N93-13205
- Euler analysis of turbofan/superfan integration for a transport aircraft p 214 N93-13206
- Recent developments in low-speed TPS-testing for engine integration drag and installed thrust reverser simulation p 160 N93-13207
- Aerodynamic integration of thrust reversers on the Fokker 100 p 160 N93-13208
- The PEP Symposium on CFD Techniques for Propulsion Applications p 214 N93-13210
- Flight analysis of air intake/engine compatibility
p 161 N93-13212
- Water tunnel studies of inlet/airframe interference phenomena p 215 N93-13216
- Some aspects of intake design, performance and integration with the airframe p 161 N93-13219
- Application of subsonic first-order panel methods for prediction of inlet and nozzle aerodynamic interactions with airframe p 130 N93-13223
- Survey on techniques used in aerodynamic nozzle/airframe integration p 161 N93-13224
- Hypersonic propulsion system force accounting p 175 N93-13229
- Integration of turbo-ramjet engines for hypersonic aircraft p 175 N93-13230
- Aerothermodynamic flow phenomena of the airframe-integrated supersonic combustion ramjet
[NASA-TM-4376] p 196 N93-15528
- Development of an engine/airframe performance matching scheme for jet engine retrofit
[AD-A258822] p 365 N93-18997
- Propelling force and resistance p 298 N93-19003
- An exploratory investigation of the flight dynamics effects of rotor rpm variations and rotor state feedback in hover
[NASA-TM-103968] p 373 N93-19380
- ENGINE ANALYZERS**
- Fault signatures obtained from fault implant tests on an F404 engine
[ASME PAPER 92-GT-82] p 348 A93-19331
- Nonlinear dynamic simulation of single- and multi-spool core engines
[AIAA PAPER 93-2580] p 1122 A93-50294
- A three-dimensional algebraic grid generation scheme for gas turbine combustors with inclined slots
[NASA-CR-191095] p 746 N93-24759
- ENGINE CONTROL**
- Integrated flight propulsion control research results using the NASA F-15 HIDE Flight Research Facility
[AIAA PAPER 92-4106] p 38 A93-11276
- Determination of YAV-8B Reaction Control System bleed flow usage
[AIAA PAPER 92-4232] p 54 A93-13330
- Design of propulsion systems for low operating costs p 55 A93-13405
- Application of model reference adaptive control to speed control system in an aeroengine p 172 A93-14498
- A minimum-time acceleration control strategy for a two-rotor aeroengine p 172 A93-14499
- Robust fault detection of jet engine sensor systems using eigenstructure assignment p 173 A93-14608
- The control of aircraft engines in the 1990's p 173 A93-15042
- An investigation of real-time diagnostic technique on aeroengine p 174 A93-16844
- Probability analysis of a method for diagnosing gas turbine engines on the basis of thermodynamic parameters p 345 A93-18337
- Active stabilization of compressor instability and surge in a working engine
[ASME PAPER 92-GT-88] p 348 A93-19335
- Improving dynamic response of a single-spool gas turbine engine using a nonlinear controller
[ASME PAPER 92-GT-392] p 355 A93-19546
- On closed-loop identification of a certain aeroengine under flight conditions p 519 A93-24026
- Model reference control of a linear plant with feedthrough element p 846 A93-37034
- Absolute stability of an automatic control system for gas turbine engines p 810 A93-39033
- Fluid-film foil bearings control engine heat p 924 A93-39949
- Demonstration of mode transition in a scramjet combustor p 899 A93-42878
- Adaptive engine stall margin control p 1108 A93-49200
- Screening studies of advanced control concepts for airbreathing engines
[AIAA PAPER 92-3320] p 1108 A93-49329
- Optical temperature compensation schemes of spectral modulation sensors for aircraft engine control p 1105 A93-49471

- Optical sensors and multiplexing for aircraft engine control p 1105 A93-49474
- On the estimation algorithm for adaptive performance optimization of turbofan engines
[AIAA PAPER 93-1823] p 1111 A93-49710
- Evaluation of a nonlinear PSC algorithm on a variable cycle engine
[AIAA PAPER 93-2077] p 1114 A93-49904
- Advanced instrumentation for next-generation aerospace propulsion control systems
[AIAA PAPER 93-2079] p 1154 A93-49906
- Application of analog computing to real-time simulation of stall and surge dynamics
[AIAA PAPER 93-2231] p 1080 A93-50037
- Benefits of variable rotor speed in integrated helicopter/engine control
[AIAA PAPER 93-3851] p 1134 A93-51438
- A study of surge control by using pulse cut-off for dual spool turbo-jet engine p 1194 A93-53862
- Developments towards versatility in digital engine control units
[ISABE 93-7088] p 1202 A93-54064
- Design of limit-tracking systems incorporating a turbofan engine with constant disturbances
[ISABE 93-7090] p 1203 A93-54066
- Development of a real time dynamic engine simulation model of a turbo fan engine
[ISABE 93-7132] p 1205 A93-54107
- Concorde propulsion: Did we get it right? The Rolls-Royce/SNECMA Olympus 593 engine reviewed
[PNR-90970] p 57 N93-11061
- Subsonic flight test evaluation of a propulsion system parameter estimation process for the F100 engine
[NASA-TM-4426] p 175 N93-13155
- Electro-optic architecture (EOA) for sensors and actuators in aircraft propulsion systems
[NASA-CR-182270] p 233 N93-15116
- Integrated engine control and monitoring with experiences derived from OLMOS p 178 N93-15168
- Real-time in-flight engine performance and health monitoring techniques for flight research application p 169 N93-15169
- Evaluation of advanced displays for engine monitoring and control
[NASA-CR-191418] p 718 N93-24764
- Screening studies of advanced control concepts for airbreathing engines
[NASA-TM-106042] p 721 N93-25079
- A modified approach to controller partitioning
[NASA-TM-106167] p 848 N93-28051
- ENGINE COOLANTS**
- Hot streaks and phantom cooling in a turbine rotor passage. II - Combined effects and analytical modelling
[ASME PAPER 92-GT-76] p 401 A93-19326
- Influence of surface heating condition on local heat transfer in a rotating square channel with smooth walls and radial outward flow
[ASME PAPER 92-GT-188] p 402 A93-19413
- Life cycle assessment of an impingement-cooled gas turbine blade
[AIAA PAPER 92-4716] p 358 A93-20321
- Operation of a cross-flow heat exchanger with partial recirculation of one of the coolants p 833 A93-39051
- Some recommendations concerning the prevention of fuel boiling in the igniters of the combustion chambers of gas turbine engines p 812 A93-39200
- Numerical analysis of high aspect ratio cooling passage flow and heat transfer
[AIAA PAPER 93-1829] p 1153 A93-49714
- Chimera grids in the simulation of three-dimensional flowfields in turbine-blade-coolant passages
[AIAA PAPER 93-2559] p 1157 A93-50280
- ENGINE DESIGN**
- Potent Trent p 53 A93-11419
- Advanced three-shaft engines - Configured for reliability, efficiency and growth p 53 A93-12236
- A design approach to high Mach number scramjet performance
[AIAA PAPER 92-4248] p 55 A93-13360
- Effects of turbine cooling assumptions on performance and sizing of high-speed civil transport
[AIAA PAPER 92-4217] p 55 A93-13383
- Inlet design using a blend of experimental and computational techniques p 114 A93-14210
- Elimination of overtemperature in turbojet p 172 A93-14481
- Hybrid real-time simulation of a two-rotor engine p 172 A93-14497
- The integral starter/generator development progress
[SAE PAPER 920967] p 173 A93-14629
- The control of aircraft engines in the 1990's p 173 A93-15042
- Propulsion of a supersonic transport: What are the challenges? II - Achievements p 174 A93-16852

Effect of design and service-related factors on the formation of combustion residues in the fuel nozzles of gas turbine engines p 345 A93-18342

Aero-engine reliability - A GE view p 345 A93-18782

Aspects of turbine blade design for integrity p 345 A93-18784

Reliability and safety considerations in engine management systems design p 346 A93-18786

Design features of the GTD 8000 and GTD 15000 marine gas turbine engines [ASME PAPER 92-GT-15] p 400 A93-19287

The design and evaluation of a high pressure ratio radial turbine [ASME PAPER 92-GT-93] p 349 A93-19339

An update on the development of the T407/GLC38 modern technology gas turbine engine [ASME PAPER 92-GT-147] p 351 A93-19375

Optimization of a multistage axial compressor stochastic approach [ASME PAPER 92-GT-163] p 351 A93-19389

Computational techniques for probabilistic analysis of turbomachinery [ASME PAPER 92-GT-167] p 351 A93-19393

Aerodynamic and performance analysis of a radial transonic impeller for a 9:1 pressure ratio compressor [ASME PAPER 92-GT-183] p 352 A93-19408

MTR390 - Engine for the future [ASME PAPER 92-GT-250] p 353 A93-19459

Conceptual design of turbo-accelerator for HST combined cycle engine [ASME PAPER 92-GT-253] p 353 A93-19462

An optimisation-matching procedure for variable cycle jet engines [ASME PAPER 92-GT-406] p 356 A93-19555

A scoping study for hypersonic transport propulsion systems [ASME PAPER 92-GT-409] p 356 A93-19558

Using contra-rotating rotors for decreasing sizes and component number in small GTE [ASME PAPER 92-GT-414] p 356 A93-19562

Optimization of a multistage axial compressor in a gas turbine engine system [ASME PAPER 92-GT-424] p 357 A93-19572

An efficient constraint to account for mistuning effects in the optimal design of engine rotors [AIAA PAPER 92-4711] p 358 A93-20280

Concurrent optimization of airframe and engine design parameters [AIAA PAPER 92-4713] p 323 A93-20281

Structural tailoring of aircraft engine blade subject to ice impact constraints [AIAA PAPER 92-4710] p 358 A93-20319

APPLE - An aeroelastic analysis system for turbomachines and propfans [AIAA PAPER 92-4712] p 358 A93-20320

Evaluation of brush seals for limited-life engines p 411 A93-21665

Hypersonic turbulent expansion-corner flow with shock impingement [AIAA PAPER 92-5101] p 274 A93-22371

Experimental results of shock trains in rectangular ducts [AIAA PAPER 92-5103] p 274 A93-22373

A graphical user-interface for propulsion system analysis [AIAA PAPER 93-0223] p 440 A93-23699

Comparison of experimental ground testing and computational fluid dynamics for the re-engined 727-100 center engine inlet [AIAA PAPER 92-3920] p 462 A93-24294

Analytical investigation of a regeneratively cooled scramjet engine [AIAA PAPER 93-0739] p 519 A93-24829

Design of an advanced nacelle for a very high bypass ratio engine p 505 A93-25362

Advances in the design of jet engine test facilities for military aircraft in Australia p 529 A93-28491

Compressor surge and stall --- Book [ISBN 0-933283-05-9] p 482 A93-29780

Optimization of composite engine structures for mechanical and thermal loads [AIAA PAPER 93-1583] p 719 A93-34115

Improved static and dynamic performance of helicopter powerplant p 809 A93-35928

T55 engine - The challenge of torque measurement p 809 A93-35929

The application of CFD to turbomachine design - Past and future p 769 A93-38130

Advanced Tupolev twinjet combines Russian and Western technologies p 802 A93-38565

Selection of the scheme and optimal parameters of the turbine of a high-temperature bypass engine with a low bypass ratio p 811 A93-39180

Expert evaluation of the technological level of aviation gas turbine engine designs p 811 A93-39187

Effect of gasdynamic parameters on the specific weight of gas-turbine aircraft engines p 899 A93-42372

Selection of the turbofan engine size p 899 A93-42379

Research on supersonic combustion p 899 A93-42877

Demonstration of mode transition in a scramjet combustor p 899 A93-42878

A damage tolerance approach for management of aging gas turbine engines p 1001 A93-45779

Optimization of a highly-loaded axial splittier rotor design p 1002 A93-46931

Improving the design of the main fuel pump of Turbo-Jet 7 p 1107 A93-48555

An efficient liner cooling scheme for advanced small gas turbine combustors [AIAA PAPER 93-1763] p 1109 A93-49660

Experimental evaluation of a cooled radial-inflow turbine [AIAA PAPER 93-1795] p 1110 A93-49685

Fiber reinforced structures for turbine engine fragment containment [AIAA PAPER 93-1816] p 1110 A93-49704

Analysis of turbine engine rotor containment and shielding structures [AIAA PAPER 93-1817] p 1110 A93-49705

CFD analysis and testing on a twin inlet ramjet [AIAA PAPER 93-1839] p 1075 A93-49723

Modern propeller systems for advanced turboprop aircraft [AIAA PAPER 93-1846] p 1111 A93-49727

CFD applications in an aeropropulsion test environment [AIAA PAPER 93-1924] p 1112 A93-49790

Proptan engines [AIAA PAPER 93-1981] p 1112 A93-49828

Numerical simulations of a pulsed detonation wave augmentation device [AIAA PAPER 93-1985] p 1112 A93-49832

A simplified representation of the off-design characteristics of high speed, high pressure ratio axial turbomachinery stages [AIAA PAPER 93-2257] p 1081 A93-50055

Study of a circular cross section thrust augmenting ejector [AIAA PAPER 93-2439] p 1118 A93-50191

Experimental studies of aerodynamic performances of hypersonic scramjet in impulse hot-shot tunnel [AIAA PAPER 93-2446] p 1120 A93-50198

Design and investigation of the stand and flying scramjet models - Conceptions and results of experiments [AIAA PAPER 93-2447] p 1120 A93-50199

Unique development testing at Allison Gas Turbine [AIAA PAPER 93-2450] p 1138 A93-50200

Analytic methods for design of wave cycles for wave rotor core engines [AIAA PAPER 93-2523] p 1121 A93-50253

Developments in silicon carbide for aircraft propulsion system applications [AIAA PAPER 93-2581] p 1157 A93-50295

Component and Engine Structural Assessment Research (CAESAR) [AIAA PAPER 93-2609] p 1122 A93-50316

Fusion-electric propulsion for hypersonic flight [AIAA PAPER 93-2611] p 1142 A93-50318

The well made engine p 1122 A93-50352

A study of a direct-injection stratified-charge rotary engine for motor vehicle application [SAE PAPER 930677] p 1158 A93-50524

New calculation methods contribution on turbomachinery design and development [ONERA, TP NO. 1993-60] p 1092 A93-51940

Research and development of aircraft engine in Japan - Historical review [ISABE 93-7000] p 1227 A93-53977

The challenge of IHPTET --- Integrated High Performance Turbine Engine Technology [ISABE 93-7001] p 1194 A93-53978

Design and technology for engine manufacture --- for Rolls-Royce aerospace business [ISABE 93-7002] p 1194 A93-53979

Propulsion technology challenges for turn-of-the-century commercial aircraft [ISABE 93-7003] p 1194 A93-53980

Mach 5 turboramjet requirements and design approach [ISABE 93-7015] p 1194 A93-53991

Development study on Air Turbo Ramjet engine for a future space plane [ISABE 93-7016] p 1195 A93-53992

Conceptual design study on combined-cycle engine for hypersonic transport [ISABE 93-7018] p 1195 A93-53994

Energy management --- aircraft propulsion system performance [ISABE 93-7019] p 1195 A93-53995

An ultra low NO(x) pilot combustor for staged low NO(x) combustion [ISABE 93-7020] p 1195 A93-53996

Low NO(x) combustor development using aerodynamic staging [ISABE 93-7021] p 1195 A93-53997

Design and testing methods of high performance combustors for airbreathing engines [ISABE 93-7024] p 1196 A93-54000

Design of high-load aviation turbomachines using modern 3D computational methods [ISABE 93-7032] p 1196 A93-54008

The effects of end-bend regulations of compressor blade on the outlet flow field [ISABE 93-7033] p 1185 A93-54009

CFD for ramjet and scramjet powered vehicles [ISABE 93-7035] p 1197 A93-54011

The design and development of an afterburner [ISABE 93-7041] p 1198 A93-54017

Thermal design and analysis of an exhaust diffuser unit in a ceramic composite [ISABE 93-7060] p 1220 A93-54036

Axial flow compressors - Mechanical design trends [ISABE 93-7061] p 1199 A93-54037

Thermal fatigue life assessment of a convection-cooled gas turbine blade [ISABE 93-7062] p 1199 A93-54038

Research and development of a turbo-accelerator for super/hypersonic transport [ISABE 93-7066] p 1200 A93-54042

Research and development of high pressure compressor for SST and HST engine [ISABE 93-7068] p 1186 A93-54044

Test results of the hydrogen fueled model combustor for the air turbo ramjet engine [ISABE 93-7082] p 1201 A93-54058

New developments with the V2500 engine [ISABE 93-7085] p 1202 A93-54061

Aerodynamic inverse design and analysis for a full engine [ISABE 93-7086] p 1186 A93-54062

Performance and configuration analysis of jet-engine off-design behavior [ISABE 93-7087] p 1202 A93-54063

Design of limit-tracking systems incorporating a turbofan engine with constant disturbances [ISABE 93-7090] p 1203 A93-54066

Structural integrity validation of limited-life engines [ISABE 93-7131] p 1205 A93-54106

A diesel powerplant development program for airships [AIAA PAPER 93-4038] p 1246 A93-54609

Performance simulation of a combustion engine charged by a variable geometry turbocharger. I - Prerequisites, boundary conditions and model development. II - Simulation algorithm, computed results p 1256 A93-54648

Future aero engine design trade offs p 1246 A93-54836

All-composite fan blade for advanced ducted engines p 1246 A93-54837

Potential use of alternative fuels in aviation p 1243 A93-54838

The Eurojet EJ200 engine p 1246 A93-54839

Combustor development for advanced helicopter engines p 1246 A93-54841

ADP - Engine concept of the future p 1246 A93-54842

Low-frequency combustion instability mechanisms in a side-dump combustor p 1247 A93-55220

Turbofan propulsion simulator p 1247 A93-55493

Small gas turbines in the 21st century p 1247 A93-55494

Preliminary design of experimental sub-scale scramjet engine [AAS PAPER 91-639] p 1247 A93-55816

Analytical and experimental investigation of flow through a turbine vane cascade p 1248 A93-56348

Engine for change p 1248 A93-56350

LV software for supersonic flow analysis [NASA-CR-190911] p 16 N93-10069

Compound cycle engine for helicopter application [NASA-CR-180824] p 55 N93-10348

SAPNEW: Parallel finite element code for thin shell structures on the Alliant FX/80 [NASA-CR-190663] p 84 N93-10372

An interactive preprocessor for the NASA engine performance program [NASA-TM-105786] p 56 N93-10983

An experimental evaluation of prediction methods for contrafans [PNR-90924] p 56 N93-11023

The prediction of convective heat transfer in rotating square ducts [PNR-90929] p 85 N93-11025

A test facility for the thermofluid-dynamics of gas bearing lubrication films [PNR-90897] p 72 N93-11032

On the basis of experience: Built in product reliability [PNR-90932] p 85 N93-11034

Rolls-Royce civil engine technology [PNR-90936] p 56 N93-11036

The Trent: Towards greater thrust [PNR-90937] p 56 N93-11037

From RB211 to Trent: An ongoing development strategy [PNR-90938] p 56 N93-11038

Introduction to the Rolls-Royce design process [PNR-90939] p 57 N93-11039

Concorde propulsion: Did we get it right? The Rolls-Royce/SNECMA Olympus 593 engine reviewed [PNR-90970] p 57 N93-11061

Simultaneous engineering in the design of aero engines [PNR-90973] p 57 N93-11062

The Trent family of engines [PNR-90974] p 58 N93-11063

Advanced three-shaft engines: Configured for reliability, efficiency, and growth [PNR-90986] p 58 N93-11068

The development of the Rolls-Royce Trent aero gas turbine [PNR-90949] p 58 N93-11108

A European collaborative NLF nacelle flight demonstrator [PNR-90992] p 20 N93-11113

The use of simultaneous engineering for the design and manufacture of the low pressure turbine for the Rolls-Royce Trent engine [PNR-90887] p 59 N93-11206

Simultaneous engineering in aero gas turbine design and manufacture [PNR-90890] p 59 N93-11208

The engine design engine. A clustered computer platform for the aerodynamic inverse design and analysis of a full engine [NASA-TM-105838] p 21 N93-11223

A concept for a counterrotating fan with reduced tone noise [NASA-TM-105736] p 101 N93-11370

Concurrent optimization of airframe and engine design parameters [NASA-TM-105908] p 60 N93-12402

Investigation of advanced counterrotation blade configuration concepts for high speed turboprop systems. Task 4: Advanced fan section aerodynamic analysis [NASA-CR-187128] p 174 N93-12695

Alternative systems for fuel gas boosters for small gas turbine engines [PB92-223049] p 212 N93-12977

An investigation of jet engine test cell aerodynamics by means of scale model test studies with comparisons to full-scale test results p 193 N93-14060

Engine technologies for future spaceplanes [ETN-92-92732] p 177 N93-15143

Prediction of the performances in combustion of ramjets and stato-rockets by isothermal experiments and modeling p 363 N93-17622

SNECMA M88 engine development status [ASME-90-GT-118] p 363 N93-17849

Improving military transport aircraft through highly integrated engine-wing design [DS-1607] p 333 N93-17850

Turbine engine combustor design at SNECMA [DS-2129] p 363 N93-17851

The technological evolution of high thrust turbine engines [DS-1881] p 364 N93-17882

Design of the advanced regional aircraft, the DART-75 [NASA-CR-192044] p 333 N93-17972

Development of an engine/airframe performance matching scheme for jet engine retrofit [AD-A258822] p 365 N93-18997

What is the progress in propulsion? p 298 N93-19006

Nozzle/cowl optimization for a hypersonic vehicle on a typical trajectory [AD-A258827] p 341 N93-19089

Role of wind tunnel tests and CFD analysis for the development of aero-engines in IHI p 365 N93-19326

Research in robust control for hypersonic vehicles [NASA-CR-192127] p 527 N93-20296

Satisfying the customer's requirements [PNR-90988] p 521 N93-20735

Applications of active adaptive noise control to jet engines [NASA-CR-192277] p 522 N93-21210

Supersonic transport: Which material for the engine [DS-2023] p 522 N93-21459

Engine driven chiller and thermal storage integration (Large tonnage engine driven chiller development) [PB92-227891] p 555 N93-21465

Structural Tailoring of Advanced Turboprops (STAT). Theoretical manual [NASA-CR-191017] p 556 N93-22005

A preliminary sizing method for unmanned aircraft using multi-variate optimization p 714 N93-25408

Design and performance of nozzle-less volute casings for inward flow radial turbines p 722 N93-25471

Optimized scramjet engine integration on a waverider airframe p 722 N93-25480

Development of a pulse ramjet based on twin valveless pulse combustors coupled to operate in antiphase p 814 N93-27186

Experimental evaluation of a cooled radial-inflow turbine [NASA-TM-106230] p 816 N93-28697

Use of local x ray computerized tomography for high-resolution, region-of-interest inspection of large ceramic components for engines [DE93-005564] p 843 N93-28943

Heat transfer and aerodynamics of a 3D design nozzle guide vane tested in the Pyestock Isentropic Light Piston Facility p 901 N93-29928

Aero-thermal design of a cooled transonic NGV and comparison with experimental results p 904 N93-29957

Propulsion technology challenges for turn-of-the-century commercial aircraft [NASA-TM-106192] p 1005 N93-32351

Analytical and experimental investigations of the oblique detonation wave engine concept [NASA-TM-102839] p 1006 N93-32374

ENGINE FAILURE

A model-based monitoring system for turbine engines [SAE PAPER 921006] p 206 A93-14639

Fewest-fault integral optimization algorithm for engine fault diagnosis p 173 A93-15343

Calculation of the parameters of a crane helicopter with one disabled engine p 366 A93-18381

Optimal takeoff of a helicopter for category A V/STOL operations p 525 A93-28611

Compressor surge and stall --- Book [ISBN 0-933283-05-9] p 482 A93-29780

Extended range operations of two and three turbofan engine airplanes p 802 A93-37391

A practical course in aircraft maintenance. I - The powerplant --- Russian book p 811 A93-39175

Fiber reinforced structures for turbine engine fragment containment [AIAA PAPER 93-1816] p 1110 A93-49704

Analysis of turbine engine rotor containment and shielding structures [AIAA PAPER 93-1817] p 1110 A93-49705

Turbine Engine Diagnostics (TED) system [AIAA PAPER 93-1818] p 1110 A93-49706

Selection of a method for protecting aircraft gas turbine engines against damage by foreign objects (Mathematical models) p 1193 A93-53554

Real-time in-flight engine performance and health monitoring techniques for flight research application p 169 N93-15169

RB199 engine oil system failure diagnostics by comparison of measured and calculated oil consumption using the OLMOS on-board monitoring system p 178 N93-15173

Experimental analysis of steady-state and dynamic monitoring of power shaft turbines p 178 N93-15176

ENGINE INLETS

Evaluation and application of the Baldwin-Lomax turbulence model in two-dimensional, unsteady, compressible boundary layers with and without separation in engine inlets [AIAA PAPER 92-3676] p 111 A93-14118

Experimental investigation of an axisymmetric hypersonic scramjet inlet for laser propulsion p 122 A93-14515

Application of laminar flow to aero engine nacelles p 128 A93-17256

Rim seal experiments and analysis of a rotor-stator system with nonaxisymmetric main flow [ASME PAPER 92-GT-160] p 402 A93-19387

Investigation of a two-dimensional scramjet inlet, freestream M = 8-18 and Tsub 0 = 4100 K p 270 A93-21669

Evaluation and application of the Baldwin-Lomax turbulence model in two-dimensional, unsteady, compressible boundary layers with and without separation in engine inlets [AIAA PAPER 92-3676] p 414 A93-22509

Results of Low Power Deicer tests on a swept inlet component in the NASA Lewis Icing Research Tunnel [AIAA PAPER 93-0032] p 327 A93-22551

Icing testing of a large full-scale inlet at the Arnold Engineering Development Center [AIAA PAPER 93-0299] p 376 A93-22697

Comparison of experimental ground testing and computational fluid dynamics for the re-engined 727-100 center engine inlet [AIAA PAPER 92-3920] p 462 A93-24294

Acoustic mode measurements in the inlet of a model turbofan using a continuously rotating rake [AIAA PAPER 93-0598] p 563 A93-24783

An experimental parametric study of geometric, Reynolds number, and ratio of specific heats effects in three-dimensional sidewall compression scramjet inlets at Mach 6 [AIAA PAPER 93-0740] p 466 A93-24830

Parameter effects on turbulent swirling flames in combustors p 534 A93-25911

Solution of Euler equations for complex forebody-inlet combinations p 680 A93-33730

Foreign object impact assessment of a high-Mach engine inlet [AIAA PAPER 93-1630] p 711 A93-34158

Study on vortex generator flow control for the management of inlet distortion p 689 A93-34488

CFD analysis of the X-29 inlet at high angle of attack p 958 A93-45140

A lag model for turbulent boundary layers developing over rough bleed surfaces [AIAA PAPER 93-2988] p 1052 A93-48181

Effects of side-inlet angle in a three-dimensional side-dump combustor p 1109 A93-49610

Real-time simulation of maneuverable aircraft flight conditions on altitude test cell [AIAA PAPER 93-1845] p 1137 A93-49726

3-D viscous flow CFD analysis of the propeller effect on an advanced ducted propeller subsonic inlet [AIAA PAPER 93-1847] p 1075 A93-49728

Smoke measurements inside a gas turbine combustor [AIAA PAPER 93-2070] p 1113 A93-49902

Experimental determination of the bulk swirl attenuation between two axial stations in the LM2500 inlet bellmouth [AIAA PAPER 93-2203] p 1155 A93-50015

Low speed test results of subsonic, turbofan scarf inlets [AIAA PAPER 93-2301] p 1082 A93-50086

A new cooling system for ultra high temperature turbines [ISABE 93-7073] p 1201 A93-54049

Wind tunnel tests of the model of intake-airframe integration [ISABE 93-7101] p 1192 A93-54077

Starting characteristics of scramjet inlets [ISABE 93-7105] p 1203 A93-54081

Evaluation of turbofan exhaust systems from scale model test data [ISABE 93-7109] p 1204 A93-54085

Low-frequency combustion instability mechanisms in a side-dump combustor p 1247 A93-55220

Turbofan propulsion simulator p 1247 A93-55493

Evaluation and application of the Baldwin-Lomax turbulence model in two-dimensional, unsteady, compressible boundary layers with and without separation in engine inlets [NASA-TM-105810] p 82 N93-10087

Application of laminar flow to aero engine nacelles [PNR-90916] p 20 N93-11020

Mach 4 testing of scramjet inlet models [NAL-TR-1137] p 26 N93-12369

Aerodynamic Engine/Airframe Integration for High Performance Aircraft and Missiles [AGARD-CP-498] p 213 N93-13199

Test techniques for engine/airframe integration p 213 N93-13200

The influence of intake swirl distortion on the steady-state performance of a low bypass, twin-spool engine p 214 N93-13211

Flight analysis of air intake/engine compatibility p 161 N93-13212

Water tunnel studies of inlet/airframe interference phenomena p 215 N93-13216

Some aspects of intake design, performance and integration with the airframe p 161 N93-13219

Application of subsonic first-order panel methods for prediction of inlet and nozzle aerodynamic interactions with airframe p 130 N93-13223

Flow prediction for three-dimensional intakes and ducts using viscous-inviscid interaction methods p 218 N93-13953

Results of low power deicer tests on a swept inlet component in the NASA Lewis icing research tunnel [NASA-TM-105968] p 138 N93-14911

Acoustic mode measurements in the inlet of a model turbofan using a continuously rotating rake [NASA-TM-105989] p 362 N93-16705

The effect of aircraft inlets on the behaviour of aero engine axial flow compressors p 422 N93-18722

- Stall transients including effects of inlet distortion and intake geometry p 423 N93-18726
- The 3D Navier-Stokes calculation of flow about scramjet inlet with strut p 301 N93-19298
- Computational parametric study of sidewall-compression scramjet inlet performance at Mach 10 [NASA-TM-4411] p 552 N93-20299
- An assessment of inlet total-pressure distortion requirements for the Compressor Research Facility (CFR) [AD-A262299] p 815 N93-27679
- The 3-D viscous flow CFD analysis of the propeller effect on an advanced ducted propeller subsonic inlet [NASA-TM-106240] p 900 N93-29162
- Solution of Euler equations for forebody-inlet ensemble of aircraft at high angle of attack [AD-A263905] p 876 N93-29862
- The influence of non-uniform spanwise inlet temperature on turbine rotor heat transfer p 901 N93-29932
- Instrumentation for in-flight acoustic measurements in an engine inlet duct of a Fokker 100 aircraft [NLR-TP-91200-U] p 1001 N93-32332
- ### ENGINE MONITORING INSTRUMENTS
- Vibration monitoring and fault diagnosis of inflight aircraft engines p 170 A93-14176
- A model-based monitoring system for turbine engines [SAE PAPER 921006] p 206 A93-14639
- Onboard maintenance monitoring systems in modern aircraft p 167 A93-15047
- Development of a model-based monitoring system for turbine and rocket engines p 195 A93-16412
- Fault signatures obtained from fault implant tests on an F404 engine [ASME PAPER 92-GT-82] p 348 A93-19331
- On-board condition management for aircraft gas turbines [ASME PAPER 92-GT-416] p 357 A93-19564
- High temperature thin film strain gauges [ONERA, TP NO. 1992-171] p 542 A93-25346
- On-board maintenance aids p 784 A93-39538
- Advanced instrumentation for next-generation aerospace propulsion control systems [AIAA PAPER 93-2079] p 1154 A93-49906
- Proceedings of the 16th Symposium on Aircraft Integrated Monitoring Systems [DLR-MITT-92-01] p 167 N93-15152
- DAR-2: On-board data acquisition system for aircraft engines p 169 N93-15166
- Integrated engine control and monitoring with experiences derived from OLMOS p 178 N93-15168
- Royal Air Force experience of the Harrier information management system p 234 N93-15170
- Monitoring of powerplants in advanced commercial aircraft p 178 N93-15171
- EJ 200 engine monitoring system: On- and off-board data capture, analysis, and management system p 178 N93-15172
- A philosophy for integrated monitoring system design p 178 N93-15174
- Experimental analysis of steady-state and dynamic monitoring of power shaft turbines p 178 N93-15176
- Evaluation of advanced displays for engine monitoring and control [NASA-CR-191418] p 718 N93-24764
- ### ENGINE NOISE
- An experimental study of a method for reducing the jet noise of bypass engines using mechanical flow mixers p 53 A93-12810
- Feasibility study on single bypass variable cycle engine with ejector [AIAA PAPER 92-4268] p 55 A93-13366
- Comparison of advanced turboprop interior noise control ground and flight test data p 444 A93-19136
- Helicopter main rotor/tail rotor noise radiation characteristics from scaled model rotor experiments in the DNW p 445 A93-19142
- Active aerodynamic control of wake-airfoil interaction noise - Theory p 445 A93-19154
- Experimental investigation of tip clearance noise in axial flow machines p 445 A93-19155
- Experimental determination of the main noise sources in a profan model by analysis of the acoustic spinning modes in the exit plane p 449 A93-19214
- Radiated noise of ducted fans p 450 A93-19215
- Wing vortex refraction effects from BAC 1-11 flight tests p 450 A93-19226
- Active control of fan noise from a turbofan engine [AIAA PAPER 93-0597] p 452 A93-23323
- Acoustic mode measurements in the inlet of a model turbofan using a continuously rotating rake [AIAA PAPER 93-0598] p 563 A93-24783
- Technical solutions to reduce and to control the noise load in the Netherlands — generated by aircraft engines p 564 A93-28492
- Toward the silent helicopter [ONERA, TP NO. 1992-229] p 851 A93-38774
- Free shear layer control and its application to fan noise [AIAA PAPER 93-3242] p 965 A93-46787
- Localization of noise sources in the exhaust jet of a turbofan engine p 1003 A93-47509
- An acoustic suppressor for the jet noise of a turbojet engine p 1003 A93-47510
- Rotor wake/stator interaction noise - Predictions vs data p 1174 A93-52447
- The acoustics of axial compressors p 1226 A93-53615
- Control of supersonic throughflow turbomachines discrete frequency noise generation by aerodynamic detuning p 1248 A93-55860
- Nozzle installation effects on the noise from supersonic exhaust plumes p 100 N93-10681
- Combustion noise and combustion instabilities in propulsion systems p 100 N93-10682
- Reduction of propeller noise by active noise control p 101 N93-10692
- An experimental evaluation of prediction methods for contrafans [PNR-90924] p 56 N93-11023
- A concept for a counterrotating fan with reduced tone noise [NASA-TM-105736] p 101 N93-11370
- Publications on acoustics research at the Langley Research Center, January 1987 - September 1992 [NASA-TM-107674] p 102 N93-12080
- Evaluation of acoustic impedance models for a perforated plate [NAL-TR-1133] p 102 N93-12375
- Air Force procedure for predicting noise around airbases: Noise exposure model (Noisemap) [AD-A255769] p 224 N93-14655
- Experimental investigation of an ejector-powered free-jet facility [NASA-TM-105868] p 291 N93-16704
- Acoustic mode measurements in the inlet of a model turbofan using a continuously rotating rake [NASA-TM-105989] p 362 N93-16705
- Engine exhaust characteristics evaluation in support of aircraft acoustic testing [NASA-TM-104263] p 1005 N93-32220
- ### ENGINE PARTS
- An evaluation system for impact damage and erosion of ceramic gas turbine components p 79 A93-12229
- A mathematical model to determine the health of components based on SOAP data — spectrometric oil analysis program p 53 A93-12238
- Midhani alloys in aeronautical service p 70 A93-12368
- Stirling engine - Available tools for long-life assessment — for space propulsion p 195 A93-13824
- Experimental techniques for the assessment of fuel thermal stability p 197 A93-14504
- A unified approach to the construction of the throttle characteristics of postrepair turbojet engines, with the NK8-2U engine used as an example p 345 A93-18372
- Lifting philosophies for aero engine fracture critical parts p 345 A93-18783
- Testing for integrity — of aircraft gas turbine engines p 346 A93-18785
- Coupled multi-disciplinary simulation of composite engine structures in propulsion environment [ASME PAPER 92-GT-6] p 346 A93-19279
- Extending the fatigue life of aircraft engine components by hole cold expansion technology [ASME PAPER 92-GT-77] p 401 A93-19327
- Achieving manufacturing excellence for gas turbine components through focused implementation of technology [ASME PAPER 92-GT-139] p 401 A93-19371
- Flexible manufacturing of aircraft engine parts [ASME PAPER 92-GT-229] p 404 A93-19446
- TEMPER - A gas-path analysis tool for commercial jet engines [ASME PAPER 92-GT-315] p 354 A93-19501
- Ceramics for aero-engine applications [ASME PAPER 92-GT-439] p 388 A93-19581
- Results of Low Power Deicer tests on a swept inlet component in the NASA Lewis Icing Research Tunnel [AIAA PAPER 93-0032] p 327 A93-22551
- Quality of the surface layer and operating properties of aircraft engine components p 834 A93-39061
- Prediction and control of the service-related properties of parts at the technological preparation stage and during the manufacture process — of aircraft engine components p 834 A93-39062
- Characteristics of friction and wear in flight vehicle engine components p 811 A93-39075
- Automated measurement of residual stresses in the surface layer of parts p 834 A93-39081
- Effect of a deformed electric field on the precision of the electrochemical machining of gas turbine engine components p 835 A93-39094
- Life analysis of a gas turbine fan disc p 897 A93-40803
- Evaluation of metallurgical degradation on gas turbine components p 915 A93-40804
- New corrosion resistant nickel-base super-alloys and technological processes of casting gas turbines parts with directional single crystal and regulable equiaxial minimized microporosity structure p 916 A93-40811
- Numerical simulation of aerothermodynamics processes in gas turbine engine components p 1002 A93-46939
- Improving the design of the main fuel pump of Turbo-Jet 7 p 1107 A93-48555
- Turbine Engine Diagnostics (TED) system [AIAA PAPER 93-1818] p 1110 A93-49706
- Aero-engine component damping estimation from full-scale aeromechanical test data [AIAA PAPER 93-1873] p 1112 A93-49748
- High speed, heavily loaded and precision aircraft type epicyclic gear system dynamic analysis overview and special considerations [AIAA PAPER 93-2151] p 1154 A93-49968
- A simplified representation of the off-design characteristics of high speed, high pressure ratio axial turbomachinery stages [AIAA PAPER 93-2257] p 1081 A93-50055
- Developments in silicon carbide for aircraft propulsion system applications [AIAA PAPER 93-2581] p 1157 A93-50295
- Component and Engine Structural Assessment Research (CAESAR) [AIAA PAPER 93-2609] p 1122 A93-50316
- Computer aided design of turbo-machinery components p 1166 A93-50489
- The application of diffusion bonding in the manufacture of aeroengine components p 1217 A93-53514
- Corrosion of ceramic matrix composites [ONERA, TP NO. 1993-82] p 1213 A93-53602
- Theoretical and experimental investigations concerning the structural integrity of aeroengine compressor discs p 56 N93-10539
- Neutron diffraction residual stress studies for aero-engine component applications [PNR-90908] p 85 N93-11014
- Testing for integrity [PNR-90927] p 56 N93-11024
- The application of manufacturing systems engineering for aero engine gears [PNR-90944] p 86 N93-11054
- The Trent family of engines [PNR-90974] p 58 N93-11063
- Small particle impact damage in carbon-carbon composites [PNR-90948] p 73 N93-11107
- Ceramic Technology Project [DE92-018748] p 73 N93-11442
- High temperature rectifiers and MOS devices in 6H-silicon carbide [AD-A254725] p 90 N93-12340
- Thermal barrier coating life prediction model development, phase 2 [NASA-CR-189111] p 198 N93-12589
- Results of low power deicer tests on a swept inlet component in the NASA Lewis icing research tunnel [NASA-TM-105968] p 138 N93-14911
- Preliminary analysis of the J-52 aircraft engine component improvement program [AD-A257640] p 363 N93-17686
- Control of in-service damage: Application to aircraft engines [DS-2027] p 364 N93-18151
- Integrity testing of brush seal in shroud ring of T-700 engine [NASA-TM-105863] p 421 N93-18380
- Materials development program, ceramic technology project addendum to program plan: Cost effective ceramics for heat engines [DE93-003663] p 394 N93-18537
- Creep fatigue life prediction for engine hot section materials (isotropic) [NASA-CR-189221] p 364 N93-18578
- Multidisciplinary tailoring of hot composite structures [NASA-TM-106027] p 550 N93-19971
- Supersonic transport: Which material for the engine [DS-2023] p 522 N93-21459
- JPRS report: Science and technology. Central Eurasia: Engineering and equipment [JPRS-UEQ-92-003] p 749 N93-25427
- Design and performance of nozzle-less volute casings for inward flow radial turbines p 722 N93-25471
- Advanced bristle seals for gas turbine engines [AD-A261296] p 752 N93-26564

- Estimating characteristic life and reliability of an aircraft engine component improvement in the early stages of the implementation process
[AD-A262118] p 815 N93-28184
- An analysis of the correlation between the J52 engine component improvement program and improved maintenance parameters
[AD-A262062] p 816 N93-28984
- Improved silicon nitride for advanced heat engines
[NASA-CR-182193] p 917 N93-29451
- Heat transfer and aerodynamics of a 3D design nozzle guide vane tested in the Pyestock Isentropic Light Piston Facility
p 901 N93-29928
- Thermal effects of a coolant film along the suction side of a high pressure turbine nozzle guide vane
p 901 N93-29930
- Characterization of ceramic composite materials for gas turbine applications
[DE93-009719] p 905 N93-30168
- ### ENGINE STARTERS
- The integral starter/generator development progress
[SAE PAPER 920967] p 173 A93-14629
- Nickel hydrogen batteries for terrestrial applications
p 557 A93-26005
- Approach of modeling continuous turbine engine operation from startup to shutdown
p 721 A93-34495
- A study of the effect of the working medium on the start-up characteristic of an aviation gas turbine engine
p 811 A93-39037
- Gas turbine starter (jet fuel starter) specification
[SAE AS 1606] p 1124 A93-52171
- ### ENGINE TESTING LABORATORIES
- AEDC H2 Facility - New test capabilities for hypersonic air-breathing vehicles
[AIAA PAPER 93-2781] p 1012 A93-46525
- A large hemi-anechoic enclosure for community-compatible aeroacoustic testing of aircraft propulsion systems
[NASA-TM-106015] p 760 N93-26551
- An assessment of inlet total-pressure distortion requirements for the Compressor Research Facility (CFR)
[AD-A262299] p 815 N93-27679
- The USAF Advanced Turbine Aerothermal Research Rig (ATARRR)
p 911 N93-29945
- ### ENGINE TESTS
- Research of starting test of the small turbojet in simulated altitude condition
p 53 A93-11870
- Parametric diagnostics of the steady states of gas turbine engines
p 54 A93-12815
- A unified approach to the construction of the throttle characteristics of postrepair turbojet engines, with the NK8-2U engine used as an example
p 345 A93-18372
- Testing for integrity --- of aircraft gas turbine engines
p 346 A93-18785
- Design and rotor performance of a 5:1 mixed-flow supersonic compressor
[ASME PAPER 92-GT-73] p 348 A93-19323
- Engine testing of a prototype low NO(x) gas turbine combustor
[ASME PAPER 92-GT-116] p 401 A93-19352
- Turbine blade vibration monitoring system
[ASME PAPER 92-GT-159] p 402 A93-19386
- The dynamic characteristics of a high pressure turbine stage in a transient wind tunnel
[ASME PAPER 92-GT-166] p 375 A93-19392
- Arc jet testing in NASA Ames Research Center thermophysics facilities
[AIAA PAPER 92-5041] p 385 A93-22315
- Issues associated with long-duration high-enthalpy scramjet combustor testing
p 721 A93-34497
- Use of PCs in controlling simulated altitude environmental test conditions in support of turbine engine testing
p 846 A93-37856
- GE90 program moves into high gear
p 810 A93-38701
- Demonstration of mode transition in a scramjet combustor
p 899 A93-42878
- AEDC H2 Facility - New test capabilities for hypersonic air-breathing vehicles
[AIAA PAPER 93-2781] p 1012 A93-46525
- CFD analysis and testing on a twin inlet ramjet
[AIAA PAPER 93-1839] p 1075 A93-49723
- Aero-engine component damping estimation from full-scale aeromechanical test data
[AIAA PAPER 93-1873] p 1112 A93-49748
- Gasdynamics of hydrogen-fueled scramjet combustors
[AIAA PAPER 93-2145] p 1115 A93-49962
- Development and use of hydrogen-air torches in an altitude facility
[AIAA PAPER 93-2176] p 1137 A93-49988
- Improved data validation and quality assurance in turbine engine test facilities
[AIAA PAPER 93-2178] p 1137 A93-49990
- Subscale validation of a freejet inlet-engine test capability
[AIAA PAPER 93-2179] p 1138 A93-49991
- Application of analog computing to real-time simulation of stall and surge dynamics
[AIAA PAPER 93-2231] p 1080 A93-50037
- Review of NASA's Hypersonic Research Engine Project
[AIAA PAPER 93-2323] p 1116 A93-50103
- In-stream measurements of combustion during Mach 5 to 7 tests of the Hypersonic Research Engine (HRE)
[AIAA PAPER 93-2324] p 1116 A93-50104
- Unique development testing at Allison Gas Turbine
[AIAA PAPER 93-2450] p 1138 A93-50200
- Engine testing at simulated altitude conditions
[AIAA PAPER 93-2452] p 1120 A93-50201
- Recent successes in modifying several existing jet engine test cells to accommodate large, high-bypass turbofan engines
[AIAA PAPER 93-2542] p 1139 A93-50266
- F405 engine in-flight thrust methodology development for the T-45A flight test program
[AIAA PAPER 93-2544] p 1121 A93-50268
- Design and testing methods of high performance combustors for airbreathing engines
[ISABE 93-7024] p 1196 A93-54000
- Variable cycle engine concept
[ISABE 93-7065] p 1200 A93-54041
- Effect of nozzle design on the performance of a highly loaded turbine stage
[ISABE 93-7096] p 1203 A93-54072
- Improved flow measurement with simultaneous period/frequency recording --- in turbojet engines
p 1254 A93-54381
- An updated data acquisition and processing system for turbine engine testing
p 1250 A93-54389
- Uncertainty assessments for engine thrust derived from two methods
p 1254 A93-54392
- Thermal effects testing at the National Solar Thermal Test Facility
p 1255 A93-54402
- Noise studies for environmental impact assessment of an outdoor engine test facility
p 99 N93-10672
- An experimental evaluation of prediction methods for contrails
[PNR-90924] p 56 N93-11023
- Testing for integrity
[PNR-90927] p 56 N93-11024
- The development of the Rolls-Royce Trent aero gas turbine
[PNR-90949] p 58 N93-11108
- Design of a high-temperature experiment for evaluating advanced structural materials
[NASA-TM-105833] p 88 N93-11624
- The influence of intake swirl distortion on the steady-state performance of a low bypass, twin-spool engine
p 214 N93-13211
- Flight analysis of air intake/engine compatibility
p 161 N93-13212
- An investigation of jet engine test cell aerodynamics by means of scale model test studies with comparisons to full-scale test results
p 193 N93-14060
- Propulsion and Energetics Panel Working Group 20 on Test Cases for Engine Life Assessment Technology
[AGARD-AR-308] p 176 N93-14890
- Introduction to test cases for engine life assessment technology
p 176 N93-14891
- Engine life assessment test case TF41 LP compressor shaft torsional fatigue
p 177 N93-14896
- SNECMA M88 engine development status
[ASME-90-GT-118] p 363 N93-17849
- Advanced Turbine Technology Applications Project (ATTAP)
[NASA-CR-189228] p 455 N93-18762
- External stress-corrosion cracking of a 1.22-m-diameter type 316 stainless steel air valve
[NASA-TP-3190] p 737 N93-26201
- Development and demonstration of a new filter system to control emissions during jet engine testing
[AD-A261203] p 755 N93-26243
- A large hemi-anechoic enclosure for community-compatible aeroacoustic testing of aircraft propulsion systems
[NASA-TM-106015] p 760 N93-26551
- Heat transfer and aerodynamics of a 3D design nozzle guide vane tested in the Pyestock Isentropic Light Piston Facility
p 901 N93-29928
- Thermal effects of a coolant film along the suction side of a high pressure turbine nozzle guide vane
p 901 N93-29930
- The influence of non-uniform spanwise inlet temperature on turbine rotor heat transfer
p 901 N93-29932
- Measurement of turbulent spots and intermittency modelling at gas-turbine conditions
p 902 N93-29934
- Fractographic and microstructural analysis of fatigue crack growth in Ti-6Al-4V fan disc forgings
p 1004 N93-31742
- Low cycle fatigue behaviour of titanium disc alloys
p 1004 N93-31745
- Hypersonic engine component experiments in high heat flux, supersonic flow environment
[NASA-TM-106273] p 1032 N93-31860
- ### ENGINEERING
- Scientific and engineering research facilities at universities and colleges: 1992
[NSF-92-325] p 192 N93-13407
- JPRS report: Science and technology. Central Eurasia: Engineering and equipment
[JPRS-UEQ-93-004] p 930 N93-29090
- ### ENGINEERING MANAGEMENT
- Simultaneous engineering in the design of aero engines
[PNR-90973] p 57 N93-11062
- The use of simultaneous engineering for the design and manufacture of the low pressure turbine for the Rolls-Royce Trent engine
[PNR-90887] p 59 N93-11206
- Innovation in engineering
[PNR-90889] p 59 N93-11207
- Simultaneous engineering in aero gas turbine design and manufacture
[PNR-90890] p 59 N93-11208
- Aviation production engineering: Selected articles
[AD-A261231] p 764 N93-27056
- ### ENGINEERS
- Dr. Alexander H. Flax: Technologist of aeronautics
[AD-A258441] p 456 N93-17890
- ### ENTHALPY
- On the conservation of rothalpy in turbomachines
[ASME PAPER 92-GT-217] p 252 A93-19439
- Transition on a sharp cone at high enthalpy - New measurements in the shock tunnel T5 at GALTIC
[AIAA PAPER 93-0343] p 281 A93-23030
- Increase in stagnation pressure and enthalpy in shock tunnels
[AIAA PAPER 93-0350] p 377 A93-23035
- An Euler code with new energy equation and new enthalpy damping approach
p 686 A93-34352
- Issues associated with long-duration high-enthalpy scramjet combustor testing
p 721 A93-34497
- High-temperature supersonic combustion testing with optical diagnostics
p 730 A93-34498
- A combined facility of ballistic range and shock tunnel using a fast action valve
p 1012 A93-45532
- Aerothermodynamic heating due to shock wave/laminar boundary-layer interactions in high-enthalpy hypersonic flow
[AIAA PAPER 93-3135] p 1064 A93-48299
- Increase of stagnation pressure and enthalpy in shock tunnels
p 295 N93-18086
- Some implications of a differential turbomachinery equation with viscous correction
[AD-A264693] p 935 N93-30571
- ### ENTROPY
- The effect of shock motion on entropy production
[AIAA PAPER 93-0665] p 465 A93-24777
- Model for entropy production and pressure variation in confined turbulent mixing
p 1071 A93-49014
- Investigations on entropy layer along hypersonic hyperboloids using a defect boundary layer
p 787 N93-27462
- ### ENVIRONMENT EFFECTS
- Technical solutions to reduce and to control the noise load in the Netherlands --- generated by aircraft engines
p 564 A93-28492
- The costs of noise at the new Munich airport
p 558 A93-28493
- Air traffic noise monitoring in and around Lisbon Airport
p 564 A93-28494
- Short-term atmospheric effects of high-altitude aircraft emissions
p 559 A93-28865
- Potential impact of combined NO(x) and SO(x) emissions from future High Speed Civil Transport aircraft on stratospheric aerosols and ozone
p 753 A93-35372
- The impact of air traffic on the atmospheric environment
p 936 A93-42659
- Activities report of Lufthansa
[ETN-92-92100] p 28 N93-11319
- Stratospheric aircraft: Impact on the stratosphere?
[DE92-016997] p 94 N93-12104
- The 1990 high-speed civil transport studies. Summary report
[NASA-CR-189619] p 330 N93-16999
- Aerospace-plane flights and stratospheric ozone: Review and preliminary assessment of the National Aerospace Plane (NASP) operations
[RAND/N-3464-AF] p 755 N93-26327
- Air Traffic and Environment
[GSF-BAND-8] p 1034 N93-31925
- Effects of air traffic on nature and environment in the neighborhood of airports by example of the Munich 2 Airport (Germany)
p 1035 N93-31932

ENVIRONMENT POLLUTION

- Computation of wake/exhaust mixing downstream of advanced transport aircraft
[AIAA PAPER 93-2944] p 1162 A93-48141
- AQUIS: A PC-based air quality and permit information system
[DE92-040092] p 434 N93-18587
- The atmospheric effects of stratospheric aircraft. Report of the 1992 Models and Measurements Workshop. Volume 1: Workshop objectives and summary
[NASA-RP-1292-VOL-1] p 754 N93-25157
- The atmospheric effects of stratospheric aircraft. Report of the 1992 Models and Measurements Workshop. Volume 2: Comparisons with global atmospheric measurements
[NASA-RP-1292-VOL-2] p 754 N93-25158
- The atmospheric effects of stratospheric aircraft. Report of the 1992 Models and Measurements Workshop. Volume 3: Special diagnostic studies
[NASA-RP-1292-VOL-3] p 754 N93-25159
- The ecological balance of Swissair: An example of waste management
p 1035 N93-31930
- Effects of air traffic on nature and environment in the neighborhood of airports by example of the Munich 2 Airport (Germany)
p 1035 N93-31932

ENVIRONMENT PROTECTION

- European environmental studies focus on impact of engine emissions
p 92 A93-10730
- Water instead of chemical corrosives against aircraft paint - Environment-friendly paint-stripping methods could mean drastic cost reductions for the aircraft industry
p 239 A93-21850
- AQUIS: A PC-based air quality and permit information system
[DE92-040092] p 434 N93-18587
- Making clean gasoline: The effect on jet fuels
[AD-A264302] p 1019 N93-32085

ENVIRONMENT SIMULATION

- Corrosion resistance of Inconel Alloy 617 in simulated gas turbine environments
[ASME PAPER 92-GT-142] p 388 A93-19374
- Some questions of scale in simulation, and a few answers
p 939 A93-42830
- Implementation of expert systems within an interactive tactical environment
[AIAA PAPER 93-3583] p 1223 A93-52678
- Pseudo Aircraft Systems - A multi-aircraft simulation system for air traffic control research
[AIAA PAPER 93-3585] p 1209 A93-52679
- Development of a large-scale, outdoor, ground-based test capability for evaluating the effect of rain on airfoil lift
[NASA-TM-4420] p 779 N93-26899

ENVIRONMENTAL SIMULATORS

- A synthetic environment flight simulator: The AFIT virtual cockpit
[AD-A259220] p 530 N93-20576

ENVIRONMENTAL CHEMISTRY

- The atmospheric effects of stratospheric aircraft. Report of the 1992 Models and Measurements Workshop. Volume 1: Workshop objectives and summary
[NASA-RP-1292-VOL-1] p 754 N93-25157
- The atmospheric effects of stratospheric aircraft. Report of the 1992 Models and Measurements Workshop. Volume 2: Comparisons with global atmospheric measurements
[NASA-RP-1292-VOL-2] p 754 N93-25158
- The atmospheric effects of stratospheric aircraft. Report of the 1992 Models and Measurements Workshop. Volume 3: Special diagnostic studies
[NASA-RP-1292-VOL-3] p 754 N93-25159

ENVIRONMENTAL CONTROL

- Testing of an energy efficient environmental control system for a patrol-type aircraft
[SAE PAPER 92-1225] p 890 A93-41399
- Rotorcraft en route ATC route standards
[AD-A249129] p 35 N93-10323
- Three-dimensional water droplet trajectory code validation using an ECS inlet geometry
[NASA-CR-191097] p 791 N93-27267

ENVIRONMENTAL MONITORING

- Mathematical modeling and control law development for the atmospheric monitoring and control system of the Controlled Environment Research Chamber (CERC) at NASA Ames Research Center
[AD-A261978] p 911 N93-29436

ENVIRONMENTAL SURVEYS

- Noise studies for environmental impact assessment of an outdoor engine test facility
p 99 N93-10672
- Aerodynamic design and synthesis of the oblique flying wing supersonic transport
p 713 N93-24768
- The ecological balance of Swissair: An example of waste management
p 1035 N93-31930

ENVIRONMENTAL TESTS

- A study of the flexural properties of carbon-epoxy composites in certain environments
p 390 A93-21999

- Environmental conditions for certification testing of helicopter advanced composite main rotor components
p 824 A93-36003

- Use of PCs in controlling simulated altitude environmental test conditions in support of turbine engine testing
p 846 A93-37856

- Environmental definition of a multi-platform avionics system
p 896 A93-42855

- Durability properties for adhesively bonded structural aerospace applications
p 1217 A93-53515

- Helicopter operations in severe environments; Proceedings of the Conference, London, United Kingdom, June 4, 1992
[ISBN 1-85768-045-6] p 1175 A93-54287

- Environmental effects of operations during Desert Shield/Desert Storm
p 1190 A93-54291

- Development of a tethered satellite force transducer
p 1251 A93-54368

- Status of R&D of high-performance materials for severe environments (Composite materials)
p 1253 A93-54728

EPICYCLOIDS

- High speed, heavily loaded and precision aircraft type epicyclic gear system dynamic analysis overview and special considerations
[AIAA PAPER 93-2151] p 1154 A93-49968

EPOXY MATRIX COMPOSITES

- Tailoring concepts for improved structural performance of rotorcraft flexbeams
p 207 A93-14811
- Evaluation of decomposition kinetic coefficients for a fiber-reinforced intumescent-epoxy
[AIAA PAPER 93-1856] p 1144 A93-49734
- Design and manufacture for producibility of carbon fiber/epoxy composite aircraft skins
[SME PAPER EM93-104] p 1043 A93-51732
- GARTUR damage mechanics for composite materials: Analytical/experimental research on delaminations
p 537 N93-21513
- Effects of intra- and inter-laminar resin content on the mechanical properties of toughened composite materials
p 921 N93-30845

EQUATIONS OF MOTION

- Optimal lateral maneuvering for microburst encounters during final approach
p 183 A93-14350
- Structural non-linearity effects on flutter of a swept wing in transonic flows
p 410 A93-20714
- Stability of the vertical autorotation of a single-winged samara
p 274 A93-22443
- A simplified wing rock prediction method
[AIAA PAPER 93-3662] p 1128 A93-48342
- Aircraft with single axis aerodynamically deployed wings
[AIAA PAPER 93-3673] p 1129 A93-48350
- Initial development of a research flight simulator software
[AIAA PAPER 93-3590] p 1223 A93-52683
- Development of the wake behind a circular cylinder impulsively started into rotatory and rectilinear motion
p 1236 A93-55736
- Flexible rotorcraft system dynamics with time-variant contact conditions
p 340 N93-19034
- Reference equations of motion for automatic rendezvous and capture
[NASA-CR-185676] p 914 N93-29652
- On the dynamics of aeroelastic oscillators with one degree of freedom
[REPT-92-96] p 1040 N93-31653

EQUATIONS OF STATE

- Analysis of hypersonic nozzles including vibrational nonequilibrium and intermolecular force effects
p 861 A93-41916
- The numerical errors in inverse simulation
[AIAA PAPER 93-3588] p 1223 A93-52681

EQUILIBRIUM EQUATIONS

- Structure-attached corotational fluid grid for transient aerodynamic computations
p 480 A93-29326
- Application of differential quadrature to the analysis of static aerodynamic phenomena
[AIAA PAPER 93-1505] p 711 A93-34044
- The minimal multiplier method in calculations of the stability, limiting vibration cycles, and limiting states of nonlinearly deformed structures
p 836 A93-39176

EQUILIBRIUM FLOW

- The stagnation line solution of the equilibrium flow with radiation and mass injection
p 680 A93-33733
- Reactive and inert inviscid flow solutions by quasi-linear formulations and shock fitting
p 927 A93-42625
- A high-order streamline Godunov scheme for steady hypersonic equilibrium flows
[AIAA PAPER 93-2997] p 1053 A93-48187
- A collocated finite volume method for predicting flows at all speeds
p 1087 A93-51736
- Numerical studies of Mach reflection with air chemistry
p 1233 A93-54815

EQUIPMENT

- JPRS report: Science and technology. Central Eurasia: Engineering and equipment
[JPRS-UEQ-93-004] p 930 N93-29090

EQUIPMENT SPECIFICATIONS

- Laboratory for modelling of prospective board equipment systems for aircraft
p 374 A93-18529
- Mil-Prime specification for parachutes
[AIAA PAPER 93-1247] p 677 A93-35184
- Document for 270 Voltage Direct Current (270 V dc) System
[SAE ARP 4729] p 1160 A93-52170
- Gas turbine starter (jet fuel starter) specification
[SAE AS 1606] p 1124 A93-52171

EQUIVALENCE

- A preliminary study of the effect of equivalence ratio on a low emissions gas turbine combustor using KIVA-2
[DE92-018616] p 215 N93-13321

EROSION

- An evaluation system for impact damage and erosion of ceramic gas turbine components
p 79 A93-12229
- Erosion resistant titanium nitride coating for turbine compressor applications
[ASME PAPER 92-GT-417] p 388 A93-19565
- The chemistry of Saudi Arabian sand - A deposition problem on helicopter turbine airfoils
p 1216 A93-53468
- Erosion predictions and measurements of high-temperature coatings and superalloys used in turbomachines
p 74 N93-12189

EROSIVE BURNING

- Erosion characteristics of ceramic particulate and whisker reinforced aluminum composites
[ASME PAPER 92-GT-369] p 388 A93-19532

ERROR ANALYSIS

- Transmission error and load distribution analysis of spur and double helical gear pairs used in a split path helicopter transmission design
p 549 A93-29426
- Application of parafoils to microwave landing system siting
[AIAA PAPER 93-1213] p 702 A93-35162
- Comments on experiments for computational validation for fluid dynamic predictions
p 927 A93-42578
- Measurements of SSR bearing errors due to site obstructions --- Secondary Surveillance Radar
p 883 A93-43407
- The numerical errors in inverse simulation
[AIAA PAPER 93-3588] p 1223 A93-52681
- An improved calibration technique for wind tunnel model attitude sensors
p 1253 A93-54356
- Static and dynamic errors in heat flux measurements
p 1254 A93-54366
- Uncertainty of derived results on X-Y plots --- in gas turbine engines
p 1261 A93-54382
- Uncertainty assessments for engine thrust derived from two methods
p 1254 A93-54392
- Instrumentation and data acquisition system for the C.I.R.A. Transonic Pilot Tunnel
p 1250 A93-54395
- Estimation of aerodynamic characteristics from flight-test data. IV - Principal component analysis and perpendicular error method
p 1241 A93-54551
- Uncertainty estimates for pressure sensitive paint measurements
p 1258 A93-55369
- Conditioned based machinery maintenance (helicopter fault detection)
[AD-A255796] p 329 N93-16396
- A critical analysis of the accuracy of several numerical techniques for combustion kinetic rate equations
[NASA-TP-3315] p 362 N93-16941
- A multi-faceted engineering study of aerodynamic errors of the Service Aircraft Instrumentation Package (SAIP)
[AD-A258059] p 293 N93-17677
- The human factor problem in the Canadian Forces aviation
p 491 N93-19657
- The use of multiple models in case-based diagnosis
p 759 N93-25969
- Information-based criteria of terrain navigability. Part 1: Data-base analysis
p 793 N93-27178
- Efficient fault diagnosis of helicopter gearboxes
[NASA-TM-106253] p 1032 N93-31846

ERROR CORRECTING CODES

- Analysis and correction of ionospheric time delay for differential GPS
p 498 A93-24028
- MSC/NASTRAN structure optimization test module version 67 (preliminary)
[REPT-5-191025] p 554 N93-20907

ERROR DETECTION CODES

- Robust fault detection of jet engine sensor systems using eigenstructure assignment
p 173 A93-14608
- Differential GPS autonomous failure detection
p 314 A93-21152
- Neural network fault diagnosis of a turbofan engine
[ISABE 93-7091] p 1203 A93-54067

ERRORS

- Airborne gravimetry, altimetry, and GPS navigation errors
p 1240 A93-55975

- Air traffic control visual scanning
[DOT/FAA/CT-TN92/16] p 35 N93-10459
- A monitor for the laboratory evaluation of control integrity in digital control systems operating in harsh electromagnetic environments
[NASA-TM-4402] p 65 N93-12304
- Motion errors and compensation possibilities
p 212 N93-13052
- Accidents and errors: A review of recent UK Army Air Corps accidents
p 495 N93-19701
- An experimental health monitoring unit for GPS and GLONASS
p 706 N93-25018
- The effect of clock, media, and station location errors on Doppler measurement accuracy
p 885 N93-29588
- An analysis of en route controller-pilot voice communications
[AD-A264784] p 935 N93-30611
- ERS-1 (ESA SATELLITE)**
- ERS-1 directional wave spectra validation with the airborne SAR PHARS
[BCRS-92-18] p 937 N93-31010
- ESCAPE SYSTEMS**
- Zvezda - The Russian pioneer in the field of life-support and escape systems for aeronautics and space
p 195 A93-16878
- How to enhance safety for future space transportation systems
p 1015 A93-45444
- Facilities and capabilities catalog for landing and escape systems
[NASA-RP-1282] p 196 N93-14495
- ESSENTIALLY NON-OSCILLATORY SCHEMES**
- Application of high-order accurate essentially nonoscillatory schemes to two-dimensional compressible viscous flows
[AIAA PAPER 93-0879] p 470 A93-24940
- Uniform high-order spectral methods for one- and two-dimensional Euler equations
p 476 A93-27068
- Numerical experiments with nonoscillatory schemes using Eulerian and new Lagrangian formulations
p 862 A93-42432
- A multigrid nonoscillatory method for computing high speed flows
[AIAA PAPER 93-3319] p 958 A93-45103
- Comparison of ENO and TVD schemes for the parabolized Navier-Stokes equations
[AIAA PAPER 93-2970] p 1049 A93-48164
- ESTIMATES**
- Uncertainty estimates for pressure sensitive paint measurements
p 1258 A93-55369
- ESTIMATING**
- Scientific and engineering research facilities at universities and colleges: 1992
[NSF-92-325] p 192 N93-13407
- Robust controller and estimator design using minimax methods
p 229 N93-13925
- Estimation of rate of climb
[ESDU-92019] p 164 N93-14541
- Estimating the regional economic significance of airports
[AD-A257658] p 382 N93-17793
- Vertical wind estimation from horizontal wind measurements
p 489 N93-19604
- Prediction of success from training
p 495 N93-19702
- Failure identification using multiple model adaptive estimation for the LAMBDA flight vehicle
[AD-A259137] p 527 N93-20596
- Estimating turbine limit load
[NASA-CR-191105] p 699 N93-25883
- Practical input optimization for aircraft parameter estimation experiments
[NASA-CR-191462] p 820 N93-27264
- A laboratory study of subjective response to sonic booms measured at White Sands Missile Range
[NASA-TM-107746] p 852 N93-27272
- Estimating characteristic life and reliability of an aircraft engine component improvement in the early stages of the implementation process
[AD-A262118] p 815 N93-28184
- Subjective response to simulated sonic booms with ground reflections
[NASA-TM-107764] p 852 N93-28692
- ETCHING**
- Photoelectrochemical etching of high aspect ratio submillimeter waveguide filters from $n(+)$ GaAs wafers
p 409 A93-20644
- ETHYL ALCOHOL**
- Postmortem alcohol production in fatal aircraft accidents
[AD-A255766] p 143 N93-14026
- ETHYLENE**
- Parameters influencing the hot-spot ignition of aviation fuel/air and ethylene/air mixtures
p 704 N93-24886
- EULER EQUATIONS OF MOTION**
- A split-matrix Runge-Kutta type space marching procedure
p 8 A93-11921
- Calculation of separated axisymmetric flow past bodies by solving Euler equations in the inner vortex region
p 14 A93-12975
- Accelerated method of the Euler equation solution in transonic airfoil flow problem
p 113 A93-14193
- MELINA - A multi-block, multi-grid 3D Euler code with sub block technique for local mesh refinement
p 115 A93-14217
- A flux-difference finite volume method for steady Euler equations on adaptive unstructured grids
p 116 A93-14277
- Parallel implementation of the feature associated mesh embedding method for the 2D-Euler equations (FAME2D)
p 225 A93-14278
- Euler solutions simulating strong shock waves and vortex phenomena over 3D wings
p 121 A93-14392
- Dispersion-relation-preserving schemes for computational aeroacoustics
p 244 A93-19151
- Assessment of a 3-D Euler code for subsonic turbine vane flows and study of the non radial blade stacking
[ASME PAPER 92-GT-63] p 247 A93-19313
- Calculation of three-dimensional unsteady flows in turbomachinery using the linearized harmonic Euler equations
[ASME PAPER 92-GT-136] p 249 A93-19368
- Advances in the numerical integration of the 3-D Euler equations in vibrating cascades
[ASME PAPER 92-GT-170] p 351 A93-19396
- Numerical research on flows in nonuniform cascades
[ASME PAPER 92-GT-276] p 253 A93-19469
- Investigation of tip clearance phenomena in an axial compressor cascade using Euler and Navier-Stokes procedures
[ASME PAPER 92-GT-299] p 255 A93-19489
- A solution scheme for the Euler equations based on a multi-dimensional wave model
[AIAA PAPER 93-0065] p 261 A93-20178
- A new rotated upwind difference scheme for the Euler equations
[AIAA PAPER 93-0066] p 261 A93-20179
- Flux limiters in a rotated upwind scheme for the Euler equations
[AIAA PAPER 93-0067] p 262 A93-20180
- Comparison of limiters in flux-split algorithms for Euler equations
[AIAA PAPER 93-0068] p 262 A93-20181
- Accurate solution of the 2D Euler equations with an efficient cell-vertex upwind scheme
[AIAA PAPER 93-0071] p 262 A93-20183
- Numerical prediction of instabilities in transonic internal flows using an Euler TVD code
[AIAA PAPER 93-0072] p 262 A93-20184
- A gridless Euler/Navier-Stokes solution algorithm for complex-aircraft applications
[AIAA PAPER 93-0333] p 268 A93-21107
- Development of a flexible and efficient multigrid-based multiblock flow solver
[AIAA PAPER 93-0677] p 269 A93-21117
- The modelling of aerodynamic flows by solution of the Euler equations on mixed polyhedral grids
p 269 A93-21218
- Cascade flow calculations by a multigrid Euler method
p 270 A93-21662
- Numerical simulation of unsteady transonic nozzle flows
p 272 A93-22230
- Solution schemes for stage-by-stage dynamic compression system modeling
[AIAA PAPER 93-0154] p 275 A93-22592
- 3-D adaptive grid-embedding Euler technique
[AIAA PAPER 93-0330] p 415 A93-23021
- Euler computations of rotor-stator interaction in turbomachinery cascades using adaptive triangular meshes
[AIAA PAPER 93-0386] p 282 A93-23065
- Single passage Euler analysis of oscillating cascade unsteady aerodynamics for arbitrary interblade phase angle
[AIAA PAPER 93-0389] p 282 A93-23067
- An installed nacelle design method using multiblock Euler solver
[AIAA PAPER 93-0528] p 284 A93-23269
- Numerical simulation of three-dimensional supersonic flows using Euler and boundary layer solvers
[AIAA PAPER 93-0531] p 284 A93-23272
- Performance of compressible flow codes at low Mach numbers
p 287 A93-23540
- Acoustic flux vector splitting scheme for Euler equations
p 460 A93-24078
- An implicit finite difference algorithm for two dimensional Euler equation
p 461 A93-24085
- Three-dimensional unstructured grid Euler method applied to turbine blades
[AIAA PAPER 93-0196] p 461 A93-24233
- Exact-gradient shape optimization of a 2-D Euler flow
p 462 A93-24308
- Numerical investigations on airfoil performance subjected to aerodynamic interference from an upstream airfoil
[AIAA PAPER 93-0639] p 463 A93-24754
- A moving mesh system for the calculation of unsteady flows
[AIAA PAPER 93-0641] p 464 A93-24756
- A new procedure for dynamic adaption of three-dimensional unstructured grids
[AIAA PAPER 93-0672] p 560 A93-24780
- A physically guided zonal approach for two-dimensional aeroflow flows
[AIAA PAPER 93-0790] p 468 A93-24869
- Viscous flow computations of flow field around an advanced propeller
[AIAA PAPER 93-0873] p 469 A93-24934
- Investigation of methods for modeling propeller-induced flow fields
[AIAA PAPER 93-0874] p 469 A93-24935
- A comparison of 'new' and 'old' flux-splitting schemes for the Euler equations
[AIAA PAPER 93-0876] p 470 A93-24937
- Recent developments in high order K-exact reconstruction on unstructured meshes
[AIAA PAPER 93-0668] p 475 A93-25546
- Characteristic multigrid method application to solve the Euler equations with unstructured and unnnested grids
p 476 A93-27065
- Euler study on porous transonic airfoils with a view toward multiport design
p 479 A93-28604
- Linearized Euler predictions of unsteady aerodynamic loads in cascades
p 480 A93-29318
- Euler solutions to nonlinear acoustics of non-lifting rotor blades
p 568 A93-29433
- Finite-volume-TVD scheme for 3-D Euler transonic flow computations in rotating curvilinear coordinates
p 679 A93-33709
- Euler solution for wing-body combination at supersonic speeds
p 680 A93-33722
- Solution of Euler equations for complex forebody-inlet combinations
p 680 A93-33730
- A kind of improved flux-split method for solving the Euler equations
p 681 A93-33739
- Wing flutter boundary prediction using unsteady Euler aerodynamic method
[AIAA PAPER 93-1422] p 739 A93-33975
- An Euler code with new energy equation and new enthalpy damping approach
p 686 A93-34352
- Nonreflecting boundary conditions of three-dimensional Euler equation calculations for strut cascades
p 689 A93-34491
- Results from a conical Euler methodology developed for unsteady vortical flows
p 692 A93-35612
- A finite-volume Euler solver for computing rotary-wing aerodynamics on unstructured meshes
p 765 A93-35935
- Unsteady blade pressures on a propfan at takeoff - Euler analysis and flight data
p 810 A93-37389
- Unsteady analysis of helicopter rotor
p 770 A93-38193
- Transonic and supersonic flow calculations around aircrafts using a multidomain Euler code
[ONERA, TP NO. 1992-137] p 772 A93-38610
- Unsteady transonic two-dimensional Euler solutions using finite elements
p 778 A93-39412
- Comparison of coordinate-invariant and coordinate-aligned upwinding for the Euler equations
[AIAA PAPER 93-3306] p 858 A93-41053
- International Symposium on Computational Fluid Dynamics, 4th, Univ. of California, Davis, Sept. 9-12, 1991, Selected Papers
p 862 A93-42426
- A multidimensional generalization of Roe's flux difference splitter for the Euler equations
p 863 A93-42437
- Solution of the Euler equations around a double ellipsoidal shape using unstructured meshes and including real gas effects
p 867 A93-42604
- Computation of the hypersonic flow over a double ellipsoid
p 868 A93-42610
- Inviscid finite-volume lambda formulation
p 872 A93-42888
- A finite-volume Euler solver for computing rotary-wing aerodynamics on unstructured meshes
p 874 A93-43782
- A multi-dimensional kinetic-based upwind solver for the Euler equations
[AIAA PAPER 93-3303] p 950 A93-45001
- New upwind dissipation models with a multidimensional approach
[AIAA PAPER 93-3304] p 950 A93-45002
- Solution of the Euler and Navier Stokes equations on parallel processors using a transposed/Thomas ADI Algorithm
[AIAA PAPER 93-3310] p 1036 A93-45006

- An implicit time-marching procedure for high speed flow
[AIAA PAPER 93-3315] p 951 A93-45011
Progress in local preconditioning of the Euler and Navier-Stokes equations
[AIAA PAPER 93-3328] p 952 A93-45022
Numerical wave propagation and steady state solutions. II - Bulk Viscosity Damping
[AIAA PAPER 93-3331] p 953 A93-45025
Euler solutions for blunt bodies using triangular meshes - Artificial viscosity forms and numerical boundary conditions
[AIAA PAPER 93-3333] p 953 A93-45027
Surface boundary conditions for the numerical solution of the Euler equations
[AIAA PAPER 93-3334] p 953 A93-45028
An accuracy assessment of Cartesian-mesh approaches for the Euler equations
[AIAA PAPER 93-3335] p 953 A93-45029
An efficient method to calculate rotor flow in hover and forward flight
[AIAA PAPER 93-3336] p 953 A93-45030
Three-dimensional unstructured grid Euler computations using a fully-implicit, upwind method
[AIAA PAPER 93-3337] p 953 A93-45031
A 3D unstructured adaptive multigrid scheme for the Euler equations
[AIAA PAPER 93-3339] p 954 A93-45033
Numerical vorticity capturing for vortex-solid body interaction problems
[AIAA PAPER 93-3343] p 954 A93-45037
Multigrid convergence of an implicit symmetric relaxation scheme
[AIAA PAPER 93-3357] p 954 A93-45051
Implicit multigrid Euler solutions with symmetric Total-Variation-Diminishing dissipation
[AIAA PAPER 93-3358] p 955 A93-45052
A 3-D finite-volume scheme for the Euler equations on adaptive tetrahedral grids
[AIAA PAPER 93-3359] p 956 A93-45083
A novel algorithm for the solution of compressible Euler equations in wave/particle split (WPS) form
p 957 A93-45093
Direct and iterative algorithms for the three-dimensional Euler equations
[AIAA PAPER 93-3378] p 957 A93-45102
A singularities tracking conservation law scheme for compressible duct flows
p 960 A93-45542
Hypersonic flow calculations using a multidomain MUSCL Euler solver
p 960 A93-45547
A multiblock, multigrid solution procedure for multielement airfoils
p 967 A93-46812
On the shock-fitting scheme of Hall-Crawley for time-linearized time-harmonic flows using Euler equations
p 972 A93-46946
Numerical solution of steady and unsteady Euler equations
p 973 A93-46988
A new flux splitting scheme
p 973 A93-47189
Computation of passively controlled transonic wing
[AIAA PAPER 93-3474] p 981 A93-47253
The application of an Euler method and a Navier Stokes method to the vortical flow about a delta wing
[AIAA PAPER 93-3510] p 984 A93-47276
Solution of the Euler equations for airfoils using asymptotic methods
p 1045 A93-48130
Numerical solution of the Euler equations for complex aerodynamic configurations using an edge-based finite element scheme
[AIAA PAPER 93-2933] p 1046 A93-48131
High resolution numerical simulation of the linearized Euler equations in conservation law form
[AIAA PAPER 93-2934] p 1148 A93-48132
A computational and experimental investigation of a delta wing with vertical tails
[AIAA PAPER 93-3009] p 1054 A93-48199
Dynamic-overlapped-grid simulation of aerodynamically determined relative motion
[AIAA PAPER 93-3018] p 1055 A93-48205
Three-dimensional time-marching aeroelastic analyses using an unstructured-grid Euler method
p 1100 A93-49012
Euler calculations of unsteady interaction of advancing rotor with a line vortex
p 1071 A93-49016
Turbofan flowfield simulation using Euler equations with body forces
[AIAA PAPER 93-1978] p 1078 A93-49825
Multistage turbomachinery flow solutions using three-dimensional implicit Euler method
[AIAA PAPER 93-2382] p 1083 A93-50150
A fourth-order MUSCL finite-difference scheme for solving the unsteady compressible Euler equations
p 1086 A93-51121
Numerical solutions of Euler equations by using a new flux vector splitting scheme
p 1087 A93-51740
Calculation of compressible gas flow on optimal difference grids
p 1091 A93-51902
- Implicit schemes for unsteady Euler equations on unstructured meshes
[ONERA, TP NO. 1993-64] p 1171 A93-51944
Flux-vector splitting for compressible low Mach number flow
p 1093 A93-52001
Euler analysis of forebody-strake vortex flows at supersonic speeds
p 1094 A93-52429
A dual-Euler method for solving all-attitude angles of the aircraft
[AIAA PAPER 93-3589] p 1223 A93-52682
An implicit difference scheme of Euler equation for unsteady transonic flow
p 1182 A93-53852
Numerical simulation of ramjet and scramjet combustion using two-dimensional Euler equations with finite rate chemistry
[ISABE 93-7083] p 1202 A93-54059
Recent developments performed at ONERA for the simulation of 3D inviscid and viscous flows in turbomachinery by the solution of Euler and Navier-Stokes equations
[ISABE 93-7094] p 1186 A93-54070
Locally implicit total variation diminishing schemes on mixed quadrilateral-triangular meshes
p 1235 A93-55356
A frontal approach for internal node generation in Delaunay triangulations
p 1262 A93-56403
Improved numerical simulation of Euler equations
p 83 A93-10309
Investigation of interference phenomena of modern wing-mounted high-bypass-ratio engines by the solution of the Euler-equations
p 213 A93-13204
Euler analysis of turbofan/superfan integration for a transport aircraft
p 214 A93-13206
Numerical simulation of the acoustic instability in the spatially developing, confined, supersonic mixing layer
p 132 A93-13521
Comparison of solution of various Euler solvers and one Navier-Stokes solver for the flow about a sharp-edged cropped delta wing
[NLR-TP-90340-U] p 418 A93-16411
Current European rotorcraft research activities on development of advanced CFD methods for the design of rotor blades (BRITE/EURAM DACRO project)
[MBB-UD-0601-91-PUB] p 293 A93-17568
Application of an Euler-equation method to a sharp-edged delta wing configuration with vortex flow
[NLR-TP-91306] p 294 A93-17809
Computational Fluid Dynamics, volume 2
[VKI-LS-1992-04-VOL-2] p 421 A93-18563
Validation of central and upwind 3D compressible flow solvers
p 421 A93-18564
Exact-gradient shape optimization of a 2D Euler flow
[INRIA-RR-1540] p 422 A93-18623
Numerical methods for aerothermodynamic design of hypersonic space transport vehicles
[MBB-FE-211-S-PUB-0481] p 514 A93-21056
A contribution to the great Riemann solver debate
[NASA-CR-191409] p 694 A93-25083
- EULER-LAGRANGE EQUATION**
Control of numerical diffusion in computational modeling of vortex flows
p 9 A93-12156
Periodic Euler and Navier-Stokes solutions about oscillating airfoils
p 241 A93-17799
A new Lagrangian method for steady supersonic flow computation. II - Slip-line resolution. III - Strong shocks
p 243 A93-18855
Implicit Euler calculation of supersonic vortex wake/engine plume interaction
[AIAA PAPER 93-0656] p 540 A93-24769
Computing 3-D steady supersonic flow via a new Lagrangian approach
[AIAA PAPER 93-0891] p 471 A93-24951
A comparison between centered and upwind schemes for two-phase compressible flows
[AIAA PAPER 93-2346] p 1083 A93-50120
A Eulerian/Lagrangian modelling to calculate the evolution of a water droplets spray
[ISABE 93-7121] p 1221 A93-54096
Stochastic finite element analysis for high speed rotors
p 554 A93-20696
- EUROPE**
Critical considerations on European air transport politics
p 103 A93-12718
The creation of a Community cabotage area in the European Community and its implications for the US bilateral aviation system
p 104 A93-13423
Air transport within the European single market - How will it look after 1992? A suggested view on the future
p 104 A93-13424
European navigation into the 21st century: Proceedings of the Conference, London, United Kingdom, Feb. 12, 1991
[ISBN 0-903409-82-8] p 311 A93-17751
European navigation into the 21st century - Frequency considerations
p 311 A93-17754
- European aerospace science and technology, 1992: A bibliography with indexes
[NASA-SP-7105] p 949 A93-32404
- EUROPEAN AIRBUS**
A330 - Completing the family
p 40 A93-11418
Advanced technology and the pilot
p 45 A93-13412
Maintainable A330
p 107 A93-13957
Aerelastic investigations as applied to Airbus airplanes
p 155 A93-14280
High capacity aircraft
p 157 A93-14395
Advanced technology constant challenge and evolutionary process
p 109 A93-15054
Composite wing results of Deutsche Airbus technology program
p 109 A93-15808
Toulouse - Flight tests of the Airbus A340
p 159 A93-16859
Taking to the skies under hydrogen power - Deutsche Aerospace Airbus studies the use of alternative fuels for civil aviation
p 677 A93-34947
Airbus or the revival of European civil aviation
p 856 A93-42655
Evaluation methodologies applied for pressurized fuselages of Airbus A/C
p 948 A93-45796
Monitoring of powerplants in advanced commercial aircraft
p 178 A93-15171
Airbus Industrie TCAS experience
p 152 A93-15186
- EVALUATING (TRANSPORTATION)**
Effects of seating configuration and number of type 3 exits on emergency aircraft evacuation
[AD-A256616] p 143 A93-14277
- EVALUATION**
Measuring flight test progress on large scale development programs
[AIAA PAPER 92-4070] p 37 A93-11257
An experimental evaluation of prediction methods for contrails
[PNR-90924] p 56 A93-11023
High Capacity Voice Recorder (HCVR) Operational Test and Evaluation (OT/E) integration test report
[DOT/FAA/CT-TN92/30] p 88 A93-11460
Experimental evaluation of candidate graphical microburst alert displays
p 145 A93-14853
Results of in-service evaluation of wind shear systems
p 146 A93-14856
In-service evaluation of wind shear systems
p 146 A93-14857
Proposed action plan to improve ADM effectiveness, part 3: Developing a new ADM paradigm on which to build advanced or expert decision making training
p 148 A93-15026
An approach to evaluating reactive airborne wind shear systems
p 489 A93-19600
Test techniques for evaluating flight displays
[NASA-TM-103947] p 516 A93-21810
- EVAPORATION**
Diffusion controlled evaporation of a multicomponent droplet - Theoretical studies on the importance of variable liquid properties
p 1021 A93-44224
- EVASIVE ACTIONS**
Application of the receding horizon strategy to singularly perturbed pursuit-evasion problems
p 369 A93-22980
- EVOKED RESPONSE (PSYCHOPHYSIOLOGY)**
Use of microprocessor-based simulator technology and MEG/EEG measurement techniques in pilot emergency-maneuver training
p 530 A93-19706
- EVOLUTION (DEVELOPMENT)**
Evolution of helicopters and the status of technology in India
p 2 A93-12234
Vorticity dynamics in spatially developing rectangular jets
[AIAA PAPER 93-3286] p 969 A93-46842
- EXCIMER LASERS**
Aerodynamic phenomena in high pulse repetition rate XeCl laser
p 1150 A93-48806
- EXCITATION**
Employment of radicals and excited state species for supersonic combustion photochemical ignition of premixed hydrogen/oxygen mixtures with ArF laser
p 73 A93-11135
In-flight structural mode excitation system for flutter testing
p 526 A93-19915
The natural excitation technique (NExT) for modal parameter extraction from operating wind turbines
[DE93-010611] p 845 A93-28603
- EXHAUST DIFFUSERS**
Allowing for the effect of flow nonisothermality on total pressure losses in the afterburner diffusers of augmented turbofan engines
p 53 A93-12811
Transonic discharge flows around diffuser vanes from a centrifugal impeller
[ISABE 93-7053] p 1185 A93-54029
Thermal design and analysis of an exhaust diffuser unit in a ceramic composite
[ISABE 93-7060] p 1220 A93-54038

- Aero engine ceramics: The vision, the reality, and the progress [PNR-90983] p 72 N93-11066
Cooling predictions in turbofan engine components p 905 N93-29964

EXHAUST EMISSION

- European environmental studies focus on impact of engine emissions p 92 A93-10730
Turbine engine developers explore ways to lower NO(x) emission levels p 52 A93-10732
ICAO analyses trends in fuel consumption by world's airlines p 1 A93-10733
Modification of combustor stoichiometry distribution for reduced NO(x) emission from aircraft engines [ASME PAPER 92-GT-108] p 349 A93-19346
Emissions reduction by varying the swirler airflow split in advanced gas turbine combustors [ASME PAPER 92-GT-110] p 349 A93-19347
Three-dimensional gas turbine combustor emissions modeling [ASME PAPER 92-GT-129] p 350 A93-19363
Aircraft turbine engine NOx emission limits - Status and trends [ASME PAPER 92-GT-415] p 357 A93-19563
Development of an optical sensor for active control of a gas turbine combustor [AIAA PAPER 93-0118] p 360 A93-22568
Three-dimensional NOx modeling for rich/lean combustor [AIAA PAPER 93-0251] p 360 A93-22660
Control of contaminants in gas turbines with variable-flow combustion chambers and hydrogen addition p 520 A93-27478
Short-term atmospheric effects of high-altitude aircraft emissions p 559 A93-28865
Quiet operations key to MD-90 success p 708 A93-33700
Potential impact of combined NO(x) and SO(x) emissions from future High Speed Civil Transport aircraft on stratospheric aerosols and ozone p 753 A93-35372
The impact of air traffic on the atmospheric environment p 936 A93-42659
Absolute intensity measurements of impurity emissions in a shock tunnel and their consequences for laser-induced fluorescence experiments p 1147 A93-48044
Atmospheric aerosols due to aircraft and ecological problems p 1162 A93-48846
An analytical study of dilution jet mixing in a cylindrical duct [AIAA PAPER 93-2043] p 1113 A93-49876
Three-dimensional emission modeling for diffusion flame, rich/lean, and lean gas turbine combustors [AIAA PAPER 93-2338] p 1117 A93-50115
Emission characteristics of a model gas turbine combustor at practical conditions [ISABE 93-7023] p 1196 A93-53999
NO(y) from sub-sonic aircraft emissions - A global three-dimensional model study p 1261 A93-56236
Stratospheric aircraft exhaust plume and wake chemistry studies [NASA-CR-189688] p 94 N93-12299
A preliminary study of the effect of equivalence ratio on a low emissions gas turbine combustor using KIVA-2 [DE92-018616] p 215 N93-13321
The 1990 high-speed civil transport studies [NASA-CR-189618] p 330 N93-16947
The 1990 high-speed civil transport studies. Summary report [NASA-CR-189619] p 330 N93-16999
Development and demonstration of a new filter system to control emissions during jet engine testing [AD-A261203] p 755 N93-26243
Particulate emissions from gas turbine engines [AD-A261374] p 725 N93-26339
CFD mixing analysis of axially opposed rows of jets injected into confined crossflow [NASA-TM-106179] p 813 N93-27128
An analytical study of dilution jet mixing in a cylindrical duct [NASA-TM-106181] p 814 N93-27160
Climatic effects of turbofan emissions in the stratosphere and the higher troposphere p 1035 N93-31927
Effects of commercial flight pollution on human health p 1035 N93-31931
- # EXHAUST FLOW SIMULATION
- Recent advances in jet simulation techniques for flight vehicles p 66 A93-12656
The cryogenic approach to simulating hot jet in transonic wind-tunnel testing p 117 A93-14297
Prediction of the radiation characteristic of a helicopter exhaust jet p 172 A93-14494
A numerical study on the radiation characteristic of an elliptical exhaust jet p 174 A93-16236
Using a full potential solver for propulsion system exhaust simulation p 689 A93-34487

- Hypersonic single expansion ramp nozzle simulations p 777 A93-39254
Scramjet nozzle experiment with hypersonic external flow p 899 A93-42879
Effects of flow-path variations on internal reversing flow in a tailpipe offtake configuration for ASTOVL aircraft [AIAA PAPER 93-2438] p 1118 A93-50190
Computational effects of inlet representation on powered hypersonic, airbreathing models p 1094 A93-52427
Assessment of a flow-through balance for hypersonic wind tunnel models with scramjet exhaust flow simulation [NASA-TM-4441] p 779 N93-27005
Effects of flow-path variations on internal reversing flow in a tailpipe offtake configuration for ASTOVL aircraft [NASA-TM-106149] p 900 N93-29065

EXHAUST GASES

- A study of a pulsed electrical field near the jet of a turbojet engine p 52 A93-10179
Recent advances in jet simulation techniques for flight vehicles p 66 A93-12656
Infrared flow visualization of V/STOL aircraft [AIAA PAPER 92-4253] p 80 A93-13343
DNW test highlights related to aircraft environment p 190 A93-14274
NO(x) sensitivities for gas turbine engines operated on lean-premixed combustion and conventional diffusion flames [ASME PAPER 92-GT-115] p 349 A93-19351
Engine testing of a prototype low NO(x) gas turbine combustor [ASME PAPER 92-GT-116] p 401 A93-19352
Ignition and exhaust emission characteristics of spray combustion in a pre-chamber type vortex combustor [ASME PAPER 92-GT-119] p 350 A93-19355
Ramjet NOx emission - Use of a 3D CFD method for the combustor design of a super/hyper-sonic transport propulsion system [ASME PAPER 92-GT-255] p 353 A93-19464
Measurements of jet aircraft emissions at cruise altitude. I - The odd-nitrogen gases NO, NO2, HNO2 and HNO3 p 556 A93-24391
The possibility of reducing the emission of benzo(a)pyrene with the exhaust gases of aviation gas turbine engines by water injection into the combustion chamber p 812 A93-39201
Toward the second-generation supersonic transport [ONERA, TP NO. 1993-26] p 890 A93-41038
Plume and wake dynamics, mixing, and chemistry behind a high speed civil transport aircraft p 1034 A93-45139
Localization of noise sources in the exhaust jet of a turbofan engine p 1003 A93-47509
Computation of wake/exhaust mixing downstream of advanced transport aircraft [AIAA PAPER 93-2944] p 1162 A93-48141
CFD code calibration and inlet-fairing effects on a 3D hypersonic powered-simulation model [AIAA PAPER 93-3041] p 1056 A93-48222
NO(x) scavenging on carbonaceous aerosol surfaces in aircraft exhaust plumes. I [AIAA PAPER 93-2343] p 1164 A93-50117
Development of an advanced exhaust mixer for a high bypass ratio turbofan engine [AIAA PAPER 93-2435] p 1118 A93-50188
Flight-determined engine exhaust characteristics of an F404 engine in an F-18 airplane [AIAA PAPER 93-2543] p 1121 A93-50267
NO(x) reduction additives for aircraft gas turbine engines [AIAA PAPER 93-2594] p 1122 A93-50306
Calculation of a plane supersonic jet simulating the exhaust jet of a hypersonic flight vehicle engine p 1103 A93-51912
Estimation of the parameters of the electrodynamic system engine-exhaust jet p 1193 A93-52965
The prediction of thermal NO(x) in gas turbine exhausts [ISABE 93-7022] p 1195 A93-53998
Measurement and prediction of flow in a gas turbine engine exhaust plume [ISABE 93-7113] p 1204 A93-54088
Effect of jet engine exhaust on SOFIA straight flight performance --- Stratospheric Observatory For Infrared Astronomy p 1263 A93-55178
Stratospheric aircraft: Impact on the stratosphere? [DE92-016997] p 94 N93-12104
Stratospheric aircraft exhaust plume and wake chemistry studies [NASA-CR-189688] p 94 N93-12299
An experimental study of under-expanded jets p 696 N93-25467
Development and demonstration of a new filter system to control emissions during jet engine testing [AD-A261203] p 755 N93-26243

- Improved selective catalytic NOx control technology for compressor station reciprocating engines [PB93-158566] p 755 N93-26529
Assessment of a flow-through balance for hypersonic wind tunnel models with scramjet exhaust flow simulation [NASA-TM-4441] p 779 N93-27005
Generation of carbon monoxide in compartment fires [PB93-146702] p 880 N93-29211

EXHAUST NOZZLES

- A system for washing the combustion chamber nozzles and flow path components of the NK-8-2U engine during service p 373 A93-18357
Optimization aspects of an ejector type hypersonic thrust nozzle [ASME PAPER 92-GT-402] p 355 A93-19551
Design of exhaust nozzles using GA optimized neural networks [AIAA PAPER 93-0410] p 361 A93-23331
Commercial turbofan engine exhaust nozzle flow analyses p 689 A93-34489
Crack simulation and life assessment of gas turbine nozzles p 915 A93-40805
Thrust vectoring control from underexpanded asymmetric nozzles [AIAA PAPER 93-3261] p 968 A93-46827
In-stream measurements of combustion during Mach 5 to 7 tests of the Hypersonic Research Engine (HRE) [AIAA PAPER 93-2324] p 1116 A93-50104
Static internal performance tests of single expansion ramp nozzle concepts designed with LO considerations [AIAA PAPER 93-2429] p 1117 A93-50185
Performance characteristics of a variable-area vane nozzle for vectoring an ASTOVL exhaust jet up to 45 deg [AIAA PAPER 93-2437] p 1118 A93-50189
Effects of flow-path variations on internal reversing flow in a tailpipe offtake configuration for ASTOVL aircraft [AIAA PAPER 93-2438] p 1118 A93-50190
Flight-determined engine exhaust characteristics of an F404 engine in an F-18 airplane [AIAA PAPER 93-2543] p 1121 A93-50267
IHPTET exhaust nozzle technology demonstrator --- integrated high performance turbine energy technology [AIAA PAPER 93-2569] p 1121 A93-50287
Internal performance of Highly Integrated Deployable Exhaust Nozzles [AIAA PAPER 93-2570] p 1084 A93-50288
Advanced aerodynamic airframe/nozzle integration [ISABE 93-7099] p 1187 A93-54075
Evaluation of turbofanjet exhaust systems from scale model test data [ISABE 93-7109] p 1204 A93-54085
Observation of fluctuation of 2D-nozzle flows [ISABE 93-7110] p 1204 A93-54086
Nozzle installation effects on the noise from supersonic exhaust plumes p 100 N93-10681
Survey on techniques used in aerodynamic nozzle/airframe integration p 161 N93-13224
CFD calibration for three-dimensional nozzle/afterbody configurations p 215 N93-13226
Supersonic investigation of two dimensional hypersonic exhaust nozzles [NASA-TM-105687] p 179 N93-15342
Experimental investigation of an ejector-powered free-jet facility [NASA-TM-105688] p 291 N93-16704
Performance characteristics of a variable-area vane nozzle for vectoring an ASTOVL exhaust jet up to 45 deg [NASA-TM-106114] p 813 N93-27131
Effects of flow-path variations on internal reversing flow in a tailpipe offtake configuration for ASTOVL aircraft [NASA-TM-106149] p 900 N93-29065
Evaluation of four advanced nozzle concepts for short takeoff and landing performance [NASA-TP-3314] p 875 N93-29165
- # EXHAUST SYSTEMS
- The acoustic response of altitude test facility exhaust systems to axisymmetric and two-dimensional turbine engine exhaust plumes p 449 A93-19209
Experimental investigation of exhaust system mixers for a high bypass turbofan engine [AIAA PAPER 93-0022] p 357 A93-20140
Numerical investigation of flow field in a turbine volute [AIAA PAPER 93-0155] p 542 A93-25505
Computational study of advanced exhaust system transition ducts with experimental validation p 689 A93-34490
An experimental study of thrust reverser models --- of axisymmetric exhaust systems of aerojet engines p 812 A93-39195
Exhaust system model test and research p 1107 A93-48525

F

- Development and use of hydrogen-air torches in an altitude facility
[AIAA PAPER 93-2176] p 1137 A93-49988
- Effects of flow-path variations on internal reversing flow in a tailpipe offtake configuration for ASTOVL aircraft
[AIAA PAPER 93-2438] p 1118 A93-50190
- Effects of flow-path variations on internal reversing flow in a tailpipe offtake configuration for ASTOVL aircraft
[NASA-TM-106149] p 900 A93-29065
- EXHAUST VELOCITY**
Engine exhaust characteristics evaluation in support of aircraft acoustic testing
[NASA-TM-104263] p 1005 A93-32220
- EXISTENCE THEOREMS**
An existence theorem for a free boundary problem of hypersonic flow theory p 857 A93-40405
- EXPANSION**
The effect of expansion on the large scale structure of a compressible turbulent boundary layer
[AIAA PAPER 93-2991] p 1052 A93-48183
- EXPERIMENT DESIGN**
An analytically designed subcomponent test to reproduce the failure of a composite wing box beam
[AIAA PAPER 93-1344] p 709 A93-33914
- A combined experimental and theoretical study of laminar flow control with particular relevance to aero engine nacelles
[PNR-90991] p 20 A93-11070
- Construction and testing of simple airfoils to demonstrate structural design, materials choice, and composite concepts p 879 A93-30979
- EXPERT SYSTEMS**
The employment of artificial intelligence for analyzing air accidents p 226 A93-14375
- Development of a prototype of an expert system for the design of comprehensive scientific-technical development programs for civil aviation p 434 A93-18373
- Expert systems for maintenance engineering p 434 A93-18762
- The Royal Air Force experience of artificial intelligence aircraft maintenance p 435 A93-18764
- Knowledge based systems and avionics equipment failure diagnosis p 238 A93-18765
- Advanced expert systems increase aircraft maintenance efficiency - An overview p 238 A93-18767
- Expert systems for the simulation of gas turbine engines
[ASME PAPER 92-GT-408] p 435 A93-19557
- An integrated knowledge system for wind tunnel testing - Project Engineers' Intelligent Assistant
[AIAA PAPER 93-0560] p 377 A93-23297
- Increased safety through knowledge-based pilot assistance p 518 A93-27499
- Development of an expert system for cockpit emergency procedures p 845 A93-35915
- A theoretical study on the ETHYLENE system - A fuzzy diagnostic expert system for large rotating machinery p 846 A93-36327
- System Status - The diagnostic edge of the pilot's associate p 808 A93-37853
- Expert system for redundancy and reconfiguration management p 938 A93-42785
- Design of a rule-based fuzzy controller for the pitch axis of an unmanned research vehicle p 907 A93-42807
- TEAMS - Technical expert aircraft maintenance system p 941 A93-42865
- The use of genetic algorithms in the design of fuzzy logic controllers p 1167 A93-50779
- Intelligent systems of flight-vehicle control p 1167 A93-50951
- Definition of the structure of expert preferences for the multicriterial analysis of control systems p 1168 A93-50953
- Generation of a plant description dictionary based on expert survey data p 1168 A93-50956
- Control problem for a plant with artificial intelligence p 1168 A93-50960
- Control theoretic approach to air traffic conflict resolution
[AIAA PAPER 93-3832] p 1097 A93-51421
- Implementation of expert systems within an interactive tactical environment
[AIAA PAPER 93-3583] p 1223 A93-52678
- Expert Systems for the simulation of turbofan engines
[ISABE 93-7133] p 1225 A93-54108
- A knowledge-based blackboard system to interpret graphical data from vibration tests of gas turbines
[PNR-90993] p 59 A93-11114
- Artificial intelligence and CFD: Expert systems for the design of airfoils and for grid generation
[DIGE-EST-TN-016] p 48 A93-11161
- Design of an Ada expert system shell for the VHSIC avionics modular flight processor p 98 A93-11947
- DESAID (the development of an expert system for aircraft initial design) p 163 A93-14448

- Failure diagnostic with MAINTEx based on AIMS at Swissair p 110 A93-15181
- Design for tactical situation awareness display
[AD-A256194] p 170 A93-15235
- An investigation of the influence of advanced aircraft diagnostics on the technological sophistication of maintenance personnel
[AD-A258888] p 240 A93-18887
- An investigation of discovery-based learning in the route planning domain
[AD-A259141] p 513 A93-20560
- Application of artificial neural networks to the design optimization of aerospace structural components
[NASA-TM-4389] p 555 A93-21831
- Spurious symptom reduction in fault monitoring
[NASA-CR-191453] p 942 A93-29192
- Development of a concept formulation process aid for analyzing training requirements and developing training devices
[AD-A263579] p 912 A93-29972
- Airspace Design Expert System (ADES), a 2D/3D mapping and modelling tool incorporating an expert system for use in instrument approach design p 888 A93-30357
- Investigation of advanced technology for airway facilities maintenance training
[DOT/FAA/CT-TN92/24] p 994 A93-32336
- EXPLOSIONS**
Transient/structural analysis of a combustor under explosive loads
[NASA-TM-107660] p 420 A93-17779
- EXPLOSIVE DECOMPRESSION**
Aircraft accident report: Explosive decompression-loss of cargo door in flight, United Airlines Flight 811, Boeing 747-122, N4713U, Honolulu, HI, 24 February 1989
[PB92-910402] p 28 A93-12193
- EXPLOSIVE DEVICES**
Proceedings of the First International Symposium on Explosive Detection Technology
[DOT/FAA/CT-92/11] p 496 A93-21856
- The UK perspective on aviation security p 496 A93-21858
- EXPLOSIVES**
Proceedings of the First International Symposium on Explosive Detection Technology
[DOT/FAA/CT-92/11] p 496 A93-21856
- Insights into US domestic aviation p 496 A93-21859
- Principles of nuclear-based explosive detection systems p 497 A93-21861
- A review of the development of a luggage explosive detection system p 497 A93-21862
- A transportable luggage examination system based on neutron interrogation p 497 A93-21863
- PFNA technique for the detection of explosives p 497 A93-21865
- A pulsed fast-thermal neutron interrogation system p 497 A93-21866
- Explosive detection system based on Electronic Neutron Generator (ENG) p 497 A93-21870
- Experience with explosive detection systems in airports p 498 A93-21895
- Automatic detection of explosives using x ray imaging p 880 A93-30275
- Explosives detection systems for airport security gas chromatographic based devices p 881 A93-30276
- EXPLOSURE**
Effect of sonic boom asymmetry on subjective loudness
[NASA-TM-107708] p 453 A93-16755
- EXTERNAL STORE SEPARATION**
Wind tunnel test techniques for UAV separation investigations
[AIAA PAPER 93-0626] p 524 A93-24743
- EXTERNAL STORES**
Transition of flutter mode of two-dimensional wing with external store p 41 A93-11818
- Effects of the pylon pitching stiffness on wing-store flutter p 41 A93-11820
- Geometry based Delaunay tetrahedralization and mesh movement strategies for multi-body CFD
[AIAA PAPER 92-4575] p 15 A93-13309
- Effects of pylon yaw and lateral stiffness on the flutter of a delta wing with external store p 800 A93-36330
- EXTERNAL TANKS**
Design optimization of natural laminar flow bodies in compressible flow
[NASA-CR-4478] p 292 A93-16940
- EXTRAPOLATION**
Superresolution radar imaging with linear prediction data extrapolation p 342 A93-20851
- The numerical solution of low Mach number flow in confined regions by Richardson extrapolation
[TRITA-NA-9207] p 789 A93-29005

F-104 AIRCRAFT

- Load experience variability of fighter aircraft
[NLR-TP-89172-U] p 514 A93-20742

F-106 AIRCRAFT

- Flight test operations using an F-106B research airplane modified with a wing leading-edge vortex flap
[AIAA PAPER 92-4094] p 42 A93-13261
- Vortex features of F-106B aircraft at subsonic speeds
[AIAA PAPER 93-3471] p 859 A93-41058

F-111 AIRCRAFT

- Reinforcement of the F-111 wing pivot fitting with a boron/epoxy doubler system - Materials engineering aspects p 1214 A93-54241

F-117A AIRCRAFT

- Flight management system on the F-117A p 908 A93-42815
- The development of aircraft in the Lockheed Skunk Works from 1954 to 1991 p 805 A93-27168

F-14 AIRCRAFT

- F-14A aircraft low-speed maneuvering aerodynamics
[AIAA PAPER 93-0523] p 283 A93-23265
- F-14D flight director development, test, and evaluation p 803 A93-38840
- Identification of a full subsonic envelope nonlinear aerodynamic model of the F-14 aircraft
[AIAA PAPER 93-3634] p 1065 A93-48319
- A neural network prototype for predicting F-14B strains at the B.L. 10 longeron
[AD-A255272] p 165 A93-15004

F-15 AIRCRAFT

- Integrated flight propulsion control research results using the NASA F-15 HIDEC Flight Research Facility
[AIAA PAPER 92-4106] p 38 A93-11276
- Flight testing and simulation of an F-15 airplane using throttles for flight control
[AIAA PAPER 92-4109] p 39 A93-11278
- Composite 'Exoskin' doubler extends F-15 Vertical Tail fatigue life
[AIAA PAPER 93-1341] p 709 A93-33911
- Design optimization study for F-15 propulsion/forward fairing compatibility p 1003 A93-47291
- Preliminary flight test results of a fly-by-throttle emergency flight control system on an F-15 airplane
[AIAA PAPER 93-1820] p 1100 A93-49708
- Identification of integrated airframe-propulsion effects on an F-15 aircraft for application to drag minimization
[AIAA PAPER 93-3764] p 1101 A93-51359
- Performance-seeking control - Program overview and future directions p 1102 A93-51360
- An examination of wing rock for the F-15
[AD-A256613] p 188 A93-14252
- Add-on damping treatment for the F-15 upper-outer wing skin
[AD-A258470] p 337 A93-18248
- F-15 composite engine access door p 920 A93-30442

F-16 AIRCRAFT

- Feasibility study of an active aeroelastic control system for the F-16 aircraft p 181 A93-14224
- AFTI/F-16 night close air support system testing p 808 A93-38841
- F-16 Digital Flight Control System improvements p 818 A93-38843
- Multiple model adaptive estimation applied to the VISTA F-16 flight control system with actuator and sensor failures p 907 A93-42806
- Decreasing F-16 nozzle drag using computational fluid dynamics
[AIAA PAPER 93-2572] p 1084 A93-50289
- Prismatic grid generation for three-dimensional complex geometries p 1178 A93-53217
- Overview of supersonic laminar flow control research on the F-16XL ships 1 and 2
[NASA-TM-104257] p 20 A93-11221
- Evaluation of CKU-5/A ejection seat catapults under varied acceleration levels
[AD-A248021] p 29 A93-12489
- Determination of stresses on laminated aircraft transparencies by the strain gage-hole drilling and sectioning method
[AD-A255548] p 164 A93-14571
- Multiple model adaptive estimation applied to the VISTA F-16 with actuator and sensor failures
[AD-A256444] p 188 A93-14608
- Strategies for optimal control design of normal acceleration command following on the F-16
[AD-A258975] p 373 A93-19095
- Human factors causes and management strategies in US Air Force F-16 mishaps 1984-present p 492 A93-19673
- F-16 accidents: The Norwegian experience p 492 A93-19674

- Category A F-16 accidents in the Belgian Air Force
p 492 N93-19675
- Combat and training aircraft class A mishaps in the Belgian Air Force 1970-1990
p 492 N93-19677
- Supersonic aerodynamic characteristics of an advanced F-16 derivative aircraft configuration
[NASA-TP-3355] p 989 N93-31733
- F-18 AIRCRAFT**
- The F-18 High Alpha Research Vehicle - A high-angle-of-attack testbed aircraft
[AIAA PAPER 92-4121] p 42 A93-13273
- A thermal analysis of an F/A-18 wing section for actuator thermal management
[SAE PAPER 921023] p 158 A93-14650
- Breaking the stall barrier
p 159 A93-17502
- Doppler global velocimetry measurements of the vortical flow above an F/A-18
[AIAA PAPER 93-0414] p 415 A93-23333
- De-Dopplerization of aircraft acoustic signals
[AIAA PAPER 93-0737] p 563 A93-24827
- Multiblock Navier-Stokes solutions about the F/A-18 wing-LEX-fuselage configuration
p 767 A93-37378
- Reconnaissance capable F/A-18D optical and infrared window antifog systems
[SAE PAPER 921182] p 890 A93-41361
- Actuated forebody strake controls for the F-18 high alpha research vehicle
[AIAA PAPER 93-3675] p 1006 A93-44233
- Forebody vortex control on an F/A-18 using small, rotatable 'tip-strakes'
[AIAA PAPER 93-3450] p 1009 A93-47236
- A wind tunnel investigation of the pressure distribution on an F/A-18 wing
[AIAA PAPER 93-3468] p 980 A93-47249
- F/A-18 departure recovery improvement evaluation
[AIAA PAPER 93-3671] p 1129 A93-48349
- Installed F/A-18 inlet flow calculations at 60 deg angle-of-attack and 10 deg side slip
[AIAA PAPER 93-1806] p 1074 A93-49695
- Development of the F/A-18 E/F air induction system
[AIAA PAPER 93-2152] p 1101 A93-49969
- Flight-determined engine exhaust characteristics of an F404 engine in an F-18 airplane
[AIAA PAPER 93-2543] p 1121 A93-50267
- Active control for fin buffet alleviation
[AIAA PAPER 93-3817] p 1133 A93-51408
- Unsteady pressure and load measurements on an F/A-18 vertical fin
p 1095 A93-52451
- Design and implementation of digital filters for analysis of F/A-18 flight test data
[AD-A253447] p 17 N93-10342
- A summary of the forebody high-angle-of-attack aerodynamics research on the F-18 and the X-29A aircraft
[NASA-TM-104261] p 25 N93-12353
- Determination of the stability and control derivatives of the F/A-18 HARV from flight data using the maximum likelihood method
[NASA-CR-191216] p 186 N93-12903
- A stochastic optimal feedforward and feedback control methodology for superagility
[NASA-CR-4471] p 229 N93-13370
- The F-18 systems research aircraft facility
[NASA-TM-4433] p 381 N93-16753
- Identification and control of non-linear time-varying dynamical systems using artificial neural networks
[AD-A257595] p 372 N93-18193
- Longitudinal-control design approach for high-angle-of-attack aircraft
[NASA-TP-3302] p 373 N93-19108
- Flight and wind-tunnel calibrations of a flush airdata sensor at high angles of attack and sideslip and at supersonic Mach numbers
[NASA-TM-104265] p 344 N93-19110
- Status of the Fiber Optic Control System Integration (FOCSI) program
[NASA-TM-106151] p 841 N93-28053
- Modal survey of a full-scale F-18 wind tunnel model
[AD-A262482] p 875 N93-29410
- Flight control system design factors for applying automated testing techniques
[NASA-TM-4242] p 910 N93-30764
- F-28 TRANSPORT AIRCRAFT**
- Results of review of Fokker F 28 'Fellowship' maintenance program
p 948 A93-45793
- F-4 AIRCRAFT**
- Human factors causes and management strategies in US Air Force F-16 mishaps 1984-present
p 492 N93-19673
- FABRICATION**
- A tooling trend at BCA - What and why
[SME PAPER EM92-111] p 202 A93-14114
- A new production technology for complex-shaped structural elements 'creep forming'
p 202 A93-14175
- The modeling of forging and precision-casting forming processes
p 207 A93-15030
- Experiences in fabrication of a waverider model for wind tunnel testing
[AIAA PAPER 93-0510] p 328 A93-23257
- Air cell --- model aircraft power supplies
[CA-PATENT-APPL-SN-2001346] p 83 N93-10368
- A domain-specific design architecture for composite material design and aircraft part redesign
p 442 N93-17522
- Add-on damping treatment for the F-15 upper-outer wing skin
[AD-A258470] p 337 N93-18248
- Advanced Turbine Technology Applications Project (ATTAP)
[NASA-CR-189228] p 455 N93-18762
- Improved ceramic slip casting technique --- application to aircraft model fabrication
[NASA-CASE-LAR-14471-1] p 536 N93-20041
- Fabrication of composite proplan blades for a cruise missile wind tunnel model
[NASA-TM-105270] p 752 N93-26202
- Research support for the Laboratory for Lightwave Technology
[AD-A261488] p 760 N93-26343
- A unified approach for composite cost reporting and prediction in the ACT program
p 920 N93-30441
- Advanced fiber placement of composite fuselage structures
p 923 N93-30864
- FABRICS**
- Experimental and analytical investigation of dynamic characteristics of extension-twist-coupled composite tubular spars
[NASA-TP-3225] p 553 N93-20585
- FABRY-PEROT INTERFEROMETERS**
- Optical temperature compensation schemes of spectral modulation sensors for aircraft engine control
p 1105 A93-49471
- FACE CENTERED CUBIC LATTICES**
- Markov fatigue in single crystal airfoils
[ASME PAPER 92-GT-95] p 387 A93-19341
- Designing new multi-phase intermetallic materials based on phase compatibility considerations
[ONERA, TP NO. 1992-131] p 772 A93-38605
- FACTORIZATION**
- Transonic profile design in curvilinear coordinates using an approximate factorization algorithm
p 7 A93-10778
- Methodology for sensitivity analysis, approximate analysis, and design optimization in CFD for multidisciplinary applications
[NASA-CR-192172] p 552 N93-20297
- FAIL-SAFE SYSTEMS**
- A structural reliability evaluation of fail-safe helicopter dynamic components
p 506 A93-27952
- FAILURE**
- US Army helicopter inertia reel locking failures
p 493 N93-19689
- Failure identification using multiple model adaptive estimation for the LAMBDA flight vehicle
[AD-A259137] p 527 N93-20596
- Multi-parameter optimization tool for low-cost commercial fuselage crown designs
p 922 N93-30858
- FAILURE ANALYSIS**
- An application of fuzzy logic and Dempster-Shafer theory to failure detection and identification
p 96 A93-13079
- Super Puma MK II - Rotor and gearbox fatigue
p 46 A93-13636
- Study on fracture failure of turbine blades in a series of turbojets
p 205 A93-14493
- Expert systems for maintenance engineering
p 434 A93-18762
- Knowledge based systems and avionics equipment failure diagnosis
p 238 A93-18765
- Nonlinear response of a clamped beam and plate to high levels of excitation
p 397 A93-19141
- A review of crack propagation under unsteady loading
p 399 A93-19207
- Differential GPS autonomous failure detection
p 314 A93-21152
- Finding fault with avionics
p 410 A93-21629
- Anti-icing failure detection instrumentation using realtime optical measurement of anti-icing fluid properties
[AIAA PAPER 93-0748] p 540 A93-24836
- An experimental and analytical investigation on the response of GR/EP composite I-beams
p 546 A93-27975
- An analytically designed subcomponent test to reproduce the failure of a composite wing box beam
[AIAA PAPER 93-1344] p 709 A93-33914
- Hammerhead aeroelastic stability revisited
[AIAA PAPER 93-1477] p 740 A93-34022
- A theoretical study on the ETHYLENE system - A fuzzy diagnostic expert system for large rotating machinery
p 846 A93-36327
- A practical course in aircraft maintenance. I - The powerplant --- Russian book
p 811 A93-39175
- Review of crack propagation under unsteady loading
p 837 A93-39416
- Computer-aided design of avionics diagnostics algorithms
p 941 A93-42863
- Lightweight aircraft turbine protection
[AIAA PAPER 93-1815] p 1110 A93-49703
- Turbine Engine Diagnostics (TED) system
[AIAA PAPER 93-1818] p 1110 A93-49706
- A new approach to robust fault detection and identification
p 1166 A93-50631
- Aircraft failure detection and identification using neural networks
[AIAA PAPER 93-3869] p 1171 A93-51455
- Fault detection, isolation, and reconfiguration for aircraft using neural networks
[AIAA PAPER 93-3870] p 1135 A93-51456
- Durability properties for adhesively bonded structural aerospace applications
p 1217 A93-53515
- Fault tolerant navigation for aircraft landing
p 1191 A93-53866
- Thermal barrier coating life prediction model development, phase 2
[NASA-CR-189111] p 198 N93-12589
- Reanalysis of multiple-wheel landing gear traffic tests
[AD-A256593] p 194 N93-14238
- Reliability of stiffened structural panels: Two examples
[NASA-TM-107687] p 219 N93-14483
- Sensor fault detection using nonlinear observer and polynomial classifier
p 170 N93-15182
- Neural network based condition monitoring
p 230 N93-15183
- Stress corrosion susceptibility of ultra-high strength steels for Naval aircraft applications
[AD-A256126] p 199 N93-15189
- Multiple model adaptive estimation applied to the VISTA F-16 with actuator and sensor failures, volume 2
[AD-A256569] p 371 N93-16165
- Preliminary analysis of the J-52 aircraft engine component improvement program
[AD-A257640] p 363 N93-17686
- Transient/structural analysis of a combustor under explosive loads
[NASA-TM-107660] p 420 N93-17779
- Application of a neural network as a potential aid in predicting NTF pump failure
[NASA-TM-107667] p 442 N93-18332
- A procedure for defining lightning risk to air vehicles
p 703 N93-24885
- External stress-corrosion cracking of a 1.22-m-diameter type 316 stainless steel air valve
[NASA-TP-3190] p 737 N93-26201
- Thermally induced stresses in a composite exposed to fire
[AD-A261714] p 737 N93-26371
- Structural tailoring of aircraft engine blade subject to ice impact constraints
[NASA-TM-106033] p 838 N93-26999
- Fault detection of helicopter gearboxes using the multi-valued influence matrix method
[NASA-TM-106100] p 838 N93-27069
- Estimating characteristic life and reliability of an aircraft engine component improvement in the early stages of the implementation process
[AD-A262118] p 815 N93-28184
- Evaluation of category 3 MLS designs
p 888 N93-30358
- Structural response of bead-stiffened thermoplastic shear webs
p 923 N93-30873
- An overview of the crash dynamics failure behavior of metal and composite aircraft structures
p 923 N93-30875
- FAILURE MODES**
- Common failure modes for composite aircraft structures due to secondary loads
p 207 A93-14812
- A study of the flexural properties of carbon-epoxy composites in certain environments
p 390 A93-21999
- Multiple model adaptive estimation applied to the VISTA F-16 flight control system with actuator and sensor failures
p 907 A93-42806
- A study of the effects of tolerances on rigging screws, turnbuckles, and associated components in BS4429: 1987
[NPL-DMM(A)-53] p 86 N93-11326
- Deformation mechanisms of NiAl cyclically deformed near the brittle-to-ductile transformation temperature
[NASA-CR-191649] p 391 N93-15830
- Aviation safety research at the National Institute for Aviation Research Wichita State University: A report to the FAA Technical Center
[NIAR-92-2] p 310 N93-16455
- Moderate interaction in stiffened composite shells under combined mechanical and thermal loadings
p 419 N93-16793
- Transient/structural analysis of a combustor under explosive loads
[NASA-TM-107660] p 420 N93-17779

Detection of spoofing, jamming, or failure of a Global Positioning System (GPS)
[AD-A259023] p 319 N93-18951

FAIRINGS

Close-up analysis of aircraft ice accretion
[AIAA PAPER 93-0029] p 309 A93-23239
Design optimization study for F-15 propulsion/forward fairing compatibility
[AIAA PAPER 93-3484] p 1003 A93-47291
Close-up analysis of aircraft ice accretion
[NASA-TM-105952] p 148 N93-15360
Aerodynamic analysis of hypersonic waverider aircraft
[NASA-CR-192981] p 780 N93-27093

FALSE ALARMS

Effective 406-MHz ELT demonstrates the potential to save more lives p 311 A93-18543
False alarm probability determination for the Honeywell Hexad Fault-Tolerant INS p 342 A93-21193
Detection performance of digital polarity sampled phase reversal code pulse compressors
[AD-A262930] p 842 N93-28289

FAN BLADES

A data processing and measuring system with a traversing probe for studying flow in the rotating impeller of an axial-flow fan p 75 A93-10032
Computer aided aerodynamic design of high pressure axial flow fan blade element p 16 A93-13649
Acoustic performance of low pressure axial fan rotors with different blade chord length and radial load distribution p 449 A93-19212
Coupled multi-disciplinary simulation of composite engine structures in propulsion environment
[ASME PAPER 92-GT-6] p 346 A93-19279
A study of stall in a low hub/tip ratio fan
[ASME PAPER 92-GT-85] p 248 A93-19334
Advanced Ducted Engines - Impact of unsteady aerodynamics on fan vibration properties
[ASME PAPER 92-GT-228] p 252 A93-19445
Flow studies in ducted twin-rotor contra-rotating axial flow fans p 258 A93-19545
Application of a dynamic compression system model to a low aspect ratio fan - Casing treatment and distortion
[AIAA PAPER 93-1871] p 1111 A93-49746
The 'Rolls-Royce' way of validating fan integrity
[AIAA PAPER 93-2602] p 1122 A93-50311
Effects of blade geometry and mode shape on fan flutter
[ISABE 93-7028] p 1196 A93-54004
Investigation of the flow field through a variable pitch fan rotor with an inlet total pressure distortion
[ISABE 93-7029] p 1184 A93-54005
Navier-Stokes computation of the three dimensional flow fields through a transonic fan blade
[ISABE 93-7030] p 1184 A93-54006
Performance improvement by forward-skewed blading of axial fan moving blades
[ISABE 93-7055] p 1185 A93-54031
A concept for a counterrotating fan with reduced tone noise
[NASA-TM-105736] p 101 N93-11370
Investigation of advanced counterrotation blade configuration concepts for high speed turboprop systems. Task 4: Advanced fan section aerodynamic analysis
[NASA-CR-187128] p 174 N93-12695
Static pressure measurements of the shock-boundary layer interaction in a simulated fan passage
[AD-A256724] p 361 N93-15979
Aerodynamic design and analysis of fans using 3D computational codes
[DS-2140] p 294 N93-17880
Model fan passage flow simulation
[AD-A261613] p 752 N93-26167
Blasim: A computational tool to assess ice impact damage on engine blades
[NASA-TM-106225] p 1031 N93-31193

FANS

Performance analysis of supersonic through-flow fan by the lifting surface theory. I - Disturbance flow field and determination of blade loadings p 267 A93-20929
Rotating stall inception in fans of low hub-tip ratio p 136 N93-14479

FAR FIELDS

An improved far field drag calculation method for nonlinear CFD codes
[AIAA PAPER 93-3417] p 975 A93-47213
Attenuation of airplane wake vortices by excitation of far-field instability
[AIAA PAPER 93-3511] p 984 A93-47277
Far field rotor noise
[AD-A260703] p 759 N93-25651
Unsteady airfoil flow solutions on moving zonal grids
[AD-A261925] p 701 N93-26198

FARM CROPS

Canonical correlation relationships among spectral and phytometric variables for twenty winter wheat fields p 433 A93-22992

FAST FOURIER TRANSFORMATIONS

Aero-optical phase measurements using Fourier transform holographic interferometry p 549 A93-29302

FAST NEUTRONS

PFNA technique for the detection of explosives p 497 N93-21865

FASTENERS

Getting it together p 78 A93-11682
Influence of modelling loading on stress distribution in turbomachinery blade fastening in case of FEM p 520 A93-27296
MOI - Magneto-optic/eddy current imaging p 927 A93-41751
A method for calculating the aerodynamic and mass characteristics of coaxial rotors with rigid blade fastening (the ABC system) p 1071 A93-49323
On design methods for bolted joints in composite aircraft structures p 1158 A93-50430

FATIGUE (MATERIALS)

Aeronautical fatigue: Key to safety and structural integrity; Proceedings of the 16th ICAF Symposium, Tokyo, Japan, May 22-24, 1991
[ISBN 4-9900181-1-7] p 80 A93-13626
Aircraft tracking optimization of parameters selection p 3 A93-13628
Maintaining the safety of an aging fleet of aircraft p 3 A93-13632
Fleet fatigue cracking threshold prediction p 3 A93-13633
A review of aging aircraft technology - An I.A.I. perspective p 3 A93-13634
Super Puma MK II - Rotor and gearbox fatigue p 46 A93-13636
Bulging of fatigue cracks in a pressurized aircraft fuselage p 81 A93-13639
Effects of prior fatigue damage on crack propagation rates in 2024-T351 aluminum alloy p 71 A93-13640
Fatigue qualification of high thickness composite rotor components p 81 A93-13646
Post buckling of laminated composite stiffened curved panels subjected to cyclic shear and compression p 204 A93-14334
Improving anti-fatigue optimum design through AI-search strategy p 208 A93-15342
Acquiring tail load spectra from in-flight measurements [AIAA PAPER 93-1607] p 711 A93-34137
Ensuring the reliability and service life of flight vehicle structures by engineering methods p 745 A93-35276
Ways of increasing the service life and reliability of bolted joints p 745 A93-35281
Effect of overloads on the service life of the structural elements of aircraft p 746 A93-35289
Evaluation of the fatigue behavior of discontinuous and continuous fiber thermoplastic composite laminates p 824 A93-36005
Damage tolerance assessment of the fighter aircraft 37 Vigen main wing attachment p 802 A93-37390
Monitoring load experience of individual aircraft p 1103 A93-52450
Aspects of fatigue affecting the design and maintenance of modern military aircraft p 1043 A93-52548
Mechanisms and modelling of environment-dependent fatigue crack growth in a nickel based superalloy [AD-A253967] p 71 N93-10717
Development of the neutron diffraction technique for the determination of near surface residual stresses in critical gas turbine components p 58 N93-11112
LARZAC HP turbine disk crack initiation and propagation spin pit test p 176 N93-14892
In-service considerations affecting component life p 177 N93-14898
Fatigue propagation behaviour of short cracks in titanium alloys p 392 N93-16637
Fatigue propagation behaviour of short cracks in aluminum alloys p 392 N93-16641
Review of aeronautical fatigue investigations in the Netherlands during the period March 1989 - March 1991 [NLR-TP-91092-U] p 331 N93-17535
Fatigue of turboengine discs p 364 N93-18149
Add-on damping treatment for the F-15 upper-outer wing skin p 337 N93-18248
Application of the cyclic J-integral to fatigue crack propagation p 839 N93-27182
Ultra-high temperature assessment study: Ceramic matrix composites p 826 N93-28592

Material characterization and fractographic examination of Ti-17 fatigue crack growth specimens for SMP SC33 p 1004 N93-31744
Fatigue crack growth results for Ti-6Al-4V, IMI 685, and Ti-17 p 1004 N93-31746

FATIGUE LIFE

On the fatigue life of M50 NiL rolling bearings p 78 A93-11346
Rotorcraft reliability and maintainability - A CAA view of future trends p 45 A93-13407
Damage severity of monitored fatigue load spectra p 154 A93-14253
The method for developing F-by-F load spectra of fighter aircraft based on manoeuvres p 154 A93-14254
Aircraft fatigue failures and tasks of structural reliability analysis p 210 A93-16246
Accelerated corrosion fatigue test methods for aging aircraft p 198 A93-16623
Refinement of algorithms for calculating the remaining life from magnetic recording instrument data - for IL-86 aircraft wing p 320 A93-18330
Justification for the linear recording of fatigue damage summation for aircraft structures under operating conditions p 320 A93-18331
Characteristics of fatigue crack growth under the service-spectrum loading of the tail boom of a helicopter p 321 A93-18339
The prediction of nonlinear dynamic loads on helicopters from flight variables using artificial neural networks p 322 A93-19231
Extending the fatigue life of aircraft engine components by hole cold expansion technology p 401 A93-19327
[ASME PAPER 92-GT-77] A method and a software for constructing F-by-F random load spectrum p 506 A93-27375
Estimation of the life of aircraft structures under stochastic steady state loading p 545 A93-27620
Composite 'Exoskin' doubler extends F-15 Vertical Tail fatigue life p 709 A93-33911
[AIAA PAPER 93-1341] Effect of a combination of design and process-related factors on the fatigue strength of bolted joints in acoustically loaded aircraft structures p 745 A93-35278
A method for estimating the survivability of bodies of revolution p 745 A93-35287
Enhancing the performance of aircraft engine blades by surface hardening p 811 A93-39072
Effect of ion treatments on the fatigue strength of blades p 811 A93-39073
Life analysis of a gas turbine fan disc p 897 A93-40803
Crack simulation and life assessment of gas turbine nozzles p 915 A93-40805
Life prediction - Thermal fatigue from isothermal data p 916 A93-40807
Dependence of the service life of a wing on its strength uniformity and landing gear location p 891 A93-42377
Recent advances of time domain approach for nonlinear response and sonic fatigue p 1022 A93-45106
How likely is multiple site damage? p 1027 A93-45791
Repairs to damage tolerant aircraft p 948 A93-45799
Problems of the strength and fatigue of the elements of aircraft structures p 1029 A93-47076
Design for cyclic loading endurance of composites p 1216 A93-53395
Clean melting and the removal of defects from aero-engine materials p 1217 A93-53503
Thermal fatigue life assessment of a convection-cooled gas turbine blade p 1199 A93-54038
[ISABE 93-7062] Rotor fatigue monitoring data acquisition system p 1261 A93-54353
The crack initiation approach for durability analysis p 1259 A93-55585
Human engineering issues for data link systems p 1260 A93-55874
Fatigue life under random load history derived from exceedance curves using different algorithms p 1260 A93-56544
An evaluation of a method of reconstituting fatigue loading from Rainflow counting [RAE-TR-89057] p 82 N93-10198
A finite element method for nonlinear panel flutter p 84 N93-10472
Verification of rain-flow reconstructions of a variable amplitude load history [NASA-CR-189670] p 91 N93-12411
Structural fatigue aspects of the P-3 Orion [ARL-STRUC-TM-558] p 161 N93-13256
Engine life assessment test case TF41 LP compressor shaft torsional fatigue p 177 N93-14896

- Review of aeronautical fatigue investigation activities developed in Alenia-GAT during the period May 1990 - March 1991 [ETN-92-92884] p 329 N93-16287
- Federal Aviation Administration pavement modeling p 379 N93-16315
- Statistical fatigue analysis of the SH-60B servo beam rail component [AD-A257474] p 332 N93-17660
- Fatigue of turboengine discs [DS-2136] p 364 N93-18149
- Study of statistical variations of load spectra and material properties on aircraft fatigue life [AD-A257961] p 339 N93-18451
- Creep fatigue life prediction for engine hot section materials (isotropic) [NASA-CR-189221] p 364 N93-18578
- Assessment of helicopter component statistical reliability computations [AD-A258931] p 510 N93-19447
- Load experience variability of fighter aircraft [NLR-TP-89172-U] p 514 N93-20742
- Stress calculation for the Sandia 34-meter wind turbine using the local circulation method and turbulent wind [DE93-004480] p 560 N93-22045
- An overview of elevated temperature damage mechanisms and fatigue behavior of a unidirectional SCS-6/Ti-15-3 composite [NASA-TM-106131] p 825 N93-26702
- Damage severity of monitored fatigue load spectra [NLR-TP-92009-U] p 999 N93-32205
- Low cycle fatigue behaviour of titanium disc alloys [NLR-TP-91346-U] p 1006 N93-32372
- FATIGUE TESTS**
- Stochastic computational mechanics for aerospace structures p 78 A93-12157
- Microstructural study of aluminide surface coatings on single crystal nickel base superalloy substrates p 70 A93-12771
- The role of fatigue testing in the design, development and certification of the ATR 42/72 p 46 A93-13637
- The method for developing F-by-F load spectra of fighter aircraft based on manoeuvres p 154 A93-14254
- Researches on sonic fatigue of the air-inlet duct of XX aircraft p 154 A93-14256
- In-flight tailload measurements p 155 A93-14285
- Toulouse - Flight tests of the Airbus A340 p 159 A93-16859
- Selection of the time scale for preventive measures under service conditions p 237 A93-18375
- Crack growth and repair of multi-site damage of fuselage lap joints p 547 A93-28291
- Application of generalized force determination to a full scale low cycle fatigue test of the SH-2G helicopter p 795 A93-35949
- Aspects of aging aircraft - A transatlantic view p 1026 A93-45776
- NASA airframe structural integrity program p 1026 A93-45782
- Evaluation methodologies applied for pressurized fuselages of Airbus A/C p 948 A93-45796
- Case study and simulation of fatigue damages and DTE of aging aircraft - A review of researches in Japan p 948 A93-45800
- Brush seal low surface speed hard-rub characteristics [AIAA PAPER 93-2534] p 1156 A93-50261
- Carbon composite repairs of helicopter metallic primary structures p 1101 A93-50429
- The application of diffusion bonding in the manufacture of aeroengine components p 1217 A93-53514
- Rotor fatigue monitoring data acquisition system p 1261 A93-54353
- Short fatigue crack growth in a nickel-base superalloy at room and elevated temperature [PNR-90892] p 72 N93-11031
- Measured data for the Sandia 34-meter vertical axis wind turbine [DE92-019807] p 94 N93-12075
- Fatigue crack growth in AerMet 100 steel [AD-A249068] p 74 N93-12248
- Review of aeronautical fatigue investigation activities developed in Alenia-GAT during the period May 1990 - March 1991 [ETN-92-92884] p 329 N93-16287
- Review of aeronautical fatigue investigations in the Netherlands during the period March 1989 - March 1991 [NLR-TP-91092-U] p 331 N93-17535
- Damage tolerance behaviour of aluminium-lithium sheet alloys [NLR-TP-91244-U] p 392 N93-17540
- Flight simulation and constant amplitude fatigue crack growth in aluminium-lithium sheet and plate [NLR-TP-91104-U] p 331 N93-17562
- Creep fatigue life prediction for engine hot section materials (isotropic) [NASA-CR-189221] p 364 N93-18578
- An improved method of structural dynamic test design for ground flying and its application to the SH-2F and SH-2G helicopters p 512 N93-19928
- Damage tolerance of a helicopter rotor high-strength steel p 555 N93-21322
- GARTEUR damage mechanics for composite materials: Analytical/experimental research on delaminations p 537 N93-21513
- General aviation aircraft: Normal acceleration data analysis and collection project [DOT/FAA/CT-91/20] p 713 N93-24739
- Brush seal low surface speed hard-rub characteristics [NASA-TM-106169] p 838 N93-27132
- AGARD Engine Disc Cooperative Test Programme [AGARD-R-766-ADD] p 1004 N93-31741
- Fractographic and microstructural analysis of fatigue crack growth in Ti-6Al-4V fan disc forgings p 1004 N93-31742
- Low cycle fatigue behaviour of titanium disc alloys p 1004 N93-31745
- Efficient fault diagnosis of helicopter gearboxes [NASA-TM-106253] p 1032 N93-31846
- FAULT DETECTION**
- Robust fault detection of jet engine sensor systems using eigenstructure assignment p 173 A93-14608
- The use of non-destructive testing to detect and monitor aircraft corrosion in service p 1258 A93-54896
- Enhancement of conventional NDT methods for corrosion detection in layered skins p 1258 A93-54898
- Sensor fault detection using nonlinear observer and polynomial classifier p 170 N93-15182
- Conditioned based machinery maintenance (helicopter fault detection) [AD-A255796] p 329 N93-16396
- Fault detection of helicopter gearboxes using the multi-valued influence matrix method [NASA-TM-106100] p 838 N93-27069
- FAULT TOLERANCE**
- A fault-tolerant air data/inertial reference system p 50 A93-10982
- False alarm probability determination for the Honeywell Hexad Fault-Tolerant INS p 342 A93-21193
- Finding fault with avionics p 410 A93-21629
- Advanced airborne 3D computer image generation systems technologies for the year 2000 p 518 A93-28176
- A fault-tolerant Air Data/Inertial Reference Unit p 807 A93-37074
- Formal verification of algorithms for critical systems p 846 A93-37623
- A performance assessment of a byzantine resilient fault-tolerant computer [AIAA PAPER 89-3064] p 938 A93-41296
- Cross channel dependency requirements of the multi-path redundant avionics suite p 928 A93-42782
- Expert system for redundancy and reconfiguration management p 938 A93-42785
- Computer-aided design of avionics diagnostics algorithms p 941 A93-42863
- Risk analysis for aging aircraft fleets p 1025 A93-45775
- The civil Damage Tolerance Requirements in theory and practice p 1026 A93-45777
- A damage tolerance approach for management of aging gas turbine engines p 1001 A93-45779
- Evaluation methodologies applied for pressurized fuselages of Airbus A/C p 948 A93-45796
- Repairs to damage tolerant aircraft p 948 A93-45799
- A new approach to robust fault detection and identification p 1166 A93-50631
- Fault detection, isolation, and reconfiguration for aircraft using neural networks [AIAA PAPER 93-3870] p 1135 A93-51456
- Characterization of the faulted behavior of digital computers and fault tolerant systems p 1224 A93-52762
- Fault tolerant navigation for aircraft landing p 1191 A93-53866
- Intelligent diagnostics systems p 98 N93-11931
- A monitor for the laboratory evaluation of control integrity in digital control systems operating in harsh electromagnetic environments [NASA-TM-4402] p 65 N93-12304
- Analysis of fault-tolerant neurocontrol architectures [NASA-TM-105898] p 65 N93-12305
- Formal design specification of a Processor Interface Unit [NASA-CR-189698] p 99 N93-12538
- A brief overview of NASA Langley's research program in formal methods p 228 N93-12958
- Summary: Experimental validation of real-time fault-tolerant systems [NASA-CR-190985] p 175 N93-13697
- Conditioned based machinery maintenance (helicopter fault detection) [AD-A255796] p 329 N93-16396
- Spurious symptom reduction in fault monitoring [NASA-CR-191453] p 942 N93-29192
- Development and flight testing of a fault-tolerant fly-by-light yaw control system p 1010 N93-31280
- FEASIBILITY**
- A feasibility study of using Langley 0.3-m transonic cryogenic tunnel sidewall boundary-layer removal system for heavy gas testing [NASA-CR-191438] p 747 N93-25087
- FEASIBILITY ANALYSIS**
- Accuracy analysis on image matching guidance systems p 62 A93-12653
- Photoluminescent thermography - Feasibility study with pointwise measurements p 211 A93-16861
- Vision-based range estimation using helicopter flight data p 151 A93-17501
- The design of test-section inserts for higher speed aerodynamic testing in the Ames 80- by 120-Foot Wind Tunnel p 374 A93-19149
- Vision-based range estimation using helicopter flight data p 317 A93-21525
- ASTOVL model engine simulators for wind tunnel research p 192 N93-13213
- Application of a flush airdata sensing system to a wing leading edge (LE-FADS) [NASA-TM-104267] p 518 N93-20163
- FEATHERING**
- Numerical study of advanced rotor blades p 23 N93-11899
- FEDERAL BUDGETS**
- National Aeronautics and Space Administration Authorization Act, fiscal year 1993 [S-REPT-102-364] p 234 N93-13798
- NASA authorization, 1993, volume 2 [GPO-56-943-VOL-2] p 234 N93-13799
- NASA's fiscal year 1993 budget [S-HRG-102-707] p 234 N93-13800
- National Aeronautics and Space Administration p 454 N93-17091
- FEEDBACK CONTROL**
- Nonlinear feedback control of highly manoeuvrable aircraft p 40 A93-11654
- Output feedback control for output tracking of nonlinear uncertain systems p 96 A93-13177
- Robust control of an aeroelastic system modeled by a singular integro-differential equation p 97 A93-13197
- Integrated aerodynamics and control system design for tailless aircraft [AIAA PAPER 92-4604] p 42 A93-13284
- Design of a full time wing leveler system using tab driven aileron controls [AIAA PAPER 92-4193] p 63 A93-13345
- Analysis and feedback control of aircraft flight in wind shear p 183 A93-14349
- Optimal lateral maneuvering for microburst encounters during final approach p 183 A93-14350
- Analysis of airframe and engine control interactions and integrated flight/p propulsion control p 185 A93-14596
- Synthesis of robust motion stabilization laws for flight vehicles p 227 A93-16777
- Improving dynamic response of a single-spool gas turbine engine using a nonlinear controller [ASME PAPER 92-GT-392] p 355 A93-19546
- Development of an optical sensor for active control of a gas turbine combustor [AIAA PAPER 93-0118] p 360 A93-22568
- Extended linear quadratic Gaussian control under randomly varying distributed delays p 439 A93-22854
- Discrete-time LTR synthesis of delayed control systems p 439 A93-22855
- A new flight control design scheme using optimal dynamic output feedback p 368 A93-22883
- Dynamical variable structure control of a helicopter in vertical flight p 369 A93-22887
- Design of flight control systems to meet rotorcraft handling qualities specifications p 370 A93-23509
- Application of feedback linearization method in a digital restructurable flight control system p 370 A93-23514
- Design of insensitive multirate aircraft control using optimized eigenstructure assignment p 370 A93-23515
- Approximation methods for control of structural acoustics models with piezoceramic actuators p 452 A93-23744
- On closed-loop identification of a certain aeroengine under flight conditions p 519 A93-24026
- Control synthesis with incomplete, complete, and supercomplete measurements p 561 A93-27603
- Generalized guidance law for collision courses p 727 A93-34533
- Optimal discrete-time dynamic output-feedback design - A w-domain approach p 757 A93-34536

- Robustness evaluation of a flexible aircraft control system p 727 A93-34540
- A closed loop controller for BVI impulsive noise reduction by Higher Harmonic Control p 849 A93-35963
- Use of PCs in controlling simulated altitude environmental test conditions in support of turbine engine testing p 846 A93-37856
- Design philosophy for wind tunnel model positioning control systems p 822 A93-37877
- Output feedback eigenstructure assignment using two Sylvester equations p 847 A93-38214
- Robust sampled data eigenstructure assignment using the delta operator --- in relation to autopilot design p 906 A93-41889
- Quantitative feedback theory applied to the design of a rotorcraft flight control system p 906 A93-41895
- Linear quadratic Gaussian/loop transfer recovery design for a helicopter in low-speed flight p 906 A93-41896
- Applying variations of the quantitative feedback technique (QFT) to unstable, non-minimum phase aircraft dynamics models p 939 A93-42797
- Dynamic compensator design in nonlinear aerospace systems p 1036 A93-44150
- Active boundary-layer control in diffusers [AIAA PAPER 93-3255] p 966 A93-46798
- Pilots' control behavior including feedback structures identified by an improved method [AIAA PAPER 93-3669] p 1129 A93-48347
- Optical sensors and multiplexing for aircraft engine control p 1105 A93-49474
- Automatic carrier landing system utilizing aircraft sensors p 1097 A93-49590
- Trajectory control for a low-lift re-entry vehicle p 1141 A93-49592
- Full envelope multivariable control law synthesis for a high-performance test aircraft p 1130 A93-49595
- Reduced order proportional integral observer with application p 1166 A93-49605
- An approach to the stall monitoring in a single stage axial compressor [AIAA PAPER 93-1872] p 1112 A93-49747
- Synthesis of the optimal control of flight vehicle braking with allowance for the discrete nature of control action generation p 1169 A93-51063
- Coupling characteristics analysis of elastic vehicle --- design of modern flight control systems p 1169 A93-51189
- Control augmentation system (CAS) synthesis via adaptation and learning [AIAA PAPER 93-3728] p 1170 A93-51328
- Nonlinear command augmentation system for a high performance aircraft [AIAA PAPER 93-3777] p 1132 A93-51372
- Self-tuning guidance applied to aeroassisted plane change problems [AIAA PAPER 93-3791] p 1143 A93-51386
- A pseudo-loop design strategy for the longitudinal control of hypersonic aircraft [AIAA PAPER 93-3814] p 1132 A93-51405
- Active control for fin buffet alleviation [AIAA PAPER 93-3817] p 1133 A93-51408
- A new way of pole placement in LQR and its application to flight control [AIAA PAPER 93-3845] p 1133 A93-51433
- H(infinity) helicopter flight control law design with and without rotor state feedback [AIAA PAPER 93-3849] p 1134 A93-51436
- A new technique for nonlinear control of aircraft [AIAA PAPER 93-3881] p 1135 A93-51466
- A parameter optimization approach to controller partitioning for integrated flight/propulsion control application p 1206 A93-54268
- Longitudinal closed-loop pilot/vehicle analysis of DFBW aircraft during approach and landing p 1206 A93-54277
- Boeing 777 high lift control system p 1249 A93-55753
- Inverse simulation: A tool for the validation of simulation programs - First results --- for helicopter flight tests and control p 1249 A93-56046
- Design, test, and evaluation of three active flutter suppression controllers [NASA-TM-4338] p 63 N93-10070
- Optimal output feedback vibration control of rotor-bearing systems p 86 N93-11220
- Embedded training capabilities for the LAMPS MK 3 system [AD-A250697] p 49 N93-11838
- Computational nonlinear control [AD-A253547] p 98 N93-12258
- On stability and control of SSTD spaceplane in super- and hypersonic ascending phase [NAL-TR-1128T] p 65 N93-12361
- Air-breathing hypersonic vehicle guidance and control studies: An integrated trajectory/control analysis methodology, phase 2 [NASA-CR-189703] p 65 N93-12413
- Design philosophy for wind tunnel model positioning systems [AD-A254958] p 192 N93-12552
- A stochastic optimal feedforward and feedback control methodology for superagility [NASA-CR-4471] p 229 N93-13370
- Ideal aircraft handling quality models: Longitudinal axis [NAL-PD-FC-9203] p 187 N93-13566
- Performance and control of ascending trajectories to minimize heat load for transatmospheric aero-space planes p 133 N93-13745
- Symposium proceedings on Quantitative Feedback Theory [AD-A255527] p 187 N93-13872
- Robust controller and estimator design using minimax methods p 229 N93-13925
- Robust nonlinear feedback guidance for an aerospace plane: A geometric approach p 189 N93-14835
- Propulsion system performance resulting from an integrated flight/propulsion control design [NASA-TM-105874] p 180 N93-15525
- Modeling and control study of the NASA 0.3-meter transonic cryogenic tunnel for use with sulfur hexafluoride medium [NASA-CR-189737] p 418 N93-16379
- Design of robust suboptimal controllers for a generalized quadratic criterion [AD-A257746] p 372 N93-17670
- Low bandwidth robust controllers for flight [NASA-CR-191774] p 372 N93-17800
- Theoretical constraints in the design of multivariable control systems [NASA-CR-191900] p 442 N93-18372
- Longitudinal-control design approach for high-angle-of-attack aircraft [NASA-TP-3302] p 373 N93-19108
- Helicopter flight control system design using the linear quadratic regulator for robust eigenstructure assignment [AD-A258904] p 373 N93-19351
- An exploratory investigation of the flight dynamics effects of rotor rpm variations and rotor state feedback in hover [NASA-TM-103968] p 373 N93-19380
- Controller partitioning for integrated flight/propulsion control implementation [NASA-TM-105804] p 527 N93-21197
- Control of nonlinear systems under input constraints with applications to flight control p 729 N93-25353
- Game theoretic synthesis for robust aerospace controllers p 819 N93-27171
- Practical input optimization for aircraft parameter estimation experiments [NASA-CR-191462] p 820 N93-27264
- The design of a robust autopilot for the Archytas prototype via linear quadratic synthesis [AD-A262151] p 820 N93-27546
- Robust control of intelligent rotor [AD-A263707] p 909 N93-29985
- Turbulent drag reduction: Studies of feedback control and flow over riblets p 878 N93-30645
- FEEDFORWARD CONTROL**
- A minimum-time acceleration control strategy for a two-rotor aeroengine p 172 A93-14499
- Identification of the open loop dynamics of the T700 turboshaft engine p 809 A93-35934
- Stiffness enhancement of flight control actuator p 1006 A93-44151
- A stochastic optimal feedforward and feedback control methodology for superagility [NASA-CR-4471] p 229 N93-13370
- A contribution to the dynamic feedforward open loop control of multivariable systems and to the optimal design of command functions [DLR-FB-92-05] p 441 N93-16515
- Identification and control of non-linear time-varying dynamical systems using artificial neural networks [AD-A257595] p 372 N93-18193
- Ferroelectricity**
- Considerations for space and naval aviation applications of ferroelectric memory [AD-A261300] p 759 N93-26294
- Ferrography**
- Ferrographic analysis of polyphenyl ether fluids p 735 A93-34561
- FERRY SPACECRAFT**
- The Hermes Carrier Aircraft (HCA) p 195 A93-14347
- FIBER COMPOSITES**
- Multidisciplinary design of composite aircraft structures by Lagrange p 76 A93-10273
- The effects of crushing surface roughness on the crushing characteristics of composite tubes p 77 A93-10918
- Fourier analysis of clamped moderately thick arbitrarily laminated plates p 206 A93-14571
- Correlation of X-ray CT measurements to shear strength in pultruded composite materials p 396 A93-18618
- Structural analysis of a nonlinear problem of aeroelasticity for CFC structures p 397 A93-18989
- Ceramic matrix composites for rocket engine turbine applications [ASME PAPER 92-GT-394] p 388 A93-19547
- Structural tailoring of aircraft engine blade subject to ice impact constraints [AIAA PAPER 92-4710] p 358 A93-20319
- Development of highly loaded root end attachments for composite material high speed flying surfaces p 539 A93-24122
- High-temperature materials warm up for debut p 535 A93-28393
- Quantification of uncertainties in composites [AIAA PAPER 93-1440] p 734 A93-33989
- Stiffness, thermal expansion, and thermal bending formulation of stiffened, fiber-reinforced composite panels [AIAA PAPER 93-1569] p 741 A93-34102
- Evaluation of the fatigue behavior of discontinuous and continuous fiber thermoplastic composite laminates p 824 A93-36005
- Fiber reinforced structures for turbine engine fragment containment [AIAA PAPER 93-1816] p 1110 A93-49704
- Evaluation of decomposition kinetic coefficients for a fiber-reinforced intumescent-epoxy [AIAA PAPER 93-1856] p 1144 A93-49734
- A two-dimensional analysis of multiple matrix cracking in a laminated composite close to its characteristic damage state p 1157 A93-50405
- Preparation and characterization of continuous fiber reinforced zirconium diboride matrix composites for a leading edge material p 1211 A93-53445
- Origin of the carbon rich sliding interface in alkali containing matrix-SiC nicalon fibre composites [ONERA, TP NO. 1993-77] p 1212 A93-53598
- Materials: Toward the non-metallic engine [PNR-90915] p 56 N93-11019
- Aero engine ceramics: The vision, the reality, and the progress [PNR-90983] p 72 N93-11066
- Proceedings of the USAF Structural Integrity Program [AD-A255379] p 110 N93-14549
- Polymer infiltration studies [NASA-CR-191652] p 200 N93-15431
- The Airbus floor beam: Towards a cost-effective composite design and manufacture research project sponsored by Airbus industry [LR-677] p 329 N93-16283
- NASA advanced design program: Analysis, design, and construction of a solar powered aircraft [NASA-CR-192040] p 332 N93-17802
- Compatibility of potential reinforcing ceramics with Ni and Fe aluminides [NASA-CR-192232] p 394 N93-18784
- Mass loaded composite rotor for vibro-acoustic application [AD-D015604] p 535 N93-20016
- Numerical modelling of induced effects of lightning strike on an all composite helicopter p 703 N93-24879
- A computational approach to predicting the extent of arc root damage in CFC panels p 735 N93-24890
- Comparison of the damage for various types of fibre reinforced composites due to different lightning test standards (MIL-STD-1757A, German military VG-standard 96903) p 736 N93-24891
- Zoning of aircraft by electric field modelling p 704 N93-24894
- Structural tailoring of aircraft engine blade subject to ice impact constraints [NASA-TM-106033] p 838 N93-26999
- Characterization of ceramic composite materials for gas turbine applications [DE93-009719] p 905 N93-30168
- First NASA Advanced Composites Technology Conference, part 2 [NASA-CP-3104-PT-2] p 921 N93-30841
- Advanced fiber placement of composite fuselage structures p 923 N93-30864
- FIBER OPTICS**
- Fiber optic-based laser vapor screen flow visualization systems for aerodynamic research in larger-scale subsonic and transonic wind tunnels p 408 A93-20298
- Embedded fiber optic sensors in large structures p 410 A93-21085
- Application issues of fiber optic sensors in aircraft structures p 410 A93-21094
- Fiber-optic interferometric sensors for measurements of pressure fluctuations - Experimental evaluation [AIAA PAPER 93-0738] p 540 A93-24828

- Embedded Bragg grating fiber optic sensor for composite flexbeams p 828 A93-37350
- Repair and maintenance of fiber optic data links on Navy aircraft p 1172 A93-48538
- Sources and detectors for fiber communications; Proceedings of the Meeting, Boston, MA, Sept. 8, 9, 1992 p 1151 A93-49455
- [SPIE-1788] p 1151 A93-49455
- Specialty fiber optic systems for mobile platforms and plastic optical fibers; Proceedings of the Meeting, Boston, MA, Sept. 9-11, 1992 p 1105 A93-49462
- [SPIE-1799] p 1105 A93-49462
- Fiber optic position sensors --- in aircraft flight control systems p 1105 A93-49465
- Ladar fiber optic sensor system for aircraft applications p 1105 A93-49467
- Compact high reliability fiber coupled laser diodes for avionics and related applications p 1152 A93-49470
- Optical temperature compensation schemes of spectral modulation sensors for aircraft engine control p 1105 A93-49471
- Implementation of fiber optic technology in flight controls p 1105 A93-49473
- Optical sensors and multiplexing for aircraft engine control p 1105 A93-49474
- Optical actuators for fly-by-light applications p 1172 A93-49475
- Flight testing of a fiber optic temperature sensor p 1105 A93-49476
- New concepts for fiber optic position sensors p 1106 A93-49477
- Fiber optics for aircraft entertainment systems p 1172 A93-49478
- An internetworking router for avionics applications --- Bridge/Router unit in fiber optics aircraft communication p 1097 A93-49479
- An introduction to the onboard LAN (OLAN) p 1166 A93-49480
- Fiber-optic technology for transport aircraft p 1173 A93-50488
- The LN-200 fiber gyro based tactical grade IMU [AIAA PAPER 93-3798] p 1106 A93-51391
- Dynamic attitude measurement system [AIAA PAPER 93-3801] p 1139 A93-51393
- Sensors with centroid based common sensing scheme and their multiplexing --- fiber optic sensors in aircraft and aircraft engine applications p 1192 A93-52994
- Multiplexing electro-optic architectures for advanced aircraft integrated flight control systems [NASA-CR-182268] p 187 N93-13735
- Electro-optic architecture for servicing sensors and actuators in advanced aircraft propulsion systems [NASA-CR-182269] p 232 N93-13762
- Electro-optic architecture (EOA) for sensors and actuators in aircraft propulsion systems [NASA-CR-182270] p 233 N93-15116
- Smart materials p 536 N93-20624
- Research support for the Laboratory for Lightwave Technology [AD-A261488] p 760 N93-26343
- Status of the Fiber Optic Control System Integration (FOCSI) program [NASA-TM-106151] p 841 N93-28053
- Development and flight testing of a fault-tolerant fly-by-light yaw control system p 1010 N93-31280
- FIBER ORIENTATION**
- Inelasticity effect in a unidirectional boron/aluminum composite under uniaxial tension p 825 A93-39024
- FIBER STRENGTH**
- The Airbus floor beam: Towards a cost-effective composite design and manufacture research project sponsored by Airbus industry [LR-677] p 329 N93-16283
- FIBER VOLUME FRACTION**
- Low leakage fiber metal seals [ASME PAPER 92-GT-141] p 402 A93-19373
- FIELD EFFECT TRANSISTORS**
- Surface emitting lasers for avionics applications p 1259 A93-55756
- High temperature rectifiers and MOS devices in 6H-silicon carbide [AD-A254725] p 90 N93-12340
- FIELD OF VIEW**
- Optical design of a wide-angle simulator probe p 211 A93-17140
- Design of an optimal single reflective holographic helmet display element p 517 A93-26886
- Investigation of the radiance from the leading edge of a wing [AIAA PAPER 93-2728] p 1039 A93-46482
- FIELD THEORY (PHYSICS)**
- CRAASH - A coordinated collision avoidance system [ONERA, TP NO. 1993-84] p 1191 A93-53604
- FIGHTER AIRCRAFT**
- Getting it together p 78 A93-11682
- Aircraft model for multicriterial analysis in decision making [AIAA PAPER 92-4192] p 44 A93-13370
- The method for developing F-by-F load spectra of fighter aircraft based on maneuvers p 154 A93-14254
- Stability considerations for enhanced manoeuvrability - An overview p 184 A93-14397
- The influence of fighter agility on air combat effectiveness p 184 A93-14398
- Comparison of algebraic turbulence models for afterbody flows with jet exhaust p 123 A93-14554
- Design of reduced-order observers with precise loop transfer recovery p 184 A93-14587
- Prediction of engine casing temperature of fighter aircraft for infrared signature studies [SAE PAPER 920961] p 206 A93-14627
- Zvezda - The Russian pioneer in the field of life-support and escape systems for aeronautics and space p 195 A93-16878
- Thrust vectoring - Theory, laboratory, and flight tests p 367 A93-21657
- Numerical simulation of dynamic lift enhancement using oscillatory leading edge flaps [AIAA PAPER 93-0186] p 276 A93-22611
- Application of structured singular value synthesis to a fighter aircraft p 368 A93-22865
- Dynamic stall on a three-dimensional rectangular wing [AIAA PAPER 93-0637] p 463 A93-24753
- Mathematical phenomenology for thrust-vectoring-induced agility comparisons p 525 A93-28613
- Computational study of advanced exhaust system transition ducts with experimental validation p 689 A93-34490
- Damage tolerance assessment of the fighter aircraft 37 Vigen main wing attachment p 802 A93-37390
- Output feedback eigenstructure assignment using two Sylvester equations p 847 A93-38214
- F/A-18 controls released departure recovery - Flight test evaluation p 803 A93-38839
- Analytical development of an equivalent system mismatch function --- for longitudinal axis of fighter aircraft in nonterminal flight phase p 906 A93-41890
- Workshop on hypersonic flows for reentry problems January 22-25th 1990 (Antibes) - Inaugural address p 856 A93-42577
- ARPA starts push for joint-service ASTOVL p 856 A93-43625
- Effect of canard oscillations on the vortical flowfield of a X-31A-like fighter model in dynamic motion [AIAA PAPER 93-3427] p 1008 A93-47222
- Attenuation of airplane wake vortices by excitation of far-field instability [AIAA PAPER 93-3511] p 984 A93-47277
- A qualitative assessment of control effectors on an advanced fighter configuration [AIAA PAPER 93-3627] p 1127 A93-48312
- Effect of rotary atmospheric gusts on fighter airplane [AIAA PAPER 93-3644] p 1127 A93-48328
- Screening studies of advanced control concepts for airbreathing engines [AIAA PAPER 92-3320] p 1108 A93-49329
- Investigation of high-alpha lateral-directional control power requirements for high-performance aircraft [AIAA PAPER 93-3647] p 1130 A93-49519
- Application of structured singular value synthesis to a fighter aircraft p 1130 A93-49594
- Full envelope multivariable control law synthesis for a high-performance test aircraft p 1130 A93-49595
- Wind tunnel results for an advanced fighter configuration employing transverse thrust for enhanced STOL capability [AIAA PAPER 93-1933] p 1100 A93-49796
- Quasi-optimal steady state and transient maneuvers with and without thrust vectoring [AIAA PAPER 93-3778] p 1132 A93-51373
- Design of a controller for a high performance fighter aircraft using Robust Inverse Dynamics Estimation (RIDE) [AIAA PAPER 93-3779] p 1132 A93-51374
- Monitoring load experience of individual aircraft p 1103 A93-52450
- Low aspect ratio wing code validation experiment p 1176 A93-53202
- A parameter optimization approach to controller partitioning for integrated flight/propulsion control application p 1206 A93-54268
- Vectoring jet effects on the flow and aerodynamic behaviors of fighter model p 1241 A93-54590
- Fighting for air p 1243 A93-54650
- Vectoring thrust and two-dimensional nozzle p 1247 A93-54863
- Bear facts --- Soviet Tu-95 aircraft p 1229 A93-55175
- Overview of high performance aircraft propulsion research [NASA-TM-105839] p 59 N93-11530
- Application of eigenstructure assignment to the control of powered lift combat aircraft p 64 N93-11871
- Specification of adaptive aiding systems [AD-A254537] p 159 N93-12602
- The PEP Symposium on CFD Techniques for Propulsion Applications p 214 N93-13210
- Some aspects of intake design, performance and integration with the airframe p 161 N93-13219
- CFD calibration for three-dimensional nozzle/afterbody configurations p 215 N93-13226
- Propulsion integration results of the STOL and Maneuver Technology Demonstrator p 161 N93-13228
- Ideal aircraft handling quality models: Longitudinal axis [NAL-PD-FC-9203] p 187 N93-13566
- Electro-optic architecture for servicing sensors and actuators in advanced aircraft propulsion systems [NASA-CR-182269] p 232 N93-13762
- Pressure distribution for the wing of the YAV-8B airplane; with and without pylons [NASA-TM-4429] p 136 N93-14451
- Standardization of precipitation static test methods and equipment for the Navy [AD-A257025] p 165 N93-15361
- F/A-18 controls released departure recovery flight test evaluation [AD-A256522] p 189 N93-15396
- Design of robust suboptimal controllers for a generalized quadratic criterion [AD-A257746] p 372 N93-17670
- Air accidents in the French Air Force p 492 N93-19676
- Combat and training aircraft class A mishaps in the Belgian Air Force 1970-1990 p 492 N93-19677
- YF-22A prototype advanced tactical fighter demonstration/validation flight test program overview p 511 N93-19906
- In-flight structural mode excitation system for flutter testing p 526 N93-19915
- Testing of an automatic, low altitude, all terrain ground collision avoidance system p 502 N93-19924
- Application of the Euler method EULFLEX to a fighter-type airplane configuration at transonic speed [MBB-FE-211-S-PUB-0489-A] p 484 N93-21059
- Allowable compression strength for CFRP-components of fighter aircraft determined by CAI-test [MBB-FE-221-S-PUB-0483] p 537 N93-21462
- Allowable compression strength for CFRP-components of fighter aircraft determined by CAI-test p 537 N93-21531
- Screening studies of advanced control concepts for airbreathing engines [NASA-TM-106042] p 721 N93-25079
- ASTOVL combat aircraft design synthesis and optimization p 717 N93-25704
- An analysis of the reliability and maintainability of the Jian 6 and Jian 7 aircraft and ways to improve them [AD-A261060] p 678 N93-26238
- The generation of side force by distributed suction [NASA-CR-193129] p 839 N93-27151
- YF-22A prototype advanced tactical fighter demonstration/validation flight test program overview p 805 N93-27173
- Damage severity of monitored fatigue load spectra [NLR-TP-92009-U] p 999 N93-32205
- Development of a method to predict transonic limit cycle oscillation characteristics of fighter aircraft [NLR-TP-91359-U] p 999 N93-32338
- FIGURE OF MERIT**
- Aircraft concept optimization using the global sensitivity approach and parametric multiobjective figures of merit [AIAA PAPER 92-4221] p 45 A93-13381
- Aero-space plane figures of merit [AIAA PAPER 92-5058] p 385 A93-22328
- Design of high speed propellers using multiobjective optimization techniques p 336 N93-18065
- Optimum design of high speed prop rotors including the coupling of performance, aeroelastic stability and structures p 337 N93-18066
- FILM COOLING**
- Heat transfer, adiabatic effectiveness, and injectant distributions downstream of a single row and two staggered rows of compound angle film-cooling holes p 201 A93-13976
- Influence of high mainstream turbulence on leading edge film cooling heat transfer - Effect of film hole spacing p 207 A93-15068
- Behaviors of the laterally injected jet in film cooling - Measurements of surface temperature and velocity/temperature field within the jet [ASME PAPER 92-GT-180] p 402 A93-19405
- Heat transfer in serpentine flow passages with rotation [ASME PAPER 92-GT-190] p 403 A93-19415

- Discharge coefficients of holes angled to the flow direction
[ASME PAPER 92-GT-192] p 403 A93-19417
Internal cooling passage heat transfer near the entrance to a film cooling hole - Experimental and computational results
[ASME PAPER 92-GT-241] p 404 A93-19450
Computational analysis of hypersonic shock wave/wall jet interaction
[AIAA PAPER 93-0604] p 269 A93-21113
Evaluation of scramjet nozzle configurations and film cooling for reduction of wall heating
[AIAA PAPER 93-0744] p 358 A93-21118
Numerical simulation of turbine 'hot spot' alleviation using film cooling
p 744 A93-34476
Gas dynamics of cooled turbines - Russian book
[ISBN 5-217-00809-1] p 721 A93-35685
Numerical analysis of aerodynamic losses in film-cooled vane cascade
p 1066 A93-48517
Experimental study on heat transfer of separated impingement jets in short distance
p 1149 A93-48518
The study of experimental turboramjets - Heat state and cooling problems
[AIAA PAPER 93-1989] p 1112 A93-49834
Verification of the TOTLOS method for calculating aerodynamic loss in film-cooled turbine cascade
p 1087 A93-51191
Effect of film cooling/regenerative cooling on scramjet engine performances
[ISABE 93-7036] p 1197 A93-54012
Impingement cooling with film coolant extraction in the airfoil leading edge regions
[ISABE 93-7078] p 1220 A93-54054
Leading edge film cooling heat transfer including the effect of mainstream turbulence
p 23 N93-11886
Investigation of hot streak migration and film cooling effects on heat transfer in rotor/stator interacting flows, report 1
[AD-A250688] p 102 N93-12490
Hydrodynamic effects on heat transfer for film-cooled turbine blades
[AD-A257291] p 361 N93-16080
Measurements and computations of external heat transfer and film cooling in turbines
[RAE-TM-P-1223] p 722 N93-25455
Determination of surface heat transfer and film cooling effectiveness in unsteady wake flow conditions
p 902 N93-29933
The effect of main stream flow angle on flame tube film cooling
p 932 N93-29953
Impingement/effusion cooling
p 932 N93-29954
The aerodynamic effect of coolant ejection in the leading edge region of a film-cooled turbine blade
p 904 N93-29958
Modeling of a turbulent flow in the presence of discrete partial cooling jets
p 904 N93-29960
A Navier-Stokes solver with different turbulence models applied to film-cooled turbine cascades
p 904 N93-29962
Cooling predictions in turbofan engine components
p 905 N93-29964

FILM THICKNESS

- NASA balloon design and flight - Philosophy and criteria
p 40 A93-11363

FINANCE

- Poland civil aviation master plan and investment program: Executive summary
[PB92-213685] p 459 N93-21342

FINANCIAL MANAGEMENT

- MPC75 as the forerunner of a new regional aircraft family
p 37 A93-10776

FINITE DIFFERENCE THEORY

- An effective multigrid method for high-speed flows
p 6 A93-10533
Multizone Navier-Stokes computations for a transonic projectile using McCormack finite difference method
p 113 A93-14192
A flux-difference finite volume method for steady Euler equations on adaptive unstructured grids
p 116 A93-14277
An AF3 algorithm for the calculation of transonic nonconservative full potential flows over wings or wing/body combinations
p 125 A93-15341
Effect of real air properties on integral aerodynamic characteristics
p 242 A93-18241
Matrix difference equation analysis of coupled structural-acoustic models for aircraft fuselage vibration and interior noise reduction
p 446 A93-19172
Calculation of turbulent flow for an enclosed rotating cone
[ASME PAPER 92-GT-70] p 400 A93-19320
Meridional flow calculation using advanced CFD techniques
[ASME PAPER 92-GT-325] p 256 A93-19509

- Optimal circumferential placement of cylindrical thermocouple probes for reduction of excitation forces
[ASME PAPER 92-GT-423] p 406 A93-19571
Coupled finite-difference/finite-element approach for wing-body aeroelasticity
[AIAA PAPER 92-4680] p 409 A93-20302
Flight vehicle aerodynamics calculated by a Galerkin finite element/finite difference method
p 266 A93-20738
Newton-like methods for fast high resolution simulation of hypersonic viscous flows
p 437 A93-20740
Air flow dynamics around an airfoil by the stabilized finite difference method
p 266 A93-20741
Flow around two circular cylinders by the random-vortex method
p 271 A93-21925
Computations of a twin-jet impingement on a flat surface
p 271 A93-22227
Direct numerical simulation of turbulent flow in a square duct
[AIAA PAPER 93-0198] p 277 A93-22618
An implicit finite difference algorithm for two dimensional Euler equation
p 461 A93-24085
Numerical simulations of a high Mach number jet flow
[AIAA PAPER 93-0653] p 540 A93-24766
A multilevel composite grid method for fluid flow computations
[AIAA PAPER 93-0768] p 541 A93-24852
Artificial viscosity models for the Navier-Stokes equations and their effect in drag prediction
[AIAA PAPER 93-0193] p 473 A93-25511
A kind of improved flux-split method for solving the Euler equations
p 681 A93-33739
Calculation of compressible boundary layers by a hybrid finite element method
p 692 A93-35613
An implicit finite-difference algorithm for the numerical simulation of supersonic flow over blunt bodies
p 770 A93-38325
Calculation of the effect of the shock wave of a delta wing on a second wing at supersonic velocities
p 776 A93-39141
Estimation of wing stability in flow from the characteristics of the transient process
p 836 A93-39177
Computational results for 2-D and 3-D ramp flows with an upwind Navier-Stokes solver
p 866 A93-42592
Implicit upwind finite-difference simulation of laminar hypersonic flow over a 2D ramp
p 867 A93-42600
Direct periodic solutions of rotor free wake calculations
p 874 A93-43781
A perspective on a quarter century of CFD research
[AIAA PAPER 93-3291] p 1021 A93-44995
Dynamic overset grid communication on distributed memory parallel processors
[AIAA PAPER 93-3311] p 1036 A93-45007
An implicit time-marching procedure for high speed flow
[AIAA PAPER 93-3315] p 951 A93-45011
Pseudo-compressibility methods for the incompressible flow equations
[AIAA PAPER 93-3329] p 952 A93-45023
Virtual zone Navier-Stokes computations for oscillating control surfaces
[AIAA PAPER 93-3363] p 955 A93-45056
Euler calculations of unsteady interaction of advancing rotor with a line vortex
p 1071 A93-49016
A fourth-order MUSCL finite-difference scheme for solving the unsteady compressible Euler equations
p 1086 A93-51121
An economical difference factorization algorithm for the numerical calculation of the system of equations for a thin viscous shock layer
p 1091 A93-51880
Calculation of compressible gas flow on optimal difference grids
p 1091 A93-51902
A finite difference study of the aerodynamic characteristics of wing profiles at transonic velocities
p 1091 A93-51903
A time-accurate high-resolution TVD scheme for solving the Navier-Stokes equations
p 1093 A93-52006
Calculation of a compressible three-dimensional boundary layer on a swept wing
p 1179 A93-53551
Numerical study of supersonic flow over a backward step with transverse injection
p 1182 A93-53853
Development of the wake behind a circular cylinder impulsively started into rotatory and rectilinear motion
p 1236 A93-55736
Numerical study of advanced rotor blades
p 23 N93-11899
New acceleration potential method for supersonic unsteady aerodynamics of lifting surfaces, further extension of the nonplanar supersonic doublet point method, and nonlinear, nongradient optimized rational function approximations for supersonic, transient response unsteady aerodynamics
p 25 N93-12344
BLSTA: A boundary layer code for stability analysis
[NASA-CR-4481] p 220 N93-14797

- Finite-difference solution for laminar or turbulent boundary layer flow over axisymmetric bodies with ideal gas, CF4, or equilibrium air chemistry
[NASA-TP-3271] p 222 N93-15434
Volume 2: Explicit, multistage upwind schemes for Euler and Navier-Stokes equations
[NASA-CR-191647] p 418 N93-16558
CFD analysis on control of secondary losses in STME LOX turbines with endwall fences
p 419 N93-17289
Modelling of interfacial and thermocline waves
[AERO-REPT-9209] p 420 N93-18103
Computation of internal flows using unstructured triangular meshes
p 299 N93-19276
Analysis of a 2-D airfoil motion flying in-proximity-to a wavy-wall surface: Finite difference method
p 300 N93-19282
Numerical simulation of a high Mach number jet flow
[NASA-TM-105985] p 551 N93-20057
Aerothermodynamic properties of hypersonic flows over radiation-adiabatic surfaces
[DLR-FB-91-42] p 485 N93-21761
Numerical modelling of induced effects of lightning strike on an all composite helicopter
p 703 N93-24879
High-order cyclo-difference techniques: An alternative to finite differences
[NASA-TM-107745] p 693 N93-25074
A hybrid multigrid technique for computing steady-state solutions to supersonic flows
p 700 N93-26078
Godunov-type schemes applied to detonation flows
[NASA-CR-191447] p 780 N93-27090
Numerical simulation of free shear flows: Towards a predictive computational aeroacoustics capability
[NASA-CR-191015] p 781 N93-27097
Recent progress in the analysis of iced airfoils and wings
p 784 N93-27441

FINITE ELEMENT METHOD

- Optimized/adapted finite elements for structural shape optimization
p 77 A93-10971
Numerical simulations of high speed inlet flows
p 115 A93-14246
Aeroelastic stability characteristics of composite cylindrical shells by the finite element method
p 203 A93-14312
Structural optimization in preliminary aircraft design - A finite-element approach
p 226 A93-14340
The rotor blade flap bending problem - An analytical test case
p 158 A93-14783
A finite element study of incompressible flows past oscillating cylinders and airfoils
p 241 A93-17750
Sonic fatigue analysis of an aircraft wing flap by the matrix difference equation method
p 399 A93-19208
Radiated noise of ducted fans
p 450 A93-19215
Accuracy and efficiency assessments for a weak statement CFD algorithm for high-speed aerodynamics
[ASME PAPER 92-GT-433] p 435 A93-19576
p-version finite element modeling for NDE
p 407 A93-19699
Coupled finite-difference/finite-element approach for wing-body aeroelasticity
[AIAA PAPER 92-4680] p 409 A93-20302
Flight vehicle aerodynamics calculated by a Galerkin finite element/finite difference method
p 266 A93-20738
A method of finite element dynamic model optimization
p 367 A93-20812
On some recent advances in multidisciplinary analysis of hypersonic vehicles
[AIAA PAPER 92-5026] p 438 A93-22302
Study of flow phenomena in high speed intakes
[AIAA PAPER 92-5029] p 272 A93-22304
Damage detection in smart structures using neural networks and finite-element analyses
p 438 A93-22540
Discontinuous Galerkin finite element method for two dimensional conservation laws
[AIAA PAPER 93-0337] p 281 A93-23026
Unsteady compressible airfoil aerodynamics using an adaptive time-discontinuous GLS finite element method
[AIAA PAPER 93-0339] p 281 A93-23027
Investigation of an electrothermal de-icer pad using a three-dimensional finite element simulation
[AIAA PAPER 93-0397] p 327 A93-23072
High accuracy computation of fluid-structure interaction in transonic cascades
[AIAA PAPER 93-0485] p 287 A93-23387
Finite element nonlinear panel flutter with arbitrary temperatures in supersonic flow
p 417 A93-23555
Fully automatic FEM data pre-processing for aeronautical electrical machine
p 538 A93-24030
Comprehensive analysis of bearingless rotors - Model development and experimental correlation of modes, response, trim and stability
[AIAA PAPER 93-0624] p 504 A93-24741

- Numerical investigations on airfoil performance subjected to aerodynamic interference from an upstream airfoil
[AIAA PAPER 93-0639] p 463 A93-24754
- Finite element analysis of the Scramaccelerator with finite rate chemistry
[AIAA PAPER 93-0745] p 540 A93-24833
- TGV tunnel entry simulations using a finite element code with automatic remeshing
[AIAA PAPER 93-0890] p 471 A93-24950
- Europe adapts CST to its needs -- computational structures technology for aerospace industry
p 560 A93-25088
- The numerical simulation of the hydrodynamic field from the pump impellers zone by means of the finite element method
p 476 A93-26905
- Influence of modelling loading on stress distribution in turbomachinery blade fastening in case of FEM
p 520 A93-27296
- An accurate nonlinear finite element analysis and test correlation of a stiffened composite wing panel
p 546 A93-27968
- Enhancements to modal testing using finite elements
p 548 A93-29258
- Expanding test mode shapes for better visualization
p 549 A93-29264
- Application of FEM model correlation and updating techniques on an aircraft using test data of a ground vibration survey
p 509 A93-29267
- Finite element computation of compressible flows with the SUPG formulation
p 482 A93-29774
- A new parallel-vector finite element analysis software on distributed-memory computers
[AIAA PAPER 93-1307] p 756 A93-33883
- Advanced transparency development for USAF aircraft
[AIAA PAPER 93-1391] p 710 A93-33954
- Dynamic analysis of multiple row fuselage stiffened structures
[AIAA PAPER 93-1438] p 710 A93-33987
- Application of a p-version finite element code to analysis of cracks
[AIAA PAPER 93-1450] p 740 A93-33999
- Analysis of interlaminar stresses in symmetric and unsymmetric laminates under various loadings
[AIAA PAPER 93-1511] p 740 A93-34050
- Foreign object impact assessment of a high-Mach engine inlet
[AIAA PAPER 93-1630] p 711 A93-34158
- Recent developments in equivalent plate modeling for wing shape optimization
[AIAA PAPER 93-1647] p 742 A93-34172
- Recent advances in the numerical analysis of ram air wings - The three dimensional simulation code 'PARA3D'
[AIAA PAPER 93-1203] p 702 A93-35154
- Calculation of compressible boundary layers by a hybrid finite element method
p 692 A93-35613
- Deforming grid variational principle for unsteady small disturbance flows in cascades
p 692 A93-35623
- Effects on load distribution in a helicopter rotor support structure associated with various boundary configurations
p 796 A93-35951
- Aeroelastic behavior of composite rotor blades with swept tips
p 827 A93-35978
- Modal analysis of multistage gear systems coupled with gearbox vibrations
p 827 A93-36588
- Transonic panel flutter
[AIAA PAPER 93-1476] p 829 A93-37438
- Structured grid variational adaption - Reaching the limit?
[ONERA, TP NO. 1992-114] p 771 A93-38590
- Unsteady transonic two-dimensional Euler solutions using finite elements
p 778 A93-39412
- Large-amplitude finite element flutter analysis of composite panels in hypersonic flow
p 837 A93-39417
- Supersonic flutter analysis of composite plates and shells
p 837 A93-39419
- A software for optimum design of an aircraft structure
p 938 A93-40495
- The finite element method in the 1990's
[ISBN 0-387-54930-7] p 925 A93-40823
- Application of the Galerkin/least-squares formulation to the analysis of hypersonic flows. II - Flow past a double ellipse
p 868 A93-42608
- The application of an adaptive unstructured grid method to the solution of hypersonic flows past double ellipse and double ellipsoid configurations
p 868 A93-42609
- Numerical simulation of hypersonic flow over a double ellipse using a Taylor-Galerkin finite element formulation with adaptive grids
p 868 A93-42617
- Inviscid calculations by an upwind finite element method of hypersonic flows over a double (single) ellipse
p 869 A93-42626
- Simplified finite element representation of fuselage frames with flexible castellations
p 892 A93-43570
- A multibody formulation for helicopter structural dynamic analysis
p 892 A93-43776
- An adaptive finite element method for turbulent free shear flow past a propeller
[AIAA PAPER 93-3388] p 956 A93-45079
- The free vibration of cylindrically-curved rectangular panels
p 1022 A93-45113
- Effect of temperature on nonlinear two-dimensional panel flutter using finite elements
p 1022 A93-45133
- Effect of stiffness characteristics on the response of composite grid-stiffened structures
p 1022 A93-45148
- Vibration analysis of composite wing with tip mass using finite elements
p 1023 A93-45175
- Finite element solution of the 3D compressible Navier-Stokes equations by a velocity-vorticity method
p 974 A93-47196
- Numerical solution of the Euler equations for complex aerodynamic configurations using an edge-based finite element scheme
[AIAA PAPER 93-2933] p 1046 A93-48131
- Fluid-structural interactions using Navier-Stokes flow equations coupled with shell finite element structures
[AIAA PAPER 93-3087] p 1099 A93-48261
- Numerical simulation of a blast inside a Boeing 747
[AIAA PAPER 93-3091] p 1099 A93-48265
- Dynamic analysis of a gear drive system in an engine
p 1149 A93-48514
- Implicit schemes for unsteady Euler equations on unstructured meshes
[ONERA, TP NO. 1993-64] p 1171 A93-51944
- Efficient finite element method for aircraft deicing problems
p 1103 A93-52443
- Vector unsymmetric eigenvalue solver for nonlinear flutter analysis on high-performance computers
p 1160 A93-52449
- Stringer peeling effects at stiffened composite panels in the postbuckling range
p 1160 A93-52453
- A nonlinear finite element of an arbitrary beam
p 1215 A93-52939
- A finite element for modeling skins of composite materials
p 1215 A93-52979
- Flutter analysis of stiffened laminated composite plates and shells in supersonic flow
p 1216 A93-53224
- Mathematical modeling of the three-dimensional temperature fields of turbine blades
p 1216 A93-53329
- Total quality management of forged products through finite element simulation
p 1217 A93-53493
- Calculation of flow fields near a lifting wing
p 1179 A93-53552
- Finite element analysis of natural vibrations of an aeroplane with asymmetric variable wing geometry
p 1218 A93-53776
- New approximate method of stress analysis for bladed rotating discs
[ISABE 93-7059] p 1219 A93-54035
- Development of computational solid mechanics and its application in aerospace engineering
p 1255 A93-54419
- Optimization of large scale systems in elasticity
p 1255 A93-54544
- Discontinuous Galerkin finite element method for Euler and Navier-Stokes equations
p 1235 A93-55357
- Comparison of radiated noise from shrouded and unshrouded propellers
p 1264 A93-55861
- Computation of hypersonic high-temperature nozzle flow
p 1238 A93-56040
- Numerical study of slightly compressible Navier-Stokes simulation of blade-vortex interaction
p 1239 A93-56216
- SAPNEW: Parallel finite element code for thin shell structures on the Alliant FX/80
[NASA-CR-190663] p 84 A93-10372
- A finite element method for nonlinear panel flutter
p 84 A93-10472
- Numerical study for the study of medium speed internal noise problems
[DILC-EST-TN-200] p 101 A93-11156
- Thermostructural applications of heat pipes for cooling leading edges of high-speed aerospace vehicles
p 91 A93-12460
- The Fourth Workshop on Dynamics and Aeroelastic Stability Modeling of Rotorcraft Systems
[AD-A255065] p 50 A93-12485
- Trim analysis by shooting and finite elements and Floquet eigenanalysis by QR and subspace iterations in helicopter dynamics
p 163 A93-13914
- Experimental and analytical investigation of the vibration characteristics of a remotely piloted helicopter
[AD-A256131] p 163 A93-14248
- A finite element model for analysis of thermoviscoelastic behavior of hypersonic leading edge structures subject to intense aerothermal heating
p 137 A93-14631
- SAPNEW: Parallel finite element code for thin shell structures on the Alliant FX-80
[NASA-CR-189212] p 220 A93-14799
- Stability of elastically tailored rotor blades
p 164 A93-14828
- Time-dependent predictions and analysis of turbine cascade data in the transonic flow region
[PNR-90957] p 139 A93-15489
- Optimization of an internally finned rotating heat pipe
[AD-A256725] p 453 A93-15980
- Development of user guidelines for a three-dimensional finite element pavement model
p 379 A93-16311
- Thermoviscoelastic analysis of pavements
p 379 A93-16313
- FAA unified pavement analysis 3-D finite element method
p 379 A93-16314
- Development of a unified airport pavement analysis and design system
p 380 A93-16317
- Unified airport pavement design procedure
p 380 A93-16318
- Mathematical optimization: A powerful tool for aircraft design
[MBB-FE-2-S-PUB-478] p 331 A93-17564
- Practical architecture of design optimisation software for aircraft structures taking the MBB-LAGRANGE code as an example
[MBB-FE-251-S-PUB-479] p 331 A93-17565
- Influence of cross section variations on the structural behaviour of composite rotor blades
[MBB-UD-0602-91-PUB] p 332 A93-17569
- Transient/structural analysis of a combustor under explosive loads
[NASA-TM-107660] p 420 A93-17779
- Interlaminar stress analysis at the skin/stiffener interface of a grid-stiffened composite panel
[NASA-CR-192177] p 393 A93-17920
- H-P adaptive methods for finite element analysis of aerothermal loads in high-speed flows
[NASA-CR-189739] p 420 A93-18093
- Basic research on design analysis methods for rotorcraft vibrations
[NASA-CR-191917] p 422 A93-18576
- A Blottner type numerical model for nonequilibrium viscous hypersonic flows in upwind finite elements
[INRIA-RR-1476] p 297 A93-18648
- Flexible rotorcraft system dynamics with time-variant contact conditions
p 340 A93-19034
- Computation of internal flows using unstructured triangular meshes
p 299 A93-19276
- Multidisciplinary tailoring of hot composite structures
[NASA-TM-106027] p 550 A93-19971
- The semi-discrete Galerkin finite element modelling of compressible viscous flow past an airfoil
[NASA-CR-192161] p 483 A93-20018
- Advanced adaptive computational methods for Navier-Stokes simulations in rotorcraft aerodynamics
[NASA-CR-192282] p 483 A93-20256
- Adaptivity-fluids-localization. The challenge to computational mechanics
p 553 A93-20618
- Resonant response analysis of a high speed gear
p 553 A93-20662
- Stochastic finite element analysis for high speed rotors
p 554 A93-20696
- The NASA/industry Design Analysis Methods for Vibrations (DAMVIBS) program: Boeing Helicopters airframe finite element modeling
p 515 A93-21313
- The NASA/industry Design Analysis Methods for Vibrations (DAMVIBS) program: McDonnell-Douglas Helicopter Company achievements
p 515 A93-21314
- The NASA/industry Design Analysis Methods for Vibrations (DAMVIBS) program: Sikorsky Aircraft: Advances toward interacting with the airframe design process
p 515 A93-21315
- GARTEUR damage mechanics for composite materials: Analytical/experimental research on delaminations
p 537 A93-21513
- Structural Tailoring of Advanced Turboprops (STAT). Theoretical manual
[NASA-CR-191017] p 556 A93-22005
- Numerical study of cavity natural convection flow with augmenting and counteracting effects by projection finite element method
p 749 A93-25540
- Thermally induced stresses in a composite exposed to fire
[AD-A261714] p 737 A93-26371
- Testing a wheeled landing gear system for the TH-57 helicopter
[AD-A262152] p 806 A93-27547
- Homenthalpic-flow approach for hypersonic inviscid non-equilibrium flows
[INRIA-RR-1652] p 788 A93-28440
- Stabilized space-time finite element formulations for unsteady incompressible flows involving fluid-body interactions
p 843 A93-29040
- Nonlinear analyses of composite aerospace structures in sonic fatigue
[NASA-CR-193124] p 930 A93-29154

- Quiet by design: Numerical acousto-elastic analysis of aircraft structures (ISBN-90-386-0042-9) p 893 N93-29268
- Static and dynamic large deflection flexural response of graphite-epoxy beams (NASA-CR-4118) p 934 N93-30374
- Design and analysis of grid stiffened concepts for aircraft composite primary structural applications p 922 N93-30861
- A comparison of classical mechanics models and finite element simulation of elastically tailored wing boxes p 922 N93-30863
- Multiple methods integration for structural mechanics analysis and design p 923 N93-30867
- Structural design using neural networks p 942 N93-31029
- Development of nose structure of a reconnaissance container for a supersonic jet aircraft [MBB-LME-242-S-PUB-0451] p 998 N93-31046
- Blasim: A computational tool to assess ice impact damage on engine blades (NASA-TM-106225) p 1031 N93-31193
- Civil tiltrotor transport point design: Model 940A (NASA-CR-191446) p 1019 N93-32234
- FINITE VOLUME METHOD**
- The numerical study of 3-D flow past control surfaces (AIAA PAPER 92-4650) p 14 A93-13305
- Adaptive multigrid for the steady Euler equations p 201 A93-13988
- Numerical computations of turbomachinery cascade turbulent flows with shocks by using multigrid scheme p 112 A93-14167
- A flux-difference finite volume method for steady Euler equations on adaptive unstructured grids p 116 A93-14277
- The accuracy of cell vertex finite volume methods on quadrilateral meshes p 227 A93-14526
- Secondary flows in a transonic cascade - Validation of a 3-D Navier-Stokes code [ASME PAPER 92-GT-62] p 247 A93-19312
- Flux limiters in a rotated upwind scheme for the Euler equations (AIAA PAPER 93-0067) p 262 A93-20180
- Cascade flow calculations by a multigrid Euler method p 270 A93-21662
- Evaluation of a CFD code for analysis of normal-shock trains (AIAA PAPER 93-0292) p 279 A93-22692
- Numerical solution of inviscid hypersonic flow around a conically-derived waverider (AIAA PAPER 93-0320) p 280 A93-23012
- High accuracy computation of fluid-structure interaction in transonic cascades (AIAA PAPER 93-0485) p 287 A93-23387
- Performance of compressible flow codes at low Mach numbers p 287 A93-23540
- Adaptive finite volume upwind approach on mixed quadrilateral-triangular meshes p 287 A93-23542
- A calculation method for the three-dimensional boundary-layer equations in integral form (AIAA PAPER 93-0786) p 541 A93-24868
- Computation of inviscid flowfield around 3-D aerospace vehicles and comparison with experimental and flight data (AIAA PAPER 93-0885) p 470 A93-24944
- Development of a robust pressure-based numerical scheme for spray combustion applications (AIAA PAPER 93-0902) p 560 A93-24960
- Recent developments in high order K-exact reconstruction on unstructured meshes (AIAA PAPER 93-0668) p 475 A93-25546
- A time dependent method in finite volume for transonic diffuser turbulent flows p 476 A93-27368
- A numerical study of mixing in supersonic combustors with hypermixing injectors (AIAA PAPER 93-0215) p 520 A93-27801
- Finite-volume-TVD scheme for 3-D Euler transonic flow computations in rotating curvilinear coordinates p 679 A93-33709
- Convenient method to convert two-dimensional CFD codes into axisymmetric ones p 689 A93-34499
- A finite-volume Euler solver for computing rotary-wing aerodynamics on unstructured meshes p 765 A93-35935
- Structured grid variational adaption - Reaching the limit? (ONERA, TP NO. 1992-114) p 771 A93-38590
- Enhanced numerical inviscid and viscous fluxes for cell centered finite volume schemes p 864 A93-42444
- Adaptive mesh embedding for reentry flow problems p 869 A93-42619
- Finite volume 3DNS and PNS solutions of hypersonic viscous flow around a delta wing using Osher's flux difference splitting p 870 A93-42633
- Treatment of vortex sheets for the transonic full-potential equation p 871 A93-42870

- Inviscid finite-volume lambda formulation p 872 A93-42888
- Numerical solution of axisymmetric heat conduction problems using finite control volume technique p 928 A93-42909
- A finite-volume Euler solver for computing rotary-wing aerodynamics on unstructured meshes p 874 A93-43782
- A perspective on a quarter century of CFD research (AIAA PAPER 93-3291) p 1021 A93-44995
- Dynamic overset grid communication on distributed memory parallel processors (AIAA PAPER 93-3311) p 1036 A93-45007
- Adaptive-prismatic-grid method for external viscous flow computations (AIAA PAPER 93-3314) p 951 A93-45010
- A 3-D finite-volume scheme for the Euler equations on adaptive tetrahedral grids p 956 A93-45083
- Direct and iterative algorithms for the three-dimensional Euler equations (AIAA PAPER 93-3378) p 957 A93-45102
- Hypersonic flow calculations using a multidomain MUSCL Euler solver p 960 A93-45547
- Multi-zonal Navier-Stokes code with the LU-SGS scheme (AIAA PAPER 93-2965) p 1148 A93-48159
- Numerical solution of Navier-Stokes equations and k-omega turbulence model equations using a staggered upwind method (AIAA PAPER 93-2968) p 1049 A93-48162
- A family of multiblock codes for computational aerothermodynamics - Application to complete vehicle hypersonic flows (AIAA PAPER 93-3042) p 1056 A93-48223
- A detailed study of mean-flow solutions for stability analysis of transitional flows (AIAA PAPER 93-3052) p 1057 A93-48232
- Upwind finite-volume Navier-Stokes computations on unstructured triangular meshes p 1070 A93-49011
- The computation over unstructured grids of inviscid hypersonic reactive flow by upwind finite-volume schemes p 1073 A93-49532
- A staggered finite volume scheme for solving cascade flow with a two-equation model of turbulence (AIAA PAPER 93-1912) p 1076 A93-49779
- Numerical aspects of a block structured compressible flow solver p 1169 A93-51279
- Flow-vector splitting for compressible low Mach number flow p 1093 A93-52001
- Upwind-biased, point-implicit relaxation strategies for hypersonic flowfield simulations on supercomputers p 1175 A93-52770
- Numerical simulation of gas turbine combustors with complex geometries (ISABE 93-7128) p 1204 A93-54103
- Locally implicit total variation diminishing schemes on mixed quadrilateral-triangular meshes p 1235 A93-55356
- Three-dimensional mesh embedding for the Navier-Stokes equations using upwind control volumes p 1239 A93-56402
- Analysis of wing-body junction flowfields using the incompressible Navier-Stokes equations, volumes 1 and 2 p 17 N93-10320
- Unsteady three-dimensional thin-layer Navier-Stokes solutions for turbomachinery in transonic flow p 218 N93-14025
- A numerical study of mixing in supersonic combustors with hypermixing injectors (NASA-CR-191027) p 294 N93-17884
- Validation of central and upwind 3D compressible flow solvers p 421 N93-18564
- Application of the Euler method EULFLEX to a fighter-type airplane configuration at transonic speed (MBB-FE-211-S-PUB-0469-A) p 484 N93-21059
- Homenthalpic-flow approach for hypersonic inviscid non-equilibrium flows (INRIA-RR-1652) p 788 N93-28440
- Ablation problems using a finite control volume technique (DE93-009861) p 942 N93-29187
- The ViB-code to simulate 3-D stator/rotor flow in axial turbines (DLR-FB-92-19) p 1003 N93-31170
- FINNED BODIES**
- Steady and quasisteady resonant lock-in of finned projectiles p 61 A93-12012
- The influence of the fuselage on high alpha vortical flows and the subsequent effect on fin buffeting p 116 A93-14263
- The suppression of single-fin buffeting using tangential leading edge blowing on a delta wing p 270 A93-21677
- Calculations on a double-fin turbulent interaction at high speed (AIAA PAPER 93-3432) p 977 A93-47224

- Waveriders with finlets (AIAA PAPER 93-3442) p 978 A93-47231
- Intense studies on unsteady secondary separations and oscillating shock waves in three-dimensional shock waves/turbulent boundary layer interaction regions induced by sharp and blunt fins (AIAA PAPER 93-2939) p 1046 A93-48137
- Analysis of missile configurations with wrap-around fins using computational fluid dynamics (AIAA PAPER 93-3631) p 1064 A93-48316
- Development of an accuracy criteria for body-on-fin carryover interference (AIAA PAPER 93-3633) p 1065 A93-48318
- The effect of orthogonal-mode rotation on forced convection in a circular-sectioned tube fitted with full circumferential transverse ribs p 932 N93-29937
- Low-speed wind tunnel study of the direct side-force characteristics of a joined-wing airplane with an upper fin (DE93-767966) p 988 N93-31189
- Navier-Stokes computations for kinetic energy projectiles in steady coning motion: A predictive capability for pitch damping (AD-A264111) p 1033 N93-32028
- FINS**
- Iterative temperature calculation method for rectangular sandwich panel fins p 76 A93-10667
- A vortex control technique for the attenuation of fin buffet p 121 A93-14408
- Effects of substrate anisotropy on coupled bilateral finlines p 208 A93-15409
- Experimental investigation of vortex-fin interaction (AIAA PAPER 93-0050) p 260 A93-20163
- A study of hypersonic swept shock wave/turbulent boundary layer interactions using a conical Navier-Stokes code (AIAA PAPER 92-5050) p 273 A93-22322
- Development and application of a nonlinear fin mixer p 368 A93-22869
- Near-field behavior of a tip vortex p 288 A93-23549
- Correlation of interaction sweepback effects on unsteady shock-induced turbulent separation (AIAA PAPER 93-0776) p 475 A93-25550
- Joining carbon composite fins to metal heat pipes using ion beam techniques p 543 A93-25979
- A study on three-dimensional shock wave/turbulent boundary layer interaction induced by sweepback sharp fins at supersonic flow p 684 A93-34274
- Correlation of conical interactions induced by sharp fins and semicones p 692 A93-35635
- A model for calculating the element of a high-temperature heat exchanger with spiral-wire fins p 833 A93-39046
- A heat transfer element of a high-temperature heat exchanger p 833 A93-39047
- The experimental study of the effect of sweepback angles and the front shape of the fin on reduction of shock wave/turbulent boundary layer interaction region p 858 A93-40431
- Computation of crossing shock/turbulent boundary layer interaction at Mach 8.3 p 961 A93-45726
- Control of unsteady shock-induced turbulent boundary layer separation upstream of blunt fins (AIAA PAPER 93-3281) p 969 A93-46839
- Curvature and leading edge sweep back effects on grid fin aerodynamic characteristics (AIAA PAPER 93-3480) p 981 A93-47258
- Effects of junction modifications on sharp-fin-induced shock wave/boundary layer interaction (AIAA PAPER 93-2935) p 1046 A93-48133
- An experimental study of the effects of deformable tip on the performance of fins and finite wings (AIAA PAPER 93-3000) p 1053 A93-48190
- Flowfield dynamics in blunt fin-induced shock wave/turbulent boundary layer interactions (AIAA PAPER 93-3133) p 1063 A93-48298
- Unsteady pressure and load measurements on an F/A-18 vertical fin p 1095 A93-52451
- Correlative behaviours of shock/boundary layer interaction induced by sharp fin and semicone p 1230 A93-54581
- Extended surface heat sinks for electronic components: A computer optimization (AD-A256134) p 218 N93-14254
- Optimization of an internally finned rotating heat pipe (AD-A256725) p 453 N93-15980
- A90 project: Design of a composite fin (ETN-92-92773) p 329 N93-16562
- Contribution of ventral fins to sideforce and yawing moment derivatives due to sideslip at low angle of attack (ESDU-92029) p 291 N93-16638
- Two-dimensional fin analysis p 750 N93-25737
- Joining carbon composite fins to titanium heat pipes (AD-A261970) p 825 N93-27667
- Articulated fin/wing control system (AD-D015712) p 909 N93-29278

FIR FILTERS

- Design and implementation of digital filters for analysis of F/A-18 flight test data
[AD-A253447] p 17 N93-10342

FIRE CONTROL

- Integrated fire control simulation systems p 1192 A93-53876
LONGBOW - Force multiplier for continuous operations p 1175 A93-54295
Narrow-body aircraft water spray optimization study [DOT/FAA/CT-TN93/3] p 705 N93-25224

FIRE EXTINGUISHERS

- Hand-held cabin fire extinguishers - Transport aircraft [SAE ARP 4712] p 1096 A93-52168
The effectiveness of hand-held fire extinguishers on cargo container fires [DOT/FAA/CT-TN92/42] p 496 N93-21821

FIRE FIGHTING

- Red-hot simulation p 1209 A93-53774
The effectiveness of hand-held fire extinguishers on cargo container fires [DOT/FAA/CT-TN92/42] p 496 N93-21821
Narrow-body aircraft water spray optimization study [DOT/FAA/CT-TN93/3] p 705 N93-25224

FIRE PREVENTION

- Maintenance of the liquid and gas systems of the IL-76 aircraft p 804 A93-39203
Hand-held cabin fire extinguishers - Transport aircraft [SAE ARP 4712] p 1096 A93-52168
Aircraft wing compartment liner concept to reduce fuel spillage [DOT/FAA/CT-TN92/34] p 331 N93-17219

FIRES

- Correlations between engineering, medical and behavioural aspects in fire-related aircraft accidents p 494 N93-19693
A model study of the aircraft cabin environment resulting from in-flight fires [DOT/FAA/CT-90/22] p 496 N93-21557
The effectiveness of hand-held fire extinguishers on cargo container fires [DOT/FAA/CT-TN92/42] p 496 N93-21821
Thermally induced stresses in a composite exposed to fire [AD-A261714] p 737 N93-26371
Ventilation effects on smoke and temperature in an aircraft cabin quarter-scale model [DOT/FAA/CT-89/25] p 791 N93-28055
Generation of carbon monoxide in compartment fires [PB93-146702] p 880 N93-29211

FIXED WINGS

- Experience with boundary element methods to calculate the aerodynamic characteristics of aircraft p 243 A93-19130
Survey - Applications of structural optimization methods to fixed wing aircraft and spacecraft [AIAA PAPER 92-4726] p 325 A93-20328
CWAS - Clean wing advisory system: A new approach to ice detection [AIAA PAPER 93-0747] p 516 A93-24835
Flutter calculations for fixed and rotating wings with state-space inflow dynamics [AIAA PAPER 93-1300] p 709 A93-33877
Bending-torsion flutter of linear viscoelastic wings including structural damping [AIAA PAPER 93-1475] p 711 A93-34021
Introduction of the M-85 high-speed rotorcraft concept p 797 A93-35980
Detection and classification of acoustic signals from fixed-wing aircraft p 850 A93-37032
Applications to fixed-wing aircraft and spacecraft p 996 A93-45432
Skin-friction topology over a surface mounted semi-ellipsoidal wing at incidence p 1178 A93-53216
An aerodynamic model for the longitudinal motion of flight training devices p 1207 A93-54278
Finite-state inflow applied to aeroelastic flutter of fixed and rotating wings p 188 N93-14830
The S.T.O.R.M. (tm): Air transport system design simulation [NASA-CR-192070] p 338 N93-18349
The testing of fixed wing tanker and receiver aircraft to establish their air-to-air refuelling capabilities, volume 11 [AGARD-AG-300-VOL-11] p 514 N93-21305
Unsteady airfoil flow solutions on moving zonal grids [AD-A261925] p 701 N93-26198

FIXTURES

- Approaches to control of the large angle magnetic suspension test fixture [NASA-CR-191890] p 381 N93-16695
Large angle magnetic suspension test fixture [NASA-CR-193123] p 1015 N93-31836

FLAME HOLDERS

- Recent progress in the implementation of active combustion control p 171 A93-14272

A numerical study of slit V-gutter flows

- p 171 A93-14273
Flow measurements behind V-gutter under non-combusting condition [AIAA PAPER 93-0020] p 408 A93-20139
A numerical simulation of a scram jet combustor flow p 810 A93-38181
Isothermal flow characteristics behind V-shape gutter with and without injection [ISABE 93-7040] p 1198 A93-54016
Large eddy simulation of turbulent combustion behind flame holders [ISABE 93-7042] p 1198 A93-54018
The combustion performance of methane-fueled ram combustor [ISABE 93-7079] p 1201 A93-54055
Development of advanced carbon-carbon annular flameholders for gas turbines [PNR-90947] p 58 N93-11106

FLAME PROPAGATION

- On the structure and response of aerodynamically-strained planar premixed flames [AIAA PAPER 93-0246] p 390 A93-22657
Induced Mach wave-flame interactions in laminar supersonic fuel jets p 475 A93-26183
Oxides of nitrogen emissions from turbulent hydrocarbon/air jet diffusion flames, phase 2 [PB93-152478] p 756 N93-26533
Nitric oxide formation in a lean, premixed-prevaporized jet A/air flame tube: An experimental and analytical study [NASA-TM-105722] p 844 N93-27012
Effects of buoyancy on gas jet diffusion flames [NASA-CR-191109] p 935 N93-31031

FLAME SPECTROSCOPY

- A mathematical model to determine the health of components based on SOAP data --- spectrometric oil analysis program p 53 A93-12238

FLAME SPRAYING

- Combustion of microemulsion sprays [AIAA PAPER 93-0131] p 390 A93-22578

FLAME STABILITY

- Combustion study on methane-fuel Laboratory Scaled Ram Combustor [ASME PAPER 92-GT-413] p 356 A93-19561
Investigation of flame stabilizers in the form of perforated grids p 1003 A93-47513
A study on 3-D velocity distribution of isothermal flows behind an afterburner flame stabilizer [ISABE 93-7039] p 1197 A93-54015

FLAME TEMPERATURE

- A preliminary study of the effect of equivalence ratio on a low emissions gas turbine combustor using KIVA-2 [DE92-018616] p 215 N93-13321
Nitric oxide formation in a lean, premixed-prevaporized jet A/air flame tube: An experimental and analytical study [NASA-TM-105722] p 844 N93-27012

FLAMEOUT

- Effects of back-pressure in a lean blowout research combustor [ASME PAPER 92-GT-81] p 387 A93-19330
An optical flameout detection system for NASA Langley's 8-Foot High Temperature Tunnel p 1254 A93-54372

FLAMES

- Chemical kinetic and aerodynamic structures of flames [AD-A256015] p 391 N93-15931

FLANGES

- Design and analysis of curved composite components for rotorcraft fuselage frames p 716 N93-25701

FLAPPING

- The rotor blade flap bending problem - An analytical test case p 158 A93-14783
An aerodynamic model for flapping-wing flight p 858 A93-40470
Numerical study of advanced rotor blades p 23 N93-11899

- User's Guide for the NREL Force and Loads Analysis Program [DE92-010579] p 216 N93-13524
User's Guide for the NREL Teetering Rotor Analysis Program (STRAP) [DE92-010580] p 216 N93-13525

- Drag due to gaps round undeflected trailing-edge controls and flaps at subsonic speeds [ESDU-92039] p 290 N93-16634
An interactive boundary-layer approach to multielement airfoils at high lift p 785 N93-27445

FLAPS (CONTROL SURFACES)

- Subsonic high-lift flight research on the NASA Transport System Research Vehicle (TSRV) [AIAA PAPER 92-4103] p 38 A93-11275
On the configuration buffet of a transport aircraft p 117 A93-14298

- In-flight surface-flow measurements on a subsonic transport high-lift flap system p 166 A93-14327
Phase II simulation evaluation of the flying qualities of two tilt-wing flap control concepts [SAE PAPER 920988] p 185 A93-14635

- A study of flow separation on an oscillating flap at Mach number 2.4 [AIAA PAPER 93-0436] p 286 A93-23350

- Numerical prediction of flap losses in a transonic wind tunnel p 288 A93-23552

- Pilot test of a low Reynolds number DTE-airfoil [AIAA PAPER 93-0643] p 464 A93-24758

- Hysteresis effects on wind tunnel measurements of a two-element airfoil [AIAA PAPER 93-0646] p 464 A93-24761

- An investigation of helicopter rotor blade flap vibratory loads p 796 A93-35975

- Flap-lag damping in hover and forward flight with a three-dimensional wake p 797 A93-35979

- Experimental investigation of spherical-convergent-flap thrust-vectoring two-dimensional plug nozzles [AIAA PAPER 93-2431] p 898 A93-41045

- Application of leading-edge vortex manipulations to reduce wing rock amplitudes p 1007 A93-45152

- Navier-Stokes simulations of the Shuttle Orbiter aerodynamic characteristics with emphasis on pitch trim and bodyflap [AIAA PAPER 93-2814] p 965 A93-46552

- Identification of actuation system and aerodynamic effects of direct-lift-control flaps p 1103 A93-52435

- Research requirements for a real-time flight measurements and data analysis system for subsonic transport high-lift research p 1244 A93-54391

- Boeing 777 high lift control system p 1249 A93-55753

- Initial piloted simulation study of geared flap control for tilt-wing V/STOL aircraft [NASA-TM-103872] p 64 N93-10741

- Boundary-layer measurements on a high Reynolds number three-element airfoil p 292 N93-16787

FLASH POINT

- Some physico-chemical characteristics of lubricating oil used in gas turbines p 70 A93-12202

FLASKS

- Application of a sulphur-doped alkane system to the study of thermal oxidation of jet fuels [ASME PAPER 92-GT-122] p 387 A93-19356

FLAT PLATES

- Calculation of a gas-dispersion laminar boundary layer on a plate with allowance for liquid film formation p 76 A93-10148

- Example of the Couette iceform design model - Flat plate iceformation p 207 A93-15070

- Measurement of a one-dimensional mobility using a laser-Doppler velocimeter p 210 A93-16647

- Numerical simulation of a three-dimensional wave packet in a growing flat plate boundary layer p 128 A93-17265

- Applications of laser techniques in fluid mechanics p 395 A93-17765

- A comparison of the drag-reducing benefits of riblets in internal and external flows p 395 A93-18054

- Experiments on the active control of boundary layer transition p 243 A93-19133

- Hypersonic flow separation in shock wave boundary layer interactions [ASME PAPER 92-GT-205] p 251 A93-19429

- Measurements of the effect of free-stream turbulence length scale on heat transfer [ASME PAPER 92-GT-244] p 405 A93-19453

- Numerical analysis of two-dimensional flows around elliptic wings above a flat plate p 267 A93-20924

- Experimental study on the characteristics of the near wake of a rotating flat plate. III - Influence of the shape near the trailing edge on periodic-velocity-fluctuation phenomena p 451 A93-21727

- A numerical investigation of a subsonic jet in a crossflow [AIAA PAPER 93-0870] p 469 A93-24931

- Boundary-layer transition extent measurements on a cone and flat plate at Mach 3.5 [AIAA PAPER 93-0342] p 474 A93-25517

- The coherent structure in a corner turbulent boundary layer p 548 A93-28575

- Analysis of thermal ignition in supersonic flat-plate boundary layers p 769 A93-37933

- Evaluation of an RNG-based algebraic turbulence model p 863 A93-42436

- An experimental contribution to the flat plate 2D compression ramp, shock/boundary layer interaction problem at Mach 14 - Test case 3.7 p 865 A93-42590

- Analytical study on plate edge noise (Noise generation from tandemly situated trailing and leading edges) p 1038 A93-45561

- Computation of crossing shock/turbulent boundary layer interaction at Mach 8.3 p 961 A93-45726
- A systems approach to a DSMC calculation of a control jet interaction experiment p 964 A93-46538 [AIAA PAPER 93-2798]
- On dynamics of the juncture vortex p 980 A93-47252 [AIAA PAPER 93-3473]
- An analytical description of hypersonic boundary layer stability p 1051 A93-48174 [AIAA PAPER 93-2981]
- A study on aerodynamic sound generated by interaction of jet and plate p 1171 A93-48288 [AIAA PAPER 93-3118]
- Numerical simulation of unsteady flow induced by a flat plate moving near ground p 1094 A93-52432
- Experimental evaluation of flat plate boundary layer growth over an anti-icing fluid film p 1140 A93-52645
- Transition correlation in subsonic flow over a flat plate p 1178 A93-53231
- Numerical analysis of a flat plate in a pitching motion. II - Effect on the flow of the position of the pivot, etc p 1181 A93-53798
- The unsteady flow past a supersonic splitter plate [ISABE 93-7047] p 1185 A93-54023
- Experimental investigation of boundary layer transition on a flat plate with C4 leading edge [ISABE 93-7123] p 1222 A93-54098
- Application of a vectorized particle simulation to the study of plates and wedges in high-speed rarefied flow p 133 A93-13746
- Analysis of a 2-D airfoil motion flying in-proximity-to a wavy-wall surface: Finite difference method p 300 A93-19282
- Prediction of vortex breakdown on a delta wing p 787 A93-27459
- Vortex structure and mass transfer near the base of a cylinder and a turbine blade p 901 A93-29929
- Modeling of a turbulent flow in the presence of discrete parietal cooling jets p 904 A93-29960
- Design and analysis of grid stiffened concepts for aircraft composite primary structural applications p 922 A93-30861
- FLAT SURFACES**
- Computations of a twin-jet impingement on a flat surface p 271 A93-22227
- Prediction of fatigue crack growth kinetics in the plane structural elements of aircraft in the biaxial stress state p 1025 A93-45670
- Effect of the size of a plane obstacle on self-oscillations generated in an underexpanded supersonic jet p 1068 A93-48849
- FLEXIBILITY**
- Scientific visualization using the Flow Analysis Software Toolkit (FAST) p 758 A93-25600
- FLEXIBLE BODIES**
- Vibration control algorithms for flexible rotors p 95 A93-10741
- A method of calculating elastic curve of semiflexible plate nozzle p 66 A93-12097
- Optimal vibration control for a flexible rotor with gyroscopic effects p 98 A93-13420
- Optimum balancing of flexible rotor p 205 A93-14489
- Tailoring concepts for improved structural performance of rotorcraft flexbeams p 207 A93-14811
- Time-variant analysis of rotorcraft systems dynamics - An exploitation of vector processors p 416 A93-23512
- Unsteady transonic potential flow over a flexible fuselage [AIAA PAPER 93-1593] p 683 A93-34124
- Experimental and theoretical study for nonlinear aeroelastic behavior of a flexible rotor blade p 837 A93-39422
- Analysis on space shape and tension distribution of towed flexible cables p 1043 A93-48554
- Dynamic simulation of flexible body systems by the vector solution method p 553 A93-20666
- Direct solutions of the Navier-Stokes equations with application to static aeroelasticity p 748 A93-25259
- FLEXIBLE WINGS**
- Dynamic analysis of rotor flexbeams based on nonlinear anisotropic shell models p 743 A93-34261
- The development of an efficient ornithopter wing p 873 A93-43685
- Aeroelastic computation for a flexible airfoil using the small perturbation method comparison with wind-tunnel results [ONERA, TP NO. 1993-43] p 987 A93-47448
- Design, test, and evaluation of three active flutter suppression controllers [NASA-TM-4338] p 63 A93-10070
- Active flutter suppression using dipole filters [NASA-TM-107594] p 186 A93-13367
- An aeroelastic model structure investigation for a manned real-time rotorcraft simulation p 693 A93-24756
- FLIGHT**
- The NASA High-Speed Research Program p 330 A93-16761
- FLIGHT ALTITUDE**
- Flight management systems information exchange with AERA to support future air traffic control concepts --- Automated En Route ATC p 31 A93-11008
- Analysis and feedback control of aircraft flight in wind shear p 183 A93-14349
- Optimal cruise performance p 802 A93-37394
- The development of a prototype aircraft height monitoring unit utilizing an SSR-based difference in time of arrival technique p 884 A93-43432
- First moves towards an 'intelligent' GPWS p 896 A93-43624
- European studies to investigate the feasibility of using 1000 ft vertical separation minima above FL(290). III - Further results and overall conclusions p 992 A93-45166
- The fuel/timing problem in a computer-aided flight preparation system for civil aircraft p 996 A93-45672
- Calculation of safe altitudes p 991 A93-45675
- Real-time simulation of maneuverable aircraft flight conditions on altitude test cell [AIAA PAPER 93-1845] p 1137 A93-49726
- Neutron-induced single event upsets in static RAMs observed at 10 KM flight altitude p 1158 A93-50561
- Single event upset in avionics p 1158 A93-50566
- Clustering methods for removing outliers from vision-based range estimates p 1171 A93-51648
- Aerothermodynamics of the high-altitude flight p 1089 A93-51783
- A radar altitude and line of sight attachment [AIAA PAPER 93-3587] p 1223 A93-52680
- Flight safety in Europe p 1227 A93-53726
- A study of viscous interaction effects on hypersonic waveriders p 135 A93-14160
- A concluding study of the altitude determination deficiencies of the Service Aircraft Instrumentation Package (SAIP) [AD-A263515] p 897 A93-29971
- Radiation exposure in aircraft p 1035 A93-31928
- FLIGHT CHARACTERISTICS**
- Multiple input/multiple output (MIMO) analysis procedures with applications to flight data p 60 A93-10777
- Solid state flight data recorders and their application in the flight operation analysis p 166 A93-14200
- Application of flight data for diagnostic purposes p 166 A93-14295
- Estimation of the probability of large flight parameters deviations p 184 A93-14399
- Phase II simulation evaluation of the flying qualities of two tilt-wing flap control concepts [SAE PAPER 920988] p 185 A93-14635
- Agility potential --- flight qualities and maneuverability of rotorcraft and V/STOL aircraft [SAE PAPER 921016] p 185 A93-14645
- Application of structured singular value synthesis to a fighter aircraft p 368 A93-22865
- Aeromechanical stability of a bearingless composite rotor in forward flight [AIAA PAPER 93-1305] p 726 A93-33881
- Impact of aeroelasticity on propulsion and longitudinal flight dynamics of an air-breathing hypersonic vehicle [AIAA PAPER 93-1367] p 733 A93-33934
- Design of the variable pitch fan for the McDonnell Douglas MD 520N helicopter equipped with the NOTAR system p 794 A93-35908
- Antitorque safety and the RAH-66 Fantail p 795 A93-35912
- Introduction of the M-85 high-speed rotorcraft concept p 797 A93-35980
- Flight Deflection Measurement System p 808 A93-37885
- Application of European CFD methods for helicopter rotors in forward flight [ONERA, TP NO. 1992-125] p 772 A93-38599
- The navigation and flying equipment of the Yak-42 aircraft --- Russian book p 792 A93-39204
- Analytical development of an equivalent system mismatch function --- for longitudinal axis of fighter aircraft in nonterminal flight phase p 906 A93-41890
- Adaptive waveform selection with a neural network p 942 A93-43470
- An efficient method to calculate rotor flow in hover and forward flight [AIAA PAPER 93-3336] p 953 A93-45030
- A set of IBM PC software for processing helicopter flight tests data to determine the flight performance characteristics p 1037 A93-45661
- General concepts related to the determination of the individual flight performance characteristics of aircraft for establishing fuel consumption standards and optimal flight regimes p 996 A93-45673
- Flight data for the Cryogenic Heat Pipe (CRYOHP) Experiment [AIAA PAPER 93-2735] p 1027 A93-46488
- Survey of nonequilibrium re-entry heating for entry flight conditions [AIAA PAPER 93-3230] p 1039 A93-46682
- Free-wake computation of helicopter rotor flowfields in forward flight [AIAA PAPER 93-3079] p 1059 A93-48253
- AIAA Atmospheric Flight Mechanics Conference, Monterey, CA, Aug. 9-11, 1993, Technical Papers p 1125 A93-48301
- Parameter estimates of an aeroelastic aircraft as affected by model simplifications [AIAA PAPER 93-3640] p 1127 A93-48325
- A new flying qualities criterion for flying wings [AIAA PAPER 93-3668] p 1128 A93-48346
- Dynamic model testing of the X-31 configuration for high-angle-of-attack flight dynamics research [AIAA PAPER 93-3674] p 1129 A93-48351
- Vision based techniques for rotorcraft low altitude flight p 1097 A93-49351
- Application of structured singular value synthesis to a fighter aircraft p 1130 A93-49594
- Quasi-optimal steady state and transient maneuvers with and without thrust vectoring [AIAA PAPER 93-3778] p 1132 A93-51373
- Longitudinal and lateral-directional flying qualities investigation of high-order characteristics for advanced-technology transports [AIAA PAPER 93-3815] p 1133 A93-51406
- Initial results of an in-flight investigation of longitudinal flying qualities for augmented, large transports in approach and landing [AIAA PAPER 93-3816] p 1133 A93-51407
- Application of eigenstructure assignment to the control of powered lift combat aircraft p 64 A93-11871
- X-29 linear aerodynamic perturbation model [AD-A254810] p 160 A93-12752
- Trim analysis by shooting and finite elements and Floquet eigenanalysis by QR and subspace iterations in helicopter dynamics p 163 A93-13914
- A simulation model of atmospheric turbulence for rotorcraft applications p 224 A93-14588
- Identification of system dynamics of a high incidence research model [RR-407] p 339 A93-18507
- Helicopters in action p 340 A93-19005
- Flight simulator for hypersonic vehicle and a study of NASP handling qualities p 530 A93-19456
- A simulation study on take-off and landing dynamics of the aircraft of a fly-by-wire control system [AD-A259286] p 510 A93-19849
- Lessons learned from an historical look at flight testing p 511 A93-19904
- Failure identification using multiple model adaptive estimation for the LAMBDA flight vehicle [AD-A259137] p 527 A93-20596
- Applications of stress envelope concepts to aircraft EMP and lightning survivability p 704 A93-24898
- A modified approach to controller partitioning [NASA-TM-106167] p 848 A93-28051
- Project ARES 2: High-altitude battery-powered aircraft p 894 A93-29715
- The DLR test aircraft in the FZ-BS, -VFV 614/ATTAS, Dornier DO 228-101, MBB BO105 S-3 p 1018 A93-31272
- FLIGHT CONDITIONS**
- Effect of flight conditions on the sound insulation of the aircraft passenger compartment p 42 A93-12978
- Stratospheric turbulence measurements and models for aerospace plane design [AIAA PAPER 92-5072] p 433 A93-22342
- Identification of noise sources based on experimental amplitude-frequency noise characteristics of aircraft p 851 A93-39040
- Aeroelastic response, loads, and stability of a composite rotor in forward flight p 906 A93-41919
- Dependence of the service life of a wing on its strength uniformity and landing gear location p 891 A93-42377
- The use of digital map data to provide enhanced navigation and displays for poor weather penetration and recovery p 992 A93-45165
- The influence of nocturnal aircraft noise on sleep and on catecholamine secretion p 1163 A93-49554
- Real-time simulation of maneuverable aircraft flight conditions on altitude test cell [AIAA PAPER 93-1845] p 1137 A93-49726
- Evaluation of a nonlinear PSC algorithm on a variable cycle engine [AIAA PAPER 93-2077] p 1114 A93-49904

- Stratospheric turbulence measurements and models for aerospace plane design p 223 N93-13288 [NASA-TM-104262]
- Special investigation report: Piper Aircraft Corporation PA-46 Malibu/Mirage Accidents/Incident, 31 May 1989 - 17 March 1991 p 149 N93-15577 [PB92-917007]
- Aeroelastic response and aeromechanical stability of helicopters with elastically coupled composite rotor blades p 715 N93-25530
- Preliminary evaluation of aviation-impact variables derived from numerical models p 1034 N93-31202 [PB93-190197]
- FLIGHT CONTROL**
- Aspects of multivariable flight control law design for helicopters using eigenstructure assignment p 60 A93-10916
- The derivation of path following error and control motion noise filters for the reduction of Global Positioning System flight test data p 32 A93-11022
- Limit of sampling periods for nonlinear flight trajectory controller of aircraft p 61 A93-11207
- Handling qualities flight test techniques and analyses used with the proposed MIL-H-8501B [AIAA PAPER 92-4081] p 61 A93-11264
- Integrated flight propulsion control research results using the NASA F-15 HIDECA Flight Research Facility [AIAA PAPER 92-4106] p 38 A93-11276
- Flight testing and simulation of an F-15 airplane using throttles for flight control [AIAA PAPER 92-4109] p 39 A93-11278
- Research on the stability and control of soaring birds [AIAA PAPER 92-4122] p 61 A93-11284
- Nonlinear feedback control of highly manoeuvrable aircraft p 40 A93-11654
- The application of optimal robust control in control system design of flying vehicles p 95 A93-11791
- Options for control and navigation of unmanned aircraft p 34 A93-12124
- Design of an adaptive flight control system with uncertainties p 95 A93-12322
- A maximum likelihood method for flight test data compatibility check p 95 A93-12732
- Discrete time H(infinity) control laws for a high performance helicopter p 96 A93-13007
- The F-18 High Alpha Research Vehicle - A high-angle-of-attack testbed aircraft [AIAA PAPER 92-4121] p 42 A93-13273
- Synthesis of a helicopter nonlinear flight controller using approximate model inversion [AIAA PAPER 92-4468] p 62 A93-13280
- Linear and nonlinear aircraft flight control for the AIAA Controls Design Challenge [AIAA PAPER 92-4628] p 62 A93-13286
- Design of a full time wing leveler system using tab driven aileron controls [AIAA PAPER 92-4193] p 63 A93-13345
- A stability augmentation system for student designed remotely-piloted vehicles [AIAA PAPER 92-4261] p 63 A93-13365
- Advanced technology and the pilot p 45 A93-13412
- Systems integration test laboratory - Application and experiences p 190 A93-13910
- Lockheed adopts media blast dry stripping for the C-130 [SAE PAPER 920949] p 107 A93-14092
- Flight path optimization and suboptimal control laws synthesis for transport mission of maneuverable aircraft p 180 A93-14160
- Integration of flight control and carrier landing aid system [ONERA, TP NO. 1993-6] p 181 A93-14187
- Digital fly-by-wire system for BK117 FBW research helicopter p 181 A93-14209
- Feasibility study of an active aeroelastic control system for the F-16 aircraft p 181 A93-14224
- Variable structure controller design and its real-time analysis for microprocessor-based flight control systems p 181 A93-14229
- An adaptive algorithm for estimation of a state vector in the system of remotely-piloted aircraft control using Kalman filter p 181 A93-14232
- Hetero-redundant architecture with Kalman filter for input processing in flight control system p 182 A93-14293
- The Hermes Carrier Aircraft (HCA) p 195 A93-14347
- Flight-determined benefits of integrated flight-propulsion control systems p 183 A93-14370
- Design of digital multiple model-following integrated flight-propulsion control systems p 183 A93-14371
- Numerical study of jet interaction at super- and hypersonic speeds for flight vehicle control p 184 A93-14379
- The integrated actuation package approach to primary flight control [SAE PAPER 920968] p 185 A93-14630
- Improvement in application of eigenstructure assignment to flight control system design p 227 A93-15406
- Solution of the terminal guidance problem for a flight vehicle using analytical mechanics methods p 228 A93-16778
- A 'low-cost' full flight simulator for basic IFR training p 374 A93-18776
- Validation of vision-based obstacle detection algorithms for low-altitude helicopter flight p 374 A93-19077
- Recent aircraft accidents p 307 A93-20819
- Closed form solutions of constrained trajectories - Application in optimal ascent of aerospace plane [AIAA PAPER 92-5012] p 385 A93-22288
- Robust control of the separation of hypersonic lifting vehicles [AIAA PAPER 92-5013] p 385 A93-22289
- Atmospheric reentry flight test of winged space vehicle [AIAA PAPER 92-5053] p 385 A93-22324
- Aerodynamic foundations for use of unsteady aerodynamic effects in flight control [AIAA PAPER 93-0188] p 276 A93-22613
- Robust stabilization based on topological connectedness p 438 A93-22830
- Extended linear quadratic Gaussian control under randomly varying distributed delays p 439 A93-22854
- Nonlinear aircraft flight control using dynamic inversion p 368 A93-22868
- Refined H-infinity controller design for rotorcraft flight control p 368 A93-22882
- A new flight control design scheme using optimal dynamic output feedback p 368 A93-22883
- Turbulence/gust alleviation using spoiler control p 369 A93-22886
- Parameter optimization for an H2 problem with multivariable gain and phase margin constraints p 439 A93-22971
- Design of flight control systems to meet rotorcraft handling qualities specifications p 370 A93-23509
- Flight simulator fidelity assessment in a rotorcraft lateral translation maneuver p 378 A93-23510
- Application of feedback linearization method in a digital restructurable flight control system p 370 A93-23514
- Failure-accommodating neural network flight control [AIAA PAPER 92-4394] p 523 A93-24495
- Pilot control identification using Minimum Model Error estimation [AIAA PAPER 92-4421] p 523 A93-24497
- Robust integrated flight/propulsion control design for a STOVL aircraft using H-infinity control design techniques p 524 A93-26432
- The aerodynamic loads on aircraft components in violent longitudinal manoeuvres p 476 A93-26898
- A treatment to flight controller nonlinearity effects - An adaptive compensator approach p 524 A93-26948
- Autonomous guidance, navigation and control bridging program plan p 532 A93-27046
- Control synthesis with incomplete, complete, and supercomplete measurements p 561 A93-27603
- A study of the problem of developing a weakly invariant flight vehicle control system p 561 A93-27688
- Application of advanced guidance and navigation systems to flight control of aircraft and future space vehicles p 500 A93-28153
- Flying qualities of the Hermes spaceplane and the shape definition process p 532 A93-28437
- Algorithms and automated techniques for the design of control systems for moving objects p 562 A93-29690
- Robustness evaluation of a flexible aircraft control system p 727 A93-34540
- Synthesis and evaluation of an H2 control law for a hovering helicopter p 728 A93-34542
- Parafoli steady turn response to control input [AIAA PAPER 93-1241] p 728 A93-35180
- Parachute canopy control and guidance training requirements and methodology [AIAA PAPER 93-1255] p 703 A93-35188
- Effects of higher order dynamics on helicopter flight control law design p 816 A93-35959
- ATHeS - A helicopter in-flight simulator with high bandwidth capability p 821 A93-35988
- Design and evaluation of a robust dynamic neurocontroller for a multivariable aircraft control problem p 817 A93-37004
- Actuator and aerodynamic modeling for high-angle-of-attack aeroservoelasticity [AIAA PAPER 93-1419] p 818 A93-37433
- Formal verification of algorithms for critical systems p 846 A93-37623
- Nonlinear analysis and flight dynamics [ONERA, TP NO. 1992-83] p 818 A93-38568
- F/A-18 controls released departure recovery - Flight test evaluation p 803 A93-38839
- F-14D flight director development, test, and evaluation p 803 A93-38840
- AFTI/F-16 night close air support system testing p 808 A93-38841
- F-16 Digital Flight Control System improvements p 818 A93-38843
- The SAAB 2000 initial flight test - Status report p 804 A93-38847
- Constrained control allocation p 938 A93-41891
- Quantitative feedback theory applied to the design of a rotorcraft flight control system p 906 A93-41895
- Applying variations of the quantitative feedback technique (QFT) to unstable, non-minimum phase aircraft dynamics models p 939 A93-42797
- Reliability assessment for self-repairing flight control systems p 907 A93-42804
- Multiple model adaptive estimation applied to the VISTA F-16 flight control system with actuator and sensor failures p 907 A93-42806
- Direct optical control - A lightweight backup consideration p 907 A93-42808
- Design of robust digital model-following flight control systems p 907 A93-42810
- Design of reconfigurable digital multiple model-following flight control systems p 908 A93-42811
- Pilot-in-the-loop analysis of propulsive-only flight control systems p 908 A93-42812
- Flight management system on the F-117A p 908 A93-42815
- Active algorithms for controlling the rotational motion of flight vehicles p 908 A93-43079
- Synthesis of a data processing and measuring system for flight vehicle control systems p 908 A93-43102
- Estimation of the service periods for complex systems in the case of a priori indeterminacy of system reliability data --- for radio electronic equipment of onboard navigation and landing p 856 A93-43109
- Real time PRF control system for SAR p 884 A93-43464
- First moves towards an 'intelligent' GPWS p 896 A93-43624
- Fundamentals of flight vehicle design --- Russian book [ISBN 5-217-01299-4] p 893 A93-43831
- Stiffness enhancement of flight control actuator p 1006 A93-44151
- Classification of the principal fuel saving methods in flight operations p 996 A93-45660
- An overview of recent subsonic laminar flow control flight experiments [AIAA PAPER 93-2987] p 1052 A93-48180
- Status of the validation of high-angle-of-attack nose-down pitch control margin design guidelines [AIAA PAPER 93-3623] p 1126 A93-48308
- Pilots' control behavior including feedback structures identified by an improved method [AIAA PAPER 93-3669] p 1129 A93-48347
- Efforts to reduce CFIT accidents should address failures of the aviation system itself p 1096 A93-49280
- Preliminary flight test results of a fly-by-throttle emergency flight control system on an F-15 airplane [AIAA PAPER 93-1820] p 1100 A93-49708
- Intelligent systems of flight-vehicle control p 1167 A93-50951
- Behavior of the particular quality characteristics of an intelligent flight vehicle control system in a multicriterial formulation p 1168 A93-50952
- Definition of the structure of expert preferences for the multicriterial analysis of control systems p 1168 A93-50953
- Multilevel intelligent control systems for flight vehicles p 1168 A93-50955
- Generation of a plant description dictionary based on expert survey data p 1168 A93-50956
- Architecture of multiprocessor data processing machines and dispatching of the knowledge acquisition process in flight control p 1168 A93-50958
- Optimization of algorithms for information processing and control p 1169 A93-51062
- Synthesis of the optimal control of flight vehicle braking with allowance for the discrete nature of control action generation p 1169 A93-51063
- Optimal structure of discrete algorithms of finite-dimensional continuous-discrete filtering in the presence of Markov noise p 1169 A93-51065
- Coupling characteristics analysis of elastic vehicle --- design of modern flight control systems p 1169 A93-51189
- A U-D factorization-based adaptive extended Kalman filter and its application to flight state estimation p 1169 A93-51198
- Control augmentation system (CAS) synthesis via adaptation and learning [AIAA PAPER 93-3728] p 1170 A93-51328
- A Hopfield neural network for adaptive control [AIAA PAPER 93-3729] p 1130 A93-51329
- The application of intelligent search strategies to robust flight control for hypersonic vehicles [AIAA PAPER 93-3732] p 1143 A93-51331

Robust control of hypersonic vehicles considering propulsive and aeroelastic effects
[AIAA PAPER 93-3762] p 1131 A93-51357

Application of controller partitioning optimization procedure to integrated flight/propulsion control design for a STOV aircraft
[AIAA PAPER 93-3766] p 1131 A93-51361

Robust, nonlinear, high angle-of-attack control design for a supermaneuverable vehicle
[AIAA PAPER 93-3774] p 1131 A93-51369

Cancellation control law for lateral-directional dynamics of a supermaneuverable aircraft
[AIAA PAPER 93-3775] p 1131 A93-51370

Design of a flight control system for a highly maneuverable aircraft using mu synthesis
[AIAA PAPER 93-3776] p 1132 A93-51371

Nonlinear command augmentation system for a high performance aircraft
[AIAA PAPER 93-3777] p 1132 A93-51372

Design of a controller for a high performance fighter aircraft using Robust Inverse Dynamics Estimation (RIDE)
[AIAA PAPER 93-3779] p 1132 A93-51374

Reentry control to a drag vs. energy profile
[AIAA PAPER 93-3790] p 1143 A93-51385

Self-tuning guidance applied to aerostated plane change problems
[AIAA PAPER 93-3791] p 1143 A93-51386

Order reduction of aeroelastic models through LK transformation and Riccati iteration
[AIAA PAPER 93-3795] p 1159 A93-51388

Integrated flight/propulsion control - Subsystem specifications for performance
[AIAA PAPER 93-3808] p 1132 A93-51400

A comparative study of multivariable robustness analysis methods as applied to integrated flight and propulsion control
[AIAA PAPER 93-3809] p 1102 A93-51401

TVC control for the AIAA design challenge airplane
[AIAA PAPER 93-3810] p 1122 A93-51402

Antiwindup analysis and design approaches for MIMO systems
[AIAA PAPER 93-3811] p 1123 A93-51403

A comparison of two multi-variable integrator windup protection schemes
[AIAA PAPER 93-3812] p 1123 A93-51404

A new way of pole placement in LQR and its application to flight control
[AIAA PAPER 93-3845] p 1133 A93-51433

Adaptive quadratic stabilization control with application to flight controller design
[AIAA PAPER 93-3847] p 1133 A93-51434

Optimal symmetric trajectories over a fixed-time domain
[AIAA PAPER 93-3848] p 1133 A93-51435

H(infinity) helicopter flight control law design with and without rotor state feedback
[AIAA PAPER 93-3849] p 1134 A93-51436

Benefits of variable rotor speed in integrated helicopter/engine control
[AIAA PAPER 93-3851] p 1134 A93-51438

Automated control of aircraft in formation flight
[AIAA PAPER 93-3852] p 1134 A93-51439

Approximate decoupling flight control system design with output feedback for nonlinear systems
[AIAA PAPER 93-3880] p 1135 A93-51465

Genetic design of digital model-following flight-control systems
[AIAA PAPER 93-3883] p 1135 A93-51468

Liquid rocket propulsion applied to manned aircraft - In historical perspective
p 1174 A93-51497

Clustering methods for removing outliers from vision-based range estimates
p 1171 A93-51648

Non-linear flight dynamics
[ONERA, TP NO. 1993-109] p 1206 A93-53621

A parameter optimization approach to controller partitioning for integrated flight/propulsion control application
p 1206 A93-54268

Predevelopment of a flight control system for a small civil aircraft
p 1249 A93-56031

Modeling and model simplification of aeroelastic vehicles: An overview
[NASA-TM-107691] p 64 A93-12216

Formal representation of the requirements for an Advanced Subsonic Civil Transport (ASCT) flight control system
[NASA-CR-189699] p 98 A93-12346

On stability and control of SSTO spaceplane in super- and hypersonic ascending phase
[NAL-TR-1128T] p 65 A93-12361

An optical fiber multi-terminal data bus system for aircraft
[NAL-TR-1125] p 52 A93-12370

A brief overview of NASA Langley's research program in formal methods
p 228 A93-12958

A stochastic optimal feedforward and feedback control methodology for superagility
[NASA-CR-4471] p 229 A93-13370

Aircraft accident/incident summary report: Controlled flight into terrain, Bruno's Inc., Beechjet, N25BR, Rome, Georgia, December 11, 1991
[PB92-910404] p 143 A93-13470

Formulation and validation of high-order mathematical models of helicopter flight dynamics
p 162 A93-13821

Robust nonlinear feedback guidance for an aerospace plane: A geometric approach
p 189 A93-14835

Taxonomy of flight variables
p 147 A93-15022

F/A-18 controls released departure recovery flight test evaluation
[AD-A256522] p 189 A93-15396

Multiple model adaptive estimation applied to the VISTA F-16 with actuator and sensor failures, volume 2
[AD-A256569] p 371 A93-16165

Developing a control system for ARES 2
p 371 A93-16769

Using software metrics and software reliability models to attain acceptable quality software for flight and ground support software for avionic systems
p 442 A93-17305

Low bandwidth robust controllers for flight
[NASA-CR-191774] p 372 A93-17800

Theoretical constraints in the design of multivariable control systems
[NASA-CR-191900] p 442 A93-18372

Manual flying of curved precision approaches to landing with electromechanical instrumentation. A piloted simulation study
[NASA-TP-3255] p 344 A93-18408

Strategies for optimal control design of normal acceleration command following on the F-16
[AD-A256975] p 373 A93-19095

Longitudinal-control design approach for high-angle-of-attack aircraft
[NASA-TP-3302] p 373 A93-19108

Helicopter flight control system design using the linear quadratic regulator for robust eigenstructure assignment
[AD-A256904] p 373 A93-19351

An exploratory investigation of the flight dynamics effects of rotor rpm variations and rotor state feedback in hover
[NASA-TM-103968] p 373 A93-19380

Generation of helicopter roll axis bandwidth data through ground-based and in-flight simulation
p 511 A93-19909

X-31A high angle of attack and initial post stall flight testing
p 511 A93-19911

Method for developing the RAFALE flight control system
p 512 A93-19912

In-flight structural mode excitation system for flutter testing
p 526 A93-19915

Fly-by voice, a technology demonstration
p 526 A93-19918

Guidance and flight control law development for hypersonic vehicles
[NASA-CR-192102] p 526 A93-19960

Research in robust control for hypersonic vehicles
[NASA-CR-192127] p 527 A93-20296

URV flight test of an Ada implemented self-repairing flight control system
[AD-A259205] p 527 A93-20551

Controller partitioning for integrated flight/propulsion control implementation
[NASA-TM-105804] p 527 A93-21197

Prediction of forces and moments for hypersonic flight vehicle control effectors
[NASA-CR-193033] p 728 A93-24762

Robust nonlinear control of vectored thrust aircraft
[NASA-CR-192727] p 728 A93-25199

Aerodynamic foundations for use of unsteady aerodynamic effects in flight control
p 695 A93-25274

Control of nonlinear systems under input constraints with applications to flight control
p 729 A93-25353

Use of high performance networks and supercomputers for real-time flight simulation
p 731 A93-25574

Low bandwidth robust controllers for flight
[NASA-CR-193085] p 819 A93-27156

New adaptive controllers for aircraft
p 847 A93-27180

Design, analysis, and control of large transport aircraft utilizing engine thrust as a backup system for the primary flight controls
[NASA-CR-192938] p 820 A93-27308

Advanced Transport Operating System (ATOPS) Flight Management/Flight Controls (FM/FC) software description
[NASA-CR-191457] p 808 A93-28621

A real-time, hardware-in-the-loop simulation of an unmanned aerial research vehicle
[AD-A262477] p 893 A93-29409

Reference equations of motion for automatic rendezvous and capture
[NASA-CR-185676] p 914 A93-29652

Virtual reality flight control display with six-degree-of-freedom controller and spherical orientation overlay
[NASA-CASE-NPO-18733-1-CU] p 897 A93-30416

Analytical foundations of gain scheduling
[AD-A264682] p 909 A93-30550

Flight control system design factors for applying automated testing techniques
[NASA-TM-4242] p 910 A93-30764

Ground installations for preparation and evaluation of flight tests
p 1014 A93-31274

ATTAS experimental-cockpit and ATMOS for component and system investigations in flight guidance
p 1014 A93-31276

Ground- and satellite-derived flight-path measurements as demonstrated in the AFES Avionics Flight Evaluation System (AFES)
p 993 A93-31281

Installations and methods for measurement of aircraft radio components and systems
p 1031 A93-31284

Current projects in Fuzzy Control
p 1038 A93-31442

FLIGHT CREWS

Jeppesen worldwide electronic NOTAM service --- Notice to Airmen
p 1 A93-11020

Flight simulator research into advanced MLS approach and departure procedures
p 149 A93-14234

Aircraft integrated management
p 141 A93-14376

Flight safety and human errors
p 141 A93-16860

Concept of closed-circuit TV system for transport aircraft under examination
p 306 A93-18542

Survey of helmet tracking technologies
p 517 A93-26882

Concept feasibility demonstration for the Army Cockpit Delethalization Program
p 795 A93-35916

British Airways ETOPs flight planning system
p 990 A93-45164

Efforts to reduce CFIT accidents should address failures of the aviation system itself
p 1096 A93-49280

Adaptive automation and human performance: Multi-task performance characteristics
[AD-A254596] p 186 A93-12578

Does cockpit management training reduce aircrew error?
p 146 A93-15014

Trans-cockpit authority gradient in Navy/Marine aircraft mishaps
p 146 A93-15016

A cognitive model for training decision making in aircrews
p 147 A93-15020

Taxonomy of flight variables
p 147 A93-15022

Shared mental models and crew decision making
p 147 A93-15023

Cockpit resource management proficiency as a factor of primary flight training
[AD-A256995] p 328 A93-16262

Special investigation report: Flight attendant training and performance during emergency situations
[PB92-917006] p 310 A93-16834

An investigation of the influence of advanced aircraft diagnostics on the technological sophistication of maintenance personnel
[AD-A258988] p 240 A93-18887

On the typography of flight-deck documentation
[NASA-CR-177605] p 571 A93-19970

Part 1: Executive summary
p 857 A93-30674

The X-15/HL-20 operations support comparison
[NASA-TM-4453] p 1017 A93-32379

FLIGHT ENVELOPES

Icing effects on aircraft stability and control determined from flight data - Preliminary results
[AIAA PAPER 93-0398] p 370 A93-23073

Flying qualities of the Hermes spaceplane and the shape definition process
p 532 A93-28437

Identification of a full subsonic envelope nonlinear aerodynamic model of the F-14 aircraft
[AIAA PAPER 93-3634] p 1065 A93-48319

Development of flying qualities and agility evaluation maneuvers
[AIAA PAPER 93-3645] p 1127 A93-48329

Aerothermal ablation characterization of selected external insulator candidates
[AIAA PAPER 93-1857] p 1145 A93-49735

TVC control for the AIAA design challenge airplane
[AIAA PAPER 93-3810] p 1122 A93-51402

Envelope function - A tool for analyzing flutter data
p 1136 A93-52455

Icing effects on aircraft stability and control determined from flight data: Preliminary results
[NASA-TM-105977] p 188 A93-14831

Natural laminar flow test in-flight visualization
p 482 A93-19921

FLIGHT HAZARDS

Lidar windshear detection for commercial aircraft
p 341 A93-17864

Sensing a change in the wind
p 307 A93-21627

- A 'new age' in aviation weather forecasting p 427 A93-22123
- Two and three-dimensional prediffuser combustor studies with air-water mixture p 390 A93-22652 [AIAA PAPER 93-0240]
- Atmospheric turbulence aloft - A review of possible methods for detection, warning, and validation of prediction models p 557 A93-24914 [AIAA PAPER 93-0847]
- Aviation safety can benefit from simulation of the dispersion of hazardous material p 487 A93-27393
- Potential hazard of aircraft wake vortices in ground effect with crosswind p 479 A93-28606
- Antitorque safety and the RAH-66 Fantail p 795 A93-35912
- Measurements in 80- by 120-foot wind tunnel of hazard posed by lift-generated wakes p 1014 A93-47281 [AIAA PAPER 93-3518]
- Wind tunnel investigation of wind shear effect on turning flight p 1127 A93-48326 [AIAA PAPER 93-3641]
- A wind shear hazard window useful in studying the effect of wind shear on the airplane during the landing approach p 1127 A93-48327 [AIAA PAPER 93-3643]
- The Orlando TDWR testbed and airborne wind shear data comparison results p 145 A93-14851
- Adverse weather test site selection study [AD-A259012] p 339 A93-18895
- Air/ground wind shear information integration: Flight test results p 488 A93-19594
- Wind shear hazard determination p 488 A93-19597
- Acquisition and use of Orlando, Florida and Continental Airbus radar flight test data p 489 A93-19603
- Vertical wind estimation from horizontal wind measurements p 489 A93-19604
- Microburst characteristics determined from 1988-1991 TDWR testbed measurements p 490 A93-19605
- Ground clutter measurements using the NASA airborne doppler radar: Description of clutter at the Denver and Philadelphia airports p 490 A93-19608
- The 1992 International Aerospace and Ground Conference on Lightning and Static Electricity: Addendum p 753 A93-24875 [DOT/FAA/CT-92/20-ADD-1]
- Digitization of analog data from in-flight lightning strikes p 753 A93-24884
- Lightning phenomenology bases for full threat return stroke occurrence following extended leader sweep at flight altitudes p 754 A93-24895
- Applications of stress envelope concepts to aircraft EMP and lightning survivability p 704 A93-24898
- Development of models for predicting the triggering of lightning by launch vehicles p 734 A93-24899
- PROAV Cable Warning System (CWS) - U.S. Army aircraft integration assessment and OCONUS field evaluation p 705 A93-26263 [AD-A261233]
- A statistical characterization of Denver-area microbursts p 845 A93-27675 [AD-A262127]
- Airborne derivation of microburst alerts from ground-based Terminal Doppler Weather Radar information: A flight evaluation p 1000 A93-32223 [NASA-TM-108990]
- FLIGHT INSTRUMENTS**
- Helicopter approaches in low visibility using RGPS and EFIS --- EFIS - Electronic Flight Instrumentation System p 142 A93-17309
- Dual control vibration tests of flight hardware p 545 A93-27782
- Flight simulator evaluation of D-size liquid crystal flat panel displays p 52 A93-12367 [NAL-TR-1136]
- Liquid crystal flat panel display evaluation tests using a flight simulator p 52 A93-12383 [NAL-TR-1122]
- Proceedings of the 16th Symposium on Aircraft Integrated Monitoring Systems p 167 A93-15152 [DLR-MITT-92-01]
- Sensor fault detection using nonlinear observer and polynomial classifier p 170 A93-15182
- A multi-faceted engineering study of aerodynamic errors of the Service Aircraft Instrumentation Package (SAIP) p 293 A93-17677 [AD-A258059]
- Development of a flight instrument package p 719 A93-25783 [AD-A260830]
- Aircraft accident report: Tomy International, Inc., d/b/a Scenic Air Tours flight 22, Beech Model E18S, N342E in-flight collision with terrain, Mount Haleakala, Maui, Hawaii, 22 April 1992 p 705 A93-25827 [PB93-910401]
- Design, fabrication, and testing of a three-dimensional acoustic orientation instrument (3-D AOI): Drawings, engineering and associated lists (conceptual and development design) p 760 A93-25915 [AD-A260934]
- YF-22A prototype advanced tactical fighter demonstration/validation flight test program overview p 805 A93-27173
- Optical technologies for UV remote sensing instruments p 853 A93-28788
- FLIGHT LOAD RECORDERS**
- Refinement of algorithms for calculating the remaining life from magnetic recording instrument data --- for IL-86 aircraft wing p 320 A93-18330
- The FAA/NASA flight loads monitoring program - The prototype system and its benefits for the aviation community p 486 A93-25125
- AH-64A rotating load usage monitoring from fixed system information p 507 A93-27953
- Load variability of a two-bladed helicopter p 507 A93-27954
- FLIGHT MANAGEMENT SYSTEMS**
- Flight management systems information exchange with AERA to support future air traffic control concepts --- Automated En Route ATC p 31 A93-11008
- Advanced technology and the pilot p 45 A93-13412
- Aircrew integrated management p 141 A93-14376
- Flight management systems p 311 A93-17757
- Vertical guidance for a Lockheed L1011-100 using optimal dynamic interpolation p 369 A93-22884
- Position reporting using GPS/OMEGA and INS p 498 A93-25173
- The role of flight management in future air traffic control p 499 A93-27909
- Terminal area traffic management p 317 A93-16213 [LR-684]
- NARSIM and EFMS: Tools for research on integrated ATM p 319 A93-17954 [NLR-TP-89336-U]
- Piloted simulation of an air-ground profile negotiation process in a time-based Air Traffic Control environment p 707 A93-26087 [NASA-TM-107748]
- Avionics systems architectures p 808 A93-27169
- Advanced Transport Operating System (ATOPS) Flight Management/Flight Controls (FM/FC) software description p 808 A93-28621 [NASA-CR-191457]
- Instigation and processing of flight tests in DLR p 998 A93-31275
- Testing of an experimental FMS p 998 A93-31277
- FLIGHT MECHANICS**
- The science of flight - Pilot-oriented aerodynamics --- Book p 240 A93-17526 [ISBN 0-8138-0398-5]
- Problems in the aerodynamics and dynamics of flight vehicles in the light of K.E. Tsiolkovsky's ideas; Lectures Devoted to K.E. Tsiolkovsky's Ideas, 25th, Kaluga, Russia, Sept. 11-14, 1990, Transactions --- Russian book p 237 A93-18376
- Solution of trajectory optimization methods using the Pontriagin maximum principle p 366 A93-18378
- Aerodynamic foundations for use of unsteady aerodynamic effects in flight control p 276 A93-22613 [AIAA PAPER 93-0188]
- Helicopters - Handbook --- Russian book p 458 A93-28874 [ISBN 5-203-00804-3]
- Optimization of endurance performance --- of aircraft p 713 A93-34400
- Zero-gravity atmospheric flight by robust nonlinear inverse dynamics p 728 A93-34550
- Investigation of the flight mechanics simulation of a hovering helicopter p 798 A93-35990
- Flight efficiency theory p 812 A93-39202
- Problems in the aerodynamics of flight vehicles and their parts p 1068 A93-48901
- Problems in the aerodynamics of flight vehicles and their components p 1091 A93-51901
- Solution of the boundary value problem in flight dynamics by the opposite motion method p 1206 A93-52944
- Non-linear flight dynamics p 1206 A93-53621 [ONERA, TP NO. 1993-109]
- An exploratory investigation of the flight dynamics effects of rotor rpm variations and rotor state feedback in hover p 373 A93-19380 [NASA-TM-103968]
- Flight Testing p 510 A93-19901 [AGARD-CP-519]
- The testing of fixed wing tanker and receiver aircraft to establish their air-to-air refuelling capabilities, volume 11 p 514 A93-21305 [AGARD-AG-300-VOL-11]
- Program of research in flight dynamics in the JIAFS at NASA-Langley Research Center p 484 A93-21562 [NASA-CR-191885]
- Flight mechanical model for performance calculations and interactions between flight vehicle and ramjet in regard to the flight orbit p 893 A93-29464 [ESA-TT-1267]
- FLIGHT OPERATIONS**
- Jet streams and associated turbulence and their effects on air transport flight operations p 154 A93-14231
- Design of an air traffic computer simulation system to support investigation of civil tiltrotor aircraft operations p 36 A93-11139 [NASA-CR-190811]
- In-service evaluation of wind shear systems p 146 A93-14857
- Proceedings of the 16th Symposium on Aircraft Integrated Monitoring Systems p 167 A93-15152 [DLR-MITT-92-01]
- New rotor trim and balance system for helicopter usage monitoring p 169 A93-15180
- Terminal area forecasts FY 1992 - 2005 p 149 A93-15390 [AD-A255797]
- Terminal area traffic management p 317 A93-16213 [LR-684]
- Pre-flight risk assessment in Emergency Medical Service (EMS) helicopters p 494 A93-19692
- Expedient repair of structural facilities p 731 A93-25656 [AD-A260727]
- Design of an air traffic computer simulation system to support investigation of civil tiltrotor aircraft operations p 707 A93-26052 [NASA-CR-192920]
- FLIGHT OPTIMIZATION**
- Enhancement of endurance performance by periodic optimal camber control p 727 A93-34541
- Results of operational testing of a system for computing optimal flight regimes --- of aircraft flight p 996 A93-45665
- The fuel/timing problem in a computer-aided flight preparation system for civil aircraft p 996 A93-45672
- General concepts related to the determination of the individual flight performance characteristics of aircraft for establishing fuel consumption standards and optimal flight regimes p 996 A93-45673
- Computer-aided study of flight regimes and fuel consumption for helicopter flight operations p 997 A93-45674
- Performance-seeking control - Program overview and future directions p 1102 A93-51360 [AIAA PAPER 93-3765]
- Application of controller partitioning optimization procedure to integrated flight/propulsion control design for a STOLV aircraft p 1131 A93-51361 [AIAA PAPER 93-3766]
- Quasi-optimal steady state and transient maneuvers with and without thrust vectoring p 1132 A93-51373 [AIAA PAPER 93-3778]
- Minimum-time flight paths of supersonic aircraft p 160 A93-13140
- Optimal thrust magnitude on a singular arc in atmospheric flight p 758 A93-25410
- Practical input optimization for aircraft parameter estimation experiments p 820 A93-27264 [NASA-CR-191462]
- FLIGHT PATHS**
- Automatic dependent surveillance (ADS) Pacific engineering trials (PET) p 30 A93-10999
- Flight management systems information exchange with AERA to support future air traffic control concepts --- Automated En Route ATC p 31 A93-11008
- The derivation of path following error and control motion noise filters for the reduction of Global Positioning System flight test data p 32 A93-11022
- Advanced technology and the pilot p 45 A93-13412
- Flight path optimization and suboptimal control laws synthesis for transport mission of maneuverable aircraft p 180 A93-14160
- Radiation safety in aircraft operations p 141 A93-14221
- Analysis and development of a total energy control system for a large transport aircraft p 183 A93-14372
- Estimation of the probability of large flight parameters deviations p 184 A93-14395
- A new method for calculation of helicopter maneuvering flight p 184 A93-14401
- Wind identification along a flight trajectory. I - 3D-kinematic approach p 223 A93-16324
- Validation of vision-based obstacle detection algorithms for low-altitude helicopter flight p 374 A93-19077
- Maximum hail concentration that can be met by an aircraft in stormy precipitations p 430 A93-22152
- Turbulence avoidance p 309 A93-22160
- Closed form solutions of constrained trajectories - Application in optimal ascent of aerospace plane p 385 A93-22288 [AIAA PAPER 92-5012]
- Unsteady panel method for flows with multiple bodies moving along various paths p 539 A93-24755 [AIAA PAPER 93-0640]
- The value of GNSS to aircraft operators p 498 A93-25172

Aviation safety can benefit from simulation of the dispersion of hazardous material p 487 A93-27393

A data processing and control system for countering wind shear p 524 A93-27604

Managing the world's air traffic p 501 A93-28392

Wind identification along a flight trajectory. II - 2D-kinematic approach p 524 A93-28469

A constrained flight route monitor system in terminal control area for air traffic control p 882 A93-42816

Approximation of a flight vehicle trajectory using Walsh functions p 909 A93-43106

Real time PRF control system for SAR p 884 A93-43464

Wind identification along a flight trajectory. III - 2D dynamic approach p 1007 A93-45401

A method of wind shear detection for powered-lift STOL aircraft [AIAA PAPER 93-3667] p 1104 A93-48345

Pilots' control behavior including feedback structures identified by an improved method [AIAA PAPER 93-3669] p 1129 A93-48347

Prediction and planning of a flight vehicle route in the presence of motion inhibiting factors p 1130 A93-50961

A technique for the measurement of cloud structure on centimeter scales p 1158 A93-51243

A pseudo-loop design strategy for the longitudinal control of hypersonic aircraft p 1132 A93-51405

Clustering methods for removing outliers from vision-based range estimates p 1171 A93-51648

Analysis of a turning point problem in flight trajectory optimization p 1210 A93-52885

Optimal trajectories for hypersonic launch vehicles p 1251 A93-54563

Guidance and control of HOPE (H-II orbiting plane) [AAS PAPER 91-653] p 1252 A93-55825

Requirements for airborne vector gravimetry p 1241 A93-55976

A simplified numerical procedure to compute the optimal trajectory of an aircraft p 48 A93-11719

Accuracy improvement of linear estimated motion using differential type sensors [NAL-TR-1135] p 91 A93-12365

Minimum-time flight paths of supersonic aircraft p 160 A93-13140

En route air traffic controllers use of flight progress strips: A graph-theoretic analysis [AD-A259062] p 319 A93-18927

Design concepts for the development of cooperative problem-solving systems p 707 A93-25261

[NASA-CR-192708] Control and optimization of aircraft trajectories p 729 A93-25543

Flight mechanical model for performance calculations and interactions between flight vehicle and ramjet in regard to the flight orbit [ESA-TT-1267] p 893 A93-29464

Two simulation studies of precision runway monitoring of independent approaches to closely spaced parallel runways [AD-A263433] p 911 A93-29815

Ground- and satellite-derived flight-path measurements as demonstrated in the AFES Avionics Flight Evaluation System (AFES) p 993 A93-31281

On-board derived flight-path measurement as demonstrated by an ILS measurement system p 994 A93-31282

Flight evaluation of a computer aided low-altitude helicopter flight guidance system [NASA-TM-103998] p 994 A93-32225

FLIGHT PLANS

Optimization of time saving in navigation through an area of variable flow p 34 A93-12125

British Airways ETOPs flight planning system p 990 A93-45164

European studies to investigate the feasibility of using 1000 ft vertical separation minima above FL(290). III - Further results and overall conclusions p 992 A93-45166

Prediction and planning of a flight vehicle route in the presence of motion inhibiting factors p 1130 A93-50961

Future FAA telecommunications plan [AD-A249133] p 89 A93-11760

A database approach to aircraft carrier airplan production [AD-A257737] p 240 A93-17666

National Airspace System flight planning operational concept NAS-SR-131 [PB93-124659] p 310 A93-18031

Design of a cooperative problem-solving system for enroute flight planning: An empirical study of its use by airline dispatchers [NASA-CR-192709] p 707 A93-25330

Application and integration of diverse technology in an aviation system: The National Aeronautical Information Processing System p 887 A93-30339

FLIGHT RECORDERS

Solid state flight data recorders and their application in the flight operation analysis p 166 A93-14200

Onboard maintenance monitoring systems in modern aircraft p 167 A93-15047

The static-memory crash recorders p 167 A93-15048

A summary of investigations of severe turbulence incidents using airline flight records p 308 A93-22153

Software support for a computerized air situation documentation system p 941 A93-43115

A localizer design to improve missed approach guidance p 992 A93-44143

Characteristics of the detection of overloads in the center of mass of Il-76 and An-12 aircraft due to runway irregularities by a standard on-board recorder p 1008 A93-45666

Digital flight recorded data - A method of estimating down draft from digital flight recorded data p 1241 A93-54559

Proceedings of the 16th Symposium on Aircraft Integrated Monitoring Systems [DLR-MITT-92-01] p 167 A93-15152

Discussion for the ideal AIMS p 167 A93-15153

Flight data and flight safety in SAS p 168 A93-15156

Detection of technical states with aircraft p 168 A93-15159

Rewritable optical disk: Application to flight recording p 221 A93-15160

Indian experience in flight data readout and analysis p 168 A93-15161

Czechoslovak development and experience in flight data recorder readout and analysis p 168 A93-15162

Software for flight recorder data evaluation developed by Lufthansa p 230 A93-15163

The FAIR (Flight Animated and Interactive Reconstruction) tool p 148 A93-15164

The SIROM flight data recorder and evaluation system p 168 A93-15165

Solid state flight data recorder with rapid data access p 221 A93-15167

EJ 200 engine monitoring system: On- and off-board data capture, analysis, and management system p 178 A93-15172

Helicopter flight data recorder and health and usage monitoring system p 169 A93-15178

Helicopter health monitoring: Current practice and future trends p 169 A93-15179

FLIGHT SAFETY

Design and conduct of a windshear detection flight experiment [AIAA PAPER 92-4092] p 38 A93-11268

Breaking through the 10 exp 6 barrier --- decreasing aircraft accident fatality rate per million flight hours p 27 A93-11498

Joint NASA/USAF Airborne Field Mill Program - Operation and safety considerations during flights of a Lear 28 airplane in adverse weather [AIAA PAPER 92-4093] p 93 A93-13262

Preliminary design features of the RASCAL - A NASA/Army rotorcraft in-flight simulator [AIAA PAPER 92-4175] p 42 A93-13311

Advanced cockpit technology in the real world p 2 A93-13409

TCAS II testing conflicts and resolutions p 165 A93-14158

The methods of reducing impact loads on occupants in the civil aircraft crash condition p 140 A93-14220

Aircrew integrated management p 141 A93-14376

Tomorrow's security p 141 A93-15058

Flight safety and human errors p 141 A93-16860

Automation of aircraft service testing tasks using the automatic control system Bezopasnost'-3 p 306 A93-18345

Search strategies for a sequence of baseline indices for building sections of a flight-safety automatic control system in the interactive mode p 306 A93-18346

The role of simulation in determining safe aircraft landing separation criteria p 306 A93-18712

Engine Health Monitoring p 346 A93-18787

Distribution of aviation weather graphics via airline communications networks p 426 A93-22113

The importance of proper aviation weather dissemination to pilots - An airline captain's perspective p 308 A93-22115

Preliminary results of the detection of clear air turbulence by the Wind Profiler Demonstration Network p 427 A93-22119

Developing the Aviation Gridded Forecast System p 427 A93-22124

The Aviation Weather Products Generator p 428 A93-22125

Integrated Terminal Weather System (ITWS)

FAA weather processor programs - Real-time dissemination of weather information to aviation end-users p 428 A93-22131

Impact of weather on aviation - A global view p 308 A93-22143

Operational aviation weather service requirements p 429 A93-22145

Buoyancy wave hazards to aviation p 430 A93-22151

Extremely low level jet in the evening in Kanto Plain p 430 A93-22159

Terminal forecast amendments - A 'cloudy' issue --- valid for up to 24 hours for airport areas p 431 A93-22167

An automated system for the measurement of slant visual range p 413 A93-22176

Anemometer siting criteria for low level wind shear alert system p 413 A93-22178

Seasonal weather hazards p 431 A93-22180

Human factors in crashes of commuter airplanes p 486 A93-24048

Aircraft icing problems - After 50 years [AIAA PAPER 93-0392] p 486 A93-24239

Aviation safety can benefit from simulation of the dispersion of hazardous material p 487 A93-27393

Wind shear alert system brings safety improvements to major U.S. airports p 529 A93-27396

Increased safety through knowledge-based pilot assistance p 518 A93-27499

Volcanic clouds --- aircraft hazards p 487 A93-28196

Flight safety in a perturbed atmosphere --- Russian book [ISBN 5-277-00815-2] p 487 A93-29431

Antitorque safety and the RAH-66 Fantail p 795 A93-35912

Extended range operations of two and three turbofan engined airplanes p 802 A93-37391

Critical dispatch - A pilot's view p 790 A93-39541

Parameter selection of electro-impulse de-icing systems p 889 A93-40493

Progress and taboos in flight safety - Human-factors research in air transportation p 879 A93-42654

A constrained flight route monitor system in terminal control area for air traffic control p 882 A93-42816

Airport surveillance radar design for increased air traffic p 883 A93-43410

European studies to investigate the feasibility of using 1000 ft vertical separation minima above FL(290). III - Further results and overall conclusions p 992 A93-45166

Vortex flap flight test operations, a safe approach p 995 A93-45168

How to enhance safety for future space transportation systems p 1015 A93-45444

Calculation of the position of aircraft center of gravity on an IBM PC p 996 A93-45671

Calculation of safe altitudes p 991 A93-45675

Towards quantitative non-destructive evaluation of aging aircraft p 1025 A93-45773

Wind-shear endurance capability for powered-lift aircraft [AIAA PAPER 93-3670] p 1129 A93-48348

Behavior of the particular quality characteristics of an intelligent flight vehicle control system in a multicritical formulation p 1168 A93-50952

Atmospheric disturbances over mountains and the flight safety p 1164 A93-51856

Flight safety in Europe p 1227 A93-53726

Unusual attitudes - Helicopters and instrument flight p 1240 A93-54550

A study on low level windshear hazard index p 1240 A93-55414

Promoting general aviation safety - A revision of pilot negligence law p 1265 A93-56540

UK airmisses involving commercial air transport, May-August 1991 [ETN-92-92260] p 28 A93-11357

UK airmisses involving commercial air transport, January-April 1991 [ETN-92-92261] p 87 A93-11358

Activities report of the German Institute for Flight Safety [ETN-92-92272] p 28 A93-11375

Proceedings of the National Weather Service Aviation Workshop: Postprint volume [PB92-176148] p 94 A93-11803

Aircraft accident report: Britt Airways, Inc., d/b/a, Continental Express Flight 2574, in-flight structural breakup, EMB-120RT, N33701, Eagle Lake, Texas, September 11, 1991 [PB92-910405] p 143 A93-13426

Aviation accidents, incidents, and violations: Psychological predictors among US pilots p 144 A93-14693

SUBJECT INDEX

Trans-cockpit authority gradient in Navy/Marine aircraft mishaps p 146 N93-15016

Embedded ADM reduces helicopter human error accidents p 147 N93-15024

Flight data and flight safety in SAS p 168 N93-15156

The FAIR (Flight Animated and Interactive Reconstruction) tool p 148 N93-15164

Sensor fault detection using nonlinear observer and polynomial classifier p 170 N93-15182

Neural network based condition monitoring p 230 N93-15183

Airbus Industrie TCAS experience p 152 N93-15186

Special investigation report: Piper Aircraft Corporation PA-46 Malibu/Mirage Accidents/Incident, 31 May 1989 - 17 March 1991 p 149 N93-15577

[PB92-917007] p 149 N93-15577

Report to Congress: Long-term availability of adequate airport system capacity p 319 N93-18202

[AD-A258209] p 319 N93-18202

An investigation of a prototype OASYS effectiveness in maneuvering flight p 338 N93-18339

[AD-A257901] p 338 N93-18339

An approach to evaluating reactive airborne wind shear systems p 489 N93-19600

RDR-4B doppler weather radar with forward looking wind shear detection capability p 489 N93-19601

How do we investigate the human factor in aircraft accidents? p 491 N93-19655

737-400 at Kegworth, 8 January 1989: The AALB investigation p 491 N93-19661

Towards an integrated approach to proactive monitoring and accident prevention p 495 N93-19700

Prediction of success from training p 495 N93-19702

Aviation safety: Problems persist in FAA's inspection program. Report to the Chairman, Subcommittee on Aviation, Committee on Public Works and Transportation, House of Representatives p 495 N93-19841

[GAO/RCED-92-14] p 495 N93-19841

Aviation safety: Users differ in views of collision avoidance system and cite problems. Report to the Chairman, Subcommittee on Investigations and Oversight, Committee on Science, Space, and Technology, House of Representatives p 502 N93-19843

[GAO/RCED-92-113] p 502 N93-19843

On the typography of flight-deck documentation p 571 N93-19970

[NASA-CR-177605] p 571 N93-19970

A pulsed fast-thermal neutron interrogation system p 497 N93-21866

The 1992 International Aerospace and Ground Conference on Lightning and Static Electricity: Addendum p 753 N93-24875

[DOT/FAA/CT-92/20-ADD-1] p 753 N93-24875

Lightning phenomenology bases for full threat return stroke occurrence following extended leader sweep at flight altitudes p 754 N93-24895

The ATC evaluation of the prototype Airport Surveillance Radar Wind Shear Processor (ASR-WSP) at Orlando International Airport p 748 N93-25210

[DOT/FAA/CT-TN92/48] p 748 N93-25210

Aircraft accident report: Tomy International, Inc., d/b/a Scenic Air Tours flight 22, Beech Model E18S, N342E in-flight collision with terrain, Mount Haleakala, Maui, Hawaii, 22 April 1992 p 705 N93-25827

[PB93-910401] p 705 N93-25827

PROAV Cable Warning System (CWS) - U.S. Army aircraft integration assessment and OCONUS field evaluation p 705 N93-26263

[AD-A261233] p 705 N93-26263

FAA international conference on airplane ground deicing p 880 N93-29286

[AD-A263617] p 880 N93-29286

Airborne derivation of microburst alerts from ground-based Terminal Doppler Weather Radar information: A flight evaluation p 1000 N93-32223

[NASA-TM-108990] p 1000 N93-32223

UK airmisses involving commercial air transport, September - December 1991 p 992 N93-32409

[ETN-93-93930] p 992 N93-32409

FLIGHT SIMULATION

Design and implementation of a flight simulation system --- Book p 66 A93-12216

Pilot/Vehicle display development from simulation to flight p 51 A93-13310

[AIAA PAPER 92-4174] p 51 A93-13310

Piloted simulation study of two tilt-wing control concepts p 63 A93-13338

[AIAA PAPER 92-4236] p 63 A93-13338

Numerical simulation of STOL operations using thrust-vectoring p 15 A93-13342

[AIAA PAPER 92-4254] p 15 A93-13342

Flight simulation and constant amplitude fatigue crack growth in aluminum-lithium sheet and plate p 71 A93-13644

FLIGHT SIMULATION

Design philosophies of the Basic Research Simulator p 191 A93-14414

Effect of stress level of gust cycles on fatigue crack propagation behavior (Acceleration and retardation of crack propagation under simplified flight simulation loading) p 198 A93-17033

Optical design of a wide-angle simulator probe p 211 A93-17140

The role of simulation in determining safe aircraft landing separation criteria p 306 A93-18712

Developing control strategies for ASTOVL aircraft p 366 A93-18777

Parallel rotorcraft flight simulation [AIAA PAPER 93-0623] p 524 A93-24740

Utilizing a microcomputer based flight simulation in teaching human factors in aviation p 570 A93-27165

A generic harmonic rotor model for helicopter flight simulation p 506 A93-27480

Improvements in hover display dynamics for a combat helicopter p 727 A93-34257

AHS, Annual Forum, 48th, Washington, June 3-5, 1992, Proceedings, Vols. 1 & 2 p 763 A93-35901

Handling qualities testing using the mission oriented requirements of ADS-33C p 817 A93-35961

Investigation of the flight mechanics simulation of a hovering helicopter p 798 A93-35990

Analytical development of an equivalent system mismatch function --- for longitudinal axis of fighter aircraft in nonterminal flight phase p 906 A93-41890

Inverse simulation of large-amplitude aircraft maneuvers p 906 A93-41893

Real-time parameter identification applied to flight simulation p 1006 A93-44142

Numerical experiment of the flight trajectory simulation by fluid dynamics and flight dynamics coupling [AIAA PAPER 93-3324] p 952 A93-45018

Moving body overset grid methods for complete aircraft tiltrotor simulations [AIAA PAPER 93-3350] p 954 A93-45044

Use of Convex supercomputers for flight simulation at NASA Langley p 1013 A93-46806

An advanced parallel rotorcraft flight simulation model - Stability characteristics and handling qualities [AIAA PAPER 93-3618] p 1125 A93-48305

On the use of back propagation with feed-forward neural networks for the aerodynamic estimation problem [AIAA PAPER 93-3638] p 1165 A93-48323

Parameter estimates of an aeroelastic aircraft as affected by model simplifications [AIAA PAPER 93-3640] p 1127 A93-48325

Wind-shear endurance capability for powered-lift aircraft [AIAA PAPER 93-3670] p 1129 A93-48348

Simulation of hypersonic flight - A concerted European effort p 1136 A93-49301

Real-time simulation of maneuverable aircraft flight conditions on altitude test cell [AIAA PAPER 93-1845] p 1137 A93-49726

Longitudinal and lateral-directional flying qualities investigation of high-order characteristics for advanced-technology transports [AIAA PAPER 93-3815] p 1133 A93-51406

Development of advanced approach and departure procedures [AIAA PAPER 93-3833] p 1098 A93-51422

AIAA Flight Simulation Technologies Conference, Monterey, CA, Aug. 9-11, 1993, Technical Papers p 1207 A93-52651

Evolution of flight simulation [AIAA PAPER 93-3545] p 1207 A93-52652

Internally coherent system of innovation - The case of flight simulation [AIAA PAPER 93-3548] p 1226 A93-52653

An advanced rotorcraft flight simulation model - Parallel implementation and performance analysis [AIAA PAPER 93-3550] p 1222 A93-52654

Methodology for integration of digital control loaders in aircraft simulators [AIAA PAPER 93-3551] p 1207 A93-52655

Dynamic simulation fidelity improvement using transfer function state extrapolation [AIAA PAPER 93-3552] p 1222 A93-52656

A high fidelity video delivery system for real-time flight simulation research [AIAA PAPER 93-3558] p 1214 A93-52659

Hybrid complex of the aircraft intellectualized control systems simulation at the stage of their research projecting [AIAA PAPER 93-3559] p 1222 A93-52660

Visual weather simulation using meteorological databases [AIAA PAPER 93-3566] p 1207 A93-52665

A primary flight display for four-dimensional guidance and navigation influence of tunnel size and level of additional information on pilot performance and control behaviour [AIAA PAPER 93-3570] p 1208 A93-52668

The development of SIMONA - A simulator facility for advanced research into simulation techniques, motion system control and navigation systems technologies [AIAA PAPER 93-3574] p 1208 A93-52670

Semi-full-scale dynamic simulation complex on the basis of centrifuge [AIAA PAPER 93-3577] p 1208 A93-52673

Representation of vehicle location in networked simulations [AIAA PAPER 93-3582] p 1214 A93-52677

A radar altitude and line of sight attachment [AIAA PAPER 93-3587] p 1223 A93-52680

A dual-Euler method for solving all-attitude angles of the aircraft [AIAA PAPER 93-3589] p 1223 A93-52682

Initial development of a research flight simulator software [AIAA PAPER 93-3590] p 1223 A93-52683

Enhancing real-time flight simulation execution by intercepting Run-Time Library calls [AIAA PAPER 93-3591] p 1224 A93-52684

Reusable code for helicopter simulation [AIAA PAPER 93-3594] p 1224 A93-52686

Flight update of aerodynamic math model [AIAA PAPER 93-3596] p 1224 A93-52687

How to consider simulation fidelity and validity for an engineering simulator [AIAA PAPER 93-3598] p 1209 A93-52688

USAF in-flight simulation - A cost-effective operating approach [AIAA PAPER 93-3604] p 1175 A93-52690

A rapid prototyping system for inflight simulation using the Calspan Learjet 25 [AIAA PAPER 93-3606] p 1191 A93-52691

Flight simulation - An overview p 1209 A93-53768

Flight research simulation takes off p 1192 A93-53769

Networks extend simulation's reach p 1225 A93-53770

Removing the risk from rotorcraft testing p 1192 A93-53772

An aerodynamic model for the longitudinal motion of flight training devices p 1207 A93-54278

Inverse simulation: A tool for the validation of simulation programs - First results --- for helicopter flight tests and control p 1249 A93-56046

Initial piloted simulation study of geared flap control for tilt-wing V/STOL aircraft [NASA-TM-103872] p 64 N93-10741

Design of an air traffic computer simulation system to support investigation of civil tiltrotor aircraft operations [NASA-CR-190811] p 36 N93-11139

Simulation analysis of a cable-mount system used for dynamic wind tunnel tests [NAL-TR-1127] p 68 N93-12359

Accuracy improvement of linear estimated motion using differential type sensors [NAL-TR-1135] p 91 N93-12365

Flight simulator evaluation of D-size liquid crystal flat panel displays [NAL-TR-1136] p 52 N93-12367

Adaptive automation and human performance: Multi-task performance characteristics [AD-A254596] p 186 N93-12578

The modelling of turbulence and downbursts for flight simulators p 193 N93-13542

Advantages of using a projected head-up display in a flight simulator [AD-A255332] p 194 N93-14559

Flight testing: Past, present, and future p 164 N93-14615

Flight simulation leaves the ground p 194 N93-14616

Hot experimental technique: A new requirement of aerothermodynamics [MBB-FE-202-S-PUB-480] p 293 N93-17543

Flight simulation and constant amplitude fatigue crack growth in aluminum-lithium sheet and plate [NLR-TP-91104-U] p 331 N93-17562

Flight simulation evaluation of the flyability of curved MLS approaches with wide-body aircraft [NLR-TP-90238-U] p 382 N93-17875

Trade-offs arising from mixture of color cueing and monocular, binocular, and stereoscopic cueing information for simulated rotorcraft flight [NASA-TP-3268] p 338 N93-18333

Theoretical constraints in the design of multivariable control systems [NASA-CR-191900] p 442 N93-18372

Flight simulator for hypersonic vehicle and a study of NASP handling qualities p 530 N93-19456

- Use of microprocessor-based simulator technology and MEG/EEG measurement techniques in pilot emergency-maneuver training p 530 N93-19706
- A simulation study on take-off and landing dynamics of the aircraft of a fly-by-wire control system [AD-A259286] p 510 N93-19849
- Generation of helicopter roll axis bandwidth data through ground-based and in-flight simulation p 511 N93-19909
- Method for developing the RAFALE flight control system p 512 N93-19912
- On-line aircraft state and parameter estimation p 512 N93-19929
- The flight test and data analysis program for the development of a Boeing/De Havilland Dash 8 simulator model p 512 N93-19930
- A synthetic environment flight simulator: The AFIT virtual cockpit [AD-A259220] p 530 N93-20576
- A simulator study into low speed longitudinal handling qualities of ACT transport aircraft [NLR-TP-89387-U] p 527 N93-20743
- An aeroelastic model structure investigation for a manned real-time rotorcraft simulation p 693 N93-24756
- Use of high performance networks and supercomputers for real-time flight simulation p 731 N93-25574
- Piloted simulation of an air-ground profile negotiation process in a time-based Air Traffic Control environment [NASA-TM-107748] p 707 N93-26087
- A real-time, hardware-in-the-loop simulation of an unmanned aerial research vehicle [AD-A262477] p 893 N93-29409
- Three-dimensional graphical representation of objects according to movement data in real-time [ESA-TT-1258] p 942 N93-30104
- Virtual reality flight control display with six-degree-of-freedom controller and spherical orientation overlay [NASA-CASE-NPO-18733-1-CU] p 897 N93-30416
- Simulators for corporate pilot training and evaluation p 912 N93-30678
- Helicopter simulator qualification p 912 N93-30681
- Helicopter simulation: Making it work p 912 N93-30682
- Helicopter training simulators: Key market factors p 912 N93-30683
- Validation and upgrading of physically based mathematical models p 942 N93-30688
- Frequency-response techniques for documentation and improvement of rotorcraft simulators p 913 N93-30689
- Bandwidth and SIMDUCE as simulator fidelity criteria p 913 N93-30690
- Methodology development for evaluation of selective-fidelity rotorcraft simulation p 913 N93-30691
- Testing of an experimental FMS p 998 N93-31277
- Pallet for helicopter test instrumentation p 1000 N93-31279
- Fractographic and microstructural analysis of fatigue crack growth in Ti-6Al-4V fan disc forgings p 1004 N93-31742
- A high-fidelity, six-degree-of-freedom batch simulation environment for tactical guidance research and evaluation [NASA-TM-4440] p 1010 N93-32380
- FLIGHT SIMULATORS**
- Flight testing and simulation of an F-15 airplane using throttles for flight control [AIAA PAPER 92-4109] p 39 A93-11278
- Design and implementation of a flight simulation system — Book p 66 A93-12216
- Preliminary design features of the RASCAL - A NASA/Army rotorcraft in-flight simulator [AIAA PAPER 92-4175] p 42 A93-13311
- Why simulators don't fly like the airplane: Data - An update with examples from the C-141B program [AIAA PAPER 92-4161] p 66 A93-13312
- Helicopter in-flight simulator ATHeS - A multipurpose testbed and its utilization [AIAA PAPER 92-4173] p 43 A93-13315
- Flight simulator research into advanced MLS approach and departure procedures p 149 A93-14234
- Flight simulator development in China p 191 A93-14410
- A simulator solution for the parachute canopy control and guidance training problem [SAE PAPER 920984] p 191 A93-14634
- Helicopter automatic flight control systems for all weather operations - EH101 and beyond p 186 A93-17310
- Model of a map indicator p 341 A93-18532
- Progress towards common standards for flight simulator qualification p 374 A93-18774

- A 'low-cost' full flight simulator for basic IFR training p 374 A93-18776
- Using system identification to improve the performance of a low-cost flight simulator p 369 A93-22885
- Flight simulator fidelity assessment in a rotorcraft lateral translation maneuver p 378 A93-23510
- Parachute canopy control and guidance training requirements and methodology [AIAA PAPER 93-1255] p 703 A93-35188
- ATHeS - A helicopter in-flight simulator with high bandwidth capability p 821 A93-35988
- Evaluation of tilt rotor aircraft design utilizing a realtime interactive simulation p 798 A93-35989
- Recent improvements on the Dynamic Flight Simulator p 1011 A93-45167
- A method of wind shear detection for powered-lift STOL aircraft [AIAA PAPER 93-3667] p 1104 A93-48345
- Use of full flight simulator technology enhances classroom training sessions p 1136 A93-49277
- A survey of position trackers p 1151 A93-49396
- The challenges of simulating wake vortex encounters and assessing separation criteria [AIAA PAPER 93-3568] p 1096 A93-49518
- Development of advanced approach and departure procedures [AIAA PAPER 93-3833] p 1098 A93-51422
- International standards for the qualification of airplane flight simulators; Conference, London, United Kingdom, Jan. 16, 17, 1992, Document Approved (ISBN 1-85768-040-5) p 1140 A93-51934
- AIAA Flight Simulation Technologies Conference, Monterey, CA, Aug. 9-11, 1993, Technical Papers p 1207 A93-52651
- Evolution of flight simulation [AIAA PAPER 93-3545] p 1207 A93-52652
- Internally coherent system of innovation - The case of flight simulation [AIAA PAPER 93-3548] p 1226 A93-52653
- Methodology for integration of digital control loaders in aircraft simulators [AIAA PAPER 93-3551] p 1207 A93-52655
- Dynamic simulation fidelity improvement using transfer function state extrapolation [AIAA PAPER 93-3552] p 1222 A93-52656
- Transport delay compensation - An inexpensive alternative to increasing image generator update rate [AIAA PAPER 93-3563] p 1223 A93-52663
- Visual weather simulation using meteorological databases [AIAA PAPER 93-3566] p 1207 A93-52665
- The development of SIMONA - A simulator facility for advanced research into simulation techniques, motion system control and navigation systems technologies [AIAA PAPER 93-3574] p 1208 A93-52670
- Development and operation of a real-time simulation at the NASA Ames Vertical Motion Simulator [AIAA PAPER 93-3575] p 1208 A93-52671
- Semi-full-scale dynamic simulation complex on the basis of centrifuge [AIAA PAPER 93-3577] p 1208 A93-52673
- Simulation motion effect on single axis compensatory tracking [AIAA PAPER 93-3579] p 1208 A93-52675
- Pilot evaluations of augmented flight simulator motion [AIAA PAPER 93-3580] p 1208 A93-52676
- Implementation of expert systems within an interactive tactical environment [AIAA PAPER 93-3583] p 1223 A93-52678
- Initial development of a research flight simulator software [AIAA PAPER 93-3590] p 1223 A93-52683
- Flight update of aerodynamic math model [AIAA PAPER 93-3596] p 1224 A93-52687
- How to consider simulation fidelity and validity for an engineering simulator [AIAA PAPER 93-3598] p 1209 A93-52688
- USAF in-flight simulation - A cost-effective operating approach [AIAA PAPER 93-3604] p 1175 A93-52690
- A rapid prototyping system for inflight simulation using the Calspan Learjet 25 [AIAA PAPER 93-3606] p 1191 A93-52691
- Flight simulation - An overview p 1209 A93-53768
- Networks extend simulation's reach p 1225 A93-53770
- Engineering simulators enhance 777 development p 1192 A93-53771
- Removing the risk from rotorcraft testing p 1192 A93-53772
- Flight simulator evaluation of D-size liquid crystal flat panel displays [NAL-TR-1136] p 52 N93-12367
- Liquid crystal flat panel display evaluation tests using a flight simulator [NAL-TR-1122] p 52 N93-12368

- Advantages of using a projected head-up display in a flight simulator [AD-A255332] p 194 N93-14559
- Flight simulation leaves the ground p 194 N93-14616
- Multiple model adaptive estimation applied to the VISTA F-16 with actuator and sensor failures, volume 2 [AD-A256569] p 371 N93-16165
- Simulator motion [AD-A257683] p 381 N93-17687
- Trade-offs arising from mixture of color cueing and monocular, binoptic, and stereoscopic cueing information for simulated rotorcraft flight [NASA-TP-3268] p 338 N93-18333
- Flight simulator for hypersonic vehicle and a study of NASP handling qualities p 530 N93-19456
- A synthetic environment flight simulator: The AFIT virtual cockpit [AD-A259220] p 530 N93-20576
- Measurement of modulation transfer functions of simulator displays [AD-A259401] p 530 N93-21268
- Preliminary studies of planning and flight strip use as air traffic controller memory aids [DOT/FAA/CT-TN92/22] p 503 N93-21759
- An aeroelastic model structure investigation for a manned real-time rotorcraft simulation p 693 N93-24756
- Evaluation of advanced displays for engine monitoring and control [NASA-CR-191418] p 716 N93-24764
- Use of high performance networks and supercomputers for real-time flight simulation p 731 N93-25574
- Rendering the out-the-window view for the AFIT virtual cockpit [AD-A262599] p 823 N93-28467
- Toward reusable graphics components in Ada [AD-A262568] p 849 N93-28577
- Part 1: Executive summary p 857 N93-30674
- Helicopter simulator standards p 912 N93-30675
- Simulators for corporate pilot training and evaluation p 912 N93-30678
- Helicopter simulator qualification p 912 N93-30681
- Helicopter simulation: Making it work p 912 N93-30682
- Determining the transferability of flight simulator data p 913 N93-30685
- Progress through precedent: Going where no helicopter simulator has gone before p 913 N93-30686
- Transfer of training and simulator qualification or myth and folklore in helicopter simulation p 913 N93-30687
- Frequency-response techniques for documentation and improvement of rotorcraft simulators p 913 N93-30689
- Bandwidth and SIMDUCE as simulator fidelity criteria p 913 N93-30690
- Methodology development for evaluation of selective-fidelity rotorcraft simulation p 913 N93-30691
- The DLR test aircraft in the FZ-BS, -VFW 614/ATTAS, Dornier DO 228-101, MBB BO105 S-3 p 1018 N93-31272
- FLIGHT STABILITY TESTS**
- Research on the stability and control of soaring birds [AIAA PAPER 92-4122] p 61 A93-11284
- Aerodynamic characteristics of the MMPT ATD vehicle at high angles of attack [AIAA PAPER 93-3493] p 982 A93-47265
- Experimental analysis of rotary derivatives on a modern aircraft configuration [AIAA PAPER 93-3514] p 985 A93-47278
- FLIGHT TEST INSTRUMENTS**
- A European collaborative NLF nacelle flight demonstrator [PNR-90992] p 20 N93-11113
- Flight Testing [AGARD-CP-519] p 510 N93-19901
- The application of phase tracking GPS for flight test trajectory determination [NLR-TP-91349-U] p 994 N93-32337
- FLIGHT TESTS**
- Automatic dependent surveillance (ADS) Pacific engineering trials (PET) p 30 A93-10999
- Differential GPS/inertial navigation approach/landing flight test results p 32 A93-11019
- AIAA Biennial Flight Test Conference, 6th, Hilton Head Island, SC, Aug. 24-26, 1992, Selected Papers p 37 A93-11251
- Flight testing in the 90's [AIAA PAPER 92-4123] p 102 A93-11256
- Measuring flight test progress on large scale development programs [AIAA PAPER 92-4070] p 37 A93-11257

SUBJECT INDEX

Real-time capture, archiving, retrieval, processing, and presentation of large quantities of flight test/research information
[AIAA PAPER 92-4073] p 95 A93-11258

Flight test and wind-tunnel study of a scaled unmanned air vehicle
[AIAA PAPER 92-4075] p 37 A93-11260

Phase I flight test of MIAG advanced development model
[AIAA PAPER 92-4076] p 95 A93-11261

Flight testing of an electric powered vehicle
[AIAA PAPER 92-4077] p 37 A93-11262

Handling qualities flight test techniques and analyses used with the proposed MIL-H-8501B
[AIAA PAPER 92-4081] p 61 A93-11264

Effects of thrust line offset on neutral point determination in stability flight testing
[AIAA PAPER 92-4082] p 61 A93-11265

Flying qualities of a remotely piloted vehicle
[AIAA PAPER 92-4083] p 61 A93-11266

Design and conduct of a windshear detection flight experiment
[AIAA PAPER 92-4092] p 38 A93-11268

757 fly-by-wire demonstrator flight test
[AIAA PAPER 92-4099] p 38 A93-11271

In-flight flow visualization results from the X-29A aircraft at high angles of attack
[AIAA PAPER 92-4102] p 38 A93-11272

Flight test results from a supercritical mission adaptive wing with smooth variable camber
[AIAA PAPER 92-4101] p 38 A93-11274

Subsonic high-lift flight research on the NASA Transport System Research Vehicle (TSRV)
[AIAA PAPER 92-4103] p 38 A93-11275

Integrated flight propulsion control research results using the NASA F-15 HIDE Flight Research Facility
[AIAA PAPER 92-4106] p 38 A93-11276

Pitch control margin at high angle of attack - Quantitative requirements (flight test correlation with simulation predictions)
[AIAA PAPER 92-4107] p 39 A93-11277

Flight testing and simulation of an F-15 airplane using throttles for flight control
[AIAA PAPER 92-4109] p 39 A93-11278

Flight experience with lightweight, low-power miniaturized instrumentation systems
[AIAA PAPER 92-4111] p 39 A93-11280

The development of an airborne information management system for flight test
[AIAA PAPER 92-4113] p 51 A93-11281

Flight test evaluation of precision-code differential GPS for terminal approach and landing
[AIAA PAPER 92-4121] p 33 A93-11294

The Superpressure Stratospheric Vehicle
[AIAA PAPER 92-4107] p 39 A93-11357

NASA Long Duration Balloon capability development project
[AIAA PAPER 92-4109] p 2 A93-11370

A maximum likelihood method for flight test data compatibility check
[AIAA PAPER 92-4094] p 95 A93-12732

Flight test operations using an F-106B research airplane modified with a wing leading-edge vortex flap
[AIAA PAPER 92-4094] p 42 A93-13261

Flight evaluation of a stagnation detection hot-film sensor
[AIAA PAPER 92-4085] p 51 A93-13253

Design and utilization of a Flight Test Engineering Database Management System at the NASA Dryden Flight Research Facility
[AIAA PAPER 92-4072] p 97 A93-13264

Recent flight-test results of optical airdata techniques
[AIAA PAPER 92-4086] p 51 A93-13265

B-2 flight test program - An update
[AIAA PAPER 92-4118] p 42 A93-13266

Test pilot's notes on flying the Low Altitude/Airspeed Unmanned Research Aircraft (LAURA)
[AIAA PAPER 92-4078] p 42 A93-13269

Airspeed calibration using GPS
[AIAA PAPER 92-4090] p 51 A93-13272

The F-18 High Alpha Research Vehicle - A high-angle-of-attack testbed aircraft
[AIAA PAPER 92-4121] p 42 A93-13273

Helicopter in-flight simulator ATHeS - A multipurpose testbed and its utilization
[AIAA PAPER 92-4173] p 43 A93-13315

Piloted simulation evaluation of pitch control designs for highly augmented STOL aircraft
[AIAA PAPER 92-4234] p 63 A93-13328

Determination of YAV-8B Reaction Control System bleed flow usage
[AIAA PAPER 92-4232] p 54 A93-13330

Reliability testing of the EH101
[AIAA PAPER 92-4232] p 45 A93-13406

Drag/thrust estimation via aircraft performance flight testing
[AIAA PAPER 92-4232] p 156 A93-14322

Parameter estimation techniques for flight flutter test analysis
[AIAA PAPER 92-4232] p 156 A93-14324

The integrated actuation package approach to primary flight control
[SAE PAPER 920968] p 185 A93-14630

Development of a hydrogen external burning flight test experiment on the NASA Dryden SR-71A aircraft
[SAE PAPER 920997] p 157 A93-14638

HUD Guidance for the ASKA Experimental STOL Aircraft using Radar Position Information
[SAE PAPER 921041] p 150 A93-14661

Tiltrotor Research Aircraft composite blade repairs - Lessons learned
p 108 A93-14819

Toulouse - Flight tests of the Airbus A340
p 159 A93-16859

Estimation of aerodynamic characteristics from flight test data. II - Analysis methods under in-flight wind tunnel test concept
p 191 A93-16934

The certification of head up displays for category 3 operation
p 142 A93-17304

The development and implementation of a head-up guidance system (HGS) for manual CAT III landings
p 151 A93-17306

Helicopter automatic flight control systems for all weather operations - EH101 and beyond
p 186 A93-17310

Vision-based range estimation using helicopter flight data
p 151 A93-17501

Breaking the stall barrier
p 159 A93-17502

Acoustic flight test experience with the XV-15 Tiltrotor aircraft with the Advanced Technology Blade (ATB)
p 445 A93-19143

Noise evaluation of light propeller-driven aircraft
p 398 A93-19189

Vibro-acoustic analysis of propeller aircraft, integrating advanced experimental modeling with in-flight data analysis
p 451 A93-19230

Rudder and elevator effects on the incipient spin characteristics of a typical general aviation training aircraft
[AIAA PAPER 93-0016] p 367 A93-20138

GPS/GLONASS flight test, lab test and coverage analysis tests
p 313 A93-21143

Results from a GPS Shuttle Training Aircraft flight test
p 384 A93-21148

A statistical comparison of differential GPS and laser generated time, space positioning information for aircraft flight testing
p 316 A93-21199

Vision-based range estimation using helicopter flight data
p 317 A93-21525

Thrust vectoring - Theory, laboratory, and flight tests
p 367 A93-21657

Overview of Japanese aerospace plane
[AIAA PAPER 92-5005] p 384 A93-22282

Some aspects of the aerodynamic methodology in hypersonic vehicle concept studies
[AIAA PAPER 92-5027] p 272 A93-22303

CFD comparisons with wind tunnel and flight data for the X-15
[AIAA PAPER 92-5047] p 273 A93-22319

Atmospheric reentry flight test of winged space vehicle
[AIAA PAPER 92-5053] p 385 A93-22324

The Air Force Flight Test Center artificial icing and rain testing capability upgrade program
[AIAA PAPER 93-0295] p 376 A93-22695

The X-15 airplane - Lessons learned
[AIAA PAPER 93-0309] p 456 A93-23005

Icing effects on aircraft stability and control determined from flight data - Preliminary results
[AIAA PAPER 93-0398] p 370 A93-23073

The effects of hypersonic flight test requirements on research vehicle design
[AIAA PAPER 93-0511] p 386 A93-23258

Liquid water content measurements using the Phase Doppler Particle Analyzer in the NASA Lewis Icing Research Tunnel
[AIAA PAPER 93-0298] p 378 A93-23698

Analysis of flight flutter test data
p 523 A93-23839

Operational and research aspects of a radio-controlled model flight test program
[AIAA PAPER 93-0625] p 504 A93-24742

Signal processing of jet noise from flyover test data
[AIAA PAPER 93-0736] p 563 A93-24826

CWAS - Clean wing advisory system: A new approach to ice detection
[AIAA PAPER 93-0747] p 516 A93-24835

High-performance aircraft propulsion research
p 529 A93-27904

Laminar-flow instrumentation for wind-tunnel and flight experiments
p 479 A93-28605

Development and validation of 'quiet tail rotor' technology
p 567 A93-29416

Validation of high frequency airload calculations using full scale flight test acoustic data
p 567 A93-29417

NOTAR system - A quiet character
p 567 A93-29418

FLIGHT TESTS

Acoustic characteristics of advanced model rotor systems
p 567 A93-29419

Prediction of helicopter component loads using neural networks
[AIAA PAPER 93-1301] p 756 A93-33878

Aeromechanical stability of helicopters with composite rotor blades in forward flight
p 794 A93-35904

Overview of Tiger dynamics validation program
p 794 A93-35907

Interactional aerodynamic effects on rotor performance in hover and forward flight
p 766 A93-35941

Side-by-side hover performance comparison of MDHC 500 NOTAR and tail rotor anti-torque systems
p 796 A93-35956

Handling qualities testing using the mission oriented requirements of ADS-33C
p 817 A93-35961

Advanced Technology Blade testing on the XV-15 Tilt Rotor Research Aircraft
p 799 A93-36020

V-22 tiltrotor Flight Test Development
p 800 A93-36021

The V-22 for SOF
p 800 A93-36026

Evaluation and extension of the flutter-margin method for flight flutter prediction
p 828 A93-37393

A data reduction system for processing instrumented flight test data
p 847 A93-37866

Validation of R85/METAR on the Puma RAE flight tests
[ONERA, TP NO. 1992-123] p 802 A93-38597

F/A-18 controls released departure recovery - Flight test evaluation
p 803 A93-38839

B-2 flight test update
p 803 A93-38844

The SAAB 2000 initial flight test - Status report
p 804 A93-38847

A study of the interaction between a wake vortex and an encountering airplane
[AIAA PAPER 93-3642] p 858 A93-40714

Effects of equipment calibration, test flight procedures and analysis methods on the accuracy of ILS glide path measurements - Book
p 881 A93-41600

Laminar flow flight experiments - A review
p 890 A93-41778

Flight research on natural laminar flow applications
p 890 A93-41779

Validation of engineering methods for predicting hypersonic vehicle control forces and moments
p 906 A93-41897

Experimental and algorithmic means of identifying mathematical models of flight vehicle
p 909 A93-43103

Application of two chaos methods to Higher Harmonic Control data - for suppression of helicopter vibration
p 909 A93-43783

A convective and radiative heat transfer analysis for the FIRE II forebody
[AIAA PAPER 93-3194] p 1021 A93-44231

Optical correlator field test results
p 1038 A93-44458

Zero-thrust glide testing for drag and propulsive efficiency of propeller aircraft
p 995 A93-45143

Vortex flap flight test operations, a safe approach
p 995 A93-45168

Determination of the takeoff and landing characteristics of aircraft by using a conditional polar
p 1007 A93-45662

Flow visualization of mast-mounted-sight/main rotor aerodynamic interactions
[AIAA PAPER 93-3517] p 1009 A93-47280

Estimation of neutral and maneuver points of aircraft by dynamic maneuvers
[AIAA PAPER 93-3620] p 1126 A93-48307

Estimation of aerodynamic coefficients using neural networks
[AIAA PAPER 93-3639] p 1165 A93-48324

Development of flying qualities and agility evaluation maneuvers
[AIAA PAPER 93-3645] p 1127 A93-48329

A simplified wing rock prediction method
[AIAA PAPER 93-3662] p 1128 A93-48342

Aeroelastic effects on the B-2 maneuver response
[AIAA PAPER 93-3664] p 1128 A93-48344

A new flying qualities criterion for flying wings
[AIAA PAPER 93-3668] p 1128 A93-48346

F/A-18 departure recovery improvement evaluation
[AIAA PAPER 93-3671] p 1129 A93-48349

On engine parameter estimation with flight test data
p 1107 A93-48520

Flight testing of a fiber optic temperature sensor
p 1105 A93-49476

Two-dimensional computational analysis of a transport high-lift system and a comparison with flight-test results
[AIAA PAPER 93-3533] p 1072 A93-49517

Preliminary flight test results of a fly-by-throttle emergency flight control system on an F-15 airplane
[AIAA PAPER 93-1820] p 1100 A93-49708

- Review of NASA's Hypersonic Research Engine Project
[AIAA PAPER 93-2323] p 1116 A93-50103
- Flight-determined engine exhaust characteristics of an F404 engine in an F-18 airplane
[AIAA PAPER 93-2543] p 1121 A93-50267
- F405 engine in-flight thrust methodology development for the T-45A flight test program
[AIAA PAPER 93-2544] p 1121 A93-50268
- X-29 high-angle-of-attack flight testing
p 1101 A93-50487
- Performance-seeking control - Program overview and future directions
[AIAA PAPER 93-3765] p 1102 A93-51360
- Initial results of an in-flight investigation of longitudinal flying qualities for augmented, large transports in approach and landing
[AIAA PAPER 93-3816] p 1133 A93-51407
- Correction of a method for calculating the noise levels of aircraft at control points during acoustic flight testing
p 1102 A93-51758
- Identification of actuation system and aerodynamic effects of direct-lift-control flaps
p 1103 A93-52435
- Instrumentation and telemetry systems for free-flight drop model testing
p 1209 A93-52754
- A method for the spectral-time identification of the longitudinal and lateral motions of an aircraft
p 1205 A93-52942
- Identification of the phase characteristics and wind-induced perturbations of an aircraft from flight test results
p 1206 A93-52943
- Complementary role of ground testing, flight testing, and computations in aerospace plane propulsion development
[ISABE 93-7034] p 1197 A93-54010
- Longitudinal closed-loop pilot/vehicle analysis of DFBW aircraft during approach and landing
p 1206 A93-54277
- Estimation of aerodynamic characteristics from flight-test data. IV - Principal component analysis and perpendicular error method
p 1241 A93-54551
- Estimation of aerodynamic characteristics from flight-test data. V - Effects of gust and its time lag
p 1230 A93-54560
- Airship applications of modern flight test techniques
[AIAA PAPER 93-4035] p 1242 A93-54606
- Inverse simulation: A tool for the validation of simulation programs - First results --- for helicopter flight tests and control
p 1249 A93-56046
- West powers East
p 1244 A93-56349
- Design and implementation of digital filters for analysis of F/A-18 flight test data
p 17 A93-10342
- [AD-A253447] p 17 A93-10342
- Appraisal of digital terrain elevation data for low-altitude flight
[NASA-TM-103896] p 35 A93-10745
- Flight test and analysis procedures for new handling criteria
[RAE-TM-FM-26] p 47 A93-10803
- A European collaborative NLF nacelle flight demonstrator
[PNR-90992] p 20 A93-11113
- Correlation of forebody pressures and aircraft yawing moments on the X-29A aircraft at high angles of attack
[NASA-TM-4417] p 22 A93-11532
- Hybrid guidance for maneuvering flight vehicles
[AD-A254110] p 69 A93-11798
- Flight test results from a supercritical mission adaptive wing with smooth variable camber
[NASA-TM-4415] p 49 A93-11863
- Flight test progress of the STOL research aircraft ASKA
[NAL-TM-643] p 49 A93-12354
- Subsonic flight test evaluation of a propulsion system parameter estimation process for the F100 engine
[NASA-TM-4426] p 175 A93-13155
- Flight analysis of air intake/engine compatibility
p 161 A93-13212
- National Aero-Space Plane: Key issues facing the program. Testimony before the Subcommittee on Technology and Competitiveness, Committee on Science, Space, and Technology, House of Representatives
[GAO/T-NSIAD-92-26] p 161 A93-13253
- Pressure distribution for the wing of the YAV-8B airplane; with and without pylons
[NASA-TM-4429] p 136 A93-14451
- Flight testing: Past, present, and future
p 164 A93-14615
- Icing effects on aircraft stability and control determined from flight data: Preliminary results
[NASA-TM-105977] p 188 A93-14831
- NASA/LMSC coherent LIDAR airborne shear sensor: System capabilities and flight test plans
p 144 A93-14847
- A neural network prototype for predicting F-14B strains at the B.L. 10 longeron
[AD-A255272] p 165 A93-15004
- F/A-18 controls released departure recovery flight test evaluation
[AD-A256522] p 189 A93-15396
- Multiple model adaptive estimation applied to the VISTA F-16 with actuator and sensor failures, volume 2
[AD-A256569] p 371 A93-16165
- Pilot weather advisor
[NASA-CR-189723] p 318 A93-16692
- Integrated helmet system testing for a nightflying helicopter
[MBB-UD-0604-91-PUB] p 343 A93-17570
- A multi-faceted engineering study of aerodynamic errors of the Service Aircraft Instrumentation Package (SAIP)
[AD-A258059] p 293 A93-17677
- Manual flying of curved precision approaches to landing with electromechanical instrumentation. A piloted simulation study
[NASA-TP-3255] p 344 A93-18408
- Operational and research aspects of a radio-controlled model flight test program
[NASA-TM-104266] p 339 A93-18616
- Adverse weather test site selection study
[AD-A259012] p 339 A93-18895
- Flight and wind-tunnel calibrations of a flush airdata sensor at high angles of attack and sideslip and at supersonic Mach numbers
[NASA-TM-104265] p 344 A93-19110
- Airborne Wind Shear Detection and Warning Systems: Fourth Combined Manufacturers' and Technologists' Conference, part 1
[NASA-CP-10105-PT-1] p 488 A93-19590
- Program overview: 1991 flight test objectives
p 488 A93-19591
- Flight test operations
p 488 A93-19592
- Air/ground wind shear information integration: Flight test results
p 488 A93-19594
- Airborne doppler radar research at Rockwell International
p 489 A93-19602
- Acquisition and use of Orlando, Florida and Continental Airbus radar flight test data
p 489 A93-19603
- NASA airborne radar wind shear detection algorithm and the detection of wet microbursts in the vicinity of Orlando, Florida
p 490 A93-19611
- Signal processing for airborne doppler radar detection of hazardous wind shear as applied to NASA 1991 radar flight experiment data
p 490 A93-19612
- A simulation study on take-off and landing dynamics of the aircraft of a fly-by-wire control system
[AD-A259286] p 510 A93-19849
- Flight Testing
[AGARD-CP-519] p 510 A93-19901
- Flight tests of the transport aircraft viewed from the industrial standpoint
p 510 A93-19903
- Lessons learned from an historical look at flight testing
p 511 A93-19904
- YF-22A prototype advanced tactical fighter demonstration/validation flight test program overview
p 511 A93-19906
- Generation of helicopter roll axis bandwidth data through ground-based and in-flight simulation
p 511 A93-19909
- AM-X high angle of attack flight test experience (single and two seat versions)
p 511 A93-19910
- X-31A high angle of attack and initial post stall flight testing
p 511 A93-19911
- Method for developing the RAFALE flight control system
p 512 A93-19912
- On automated analysis of flight test data
p 512 A93-19913
- System identification for X-31A project support: Lessons learned so far
p 512 A93-19914
- Overview of the NASA Dryden Flight Research Facility aeronautical flight projects testing
p 512 A93-19916
- Testing of an automatic, low altitude, all terrain ground collision avoidance system
p 502 A93-19924
- RAMSES: Multi-spectral experimental radar station installed on board the Transall
p 550 A93-19925
- Development and flight testing of a surface pressure measurement installation on the EAP demonstrator aircraft
p 550 A93-19927
- The flight test and data analysis program for the development of a Boeing/De Havilland Dash 8 simulator model
p 512 A93-19930
- URV flight test of an Ada implemented self-repairing flight control system
[AD-A259205] p 527 A93-20551
- The testing of fixed wing tanker and receiver aircraft to establish their air-to-air refuelling capabilities, volume 11
[AGARD-AG-300-VOL-11] p 514 A93-21305
- Program of research in flight dynamics in the JIAFS at NASA-Langley Research Center
[NASA-CR-191885] p 484 A93-21562
- An aeroelastic model structure investigation for a manned real-time rotorcraft simulation
p 693 A93-24756
- In-flight evaluation of noise levels and assessment of active noise reduction systems in the Seahawk S-70B-2 helicopter
[AD-A260689] p 759 A93-25649
- Development of a flight instrument package
[AD-A260830] p 719 A93-25783
- YF-22A prototype advanced tactical fighter demonstration/validation flight test program overview
p 805 A93-27173
- Practical input optimization for aircraft parameter estimation experiments
[NASA-CR-191462] p 820 A93-27264
- Status of the Fiber Optic Control System Integration (FOCSI) program
[NASA-TM-106151] p 841 A93-28053
- Flight evaluation of a computer aided low-altitude helicopter flight guidance system
p 820 A93-28869
- Helicopter approach capability using the differential global positioning system
[NASA-CR-193183] p 793 A93-28936
- Design study to simulate the development of a commercial transportation system
p 894 A93-29718
- A concluding study of the altitude determination deficiencies of the Service Aircraft Instrumentation Package (SAIP)
[AD-A263515] p 897 A93-29971
- Vortex wake characteristics of B757-200 and B767-200 aircraft using the tower fly-by technique
[PB93-180255] p 878 A93-30387
- Vortex wake characteristics of B757-200 and B767-200 aircraft using the tower fly-by technique
[PB93-180263] p 878 A93-30388
- Determining the transferability of flight simulator data
p 913 A93-30685
- Flight test of avionics and air-traffic control systems
[ESA-TT-1279] p 993 A93-31271
- The DLR test aircraft in the FZ-BS, -VFW 614/ATTAS, Dornier DO 228-101, MBB BO105 S-3
p 1018 A93-31272
- Ground installations for preparation and evaluation of flight tests
p 1014 A93-31274
- Instigation and processing of flight tests in DLR
p 998 A93-31275
- Testing of an experimental FMS
p 998 A93-31277
- Pallet for helicopter test instrumentation
p 1000 A93-31279
- Development and flight testing of a fault-tolerant fly-by-light yaw control system
p 1010 A93-31280
- Ground- and satellite-derived flight-path measurements as demonstrated in the AFES Avionics Flight Evaluation System (AFES)
p 993 A93-31281
- Installations and methods for measurement of aircraft radio components and systems
p 1031 A93-31284
- Effects of an aft facing step on the surface of a laminar flow glider wing
[NASA-CR-193302] p 990 A93-31855
- Engine exhaust characteristics evaluation in support of aircraft acoustic testing
[NASA-TM-104263] p 1005 A93-32220
- Airborne derivation of microburst alerts from ground-based Terminal Doppler Weather Radar information: A flight evaluation
[NASA-TM-108990] p 1000 A93-32223
- Flight evaluation of a computer aided low-altitude helicopter flight guidance system
[NASA-TM-103998] p 994 A93-32225
- Instrumentation for in-flight acoustic measurements in an engine inlet duct of a Fokker 100 aircraft
[NLR-TP-91200-U] p 1001 A93-32332
- Evaluation of the flyability of MLS curved approaches for wide-body aircraft
[NLR-TP-91396-U] p 999 A93-32416
- FLIGHT TIME**
- Trans-oceanic, polar patrol balloons and future prospects
p 26 A93-11366
- Long-duration balloon flights in the middle stratosphere
p 40 A93-11369
- NASA Long Duration Balloon capability development project
p 2 A93-11370
- Concept for an open-neck stratospheric balloon with long-duration flight capability
p 40 A93-11371
- Trans-oceanic balloon flight over east China sea
p 27 A93-11372
- Optimization of time saving in navigation through an area of variable flow
p 34 A93-12125
- On the maximum range of flying wings
[AIAA PAPER 92-4223] p 504 A93-24492
- The fuel/timing problem in a computer-aided flight preparation system for civil aircraft
p 996 A93-45672
- General concepts related to the determination of the individual flight performance characteristics of aircraft for establishing fuel consumption standards and optimal flight regimes
p 996 A93-45673

SUBJECT INDEX

- Computer-aided study of flight regimes and fuel consumption for helicopter flight operations p 997 A93-45674
- Minimum time turn of a helicopter p 1248 A93-54554
- General aviation aircraft: Normal acceleration data analysis and collection project [DOT/FAA/CT-91/20] p 713 N93-24739
- ### FLIGHT TRAINING
- A simulator solution for the parachute canopy control and guidance training problem [SAE PAPER 920984] p 191 A93-14634
- A 'low-cost' full flight simulator for basic IFR training p 374 A93-18776
- F/A-18 controls released departure recovery - Flight test evaluation p 803 A93-38839
- Innovative bagging techniques on a composite P-51 Mustang replica p 1191 A93-53405
- F/A-18 controls released departure recovery flight test evaluation [AD-A256522] p 189 N93-15396
- Cockpit resource management proficiency as a factor of primary flight training [AD-A256995] p 328 N93-16262
- Functional requirements of an advanced instructional design advisor: Simulation authoring, Volume 3 [AD-A256650] p 440 N93-16500
- Special investigation report: Flight attendant training and performance during emergency situations [PB92-917006] p 310 N93-16834
- Prediction of success from training p 495 N93-19702
- Measurement of modulation transfer functions of simulator displays [AD-A259401] p 530 N93-21268
- Performance-based testing and success in Naval advanced flight training [AD-A260838] p 717 N93-25933
- ### FLIGHT VEHICLES
- Software for the control of measurement data acquisition, processing, and monitoring during strength testings p 94 A93-10042
- A study of the possibility of the parallel execution of a program for calculating the aerodynamic characteristics of flight vehicles using an improved panel method p 95 A93-10045
- Recent advances in jet simulation techniques for flight vehicles p 66 A93-12656
- A nomographic model for multicriterial optimization during the design of a flight vehicle powerplant p 95 A93-12821
- Numerical study of jet interaction at super- and hypersonic speeds for flight vehicle control p 184 A93-14379
- Simulation of a hypersonic flow over vehicles at low Reynolds numbers p 120 A93-14381
- Modeling of human operator actions in the stochastic trajectory tracking problem for a dynamic plant p 228 A93-16783
- A new method for determining the number of flight vehicle prototypes subject to full-scale testing p 434 A93-18316
- The use of subscale models to predict self-induced oscillations of flight vehicles [AIAA PAPER 93-0093] p 264 A93-20199
- Aeroelastic model design using structural optimization [AIAA PAPER 92-4730] p 409 A93-20329
- High-performance computing for flight vehicles; Proceedings of the Symposium, Washington, Dec. 7-9, 1992 p 437 A93-20701
- Flight vehicle aerodynamics calculated by a Galerkin finite element/finite difference method p 266 A93-20738
- A set of application programs for the smoothing of curves and surfaces by the method of monoidal transformations in the geometric module of a CAD system for the design of flight vehicles p 561 A93-27629
- Algorithms and automated techniques for the design of control systems for moving objects p 562 A93-29690
- A design concept for a flight vehicle computer system with artificial intelligence elements p 757 A93-35663
- Comments on experiments for computational validation for fluid dynamic predictions p 927 A93-42578
- Active algorithms for controlling the rotational motion of flight vehicles p 908 A93-43079
- Synthesis of a data processing and measuring system for flight vehicle control systems p 908 A93-43102
- Experimental and algorithmic means of identifying mathematical models of flight vehicle p 909 A93-43103
- Approximation of a flight vehicle trajectory using Walsh functions p 909 A93-43106
- Visualization and view simulation based on transputers p 1037 A93-45150

- Numerical simulation of upstream disturbance on flows around a slender body [AIAA PAPER 93-2956] p 1047 A93-48150
- Experimental simulation of the aerodynamic heating of bodies in a molecular region p 1090 A93-51871
- Certain improved algorithms for calculating the aerodynamic characteristics of flight vehicles in free-molecular flow p 1090 A93-51872
- Problems in the aerodynamics of flight vehicles and their components p 1091 A93-51901
- ### FLIR DETECTORS
- Infrared detection of high altitude clear air turbulence [AIAA PAPER 93-0852] p 557 A93-24916
- Visual field information in Nap-of-the-Earth flight by teleoperated Helmet-Mounted Displays p 517 A93-26884
- ### FLOORS
- Energy-absorbing-beam design for composite aircraft subfloors [AIAA PAPER 93-1339] p 709 A93-33909
- ### FLOQUET THEOREM
- Trim analysis by shooting and finite elements and Floquet eigenanalysis by QR and subspace iterations in helicopter dynamics p 163 N93-13914
- ### FLOW CHARACTERISTICS
- Effect of wall heating on a supersonic turbulent boundary layer p 11 A93-12429
- Effect of heat supply on the gasdynamic parameters of gas flow in Laval nozzles p 12 A93-12760
- Effect of the drag of the front body on the restructuring of flow between two bodies in the path of supersonic flow, with one body located in the wake of the other p 14 A93-12973
- Stirling engine - Available tools for long-life assessment --- for space propulsion p 195 A93-13824
- Flow characteristics of an S-shaped inlet at high incidence p 114 A93-14213
- The use of a deep honeycomb to achieve high flow quality in the ARA 9 ft x 8 ft Transonic Wind Tunnel p 190 A93-14276
- A low speed wind-tunnel with extreme flow quality - Design and tests p 190 A93-14352
- Generation of flow disturbances in transonic wind tunnels p 119 A93-14354
- A wide-range axial-flow compressor stage performance model [ASME PAPER 92-GT-58] p 348 A93-19308
- The use of interferometry in the study of rotorcraft aerodynamics p 407 A93-19914
- Investigation of the dynamic inflow's influence on rotor control derivatives p 266 A93-20802
- Two-dimensional cascade tests of MCA blades in the high transonic Mach number region. V - Effect of space/chord ratio on the parameters of cascade performance p 267 A93-20930
- Flow field characteristics of an axisymmetric sudden-expansion pipe flow with different initial swirl distribution p 411 A93-21688
- Doppler global velocimetry measurements of the vortical flow above an F/A-18 [AIAA PAPER 93-0414] p 415 A93-23333
- Effects of free-stream turbulence on boundary-layer transition [AIAA PAPER 93-0488] p 416 A93-23390
- Eduction of swirling structure using the velocity gradient tensor p 416 A93-23547
- Numerical study of an axisymmetric turbulent jet-impingement flow [AIAA PAPER 93-0652] p 543 A93-25545
- Visualization and analysis of supersonic flow in rotating turbine stage. II - Analysis of the flow into the moving blades and their exit flow p 476 A93-27442
- A method for calculating the characteristics of plane compressor cascades for different values of the Reynolds criterion p 545 A93-27616
- Three-dimensional flow past an ogival-cylindrical body in combination with a delta wing p 478 A93-27636
- A method of predicting quasi-steady aerodynamics for flutter analysis of high speed vehicles using steady CFD calculations [AIAA PAPER 93-1364] p 682 A93-33931
- Intermode exchange in a supersonic boundary layer p 691 A93-35346
- A heat transfer element of a high-temperature heat exchanger p 833 A93-39047
- Flow past three-dimensional irregularities in a hypersonic boundary layer on a cooled body p 775 A93-39119
- Underexpanded boundary jet in a wake flow p 775 A93-39123
- Hypersonic flows for reentry problems. Vols. 1 & 2 [ISBN 0-387-54428-3] p 864 A93-42576
- The countercurrent mixing layer - Strategies for shear-layer control [AIAA PAPER 93-3260] p 968 A93-46826

FLOW CHARACTERISTICS

- Heat transfer on blunt cones in nonuniform supersonic flow in the presence of gas injection from the surface p 972 A93-46975
- A flowfield study of a close-coupled canard configuration [AIAA PAPER 93-3499] p 983 A93-47269
- An investigation of shock wave turbulent boundary layer interaction with bleed through slanted slots [AIAA PAPER 93-2992] p 1052 A93-48184
- Some stability characteristics of the boundary layer on a yawed cone [AIAA PAPER 93-3048] p 1057 A93-48228
- Flow field characteristics of a complex blade tip at high angles of attack [AIAA PAPER 93-3083] p 1060 A93-48257
- An experimental investigation of endwall flow control in a compressor plane cascade wind tunnel p 1066 A93-48512
- Effects of side-inlet angle in a three-dimensional side-dump combustor p 1109 A93-49610
- Numerical simulations of the unstart phenomenon in a supersonic inlet/diffuser [AIAA PAPER 93-2239] p 1081 A93-50041
- Flow investigation of a low-speed-operated centrifugal compressor over a flow range including zero flow [AIAA PAPER 93-2240] p 1155 A93-50042
- Effects of flow-path variations on internal reversing flow in a tailpipe offtake configuration for ASTOVL aircraft [AIAA PAPER 93-2438] p 1118 A93-50190
- The development of a large annular facility for testing gas turbine combustor diffuser systems [AIAA PAPER 93-2546] p 1139 A93-50269
- An experimental study of the dynamic effect of a supersonic underexpanded jet on a plane surface parallel to the nozzle axis p 1092 A93-51913
- Estimation of the change of axial-flow compressor characteristics during long-term service p 1193 A93-52949
- Isothermal flow characteristics behind V-shape gutter with and without injection [ISABE 93-7040] p 1198 A93-54016
- Correlations for flow property variation at outlet of a centrifugal impeller [ISABE 93-7054] p 1185 A93-54030
- Research requirements for a real-time flight measurements and data analysis system for subsonic transport high-lift research p 1244 A93-54391
- Development of separation due to interaction between a shock wave and a turbulent boundary layer perturbed by rarefaction waves p 1233 A93-55019
- Hypersonic inlet efficiency revisited p 16 N93-10012
- Characteristics of separated flows including cavitation effects p 84 N93-10874
- Dynamical effects of suction/heating on turbulent boundary layers [AD-A248459] p 87 N93-11416
- Flight test results from a supercritical mission adaptive wing with smooth variable camber [NASA-TM-4415] p 49 N93-11863
- Overview on test cases for computation of internal flows in turbomachines p 214 N93-13209
- Effects of forebody strakes and Mach number on overall aerodynamic characteristics of configuration with 55 deg cropped delta wing [NASA-TP-3253] p 131 N93-13353
- Chaotic vortical motion in the near region of a plane jet p 131 N93-13493
- The unsteady aerodynamics of a delta wing undergoing large-amplitude pitching motions p 134 N93-13929
- Parametric study of air sampling cyclones p 135 N93-14173
- Pressure distribution for the wing of the YAV-8B airplane; with and without pylons [NASA-TM-4429] p 136 N93-14451
- Control of low-speed turbulent separated flow over a backward-facing ramp p 219 N93-14475
- Wake similarity and vortex formation for two-dimensional bluff bodies p 138 N93-15101
- Natural laminar flow test in-flight visualization p 482 N93-19921
- Mean flow interactions of a counter-rotating propeller p 552 N93-20289
- The influence of the rotor test facilities ROTEST and ROTOS on the rotor inflow [DLR-MITT-91-16] p 522 N93-21173
- A numerical and experimental studies of flow characteristics in centrifugal fans p 695 N93-25339
- Effect of pylon cross-sectional geometries on propulsion integration for a low-wing transport [NASA-TP-3333] p 788 N93-28070
- Effects of flow-path variations on internal reversing flow in a tailpipe offtake configuration for ASTOVL aircraft [NASA-TM-106149] p 900 N93-29065
- Flow phenomena in turbomachines [AD-A263049] p 930 N93-29141

- Cooling geometry optimization using liquid crystal technique p 902 A93-29939
- Flow and heat transfer between gas-turbine discs p 903 A93-29950
- Three-dimensional fiber-optic LDV measurements in the endwall region of a linear cascade of controlled-diffusion stator blades [AD-A263513] p 933 A93-29968
- Vortex wake characteristics of B757-200 and B767-200 aircraft using the tower fly-by technique [PB93-180255] p 878 A93-30387
- Vortex wake characteristics of B757-200 and B767-200 aircraft using the tower fly-by technique [PB93-180263] p 878 A93-30388
- Penn State axial flow turbine facility: Performance and nozzle flow field p 1032 A93-31588
- The prediction of noise from co-axial jets [ISVR-TR-215] p 1040 A93-32339
- FLOW COEFFICIENTS**
- Low area ratio aircraft fuel jet-pump performances with and without cavitation p 272 A93-22264
- The effect of Reynolds number on control of forebody asymmetry by suction and bleed [AIAA PAPER 93-3265] p 968 A93-46831
- Performance parameters and assessment p 81 A93-10052
- Rotating stall: Modeling-measurement techniques; unsteady loss-unsteady flow field p 424 A93-18732
- Experimental effects of wing location on wing-body pressures at supersonic speeds [NASA-TM-4434] p 700 A93-26085
- FLOW DEFLECTION**
- One-dimensional methods for accurate prediction of off-design performance behavior of axial turbines [ASME PAPER 92-GT-54] p 347 A93-19304
- Nonlocal vs. local instability of compressible flows including body metric, flow divergence and 3D-wave propagation [AIAA PAPER 93-2982] p 1051 A93-48175
- Effect of the size of a plane obstacle on self-oscillations generated in an underexpanded supersonic jet p 1068 A93-48849
- FLOW DIRECTION INDICATORS**
- Experimental investigations of the time and flow-direction responses of shear-stress-sensitive liquid crystal coatings [AIAA PAPER 93-0181] p 542 A93-25508
- FLOW DISTORTION**
- A study of the effect of nonstationary perturbations on flow in the front separation region p 5 A93-10150
- Flow characteristics of an S-shaped inlet at high incidence p 114 A93-14213
- A digital simulation and its experimental investigation for the response of gas-turbine engines to intake flow distortion p 120 A93-14366
- Instability of local separated flows with respect to small-amplitude perturbations p 125 A93-15254
- Experimental study of controlled tip disturbance effect on flow asymmetry p 211 A93-17417
- Recess vane passive stall control [ASME PAPER 92-GT-36] p 246 A93-19296
- Estimation of the maximum values of instantaneous distortion index DC sub theta --- of fluid flow p 266 A93-20806
- A new technique for analysis of unsteady aerodynamic responses of cascade airfoils with blunt leading edge. I - Theory p 267 A93-20909
- Performance analysis of supersonic through-flow fan by the lifting surface theory. I - Disturbance flow field and determination of blade loadings p 267 A93-20929
- Conventional skin friction measurement techniques for strongly perturbed supersonic turbulent boundary layers p 271 A93-21863
- Flow quality improvement in a high speed blowdown wind tunnel [AIAA PAPER 93-0353] p 377 A93-23038
- Vortex distortion during vortex-surface interaction in a Mach 3 stream [AIAA PAPER 93-0761] p 467 A93-24846
- Calculation of three-dimensional supersonic flow past lifting surfaces p 477 A93-27607
- Interaction of Tollmien-Schlichting waves with localized disturbances p 545 A93-27637
- The effect of Reynolds number on control of forebody asymmetry by suction and bleed [AIAA PAPER 93-3265] p 968 A93-46831
- Numerical simulation of upstream disturbance on flows around a slender body [AIAA PAPER 93-2956] p 1047 A93-48150
- Development of resonance perturbations in a supersonic jet p 1088 A93-51772
- Modeling the flow around a body via the solution of the relaxational kinetic equation p 1089 A93-51868
- Calculation of compressible gas flow on optimal difference grids p 1091 A93-51902

- A study of optical distortions arising in radiation transmission through cavities with gas flow around them p 1225 A93-52945
- Review of stall, surge and active control in axial compressors [ISABE 93-7011] p 1184 A93-53987
- An investigation of post stall transients and recoverability of axial compression systems [ISABE 93-7012] p 1184 A93-53988
- Quantitative Knudsen-number dependences of density disturbances in front of obstructions in supersonic divergent flows p 1239 A93-56220
- The role of turbomachinery testing for stability in distorted flow [PNR-90943] p 57 A93-11040
- Experimental and numerical examinations of the influence of inlet distortion perturbations on the working behavior of turbofan compressors [ETN-93-92733] p 364 A93-18628
- Stall transients including effects of inlet distortion and intake geometry p 423 A93-18726
- FLOW DISTRIBUTION**
- A data processing and measuring system with a traversing probe for studying flow in the rotating impeller of an axial-flow fan p 75 A93-10032
- Effect of a large-scale inhomogeneity of the incoming flow on flow in a plane turbine cascade p 6 A93-10189
- An effective multigrid method for high-speed flows p 6 A93-10533
- Flow problems posed by reentry in planetary atmospheres p 11 A93-12432
- Experimental research for the discharge flow of a centrifugal impeller and the flowfield in the vaneless diffuser p 11 A93-12454
- Effect of hub treatment on performance of an axial flow compressor p 53 A93-12736
- Infrared flow visualization of V/STOL aircraft [AIAA PAPER 92-4253] p 80 A93-13343
- Probing questions for aerodynamic testing p 80 A93-13437
- Heat transfer, adiabatic effectiveness, and injectant distributions downstream of a single row and two staggered rows of compound angle film-cooling holes p 201 A93-13976
- Navier-Stokes analysis of turbine blade heat transfer and performance p 201 A93-13978
- Application of multigrid and adaptive grid embedding to the two-dimensional flux-split Euler equations p 202 A93-13990
- Flow structures around a constant-rate pitching airfoil and mechanism of dynamic stall p 118 A93-14332
- Experimental investigations of the separation behavior in 3D shock wave/turbulent boundary-layer interactions p 119 A93-14345
- Interactive hypersonic waverider design and optimization p 119 A93-14348
- Viscous flow field prediction in axisymmetric passages p 204 A93-14478
- Digital simulation of transonic flow fields in a planar nozzle p 122 A93-14479
- Confined jet thrust vector control nozzle studies p 172 A93-14516
- Study on vortex flow control of inlet distortion p 122 A93-14520
- Modeling of interfaces in problems of flow of a ponderable fluid past a wing profile p 124 A93-15189
- Method and results of studies of flow past supersonic flight vehicles at moderate and large angles of attack p 242 A93-18377
- Flow field measurements in a turbulent free jet issuing from a sharp-edged square slot p 244 A93-19158
- Flowfield measurements for a supersonic mixer ejector in forward flight p 399 A93-19217
- Aerodynamic performance of a transonic low aspect ratio turbine nozzle [ASME PAPER 92-GT-31] p 245 A93-19291
- Turbulence evaluation within the secondary flow region of a turbine cascade [ASME PAPER 92-GT-60] p 247 A93-19310
- Experimental and computational investigation of flow in catalytic monolith channels [ASME PAPER 92-GT-118] p 387 A93-19354
- Experimental and computational investigation of the NASA Low-Speed Centrifugal Compressor flow field [ASME PAPER 92-GT-213] p 252 A93-19436
- A comparison of the measured and predicted flowfield in a modern fan-bypass configuration [ASME PAPER 92-GT-298] p 254 A93-19488
- Direct measurements of skin friction in supersonic combustion flow fields [ASME PAPER 92-GT-320] p 405 A93-19506
- The computation of internal flow fields in centrifugal compressor impellers p 259 A93-20120

- Constrained optimization of three-dimensional hypersonic vehicle configurations [AIAA PAPER 93-0039] p 260 A93-20152
- Flow field characteristics of an axisymmetric sudden-expansion pipe flow with different initial swirl distribution p 411 A93-21688
- 3-D LDV measurements over a delta wing in pitch-up motion [AIAA PAPER 93-0185] p 275 A93-22610
- Direct numerical simulation of turbulent flow in a square duct [AIAA PAPER 93-0198] p 277 A93-22618
- LDV flowfield measurements on a straight and swept wing with a simulated ice accretion [AIAA PAPER 93-0300] p 280 A93-23001
- Numerical simulation of flow past the X24C reentry vehicle [AIAA PAPER 93-0319] p 280 A93-23011
- Flowfield computations over the Space Shuttle Orbiter with a proposed canard at a Mach number of 5.8 and 50 degrees angle of attack [AIAA PAPER 93-0322] p 281 A93-23014
- CFD analysis of hypersonic chemically reacting flowfields around a generic shape [AIAA PAPER 93-0323] p 281 A93-23015
- 3D Euler flow solutions using unstructured Cartesian and prismatic grids [AIAA PAPER 93-0331] p 281 A93-23022
- Comparison of predictions with measurements for a quiet supersonic tunnel [AIAA PAPER 93-0344] p 376 A93-23031
- Flow quality improvement in a high speed blowdown wind tunnel [AIAA PAPER 93-0353] p 377 A93-23038
- Ice accretion and performance degradation calculations with LEWICE/NS [AIAA PAPER 93-0173] p 310 A93-23244
- Calculation of the flowfield around an airfoil with spoiler [AIAA PAPER 93-0527] p 284 A93-23268
- Estimation of unsteady lift on a pitching airfoil from wake velocity surveys [AIAA PAPER 93-0437] p 286 A93-23351
- Initial acceleration effects on the flow field development around rapidly pitching airfoils [AIAA PAPER 93-0438] p 286 A93-23352
- Direct boundary value solution of wave rotor flow fields [AIAA PAPER 93-0483] p 415 A93-23385
- Nonlinear relaxation/quasi-Newton algorithm for the compressible Navier-Stokes equations p 287 A93-23541
- Doppler global velocimetry - The next generation? [AIAA PAPER 92-3897] p 539 A93-24486
- Navier-Stokes computations and experimental comparisons for multielement airfoil configurations [AIAA PAPER 93-0645] p 464 A93-24760
- Mean flowfield structure of a three-dimensional supersonic turbulent boundary layer [AIAA PAPER 93-0661] p 465 A93-24774
- Navier-Stokes calculations for the unsteady flowfield of turbomachinery [AIAA PAPER 93-0676] p 465 A93-24786
- Pressure-based high-order TVD methodology for dynamic stall simulation [AIAA PAPER 93-0680] p 466 A93-24788
- Interaction strength and model geometry effects on the structure of crossing-shock wave/turbulent boundary-layer interactions [AIAA PAPER 93-0780] p 467 A93-24862
- Three dimensional near field behavior of a tip vortex developing on an elliptic foil [AIAA PAPER 93-0865] p 468 A93-24927
- A simple criterion for vortex breakdown [AIAA PAPER 93-0866] p 469 A93-24928
- Viscous flow computations of flow field around an advanced propeller [AIAA PAPER 93-0873] p 469 A93-24934
- Investigation of methods for modeling propeller-induced flow fields [AIAA PAPER 93-0874] p 469 A93-24935
- Computation of inviscid flowfield around 3-D aerospace vehicles and comparison with experimental and flight data [AIAA PAPER 93-0885] p 470 A93-24944
- Experimental and numerical delta wing study at high angles of attack and sideslip [AIAA PAPER 92-2713] p 473 A93-24990
- Numerical investigation of flow field in a turbine vane [AIAA PAPER 93-0155] p 542 A93-25505
- The numerical simulation of the hydrodynamic field from the pump impellers zone by means of the finite element method p 476 A93-26905
- Current status of computational methods for transonic unsteady aerodynamics and aeroelastic applications p 480 A93-29175

- Flowfield analysis of modern helicopter rotors in hover by Navier-Stokes method p 481 A93-29435
- Flow visualization and flow field measurements of a 1/12 scale tilt rotor aircraft in hover p 482 A93-29441
- Pressure fluctuations on the surface of two circular cylinders in tandem arrangements at high Reynolds numbers p 679 A93-33718
- Solution of Euler equations for complex forebody-inlet combinations p 680 A93-33730
- The use of artificial intelligence for buffet environments [AIAA PAPER 93-1534] p 727 A93-34071
- Experimental supersonic hydrogen combustion employing staged injection behind a rearward-facing step p 744 A93-34496
- A study of flow structure and heat transfer intensity in the vicinity of an expanding step on a plate p 691 A93-35268
- Study of supersonic intersection flowfield at modified wing-body junctions p 692 A93-35621
- Computational investigation of a pneumatic forebody flow control concept p 768 A93-37383
- Unsteady analysis of helicopter rotor p 770 A93-38193
- Numerical study on atom-molecule radiation flowfield around a hypersonic blunt body p 770 A93-38434
- Instantaneous structure of vortex breakdown on a delta wing via particle image velocimetry p 779 A93-39428
- Velocity vector LDA measurement inside a pitched blade impeller p 924 A93-40390
- FUM - An efficient MMB solver for steady inviscid flows p 862 A93-42431
- Solution of three-dimensional supersonic flowfields via adapting unstructured meshes p 863 A93-42442
- Enhanced numerical inviscid and viscous fluxes for cell centered finite volume schemes p 864 A93-42444
- Comments on experiments for computational validation for fluid dynamic predictions p 927 A93-42578
- Hypersonic stability and transition p 864 A93-42579
- CFD for hypersonic propulsion p 865 A93-42585
- Inviscid calculations by an upwind finite element method of hypersonic flows over a double (single) ellipse p 869 A93-42626
- Research on supersonic combustion p 899 A93-42877
- An experimental study of a turbulent wing-body junction and wake flow p 873 A93-43541
- Transonic shockwave/turbulent boundary layer interactions on a porous surface p 873 A93-43686
- Further study of high speed single free jets p 873 A93-43687
- A computational investigation of fuel mixing in a hypersonic scramjet [AIAA PAPER 93-2994] p 1001 A93-44230
- Three-dimensional calculation of a hydrogen jet injection into a supersonic air flow p 950 A93-44374
- Effects of spatial order of accuracy on the computation of vortical flowfields [AIAA PAPER 93-3371] p 955 A93-45064
- CFD analysis of the X-29 inlet at high angle of attack p 958 A93-45140
- Organized structure in a compressible turbulent shear layer p 961 A93-45730
- Some measurements on dependence of rectangular cylinder drag on elevation p 1025 A93-45745
- Low-to-high altitude predictions of three-dimensional ablative re-entry flowfields p 1027 A93-46407
- Enhancements to viscous-shock-layer technique p 962 A93-46408
- Vorticity dynamics in spatially developing rectangular jets [AIAA PAPER 93-3286] p 969 A93-46842
- The practical application of solution-adaption to the numerical simulation of complex turbomachinery problems p 970 A93-46916
- Inverse problem using S2-S1 approach for the design of the turbomachine with splitter blades p 971 A93-46929
- Effect of canard oscillations on the vortical flowfield of a X-31A-like fighter model in dynamic motion [AIAA PAPER 93-3427] p 1008 A93-47222
- Experimental and computational investigations of the flowfield around the F117A [AIAA PAPER 93-3508] p 984 A93-47274
- Navier-Stokes calculations of rotating BERP planform blade flowfields [AIAA PAPER 93-3527] p 986 A93-47286
- The effect of expansion on the large scale structure of a compressible turbulent boundary layer [AIAA PAPER 93-2991] p 1052 A93-48183
- A computational study of wingtip vortex flowfield [AIAA PAPER 93-3010] p 1054 A93-48200
- Investigation of the flowfield over parallel-arranged launch vehicles [AIAA PAPER 93-3060] p 1058 A93-48237
- The use of triangular elements in panel methods for calculating flow past flight vehicles p 1068 A93-48904
- Numerical calculation of polars and heat transfer for supersonic three-dimensional flow past wings with allowance for radiation p 1068 A93-48905
- Calculation of subsonic flow of a gas past an airfoil p 1068 A93-48908
- Effects of external excitation on the leading-edge separation flowfield p 1071 A93-49198
- Investigation of nacelle upper cowl flow separation using on- and off-body flow visualization techniques p 1072 A93-49507
- Flow analysis and design optimization methods for nozzle-afterbody of a hypersonic vehicle p 1073 A93-49531
- Calculation of scramjet inlet with thick boundary-layer ingestion [AIAA PAPER 93-1836] p 1074 A93-49720
- Rotor-rotor interaction for counter-rotating fans. I - Three dimensional flowfield measurements [AIAA PAPER 93-1848] p 1075 A93-49729
- Unsteady aerodynamic flow phenomena in a transonic compressor stage [AIAA PAPER 93-1868] p 1075 A93-49743
- Summary of the GASP code application and evaluation effort for scramjet combustor flowfields [AIAA PAPER 93-1973] p 1077 A93-49820
- Turbofan flowfield simulation using Euler equations with body forces [AIAA PAPER 93-1978] p 1078 A93-49825
- Computation of the flow field in an annular gas turbine combustor [AIAA PAPER 93-2074] p 1113 A93-49903
- Experimental investigation of slot injection into supersonic flow with an adverse pressure gradient [AIAA PAPER 93-2442] p 1119 A93-50194
- Experimental and numerical study of swept ramp injection into a supersonic flowfield [AIAA PAPER 93-2445] p 1119 A93-50197
- Three-dimensional numerical simulation of gradual opening in a wave rotor passage [AIAA PAPER 93-2526] p 1156 A93-50254
- Navier-Stokes analysis of radial turbine rotor performance [AIAA PAPER 93-2555] p 1121 A93-50277
- Chimera grids in the simulation of three-dimensional flowfields in turbine-blade-coolant passages [AIAA PAPER 93-2559] p 1157 A93-50280
- Spline-collocation solution of a Fredholm equation of the second kind in the problem of flow past an airfoil p 1092 A93-51904
- Calculation of supersonic flow past a body of revolution with a piecewise linear distribution of singularities at its axis p 1092 A93-51910
- Flowfield simulation about the stratospheric observatory for infrared astronomy p 1095 A93-52446
- Measurements and computational analysis of heat transfer and flow in a simulated turbine blade internal cooling passage [AIAA PAPER 93-1797] p 1218 A93-53585
- Laser velocimeter measurements of the flow field generated by a forward-swept propfan during flutter [AIAA PAPER 93-2919] p 1180 A93-53591
- Investigation of the flow field through a variable pitch fan rotor with an inlet total pressure distortion [ISABE 93-7029] p 1184 A93-54005
- Navier-Stokes computation of the three dimensional flow fields through a transonic fan blade [ISABE 93-7030] p 1184 A93-54006
- Tip clearance effects on the flow field of an axial turbine rotor blade cascade [ISABE 93-7057] p 1185 A93-54033
- Navier-Stokes analysis of turbine flowfield and external heat transfer [ISABE 93-7075] p 1186 A93-54051
- Finite-rate H₂/air combustion effects in CRJ for hypersonic launchers [ISABE 93-7084] p 1202 A93-54060
- Experimental analysis of turbine rotor flow at design and off-design conditions [ISABE 93-7092] p 1186 A93-54068
- On the numerical simulation of the two-dimensional flow field around a hypersonic air-intake-compressibility effects [ISABE 93-7100] p 1187 A93-54076
- Study on flow field around slender diamond cone traveling at hypersonic speed p 1189 A93-54314
- The effects of reaction rate constants and catalytic wall on the hypersonic flow field over blunt bodies p 1230 A93-54586
- Three-dimensional flow analysis of a four-stage transonic axial compressor with inlet guide vanes p 1232 A93-54643
- Rotor/stator flow coupling in turbomachines p 1232 A93-54647
- Results about the structure of the shock wave reflection process for strong incoming shock waves p 1233 A93-54810
- A general introduction to aeroacoustics and atmospheric sound p 1264 A93-55852
- Analytical and experimental investigation of flow through a turbine vane cascade p 1248 A93-56348
- The integration of geometric modeling into an inverse design method and application of a PC-based inverse design method and comparison with test results p 81 N93-10058
- Forced unsteady separated flows on a 45 degree delta wing p 82 N93-10305
- Analysis of wing-body junction flowfields using the incompressible Navier-Stokes equations, volumes 1 and 2 p 17 N93-10320
- Explicit Navier-Stokes computation of turbomachinery flows p 83 N93-10370
- LDV Measurements of unsteady flow fields in radial turbine [AD-A253592] p 19 N93-10648
- Effect of planform and body on supersonic aerodynamics of multibody configurations [NASA-TP-3212] p 19 N93-10824
- Compressible and incompressible fluid seals: Influence on rotorodynamic response and stability [NASA-CR-190746] p 85 N93-10891
- Experimental study of the flow field inside a whirling annular seal p 85 N93-10892
- The hemisphere-cylinder at an angle of attack p 21 N93-11250
- Experimental investigation of the effects of aft blowing with various nozzle exit geometries on a 3.0 caliber tangent ogive at high angles of attack: Forebody pressure distributions [NASA-CR-190935] p 22 N93-11605
- An experimental study of flow patterns and endwall heat transfer upstream of a surface-mounted rectangular obstruction in a turbulent boundary layer p 89 N93-11698
- Effects of sweep on the physics of unsteady shock-induced turbulent separated flows [AD-A247035] p 22 N93-11742
- Numerical analysis of the flow fields in a RQL gas turbine combustor [DE92-017509] p 89 N93-11767
- A wall interference assessment/correction system [NASA-CR-190617] p 68 N93-11910
- An investigation of the effects of aft blowing on a 3.0 caliber tangent ogive body at high angles of attack [NASA-CR-190934] p 24 N93-12004
- A general introduction to aeroacoustics and atmospheric sound [NASA-CR-189717] p 102 N93-12021
- Unsteady propeller/wing aerodynamic interactions p 24 N93-12190
- Solution of nonlinear flow equations for complex aerodynamic shapes [NASA-CR-190979] p 90 N93-12329
- Studies of a flat wake rotor theory [NASA-CR-190936] p 25 N93-12343
- A summary of the forebody high-angle-of-attack aerodynamics research on the F-18 and the X-29A aircraft [NASA-TM-104261] p 25 N93-12353
- Experiments and analysis concerning the use of external burning to reduce aerospace vehicle transonic drag p 70 N93-12537
- A numerical study of hypersonic flow with strong surface blowing p 129 N93-13128
- Application of a solution adaptive grid to flow over an embedded cavity p 130 N93-13141
- Detailed analysis of wing-nacelle interaction for commercial transport aircraft p 213 N93-13203
- Investigation of interference phenomena of modern wing-mounted high-bypass-ratio engines by the solution of the Euler-equations p 213 N93-13204
- Euler analysis of turbofan/superfan integration for a transport aircraft p 214 N93-13206
- Recent developments in low-speed TPS-testing for engine integration drag and installed thrust reverser simulation p 160 N93-13207
- Investigation of the flowfield around an isolated bypass engine with fan and core jet p 215 N93-13227
- Mathematical problems in inviscid hypersonic flow p 131 N93-13451
- Velocity and temperature measurements in a non-premixed reacting flow behind a backward facing step p 132 N93-13632
- Planar measurement of flow field parameters in nonreacting supersonic flows with laser-induced iodine fluorescence p 133 N93-13801
- Assessment of potential aerodynamic benefits from spanwise blowing at the wing tip p 134 N93-13822

An experimental/computational study of heat transfer in sharp fin induced shock wave/turbulent boundary layer interactions at low hypersonic Mach numbers

p 217 N93-13826

Overall effects of separation on thin aerofoils

[ISBN-0-315-67464-4] p 135 N93-13930

Flow prediction for three-dimensional intakes and ducts using viscous-inviscid interaction methods

p 218 N93-13953

Unsteady three-dimensional thin-layer Navier-Stokes solutions for turbomachinery in transonic flow

p 218 N93-14025

Navier-Stokes flowfield computation of wing/rotor interaction for a tilt rotor aircraft in hover

p 135 N93-14035

Direct prediction of a separation boundary for aerofoils using a viscous-coupled calculation method

[ESDU-92008] p 136 N93-14516

Investigations of detail design issues for the high speed acoustic wind tunnel using a 60th scale model tunnel. Part 2: Tests with the closed circuit

[NASA-CR-191672] p 137 N93-14738

Estimation of unsteady lift on a pitching airfoil from wake velocity surveys

[NASA-TM-105947] p 138 N93-14791

L.D.V. measurements of unsteady flow fields in radial turbine

[AD-A255728] p 221 N93-15065

An experimental investigation of base bleed effect on the wake turbulent structure behind a two-dimensional blunt model

[MPIS-9/1991] p 139 N93-15131

Flowfield study of a close-coupled canard configuration

[AD-A256311] p 139 N93-15245

An experimental and analytical study of TIP clearance effects in axial flow compressors

[AD-A256434] p 179 N93-15337

Ice accretion and performance degradation calculations with LEWICE/NS

[NASA-TM-105972] p 148 N93-15354

An integral equation solution for multistage turbomachinery design calculations

[NASA-TM-105970] p 179 N93-15521

Investigation of the aerothermodynamics of hypervelocity reacting flows in the ram accelerator

[NASA-CR-191715] p 140 N93-15588

Detailed near surface flow about yawed, stranded cables

[AD-A257382] p 418 N93-15857

Computational investigations of a NACA 0012 airfoil in low Reynolds number flows

[AD-A257300] p 288 N93-15920

Experimental and numerical investigation of vortex flow over a 76/60-deg double-delta wing

[LR-680] p 289 N93-16210

An advanced graphics-interactive system for a multi-block structured grid generation within an industrial environment

[ETN-92-92885] p 440 N93-16288

Comparison of solution of various Euler solvers and one Navier-Stokes solver for the flow about a sharp-edged cropped delta wing

[NLR-TP-90340-U] p 418 N93-16411

Hypersonic flows including real gas effects

[AERO-REPT-9112] p 289 N93-16467

Interferometric reconstruction of three-dimensional high-speed aerodynamic flows

p 291 N93-16765

Flowfield computations over the Space Shuttle orbiter with a proposed canard at a Mach number of 5.8 and 50 deg angle of attack

[AD-A258058] p 293 N93-17756

An experimental investigation of interacting wing-tip vortex pairs

[AD-A258471] p 295 N93-18272

A wall interference assessment/correction system

[NASA-CR-191889] p 296 N93-18384

Simulation of unsteady rotational flow over propfan configuration

[NASA-CR-192234] p 296 N93-18585

Axial Flow Compressors, volume 1

[VKI-LS-1992-02-VOL-1] p 422 N93-18721

A numerical simulations of inner flow of scramjet

p 304 N93-19318

Computation of H₂/air reacting flowfields in drag-reduction external combustion

[NASA-CR-191071] p 536 N93-20237

An experimental investigation of a round turbulent jet in a cross-flow

p 553 N93-20689

Experiments on smooth cantilevered circular cylinders in a low-turbulence uniform flow. Part 2: Fluctuating loads on a cantilever of aspect ratio 30

[PB93-110500] p 555 N93-21382

Aerothermodynamic properties of hypersonic flows over radiation-adiabatic surfaces

[DLR-FB-91-42] p 485 N93-21761

Experimental investigations on wing-body combinations and their components at high angles of attack in the subsonic and transonic speed range

[DLR-FB-91-43] p 516 N93-21762

A three-dimensional algebraic grid generation scheme for gas turbine combustors with inclined slots

[NASA-CR-191095] p 746 N93-24759

Computational study of the aerodynamics and control by blowing of asymmetric vortical flows over delta wings

p 693 N93-24772

Surface and flow field measurements in a symmetric crossing shock wave/turbulent boundary-layer interaction

[NASA-TM-106086] p 693 N93-24911

Combined LAURA-UPS hypersonic solution procedure

[NASA-TM-107682] p 747 N93-25176

An experimental study of the sources of fluctuating pressure loads beneath swept shock/boundary-layer interactions

[NASA-CR-192918] p 749 N93-25266

A numerical and experimental studies of flow characteristics in centrifugal fans

p 695 N93-25339

Optimized scramjet engine integration on a waverider airframe

p 722 N93-25480

Experimental and computational investigation of helium injection into air at supersonic and hypersonic speeds

p 696 N93-25487

A new LU-SGS flow solver for calculating reentry flows

p 698 N93-25759

Visualization of a Mach 2 reacting flow using Planar Laser-Induced Fluorescence (PLIF)

p 731 N93-26006

The blade curving effects in a turbine stator cascade with low aspect ratio

[AD-A261083] p 725 N93-26239

Adjoint methods for aerodynamic wing design

[NASA-CR-193086] p 805 N93-27089

Towards an analytical treatment of the aerostatic problem of a circular wing

p 781 N93-27214

Leading edge vortices in a chordwise periodic flow

p 782 N93-27218

Effect of vortex behavior on loads acting on a 65 deg delta wing oscillating in roll at high incidence

p 782 N93-27220

Stability investigations of airfoil flow by global analysis

p 783 N93-27436

Aerodynamics of a finite wing with simulated ice

p 784 N93-27437

A composite structured/unstructured-mesh Euler method for complex airfoil shapes

p 784 N93-27439

Comparison of reacting and non-reacting shear layers at a high subsonic Mach number

[NASA-TM-106198] p 814 N93-27610

Direct measurements of skin friction in supersonic combustion flow fields

[AD-A262878] p 825 N93-28226

Homenthalpic-flow approach for hypersonic inviscid non-equilibrium flows

[INRIA-RR-1652] p 788 N93-28440

The ground vortex flow field associated with a jet in a cross flow impinging on a ground plane for uniform and annular turbulent axisymmetric jets

[NASA-CR-4513] p 789 N93-28449

Navier-Stokes analysis of radial turbine rotor performance

[NASA-CR-191153] p 815 N93-28609

Preliminary design of an intermittent smoke flow visualization system

[NASA-CR-186027] p 806 N93-28693

Stabilized space-time finite element formulations for unsteady incompressible flows involving fluid-body interactions

p 843 N93-29040

Three-dimensional numerical simulation of gradual opening in a wave rotor passage

[NASA-CR-191157] p 900 N93-29072

An experimental study of flow over a 6 to 1 prolate spheroid at incidence

p 874 N93-29124

Development of an unstructured solution adaptive method for the quasi-three-dimensional Euler and Navier-Stokes equations

[NASA-CR-193241] p 930 N93-29213

Vortex structure and mass transfer near the base of a cylinder and a turbine blade

p 901 N93-29929

The effect of main stream flow angle on flame tube film cooling

p 932 N93-29953

The aerodynamic effect of coolant ejection in the leading edge region of a film-cooled turbine blade

p 904 N93-29958

Turbulence characteristics of an axisymmetric reacting flow

[NASA-CR-4110] p 877 N93-30373

Topology and grid adaption for high-speed flow computations

[NASA-CR-4216] p 934 N93-30375

Computation of a delta-wing roll-and-hold maneuver

[AD-A264704] p 909 N93-30498

Strong parallel blade-vortex interaction and noise propagation in helicopter flight

p 944 N93-30980

TDLM: A Transonic Doublet Lattice Method for 3D potential unsteady transonic flow calculation

[DLR-FB-92-25] p 988 N93-31171

Penn State axial flow turbine facility: Performance and nozzle flow field

p 1032 N93-31588

Measurements and computational analysis of heat transfer and flow in a simulated turbine blade internal cooling passage

[NASA-TM-106189] p 1032 N93-31647

Reynolds number influences in aeronautics

[NASA-TM-107730] p 989 N93-31732

FLOW EQUATIONS

Modeling of interfaces in problems of flow of a ponderable fluid past a wing profile

p 124 A93-15189

A method for calculating supersonic three-dimensional flows in pyramidal nozzles

p 125 A93-15216

Meridional flow calculation using advanced CFD techniques

[ASME PAPER 92-GT-325] p 256 A93-19509

An approximately factored incremental strategy for calculating consistent discrete aerodynamic sensitivity derivatives

[AIAA PAPER 92-4746] p 265 A93-20344

The prediction of riblet behaviour with a low-Reynolds number k-epsilon model

p 270 A93-21720

The development of a CFD potential method for the analysis of tilt-rotors

p 481 A93-29434

Airfoil shape optimization using sensitivity analysis on viscous flow equations

p 682 A93-33755

Instability of rectangular jets

p 720 A93-34410

Modeling of linear isentropic flow systems

p 828 A93-37046

VSL analysis of nonequilibrium flows around a hypersonic body

p 769 A93-38146

Pseudo-compressibility methods for the incompressible flow equations

[AIAA PAPER 93-3329] p 952 A93-45023

Burnett solutions along the stagnation line of a cooled cylinder in low-density hypersonic flows

[AIAA PAPER 93-2726] p 962 A93-46480

Application of a two-equation turbulence model for high speed compressible flows using unstructured grids

[AIAA PAPER 93-3029] p 1056 A93-48213

Fluid-structural interactions using Navier-Stokes flow equations coupled with shell finite element structures

[AIAA PAPER 93-3087] p 1099 A93-48261

On numerical solutions of Burnett equations for hypersonic flow past 2-D circular blunt leading edges in continuum transition regime

[AIAA PAPER 93-3092] p 1060 A93-48266

Some Fuchs-type equations in fluid mechanics

p 1165 A93-48967

Numerical modeling of flow in a hypersonic laminar boundary layer

p 1086 A93-50967

Supersonic flow past a cone with heat transfer near its tip

p 1089 A93-51780

Calculation of flow fields near a lifting wing

p 1179 A93-53552

The streamline throughflow method of axial turbomachinery flow analysis

[ISABE 93-7031] p 1184 A93-54007

Recent advances in steady compressible aerodynamic sensitivity analysis

p 1236 A93-55400

The prediction of convective heat transfer in rotating square ducts

[PNR-90929] p 85 N93-11025

Solution of nonlinear flow equations for complex aerodynamic shapes

[NASA-CR-190979] p 90 N93-12329

An experimental and computational investigation of slender wings undergoing wing rock

p 187 N93-13915

Time-dependent predictions and analysis of turbine cascade data in the transonic flow region

[PNR-90957] p 139 N93-15489

An integral equation solution for multistage turbomachinery design calculations

[NASA-TM-105970] p 179 N93-15521

Application of the Euler method EULFLEX to a fighter-type airplane configuration at transonic speed

[MBB-FE-211-S-PUB-0489-A] p 484 N93-21059

Godunov-type schemes applied to detonation flows

[NASA-CR-191447] p 780 N93-27090

FLOW GEOMETRY

Hemispherical and spherical flow parameter detectors

p 75 A93-10044

Numerical modeling of supersonic flows past wings of different aspect ratios over a wide range of angles of attack within the framework of the plane section law

p 5 A93-10141

Influence of surface heat flux ratio on heat transfer augmentation in square channels with parallel, crossed, and V-shaped angled ribs

p 201 A93-13981

Further studies on the asymmetrical flow past yawed cylinders p 118 A93-14304

Noncoaxial mixing in a rectangular duct p 205 A93-14518

Marching grid generation for external viscous flow problems p 228 A93-16979

Instability of rectangular jets p 398 A93-19157

The extension of a solution-adaptive 3D Navier-Stokes solver towards geometries of arbitrary complexity [ASME PAPER 92-GT-363] p 257 A93-19527

Transitional characteristics of vortices issued from a body which creates asymmetric flow field - In a case of thin symmetrical airfoil with angle of attack under rotational oscillation of small amplitude p 267 A93-20923

On the structure and response of aerodynamically-strained planar premixed flames [AIAA PAPER 93-0246] p 390 A93-22657

Numerical prediction of flap losses in a transonic wind tunnel p 288 A93-23552

A coupled multi-block solution procedure for spray combustion in complex geometries [AIAA PAPER 93-0108] p 539 A93-24230

Prediction of asymmetric vortical flows around slender bodies using Navier-Stokes equations p 478 A93-27925

Numerical study on the interaction of supersonic flow past a wedge and free jet p 479 A93-28574

Viscous-inviscid interaction coupled calculation of three-dimensional turbulent separated flow over dents p 681 A93-33748

A comparison between numerical models and measurements in a Kaplan turbine guide vanes p 685 A93-34339

Instability of rectangular jets p 720 A93-34410

Structured grid variational adaption - Reaching the limit? [ONERA, TP NO. 1992-114] p 771 A93-38590

Effect of the thermodynamic air model on the aerodynamic characteristics of profiles with bends p 776 A93-39136

Comparison of coordinate-invariant and coordinate-aligned upwinding for the Euler equations [AIAA PAPER 93-3306] p 858 A93-41053

Symmetry breaking in vortical flows over cones - Theory and numerical experiments [AIAA PAPER 93-3408] p 859 A93-41056

An accuracy assessment of Cartesian-mesh approaches for the Euler equations [AIAA PAPER 93-3335] p 953 A93-45029

Time-accurate simulation of a self-excited oscillatory supersonic external flow with a multi-block solution-adaptive mesh algorithm [AIAA PAPER 93-3387] p 956 A93-45078

Simulation of flow past complex geometries using a parallel implicit incompressible flow solver p 957 A93-45095

Air dissociation effects on aerodynamic characteristics of an aerospace plane p 959 A93-45149

Formation of shock waves in transient base flow p 1023 A93-45460

Effects of bleed-hole geometry and plenum pressure on three-dimensional shock-wave/boundary-layer/bleed interactions [AIAA PAPER 93-3259] p 967 A93-46800

Multigrid methods for calculating 3D flows in complex geometries p 973 A93-46984

Trajectory mapping of quasi-periodic structures in a vortex flow [AIAA PAPER 93-2914] p 1044 A93-48116

Shock-wave/boundary layer interactions at hypersonic speeds by an implicit Navier-Stokes solver [AIAA PAPER 93-2938] p 1046 A93-48136

Intake flow modeling in a four stroke diesel using KIVA3 [AIAA PAPER 93-2952] p 1148 A93-48146

An initial comparison of CFD with experiment for a geometrically simplified STOVL model [AIAA PAPER 93-3059] p 1058 A93-48236

Experimental investigation on patterned blades of compressor p 1066 A93-48515

An experimental study of a compound supersonic jet p 1069 A93-48914

Thoughts on conical flow asymmetry p 1070 A93-49003

Effect of curvature on stationary crossflow instability of a three-dimensional boundary layer p 1070 A93-49010

Turbofan flowfield simulation using Euler equations with body forces [AIAA PAPER 93-1978] p 1078 A93-49825

The turbulence and mixing characteristics of the complex flow in a simulated augmentor p 1123 A93-51642

Velocity fluctuation based on the difference in the flow pattern in the channels of a centrifugal impeller p 1182 A93-53842

Three-dimensional separated flow over a prolate spheroid p 1235 A93-55379

Stall transients including effects of inlet distortion and intake geometry p 423 A93-18726

On the disturbances development in the supersonic boundary layer p 484 A93-20686

FLOW MEASUREMENT

Probing questions for aerodynamic testing p 80 A93-13437

In-flight surface-flow measurements on a subsonic transport high-lift flap system p 166 A93-14327

Flow field measurements in a turbulent free jet issuing from a sharp-edged square slot p 244 A93-19158

Three dimensional transonic flow measurements in an axial turbine with conical walls [ASME PAPER 92-GT-61] p 247 A93-19311

Measurement of unsteady flow and heat transfer in a linear turbine cascade [ASME PAPER 92-GT-323] p 256 A93-19507

Flow measurements behind V-gutter under non-combusting condition [AIAA PAPER 93-0020] p 408 A93-20139

Streamwise variation of mean velocity field for the turbulent boundary layer interacting with controlled longitudinal vortex arrays p 267 A93-20933

Measurements in the near-field of a turbulent wingtip vortex [AIAA PAPER 93-0551] p 285 A93-23290

Time-dependent 3-component laser-Doppler-anemometer and simultaneous position measurements in the flow of an aircraft engine p 538 A93-23809

Seed particle response and size characterization in high speed flows p 459 A93-23811

Corrections to fringe distortion due to flow density gradients in optical interferometry [AIAA PAPER 93-0631] p 539 A93-24748

Three dimensional near field behavior of a tip vortex developing on an elliptic foil [AIAA PAPER 93-0865] p 468 A93-24927

Boundary-layer transition extent measurements on a cone and flat plate at Mach 3.5 [AIAA PAPER 93-0342] p 474 A93-25517

Laminar-flow instrumentation for wind-tunnel and flight experiments p 479 A93-28605

Two-dimensional laser velocimetry for the study of dual-flow jets with flight effect in the CEPPA 19 anechoic wind tunnel [ONERA, TP NO. 1992-144] p 831 A93-38614

Intrusive and nonintrusive measurements of flow properties in arc jets p 943 A93-42584

Flow field measurements in a crossing shockwave turbulent boundary layer interaction at Mach 3 [AIAA PAPER 93-3434] p 977 A93-47226

Laser holographic interferometric measurements of the flow behind a rearward facing step [AIAA PAPER 93-3515] p 985 A93-47279

The development of swirl five-hole probe p 987 A93-47341

Flowfield measurements about a multi-element airfoil at high Reynolds numbers [AIAA PAPER 93-3137] p 1064 A93-48300

Experimental study on turbulent two-phase flow in a dual-inlet side dump combustor p 1106 A93-48506

Investigation of flows in a controlled diffusion airfoil cascade passage p 1071 A93-49188

Stator relative, rotor blade-to-blade near wall flow in a multistage axial compressor with tip clearance variation [AIAA PAPER 93-2389] p 1083 A93-50154

Pressure distribution measurement around hypersonic delta winged semicone - Measurement by means of magnet tape p 1176 A93-53193

Observations of liquid jets injected into a highly accelerated supersonic boundary layer p 1177 A93-53214

Design and testing methods of high performance combustors for airbreathing engines [ISABE 93-7024] p 1196 A93-54000

Isothermal flow characteristics behind V-shape gutter with and without injection [ISABE 93-7040] p 1198 A93-54016

Large eddy simulation of turbulent combustion behind flame holders [ISABE 93-7042] p 1198 A93-54018

Correlations for flow property variation at outlet of a centrifugal impeller [ISABE 93-7054] p 1185 A93-54030

Improved flow measurement with simultaneous period/frequency recording --- in turbojet engines p 1254 A93-54381

Measurement of turbulent boundary layer in transonic flow p 1236 A93-55411

LV software for supersonic flow analysis [NASA-CR-190911] p 16 N93-10069

Method of remotely characterizing thermal properties of a sample [NASA-CASE-LAR-13508-3-CU] p 67 N93-11057

Operating experience using venturi flow meters at liquid helium temperature [DE92-014693] p 90 N93-12140

The jet behaviour of an actual high-bypass engine as determined by LDA-measurements in ground tests p 175 N93-13218

Airfoil-vortex interaction and the wake of an oscillating airfoil p 134 N93-13803

Hot film wall shear instrumentation for compressible boundary layer transition research [NASA-CR-191360] p 294 N93-17855

An experimental study of a turbulent boundary layer in the trailing edge region of a circulation-control airfoil [NASA-CR-191262] p 295 N93-17934

Reflection type skin friction meter [NASA-CASE-LAR-14520-1-SB] p 296 N93-18275

Electron beam probing of blow-down hypersonic flows [ONERA-NT-1992-7] p 298 N93-18701

Surface and flow field measurements in a symmetric crossing shock wave/turbulent boundary-layer interaction [NASA-TM-106086] p 693 N93-24911

An investigation of laser velocimetry measurements within high speed, complex flows p 748 N93-25237

An investigation on planar velocimetry by spatial cross-correlation p 697 N93-25664

Method of measuring cross-flow vortices by use of an array of hot-film sensors [NASA-CASE-LAR-14824-1-SB] p 751 N93-26000

Trailing vortex/tree-surface interaction [AD-A261654] p 701 N93-26195

Optically smart surfaces survivability testing at Mach 3 [AD-A261785] p 760 N93-26566

Analysis of fluctuating static pressure measurements in a large high Reynolds number transonic cryogenic wind tunnel [NASA-TM-108722] p 823 N93-27142

Experimental study of heat transfer close to a plane wall heated in the presence of multiple injections (subsonic flow) p 901 N93-29931

Turbulence characteristics of an axisymmetric reacting flow [NASA-CR-4110] p 877 N93-30373

Compressible turbulence in a high-speed high Reynolds number mixing layer p 878 N93-30583

Turbulence measurement in a reacting and non-reacting shear layer at a high subsonic Mach number [NASA-TM-106186] p 989 N93-31839

FLOW RESISTANCE

A fuel-oil matrix heat exchanger p 833 A93-39052

Effect of rotation on heat transfer and hydraulic resistance in the radial cooling channels of turbine rotor blades p 1215 A93-52950

Pressure field and drag of a single cavity with rounded and sharp edges p 1258 A93-55018

FLOW STABILITY

Viscous instability of hypersonic flow past a wedge p 4 A93-10137

Experimental study of crossflow instability and laminar-turbulent transition on a swept wing p 115 A93-14250

Instability of local separated flows with respect to small-amplitude perturbations p 125 A93-15254

On the cross-flow instability near a rotating disk p 128 A93-17264

Laminar flow research in the 1940-1950s - A personal recollection p 235 A93-17271

Experimental study of controlled tip disturbance effect on flow asymmetry p 211 A93-17417

Experiments on the active control of boundary layer transition p 243 A93-19133

Unsteady pressures under impinging jets in crossflows p 399 A93-19220

Stability of fully developed rotating stall [ASME PAPER 92-GT-57] p 348 A93-19307

Evaluation of approaches to active compressor surge stabilization [ASME PAPER 92-GT-182] p 352 A93-19407

A unified model for rotating stall and surge p 259 A93-20119

Numerical prediction of instabilities in transonic internal flows using an Euler TVD code [AIAA PAPER 93-0072] p 262 A93-20184

Effect of micron-sized roughness on transition in swept-wing flows [AIAA PAPER 93-0076] p 262 A93-20188

Viscous and inviscid instabilities of a trailing vortex p 268 A93-21042

Prediction of rotor dynamic destabilizing forces in axial flow compressors p 272 A93-22263

Flow stability issues in supersonic inlet flow analyses [AIAA PAPER 93-0290] p 279 A93-22690

- Effects of free-stream turbulence on boundary-layer transition
[AIAA PAPER 93-0488] p 416 A93-23390
- Numerical experiments on the stability of leading edge boundary layer flow - A two-dimensional linear study p 477 A93-27475
- Finite element computation of compressible flows with the SUPG formulation p 482 A93-29774
- Instability of rectangular jets p 720 A93-34410
- Temperature and suction effects on the instability of an infinite swept attachment line p 691 A93-35486
- Laminar flow control - Introduction and overview p 859 A93-41777
- Wave interaction theory and LFC p 860 A93-41781
- Hypersonic stability and transition p 864 A93-42579
- Stability conditions for a transonic decelerating flow in a duct p 872 A93-43027
- Effect of nonaxisymmetric forcing on a swirling jet with vortex breakdown
[AIAA PAPER 93-3251] p 1028 A93-46796
- Transition in supersonic flow past axisymmetric bodies p 967 A93-46817
- The prediction and the active control of surge in multi-stage axial-flow compressors p 1002 A93-46945
- Nonlocal vs. local instability of compressible flows including body metric, flow divergence and 3D-wave propagation
[AIAA PAPER 93-2982] p 1051 A93-48175
- Transition for three-dimensional boundary layers on wings in the transonic regime
[AIAA PAPER 93-3049] p 1057 A93-48229
- A detailed study of mean-flow solutions for stability analysis of transitional flows
[AIAA PAPER 93-3052] p 1057 A93-48232
- Audio post-processing for shear layer calculations
[AIAA PAPER 93-3075] p 1059 A93-48250
- 2-D theoretical analysis of circumferential grooved casing treatment p 1066 A93-48501
- Effect of steady-state circumferential pressure and temperature distortions on compressor stability p 1106 A93-48503
- Secondary instability mechanisms in compressible axisymmetric boundary layers p 1070 A93-49009
- Analysis of the stability characteristics of hypersonic flow of a detonable gas mixture in the stagnation region of a blunt body
[AIAA PAPER 93-1918] p 1076 A93-49784
- Compressor unsteady aerodynamic response to rotating stall and surge excitations
[AIAA PAPER 93-2087] p 1079 A93-49914
- A model for the selective amplification of spatially coherent waves in a centrifugal compressor on the verge of rotating stall
[AIAA PAPER 93-2236] p 1080 A93-50039
- Flow investigation of a low-speed-operated centrifugal compressor over a flow range including zero flow
[AIAA PAPER 93-2240] p 1155 A93-50042
- Steady transonic weakly perturbed flows in a vibrationally relaxing gas p 1088 A93-51768
- Observation of fluctuation of 2D-nozzle flows
[ISABE 93-7110] p 1204 A93-54086
- Instability of a supersonic vortex sheet inside a circular duct p 1234 A93-55142
- Comparison of confined, compressible, spatially developing mixing layers with temporal mixing layers p 1234 A93-55352
- Development and computation of continuum higher order constitutive relations for high-altitude hypersonic flow p 132 A93-13578
- Design optimization of natural laminar flow bodies in compressible flow
[NASA-CR-4478] p 292 A93-16940
- The stability of a trailing-line vortex in compressible flow
[NASA-CR-189738] p 298 A93-18771
- Crossflow stability and transition experiments in a swept-wing flow
[NASA-TM-108650] p 555 A93-21819
- Instability of flow in a streamwise corner
[NASA-CR-191410] p 694 A93-25153
- Stationary crossflow instability on an infinite swept wing p 699 A93-25865
- Active stabilization of aeromechanical systems
[AD-A261366] p 725 A93-26335
- Godunov-type schemes applied to detonation flows
[NASA-CR-191447] p 780 A93-27090
- Airfoil stability in turbulent flow p 781 A93-27212
- Stability investigations of airfoil flow by global analysis p 783 A93-27436
- Discrete-vortex simulation of pulsating flow on a turbulent leading-edge separation bubble p 787 A93-27457
- FLOW THEORY**
- Numerical solution of a free-boundary problem in hypersonic flow theory - Nonequilibrium viscous shock layers p 8 A93-11920

- Lord Rayleigh and hydrodynamic similarity p 211 A93-17408
- Performance analysis of supersonic through-flow fan by the lifting surface theory. I - Disturbance flow field and determination of blade loadings p 267 A93-20929
- Nonsteady, one-dimensional, internal, compressible flows - Theory and applications --- Book
[ISBN 0-19-507358-4] p 548 A93-28749
- A one-dimensional theory for supersonic gas jets above the critical pressure p 774 A93-39115
- An existence theorem for a free boundary problem of hypersonic flow theory p 857 A93-40405
- Newtonian and hypersonic flows over oscillating bodies of revolution. II - Parabolic bodies p 872 A93-42931
- Hypersonic, turbulent viscous interaction past an expansion corner
[AIAA PAPER 93-2985] p 1051 A93-48178
- A wake singularity potential flow model for airfoils experiencing trailing-edge stall p 1067 A93-48544
- A combined experimental and theoretical study of laminar flow control with particular relevance to aero engine nacelles
[PNR-90991] p 20 N93-11070
- Numerical investigations into the base drag of various wedges using the base flow model developed by Mauri Tanner
[REPT-B-36] p 26 N93-12414
- Adjoint methods for aerodynamic wing design
[NASA-CR-193086] p 805 N93-27089
- FLOW VELOCITY**
- A transfer standard of an air flow rate unit VET 150-2-87 p 66 A93-10049
- Direct numerical simulation of laminar breakdown in high-speed, axisymmetric boundary layers p 8 A93-11527
- Numerical simulations of high-speed flows about waveriders with sharp leading edges p 9 A93-12007
- Numerical analysis of the 3-D turbulent flow in an S-shaped diffuser p 116 A93-14252
- Correlation of mean velocity measurements downstream of a swept backward-facing step p 123 A93-14552
- Excitation of velocity fluctuations and noise in a wind tunnel p 444 A93-18242
- Forcing function effects on unsteady aerodynamic gust response. I - Forcing functions
[ASME PAPER 92-GT-174] p 251 A93-19400
- The problem of dynamic stall simulation revisited
[AIAA PAPER 93-0091] p 264 A93-20197
- Inlet velocity profile effects on turbulent swirling flow predictions
[AIAA PAPER 93-0133] p 274 A93-22580
- Doppler global velocimetry measurements of the vortical flow above an F/A-18
[AIAA PAPER 93-0414] p 415 A93-23333
- Engineering approach to the prediction of shock patterns in bounded high-speed flows p 287 A93-23545
- Eduction of swirling structure using the velocity gradient tensor p 416 A93-23547
- Effect of a rotating propeller on the separation angle of attack
[AIAA PAPER 93-0017] p 472 A93-24978
- Introduction of small velocity and pressure variation into a stationary compressible fluid p 473 A93-25060
- On the accurate prediction of the wall-normal velocity in compressible boundary-layer flow p 477 A93-27474
- Experience with the use of liquid crystals in conjunction with the filament method is studying the structure of supersonic flow downstream of a plane step p 478 A93-27639
- Application of particle image velocimetry in high-speed separated flows p 549 A93-29304
- Two-dimensional laser velocimetry for the study of dual-flow jets with flight effect in the CEPRA 19 anechoic wind tunnel
[ONERA, TP NO. 1992-144] p 831 A93-38614
- Analysis of turbulence in supersonic flows by means of laser velocimetry
[ONERA, TP NO. 1992-148] p 773 A93-38729
- Velocity and vorticity distributions over an oscillating airfoil under compressible dynamic stall p 778 A93-39403
- Experimental investigation of the management of large-sized drops and the onset of Marangoni-convection p 926 A93-41700
- Strong vortex/boundary layer interactions. I - Vortices high p 930 A93-43539
- An implicit time-marching procedure for high speed flow
[AIAA PAPER 93-3315] p 951 A93-45011
- A multiblock, multigrid solution procedure for multi-element airfoils p 967 A93-46812
- Mathematical model for the effect of turbulent velocity pulsations on the stability of a powerplant p 1003 A93-47508

- SCV measurements in the wake of a rotor in hover and forward flight
[AIAA PAPER 93-3080] p 1059 A93-48254
- Correlation of unsteady pressure and inflow velocity fields of a pitching rotor blade
[AIAA PAPER 93-3082] p 1060 A93-48256
- Formulas for determining the induced velocity in the direct and inverse rotor problems p 1071 A93-49324
- Nonintrusive, multipoint velocity measurements in high-pressure combustion flows
[AIAA PAPER 93-2032] p 1145 A93-49867
- Gravity sensitivity of a resistojet water vaporizer
[AIAA PAPER 93-2402] p 1156 A93-50167
- Three-dimensional flow field in a turbine nozzle passage
[AIAA PAPER 93-2556] p 1084 A93-50278
- Self-excitation of intense oscillations in flow inside a wind tunnel with an open test section p 1091 A93-51883
- Experimental study of the flow field inside a whirling annular seal p 85 N93-10892
- The measurement of the velocity field induced by a gust generator in a closed-circuit subsonic wind-tunnel
[RAE-TM-MAT/STR-1102] p 67 N93-11435
- The convection speed of the dynamic stall vortex
[AD-A247258] p 21 N93-11464
- Operating experience using venturi flow meters at liquid helium temperature
[DE92-014693] p 90 N93-12140
- Studies of a flat wake rotor theory
[NASA-CR-190936] p 25 N93-12343
- The jet behaviour of an actual high-bypass engine as determined by LDA-measurements in ground tests p 175 N93-13218
- Velocity and temperature measurements in a non-premixed reacting flow behind a backward facing step p 132 N93-13632
- Dynamics of vortex rings in cross-flow p 134 N93-13917
- Parametric study of air sampling cyclones p 135 N93-14173
- Effect of a rotating propeller on the separation angle of attack and distortion in ducted propeller inlets
[NASA-TM-105935] p 290 N93-16625
- Wind tunnel seeding particles for laser velocimeter p 292 N93-16770
- Effect of Reynolds number on the standards of a simplified anemometric probe
[IMFL-91-31] p 293 N93-17542
- Gravity sensitivity of a resistojet water vaporizer
[NASA-TM-106220] p 914 N93-29194
- Turbulence characteristics of an axisymmetric reacting flow
[NASA-CR-4110] p 877 N93-30373
- The influence of variable flow velocity on unsteady airfoil behavior
[DLR-FB-92-22] p 988 N93-31320
- FLOW VISUALIZATION**
- Ship airwake measurement and flow visualization
[AIAA PAPER 92-4088] p 7 A93-11267
- In-flight flow visualization results from the X-29A aircraft at high angles of attack
[AIAA PAPER 92-4102] p 38 A93-11272
- Infrared flow visualization of V/STOL aircraft
[AIAA PAPER 92-4253] p 80 A93-13343
- The influence of the fuselage on high alpha vortical flows and the subsequent effect on fin buffeting p 116 A93-14263
- A low-speed wind tunnel study of vortex interaction control techniques on a chine-forebody/delta-wing configuration p 122 A93-14409
- Visualization and analysis of supersonic flow in rotating turbine stage. I - Influence of shock wave between stationary and moving blades p 126 A93-15449
- Partially exposed polymer dispersed liquid crystals for boundary layer investigations p 399 A93-19250
- Compressible flow pressure losses in wye-junctions
[ASME PAPER 92-GT-71] p 248 A93-19321
- Separated flow in a low speed two-dimensional cascade. I - Flow visualization and time-mean velocity measurements
[ASME PAPER 92-GT-356] p 257 A93-19521
- The use of interferometry in the study of rotorcraft aerodynamics p 407 A93-19914
- Numerical analysis of a chined forebody with asymmetric strakes
[AIAA PAPER 93-0051] p 260 A93-20164
- The aerodynamic effects of sideslip on double delta wings
[AIAA PAPER 93-0053] p 261 A93-20166
- An experimental investigation of twin fin buffeting and suppression
[AIAA PAPER 93-0054] p 261 A93-20167
- Flow visualization studies on sidewall effects in two dimensional transonic airfoil testing
[AIAA PAPER 93-0090] p 263 A93-20196

- Fiber optic-based laser vapor screen flow visualization systems for aerodynamic research in larger-scale subsonic and transonic wind tunnels p 408 A93-20298
- Holographic interferometric investigation of shock wave interaction with a ramp p 271 A93-21921
- Visualization of vortical flows with yet another post-processor [AIAA PAPER 93-0222] p 415 A93-22638
- Experimental and numerical investigation of Mach 2.5 supersonic mixed compression inlet [AIAA PAPER 93-0289] p 279 A93-22689
- Validation of a Navier-Stokes code using a (k,epsilon) turbulence model applied to a three-dimensional transonic channel [AIAA PAPER 93-0293] p 279 A93-22693
- Isolator-combustor interaction in a dual-mode scramjet engine [AIAA PAPER 93-0358] p 360 A93-23041
- Measurements in the near-field of a turbulent wingtip vortex [AIAA PAPER 93-0551] p 285 A93-23290
- Experimental investigation of rotor/lifting surface interactions [AIAA PAPER 93-0871] p 469 A93-24932
- Experimental investigations of the time and flow-direction responses of shear-stress-sensitive liquid crystal coatings [AIAA PAPER 93-0181] p 542 A93-25508
- Visualization and analysis of supersonic flow in rotating turbine stage. II - Analysis of the flow into the moving blades and their exit flow p 476 A93-27442
- Flow visualization and flow field measurements of a 1/12 scale tilt rotor aircraft in hover p 482 A93-29441
- A study of the rotor wake of a small-scale rotor model in forward flight using laser light sheet flow visualization with comparisons to analytical models p 766 A93-35957
- Shadowgraph flow visualization of isolated titrator and rotor/wing wakes p 767 A93-35996
- Contribution of visualization to the study of unsteady aspects of vortex breakdown [ONERA, TP NO. 1992-93] p 771 A93-38576
- Schlieren device and holographic interferometer for hypersonic flow visualization [ONERA, TP NO. 1992-160] p 832 A93-38739
- The experimental study of the effect of sweptback angles and the front shape of the fin on reduction of shock wave/turbulent boundary layer interaction region p 858 A93-40431
- Aerodynamic investigation with focusing schlieren in a cryogenic wind tunnel [AIAA PAPER 93-3485] p 910 A93-41059
- Experimental investigation of the management of large-sized drops and the onset of Marangoni-convection p 926 A93-41700
- Experimental study of the flow around a double ellipsoid configuration p 867 A93-42603
- Visualisation and analysis of three dimensional transonic flows by holographic interferometry p 1020 A93-44194
- Particle imaging techniques and applications p 1020 A93-44195
- Aerodynamic heating phenomenon in three dimensional shock wave/turbulent boundary layer interaction induced by sweptback fins in hypersonic flows p 960 A93-45507
- Observations of large-scale structures in wakes behind axisymmetric bodies p 965 A93-46748
- A visual study of recessed angled spanwise blowing method on a delta wing [AIAA PAPER 93-3246] p 966 A93-46791
- Control of a supersonic reattaching shear layer [AIAA PAPER 93-3248] p 966 A93-46793
- A three dimensional view of velocity using lasers p 1028 A93-46822
- An investigation of the effects of a rear stagnation jet on the wake behind a cylinder [AIAA PAPER 93-3274] p 969 A93-46835
- The three dimensional flow in a compressor cascade at design and off-design conditions p 971 A93-46927
- Application of the shadowgraph flow visualization technique to a full-scale helicopter rotor in hover and forward flight [AIAA PAPER 93-3411] p 1030 A93-47208
- A visualization study of the vortical flow over a double-delta wing in dynamic motion [AIAA PAPER 93-3425] p 976 A93-47220
- A visualizing method of streamlines around hypersonic vehicles [AIAA PAPER 93-3440] p 1014 A93-47230
- On dynamics of the juncture vortex [AIAA PAPER 93-3473] p 980 A93-47252
- Effect of leeward flow dividers on the wing rock of a delta wing [AIAA PAPER 93-3492] p 982 A93-47264
- Flow control over delta wings at high angles of attack [AIAA PAPER 93-3494] p 983 A93-47266
- Flow visualization of mast-mounted-sight/main rotor aerodynamic interactions [AIAA PAPER 93-3517] p 1009 A93-47280
- Computer-aided light sheet flow visualization [AIAA PAPER 93-2915] p 1147 A93-48117
- The effect of expansion on the large scale structure of a compressible turbulent boundary layer [AIAA PAPER 93-2991] p 1052 A93-48183
- A qualitative assessment of control effectors on an advanced fighter configuration [AIAA PAPER 93-3627] p 1127 A93-48312
- Investigation of nacelle upper cowl flow separation using on- and off-body flow visualization techniques p 1072 A93-49507
- 3-dimensional interactions in the rotor of an axial turbine [AIAA PAPER 93-2255] p 1081 A93-50053
- Fluidic scale model multi-plane thrust vector control test results [AIAA PAPER 93-2433] p 1117 A93-50187
- Unsteady aerodynamic behavior of an airfoil with and without a slot p 1093 A93-52007
- Unsteady wing surface pressures in the wake of a propeller p 1095 A93-52436
- Skin-friction topology over a surface mounted semi-ellipsoidal wing at incidence p 1178 A93-53216
- A preliminary investigation of the control of separated flow by means of excitation p 1182 A93-53859
- Observation of fluctuation of 2D-nozzle flows [ISABE 93-7110] p 1204 A93-54086
- LIF visualization of 3-dimensional hypersonic mixing [ISABE 93-7114] p 1221 A93-54089
- Results about the structure of the shock wave reflection process for strong incoming shock waves p 1233 A93-54810
- Three-dimensional simulations of compressible mixing layers - Visualizations and statistical analysis p 1235 A93-55360
- On the analysis of an impinging jet on ground effects p 1260 A93-56339
- Tilt rotor hover aeroacoustics [NASA-CR-177598] p 99 A93-10458
- An experimental study of flow patterns and endwall heat transfer upstream of a surface-mounted rectangular obstruction in a turbulent boundary layer p 89 A93-11698
- The 13 ft by 9 ft low speed wind tunnel facility at DRA (Aerospace Division) Bedford (England) [RAE-TM-AERO-2228] p 23 A93-11883
- An investigation of the effects of aft blowing on a 3.0 caliber tangent ogive body at high angles of attack [NASA-CR-190934] p 24 A93-12004
- Unsteady propeller/wing aerodynamic interactions p 24 A93-12190
- An experimental study of the relationship between forces and moments and vortex breakdown on a pitching delta wing p 49 A93-12206
- A summary of the forebody high-angle-of-attack aerodynamics research on the F-18 and the X-29A aircraft [NASA-TM-104261] p 25 A93-12353
- In-flight flow visualization results from the X-29A aircraft at high angles of attack [NASA-TM-4430] p 131 A93-13322
- Subsonic aerodynamic research laboratory [AD-A256060] p 137 A93-14661
- Detailed near surface flow about yawed, stranded cables [AD-A257382] p 418 A93-15857
- An advanced graphics-interactive system for a multi-block structured grid generation within an industrial environment [ETN-92-92885] p 440 A93-16288
- Three dimensional boundary-layer transition on a swept wing p 419 A93-16818
- Experiments on swept-wing boundary-layer transition p 419 A93-16829
- Combustion instabilities in a side-dump model ramjet combustor p 362 A93-17613
- A computational and experimental investigation of the propulsive and lifting characteristics of oscillating airfoils and airfoil combinations in incompressible flow [AD-A258019] p 294 A93-17819
- An experimental investigation of interacting wing-tip vortex pairs [AD-A258471] p 295 A93-18272
- Influence of the physical modelling of viscous terms on hypersonic flow computations [INRIA-RR-1493] p 297 A93-18652
- Proceedings of the Ninth NAL Symposium on Aircraft Computational Aerodynamics [NAL-SP-16] p 299 A93-19273
- Wind tunnel tests and CFD in Fuji Heavy Industries p 304 A93-19323
- Wind tunnel testing and CFD simulation in Mitsubishi Heavy Industries p 305 A93-19325
- Natural laminar flow test in-flight visualization p 482 A93-19921
- Aerothermodynamic properties of hypersonic flows over radiation-adiabatic surfaces [DLR-FB-91-42] p 485 A93-21761
- Flow visualizations of perpendicular blade vortex interactions [NASA-CR-192725] p 748 A93-25208
- Scientific visualization using the Flow Analysis Software Toolkit (FAST) p 758 A93-25600
- An investigation of photothermal velocimetry for application to transient, high-speed gas flows p 698 A93-25720
- Aerodynamics of a finite wing with simulated ice p 784 A93-27437
- Studies of origin of three-dimensionality in laminar wakes [AD-A262281] p 841 A93-28242
- The ground vortex flow field associated with a jet in a cross flow impinging on a ground plane for uniform and annular turbulent axisymmetric jets [NASA-CR-4513] p 789 A93-28449
- Preliminary design of an intermittent smoke flow visualization system [NASA-CR-186027] p 806 A93-28693
- Flow visualization on helicopter blades using acenaphthen [ESA-TT-1255] p 931 A93-29273
- Vortex structure and mass transfer near the base of a cylinder and a turbine blade p 901 A93-29929
- The aerodynamic effect of coolant ejection in the leading edge region of a film-cooled turbine blade p 904 A93-29958
- Contribution to the study of the interaction between acoustic waves and coherent structures induced by a prismatic cylinder in a rectangular cavity [ONERA-NT-1990-10] p 918 A93-30203
- A break-down of sting interference effects [NLR-TP-91220-U] p 1014 A93-31042
- ### FLOWMETERS
- Hemispherical and spherical flow parameter detectors p 75 A93-10044
- Experience with the use of liquid crystals in conjunction with the filament method in studying the structure of supersonic flow downstream of a plane step p 478 A93-27639
- Improved flow measurement with simultaneous period/frequency recording --- in turbojet engines p 1254 A93-54381
- Operating experience using venturi flow meters at liquid helium temperature [DE92-014693] p 90 A93-12140
- ### FLUID DYNAMICS
- Experimental study of dynamic fluid forces and moments for a long annular seal p 209 A93-15684
- Canadian low-gravity research using parabolic aircraft p 384 A93-21908
- Forcing function generator fluid dynamic effects on compressor blade gust response [AIAA PAPER 93-0157] p 275 A93-22594
- An overview on practical application of helicopter noise certification rules p 487 A93-29442
- An efficient procedure for cascade aeroelastic stability determination using nonlinear, time-marching aerodynamic solvers [AIAA PAPER 93-1631] p 719 A93-34159
- Numerical Fluid Dynamics Symposium, 5th, Tokyo, Japan, Dec. 19-21, 1991, Proceedings p 830 A93-38126
- Natural laminar flow and laminar flow control [ISBN 0-387-97737-6] p 859 A93-41776
- An investigation of post stall transients and recoverability of axial compression systems [ISABE 93-7012] p 1184 A93-53988
- Fluid dynamics and convective heat transfer in impinging jets through implementation of a high resolution liquid crystal technique [ISABE 93-7077] p 1220 A93-54053
- A plume-induced boundary layer separation experiment [AD-A255397] p 220 A93-14677
- Experimental analysis of the aeroacoustics of cascaded airfoils [AD-A257945] p 420 A93-18121
- Experimental and numerical examinations of the influence of inlet distortion perturbations on the working behavior of turbocompressors [ETN-93-92733] p 364 A93-18628
- Scientific visualization using the Flow Analysis Software Toolkit (FAST) p 758 A93-25600
- Fundamental studies of droplet interactions in dense sprays [AD-A261165] p 737 A93-25948

- Studies of origin of three-dimensionality in laminar wakes
 [AD-A262281] p 841 N93-28242
 JPRS report: Science and technology. Central Eurasia: Engineering and equipment
 [JPRS-UEQ-93-004] p 930 N93-29090
 Generation of carbon monoxide in compartment fires
 [PB93-146702] p 880 N93-29211
 Measurement of turbulent spots and intermittency modelling at gas-turbine conditions p 902 N93-29934

FLUID FILMS

- Two-directional skin friction measurement utilizing a compact internally mounted thin-liquid-film skin friction meter
 [AIAA PAPER 93-0180] p 414 A93-22608
 Dynamics of the behavior of nematic films in gasdynamic flows p 746 A93-35345
 Fuel film formation in the fuel-air premixer of the combustion chamber p 812 A93-39193
 Fluid-film foil bearings control engine heat p 924 A93-39949
 Testing of a high performance compressor discharge seal
 [AIAA PAPER 93-1997] p 1153 A93-49840
 Liquid hydrogen foil-bearing turbopump
 [AIAA PAPER 93-2537] p 1156 A93-50264
 Experimental evaluation of flat plate boundary layer growth over an anti-icing fluid film p 1140 A93-52645
 A test facility for the thermofluid-dynamics of gas bearing lubrication films
 [PNR-90897] p 72 N93-11032

FLUID FILTERS

- Design characteristics of the functional systems of aircraft and prediction of their technical condition p 320 A93-18334

FLUID FLOW

- Tracking flow features using overset grids
 [AIAA PAPER 93-0197] p 276 A93-22617
 Fluid flows around cascades p 479 A93-28518
 Physical effects of vegetation on wind-blown sand in the coastal environments of Florida
 [PB92-188424] p 93 N93-11702
 Grid sensitivity for aerodynamic optimization and flow analysis
 [NASA-CR-192980] p 694 N93-25117
 Kinetics and energy transfer in nonequilibrium fluid flows
 [AD-A263612] p 875 N93-29284
 Multiparticle imaging technique for two-phase fluid flows using pulsed laser speckle velocimetry
 [DE93-011734] p 935 N93-30489
 Reynolds number influences in aeronautics
 [NASA-TM-107730] p 989 N93-31732

FLUID INJECTION

- Behaviors of the laterally injected jet in film cooling - Measurements of surface temperature and velocity/temperature field within the jet
 [ASME PAPER 92-GT-180] p 402 A93-19405
 Control of vortices on a delta wing by leading-edge injection p 860 A93-41906
 Two-dimensional and three-dimensional mixing flow structures with injected through slotted nozzle and circular nozzle into supersonic flows
 [ISABE 93-7117] p 1221 A93-54092
 Modeling of a turbulent flow in the presence of discrete parietal cooling jets p 904 N93-29960
 A Navier-Stokes solver with different turbulence models applied to film-cooled turbine cascades p 904 N93-29962

FLUID JETS

- Calculation of three-dimensional turbulent jets propagating behind nozzles of rectangular cross section p 6 A93-10192
 An experimental investigation on the combustor with bypass flow in integral liquid fuel ramjet p 174 A93-16235
 Characteristics of liquid jet atomization across a high-speed airstream. I - Experiment on shape of spray, spatial distribution of injected liquid and Sauter mean diameter p 411 A93-21743
 Characteristics of liquid jet atomization across a high-speed airstream. II - Calculation of spatial distribution of liquid, variation of drop diameter and drop trajectory p 412 A93-21744
 Penetration and mixing of bubbling liquid jets from multiple injectors normal to a supersonic air stream
 [AIAA PAPER 92-5060] p 413 A93-22330
 Experimental investigation of crossflow jet mixing in a rectangular duct
 [NASA-TM-106152] p 812 N93-27026
 Experimental study of cross flow mixing in cylindrical and rectangular ducts
 [NASA-CR-187141] p 815 N93-27680

FLUID MECHANICS

- Applications of laser techniques in fluid mechanics p 395 A93-17765

- Nonsteady, one-dimensional, internal, compressible flows - Theory and applications - Book
 [ISBN 0-19-507358-4] p 548 A93-28749
 The status of CFD - An Air Force perspective
 [AIAA PAPER 93-3293] p 1021 A93-44997
 The fluid physics of parachute inflation p 1189 A93-54347

- The Goldstein Aeronautical Engineering Research Laboratory
 [AERO-REPT-9109] p 240 N93-16465
 Lift and drag forces on droplets and particles in wall-bounded shear flows
 [DE93-002678] p 419 N93-17761
 Combined experiment, phase 1
 [DE93-000012] p 485 N93-21766
 Development and application of computational aerothermodynamics flowfield computer codes
 [NASA-CR-192940] p 692 N93-24736
 Current research activities: Applied and numerical mathematics, fluid mechanics, experiments in transition and turbulence and aerodynamics, and computer science
 [NASA-CR-191408] p 758 N93-25084
 Unsteady vortex loop/dipole theory applied to the work and acoustics of an ideal low speed propeller
 [AD-A264057] p 876 N93-29891

FLUID-SOLID INTERACTIONS

- Three-dimensional flow over two spheres placed side by side p 539 A93-24412
 Apparent mass effects on parafoil dynamics
 [AIAA PAPER 93-1236] p 690 A93-35177
 A study of the interaction between a wake vortex and an encountering airplane
 [AIAA PAPER 93-3642] p 858 A93-40714
 Stability analysis of dynamic meshes for transient aerodynamic computations
 [AIAA PAPER 93-3325] p 1022 A93-45019
 Analytical study on plate edge noise (Noise generation from tandemly situated trailing and leading edges)
 p 1038 A93-45561
 Fluid-structural interactions using Navier-Stokes flow equations coupled with shell finite element structures
 [AIAA PAPER 93-3087] p 1099 A93-48261
 Effect of the size of a plane obstacle on self-oscillations generated in an underexpanded supersonic jet
 p 1068 A93-48849

FLUIDICS

- Fluidic scale model multi-plane thrust vector control test results
 [AIAA PAPER 93-2433] p 1117 A93-50187

FLUIDIZED BED PROCESSORS

- Advanced turbine design for coal-fueled engines
 [DE93-000224] p 554 N93-21254

FLUORESCENCE

- Characterization of electron beam propagation for hypersonic flight research applications
 [AIAA PAPER 92-5087] p 452 A93-22357

FLUORINE

- Mixing and reaction in the subsonic 2-D turbulent free shear layer p 289 N93-16508

FLUOROCARBONS

- COF₂ radiation from an air-TEFLO wake p 12 A93-12659

FLUTTER

- Flutter of grouped turbine blades
 [ASME PAPER 92-GT-227] p 404 A93-19444
 The vibration and flutter of composite material laminate p 543 A93-26617
 Elementary stall flutter of an aircraft wing p 545 A93-27289
 Backward bifurcation for structural divergence of a wing section p 526 A93-29351
 Experimental unsteady pressures at flutter on the Supercritical Wing Benchmark Model
 [AIAA PAPER 93-1592] p 683 A93-34123
 Unsteady aerodynamics and flutter of propfans using a three-dimensional Full-Potential Solver
 [AIAA PAPER 93-1633] p 720 A93-34161
 Effects of pylon yaw and lateral stiffness on the flutter of a delta wing with external store p 800 A93-36330
 Investigation of subharmonic response of limit cycle flutter of wing-store system p 800 A93-36339
 Supersonic turbomachine rotor flutter control by aerodynamic detuning p 899 A93-42884
 Use of eigenvectors in the solution of the flutter equation p 1022 A93-45151
 Computational analysis of nonlinear aeroelastic phenomena during stall flutter of cascaded airfoils
 [AIAA PAPER 93-2082] p 1079 A93-49909
 Unsteady aerodynamics and flutter based on the potential equation p 1079 A93-49913
 Laser velocimeter measurements of the flow field generated by a forward-swept propfan during flutter
 [AIAA PAPER 93-2919] p 1180 A93-53591

- Nonlinear stall flutter of wings with bending-torsion coupling
 [AD-A254323] p 186 N93-12959
 Active flutter suppression using dipole filters
 [NASA-TM-107594] p 186 N93-13367
 Transonic aeroelastic analysis of systems with structural nonlinearities p 217 N93-13769
 An investigation of the dynamic response of lifting surfaces with concentrated structural nonlinearities p 162 N93-13807
 A compilation of the mathematics leading to the doublet lattice method
 [AD-A256304] p 136 N93-14441
 Multi-disciplinary optimization of aeroservoelastic systems
 [NASA-CR-191255] p 220 N93-14766
 Finite-state inflow applied to aeroelastic flutter of fixed and rotating wings p 188 N93-14830
 On flutter behavior of a 2-D compressor cascade in incompressible flow p 418 N93-16543
 Introduction to Flutter of Winged Aircraft, volume 1
 [VKI-LS-1992-01] p 372 N93-18142
 The unified method of aeroelasticity p 372 N93-18143
 In-flight structural mode excitation system for flutter testing p 526 N93-19915
 The influence of structural optimization on the aeroelastic properties of a vertical tail
 [AD-A259140] p 513 N93-20575
 Analytical and experimental investigation of flutter suppression by piezoelectric actuation
 [NASA-TP-3241] p 513 N93-20584
 Airfoil stability in turbulent flow p 781 N93-27212
 Integrated structural design, vibration control, and aeroelastic tailoring by multiobjective optimization p 1030 N93-31137
 TDLM: A Transonic Doublet Lattice Method for 3D potential unsteady transonic flow calculation
 [DLR-FB-92-25] p 988 N93-31171
- FLUTTER ANALYSIS
- Transition of flutter mode of two-dimensional wing with external store p 41 A93-11818
 Effects of the pylon pitching stiffness on wing-store flutter p 41 A93-11820
 Subharmonic bifurcation analysis of wing with store flutter p 78 A93-12098
 Nonlinear problems of aeroelasticity p 78 A93-12153
 Integrated control law synthesis of gust load alleviation and flutter margin augmentation for a transport aircraft p 182 A93-14281
 An investigation of mode shift flutter suppression scheme for empennages p 182 A93-14288
 Application of vibration-and-flutter integration analysis system for a trainer p 226 A93-14311
 Parameter estimation techniques for flight flutter test analysis p 156 A93-14324
 On orthogonal search method of flutter analysis p 208 A93-15402
 Geometrically nonlinear local flutter analysis of supersonic airplane skin plates in the potential supersonic flow
 [ISAB 83-01-10939-4] p 394 A93-17569
 Coupled 3-D aeroelastic stability analysis of bladed disks
 [ASME PAPER 92-GT-171] p 351 A93-19397
 Flutter calculations for a system with interacting nonlinearities p 409 A93-20304
 Aeroservoelasticity in HISAIR - High Speed Airframe Integration Research
 [AIAA PAPER 92-4719] p 324 A93-20322
 An approach to tiltrotor wing aeroservoelastic optimization through increased productivity
 [AIAA PAPER 92-4781] p 326 A93-20371
 Flutter optimization of large transport aircraft
 [AIAA PAPER 92-4795] p 326 A93-20381
 Structural non-linearity effects on flutter of a swept wing in transonic flows p 410 A93-20714
 Optimal control law synthesis for flutter suppression using active acoustic excitations p 370 A93-23516
 Modeling, analysis, and prediction of flutter at transonic speeds p 416 A93-23553
 Analysis of flight flutter test data p 523 A93-23839
 Direct multivariable adaptive controller with application to wing flutter p 524 A93-26946
 Current status of computational methods for transonic unsteady aerodynamics and aeroelastic applications p 480 A93-29175
 Signal processing and system identification techniques for flutter test data analysis p 529 A93-29282
 Flutter calculations for fixed and rotating wings with state-space inflow dynamics
 [AIAA PAPER 93-1300] p 709 A93-33877

Vibration and flutter of stiff-inplane elastically tailored composite rotor blades
[AIAA PAPER 93-1302] p 725 A93-33879

Aeroelastic character of a National Aerospace Plane demonstrator concept
[AIAA PAPER 93-1314] p 732 A93-33890

A method of predicting quasi-steady aerodynamics for flutter analysis of high speed vehicles using steady CFD calculations
[AIAA PAPER 93-1364] p 682 A93-33931

Aerothermoelastic analysis of a NASP demonstrator model
[AIAA PAPER 93-1366] p 733 A93-33933

Structural modeling of low-aspect ratio composite wings
[AIAA PAPER 93-1371] p 739 A93-33937

Wing flutter boundary prediction using unsteady Euler aerodynamic method
[AIAA PAPER 93-1422] p 739 A93-33975

Bending-torsion flutter of linear viscoelastic wings including structural damping
[AIAA PAPER 93-1475] p 711 A93-34021

Exact flutter solution of advanced anisotropic composite cantilevered wing structures
[AIAA PAPER 93-1535] p 727 A93-34072

In-flight investigation of a rotating cylinder-based structural excitation system for flutter testing
[AIAA PAPER 93-1537] p 711 A93-34074

X-31A flight flutter test excitation by control surfaces
[AIAA PAPER 93-1538] p 727 A93-34075

Sensitivity analysis of flutter response of a typical section and a wing in transonic flow
[AIAA PAPER 93-1646] p 742 A93-34171

Aeroelastic challenges for a High Speed Civil Transport
[AIAA PAPER 93-1478] p 712 A93-34240

Evaluation and extension of the flutter-margin method for flight flutter prediction
[AIAA PAPER 93-1478] p 712 A93-34240

A flutter investigation of all-moveable NASP-like wings at hypersonic speeds
[AIAA PAPER 93-1315] p 769 A93-37427

Hypersonic flutter of a curved shallow panel with aerodynamic heating
[AIAA PAPER 93-1318] p 829 A93-37428

Transonic panel flutter
[AIAA PAPER 93-1476] p 829 A93-37438

Nonlinear flutter of composite plates with damage evolution
[AIAA PAPER 93-1546] p 829 A93-37441

Supersonic flutter analysis of composite plates and shells
[AIAA PAPER 93-1546] p 829 A93-37441

Experimental and theoretical study for nonlinear aeroelastic behavior of a flexible rotor blade
[AIAA PAPER 93-1546] p 829 A93-37441

Effect of structural uncertainties on flutter analysis
[AIAA PAPER 93-1546] p 829 A93-37441

Subsonic/transonic cascade flutter using a full-potential solver
[AIAA PAPER 93-1546] p 829 A93-37441

Supersonic panel flutter analysis of shallow shells
[AIAA PAPER 93-1546] p 829 A93-37441

Virtual zone Navier-Stokes computations for oscillating control surfaces
[AIAA PAPER 93-3363] p 955 A93-45056

Flutter analysis of composite panels on many supports
[AIAA PAPER 93-3363] p 955 A93-45056

Prediction of three-dimensional low frequency unsteady transonic flow and forced vibration in axial turbine stages
[AIAA PAPER 93-3363] p 955 A93-45056

Calculation of AGARD Wing 445.6 flutter using Navier-Stokes aerodynamics
[AIAA PAPER 93-3476] p 981 A93-47255

Stability of fluttered panels subjected to in-plane harmonic forces
[AIAA PAPER 93-2084] p 1114 A93-49911

Blade row interaction effects on flutter and forced response
[AIAA PAPER 93-2084] p 1114 A93-49911

Envelope function - A tool for analyzing flutter data
[AIAA PAPER 93-2084] p 1114 A93-49911

Nonlinear aspects of transonic aeroelasticity
[AIAA PAPER 93-2084] p 1114 A93-49911

Flutter analysis of stiffened laminated composite plates and shells in supersonic flow
[AIAA PAPER 93-2084] p 1114 A93-49911

Effects of blade geometry and mode shape on fan flutter
[AIAA PAPER 93-2084] p 1114 A93-49911

The unsteady flow past a supersonic splitter plate
[AIAA PAPER 93-2084] p 1114 A93-49911

Consideration of mass elements of the control system in a flutter analysis
[AIAA PAPER 93-2084] p 1114 A93-49911

The whirl-flutter problem in aircraft construction
[AIAA PAPER 93-2084] p 1114 A93-49911

A finite element method for nonlinear panel flutter
[AIAA PAPER 93-2084] p 1114 A93-49911

Control of panel flutter at high supersonic speed
[AIAA PAPER 93-2084] p 1114 A93-49911

Multi-disciplinary optimization of aeroservoelastic systems
[NASA-CR-191255] p 220 N93-14766

Beyond the frequency limits of time-linearized methods
[NLR-TP-91216-U] p 295 N93-17929

Introduction to Flutter of Winged Aircraft, volume 1
[VKI-LS-1992-01] p 372 N93-18142

The unified method of aeroelasticity
[NLR-TP-91216-U] p 295 N93-17929

Simulation of unsteady rotational flow over propfan configuration
[NASA-CR-192234] p 296 N93-18585

Formulation of a structural model for flutter analysis of low aspect ratio composite aircraft wings
[NLR-TP-91216-U] p 295 N93-17929

Fluid/structures interactions. Aircraft considerations
[NLR-TP-91216-U] p 295 N93-17929

FLUX DENSITY
Variable-speed generators with flux weakening
[NLR-TP-91216-U] p 295 N93-17929

FLUX VECTOR SPLITTING
A multi-zonal local solution methodology for the accelerated solution of the turbulent Navier-Stokes equations
[AIAA PAPER 93-0068] p 262 A93-20181

Comparison of limiters in flux-split algorithms for Euler equations
[AIAA PAPER 93-0068] p 262 A93-20181

Solution schemes for stage-by-stage dynamic compression system modeling
[AIAA PAPER 93-0154] p 275 A93-22592

Numerical solution of inviscid hypersonic flow around a conically-derived waverider
[AIAA PAPER 93-0320] p 280 A93-23012

Nonlinear relaxation/quasi-Newton algorithm for the compressible Navier-Stokes equations
[AIAA PAPER 93-0320] p 280 A93-23012

Acoustic flux vector splitting scheme for Euler equations
[AIAA PAPER 93-0876] p 470 A93-24937

A comparison of 'new' and 'old' flux-splitting schemes for the Euler equations
[AIAA PAPER 93-0876] p 470 A93-24937

Computation of inviscid flowfield around 3-D aerospace vehicles and comparison with experimental and flight data
[AIAA PAPER 93-0885] p 470 A93-24944

An upwind, kinetic flux-vector splitting method for flows in chemical and thermal non-equilibrium
[AIAA PAPER 93-0894] p 472 A93-24954

Hypersonic nonequilibrium flow computations using the Roe flux-difference split scheme
[AIAA PAPER 93-0894] p 472 A93-24954

Accuracy of flux-split algorithms in high-speed viscous flows
[AIAA PAPER 93-0894] p 472 A93-24954

Computation of hypersonic flow over a sphere using kinetic flux vector splitting scheme with equilibrium chemistry
[AIAA PAPER 93-0894] p 472 A93-24954

Enhanced numerical inviscid and viscous fluxes for cell centered finite volume schemes
[AIAA PAPER 93-0894] p 472 A93-24954

Finite volume 3DNS and PNS solutions of hypersonic viscous flow around a delta wing using Osher's flux difference splitting
[AIAA PAPER 93-3302] p 950 A93-45000

Field by field hybrid upwind splitting methods
[AIAA PAPER 93-3302] p 950 A93-45000

Computation of shock diffraction in external and internal flows
[AIAA PAPER 93-3302] p 950 A93-45000

A new flux splitting scheme
[AIAA PAPER 93-3302] p 950 A93-45000

A three-dimensional pressure flux-split RNS application to sub/supersonic flow in inlets and ducts
[AIAA PAPER 93-3063] p 1058 A93-48239

Numerical solutions of Euler equations by using a new flux vector splitting scheme
[AIAA PAPER 93-3063] p 1058 A93-48239

Flux-vector splitting for compressible low Mach number flow
[AIAA PAPER 93-3063] p 1058 A93-48239

An implicit difference scheme of Euler equation for unsteady transonic flow
[AIAA PAPER 93-3063] p 1058 A93-48239

Unsteady three-dimensional thin-layer Navier-Stokes solutions for turbomachinery in transonic flow
[AIAA PAPER 93-3063] p 1058 A93-48239

Volume 2: Explicit, multistage upwind schemes for Euler and Navier-Stokes equations
[NASA-CR-191647] p 418 N93-16558

Validation of central and upwind 3D compressible flow solvers
[NASA-CR-191647] p 418 N93-16558

Homenthalpic-flow approach for hypersonic inviscid non-equilibrium flows
[INRIA-RR-1652] p 788 N93-28440

FLY ASH
The aeronautical volcanic ash problem
[NLR-TP-91200-U] p 1001 N93-32332

Volcanic ash and aircraft operations
[NLR-TP-91200-U] p 1001 N93-32332

FLY BY LIGHT CONTROL
Direct optical control - A lightweight backup consideration
[NLR-TP-91200-U] p 1001 N93-32332

Specialty fiber optic systems for mobile platforms and plastic optical fibers; Proceedings of the Meeting, Boston, MA, Sept. 9-11, 1992
[SPIE-1799] p 1105 A93-49462

Fiber optic position sensors --- in aircraft flight control systems
[SPIE-1799] p 1105 A93-49462

Desirable characteristics for rotorcraft optical components
[SPIE-1799] p 1105 A93-49462

Ladar fiber optic sensor system for aircraft applications
[SPIE-1799] p 1105 A93-49462

Implementation of fiber optic technology in flight controls
[SPIE-1799] p 1105 A93-49462

Optical actuators for fly-by-light applications
[SPIE-1799] p 1105 A93-49462

Multiplexing electro-optic architectures for advanced aircraft integrated flight control systems
[NASA-CR-182268] p 187 N93-13735

FLY BY WIRE CONTROL
757 fly-by-wire demonstrator flight test
[AIAA PAPER 92-4099] p 38 A93-11271

Digital fly-by-wire system for BK117 FBW research helicopter
[AIAA PAPER 92-4099] p 38 A93-11271

Design and robustness issues for highly augmented helicopter controls
[AIAA PAPER 92-4099] p 38 A93-11271

A longitudinal control law integrating flight controls and engine controls
[AIAA PAPER 92-4099] p 38 A93-11271

Development status of the RAH-66 Comanche
[AIAA PAPER 92-4099] p 38 A93-11271

Direct optical control - A lightweight backup consideration
[AIAA PAPER 92-4099] p 38 A93-11271

The all-electric aircraft - In your future?
[AIAA PAPER 92-4099] p 38 A93-11271

Preliminary flight test results of a fly-by-throttle emergency flight control system on an F-15 airplane
[AIAA PAPER 93-1820] p 1100 A93-49708

Harmonic oscillation in FBW system
[AIAA PAPER 93-1820] p 1100 A93-49708

A simulation study on take-off and landing dynamics of fly-by-wire control system aircraft
[AIAA PAPER 93-1820] p 1100 A93-49708

Boeing 777 high lift control system
[AIAA PAPER 93-1820] p 1100 A93-49708

Predevelopment of a flight control system for a small civil aircraft
[AIAA PAPER 93-1820] p 1100 A93-49708

Multiple model adaptive estimation applied to the VISTA F-16 with actuator and sensor failures
[AIAA PAPER 93-1820] p 1100 A93-49708

A simulation study on take-off and landing dynamics of the aircraft of a fly-by-wire control system
[AIAA PAPER 93-1820] p 1100 A93-49708

A simulator study into low speed longitudinal handling qualities of ACT transport aircraft
[AIAA PAPER 93-1820] p 1100 A93-49708

Robust crossfeed design for hovering rotorcraft
[NASA-CR-193107] p 805 N93-27241

Project ARES 2: High-altitude battery-powered aircraft
[NASA-CR-193107] p 805 N93-27241

Development and flight testing of a fault-tolerant fly-by-light yaw control system
[NASA-CR-193107] p 805 N93-27241

FLYING PLATFORMS
Accuracy of GPS-derived acceleration from moving platform tests
[NASA-CR-193107] p 805 N93-27241

Meeting review: Third NCAR Research Aircraft Fleet Workshop
[NASA-CR-193107] p 805 N93-27241

The real aperture antenna of SAR, a key element for performance
[NASA-CR-193107] p 805 N93-27241

FLYWHEELS
A study upon structural optimization of elastic rotors for mechanical systems
[INPE-5376-TDI/471] p 83 N93-10310

FOG
Sea fog and stratus - A major aviation hazard in the northern Gulf of Mexico
[SAE PAPER 921130] p 895 A93-41318

Sea fog and stratus - A major aviation and marine hazard in the northern Gulf of Mexico
[SAE PAPER 921130] p 895 A93-41318

Engineering a visual system for seeing through fog
[SAE PAPER 921130] p 895 A93-41318

Reconnaissance capable F/A-18D optical and infrared window antifog systems
[SAE PAPER 921130] p 895 A93-41318

FOIL BEARINGS
Fluid-film foil bearings control engine heat
[SAE PAPER 921130] p 895 A93-41318

FOKKER AIRCRAFT
Aerodynamic integration of thrust reversers on the Fokker 100
[ISBN-90-6275-670-0] p 240 N93-19002

Professor Wittenberg: His speciality and versatility
[ISBN-90-6275-670-0] p 240 N93-19002

Aircraft performance in practice
[ISBN-90-6275-670-0] p 240 N93-19002

Instrumentation for in-flight acoustic measurements in an engine inlet duct of a Fokker 100 aircraft
[NLR-TP-91200-U] p 1001 N93-32332

FORCE DISTRIBUTION
Review of the normal force fluctuations of aerofoils with separated flow
[NLR-TP-91200-U] p 1001 N93-32332

- Post-critical behaviour of a tapered cantilever column subjected to a uniformly distributed tangential follower force p 831 A93-38431
- Comparison of some direct multi-point force appropriation methods p 928 A93-43338
- Consideration of mass elements of the control system in a flutter analysis p 1249 A93-56217
- Harmonic analysis of the aerodynamic forces on a Darrieus rotor p 18 N93-10551
- Hypersonic propulsion system force accounting p 175 N93-13229
- Analysis of wind-tunnel data for elliptic cross-sectioned forebodies at Mach numbers 0.4 to 5.0 p 782 N93-27221

FORCED CONVECTION

- Augmentation of turbulent heat transfer with a vortex generator attached to a LEBU plate p 411 A93-21729
- The effect of orthogonal-mode rotation on forced convection in a circular-sectioned tube fitted with full circumferential transverse ribs p 932 N93-29937
- Turbulent flow and heat transfer in idealized blade cooling passages p 902 N93-29938
- Performance of thermal adhesives in forced convection p 924 N93-30974

FORCED VIBRATION

- Subharmonic bifurcation analysis of wing with store flutter p 78 A93-12098
- Active control of the shear layer on a static airfoil [AIAA PAPER 93-0442] p 286 A93-23353
- Experimental and theoretical study for nonlinear aeroelastic behavior of a flexible rotor blade p 837 A93-39422
- The effects of forced oscillations on the performance of airfoils [AIAA PAPER 93-3264] p 968 A93-46829
- Prediction of three-dimensional low frequency unsteady transonic flow and forced vibration in axial turbine stages p 971 A93-46934
- Unsteady aerodynamic models for maneuvering aircraft [AIAA PAPER 93-3626] p 1126 A93-48311
- Development of nonlinear aerodynamic models for unsteady responses p 19 N93-10845
- Dynamic simulation of flexible body systems by the vector solution method p 553 N93-20666
- Stochastic finite element analysis for high speed rotors p 554 N93-20696
- Helicopter forced response vibration analysis method RTVIB20 [AD-A261809] p 730 N93-26260

FOREBODIES

- Correlation of forebody pressures and aircraft yawing moments on the X-29A aircraft at high angles of attack [AIAA PAPER 92-4105] p 38 A93-11273
- Lateral aerodynamics characteristics of forebodies at high angle of attack in subsonic and transonic flows p 118 A93-14302
- A low-speed wind tunnel study of vortex interaction control techniques on a chine-forebody/delta-wing configuration p 122 A93-14409
- A sensitivity study for pneumatic vortex control on a chined forebody [AIAA PAPER 93-0049] p 260 A93-20162
- Numerical analysis of a chined forebody with asymmetric strakes [AIAA PAPER 93-0051] p 260 A93-20164
- Quantitative laser velocimetry measurements in the hypersonic regime by the integration of experimental and computational analysis [AIAA PAPER 93-0089] p 263 A93-20195
- Application of space-marching methods to hypersonic forebody flow fields [AIAA PAPER 92-5030] p 272 A93-22305
- An estimate of the 'doomed propellant fraction' for a Superdetonative Ram Accelerator p 385 A93-23042
- Stability theory and transition prediction applied to a general aviation fuselage p 479 A93-28601
- Computational investigation of a pneumatic forebody flow control concept p 768 A93-37383
- Actuated forebody strake controls for the F-18 high alpha research vehicle [AIAA PAPER 93-3675] p 1006 A93-44233
- The effect of Reynolds number on control of forebody asymmetry by suction and bleed [AIAA PAPER 93-3265] p 968 A93-46831
- AIAA Applied Aerodynamics Conference, 11th, Monterey, CA, Aug. 9-11, 1993, Technical Papers. Pts. 1 & 2 p 974 A93-47201
- Tangential Forebody Blowing-yaw control at high alpha [AIAA PAPER 93-3406] p 1008 A93-47205
- Side-force control on a forebody of diamond cross-section at high angles of attack [AIAA PAPER 93-3407] p 1008 A93-47206

- Forebody vortex control with jet and slot blowing on an F/A-18 [AIAA PAPER 93-3449] p 1009 A93-47235
- Forebody vortex control on an F/A-18 using small, rotatable 'tip-strakes' [AIAA PAPER 93-3450] p 1009 A93-47236
- Navier-Stokes simulation of external/internal transonic flow on the forebody/inlet of the AV-8B Harrier II [AIAA PAPER 93-3057] p 1058 A93-48234
- Engineering method for calculating inlet face property profiles on high speed vehicle forebodies [AIAA PAPER 93-3113] p 1062 A93-48283
- Lateral control at high angles of attack using pneumatic blowing through a chined forebody [AIAA PAPER 93-3624] p 1126 A93-48309
- Euler analysis of forebody-strake vortex flows at supersonic speeds p 1094 A93-52429
- Correlation of forebody pressures and aircraft yawing moments on the X-29A aircraft at high angles of attack [NASA-TM-4417] p 22 N93-11532
- A summary of the forebody high-angle-of-attack aerodynamics research on the F-18 and the X-29A aircraft [NASA-TM-104261] p 25 N93-12353
- Effects of forebody strakes and Mach number on overall aerodynamic characteristics of configuration with 55 deg cropped delta wing [NASA-TP-3253] p 131 N93-13353
- Flight and wind-tunnel calibrations of a flush airdata sensor at high angles of attack and sideslip and at supersonic Mach numbers [NASA-TM-104265] p 344 N93-19110
- Sensitivity calculations for a 2D, inviscid, supersonic forebody problem [NASA-CR-191444] p 779 N93-27004
- Analysis of wind-tunnel data for elliptic cross-sectioned forebodies at Mach numbers 0.4 to 5.0 p 782 N93-27221
- Solution of Euler equations for forebody-inlet ensemble of aircraft at high angle of attack [AD-A263905] p 876 N93-29862
- FORECASTING**
- Methods of economic evaluation - Forecasting critique [AIAA PAPER 92-4285] p 570 A93-24300
- Meeting review: Third NCAR Research Aircraft Fleet Workshop [PB92-222710] p 223 N93-12818
- Terminal area forecasts FY 1992 - 2005 [AD-A255797] p 149 N93-15390
- Poland civil aviation master plan and investment program: Executive summary [PB92-213685] p 459 N93-21342
- Poland civil aviation master plan and investment program [PB92-213693] p 459 N93-21343
- FORESTS**
- Large-eddy simulation of turbulent flow above and within a forest p 92 A93-11404
- FORGING**
- The modeling of forging and precision-casting forming processes p 207 A93-15030
- Total quality management of forged products through finite element simulation p 1217 A93-53493
- FORM FACTORS**
- Effects of blade geometry and mode shape on fan flutter [ISABE 93-7028] p 1196 A93-54004
- FORMALISM**
- Formalization of the problem of preliminary aircraft design p 891 A93-42375
- FORMING TECHNIQUES**
- Mechanical testing analyses of new aluminium alloy SPF typical-parts in aircraft p 196 A93-14174
- A new production technology for complex-shaped structural elements 'creep forming' p 202 A93-14175
- A new method to study the forming process of complicated sheetmetal aero-parts p 204 A93-14363
- Thermoplastic composite parts manufacture at Du Pont [SME PAPER EM93-106] p 1159 A93-51728
- Structural applications of Avimid K3B LDF thermoplastic composites -- for advanced aircraft p 1216 A93-53429
- Consolidation of graphite thermoplastic textile preforms for primary aircraft structure p 919 N93-30439
- FOUNDATIONS**
- Identification and conversion of foundation parameters for airport pavement p 538 A93-24035
- FOURIER ANALYSIS**
- Fourier analysis of clamped moderately thick arbitrarily laminated plates p 206 A93-14571
- Blade excitation by circumferentially asymmetric rotating stall in centrifugal compressors [ASME PAPER 92-GT-148] p 351 A93-19376

- Optimal circumferential placement of cylindrical thermocouple probes for reduction of excitation forces [ASME PAPER 92-GT-423] p 406 A93-19571
- Thrust imparted to an airfoil by passage through a sinusoidal upwash field p 1178 A93-53219
- Nonlinear aeroelasticity of composite structures [AD-A254285] p 47 N93-10842
- Development of nonlinear aerodynamic models for unsteady responses p 19 N93-10845
- FOURIER SERIES**
- Numerical optimization methods for variational inverse boundary value problems of aerodynamics p 1088 A93-51771
- FOURIER TRANSFORMATION**
- Equivalent deterministic inputs for atmospheric turbulence p 183 A93-14351
- Receptivity of three-dimensional boundary layers [AIAA PAPER 93-0074] p 262 A93-20186
- FRACTOGRAPHY**
- A study of the flexural properties of carbon-epoxy composites in certain environments p 390 A93-21999
- Flight simulation and constant amplitude fatigue crack growth in aluminum-lithium sheet and plate [NLR-TP-91104-U] p 331 N93-17562
- AGARD Engine Disc Cooperative Test Programme [AGARD-R-766-ADD] p 1004 N93-31741
- Fractographic and microstructural analysis of fatigue crack growth in Ti-6Al-4V fan disc forgings p 1004 N93-31742
- Fractographic investigation of IMI 685 crack propagation specimens for SMP SC33 p 1004 N93-31743
- Material characterization and fractographic examination of Ti-17 fatigue crack growth specimens for SMP SC33 p 1004 N93-31744
- FRACTURE MECHANICS**
- Stochastic computational mechanics for aerospace structures p 78 A93-12157
- An evaluation system for impact damage and erosion of ceramic gas turbine components p 79 A93-12229
- Bulging of fatigue cracks in a pressurized aircraft fuselage p 81 A93-13639
- Flight simulation and constant amplitude fatigue crack growth in aluminum-lithium sheet and plate p 71 A93-13644
- A synthesized method in durability analysis p 203 A93-14286
- Study on fracture failure of turbine blades in a series of turbojets p 205 A93-14493
- Lifting philosophies for aero engine fracture critical parts p 345 A93-18783
- Fracture of highway and airport pavements p 547 A93-28290
- Crack growth and repair of multi-site damage of fuselage lap joints p 547 A93-28291
- Analysis of the friction and wear mechanisms of multilayered plasma-sprayed ceramic coatings p 548 A93-28567
- Tapered geometries for improved crashworthiness under side loads p 743 A93-34259
- Crack growth/damage tolerance analysis methods as applied to V-22 fuselage and empennage p 795 A93-35948
- Evaluation of the fatigue behavior of discontinuous and continuous fiber thermoplastic composite laminates p 824 A93-36005
- Methodology for studying the fracture of aircraft structures in static tests p 801 A93-36785
- Load-bearing capacity of an aircraft wing based on the condition of compressed surface fracture p 801 A93-36794
- High temperature fracture mechanism of gas-pressure sintered silicon nitride p 825 A93-38893
- Crack analysis using discontinuous boundary elements p 925 A93-40775
- Characterization of delamination and fiber fractures in carbon fiber reinforced plastics induced from impact p 915 A93-40787
- Applications of advanced fracture mechanics to fuselage p 1026 A93-45787
- A laboratory study of fracture in the presence of lap splice multiple site damage p 1027 A93-45790
- A study of damage tolerance of the landing gear structure p 1219 A93-53881
- Reinforcement of the F-111 wing pivot fitting with a boron/epoxy doubler system - Materials engineering aspects p 1214 A93-54241
- Mechanisms and modelling of environment-dependent fatigue crack growth in a nickel based superalloy [AD-A253967] p 71 N93-10717
- Fatigue in single crystal nickel superalloys [AD-A254603] p 74 N93-12237
- Verification of rain-flow reconstructions of a variable amplitude load history [NASA-CR-189670] p 91 N93-12411
- State of the art review of rutting and cracking in pavements p 380 N93-16316

- Fatigue in single crystal nickel superalloys
[AD-A258038] p 393 N93-17704
- Numerical determination of the residual strength of battle damaged composite plates p 537 N93-21533
- Fatigue in single crystal nickel superalloys
[AD-A261742] p 737 N93-26282
- Application of the cyclic J-integral to fatigue crack propagation p 839 N93-27182
- NASA-UVA Light Aerospace Alloy and Structures Technology Program (LA2ST)
[NASA-CR-193412] p 1019 N93-31739
- Fractographic and microstructural analysis of fatigue crack growth in Ti-6Al-4V fan disc forgings p 1004 N93-31742
- Fractographic investigation of IMI 685 crack propagation specimens for SMP SC33 p 1004 N93-31743
- Fatigue in single crystal nickel superalloys
[AD-A265451] p 1019 N93-31795
- FRACTURE STRENGTH**
- Damage tolerance assessment on the multisite cracks for the YS-11 aircraft p 46 A93-13642
- PAA-core aluminum honeycomb - An end user's evaluation p 209 A93-15738
- Crack growth under conditions of service loading p 396 A93-18370
- Research and development of ceramic turbine wheels [ASME PAPER 92-GT-295] p 354 A93-19485
- INCOLOY 908, a low coefficient of expansion alloy for high-strength cryogenic applications. I. Physical metallurgy p 534 A93-25686
- High temperature corrosion resistant bearing steel development [AIAA PAPER 93-2000] p 1145 A93-49842
- Fatigue crack growth in AerMet 100 steel [AD-A249068] p 74 N93-12248
- Reanalysis of multiple-wheel landing gear traffic tests [AD-A256593] p 194 N93-14238
- Damage tolerance behaviour of aluminium-lithium sheet alloys [NLR-TP-91244-U] p 392 N93-17540
- Damage tolerance of a helicopter rotor high-strength steel p 555 N93-21322
- Improved silicon nitride for advanced heat engines [NASA-CR-182193] p 917 N93-29451
- Effects of intra- and inter-laminar resin content on the mechanical properties of toughened composite materials p 921 N93-30845
- NASA-UVA Light Aerospace Alloy and Structures Technology Program (LA2ST)
[NASA-CR-193412] p 1019 N93-31739
- FRACTURES (MATERIALS)**
- Nondestructive evaluation of ceramic and metal matrix composites for NASA's HITEMP and enabling propulsion materials programs [NASA-TM-105807] p 85 N93-10963
- FRACTURING**
- Fatigue in single crystal nickel superalloys [AD-A254704] p 198 N93-12746
- Fatigue in single crystal nickel superalloys [AD-A259191] p 536 N93-20275
- FRANCE**
- French aerospace equipment p 1041 N93-31734
- FREDHOLM EQUATIONS**
- Spline-collocation solution of a Fredholm equation of the second kind in the problem of flow past an airfoil p 1092 A93-51904
- FREE BOUNDARIES**
- Numerical solution of a free-boundary problem in hypersonic flow theory - Nonequilibrium viscous shock layers p 8 A93-11920
- A fast multigrid method for solving incompressible hydrodynamic problems with free surfaces [AIAA PAPER 93-0767] p 540 A93-24851
- Interaction of a streamwise vortex with a free surface [AIAA PAPER 93-0556] p 543 A93-25539
- An existence theorem for a free boundary problem of hypersonic flow theory p 857 A93-40405
- FREE CONVECTION**
- Performance of thermal adhesives in forced convection p 924 N93-30974
- FREE FLIGHT**
- A joint Soviet-Bulgarian scientific program for free-flight and tethered aerostat observations p 2 A93-11374
- Simulation analysis of a cable-mount system used for dynamic wind tunnel tests p 68 N93-12359
- Design and implementation of fuzzy logic controllers [NASA-CR-193268] p 1038 N93-31649
- FREE FLOW**
- Control of numerical diffusion in computational modeling of vortex flows p 9 A93-12156
- An experimental study for interaction flow between shock wave and turbulent boundary layer p 120 A93-14355
- Measurements of the effect of free-stream turbulence length scale on heat transfer [ASME PAPER 92-GT-244] p 405 A93-19453
- The effects of incident turbulence and moving wakes on laminar heat transfer in gas turbines [ASME PAPER 92-GT-377] p 406 A93-19535
- Quantitative laser velocimetry measurements in the hypersonic regime by the integration of experimental and computational analysis [AIAA PAPER 93-0089] p 263 A93-20195
- Control of pressure fluctuations in the reattachment region of a supersonic free shear layer [AIAA PAPER 93-0385] p 282 A93-23064
- Nonplanar Doublet-Point method for supersonic unsteady aerodynamics [AIAA PAPER 93-1588] p 682 A93-34120
- Aerodynamic shape optimization using preconditioned conjugate gradient methods [AIAA PAPER 93-3322] p 952 A93-45016
- Visual observations of supersonic transverse jets p 965 A93-46750
- Instability of three-dimensional supersonic boundary layer p 973 A93-46987
- Supersonic vortex breakdown over a delta wing in transonic flow [AIAA PAPER 93-3472] p 980 A93-47251
- An adaptive grid/Navier-Stokes methodology for the calculation of nozzle afterbody base flows with a supersonic freestream [AIAA PAPER 93-1922] p 1076 A93-49788
- Hypersonic inlet efficiency revisited p 16 N93-10012
- Application of a vectorized particle simulation to the study of plates and wedges in high-speed rarefied flow p 133 N93-13746
- Bypass transition in compressible boundary layers p 417 N93-15801
- Experimental investigation of the aerodynamics of independently rotating cylindrical shells [AD-A258917] p 305 N93-19340
- Increased heat transfer to elliptical leading edges due to spanwise variations in the freestream momentum: Numerical and experimental results [NASA-TM-106150] p 838 N93-27020
- Discrete-vortex simulation of pulsating flow on a turbulent leading-edge separation bubble p 787 N93-27457
- Prediction of vortex breakdown on a delta wing p 787 N93-27459
- Heat transfer with moderate free stream turbulence p 932 N93-29936
- The influence of variable flow velocity on unsteady airfoil behavior [DLR-FB-92-22] p 988 N93-31320
- FREE JETS**
- Calculation of three-dimensional turbulent jets propagating behind nozzles of rectangular cross section p 6 A93-10192
- Excitation of velocity fluctuations and noise in a wind tunnel p 444 A93-18242
- Flow field measurements in a turbulent free jet issuing from a sharp-edged square slot p 244 A93-19158
- Experiments on rarefied supersonic free jets using impact probes p 461 A93-24091
- Numerical study on the interaction of supersonic flow past a wedge and free jet p 479 A93-28574
- Further study of high speed single free jets p 873 A93-43687
- An experimental study of a compound supersonic jet p 1069 A93-48914
- Subscale validation of a freejet inlet-engine test capability [AIAA PAPER 93-2179] p 1138 A93-49991
- C-2 subsonic freejet development and demonstration [AIAA PAPER 93-2180] p 1138 A93-49992
- An approach to in-situ analysis of scramjet combustor behavior [AIAA PAPER 93-2328] p 1116 A93-50108
- Streamwise vorticity generation and mixing enhancement in free jets by 'delta-tabs' [AIAA PAPER 93-3253] p 1180 A93-53592
- Experimental investigation of an ejector-powered free-jet facility [NASA-TM-105868] p 291 N93-16704
- Streamwise vorticity generation and mixing enhancement in free jets by delta-tabs [NASA-TM-106235] p 988 N93-31648
- FREE MOLECULAR FLOW**
- Calculation of the aerodynamic characteristics of bodies with meshlike surfaces in hypersonic rarefied-gas flow p 1090 A93-51870
- Experimental simulation of the aerodynamic heating of bodies in a molecular region p 1090 A93-51871
- Certain improved algorithms for calculating the aerodynamic characteristics of flight vehicles in free-molecular flow p 1090 A93-51872
- Rarefied-flow Shuttle aerodynamics model [NASA-TM-107698] p 458 N93-19976
- Hypersonic panel flutter in a rarefied atmosphere [NASA-CR-4514] p 780 N93-27084
- FREE VIBRATION**
- Analysis of complicated plates by a nine-node spline plate element p 206 A93-14616
- Nonlinear large amplitude vibration of composite helicopter blade at large static deflection p 713 A93-35630
- The free vibration of cylindrically-curved rectangular panels p 1022 A93-45113
- Optimization of an aeroelastic system using the dynamic stability condition p 1029 A93-47085
- Dynamic analysis of a pre-and-post ice impacted blade [NASA-TM-105829] p 90 N93-12197
- Experimental and analytical investigation of the vibration characteristics of a remotely piloted helicopter [AD-A256131] p 163 N93-14248
- Stochastic finite element analysis for high speed rotors p 554 N93-20696
- FREE WING AIRCRAFT**
- An ultralight free-wing aircraft design study [AIAA PAPER 92-4194] p 44 A93-13371
- FREE-PISTON ENGINES**
- Free-piston Stirling coolers for intermediate lift temperatures p 543 A93-26062
- Performance considerations in the operation of free-piston driven hypersonic test facilities p 1011 A93-45497
- Free piston facilities with air driver gas p 1011 A93-45528
- Hypervelocity flows of argon produced in a free piston driven expansion tube p 1012 A93-45530
- Double diaphragm driven free piston expansion tube p 1016 A93-45533
- Computational fluid dynamics code validation using a free piston hypervelocity shock tunnel p 960 A93-45545
- FREEZING**
- Developments in icing test techniques for aerospace applications in the RAE Pyestock (England) altitude test facility [RAE-TM-P-1214] p 48 N93-11485
- Mathematical model of frost heave and thaw settlement in pavements [CRR-LEPT-93-2] p 912 N93-30103
- FREQUENCY HOPPING**
- Digital hopping GPS/GLONASS receiver p 312 A93-21128
- FREQUENCY MODULATION**
- Demonstration of an integrated, active 4 x 4 photonic crossbar p 211 A93-17392
- Robust method for estimating the parameters of a linear FM waveform p 1147 A93-47650
- FREQUENCY RANGES**
- An aeroelastic model structure investigation for a manned real-time rotorcraft simulation p 693 N93-24756
- FREQUENCY RESPONSE**
- Development of a system for aerodynamic fast-response probe measurements p 203 A93-14325
- Subharmonic and harmonic forced response of the wake of a circular cylinder p 288 A93-23565
- A frequency domain theory for structural identification p 930 A93-43778
- Digital data acquisition and preliminary instrumentation study for the F-16 laminar flow control vehicle p 292 N93-16784
- Hot film wall shear instrumentation for compressible boundary layer transition research, [NASA-CR-191360] p 294 N93-17855
- Frequency-response techniques for documentation and improvement of rotorcraft simulators p 913 N93-30689
- FREQUENCY REUSE**
- Three-dimensional cellular systems for aeronautical mobile radio communications p 502 A93-29639
- FREQUENCY STABILITY**
- Correction of the frequency characteristic of the waveguide circuit of an acoustic-jet temperature transducer p 832 A93-39036
- FRETING**
- The fretting damage and effect of temperature in typical joint of aircraft construction p 203 A93-14196
- FRICTION**
- Analysis of the friction and wear mechanisms of multilayered plasma-sprayed ceramic coatings p 548 A93-28567
- Effects of foundation excitation on multiple rub interactions in turbomachinery p 1260 A93-55996
- FRICTION DRAG**
- Effect of longitudinal microribbing on the drag of a body of revolution p 5 A93-10147

- Recent developments in international laminar flow research programs for transport aircraft
[ONERA, TP NO. 1992-163] p 457 A93-26878
- Development of a skin friction gauge for use in an impulse facility p 1024 A93-45526
- Overall effects of separation on thin aerofoils
[ISBN-0-315-67464-4] p 135 N93-13930
- Analysis and evaluation of an integrated laminar flow control propulsion system
[NASA-CR-192162] p 551 N93-20268
- FRICTION FACTOR**
- Analysis and evaluation of an integrated laminar flow control propulsion system
[NASA-CR-192162] p 551 N93-20268
- FRICTION MEASUREMENT**
- On the measurements of the skin friction in 3-D flows - Application to a complete 3-D shear layer flow p 118 A93-14329
- Conventional skin friction measurement techniques for strongly perturbed supersonic turbulent boundary layers p 271 A93-21863
- Two-directional skin friction measurement utilizing a compact internally mounted thin-liquid-film skin friction meter
[AIAA PAPER 93-0180] p 414 A93-22608
- Development of a skin friction gauge for use in an impulse facility p 1024 A93-45526
- Direct measurements of skin friction in a scramjet combustor
[AIAA PAPER 93-2443] p 1119 A93-50195
- Reflection type skin friction meter
[NASA-CASE-LAR-14520-1-SB] p 296 N93-18275
- FRICTION REDUCTION**
- Effect of longitudinal microribbing on the drag of a body of revolution p 5 A93-10147
- Some aspects of the design of combination landing gear — for stable aircraft motion on runways p 891 A93-42374
- Analysis and evaluation of an integrated laminar flow control propulsion system
[NASA-CR-192162] p 551 N93-20268
- FRICTION WELDING**
- Friction surfacing and linear friction welding p 1217 A93-53499
- FROST**
- Performance degradation due to hoar frost on lifting surfaces p 305 A93-17798
- Effect of underwing frost on transport aircraft takeoff performance
[DOT/FAA/CT-TN93/9] p 791 N93-27252
- Mathematical model of frost heave and thaw settlement in pavements
[CRREL-REPT-93-2] p 912 N93-30103
- FUEL CELLS**
- Support of composite fuel cells
[SME PAPER EM92-101] p 152 A93-14102
- Fuel cell powered electric propulsion for HALE aircraft
[ASME PAPER 92-GT-404] p 356 A93-19553
- FUEL COMBUSTION**
- Mixing and combustion studies using discrete orifice injection at hypervelocity flight conditions p 205 A93-14523
- Numerical simulation of shock-induced combustion/detonation p 410 A93-20719
- Combustion of microemulsion sprays
[AIAA PAPER 93-0131] p 390 A93-22578
- Consideration of the completeness of combustion and dissociation and recombination processes in mathematical models of jet engines for high supersonic flight velocities p 520 A93-27627
- Polyethylene pyrolysis model for combustion calculations in solid fuel ramjets p 520 A93-27739
- Ignition process of fuel droplet arrays in a supersonic flowfield p 535 A93-27766
- Choice of the heating system for high-temperature generators using chemical fuel p 559 A93-29660
- On the stability of the process of formation of combustion generated particles by coagulation and simultaneous shrinkage due to particle oxidation
[AIAA PAPER 93-2478] p 1146 A93-50220
- Periodic chemical energy release for active combustion control
[ISABE 93-7043] p 1198 A93-54019
- Velocity and temperature measurements in a non-premixed reacting flow behind a backward facing step p 132 A93-13632
- A procedure for defining lightning risk to air vehicles p 703 A93-24885
- Parameters influencing the hot-spot ignition of aviation fuel/air and ethylene/air mixtures p 704 A93-24886
- Fuel injector: Air swirl characterization aerothermal modeling, phase 2, volume 2
[NASA-CR-189193-VOL-2] p 721 N93-25106

- Nitric oxide formation in a lean, premixed-prevaporized jet A/air flame tube: An experimental and analytical study
[NASA-TM-105722] p 844 N93-27012
- Development of a pulse ramjet based on twin valveless pulse combustors coupled to operate in antiphase p 814 N93-27186
- Generation of carbon monoxide in compartment fires
[PB93-146702] p 880 N93-29211
- FUEL CONSUMPTION**
- ICAO analyses trends in fuel consumption by world's airlines p 1 A93-10733
- The multi-heat addition turbine engine
[AIAA PAPER 92-4272] p 54 A93-13334
- Optimizing the cruising fuel efficiency of commercial aircraft on the basis of flight manual data p 321 A93-18351
- Calculation of fuel economy for the Tu-154 aircraft in relation to the washing of the NK-8-2U engine at civil aviation maintenance facilities p 345 A93-18356
- A compact, intercooled and regenerated gas turbine for HALE applications
[ASME PAPER 92-GT-401] p 355 A93-19550
- High pressure ratio intercooled turboprop study
[ASME PAPER 92-GT-405] p 356 A93-19554
- A study of aerodynamic performance of a contra-rotating axial compressor stage p 463 A93-24524
- Enhancement of endurance performance by periodic optimal camber control p 727 A93-34541
- Some contributions to propulsion theory - Fuel consumption formulae and general range equation p 713 A93-34850
- Determination of the takeoff characteristics of jet engines during the preliminary design of aircraft p 892 A93-42378
- Selection of the turbofan engine size p 899 A93-42379
- Singular arcs for blunt endoatmospheric vehicles p 1015 A93-44380
- Classification of the principal fuel saving methods in flight operations p 996 A93-45660
- Results of operational testing of a system for computing optimal flight regimes — of aircraft flight p 996 A93-45665
- The fuel/timing problem in a computer-aided flight preparation system for civil aircraft p 996 A93-45672
- General concepts related to the determination of the individual flight performance characteristics of aircraft for establishing fuel consumption standards and optimal flight regimes p 996 A93-45673
- Computer-aided study of flight regimes and fuel consumption for helicopter flight operations p 997 A93-45674
- High speed propeller acoustics and aerodynamics - A boundary element approach p 967 A93-46804
- An analysis of air-turbo-rocket performance
[AIAA PAPER 93-1982] p 1141 A93-49829
- The study of experimental turboramjets - Heat state and cooling problems
[AIAA PAPER 93-1989] p 1112 A93-49834
- A study of a direct-injection stratified-charge rotary engine for motor vehicle application
[SAE PAPER 930677] p 1158 A93-50524
- An investigation of the fuel-optimal periodic trajectories of a hypersonic vehicle
[AIAA PAPER 93-3753] p 1101 A93-51349
- Compound cycle engine for helicopter application
[NASA-CR-180824] p 55 N93-10348
- Civil aircraft engines: The next generation
[PNR-90962] p 58 N93-11085
- RB199 engine oil system failure diagnostics by comparison of measured and calculated oil consumption using the OLMOS on-board monitoring system p 178 N93-15173
- Development of an engine/airframe performance matching scheme for jet engine retrofit
[AD-A258822] p 365 N93-18997
- Regression rate mechanism in a solid fuel ramjet p 814 N93-27185
- FUEL CONTAMINATION**
- Effect of design and service-related factors on the formation of combustion residues in the fuel nozzles of gas turbine engines p 345 A93-18342
- Calculation of fuel economy for the Tu-154 aircraft in relation to the washing of the NK-8-2U engine at civil aviation maintenance facilities p 345 A93-18356
- Effect of a metal deactivator fuel additive on fuel deposition in fuel atomizers at high temperature
[AD-A260915] p 736 N93-25914
- FUEL CONTROL**
- Generic developmental turbojet fuel control p 172 A93-14519
- Optimizing the cruising fuel efficiency of commercial aircraft on the basis of flight manual data p 321 A93-18351

- The required damping and control process quality in a fuel pressure regulator p 810 A93-39034
- Some recommendations concerning the prevention of fuel boiling in the igniters of the combustion chambers of gas turbine engines p 812 A93-39200
- Surge recovery and compressor working line control using compressor exit Mach number measurement p 897 A93-40435
- Algorithmic method for optimizing the precision characteristics of a fuel metering system p 999 A93-45681
- Simplified mathematical model and digital simulation of aeroengine p 1106 A93-48511
- A new type of fuel control model p 1108 A93-49204
- A study of surge control by using pulse cut-off for dual spool turbojet engine p 1194 A93-53862
- Action composition for the animation of natural language instructions p 228 N93-12554
- FUEL CORROSION**
- Effect of aqueous solutions of water-crystallization inhibiting fluids on Thiokol-based sealants p 1017 A93-45689
- FUEL FLOW**
- Vaporizer performance p 79 A93-12784
- Results of high temperature JP-7 cracking assessment
[AIAA PAPER 93-0806] p 533 A93-24882
- USAF supercritical hydrocarbon fuels interests
[AIAA PAPER 93-0807] p 533 A93-24883
- Fuel film formation in the fuel-air premixer of the combustion chamber p 812 A93-39193
- Performance-seeking control - Program overview and future directions
[AIAA PAPER 93-3765] p 1102 A93-51360
- Improved flow measurement with simultaneous period/frequency recording — in turbojet engines p 1254 A93-54381
- Uncertainty of derived results on X-Y plots — in gas turbine engines p 1261 A93-54382
- Propulsion system performance resulting from an integrated flight/propulsion control design
[NASA-TM-105874] p 180 N93-15525
- FUEL INJECTION**
- An experimental investigation of hydrogen-fueled supersonic combustor p 53 A93-12733
- A study of dynamic characteristics of axial compression systems by heat addition p 202 A93-14168
- Mixing and combustion studies using discrete orifice injection at hypervelocity flight conditions p 205 A93-14523
- Innovative high temperature aircraft engine fuel nozzle design
[ASME PAPER 92-GT-132] p 350 A93-19365
- Design features influencing the distribution of fuel within the spray from an air blast fuel injector
[ASME PAPER 92-GT-235] p 353 A93-19448
- Effects of compression and expansion ramp fuel injector configuration on scramjet combustion and heat transfer
[AIAA PAPER 93-0609] p 358 A93-21114
- Effects of injector geometry on scramjet combustor performance p 359 A93-21670
- Characteristics of liquid jet atomization across a high-speed airstream. I - Experiment on shape of spray, spatial distribution of injected liquid and Sauter mean diameter p 411 A93-21743
- Dual transverse injection of H2 gas into Mach 1.8 flows at University Komaba wind tunnel p 376 A93-21833
- Penetration and mixing of bubbling liquid jets from multiple injectors normal to a supersonic air stream
[AIAA PAPER 92-5060] p 413 A93-22330
- Numerical and experimental investigation of mixing enhancement in scramjets
[AIAA PAPER 92-5063] p 414 A93-22333
- Data analysis of the parametric scramjet combustor experiments conducted in the Calspan 96 inch shock tunnel - 4th entry
[AIAA PAPER 92-5098] p 359 A93-22368
- Some issues concerning active control of combustion instability in a ramjet
[AIAA PAPER 93-0116] p 360 A93-22566
- An optical comparison of wall and axial injection for high enthalpy reacting scramjet flows
[AIAA PAPER 93-0357] p 377 A93-23040
- Induced Mach wave-flame interactions in laminar supersonic fuel jets p 475 A93-26183
- Effect of combustion on the interaction of an underexpanded wall hydrogen jet with supersonic flow in a plane duct p 534 A93-27658
- A numerical study of mixing in supersonic combustors with hypermixing injectors
[AIAA PAPER 93-0215] p 520 A93-27801
- The stagnation line solution of the equilibrium flow with radiation and mass injection p 680 A93-33733

Experimental supersonic hydrogen combustion employing staged injection behind a rearward-facing step p 744 A93-34496

Investigation of a contoured wall injector for hypervelocity mixing augmentation p 837 A93-39407

Thermal analysis of a shower-head burner [SAE PAPER 921226] p 898 A93-41400

A computational investigation of fuel mixing in a hypersonic scramjet [AIAA PAPER 93-2994] p 1001 A93-44230

Correlation of droplet behavior with gas-phase structures in a gas turbine combustor [AIAA PAPER 93-1767] p 1152 A93-49663

Scramjet fuel mixing enhancement by cross-stream pressure gradients [AIAA PAPER 93-2139] p 1114 A93-49957

A review of supersonic combustion research at AEDC with hypersonic application [AIAA PAPER 93-2326] p 1116 A93-50106

An approach to in-situ analysis of scramjet combustor behavior [AIAA PAPER 93-2328] p 1116 A93-50108

Experimental investigation of slot injection into supersonic flow with an adverse pressure gradient [AIAA PAPER 93-2442] p 1119 A93-50194

Experimental and numerical study of swept ramp injection into a supersonic flowfield [AIAA PAPER 93-2445] p 1119 A93-50197

A study of a direct-injection stratified-charge rotary engine for motor vehicle application [SAE PAPER 930677] p 1158 A93-50524

A study of self-ignition of methane-hydrogen mixture fuel injected into high enthalpy supersonic airstreams [ISABE 93-7049] p 1213 A93-54025

Ignition and combustion performance of a scramjet combustor with a fuel injection strut [ISABE 93-7050] p 1199 A93-54026

Numerical method for simulating fluid-dynamic and heat-transfer changes in jet-engine injector feed-arm due to fouling p 1245 A93-54467

A preliminary study of the effect of equivalence ratio on a low emissions gas turbine combustor using KIVA-2 [DE92-018616] p 215 N93-13321

Turbine engine combustor design at SNECMA [DS-2129] p 363 N93-17851

A numerical study of mixing in supersonic combustors with hypermixing injectors [NASA-CR-191027] p 294 N93-17884

Fuel injector: Air swirl characterization aerothermal modeling, phase 2, volume 1 [NASA-CR-189193-VOL-1] p 721 N93-24754

Analytical and experimental investigations of the oblique detonation wave engine concept [NASA-TM-102839] p 1006 N93-32374

FUEL PUMPS

A study of the effect of the working medium on the start-up characteristic of an aviation gas turbine engine p 811 A93-39037

Fluid-film foil bearings control engine heat p 924 A93-39949

Improving the design of the main fuel pump of Turbo-Jet 7 p 1107 A93-48555

Design and test of a small two stage counter-rotating turbine for rocket engine application [AIAA PAPER 93-2136] p 1142 A93-49954

Three-dimensional analysis of the Pratt and Whitney alternate design SSME fuel turbine p 1031 N93-31584

FUEL SPRAYS

Experimental techniques for the assessment of fuel thermal stability p 197 A93-14504

Ignition and exhaust emission characteristics of spray combustion in a pre-chamber type vortex combustor [ASME PAPER 92-GT-119] p 350 A93-19355

Design features influencing the distribution of fuel within the spray from an air blast fuel injector [ASME PAPER 92-GT-235] p 353 A93-19448

Characteristics of liquid jet atomization across a high-speed airstream. I - Experiment on shape of spray, spatial distribution of injected liquid and Sauter mean diameter p 411 A93-21743

Characteristics of liquid jet atomization across a high-speed airstream. II - Calculation of spatial distribution of liquid, variation of drop diameter and drop trajectory p 412 A93-21744

Development of a robust pressure-based numerical scheme for spray combustion applications [AIAA PAPER 93-0902] p 560 A93-24960

Computations of spray, fuel-air mixing, and combustion in a lean-premixed-prevaporized combustor [AIAA PAPER 93-2069] p 1153 A93-49901

Dual-spray airblast fuel nozzle for advanced small gas turbine combustors [AIAA PAPER 93-2336] p 1116 A93-50113

Blowout of turbulent disc/pilot stabilized jet diffusion flames [ISABE 93-7026] p 1213 A93-54002

Fuel Injector: Air swirl characterization aerothermal modeling, phase 2, volume 2 [NASA-CR-189193-VOL-2] p 721 N93-25106

Fundamental studies of droplet interactions in dense sprays [AD-A261165] p 737 N93-25948

Modeling the effects of drop drag and breakup on fuel sprays [AD-A263650] p 931 N93-29388

FUEL SYSTEMS

Integrated utilities management system for aircraft p 153 A93-14208

RB199 engine oil system failure diagnostics by comparison of measured and calculated oil consumption using the OLMOS on-board monitoring system p 178 N93-15173

Aircraft wing compartment liner concept to reduce fuel spillage [DOT/FAA/CT-TN92/34] p 331 N93-17219

FUEL TANKS

Selecting a method for sealing riveted joints in fuel compartments p 746 A93-35295

Algorithmic method for optimizing the precision characteristics of a fuel metering system p 999 A93-45681

Effect of aqueous solutions of water-crystallization inhibiting fluids on Thiocol-based sealants p 1017 A93-45689

FUEL TESTS

Use of alternative fuels for aviation p 196 A93-14292

Studies of jet thermal stability in a flowing system [ASME PAPER 92-GT-106] p 401 A93-19344

Liquid flow reactor and method of using [AD-D015392] p 222 N93-15232

Interferometric JFTOT tube deposit measuring device [AD-D015599] p 536 N93-20247

FUEL-AIR RATIO

An experimental investigation of hydrogen-fueled supersonic combustor p 53 A93-12733

Scramjet combustor and nozzle computations p 171 A93-14243

Carbon monoxide emissions in lean premixed combustion p 197 A93-14503

Design features influencing the distribution of fuel within the spray from an air blast fuel injector [ASME PAPER 92-GT-235] p 353 A93-19448

Simplified jet fuel reaction mechanism for lean burn combustion application [AIAA PAPER 93-0021] p 390 A93-23238

Fuel film formation in the fuel-air premixer of the combustion chamber p 812 A93-39193

Demonstration of mode transition in a scramjet combustor p 899 A93-42878

Computations of spray, fuel-air mixing, and combustion in a lean-premixed-prevaporized combustor [AIAA PAPER 93-2069] p 1153 A93-49901

Vortex generation and mixing in three-dimensional supersonic combustors [AIAA PAPER 93-2144] p 1115 A93-49961

Gasdynamics of hydrogen-fueled scramjet combustors [AIAA PAPER 93-2145] p 1115 A93-49962

Standing normal detonations and oblique detonations for propulsion [AIAA PAPER 93-2325] p 1116 A93-50105

Some supersonic and hypersonic research at GASL in the 1960s and 70s [AIAA PAPER 93-2327] p 1145 A93-50107

A study of a direct-injection stratified-charge rotary engine for motor vehicle application [SAE PAPER 930677] p 1158 A93-50524

Hypersonic shock-induced combustion ramjet performance analysis [ISABE 93-7037] p 1197 A93-54013

LIF visualization of 3-dimensional hypersonic mixing [ISABE 93-7114] p 1221 A93-54089

Enhanced fuel-air mixing in hypersonic engines [ISABE 93-7115] p 1221 A93-54090

Experiments and analysis concerning the use of external burning to reduce aerospace vehicle transonic drag p 70 N93-12537

Simplified jet-A kinetic mechanism for combustor application [NASA-TM-105940] p 200 N93-15504

Turbulence characteristics of an axisymmetric reacting flow [NASA-CR-4110] p 877 N93-30373

FUELS

X ray diffraction and electron microscope studies of Yttria Stabilized Zirconia (YSZ) ceramic coatings exposed to vanadia [AD-A258055] p 392 N93-17676

Development of a method to determine the autoxidation of turbine fuels [AD-A260578] p 736 N93-25902

FULL SCALE TESTS

A new method for determining the number of flight vehicle prototypes subject to full-scale testing p 434 A93-18316

Unsteady aerodynamics in airplane stall-spin departure [AIAA PAPER 93-0622] p 523 A93-24739

Validation of high frequency airload calculations using full scale flight test acoustic data p 567 A93-29417

Application of the shadowgraph flow visualization technique to a full-scale helicopter rotor in hover and forward flight [AIAA PAPER 93-3411] p 1030 A93-47208

Performance results from a test of an S-76 rotor in the NASA Ames 80- by 120-foot wind tunnel [AIAA PAPER 93-3414] p 975 A93-47211

Flight test progress of the STOL research aircraft ASKA [NAL-TM-643] p 49 N93-12354

Aerodynamic integration of thrust reversers on the Fokker 100 p 160 N93-13208

An investigation of jet engine test cell aerodynamics by means of scale model test studies with comparisons to full-scale test results p 193 N93-14060

Narrow-body aircraft water spray optimization study [DOT/FAA/CT-TN93/3] p 705 N93-25224

Modal survey of a full-scale F-18 wind tunnel model [AD-A262482] p 875 N93-29410

FUNCTION GENERATORS

Forcing function generator fluid dynamic effects on compressor blade stall response [AIAA PAPER 93-0157] p 275 A93-22594

FUNCTIONAL ANALYSIS

Definition of the 2005 flight deck environment [NASA-CR-4479] p 343 N93-16693

FUNCTIONAL DESIGN SPECIFICATIONS

Design characteristics of the functional systems of aircraft and prediction of their technical condition p 320 A93-18334

Structure of a knowledge base used in the computerized synthesis of aircraft layout p 891 A93-42373

Integrated flight/propulsion control - Subsystem specifications for performance [AIAA PAPER 93-3808] p 1132 A93-51400

Gas turbine starter (jet fuel starter) specification [SAE AS 1606] p 1124 A93-52171

Crashworthy landing gear design [SAE AIR 4566] p 1103 A93-52175

Formal design specification of a Processor Interface Unit [NASA-CR-189698] p 99 N93-12538

Definition of the 2005 flight deck environment [NASA-CR-4479] p 343 N93-16693

US Army helicopter inertia reel locking failures p 493 N93-19689

FUNCTIONALLY GRADIENT MATERIALS

Application of functionally gradient materials to scramjet engines [ISABE 93-7063] p 1200 A93-54039

Thermal barrier design of gamma-TiAl Functionally Gradient Materials (FGMs) for scramjet engine applications p 1246 A93-54556

FUNCTIONS (MATHEMATICS)

Issues in large-scale optimization with expensive functions p 437 A93-20708

FURNACES

FNAS modify matrix and transparent experiments [NASA-CR-184442] p 198 N93-13311

FUSELAGES

Bulging of fatigue cracks in a pressurized aircraft fuselage p 81 A93-13639

Damage tolerance assessment on the multisite cracks for the YS-11 aircraft p 46 A93-13642

Nonlinear rotor-fuselage coupled response to generic periodic control modes using advanced computation techniques p 153 A93-14226

The influence of the fuselage on high alpha vortical flows and the subsequent effect on fin buffeting p 116 A93-14263

The numerical calculation for the coupling of multiple propeller discrete noise and its interaction with the fuselage boundary p 231 A93-14268

The influence of rotor and fuselage wakes on rotorcraft stability and control p 183 A93-14373

Active control of interior noise in model aircraft fuselages using piezoceramic actuators p 231 A93-14540

The design development of the monolithic CFRP centre fuselage skin of the European fighter aircraft p 159 A93-15782

The production of a monolithic CFRP fuselage skin for the European Fighter Aircraft p 109 A93-15810

Experimental investigations into composite fuselage impact damage resistance and post-impact compression behavior p 159 A93-15812

Sound transmission through stiffened double-panel structures lined with elastic porous materials p 444 A93-19139

Matrix difference equation analysis of coupled structural-acoustic models for aircraft fuselage vibration and interior noise reduction p 446 A93-19172

Active control of sound transmission through stiff lightweight composite fuselage constructions p 447 A93-19187

Experimental and analytical investigations of fuselage modal characteristics and structural-acoustic coupling p 451 A93-19229

Automation of disbond detection in aircraft fuselage through thermal image processing p 407 A93-19598

Experimental measurement of structural intensity on an aircraft fuselage p 544 A93-26999

Crack growth and repair of multi-site damage of fuselage lap joints p 547 A93-28291

Stability theory and transition prediction applied to a general aviation fuselage p 479 A93-28601

Dynamic analysis of multiple row fuselage stiffened structures [AIAA PAPER 93-1438] p 710 A93-33987

Unsteady transonic potential flow over a flexible fuselage [AIAA PAPER 93-1593] p 683 A93-34124

The development of the coupled rotor-fuselage model (CRFM) p 794 A93-35903

Navier-Stokes correlations to fuselage wind tunnel test data p 765 A93-35937

Helicopter aerodynamics research techniques and rotor-fuselage interaction analysis p 765 A93-35938

Crack growth/damage tolerance analysis methods as applied to V-22 fuselage and empennage p 795 A93-35948

Coupled rotor fuselage mode shapes - A tool in understanding helicopter response p 797 A93-35977

The development of a crashworthy composite fuselage and landing gear p 799 A93-36001

Efficiency of using longitudinal and circumferential bands in the structures of an airtight fuselage p 801 A93-36795

Effect of the aerodynamic interference of the rotor and the fuselage on the power requirements for the horizontal flight of a helicopter p 819 A93-39179

The experimental investigation of combination effect by using injection effect of aeroengine jet exhaust p 898 A93-41742

Noise transmission of skin-stringer panels using a decaying wave method p 943 A93-41929

Optimization of equipment layout in the fuselage of maneuverable aircraft p 891 A93-42370

Simplified finite element representation of fuselage frames with flexible castellations p 892 A93-43570

Towards quantitative non-destructive evaluation of aging aircraft p 1025 A93-45773

Computational schemes for integrity analyses of fuselage panels in aging airplanes p 1025 A93-45774

Fuselage longitudinal splice design p 997 A93-45784

Representation and probability issues in the simulation of multi-site damage p 1026 A93-45785

Applications of advanced fracture mechanics to fuselage p 1026 A93-45787

Axial crack propagation and arrest in pressurized fuselage p 1026 A93-45788

Effects of floor location on response of composite fuselage frames p 997 A93-46809

Thermal control of a lidar laser system using a non-conventional ram air heat exchanger p 1028 A93-46821

CFD drag predictions for a wide body transport fuselage with flight test verification [AIAA PAPER 93-3418] p 976 A93-47214

National Aerospace Plane Integrated Fuselage/Cryotank Risk Reduction program [AIAA PAPER 93-2564] p 1142 A93-50284

Design and manufacture for producibility of carbon fiber/epoxy composite aircraft skins [SME PAPER EM93-104] p 1043 A93-51732

Calculation of the position of the flow separation line in an analog model of flow past a body p 1176 A93-52958

Structural-acoustic coupling in aircraft fuselage structures p 1243 A93-55856

Correlation of forebody pressures and aircraft yawing moments on the X-29A aircraft at high angles of attack [NASA-TM-4417] p 22 N93-11532

Evaluation of alternatives for increasing A-7D rearward visibility [AD-A255071] p 50 N93-12488

Probabilistic evaluation of fuselage-type composite structures [NASA-TM-105881] p 212 N93-12735

Stress calculations on the window section of an all-composite aircraft fuselage [LR-688] p 328 N93-16215

Design optimization of natural laminar flow bodies in compressible flow [NASA-CR-4478] p 292 N93-16940

Damage tolerance assessment of boron/epoxy repairs to fuselage lap joints [AD-A258383] p 338 N93-18257

Alternative equipment test procedures for simultaneous current injection on multiple cable bundles p 747 N93-24903

Tangential fuselage blowing on an ogive cylinder p 697 N93-25545

Design and analysis of curved composite components for rotorcraft fuselage frames p 716 N93-25701

Quiet by design: Numerical acousto-elastic analysis of aircraft structures [ISBN-90-386-0042-9] p 893 N93-29268

Advanced technology commercial fuselage structure p 918 N93-30432

Design and manufacturing concepts for thermoplastic structures p 919 N93-30434

Structural evaluation of curved stiffened composite panels fabricated using a THERM-Xsm process p 919 N93-30435

Noise transmission properties and control strategies for composite structures p 919 N93-30436

Cost studies for commercial fuselage crown designs p 920 N93-30440

Fabrication of the V-22 composite AFT fuselage using automated fiber placement p 920 N93-30443

Effects of intra- and inter-laminar resin content on the mechanical properties of toughened composite materials p 921 N93-30845

Mechanical and analytical screening of braided composites for transport fuselage applications p 922 N93-30855

Developments in impact damage modeling for laminated composite structures p 922 N93-30857

Multi-parameter optimization tool for low-cost commercial fuselage crown designs p 922 N93-30858

Design and analysis of grid stiffened concepts for aircraft composite primary structural applications p 922 N93-30861

Advanced fiber placement of composite fuselage structures p 923 N93-30864

Process and assembly plans for low cost commercial fuselage structure p 923 N93-30865

FUSION WELDING

Structural applications of Avimid K3B LDF thermoplastic composites --- for advanced aircraft p 1216 A93-53429

FUZZY SETS

An application of fuzzy logic and Dempster-Shafer theory to failure detection and identification p 96 A93-13079

A fuzzy dynamic analysis method for aeromaintenance system p 225 A93-14177

Design of a rule-based fuzzy controller for the pitch axis of an unmanned research vehicle p 907 A93-42807

Optimization using fuzzy set theory p 1037 A93-45431

The use of genetic algorithms in the design of fuzzy logic controllers p 1167 A93-50779

Fuzzy logic control algorithm for suppressing E-6A Long Trailing Wire Antenna wind shear induced oscillations [AIAA PAPER 93-3868] p 1171 A93-51454

Design and implementation of fuzzy logic controllers [NASA-CR-193268] p 1038 N93-31649

FUZZY SYSTEMS

Controller design using fuzzy logic - A case study p 756 A93-33793

A theoretical study on the ETHYLENE system - A fuzzy diagnostic expert system for large rotating machinery p 846 A93-36327

Using fuzzy behaviors for the outdoor navigation of a car with low-resolution sensors [DE93-002428] p 706 N93-25120

Current projects in Fuzzy Control p 1038 N93-31442

Design and implementation of fuzzy logic controllers [NASA-CR-193268] p 1038 N93-31649

G**GALERKIN METHOD**

Flight vehicle aerodynamics calculated by a Galerkin finite element/finite difference method p 266 A93-20738

Discontinuous Galerkin finite element method for two dimensional conservation laws [AIAA PAPER 93-0337] p 281 A93-23026

Unsteady compressible airfoil aerodynamics using an adaptive time-discontinuous GLS finite element method [AIAA PAPER 93-0339] p 281 A93-23027

Finite element computation of compressible flows with the SUPG formulation p 482 A93-29774

Calculation of numerical boundary measure for wavelet-Galerkin approximations in aeroelasticity [AIAA PAPER 93-1539] p 741 A93-34076

Application of the Galerkin/least-squares formulation to the analysis of hypersonic flows. I - Flow over a two-dimensional ramp p 866 A93-42593

Application of the Galerkin/least-squares formulation to the analysis of hypersonic flows. II - Flow past a double ellipse p 868 A93-42608

Numerical simulation of hypersonic flow over a double ellipse using a Taylor-Galerkin finite element formulation with adaptive grids p 868 A93-42617

Semi-discrete Galerkin solution of the compressible boundary-layer equations with viscous-inviscid interaction [AIAA PAPER 93-3520] p 985 A93-47282

Discontinuous Galerkin finite element method for Euler and Navier-Stokes equations p 1235 A93-55357

The semi-discrete Galerkin finite element modelling of compressible viscous flow past an airfoil [NASA-CR-192161] p 483 N93-20018

Multiple methods integration for structural mechanics analysis and design p 923 N93-30867

GALLIUM ARSENIDES

Photoelectrochemical etching of high aspect ratio submillimeter waveguide filters from n(+) GaAs wafers p 409 A93-20644

Reconfigurable photonic data networks for military aircraft p 928 A93-42783

GAME THEORY

Solution of trajectory optimization methods using the Pontriagin maximum principle p 366 A93-18378

Application of the receding horizon strategy to singularly perturbed pursuit-evasion problems p 369 A93-22980

A data processing and control system for counteracting wind shear p 524 A93-27604

Game theoretic synthesis for robust aerospace controllers p 819 N93-27171

Artificial intelligence methodologies in flight related differential game, control and optimization problems [AD-A262405] p 848 A93-28498

GAMMA RAY ASTRONOMY

The GRAD Supernova Observer - First Flight of a very large balloon over Antarctica p 27 A93-11367

GAMMA RAY SPECTROMETERS

A transportable luggage examination system based on neutron interrogation p 497 N93-21863

PFNA technique for the detection of explosives p 497 N93-21865

GAMMA RAYS

A review of the development of a luggage explosive detection system p 497 N93-21862

A pulsed fast-thermal neutron interrogation system p 497 N93-21866

GAPS

The frequency of incipient vortex-shedding from a circular cylinder in a laminar boundary layer (The effect of the gap ratio on the vortex shedding frequency) p 126 A93-15488

Shock formation in overexpanded tip leakage flow [ASME PAPER 92-GT-1] p 245 A93-19276

GAS ANALYSIS

Parametric study of air sampling cyclones p 135 N93-14173

GAS ATOMIZATION

Experimental and theoretical investigation of a research atomizer/combustion chamber configuration [ASME PAPER 92-GT-137] p 401 A93-19369

GAS BEARINGS

An externally pressurized air bearing system, journals and thrust, for application to small turbomachinery [ASME PAPER 92-GT-382] p 406 A93-19539

A test facility for the thermofluid-dynamics of gas bearing lubrication films [PNR-90897] p 72 N93-11032

GAS CHROMATOGRAPHY

Some physico-chemical characteristics of lubricating oil used in gas turbines p 70 A93-12202

Gas analysis system for the Eight Foot High Temperature Tunnel p 822 A93-37875

Summer research program (1992). High School Apprenticeship Program (HSAP) reports. Volume 16: Arnold Engineering Development Center Civil Engineering Laboratory [AD-A262024] p 945 N93-29396

Explosives detection systems for airport security gas chromatographic based devices p 881 N93-30276

GAS COMPOSITION

Predicted aircraft effects on stratospheric ozone p 93 N93-11096

GAS COOLING

- A fuel-oil matrix heat exchanger p 833 A93-39052
Coupling of 3D-Navier-Stokes external flow calculations and internal 3D-heat conduction calculations for cooled turbine blades p 904 N93-29961

GAS DENSITY

- Characterization of electron beam propagation for hypersonic flight research applications [AIAA PAPER 92-5087] p 452 A93-22357

- An investigation on the use of a heavy gas to improve the performance of the equilibrium interface technique in shock tube flows [AIAA PAPER 93-2017] p 1078 A93-49855

GAS DETECTORS

- Explosives detection systems for airport security gas chromatographic based devices p 881 N93-30276

GAS DISCHARGE TUBES

- A novel development of the Ludwieg tube, for extended test duration p 1011 A93-45529

GAS DISSOCIATION

- A computer simulation of the production of an artificially ionized layer using the Arecibo facility [DE93-010817] p 937 N93-30487

GAS DYNAMICS

- Free piston shock tunnels - Developments and capabilities p 66 A93-12316

- Effect of heat supply on the gasdynamic parameters of gas flow in Laval nozzles p 12 A93-12760

- Allowing for the effect of flow nonisothermality on total pressure losses in the afterburner diffusers of augmented turbofan engines p 53 A93-12811

- Parametric diagnostics of the steady states of gas turbine engines p 54 A93-12815

- Shedding new light on gas dynamics p 80 A93-13435

- Supersonic combustion and gasdynamic of scramjet p 170 A93-14242

- Flux limiters in a rotated upwind scheme for the Euler equations [AIAA PAPER 93-0067] p 262 A93-20180

- Uniform high-order spectral methods for one- and two-dimensional Euler equations p 476 A93-27068

- Dynamics of the behavior of nematic films in gasdynamic flows p 746 A93-35345

- Gas dynamics of cooled turbines --- Russian book [ISBN 5-217-00809-1] p 721 A93-35685

- Supersonic flow of a gas over a semiinfinite plate with small-scale harmonic spanwise oscillations p 775 A93-39118

- Problems in physical gas dynamics p 775 A93-39126

- Kinetic theory of nonequilibrium flows of gas and disperse media with internal degrees of freedom and chemical reactions p 851 A93-39127

- Kinetic theory of hypersonic flows of a viscous gas p 775 A93-39130

- Asymptotic structure of a limiting hypersonic flow in a shock wave p 776 A93-39131

- The problem of two Coulomb centers and its applications in physical aerodynamics p 776 A93-39132

- Nonequilibrium limiting hypersonic flow of a gas past three-dimensional tapered bodies with a separated shock p 776 A93-39133

- Numerical study of spontaneous nitrogen condensation in the axisymmetric hypersonic nozzles of wind tunnels p 777 A93-39143

- Flow density distribution in a two-phase submerged jet p 836 A93-39144

- Modeling of flow in a pulsed shock tunnel p 777 A93-39152

- Effect of gasdynamic parameters on the specific weight of gas-turbine aircraft engines p 899 A93-42372

- Gas-kinetical and Navier-Stokes simulations of reentry flows p 865 A93-42582

- Computation of thermochemical nonequilibrium flows around a simple and a double ellipse p 869 A93-42629

- Shock waves; Proceedings of the 18th International Symposium, Sendai, Japan, July 21-26, 1991. Vols. 1 & 2 [ISBN 0-387-55686-9] p 1023 A93-45451

- Shock tube validation experiments for the simulation of ram-accelerator-related combustion and gasdynamic problems p 1016 A93-45499

- Double diaphragm driven free piston expansion tube p 1016 A93-45533

- Experimental study on turbulent two-phase flow in a dual-inlet side dump combustor p 1106 A93-48506

- Experimental investigation on effect of solid particles on blade pressure distribution in compressor cascade flow p 1066 A93-48513

- Calculation of subsonic flow of a gas past an airfoil p 1068 A93-48908

- Some Fuchs-type equations in fluid mechanics p 1165 A93-48967

- Three-dimensional hypersonic flow of a gas past wings p 1069 A93-48971

- Gasdynamics of hydrogen-fueled scramjet combustors [AIAA PAPER 93-2145] p 1115 A93-49962

- Three-dimensional numerical simulation of gradual opening in a wave rotor passage [AIAA PAPER 93-2526] p 1156 A93-50254

- Stability of oriented differences for central differences in a program for calculating smooth supersonic flows p 1085 A93-50966

- Steady transonic weakly perturbed flows in a vibrationally relaxing gas p 1088 A93-51768

- Steady state supersonic flows of a vibrationally excited gas past thin bodies p 1089 A93-51818

- Calculation of compressible gas flow on optimal difference grids p 1091 A93-51902

- Determination of the aerodynamic characteristics of thin bodies of revolution with an arbitrary number of cantilever surfaces in inhomogeneous flow p 1092 A93-51911

- Calculation of a plane supersonic jet simulating the exhaust jet of a hypersonic flight vehicle engine p 1103 A93-51912

- Comparison of gasdynamic models in hypersonic flow p 1179 A93-53315

- Recent advances in computational analysis of hypersonic vehicles p 1179 A93-53364

- The design and development of an afterburner [ISABE 93-7041] p 1198 A93-54017

- Development and computation of continuum higher order constitutive relations for high-altitude hypersonic flow p 132 A93-13578

- Upgrade and extension of the data acquisition system for propulsion and gas dynamic laboratories [AD-A256836] p 235 N93-15637

- Hypersonic flows including real gas effects [AERO-REPT-9112] p 289 N93-16467

- Comparison of methodologies for describing relaxation in nonequilibrium gaseous systems p 419 N93-16786

- Generic hypersonic vehicle performance model [NASA-CR-192953] p 714 N93-25162

- Supersonic shock wave/vortex interaction [NASA-CR-192917] p 695 N93-25249

- Gordon-type schemes applied to detonation flows [NASA-CR-191447] p 780 N93-27090

- Analysis of unsteady wave processes in a rotating channel [NASA-CR-191154] p 816 N93-28617

- Three-dimensional numerical simulation of gradual opening in a wave rotor passage [NASA-CR-191157] p 900 N93-29072

GAS EXPANSION

- Direct numerical simulation of nitric oxide evolution in underexpanded jets [ASME PAPER 92-GT-372] p 355 A93-19534

- Comparison of continuum and particle simulations of expanding rarefied flows [AIAA PAPER 93-0728] p 466 A93-24818

- A novel development of the Ludwieg tube, for extended test duration p 1011 A93-45529

- Hypervelocity flows of argon produced in a free piston driven expansion tube p 1012 A93-45530

- Double diaphragm driven free piston expansion tube p 1016 A93-45533

- Effects of nozzle contour on the aerodynamic characteristics of underexpanded annular impinging jets p 1024 A93-45563

- Exploratory study of shock reflection near an expansion corner [AIAA PAPER 93-3132] p 1063 A93-48297

GAS FLOW

- A method for determining the aerodynamic coefficients of asymmetric bodies with allowance for nonlinear influence factors of the body shape p 5 A93-10142

- Monotonicity characteristics of some plane vortex flows of incompressible fluids and subsonic gas flows p 13 A93-12932

- A comparison of upwind schemes for computation of three-dimensional hypersonic real-gas flows [AIAA PAPER 92-4350] p 15 A93-13306

- TEMPER - A gas-path analysis tool for commercial jet engines [ASME PAPER 92-GT-315] p 354 A93-19501

- An improved numerical model for wave rotor design and analysis [AIAA PAPER 93-0482] p 361 A93-23384

- Comparison of continuum and particle simulations of expanding rarefied flows [AIAA PAPER 93-0728] p 466 A93-24818

- Determination of gas flow rate in a duct from measured static pressures p 520 A93-27625

- Numerical analysis for chemically non-equilibrium flow p 770 A93-38148

- The use of aviation gas-liquid heat exchangers employing heat pipes p 833 A93-39050

- Computation of thermochemical nonequilibrium flows around a simple and a double ellipse p 869 A93-42629

- Rarefied gas flow around a 3D-delta-wing p 870 A93-42639

- On the accuracy and efficiency of CFD methods in real gas hypersonics p 871 A93-42869

- An overview of Ames experimental aerothermodynamics p 1011 A93-45496

- Computation of shock diffraction in external and internal flows p 1024 A93-45537

- A report on the status of MHD hypersonic ground test technology in Russia [AIAA PAPER 93-3193] p 1012 A93-46656

- Requirements for facilities and measurement techniques to support CFD development for hypersonic aircraft p 1014 A93-47024

- An investigation on the use of a heavy gas to improve the performance of the equilibrium interface technique in shock tube flows [AIAA PAPER 93-2017] p 1078 A93-49855

- A study of optical distortions arising in radiation transmission through cavities with gas flow around them p 1225 A93-52945

- Direct simulation of reacting fuel gas flows in a supersonic mixing layer [ISABE 93-7072] p 1201 A93-54048

- Steady-state supersonic flow of a vibrationally excited gas past a slender body of revolution at a small angle of attack p 1233 A93-55014

- Relaxation of discrete rotational energy distributions using a Monte Carlo method p 1234 A93-55146

- Experimental investigation of effect of particles on blade pressure distribution in impulse cascade flow p 1236 A93-55398

- Algebraic determination of the shock wave shape in axisymmetric flow over a circular cylinder p 1237 A93-56030

- An improved numerical model for wave rotor design and analysis [NASA-TM-105915] p 60 N93-12418

- Mathematical problems in inviscid hypersonic flow p 131 N93-13451

- Control of asymmetric jet [AD-A255967] p 219 N93-14400

- Rarefied gas numerical wind tunnel, Part 7: OREX p 382 N93-19280

- An investigation of photothermal velocimetry for application to transient, high-speed gas flows p 698 N93-25720

- Modeling the effects of drop drag and breakup on fuel sprays [AD-A263650] p 931 N93-29388

- Heat transfer with moderate free stream turbulence p 932 N93-29936

GAS GENERATORS

- Combined engines for hypersonic flight p 171 A93-14244

- Using contra-rotating rotors for decreasing sizes and component number in small GTE [ASME PAPER 92-GT-414] p 356 A93-19562

- An improved numerical model for wave rotor design and analysis [AIAA PAPER 93-0482] p 361 A93-23384

- The integration of geometric modeling into an inverse design method and application of a PC-based inverse design method and comparison with test results p 81 N93-10058

- An improved numerical model for wave rotor design and analysis [NASA-TM-105915] p 60 N93-12418

- GAS GUNS

- Characterization of the performance of shock-tube wind tunnels [AIAA PAPER 93-0351] p 377 A93-23036

- Analysis and demonstration of a Scramaccelerator system [AIAA PAPER 93-2183] p 1142 A93-49995

GAS HEATING

- AEDC expanded flow arc facility (HEAT-H2) description and calibration p 821 A93-37872

GAS INJECTION

- Two-phase injection from the front surface of a blunt body in hypersonic flow p 241 A93-18233

- Workshop report - A validation study of Navier-Stokes codes for transverse injection into a Mach 2 flow p 270 A93-21330

- Dual transverse injection of H2 gas into Mach 1.8 flows at University Komaba wind tunnel p 376 A93-21833

- A study of the temperature of bodies in the flow-around regime in the case of surface gas injection p 691 A93-35344

- The numerical model of supersonic air flow field with hydrogen transverse injection p 859 A93-41736

- The experimental investigation of combination effect by using injection effect of aeroengine jet exhaust
p 898 A93-41742
- Three-dimensional calculation of a hydrogen jet injection into a supersonic air flow
p 950 A93-44374
- Performance improvement of gas turbine with steam injection
p 1107 A93-48523
- Tandem transverse hydrogen gas injection into a supersonic airflow
[ISABE 93-7069] p 1201 A93-54045
- Numerical and experimental study on two- and three-dimensional supersonic flow field with hydrogen injection
[ISABE 93-7118] p 1188 A93-54093
- Projectile base bleed technology. Part 2: User's guide CMINT computer code, version 5.04-BRL
[AD-A258630] p 551 N93-19999
- Experimental and computational investigation of helium injection into air at supersonic and hypersonic speeds
p 696 N93-25487
- Workshop Report: A validation study of Navier-Stokes codes for transverse injection into a Mach 2 flow
p 751 N93-26008
- Oxides of nitrogen emissions from turbulent hydrocarbon/air jet diffusion flames, phase 2
[PB93-152478] p 756 N93-26533
- In-situ bioventing: Two US EPA and Air Force sponsored field studies
[PB93-194231] p 1035 N93-32089
- GAS IONIZATION**
- Numerical modeling of ionization in nonequilibrium nitrogen flows in hypersonic nozzles
p 836 A93-39137
- Test results of the effects of air ionization on cigarette smoke particulate levels within a commercial airplane
[SAE PAPER 92-1183] p 855 A93-41362
- GAS JETS**
- Shock wave ahead of a liquid jet in supersonic cross flow
p 477 A93-27605
- A one-dimensional theory for supersonic gas jets above the critical pressure
p 774 A93-39115
- An experimental study of the three-dimensional interaction of a transverse jet with hypersonic flow
p 777 A93-39150
- Noise reduction of supersonic heated jet with jet mixing enhancement by tabs
[ISABE 93-7046] p 1198 A93-54022
- Mechanisms of sound generation in subsonic jets
p 101 N93-10688
- Experimental and computational investigation of helium injection into air at supersonic and hypersonic speeds
p 696 N93-25487
- Plume effects on the flow around a blunt cone at hypersonic speeds
p 787 N93-27460
- Effects of buoyancy on gas jet diffusion flames
[NASA-CR-191109] p 935 N93-31031
- GAS LUBRICANTS**
- Testing of a high performance compressor discharge seal
[AIAA PAPER 93-1997] p 1153 A93-49840
- GAS MIXTURES**
- Hypersonic chemically reacting flow of a reentry body
p 769 A93-38147
- Convective heat-transfer rate distributions over a 140 deg blunt cone at hypersonic speeds in different gas environments
[AIAA PAPER 93-2787] p 1027 A93-46529
- Development and use of hydrogen-air torches in an altitude facility
[AIAA PAPER 93-2176] p 1137 A93-49988
- Development of an advanced exhaust mixer for a high bypass ratio turbofan engine
[AIAA PAPER 93-2435] p 1118 A93-50188
- Thermodynamic aspects of model testing in cryogenic wind tunnels
p 1251 A93-56222
- GAS PATH ANALYSIS**
- A philosophy for integrated monitoring system design
p 178 N93-15174
- Some experiments and ideas on GPA before reaching steady state of engine
p 178 N93-15175
- GAS PRESSURE**
- Effect of heat supply on the gasdynamic parameters of gas flow in Laval nozzles
p 12 A93-12760
- GAS TEMPERATURE**
- Attempt to evaluate the computations for test case 6.1 - Cold hypersonic flow past ellipsoidal shapes
p 869 A93-42620
- Flight testing of a fiber optic temperature sensor
p 1105 A93-49476
- Noise reduction of supersonic heated jet with jet mixing enhancement by tabs
[ISABE 93-7046] p 1198 A93-54022
- An evaluation of thermal energy storage options for precooled gas turbine inlet air
[DE93-005980] p 754 N93-24975

GAS TURBINE ENGINES

- Some physico-chemical characteristics of lubricating oil used in gas turbines
p 70 A93-12202
- An evaluation system for impact damage and erosion of ceramic gas turbine components
p 79 A93-12229
- Vaporizer performance
p 79 A93-12784
- Parametric diagnostics of the steady states of gas turbine engines
p 54 A93-12815
- Evaluation of the efficiency of the direct search method in solving the problem of numerical calculation of the complex hydraulic cooling systems of aviation gas turbine engines
p 54 A93-12818
- A method for estimating the technico-economic efficiency of measures increasing the reliability of gas turbine engines in service
p 54 A93-12822
- Stirling engine - Available tools for long-life assessment --- for space propulsion
p 195 A93-13824
- Heat transfer, adiabatic effectiveness, and injectant distributions downstream of a single row and two staggered rows of compound angle film-cooling holes
p 201 A93-13976
- Comparison of heat transfer measurements with computations for turbulent flow around a 180 deg bend
p 201 A93-13980
- Advancements in aircraft gas turbine engines - Past and future
p 170 A93-14153
- Inlet design using a blend of experimental and computational techniques
p 114 A93-14210
- Numerical simulation of turbulent reacting flows in combustion chambers
p 171 A93-14271
- A digital simulation and its experimental investigation for the response of gas-turbine engines to intake flow distortion
p 120 A93-14366
- Carbon monoxide emissions in lean premixed combustion
p 197 A93-14503
- The development of titanium alloys for gas turbines
p 197 A93-15031
- Probability analysis of a method for diagnosing gas turbine engines on the basis of thermogasdynamic parameters
p 345 A93-18337
- Effect of design and service-related factors on the formation of combustion residues in the fuel nozzles of gas turbine engines
p 345 A93-18342
- A system for washing the combustion chamber nozzles and flow path components of the NK-8-2U engine during service
p 373 A93-18357
- Vibrational monitoring and diagnostics of the technical condition of gas turbine engines at civil aviation repair facilities
p 374 A93-18362
- Safety through integrity and reliability --- for passenger and military aircraft
p 239 A93-18779
- Lifting philosophies for aero engine fracture critical parts
p 345 A93-18783
- Aspects of turbine blade design for integrity
p 345 A93-18784
- Testing for integrity --- of aircraft gas turbine engines
p 346 A93-18785
- Design features of the GTD 8000 and GTD 15000 marine gas turbine engines
[ASME PAPER 92-GT-15] p 400 A93-19287
- Influence of a thermal barrier coating on the performance of a turboprop engine
[ASME PAPER 92-GT-38] p 347 A93-19297
- Electromechanical measurement of turbomachinery blade tip-to-casing running clearance
[ASME PAPER 92-GT-50] p 400 A93-19303
- A wide-range axial-flow compressor stage performance model
[ASME PAPER 92-GT-58] p 348 A93-19308
- Hot streaks and phantom cooling in a turbine rotor passage. II - Combined effects and analytical modelling
[ASME PAPER 92-GT-76] p 401 A93-19326
- Effects of back-pressure in a lean blowout research combustor
[ASME PAPER 92-GT-81] p 387 A93-19330
- Fault signatures obtained from fault implant tests on an F404 engine
[ASME PAPER 92-GT-82] p 348 A93-19331
- The effect of compressor rotor tip crops on turbofan engine performance
[ASME PAPER 92-GT-83] p 348 A93-19332
- The design and evaluation of a high pressure ratio radial turbine
[ASME PAPER 92-GT-93] p 349 A93-19339
- Emissions reduction by varying the swirler airflow split in advanced gas turbine combustors
[ASME PAPER 92-GT-110] p 349 A93-19347
- NO(x) sensitivities for gas turbine engines operated on lean-premixed combustion and conventional diffusion flames
[ASME PAPER 92-GT-115] p 349 A93-19351
- Engine testing of a prototype low NO(x) gas turbine combustor
[ASME PAPER 92-GT-116] p 401 A93-19352

- Experimental and computational investigation of flow in catalytic monolith channels
[ASME PAPER 92-GT-118] p 387 A93-19354
- Investigation of combustion structure inside low NO(x) combustors for a 1500 C-class gas turbine
[ASME PAPER 92-GT-123] p 350 A93-19357
- Three-dimensional gas turbine combustor emissions modeling
[ASME PAPER 92-GT-129] p 350 A93-19363
- Coherent anti-Stokes Raman scattering (CARS) thermometry in a model gas turbine can combustor
[ASME PAPER 92-GT-134] p 387 A93-19366
- The combustion of droplets within gas turbine combustors - Some recent observations on combustor efficiency
[ASME PAPER 92-GT-135] p 388 A93-19367
- Experimental and theoretical investigation of a research atomizer/combustion chamber configuration
[ASME PAPER 92-GT-137] p 401 A93-19369
- Achieving manufacturing excellence for gas turbine components through focused implementation of technology
[ASME PAPER 92-GT-139] p 401 A93-19371
- Corrosion resistance of Inconel Alloy 617 in simulated gas turbine environments
[ASME PAPER 92-GT-142] p 388 A93-19374
- An update on the development of the T407/GLC38 modern technology gas turbine engine
[ASME PAPER 92-GT-147] p 351 A93-19375
- Techniques for aerodynamic loss measurement of transonic turbine cascades with trailing-edge region coolant ejection
[ASME PAPER 92-GT-157] p 250 A93-19384
- Transonic flow through turbine cascades with nonuniform pitch
[ASME PAPER 92-GT-158] p 250 A93-19385
- Rim seal experiments and analysis of a rotor-stator system with nonaxisymmetric main flow
[ASME PAPER 92-GT-160] p 402 A93-19387
- The dynamic characteristics of a high pressure turbine stage in a transient wind tunnel
[ASME PAPER 92-GT-166] p 375 A93-19392
- Heat transfer in serpentine flow passages with rotation
[ASME PAPER 92-GT-190] p 403 A93-19415
- Heat transfer in rotating serpentine passages with trips skewed to the flow
[ASME PAPER 92-GT-191] p 403 A93-19416
- Discharge coefficients of holes angled to the flow direction
[ASME PAPER 92-GT-192] p 403 A93-19417
- Tip clearance effect on heat transfer and leakage flows on the shroud-wall surface in an axial flow turbine
[ASME PAPER 92-GT-200] p 403 A93-19425
- The evolution of thermal barrier coatings in gas turbine engine applications
[ASME PAPER 92-GT-203] p 388 A93-19427
- Scaling of the two-phase flow downstream of a gas turbine combustor swirl cup - Mean quantities
[ASME PAPER 92-GT-207] p 404 A93-19431
- Heat transfer and aerodynamics of a high rim speed turbine nozzle guide vane with profiled end walls
[ASME PAPER 92-GT-243] p 253 A93-19452
- An experimental investigation of convective heat transfer at the leading edge of a gas turbine airfoil
[ASME PAPER 92-GT-248] p 405 A93-19457
- The role of laminar-turbulent transition in gas turbine engines - A discussion
[ASME PAPER 92-GT-301] p 255 A93-19491
- Powder metallurgy repair of turbine components
[ASME PAPER 92-GT-312] p 354 A93-19500
- TEMPER - A gas-path analysis tool for commercial jet engines
[ASME PAPER 92-GT-315] p 354 A93-19501
- The comparison of different simplified mathematical models of the gas turbine combustion chamber as an object of temperature and pressure control
[ASME PAPER 92-GT-347] p 354 A93-19518
- Performance of gas turbine compressor cleaners
[ASME PAPER 92-GT-360] p 355 A93-19524
- Models for predicting the performance of Brayton-cycle engines
[ASME PAPER 92-GT-361] p 355 A93-19525
- An automated flow line for gas turbine blade repair
[ASME PAPER 92-GT-367] p 375 A93-19531
- Effective sealing of a disk cavity using a double-toothed rim seal
[ASME PAPER 92-GT-379] p 406 A93-19537
- Improving dynamic response of a single-spool gas turbine engine using a nonlinear controller
[ASME PAPER 92-GT-392] p 355 A93-19546
- Ceramic matrix composites for rocket engine turbine applications
[ASME PAPER 92-GT-394] p 388 A93-19547
- A compact, intercooled and regenerated gas turbine for HALE applications
[ASME PAPER 92-GT-401] p 355 A93-19550

- An optimisation-matching procedure for variable cycle jet engines
[ASME PAPER 92-GT-406] p 356 A93-19555
- Some aspects of variable geometry gas turbine operation
[ASME PAPER 92-GT-407] p 356 A93-19556
- Expert systems for the simulation of gas turbine engines
[ASME PAPER 92-GT-408] p 435 A93-19557
- Using contra-rotating rotors for decreasing sizes and component number in small GTE
[ASME PAPER 92-GT-414] p 356 A93-19562
- Optimal circumferential placement of cylindrical thermocouple probes for reduction of excitation forces
[ASME PAPER 92-GT-423] p 406 A93-19571
- Optimization of a multistage axial compressor in a gas turbine engine system
[ASME PAPER 92-GT-424] p 357 A93-19572
- Ceramics for aero-engine applications
[ASME PAPER 92-GT-439] p 388 A93-19581
- An efficient constraint to account for mistuning effects in the optimal design of engine rotors
[AIAA PAPER 92-4711] p 358 A93-20280
- APPLE - An aeroelastic analysis system for turbomachines and propfans
[AIAA PAPER 92-4712] p 358 A93-20320
- Life cycle assessment of an impingement-cooled gas turbine blade
[AIAA PAPER 92-4716] p 358 A93-20321
- Influences on the sprays formed by high-shear fuel nozzle/swirler assemblies
p 411 A93-21653
- Evaluation of brush seals for limited-life engines
p 411 A93-21665
- Combustion performance of a hydrogen-fueled small combustor for a micro gas turbine
p 389 A93-21731
- Development of an optical sensor for active control of a gas turbine combustor
[AIAA PAPER 93-0118] p 360 A93-22568
- Inlet velocity profile effects on turbulent swirling flow predictions
[AIAA PAPER 93-0133] p 274 A93-22580
- Two and three-dimensional prediffuser combustor studies with air-water mixture
[AIAA PAPER 93-0240] p 390 A93-22652
- CARS thermometry in a liquid fueled model combustor
[AIAA PAPER 93-0366] p 390 A93-23047
- An improved numerical model for wave rotor design and analysis
[AIAA PAPER 93-0482] p 361 A93-23384
- A graphical user-interface for propulsion system analysis
[AIAA PAPER 93-0223] p 440 A93-23699
- Driven cavity simulation of turbomachine blade flows with vortex control
[AIAA PAPER 93-0390] p 461 A93-24238
- Life assessment of gas turbine bucket coating based on degradation analysis
p 533 A93-24464
- Heat pipe turbine vane cooling
p 519 A93-26114
- Control of contaminants in gas turbines with variable-flow combustion chambers and hydrogen addition
p 520 A93-27478
- Determination of gas flow rate in a duct from measured static pressures
p 520 A93-27625
- Calculating the cutting depth during the milling of large gas turbine engine blades
p 545 A93-27628
- Isothermal oxidation behavior of alpha-2 titanium aluminide alloys
p 535 A93-29563
- Numerical simulation of turbine 'hot spot' alleviation using film cooling
p 744 A93-34476
- Improved static and dynamic performance of helicopter powerplant
p 809 A93-35928
- Model reference control of a linear plant with feedthrough element
p 846 A93-37034
- Absolute stability of an automatic control system for gas turbine engines
p 810 A93-39033
- Heat exchangers of gas turbine engines
p 833 A93-39044
- Calculation of a collector-type annular plate heat exchanger
p 833 A93-39045
- Development of a process for fabricating a plate heat exchanger for the heat recovery system of gas turbine engines
p 834 A93-39053
- Determination of the dynamic characteristics of heat exchangers for the heat recovery system of gas turbine engines
p 834 A93-39054
- Solution of the problem of determining the dynamic characteristics of the cross-flow heat exchanger of the heat recovery system of gas turbine engines
p 834 A93-39055
- Effect of a deformed electric field on the precision of the electrochemical machining of gas turbine engine components
p 835 A93-39094
- Increasing the efficiency of the electrochemical dimensional machining of gas turbine engine blades of EP718VD alloy
p 835 A93-39095
- Increasing the durability of gas turbine engine compressor blades by using a combined hardening/finishing treatment to control the stressed state of the surface layer
p 835 A93-39099
- Effect of the technological process structure on residual stress distribution in the blade foil of gas turbine engines
p 836 A93-39106
- Modeling of the multiparameter assembly of engineering products for a specified priority of output geometrical parameters
p 836 A93-39109
- A practical course in aircraft maintenance. I - The powerplant --- Russian book
p 811 A93-39175
- Expert evaluation of the technological level of aviation gas turbine engine designs
p 811 A93-39187
- Some recommendations concerning the prevention of fuel boiling in the igniters of the combustion chambers of gas turbine engines
p 812 A93-39200
- The possibility of reducing the emission of benzo(a)pyrene with the exhaust gases of aviation gas turbine engines by water injection into the combustion chamber
p 812 A93-39201
- Recent evolution of gas turbine materials and the development of models for life prediction
p 915 A93-40802
- Life analysis of a gas turbine fan disc
p 897 A93-40803
- Evaluation of metallurgical degradation on gas turbine components
p 915 A93-40804
- Crack simulation and life assessment of gas turbine nozzles
p 915 A93-40805
- Life prediction - Thermal fatigue from isothermal data
p 916 A93-40807
- New corrosion resistant nickel-base super-alloys and technological processes of casting gas turbines parts with directional single crystal and regulable equiaxial minimized microporosity structure
p 916 A93-40811
- Concurrent field service and laboratory testing as a means of improving reliability in creep-rupture applications
p 916 A93-40814
- Influence of stator-rotor gap on axial-turbine unsteady forcing functions
p 899 A93-41918
- Effect of gasdynamic parameters on the specific weight of gas-turbine aircraft engines
p 899 A93-42372
- Selection of the powerplant for a thermoplane
p 899 A93-42380
- Diffusion controlled evaporation of a multicomponent droplet - Theoretical studies on the importance of variable liquid properties
p 1021 A93-44224
- A damage tolerance approach for management of aging gas turbine engines
p 1001 A93-45779
- Optimization of a highly-loaded axial splittler rotor design
p 1002 A93-46931
- Numerical simulation of aerothermodynamics processes in gas turbine engine components
p 1002 A93-46939
- Modelling three-dimensional gas-turbine-combustor model flow using second-moment closure
[AIAA PAPER 93-3104] p 1149 A93-48277
- Acoustical properties of sound absorbing structures at high temperature
p 1172 A93-48522
- Performance improvement of gas turbine with steam injection
p 1107 A93-48523
- Experimental research on a semiwater-gas-fired gas-turbine
p 1107 A93-48524
- An optimization method for statistical ascertainment of the most probable peak temperature at combustor exit
p 1108 A93-49195
- Screening studies of advanced control concepts for airbreathing engines
[AIAA PAPER 92-3320] p 1108 A93-49329
- Mixing in the dome region of a staged gas turbine combustor
p 1109 A93-49612
- Carbon/silicon carbide composite materials in advanced unmanned gas turbine engine combustors
[AIAA PAPER 93-1761] p 1144 A93-49658
- Effect of geometry, bleed rates and flow splits on pressure recovery of a canted hybrid vortex-controlled diffuser
[AIAA PAPER 93-1762] p 1109 A93-49659
- An efficient liner cooling scheme for advanced small gas turbine combustors
[AIAA PAPER 93-1763] p 1109 A93-49660
- Correlation of droplet behavior with gas-phase structures in a gas turbine combustor
[AIAA PAPER 93-1767] p 1152 A93-49663
- Fiber reinforced structures for turbine engine fragment containment
[AIAA PAPER 93-1816] p 1110 A93-49704
- Turbine Engine Diagnostics (TED) system
[AIAA PAPER 93-1818] p 1110 A93-49706
- Vane optimization for maximum efficiency using design of experiments
[AIAA PAPER 93-1867] p 1111 A93-49742
- The effects of turbulence modeling on the numerical simulation of confined swirling flows
[AIAA PAPER 93-1976] p 1078 A93-49823
- Hysteresis and bristle stiffening effects of conventional brush seals
[AIAA PAPER 93-1996] p 1153 A93-49839
- Testing of a high performance compressor discharge seal
[AIAA PAPER 93-1997] p 1153 A93-49840
- High temperature corrosion resistant bearing steel development
[AIAA PAPER 93-2000] p 1145 A93-49842
- An analytical study of dilution jet mixing in a cylindrical duct
[AIAA PAPER 93-2043] p 1113 A93-49876
- User-friendly codes for the training on gas turbine engines
[AIAA PAPER 93-2051] p 1166 A93-49884
- Computations of spray, fuel-air mixing, and combustion in a lean-premixed-prevaporized combustor
[AIAA PAPER 93-2069] p 1153 A93-49901
- Smoke measurements inside a gas turbine combustor
[AIAA PAPER 93-2070] p 1113 A93-49902
- Computation of the flow field in an annular gas turbine combustor
[AIAA PAPER 93-2074] p 1113 A93-49903
- C-2 subsonic freejet development and demonstration
[AIAA PAPER 93-2180] p 1138 A93-49992
- Integrated CFD modeling of gas turbine combustors
[AIAA PAPER 93-2196] p 1115 A93-50008
- Experimental determination of the bulk swirl attenuation between two axial stations in the LM2500 inlet bellmouth
[AIAA PAPER 93-2203] p 1155 A93-50015
- A simplified representation of the off-design characteristics of high speed, high pressure ratio axial turbomachinery stages
[AIAA PAPER 93-2257] p 1081 A93-50055
- Dual-spray airblast fuel nozzle for advanced small gas turbine combustors
[AIAA PAPER 93-2336] p 1116 A93-50113
- Three-dimensional emission modeling for diffusion flame, rich/lean, and lean gas turbine combustors
[AIAA PAPER 93-2338] p 1117 A93-50115
- Effects of flow-path variations on internal reversing flow in a tailpipe offtake configuration for ASTOVL aircraft
[AIAA PAPER 93-2438] p 1118 A93-50190
- Unique development testing at Allison Gas Turbine
[AIAA PAPER 93-2450] p 1138 A93-50200
- Implementation of an infrared thermal imaging system to measure temperature in a gas turbine engine
[AIAA PAPER 93-2469] p 1120 A93-50215
- The development of a large annular facility for testing gas turbine combustor diffuser systems
[AIAA PAPER 93-2546] p 1139 A93-50269
- Nonlinear dynamic simulation of single- and multi-spool core engines
[AIAA PAPER 93-2580] p 1122 A93-50294
- NO(x) reduction additives for aircraft gas turbine engines
[AIAA PAPER 93-2594] p 1122 A93-50306
- Scalar characteristics in a liquid-fueled combustor with curved exit nozzle
p 1123 A93-51643
- Measurements of gas composition and temperature inside a can type model combustor
p 1123 A93-51644
- Numerical model for predictions of reverse flow combustor aerothermal characteristics
p 1123 A93-51645
- Gas turbine starter (jet fuel starter) specification
[SAE AS 1606] p 1124 A93-52171
- Progress towards understanding and predicting heat transfer in the turbine gas path
p 1215 A93-52751
- Selection of a method for protecting aircraft gas turbine engines against damage by foreign objects (Mathematical models)
p 1193 A93-53534
- High temperature heat exchangers for gas turbines and future hypersonic air breathing propulsion
[ONERA, TP NO. 1993-75] p 1218 A93-53596
- Design and technology for engine manufacture --- for Rolls-Royce aerospace business
[ISABE 93-7002] p 1194 A93-53979
- Propulsion technology challenges for turn-of-the-century commercial aircraft
[ISABE 93-7003] p 1194 A93-53980
- The prediction of thermal NO(x) in gas turbine exhausts
[ISABE 93-7022] p 1195 A93-53998
- Emission characteristics of a model gas turbine combustor at practical conditions
[ISABE 93-7023] p 1196 A93-53999
- Design of high-load aviation turbomachines using modern 3D computational methods
[ISABE 93-7032] p 1196 A93-54008
- Thermal fatigue life assessment of a convection-cooled gas turbine blade
[ISABE 93-7062] p 1199 A93-54038
- A new cooling system for ultra high temperature turbines
[ISABE 93-7073] p 1201 A93-54049

New developments with the V2500 engine
[ISABE 93-7085] p 1202 A93-54061
Thermodynamic and neural network computer modelling of implanted component faults in a gas turbine engine
[ISABE 93-7089] p 1202 A93-54065
Experimental analysis of turbine rotor flow at design and off-design conditions
[ISABE 93-7092] p 1186 A93-54068
A finite element code for gas turbine combustor flow with Stretched Laminar Flamelet modelling
[ISABE 93-7127] p 1204 A93-54102
Numerical simulation of gas turbine combustors with complex geometries
[ISABE 93-7128] p 1204 A93-54103
Mixing of multiple jets with a confined subsonic crossflow
p 1189 A93-54324
Uncertainty of derived results on X-Y plots — in gas turbine engines
p 1261 A93-54382
Prediction of rotating disc flow and heat transfer in gas turbine engines
p 1256 A93-54634
Effects of turn region treatments on pressure loss through sharp 180-degree bends
p 1256 A93-54636
Presence and future of the electro-chemical processes in aero-engine production
p 1257 A93-54840
Small gas turbines in the 21st century
p 1247 A93-55494
Compound cycle engine for helicopter application
[NASA-CR-180824] p 55 N93-10348
Noise studies for environmental impact assessment of an outdoor engine test facility
p 99 N93-10672
An interactive preprocessor for the NASA engine performance program
[NASA-TM-105786] p 56 N93-10983
Materials: Toward the non-metallic engine
[PNR-90915] p 56 N93-11019
Testing for integrity
[PNR-90927] p 56 N93-11024
The prediction of convective heat transfer in rotating square ducts
[PNR-90929] p 85 N93-11025
A test facility for the thermofluid-dynamics of gas bearing lubrication films
[PNR-90987] p 72 N93-11032
On the basis of experience: Built in product reliability
[PNR-90932] p 85 N93-11034
Simultaneous engineering in the design of aero engines
[PNR-90973] p 57 N93-11062
Maintainability of large gas turbine aero engines
[PNR-90987] p 58 N93-11069
Advanced materials in gas turbine engines: An assessment
[PNR-90946] p 58 N93-11105
Development of advanced carbon-carbon annular flameholders for gas turbines
[PNR-90947] p 58 N93-11106
Small particle impact damage in carbon-carbon composites
[PNR-90948] p 73 N93-11107
The development of the Rolls-Royce Trent aero gas turbine
[PNR-90949] p 58 N93-11108
Development of the neutron diffraction technique for the determination of near surface residual stresses in critical gas turbine components
[PNR-90984] p 58 N93-11112
Simultaneous engineering in aero gas turbine design and manufacture
[PNR-90890] p 59 N93-11208
Numerical analysis of the flow fields in a RQL gas turbine combustor
[DE92-017509] p 89 N93-11767
Erosion predictions and measurements of high-temperature coatings and superalloys used in turbomachines
p 74 N93-12189
An improved numerical model for wave rotor design and analysis
[NASA-TM-105915] p 60 N93-12418
Investigation of hot streak migration and film cooling effects on heat transfer in rotor/stator interacting flows, report 1
[AD-A250688] p 102 N93-12490
AFOSR Contractors Meeting in Propulsion
[AD-A254484] p 195 N93-12575
Thermal barrier coating life prediction model development, phase 2
[NASA-CR-189111] p 198 N93-12589
Alternative systems for fuel gas boosters for small gas turbine engines
[PB92-223049] p 212 N93-12977
Overview on test cases for computation of internal flows in turbomachines
p 214 N93-13209
A preliminary study of the effect of equivalence ratio on a low emissions gas turbine combustor using KIVA-2
[DE92-018616] p 215 N93-13321

Propulsion and Energetics Panel Working Group 20 on Test Cases for Engine Life Assessment Technology
[AGARD-AR-308] p 176 N93-14890
Introduction to test cases for engine life assessment technology
p 176 N93-14891
LARZAC HP turbine disk crack initiation and propagation spin pit test
p 176 N93-14892
RB 199 high pressure compressor stage 3 spin pit tests
p 176 N93-14893
CF6-6 high pressure compressor stage 5 locking slot crack propagation spin pit test
p 176 N93-14894
RB211-524B disc and drive cones hot cyclic spinning test
p 177 N93-14895
F100 second stage fan disk bothole crack propagation ferris wheel test
p 177 N93-14897
In-service considerations affecting component life
p 177 N93-14898
Some experiments and ideas on GPA before reaching steady state of engine
p 178 N93-15175
Experimental analysis of steady-state and dynamic monitoring of power shaft turbines
p 178 N93-15176
Bypass transition in compressible boundary layers
p 417 N93-15801
X ray diffraction and electron microscope studies of Yttria Stabilized Zirconia (YSZ) ceramic coatings exposed to vanadia
[AD-A258055] p 392 N93-17676
Advanced Turbine Technology Applications Project (ATTAP)
[NASA-CR-189228] p 455 N93-18762
Active stabilization to prevent surge in centrifugal compression systems
[NASA-CR-191625] p 424 N93-18862
Advanced turbine design for coal-fueled engines
[DE93-000224] p 554 N93-21254
A three-dimensional algebraic grid generation scheme for gas turbine combustors with inclined slots
[NASA-CR-191095] p 746 N93-24759
Screening studies of advanced control concepts for airbreathing engines
[NASA-TM-106042] p 721 N93-25079
JPFR report: Science and technology. Central Eurasia: Engineering and equipment
[JPFR-UEQ-92-003] p 749 N93-25427
Gas turbine system simulation: An object-oriented approach
[NASA-TM-106044] p 723 N93-25673
Simulation of aircraft gas turbine engine
p 723 N93-25751
Active stabilization of aeromechanical systems
[AD-A261366] p 725 N93-26335
Particulate emissions from gas turbine engines
[AD-A261374] p 725 N93-26339
Advanced bristle seals for gas turbine engines
[AD-A261296] p 752 N93-26564
Nitric oxide formation in a lean, premixed-prevaporized jet A/air flame tube: An experimental and analytical study
[NASA-TM-105722] p 844 N93-27012
An analytical study of dilution jet mixing in a cylindrical duct
[NASA-TM-106181] p 814 N93-27160
Effects of flow-path variations on internal reversing flow in a tailpipe offtake configuration for ASTOVL aircraft
[NASA-TM-106149] p 900 N93-29065
Spurious symptom reduction in fault monitoring
[NASA-CR-191453] p 942 N93-29192
Microwave processing of silicon nitride for advanced gas turbine applications
[DE93-007910] p 917 N93-29767
Keynote address: Unsteady, multimode transition in gas turbine engines
p 901 N93-29927
Heat transfer and aerodynamics of a 3D design nozzle guide vane tested in the Pyestock Isentropic Light Piston Facility
p 901 N93-29928
Thermal effects of a coolant film along the suction side of a high pressure turbine nozzle guide vane
p 901 N93-29930
The influence of non-uniform spanwise inlet temperature on turbine rotor heat transfer
p 901 N93-29932
Measurement of turbulent spots and intermittency modelling at gas-turbine conditions
p 902 N93-29934
Heat transfer in high turbulence flows: A 2-D planar wall jet
p 932 N93-29935
Heat transfer with moderate free stream turbulence
p 932 N93-29936
Prediction of jet impingement cooling scheme characteristics (airfoil leading edge application)
p 932 N93-29941
Local heat transfer measurement with liquid crystals on rotating surfaces including non-axisymmetric cases
p 902 N93-29943
The USAF Advanced Turbine Aerothermal Research Rig (ATARR)
p 911 N93-29945
Aerothermic calculations of flows in interdisc cavities of turbines
p 903 N93-29947

Modelling thermal behaviour of turbomachinery discs and casings
p 903 N93-29949
Flow and heat transfer between gas-turbine discs
p 903 N93-29950
Heat transfer and leakage in high-speed rotating stepped labyrinth seals
p 903 N93-29951
The effect of main stream flow angle on flame tube film cooling
p 932 N93-29953
Impingement/effusion cooling
p 932 N93-29954
Characterization of ceramic composite materials for gas turbine applications
p 905 N93-30168
Fatigue in single crystal nickel superalloys
[AD-A265451] p 1019 N93-31795
Propulsion technology challenges for turn-of-the-century commercial aircraft
[NASA-TM-106192] p 1005 N93-32351
GAS TURBINES
Visualization and analysis of supersonic flow in rotating turbine stage. I - Influence of shock wave between stationary and moving blades
p 126 A93-15449
Shock formation in overexpanded tip leakage flow
[ASME PAPER 92-GT-1] p 245 A93-19276
Aerodynamic performance of a transonic low aspect ratio turbine nozzle
[ASME PAPER 92-GT-31] p 245 A93-19291
A systems dynamics approach to modeling gas turbine combustor wear
[ASME PAPER 92-GT-47] p 347 A93-19300
Experimental analysis of transonic flow through the variable nozzle of a radial inflow turbine
[ASME PAPER 92-GT-90] p 248 A93-19336
The effects of incident turbulence and moving wakes on laminar heat transfer in gas turbines
[ASME PAPER 92-GT-377] p 406 A93-19535
On-board condition management for aircraft gas turbines
[ASME PAPER 92-GT-416] p 357 A93-19564
Machinery arrangements for small VTOL transport aircraft
p 713 A93-34848
Gas dynamics of cooled turbines — Russian book
[ISBN 5-217-00809-1] p 721 A93-35685
Hierarchical development of three direct-design methods for two-dimensional axial-turbomachinery cascades
p 812 A93-39271
A knowledge-based blackboard system to interpret graphical data from vibration tests of gas turbines
[PNR-90993] p 59 N93-11114
Heat transfer and aerodynamics of a high rim speed turbine nozzle guide vane with profiled end walls
[AD-A258346] p 295 N93-17991
Multi-heat addition turbine engine
[NASA-CASE-LEW-15094-1] p 522 N93-22034
An evaluation of thermal energy storage options for precooled gas turbine inlet air
[DE93-005980] p 754 N93-24975
Radial inflow turbine study
[AD-A260767] p 724 N93-25917
Fatigue in single crystal nickel superalloys
[AD-A261742] p 737 N93-26282
Experimental investigation of crossflow jet mixing in a rectangular duct
[NASA-TM-106152] p 812 N93-27026
By-passing of heat exchangers in gas turbines
p 814 N93-27189
Use of local x ray computerized tomography for high-resolution, region-of-interest inspection of large ceramic components for engines
[DE93-005564] p 843 N93-28943
Flow phenomena in turbomachines
[AD-A263049] p 930 N93-29141
Heat Transfer and Cooling in Gas Turbines
[AGARD-CP-527] p 901 N93-29926
The effect of orthogonal-mode rotation on forced convection in a circular-sectioned tube fitted with full circumferential transverse ribs
p 932 N93-29937
Coupling of 3D-Navier-Stokes external flow calculations and internal 3D-heat conduction calculations for cooled turbine blades
p 904 N93-29961
GAS-METAL INTERACTIONS
Gas phase hydrogen permeation in a Ni-Fe-Co superalloy
p 735 A93-34510
GAS-SOLID INTERACTIONS
Energetics of gas-surface interactions in transitional flows at entry velocities
p 778 A93-39259
GAS-SOLID INTERFACES
Scattering kernels for gas-surface interaction
p 943 A93-42580
GASDYNAMIC LASERS
Autonomous mobile laser complex
p 395 A93-17767
GASEOUS FUELS
Use of alternative fuels for aviation
p 196 A93-14292
Experimental research on a semiwater-gas-fired gas-turbine
p 1107 A93-48524

SUBJECT INDEX

- Mixing enhancement and combustion of gaseous fuel in a supersonic combustor
[AIAA PAPER 93-2143] p 1114 A93-49960
- GASEOUS ROCKET PROPELLANTS**
An estimate of the 'doomed propellant fraction' for a Superdetonative Ram Accelerator
[AIAA PAPER 93-0359] p 385 A93-23042
- GASKETS**
Hermetic sealing and EMI shielding gasket
[AD-D015359] p 199 N93-13414
- GASOLINE**
Making clean gasoline: The effect on jet fuels
[AD-A264302] p 1019 N93-32085
- GAU-2 AIRFOIL**
Flowfield measurements of a two-element airfoil with large separation
p 480 A93-29307
- GEAR**
Dynamic analysis of a gear drive system in aeroengine
p 1149 A93-48514
- GEAR TEETH**
Radiation mechanism for the aerodynamic sound of gears - An explanation for the radiation process by air flow observation
p 451 A93-21859
Some characteristics of the design of heads for the cutting of bevel gears with negative curvature of the circular-arc tooth line
p 835 A93-39093
Low-noise, high-strength, spiral-bevel gears for helicopter transmissions
[AIAA PAPER 93-2149] p 1154 A93-49966
Multilevel solution of the elastohydrodynamic lubrication of concentrated contacts in spiroid gears
p 1161 A93-52606
Computational gearing mechanics
[NASA-CR-191127] p 751 N93-25884
Face-gear drives: Design, analysis, and testing for helicopter transmission applications
[NASA-TM-106101] p 839 N93-27133
- GEARS**
Dynamic characteristics of two new vibration modes of the disk-shell shaped gear
p 204 A93-14484
Parametric study of the gear blank structure in helicopter transmission design
p 546 A93-27973
Acoustical analysis of gear housing vibration
p 567 A93-29420
Modal analysis of multistage gear systems coupled with gearbox vibrations
p 827 A93-36588
Initial test results of 40,000 horsepower fan drive gear system for advanced ducted propulsion systems
[AIAA PAPER 93-2146] p 1154 A93-49963
Low-noise, high-strength, spiral-bevel gears for helicopter transmissions
[AIAA PAPER 93-2149] p 1154 A93-49966
High speed, heavily loaded and precision aircraft type epicyclic gear system dynamic analysis overview and special considerations
[AIAA PAPER 93-2151] p 1154 A93-49968
Multilevel solution of the elastohydrodynamic lubrication of concentrated contacts in spiroid gears
p 1161 A93-52606
The application of manufacturing systems engineering for aero engine gears
[PNR-90944] p 86 N93-11054
Time-frequency domain analysis of vibration signals for machinery diagnostics. 3: The present power spectral density
[OUEL-1911/92] p 89 N93-11707
Conditioned based machinery maintenance (helicopter fault detection)
[AD-A255796] p 329 N93-16396
Flexible rotorcraft system dynamics with time-variant contact conditions
p 340 N93-19034
Resonant response analysis of a high speed gear
p 553 N93-20662
Computational gearing mechanics
[NASA-CR-191127] p 751 N93-25884
Fault detection of helicopter gearboxes using the multi-valued influence matrix method
[NASA-TM-106100] p 838 N93-27069
Sikorsky Aircraft Advanced Rotorcraft Transmission (ART) program
[NASA-CR-191079] p 840 N93-27268
Efficient fault diagnosis of helicopter gearboxes
[NASA-TM-106253] p 1032 N93-31846
- GELLED PROPELLANTS**
Atomization of JP-10/B4C gelled slurry fuel
[AD-A256827] p 391 N93-15686
- GENERAL AVIATION AIRCRAFT**
General aviation turbine markets - An economic overview
[AIAA PAPER 92-4191] p 103 A93-13369
Adaptive optimization of general aviation aircraft
[AIAA PAPER 92-4195] p 44 A93-13372
A guidance display system for single pilot operation
[AIAA PAPER 92-4196] p 51 A93-13373

- Rudder and elevator effects on the incipient spin characteristics of a typical general aviation training aircraft
[AIAA PAPER 93-0016] p 367 A93-20138
Weather-related accidents in the Canadian aviation industry - An analysis of the chief contributory factors
p 307 A93-22106
Design development for advanced general aviation aircraft. II
p 897 A93-40475
Ilyushin takes on the market
p 945 A93-43623
A localizer design to improve missed approach guidance
p 992 A93-44143
Two leading-edge droop modifications for tailoring stall characteristics of a general aviation trainer configuration
p 1008 A93-46807
Analysis of wing-body junction flowfields using the incompressible Navier-Stokes equations, volumes 1 and 2
p 17 N93-10320
Terminal area forecasts FY 1992 - 2005
[AD-A255797] p 149 N93-15390
Pilot weather advisor
[NASA-CR-189723] p 318 N93-16692
Proceedings of the AIAA/FAA Joint Symposium on General Aviation Systems
[AD-A257780] p 240 N93-17732
Use of microprocessor-based simulator technology and MEG/EEG measurement techniques in pilot emergency-maneuver training
p 530 N93-19706
General aviation aircraft: Normal acceleration data analysis and collection project
[DOT/FAA/CT-91/20] p 713 N93-24739
Lightning data acquisition
p 753 N93-24883
Annual review of aircraft accident data: US general aviation calendar year 1989
[PB93-160687] p 790 N93-27033
Preliminary design studies of an advanced general aviation aircraft
p 894 N93-29717
Reaction to aircraft noise near general aviation airfields
[DORA-8203] p 1040 N93-32377
- GENERAL OVERVIEWS**
An overview of aeroelasticity studies for the National Aero-Space Plane
[AIAA PAPER 93-1313] p 732 A93-33889
Overview of Tiger dynamics validation program
p 794 A93-35907
Laminar flow control - Introduction and overview
p 859 A93-41777
Laminar flow flight experiments - A review
p 890 A93-41778
A perspective on a quarter century of CFD research
[AIAA PAPER 93-3291] p 1021 A93-44995
Airship insurance in London
[AIAA PAPER 93-4043] p 1265 A93-54611
- GENETIC ALGORITHMS**
Design of exhaust nozzles using GA optimized neural networks
[AIAA PAPER 93-0410] p 361 A93-23331
The use of genetic algorithms in the design of fuzzy logic controllers
p 1167 A93-50779
Genetic design of digital model-following flight-control systems
[AIAA PAPER 93-3883] p 1135 A93-51468
- GEODESY**
Repair, evaluation, maintenance, and rehabilitation research program. Continuous Deformation Monitoring System (CDMS)
[AD-A261833] p 708 N93-26274
- GEODETIC COORDINATES**
Experiences with two GPS receivers in northern Europe
[NLR-TP-91168-U] p 993 N93-31120
- GEOLOGICAL SURVEYS**
Land subsidence and problems affecting land use at Edwards Air Force Base and vicinity, California, 1990
[PB93-182236] p 1036 N93-32191
- GEOLOGY**
Meeting review: Third NCAR Research Aircraft Fleet Workshop
[PB92-222710] p 223 N93-12818
- GEOMETRIC DILUTION OF PRECISION**
Effect of terrain masking on GPS position dilution of precision
p 317 A93-21824
- GEOMETRICAL ACOUSTICS**
Propagation of high frequency jet noise using geometric acoustics
[AIAA PAPER 93-0147] p 452 A93-23241
Propagation of high frequency jet noise using geometric acoustics
[NASA-TM-106013] p 233 N93-15575
- GEOMETRY**
Example of the Couette iceform design model - Flat plate iceformation
p 207 A93-15070
Effect of boundary conditions and panel geometry on the response of laminated panels subjected to transverse pressure loads
p 1259 A93-55674

GLOBAL POSITIONING SYSTEM

- GEOPHYSICS**
Meeting review: Third NCAR Research Aircraft Fleet Workshop
[PB92-222710] p 223 N93-12818
- GESTROPHIC WIND**
Surface shear stress estimates from geostrophic winds for use in sensible and latent heat flux formulations
p 936 N93-30044
- GEOSYNCHRONOUS ORBITS**
Receiver Autonomous Integrity Monitoring (RAIM) availability for supplemental GPS navigation
p 312 A93-18554
- GERMAN SPACE PROGRAM**
DLR research program overview on airport surface movement guidance and control
p 499 A93-27912
Modern helicopter technologies at MBB and the application in future programmes
[MBB-UD-0599-91-PUB] p 331 N93-17566
Technology transfer: Potential of BMFT concept for hypersonics
[MBB-LME-202-S-PUB-0505] p 1041 N93-31045
- GERMANY**
Stumbling blocks for airport construction in the new German federal states
p 1227 A93-53727
Activities report of Lufthansa
[ETN-92-92100] p 28 N93-11319
Activities report of the German Institute for Flight Safety
[ETN-92-92272] p 28 N93-11375
- GLASS**
A study of the effect of the support fastening compliance on the stress-strain state of aircraft transparencies
p 997 A93-47079
- GLASS FIBERS**
Tiltrotor Research Aircraft composite blade repairs - Lessons learned
p 108 A93-14819
Nonlinear deformation mechanics of multilayer transparency elements - Some calculation results --- for aircraft portholes
p 1191 A93-52937
Fiber pulling apparatus modification
[NASA-CR-184498] p 220 N93-14763
- GLASS TRANSITION TEMPERATURE**
A study of the origin of residual stresses and strains in the transparencies of supersonic aircraft
p 801 A93-36784
- GLAZES**
Results of a low power ice protection system test and a new method of imaging data analysis
p 795 A93-35932
- GLIDE PATHS**
Helicopter approaches in low visibility using RGPS and EFIS --- EFIS - Electronic Flight Instrumentation System
p 142 A93-17309
Laser Centerline Localizer and Laser Glideslope Indicator for visual guidance on approach to landing
p 500 A93-28156
Effects of equipment calibration, test flight procedures and analysing methods on the accuracy of ILS glide path measurements --- Book
p 881 A93-41600
Effect of wet snow on the null-reference ILS system
p 1097 A93-50660
Alternative solution to optimum gliding velocity in a steady head wind or tail wind
p 1136 A93-52458
ILS mathematical modeling study of an ILS glide slope proposed for runway 19L at the Meridian Naval Air Station, Mississippi
[DOT/FAA/CT-TN93/8] p 705 N93-24741
Evaluation of four advanced nozzle concepts for short takeoff and landing performance
[NASA-TP-3314] p 875 N93-29165
- GLIDERS**
A sensitivity analysis of the stability of a tug-rope-sailplane system
p 184 A93-14400
Flutter calculations for a system with interacting nonlinearities
[AIAA PAPER 92-4682] p 409 A93-20304
Modeling and analysis of the winch launch of a glider
p 528 A93-27294
A new flying qualities criterion for flying wings
[AIAA PAPER 93-3668] p 1128 A93-48346
Longitudinal dynamics of a towed sailplane
p 1130 A93-49577
Effects of an aft facing step on the surface of a laminar flow glider wing
[NASA-CR-193302] p 990 N93-31855
- GLIDING**
Zero-thrust glide testing for drag and propulsive efficiency of propeller aircraft
p 995 A93-45143
Alternative solution to optimum gliding velocity in a steady head wind or tail wind
p 1136 A93-52458
- GLOBAL POSITIONING SYSTEM**
Progress towards joint civil use of GPS and GLONASS
p 29 A93-10977
Civil standardization of the Global Positioning System for the aviation community
p 29 A93-10981

- Measurement technique for Loran-C pulse wave distortion measures and performance in an environment of noise p 29 A93-10988
- Development of a TRN/INS/GPS integrated navigation system p 30 A93-11004
- Integration of full scale development aircraft GPS user equipment (AN/ARN-151) with Doppler radar systems p 31 A93-11012
- Architectures and GPS/INS integration - Impact on mission accomplishment p 31 A93-11013
- Design, capabilities, and performance of the miniaturized airborne GPS receiver p 32 A93-11014
- The Texas Instruments/Honeywell GPS Guidance Package p 32 A93-11015
- Differential GPS/inertial navigation approach/landing flight test results p 32 A93-11019
- The derivation of path following error and control motion noise filters for the reduction of Global Positioning System flight test data p 32 A93-11022
- Real time DGPS service for precise positioning - Activities in the Federal Republic of Germany p 1 A93-11027
- Maintaining high accuracy GPS positioning 'on the fly' - using traverse closures, residual analysis, inertial navigation in aircraft p 2 A93-11028
- Achieving modularity with tightly-coupled GPS/INS p 33 A93-11032
- Receiver autonomous integrity monitoring (RAIM) capability for sole-means GPS navigation in the oceanic phase of flight p 33 A93-11035
- GPS integrity monitoring and system improvement with ground station and multistationary satellite support p 33 A93-11044
- Flight test evaluation of precision-code differential GPS for terminal approach and landing p 33 A93-11294
- Multipath effects on GPS code phase measurements p 34 A93-11295
- Statistical validation for GPS integrity test p 34 A93-11297
- The use of satellite geometry for prevention of cycle slips in a GPS processor p 34 A93-11298
- Airspeed calibration using GPS [AIAA PAPER 92-4090] p 51 A93-13272
- Precision increasing and integrity monitoring of navigation data for GPS/inertial hybrid solution p 149 A93-14157
- Investigation of precise approach and landing of civil aircraft using integrated system based on GPS p 180 A93-14159
- Helicopter approaches in low visibility using RGPS and EFIS - EFIS - Electronic Flight Instrumentation System p 142 A93-17309
- Airborne trials of Loran-C p 111 A93-17756
- Receiver Autonomous Integrity Monitoring (RAIM) availability for supplemental GPS navigation p 312 A93-18554
- The GPS system - Satellite radio-navigation p 312 A93-20008
- Description and capabilities of the Navcore-V GPS receiver engine p 312 A93-21127
- Digital hopping GPS/GLONASS receiver p 312 A93-21128
- USCG HU-25A/GPS integration p 313 A93-21130
- The effects of ionospheric errors on single-frequency GPS users p 313 A93-21141
- Integrated use of GPS and GLONASS in civil aviation navigation. II - Experience with GLONASS p 313 A93-21142
- GPS/GLONASS flight test, lab test and coverage analysis tests p 313 A93-21143
- Airport navigation and surveillance using GPS and ADS p 313 A93-21145
- Guidance accuracy considerations for realtime GPS interferometry p 342 A93-21146
- Performance analysis of a miniaturized airborne GPS receiver p 313 A93-21147
- Results from a GPS Shuttle Training Aircraft flight test p 384 A93-21148
- Differential GPS autonomous failure detection p 314 A93-21152
- Errors in long distance kinematic GPS p 314 A93-21154
- Update on GPS integrity requirements of the RTCA MOPS p 314 A93-21155
- Work performed in the United Kingdom to establish the feasibility of RAIM in a GPS receiver in flight p 314 A93-21157
- A new algorithm of Receiver Autonomous Integrity Monitoring (RAIM) for GPS navigation p 314 A93-21161
- Statistical quality control for kinematic GPS positioning p 314 A93-21162
- Decision making for a public differential GPS service p 314 A93-21165
- GPS continuity - Initial findings p 314 A93-21167
- Institute of Navigation, National Technical Meeting, San Diego, CA, Jan. 27-29, 1992, Proceedings p 315 A93-21176
- INS/DGPS integration for trajectory determination of a test vehicle p 315 A93-21178
- Planning for complementary MLS/GPS operations p 315 A93-21180
- MIAS, the integration of MLS with DGPS/DLoran-C p 315 A93-21181
- GPS availability and reliability for aircraft precision approach p 315 A93-21182
- Analysis of DGPS/INS and MLS/INS final approach navigation errors and control performance data p 315 A93-21183
- Guidelines for NAVSTAR GPS embedded receiver applications p 315 A93-21184
- On the selection of a GPS validity indicator for aircraft navigation in the National Airspace System (NAS) p 316 A93-21186
- The applications, benefits, and issues of employing GPS and Glonass with Automatic Dependent Surveillance p 316 A93-21188
- Terminal area surveillance using GPS p 316 A93-21190
- A statistical comparison of differential GPS and laser generated time, space positioning information for aircraft flight testing p 316 A93-21199
- Differential GPS control of Starcar 2 p 317 A93-21201
- Analysis of a high-performance C/A-code GPS receiver in kinematic mode p 317 A93-21822
- A baseline GPS RAIM scheme and a note on the equivalence of three RAIM methods p 317 A93-21823
- Effect of terrain masking on GPS position dilution of precision p 317 A93-21824
- Analysis and correction of ionospheric time delay for differential GPS p 498 A93-24028
- Position reporting using GPS/OMEGA and INS p 498 A93-25173
- Data communication for airborne differential GPS/GLONASS application p 499 A93-27910
- Integration of a course and position reference system with GPS p 499 A93-27911
- Application of new GPS aircraft control/display system to topographic mapping of the Greenland ice cap p 499 A93-28152
- Application of advanced guidance and navigation systems to flight control of aircraft and future space vehicles p 500 A93-28153
- The high accuracy applications of the GPS system to static positioning p 500 A93-28193
- GNSS - A global system of satellite-aided navigation p 500 A93-28194
- Differential GPS and its applications in the aeronautical realm p 500 A93-28195
- Application of parafoils to microwave landing system siting [AIAA PAPER 93-1213] p 702 A93-35162
- GPS autoland considerations p 792 A93-38203
- Augmentation of a navigation reference system with differential global positioning system pseudorange measurements p 881 A93-42798
- Receiver Autonomous Integrity Monitoring (RAIM) of GPS and GLONASS p 993 A93-46891
- Ongoing GPS experiments demonstrate potential of satellite navigation technology p 1097 A93-49278
- Overview of the FAA's differential GPS CAT III technical feasibility demonstration program p 1098 A93-51425
- [AIAA PAPER 93-3836] p 1098 A93-51425
- Multiple receiver, zero-length baseline kinematic GPS positioning techniques for airborne gravity measurement p 1240 A93-55974
- Airborne gravimetry, altimetry, and GPS navigation errors p 1240 A93-55975
- Requirements for airborne vector gravimetry p 1241 A93-55976
- Integrated DGPS/IMU systems for airborne navigation in Poland p 1241 A93-56049
- Proposed revisions to RTCM SC-104 recommended standards for differential NAVSTAR/GPS service for carrier phase applications [AD-A255276] p 152 A93-15005
- Correction of inertial measurements using GPS updates for underwater navigation [AD-A257329] p 317 A93-15988
- Multipath effects in a Global Positioning Satellite system receiver p 318 A93-17311
- Navstar global positioning system: Introduction and status [NLR-TP-91008-U] p 318 A93-17559
- GPS Interferometry [NASA-CR-192301] p 319 A93-18873
- Detection of spoofing, jamming, or failure of a Global Positioning System (GPS) [AD-A259023] p 319 A93-18951
- A model of Global Positioning System (GPS) Master Control Station (MCS) operations [AD-A258846] p 320 A93-19067
- Development of a realtime DGPS system [DLR-MITT-92-06] p 503 A93-20749
- An experimental health monitoring unit for GPS and GLONASS p 706 A93-25018
- Methodology investigation: Global Positioning System integration (GPS) [AD-A261054] p 708 A93-26237
- Repair, evaluation, maintenance, and rehabilitation research program. Continuous Deformation Monitoring System (CDMS) [AD-A261833] p 708 A93-26274
- Follow-on operational test and evaluation of the NAVSTAR global positioning system air integration/installation program [AD-A263067] p 793 A93-27925
- Flight evaluation of a computer aided low-altitude helicopter flight guidance system p 820 A93-28869
- Helicopter approach capability using the differential global positioning system (NASA-CR-193183) p 793 A93-28936
- System analysis for a kinematic positioning system based on the global positioning system [AD-A262830] p 885 A93-29468
- Embedded GPS: The Canadian Marconi approach p 886 A93-30330
- Attitude determination using GPS: Development of an all solid-state guidance, navigation, and control sensor for air and space vehicles based on the global positioning system p 888 A93-30605
- Design and implementation of a Global Positioning System (GPS) supported area navigation system with electronic airway [ILR-MITT-275(1992)] p 889 A93-30671
- Experiences with two GPS receivers in northern Europe [NLR-TP-91168-U] p 993 A93-31120
- The application of phase tracking GPS for flight test trajectory determination [NLR-TP-91349-U] p 994 A93-32337
- GLOBAL TRACKING NETWORK**
- The high accuracy applications of the GPS system to static positioning p 500 A93-28193
- GLOBAL WARMING**
- ICAO analyses trends in fuel consumption by world's airlines p 1 A93-10733
- GOERTLER INSTABILITY**
- Detection of Goertler vortices in hypersonic flow p 120 A93-14382
- Coriolis effects on Goertler vortices in the boundary-layer flow on concave wall p 123 A93-14564
- Goertler instability and hypersonic quiet nozzle design p 480 A93-29155
- GOGGLES**
- Royal Air Force support helicopters - Night operations p 1190 A93-54293
- GONDOLAS**
- Resonance frequencies of a gondola submitted to a forced rotation under a stratospheric balloon p 27 A93-11384
- GOVERNMENT PROCUREMENT**
- Hovering decisions - development of EH101 helicopter p 46 A93-13700
- Applying commercial style acquisition practices to the procurement of commercially available aircraft [AD-A258143] p 455 A93-18087
- GOVERNMENT/INDUSTRY RELATIONS**
- The Federal Aviation Administration (FAA) and the National Weather Service (NWS) modernization programs - Catalysts for change in weather services p 427 A93-22114
- The NASA/industry design analysis methods for vibrations (DAMVIBS) program - Accomplishments and contributions p 508 A93-27971
- Space policy 2000 p 1174 A93-50333
- GRADIENTS**
- Exact-gradient shape optimization of a 2D Euler flow [INRIA-RR-1540] p 422 A93-18623
- Investigations on entropy layer along hypersonic hyperboloids using a defect boundary layer p 787 A93-27462
- GRAIN SIZE**
- Effects of grain size and carbides on the creep resistance and rupture properties of a conventionally cast nickel-base superalloy p 389 A93-21699
- GRAPH THEORY**
- Graph-theory studies of the possibility of occurrence of flight accidents and incidents during the take-off under special operating conditions p 306 A93-18365
- Algorithms for constructing models of the interaction of diagnostic systems with reserved aviation equipment p 847 A93-39043

SUBJECT INDEX

- En route air traffic controllers use of flight progress strips:
A graph-theoretic analysis [AD-A259062] p 319 N93-18927
- GRAPHICAL USER INTERFACE**
A graphical user-interface for propulsion system analysis [AIAA PAPER 93-0223] p 440 A93-23699
- GRAPHITE**
Oxidation-resistant high-temperature materials p 915 A93-40362
Consolidation of graphite thermoplastic textile preforms for primary aircraft structure p 919 N93-30439
- GRAPHITE-EPOXY COMPOSITES**
Support of composite fuel cells [SME PAPER EM92-101] p 152 A93-14102
Commercial airplane primary structure [SME PAPER EM92-115] p 107 A93-14112
Compression after impact (CAI) properties of CF/PEEK (APC-2) and conventional CF/epoxy stiffened panels p 196 A93-14307
Sandwich construction in the Starship p 159 A93-15737
A study of the flexural properties of carbon-epoxy composites in certain environments p 390 A93-21999
Repair of delaminations and impact damage in composite aircraft structures p 457 A93-24107
Coupled composite rotor blades under bending and torsional loads p 546 A93-27970
An experimental and analytical investigation on the response of GR/EP composite I-frames p 546 A93-27975
Tapered geometries for improved crashworthiness under side loads p 743 A93-34259
Nonlinear large amplitude vibration of composite helicopter blade at large static deflection p 713 A93-35630
Environmental conditions for certification testing of helicopter advanced composite main rotor components p 824 A93-36003
Design and manufacture for producibility of carbon fiber/epoxy composite aircraft skins [SME PAPER EM93-104] p 1043 A93-51732
Stringer peeling effects at stiffened composite panels in the postbuckling range p 1160 A93-52453
The characterization and development of materials for advanced textile composites p 1211 A93-53434
Effect of boundary conditions and panel geometry on the response of laminated panels subjected to transverse pressure loads p 1259 A93-55674
Damping in aerospace composite materials p 1260 A93-55869
Nonlinear aeroelasticity of composite structures [AD-A254285] p 47 N93-10842
Reliability of stiffened structural panels: Two examples [NASA-TM-107687] p 219 N93-14483
Experimental and analytical investigation of dynamic characteristics of extension-twist-coupled composite tubular spars [NASA-TP-3225] p 553 N93-20585
Fabrication of composite propfan blades for a cruise missile wind tunnel model [NASA-TM-105270] p 752 N93-26202
Thermally induced stresses in a composite exposed to fire p 737 N93-26371
Structural tailoring of aircraft engine blade subject to ice impact constraints [NASA-TM-106033] p 838 N93-26999
Static and dynamic large deflection flexural response of graphite-epoxy beams [NASA-CR-4118] p 934 N93-30374
Mechanical and analytical screening of braided composites for transport fuselage applications p 922 N93-30855
- GRATINGS (SPECTRA)**
Embedded Bragg grating fiber optic sensor for composite flexbeams p 828 A93-37350
- GRAVIMETERS**
Airborne gravimetry from a light aircraft p 1245 A93-55972
Accuracy of GPS-derived acceleration from moving platform tests p 1240 A93-55973
Multiple receiver, zero-length baseline kinematic GPS positioning techniques for airborne gravity measurement p 1240 A93-55974
Requirements for airborne vector gravimetry p 1241 A93-55976
Airborne vector gravimetry with an aided inertial survey system p 1241 A93-55977
- GRAVIMETRY**
Airborne gravimetry, altimetry, and GPS navigation errors p 1240 A93-55975
- GRAVITATION**
Gravity sensitivity of a resistojel water vaporizer [AIAA PAPER 93-2402] p 1156 A93-50167

- Gravity sensitivity of a resistojel water vaporizer [NASA-TM-106220] p 914 N93-29194
- GRAVITATIONAL EFFECTS**
Stability of the vapour phase in a rotating two-phase fluid system subjected to different gravitational intensities p 926 A93-41714
Gravity sensitivity of a resistojel water vaporizer [AIAA PAPER 93-2402] p 1156 A93-50167
Fiber pulling apparatus modification [NASA-CR-184498] p 220 N93-14763
Vibration isolation technology: An executive summary of systems development and demonstration [NASA-TM-105937] p 110 N93-15573
Numerical study of cavity natural convection flow with augmenting and counteracting effects by projection finite element method p 749 N93-25540
Gravity sensitivity of a resistojel water vaporizer [NASA-TM-106220] p 914 N93-29194
- GRAVITY ANOMALIES**
Airborne gravimetry from a light aircraft p 1245 A93-55972
Requirements for airborne vector gravimetry p 1241 A93-55976
- GRAVITY GRADIOMETERS**
Controlling common mode stabilization errors in airborne gravity gradiometry p 1245 A93-55978
- GRAVITY PROBE B**
Aeronomy coexperiments on drag-free satellites with proportional thrusters: GP-B and STEP p 195 N93-13922
- GRAZING INCIDENCE**
Grazing angle dependency of SAR imagery p 884 A93-43455
- GREASES**
Improved lubricating greases for aircraft wheel bearings [SAE PAPER 921038] p 197 A93-14658
- GRID GENERATION (MATHEMATICS)**
Two modified versions of Hsu-Lee's elliptic solver of grid generation p 95 A93-11085
Grid-characteristic method for calculating a three-dimensional boundary layer on the bounding surfaces of the blade passage of a turbomachine p 13 A93-12808
Unstructured grid solutions to a wing/pylon/store configuration using VGRID3D/USM3D [AIAA PAPER 92-4572] p 14 A93-13303
Geometry based Delaunay tetrahedralization and mesh movement strategies for multi-body CFD [AIAA PAPER 92-4575] p 15 A93-13309
Hybrid grid approach to study dynamic stall p 122 A93-14548
Marching grid generation for external viscous flow problems p 228 A93-16979
The extension of a solution-adaptive 3D Navier-Stokes solver towards geometries of arbitrary complexity [ASME PAPER 92-GT-363] p 257 A93-19527
Grid generation for three-dimensional turbomachinery geometries including tip clearance p 270 A93-21658
Study of flow phenomena in high speed intakes [AIAA PAPER 92-5029] p 272 A93-22304
Grid and design variables sensitivity analyses for NACA four-digit wing-sections [AIAA PAPER 93-0195] p 276 A93-22616
Aircraft grid generation using interactive environment [AIAA PAPER 93-0224] p 438 A93-22639
3D Euler flow solutions using unstructured Cartesian and prismatic grids [AIAA PAPER 93-0331] p 281 A93-23022
Ice accretion and performance degradation calculations with LEWICE/NS [AIAA PAPER 93-0173] p 310 A93-23244
Multi-block grid generation for complete aircraft configurations p 460 A93-23838
A two-dimensional elliptic grid generator for a wing-body section involving grid control functions p 460 A93-24083
Hybrid prismatic/tetrahedral grid generation for complex 3-D geometries [AIAA PAPER 93-0669] p 465 A93-24778
Unstructured 3D Delaunay mesh generation applied to planes, trains and automobiles [AIAA PAPER 93-0673] p 560 A93-24781
A fully implicit Navier-Stokes algorithm using an unstructured grid and flux difference splitting [AIAA PAPER 93-0875] p 470 A93-24936
TGV tunnel entry simulations using a finite element code with automatic remeshing [AIAA PAPER 93-0890] p 471 A93-24950
MESH3D - A tool for the construction of three-dimensional meshes [ONERA, TP NO. 1992-164] p 561 A93-25339
Solution-adaptive and quality-enhancing grid generation p 480 A93-28610
Linearized Euler predictions of unsteady aerodynamic loads in cascades p 480 A93-29318

GRID GENERATION (MATHEMATICS)

- Adaptive grid generation using optimal control theory p 770 A93-38187
- Unsteady analysis of helicopter rotor p 770 A93-38193
- Structured grid variational adaption - Reaching the limit? [ONERA, TP NO. 1992-114] p 771 A93-38590
Development of a transonic Euler method for complete aircraft configurations p 779 A93-39721
Computational results for 2-D and 3-D ramp flows with an upwind Navier-Stokes solver p 866 A93-42592
Generation of unstructured tetrahedral meshes by advancing front technique p 1021 A93-44206
Unstructured grids on NURBS surfaces - NonUniform Rational B-Splines [AIAA PAPER 93-3454] p 949 A93-44232
Mesh generation for the computation of flowfields over complex aerodynamic shapes p 995 A93-44888
A 3D unstructured adaptive multigrid scheme for the Euler equations [AIAA PAPER 93-3339] p 954 A93-45033
A three-dimensional Delaunay unstructured grid generator and flow solver for bodies in relative motion [AIAA PAPER 93-3349] p 954 A93-45043
A graphically interactive approach to structured and unstructured surface grid quality analysis [AIAA PAPER 93-3351] p 954 A93-45045
Visual grid quality assessment for 3D unstructured meshes [AIAA PAPER 93-3352] p 1036 A93-45046
Techniques for the visual evaluation of computational grids [AIAA PAPER 93-3353] p 1037 A93-45047
Adaptive Cartesian grid methods for representing geometry in inviscid compressible flow [AIAA PAPER 93-3385] p 955 A93-45076
3D automatic Cartesian grid generation for Euler flows [AIAA PAPER 93-3386] p 956 A93-45077
An adaptive finite element method for turbulent free shear flow past a propeller [AIAA PAPER 93-3388] p 956 A93-45079
Adaptive inviscid flow solutions for aerospace geometries on efficiently generated unstructured tetrahedral meshes [AIAA PAPER 93-3390] p 956 A93-45081
A simulation technique for 2-D unsteady inviscid flows around arbitrarily moving and deforming bodies of arbitrary geometry [AIAA PAPER 93-3391] p 956 A93-45082
A 3-D finite-volume scheme for the Euler equations on adaptive tetrahedral grids p 956 A93-45083
An upwind multigrid algorithm for calculating flows on unstructured grids p 957 A93-45088
Single block three-dimensional volume grids about complex aerodynamic vehicles p 957 A93-45099
Advancing-layers method for generation of unstructured viscous grids p 957 A93-45101
Adaptive refinement-coarsening scheme for three-dimensional unstructured meshes p 961 A93-45735
The practical application of solution-adaption to the numerical simulation of complex turbomachinery problems p 970 A93-46916
Intensive industrial use of 3D Euler numerical methods for axial flow turbine analysis and design p 1002 A93-46943
Near-field supersonic flow predictions by an adaptive unstructured tetrahedral grid solver [AIAA PAPER 93-3430] p 977 A93-47223
Unstructured grid generation using interactive three-dimensional boundary and efficient three-dimensional volume methods [AIAA PAPER 93-3452] p 1037 A93-47237
Unstructured viscous grid generation by advancing-layers method [AIAA PAPER 93-3453] p 979 A93-47238
Grid and aerodynamic sensitivity analyses of airplane components [AIAA PAPER 93-3475] p 981 A93-47254
A computational study of wingtip vortex flowfield [AIAA PAPER 93-3010] p 1054 A93-48200
Turbopfan flowfield simulation using Euler equations with body forces [AIAA PAPER 93-1978] p 1078 A93-49825
3-D turbomachinery Euler and Navier-Stokes calculations with a multidomain cell-centered approach [AIAA PAPER 93-2576] p 1085 A93-50292
Prismatic grid generation for three-dimensional complex geometries p 1178 A93-53217
The construction of nearly orthogonal multiblock grids for compressible flow simulation p 1219 A93-53847
The body-fitted coordinates generation for multi-element airfoils p 1231 A93-54598
A frontal approach for internal node generation in Delaunay triangulations p 1262 A93-56403

- Sweepline algorithm for unstructured-grid generation on two-dimensional non-convex domains p 1262 A93-56413
- Interactive grid generation program for CAP-TSD [NASA-TM-102705] p 17 N93-10349
- Artificial intelligence and CFD: Expert systems for the design of airfoils and for grid generation [DIGE-EST-TN-016] p 48 N93-11161
- Solution of compressible Navier-Stokes equations using spectral methods on arbitrary two-dimensional domains p 218 N93-14041
- Ice accretion and performance degradation calculations with LEWICE/NS [NASA-TM-105972] p 148 N93-15354
- An advanced graphics-interactive system for a multi-block structured grid generation within an industrial environment [ETN-92-92885] p 440 N93-16288
- Application of the Euler method EUFLEX to a fighter-type airplane configuration at transonic speed [MBB-FE-211-S-PUB-0489-A] p 484 N93-21059
- A three-dimensional algebraic grid generation scheme for gas turbine combustors with inclined slots [NASA-CR-191095] p 746 N93-24759
- A comparison using APPL and PVM for a parallel implementation of an unstructured grid generation program [NASA-CR-191425] p 757 N93-25073
- A contribution to the great Riemann solver debate [NASA-CR-191409] p 694 N93-25083
- Grid sensitivity for aerodynamic optimization and flow analysis [NASA-CR-192980] p 694 N93-25117
- Unstructured viscous grid generation by advancing-front method [NASA-CR-191449] p 780 N93-27067
- Unstructured mesh algorithms for aerodynamic calculations p 785 N93-27444
- Assessment of computational issues associated with analysis of high-lift systems p 785 N93-27449
- Adaptive EAGLE dynamic solution adaptation and grid quality enhancement p 788 N93-27464
- Ship viscous flow: A report on the 1990 SSPA-IIHR Workshop p 840 N93-27466
- Topology and grid adaption for high-speed flow computations [NASA-CR-4216] p 934 N93-30375
- The VIB-code to simulate 3-D stator/rotor flow in axial turbines [DLR-FB-92-19] p 1003 N93-31170
- ### GRIDS
- Optimal conditions for flow turbulence reduction by a set of grids p 836 A93-39122
- Curvature and leading edge sweep back effects on grid fin aerodynamic characteristics [AIAA PAPER 93-3480] p 981 A93-47258
- ### GROOVES
- Wind-tunnel tests of an inclined cylinder having helical grooves [AIAA PAPER 93-3456] p 979 A93-47239
- Experimental study of the effect of helical grooves on an infinite cylinder [AD-A260890] p 751 N93-25912
- ### GROUND BASED CONTROL
- Air Traffic Control ground movement control in low visibility p 151 A93-17308
- A reactive approach for distributed air traffic control [ONERA, TP NO. 1993-83] p 1190 A93-53603
- Airport stand assignment model [TT-9104] p 67 N93-11728
- The effect of TCAS interrogations on the Chicago O'Hare ATCRBS system [DOT/FAA/CT-92/22] p 318 N93-16498
- Mission planning systems for tactical aircraft (pre-flight and in-flight) [AGARD-AR-313] p 496 N93-21187
- Piloted simulation of an air-ground profile negotiation process in a time-based Air Traffic Control environment [NASA-TM-107748] p 707 N93-26087
- ### GROUND CREWS
- The benefits of ground maintenance simulators p 238 A93-18757
- An investigation of the influence of advanced aircraft diagnostics on the technological sophistication of maintenance personnel [AD-A258988] p 240 N93-18887
- The X-15/HL-20 operations support comparison [NASA-TM-4453] p 1017 N93-32379
- ### GROUND EFFECT (AERODYNAMICS)
- Small scale jet effects and hot gas ingestion investigations at NASA Ames [AIAA PAPER 92-4252] p 67 A93-13339
- A study of the effect of a moving ground belt on the vortex created by a jet impinging on the ground in a cross flow [AIAA PAPER 92-4250] p 15 A93-13361
- Ground vortex formation for uniform and nonuniform jets impinging on a ground plane [AIAA PAPER 92-4251] p 80 A93-13362
- A study of propeller/wing interaction including the effect of ground proximity p 113 A93-14190
- Unsteady pressures under impinging jets in crossflows p 399 A93-19220
- Two-, three-, and four-poster jets in cross flow [AIAA PAPER 93-0023] p 408 A93-20141
- Unsteady effects of camber on the aerodynamic characteristics of a thin airfoil moving near the ground p 270 A93-21719
- Lift enhancement of ground-effect wing. I - Results of screening tests of various concepts p 271 A93-21737
- Lift enhancement of ground-effect wing. II - Experimental investigation of the power augmented ram wing in ground effect through the wind tunnel p 271 A93-21738
- A study of single jet impingement ground effect lift loss [AIAA PAPER 93-0869] p 469 A93-24930
- Microchannel plate modal gain variations with temperature p 477 A93-27445
- Potential hazard of aircraft wake vortices in ground effect with crosswind p 479 A93-28606
- Ground effect on the take-off characteristics of sea-based aircraft p 679 A93-33706
- Analysis of slender bodies of revolution with an angle of attack in extreme ground effect p 679 A93-33716
- Tip vortex geometry of a hovering helicopter rotor in ground effect p 893 A93-43779
- Effect of ground and ceiling planes on shape of energized wakes [AIAA PAPER 93-3410] p 974 A93-47207
- Unsteady ground effects on aerodynamic coefficients of finite wings with camber [AIAA PAPER 93-3423] p 976 A93-47218
- The moving wall effect vis-a-vis other dynamic stall flow mechanisms [AIAA PAPER 93-3424] p 1008 A93-47219
- Calculation of V/STOL aircraft aerodynamics with deflected jets in ground effect [AIAA PAPER 93-3530] p 986 A93-47287
- Numerical simulation of unsteady flow induced by a flat plate moving near ground p 1094 A93-52432
- On the analysis of an impinging jet on ground effects p 1260 A93-56339
- ### GROUND EFFECT (COMMUNICATIONS)
- Systems issues in airborne Doppler radar/LIDAR certification p 145 N93-14855
- Ground clutter measurements using the NASA airborne doppler radar: Description of clutter at the Denver and Philadelphia airports p 490 N93-19608
- Comparison of simulated and actual wind shear radar data products p 490 N93-19610
- Signal processing for airborne doppler radar detection of hazardous wind shear as applied to NASA 1991 radar flight experiment data p 490 N93-19612
- ### GROUND EFFECT MACHINES
- Aerodynamic environment of an advanced short takeoff and vertical landing aircraft in hover p 231 A93-14539
- Lift enhancement of ground-effect wing. I - Results of screening tests of various concepts p 271 A93-21737
- Lift enhancement of ground-effect wing. II - Experimental investigation of the power augmented ram wing in ground effect through the wind tunnel p 271 A93-21738
- Compressible flow in a hovercraft air cushion p 480 A93-29316
- Russians completing new ground-effect vehicle p 853 A93-38535
- Canadian experience with air cushion vehicle skirts p 837 A93-39722
- On hovercraft overwater heave stability p 1219 A93-53819
- Kelvin-Helmholtz wave generation beneath hovercraft skirts p 1219 A93-53820
- ### GROUND HANDLING
- Loads at the nose landing gears of civil transport aircraft during towbarless towing operations p 45 A93-13629
- The human factors aspects of aircraft ground handling p 237 A93-18756
- ### GROUND OPERATIONAL SUPPORT SYSTEM
- The X-15/HL-20 operations support comparison [NASA-TM-4453] p 1017 N93-32379
- ### GROUND RESONANCE
- Influence of pitch-lag coupling on damping requirements to stabilize 'ground/air resonance' p 158 A93-14784
- The cusp catastrophe and the stability problem of helicopter ground resonance p 1099 A93-48059
- Rigid body mode identification of the PAH-2 helicopter using the eigensystem realization algorithm [NASA-TM-107690] p 88 N93-11544
- ### GROUND SPEED
- Aircraft turns into and down wind [AERO-REPT-9201] p 337 N93-18131
- ### GROUND STATIONS
- GPS integrity monitoring and system improvement with ground station and multistationary satellite support p 33 A93-11044
- Appraisal of digital terrain elevation data for low-altitude flight [NASA-TM-103896] p 35 N93-10745
- ### GROUND SUPPORT EQUIPMENT
- Steering system of a vehicle, such as a snow removing machine for airfields [CA-PATENT-APPL-SN-1293201] p 83 N93-10367
- Waterborne polyurethane binder resins for compliant aircraft coatings p 199 N93-14573
- The Teledyne controls aircraft condition monitoring system p 168 N93-15155
- Ground Support Equipment (GSE) for Aircraft Condition Monitoring System (ACMS) p 110 N93-15158
- ### GROUND SUPPORT SYSTEMS
- A proposed multi-modal FM/CW aircraft radar for use during ground operations p 206 A93-14678
- Failure diagnostic with MAINTEx based on AIMS at Swissair p 110 N93-15181
- Personal computer based test- and emulation equipment for maintenance and ground support p 110 N93-15185
- Using software metrics and software reliability models to attain acceptable quality software for flight and ground support software for avionics systems p 442 N93-17305
- An approach to evaluating reactive airborne wind shear systems p 489 N93-19600
- ### GROUND TESTS
- Effects of vitiated air on the results of ground tests of scramjet combustor p 173 A93-16234
- Comparison of advanced turboprop interior noise control ground and flight test data p 444 A93-19136
- Air/helium ground-test simulation pertinent to the definition of slender body hypersonic aerodynamics [AIAA PAPER 93-0318] p 268 A93-21106
- Comparison of experimental ground testing and computational fluid dynamics for the re-engined 727-100 center engine inlet [AIAA PAPER 92-3920] p 462 A93-24294
- Trends in international aerospace ground test facilities [AIAA PAPER 93-0348] p 528 A93-25518
- Ground vibration test on Piaggio P. 180 aircraft - Comparison between two modal test methods p 509 A93-29246
- Application of FEM model correlation and updating techniques on an aircraft using test data of a ground vibration survey p 509 A93-29267
- Hover testing a demonstrated and cost-effective risk reduction tool [AIAA PAPER 93-2677] p 913 A93-42234
- Development and operation of new arc heater technology for a large-scale scramjet propulsion test facility [AIAA PAPER 93-2786] p 1016 A93-46528
- A report on the status of MHD hypersonic ground test technology in Russia [AIAA PAPER 93-3193] p 1012 A93-46656
- Langley proposed advanced hypervelocity aerophysics facility - A status report p 1013 A93-47015
- Advancing the state of the art hypersonic testing - HYTEST/MTMI [AIAA PAPER 93-2023] p 1113 A93-49860
- Ground test simulation fidelity of turbine engine airstarts [AIAA PAPER 93-2173] p 1137 A93-49986
- Recent successes in modifying several existing jet engine test cells to accommodate large, high-bypass turbofan engines [AIAA PAPER 93-2542] p 1139 A93-50266
- Complementary role of ground testing, flight testing, and computations in aerospace plane propulsion development [ISABE 93-7034] p 1197 A93-54010
- Novel nozzle p 1245 A93-54450
- A preliminary study associated with the experimental measurement of the aero-optic characteristics of hypersonic configurations [AD-A253792] p 24 N93-12063
- The jet behaviour of an actual high-bypass engine as determined by LDA-measurements in ground tests p 175 N93-13218
- Technology benefits and ground test facilities for high-speed civil transport development [NASA-TM-107670] p 378 N93-15790
- Hot experimental technique: A new requirement of aerothermodynamics [MBB-FE-202-S-PUB-480] p 293 N93-17543
- Flight Testing [AGARD-CP-519] p 510 N93-19901

SUBJECT INDEX

Development of a large-scale, outdoor, ground-based test capability for evaluating the effect of rain on airfoil lift
[NASA-TM-4420] p 779 N93-26899

The HYDICE instrument design and its application to planetary instruments p 842 N93-28766

Flight test of avionic and air-traffic control systems [ESA-TT-1279] p 993 N93-31271

Ground installations for preparation and evaluation of flight tests p 1014 N93-31274

GROUND WAVE PROPAGATION
Effect of skywave interference on the coverage of Loran-C p 33 A93-11095

GROUND WIND
The dynamics of microbursts as revealed by Doppler radar observations and numerical simulations p 432 A93-22196

Surface drag instabilities in the atmospheric boundary layer p 1163 A93-49069

GROUND-AIR-GROUND COMMUNICATION
A minimum rate of position reporting in the future oceanic air traffic control system p 30 A93-11006

Data communication for airborne differential GPS/GLONASS application p 499 A93-27910

FAA Technical Center Aeronautical Data Link Research Plan [DOT/FAA/CT-92/23] p 417 N93-15698

Enhancing availability, performance, and flexibility of air traffic control air-ground services p 887 N93-30353

Testing concept of a taxiing control system, summary p 1010 N93-31278

GROUP THEORY
Evaluation of RNG algebraic turbulence models for boundary layers p 684 A93-34331

GRUMMAN AIRCRAFT
The benefits of Maglev technology [AIAA PAPER 93-2949] p 1174 A93-48145

GUIDANCE (MOTION)
Accuracy analysis on image matching guidance systems p 62 A93-12653

A simulator solution for the parachute canopy control and guidance training problem [SAE PAPER 920984] p 191 A93-14634

GUIDANCE SENSORS
The Texas Instruments/Honeywell GPS Guidance Package p 32 A93-11015

Sensors and sensor systems for guidance and navigation; Proceedings of the Meeting, Orlando, FL, Apr. 2, 3, 1991 [SPIE-1478] p 532 A93-27043

DLR research program overview on airport surface movement guidance and control p 499 A93-27912

Sensors and sensor systems for guidance and navigation II; Proceedings of the Meeting, Orlando, FL, Apr. 22, 23, 1992 [SPIE-1694] p 547 A93-28151

GUIDE VANES
Aerodynamic design of pivotable nozzle vanes for radial-inflow turbines [ASME PAPER 92-GT-94] p 349 A93-19340

Heat transfer and aerodynamics of a high rim speed turbine nozzle guide vane with profiled end walls [ASME PAPER 92-GT-243] p 253 A93-19452

Ingestion into the upstream wheel-space of an axial turbine stage [ASME PAPER 92-GT-303] p 354 A93-19493

Rotor blade unsteady aerodynamic gust response to inlet guide vane wakes [ASME PAPER 91-GT-129] p 475 A93-26897

A comparison between numerical models and measurements in a Kaplan turbine guide vanes p 685 A93-34339

Three dimensional aero-thermal characteristics of a high pressure turbine nozzle guide vane p 1002 A93-46942

Intensive industrial use of 3D Euler numerical methods for axial flow turbine analysis and design p 1002 A93-46943

Viscous analysis of high pressure turbine inlet guide vane flow including cooling injections [AIAA PAPER 93-1798] p 1074 A93-49687

Numerical study on inception of stall cells in rotating stall [ISABE 93-7007] p 1183 A93-53983

Comparison of radiated noise from shrouded and unshrouded propellers p 1264 A93-55861

L.D.V. measurements of unsteady flow fields in radial turbine [AD-A255728] p 221 N93-15065

Heat transfer and aerodynamics of a high rim speed turbine nozzle guide vane with profiled end walls [AD-A258346] p 295 N93-17991

Heat transfer and aerodynamics of a 3D design nozzle guide vane tested in the Pyestock Isentropic Light Piston Facility p 901 N93-29928

Thermal effects of a coolant film along the suction side of a high pressure turbine nozzle guide vane p 901 N93-29930

Aero-thermal design of a cooled transonic NGV and comparison with experimental results p 904 N93-29857

Coupling of 3D-Navier-Stokes external flow calculations and internal 3D-heat conduction calculations for cooled turbine blades p 904 N93-29961

GUN LAUNCHERS
Initiation of combustion in the thermally choked ram accelerator p 1016 A93-45501

GUST ALLEVIATORS
Turbulence/gust alleviation using spoiler control p 369 A93-22886

Simultaneous structure/control design optimization of a wing structure with a gust load alleviation system p 525 A93-28616

GUST LOADS
A proposal concerning the dynamic analysis method of continuous gust design rules p 181 A93-14197

Integrated control law synthesis of gust load alleviation and flutter margin augmentation for a transport aircraft p 182 A93-14281

Forcing function effects on unsteady aerodynamic gust response. I - Forcing functions [ASME PAPER 92-GT-174] p 251 A93-19400

Forcing function effects on unsteady aerodynamic gust response. II - Low solidity airfoil row response [ASME PAPER 92-GT-175] p 251 A93-19401

Unsteady aerodynamics and gust response in compressors and turbines [ASME PAPER 92-GT-422] p 258 A93-19570

Detection of microburst-related gust fronts using Doppler radar p 427 A93-22118

Improvement in gust front algorithm detection capability using reflectivity thin lines versus azimuthal shears p 427 A93-22120

A fine structure of the gust front observed with sonic anemometer p 430 A93-22158

An improved gust front detection algorithm for the TDWR p 432 A93-22191

Forcing function generator fluid dynamic effects on compressor blade gust response [AIAA PAPER 93-0157] p 275 A93-22594

Rotor blade unsteady aerodynamic gust response to inlet guide vane wakes [ASME PAPER 91-GT-129] p 475 A93-26897

Simultaneous structure/control design optimization of a wing structure with a gust load alleviation system p 525 A93-28616

Further studies using matched filter theory and stochastic simulation for gust loads prediction [AIAA PAPER 93-1365] p 726 A93-33932

Estimation of wing stability in flow from the characteristics of the transient process p 836 A93-39177

Alternative approximations for integrated control/structure aeroservoelastic synthesis p 819 A93-39418

A wind shear hazard window useful in studying the effect of wind shear on the airplane during the landing approach [AIAA PAPER 93-3643] p 1127 A93-48327

Effect of rotary atmospheric gusts on fighter airplane [AIAA PAPER 93-3644] p 1127 A93-48328

Investigation of roll requirements for carrier approach [AIAA PAPER 93-3649] p 1128 A93-48332

Response of B-2 aircraft to nonuniform spanwise turbulence p 1135 A93-52437

Computation of maximized gust loads for nonlinear aircraft using matched-filter-based schemes p 1136 A93-52452

Forcing function modeling for flow induced vibration [ISABE 93-7027] p 1196 A93-54003

Estimation of aerodynamic characteristics from flight-test data. V - Effects of gust and its time lag p 1230 A93-54560

An airfoil in transonic flow in the presence of wind gusts and weak shock waves p 1233 A93-55015

Flight simulation and constant amplitude fatigue crack growth in aluminum-lithium sheet and plate [NLR-TP-91104-U] p 331 N93-17562

GUSTS
Effect of stress level of gust cycles on fatigue crack propagation behavior (Acceleration and retardation of crack propagation under simplified flight simulation loading) p 198 A93-17033

Stratospheric turbulence measurements and models for aerospace plane design [AIAA PAPER 92-5072] p 433 A93-22342

Lift and pitching moment measurements in vertical gusts p 906 A93-42259

The measurement of the velocity field induced by a gust generator in a closed-circuit subsonic wind-tunnel [RAE-TM-MAT/STR-1102] p 67 N93-11435

HANDLING EQUIPMENT

Stratospheric turbulence measurements and models for aerospace plane design [NASA-TM-104262] p 223 N93-13288

Multi-disciplinary optimization of aeroservoelastic systems [NASA-CR-191255] p 220 N93-14766

General aviation aircraft: Normal acceleration data analysis and collection project [DOT/FAA/CT-91/20] p 713 N93-24739

GYROCOMPASSES
Damping of a gyro horizon-compass with arbitrary displacement of the suspension point p 1025 A93-45684

GYRODAMPERS
Damping of a gyro horizon-compass with arbitrary displacement of the suspension point p 1025 A93-45684

GYROSCOPIC COUPLING
Optimum design of rotor-bearing systems with eigenvalue constraints [ASME PAPER 92-GT-307] p 405 A93-19497

GYROSCOPIC PENDULUMS
Damping of a gyro horizon-compass with arbitrary displacement of the suspension point p 1025 A93-45684

GYROSCOPIC STABILITY
Improving the service characteristics of an aircraft through the gyroscopic damping of its structure p 366 A93-18363

H

H-INFINITY CONTROL
Refined H-infinity controller design for rotorcraft flight control p 368 A93-22882

Robust integrated flight/p propulsion control design for a STOVL aircraft using H-infinity control design techniques p 524 A93-26432

Design of a flight control system for a highly maneuverable aircraft using mu synthesis [AIAA PAPER 93-3776] p 1132 A93-51371

H(infinity) helicopter flight control law design with and without rotor state feedback [AIAA PAPER 93-3849] p 1134 A93-51436

Design of a helicopter control system to meet handling quality specifications using H(infinity) techniques [AIAA PAPER 93-3850] p 1134 A93-51437

A problem formulation for glideslope tracking in wind shear using advanced robust control techniques [NASA-TM-104164] p 64 N93-11176

Strategies for optimal control design of normal acceleration command following on the F-16 [AD-A258975] p 373 N93-19095

H-53 HELICOPTER
Sikorsky Aircraft Advanced Rotorcraft Transmission (ART) program [NASA-CR-191079] p 840 N93-27268

H-60 HELICOPTER
A critical assessment of UH-60 main rotor blade airfoil data [AIAA PAPER 93-3413] p 975 A93-47210

Statistical fatigue analysis of the SH-60B servo beam rail component [AD-A257474] p 332 N93-17660

HAFNIUM OXIDES
Microstructure of yttria stabilized zirconia-hafnia plasma sprayed thermal barrier coatings [ONERA, TP NO. 1993-54] p 1146 A93-51936

HAIL
Slicing model for foreign soft-body objects impacting on blade rows p 28 A93-12372

Studies into the hail ingestion characteristics of turbofan engines [AIAA PAPER 93-2174] p 1115 A93-49987

HAILSTORMS
Maximum hail concentration that can be met by an aircraft in stormy precipitations p 430 A93-22152

HAMILTON-JACOBI EQUATION
Matched asymptotic expansion of the Hamilton-Jacobi-Bellman equation for aeroassisted plane-change maneuvers [AIAA PAPER 93-3752] p 1143 A93-51348

HAMMERHEAD CONFIGURATION
Hammerhead aeroelastic stability revisited [AIAA PAPER 93-1477] p 740 A93-34022

HANDBOOKS
Wright Laboratory research and development facilities handbook [AD-A258746] p 572 N93-20403

Particulate emissions from gas turbine engines [AD-A261374] p 725 N93-26339

HANDLING EQUIPMENT
A simulator study into low speed longitudinal handling qualities of ACT transport aircraft [NLR-TP-89387-U] p 527 N93-20743

- Transmission system for a transfer device gripping a double wheel
[CA-PATENT-APPL-SN-2024585] p 731 N93-25178
- HANG GLIDERS**
- Combining direct and indirect methods in optimal control: Range maximization of a hang glider
[REPT-313] p 371 N93-16618
- HARDENING (MATERIALS)**
- Enhancing the performance of aircraft engine blades by surface hardening p 811 A93-39072
- Increasing the durability of gas turbine engine compressor blades by using a combined hardening/finishing treatment to control the stressed state of the surface layer p 835 A93-39099
- Hardening/finishing treatment of compressor blades using a machine with planetary container motion p 835 A93-39102
- A mathematical model of the vibrational impact hardening of parts p 837 A93-39185
- HARDWARE**
- Design philosophies of the Basic Research Simulator p 191 A93-14414
- Dual control vibration tests of flight hardware p 545 A93-27782
- The importance of configuration management - An overview with test program sets p 853 A93-35926
- HARMONIC ANALYSIS**
- Harmonic analysis of the aerodynamic forces on a Darrieus rotor p 18 N93-10551
- HARMONIC CONTROL**
- Nonlinear rotor-fuselage coupled response to generic periodic control modes using advanced computation techniques p 153 A93-14226
- HHC study in the DNW to reduce BVI noise - An analysis p 565 A93-29405
- A closed loop controller for BVI impulsive noise reduction by Higher Harmonic Control p 849 A93-35963
- Performance of higher harmonic control algorithms for helicopter vibration reduction p 890 A93-41904
- Application of two chaos methods to Higher Harmonic Control data --- for suppression of helicopter vibration p 909 A93-43783
- Experimental and analytical investigation of the vibration characteristics of a remotely piloted helicopter
[AD-A256131] p 163 N93-14248
- HARMONIC EXCITATION**
- Subharmonic bifurcation analysis of wing with store flutter p 78 A93-12098
- HARMONIC FUNCTIONS**
- Calculation of three-dimensional unsteady flows in turbomachinery using the linearized harmonic Euler equations
[ASME PAPER 92-GT-136] p 249 A93-19368
- HARMONIC MOTION**
- Analytic continuation of Pade approximations to the unsteady kernel functions to obtain a better understanding of the analytic continuation of Pade approximations to unsteady parameters in general p 117 A93-14283
- HARMONIC OSCILLATION**
- A low-speed aerodynamic model for harmonically oscillating aircraft configurations p 8 A93-11500
- Subharmonic and harmonic forced response of the wake of a circular cylinder p 288 A93-23565
- Incompressible potential flow calculation about harmonically oscillating three-dimensional configurations p 461 A93-24089
- Investigation of subharmonic response of limit cycle flutter of wing-store system p 800 A93-36339
- Stability of fluttered panels subjected to in-plane harmonic forces p 1151 A93-49017
- Streaming vorticity flux from oscillating walls with finite amplitude p 1160 A93-52517
- Harmonic oscillation in FBW system p 1206 A93-53877
- Development of nonlinear aerodynamic models for unsteady responses p 19 N93-10845
- HARMONIC RADIATION**
- An optimal detection algorithm for harmonic interference signals in Loran-C p 993 A93-46889
- HARMONICS**
- A generic harmonic rotor model for helicopter flight simulation p 506 A93-27480
- HARNESSES**
- High voltage quick-disconnect harness system for helmet-mounted displays p 516 A93-25922
- HARRIER AIRCRAFT**
- Navier-Stokes simulation of external/internal transonic flow on the forebody/inlet of the AV-8B Harrier II
[AIAA PAPER 93-3057] p 1058 A93-48234
- Evolution of the SIIIS-3 Ejection Seat into a Reduced Weight (RW) ejection seat p 1239 A93-54549
- Pressure distribution for the wing of the YAV-8B airplane, with and without pylons
[NASA-TM-4429] p 136 N93-14451
- Royal Air Force experience of the Harrier information management system p 234 N93-15170

HASTELLOY (TRADEMARK)

- Evaluation of metallurgical degradation on gas turbine components p 915 A93-40804

HAZARDS

- The Orlando TDWR testbed and airborne wind shear date comparison results p 145 N93-14851
- T-38 forward windshield development and performance demonstration report
[AD-A259240] p 513 N93-20579
- Proceedings of the Aircraft Wake Vortices conference, volume 1
[PB93-126449] p 485 N93-21796
- Proceedings of the Aircraft Wake Vortices conference, volume 2
[PB93-127728] p 559 N93-21799
- A review of civil aviation propeller-to-person accidents: 1980-1989
[AD-A260695] p 705 N93-25896

HAZE

- Uplink laser propagation measurements through the sea surface, haze and clouds
[AD-A264687] p 935 N93-30553

HEAD (ANATOMY)

- The effectiveness of airbags in reducing the severity of head injury from gunsight strikes in attack helicopters p 494 N93-19691

HEAD-UP DISPLAYS

- Requirements for integrated flight and traffic management during final approach p 31 A93-11009
- Trends of the airborne cockpit display format p 50 A93-11203
- HUD Guidance for the ASKA Experimental STOL Aircraft using Radar Position Information
[SAE PAPER 921041] p 150 A93-14661
- Fixed and rotary wing all weather operations system requirements p 142 A93-17303
- The certification of head up displays for category 3 operation p 142 A93-17304
- A review of alternative philosophies --- methods for operating in ICAO category 3 weather conditions p 142 A93-17305
- The development and implementation of a head-up guidance system (HGS) for manual CAT III landings p 151 A93-17306
- F-14D flight director development, test, and evaluation p 803 A93-38840
- Displaying the night p 1244 A93-55297
- Advantages of using a projected head-up display in a flight simulator
[AD-A255332] p 194 N93-14559
- Simulator evaluation of displays for a revised takeoff performance monitoring system
[NASA-TP-3270] p 189 N93-15366
- Test techniques for evaluating flight displays
[NASA-TM-103947] p 516 N93-21810

HEARING

- In-flight evaluation of noise levels and assessment of active noise reduction systems in the Seahawk S-70B-2 helicopter
[AD-A260689] p 759 N93-25649
- Design, fabrication, and testing of a three-dimensional acoustic orientation instrument (3-D AOI): Drawings, engineering and associated lists (conceptual and development design)
[AD-A260934] p 760 N93-25915

HEAT ENGINES

- The multi-heat addition turbine engine
[AIAA PAPER 92-4272] p 54 A93-13334
- Materials development program, ceramic technology project addendum to program plan: Cost effective ceramics for heat engines
[DE93-003663] p 394 N93-18537
- Process optimization of Hexoloy SX-SiC towards improved mechanical properties
[DE93-007913] p 826 N93-28564

HEAT EXCHANGERS

- Studies of jet thermal stability in a flowing system
[ASME PAPER 92-GT-106] p 401 A93-19344
- Heat exchangers of gas turbine engines p 833 A93-39044
- Calculation of a collector-type annular plate heat exchanger p 833 A93-39045
- A model for calculating the element of a high-temperature heat exchanger with spiral-wire fins p 833 A93-39046
- A heat transfer element of a high-temperature heat exchanger p 833 A93-39047
- The use of aviation gas-liquid heat exchangers employing heat pipes p 833 A93-39050
- Operation of a cross-flow heat exchanger with partial recirculation of one of the coolants p 833 A93-39051
- A fuel-oil matrix heat exchanger p 833 A93-39052
- Development of a process for fabricating a plate heat exchanger for the heat recovery system of gas turbine engines p 834 A93-39053

- Determination of the dynamic characteristics of heat exchangers for the heat recovery system of gas turbine engines p 834 A93-39054
- Solution of the problem of determining the dynamic characteristics of the cross-flow heat exchanger of the heat recovery system of gas turbine engines p 834 A93-39055
- A method for calculating the dynamic characteristics of heat exchangers with single-phase cryogenic coolants p 851 A93-39057
- Study on dynamic characteristics of heat exchanger p 924 A93-40492
- Thermal control of a lidar laser system using a non-conventional ram air heat exchanger p 1028 A93-46821
- High temperature heat exchangers for gas turbines and future hypersonic air breathing propulsion
[ONERA, TP NO. 1993-75] p 1218 A93-53596
- Characteristics of heat exchanger in supersonic/subsonic flows
[ISABE 93-7119] p 1221 A93-54094
- Compact heat exchanger fitted to engines of the inverted type
[ISABE 93-7120] p 1221 A93-54095
- An evaluation of thermal energy storage options for precooled gas turbine inlet air
[DE93-005980] p 754 A93-24975
- By-passing of heat exchangers in gas turbines p 814 N93-27189

HEAT FLUX

- Evaluation of 2D scramjet nozzle performance p 52 A93-11209
- Influence of surface heat flux ratio on heat transfer augmentation in square channels with parallel, crossed, and V-shaped angled ribs p 201 A93-13981
- Experimental investigation of hydrogen burning and heat transfer in annular duct at supersonic velocity p 171 A93-14247
- Direct measurements of skin friction in supersonic combustion flow fields
[ASME PAPER 92-GT-320] p 405 A93-19506
- Spatial and temporal variations of the fluxes of carbon dioxide and sensible and latent heat over the FIFE site p 425 A93-20586
- FIFE atmospheric boundary layer budget methods p 426 A93-20591
- Heat flux microsensor measurements
[AIAA PAPER 92-5038] p 413 A93-22312
- The effect of entrance radius and film injection on wall heating in scramjet nozzles p 360 A93-22505
- Time-resolved surface heat flux measurements in the wing/body junction vortex
[AIAA PAPER 93-0918] p 472 A93-24972
- Thin gradient heat fluxmeters developed at ONERA
[ONERA, TP NO. 1992-87] p 831 A93-38571
- Microsensors for high heat flux measurements p 928 A93-42920
- Effects of longitudinal vortex generators on heat transfer and flow loss in turbulent channel flows p 1021 A93-44222
- An approximate method for calculating heating rates on three-dimensional vehicles
[AIAA PAPER 93-2881] p 949 A93-44228
- Applications of infrared measurement technique in hypersonic facilities p 1024 A93-45505
- A preliminary investigation of the Helmholtz resonator concept for heat flux reduction
[AIAA PAPER 93-2742] p 963 A93-46493
- Progress towards understanding and predicting heat transfer in the turbine gas path p 1215 A93-52751
- Application of functionally gradient materials to scramjet engines
[ISABE 93-7063] p 1200 A93-54039
- Static and dynamic errors in heat flux measurements p 1254 A93-54366
- Heat loads as key problem of hypersonic flight
[MBB-FE-202-S-PUB-0486] p 484 N93-21054
- Surface shear stress estimates from geostrophic winds for use in sensible and latent heat flux formulations p 936 N93-30044
- Hypersonic engine component experiments in high heat flux, supersonic flow environment
[NASA-TM-106273] p 1032 N93-31860
- HEAT GENERATION**
- Development of a process for fabricating a plate heat exchanger for the heat recovery system of gas turbine engines p 834 A93-39053
- HEAT MEASUREMENT**
- Digital image processing applied to heat transfer measurement in hypersonic wind tunnel
[ONERA, TP NO. 1992-118] p 831 A93-38593
- Microsensors for high heat flux measurements p 928 A93-42920
- Static and dynamic errors in heat flux measurements p 1254 A93-54366

SUBJECT INDEX

Study of optical techniques for the Ames unitary wind tunnel. Part 5: Infrared imagery
[NASA-CR-191385] p 194 N93-14809

HEAT OF COMBUSTION

Choice of the heating system for high-temperature generators using chemical fuel p 559 A93-29660
Energy management --- aircraft propulsion system performance
[ISABE 93-7019] p 1195 A93-53995

HEAT OF VAPORIZATION

Evaporation and specific heats of motor fuels p 71 A93-12823

HEAT PIPES

Niobium alloy heat pipes for use in oxidizing environments p 200 A93-13791
A thermal analysis of an F/A-18 wing section for actuator thermal management p 158 A93-14650
[SAE PAPER 92-023] p 158 A93-14650
Joining carbon composite fins to metal heat pipes using ion beam techniques p 543 A93-25979
Heat pipe turbine vane cooling p 519 A93-26114
The use of aviation gas-liquid heat exchangers employing heat pipes p 833 A93-39050
Flight data for the Cryogenic Heat Pipe (CRYOHP) Experiment
[AIAA PAPER 93-2735] p 1027 A93-46488
Conjugate modeling of high-temperature nosecon and wing leading edge heat pipes p 1259 A93-55465
Thermostructural applications of heat pipes for cooling leading edges of high-speed aerospace vehicles p 91 N93-12460
Optimization of an internally finned rotating heat pipe [AD-A256725] p 453 N93-15980
Joining carbon composite fins to titanium heat pipes [AD-A261970] p 825 N93-27667

HEAT PUMPS

Electro-modulated control of supply pressure in hydraulic systems p 412 A93-21842
[SAE PAPER 91-2119] p 412 A93-21842
Variable speed rotary compressor and adjustable speed drive efficiencies measured in the laboratory [DE92-040026] p 222 N93-15278

HEAT RADIATORS

High pressure ratio intercooled turboprop study [ASME PAPER 92-GT-405] p 356 A93-19554

HEAT RESISTANT ALLOYS

Raising the high temperature limit of the nickel-iron-base superalloy p 70 A93-12114
Midhani alloys in aeronautical service p 70 A93-12368
The development of titanium alloys for gas turbines p 197 A93-15031
Markov fatigue in single crystal airfoils [ASME PAPER 92-GT-95] p 387 A93-19341
Powder metallurgy repair of turbine components [ASME PAPER 92-GT-312] p 354 A93-19500
Effects of grain size and carbides on the creep resistance and rupture properties of a conventionally cast nickel-base superalloy p 389 A93-21699
Gas phase hydrogen permeation in a Ni-Fe-Co superalloy p 735 A93-34510
Resource conservation and improvement of the service characteristics of castings of high-temperature nickel alloys through a high-temperature melt treatment p 824 A93-36718
Designing new multi-phase intermetallic materials based on phase compatibility considerations [ONERA, TP NO. 1992-131] p 772 A93-38605
Materials problems connected with the propulsion of supersonic air carriers [ONERA, TP NO. 1992-157] p 824 A93-38736
Recent evolution of gas turbine materials and the development of models for life prediction p 915 A93-40802
Crack simulation and life assessment of gas turbine nozzles p 915 A93-40805
Life prediction - Thermal fatigue from isothermal data p 916 A93-40807
Creep crack growth and tail part behavior of low alloy steels and Ni based super alloy p 916 A93-40808
New corrosion resistant nickel-base super-alloys and technological processes of casting gas turbines parts with directional single crystal and regulable equiaxial minimized microporosity structure p 916 A93-40811
Concurrent field service and laboratory testing as a means of improving reliability in creep-rupture applications p 916 A93-40814
Effect of environment on creep-fatigue crack propagation in turbine disc superalloys [ONERA, TP NO. 1993-5] p 916 A93-41023
Infrared thermography of plastic instabilities in a single crystal superalloy [ONERA, TP NO. 1993-18] p 916 A93-41031
Boeing 777 gets a boost from titanium p 1018 A93-45987

Measurements of dynamic Young's modulus and damping in single crystals of a nickel-based superalloy as a function of temperature p 1147 A93-52513
Clean melting and the removal of defects from aero-engine materials p 1217 A93-53503
Material requirements for the High Speed Civil Transport [ISABE 93-7067] p 1200 A93-54043
Ultra-high temperature materials in the research and development of super/hypersonic transport propulsion system p 1252 A93-54712
Mechanisms and modelling of environment-dependent fatigue crack growth in a nickel based superalloy [AD-A253967] p 71 N93-10717
Erosion predictions and measurements of high-temperature coatings and superalloys used in turbomachines p 74 N93-12189
Fatigue in single crystal nickel superalloys [AD-A254603] p 74 N93-12237
Fatigue in single crystal nickel superalloys [AD-A254704] p 198 N93-12746
HIP consolidation of aluminum-rich intermetallic alloys and their composites [NAWCADWAR-92003-60] p 199 N93-14726
Fiber reinforced composites: A new class of glass and glass ceramic materials for thermomechanical applications [REPT-921-430-104] p 200 N93-15490
Deformation mechanisms of NiAl cyclically deformed near the brittle-to-ductile transformation temperature [NASA-CR-191649] p 391 N93-15830
Fatigue in single crystal nickel superalloys [AD-A258038] p 393 N93-17704
Supersonic transport: Which material for the engine [DS-2023] p 522 N93-21459
Selection criteria for metallic high temperature structural materials in hypersonic flying equipment [MBB-LME-221-HYPAC-PUB-2-A] p 515 N93-21479
Fatigue in single crystal nickel superalloys [AD-A260709] p 736 N93-25843
Fatigue in single crystal nickel superalloys [AD-A261742] p 737 N93-26282
Platinum-modified diffusion aluminide coatings on nickel-base superalloys p 917 N93-29981
Fatigue in single crystal nickel superalloys [AD-A265451] p 1019 N93-31795

HEAT SINKS

USAF supercritical hydrocarbon fuels interests [AIAA PAPER 93-0807] p 533 A93-24883
Heat pipe turbine vane cooling p 519 A93-26114
Extended surface heat sinks for electronic components: A computer optimization [AD-A256134] p 218 N93-14254
Performance of thermal adhesives in forced convection p 924 N93-30974

HEAT SOURCES

USAF supercritical hydrocarbon fuels interests [AIAA PAPER 93-0807] p 533 A93-24883

HEAT STORAGE

Enhanced heat transport in environmental systems using microencapsulated phase change materials [SAE PAPER 92-1224] p 926 A93-41398
Engine driven chiller and thermal storage integration (Large tonnage engine driven chiller development) [PB92-227891] p 555 N93-21465
An evaluation of thermal energy storage options for precooled gas turbine inlet air [DE93-005980] p 754 N93-24975

HEAT TRANSFER

Recent refinements and increased capabilities in balloon vertical performance analysis p 40 A93-11361
Experiments on Space Shuttle Orbiter models in a free piston shock tunnel p 7 A93-11497
Effect of wall heating on a supersonic turbulent boundary layer p 11 A93-12429
Effect of heat supply on the gasdynamic parameters of gas flow in Laval nozzles p 12 A93-12760
Vaporizer performance p 79 A93-12784
The conceptual study of supersonic transport structure [AIAA PAPER 92-4219] p 43 A93-13348
Heat transfer, adiabatic effectiveness, and injectant distributions downstream of a single row and two staggered rows of compound angle film-cooling holes p 201 A93-13976
Navier-Stokes analysis of turbine blade heat transfer and performance p 201 A93-13978
Comparison of heat transfer measurements with computations for turbulent flow around a 180 deg bend p 201 A93-13980
Experimental investigation of hydrogen burning and heat transfer in annular duct at supersonic velocity p 171 A93-14247
Heat transfer performance comparisons of five different rectangular channels with parallel angled ribs p 397 A93-18752

HEAT TRANSFER

Hot streaks and phantom cooling in a turbine rotor passage. II - Combined effects and analytical modelling [ASME PAPER 92-GT-76] p 401 A93-19326
Surface-curvature-distribution effects on turbine-cascade performance [ASME PAPER 92-GT-84] p 248 A93-19333
Innovative high temperature aircraft engine fuel nozzle design [ASME PAPER 92-GT-132] p 350 A93-19365
The dynamic characteristics of a high pressure turbine stage in a transient wind tunnel [ASME PAPER 92-GT-166] p 375 A93-19392
Effect of trailing-edge ejection on local heat (mass) transfer in pin fin cooling channels in turbine blades [ASME PAPER 92-GT-178] p 352 A93-19404
Heat transfer in serpentine flow passages with rotation [ASME PAPER 92-GT-190] p 403 A93-19415
Heat transfer in rotating serpentine passages with trips skewed to the flow [ASME PAPER 92-GT-191] p 403 A93-19416
An experimental study of heat transfer in a large-scale turbine rotor passage [ASME PAPER 92-GT-195] p 403 A93-19420
Internal cooling passage heat transfer near the entrance to a film cooling hole - Experimental and computational results [ASME PAPER 92-GT-241] p 404 A93-19450
Heat transfer and aerodynamics of a high rim speed turbine nozzle guide vane with profiled end walls [ASME PAPER 92-GT-243] p 253 A93-19452
Measurements of the effect of free-stream turbulence length scale on heat transfer [ASME PAPER 92-GT-244] p 405 A93-19453
Aircraft experiments on microgravity pool boiling - Vapor-liquid behaviour and heat transfer characteristics in boiling of n-pentane, CFC-113 and water p 410 A93-20920
Effects of compression and expansion ramp fuel injector configuration on scramjet combustion and heat transfer [AIAA PAPER 93-0609] p 358 A93-21114
An algebraic turbulence model for three-dimensional viscous flows [AIAA PAPER 93-0083] p 274 A93-22552
Close-up analysis of aircraft ice accretion [AIAA PAPER 93-0029] p 309 A93-23239
The design of a senior-level CAD course with emphasis on fluid/thermal systems [AIAA PAPER 93-0426] p 454 A93-23344
A model for calculating the element of a high-temperature heat exchanger with spiral-wire fins p 833 A93-39046
A fuel-oil matrix heat exchanger p 833 A93-39052
Determination of the dynamic characteristics of heat exchangers for the heat recovery system of gas turbine engines p 834 A93-39054
Solution of the problem of determining the dynamic characteristics of the cross-flow heat exchanger of the heat recovery system of gas turbine engines p 834 A93-39055
Modeling of the physicochemical processes of nonequilibrium heat transfer in the subsonic jets of an induction plasmatron p 836 A93-39147
Enhanced heat transport in environmental systems using microencapsulated phase change materials [SAE PAPER 92-1224] p 926 A93-41398
Applications of liquid crystal surface thermography to hypersonic flow p 1023 A93-45504
Solution strategy for three-dimensional configurations at hypersonic speeds p 962 A93-46406
Thermal analysis of an arc heater electrode with a rotating arc foot [AIAA PAPER 93-2855] p 1028 A93-46590
Analysis of the effect of surface heating on boundary layer development over an NLS-0215 airfoil [AIAA PAPER 93-3437] p 978 A93-47229
Computation of hypersonic flow past blunt body for nonequilibrium weakly ionized air [AIAA PAPER 93-2995] p 1053 A93-48185
Experimental study on heat transfer of separated impinging jets in short distance p 1149 A93-48518
Heat Transfer and Fluid Mechanics Institute, 33rd, California State Univ., Sacramento, June 3, 4, 1993, Proceedings p 1152 A93-49505
Numerical analysis of high aspect ratio cooling passage flow and heat transfer [AIAA PAPER 93-1829] p 1153 A93-49714
The study of experimental turboramjets - Heat state and cooling problems [AIAA PAPER 93-1989] p 1112 A93-49834
High Reynolds number and turbulence effects on aerodynamics and heat transfer in a turbine cascade [AIAA PAPER 93-2252] p 1155 A93-50050
Chimera grids in the simulation of three-dimensional flowfields in turbine-blade-coolant passages [AIAA PAPER 93-2559] p 1157 A93-50280

- Effect of rotation on heat transfer and hydraulic resistance in the radial cooling channels of turbine rotor blades p 1215 A93-52950
- Measurements and computational analysis of heat transfer and flow in a simulated turbine blade internal cooling passage [AIAA PAPER 93-1797] p 1218 A93-53585
- Navier-Stokes analysis of turbine flowfield and external heat transfer [ISABE 93-7075] p 1186 A93-54051
- Numerical method for simulating fluid-dynamic and heat-transfer changes in jet-engine injector feed-arm due to fouling p 1245 A93-54467
- Heat transfer in a five-pass irregular channel with and without pin-fins p 1256 A93-54633
- Prediction of rotating disc flow and heat transfer in gas turbine engines p 1256 A93-54634
- Hypersonic flow of a gas past wing with heat transfer p 1234 A93-55030
- Local heat transfer distribution in a rotating serpentine rib-roughened flow passage p 1259 A93-55459
- Radial turbine cooling p 82 N93-10061
- Flow over a leading edge with distributed roughness p 18 N93-10549
- Experimental heat transfer results in turbine stators and rotors and a comparison with theory [PNR-90945] p 57 N93-11055
- An experimental study of flow patterns and endwall heat transfer upstream of a surface-mounted rectangular obstruction in a turbulent boundary layer p 89 N93-11698
- Investigation of hot streak migration and film cooling effects on heat transfer in rotor/stator interacting flows, report 1 [AD-A250688] p 102 N93-12490
- Simulation of two-dimensional icing, de-icing and anti-icing phenomena p 142 N93-13364
- An experimental/computational study of heat transfer in sharp fin induced shock wave/turbulent boundary layer interactions at low hypersonic Mach numbers p 217 N93-13826
- An algebraic turbulence model for three-dimensional viscous flows [NASA-TM-105931] p 110 N93-14102
- Close-up analysis of aircraft ice accretion [NASA-TM-105952] p 148 N93-15360
- Finite-difference solution for laminar or turbulent boundary layer flow over axisymmetric bodies with ideal gas, CF₄, or equilibrium air chemistry [NASA-TP-3271] p 222 N93-15434
- Hydrodynamic effects on heat transfer for film-cooled turbine blades [AD-A257291] p 361 N93-16080
- Heat transfer and aerodynamics of a high rim speed turbine nozzle guide vane with profiled end walls [AD-A258346] p 295 N93-17991
- Numerical analysis of the flow in a turbulated rectangular duct simulating the cooling passages in a turbine blade [AD-A257855] p 420 N93-18305
- Multidisciplinary tailoring of hot composite structures [NASA-TM-106027] p 550 N93-19971
- Multi-heat addition turbine engine [NASA-CASE-LEW-15094-1] p 522 N93-22034
- Measurements and computations of external heat transfer and film cooling in turbines [RAE-TM-P-1223] p 722 N93-25455
- Heat transfer measurements in swept shock wave/turbulent boundary-layer interactions p 750 N93-25705
- Two-dimensional fin analysis p 750 N93-25737
- Uniform roughness studies [WL-TR-92-3041] p 751 N93-25951
- Flow control of low heat load turbine airfoils [AD-A260941] p 724 N93-26219
- Influence of supercritical conditions on pre-combustion chemistry and transport behavior of jet fuels [AD-A261813] p 737 N93-26268
- Increased heat transfer to elliptical leading edges due to spanwise variations in the freestream momentum: Numerical and experimental results [NASA-TM-106150] p 838 N93-27020
- Regression rate mechanism in a solid fuel ramjet p 814 N93-27185
- Flow phenomena in turbomachines [AD-A263049] p 930 N93-29141
- High Reynolds number and turbulence effects on aerodynamics and heat transfer in a turbine cascade [NASA-TM-106187] p 930 N93-29157
- Heat Transfer and Cooling in Gas Turbines [AGARD-CP-527] p 901 N93-29926
- Heat transfer and aerodynamics of a 3D design nozzle guide vane tested in the Pyestock Isentropic Light Piston Facility p 901 N93-29928
- Experimental study of heat transfer close to a plane wall heated in the presence of multiple injections (subsonic flow) p 901 N93-29931
- The influence of non-uniform spanwise inlet temperature on turbine rotor heat transfer p 901 N93-29932
- Determination of surface heat transfer and film cooling effectiveness in unsteady wake flow conditions p 902 N93-29933
- Measurement of turbulent spots and intermittency modelling at gas-turbine conditions p 902 N93-29934
- Heat transfer in high turbulence flows: A 2-D planar wall jet p 932 N93-29935
- Heat transfer with moderate free stream turbulence p 932 N93-29936
- Cooling geometry optimization using liquid crystal technique p 902 N93-29939
- Prediction of jet impingement cooling scheme characteristics (airfoil leading edge application) p 932 N93-29941
- Local heat transfer measurement with liquid crystals on rotating surfaces including non-axisymmetric cases p 902 N93-29943
- Transient thermal behaviour of a compressor rotor with axial cooling air flow and co-rotating or contra-rotating shaft p 903 N93-29946
- Flow and heat transfer between gas-turbine discs p 903 N93-29950
- Heat transfer and leakage in high-speed rotating stepped labyrinth seals p 903 N93-29951
- Impingement/effusion cooling p 932 N93-29954
- Coupling of 3D-Navier-Stokes external flow calculations and internal 3D-heat conduction calculations for cooled turbine blades p 904 N93-29961
- Navier-Stokes analysis of three-dimensional flow and heat transfer inside turbine blade rows p 905 N93-29963
- Parametric studies of shock wave/boundary layer interactions over 2D compression corners at Mach 6 [VKI-TN-181] p 988 N93-31538
- Overview of aerothermodynamic loads definition study p 1016 N93-31583
- Measurements and computational analysis of heat transfer and flow in a simulated turbine blade internal cooling passage [NASA-TM-106189] p 1032 N93-31647
- ### HEAT TRANSFER COEFFICIENTS
- Two modified versions of Hsu-Lee's elliptic solver of grid generation p 95 A93-11085
- A study of heat transfer from a disk in a rotating cavity with axial and radial-axial flow of a liquid p 54 A93-12812
- Influence of surface heat flux ratio on heat transfer augmentation in square channels with parallel, crossed, and V-shaped angled ribs p 201 A93-13981
- Computation of laminar flow and heat transfer over an enclosed rotating disk with and without jet impingement p 201 A93-13982
- Influence of high mainstream turbulence on leading edge film cooling heat transfer - Effect of film hole spacing p 207 A93-15068
- Influence of surface heating condition on local heat transfer in a rotating square channel with smooth walls and radial outward flow [ASME PAPER 92-GT-188] p 402 A93-19413
- Heat transfer in rotating serpentine passages with trips skewed to the flow [ASME PAPER 92-GT-191] p 403 A93-19416
- Measurement of unsteady flow and heat transfer in a linear turbine cascade [ASME PAPER 92-GT-323] p 256 A93-19507
- Rotor cavity flow and heat transfer with inlet swirl and radial outflow of cooling air [ASME PAPER 92-GT-378] p 406 A93-19536
- Turbulence modeling for complex hypersonic flows [AIAA PAPER 93-0200] p 277 A93-22620
- Advancements in the LEWICE Ice Accretion Model [AIAA PAPER 93-0171] p 309 A93-23243
- Infrared thermography for hot-shot wind tunnel [ONERA, TP NO. 1992-103] p 831 A93-38583
- A heat transfer element of a high-temperature heat exchanger p 833 A93-39047
- The use of aviation gas-liquid heat exchangers employing heat pipes p 833 A93-39050
- A method for calculating the dynamic characteristics of heat exchangers with single-phase cryogenic coolants p 851 A93-39057
- Selection of the powerplant for a thermoplane p 899 A93-42380
- Measurements and computational analysis of heat transfer and flow in a simulated turbine blade internal cooling passage [AIAA PAPER 93-1797] p 1218 A93-53585
- Heat transfer and material temperature conditions in the leading edge area of impingement-cooled turbine vanes [ISABE 93-7076] p 1220 A93-54052
- Impingement cooling with film coolant extraction in the airfoil leading edge regions [ISABE 93-7078] p 1220 A93-54054
- Leading edge film cooling heat transfer including the effect of mainstream turbulence p 23 N93-11886
- Thermal effects of a coolant film along the suction side of a high pressure turbine nozzle guide vane p 9C1 N93-29930
- Cooling geometry optimization using liquid crystal technique p 902 N93-29939
- Prediction of jet impingement cooling scheme characteristics (airfoil leading edge application) p 932 N93-29941
- Measurements and computational analysis of heat transfer and flow in a simulated turbine blade internal cooling passage [NASA-TM-106189] p 1032 N93-31647
- ### HEAT TRANSMISSION
- A computational approach to predicting the extent of arc root damage in CFC panels p 735 N93-24890
- Overview of aerothermodynamic loads definition study p 1016 N93-31583
- ### HEAT TREATMENT
- Resource conservation and improvement of the service characteristics of castings of high-temperature nickel alloys through a high-temperature melt treatment p 824 A93-36718
- Structural stability of 'beta-CEZ' alloy [ONERA, TP NO. 1992-106] p 824 A93-38586
- Total quality management of forged products through finite element simulation p 1217 A93-53493
- Fractographic investigation of IMI 685 crack propagation specimens for SMP SC33 p 1004 N93-31743
- ### HEATERS
- Performance of thermal adhesives in forced convection p 924 N93-30974
- ### HEATING
- Numerical modeling of runback water on ice protected aircraft surfaces p 840 N93-27438
- ### HEATING EQUIPMENT
- Characteristics of the flame air heater of a hypersonic wind tunnel p 1140 A93-51884
- ### HEAVING
- On hovercraft overwater heave stability p 1219 A93-53819
- Kelvin-Helmholtz wave generation beneath hovercraft skirts p 1219 A93-53820
- Mathematical model of frost heave and thaw settlement in pavements [CRREL-REPT-93-2] p 912 N93-30103
- ### HEAVY LIFT HELICOPTERS
- Using helicopters for transporting large and heavy loads p 306 A93-18350
- ### HEAVY LIFT LAUNCH VEHICLES
- Hammerhead aeroelastic stability revisited [AIAA PAPER 93-1477] p 740 A93-34022
- MAKS - Eastern promise? --- multi-purpose aerospace system p 733 A93-34266
- ### HELICAL FLOW
- A simple criterion for vortex breakdown [AIAA PAPER 93-0866] p 469 A93-24928
- ### HELICOPTER CONTROL
- Multiple input/multiple output (MIMO) analysis procedures with applications to flight data p 60 A93-10777
- Aspects of multivariable flight control law design for helicopters using eigenstructure assignment p 60 A93-10916
- Discrete time H(infinity) control laws for a high performance helicopter p 96 A93-13007
- Synthesis of a helicopter nonlinear flight controller using approximate model inversion [AIAA PAPER 92-4468] p 62 A93-13280
- Helicopter in-flight simulator ATHeS - A multipurpose testbed and its utilization [AIAA PAPER 92-4173] p 43 A93-13315
- Digital fly-by-wire system for BK117 FBW research helicopter p 181 A93-14209
- The influence of rotor and fuselage wakes on rotorcraft stability and control p 183 A93-14373
- Design and robustness issues for highly augmented helicopter controls p 185 A93-14594
- Helicopter automatic flight control systems for all weather operations - EH101 and beyond p 186 A93-17310
- Validation of vision-based obstacle detection algorithms for low-altitude helicopter flight p 374 A93-19077
- Refined H-infinity controller design for rotorcraft flight control p 368 A93-22882
- Dynamical variable structure control of a helicopter in vertical flight p 369 A93-22887
- Design of flight control systems to meet rotorcraft handling qualities specifications p 370 A93-23509
- Three-dimensional modeling and control of a twin-lift helicopter system p 370 A93-23511
- Optimal takeoff of a helicopter for category A V/STOL operations p 525 A93-28611

- Prediction of helicopter component loads using neural networks
[AIAA PAPER 93-1301] p 756 A93-33878
- Vibration and flutter of stiff-inplane elastically tailored composite rotor blades
[AIAA PAPER 93-1302] p 725 A93-33879
- Full-scale wind tunnel investigation of a helicopter individual blade control system
[AIAA PAPER 93-1361] p 726 A93-33929
- Improvements in hover display dynamics for a combat helicopter
p 727 A93-34257
- Synthesis and evaluation of an H2 control law for a hovering helicopter
p 728 A93-34542
- Automatic guidance and control laws for helicopter obstacle avoidance
p 728 A93-35518
- Design of the variable pitch fan for the McDonnell Douglas MD 520N helicopter equipped with the NOTAR system
p 794 A93-35908
- Effects of higher order dynamics on helicopter flight control law design
p 816 A93-35959
- Digital resolver for helicopter model blade motion analysis
p 830 A93-37878
- Quantitative feedback theory applied to the design of a rotorcraft flight control system
p 906 A93-41895
- Linear quadratic Gaussian/loop transfer recovery design for a helicopter in low-speed flight
p 906 A93-41896
- Performance of higher harmonic control algorithms for helicopter vibration reduction
p 890 A93-41904
- Helicopter control law based on sliding mode with model following
p 907 A93-42559
- Application of two chaos methods to higher harmonic control data --- for suppression of helicopter vibration
p 909 A93-43783
- H(infinity) helicopter flight control law design with and without rotor state feedback
[AIAA PAPER 93-3849] p 1134 A93-51436
- Design of a helicopter control system to meet handling quality specifications using H(infinity) techniques
[AIAA PAPER 93-3850] p 1134 A93-51437
- Benefits of variable rotor speed in integrated helicopter/engine control
[AIAA PAPER 93-3851] p 1134 A93-51438
- A test bench for rotorcraft hover control
[AIAA PAPER 93-3853] p 1140 A93-51440
- Vision based obstacle detection and grouping for helicopter guidance
[AIAA PAPER 93-3871] p 1098 A93-51457
- Removing the risk from rotorcraft testing
p 1192 A93-53772
- Minimum time turn of a helicopter
p 1248 A93-54554
- Multirate and event-driven Kalman filters for helicopter flight
p 1245 A93-55760
- Inverse simulation: A tool for the validation of simulation programs - First results --- for helicopter flight tests and control
p 1249 A93-56046
- Flight test and analysis procedures for new handling criteria
[RAE-TM-FM-26] p 47 N93-10803
- Trim analysis by shooting and finite elements and Floquet eigenanalysis by QR and subspace iterations in helicopter dynamics
p 163 N93-13914
- Ground based simulation evaluation of the effects of time delays and motion on rotorcraft handling qualities
[AD-A256921] p 328 N93-16186
- Helicopter installations: From motor to rotor
[LR-675] p 329 N93-16345
- Developing a control system for ARES 2
p 371 N93-16769
- Mission oriented investigation of handling qualities through simulation
[MBB-UD-0600-91-PUB] p 332 N93-17567
- An investigation of a prototype OASYS effectiveness in maneuvering flight
[AD-A257901] p 338 N93-18339
- Helicopter flight control system design using the linear quadratic regulator for robust eigenstructure assignment
[AD-A258904] p 373 N93-19351
- An exploratory investigation of the flight dynamics effects of rotor rpm variations and rotor state feedback in hover
[NASA-TM-103968] p 373 N93-19380
- Generation of helicopter roll axis bandwidth data through ground-based and in-flight simulation
p 511 N93-19809
- Discrete range clustering using Monte Carlo methods
[NASA-TM-104004] p 706 N93-24914
- Helicopter low-speed yaw control
[NASA-CASE-LAR-14219-1] p 729 N93-25998
- Image-based ranging and guidance for rotorcraft
[NASA-CR-177608] p 708 N93-26549
- Development and flight testing of a fault-tolerant fly-by-light yaw control system
p 1010 N93-31280
- Current projects in Fuzzy Control
p 1038 N93-31442
- ### HELICOPTER DESIGN
- Test and analysis of an advanced technology landing gear
p 37 A93-10917
- Evolution of helicopters and the status of technology in India
p 2 A93-12234
- Discrete time H(infinity) control laws for a high performance helicopter
p 96 A93-13007
- Preliminary design features of the RASCAL - A NASA/Army rotorcraft in-flight simulator
[AIAA PAPER 92-4175] p 42 A93-13311
- Reaction drive rotors - Lessons learned (Hero had a good idea - But) --- jet helicopter performance
[AIAA PAPER 92-4279] p 55 A93-13352
- Reliability testing of the EH101
p 45 A93-13406
- Rotorcraft reliability and maintainability - A CAA view of future trends
p 45 A93-13407
- Super Panda MK II - Rotor and gearbox fatigue
p 46 A93-13636
- Hovering decisions --- development of EH101 helicopter
p 46 A93-13700
- Application of CAD system in geometric modeling for helicopter preliminary design
p 153 A93-14203
- The influence of main design parameters on helicopter air resonance and its source of instability
p 154 A93-14261
- Design and fabrication of a composite transmission housing for a helicopter tail rotor
p 156 A93-14339
- Characteristics of fatigue crack growth under the service-spectrum loading of the tail boom of a helicopter
p 321 A93-18339
- Using helicopters for transporting large and heavy loads
p 306 A93-18350
- Lynx: High performance - Low noise
p 322 A93-19185
- Multidisciplinary optimization of helicopter rotor blades including design variable sensitivity
[AIAA PAPER 92-4783] p 323 A93-20289
- Multidisciplinary analysis and sensitivity derivatives for isolated helicopter rotors in hover
[AIAA PAPER 92-4696] p 324 A93-20308
- Development of a structural optimization capability for the aeroelastic tailoring of composite rotor blades with straight and swept tips
[AIAA PAPER 92-4779] p 326 A93-20370
- Vibration reduction for helicopter airframes - An application of the general-purpose structural optimization program STARS
[AIAA PAPER 92-4782] p 326 A93-20372
- Advancing helicopters
p 327 A93-21836
- Fifty years of tandem rotor helicopter engineering
p 504 A93-25250
- A structural reliability evaluation of fail-safe helicopter dynamic components
p 506 A93-27952
- Progress in the application of a non-linear programming methodology to the design of a low-vibration airframe
p 507 A93-27959
- Novel approaches to complex geometry structure
p 546 A93-27969
- Experiences at Langley Research Center in the application of optimization techniques to helicopter airframes for vibration reduction
p 508 A93-27972
- Parametric study of the gear blank structure in helicopter transmission design
p 546 A93-27973
- Transmission error and load distribution analysis of spur and double helical gear pairs used in a split path helicopter transmission design
p 549 A93-29426
- Active control of helicopter transmission noise
p 568 A93-29428
- Damage tolerance evaluation of new manufacturing techniques for composite helicopter drive shafts
[AIAA PAPER 93-1400] p 739 A93-33960
- An automated mode tracking strategy --- dynamic structural analysis of helicopter structures
[AIAA PAPER 93-1414] p 739 A93-33970
- Improvements in hover display dynamics for a combat helicopter
p 727 A93-34257
- A modal-based procedure for efficiently predicting low vibration rotor designs
p 712 A93-34262
- Comanche airframe design - The PDT approach
p 744 A93-34469
- Developing the MD Explorer
p 744 A93-34472
- Overview of Tiger dynamics validation program
p 794 A93-35907
- Design of the variable pitch fan for the McDonnell Douglas MD 520N helicopter equipped with the NOTAR system
p 794 A93-35908
- PDT approach for developing RAH-66 Comanche airframe systems
p 795 A93-35909
- A vibration monitoring acquisition and diagnostic system for helicopter drive train bench tests
p 826 A93-35930
- A High Deflection Diaphragm concept (HDD) for power transmission shafting
p 826 A93-35931
- Navier-Stokes correlations to fuselage wind tunnel test data
p 765 A93-35937
- A Taguchi analysis of helicopter maneuverability and agility
p 763 A93-35944
- Application of generalized force determination to a full scale low cycle fatigue test of the SH-2G helicopter
p 795 A93-35949
- Effects on load distribution in a helicopter rotor support structure associated with various boundary configurations
p 796 A93-35951
- Thermoplastic applications in helicopter components
p 796 A93-35952
- MI-26 autorotational landings
p 816 A93-35955
- Side-by-side hover performance comparison of MDHC 500 NOTAR and tail rotor anti-torque systems
p 796 A93-35956
- Optimum design of high speed prop-rotors using a multidisciplinary approach
p 798 A93-35985
- A parametric study of real time mathematical modeling incorporating dynamic wake and elastic blades
p 798 A93-35986
- Helicopter rotor disk and Blade Element comparison
p 799 A93-35991
- Development and validation of a comprehensive real time AH-64 Apache simulation model
p 799 A93-35992
- Rotor blade airfoil design by numerical optimization and unsteady calculations
[ONERA, TP NO. 1992-65] p 766 A93-35993
- An application of knowledge-based engineering to composite tooling design
p 846 A93-36010
- The Cabri two-seat helicopter - Design and first flights
p 799 A93-36019
- Blade twist-design of experiment
p 800 A93-36025
- Optimal design of honeycomb sandwich shell aircraft structures of composite materials
p 828 A93-36800
- Development status of the RAH-66 Comanche
p 803 A93-38838
- Investigation of helicopter air resonance in hover by complex coordinates and mutual excitation analysis
p 893 A93-43777
- A frequency domain theory for structural identification
p 930 A93-43778
- Carbon composite repairs of helicopter metallic primary structures
p 1101 A93-50429
- Finite state aeroelastic model for use in rotor design optimization
p 1104 A93-52454
- The development of a new air filtration system for the Alouette III helicopter
[ISABE 93-7048] p 1199 A93-54024
- Royal Navy helicopter operations in the maritime environment
p 1190 A93-54290
- The T700 ... from salt spray to sand blast
p 1205 A93-54292
- The quiet helicopter; Proceedings of the Conference, London, United Kingdom, Mar. 17, 1992
[ISBN 1-85768-020-0] p 1262 A93-54718
- Helicopter noise certification
p 1262 A93-54720
- Helicopter noise reduction programme - AGUSTA achievements
p 1262 A93-54721
- Noise characteristics of helicopters with the NOTAR anti-torque system
p 1262 A93-54722
- A new methodology for helicopter internal noise reduction application to the AS332 L2
p 1243 A93-54723
- European research into helicopter internal noise
p 1243 A93-54724
- Review of helicopter noise research in Europe
p 1263 A93-54725
- Split torque transmission load sharing
[NASA-TM-105884] p 212 N93-12736
- Helicopter installations: From motor to rotor
[LR-675] p 329 N93-16345
- Test and integration concept for complex helicopter avionic systems
[MBB-UD-0605-91-PUB] p 343 N93-17547
- Modern helicopter technologies at MBB and the application in future programmes
[MBB-UD-0599-91-PUB] p 331 N93-17566
- Mission oriented investigation of handling qualities through simulation
[MBB-UD-0600-91-PUB] p 332 N93-17567
- Current European rotorcraft research activities on development of advanced CFD methods for the design of rotor blades (BRITE/EURAM DACRO project)
[MBB-UD-0601-91-PUB] p 293 N93-17568
- RPH preliminary design, trend analysis and initial analysis of the NPS hummingbird
[AD-A257854] p 338 N93-18304
- The S.T.o.R.M. (tm): Air transport system design simulation
[NASA-CR-192070] p 338 N93-18349
- Helicopters in action
p 340 N93-19005
- Rotor design optimization using a free wake analysis
[NASA-CR-177612] p 693 N93-25075
- Face-gear drives: Design, analysis, and testing for helicopter transmission applications
[NASA-TM-106101] p 839 N93-27133

- Robust crossfeed design for hovering rotorcraft
[NASA-CR-193107] p 805 N93-27241
- HELICOPTER ENGINES**
- Design of propulsion systems for low operating costs
p 55 A93-13405
- Experimental study of the acoustic spinning modes generated by a helicopter turboshaft engine
[ONERA, TP NO. 1992-141] p 230 A93-14266
- A numerical study on the radiation characteristic of an elliptical exhaust jet
p 174 A93-16236
- Calculation of the parameters of a crane helicopter with one disabled engine
p 366 A93-18381
- Helicopter main rotor/tail rotor noise radiation characteristics from scaled model rotor experiments in the DNW
p 445 A93-19142
- Aerodesign and performance analysis of a radial transonic impeller for a 9:1 pressure ratio compressor
[ASME PAPER 92-GT-183] p 352 A93-19408
- MTR390 - Engine for the future
[ASME PAPER 92-GT-250] p 353 A93-19459
- Numerical forecasting of liquid water content to assess airframe icing risk
p 429 A93-22147
- Helicopter plume detection by using an ultranarrow-band noncoherent laser Doppler velocimeter
p 542 A93-25198
- Fifty years of tandem rotor helicopter engineering
p 504 A93-25250
- Continuous judgment of helicopter noise - On the validity of Leq and Zwicker's method (ISO 532B)
p 558 A93-28478
- Improved static and dynamic performance of helicopter powerplant
p 809 A93-35928
- Identification of the open loop dynamics of the T700 turboshaft engine
p 809 A93-35934
- Particle dynamics simulations in inlet separator with an experimentally based bounce model
[AIAA PAPER 93-2156] p 1115 A93-49972
- Analytic methods for design of wave cycles for wave rotor core engines
p 1121 A93-50253
- The chemistry of Saudi Arabian sand - A deposition problem on helicopter turbine airfoils
p 1216 A93-53468
- The T700 ... from salt spray to sand blast
p 1205 A93-54292
- Combustor development for advanced helicopter engines
p 1246 A93-54841
- Measuring risk in single-engine and twin-engine helicopters
p 148 A93-15025
- Onboard System Evaluation of Rotors Vibration, Engines (OBSERVE) monitoring system
[AD-A255366] p 165 N93-15227
- Helicopter installations: From motor to rotor
[LR-675] p 329 N93-16345
- Analysis of consolidation of intermediate level maintenance for Atlantic Fleet T700-GE-401 engines
[AD-A257754] p 363 N93-17695
- Integrity testing of brush seal in shroud ring of T-700 engine
p 421 N93-18380
- HELICOPTER PERFORMANCE**
- Experimental study of rotor wake/body interactions in hover
p 124 A93-14782
- Influence of pitch-lag coupling on damping requirements to stabilize 'ground/air resonance'
p 158 A93-14784
- The prediction of nonlinear dynamic loads on helicopters from flight variables using artificial neural networks
p 322 A93-19231
- Passive range sensor refinement using texture and segmentation
p 544 A93-27044
- Problems in the modeling of helicopter flight
p 506 A93-27293
- Helicopters - Handbook --- Russian book
[ISBN 5-203-00804-3] p 458 A93-28874
- Helicopter noise standards - Requirements, compliance, and improvements
p 569 A93-29443
- Frequency-domain identification of BO 105 derivative models with rotor degrees of freedom
p 712 A93-34263
- Configuration management impacts on customer support and satisfaction
p 853 A93-35922
- An advanced method for predicting the performance of helicopter propulsion system ejectors
p 809 A93-35933
- The strake - A simple means for directional control improvement
p 802 A93-37997
- A numerical procedure for aerodynamic optimization of helicopter rotor blades
[ONERA, TP NO. 1992-121] p 771 A93-38595
- A set of IBM PC software for processing helicopter flight tests data to determine the flight performance characteristics
p 1037 A93-45661
- Computer-aided study of flight regimes and fuel consumption for helicopter flight operations
p 997 A93-45674

- Performance results from a test of an S-76 rotor in the NASA Ames 80- by 120-foot wind tunnel
[AIAA PAPER 93-3414] p 975 A93-47211
- Helicopter operations in severe environments; Proceedings of the Conference, London, United Kingdom, June 4, 1992
[ISBN 1-85768-045-6] p 1175 A93-54287
- Arctic environment - Helicopter operations in cold climates
p 1189 A93-54288
- Operating helicopters in a demanding environment - Mountain flying/high evaluations
p 1190 A93-54289
- Avionic systems in support of covert helicopter operations
p 1193 A93-54294
- LONGBOW - Force multiplier for continuous operations
p 1175 A93-54295
- Flight test and analysis procedures for new handling criteria
[RAE-TM-FM-26] p 47 N93-10803
- Trim analysis by shooting and finite elements and Floquet eigenanalysis by QR and subspace iterations in helicopter dynamics
p 163 N93-13914
- Helicopter health monitoring: Current practice and future trends
p 169 N93-15179
- New rotor trim and balance system for helicopter usage monitoring
p 169 N93-15180
- Ground based simulation evaluation of the effects of time delays and motion on rotorcraft handling qualities
[AD-A256921] p 328 N93-16186
- Helicopters in action
p 340 N93-19005
- HELICOPTER PROPELLER DRIVE**
- Damage tolerance evaluation of new manufacturing techniques for composite helicopter drive shafts
[AIAA PAPER 93-1400] p 739 A93-33960
- Low-noise, high-strength, spiral-bevel gears for helicopter transmissions
[AIAA PAPER 93-2149] p 1154 A93-49966
- Split torque transmission load sharing
[NASA-TM-105884] p 212 N93-12736
- Flexible rotorcraft system dynamics with time-variant contact conditions
p 340 N93-19034
- Fault detection of helicopter gearboxes using the multi-valued influence matrix method
[NASA-TM-106100] p 838 N93-27069
- Face-gear drives: Design, analysis, and testing for helicopter transmission applications
[NASA-TM-106101] p 839 N93-27133
- Sikorsky Aircraft Advanced Rotorcraft Transmission (ART) program
[NASA-CR-191079] p 840 N93-27268
- HELICOPTER TAIL ROTORS**
- Super Puma MK II - Rotor and gearbox fatigue
p 46 A93-13636
- Design and fabrication of a composite transmission housing for a helicopter tail rotor
p 156 A93-14339
- Continuous judgment of helicopter noise - On the validity of Leq and Zwicker's method (ISO 532B)
p 558 A93-28478
- Overview of Tiger dynamics validation program
p 794 A93-35907
- Antitorque safety and the RAH-66 Fantail
p 795 A93-35912
- Effects of ingested atmospheric turbulence on measured tail rotor acoustics
p 849 A93-35964
- Toward the silent helicopter
[ONERA, TP NO. 1992-229] p 851 A93-38774
- Noise characteristics of helicopters with the NOTAR anti-torque system
p 1262 A93-54722
- Current European rotorcraft research activities on development of advanced CFD methods for the design of rotor blades (BRITE/EURAM DACRO project)
[MBB-UD-0601-91-PUB] p 293 N93-17568
- Influence of cross section variations on the structural behaviour of composite rotor blades
[MBB-UD-0602-91-PUB] p 332 N93-17569
- HELICOPTER WAKES**
- Flowfield analysis of modern helicopter rotors in hover by Navier-Stokes method
p 481 A93-29435
- Recent developments in rotor wake modeling for helicopter noise prediction
p 481 A93-29437
- Effect of an unsteady three-dimensional wake on elastic blade-flapping eigenvalues in hover
p 683 A93-34260
- TURNs - A free-wake Euler/Navier-Stokes numerical method for helicopter rotors
p 692 A93-35634
- Aerodynamic rotor loads prediction method with free wake for low speed descent flights
[ONERA, TP NO. 1992-122] p 772 A93-38596
- Blade-vortex interaction noise - Prediction and comparison with flight and wind tunnel tests
[ONERA, TP NO. 1992-126] p 851 A93-38600
- Efficient free wake calculations using analytical/numerical matching
p 874 A93-43780
- Direct periodic solutions of rotor free wake calculations
p 874 A93-43781
- Wake structure of a helicopter rotor in forward flight
p 958 A93-45138

- Free-wake computation of helicopter rotor flowfields in forward flight
[AIAA PAPER 93-3079] p 1059 A93-48253
- Summary of the interaction of a rotor wake with a circular cylinder
[AIAA PAPER 93-3084] p 1060 A93-48258
- Acoustic noise generation at the air/ocean boundary
[DREA-CR-90-445] p 99 N93-10642
- Studies of a flat wake rotor theory
[NASA-CR-190936] p 25 N93-12343
- The Application of CFD to rotary wing flow problems
[NASA-TM-102803] p 139 N93-15483
- HELICOPTERS**
- Helicopter in-flight simulator ATTHes - A multipurpose testbed and its utilization
[AIAA PAPER 92-4173] p 43 A93-13315
- A new method for calculation of helicopter maneuvering flight
p 184 A93-14401
- Prediction of the radiation characteristic of a helicopter exhaust jet
p 172 A93-14494
- Optical microphone for the detection of hidden helicopters
p 205 A93-14542
- Tiltrotor Research Aircraft composite blade repairs - Lessons learned
p 108 A93-14819
- Vision-based range estimation using helicopter flight data
p 151 A93-17501
- Helicopter noise prediction - The current status and future direction
p 448 A93-19202
- Vision-based range estimation using helicopter flight data
p 317 A93-21525
- Reducing helicopter operating costs
p 486 A93-25249
- A generic harmonic rotor model for helicopter flight simulation
p 506 A93-27480
- The NASA/industry design analysis methods for vibrations (DAMVIBS) program - Accomplishments and contributions
p 508 A93-27971
- Advanced composite helicopter MISERS GOLD test/analysis
p 508 A93-27974
- Human response to helicopter noise - A test of A-weighting
p 567 A93-29424
- Optimal open multistep discretization formulas for real-time simulation
p 757 A93-34539
- Aeromechanical stability of helicopters with composite rotor blades in forward flight
p 794 A93-35904
- On the effect of pitch/mast-bending coupling on whirl-mode stability
p 794 A93-35906
- MIDAS technology transfer
p 845 A93-35920
- A finite-volume Euler solver for computing rotary-wing aerodynamics on unstructured meshes
p 765 A93-35935
- Helicopter aerodynamics research techniques and rotor-fuselage interaction analysis
p 765 A93-35938
- A closed loop controller for BVI impulsive noise reduction by Higher Harmonic Control
p 849 A93-35963
- An analysis on high speed impulsive noise of transonic helicopter rotor
p 849 A93-35965
- An investigation of helicopter rotor blade flap vibratory loads
p 796 A93-35975
- Application of component mode synthesis to modeling the dynamic response of Bearingless Main Rotors
p 796 A93-35976
- Coupled rotor fuselage mode shapes - A tool in understanding helicopter response
p 797 A93-35977
- Introduction of the M-85 high-speed rotorcraft concept
p 797 A93-35980
- Helicopter response to atmospheric turbulence
p 817 A93-35987
- ATTHes - A helicopter in-flight simulator with high bandwidth capability
p 821 A93-35988
- Environmental conditions for certification testing of helicopter advanced composite main rotor components
p 824 A93-36003
- Nonlinear analysis of composite thin-walled helicopter blades
p 827 A93-36006
- Valisys - A new quality assurance tool
p 845 A93-36007
- Some considerations on indication means for helicopter pilot vision systems
p 807 A93-36018
- Laser velocimetry around helicopter blades in the DNW wind tunnel of the NLR
[ONERA, TP NO. 1992-143] p 831 A93-38613
- The ring laser gyro and its applications
p 927 A93-42657
- Design of aircraft, helicopters, and aviation engines --- Russian book
[ISBN 5-277-01192-7] p 947 A93-44508
- Helicopter external noise prediction and reduction
[ONERA, TP NO. 1993-48] p 1039 A93-47450
- Reusable code for helicopter simulation
[AIAA PAPER 93-3594] p 1224 A93-52686
- Analysis of spatial motion dynamics of a helicopter for various models of the induced velocity field
p 1191 A93-53721
- Optimization of sandwich structures with respect to local instabilities with MBB-LAGRANGE
p 1255 A93-54540

SUBJECT INDEX

Unusual attitudes - Helicopters and instrument flight
p 1240 A93-54550

Helicopter noise - Public perspective
p 1261 A93-54719

Rotorcraft en route ATC route standards
[AD-A249129] p 35 N93-10323

Compound cycle engine for helicopter application
[NASA-CR-180824] p 55 N93-10348

Appraisal of digital terrain elevation data for low-altitude flight
[NASA-TM-103896] p 35 N93-10745

Flight test and analysis procedures for new handling criteria
[RAE-TM-FM-26] p 47 N93-10803

Contributions to the experimental investigation of rotor/body aerodynamic interactions p 20 N93-10877

Rotorcraft health and usage monitoring systems: A literature survey
[DOT/FAA/RD-91/6] p 48 N93-11461

Time-frequency domain analysis of vibration signals for machinery diagnostics. 3: The present power spectral density
[OUEL-1991/92] p 89 N93-11707

Embedded training capabilities for the LAMPS MK 3 system
[AD-A250697] p 49 N93-11838

Integration of radar altimeter, precision navigation, and digital terrain data for low-altitude flight
[NASA-TM-103958] p 36 N93-12320

Verification of rain-flow reconstructions of a variable amplitude load history
[NASA-CR-189670] p 91 N93-12411

Formulation and validation of high-order mathematical models of helicopter flight dynamics
p 162 N93-13821

Experimental and analytical investigation of the vibration characteristics of a remotely piloted helicopter
[AD-A256131] p 163 N93-14248

Workshop on Aeronautical Decision Making (ADM). Volume 2: Plenary Session With Presentations and Proposed Action Plan
[DOT/FAA/RD-92/14-VOL-2] p 146 N93-15013

Embedded ADM reduces helicopter human error accidents
p 147 N93-15024

Measuring risk in single-engine and twin-engine helicopters
p 148 N93-15025

Helicopter flight data recorder and health and usage monitoring system
p 169 N93-15178

Modeling limits of the EMV analysis program CONCEPT by example of the influence of a helicopter structure on a frame antenna
[MBB-UD-0614-92-PUB] p 223 N93-15487

Helicopter installations: From motor to rotor
[LR-675] p 329 N93-16345

Conditioned based machinery maintenance (helicopter fault detection)
[AD-A255796] p 329 N93-16396

Measurement of the dynamic undercarriage response of a Sikorsky S-70B-2 helicopter: Instrumentation and test methods: Flight mechanics technical memorandum
[AD-A256319] p 329 N93-16404

Relationship between mechanical-property and energy-absorption trends for composite tubes
[NASA-TP-3284] p 392 N93-16537

Modern helicopter technologies at MBB and the application in future programmes
[MBB-UD-0599-91-PUB] p 331 N93-17566

Integrated helmet system testing for a nightflying helicopter
[MBB-UD-0604-91-PUB] p 343 N93-17570

Open airscrew VTOL concepts
[NASA-CR-177603] p 240 N93-17883

The S.T.o.R.M. (tm): Air transport system design simulation
[NASA-CR-192070] p 338 N93-18349

Basic research on design analysis methods for rotorcraft vibrations
[NASA-CR-191917] p 422 N93-18576

Numerical investigation of swirl-airfoil interactions in transonic area
[MPIS-8/1991] p 297 N93-18627

Professor Wittenberg: His speciality and versatility
[ISBN-90-6275-670-0] p 240 N93-19002

Helicopters in action
p 340 N93-19005

Wind tunnel test and CFD in Kawasaki Heavy Industries, Gifu
p 304 N93-19324

An exploratory investigation of the flight dynamics effects of rotor rpm variations and rotor state feedback in hover
[NASA-TM-103968] p 373 N93-19380

Assessment of helicopter component statistical reliability computations
[AD-A258931] p 510 N93-19447

Royal Naval helicopter ditching experience
p 492 N93-19684

Canadian Forces helicopter ditchings: 1952-1990
p 493 N93-19685

Helicopter accidents over water in the national navy: Epidemiological study over the period 1980-1991
p 493 N93-19686

Helicopter crash survival at sea: United States Navy/Marine Corps experience 1977-1990
p 493 N93-19687

US Army helicopter inertia reel locking failures
p 493 N93-19689

Pre-flight risk assessment in Emergency Medical Service (EMS) helicopters
p 494 N93-19692

Generation of helicopter roll axis bandwidth data through ground-based and in-flight simulation
p 511 N93-19909

Fly-by voice, a technology demonstration
p 526 N93-19918

An improved method of structural dynamic test design for ground flying and its application to the SH-2F and SH-2G helicopters
p 512 N93-19928

Advanced adaptive computational methods for Navier-Stokes simulations in rotorcraft aerodynamics
[NASA-CR-192282] p 483 N93-20256

HELITRAK: A helicopter-tracking receiver system for television outside broadcast links
[BBC-RD-1992/5] p 552 N93-20573

The NASA/industry Design Analysis Methods for Vibrations (DAMVIBS) program: Boeing Helicopters airframe finite element modeling
p 515 N93-21313

The NASA/industry Design Analysis Methods for Vibrations (DAMVIBS) program: McDonnell-Douglas Helicopter Company achievements
p 515 N93-21314

Numerical modelling of induced effects of lightning strike on an all composite helicopter
p 703 N93-24879

Aeroelastic response and aeromechanical stability of helicopters with elastically coupled composite rotor blades
p 715 N93-25530

Structural dynamic analysis of bearingless rotor blade
p 717 N93-25719

Computational gearing mechanics
[NASA-CR-191127] p 751 N93-25884

Helicopter low-speed yaw control
[NASA-CASE-LAR-14219-1] p 729 N93-25998

Helicopter forced response vibration analysis method RTVIB20
[AD-A261809] p 730 N93-26260

PROAV Cable Warning System (CWS) - U.S. Army aircraft integration assessment and OCONUS field evaluation
[AD-A261233] p 705 N93-26263

Some recent applications of Navier-Stokes codes to rotorcraft
p 786 N93-27452

Dynamic System Coupler Program (DYSCO 4.1). Volume 1: Theoretical manual
[AD-B131156L] p 848 N93-27531

Testing a wheeled landing gear system for the TH-57 helicopter
[AD-A262152] p 806 N93-27547

Dynamic System Coupler Program (DYSCO 4.1). Volume 2: User's manual
[AD-B131157L] p 848 N93-27589

Dynamic System Coupler Program (DYSCO 4.1). Volume 3: User's manual supplement
[AD-B131158L] p 848 N93-27590

Flight evaluation of a computer aided low-altitude helicopter flight guidance system
p 820 N93-28869

Helicopter approach capability using the differential global positioning system
[NASA-CR-193183] p 793 N93-28936

A passive infrared ice detection technique for helicopter applications
[NASA-CR-193187] p 880 N93-29152

Aerodynamic characteristics of a rotorcraft airfoil designed for the tip region of a main rotor blade
[NASA-TM-4264] p 876 N93-29450

External acoustical noise measurements for aviation systems
[AD-A263138] p 943 N93-29480

Models for performance assessment of HF antennas on the CH-135/Twin Huey helicopter
p 933 N93-30291

NASA/FAA helicopter simulator workshop
[NASA-CP-3156] p 857 N93-30673

Part 1: Executive summary
p 857 N93-30674

Helicopter simulator standards
p 912 N93-30675

Helicopter simulator qualification
p 912 N93-30681

Helicopter simulation: Making it work
p 912 N93-30682

Helicopter training simulators: Key market factors
p 912 N93-30683

Progress through precedent: Going where no helicopter simulator has gone before
p 913 N93-30686

Transfer of training and simulator qualification or myth and folklore in helicopter simulation
p 913 N93-30687

Validation and upgrading of physically based mathematical models
p 942 N93-30688

HEMISPHERE CYLINDER BODIES

Frequency-response techniques for documentation and improvement of rotorcraft simulators
p 913 N93-30689

Bandwidth and SIMDUCE as simulator fidelity criteria
p 913 N93-30690

Methodology development for evaluation of selective-fidelity rotorcraft simulation
p 913 N93-30691

Strong parallel blade-vortex interaction and noise propagation in helicopter flight
p 944 N93-30980

Advanced electromagnetic methods for aerospace vehicles
[NASA-CR-193468] p 936 N93-31036

Operation of the helicopter antenna radiation prediction code
[NASA-CR-193259] p 1030 N93-31110

The DLR test aircraft in the FZ-BS, -YFW 614/ATTAS, Dornier DO 228-101, MBB BO105 S-3
p 1018 N93-31272

Pallet for helicopter test instrumentation
p 1000 N93-31279

Efficient fault diagnosis of helicopter gearboxes
[NASA-TM-106253] p 1032 N93-31846

Flight evaluation of a computer aided low-altitude helicopter flight guidance system
[NASA-TM-103998] p 994 N93-32225

HELIOSTATS
Thermal effects testing at the National Solar Thermal Test Facility
p 1255 A93-54402

Wind load design methods for ground-based heliostats and parabolic dish collectors
[DE93-002737] p 433 N93-15839

HELIOTRONS
Beta-limiting phenomena in high-aspect-ratio toroidal helical plasmas
[NIFS-188] p 569 N93-20546

HELIPORTS
Helicopter noise - Public perspective
p 1261 A93-54719

HELIUM
Advanced technologies airships
p 108 A93-14183

Brush seal leakage performance with gaseous working fluids at static and low rotor speed conditions
[ASME PAPER 92-GT-304] p 405 A93-19494

Experimental and computational investigation of helium injection into air at supersonic and hypersonic speeds
p 696 N93-25487

HELIUM-NEON LASERS
Turbine blade vibration monitoring system
[ASME PAPER 92-GT-159] p 402 A93-19386

HELMET MOUNTED DISPLAYS
High voltage quick-disconnect harness system for helmet-mounted displays
p 516 A93-25922

Survey of helmet tracking technologies
p 517 A93-26882

Visual field information in Nap-of-the-Earth flight by teleoperated Helmet-Mounted displays
p 517 A93-26884

Design of an optimal single reflective holographic helmet display element
p 517 A93-26886

Performance considerations for high-definition head-mounted displays
p 518 A93-27242

Miniature display technologies for integrated helmet systems
p 718 A93-34819

Some considerations on indication means for helicopter pilot vision systems
p 807 A93-36018

Displaying the night
p 1244 A93-55297

Integration of an integrated helmet system for PAH 2
p 1244 A93-55298

Integrated helmet system testing for a nightflying helicopter
[MBB-UD-0604-91-PUB] p 343 N93-17570

Trade-offs arising from mixture of color cueing and monocular, binocular, and stereoscopic cueing information for simulated rotorcraft flight
[NASA-TP-3268] p 338 N93-18333

Test techniques for evaluating flight displays
[NASA-TM-103947] p 516 N93-21810

HELMETS
Helmet Mounted Sight and display testing
p 517 A93-26883

Integrated helmet system testing for a nightflying helicopter
[MBB-UD-0604-91-PUB] p 343 N93-17570

In-flight evaluation of noise levels and assessment of active noise reduction systems in the Seahawk S-70B-2 helicopter
[AD-A260689] p 759 N93-25649

HELMHOLTZ RESONATORS
A preliminary investigation of the Helmholtz resonator concept for heat flux reduction
[AIAA PAPER 93-2742] p 963 A93-46493

HEMISPHERE CYLINDER BODIES
The hemisphere-cylinder in dynamic pitch-up motions
[AIAA PAPER 93-2963] p 1048 A93-48157

- The hemisphere-cylinder at an angle of attack
p 21 N93-11250
- HERMES MANNED SPACEPLANE**
Computational methods applied to the aerodynamics of spaceplanes and launchers
[ONERA, TP NO. 1992-140] p 114 A93-14216
The Hermes Carrier Aircraft (HCA)
p 195 A93-14347
Validation of aerodynamic simulation methods for Hermes spaceplane and future hypersonic vehicles
[AIAA PAPER 92-5065] p 273 A93-22335
CFD analysis of hypersonic chemically reacting flowfields around a generic shape
[AIAA PAPER 93-0323] p 281 A93-23015
Flying qualities of the Hermes spaceplane and the shape definition process
p 532 A93-28437
A family of multiblock codes for computational aerothermodynamics - Application to complete vehicle hypersonic flows
[AIAA PAPER 93-3042] p 1056 A93-48223
Aerodynamic calculation of complex three-dimensional configurations
p 1094 A93-52426
- HERMETIC SEALS**
Selecting a method for sealing riveted joints in fuel compartments
p 746 A93-35295
Effect of aqueous solutions of water-crystallization inhibiting fluids on Thiokol-based sealants
p 1017 A93-45689
Hermetic sealing and EMI shielding gasket
[AD-D015359] p 199 N93-13414
- HEURISTIC METHODS**
Scheduling of an aircraft fleet
p 443 N93-18665
- HIERARCHIES**
Aircraft optimization by a system approach - Achievements and trends
p 153 A93-14205
- HIGH ACCELERATION**
Evaluation of CKU-5/A ejection seat catapults under varied acceleration levels
[AD-A248021] p 29 N93-12489
- HIGH ALTITUDE**
Fuel cell powered electric propulsion for HALE aircraft
[ASME PAPER 92-GT-404] p 356 A93-19553
The effect of extreme altitude on parachute filling distance
[AIAA PAPER 93-1207] p 702 A93-35158
Stabilization of the Burnett equations and application to hypersonic flows
p 778 A93-39410
Viscous hypersonic shock-shock interaction on a blunt body at high altitude
p 962 A93-46477
Aerodynamics of Shuttle Orbiter at high altitudes
[AIAA PAPER 93-2815] p 965 A93-46553
Aerothermodynamics of the high-altitude flight
p 1089 A93-51783
Development and computation of continuum higher order constitutive relations for high-altitude hypersonic flow
p 132 N93-13578
- HIGH ALTITUDE BALLOONS**
The unrealized potential for heavy balloon payloads
p 39 A93-11359
Long-duration balloon flights in the middle stratosphere
p 40 A93-11369
Concept for an open-neck stratospheric balloon with long-duration flight capability
p 40 A93-11371
Polar Patrol Balloon Experiment in Antarctica
p 27 A93-11373
A joint Soviet-Bulgarian scientific program for free-flight and tethered aerostat observations
p 2 A93-11374
Resonance frequencies of a gondola submitted to a forced rotation under a stratospheric balloon
p 27 A93-11384
- HIGH ALTITUDE ENVIRONMENTS**
Higher-order viscous shock-layer solutions for high altitude flows
[AIAA PAPER 93-2724] p 858 A93-41050
- HIGH ALTITUDE PRESSURE**
High pressure ratio intercooled turboprop study
[ASME PAPER 92-GT-405] p 356 A93-19554
- HIGH ALTITUDE TESTS**
Above the sky — high altitude flight in ER-2 aircraft
p 1044 A93-52614
- HIGH ASPECT RATIO**
Influence of second-order boundary layer effects in hypersonic flow past blunt cones of large aspect ratio
p 241 A93-18238
A method for the optimum design of a large-aspect-ratio wing
p 828 A93-36793
An experimental study of droop leading edge modifications on high and low aspect ratio wings up to 50 deg angle of attack
[AIAA PAPER 93-3496] p 983 A93-47268
Numerical analysis of high aspect ratio cooling passage flow and heat transfer
[AIAA PAPER 93-1829] p 1153 A93-49714
- Beta-limiting phenomena in high-aspect-ratio toroidal helical plasmas
[NIFS-188] p 569 N93-20546
- HIGH ENERGY FUELS**
What is the progress in propulsion?
p 298 N93-19006
- HIGH PASS FILTERS**
Photoelectrochemical etching of high aspect ratio submillimeter waveguide filters from n(+) GaAs wafers
p 409 A93-20644
Design and implementation of digital filters for analysis of F/A-18 flight test data
[AD-A253447] p 17 N93-10342
- HIGH POWER LASERS**
Aerodynamic phenomena in high pulse repetition rate XeCl laser
p 1150 A93-48806
Laser and skill enhance results
p 1257 A93-54843
- HIGH PRESSURE**
New experiments in a 120-mm ram accelerator at high pressures
[AIAA PAPER 93-2589] p 1142 A93-50301
Research and development of high pressure compressor for SST and HST engine
[ISABE 93-7068] p 1186 A93-54044
CF-6 high pressure compressor stage 5 locking slot crack propagation spin pit test
p 176 N93-14894
Field evaluation of six protective coatings applied to T-56 turbine blades after 2000 hours of engine use
[AD-A261112] p 522 N93-21316
Heat transfer and aerodynamics of a 3D design nozzle guide vane tested in the Pyestock Isentropic Light Piston Facility
p 901 N93-29928
- HIGH RESOLUTION**
High-resolution displays and projection systems; Proceedings of the Meeting, San Jose, CA, Feb. 11, 12, 1992
[SPIE-1664] p 544 A93-27237
Performance considerations for high-definition head-mounted displays
p 518 A93-27242
ISAR motion compensation and superresolution imaging of aircraft
p 928 A93-42793
Studies of superresolution range-Doppler imaging
p 928 A93-43344
Fluid dynamics and convective heat transfer in impinging jets through implementation of a high resolution liquid crystal technique
[ISABE 93-7077] p 1220 A93-54053
Motion errors and compensation possibilities
p 212 N93-13052
- HIGH REYNOLDS NUMBER**
Preliminary assessment of tunnel wall interference in the NDA cryogenic wind tunnel
[AIAA PAPER 93-0421] p 285 A93-23340
Compressible turbulence measurements in a high-speed high Reynolds number mixing layer
[AIAA PAPER 93-0660] p 465 A93-24773
Flowfield measurements of a two-element airfoil with large separation
p 480 A93-29307
Vortex generators used to control laminar separation bubbles
p 768 A93-37381
Domain splitting explicit time marching scheme for simulation of unsteady high Reynolds number flow
p 830 A93-38140
Wave interaction theory and LFC
p 860 A93-41781
Grid-refinement study of hypersonic laminar flow over a 2-D ramp
p 866 A93-42597
Experimental study of the flow around a double ellipsoid configuration
p 867 A93-42603
Numerical simulation of vortex shedding past triangular cylinders at high Reynolds number using a k-epsilon turbulence model
p 871 A93-42873
Three-dimensional vortex method for parachutes
p 872 A93-42874
Adaptive-prismatic-grid method for external viscous flow computations
[AIAA PAPER 93-3314] p 951 A93-45010
Simulation of flow past complex geometries using a parallel implicit incompressible flow solver
p 957 A93-45095
Comparative wind tunnel tests at high Reynolds numbers of NACA 64 621 airfoils with two airfoil configurations
p 967 A93-46823
Prediction of stall and post-stall behavior of airfoils at low and high Reynolds numbers
[AIAA PAPER 93-3502] p 983 A93-47270
Flowfield measurements about a multi-element airfoil at high Reynolds numbers
[AIAA PAPER 93-3137] p 1064 A93-48300
High Reynolds number and turbulence effects on aerodynamics and heat transfer in a turbine cascade
[AIAA PAPER 93-2252] p 1155 A93-50050
A new and working automatic calibration machine for wind tunnel internal force balances
[AIAA PAPER 93-2467] p 1138 A93-50214
- A study of incipient separation limits for shock-induced boundary layer separation for Mach 6 high Reynolds flow
[AIAA PAPER 93-2481] p 1084 A93-50222
Zonal-local solution method for the turbulent Navier-Stokes equations
p 1177 A93-53205
Analysis of high Reynolds number inviscid/viscid interactions in cascades
p 1234 A93-55351
Time dependent heat transfer rates in high Reynolds number hypersonic flowfields
p 216 N93-13664
Flow prediction for three-dimensional intakes and ducts using viscous-inviscid interaction methods
p 218 N93-13953
A realizable Reynolds stress algebraic equation model
[NASA-TM-105993] p 290 N93-16596
Boundary-layer measurements on a high Reynolds number three-element airfoil
p 292 N93-16787
Methodology for sensitivity analysis, approximate analysis, and design optimization in CFD for multidisciplinary applications
[NASA-CR-192172] p 552 N93-20297
Analysis of fluctuating static pressure measurements in a large high Reynolds number transonic cryogenic wind tunnel
[NASA-TM-108722] p 823 N93-27142
Investigation of forced unsteady separated flows using velocity-vorticity form of Navier-Stokes equations
p 840 N93-27451
Simultaneous mapping of the unsteady flow fields by Particle Displacement Velocimetry (PDV)
p 786 N93-27454
High Reynolds number and turbulence effects on aerodynamics and heat transfer in a turbine cascade
[NASA-TM-106187] p 930 N93-29157
High-Reynolds-number test of a 5-percent-thick low-aspect-ratio semispan wing in the Langley 0.3-meter transonic cryogenic tunnel: Wing pressure distributions
[NASA-TM-4227] p 875 N93-29449
Vortex shedding by blunt/bluff bodies at high Reynolds numbers. Volume 4: Rectangles
[AD-A264154] p 877 N93-30151
Vortex shedding by blunt/bluff bodies at high Reynolds numbers. Volume 1: Data analysis
[AD-A264151] p 877 N93-30171
Vortex shedding by Blunt/Bluff bodies at high Reynolds numbers. Volume 2: Cylinders, octagon, hexagon
[AD-A264152] p 877 N93-30172
Vortex shedding by blunt/bluff bodies at high Reynolds numbers. Volume 3: Cubes
[AD-A264153] p 877 N93-30173
Compressible turbulence in a high-speed high Reynolds number mixing layer
p 878 N93-30583
- HIGH SPEED**
Introduction of the M-85 high-speed rotorcraft concept
p 797 A93-35980
Modeling of linear isentropic flow systems
p 828 A93-37046
Further study of high speed single free jets
p 873 A93-43687
Investigation of advanced counterrotation blade configuration concepts for high speed turboprop systems. Task 4: Advanced fan section aerodynamic analysis
[NASA-CR-187128] p 174 N93-12695
Upgrade and extension of the data acquisition system for propulsion and gas dynamic laboratories
[AD-A256836] p 235 N93-15637
The NASA High-Speed Research Program
p 330 N93-16761
Investigation of advanced counterrotation blade configuration concepts for high speed turboprop systems. Task 5: Unsteady counterrotation ducted propfan analysis. Computer program user's manual
[NASA-CR-187125] p 521 N93-20583
An investigation of photothermal velocimetry for application to transient, high-speed gas flows
p 698 N93-25720
The development of a parachute system for aerial delivery from high speed cargo aircraft
[DE93-008339] p 790 N93-29035
The HSCST mission analysis of waverider designs
[NASA-CR-193467] p 879 N93-31037
- HIGH STRENGTH**
High-strength combination fasteners for joint assembly in aircraft structures
p 745 A93-35283
- HIGH STRENGTH ALLOYS**
Structure of martensite in titanium alloy Ti-6Al-1.6Zr-3.3Mo-0.3Si
p 916 A93-43616
- HIGH STRENGTH STEELS**
Stress corrosion susceptibility of ultra-high strength steels for Naval aircraft applications
[AD-A256126] p 199 N93-15189
- HIGH TEMPERATURE**
High temperature thin film strain gauges
[ONERA, TP NO. 1992-171] p 542 A93-25346

SUBJECT INDEX

- High temperature heat exchangers for gas turbines and future hypersonic air breathing propulsion
[ONERA, TP NO. 1993-75] p 1218 A93-53596
- Studies on coolant problems in aeronautical turbine cascades
[ISABE 93-7074] p 1220 A93-54050
- Mechanisms and modelling of environment-dependent fatigue crack growth in a nickel based superalloy
[AD-A253967] p 71 A93-10717
- Deformation mechanisms of NiAl cyclically deformed near the brittle-to-ductile transformation temperature
[NASA-CR-191649] p 391 A93-15830
- ### HIGH TEMPERATURE AIR
- Innovative high temperature aircraft engine fuel nozzle design
[ASME PAPER 92-GT-132] p 350 A93-19365
- Reacting gas and surface coupling in high temperature air flows
p 686 A93-34353
- AEDC expanded flow arc facility (HEAT-H2) description and calibration
p 821 A93-37872
- An experimental study of the air drying process in air coolers
p 834 A93-39059
- Thermal analysis of a shower-head burner
[SAE PAPER 921226] p 898 A93-41400
- Free piston facilities with air driver gas
p 1011 A93-45528
- Characteristics of the flame air heater of a hypersonic wind tunnel
p 1140 A93-51884
- Numerical modeling of runback water on ice protected aircraft surfaces
p 840 A93-27438
- Experimental study of heat transfer close to a plane wall heated in the presence of multiple injections (subsonic flow)
p 901 A93-29931
- ### HIGH TEMPERATURE ENVIRONMENTS
- Measurement of aerodynamic forces at high temperatures
p 75 A93-10030
- Niobium alloy heat pipes for use in oxidizing environments
p 200 A93-13791
- A very efficient tool for the structural analysis of hypersonic vehicles under high temperature aspects
p 203 A93-14194
- Development of polyimide adhesives for 371 C (700 F) structural performance for aerospace bonding applications - FM 680 system
p 198 A93-15757
- The effects of temperature on supersonic jet noise emission
p 446 A93-19159
- Acoustic properties of supersonic helium/air jets at low Reynolds numbers
p 446 A93-19160
- Innovative high temperature aircraft engine fuel nozzle design
[ASME PAPER 92-GT-132] p 350 A93-19365
- Results of high temperature JP-7 cracking assessment
[AIAA PAPER 93-0806] p 533 A93-24882
- Processing of high temperature carbon fiber reinforced polymers
[SME PAPER EM92-215] p 925 A93-40654
- Acoustical properties of sound absorbing structures at high temperature
p 1172 A93-48522
- The properties of newly developed highly damage tolerant and easy handleable carbon fiber/modified bismaleimide prepreg system
p 1212 A93-53448
- Overview of NASA's advanced high temperature engine materials technology program
p 1212 A93-53453
- Thermal design and analysis of an exhaust diffuser unit in a ceramic composite
[ISABE 93-7060] p 1220 A93-54036
- Development of MIL-H-53119, -54 C to 175 C high-temperature nonflammable hydraulic fluid for Air Force systems
p 1214 A93-54250
- An optical flameout detection system for NASA Langley's 8-Foot High Temperature Tunnel
p 1254 A93-54372
- Materials: Toward the non-metallic engine
[PNR-90915] p 56 A93-11019
- Design of a high-temperature experiment for evaluating advanced structural materials
[NASA-TM-105833] p 88 A93-11624
- High temperature rectifiers and MOS devices in 6H-silicon carbide
p 90 A93-12340
- High-temperature strain measurement techniques: Current developments and challenges
p 217 A93-13669
- RB211-524B disc and drive cones hot cyclic spinning test
p 177 A93-14895
- ### HIGH TEMPERATURE FLUIDS
- A model for calculating the element of a high-temperature heat exchanger with spiral-wire fins
p 833 A93-39046
- A heat transfer element of a high-temperature heat exchanger
p 833 A93-39047
- ### HIGH TEMPERATURE GASES
- Investigation of combustion structure inside low NO(x) combustors for a 1500 C-class gas turbine
[ASME PAPER 92-GT-123] p 350 A93-19357

- Gas dynamics of cooled turbines --- Russian book
[ISBN 5-217-00809-1] p 721 A93-35685
- Gas analysis system for the Eight Foot High Temperature Tunnel
p 822 A93-37875
- Selection of the scheme and optimal parameters of the turbine of a high-temperature bypass engine with a low bypass ratio
p 811 A93-39180
- Microsensors for high heat flux measurements
p 928 A93-42920
- An overview of Ames experimental aerothermodynamics
p 1011 A93-45496
- Subscale hot-fire testing of a formed platelet liner
[AIAA PAPER 93-1827] p 1141 A93-49713
- Nonintrusive, multipoint velocity measurements in high-pressure combustion flows
[AIAA PAPER 93-2032] p 1145 A93-49867
- Development of an advanced exhaust mixer for a high bypass ratio turbofan engine
[AIAA PAPER 93-2435] p 1118 A93-50188
- Non-self-similarity of a boundary layer flow of a high-temperature gas in a Laval nozzle
p 1176 A93-52946
- A new cooling system for ultra high temperature turbines
[ISABE 93-7073] p 1201 A93-54049
- Computation of hypersonic high-temperature nozzle flow
p 1238 A93-56040
- Computational study of real gas effects in high speed high temperature flow, volume 2
[AERO-REPT-9203-VOL-2] p 289 A93-16470
- ### HIGH TEMPERATURE LUBRICANTS
- Coking characteristics of polyphenyl ether lubricants using a Static Coker and a Micro Carbon Residue Tester
p 77 A93-11341
- ### HIGH TEMPERATURE RESEARCH
- Current research in oxidation-resistant carbon-carbon composites at NASA, Langley Research Center
p 74 A93-12456
- ### HIGH TEMPERATURE SUPERCONDUCTORS
- Lifting forces acting on magnets placed above a superconducting plane
p 79 A93-12332
- ### HIGH TEMPERATURE TESTS
- Raising the high temperature limit of the nickel-iron-base superalloy
p 70 A93-12114
- Ceramic coatings enhance material performance
p 71 A93-13648
- Characterization of the performance of shock-tube wind tunnels
[AIAA PAPER 93-0351] p 377 A93-23036
- A hot dynamic seal rig for measuring hypersonic engine seal durability and flow performance
[AIAA PAPER 93-1346] p 738 A93-33916
- Effect of environment on creep-fatigue crack propagation in turbine disc superalloys
[ONERA, TP NO. 1993-5] p 916 A93-41023
- Stress relaxation of low pressure plasma-sprayed NiCrAlY alloys
p 1211 A93-52870
- Conjugate modeling of high-temperature nosecone and wing leading edge heat pipes
p 1259 A93-55465
- Erosion predictions and measurements of high-temperature coatings and superalloys, used in turbomachines
p 74 A93-12189
- An overview of elevated temperature damage mechanisms and fatigue behavior of a unidirectional SCS-6/Ti-15-3 composite
[NASA-TM-106131] p 825 A93-26702
- NASA-UVA Light Aerospace Alloy and Structures Technology Program (LA2ST)
[NASA-CR-193412] p 1019 A93-31739
- Hypersonic engine component experiments in high heat flux, supersonic flow environment
[NASA-TM-106273] p 1032 A93-31860
- ### HIGH THRUST
- Design and technology for engine manufacture --- for Rolls-Royce aerospace business
[ISABE 93-7002] p 1194 A93-53979
- From RB211 to Trent: An ongoing development strategy
[PNR-90938] p 56 A93-11038
- ### HIGHLY MANEUVERABLE AIRCRAFT
- Nonlinear feedback control of highly manoeuvrable aircraft
p 40 A93-11654
- Pilot/Vehicle display development from simulation to flight
[AIAA PAPER 92-4174] p 51 A93-13310
- RISK - Interactive multidisciplinary system for designing airframes
p 226 A93-14337
- Pressure measurements on a pitching airfoil in a water channel
[AIAA PAPER 93-0184] p 473 A93-25510
- Investigation of high-alpha lateral-directional control power requirements for high-performance aircraft
[AIAA PAPER 93-3647] p 1130 A93-49519
- Real-time simulation of maneuverable aircraft flight conditions on altitude test cell
[AIAA PAPER 93-1845] p 1137 A93-49726

HOLOGRAPHIC INTERFEROMETRY

- Robust, nonlinear, high angle-of-attack control design for a supermaneuverable vehicle
[AIAA PAPER 93-3774] p 1131 A93-51369
- Cancellation control law for lateral-directional dynamics of a supermaneuverable aircraft
[AIAA PAPER 93-3775] p 1131 A93-51370
- Design of a flight control system for a highly maneuverable aircraft using mu synthesis
[AIAA PAPER 93-3776] p 1132 A93-51371
- Stability analysis through bifurcation theory. I, II
[ONERA, TP NO. 1993-108] p 1225 A93-53620
- Advanced aircraft with thrust vector control
[MBB-FE-1-SUB-0504] p 998 A93-31043
- ### HILBERT SPACE
- Linear quadratic tracking problems in Hilbert space - Application to optimal active noise suppression
p 1224 A93-52763
- ### HILSCH TUBES
- The development of a new air filtration system for the Alouette III helicopter
[ISABE 93-7048] p 1199 A93-54024
- ### HISTORIES
- Winds of change: Expanding the frontiers of flight. Langley Research Center's 75 years of accomplishment, 1917-1992
[NASA-NP-130] p 104 A93-11100
- The V-22 Osprey: A case analysis
[AD-A256445] p 164 A93-14601
- Aeronautics in NACA and NASA
[NASA-NP-156] p 678 A93-26422
- ### HODOGRAPHS
- Supercritical wing design, a three dimensional hodograph approach
[AIAA PAPER 92-2657] p 472 A93-24986
- Hodograph analysis in aircraft trajectory optimization
[AIAA PAPER 93-3742] p 1101 A93-51338
- ### HOLE GEOMETRY (MECHANICS)
- Theory of the machining of polyhedral holes by plunge cutting
p 835 A93-39091
- Laser and skill enhance results
p 1257 A93-54843
- RB211-524B disc and drive cones hot cyclic spinning test
p 177 A93-14895
- ### HOLES (MECHANICS)
- Extending the fatigue life of aircraft engine components by hole cold expansion technology
[ASME PAPER 92-GT-77] p 401 A93-19327
- Discharge coefficients of holes angled to the flow direction
[ASME PAPER 92-GT-192] p 403 A93-19417
- Internal cooling passage heat transfer near the entrance to a film cooling hole - Experimental and computational results
[ASME PAPER 92-GT-241] p 404 A93-19450
- A laboratory study of fracture in the presence of lap splice multiple site damage
p 1027 A93-45790
- Reliability of stiffened structural panels: Two examples
[NASA-TM-107687] p 219 A93-14483
- RB 199 high pressure compressor stage 3 spin pit tests
p 176 A93-14893
- F100 second stage fan disk bolt-hole crack propagation ferris wheel test
p 177 A93-14897
- The aerodynamic performance of laser drilled sheets
[AERO-REPT-9204] p 484 A93-20806
- ### HOLOGRAPHIC INTERFEROMETRY
- Double mode behaviour of bladed disk assemblies in the resonance frequency range, visualized by means of holographic interferometry
[ASME PAPER 92-GT-438] p 357 A93-19580
- A rapid procedure for obtaining time-average interferograms of vibrating bodies
p 412 A93-21857
- Holographic interferometric investigation of shock wave interaction with a ramp
p 271 A93-21921
- Aero-optical phase measurements using Fourier transform holographic interferometry
p 549 A93-29302
- Schlieren device and holographic interferometer for hypersonic flow visualization
[ONERA, TP NO. 1992-160] p 832 A93-38739
- Evaluation by holographic interferometry of impact damage in composite aeronautical structures
p 1020 A93-44193
- Visualisation and analysis of three dimensional transonic flows by holographic interferometry
p 1020 A93-44194
- Progress in industrial holography in France
p 1020 A93-44197
- Laser holographic interferometric measurements of the flow behind a rearward facing step
[AIAA PAPER 93-3515] p 985 A93-47279
- Interferometric reconstruction of three-dimensional high-speed aerodynamic flows
p 291 A93-16765
- Study of optical techniques for the Ames unitary wind tunnel: Digital image processing, part 6
[NASA-CR-192164] p 382 A93-18766

HOLOGRAPHY

- Video holography and laser vibrometry...The dynamic duo p 210 A93-16611
- Optically smart surfaces for aerodynamic measurements [AIAA PAPER 92-3895] p 539 A93-24484
- Design of an optimal single reflective holographic helmet display element p 517 A93-26886
- Particle imaging techniques and applications p 1020 A93-44195
- Progress in industrial holography in France p 1020 A93-44197
- Ultra wide band 3-D cross section (RCS) holography [DE92-019133] p 89 A93-11802
- Optically smart surfaces survivability testing at Mach 3 [AD-A261785] p 760 A93-26566

HONEYCOMB CORES

- Tiltrotor Research Aircraft composite blade repairs - Lessons learned p 108 A93-14819
- Sandwich construction in the Starship p 159 A93-15737

HONEYCOMB STRUCTURES

- The use of a deep honeycomb to achieve high flow quality in the ARA 9 ft x 8 ft Transonic Wind Tunnel p 190 A93-14276
- PAA-core aluminum honeycomb - An end user's evaluation p 209 A93-15738
- Optimal design of honeycomb sandwich shell aircraft structures of composite materials p 828 A93-36800
- Integrity testing of brush seal in shroud ring of T-700 engine [NASA-TM-105863] p 421 A93-18380

HORIZONTAL DISTRIBUTION

- The onset of disintegration and corona in water drops falling at terminal velocity in horizontal electric fields p 1163 A93-49130

HORIZONTAL FLIGHT

- Effect of the aerodynamic interference of the rotor and the fuselage on the power requirements for the horizontal flight of a helicopter p 819 A93-39179
- Selection of the powerplant for a thermoplane p 899 A93-42380
- An experimental and a theoretical investigation of rotor pitch damping using a model rotor p 47 A93-10322
- Contributions to the experimental investigation of rotor/body aerodynamic interactions p 20 A93-10877
- The effect of wake dynamics on rotor eigenvalues in forward flight p 137 A93-14595
- The Application of CFD to rotary wing flow problems [NASA-TM-102803] p 139 A93-15483
- Fundamentals of adaptive anticipation techniques for the detection of threatening air traffic conflicts: Investigation of the horizontal proximity situation in the case of expected heading changes p 503 A93-21004
- Aeroelastic response and aeromechanical stability of helicopters with elastically coupled composite rotor blades p 715 A93-25530
- Development and testing of the digital control system for the Archytas unmanned air vehicle [AD-A261656] p 729 A93-26196

HORIZONTAL SPACECRAFT LANDING

- Takeoff and landing analysis methodology for an airbreathing space booster p 914 A93-42927

HORIZONTAL TAIL SURFACES

- Apparatus and method for improving spin recovery on aircraft [NASA-CASE-LAR-14747-1] p 526 A93-20039

HORSEPOWER

- Electro-modulated control of supply pressure in hydraulic systems [SAE PAPER 912119] p 412 A93-21842

HORSESHOE VORTICES

- Experimental study on the three dimensional flow within a compressor cascade with tip clearance. I - Velocity and pressure fields [ASME PAPER 92-GT-215] p 258 A93-19574
- Time-resolved surface heat flux measurements in the wing/body junction vortex [AIAA PAPER 93-0918] p 472 A93-24972
- An experimental study of a turbulent wing-body junction and wake flow p 873 A93-43541
- On dynamics of the juncture vortex [AIAA PAPER 93-3473] p 980 A93-47252

HOT CORROSION

- Hot end cleaning - Corrosion pitting of turbine discs [SAE PAPER 920930] p 202 A93-14081
- High temperature corrosion resistant bearing steel development [AIAA PAPER 93-2000] p 1145 A93-49842
- Advanced turbine design for coal-fueled engines [DE93-000224] p 554 A93-21254
- Platinum-modified diffusion aluminide coatings on nickel-base superalloys [AD-A263597] p 917 A93-29981

HOT ISOSTATIC PRESSING

- HIP consolidation of aluminum-rich intermetallic alloys and their composites [NAWCADWAR-92003-60] p 199 A93-14726

HOT SURFACES

- Influence of surface heating condition on local heat transfer in a rotating square channel with smooth walls and radial outward flow [ASME PAPER 92-GT-188] p 402 A93-19413
- Hot experimental technique: A new requirement of aerothermodynamics [MBB-FE-202-S-PUB-480] p 293 A93-17543

HOT-FILM ANEMOMETERS

- Flight evaluation of a stagnation detection hot-film sensor [AIAA PAPER 92-4085] p 51 A93-13263
- Calibration of thermal anemometer at very low Reynolds numbers under microgravity p 926 A93-41729
- Surface hot-film method for the measurement of transition, separation and reattachment points [AIAA PAPER 93-2918] p 1148 A93-48120
- 3-dimensional interactions in the rotor of an axial turbine [AIAA PAPER 93-2255] p 1081 A93-50053
- Hot film wall shear instrumentation for compressible boundary layer transition research [NASA-CR-191360] p 294 A93-17855
- The experimental study of transition and leading edge contamination of swept wings [LIB-TRANS-2197] p 782 A93-27274

HOT-WIRE ANEMOMETERS

- Calibration of thermal anemometer at very low Reynolds numbers under microgravity p 926 A93-41729
- An experimental study of flow patterns and endwall heat transfer upstream of a surface-mounted rectangular obstruction in a turbulent boundary layer p 89 A93-11698

HOT-WIRE FLOWMETERS

- Unsteady turbulent skin-friction measurement in an adverse pressure gradient p 206 A93-14545
- Experimental studies of the turbulent structure of supersonic mixing layers [AIAA PAPER 93-0217] p 278 A93-22633

HOUSINGS

- Design and fabrication of a composite transmission housing for a helicopter tail rotor p 156 A93-14339
- Acoustical analysis of gear housing vibration p 567 A93-29420

HOVERCRAFT GROUND EFFECT MACHINES

- The legal status of ekranoplanes p 453 A93-20900

HOVERING

- Small scale jet effects and hot gas ingestion investigations at NASA Ames [AIAA PAPER 92-4252] p 67 A93-13339
- Experimental study of rotor wake/body interactions in hover p 124 A93-14782
- Multidisciplinary analysis and sensitivity derivatives for isolated helicopter rotors in hover [AIAA PAPER 92-4696] p 324 A93-20308
- Conceptual assessment of two high-speed rotorcraft p 508 A93-28612
- Far-field hover acoustic characteristics of the XV-15 tiltrotor aircraft with Advanced Technology Blades p 566 A93-29412
- Euler solutions to nonlinear acoustics of non-lifting rotor blades p 568 A93-29433
- Flowfield analysis of modern helicopter rotors in hover by Navier-Stokes method p 481 A93-29435
- Flow visualization and flow field measurements of a 1/12 scale tilt rotor aircraft in hover p 482 A93-29441
- Improvements in hover display dynamics for a combat helicopter p 727 A93-34257
- Effect of an unsteady three-dimensional wake on elastic blade-flapping eigenvalues in hover p 683 A93-34260
- Synthesis and evaluation of an H2 control law for a hovering helicopter p 728 A93-34542
- Introduction of the M-85 high-speed rotorcraft concept p 797 A93-35980
- Investigation of the flight mechanics simulation of a hovering helicopter p 798 A93-35990
- Shadowgraph flow visualization of isolated tiltrotor and rotor/wing wakes p 767 A93-35996
- Hover performance analysis of advanced rotor blades p 767 A93-35998
- Hover testing a demonstrated and cost-effective risk reduction tool [AIAA PAPER 93-2677] p 913 A93-42234
- Tip vortex geometry of a hovering helicopter rotor in ground effect p 893 A93-43779
- Free-wake computation of helicopter rotor flowfields in forward flight [AIAA PAPER 93-3079] p 1059 A93-48253
- SCV measurements in the wake of a rotor in hover and forward flight [AIAA PAPER 93-3080] p 1059 A93-48254

- A test bench for rotorcraft hover control [AIAA PAPER 93-3853] p 1140 A93-51440
- Data acquisition for aeroelastic testing at the NASA Langley Transonic Dynamics Facility p 1250 A93-54397
- An experimental and a theoretical investigation of rotor pitch damping using a model rotor p 47 A93-10322
- Tilt rotor hover aeroacoustics [NASA-CR-177598] p 99 A93-10458
- Contributions to the experimental investigation of rotor/body aerodynamic interactions p 20 A93-10877
- Navier-Stokes flowfield computation of wing/rotor interaction for a tilt rotor aircraft in hover p 135 A93-14035
- Stability of elastically tailored rotor blades p 164 A93-14828
- Finite-state inflow applied to aeroelastic flutter of fixed and rotating wings p 188 A93-14830
- The Application of CFD to rotary wing flow problems [NASA-TM-102803] p 139 A93-15483
- Ground based simulation evaluation of the effects of time delays and motion on rotorcraft handling qualities [AD-A256921] p 328 A93-16186
- Helicopter flight control system design using the linear quadratic regulator for robust eigenstructure assignment [AD-A258904] p 373 A93-19351
- An exploratory investigation of the flight dynamics effects of rotor rpm variations and rotor state feedback in hover [NASA-TM-103968] p 373 A93-19380
- Application of finite-state inflow to flap-lag-torsion damping in hover p 714 A93-25486
- Aeroelastic response and aeromechanical stability of helicopters with elastically coupled composite rotor blades p 715 A93-25530
- Jet-induced ground effects on a parametric flat-plate model in hover [NASA-TM-104001] p 700 A93-26099
- Transition aerodynamics for 20-percent-scale VTOL unmanned aerial vehicle [NASA-TM-4419] p 779 A93-27032
- Current projects in Fuzzy Control p 1038 A93-31442

HOVERING STABILITY

- Navier-Stokes computation of wing/rotor interaction for a tilt rotor in hover p 122 A93-14537
- Aeroacoustic environment of an advanced short takeoff and vertical landing aircraft in hover p 231 A93-14539
- Influence of pitch-lag coupling on damping requirements to stabilize 'ground/air resonance' p 158 A93-14784
- Flutter calculations for fixed and rotating wings with state-space inflow dynamics [AIAA PAPER 93-1300] p 709 A93-33877
- Aeromechanical stability of helicopters with composite rotor blades in forward flight p 794 A93-35904
- Numerical simulation of a hovering rotor using embedded grids p 765 A93-35936
- Interactional aerodynamic effects on rotor performance in hover and forward flight p 766 A93-35941
- Side-by-side hover performance comparison of MDHC 500 NOTAR and tail rotor anti-torque systems p 796 A93-35956
- Flap-lag damping in hover and forward flight with a three-dimensional wake p 797 A93-35979
- An efficient method to calculate rotor flow in hover and forward flight [AIAA PAPER 93-3336] p 953 A93-45030
- Navier-Stokes calculations of rotating BERP platform blade flowfields [AIAA PAPER 93-3527] p 986 A93-47286

HTPB PROPELLANTS

- Regression rate mechanism in a solid fuel ramjet p 814 A93-27185

HUBS

- Effect of hub treatment on performance of an axial flow compressor p 53 A93-12736
- Super Puma MK II - Rotor and gearbox fatigue p 46 A93-13636
- Fatigue qualification of high thickness composite rotor components p 81 A93-13646
- A study of stall in a low hub/tip ratio fan [ASME PAPER 92-GT-85] p 248 A93-19334
- Sources of helicopter rotor hub inplane shears [AIAA PAPER 93-1358] p 709 A93-33927

HUGONOT EQUATION OF STATE

- Hugoniot analysis of the ram accelerator p 1023 A93-45500

HULLS (STRUCTURES)

- Simultaneous mapping of the unsteady flow fields by Particle Displacement Velocimetry (PDV) p 786 A93-27454

HUMAN FACTORS ENGINEERING

- Advanced technology and the pilot p 45 A93-13412
- Human factors of aircraft cabin safety p 140 A93-14218
- Progress and taboos in air safety orientations of research in human factors in air transport p 141 A93-14374

Aircrew integrated management p 141 A93-14376
Experimental working position simulator to analyse, develop and optimize concepts for computer-aided Air Traffic Management p 191 A93-14412
The application of human factors engineering at General Electric Aircraft Engines [SAE PAPER 921039] p 108 A93-14659
Control of the pilot-system interface p 166 A93-15040
Model of a map indicator p 341 A93-18532
Key trends in human factors of aircraft maintenance; Proceedings of the Conference, London, United Kingdom, Oct. 31, 1991 p 237 A93-18754
[ISBN 1-85768-0057]
The designs for safety — considering human factors in aircraft maintenance p 321 A93-18755
The human factors aspects of aircraft ground handling p 237 A93-18756
The National Plan for Aviation Human Factors - Maintenance research issues p 457 A93-27132
Ongoing and planned R&D efforts in airway facilities maintenance p 458 A93-27134
The development of the Boeing Human Model p 561 A93-27150
Utilizing a microcomputer based flight simulation in teaching human factors in aviation p 570 A93-27165
Using TRACON as a teaching tool p 571 A93-27166
Spatial orientation and wayfinding in airport passenger terminals - Implications for environmental design p 487 A93-27168
Performance considerations for high-definition head-mounted displays p 518 A93-27242
AHS, Annual Forum, 48th, Washington, June 3-5, 1992, Proceedings, Vols. 1 & 2 p 763 A93-35901
MIDAS technology transfer p 845 A93-35920
Progress and taboos in flight safety - Human-factors research in air transportation p 879 A93-42654
Pilot task monitoring using neural networks p 940 A93-42846
International standards for the qualification of airplane flight simulators; Conference, London, United Kingdom, Jan. 16, 17, 1992, Document Approved [ISBN 1-85768-040-5] p 1140 A93-51934
AIAA Flight Simulation Technologies Conference, Monterey, CA, Aug. 9-11, 1993, Technical Papers p 1207 A93-52651
Effect of lift-to-drag ratio in pilot rating of the HL-20 landing task p 1210 A93-53738
Integration of an integrated helmet system for PAH 2 p 1244 A93-55298
Methods and principles for determining task dependent interface content [NASA-CR-190837] p 36 A93-10961
Design of instrument approach procedure charts: Comprehension speed of missed approach instructions coded in text or icons p 36 A93-11252
[PB92-205673]
Action composition for the animation of natural language instructions p 228 A93-12554
[AD-A254963]
Workshop on Aeronautical Decision Making (ADM). Volume 2: Plenary Session With Presentations and Proposed Action Plan [DOT/FAA/RD-92/14-VOL-2] p 146 A93-15013
Does cockpit management training reduce aircrew error? p 146 A93-15014
Cockpit decision making p 146 A93-15015
Trans-cockpit authority gradient in Navy/Marine aircraft mishaps p 146 A93-15016
A cognitive model for training decision making in aircrews p 147 A93-15020
Elements of a theory of natural decision making p 147 A93-15021
Taxonomy of flight variables p 147 A93-15022
Shared mental models and crew decision making p 147 A93-15023
Embedded ADM reduces helicopter human error accidents p 147 A93-15024
Proposed action plan to improve ADM effectiveness, part 3: Developing a new ADM paradigm on which to build advanced or expert decision making training p 148 A93-15026
FAA Technical Center Aeronautical Data Link Research Plan p 417 A93-15698
[DOT/FAA/CT-92/23]
Aviation safety research at the National Institute for Aviation Research Wichita State University: A report to the FAA Technical Center p 310 A93-16455
[NIAR-92-2]
Integrated helmet system testing for a nightflying helicopter p 343 A93-17570
[MBB-UD-0604-91-PUB]
Aircraft Accidents: Trends in Aerospace Medical Investigation Techniques p 490 A93-19653
[AGARD-CP-532]

How do we investigate the human factor in aircraft accidents? p 491 A93-19655
A method for investigating human factor aspects of military aircraft accidents p 491 A93-19656
The human factor problem in the Canadian Forces aviation p 491 A93-19657
Underlying causes of accidents: Casual networks p 491 A93-19658
Aid in investigation by figure animation p 491 A93-19659
Human factors causes and management strategies in US Air Force F-16 mishaps 1984-present p 492 A93-19673
F-16 accidents: The Norwegian experience p 492 A93-19674
Category A F-16 accidents in the Belgian Air Force p 492 A93-19675
Air accidents in the French Air Force p 492 A93-19676
Combat and training aircraft class A mishaps in the Belgian Air Force 1970-1990 p 492 A93-19677
Underlying causes of human error in US Army rotary wind accidents p 492 A93-19678
Accidents and errors: A review of recent UK Army Air Corps accidents p 495 A93-19701
Liquid crystal displays replacing the CRT and CLE of future cockpits p 518 A93-19783
Lessons learned from an historical look at flight testing p 511 A93-19904
On the typography of flight-deck documentation [NASA-CR-177605] p 571 A93-19970
Mission planning systems for tactical aircraft (pre-flight and in-flight) p 496 A93-21187
[AGARD-AR-313]
Crashworthiness of composite seats for civil aircraft p 703 A93-24773
HUMAN FACTORS LABORATORIES
The National Plan for Aviation Human Factors - Maintenance research issues p 457 A93-27132
Ongoing and planned R&D efforts in airway facilities maintenance p 458 A93-27134
HUMAN PERFORMANCE
The National Plan for Aviation Human Factors - Maintenance research issues p 457 A93-27132
Evolution of European air space toward precision navigation (P/RNAV) p 882 A93-43369
Adaptive automation and human performance: Multi-task performance characteristics [AD-A254596] p 186 A93-12578
Performance of color-dependent tasks of air traffic control specialists as a function of type and degree of color vision deficiency [AD-A256614] p 151 A93-14275
Elements of a theory of natural decision making p 147 A93-15021
Proposed action plan to improve ADM effectiveness, part 3: Developing a new ADM paradigm on which to build advanced or expert decision making training p 148 A93-15026
Simulator motion [AD-A257683] p 381 A93-17687
An investigation of the influence of advanced aircraft diagnostics on the technological sophistication of maintenance personnel [AD-A259988] p 240 A93-18887
Underlying causes of human error in US Army rotary wind accidents p 492 A93-19678
Helicopter accidents over water in the national navy: Epidemiological study over the period 1980-1991 p 493 A93-19686
Accidents and errors: A review of recent UK Army Air Corps accidents p 495 A93-19701
Comparison of performance on the Shipley Institute of Living Scale, Air Traffic Control Specialist Selection Test, and FAA Academy Screen [AD-A259249] p 502 A93-20582
Performance-based testing and success in Naval advanced flight training p 717 A93-25933
Aircraft accident report: Controlled collision with terrain GP Express Airlines, Inc., Flight 861, A Beechcraft C99, N118GP, Anniston, Alabama, 8 June 1992 [PB93-910403] p 790 A93-27035
HUMAN REACTIONS
Influence of aircraft noise on speech intelligibility p 558 A93-28483
Preliminary results from a study of community response to noise from military aircraft exercise p 558 A93-28484
Night aircraft noise index and sleep research results p 558 A93-28485
Final results from a study of community response to aircraft noise around Oslo Airport Fornebu p 558 A93-28486
Fatigue effects of noise among airplane mechanics p 558 A93-28495

Noise-induced reaction in a work community adjacent to aircraft runways - The Royal Australian Airforce p 559 A93-28496
Reaction to aircraft noise near general aviation airfields [DORA-8203] p 1040 A93-32377
HURRICANES
An unmanned aircraft for dropwindsone deployment and hurricane reconnaissance p 677 A93-34587
Comparison of three methods to deduce three-dimensional wind fields in a hurricane with airborne Doppler radar p 844 A93-37691
HYBRID COMPOSITES
Nonlinear analyses of composite aerospace structures in sonic fatigue [NASA-CR-193124] p 930 A93-29154
HYBRID PROPULSION
Engine technologies for future spaceplanes [ETN-92-92732] p 177 A93-15143
HYDRAULIC CONTROL
Design characteristics of the functional systems of aircraft and prediction of their technical condition p 320 A93-18334
A method for evaluating the technical condition of hydraulic control boosters without their disassembly — repair of aircraft systems p 395 A93-18335
Characteristics of the diagnostics of booster system components p 321 A93-18361
Monitoring the purity of the working fluids of aircraft hydraulic systems during service p 321 A93-18367
The Boeing 747-400 upper rudder control system with triple tandem valve [SAE PAPER 912133] p 327 A93-21843
Design, analysis, and control of large transport aircraft utilizing engine thrust as a backup system for the primary flight controls [NASA-CR-192938] p 820 A93-27308
HYDRAULIC EQUIPMENT
Evaluation of the efficiency of the direct search method in solving the problem of numerical calculation of the complex hydraulic cooling systems of aviation gas turbine engines p 54 A93-12818
Integrated utilities management system for aircraft p 153 A93-14208
Advanced aerospace hydraulic systems and components [SAE SP-885] p 412 A93-21840
Electro-modulated control of supply pressure in hydraulic systems [SAE PAPER 912119] p 412 A93-21842
HYDRAULIC FLUIDS
Monitoring the purity of the working fluids of aircraft hydraulic systems during service p 321 A93-18367
Development of MIL-H-53119, -54 C to 175 C high-temperature nonflammable hydraulic fluid for Air Force systems p 1214 A93-54250
HYDRAULIC JETS
Water instead of chemical corrosives against aircraft paint - Environment-friendly paint-stripping methods could mean drastic cost reductions for the aircraft industry p 239 A93-21850
Ultra-high pressure water jet technology - An overview of a new process for aerospace paint stripping [SME PAPER AD92-196] p 855 A93-40661
HYDRAULIC TEST TUNNELS
A qualitative assessment of control effectors on an advanced fighter configuration [AIAA PAPER 93-3627] p 1127 A93-48312
Wind tunnel tests and CFD in Fuji Heavy Industries p 304 A93-19323
HYDRIDES
Application of vanadium hydride compressors for Joule-Thomson cryocoolers p 1149 A93-48616
HYDROCARBON COMBUSTION
Three-dimensional gas turbine combustor emissions modeling [ASME PAPER 92-GT-129] p 350 A93-19363
Chemical kinetic and aerodynamic structures of flames [AD-A256015] p 391 A93-15931
HYDROCARBON FUELS
USAF supercritical hydrocarbon fuels interests [AIAA PAPER 93-0807] p 533 A93-24883
A hypersonic waverider research vehicle [AIAA PAPER 93-0402] p 505 A93-25522
Design and investigation of the stand and flying scramjet models - Conceptions and results of experiments [AIAA PAPER 93-2447] p 1120 A93-50199
A study of self-ignition of methane-hydrogen mixture fuel injected into high enthalpy supersonic airstreams [ISABE 93-7049] p 1213 A93-54025
High density strained hydrocarbon fuels for air breathing propulsion [ISABE 93-7081] p 1213 A93-54057
Liquid flow reactor and method of using [AD-D015392] p 222 A93-15232

- Fundamental studies of droplet interactions in dense sprays
[AD-A261165] p 737 N93-25948
- HYDROCARBONS**
Viscosity of aviation fuel components - Aromatic hydrocarbons (alkyl benzenes) p 1211 A93-52961
- HYDRODYNAMIC RAM EFFECT**
Ribless ram air parachute
[AD-D015351] p 20 N93-11050
- HYDRODYNAMICS**
Hydrodynamic effects on heat transfer for film-cooled turbine blades
[AD-A257291] p 361 N93-16080
Combustion instabilities in a side-dump model ramjet combustor p 362 N93-17613
Articulated fin/wing control system p 909 N93-29278
[AD-D015712] p 909 N93-29278
On the verification of a theory for sculling propulsion [ETN-93-94040] p 1031 N93-31519
- HYDROFOILS**
Rotation and cavitation of a marginal vortex p 11 A93-12433
Design features of the GTD 8000 and GTD 15000 marine gas turbine engines
[ASME PAPER 92-GT-15] p 400 A93-19287
- HYDROGEN**
Role of hydrogen/air chemistry in nozzle performance for a hypersonic propulsion system p 359 A93-21668
The numerical model of supersonic air flow field with hydrogen transverse injection p 859 A93-41736
Slush hydrogen quantity gaging and mixing for the National Aerospace Plane p 1150 A93-48635
Development and use of hydrogen-air torches in an altitude facility p 1137 A93-49988
Kinetic scheme selection in describing detonation in an H₂-air mixture behind shock waves p 1253 A93-55032
Experiments and analysis concerning the use of external burning to reduce aerospace vehicle transonic drag p 70 N93-12537
Mixing and reaction in the subsonic 2-D turbulent free shear layer p 289 N93-16508
Numerical study on transverse hydrogen injection into a supersonic flowfield p 302 N93-19311
- HYDROGEN EMBRITTLEMENT**
Gas phase hydrogen permeation in a Ni-Fe-Co superalloy p 735 A93-34510
Hydrogen-induced stress corrosion cracking susceptibility analysis of pitch links from the AH-64 Apache helicopter p 736 N93-25895
- HYDROGEN FUELS**
An experimental investigation of hydrogen-fueled supersonic combustor p 53 A93-12733
Combustion performance of a hydrogen-fueled small combustor for a micro gas turbine p 389 A93-21731
Dual transverse injection of H₂ gas into Mach 1.8 flows at University Komaba wind tunnel p 376 A93-21833
PDF prediction of supersonic hydrogen flames p 391 A93-23358
[AIAA PAPER 93-0448] p 391 A93-23358
Analytical comparison of convective heat transfer correlations in supercritical hydrogen p 416 A93-23477
A hypersonic waverider research vehicle p 505 A93-25522
[AIAA PAPER 93-0402] p 505 A93-25522
Taking to the skies under hydrogen power - Deutsche Aerospace Airbus studies the use of alternative fuels for civil aviation p 677 A93-34947
Gasdynamics of hydrogen-fueled scramjet combustors [AIAA PAPER 93-2145] p 1115 A93-49962
Modeling of turbulent supersonic H₂-air combustion with a multivariate beta PDF [AIAA PAPER 93-2198] p 1155 A93-50010
An approach to in-situ analysis of scramjet combustor behavior [AIAA PAPER 93-2328] p 1116 A93-50108
Design and investigation of the stand and flying scramjet models - Conceptions and results of experiments [AIAA PAPER 93-2447] p 1120 A93-50199
Energy management --- aircraft propulsion system performance p 1195 A93-53995
[ISABE 93-7019] p 1195 A93-53995
Hypersonic shock-induced combustion ramjet performance analysis p 1197 A93-54013
[ISABE 93-7037] p 1197 A93-54013
A study of self-ignition of methane-hydrogen mixture fuel injected into high enthalpy supersonic airstreams [ISABE 93-7049] p 1213 A93-54025
Experimental Investigation of Nozzle/Plume Aerodynamics at Hypersonic Speeds [NASA-CR-191368] p 386 N93-18085
Computation of H₂/air reacting flowfields in drag-reduction external combustion [NASA-CR-191071] p 536 N93-20237

HYDROGEN OXYGEN ENGINES

- Integrated air separation and propulsion system for aerospace plane with atmospheric oxygen collection [SAE PAPER 920974] p 195 A93-14633
Ceramic matrix composites for rocket engine turbine applications [ASME PAPER 92-GT-394] p 388 A93-19547
Finite-rate H₂/air combustion effects in CRJ for hypersonic launchers [ISABE 93-7084] p 1202 A93-54060
Compact heat exchanger fitted to engines of the inverted type [ISABE 93-7120] p 1221 A93-54095
Hypersonic engine component experiments in high heat flux, supersonic flow environment [NASA-TM-106273] p 1032 N93-31860
- HYDROGRAPHY**
System analysis for a kinematic positioning system based on the global positioning system [AD-A262830] p 885 N93-29468
- HYDROMECHANICS**
Electro-modulated control of supply pressure in hydraulic systems [SAE PAPER 912119] p 412 A93-21842
A study of the stability of the acceleration circuit of the hydro-mechanical automatic control system of an aviation gas turbine engine p 810 A93-39028
- HYDROMETEOROLOGY**
Hydrometeor identification using cross polar radar measurements and aircraft verification p 844 A93-37719
- HYDROPLANES (SURFACES)**
Experiments on low aspect ratio hydroplanes to measure lift under static and dynamic conditions [ARE-TM(UHR)-90306] p 21 N93-11365
Lift coefficient of a randomly oscillating hydroplane [DRA/MAR-TM(MTH)-91320] p 21 N93-11377
- HYDROSTATIC PRESSURE**
Silicon differential pressure transducer line pressure effects and compensation p 830 A93-37890
- HYDROXYL RADICALS**
Planar imaging of OH density distributions in a supersonic combustion tunnel [AIAA PAPER 93-0042] p 389 A93-20155
Laser selection criteria for OH fluorescence measurements in supersonic combustion test facilities p 549 A93-29315
Comparison of NO and OH PLIF temperature measurements in a scramjet model flowfield [AIAA PAPER 93-2035] p 1113 A93-49870
An aircraft instrument design for in situ tropospheric OH measurements by laser induced fluorescence at low pressures p 1159 A93-51528
- HYPERBARIC CHAMBERS**
High-pressure hypervelocity electrothermal wind-tunnel performance study and subscale tests p 1137 A93-49617
- HYPERBOLIC DIFFERENTIAL EQUATIONS**
The accuracy of cell vertex finite volume methods on quadrilateral meshes p 227 A93-14526
Solution of the problem of determining the dynamic characteristics of the cross-flow heat exchanger of the heat recovery system of gas turbine engines p 834 A93-39055
- HYPERCUBE MULTIPROCESSORS**
Implementation of BMLC computer model on hypercube systems --- Baseline Microwave Landing System p 32 A93-11024
[FFA-TN-1992-37] p 843 N93-28994
- HYPERSONIC AIRCRAFT**
Near-optimal energy transitions for energy-state trajectories of hypersonic aircraft [AIAA PAPER 92-4300] p 69 A93-13276
Integration of turbo-expander- and turbo-ramjet-engines in hypersonic vehicles [ASME PAPER 92-GT-204] p 353 A93-19428
Conceptual design of turbo-accelerator for HST combined cycle engine [ASME PAPER 92-GT-253] p 353 A93-19462
Some topics of research on hypersonic airbreathing engines at National Aerospace Laboratory [ASME PAPER 92-GT-256] p 353 A93-19465
A scoping study for hypersonic transport propulsion systems [ASME PAPER 92-GT-409] p 356 A93-19558
Air-breathing hypersonic cruise - Prospects for Mach 4.7 waverider aircraft [ASME PAPER 92-GT-437] p 384 A93-19579
Structural Tailoring/Analysis for Hypersonic Components - A computational simulation [AIAA PAPER 92-4722] p 325 A93-20324
Analytical comparison of convective heat transfer correlations in supercritical hydrogen p 416 A93-23477

- The structure and material testing facility needed for future SST/HST development [AIAA PAPER 92-3887] p 528 A93-24481
Current technologies for waverider aircraft [AIAA PAPER 93-0400] p 505 A93-25521
Interference of an oblique shock with a shock layer on a blunt edge for small Reynolds numbers p 775 A93-39120
Computational fluid dynamics for hypersonic airbreathing aircraft p 865 A93-42581
A computational investigation of fuel mixing in a hypersonic scramjet [AIAA PAPER 93-2994] p 1001 A93-44230
Active control of aerothermoelastic effects for a conceptual hypersonic aircraft p 1007 A93-45137
Supersonic/hypersonic aerodynamic methods for aircraft design and analysis p 967 A93-46816
Requirements for facilities and measurement techniques to support CFD development for hypersonic aircraft p 1014 A93-47024
Interpretation of waverider performance data using computational fluid dynamics [AIAA PAPER 93-2921] p 1044 A93-48122
Hypersonic configuration optimization with an Euler/boundary layer coupling technique [AIAA PAPER 93-3116] p 1062 A93-48286
An experimental study of the thrust and aerodynamic characteristics of an operating ramjet engine in a blowdown wind tunnel p 1107 A93-48828
Future technology aim of the National Aerospace Plane Program [AIAA PAPER 93-1988] p 1141 A93-49833
Review of NASA's Hypersonic Research Engine Project [AIAA PAPER 93-2323] p 1116 A93-50103
Aircraft cryogenic fuel system design issues [AIAA PAPER 93-2567] p 1121 A93-50285
A pseudo-loop design strategy for the longitudinal control of hypersonic aircraft [AIAA PAPER 93-3814] p 1132 A93-51405
Effect of boundary layer suction on the thrust and aerodynamic efficiency of a hypersonic flight vehicle p 1176 A93-52959
Mach 5 turboramjet requirements and design approach [ISABE 93-7015] p 1194 A93-53991
Conceptual design study on combined-cycle engine for hypersonic transport [ISABE 93-7018] p 1195 A93-53994
Research and development of a turbo-accelerator for super/hypersonic transport [ISABE 93-7066] p 1200 A93-54042
Research and development of high pressure compressor for SST and HST engine [ISABE 93-7068] p 1186 A93-54044
Ultra-high temperature materials in the research and development of super/hypersonic transport propulsion system p 1252 A93-54712
Control of supersonic throughflow turbomachines discrete frequency noise generation by aerodynamic detuning p 1248 A93-55860
Integration of turbo-ramjet engines for hypersonic aircraft p 175 N93-13230
Hypersonic reconnaissance aircraft [NASA-CR-192049] p 333 N93-17804
A manned hypersonic reconnaissance vehicle which does not require airborne fueling p 333 N93-17888
Advanced hypersonic aircraft design [NASA-CR-192046] p 334 N93-18037
Operational and research aspects of a radio-controlled model flight test program [NASA-TM-104266] p 339 N93-18616
Aerodynamic analysis of hypersonic waverider aircraft [NASA-CR-192981] p 780 N93-27093
Hypersonics revisited p 781 N93-27167
Calculations on unsteady type 4 interaction at Mach 8 [AD-A265214] p 990 N93-32004
Analytical and experimental investigations of the oblique detonation wave engine concept [NASA-TM-102839] p 1006 N93-32374
- HYPERSONIC BOUNDARY LAYER**
Detection of Goertler vortices in hypersonic flow p 120 A93-14382
Unstable branches of a hypersonic, chemically reacting boundary layer p 128 A93-17262
The asymptotic theory of hypersonic boundary-layer stability p 462 A93-24409
The long-wave limit in the asymptotic theory of hypersonic boundary-layer stability p 462 A93-24410
On high speed turbulence modeling of shock-wave boundary-layer interaction [AIAA PAPER 93-0778] p 541 A93-24860
On the breakdown of a hypersonic laminar boundary layer [AIAA PAPER 93-0896] p 472 A93-24956

- A new model for super/hypersonic turbulent boundary layers
[AIAA PAPER 93-0897] p 472 A93-24957
- Shock/boundary layer interaction in a hypersonic flow in the presence of an entropy layer
[ONERA, TP NO. 1992-181] p 773 A93-38743
- Flow past three-dimensional irregularities in a hypersonic boundary layer on a cooled body p 775 A93-39119
- High-speed turbulence modeling of shock-wave/boundary-layer interaction p 927 A93-41910
- Experiments on shock-wave/boundary-layer interactions produced by two-dimensional ramps and three-dimensional obstacles p 865 A93-42589
- An experimental contribution to the flat plate 2D compression ramp, shock/boundary layer interaction problem at Mach 14 - Test case 3.7 p 865 A93-42590
- Aerodynamic heating in the vicinity of hypersonic, axisymmetric, shock-wave boundary-layer interactions [AIAA PAPER 93-2766] p 963 A93-46512
- Passive control of shock wave/boundary layer interaction at hypersonic speed [AIAA PAPER 93-3249] p 966 A93-46794
- Scaling of incipient separation in high speed laminar flows [AIAA PAPER 93-3435] p 978 A93-47227
- Experimental study of shock wave and hypersonic boundary layer interactions near a convex corner [AIAA PAPER 93-2980] p 1051 A93-48173
- An analytical description of hypersonic boundary layer stability [AIAA PAPER 93-2981] p 1051 A93-48174
- Second-order effects in hypersonic laminar boundary layers p 1073 A93-49529
- Real gas effects in two- and three-dimensional hypersonic, laminar boundary layers p 1073 A93-49530
- Numerical modeling of flow in a hypersonic laminar boundary layer p 1086 A93-50967
- Calculation of perturbation propagation upstream in a hypersonic laminar boundary layer p 1086 A93-50968
- Separation phenomenon in a hypersonic flow with strong wall cooling - Subcritical regime p 1189 A93-54266
- Vibration excitation in laminar hypersonic boundary layers p 1237 A93-56028
- Experimental investigations of hypersonic shock-boundary layer interaction p 1238 A93-56037
- Time dependent heat transfer rates in high Reynolds number hypersonic flowfields p 216 A93-13664
- Modeling variable blowing on a slender cone in hypersonic flow p 138 A93-14836
- Reynolds number influences in aeronautics [NASA-TM-107730] p 989 A93-31732
- ### **HYPERSONIC COMBUSTION**
- In-stream measurements of combustion during Mach 5 to 7 tests of the Hypersonic Research Engine (HRE) [AIAA PAPER 93-2324] p 1116 A93-50104
- A review of supersonic combustion research at AEDC with hypersonic application [AIAA PAPER 93-2326] p 1116 A93-50106
- Hypersonic shock-induced combustion ramjet performance analysis [ISABE 93-7037] p 1197 A93-54013
- Enhanced fuel-air mixing in hypersonic engines [ISABE 93-7115] p 1221 A93-54090
- Shock enhancement and control of hypersonic combustion [AD-A254295] p 72 A93-10843
- ### **HYPERSONIC FLIGHT**
- A design approach to high Mach number scramjet performance [AIAA PAPER 92-4248] p 55 A93-13360
- Fluid/chemistry modeling for hypersonic flight analysis p 111 A93-14120
- Combined engines for hypersonic flight p 171 A93-14244
- Experimental investigation of aerothermal problems associated with hypersonic flight of HST p 120 A93-14380
- The United States in the conquest of the hypersonic p 109 A93-15056
- Overview of the Japanese National Project for Super/Hyper-Sonic Transport propulsion system [ASME PAPER 92-GT-252] p 239 A93-19461
- Nonequilibrium excitation of internal molecular degrees of freedom in the shock layer during hypersonic flight p 412 A93-21922
- Keynote address - Advanced Technology demonstrators, prototypes and hypersonic flight [AIAA PAPER 92-4999] p 456 A93-22276
- Closed form solutions of constrained trajectories - Application in optimal ascent of aerospace plane [AIAA PAPER 92-5012] p 385 A93-22288
- On the coupled thermomechanical analysis of hypersonic flight vehicle structures [AIAA PAPER 92-5018] p 413 A93-22294
- Characterization of electron beam propagation for hypersonic flight research applications [AIAA PAPER 92-5087] p 452 A93-22357
- The X-15 airplane - Lessons learned [AIAA PAPER 93-0309] p 456 A93-23005
- A comparison of hypersonic flight and prediction results [AIAA PAPER 93-0311] p 280 A93-23006
- Application of CFD to a generic hypersonic flight research study [AIAA PAPER 93-0312] p 280 A93-23007
- Numerical simulation of flow past the X24C reentry vehicle [AIAA PAPER 93-0319] p 280 A93-23011
- Flowfield computations over the Space Shuttle Orbiter with a proposed canard at a Mach number of 5.8 and 50 degrees angle of attack [AIAA PAPER 93-0322] p 281 A93-23014
- Characterization of the performance of shock-tube wind tunnels [AIAA PAPER 93-0351] p 377 A93-23036
- The effects of hypersonic flight test requirements on research vehicle design [AIAA PAPER 93-0511] p 386 A93-23258
- Pulsed detonation engine experimental and theoretical review [AIAA PAPER 92-3168] p 531 A93-24478
- A study of compressible turbulence [AIAA PAPER 93-0659] p 465 A93-24772
- NASP - Waveriders in a hypersonic sky. I p 532 A93-25355
- NASP - Waveriders in a hypersonic sky. II p 532 A93-25359
- NASA's hypersonic flight research program [AIAA PAPER 93-0308] p 457 A93-25516
- Reaction zone structure for strong, weak overdriven, and weak underdriven oblique detonations p 746 A93-35492
- Hypersonic flutter of a curved shallow panel with aerodynamic heating [AIAA PAPER 93-1318] p 829 A93-37428
- Shock/boundary layer interaction in a hypersonic flow in the presence of an entropy layer [ONERA, TP NO. 1992-181] p 773 A93-38743
- CFD for hypersonic propulsion p 865 A93-42585
- Research on supersonic combustion p 899 A93-42877
- A convective and radiative heat transfer analysis for the FIRE II forebody [AIAA PAPER 93-3194] p 1021 A93-44231
- Double diaphragm driven free piston expansion tube p 1016 A93-45533
- Solution strategy for three-dimensional configurations at hypersonic speeds p 962 A93-46406
- Non-equilibrium thermal radiation from air shock layers modelled with the Direct Simulation Monte Carlo method [AIAA PAPER 93-2805] p 1028 A93-46544
- Simulation of hypersonic flight - A concerted European effort p 1136 A93-49301
- Analytical solutions to constrained hypersonic flight trajectories p 1141 A93-49596
- Hypersonic ignition and thrust production in a scramjet [AIAA PAPER 93-2444] p 1119 A93-50196
- An investigation of the fuel-optimal periodic trajectories of a hypersonic vehicle [AIAA PAPER 93-3753] p 1101 A93-51349
- Dynamics of hypersonic flight vehicles exhibiting significant aeroelastic and aeropropulsive interactions [AIAA PAPER 93-3763] p 1131 A93-51358
- Aerothermodynamics of the high-altitude flight p 1089 A93-51783
- Aerodynamic heating environment definition/thermal protection system selection for the HL-20 p 1181 A93-53739
- HL-20 computational fluid dynamics analysis p 1181 A93-53740
- Studies on methane-fuel ram combustor for HST combined cycle engine [ISABE 93-7080] p 1201 A93-54056
- Finite-rate H₂/air combustion effects in CRJ for hypersonic launchers [ISABE 93-7084] p 1202 A93-54060
- LIF visualization of 3-dimensional hypersonic mixing [ISABE 93-7114] p 1221 A93-54089
- Enhanced fuel-air mixing in hypersonic engines [ISABE 93-7115] p 1221 A93-54090
- Numerical study of nitric oxide formation in a hypersonic ramjet engine [ISABE 93-7125] p 1204 A93-54100
- Heat loads as key problem of hypersonic flight p 1222 A93-54276
- Development of a tethered satellite force transducer p 1251 A93-54368
- An optical flameout detection system for NASA Langley's 8-Foot High Temperature Tunnel p 1254 A93-54372
- Hypersonic inlet efficiency revisited p 16 A93-10012
- On stability and control of SSTD spaceplane in super- and hypersonic ascending phase [NAL-TR-1128T] p 65 A93-12361
- Hypersonic propulsion system force accounting p 175 A93-13229
- High-temperature strain measurement techniques: Current developments and challenges p 217 A93-13669
- Engine technologies for future spaceplanes [ETN-92-92732] p 177 A93-15143
- Hot experimental technique: A new requirement of aerothermodynamics [MBB-FE-202-S-PUB-480] p 293 A93-17543
- Analytical solutions to constrained hypersonic flight trajectories [NASA-CR-191987] p 297 A93-18602
- Numerical calculation of flow field in supersonic combustion chamber p 304 A93-19317
- Turbulence modeling for hypersonic flight [NASA-CR-192288] p 483 A93-20235
- Heat loads as key problem of hypersonic flight [MBB-FE-202-S-PUB-0486] p 484 A93-21054
- Development of a non-linear simulation for generic hypersonic vehicles - ASUHS1 [NASA-CR-192710] p 516 A93-22003
- Trajectory optimization for the National aerospace plane [NASA-CR-192954] p 716 A93-25670
- Information requirements analyses for transatmospheric vehicles [AD-A261189] p 718 A93-25949
- Evaluation of candidate working fluid formulations for the electrothermal-chemical wind tunnel [NASA-CR-193366] p 1015 A93-31848
- Hypersonic engine component experiments in high heat flux, supersonic flow environment [NASA-TM-106273] p 1032 A93-31860
- ### **HYPERSONIC FLOW**
- Approximate methods for heat flows toward the surface of three-dimensional bodies p 4 A93-10080
- Viscous instability of hypersonic flow past a wedge p 4 A93-10137
- Calculation of a three-dimensional boundary layer at the lee side of a finite-span delta wing in the case of viscous interaction with hypersonic flow p 5 A93-10143
- An effective multigrid method for high-speed flows p 8 A93-10533
- An implicit multigrid scheme for hypersonic strong-interaction flowfields p 6 A93-10534
- Transport processes in hypersonic flows p 7 A93-11302
- Numerical solution of a free-boundary problem in hypersonic flow theory - Nonequilibrium viscous shock layers p 8 A93-11920
- A split-matrix Runge-Kutta type space marching procedure p 8 A93-11921
- Flow problems posed by reentry in planetary atmospheres p 11 A93-12432
- Shock wave interference on a wing with a partition at hypersonic velocities p 13 A93-12839
- A comparison of upwind schemes for computation of three-dimensional hypersonic real-gas flows [AIAA PAPER 92-4350] p 15 A93-13306
- Condensation of nitrogen in hypersonic flows - Measurements confirm a theoretical model p 111 A93-13945
- Simulation of a hypersonic flow over vehicles at low Reynolds numbers p 120 A93-14381
- Detection of Goertler vortices in hypersonic flow p 120 A93-14382
- Analytical solutions for hypersonic flow past slender power-law bodies at small angle of attack p 122 A93-14550
- Calculation of radiant energy transfer in hypersonic flow past blunt bodies using the P1 and P2 approximations of the spherical harmonic method p 124 A93-15209
- Two-phase injection from the front surface of a blunt body in hypersonic flow p 241 A93-18233
- Influence of second-order boundary layer effects in hypersonic flow past blunt cones of large aspect ratio p 241 A93-18238
- Effect of real air properties on integral aerodynamic characteristics p 242 A93-18241
- Accuracy and efficiency assessments for a weak statement CFD algorithm for high-speed aerodynamics [ASME PAPER 92-GT-433] p 435 A93-19576
- Quantitative laser velocimetry measurements in the hypersonic regime by the integration of experimental and computational analysis [AIAA PAPER 93-0089] p 263 A93-20195

- Design of a wing shape for study of hypersonic crossflow transition in flight p 265 A93-20713
- Newton-like methods for fast high resolution simulation of hypersonic viscous flows p 437 A93-20740
- Investigation of a two-dimensional scramjet inlet, freestream $M = 8-18$ and $T_{sub} = 4100$ K p 270 A93-21669
- Application of space-marching methods to hypersonic forebody flow fields p 272 A93-22305
- [AIAA PAPER 92-5030] The Burnett shock structures in low density hypersonic flows p 273 A93-22320
- [AIAA PAPER 92-5048] A study of hypersonic swept shock wave/turbulent boundary layer interactions using a conical Navier-Stokes code p 273 A93-22322
- [AIAA PAPER 92-5050] Hypersonic turbulent expansion-corner flow with shock impingement p 274 A93-22371
- [AIAA PAPER 92-5101] Turbulence modeling for complex hypersonic flows p 277 A93-22620
- [AIAA PAPER 93-0200] Numerical solution of inviscid hypersonic flow around a conically-derived waverider p 280 A93-23012
- [AIAA PAPER 93-0320] Expanding the waverider design space using general supersonic and hypersonic generating flows p 283 A93-23253
- [AIAA PAPER 93-0505] Three-dimensional hypersonic shock wave/turbulent boundary-layer interactions p 287 A93-23533
- Numerical computation of viscous hypersonic flow around spherically blunted cones at angle of attack p 460 A93-24082
- Multigrid techniques for hypersonic viscous flows p 467 A93-24855
- [AIAA PAPER 93-0771] Hypersonic crossing shock-wave/turbulent-boundary-layer interactions p 467 A93-24863
- [AIAA PAPER 93-0781] Application of high-order accurate essentially nonoscillatory schemes to two-dimensional compressible viscous flows p 470 A93-24940
- [AIAA PAPER 93-0879] Hypersonic inviscid and viscous flow computations with a new optimized thermodynamic equilibrium model p 471 A93-24953
- [AIAA PAPER 93-0893] The application and analysis of liquid crystal thermographs in short duration hypersonic flow p 542 A93-25509
- [AIAA PAPER 93-0182] Hypersonic viscous flow simulations p 478 A93-27926
- Numerical study of the flow establishment time in hypersonic shock tunnels p 480 A93-29153
- A hot dynamic seal rig for measuring hypersonic engine seal durability and flow performance p 738 A93-33916
- [AIAA PAPER 93-1346] Evaluation of RNG algebraic turbulence models for boundary layers p 684 A93-34331
- Numerical simulation of hypersonic rarefied gas flow over blunt bodies p 687 A93-34356
- Numerical simulation of two-dimensional compressible flows p 687 A93-34357
- Reactive and dissipative hypersonic flow in a wind tunnel nozzle p 687 A93-34358
- Hypersonic nonequilibrium flow computations using the Roe flux-difference split scheme p 692 A93-35609
- Numerical analysis for chemically non-equilibrium flow p 770 A93-38148
- Numerical study on atom-molecule radiation flowfield around a hypersonic blunt body p 770 A93-38434
- Viscous nonequilibrium flow calculations [ONERA, TP NO. 1992-89] p 771 A93-38573
- Schlieren device and holographic interferometer for hypersonic flow visualization [ONERA, TP NO. 1992-160] p 832 A93-38739
- Shock wave/boundary layer interaction in a two-dimensional laminar hypersonic flow [ONERA, TP NO. 1992-182] p 773 A93-38744
- Kinetic theory of hypersonic flows of a viscous gas p 775 A93-39130
- Asymptotic structure of a limiting hypersonic flow in a shock wave p 776 A93-39131
- Nonequilibrium limiting hypersonic flow of a gas past three-dimensional tapered bodies with a separated shock p 776 A93-39133
- An approximate method for calculating nonequilibrium flows near blunt bodies p 776 A93-39134
- Hypersonic limiting flows of a relaxing gas with pressure changes in the main approximation p 776 A93-39135
- Flow density distribution in a two-phase submerged jet p 836 A93-39144
- Nonequilibrium heat transfer near the critical point of blunt bodies p 777 A93-39145
- An experimental study of the three-dimensional interaction of a transverse jet with hypersonic flow p 777 A93-39150
- Computational flow predictions for hypersonic drag devices p 777 A93-39257
- Stabilization of the Burnett equations and application to hypersonic flows p 778 A93-39410
- Large-amplitude finite element flutter analysis of composite panels in hypersonic flow p 837 A93-39417
- Newtonian and hypersonic flows over oscillating bodies of revolution. I - Circular cones p 857 A93-39942
- An existence theorem for a free boundary problem of hypersonic flow theory p 857 A93-40405
- Infrared thermography characterization of Goertler vortex type patterns in hypersonic flows [ONERA, TP NO. 1993-13] p 925 A93-41029
- Damping of surface pressure fluctuations in hypersonic turbulent flow past expansion corners p 860 A93-41914
- Computation of hypersonic flow over a sphere using kinetic flux vector splitting scheme with equilibrium chemistry p 861 A93-42260
- International Symposium on Computational Fluid Dynamics, 4th, Univ. of California, Davis, Sept. 9-12, 1991, Selected Papers p 862 A93-42426
- FUM - An efficient MMB solver for steady inviscid flows p 862 A93-42431
- Thermo-chemical models for hypersonic flows p 863 A93-42433
- Simulation of nonequilibrium hypersonic flows p 863 A93-42443
- Equilibrium and nonequilibrium modeling of hypersonic inviscid flows p 864 A93-42448
- Workshop on hypersonic flows for reentry problems January 22-25th 1990 (Antibes) - Inaugural address p 856 A93-42577
- Computational fluid dynamics for hypersonic airbreathing aircraft p 865 A93-42581
- Computation of hypersonic turbulent flow over a rearward facing step p 865 A93-42587
- Hypersonic cone flow predictions using an implicit upwind space-marching code p 865 A93-42588
- Viscous, 2-D, laminar hypersonic flows over compression ramps p 866 A93-42591
- Computational results for 2-D and 3-D ramp flows with an upwind Navier-Stokes solver p 866 A93-42592
- Application of the Galerkin/least-squares formulation to the analysis of hypersonic flows. I - Flow over a two-dimensional ramp p 866 A93-42593
- Computation of flows over 2D ramps p 866 A93-42595
- Hypersonic viscous flow over two-dimensional ramps p 866 A93-42596
- Grid-refinement study of hypersonic laminar flow over a 2-D ramp p 866 A93-42597
- Computational results for flows over compression ramps p 866 A93-42599
- Implicit upwind finite-difference simulation of laminar hypersonic flow over a 2D ramp p 867 A93-42600
- A synthesis of results on the calculation of flow over a 2D ramp and a 3D obstacle - Antibes test cases 3 and 4 p 867 A93-42601
- Experimental study of the longitudinal hypersonic corner flow field - HERMES-R&D research program, problem no. 5 p 867 A93-42602
- Experimental study of the flow around a double ellipsoid configuration p 867 A93-42603
- An upwind relaxation method for hypersonic viscous flows over a double-ellipsoidal body p 867 A93-42606
- Navier-Stokes calculations over a double ellipse and a double ellipsoid by an implicit non-centered method p 867 A93-42607
- Application of the Galerkin/least-squares formulation to the analysis of hypersonic flows. II - Flow past a double ellipse p 868 A93-42608
- The application of an adaptive unstructured grid method to the solution of hypersonic flows past double ellipse and double ellipsoid configurations p 868 A93-42609
- Computation of the hypersonic flow over a double ellipsoid p 868 A93-42610
- Numerical simulation of laminar hypersonic flow past a double-ellipsoid p 868 A93-42612
- 2D hypersonic viscous flow past a double ellipse geometry p 868 A93-42613
- Hypersonic flows over a double or simple ellipse p 868 A93-42614
- Viscous and inviscid hypersonic flow about a double ellipsoid p 868 A93-42616
- Numerical simulation of hypersonic flow over a double ellipse using a Taylor-Galerkin finite element formulation with adaptive grids p 868 A93-42617
- Hypersonic viscous flow past double ellipse and past double ellipsoid - Numerical results p 868 A93-42618
- Adaptive mesh embedding for reentry flow problems p 869 A93-42619
- Attempt to evaluate the computations for test case 6.1 - Cold hypersonic flow past ellipsoidal shapes p 869 A93-42620
- A contribution to the prediction of hypersonic non-equilibrium flows p 869 A93-42624
- Problem 6.4.1 - Rarefied flow around a double ellipse p 869 A93-42630
- The hypersonic double ellipse in rarefied flow p 869 A93-42631
- Leeside flow over delta wing at $M = 7.15$ - Experimental results for test case 7.1.2 p 870 A93-42632
- Finite volume 3DNS and PNS solutions of hypersonic viscous flow around a delta wing using Osher's flux difference splitting p 870 A93-42633
- Inviscid hypersonic flow over a delta wing p 870 A93-42634
- Hypersonic leeside delta-wing-flow computations using centered schemes p 870 A93-42635
- Experimental density flowfields over a delta wing located in rarefied hypersonic flows p 870 A93-42637
- Experiments on the heat transfer and on the aerodynamic coefficients of a delta wing in rarefied hypersonic flows p 870 A93-42638
- Rarefied gas flow around a 3D-deltawing p 870 A93-42639
- Appraisal of the rarefied flow computations (problems 6.4.1 and 7.2.1) p 871 A93-42640
- On the accuracy and efficiency of CFD methods in real gas hypersonics p 871 A93-42869
- Scramjet nozzle experiment with hypersonic external flow p 899 A93-42879
- Newtonian and hypersonic flows over oscillating bodies of revolution. II - Parabolic bodies p 872 A93-42931
- Zonally-decoupled DSMC solutions of hypersonic blunt body wake flows [AIAA PAPER 93-2808] p 949 A93-44227
- Shock waves; Proceedings of the 18th International Symposium, Sendai, Japan, July 21-26, 1991. Vols. 1 & 2 [ISBN 0-387-55686-9] p 1023 A93-45451
- An overview of Ames experimental aerothermodynamics p 1011 A93-45496
- Applications of liquid crystal surface thermography to hypersonic flow p 1023 A93-45504
- Aerodynamic heating phenomenon in three dimensional shock wave/turbulent boundary layer interaction induced by sweptback fins in hypersonic flows p 960 A93-45507
- A combined facility of ballistic range and shock tunnel using a fast action valve p 1012 A93-45532
- Computational fluid dynamics code validation using a free piston hypervelocity shock tunnel p 960 A93-45545
- Hypersonic flow calculations using a multidomain MUSCL Euler solver p 960 A93-45547
- Viscous hypersonic shock-shock interaction on a blunt body at high altitude [AIAA PAPER 93-2722] p 962 A93-46477
- Hypersonic stagnation line merged layer flow on blunt axisymmetric bodies of arbitrary shape [AIAA PAPER 93-2723] p 962 A93-46478
- PNS predictions of axisymmetric hypersonic blunt-body and afterbody flowfields [AIAA PAPER 93-2725] p 962 A93-46479
- Burnett solutions along the stagnation line of a cooled cylinder in low-density hypersonic flows [AIAA PAPER 93-2726] p 962 A93-46480
- Convective heat-transfer rate distributions over a 140 deg blunt cone at hypersonic speeds in different gas environments [AIAA PAPER 93-2787] p 1027 A93-46529
- Flow resolution and domain of influence in rarefied hypersonic blunt-body flows [AIAA PAPER 93-2806] p 964 A93-46546
- Comparisons between DSMC and the Navier-Stokes equations for reentry flows [AIAA PAPER 93-2810] p 964 A93-46549
- Experiments on shock wave/boundary layer interaction in hypersonic flow p 970 A93-46888
- The three-dimensional representation of the pressure distribution on wedged delta wings with supersonic leading edges in supersonic-hypersonic flow p 973 A93-46989
- Computational analysis of off-design waveriders [AIAA PAPER 93-3488] p 982 A93-47262
- CFD study of the flowfield due to a supersonic jet exiting into a hypersonic stream from a conical surface. II [AIAA PAPER 93-2926] p 1045 A93-48127
- Hypersonic flow past open cavities [AIAA PAPER 93-2969] p 1049 A93-48163
- Comparison of ENO and TVD schemes for the parabolized Navier-Stokes equations [AIAA PAPER 93-2970] p 1049 A93-48164
- Instability of hypersonic flow past blunt cones - Effects of mean flow variations [AIAA PAPER 93-2983] p 1051 A93-48176

- Aerodynamic heating with boundary layer transition and heat protection with mass addition on blunt body in hypersonic flows
[AIAA PAPER 93-2984] p 1051 A93-48177
- Hypersonic, turbulent viscous interaction past an expansion corner
[AIAA PAPER 93-2985] p 1051 A93-48178
- A finite element and symbolic method for studying laminar boundary layers of real gases in equilibrium at Mach numbers to 30
[AIAA PAPER 93-2986] p 1052 A93-48179
- Computation of hypersonic flow past blunt body for nonequilibrium weakly ionized air
[AIAA PAPER 93-2995] p 1053 A93-48185
- A high-order streamline Godunov scheme for steady hypersonic equilibrium flows
[AIAA PAPER 93-2997] p 1053 A93-48187
- The prediction of viscous nonequilibrium hypersonic flows about ablating configurations using an upwind parabolized Navier-Stokes code
[AIAA PAPER 93-2998] p 1053 A93-48188
- Multi-block calculations for flows in local chemical equilibrium
[AIAA PAPER 93-2999] p 1053 A93-48189
- Application of a two-equation turbulence model for high speed compressible flows using unstructured grids
[AIAA PAPER 93-3029] p 1056 A93-48213
- CFD code calibration and inlet-fairing effects on a 3D hypersonic powered-simulation model
[AIAA PAPER 93-3041] p 1056 A93-48222
- A family of multiblock codes for computational aerothermodynamics - Application to complete vehicle hypersonic flows
[AIAA PAPER 93-3042] p 1056 A93-48223
- CARS studies in hypersonic flows
[AIAA PAPER 93-3047] p 1144 A93-48227
- Investigation of the flowfield over parallel-arranged launch vehicles
[AIAA PAPER 93-3060] p 1058 A93-48237
- Use of shear-stress-sensitive, temperature-insensitive liquid crystals for boundary layer transition detection in hypersonic flows
[AIAA PAPER 93-3070] p 1059 A93-48245
- On numerical solutions of Burnett equations for hypersonic flow past 2-D circular blunt leading edges in continuum transition regime
[AIAA PAPER 93-3092] p 1060 A93-48266
- DSMC numerical investigation of rarefied compression corner flow
[AIAA PAPER 93-3096] p 1061 A93-48270
- Hypersonic configuration optimization with an Euler/boundary layer coupling technique
[AIAA PAPER 93-3116] p 1062 A93-48286
- Abnormal peaks of increased heat-transfer on the blunt delta wing in the hypersonic flow
[AIAA PAPER 93-3129] p 1063 A93-48294
- Aerothermodynamic heating due to shock wave/laminar boundary-layer interactions in high-enthalpy hypersonic flow
[AIAA PAPER 93-3135] p 1064 A93-48299
- Three-dimensional hypersonic flow of a gas past wings
p 1069 A93-48971
- Hypersonic flow past a low-aspect-ratio triangular plate at large angles of attack
p 1069 A93-48974
- Multigrid techniques for hypersonic viscous flows
p 1071 A93-49027
- Computational methods in hypersonic aerodynamics
[ISBN 0-7923-1673-8] p 1072 A93-49521
- Introduction to the physical aspects of hypersonic aerodynamics
p 1072 A93-49522
- Computational methods for viscous hypersonic flows
p 1152 A93-49523
- Efficient multigrid computation of steady hypersonic flows
p 1152 A93-49527
- Flow analysis and design optimization methods for nozzle-afterbody of a hypersonic vehicle
p 1073 A93-49531
- The computation over unstructured grids of inviscid hypersonic reactive flow by upwind finite-volume schemes
p 1073 A93-49532
- Calculation of scramjet inlet with thick boundary-layer ingestion
[AIAA PAPER 93-1836] p 1074 A93-49720
- Analysis of the stability characteristics of hypersonic flow of a detonable gas mixture in the stagnation region of a blunt body
[AIAA PAPER 93-1918] p 1076 A93-49784
- Numerical study of the transient flow in the driven tube and the nozzle section of a shock tunnel
[AIAA PAPER 93-2018] p 1078 A93-49856
- A study of incipient separation limits for shock-induced boundary layer separation for Mach 6 high Reynolds flow
[AIAA PAPER 93-2481] p 1084 A93-50222
- The problem of viscous hypersonic flow past blunt bodies in the spreading plane
p 1086 A93-50969
- Optimal wing shapes in a hypersonic nonequilibrium flow
p 1088 A93-51770
- Heat transfer on tip fins in hypersonic flow
p 1088 A93-51775
- A study of turbulent flow in a viscous shock layer in the case of gas flow past oblong blunt bodies
p 1089 A93-51820
- Approximate calculation of the aerodynamic characteristics of simple bodies in hypersonic rarefied-gas flow
p 1090 A93-51869
- Calculation of the aerodynamic characteristics of bodies with meshlike surfaces in hypersonic rarefied-gas flow
p 1090 A93-51870
- Effect of Reynolds number on the aerodynamic characteristics of a semicone with a wing in the case of hypersonic flow velocities
p 1090 A93-51878
- Investigation of the structure of a multicomponent viscous shock layer
p 1090 A93-51879
- An extended insight into hypersonic flow phenomena using numerical methods
p 1093 A93-51999
- Numerical simulation of shock/shock and shock-wave/boundary-layer interactions in hypersonic flows
p 1093 A93-52000
- Upwind-biased, point-implicit relaxation strategies for hypersonic flowfield simulations on supercomputers
p 1175 A93-52770
- Pressure distribution measurement around hypersonic delta winged semicone - Measurement by means of magnet tape
p 1176 A93-53193
- Space marching calculations about hypersonic configurations using a solution-adaptive mesh algorithm
p 1177 A93-53212
- Application of the small parameter method to the problem of three-dimensional flow of a viscous gas past bodies
p 1178 A93-53314
- Comparison of gasdynamic models in hypersonic flow
p 1179 A93-53315
- Shock shapes around slender diamond cones traveling at hypersonic speed
p 1181 A93-53840
- Numerical solution of N-S equations for hypersonic flow over capsule-type vehicles
p 1182 A93-53858
- Numerical simulation of a two-dimensional supersonic mixed-compression inlet
[ISABE 93-7107] p 1188 A93-54083
- Separation phenomenon in a hypersonic flow with strong wall cooling - Subcritical regime
p 1189 A93-54266
- Computation of nonequilibrium hypersonic flowfields around hemisphere cylinders
p 1229 A93-54469
- The effects of reaction rate constants and catalytic wall on the hypersonic flow field over blunt bodies
p 1230 A93-54586
- Numerical studies of Mach reflection with air chemistry
p 1233 A93-54815
- Hypersonic flow of a gas past wing with heat transfer
p 1234 A93-55030
- Supersonic and hypersonic flow computations for the research configuration ELAC 1 and comparison to experimental data
p 1237 A93-56034
- Computation of viscous hypersonic non-equilibrium blunt body flow
p 1238 A93-56038
- Employment of radicals and excited state species for supersonic combustion photochemical ignition of premixed hydrogen/oxygen mixtures with ArF laser
p 73 N93-11135
- A preliminary study associated with the experimental measurement of the aero-optic characteristics of hypersonic configurations
[AD-A253792] p 24 N93-12063
- A numerical study of hypersonic flow with strong surface blowing
p 129 N93-13128
- Mathematical problems in inviscid hypersonic flow
p 131 N93-13451
- Development and computation of continuum higher order constitutive relations for high-altitude hypersonic flow
p 132 N93-13578
- Time dependent heat transfer rates in high Reynolds number hypersonic flowfields
p 216 N93-13664
- Application of a vectorized particle simulation to the study of plates and wedges in high-speed rarefied flow
p 133 N93-13746
- Computational analysis of hypersonic flows past elliptic-cone waveriders
[NASA-CR-191304] p 138 N93-14767
- Modeling variable blowing on a slender cone in hypersonic flow
p 138 N93-14836
- Transition induced normal forces and their effects on the aerodynamic characteristics of slender sharp cones
[AD-A256802] p 288 N93-15889
- Hypersonic flows including real gas effects
[AERO-REPT-9112] p 289 N93-16467
- Computational study of real gas effects in high speed high temperature flow, volume 2
[AERO-REPT-9203-VOL-2] p 289 N93-16470
- Hot experimental technique: A new requirement of aerothermodynamics
[MBB-FE-202-S-PUB-480] p 293 N93-17543
- H-P adaptive methods for finite element analysis of aerothermal loads in high-speed flows
[NASA-CR-189739] p 420 N93-18093
- Hypersonic flows as related to the national aerospace plane
[NASA-CR-191980] p 296 N93-18378
- Computational Fluid Dynamics, volume 2
[VKI-LS-1992-04-VOL-2] p 421 N93-18563
- A Blottner type numerical model for nonequilibrium viscous hypersonic flows in upwind finite elements
[INRIA-RR-1476] p 297 N93-18648
- Influence of the physical modelling of viscous terms on hypersonic flow computations
[INRIA-RR-1493] p 297 N93-18652
- Electron beam probing of blow-down hypersonic flows
[ONERA-NT-1992-7] p 298 N93-18701
- A simple grid generation technique for hypersonic flow around complex configuration
p 299 N93-19275
- Numerical computations using multi-domain technique
p 299 N93-19277
- The role of computational fluid dynamics in aeronautical engineering. 9: Analysis of hypersonic equilibrium air flow
p 301 N93-19294
- Numerical calculation of hypersonic non-equilibrium flow around OREX
p 301 N93-19296
- Numerical simulation of hypersonic flow around H-2 Orbiting Plane (HOPE), part 3
p 301 N93-19297
- Numerical calculation of flow field in supersonic combustion chamber
p 304 N93-19317
- Issues and approach to develop validated analysis tools for hypersonic flows: One perspective
[NASA-TM-103937] p 305 N93-19379
- Computational analysis of hypersonic flows past generalized cone-derived waveriders
p 483 N93-20288
- Aerothermodynamic properties of hypersonic flows over radiation-adiabatic surfaces
[DLR-FB-91-42] p 485 N93-21761
- Development and application of computational aerothermodynamics flowfield computer codes
[NASA-CR-192940] p 692 N93-24736
- Prediction of forces and moments for hypersonic flight vehicle control effectors
[NASA-CR-193033] p 728 N93-24762
- An investigation of laser velocimetry measurements within high speed, complex flows
p 748 N93-25237
- Experimental and computational investigation of helium injection into air at supersonic and hypersonic speeds
p 696 N93-25487
- Assessment of computational issues associated with analysis of high-lift systems
p 785 N93-27449
- Topology and grid adaption for high-speed flow computations
[NASA-CR-4216] p 934 N93-30375
- Calculations on unsteady type 4 interaction at Mach 8
[AD-A265214] p 990 N93-32004
- HYPERSONIC FORCES**
Hypersonic propulsion system force accounting
p 175 N93-13229
- HYPERSONIC GLIDERS**
Guidance law based on piecewise constant control for hypersonic gliders
[AIAA PAPER 93-3888] p 1144 A93-51472
- HYPERSONIC HEAT TRANSFER**
Heat loads as key problem of hypersonic flight
p 1222 A93-54276
- Time dependent heat transfer rates in high Reynolds number hypersonic flowfields
p 216 N93-13664
- Hypersonics revisited
p 781 N93-27167
- HYPERSONIC INLETS**
Study of flow phenomena in high speed intakes
[AIAA PAPER 92-5029] p 272 A93-22304
- Techniques for the measurement of scramjet inlet performance at hypersonic speeds
[AIAA PAPER 92-5104] p 274 A93-22374
- Hypersonic shock-wave/turbulent-boundary-layer interactions
[AIAA PAPER 93-0781] p 467 A93-24863
- Computational effects of inlet representation on powered hypersonic, airbreathing models
p 1094 A93-52427
- On the numerical simulation of the two-dimensional flow field around a hypersonic air-intake-compressibility effects
[ISABE 93-7100] p 1187 A93-54076
- Numerical studies of Mach reflection with air chemistry
p 1233 A93-54815
- Hypersonic inlet efficiency revisited
p 16 N93-10012
- HYPERSONIC NOZZLES**
Aerodynamic design of axisymmetric hypersonic wind-tunnel nozzles using a least-squares/parabolized Navier-Stokes procedure
p 9 A93-12011
- Optimization aspects of an ejector type hypersonic thrust nozzle
[ASME PAPER 92-GT-402] p 355 A93-19551

- Evaluation of scramjet nozzle configurations and film cooling for reduction of wall heating
[AIAA PAPER 93-0744] p 358 A93-21118
- Role of hydrogen/air chemistry in nozzle performance for a hypersonic propulsion system p 359 A93-21668
- Goertler instability and hypersonic quiet nozzle design p 480 A93-29155
- Numerical simulation of starting process in a hypersonic nozzle p 684 A93-34275
- Numerical modeling of ionization in nonequilibrium nitrogen flows in hypersonic nozzles p 836 A93-39137
- Calculation of the effect of flow conicity in a hypersonic nozzle on the aerodynamics of a flight vehicle model p 776 A93-39142
- Numerical study of spontaneous nitrogen condensation in the axisymmetric hypersonic nozzles of wind tunnels p 777 A93-39143
- Analysis of hypersonic nozzles including vibrational nonequilibrium and intermolecular force effects p 861 A93-41916
- A strategy for the optimal design of nozzle contours [AIAA PAPER 93-2720] p 962 A93-46476
- Flow calibration of two hypersonic nozzles in the AEDC HEAT-H2 high-enthalpy arc-heated wind tunnel [AIAA PAPER 93-2782] p 1012 A93-46526
- Numerical study of the transient flow in the driven tube and the nozzle section of a shock tunnel [AIAA PAPER 93-2018] p 1078 A93-49856
- Computation of hypersonic high-temperature nozzle flow p 1238 A93-56040
- Hypervelocity scramjet combustor-nozzle analysis and design [NASA-CR-190965] p 60 N93-12214
- Supersonic investigation of two dimensional hypersonic exhaust nozzles [NASA-TM-105687] p 179 N93-15342
- Design of a nozzle for a hypersonic wind tunnel [AERO-REPT-9113] p 381 N93-16468
- ### HYPERSONIC REENTRY
- Taking into account surface roughness in computing hypersonic re-entry body p 686 A93-34354
- Numerical simulation of hypersonic rarefied gas flow over blunt bodies p 687 A93-34356
- VSL analysis of nonequilibrium flows around a hypersonic body p 769 A93-38146
- Hypersonic chemically reacting flow of a reentry body p 769 A93-38147
- Computational flow predictions for hypersonic drag devices p 777 A93-39257
- Hypersonic flows for reentry problems. Vols. 1 & 2 [ISBN 0-387-54428-3] p 864 A93-42576
- Workshop on hypersonic flows for reentry problems January 22-25th 1990 (Antibes) - Inaugural address p 856 A93-42577
- Gas-kinetic and Navier-Stokes simulations of reentry flows p 865 A93-42582
- Experimental study of the longitudinal hypersonic corner flow field - HERMES-R&D research program, problem no. 5 p 867 A93-42602
- Navier-Stokes calculations over a double ellipse and a double ellipsoid by an implicit non-centered method p 867 A93-42607
- Adaptive mesh embedding for reentry flow problems p 869 A93-42619
- Low-to-high altitude predictions of three-dimensional ablative re-entry flowfields p 1027 A93-46407
- Two-layer convective heating prediction procedures and sensitivities for blunt body reentry vehicles [AIAA PAPER 93-2763] p 963 A93-46509
- Monte Carlo simulation of radiating reentry flows [AIAA PAPER 93-2809] p 964 A93-46548
- Comparisons between DSMC and the Navier-Stokes equations for reentry flows p 964 A93-46549
- Experiments on shock wave/boundary layer interaction in hypersonic flow p 970 A93-46888
- Effects of wall conditions on chemically nonequilibrium shock-layer flow over hypersonic reentry bodies p 970 A93-46908
- Hypersonic vehicle research by using a large shock tunnel [AAS PAPER 91-607] p 1250 A93-55841
- A hybrid multigrid technique for computing steady-state solutions to supersonic flows p 700 N93-26078
- ### HYPERSONIC SHOCK
- A unified hypersonic/supersonic method for aeroelastic applications including shock-unsteady wave interaction [AIAA PAPER 93-1317] p 738 A93-33892
- On the compression process in a free-piston shock-tunnel p 1136 A93-48041
- Investigation of a hypersonic crossing shock wave/turbulent boundary layer interaction p 1044 A93-48043
- An investigation on the use of a heavy gas to improve the performance of the equilibrium interface technique in shock tube flows [AIAA PAPER 93-2017] p 1078 A93-49855
- Hypersonic shock-induced combustion ramjet performance analysis [ISABE 93-7037] p 1197 A93-54013
- Experimental investigations of hypersonic shock-boundary layer interaction p 1238 A93-56037
- ### HYPERSONIC SPEED
- Increasing the lift-drag ratio of wings of small aspect ratio at hypersonic velocities p 13 A93-12933
- Numerical study of jet interaction at super- and hypersonic speeds for flight vehicle control p 184 A93-14379
- Hypersonic flow separation in shock wave boundary layer interactions [ASME PAPER 92-GT-205] p 251 A93-19429
- Ramjet NOx emission - Use of a 3D CFD method for the combustor design of a super/hyper-sonic transport propulsion system [ASME PAPER 92-GT-255] p 353 A93-19464
- Overview of Japanese aerospace plane [AIAA PAPER 92-5005] p 384 A93-22282
- Flight performance of hypersonic minor circle turning maneuvers [AIAA PAPER 93-0627] p 531 A93-24744
- Numerical simulation of crossing/turbulent boundary layer interaction at Mach 8.3 comparison of zero and two-equation turbulence models [AIAA PAPER 93-0779] p 467 A93-24861
- Plume effects at hypersonic speeds p 959 A93-45494
- Solution strategy for three-dimensional configurations at hypersonic speeds p 962 A93-46406
- Standing normal detonations and oblique detonations for propulsion [AIAA PAPER 93-2325] p 1116 A93-50105
- Heat loads as key problem of hypersonic flight p 1222 A93-54276
- Study on flow field around slender diamond cone traveling at hypersonic speed p 1189 A93-54314
- An experimental/computational study of heat transfer in sharp fin induced shock wave/turbulent boundary layer interactions at low hypersonic Mach numbers p 217 N93-13826
- Supersonic investigation of two dimensional hypersonic exhaust nozzles [NASA-TM-105687] p 179 N93-15342
- Flowfield computations over the Space Shuttle orbiter with a proposed canard at a Mach number of 5.8 and 50 deg angle of attack [AD-A258058] p 293 N93-17756
- Experimental Investigation of Nozzle/Plume Aerodynamics at Hypersonic Speeds [NASA-CR-191368] p 386 N93-18085
- SR-SCARLET 1: Peregrin [NASA-CR-192048] p 337 N93-18155
- The effects of viscosity on a conically derived waverider [AD-A259019] p 424 N93-19101
- Computational parametric study of sidewall-compression scramjet inlet performance at Mach 10 [NASA-TM-4411] p 552 N93-20299
- Combined LAURA-UPS hypersonic solution procedure [NASA-TM-107682] p 747 N93-25176
- Plume effects on the flow around a blunt cone at hypersonic speeds p 787 N93-27460
- Hypersonic lateral and directional stability characteristics of aerossist flight experiment configuration in air and CF4 [NASA-TM-4435] p 875 N93-29166
- Calculations on unsteady type 4 interaction at Mach 8 [AD-A265214] p 990 N93-32004
- ### HYPERSONIC TEST APPARATUS
- Techniques for the measurement of scramjet inlet performance at hypersonic speeds [AIAA PAPER 92-5104] p 274 A93-22374
- Langley 8-foot high-temperature tunnel oxygen measurement system p 1010 A93-44892
- Advancing the state of the art hypersonic testing - HYTEST/MTMI [AIAA PAPER 93-2023] p 1113 A93-49860
- Experimental studies in the Aachen hypersonic shock tunnel p 1251 A93-56032
- ### HYPERSONIC VEHICLES
- Viscous shock-layer numerical calculations of three dimensional nonequilibrium flows over hypersonic blunt bodies at high angle of attack p 12 A93-12651
- A very efficient tool for the structural analysis of hypersonic vehicles under high temperature analysis p 203 A93-14194
- Research and applications in structural dynamics and aeroelasticity p 153 A93-14223
- Hypersonic design p 156 A93-14346
- High speed aircraft tire dynamics/issues [SAE PAPER 921037] p 158 A93-14657
- Integration of turbo-expander- and turbo-ramjet-engines in hypersonic vehicles [ASME PAPER 92-GT-204] p 353 A93-19428
- Balance of moments for hypersonic vehicles [ASME PAPER 92-GT-251] p 253 A93-19460
- Constrained optimization of three-dimensional hypersonic vehicle configurations [AIAA PAPER 93-0039] p 260 A93-20152
- Analysis of the NASA Hypersonic Wing Test Structure [AIAA PAPER 92-4724] p 409 A93-20326
- Numerical simulation of shock-induced combustion/detonation p 410 A93-20719
- Design of a hypersonic waverider-derived airplane [AIAA PAPER 93-0401] p 384 A93-21108
- Role of hydrogen/air chemistry in nozzle performance for a hypersonic propulsion system p 359 A93-21668
- Evaluation of some significant issues affecting trajectory and control management for air-breathing hypersonic vehicles [AIAA PAPER 92-5011] p 384 A93-22287
- Robust control of the separation of hypersonic lifting vehicles [AIAA PAPER 92-5013] p 385 A93-22289
- On the coupled thermomechanical analysis of hypersonic flight vehicle structures [AIAA PAPER 92-5018] p 413 A93-22294
- An aerospace plane as a detonation wave ramjet/airframe integrated waverider [AIAA PAPER 92-5022] p 272 A93-22298
- On some recent advances in multidisciplinary analysis of hypersonic vehicles [AIAA PAPER 92-5026] p 438 A93-22302
- Some aspects of the aerodynamic methodology in hypersonic vehicle concept studies [AIAA PAPER 92-5027] p 272 A93-22303
- German university research in hypersonics [AIAA PAPER 92-5033] p 239 A93-22307
- A historical perspective on hypersonic research at the NACA/NASA Langley Research Center (1944-1984) [AIAA PAPER 92-5034] p 456 A93-22308
- Validation of aerodynamic simulation methods for Hermes spaceplane and future hypersonic vehicles [AIAA PAPER 92-5065] p 273 A93-22335
- Development and application of GASP 2.0 [AIAA PAPER 92-5067] p 438 A93-22337
- Engine/airframe integration for waverider cruise vehicles [AIAA PAPER 93-0507] p 283 A93-23254
- Stability and control of hypersonic waveriders [AIAA PAPER 93-0508] p 370 A93-23255
- Analysis of a hypersonic waverider research vehicle with a hydrocarbon scramjet engine [AIAA PAPER 93-0509] p 386 A93-23256
- Experiences in fabrication of a waverider model for wind tunnel testing [AIAA PAPER 93-0510] p 328 A93-23257
- The effects of hypersonic flight test requirements on research vehicle design [AIAA PAPER 93-0511] p 386 A93-23258
- A re-evaluation of the waverider design process [AIAA PAPER 93-0404] p 440 A93-23326
- Hypersonic waveriders - Where do we stand? [AIAA PAPER 93-0399] p 474 A93-25520
- A hypersonic waverider research vehicle [AIAA PAPER 93-0402] p 505 A93-25522
- Propulsion/airframe integration issues for waverider aircraft [AIAA PAPER 93-0506] p 505 A93-25533
- Impact of aeroelasticity on propulsion and longitudinal flight dynamics of an air-breathing hypersonic vehicle [AIAA PAPER 93-1367] p 733 A93-33934
- Supersonic aeroelastic instability results for a NASP-like wing model [AIAA PAPER 93-1369] p 682 A93-33935
- A flutter investigation of all-moveable NASP-like wings at hypersonic speeds [AIAA PAPER 93-1315] p 769 A93-37427
- Experiments on shock wave-boundary layer interaction at high Mach number with entropy layer effect [ONERA, TP NO. 1992-101] p 771 A93-38581
- Engineering method for calculating surface pressures and heating rates on vehicles with embedded shocks p 777 A93-39255
- Shock interference prediction using direct simulation Monte Carlo p 778 A93-39258
- Hypersonic propulsion - Breaking the thermal barrier p 897 A93-40437
- Application of the multigrid solution technique to hypersonic entry vehicles [AIAA PAPER 93-2721] p 858 A93-41049
- Validation of engineering methods for predicting hypersonic vehicle control forces and moments p 906 A93-41897
- Hypersonic stability and transition p 864 A93-42579

- Inviscid calculations by an upwind finite element method of hypersonic flows over a double (single) ellipse
p 669 A93-42626
- Development of a skin friction gauge for use in an impulse facility
p 1024 A93-45526
- AEDC H2 Facility - New test capabilities for hypersonic air-breathing vehicles
[AIAA PAPER 93-2781] p 1012 A93-46525
- Actively cooled panel testing perils, problems, and pitfalls --- for aerospace vehicles
p 1028 A93-46802
- A visualizing method of streamlines around hypersonic vehicles
[AIAA PAPER 93-3440] p 1014 A93-47230
- Waveriders with finlets
[AIAA PAPER 93-3442] p 978 A93-47231
- Aerodynamic design of a hypersonic body with a constant favorable pressure gradient
[AIAA PAPER 93-3444] p 978 A93-47232
- Shock-wave/boundary layer interactions at hypersonic speeds by an implicit Navier-Stokes solver
[AIAA PAPER 93-2938] p 1046 A93-48136
- Application of parabolized Navier-Stokes technique for high-L/D, hypersonic vehicle design
[AIAA PAPER 93-2948] p 1047 A93-48144
- Developing a data base for the calibration and validation of hypersonic CFD codes - Sharp cones
[AIAA PAPER 93-3044] p 1057 A93-48224
- The European Data Base - A new CFD validation tool for the design of space vehicles
[AIAA PAPER 93-3045] p 1057 A93-48225
- A study of turbulence in rarefied gases
[AIAA PAPER 93-3097] p 1061 A93-48271
- Engineering method for calculating inlet face property profiles on high speed vehicle forebodies
[AIAA PAPER 93-3113] p 1062 A93-48283
- Approximate method for the aerodynamic design of flight vehicles for high supersonic flight speeds
p 1069 A93-48966
- Hypersonic aerodynamic characteristics for Langley Test Technique Demonstrator
[AIAA PAPER 93-3443] p 1072 A93-49516
- Flow analysis and design optimization methods for nozzle-afterbody of a hypersonic vehicle
p 1073 A93-49531
- Harnessing nitrous oxide for elevation of temperature and pressure in piston facilities
[AIAA PAPER 93-2016] p 1137 A93-49854
- Advanced instrumentation for next-generation aerospace propulsion control systems
[AIAA PAPER 93-2079] p 1154 A93-49906
- Experimental studies of aerodynamic performances of hypersonic scramjet in impulse hot-shot tunnel
[AIAA PAPER 93-2446] p 1120 A93-50198
- A numerical study of the unsteady processes associated with the type IV shock interaction
[AIAA PAPER 93-2479] p 1083 A93-50221
- The application of intelligent search strategies to robust flight control for hypersonic vehicles
[AIAA PAPER 93-3732] p 1143 A93-51331
- An investigation of the fuel-optimal periodic trajectories of a hypersonic vehicle
[AIAA PAPER 93-3753] p 1101 A93-51349
- Robust control of hypersonic vehicles considering propulsive and aeroelastic effects
[AIAA PAPER 93-3762] p 1131 A93-51357
- Dynamics of hypersonic flight vehicles exhibiting significant aeroelastic and aeropropulsive interactions
[AIAA PAPER 93-3763] p 1131 A93-51358
- Self-tuning guidance applied to aeroassisted plane change problems
[AIAA PAPER 93-3791] p 1143 A93-51386
- Experimental studies of supersonic flow past wedges with longitudinal slots on the windward side
p 1089 A93-51786
- Calculation of a plane supersonic jet simulating the exhaust jet of a hypersonic flight vehicle engine
p 1103 A93-51912
- Computational effects of inlet representation on powered hypersonic, airbreathing models
p 1094 A93-52427
- Recent advances in computational analysis of hypersonic vehicles
p 1179 A93-53364
- Evaluation of 2D ceramic matrix composites in aeroconvective environments
p 1212 A93-53459
- High temperature heat exchangers for gas turbines and future hypersonic air breathing propulsion
[ONERA, TP NO. 1993-75] p 1218 A93-53596
- Optimal trajectories for hypersonic launch vehicles
p 1251 A93-54563
- Hypersonic vehicle research by using a large shock tunnel
[AAS PAPER 91-607] p 1250 A93-55841
- Low-speed aerodynamics of the hypersonic research configuration ELAC I
p 1237 A93-56035
- Flow computation for the hypersonic configuration ELAC I at low speeds and large incidence
p 1238 A93-56036
- Air-breathing hypersonic vehicle guidance and control studies: An integrated trajectory/control analysis methodology, phase 2
[NASA-CR-189703] p 65 N93-12413
- Current research in oxidation-resistant carbon-carbon composites at NASA, Langley Research Center
p 74 N93-12456
- Thermal control/oxidation resistant coatings for titanium-based alloys
p 74 N93-12457
- A numerical study of hypersonic flow with strong surface blowing
p 129 N93-13128
- Application of a vectorized particle simulation to the study of plates and wedges in high-speed rarefied flow
p 133 N93-13746
- A study of viscous interaction effects on hypersonic waveriders
p 135 N93-14160
- Nozzle/cowl optimization for a hypersonic vehicle on a typical trajectory
[AD-A258827] p 341 N93-19089
- The effects of viscosity on a conically derived waverider
[AD-A259019] p 424 N93-19101
- A simple grid generation technique for hypersonic flow around complex configuration
p 299 N93-19275
- Flight simulator for hypersonic vehicle and a study of NASP handling qualities
p 530 N93-19456
- Lumped mass modelling for the dynamic analysis of aircraft structures
p 510 N93-19460
- Guidance and flight control law development for hypersonic vehicles
[NASA-CR-192102] p 526 N93-19960
- Rarefied-flow Shuttle aerodynamics model
[NASA-TM-107698] p 458 N93-19976
- Computation of H2/air reacting flowfields in drag-reduction external combustion
[NASA-CR-191071] p 536 N93-20237
- Research in robust control for hypersonic vehicles
[NASA-CR-192127] p 527 N93-20296
- Numerical methods for aerothermodynamic design of hypersonic space transport vehicles
[MBB-FE-211-S-PUB-0481] p 514 N93-21056
- Selection criteria for metallic high temperature structural materials in hypersonic flying equipment
[MBB-LME-221-HYPAC-PUB-2-A] p 515 N93-21479
- Development of a non-linear simulation for generic hypersonic vehicles - ASUHS1
[NASA-CR-192710] p 516 N93-22003
- Prediction of forces and moments for hypersonic flight vehicle control effectors
[NASA-CR-193033] p 728 N93-24762
- Generic hypersonic vehicle performance model
[NASA-CR-192953] p 714 N93-25162
- Combined LAURA-UPS hypersonic solution procedure
[NASA-TM-107682] p 747 N93-25176
- Optimized scramjet engine integration on a waverider airframe
p 722 N93-25480
- Supersonic aeroelastic instability results for a NASP-like wing model
[NASA-TM-107739] p 718 N93-26553
- Parametric studies of shock wave/boundary layer interactions over 2D compression corners at Mach 6
[VKI-TN-181] p 988 N93-31538
- HYPERSONIC WAKES**
- COF2 radiation from an air-tylon wake
p 12 A93-12659
- Near wake structure for a generic ASTV configuration
[AIAA PAPER 93-0271] p 268 A93-21103
- Calculation of optical and electric characteristics from hypersonic blunt-body wakes
p 680 A93-33729
- A numerical inversion method for determining aerodynamic effects on particulate exhaust plumes from onboard irradiance data
p 823 A93-37482
- Zonally-decoupled DSMC solutions of hypersonic blunt body wake flows
[AIAA PAPER 93-2808] p 949 A93-44227
- Hypersonic blunt body wake computations using DSMC and Navier-Stokes solvers
[AIAA PAPER 93-2807] p 964 A93-46547
- Determination of the $N_2(+)+e$ recombination rate constant from ballistic experiments
p 1234 A93-55026
- HYPERSONIC WIND TUNNELS**
- Numerical simulations of high speed inlet flows
p 115 A93-14246
- An experimental study for interaction flow between shock wave and turbulent boundary layer
p 120 A93-14355
- Photoluminescent thermography - Feasibility study with pointwise measurements
p 211 A93-16861
- Near wake structure for a generic ASTV configuration
[AIAA PAPER 93-0271] p 268 A93-21103
- Air/helium ground-test simulation pertinent to the definition of slender body hypersonic aerodynamics
[AIAA PAPER 93-0318] p 268 A93-21106
- Power generation source for an electrothermal hypersonic wind tunnel
[AIAA PAPER 92-5045] p 376 A93-22317
- Numerical study of the flow establishment time in hypersonic shock tunnels
p 480 A93-29153
- Goertler instability and hypersonic quiet nozzle design
p 480 A93-29155
- Aero-optical phase measurements using Fourier transform holographic interferometry
p 549 A93-29302
- Calculations of viscous nonequilibrium flows in nozzles
[ONERA, TP NO. 1992-91] p 771 A93-38574
- Infrared thermography for hot-shot wind tunnel
[ONERA, TP NO. 1992-103] p 831 A93-38583
- Digital image processing applied to heat transfer measurement in hypersonic wind tunnel
[ONERA, TP NO. 1992-118] p 831 A93-38593
- Numerical study of spontaneous nitrogen condensation in the axisymmetric hypersonic nozzles of wind tunnels
p 777 A93-39143
- Hypersonic single expansion ramp nozzle simulations
p 777 A93-39254
- Quasi monodimensional inviscid non equilibrium nozzle flow computation
p 927 A93-42646
- Shock tube application - High enthalpy European wind tunnels
p 1011 A93-45452
- Plume effects at hypersonic speeds
p 959 A93-45494
- An overview of Ames experimental aerothermodynamics
p 1011 A93-45496
- Performance considerations in the operation of free-piston driven hypersonic test facilities
p 1011 A93-45497
- Applications of infrared measurement technique in hypersonic facilities
p 1024 A93-45505
- A laser induced fluorescence system for the high enthalpy shock tunnel (HEG) in Goettingen
p 1024 A93-45506
- Flow calibration of two hypersonic nozzles in the AEDC HEAT-H2 high-enthalpy arc-heated wind tunnel
[AIAA PAPER 93-2782] p 1012 A93-46526
- A report on the status of MHD hypersonic ground test technology in Russia
[AIAA PAPER 93-3193] p 1012 A93-46656
- Experimental study of transitional axisymmetric shock-boundary layer interactions at Mach 5
[AIAA PAPER 93-3131] p 1063 A93-48296
- Simulation of hypersonic flight - A concerted European effort
p 1136 A93-49301
- In-stream measurements of combustion during Mach 5 to 7 tests of the Hypersonic Research Engine (HRE)
[AIAA PAPER 93-2324] p 1116 A93-50104
- Aerothermodynamics of the high-altitude flight
p 1089 A93-51783
- Characteristics of the flame air heater of a hypersonic wind tunnel
p 1140 A93-51884
- Design of a nozzle for a hypersonic wind tunnel
[AERO-REPT-9113] p 381 N93-16468
- Photoluminescent thermography in hypersonic blowdown wind tunnel: Feasibility study with pinpoint measurement
[ONERA-NT-1992-8] p 297 N93-18617
- Assessment of a flow-through balance for hypersonic wind tunnel models with scramjet exhaust flow simulation
[NASA-TM-4441] p 779 N93-27005
- Evaluation of candidate working fluid formulations for the electrothermal-chemical wind tunnel
[NASA-CR-193366] p 1015 N93-31848
- HYPERSONICS**
- Air/helium ground-test simulation pertinent to the definition of slender body hypersonic aerodynamics
[AIAA PAPER 93-0318] p 268 A93-21106
- CFD for hypersonic propulsion
p 865 A93-42585
- Flow analysis and design optimization methods for nozzle-afterbody of a hypersonic vehicle
p 1073 A93-49531
- Hypersonic panel flutter in a rarefied atmosphere
p 188 N93-13928
- Numerical simulation of hypersonic aerodynamics and the computational needs for the design of an aerospace plane
[AD-A260681] p 699 N93-25894
- Hypersonic panel flutter in a rarefied atmosphere
[NASA-CR-4514] p 780 N93-27084
- The Center of Excellence for Hypersonics Training and Research at the University of Texas at Austin
[NASA-CR-193070] p 781 N93-27126
- Hypersonics revisited
p 781 N93-27167
- Investigations on entropy layer along hypersonic hyperboloids using a defect boundary layer
p 787 N93-27462

- Hypersonic lateral and directional stability characteristics of aerospace flight experiment configuration in air and CF4
[NASA-TM-4435] p 875 N93-29166
- Technology transfer: Potential of BMFT concept for hypersonics
[MBB-LME-202-S-PUB-0505] p 1041 N93-31045
- Evaluation of candidate working fluid formulations for the electrothermal-chemical wind tunnel
[NASA-CR-193366] p 1015 N93-31848
- HYPERVELOCITY**
- Hypervelocity scramjet combustor-nozzle analysis and design
[NASA-CR-190965] p 60 N93-12214
- HYPERVELOCITY FLOW**
- Mixing and combustion studies using discrete orifice injection at hypervelocity flight conditions
p 205 A93-14523
- Transition on a sharp cone at high enthalpy - New measurements in the shock tunnel T5 at GARCIT
[AIAA PAPER 93-0343] p 281 A93-23030
- Investigation of a contoured wall injector for hypervelocity mixing augmentation
p 837 A93-39407
- Millisecond aerodynamic force measurement with side-jet model in the ISL shock tunnel
p 822 A93-39414
- Hypervelocity flows of argon produced in a free piston driven expansion tube
p 1012 A93-45530
- Absolute intensity measurements of impurity emissions in a shock tunnel and their consequences for laser-induced fluorescence experiments
p 1147 A93-48044
- Drag measurements on blunt cones and a scramjet vehicle in hypervelocity flow
[AIAA PAPER 93-2979] p 1050 A93-48172
- Shock tunnel experiments and approximative methods on hypervelocity side-jet control effectiveness
[AIAA PAPER 93-1929] p 1077 A93-49794
- Research activity at the shock tube facility at NASA Ames
p 1252 A93-54804
- Nonequilibrium shock layer radiation in a simulated Titan atmosphere
p 1233 A93-54805
- Investigation of the aerothermodynamics of hypervelocity reacting flows in the ram accelerator
[NASA-CR-191715] p 140 N93-15588
- Comparison of methodologies for describing relaxation in nonequilibrium gaseous systems
p 419 N93-16786
- Issues and approach to develop validated analysis tools for hypersonic flows: One perspective
[NASA-TM-103937] p 305 N93-19379
- HYPERVELOCITY GUNS**
- New experiments in a 120-mm ram accelerator at high pressures
[AIAA PAPER 93-2589] p 1142 A93-50301
- HYPERVELOCITY PROJECTILES**
- Upgrade of ballistic range facilities at AEDC - Two-thirds complete
[AIAA PAPER 93-0349] p 377 A93-23034
- Langley proposed advanced hypervelocity aerophysics facility - A status report
p 1013 A93-47015
- New experiments in a 120-mm ram accelerator at high pressures
[AIAA PAPER 93-2589] p 1142 A93-50301
- Investigation of the aerothermodynamics of hypervelocity reacting flows in the ram accelerator
[NASA-CR-191715] p 140 N93-15588
- HYPERVELOCITY WIND TUNNELS**
- Computational fluid dynamics code validation using a free piston hypervelocity shock tunnel
p 960 A93-45545
- Measurement and analysis of nitric oxide radiation in an arc-jet flow
[AIAA PAPER 93-2800] p 1016 A93-46540
- High-pressure hypervelocity electrothermal wind-tunnel performance study and subscale tests
p 1137 A93-49617
- HYSTERESIS**
- Hysteresis effects on wind tunnel measurements of a two-element airfoil
[AIAA PAPER 93-0646] p 464 A93-24761
- Hysteresis and bristle stiffening effects of conventional brush seals
[AIAA PAPER 93-1996] p 1153 A93-49839
- The aerodynamic characteristics of the Gottingen 797 and Wortmann FX63-137 aerofoil sections at very low Reynolds numbers
p 295 N93-18128
- Numerical simulation of unsteady large scale separated flow around oscillating airfoil
p 300 N93-19285
- ICE**
- Dynamic analysis of a pre-and-post ice impacted blade
[NASA-TM-105829] p 90 N93-12197
- Root damage analysis of aircraft engine blade subject to ice impact
[NASA-TM-105779] p 222 N93-15343
- An evaluation of thermal energy storage options for precooled gas turbine inlet air
[DE93-005980] p 754 N93-24975
- Structural tailoring of aircraft engine blade subject to ice impact constraints
[NASA-TM-106033] p 838 N93-26999
- Aircraft ice detectors and related technologies for onground and inflight applications
[DOT/FAA/CT-92/27] p 791 N93-27269
- Experimental and computational ice shapes and resulting drag increase for a NACA 0012 airfoil
p 784 N93-27440
- Recent progress in the analysis of iced airfoils and wings
p 784 N93-27441
- Interaction between ice and propeller
[VTT-TIED-1281] p 841 N93-27832
- A passive infrared ice detection technique for helicopter applications
[NASA-CR-193187] p 880 N93-29152
- Blasim: A computational tool to assess ice impact damage on engine blades
[NASA-TM-106225] p 1031 N93-31193
- ICE CLOUDS**
- The Air Force Flight Test Center artificial icing and rain testing capability upgrade program
[AIAA PAPER 93-0295] p 376 A93-22695
- Liquid water content measurements using the Phase Doppler Particle Analyzer in the NASA Lewis Icing Research Tunnel
[AIAA PAPER 93-0298] p 378 A93-23698
- Identification of icing water clouds by NOAA AVHRR satellite data
[DLR-FB-92-11] p 434 N93-16477
- Natural and augmented snowfall growth processes and their interactions with the natural and modified aerosol
[PB93-153096] p 755 N93-25874
- ICE ENVIRONMENTS**
- Arctic environment - Helicopter operations in cold climates
p 1189 A93-54288
- ICE FORMATION**
- Example of the Couette iceform design model - Flat plate iceformation
p 207 A93-15070
- Micro-physical models for simulating realistic ice accretions
[AIAA PAPER 93-0025] p 307 A93-20143
- Prediction of the ice accretion with viscous effects on aircraft wings
[AIAA PAPER 93-0027] p 307 A93-20145
- A proposed icing severity index based upon meteorology
p 429 A93-22136
- Ice prediction systems for runways
p 376 A93-22174
- LEWICE droplet trajectory calculations on a parallel computer
[AIAA PAPER 93-0172] p 438 A93-22604
- Icing effects on aircraft stability and control determined from flight data - Preliminary results
[AIAA PAPER 93-0398] p 370 A93-23073
- Close-up analysis of aircraft ice accretion
[AIAA PAPER 93-0029] p 309 A93-23239
- Advancements in the LEWICE Ice Accretion Model
[AIAA PAPER 93-0171] p 309 A93-23243
- Ice accretion and performance degradation calculations with LEWICE/NS
[AIAA PAPER 93-0173] p 310 A93-23244
- Ice accretion prediction for a typical commercial transport aircraft
[AIAA PAPER 93-0174] p 310 A93-23245
- An overview of shed ice impact studies in the NASA Lewis Icing Research Tunnel
[AIAA PAPER 93-0301] p 283 A93-23247
- CWAS - Clean wing advisory system: A new approach to ice detection
[AIAA PAPER 93-0747] p 516 A93-24835
- Anti-icing failure detection instrumentation using realtime optical measurement of anti-icing fluid properties
[AIAA PAPER 93-0748] p 540 A93-24836
- Field studies of hold-over-times for type II anti-icing fluids - Results and insights
[AIAA PAPER 93-0749] p 486 A93-24837
- Experimental assessment of airframe damage due to impacting ice
[AIAA PAPER 93-0751] p 504 A93-24838
- BLASIM - A computational tool to assess ice impact damage on engine blades
[AIAA PAPER 93-1638] p 720 A93-34165
- Results of a low power ice protection system test and a new method of imaging data analysis
p 795 A93-35932
- Compact heat exchanger fitted to engines of the inverted type
[ISABE 93-7120] p 1221 A93-54095
- Icing Research Tunnel rotating bar calibration measurement system
p 1255 A93-54398
- Developments in icing test techniques for aerospace applications in the RAE Pyestock (England) altitude test facility
[RAE-TM-P-1214] p 48 N93-11485
- Simulation of two-dimensional icing, de-icing and anti-icing phenomena
p 142 N93-13364
- Icing effects on aircraft stability and control determined from flight data: Preliminary results
[NASA-TM-105977] p 188 N93-14831
- Ice accretion and performance degradation calculations with LEWICE/NS
[NASA-TM-105972] p 148 N93-15354
- Close-up analysis of aircraft ice accretion
[NASA-TM-105952] p 148 N93-15360
- An overview of shed ice impact in the NASA Lewis Icing Research Tunnel
[NASA-TM-105969] p 139 N93-15404
- Ice accretion prediction for a typical commercial transport aircraft
[NASA-TM-105976] p 149 N93-15522
- Identification of icing water clouds by NOAA AVHRR satellite data
[DLR-FB-92-11] p 434 N93-16477
- Effect of underwing frost on transport aircraft takeoff performance
[DOT/FAA/CT-TN93/9] p 791 N93-27252
- Three-dimensional water droplet trajectory code validation using an ECS inlet geometry
[NASA-CR-191097] p 791 N93-27267
- Aircraft ice detectors and related technologies for onground and inflight applications
[DOT/FAA/CT-92/27] p 791 N93-27269
- Experimental and computational ice shapes and resulting drag increase for a NACA 0012 airfoil
p 784 N93-27440
- Recent progress in the analysis of iced airfoils and wings
p 784 N93-27441
- A passive infrared ice detection technique for helicopter applications
[NASA-CR-193187] p 880 N93-29152
- ICE MAPPING**
- Dual-band infrared imaging applications: Locating buried minefields, mapping sea ice, and inspecting aging aircraft
[DE93-000516] p 453 N93-17225
- ICE NUCLEI**
- Icing prevention by ultrasonic nucleation of supercooled water droplets in front of subsonic aircraft
[AD-A258212] p 142 N93-12816
- ICE PREVENTION**
- Results of Low Power Deicer tests on a swept inlet component in the NASA Lewis Icing Research Tunnel
[AIAA PAPER 93-0032] p 327 A93-22551
- Surface roughness due to residual ice in the use of low power deicing systems
[AIAA PAPER 93-0031] p 282 A93-23240
- Numerical modeling of anti-icing systems and comparison to test results on a NACA 0012 airfoil
[AIAA PAPER 93-0170] p 327 A93-23242
- Results of a low power ice protection system test and a new method of imaging data analysis
p 795 A93-35932
- Experimental evaluation of flat plate boundary layer growth over an anti-icing fluid film
p 1140 A93-52645
- Icing prevention by ultrasonic nucleation of supercooled water droplets in front of subsonic aircraft
[AD-A258212] p 142 N93-12816
- Simulation of two-dimensional icing, de-icing and anti-icing phenomena
p 142 N93-13364
- Results of low power deicer tests on a swept inlet component in the NASA Lewis icing research tunnel
[NASA-TM-105968] p 138 N93-14911
- Surface roughness due to residual ice in the use of low power deicing systems
[NASA-TM-105971] p 139 N93-15338
- Numerical modeling of anti-icing systems and comparison to test results on a NACA 0012 airfoil
[NASA-TM-105975] p 148 N93-15345
- Numerical modeling of runback water on ice protected aircraft surfaces
p 840 N93-27438
- FAA international conference on airplane ground deicing
[AD-A263617] p 880 N93-29286
- IDEAL FLUIDS**
- Axisymmetric vortex sheet roll-up
p 788 N93-28078
- IDEAL GAS**
- Flux limiters in a rotated upwind scheme for the Euler equations
[AIAA PAPER 93-0067] p 262 A93-20180
- An improved numerical model for wave rotor design and analysis
[AIAA PAPER 93-0482] p 361 A93-23384
- Subsonic potential flow and the transonic controversy
p 479 A93-28544

- Intermode exchange in a supersonic boundary layer
p 691 A93-35346
- Requirements for facilities and measurement techniques to support CFD development for hypersonic aircraft
p 1014 A93-47024
- Algebraic determination of the shock wave shape in axisymmetric flow over a circular cylinder
p 1237 A93-56030
- An improved numerical model for wave rotor design and analysis
[NASA-TM-105915] p 60 A93-12418
- Navier-Stokes simulations of unsteady transonic flow phenomena
[NASA-TM-103962] p 129 A93-12721
- Mathematical problems in inviscid hypersonic flow
p 131 A93-13451
- Combined LAURA-UPS hypersonic solution procedure
[NASA-TM-107682] p 747 A93-25176
- IFF SYSTEMS (IDENTIFICATION)**
- An SSR/IFF Environment Model --- Secondary Surveillance Radar p 883 A93-43406
- IGNITION**
- Comment on "Experimental study on autoignition in a scramjet combustor" p 172 A93-14525
- Ignition and spread of combustion within a supersonic boundary layer p 535 A93-27732
- Ignition process of fuel droplet arrays in a supersonic flowfield p 535 A93-27766
- Ignition analysis of unpremixed reactants with chain mechanism in a supersonic mixing layer
p 735 A93-35619
- Initiation of combustion in the thermally choked ram accelerator p 1016 A93-45501
- Development and use of hydrogen-air torches in an altitude facility
[AIAA PAPER 93-2176] p 1137 A93-49988
- Boron particle ignition in high-speed flow
[AIAA PAPER 93-2202] p 1145 A93-50014
- Shock enhancement and control of hypersonic combustion
[AD-A254295] p 72 A93-10843
- A k-omega-multivariate beta PDF for supersonic combustion
[NASA-CR-191930] p 537 A93-21749
- IGNITION LIMITS**
- Ignition and exhaust emission characteristics of spray combustion in a pre-chamber type vortex combustor
[ASME PAPER 92-GT-119] p 350 A93-19355
- A study of self-ignition of methane-hydrogen mixture fuel injected into high enthalpy supersonic airstreams
[ISABE 93-7049] p 1213 A93-54025
- IGNITION TEMPERATURE**
- Analysis of thermal ignition in supersonic flat-plate boundary layers p 769 A93-37933
- Some recommendations concerning the prevention of fuel boiling in the igniters of the combustion chambers of gas turbine engines p 812 A93-39200
- Ignition of boron particles coated by a thin titanium film
[AIAA PAPER 93-2201] p 1145 A93-50013
- Ignition and combustion performance of a scramjet combustor with a fuel injection strut
[ISABE 93-7050] p 1199 A93-54026
- Employment of radicals and excited state species for supersonic combustion photochemical ignition of premixed hydrogen/oxygen mixtures with ArF laser
p 73 A93-11135
- ILLUMINATION**
- Nonlinear deformation mechanics of multilayer transparency elements - Some calculation results --- for aircraft portholes p 1191 A93-52937
- ILLUMINATORS**
- Bistatic radar using satellite-borne illuminators of opportunity p 914 A93-43437
- ILYUSHIN AIRCRAFT**
- Analysis of random components during measurements in the computerized diagnostic system Anaz-86
p 321 A93-18344
- Assessment of flight data in real time
p 341 A93-18364
- Propulsion system simulator with propan for tests on a large scale model of IL-114 airplane in a full-size wind tunnel of TsAGI p 1013 A93-46933
- IMAGE ANALYSIS**
- Accuracy analysis on image matching guidance systems p 62 A93-12653
- Passive range estimation for rotorcraft low-altitude flight p 948 A93-46608
- Computer-aided light sheet flow visualization
[AIAA PAPER 93-2915] p 1147 A93-48117
- Passive range estimation for rotorcraft low-altitude flight p 1190 A93-52881
- Automated extraction of aircraft runway patterns from radar imagery
[AD-A254258] p 68 A93-11751
- Image-based ranging and guidance for rotorcraft
[NASA-CR-177608] p 708 A93-26549
- Automatic detection of explosives using x ray imaging p 880 A93-30275
- IMAGE INTENSIFIERS**
- Integrated helmet system testing for a nightflying helicopter
[MBB-UD-0604-91-PUB] p 343 A93-17570
- IMAGE MOTION COMPENSATION**
- Research on ISAR motion compensation and imaging by modeling electromagnetic data p 342 A93-20852
- ISAR motion compensation and superresolution imaging of aircraft p 928 A93-42793
- Motion compensation in a time domain SAR processor p 885 A93-43466
- IMAGE PROCESSING**
- Planar imaging of OH density distributions in a supersonic combustion tunnel
[AIAA PAPER 93-0042] p 389 A93-20155
- The ISAR image-formation results of Boeing-727
p 342 A93-20857
- Vision-based recursive estimation of rotorcraft obstacle locations p 343 A93-22851
- Passive range sensor refinement using texture and segmentation p 544 A93-27044
- A fast algorithm for image-based ranging p 544 A93-27045
- Results of a low power ice protection system test and a new method of imaging data analysis p 795 A93-35932
- Digital image processing applied to heat transfer measurement in hypersonic wind tunnel
[ONERA, TP NO. 1992-118] p 831 A93-38593
- Topographic mapping using a Ku-band airborne elevation interferometer p 896 A93-42786
- ISAR motion compensation and superresolution imaging of aircraft p 928 A93-42793
- Visualization and view simulation based on transputers p 1037 A93-45150
- The Airborne Ocean Color Imager - System description and image processing p 1157 A93-50369
- Terrain modeling for real-time photo-texture based visual simulation
[AIAA PAPER 93-3607] p 1214 A93-52667
- A radar altitude and line of sight attachment
[AIAA PAPER 93-3587] p 1223 A93-52680
- Texture as a visual cueing element in computer image generation. I - Representation of the sea surface
[AIAA PAPER 93-3560] p 1214 A93-52695
- Automated extraction of aircraft runway patterns from radar imagery
[AD-A254258] p 68 A93-11751
- Ultra wide band 3-D cross section (RCS) holography
[DE92-019133] p 89 A93-11802
- Realization of real time graphics in vehicles with high dynamic motion
[ETN-93-92739] p 443 A93-18630
- Study of optical techniques for the Ames unitary wind tunnel: Digital image processing, part 6
[NASA-CR-192164] p 382 A93-18766
- Measurement of modulation transfer functions of simulator displays
[AD-A259401] p 530 A93-21268
- On-board derived flight-path measurement as demonstrated by an ILS measurement system p 994 A93-31282
- Testing of an experimental system for image reconnaissance p 1040 A93-31283
- Expansion-based passive ranging
[NASA-TM-104025] p 994 A93-32348
- IMAGE RESOLUTION**
- Superresolution radar imaging with linear prediction data extrapolation p 342 A93-20851
- Synchronous X-ray Sinography for nondestructive imaging of turbine engines under load
[AIAA PAPER 93-1819] p 1153 A93-49707
- Motion errors and compensation possibilities p 212 A93-13052
- X ray microscopy resource center at the Advanced Light Source
[DE93-010449] p 911 A93-29869
- IMAGE VELOCITY SENSORS**
- Application of particle image velocimetry in high-speed separated flows p 549 A93-29304
- IMAGERY**
- The HYDICE instrument design and its application to planetary instruments p 842 A93-28766
- IMAGING RADAR**
- Results from a VHF impulse synthetic-aperture radar p 501 A93-28219
- IMAGING TECHNIQUES**
- Measurement of shed vorticity and circulation from rotating aerofoil by particle image velocimetry p 538 A93-23804
- Advanced airborne 3D computer image generation systems technologies for the year 2000 p 518 A93-28176
- Laser selection criteria for OH fluorescence measurements in supersonic combustion test facilities p 549 A93-29315
- Results of a low power ice protection system test and a new method of imaging data analysis p 795 A93-35932
- MOI - Magneto-optic/eddy current imaging p 927 A93-41751
- Studies of superresolution range-Doppler imaging p 928 A93-43344
- Method of remotely characterizing thermal properties of a sample
[NASA-CASE-LAR-13508-3-CU] p 67 A93-11057
- Magneto-optic imaging inspection of selected corrosion specimens
[DOT/FAA/CT-TN92/20] p 88 A93-11617
- Planar measurement of flow field parameters in nonreacting supersonic flows with laser-induced iodine fluorescence p 133 A93-13801
- Dual-band infrared imaging applications: Locating buried minefields, mapping sea ice, and inspecting aging aircraft
[DE93-000516] p 453 A93-17225
- IR imaging for combustion characteristics and optical properties of boron/boron oxide
[AD-A257747] p 393 A93-17693
- Study of optical techniques for the Ames unitary wind tunnel, part 7
[NASA-CR-192165] p 382 A93-18520
- Study of optical techniques for the Ames unitary wind tunnel: Digital image processing, part 6
[NASA-CR-192164] p 382 A93-18766
- An investigation of photothermal velocimetry for application to transient, high-speed gas flows p 698 A93-25720
- Small satellites and RPA's in global-change research
[AD-A260762] p 755 A93-25837
- A model-based approach for detection of objects in low resolution passive millimeter wave images
[NASA-CR-193161] p 808 A93-28418
- Preliminary design of an intermittent smoke flow visualization system
[NASA-CR-186027] p 806 A93-28693
- Multiparticle imaging technique for two-phase fluid flows using pulsed laser speckle velocimetry
[DE93-011734] p 935 A93-30489
- IMPACT DAMAGE**
- An evaluation system for impact damage and erosion of ceramic gas turbine components p 79 A93-12229
- Slicing model for foreign soft-body objects impacting on blade rows p 28 A93-12372
- Dynamic analysis of a pre-and-post ice impacted blade
[AIAA PAPER 92-4273] p 54 A93-13333
- Compression after impact (CAI) properties of CF/PEEK (APC-2) and conventional CF/epoxy stiffened panels p 196 A93-14307
- An impact dynamics investigation on some problems in bird strike on windshields of high speed aircraft p 197 A93-15346
- Experimental investigations into composite fuselage impact damage resistance and post-impact compression behavior p 159 A93-15812
- Repair of delaminations and impact damage in composite aircraft structures p 457 A93-24107
- Experimental assessment of airframe damage due to impacting ice
[AIAA PAPER 93-0751] p 504 A93-24838
- An experimental and analytical investigation on the response of GR/EP composite I-frames p 546 A93-27975
- Rapid detection and quantification of impact damage in composite structures p 547 A93-27978
- Delaminations of barely visible impact damage in CFRP laminates p 737 A93-33798
- Foreign object impact assessment of a high-Mach engine inlet
[AIAA PAPER 93-1630] p 711 A93-34158
- BLASIM - A computational tool to assess ice impact damage on engine blades
[AIAA PAPER 93-1638] p 720 A93-34165
- Evaluation by holographic interferometry of impact damage in composite aeronautical structures p 1020 A93-44193
- Small particle impact damage in carbon-carbon composites
[PNR-90948] p 73 A93-11107
- Dynamic analysis of a pre-and-post ice impacted blade
[NASA-TM-105829] p 90 A93-12197
- Allowable compression strength for CFRP-components of fighter aircraft determined by CAI-test
[MBB-FE-221-S-PUB-0483] p 537 A93-21462

GARTEUR damage mechanics for composite materials: Analytical/experimental research on delaminations p 537 N93-21513

Numerical determination of the residual strength of battle damaged composite plates p 537 N93-21533

Expedient repair of structural facilities [AD-A260727] p 731 N93-25656

Structural tailoring of aircraft engine blade subject to ice impact constraints p 838 N93-26999

[NASA-TM-106033] Developments in impact damage modeling for laminated composite structures p 922 N93-30857

Consideration of impact damages by dimensioning CFC (Carbon Fiber Reinforced Composites) components [MBB-FE-221-S-PUB-0501] p 1018 N93-31044

Blasim: A computational tool to assess ice impact damage on engine blades [NASA-TM-106225] p 1031 N93-31193

IMPACT LOADS

Bird impact dynamic response analysis for aircraft arc windshield p 41 A93-11815

The methods of reducing impact loads on occupants in the civil aircraft crash condition p 140 A93-14220

New model of bird impact response analysis and its engineering solution p 156 A93-14336

Effect of bird impact load types on blade response p 174 A93-16846

Numerical modeling of the impact of a bird against aircraft transparencies p 801 A93-36797

A mathematical model of the vibrational impact hardening of parts p 837 A93-39185

Characterization of delamination and fiber fractures in carbon fiber reinforced plastics induced from impact p 915 A93-40787

Characteristics of the detection of overloads in the center of mass of IL-76 and An-12 aircraft due to runway irregularities by a standard on-board recorder p 1008 A93-45666

Aircraft monitoring of the planeness of the existing and new runways p 991 A93-45668

Static and dynamic large deflection flexural response of graphite-epoxy beams p 934 A93-30374

[NASA-CR-4118] Blasim: A computational tool to assess ice impact damage on engine blades [NASA-TM-106225] p 1031 N93-31193

IMPACT RESISTANCE

Experimental investigations into composite fuselage impact damage resistance and post-impact compression behavior p 159 A93-15812

Advanced transparency development for USAF aircraft [AIAA PAPER 93-1391] p 710 A93-33954

Response of laminated composite plates to low-speed impact by airgun-propelled and dropped-weight impactors p 739 A93-33962

[AIAA PAPER 93-1402] Low velocity impact in a graphite/PEEK [AIAA PAPER 93-1403] p 734 A93-33963

IMPACT STRENGTH

Test and analysis of an advanced technology landing gear p 37 A93-10917

IMPACT TESTS

An overview of shed ice impact studies in the NASA Lewis Icing Research Tunnel [AIAA PAPER 93-0301] p 283 A93-23247

Delaminations of barely visible impact damage in CFRP laminates p 737 A93-33798

Advanced transparency development for USAF aircraft [AIAA PAPER 93-1391] p 710 A93-33954

The application of diffusion bonding in the manufacture of aeroengine components p 1217 A93-53514

Instrumentation and data acquisition for full-scale aircraft crash testing p 1250 A93-54399

An overview of shed ice impact in the NASA Lewis Icing Research Tunnel [NASA-TM-105969] p 139 N93-15404

IMPACT TOLERANCES

Consideration of impact damages by dimensioning CFC (Carbon Fiber Reinforced Composites) components [MBB-FE-221-S-PUB-0501] p 1018 N93-31044

IMPELLERS

A data processing and measuring system with a traversing probe for studying flow in the rotating impeller of an axial-flow fan p 75 A93-10032

Experimental research for the discharge flow of a centrifugal impeller and the flowfield in the vaneless diffuser p 11 A93-12454

Axial length influence on the performance of centrifugal impellers p 205 A93-14517

Unsteady pressure measurements in a rotating centrifugal impeller [ASME PAPER 92-GT-152] p 402 A93-19379

Aerodesign and performance analysis of a radial transonic impeller for a 9:1 pressure ratio compressor [ASME PAPER 92-GT-183] p 352 A93-19408

Development and industrial application of the 'all-over-controlled vortex distribution method' for designing radial and mixed flow impellers [ASME PAPER 92-GT-262] p 405 A93-19466

A CAD computer system for centrifugal compressor impeller with transonic inflow p 259 A93-20118

Advanced direct-design procedure for centrifugal impellers p 411 A93-21659

Dynamics of a high speed impeller - Analysis and experimental verification [AIAA PAPER 93-1362] p 743 A93-34239

Velocity vector LDA measurement inside a pitched blade impeller p 924 A93-40390

Processing integral impeller 4-coordinate numerically controlled milling machine p 926 A93-41749

Effect of radial distortion on the performance of a centrifugal compressor p 861 A93-42256

Numerical modelling of viscous turbomachinery flows with a pressure correction method p 723 N93-25702

IMPINGEMENT

Shock interference prediction using direct simulation Monte Carlo p 778 A93-39258

Three-dimensional water droplet trajectory code validation using an ECS inlet geometry [NASA-CR-191097] p 791 N93-27267

Local heat transfer measurement with liquid crystals on rotating surfaces including non-axisymmetric cases p 902 N93-29943

IMPULSES

A plate loaded by a transverse impulse force and in-plane forces p 828 A93-36799

Development of a skin friction gauge for use in an impulse facility p 1024 A93-45526

IN SITU MEASUREMENT

Aircraft lightning initiation and interception from in situ electric measurements and fast video observations p 140 A93-14064

Advanced diagnostics for in situ measurement of particle formation and deposition in thermally stressed jet fuels [AIAA PAPER 93-0363] p 390 A93-23045

An approach to in-situ analysis of scramjet combustor behavior [AIAA PAPER 93-2328] p 1116 A93-50108

An aircraft instrument design for in situ tropospheric OH measurements by laser induced fluorescence at low pressures p 1159 A93-51528

In situ material characterization for pavement evaluation by the Spectral-Analysis-of-Surface-Waves (SASW) method [AD-A255660] p 194 A93-14128

NASA wind shear flight test in situ results p 488 N93-19593

Comparison of the electrical charging and discharging environments of multiple aircraft-borne electric-field measurement systems p 704 N93-24887

IN-FLIGHT MONITORING

Aircraft tracking optimization of parameters selection p 3 A93-13628

Vibration monitoring and fault diagnosis of inflight aircraft engines p 170 A93-14176

In-flight tailload measurements p 155 A93-14285

Development of a model-based monitoring system for turbine and rocket engines p 195 A93-16412

Assessment of flight data in real time p 341 A93-18364

Crack growth under conditions of service loading p 396 A93-18370

Engine Health Monitoring p 346 A93-18787

AH-64A rotating load usage monitoring from fixed system information p 507 A93-27953

Tiltrotor interior noise characteristics p 509 A93-29421

In-flight investigation of a rotating cylinder-based structural excitation system for flutter testing [AIAA PAPER 93-1537] p 711 A93-34074

Acquiring tail load spectra from in-flight measurements [AIAA PAPER 93-1607] p 711 A93-34137

F405 engine in-flight thrust methodology development for the T-45A flight test program [AIAA PAPER 93-2544] p 1121 A93-50268

Estimation of aerodynamic characteristics from flight-test data. IV - Principal component analysis and perpendicular error method p 1241 A93-54551

Flight test progress of the STOL research aircraft ASKA [NAL-TM-643] p 49 N93-12354

Proceedings of the 18th Symposium on Aircraft Integrated Monitoring Systems [DLR-MITT-92-01] p 167 N93-15152

Discussion for the ideal AIMS p 167 N93-15153

Software flexibility and configuration control for the A340/A330 Aircraft Condition Monitoring System (ACMS) p 167 N93-15154

The Teledyne controls aircraft condition monitoring system p 168 N93-15155

Flight data and flight safety in SAS p 168 N93-15156

Detection of technical states with aircraft p 168 N93-15159

Integrated engine control and monitoring with experiences derived from OLMOS p 178 N93-15168

Real-time in-flight engine performance and health monitoring techniques for flight research application p 169 N93-15169

Monitoring of powerplants in advanced commercial aircraft p 178 N93-15171

EJ 200 engine monitoring system: On- and off-board data capture, analysis, and management system p 178 N93-15172

RB199 engine oil system failure diagnostics by comparison of measured and calculated oil consumption using the OLMOS on-board monitoring system p 178 N93-15173

A philosophy for integrated monitoring system design p 178 N93-15174

Modelling the engine temperature distribution between shut down and restart for life usage monitoring p 169 N93-15177

Helicopter flight data recorder and health and usage monitoring system p 169 N93-15178

Helicopter health monitoring: Current practice and future trends p 169 N93-15179

New rotor trim and balance system for helicopter usage monitoring p 169 N93-15180

Failure diagnostic with MAINTEx based on AIMS at Swissair p 110 N93-15181

Neural network based condition monitoring p 230 N93-15183

Personal computer based test- and emulation equipment for maintenance and ground support p 110 N93-15185

Airbus Industrie TCAS experience p 152 N93-15186

Three-dimensional numerical simulation of the 20 June 1991, Orlando microburst p 488 N93-19598

Load experience variability of fighter aircraft [NLR-TP-89172-U] p 514 N93-20742

Digitization of analog data from in-flight lightning strikes p 753 N93-24884

Comparison of the electrical charging and discharging environments of multiple aircraft-borne electric-field measurement systems p 704 N93-24887

Flow prediction over a transport multi-element high-lift system and comparison with flight measurements p 785 N93-27448

Spurious symptom reduction in fault monitoring [NASA-CR-191453] p 942 N93-29192

INCIDENCE

Flow computation for the hypersonic configuration ELAC I at low speeds and large incidence p 1238 A93-56036

INCOMPRESSIBLE BOUNDARY LAYER

A numerical solution of the asymptotic problem of boundary layer separation in an incompressible liquid upstream of the corner point of a body p 965 A93-46699

Roughness-induced generation of crossflow vortices in three-dimensional boundary layers [NASA-CR-4505] p 780 N93-27096

The remarkable ability of turbulence model equations to describe transition p 783 N93-27432

INCOMPRESSIBLE FLOW

Optimal control of lift/drag ratios on a rotating cylinder p 76 A93-10275

A low-speed aerodynamic model for harmonically oscillating aircraft configurations p 8 A93-11500

A method for calculating flow past an arbitrary airfoil profile in the presence of flow separation p 13 A93-12807

Nonstationary flow of a viscous incompressible fluid past an airfoil p 79 A93-12922

Generalized multipoint inverse airfoil design p 122 A93-14541

Instability of the periodic deflection of a panel surface in a turbulent boundary layer p 208 A93-15188

A conformal-integral method for solving the direct problem in turbomachine cascade aerodynamics p 125 A93-15217

A finite element study of incompressible flows past oscillating cylinders and aerofoils p 241 A93-17750

Simulation of the secondary air system of aero engines [ASME PAPER 92-GT-68] p 348 A93-19318

Aerodynamic design of pivotable nozzle vanes for radial-inflow turbines [ASME PAPER 92-GT-94] p 349 A93-19340

An inviscid-viscous interaction approach to the calculation of dynamic stall initiation on airfoils [ASME PAPER 92-GT-128] p 249 A93-19362

A three-dimensional inviscid flow solver in Chimera flow simulation
[AIAA PAPER 93-0190] p 276 A93-22614

The three-dimensional separated flow structure in a variable aspect ratio sudden expansion duct
[AIAA PAPER 93-0213] p 278 A93-22630

Aerodynamic analysis of flapping wing propulsion
[AIAA PAPER 93-0484] p 286 A93-23386

Numerical modeling of leading edge separated flow at incompressible speeds p 460 A93-24079

Incompressible potential flow calculation about harmonically oscillating three-dimensional configurations p 461 A93-24089

A fast multigrid method for solving incompressible hydrodynamic problems with free surfaces
[AIAA PAPER 93-0767] p 540 A93-24851

Incompressible flow computation of forces and moments on bodies of revolution at incidence
[AIAA PAPER 93-0787] p 541 A93-24867

Numerical study of an axisymmetric turbulent jet-impingement flow
[AIAA PAPER 93-0652] p 543 A93-25545

Solution-adaptive and quality-enhancing grid generation p 480 A93-28610

Karman vortex street-airfoil interaction p 678 A93-33703

An analysis of the post-instability behaviour of a two-dimensional airfoil with a structural nonlinearity
[AIAA PAPER 93-1474] p 726 A93-34020

Calculation of laminar and turbulent asymmetric wakes p 684 A93-34318

Permeable airfoils in incompressible flow p 768 A93-37401

Turbulent flow simulation around the aeroflow with pseudo-compressibility p 830 A93-38155

Numerical calculation of separated flows around wing section in unsteady motion by using incompressible Navier-Stokes equations p 770 A93-38158

Laser-velocimeter study of vortex breakdown on a 70-deg swept delta wing in incompressible flow
[ONERA, TP NO. 1992-147] p 773 A93-38728

A viscous-inviscid solver for high-lift incompressible flows over multi-element airfoils at deep separation conditions
[ONERA, TP NO. 1992-183] p 774 A93-38745

Pseudo-compressibility methods for the incompressible flow equations p 952 A93-45023

Numerical wave propagation and steady state solutions. II - Bulk Viscosity Damping
[AIAA PAPER 93-3331] p 953 A93-45025

Simulation of flow past complex geometries using a parallel implicit incompressible flow solver p 957 A93-45095

Numerical analysis of airfoil cascades subjected to unsteady flow p 972 A93-46944

Two dimensional incompressible flow through a vibrating bladed disc - Theoretical model p 973 A93-46991

Numerical simulation of incompressible viscous flow around a propeller p 984 A93-47271

A computational study of wingtip vortex flowfield
[AIAA PAPER 93-3010] p 1054 A93-48200

A wake singularity potential flow model for airfoils experiencing trailing-edge stall p 1067 A93-48544

Pressure pulsations on a delta wing in incompressible flow p 1069 A93-48912

A new technique for analysis of unsteady aerodynamic responses of cascade airfoils with blunt leading edge - Unsteady aerodynamic responses of the cascade in incompressible flow p 1086 A93-51122

Spline-collocation solution of a Fredholm equation of the second kind in the problem of flow past an airfoil p 1092 A93-51904

Efficient simulation of incompressible viscous flow over single and multi-element airfoils p 1095 A93-52448

The effects of fixed rotor tilt on the rotordynamic coefficients of incompressible flow annular seals p 1161 A93-52601

Improved numerical simulation of Euler equations p 83 A93-10309

Analysis of wing-body junction flowfields using the incompressible Navier-Stokes equations, volumes 1 and 2 p 17 A93-10320

Multi-point inverse design of isolated airfoils and airfoils in cascade in incompressible flow p 163 A93-14462

On flutter behavior of a 2-D compressor cascade in incompressible flow p 418 A93-16543

[DLR-FB-91-26] p 418 A93-16543

A computational and experimental investigation of the propulsive and lifting characteristics of oscillating airfoils and airfoil combinations in incompressible flow
[AD-A258019] p 294 A93-17819

Instability of flow in a streamwise corner
[NASA-CR-191410] p 694 A93-25153

Efficient simulation of incompressible viscous flow over multi-element airfoils p 784 A93-27443

The numerical solution of low Mach number flow in confined regions by Richardson extrapolation
[TRITA-NA-9207] p 789 A93-29005

Stabilized space-time finite element formulations for unsteady incompressible flows involving fluid-body interactions p 843 A93-29040

A parallel implicit incompressible flow solver using unstructured meshes
[AD-A263395] p 931 A93-29851

INCOMPRESSIBLE FLUIDS

Calculation of three-dimensional turbulent jets propagating behind nozzles of rectangular cross section p 6 A93-10192

Monotonicity characteristics of some plane vortex flows of incompressible fluids and subsonic gas flows p 13 A93-12932

Oblique wave evolution in a plane subsonic boundary layer p 124 A93-15178

Modeling of interfaces in problems of flow of a ponderable fluid past a wing profile p 124 A93-15189

Compressible and incompressible fluid seals: Influence on rotordynamic response and stability
[NASA-CR-190746] p 85 A93-10891

INCONEL (TRADEMARK)

Corrosion resistance of Inconel Alloy 617 in simulated gas turbine environments
[ASME PAPER 92-GT-142] p 388 A93-19374

INDEPENDENT VARIABLES

Probabilistic assessment of composite structures
[NASA-TM-106024] p 825 A93-27092

INDEXES (DOCUMENTATION)

AGARD index of publications, 1989-1991
[AGARD-INDEX-89-91] p 104 A93-10610

Index to NASA news releases and speeches, 1991
[NASA-TM-108004] p 104 A93-10815

Index to NASA news releases and speeches, 1990
[NASA-TM-108003] p 104 A93-10872

USA aviation digest index, 1989, volume 11
[AD-A258673] p 571 A93-20388

Index to USA aviation digest, 1990
[AD-A258678] p 572 A93-20389

Index to USA aviation digest, 1991
[AD-A258679] p 572 A93-20390

European aerospace science and technology, 1992: A bibliography with indexes
[NASA-SP-7105] p 949 A93-32404

INDUCED DRAG

Effect of wing planforms on induced drag reduction p 127 A93-16932

Computation of induced drag for elliptical and crescent-shaped wings p 958 A93-45136

Effect of the wing planform on the optimal deformation of the middle surface p 1150 A93-48909

Minimization of the induced drag of nonplanar lifting systems p 1068 A93-48910

Nonplanar wings with a minimum induced drag p 1089 A93-51779

A study of the aerodynamics of a wing with end slots p 1092 A93-51907

Induced drag of a crescent wing planform p 1094 A93-52430

Assessment of potential aerodynamic benefits from spanwise blowing at the wing tip p 134 A93-13822

Quantitative three-dimensional low-speed wake surveys p 785 A93-27447

INDUSTRIAL MANAGEMENT

Activities report of Lufthansa
[ETN-92-92100] p 28 A93-11319

The airline quality report, 1992
[NIAR-92-11] p 310 A93-18036

INDUSTRIAL PLANTS

Flexible manufacturing of aircraft engine parts
[ASME PAPER 92-GT-229] p 404 A93-19446

INDUSTRIAL SAFETY

Advantages of a one-part resin system for processing aerospace parts by Resin Transfer Molding (RTM)
[SME PAPER EM93-112] p 1159 A93-51729

INDUSTRIES

Industry survey of space system cost benefits from New Ways Of Doing Business p 454 A93-17325

Pre-flight risk assessment in Emergency Medical Service (EMS) helicopters p 494 A93-19692

NASA SBIR abstracts of 1990 phase 1 projects
[NASA-TM-108145] p 572 A93-21794

INELASTIC SCATTERING

Scattering kernels for gas-surface interaction p 943 A93-42580

PFNA technique for the detection of explosives p 497 A93-21865

INEQUALITIES

Design of a low sensitivity and norm multivariable controller using eigenstructure assignment and the method of inequalities
[AIAA PAPER 93-3802] p 1170 A93-51394

Combining direct and indirect methods in optimal control: Range maximization of a hang glider
[REPT-313] p 371 A93-16618

INERTIA

Vibration isolation technology: An executive summary of systems development and demonstration
[NASA-TM-105937] p 110 A93-15573

US Army helicopter inertia reel locking failures p 493 A93-19689

INERTIAL GUIDANCE

Sensor alignment Kalman filters for inertial stabilization systems p 50 A93-11018

Analysis of DGPS/INS and MLS/INS final approach navigation errors and control performance data p 315 A93-21183

Hybrid guidance for maneuvering flight vehicles
[AD-A254110] p 69 A93-11788

INERTIAL NAVIGATION

Precision navigation with an integrated navigation system p 29 A93-10782

Development of a TRN/INS/GPS integrated navigation system p 30 A93-11004

Architectures and GPS/INS integration - Impact on mission accomplishment p 31 A93-11013

Differential GPS/inertial navigation approach/landing flight test results p 32 A93-11019

Maintaining high accuracy GPS positioning 'on the fly' --- using traverse closures, residual analysis, inertial navigation in aircraft p 92 A93-11028

Achieving modularity with tightly-coupled GPS/INS p 33 A93-11032

Precision increasing and integrity monitoring of navigation data for GPS/inertial hybrid solution p 149 A93-14157

BUAA inertial terrain-aided navigation (BITAN) algorithm p 149 A93-14235

Flight management systems p 311 A93-17757

Institute of Navigation, National Technical Meeting, San Diego, CA, Jan. 27-29, 1992, Proceedings p 315 A93-21176

INS/DGPS integration for trajectory determination of a test vehicle p 315 A93-21178

False alarm probability determination for the Honeywell Hexad Fault-Tolerant INS p 342 A93-21193

The value of GNSS to aircraft operators p 498 A93-25172

Position reporting using GPS/OMEGA and INS p 498 A93-25173

Integration of a course and position reference system with GPS p 499 A93-27911

Application of advanced guidance and navigation systems to flight control of aircraft and future space vehicles p 500 A93-28153

The ring laser gyro and its applications p 927 A93-42657

Augmentation of a navigation reference system with differential global positioning system pseudorange measurements p 881 A93-42798

Adaptive filtering of Doppler velocimeter errors due to the characteristics of the reflecting surface p 992 A93-45650

Guidance and control of HOPE (H-II orbiting plane)
[AAS PAPER 91-653] p 1252 A93-55825

Airborne vector gravimetry with an aided inertial survey system p 1241 A93-55977

Correction of inertial measurements using GPS updates for underwater navigation
[AD-A257329] p 317 A93-15988

Flight evaluation of a computer aided low-altitude helicopter flight guidance system p 820 A93-28869

System analysis for a kinematic positioning system based on the global positioning system
[AD-A262830] p 885 A93-29468

High reliability, maintenance-free INS battery development
[AD-A264521] p 934 A93-30406

On-board derived flight-path measurement as demonstrated by an ILS measurement system p 994 A93-31282

INERTIAL PLATFORMS

The Texas Instruments/Honeywell GPS Guidance Package p 32 A93-11015

The LN-200 fiber gyro based tactical grade IMU
[AIAA PAPER 93-3798] p 1106 A93-51391

Controlling common mode stabilization errors in airborne gravity gradiometry p 1245 A93-55978

Integrated DGPS/IMU systems for airborne navigation in Poland p 1241 A93-56049

INERTIAL REFERENCE SYSTEMS

A fault-tolerant air data/inertial reference system p 50 A93-10982

A fault-tolerant Air Data/Inertial Reference Unit p 807 A93-37074

GPS autoland considerations p 792 A93-38203

INFERENCE

Design of an Ada expert system shell for the VHSIC avionics modular flight processor p 98 N93-11947

INFILTRATION

Polymer infiltration studies [NASA-CR-191652] p 200 N93-15431

INFINITE SPAN WINGS

Stationary crossflow instability on an infinite swept wing p 699 N93-25865

INFLATABLE STRUCTURES

Stable cross type parachute with inflation aid [AIAA PAPER 93-1201] p 702 A93-35152
Development testing of large ram air inflated wings [AIAA PAPER 93-1204] p 702 A93-35155
A simple, approximate model of parachute inflation [AIAA PAPER 93-1206] p 702 A93-35157
The effect of extreme altitude on parachute filling distance [AIAA PAPER 93-1207] p 702 A93-35158
Radial reefing method for accelerated and controlled parachute opening [AIAA PAPER 93-1209] p 702 A93-35159
Comparison of electrostatic and aerodynamic forces during parachute opening [AIAA PAPER 93-1210] p 689 A93-35160
The fluid physics of parachute inflation p 1189 A93-54347

INFLATING

Comparison of electrostatic and aerodynamic forces during parachute opening [AIAA PAPER 93-1210] p 689 A93-35160
Methods and results of theoretical investigations for high-speed parachute systems [AIAA PAPER 93-1227] p 690 A93-35173
Computation of aeroelastic characteristics and stress-strained state of parachutes [AIAA PAPER 93-1237] p 744 A93-35178
A simple, approximate model of parachute inflation [DE93-002465] p 694 A93-25121
A computational model that couples aerodynamic and structural dynamic behavior of parachutes during the opening process [AD-A264115] p 877 N93-30119

INFORMATION

Information requirements analyses for transatmospheric vehicles [AD-A261189] p 718 N93-25949

INFORMATION DISSEMINATION

Jeppesen worldwide electronic NOTAM service --- Notice to Airmen p 1 A93-11020

INFORMATION FLOW

Optimization of algorithms for information processing and control p 1169 A93-51062
Information systems for airport operations [TT-9202] p 152 N93-14729

INFORMATION MANAGEMENT

Real-time capture, archiving, retrieval, processing, and presentation of large quantities of flight test/research information [AIAA PAPER 92-4073] p 95 A93-11258
The development of an airborne information management system for flight test [AIAA PAPER 92-4113] p 51 A93-11281
Developing the Aviation Gridded Forecast System p 427 A93-22124
Weather information requirements for Terminal Air Traffic Control Automation p 429 A93-22146
Methods and principles for determining task dependent interface content [NASA-CR-190837] p 36 N93-10961
Royal Air Force experience of the Harrier information management system p 234 N93-15170
Design for tactical situation awareness display [AD-A256194] p 170 N93-15235

INFORMATION RETRIEVAL

Reusable Ada avionics software packages library system p 944 A93-42828

INFORMATION SYSTEMS

Jeppesen worldwide electronic NOTAM service --- Notice to Airmen p 1 A93-11020
Methods and equipment for data processing and acquisition in information management systems p 856 A93-43101
Generation of a plant description dictionary based on expert survey data p 1168 A93-50956
Methods and principles for determining task dependent interface content [NASA-CR-190837] p 36 N93-10961
Information systems for airport operations [TT-9202] p 152 N93-14729
Royal Air Force experience of the Harrier information management system p 234 N93-15170
AQUIS: A PC-based air quality and permit information system [DE92-040092] p 434 N93-18587

Handling and using information systems with new technology [PNR-90910] p 572 N93-20734

The use of multiple models in case-based diagnosis p 759 N93-25969

Meteorological information for aviation: A systems approach p 937 N93-30298

Application and integration of diverse technology in an aviation system: The National Aeronautics Information Processing System p 887 N93-30339

International aircraft operator information system [DOT/FAA/CT-93/4] p 949 N93-32232

INFORMATION TRANSFER

Jeppesen worldwide electronic NOTAM service --- Notice to Airmen p 1 A93-11020
FAA weather processor programs - Real-time dissemination of weather information to aviation end-users p 428 A93-22131
MIST - A remote briefing system p 437 A93-22132
Automated Weather Distribution System (AWDS) for support of global aviation p 428 A93-22134
The National Plan for Aviation Human Factors - Maintenance research issues p 457 A93-27132
Handling and using information systems with new technology [PNR-90910] p 572 N93-20734

INFRARED DETECTORS

IR window damage measured by reflective scatter p 851 A93-39544
Reconnaissance capable F/A-18D optical and infrared window antifog systems [SAE PAPER 921182] p 890 A93-41361
IR sensors; Proceedings of the Conference, London, United Kingdom, Feb. 18, 1992 [ISBN 1-85768-010-3] p 1244 A93-55294
Future trends in IR sensors p 1258 A93-55295
Displaying the night p 1244 A93-55297
Passive IR surveillance for helicopter systems - The Sea Owl equipment p 1244 A93-55299
Flight test operations p 488 N93-19592
Three-dimensional numerical simulation of the 20 June 1991, Orlando microburst p 488 N93-19598
Small satellites and RPA's in global-change research [AD-A260762] p 755 N93-25837
The infrared measurement for the reentry-body-translation [AD-A263100] p 914 N93-29134
A passive infrared ice detection technique for helicopter applications [NASA-CR-193187] p 880 N93-29152

INFRARED FILTERS

IR imaging for combustion characteristics and optical properties of boron/boron oxide [AD-A257747] p 393 N93-17693

INFRARED IMAGERY

Infrared flow visualization of V/STOL aircraft [AIAA PAPER 92-4253] p 80 A93-13343
Recent developments in compressor-based Joule-Thomson cooling --- of thermal imaging equipment in ground and helicopter-borne applications p 547 A93-28244
Infrared thermography for hot-shot wind tunnel [ONERA, TP NO. 1992-103] p 831 A93-38583
Infrared thermography characterization of Goertler vortex type patterns in hypersonic flows [ONERA, TP NO. 1993-13] p 925 A93-41029
Engineering a visual system for seeing through fog [SAE PAPER 921130] p 895 A93-41318
Applications of IR imagery to thermal evaluations [SAE PAPER 921223] p 926 A93-41397
Implementation of an infrared thermal imaging system to measure temperature in a gas turbine engine [AIAA PAPER 93-2469] p 1120 A93-50215
Study of optical techniques for the Ames unitary wind tunnel. Part 5: Infrared imagery [NASA-CR-191385] p 194 N93-14809
Dual-band infrared imaging applications: Locating buried minefields, mapping sea ice, and inspecting aging aircraft [DE93-000516] p 453 N93-17225
IR imaging for combustion characteristics and optical properties of boron/boron oxide [AD-A257747] p 393 N93-17693
Small satellites and RPA's in global-change research [AD-A260762] p 755 N93-25837

INFRARED INSPECTION

Applications of infrared measurement technique in hypersonic facilities p 1024 A93-45505

INFRARED INSTRUMENTS

Advanced technology wind shear prediction system evaluation p 146 N93-14858

INFRARED LASERS

A high resolution airborne multisensor system p 343 A93-21966
Scanning Laser Aircraft Surveillance System for carrier flight operations p 500 A93-28157

INFRARED RADIATION

COF2 radiation from an air-tyeflon wake p 12 A93-12659
The infrared measurement for the reentry-body-translation [AD-A263100] p 914 N93-29134

INFRARED SCANNERS

Applications of IR imagery to thermal evaluations [SAE PAPER 921223] p 926 A93-41397

INFRARED SIGNATURES

Prediction of engine casing temperature of fighter aircraft for infrared signature studies [SAE PAPER 920961] p 206 A93-14627
A passive infrared ice detection technique for helicopter applications [NASA-CR-193187] p 880 N93-29152

INFRARED SPECTRA

Remote sensing cloud properties from high spectral resolution infrared observations p 1034 A93-46780
Measurement of aerodynamic shear stress using side chain liquid crystal polymers [AD-A254312] p 72 N93-10770

INFRARED SPECTROMETERS

Preliminary results of the ISM campaign - The Landes, South West France p 1161 A93-47553

INFRARED SUPPRESSION

A numerical study on the radiation characteristic of an elliptical exhaust jet p 174 A93-16236

INFRARED TELESCOPES

Utilization of CAD/CAE for concurrent design of structural aircraft components [AIAA PAPER 93-1466] p 710 A93-34014
Effect of jet engine exhaust on SOFIA stratospheric performance --- Stratospheric Observatory For Infrared Astronomy p 1263 A93-55178

INFRARED WINDOWS

Thermal shock capabilities of infrared dome materials p 70 A93-11454
Reconnaissance capable F/A-18D optical and infrared window antifog systems [SAE PAPER 921182] p 890 A93-41361
Remote sensing cloud properties from high spectral resolution infrared observations p 1034 A93-46780

INGESTION

Ingestion into the upstream wheelspace of an axial turbine stage [ASME PAPER 92-GT-303] p 354 A93-19493
Wake ingestion propulsion benefit p 411 A93-21660

INGESTION (ENGINES)

Small scale jet effects and hot gas ingestion investigations at NASA Ames [AIAA PAPER 92-4252] p 67 A93-13339
Two and three-dimensional prediffuser combustor studies with air-water mixture [AIAA PAPER 93-0240] p 390 A93-22652
An experimental study of the effects of body-side compression on forward swept sidewall compression inlets ingesting a turbulent boundary layer [AIAA PAPER 93-3125] p 1072 A93-49515
Studies into the hail ingestion characteristics of turbofan engines [AIAA PAPER 93-2174] p 1115 A93-49987
Three-dimensional prediffuser combustor studies with air-water mixture [AIAA PAPER 93-2474] p 1120 A93-50217
Transient performance of fan engine with water ingestion [NASA-CR-190778] p 677 N93-25134

INJECTION

Experimental study of heat transfer close to a plane wall heated in the presence of multiple injections (subsonic flow) p 901 N93-29931

INJECTION MOLDING

Improved silicon nitride for advanced heat engines [NASA-CR-182193] p 917 N93-29451
Resin transfer molding for advanced composite primary aircraft structures p 919 N93-30438

INJECTORS

Mixing and combustion studies using discrete orifice injection at hypervelocity flight conditions p 205 A93-14523
A numerical study of mixing in supersonic combustors with hypermixing injectors [AIAA PAPER 93-0215] p 520 A93-27801
A numerical study of mixing in supersonic combustors with hypermixing injectors [NASA-CR-191027] p 294 N93-17884

INJURIES

Federal preemption in commercial aviation - Tort litigation under 49 U.S.C. section 1305 p 944 A93-42997
No rescue in sight for Warsaw plaintiffs from either courts or legislature - Montreal Protocol 3 draws in committee p 945 A93-42999

- Air carriers' liability for passenger injury or death - The Japanese Initiative and Response to the recent EC Consultation Paper p 1226 A93-52930
- 737-400 at Kegworth, 8 January 1989: The AAIB investigation p 491 N93-19661
- US Army's aviation life support equipment retrieval program real world design successes from proactive investigation p 494 N93-19690
- ### INLET AIRFRAME CONFIGURATIONS
- Starting and test rhombus characteristics of two-dimensional supersonic free-jet nozzle/generic supersonic aircraft inlet configurations [AIAA PAPER 92-5091] p 273 A93-22361
- Development of the F/A-18 E/F air induction system [AIAA PAPER 93-2152] p 1101 A93-49969
- A comparative study of Full Navier-Stokes and Reduced Navier-Stokes analyses for separating flows within a diffusing inlet S-duct [AIAA PAPER 93-2154] p 1079 A93-49970
- Aerodynamic Engine/Airframe integration for High Performance Aircraft and Missiles [AGARD-CP-498] p 213 N93-13199
- Solution of Euler equations for forebody-inlet ensemble of aircraft at high angle of attack [AD-A263905] p 876 N93-29862
- ### INLET FLOW
- Flow characteristics of an S-shaped inlet at high incidence p 114 A93-14213
- Numerical simulations of high speed inlet flows p 115 A93-14246
- Shock formation in overexpanded tip leakage flow [ASME PAPER 92-GT-1] p 245 A93-19276
- Experimental analysis of transonic flow through the variable nozzle of a radial inflow turbine [ASME PAPER 92-GT-90] p 248 A93-19336
- The design and evaluation of a high pressure ratio radial turbine [ASME PAPER 92-GT-93] p 349 A93-19339
- Balance of moments for hypersonic vehicles [ASME PAPER 92-GT-251] p 253 A93-19460
- Rotor cavity flow and heat transfer with inlet swirl and radial outflow of cooling air [ASME PAPER 92-GT-378] p 406 A93-19536
- A CAD computer system for centrifugal compressor impeller with transonic inflow p 259 A93-20118
- Quantitative laser velocimetry measurements in the hypersonic regime by the integration of experimental and computational analysis [AIAA PAPER 93-0089] p 263 A93-20195
- Unsteady loads measurements in a generic high speed engine model by means of recessed transducers [AIAA PAPER 93-0287] p 342 A93-21104
- Flow field characteristics of an axisymmetric sudden-expansion pipe flow with different initial swirl distribution p 411 A93-21688
- Holographic interferometric investigation of shock wave interaction with a ramp p 271 A93-21921
- Inlet velocity profile effects on turbulent swirling flow predictions [AIAA PAPER 93-0133] p 274 A93-22580
- Experimental and numerical investigation of Mach 2.5 supersonic mixed compression inlet p 279 A93-22689
- Flow stability issues in supersonic inlet flow analyses [AIAA PAPER 93-0290] p 279 A93-22690
- Hypersonic crossing shock-wave/turbulent-boundary-layer interactions [AIAA PAPER 93-0781] p 467 A93-24863
- Effect of a rotating propeller on the separation angle of attack [AIAA PAPER 93-0017] p 472 A93-24978
- Rotor blade unsteady aerodynamic gust response to inlet guide vane wakes [ASME PAPER 91-GT-129] p 475 A93-26897
- Inlet turbulence distortion and viscous flow development in a controlled-diffusion compressor cascade at very high incidence p 688 A93-34485
- Supersonic turbomachine rotor flutter control by aerodynamic detuning p 899 A93-42884
- Modeling supersonic inlet boundary-layer bleed roughness p 872 A93-42891
- CFD analysis of the X-29 inlet at high angle of attack p 958 A93-45140
- Intake flow modeling in a four stroke diesel using KIVA3 [AIAA PAPER 93-2952] p 1148 A93-48146
- CFD code calibration and inlet-fairing effects on a 3D hypersonic powered-simulation model [AIAA PAPER 93-3041] p 1056 A93-48222
- Navier-Stokes simulation of external/internal transonic flow on the forebody/inlet of the AV-8B Harrier II [AIAA PAPER 93-3057] p 1058 A93-48234
- Correlation of unsteady pressure and inflow velocity fields of a pitching rotor blade [AIAA PAPER 93-3082] p 1060 A93-48256
- Engineering method for calculating inlet face property profiles on high speed vehicle forebodies [AIAA PAPER 93-3113] p 1062 A93-48283
- Experimental study on turbulent two-phase flow in a dual-inlet side dump combustor p 1106 A93-48506
- Installed F/A-18 inlet flow calculations at 60 deg angle-of-attack and 10 deg side slip [AIAA PAPER 93-1806] p 1074 A93-49695
- Calculation of scramjet inlet with thick boundary-layer ingestion [AIAA PAPER 93-1836] p 1074 A93-49720
- Numerical study of the performance of swept, curved compression surface scramjet inlets [AIAA PAPER 93-1837] p 1074 A93-49721
- Real-time simulation of maneuverable aircraft flight conditions on altitude test cell [AIAA PAPER 93-1845] p 1137 A93-49726
- 3-D viscous flow CFD analysis of the propeller effect on an advanced ducted propeller subsonic inlet [AIAA PAPER 93-1847] p 1075 A93-49728
- Stall inception in single stage, high-speed compressors with straight and swept leading edges [AIAA PAPER 93-1870] p 1076 A93-49745
- A comparative study of Full Navier-Stokes and Reduced Navier-Stokes analyses for separating flows within a diffusing inlet S-duct [AIAA PAPER 93-2154] p 1079 A93-49970
- Particle dynamics simulations in inlet separator with an experimentally based bounce model [AIAA PAPER 93-2156] p 1115 A93-49972
- Experimental determination of the bulk swirl attenuation between two axial stations in the LM2500 inlet bellmouth [AIAA PAPER 93-2203] p 1155 A93-50015
- Numerical simulations of the unstart phenomenon in a supersonic inlet/diffuser [AIAA PAPER 93-2239] p 1081 A93-50041
- Simulation of propulsion system's transient response to planar wave inlet distortion and the effect of compressor wear [AIAA PAPER 93-2384] p 1117 A93-50152
- 3D PARC Navier-Stokes analysis of an HSCT suppressor nozzle secondary inlet lip and duct [AIAA PAPER 93-2568] p 1084 A93-50286
- A study of the stability of vortical structures in supersonic inlets [ISABE 93-7103] p 1187 A93-54079
- Off-design performance of scramjet nozzles [ISABE 93-7108] p 1203 A93-54084
- An experimental investigation of the flow in a diffusing S-duct [NASA-TM-105809] p 60 N93-12077
- Some aspects of intake design, performance and integration with the airframe p 161 N93-13219
- Comparative performance tests of a pitot-inlet in several European wind-tunnels at subsonic and supersonic speeds p 130 N93-13221
- Flow prediction for three-dimensional intakes and ducts using viscous-inviscid interaction methods p 218 N93-13953
- Effect of a rotating propeller on the separation angle of attack and distortion in ducted propeller inlets [NASA-TM-105935] p 290 N93-16625
- Experimental and numerical examinations of the influence of inlet distortion perturbations on the working behavior of turbofan compressors [ETN-93-92733] p 364 N93-18628
- Stall transients including effects of inlet distortion and intake geometry p 423 N93-18726
- Nozzle diffuser for use with an open test section of a wind tunnel [NASA-CASE-LAR-14424-1-SB] p 731 N93-25996
- The 3-D viscous flow CFD analysis of the propeller effect on an advanced ducted propeller subsonic inlet [NASA-TM-106240] p 900 N93-29162
- Solution of Euler equations for forebody-inlet ensemble of aircraft at high angle of attack [AD-A263905] p 876 N93-29862
- Three-dimensional flow calculations inside SSME GGGT first stage blade rows p 1017 N93-31585
- ### INLET NOZZLES
- Comment on 'Experimental study on autoignition in a scramjet combustor' p 172 A93-14525
- Theoretical investigation of combustion characteristics in ram-jet dump combustor with side-inlet p 346 A93-19121
- Starting and test rhombus characteristics of two-dimensional supersonic free-jet nozzle/generic supersonic aircraft inlet configurations [AIAA PAPER 92-5091] p 273 A93-22361
- ASTOVL model engine simulators for wind tunnel research p 192 N93-13213
- Application of subsonic first-order panel methods for prediction of inlet and nozzle aerodynamic interactions with airframe p 130 N93-13223
- Nozzle diffuser for use with an open test section of a wind tunnel [NASA-CASE-LAR-14424-1-SB] p 731 N93-25996
- ### INLET PRESSURE
- Viscous analysis of high pressure turbine inlet guide vane flow including cooling injections [AIAA PAPER 93-1798] p 1074 A93-49687
- Investigation of the flow field through a variable pitch fan rotor with an inlet total pressure distortion [ISABE 93-7029] p 1184 A93-54005
- A novel-high-performance system for recording and analysing instantaneous total pressure distortion in air intakes p 214 N93-13215
- An assessment of inlet total-pressure distortion requirements for the Compressor Research Facility (CFR) [AD-A262299] p 815 N93-27679
- ### INLET TEMPERATURE
- Experimental investigation of an axisymmetric hypersonic scramjet inlet for laser propulsion p 122 A93-14515
- Behaviors of the laterally injected jet in film cooling - Measurements of surface temperature and velocity/temperature field within the jet [ASME PAPER 92-GT-180] p 402 A93-19405
- Effective sealing of a disk cavity using a double-toothed rim seal [ASME PAPER 92-GT-379] p 406 A93-19537
- Initial results from the NASA Lewis wave rotor experiment [AIAA PAPER 93-2521] p 1193 A93-53589
- Heat transfer and material temperature conditions in the leading edge area of impingement-cooled turbine vanes [ISABE 93-7076] p 1220 A93-54052
- Measurements and computations of external heat transfer and film cooling in turbines [RAE-TM-P-1223] p 722 N93-25455
- Nitric oxide formation in a lean, premixed-prevaporized jet A/air flame tube: An experimental and analytical study [NASA-TM-105722] p 844 N93-27012
- Flow phenomena in turbomachines [AD-A263049] p 930 N93-29141
- The influence of non-uniform spanwise inlet temperature on turbine rotor heat transfer p 901 N93-29932
- Initial results from the NASA-Lewis wave rotor experiment [NASA-TM-106148] p 1005 N93-32368
- ### INSERTS
- The design of test-section inserts for higher speed aerodynamic testing in the Ames 80- by 120-Foot Wind Tunnel p 374 A93-19149
- ### INSPECTION
- Aging review of the YS-11 aircraft p 46 A93-13635
- Damage tolerance assessment on the multiple cracks for the YS-11 aircraft p 46 A93-13642
- Titrotor Research Aircraft composite blade repairs - Lessons learned p 108 A93-14819
- Looking and seeing - A practical problem - aircraft maintenance and inspection p 238 A93-18758
- Aircraft safety evaluation p 1043 A93-50486
- Eddy current inspection of open fastener holes in aluminum aircraft structure [SAE ARP 4402] p 1160 A93-52167
- Aircraft accident report: Atlantic Southeast Airlines, Inc. Flight 2311, uncontrolled collision with terrain, an Embraer EMB-120, N270AS, Brunswick, Georgia, 5 April 1991 [PB92-910403] p 28 N93-11471
- Integrated Blade Inspection System (IBIS) upgrade study [AD-A258912] p 365 N93-19356
- Aviation safety: Problems persist in FAA's inspection program. Report to the Chairman, Subcommittee on Aviation, Committee on Public Works and Transportation, House of Representatives [GAO/RCED-92-14] p 495 N93-19841
- Nondestructive inspection of in-service aircraft [ETN-93-93059] p 496 N93-20928
- Damage detection by Acousto-Ultrasonic Location (AUL) p 555 N93-21529
- Reliability assessment at airline inspection facilities. Volume 1: A generic protocol for inspection reliability experiments [DOT/FAA/CT-92/12-VOL-1] p 704 N93-25110
- Reliability assessment at airline inspection facilities. Volume 2: Protocol for an eddy current inspection reliability experiment [DOT/FAA/CT-92/12-VOL-2] p 842 N93-28685
- ### INSTALLING
- Requirements for soldered electrical connections [NHB-5300.4(3A-2)] p 212 N93-12674
- Development and flight testing of a surface pressure measurement installation on the EAP demonstrator aircraft p 550 N93-19927

INSTRUCTION SETS (COMPUTERS)

Action composition for the animation of natural language instructions
[AD-A254963] p 228 N93-12554

INSTRUMENT APPROACH

Complementary MLS and GNSS operations p 384 A93-21160
MIAS, the integration of MLS with DGPS/DLoran-C p 315 A93-21181

GPS availability and reliability for aircraft precision approach p 315 A93-21182
Analysis of DGPS/INS and MLS/INS final approach navigation errors and control performance data p 315 A93-21183

Piloted simulator investigations of a civil tilt-rotor aircraft on steep instrument approaches p 800 A93-36023
F-14D flight director development, test, and evaluation p 803 A93-38840

Design of instrument approach procedure charts: Comprehension speed of missed approach instructions coded in text or icons p 36 N93-11252
[PB92-205673]

DME-derived positions compared with MLS- and ILS-derived positions p 318 N93-16343
[NLR-TP-90119-U]

The dependent converging instrument approach procedure: An analysis of its safety and applicability [DOE/FAA/RD-93/6] p 707 N93-25456

INSTRUMENT COMPENSATION

AEDC expanded flow arc facility (HEAT-H2) description and calibration p 821 A93-37872
A new and working automatic calibration machine for wind tunnel internal force balances [AIAA PAPER 93-2467] p 1138 A93-50214

INSTRUMENT ERRORS

A maximum likelihood method for flight test data compatibility check p 95 A93-12732
Analysis of random components during measurements in the computerized diagnostic system Analiz-86 p 321 A93-18344

Effect of a deformed electric field on the precision of the electrochemical machining of gas turbine engine components p 835 A93-39094
Instrumentation and data acquisition system for the C.I.R.A. Transonic Pilot Tunnel p 1250 A93-54395

Airborne vector gravimetry with an aided inertial survey system p 1241 A93-55977
Controlling common mode stabilization errors in airborne gravity gradiometry p 1245 A93-55978

Aircraft accident report: Tomy International, Inc., d/b/a Scenic Air Tours flight 22, Beech Model E18S, N342E in-flight collision with terrain, Mount Haleakala, Maui, Hawaii, 22 April 1992 [PB93-910401] p 705 N93-25827

A break-down of sting interference effects [NLR-TP-91220-U] p 1014 N93-31042

INSTRUMENT FLIGHT RULES

The dependent converging instrument approach procedure [AIAA PAPER 93-3835] p 1098 A93-51424

Unusual attitudes - Helicopters and instrument flight p 1240 A93-54550
Rotorcraft en route ATC route standards [AD-A249129] p 35 N93-10323

INSTRUMENT LANDING SYSTEMS

Investigation of precise approach and landing of civil aircraft using integrated system based on GPS p 180 A93-14159

Landing guidance systems for CAT III operations p 151 A93-17307
Synthetic vision - A view in the fog p 792 A93-37068

F-14D flight director development, test, and evaluation p 803 A93-38840
Effects of equipment calibration, test flight procedures and analyzing methods on the accuracy of ILS glide path measurements - Book p 881 A93-41600

A localizer design to improve missed approach guidance p 992 A93-44143
Effect of wet snow on the null-reference ILS system p 1097 A93-50660

Overview of the FAA's differential GPS CAT III technical feasibility demonstration program [AIAA PAPER 93-3836] p 1098 A93-51425

ILS mathematical modeling study of the effects of an ASR-9 structure at the Long Island MacArthur Airport, Islip, NY [DOT/FAA/CT-TN92/25] p 192 N93-12668

DME-derived positions compared with MLS- and ILS-derived positions p 318 N93-16343
[NLR-TP-90119-U]

ILS mathematical modeling study of an ILS glide slope proposed for runway 19L at the Meridian Naval Air Station, Mississippi [DOT/FAA/CT-TN93/8] p 705 N93-24741

The ILS mathematical modeling study of the Runway 10 ILS Localizer at Luis Munoz Marin International Airport, San Juan, Puerto Rico [DOT/FAA/CT-TN93/10] p 792 N93-27017

Two simulation studies of precision runway monitoring of independent approaches to closely spaced parallel runways [AD-A263433] p 911 N93-29815

On-board derived flight-path measurement as demonstrated by an ILS measurement system p 994 N93-31282

INSTRUMENT PACKAGES

The Texas Instruments/Honeywell GPS Guidance Package p 32 A93-11015

Development of a flight instrument package [AD-A260830] p 719 N93-25783

INSULATION

Aerothermal ablative characterization of selected external insulator candidates [AIAA PAPER 93-1857] p 1145 A93-49735

A new methodology for helicopter internal noise reduction application to the AS332 L2 p 1243 A93-54723

INSURANCE (CONTRACTS)

Airship insurance in London [AIAA PAPER 93-4043] p 1265 A93-54611

INTAKE SYSTEMS

Study on vortex flow control of inlet distortion p 122 A93-14520
Techniques for the measurement of scramjet inlet performance at hypersonic speeds [AIAA PAPER 92-5104] p 274 A93-22374

Applying and validating the RANS-3D flow-solver for evaluating a subsonic serpentine diffuser geometry [AIAA PAPER 93-2157] p 1079 A93-49973

Subscale validation of a freejet inlet-engine test capability [AIAA PAPER 93-2179] p 1138 A93-49991

High speed test results of subsonic, turbofan scarf inlets [AIAA PAPER 93-2302] p 1082 A93-50087

INTEGRAL EQUATIONS

Robust control of an aeroelastic system modeled by a singular integro-differential equation p 97 A93-13197
One-dimensional methods for accurate prediction of off-design performance behavior of axial turbines [ASME PAPER 92-GT-54] p 347 A93-19304

Calculation of turbulent flow for an enclosed rotating cone [ASME PAPER 92-GT-70] p 400 A93-19320

Analytical expression of dissipation integral for kinetic energy integral equation --- calculation of turbulent compressible boundary layer in aerodynamics p 1183 A93-53860

An integral equation solution for multistage turbomachinery design calculations [NASA-TM-105970] p 179 N93-15521

INTEGRAL ROCKET RAMJETS

Analysis of thrust modulation of ram-rockets by a vortex valve p 814 N93-27187

INTEGRAL TRANSFORMATIONS

A method for the spectral-time identification of the longitudinal and lateral motions of an aircraft p 1205 A93-52942

INTEGRATED ENERGY SYSTEMS

Discussion for the ideal AIMS p 167 N93-15153

INTEGRATED MISSION CONTROL CENTER

The effect of TCAS interrogations on the Chicago O'Hare ATCRBS system [DOT/FAA/CT-92/22] p 318 N93-16498

INTEGRATED OPTICS

Integrated optoelectronics for communication and processing; Proceedings of the Meeting, Boston, MA, Sept. 3, 4, 1991 [SPIE-1582] p 1158 A93-51250

Smart materials p 536 N93-20624

INTEGRITY

Aeronautical fatigue: Key to safety and structural integrity; Proceedings of the 16th ICAF Symposium, Tokyo, Japan, May 22-24, 1991 [ISBN 4-9900181-1-7] p 80 A93-13626

Structural integrity challenges p 3 A93-13627
Aero engine reliability, integrity and safety; Proceedings of the Conference, Bristol, United Kingdom, Oct. 17, 18, 1991 [ISBN 0-903409-70-4] p 345 A93-18778

Safety through integrity and reliability --- for passenger and military aircraft p 239 A93-18779

Aspects of turbine blade design for integrity p 345 A93-18784
Testing for integrity --- of aircraft gas turbine engines p 346 A93-18785

Computational schemes for integrity analyses of fuselage panels in aging airplanes p 1025 A93-45774
Structural integrity of aging airplanes - A perspective p 948 A93-45789

Test facility for evaluation of structural integrity of stiffened and jointed aircraft curved panels p 1012 A93-45794

Receiver Autonomous Integrity Monitoring (RAIM) of GPS and GLONASS p 993 A93-46891

Testing for integrity [PNR-90927] p 56 N93-11024

An experimental health monitoring unit for GPS and GLONASS p 706 N93-25018

INTELLIGENCE TESTS

Comparison of performance on the Shipley Institute of Living Scale, Air Traffic Control Specialist Selection Test, and FAA Academy Screen [AD-A259249] p 502 N93-20582

INTELLIGIBILITY

Influence of aircraft noise on speech intelligibility p 558 A93-28483

INTERACTIONAL AERODYNAMICS

Intensification of flow mixing behind an oblique shock wave p 4 A93-10138

An asymptotic model of a closed separation region in supersonic flow p 4 A93-10139

Calculation of a three-dimensional boundary layer at the lee side of a finite-span delta wing in the case of viscous interaction with hypersonic flow p 5 A93-10143

On improving adequacy of modeling in wind tunnel problems p 6 A93-10404

An implicit multigrid scheme for hypersonic strong-interaction flowfields p 6 A93-10534

Transonic profile design in curvilinear coordinates using an approximate factorization algorithm p 7 A93-10778

Nonlinear aeroelasticity and chaos p 79 A93-12165

An aerodynamic model of multiple lifting surfaces including wake deformation and tip effect p 10 A93-12366

Numerical simulation for aeroelasticity in turbomachines with vortex method. I - Theory and method p 53 A93-12452

Aerospace - Collected translations of selected papers, 1992 p 2 A93-12726

A comparative analysis of algorithms for solving systems of high-order linear algebraic equations p 96 A93-12977

An analysis of helicopter dynamic response to turbulence using fuselage and blade element atmospheric sampling techniques [AIAA PAPER 92-4148] p 43 A93-13314

Over wing propeller aerodynamics p 113 A93-14189

A study of propeller/wing interaction including the effect of ground proximity p 113 A93-14190

Study of aeroservoelastic stability of an aircraft p 182 A93-14259

The influence of main design parameters on helicopter air resonance and its source of instability p 154 A93-14261

An interactive numerical procedure for rotor aeroelastic stability analysis using elastic lifting surface p 155 A93-14313

Modelling for aileron induced unsteady aerodynamic effects for parameter estimation p 118 A93-14323

Wing rock of lifting systems p 118 A93-14330

An experimental study for interaction flow between shock wave and turbulent boundary layer p 120 A93-14355

Experimental and theoretical studies of helicopter rotor-fuselage interaction [ONERA, TP NO. 1992-142] p 120 A93-14356

Numerical study of jet interaction at super- and hypersonic speeds for flight vehicle control p 184 A93-14379

Supersonic wing/body interference p 121 A93-14391

A vortex control technique for the attenuation of fin buffet p 121 A93-14408

Navier-Stokes computation of wing/rotor interaction for a tilt rotor in hover p 122 A93-14537

Analytical solutions for hypersonic flow past slender power-law bodies at small angle of attack p 122 A93-14550

Comparison of algebraic turbulence models for afterbody flows with jet exhaust p 123 A93-14554

Determination of vortex burst location on delta wings from surface pressure measurements p 123 A93-14557

Coriolis effects on Goertler vortices in the boundary-layer flow on concave wall p 123 A93-14564

Flow past a finite-span wing in the presence of external acoustic loading p 127 A93-16707

Active aerodynamic control of wake-airfoil interaction noise - Experiment p 445 A93-19153

Active aerodynamic control of wake-airfoil interaction noise - Theory p 445 A93-19154

Numerical analysis of acoustic effect of rotor wakes in rotor-stator interaction p 447 A93-19182

- Nonlinear response and sonic fatigue of high speed aircraft p 399 A93-19211
- Wing vortex refraction effects from BAC 1-11 flight tests p 450 A93-19226
- Prediction of 2D viscous transonic flow in compressor cascades using a semi-empirical shock/boundary-layer interaction method [ASME PAPER 92-GT-277] p 253 A93-19470
- Blade loading of transonic circular cascade diffuser p 267 A93-20919
- Transitional characteristics of vortices issued from a body which creates asymmetric flow field - In a case of thin symmetrical airfoil with angle of attack under rotational oscillation of small amplitude p 267 A93-20923
- Holographic interferometric investigation of shock wave interaction with a ramp p 271 A93-21921
- Hypersonic turbulent expansion-corner flow with shock impingement [AIAA PAPER 92-5101] p 274 A93-22371
- Study on steady and unsteady unstart phenomena due to compound choking and/or fluctuations in combustor of scramjet engines [AIAA PAPER 92-5102] p 359 A93-22372
- A parametric study of bleed in shock boundary layer interactions [AIAA PAPER 93-0294] p 280 A93-22694
- A comparison of hypersonic flight and prediction results [AIAA PAPER 93-0311] p 280 A93-23006
- Wall pressure fluctuations beneath swept shock wave/boundary layer interactions [AIAA PAPER 93-0384] p 282 A93-23063
- High accuracy computation of fluid-structure interaction in transonic cascades [AIAA PAPER 93-0485] p 287 A93-23387
- Three-dimensional hypersonic shock wave/turbulent boundary-layer interactions p 287 A93-23533
- Engineering approach to the prediction of shock patterns in bounded high-speed flows p 287 A93-23545
- Shock/boundary-layer interaction control with vortex generators and passive cavity p 287 A93-23546
- Direct solution of two-dimensional Navier-Stokes equations for static aeroelasticity problems p 417 A93-23554
- Subharmonic and harmonic forced response of the wake of a circular cylinder p 288 A93-23565
- A Laser Doppler Anemometry study of a supersonic jet in a low speed cross-flow p 459 A93-23807
- Experimental investigation of a 2D parallel vortex/airfoil interaction p 538 A93-23808
- Unsteady panel method for flows with multiple bodies moving along various paths [AIAA PAPER 93-0640] p 539 A93-24755
- Implicit Euler calculation of supersonic vortex wake/engine plume interaction [AIAA PAPER 93-0656] p 540 A93-24769
- Vortex distortion during vortex-surface interaction in a Mach 3 stream [AIAA PAPER 93-0761] p 467 A93-24846
- Interaction strength and model geometry effects on the structure of crossing-shock wave/turbulent boundary-layer interactions [AIAA PAPER 93-0780] p 467 A93-24862
- Vortex/surface interaction [AIAA PAPER 93-0863] p 468 A93-24925
- Experimental investigation of rotor/lifting surface interactions [AIAA PAPER 93-0871] p 469 A93-24932
- Time-resolved surface heat flux measurements in the wing/body junction vortex [AIAA PAPER 93-0918] p 472 A93-24972
- Shock wave ahead of a liquid jet in supersonic cross flow p 477 A93-27605
- Interaction of Tollmien-Schlichting waves with localized disturbances p 545 A93-27637
- Numerical study on the interaction of supersonic flow past a wedge and free jet p 479 A93-28574
- Potential hazard of aircraft wake vortices in ground effect with crosswind p 479 A93-28606
- A study of blade-vortex interaction sound generation and directionality p 565 A93-29402
- Experimental study of a single strong vortex-airfoil interaction p 481 A93-29432
- Flowfield analysis of modern helicopter rotors in hover by Navier-Stokes method p 481 A93-29435
- Flow visualization and flow field measurements of a 1/12 scale tilt rotor aircraft in hover p 482 A93-29441
- Karman vortex street-airfoil interaction p 678 A93-33703
- On the favorable interference in the supersonic flow p 679 A93-33713
- Active control of vibratory airloads induced by helicopter rotor-fuselage interactions [AIAA PAPER 93-1363] p 726 A93-33930
- Acoustics due to flow-structural interaction and its transmission through a double-panel in high-speed cruising flight [AIAA PAPER 93-1431] p 710 A93-33981
- A study on two-dimensional and three-dimensional secondary jet interactions with a supersonic flow p 683 A93-34273
- A study on three-dimensional shock wave/turbulent boundary layer interaction induced by sweptback sharp fins at supersonic flow p 684 A93-34274
- The interaction between a steady jet flow and a supersonic blade tip p 688 A93-34415
- Multipassage three-dimensional Navier-Stokes simulation of turbine rotor-stator interaction p 688 A93-34484
- Wall jets created by single and twin high pressure jet impingement p 744 A93-34847
- Calculation of the irregular interaction of shock waves p 691 A93-35339
- Helicopter aerodynamics research techniques and rotor-fuselage interaction analysis p 765 A93-35938
- Vortex methods for the computational analysis of rotor/body interaction p 765 A93-35939
- Three-dimensional calculations of rotor-airframe interaction in forward flight p 795 A93-35940
- Interactional aerodynamic effects on rotor performance in hover and forward flight p 766 A93-35941
- Transonic blade-vortex interactions - Noise reduction p 850 A93-37396
- Asymptotic structure of a limiting hypersonic flow in a shock wave p 776 A93-39131
- Calculation of the effect of the shock wave of a delta wing on a second wing at supersonic velocities p 776 A93-39141
- An experimental study of the three-dimensional interaction of a transverse jet with hypersonic flow p 777 A93-39150
- Passive control of a shock wave/turbulent boundary layer interaction in a transonic flow p 858 A93-40444
- Experiments on shock-wave/boundary-layer interactions produced by two-dimensional ramps and three-dimensional obstacles p 865 A93-42589
- Experimental study of the longitudinal hypersonic corner flow field - HERMES-R&D research program, problem no. 5 p 867 A93-42602
- An adaptive finite element method for turbulent free shear flow past a propeller [AIAA PAPER 93-3388] p 956 A93-45079
- Viscous hypersonic shock-shock interaction on a blunt body at high altitude [AIAA PAPER 93-2722] p 962 A93-46477
- A numerical solution of the asymptotic problem of boundary layer separation in an incompressible liquid upstream of the corner point of a body p 965 A93-46699
- Numerical simulation of wing-wall juncture flow for a pitching wing [AIAA PAPER 93-3401] p 974 A93-47203
- Tangential Forebody Blowing-yaw control at high alpha [AIAA PAPER 93-3406] p 1008 A93-47205
- A visualization study of the vortical flow over a double-delta wing in dynamic motion [AIAA PAPER 93-3425] p 976 A93-47220
- Calculations on a double-fin turbulent interaction at high speed [AIAA PAPER 93-3432] p 977 A93-47224
- A Laplace interaction law for the computation of viscous airfoil flow in low and high speed aerodynamics [AIAA PAPER 93-3462] p 979 A93-47244
- Flow visualization of mast-mounted-sight/main rotor aerodynamic interactions [AIAA PAPER 93-3517] p 1009 A93-47280
- Semi-discrete Galerkin solution of the compressible boundary-layer equations with viscous-inviscid interaction [AIAA PAPER 93-3520] p 985 A93-47282
- Normal shock wave oscillations in supersonic diffusers p 1044 A93-48042
- Investigation of a hypersonic crossing shock wave/turbulent boundary layer interaction p 1044 A93-48043
- A numerical investigation of supersonic strut/airfoil interactions in annular flow with varying strut thickness [AIAA PAPER 93-2927] p 1045 A93-48128
- Effects of junction modifications on sharp-fin-induced shock wave/boundary layer interaction [AIAA PAPER 93-2935] p 1046 A93-48133
- Shock-wave/boundary layer interactions at hypersonic speeds by an implicit Navier-Stokes solver [AIAA PAPER 93-2938] p 1046 A93-48136
- Intense studies on unsteady secondary separations and oscillating shock waves in three-dimensional shock waves/turbulent boundary layer interaction regions induced by sharp and blunt fins [AIAA PAPER 93-2939] p 1046 A93-48137
- Improvement of conical similarity rule in swept shock wave/boundary layer interaction [AIAA PAPER 93-2941] p 1046 A93-48139
- Shock-vortex interaction over a 65-degree delta wing in transonic flow [AIAA PAPER 93-2973] p 1049 A93-48167
- Experimental study of shock wave and hypersonic boundary layer interactions near a convex corner [AIAA PAPER 93-2980] p 1051 A93-48173
- Nonlocal vs. local instability of compressible flows including body metric, flow divergence and 3D-wave propagation [AIAA PAPER 93-2982] p 1051 A93-48175
- Hypersonic, turbulent viscous interaction past an expansion corner [AIAA PAPER 93-2985] p 1051 A93-48178
- Effects of boundary layer bleed on swept-shock/boundary layer interaction [AIAA PAPER 93-2989] p 1052 A93-48182
- An investigation of shock wave turbulent boundary layer interaction with bleed through slanted slots [AIAA PAPER 93-2992] p 1052 A93-48184
- An experimental study of the effects of deformable tip on the performance of fins and finite wings [AIAA PAPER 93-3000] p 1053 A93-48190
- Simulation of DD-963 ship airwake by Navier-Stokes method [AIAA PAPER 93-3002] p 1053 A93-48192
- A computational and experimental investigation of a delta wing with vertical tails [AIAA PAPER 93-3009] p 1054 A93-48199
- A viscous-inviscid interaction method for 2-D unsteady, compressible flows [AIAA PAPER 93-3019] p 1055 A93-48206
- A fast robust viscous-inviscid interaction solver for transonic flow about wing/body configurations on the basis of full potential theory [AIAA PAPER 93-3026] p 1056 A93-48211
- Application of a two-equation turbulence model for high speed compressible flows using unstructured grids [AIAA PAPER 93-3029] p 1056 A93-48213
- An initial comparison of CFD with experiment for a geometrically simplified STOVL model [AIAA PAPER 93-3059] p 1058 A93-48236
- Laser Interferometer Skin-Friction measurements of crossing-shock wave/turbulent boundary-layer interactions [AIAA PAPER 93-3072] p 1148 A93-48247
- Summary of the interaction of a rotor wake with a circular cylinder [AIAA PAPER 93-3084] p 1060 A93-48258
- A study on aerodynamic sound generated by interaction of jet and plate [AIAA PAPER 93-3118] p 1171 A93-48288
- Numerical simulation of a shock wave/turbulent boundary layer interaction in a duct [AIAA PAPER 93-3127] p 1063 A93-48293
- Experimental study of transitional axisymmetric shock-boundary layer interactions at Mach 5 [AIAA PAPER 93-3131] p 1063 A93-48296
- Exploratory study of shock reflection near an expansion corner [AIAA PAPER 93-3132] p 1063 A93-48297
- Flowfield dynamics in blunt fin-induced shock wave/turbulent boundary layer interactions [AIAA PAPER 93-3133] p 1063 A93-48298
- A study of the interaction of a nonstationary shock wave with a boundary layer on a plate in the transition regime p 1150 A93-48850
- An experimental study of a compound supersonic jet p 1069 A93-48914
- Approximate method for the aerodynamic design of flight vehicles for high supersonic flight speeds p 1069 A93-48966
- Euler calculations of unsteady interaction of advancing rotor with a line vortex p 1071 A93-49016
- Analysis of a high bypass ratio engine installation using the chimera domain decomposition technique [AIAA PAPER 93-1808] p 1100 A93-49697
- Investigation of a strut/airfoil interaction in supersonic annular flow [AIAA PAPER 93-1925] p 1076 A93-49791
- The numerical calculation on the flowfields of transverse jet interaction in the base of vehicle at supersonic speeds [AIAA PAPER 93-1931] p 1077 A93-49795
- 3-D Euler simulation of vane-blade interaction in a transonic turbine [AIAA PAPER 93-2256] p 1081 A93-50054
- A numerical study of the unsteady processes associated with the type IV shock interaction [AIAA PAPER 93-2479] p 1083 A93-50221
- Numerical modeling of flow in a hypersonic laminar boundary layer p 1086 A93-50967
- On boundary-layer transition in transonic flow p 1087 A93-51280

- Dynamics of hypersonic flight vehicles exhibiting significant aerodynamic and aeropropulsive interactions [AIAA PAPER 93-3763] p 1131 A93-51358
- Development of resonance perturbations in a supersonic jet p 1088 A93-51772
- An economical difference factorization algorithm for the numerical calculation of the system of equations for a thin viscous shock layer p 1091 A93-51880
- Determination of the aerodynamic characteristics of thin bodies of revolution with an arbitrary number of cantilever surfaces in inhomogeneous flow p 1092 A93-51911
- Numerical simulation of shock/shock and shock-wave/boundary-layer interactions in hypersonic flows p 1093 A93-52000
- Computation of subsonic viscous and transonic viscous-inviscid unsteady flow p 1094 A93-52012
- Rotor wake/stator interaction noise - Predictions vs data p 1174 A93-52447
- Active aerodynamic control of wake-airfoil interaction noise - Experiment p 1225 A93-53206
- Analytical expression of dissipation integral for kinetic energy integral equation --- calculation of turbulent compressible boundary layer in aerodynamics p 1183 A93-53860
- Transonic area rule about lifting configurations p 1183 A93-53868
- A 2-D compressible N-S simulation of starting- and stalling-flows in a compressor cascades system [ISABE 93-7006] p 1183 A93-53982
- Transonic discharge flows around diffuser vanes from a centrifugal impeller p 1185 A93-54029
- Effects of wake interaction of two turbine cascades on secondary/tip-leakage flows and losses [ISABE 93-7058] p 1185 A93-54034
- Study on flow field around slender diamond cone traveling at hypersonic speed p 1189 A93-54314
- A method for aerodynamic calculation by placing linear vari-strength vortex panels on airfoil contour p 1231 A93-54597
- An airfoil in transonic flow in the presence of wind gusts and weak shock waves p 1233 A93-55015
- Development of separation due to interaction between a shock wave and a turbulent boundary layer perturbed by rarefaction waves p 1233 A93-55019
- An improved multiple line-vortex method for simulation of separated vortices of slender wings p 1236 A93-55412
- Comparison of radiated noise from shrouded and unshrouded propellers p 1264 A93-55861
- Experimental investigations of hypersonic shock-boundary layer interaction p 1238 A93-56037
- Numerical study of slightly compressible Navier-Stokes simulation of blade-vortex interaction p 1239 A93-56216
- Interaction of compressible vortices with a rigid plate p 1239 A93-56219
- Effect of planform and body on supersonic aerodynamics of multibody configurations [NASA-TP-3212] p 119 A93-10824
- Contributions to the experimental investigation of rotor/body aerodynamic interactions p 20 A93-10877
- Unsteady propeller/wing aerodynamic interactions p 24 A93-12190
- Aerodynamic Engine/Airframe Integration for High Performance Aircraft and Missiles [AGARD-CP-498] p 213 A93-13199
- Detailed analysis of wing-nacelle interaction for commercial transport aircraft p 213 A93-13203
- Recent developments in low-speed TPS-testing for engine integration drag and installed thrust reverser simulation p 160 A93-13207
- Aerodynamic integration of thrust reversers on the Fokker 100 p 160 A93-13208
- Water tunnel studies of inlet/airframe interference phenomena p 215 A93-13216
- AGARD WG13 aerodynamics of high speed air intakes: Assessment of CFD results p 215 A93-13220
- Airfoil-vortex interaction and the wake of an oscillating airfoil p 134 A93-13803
- Navier-Stokes flowfield computation of wing/rotor interaction for a tilt rotor aircraft in hover p 135 A93-14035
- A study of viscous interaction effects on hypersonic waveriders p 135 A93-14160
- Pressure distribution for the wing of the YAV-8B airplane; with and without pylons p 136 A93-14451
- A computational and experimental investigation of the propulsive and lifting characteristics of oscillating airfoils and airfoil combinations in incompressible flow [AD-A258019] p 294 A93-17819
- Pitching moment of low aspect ratio wing-body combinations up to high angles of attack at supersonic speeds [ESDU-92043] p 333 A93-17958
- Mean flow interactions of a counter-rotating propeller p 552 A93-20289
- INTERACTIONS**
- Interaction between ice and propeller [VTI-TIED-1281] p 841 A93-27832
- INTERACTIVE CONTROL**
- Performance prediction of the interacting multiple model algorithm p 439 A93-22926
- Passive control of coherent vortices in compressible mixing layers p 968 A93-46828
- [AIAA PAPER 93-3262] p 968 A93-46828
- Implementation of expert systems within an interactive tactical environment p 1223 A93-52678
- [AIAA PAPER 93-3583] p 1223 A93-52678
- An interactive preprocessor for the NASA engine performance program [NASA-TM-105786] p 56 A93-10983
- INTERCEPTION**
- Optimal finite-thrust time-bounded direct-ascent interception p 734 A93-25272
- INTERFERENCE**
- Wall-signature methods for high speed wind tunnel wall interference corrections p 375 A93-20803
- INTERFERENCE IMMUNITY**
- Relative sensitivity of Loran-C phase tracking and cycle selection to CWI p 792 A93-36502
- Carrier wave signals interfering with Loran-C [ETN-92-92528] p 318 A93-17584
- INTERFERENCE LIFT**
- Thrust imparted to an airfoil by passage through a sinusoidal upwash field p 1178 A93-53219
- INTERFEROMETERS**
- Topographic mapping using a Ku-band airborne elevation interferometer p 896 A93-42786
- INTERFEROMETRY**
- The use of interferometry in the study of rotorcraft aerodynamics p 407 A93-19914
- Guidance accuracy considerations for realtime GPS interferometry p 342 A93-21146
- Interferometric investigations of compressible dynamic stall over a transiently pitching airfoil [AIAA PAPER 93-0211] p 278 A93-22628
- Corrections to fringe distortion due to flow density gradients in optical interferometry [AIAA PAPER 93-0631] p 539 A93-24748
- GPS Interferometry [NASA-CR-192301] p 319 A93-18873
- Interferometric JFTOT tube deposit measuring device [AD-D015599] p 536 A93-20247
- INTERGRANULAR CORROSION**
- Ultrasonic thickness measurement using the angle technique p 542 A93-23535
- Mechanisms and modelling of environment-dependent fatigue crack growth in a nickel based superalloy [AD-A253967] p 71 A93-10717
- INTERLAMINAR STRESS**
- Common failure modes for composite aircraft structures due to secondary loads p 207 A93-14812
- Impact ice interface shear stresses caused by blade bending and twisting [AIAA PAPER 93-0030] p 307 A93-20147
- Analysis of interlaminar stresses in symmetric and unsymmetric laminates under various loadings [AIAA PAPER 93-1511] p 740 A93-34050
- INTERLAYERS**
- Interlaminar stress analysis at the skin/stiffener interface of a grid-stiffened composite panel [NASA-CR-192177] p 393 A93-17920
- INTERMETALLICS**
- Technical note - Plasma-sprayed ceramic thermal barrier coatings for smooth intermetallic alloys p 209 A93-15702
- Isothermal oxidation behavior of alpha-2 titanium aluminide alloys p 535 A93-29563
- Potential and prospects of intermetallic materials for applications in the aerospace industry [ONERA, TP NO. 1992-99] p 824 A93-38580
- Designing new multi-phase intermetallic materials based on phase compatibility considerations [ONERA, TP NO. 1992-131] p 772 A93-38605
- Chemical stability of titanium diboride reinforcement in nickel aluminide matrices p 1147 A93-52473
- Overview of NASA's advanced high temperature engine materials technology program p 1212 A93-53453
- Material requirements for the High Speed Civil Transport [ISABE 93-7067] p 1200 A93-54043
- Thermal barrier design of gamma-TiAl Functionally Graded Materials (FGMs) for scramjet engine applications p 1246 A93-54556
- HIP consolidation of aluminum-rich intermetallic alloys and their composites [NAWCADWAR-92003-60] p 199 A93-14726
- INTERMITTENCY**
- Measurement of turbulent spots and intermittency modelling at gas-turbine conditions p 902 A93-29934
- INTERNAL COMBUSTION ENGINES**
- Intake flow modeling in a four stroke diesel using KIVA3 [AIAA PAPER 93-2952] p 1148 A93-48146
- Materials development program, ceramic technology project addendum to program plan: Cost effective ceramics for heat engines [DE93-003663] p 394 A93-18537
- Engine driven chiller and thermal storage integration (Large tonnage engine driven chiller development) [PB92-227891] p 555 A93-21465
- Improved selective catalytic NOx control technology for compressor station reciprocating engines [PB93-158566] p 755 A93-26529
- INTERNAL COMPRESSION INLETS**
- Effect of radial distortion on the performance of a centrifugal compressor p 861 A93-42256
- INTERNATIONAL COOPERATION**
- Spanish-Indonesian cooperation in the development, production, certification and marketing of CN-235 commuter aircraft p 108 A93-14156
- In the pursuit of a single European air traffic control system p 150 A93-15053
- International Conference on Aviation Weather Systems, 4th, Paris, France, June 24-28, 1991, Preprints p 426 A93-22101
- Keynote address - Advanced Technology demonstrators, prototypes and hypersonic flight [AIAA PAPER 92-4999] p 456 A93-22276
- Terrorism and air-specific perils and the liability of air freight carriers under Article 17 of the Warsaw Agreement p 570 A93-24252
- Will aerospace plane development go international? p 1043 A93-49331
- What can Japan teach the U.S. about composites? p 1144 A93-49336
- Implications of European legislation post 1992; Proceedings of the Conference, London, United Kingdom, Mar. 12, 1992 p 1043 A93-50353
- [ISBN 1-85768-015-4] p 1043 A93-50353
- Flight safety in Europe p 1227 A93-53726
- Europe's new windtunnel p 1210 A93-54275
- West powers East p 1244 A93-56349
- Civil aircraft engines: The next generation [PNR-90962] p 58 A93-11085
- Coordinating Council, Fourth Meeting: NACA Documents Database Project [NASA-TM-108017] p 234 A93-12671
- Contributions to the American Meteorological Society's 26th International Conference on Radar Meteorology [AD-A263385] p 936 A93-29257
- INTERNATIONAL RELATIONS**
- Air transport and the environment - Regulating aircraft noise p 1226 A93-52931
- INTERNATIONAL TRADE**
- Defence electronics industry profile, 1990-1991 [CTN-92-60515] p 84 A93-10653
- INTERPLANETARY SPACECRAFT**
- Conceptual design of a Mars transportation system [NASA-CR-192039] p 420 A93-18047
- INTERPOLATION**
- Vertical guidance for a Lockheed L1011-100 using optimal dynamic interpolation p 369 A93-22884
- Uniform high-order spectral methods for one- and two-dimensional Euler equations p 476 A93-27068
- Unsteady airfoil flow solutions on moving zonal grids [AD-A261925] p 701 A93-26198
- INTERPROCESSOR COMMUNICATION**
- Onboard Connectivity Network for command and control aircraft p 1166 A93-49481
- Formal design specification of a Processor Interface Unit [NASA-CR-189698] p 99 A93-12538
- INVENTORIES**
- World jet airplane inventory at year-end 1992 [PB93-174324] p 765 A93-27405
- World commercial aircraft accidents [DE93-010892] p 791 A93-28571
- INVENTORY MANAGEMENT**
- Desert store --- of mothballed commercial jet aircraft p 1229 A93-54866
- INVERSE KINEMATICS**
- Turbulence/gust alleviation using spoiler control p 369 A93-22886
- Zero-gravity atmospheric flight by robust nonlinear inverse dynamics p 728 A93-34550
- Design of a controller for a high performance fighter aircraft using Robust Inverse Dynamics Estimation (RIDE) [AIAA PAPER 93-3779] p 1132 A93-51374
- INVERSIONS**
- Synthesis of a helicopter nonlinear flight controller using approximate model inversion [AIAA PAPER 92-4468] p 62 A93-13280

- A numerical inversion method for determining aerodynamic effects on particulate exhaust plumes from onboard irradiance data p 823 A93-37482
- INVESTMENT CASTING**
X-ray computed tomography for casting development [AD-A261786] p 752 N93-26526
Use of titanium castings without a casting factor [AD-A264114] p 1018 N93-31192
- INVISCID FLOW**
A low-speed aerodynamic model for harmonically oscillating aircraft configurations p 8 A93-11500
Unstructured grid solutions to a wing/pylon/store configuration using VGRID3D/USM3D [AIAA PAPER 92-4572] p 14 A93-13303
Nozzle flow computations using the Euler equations p 112 A93-14170
Generalized multipoint inverse airfoil design p 122 A93-14541
A conformal-integral method for solving the direct problem in turbomachine cascade aerodynamics p 125 A93-15217
Strong coupling between inviscid fluid and boundary layer for airfoils with a sharp edge. II - 2D unsteady case for isolated airfoil and straight blade cascade p 126 A93-16473
Periodic Euler and Navier-Stokes solutions about oscillating airfoils p 241 A93-17799
Longitudinal vortex control - Techniques and applications (The 32nd Lanchester Lecture) p 242 A93-18526
Aerodynamic design of turbomachinery blading in three-dimensional flow - An application to radial inflow turbines [ASME PAPER 92-GT-74] p 248 A93-19324
Aerodynamic design of pivotable nozzle vanes for radial-inflow turbines [ASME PAPER 92-GT-94] p 349 A93-19340
Viscous and inviscid instabilities of a trailing vortex p 268 A93-21042
A three-dimensional inviscid flow solver in Chimera flow simulation [AIAA PAPER 93-0190] p 276 A93-22614
Numerical solution of inviscid hypersonic flow around a conically-derived waverider p 280 A93-23012
3D Euler flow solutions using unstructured Cartesian and prismatic grids [AIAA PAPER 93-0331] p 281 A93-23022
Adaptive finite volume upwind approach on mixed quadrilateral-triangular meshes p 287 A93-23542
Shock oscillation in two-dimensional, inviscid, unsteady channel flow p 288 A93-23563
Acoustic flux vector splitting scheme for Euler equations p 460 A93-24078
NO22D - A two dimensional explicit inviscid upwind code for convergent divergent nozzles p 460 A93-24080
Finite element analysis of the Scramaccelerator with finite rate chemistry [AIAA PAPER 93-0745] p 540 A93-24833
Vortical solutions in supersonic corner flows [AIAA PAPER 93-0760] p 466 A93-24845
Hypersonic inviscid and viscous flow computations with a new optimized thermodynamic equilibrium model [AIAA PAPER 93-0893] p 471 A93-24953
Characteristic multigrid method application to solve the Euler equations with unstructured and unnested grids p 476 A93-27065
Uniform high-order spectral methods for one- and two-dimensional Euler equations p 476 A93-27068
The analysis and computation of viscous-inviscid interactive problem for three dimensional transonic flow p 681 A93-33741
Viscous-inviscid interaction coupled calculation of three-dimensional turbulent separated flow over dents p 681 A93-33748
Numerical simulation of inviscid transonic flow over two-dimensional slender bodies p 686 A93-34348
Efficient hybrid scheme for the analysis of counter-rotating propellers p 688 A93-34483
Experimental validation of a discrete vortex method for inviscid axisymmetric flow around parachute canopies [AIAA PAPER 93-1216] p 689 A93-35165
Apparent mass effects on parafoil dynamics [AIAA PAPER 93-1236] p 690 A93-35177
Modeling of linear isentropic flow systems p 828 A93-37046
Inviscid instability of a skewed compressible mixing layer p 769 A93-37941
Numerical analysis for chemically non-equilibrium flow p 770 A93-38148
A viscous-inviscid solver for high-lift incompressible flows over multi-element airfoils at deep separation conditions [ONERA, TP NO. 1992-183] p 774 A93-38745
Viscous-inviscid calculation of high-lift separated compressible flows over airfoils and wings [ONERA, TP NO. 1992-184] p 774 A93-38746
Transonic aerodynamics including strong effects from heat addition p 862 A93-42428
FUM - An efficient MMB solver for steady inviscid flows p 862 A93-42431
Enhanced numerical inviscid and viscous flows for cell centered finite volume schemes p 864 A93-42444
Viscous and inviscid hypersonic flow about a double ellipsoid p 868 A93-42616
A contribution to the prediction of hypersonic non-equilibrium flows p 869 A93-42624
Reactive and inert inviscid flow solutions by quasi-linear formulations and shock fitting p 927 A93-42625
Inviscid calculations by an upwind finite element method of hypersonic flows over a double (single) ellipse p 869 A93-42626
Contribution to Problem 6 using an upwind Euler solver with unstructured meshes p 869 A93-42627
Inviscid hypersonic flow over a delta wing p 870 A93-42634
Hypersonic leeside delta-wing-flow computations using centered schemes p 870 A93-42635
Evaluation of contributions for test case 7.1.1 and 7.1.2 p 870 A93-42636
Quasi monodimensional inviscid non equilibrium nozzle flow computation p 927 A93-42646
The status of CFD - An Air Force perspective [AIAA PAPER 93-3293] p 1021 A93-44997
Computations of inviscid compressible flows using fluctuation-splitting on triangular meshes [AIAA PAPER 93-3301] p 950 A93-44999
Euler solutions for blunt bodies using triangular meshes - Artificial viscosity forms and numerical boundary conditions [AIAA PAPER 93-3333] p 953 A93-45027
Surface boundary conditions for the numerical solution of the Euler equations [AIAA PAPER 93-3334] p 953 A93-45028
Implicit multigrid Euler solutions with symmetric Total-Variation-Diminishing dissipation [AIAA PAPER 93-3358] p 955 A93-45052
Adaptive Cartesian grid methods for representing geometry in inviscid compressible flow [AIAA PAPER 93-3385] p 955 A93-45076
3D automatic Cartesian grid generation for Euler flows [AIAA PAPER 93-3386] p 956 A93-45077
Adaptive inviscid flow solutions for aerospace geometries on efficiently generated unstructured tetrahedral meshes [AIAA PAPER 93-3390] p 956 A93-45081
A simulation technique for 2-D unsteady inviscid flows around arbitrarily moving and deforming bodies of arbitrary geometry [AIAA PAPER 93-3391] p 956 A93-45082
An upwind multigrid algorithm for calculating flows on unstructured grids p 957 A93-45088
Advancing-layers method for generation of unstructured viscous grids p 957 A93-45101
Comment on 'Flow near the trailing edge of an airfoil' p 961 A93-45754
Application of an engineering inviscid-boundary layer method to slender three-dimensional vehicle forebodies [AIAA PAPER 93-2793] p 963 A93-46534
A multiblock, multigrid solution procedure for multielement airfoils p 967 A93-46812
3D/quasi-3D trans- and supersonic flow calculation in advanced centrifugal/axial compressor stages p 972 A93-46936
Numerical analysis of airfoil cascades subjected to unsteady flow p 972 A93-46944
Unstructured viscous grid generation by advancing-layers method [AIAA PAPER 93-3453] p 979 A93-47238
Calculating crossflow separation using boundary layer computations coupled with an inviscid method [AIAA PAPER 93-3459] p 979 A93-47242
Asymmetric vortical solutions in supersonic corners - Steady 3D space-marching versus time-dependent conical results [AIAA PAPER 93-2957] p 1047 A93-48151
A viscous-inviscid interaction method for 2-D unsteady, compressible flows p 1055 A93-48206
Clebsch variable model for unsteady inviscid transonic flow with strong shock waves [AIAA PAPER 93-3025] p 1055 A93-48210
A fast robust viscous-inviscid interaction solver for transonic flow about wing/body configurations on the basis of full potential theory [AIAA PAPER 93-3026] p 1056 A93-48211
Upwind finite-volume Navier-Stokes computations on unstructured triangular meshes p 1070 A93-49011
Vortical solutions in supersonic corner flows p 1071 A93-49015
Numerical study of the transient flow in the driven tube and the nozzle section of a shock tunnel [AIAA PAPER 93-2018] p 1078 A93-49856
Three-dimensional numerical simulation of gradual opening in a wave rotor passage [AIAA PAPER 93-2526] p 1156 A93-50254
Stagnation point computations of nonequilibrium inviscid blunt body flow p 1093 A93-52005
Euler/experiment correlations of sonic boom pressure signatures p 1095 A93-52439
Construction of wakes in the discrete vortex method p 1179 A93-53333
Kelvin-Helmholtz wave generation beneath hovercraft skirts p 1219 A93-53820
The streamline throughflow method of axial turbomachinery flow analysis [ISABE 93-7031] p 1184 A93-54007
Hypersonic shock-induced combustion ramjet performance analysis [ISABE 93-7037] p 1197 A93-54013
Analysis of high Reynolds number inviscid/viscid interactions in cascades p 1234 A93-55351
Locally implicit total variation diminishing schemes on mixed quadrilateral-triangular meshes p 1235 A93-55356
Investigation of the flowfield around an isolated bypass engine with fan and core jet p 215 A93-13227
Mathematical problems in inviscid hypersonic flow p 131 A93-13451
Flow prediction for three-dimensional intakes and ducts using viscous-inviscid interaction methods p 218 A93-13953
Pressure drag and lift contributions for blunted forebodies of fineness ratio 2.0 in transonic flow (M infinity less than or equal to 1.4) [ESDU-89033] p 136 A93-14515
Computational analysis of hypersonic flows past elliptic-cone waveriders [NASA-CR-191304] p 138 A93-14767
An integral equation solution for multistage turbomachinery design calculations [NASA-TM-105970] p 179 A93-15521
Increase of stagnation pressure and enthalpy in shock tunnels p 295 A93-18086
The stability of a trailing-line vortex in compressible flow [NASA-CR-189738] p 298 A93-18771
Computation of internal flows using unstructured triangular meshes p 299 A93-19276
Analysis of a 2-D airfoil motion in proximity-to-a wavy-wall surface: Lifting-surface-method p 300 A93-19281
Numerical simulations of supersonic flow by a fourth-order compact MUSCL TVD scheme p 302 A93-19308
Analytical and numerical study on steady Mach reflection p 302 A93-19309
Shock-dependent, optimum thrust wings in supersonic flow p 483 A93-20169
Advanced adaptive computational methods for Navier-Stokes simulations in rotorcraft aerodynamics [NASA-CR-192282] p 483 A93-20256
Navier-Stokes simulations of unsteady transonic flow phenomena p 697 A93-25542
Unstructured viscous grid generation by advancing-front method [NASA-CR-191449] p 780 A93-27067
Recent progress in the analysis of iced airfoils and wings p 784 A93-27441
Unstructured mesh algorithms for aerodynamic calculations p 785 A93-27444
Calculation of fully three-dimensional separated flow with an unsteady viscous-inviscid interaction method p 786 A93-27455
Investigations on entropy layer along hypersonic hyperboloids using a defect boundary layer p 787 A93-27462
Three-dimensional numerical simulation of gradual opening in a wave rotor passage [NASA-CR-191157] p 900 A93-29072
Development of an unstructured solution adaptive method for the quasi-three-dimensional Euler and Navier-Stokes equations p 930 A93-29213
Solution of Euler equations for forebody-inlet ensemble of aircraft at high angle of attack [AD-A263905] p 876 A93-29862
Numerical simulation of the flow in a 1:57-scale axisymmetric model of a large blast simulator [AD-A265551] p 1015 A93-31916
NLR inviscid transonic unsteady loads prediction methods in aeroelasticity [NLR-TP-91410-U] p 990 A93-32358

IODINE

Planar measurement of flow field parameters in nonreacting supersonic flows with laser-induced iodine fluorescence p 133 N93-13801

ION BEAMS

Joining carbon composite fins to titanium heat pipes [AD-A261970] p 825 N93-27667

ION IMPLANTATION

Effect of ion treatments on the fatigue strength of blades p 811 A93-39073

IONIZATION

A novel aircraft-based tandem mass spectrometer for atmospheric ion and trace gas measurements p 925 A93-40672

IONIZED GASES

Computation of hypersonic flow past blunt body for nonequilibrium weakly ionized air [AIAA PAPER 93-2995] p 1053 A93-48185

DSMC simulation of ionized rarefied flows [AIAA PAPER 93-3095] p 1061 A93-48269

IONOSPHERIC PROPAGATION

The effects of ionospheric errors on single-frequency GPS users p 313 A93-21141

Analysis and correction of ionospheric time delay for differential GPS p 498 A93-24028

Propagation results of aeronautical satellite communication experiments using INMARSAT satellite p 533 A93-29607

IRON ALLOYS

Raising the high temperature limit of the nickel-iron-base superalloy p 70 A93-12114

INCOLOY 908, a low coefficient of expansion alloy for high-strength cryogenic applications. I - Physical metallurgy p 534 A93-25686

IRRADIANCE

A numerical inversion method for determining aerodynamic effects on particulate exhaust plumes from onboard irradiance data p 823 A93-37482

ISENTROPIC PROCESSES

Diagnostic studies of clear air turbulence in isentropic coordinates p 430 A93-22154

Mean flowfield structure of a three-dimensional supersonic turbulent boundary layer [AIAA PAPER 93-0661] p 465 A93-24774

Modeling of linear isentropic flow systems p 828 A93-37046

ISOLATORS

Experimental results of shock trains in rectangular ducts p 274 A93-22373

ISOPARAMETRIC FINITE ELEMENTS

A nonlinear finite element of an arbitrary beam p 1215 A93-52939

ISOTHERMAL FLOW

Three component LDV velocity measurements in a can type research combustor for CFD validation. I - Isothermal p 350 A93-19370

Determination of heat transfer to flow in a duct with a pseudodiscontinuity p 1179 A93-53365

A study on 3-D velocity distribution of isothermal flows behind an afterburner flame stabilizer [ISABE 93-7039] p 1197 A93-54015

Isothermal flow characteristics behind V-shape gutter with and without injection [ISABE 93-7040] p 1198 A93-54016

ISOTHERMAL PROCESSES

Isothermal oxidation behavior of alpha-2 titanium aluminide alloys p 535 A93-29563

ISOTROPIC MEDIA

Propagation of transverse anti-plane waves in orthotropic layers p 412 A93-21878

Crack models for a transversely isotropic medium p 557 A93-24566

ISOTROPY

Creep fatigue life prediction for engine hot section materials (isotropic) [NASA-CR-189221] p 364 N93-18578

ITERATION

Propagation of high frequency jet noise using geometric acoustics [AIAA PAPER 93-0147] p 452 A93-23241

Sensitivity analysis of a wing aeroelastic response p 958 A93-45142

An approach to constrained aerodynamic design with application to airfoils [NASA-TP-3260] p 24 N93-12321

Propagation of high frequency jet noise using geometric acoustics [NASA-TM-106013] p 233 N93-15575

Combining direct and indirect methods in optimal control: Range maximization of a hang glider [REPT-313] p 371 N93-16618

ITERATIVE SOLUTION

Iterative temperature calculation method for rectangular sandwich panel fins p 76 A93-10667

Multiple input/multiple output (MIMO) analysis procedures with applications to flight data p 60 A93-10777

Some special purpose preconditioners for conjugate gradient-like methods applied to CFD p 772 A93-38638

Analysis of implicit treatments for a centred Euler solver p 864 A93-42449

Direct and iterative algorithms for the three-dimensional Euler equations [AIAA PAPER 93-3378] p 957 A93-45102

An iterative multidisciplinary analysis for rotor blade shape determination [AIAA PAPER 93-2085] p 1114 A93-49912

Trim analysis by shooting and finite elements and Floquet eigenanalysis by QR and subspace iterations in helicopter dynamics p 163 N93-13914

Combining direct and indirect methods in optimal control: Range maximization of a hang glider [REPT-313] p 371 N93-16618

Methodology for sensitivity analysis, approximate analysis, and design optimization in CFD for multidisciplinary applications [NASA-CR-192172] p 552 N93-20297

J

J INTEGRAL

Application of the cyclic J-integral to fatigue crack propagation p 839 N93-27182

J-52 ENGINE

Preliminary analysis of the J-52 aircraft engine component improvement program [AD-A257640] p 363 N93-17686

An analysis of the correlation between the J52 engine component improvement program and improved maintenance parameters [AD-A262062] p 816 N93-28984

JACOBI MATRIX METHOD

Time-variant analysis of rotorcraft systems dynamics - An exploitation of vector processors p 416 A93-23512

Jacobian update strategies for quadratic and near-quadratic convergence of Newton and Newton-like implicit schemes [AIAA PAPER 93-0878] p 470 A93-24939

Computation of internal flows using unstructured triangular meshes p 299 N93-19276

JAPANESE SPACE PROGRAM

Test results on air turbo ramjet for a futurespace plane [AIAA PAPER 92-5054] p 359 A93-22325

Guidance and control of HOPE (H-II orbiting plane) [AAS PAPER 91-653] p 1252 A93-55825

JAPANESE SPACECRAFT

Research on combined HOPE navigation technology p 533 N93-20428

JET AIRCRAFT

General aviation turbine markets - An economic overview [AIAA PAPER 92-4191] p 103 A93-13369

Civil spin-off from military aircraft cockpit research p 45 A93-13415

Annual Paul E. Hemke Lecture in aerospace engineering p 107 A93-14067

The Royal Air Force experience of artificial intelligence aircraft maintenance p 435 A93-18764

The noise of jet aircraft flying with high speeds at low altitudes p 450 A93-19218

Numerical simulation of jet noise p 265 A93-20716

Measurements of jet aircraft emissions at cruise altitude. I - The odd-nitrogen gases NO, NO2, HNO2 and HNO3 p 556 A93-24391

On the maximum range of flying wings [AIAA PAPER 92-4223] p 504 A93-24492

Aging jet transport structural evaluation programs p 947 A93-45781

A study on low level windshear hazard index p 1240 A93-55414

Estimation of rate of climb [ESDU-92019] p 164 N93-14541

Calculation of noise emission caused by jet aircraft during takeoff, approach and horizontal flyover [DLR-MITT-91-15] p 569 N93-21368

World jet airplane inventory at year-end 1992 [PB93-174324] p 765 N93-27405

JET AIRCRAFT NOISE

Prediction of jet mixing noise in high-speed flight p 450 A93-19216

Propagation of high frequency jet noise using geometric acoustics [AIAA PAPER 93-0147] p 452 A93-23241

Acoustic mode measurements in the inlet of a model turbofan using a continuously rotating rake [AIAA PAPER 93-0598] p 563 A93-24783

Computation of supersonic jet noise under imperfectly expanded conditions [AIAA PAPER 93-0735] p 563 A93-24825

Signal processing of jet noise from flyover test data [AIAA PAPER 93-0736] p 563 A93-24826

De-Dopplerization of aircraft acoustic signals [AIAA PAPER 93-0737] p 563 A93-24827

Noise reduction programs for in-service jet transports p 521 A93-28479

Preliminary experiments on active control of fan noise from a turbofan engine p 759 A93-34957

Elements of NASA's high-speed research program [AIAA PAPER 93-2942] p 947 A93-45155

Comparison of flyover noise data from aircraft at high subsonic speeds with prediction p 100 N93-10674

Nozzle installation effects on the noise from supersonic exhaust plumes p 100 N93-10681

Combustion noise and combustion instabilities in propulsion systems p 100 N93-10682

The prediction of noise radiation from supersonic elliptic jets p 100 N93-10684

Prediction of jet mixing noise for high subsonic flight speeds p 100 N93-10685

Mechanisms of sound generation in subsonic jets p 101 N93-10688

A concept for a counterrotating fan with reduced tone noise [NASA-TM-105736] p 101 N93-11370

Computation of supersonic jet noise under imperfectly expanded conditions [NASA-TM-105961] p 233 N93-15430

Propagation of high frequency jet noise using geometric acoustics [NASA-TM-106013] p 233 N93-15575

Acoustic mode measurements in the inlet of a model turbofan using a continuously rotating rake [NASA-TM-105989] p 362 N93-16705

Numerical simulation of a high Mach number jet flow [NASA-TM-105985] p 551 N93-20057

Jet mixer noise suppressor using acoustic feedback [NASA-CASE-LEW-15170-1] p 853 N93-28953

Some aspects of the aeroacoustics of high-speed jets [NASA-CR-191458] p 843 N93-28975

Engine exhaust characteristics evaluation in support of aircraft acoustic testing [NASA-TM-104263] p 1005 N93-32220

Control of jet noise [NASA-CR-193552] p 1040 N93-32221

The prediction of noise from co-axial jets [ISVR-TR-215] p 1040 N93-32339

JET CONTROL

A systems approach to a DSMC calculation of a control jet interaction experiment [AIAA PAPER 93-2798] p 964 A93-46538

Shock tunnel experiments and approximate methods on hypervelocity side-jet control effectiveness [AIAA PAPER 93-1929] p 1077 A93-49794

Applications of active adaptive noise control to jet engines [NASA-CR-192277] p 522 N93-21210

JET ENGINE FUELS

Studies of jet thermal stability in a flowing system [ASME PAPER 92-GT-106] p 401 A93-19344

Application of a sulphur-doped alkane system to the study of thermal oxidation of jet fuels [ASME PAPER 92-GT-122] p 387 A93-19356

Advanced diagnostics for in situ measurement of particle formation and deposition in thermally stressed jet fuels [AIAA PAPER 93-0363] p 390 A93-23045

Simplified jet fuel reaction mechanism for lean burn combustion application [AIAA PAPER 93-0021] p 390 A93-23238

Results of high temperature JP-7 cracking assessment [AIAA PAPER 93-0806] p 533 A93-24882

Effects of thermal history and jet fuel absorption on the properties of APC-2 p 534 A93-25252

Measurements of wear and acoustic emission from fuel-wetted surfaces p 744 A93-34925

Analysis of jet fuel thermal oxidation deposits by spectral fluorometric technique p 1253 A93-55697

Simplified jet-A kinetic mechanism for combustor application [NASA-TM-105940] p 200 N93-15504

A condensed phase test cell assembly for the System for Thermal Diagnostic Studies (STDS) [AD-A260578] p 393 N93-18242

Interferometric JFTOT tube deposit measuring device [AD-D015599] p 536 N93-20247

Development of a method to determine the autooxidation of turbine fuels [AD-A260578] p 736 N93-25902

Influence of supercritical conditions on pre-combustion chemistry and transport behavior of jet fuels [AD-A261813] p 737 N93-26268

- Oxides of nitrogen emissions from turbulent hydrocarbon/air jet diffusion flames, phase 2 [PB93-152478] p 756 N93-26533
- Advanced thermally-stable, coal-derived, jet fuels program: Experiment system and model development [AD-A262747] p 917 N93-29402
- ### JET ENGINES
- Numerical solution of dynamic equations arising in a jet engine simulation p 53 A93-12237
- Hot end cleaning - Corrosion pitting of turbine discs [SAE PAPER 920930] p 202 A93-14081
- Evaluation and application of the Baldwin-Lomax turbulence model in two-dimensional, unsteady, compressible boundary layers with and without separation in engine inlets [AIAA PAPER 92-3676] p 111 A93-14118
- Study on vortex flow control of inlet distortion p 122 A93-14520
- Robust fault detection of jet engine sensor systems using eigenstructure assignment p 173 A93-14608
- Philosophical approach to the basic understanding of the mechanics of jet propulsion [SAE PAPER 920960] p 173 A93-14626
- Prediction of engine casing temperature of fighter aircraft for infrared signature studies [SAE PAPER 920961] p 206 A93-14627
- Fewest-fault integral optimization algorithm for engine fault diagnosis p 173 A93-15343
- Welding wire selection critical to jet engine repair work p 208 A93-15375
- Autonomous mobile laser complex p 395 A93-17767
- Measurement of the center-of-gravity using X-ray computed tomography p 396 A93-18619
- Simulation of the secondary air system of aero engines [ASME PAPER 92-GT-68] p 348 A93-19318
- TEMPER - A gas-path analysis tool for commercial jet engines [ASME PAPER 92-GT-315] p 354 A93-19501
- Direct numerical simulation of nitric oxide evolution in underexpanded jets [ASME PAPER 92-GT-372] p 355 A93-19534
- An optimisation-matching procedure for variable cycle jet engines [ASME PAPER 92-GT-406] p 356 A93-19555
- A rapid procedure for obtaining time-average interferograms of vibrating bodies p 412 A93-21857
- Evaluation and application of the Baldwin-Lomax turbulence model in two-dimensional, unsteady, compressible boundary layers with and without separation in engine inlets [AIAA PAPER 92-3676] p 414 A93-22509
- Pulsed detonation engine experimental and theoretical review [AIAA PAPER 92-3168] p 531 A93-24478
- Rocket engine versus jet engine comparison [AIAA PAPER 92-3686] p 531 A93-24479
- Real-time optical measurement of alkali species in air for jet engine corrosion testing [AIAA PAPER 93-0791] p 541 A93-24870
- Consideration of the completeness of combustion and dissociation and recombination processes in mathematical models of jet engines for high supersonic flight velocities p 520 A93-27627
- Advances in the design of jet engine test facilities for military aircraft in Australia p 529 A93-28491
- Some contributions to propulsion theory - Fuel consumption formulae and general range equation p 713 A93-34850
- Identification of the open loop dynamics of the T700 turbohaft engine p 809 A93-35934
- Flight efficiency theory p 812 A93-39202
- Some contributions to propulsion theory - The Stream Force Theorem and applications to propulsion p 924 A93-40472
- Supersonic laminar flow control p 860 A93-41782
- Determination of the takeoff characteristics of jet engines during the preliminary design of aircraft p 892 A93-42378
- The use of streamwise vorticity to enhance ejector performance [AIAA PAPER 93-3247] p 966 A93-46792
- Experimental and numerical study of transonic turbine cascade flow [AIAA PAPER 93-3064] p 1059 A93-48240
- Investigation of nacelle upper cowl flow separation using on- and off-body flow visualization techniques p 1072 A93-49507
- Pyrometer for turbine applications in the presence of reflection and combustion [AIAA PAPER 93-2374] p 1156 A93-50143
- Estimation of the parameters of the electrodynamic system engine-exhaust jet p 1193 A93-52965
- Initial results from the NASA Lewis wave rotor experiment [AIAA PAPER 93-2521] p 1193 A93-53589
- The design and development of an afterburner [ISABE 93-7041] p 1198 A93-54017
- Performance and configuration analysis of jet-engine off-design behavior [ISABE 93-7087] p 1202 A93-54063
- Uncertainty assessments for engine thrust derived from two methods p 1254 A93-54392
- Numerical method for simulating fluid-dynamic and heat-transfer changes in jet-engine injector feed-arm due to fouling p 1245 A93-54467
- Effect of jet engine exhaust on SOFIA straight performance --- Stratospheric Observatory For Infrared Astronomy p 1263 A93-55178
- Evaluation and application of the Baldwin-Lomax turbulence model in two-dimensional, unsteady, compressible boundary layers with and without separation in engine inlets [NASA-TM-105810] p 82 N93-10087
- Mechanisms and modelling of environment-dependent fatigue crack growth in a nickel based superalloy [AD-A253967] p 71 N93-10717
- The Trent family of engines [PNR-90974] p 58 N93-11063
- A concept for a counterrotating fan with reduced tone noise [NASA-TM-105736] p 101 N93-11370
- An investigation of jet engine test cell aerodynamics by means of scale model test studies with comparisons to full-scale test results p 193 N93-14060
- Development of an engine/airframe performance matching scheme for jet engine retrofit [AD-A258822] p 365 N93-18997
- Numerical simulation of the flow through non-uniform airfoil cascade p 302 N93-19310
- Numerical study on transverse hydrogen injection into a supersonic flowfield p 302 N93-19311
- Integrated Blade Inspection System (IBIS) upgrade study [AD-A258912] p 365 N93-19356
- Applications of active adaptive noise control to jet engines [NASA-CR-192277] p 522 N93-21210
- External stress-corrosion cracking of a 1.22-m-diameter type 316 stainless steel air valve [NASA-TP-3190] p 737 N93-26201
- Development and demonstration of a new filter system to control emissions during jet engine testing [AD-A261203] p 755 N93-26243
- Initial results from the NASA-Lewis wave rotor experiment [NASA-TM-106148] p 1005 N93-32368
- ### JET EXHAUST
- Recent advances in jet simulation techniques for flight vehicles p 66 A93-12656
- Ground vortex formation for uniform and nonuniform jets impinging on a ground plane [AIAA PAPER 92-4251] p 80 A93-13362
- Comparison of algebraic turbulence models for afterbody flows with jet exhaust p 123 A93-14554
- The experimental investigation of combination effect by using injection effect of aeroengine jet exhaust p 898 A93-41742
- Flow and heat transfer in a turbulent boundary layer through skewed and pitched jets p 1151 A93-49007
- ### JET FLAPS
- Wind tunnel investigation of a twin-engine jet transport semi-span model with upper surface blown jet flap [NAL-TR-1134] p 26 N93-12503
- ### JET FLOW
- Experimental study of condensation vapor-air jets p 76 A93-10180
- Self-excited oscillations at supersonic off-design jet outflow p 6 A93-10402
- An experimental study of a method for reducing the jet noise of bypass engines using mechanical flow mixers p 53 A93-12810
- Effect of the powerplant configuration on the air flow rate of the jet shield p 54 A93-12820
- Small scale jet effects and hot gas ingestion investigations at NASA Ames [AIAA PAPER 92-4252] p 67 A93-13339
- The cryogenic approach to simulating hot jet in transonic wind-tunnel testing p 117 A93-14297
- Numerical study of jet interaction at super- and hypersonic speeds for flight vehicle control p 184 A93-14379
- Prediction of the radiation characteristic of a helicopter exhaust jet p 172 A93-14494
- Confined jet thrust vector control nozzle studies p 172 A93-14516
- A numerical study on the radiation characteristic of an elliptical exhaust jet p 174 A93-16236
- Instability of rectangular jets p 398 A93-19157
- On the scaling of small-scale jet noise to large scale p 448 A93-19195
- Behaviors of the laterally injected jet in film cooling - Measurements of surface temperature and velocity/temperature field within the jet [ASME PAPER 92-GT-180] p 402 A93-19405
- Direct numerical simulation of nitric oxide evolution in underexpanded jets [ASME PAPER 92-GT-372] p 355 A93-19534
- Accuracy considerations in the computational analysis of jet noise [AIAA PAPER 93-0146] p 451 A93-19804
- Two-, three-, and four-poster jets in cross flow [AIAA PAPER 93-0023] p 408 A93-20141
- Characteristics of liquid jet atomization across a high-speed airstream. I - Experiment on shape of spray, spatial distribution of injected liquid and Sauter mean diameter p 411 A93-21743
- Numerical simulation of the turbulent flow in round jets [AIAA PAPER 93-0199] p 277 A93-22619
- Investigation on bi-flat jet separated flow in a rectangular combustor p 459 A93-23778
- Numerical simulations of a high Mach number jet flow [AIAA PAPER 93-0653] p 540 A93-24766
- A numerical investigation of a subsonic jet in a crossflow [AIAA PAPER 93-0870] p 469 A93-24931
- Experimental and numerical investigations of the vortex-flame interactions in a driven jet diffusion flame [AIAA PAPER 93-0455] p 534 A93-25532
- Compressible flow in a hovercraft air cushion p 480 A93-29316
- Simulation for hot jet by cryogenic wind tunnels p 730 A93-33750
- A study on two-dimensional and three-dimensional secondary jet interactions with a supersonic flow p 683 A93-34273
- Instability of rectangular jets p 720 A93-34410
- Effects of blowing on delta wing vortices during dynamic pitching p 768 A93-37384
- A numerical simulation of a scram jet combustor flow p 810 A93-38181
- Phenomenology and simplified modeling of a vortex wake generated by a transverse jet [ONERA, TP NO. 1992-194] p 774 A93-38755
- Flow density distribution in a two-phase submerged jet p 836 A93-39144
- Modeling of the physicochemical processes of nonequilibrium heat transfer in the subsonic jets of an induction plasmatron p 836 A93-39147
- Hypersonic single expansion ramp nozzle simulations p 777 A93-39254
- Study of mixing flow field of a jet in a supersonic cross flow. I - Experimental facilities and preliminary experiments p 857 A93-40430
- Intrusive and nonintrusive measurements of flow properties in arc jets p 943 A93-42584
- Three-dimensional calculation of a hydrogen jet injection into a supersonic air flow p 950 A93-44374
- Effect of nonaxisymmetric forcing on a swirling jet with vortex breakdown [AIAA PAPER 93-3251] p 1028 A93-46796
- An investigation of the effects of a rear stagnation jet on the wake behind a cylinder [AIAA PAPER 93-3274] p 969 A93-46835
- Vorticity dynamics in spatially developing rectangular jets [AIAA PAPER 93-3286] p 969 A93-46842
- Forebody vortex control with jet and slot blowing on an F/A-18 [AIAA PAPER 93-3449] p 1009 A93-47235
- Calculation of V/STOL aircraft aerodynamics with deflected jets in ground effect [AIAA PAPER 93-3530] p 986 A93-47287
- Effects of aft geometry on vortex behavior and force production by a tangential jet on a body at high alpha [AIAA PAPER 93-2961] p 1048 A93-48155
- An initial comparison of CFD with experiment for a geometrically simplified STOVL model [AIAA PAPER 93-3059] p 1058 A93-48236
- Modelling three-dimensional gas-turbine-combustor model flow using second-moment closure [AIAA PAPER 93-3104] p 1149 A93-48277
- Effects of a rear stagnation jet on the wake behind a cylinder p 1151 A93-49026
- Shock tunnel experiments and approximative methods on hypervelocity side-jet control effectiveness [AIAA PAPER 93-1929] p 1077 A93-49794
- Molecular mixing of jets in supersonic flow [AIAA PAPER 93-2021] p 1078 A93-49858
- Acoustic intensity of nonisothermal coaxial jets with an inverted velocity profile p 1124 A93-51759
- Construction of wakes in the discrete vortex method p 1179 A93-53333

- Blowout of turbulent disc/pilot stabilized jet diffusion flames
[ISABE 93-7026] p 1213 A93-54002
- Observation of fluctuation of 2D-nozzle flows
[ISABE 93-7110] p 1204 A93-54086
- Mixing of multiple jets with a confined subsonic crossflow
p 1189 A93-54324
- Vectoring jet effects on the flow and aerodynamic behaviors of fighter model
p 1241 A93-54590
- Chaotic vortical motion in the near region of a plane jet
p 131 A93-13493
- Dynamics of vortex rings in cross-flow
p 134 A93-13917
- Control of asymmetric jet
[AD-A255967] p 219 N93-14400
- Numerical simulation of a high Mach number jet flow
[NASA-TM-105985] p 551 N93-20057
- An experimental investigation of a round turbulent jet in a cross-flow
p 553 N93-20689
- Experimental and computational investigation of helium injection into air at supersonic and hypersonic speeds
p 696 N93-25487
- Oxides of nitrogen emissions from turbulent hydrocarbon/air jet diffusion flames, phase 2
[PB93-152478] p 756 N93-26533
- The ground vortex flow field associated with a jet in a cross flow impinging on a ground plane for uniform and annular turbulent axisymmetric jets
p 789 N93-28449
- Experimental study of heat transfer close to a plane wall heated in the presence of multiple injections (subsonic flow)
p 901 N93-29931
- Heat transfer in high turbulence flows: A 2-D planar wall jet
p 932 N93-29935
- Modeling of a turbulent flow in the presence of discrete parietal cooling jets
p 904 N93-29960
- Effects of buoyancy on gas jet diffusion flames
[NASA-CR-191109] p 935 N93-31031
- JET IMPINGEMENT**
- A study of the effect of a moving ground belt on the vortex created by a jet impinging on the ground in a cross flow
[AIAA PAPER 92-4250] p 15 A93-13361
- Ground vortex formation for uniform and nonuniform jets impinging on a ground plane
[AIAA PAPER 92-4251] p 80 A93-13362
- Computation of laminar flow and heat transfer over an enclosed rotating disk with and without jet impingement
p 201 A93-13982
- Breakdown of steady state axisymmetric flow in a shock layer formed as a result of the impingement of a supersonic underexpanded jet on a perpendicular plane obstacle
p 241 A93-18230
- Unsteady pressures under impinging jets in crossflows
p 399 A93-19220
- Computations of a twin-jet impingement on a flat surface
p 271 A93-22227
- A study of single jet impingement ground effect lift loss
[AIAA PAPER 93-0869] p 469 A93-24930
- Numerical study of an axisymmetric turbulent jet-impingement flow
[AIAA PAPER 93-0652] p 543 A93-25545
- Wall jets created by single and twin high pressure jet impingement
p 744 A93-34847
- Effects of nozzle contour on the aerodynamic characteristics of underexpanded annular impinging jets
p 1024 A93-45563
- Vortex developments over steady and accelerated airfoils incorporating a trailing edge jet
[AIAA PAPER 93-3008] p 1054 A93-48198
- Experimental study on heat transfer of separated impingement jets in short distance
p 1149 A93-48518
- Heat transfer and material temperature conditions in the leading edge area of impingement-cooled turbine vanes
[ISABE 93-7076] p 1220 A93-54052
- Fluid dynamics and convective heat transfer in impinging jets through implementation of a high resolution liquid crystal technique
[ISABE 93-7077] p 1220 A93-54053
- Impingement cooling with film coolant extraction in the airfoil leading edge regions
[ISABE 93-7078] p 1220 A93-54054
- On the analysis of an impinging jet on ground effects
p 1260 A93-56339
- Nozzle installation effects on the noise from supersonic exhaust plumes
p 100 N93-10681
- Combustion instabilities in a side-dump model ramjet combustor
p 382 N93-17613
- Reduction in size and unsteadiness of a VTOL ground vortex by ground fences
[NASA-CR-192997] p 700 N93-26049
- Prediction of jet impingement cooling scheme characteristics (airfoil leading edge application)
p 932 N93-29941

JET MIXING FLOW

- Intensification of flow mixing behind an oblique shock wave
p 4 A93-10138
- Numerical simulation of compressible mixing zones
p 10 A93-12427
- Noncoaxial mixing in a rectangular duct
p 205 A93-14518
- On the scaling of small-scale jet noise to large scale
p 448 A93-19195
- Experimental investigations and efficiency prediction of jet noise reduction techniques
p 449 A93-19206
- Prediction of jet mixing noise in high-speed flight
p 450 A93-19216
- Flowfield measurements for a supersonic mixer ejector in forward flight
p 399 A93-19217
- Analysis of jet/wake mixing in a vaneless diffuser
[ASME PAPER 92-GT-418] p 258 A93-19566
- Characteristics of liquid jet atomization across a high-speed airstream. I - Experiment on shape of spray, spatial distribution of injected liquid and Sauter mean diameter
p 411 A93-21743
- Characteristics of liquid jet atomization across a high-speed airstream. II - Calculation of spatial distribution of liquid, variation of drop diameter and drop trajectory
p 412 A93-21744
- Penetration and mixing of bubbling liquid jets from multiple injectors normal to a supersonic air stream
[AIAA PAPER 92-5060] p 413 A93-22330
- Optimization of circular orifice jets mixing into a heated crossflow in a cylindrical duct
[AIAA PAPER 93-0249] p 361 A93-23246
- A numerical study of mixing in supersonic combustors with hypermixing injectors
[AIAA PAPER 93-0215] p 520 A93-27801
- Numerical study on the interaction of supersonic flow past a wedge and free jet
p 479 A93-28574
- Free shear layer control and its application to fan noise
[AIAA PAPER 93-3242] p 965 A93-46787
- An analytical study of dilution jet mixing in a cylindrical duct
[AIAA PAPER 93-2043] p 1113 A93-49876
- Some supersonic and hypersonic research at GASL in the 1960s and 70s
[AIAA PAPER 93-2327] p 1145 A93-50107
- Comparison of the initial development of shear layers in two-dimensional and axisymmetric ejector configurations
[AIAA PAPER 93-2441] p 1119 A93-50193
- Streamwise vorticity generation and mixing enhancement in free jets by 'delta-tabs'
[AIAA PAPER 93-3253] p 1180 A93-53592
- Noise reduction of supersonic heated jet with jet mixing enhancement by tabs
[ISABE 93-7046] p 1198 A93-54022
- Two-dimensional and three-dimensional mixing flow structures with injected through slotted nozzle and circular nozzle into supersonic flows
[ISABE 93-7117] p 1221 A93-54092
- Numerical and experimental study on two- and three-dimensional supersonic flow field with hydrogen injection
[ISABE 93-7118] p 1188 A93-54093
- Enhancement of mixing in high-speed heated jets using a counterflowing nozzle
p 1235 A93-55359
- The prediction of noise radiation from supersonic elliptic jets
p 100 N93-10684
- Prediction of jet mixing noise for high subsonic flight speeds
p 100 N93-10685
- Mechanisms of sound generation in subsonic jets
p 101 N93-10688
- Control of asymmetric jet
[AD-A255967] p 219 N93-14400
- Optimization of circular orifice jets mixing into a heated cross flow in a cylindrical duct
[NASA-TM-105984] p 179 N93-15359
- A numerical study of mixing in supersonic combustors with hypermixing injectors
[NASA-CR-191027] p 294 N93-17884
- Experimental and computational investigation of helium injection into air at supersonic and hypersonic speeds
p 696 N93-25487
- Experimental investigation of crossflow jet mixing in a rectangular duct
[NASA-TM-106152] p 812 N93-27026
- CFD mixing analysis of axially opposed rows of jets injected into confined crossflow
[NASA-TM-106179] p 813 N93-27128
- An analytical study of dilution jet mixing in a cylindrical duct
[NASA-TM-106181] p 814 N93-27160
- Experimental study of cross flow mixing in cylindrical and rectangular ducts
[NASA-CR-187141] p 815 N93-27680

- Streamwise vorticity generation and mixing enhancement in free jets by delta-tabs
[NASA-TM-106235] p 988 N93-31648
- Enhanced mixing of a rectangular supersonic jet by natural and induced screech
[NASA-TM-106245] p 989 N93-31672
- The prediction of noise from co-axial jets
[ISVR-TR-215] p 1040 N93-32339
- JET NOZZLES**
- Feasibility study on single bypass variable cycle engine with ejector
[AIAA PAPER 92-4268] p 55 A93-13366
- Arc jet testing in NASA Ames Research Center thermophysics facilities
[AIAA PAPER 92-5041] p 385 A93-22315
- Further study of high speed single free jets
p 873 A93-43687
- Flow calibration of two hypersonic nozzles in the AEDC HEAT-H2 high-enthalpy arc-heated wind tunnel
[AIAA PAPER 93-2782] p 1012 A93-46526
- Control of asymmetric jet
[AD-A255967] p 219 N93-14400
- JET PROPULSION**
- Philosophical approach to the basic understanding of the mechanics of jet propulsion
[SAE PAPER 920960] p 173 A93-14626
- Thrust vectoring - Theory, laboratory, and flight tests
p 367 A93-21657
- Some contributions to propulsion theory - The Stream Force Theorem and applications to propulsion
p 924 A93-40472
- The turbulence and mixing characteristics of the complex flow in a simulated augmentor
p 1123 A93-51642
- Scalar characteristics in a liquid-fuelled combustor with curved exit nozzle
p 1123 A93-51643
- Measurements of gas composition and temperature inside a can type model combustor
p 1123 A93-51644
- Engine technology challenges for a 21st Century High-Speed Civil Transport
[ISABE 93-7064] p 1200 A93-54040
- Ultra-high temperature materials in the research and development of super/hypersonic transport propulsion system
p 1252 A93-54712
- Vectoring thrust and two-dimensional nozzle
p 1247 A93-54863
- Concorde propulsion: Did we get it right? The Rolls-Royce/SNECMA Olympus 593 engine reviewed
[PNR-90970] p 57 N93-11061
- Engine technology challenges for a 21st Century High-Speed Civil Transport
[NASA-TM-106216] p 1004 N93-31671
- JET PUMPS**
- Low area ratio aircraft fuel jet-pump performances with and without cavitation
p 272 A93-22264
- JET STREAMS (METEOROLOGY)**
- Jet streams and associated turbulence and their effects on air transport flight operations
p 154 A93-14231
- Extremely low level jet in the evening in Kanto Plain
p 430 A93-22159
- Recent experiment focuses on operational impact of jet stream forecast errors
p 487 A93-27394
- JET THRUST**
- Confined jet thrust vector control nozzle studies
p 172 A93-14516
- Flight efficiency theory
p 812 A93-39202
- Determination of the takeoff characteristics of jet engines during the preliminary design of aircraft
p 892 A93-42378
- Wind tunnel results for an advanced fighter configuration employing transverse thrust for enhanced STOL capability
[AIAA PAPER 93-1933] p 1100 A93-49796
- Hypersonic ignition and thrust production in a scramjet
[AIAA PAPER 93-2444] p 1119 A93-50196
- Numerical study of a delta planform with multiple jets in ground effect
[SAE PAPER 892283] p 1176 A93-53200
- Uncertainty assessments for engine thrust derived from two methods
p 1254 A93-54392
- JET VANES**
- Heat pipe turbine vane cooling
p 519 A93-26114
- Numerical analysis of aerodynamic losses in film-cooled vane cascade
p 1066 A93-48517
- JOINED WINGS**
- Structural optimization for joined-wing synthesis
[AIAA PAPER 92-4761] p 325 A93-20356
- Structural and aerodynamic optimization of joined-wing aircraft
p 715 N93-25526
- JOINING**
- Simplified finite element representation of fuselage frames with flexible castellations
p 892 A93-43570
- JOINTS (JUNCTIONS)**
- Compressible flow pressure losses in wye-junctions
[ASME PAPER 92-GT-71] p 248 A93-19321

- Coupling conditions for substructures with varying idealization p 1029 A93-47078
- The technical background to standards for shackles [NPL-DMM(A)-51] p 86 N93-11325
- An experimental examination of the thermal and acoustic environments on runway joint seals [AD-A257965] p 382 N93-17734
- JOULE-THOMSON EFFECT**
- Recent developments in compressor-based Joule-Thomson cooling — of thermal imaging equipment in ground and helicopter-borne applications p 547 A93-28244
- Application of vanadium hydride compressors for Joule-Thomson cryocoolers p 1149 A93-48616
- JOURNAL BEARINGS**
- An externally pressurized air bearing system, journals and thrust, for application to small turbomachinery [ASME PAPER 92-GT-382] p 406 A93-19539
- Online vibration control of a flexible rotor/bearing system p 219 N93-14468
- JP-4 JET FUEL**
- Making clean gasoline: The effect on jet fuels [AD-A264302] p 1019 N93-32085
- JP-5 JET FUEL**
- Effect of a metal deactivator fuel additive on fuel deposition in fuel atomizers at high temperature [AD-A260915] p 736 N93-25914
- JP-8 JET FUEL**
- Making clean gasoline: The effect on jet fuels [AD-A264302] p 1019 N93-32085
- K**
- K-EPSILON TURBULENCE MODEL**
- Comparison of heat transfer measurements with computations for turbulent flow around a 180 deg bend p 201 A93-13980
- Numerical simulation of turbulent reacting flows in combustion chambers p 171 A93-14271
- Theoretical investigation of combustion characteristics in ram-jet dump combustor with side-inlet p 346 A93-19121
- An investigation of turbulence modelling in transonic fans including a novel implementation of an implicit k-epsilon turbulence model [ASME PAPER 92-GT-308] p 256 A93-19498
- Three-dimensional Navier-Stokes computations of transonic fan flow using an explicit flow solver and an implicit k-epsilon solver [ASME PAPER 92-GT-309] p 256 A93-19499
- The computation of internal flow fields in centrifugal compressor impellers p 259 A93-20120
- The prediction of riblet behaviour with a low-Reynolds number k-epsilon model p 270 A93-21720
- Validation of a Navier-Stokes code using a (k,epsilon) turbulence model applied to a three-dimensional transonic channel [AIAA PAPER 93-0293] p 279 A93-22693
- Numerical simulation of crossing/turbulent boundary layer interaction at Mach 8.3 comparison of zero and two-equation turbulence models [AIAA PAPER 93-0779] p 467 A93-24861
- Compressible flow calculations using a two-equation turbulence model and unstructured grids p 686 A93-34351
- Turbulent flow simulation around the aerofoil with pseudo-compressibility p 830 A93-38155
- Numerical simulation of vortex shedding past triangular cylinders at high Reynolds number using a k-epsilon turbulence model p 871 A93-42873
- Variant bi-conjugate gradient methods for the compressible Navier-Stokes solver with a two-equation model of turbulence [AIAA PAPER 93-3316] p 951 A93-45012
- Computation of crossing shock/turbulent boundary layer interaction at Mach 8.3 p 961 A93-45726
- A pointwise version of the Baldwin-Barth turbulence model [AIAA PAPER 93-3523] p 985 A93-47284
- Some practical turbulence modeling options for Reynolds-averaged full Navier-Stokes calculations of three-dimensional flows [AIAA PAPER 93-2964] p 1048 A93-48158
- Numerical solution of Navier-Stokes equations and k-omega turbulence model equations using a staggered upwind method [AIAA PAPER 93-2968] p 1049 A93-48162
- High lift airfoil flow simulation using a wall-corrected Algebraic Stress Model [AIAA PAPER 93-3109] p 1061 A93-48280
- A two layer k-epsilon computation of transonic viscous flow including separation over the DLR-F5 wing [AIAA PAPER 93-3110] p 1061 A93-48281

- A staggered finite volume scheme for solving cascade flow with a two-equation model of turbulence [AIAA PAPER 93-1912] p 1076 A93-49779
- An unstructured adaptive quadrilateral mesh-based scheme for viscous turbomachinery flow calculations [AIAA PAPER 93-1975] p 1077 A93-49822
- The effects of turbulence modeling on the numerical simulation of confined swirling flows [AIAA PAPER 93-1976] p 1078 A93-49823
- Numerical analysis of flow within cascade with tip clearance p 1176 A93-53192
- Low-Reynolds-number k-epsilon model for unsteady turbulent boundary-layer flows p 1177 A93-53208
- 3D laminar and 2D turbulent computations with the Navier-Stokes solver FLU3M [ONERA, TP NO. 1993-105] p 1180 A93-53618
- Explicit Navier-Stokes computation of turbomachinery flows p 83 N93-10370
- A realizable Reynolds stress algebraic equation model [NASA-TM-105993] p 290 N93-16596
- Fuel injector: Air swirl characterization aerothermal modeling, phase 2, volume 1 [NASA-CR-189193-VOL-1] p 721 N93-24754
- Fuel Injector: Air swirl characterization aerothermal modeling, phase 2, volume 2 [NASA-CR-189193-VOL-2] p 721 N93-25106
- Studies in air/air supersonic mixing layers p 700 N93-26007
- The remarkable ability of turbulence model equations to describe transition p 783 N93-27432
- Turbulent flow and heat transfer in idealized blade cooling passages p 902 N93-29938
- Modeling of a turbulent flow in the presence of discrete parietal cooling jets p 904 N93-29960
- Turbulence characteristics of an axisymmetric reacting flow [NASA-CR-4110] p 877 N93-30373
- The numerical simulation of circulation controlled airfoil flowfields p 879 N93-30947
- Numerical simulation of the flow in a 1:57-scale axisymmetric model of a large blast simulator [AD-A265551] p 1015 N93-31916
- KALMAN FILTERS**
- Precision navigation with an integrated navigation system p 29 A93-10782
- Sensor alignment Kalman filters for inertial stabilization systems p 50 A93-11018
- An adaptive algorithm for estimation of a state vector in the system of remotely-piloted aircraft control using Kalman filter p 181 A93-14232
- BUAA inertial terrain-aided navigation (BITAN) algorithm p 149 A93-14235
- A new aircraft integrated positioning and communication system based on satellite p 150 A93-14236
- Hetero-redundant architecture with Kalman filter for input processing in flight control system p 182 A93-14293
- Vision-based range estimation using helicopter flight data p 151 A93-17501
- Vision-based range estimation using helicopter flight data p 317 A93-21525
- Track moving emitters with Kalman processing p 317 A93-22275
- Vision-based recursive estimation of rotorcraft obstacle locations p 343 A93-22851
- A nonsearch adaptive control system with a reference model and derivative measurement p 561 A93-26838
- Augmentation of a navigation reference system with differential global positioning system pseudorange measurements p 881 A93-42798
- Passive range estimation for rotorcraft low-altitude flight p 948 A93-46608
- A U-D factorization-based adaptive extended Kalman filter and its application to flight state estimation p 1169 A93-51198
- Identification of nonlinear mechanical systems using combined state and parameter evaluation p 1224 A93-52732
- Passive range estimation for rotorcraft low-altitude flight p 1190 A93-52881
- A monitor for the laboratory evaluation of control integrity in digital control systems operating in harsh electromagnetic environments [NASA-TM-4402] p 65 N93-12304
- Integration of radar altimeter, precision navigation, and digital terrain data for low-altitude flight [NASA-TM-103958] p 36 N93-12320
- Accuracy improvement of linear estimated motion using differential type sensors p 91 N93-12365
- Multiple model adaptive estimation applied to the VISTA F-16 with actuator and sensor failures [AD-A256444] p 188 N93-14608
- Correction of inertial measurements using GPS updates for underwater navigation [AD-A257329] p 317 N93-15988

- Multiple model adaptive estimation applied to the VISTA F-16 with actuator and sensor failures, volume 2 [AD-A256569] p 371 N93-16165
- Detection of spoofing, jamming, or failure of a Global Positioning System (GPS) [AD-A259023] p 319 N93-18951
- Failure identification using multiple model adaptive estimation for the LAMBDA flight vehicle [AD-A259137] p 527 N93-20596
- System for calibrating a gyro navigator [AD-D015668] p 708 N93-26093
- KARMAN VORTEX STREET**
- Karman vortex street-airfoil interaction p 678 A93-33703
- On computing vortex asymmetries about cones at angle of attack using the conical Navier-Stokes equations [AIAA PAPER 93-3628] p 1064 A93-48313
- Experimental investigation into the mechanism of discrete frequency noise (DFN) generation from a NACA 0012 blade p 1225 A93-53194
- The leading edge vortex of a rotating stall cell [ISABE 93-7009] p 1183 A93-53985
- Effect of passive flow-control devices on turbulent low-speed base flow p 82 N93-10304
- Rotating stall cell and Von Karman vortex street: A meteorological theory p 424 N93-18734
- Studies of origin of three-dimensionality in laminar wakes [AD-A262281] p 841 N93-28242
- KEELS**
- Effects of intra- and inter-laminar resin content on the mechanical properties of toughened composite materials p 921 N93-30845
- KELVIN-HELMHOLTZ INSTABILITY**
- The effects of temperature on supersonic jet noise emission p 446 A93-19159
- Numerical simulation of the turbulent flow in round jets [AIAA PAPER 93-0199] p 277 A93-22619
- Active forcing of an axisymmetric leading-edge turbulent separation bubble [AIAA PAPER 93-3245] p 966 A93-46790
- Kelvin-Helmholtz wave generation beneath hovercraft skirts p 1219 A93-53820
- Comparison of confined, compressible, spatially developing mixing layers with temporal mixing layers p 1234 A93-55352
- KEPLER LAWS**
- Singular arcs for blunt endoatmospheric vehicles p 1015 A93-44380
- KERNEL FUNCTIONS**
- Analytic continuation of Pade approximations to the unsteady kernel functions to obtain a better understanding of the analytic continuation of Pade approximations to unsteady parameters in general p 117 A93-14283
- Scattering kernels for gas-surface interaction p 943 A93-42580
- KEROSENE**
- Supersonic combustion and gasdynamic of scramjet p 170 A93-14242
- Design features influencing the distribution of fuel within the spray from an air blast fuel injector [ASME PAPER 92-GT-235] p 353 A93-19448
- KEVLAR (TRADEMARK)**
- The development and evaluation of advanced Kevlar sandwich structure for application to rotorcraft airframes p 546 A93-27965
- KINEMATIC EQUATIONS**
- Wind identification along a flight trajectory. I - 3D-kinematic approach p 223 A93-16324
- Kinematics of aeroinertial aircraft rotation p 819 A93-39192
- Kinematic domain decomposition for boundary-motion-induced flow simulations p 1028 A93-46811
- Kinematics and aerodynamics of the velocity vector roll [AIAA PAPER 93-3625] p 1126 A93-48310
- KINEMATICS**
- Studies in air/air supersonic mixing layers p 700 N93-26007
- System analysis for a kinematic positioning system based on the global positioning system [AD-A262830] p 885 N93-29468
- KINETIC ENERGY**
- Jet streams and associated turbulence and their effects on air transport flight operations p 154 A93-14231
- Aircraft braking systems p 995 A93-44850
- Thrust imparted to an airfoil by passage through a sinusoidal upwash field p 1178 A93-53219
- Analytical expression of dissipation integral for kinetic energy integral equation — calculation of turbulent compressible boundary layer in aerodynamics p 1183 A93-53860
- The energy dissipation in a rotating stall cell [ISABE 93-7010] p 1183 A93-53986

Navier-Stokes computations for kinetic energy projectiles in steady coning motion: A predictive capability for pitch damping
[AD-A264111] p 1033 N93-32028

KINETIC EQUATIONS

An approximate method for calculating nonequilibrium flows near blunt bodies p 776 A93-39134
A multi-dimensional kinetic-based upwind solver for the Euler equations
[AIAA PAPER 93-3303] p 950 A93-45001
Modeling the flow around a body via the solution of the relaxational kinetic equation p 1089 A93-51868
Turbulence and chaos in classical and quantum systems p 232 N93-14144

KINETIC THEORY

Problems in physical gas dynamics p 775 A93-39126
Kinetic theory of nonequilibrium flows of gas and disperse media with internal degrees of freedom and chemical reactions p 851 A93-39127
Kinetic theory of hypersonic flows of a viscous gas p 775 A93-39130
A computer simulation of the production of an artificially ionized layer using the Arecibo facility
[DE93-010817] p 937 N93-30487

KNOWLEDGE BASED SYSTEMS

An application of knowledge-based engineering to composite tooling design p 846 A93-36010
System Status - The diagnostic edge of the pilot's associate p 808 A93-37853
A constrained flight route monitor system in terminal control area for air traffic control p 882 A93-42816

KNOWLEDGE BASES (ARTIFICIAL INTELLIGENCE)

Artificial intelligence techniques for improving aircraft maintenance efficiency; Proceedings of the Conference, London, United Kingdom, Feb. 21, 1991
[ISBN 0-903409-84-4] p 238 A93-18761
Expert systems for the simulation of gas turbine engines
[ASME PAPER 92-GT-408] p 435 A93-19557
Structure of a knowledge base used in the computerized synthesis of aircraft layout p 891 A93-42373
Intelligent systems of flight-vehicle control p 1167 A93-50951
Generation of a plant description dictionary based on expert survey data p 1168 A93-50956
Architecture of multiprocessor data processing machines and dispatching of the knowledge acquisition process in flight control p 1168 A93-50958
Control problem for a plant with artificial intelligence p 1168 A93-50960
A knowledge-based blackboard system to interpret graphical data from vibration tests of gas turbines
[PNR-90993] p 59 N93-11114
Artificial intelligence and CFD: Expert systems for the design of airfoils and for grid generation
[DIGE-EST-TN-016] p 48 N93-11161
A domain-specific design architecture for composite material design and aircraft part redesign p 442 N93-17522

KNOWLEDGE REPRESENTATION

Representation and presentation of requirements knowledge p 228 A93-17389
A theoretical study on the ETHYLENE system - A fuzzy diagnostic expert system for large rotating machinery p 846 A93-36327
Functional requirements of an advanced instructional design advisor: Simulation authoring, Volume 3
[AD-A256650] p 440 N93-16500

KNUDSEN FLOW

Calculation of flow of a rarefied gas past a sphere for an arbitrary Knudsen number p 124 A93-15146
Near wake structure for a generic ASTV configuration
[AIAA PAPER 93-0271] p 268 A93-21103
Aerodynamics of Shuttle Orbiter at high altitudes
[AIAA PAPER 93-2815] p 965 A93-46553
Application of a vectorized particle simulation to the study of plates and wedges in high-speed rarefied flow p 133 N93-13746

KOLMOGOROV THEORY

A pointwise version of the Baldwin-Barth turbulence model
[AIAA PAPER 93-3523] p 985 A93-47284

KUTTA-JOUKOWSKI CONDITION

A method for the prediction of induced drag for planar and nonplanar wings
[AIAA PAPER 93-3420] p 976 A93-47216

LABORATORIES

The Goldstein Aeronautical Engineering Research Laboratory
[AERO-REPT-9109] p 240 N93-16465

LABORATORY EQUIPMENT

The start of the laboratory - The beginnings of the MIT Instrumentation Laboratory p 235 A93-17326

LABYRINTH SEALS

Evaluation of brush seals for limited-life engines p 411 A93-21665
Heat Transfer and Cooling in Gas Turbines
[AGARD-CP-527] p 901 N93-29926
Heat transfer and leakage in high-speed rotating stepped labyrinth seals p 903 N93-29951

LAGRANGE COORDINATES

Quasi-one-dimensional modelling of free-piston shock tunnels
[AIAA PAPER 93-0352] p 377 A93-23037

LAGRANGIAN FUNCTION

An extended Lagrangian method
[AIAA PAPER 93-3305] p 951 A93-45003

LAMINAR BOUNDARY LAYER

Calculation of a gas-dispersion laminar boundary layer on a plate with allowance for liquid film formation p 76 A93-10148

Evaluation of 2D scramjet nozzle performance p 52 A93-11209

Compressible laminar and turbulent boundary layer computation for the three-dimensional wing p 12 A93-12735

A study of the laminar-turbulent transition in a boundary layer and separation on cones at supersonic velocities p 14 A93-12974

Hybrid laminar flow control applied to advanced turbofan engine nacelles
[SAE PAPER 920962] p 123 A93-14628

Oblique wave evolution in a plane subsonic boundary layer p 124 A93-15178

Instability of local separated flows with respect to small-amplitude perturbations p 125 A93-15254

The frequency of incipient vortex-shedding from a circular cylinder in a laminar boundary layer (The effect of the gap ratio on the vortex shedding frequency) p 126 A93-15488

Engineering aspects of laminar flow research at Handley Page p 235 A93-17275

Experimental investigation of laminar to turbulent boundary layer transition with separation bubbles at low Reynolds number p 128 A93-17277

On the coupling between a supersonic boundary layer and a flexible surface p 243 A93-19132

Boundary layer effects on the transonic flow in a straight turbine cascade
[ASME PAPER 92-GT-155] p 249 A93-19382

Calculation of three-dimensional boundary layers on rotor blades using integral methods
[ASME PAPER 92-GT-210] p 252 A93-19433

Measurement of unsteady flow and heat transfer in a linear turbine cascade
[ASME PAPER 92-GT-323] p 256 A93-19507

Stability and transition on swept wings
[AIAA PAPER 93-0078] p 263 A93-20190

Transition on a sharp cone at high enthalpy - New measurements in the shock tunnel T5 at GALCIT
[AIAA PAPER 93-0343] p 281 A93-23030

Development of the NASA-Ames low disturbance supersonic wind tunnel for transition research up to Mach 2.5
[AIAA PAPER 92-3909] p 462 A93-24488

On the breakdown of a hypersonic laminar boundary layer
[AIAA PAPER 93-0896] p 472 A93-24956

A method for calculating the characteristics of plane compressor cascades for different values of the Reynolds criterion p 545 A93-27616

Inviscid instability of a skewed compressible mixing layer p 769 A93-37941

Experiments on shock wave-boundary layer interaction at high Mach number with entropy layer effect
[ONERA, TP NO. 1992-101] p 771 A93-38581

Shock wave/boundary layer interaction in a two-dimensional laminar hypersonic flow
[ONERA, TP NO. 1992-182] p 773 A93-38744

The determination of hybrid analytical-numerical solutions for the three-dimensional compressible boundary layer p 1029 A93-46979

Experimental study of the effect of external turbulence and the shape of the surface on the characteristics of laminar and transition boundary layers p 987 A93-47522

A finite element and symbolic method for studying laminar boundary layers of real gases in equilibrium at Mach numbers to 30
[AIAA PAPER 93-2986] p 1052 A93-48179

Bypass transition in two- and three-dimensional boundary layers
[AIAA PAPER 93-3050] p 1057 A93-48230

Aerothermodynamic heating due to shock wave/laminar boundary-layer interactions in high-enthalpy hypersonic flow
[AIAA PAPER 93-3135] p 1064 A93-48299

A study of the effect of surface riblets on the evolution of a solitary wave packet (λ vortex) in a laminar boundary layer p 1067 A93-48827

A study of the interaction of a nonstationary shock wave with a boundary layer on a plate in the transition regime p 1150 A93-48850

Second-order effects in hypersonic laminar boundary layers p 1073 A93-49529

Real gas effects in two- and three-dimensional hypersonic, laminar boundary layers p 1073 A93-49530

Nontraditional methods of controlling the stability of a laminar subsonic boundary layer p 1085 A93-50962

Numerical modeling of flow in a hypersonic laminar boundary layer p 1086 A93-50967

Calculation of perturbation propagation upstream in a hypersonic laminar boundary layer p 1086 A93-50968

Laminarization of the boundary layer on a vibrating wing p 1089 A93-51776

An experimental investigation on laminar boundary layer separation over a backward-facing step p 1230 A93-54588

Vibration excitation in laminar hypersonic boundary layers p 1237 A93-56028

Overview of supersonic laminar flow control research on the F-16XL ships 1 and 2
[NASA-TM-104257] p 20 N93-11221

The hemisphere-cylinder at an angle of attack p 21 N93-11250

Laminar boundary-layer breakdown
[AD-A254489] p 90 N93-12162

Application of a solution adaptive grid to flow over an embedded cavity p 130 N93-13141

BLSTA: A boundary layer code for stability analysis
[NASA-CR-4481] p 220 N93-14797

Analysis and evaluation of an integrated laminar flow control propulsion system
[NASA-CR-192162] p 551 N93-20268

Swept wing attachment line contamination fence
[NASA-CASE-LAR-13400-1] p 485 N93-22015

High-lift aerodynamics: Prospects and plans p 784 N93-27442

Keynote address: Unsteady, multimode transition in gas turbine engines p 901 N93-29927

Measurement of turbulent spots and intermittency modelling at gas-turbine conditions p 902 N93-29934

Effects of an aft facing step on the surface of a laminar flow glider wing
[NASA-CR-193302] p 990 N93-31855

LAMINAR FLOW

Boundary layer separation in a corner formed by two planes p 6 A93-10188

An effective multigrid method for high-speed flows p 6 A93-10533

Measurement of attachment-line location in a wind-tunnel and in supersonic flight
[AIAA PAPER 92-4089] p 39 A93-11285

Numerical dissipation in F3D thin-layer Navier-Stokes solution for flows with wall transpiration p 9 A93-12010

Computation of laminar flow and heat transfer over an enclosed rotating disk with and without jet impingement p 201 A93-13982

Cobra maneuver considerations p 182 A93-14306

In-flight detection of flow separation, stagnation, and transition p 166 A93-14326

Application of laminar flow to aero engine nacelles p 128 A93-17256

Scramjet fuel-air mixing establishment in a pulse facility p 359 A93-21667

What makes the Cobra maneuver possible?
[AIAA PAPER 93-0183] p 367 A93-22609

Unsteady laminar separation on low-Reynolds-number airfoils
[AIAA PAPER 93-0209] p 278 A93-22627

Streamwise vortex meander in a plane mixing layer
[AIAA PAPER 93-0553] p 285 A93-23292

A Navier-Stokes simulation of vortex shedding from square cylinder in unconfined domain p 538 A93-24084

An upwind formulation for the solution of thin-layer Navier-Stokes equations p 461 A93-24088

Three-dimensional flow simulation over axisymmetric bodies using Navier-Stokes equations at hypersonic Mach numbers p 461 A93-24090

The asymptotic theory of hypersonic boundary-layer stability p 462 A93-24409

L**L-1011 AIRCRAFT**

Vertical guidance for a Lockheed L1011-100 using optimal dynamic interpolation p 369 A93-22884

Artificial viscosity models for the Navier-Stokes equations and their effect in drag prediction [AIAA PAPER 93-0193] p 473 A93-25511

Induced Mach wave-flame interactions in laminar supersonic fuel jets p 475 A93-26183

Recent developments in international laminar flow research programs for transport aircraft [ONERA, TP NO. 1992-163] p 457 A93-26878

Laminar-flow instrumentation for wind-tunnel and flight experiments p 479 A93-28605

Goertler instability and hypersonic quiet nozzle design p 480 A93-29155

The numerical calculation and application of compressible boundary layers on laminar-flow-control and natural-laminar-flow wings p 680 A93-33727

Numerical methods in laminar and turbulent flow; Proceedings of the 7th International Conference, Stanford Univ., CA, July 15-19, 1991. Vol. 7, pts. 1 & 2 [ISBN 0-906674-77-8] p 743 A93-34301

Calculation of compressible boundary layers by a hybrid finite element method p 692 A93-35613

A data system for the observation of flow conditions on an aircraft wing p 808 A93-37882

An implicit finite-difference algorithm for the numerical simulation of supersonic flow over blunt bodies p 770 A93-38325

Supersonic vortical flows around an ogive-cylinder - Laminar and turbulent computations [ONERA, TP NO. 1992-111] p 771 A93-38588

Natural laminar flow and laminar flow control [ISBN 0-387-97737-6] p 859 A93-41776

Laminar flow control - Introduction and overview p 859 A93-41777

Laminar flow flight experiments - A review p 890 A93-41778

Flight research on natural laminar flow applications p 890 A93-41779

Subsonic natural-laminar-flow airfoils p 860 A93-41780

Accuracy of flux-split algorithms in high-speed viscous flows p 860 A93-41912

Viscous, 2-D, laminar hypersonic flows over compression ramps p 866 A93-42591

The application of an adaptive upwind unstructured grid solution algorithm to the simulation of compressible laminar viscous flows over compression corners p 866 A93-42594

Grid-refinement study of hypersonic laminar flow over a 2-D ramp p 866 A93-42597

Implicit upwind finite-difference simulation of laminar hypersonic flow over a 2D ramp p 867 A93-42600

Numerical simulation of laminar hypersonic flow past a double-ellipsoid p 868 A93-42612

Attempt to evaluate the computations for test case 6.1 - Cold hypersonic flow past ellipsoidal shapes p 869 A93-42620

Evaluation of contributions for test case 7.1.1 and 7.1.2 p 870 A93-42636

An upwind multigrid algorithm for calculating flows on unstructured grids p 957 A93-45088

Active flow control with neural networks [AIAA PAPER 93-3273] p 1037 A93-46834

Vorticity dynamics in spatially developing rectangular jets [AIAA PAPER 93-3286] p 969 A93-46842

Method of characteristics for computing three-dimensional boundary layers p 970 A93-46886

Scaling of incipient separation in high speed laminar flows [AIAA PAPER 93-3435] p 978 A93-47227

Development of an innovative natural laminar flow wing concept for high-speed civil transports [AIAA PAPER 93-3466] p 980 A93-47247

Application of natural laminar flow to a supersonic transport concept [AIAA PAPER 93-3467] p 997 A93-47248

Instability of hypersonic flow past blunt cones - Effects of mean flow variations [AIAA PAPER 93-2983] p 1051 A93-48176

A laminar flow rotor for a radial inflow turbine [AIAA PAPER 93-1796] p 1074 A93-49686

High Reynolds number and turbulence effects on aerodynamics and heat transfer in a turbine cascade [AIAA PAPER 93-2252] p 1155 A93-50050

Multigrid Navier-Stokes calculations for three-dimensional cascades p 1177 A93-53209

3D laminar and 2D turbulent computations with the Navier-Stokes solver FLU3M [ONERA, TP NO. 1993-105] p 1180 A93-53618

Reynolds number dependence of the drag coefficient for laminar flow through fine-scale photetched screens p 1218 A93-53815

A finite element code for gas turbine combustor flow with Stretched Laminar Flamelet modelling [ISABE 93-7127] p 1204 A93-54102

Supersonic and hypersonic flow computations for the research configuration ELAC I and comparison to experimental data p 1237 A93-56034

Application of laminar flow to aero engine nacelles [PNR-90916] p 20 N93-11020

A combined experimental and theoretical study of laminar flow control with particular relevance to aero engine nacelles [PNR-90991] p 20 N93-11070

A European collaborative NLF nacelle flight demonstrator [PNR-90992] p 20 N93-11113

Overview of supersonic laminar flow control research on the F-16XL ships 1 and 2 [NASA-TM-104257] p 20 N93-11221

Experimental investigation of the effects of aft blowing with various nozzle exit geometries on a 3.0 caliber tangent ogive at high angles of attack: Forebody pressure distributions [NASA-CR-190935] p 22 N93-11605

Boundary layer relaminarization device [NASA-CASE-LAR-14470-1] p 23 N93-11876

Finite-difference solution for laminar or turbulent boundary layer flow over axisymmetric bodies with ideal gas, CF₄, or equilibrium air chemistry [NASA-TP-3271] p 222 N93-15434

Digital data acquisition and preliminary instrumentation study for the F-16 laminar flow control vehicle p 292 N93-16784

Design optimization of natural laminar flow bodies in compressible flow [NASA-CR-4478] p 292 N93-16940

Modeling the transition region [NASA-CR-4492] p 298 N93-19015

Natural laminar flow test in-flight visualization p 482 N93-19921

Combined LAURA-UPS hypersonic solution procedure [NASA-TM-107682] p 747 N93-25176

Stationary crossflow instability on an infinite swept wing p 699 N93-25865

Increased heat transfer to elliptical leading edges due to spanwise variations in the freestream momentum: Numerical and experimental results [NASA-TM-106150] p 838 N93-27020

The generation of side force by distributed suction [NASA-CR-193129] p 839 N93-27151

The remarkable ability of turbulence model equations to describe transition p 783 N93-27432

Investigation of forced unsteady separated flows using velocity-vorticity form of Navier-Stokes equations p 840 N93-27451

Studies of origin of three-dimensionality in laminar wakes [AD-A262281] p 841 N93-28242

High Reynolds number and turbulence effects on aerodynamics and heat transfer in a turbine cascade [NASA-TM-106187] p 930 N93-29157

Flow visualization on helicopter blades using acenaphthen [ESA-TT-1255] p 931 N93-29273

Effects of buoyancy on gas jet diffusion flames [NASA-CR-191109] p 935 N93-31031

Effects of an aft facing step on the surface of a laminar flow glider wing [NASA-CR-193302] p 990 N93-31855

Selected experiments in laminar flow: An annotated bibliography [NASA-TM-103989] p 990 N93-32226

LAMINAR FLOW AIRFOILS

Laminar flow research in the 1940-1950s - A personal recollection p 235 A93-17271

An approximately factored incremental strategy for calculating consistent discrete aerodynamic sensitivity derivatives [AIAA PAPER 92-4746] p 265 A93-20344

Dornier 228 experimental with laminar wing p 506 A93-27500

Vortex generators used to control laminar separation bubbles p 768 A93-37381

An overview of recent subsonic laminar flow control flight experiments [AIAA PAPER 93-2987] p 1052 A93-48180

Natural laminar flow test in-flight visualization p 482 N93-19921

LAMINAR HEAT TRANSFER

The effects of incident turbulence and moving wakes on laminar heat transfer in gas turbines [ASME PAPER 92-GT-377] p 406 A93-19535

Plume effects on the flow around a blunt cone at hypersonic speeds p 787 N93-27460

LAMINAR WAKES

Spreadsheet microcomputer numerical method for the compressible laminar wake flow p 684 A93-34308

Calculation of laminar and turbulent asymmetric wakes p 684 A93-34318

Studies of origin of three-dimensionality in laminar wakes [AD-A262281] p 841 N93-28242

LAMINATES

Nonlinear deformation mechanics of multilayer transparency elements - General theory relations p 79 A93-12800

Fatigue qualification of high thickness composite rotor components p 81 A93-13646

Fundamentals of composite repair [SME PAPER EM92-100] p 196 A93-14101

Post buckling of laminated composite stiffened curved panels subjected to cyclic shear and compression p 204 A93-14334

Contact analysis for riveted and bolted joints of composite laminates p 204 A93-14384

Stiffness design method of symmetric laminates using lamination parameters p 206 A93-14569

Fourier analysis of clamped moderately thick arbitrarily laminated plates p 206 A93-14571

Tailoring concepts for improved structural performance of rotorcraft flexbeams p 207 A93-14811

Propagation of transverse anti-plane waves in orthotropic layers p 412 A93-21878

Model multilayer structured composites p 533 A93-24509

The vibration and flutter of composite material laminate p 543 A93-26617

Global/local interlaminar stress analysis of a grid-stiffened composite panel p 548 A93-28543

Thermomechanical postbuckling analysis of laminated composite shells [AIAA PAPER 93-1337] p 738 A93-33907

Response of laminated composite plates to low-speed impact by airgun-propelled and dropped-weight impactors [AIAA PAPER 93-1402] p 739 A93-33962

Analysis of interlaminar stresses in symmetric and unsymmetric laminates under various loadings [AIAA PAPER 93-1511] p 740 A93-34050

A refined structural model of composite aircraft wings for the enhancement of vibrational and aeroelastic response characteristics [AIAA PAPER 93-1536] p 740 A93-34073

Dynamic analysis of rotor flexbeams based on nonlinear anisotropic shell models p 743 A93-34261

Aeromechanical stability of helicopters with composite rotor blades in forward flight p 794 A93-35904

Evaluation of the fatigue behavior of discontinuous and continuous fiber thermoplastic composite laminates p 824 A93-36005

Nonlinear analysis of composite thin-walled helicopter blades p 827 A93-36006

Shape sensitivities and approximations of modal response of laminated skew plates p 829 A93-37403

A two-dimensional analysis of multiple matrix cracking in a laminated composite close to its characteristic damage state p 1157 A93-50405

Nonlinear deformation mechanics of multilayer transparency elements - Some calculation results -- for aircraft portholes p 1191 A93-52937

Flutter analysis of stiffened laminated composite plates and shells in supersonic flow p 1216 A93-53224

Enhancement of conventional NDT methods for corrosion detection in layered skins p 1258 A93-54898

Effect of boundary conditions and panel geometry on the response of laminated panels subjected to transverse pressure loads p 1259 A93-55674

Probabilistic evaluation of fuselage-type composite structures [NASA-TM-105881] p 212 N93-12735

Determination of stresses on laminated aircraft transparencies by the strain gage-hole drilling and sectioning method [AD-A255548] p 164 A93-14571

Stress calculations on the window section of an all-composite aircraft fuselage [LR-688] p 328 N93-16215

Relationship between mechanical-property and energy-absorption trends for composite tubes [NASA-TP-3284] p 392 N93-16537

A90 project: Design of a composite fin [ETN-92-92773] p 329 N93-16562

Interlaminar stress analysis at the skin/stiffener interface of a grid-stiffened composite panel [NASA-CR-192177] p 393 N93-17920

Damage detection by Acousto-Ultrasonic Location (AUL) p 555 A93-21529

Design and analysis of curved composite components for rotorcraft fuselage frames p 716 N93-25701

Structural tailoring of aircraft engine blade subject to ice impact constraints [NASA-TM-106033] p 838 N93-26999

Probabilistic assessment of composite structures [NASA-TM-106024] p 825 N93-27092

- First NASA Advanced Composites Technology Conference, part 2
[NASA-CP-3104-PT-2] p 921 A93-30841
- Effects of intra- and inter-laminar resin content on the mechanical properties of toughened composite materials p 921 A93-30845
- Developments in impact damage modeling for laminated composite structures p 922 A93-30857
- Advanced fiber placement of composite fuselage structures p 923 A93-30864
- LAND ICE**
- Application of new GPS aircraft control/display system to topographic mapping of the Greenland ice cap p 499 A93-28152
- LAND MOBILE SATELLITE SERVICE**
- LOCSTAR - A satellite radiodetermination system for Europe p 150 A93-15037
- LAND SURFACE TEMPERATURE**
- Variability of geophysical parameters from aircraft radiance measurements for FIFE p 426 A93-20622
- LAND USE**
- Control of land use near airports is best means of reducing impact of aircraft noise p 571 A93-29575
- Land subsidence and problems affecting land use at Edwards Air Force Base and vicinity, California, 1990 [PB93-182236] p 1036 A93-32191
- LANDAU-GINZBURG EQUATIONS**
- The onset of vortex turbulence p 788 A93-28251
- LANDING**
- Navier-Stokes computations and experimental comparisons for multielement airfoil configurations [AIAA PAPER 93-0645] p 464 A93-24760
- A study of the problem of developing a weakly invariant flight vehicle control system p 561 A93-27688
- Example of statistical techniques applied to analysis of landing ground roll distance measurements (linear regression, correlation coefficient and F-test) [ESDU-92021] p 330 A93-16635
- LANDING AIDS**
- Integration of flight control and carrier landing aid system [ONERA, TP NO. 1993-6] p 181 A93-14187
- Development of laser conducting landing system p 150 A93-14320
- Fixed and rotary wing all weather operations system requirements p 142 A93-17303
- Landing guidance systems for CAT III operations p 151 A93-17307
- A history of visual approach guidance indicator systems in Australia p 498 A93-25171
- A study of the problem of developing a weakly invariant flight vehicle control system p 561 A93-27688
- Facilities and capabilities catalog for landing and escape systems [NASA-RP-1282] p 196 A93-14495
- LANDING GEAR**
- Test and analysis of an advanced technology landing gear p 37 A93-10917
- Wheel shimmy analysis for main landing gear of aircraft p 41 A93-11809
- Loads at the nose landing gears of civil transport aircraft during towbarless towing operations p 45 A93-13629
- Integrated utilities management system for aircraft p 153 A93-14208
- The simulation of aircraft landing gear dynamics p 155 A93-14318
- Some dynamic problems in design of aircraft landing gear p 155 A93-14321
- A methodological approach to the development of service and technical specifications for an actively controlled multistrut landing gear p 321 A93-18349
- Expanding the operation scope of aircraft through the use of air-cushion landing gear p 321 A93-18354
- Scanning Laser Aircraft Surveillance System for carrier flight operations p 500 A93-28157
- Transmission error and load distribution analysis of spur and double helical gear pairs used in a split path helicopter transmission design p 549 A93-29426
- Determination of tire-wheel interface pressure distribution for aircraft wheels [AIAA PAPER 93-1343] p 709 A93-33913
- The development of a crashworthy composite fuselage and landing gear p 799 A93-36001
- A nonlinear analysis methodology for the design of skid landing gears p 799 A93-36004
- The investigation of limit cycle amplitude of nonlinear nose gear p 800 A93-36342
- Some aspects of the design of combination landing gear --- for stable aircraft motion on runways p 891 A93-42374
- Computerized synthesis of three-dimensional kinematic landing gear schemes with a single turning axis p 891 A93-42376
- Dependence of the service life of a wing on its strength uniformity and landing gear location p 891 A93-42377

- Electrorheologically controlled landing gear p 1021 A93-44851
- Determination of the vertical velocity component of aircraft landing on an airfield with a longitudinally sloping runway p 1007 A93-45664
- Operating an aircraft during the landing on an airfield with a substantial longitudinal macroslope of the runway p 1008 A93-45667
- Beyond steel - TMCs for lighter landing gear p 1100 A93-49337
- Crashworthy landing gear design [SAE AIR 4566] p 1103 A93-52175
- A study of damage tolerance of the landing gear structure p 1219 A93-53881
- NASA Langley's Aircraft Landing Dynamics Facility p 1250 A93-54400
- Optimization of oleo-pneumatic shock absorber of aircraft p 1243 A93-55415
- Fatigue crack growth in AerMet 100 steel [AD-A249068] p 74 A93-12248
- Reanalysis of multiple-wheel landing gear traffic tests [AD-A256593] p 194 A93-14238
- Stress corrosion susceptibility of ultra-high strength steels for Naval aircraft applications [AD-A256126] p 199 A93-15189
- Aircraft landing gear shimmy p 340 A93-19029
- Testing a wheeled landing gear system for the TH-57 helicopter [AD-A262152] p 806 A93-27547
- LANDING INSTRUMENTS**
- Differential GPS/inertial navigation approach/landing flight test results p 32 A93-11019
- Airborne MLS equipment p 312 A93-18555
- Synthetic vision - A view in the fog p 792 A93-37068
- A vision-based method for autonomous landing p 1190 A93-53172
- Manual flying of curved precision approaches to landing with electromechanical instrumentation. A piloted simulation study [NASA-TP-3255] p 344 A93-18408
- LANDING RADAR**
- SIR technology helps ensure safe landings for NASA --- Subsurface Interface Radar p 384 A93-21765
- LANDING SIMULATION**
- The simulation of aircraft landing gear dynamics p 155 A93-14318
- Manual flying of curved precision approaches to landing with electromechanical instrumentation. A piloted simulation study [NASA-TP-3255] p 344 A93-18408
- LANDING SITES**
- In situ material characterization for pavement evaluation by the Spectral-Analysis-of-Surface-Waves (SASW) method [AD-A255660] p 194 A93-14128
- LANDING SPEED**
- Energy method for analysis of measured airspeed change in landing airborne manoeuvre [ESDU-92020] p 335 A93-18042
- LANDSAT SATELLITES**
- National Aeronautics and Space Administration p 454 A93-17091
- LAP JOINTS**
- Comparison of heating protocols for detection of disbonds in lap joints p 396 A93-18627
- Assessment of aircraft structural integrity by detecting disbonds through ultrasonic scanning p 406 A93-19587
- Ultrasonic NDE of adhesive and sealant bonded aluminum lap-splices p 407 A93-19595
- Automation of disbond detection in aircraft fuselage through thermal image processing p 407 A93-19598
- Crack growth and repair of multi-site damage of fuselage lap joints p 547 A93-28291
- Bonded repair of multi-site damage p 947 A93-45786
- Applications of advanced fracture mechanics to fuselage p 1026 A93-45787
- A laboratory study of fracture in the presence of lap splice multiple site damage p 1027 A93-45790
- Test facility for evaluation of structural integrity of stiffened and jointed aircraft curved panels p 1012 A93-45794
- Estimation of requirements of inspection intervals for panels susceptible to Multiple Site Damage p 948 A93-45795
- Damage tolerance assessment of boron/epoxy repairs to fuselage lap joints [AD-A258383] p 338 A93-18257
- Investigation of corrosion in aluminum/adhesive lap-splices using pulse-echo ultrasonic techniques [DE93-008074] p 749 A93-25518

LAPLACE EQUATION

- ISAC - A tool for aeroservoelastic modeling and analysis --- Interaction of Structures, Aerodynamics, and Control [AIAA PAPER 93-1421] p 726 A93-33974
- A Laplace interaction law for the computation of viscous airfoil flow in low and high speed aerodynamics [AIAA PAPER 93-3462] p 979 A93-47244

LAPLACE TRANSFORMATION

- Calculation of the passive noise power for onboard single-pulse automatic direction tracking systems p 882 A93-43111

LAPSE RATE

- Matching engine and aircraft lapse rates for the HSCT [AIAA PAPER 93-1809] p 1100 A93-49698

LARGE SPACE STRUCTURES

- Technical needs and research opportunities provided by projected aeronautical and space systems [NASA-CR-192124] p 386 A93-16629

LASER ALTIMETERS

- Mapping new and old worlds with laser altimetry p 1034 A93-45699

LASER ANEMOMETERS

- Experimental and computational investigation of the NASA Low-Speed Centrifugal Compressor flow field [ASME PAPER 92-GT-213] p 252 A93-19436
- Seeding materials for use in laser anemometry [AIAA PAPER 93-0006] p 389 A93-20129
- Application of particle image velocimetry in high-speed separated flows p 549 A93-29304
- Experimental analysis of turbine rotor flow at design and off-design conditions [ISABE 93-7092] p 1186 A93-54068
- Experimental study of the flow field inside a whirling annular seal p 85 A93-10892
- The jet behaviour of an actual high-bypass engine as determined by LDA-measurements in ground tests p 175 A93-13218

LASER APPLICATIONS

- Video holography and laser vibrometry...The dynamic duo p 210 A93-18611
- Applications of laser techniques in fluid mechanics p 395 A93-17765
- Autonomous mobile laser complex p 395 A93-17767
- Fiber optic-based laser vapor screen flow visualization systems for aerodynamic research in larger-scale subsonic and transonic wind tunnels p 408 A93-20298
- Liquid water content measurements using the Phase Doppler Particle Analyzer in the NASA Lewis Icing Research Tunnel [AIAA PAPER 93-0298] p 378 A93-23698
- A study of the rotor wake of a small-scale rotor model in forward flight using laser light sheet flow visualization with comparisons to analytical models p 766 A93-35957

- Method of remotely characterizing thermal properties of a sample [NASA-CASE-LAR-13508-3-CU] p 67 A93-11057

- Research support for the Laboratory for Lightwave Technology [AD-A261488] p 760 A93-26343

- Uplink laser propagation measurements through the sea surface, haze and clouds [AD-A264687] p 935 A93-30553

LASER ARRAYS

- Diffraction limited collimating optics for high aspect ratio laser diode arrays p 1172 A93-48411
- Integrated optoelectronics for communication and processing: Proceedings of the Meeting, Boston, MA, Sept. 3, 4, 1991 [SPIE-1582] p 1158 A93-51250

LASER BEAMS

- Shedding new light on gas dynamics p 80 A93-13435
- Development of laser conducting landing system p 150 A93-14320
- Misalignments of airborne laser beams due to mechanical vibrations p 394 A93-17762
- Laser Centerline Localizer and Laser Glideslope Indicator for visual guidance on approach to landing p 500 A93-28156
- Scanning Laser Aircraft Surveillance System for carrier flight operations p 500 A93-28157
- Diffraction limited collimating optics for high aspect ratio laser diode arrays p 1172 A93-48411
- Supersonic flow past energy release regions p 1069 A93-48973

LASER CAVITIES

- Surface emitting lasers for avionics applications p 1259 A93-55756

LASER CUTTING

- Effect of the proximity of the machined surface on the discharge coefficients of laser cutter nozzles p 79 A93-12809
- Case studies - Applications of laser systems for cutting and welding aerospace parts p 1217 A93-53498

LASER DOPPLER VELOCIMETERS

- Experimental and theoretical studies of helicopter rotor-fuselage interaction
[ONERA, TP NO. 1992-142] p 120 A93-14356
- Optical microphone for the detection of hidden helicopters p 205 A93-14542
- Measurement of a one-dimensional mobility using a laser-Doppler velocimeter p 210 A93-16647
- Detection and parameter estimation of atmospheric turbulence by ground-based and airborne CO₂ Doppler lidars p 395 A93-17862
- Experimental and theoretical investigation of a research atomizer/combustion chamber configuration
[ASME PAPER 92-GT-137] p 401 A93-19369
- Three component LDV velocity measurements in a can type research combustor for CFD validation. I - Isothermal
[ASME PAPER 92-GT-138] p 350 A93-19370
- Measurement of the three-dimensional tip region flowfield in an axial compressor p 252 A93-19434
- Seeding materials for use in laser anemometry
[AIAA PAPER 93-0006] p 389 A93-20129
- Flow measurements behind V-gutter under non-combusting condition p 408 A93-20139
- Quantitative laser velocimetry measurements in the hypersonic regime by the integration of experimental and computational analysis
[AIAA PAPER 93-0089] p 263 A93-20195
- 3-D LDV measurements over a delta wing in pitch-up motion p 275 A93-22610
- Experimental studies of the turbulent structure of supersonic mixing layers
[AIAA PAPER 93-0217] p 278 A93-22633
- LDV flowfield measurements on a straight and swept wing with a simulated ice accretion p 280 A93-23001
- Doppler global velocimetry measurements of the vortical flow above an F/A-18 p 415 A93-23333
- A Laser Doppler Anemometry study of a supersonic jet in a low speed cross-flow p 459 A93-23807
- Experimental investigation of a 2D parallel vortex/airfoil interaction p 538 A93-23808
- Time-dependent 3-component laser-Doppler-anemometer and simultaneous position measurements in the flow of an aircraft engine p 538 A93-23809
- Seed particle response and size characterization in high speed flows p 459 A93-23811
- Doppler global velocimetry - The next generation? p 539 A93-24486
- Helicopter plume detection by using an ultranarrow-band noncoherent laser Doppler velocimeter p 542 A93-25198
- Interaction of a streamwise vortex with a free surface
[AIAA PAPER 93-0556] p 543 A93-25539
- Recent developments in rotor wake modeling for helicopter noise prediction p 481 A93-29437
- Inlet turbulence distortion and viscous flow development in a controlled-diffusion compressor cascade at very high incidence p 688 A93-34485
- Velocity vector LDA measurement inside a pitched blade impeller p 924 A93-40390
- Experimental investigation of leading edge vortices using LDA p 861 A93-42254
- A three dimensional view of velocity using lasers p 1028 A93-46822
- The hemisphere-cylinder in dynamic pitch-up motions
[AIAA PAPER 93-2963] p 1048 A93-48157
- Experimental study of 3-D separation on a large scale model
[AIAA PAPER 93-3007] p 1053 A93-48197
- Swirling flows in a contoured-wall combustion chamber
[AIAA PAPER 93-1765] p 1073 A93-49661
- Three-dimensional flow field in a turbine nozzle passage p 1084 A93-50278
- Isothermal flow characteristics behind V-shape gutter with and without injection
[ISABE 93-7040] p 1198 A93-54016
- Large eddy simulation of turbulent combustion behind flame holders
[ISABE 93-7042] p 1198 A93-54018
- Low-speed aerodynamics of the hypersonic research configuration ELAC I p 1237 A93-56035
- On the analysis of an impinging jet on ground effects p 1260 A93-56339
- LV software for supersonic flow analysis
[NASA-CR-190911] p 16 N93-10069
- LDV Measurements of unsteady flow fields in radial turbine
[AD-A253592] p 19 N93-10648

- Experimental study of the flow field inside a whirling annular seal p 85 N93-10892
- An experimental study of flow patterns and endwall heat transfer upstream of a surface-mounted rectangular obstruction in a turbulent boundary layer p 89 N93-11698
- The jet behaviour of an actual high-bypass engine as determined by LDA-measurements in ground tests p 175 N93-13218
- Airfoil-vortex interaction and the wake of an oscillating airfoil p 134 N93-13803
- Wind tunnel seeding particles for laser velocimeter p 292 N93-16770
- An experimental study of a turbulent boundary layer in the trailing edge region of a circulation-control airfoil
[NASA-CR-191262] p 295 N93-17934
- An investigation of laser velocimetry measurements within high speed, complex flows p 748 N93-25237
- Trailing vortex/free-surface interaction
[AD-A261654] p 701 N93-26195
- Three-dimensional fiber-optic LDV measurements in the endwall region of a linear cascade of controlled-diffusion stator blades p 933 N93-29968
- Multiparticle imaging technique for two-phase fluid flows using pulsed laser speckle velocimetry
[DE93-011734] p 935 N93-30489
- LASER DRILLING**
Laser and skill enhance results p 1257 A93-54843
- The aerodynamic performance of laser drilled sheets
[AERO-REPT-9204] p 484 N93-20806
- LASER GUIDANCE**
Laser Centerline Localizer and Laser Glideslope Indicator for visual guidance on approach to landing p 500 A93-28156
- LASER GYROSCOPES**
The ring laser gyro and its applications p 927 A93-42657
- LASER INDUCED FLUORESCENCE**
Progress in laser spectroscopic techniques for aerodynamic measurements - An overview p 549 A93-29308
- Laser selection criteria for OH fluorescence measurements in supersonic combustion test facilities p 549 A93-29315
- A laser induced fluorescence system for the high enthalpy shock tunnel (HEG) in Goettingen p 1024 A93-45506
- Absolute intensity measurements of impurity emissions in a shock tunnel and their consequences for laser-induced fluorescence experiments p 1147 A93-48044
- Comparison of NO and OH PLIF temperature measurements in a scramjet model flowfield
[AIAA PAPER 93-2035] p 1113 A93-49870
- An aircraft instrument design for in situ tropospheric OH measurements by laser induced fluorescence at low pressures p 1159 A93-51528
- LIF visualization of 3-dimensional hypersonic mixing
[ISABE 93-7114] p 1221 A93-54089
- Planar measurement of flow field parameters in nonreacting supersonic flows with laser-induced iodine fluorescence p 133 N93-13801
- Visualization of a Mach 2 reacting flow using Planar Laser-Induced Fluorescence (PLIF) p 731 N93-26006
- Simultaneous mapping of the unsteady flow fields by Particle Displacement Velocimetry (PDV) p 786 N93-27454
- LASER INTERFEROMETRY**
Laser holographic interferometric measurements of the flow behind a rearward facing step
[AIAA PAPER 93-3515] p 985 A93-47279
- Laser Interferometer Skin-Friction measurements of crossing-shock wave/turbulent boundary-layer interactions
[AIAA PAPER 93-3072] p 1148 A93-48247
- A study of optical distortions arising in radiation transmission through cavities with gas flow around them p 1225 A93-52945
- Study of optical techniques for the Ames unitary wind tunnel: Digital image processing, part 6
[NASA-CR-192164] p 382 N93-18766
- LASER OUTPUTS**
Surface emitting lasers for avionics applications p 1259 A93-55756
- Uplink laser propagation measurements through the sea surface, haze and clouds
[AD-A264687] p 935 N93-30553
- LASER PROPULSION**
Experimental investigation of an axisymmetric hypersonic scramjet inlet for laser propulsion p 122 A93-14515
- LASER RANGER/TRACKER**
Ground- and satellite-derived flight-path measurements as demonstrated in the AFES Avionics Flight Evaluation System (AFES) p 993 N93-31281

LASER SPECTROMETERS

- Remote sensing of O₂ in a supersonic combustor using diode lasers and fiber optics
[AIAA PAPER 92-5090] p 414 A93-22360

LASER SPECTROSCOPY

- Shedding new light on gas dynamics p 80 A93-13435
- Progress in laser spectroscopic techniques for aerodynamic measurements - An overview p 549 A93-29308

CARS studies in hypersonic flows

- [AIAA PAPER 93-3047] p 1144 A93-48227

LASER TARGET INTERACTIONS

- Shedding new light on gas dynamics p 80 A93-13435

LASER WELDING

- Case studies - Applications of laser systems for cutting and welding aerospace parts p 1217 A93-53498

LASER WINDOWS

- Compound curvature laser window development
[AIAA PAPER 93-2177] p 1173 A93-49989

LATENT HEAT

- Spatial and temporal variations of the fluxes of carbon dioxide and sensible and latent heat over the FIFE site p 425 A93-20586
- A passive infrared ice detection technique for helicopter applications
[NASA-CR-193187] p 880 N93-29152
- Surface shear stress estimates from geostrophic winds for use in sensible and latent heat flux formulations p 936 N93-30044

LATERAL CONTROL

- Computational investigation of a pneumatic forebody flow control concept p 768 A93-37383
- Actuated forebody strake controls for the F-18 high alpha research vehicle
[AIAA PAPER 93-3675] p 1006 A93-44233
- Tangential Forebody Blowing-yaw control at high alpha
[AIAA PAPER 93-3406] p 1008 A93-47205
- Side-force control on a forebody of diamond cross-section at high angles of attack
[AIAA PAPER 93-3407] p 1008 A93-47206
- The benefits of Maglev technology
[AIAA PAPER 93-2949] p 1174 A93-48145
- Lateral control at high angles of attack using pneumatic blowing through a chined forebody
[AIAA PAPER 93-3624] p 1126 A93-48309
- Development of lateral-directional departure criteria
[AIAA PAPER 93-3650] p 1128 A93-48333
- F/A-18 departure recovery improvement evaluation
[AIAA PAPER 93-3671] p 1129 A93-48349
- Investigation of high-alpha lateral-directional control power requirements for high-performance aircraft
[AIAA PAPER 93-3647] p 1130 A93-49519
- Cancellation control law for lateral-directional dynamics of a supermaneuverable aircraft
[AIAA PAPER 93-3775] p 1131 A93-51370
- Longitudinal and lateral-directional flying qualities investigation of high-order characteristics for advanced-technology transports
[AIAA PAPER 93-3815] p 1133 A93-51406
- A method for the spectral-time identification of the longitudinal and lateral motions of an aircraft p 1205 A93-52942
- Optimal output feedback vibration control of rotor-bearing systems p 86 N93-11220
- Low bandwidth robust controllers for flight
[NASA-CR-193085] p 819 N93-27156
- Experiments in the control of wing rock at high angle of attack using tangential leading edge blowing p 1009 N93-31068

LATERAL OSCILLATION

- Further analysis of high-rate rolling experiments of a 65 deg delta wing p 523 A93-24737
- The investigation of limit cycle amplitude of nonlinear nose gear p 800 A93-36342

LATERAL STABILITY

- Lateral aerodynamics characteristics of forebodies at high angle of attack in subsonic and transonic flows p 118 A93-14302
- Calculation of transonic longitudinal and lateral-directional characteristics of aircraft by the small disturbance theory
[AIAA PAPER 93-3617] p 1125 A93-48304
- Effects of forebody strakes and Mach number on overall aerodynamic characteristics of configuration with 55 deg cropped delta wing
[NASA-TP-3253] p 131 N93-13353
- Hypersonic lateral and directional stability characteristics of aerobassist flight experiment configuration in air and CF4
[NASA-TM-4435] p 875 N93-29166

LATTICES (MATHEMATICS)

- A compilation of the mathematics leading to the doublet lattice method
[AD-A256304] p 136 N93-14441
TDLM: A Transonic Doublet Lattice Method for 3D potential unsteady transonic flow calculation
[DLR-FB-92-25] p 988 N93-31171

LAUNCH VEHICLE CONFIGURATIONS

- Near-term two-stage-to-orbit, fully reusable, horizontal take-off/landing launch vehicle p 1015 A93-45441
Optimal trajectories for hypersonic launch vehicles p 1251 A93-54563

LAUNCH VEHICLES

- Cross channel dependency requirements of the multi-path redundant avionics suite p 928 A93-42782
Takeoff and landing analysis methodology for an airbreathing space booster p 914 A93-42927
Code validation for high speed flow simulation over the VLS launcher fairing — Brazilian satellite launch vehicles [AIAA PAPER 93-3046] p 1057 A93-48226
Investigation of the flowfield over parallel-arranged launch vehicles [AIAA PAPER 93-3060] p 1058 A93-48237
Development of models for predicting the triggering of lightning by launch vehicles p 734 A93-24899

LAUNCHERS

- Analysis and demonstration of a Scramaccelerator system [AIAA PAPER 93-2183] p 1142 A93-49995

LAUNCHING

- The improvement of the static launch method in Japan p 26 A93-11364
Modeling and analysis of the winch launch of a glider p 528 A93-27294

LAW (JURISPRUDENCE)

- Recent developments in aviation case law p 569 A93-23870
The role of the radiologist in the medicolegal procedure after an aviation accident p 853 A93-39701

LAY-UP

- Wet layup materials for repair of bismaleimide composites p 1212 A93-53451
Advanced fiber placement of composite fuselage structures p 923 N93-30864

LAYOUTS

- Optimization of equipment layout in the fuselage of maneuverable aircraft p 891 A93-42370
On the typography of flight-deck documentation [NASA-CR-177605] p 571 N93-19970

LEAD ACID BATTERIES

- High reliability, maintenance-free INS battery development [AD-A264521] p 934 N93-30406

LEADING EDGE FLAPS

- Flight test operations using an F-106B research airplane modified with a wing leading-edge vortex flap [AIAA PAPER 92-4094] p 42 A93-13261
Numerical simulation of dynamic lift enhancement using oscillatory leading edge flaps [AIAA PAPER 93-0186] p 276 A93-22611
Vortex flap flight test operations, a safe approach p 995 A93-45168
Vortex capture by a two-dimensional airfoil with a small oscillating leading-edge flap [AIAA PAPER 93-3266] p 968 A93-46830
Separated flowfield and lift on an airfoil with an oscillating leading-edge flap [AIAA PAPER 93-3422] p 976 A93-47217
A preliminary investigation of the control of separated flow by means of excitation p 1182 A93-53859
Maximum lift of wings with leading-edge devices and trailing-edge flaps deployed [ESDU-92031] p 290 N93-16522
Conical Euler analysis and active roll suppression for unsteady vortical flows about rolling delta wings [NASA-TP-3259] p 701 N93-26134

LEADING EDGE SLATS

- Flowfield measurements about a multi-element airfoil at high Reynolds numbers [AIAA PAPER 93-3137] p 1064 A93-48300
Unsteady aerodynamic behavior of an airfoil with and without a slat p 1093 A93-52007
Effect of underwing frost on transport aircraft takeoff performance [DOT/FAA/CT-TN93/9] p 791 N93-27252

LEADING EDGE SWEEP

- Effect of planform and body on supersonic aerodynamics of multibody configurations [NASA-TP-3212] p 19 N93-10824
Computational parametric study of sidewall-compression scramjet inlet performance at Mach 10 [NASA-TM-4411] p 552 N93-20299

LEADING EDGES

- Shock wave interference on a wing with a partition at hypersonic velocities p 13 A93-12839

- Increasing the lift-drag ratio of wings of small aspect ratio at hypersonic velocities p 13 A93-12933
Practical considerations in waverider applications [AIAA PAPER 92-4247] p 43 A93-13326
Wing rock of lifting systems p 118 A93-14330
Leading edge vortices in a chordwise periodic flow p 119 A93-14333
Influence of high mainstream turbulence on leading edge film cooling heat transfer - Effect of film hole spacing p 207 A93-15068
Subsonic separated flow past slender delta wings p 124 A93-15109
Instability of local separated flows with respect to small-amplitude perturbations p 125 A93-15254
Heat transfer and turbulence in a turbulated blade cooling circuit [ASME PAPER 92-GT-187] p 402 A93-19412
An experimental investigation of convective heat transfer at the leading edge of a gas turbine airfoil [ASME PAPER 92-GT-248] p 405 A93-19457
Investigation of leading edge ice accretion with cyclical pneumatic boot inflation [AIAA PAPER 93-0007] p 306 A93-20130
Active control of wing rock of a delta wing at post-stall using tangential leading edge blowing [AIAA PAPER 93-0056] p 367 A93-20169
The suppression of single-fin buffeting using tangential leading edge blowing on a delta wing p 270 A93-21677
CFD zonal modeling of leading-edge ice effects for a complete aircraft [AIAA PAPER 93-0167] p 275 A93-22601
Improvement of the ONERA 3D icing code, comparison with 3D experimental shapes [AIAA PAPER 93-0169] p 275 A93-22603
Measurements of circulation and vorticity in the leading-edge vortex of a delta wing p 288 A93-23548
Numerical modeling of leading edge separated flow at incompressible speeds p 460 A93-24079
Effect of leading-edge porosity on blade-vortex interaction noise [AIAA PAPER 93-0601] p 563 A93-24727
Application of a flush airdata sensing system to a wing leading edge (LE-FADS) [AIAA PAPER 93-0634] p 516 A93-24750
A simple criterion for vortex breakdown [AIAA PAPER 93-0866] p 469 A93-24928
Numerical experiments on the stability of leading edge boundary layer flow - A two-dimensional linear study p 477 A93-27475
Experiments on a 60 deg delta wing with vortex flaps and vortex plates p 477 A93-27482
Wave resistance of swept wings with supersonic edges p 478 A93-27624
Role of leading-edge vortex flows in prop-fan interaction noise p 565 A93-28614
Transonic flow around the leading edge of a thin airfoil with a parabolic nose p 688 A93-34405
Oblique shock formation in impulsively started wedge flows p 692 A93-35636
Multiblock Navier-Stokes solutions about the F/A-18 wing-LEX-fuselage configuration p 767 A93-37378
Slender wing rock revisited p 768 A93-37386
Interference of an oblique shock with a shock layer on a blunt edge for small Reynolds numbers p 775 A93-39120
Aerodynamics of maneuvering slender wings with leading-edge separation p 778 A93-39401
Control of vortices on a delta wing by leading-edge injection p 860 A93-41906
Experimental investigation of leading edge vortices using LDA p 861 A93-42254
Effects of spatial order of accuracy on the computation of vortical flowfields [AIAA PAPER 93-3371] p 955 A93-45064
Application of leading-edge vortex manipulations to reduce wing rock amplitudes p 1007 A93-45152
Leading-edge transition and relaminarization phenomena on a subsonic high-lift system [AIAA PAPER 93-3140] p 959 A93-45154
Analytical study on plate edge noise (Noise generation from tandemly situated trailing and leading edges) p 1038 A93-45561
Instantaneous topology of the unsteady leading-edge vortex at high angle of attack p 961 A93-45728
Investigation of the radiance from the leading edge of a wing [AIAA PAPER 93-2728] p 1039 A93-46482
A viscous shock-layer analysis of 2-D and axisymmetric flows [AIAA PAPER 93-2751] p 963 A93-46500
Two leading-edge droop modifications for tailoring stall characteristics of a general aviation trainer configuration p 1008 A93-46807

- The effects of forced oscillations on the performance of airfoils [AIAA PAPER 93-3264] p 968 A93-46829
Control of the dynamic-stall vortex over a pitching airfoil by leading-edge suction [AIAA PAPER 93-3267] p 969 A93-46832
The three-dimensional representation of the pressure distribution on wedged delta wings with supersonic leading edges in supersonic-hypersonic flow p 973 A93-46989
Aerodynamic characteristics of a delta wing with a body-hinged leading-edge extension [AIAA PAPER 93-3446] p 978 A93-47233
Boundary layer effects on the flow of a leading edge vortex [AIAA PAPER 93-3463] p 980 A93-47245
Curvature and leading edge sweep back effects on grid fin aerodynamic characteristics [AIAA PAPER 93-3480] p 981 A93-47258
Nonslender waveriders [AIAA PAPER 93-3487] p 982 A93-47261
An experimental study of droop leading edge modifications on high and low aspect ratio wings up to 50 deg angle of attack [AIAA PAPER 93-3496] p 983 A93-47268
Experimental and computational investigations of the flowfield around the F117A [AIAA PAPER 93-3508] p 984 A93-47274
Characteristics of deformable leading edge for high performance helicopter rotor [AIAA PAPER 93-3526] p 986 A93-47285
On numerical solutions of Burnett equations for hypersonic flow past 2-D circular blunt leading edges in continuum transition regime [AIAA PAPER 93-3092] p 1060 A93-48266
Flow physics of critical states for rolling delta wings [AIAA PAPER 93-3683] p 1129 A93-48355
An experimental investigation of endwall flow control in a compressor plane cascade wind tunnel p 1066 A93-48512
Effects of external excitation on the leading-edge separation flowfield p 1071 A93-49198
Stall inception in single stage, high-speed compressors with straight and swept leading edges [AIAA PAPER 93-1870] p 1076 A93-49745
Brush seal low surface speed hard-rub characteristics [AIAA PAPER 93-2534] p 1156 A93-50261
A new technique for analysis of unsteady aerodynamic responses of cascade airfoils with blunt leading edge - Unsteady aerodynamic responses of the cascade in incompressible flow p 1086 A93-51122
Laminarization of the boundary layer on a vibrating wing p 1089 A93-51776
Euler analysis of forebody-strake vortex flows at supersonic speeds p 1094 A93-52429
Unsteady wing surface pressures in the wake of a propeller p 1095 A93-52436
Effect of leading-edge geometry on delta wing unsteady aerodynamics p 1095 A93-52457
Preparation and characterization of continuous fiber reinforced zirconium diboride matrix composites for a leading edge material p 1211 A93-53445
Wet layup materials for repair of bismaleimide composites p 1212 A93-53451
The leading edge vortex of a rotating stall cell [ISABE 93-7009] p 1183 A93-53985
Heat transfer and material temperature conditions in the leading edge area of impingement-cooled turbine vanes [ISABE 93-7076] p 1220 A93-54052
Impingement cooling with film coolant extraction in the airfoil leading edge regions [ISABE 93-7078] p 1220 A93-54054
Experimental investigation of boundary layer transition on a flat plate with C4 leading edge [ISABE 93-7123] p 1222 A93-54098
The effect of outboard leading-edge bluntness of double-delta wing on its aerodynamic characteristics p 1230 A93-54589
Conjugate modeling of high-temperature nosecap and wing leading edge heat pipes p 1259 A93-55465
Pressure measurements at supersonic speeds on the research configuration ELAC I p 1237 A93-56033
Low-speed aerodynamics of the hypersonic research configuration ELAC I p 1237 A93-56035
Hypersonic inlet efficiency revisited p 16 N93-10012
Flow over a leading edge with distributed roughness p 18 N93-10549
The convection speed of the dynamic stall vortex [AD-A247258] p 21 N93-11464
Flight test results from a supercritical mission adaptive wing with smooth variable camber [NASA-TM-4415] p 49 N93-11863
Boundary layer relaminarization device [NASA-CASE-LAR-14470-1] p 23 N93-11876

- An approach to constrained aerodynamic design with application to airfoils
[NASA-TP-3260] p 24 N93-12321
- Thermostructural applications of heat pipes for cooling leading edges of high-speed aerospace vehicles
p 91 N93-12460
- A finite element model for analysis of thermoviscoplastic behavior of hypersonic leading edge structures subject to intense aerothermal heating
p 137 N93-14631
- Computational analysis of hypersonic flows past elliptic-cone waveriders
[NASA-CR-191304] p 138 N93-14767
- BLSTA: A boundary layer code for stability analysis
[NASA-CR-4481] p 220 N93-14797
- Analysis of in-flight structural failures of P-3C wing leading edge segments
[AD-A256212] p 165 N93-15238
- Flowfield study of a close-coupled canard configuration
[AD-A256311] p 139 N93-15245
- Root damage analysis of aircraft engine blade subject to ice impact
[NASA-TM-105779] p 222 N93-15343
- Navier-Stokes calculation of transonic flow past the NTF 65-deg delta wing
p 292 N93-16797
- Two- and three-dimensional blade vortex interactions
[NASA-CR-177567] p 293 N93-16942
- The effect of surface suction near the leading edge of a swept-back wing
[AERO-REPT-9205] p 484 N93-20807
- Swept wing attachment line contamination fence
[NASA-CASE-LAR-13400-1] p 485 N93-22015
- The transient development of vortices over delta wings
p 695 N93-25269
- Numerical simulation of leading-edge receptivity to freestream vorticity
p 696 N93-25388
- Structural tailoring of aircraft engine blade subject to ice impact constraints
[NASA-TM-106033] p 838 N93-26999
- Increased heat transfer to elliptical leading edges due to spanwise variations in the freestream momentum: Numerical and experimental results
[NASA-TM-106150] p 838 N93-27020
- Brush seal low surface speed hard-rub characteristics
[NASA-TM-106169] p 838 N93-27132
- Leading edge vortices in a chordwise periodic flow
p 782 N93-27218
- The experimental study of transition and leading edge contamination of swept wings
[LIB-TRANS-2197] p 782 N93-27274
- Three-dimensional compressible stability-transition calculations using the spatial theory
p 783 N93-27431
- Aerodynamics of a finite wing with simulated ice
p 784 N93-27437
- Discrete-vortex simulation of pulsating flow on a turbulent leading-edge separation bubble
p 787 N93-27457
- Prediction of vortex breakdown on a delta wing
p 787 N93-27459
- Prediction of jet impingement cooling scheme characteristics (airfoil leading edge application)
p 932 N93-29941
- Topology and grid adaption for high-speed flow computations
[NASA-CR-4216] p 934 N93-30375
- Experiments in the control of wing rock at high angle of attack using tangential leading edge blowing
p 1009 N93-31068
- LEAF AREA INDEX**
Assessing spatial and seasonal variations in grasslands with spectral reflectances from a helicopter platform
p 426 N93-20621
- LEAKAGE**
Low leakage fiber metal seals
[ASME PAPER 92-GT-141] p 402 N93-19373
- Brush seal leakage performance with gaseous working fluids at static and low rotor speed conditions
[ASME PAPER 92-GT-304] p 405 N93-19494
- Evaluation of brush seals for limited-life engines
p 411 N93-21665
- Brush seal low surface speed hard-rub characteristics
[AIAA PAPER 93-2534] p 1156 N93-50261
- Interconversion of two kinds of methods for cabin leakage test
p 1192 N93-53874
- Brush seal bristle flexure and hard-rub characteristics
[NASA-TM-105864] p 421 N93-18321
- Inward contaminant leakage tests of the S-Tron Corporation emergency escape breathing device. Phase 1: Tests of the original design. Phase 2: Tests with the redesigned neck seal
[DOT/FAA/AM-92/18] p 704 N93-25205
- Brush seal low surface speed hard-rub characteristics
[NASA-TM-106169] p 838 N93-27132
- Heat transfer and leakage in high-speed rotating stepped labyrinth seals
p 903 N93-29951
- LEAR JET AIRCRAFT**
Joint NASA/USAF Airborne Field Mill Program - Operation and safety considerations during flights of a Lear 28 airplane in adverse weather
[AIAA PAPER 92-4093] p 93 N93-13262
- A rapid prototyping system for inflight simulation using the Calspan Learjet 25
[AIAA PAPER 93-3606] p 1191 N93-52691
- LEARNING**
Total Quality Management in curriculum development
[AIAA PAPER 93-0326] p 454 N93-23018
- A comparison between the impact of noise from aircraft, road traffic and trains on long-term recall and recognition of a text in children aged 12-14 years
p 1163 N93-49552
- LEARNING THEORY**
The analysis of expert performance in the redesign of the en route air traffic control curriculum
p 571 N93-27189
- Control augmentation system (CAS) synthesis via adaptation and learning
[AIAA PAPER 93-3728] p 1170 N93-51328
- LEAST SQUARES METHOD**
Aerodynamic design of axisymmetric hypersonic wind-tunnel nozzles using a least-squares/parabolized Navier-Stokes procedure
p 9 N93-12011
- Unsteady compressible airfoil aerodynamics using an adaptive time-discontinuous GLS finite element method
[AIAA PAPER 93-0339] p 281 N93-23027
- Application of the Galerkin/least-squares formulation to the analysis of hypersonic flows. I - Flow over a two-dimensional ramp
p 866 N93-42593
- Application of the Galerkin/least-squares formulation to the analysis of hypersonic flows. II - Flow past a double ellipse
p 868 N93-42608
- Studies of superresolution range-Doppler imaging
p 928 N93-43344
- Computer program for calculating and fitting thermodynamic functions
[NASA-RP-1271] p 231 N93-12967
- Automatic pulse shaping with the AN/FPN-42 and AN/FPN-44A Loran-C transmitters
[AD-A257860] p 319 N93-18309
- LECTURES**
Index to NASA news releases and speeches, 1991
[NASA-TM-108004] p 104 N93-10815
- Index to NASA news releases and speeches, 1990
[NASA-TM-108003] p 104 N93-10872
- Special publication of National Aerospace Laboratory
[DE93-716176] p 239 N93-15946
- Lanchester: The man
[AERO-REPT-9111] p 456 N93-16464
- LEGAL LIABILITY**
Handling the legal consequences of aviation disasters - Passenger compensation
[ISBN 3-452-22293-4] p 103 N93-11411
- Recent developments in aviation case law
p 569 N93-23870
- Obstacles to increasing airspace - Jumping through environmental law hoops
p 569 N93-23872
- Responsibility and assignment of roles on overlong flights
p 570 N93-24253
- Federal preemption in commercial aviation - Tort litigation under 49 U.S.C. section 1305
p 944 N93-42997
- The Foreign Sovereign Immunities Act of 1976 - Misjoinder, nonjoinder, and collusive joinder
p 944 N93-42998
- No rescue in sight for Warsaw plaintiffs from either courts or legislature - Montreal Protocol 3 drowns in committee
p 945 N93-42999
- Air carriers' liability for passenger injury or death - The Japanese Initiative and Response to the recent EC Consultation Paper
p 1226 N93-52930
- A general framework for analyzing choice-of-law problems in air crash litigation
p 1265 N93-56537
- LEGENDRE FUNCTIONS**
The Generalized Legendre-Clebsch Condition on state/control constrained arcs
[AIAA PAPER 93-3746] p 1170 N93-51342
- LENNARD-JONES POTENTIAL**
Monte Carlo simulation of normal shock wave. Part 1: Lennard-Jones potential
p 300 N93-19279
- LENS DESIGN**
Diffraction limited collimating optics for high aspect ratio laser diode arrays
p 1172 N93-48411
- LENSES**
A preliminary study associated with the experimental measurement of the aero-optic characteristics of hypersonic configurations
[AD-A253792] p 24 N93-12063
- LETHALITY**
Comparison of toxicity rankings of six aircraft cabin polymers by lethality and by incapacitation in rats
p 26 N93-10328
- LEVITATION**
A magnetic suspension system with a large angular range
p 1139 N93-51295
- Forces on a magnet moving past figure-eight coils
[DE93-009965] p 943 N93-29189
- LIAPUNOV FUNCTIONS**
Control design for robust eigenstructure assignment in linear uncertain systems
p 97 N93-13241
- The application of intelligent search strategies to robust flight control for hypersonic vehicles
[AIAA PAPER 93-3732] p 1143 N93-51331
- Control of nonlinear systems under input constraints with applications to flight control
p 729 N93-25353
- LIBRARIES**
Design recovery for software library population
[AD-A259292] p 572 N93-20611
- Summer research program (1992). High School Apprenticeship Program (HSAP) reports. Volume 16: Arnold Engineering Development Center Civil Engineering Laboratory
[AD-A262024] p 945 N93-29396
- LIFE (DURABILITY)**
Stirling engine - Available tools for long-life assessment --- for space propulsion
p 195 N93-13824
- A hot dynamic seal rig for measuring hypersonic engine seal durability and flow performance
[AIAA PAPER 93-1346] p 738 N93-33916
- Risk analysis for aging aircraft fleets
p 1025 N93-45775
- A damage tolerance approach for management of aging gas turbine engines
p 1001 N93-45779
- The crack initiation approach for durability analysis
p 1259 N93-55585
- Thermal barrier coating life prediction model development, phase 2
[NASA-CR-189111] p 198 N93-12589
- Propulsion and Energetics Panel Working Group 20 on Test Cases for Engine Life Assessment Technology
[AGARD-AR-308] p 176 N93-14890
- Introduction to test cases for engine life assessment technology
p 176 N93-14891
- LARZAC HP turbine disk crack initiation and propagation spin pit test
p 176 N93-14892
- RB 199 high pressure compressor stage 3 spin pit tests
p 176 N93-14893
- CF6-6 high pressure compressor stage 5 locking slot crack propagation spin pit test
p 176 N93-14894
- F100 second stage fan disk bolthole crack propagation ferris wheel test
p 177 N93-14897
- In-service considerations affecting component life
p 177 N93-14898
- Turbomachinery and potential computations
[DS-2026] p 363 N93-17740
- Control of in-service damage: Application to aircraft engines
[DS-2027] p 364 N93-18151
- LIFE CYCLE COSTS**
Designing to aircraft system effectiveness/cost/time with VERT - The system analysis method for aircraft
p 153 N93-14204
- Life cycle assessment of an impingement-cooled gas turbine blade
[AIAA PAPER 92-4716] p 358 N93-20321
- Acoustic emission technology for smart structures
p 1263 N93-55331
- Alternative systems for fuel gas boosters for small gas turbine engines
[PB92-223049] p 212 N93-12977
- LIFE SCIENCES**
Canadian low-gravity research using parabolic aircraft
p 384 N93-21908
- LIFE SPAN**
MPC75 - The evolution of a new regional airliner for the late nineties
p 155 N93-14289
- LIFE SUPPORT SYSTEMS**
Zvezda - The Russian pioneer in the field of life-support and escape systems for aeronautics and space
p 195 N93-16878
- US Army's aviation life support equipment retrieval program real world design successes from proactive investigation
p 494 N93-19690
- Mathematical modeling and control law development for the atmospheric monitoring and control system of the Controlled Environment Research Chamber (CERC) at NASA Ames Research Center
[AD-A261978] p 911 N93-29436
- LIFT**
Subsonic high-lift flight research on the NASA Transport System Research Vehicle (TSRV)
[AIAA PAPER 92-4103] p 38 N93-11275
- Lifting forces acting on magnets placed above a superconducting plane
p 79 N93-12332
- A method for calculating flow past an arbitrary airfoil profile in the presence of flow separation
p 13 N93-12807

- HSCT high-lift aerodynamic technology requirements [AIAA PAPER 92-4228] p 44 A93-13355
- Aerodynamic characteristics of transport airplanes in low speed configuration p 113 A93-14172
- Wing rock of lifting systems p 118 A93-14330
- Generalized vortex lattice method for oscillating lifting surfaces in subsonic flow p 123 A93-14555
- Performance degradation due to hoar frost on lifting surfaces p 305 A93-17798
- Aerodynamic degradation due to distributed roughness on high lift configuration [AIAA PAPER 93-0028] p 260 A93-20146
- Lift enhancement of ground-effect wing. I - Results of screening tests of various concepts p 271 A93-21737
- Estimation of unsteady lift on a pitching airfoil from wake velocity surveys [AIAA PAPER 93-0437] p 286 A93-23351
- Three-dimensional modeling and control of a twin-lift helicopter system p 370 A93-23511
- Pilot test of a low Reynolds number DTE-airfoil [AIAA PAPER 93-0643] p 464 A93-24758
- Two-dimensional Navier-Stokes analysis of high-lift multi-element airfoils using the q-omega turbulence model [AIAA PAPER 93-0679] p 466 A93-24787
- A study of single jet impingement ground effect lift loss [AIAA PAPER 93-0869] p 469 A93-24930
- Free-piston Stirling coolers for intermediate lift temperatures p 543 A93-26062
- Calculation of the flow around a high-lift airfoil using an explicit code and an algebraic Reynolds stress model p 685 A93-34344
- Indicial lift approximations for two-dimensional subsonic flow as obtained from oscillatory measurements p 768 A93-37385
- Permeable airfoils in incompressible flow p 768 A93-37401
- A viscous-inviscid solver for high-lift incompressible flows over multi-element airfoils at deep separation conditions [ONERA, TP NO. 1992-183] p 774 A93-38745
- Lifting line theory for supersonic flow applications p 778 A93-39402
- Lift and pitching moment measurements in vertical gusts p 906 A93-42259
- The three-dimensional representation of the lift and pitching moment coefficients on wedged rectangular wings in supersonic flow p 973 A93-46990
- AIAA Applied Aerodynamics Conference, 11th, Monterey, CA, Aug. 9-11, 1993, Technical Papers. Pts. 1 & 2 p 974 A93-47201
- A critical assessment of UH-60 main rotor blade airfoil data [AIAA PAPER 93-3413] p 975 A93-47210
- Separated flowfield and lift on an airfoil with an oscillating leading-edge flap [AIAA PAPER 93-3422] p 976 A93-47217
- Measurements in 80- by 120-foot wind tunnel of hazard posed by lift-generated wakes [AIAA PAPER 93-3518] p 1014 A93-47281
- Two-dimensional computational analysis of a transport high-lift system and a comparison with flight-test results [AIAA PAPER 93-3533] p 1072 A93-49517
- Wind tunnel results for an advanced fighter configuration employing transverse thrust for enhanced STOL capability [AIAA PAPER 93-1933] p 1100 A93-49796
- Identification of actuation system and aerodynamic effects of direct-lift-control flaps p 1103 A93-52435
- Transonic area rule about lifting configurations p 1183 A93-53868
- Research requirements for a real-time flight measurements and data analysis system for subsonic transport high-lift research p 1244 A93-54391
- Determination of the transonic flow field around an airfoil section for a given lift force coefficient p 1239 A93-56215
- Forced unsteady separated flows on a 45 degree delta wing [AD-A253146] p 82 A93-10305
- Control of lift and drag in unsteady flows [AD-A253146] p 17 A93-10340
- A method of testing two-dimensional airfoils [AD-A253210] p 17 A93-10375
- Experiments on low aspect ratio hydroplanes to measure lift under static and dynamic conditions [ARE-TM(UHR)-90306] p 21 A93-11365
- Lift coefficient of a randomly oscillating hydroplane [DRA/MAR-TM(MTH)-91320] p 21 A93-11377
- A wind tunnel investigation to determine buffet countermeasures for STOL aircraft alpha-sweep flight testing [NAL-TR-1129] p 65 A93-12362
- Dynamic stall effects on hingeless rotor stability with experimental correlation p 129 A93-13010
- Investigation of interference phenomena of modern wing-mounted high-bypass-ratio engines by the solution of the Euler-equations p 213 A93-13204
- Pressure drag and lift contributions for blunted forebodies of fineness ratio 2.0 in transonic flow (M infinity less than or equal to 1.4) [ESDU-89033] p 136 A93-14515
- Estimation of unsteady lift on a pitching airfoil from wake velocity surveys [NASA-TM-105947] p 138 A93-14791
- Maximum lift of wings with leading-edge devices and trailing-edge flaps deployed [ESDU-92031] p 290 A93-16522
- A computational and experimental investigation of the propulsive and lifting characteristics of oscillating airfoils and airfoil combinations in incompressible flow [AD-A258019] p 294 A93-17819
- The aerodynamic characteristics of the Gottingen 797 and Wortmann FX63-137 aerofoil sections at very low Reynolds numbers [ETN-93-92999] p 295 A93-18128
- An experimental investigation of a finite circulation control wing [AD-A259044] p 340 A93-18896
- An analysis of lift forces on aerosols in a wall bounded turbulent shear flow [DE93-003362] p 747 A93-24963
- Aerodynamic foundations for use of unsteady aerodynamic effects in flight control p 695 A93-25274
- Towards an analytical treatment of the aerostatic problem of a circular wing p 781 A93-27214
- Leading edge vortices in a chordwise periodic flow p 782 A93-27218
- Effect of pylon cross-sectional geometries on propulsion integration for a low-wing transport [NASA-TP-3333] p 788 A93-28070
- Unsteady vortex loop/dipole theory applied to the work and acoustics of an ideal low speed propeller [AD-A264057] p 876 A93-29891
- LIFT AUGMENTATION**
- Numerical simulation of dynamic lift enhancement using oscillatory leading edge flaps [AIAA PAPER 93-0186] p 276 A93-22611
- Lift enhancement of an airfoil using a Gurney flap and vortex generators [AIAA PAPER 93-0647] p 464 A93-24762
- Optimization of the parameters of the lift-augmentation devices of the wing of a maneuverable aircraft equipped with an active load-reduction system p 804 A93-39189
- Lift enhancement due to unsteady aerodynamics [AIAA PAPER 93-3538] p 986 A93-47289
- Lift enhancement using a close-coupled oscillating canard [AD-A257877] p 296 A93-18336
- Tailored composite wings with elastically produced chordwise camber p 923 A93-30876
- The numerical simulation of circulation controlled airfoil flowfields p 879 A93-30947
- LIFT DEVICES**
- An aerodynamic model of multiple lifting surfaces including wake deformation and tip effect p 10 A93-12366
- Maximizing the critical Mach number for lifting wing profiles p 13 A93-12841
- Effects of icing on the aerodynamic performance of high lift airfoils [AIAA PAPER 93-0026] p 259 A93-20144
- Aerodynamic degradation due to distributed roughness on high lift configuration [AIAA PAPER 93-0028] p 260 A93-20146
- Progress in high-lift aerodynamic calculations [AIAA PAPER 93-0194] p 474 A93-25512
- Nonplanar Doublet-Point method for supersonic unsteady aerodynamics [AIAA PAPER 93-1588] p 682 A93-34120
- High lift multiple element airfoil analysis with unstructured grids [AIAA PAPER 93-3478] p 981 A93-47256
- Supersonic flow past a rectangular wing of finite thickness p 1086 A93-50972
- Free streamline-boundary layer analysis for separated flow over an airfoil p 1239 A93-56327
- A study of the effects of tolerances on rigging screws, turnbuckles, and associated components in BS4429: 1987 [NPL-DMM(A)-53] p 86 A93-11326
- Lanchester: The man [AERO-REPT-9111] p 456 A93-16464
- Maximum lift of wings with leading-edge devices and trailing-edge flaps deployed [ESDU-92031] p 290 A93-16522
- Analysis of a 2-D airfoil motion flying in-proximity-to a wavy-wall surface: Lifting-surface-method p 300 A93-19281
- Analysis of a 2-D airfoil motion flying in-proximity-to a wavy-wall surface: Finite difference method p 300 A93-19282
- LIFT DRAG RATIO**
- Optimal control of lift/drag ratios on a rotating cylinder p 76 A93-10275
- Increasing the lift-drag ratio of wings of small aspect ratio at hypersonic velocities p 13 A93-12933
- Aerodynamic characteristics of a next generation high-speed civil transport [AIAA PAPER 92-4229] p 15 A93-13356
- Improving the lift to drag characteristics of low boom configuration [AIAA PAPER 92-4218] p 16 A93-13380
- A re-evaluation of the waverider design process [AIAA PAPER 93-0404] p 440 A93-23326
- Problems in the optimum design of a wing profile for nonseparated flow over a range of angles of attack p 477 A93-27614
- Enhancement of endurance performance by periodic optimal camber control p 727 A93-34541
- Some contributions to propulsion theory - Fuel consumption formulae and general range equation p 713 A93-34850
- Inviscid hypersonic flow over a delta wing p 870 A93-42634
- Curvature and leading edge sweep back effects on grid fin aerodynamic characteristics [AIAA PAPER 93-3480] p 981 A93-47258
- Non slender waveriders [AIAA PAPER 93-3487] p 982 A93-47261
- Application of parabolized Navier-Stokes technique for high-L/D, hypersonic vehicle design [AIAA PAPER 93-2948] p 1047 A93-48144
- Experimental studies of supersonic flow past wedges with longitudinal slots on the windward side p 1089 A93-51786
- A study of air intake parameters on the aerodynamic characteristics of a parasail p 1092 A93-51908
- Effect of lift-to-drag ratio in pilot rating of the HL-20 landing task p 1210 A93-53738
- The aerodynamic characteristics of the Gottingen 797 and Wortmann FX63-137 aerofoil sections at very low Reynolds numbers [ETN-93-92999] p 295 A93-18128
- LIFT FANS**
- Calculations of aerodynamic forces on a wing with thrust using BEM p 300 A93-19286
- LIFTING BODIES**
- Separation control and lift enhancement on airfoil using unsteady excitations p 118 A93-14305
- An interactive numerical procedure for rotor aerodynamic stability analysis using elastic lifting surface p 155 A93-14313
- Lifting surface theory for steady aerodynamic analysis of ducted counter rotation propfan [ASME PAPER 92-GT-14] p 347 A93-18286
- Performance analysis of supersonic through-flow fan by the lifting surface theory. I - Disturbance flow field and determination of blade loadings p 267 A93-20929
- Robust control of the separation of hypersonic lifting vehicles [AIAA PAPER 92-5013] p 385 A93-22289
- Aerodynamic forces and moments on a dihedral swept wing in a translation with attack and side-slip angle p 476 A93-26903
- Calculation of three-dimensional supersonic flow past lifting surfaces p 477 A93-27607
- An experimental and analytical study of a lifting-body wind-tunnel model exhibiting body-freedom flutter [AIAA PAPER 93-1316] p 732 A93-33891
- Prandtl theory applied to paraglider aerodynamics [AIAA PAPER 93-1220] p 690 A93-35169
- Optimization of the stiffness and mass characteristics of lifting surface structures modeled by an elastic beam p 827 A93-36789
- S-plane aerodynamics of nonplanar lifting surfaces p 958 A93-45134
- Minimization of the induced drag of nonplanar lifting systems p 1068 A93-48910
- Aerodynamic characteristics of the HL-20 p 1181 A93-53738
- New acceleration potential method for supersonic unsteady aerodynamics of lifting surfaces, further extension of the nonplanar supersonic doublet point method, and nonlinear, nongradient optimized rational function approximations for supersonic, transient response unsteady aerodynamics p 25 A93-12344
- SR-SCARLET 1: Peregrin [NASA-CR-192048] p 337 A93-18155
- Panel methods for aerodynamic analysis and design [NLR-TP-91404-U] p 990 A93-32357
- LIFTING REENTRY VEHICLES**
- Six-degree-of-freedom guidance and control-entry analysis of the HL-20 p 1210 A93-53737

SUBJECT INDEX

- Aerodynamic heating environment definition/thermal protection system selection for the HL-20
p 1181 A93-53739
- HL-20 computational fluid dynamics analysis
p 1181 A93-53740
- HL-20 operations and support requirements for the Personnel Launch System mission
p 1210 A93-53745
- The X-15/HL-20 operations support comparison [NASA-TM-4453]
p 1017 N93-32379
- LIFTING ROTORS**
Studies of a flat wake rotor theory [NASA-CR-190936]
p 25 N93-12343
- LIGHT AIRCRAFT**
Using ultralight flight vehicles for large-scale aerial photography
p 92 A93-10098
- A civil aircraft industry for India
p 2 A93-12233
- Noise evaluation of light propeller-driven aircraft
p 398 A93-19189
- Flutter calculations for a system with interacting nonlinearities [AIAA PAPER 92-4682]
p 409 A93-20304
- Machinery arrangements for small VTOL transport aircraft
p 713 A93-34848
- A nonlinear control strategy for robust sliding mode performance in the presence of unmatched uncertainty
p 938 A93-42556
- Zero-thrust glide testing for drag and propulsive efficiency of propeller aircraft
p 995 A93-45143
- Lightweight aircraft turbine protection [AIAA PAPER 93-1815]
p 1110 A93-49703
- Analysis of wing-body junction flowfields using the incompressible Navier-Stokes equations, volumes 1 and 2
p 17 N93-10320
- NASA advanced design program: Analysis, design, and construction of a solar powered aircraft [NASA-CR-192040]
p 332 N93-17802
- LIGHT ALLOYS**
NASA-UVA light aerospace alloy and structure technology program supplement: Aluminum-based materials for high speed aircraft [NASA-CR-4517]
p 1019 N93-31643
- NASA-UVA Light Aerospace Alloy and Structures Technology Program (LA2ST)
p 1019 N93-31739
- LIGHT BEAMS**
Sensors with centroid based common sensing scheme and their multiplexing --- fiber optic sensors in aircraft and aircraft engine applications
p 1192 A93-52994
- LIGHT EMITTING DIODES**
Miniature display technologies for integrated helmet systems
p 718 A93-34819
- LIGHT GAS GUNS**
Upgrade of ballistic range facilities at AEDC - Two-thirds complete [AIAA PAPER 93-0349]
p 377 A93-23034
- LIGHT HELICOPTERS**
Comanche airframe design - The PDT approach
p 744 A93-34469
- PDT approach for developing RAH-66 Comanche airframe systems
p 795 A93-35909
- Concept feasibility demonstration for the Army Cockpit Delethalization Program
p 795 A93-35916
- LIGHT MODULATION**
Miniature display technologies for integrated helmet systems
p 718 A93-34819
- Optical temperature compensation schemes of spectral modulation sensors for aircraft engine control
p 1105 A93-49471
- Optical sensors and multiplexing for aircraft engine control
p 1105 A93-49474
- LIGHT SCATTERING**
IR window damage measured by reflective scatter
p 851 A93-39544
- Aureole lidar - Instrument design, data analysis, and comparison with aircraft spectrometer measurements
p 1160 A93-52419
- LIGHT SOURCES**
Undulator Spectromicroscopy Facility at the Advanced Light Source [DE93-007964]
p 823 N93-28490
- X ray microscopy resource center at the Advanced Light Source [DE93-010449]
p 911 N93-29869
- LIGHT TRANSMISSION**
Position sensor with two wavelength time domain multiplexing for civil aircraft application
p 1104 A93-49432
- LIGHT TRANSPORT AIRCRAFT**
Human factors in crashes of commuter airplanes
p 486 A93-24048
- LIGHTHILL METHOD**
Shock waves and the Ffowcs Williams-Hawkins equation
p 480 A93-29411

LIGHTNING

- Joint NASA/USAF Airborne Field Mill Program - Operation and safety considerations during flights of a Lear 28 airplane in adverse weather [AIAA PAPER 92-4093]
p 93 A93-13262
- Aircraft lightning initiation and interception from in situ electric measurements and fast video observations
p 140 A93-14064
- Support of composite fuel cells [SME PAPER EM92-101]
p 152 A93-14102
- Electrostatic discharges [ONERA, TP NO. 1992-82]
p 844 A93-38567
- Mechanical damage to aircraft structures from lightning strikes
p 879 A93-40432
- A monitor for the laboratory evaluation of control integrity in digital control systems operating in harsh electromagnetic environments [NASA-TM-4402]
p 65 N93-12304
- The 1992 International Aerospace and Ground Conference on Lightning and Static Electricity: Addendum [DOT/FAA/CT-92/20-ADD-1]
p 753 N93-24875
- Numerical modelling of induced effects of lightning strike on an all composite helicopter
p 703 N93-24879
- Zoning of aircraft: A review of the definitions
p 703 N93-24880
- Lightning data acquisition
p 753 N93-24883
- Digitization of analog data from in-flight lightning strikes
p 753 N93-24884
- A procedure for defining lightning risk to air vehicles
p 703 N93-24885
- Parameters influencing the hot-spot ignition of aviation fuel/air and ethylene/air mixtures
p 704 N93-24886
- A computational approach to predicting the extent of arc root damage in CFC panels
p 735 N93-24890
- Comparison of the damage for various types of fibre reinforced composites due to different lightning test standards (MIL-STD-1757A, German military VG-standard 96903)
p 736 N93-24891
- Zoning of aircraft by electric field modelling
p 704 N93-24894
- Lightning phenomenology bases for full threat return stroke occurrence following extended leader sweep at flight altitudes
p 754 N93-24895
- Applications of stress envelope concepts to aircraft EMP and lightning survivability
p 704 N93-24898
- Development of models for predicting the triggering of lightning by launch vehicles
p 734 N93-24899
- A single-point warning system for thunderstorms and electric fields
p 747 N93-24900
- LIGHTNING SUPPRESSION**
Lightning protection of composite structure
p 141 A93-15801
- HIRF and lightning --- EMC of aircraft systems and installations for safe operation
p 764 A93-39539
- LINE OF SIGHT**
Survey of helmet tracking technologies
p 517 A93-26882
- New analytical solutions for proportional navigation
p 728 A93-34545
- Exact closed-form solution of generalized proportional navigation
p 1130 A93-49598
- A radar altitude and line of sight attachment [AIAA PAPER 93-3587]
p 1223 A93-52680
- LINE OF SIGHT COMMUNICATION**
Airsip/U.S. naval vessels UHF communications relay demonstration [AIAA PAPER 93-4032]
p 1240 A93-54604
- LINEAR EQUATIONS**
A comparative analysis of algorithms for solving systems of high-order linear algebraic equations
p 96 A93-12977
- Aerodynamic shape optimization via sensitivity analysis on decomposed computational domains [AIAA PAPER 92-4698]
p 265 A93-20310
- Three-dimensional Navier-Stokes analysis of the tip clearance flow in linear turbine cascades [AIAA PAPER 93-0391]
p 282 A93-23068
- Application of feedback linearization method in a digital restructurable flight control system
p 370 A93-23514
- Some Fuchs-type equations in fluid mechanics
p 1165 A93-48967
- Three-dimensional Navier-Stokes analysis of tip clearance flow in linear turbine cascades
p 1235 A93-55364
- LINEAR PREDICTION**
Superresolution radar imaging with linear prediction data extrapolation
p 342 A93-20851
- Limitations of linear theory for sonic boom calculations
p 850 A93-37380
- Studies of superresolution range-Doppler imaging
p 928 A93-43344
- LINEAR PROGRAMMING**
Development and application of a nonlinear fin mixer
p 368 A93-22869

LINEARIZATION

- Selection of a method for protecting aircraft gas turbine engines against damage by foreign objects (Mathematical models)
p 1193 A93-53554
- LINEAR QUADRATIC GAUSSIAN CONTROL**
Integrated control law synthesis of gust load alleviation and flutter margin augmentation for a transport aircraft
p 182 A93-14281
- Extended linear quadratic Gaussian control under randomly varying distributed delays
p 439 A93-22854
- Parameter optimization for an H2 problem with multivariable gain and phase margin constraints
p 439 A93-22971
- On the order reduction of LQG designed controllers [AIAA PAPER 93-1420]
p 756 A93-33973
- Linear quadratic Gaussian/loop transfer recovery design for a helicopter in low-speed flight
p 906 A93-41896
- Design, test, and evaluation of three active flutter suppression controllers [NASA-TM-4338]
p 63 N93-10070
- Robust controller and estimator design using minimax methods
p 229 N93-13925
- Strategies for optimal control design of normal acceleration command following on the F-16 [AD-A258975]
p 373 N93-19095
- Improvements to LQGI/LTR methodology for plants with lightly damped or low frequency poles [AD-A258841]
p 443 N93-19112
- LINEAR QUADRATIC REGULATOR**
The application of optimal robust control in control system design of flying vehicles
p 95 A93-11791
- Robust digital control of a high-performance engine --- F-100 turbofan
p 359 A93-21792
- Extended linear quadratic Gaussian control under randomly varying distributed delays
p 439 A93-22854
- Approximation methods for control of structural acoustics models with piezoceramic actuators
p 452 A93-23744
- On the order reduction of LQG designed controllers [AIAA PAPER 93-1420]
p 756 A93-33973
- Full envelope multivariable control law synthesis for a high-performance test aircraft
p 1130 A93-49595
- A new way of pole placement in LQR and its application to flight control [AIAA PAPER 93-3845]
p 1133 A93-51433
- Adaptive quadratic stabilization control with application to flight controller design [AIAA PAPER 93-3847]
p 1133 A93-51434
- Linear quadratic tracking problems in Hilbert space - Application to optimal active noise suppression
p 1224 A93-52763
- Optimal output feedback vibration control of rotor-bearing systems
p 86 N93-11220
- Design of robust suboptimal controllers for a generalized quadratic criterion [AD-A257746]
p 372 N93-17670
- Helicopter flight control system design using the linear quadratic regulator for robust eigenstructure assignment [AD-A258904]
p 373 N93-19351
- An exploratory investigation of the flight dynamics effects of rotor rpm variations and rotor state feedback in hover [NASA-TM-103968]
p 373 N93-19380
- Game theoretic synthesis for robust aerospace controllers
p 819 N93-27171
- The design of a robust autopilot for the Archytas prototype via linear quadratic synthesis [AD-A262151]
p 820 N93-27546
- LINEAR SYSTEMS**
Control design for robust eigenstructure assignment in linear uncertain systems
p 97 A93-13241
- Linear and nonlinear aircraft flight control for the AIAA Controls Design Challenge [AIAA PAPER 92-4628]
p 62 A93-13286
- Stochastic measures of performance robustness in aircraft control systems
p 185 A93-14595
- Performance prediction of the interacting multiple model algorithm
p 439 A93-22926
- Observability analysis of piece-wise constant systems. I - Theory
p 501 A93-29599
- Model reference control of a linear plant with feedthrough element
p 846 A93-37034
- Modeling of linear isentropic flow systems
p 828 A93-37046
- Output feedback eigenstructure assignment using two Sylvester equations
p 847 A93-38214
- Design of a low sensitivity and norm multivariable controller using eigenstructure assignment and the method of inequalities [AIAA PAPER 93-3802]
p 1170 A93-51394
- LINEARIZATION**
Identification of weakly nonlinear dynamic systems by means of random excitations
p 227 A93-16472
- Three-dimensional modeling and control of a twin-lift helicopter system
p 370 A93-23511
- A multidimensional generalization of Roe's flux difference splitter for the Euler equations
p 863 A93-42437

- Computational nonlinear control
[AD-A253547] p 98 N93-12258
Prediction of unsteady flows in turbomachinery using the linearized Euler equations on deforming grids
[NASA-CR-192919] p 747 N93-25109
- LININGS**
The design and commissioning of an acoustic liner for propeller noise testing in the ARA transonic wind tunnel [PNR-90880] p 101 N93-11204
Consecutive plate acoustic suppressor apparatus and methods
[NASA-CASE-LEW-15430-1] p 453 N93-17051
Aircraft wing compartment liner concept to reduce fuel spillage
[DOT/FAA/CT-TN92/34] p 331 N93-17219
- LIOUVILLE EQUATIONS**
Turbulence and chaos in classical and quantum systems p 232 N93-14144
- LIQUEFACTION**
Integrated air separation and propulsion system for aerospace plane with atmospheric oxygen collection
[SAE PAPER 920974] p 195 A93-14633
- LIQUEFIED NATURAL GAS**
Use of alternative fuels for aviation p 196 A93-14292
- LIQUID BEARINGS**
Liquid hydrogen foil-bearing turbopump
[AIAA PAPER 93-2537] p 1156 A93-50264
- LIQUID COOLING**
Preliminary design of experimental sub-scale scramjet engine
[AAS PAPER 91-639] p 1247 A93-55816
- LIQUID CRYSTALS**
A large flat panel multifunction display for military and space applications p 77 A93-10963
Partially exposed polymer dispersed liquid crystals for boundary layer investigations p 399 A93-19250
Experimental investigations of the time and flow-direction responses of shear-stress-sensitive liquid crystal coatings
[AIAA PAPER 93-0181] p 542 A93-25508
The application and analysis of liquid crystal thermographs in short duration hypersonic flow
[AIAA PAPER 93-0182] p 542 A93-25509
Experience with the use of liquid crystals in conjunction with the filament method is studying the structure of supersonic flow downstream of a plane step p 478 A93-27639
Miniature display technologies for integrated helmet systems p 718 A93-34819
Dynamics of the behavior of nematic films in gasdynamic flows p 746 A93-35345
Applications of liquid crystal surface thermography to hypersonic flow p 1023 A93-45504
Use of shear-stress-sensitive, temperature-insensitive liquid crystals for boundary layer transition detection in hypersonic flows p 1059 A93-48245
Fluid dynamics and convective heat transfer in impinging jets through implementation of a high resolution liquid crystal technique
[ISABE 93-7077] p 1220 A93-54053
Measurement of aerodynamic shear stress using side chain liquid crystal polymers
[AD-A254312] p 72 N93-10770
Liquid crystal displays replacing the CRT and CLE of future cockpits p 518 N93-19783
Cooling geometry optimization using liquid crystal technique p 902 N93-29939
Local heat transfer measurement with liquid crystals on rotating surfaces including non-axisymmetric cases p 902 N93-29943
- LIQUID FLOW**
The use of aviation gas-liquid heat exchangers employing heat pipes p 833 A93-39050
Operating experience using venturi flow meters at liquid helium temperature
[DE92-014693] p 90 N93-12140
- LIQUID FUELS**
Evaporation and specific heats of motor fuels p 71 A93-12823
Viscosity of aviation fuel components (n-alkanes) p 71 A93-12824
An experimental investigation on the combustor with bypass flow in integral liquid fuel ramjet p 174 A93-16235
CARS thermometry in a liquid fueled model combustor
[AIAA PAPER 93-0366] p 390 A93-23047
Scalar characteristics in a liquid-fuelled combustor with curved exit nozzle p 1123 A93-51643
Measurements of gas composition and temperature inside a can type model combustor p 1123 A93-51644
Liquid flow reactor and method of using
[AD-D015392] p 222 N93-15232
- LIQUID HELIUM**
Operating experience using venturi flow meters at liquid helium temperature
[DE92-014693] p 90 N93-12140
- LIQUID HYDROGEN**
Design of a hydrogen test facility p 532 A93-25993
Taking to the skies under hydrogen power - Deutsche Aerospace Airbus studies the use of alternative fuels for civil aviation p 677 A93-34947
Liquid hydrogen foil-bearing turbopump
[AIAA PAPER 93-2537] p 1156 A93-50264
- LIQUID INJECTION**
Shock wave ahead of a liquid jet in supersonic cross flow p 477 A93-27605
Observations of liquid jets injected into a highly accelerated supersonic boundary layer p 1177 A93-53214
Apparatus for reduction of vibration in liquid-injected gas compressor system
[AD-D015607] p 554 N93-20772
- LIQUID PHASES**
Liquid water profiling using remote sensor observations p 429 A93-22150
A condensed phase test cell assembly for the System for Thermal Diagnostic Studies (STDs)
[AD-A258463] p 393 N93-18242
The WINCOF-I code: Detailed description
[NASA-CR-190779] p 677 N93-24760
- LIQUID PROPELLANT ROCKET ENGINES**
Rocket engine versus jet engine comparison
[AIAA PAPER 92-3686] p 531 A93-24479
Liquid rocket propulsion applied to manned aircraft - In historical perspective p 1174 A93-51497
- LIQUID ROCKET PROPELLANTS**
Nozzle effects on linear stability behaviour of combustors
[ISABE 93-7044] p 1198 A93-54020
- LIQUID-GAS MIXTURES**
Calculation of a gas-dispersion laminar boundary layer on a plate with allowance for liquid film formation p 76 A93-10148
Design features influencing the distribution of fuel within the spray from an air blast fuel injector
[ASME PAPER 92-GT-235] p 353 A93-19448
Parameters influencing the hot-spot ignition of aviation fuel/air and ethylene/air mixtures p 704 N93-24886
Flow visualizations of perpendicular blade vortex interactions
[NASA-CR-192725] p 748 N93-25208
- LIQUID-SOLID INTERFACES**
Modeling of interfaces in problems of flow of a ponderable fluid past a wing profile p 124 A93-15189
High accuracy computation of fluid-structure interaction in transonic cascades
[AIAA PAPER 93-0485] p 287 A93-23387
Determination of the shape of a wing profile in boundary layer flow with a given velocity diagram p 1067 A93-48844
- LIQUID-VAPOR INTERFACES**
Aircraft experiments on microgravity pool boiling - Vapor-liquid behaviour and heat transfer characteristics in boiling of n-pentane, CFC-113 and water p 410 A93-20920
Kelvin-Helmholtz wave generation beneath hovercraft skirts p 1219 A93-53820
The WINCOF-I code: Detailed description
[NASA-CR-190779] p 677 N93-24760
- LITHIUM ALLOYS**
Damage tolerance behaviour of aluminium-lithium sheet alloys
[NLR-TP-91244-U] p 392 N93-17540
Flight simulation and constant amplitude fatigue crack growth in aluminum-lithium sheet and plate
[NLR-TP-91104-U] p 331 N93-17562
Accelerated and real-time corrosion testing of aluminum-lithium alloys
[NLR-TP-91203-U] p 1020 N93-32385
- LITHOGRAPHY**
Rapid wind tunnel prototype using stereolithography and equivalent technologies p 191 A93-14365
- LOAD CARRYING CAPACITY**
A study of the strength of a closed system of wings p 828 A93-36792
Load-bearing capacity of an aircraft wing based on the condition of compressed surface fracture p 801 A93-36794
A study of the effect of the static aeroelasticity of a swept wing on its weight response p 801 A93-36798
Selection of the primary aircraft structure at the preliminary design stage p 891 A93-42371
- LOAD DISTRIBUTION (FORCES)**
Mixed mode stress intensity-factors in transversely loaded plates p 200 A93-13943
Common failure modes for composite aircraft structures due to secondary loads p 207 A93-14812
- Characteristics of fatigue crack growth under the service-spectrum loading of the tail boom of a helicopter p 321 A93-18339
Acoustic performance of low pressure axial fan rotors with different blade chord length and radial load distribution p 449 A93-19212
Blade loading and shock wave in a transonic circular cascade diffuser p 246 A93-19294
[ASME PAPER 92-GT-34] p 246 A93-19294
Design of advanced beams considering elasto-plastic behaviour of material p 544 A93-26904
Influence of modelling loading on stress distribution in turbomachinery blade fastening in case of FEM p 520 A93-27296
Acquiring tail load spectra from in-flight measurements
[AIAA PAPER 93-1607] p 711 A93-34137
Efficient sensitivity analysis for rotary-wing aeromechanical problems
[AIAA PAPER 93-1648] p 711 A93-34173
Tapered geometries for improved crashworthiness under side loads p 743 A93-34259
Effects on load distribution in a helicopter rotor support structure associated with various boundary configurations p 796 A93-35951
Buckling of open-section bead-stiffened composite panels p 1157 A93-50420
On design methods for bolted joints in composite aircraft structures p 1158 A93-50430
Aircraft safety evaluation p 1043 A93-50486
An improved method for determining force balance calibration accuracy p 1254 A93-54369
Structural analysis of the light weight hard nose of the 71M aerostat
[AIAA PAPER 93-4037] p 1255 A93-54608
The crack initiation approach for durability analysis p 1259 A93-55585
Split torque transmission load sharing
[NASA-TM-105884] p 212 N93-12736
A discussion of the results of the rainfall counting of a wide range of dynamics associated with the simultaneous operation of adjacent wind turbines
[DE93-000016] p 434 N93-18705
- LOAD TESTS**
Testing for integrity --- of aircraft gas turbine engines p 346 A93-18785
Nonlinear response of a clamped beam and plate to high levels of excitation p 397 A93-19141
Testing for integrity
[PNR-90927] p 56 N93-11024
Verification of rain-flow reconstructions of a variable amplitude load history
[NASA-CR-189670] p 91 N93-12411
Load test set-up for the Airmass Sunburst Ultra-Light Aircraft p 895 N93-29776
- LOADING MOMENTS**
Incompressible flow computation of forces and moments on bodies of revolution at incidence
[AIAA PAPER 93-0787] p 541 A93-24867
- LOADING RATE**
Damage severity of monitored fatigue load spectra p 154 A93-14253
The method for developing F-by-F load spectra of fighter aircraft based on manoeuvres p 154 A93-14254
In-flight tailload measurements p 155 A93-14285
Effect of stiffness characteristics on the response of composite grid-stiffened structures p 1022 A93-45148
Load rating for a delta wing box based on a reliability criterion p 1030 A93-47093
- LOADS (FORCES)**
Aircraft tracking optimization of parameters selection p 3 A93-13628
Loads at the nose landing gears of civil transport aircraft during towbarless towing operations p 45 A93-13629
Thermomechanical postbuckling analysis of laminated composite shells
[AIAA PAPER 93-1337] p 738 A93-33907
Application of generalized force determination to a full scale low cycle fatigue test of the SH-2G helicopter p 795 A93-35949
Post-critical behaviour of a tapered cantilever column subjected to a uniformly distributed tangential follower force p 831 A93-38431
Blade row interaction effects on compressor measurements p 900 A93-42885
Using spectral analysis for estimating the effect of runway irregularities on the loading of transport aircraft structures p 996 A93-45669
An evaluation of a method of reconstituting fatigue loading from Rainflow counting
[RAE-TR-89057] p 82 N93-10198
The technical background to standards for eyebolts
[NPL-DMM(A)-52] p 87 N93-11327
Reanalysis of multiple-wheel landing gear traffic tests
[AD-A256593] p 194 N93-14238
A90 project: Design of a composite fin
[ETN-92-92773] p 329 N93-16562

- Review of aeronautical fatigue investigations in the Netherlands during the period March 1989 - March 1991 [NLR-TP-91092-U] p 331 N93-17535
- Estimating turbine limit load [NASA-CR-191105] p 699 N93-25883
- Interaction between ice and propeller [VTT-TIED-1281] p 841 N93-27832
- AGARD Engine Disc Cooperative Test Programme [AGARD-R-766-ADD] p 1004 N93-31741
- Fatigue crack growth results for Ti-6Al-4V, IMI 685, and Ti-17 p 1004 N93-31746
- LOCAL AREA NETWORKS**
- An interneting brouter for avionics applications — Bridge/Router unit in fiber optics aircraft communication p 1097 A93-49479
- An introduction to the onboard LAN (OLAN) p 1166 A93-49480
- Fiber-optic technology for transport aircraft p 1173 A93-50488
- Pseudo Aircraft Systems - A multi-aircraft simulation system for air traffic control research [AIAA PAPER 93-3585] p 1209 A93-52679
- The engine design engine. A clustered computer platform for the aerodynamic inverse design and analysis of a full engine [NASA-TM-105838] p 21 N93-11223
- LOCKING**
- US Army helicopter inertia reel locking failures p 493 N93-19689
- LOG PERIODIC ANTENNAS**
- ILS mathematical modeling study of the effects of an ASR-9 structure at the Long Island MacArthur Airport, Islip, NY [DOT/FAA/CT-TN92/25] p 192 N93-12668
- The ILS mathematical modeling study of the Runway 10 ILS Localizer at Luis Munoz Marin International Airport, San Juan, Puerto Rico [DOT/FAA/CT-TN93/10] p 792 N93-27017
- LOGIC DESIGN**
- Design and implementation of fuzzy logic controllers [NASA-CR-193268] p 1038 N93-31649
- LOGISTICS**
- A review of aging aircraft technology - An I.A.I. perspective p 3 A93-13634
- Technical operating report on the Data Integration and Collection Environment (DICE) instrumentation system design [AD-A258444] p 455 N93-17891
- LOGISTICS MANAGEMENT**
- Logistic Support Analysis - An integrated approach to configuration management p 763 A93-35924
- Management of Automatic Data Processing (ADP) system documentation in the Department of Defense [AD-A258507] p 571 N93-20048
- LONGERONS**
- A neural network prototype for predicting F-14B strains at the B.L. 10 longeron [AD-A255272] p 165 N93-15004
- LONGITUDINAL CONTROL**
- Pitch control margin at high angle of attack - Quantitative requirements (flight test correlation with simulation predictions) p 39 A93-11277
- [AIAA PAPER 92-4107] p 39 A93-11277
- Piloted simulation study of two tilt-wing control concepts [AIAA PAPER 92-4236] p 63 A93-13338
- A longitudinal control law integrating flight controls and engine controls p 186 A93-15046
- Flying qualities of the Hermes spaceplane and the shape definition process p 532 A93-28437
- Full-scale wind tunnel investigation of a helicopter individual blade control system [AIAA PAPER 93-1361] p 726 A93-33929
- Pilot-in-the-loop analysis of propulsive-only flight control systems p 908 A93-42812
- F/A-18 departure recovery improvement evaluation [AIAA PAPER 93-3671] p 1129 A93-48349
- Use of neural networks in control of high-alpha maneuvers p 1130 A93-49593
- Design of a flight control system for a highly maneuverable aircraft using mu synthesis [AIAA PAPER 93-3776] p 1132 A93-51371
- A pseudo-loop design strategy for the longitudinal control of hypersonic aircraft [AIAA PAPER 93-3814] p 1132 A93-51405
- Longitudinal and lateral-directional flying qualities investigation of high-order characteristics for advanced-technology transports [AIAA PAPER 93-3815] p 1133 A93-51406
- A method for the spectral-time identification of the longitudinal and lateral motions of an aircraft p 1205 A93-52942
- Longitudinal closed-loop pilot/vehicle analysis of DFBW aircraft during approach and landing p 1206 A93-54277
- Pitch control trimming system for canard design aircraft [CA-PATENT-APPL-SN-2013236] p 63 N93-10374
- Ideal aircraft handling quality models: Longitudinal axis [NAL-PD-FC-9203] p 187 N93-13566
- Longitudinal-control design approach for high-angle-of-attack aircraft [NASA-TP-3302] p 373 N93-19108
- Control of nonlinear systems under input constraints with applications to flight control p 729 N93-25353
- New adaptive controllers for aircraft p 847 N93-27180
- LONGITUDINAL STABILITY**
- The aerodynamic loads on aircraft components in violent longitudinal manoeuvres p 476 A93-26898
- Impact of aeroelasticity on propulsion and longitudinal flight dynamics of an air-breathing hypersonic vehicle [AIAA PAPER 93-1367] p 733 A93-33934
- An acceleration technique for time accurate calculations — of unsteady flow around pitching delta wings p 957 A93-45092
- Calculation of transonic longitudinal and lateral-directional characteristics of aircraft by the small disturbance theory [AIAA PAPER 93-3617] p 1125 A93-48304
- Estimation of neutral and maneuver points of aircraft by dynamic maneuvers [AIAA PAPER 93-3620] p 1126 A93-48307
- Longitudinal dynamics of a towed sailplane p 1130 A93-49577
- An aerodynamic model for the longitudinal motion of flight training devices p 1207 A93-54278
- Aerodynamic integration of thrust reversers on the Fokker 100 p 160 N93-13208
- Effects of forebody strakes and Mach number on overall aerodynamic characteristics of configuration with 55 deg cropped delta wing [NASA-TP-3253] p 131 N93-13353
- LONGITUDINAL WAVES**
- Flow and heat transfer in a turbulent boundary layer through skewed and pitched jets p 1151 A93-49007
- LOOP ANTENNAS**
- Corroboration of a moment-method calculation of the maximum mutual coupling between two HF antennas mounted on a helicopter p 881 A93-40332
- ELF, VLF and LF radiation from a very large loop antenna with a mountain core p 924 A93-40334
- LORAN C**
- Merger and acquisition - Enhancing Loran propagation technology with artificial intelligence p 29 A93-10987
- Measurement technique for Loran-C pulse wave distortion measures and performance in an environment of noise p 29 A93-10988
- Effect of skywave interference on the coverage of Loran-C p 33 A93-11095
- Airborne trials of Loran-C p 311 A93-17756
- Analysis of Loran-C performance in the Pemberton area, B.C. p 311 A93-17797
- MIAS, the integration of MLS with DGPS/DLoran-C p 315 A93-21181
- Relative sensitivity of Loran-C phase tracking and cycle selection to CWI p 792 A93-36502
- An optimal detection algorithm for harmonic interference signals in Loran-C p 993 A93-46889
- Rotorcraft en route ATC route standards [AD-A249129] p 35 N93-10323
- Carrier wave signals interfering with Loran-C [ETN-92-92528] p 318 N93-17584
- Automatic pulse shaping with the AN/FPN-42 and AN/FPN-44A Loran-C transmitters [AD-A257860] p 319 N93-18309
- LOSSES**
- Initial results from the NASA Lewis wave rotor experiment [AIAA PAPER 93-2521] p 1193 A93-53589
- Rotating stall: Modeling-measurement techniques; unsteady loss-unsteady flow field p 424 N93-18732
- World commercial aircraft accidents [DE93-010892] p 791 N93-28571
- Initial results from the NASA-Lewis wave rotor experiment [NASA-TM-106148] p 1005 N93-32368
- LOSSY MEDIA**
- Receiving and scattering characteristics of an imaged monopole beneath a lossy sheet p 1158 A93-50543
- LOUDNESS**
- Loudness versus level of aircraft noise p 557 A93-28477
- Laboratory study of effects of sonic boom shaping on subjective loudness and acceptability [NASA-TP-3269] p 102 N93-11620
- Effect of sonic boom asymmetry on subjective loudness [NASA-TM-107708] p 453 N93-16755
- Loudness and annoyance response to simulated outdoor and indoor sonic booms [NASA-TM-107756] p 852 N93-27271
- A laboratory study of subjective response to sonic booms measured at White Sands Missile Range [NASA-TM-107746] p 852 N93-27272
- Subjective response to simulated sonic booms with ground reflections [NASA-TM-107764] p 852 N93-28692
- LOUDSPEAKERS**
- Cabin noise source-path identification for AD-200 ultralight aircraft p 444 A93-19138
- LOUVERS**
- Experimental analysis of the aeroacoustics of cascaded airfoils [AD-A257945] p 420 N93-18121
- LOW ALTITUDE**
- Test pilot's notes on flying the Low Altitude/Airspeed Unmanned Research Aircraft (LAURA) [AIAA PAPER 92-4078] p 42 A93-13269
- Validation of vision-based obstacle detection algorithms for low-altitude helicopter flight p 374 A93-19077
- The noise of jet aircraft flying with high speeds at low altitudes p 450 A93-19218
- Stable cross type parachute with inflation aid [AIAA PAPER 93-1201] p 702 A93-35152
- Radial reefing method for accelerated and controlled parachute opening [AIAA PAPER 93-1209] p 702 A93-35159
- Passive range estimation for rotorcraft low-altitude flight p 948 A93-46608
- Results of a low-altitude flight noise study in Germany - Acute extraural effects p 1163 A93-49557
- Passive range estimation for rotorcraft low-altitude flight p 1190 A93-52881
- Appraisal of digital terrain elevation data for low-altitude flight [NASA-TM-103896] p 35 N93-10745
- Integration of radar altimeter, precision navigation, and digital terrain data for low-altitude flight [NASA-TM-103958] p 36 N93-12320
- Testing of an automatic, low altitude, all terrain ground collision avoidance system p 502 N93-19924
- T-38 forward windshield development and performance demonstration report [AD-A259240] p 513 N93-20579
- A prediction model for noise from low-altitude military aircraft [AD-A262494] p 852 N93-27662
- LOW ASPECT RATIO**
- Increasing the lift-drag ratio of wings of small aspect ratio at hypersonic velocities p 13 A93-12933
- Low aspect ratio transonic rotors. II - Influence of location of maximum thickness on transonic compressor performance [ASME PAPER 92-GT-186] p 352 A93-19411
- An experimental study of droop leading edge modifications on high and low aspect ratio wings up to 50 deg angle of attack [AIAA PAPER 93-3496] p 983 A93-47268
- Experiments on low aspect ratio hydroplanes to measure lift under static and dynamic conditions [ARE-TM(UHR)-90306] p 21 N93-11365
- Diagnostics systems for the TBR-E tokamak [INPE-5428-RPQ/662] p 232 N93-13257
- Pitching moment of low aspect ratio wing-body combinations up to high angles of attack at supersonic speeds [ESDU-92043] p 333 N93-17958
- The blade curving effects in a turbine stator cascade with low aspect ratio [AD-A261063] p 725 N93-26239
- LOW ASPECT RATIO WINGS**
- Calculations of separated vortex flows at low speed for low-aspect-ratio wings p 264 A93-20300
- Near-field behavior of a tip vortex p 288 A93-23549
- Structural modeling of low-aspect ratio composite wings [AIAA PAPER 93-1371] p 739 A93-33937
- Three-dimensional hypersonic flow of a gas past wings p 1069 A93-48971
- Hypersonic flow past a low-aspect-ratio triangular plate at large angles of attack p 1069 A93-48974
- Low aspect ratio wing code validation experiment p 1176 A93-53202
- Aerodynamic characteristics of conical triangular-planform wings of low aspect ratio in subsonic stalled flow p 1180 A93-53574
- Formulation of a structural model for flutter analysis of low aspect ratio composite aircraft wings p 372 N93-19019
- Supersonic aeroelastic instability results for a NASP-like wing model [NASA-TM-107739] p 718 N93-26553
- Towards an analytical treatment of the aerolastic problem of a circular wing p 781 N93-27214

LOW COST

High-Reynolds-number test of a 5-percent-thick low-aspect-ratio semispan wing in the Langley 0.3-meter transonic cryogenic tunnel: Wing pressure distributions [NASA-TM-4227] p 875 N93-29449

LOW COST

Low-cost approaches to proving of high-risk fast VTOL designs [SAE PAPER 920989] p 157 A93-14636

A 'low-cost' full flight simulator for basic IFR training p 374 A93-18776

Robo-line storage: Low latency, high capacity storage systems over geographically distributed networks [NASA-CR-192910] p 758 N93-25130

Selection and static calibration of the Marsh J1678 pressure gauge p 931 N93-29779

LOW DENSITY FLOW

The Burnett shock structures in low density hypersonic flows

[AIAA PAPER 92-5048] p 273 A93-22320

Burnett solutions along the stagnation line of a cooled cylinder in low-density hypersonic flows

[AIAA PAPER 93-2726] p 962 A93-46480

Issues and approach to develop validated analysis tools for hypersonic flows: One perspective

[NASA-TM-103937] p 305 N93-19379

LOW FREQUENCIES

ELF, VLF and LF radiation from a very large loop antenna with a mountain core p 924 A93-40334

Low-frequency combustion oscillations in a model afterburner p 1193 A93-53702

The low frequency aeroacoustics of buried nozzle systems p 1205 A93-54244

LOW LEVEL TURBULENCE

Summary of findings from the PIREP-based analyses conducted during the 1988 to 1990 evaluations of TDWR-based and TDWR/LLWAS-based alert services provided to landing/departing pilots

[AD-A253859] p 93 N93-11144

LOW NOISE

Low-noise, high-strength, spiral-bevel gears for helicopter transmissions [AIAA PAPER 93-2149] p 1154 A93-49966

LOW PRESSURE

The influence of intake swirl distortion on the steady-state performance of a low bypass, twin-spool engine p 214 N93-13211

LOW REYNOLDS NUMBER

Simulation of a hypersonic flow over vehicles at low Reynolds numbers p 120 A93-14381

Experimental investigation of laminar to turbulent boundary layer transition with separation bubbles at low Reynolds number p 128 A93-17277

Acoustic properties of supersonic helium/air jets at low Reynolds numbers p 446 A93-19160

Pilot test of a low Reynolds number DTE-airfoil [AIAA PAPER 93-0643] p 464 A93-24758

On high speed turbulence modeling of shock-wave boundary-layer interaction p 541 A93-24860

An experimental study on location of transitional separation bubble on a low Reynolds numbers airfoil p 680 A93-33725

Calibration of thermal anemometer at very low Reynolds numbers under microgravity p 926 A93-41729

High-speed turbulence modeling of shock-wave/boundary-layer interaction p 927 A93-41910

Prediction of stall and post-stall behavior of airfoils at low and high Reynolds numbers p 983 A93-47270

Exploratory study of shock reflection near an expansion corner [AIAA PAPER 93-3132] p 1063 A93-48297

Calculation of scramjet inlet with thick boundary-layer ingestion [AIAA PAPER 93-1836] p 1074 A93-49720

Investigation of the effect of physical processes on heat transfer to blunt bodies at low Reynolds numbers p 1090 A93-51877

Investigation of supersonic shaped nozzles in a low-pressure wind tunnel p 1091 A93-51881

Low-Reynolds-number k-epsilon model for unsteady turbulent boundary-layer flows p 1177 A93-53208

Computational investigations of a NACA 0012 airfoil in low Reynolds number flows p 288 N93-15920

Methodology for sensitivity analysis, approximate analysis, and design optimization in CFD for multidisciplinary applications [NASA-CR-192172] p 552 N93-20297

LOW SPEED

Test pilot's notes on flying the Low Altitude/Airspeed Unmanned Research Aircraft (LAURA) [AIAA PAPER 92-4078] p 42 A93-13269

Aerodynamic characteristics of transport airplanes in low speed configuration p 113 A93-14172

A low-speed wind tunnel study of vortex interaction control techniques on a chine-forebody/delta-wing configuration p 122 A93-14409

F-14A aircraft low-speed maneuvering aerodynamics [AIAA PAPER 93-0523] p 283 A93-23265

The strake - A simple means for directional control improvement p 802 A93-37997

Aerodynamic rotor loads prediction method with free wake for low speed descent flights [ONERA, TP NO. 1992-122] p 772 A93-38596

Linear quadratic Gaussian/loop transfer recovery design for a helicopter in low-speed flight p 906 A93-41896

Effect of passive flow-control devices on turbulent low-speed base flow p 82 N93-10304

An experimental and a theoretical investigation of rotor pitch damping using a model rotor p 47 N93-10322

Helicopter low-speed yaw control [NASA-CASE-LAR-14219-1] p 729 N93-25998

Quantitative three-dimensional low-speed wake surveys p 785 N93-27447

Unsteady vortex loop/dipole theory applied to the work and acoustics of an ideal low speed propeller [AD-A264057] p 876 N93-29891

LOW SPEED WIND TUNNELS

Breakdown analysis on delta wing vortices p 7 A93-10779

The effect of wind tunnel constraint on unsteady aerodynamics experiments p 190 A93-14300

A low speed wind-tunnel with extreme flow quality - Design and tests p 190 A93-14352

Five years operational experiences with Indonesian Low Speed Tunnel (ILST) p 191 A93-14403

Experimental studies of vortex flaps and vortex plates p 121 A93-14406

On aerodynamic loading of linear compressor cascades [ASME PAPER 92-GT-275] p 253 A93-19468

Body-axis rolling motion critical states of a 65-degree delta wing [AIAA PAPER 93-0621] p 523 A93-24738

Application of a flush airdata sensing system to a wing leading edge (LE-FADS) [AIAA PAPER 93-0634] p 516 A93-24750

Dynamic stability derivatives evaluation in a low-speed wind tunnel p 821 A93-37402

Experimental analysis of rotary derivatives on a modern aircraft configuration [AIAA PAPER 93-3514] p 985 A93-47278

Lift enhancement due to unsteady aerodynamics [AIAA PAPER 93-3538] p 986 A93-47289

Analysis of stability characteristics of a high performance aircraft [AIAA PAPER 93-3616] p 1125 A93-48303

Wind tunnel investigation of wind shear effect on turning flight [AIAA PAPER 93-3641] p 1127 A93-48326

Low-speed aerodynamics of the hypersonic research configuration ELAC I p 1237 A93-56035

The 13 ft by 9 ft low speed wind tunnel facility at DRA (Aerospace Division) Bedford (England) [RAE-TM-AERO-2228] p 23 N93-11883

Simulation analysis of a cable-mount system used for dynamic wind tunnel tests [NAL-TR-1127] p 68 N93-12359

Tests of models equipped with TPS in low speed ONERA F1 pressurized wind tunnel p 213 N93-13201

Wind tunnel tests and CFD in Fuji Heavy Industries p 304 N93-19323

Determination of surface heat transfer and film cooling effectiveness in unsteady wake flow conditions p 902 N93-29933

LOW TEMPERATURE ENVIRONMENTS

Microwave processing of silicon nitride for advanced gas turbine applications [DE93-007910] p 917 N93-29767

LOW TURBULENCE

Optimal conditions for flow turbulence reduction by a set of grids p 836 A93-39122

Some key problems in the design of the NPU open-circuit low-turbulence wind tunnel p 1139 A93-51188

Subsonic aerodynamic research laboratory [AD-A256060] p 137 N93-14661

Boundary-layer measurements on a high Reynolds number three-element airfoil p 292 N93-16787

Experiments on smooth cantilevered circular cylinders in a low-turbulence uniform flow. Part 2: Fluctuating loads on a cantilever of aspect ratio 30 [PB93-110500] p 555 N93-21382

Experiments on smooth cantilevered circular cylinders in low-turbulence uniform flow. Part 1: Mean loading with aspect ratios in the range 4 to 30 [PB93-111763] p 555 N93-21383

LOW VISIBILITY

Air Traffic Control ground movement control in low visibility p 151 A93-17308

Ground visual aids - Recent research at RAE Bedford p 191 A93-17311

Synthetic vision - A view in the fog p 792 A93-37068

Multiple function sensors for Enhanced Vision application p 807 A93-37071

LOW WEIGHT

Potential aerospace applications for metal matrix composites p 389 A93-21678

Advanced composite fiber/metal pressure vessels for aircraft applications [AIAA PAPER 93-2246] p 1155 A93-50047

LOWER ATMOSPHERE

Buoyancy wave hazards to aviation p 430 A93-22151

LUBRICANT TESTS

Coking characteristics of polyphenyl ether lubricants using a Static Coker and a Micro Carbon Residue Tester p 77 A93-11341

A mathematical model to determine the health of components based on SOAP data --- spectrometric oil analysis program p 53 A93-12238

LUBRICANTS

A test facility for the thermofluid-dynamics of gas bearing lubrication films [PNR-90897] p 72 N93-11032

LUBRICATING OILS

Some physio-chemical characteristics of lubricating oil used in gas turbines p 70 A93-12202

A mathematical model to determine the health of components based on SOAP data --- spectrometric oil analysis program p 53 A93-12238

Evaporation and specific heats of motor fuels p 71 A93-12823

Improved lubricating greases for aircraft wheel bearings [SAE PAPER 921038] p 197 A93-14658

Protective properties of aviation oils p 735 A93-35299

RB199 engine oil system failure diagnostics by comparison of measured and calculated oil consumption using the OLMOS on-board monitoring system p 178 N93-15173

LUBRICATION

Multilevel solution of the elastohydrodynamic lubrication of concentrated contacts in spiroid gears p 1161 A93-52606

LUBRICATION SYSTEMS

Maintenance of the liquid and gas systems of the II-76 aircraft p 804 A93-39203

LUGS

F-14 wing lug coating investigation [AD-A257384] p 328 N93-15858

LUMINOUS INTENSITY

Video luminescent barometry - The induction period [AIAA PAPER 93-0179] p 414 A93-22607

Uncertainty estimates for pressure sensitive paint measurements p 1258 A93-55369

LUMPED PARAMETER SYSTEMS

Lumped mass modelling for the dynamic analysis of aircraft structures p 510 N93-19460

LUNAR SOIL

Fiber pulling apparatus modification [NASA-CR-184498] p 220 N93-14763

LUNAR SURFACE

Analytical study on the separation dynamics of LUNAR-A/penetrator p 1265 A93-56272

M

MACH NUMBER

Regimes of supersonic flow past the windward side of V-shaped wings p 5 A93-10144

Transport processes in hypersonic flows p 7 A93-11302

Maximizing the critical Mach number for lifting wing profiles p 13 A93-12841

A design approach to high Mach number scramjet performance [AIAA PAPER 92-4248] p 55 A93-13360

Inlet design using a blend of experimental and computational techniques p 114 A93-14210

Passive boundary-layer bleed for supersonic intakes p 114 A93-14212

Scramjet combustor and nozzle computations p 171 A93-14243

Numerical simulations of high speed inlet flows p 115 A93-14246

The ramjet engine in high speed propulsion p 174 A93-16853

Air-breathing hypersonic cruise - Prospects for Mach 4-7 waverider aircraft [ASME PAPER 92-GT-437] p 384 A93-19579

Fine control of Mach number in subsonic wind tunnel p 375 A93-20808

- High Mach number dynamic stability of blunt slender cones at angle of attack p 271 A93-21721
- Flow quality improvement in a high speed blowdown wind tunnel
- [AIAA PAPER 93-0353] p 377 A93-23038
- Preliminary assessment of tunnel wall interference in the NDA cryogenic wind tunnel
- [AIAA PAPER 93-0421] p 285 A93-23340
- Performance of compressible flow codes at low Mach numbers
- p 287 A93-23540
- Three-dimensional flow simulation over axisymmetric bodies using Navier-Stokes equations at hypersonic Mach numbers
- p 461 A93-24090
- Hysteresis effects on wind tunnel measurements of a two-element airfoil
- [AIAA PAPER 93-0646] p 464 A93-24761
- Numerical simulations of a high Mach number jet flow
- [AIAA PAPER 93-0653] p 540 A93-24766
- Vortex distortion during vortex-surface interaction in a Mach 3 stream
- [AIAA PAPER 93-0761] p 467 A93-24846
- Numerical simulation of crossing/turbulent boundary layer interaction at Mach 8.3 comparison of zero and two-equation turbulence models
- [AIAA PAPER 93-0779] p 467 A93-24861
- Sonic boom spectra of Space Shuttle Columbia landing 10 December 1990
- p 533 A93-28488
- Aerothermoelastic analysis of a NASP demonstrator model
- [AIAA PAPER 93-1366] p 733 A93-33933
- Testing techniques for straight transonic and supersonic cascades
- [ONERA, TP NO. 1992-155] p 773 A93-38734
- A French look at the future supersonic transport
- [ONERA, TP NO. 1992-209] p 803 A93-38763
- Mach disk of dual coaxial axisymmetric jets
- p 861 A93-41932
- Hypersonic cone flow predictions using an implicit upwind space-marching code
- p 865 A93-42588
- An experimental contribution to the flat plate 2D compression ramp, shock/boundary layer interaction problem at Mach 14 - Test case 3.7
- p 865 A93-42590
- Experimental study of the flow around a double ellipsoid configuration
- p 867 A93-42603
- Leeside flow over delta wing at $M = 7.15$ - Experimental results for test case 7.1.2
- p 870 A93-42632
- Evaluation of contributions for test case 7.1.1 and 7.1.2
- p 870 A93-42636
- It's time to go supersonic
- p 949 A93-44099
- Numerical wave propagation and steady state solutions. II - Bulk Viscosity Damping
- [AIAA PAPER 93-3331] p 953 A93-45025
- Flutter analysis of composite panels on many supports
- p 1022 A93-45119
- Supersonic vortex breakdown over a delta wing in transonic flow
- [AIAA PAPER 93-3472] p 980 A93-47251
- Aerodynamic characteristics of the MMPT ATD vehicle at high angles of attack
- [AIAA PAPER 93-3493] p 982 A93-47265
- Hypersonic flow past open cavities
- [AIAA PAPER 93-2969] p 1049 A93-48163
- Transition effects on compressible dynamic stall of transiently pitching airfoils
- [AIAA PAPER 93-2978] p 1050 A93-48171
- Experimental study of shock wave and hypersonic boundary layer interactions near a convex corner
- [AIAA PAPER 93-2980] p 1051 A93-48173
- An analytical description of hypersonic boundary layer stability
- [AIAA PAPER 93-2981] p 1051 A93-48174
- A finite element and symbolic method for studying laminar boundary layers of real gases in equilibrium at Mach numbers to 30
- [AIAA PAPER 93-2986] p 1052 A93-48179
- Experimental study of transitional axisymmetric shock-boundary layer interactions at Mach 5
- [AIAA PAPER 93-3131] p 1063 A93-48296
- Exploratory study of shock reflection near an expansion corner
- [AIAA PAPER 93-3132] p 1063 A93-48297
- Flowfield dynamics in blunt fin-induced shock wave/turbulent boundary layer interactions
- [AIAA PAPER 93-3133] p 1063 A93-48298
- Numerical study of the performance of swept, curved compression surface scramjet inlets
- [AIAA PAPER 93-1837] p 1074 A93-49721
- Structural design and analysis of a Mach zero to five turbo-ramjet system
- [AIAA PAPER 93-1983] p 1112 A93-49830
- The study of experimental turboramjets - Heat state and cooling problems
- [AIAA PAPER 93-1989] p 1112 A93-49834
- C-2 subsonic freejet development and demonstration
- [AIAA PAPER 93-2180] p 1138 A93-49992
- An experimental study of supersonic air-intake with 5-shock system at Mach 3
- [AIAA PAPER 93-2305] p 1082 A93-50089
- Two-dimensional numerical simulation for Mach-3 multishock air-intake with bleed systems
- [AIAA PAPER 93-2306] p 1082 A93-50090
- In-stream measurements of combustion during Mach 5 to 7 tests of the Hypersonic Research Engine (HRE)
- [AIAA PAPER 93-2324] p 1116 A93-50104
- Effects of flow-path variations on internal reversing flow in a tailpipe oftake configuration for ASTOVL aircraft
- [AIAA PAPER 93-2438] p 1118 A93-50190
- An upgraded data acquisition and processing system for the Aeropropulsion Systems Test Facility at Arnold Engineering Development Center
- [AIAA PAPER 93-2466] p 1138 A93-50213
- A study of incipient separation limits for shock-induced boundary layer separation for Mach 6 high Reynolds flow
- [AIAA PAPER 93-2481] p 1084 A93-50222
- New derivation of relationship between Mach angle and Mach number
- p 1086 A93-51190
- Multielement airfoil performance due to Reynolds and Mach number variations
- p 1095 A93-52442
- Developing numerical techniques for solving low Mach number fluid-acoustic problems
- p 1235 A93-55353
- Experimental studies in the Aachen hypersonic shock tunnel
- p 1251 A93-56032
- Experimental investigations of hypersonic shock-boundary layer interaction
- p 1238 A93-56037
- Effect of planform and body on supersonic aerodynamics of multibody configurations
- [NASA-TP-3212] p 19 A93-10824
- Effects of forebody strakes and Mach number on overall aerodynamic characteristics of configuration with 55 deg cropped delta wing
- [NASA-TP-3253] p 131 A93-13353
- An experimental/computational study of heat transfer in sharp fin induced shock wave/turbulent boundary layer interactions at low hypersonic Mach numbers
- p 217 A93-13826
- A study of viscous interaction effects on hypersonic waveriders
- p 135 A93-14160
- Pressure drag and lift contributions for blunted forebodies of fineness ratio 2.0 in transonic flow (M infinity less than or equal to 1.4)
- [ESDU-89033] p 136 A93-14515
- User manual for NASA Lewis 10 by 10 foot supersonic wind tunnel
- [NASA-TM-105626] p 194 A93-15498
- The 1990 high-speed civil transport studies
- [NASA-CR-189618] p 330 A93-16947
- Research in robust control for hypersonic vehicles
- [NASA-CR-192127] p 527 A93-20296
- Aerodynamic design and synthesis of the oblique flying wing supersonic transport
- p 713 A93-24768
- Conical Euler analysis and active roll suppression for unsteady vortical flows about rolling delta wings
- [NASA-TP-3259] p 701 A93-26134
- Analysis of fluctuating static pressure measurements in a large high Reynolds number transonic cryogenic wind tunnel
- [NASA-TM-108722] p 823 A93-27142
- Analysis of wind-tunnel data for elliptic cross-sectioned forebodies at Mach numbers 0.4 to 5.0
- p 782 A93-27221
- Reynolds and Mach number effects on multielement airfoils
- p 785 A93-27446
- Dynamic airfoil stall investigations
- p 786 A93-27453
- Effects of flow-path variations on internal reversing flow in a tailpipe oftake configuration for ASTOVL aircraft
- [NASA-TM-106149] p 900 A93-29065
- Performance characteristics of two multiaxis thrust-vectoring nozzles at Mach numbers up to 1.28
- [NASA-TP-3313] p 874 A93-29160
- Solution of Euler equations for forebody-inlet ensemble of aircraft at high angle of attack
- [AD-A263905] p 876 A93-29862
- Measurement of turbulent spots and intermittency modelling at gas-turbine conditions
- p 902 A93-29934
- Supersonic aerodynamic characteristics of an advanced F-16 derivative aircraft configuration
- [NASA-TP-3355] p 989 A93-31733
- MACH REFLECTION**
- Holographic interferometric investigation of shock wave interaction with a ramp
- p 271 A93-21921
- Calculation of the irregular interaction of shock waves
- p 691 A93-35339
- Formation of the shock reflection on a wedge
- p 1023 A93-45476
- New derivation of relationship between Mach angle and Mach number
- p 1086 A93-51190
- Results about the structure of the shock wave reflection process for strong incoming shock waves
- p 1233 A93-54810
- Numerical studies of Mach reflection with air chemistry
- p 1233 A93-54815
- Chemical nonequilibrium effects of Mach reflection
- p 1233 A93-54816
- Analytical and numerical study on steady Mach reflection
- p 302 A93-19309
- MACH-ZEHNDER INTERFEROMETERS**
- Fiber-optic interferometric sensors for measurements of pressure fluctuations - Experimental evaluation
- [AIAA PAPER 93-0738] p 540 A93-24828
- MACHINE LEARNING**
- An investigation of discovery-based learning in the route planning domain
- [AD-A259141] p 513 A93-20560
- MACHINE TOOLS**
- Prediction and control of the service-related properties of parts at the technological preparation stage and during the manufacture process --- of aircraft engine components
- p 834 A93-39062
- High-efficiency machining methods for aviation materials
- [ISBN 5-230-16902-8] p 835 A93-39084
- Theory of the machining of polyhedral holes by plunge cutting
- p 835 A93-39091
- Some characteristics of the design of heads for the cutting of bevel gears with negative curvature of the circular-arc tooth line
- p 835 A93-39093
- On machine capacitance dimensional and surface profile measurement system
- p 750 A93-25579
- MACHINERY**
- Rotating machinery - Transport phenomena; Proceedings of the 3rd International Symposium on Transport Phenomena and Dynamics of Rotating Machinery (ISROMAC-3), Honolulu, HI, Apr. 1-4, 1990 [ISBN 1-56032-147-4] p 1256 A93-54626
- MACHINING**
- Study of the method for determining residual stress induced by machining in airplane canopies made of PMMA
- p 534 A93-27366
- High-efficiency machining methods for aviation materials
- [ISBN 5-230-16902-8] p 835 A93-39084
- Some characteristics of the design of heads for the cutting of bevel gears with negative curvature of the circular-arc tooth line
- p 835 A93-39093
- Hardening/finishing treatment of compressor blades using a machine with planetary container motion
- p 835 A93-39102
- MACINTOSH PERSONAL COMPUTERS**
- Data acquisition and analysis on a Macintosh
- p 562 A93-29422
- MAGNESIUM**
- Studies of fuel-rich magnesium propellants in a small solid fuel ramjet combustor
- p 535 A93-27759
- MAGNET COILS**
- Forces on a magnet moving past figure-eight coils
- [DE93-009965] p 943 A93-29189
- MAGNETIC BEARINGS**
- Lifting forces acting on magnets placed above a superconducting plane
- p 79 A93-12332
- Magnetic bearings for cryogenic turbomachines
- p 1149 A93-48601
- Blade loss dynamics of a magnetically supported rotor
- p 1257 A93-54653
- Active magnetic bearings applied to industrial compressors
- p 841 A93-27570
- Large angle magnetic suspension test fixture
- [NASA-CR-193123] p 1015 A93-31836
- Design and application of Active Magnetic Bearings (AMB) for vibration control
- p 1033 A93-32279
- MAGNETIC COMPASSES**
- Can one do without the magnetic reference?
- p 501 A93-28197
- Development of a microcomputer-based magnetic heading sensor
- p 1160 A93-52152
- MAGNETIC CONTROL**
- Approaches to control of the large angle magnetic suspension test fixture
- [NASA-CR-191890] p 381 A93-16695
- MAGNETIC DIPOLES**
- Lifting forces acting on magnets placed above a superconducting plane
- p 79 A93-12332
- MAGNETIC FIELDS**
- Forces on a magnet moving past figure-eight coils
- [DE93-009965] p 943 A93-29189
- MAGNETIC LEVITATION VEHICLES**
- The benefits of Maglev technology
- [AIAA PAPER 93-2949] p 1174 A93-48145
- Aerodynamic forces on maglev vehicles
- [PB93-154813] p 782 A93-27413
- MAGNETIC MEASUREMENT**
- Resonance frequencies of a gondola submitted to a forced rotation under a stratospheric balloon
- p 27 A93-11384

MAGNETIC RECORDING

- Refinement of algorithms for calculating the remaining life from magnetic recording instrument data — for IL-86 aircraft wing p 320 A93-18330
Software support for a computerized air situation documentation system p 941 A93-43115

MAGNETIC SUSPENSION

- Analysis, modelling and simulation of the large-angle magnetic suspension test fixture p 375 A93-20297
A magnetic suspension system with a large angular range p 1139 A93-51295
Vibration isolation technology: An executive summary of systems development and demonstration [NASA-TM-105937] p 110 N93-15573
Approaches to control of the large angle magnetic suspension test fixture p 381 N93-16695
Forces on a magnet moving past figure-eight coils [DE93-009965] p 943 N93-29189
Large angle magnetic suspension test fixture [NASA-CR-193123] p 1015 N93-31836

MAGNETIC VARIATIONS

- Magnetic variation - A primitive concept and its hold on contemporary navigation p 32 A93-11021

MAGNETO-OPTICS

- Imaging flaws in thin metal plates using a magneto-optic device p 397 A93-18670
Helicopter plume detection by using an ultranarrow-band noncoherent laser Doppler velocimeter p 542 A93-25198
MOI - Magneto-optic/eddy current imaging p 927 A93-41751
Magneto-optic imaging inspection of selected corrosion specimens [DOT/FAA/CT-TN92/20] p 88 N93-11617

MAGNETOHYDRODYNAMIC FLOW

- A report on the status of MHD hypersonic ground test technology in Russia [AIAA PAPER 93-3193] p 1012 A93-46656

MAGNETOHYDRODYNAMIC GENERATORS

- Effects of external control circuit on coal-fired supersonic diagonal-type MHD generator p 1173 A93-49619

MAGNETOMETERS

- Development of a microcomputer-based magnetic heading sensor p 1160 A93-52152

MAGNETOPLASMA DYNAMICS

- Non-equilibrium flow in an arc heated wind tunnel p 910 A93-42642

MAINTAINABILITY

- Rotorcraft reliability and maintainability: Future design requirements; Proceedings of the Conference, London, United Kingdom, Mar. 20, 1991 [ISBN 0-903409-88-7] p 45 A93-13401
The military operator's experience of reliability and maintainability characteristics p 80 A93-13403
Aircraft designer's viewpoint of reliability and maintainability p 45 A93-13404
Rotorcraft reliability and maintainability - A CAA view of future trends p 45 A93-13407
R&M 2000 field data requirements for a SPO operation p 856 A93-42853
On the basis of experience: Built in product reliability [PNR-90932] p 85 N93-11034
Maintainability of large gas turbine aero engines [PNR-90987] p 58 N93-11069

- An analysis of the reliability and maintainability of the Jian 6 and Jian 7 aircraft and ways to improve them [AD-A261060] p 678 N93-26238
Follow-on operational test and evaluation of the NAVSTAR global positioning system air integration/installation program [AD-A263067] p 793 N93-27925

MAINTENANCE

- Tiltrotor Research Aircraft composite blade repairs - Lessons learned p 108 A93-14819
Powder metallurgy repair of turbine components [ASME PAPER 92-GT-312] p 354 A93-19500
Integrated modular avionics p 896 A93-42777
An interactive preprocessor for the NASA engine performance program [NASA-TM-105786] p 56 N93-10983
Scientific and engineering research facilities at universities and colleges: 1992 [NSF-92-325] p 192 N93-13407
Proceedings of the USAF Structural Integrity Program [AD-A255379] p 110 N93-14549
Technical operating report on the Data Integration and Collection Environment (DICE) instrumentation system design [AD-A258444] p 455 N93-17891
Handling and using information systems with new technology [PNR-90910] p 572 N93-20734
Expendable repair of structural facilities [AD-A260727] p 731 N93-25656

- An analysis of the correlation between the J52 engine component improvement program and improved maintenance parameters [AD-A262062] p 816 N93-28984

MAINTENANCE TRAINING

- The benefits of ground maintenance simulators p 238 A93-18757
Investigation of advanced technology for airway facilities maintenance training [DOT/FAA/CT-TN92/24] p 994 N93-32336

MAN MACHINE SYSTEMS

- Trends of the airborne cockpit display format p 50 A93-11203
Digital map display technology p 77 A93-11206
Control of the pilot-system interface p 166 A93-15040

- Helmet Mounted Sight and display testing p 517 A93-26883
MIDAS technology transfer p 845 A93-35920

- International standards for the qualification of airplane flight simulators; Conference, London, United Kingdom, Jan. 16, 17, 1992, Document Approved [ISBN 1-85768-040-5] p 1140 A93-51934

- Pilot evaluations of augmented flight simulator motion [AIAA PAPER 93-3580] p 1208 A93-52676
Intelligent diagnostics systems p 98 N93-11931
Specification of adaptive aiding systems [AD-A254537] p 159 N93-12602

- NARSIM and EFMS: Tools for research on integrated ATM [NLR-TP-89336-U] p 319 N93-17954

- Flight simulator for hypersonic vehicle and a study of NASP handling qualities p 530 N93-19456
Liquid crystal displays replacing the CRT and CLE of future cockpits p 518 N93-19783

- Mission planning systems for tactical aircraft (pre-flight and in-flight) [AGARD-AR-313] p 496 N93-21187

- Design and implementation of a Global Positioning System (GPS) supported area navigation system with electronic aircraft [ILR-MITT-275(1992)] p 889 N93-30671

MAN-COMPUTER INTERFACE

- An inviscid-viscous interaction approach to the calculation of dynamic stall initiation on airfoils [ASME PAPER 92-GT-128] p 249 A93-19362

- An integrated knowledge system for wind tunnel testing - Project Engineers' Intelligent Assistant [AIAA PAPER 93-0560] p 377 A93-23297

- A graphical user-interface for propulsion system analysis [AIAA PAPER 93-0223] p 440 A93-23699

- A survey of position trackers p 1151 A93-49396
Definition of the structure of expert preferences for the multicriterial analysis of control systems p 1168 A93-50953

- An evaluation of software tools for the design and development of cockpit displays [AIAA PAPER 93-3593] p 1224 A93-52685

- Methods and principles for determining task dependent interface content [NASA-CR-190837] p 36 N93-10961

- NARSIM and EFMS: Tools for research on integrated ATM [NLR-TP-89336-U] p 319 N93-17954

- Management of Automatic Data Processing (ADP) system documentation in the Department of Defense [AD-A258507] p 571 N93-20048

MANAGEMENT

- Human factors causes and management strategies in US Air Force F-16 mishaps 1984-present p 492 N93-19673

- National Airspace System: Air traffic control and airspace management operational concept NAS-SR-132 [DOT/FAA/SE-92/5] p 502 N93-20164

MANAGEMENT ANALYSIS

- A study on the marginal analysis method for the airline yield management p 487 A93-27370

- Configuration management impacts on customer support and satisfaction p 853 A93-35922

MANAGEMENT INFORMATION SYSTEMS

- The development of an airborne information management system for flight test [AIAA PAPER 92-4113] p 51 A93-11281

- Integrating the maintenance requirement maintenance ground based data systems - The missing link? p 238 A93-18760

- Intelligent diagnostics systems p 98 N93-11931
Towards an integrated approach to proactive monitoring and accident prevention p 495 N93-19700

- Management of Automatic Data Processing (ADP) system documentation in the Department of Defense [AD-A258507] p 571 N93-20048

MANAGEMENT METHODS

- A damage tolerance/life processor for structural integrity and force management p 507 A93-27962

- A database approach to aircraft carrier airplan production [AD-A257737] p 240 N93-17666

- Design of a cooperative problem-solving system for enroute flight planning: An empirical study of its use by airline dispatchers [NASA-CR-192709] p 707 N93-25330

- Aviation production engineering: Selected articles [AD-A261231] p 764 N93-27056

MANAGEMENT PLANNING

- Innovation in engineering [PNR-90889] p 59 N93-11207

- Airport stand assignment model [TT-9104] p 67 N93-11728

- Report to Congress: Long-term availability of adequate airport system capacity [AD-A258209] p 319 N93-18202

- Wright Laboratory research and development facilities handbook [AD-A258746] p 572 N93-20403

- Aircraft electrical and environmental systems, AFSCs 452x5, 454x5, and 454x6 [AD-A261213] p 717 N93-25733

- The 1991-1992 aviation system capacity plan [AD-A263436] p 911 N93-29788

MANAGEMENT SYSTEMS

- On-board condition management for aircraft gas turbines [ASME PAPER 92-GT-416] p 357 A93-19564

- Managing the world's air traffic p 501 A93-28392
Methods and equipment for data processing and acquisition in information management systems p 856 A93-43101

- Satellite navigation in traffic management p 914 A93-43549

MANEUVERABILITY

- Static aeroelastic analysis of a maneuvering aircraft with damaged wing [AIAA PAPER 92-4765] p 325 A93-20360

- Flight test and analysis procedures for new handling criteria [RAE-TM-FM-26] p 47 N93-10803

- Overview of high performance aircraft propulsion research [NASA-TM-105839] p 59 N93-11530

- Motion simulation of underwater vehicles [VTT-PUBS-97] p 443 N93-18698

- Dynamic airfoil stall investigations p 786 N93-27453

- Advanced aircraft with thrust vector control [MBB-FE-1-S-PUB-0504] p 998 N93-31043

MANEUVERABLE REENTRY BODIES

- Trajectory control for a low-lift re-entry vehicle p 1141 A93-49592

- Analysis of a turning point problem in flight trajectory optimization p 1210 A93-52885

MANEUVERS

- Parachute canopy control and guidance training requirements and methodology [AIAA PAPER 93-1255] p 703 A93-35188

- An investigation of a prototype OASYS effectiveness in maneuvering flight [AD-A257901] p 338 N93-18339

MANIPULATORS

- System identification of unstable manipulators using ERA methods - Eigensystem Realization Algorithm [AIAA PAPER 93-3842] p 1170 A93-51431

MANNED SPACECRAFT

- Aerodynamic heating environment definition/thermal protection system selection for the HL-20 p 1181 A93-53739

- HL-20 computational fluid dynamics analysis p 1181 A93-53740

MANUAL CONTROL

- Flight testing and simulation of an F-15 airplane using throttles for flight control [AIAA PAPER 92-4109] p 39 A93-11278

- A review of alternative philosophies — methods for operating in ICAO category 3 weather conditions p 142 A93-17305

- Manual flying of curved precision approaches to landing with electromechanical instrumentation. A piloted simulation study [NASA-TP-3255] p 344 N93-18408

- A simulator study into low speed longitudinal handling qualities of ACT transport aircraft [NLR-TP-89387-U] p 527 N93-20743

MANUALS

- An interactive preprocessor for the NASA engine performance program [NASA-TM-105786] p 56 N93-10983

- User manual for NASA Lewis 10 by 10 foot supersonic wind tunnel [NASA-TM-105626] p 194 N93-15498

- Flight dynamics system software development environment (FDS/SDE) tutorial [NASA-TM-108580] p 230 N93-15502
- NASA Lewis 8- by 6-foot supersonic wind tunnel user manual [NASA-TM-105771] p 730 N93-25080
- MANUFACTURING**
- Achieving manufacturing excellence for gas turbine components through focused implementation of technology [ASME PAPER 92-GT-139] p 401 A93-19371
- Effect of manufacturing deviations on performance of axial flow compressor blading [ASME PAPER 92-GT-326] p 257 A93-19510
- Ensuring the reliability and service life of flight vehicle structures by engineering methods p 745 A93-35276
- Improved Airframe Manufacturing Technology p 763 A93-35971
- Design for manufacture by resin transfer molding of composite parts for rotorcraft [SME PAPER EM93-103] p 1159 A93-51733
- The application of manufacturing systems engineering for aero engine gears [PNR-90944] p 86 N93-11054
- The use of simultaneous engineering for the design and manufacture of the low pressure turbine for the Rolls-Royce Trent engine [PNR-90887] p 59 N93-11206
- Simultaneous engineering in aero gas turbine design and manufacture [PNR-90890] p 59 N93-11208
- Optimum design of aircraft structures with manufacturing and buckling constraints p 162 N93-13815
- The Airbus floor beam: Towards a cost-effective composite design and manufacture research project sponsored by Airbus industry [LR-677] p 329 N93-16283
- YF-22A prototype advanced tactical fighter demonstration/validation flight test program overview p 511 N93-19906
- Development of cure cycles: From laboratory analysis and testing to production of large scale composites [MBB-Z-0442-92-PUB] p 536 N93-20845
- On machine capacitance dimensional and surface profile measurement system p 750 N93-25579
- Special tooling disposition for aircraft entering post production support [AD-A261614] p 678 N93-26168
- Aviation production engineering: Selected articles [AD-A261231] p 764 N93-27056
- Coherent systems in the terahertz frequency range: Elements, operation, and examples p 841 N93-27727
- Process optimization of Hexoloy SX-SiC towards improved mechanical properties [DE93-007913] p 826 N93-28564
- Lessons learned for composite structures p 920 N93-30444
- Process and assembly plans for low cost commercial fuselage structure p 923 N93-30865
- Electropneumatic actuator, phase 1 [PB93-174951] p 1033 N93-31876
- MAP MATCHING GUIDANCE**
- Hybrid guidance for maneuvering flight vehicles [AD-A254110] p 69 N93-11798
- Information-based criteria of terrain navigability. Part 1: Data-base analysis p 793 N93-27178
- MAPPING**
- Digital map display technology p 77 A93-11206
- Merging sparse optical flow and edge connectivity between image features: A representation scheme for 2-D display of scene depth p 845 N93-27179
- MAPS**
- Maps and charts for visual air navigation p 498 A93-25170
- Merging sparse optical flow and edge connectivity between image features: A representation scheme for 2-D display of scene depth p 845 N93-27179
- Aerial cartography using SICAD NAV-AIR p 1034 N93-31258
- MARANGONI CONVECTION**
- Experimental investigation of the management of large-sized drops and the onset of Marangoni-convection p 926 A93-41700
- MARINE ENVIRONMENTS**
- Royal Navy helicopter operations in the maritime environment p 1190 A93-54290
- MARINE METEOROLOGY**
- Sea fog and stratus - A major aviation and marine hazard in the northern Gulf of Mexico p 844 A93-39762
- MARINE PROPULSION**
- Experimental determination of the bulk swirl attenuation between two axial stations in the LM2500 inlet bellmouth [AIAA PAPER 93-2203] p 1155 A93-50015
- Interaction between ice and propeller [VTT-TIED-1281] p 841 N93-27832
- On the verification of a theory for sculling propulsion [ETN-93-94040] p 1031 N93-31519
- MARKET RESEARCH**
- Prospects for a second generation supersonic transport p 108 A93-14154
- Competition in a single European air transport market; Proceedings of the Conference, London, United Kingdom, Dec. 1, 1992 [ISBN 1-85768-080-4] p 458 A93-29473
- Configuration management impacts on customer support and satisfaction p 853 A93-35922
- The well made engine p 1122 A93-50352
- Defence electronics industry profile, 1990-1991 [CTN-92-60515] p 84 N93-10653
- Future regional transport aircraft market, constraints, and technology stimuli p 109 N93-13025
- The 1990 high-speed civil transport studies [NASA-TM-107669] p 330 N93-16947
- The 1990 high-speed civil transport studies. Summary report [NASA-CR-189618] p 330 N93-16999
- Design of a turbofan powered regional transport aircraft p 894 N93-29721
- Helicopter training simulators: Key market factors p 912 N93-30683
- MARKOV PROCESSES**
- Comparison of neural network and Markov random field image segmentation techniques p 397 A93-18652
- Markov fatigue in single crystal airfoils [ASME PAPER 92-GT-95] p 387 A93-19341
- The development of the speaker independent ARM continuous speech recognition system [RSRE-MEMO-4473] p 87 N93-11383
- Preliminary results on the use of linear discriminant analysis in the ARM continuous speech recognition system [RSRE-MEMO-4511] p 87 N93-11384
- The use of linear discriminant analysis in the ARM continuous speech recognition system [RSRE-MEMO-4512] p 87 N93-11385
- Fatigue in single crystal nickel superalloys [AD-A254603] p 74 N93-12237
- MARS (PLANET)**
- Conceptual design of a Mars transportation system [NASA-CR-192039] p 420 N93-18047
- MARTENSITIC TRANSFORMATION**
- Structure of martensite in titanium alloy Ti-6Al-1.6Zr-3.3Mo-0.3Si p 916 A93-43616
- MASS DISTRIBUTION**
- Stability of the vertical autorotation of a single-winged samara p 274 A93-22443
- Calculation of the position of aircraft center of gravity on an IBM PC p 996 A93-45671
- Effect of geometry, static stability, and mass distribution on the tumbling characteristics of generic flying-wing models [AIAA PAPER 93-3615] p 1125 A93-48302
- A method for calculating the aerodynamic and mass characteristics of coaxial rotors with rigid blade fastening (the ABC system) p 1071 A93-49323
- MASS FLOW**
- An investigation of post stall transients and recoverability of axial compression systems. I - A simplified method [ASME PAPER 92-GT-55] p 347 A93-19305
- Evaluation of approaches to active compressor surge stabilization [ASME PAPER 92-GT-182] p 352 A93-19407
- An optimisation-matching procedure for variable cycle jet engines [ASME PAPER 92-GT-406] p 356 A93-19555
- A comparison between numerically modelled and experimentally measured loss mechanisms in wave rotors [AIAA PAPER 93-2522] p 1120 A93-50252
- Performance parameters and assessment p 81 N93-10052
- System and method for cancelling expansion waves in a wave rotor [NASA-CASE-LEW-15218-1] p 86 N93-11172
- Numerical analysis of the flow fields in a RQL gas turbine combustor [DE92-017509] p 89 N93-11767
- Application of subsonic first-order panel methods for prediction of inlet and nozzle aerodynamic interactions with airframe p 130 N93-13223
- A numerical investigation for supersonic inlet p 303 N93-19315
- The aerodynamic performance of laser drilled sheets [AERO-REPT-9204] p 484 N93-20806
- A feasibility study of using Langley 0.3-m transonic cryogenic tunnel sidewall boundary-layer removal system for heavy gas testing [NASA-CR-191438] p 747 N93-25087
- CFD mixing analysis of axially opposed rows of jets injected into confined crossflow [NASA-TM-106179] p 813 N93-27128
- By-passing of heat exchangers in gas turbines p 814 N93-27189
- Solution of Euler equations for forebody-inlet ensemble of aircraft at high angle of attack [AD-A263905] p 876 N93-29862
- MASS FLOW RATE**
- Scramjet fuel-air mixing establishment in a pulse facility p 359 A93-21667
- Effect of radial distortion on the performance of a centrifugal compressor p 861 A93-42256
- Atomization of JP-10/B4C gelled slurry fuel [AD-A256827] p 391 N93-15686
- Experimental analysis of combustion oscillations with reference to ramjet propulsion p 392 N93-17614
- A feasibility study of using Langley 0.3-m transonic cryogenic tunnel sidewall boundary-layer removal system for heavy gas testing [NASA-CR-191438] p 747 N93-25087
- MASS RATIOS**
- Modeling of turbulent supersonic H₂-air combustion with an improved joint beta PDF [NASA-CR-191929] p 391 N93-16389
- MASS SPECTROMETERS**
- Measurements of jet aircraft emissions at cruise altitude. I - The odd-nitrogen gases NO, NO₂, HNO₂ and HNO₃ p 556 A93-24391
- A novel aircraft-based tandem mass spectrometer for atmospheric ion and trace gas measurements p 925 A93-40672
- MASS TRANSFER**
- Effect of trailing-edge ejection on local heat (mass) transfer in pin fin cooling channels in turbine blades [ASME PAPER 92-GT-178] p 352 A93-19404
- The WINCOF-I code: Detailed description [NASA-CR-190779] p 677 N93-24760
- Vortex structure and mass transfer near the base of a cylinder and a turbine blade p 901 N93-29929
- MASSIVELY PARALLEL PROCESSORS**
- Aircraft optimization by a system approach - Achievements and trends p 153 A93-14205
- A performance comparison of massively parallel Parabolized Navier-Stokes solutions [AIAA PAPER 93-0059] p 435 A93-20172
- Massively parallel aerodynamic shape optimization p 266 A93-20729
- A new parallel-vector finite element analysis software on distributed-memory computers [AIAA PAPER 93-1307] p 756 A93-33883
- MATCHED FILTERS**
- Further studies using matched filter theory and stochastic simulation for gust loads prediction [AIAA PAPER 93-1365] p 726 A93-33932
- Fast design of circular-harmonic filters using simulated annealing p 1038 A93-45556
- Computation of maximized gust loads for nonlinear aircraft using matched-filter-based schemes p 1136 A93-52452
- ACTA Aeronautica et Astronautica Sinica (selected articles) p 110 N93-13946
- [AD-A255070] p 110 N93-13946
- Detection performance of digital polarity sampled phase reversal code pulse compressors [AD-A262930] p 842 N93-28289
- MATERIAL ABSORPTION**
- Effects of thermal history and jet fuel absorption on the properties of APC-2 p 534 A93-25252
- MATERIALS SCIENCE**
- Canadian low-gravity research using parabolic aircraft p 384 A93-21908
- AIAA/ASME/ASCE/AHS/ASC Structures, Structural Dynamics, and Materials Conference, 34th and AIAA/ASME Adaptive Structures Forum, La Jolla, CA, Apr. 19-22, 1993, Technical Papers. Pts. 1-6 p 738 A93-33876
- Materials problems connected with the propulsion of supersonic air carriers [ONERA, TP NO. 1992-157] p 824 A93-38736
- Computed tomography of advanced materials and processes p 832 A93-38975
- The effects of high-pressure water on the material integrity of selected aircraft coatings and substrates [SME PAPER AD92-207] p 855 A93-40668
- Materials development for light design - A suppliers view p 915 A93-40777
- Materials processing in low gravity [NASA-CR-184421] p 91 N93-12401
- Federal Aviation Administration pavement modeling p 379 N93-16315
- Construction and testing of simple airfoils to demonstrate structural design, materials choice, and composite concepts p 879 N93-30979

MATERIALS TESTS

- Case studies in composite material structural design, manufacture and testing p 157 A93-14385
The structure and material testing facility needed for future SST/HST development p 528 A93-24481
[AIAA PAPER 92-3887]
Fiber pulling apparatus modification p 220 N93-14763
[NASA-CR-184498]
Construction and testing of simple airfoils to demonstrate structural design, materials choice, and composite concepts p 879 N93-30979

MATHEMATICAL LOGIC

- Search strategies for a sequence of baseline indices for building sections of a flight-safety automatic control system in the interactive mode p 306 A93-18346
A brief overview of NASA Langley's research program in formal methods p 228 N93-12958

MATHEMATICAL MODELS

- Numerical modeling of supersonic flows past wings of different aspect ratios over a wide range of angles of attack within the framework of the plane section law p 5 A93-10141
DME/P critical area determination on message passing processors p 31 A93-11010
A mathematical model to determine the health of components based on SOAP data — spectrometric oil analysis program p 53 A93-12238
A nomographic model for multicriterial optimization during the design of a flight vehicle powerplant p 95 A93-12821
Specification of a class of discrete event processes and their controllers p 96 A93-13078
Nonlinear aerodynamic parameter estimation and model structure identification p 15 A93-13308
[AIAA PAPER 92-4502]
Stirling engine - Available tools for long-life assessment — for space propulsion p 195 A93-13824
Application of SPEED in aviation industry p 225 A93-14178
A new aircraft integrated positioning and communication system based on satellite p 150 A93-14236
The numerical calculation for the coupling of multiple propeller discrete noise and its interaction with the fuselage boundary p 231 A93-14268
Dynamic stability, coupling and active control of elastic vehicles with unsteady aerodynamic forces modeling p 182 A93-14282
An investigation of real-time diagnostic technique on aeroengine p 174 A93-16844
Motion and decay of trailing vortices within the atmospheric surface layer p 425 A93-18548
Coupled multi-disciplinary simulation of composite engine structures in propulsion environment [ASME PAPER 92-GT-6] p 346 A93-19279
The comparison of different simplified mathematical models of the gas turbine combustion chamber as an object of temperature and pressure control [ASME PAPER 92-GT-347] p 354 A93-19518
Analysis, modelling and simulation of the large-angle magnetic suspension test fixture p 375 A93-20297
Experimental and numerical analysis of the wing rock characteristics of a 'wing-body-tail' configuration [AIAA PAPER 93-0187] p 368 A93-22612
Using system identification to improve the performance of a low-cost flight simulator p 369 A93-22885
Numerical modeling of anti-icing systems and comparison to test results on a NACA 0012 airfoil [AIAA PAPER 93-0170] p 327 A93-23242
Ice accretion prediction for a typical commercial transport aircraft p 310 A93-23245
[AIAA PAPER 93-0174]
An improved numerical model for wave rotor design and analysis p 361 A93-23384
[AIAA PAPER 93-0482]
Approximation methods for control of structural acoustics models with piezoceramic actuators p 452 A93-23744
Numerical modeling of leading edge separated flow at incompressible speeds p 460 A93-24079
Comprehensive analysis of bearingless rotors - Model development and experimental correlation of modes, response, trim and stability [AIAA PAPER 93-0624] p 504 A93-24741
A simple criterion for vortex breakdown [AIAA PAPER 93-0866] p 469 A93-24928
A new method for improved rotor free-wake convergence [AIAA PAPER 93-0872] p 469 A93-24933
Development of a model to predict electric vehicle performance over a variety of driving conditions p 570 A93-26011
Problems in the modeling of helicopter flight p 506 A93-27293
A generic harmonic rotor model for helicopter flight simulation p 506 A93-27480

- Sensitivity-based scaling for approximating structural response p 548 A93-28618
Effect of modeling techniques in the coupled rotor-body vibration analysis p 710 A93-33928
[AIAA PAPER 93-1360]
Recent developments in equivalent plate modeling for wing shape optimization p 742 A93-34172
[AIAA PAPER 93-1647]
Approach of modeling continuous turbine engine operation from startup to shutdown p 721 A93-34495
Selection of protective coatings for parts in a computer-aided design system p 746 A93-35290
A study of the rotor wake of a small-scale rotor model in forward flight using laser light sheet flow visualization with comparisons to analytical models p 766 A93-35957
A parametric study of real time mathematical modeling incorporating dynamic wake and elastic blades p 798 A93-35986
A 2-D numerical model for predicting the aerodynamic performance of the NOTAR system tailboom p 766 A93-35994
Modal analysis of multistage gear systems coupled with gearbox vibrations p 827 A93-36588
Numerical modeling of the impact of a bird against aircraft transparencies p 801 A93-36797
Robust stabilization of an aero-elastic system p 817 A93-37044
Modeling of linear isentropic flow systems p 828 A93-37046
The numerical model of supersonic air flow field with hydrogen transverse injection p 859 A93-41736
Computation of hypersonic flow over a sphere using kinetic flux vector splitting scheme with equilibrium chemistry p 861 A93-42260
Some questions of scale in simulation, and a few answers p 939 A93-42830
A new flux splitting scheme p 973 A93-47189
On the modelling of separated flows about airfoils [AIAA PAPER 93-3479] p 981 A93-47257
Mathematical model for the effect of turbulent velocity pulsations on the stability of a powerplant p 1003 A93-47508
Nonlinear aerodynamic modeling using multivariate orthogonal functions p 1065 A93-48321
[AIAA PAPER 93-3636]
Vibration characteristics of mistuned bladed disk p 1108 A93-49190
Problems in the optimization of complex engineering systems p 1165 A93-49307
An analytical study of dilution jet mixing in a cylindrical duct p 1113 A93-49876
[AIAA PAPER 93-2043]
Numerical modeling of flow in a hypersonic laminar boundary layer p 1086 A93-50967
Numerical model for predictions of reverse flow combustor aerothermal characteristics p 1123 A93-51645
Flight update of aerodynamic math model [AIAA PAPER 93-3596] p 1224 A93-52687
An experimental and a theoretical investigation of rotor pitch damping using a model rotor p 47 N93-10322
A comparative study of semi-empirical dynamic stall models p 18 N93-10544
Combustion noise and combustion instabilities in propulsion systems p 100 N93-10682
Development of nonlinear aerodynamic models for unsteady responses p 19 N93-10845
Arguments concerning wind tunnel test studies of the trim characteristics of objects with small asymmetries [AD-A254111] p 19 N93-10858
The prediction of convective heat transfer in rotating square ducts p 85 N93-11025
[PNR-90929]
The role of turbomachinery testing for stability in distorted flow p 57 N93-11040
[PNR-90943]
Experiments on low aspect ratio hydroplanes to measure lift under static and dynamic conditions [ARE-TM(UHR)-90306] p 21 N93-11365
Modeling and model simplification of aeroelastic vehicles: An overview p 64 N93-12216
[NASA-TM-107691]
Numerical investigations into the base drag of various wedges using the base flow model developed by Mauri Tanner [REPT-B-36] p 26 N93-12414
An improved numerical model for wave rotor design and analysis p 60 N93-12418
[NASA-TM-105915]
Thermostructural applications of heat pipes for cooling leading edges of high-speed aerospace vehicles p 91 N93-12460
Thermal barrier coating life prediction model development, phase 2 [NASA-CR-189111] p 198 N93-12589

- ILS mathematical modeling study of the effects of an ASR-9 structure at the Long Island MacArthur Airport, Islip, NY [DOT/FAA/CT-TN92/25] p 192 N93-12668
An investigation of the dynamic response of lifting surfaces with concentrated structural nonlinearities p 162 N93-13807
Formulation and validation of high-order mathematical models of helicopter flight dynamics p 162 N93-13821
Assessment of potential aerodynamic benefits from spanwise blowing at the wing tip p 134 N93-13822
Evaluation of three models used for predicting noise propagated long distances overground [AD-A255963] p 232 N93-14406
A compilation of the mathematics leading to the doublet lattice method [AD-A256304] p 136 N93-14441
A finite element model for analysis of thermoviscoplastic behavior of hypersonic leading edge structures subject to intense aerothermal heating p 137 N93-14631
Finite-state inflow applied to aeroelastic flutter of fixed and rotating wings p 188 N93-14830
Modeling variable blowing on a slender cone in hypersonic flow p 138 N93-14836
Aeroplane crashes on the runway: Validation and final evaluation of the method of modeling an airframe structure [IMFL-91-32] p 165 N93-15126
Numerical modeling of anti-icing systems and comparison to test results on a NASA 0012 airfoil [NASA-TM-105975] p 148 N93-15345
Ice accretion prediction for a typical commercial transport aircraft [NASA-TM-105976] p 149 N93-15522
Optimization of an internally finned rotating heat pipe [AD-A256725] p 453 N93-15980
Experimental and numerical investigation of vortex flow over a 76/60-deg double-delta wing [LR-680] p 289 N93-16210
Unified Airport Design and Analysis Concepts Workshop [DOT/FAA/RD-92/17] p 378 N93-16309
State of the art of airport pavement analysis and design p 378 N93-16310
Development of user guidelines for a three-dimensional finite element pavement model p 379 N93-16311
Federal Aviation Administration pavement modeling p 379 N93-16315
State of the art review of rutting and cracking in pavements p 380 N93-16316
Development of a unified airport pavement analysis and design system p 380 N93-16317
Unified airport pavement design procedure p 380 N93-16318
Three-dimensional stress analysis of multilayered airport pavements: Integral transform approach p 381 N93-16319
A domain-specific design architecture for composite material design and aircraft part redesign p 442 N93-17522
Mathematical optimization: A powerful tool for aircraft design [MBB-FE-2-S-PUB-478] p 331 N93-17564
Pitching moment of low aspect ratio wing-body combinations up to high angles of attack at supersonic speeds [ESDU-92043] p 333 N93-17958
Introduction to Flutter of Winged Aircraft, volume 1 [VKI-LS-1992-01] p 372 N93-18142
The unified method of aeroelasticity p 372 N93-18143
Identification of system dynamics of a high incidence research model [RR-407] p 339 N93-18507
Basic research on design analysis methods for rotorcraft vibrations [NASA-CR-191917] p 422 N93-18576
A Blotter type numerical model for nonequilibrium viscous hypersonic flows in upwind finite elements [INRIA-RR-1478] p 297 N93-18648
Influence of the physical modelling of viscous terms on hypersonic flow computations [INRIA-RR-1493] p 297 N93-18652
Stall transients including effects of inlet distortion and intake geometry p 423 N93-18726
Axial Flow Compressors, volume 2 [VKI-LS-1992-02-VOL-2] p 423 N93-18731
Rotating stall: Modeling-measurement techniques; unsteady loss-unsteady flow field p 424 N93-18732
Formulation of a structural model for flutter analysis of low aspect ratio composite aircraft wings p 372 N93-19019
Aircraft landing gear shimmy p 340 N93-19029
On-line aircraft state and parameter estimation p 512 N93-19929

The semi-discrete Galerkin finite element modelling of compressible viscous flow past an airfoil [NASA-CR-192161] p 483 N93-20018

Evaluation of candidate working fluid formulations for the electrothermal - chemical wind tunnel [NASA-CR-192196] p 530 N93-20312

Resonant response analysis of a high speed gear p 553 N93-20662

Analysis of aircraft noise levels in the vicinity of start-of-takeoff roll at Baltimore-Washington International Airport [PB92-221605] p 559 N93-21501

Modelisation and computation of composite materials p 537 N93-21518

Unsteady Navier-Stokes method for accelerated moving airfoils with separation [DLR-FB-92-03] p 485 N93-21763

ILS mathematical modeling study of an ILS glide slope proposed for runway 19L at the Meridian Naval Air Station, Mississippi [DOT/FAA/CT-TN93/8] p 705 N93-24741

Crashworthiness of composite seats for civil aircraft p 703 N93-24773

The 1992 International Aerospace and Ground Conference on Lightning and Static Electricity: Addendum [DOT/FAA/CT-92/20-ADD-1] p 753 N93-24875

Numerical modelling of induced effects of lightning strike on an all composite helicopter p 703 N93-24879

A computational approach to predicting the extent of arc root damage in CFC panels p 735 N93-24890

Zoning of aircraft by electric field modelling p 704 N93-24894

Lightning phenomenology bases for full threat return stroke occurrence following extended leader sweep at flight altitudes p 754 N93-24895

Development of models for predicting the triggering of lightning by launch vehicles p 734 N93-24899

Fuel Injector: Air swirl characterization aerothermal modeling, phase 2, volume 2 [NASA-CR-189193-VOL-2] p 721 N93-25106

Grid sensitivity for aerodynamic optimization and flow analysis [NASA-CR-192980] p 694 N93-25117

A simple, approximate model of parachute inflation [DE93-002465] p 694 N93-25121

Generic hypersonic vehicle performance model [NASA-CR-192953] p 714 N93-25162

Integrated aerodynamic-structural wing design optimization p 714 N93-25279

A numerical and experimental studies of flow characteristics in centrifugal fans p 695 N93-25339

A preliminary sizing method for unmanned aircraft using multi-variate optimisation p 714 N93-25408

Use of high performance networks and supercomputers for real-time flight simulation p 731 N93-25574

Numerical modelling of viscous turbomachinery flows with a pressure correction method p 723 N93-25702

Thermally induced stresses in a composite exposed to fire [AD-A261714] p 737 N93-26371

The ILS mathematical modeling study of the Runway 10 ILS Localizer at Luis Munoz Marin International Airport, San Juan, Puerto Rico [DOT/FAA/CT-TN93/10] p 792 N93-27017

An analytical study of dilution jet mixing in a cylindrical duct [NASA-TM-106181] p 814 N93-27160

Regression rate mechanism in a solid fuel ramjet p 814 N93-27185

Development of a pulse ramjet based on twin valveless pulse combustors coupled to operate in antiphase p 814 N93-27186

Analysis of thrust modulation of ram-rockets by a vortex valve p 814 N93-27187

Numerical modeling of runback water on ice protected aircraft surfaces p 840 N93-27438

Active magnetic bearings applied to industrial compressors p 841 N93-27570

A prediction model for noise from low-altitude military aircraft [AD-A262494] p 852 N93-27662

Homenthalpic-flow approach for hypersonic inviscid non-equilibrium flows [INRIA-RR-1652] p 788 N93-28440

An experimental study of flow over a 6 to 1 prolate spheroid at incidence p 874 N93-29124

Modeling the effects of drop drag and breakup on fuel sprays [AD-A263650] p 931 N93-29388

Advanced thermally-stable, coal-derived, jet fuels program: Experiment system and model development [AD-A262747] p 917 N93-29402

Mathematical modeling and control law development for the atmospheric monitoring and control system of the Controlled Environment Research Chamber (CERC) at NASA Ames Research Center [AD-A261978] p 911 N93-29436

Flight mechanical model for performance calculations and interactions between flight vehicle and ramjet in regard to the flight orbit [ESA-TT-1267] p 893 N93-29464

Measurement of turbulent spots and intermittency modelling at gas-turbine conditions p 902 N93-29934

Modelling thermal behaviour of turbomachinery discs and casings p 903 N93-29949

A Navier-Stokes solver with different turbulence models applied to film-cooled turbine cascades p 904 N93-29962

Mathematical model of frost heave and thaw settlement in pavements [CRREL-REPT-93-2] p 912 N93-30103

Simulation, characterization and control of forced unsteady viscous flows using Navier-Stokes equations [AD-A264333] p 934 N93-30369

Validation and upgrading of physically based mathematical models p 942 N93-30688

Structural design using neural networks p 942 N93-31029

On the verification of a theory for sculling propulsion [ETN-93-94040] p 1031 N93-31519

Crack growth prediction models p 1004 N93-31747

Large angle magnetic suspension test fixture [NASA-CR-193123] p 1015 N93-31836

MATHEMATICAL PROGRAMMING

Optimization of the parameters of the lift-augmentation devices of the wing of a maneuverable aircraft equipped with an active load-reduction system p 804 A93-39189

Nonsmooth trajectory optimization - An approach using continuous simulated annealing [AIAA PAPER 93-3657] p 1099 A93-48337

Control problem for a plant with artificial intelligence p 1168 A93-50960

MATRICES (MATHEMATICS)

An improved method of structural dynamic test design for ground flying and its application to the SH-2F and SH-2G helicopters p 512 N93-19928

A transfer matrix approach to vibration localization in mistuned blade assemblies [NASA-TM-106112] p 838 N93-27088

MATRIX MATERIALS

Advanced fiber/matrix material systems p 921 N93-30854

MATRIX METHODS

Comparison of some direct multi-point force appropriation methods p 928 A93-43338

A transfer matrix approach to vibration localization in mistuned blade assemblies [NASA-TM-106112] p 838 N93-27088

MAXIMUM LIKELIHOOD ESTIMATES

A maximum likelihood method for flight test data compatibility check p 95 A93-12732

Prospective application of neural networks in superresolution radars p 211 A93-16849

Estimation of aerodynamic characteristics from flight test data. II - Analysis methods under in-flight wind tunnel test concept p 191 A93-16934

Determination of the stability and control derivatives of the F/A-18 HARV from flight data using the maximum likelihood method [NASA-CR-191216] p 186 N93-12903

The flight test and data analysis program for the development of a Boeing/De Havilland Dash 8 simulator model p 512 N93-19930

MCDONNELL AIRCRAFT

NOTAR system - A quiet character p 567 A93-29418

MCDONNELL DOUGLAS AIRCRAFT

The smart truck --- structure, systems, avionics of C-17 airlifter p 40 A93-11420

C-17 - High-tech 'lifter from Long Beach p 713 A93-34519

MD-11 Automatic Flight System p 818 A93-37075

MEAN

General aviation aircraft: Normal acceleration data analysis and collection project [DOT/FAA/CT-91/20] p 713 N93-24739

MEASURING INSTRUMENTS

Collection of works on measuring and computing systems for research on the aerodynamics, dynamics, and strength of flight vehicles p 75 A93-10026

Probing questions for aerodynamic testing p 80 A93-13437

Aircraft measurement of electric field - Self-calibration p 753 A93-34694

Thin gradient heat fluxmeters developed at ONERA [ONERA, TP NO. 1992-87] p 831 A93-38571

Algorithmic method for optimizing the precision characteristics of a fuel metering system p 999 A93-45681

Use of shear-stress-sensitive, temperature-insensitive liquid crystals for boundary layer transition detection in hypersonic flows [AIAA PAPER 93-3070] p 1059 A93-48245

Sensors with centroid based common sensing scheme and their multiplexing --- fiber optic sensors in aircraft and aircraft engine applications p 1192 A93-52994

Sensor fault detection using nonlinear observer and polynomial classifier p 170 N93-15182

Reflection type skin friction meter [NASA-CASE-LAR-14520-1-SB] p 296 N93-18275

Program overview: 1991 flight test objectives p 488 N93-19591

Method of measuring cross-flow vortices by use of an array of hot-film sensors [NASA-CASE-LAR-14824-1-SB] p 751 N93-26000

Flow prediction over a transport multi-element high-lift system and comparison with flight measurements p 785 N93-27448

Advanced thermally-stable, coal-derived, jet fuels program: Experiment system and model development [AD-A262747] p 917 N93-29402

Selection and static calibration of the Marsh J1678 pressure gauge p 931 N93-29779

The basic measurement equipment of the DLR test aircraft p 1000 N93-31273

MECHANICAL DEVICES

Chaos in mechanical systems with especial reference to rotorcraft and missiles [AD-A263703] p 943 N93-29384

MECHANICAL DRIVES

Super Puma MK II - Rotor and gearbox fatigue p 46 A93-13636

A vibration monitoring acquisition and diagnostic system for helicopter drive train bench tests p 826 A93-35930

Variable speed rotary compressor and adjustable speed drive efficiencies measured in the laboratory [DE92-040026] p 222 N93-15278

MECHANICAL ENGINEERING

Computational nonlinear mechanics in aerospace engineering [ISBN 1-56347-044-6] p 78 A93-12151

Effect of manufacturing deviations on performance of axial flow compressor blading [ASME PAPER 92-GT-326] p 257 A93-19510

The design of a senior-level CAD course with emphasis on fluid/thermal systems [AIAA PAPER 93-0426] p 454 A93-23344

Rotating machinery - Dynamics: Proceedings of the 3rd International Symposium on Transport Phenomena and Dynamics of Rotating Machinery (ISROMAC-3), Honolulu, HI, Apr. 1-4, 1990 [ISBN 1-56032-147-4] p 1257 A93-54651

Adaptivity-fluids-localization. The challenge to computational mechanics p 553 N93-20618

MECHANICAL MEASUREMENT

Correlation of X-ray CT measurements to shear strength in pultruded composite materials p 396 A93-18618

Experimental measurement of structural intensity on an aircraft fuselage p 544 A93-26999

Embedded Bragg grating fiber optic sensor for composite flexbeams p 828 A93-37350

MECHANICAL PROPERTIES

Stirling engine - Available tools for long-life assessment --- for space propulsion p 195 A93-13824

Mechanical testing analyses of new aluminium alloy SP7 typical-parts in aircraft p 196 A93-14174

Thermoplastic and thermosetting matrix composite structures - Comparison of mechanical properties p 197 A93-15029

Effects of thermal history and jet fuel absorption on the properties of APC-2 p 534 A93-25252

Quantification of uncertainties in composites [AIAA PAPER 93-1440] p 734 A93-33989

Gas phase hydrogen permeation in a Ni-Fe-Co superalloy p 735 A93-34510

A study of the strength of a closed system of wings p 828 A93-36792

Birth of the betas p 824 A93-38200

Potential and prospects of intermetallic materials for applications in the aerospace industry [ONERA, TP NO. 1992-99] p 824 A93-38580

Shock waves; Proceedings of the 18th International Symposium, Sendai, Japan, July 21-26, 1991. Vols. 1 & 2 [ISBN 0-387-55686-9] p 1023 A93-45451

Boeing 777 gets a boost from titanium p 1018 A93-45987

Mechanical anisotropy in directionally solidified turbine blade p 1018 A93-47356

Beyond steel - TMCs for lighter landing gear p 1100 A93-49337

- Main directions of improving the quality of aluminum-lithium alloys for welded aircraft structures p 1146 A93-51104
- The characterization and development of materials for advanced textile composites p 1211 A93-53434
- Repair materials and processes for the MD-11 Composite Tailcone p 1216 A93-53452
- Evaluation of 2D ceramic matrix composites in aeroconvective environments p 1212 A93-53459
- Origin of the carbon rich sliding interface in alkali containing matrix-SiC nicalon fibre composites [ONERA, TP NO. 1993-77] p 1212 A93-53598
- Advanced materials in gas turbine engines: An assessment [PNR-90946] p 58 N93-11105
- Development of advanced carbon-carbon annular flameholders for gas turbines [PNR-90947] p 58 N93-11106
- Thermal barrier coating life prediction model development, phase 2 [NASA-CR-189111] p 198 N93-12589
- Proceedings of the USAF Structural Integrity Program [AD-A255379] p 110 N93-14549
- Micro mechanical behavior of pavements p 379 N93-16312
- Process optimization of Hexoloy SX-SiC towards improved mechanical properties [DE93-007913] p 826 N93-28564
- Characterization of ceramic composite materials for gas turbine applications [DE93-009719] p 905 N93-30168
- Use of titanium castings without a casting factor [AD-A264414] p 1018 N93-31192
- MEDICAL EQUIPMENT**
- Radiated electric field measurements in U.S. Army helicopters p 209 A93-16163
- MEDICAL SERVICES**
- Pre-flight risk assessment in Emergency Medical Service (EMS) helicopters p 494 N93-19692
- MELTING**
- Clean melting and the removal of defects from aero-engine materials p 1217 A93-53503
- Mathematical model of frost heave and thaw settlement in pavements [CRREL-REPT-93-2] p 912 N93-30103
- MELTING POINTS**
- Coking characteristics of polyphenyl ether lubricants using a Static Coker and a Micro Carbon Residue Tester p 77 A93-11341
- Viscosity of aviation fuel components (n-alkanes) p 71 A93-12824
- MEMBRANE STRUCTURES**
- Determination of the membrane and flexural shell deformations from the readings of a two-sided rosette-type strain gage p 75 A93-10047
- A viscous flow based membrane wing model [AIAA PAPER 93-2955] p 1047 A93-48149
- MEMORY**
- Preliminary studies of planning and flight strip use as air traffic controller memory aids [DOT/FAA/CT-TN92/22] p 503 N93-21759
- MEMORY (COMPUTERS)**
- Concurrent processing adaptation of aeroelastic analysis of propfans p 173 A93-14624
- The static-memory crash recorders p 167 A93-15048
- A new parallel-vector finite element analysis software on distributed-memory computers [AIAA PAPER 93-1307] p 756 A93-33883
- Dynamic overset grid communication on distributed memory parallel processors [AIAA PAPER 93-3311] p 1036 A93-45007
- The 3D Navier-Stokes flow analysis for shared and distributed memory MIMD computers [AD-A256038] p 221 N93-15187
- Considerations for space and naval aviation applications of ferroelectric memory [AD-A261300] p 759 N93-26294
- MENTAL PERFORMANCE**
- Shared mental models and crew decision making p 147 N93-15023
- Comparison of performance on the Shipley Institute of Living Scale, Air Traffic Control Specialist Selection Test, and FAA Academy Screen [AD-A259249] p 502 N93-20582
- Preliminary studies of planning and flight strip use as air traffic controller memory aids [DOT/FAA/CT-TN92/22] p 503 N93-21759
- MERIDIONAL FLOW**
- A method for optimizing the meridional passage of the rotor in centrifugal compressors p 119 A93-14344
- Meridional flow calculation using advanced CFD techniques [ASME PAPER 92-GT-325] p 256 A93-19509
- A computer program for meridional flows in multistage axial flow compressors with turbulence and multi-effects of 3-D flows p 1165 A93-49186
- MESH**
- Reduction in size and unsteadiness of a VTOL ground vortex by ground fences [NASA-CR-192997] p 700 N93-26049
- MESOSCALE PHENOMENA**
- Motion and decay of trailing vortices within the atmospheric surface layer p 425 A93-18548
- The Aviation Weather Products Generator p 428 A93-22125
- The FAA aircraft icing Forecasting Improvement Program - Validation of aircraft icing forecasts in the Denver area [AIAA PAPER 93-0393] p 309 A93-23069
- METAL AIR BATTERIES**
- Air cell - model aircraft power supplies [CA-PATENT-APPL-SN-2001346] p 83 N93-10368
- METAL BONDING**
- Stress relaxation of low pressure plasma-sprayed NiCrAlY alloys p 1211 A93-52870
- Joining carbon composite fins to titanium heat pipes [AD-A261970] p 825 N93-27667
- METAL COATINGS**
- Evaluation of simple aluminide and platinum modified aluminide coatings on high pressure turbine blades after factory engine testing - Round II [ASME PAPER 92-GT-140] p 388 A93-19372
- Life assessment of gas turbine bucket coating based on degradation analysis p 533 A93-24464
- Ignition of boron particles coated by a thin titanium film [AIAA PAPER 93-2201] p 1145 A93-50013
- METAL CUTTING**
- Calculating the cutting depth during the milling of large gas turbine engine blades p 545 A93-27628
- Prediction and control of the service-related properties of parts at the technological preparation stage and during the manufacture process - of aircraft engine components p 834 A93-39062
- METAL FATIGUE**
- On the fatigue life of M50 NiL rolling bearings p 78 A93-11346
- Effect of environment on creep-fatigue crack propagation in turbine disc superalloys [ONERA, TP NO. 1993-5] p 916 A93-41023
- Prediction of fatigue crack growth kinetics in the plane structural elements of aircraft in the biaxial stress state p 1025 A93-45670
- The effect of exfoliation corrosion on the fatigue behavior of structural aluminum alloys p 1017 A93-45778
- Clean melting and the removal of defects from aero-engine materials p 1217 A93-53503
- Fatigue in single crystal nickel superalloys [AD-A254603] p 74 N93-12237
- Fatigue crack growth in AerMet 100 steel [AD-A249068] p 74 N93-12248
- Fatigue in single crystal nickel superalloys [AD-A254704] p 198 N93-12746
- Fatigue in single crystal nickel superalloys [AD-A260709] p 736 N93-25843
- Damage tolerance assessment and usage variation analysis for C-130 aircraft in the Israeli Air Force p 839 N93-27210
- METAL FIBERS**
- Low leakage fiber metal seals [ASME PAPER 92-GT-141] p 402 A93-19373
- METAL FILMS**
- Ignition of boron particles coated by a thin titanium film [AIAA PAPER 93-2201] p 1145 A93-50013
- METAL FINISHING**
- Ultrasonic polishing p 750 N93-25580
- METAL FUELS**
- Effect of a metal deactivator fuel additive on fuel deposition in fuel atomizers at high temperature [AD-A260915] p 736 N93-25914
- METAL MATRIX COMPOSITES**
- Erosion characteristics of ceramic particulate and whisker reinforced aluminum composites [ASME PAPER 92-GT-369] p 388 A93-19532
- Potential aerospace applications for metal matrix composites p 389 A93-21678
- High-temperature materials warm up for debut p 535 A93-28393
- Potential and prospects of intermetallic materials for applications in the aerospace industry [ONERA, TP NO. 1992-99] p 824 A93-38580
- Beyond steel - TMCs for lighter landing gear p 1100 A93-49337
- Chemical stability of titanium diboride reinforcement in nickel aluminide matrices p 1147 A93-52473
- Friction surfacing and linear friction welding p 1217 A93-53499
- Status of R&D of high-performance materials for severe environments (Composite materials) p 1253 A93-54728
- Nondestructive evaluation of ceramic and metal matrix composites for NASA's HITEMP and enabling propulsion materials programs [NASA-TM-105807] p 85 N93-10963
- FNAS modify matrix and transparent experiments [NASA-CR-184442] p 198 N93-13311
- Compatibility of potential reinforcing ceramics with Ni and Fe aluminides [NASA-CR-192232] p 394 N93-18784
- An overview of elevated temperature damage mechanisms and fatigue behavior of a unidirectional SCS-6/Ti-15-3 composite [NASA-TM-106131] p 825 N93-26702
- NASA-UVA light aerospace alloy and structure technology program supplement: Aluminum-based materials for high speed aircraft [NASA-CR-4517] p 1019 N93-31643
- METAL OXIDE SEMICONDUCTORS**
- High temperature rectifiers and MOS devices in 6H-silicon carbide [AD-A254725] p 90 N93-12340
- METAL PLATES**
- Development of a process for fabricating a plate heat exchanger for the heat recovery system of gas turbine engines p 834 A93-39053
- Selection criteria for metallic high temperature structural materials in hypersonic flying equipment [MBL-LME-221-HYPAC-PUB-2-A] p 515 N93-21479
- METAL PROPELLANTS**
- Effect of a metal deactivator fuel additive on fuel deposition in fuel atomizers at high temperature [AD-A260915] p 736 N93-25914
- METAL SHEETS**
- A new method to study the forming process of complicated sheetmetal aero-parts p 204 A93-14363
- Stochastic modeling and adaptive control algorithm of brake bending p 227 A93-14417
- Imaging flaws in thin metal plates using a magneto-optic device p 397 A93-18670
- An evaluation of the pressure proof test concept for 2024-T3 aluminum alloy sheet p 1026 A93-45780
- Damage tolerance behaviour of aluminium-lithium sheet alloys [NLR-TP-91244-U] p 392 N93-17540
- The aerodynamic performance of laser drilled sheets [AERO-REPT-9204] p 484 N93-20806
- METAL SURFACES**
- Coherent X-ray imaging for corrosion evaluation - A preliminary assessment p 396 A93-18611
- Joining carbon composite fins to metal heat pipes using ion beam techniques p 543 A93-25979
- Measurements of wear and acoustic emission from fuel-wetted surfaces p 744 A93-34925
- Carbon composite repairs of helicopter metallic primary structures p 1101 A93-50429
- METAL WORKING**
- Stochastic modeling and adaptive control algorithm of brake bending p 227 A93-14417
- METALLIZING**
- Joining carbon composite fins to titanium heat pipes [AD-A261970] p 825 N93-27667
- METALLOGRAPHY**
- External stress-corrosion cracking of a 1.22-m-diameter type 316 stainless steel air valve [NASA-TP-3190] p 737 N93-26201
- METALS**
- A tooling trend at BCA - What and why [SME PAPER EM92-111] p 202 A93-14114
- METASTABLE STATE**
- The onset of vortex turbulence p 788 N93-28251
- METEOROLOGICAL CHARTS**
- The aeronautical volcanic ash problem p 309 A93-22156
- METEOROLOGICAL FLIGHT**
- Electrostatic discharges [ONERA, TP NO. 1992-82] p 844 A93-38567
- METEOROLOGICAL INSTRUMENTS**
- Principles of the design of automated meteorological support systems for aviation [ISBN 5-286-00342-7] p 151 A93-15224
- Elevated array detection and measurement of microbursts using Theta(E) p 412 A93-22173
- METEOROLOGICAL PARAMETERS**
- The Meteorological Data Collection and Reporting System - Status and future directions p 428 A93-22133
- Impact of weather on aviation - A global view p 308 A93-22143
- Weather information requirements for Terminal Air Traffic Control Automation p 429 A93-22146
- Validation of aviation weather products for the Advanced Traffic Management System p 430 A93-22161

The role of national meteorological services in aviation servicing under the final phase of the World Area Forecast System p 431 A93-22162

CWAS - Clean wing advisory system: A new approach to ice detection [AIAA PAPER 93-0747] p 516 A93-24835

Proceedings of the National Weather Service Aviation Workshop: Postprint volume [PB92-176148] p 94 A93-11803

Next Generation Weather Radar (NEXRAD) Principal User Processor (PUP) Operational Test and Evaluation (OT&E) operational test plan [DOT/FAA/CT-TN93/22] p 841 A93-28054

Meteorological information for aviation: A systems approach p 937 A93-30298

Preliminary evaluation of aviation-impact variables derived from numerical models [PB93-190197] p 1034 A93-31202

METEOROLOGICAL RADAR

1992 - The year of the radome? p 209 A93-15525

An experimental cockpit display for TDWR wind shear alerts p 343 A93-22111

Improvement in gust front algorithm detection capability using reflectivity thin lines versus azimuthal shears p 427 A93-22120

A comparison of several airborne measures of turbulence p 308 A93-22121

A 'new age' in aviation weather forecasting p 427 A93-22123

Status of the Terminal Doppler Weather Radar one year before deployment p 431 A93-22184

Terminal Doppler Weather Radar program at Denver's Stapleton International Airport during 1989 and 1990 p 432 A93-22188

A technique to correct airborne Doppler data for coordinate transformation errors using surface clutter p 807 A93-37699

Update on the NASA ER-2 Doppler radar system (EDOP) p 807 A93-37737

An integrated weather channel designed for an up-to-date ATC radar system p 929 A93-43434

Three-dimensional simulation of the Denver 11 July 1988 microburst-producing storm p 1164 A93-50373

Summary of findings from the PIREP-based analyses conducted during the 1988 to 1990 evaluations of TDWR-based and TDWR/LLWAS-based alert services provided to landing/departing pilots [AD-A253859] p 93 A93-11144

Terminal Doppler Weather Radar (TDWR) Operational Test and Evaluation (OT&E) integration test plan [DOT/FAA/CT-TN92/6] p 151 A93-13377

Birds mimicking microbursts on 2 June 1990 in Orlando, Florida [AD-A255703] p 143 A93-14024

Terminal Doppler weather radar/low-level wind shear alert system integration algorithm specification, version 1.1 [AD-A255319] p 224 A93-14547

NASA/LMSC coherent LIDAR airborne shear sensor: System capabilities and flight test plans p 144 A93-14847

Solid-state coherent laser radar wind shear measuring systems p 144 A93-14848

The Orlando TDWR testbed and airborne wind shear data comparison results p 145 A93-14851

TDWR 1991 Program Review p 145 A93-14852

Systems issues in airborne Doppler radar/LIDAR certification p 145 A93-14855

Airborne Wind Shear Detection and Warning Systems: Fourth Combined Manufacturers' and Technologists' Conference, part 1 [NASA-CP-10105-PT-1] p 488 A93-19590

Program overview: 1991 flight test objectives p 488 A93-19591

Air/ground wind shear information integration: Flight test results p 488 A93-19594

Doppler radar results p 488 A93-19595

Three-dimensional numerical simulation of the 20 June 1991, Orlando microburst p 488 A93-19598

RDR-4B doppler weather radar with forward looking wind shear detection capability p 489 A93-19601

Airborne doppler radar research at Rockwell International p 489 A93-19602

Acquisition and use of Orlando, Florida and Continental Airbus radar flight test data p 489 A93-19603

Comparison of simulated and actual wind shear radar data products p 490 A93-19610

NASA airborne radar wind shear detection algorithm and the detection of wet microbursts in the vicinity of Orlando, Florida p 490 A93-19611

Signal processing for airborne doppler radar detection of hazardous wind shear as applied to NASA 1991 radar flight experiment data p 490 A93-19612

The ATC evaluation of the prototype Airport Surveillance Radar Wind Shear Processor (ASR-WSP) at Orlando International Airport [DOT/FAA/CT-TN92/48] p 748 A93-25210

Setting values for TDWR/LLWAS 3 integration parameters [AD-A260740] p 755 A93-25645

Next Generation Weather Radar (NEXRAD) Principal User Processor (PUP) Operational Test and Evaluation (OT&E) operational test plan [DOT/FAA/CT-TN93/22] p 841 A93-28054

Contributions to the American Meteorological Society's 26th International Conference on Radar Meteorology [AD-A263385] p 936 A93-29257

Airborne derivation of microburst alerts from ground-based Terminal Doppler Weather Radar information: A flight evaluation [NASA-TM-108990] p 1000 A93-32223

METEOROLOGICAL RESEARCH AIRCRAFT

Meeting review: Third NCAR Research Aircraft Fleet Workshop [PB92-222710] p 223 A93-12818

METEOROLOGICAL SATELLITES

The Meteorologist Weather Processor for U.S. National Weather Service units at Federal Aviation Administration sites p 428 A93-22130

The role of national meteorological services in aviation servicing under the final phase of the World Area Forecast System p 431 A93-22162

METEOROLOGICAL SERVICES

Seasonal weather hazards p 431 A93-22180

Proceedings of the National Weather Service Aviation Workshop: Postprint volume [PB92-176148] p 94 A93-11803

Next Generation Weather Radar (NEXRAD) Principal User Processor (PUP) Operational Test and Evaluation (OT&E) operational test plan [DOT/FAA/CT-TN93/22] p 841 A93-28054

METHANE

Combustion study on methane-fuel Laboratory Scaled Ram Combustor [ASME PAPER 92-GT-413] p 356 A93-19561

A study of self-ignition of methane-hydrogen mixture fuel injected into high enthalpy supersonic airstreams [ISABE 93-7049] p 1213 A93-54025

Studies on methane-fuel ram combustor for HST combined cycle engine [ISABE 93-7080] p 1201 A93-54056

METHOD OF CHARACTERISTICS

Grid-characteristic method for calculating a three-dimensional boundary layer on the bounding surfaces of the blade passage of a turbomachine p 13 A93-12808

A method for calculating supersonic three-dimensional flows in pyramidal nozzles p 125 A93-15216

Method of characteristics for computing three-dimensional boundary layers p 970 A93-46886

METHOD OF MOMENTS

Corroboration of a moment-method calculation of the maximum mutual coupling between two HF antennas mounted on a helicopter p 881 A93-40332

METHODOLOGY

Development of generic helicopter performance methodology for real time mission analyses p 152 A93-14185

A multi-zonal local solution methodology for the accelerated solution of the turbulent Navier-Stokes equations p 117 A93-14279

Evaluation methodologies applied for pressurized fuselages of Airbus A/C p 948 A93-45796

Methodology for commercial engine/aircraft optimization [AIAA PAPER 93-1807] p 1166 A93-49696

An adaptive grid/Navier-Stokes methodology for the calculation of nozzle afterbody base flows with a supersonic freestream [AIAA PAPER 93-1922] p 1076 A93-49788

METHYL ALCOHOL

Fuel Injector: Air swirl characterization aerothermal modeling, phase 2, volume 2 [NASA-CR-189193-VOL-2] p 721 A93-25106

METHYL COMPOUNDS

Theoretical study of the bond dissociation energies of propyne (C₃H₄) p 230 A93-14099

MICHELSON INTERFEROMETERS

Fiber-optic interferometric sensors for measurements of pressure fluctuations - Experimental evaluation [AIAA PAPER 93-0738] p 540 A93-24828

MICROBURSTS (METEOROLOGY)

Optimal lateral maneuvering for microburst encounters during final approach p 183 A93-14350

Low-level wind-shear terminology p 426 A93-22104

Hazard assessment and cockpit presentation issues for microburst alerting systems p 308 A93-22112

Detection of microburst-related gust fronts using Doppler radar p 427 A93-22118

A quantitative method to estimate the microburst wind shear hazard to aircraft p 309 A93-22172

Elevated array detection and measurement of microbursts using Theta(E) p 412 A93-22173

Performance results and potential operational uses for the prototype TDWR microburst prediction product p 432 A93-22190

The dynamics of microbursts as revealed by Doppler radar observations and numerical simulations p 432 A93-22196

Microburst observations in tropical Australia p 432 A93-22198

Doppler radar observation of tornado and microburst around Chitose Airport p 432 A93-22199

Structure of downbursts associated with heavy rainfall observed in Tokyo p 433 A93-22200

Microbursts detection with airborne Doppler lidar p 433 A93-22201

Wind shear alert system brings safety improvements to major U.S. airports p 529 A93-27396

Microburst avoidance crew procedures for forward-looking sensor equipped aircraft [AIAA PAPER 93-3942] p 1007 A93-44234

Three-dimensional simulation of the Denver 11 July 1988 microburst-producing storm p 1164 A93-50373

Case study of a low-reflectivity pulsating microburst - Numerical simulation of the Denver, 8 July 1989, storm p 1222 A93-52898

Development of the Advance Warning Airborne System(AWAS) p 144 A93-14849

A millimeter-wave radiometer for detecting microbursts p 145 A93-14850

The Orlando TDWR testbed and airborne wind shear data comparison results p 145 A93-14851

Experimental evaluation of candidate graphical microburst alert displays p 145 A93-14853

Airborne Wind Shear Detection and Warning Systems: Fourth Combined Manufacturers' and Technologists' Conference, part 1 [NASA-CP-10105-PT-1] p 488 A93-19590

NASA wind shear flight test in situ results p 488 A93-19593

Air/ground wind shear information integration: Flight test results p 488 A93-19594

An approach to evaluating reactive airborne wind shear systems p 489 A93-19600

Vertical wind estimation from horizontal wind measurements p 489 A93-19604

Microburst characteristics determined from 1988-1991 TDWR testbed measurements p 490 A93-19605

Comparison of simulated and actual wind shear radar data products p 490 A93-19610

NASA airborne radar wind shear detection algorithm and the detection of wet microbursts in the vicinity of Orlando, Florida p 490 A93-19611

Signal processing for airborne doppler radar detection of hazardous wind shear as applied to NASA 1991 radar flight experiment data p 490 A93-19612

A statistical characterization of Denver-area microbursts [AD-A262127] p 845 A93-27675

Aircraft guidance for wind shear avoidance: Decision-making under uncertainty p 889 A93-31005

Airborne derivation of microburst alerts from ground-based Terminal Doppler Weather Radar information: A flight evaluation [NASA-TM-108990] p 1000 A93-32223

MICROCOMPUTERS

Air flow dynamics around an aerofoil by the stabilized finite difference method p 266 A93-20741

A microcomputer program for estimating low altitude wind and turbulence fields p 438 A93-22163

Utilizing a microcomputer based flight simulation in teaching human factors in aviation p 570 A93-27165

Development of a microcomputer-based magnetic heading sensor p 1160 A93-52152

MICROGRAVITY

Aircraft experiments on microgravity pool boiling - Vapor-liquid behaviour and heat transfer characteristics in boiling of n-pentane, CFC-113 and water p 410 A93-20920

Canadian low-gravity research using parabolic aircraft p 384 A93-21908

Calibration of thermal anemometer at very low Reynolds numbers under microgravity p 926 A93-41729

Flight data for the Cryogenic Heat Pipe (CRYOHP) Experiment [AIAA PAPER 93-2735] p 1027 A93-46488

Gravity sensitivity of a resistojel water vaporizer [AIAA PAPER 93-2402] p 1156 A93-50167

Materials processing in low gravity [NASA-CR-184421] p 91 A93-12401

FNAS modify matrix and transparent experiments [NASA-CR-184442] p 198 A93-13311

- Numerical study of cavity natural convection flow with augmenting and counteracting effects by projection finite element method p 749 N93-25540
Gravity sensitivity of a resistojet water vaporizer [NASA-TM-106220] p 914 N93-29184
Effects of buoyancy on gas jet diffusion flames [NASA-CR-191109] p 935 N93-31031
- MICROMECHANICS**
Integration of a course and position reference system with GPS p 499 A93-27911
Fatigue in single crystal nickel superalloys [AD-A254603] p 74 N93-12237
- MICROPARTICLES**
Simultaneous mapping of the unsteady flow fields by Particle Displacement Velocimetry (PDV) p 786 N93-27454
- MICROPHONES**
Optical microphone for the detection of hidden helicopters p 205 A93-14542
Acoustic mode measurements in the inlet of a model turbofan using a continuously rotating rake - Data collection/analysis techniques [AIAA PAPER 93-0599] p 361 A93-23324
Acoustic mode measurements in the inlet of a model turbofan using a continuously rotating rake [AIAA PAPER 93-0598] p 563 A93-24783
Acoustic mode measurements in the inlet of a model turbofan using a continuously rotating rake: Data collection/analysis techniques [NASA-TM-105936] p 179 N93-15403
Acoustic mode measurements in the inlet of a model turbofan using a continuously rotating rake [NASA-TM-105989] p 362 N93-16705
- MICROPROCESSORS**
The development of an airborne information management system for flight test [AIAA PAPER 92-4113] p 51 A93-11281
Stabilization of the dynamic characteristics of the automatic control systems of a flight vehicle p 62 A93-12802
Results of operational testing of a system for computing optimal flight regimes --- of aircraft flight p 996 A93-45665
Formal design specification of a Processor Interface Unit [NASA-CR-189698] p 99 N93-12538
Use of microprocessor-based simulator technology and MEG/EEG measurement techniques in pilot emergency-maneuver training p 530 N93-19706
A PC-based simulation of the National Transonic Facility's safety microprocessor [NASA-TM-109003] p 1038 N93-32224
- MICROSCOPES**
IR imaging for combustion characteristics and optical properties of boron/boron oxide [AD-A257747] p 393 N93-17693
X ray microscopy resource center at the Advanced Light Source [DE93-010449] p 911 N93-29869
- MICROSCOPY**
IR imaging for combustion characteristics and optical properties of boron/boron oxide [AD-A257747] p 393 N93-17693
X ray microscopy resource center at the Advanced Light Source [DE93-010449] p 911 N93-29869
- MICROSTRIP DEVICES**
The microstrip proportional counter p 549 A93-29485
- MICROSTRUCTURE**
The development of titanium alloys for gas turbines p 197 A93-15031
Birth of the betas p 824 A93-38200
Structure of martensite in titanium alloy Ti-6Al-1.6Zr-3.3Mo-0.3Si p 916 A93-43616
Boeing 777 gets a boost from titanium p 1018 A93-45987
In-service considerations affecting component life p 177 N93-14898
The beta-CEZ, a new high performance titanium alloy for aerospace engines [DS-2022] p 393 N93-17852
Modelisation and computation of composite materials p 537 N93-21518
External stress-corrosion cracking of a 1.22-m-diameter type 316 stainless steel air valve [NASA-TP-3190] p 737 N93-26201
Process optimization of Hexoloy SX-SiC towards improved mechanical properties [DE93-007913] p 826 N93-28564
Use of titanium castings without a casting factor [AD-A264414] p 1018 N93-31192
Material characterization and tractographic examination of Ti-17 fatigue crack growth specimens for SMP SC33 p 1004 N93-31744
- MICROWAVE COUPLING**
Coupling gain computation between antennas on circular cylinders at SHF/EHF frequencies p 933 N93-30309
- MICROWAVE EMISSION**
A computer simulation of the production of an artificially ionized layer using the Arecibo facility [DE93-010817] p 937 N93-30487
- MICROWAVE EQUIPMENT**
Definition study PHARUS [AD-A256560] p 221 N93-14805
- MICROWAVE IMAGERY**
A comparison of wind speed measured by the Special Sensor Microwave Imager (SSM/I) and the Geosat altimeter p 1033 A93-44862
A model-based approach for detection of objects in low resolution passive millimeter wave images [NASA-CR-193161] p 808 N93-28418
- MICROWAVE LANDING SYSTEMS**
DME/P critical area determination on message passing processors p 31 A93-11010
The Microwave Landing System - A precision approach for the future p 32 A93-11023
Implementation of BMLS computer model on hypercube systems --- Baseline Microwave Landing System p 32 A93-11024
Flight test evaluation of precision-code differential GPS for terminal approach and landing p 33 A93-11294
Landing guidance systems for CAT III operations p 151 A93-17307
Airborne MLS equipment p 312 A93-18555
Complementary MLS and GNSS operations p 384 A93-21160
Institute of Navigation, National Technical Meeting, San Diego, CA, Jan. 27-29, 1992, Proceedings p 315 A93-21176
Planning for complementary MLS/GPS operations p 315 A93-21180
MIAS, the integration of MLS with DGPS/DLoran-C p 315 A93-21181
Analysis of DGPS/INS and MLS/INS final approach navigation errors and control performance data p 315 A93-21183
An MLS for the twenty-first century p 316 A93-21197
Application of parafoils to microwave landing system siting [AIAA PAPER 93-1213] p 702 A93-35162
Half-scale modeling experience in the testing of radio navigation and landing systems p 882 A93-43112
Development of advanced approach and departure procedures [AIAA PAPER 93-3833] p 1098 A93-51422
Fault tolerant navigation for aircraft landing p 1191 A93-53866
DME-derived positions compared with MLS- and ILS-derived positions [NLR-TP-90119-U] p 318 N93-16343
Flight simulation evaluation of the flyability of curved MLS approaches with wide-body aircraft [NLR-TP-90238-U] p 382 N93-17875
Manual flying of curved precision approaches to landing with electromechanical instrumentation. A piloted simulation study [NASA-TP-3255] p 344 N93-18408
A model-based approach for detection of objects in low resolution passive millimeter wave images [NASA-CR-193161] p 808 N93-28418
Evaluation of category 3 MLS designs p 888 N93-30358
Evaluation of the flyability of MLS curved approaches for wide-body aircraft [NLR-TP-91396-U] p 999 N93-32416
- MICROWAVE POWER BEAMING**
A self-steering array for the SHARP microwave-powered aircraft p 792 A93-37090
- MICROWAVE RADIOMETERS**
Study on aircraft microwave remote sensing of sea-water surface salinity p 92 A93-12407
Liquid water profiling using remote sensor observations p 429 A93-22150
A horizontal atmospheric temperature sounder - Applications to remote sensing of atmospheric hazards p 929 A93-43502
A millimeter-wave radiometer for detecting microbursts p 145 N93-14850
- MICROWAVE SENSORS**
Ground- and satellite-derived flight-path measurements as demonstrated in the AFES Avionics Flight Evaluation System (AFES) p 993 N93-31281
- MICROWAVE SOUNDING**
PBM observations of surface soil moisture in Monsoon 90 p 1162 A93-47676
- MICROWAVES**
Microwave processing of silicon nitride for advanced gas turbine applications [DE93-007910] p 917 N93-29767
- A computer simulation of the production of an artificially ionized layer using the Arecibo facility [DE93-010817] p 937 N93-30487
- MIDAIR COLLISIONS**
New results in optimal missile avoidance analysis p 369 A93-22937
CRAASH - A coordinated collision avoidance system [ONERA, TP NO. 1993-84] p 1191 A93-53604
UK airmisses involving commercial air transport, September - December 1991 [ETN-93-83930] p 992 N93-32409
- MIDCOURSE TRAJECTORIES**
Guidance law based on piecewise constant control for hypersonic gliders [AIAA PAPER 93-3888] p 1144 A93-51472
- MIE SCATTERING**
Uplink laser propagation measurements through the sea surface, haze and clouds [AD-A264687] p 935 N93-30553
- MILITARY AIR FACILITIES**
Battle damage repairs p 239 A93-22698
AQUIS: A PC-based air quality and permit information system [DE92-040092] p 434 N93-18587
Land subsidence and problems affecting land use at Edwards Air Force Base and vicinity, California, 1990 [PB93-182236] p 1036 N93-32191
- MILITARY AIRCRAFT**
Transport resurrection p 41 A93-12434
Rotorcraft reliability and maintainability: Future design requirements; Proceedings of the Conference, London, United Kingdom, Mar. 20, 1991 [ISBN 0-903409-88-7] p 45 A93-13401
The military operator's experience of reliability and maintainability characteristics p 80 A93-13403
Civil spin-off from military aircraft cockpit research p 45 A93-13415
Structural integrity challenges p 3 A93-13627
Damage severity of monitored fatigue load spectra p 154 A93-14253
Electro-modulated control of supply pressure in hydraulic systems [SAE PAPER 912119] p 412 A93-21842
Rocket engine versus jet engine comparison [AIAA PAPER 92-3686] p 531 A93-24479
Preliminary results from a study of community response to noise from military aircraft exercise p 558 A93-28484
Advances in the design of jet engine test facilities for military aircraft in Australia p 529 A93-28491
Management miscues, delays snarl C-17 program p 760 A93-34944
Reconfigurable photonic data networks for military aircraft p 928 A93-42783
TEAMS - Technical expert aircraft maintenance system p 941 A93-42865
Trends in air power - New systems, old platforms? p 856 A93-43650
The NASA Computational Fluid Dynamics (CFD) program - Building technology to solve future challenges [AIAA PAPER 93-3292] p 1041 A93-44996
Specific features of military low-altitude flight noise - Criteria for risk of damage and physiological effects p 1164 A93-49558
Wheel and brake design and test requirements for military aircraft [SAE ARP 1493] p 1103 A93-52165
Aspects of fatigue affecting the design and maintenance of modern military aircraft p 1043 A93-52548
Europe's new windtunnel p 1210 A93-54275
A study of military aircraft and engine tactical/technical performance evaluation p 1242 A93-54596
A numerical study of aerodynamic wing design for supercritical conditions of an advanced training and military aircraft p 1238 A93-56213
Winds of change: Expanding the frontiers of flight. Langley Research Center's 75 years of accomplishment, 1917-1992 [NASA-NP-130] p 104 N93-11100
Waterborne polyurethane binder resins for compliant aircraft coatings [AD-A256246] p 199 N93-14573
A database approach to aircraft carrier airplan production [AD-A257737] p 240 N93-17666
Improving military transport aircraft through highly integrated engine-wing design [DS-1607] p 333 N93-17850
An investigation of the influence of advanced aircraft diagnostics on the technological sophistication of maintenance personnel [AD-A258988] p 240 N93-18887
Mission planning systems for tactical aircraft (pre-flight and in-flight) [AGARD-AR-313] p 496 N93-21187

SUBJECT INDEX

- Thermally induced stresses in a composite exposed to fire
[AD-A261714] p 737 N93-26371
- A prediction model for noise from low-altitude military aircraft
[AD-A262494] p 852 N93-27662
- ### MILITARY AVIATION
- The state-of-the-art of nondestructive evaluation of military runways p 375 A93-19659
- Considerations for space and naval aviation applications of ferroelectric memory
[AD-A261300] p 759 N93-26294
- ### MILITARY HELICOPTERS
- Hovering decisions --- development of EH101 helicopter p 46 A93-13700
- Development of generic helicopter performance methodology for real time mission analyses p 152 A93-14185
- Choice of materials for military helicopters p 158 A93-15028
- Radiated electric field measurements in U.S. Army helicopters p 209 A93-16163
- Lynx: High performance - Low noise p 322 A93-19185
- A retrospective of 3600 composite blades p 507 A93-27963
- Improvements in hover display dynamics for a combat helicopter p 727 A93-34257
- Comanche airframe design - The PDT approach p 744 A93-34469
- Controlling hazardous configurations in helicopter systems p 763 A93-35927
- A Taguchi analysis of helicopter maneuverability and agility p 763 A93-35944
- EH 101 ship interface trials p 796 A93-35954
- Frequency-domain identification of coupled rotor/body models of an advanced attack helicopter p 816 A93-35960
- Development status of the RAH-66 Comanche p 803 A93-38838
- Royal Navy helicopter operations in the maritime environment p 1190 A93-54290
- Environmental effects of operations during Desert Shield/Desert Storm p 1190 A93-54291
- Royal Air Force support helicopters - Night operations p 1190 A93-54293
- Avionic systems in support of covert helicopter operations p 1193 A93-54294
- Longbow - Force multiplier for continuous operations p 1175 A93-54295
- Integration of an integrated helmet system for PAH 2 p 1244 A93-55298
- Passive IR surveillance for helicopter systems - The Sea Owl equipment p 1244 A93-55299
- Compound cycle engine for helicopter application [NASA-CR-180824] p 55 N93-10348
- Rigid body mode identification of the PAH-2 helicopter using the eigensystem realization algorithm [NASA-TM-107690] p 88 N93-11544
- The Fourth Workshop on Dynamics and Aeroelastic Stability Modeling of Rotorcraft Systems [AD-A255065] p 50 N93-12485
- The effectiveness of airbags in reducing the severity of head injury from gunsight strikes in attack helicopters p 494 A93-19691
- ### MILITARY OPERATIONS
- A database approach to aircraft carrier airplan production [AD-A257737] p 240 N93-17666
- Mission planning systems for tactical aircraft (pre-flight and in-flight) [AGARD-AR-313] p 496 N93-21187
- ### MILITARY TECHNOLOGY
- Architectures and GPS/INS integration - Impact on mission accomplishment p 31 A93-11013
- Design considerations for air-to-air laser communications p 312 A93-18932
- A survey of display technologies for military aircraft cockpit applications p 517 A93-27239
- AHS, Annual Forum, 48th, Washington, June 3-5, 1992, Proceedings, Vols. 1 & 2 p 763 A93-35901
- Airship: The 'Look Out' - A versatile surveillance platform [AIAA PAPER 93-4033] p 1229 A93-54605
- Formulation and validation of high-order mathematical models of helicopter flight dynamics p 162 N93-13821
- ### MILLIMETER WAVES
- Effects of substrate anisotropy on coupled bilateral finlines p 208 A93-15409
- A millimeter-wave radiometer for detecting microbursts p 145 N93-14850
- ### MILLING
- Processing integral impeller 4-coordinate numerically controlled milling machine p 926 A93-41749

MIMD (COMPUTERS)

- A performance comparison of massively parallel Parabolized Navier-Stokes solutions [AIAA PAPER 93-0059] p 435 A93-20172
- LEWICE droplet trajectory calculations on a parallel computer [AIAA PAPER 93-0172] p 438 A93-22604
- The 3D Navier-Stokes flow analysis for shared and distributed memory MIMD computers [AD-A256038] p 221 N93-15187
- Numerical Wind Tunnel hardware p 383 N93-19289

MIMO (CONTROL SYSTEMS)

- Multiple input/multiple output (MIMO) analysis procedures with applications to flight data p 60 A93-10777
- Discrete-time LTR synthesis of delayed control systems p 439 A93-22855
- Refined H-infinity controller design for rotorcraft flight control p 368 A93-22882
- Design of insensitive multirate aircraft control using optimized eigenstructure assignment p 370 A93-23515
- Applying variations of the quantitative feedback technique (QFT) to unstable, non-minimum phase aircraft dynamics models p 939 A93-42797
- Antiwindup analysis and design approaches for MIMO systems [AIAA PAPER 93-3811] p 1123 A93-51403
- A comparison of two multi-variable integrator windup protection schemes [AIAA PAPER 93-3812] p 1123 A93-51404
- Symposium proceedings on Quantitative Feedback Theory [AD-A255527] p 187 N93-13872
- Adaptive control of nonlinear nonminimum phase systems p 229 N93-14470
- Identification and control of non-linear time-varying dynamical systems using artificial neural networks [AD-A257595] p 372 N93-18193
- Applications of active adaptive noise control to jet engines [NASA-CR-192277] p 522 N93-21210
- Robust crossfeed design for hovering rotorcraft [NASA-CR-193107] p 805 N93-27241
- ### MINIATURIZATION
- Flight experience with lightweight, low-power miniaturized instrumentation systems [AIAA PAPER 92-4111] p 39 A93-11280
- ### MINIMAX TECHNIQUE
- Maximizing the critical Mach number for lifting wing profiles p 13 A93-12841
- Robust controller and estimator design using minimax methods p 229 N93-13925
- ### MIRAGE AIRCRAFT
- Flight analysis of air intake/engine compatibility p 161 N93-13212
- ### MIRRORS
- Optical technologies for UV remote sensing instruments p 853 N93-28788
- ### MISALIGNMENT
- Misalignments of airborne laser beams due to mechanical vibrations p 394 A93-17762
- ### MISSILE BODIES
- A concurrent hybrid Navier-Stokes/Euler approach to fluid dynamic computations [AIAA PAPER 93-0789] p 468 A93-24865
- ### MISSILE CONFIGURATIONS
- Thermal shock capabilities of infrared dome materials p 70 A93-11454
- Wind tunnel investigation with an operational turbojet engine [AIAA PAPER 93-0036] p 322 A93-20150
- Computations of aerodynamic drag for turbulent transonic projectiles with and without spin [AIAA PAPER 93-3416] p 975 A93-47212
- Base drag prediction on missile configurations [AIAA PAPER 93-3629] p 1064 A93-48314
- Analysis of missile configurations with wrap-around fins using computational fluid dynamics [AIAA PAPER 93-3631] p 1064 A93-48316
- Fabrication of composite propfan blades for a cruise missile wind tunnel model [NASA-TM-105270] p 752 N93-26202
- ### MISSILE CONTROL
- Wind tunnel investigation with an operational turbojet engine [AIAA PAPER 93-0036] p 322 A93-20150
- Development and application of a nonlinear fin mixer p 368 A93-22869
- New results in optimal missile avoidance analysis p 369 A93-22937
- Sequential smoothing and filtering for maneuvering target tracking p 440 A93-22978

MIXING LAYERS (FLUIDS)

- Sensors and sensor systems for guidance and navigation II; Proceedings of the Meeting, Orlando, FL, Apr. 22, 23, 1992 [SPIE-1694] p 547 A93-28151
- New analytical solutions for proportional navigation p 728 A93-34545
- Base drag prediction on missile configurations [AIAA PAPER 93-3629] p 1064 A93-48314
- Dynamic attitude measurement system [AIAA PAPER 93-3801] p 1139 A93-51393
- ### MISSILE DESIGN
- Aerodynamic Engine/Airframe Integration for High Performance Aircraft and Missiles [AGARD-CP-498] p 213 N93-13199
- ### MISSILE TESTS
- Wind tunnel investigation with an operational turbojet engine [AIAA PAPER 93-0036] p 322 A93-20150
- ### MISSILE TRAJECTORIES
- New analytical solutions for proportional navigation p 728 A93-34545
- Development of an accuracy criteria for body-on-fin carryover interference [AIAA PAPER 93-3633] p 1065 A93-48318
- ### MISSILES
- The PEP Symposium on CFD Techniques for Propulsion Applications p 214 N93-13210
- Some aspects of intake design, performance and integration with the airframe p 161 N93-13219
- The Fifth Symposium on Numerical and Physical Aspects of Aerodynamic Flows [NASA-CR-193000] p 783 N93-27427
- Kinetics and energy transfer in nonequilibrium fluid flows [AD-A263612] p 875 N93-29284
- Chaos in mechanical systems with especial reference to rotorcraft and missiles [AD-A263703] p 943 N93-29384
- ### MISSION ADAPTIVE WINGS
- Flight test results from a supercritical mission adaptive wing with smooth variable camber [AIAA PAPER 92-4101] p 38 A93-11274
- Flight test results from a supercritical mission adaptive wing with smooth variable camber [NASA-TM-4415] p 49 N93-11863
- ### MISSION PLANNING
- Natural environment application for NASP-X-30 design and mission planning [AIAA PAPER 93-0851] p 531 A93-24915
- MAKS - Eastern promise? --- multi-purpose aerospace system p 733 A93-34266
- Mission planning systems for tactical aircraft (pre-flight and in-flight) [AGARD-AR-313] p 496 N93-21187
- ### MISTUNING (TURBOMACHINERY)
- The combined closed form-perturbation approach to the analysis of mistuned bladed disks [ASME PAPER 92-GT-125] p 350 A93-19359
- An efficient constraint to account for mistuning effects in the optimal design of engine rotors [AIAA PAPER 92-4711] p 358 A93-20280
- Aeroelastic dynamics of mistuned blade assemblies with closely spaced blade modes [AIAA PAPER 93-1628] p 810 A93-37446
- Optimization of blade arrangement in a randomly mistuned cascade using simulated annealing [AIAA PAPER 93-2254] p 1115 A93-50052
- ### MIXERS
- Experimental investigation of exhaust system mixers for a high bypass turbofan engine [AIAA PAPER 93-0022] p 357 A93-20140
- Development and application of a nonlinear fin mixer p 368 A93-22869
- Design, fabrication, and testing of a three-dimensional acoustic orientation instrument (3-D AOI): Drawings, engineering and associated lists (conceptual and development design) [AD-A260934] p 760 N93-25915
- ### MIXING
- Analysis of high speed multistage compressor throughflow using spanwise mixing [ASME PAPER 92-GT-13] p 347 A93-19285
- ### MIXING LAYERS (FLUIDS)
- Numerical simulation of compressible mixing zones p 10 A93-12427
- Experimental analysis of turbulence within supersonic mixing layers p 11 A93-12428
- Numerical and experimental investigation of mixing enhancement in scramjets [AIAA PAPER 92-5063] p 414 A93-22333
- Total-pressure loss in supersonic parallel mixing [AIAA PAPER 93-0216] p 278 A93-22632
- Experimental studies of the turbulent structure of supersonic mixing layers [AIAA PAPER 93-0217] p 278 A93-22633

- Vortical and turbulent structure of a lobed mixer free-shear layer
[AIAA PAPER 93-0219] p 415 A93-22635
- A study of compressible turbulence
[AIAA PAPER 93-0659] p 465 A93-24772
- Compressible turbulence measurements in a high-speed high Reynolds number mixing layer
[AIAA PAPER 93-0660] p 465 A93-24773
- Ignition analysis of unpremixed reactants with chain mechanism in a supersonic mixing layer
p 735 A93-35619
- Inviscid instability of a skewed compressible mixing layer
p 769 A93-37941
- A numerical study of wave propagation in a confined mixing layer by eigenfunction expansions
p 873 A93-43629
- Compressibility, exothermicity, and three dimensionality in spatially evolving reactive shear flows
p 950 A93-44375
- Enhanced mixing via geometric manipulation of a splitter plate
[AIAA PAPER 93-3244] p 966 A93-46789
- The countercurved mixing layer - Strategies for shear-layer control
[AIAA PAPER 93-3260] p 968 A93-46826
- Passive control of coherent vortices in compressible mixing layers
[AIAA PAPER 93-3262] p 968 A93-46828
- Scramjet fuel mixing enhancement by cross-stream pressure gradients
[AIAA PAPER 93-2139] p 1114 A93-49957
- Streamwise vorticity generation and mixing enhancement in free jets by 'delta-tabs'
[AIAA PAPER 93-3253] p 1180 A93-53592
- Effect of film cooling/regenerative cooling on scramjet engine performances
[ISABE 93-7036] p 1197 A93-54012
- Direct simulation of reacting fuel gas flows in a supersonic mixing layer
[ISABE 93-7072] p 1201 A93-54048
- Enhanced fuel-air mixing in hypersonic engines
[ISABE 93-7115] p 1221 A93-54090
- The experimental evaluation of annular ejector system under concurrent mixing and diffusion
p 1250 A93-54593
- Instability of a supersonic vortex sheet inside a circular duct
p 1234 A93-55142
- Comparison of confined, compressible, spatially developing mixing layers with temporal mixing layers
p 1234 A93-55352
- Three-dimensional simulations of compressible mixing layers - Visualizations and statistical analysis
p 1235 A93-55360
- Effect of the flow non-uniformity on the mixing layer at the interface of parallel supersonic flows
[ISAS-RN-646] p 128 A93-12716
- Numerical simulation of the acoustic instability in the spatially developing, confined, supersonic mixing layer
p 132 A93-13521
- Mixing and reaction in the subsonic 2-D turbulent free shear layer
p 289 A93-16508
- Initial streamwise vorticity formation in a two-stream mixing layer
p 698 A93-25752
- Jet mixer noise suppressor using acoustic feedback
[NASA-CASE-LEW-15170-1] p 853 A93-28953
- Compressible turbulence in a high-speed high Reynolds number mixing layer
p 878 A93-30583
- Streamwise vorticity generation and mixing enhancement in free jets by delta-tabs
[NASA-TM-106235] p 988 A93-31648
- Turbulence measurement in a reacting and non-reacting shear layer at a high subsonic Mach number
[NASA-TM-106186] p 989 A93-31839
- MIXING LENGTH FLOW THEORY**
- Study of mixing flow field of a jet in a supersonic cross flow. I - Experimental facilities and preliminary experiments
p 857 A93-40430
- Three-dimensional analysis of turbine rotor flow including tip clearance
[ASME PAPER 93-GT-111] p 987 A93-47446
- Mixing of multiple jets with a confined subsonic crossflow
p 1189 A93-54324
- Projectile base bleed technology. Part 2: User's guide
CMINT computer code, version 5.04-BRL
[AD-A258630] p 551 A93-19999
- Modeling of a turbulent flow in the presence of discrete parietal cooling jets
p 904 A93-29960
- MOBILE COMMUNICATION SYSTEMS**
- Capacity as a consideration for providing aeronautical mobile satellite air traffic services in the U.S. domestic airspace
p 30 A93-11007
- Three-dimensional cellular systems for aeronautical mobile radio communications
p 502 A93-29639
- MODAL RESPONSE**
- Parameter estimation techniques for flight flutter test analysis
p 156 A93-14324

- Modal analysis of unsteady aerodynamic response of subsonic annular cascade with steady loading under elastic vibration
p 126 A93-15495
- Identification of weakly nonlinear dynamic systems by means of random excitations
p 227 A93-16472
- Sonic fatigue analysis of an aircraft wing flap by the matrix difference equation method
p 399 A93-19208
- Experimental and analytical investigations of fuselage modal characteristics and structural-acoustic coupling
p 451 A93-19229
- Vibro-acoustic analysis of propeller aircraft, integrating advanced experimental modeling with in-flight data analysis
p 451 A93-19230
- Pressure fluctuation on casing wall of isolated axial compressor rotors at low flow rate
[ASME PAPER 92-GT-33] p 246 A93-19293
- An efficient constraint to account for mistuning effects in the optimal design of engine rotors
[AIAA PAPER 92-4711] p 358 A93-20280
- Examples of dynamic response optimization using MSC/NASTRAN
[AIAA PAPER 92-4814] p 436 A93-20394
- Modal analysis in the certification of a commercial aircraft
p 509 A93-29241
- Ground vibration test on Piaggio P. 180 aircraft - Comparison between two modal test methods
p 509 A93-29246
- Enhancements to modal testing using finite elements
p 548 A93-29258
- Expanding test mode shapes for better visualization
p 549 A93-29264
- Application of FEM model correlation and updating techniques on an aircraft using test data of a ground vibration survey
p 509 A93-29267
- Thermoelastic vibration test techniques
p 549 A93-29293
- A modal-based procedure for efficiently predicting low vibration rotor designs
p 712 A93-34262
- Application of component mode synthesis to modeling the dynamic response of Bearingless Main Rotors
p 796 A93-35976
- Coupled rotor fuselage mode shapes - A tool in understanding helicopter response
p 797 A93-35977
- Extraction of inherent aerodynamic lag poles for the time domain representation of modal unsteady airloads
[AIAA PAPER 93-1591] p 829 A93-37443
- Aeroelastic dynamics of mistuned blade assemblies with closely spaced blade modes
[AIAA PAPER 93-1628] p 810 A93-37446
- Modal identification of aircraft structures - ONERA methods
[ONERA, TP NO. 1992-86] p 802 A93-38570
- Vibration characteristics of mistuned bladed disk
p 1108 A93-49190
- High-frequency acoustic radiation from a curved duct of circular cross section
[ONERA, TP NO. 1993-55] p 1173 A93-51937
- The use of beam-like modal data for stiffness profile estimation by the EBS method. I - Justification and implementation --- Equivalent Beam Stiffness
p 1257 A93-54649
- Effects of foundation excitation on multiple rub interactions in turbomachinery
p 1260 A93-55996
- Modal survey of a full-scale F-18 wind tunnel model
[AD-A262482] p 875 A93-29410
- Modal measurements and propeller field excitation on acoustic full scale mockup of SAAB 340 aircraft
[FFA-TN-1992-08] p 1039 A93-31051
- MODEL REFERENCE ADAPTIVE CONTROL**
- Nonlinear time-series-based adaptive control applications
p 97 A93-13230
- Application of model reference adaptive control to speed control system in an aeroengine
p 172 A93-14498
- A nonlinear adaptive control system with a reference model and derivative measurement
p 561 A93-26838
- Model reference control of a linear plant with feedthrough element
p 846 A93-37034
- Design of robust digital model-following flight control systems
p 907 A93-42810
- Design of reconfigurable digital multiple model-following flight control systems
p 908 A93-42811
- Adaptive quadratic stabilization control with application to flight controller design
[AIAA PAPER 93-3847] p 1133 A93-51434
- Genetic design of digital model-following flight-control systems
[AIAA PAPER 93-3883] p 1135 A93-51468
- New adaptive controllers for aircraft
p 847 A93-27180
- MODULARITY**
- Achieving modularity with tightly-coupled GPS/INS
p 33 A93-11032
- MODULATION**
- Multiplexing electro-optic architectures for advanced aircraft integrated flight control systems
[NASA-CR-182268] p 187 A93-13735

MODULATION TRANSFER FUNCTION

- Measurement of modulation transfer functions of simulator displays
[AD-A259401] p 530 A93-21268
- MODULES**
- Advanced Transport Operating System (ATOPS) utility library software description
[NASA-CR-191469] p 1000 A93-32218
- MODULUS OF ELASTICITY**
- Elastic constants for unidirectional boron-epoxy composites
p 387 A93-18636
- Inelasticity effect in a unidirectional boron/aluminum composite under uniaxial tension
p 825 A93-39024
- Measurements of dynamic Young's modulus and damping in single crystals of a nickel-based superalloy as a function of temperature
p 1147 A93-52513
- In situ material characterization for pavement evaluation by the Spectral-Analysis-of-Surface-Waves (SASW) method
[AD-A255660] p 194 A93-14128
- Reanalysis of multiple-wheel landing gear traffic tests
[AD-A256593] p 194 A93-14238
- MOIRE INTERFEROMETRY**
- Optical methods of stress analysis applied to cracked components
p 1027 A93-45798
- MOISTURE CONTENT**
- Numerical forecasting of liquid water content to assess airframe icing risk
p 429 A93-22147
- The FAA aircraft Icing Forecasting Improvement Program - Validation of aircraft icing forecasts in the Denver area
[AIAA PAPER 93-0393] p 309 A93-23069
- Liquid water content measurements using the Phase Doppler Particle Analyzer in the NASA Lewis Icing Research Tunnel
[AIAA PAPER 93-0298] p 378 A93-23698
- An experimental study of the air drying process in air coolers
p 834 A93-39059
- Calculation of sandwich plates with polymer composite skins under conditions of high humidity
p 1215 A93-52968
- Repair materials and processes for the MD-11 Composite Tailcone
p 1216 A93-53452
- Natural and augmented snowfall growth processes and their interactions with the natural and modified aerosol
[PB93-153096] p 755 A93-25874
- MOLDING MATERIALS**
- Improved ceramic slip casting technique --- application to aircraft model fabrication
[NASA-CASE-LAR-14471-1] p 536 A93-20041
- MOLDS**
- Development of stitching reinforcement for transport wing panels
p 921 A93-30852
- Development of resins for composites by resin transfer molding
p 921 A93-30853
- MOLECULAR COLLISIONS**
- The hypersonic double ellipse in rarefied flow
p 869 A93-42631
- Relaxation of discrete rotational energy distributions using a Monte Carlo method
p 1234 A93-55146
- Monte Carlo simulation of normal shock wave. Part 1: Lennard-Jones potential
p 300 A93-19279
- MOLECULAR EXCITATION**
- Effect of the formation of excited oxygen molecules on the kinetics of exchange reactions and the heat flux during braking in the upper layers of the atmosphere
p 1070 A93-48975
- Steady-state supersonic flow of a vibrationally excited gas past a slender body of revolution at a small angle of attack
p 1233 A93-55014
- MOLECULAR FLOW**
- Problem 6.4.1 - Rarefied flow around a double ellipse
p 869 A93-42630
- MOLECULAR GASES**
- Calculation of flow of a rarefied gas past a sphere for an arbitrary Knudsen number
p 124 A93-15146
- Development and application of the Monte Carlo method for solving the Boltzmann equation and its models
p 1173 A93-51867
- MOLECULAR OSCILLATIONS**
- Steady state supersonic flows of a vibrationally excited gas past thin bodies
p 1089 A93-51818
- Vibration excitation in laminar hypersonic boundary layers
p 1237 A93-56028
- MOLECULAR RELAXATION**
- Nonequilibrium excitation of internal molecular degrees of freedom in the shock layer during hypersonic flight
p 412 A93-21922
- VSL analysis of nonequilibrium flows around a hypersonic body
p 769 A93-38146
- Nonequilibrium limiting hypersonic flow of a gas past three-dimensional tapered bodies with a separated shock
p 776 A93-39133
- Hypersonic limiting flows of a relaxing gas with pressure changes in the main approximation
p 776 A93-39135

Steady transonic weakly perturbed flows in a vibrationally relaxing gas p 1088 A93-51768
Modeling the flow around a body via the solution of the relaxation kinetic equation p 1089 A93-51868
Relaxation of discrete rotational energy distributions using a Monte Carlo method p 1234 A93-55146

MOLECULAR STRUCTURE
Development and application of the Monte Carlo method for solving the Boltzmann equation and its models p 1173 A93-51867

MOLTEN SALTS
Corrosion of ceramic matrix composites [ONERA, TP NO. 1993-82] p 1213 A93-53602

MOMENT DISTRIBUTION
Some unsteady fluid forces on pump impellers p 413 A93-22265
Validation of engineering methods for predicting hypersonic vehicle control forces and moments p 906 A93-41897
An analytical-experimental method for studying the strength and stability of thin-walled structures p 1029 A93-47084
Estimation of the effect of the longitudinal moment due to the engine thrust on the mass of a subsonic passenger aircraft p 1191 A93-52954
Numerical minimization of the moment coefficient of a supercritical airfoil section p 1238 A93-56214
A method of testing two-dimensional airfoils [AD-A253210] p 17 N93-10375
Development of nonlinear aerodynamic models for unsteady responses p 19 N93-10845

MOMENTS OF INERTIA
Radii effect on the translation spring constant of force transducer beams p 829 A93-37867
Estimation of aircraft inertia characteristics from bifilar pendulum test data p 1249 A93-56029
Review of initial experiments using the Hawk model, dynamic rig facility, and the CED 1401 digital data acquisition equipment [CRANFIELD-AERO-9017] p 531 N93-21406

MOMENTUM
Optimization of circular orifice jets mixing into a heated crossflow in a cylindrical duct [AIAA PAPER 93-0249] p 361 A93-23246
Optimization of circular orifice jets mixing into a heated cross flow in a cylindrical duct [NASA-TM-105984] p 179 N93-15359
Increased heat transfer to elliptical leading edges due to spanwise variations in the freestream momentum: Numerical and experimental results [NASA-TM-106150] p 838 N93-27020

MOMENTUM TRANSFER
Effect of bird impact load types on blade response p 174 A93-16846
Radial transport and momentum exchange in an axial compressor [ASME PAPER 92-GT-364] p 257 A93-19528
Root damage analysis of aircraft engine blade subject to ice impact [NASA-TM-105779] p 222 N93-15343

MONATOMIC GASES
Computer program for calculating and fitting thermodynamic functions [NASA-RP-1271] p 231 N93-12967

MONITORS
Rotorcraft health and usage monitoring systems: A literature survey [DOT/FAA/RD-91/6] p 48 N93-11461
Limited production Precision Runway Monitor (PRM) master test plan [DOT/FAA/CT-TN92/23] p 192 N93-12899
Discussion for the ideal AIMS p 167 N93-15153
Royal Air Force experience of the Harrier information management system p 234 N93-15170
An experimental health monitoring unit for GPS and GLONASS p 706 N93-25018
Advanced thermally-stable, coal-derived, jet fuels program: Experiment system and model development [AD-A262747] p 917 N93-29402
Computer-controlled alignment for a 2000-line color monitor p 886 N93-30324

MONOCULAR VISION
Trade-offs arising from mixture of color cueing and monocular, binocular, and stereoscopic cueing information for simulated rotorcraft flight [NASA-TP-3268] p 338 N93-18333

MONOPLANES
SAE Aero Design '92 [SAE PAPER 921009] p 157 A93-14641

MONOPOLE ANTENNAS
Receiving and scattering characteristics of an imaged monopole beneath a lossy sheet p 1158 A93-50543

MONOPOLES
Computation of far-field helicopter rotor tone noise [ONERA-P-1990-5] p 943 N93-30110

MONOPULSE RADAR
Radar 92: Proceedings of the International Conference, Brighton, United Kingdom, Oct. 12, 13, 1992 [ISBN 0-85296-533-2] p 929 A93-43376
Evolution of radar data processing in the French air traffic control system p 886 N93-30325

MONOTECTIC ALLOYS
FNAS modify matrix and transparent experiments [NASA-CR-184442] p 198 N93-13311

MONOTONE FUNCTIONS
Monotonicity characteristics of some plane vortex flows of incompressible fluids and subsonic gas flows p 13 A93-12932

MONTE CARLO METHOD
Computational techniques for probabilistic analysis of turbomachinery [ASME PAPER 92-GT-167] p 351 A93-19393
Near wake structure for a generic ASTV configuration [AIAA PAPER 93-0271] p 268 A93-21103
Shock interference prediction using direct simulation Monte Carlo p 778 A93-39258
Problem 6.4.1 - Rarefied flow around a double ellipse p 869 A93-42630
Zonally-decoupled DSMC solutions of hypersonic blunt body wake flows [AIAA PAPER 93-2808] p 949 A93-44227
A systems approach to a DSMC calculation of a control jet interaction experiment [AIAA PAPER 93-2798] p 964 A93-46538
Non-equilibrium thermal radiation from air shock layers modelled with the Direct Simulation Monte Carlo method [AIAA PAPER 93-2805] p 1028 A93-46544
Flow resolution and domain of influence in rarefied hypersonic blunt-body flows [AIAA PAPER 93-2806] p 964 A93-46546
Hypersonic blunt body wake computations using DSMC and Navier-Stokes solvers [AIAA PAPER 93-2807] p 964 A93-46547
Monte Carlo simulation of radiating reentry flows [AIAA PAPER 93-2809] p 964 A93-46548
Comparisons between DSMC and the Navier-Stokes equations for reentry flows [AIAA PAPER 93-2810] p 964 A93-46549
Aerodynamics of Shuttle Orbiter at high altitudes [AIAA PAPER 93-2815] p 965 A93-46553
DSMC simulation of ionized rarefied flows [AIAA PAPER 93-3095] p 1061 A93-48269
DSMC numerical investigation of rarefied compression corner flow [AIAA PAPER 93-3096] p 1061 A93-48270
Performance prediction of the interacting multiple model algorithm p 1167 A93-50638
Development and application of the Monte Carlo method for solving the Boltzmann equation and its models p 1173 A93-51867
Direct simulation of reacting fuel gas flows in a supersonic mixing layer [ISABE 93-7072] p 1201 A93-54048
Summary: Experimental validation of real-time fault-tolerant systems [NASA-CR-190985] p 175 N93-13697
Proceedings of the Ninth NAL Symposium on Aircraft Computational Aerodynamics [NAL-SP-16] p 299 N93-19273
Development and application of computational aerothermodynamics flowfield computer codes [NASA-CR-192940] p 692 N93-24736
Discrete range clustering using Monte Carlo methods [NASA-TM-104004] p 706 N93-24914
A transfer matrix approach to vibration localization in mistuned blade assemblies [NASA-TM-106112] p 838 N93-27088

MORTALITY
Breaking through the 10 exp 6 barrier --- decreasing aircraft accident fatality rate per million flight hours p 27 A93-11498
Increase in mortality rates due to aircraft noise p 1163 A93-49551
Radiation exposure in aircraft p 1035 N93-31928

MOTION PERCEPTION
Pilot evaluations of augmented flight simulator motion [AIAA PAPER 93-3580] p 1208 A93-52676

MOTION SICKNESS
A survey of position trackers p 1151 A93-49396

MOTION SIMULATION
Research on ISAR motion compensation and imaging by modeling electromagnetic data p 342 A93-20852
The development of SIMONA - A simulator facility for advanced research into simulation techniques, motion system control and navigation systems technologies [AIAA PAPER 93-3574] p 1208 A93-52670
Simulation motion effect on single axis compensatory tracking [AIAA PAPER 93-3579] p 1208 A93-52675
Pilot evaluations of augmented flight simulator motion [AIAA PAPER 93-3580] p 1208 A93-52676

Simulator motion [AD-A257683] p 381 N93-17687
Motion simulation of underwater vehicles [VTT-PUBS-97] p 443 N93-18698
Three-dimensional graphical representation of objects according to movement data in realtime [ESA-TT-1258] p 942 N93-30104

MOTION SIMULATORS
Simulator motion [AD-A257683] p 381 N93-17687

MOTION STABILITY
Control synthesis with incomplete, complete, and supercomplete measurements p 561 A93-27603
A simplified wing rock prediction method [AIAA PAPER 93-3662] p 1128 A93-48342
Effect of the atmosphere density gradient on aerodynamic stabilization p 1252 A93-55034

MOTOR VEHICLES
Steering system of a vehicle, such as a snow removing machine for airfields [CA-PATENT-APPL-SN-1293201] p 83 N93-10367

MOUNTAINS
Efforts to reduce CFIT accidents should address failures of the aviation system itself p 1096 A93-49280
Atmospheric disturbances over mountains and the flight safety p 1164 A93-51856
Aircraft accident/incident summary report: Controlled flight into terrain, Bruno's Inc., Beechjet, N25BR, Rome, Georgia, December 11, 1991 [PB92-910404] p 143 N93-13470

MOVING TARGET INDICATORS
The ISAR image-formation results of Boeing-727 p 342 A93-20857
Track moving emitters with Kalman processing p 317 A93-22275
Adaptive clutter suppression for airborne array radars using clutter subspace approximation p 883 A93-43411
Adaptive array processing for airborne radar p 883 A93-43412
Antenna design for adaptive airborne MTI p 884 A93-43440
Ongoing GPS experiments demonstrate potential of satellite navigation technology p 1097 A93-49278

MTBF
Integrated modular avionics p 896 A93-42777

MULTIGRID METHODS
An implicit multigrid scheme for hypersonic strong-interaction flowfields p 6 A93-10534
Adaptive multigrid for the steady Euler equations p 201 A93-13988
Application of multigrid and adaptive grid embedding to the two-dimensional flux-split Euler equations p 202 A93-13990
Numerical computations of turbomachinery cascade turbulent flows with shocks by using multigrid scheme p 112 A93-14167
MELINA - A multi-block, multi-grid 3D Euler code with sub block technique for local mesh refinement p 115 A93-14217
Numerical research on flows in nonuniform cascades [ASME PAPER 92-GT-276] p 253 A93-19469
Development of a flexible and efficient multigrid-based multiblock flow solver [AIAA PAPER 93-0677] p 269 A93-21117
3-D adaptive grid-embedding Euler technique [AIAA PAPER 93-0330] p 415 A93-23021
An installed nacelle design method using multiblock Euler solver [AIAA PAPER 93-0528] p 284 A93-23269
A fast multigrid method for solving incompressible hydrodynamic problems with free surfaces [AIAA PAPER 93-0767] p 540 A93-2485; A multilevel composite grid method for fluid flow computations [AIAA PAPER 93-0768] p 541 A93-24852
Multigrid techniques for hypersonic viscous flows [AIAA PAPER 93-0771] p 467 A93-24855
Characteristic multigrid method application to solve the Euler equations with unstructured and unsteady grids p 476 A93-27065
Solution-adaptive and quality-enhancing grid generation p 480 A93-28610
An Euler code with new energy equation and new enthalpy damping approach p 686 A93-34352
Characteristics of three-dimensional turbulent jets in crossflow p 772 A93-38695
Application of the multigrid solution technique to hypersonic entry vehicles [AIAA PAPER 93-2721] p 858 A93-41049
Implicit multigrid techniques for compressible flows p 862 A93-42429
Computation of flows over 2D ramps p 866 A93-42595
Multigrid calculation of three-dimensional viscous cascade flows p 872 A93-42889

A 3D unstructured adaptive multigrid scheme for the Euler equations

[AIAA PAPER 93-3339] p 954 A93-45033

Multigrid convergence of an implicit symmetric relaxation scheme

[AIAA PAPER 93-3357] p 954 A93-45051

Implicit multigrid Euler solutions with symmetric Total-Variation-Diminishing dissipation

[AIAA PAPER 93-3358] p 955 A93-45052

Adaptive inviscid flow solutions for aerospace geometries on efficiently generated unstructured tetrahedral meshes

[AIAA PAPER 93-3390] p 956 A93-45081

A 3-D finite-volume scheme for the Euler equations on adaptive tetrahedral grids

p 956 A93-45083

A simple multigrid procedure for explicit time-marching on unstructured grids

p 956 A93-45087

An upwind multigrid algorithm for calculating flows on unstructured grids

p 957 A93-45088

A multigrid nonoscillatory method for computing high speed flows

[AIAA PAPER 93-3319] p 958 A93-45103

A multiblock, multigrid solution procedure for multielement airfoils

p 967 A93-46812

Multigrid methods for calculating 3D flows in complex geometries

p 973 A93-46984

Navier-Stokes calculations for transport wing-body configurations with nacelles and struts

[AIAA PAPER 93-2945] p 1047 A93-48142

Multigrid techniques for hypersonic viscous flows

p 1071 A93-49027

Secondary flow computation by means of an inviscid multigrid Finite Volume Lambda Formulation

[AIAA PAPER 93-1974] p 1077 A93-49821

3-D turbomachinery Euler and Navier-Stokes calculations with a multidomain cell-centered approach

[AIAA PAPER 93-2576] p 1085 A93-50292

Multigrid Navier-Stokes calculations for three-dimensional cascades

p 1177 A93-53209

Volume 2: Explicit, multistage upwind schemes for Euler and Navier-Stokes equations

[NASA-CR-191647] p 418 A93-16558

Implementation of a multidomain Navier-Stokes code on the Intel iPSC2 hypercube

[FFA-TN-1992-37] p 843 A93-28994

WBNFLOW: Multi-grid/multi-block potential solver for compressible flow. User's guide

[FFA-TN-1992-43] p 1031 A93-31146

MULTIPATH TRANSMISSION

Multipath effects on GPS code phase measurements

p 34 A93-11295

Application of parafolios to microwave landing system siting

[AIAA PAPER 93-1213] p 702 A93-35162

Multipath effects in a Global Positioning Satellite system receiver

p 318 A93-17311

GPS Interferometry

[NASA-CR-192301] p 319 A93-18873

MULTIPHASE FLOW

Aeroloids and secondary flows in a transonic mixed flow turbine stage

[ASME PAPER 92-GT-72] p 248 A93-19322

Design and rotor performance of a 5:1 mixed-flow supersonic compressor

[ASME PAPER 92-GT-73] p 348 A93-19323

Optimization of circular orifice jets mixing into a heated crossflow in a cylindrical duct

[AIAA PAPER 93-0249] p 361 A93-23246

Optimization of circular orifice jets mixing into a heated cross flow in a cylindrical duct

[NASA-TM-105984] p 179 A93-15359

MULTIPLE TARGET TRACKING

A multisensor-multitarget data association algorithm for heterogeneous sensors

p 439 A93-22899

MULTIPLEXING

Sensors with centroid based common sensing scheme and their multiplexing — fiber optic sensors in aircraft and aircraft engine applications

p 1192 A93-52994

Multiplexing electro-optic architectures for advanced aircraft integrated flight control systems

[NASA-CR-182268] p 187 A93-13735

Electro-optic architecture (EOA) for sensors and actuators in aircraft propulsion systems

[NASA-CR-182270] p 233 A93-15116

The Data Multiplexing Network (DMN) phase 3 Extended Distance Data Cable (EDDC) test and evaluation

[DOT/FAA/CT-TN93/11] p 752 A93-26160

MULTIPROCESSING (COMPUTERS)

LEWICE droplet trajectory calculations on a parallel computer

[AIAA PAPER 93-0172] p 438 A93-22604

Architecture of multiprocessor data processing machines and dispatching of the knowledge acquisition process in flight control

p 1168 A93-50958

MULTIPROGRAMMING

An advanced rotorcraft flight simulation model - Parallel implementation and performance analysis

[AIAA PAPER 93-3550] p 1222 A93-52654

MULTISENSOR APPLICATIONS

Sensor alignment Kalman filters for inertial stabilization systems

p 50 A93-11018

A high resolution airborne multisensor system

p 343 A93-21966

A multisensor-multitarget data association algorithm for heterogeneous sensors

p 439 A93-22899

A multisensor-multitarget data association algorithm for heterogeneous sensors

p 1020 A93-44168

Design for tactical situation awareness display

[AD-A256194] p 170 A93-15235

Method of measuring cross-flow vortices by use of an array of hot-film sensors

[NASA-CASE-LAR-14824-1-SB] p 751 A93-26000

MULTISPECTRAL RADAR

RAMSES: Multi-spectral experimental radar station installed on board the Transall

p 550 A93-19925

MULTISTATIC RADAR

Bistatic radar using satellite-borne illuminators of opportunity

p 914 A93-43437

MULTIVARIABLE CONTROL

Aspects of multivariable flight control law design for helicopters using eigenstructure assignment

p 60 A93-10916

Direct multivariable adaptive controller with application to wing flutter

p 524 A93-26946

Design and evaluation of a robust dynamic neurocontroller for a multivariable aircraft control problem

p 617 A93-37004

Full envelope multivariable control law synthesis for a high-performance test aircraft

p 1130 A93-49595

Multilevel control systems and optimization of their structures

p 1168 A93-50954

Multilevel intelligent control systems for flight vehicles

p 1168 A93-50955

Design of a low sensitivity and norm multivariable controller using eigenstructure assignment and the method of inequalities

[AIAA PAPER 93-3802] p 1170 A93-51394

Design of limit-tracking systems incorporating a turbofan engine with constant disturbances

[ISABE 93-7090] p 1203 A93-54066

Theoretical constraints in the design of multivariable control systems

[NASA-CR-191900] p 442 A93-18372

MULTIVARIATE STATISTICAL ANALYSIS

A k-omega multivariate beta PDF for supersonic turbulent combustion

[AIAA PAPER 93-2197] p 1154 A93-50009

Modeling of turbulent supersonic H₂-air combustion with a multivariate beta PDF

[AIAA PAPER 93-2198] p 1155 A93-50010

N

N-TYPE SEMICONDUCTORS

Photoelectrochemical etching of high aspect ratio submillimeter waveguide filters from n(+) GaAs wafers

p 409 A93-20644

NACELLES

Hybrid laminar flow control applied to advanced turbofan engine nacelles

[SAE PAPER 920962] p 123 A93-14628

Application of laminar flow to aero engine nacelles

p 128 A93-17256

An installed nacelle design method using multiblock Euler solver

[AIAA PAPER 93-0528] p 284 A93-23269

Design of an advanced nacelle for a very high bypass ratio engine

p 505 A93-25362

V-22 nacelle conversion actuator

p 889 A93-40438

Investigation of nacelle upper cowl flow separation using on- and off-body flow visualization techniques

p 1072 A93-49507

On boundary-layer transition in transonic flow

p 1087 A93-51280

Second generation low order panel method and its application for a case of nacelle

p 1231 A93-54595

Application of laminar flow to aero engine nacelles

[PNR-90916] p 20 A93-11020

A combined experimental and theoretical study of laminar flow control with particular relevance to aero engine nacelles

[PNR-90991] p 20 A93-11070

A European collaborative NLF nacelle flight demonstrator

[PNR-90992] p 20 A93-11113

A wind tunnel investigation to determine buffet countermeasures for STOL aircraft alpha-sweep flight testing

[NAL-TR-1129] p 65 A93-12362

High-speed aerodynamics of upper surface blowing aircraft configurations

p 132 A93-13729

Design optimization of natural laminar flow bodies in compressible flow

[NASA-CR-4478] p 292 A93-16940

NAP-OF-THE-EARTH NAVIGATION

Visual field information in Nap-of-the-Earth flight by teleoperated Helmet-Mounted displays

p 517 A93-26884

Technologies for automating rotorcraft nap-of-the-earth flight

p 885 A93-43784

Passive range estimation for rotorcraft low-altitude flight

p 948 A93-46608

Electro-optical navigation for aircraft

p 1097 A93-50643

Passive range estimation for rotorcraft low-altitude flight

p 1190 A93-52881

Multirate and event-driven Kalman filters for helicopter flight

p 1245 A93-55760

Flight test and analysis procedures for new handling criteria

[RAE-TM-FM-26] p 47 A93-10803

Integration of radar altimeter, precision navigation, and digital terrain data for low-altitude flight

[NASA-TM-103958] p 36 A93-12320

Testing of an automatic, low altitude, all terrain ground collision avoidance system

p 502 A93-19924

Methodology investigation: Global Positioning System integration (GPS)

[AD-A261054] p 708 A93-26237

Image-based ranging and guidance for rotorcraft

[NASA-CR-177608] p 708 A93-26549

Merging sparse optical flow and edge connectivity between image features: A representation scheme for 2-D display of scene depth

p 845 A93-27179

Flight evaluation of a computer aided low-altitude helicopter flight guidance system

p 820 A93-28869

Flight evaluation of a computer aided low-altitude helicopter flight guidance system

[NASA-TM-103998] p 994 A93-32225

NAPHTHALENE

Vortex structure and mass transfer near the base of a cylinder and a turbine blade

p 901 A93-29929

NARROWBAND

Helicopter plume detection by using an ultranarrow-band noncoherent laser Doppler velocimeter

p 542 A93-25198

Scale-up of the spectra of aerodynamic pressure pulsations with narrowband maxima

p 1088 A93-51756

NASA PROGRAMS

Status of the NASA Balloon Program

p 1 A93-11365

NASA Long Duration Balloon capability development project

p 2 A93-11370

A historical perspective on hypersonic research at the NASA/NASA Langley Research Center (1944-1984)

[AIAA PAPER 92-5034] p 456 A93-22308

Update on the NASA ER-2 Doppler radar system (EDOP)

p 807 A93-37737

The NASA Computational Fluid Dynamics (CFD) program - Building technology to solve future challenges

[AIAA PAPER 93-3292] p 1041 A93-44996

Propulsion technology challenges for turn-of-the-century commercial aircraft

[ISABE 93-7003] p 1194 A93-53980

Aeronautical technologies for the twenty-first century

[NASA-CR-190918] p 4 A93-10647

Index to NASA news releases and speeches, 1991

[NASA-TM-108004] p 104 A93-10815

Index to NASA news releases and speeches, 1990

[NASA-TM-108003] p 104 A93-10872

Winds of change: Expanding the frontiers of flight. Langley Research Center's 75 years of accomplishment, 1917-1992

[NASA-NP-130] p 104 A93-11100

Coordinating Council. Fourth Meeting: NACA Documents Database Project

[NASA-TM-108017] p 234 A93-12671

Coordinating Council. Sixth Meeting: Who Are Our Key Users?

[NASA-TM-108021] p 234 A93-12672

NASA aeronautics: Research and technology program highlights

[NASA-NP-159] p 109 A93-13110

Structural dynamics branch research and accomplishments to FY 1992

[NASA-TM-105824] p 552 A93-20368

NASA SBIR abstracts of 1990 phase 1 projects

[NASA-TM-108145] p 572 A93-21794

NASA SBIR abstracts of 1991 phase 1 projects

[NASA-TM-108240] p 945 A93-29323

Research and technology objectives and plans: Summary fiscal year 1991

[NASA-TM-103086] p 946 A93-29452

First NASA Advanced Composites Technology Conference, part 2
[NASA-CP-3104-PT-2] p 921 N93-30841

Propulsion technology challenges for turn-of-the-century commercial aircraft
[NASA-TM-106192] p 1005 N93-32351

NASA SPACE PROGRAMS

NASA's hypersonic flight research program
[AIAA PAPER 93-0308] p 457 A93-25516

Evolutionary NASA - Inventors to bureaucrats
p 1174 A93-50330

International aerospace STI
p 1227 A93-53826

National Aeronautics and Space Administration
p 454 N93-17091

Aeronautics in NACA and NASA
[NASA-NP-156] p 678 N93-26422

Aeronautics and space report of the President: Fiscal year 1992 activities
p 854 N93-27041

NASTRAN

Modal analysis of multistage gear systems coupled with gearbox vibrations
p 827 A93-36588

The NASA/industry Design Analysis Methods for Vibrations (DAMVIBS) program: Boeing Helicopters airframe finite element modeling
p 515 N93-21313

Stress calculation for the Sandia 34-meter wind turbine using the local circulation method and turbulent wind
[DE93-004480] p 560 N93-22045

NASTRAN analysis for the Airmass Sunburst model 'C'
p 931 N93-29777

NATIONAL AEROSPACE PLANE PROGRAM

Fluid/chemistry modeling for hypersonic flight analysis
p 111 A93-14120

The United States in the conquest of the hypersonic
p 109 A93-15056

Subsonic static and dynamic stability characteristics of the test technique demonstrator NASP configuration
[AIAA PAPER 93-0519] p 268 A93-21111

Keynote address - Advanced Technology demonstrators, prototypes and hypersonic flight
[AIAA PAPER 92-4999] p 456 A93-22276

Supersonic dynamic stability characteristics of the test technique demonstrator NASP configuration
[AIAA PAPER 92-5009] p 367 A93-22285

Aero-space plane figures of merit
[AIAA PAPER 92-5058] p 385 A93-22328

A dynamic inversion control approach for high-Mach trajectory tracking
p 385 A93-22870

Numerical simulation of flow past the X24C reentry vehicle
[AIAA PAPER 93-0319] p 280 A93-23011

Construction of a one-third scale model of the NASP
[AIAA PAPER 93-0427] p 386 A93-23345

Natural environment application for NASP-X-30 design and mission planning
[AIAA PAPER 93-0851] p 531 A93-24915

Zen and the art of airplane sizing
p 504 A93-25174

NASP - Waveriders in a hypersonic sky. I
p 532 A93-25355

NASP - Waveriders in a hypersonic sky. II
p 532 A93-25359

An overview of aeroelasticity studies for the National Aero-Space Plane
[AIAA PAPER 93-1313] p 732 A93-33889

Aeroelastic character of a National Aerospace Plane demonstrator concept
[AIAA PAPER 93-1314] p 732 A93-33890

An experimental and analytical study of a lifting-body wind-tunnel model exhibiting body-freedom flutter
[AIAA PAPER 93-1316] p 732 A93-33891

Aerothermoelastic analysis of a NASP demonstrator model
[AIAA PAPER 93-1366] p 733 A93-33933

Supersonic aeroelastic instability results for a NASP-like wing model
[AIAA PAPER 93-1369] p 682 A93-33935

Active control of aerothermoelastic effects for a conceptual hypersonic aircraft
p 1007 A93-45137

CFD code calibration and inlet-fairing effects on a 3D hypersonic powered-simulation model
[AIAA PAPER 93-3041] p 1056 A93-48222

Investigation of the flowfield over parallel-arranged launch vehicles
[AIAA PAPER 93-3060] p 1058 A93-48237

Engineering method for calculating inlet face property profiles on high speed vehicle forebodies
[AIAA PAPER 93-3113] p 1062 A93-48283

Slush hydrogen quantity gaging and mixing for the National Aerospace Plane
p 1150 A93-48635

Future technology aim of the National Aerospace Plane Program
[AIAA PAPER 93-1988] p 1141 A93-49833

Advancing the state of the art hypersonic testing - HYTEST/MTMI
[AIAA PAPER 93-2023] p 1113 A93-49860

National Aerospace Plane Integrated
Fuselage/Cryotank Risk Reduction program
[AIAA PAPER 93-2564] p 1142 A93-50284

A configuration development strategy for the NASP
p 46 N93-10011

National Aero-Space Plane: Key issues facing the program. Testimony before the Subcommittee on Technology and Competitiveness, Committee on Science, Space, and Technology, House of Representatives
[GAO/T-NSIAD-92-26] p 161 N93-13253

High-temperature strain measurement techniques: Current developments and challenges
p 217 N93-13669

National Aeronautics and Space Administration
p 454 N93-17091

Hypersonic flows as related to the national aerospace plane
[NASA-CR-191980] p 296 N93-18378

National aero-space plane: Restructuring future research and development efforts
[AD-A258799] p 340 N93-18981

The National Aero-Space Plane program: A revolutionary concept
p 511 N93-19908

Turbulence modeling for hypersonic flight
[NASA-CR-192288] p 483 N93-20235

Trajectory optimization for the National aerospace plane
[NASA-CR-192954] p 716 N93-25670

Numerical simulation of hypersonic aerodynamics and the computational needs for the design of an aerospace plane
[AD-A260681] p 699 N93-25894

Aerospace-plane flights and stratospheric ozone: Review and preliminary assessment of the National Aerospace Plane (NASP) operations
[RAND/N-3464-AF] p 755 N93-26327

NATIONAL AIRSPACE SYSTEM

Magnetic variation - A primitive concept and its hold on contemporary navigation
p 32 A93-11021

Complementary MLS and GNSS operations
p 384 A93-21160

On the selection of a GPS validity indicator for aircraft navigation in the National Airspace System (NAS)
p 316 A93-21186

Airspace redesign - Making the GRADE
p 317 A93-21630

Statistical techniques for traffic flow management
[AIAA PAPER 93-3834] p 1098 A93-51423

A description of the Mode Select beacon system (Mode S) and its associated benefits to the National Airspace System (NAS)
[DOT/FAA/SE-92/6] p 35 N93-10738

Methods and principles for determining task dependent interface content
[NASA-CR-190837] p 36 N93-10961

Limited production Precision Runway Monitor (PRM) master test plan
[DOT/FAA/CT-TN92/23] p 192 N93-12899

Terminal Doppler Weather Radar (TDWR) Operational Test and Evaluation (OT/E) integration test plan
[DOT/FAA/CT-TN92/6] p 151 N93-13377

A NASPAC-based analysis of the delay and cost effects of the Dallas/Fort Worth metroplex plan
[DOT/FAA/CT-TN92/21] p 193 N93-13447

National Airspace System flight planning operational concept NAS-SR-131
[PB93-124659] p 310 N93-18031

National Airspace System: Air traffic control and airspace management operational concept NAS-SR-132
[DOT/FAA/SE-92/5] p 502 N93-20164

Definitional mission for civil aviation master plan for Poland
[PB92-213974] p 459 N93-21713

Runway Visual Range (RVR) Operational Test and Evaluation (OT&E) integration and OT&E operational test report
[DOT/FAA/CT-TN92/37] p 706 N93-25243

National Airspace System Performance Analysis Capability (NASPAC) simulation model
p 887 N93-30351

NATURAL GAS

Improved selective catalytic NOx control technology for compressor station reciprocating engines
[PB93-158566] p 755 N93-26529

NATURAL LANGUAGE (COMPUTERS)

Action composition for the animation of natural language instructions
[AD-A254963] p 228 N93-12554

NAVIER-STOKES EQUATION

An asymptotic model of a closed separation region in supersonic flow
p 4 A93-10139

An effective multigrid method for high-speed flows
p 6 A93-10533

An implicit multigrid scheme for hypersonic strong-interaction flowfields
p 6 A93-10534

Direct numerical simulation of laminar breakdown in high-speed, axisymmetric boundary layers
p 8 A93-11527

Numerical dissipation in F3D thin-layer Navier-Stokes solution for flows with wall transpiration
p 9 A93-12010

Aerodynamic design of axisymmetric hypersonic wind-tunnel nozzles using a least-squares/parabolized Navier-Stokes procedure
p 9 A93-12011

Effect of canard position on the longitudinal aerodynamic characteristics of a close-coupled canard-wing-body configuration
[AIAA PAPER 92-4632] p 14 A93-13304

The numerical study of 3-D flow past control surfaces
[AIAA PAPER 92-4650] p 14 A93-13305

Navier-Stokes analysis of turbine blade heat transfer and performance
p 201 A93-13978

Influence of trailing-edge grid structure on Navier-Stokes computation of turbomachinery cascade flow
p 111 A93-14078

Navier-Stokes calculations of the flow about wing-flap combinations
p 112 A93-14171

Multizone Navier-Stokes computations for a transonic projectile using MacCormack finite difference method
p 113 A93-14192

Assessment and correction of tunnel wall interference by Navier-Stokes solutions
p 116 A93-14275

A multi-zonal local solution methodology for the accelerated solution of the turbulent Navier-Stokes equations
p 117 A93-14279

Navier-Stokes computation of wing/rotor interaction for a tilt rotor in hover
p 122 A93-14537

Implicit Navier-Stokes solver for three-dimensional compressible flows
p 122 A93-14546

Periodic Euler and Navier-Stokes solutions about oscillating airfoils
p 241 A93-17799

Effect of real air properties on integral aerodynamic characteristics
p 242 A93-18241

On the coupling between a supersonic boundary layer and a flexible surface
p 243 A93-19132

Numerical analysis of acoustic effect of rotor wakes in rotor-stator interaction
p 447 A93-19182

Secondary flows in a transonic cascade - Validation of a 3-D Navier-Stokes code
[ASME PAPER 92-GT-62] p 247 A93-19312

Analysis of steady and unsteady turbine cascade flows by a locally implicit hybrid algorithm
[ASME PAPER 92-GT-127] p 249 A93-19361

Investigations on a radial compressor tandem-rotor stage with adjustable geometry
[ASME PAPER 92-GT-218] p 404 A93-19440

Navier-Stokes computation on a pivoting doors thrust reverser and comparison with tests
[ASME PAPER 92-GT-254] p 353 A93-19463

Investigation of tip clearance phenomena in an axial compressor cascade using Euler and Navier-Stokes procedures
[ASME PAPER 92-GT-299] p 255 A93-19489

Three-dimensional Navier-Stokes computations of transonic fan flow using an explicit flow solver and an implicit k-epsilon solver
[ASME PAPER 92-GT-309] p 256 A93-19499

The extension of a solution-adaptive 3D Navier-Stokes solver towards geometries of arbitrary complexity
[ASME PAPER 92-GT-363] p 257 A93-19527

Accuracy issues in the prediction of supersonic inlet flows
[ASME PAPER 92-GT-400] p 258 A93-19549

Analysis of jet/wake mixing in a vaneless diffuser
[ASME PAPER 92-GT-418] p 258 A93-19566

A novel approach to high resolution compressible cascade flow analysis using the Navier-Stokes equations
[ASME PAPER 92-GT-419] p 258 A93-19567

A performance comparison of massively parallel Parabolized Navier-Stokes solutions
[AIAA PAPER 93-0059] p 435 A93-20172

Implementation of an explicit Navier-Stokes algorithm on a distributed memory parallel computer
[AIAA PAPER 93-0063] p 261 A93-20176

Unsteady two- and three-dimensional Navier-Stokes simulations of multistage turbomachinery flows
p 266 A93-20721

Large-scale simulation of the three-dimensional Navier-Stokes equations
p 437 A93-20739

A gridless Euler/Navier-Stokes solution algorithm for complex-aircraft applications
[AIAA PAPER 93-0333] p 268 A93-21107

Development of a flexible and efficient multigrid-based multiblock flow solver
[AIAA PAPER 93-0677] p 269 A93-21117

Workshop report - A validation study of Navier-Stokes codes for transverse injection into a Mach 2 flow
p 270 A93-21330

Numerical analysis of reacting flow using finite rate chemistry models
p 389 A93-21666

Computations of a twin-jet impingement on a flat surface p 271 A93-22227

Application of space-marching methods to hypersonic forebody flow fields p 272 A93-22305

[AIAA PAPER 92-5030] p 272 A93-22305

A study of hypersonic swept shock wave/turbulent boundary layer interactions using a conical Navier-Stokes code p 273 A93-22322

[AIAA PAPER 92-5050] p 273 A93-22322

An algebraic turbulence model for three-dimensional viscous flows p 274 A93-22552

[AIAA PAPER 93-0083] p 274 A93-22552

Numerical simulation of the turbulent flow in round jets p 277 A93-22619

[AIAA PAPER 93-0199] p 277 A93-22619

The effect of Reynolds number and turbulence on airfoil aerodynamics at -90 degrees incidence p 277 A93-22624

[AIAA PAPER 93-0206] p 277 A93-22624

Aircraft grid generation using interactive environment p 438 A93-22639

[AIAA PAPER 93-0224] p 438 A93-22639

Evaluation of a CFD code for analysis of normal-shock trains p 279 A93-22692

[AIAA PAPER 93-0292] p 279 A93-22692

Validation of a Navier-Stokes code using a (K,epsilon) turbulence model applied to a three-dimensional transonic channel p 279 A93-22693

[AIAA PAPER 93-0293] p 279 A93-22693

A parametric study of bleed in shock boundary layer interactions p 280 A93-22694

[AIAA PAPER 93-0294] p 280 A93-22694

Application of CFD to a generic hypersonic flight research study p 280 A93-23007

[AIAA PAPER 93-0312] p 280 A93-23007

A hybrid structured-unstructured grid method for unsteady turbomachinery flow computations p 282 A93-23066

[AIAA PAPER 93-0387] p 282 A93-23066

Three-dimensional Navier-Stokes analysis of the tip clearance flow in linear turbine cascades p 282 A93-23068

[AIAA PAPER 93-0391] p 282 A93-23068

Ice accretion and performance degradation calculations with LEWICE/NS p 310 A93-23244

[AIAA PAPER 93-0173] p 310 A93-23244

Application of a Navier-Stokes aerodynamic method to improve fighter wing performance at maneuver flight conditions p 284 A93-23270

[AIAA PAPER 93-0529] p 284 A93-23270

Nonlinear relaxation/quasi-Newton algorithm for the compressible Navier-Stokes equations p 287 A93-23541

[AIAA PAPER 93-0529] p 287 A93-23541

A Navier-Stokes simulation of vortex shedding from square cylinder in unconfined domain p 538 A93-24084

[AIAA PAPER 93-0529] p 538 A93-24084

An upwind formulation for the solution of thin-layer Navier-Stokes equations p 461 A93-24088

[AIAA PAPER 93-0529] p 461 A93-24088

Three-dimensional flow simulation over axisymmetric bodies using Navier-Stokes equations at hypersonic Mach numbers p 461 A93-24090

[AIAA PAPER 93-0529] p 461 A93-24090

Three-dimensional Navier-Stokes calculations using solution-adapted grids p 462 A93-24240

[AIAA PAPER 93-0431] p 462 A93-24240

A numerical method for solving Navier-Stokes equations for low Mach number compressible flows p 463 A93-24672

[AIAA PAPER 93-0601] p 463 A93-24672

Effect of leading-edge porosity on blade-vortex interaction noise p 563 A93-24727

[AIAA PAPER 93-0601] p 563 A93-24727

Navier-Stokes computations and experimental comparisons for multielement airfoil configurations p 464 A93-24760

[AIAA PAPER 93-0645] p 464 A93-24760

Airfoil design using the Navier-Stokes equations p 464 A93-24763

[AIAA PAPER 93-0648] p 464 A93-24763

Navier-Stokes calculations for the unsteady flowfield of turbomachinery p 465 A93-24786

[AIAA PAPER 93-0676] p 465 A93-24786

Two-dimensional Navier-Stokes analysis of high-lift multi-element airfoils using the q-omega turbulence model p 466 A93-24787

[AIAA PAPER 93-0679] p 466 A93-24787

Comparison of continuum and particle simulations of expanding rarefied flows p 466 A93-24818

[AIAA PAPER 93-0728] p 466 A93-24818

A multilevel composite grid method for fluid flow computations p 541 A93-24852

[AIAA PAPER 93-0768] p 541 A93-24852

A concurrent hybrid Navier-Stokes/Euler approach to fluid dynamic computations p 468 A93-24865

[AIAA PAPER 93-0789] p 468 A93-24865

A physically guided zonal approach for two-dimensional aerfoil flows p 468 A93-24869

[AIAA PAPER 93-0790] p 468 A93-24869

Numerical simulation of vortex generation and capture above an airfoil p 468 A93-24926

[AIAA PAPER 93-0864] p 468 A93-24926

A fully implicit Navier-Stokes algorithm using an unstructured grid and flux difference splitting p 470 A93-24936

[AIAA PAPER 93-0875] p 470 A93-24936

Jacobian update strategies for quadratic and near-quadratic convergence of Newton and Newton-like implicit schemes p 470 A93-24939

[AIAA PAPER 93-0878] p 470 A93-24939

Application of high-order accurate essentially nonoscillatory schemes to two-dimensional compressible viscous flows p 470 A93-24940

[AIAA PAPER 93-0879] p 470 A93-24940

Aerodynamic analyses for design and education p 473 A93-24988

[AIAA PAPER 92-2664] p 473 A93-24988

Artificial viscosity models for the Navier-Stokes equations and their effect in drag prediction p 473 A93-25511

[AIAA PAPER 93-0193] p 473 A93-25511

Recent developments in high order K-exact reconstruction on unstructured meshes p 475 A93-25546

[AIAA PAPER 93-0668] p 475 A93-25546

A numerical study of mixing in supersonic combustors with hypermixing injectors p 520 A93-27801

[AIAA PAPER 93-0215] p 520 A93-27801

Investigation of vortex breakdown on delta wings using Navier-Stokes equations p 478 A93-27924

[AIAA PAPER 93-0215] p 478 A93-27924

Prediction of asymmetric vortical flows around slender bodies using Navier-Stokes equations p 478 A93-27925

[AIAA PAPER 93-0215] p 478 A93-27925

Numerical study of the flow establishment time in hypersonic shock tunnels p 480 A93-29153

[AIAA PAPER 93-0215] p 480 A93-29153

Current status of computational methods for transonic unsteady aerodynamics and aeroelastic applications p 480 A93-29175

[AIAA PAPER 93-0215] p 480 A93-29175

Flowfield analysis of modern helicopter rotors in hover by Navier-Stokes method p 481 A93-29435

[AIAA PAPER 93-0215] p 481 A93-29435

A numerical study of advanced rotor blades p 481 A93-29436

[AIAA PAPER 93-0215] p 481 A93-29436

Computation of supersonic crossflow separation using a new parabolized Navier-Stokes code p 687 A93-34355

[AIAA PAPER 93-0215] p 687 A93-34355

Dynamically adaptive grid and its applications to flow problems p 688 A93-34362

[AIAA PAPER 93-0215] p 688 A93-34362

Numerical simulation of turbine 'hot spot' alleviation using film cooling p 744 A93-34476

[AIAA PAPER 93-0215] p 744 A93-34476

Multipassage three-dimensional Navier-Stokes simulation of turbine rotor-stator interaction p 688 A93-34484

[AIAA PAPER 93-0215] p 688 A93-34484

Study on vortex generator flow control for the management of inlet distortion p 689 A93-34488

[AIAA PAPER 93-0215] p 689 A93-34488

Commercial turbofan engine exhaust nozzle flow analyses p 689 A93-34489

[AIAA PAPER 93-0215] p 689 A93-34489

Computational study of advanced exhaust system transition ducts with experimental validation p 689 A93-34490

[AIAA PAPER 93-0215] p 689 A93-34490

Hypersonic nonequilibrium flow computations using the Roe flux-difference split scheme p 692 A93-35609

[AIAA PAPER 93-0215] p 692 A93-35609

URNS - A free-wake Euler/Navier-Stokes numerical method for helicopter rotors p 692 A93-35634

[AIAA PAPER 93-0215] p 692 A93-35634

Navier-Stokes correlations to fuselage wind tunnel test data p 765 A93-35937

[AIAA PAPER 93-0215] p 765 A93-35937

Multiblock Navier-Stokes solutions about the F/A-18 wing-LEX-fuselage configuration p 767 A93-37378

[AIAA PAPER 93-0215] p 767 A93-37378

Nonequilibrium turbulence modeling study on light dynamic stall of a NACA0012 airfoil p 768 A93-37379

[AIAA PAPER 93-0215] p 768 A93-37379

Turbulent flow simulation around the aerofol with pseudo-compressibility p 830 A93-38155

[AIAA PAPER 93-0215] p 830 A93-38155

Numerical calculation of separated flows around wing section in unsteady motion by using incompressible Navier-Stokes equations p 770 A93-38158

[AIAA PAPER 93-0215] p 770 A93-38158

Supersonic vortical flows around an ogive-cylinder - Laminar and turbulent computations p 771 A93-38588

[AIAA PAPER 93-0215] p 771 A93-38588

[ONERA, TP NO. 1992-111] p 771 A93-38588

Supersonic flow of a gas over a semiinfinite plate with small-scale harmonic spanwise oscillations p 775 A93-39118

[AIAA PAPER 93-0215] p 775 A93-39118

Shock interference prediction using direct simulation Monte Carlo p 778 A93-39258

[AIAA PAPER 93-0215] p 778 A93-39258

Navier-Stokes stall predictions using an algebraic Reynolds-stress model p 778 A93-39260

[AIAA PAPER 93-0215] p 778 A93-39260

Research in unsteady aerodynamics and computational aeroelasticity at the NASA Langley Research Center p 804 A93-39498

[AIAA PAPER 93-0215] p 804 A93-39498

Prediction of static performance for single expansion ramp nozzles p 898 A93-41047

[AIAA PAPER 93-2571] p 898 A93-41047

Higher-order viscous shock-layer solutions for high altitude flows p 858 A93-41050

[AIAA PAPER 93-2724] p 858 A93-41050

International Symposium on Computational Fluid Dynamics, 4th, Univ. of California, Davis, Sept. 9-12, 1991, Selected Papers p 862 A93-42426

[AIAA PAPER 93-2724] p 862 A93-42426

Gas-kinetic and Navier-Stokes simulations of reentry flows p 865 A93-42582

[AIAA PAPER 93-2724] p 865 A93-42582

Computational results for 2-D and 3-D ramp flows with an upwind Navier-Stokes solver p 866 A93-42592

[AIAA PAPER 93-2724] p 866 A93-42592

Computation of flows over 2D ramps p 866 A93-42595

[AIAA PAPER 93-2724] p 866 A93-42595

Navier-Stokes calculations over a double ellipse and a double ellipsoid by an implicit non-centered method p 867 A93-42607

[AIAA PAPER 93-2724] p 867 A93-42607

Application of the Galerkin/least-squares formulation to the analysis of hypersonic flows. II - Flow past a double ellipse p 868 A93-42608

[AIAA PAPER 93-2724] p 868 A93-42608

Computation of the hypersonic flow over a double ellipsoid p 868 A93-42610

[AIAA PAPER 93-2724] p 868 A93-42610

Numerical simulation of laminar hypersonic flow past a double-ellipsoid p 868 A93-42612

[AIAA PAPER 93-2724] p 868 A93-42612

2D hypersonic viscous flow past a double ellipse geometry p 868 A93-42613

[AIAA PAPER 93-2724] p 868 A93-42613

Hypersonic viscous flow past double ellipse and past double ellipsoid - Numerical results p 868 A93-42618

[AIAA PAPER 93-2724] p 868 A93-42618

Computation of thermochemical nonequilibrium flows around a simple and a double ellipse p 869 A93-42629

[AIAA PAPER 93-2724] p 869 A93-42629

Finite volume 3DNS and PNS solutions of hypersonic viscous flow around a delta wing using Osher's flux difference splitting p 870 A93-42633

[AIAA PAPER 93-2724] p 870 A93-42633

Hypersonic leeside delta-wing-flow computations using centered schemes p 870 A93-42635

[AIAA PAPER 93-2724] p 870 A93-42635

On the accuracy and efficiency of CFD methods in real gas hypersonics p 871 A93-42689

[AIAA PAPER 93-2724] p 871 A93-42689

Modeling supersonic inlet boundary-layer bleed roughness p 872 A93-42891

[AIAA PAPER 93-2724] p 872 A93-42891

New upwind dissipation models with a multidimensional approach p 950 A93-45002

[AIAA PAPER 93-3304] p 950 A93-45002

Solution of the Euler and Navier-Stokes equations on parallel processors using a transposed/Thomas ADI Algorithm p 1036 A93-45006

[AIAA PAPER 93-3310] p 1036 A93-45006

Variant bi-conjugate gradient methods for the compressible Navier-Stokes solver with a two-equation model of turbulence p 951 A93-45012

[AIAA PAPER 93-3316] p 951 A93-45012

A coarse-grid correction/nonlinear relaxation algorithm for the three-dimensional, compressible Navier-Stokes equations p 951 A93-45013

[AIAA PAPER 93-3317] p 951 A93-45013

Two-dimensional CFD modeling of wave rotor flow dynamics p 952 A93-45014

[AIAA PAPER 93-3318] p 952 A93-45014

Calculation of optimum airfoils using direct solutions of the Navier-Stokes equations p 952 A93-45017

[AIAA PAPER 93-3323] p 952 A93-45017

Numerical experiment of the flight trajectory simulation by fluid dynamics and flight dynamics coupling p 952 A93-45018

[AIAA PAPER 93-3324] p 952 A93-45018

Progress in local preconditioning of the Euler and Navier-Stokes equations p 952 A93-45022

[AIAA PAPER 93-3328] p 952 A93-45022

Numerical vorticity capturing for vortex-solid body interaction problems p 954 A93-45037

[AIAA PAPER 93-3343] p 954 A93-45037

Virtual zone Navier-Stokes computations for oscillating control surfaces p 955 A93-45056

[AIAA PAPER 93-3363] p 955 A93-45056

Preconditioned domain decomposition scheme for three-dimensional aerodynamic sensitivity analysis p 957 A93-45096

[AIAA PAPER 93-3363] p 957 A93-45096

Reynolds number effects on supersonic asymmetrical flows over a cone p 958 A93-45141

[AIAA PAPER 93-3363] p 958 A93-45141

Navier-Stokes analysis of three-dimensional S-ducts p 959 A93-45146

[AIAA PAPER 93-3363] p 959 A93-45146

PNS predictions of axisymmetric hypersonic blunt-body and afterbody flowfields p 962 A93-46479

[AIAA PAPER 93-3363] p 962 A93-46479

Hypersonic blunt body wake computations using DSMC and Navier-Stokes solvers p 964 A93-46547

[AIAA PAPER 93-2807] p 964 A93-46547

Comparisons between DSMC and the Navier-Stokes equations for reentry flows p 964 A93-46549

[AIAA PAPER 93-2810] p 964 A93-46549

Kinematic domain decomposition for boundary-motion-induced flow simulations p 1028 A93-46811

[AIAA PAPER 93-2810] p 1028 A93-46811

The three dimensional flow in a compressor cascade at design and off-design conditions p 971 A93-46927

[AIAA PAPER 93-2810] p 971 A93-46927

3D viscous flow analysis in axial turbine including tip leakage phenomena p 972 A93-46940

[AIAA PAPER 93-2810] p 972 A93-46940

Navier-Stokes flow simulation in a 2D high pressure turbine cascade with a cooled slot trailing edge p 972 A93-46941

[AIAA PAPER 93-2810] p 972 A93-46941

Multigrid methods for calculating 3D flows in complex geometries p 973 A93-46984

[AIAA PAPER 93-2810] p 973 A93-46984

Numerical simulation of linear interference wave development in three-dimensional boundary layers p 1029 A93-46993

[AIAA PAPER 93-2810] p 1029 A93-46993

A new flux splitting scheme p 973 A93-47189

[AIAA PAPER 93-2810] p 973 A93-47189

Finite element solution of the 3D compressible Navier-Stokes equations by a velocity-vorticity method p 974 A93-47196

[AIAA PAPER 93-2810] p 974 A93-47196

Calculation of AGARD Wing 445.6 flutter using Navier-Stokes aerodynamics p 981 A93-47255

[AIAA PAPER 93-3476] p 981 A93-47255

Application of computational fluid dynamics in transonic aerodynamic design
[AIAA PAPER 93-3481] p 982 A93-47259

Navier-Stokes prediction of a delta wing in roll with vortex breakdown
[AIAA PAPER 93-3495] p 983 A93-47267

Numerical simulation of incompressible viscous flow around a propeller
[AIAA PAPER 93-3503] p 984 A93-47271

The application of an Euler method and a Navier Stokes method to the vortical flow about a delta wing
[AIAA PAPER 93-3510] p 984 A93-47276

A 3D Navier-Stokes analysis of a generic ground vehicle shape
[AIAA PAPER 93-3521] p 985 A93-47283

A pointwise version of the Baldwin-Barth turbulence model
[AIAA PAPER 93-3523] p 985 A93-47284

Navier-Stokes calculations of rotating BERP planform blade flowfields
[AIAA PAPER 93-3527] p 986 A93-47286

Navier-Stokes calculations for transport wing-body configurations with nacelles and struts
[AIAA PAPER 93-2945] p 1047 A93-48142

Application of parabolized Navier-Stokes technique for high-L/D, hypersonic vehicle design
[AIAA PAPER 93-2948] p 1047 A93-48144

Active control of asymmetric conical flow using spinning and rotatory oscillations
[AIAA PAPER 93-2958] p 1048 A93-48152

Effects of air geometry on vortex behavior and force production by a tangential jet on a body at high alpha
[AIAA PAPER 93-2961] p 1048 A93-48155

Some practical turbulence modeling options for Reynolds-averaged full Navier-Stokes calculations of three-dimensional flows
[AIAA PAPER 93-2964] p 1048 A93-48158

Multi-zonal Navier-Stokes code with the LU-SGS scheme
[AIAA PAPER 93-2965] p 1148 A93-48159

A numerical study of the effect of geometry variation, turbulence models, and dissipation on the flow past control surfaces
[AIAA PAPER 93-2967] p 1048 A93-48161

Numerical solution of Navier-Stokes equations and k-omega turbulence model equations using a staggered upwind method
[AIAA PAPER 93-2968] p 1049 A93-48162

Hypersonic flow past open cavities
[AIAA PAPER 93-2969] p 1049 A93-48163

Comparison of ENO and TVD schemes for the parabolized Navier-Stokes equations
[AIAA PAPER 93-2970] p 1049 A93-48164

Precise pitching airfoil computations by use of dynamic unstructured meshes
[AIAA PAPER 93-2971] p 1049 A93-48165

Computational study of vortex breakdown on a pitching delta wing
[AIAA PAPER 93-2974] p 1050 A93-48168

Computation of delta-wing roll maneuvers
[AIAA PAPER 93-2975] p 1050 A93-48169

Three-dimensional unsteady separating flows around an oscillatory forward-swept wing
[AIAA PAPER 93-2976] p 1050 A93-48170

Simulation of DD-963 ship airwake by Navier-Stokes method
[AIAA PAPER 93-3002] p 1053 A93-48192

A computational and experimental investigation of a delta wing with vertical tails
[AIAA PAPER 93-3009] p 1054 A93-48199

A solution-adaptive hybrid-grid method for the unsteady analysis of turbomachinery
[AIAA PAPER 93-3015] p 1148 A93-48204

Navier-Stokes simulation of external/internal transonic flow on the forebody/inlet of the AV-8B Harrier II
[AIAA PAPER 93-3057] p 1058 A93-48234

Unsteady Navier-Stokes simulation of the canard-wing-body ramp motion
[AIAA PAPER 93-3058] p 1058 A93-48235

Fluid-structural interactions using Navier-Stokes flow equations coupled with shell finite element structures
[AIAA PAPER 93-3087] p 1099 A93-48261

On computing vortex asymmetries about cones at angle of attack using the conical Navier-Stokes equations
[AIAA PAPER 93-3628] p 1064 A93-48313

Navier-Stokes computations on full-span wing-body configuration with oscillating control surfaces
[AIAA PAPER 93-3687] p 1065 A93-48356

Upwind finite-volume Navier-Stokes computations on unstructured triangular meshes
p 1070 A93-49011

Computational methods for viscous hypersonic flows
p 1152 A93-49523

3-D viscous flow CFD analysis of the propeller effect on an advanced ducted propeller subsonic inlet
[AIAA PAPER 93-1847] p 1075 A93-49728

An adaptive grid/Navier-Stokes methodology for the calculation of nozzle afterbody base flows with a supersonic freestream
[AIAA PAPER 93-1922] p 1076 A93-49788

An unstructured adaptive quadrilateral mesh-based scheme for viscous turbomachinery flow calculations
[AIAA PAPER 93-1975] p 1077 A93-49822

Unsteady, three-dimensional, Navier-Stokes simulations of multistage turbomachinery flows
[AIAA PAPER 93-1979] p 1153 A93-49826

A comparative study of Full Navier-Stokes and Reduced Navier-Stokes analyses for separating flows within a diffusing inlet S-duct
[AIAA PAPER 93-2154] p 1079 A93-49970

Particle dynamics simulations in inlet separator with an experimentally based bounce model
[AIAA PAPER 93-2156] p 1115 A93-49972

Applying and validating the RANS-3D flow-solver for evaluating a subsonic serpentine diffuser geometry
[AIAA PAPER 93-2157] p 1079 A93-49973

High Reynolds number and turbulence effects on aerodynamics and heat transfer in a turbine cascade
[AIAA PAPER 93-2252] p 1155 A93-50050

Development of an advanced exhaust mixer for a high bypass ratio turbofan engine
[AIAA PAPER 93-2435] p 1118 A93-50188

Navier-Stokes analysis of radial turbine rotor performance
[AIAA PAPER 93-2555] p 1121 A93-50277

3D PARC Navier-Stokes analysis of an HSCT suppressor nozzle secondary inlet lip and duct
[AIAA PAPER 93-2568] p 1084 A93-50286

Numerical aspects of a block structured compressible flow solver
p 1169 A93-51279

An extended insight into hypersonic flow phenomena using numerical methods
p 1093 A93-51999

A time-accurate high-resolution TVD scheme for solving the Navier-Stokes equations
p 1093 A93-52006

Unsteady aerodynamic behavior of an airfoil with and without a slat
p 1093 A93-52007

Transonic Navier-Stokes flow computations over wing-fuselage geometries
p 1095 A93-52456

Navier-Stokes investigation of blunt trailing-edge airfoils using O grids
p 1095 A93-52459

Numerical study of a delta planform with multiple jets in ground effect
[SAE PAPER 892283] p 1176 A93-53200

Effective treatment of the singular line boundary problem for three-dimensional grids
p 1177 A93-53204

Zonal-local solution method for the turbulent Navier-Stokes equations
p 1177 A93-53205

Multigrid Navier-Stokes calculations for three-dimensional cascades
p 1177 A93-53209

Space marching calculations about hypersonic configurations using a solution-adaptive mesh algorithm
p 1177 A93-53212

Three-dimensional Navier-Stokes/full-potential coupled analysis for viscous transonic flow
p 1178 A93-53218

3D laminar and 2D turbulent computations with the Navier-Stokes solver FLU3M
[ONERA, TP NO. 1993-105] p 1180 A93-53618

Numerical solution of N-S equations for hypersonic flow over capsule-type vehicles
p 1182 A93-53858

Navier-Stokes computation of the three dimensional flow fields through a transonic fan blade
[ISABE 93-7030] p 1184 A93-54006

Navier-Stokes analysis of turbine flowfield and external heat transfer
[ISABE 93-7075] p 1186 A93-54051

Recent developments performed at ONERA for the simulation of 3D inviscid and viscous flows in turbomachinery by the solution of Euler and Navier-Stokes equations
[ISABE 93-7094] p 1186 A93-54070

Three-dimensional flow analysis inside turbomachinery stages with steady and unsteady Navier-Stokes method
[ISABE 93-7095] p 1186 A93-54071

Three-dimensional Navier-Stokes analysis of tip clearance flow in linear turbine cascades
p 1235 A93-55364

Supersonic and hypersonic flow computations for the research configuration ELAC I and comparison to experimental data
p 1237 A93-56034

Computation of viscous hypersonic non-equilibrium blunt body flow
p 1238 A93-56038

Numerical study of slightly compressible Navier-Stokes simulation of blade-vortex interaction
p 1239 A93-56216

Three-dimensional mesh embedding for the Navier-Stokes equations using upwind control volumes
p 1239 A93-56402

Navier-Stokes dynamics and aeroelastic computations for vortical flows, buffet and aeroelastic applications
[NASA-CR-190692] p 17 N93-10098

Analysis of wing-body junction flowfields using the incompressible Navier-Stokes equations, volumes 1 and 2
p 17 N93-10320

Explicit Navier-Stokes computation of turbomachinery flows
p 83 N93-10370

Numerical study of advanced rotor blades
p 23 N93-11899

Investigation of advanced counterrotation blade configuration concepts for high speed turboprop systems. Task 4: Advanced fan section aerodynamic analysis
[NASA-CR-187128] p 174 N93-12695

Navier-Stokes simulations of unsteady transonic flow phenomena
[NASA-TM-103962] p 129 N93-12721

Application of a solution adaptive grid to flow over an embedded cavity
p 130 N93-13141

The PEP Symposium on CFD Techniques for Propulsion Applications
p 214 N93-13210

Unsteady three-dimensional thin-layer Navier-Stokes solutions for turbomachinery in transonic flow
p 218 N93-14025

Navier-Stokes flowfield computation of wing/rotor interaction for a tilt rotor aircraft in hover
p 135 N93-14035

Solution of compressible Navier-Stokes equations using spectral methods on arbitrary two-dimensional domains
p 218 N93-14041

An algebraic turbulence model for three-dimensional viscous flows
[NASA-TM-105931] p 110 N93-14102

Passive control of supersonic asymmetric vortical flows around cones
p 220 N93-14692

The 3D Navier-Stokes flow analysis for shared and distributed memory MIMD computers
[AD-A256038] p 221 N93-15187

Ice accretion and performance degradation calculations with LEWICE/NS
[NASA-TM-105972] p 148 N93-15354

Comparison of solution of various Euler solvers and one Navier-Stokes solver for the flow about a sharp-edged cropped delta wing
[NLR-TP-90340-U] p 418 N93-16411

Hypersonic flows including real gas effects
[AERO-REPT-9112] p 289 N93-16467

Volume 2: Explicit, multistage upwind schemes for Euler and Navier-Stokes equations
[NASA-CR-191647] p 418 N93-16558

Navier-Stokes calculation of transonic flow past the NTF 65-deg delta wing
p 292 N93-16797

Turbine engine combustor design at SNECMA
[DS-2129] p 363 N93-17851

A numerical study of mixing in supersonic combustors with hypermixing injectors
[NASA-CR-191027] p 294 N93-17884

H-P adaptive methods for finite element analysis of aerothermal loads in high-speed flows
[NASA-CR-189739] p 420 N93-18093

Computational Fluid Dynamics, volume 2
[VKI-LS-1992-04-VOL-2] p 421 N93-18563

Parabolized Navier-Stokes methods for hypersonic flows
p 421 N93-18565

A Blottner type numerical model for nonequilibrium viscous hypersonic flows in upwind finite elements
[INRIA-RR-1476] p 297 N93-18648

Endwall flows and blading design for axial flow compressors
p 423 N93-18730

Numerical simulations of hypersonic rarefied transition regime flows: DSMC method and Navier-Stokes computation
p 299 N93-19278

Numerical calculation of hypersonic non-equilibrium flow around OREX
p 301 N93-19296

Wind tunnel test and CFD in Kawasaki Heavy Industries, Gifu
p 304 N93-19324

Wind tunnel testing and CFD simulation in Mitsubishi Heavy Industries
p 305 N93-19325

Numerical simulation of a high Mach number jet flow
[NASA-TM-105985] p 551 N93-20057

Turbulence modeling for hypersonic flight
[NASA-CR-192288] p 483 N93-20235

Advanced adaptive computational methods for Navier-Stokes simulations in rotorcraft aerodynamics
[NASA-CR-192282] p 483 N93-20256

Methodology for sensitivity analysis, approximate analysis, and design optimization in CFD for multidisciplinary applications
[NASA-CR-192172] p 552 N93-20297

Numerical methods for aerothermodynamic design of hypersonic space transport vehicles
[MBB-FE-211-S-PUB-0481] p 514 N93-21056

Aerothermodynamic properties of hypersonic flows over radiation-adiabatic surfaces
[DLR-FB-91-42] p 485 N93-21761

Unsteady Navier-Stokes method for accelerated moving airfoils with separation
[DLR-FB-92-03] p 485 N93-21763

- Computational study of the aerodynamics and control by blowing of asymmetric vortical flows over delta wings p 693 N93-24772
- Direct solutions of the Navier-Stokes equations with application to static aeroelasticity p 748 N93-25259
- Numerical simulation of leading-edge receptivity to freestream vorticity p 696 N93-25388
- Navier-Stokes simulations of unsteady transonic flow phenomena p 697 N93-25542
- Tangential fuselage blowing on an ogive cylinder p 697 N93-25545
- Numerical modelling of viscous turbomachinery flows with a pressure correction method p 723 N93-25702
- Stationary crossflow instability on an infinite swept wing p 699 N93-25865
- Simulation of vortex bursting p 699 N93-25881
- Workshop Report: A validation study of Navier-Stokes codes for transverse injection into a Mach 2 flow p 751 N93-26008
- Unsteady airfoil flow solutions on moving zonal grids [AD-A261925] p 701 N93-26198
- Increased heat transfer to elliptical leading edges due to spanwise variations in the freestream momentum: Numerical and experimental results [NASA-TM-106150] p 838 N93-27020
- Assessment of computational issues associated with analysis of high-lift systems p 785 N93-27449
- Investigation of forced unsteady separated flows using velocity-vorticity form of Navier-Stokes equations p 840 N93-27451
- Some recent applications of Navier-Stokes codes to rotorcraft p 786 N93-27452
- Prediction of airfoil stall using Navier-Stokes equations in streamline coordinates p 787 N93-27456
- Navier-Stokes simulation of viscous, separated, supersonic flow over a projectile rotating band [AD-A263073] p 788 N93-27955
- Navier-Stokes analysis of radial turbine rotor performance [NASA-CR-191153] p 815 N93-28609
- Implementation of a multidomain Navier-Stokes code on the Intel iPSC2 hypercube [FFA-TN-1992-37] p 843 N93-28994
- The numerical solution of low Mach number flow in confined regions by Richardson extrapolation [TRITA-NA-9207] p 789 N93-29005
- High Reynolds number and turbulence effects on aerodynamics and heat transfer in a turbine cascade [NASA-TM-106187] p 930 N93-29157
- The 3-D viscous flow CFD analysis of the propeller effect on an advanced ducted propeller subsonic inlet [NASA-TM-106240] p 900 N93-29162
- Development of an unstructured solution adaptive method for the quasi-three-dimensional Euler and Navier-Stokes equations [NASA-CR-193241] p 930 N93-29213
- Aero-thermic calculations of flows in interdisc cavities of turbines p 903 N93-29947
- The aerodynamic effect of coolant ejection in the leading edge region of a film-cooled turbine blade p 904 N93-29958
- Coupling of 3D-Navier-Stokes external flow calculations and internal 3D-heat conduction calculations for cooled turbine blades p 904 N93-29961
- Navier-Stokes analysis of three-dimensional flow and heat transfer inside turbine blade rows p 905 N93-29963
- Simulation, characterization and control of forced unsteady viscous flows using Navier-Stokes equations [AD-A264333] p 934 N93-30369
- Topology and grid adaption for high-speed flow computations [NASA-CR-4216] p 934 N93-30375
- Computation of a delta-wing roll-and-hold maneuver [AD-A264704] p 909 N93-30498
- Some implications of a differential turbomachinery equation with viscous correction p 935 N93-30571
- Compressible turbulence in a high-speed high Reynolds number mixing layer p 878 N93-30583
- Strong parallel blade-vortex interaction and noise propagation in helicopter flight p 944 N93-30980
- The ViB-code to simulate 3-D stator/rotor flow in axial turbines [DLR-FB-92-19] p 1003 N93-31170
- Numerical simulation of the flow in a 1:57-scale axisymmetric model of a large blast simulator [AD-A265551] p 1015 N93-31916
- Navier-Stokes computations for kinetic energy projectiles in steady coning motion: A predictive capability for pitch damping [AD-A264111] p 1033 N93-32028
- European navigation into the 21st century: Proceedings of the Conference, London, United Kingdom, Feb. 12, 1991 [ISBN 0-903409-82-8] p 311 N93-17751
- Information-based criteria of terrain navigability. Part 1: Data-base analysis p 793 N93-27178
- Advanced Unmanned Search System (AUSS) supervisory command, control and navigation [AD-A263171] p 793 N93-28990
- ### NAVIGATION AIDS
- Magnetic variation - A primitive concept and its hold on contemporary navigation p 32 N93-11021
- Real time DGPS service for precise positioning - Activities in the Federal Republic of Germany p 1 N93-11027
- Accuracy analysis on image matching guidance systems p 62 N93-12653
- Update on GPS integrity requirements of the RTCA MOPS p 314 N93-21155
- INS/DGPS integration for trajectory determination of a test vehicle p 315 N93-21178
- Planning for complementary MLS/GPS operations p 315 N93-21180
- On the selection of a GPS validity indicator for aircraft navigation in the National Airspace System (NAS) p 316 N93-21186
- Integrated Soviet VLF/Omega Receiver design p 316 N93-21198
- Maps and charts for visual air navigation p 498 N93-25170
- A history of visual approach guidance indicator systems in Australia p 498 N93-25171
- Sensors and sensor systems for guidance and navigation; Proceedings of the Meeting, Orlando, FL, Apr. 2, 3, 1991 [SPIE-1478] p 532 N93-27043
- Can one do without the magnetic reference? p 501 N93-28197
- Augmentation of a navigation reference system with differential global positioning system pseudorange measurements p 881 N93-42798
- Evolution of European air space toward precision navigation (P/RNAV) p 882 N93-43369
- The use of digital map data to provide enhanced navigation and displays for poor weather penetration and recovery p 992 N93-45165
- Automatic navigation in the air and at sea p 1099 N93-52593
- Appraisal of digital terrain elevation data for low-altitude flight [NASA-TM-103896] p 35 N93-10745
- Flight simulator evaluation of D-size liquid crystal flat panel displays p 52 N93-12367
- Liquid crystal flat panel display evaluation tests using a flight simulator [NAL-TR-1122] p 52 N93-12383
- High reliability, maintenance-free INS battery development [AD-A264521] p 934 N93-30406
- Design and implementation of a Global Positioning System (GPS) supported area navigation system with electronic aircraft [ILR-MITT-275(1992)] p 889 N93-30671
- Aerial cartography using SICAD NAV-AIR p 1034 N93-31258
- ### NAVIGATION INSTRUMENTS
- Development of a TRN/INS/GPS integrated navigation system p 30 N93-11004
- Achieving modularity with tightly-coupled GPS/INS p 33 N93-11032
- A fault-tolerant Air Data/Inertial Reference Unit p 807 N93-37074
- A control algorithm for a navigation-landing system in the case of a priori indeterminacy of failure data p 882 N93-43108
- Fault tolerant navigation for aircraft landing p 1191 N93-53866
- System for calibrating a gyro navigator [AD-DO15668] p 708 N93-26093
- Design and implementation of a Global Positioning System (GPS) supported area navigation system with electronic aircraft [ILR-MITT-275(1992)] p 889 N93-30671
- Aerial cartography using SICAD NAV-AIR p 1034 N93-31258
- Pallet for helicopter test instrumentation p 1000 N93-31279
- ### NAVIGATION SATELLITES
- Progress towards joint civil use of GPS and GLONASS p 29 N93-10977
- Precision increasing and integrity monitoring of navigation data for GPS/inertial hybrid solution p 149 N93-14157
- Receiver Autonomous Integrity Monitoring (RAIM) availability for supplemental GPS navigation p 312 N93-18554
- Applications of space techniques to civil aviation operations p 312 N93-20007
- The value of GNSS to aircraft operators p 498 N93-25172
- Can one do without the magnetic reference? p 501 N93-28197
- Satcom Pacific Ocean trials p 501 N93-28198
- GPS autoland considerations p 792 N93-38203
- Ongoing GPS experiments demonstrate potential of satellite navigation technology p 1097 N93-49278
- An experimental health monitoring unit for GPS and GLONASS p 706 N93-25018
- System analysis for a kinematic positioning system based on the global positioning system [AD-A262830] p 885 N93-29468
- ### NAVSTAR SATELLITES
- Progress towards joint civil use of GPS and GLONASS p 29 N93-10977
- Guidelines for NAVSTAR GPS embedded receiver applications p 315 N93-21184
- Proposed revisions to RTCM SC-104 recommended standards for differential NAVSTAR/GPS service for carrier phase applications [AD-A255276] p 152 N93-15005
- Navstar global positioning system: Introduction and status [NLR-TP-91008-U] p 318 N93-17559
- A model of Global Positioning System (GPS) Master Control Station (MCS) operations [AD-A258846] p 320 N93-19067
- Follow-on operational test and evaluation of the NAVSTAR global positioning system air integration/installation program [AD-A263067] p 793 N93-27925
- ### NAVY
- Royal Navy helicopter operations in the maritime environment p 1190 N93-54290
- Standardization of precipitation static test methods and equipment for the Navy [AD-A257025] p 165 N93-15361
- ### NEAR FIELDS
- Measurements in the near-field of a turbulent wingtip vortex [AIAA PAPER 93-0551] p 285 N93-23290
- Three dimensional near field behavior of a tip vortex developing on an elliptic foil [AIAA PAPER 93-0865] p 468 N93-24927
- Near-field supersonic flow predictions by an adaptive unstructured tetrahedral grid solver [AIAA PAPER 93-3430] p 977 N93-47223
- Turbulent structure of a wingtip vortex in the near field [AIAA PAPER 93-3011] p 1054 N93-48201
- Ultra wide band 3-D cross section (RCS) holography [DE92-019133] p 89 N93-11802
- ### NEAR WAKES
- Experimental study on the characteristics of the near wake of a rotating flat plate. III - Influence of the shape near the trailing edge on periodic-velocity-fluctuation phenomena p 451 N93-21727
- The influence of the boundary layer on the subsonic near-wake of a family of bluff bodies [AIAA PAPER 93-0525] p 284 N93-23266
- Wake structure of a helicopter rotor in forward flight p 958 N93-45138
- Supersonic base flow experiments in the near-wake of a cylindrical afterbody [AIAA PAPER 93-2924] p 1045 N93-48125
- Study of the near-wake structure of a subsonic base cavity flowfield using PIV [AIAA PAPER 93-3040] p 1056 N93-48221
- Reynolds stress profiles in the near wake of an oscillating airfoil p 1236 N93-55380
- ### NETHERLANDS
- Review of aerodynamic design in the Netherlands [NLR-TP-91260-U] p 999 N93-31840
- ### NETWORK CONTROL
- Neurocontrol design and analysis for a multivariable aircraft control problem p 906 N93-41894
- ### NETWORK SYNTHESIS
- Analog simulation as part of a power supply design analysis universal platform p 543 N93-25962
- Automated design and fabrication of radio-electronic circuits p 1151 N93-49000
- Effects of external control circuit on coal-fired supersonic diagonal-type MHD generator p 1173 N93-49619
- ### NEURAL NETS
- Merger and acquisition - Enhancing Loran propagation technology with artificial intelligence p 29 N93-10987
- Multilevel control of dynamical systems using neural networks p 96 N93-13011
- Neural-network-based catastrophe avoidance control systems p 97 N93-13233
- ### NAVIGATION
- IEEE PLANS '92 - Position Location and Navigation Symposium, Monterey, CA, Mar. 24-27, 1992, Record [ISBN 0-7803-0469-1] p 29 N93-10976

- Prospective application of neural networks in superresolution radars p 211 A93-16849
- Comparison of neural network and Markov random field image segmentation techniques p 397 A93-18652
- The prediction of nonlinear dynamic loads on helicopters from flight variables using artificial neural networks p 322 A93-19231
- Aerodynamic performance optimization of a rotor blade using a neural network as the analysis [AIAA PAPER 92-4837] p 324 A93-20295
- Damage detection in smart structures using neural networks and finite-element analyses p 438 A93-22540
- Development and application of a nonlinear fin mixer p 368 A93-22869
- An application of artificial neural networks to experimental data approximation [AIAA PAPER 93-0408] p 440 A93-23330
- Design of exhaust nozzles using GA optimized neural networks [AIAA PAPER 93-0410] p 361 A93-23331
- Failure-accommodating neural network flight control [AIAA PAPER 92-4394] p 523 A93-24495
- Prediction of helicopter component loads using neural networks [AIAA PAPER 93-1301] p 756 A93-33878
- Design and evaluation of a robust dynamic neurocontroller for a multivariable aircraft control problem p 817 A93-37004
- Neural network controllers for the X29 aircraft p 817 A93-37005
- Neurocontrol design and analysis for a multivariable aircraft control problem p 906 A93-41894
- Pilot task monitoring using neural networks p 940 A93-42846
- Studies of superresolution range-Doppler imaging p 928 A93-43344
- Radar 92; Proceedings of the International Conference, Brighton, United Kingdom, Oct. 12, 13, 1992 [ISBN 0-85296-533-2] p 929 A93-43376
- Adaptive waveform selection with a neural network p 942 A93-43470
- Active flow control with neural networks [AIAA PAPER 93-3273] p 1037 A93-46834
- Neural network prediction of three-dimensional unsteady separated flow fields [AIAA PAPER 93-3426] p 977 A93-47221
- On the use of back propagation with feed-forward neural networks for the aerodynamic estimation problem [AIAA PAPER 93-3638] p 1165 A93-48323
- Estimation of aerodynamic coefficients using neural networks [AIAA PAPER 93-3639] p 1165 A93-48324
- Use of neural networks in control of high-alpha maneuvers p 1130 A93-49593
- WNN 92; Proceedings of the 3rd Workshop on Neural Networks: Academic/Industrial/NASA/Defense, Auburn Univ., AL, Feb. 10-12, 1992 and South Shore Harbour, TX, Nov. 4-6, 1992 [SPIE-1721] p 1167 A93-50726
- Control of takeoff of a hypersonic aircraft using neural networks p 1167 A93-50744
- A Hopfield neural network for adaptive control [AIAA PAPER 93-3729] p 1130 A93-51329
- Multiple radial basis function networks in modeling and control [AIAA PAPER 93-3731] p 1170 A93-51330
- Aircraft failure detection and identification using neural networks [AIAA PAPER 93-3869] p 1171 A93-51455
- Fault detection, isolation, and reconfiguration for aircraft using neural networks [AIAA PAPER 93-3870] p 1135 A93-51456
- Neural network fault diagnosis of a turbofan engine [ISABE 93-7091] p 1203 A93-54067
- Analysis of fault-tolerant neurocontrol architectures [NASA-TM-105898] p 65 A93-12305
- A neural network prototype for predicting F-14B strains at the B.L. 10 longeron [AD-A255272] p 165 A93-15004
- Neural network based condition monitoring p 230 A93-15183
- Identification and control of non-linear time-varying dynamical systems using artificial neural networks [AD-A257595] p 372 A93-18193
- Application of a neural network as a potential aid in predicting NTF pump failure [NASA-TM-107667] p 442 A93-18332
- Application of artificial neural networks to the design optimization of aerospace structural components [NASA-TM-4389] p 555 A93-21831
- Control of complex dynamic systems by neural networks p 758 A93-25611
- Robustness enhancement of neurocontroller and state estimator [NASA-TM-106028] p 819 A93-26907
- Center for Aeronautics and Space Information Sciences [NASA-CR-193140] p 848 A93-27289
- Artificial intelligence methodologies in flight related differential game, control and optimization problems [AD-A262405] p 848 A93-28498
- Spurious symptom reduction in fault monitoring [NASA-CR-191453] p 942 A93-29192
- Neural networks application to divergence-based passive ranging [NASA-TM-103981] p 885 A93-29653
- Effect of design selection on response surface performance [NASA-CR-4520] p 895 A93-29885
- Structural design using neural networks p 942 A93-31029
- NEUTRON ACTIVATION ANALYSIS**
- A review of the development of a luggage explosive detection system p 497 A93-21862
- A transportable luggage examination system based on neutron interrogation p 497 A93-21863
- PFNA technique for the detection of explosives p 497 A93-21865
- A pulsed fast-thermal neutron interrogation system p 497 A93-21866
- Experience with explosive detection systems in airports p 498 A93-21895
- NEUTRON DIFFRACTION**
- Neutron diffraction residual stress studies for aero-engine component applications [PNR-90908] p 85 A93-11014
- Development of the neutron diffraction technique for the determination of near surface residual stresses in critical gas turbine components [PNR-90984] p 58 A93-11112
- NEUTRON IRRADIATION**
- Neutron-induced single event upsets in static RAMs observed at 10 KM flight altitude p 1158 A93-50561
- NEUTRON SOURCES**
- Explosive detection system based on Electronic Neutron Generator (ENG) p 497 A93-21870
- NEWS**
- Index to NASA news releases and speeches, 1991 [NASA-TM-108004] p 104 A93-10815
- Index to NASA news releases and speeches, 1990 [NASA-TM-108003] p 104 A93-10872
- NEWTON METHODS**
- Structural optimization using Newton Modified Barrier Method [AIAA PAPER 92-4756] p 409 A93-20352
- Newton-like methods for fast high resolution simulation of hypersonic viscous flows p 437 A93-20740
- Jacobian update strategies for quadratic and near-quadratic convergence of Newton and Newton-like implicit schemes [AIAA PAPER 93-0878] p 470 A93-24939
- Using current numerical methods in a mathematical model of flight vehicle synthesis p 804 A93-39188
- Direct solutions of the Navier-Stokes equations with application to static aeroelasticity p 748 A93-25259
- NEWTON-RAPHSON METHOD**
- A robust direct-integration method for rotorcraft maneuver and periodic response p 61 A93-10919
- Numerical solution of dynamic equations arising in a jet engine simulation p 53 A93-12237
- Unstructured grids on NURBS surfaces --- NonUniform Rational B-Splines [AIAA PAPER 93-3454] p 949 A93-44232
- NEWTONIAN FLUIDS**
- Newtonian and hypersonic flows over oscillating bodies of revolution. I - Circular cones p 857 A93-39942
- NICKEL ALLOYS**
- Raising the high temperature limit of the nickel-iron-base superalloy p 70 A93-12114
- Microstructural study of aluminide surface coatings on single crystal nickel base superalloy substrates p 70 A93-12771
- Effects of grain size and carbides on the creep resistance and rupture properties of a conventionally cast nickel-base superalloy p 389 A93-21699
- INCOLOY 908, a low coefficient of expansion alloy for high-strength cryogenic applications. I - Physical metallurgy p 534 A93-25686
- Gas phase hydrogen permeation in a Ni-Fe-Co superalloy p 735 A93-34510
- Resource conservation and improvement of the service characteristics of castings of high-temperature nickel alloys through a high-temperature melt treatment p 824 A93-36718
- Designing new multi-phase intermetallic materials based on phase compatibility considerations [ONERA, TP NO. 1992-131] p 772 A93-38605
- Recent evolution of gas turbine materials and the development of models for life prediction p 915 A93-40802
- Creep crack growth and tail part behavior of low alloy steels and Ni based super alloy p 916 A93-40808
- New corrosion resistant nickel-base super-alloys and technological processes of casting gas turbines parts with directional single crystal and regulable equiaxed minimized microporosity structure p 916 A93-40811
- Microstructure of yttria stabilized zirconia-hafnia plasma sprayed thermal barrier coatings [ONERA, TP NO. 1993-54] p 1146 A93-51936
- Chemical stability of titanium diboride reinforcement in nickel aluminide matrices p 1147 A93-52473
- Measurements of dynamic Young's modulus and damping in single crystals of a nickel-based superalloy as a function of temperature p 1147 A93-52513
- Stress relaxation of low pressure plasma-sprayed NiCrAlY alloys p 1211 A93-52870
- Mechanisms and modelling of environment-dependent fatigue crack growth in a nickel based superalloy [AD-A253967] p 71 A93-10717
- Short fatigue crack growth in a nickel-base superalloy at room and elevated temperature [PNR-90892] p 72 A93-11031
- Erosion predictions and measurements of high-temperature coatings and superalloys used in turbomachines p 74 A93-12189
- Fatigue in single crystal nickel superalloys [AD-A254603] p 74 A93-12237
- Fatigue in single crystal nickel superalloys [AD-A254704] p 198 A93-12746
- Deformation mechanisms of NiAl cyclicly deformed near the brittle-to-ductile transformation temperature [NASA-CR-191649] p 391 A93-15830
- Fatigue in single crystal nickel superalloys [AD-A258038] p 393 A93-17704
- Fatigue in single crystal nickel superalloys [AD-A259191] p 536 A93-20275
- Fatigue in single crystal nickel superalloys [AD-A260709] p 736 A93-25843
- Fatigue in single crystal nickel superalloys [AD-A261742] p 737 A93-26282
- Platinum-modified diffusion aluminide coatings on nickel-base superalloys p 917 A93-29981
- Fatigue in single crystal nickel superalloys [AD-A265451] p 1019 A93-31795
- NICKEL CADMIUM BATTERIES**
- High reliability, maintenance-free INS battery development [AD-A264521] p 934 A93-30406
- NICKEL HYDROGEN BATTERIES**
- Nickel hydrogen batteries for terrestrial applications p 557 A93-26005
- NIGHT**
- Helicopter crash survival at sea: United States Navy/Marine Corps experience 1977-1990 p 493 A93-19687
- NIGHT FLIGHTS (AIRCRAFT)**
- Night aircraft noise index and sleep research results p 558 A93-28485
- Computer-based modelling of aircraft noise impact p 559 A93-28497
- Visual augmentation for night flight over featureless terrain p 806 A93-35921
- AFTI/F-16 night close air support system testing p 808 A93-38841
- Flight management system on the F-117A p 908 A93-42815
- Pilot task monitoring using neural networks p 940 A93-42846
- Royal Air Force support helicopters - Night operations p 1190 A93-54293
- Integrated helmet system testing for a nightflying helicopter [MBB-UD-0604-91-PUB] p 343 A93-17570
- NIGHT VISION**
- Royal Air Force support helicopters - Night operations p 1190 A93-54293
- Displaying the night p 1244 A93-55297
- NIOBIUM ALLOYS**
- Niobium alloy heat pipes for use in oxidizing environments p 200 A93-13791
- NITRIC OXIDE**
- Ignition and exhaust emission characteristics of spray combustion in a pre-chamber type vortex combustor [ASME PAPER 92-GT-119] p 350 A93-19355
- Three-dimensional gas turbine combustor emissions modeling [ASME PAPER 92-GT-129] p 350 A93-19363
- Ramjet NOx emission - Use of a 3D CFD method for the combustor design of a super/hyper-sonic transport propulsion system [ASME PAPER 92-GT-255] p 353 A93-19464
- Direct numerical simulation of nitric oxide evolution in underexpanded jets [ASME PAPER 92-GT-372] p 355 A93-19534

NITROGEN

- Measurement and analysis of nitric oxide radiation in an arc-jet flow
[AIAA PAPER 93-2800] p 1016 A93-46540
- Comparison of NO and OH PLIF temperature measurements in a scramjet model flowfield
[AIAA PAPER 93-2035] p 1113 A93-49870
- Numerical study of nitric oxide formation in a hypersonic ramjet engine
[ISABE 93-7125] p 1204 A93-54100
- Nitric oxide formation in a lean, premixed-prevaporized jet A/air flame tube: An experimental and analytical study
[NASA-TM-105722] p 844 N93-27012
- ### NITROGEN
- Condensation of nitrogen in hypersonic flows - Measurements confirm a theoretical model
p 111 A93-13945
- Numerical modeling of ionization in nonequilibrium nitrogen flows in hypersonic nozzles
p 836 A93-39137
- Numerical study of spontaneous nitrogen condensation in the axisymmetric hypersonic nozzles of wind tunnels
p 777 A93-39143
- CARS studies in hypersonic flows
[AIAA PAPER 93-3047] p 1144 A93-48227
- Modifications to Langley 0.3-m TCT adaptive wall software for heavy gas test medium, phase 1 studies
[NASA-CR-189736] p 291 N93-16710
- A transportable luggage examination system based on neutron interrogation
p 497 N93-21863
- ### NITROGEN IONS
- Determination of the $N_2(+) + e$ recombination rate constant from ballistic experiments
p 1234 A93-55026
- ### NITROGEN OXIDES
- European environmental studies focus on impact of engine emissions
p 92 A93-10730
- Turbine engine developers explore ways to lower NO(x) emission levels
p 52 A93-10732
- Modification of combustor stoichiometry distribution for reduced NO(x) emission from aircraft engines
[ASME PAPER 92-GT-108] p 349 A93-19346
- NO(x) sensitivities for gas turbine engines operated on lean-premixed combustion and conventional diffusion flames
[ASME PAPER 92-GT-115] p 349 A93-19351
- Engine testing of a prototype low NO(x) gas turbine combustor
[ASME PAPER 92-GT-116] p 401 A93-19352
- Investigation of combustion structure inside low NO(x) combustors for a 1500 C-class gas turbine
[ASME PAPER 92-GT-123] p 350 A93-19357
- Aircraft turbine engine NOx emission limits - Status and trends
[ASME PAPER 92-GT-415] p 357 A93-19563
- Three-dimensional NOx modeling for rich/lean combustor
[AIAA PAPER 93-0251] p 360 A93-22660
- A review of chemically reactive turbulent flow mixing mechanisms and a new design for a low NO(x) combustor
p 1109 A93-49508
- Three-dimensional emission modeling for diffusion flame, rich/lean, and lean gas turbine combustors
[AIAA PAPER 93-2338] p 1117 A93-50115
- NO(x) scavenging on carbonaceous aerosol surfaces in aircraft exhaust plumes. I
[AIAA PAPER 93-2343] p 1164 A93-50117
- NO(x) reduction additives for aircraft gas turbine engines
[AIAA PAPER 93-2594] p 1122 A93-50306
- An ultra low NO(x) pilot combustor for staged low NO(x) combustion
[ISABE 93-7020] p 1195 A93-53996
- Low NO(x) combustor development using aerodynamic staging
[ISABE 93-7021] p 1195 A93-53997
- The prediction of thermal NO(x) in gas turbine exhausts
[ISABE 93-7022] p 1195 A93-53998
- NO(y) from sub-sonic aircraft emissions - A global three-dimensional model study
p 1261 A93-56236
- Stratospheric aircraft: Impact on the stratosphere?
[DE92-01697] p 94 N93-12104
- Improved selective catalytic NOx control technology for compressor station reciprocating engines
[PB93-158566] p 755 N93-26529
- Oxides of nitrogen emissions from turbulent hydrocarbon/air jet diffusion flames, phase 2
[PB93-152478] p 756 N93-26533
- Climatic effects of turbofan emissions in the stratosphere and the higher troposphere
p 1035 N93-31927
- Effects of commercial flight pollution on human health
p 1035 N93-31931

NOAA SATELLITES

- Calibration results for NOAA-11 AVHRR channels 1 and 2 from congruent path aircraft observations
p 1143 A93-51237
- Identification of icing water clouds by NOAA AVHRR satellite data
[DLR-FB-92-11] p 434 N93-16477
- ### NOSES (STANDING WAVES)
- Analysis of complicated plates by a nine-node spline plate element
p 206 A93-14616
- ### NOISE (SOUND)
- Experimental analysis of the aeroacoustics of cascaded airfoils
[AD-A257945] p 420 N93-18121
- ### NOISE GENERATORS
- Evolving noise issue could persist into the next century
p 99 A93-10731
- Experimental study of the acoustic spinning modes generated by a helicopter turboshaft engine
[ONERA, TP NO. 1992-141] p 230 A93-14266
- A semi-empirical theory of the noise in slotted tunnels caused by diffuser suction
p 231 A93-14353
- Generation of flow disturbances in transonic wind tunnels
p 119 A93-14354
- Excitation of velocity fluctuations and noise in a wind tunnel
p 444 A93-18242
- Continuous judgment of helicopter noise - On the validity of Leq and Zwicker's method (ISO 532B)
p 558 A93-28478
- Advances in the design of jet engine test facilities for military aircraft in Australia
p 529 A93-28491
- Air traffic noise monitoring in and around Lisbon Airport
p 564 A93-28494
- Analytical study on plate edge noise (Noise generation from tandemly situated trailing and leading edges)
p 1038 A93-45561
- Some aspects of the aeroacoustics of high-speed jets
[NASA-CR-191458] p 843 N93-28975
- ### NOISE INJURIES
- Results of a low-altitude flight noise study in Germany - Acute extraaural effects
p 1163 A93-49557
- Specific features of military low-altitude flight noise - Criteria for risk of damage and physiological effects
p 1164 A93-49558
- Review - Extraaural health effects of aircraft noise
p 1164 A93-49559
- ### NOISE INTENSITY
- Experimental study of the acoustic spinning modes generated by a helicopter turboshaft engine
[ONERA, TP NO. 1992-141] p 230 A93-14266
- Generation of flow disturbances in transonic wind tunnels
p 119 A93-14354
- Noise reduction programs for in-service jet transports
p 521 A93-28479
- Influence of aircraft noise on speech intelligibility
p 558 A93-28483
- Preliminary results from a study of community response to noise from military aircraft exercise
p 558 A93-28484
- Night aircraft noise index and sleep research results
p 558 A93-28485
- Final results from a study of community response to aircraft noise around Oslo Airport Fornebu
p 558 A93-28486
- Sound exposure spectrum levels of sonic booms
p 564 A93-28489
- Technical solutions to reduce and to control the noise load in the Netherlands - generated by aircraft engines
p 564 A93-28492
- Noise-induced reaction in a work community adjacent to aircraft runways - The Royal Australian Airforce
p 559 A93-28496
- Computer-based modelling of aircraft noise impact
p 559 A93-28497
- Calculation of the passive noise power for onboard single-pulse automatic direction tracking systems
p 882 A93-43111
- Increase in mortality rates due to aircraft noise
p 1163 A93-49551
- A new methodology for helicopter internal noise reduction application to the AS332 L2
p 1243 A93-54723
- Noise studies for environmental impact assessment of an outdoor engine test facility
p 99 N93-10672
- Laboratory study of effects of sonic boom shaping on subjective loudness and acceptability
[NASA-TP-3269] p 102 N93-11620
- Experimental analysis of the aeroacoustics of cascaded airfoils
[AD-A257945] p 420 N93-18121
- Effect of personal and situational variables on noise annoyance: With special reference to implications for en route noise
[NASA-CR-189676] p 569 N93-21317

SUBJECT INDEX

- Analysis of aircraft noise levels in the vicinity of start-of-takeoff roll at Baltimore-Washington International Airport
[PB92-221605] p 559 N93-21501
- In-flight evaluation of noise levels and assessment of active noise reduction systems in the Seahawk S-70B-2 helicopter
[AD-A260689] p 759 N93-25649
- Aerospace-plane flights and stratospheric ozone: Review and preliminary assessment of the National Aerospace Plane (NASP) operations
[RAND/N-3464-AF] p 755 N93-26327
- ### NOISE MEASUREMENT
- The noise from supersonic elliptic jets
p 445 A93-19156
- Noise evaluation of light propeller-driven aircraft
p 398 A93-19189
- A contribution to noise improvements for aircraft by noise measurement evaluation
p 448 A93-19190
- Loudness versus level of aircraft noise
p 557 A93-28477
- Comparison of airport noise calculation models
p 564 A93-28480
- Final results from a study of community response to aircraft noise around Oslo Airport Fornebu
p 558 A93-28486
- Air traffic noise monitoring in and around Lisbon Airport
p 564 A93-28494
- Performance prediction of the interacting multiple model algorithm
p 1167 A93-50638
- Correction of a method for calculating the noise levels of aircraft at control points during acoustic flight testing
p 1102 A93-51758
- Some acoustic features of perforated test section walls with splitter plates
p 1226 A93-53222
- Helicopter noise certification
p 1262 A93-54720
- Comparison of flyover noise data from aircraft at high subsonic speeds with prediction
p 100 N93-10674
- Further noise measurements in a slotted cryogenic wind tunnel
[RAE-TM-AERO-2201] p 101 N93-10805
- The design and commissioning of an acoustic liner for propeller noise testing in the ARA transonic wind tunnel
[PNR-90880] p 101 N93-11204
- Evaluation of three models used for predicting noise propagated long distances overground
[AD-A255963] p 232 N93-14406
- Calculation of noise emission caused by jet aircraft during takeoff, approach and horizontal flyover
[DLR-MITT-91-15] p 569 N93-21368
- External acoustical noise measurements for aviation systems
[AD-A263138] p 943 N93-29480
- ### NOISE POLLUTION
- Control measures used to reduce community noise from civil aviation in Denmark
p 425 A93-19191
- The impact of air traffic on the atmospheric environment
p 936 A93-42659
- A comparison between the impact of noise from aircraft, road traffic and trains on long-term recall and recognition of a text in children aged 12-14 years
p 1163 A93-49552
- Review - Extraaural health effects of aircraft noise
p 1164 A93-49559
- Air transport and the environment - Regulating aircraft noise
p 1226 A93-52931
- Helicopter noise - Public perspective
p 1261 A93-54719
- Laboratory study of effects of sonic boom shaping on subjective loudness and acceptability
[NASA-TP-3269] p 102 N93-11620
- Air Force procedure for predicting noise around airbases: Noise exposure model (NoiseMap)
[AD-A255769] p 224 N93-14655
- Effects on health of noise disturbances due to air traffic
p 1035 N93-31929
- Reaction to aircraft noise near general aviation airfields
[DORA-8203] p 1040 N93-32377
- ### NOISE PREDICTION
- Computation of supersonic jet noise under imperfectly expanded conditions
[AIAA PAPER 93-0735] p 563 A93-24825
- Role of leading-edge vortex flows in prop-fan interaction noise
p 565 A93-28614
- A dynamic stiffness/boundary element method for the prediction of interior noise levels
p 1226 A93-53817
- A prediction model for the vortex shedding noise from the wake of an airfoil or axial flow fan blades
p 1265 A93-55995
- Numerical study for the study of medium speed internal noise problems
[DILC-EST-TN-200] p 101 N93-11156
- Evaluation of three models used for predicting noise propagated long distances overground
[AD-A255963] p 232 N93-14406

- Computation of supersonic jet noise under imperfectly expanded conditions
[NASA-TM-105961] p 233 N93-15430
- The prediction of noise from co-axial jets
[ISVR-TR-215] p 1040 N93-32339
- NOISE PREDICTION (AIRCRAFT)**
- The numerical calculation of aircraft propeller noise
p 174 A93-16239
- Advances in tilt rotor noise prediction
p 447 A93-19184
- The critical role of turbulence modeling in the prediction of supersonic jet structure for acoustic applications
p 398 A93-19193
- A numerical method for the prediction of quadrupole shock wave noise
p 448 A93-19201
- Helicopter noise prediction - The current status and future direction
p 448 A93-19202
- Prediction of jet mixing noise in high-speed flight
p 450 A93-19216
- The noise of jet aircraft flying with high speeds at low altitudes
p 450 A93-19218
- Comparison of airport noise calculation models
p 564 A93-28480
- The airnoise boundary concept for airport noise management
p 564 A93-28482
- Preliminary results from a study of community response to noise from military aircraft exercise
p 558 A93-28484
- AHS and Royal Aeronautical Society, Technical Specialists' Meeting on Rotorcraft Acoustics/Fluid Dynamics, Philadelphia, PA, Oct. 15-17, 1991, Proceedings
p 565 A93-29401
- High-speed helicopter rotor noise - Shock waves as a potent source of sound
p 565 A93-29403
- Sensitivity of acoustic predictions to variation of input parameters
p 565 A93-29404
- The role of blade elasticity in the prediction of blade-vortex interaction noise
p 566 A93-29406
- Theoretical modelling of rotor noise radiation
p 566 A93-29407
- The development of a prediction method for the calculation of blade-vortex interaction noise based on measured airloads
p 566 A93-29409
- The influence of quadrupole sources in the boundary layer and wake of a blade on helicopter rotor noise
p 566 A93-29410
- A comparative analysis of XV-15 tiltrotor hover test data and WOPWOP predictions incorporating the fountain effect
p 509 A93-29414
- Tiltrotor ground noise reduction from rotor parametric changes as predicted by ROTONET
p 567 A93-29415
- Validation of high frequency airload calculations using full scale flight test acoustic data
p 567 A93-29417
- Acoustical analysis of gear housing vibration
p 567 A93-29420
- Recent developments in rotor wake modelling for helicopter noise prediction
p 481 A93-29437
- A modal-based procedure for efficiently predicting low vibration rotor designs
p 712 A93-34262
- Civil tiltrotor noise impact prediction methodology
p 850 A93-35967
- Predicting rotorcraft transmission noise
p 850 A93-35968
- Limitations of linear theory for sonic boom calculations
p 850 A93-37380
- Transonic blade-vortex interactions - Noise reduction
p 850 A93-37396
- Blade-vortex interaction noise - Prediction and comparison with flight and wind tunnel tests
[ONERA, TP NO. 1992-126] p 851 A93-38600
- Helicopter external noise prediction and reduction
[ONERA, TP NO. 1993-48] p 1039 A93-47450
- Rotor wake/stator interaction noise - Predictions vs data
p 1174 A93-52447
- The quiet helicopter; Proceedings of the Conference, London, United Kingdom, Mar. 17, 1992
[ISBN 1-85768-020-0] p 1262 A93-54718
- European research into helicopter internal noise
p 1243 A93-54724
- Tilt rotor hover aeroacoustics
[NASA-CR-177598] p 99 N93-10458
- Noise studies for environmental impact assessment of an outdoor engine test facility
p 99 N93-10672
- Non-propulsive aerodynamic noise
p 99 N93-10673
- Comparison of flyover noise data from aircraft at high subsonic speeds with prediction
p 100 N93-10674
- Combustion noise and combustion instabilities in propulsion systems
p 100 N93-10682
- The prediction of noise radiation from supersonic elliptic jets
p 100 N93-10684
- Prediction of jet mixing noise for high subsonic flight speeds
p 100 N93-10685
- Air Force procedure for predicting noise around airbases: Noise exposure model (Noisemap)
[AD-A255769] p 224 N93-14655
- Tiltrotor aircraft noise: A summary of the presentations and discussions at the 1991 FAA/Georgia Tech Workshop
[DOT/FAA/RD-91/23] p 232 N93-14912
- A prediction model for noise from low-altitude military aircraft
[AD-A262494] p 852 N93-27662
- Computation of far-field helicopter rotor tone noise
[ONERA-P-1990-5] p 943 N93-30110
- NOISE PROPAGATION**
- Propagation of high frequency jet noise using geometric acoustics
[AIAA PAPER 93-0147] p 452 A93-23241
- Transmission error and load distribution analysis of spur and double helical gear pairs used in a split path helicopter transmission design
p 549 A93-29426
- Noise transmission of skin-stringer panels using a decaying wave method
p 943 A93-41929
- Comparison of radiated noise from shrouded and unshrouded propellers
p 1264 A93-55861
- Laboratory study of effects of sonic boom shaping on subjective loudness and acceptability
[NASA-TP-3269] p 102 N93-11620
- Evaluation of three models used for predicting noise propagated long distances overground
[AD-A255963] p 232 N93-14406
- Propagation of high frequency jet noise using geometric acoustics
[NASA-TM-106013] p 233 N93-15575
- Far field rotor noise
[AD-A260703] p 759 N93-25651
- Rotating rake design for unique measurement of fan-generated spinning acoustic modes
[NASA-TM-105946] p 724 N93-26161
- Noise transmission properties and control strategies for composite structures
p 919 N93-30436
- Strong parallel blade-vortex interaction and noise propagation in helicopter flight
p 944 N93-30980
- NOISE REDUCTION**
- Evolving noise issue could persist into the next century
p 99 A93-10731
- Investigation of cabin noise reduction in the Y12
p 41 A93-11816
- An experimental study of a method for reducing the jet noise of bypass engines using mechanical flow mixers
p 53 A93-12810
- Effect of flight conditions on the sound insulation of the aircraft passenger compartment
p 42 A93-12978
- Experimental study of the acoustic spinning modes generated by a helicopter turboshaft engine
[ONERA, TP NO. 1992-141] p 230 A93-14266
- DNW test highlights related to aircraft environment
p 190 A93-14274
- Comparison of advanced turboprop interior noise control ground and flight test data
p 444 A93-19136
- New design concepts for silencing aeroacoustic wind tunnels
p 445 A93-19147
- Active aerodynamic control of wake-airfoil interaction noise - Theory
p 445 A93-19154
- Experimental investigation of tip clearance noise in axial flow machines
p 445 A93-19155
- Instability of rectangular jets
p 398 A93-19157
- Assessment and design of low boom configurations for supersonic transport aircraft
p 446 A93-19163
- On sound attenuation in boundary layers
p 446 A93-19164
- Matrix difference equation analysis of coupled structural-acoustic models for aircraft fuselage vibration and interior noise reduction
p 446 A93-19172
- Evaluation of piezoceramic actuators for control of aircraft interior noise
p 447 A93-19186
- A contribution to noise improvements for aircraft by noise measurement evaluation
p 448 A93-19190
- Control measures used to reduce community noise from civil aviation in Denmark
p 425 A93-19191
- The critical role of turbulence modeling in the prediction of supersonic jet structure for acoustic applications
p 398 A93-19193
- Control of coherent structures and aero-acoustic characteristics of subsonic and supersonic turbulent jets
p 448 A93-19196
- Combined noise and flow control of supersonic jets using swirl
p 398 A93-19204
- Experimental investigations and efficiency prediction of jet noise reduction techniques
p 449 A93-19206
- Flowfield measurements for a supersonic mixer ejector in forward flight
p 399 A93-19217
- Experimental results on propeller noise attenuation using an 'active noise control' technique
p 450 A93-19223
- Reduction of propeller noise by active noise control
p 450 A93-19224
- Numerical simulation of jet noise
p 265 A93-20716
- Active control of fan noise from a turbofan engine
[AIAA PAPER 93-0597] p 452 A93-23323
- Approximation methods for control of structural acoustics models with piezoceramic actuators
p 452 A93-23744
- Investigation of cabin noise reduction in the Y12
p 506 A93-27371
- Loudness versus level of aircraft noise
p 557 A93-28477
- Noise reduction programs for in-service jet transports
p 521 A93-28479
- Alternative approach routes to runway 24 at Oslo Airport, Fornebu
p 487 A93-28481
- The airnoise boundary concept for airport noise management
p 564 A93-28482
- Night aircraft noise index and sleep research results
p 558 A93-28485
- Technical solutions to reduce and control the noise load in the Netherlands --- generated by aircraft engines
p 564 A93-28492
- The costs of noise at the new Munich airport
p 558 A93-28493
- Computer-based modelling of aircraft noise impact
p 559 A93-28497
- AHS and Royal Aeronautical Society, Technical Specialists' Meeting on Rotorcraft Acoustics/Fluid Dynamics, Philadelphia, PA, Oct. 15-17, 1991, Proceedings
p 565 A93-29401
- HHC study in the DNW to reduce BVI noise - An analysis
p 565 A93-29405
- Noise reduction for transonic blade-vortex interactions
p 566 A93-29408
- Tiltrotor ground noise reduction from rotor parametric changes as predicted by ROTONET
p 567 A93-29415
- Development and validation of 'quiet tail rotor' technology
p 567 A93-29416
- Tiltrotor interior noise characteristics
p 509 A93-29421
- ADDRAS - An integrated systems approach
p 562 A93-29423
- Active control of interior noise in a large scale cylinder using piezoelectric actuators
p 568 A93-29425
- An overview of possible and not-so-possible tasks for active control of sound and vibration
p 568 A93-29429
- Helicopter noise standards - Requirements, compliance, and improvements
p 569 A93-29443
- Quiet operations key to MD-90 success
p 708 A93-33700
- Preliminary experiments on active control of fan noise from a turbofan engine
p 759 A93-34957
- A closed loop controller for BVI impulsive noise reduction by Higher Harmonic Control
p 849 A93-35963
- Predicting rotorcraft transmission noise
p 850 A93-35968
- Transonic blade-vortex interactions - Noise reduction
p 850 A93-37396
- Toward the silent helicopter
[ONERA, TP NO. 1992-229] p 851 A93-38774
- Identification of noise sources based on experimental amplitude-frequency noise characteristics of aircraft
p 851 A93-39040
- Design verification of ground run-up noise suppressors for afterburning engines
p 910 A93-42892
- Theoretical studies of the active control of propeller induced cabin noise using secondary force inputs
p 995 A93-45124
- Elements of NASA's high-speed research program
[AIAA PAPER 93-2942] p 947 A93-45155
- Propeller noise reduction by means of unsymmetrical blade-spacing
p 1039 A93-46706
- Helicopter external noise prediction and reduction
[ONERA, TP NO. 1993-48] p 1039 A93-47450
- An acoustic suppressor for the jet noise of a turbojet engine
p 1003 A93-47510
- Pressure pulsations on a delta wing in incompressible flow
p 1069 A93-48912
- Engineering science research issues in high power density transmission dynamics for aerospace applications --- rotorcraft geared rotors
[AIAA PAPER 93-2299] p 1155 A93-50084
- Low speed test results of subsonic, turbofan scari inlets
[AIAA PAPER 93-2301] p 1082 A93-50086
- Acoustic intensity of nonisothermal coaxial jets with an inverted velocity profile
p 1124 A93-51759
- Determination of fan noise in a lined duct with flow using the Green function method
p 1124 A93-51761
- An aeroacoustic stand for evaluating the efficiency of sound-absorbing structures under conditions of acoustic wave propagation in a moving medium
p 1140 A93-51762
- Linear quadratic tracking problems in Hilbert space - Application to optimal active noise suppression
p 1224 A93-52763

- Noise reduction of supersonic heated jet with jet mixing enhancement by tabs
[ISABE 93-7046] p 1198 A93-54022
- The quiet helicopter; Proceedings of the Conference, London, United Kingdom, Mar. 17, 1992
[ISBN 1-85768-020-0] p 1262 A93-54718
- Helicopter noise - Public perspective p 1261 A93-54719
- Helicopter noise reduction programme - AGUSTA achievements p 1262 A93-54721
- Noise characteristics of helicopters with the NOTAR anti-torque system p 1262 A93-54722
- A new methodology for helicopter internal noise reduction application to the AS332 L2 p 1243 A93-54723
- Review of helicopter noise research in Europe p 1263 A93-54725
- Control of supersonic throughflow turbomachines discrete frequency noise generation by aerodynamic detuning p 1248 A93-55860
- Non-propulsive aerodynamic noise p 99 A93-10673
- Reduction of propeller noise by active noise control p 101 A93-10692
- Civil aircraft engines: The next generation [PNR-90962] p 58 A93-11085
- A concept for a counterrotating fan with reduced tone noise [NASA-TM-105736] p 101 A93-11370
- Publications on acoustics research at the Langley Research Center, January 1987 - September 1992 [NASA-TM-107674] p 102 A93-12080
- Evaluation of acoustic impedance models for a perforated plate [NAL-TR-1133] p 102 A93-12375
- Report on the final panel discussion on computational aeroacoustics [NASA-CR-189718] p 231 A93-12986
- Evaluation of three models used for predicting noise propagated long distances overground [AD-A255963] p 232 A93-14406
- Tiltrotor aircraft noise: A summary of the presentations and discussions at the 1991 FAA/Georgia Tech Workshop [DOT/FAA/RD-91/23] p 232 A93-14912
- Consecutive plate acoustic suppressor apparatus and methods [NASA-CASE-LEW-15430-1] p 453 A93-17051
- Aircraft trajectory tracking and prediction [AD-A259039] p 340 A93-18999
- Applications of active adaptive noise control to jet engines [NASA-CR-192277] p 522 A93-21210
- Calculation of noise emission caused by jet aircraft during takeoff, approach and horizontal flyover [DLR-MITT-91-15] p 569 A93-21368
- A numerical and experimental studies of flow characteristics in centrifugal fans p 695 A93-25339
- In-flight evaluation of noise levels and assessment of active noise reduction systems in the Seahawk S-70B-2 helicopter [AD-A260689] p 759 A93-25649
- Rotating rake design for unique measurement of fan-generated spinning acoustic modes [NASA-TM-105946] p 724 A93-26161
- A large hemi-anechoic enclosure for community-compatible aeroacoustic testing of aircraft propulsion systems [NASA-TM-106015] p 760 A93-26551
- Sikorsky Aircraft Advanced Rotorcraft Transmission (ART) program [NASA-CR-191079] p 840 A93-27268
- Loudness and annoyance response to simulated outdoor and indoor sonic booms [NASA-TM-107756] p 852 A93-27271
- Jet mixer noise suppressor using acoustic feedback [NASA-CASE-LEW-15170-1] p 853 A93-28953
- Quiet by design: Numerical acousto-elastic analysis of aircraft structures [ISBN-90-386-0042-9] p 893 A93-29268
- Noise transmission properties and control strategies for composite structures p 919 A93-30436
- Control of jet noise [NASA-CR-193552] p 1040 A93-32221
- NOISE SPECTRA**
- Sonic boom spectra of Space Shuttle Columbia landing 10 December 1990 p 533 A93-28488
- Sound exposure spectrum levels of sonic booms p 564 A93-28489
- Correction of a method for calculating the noise levels of aircraft at control points during acoustic flight testing p 1102 A93-51758
- Strong parallel blade-vortex interaction and noise propagation in helicopter flight p 944 A93-30980
- NOISE TOLERANCE**
- Final results from a study of community response to aircraft noise around Oslo Airport Fornebu p 425 A93-19192
- Human response to helicopter noise - A test of A-weighting p 567 A93-29424
- NOMOGRAPHS**
- A nomographic model for multicriterial optimization during the design of a flight vehicle powerplant p 95 A93-12821
- NONADIABATIC CONDITIONS**
- Hypersonic inlet efficiency revisited p 16 A93-10012
- NONDESTRUCTIVE TESTS**
- In-service inspection of commercial aircraft composite structure [SME PAPER EM92-124] p 107 A93-14116
- Coherent X-ray imaging for corrosion evaluation - A preliminary assessment p 396 A93-18611
- Correlation of X-ray CT measurements to shear strength in pultruded composite materials p 396 A93-18618
- Measurement of the center-of-gravity using X-ray computed tomography p 396 A93-18619
- Comparison of heating protocols for detection of disbands in lap joints p 396 A93-18627
- Elastic constants for unidirectional boron-epoxy composites p 387 A93-18636
- Comparison of neural network and Markov random field image segmentation techniques p 397 A93-18652
- Imaging flaws in thin metal plates using a magneto-optic device p 397 A93-18670
- An automated flow line for gas turbine blade repair [ASME PAPER 92-GT-367] p 375 A93-19531
- Review of progress in quantitative nondestructive evaluation. Vol. 11B: Proceedings of the 18th Annual Review, Brunswick, ME, July 28-Aug. 2, 1991 Vol. 11B [ISBN 0-306-44206-X] p 406 A93-19582
- Automation of disbond detection in aircraft fuselage through thermal image processing p 407 A93-19598
- The state-of-the-art of nondestructive evaluation of military runways p 375 A93-19659
- Large-area aircraft scanner p 407 A93-19693
- p-version finite element modeling for NDE p 407 A93-19699
- Rapid detection and quantification of impact damage in composite structures p 547 A93-27978
- RACE pulls for shared control --- telerobotics and automation technology for aircraft maintenance and inspection p 458 A93-29130
- Computed tomography of advanced materials and processes p 832 A93-38975
- Emerging technology for large-area scanning of aging aircraft [SME PAPER AD92-205] p 925 A93-40666
- MOI - Magneto-optic/eddy current imaging p 927 A93-41751
- Progress in industrial holography in France p 1020 A93-44197
- Towards quantitative non-destructive evaluation of aging aircraft p 1025 A93-45773
- The Civil Damage Tolerance Requirements in theory and practice p 1026 A93-45777
- Estimation of requirements of inspection intervals for panels susceptible to Multiple Site Damage p 948 A93-45795
- Synchronous X-ray Sinography for nondestructive imaging of turbine engines under load [AIAA PAPER 93-1819] p 1153 A93-49707
- Compound curvature laser window development [AIAA PAPER 93-2177] p 1173 A93-49989
- Eddy current inspection of open fastener holes in aluminum aircraft structure [SAE ARP 4402] p 1160 A93-52167
- NDT for corrosion in aerospace structures; Proceedings of the Conference, London, United Kingdom, Feb. 12, 1992 [ISBN 0-903409-99-2] p 1257 A93-54894
- The use of non-destructive testing to detect and monitor aircraft corrosion in service p 1258 A93-54896
- NDT for corrosion in aerospace structures - A review of NDT techniques p 1258 A93-54897
- Enhancement of conventional NDT methods for corrosion detection in layered skins p 1258 A93-54898
- Assessment of NDT reliability p 1258 A93-54900
- Acoustic emission technology for smart structures p 1263 A93-55331
- Nondestructive evaluation of ceramic and metal matrix composites for NASA's HITEMP and enabling propulsion materials programs [NASA-TM-105807] p 85 A93-10963
- Using NDT techniques in the maintenance of aeronautical products [REPT-921-430-102] p 88 A93-11587
- Magneto-optic imaging inspection of selected corrosion specimens [DOT/FAA/CT-TN92/20] p 88 A93-11617
- Structural fatigue aspects of the P-3 Orion [ARL-STRUC-TM-558] p 161 A93-13256
- In situ material characterization for pavement evaluation by the Spectral-Analysis-of-Surface-Waves (SASW) method [AD-A255660] p 194 A93-14128
- Proceedings of the USAF Structural Integrity Program [AD-A255379] p 110 A93-14549
- Dual-band infrared imaging applications: Locating buried minefields, mapping sea ice, and inspecting aging aircraft [DE93-000516] p 453 A93-17225
- Review of aeronautical fatigue investigations in the Netherlands during the period March 1989 - March 1991 [NLR-TP-91092-U] p 331 A93-17535
- Control of in-service damage: Application to aircraft engines [DS-2027] p 364 A93-18151
- Integrated Blade Inspection System (IBIS) upgrade study [AD-A258912] p 365 A93-19356
- Nondestructive inspection of in-service aircraft [ETN-93-93059] p 496 A93-20928
- Reliability assessment at airline inspection facilities. Volume 1: A generic protocol for inspection reliability experiments [DOT/FAA/CT-92/12-VOL-1] p 704 A93-25110
- Investigation of corrosion in aluminum/adhesive lap-splices using pulse-echo ultrasonic techniques [DE93-008074] p 749 A93-25518
- X-ray computed tomography for casting development [AD-A261786] p 752 A93-26526
- NDE of PWA 1480 single crystal turbine blade material [NASA-TM-106140] p 815 A93-27640
- Reliability assessment at airline inspection facilities. Volume 2: Protocol for an eddy current inspection reliability experiment [DOT/FAA/CT-92/12-VOL-2] p 842 A93-28685
- Use of local x ray computerized tomography for high-resolution, region-of-interest inspection of large ceramic components for engines [DE93-005564] p 843 A93-28943
- Characterization of ceramic composite materials for gas turbine applications [DE93-009719] p 905 A93-30168
- Use of titanium castings without a casting factor [AD-A264414] p 1018 A93-31192
- NONEQUILIBRIUM CONDITIONS**
- Computation of nonequilibrium radiating shock layers [AIAA PAPER 93-0144] p 414 A93-22588
- Hypersonic nonequilibrium flow computations using the Roe flux-difference split scheme p 692 A93-35609
- Nonequilibrium turbulence modeling study on light dynamic stall of a NACA0012 airfoil p 768 A93-37379
- Thermo-chemical models for hypersonic flows p 863 A93-42433
- Simulation of nonequilibrium hypersonic flows p 863 A93-42443
- Equilibrium and nonequilibrium modeling of hypersonic inviscid flows p 864 A93-42448
- Review of chemical-kinetic problems of future NASA missions. I - Earth entries p 872 A93-42899
- Computation of hypersonic flow past blunt body for nonequilibrium weakly ionized air [AIAA PAPER 93-2995] p 1053 A93-48185
- Calculation of real-gas effects on airfoil aerodynamic characteristics p 1229 A93-54477
- Research activity at the shock tube facility at NASA Ames p 1252 A93-54804
- Nonequilibrium shock layer radiation in a simulated Titan atmosphere p 1233 A93-54805
- Chemical nonequilibrium effects of Mach reflection p 1233 A93-54816
- Relaxation of discrete rotational energy distributions using a Monte Carlo method p 1234 A93-55146
- Kinetics and energy transfer in nonequilibrium fluid flows [AD-A263612] p 875 A93-29284
- NONEQUILIBRIUM FLOW**
- A comparison of 'new' and 'old' flux-splitting schemes for the Euler equations [AIAA PAPER 93-0876] p 470 A93-24937
- An upwind, kinetic flux-vector splitting method for flows in chemical and thermal non-equilibrium [AIAA PAPER 93-0894] p 472 A93-24954
- Calculation of optical and electric characteristics from hypersonic blunt-body wakes p 680 A93-33729
- Numerical analysis for chemically non-equilibrium flow p 770 A93-38148
- Viscous nonequilibrium flow calculations [ONERA, TP NO. 1992-89] p 771 A93-38573

- Calculations of viscous nonequilibrium flows in nozzles [ONERA, TP NO. 1992-91] p 771 A93-38574
- Kinetic theory of nonequilibrium flows of gas and disperse media with internal degrees of freedom and chemical reactions p 851 A93-39127
- Nonequilibrium limiting hypersonic flow of a gas past three-dimensional tapered bodies with a separated shock p 776 A93-39133
- An approximate method for calculating nonequilibrium flows near blunt bodies p 776 A93-39134
- Numerical modeling of ionization in nonequilibrium nitrogen flows in hypersonic nozzles p 836 A93-39137
- Nonequilibrium heat transfer near the critical point of blunt bodies p 777 A93-39145
- Modeling of the physicochemical processes of nonequilibrium heat transfer in the subsonic jets of an induction plasmatron p 836 A93-39147
- Higher-order viscous shock-layer solutions for high altitude flows p 858 A93-41050 [AIAA PAPER 93-2724]
- Analysis of hypersonic nozzles including vibrational nonequilibrium and intermolecular force effects p 861 A93-41916
- A contribution to the prediction of hypersonic non-equilibrium flows p 869 A93-42624
- Reactive and inert inviscid flow solutions by quasi-linear formulations and shock fitting p 927 A93-42625
- Computation of thermochemical nonequilibrium flows around a simple and a double ellipse p 869 A93-42629
- Non-equilibrium flow in an arc heated wind tunnel p 910 A93-42642
- Application of program LAURA to thermochemical nonequilibrium flow through a nozzle p 871 A93-42644
- Quasi monodimensional inviscid non equilibrium nozzle flow computation p 927 A93-42646
- Survey of nonequilibrium re-entry heating for entry flight conditions p 1039 A93-46682 [AIAA PAPER 93-3230]
- Effects of wall conditions on chemically nonequilibrium shock-layer flow over hypersonic reentry bodies p 970 A93-46908
- The prediction of viscous nonequilibrium hypersonic flows about ablating configurations using an upwind parabolized Navier-Stokes code p 1053 A93-48188 [AIAA PAPER 93-2998]
- Optimal wing shapes in a hypersonic nonequilibrium flow p 1088 A93-51770
- Stagnation point computations of nonequilibrium inviscid blunt body flow p 1093 A93-52005
- Recent advances in computational analysis of hypersonic vehicles p 1179 A93-53364
- Computation of nonequilibrium hypersonic flowfields around hemisphere cylinders p 1229 A93-54469
- Computation of viscous hypersonic non-equilibrium blunt body flow p 1238 A93-56038
- Development and computation of continuum higher order constitutive relations for high-altitude hypersonic flow p 132 A93-13578
- Computational study of real gas effects in high speed high temperature flow, volume 2 p 289 A93-16470 [AERO-REPT-9203-VOL-2]
- Comparison of methodologies for describing relaxation in nonequilibrium gaseous systems p 419 A93-16786
- A Blottner type numerical model for nonequilibrium viscous hypersonic flows in upwind finite elements [INRIA-RR-1476] p 297 A93-18648
- Influence of the physical modelling of viscous terms on hypersonic flow computations p 297 A93-18652 [INRIA-RR-1493]
- Numerical calculation of hypersonic non-equilibrium flow around OREX p 301 A93-19296
- A new LU-SGS flow solver for calculating reentry flows p 698 A93-25759
- Kinetics and energy transfer in nonequilibrium fluid flows p 875 A93-29284 [AD-A263612]
- Nonequilibrium Radiation**
- Monte Carlo simulation of radiating reentry flows [AIAA PAPER 93-2809] p 964 A93-46548
- Nonequilibrium Thermodynamics**
- An upwind, kinetic flux-vector splitting method for flows in chemical and thermal non-equilibrium [AIAA PAPER 93-0894] p 472 A93-24954
- Application of program LAURA to thermochemical nonequilibrium flow through a nozzle p 871 A93-42644
- Radiative heat transfer from non-equilibrium high-enthalpy shock layers p 1024 A93-45515
- Survey of nonequilibrium re-entry heating for entry flight conditions p 1039 A93-46682 [AIAA PAPER 93-3230]
- NONFLAMMABLE MATERIALS**
- Development of MIL-H-53119, -54 C to 175 C high-temperature nonflammable hydraulic fluid for Air Force systems p 1214 A93-54250
- NONINTRUSIVE MEASUREMENT**
- Remote sensing of O₂ in a supersonic combustor using diode lasers and fiber optics p 414 A93-22360 [AIAA PAPER 92-5090]
- Intrusive and nonintrusive measurements of flow properties in arc jets p 943 A93-42584
- Absolute intensity measurements of impurity emissions in a shock tunnel and their consequences for laser-induced fluorescence experiments p 1147 A93-48044
- Pyrometer for turbine applications in the presence of reflection and combustion p 1156 A93-50143 [AIAA PAPER 93-2374]
- LIF visualization of 3-dimensional hypersonic mixing [ISABE 93-7114] p 1221 A93-54089
- NONISENTPROPICITY**
- Numerical solution of non-isentropic transonic cascade flow by time-marching method p 679 A93-33715
- Some contributions to propulsion theory - Non-isentropic duct flow and the general drag wake traverse p 874 A93-43688
- NONISOTHERMAL PROCESSES**
- Allowing for the effect of flow nonisothermality on total pressure losses in the afterburner diffusers of augmented turbofan engines p 53 A93-12811
- NONLINEAR EQUATIONS**
- Computational nonlinear mechanics in aerospace engineering [ISBN 1-56347-044-6] p 78 A93-12151
- Nonlinear problems of aeroelasticity p 78 A93-12153
- Flutter calculations for a system with interacting nonlinearities p 409 A93-20304 [AIAA PAPER 92-4682]
- Massively parallel aerodynamic shape optimization p 266 A93-20729
- Using current numerical methods in a mathematical model of flight vehicle synthesis p 804 A93-39188
- Recent advances in steady compressible aerodynamic sensitivity analysis p 1236 A93-55400
- Improved numerical simulation of Euler equations p 83 A93-10309
- Wind tunnel spin data reduction to obtain aerodynamic spin damping coefficients by using nonlinear equation of motion p 19 A93-10811 [AD-A253880]
- Development of nonlinear aerodynamic models for unsteady responses p 19 A93-10845
- A primer on polynomial resultants [AD-A246883] p 98 A93-11463
- Solution of nonlinear flow equations for complex aerodynamic shapes [NASA-CR-190979] p 90 A93-12329
- Turbulence and chaos in classical and quantum systems p 232 A93-14144
- Special publication of National Aerospace Laboratory [DE93-716176] p 239 A93-15946
- Vortex breakdown incipience: Theoretical considerations [NASA-CR-189734] p 290 A93-16627
- NONLINEAR FEEDBACK**
- Robust nonlinear feedback guidance for an aerospace plane: A geometric approach p 189 A93-14835
- NONLINEAR PROGRAMMING**
- Progress in the application of a non-linear programming methodology to the design of a low-vibration airframe p 507 A93-27959
- Optimization using fuzzy set theory p 1037 A93-45431
- Application of artificial neural networks to the design optimization of aerospace structural components [NASA-TM-4389] p 555 A93-21831
- NONLINEAR SYSTEMS**
- Comparison of nonlinear tracking controllers for a compressible flow process p 66 A93-12224
- Output feedback control for output tracking of nonlinear uncertain systems p 96 A93-13177
- Nonlinear time-series-based adaptive control applications p 97 A93-13230
- Synthesis of a helicopter nonlinear flight controller using approximate model inversion p 62 A93-13280 [AIAA PAPER 92-4468]
- Linear and nonlinear aircraft flight control for the AIAA Controls Design Challenge p 62 A93-13286 [AIAA PAPER 92-4628]
- Generalized multipoint inverse airfoil design p 122 A93-14541
- Identification of weakly nonlinear dynamic systems by means of random excitations p 227 A93-16472
- Structural analysis of a nonlinear problem of aeroelasticity for CFC structures p 397 A93-18989
- A study on stability and response analysis of a nonlinear rotor system with mass unbalance and side load [ASME PAPER 92-GT-7] p 400 A93-19280
- Control of a high performance aircraft with unacceptable aerodynamics p 369 A93-22905
- Output tracking control of nonlinear systems with weakly non-minimum phase p 439 A93-22968
- Three-dimensional modeling and control of a twin-lift helicopter system p 370 A93-23511
- Failure-accommodating neural network flight control [AIAA PAPER 92-4394] p 523 A93-24495
- Numerical simulation of homogeneous non-Gaussian random vector fields p 561 A93-27584
- Backward bifurcation for structural divergence of a wing section p 526 A93-29351
- Extension of a nonlinear systems theory to general-frequency unsteady transonic aerodynamic responses [AIAA PAPER 93-1590] p 683 A93-34122
- The investigation of limit cycle amplitude of nonlinear nose gear p 800 A93-36342
- Nonlinear analysis and flight dynamics [ONERA, TP NO. 1992-83] p 818 A93-38568
- Recent advances of time domain approach for nonlinear response and sonic fatigue p 1022 A93-45106
- An improved far field drag calculation method for nonlinear CFD codes p 975 A93-47213 [AIAA PAPER 93-3417]
- Nonlinear command augmentation system for a high performance aircraft p 1132 A93-51372 [AIAA PAPER 93-3777]
- Approximate decoupling flight control system design with output feedback for nonlinear systems p 1135 A93-51465 [AIAA PAPER 93-3880]
- A new technique for nonlinear control of aircraft [AIAA PAPER 93-3881] p 1135 A93-51466
- Identification of actuation system and aerodynamic effects of direct-lift-control flaps p 1103 A93-52435
- Identification of nonlinear mechanical systems using combined state and parameter evaluation p 1224 A93-52732
- A study upon structural optimization of elastic rotors for mechanical systems [INPE-5376-TD/471] p 83 A93-10310
- Combustion noise and combustion instabilities in propulsion systems p 100 A93-10682
- Nonlinear aeroelasticity of composite structures [AD-A254285] p 47 A93-10842
- A primer on polynomial resultants [AD-A246883] p 98 A93-11463
- Laminar boundary-layer breakdown [AD-A254489] p 90 A93-12162
- Computational nonlinear control [AD-A253547] p 98 A93-12258
- Nonlinear stall flutter of wings with bending-torsion coupling [AD-A254323] p 186 A93-12959
- Chaotic vortical motion in the near region of a plane jet p 131 A93-13493
- Active control of combustion instability in a ramjet using large-eddy simulations [AD-A255226] p 175 A93-14111
- Adaptive control of nonlinear nonminimum phase systems p 229 A93-14470
- Automatic pulse shaping with the AN/FPN-42 and AN/FPN-44A Loran-C transmitters p 319 A93-18309 [AD-A257860]
- Robust nonlinear control of vectored thrust aircraft [NASA-CR-192727] p 728 A93-25199
- Control of nonlinear systems under input constraints with applications to flight control p 729 A93-25353
- Hypersonic panel flutter in a rarefied atmosphere [NASA-CR-4514] p 780 A93-27084
- Parameter identification for nonlinear aerodynamic systems [NASA-CR-193072] p 782 A93-27282
- Static and dynamic large deflection flexural response of graphite-epoxy beams [NASA-CR-4118] p 934 A93-30374
- NONLINEARITY**
- A treatment to flight controller nonlinearity effects - An adaptive compensator approach p 524 A93-26948
- Euler solutions to nonlinear acoustics of non-lifting rotor blades p 568 A93-29433
- Nonlinear aspects of transonic aeroelasticity p 1096 A93-52642
- A finite element method for nonlinear panel flutter p 84 A93-10472
- A field panel method for transonic flows p 18 A93-10547
- Application of eigenstructure assignment to the control of powered lift combat aircraft p 64 A93-11871
- Computational nonlinear control [AD-A253547] p 98 A93-12258

- The Fourth Workshop on Dynamics and Aeroelastic Stability Modeling of Rotorcraft Systems
[AD-A255065] p 50 N93-12485
- Transonic aeroelastic analysis of systems with structural nonlinearities p 217 N93-13769
- Identification and control of non-linear time-varying dynamical systems using artificial neural networks
[AD-A257595] p 372 N93-18193
- Development of a non-linear simulation for generic hypersonic vehicles - ASUHS1
[NASA-CR-192710] p 516 N93-22003
- Far field rotor noise
[AD-A260703] p 759 N93-25651
- Nonlinear analyses of composite aerospace structures in sonic fatigue
[NASA-CR-193124] p 930 N93-29154
- NONPARAMETRIC STATISTICS**
Statistical methods in flight vehicle control theory
p 1165 A93-49306
- NONUNIFORM FLOW**
Effect of a large-scale inhomogeneity of the incoming flow on flow in a plane turbine cascade p 6 A93-10189
- Numerical research on flows in nonuniform cascades
[ASME PAPER 92-GT-276] p 253 A93-19469
- Design of exhaust nozzles using GA optimized neural networks
[AIAA PAPER 93-0410] p 361 A93-23331
- Heat transfer on blunt cones in nonuniform supersonic flow in the presence of gas injection from the surface p 972 A93-46975
- Determination of the aerodynamic characteristics of thin bodies of revolution with an arbitrary number of cantilever surfaces in inhomogeneous flow p 1092 A93-51911
- An investigation of post stall transients and recoverability of axial compression systems p 1184 A93-53988
- Hypersonic inlet efficiency revisited p 16 N93-10012
- NONUNIFORMITY**
Oscillation of circular shock waves with upstream nonuniformity p 208 A93-15496
- The influence of non-uniform spanwise inlet temperature on turbine rotor heat transfer p 901 N93-29932
- NORMAL DENSITY FUNCTIONS**
Time-frequency domain analysis of vibration signals for machinery diagnostics. 3: The present power spectral density
[OUEL-1911/92] p 89 N93-11707
- NORMAL SHOCK WAVES**
Parametrical investigation of the interaction between turbulent wall shear layers and normal shock waves, including separation p 681 A93-33752
- Normal shock wave oscillations in supersonic diffusers p 1044 A93-48042
- Standing normal detonations and oblique detonations for propulsion
[AIAA PAPER 93-2325] p 1116 A93-50105
- AGARD WG13 aerodynamics of high speed air intakes: Assessment of CFD results p 215 N93-13220
- Monte Carlo simulation of normal shock wave. Part 1: Lennard-Jones potential p 300 N93-19279
- Supersonic shock wave/vortex interaction
[NASA-CR-192917] p 695 N93-25249
- An investigation of photothermal velocimetry for application to transient, high-speed gas flows p 698 N93-25720
- NOSE CONES**
Convective heat-transfer rate distributions over a 140 deg blunt cone at hypersonic speeds in different gas environments
[AIAA PAPER 93-2787] p 1027 A93-46529
- Computational analysis of off-design waveriders
[AIAA PAPER 93-3488] p 982 A93-47262
- Drag measurements on blunted cones and a scramjet vehicle in hypervelocity flow
[AIAA PAPER 93-2979] p 1050 A93-48172
- Instability of hypersonic flow past blunt cones - Effects of mean flow variations
[AIAA PAPER 93-2983] p 1051 A93-48176
- On computing vortex asymmetries about cones at angle of attack using the conical Navier-Stokes equations
[AIAA PAPER 93-3628] p 1064 A93-48313
- Structural analysis of the light weight hard nose of the 71M aerostat
[AIAA PAPER 93-4037] p 1255 A93-54608
- Conjugate modeling of high-temperature nose cap and wing leading edge heat pipes p 1259 A93-55465
- NOSE TIPS**
Forebody vortex control - A progress review
[AIAA PAPER 93-3540] p 986 A93-47292
- One type of automatically adjusted difference scheme with artificial viscosity to calculate ablated exterior shapes
[AD-A254108] p 19 N93-10856
- Ablation problems using a finite control volume technique
[DE93-009861] p 942 N93-29187
- NOSE WHEELS**
Loads at the nose landing gears of civil transport aircraft during towbarless towing operations p 45 A93-13629
- The investigation of limit cycle amplitude of nonlinear nose gear p 800 A93-36342
- The evolution of a nose-wheel steering system p 995 A93-44852
- Testing a wheeled landing gear system for the TH-57 helicopter
[AD-A262152] p 806 N93-27547
- NOSES (FOREBODIES)**
Numerical solution of radiative flowfield on the nose region of blunt bodies p 120 A93-14359
- Transonic flow around the leading edge of a thin airfoil with a parabolic nose p 688 A93-34405
- Simulation of ablation in Earth atmospheric entry
[AIAA PAPER 93-2789] p 1027 A93-46531
- Application of an engineering inviscid-boundary layer method to slender three-dimensional vehicle forebodies
[AIAA PAPER 93-2793] p 963 A93-46534
- CFD drag predictions for a wide body transport fuselage with flight test verification
[AIAA PAPER 93-3418] p 976 A93-47214
- Forebody vortex control - A progress review
[AIAA PAPER 93-3540] p 986 A93-47292
- Effect of forebody tangential slot blowing on flow about a full aircraft geometry p 1048 A93-48156
- Development of nose structure of a reconnaissance container for a supersonic jet aircraft
[MBB-LME-242-S-PUB-0451] p 998 N93-31046
- NOWCASTING**
Nowcasts of thunderstorm initiation and evolution p 752 A93-33773
- NOZZLE DESIGN**
Aerodynamic design of axisymmetric hypersonic wind-tunnel nozzles using a least-squares/parabolized Navier-Stokes procedure p 9 A93-12011
- Effect of nozzle design on near acoustic field of supersonic circular and rectangular jets p 448 A93-19203
- Innovative high temperature aircraft engine fuel nozzle design
[ASME PAPER 92-GT-132] p 350 A93-19365
- The optimum value of the nozzle outlet angle of turbine stages
[ASME PAPER 92-GT-224] p 404 A93-19442
- Evaluation of scramjet nozzle configurations and film cooling for reduction of wall heating
[AIAA PAPER 93-0744] p 358 A93-21118
- Starting and test rhombus characteristics of two-dimensional supersonic free-jet nozzle/generic supersonic aircraft inlet configurations
[AIAA PAPER 92-5091] p 273 A93-22361
- Design of exhaust nozzles using GA optimized neural networks
[AIAA PAPER 93-0410] p 361 A93-23331
- Goertler instability and hypersonic quiet nozzle design p 480 A93-29155
- Thrust vectoring nozzles give pilots an edge p 720 A93-34375
- A strategy for the optimal design of nozzle contours
[AIAA PAPER 93-2720] p 962 A93-46476
- Thrust vectoring control from underexpanded asymmetric nozzles
[AIAA PAPER 93-3261] p 968 A93-46827
- C-2 subsonic freejet development and demonstration
[AIAA PAPER 93-2180] p 1138 A93-49992
- Dual-spray airblast fuel nozzle for advanced small gas turbine combustors p 1116 A93-50113
- Performance characteristics of a variable-area vane nozzle for vectoring an ASTOVL exhaust jet up to 45 deg
[AIAA PAPER 93-2437] p 1118 A93-50189
- IHPET exhaust nozzle technology demonstrator - integrated high performance turbine energy technology
[AIAA PAPER 93-2569] p 1121 A93-50287
- Aerodynamics design of convergent-divergent nozzles
[AIAA PAPER 93-2574] p 1085 A93-50290
- Low-frequency combustion oscillations in a model afterburner p 1193 A93-53702
- Effect of nozzle design on the performance of a highly loaded turbine stage
[ISABE 93-7096] p 1203 A93-54072
- Optimization of afterbodies and engine nozzle by using CFD methods
[ISABE 93-7098] p 1187 A93-54074
- Advanced aerodynamic airframe/nozzle integration
[ISABE 93-7099] p 1187 A93-54075
- Design of air intakes and nozzles for transonic rotational flows
[ISABE 93-7102] p 1187 A93-54078
- Influence of chemical kinetics effects in nozzles shape design
[ISABE 93-7112] p 1188 A93-54087
- Novel nozzle p 1245 A93-54450
- Nozzle installation effects on the noise from supersonic exhaust plumes p 100 N93-10681
- Hypervelocity scramjet combustor-nozzle analysis and design
[NASA-CR-190965] p 60 N93-12214
- Survey on techniques used in aerodynamic nozzle/airframe integration p 161 N93-13224
- Design of a nozzle for a hypersonic wind tunnel
[AERO-REPT-9113] p 381 N93-16468
- Nozzle/cowl optimization for a hypersonic vehicle on a typical trajectory
[AD-A258827] p 341 N93-19089
- Performance characteristics of a variable-area vane nozzle for vectoring an ASTOVL exhaust jet up to 45 deg
[NASA-TM-106114] p 813 N93-27131
- Analytical and experimental investigation of annular propulsive nozzles p 815 N93-28391
- Heat transfer and aerodynamics of a 3D design nozzle guide vane tested in the Pyestock Isentropic Light Piston Facility p 901 N93-29928
- NOZZLE EFFICIENCY**
Development of a hydrogen external burning flight test experiment on the NASA Dryden SR-71A aircraft
[SAE PAPER 920997] p 157 A93-14638
- Role of hydrogen/air chemistry in nozzle performance for a hypersonic propulsion system p 359 A93-21668
- The effect of entrance radius and film injection on wall heating in scramjet nozzles p 360 A93-22505
- Developments in icing test techniques for aerospace applications in the RAE Pyestock (England) altitude test facility
[RAE-TM-P-1214] p 48 N93-11485
- Analytical and experimental investigation of annular propulsive nozzles
[AD-A262685] p 815 N93-28391
- NOZZLE FLOW**
A method of calculating elastic curve of semiflexible plate nozzle p 66 A93-12097
- Effect of the proximity of the machined surface on the discharge coefficients of laser cutter nozzles p 79 A93-12809
- Nozzle flow computations using the Euler equations p 112 A93-14170
- Numerical solution of 3-D turbulent flows inside of new concept nozzles p 114 A93-14211
- Digital simulation of transonic flow fields in a planar nozzle p 122 A93-14479
- Calculation of pressure ratio at nozzle exit with shock p 122 A93-14480
- A method for calculating supersonic three-dimensional flows in pyramidal nozzles p 125 A93-15216
- Study on unsymmetrical supersonic nozzle flows p 127 A93-16933
- Streamline curvature in supersonic shear layers p 244 A93-19194
- Unsteady pressures on exhaust nozzle interior surfaces - Empirical correlations for prediction p 244 A93-19219
- A numerical investigation into the nozzle flow of high by-pass turbofans
[ASME PAPER 92-GT-10] p 346 A93-19283
- Aerodynamic performance of a transonic low aspect ratio turbine nozzle
[ASME PAPER 92-GT-31] p 245 A93-19291
- The optimum value of the nozzle outlet angle of turbine stages
[ASME PAPER 92-GT-224] p 404 A93-19442
- Balance of moments for hypersonic vehicles
[ASME PAPER 92-GT-251] p 253 A93-19460
- Evaluation of scramjet nozzle configurations and film cooling for reduction of wall heating
[AIAA PAPER 93-0744] p 358 A93-21118
- Influences on the sprays formed by high-shear fuel nozzle/swirler assemblies p 411 A93-21653
- Role of hydrogen/air chemistry in nozzle performance for a hypersonic propulsion system p 359 A93-21668
- Numerical simulation of unsteady transonic nozzle flows p 272 A93-22230
- Flow quality improvement in a high speed blowdown wind tunnel
[AIAA PAPER 93-0353] p 377 A93-23038
- Real gas effects for compressible nozzle flows p 682 A93-33757
- Numerical simulation of starting process in a hypersonic nozzle p 684 A93-34275
- Spreadsheet microcomputer numerical method for the compressible laminar wake flow p 684 A93-34308
- Reactive and dissipative hypersonic flow in a wind tunnel nozzle p 687 A93-34358

Commercial turbofan engine exhaust nozzle flow analyses p 689 A93-34489
Issues associated with long-duration high-enthalpy scramjet combustor testing p 721 A93-34497
Underexpanded boundary jet in a wake flow p 775 A93-39123
Hypersonic single expansion ramp nozzle simulations p 777 A93-39254
Flip-flop jet nozzle extended to supersonic flows p 778 A93-39409
Supersonic jet control via point disturbances inside the nozzle p 861 A93-41930
CFD for hypersonic propulsion p 865 A93-42585
Application of program LAURA to thermochemical nonequilibrium flow through a nozzle p 871 A93-42644
Quasi monodimensional inviscid non equilibrium nozzle flow computation p 927 A93-42646
Scramjet nozzle experiment with hypersonic external flow p 899 A93-42879
Computation of unsteady nozzle flows p 960 A93-45543
A systems approach to a DSMC calculation of a control jet interaction experiment p 964 A93-46538
The use of streamwise vorticity to enhance ejector performance p 966 A93-46792
Numerical simulation of aerothermodynamics processes in gas turbine engine components p 1002 A93-46939
On the shock-fitting scheme of Hall-Crawley for time-linearized time-harmonic flows using Euler equations p 972 A93-46946
Absolute intensity measurements of impurity emissions in a shock tunnel and their consequences for laser-induced fluorescence experiments p 1147 A93-48044
Validation studies of scramjet nozzle performance p 1109 A93-49616
CFD validation for scramjet combustor and nozzle flows. I p 1111 A93-49724
An adaptive grid/Navier-Stokes methodology for the calculation of nozzle afterbody base flows with a supersonic freestream p 1076 A93-49788
Boundary condition procedures for CFD analyses of propulsion systems - The multi-zone problem p 1077 A93-49819
Using a diagonal implicit algorithm to calculate transonic nozzle flow p 1082 A93-50119
Performance characteristics of a variable-area vane nozzle for vectoring an ASTOVL exhaust jet up to 45 deg p 1118 A93-50189
Effects of flow-path variations on internal reversing flow in a tailpipe offtake configuration for ASTOVL aircraft p 1118 A93-50190
Three-dimensional flow field in a turbine nozzle passage p 1084 A93-50278
Decreasing F-16 nozzle drag using computational fluid dynamics p 1084 A93-50289
An experimental study of the dynamic effect of a supersonic underexpanded jet on a plane surface parallel to the nozzle axis p 1092 A93-51913
An extended insight into hypersonic flow phenomena using numerical methods p 1093 A93-51999
Flux-vector splitting for compressible low Mach number flow p 1093 A93-52001
Nozzle effects on linear stability behaviour of combustors p 1198 A93-54020
Off-design performance of scramjet nozzles p 1203 A93-54084
Observation of fluctuation of 2D-nozzle flows p 1204 A93-54086
The low frequency aeroacoustics of buried nozzle systems p 1205 A93-54244
A new method for resolving transonic nozzle flows using orthogonal stream-lines coordinate system p 1230 A93-54584
An experimental investigation of the effects of swirling flow on the performance of nozzles p 1247 A93-54859
Enhancement of mixing in high-speed heated jets using a counterflowing nozzle p 1235 A93-55359
Computation of hypersonic high-temperature nozzle flow p 1238 A93-56040
Hypervelocity scramjet combustor-nozzle analysis and design p 60 A93-12214
The jet behaviour of an actual high-bypass engine as determined by LDA-measurements in ground tests p 175 A93-13218

Control of asymmetric jet p 219 A93-14400
[AD-A255967]
Exact-gradient shape optimization of a 2D Euler flow p 422 A93-18623
[INRIA-RR-1540]
Numerical simulation of flow for a scramjet nozzle p 302 A93-19299
Performance characteristics of a variable-area vane nozzle for vectoring an ASTOVL exhaust jet up to 45 deg p 813 A93-27131
[NASA-TM-106114]
Analysis of thrust modulation of ram-rockets by a vortex valve p 814 A93-27187
Analytical and experimental investigation of annular propulsive nozzles p 815 A93-28391
[AD-A262685]
Effects of flow-path variations on internal reversing flow in a tailpipe offtake configuration for ASTOVL aircraft p 900 A93-29065
[NASA-TM-106149]
Penn State axial flow turbine facility: Performance and nozzle flow field p 1032 A93-31588
NOZZLE GEOMETRY
Variational problem of the profiling of the side walls of the supersonic section of a narrow three-dimensional nozzle p 4 A93-10140
Calculation of three-dimensional turbulent jets propagating behind nozzles of rectangular cross section p 6 A93-10192
Effect of heat supply on the gasdynamic parameters of gas flow in Laval nozzles p 12 A93-12760
Confined jet thrust vector control nozzle studies p 172 A93-14516
Aeroacoustic environment of an advanced short takeoff and vertical landing aircraft in hover p 231 A93-14539
A method for calculating supersonic three-dimensional flows in pyramidal nozzles p 125 A93-15216
Effect of nozzle design on near acoustic field of supersonic circular and rectangular jets p 448 A93-19203
Unsteady pressures on exhaust nozzle interior surfaces - Empirical correlations for prediction p 244 A93-19219
Experimental analysis of transonic flow through the variable nozzle of a radial inflow turbine p 248 A93-19336
[ASME PAPER 92-GT-90]
Optimization aspects of an ejector type hypersonic thrust nozzle p 355 A93-19551
[ASME PAPER 92-GT-402]
Measured thrust losses associated with secondary air injection through nozzle walls p 270 A93-21656
Starting and test rhombus characteristics of two-dimensional supersonic free-jet nozzle/generic supersonic aircraft inlet configurations p 273 A93-22361
[AIAA PAPER 92-5091]
Computation of supersonic jet noise under imperfectly expanded conditions p 563 A93-24825
[AIAA PAPER 93-0735]
X-29 vortex flow control tests p 804 A93-38846
Flip-flop jet nozzle extended to supersonic flows p 778 A93-39409
Experimental investigation of spherical-convergent-flap thrust-vectoring two-dimensional plug nozzles p 898 A93-41045
[AIAA PAPER 93-2431]
Prediction of static performance for single expansion ramp nozzles p 898 A93-41047
[AIAA PAPER 93-2571]
Effects of nozzle contour on the aerodynamic characteristics of underexpanded annular impinging jets p 1024 A93-45563
[AD-A258212]
A strategy for the optimal design of nozzle contours p 962 A93-46476
[AIAA PAPER 93-2720]
Thrust vectoring control from underexpanded asymmetric nozzles p 968 A93-46827
[AIAA PAPER 93-3261]
Three dimensional aero-thermal characteristics of a high pressure turbine nozzle guide vane p 1002 A93-46942
Numerical study of the transient flow in the driven tube and the nozzle section of a shock tunnel p 1078 A93-49856
[AIAA PAPER 93-2018]
Static internal performance tests of single expansion ramp nozzle concepts designed with LO considerations p 1117 A93-50185
[AIAA PAPER 93-2429]
Scale model test results for several spherical/two-dimensional nozzle concepts p 1117 A93-50186
[AIAA PAPER 93-2430]
Fluidic scale model multi-plane thrust vector control test results p 1117 A93-50187
[AIAA PAPER 93-2433]
Study of a circular cross section thrust augmenting ejector p 1118 A93-50191
[AIAA PAPER 93-2439]
Advanced aerodynamic airframe/nozzle integration p 1187 A93-54075
[ISABE 93-7099]
Influence of chemical kinetics effects in nozzles shape design p 1188 A93-54087
[ISABE 93-7112]

Two-dimensional and three-dimensional mixing flow structures with injected through slotted nozzle and circular nozzle into supersonic flows p 1221 A93-54092
[ISABE 93-7117]
Nozzle installation effects on the noise from supersonic exhaust plumes p 100 A93-10681
Experimental investigation of the effects of aft blowing with various nozzle exit geometries on a 3.0 caliber tangent ogive at high angles of attack: Forebody pressure distributions p 22 A93-11605
[NASA-CR-190935]
An investigation of the effects of aft blowing on a 3.0 caliber tangent ogive body at high angles of attack p 24 A93-12004
[NASA-CR-190934]
Supersonic investigation of two dimensional hypersonic exhaust nozzles p 179 A93-15342
[NASA-TM-105687]
Computation of supersonic jet noise under imperfectly expanded conditions p 233 A93-15430
[NASA-TM-105961]
Enhanced mixing of a rectangular supersonic jet by natural and induced screech p 989 A93-31672
[NASA-TM-106245]
NOZZLE INSERTS
Streamwise vorticity generation and mixing enhancement in free jets by 'delta-tabs' p 1180 A93-53592
[AIAA PAPER 93-3253]
Streamwise vorticity generation and mixing enhancement in free jets by delta-tabs p 988 A93-31648
[NASA-TM-106235]
NOZZLE WALLS
Development of the NASA-Ames low disturbance supersonic wind tunnel for transition research up to Mach 2.5 p 462 A93-24488
[AIAA PAPER 92-3909]
NOZZLES
Investigations of detail design issues for the high speed acoustic wind tunnel using a 60th scale model tunnel. Part 1: Tests with open circuits p 137 A93-14737
[NASA-CR-191671]
Thermal effects of a coolant film along the suction side of a high pressure turbine nozzle guide vane p 901 A93-29930
NUCLEAR ELECTRIC PROPULSION
Fusion-electric propulsion for hypersonic flight p 1142 A93-50318
[AIAA PAPER 93-2611]
NUCLEAR EXPLOSIONS
Analysis of structural dynamic response for aircraft operating in the environment of nuclear explosion shock waves p 78 A93-11810
NUCLEAR FUSION
Fusion-electric propulsion for hypersonic flight p 1142 A93-50318
[AIAA PAPER 93-2611]
NUCLEAR PROPULSION
Nuclear thermal rocket entry heating and thermal response preliminary analysis p 385 A93-23058
[AIAA PAPER 93-0378]
NUCLEAR REACTIONS
Principles of nuclear-based explosive detection systems p 497 A93-21861
NUCLEAR ROCKET ENGINES
Nuclear thermal rocket entry heating and thermal response preliminary analysis p 385 A93-23058
[AIAA PAPER 93-0378]
NUCLEATION
Ice prevention by ultrasonic nucleation of supercooled water droplets in front of subsonic aircraft p 142 A93-12816
[AD-A258212]
The onset of vortex turbulence p 788 A93-28251
NUMERICAL ANALYSIS
Numerical analysis of three-dimensional viscous flows around an advanced counterrotating propeller p 112 A93-14165
Numerical analysis of the 3-D turbulent flow in an S-shaped diffuser p 116 A93-14252
Fewest-fault integral optimization algorithm for engine fault diagnosis p 173 A93-15343
Numerical analysis of a chined forebody with asymmetric strakes p 260 A93-20164
[AIAA PAPER 93-0051]
Numerical analysis of two-dimensional flows around elliptic wings above a flat plate p 267 A93-20924
Recent advances in the numerical analysis of ram air wings - The three dimensional simulation code 'PARA3D' p 702 A93-35154
[AIAA PAPER 93-1203]
Numerical analysis for chemically non-equilibrium flow p 770 A93-38148
Numerical analysis of airfoil cascades subjected to unsteady flow p 972 A93-46944
Numerical analysis of high aspect ratio cooling passage flow and heat transfer p 1153 A93-49714
[AIAA PAPER 93-1829]
A numerical analysis of supersonic flow over an axisymmetric afterbody p 1083 A93-50121
[AIAA PAPER 93-2347]

- Developing numerical techniques for solving low Mach number fluid-acoustic problems p 1235 A93-55353
- Design problems of three-dimensional contractions — in incompressible flow p 1236 A93-55584
- Sweeping algorithm for unstructured-grid generation on two-dimensional non-convex domains p 1262 A93-56413
- Numerical analysis of the flow fields in a RQL gas turbine combustor p 89 A93-11767
- [DE92-017509] p 89 A93-11767
- Investigation of advanced counterrotation blade configuration concepts for high speed turboprop systems. Task 4: Advanced fan section aerodynamic analysis [NASA-CR-187128] p 174 A93-12695
- Aeroelastic stability and response of rotating structures [NASA-CR-191803] p 371 A93-16560
- Numerical analysis of the flow in a tubulated rectangular duct simulating the cooling passages in a turbine blade [AD-A257855] p 420 A93-18305
- Rotating stall: Modeling-measurement techniques; unsteady loss-unsteady flow field p 424 A93-18732
- On the roles of wind tunnel testing and computational fluid dynamics in the aircraft development p 341 A93-19322
- Wind shear hazard determination p 488 A93-19597
- Current research activities: Applied and numerical mathematics, fluid mechanics, experiments in transition and turbulence and aerodynamics, and computer science [NASA-CR-191408] p 758 A93-25084
- Quiet by design: Numerical acousto-elastic analysis of aircraft structures [ISBN-90-386-0042-9] p 893 A93-29266
- Transmission of sound through a rotor [NLR-TP-92014-U] p 1006 A93-32386
- NUMERICAL CONTROL**
- Vibration control algorithms for flexible rotors p 95 A93-10741
- Robust digital control of a high-performance engine — F-100 turbofan p 359 A93-21792
- Generalized guidance law for collision courses p 727 A93-34533
- Optimal discrete-time dynamic output-feedback design - A w-domain approach p 757 A93-34536
- Digital resolver for helicopter model blade motion analysis p 830 A93-37878
- Processing integral impeller 4-coordinate numerically controlled milling machine p 926 A93-41749
- Using numerical control algorithms in stabilization systems with digital correction p 941 A93-43113
- Data acquisition for aeroelastic testing at the NASA Langley Transonic Dynamics Facility p 1250 A93-54397
- Predevelopment of a flight control system for a small civil aircraft p 1249 A93-56031
- A monitor for the laboratory evaluation of control integrity in digital control systems operating in harsh electromagnetic environments [NASA-TM-4402] p 65 A93-12304
- A brief overview of NASA Langley's research program in formal methods p 228 A93-12958
- Using fuzzy behaviors for the outdoor navigation of a car with low-resolution sensors [DE93-002428] p 706 A93-25120
- NUMERICAL FLOW VISUALIZATION**
- Turbine blade cascade flows p 10 A93-12361
- Dynamic stall on a three-dimensional rectangular wing [AIAA PAPER 93-0637] p 463 A93-24753
- Unsteady panel method for flows with multiple bodies moving along various paths [AIAA PAPER 93-0640] p 539 A93-24755
- Numerical simulation and physical aspects of supersonic vortex breakdown p 1093 A93-52011
- The hemisphere-cylinder at an angle of attack p 21 A93-11250
- User's manual for Interactive Data Display System (IDDS) [NASA-TM-105572] p 441 A93-16613
- Vortex breakdown incipience: Theoretical considerations [NASA-CR-189734] p 290 A93-16627
- Modelling of interfacial and thermocline waves [AERO-REPT-9209] p 420 A93-18103
- NUMERICAL INTEGRATION**
- The numerical calculation of aircraft propeller noise p 174 A93-16239
- Advances in the numerical integration of the 3-D Euler equations in vibrating cascades [ASME PAPER 92-GT-170] p 351 A93-19396
- Investigation of the flowfield over parallel-arranged launch vehicles [AIAA PAPER 93-3060] p 1058 A93-48237
- The numerical errors in inverse simulation [AIAA PAPER 93-3588] p 1223 A93-52681

- Homenthalpic-flow approach for hypersonic inviscid non-equilibrium flows [INRIA-RR-1652] p 788 A93-28440
- NUMERICAL STABILITY**
- Stability analysis of dynamic meshes for transient aerodynamic computations [AIAA PAPER 93-3325] p 1022 A93-45019
- NUMERICAL WEATHER FORECASTING**
- Numerical forecasting of liquid water content to assess airframe icing risk p 429 A93-22147
- Sea fog and stratus - A major aviation and marine hazard in the northern Gulf of Mexico p 844 A93-39762
- Preliminary evaluation of aviation-impact variables derived from numerical models [PB93-190197] p 1034 A93-31202
- NUSSLET NUMBER**
- Transient thermal behaviour of a compressor rotor with axial cooling air flow and co-rotating or contra-rotating shaft p 903 A93-29946
- NYLON (TRADEMARK)**
- The Superpressure Stratospheric Vehicle p 39 A93-11357
- The degradation of parachutes: Age and mechanical wear [AD-A252243] p 24 A93-12179
- OBJECT-ORIENTED PROGRAMMING**
- Representation and presentation of requirements knowledge p 228 A93-17389
- Enhancing real-time flight simulation execution by intercepting Run-Time Library calls [AIAA PAPER 93-3591] p 1224 A93-52684
- Reusable code for helicopter simulation [AIAA PAPER 93-3594] p 1224 A93-52686
- Software Engineering Laboratory Ada performance study: Results and implications p 441 A93-17172
- Domain specific software design for decision aiding p 442 A93-17517
- A synthetic environment flight simulator: The AFIT virtual cockpit [AD-A259220] p 530 A93-20576
- Gas turbine system simulation: An object-oriented approach [NASA-TM-106044] p 723 A93-25673
- Toward reusable graphics components in Ada [AD-A262568] p 849 A93-28577
- OBLIQUE SHOCK WAVES**
- Intensification of flow mixing behind an oblique shock wave p 4 A93-10138
- Oblique wave evolution in a plane subsonic boundary layer p 124 A93-15178
- Shock formation in overexpanded tip leakage flow [ASME PAPER 92-GT-1] p 245 A93-19276
- Hypersonic flow separation in shock wave boundary layer interactions [ASME PAPER 92-GT-205] p 251 A93-19429
- A parametric study of bleed in shock boundary layer interactions [AIAA PAPER 93-0294] p 280 A93-22694
- Engineering approach to the prediction of shock patterns in bounded high-speed flows p 287 A93-23545
- A numerical study of unsteady supersonic compression ramp flows [AIAA PAPER 93-0883] p 470 A93-24943
- Stability of oblique detonations in RAM accelerators [AIAA PAPER 92-0089] p 541 A93-24979
- Reaction zone structure for strong, weak overdriven, and weak underdriven oblique detonations p 746 A93-35492
- Oblique shock formation in impulsively started wedge flows p 692 A93-35636
- Theoretical and experimental study of the behavior of particles passing through a shock wave [ONERA, TP NO. 1992-233] p 774 A93-38777
- Interference of an oblique shock with a shock layer on a blunt edge for small Reynolds numbers p 775 A93-39120
- A multi-dimensional kinetic-based upwind solver for the Euler equations [AIAA PAPER 93-3303] p 950 A93-45001
- Calculations on a double-fin turbulent interaction at high speed [AIAA PAPER 93-3432] p 977 A93-47224
- An investigation of shock wave turbulent boundary layer interaction with bleed through slanted slots [AIAA PAPER 93-2992] p 1052 A93-48184
- Numerical simulation of a shock wave/turbulent boundary layer interaction in a duct [AIAA PAPER 93-3127] p 1063 A93-48293
- An investigation of shock wave turbulent boundary layer interaction with bleed through normal and slanted slots [AIAA PAPER 93-2155] p 1079 A93-49971

- Standing normal detonations and oblique detonations for propulsion [AIAA PAPER 93-2325] p 1116 A93-50105
- A plume-induced boundary layer separation experiment [AD-A255397] p 220 A93-14677
- Supersonic shock wave/vortex interaction [NASA-CR-192917] p 695 A93-25249
- Analytical and experimental investigations of the oblique detonation wave engine concept [NASA-TM-102839] p 1006 A93-32374
- OBLIQUE WINGS**
- Oblique wing supersonic transport concepts [AIAA PAPER 92-4230] p 43 A93-13337
- RTJ-303: Variable geometry, oblique wing supersonic aircraft [NASA-CR-192054] p 337 A93-18166
- Aerodynamic design and synthesis of the oblique flying wing supersonic transport p 713 A93-24768
- OBSERVABILITY (SYSTEMS)**
- Output feedback control for output tracking of nonlinear uncertain systems p 96 A93-13177
- Design of reduced-order observers with precise loop transfer recovery p 184 A93-14587
- Observability analysis of piece-wise constant systems. I - Theory p 501 A93-29599
- OBSTACLE AVOIDANCE**
- Validation of vision-based obstacle detection algorithms for low-altitude helicopter flight p 374 A93-19077
- Vision-based recursive estimation of rotorcraft obstacle locations p 343 A93-22851
- Automatic guidance and control laws for helicopter obstacle avoidance p 728 A93-35518
- Technologies for automating rotorcraft nap-of-the-earth flight p 885 A93-43784
- Passive range estimation for rotorcraft low-altitude flight p 948 A93-46608
- Vision based techniques for rotorcraft low altitude flight p 1097 A93-49351
- Electro-optical navigation for aircraft p 1097 A93-50643
- Vision based obstacle detection and grouping for helicopter guidance [AIAA PAPER 93-3871] p 1098 A93-51457
- Clustering methods for removing outliers from vision-based range estimates p 1171 A93-51648
- A parallel implementation of a multisensor feature-based range-estimation method p 1099 A93-51967
- Passive range estimation for rotorcraft low-altitude flight p 1190 A93-52881
- Multirate and event-driven Kalman filters for helicopter flight p 1245 A93-55760
- An investigation of a prototype OASYS effectiveness in maneuvering flight [AD-A257901] p 338 A93-18339
- Discrete range clustering using Monte Carlo methods [NASA-TM-104004] p 706 A93-24914
- PROAV Cable Warning System (CWS) - U.S. Army aircraft integration assessment and OCONUS field evaluation [AD-A261233] p 705 A93-26263
- Merging sparse optical flow and edge connectivity between image features: A representation scheme for 2-D display of scene depth p 845 A93-27179
- OCCUPATION**
- Being an engineer - A risky occupation? Proceedings of the Conference, London, United Kingdom, June 8, 1993 [ISBN 1-85768-120-7] p 945 A93-43869
- Aircraft electrical and environmental systems, AFSCs 452x5, 454x5, and 454x6 [AD-A261213] p 717 A93-25733
- OCEAN DATA ACQUISITIONS SYSTEMS**
- ERS-1 directional wave spectra validation with the airborne SAR PHARS [BCRS-92-18] p 937 A93-31010
- OCEAN SURFACE**
- Study on aircraft microwave remote sensing of sea-water surface salinity p 92 A93-12407
- The Airborne Ocean Color Imager - System description and image processing p 1157 A93-50369
- Texture as a visual cueing element in computer image generation. I - Representation of the sea surface [AIAA PAPER 93-3560] p 1214 A93-52695
- Acoustic noise generation at the air/ocean boundary [DREA-CR-90-445] p 99 A93-10642
- Uplink laser propagation measurements through the sea surface, haze and clouds [AD-A264687] p 935 A93-30553
- OCEANOGRAPHY**
- Meeting review: Third NCAR Research Aircraft Fleet Workshop [PB92-222710] p 223 A93-12818
- OCULOMETERS**
- Air traffic control visual scanning [DOT/FAA/CT-TN92/16] p 35 A93-10459

SUBJECT INDEX

OFFSHORE PLATFORMS

Helicopters in action p 340 N93-19005

OGIVES

The influence of the boundary layer on the subsonic near-wake of a family of bluff bodies [AIAA PAPER 93-0525] p 284 A93-23266

Supersonic vortical flows around an ogive-cylinder - Laminar and turbulent computations [ONERA, TP NO. 1992-111] p 771 A93-38588

Investigation of vortex development on a pitching slender body of revolution p 1095 A93-52445

An investigation of the effects of aft blowing on a 3.0 caliber tangent ogive body at high angles of attack [NASA-CR-190934] p 24 N93-12004

Tangential fuselage blowing on an ogive cylinder p 697 N93-25545

OH-58 HELICOPTER

Load variability of a two-bladed helicopter p 507 A93-27954

Low-noise, high-strength, spiral-bevel gears for helicopter transmissions [AIAA PAPER 93-2149] p 1154 A93-49966

OIL ADDITIVES

Protective properties of aviation oils p 735 A93-35299

OIL FIELDS

Helicopters in action p 340 N93-19005

OMEGA NAVIGATION SYSTEM

Integrated Soviet VLF/Omega Receiver design p 316 A93-21198

Position reporting using GPS/OMEGA and INS p 498 A93-25173

ON-LINE SYSTEMS

Directory of factual and numeric databases of relevance to aerospace and defence R and D [AGARD-R-777] p 104 N93-11710

Multiple-function multi-input/multi-output digital control and on-line analysis [NASA-TM-107697] p 162 N93-13565

Online vibration control of a flexible rotor/bearing system p 219 N93-14468

On-line aircraft state and parameter estimation p 512 N93-19929

ONBOARD DATA PROCESSING

A fault-tolerant air data/inertial reference system p 50 A93-10982

Advanced real time integrated processors --- for Lockheed F-22 advanced tactical fighter p 50 A93-11000

On-board condition management for aircraft gas turbines [ASME PAPER 92-GT-416] p 357 A93-19564

A distributed, message-based, airspace environment p 313 A93-21144

Software flexibility and configuration control for the A340/A330 Aircraft Condition Monitoring System (ACMS) p 167 N93-15154

Flight data and flight safety in SAS p 168 N93-15156

The SIROM flight data recorder and evaluation system p 168 N93-15165

DAR-2: On-board data acquisition system for aircraft engines p 169 N93-15166

EJ 200 engine monitoring system: On- and off-board data capture, analysis, and management system p 178 N93-15172

RB199 engine oil system failure diagnostics by comparison of measured and calculated oil consumption using the OLMOS on-board monitoring system p 178 N93-15173

Realization of real time graphics in vehicles with high dynamic motion [ETN-93-92739] p 443 N93-18630

Avionics systems architectures p 808 N93-27169

ONBOARD EQUIPMENT

Characteristics of the detection of overloads in the center of mass of IL-76 and An-12 aircraft due to runway irregularities by a standard on-board recorder p 1008 A93-45666

Onboard Connectivity Network for command and control aircraft p 1166 A93-49481

DAR-2: On-board data acquisition system for aircraft engines p 169 N93-15166

Integrated engine control and monitoring with experiences derived from OLMOS p 178 N93-15168

Royal Air Force experience of the Harrier information management system p 234 N93-15170

EJ 200 engine monitoring system: On- and off-board data capture, analysis, and management system p 178 N93-15172

On-board derived flight-path measurement as demonstrated by an ILS measurement system p 994 N93-31282

ONE DIMENSIONAL FLOW

The Burnett shock structures in low density hypersonic flows [AIAA PAPER 92-5048] p 273 A93-22320

Isolator-combustor interaction in a dual-mode scramjet engine [AIAA PAPER 93-0358] p 360 A93-23041

Nonsteady, one-dimensional, internal, compressible flows - Theory and applications --- Book [ISBN 0-19-507358-4] p 548 A93-28749

A one-dimensional theory for supersonic gas jets above the critical pressure p 774 A93-39115

Quasi monodimensional inviscid non equilibrium nozzle flow computation p 927 A93-42646

Some contributions to propulsion theory - Non-isentropic duct flow and the general drag wake traverse p 874 A93-43688

OPEN CHANNEL FLOW

Self-excitation of intense oscillations in flow inside a wind tunnel with an open test section p 1091 A93-51883

OPENINGS

A Rayleigh-Ritz analysis methodology for cutouts in composite structures p 923 N93-30869

OPERATING COSTS

Design of propulsion systems for low operating costs p 55 A93-13405

High capacity aircraft p 157 A93-14395

Influence of a thermal barrier coating on the performance of a turbo-prop engine [ASME PAPER 92-GT-38] p 347 A93-19297

Reducing helicopter operating costs p 486 A93-25249

Comparison of all-electric secondary power systems for civil transport p 519 A93-25997

Future aero engine design trade offs p 1246 A93-54836

Comparison of all-electric secondary power systems for civil subsonic transports [NASA-TM-105852] p 55 N93-10456

Future regional transport aircraft market, constraints, and technology stimuli [NASA-TM-107669] p 109 N93-13025

OPERATING TEMPERATURE

The multi-heat addition turbine engine [AIAA PAPER 92-4272] p 54 A93-13334

Niobium alloy heat pipes for use in oxidizing environments p 200 A93-13791

Studies on coolant problems in aeronautical turbine cascades [ISABE 93-7074] p 1220 A93-54050

Modelling the engine temperature distribution between shut down and restart for life usage monitoring p 169 N93-15177

OPERATIONAL HAZARDS

The hazard and alarm of windshear p 141 A93-14317

Impact of weather on aviation - A global view p 308 A93-22143

An evaluation of aircraft icing forecasts for the continental United States p 429 A93-22149

Buoyancy wave hazards to aviation p 430 A93-22151

OPERATIONS RESEARCH

IOPS advisor: Research in progress on knowledge-intensive methods for irregular operations airline scheduling p 443 N93-18686

OPERATOR PERFORMANCE

Modeling of human operator actions in the stochastic trajectory tracking problem for a dynamic plant p 228 A93-16783

Adaptive automation and human performance: Multi-task performance characteristics [AD-A254596] p 186 N93-12578

OPERATORS (PERSONNEL)

The military operator's experience of reliability and maintainability characteristics p 80 A93-13403

OPTICAL COMMUNICATION

Optical interconnection and packaging technologies for advanced avionics systems p 77 A93-10960

Design considerations for air-to-air laser communications p 312 A93-18932

Diffraction limited collimating optics for high aspect ratio laser diode arrays p 1172 A93-48411

Repair and maintenance of fiber optic data links on Navy aircraft p 1172 A93-48538

Sources and detectors for fiber communications; Proceedings of the Meeting, Boston, MA, Sept. 8, 9, 1992 [SPIE-1788] p 1151 A93-49455

Uplink laser propagation measurements through the sea surface, haze and clouds [AD-A264687] p 935 N93-30553

OPTICAL COMPUTERS

Optical correlator field test results p 1038 A93-44458

OPTICAL MEASURING INSTRUMENTS

OPTICAL CORRELATORS

Optical correlator field test results p 1038 A93-44458

OPTICAL COUPLING

Optical interconnection and packaging technologies for advanced avionics systems p 77 A93-10960

An optical fiber multi-terminal data bus system for aircraft [NAL-TR-1125] p 52 N93-12370

OPTICAL DATA PROCESSING

Optical methods of stress analysis applied to cracked components p 1027 A93-45798

OPTICAL DISKS

Rewritable optical disk: Application to flight recording p 221 N93-15160

Handling and using information systems with new technology [PNR-90910] p 572 N93-20734

OPTICAL EQUIPMENT

Desirable characteristics for rotorcraft optical components p 1172 A93-49466

OPTICAL FIBERS

Optical interconnection and packaging technologies for advanced avionics systems p 77 A93-10960

Application issues of fiber optic sensors in aircraft structures p 410 A93-21094

Integration of a course and position reference system with GPS p 499 A93-27911

Position sensor with two wavelength time domain multiplexing for civil aircraft application p 1104 A93-49432

An optical fiber multi-terminal data bus system for aircraft [NAL-TR-1125] p 52 N93-12370

Electro-optic architecture (EOA) for sensors and actuators in aircraft propulsion systems [NASA-CR-182270] p 233 N93-15116

Research support for the Laboratory for Lightwave Technology [AD-A261488] p 760 N93-26343

OPTICAL FILTERS

The history and development of coated Contrast Enhancement Filters for cockpit displays p 564 A93-28180

An optical fiber based position sensor with immunity to temperature variation p 743 A93-34287

Fast design of circular-harmonic filters using simulated annealing p 1038 A93-45556

OPTICAL FLOW (IMAGE ANALYSIS)

Neural networks application to divergence-based passive ranging [NASA-TM-103981] p 885 N93-29653

Expansion-based passive ranging [NASA-TM-104025] p 994 N93-32348

OPTICAL GYROSCOPES

The LN-200 fiber gyro based tactical grade IMU [AIAA PAPER 93-3798] p 1106 A93-51391

OPTICAL MATERIALS

Thermal shock capabilities of infrared dome materials p 70 A93-11454

Measurement of aerodynamic shear stress using side chain liquid crystal polymers [AD-A254312] p 72 N93-10770

Optically smart surfaces survivability testing at Mach 3 [AD-A261785] p 760 N93-26566

OPTICAL MEASUREMENT

Recent flight-test results of optical airdata techniques [AIAA PAPER 92-4086] p 51 A93-13265

Optically smart surfaces for aerodynamic measurements [AIAA PAPER 92-3895] p 539 A93-24484

Anti-icing failure detection instrumentation using real-time optical measurement of anti-icing fluid properties [AIAA PAPER 93-0748] p 540 A93-24836

Real-time optical measurement of alkali species in air for jet engine corrosion testing [AIAA PAPER 93-0791] p 541 A93-24870

Reflection type skin friction meter [NASA-CASE-LAR-14520-1-SB] p 296 N93-18275

Interferometric JFTOT tube deposit measuring device [AD-D015599] p 536 N93-20247

Optical blade vibration measurement [ETN-93-93454] p 905 N93-29999

OPTICAL MEASURING INSTRUMENTS

Turbine blade vibration monitoring system [ASME PAPER 92-GT-159] p 402 A93-19386

Embedded fiber optic sensors in large structures p 410 A93-21085

Application issues of fiber optic sensors in aircraft structures p 410 A93-21094

Fiber-optic interferometric sensors for measurements of pressure fluctuations - Experimental evaluation [AIAA PAPER 93-0738] p 540 A93-24828

An optical fiber based position sensor with immunity to temperature variation p 743 A93-34287

- Embedded Bragg grating fiber optic sensor for composite flexbeams p 828 A93-37350
 Reconnaissance capable F/A-18D optical and infrared window antifog systems p 890 A93-41361
 [SAE PAPER 921182]
 Stray radiation in optical systems II; Proceedings of the Meeting, San Diego, CA, July 20-22, 1992 [SPIE-1753] p 1263 A93-55176
 Multiplexing electro-optic architectures for advanced aircraft integrated flight control systems [NASA-CR-182268] p 187 N93-13735
 Study of optical techniques for the Ames unitary wind tunnel: Digital image processing, part 6 [NASA-CR-192164] p 382 N93-18766
 Smart materials p 536 N93-20624
 Status of the Fiber Optic Control System Integration (FOCSI) program [NASA-TM-106151] p 841 N93-28053

OPTICAL PATHS

- Corrections to fringe distortion due to flow density gradients in optical interferometry [AIAA PAPER 93-0631] p 539 A93-24748

OPTICAL PROPERTIES

- Measurement of aerodynamic shear stress using side chain liquid crystal polymers [AD-A254312] p 72 N93-10770
 A preliminary study associated with the experimental measurement of the aero-optic characteristics of hypersonic configurations [AD-A253792] p 24 N93-12063
 IR imaging for combustion characteristics and optical properties of boron/boron oxide [AD-A257747] p 393 N93-17693

OPTICAL RADAR

- Detection and parameter estimation of atmospheric turbulence by ground-based and airborne CO₂ Doppler lidars p 395 A93-17862
 Lidar windshear detection for commercial aircraft p 341 A93-17864
 Volume-imaging lidar observations of the convective structure surrounding the flight path of a flux-measuring aircraft p 425 A93-20579
 An automated system for the measurement of slant visual range p 413 A93-22176
 Microbursts detection with airborne Doppler lidar p 433 A93-22201
 New slant visual range measuring device promises improved airport operations p 529 A93-27395
 Ladar fiber optic sensor system for aircraft applications p 1105 A93-49467
 New concepts for fiber optic position sensors p 1106 A93-49477
 Aureole lidar - Instrument design, data analysis, and comparison with aircraft spectrometer measurements p 1160 A93-52419
 Study of artificial and natural turbulence in atmospheric boundary layer with a CW Doppler CO₂ lidar p 1257 A93-54799
 Flight test operations p 488 N93-19592
 Vertical wind estimation from horizontal wind measurements p 489 N93-19604

OPTICAL REFLECTION

- Reflection type skin friction meter [NASA-CASE-LAR-14520-1-SB] p 296 N93-18275

OPTICAL SWITCHING

- Demonstration of an integrated, active 4 x 4 photonic crossbar p 211 A93-17392

OPTICAL TRACKING

- Differential GPS/inertial navigation approach/landing flight test results p 32 A93-11019
 Unorthodoxy rising - VTOL p 1 A93-11250

OPTICS

- Study of optical techniques for the Ames unitary wind tunnel, part 7 [NASA-CR-192165] p 382 N93-18520
 JPRS report: Science and technology, Central Eurasia: Engineering and equipment [JPRS-UEQ-93-004] p 930 N93-29090

OPTIMAL CONTROL

- Optimal control of lift/drag ratios on a rotating cylinder p 76 A93-10275
 Nonlinear feedback control of highly manoeuvrable aircraft p 40 A93-11654
 The application of optimal robust control in control system design of flying vehicles p 95 A93-11791
 Discrete time H(infinity) control laws for a high performance helicopter p 96 A93-13007
 H(infinity) optimal controllers for a distributed model of an unstable aircraft p 62 A93-13247
 Near-optimal energy transitions for energy-state trajectories of hypersonic aircraft [AIAA PAPER 92-4300] p 69 A93-13276
 Optimal vibration control for a flexible rotor with gyroscopic effects p 98 A93-13420

- Integrated control law synthesis of gust load alleviation and flutter margin augmentation for a transport aircraft p 182 A93-14281

- Design and robustness issues for highly augmented helicopter controls p 185 A93-14594
 Solution of the terminal guidance problem for a flight vehicle using analytical mechanics methods p 228 A93-16778

- Vibrational monitoring and diagnostics of the technical condition of gas turbine engines at civil aviation repair facilities p 374 A93-18362

- Analysis of the pump station of an aircraft hydraulic system as a subject of diagnosis p 321 A93-18374
 Evaluation of some significant issues affecting trajectory and control management for air-breathing hypersonic vehicles [AIAA PAPER 92-5011] p 384 A93-22287

- Parameter optimization for an H2 problem with multivariable gain and phase margin constraints p 439 A93-22971

- Design of insensitive multirate aircraft control using optimized eigenstructure assignment p 370 A93-23515

- Optimal control law synthesis for flutter suppression using active acoustic excitations p 370 A93-23516
 Active aircraft recovery from a spin p 524 A93-27295

- Control synthesis with incomplete, complete, and supercomplete measurements p 561 A93-27603
 Calculating the cutting depth during the milling of large gas turbine engine blades p 545 A93-27628
 An identification method for dynamic systems with delay p 562 A93-27689

- Optimal takeoff of a helicopter for category A V/STOL operations p 525 A93-28611

- Optimization of endurance performance --- of aircraft p 713 A93-34400

- Optimal open multistep discretization formulas for real-time simulation p 757 A93-34539

- Enhancement of endurance performance by periodic optimal camber control p 727 A93-34541

- An algorithm with prediction in a control problem with functional constraints p 757 A93-35307

- Numerical computation and approximations of H(infinity) optimal controllers for a 2-parameter distributed model of an unstable aircraft p 817 A93-37040

- Adaptive grid generation using optimal control theory p 770 A93-38187

- Analytical development of an equivalent system mismatch function --- for longitudinal axis of fighter aircraft in nonterminal flight phase p 906 A93-41890

- Neurocontrol design and analysis for a multivariable aircraft control problem p 906 A93-41894

- Periodic maximum range cruise with singular control p 890 A93-41903

- The UTA autonomous aerial vehicle - Automatic control and navigation p 908 A93-42813

- Singular arcs for blunt endoatmospheric vehicles p 1015 A93-44380

- Algorithmic method for optimizing the precision characteristics of a fuel metering system p 999 A93-45681

- The prediction and the active control of surge in multi-stage axial-flow compressors p 1002 A93-46945

- Aircraft control requirements and achievable dynamics prediction [AIAA PAPER 93-3648] p 1128 A93-48331

- Nonsmooth trajectory optimization - An approach using continuous simulated annealing [AIAA PAPER 93-3657] p 1099 A93-48337

- Optimum poststall turning and supersonic turning [AIAA PAPER 93-3659] p 1128 A93-48339

- Statistical methods in flight vehicle control theory p 1165 A93-49306

- Problems in the optimization of complex engineering systems p 1165 A93-49307

- Automatic carrier landing system utilizing aircraft sensors p 1097 A93-49590

- On the estimation algorithm for adaptive performance optimization of turbofan engines [AIAA PAPER 93-1823] p 1111 A93-49710

- Evaluation of a nonlinear PSC algorithm on a variable cycle engine [AIAA PAPER 93-2077] p 1114 A93-49904

- Multilevel control systems and optimization of their structures p 1168 A93-50954

- Multilevel intelligent control systems for flight vehicles p 1168 A93-50955

- Optimization of algorithms for information processing and control p 1169 A93-51062

- A Hopfield neural network for adaptive control [AIAA PAPER 93-3729] p 1130 A93-51329

- Hodograph analysis in aircraft trajectory optimization [AIAA PAPER 93-3742] p 1101 A93-51338

- The Generalized Legendre-Clebsch Condition on state/control constrained arcs [AIAA PAPER 93-3746] p 1170 A93-51342

- Near-optimal, asymptotic tracking in control problems involving state-variable inequality constraints [AIAA PAPER 93-3748] p 1170 A93-51344

- Matched asymptotic expansion of the Hamilton-Jacobi-Bellman equation for aeroassisted plane-change maneuvers [AIAA PAPER 93-3752] p 1143 A93-51348

- Performance-seeking control - Program overview and future directions [AIAA PAPER 93-3765] p 1102 A93-51360

- Guidance law based on piecewise constant control for hypersonic gliders [AIAA PAPER 93-3888] p 1144 A93-51472

- Optimal performance of airplanes flying through windshear [AIAA PAPER 93-3846] p 1102 A93-51480

- Linear quadratic tracking problems in Hilbert space - Application to optimal active noise suppression p 1224 A93-52763

- Optimal control of the rocking and damping of swings p 1263 A93-54998

- Optimal output feedback vibration control of rotor-bearing systems p 86 N93-11220

- Subsonic flight test evaluation of a propulsion system parameter estimation process for the F100 engine [NASA-TM-4426] p 175 N93-13155

- A stochastic optimal feedforward and feedback control methodology for superagility [NASA-CR-4471] p 229 N93-13370

- Robust controller and estimator design using minimax methods p 229 N93-13925

- A contribution to the dynamic feedforward open loop control of multivariable systems and to the optimal design of command functions [DLR-FB-92-05] p 441 N93-16515

- Combining direct and indirect methods in optimal control: Range maximization of a hang glider [REPT-313] p 371 N93-16618

- Design of robust suboptimal controllers for a generalized quadratic criterion [AD-A257746] p 372 N93-17670

- Automatic pulse shaping with the AN/FPN-42 and AN/FPN-44A Loran-C transmitters [AD-A257860] p 319 N93-18309

- Strategies for optimal control design of normal acceleration command following on the F-16 [AD-A258975] p 373 N93-19095

- Guidance and flight control law development for hypersonic vehicles [NASA-CR-192102] p 526 N93-19960

- Optimal finite-thrust time-bounded direct-ascent interception p 734 N93-25272

- Optimal thrust magnitude on a singular arc in atmospheric flight p 758 N93-25410

- Control and optimization of aircraft trajectories p 729 N93-25543

- Artificial intelligence methodologies in flight related differential game, control and optimization problems [AD-A262405] p 848 N93-28498

- Integrated structural design, vibration control, and aeroelastic tailoring by multiobjective optimization p 1030 N93-31137

- Optimization

- Optimized/adapted finite elements for structural shape optimization p 77 A93-10971

- Optimization of time saving in navigation through an area of variable flow p 34 A93-12125

- A nomographic model for multicriterial optimization during the design of a flight vehicle powerplant p 95 A93-12821

- Optimization-based linear and nonlinear design methodologies for aircraft control. II - Final simulations [AIAA PAPER 92-4627] p 62 A93-13285

- Adaptive optimization of general aviation aircraft [AIAA PAPER 92-4195] p 44 A93-13372

- Aircraft concept optimization using the global sensitivity approach and parametric multiobjective figures of merit [AIAA PAPER 92-4221] p 45 A93-13381

- Multi-point design of transonic airfoils using optimization [AIAA PAPER 92-4225] p 16 A93-13382

- Optimality-based control laws for real-time aircraft control via parameter optimization p 180 A93-14161

- Aircraft optimization by a system approach - Achievements and trends p 153 A93-14205

- Engineering optimization of aeronautical structures p 154 A93-14227

- Structural optimization in preliminary aircraft design - A finite-element approach p 226 A93-14340

- A method for optimizing the meridional passage of the rotor in centrifugal compressors p 119 A93-14344
- Interactive hypersonic waverider design and optimization p 119 A93-14348
- Optimal lateral maneuvering for microburst encounters during final approach p 183 A93-14350
- A method for optimizing the meridional passage in a centrifugal compressor p 204 A93-14483
- Improving anti-fatigue optimum design through AI-search strategy p 208 A93-15342
- Fewest-fault integral optimization algorithm for engine fault diagnosis p 173 A93-15343
- Structural optimization of a cantilevered rotating beam p 210 A93-16248
- Optimization of a multistage axial compressor stochastic approach [ASME PAPER 92-GT-163] p 351 A93-19389
- Optimum design of rotor-bearing systems with eigenvalue constraints [ASME PAPER 92-GT-307] p 405 A93-19497
- A compact, intercooled and regenerated gas turbine for HALE applications [ASME PAPER 92-GT-401] p 355 A93-19550
- Optimization aspects of an ejector type hypersonic thrust nozzle [ASME PAPER 92-GT-402] p 355 A93-19551
- Optimization of a multistage axial compressor in a gas turbine engine system [ASME PAPER 92-GT-424] p 357 A93-19572
- Constrained optimization of three-dimensional hypersonic vehicle configurations [AIAA PAPER 93-0039] p 260 A93-20152
- An efficient approach to optimal aerodynamic design. I - Analytic geometry and aerodynamic sensitivities [AIAA PAPER 93-0099] p 264 A93-20204
- An efficient approach to optimal aerodynamic design. II - Implementation and evaluation [AIAA PAPER 93-0100] p 264 A93-20205
- Development of the quasi-procedural method for use in aircraft configuration optimization [AIAA PAPER 92-4693] p 322 A93-20278
- Aeroelastic optimization of a composite helicopter rotor [AIAA PAPER 92-4780] p 323 A93-20287
- Optimization of anisotropic structures considering strength, stiffness and aeroelastic constraints [AIAA PAPER 92-4796] p 408 A93-20291
- Structural optimization with frequency constraints - A review [AIAA PAPER 92-4813] p 408 A93-20293
- Aerodynamic performance optimization of a rotor blade using a neural network as the analysis [AIAA PAPER 92-4837] p 324 A93-20295
- AIAA/USAF/NASA/OAI Symposium on Multidisciplinary Analysis and Optimization, 4th, Cleveland, OH, Sept. 21-23, 1992, Technical Papers. Pts. 1 & 2 p 435 A93-20301
- A multi-point optimization for transonic airfoil design [AIAA PAPER 92-4681] p 264 A93-20303
- Improving the efficiency of aerodynamic shape optimization procedures [AIAA PAPER 92-4697] p 264 A93-20309
- Aerodynamic shape optimization via sensitivity analysis on decomposed computational domains [AIAA PAPER 92-4698] p 265 A93-20310
- Multidisciplinary propulsion simulation using NPSS [AIAA PAPER 92-4709] p 435 A93-20318
- Preliminary wing design of a high speed civil transport aircraft by multilevel decomposition techniques [AIAA PAPER 92-4721] p 325 A93-20323
- Structural Tailoring/Analysis for Hypersonic Components - A computational simulation [AIAA PAPER 92-4722] p 325 A93-20324
- Survey - Applications of structural optimization methods to fixed wing aircraft and spacecraft [AIAA PAPER 92-4726] p 325 A93-20328
- Aeroelastic model design using structural optimization [AIAA PAPER 92-4730] p 409 A93-20329
- On alternative problem formulations for multidisciplinary design optimization [AIAA PAPER 92-4752] p 436 A93-20350
- Observations on computational methodologies for use in large-scale, gradient-based, multidisciplinary design [AIAA PAPER 92-4753] p 436 A93-20351
- Structural optimization using Newton Modified Barrier Method [AIAA PAPER 92-4756] p 409 A93-20352
- Structural optimization for joined-wing synthesis [AIAA PAPER 92-4761] p 325 A93-20356
- Recent advances in integrated multidisciplinary optimization of rotorcraft [AIAA PAPER 92-4777] p 325 A93-20369
- Development of a structural optimization capability for the aeroelastic tailoring of composite rotor blades with straight and swept tips [AIAA PAPER 92-4779] p 326 A93-20370
- An approach to tiltrotor wing aeroservoelastic optimization through increased productivity [AIAA PAPER 92-4781] p 326 A93-20371
- Flutter optimization of large transport aircraft [AIAA PAPER 92-4795] p 326 A93-20381
- Examples of dynamic response optimization using MSC/NASTRAN [AIAA PAPER 92-4814] p 436 A93-20394
- Design vector parallelization to speedup the structural optimization process [AIAA PAPER 92-4834] p 436 A93-20411
- Analytical formulation of optimum rotor interdisciplinary design with a three-dimensional wake [AIAA PAPER 92-4778] p 265 A93-20416
- Issues in large-scale optimization with expensive functions p 437 A93-20708
- Massively parallel aerodynamic shape optimization p 266 A93-20729
- A method of finite element dynamic model optimization p 367 A93-20812
- Grid and design variables sensitivity analyses for NACA four-digit wing-sections [AIAA PAPER 93-0195] p 276 A93-22616
- The design of optimized airfoils in subcritical flow [AIAA PAPER 93-0532] p 285 A93-23273
- Design of exhaust nozzles using GA optimized neural networks [AIAA PAPER 93-0410] p 361 A93-23331
- Exact-gradient shape optimization of a 2-D Euler flow p 462 A93-24308
- Airfoil design using the Navier-Stokes equations [AIAA PAPER 93-0648] p 464 A93-24763
- Regional fanjet aircraft optimization studies p 508 A93-28602
- Sensitivity-based scaling for approximating structural response p 548 A93-28618
- Airfoil shape optimization using sensitivity analysis on viscous flow equations p 682 A93-33755
- An inverse method for computation of structural stiffness distributions of aeroelastically optimized wings [AIAA PAPER 93-1540] p 741 A93-34077
- Optimization of composite engine structures for mechanical and thermal loads [AIAA PAPER 93-1583] p 719 A93-34115
- A new sensitivity analysis for structural optimization of composite rotor blades [AIAA PAPER 93-1644] p 742 A93-34169
- Mathematical statement of the problem of optimizing the design of an airframe for ease of manufacture p 745 A93-35286
- Modeling and optimization of aircraft assembly --- Russian book [ISBN 5-217-00808-3] p 677 A93-35677
- On design and optimization of curved composite beams p 826 A93-35953
- Optimum design of high speed prop-rotors using a multidisciplinary approach p 798 A93-35985
- Rotor blade airfoil design by numerical optimization and unsteady calculations [ONERA, TP NO. 1992-65] p 766 A93-35993
- Stress-strain analysis and optimal design of aircraft structures p 827 A93-36782
- Methodology for studying the fracture of aircraft structures in static tests p 801 A93-36785
- Optimization of the stiffness and mass characteristics of lifting surface structures modeled by an elastic beam p 827 A93-36789
- A method for the optimum design of a large-aspect-ratio wing p 828 A93-36793
- Optimal design of honeycomb sandwich shell aircraft structures of composite materials p 828 A93-36800
- Optimal takeoff procedures for a transport category tiltrotor p 802 A93-37377
- Integrated structure/control/aerodynamic synthesis of actively controlled composite wings p 818 A93-37392
- Optimal cruise performance p 802 A93-37394
- A numerical procedure for aerodynamic optimization of helicopter rotor blades [ONERA, TP NO. 1992-121] p 771 A93-38595
- Optimal design of centered squeeze film dampers p 831 A93-38629
- Expert evaluation of the technological level of aviation gas turbine engine designs p 811 A93-39187
- Optimisation of constant altitude-constant airspeed flight for piston-prop aircraft p 889 A93-40473
- A software for optimum design of an aircraft structure p 938 A93-40495
- Evolution of European air space toward precision navigation (P/RNAV) p 882 A93-43369
- Aerodynamic shape optimization using preconditioned conjugate gradient methods [AIAA PAPER 93-3322] p 952 A93-45016
- Calculation of optimum airfoils using direct solutions of the Navier-Stokes equations [AIAA PAPER 93-3323] p 952 A93-45017
- Preconditioned domain decomposition scheme for three-dimensional aerodynamic sensitivity analysis p 957 A93-45096
- Recent improvements on the Dynamic Flight Simulator p 1011 A93-45167
- Optimization using fuzzy set theory p 1037 A93-45431
- Applications to fixed-wing aircraft and spacecraft p 996 A93-45432
- A strategy for the optimal design of nozzle contours [AIAA PAPER 93-2720] p 962 A93-46476
- An optimal detection algorithm for harmonic interference signals in Loran-C p 993 A93-46889
- Optimization of an aeroelastic system using the dynamic stability condition p 1029 A93-47085
- Grid and aerodynamic sensitivity analyses of airplane components [AIAA PAPER 93-3475] p 981 A93-47254
- Design optimization study for F-15 propulsion/forward fairing compatibility [AIAA PAPER 93-3484] p 1003 A93-47291
- Shape optimization for aerodynamic efficiency and low observability [AIAA PAPER 93-3115] p 1062 A93-48285
- Hypersonic configuration optimization with an Euler/boundary layer coupling technique [AIAA PAPER 93-3116] p 1062 A93-48286
- An optimization method for statistical ascertainment of the most probable peak temperature at combustor exit p 1108 A93-49195
- Flow analysis and design optimization methods for nozzle-afterbody of a hypersonic vehicle p 1073 A93-49531
- Methodology for commercial engine/aircraft optimization [AIAA PAPER 93-1807] p 1166 A93-49696
- Dual Engine application of the Performance Seeking Control algorithm [AIAA PAPER 93-1822] p 1110 A93-49709
- Vane optimization for maximum efficiency using design of experiments [AIAA PAPER 93-1867] p 1111 A93-49742
- Optimization of blade arrangement in a randomly mistuned cascade using simulated annealing [AIAA PAPER 93-2254] p 1115 A93-50052
- Computer aided design of turbo-machinery components p 1166 A93-50489
- WNN 92: Proceedings of the 3rd Workshop on Neural Networks: Academic/Industrial/NASA/Defense, Auburn Univ., AL, Feb. 10-12, 1992 and South Shore Harbour, TX, Nov. 4-6, 1992 p 1167 A93-50726
- Computation of maximized gust loads for nonlinear aircraft using matched-filter-based schemes p 1136 A93-52452
- Finite state aeroelastic model for use in rotor design optimization p 1104 A93-52454
- Alternative solution to optimum gliding velocity in a steady head wind or tail wind p 1136 A93-52458
- Optimization of afterbodies and engine nozzle by using CFD methods [ISABE 93-7098] p 1187 A93-54074
- Optimization of sandwich structures with respect to local instabilities with MBB-LAGRANGE p 1255 A93-54540
- Optimization of large scale systems in elasticity p 1255 A93-54544
- A diesel powerplant development program for airships [AIAA PAPER 93-4038] p 1246 A93-54609
- Optimization of oleo-pneumatic shock absorber of aircraft p 1243 A93-55415
- Recent advances in multidisciplinary optimization of rotorcraft [NASA-TM-107665] p 47 A93-10968
- Innovation in engineering [PNR-90889] p 59 A93-11207
- The role of under-determined approximations in engineering and science application p 441 A93-16763
- Multidisciplinary design optimization using response surface analysis p 330 A93-16796
- Design optimization of natural laminar flow bodies in compressible flow [NASA-CR-4478] p 292 A93-16940
- Mathematical optimization: A powerful tool for aircraft design [MBB-FE-2-S-PUB-478] p 331 A93-17564
- Practical architecture of design optimisation software for aircraft structures taking the MBB-LAGRANGE code as an example [MBB-FE-251-S-PUB-479] p 331 A93-17565
- Turbomachinery and potential computations [DS-2026] p 363 A93-17740
- Aerodynamic design and analysis of fans using 3D computational codes [DS-2140] p 294 A93-17880

- CFD-based approximation concepts for aerodynamic design optimization with application to a 2-D scramjet vehicle
[AD-A258084] p 333 N93-17893
- Optimum Design of High Speed Prop-Rotors
[NASA-CR-190915] p 336 N93-18064
- Design of high speed propellers using multiobjective optimization techniques p 336 N93-18065
- Optimum design of high speed prop rotors including the coupling of performance, aeroelastic stability and structures p 337 N93-18066
- MSC/NASTRAN structure optimization test module version 67 (preliminary) p 554 N93-20907
- Optimization and sensitivity computations for the conception of internal ventilation system in the aircraft engine [ETN-93-93375] p 521 N93-20913
- Grid sensitivity for aerodynamic optimization and flow analysis [NASA-CR-192980] p 694 N93-25117
- Integrated aerodynamic-structural wing design optimization p 714 N93-25279
- A preliminary sizing method for unmanned aircraft using multi-variate optimization p 714 N93-25408
- A computational aerodynamic design optimization method using sensitivity analysis p 716 N93-25552
- Techniques for designing rotorcraft control systems [NASA-CR-192960] p 729 N93-26046
- Sensitivity calculations for a 2D, inviscid, supersonic forebody problem [NASA-CR-191444] p 779 N93-27004
- Multidisciplinary design optimization: An emerging new engineering discipline [NASA-TM-107761] p 806 N93-27258
- Optimal design and imperfection sensitivity of nonlinear shell structures [FFA-TN-1992-30] p 1030 N93-31123
- Integrated structural design, vibration control, and aeroelastic tailoring by multiobjective optimization p 1030 N93-31137
- Review of aerodynamic design in the Netherlands [NLR-TP-91260-U] p 999 N93-31840
- ### OPTOELECTRONIC DEVICES
- Passive range sensor refinement using texture and segmentation p 544 A93-27044
- Integrated optoelectronics for communication and processing; Proceedings of the Meeting, Boston, MA, Sept. 3, 4, 1991 [SPIE-1582] p 1158 A93-51250
- Discrete range clustering using Monte Carlo methods [NASA-TM-104004] p 706 N93-24914
- ### ORBIT CALCULATION
- Computation of optimal low- and medium-thrust orbit transfers [AIAA PAPER 93-3855] p 1144 A93-51442
- The effect of clock, media, and station location errors on Doppler measurement accuracy p 885 N93-29588
- ### ORBITAL MANEUVERS
- Optimal impulsive interorbital transfers with aerodynamic maneuvers p 1141 A93-48838
- Matched asymptotic expansion of the Hamilton-Jacobi-Bellman equation for aeroassisted plane-change maneuvers [AIAA PAPER 93-3752] p 1143 A93-51348
- Analysis of a turning point problem in flight trajectory optimization p 1210 A93-52885
- ### ORBITAL RENDEZVOUS
- Reference equations of motion for automatic rendezvous and capture [NASA-CR-185676] p 914 N93-29652
- ### ORGANIC LIQUIDS
- Effect of aqueous solutions of water-crystallization inhibiting fluids on Thiokol-based sealants p 1017 A93-45689
- ### ORIFICE FLOW
- Effects of injector geometry on scramjet combustor performance p 359 A93-21670
- An analytical study of dilution jet mixing in a cylindrical duct [AIAA PAPER 93-2043] p 1113 A93-49876
- An analytical study of dilution jet mixing in a cylindrical duct [NASA-TM-106181] p 814 N93-27160
- ### ORTHOGONAL FUNCTIONS
- On orthogonal search method of flutter analysis p 208 A93-15402
- Nonlinear aerodynamic modeling using multivariate orthogonal functions [AIAA PAPER 93-3636] p 1065 A93-48321
- ### ORTHOTROPIC PLATES
- Propagation of transverse anti-plane waves in orthotropic layers p 412 A93-21878
- Hypersonic flutter of a curved shallow panel with aerodynamic heating [AIAA PAPER 93-1318] p 829 A93-37428
- Nonlinear flutter of orthotropic composite panel under aerodynamic heating p 1025 A93-45740
- ### OSCILLATING CYLINDERS
- A finite element study of incompressible flows past oscillating cylinders and aerofoils p 241 A93-17750
- Stabilized space-time finite element formulations for unsteady incompressible flows involving fluid-body interactions p 843 N93-29040
- ### OSCILLATING FLOW
- Self-excited oscillations at supersonic off-design jet outflow p 6 A93-10402
- Numerical analysis of two-dimensional turbulent flows through an oscillating cascade p 126 A93-15494
- Oscillation of circular shock waves with upstream nonuniformity p 208 A93-15496
- Periodic Euler and Navier-Stokes solutions about oscillating airfoils p 241 A93-17799
- A unified model for rotating stall and surge p 259 A93-20119
- Transonic shock oscillations calculated with a new interactive boundary layer coupling method [AIAA PAPER 93-0777] p 269 A93-21119
- Single passage Euler analysis of oscillating cascade unsteady aerodynamics for arbitrary interblade phase angle [AIAA PAPER 93-0389] p 282 A93-23067
- Shock oscillation in two-dimensional, inviscid, unsteady channel flow p 288 A93-23563
- The effect of Reynold's number on a natural low frequency flow oscillation over an airfoil near stall [AIAA PAPER 92-4040] p 463 A93-24489
- The effect of shock motion on entropy production [AIAA PAPER 93-0665] p 465 A93-24777
- Oscillatory blowing, a tool to delay boundary layer separation [AIAA PAPER 93-0440] p 474 A93-25529
- Fluid flows around cascades p 479 A93-28518
- Modeling of flow in a pulsed shock tunnel p 777 A93-39152
- Flip-flop jet nozzle extended to supersonic flows p 778 A93-39409
- Low-frequency flow oscillation over airfoils near stall p 861 A93-41931
- Oscillations of circular shock waves with upstream disturbance p 1023 A93-45463
- The countercurrent mixing layer - Strategies for shear-layer control [AIAA PAPER 93-3260] p 968 A93-45826
- Normal shock wave oscillations in supersonic diffusers p 1044 A93-48042
- Intense studies on unsteady secondary separations and oscillating shock waves in three-dimensional shock waves/turbulent boundary layer interaction regions induced by sharp and blunt fins [AIAA PAPER 93-2939] p 1046 A93-48137
- Active control of asymmetric conical flow using spinning and rotatory oscillations [AIAA PAPER 93-2958] p 1048 A93-48152
- A simplified approach for control of rotating stall. I - Theoretical development [AIAA PAPER 93-2229] p 1080 A93-50035
- Laminarization of the boundary layer on a vibrating wing p 1089 A93-51776
- Self-excitation of intense oscillations in flow inside a wind tunnel with an open test section p 1091 A93-51883
- Production of oscillatory flow in wind tunnels p 1218 A93-53812
- Study of a pulse ramjet based on twin valveless combustors coupled to operate in antiphase [ISABE 93-7038] p 1197 A93-54014
- Oscillatory blowing - A tool to delay boundary-layer separation p 1235 A93-55362
- Forced unsteady separated flows on a 45 degree delta wing p 82 N93-10305
- ### OSCILLATIONS
- Oscillations of circular shock waves with upstream disturbance p 1023 A93-45463
- Experiments on low aspect ratio hydroplanes to measure lift under static and dynamic conditions [ARE-TM(UHR)-90306] p 21 N93-11365
- Lift coefficient of a randomly oscillating hydroplane [DRA/MAR-TM(MTH)-91320] p 21 N93-11377
- A laboratory investigation of raindrop oscillations p 224 A93-13790
- Aircraft landing gear shimmy p 340 N93-19029
- JPRS report: Science and technology. Central Eurasia: Engineering and equipment [JPRS-UEQ-92-003] p 749 N93-25427
- The natural excitation technique (NEXt) for modal parameter extraction from operating wind turbines [DE93-010611] p 845 N93-28603
- Chaos in mechanical systems with special reference to rotorcraft and missiles [AD-A263703] p 943 N93-28384
- ### OSCILLATORS
- On the dynamics of aeroelastic oscillators with one degree of freedom [REPT-92-96] p 1040 N93-31653
- ### OUTLET FLOW
- The optimum value of the nozzle outlet angle of turbine stages [ASME PAPER 92-GT-224] p 404 A93-19442
- The effects of end-bend regulations of compressor blade on the outlet flow field [ISABE 93-7033] p 1185 A93-54009
- Transonic discharge flows around diffuser vanes from a centrifugal impeller [ISABE 93-7053] p 1185 A93-54029
- Correlations for flow property variation at outlet of a centrifugal impeller [ISABE 93-7054] p 1185 A93-54030
- ### OXIDATION
- Application of a sulphur-doped alkane system to the study of thermal oxidation of jet fuels [ASME PAPER 92-GT-122] p 387 A93-19356
- Static tests of jet fuel thermal and oxidative stability p 389 A93-21651
- Analysis of jet fuel thermal oxidation deposits by spectral fluorometric technique p 1253 A93-55697
- Mechanisms and modelling of environment-dependent fatigue crack growth in a nickel based superalloy [AD-A253967] p 71 N93-10717
- Current research in oxidation-resistant carbon-carbon composites at NASA. Langley Research Center p 74 N93-12456
- Thermal control/oxidation resistant coatings for titanium-based alloys p 74 N93-12457
- ### OXIDATION RESISTANCE
- Ceramic coatings enhance material performance p 71 A93-13648
- Niobium alloy heat pipes for use in oxidizing environments p 200 A93-13791
- Isothermal oxidation behavior of alpha-2 titanium aluminide alloys p 535 A93-29563
- Oxidation-resistant high-temperature materials p 915 A93-40362
- Small particle impact damage in carbon-carbon composites [PNR-90948] p 73 N93-11107
- Current research in oxidation-resistant carbon-carbon composites at NASA. Langley Research Center p 74 N93-12456
- Thermal control/oxidation resistant coatings for titanium-based alloys p 74 N93-12457
- Selection criteria for metallic high temperature structural materials in hypersonic flying equipment [MBB-LME-221-HYPAC-PUB-2-A] p 515 N93-21479
- Ultrahigh temperature assessment study: Ceramic matrix composites [AD-A262740] p 826 A93-28592
- Platinum-modified diffusion aluminide coatings on nickel-base superalloys [AD-A263597] p 917 N93-29981
- ### OXIDES
- Research support for the Laboratory for Lightwave Technology [AD-A261488] p 760 N93-26343
- ### OXYGEN
- Langley 8-foot high-temperature tunnel oxygen measurement system p 1010 A93-44892
- Effect of the formation of excited oxygen molecules on the kinetics of exchange reactions and the heat flux during braking in the upper layers of the atmosphere p 1070 A93-48975
- Rotational CARS measurements in a rotating cavity with axial throughflow of cooling air: Oxygen concentration measurements [PNR-90935] p 72 N93-11035
- In-situ bioventing: Two US EPA and Air Force sponsored field studies [PB93-194231] p 1035 N93-32089
- ### OXYGEN ANALYZERS
- Langley 8-foot high-temperature tunnel oxygen measurement system p 1010 A93-44892
- ### OXYGEN SPECTRA
- Remote sensing of O₂ in a supersonic combustor using diode lasers and fiber optics [AIAA PAPER 92-5090] p 414 A93-22360
- ### OZONE
- European environmental studies focus on impact of engine emissions p 92 A93-10730
- Turbine engine developers explore ways to lower NO(x) emission levels p 52 A93-10732
- Kinetic scheme selection in describing detonation in an H₂-air mixture behind shock waves p 1253 A93-55032
- Predicted aircraft effects on stratospheric ozone p 93 N93-11096

- Impact of supersonic and subsonic aircraft on ozone: Including heterogeneous chemical reaction mechanisms [DE92-019619] p 224 N93-13655
- Making clean gasoline: The effect on jet fuels [AD-A264302] p 1019 N93-32085
- OZONE DEPLETION**
- Potential impact of combined NO(x) and SO(x) emissions from future High Speed Civil Transport aircraft on stratospheric aerosols and ozone p 753 A93-35372
- Implications of three-dimensional tracer studies for two-dimensional assessments of the impact of supersonic aircraft on stratospheric ozone p 936 A93-41269
- Engine technology challenges for a 21st Century High-Speed Civil Transport [ISABE 93-7064] p 1200 A93-54040
- Stratospheric aircraft: Impact on the stratosphere? [DE92-016997] p 94 N93-12104
- Aerospace-plane flights and stratospheric ozone: Review and preliminary assessment of the National Aerospace Plane (NASP) operations [RAND/N-3464-AF] p 755 N93-26327
- Engine technology challenges for a 21st Century High-Speed Civil Transport [NASA-TM-106216] p 1004 N93-31671
- OZONOSPHERE**
- Impact of supersonic and subsonic aircraft on ozone: Including heterogeneous chemical reaction mechanisms [DE92-019619] p 224 N93-13655

P

- P-3 AIRCRAFT**
- Structural fatigue aspects of the P-3 Orion [ARL-STRUC-TM-558] p 161 N93-13256
- Analysis of in-flight structural failures of P-3C wing leading edge segments [AD-A256212] p 165 N93-15238
- Uplink laser propagation measurements through the sea surface, haze and clouds [AD-A264687] p 935 N93-30553
- P-51 AIRCRAFT**
- Innovative bagging techniques on a composite P-51 Mustang replica p 1191 A93-53405
- PAINTS**
- Water instead of chemical corrosives against aircraft paint - Environment-friendly paint-stripping methods could mean drastic cost reductions for the aircraft industry p 239 A93-21850
- Data analysis techniques for pressure- and temperature-sensitive paint [AIAA PAPER 93-0176] p 414 A93-22605
- Aerodynamic applications of pressure sensitive paint p 549 A93-29301
- Ultra-high pressure water jet technology - An overview of a new process for aerospace paint stripping [SME PAPER AD92-196] p 855 A93-40661
- Robotic aircraft painting with SAFARI [SME PAPER AD92-198] p 855 A93-40662
- Sensor-adaptive control for aircraft paint stripping [SME PAPER AD92-200] p 855 A93-40663
- Automated Laser Paint Stripping (ALPS) [SME PAPER AD92-206] p 855 A93-40667
- Uncertainty estimates for pressure sensitive paint measurements p 1258 A93-55369
- F-14 wing lug coating investigation [AD-A257384] p 328 N93-15858
- PANEL FLUTTER**
- Instability of the periodic deflection of a panel surface in a turbulent boundary layer p 208 A93-15188
- Geometrically nonlinear local flutter analysis of supersonic airplane skin plates in the potential supersonic flow [ISBN 83-01-10939-4] p 394 A93-17569
- Finite element nonlinear panel flutter with arbitrary temperatures in supersonic flow p 417 A93-23555
- A unified hypersonic/supersonic method for aeroelastic applications including shock-unsteady wave interaction [AIAA PAPER 93-1317] p 738 A93-33892
- Large-amplitude finite element flutter analysis of composite panels in hypersonic flow p 837 A93-39417
- Effect of temperature on nonlinear two-dimensional panel flutter using finite elements p 1022 A93-45133
- Nonlinear flutter of orthotropic composite panel under aerodynamic heating p 1025 A93-45740
- Vector unsymmetric eigenequation solver for nonlinear flutter analysis on high-performance computers p 1160 A93-52449
- A finite element method for nonlinear panel flutter p 84 N93-10472
- Control of panel flutter at high supersonic speed p 47 N93-10900
- Hypersonic panel flutter in a rarefied atmosphere p 188 N93-13928

- Hypersonic panel flutter in a rarefied atmosphere [NASA-CR-4514] p 780 N93-27084
- PANEL METHOD (FLUID DYNAMICS)**
- A study of the possibility of the parallel execution of a program for calculating the aerodynamic characteristics of flight vehicles using an improved panel method p 95 A93-10045
- Wing pressure loads in canard configurations - A comparison between numerical results and experimental data p 7 A93-11499
- Design of manoeuvrable simple and complex planform transonic wings with attained thrust-, panel- and Euler-methods p 117 A93-14301
- Boundary-layer induced noise in aircraft p 444 A93-19137
- Comparison of PMARC and analytic results for two-dimensional unsteady airfoils [AIAA PAPER 93-0636] p 463 A93-24752
- Unsteady panel method for flows with multiple bodies moving along various paths [AIAA PAPER 93-0640] p 539 A93-24755
- Aerodynamic analyses for design and education [AIAA PAPER 92-2664] p 473 A93-24988
- S-plane aerodynamics of nonplanar lifting surfaces p 958 A93-45134
- Time domain panel method for wings p 958 A93-45135
- CFD analysis of the X-29 inlet at high angle of attack p 958 A93-45140
- On the legitimacy and accuracy of downwash computations by panel methods on 3D wings p 970 A93-46885
- Computation of wake roll-up for complete aircraft configurations [AIAA PAPER 93-3509] p 984 A93-47275
- The use of triangular elements in panel methods for calculating flow past flight vehicles p 1068 A93-48904
- Induced drag of a crescent wing planform p 1094 A93-52430
- Second generation low order panel method and its application for a case of nacelle p 1231 A93-54595
- Flow computation for the hypersonic configuration ELAC I at low speeds and large incidence p 1238 A93-56036
- A field panel method for transonic flows p 18 N93-10547
- Numerical investigations into the base drag of various wedges using the base flow model developed by Mauri Tanner [REPT-B-36] p 26 N93-12414
- Aerodynamic analysis of slipstream/wing/nacelle interference for preliminary design of aircraft configurations p 130 N93-13205
- Application of subsonic first-order panel methods for prediction of inlet and nozzle aerodynamic interactions with airframe p 130 N93-13223
- Analysis and design of planar and non-planar wings for induced drag minimization [NASA-CR-191274] p 131 N93-13463
- Development of a computer assisted toolbox for aerodynamic design of aircraft at subcritical conditions with application to three-surface and canard aircraft [ISBN-90-6275-768-5] p 441 N93-16567
- Practical architecture of design optimisation software for aircraft structures taking the MBB-LAGRANGE code as an example [MBB-FE-251-S-PUB-479] p 331 N93-17565
- The influence of the rotor test facilities ROTEST and ROTOS on the rotor inflow [DLR-MITT-91-16] p 522 N93-21173
- Further development of the CANAERO computer code to include a time-stepping capability [DREA-CR-91-478] p 562 N93-21820
- TDL: A Transonic Doublet Lattice Method for 3D potential unsteady transonic flow calculation [DLR-FB-92-25] p 988 N93-31171
- Panel methods for aerodynamic analysis and design [NLR-TP-91404-U] p 990 N93-32357
- PANELS**
- A new production technology for complex-shaped structural elements 'creep forming' p 202 A93-14175
- Nonlinear vibration and radiation from a panel with transition to chaos p 205 A93-14543
- Dynamics of skin-stringer panels using modified wave methods p 206 A93-14561
- Nonlinear aeroelastic response of panels [AIAA PAPER 93-1599] p 741 A93-34130
- Stress-strain state of the elements of a single-stringer riveted panel p 746 A93-35288
- Evaluation of thermoplastic stiffened panels for application to rotorcraft airframes p 827 A93-36000
- Transonic panel flutter [AIAA PAPER 93-1476] p 829 A93-37438
- Noise transmission of skin-stringer panels using a decaying wave method p 943 A93-41929

- Supersonic panel flutter analysis of shallow shells p 927 A93-41935
- An experimental system for studying the vibrations and acoustic emission of cylindrical shells and panels in a field of turbulent pressure pulsations p 1140 A93-51754
- Effect of boundary conditions and panel geometry on the response of laminated panels subjected to transverse pressure loads p 1259 A93-55674
- Interlaminar stress analysis at the skin/stiffener interface of a grid-stiffened composite panel [NASA-CR-192177] p 393 N93-17920
- Liquid crystal displays replacing the CRT and CLE of future cockpits p 518 N93-19783
- A computational approach to predicting the extent of arc root damage in CFC panels p 735 N93-24890
- Multi-parameter optimization tool for low-cost commercial fuselage crown designs p 922 N93-30858
- Optimization of composite sandwich cover panels subjected to compressive loadings p 922 N93-30862
- Advanced fiber placement of composite fuselage structures p 923 N93-30864
- PARABOLIC BODIES**
- Newtonian and hypersonic flows over oscillating bodies of revolution. II - Parabolic bodies p 872 A93-42931
- PARABOLIC DIFFERENTIAL EQUATIONS**
- A performance comparison of massively parallel Parabolized Navier-Stokes solutions [AIAA PAPER 93-0059] p 435 A93-20172
- Transition studies for swept wing flows using PSE --- parabolized stability equations [AIAA PAPER 93-0077] p 263 A93-20189
- Computation of supersonic crossflow separation using a new parabolized Navier-Stokes code p 687 A93-34355
- PNS predictions of axisymmetric hypersonic blunt-body and afterbody flowfields [AIAA PAPER 93-2725] p 962 A93-46479
- Application of a parabolized Navier-Stokes code to an HSCT configuration and comparison to wind tunnel test data [AIAA PAPER 93-3537] p 986 A93-47288
- Application of parabolized Navier-Stokes technique for high-L/D, hypersonic vehicle design [AIAA PAPER 93-2948] p 1047 A93-48144
- Comparison of ENO and TVD schemes for the parabolized Navier-Stokes equations [AIAA PAPER 93-2970] p 1049 A93-48164
- An economical difference factorization algorithm for the numerical calculation of the system of equations for a thin viscous shock layer p 1091 A93-51880
- Parabolized Navier-Stokes methods for hypersonic flows p 421 N93-18565
- PARABOLIC FLIGHT**
- Canadian low-gravity research using parabolic aircraft p 384 A93-21908
- Experimental investigation of the management of large-sized drops and the onset of Marangoni-convection p 926 A93-41700
- PARABOLIC REFLECTORS**
- Wind load design methods for ground-based heliostats and parabolic dish collectors [DE93-002737] p 433 N93-15839
- PARACHUTE DESCENT**
- Payload vehicle aerodynamic re-entry analysis p 69 A93-12004
- A simulator solution for the parachute canopy control and guidance training problem [SAE PAPER 920984] p 191 A93-14634
- Stable cross type parachute with inflation aid [AIAA PAPER 93-1201] p 702 A93-35152
- Radial reefing method for accelerated and controlled parachute opening [AIAA PAPER 93-1209] p 702 A93-35159
- Comparison of electrostatic and aerodynamic forces during parachute opening [AIAA PAPER 93-1210] p 689 A93-35160
- Experimental validation of a discrete vortex method for inviscid axisymmetric flow around parachute canopies [AIAA PAPER 93-1216] p 689 A93-35165
- Methods and results of theoretical investigations for high-speed parachute systems [AIAA PAPER 93-1227] p 690 A93-35173
- The development of a parachute system for aerial delivery from high speed cargo aircraft [AIAA PAPER 93-1232] p 703 A93-35174
- Computation of aeroelastic characteristics and stress-strained state of parachutes [AIAA PAPER 93-1237] p 744 A93-35178
- The stability and aerodynamic performances of clusters of small cruciform parachutes [AIAA PAPER 93-1242] p 690 A93-35181
- Influence of the canopy-payload coupling on the dynamic stability in pitch of a parachute system [AIAA PAPER 93-1248] p 690 A93-35185

- Parachute canopy control and guidance training requirements and methodology
[AIAA PAPER 93-1255] p 703 A93-35188
Effect of anomalous aerodynamic heating during the descent of a parachute along a trajectory
p 1069 A93-48924
The fluid physics of parachute inflation
p 1189 A93-54347
A simple, approximate model of parachute inflation
[DE93-002465] p 694 A93-25121
- PARACHUTE FABRICS**
Radial reefing method for accelerated and controlled parachute opening
[AIAA PAPER 93-1209] p 702 A93-35159
The fluid physics of parachute inflation
p 1189 A93-54347
Ribless ram air parachute
[AD-D015531] p 20 A93-11050
High efficiency, low weight and volume energy absorbent seam
[AD-D015531] p 554 A93-20765
- PARACHUTES**
Scientific ballooning payload termination loads
p 27 A93-11383
A simple, approximate model of parachute inflation
[AIAA PAPER 93-1206] p 702 A93-35157
The effect of extreme altitude on parachute filling distance
[AIAA PAPER 93-1207] p 702 A93-35158
Mil-Prime specification for parachutes
[AIAA PAPER 93-1247] p 677 A93-35184
Three-dimensional vortex method for parachutes
p 872 A93-42874
Ribless ram air parachute
[AD-D015531] p 20 A93-11050
The degradation of parachutes: Age and mechanical wear
[AD-A252243] p 24 A93-12179
High efficiency, low weight and volume energy absorbent seam
[AD-D015531] p 554 A93-20765
The development of a parachute system for aerial delivery from high speed cargo aircraft
[DE93-008339] p 790 A93-29035
A computational model that couples aerodynamic and structural dynamic behavior of parachutes during the opening process
[AD-A264115] p 877 A93-30119
- PARALLEL COMPUTERS**
Parallel computation of 3-D Navier-Stokes flowfields for supersonic vehicles
[AIAA PAPER 93-0064] p 261 A93-20177
Unsteady flow simulation on a parallel computer
p 1022 A93-45089
On the use of back propagation with feed-forward neural networks for the aerodynamic estimation problem
[AIAA PAPER 93-3638] p 1165 A93-48323
The 3D Navier-Stokes flow analysis for shared and distributed memory MIMD computers
[AD-A256038] p 221 A93-15187
Numerical Wind Tunnel: Requirements and the outline
p 383 A93-19288
The operating system for Numerical Wind Tunnel
p 383 A93-19290
The language processor system for the Numerical Wind Tunnel
p 383 A93-19291
- PARALLEL FLOW**
Performance characteristics of a variable-area vane nozzle for vectoring an ASTOVL exhaust jet up to 45 deg
[AIAA PAPER 93-2437] p 1118 A93-50189
Effect of the flow non-uniformity on the mixing layer at the interface of parallel supersonic flows
[ISAS-RN-646] p 128 A93-12716
On the disturbances development in the supersonic boundary layer
p 484 A93-20686
Performance characteristics of a variable-area vane nozzle for vectoring an ASTOVL exhaust jet up to 45 deg
[NASA-TM-106114] p 813 A93-27131
A parallel implicit incompressible flow solver using unstructured meshes
[AD-A263395] p 931 A93-29851
- PARALLEL PLATES**
Further studies on the asymmetrical flow past yawed cylinders
p 118 A93-14304
Consecutive plate acoustic suppressor apparatus and methods
[NASA-CASE-LEW-15430-1] p 453 A93-17051
- PARALLEL PROCESSING (COMPUTERS)**
A study of the possibility of the parallel execution of a program for calculating the aerodynamic characteristics of flight vehicles using an improved panel method
p 95 A93-10045
The new challenge of computational aerodynamics
p 112 A93-14169
- Parallel implementation of the feature associated mesh embedding method for the 2D-Euler equations (FAME2D)
p 225 A93-14278
Design vector parallelization to speedup the structural optimization process
[AIAA PAPER 92-4834] p 436 A93-20411
LEWICE droplet trajectory calculations on a parallel computer
[AIAA PAPER 93-0172] p 438 A93-22604
Parallel rotorcraft flight simulation
[AIAA PAPER 93-0623] p 524 A93-24740
An integrated flow simulation system on a parallel computer. I - Basic concept. II - The flow solver
p 688 A93-34370
CFD development and a future high speed computer
p 847 A93-38128
Research in unsteady aerodynamics and computational aeroelasticity at the NASA Langley Research Center
p 804 A93-39498
Solution of the Euler and Navier Stokes equations on parallel processors using a transposed/Thomas ADI Algorithm
[AIAA PAPER 93-3310] p 1036 A93-45006
Dynamic overset grid communication on distributed memory parallel processors
[AIAA PAPER 93-3311] p 1036 A93-45007
Simulation of flow past complex geometries using a parallel implicit incompressible flow solver
p 957 A93-45095
Visualization and view simulation based on transputers
p 1037 A93-45150
An advanced parallel rotorcraft flight simulation model - Stability characteristics and handling qualities
[AIAA PAPER 93-3618] p 1125 A93-48305
An advanced rotorcraft flight simulation model - Parallel implementation and performance analysis
[AIAA PAPER 93-3550] p 1222 A93-52654
SAPNEW: Parallel finite element code for thin shell structures on the Alliant FX/80
[NASA-CR-190663] p 84 A93-10372
The engine design engine. A clustered computer platform for the aerodynamic inverse design and analysis of a full engine
[NASA-TM-105838] p 21 A93-11223
Analysis of fault-tolerant neurocontrol architectures
[NASA-TM-105898] p 65 A93-12305
Turbomachinery CFD on parallel computers
[NASA-TM-105932] p 228 A93-13154
SAPNEW: Parallel finite element code for thin shell structures on the Alliant FX-80
[NASA-CR-189212] p 220 A93-14799
Identification and control of non-linear time-varying dynamical systems using artificial neural networks
[AD-A257595] p 372 A93-18193
The operating system for Numerical Wind Tunnel
p 383 A93-19290
The language processor system for the Numerical Wind Tunnel
p 383 A93-19291
A comparison using APPL and PVM for a parallel implementation of an unstructured grid generation program
[NASA-CR-191425] p 757 A93-25073
Implementation of a multidomain Navier-Stokes code on the Intel iPSC2 hypercube
[FFA-TN-1992-37] p 843 A93-28994
- PARALLEL PROGRAMMING**
Implementation of an explicit Navier-Stokes algorithm on a distributed memory parallel computer
[AIAA PAPER 93-0063] p 261 A93-20176
- PARAMETER IDENTIFICATION**
Nonlinear multi-point modelling and parameter estimation of the DO 28 research aircraft
p 41 A93-12727
An application of fuzzy logic and Dempster-Shafer theory to failure detection and identification
p 96 A93-13079
Nonlinear aerodynamic parameter estimation and model structure identification
[AIAA PAPER 92-4502] p 15 A93-13308
Parameter estimation techniques for flight flutter test analysis
p 156 A93-14324
Calculation of the parameters of a crane helicopter with one disabled engine
p 366 A93-18381
Icing effects on aircraft stability and control determined from flight data - Preliminary results
[AIAA PAPER 93-0398] p 370 A93-23073
Identification and conversion of foundation parameters for airport pavement
p 538 A93-24035
Comment on 'Equation decoupling - A new approach to the aerodynamic identification of unstable aircraft'
p 818 A93-37406
Real-time parameter identification applied to flight simulation
p 1006 A93-44142
Aileron and sideslip-induced unsteady aerodynamic modeling for lateral parameter estimation
p 1007 A93-45144
- Parameter estimates of an aeroelastic aircraft as affected by model simplifications
[AIAA PAPER 93-3640] p 1127 A93-48325
On engine parameter estimation with flight test data
p 1107 A93-48520
Identification of integrated airframe-propulsion effects on an F-15 aircraft for application to drag minimization
[AIAA PAPER 93-3764] p 1101 A93-51359
Identification of nonlinear mechanical systems using combined state and parameter evaluation
p 1224 A93-52732
A method for the spectral-time identification of the longitudinal and lateral motions of an aircraft
p 1205 A93-52942
Estimation of the parameters of the electrodynamic system engine-exhaust jet
p 1193 A93-52965
Flight testing: Past, present, and future
p 164 A93-14615
Icing effects on aircraft stability and control determined from flight data: Preliminary results
[NASA-TM-105977] p 188 A93-14831
Practical input optimization for aircraft parameter estimation experiments
[NASA-CR-191462] p 820 A93-27264
Parameter identification for nonlinear aerodynamic systems
[NASA-CR-193072] p 782 A93-27282
The basic measurement equipment of the DLR test aircraft
p 1000 A93-31273
- PARAMETERIZATION**
Parameter optimization for an H2 problem with multivariable gain and phase margin constraints
p 439 A93-22971
- PARAWINGS**
Application of parafoils to microwave landing system siting
[AIAA PAPER 93-1213] p 702 A93-35162
Apparent mass effects on parafoil dynamics
[AIAA PAPER 93-1236] p 690 A93-35177
Parafoil steady turn response to control input
[AIAA PAPER 93-1241] p 728 A93-35180
A study of the effect of the shape of a parasail on its lift-drag ratio
p 1069 A93-48913
- PARTIAL DIFFERENTIAL EQUATIONS**
Observations on computational methodologies for use in large-scale, gradient-based, multidisciplinary design
[AIAA PAPER 92-4753] p 436 A93-20351
Modeling of linear isentropic flow systems
p 828 A93-37046
Improved numerical simulation of Euler equations
p 83 A93-10309
- PARTIAL PRESSURE**
Partial admission and unsteady flow in radial turbines
p 81 A93-10059
Development of a method to determine the autooxidation of turbine fuels
[AD-A260578] p 736 A93-25902
- PARTICLE ACCELERATION**
Seed particle response and size characterization in high speed flows
p 459 A93-23811
- PARTICLE ACCELERATORS**
Explosive detection system based on Electronic Neutron Generator (ENG)
p 497 A93-21870
- PARTICLE CHARGING**
Comparison of the electrical charging and discharging environments of multiple aircraft-borne electric-field measurement systems
p 704 A93-24887
- PARTICLE IMAGE VELOCIMETRY**
Particle imaging techniques and applications
p 1020 A93-44195
Study of the near-wake structure of a subsonic base cavity flowfield using PIV
[AIAA PAPER 93-3040] p 1056 A93-48221
- PARTICLE IN CELL TECHNIQUE**
Comparison of continuum and particle simulations of expanding rarefied flows
[AIAA PAPER 93-0728] p 466 A93-24818
The hypersonic double ellipse in rarefied flow
p 869 A93-42631
- PARTICLE LADEN JETS**
An electrostatic probe for determining particle characteristics in disperse flow
p 76 A93-10178
Application of particle image velocimetry in high-speed separated flows
p 549 A93-29304
- PARTICLE MASS**
Ignition of boron particles coated by a thin titanium film
[AIAA PAPER 93-2201] p 1145 A93-50013
- PARTICLE MOTION**
Lift and drag forces on droplets and particles in wall-bounded shear flows
[DE93-002678] p 419 A93-17761
An investigation of laser velocimetry measurements within high speed, complex flows
p 748 A93-25237

PARTICLE SIZE DISTRIBUTION

- Seeding materials for use in laser anemometry
[AIAA PAPER 93-0006] p 389 A93-20129
- Seed particle response and size characterization in high speed flows p 459 A93-23811
- Particulates and aerosols characterized in real time for harsh environments using the UMR mobile aerosol sampling system (MASS)
[AIAA PAPER 93-2344] p 1156 A93-50118
- On the stability of the process of formation of combustion generated particles by coagulation and simultaneous shrinkage due to particle oxidation
[AIAA PAPER 93-2478] p 1146 A93-50220
- Experimental investigation of effect of particles on blade pressure distribution in impulse cascade flow p 1236 A93-55398

PARTICLE TRAJECTORIES

- Tracking of raindrops in flow over an airfoil
[AIAA PAPER 93-0168] p 275 A93-22602
- LEWICE droplet trajectory calculations on a parallel computer
[AIAA PAPER 93-0172] p 438 A93-22604
- Three-dimensional water droplet trajectory code validation using an ECS inlet geometry
[NASA-CR-191097] p 791 A93-27267

PARTICLES

- Liquid flow reactor and method of using
[AD-D015392] p 222 A93-15232
- Wind tunnel seeding particles for laser velocimeter p 292 A93-16770

PARTICULATE REINFORCED COMPOSITES

- Erosion characteristics of ceramic particulate and whisker reinforced aluminum composites
[ASME PAPER 92-GT-369] p 388 A93-19532

PARTICULATES

- Theoretical and experimental study of the behavior of particles passing through a shock wave
[ONERA, TP NO. 1992-233] p 774 A93-38777
- Particulates and aerosols characterized in real time for harsh environments using the UMR mobile aerosol sampling system (MASS)
[AIAA PAPER 93-2344] p 1156 A93-50118
- Particulate emissions from gas turbine engines
[AD-A261374] p 725 A93-26339

PARTITIONS (MATHEMATICS)

- Drag and drag partition on rough surfaces p 79 A93-12460
- Application of controller partitioning optimization procedure to integrated flight/propulsion control design for a STOLV aircraft
[AIAA PAPER 93-3766] p 1131 A93-51361

PASSENGER AIRCRAFT

- Handling the legal consequences of aviation disasters - Passenger compensation
[ISBN 3-452-22293-4] p 103 A93-11411
- Effect of flight conditions on the sound insulation of the aircraft passenger compartment p 42 A93-12978
- The methods of reducing impact loads on occupants in the civil aircraft crash condition p 140 A93-14220
- Integration of high bypass ratio engines on modern transonic wings for regional aircraft p 506 A93-27479
- Advanced Tupolev twinjet combines Russian and Western technologies p 802 A93-38565
- Tobacco smoking in aircraft - A fog of legal rhetoric? p 944 A93-40474
- Test results of the effects of air ionization on cigarette smoke particulate levels within a commercial airplane
[SAE PAPER 921183] p 855 A93-41362
- Determination of the natural vibrations of an acoustic medium in the cabin of a passenger aircraft by the finite element method p 1102 A93-51752
- Cabin accommodations for passengers with ambulatory disabilities - Transport category aircraft
[SAE ARP 4387] p 1103 A93-52166
- Estimation of the effect of the longitudinal moment due to the engine thrust on the mass of a subsonic passenger aircraft p 1191 A93-52954
- Russian survivor --- Tu-334 aircraft p 1243 A93-54867
- Rolls-Royce civil engine technology
[PNR-90936] p 56 A93-11036
- The Trent: Towards greater thrust
[PNR-90937] p 56 A93-11037
- Effects of seating configuration and number of type 3 exits on emergency aircraft evacuation
[AD-A256616] p 143 A93-14277
- The design of a long range megatransport aircraft
[NASA-CR-192077] p 332 A93-17711
- Design of the advanced regional aircraft, the DART-75
[NASA-CR-192044] p 333 A93-17972
- MM-122: High speed civil transport
[NASA-CR-192011] p 334 A93-17974
- Phoenix: Preliminary design of a high speed civil transport
[NASA-CR-192024] p 334 A93-17976

- Tesseract: Supersonic business transport
[NASA-CR-192072] p 334 A93-17977
- Eagle RTS: A design for a regional transport aircraft
[NASA-CR-192032] p 334 A93-18017
- A second-generation high speed civil transport: Stingray
[NASA-CR-192022] p 336 A93-18059
- The Trojan --- supersonic transport
[NASA-CR-192013] p 336 A93-18060
- Preliminary design of a high speed civil transport: The Opus 0-001
[NASA-CR-192018] p 336 A93-18061
- RTJ-303: Variable geometry, oblique wing supersonic aircraft
[NASA-CR-192054] p 337 A93-18166
- Longitudinal acceleration test of overhead luggage bins in a transport airframe section p 991 A93-31652
- Civil tiltrotor transport point design: Model 940A
[NASA-CR-191446] p 1019 A93-32234

PASSENGERS

- Spatial orientation and wayfinding in airport passenger terminals - Implications for environmental design p 487 A93-27168
- An investigation of ground access mode choice for departing passengers
[TT-9201] p 67 A93-11224
- A transportable luggage examination system based on neutron interrogation p 497 A93-21863

PASSIVE L-BAND RADIOMETERS

- PBMR observations of surface soil moisture in Monsoon 90 p 1162 A93-47676

PATHOLOGICAL EFFECTS

- Results of a low-altitude flight noise study in Germany - Acute extraneous effects p 1163 A93-49557
- Effects of commercial flight pollution on human health p 1035 A93-31931

PATTERN RECOGNITION

- A formalization and implementation of topological visual navigation in two dimensions p 435 A93-19101
- Visual augmentation for night flight over featureless terrain p 806 A93-35921
- Fast design of circular-harmonic filters using simulated annealing p 1038 A93-45556
- WNN 92: Proceedings of the 3rd Workshop on Neural Networks: Academic/Industrial/NASA/Defense, Auburn Univ., AL, Feb. 10-12, 1992 and South Shore Harbour, TX, Nov. 4-6, 1992 p 1167 A93-50726
- Automated extraction of aircraft runway patterns from radar imagery
[AD-A254258] p 68 A93-11751
- Advances in speech processing p 550 A93-19771
- Neural networks application to divergence-based passive ranging
[NASA-TM-103981] p 885 A93-29653
- Classification of radar clutter in an air traffic control environment p 886 A93-30299
- Efficient fault diagnosis of helicopter gearboxes
[NASA-TM-106253] p 1032 A93-31846

PAVEMENTS

- The state-of-the-art of nondestructive evaluation of military runways p 375 A93-19659
- Identification and conversion of foundation parameters for airport pavement p 538 A93-24035
- In situ material characterization for pavement evaluation by the Spectral-Analysis-of-Surface-Waves (SASW) method
[AD-A255660] p 194 A93-14128
- Reanalysis of multiple-wheel landing gear traffic tests
[AD-A256593] p 194 A93-14238
- Unified Airport Design and Analysis Concepts Workshop
[DOT/FAA/RD-92/17] p 378 A93-16309
- State of the art of airport pavement analysis and design p 378 A93-16310
- Development of user guidelines for a three-dimensional finite element pavement model p 379 A93-16311
- Micro mechanical behavior of pavements p 379 A93-16312
- Thermoviscoelastic analysis of pavements p 379 A93-16313
- FAA unified pavement analysis 3-D finite element method p 379 A93-16314
- Federal Aviation Administration pavement modeling p 379 A93-16315
- State of the art review of rutting and cracking in pavements p 380 A93-16316
- Development of a unified airport pavement analysis and design system p 380 A93-16317
- Unified airport pavement design procedure p 380 A93-16318
- Three-dimensional stress analysis of multilayered airport pavements: Integral transform approach p 381 A93-16319

- State-of-the-art survey of flexible pavement crack sealing procedures in the United States
[AD-A258050] p 382 A93-17708
- Mathematical model of frost heave and thaw settlement in pavements
[CRREL-REPT-93-2] p 912 A93-30103

PAYLOADS

- Influence of the canopy-payload coupling on the dynamic stability in pitch of a parachute system
[AIAA PAPER 93-1248] p 690 A93-35185
- National Aeronautics and Space Administration p 454 A93-17091

PEEK

- Compression after impact (CAI) properties of CF/PEEK (APC-2) and conventional CF/epoxy stiffened panels p 196 A93-14307
- Effects of thermal history and jet fuel absorption on the properties of APC-2 p 534 A93-25252
- Low velocity impact in a graphite/PEEK
[AIAA PAPER 93-1403] p 734 A93-33963
- Consolidation of graphite thermoplastic textile preforms for primary aircraft structure p 919 A93-30439
- Advanced fiber/matrix material systems p 921 A93-30854

PEELING

- Water instead of chemical corrosives against aircraft paint - Environment-friendly paint-stripping methods could mean drastic cost reductions for the aircraft industry p 239 A93-21850
- Ultra-high pressure water jet technology - An overview of a new process for aerospace paint stripping
[SME PAPER AD92-196] p 855 A93-40661
- Automated Laser Paint Stripping (ALPS)
[SME PAPER AD92-206] p 855 A93-40667

PELLETS

- Lockheed adopts media blast dry stripping for the C-130
[SAE PAPER 920949] p 107 A93-14092

PENDULUMS

- Estimation of aircraft inertia characteristics from bifilar pendulum test data p 1249 A93-56029
- JPRS report: Science and technology. Central Eurasia: Engineering and equipment
[JPRS-UEQ-92-003] p 749 A93-25427

PENETRANTS

- NDE of PWA 1480 single crystal turbine blade material
[NASA-TM-106140] p 815 A93-27640

PENETRATION

- Analytical study on the separation dynamics of LUNAR-A/penetrator p 1265 A93-56272

PENTANES

- Aircraft experiments on microgravity pool boiling - Vapor-liquid behaviour and heat transfer characteristics in boiling of n-pentane, CFC-113 and water p 410 A93-20920

PERFORATED PLATES

- Photoelastic stress analysis of skewed cutout in a sandwich skew plate subjected to inplane and transverse eccentric load p 210 A93-16604
- Forcing function effects on unsteady aerodynamic gust response. I - Forcing functions
[ASME PAPER 92-GT-174] p 251 A93-19400
- Forcing function effects on unsteady aerodynamic gust response. II - Low solidity airfoil row response
[ASME PAPER 92-GT-175] p 251 A93-19401
- Design and fabrication of panels with cutouts p 1215 A93-52973
- Evaluation of acoustic impedance models for a perforated plate
[NAL-TR-1133] p 102 A93-12375
- Stress calculations on the window section of an all-composite aircraft fuselage p 328 A93-16215
- The aerodynamic performance of laser drilled sheets
[AERO-REPT-9204] p 484 A93-20806

PERFORMANCE

- The design of test-section inserts for higher speed aeroacoustic testing in the Ames 80- by 120-Foot Wind Tunnel p 374 A93-19149
- Experience with explosive detection systems in airports p 498 A93-21895

PERFORMANCE PREDICTION

- Implementation of BMLS computer model on hypercube systems --- Baseline Microwave Landing System p 32 A93-11024
- Recent refinements and increased capabilities in balloon vertical performance analysis p 40 A93-11361
- A prediction of the stalling for wings with rear separation p 116 A93-14264
- Stochastic measures of performance robustness in aircraft control systems p 185 A93-14595
- One-dimensional methods for accurate prediction of off-design performance behavior of axial turbines
[ASME PAPER 92-GT-54] p 347 A93-19304

A wide-range axial-flow compressor stage performance model
[ASME PAPER 92-GT-58] p 348 A93-19308

Computational techniques for probabilistic analysis of turbomachinery
[ASME PAPER 92-GT-167] p 351 A93-19393

An analysis system for blade forced response
[ASME PAPER 92-GT-172] p 352 A93-19398

Transition prediction in attached and separated shear layers using an integral method
[ASME PAPER 92-GT-281] p 253 A93-19473

Separated flow in a low speed two-dimensional cascade. II - Cascade performance
[ASME PAPER 92-GT-357] p 257 A93-19522

Models for predicting the performance of Brayton-cycle engines
[ASME PAPER 92-GT-361] p 355 A93-19525

Flow studies in ducted twin-rotor contra-rotating axial flow fans
[ASME PAPER 92-GT-390] p 258 A93-19545

Accuracy issues in the prediction of supersonic inlet flows
[ASME PAPER 92-GT-400] p 258 A93-19549

On-board condition management for aircraft gas turbines
[ASME PAPER 92-GT-416] p 357 A93-19564

The use of subscale models to predict self-induced oscillations of flight vehicles
[AIAA PAPER 93-0093] p 264 A93-20199

High-performance computing for flight vehicles; Proceedings of the Symposium, Washington, Dec. 7-9, 1992 p 437 A93-20701

Aerothermodynamic analysis of combined-cycle propulsion systems p 359 A93-21671

Performance results and potential operational uses for the prototype TDWR microburst prediction product p 432 A93-22190

Some aspects of the aerodynamic methodology in hypersonic vehicle concept studies
[AIAA PAPER 92-5027] p 272 A93-22303

Inlet velocity profile effects on turbulent swirling flow predictions
[AIAA PAPER 93-0133] p 274 A93-22580

Numerical prediction of aerodynamic noise radiated from low Mach number turbulent wake
[AIAA PAPER 93-0145] p 452 A93-22589

Prediction of active control of subsonic centrifugal compressor rotating stall
[AIAA PAPER 93-0153] p 274 A93-22591

Performance prediction of the interacting multiple model algorithm p 439 A93-22926

Pdf prediction of supersonic hydrogen flames
[AIAA PAPER 93-0448] p 391 A93-23358

BIPS Turboalternator-Compressor characteristics and application to the NASA Solar Dynamic Ground Demonstration Program p 532 A93-25965

Development of a model to predict electric vehicle performance over a variety of driving conditions p 570 A93-26011

Prediction of helicopter component loads using neural networks
[AIAA PAPER 93-1301] p 756 A93-33878

A method of predicting quasi-steady aerodynamics for flutter analysis of high speed vehicles using steady CFD calculations
[AIAA PAPER 93-1364] p 682 A93-33931

An advanced method for predicting the performance of helicopter propulsion system ejectors p 809 A93-35933

Interactional aerodynamic effects on rotor performance in hover and forward flight p 766 A93-35941

A 2-D numerical model for predicting the aerodynamic performance of the NOTAR system tailboom p 766 A93-35994

Hover performance analysis of advanced rotor blades p 767 A93-35998

A numerical procedure for aerodynamic optimization of helicopter rotor blades
[ONERA, TP NO. 1992-121] p 771 A93-38595

Prediction of static performance for single expansion ramp nozzles
[AIAA PAPER 93-2571] p 898 A93-41047

Analytical development of an equivalent system mismatch function --- for longitudinal axis of fighter aircraft in nonterminal flight phase p 906 A93-41890

Hypersonic cone flow predictions using an implicit upwind space-marching code p 865 A93-42588

A contribution to the prediction of hypersonic non-equilibrium flows p 869 A93-42624

Performance data of the new free-piston shock tunnel T5 at GALCIT p 1011 A93-45498

Thermal control of a lidar laser system using a non-conventional ram air heat exchanger p 1028 A93-46821

Navier-Stokes prediction of a delta wing in roll with vortex breakdown
[AIAA PAPER 93-3495] p 983 A93-47267

Prediction of stall and post-stall behavior of airfoils at low and high Reynolds numbers
[AIAA PAPER 93-3502] p 983 A93-47270

A study of the rotary balance technique for predicting pitch damping
[AIAA PAPER 93-3619] p 1125 A93-48306

Base drag prediction on missile configurations
[AIAA PAPER 93-3629] p 1064 A93-48314

Development of an accuracy criteria for body-on-fin carryover interference
[AIAA PAPER 93-3633] p 1065 A93-48318

Aircraft control requirements and achievable dynamics prediction
[AIAA PAPER 93-3648] p 1128 A93-48331

A blade element method for predicting the off-design performance of compressors p 1107 A93-49187

Frontally tapered squared trench casing treatment for improvement of compressor performance p 1108 A93-49202

Turbine Engine Diagnostics (TED) system
[AIAA PAPER 93-1818] p 1110 A93-49706

Integrated flight/propulsion control - Subsystem specifications for performance
[AIAA PAPER 93-3808] p 1132 A93-51400

Numerical model for predictions of reverse flow combustor aerothermal characteristics p 1123 A93-51645

How to consider simulation fidelity and validity for an engineering simulator
[AIAA PAPER 93-3598] p 1209 A93-52688

Thermodynamic and neural network computer modelling of implanted component faults in a gas turbine engine
[ISABE 93-7089] p 1202 A93-54065

A study of military aircraft and engine tactical/technical performance evaluation p 1242 A93-54596

Prediction of rotating disc flow and heat transfer in gas turbine engines p 1256 A93-54634

Effects of foundation excitation on multiple rub interactions in turbomachinery p 1260 A93-55996

An interactive preprocessor for the NASA engine performance program
[NASA-TM-105786] p 56 A93-10983

An investigation of two-propeller tilt wing V/STOL aircraft flight characteristics
[AD-A257751] p 332 A93-17694

Low bandwidth robust controllers for flight
[NASA-CR-191774] p 372 A93-17800

Rotor design optimization using a free wake analysis
[NASA-CR-177612] p 693 A93-25075

Transient performance of fan engine with water ingestion
[NASA-CR-190778] p 677 A93-25134

The effects of reaction on axial compressor performance p 724 A93-25882

Flight mechanical model for performance calculations and interactions between flight vehicle and ramjet in regard to the flight orbit
[ESA-TT-1267] p 893 A93-29464

PERFORMANCE TESTS

Drag/thrust estimation via aircraft performance flight testing p 156 A93-14322

Braking, steering, and wear performance of radial-belted and bias-ply aircraft tires
[SAE PAPER 921036] p 158 A93-14656

Development of polyimide adhesives for 371 C (700 F) structural performance for aerospace bonding applications - FM 680 system p 198 A93-15757

Analysis of the NASA Hypersonic Wing Test Structure
[AIAA PAPER 92-4724] p 409 A93-20326

Development of a six component flexured two shell internal-strain gage balance
[AIAA PAPER 93-0793] p 541 A93-24872

Helmet Mounted Sight and display testing p 517 A93-26883

Internal performance characteristics of vectored axisymmetric ejector nozzles
[AIAA PAPER 93-2432] p 898 A93-41046

The effects of forced oscillations on the performance of airfoils
[AIAA PAPER 93-3264] p 968 A93-46829

Characteristics of deformable leading edge for high performance helicopter rotor
[AIAA PAPER 93-3526] p 986 A93-47285

Exhaust system model test and research p 1107 A93-48525

Test results of an orifice pulse tube refrigerator p 1149 A93-48612

Validation studies of scramjet nozzle performance p 1109 A93-49616

High-pressure hypervelocity electrothermal wind-tunnel performance study and subscale tests p 1137 A93-49617

Carbon/silicon carbide composite materials in advanced unmanned gas turbine engine combustors
[AIAA PAPER 93-1761] p 1144 A93-49658

An investigation on the use of a heavy gas to improve the performance of the equilibrium interface technique in shock tube flows
[AIAA PAPER 93-2017] p 1078 A93-49855

Ground test simulation fidelity of turbine engine airstarts
[AIAA PAPER 93-2173] p 1137 A93-49986

Static internal performance tests of single expansion ramp nozzle concepts designed with LO considerations
[AIAA PAPER 93-2429] p 1117 A93-50185

Performance characteristics of a variable-area vane nozzle for vectored an ASTOVL exhaust jet up to 45 deg
[AIAA PAPER 93-2437] p 1118 A93-50189

Internal performance of Highly Integrated Deployable Exhaust Nozzles
[AIAA PAPER 93-2570] p 1084 A93-50288

New experiments in a 120-mm ram accelerator at high pressures
[AIAA PAPER 93-2589] p 1142 A93-50301

International standards for the qualification of airplane flight simulators; Conference, London, United Kingdom, Jan. 16, 17, 1992, Document Approved (ISBN 1-85768-040-5) p 1140 A93-51934

Uncertainty of derived results on X-Y plots --- in gas turbine engines p 1261 A93-54382

Uncertainty assessments for engine thrust derived from two methods p 1254 A93-54392

Instrumentation and data acquisition system for the C.I.R.A. Transonic Pilot Tunnel p 1250 A93-54395

Effect of jet engine exhaust on SOFIA stratospheric performance --- Stratospheric Observatory For Infrared Astronomy p 1263 A93-55178

A test facility for the thermofluid-dynamics of gas bearing lubrication films
[PNR-90897] p 72 A93-11032

The role of turbomachinery testing for stability in distorted flow
[PNR-90943] p 57 A93-11040

The development of the Rolls-Royce Trent aero gas turbine
[PNR-90949] p 58 A93-11108

The technical background to standards for shackles
[NPL-DMM(A)-51] p 86 A93-11325

High Capacity Voice Recorder (HCVR) Operational Test and Evaluation (OT/E) integration test report
[DOT/FAA/CT-TN92/30] p 88 A93-11460

Embedded training capabilities for the LAMPS MK 3 system
[AD-A250697] p 49 A93-11838

Measured data for the Sandia 34-meter vertical axis wind turbine
[DE92-019807] p 94 A93-12075

Evaluation of CKU-5/A ejection seat catapults under varied acceleration levels
[AD-A248021] p 29 A93-12489

Limited production Precision Runway Monitor (PRM) master test plan
[DOT/FAA/CT-TN92/23] p 192 A93-12899

Comparative performance tests of a pitot-inlet in several European wind-tunnels at subsonic and supersonic speeds p 130 A93-13221

Terminal Doppler Weather Radar (TDWR) Operational Test and Evaluation (OT/E) integration test plan
[DOT/FAA/CT-TN92/6] p 151 A93-13377

Facilities and capabilities catalog for landing and escape systems
[NASA-RP-1282] p 196 A93-14495

The Orlando TDWR testbed and airborne wind shear date comparison results p 145 A93-14851

Measurement of the dynamic undercarriage response of a Sikorsky S-70B-2 helicopter: Instrumentation and test methods: Flight mechanics technical memorandum
[AD-A256319] p 329 A93-16404

Test and integration concept for complex helicopter avionic systems
[MBB-UD-0605-91-PUB] p 343 A93-17547

Integrated helmet system testing for a nightflying helicopter
[MBB-UD-0604-91-PUB] p 343 A93-17570

Role of wind tunnel tests and CFD analysis for the development of aero-engines in IHI p 365 A93-19326

An approach to evaluating reactive airborne wind shear systems p 489 A93-19600

In-flight structural mode excitation system for flutter testing p 526 A93-19915

Testing of an automatic, low altitude, low terrain ground collision avoidance system p 502 A93-19924

A procedure for defining lightning risk to air vehicles p 703 A93-24885

Performance-based testing and success in Naval advanced flight training
[AD-A260838] p 717 A93-25933

- The Data Multiplexing Network (DMN) phase 3 Extended Distance Data Cable (EDDC) test and evaluation [DOT/FAA/CT-TN93/11] p 752 N93-26160
- Performance characteristics of a variable-area vane nozzle for vectoring an ASTOVL exhaust jet up to 45 deg [NASA-TM-106114] p 813 N93-27131
- Time delay measurements of current primary FAA air/ground transmitters and receivers [DOT/FAA/CT-TN93/14] p 842 N93-28555
- Data Multiplexing Network (DMN) equipment Operational Test and Evaluation (OT&E) integration test report [AD-A263172] p 942 N93-29490
- Testing of an experimental FMS p 998 N93-31277
- PERIODIC FUNCTIONS**
- Direct periodic solutions of rotor free wake calculations p 874 A93-43781
- PERIODIC VARIATIONS**
- Periodic maximum range cruise with singular control p 890 A93-41903
- PERIODICALS**
- USA aviation digest index, 1989, volume 11 [AD-A258673] p 571 N93-20388
- Index to USA aviation digest, 1990 [AD-A258678] p 572 N93-20389
- PERMANENT MAGNETS**
- Lifting forces acting on magnets placed above a superconducting plane p 79 A93-12332
- Variable-speed generators with flux weakening p 750 N93-25599
- Forces on a magnet moving past figure-eight coils [DE93-009965] p 943 N93-29189
- PERMEABILITY**
- Permeable airfoils in incompressible flow p 768 A93-37401
- PEROXIDES**
- Development of a method to determine the autoxidation of turbine fuels [AD-A260578] p 736 N93-25902
- PERSHING MISSILE**
- Evaluation of three models used for predicting noise propagated long distances overground [AD-A255963] p 232 N93-14406
- PERSONAL COMPUTERS**
- Generic developmental turbojet fuel control p 172 A93-14519
- Use of PCs in controlling simulated altitude environmental test conditions in support of turbine engine testing p 846 A93-37856
- A set of IBM PC software for processing helicopter flight tests data to determine the flight performance characteristics p 1037 A93-45661
- The integration of geometric modeling into an inverse design method and application of a PC-based inverse design method and comparison with test results p 81 N93-10058
- Personal computer based test- and emulation equipment for maintenance and ground support p 110 N93-15185
- Development of a menu driven materials data base for use on personal computers: Aircraft structures technical memorandum [AD-A256317] p 392 N93-16403
- Development and testing of the digital control system for the Archytas unmanned air vehicle [AD-A261656] p 729 N93-26196
- A PC-based simulation of the National Transonic Facility's safety microprocessor [NASA-TM-109003] p 1038 N93-32224
- PERSONNEL**
- Comparison of performance on the Shipley Institute of Living Scale, Air Traffic Control Specialist Selection Test, and FAA Academy Screen [AD-A259249] p 502 N93-20582
- Aircraft electrical and environmental systems, AFSCs 452x5, 454x5, and 454x6 [AD-A261213] p 717 N93-25733
- PERSONNEL DEVELOPMENT**
- Future availability of aircraft maintenance personnel p 570 A93-27133
- PERSONNEL MANAGEMENT**
- Aviation production engineering: Selected articles [AD-A261231] p 764 N93-27056
- PERSONNEL SELECTION**
- Identifying ability requirements for operators of future automated air traffic control systems [AD-A256615] p 152 N93-14276
- PERTURBATION**
- IOPS advisor: Research in progress on knowledge-intensive methods for irregular operations airline scheduling p 443 N93-18686
- PERTURBATION THEORY**
- Calculation of transonic flow over bodies of varying complexity using Singular Perturbation Method p 116 A93-14265
- Method of simulating unsteady turbomachinery flows with multiple perturbations p 123 A93-14556
- Receptivity of three-dimensional boundary layers [AIAA PAPER 93-0074] p 262 A93-20186
- Evolution of a three-dimensional nonequilibrium boundary layer in a dihedral angle behind a perturbation source p 872 A93-43013
- Calculation of transonic longitudinal and lateral-directional characteristics of aircraft by the small disturbance theory [AIAA PAPER 93-3617] p 1125 A93-48304
- A simplified wing rock prediction method [AIAA PAPER 93-3662] p 1128 A93-48342
- Calculation of perturbation propagation upstream in a hypersonic laminar boundary layer p 1086 A93-50968
- Analysis of spatial motion dynamics of a helicopter for various models of the induced velocity field p 1191 A93-53721
- Current European rotorcraft research activities on development of advanced CFD methods for the design of rotor blades (BRITE/EURAM DACRO project) [MBB-UD-0601-91-PUB] p 293 N93-17568
- PHASE CHANGE MATERIALS**
- Enhanced heat transport in environmental systems using microencapsulated phase change materials [SAE PAPER 921224] p 926 A93-41398
- PHASE ERROR**
- Relative sensitivity of Loran-C phase tracking and cycle selection to CWI p 792 A93-36502
- PHASE LOCKED SYSTEMS**
- New algorithms for hyperbolic radionavigation p 881 A93-40359
- PHASE MODULATION**
- Analysis of the effects of blade pitch on the radar return signal from rotating aircraft blades p 885 A93-43476
- PHASE STABILITY (MATERIALS)**
- Raising the high temperature limit of the nickel-iron-base superalloy p 70 A93-12114
- Structural stability of 'beta-CEZ' alloy [ONERA, TP NO. 1992-106] p 824 A93-38586
- Designing new multi-phase intermetallic materials based on phase compatibility considerations [ONERA, TP NO. 1992-131] p 772 A93-38605
- PHASE TRANSFORMATIONS**
- Investigation of an electrothermal de-icer pad using a three-dimensional finite element simulation [AIAA PAPER 93-0397] p 327 A93-23072
- Transonic aerodynamics including strong effects from heat addition p 862 A93-42428
- Efficient finite element method for aircraft deicing problems p 1103 A93-52443
- PHASED ARRAYS**
- A self-steering array for the SHARP microwave-powered aircraft p 792 A93-37090
- A dual polarised active phased array antenna with low cross polarisation for a polarimetric airborne SAR p 883 A93-43401
- Airport surveillance radar design for increased air traffic p 883 A93-43410
- Antenna design for adaptive airborne MTI p 884 A93-43440
- The PHARUS project, first results of the realization phase --- Phased Array Universal SAR p 884 A93-43454
- Motion compensation in a time domain SAR processor p 885 A93-43466
- Adaptive waveform selection with a neural network p 942 A93-43470
- The realization phase of the PHARUS project --- Phased ARray Universal SAR p 1162 A93-47658
- Definition study PHARUS [AD-A256560] p 221 N93-14805
- PHOTOCHEMICAL REACTIONS**
- Employment of radicals and excited state species for supersonic combustion photochemical ignition of premixed hydrogen/oxygen mixtures with ArF laser p 73 N93-11135
- PHOTOELASTIC ANALYSIS**
- Photoelastic stress analysis of skewed cutout in a sandwich skew plate subjected to inplane and transverse eccentric load p 210 A93-16604
- PHOTOELASTICITY**
- Optical methods of stress analysis applied to cracked components p 1027 A93-45798
- PHOTOELECTROCHEMISTRY**
- Photoelectrochemical etching of high aspect ratio submillimeter waveguide filters from n(+) GaAs wafers p 409 A93-20644
- PHOTOGRAPHIC MEASUREMENT**
- Flight Deflection Measurement System p 808 A93-37885
- PHOTOINTERPRETATION**
- Vision based obstacle detection and grouping for helicopter guidance [AIAA PAPER 93-3871] p 1098 A93-51457
- PHOTOLUMINESCENCE**
- Photoluminescent thermography - Feasibility study with pointwise measurements p 211 A93-16861
- Video luminescent barometry - The induction period [AIAA PAPER 93-0179] p 414 A93-22607
- Aerodynamic applications of pressure sensitive paint p 549 A93-29301
- Uncertainty estimates for pressure sensitive paint measurements p 1258 A93-55369
- Photoluminescent thermography in hypersonic blowdown wind tunnel: Feasibility study with pinpoint measurement [ONERA-NT-1992-8] p 297 N93-18617
- PHOTOMAPPING**
- Mapping new and old worlds with laser altimetry p 1034 A93-45699
- PHOTON BEAMS**
- Poster session: Fifth Users Meeting for the Advanced Photon Source [DE93-006019] p 732 N93-26498
- PHOTONICS**
- Demonstration of an integrated, active 4 x 4 photonic crossbar p 211 A93-17392
- Reconfigurable photonic data networks for military aircraft p 928 A93-42783
- PHOTORECONNAISSANCE**
- Development of nose structure of a reconnaissance container for a supersonic jet aircraft [MBB-LME-242-S-PUB-0451] p 998 N93-31046
- PHOTOVOLTAIC CONVERSION**
- Nickel hydrogen batteries for terrestrial applications p 557 A93-26005
- Development of a model to predict electric vehicle performance over a variety of driving conditions p 570 A93-26011
- Computational and experimental investigation of a solar energy system for an atmospheric flight vehicle p 521 A93-29655
- PHYSICAL OPTICS**
- ILS mathematical modeling study of an ILS glide slope proposed for runway 19L at the Meridian Naval Air Station, Mississippi [DOT/FAA/CT-TN93/8] p 705 N93-24741
- PHYSICAL PROPERTIES**
- Resource conservation and improvement of the service characteristics of castings of high-temperature nickel alloys through a high-temperature melt treatment p 824 A93-36718
- PHYSICIANS**
- The role of the radiologist in the medicolegal procedure after an aviation accident p 853 A93-39701
- PHYSICS**
- Flow physics of critical states for rolling delta wings [AIAA PAPER 93-3683] p 1129 A93-48355
- PHYSIOLOGICAL EFFECTS**
- Specific features of military low-altitude flight noise - Criteria for risk of damage and physiological effects p 1164 A93-49558
- Review - Extraaural health effects of aircraft noise p 1164 A93-49559
- Sonic boom problem for future highspeed aircraft [ONERA-NT-1990-3] p 876 A93-30020
- Effects on health of noise disturbances due to air traffic p 1035 A93-31929
- PHYSIOLOGICAL RESPONSES**
- Results of a low-altitude flight noise study in Germany - Acute extraaural effects p 1163 A93-49557
- Autogenic-feedback training improves pilot performance during emergency flying conditions [NASA-TM-104005] p 790 N93-27076
- PHYSIOLOGY**
- A method for investigating human factor aspects of military aircraft accidents p 491 A93-19656
- PICTURE TUBES**
- Computer-controlled alignment for a 2000-line color monitor p 886 A93-30324
- PIEZOELECTRIC CERAMICS**
- Approximation methods for control of structural acoustics models with piezoceramic actuators p 452 A93-23744
- PIEZOELECTRIC CRYSTALS**
- Actuation strain decoupling through enhanced directional attachment in plates and aerodynamic surfaces p 394 A93-17727
- PIEZOELECTRIC TRANSDUCERS**
- Modal sensors and actuators for individual blade control [AIAA PAPER 93-1703] p 712 A93-34225
- PIEZOELECTRICITY**
- Active control of interior noise in a large scale cylinder using piezoelectric actuators p 568 A93-29425
- Control of panel flutter at high supersonic speed p 47 N93-10900
- Analytical and experimental investigation of flutter suppression by piezoelectric actuation [NASA-TP-3241] p 513 N93-20584

PILOT ERROR

- Review of human error accidents in civil aviation
p 27 A93-12367
- Flight safety and human errors p 141 A93-16860
- Human factors in crashes of commuter airplanes
p 486 A93-24048
- The development of an Altitude Awareness Program -
An integrated approach p 486 A93-27136
- Development of an expert system for cockpit emergency
procedures p 845 A93-35915
- Promoting general aviation safety - A revision of pilot
negligence law p 1265 A93-56540
- Aircraft accident report: Tomy International, Inc., d/b/a
Scenic Air Tours flight 22, Beech Model E18S, N342E
in-flight collision with terrain, Mount Haleakala, Maui,
Hawaii, 22 April 1992
[PB93-910401] p 705 N93-25827
- Autogenic-feedback training improves pilot performance
during emergency flying conditions
[NASA-TM-104005] p 790 N93-27076
- PILOT PERFORMANCE**
- Review of human error accidents in civil aviation
p 27 A93-12367
- The certification of head up displays for category 3
operation p 142 A93-17304
- The development of an Altitude Awareness Program -
An integrated approach p 486 A93-27136
- Increased safety through knowledge-based pilot
assistance p 518 A93-27499
- Some considerations on indication means for helicopter
pilot vision systems p 807 A93-36018
- Critical dispatch - A pilot's view p 790 A93-39541
- Progress and taboos in flight safety - Human-factors
research in air transportation p 879 A93-42654
- Pilot task monitoring using neural networks
p 940 A93-42846
- Pilots' control behavior including feedback structures
identified by an improved method
[AIAA PAPER 93-3669] p 1129 A93-48347
- A primary flight display for four-dimensional guidance
and navigation influence of tunnel size and level of
additional information on pilot performance and control
behaviour
[AIAA PAPER 93-3570] p 1208 A93-52668
- Simulation motion effect on single axis compensatory
tracking
[AIAA PAPER 93-3579] p 1208 A93-52675
- Effect of lift-to-drag ratio in pilot rating of the HL-20
landing task p 1210 A93-53738
- Advanced terrain displays to transport category
aircraft
[PB92-197136] p 35 N93-10065
- Design of instrument approach procedure charts:
Comprehension speed of missed approach instructions
coded in text or icons
[PB92-205673] p 36 N93-11252
- Theory and design of adaptive automation in aviation
systems
[AD-A254595] p 160 N93-12613
- How expert pilots think p 147 N93-15017
- Methodology for studying and training expertise
p 147 N93-15018
- Simulator evaluation of displays for a revised takeoff
performance monitoring system
[NASA-TP-3270] p 189 N93-15366
- Ground based simulation evaluation of the effects of
time delays and motion on rotorcraft handling qualities
[AD-A256921] p 328 N93-16186
- Simulator motion
[AD-A257683] p 381 N93-17687
- Autogenic-feedback training improves pilot performance
during emergency flying conditions
[NASA-TM-104005] p 790 N93-27076
- PILOT SELECTION**
- Performance-based testing and success in Naval
advanced flight training
[AD-A260838] p 717 N93-25933
- PILOT TRAINING**
- Flight testing in the 90's
[AIAA PAPER 92-4123] p 102 A93-11256
- Helicopter in-flight simulator ATTHes - A multipurpose
testbed and its utilization
[AIAA PAPER 92-4173] p 43 A93-13315
- Low-level wind-shear terminology p 426 A93-22104
- An index of resource materials for aviation meteorology
education and training p 453 A93-22105
- New initiatives for aviation meteorology training - 1989
through 1991 p 307 A93-22109
- Improving weather questions on Federal Aviation
Administration exams p 308 A93-22110
- Aircraft icing problems - After 50 years
[AIAA PAPER 93-0392] p 486 A93-24239
- A context-based introduction to aircraft radio
communications p 570 A93-27164
- Development of an expert system for cockpit emergency
procedures p 845 A93-35915

- Progress and taboos in flight safety - Human-factors
research in air transportation p 879 A93-42654
- Evolution of flight simulation
[AIAA PAPER 93-3545] p 1207 A93-52652
- The modelling of turbulence and downbursts for flight
simulators p 193 N93-13542
- Does cockpit management training reduce aircrew
error? p 146 N93-15014
- Cockpit decision making p 146 N93-15015
- How expert pilots think p 147 N93-15017
- Methodology for studying and training expertise
p 147 N93-15018
- Enhanced Aeronautical Resource Management training
alternatives p 147 N93-15019
- Embedded ADM reduces helicopter human error
accidents p 147 N93-15024
- Measuring risk in single-engine and twin-engine
helicopters p 148 N93-15025
- Combat and training aircraft class A mishaps in the
Belgian Air Force 1970-1990 p 492 N93-19677
- Underlying causes of human error in US Army rotary
wing accidents p 492 N93-19678
- Prediction of success from training
p 495 N93-19702
- Use of microprocessor-based simulator technology and
MEG/EEG measurement techniques in pilot
emergency-maneuver training p 530 N93-19706
- Autogenic-feedback training improves pilot performance
during emergency flying conditions
[NASA-TM-104005] p 790 N93-27076
- Part 1: Executive summary p 857 N93-30674
- Helicopter simulator standards p 912 N93-30675
- Simulators for corporate pilot training and evaluation
p 912 N93-30678
- Helicopter simulator qualification p 912 N93-30681
- Helicopter simulation: Making it work
p 912 N93-30682
- Helicopter training simulators: Key market factors
p 912 N93-30683
- Determining the transferability of flight simulator data
p 913 N93-30685
- Progress through precedent: Going where no helicopter
simulator has gone before p 913 N93-30686
- Transfer of training and simulator qualification or myth
and folklore in helicopter simulation p 913 N93-30687
- PILOTLESS AIRCRAFT**
- Unorthodoxy rising - VTOL p 1 A93-11250
- Flight test and wind-tunnel study of a scaled unmanned
air vehicle
[AIAA PAPER 92-4075] p 37 A93-11260
- Phase I flight test of MIAG advanced development
model
[AIAA PAPER 92-4076] p 95 A93-11261
- Flight testing of an electric powered vehicle
[AIAA PAPER 92-4077] p 37 A93-11262
- Flying qualities of a remotely piloted vehicle
[AIAA PAPER 92-4083] p 61 A93-11266
- Options for control and navigation of unmanned
aircraft p 34 A93-12124
- Test pilot's notes on flying the Low Altitude/Airspeed
Unmanned Research Aircraft (LAURA)
[AIAA PAPER 92-4078] p 42 A93-13269
- A fast algorithm for obtaining dense depth maps for
high speed navigation p 435 A93-19080
- A formalization and implementation of topological visual
navigation in two dimensions p 435 A93-19101
- Wind tunnel test techniques for UAV separation
investigations
[AIAA PAPER 93-0626] p 524 A93-24743
- The PAVE PACE integrated RF architecture for next
generation avionics p 896 A93-42784
- Design of a rule-based fuzzy controller for the pitch axis
of an unmanned research vehicle p 907 A93-42807
- The UTA autonomous aerial vehicle - Automatic control
and navigation p 908 A93-42813
- Air cell - model aircraft power supplies
[CA-PATENT-APPL-SN-2001346] p 83 N93-10368
- A preliminary sizing method for unmanned aircraft using
multi-variate optimisation p 714 N93-25408
- Development and testing of the Perseus
proof-of-concept aircraft
[DE93-010121] p 806 N93-28586
- A real-time, hardware-in-the-loop simulation of an
unmanned aerial research vehicle
[AD-A262477] p 893 N93-29409
- PILOTS**
- Aviation accidents, incidents, and violations:
Psychological predictors among US pilots
p 144 N93-14693
- Aircraft accident report: Tomy International, Inc., d/b/a
Scenic Air Tours flight 22, Beech Model E18S, N342E
in-flight collision with terrain, Mount Haleakala, Maui,
Hawaii, 22 April 1992
[PB93-910401] p 705 N93-25827

PILOTS (PERSONNEL)

- An analysis of en route controller-pilot voice
communications
[AD-A264784] p 935 N93-30611
- PINS**
- Effect of trailing-edge ejection on local heat (mass)
transfer in pin fin cooling channels in turbine blades
[ASME PAPER 92-GT-178] p 352 A93-19404
- Heat transfer in a five-pass irregular channel with and
without pin-fins p 1256 A93-54633
- PIPE FLOW**
- A comparison of the drag-reducing benefits of riblets
in internal and external flows p 395 A93-18054
- Simulation of the secondary air system of aero
engines
[ASME PAPER 92-GT-68] p 348 A93-19318
- Flow field characteristics of an axisymmetric
sudden-expansion pipe flow with different initial swirl
distribution p 411 A93-21688
- Calculations of viscous nonequilibrium flows in nozzles
[ONERA, TP NO. 1992-91] p 771 A93-38574
- Drag characteristics of extra-thin-fin-riblets in an air flow
conduit p 1151 A93-49240
- A comparison between numerically modelled and
experimentally measured loss mechanisms in wave
rotors
[AIAA PAPER 93-2522] p 1120 A93-50252
- The remarkable ability of turbulence model equations
to describe transition p 783 N93-27432
- PIPER AIRCRAFT**
- Special investigation report: Piper Aircraft Corporation
PA-46 Malibu/Mirage Accidents/Incident, 31 May 1989 -
17 March 1991
[PB92-917007] p 149 N93-15577
- PIPES (TUBES)**
- The effects of crushing surface roughness on the
crushing characteristics of composite tubes
p 77 A93-10918
- PISTON ENGINES**
- Harnessing nitrous oxide for elevation of temperature
and pressure in piston facilities
[AIAA PAPER 93-2016] p 1137 A93-49854
- A preliminary sizing method for unmanned aircraft using
multi-variate optimisation p 714 N93-25408
- Improved selective catalytic NOx control technology for
compressor station reciprocating engines
[PB93-158566] p 755 N93-26529
- PISTONS**
- Experiments on Space Shuttle Orbiter models in a free
piston shock tunnel p 7 A93-11497
- Free piston shock tunnels - Developments and
capabilities p 66 A93-12316
- PITCH**
- A study on aerodynamic sound generated by interaction
of jet and plate
[AIAA PAPER 93-3118] p 1171 A93-48288
- PITCH (INCLINATION)**
- Dynamic characteristics of an airfoil at high speed
change of pitch angle p 10 A93-12324
- Pitched simulation evaluation of pitch control designs
for highly augmented STOVL aircraft
[AIAA PAPER 92-4234] p 63 A93-13328
- Influence of pitch-lag coupling on damping requirements
to stabilize 'ground/air resonance' p 158 A93-14784
- Incidence angle and pitch-chord effects on secondary
flows downstream of a turbine cascade
[ASME PAPER 92-GT-184] p 251 A93-19409
- Interferometric investigations of compressible dynamic
stall over a transiently pitching airfoil
[AIAA PAPER 93-0211] p 278 A93-22628
- Investigation of the aircraft spin via sensitivity analysis
p 524 A93-27300
- Modeling and control design of a wind tunnel model
support p 529 A93-29281
- Velocity vector LDA measurement inside a pitched blade
impeller p 924 A93-40390
- Design of a rule-based fuzzy controller for the pitch axis
of an unmanned research vehicle p 907 A93-42807
- Determination of the vertical velocity component of
aircraft landing on an airfield with a longitudinally sloping
runway p 1007 A93-45664
- Initial acceleration effects on flow evolution around
airfoils pitching to high angles of attack
p 961 A93-45750
- Navier-Stokes simulations of the Shuttle Orbiter
aerodynamic characteristics with emphasis on pitch trim
and bodyflap
[AIAA PAPER 93-2814] p 965 A93-46552
- Precise pitching airfoil computations by use of dynamic
unstructured meshes
[AIAA PAPER 93-2971] p 1049 A93-48165
- Tip vortex, stall vortex, and separation observations on
pitching three-dimensional wings
[AIAA PAPER 93-2972] p 1049 A93-48166

- Computational study of vortex breakdown on a pitching delta wing
[AIAA PAPER 93-2974] p 1050 A93-48168
- Transition effects on compressible dynamic stall of transiently pitching airfoils
[AIAA PAPER 93-2978] p 1050 A93-48171
- Correlation of unsteady pressure and inflow velocity fields of a pitching rotor blade
[AIAA PAPER 93-3082] p 1060 A93-48256
- Status of the validation of high-angle-of-attack nose-down pitch control margin design guidelines
[AIAA PAPER 93-3623] p 1126 A93-48308
- Flow and heat transfer in a turbulent boundary layer through skewed and pitched jets
[AIAA PAPER 93-49007] p 1151 A93-49007
- A pseudo-loop design strategy for the longitudinal control of hypersonic aircraft
[AIAA PAPER 93-3814] p 1132 A93-51405
- An experimental and a theoretical investigation of rotor pitch damping using a model rotor
[AIAA PAPER 93-4032] p 47 N93-10322
- New adaptive controllers for aircraft
p 847 N93-27180
- PITCHING MOMENTS**
- Effects of thrust line offset on neutral point determination in stability flight testing
[AIAA PAPER 92-4082] p 61 A93-11265
- Effects of the pylon pitching stiffness on wing-store flutter
[AIAA PAPER 93-0434] p 41 A93-11820
- Flow structures around a constant-rate pitching airfoil and mechanism of dynamic stall
[AIAA PAPER 93-0434] p 118 A93-14332
- Balance of moments for hypersonic vehicles
[ASME PAPER 92-GT-251] p 253 A93-19460
- A new semiempirical method for computing nonlinear angle-of-attack aerodynamics on wing-body-tail configurations
[AIAA PAPER 93-0034] p 260 A93-20148
- Estimation of unsteady lift on a pitching airfoil from wake velocity surveys
[AIAA PAPER 93-0437] p 286 A93-23351
- Initial acceleration effects on the flow field development around rapidly pitching airfoils
[AIAA PAPER 93-0438] p 286 A93-23352
- Pressure measurements on a pitching airfoil in a water channel
[AIAA PAPER 93-0184] p 473 A93-25510
- Structure of vortex breakdown on a pitching delta wing
[AIAA PAPER 93-0434] p 474 A93-25528
- Schlieren studies of compressibility effects on dynamic stall of transiently pitching airfoils
[AIAA PAPER 93-0434] p 480 A93-28608
- On the effect of pitch/mast-bending coupling on whirl-mode stability
[AIAA PAPER 93-0434] p 794 A93-35906
- Lift and pitching moment measurements in vertical gusts
[AIAA PAPER 93-0434] p 906 A93-42259
- Aerodynamics of Shuttle Orbiter at high altitudes
[AIAA PAPER 93-2815] p 965 A93-46553
- Control of the dynamic-stall vortex over a pitching airfoil by leading-edge suction
[AIAA PAPER 93-3267] p 969 A93-46832
- The three-dimensional representation of the lift and pitching moment coefficients on wedged rectangular wings in supersonic flow
[AIAA PAPER 93-3267] p 973 A93-46990
- A study of the rotary balance technique for predicting pitch damping
[AIAA PAPER 93-3619] p 1125 A93-48306
- Investigation of vortex development on a pitching slender body of revolution
[AIAA PAPER 93-3619] p 1095 A93-52445
- Numerical analysis of a flat plate in a pitching motion. II - Effect on the flow of the position of the pivot, etc
[AIAA PAPER 93-3619] p 1181 A93-53798
- Investigation of the flow field through a variable pitch fan rotor with an inlet total pressure distortion
[ISABE 93-7029] p 1184 A93-54005
- A method of testing two-dimensional airfoils
[AD-A253210] p 17 N93-10375
- Dynamic stall effects on hingeless rotor stability with experimental correlation
[AD-A253210] p 129 N93-13010
- Multi-point inverse design of isolated airfoils and airfoils in cascade in incompressible flow
[AD-A253210] p 163 N93-14462
- Estimation of unsteady lift on a pitching airfoil from wake velocity surveys
[NASA-TM-105947] p 138 N93-14791
- Pitching moment of low aspect ratio wing-body combinations up to high angles of attack at supersonic speeds
[ESDU-92043] p 333 N93-17958
- An experimental investigation of a finite circulation control wing
[AD-A259044] p 340 N93-18896
- Analysis of wind-tunnel data for elliptic cross-sectioned forebodies at Mach numbers 0.4 to 5.0
[NASA-TM-3314] p 782 N93-27221
- Evaluation of four advanced nozzle concepts for short takeoff and landing performance
[NASA-TM-3314] p 875 N93-29165
- Aerodynamic characteristics of a rotorcraft airfoil designed for the tip region of a main rotor blade
[NASA-TM-4264] p 876 N93-29450
- Construction, wind tunnel testing and data analysis for a 1/5 scale ultra-light wing model
[SAE PAPER 920930] p 876 N93-29778
- PITOT TUBES**
- Millisecond aerodynamic force measurement with side-jet model in the ISL shock tunnel
[SAE PAPER 920930] p 822 A93-39414
- Some contributions to propulsion theory - Non-isentropic duct flow and the general drag wake traverse
[SAE PAPER 920930] p 874 A93-43688
- Comparative performance tests of a pitot-inlet in several European wind-tunnels at subsonic and supersonic speeds
[SAE PAPER 920930] p 130 N93-13221
- PITTING**
- Hot end cleaning - Corrosion pitting of turbine discs
[SAE PAPER 920930] p 202 A93-14081
- PIXELS**
- A large flat panel multifunction display for military and space applications
[SAE PAPER 920930] p 77 A93-10963
- PLANAR STRUCTURES**
- Analysis and design of planar and non-planar wings for induced drag minimization
[NASA-CR-191274] p 131 N93-13463
- PLANE STRESS**
- Photoelastic stress analysis of skewed cutout in a sandwich skew plate subjected to inplane and transverse eccentric load
[SAE PAPER 920930] p 210 A93-16604
- A finite element for modeling skins of composite materials
[SAE PAPER 920930] p 1215 A93-52979
- PLANE WAVES**
- On the coupling between a supersonic boundary layer and a flexible surface
[SAE PAPER 920930] p 243 A93-19132
- Design of an optimal single reflective holographic helmet display element
[SAE PAPER 920930] p 517 A93-26886
- Simulation of propulsion system's transient response to planar wave inlet distortion and the effect of compressor wear
[AIAA PAPER 93-2384] p 1117 A93-50152
- PLANETARY ATMOSPHERES**
- Flow problems posed by reentry in planetary atmospheres
[AIAA PAPER 93-2384] p 11 A93-12432
- PLANETARY BOUNDARY LAYER**
- Volume-imaging lidar observations of the convective structure surrounding the flight path of a flux-measuring aircraft
[AIAA PAPER 93-2384] p 425 A93-20579
- PLANETARY LANDING**
- A fast algorithm for image-based ranging
[AIAA PAPER 93-2384] p 544 A93-27045
- PLANFORMS**
- Recent developments in equivalent plate modeling for wing shape optimization
[AIAA PAPER 93-1647] p 742 A93-34172
- Lift and pitching moment measurements in vertical gusts
[AIAA PAPER 93-1647] p 906 A93-42259
- Numerical study of a delta planform with multiple jets in ground effect
[SAE PAPER 892283] p 1176 A93-53200
- Effect of planform and body on supersonic aerodynamics of multi-body configurations
[NASA-TM-3212] p 19 N93-10824
- Flowfield study of a close-coupled canard configuration
[AD-A256311] p 139 N93-15245
- PLASMA ACCELERATION**
- A report on the status of MHD hypersonic ground test technology in Russia
[AIAA PAPER 93-3193] p 1012 A93-46656
- PLASMA DIAGNOSTICS**
- Non-equilibrium flow in an arc heated wind tunnel
[INPE-5428-RPQ/662] p 910 A93-42642
- Diagnostics systems for the TBR-E tokamak
[INPE-5428-RPQ/662] p 232 N93-13257
- Coherent systems in the terahertz frequency range: Elements, operation, and examples
[INPE-5428-RPQ/662] p 841 N93-27727
- PLASMA INTERACTIONS**
- Evaluation of candidate working fluid formulations for the electrothermal - chemical wind tunnel
[NASA-CR-192196] p 530 N93-20312
- PLASMA OSCILLATIONS**
- Beta-limiting phenomena in high-aspect-ratio toroidal helical plasmas
[NIFS-188] p 569 N93-20546
- PLASMA PRESSURE**
- Beta-limiting phenomena in high-aspect-ratio toroidal helical plasmas
[NIFS-188] p 569 N93-20546
- PLASMA PROPULSION**
- AFOSR Contractors Meeting in Propulsion
[AD-A254484] p 195 N93-12575
- PLASMA SPRAYING**
- Technical note - Plasma-sprayed ceramic thermal barrier coatings for smooth intermetallic alloys
[SAE PAPER 920930] p 209 A93-15702
- Analysis of the friction and wear mechanisms of multilayered plasma-sprayed ceramic coatings
[SAE PAPER 920930] p 548 A93-28567
- Microstructure of yttria stabilized zirconia-hafnia plasma sprayed thermal barrier coatings
[ONERA, TP NO. 1993-54] p 1146 A93-51936
- Stress relaxation of low pressure plasma-sprayed NiCrAlY alloys
[ONERA, TP NO. 1993-54] p 1211 A93-52870
- PLASMATRONS**
- Modeling of the physicochemical processes of nonequilibrium heat transfer in the subsonic jets of an induction plasmatron
[ONERA, TP NO. 1993-54] p 836 A93-39147
- PLASTIC AIRCRAFT STRUCTURES**
- Fundamentals of composite repair
[SME PAPER EM92-100] p 196 A93-14101
- In-service inspection of commercial aircraft composite structure
[SME PAPER EM92-124] p 107 A93-14116
- Counting the cost of composites
[SME PAPER EM92-124] p 107 A93-14117
- Design and fabrication of a composite transmission housing for a helicopter tail rotor
[SME PAPER EM92-124] p 156 A93-14339
- Tailoring concepts for improved structural performance of rotorcraft flexbeams
[SME PAPER EM92-124] p 207 A93-14811
- Adaptive aeroelastic composite wings - Control and optimization issues
[SME PAPER EM92-124] p 185 A93-14818
- Thermoplastic and thermosetting matrix composite structures - Comparison of mechanical properties
[SME PAPER EM92-124] p 197 A93-15029
- Evaluation by holographic interferometry of impact damage in composite aeronautical structures
[SME PAPER EM92-124] p 1020 A93-44193
- Design and manufacture for producibility of carbon fiber/epoxy composite aircraft skins
[SME PAPER EM93-104] p 1043 A93-51732
- Design for manufacture by resin transfer molding of composite parts for rotorcraft
[SME PAPER EM93-103] p 1159 A93-51733
- An experimental study of reinforced panels of composite materials
[SME PAPER EM93-103] p 1215 A93-52975
- All-composite fan blade for advanced ducted engines
[SME PAPER EM93-103] p 1246 A93-54837
- The Airbus floor beam: Towards a cost-effective composite design and manufacture research project sponsored by Airbus industry
[LR-677] p 329 N93-16283
- A90 project: Design of a composite fin
[ETN-92-92773] p 329 N93-16562
- PLASTIC DEFORMATION**
- Aeroplane crashes on the runway: Validation and final evaluation of the method of modeling an airframe structure
[IMFL-91-32] p 165 N93-15126
- PLASTIC PROPELLANTS**
- Regression rate mechanism in a solid fuel ramjet
[IMFL-91-32] p 814 N93-27185
- PLASTIC PROPERTIES**
- Infrared thermography of plastic instabilities in a single crystal superalloy
[ONERA, TP NO. 1993-18] p 916 A93-41031
- PLASTICS**
- Specialty fiber optic systems for mobile platforms and plastic optical fibers; Proceedings of the Meeting, Boston, MA, Sept. 9-11, 1992
[SPIE-1799] p 1105 A93-49462
- PLATE THEORY**
- Analysis of complicated plates by a nine-node spline plate element
[AIAA PAPER 93-1413] p 206 A93-14616
- Lessons from application of equivalent plate structural modeling to an HSCT wing
[AIAA PAPER 93-1413] p 739 A93-33969
- Recent developments in equivalent plate modeling for wing shape optimization
[AIAA PAPER 93-1647] p 742 A93-34172
- Nonlinear flutter of composite plates with damage evolution
[AIAA PAPER 93-1546] p 829 A93-37441
- Effect of boundary conditions and panel geometry on the response of laminated panels subjected to transverse pressure loads
[AIAA PAPER 93-1546] p 1259 A93-55674
- Analytical and experimental investigation of flutter suppression by piezoelectric actuation
[NASA-TP-3241] p 513 N93-20584
- PLATES (STRUCTURAL MEMBERS)**
- A method of calculating elastic curve of semiflexible plate nozzle
[AIAA PAPER 93-1546] p 66 A93-12097
- Supersonic flutter analysis of composite plates and shells
[AIAA PAPER 93-1546] p 837 A93-39419
- Stability of fluttered panels subjected to in-plane harmonic forces
[AIAA PAPER 93-1546] p 1151 A93-49017
- Analytical and experimental investigation of flutter suppression by piezoelectric actuation
[NASA-TP-3241] p 513 N93-20584
- Numerical determination of the residual strength of battle damaged composite plates
[AIAA PAPER 93-1546] p 537 N93-21533
- PLATINUM**
- Evaluation of simple aluminide and platinum modified aluminide coatings on high pressure turbine blades after factory engine testing - Round II
[ASME PAPER 92-GT-140] p 388 A93-19372

Platinum-modified diffusion aluminide coatings on nickel-base superalloys
[AD-A263597] p 917 N93-29981

PLATINUM ALLOYS

Life assessment of gas turbine bucket coating based on degradation analysis p 533 A93-24464
Field evaluation of six protective coatings applied to T-56 turbine blades after 2000 hours of engine use
[AD-A261112] p 522 N93-21316

PLATINUM COMPOUNDS

Video luminescent barometry - The induction period
[AIAA PAPER 93-0179] p 414 A93-22607

PLENUM CHAMBERS

Effects of bleed-hole geometry and plenum pressure on three-dimensional shock-wave/boundary-layer/bleed interactions
[AIAA PAPER 93-3259] p 967 A93-46800
Further noise measurements in a slotted cryogenic wind tunnel
[RAE-TM-AERO-2201] p 101 N93-10805

PLUGS

Experimental investigation of spherical-convergent-flap thrust-vectoring two-dimensional plug nozzles
[AIAA PAPER 93-2431] p 898 A93-41045

PLUMES

The composite shape and structure of coherent eddies in the convective boundary layer p 93 A93-12643
The acoustic response of altitude test facility exhaust systems to axisymmetric and two-dimensional turbine engine exhaust plumes p 449 A93-19209
Volume-imaging lidar observations of the convective structure surrounding the flight path of a flux-measuring aircraft p 425 A93-20579
Remote sensing of volcanic ash hazards to aircraft p 556 A93-24213
Implicit Euler calculation of supersonic vortex wake/engine plume interaction
[AIAA PAPER 93-0656] p 540 A93-24769
Helicopter plume detection by using an ultranarrow-band noncoherent laser Doppler velocimeter p 542 A93-25198
Hypersonic single expansion ramp nozzle simulations p 777 A93-39254
Plume effects at hypersonic speeds p 959 A93-45494
NO(x) scavenging on carbonaceous aerosol surfaces in aircraft exhaust plumes. I
[AIAA PAPER 93-2343] p 1164 A93-50117
Measurement and prediction of flow in a gas turbine engine exhaust plume
[ISABE 93-7113] p 1204 A93-54088
Nozzle installation effects on the noise from supersonic exhaust plumes p 100 N93-10681
Stratospheric aircraft exhaust plume and wake chemistry studies
[NASA-CR-189688] p 94 N93-12299
A plume-induced boundary layer separation experiment
[AD-A255397] p 220 N93-14677
Plume effects on the flow around a blunted cone at hypersonic speeds p 787 N93-27460

PLY ORIENTATION
Structural tailoring of aircraft engine blade subject to ice impact constraints
[NASA-TM-106033] p 838 N93-26999

PNEUMATIC CIRCUITS
A pressure distribution measuring system with pneumatic switches and automatic band selection p 75 A93-10029

PNEUMATIC CONTROL
A sensitivity study for pneumatic vortex control on a chined forebody
[AIAA PAPER 93-0049] p 260 A93-20162
Computational investigation of a pneumatic forebody flow control concept p 768 A93-37383
Side force augmentation at high angle of attack from pneumatic vortex flow control
[AIAA PAPER 93-2959] p 1124 A93-48153
Lateral control at high angles of attack using pneumatic blowing through a chined forebody
[AIAA PAPER 93-3624] p 1126 A93-48309
Quantitative-force measurements of pneumatic control on a wing/stroke model
[AD-A257343] p 289 N93-16157

PNEUMATIC EQUIPMENT
Optimization of pneumatic subsystems for transport aircraft p 159 A93-15049
Control of the quality of dynamic processes in the valves of power-generating equipment p 832 A93-39030

PNEUMATIC PROBES
A pressure distribution measuring system with pneumatic switches and automatic band selection p 75 A93-10029
A data processing and measuring system with a traversing probe for studying flow in the rotating impeller of an axial-flow fan p 75 A93-10032

PNEUMATICS

Electropneumatic actuator, phase 1
[PB93-174951] p 1033 N93-31876

POINT DEFECTS

The onset of vortex turbulence p 788 N93-28251

POINT SOURCES

The future of area navigation in Western Europe p 311 A93-17752

POINT TO POINT COMMUNICATION

Onboard Connectivity Network for command and control aircraft p 1166 A93-49481

POISSON DENSITY FUNCTIONS

Numerical simulation of homogeneous non-Gaussian random vector fields p 561 A93-27584

POISSON EQUATION

Navier-Stokes simulation of viscous, separated, supersonic flow over a projectile rotating band
[AD-A263073] p 788 N93-27955

POLAND

Poland civil aviation master plan and investment program: Executive summary
[PB92-213685] p 459 N93-21342

Poland civil aviation master plan and investment program
[PB92-213693] p 459 N93-21343

Definitional mission for civil aviation master plan for Poland
[PB92-213974] p 459 N93-21713

POLAR NAVIGATION

History of aerial polar navigation p 104 A93-11300

POLARIMETRY

The realization phase of the PHARUS project --- Phased A-Ray Universal SAR p 1162 A93-47658

POLARITY

Detection performance of digital polarity sampled phase reversal code pulse compressors
[AD-A262930] p 842 N93-28289

POLICIES

Space policy 2000 p 1174 A93-50333
Proceedings of the First International Symposium on Explosive Detection Technology
[DOT/FAA/CT-92/11] p 496 N93-21856

POLISHING

Ultrasonic polishing p 750 N93-25580

POLLUTION CONTROL

Modification of combustor stoichiometry distribution for reduced NO(x) emission from aircraft engines
[ASME PAPER 92-GT-108] p 349 A93-19346

Control of contaminants in gas turbines with variable-flow combustion chambers and hydrogen addition p 520 A93-27478

Civil aircraft engines: The next generation
[PNR-90962] p 58 N93-11085

Activities report of Lufthansa
[ETN-92-92100] p 28 N93-11319

The 1990 high-speed civil transport studies
[NASA-CR-189618] p 330 N93-16947

The 1990 high-speed civil transport studies. Summary report
[NASA-CR-189619] p 330 N93-16999

AQUIS: A PC-based air quality and permit information system
[DE92-040092] p 434 N93-18587

Development and demonstration of a new filter system to control emissions during jet engine testing
[AD-A261203] p 755 N93-26243

Improved selective catalytic NOx control technology for compressor station reciprocating engines
[PB93-158566] p 755 N93-26529

In-situ bioventing: Two US EPA and Air Force sponsored field studies
[PB93-194231] p 1035 N93-32089

POLLUTION MONITORING
AQUIS: A PC-based air quality and permit information system
[DE92-040092] p 434 N93-18587

POLYATOMIC GASES
Problems in physical gas dynamics p 775 A93-39126

Kinetic theory of nonequilibrium flows of gas and disperse media with internal degrees of freedom and chemical reactions p 851 A93-39127

POLYETHYLENES

The unrealized potential for heavy balloon payloads p 39 A93-11359

Polyethylene pyrolysis model for combustion calculations in solid fuel ramjets p 520 A93-27739

POLYIMIDE RESINS
Development of polyimide adhesives for 371 C (700 F) structural performance for aerospace bonding applications - FM 680 system p 198 A93-15757

POLYIMIDES
Structural applications of Avimid K3B LDF thermoplastic composites --- for advanced aircraft p 1216 A93-53429

Advanced fiber/matrix material systems p 921 N93-30854

POLYMER MATRIX COMPOSITES

Lightning protection of composite structure p 141 A93-15801

Computer-aided cure optimization p 209 A93-15804

Model multilayer structured composites p 533 A93-24509

Evaluation of the fatigue behavior of discontinuous and continuous fiber thermoplastic composite laminates p 824 A93-36005

A two-dimensional analysis of multiple matrix cracking in a laminated composite close to its characteristic damage state p 1157 A93-50405

Calculation of sandwich plates with polymer composite skins under conditions of high humidity p 1215 A93-52968

Overview of NASA's advanced high temperature engine materials technology program p 1212 A93-53453

HOPE and its thermal protection systems p 1252 A93-54711

The Airbus floor beam: Towards a cost-effective composite design and manufacture research project sponsored by Airbus industry p 329 N93-16283

POLYMERIC FILMS

The Superpressure Stratospheric Vehicle p 39 A93-11357

The unrealized potential for heavy balloon payloads p 39 A93-11359

Video luminescent barometry - The induction period
[AIAA PAPER 93-0179] p 414 A93-22607

Thin gradient heat fluxmeters developed at ONERA [ONERA, TP NO. 1992-87] p 831 A93-38571

Waterborne polyurethane binder resins for compliant aircraft coatings
[AD-A256246] p 199 N93-14573

POLYMERS

Comparison of toxicity rankings of six aircraft cabin polymers by lethality and by incapacitation in rats p 26 A93-10328

Measurement of aerodynamic shear stress using side chain liquid crystal polymers p 72 N93-10770

POLYMETHYL METHACRYLATE
Study of the method for determining residual stress induced by machining in airplane canopies made of PMMA p 534 A93-27366

POLYNOMIALS
Uniform high-order spectral methods for one- and two-dimensional Euler equations p 476 A93-27068

Interactive grid generation program for CAP-TSD [NASA-TM-102705] p 17 N93-10349

A primer on polynomial resultants
[AD-A246883] p 98 N93-11463

Effect of design selection on response surface performance
[NASA-CR-4520] p 895 N93-29885

POLYPHENYL ETHER
Coking characteristics of polyphenyl ether lubricants using a Static Coker and a Micro Carbon Residue Tester p 77 A93-11341

Ferrographic analysis of polyphenyl ether fluids p 735 A93-34561

POLYSTYRENE
Seeding materials for use in laser anemometry
[AIAA PAPER 93-0006] p 389 A93-20129

POLYURETHANE FOAM
Generation of carbon monoxide in compartment fires
[PB93-146702] p 880 N93-29211

POLYURETHANE RESINS
Hermetic sealing and EMI shielding gasket
[AD-D015359] p 199 N93-13414

Waterborne polyurethane binder resins for compliant aircraft coatings
[AD-A256246] p 199 N93-14573

POROSITY
Crack models for a transversely isotropic medium p 557 A93-24566

Effect of leading-edge porosity on blade-vortex interaction noise
[AIAA PAPER 93-0601] p 563 A93-24727

Transonic shockwave/turbulent boundary layer interactions on a porous surface p 873 A93-43686

Nondestructive evaluation of ceramic and metal matrix composites for NASA's HITEMP and enabling propulsion materials programs
[NASA-TM-105807] p 85 N93-10963

Computation of transonic flow over a porous surface projectile p 696 N93-25409

POROUS BOUNDARY LAYER CONTROL
Numerical solution of the integral equations of the aerodynamics of porous surfaces p 13 A93-12768

Flow studies in ducted twin-rotor contra-rotating axial flow fans
[ASME PAPER 92-GT-390] p 258 A93-19545

- Shock/boundary-layer interaction control with vortex generators and passive cavity p 287 A93-23546
- A lag model for turbulent boundary layers developing over rough bleed surfaces [AIAA PAPER 93-2988] p 1052 A93-48181
- ### POROUS MATERIALS
- Effect of airfoil porosity on the shock wave position and intensity at transonic velocities p 241 A93-18222
- Low leakage fiber metal seals [ASME PAPER 92-GT-141] p 402 A93-19373
- The effectiveness of porous squeeze film dampers for suppressing nonsynchronous motions p 545 A93-27316
- Euler study on porous transonic airfoils with a view toward multipoint design p 479 A93-28604
- Acoustical properties of sound absorbing structures at high temperature p 1172 A93-48522
- ### POROUS WALLS
- Numerical solution of the integral equations of the aerodynamics of porous surfaces p 13 A93-12768
- Sound transmission through stiffened double-panel structures lined with elastic porous materials p 444 A93-19139
- Some acoustic features of perforated test section walls with splitter plates p 1226 A93-53222
- ### POSITION (LOCATION)
- IEEE PLANS '92 - Position Location and Navigation Symposium, Monterey, CA, Mar. 24-27, 1992, Record [ISBN 0-7803-0469-1] p 29 A93-10976
- Lessons learned during testing of the Enhanced Position Location Reporting System (EPLRS) p 77 A93-10996
- Automatic dependant surveillance focus of civil avionics integration p 30 A93-10998
- Automatic dependent surveillance (ADS) Pacific engineering trials (PET) p 30 A93-10999
- A minimum rate of position reporting in the future oceanic air traffic control system p 30 A93-11006
- Investigation on air refueling scheduling p 108 A93-14315
- LOCSTAR - A satellite radiodetermination system for Europe p 150 A93-15037
- Time-dependent 3-component laser-Doppler-anemometer and simultaneous position measurements in the flow of an aircraft engine p 538 A93-23809
- New concepts in remote sensing and geolocation p 556 A93-24173
- A localizer design to improve missed approach guidance p 992 A93-44143
- Representation of vehicle location in networked simulations p 1214 A93-52677
- [AIAA PAPER 93-3582] Multiple receiver, zero-length baseline kinematic GPS positioning techniques for airborne gravity measurement p 1240 A93-55974
- ILS mathematical modeling study of the effects of an ASR-9 structure at the Long Island MacArthur Airport, Islip, NY [DOT/FAA/CT-TN92/25] p 192 N93-12668
- An experimental health monitoring unit for GPS and GLONASS p 706 N93-25018
- Optimal finite-thrust time-bounded direct-ascent interception p 734 N93-25272
- Visualization of a Mach 2 reacting flow using Planar Laser-Induced Fluorescence (PLIF) p 731 N93-26006
- A transfer matrix approach to vibration localization in mistuned blade assemblies [NASA-TM-106112] p 838 N93-27088
- ### POSITION (TITLE)
- Annual Paul E. Hemke Lecture in aerospace engineering p 107 A93-14067
- ### POSITION ERRORS
- The derivation of path following error and control motion noise filters for the reduction of Global Positioning System flight test data p 32 A93-11022
- Receiver autonomous integrity monitoring (RAIM) capability for sole-means GPS navigation in the oceanic phase of flight p 33 A93-11035
- Differential GPS autonomous failure detection p 314 A93-21152
- Analysis of DGPS/INS and MLS/INS final approach navigation errors and control performance data p 315 A93-21183
- Data communication for airborne differential GPS/GLONASS application p 499 A93-27910
- DME-derived positions compared with MLS- and ILS-derived positions [NLR-TP-90119-U] p 318 N93-16343
- Information-based criteria of terrain navigability. Part 1: Data-base analysis p 793 N93-27178
- Experiences with two GPS receivers in northern Europe [NLR-TP-91168-U] p 993 N93-31120
- ### POSITION INDICATORS
- The high accuracy applications of the GPS system to static positioning p 500 A93-28193
- An optical fiber based position sensor with immunity to temperature variation p 743 A93-34287
- Fiber optic position sensors --- in aircraft flight control systems p 1105 A93-49465
- Desirable characteristics for rotorcraft optical components p 1172 A93-49466
- Ladar fiber optic sensor system for aircraft applications p 1105 A93-49467
- New concepts for fiber optic position sensors p 1106 A93-49477
- System for calibrating a gyro navigator [AD-D015668] p 708 N93-26093
- ### POSITION SENSING
- A survey of position trackers p 1151 A93-49396
- Position sensor with two wavelength time domain multiplexing for civil aircraft application p 1104 A93-49432
- Fiber optic position sensors --- in aircraft flight control systems p 1105 A93-49465
- Desirable characteristics for rotorcraft optical components p 1172 A93-49466
- Ladar fiber optic sensor system for aircraft applications p 1105 A93-49467
- New concepts for fiber optic position sensors p 1106 A93-49477
- Accuracy improvement of linear estimated motion using differential type sensors [NAL-TR-1135] p 91 N93-12365
- ### POSITIONING
- The GPS system - Satellite radio-navigation p 312 A93-20008
- A distributed, message-based, airspace environment p 313 A93-21144
- Modeling and control design of a wind tunnel model support p 529 A93-29281
- Overview of the FAA's differential GPS CAT III technical feasibility demonstration program [AIAA PAPER 93-3836] p 1098 A93-51425
- GPS Interferometry [NASA-CR-192301] p 319 N93-18873
- System analysis for a kinematic positioning system based on the global positioning system [AD-A262830] p 885 N93-29468
- ### POSITIONING DEVICES (MACHINERY)
- Design philosophy for wind tunnel model positioning control systems p 822 A93-37877
- Design philosophy for wind tunnel model positioning systems [AD-A254958] p 192 N93-12552
- ### POTENTIAL FLOW
- Numerical solution of transonic full-potential-equivalent equations in von Mises co-ordinates p 111 A93-14080
- A fast method for calculating three-dimensional transonic potential flows in turbomachine blade rows p 125 A93-15215
- Optimal circumferential placement of cylindrical thermocouple probes for reduction of excitation forces [ASME PAPER 92-GT-423] p 406 A93-19571
- Incompressible potential flow calculation about harmonically oscillating three-dimensional configurations p 461 A93-24089
- Subsonic potential flow and the transonic controversy p 479 A93-28544
- Unsteady transonic potential flow over a flexible fuselage [AIAA PAPER 93-1593] p 683 A93-34124
- Transonic flow around the leading edge of a thin airfoil with a parabolic nose p 688 A93-34405
- Application of a full potential code to the definition of a transonic test section [ONERA, TP NO. 1992-84] p 822 A93-38569
- Treatment of vortex sheets for the transonic full-potential equation p 871 A93-42870
- A wake singularity potential flow model for airfoils experiencing trailing-edge stall p 1067 A93-48544
- Aerodynamic investigation of radial turbines using computational methods p 81 N93-10056
- Numerical investigations into the base drag of various wedges using the base flow model developed by Mauri Tanner [REPT-B-36] p 26 N93-12414
- Overall effects of separation on thin aeroflows [ISBN-0-315-67464-4] p 135 N93-13930
- A compilation of the mathematics leading to the doublet lattice method [AD-A256304] p 136 N93-14441
- Application of the program profile for the design of low-speed, low-observable configuration airfoils [AD-A258842] p 305 N93-19364
- Unsteady vortex loop/dipole theory applied to the work and acoustics of an ideal low speed propeller [AD-A264057] p 876 N93-29891
- ### POTENTIAL THEORY
- The development of a CFD potential method for the analysis of tilt-rotors p 481 A93-29434
- A fast robust viscous-inviscid interaction solver for transonic flow about wing/body configurations on the basis of full potential theory [AIAA PAPER 93-3026] p 1056 A93-48211
- Current European rotorcraft research activities on development of advanced CFD methods for the design of rotor blades (BRITE/EURAM DACRO project) [MBB-UD-0601-91-PUB] p 293 N93-17568
- ### POWDER (PARTICLES)
- Polymer infiltration studies [NASA-CR-191652] p 200 N93-15431
- Process optimization of Hexoloy SX-SiC towards improved mechanical properties [DE93-007913] p 826 N93-28564
- Advanced fiber/matrix material systems p 921 N93-30854
- ### POWDER METALLURGY
- Powder metallurgy repair of turbine components [ASME PAPER 92-GT-312] p 354 A93-19500
- ### POWER CONDITIONING
- Development of a model to predict electric vehicle performance over a variety of driving conditions p 570 A93-26011
- ### POWER CONVERTERS
- A new resonant link aircraft power generating system p 809 A93-36266
- ### POWER EFFICIENCY
- Advanced three-shaft engines - Configured for reliability, efficiency and growth p 53 A93-12236
- Effect of the aerodynamic interference of the rotor and the fuselage on the power requirements for the horizontal flight of a helicopter p 819 A93-39179
- Expert evaluation of the technological level of aviation gas turbine engine designs p 811 A93-39187
- Flight efficiency theory p 812 A93-39202
- Optimization of the blade angle of the AV-2 propeller for improving the flight performance characteristics of An-2 aircraft p 996 A93-45663
- Performance improvement of gas turbine with steam injection p 1107 A93-48523
- The combined effect of clearances and peripheral overlaps on the efficiency of microturbines with shrouded rotors p 1193 A93-52963
- Small gas turbines in the 21st century p 1247 A93-55494
- ### POWER LINES
- PROAV Cable Warning System (CWS) - U.S. Army aircraft integration assessment and OCONUS field evaluation [AD-A261233] p 705 N93-26263
- ### POWER LOSS
- The flow lag angle in the rotor of a centrifugal compressor with allowance for viscosity effects p 1179 A93-53555
- ### POWER SERIES
- Flexure-torsion behavior of prismatic beams. I - Section properties via power series p 417 A93-23557
- ### POWER SPECTRA
- Equivalent deterministic inputs for atmospheric turbulence p 183 A93-14351
- Turbulent structure in a vortex wake shed from an inclined circular cylinder p 125 A93-15443
- Detection and classification of acoustic signals from fixed-wing aircraft p 850 A93-37032
- Time-frequency domain analysis of vibration signals for machinery diagnostics. 3: The present power spectral density [OUEL-1911/92] p 89 N93-11707
- Vortex shedding by blunt/bluff bodies at high Reynolds numbers. Volume 4: Rectangles [AD-A264154] p 877 N93-30151
- Vortex shedding by blunt/bluff bodies at high Reynolds numbers. Volume 1: Data analysis [AD-A264151] p 877 N93-30171
- Vortex shedding by Blunt/Bluff bodies at high Reynolds numbers. Volume 2: Cylinders, octagon, hexagon [AD-A264152] p 877 N93-30172
- Vortex shedding by blunt/bluff bodies at high Reynolds numbers. Volume 3: Cubes [AD-A264153] p 877 N93-30173
- ### POWER SUPPLIES
- Autonomous mobile laser complex p 395 A93-17767
- High reliability, maintenance-free INS battery development [AD-A264521] p 934 N93-30406
- ### POWER SUPPLY CIRCUITS
- Effects of external control circuit on coal-fired supersonic diagonal-type MHD generator p 1173 A93-49619
- ### POWER TRANSMISSION
- A High Deflection Diaphragm concept (HDD) for power transmission shafting p 826 A93-35931
- ### POWERED LIFT AIRCRAFT
- A method of wind shear detection for powered-lift STOL aircraft [AIAA PAPER 93-3667] p 1104 A93-48345

- Wind-shear endurance capability for powered-lift aircraft
[AIAA PAPER 93-3670] p 1129 A93-48348
Effects of flow-path variations on internal reversing flow in a tailpipe offtake configuration for ASTOVL aircraft
[AIAA PAPER 93-2438] p 1118 A93-50190
Application of eigenstructure assignment to the control of powered lift combat aircraft p 64 A93-11871
Experimental performance of a ventral nozzle with pitch and yaw vectoring capability for SSTOVL aircraft
[NASA-TM-106054] p 722 A93-25129
Effects of flow-path variations on internal reversing flow in a tailpipe offtake configuration for ASTOVL aircraft
[NASA-TM-106149] p 900 A93-29065
- POWERED MODELS**
Tests of models equipped with TPS in low speed ONERA F1 pressurized wind tunnel p 213 N93-13201
Recent developments in low-speed TPS-testing for engine integration drag and installed thrust reverser simulation p 160 N93-13207
- POYNTING THEOREM**
Solution of trajectory optimization methods using the Pontriagin maximum principle p 366 A93-18378
- PRANDTL-MEYER EXPANSION**
Observations of liquid jets injected into a highly accelerated supersonic boundary layer p 1177 A93-53214
- PREBURNERS**
Overview of aerothermodynamic loads definition study p 1016 N93-31583
- PRECIPITATION (METEOROLOGY)**
Hydrometeor identification using cross polar radar measurements and aircraft verification p 844 A93-37719
Update on the NASA ER-2 Doppler radar system (EDOP) p 807 A93-37737
Behavior of precipitating water drops under the influence of electrical and aerodynamical forces p 1034 A93-45176
- PRECIPITATION HARDENING**
Structural stability of 'beta-CEZ' alloy
[ONERA, TP NO. 1992-106] p 824 A93-38586
- PRECIPITATION PARTICLE MEASUREMENT**
Maximum hail concentration that can be met by an aircraft in stormy precipitations p 430 A93-22152
- PRECONDITIONING**
Preconditioned domain decomposition scheme for three-dimensional aerodynamic sensitivity analysis p 957 A93-45096
- PRECOOLING**
Characteristics of heat exchanger in supersonic/subsonic flows
[ISABE 93-7119] p 1221 A93-54094
An evaluation of thermal energy storage options for precooling gas turbine inlet air
[DE93-005980] p 754 A93-24975
- PREDICTION ANALYSIS TECHNIQUES**
Prediction of the inception of rotating stall for multistage axial flow compressors p 12 A93-12731
Stirling engine - Available tools for long-life assessment for space propulsion p 195 A93-13824
Aircraft fatigue failures and tasks of structural reliability analysis p 210 A93-16246
Numerical prediction of instabilities in transonic internal flows using an Euler TVD code
[AIAA PAPER 93-0072] p 262 A93-20184
Prediction of fluctuating pressure in attached and separated compressible flow
[AIAA PAPER 93-0286] p 279 A93-22687
Further studies using matched filter theory and stochastic simulation for gust loads prediction
[AIAA PAPER 93-1365] p 726 A93-33932
Evaluation and extension of the flutter-margin method for flight flutter prediction p 828 A93-37393
Numerical prediction of aerodynamic sound using large eddy simulation p 850 A93-38150
On the possibility of singularities in the acoustic field of supersonic sources when BEM is applied to a wave equation p 1039 A93-46805
The prediction and the active control of surge in multi-stage axial-flow compressors p 1002 A93-46945
Verification of rain-flow reconstructions of a variable amplitude load history
[NASA-CR-189670] p 91 A93-12411
The Fourth Workshop on Dynamics and Aeroelastic Stability Modeling of Rotorcraft Systems
[AD-A255065] p 50 A93-12485
Thermal barrier coating life prediction model development, phase 2 p 198 A93-12589
Analysis and design of planar and non-planar wings for induced drag minimization
[NASA-CR-191274] p 131 A93-13463
Evaluation of three models used for predicting noise propagated long distances overground
[AD-A255963] p 232 A93-14406
- Reliability of stiffened structural panels: Two examples
[NASA-TM-107687] p 219 A93-14483
Advanced technology wind shear prediction system evaluation p 146 A93-14858
LARZAC HP turbine disk crack initiation and propagation spin pit test p 176 A93-14892
Drag due to gaps round undeflected trailing-edge controls and flaps at subsonic speeds
[ESDU-92039] p 290 A93-16634
Application of a neural network as a potential aid in predicting NTF pump failure
[NASA-TM-107667] p 442 A93-18332
Creep fatigue life prediction for engine hot section materials (isotropic)
[NASA-CR-189221] p 364 A93-18578
The 1992 International Aerospace and Ground Conference on Lightning and Static Electricity: Addendum
[DOT/FAA/CT-92/20-ADD-1] p 753 A93-24875
A computational approach to predicting the extent of arc root damage in CFC panels p 735 A93-24890
Development of models for predicting the triggering of lightning by launch vehicles p 734 A93-24899
Numerical simulation of free shear flows: Towards a predictive computational aeroacoustics capability
[NASA-CR-191015] p 781 A93-27097
Three-dimensional water droplet trajectory code validation using an ECS inlet geometry
[NASA-CR-191097] p 791 A93-27267
Loudness and annoyance response to simulated outdoor and indoor sonic booms
[NASA-TM-107756] p 852 A93-27271
Heat Transfer and Cooling in Gas Turbines
[AGARD-CP-527] p 901 A93-29926
Mathematical model of frost heave and thaw settlement in pavements
[CRREL-REPT-93-2] p 912 A93-30103
First NASA Advanced Composites Technology Conference, part 2
[NASA-CP-3104-PT-2] p 921 A93-30841
Navier-Stokes computations for kinetic energy projectiles in steady coning motion: A predictive capability for pitch damping p 1033 A93-32028
Development of a method to predict transonic limit cycle oscillation characteristics of fighter aircraft
[NLR-TP-91359-U] p 999 A93-32338
- PREDICTIONS**
Aviation accidents, incidents, and violations: Psychological predictors among US pilots p 144 A93-14693
Development of the Advance Warning Airborne System(AWAS) p 144 A93-14849
In-service evaluation of wind shear systems p 146 A93-14857
Advanced technology wind shear prediction system evaluation p 146 A93-14858
A neural network prototype for predicting F-14B strains at the B.L. 10 longeron p 165 A93-15004
Contribution of ventral fins to sideforce and yawing moment derivatives due to sideslip at low angle of attack
[ESDU-92029] p 291 A93-16638
Prediction of success from training p 495 A93-19702
Comparison of performance on the Shiley Institute of Living Scale, Air Traffic Control Specialist Selection Test, and FAA Academy Screen
[AD-A259249] p 502 A93-20582
Fundamentals of adaptive anticipation techniques for the detection of threatening air traffic conflicts: Investigation of the horizontal proximity situation in the case of expected heading changes
[DLR-MITT-91-21] p 503 A93-21004
The transition prediction toolkit: LST, SIT, PSE, DNS, and LES p 783 A93-27429
Developments in impact damage modeling for laminated composite structures p 922 A93-30857
- PREDICTOR-CORRECTOR METHODS**
A new method for improved rotor free-wake convergence
[AIAA PAPER 93-0872] p 469 A93-24933
Enhancements to viscous-shock-layer technique p 962 A93-46408
An experimental evaluation of prediction methods for contrafans
[PNR-90924] p 56 A93-11023
Volume 2: Explicit, multistage upwind schemes for Euler and Navier-Stokes equations
[NASA-CR-191647] p 418 A93-16558
- PREFLIGHT ANALYSIS**
The fuel/timing problem in a computer-aided flight preparation system for civil aircraft p 996 A93-45672
- PREFLIGHT OPERATIONS**
Calculation of the position of aircraft center of gravity on an IBM PC p 996 A93-45671
- PREFORMS**
3-D braided preforms; cost to manufacture: Magnawave. I - Identifying cost factors p 1226 A93-53423
Consolidation of graphite thermoplastic textile preforms for primary aircraft structure p 919 A93-30439
- PREMIXED FLAMES**
Recent progress in the implementation of active combustion control p 171 A93-14272
Carbon monoxide emissions in lean premixed combustion p 197 A93-14503
NO(x) sensitivities for gas turbine engines operated on lean-premixed combustion and conventional diffusion flames
[ASME PAPER 92-GT-115] p 349 A93-19351
On the structure and response of aerodynamically-strained planar premixed flames
[AIAA PAPER 93-0246] p 390 A93-22657
Pd prediction of supersonic hydrogen flames
[AIAA PAPER 93-0448] p 391 A93-23358
A coupled multi-block solution procedure for spray combustion in complex geometries
[AIAA PAPER 93-0108] p 539 A93-24230
Computations of spray, fuel-air mixing, and combustion in a lean-premixed-prevaporized combustor
[AIAA PAPER 93-2069] p 1153 A93-49901
The prediction of thermal NO(x) in gas turbine exhausts
[ISABE 93-7022] p 1195 A93-53998
Large eddy simulation of turbulent combustion behind flame holders
[ISABE 93-7042] p 1198 A93-54018
Chemical kinetic and aerodynamic structures of flames
[AD-A256015] p 391 A93-15931
Oxides of nitrogen emissions from turbulent hydrocarbon/air jet diffusion flames, phase 2
[PB93-152478] p 756 A93-26533
- PREMIXING**
Employment of radicals and excited state species for supersonic combustion photochemical ignition of premixed hydrogen/oxygen mixtures with ArF laser p 73 N93-11135
- PREPREGS**
The characterization and development of materials for advanced textile composites p 1211 A93-53434
The properties of newly developed highly damage tolerant and easy handleable carbon fiber/modified bismaleimide prepreg system p 1212 A93-53448
Wet layup materials for repair of bismaleimide composites p 1212 A93-53451
Repair materials and processes for the MD-11 Composite Tailcone p 1216 A93-53452
Experimental and analytical investigation of dynamic characteristics of extension-twist-coupled composite tubular spars
[NASA-TP-3225] p 553 A93-20585
Design, analysis, and fabrication of the technology integration box beam p 919 A93-30433
Development of resins for composites by resin transfer molding p 921 A93-30853
Advanced fiber placement of composite fuselage structures p 923 A93-30864
- PREPROCESSING**
An interactive preprocessor for the NASA engine performance program
[NASA-TM-105786] p 56 A93-10983
- PRESIDENTIAL REPORTS**
Aeronautics and space report of the President: Fiscal year 1992 activities p 854 A93-27041
- PRESSURE**
Time-dependent predictions and analysis of turbine cascade data in the transonic flow region
[PNR-90957] p 139 A93-15489
- PRESSURE CHAMBERS**
On the compression process in a free-piston shock-tunnel p 1136 A93-48041
- PRESSURE DISTRIBUTION**
A pressure distribution measuring system with pneumatic switches and automatic band selection p 75 A93-10029
Wing pressure loads in canard configurations - A comparison between numerical results and experimental data p 7 A93-11499
Experimental investigations of the separation behavior in 3D shock wave/turbulent boundary-layer interactions p 119 A93-14345
Toward an integration of aerodynamics and aeroacoustics of rotors p 243 A93-19127
Unsteady pressures under impinging jets in crossflows p 399 A93-19220

Experimental and theoretical analysis of the flow in a centrifugal compressor volute
[ASME PAPER 92-GT-30] p 400 A93-19290

Pressure fluctuation on casing wall of isolated axial compressor rotors at low flow rate
[ASME PAPER 92-GT-33] p 246 A93-19293

Massively parallel aerodynamic shape optimization
p 266 A93-20729

Control of pressure fluctuations in the reattachment region of a supersonic free shear layer
[AIAA PAPER 93-0385] p 282 A93-23064

Vortex/surface interaction
[AIAA PAPER 93-0863] p 468 A93-24925

Pressure measurements on a pitching airfoil in a water channel
[AIAA PAPER 93-0184] p 473 A93-25510

Pressure fluctuations on the surface of two circular cylinders in tandem arrangements at high Reynolds numbers
p 679 A93-33718

Determination of tire-wheel interface pressure distribution for aircraft wheels
[AIAA PAPER 93-1343] p 709 A93-33913

Sensitivity analysis of aeroelastic response of a wing using piecewise pressure representation
[AIAA PAPER 93-1645] p 742 A93-34170

Hypersonic limiting flows of a relaxing gas with pressure changes in the main approximation
p 776 A93-39135

Engineering method for calculating surface pressures and heating rates on vehicles with embedded shocks
p 777 A93-39255

Damping of surface pressure fluctuations in hypersonic turbulent flow past expansion corners
p 860 A93-41914

Results from a set of low speed blade-vortex interaction experiments
p 872 A93-43540

Unstructured grids for sonic-boom analysis
[AIAA PAPER 93-2929] p 949 A93-44229

Performance data of the new free-piston shock tunnel T5 at GALCIT
p 1011 A93-45498

Effect of nonaxisymmetric forcing on a swirling jet with vortex breakdown
[AIAA PAPER 93-3251] p 1028 A93-46796

Adaptation of a 3-D pressure correction Navier-Stokes solver for the accurate modelling of tip clearance flows
p 971 A93-46932

A wind tunnel investigation of the pressure distribution on an F/A-18 wing
[AIAA PAPER 93-3468] p 980 A93-47249

Code validation for high speed flow simulation over the VLS launcher fairing --- Brazilian satellite launch vehicles
[AIAA PAPER 93-3046] p 1057 A93-48226

Experimental investigation on effect of solid particles on blade pressure distribution in compressor cascade flow
p 1066 A93-48513

Periodic vortex shedding over delta wings
p 1070 A93-49002

Model for entropy production and pressure variation in confined turbulent mixing
p 1071 A93-49014

Thrust loss due to supersonic mixing
[AIAA PAPER 93-2140] p 1114 A93-49958

High Reynolds number and turbulence effects on aerodynamics and heat transfer in a turbine cascade
[AIAA PAPER 93-2252] p 1155 A93-50050

An experimental study of the dynamic effect of a supersonic underexpanded jet on a plane surface parallel to the nozzle axis
p 1092 A93-51913

The effects of fixed rotor tilt on the rotorodynamic coefficients of incompressible flow annular seals
p 1161 A93-52601

Pressure distribution measurement around hypersonic delta winged semicone - Measurement by means of magnet tape
p 1176 A93-53193

Moving wall effects in transverse subsonic flow past a rotating cylinder
p 1179 A93-53573

Spectral analysis of unsteady surface pressure on a pusher propeller
p 1232 A93-54646

Pressure field and drag of a single cavity with rounded and sharp edges
p 1258 A93-55018

Analysis of wing-body junction flowfields using the incompressible Navier-Stokes equations, volumes 1 and 2
p 17 N93-10320

A combined experimental and theoretical study of laminar flow control with particular relevance to aero engine nacelles
[PNR-90991] p 20 N93-11070

Correlation of forebody pressures and aircraft yawing moments on the X-29A aircraft at high angles of attack
[NASA-TM-4417] p 22 N93-11532

Experimental investigation of the effects of aft blowing with various nozzle exit geometries on a 3.0 caliber tangent ogive at high angles of attack: Forebody pressure distributions
[NASA-CR-190935] p 22 N93-11605

Effects of sweep on the physics of unsteady shock-induced turbulent separated flows
[AD-A247035] p 22 N93-11742

Flight test results from a supercritical mission adaptive wing with smooth variable camber
[NASA-TM-4415] p 49 N93-11863

A wall interference assessment/correction system
[NASA-CR-190617] p 68 N93-11910

An investigation of the effects of aft blowing on a 3.0 caliber tangent ogive body at high angles of attack
[NASA-CR-190934] p 24 N93-12004

Unsteady propeller/wing aerodynamic interactions
p 24 N93-12190

An approach to constrained aerodynamic design with application to airfoils
[NASA-TP-3260] p 24 N93-12321

A numerical study of hypersonic flow with strong surface blowing
p 129 N93-13128

Application of a solution adaptive grid to flow over an embedded cavity
p 130 N93-13141

An experimental/computational study of heat transfer in sharp fin induced shock wave/turbulent boundary layer interactions at low hypersonic Mach numbers
p 217 N93-13826

Pressure distribution for the wing of the YAV-8B airplane; with and without pylons
[NASA-TM-4429] p 136 N93-14451

Pressure drag and lift contributions for blunted forebodies of fineness ratio 2.0 in transonic flow (M infinity less than or equal to 1.4)
[ESDU-89033] p 136 N93-14515

Detailed near surface flow about yawed, stranded cables
[AD-A257382] p 418 N93-15857

Static pressure measurements of the shock-boundary layer interaction in a simulated fan passage
[AD-A256724] p 361 N93-15979

Preliminary efforts toward development of data handling and analysis software for unsteady flow measurements: An application for aeroelastic transonic flow configurations
p 291 N93-16768

Navier-Stokes calculation of transonic flow past the NTF 65-deg delta wing
p 292 N93-16797

Hypersonic flows as related to the national aerospace plane
[NASA-CR-191980] p 296 N93-18378

Experimental and numerical examinations of the influence of inlet distortion perturbations on the working behavior of turbofan compressors
[ETN-93-92733] p 364 N93-18628

Experimental investigation of rotating stall in a mismatched three stage axial flow compressor
p 423 N93-18727

Performance of controlled diffusion blades
p 424 N93-18735

Numerical investigation of performance degradation of wings and rotors due to icing
[NASA-CR-192233] p 339 N93-18783

Numerical computations using multi-domain technique
p 299 N93-19277

Analysis of a 2-D airfoil motion flying in-proximity-to a wavy-wall surface: Finite difference method
p 300 N93-19282

Numerical study on transverse hydrogen injection into a supersonic flowfield
p 302 N93-19311

Wind tunnel wall interference correction at subsonic speeds
p 304 N93-19320

Wind tunnel testing and CFD simulation in Mitsubishi Heavy Industries
p 305 N93-19325

The aerodynamic performance of laser drilled sheets
[AERO-REPT-9204] p 484 N93-20806

HSCT mission analysis of waverider designs
[NASA-CR-192193] p 515 N93-21646

Surface and flow field measurements in a symmetric crossing shock wave/turbulent boundary-layer interaction
[NASA-TM-106086] p 693 N93-24911

Generic hypersonic vehicle performance model
[NASA-CR-192953] p 714 N93-25162

An experimental study of the sources of fluctuating pressure loads beneath swept shock/boundary-layer interactions
[NASA-CR-192918] p 749 N93-25266

The transient development of vortices over delta wings
p 695 N93-25269

Experimental effects of wing location on wing-body pressures at supersonic speeds
[NASA-TM-4434] p 700 N93-26085

Model fan passage flow simulation
[AD-A261613] p 752 N93-26167

Towards an analytical treatment of the aerodynamic problem of a circular wing
p 781 N93-27214

Effect of vortex behavior on loads acting on a 65 deg delta wing oscillating in roll at high incidence
p 782 N93-27220

Flow prediction over a transport multi-element high-lift system and comparison with flight measurements
p 785 N93-27448

Unsteady transition measurements on a pitching three-dimensional wing
p 820 N93-27450

Navier-Stokes simulation of viscous, separated, supersonic flow over a projectile rotating band
[AD-A263073] p 788 N93-27955

Transonic flows on an oscillating airfoil and their effect on the flutter-boundary
[DLR-FB-92-08] p 790 N93-29006

High Reynolds number and turbulence effects on aerodynamics and heat transfer in a turbine cascade
[NASA-TM-106187] p 930 N93-29157

Performance characteristics of two multiaxis thrust-vectoring nozzles at Mach numbers up to 1.28
[NASA-TP-3313] p 874 N93-29160

High-Reynolds-number test of a 5-percent-thick low-aspect-ratio semispan wing in the Langley 0.3-meter transonic cryogenic tunnel: Wing pressure distributions
[NASA-TM-4227] p 875 N93-29449

Determination of surface heat transfer and film cooling effectiveness in unsteady wake flow conditions
p 902 N93-29933

The aerodynamic effect of coolant ejection in the leading edge region of a film-cooled turbine blade
p 904 N93-29958

PRESSURE DRAG

Pressure drag and lift contributions for blunted forebodies of fineness ratio 2.0 in transonic flow (M infinity less than or equal to 1.4)
[ESDU-89033] p 136 N93-14515

Experiments on smooth cantilevered circular cylinders in low-turbulence uniform flow. Part 1: Mean loading with aspect ratios in the range 4 to 30
[PB93-11763] p 555 N93-21383

PRESSURE DROP

Allowing for the effect of flow nonisothermality on total pressure losses in the afterburner diffusers of augmented turbofan engines
p 53 A93-12811

Compressible flow pressure losses in wye-junctions
[ASME PAPER 92-GT-71] p 248 A93-19321

Techniques for aerodynamic loss measurement of transonic turbine cascades with trailing-edge region coolant ejection
[ASME PAPER 92-GT-157] p 250 A93-19384

Total-pressure loss in supersonic parallel mixing
[AIAA PAPER 93-0216] p 278 A93-22632

An experimental study of thrust reverser models --- of axisymmetric exhaust systems of aerjet engines
p 812 A93-39195

Exhaust system model test and research
p 1107 A93-48525

A new type of fuel control model
p 1108 A93-49204

The development of a new air filtration system for the Alouette III helicopter
[ISABE 93-7048] p 1199 A93-54024

Effects of turn region treatments on pressure loss through sharp 180-degree bends
p 1256 A93-54636

PRESSURE EFFECTS

Effects of back-pressure in a lean blowout research combustor
[ASME PAPER 92-GT-81] p 387 A93-19330

Wall jets created by single and twin high pressure jet impingement
p 744 A93-34847

Silicon differential pressure transducer line pressure effects and compensation
p 830 A93-37890

The effects of high-pressure water on the material integrity of selected aircraft coatings and substrates
[SME PAPER AD92-207] p 855 A93-40668

The Langley 8-ft transonic pressure tunnel laminar-flow-control experiment
p 910 A93-41783

Effect of the flow non-uniformity on the mixing layer at the interface of parallel supersonic flows
[ISAS-RN-646] p 128 N93-12716

A novel-high-performance system for recording and analysing instantaneous total pressure distortion in air intakes
p 214 N93-13215

PRESSURE GAGES

A multi-faceted engineering study of aerodynamic errors of the Service Aircraft Instrumentation Package (SAIP)
[AD-A258059] p 293 N93-17677

Selection and static calibration of the Marsh J1678 pressure gauge
p 931 N93-29779

PRESSURE GRADIENTS

Unsteady turbulent skin-friction measurement in an adverse pressure gradient
p 206 A93-14545

The effect of entrance radius and film injection on wall heating in scramjet nozzles
p 360 A93-22505

Total-pressure loss in supersonic parallel mixing
[AIAA PAPER 93-0216] p 278 A93-22632

Hypersonic stability and transition
p 864 A93-42579

Aerodynamic design of a hypersonic body with a constant favorable pressure gradient
[AIAA PAPER 93-3444] p 978 A93-47232

A lag model for turbulent boundary layers developing over rough bleed surfaces
[AIAA PAPER 93-2988] p 1052 A93-48181

- Calculation of the parameters of instability waves in the preseparation region p 1067 A93-48826
 Determination of the aerodynamic balance efficiency of aircraft p 1130 A93-48903
 Investigation of supersonic shaped nozzles in a low-pressure wind tunnel p 1091 A93-51881
 The reduction of skin friction by riblets under the influence of an adverse pressure gradient p 1218 A93-53810
 Effect of the flow non-uniformity on the mixing layer at the interface of parallel supersonic flows [ISAS-RN-646] p 128 A93-12716
 Flow prediction over a transport multi-element high-lift system and comparison with flight measurements p 785 A93-27448
 Heat transfer with moderate free stream turbulence p 932 A93-29936

PRESSURE MEASUREMENT

- A pressure distribution measuring system with pneumatic switches and automatic band selection p 75 A93-10029
 Experiments on Space Shuttle Orbiter models in a free piston shock tunnel p 7 A93-11497
 Extending the useful frequency of 'rigid' wind tunnel models with active control p 190 A93-14299
 Determination of vortex burst location on delta wings from surface pressure measurements p 123 A93-14557
 The effects of blade loading in radial and mixed flow turbines [ASME PAPER 92-GT-92] p 349 A93-19338
 Unsteady pressure measurements in a rotating centrifugal impeller [ASME PAPER 92-GT-152] p 402 A93-19379
 Unsteady pressure measurements on the rotor of a model turbine stage in a transient flow facility [ASME PAPER 92-GT-156] p 250 A93-19383
 Separated flow in a low speed two-dimensional cascade. II - Cascade performance [ASME PAPER 92-GT-357] p 257 A93-19522
 Experimental investigation of vortex-fin interaction [AIAA PAPER 93-0050] p 260 A93-20163
 The aerodynamic effects of sideslip on double delta wings [AIAA PAPER 93-0053] p 261 A93-20166
 Unsteady loads measurements in a generic high speed engine model by means of recessed transducers [AIAA PAPER 93-0287] p 342 A93-21104
 Data analysis techniques for pressure- and temperature-sensitive paint [AIAA PAPER 93-0176] p 414 A93-22605
 Video luminescent barometry - The induction period [AIAA PAPER 93-0179] p 414 A93-22607
 Validation of a Navier-Stokes code using a (k, ϵ) turbulence model applied to a three-dimensional transonic channel p 279 A93-22693
 Wall pressure fluctuations beneath swept shock wave/boundary layer interactions [AIAA PAPER 93-0384] p 282 A93-23063
 A study of flow separation on an oscillating flap at Mach number 2.4 [AIAA PAPER 93-0436] p 286 A93-23350
 Fiber-optic interferometric sensors for measurements of pressure fluctuations - Experimental evaluation [AIAA PAPER 93-0738] p 540 A93-24828
 An examination of vortex convection effects during blade-vortex interaction p 473 A93-25360
 Pressure measurements on a pitching airfoil in a water channel [AIAA PAPER 93-0184] p 473 A93-25510
 Aerodynamic applications of pressure sensitive paint p 549 A93-29301
 Comparative wind tunnel tests at high Reynolds numbers of NACA 64 621 airfoils with two aileron configurations p 967 A93-46823
 In-stream measurements of combustion during Mach 5 to 7 tests of the Hypersonic Research Engine (HRE) [AIAA PAPER 93-2324] p 1116 A93-50104
 Stall inception in a multi-stage high speed axial compressor [AIAA PAPER 93-2386] p 1117 A93-50153
 Three-dimensional flow field in a turbine nozzle passage [AIAA PAPER 93-2556] p 1084 A93-50278
 Unsteady wing surface pressures in the wake of a propeller p 1095 A93-52436
 Unsteady pressure and load measurements on an F/A-18 vertical fin p 1095 A93-52451
 Boundary layer and pressure measurements on a cylinder with unsteady circulation control p 1177 A93-53207
 Development of a dynamic pressure response calibrator p 1254 A93-54362
 Uncertainty estimates for pressure sensitive paint measurements p 1258 A93-55369

- Pressure measurements at supersonic speeds on the research configuration ELAC I p 1237 A93-56033
 The hemisphere-cylinder at an angle of attack p 21 N93-11250
 An experimental study of flow patterns and endwall heat transfer upstream of a surface-mounted rectangular obstruction in a turbulent boundary layer p 89 N93-11698
 Operating experience using venturi flow meters at liquid helium temperature [DE92-014693] p 90 N93-12140
 Planar measurement of flow field parameters in nonreacting supersonic flows with laser-induced iodine fluorescence p 133 N93-13801
 Flowfield study of a close-coupled canard configuration [AD-A256311] p 139 N93-15245
 Upgrade and extension of the data acquisition system for propulsion and gas dynamic laboratories [AD-A256836] p 235 N93-15637
 Static pressure measurements of the shock-boundary layer interaction in a simulated fan passage [AD-A256724] p 361 N93-15979
 Development and flight testing of a surface pressure measurement installation on the EAP demonstrator aircraft p 550 N93-19927
 Experiments on smooth cantilevered circular cylinders in a low-turbulence uniform flow. Part 2: Fluctuating loads on a cantilever of aspect ratio 30 [PB93-110500] p 555 N93-21382
 Combined experiment, phase 1 [DE93-000012] p 485 N93-21766
 Surface and flow field measurements in a symmetric crossing shock wave/turbulent boundary-layer interaction [NASA-TM-106086] p 693 N93-24911
 An experimental study of the sources of fluctuating pressure loads beneath swept shock/boundary-layer interactions [NASA-CR-192918] p 749 N93-25266
 The transient development of vortices over delta wings p 695 N93-25269
 Experimental effects of wing location on wing-body pressures at supersonic speeds [NASA-TM-4434] p 700 N93-26085
 Jet-induced ground effects on a parametric flat-plate model in hover [NASA-TM-104001] p 700 N93-26099
 Analysis of fluctuating static pressure measurements in a large high Reynolds number transonic cryogenic wind tunnel [NASA-TM-108722] p 823 N93-27142
 Selection and static calibration of the Marsh J1678 pressure gauge p 931 N93-29779
- PRESSURE OSCILLATIONS**
 Recent progress in the implementation of active combustion control p 171 A93-14272
 Extending the useful frequency of 'rigid' wind tunnel models with active control p 190 A93-14299
 Experiments on the active control of boundary layer transition p 243 A93-19133
 On space correlation of pressure pulsations on the streamlined surface before a step p 244 A93-19135
 Pressure fluctuation on casing wall of isolated axial compressor rotors at low flow rate [ASME PAPER 92-GT-33] p 246 A93-19293
 Unsteady pressure measurements in a rotating centrifugal impeller [ASME PAPER 92-GT-152] p 402 A93-19379
 Unsteady pressure measurements on the rotor of a model turbine stage in a transient flow facility [ASME PAPER 92-GT-156] p 250 A93-19383
 Prediction of fluctuating pressure in attached and separated compressible flow [AIAA PAPER 93-0286] p 279 A93-22687
 Unsteady vortex dynamics and surface pressure topologies on a pitching wing [AIAA PAPER 93-0435] p 286 A93-23349
 Fiber-optic interferometric sensors for measurements of pressure fluctuations - Experimental evaluation [AIAA PAPER 93-0738] p 540 A93-24828
 Introduction of small velocity and pressure variation into a stationary compressible fluid p 473 A93-25060
 Development update for the NASA Ames 16-Inch Shock Tunnel Facility p 822 A93-37873
 Computational models of dampers for computer-aided design p 832 A93-39032
 Correction of the frequency characteristic of the waveguide circuit of an acoustic-jet temperature transducer p 832 A93-39036
 A study of the effect of the working medium on the start-up characteristic of an aviation gas turbine engine p 811 A93-39037
 On the compression process in a free-piston shock-tunnel p 1136 A93-48041

- Correlation of unsteady pressure and inflow velocity fields of a pitching rotor blade [AIAA PAPER 93-3082] p 1060 A93-48256
 Effect of steady-state circumferential pressure and temperature distortions on compressor stability p 1106 A93-48503
 Pressure pulsations on a delta wing in incompressible flow p 1069 A93-48912
 Stall inception in single stage, high-speed compressors with straight and swept leading edges [AIAA PAPER 93-1870] p 1076 A93-49745
 An experimental system for studying the vibrations and acoustic emission of cylindrical shells and panels in a field of turbulent pressure pulsations p 1140 A93-51754
 A study of pressure fluctuations on the surface of a delta wing near the sharp leading edge p 1091 A93-51882
 Production of oscillatory flow in wind tunnels p 1218 A93-53812
 Investigation of the flow field through a variable pitch fan rotor with an inlet total pressure distortion [ISABE 93-7029] p 1184 A93-54005
 Further noise measurements in a slotted cryogenic wind tunnel [RAE-TM-AERO-2201] p 101 N93-10805
 The combustion time lag and its role in ramjet combustion instability p 73 N93-11137
 Experimental analysis of combustion oscillations with reference to ramjet propulsion p 392 N93-17614
 An experimental study of the sources of fluctuating pressure loads beneath swept shock/boundary-layer interactions [NASA-CR-192918] p 749 N93-25266
 An assessment of inlet total-pressure distortion requirements for the Compressor Research Facility (CFR) [AD-A262299] p 815 N93-27679
 Strong parallel blade-vortex interaction and noise propagation in helicopter flight p 944 N93-30980
- PRESSURE PULSES**
 Spectra of pressure pulsations on the surface of a cone in the transition region at supersonic flow velocities p 1088 A93-51755
 Scale-up of the spectra of aerodynamic pressure pulsations with narrowband maxima p 1088 A93-51756
 Two- and three-dimensional blade vortex interactions [NASA-CR-177567] p 293 N93-16942
- PRESSURE RATIO**
 Calculation of pressure ratio at nozzle exit with shock p 122 A93-14480
 High pressure ratio intercooled turbo-prop study [ASME PAPER 92-GT-405] p 356 A93-19554
 Internal performance characteristics of vectored axisymmetric ejector nozzles [AIAA PAPER 93-2432] p 898 A93-41046
 Thrust vectoring control from underexpanded asymmetric nozzles [AIAA PAPER 93-3261] p 968 A93-46827
 Averaging techniques for steady and unsteady calculations of a transonic fan stage [AIAA PAPER 93-3065] p 1059 A93-48241
 Investigation of the flowfield around an isolated bypass engine with fan and core jet p 215 N93-13227
 Pressure drag and lift contributions for blunt forebodies of fineness ratio 2.0 in transonic flow (M infinity less than or equal to 1.4) [ESDU-89033] p 136 N93-14515
 Supersonic investigation of two dimensional hypersonic exhaust nozzles [NASA-TM-105687] p 179 N93-15342
 Experimental performance of a ventral nozzle with pitch and yaw vectoring capability for SSTOVL aircraft [NASA-TM-106054] p 722 N93-25129
 Estimating turbine limit load [NASA-CR-191105] p 699 N93-25883
 Performance characteristics of two multiaxis thrust-vectoring nozzles at Mach numbers up to 1.28 [NASA-TP-3313] p 874 N93-29160
- PRESSURE RECOVERY**
 Active boundary-layer control in diffusers [AIAA PAPER 93-2555] p 966 A93-46798
 Two-dimensional numerical simulation for Mach-3 multishock air-intake with bleed systems [AIAA PAPER 93-2306] p 1082 A93-50090
 Mach 4 testing of scramjet inlet models [NAL-TR-1137] p 26 N93-12369
 Investigations of detail design issues for the high speed acoustic wind tunnel using a 60th scale model tunnel. Part 1: Tests with open circuits [NASA-CR-191671] p 137 N93-14737
- PRESSURE REDUCTION**
 Modeling of flow in a pulsed shock tunnel p 777 A93-39152

Effects of bleed-hole geometry and plenum pressure on three-dimensional shock-wave/boundary-layer/bleed interactions
[AIAA PAPER 93-3259] p 967 A93-46800

An investigation of shock wave turbulent boundary layer interaction with bleed through normal and slanted slots
[AIAA PAPER 93-2155] p 1079 A93-49971

Two-dimensional numerical simulation for Mach-3 multishock air-intake with bleed systems
[AIAA PAPER 93-2306] p 1082 A93-50090

PRESSURE REGULATORS

The required damping and control process quality in a fuel pressure regulator p 810 A93-39034

PRESSURE SENSORS

Hemispherical and spherical flow parameter detectors p 75 A93-10044

Development of a system for aerodynamic fast-response probe measurements p 203 A93-14325

Wind tunnel operator aimed comparison between two electronic pressure scanner systems p 830 A93-37876

Silicon differential pressure transducer line pressure effects and compensation p 830 A93-37890

Calibration of a transonic 5-hole probe for a multi-element airfoil cascade facility p 1138 A93-50216

[AIAA PAPER 93-2471] p 1254 A93-54362

Development of a dynamic pressure response calibrator p 1254 A93-54362

Wind tunnel operator aimed comparison between two electronic pressure scanner systems p 67 N93-11225

[DLAS-EST-TR-040] p 214 A93-13215

A novel-high-performance system for recording and analysing instantaneous total pressure distortion in air intakes p 214 A93-13215

PRESSURE VESSELS

Nuclear thermal rocket entry heating and thermal response preliminary analysis p 385 A93-23058

[AIAA PAPER 93-0378] p 557 A93-26005

Nickel hydrogen batteries for terrestrial applications p 557 A93-26005

Advanced composite fiber/metal pressure vessels for aircraft applications p 1155 A93-50047

[AIAA PAPER 93-2246] p 1155 A93-50047

PRESSURIZED CABINS

Bulging of fatigue cracks in a pressurized aircraft fuselage p 81 A93-13639

Cabin accommodations for passengers with ambulatory disabilities - Transport category aircraft [SAE ARP 4387] p 1103 A93-52166

PRESSURIZING

Axial length influence on the performance of centrifugal impellers p 205 A93-14517

An evaluation of the pressure proof test concept for 2024-T3 aluminium alloy sheet p 1026 A93-45780

Axial crack propagation and arrest in pressurized fuselage p 1026 A93-45788

Evaluation methodologies applied for pressurized fuselages of Airbus A/C p 948 A93-45796

PRIMERS (COATINGS)

"No VOC" water-borne corrosion resistant primers for aerospace bonding applications p 1211 A93-53419

Evaluation of water-borne adhesive bonding primers for use on the advanced aircraft material aluminum-lithium p 1211 A93-53420

PRINCIPAL COMPONENTS ANALYSIS

Estimation of aerodynamic characteristics from flight-test data. IV - Principal component analysis and perpendicular error method p 1241 A93-54551

PRISMS

Flexure-torsion behavior of prismatic beams. I - Section properties via power series p 417 A93-23557

Prismatic grid generation for three-dimensional complex geometries p 1178 A93-53217

The HYDICE instrument design and its application to planetary instruments p 842 A93-28766

PROBABILITY DENSITY FUNCTIONS

The combined closed form-perturbation approach to the analysis of mistuned bladed disks p 350 A93-19359

PDF prediction of supersonic hydrogen flames [AIAA PAPER 93-0448] p 391 A93-23358

A k-omega multivariate beta PDF for supersonic turbulent combustion p 1154 A93-50009

[AIAA PAPER 93-2197] p 1154 A93-50009

Modeling of turbulent supersonic H₂-air combustion with a multivariate beta PDF p 1155 A93-50010

[AIAA PAPER 93-2198] p 1216 A93-53395

Design for cyclic loading endurance of composites p 1216 A93-53395

Modeling of turbulent supersonic H₂-air combustion with an improved joint beta PDF p 391 A93-16389

[NASA-CR-191929] p 391 A93-16389

PROBABILITY DISTRIBUTION FUNCTIONS

Computational techniques for probabilistic analysis of turbomachinery [ASME PAPER 92-GT-167] p 351 A93-19393

Optimal structure of discrete algorithms of finite-dimensional continuous-discrete filtering in the presence of Markov noise p 1169 A93-51065

Probabilistic evaluation of fuselage-type composite structures [NASA-TM-105881] p 212 N93-12735

PROBABILITY THEORY

Estimation of the probability of large flight parameters deviations p 184 A93-14399

Probability analysis of a method for diagnosing gas turbine engines on the basis of thermogasdynamic parameters p 345 A93-18337

Probabilistic turbine blade tip durability analysis [AIAA PAPER 93-1383] p 719 A93-33946

Quantification of uncertainties in composites [AIAA PAPER 93-1440] p 734 A93-33989

Probabilistically configured adaptive composite structures [AIAA PAPER 93-1679] p 743 A93-34191

Representation and probability issues in the simulation of multi-site damage p 1026 A93-45785

Assessment of helicopter component statistical reliability computations [AD-A258931] p 510 N93-19447

PROBLEM SOLVING

A comparative analysis of algorithms for solving systems of high-order linear algebraic equations p 96 A93-12977

Experimental study of the longitudinal hypersonic corner flow field - HERMES-R&D research program, problem no. 5 p 867 A93-42602

Design concepts for the development of cooperative problem-solving systems [NASA-CR-192708] p 707 N93-25261

Design of a cooperative problem-solving system for enroute flight planning: An empirical study of its use by airline dispatchers [NASA-CR-192709] p 707 N93-25330

PROCESS CONTROL (INDUSTRY)

Flexible manufacturing of aircraft engine parts [ASME PAPER 92-GT-229] p 404 A93-19446

Coherent systems in the terahertz frequency range: Elements, operation, and examples p 841 N93-27727

Process optimization of Hexoloy SX-SiC towards improved mechanical properties [DE93-007913] p 826 N93-28564

PRODUCT DEVELOPMENT

A330 - Completing the family p 40 A93-11418

Potent Trent p 53 A93-11419

The smart truck --- structure, systems, avionics of C-17 airlifter p 40 A93-11420

B-2 flight test program - An update [AIAA PAPER 92-4118] p 42 A93-13266

Pilot/Vehicle display development from simulation to flight [AIAA PAPER 92-4174] p 51 A93-13310

Design for global competition - The Boeing 777 [AIAA PAPER 92-4190] p 2 A93-13368

The role of fatigue testing in the design, development and certification of the ATR 42/72 p 46 A93-13637

Maintainable A330 p 107 A93-13957

Spanish-Indonesian cooperation in the development, production, certification and marketing of CN-235 commuter aircraft p 108 A93-14156

The integral starter/generator development progress [SAE PAPER 92-0967] p 173 A93-14629

The design development of the monolithic CFRP centre fuselage skin of the European fighter aircraft p 159 A93-15782

The production of a monolithic CFRP fuselage skin for the European Fighter Aircraft p 109 A93-15810

Potential aerospace applications for metal matrix composites p 389 A93-21678

PDT approach for developing RAH-66 Comanche airframe systems p 795 A93-35909

Prediction and control of the service-related properties of parts at the technological preparation stage and during the manufacture process --- of aircraft engine components p 834 A93-39062

Modeling of the multiparameter assembly of engineering products for a specified priority of output geometrical parameters p 836 A93-39109

C-17 should fulfill USAF airlift mission p 805 A93-39599

Airbus or the revival of European civil aviation p 856 A93-42655

Near-term two-stage-to-orbit, fully reusable, horizontal take-off/landing launch vehicle p 1015 A93-45441

Development methodology for contemporary avionics systems [SAE PAPER 931591] p 1104 A93-49340

Engineering simulators enhance 777 development p 1192 A93-53771

Removing the risk from rotorcraft testing p 1192 A93-53772

Evolution of the SIIIS-3 Ejection Seat into a Reduced Weight (RW) ejection seat p 1239 A93-54549

Future aero engine design trade offs p 1246 A93-54836

The Eurojet EJ200 engine p 1246 A93-54839

Combustor development for advanced helicopter engines p 1246 A93-54841

Rolls-Royce civil engine technology [PNR-90936] p 56 N93-11036

The Trent: Towards greater thrust [PNR-90937] p 56 N93-11037

Introduction to the Rolls-Royce design process [PNR-90939] p 57 N93-11039

Simultaneous engineering in the design of aero engines [PNR-90973] p 57 N93-11062

The Trent family of engines [PNR-90974] p 58 N93-11063

Advanced materials in gas turbine engines: An assessment [PNR-90946] p 58 N93-11105

The development of the Rolls-Royce Trent aero gas turbine [PNR-90949] p 58 N93-11108

The use of simultaneous engineering for the design and manufacture of the low pressure turbine for the Rolls-Royce Trent engine [PNR-90887] p 59 N93-11206

Innovation in engineering [PNR-90889] p 59 N93-11207

Simultaneous engineering in aero gas turbine design and manufacture [PNR-90890] p 59 N93-11208

The changing nature of design [PNR-91011] p 48 N93-11334

Software Engineering Laboratory Ada performance study: Results and implications p 441 N93-17172

SNEMA M88 engine development status [ASME-90-GT-118] p 363 N93-17849

The beta-CEZ, a new high performance titanium alloy for aerospace engines [DS-2022] p 393 N93-17852

YF-22A prototype advanced tactical fighter demonstration/validation flight test program overview p 511 N93-19906

The NASA SBIR product catalog [NASA-TM-108242] p 945 N93-29322

PRODUCTION COSTS

Future regional transport aircraft market, constraints, and technology stimuli [NASA-TM-107669] p 109 N93-13025

PRODUCTION ENGINEERING

Cost effective process selection for composite structure [SME PAPER EM93-100] p 1043 A93-51727

Advantages of a one-part resin system for processing aerospace parts by Resin Transfer Molding (RTM) [SME PAPER EM93-112] p 1159 A93-51729

Presence and future of the electro-chemical processes in aero-engine production p 1257 A93-54840

Introduction to the Rolls-Royce design process [PNR-90939] p 57 N93-11039

Simultaneous engineering in the design of aero engines [PNR-90973] p 57 N93-11062

The use of simultaneous engineering for the design and manufacture of the low pressure turbine for the Rolls-Royce Trent engine [PNR-90887] p 59 N93-11206

Innovation in engineering [PNR-90889] p 59 N93-11207

Industry survey of space system cost benefits from New Ways Of Doing Business p 454 A93-17325

Aviation production engineering: Selected articles [AD-A261231] p 764 N93-27056

PRODUCTION MANAGEMENT

Achieving manufacturing excellence for gas turbine components through focused implementation of technology [ASME PAPER 92-GT-139] p 401 A93-19371

Flexible manufacturing of aircraft engine parts [ASME PAPER 92-GT-229] p 404 A93-19446

Introduction to the Rolls-Royce design process [PNR-90939] p 57 N93-11039

Software Management Environment (SME) installation guide [NASA-TM-108578] p 230 N93-15578

PRODUCTION PLANNING

Achieving manufacturing excellence for gas turbine components through focused implementation of technology [ASME PAPER 92-GT-139] p 401 A93-19371

PRODUCTS

- Report to the Chairman, Legislation, and National Security Subcommittee, Committee on Government Operations, House of Representatives. Unmanned aerial vehicles: More testing needed before production of short-range system
[AD-A259473] p 513 N93-20245
- Special tooling disposition for aircraft entering post production support
[AD-A261614] p 678 N93-26168
- PRODUCTS**
The NASA SBIR product catalog
[NASA-TM-108242] p 945 N93-29322
- PROFILES**
On machine capacitance dimensional and surface profile measurement system p 750 N93-25579
- PROFILOMETERS**
Aircraft monitoring of the planeness of the existing and new runways p 991 A93-45668
- PROGRAM VERIFICATION (COMPUTERS)**
Formal verification of algorithms for critical systems p 846 A93-37623
Avionics software performance p 939 A93-42822
Low aspect ratio wing code validation experiment p 1176 A93-53202
- PROGRAMMING**
Numerical Wind Tunnel: Requirements and the outline p 383 N93-19288
- PROGRAMMING ENVIRONMENTS**
Flight dynamics system software development environment (FDS/SDE) tutorial
[NASA-TM-108580] p 230 N93-15502
Software Management Environment (SME) installation guide
[NASA-TM-108578] p 230 N93-15578
Data collection procedures for the Software Engineering Laboratory (SEL) database
[NASA-TM-108579] p 230 N93-15579
Software Engineering Laboratory Ada performance study: Results and implications p 441 N93-17172
- PROGRAMMING LANGUAGES**
Application of SPEED in aviation industry p 225 A93-14178
User-friendly codes for the training on gas turbine engines
[AIAA PAPER 93-2051] p 1166 A93-49884
Formal representation of the requirements for an Advanced Subsonic Civil Transport (ASCT) flight control system
[NASA-CR-189699] p 98 N93-12346
- PROJECT MANAGEMENT**
Management miscues, delays snarl C-17 program p 760 A93-34944
The importance of configuration management - An overview with test program sets p 853 A93-35926
Report to Congress: State Block Grant Program
[AD-A254569] p 193 N93-13882
The V-22 Osprey: A case analysis
[AD-A256445] p 164 N93-14601
National Airspace System flight planning operational concept NAS-SR-131
[PB93-124659] p 310 N93-18031
A model of Global Positioning System (GPS) Master Control Station (MCS) operations
[AD-A258846] p 320 N93-19067
- PROJECT PLANNING**
Limited production Precision Runway Monitor (PRM) master test plan
[DOT/FAA/CT-TN92/23] p 192 N93-12899
Scientific and engineering research facilities at universities and colleges: 1992
[NSF-92-325] p 192 N93-13407
Exodus: Prime Mover
[NASA-CR-192051] p 332 N93-17803
SNECMA M88 engine development status
[ASME-90-GT-118] p 363 N93-17849
Materials development program, ceramic technology project addendum to program plan: Cost effective ceramics for heat engines
[DE93-003663] p 394 N93-18537
Rotorcraft master plan p 857 N93-30677
- PROJECTILES**
Steady and quasisteady resonant lock-in of finned projectiles p 61 A93-12012
Multizone Navier-Stokes computations for a transonic projectile using MacCormack finite difference method p 113 A93-14192
Finite element analysis of the Scramaccelerator with finite rate chemistry
[AIAA PAPER 93-0745] p 540 A93-24833
Projectile base bleed technology. Part 2: User's guide CMINT computer code, version 5.04-BRL
[AD-A258630] p 551 N93-19999
Numerical determination of the residual strength of battle damaged composite plates p 537 N93-21533
Computation of transonic flow over a porous surface projectile p 696 N93-25409

- Navier-Stokes simulation of viscous, separated, supersonic flow over a projectile rotating band
[AD-A263073] p 788 N93-27955
- Navier-Stokes computations for kinetic energy projectiles in steady coning motion: A predictive capability for pitch damping
[AD-A264111] p 1033 N93-32028
- PROJECTORS**
High-resolution displays and projection systems: Proceedings of the Meeting, San Jose, CA, Feb. 11, 12, 1992
[SPIE-1664] p 544 A93-27237
Advantages of using a projected head-up display in a flight simulator
[AD-A255332] p 194 N93-14559
- PROLATE SPHEROIDS**
Three-dimensional separated flow over a prolate spheroid p 1235 A93-55379
An experimental study of flow over a 6 to 1 prolate spheroid at incidence p 874 N93-29124
- PROP-FAN TECHNOLOGY**
Aeroacoustic wind tunnel testing of a counterrotating shrouded propfan-model p 449 A93-19213
Experimental determination of the main noise sources in a propfan model by analysis of the acoustic spinning modes in the exit plane p 449 A93-19214
An assessment of wake structure behind forward swept and aft swept propfans at high loading p 245 A93-19222
Lifting surface theory for steady aerodynamic analysis of ducted counter rotation propfan
[ASME PAPER 92-GT-14] p 347 A93-19286
APPLE - An aeroelastic analysis system for turbomachinery and propfans
[AIAA PAPER 92-4712] p 358 A93-20320
Navier-Stokes calculations for the unsteady flowfield of turbomachinery
[AIAA PAPER 93-0676] p 465 A93-24786
Zen and the art of airplane sizing p 504 A93-25174
Role of leading-edge vortex flows in prop-fan interaction noise p 565 A93-28614
Experimental investigation of counter-rotating propfan flutter at cruise conditions
[AIAA PAPER 93-1632] p 720 A93-34160
Unsteady aerodynamics and flutter of propfans using a three-dimensional Full-Potential Solver
[AIAA PAPER 93-1633] p 720 A93-34161
On the static stability of forward swept propfans
[AIAA PAPER 93-1634] p 720 A93-34162
Unsteady blade pressures on a propfan at takeoff - Euler analysis and flight data p 810 A93-37389
Propulsion system simulator with propfan for tests on a large scale model of IL-114 airplane in a full-size wind tunnel of TsAGI p 1013 A93-46933
Propfan engines
[AIAA PAPER 93-1981] p 1112 A93-49828
Unsteady aerodynamics and flutter based on the potential equation
[AIAA PAPER 93-2086] p 1079 A93-49913
ADP - Engine concept of the future p 1246 A93-54842
Investigation of advanced counterrotation blade configuration concepts for high speed turboprop systems. Task 4: Advanced fan section aerodynamic analysis
[NASA-CR-187128] p 174 N93-12695
Simulation of unsteady rotational flow over propfan configuration
[NASA-CR-192234] p 296 N93-18585
Investigation of advanced counterrotation blade configuration concepts for high speed turboprop systems. Task 4: Advanced fan section aerodynamic analysis computer program user's manual
[NASA-CR-187127] p 364 N93-18702
Investigation of advanced counterrotation blade configuration concepts for high speed turboprop systems. Task 5: Unsteady counterrotation ducted propfan analysis. Computer program user's manual
[NASA-CR-187125] p 521 N93-20583
Investigation of advanced counterrotation blade configuration concepts for high speed turboprop systems. Task 5: Unsteady counterrotation ducted propfan analysis
[NASA-CR-187126] p 521 N93-20773
Structural Tailoring of Advanced Turboprops (STAT). Theoretical manual
[NASA-CR-191017] p 556 N93-22005
Fabrication of composite propfan blades for a cruise missile wind tunnel model
[NASA-TM-105270] p 752 N93-26202
In-flight near- and far-field acoustic data measured on the Propfan Test Assessment (PTA) testbed and with an adjacent aircraft
[NASA-TM-103719] p 852 N93-27058
User's manual for UCAP: Unified Counter-Rotation Aero-Acoustics Program
[NASA-CR-191034] p 852 N93-27148

SUBJECT INDEX

- PROPAGATION MODES**
Acoustic mode measurements in the inlet of a model turbofan using a continuously rotating rake
[AIAA PAPER 93-0598] p 563 A93-24783
Acoustic mode measurements in the inlet of a model turbofan using a continuously rotating rake
[NASA-TM-105989] p 362 N93-16705
- PROPAGATION VELOCITY**
Prediction of fatigue crack growth kinetics in the plane structural elements of aircraft in the biaxial stress state p 1025 A93-45670
- PROPANE**
Turbulence characteristics of an axisymmetric reacting flow
[NASA-CR-4110] p 877 N93-30373
- PROPELLANT COMBUSTION**
Experiments and analysis concerning the use of external burning to reduce aerospace vehicle transonic drag p 70 N93-12537
Combustion in supersonic flows p 199 N93-14627
Investigation of the aerothermodynamics of hypervelocity reacting flows in the ram accelerator
[NASA-CR-191715] p 140 N93-15588
- PROPELLANT DECOMPOSITION**
Numerical method for simulating fluid-dynamic and heat-transfer changes in jet-engine injector feed-arm due to fouling p 1245 A93-54467
Regression rate mechanism in a solid fuel ramjet p 814 N93-27185
Advanced thermally-stable, coal-derived, jet fuels program: Experiment system and model development
[AD-A262747] p 917 N93-29402
- PROPELLANT EXPLOSIONS**
Pulsed detonation engine experimental and theoretical review
[AIAA PAPER 92-3168] p 531 A93-24478
- PROPELLANT PROPERTIES**
Advanced diagnostics for in situ measurement of particle formation and deposition in thermally stressed jet fuels
[AIAA PAPER 93-0363] p 390 A93-23045
- PROPELLANT STORAGE**
Design and investigation of the stand and flying scramjet models - Conceptions and results of experiments
[AIAA PAPER 93-2447] p 1120 A93-50199
- PROPELLANT TESTS**
Advanced diagnostics for in situ measurement of particle formation and deposition in thermally stressed jet fuels
[AIAA PAPER 93-0363] p 390 A93-23045
- PROPELLANTS**
Hugoniot analysis of the ram accelerator p 1023 A93-45500
- PROPELLER BLADES**
On the use of the method of matched asymptotic expansions in propeller aerodynamics and acoustics p 8 A93-11553
Over wing propeller aerodynamics p 113 A93-14189
A study of propeller/wing interaction including the effect of ground proximity p 113 A93-14190
Cruise noise of an advanced propeller with swirl recovery vanes p 564 A93-28609
BLASIM - A computational tool to assess ice impact damage on engine blades
[AIAA PAPER 93-1638] p 720 A93-34165
Analysis of the effects of blade pitch on the radar return signal from rotating aircraft blades p 885 A93-43476
Theoretical studies of the active control of propeller induced cabin noise using secondary force inputs p 995 A93-45124
High speed propeller acoustics and aerodynamics - A boundary element approach p 967 A93-46804
Acoustic experiments of two scaled-model propellers on the ground p 1172 A93-48507
Formulas for determining the induced velocity in the direct and inverse rotor problems p 1071 A93-49324
The effect of unsteady blade loading on the aeroacoustics of a pusher propeller
[AIAA PAPER 93-1805] p 1173 A93-49694
Spectral analysis of unsteady surface pressure on a pusher propeller p 1232 A93-54646
Root damage analysis of aircraft engine blade subject to ice impact
[NASA-TM-105779] p 222 N93-15343
A review of civil aviation propeller-to-person accidents: 1980-1989 p 705 N93-25896
Interaction between ice and propeller
[VTT-TIED-1281] p 841 N93-27832
An integrated optimum design approach for high speed prop-rotors including acoustic constraints
[NASA-CR-193222] p 893 N93-29153
Project ARES 2: High-altitude battery-powered aircraft p 894 N93-29715
Unsteady vortex loop/dipole theory applied to the work and acoustics of an ideal low speed propeller
[AD-A264057] p 876 N93-29891

PROPELLER EFFICIENCY

- Efficient hybrid scheme for the analysis of counter-rotating propellers p 688 A93-34483
On the verification of a theory for sculling propulsion [ETN-93-94040] p 1031 N93-31519

PROPELLER FANS

- Concurrent processing adaptation of aeroelastic analysis of propfans p 173 A93-14624
Lifting surface theory for steady aerodynamic analysis of ducted counter rotation propfan [ASME PAPER 92-GT-14] p 347 A93-19286
Unsteady blade pressures on a propfan at takeoff - Euler analysis and flight data p 810 A93-37389
Laser velocimeter measurements of the flow field generated by a forward-swept propfan during flutter [AIAA PAPER 93-2919] p 1180 A93-53591
Investigation of advanced counterrotation blade configuration concepts for high speed turboprop systems. Task 5: Unsteady counterrotation ducted propfan analysis. Computer program user's manual [NASA-CR-187125] p 521 N93-20583
Investigation of advanced counterrotation blade configuration concepts for high speed turboprop systems. Task 5: Unsteady counterrotation ducted propfan analysis [NASA-CR-187126] p 521 N93-20773
Structural Tailoring of Advanced Turboprops (STAT). Theoretical manual [NASA-CR-191017] p 556 N93-22005
A numerical and experimental studies of flow characteristics in centrifugal fans p 695 N93-25339
Fabrication of composite propfan blades for a cruise missile wind tunnel model [NASA-TM-105270] p 752 N93-26202
In-flight near- and far-field acoustic data measured on the Propfan Test Assessment (PTA) testbed and with an adjacent aircraft [NASA-TM-103719] p 852 N93-27058
User's manual for UCAP: Unified Counter-Rotation Aero-Acoustics Program [NASA-CR-191034] p 852 N93-27148

PROPELLER NOISE

- The numerical calculation for the coupling of multiple propeller discrete noise and its interaction with the fuselage boundary p 231 A93-14268
The numerical calculation of aircraft propeller noise p 174 A93-16239
Cabin noise source-path identification for AD-200 ultralight aircraft p 444 A93-19138
Noise evaluation of light propeller-driven aircraft p 398 A93-19189
Forward rotor vortex effects on counter rotating propeller noise p 245 A93-19221
Experimental results on propeller noise attenuation using an 'active noise control' technique p 450 A93-19223
Reduction of propeller noise by active noise control p 450 A93-19224
Vibro-acoustic analysis of propeller aircraft, integrating advanced experimental modeling with in-flight data analysis p 451 A93-19230
Cruise noise of an advanced propeller with swirl recovery vanes p 564 A93-28609
Toward the silent helicopter [ONERA, TP NO. 1992-229] p 851 A93-38774
Theoretical studies of the active control of propeller induced cabin noise using secondary force inputs p 995 A93-45124
High speed propeller acoustics and aerodynamics - A boundary element approach p 967 A93-46804
Noise and vibration analysis in propeller aircraft by advanced experimental modeling techniques p 1264 A93-55862
Reduction of propeller noise by active noise control p 101 N93-10692
The design and commissioning of an acoustic liner for propeller noise testing in the ARA transonic wind tunnel [PNR-90880] p 101 N93-11204
In-flight near- and far-field acoustic data measured on the Propfan Test Assessment (PTA) testbed and with an adjacent aircraft [NASA-TM-103719] p 852 N93-27058
Modal measurements and propeller field excitation on acoustic full scale mockup of SAAB 340 aircraft [FFA-TN-1992-08] p 1039 N93-31051

PROPELLER SLIPSTREAMS

- Investigation of methods for modeling propeller-induced flow fields [AIAA PAPER 93-0874] p 469 A93-24935
Treatment of vortex sheets for the transonic full-potential equation p 871 A93-42870
Unsteady wing surface pressures in the wake of a propeller p 1095 A93-52436
Unsteady propeller/wing aerodynamic interactions p 24 N93-12190

- Aerodynamic analysis of slipstream/wing/nacelle interference for preliminary design of aircraft configurations p 130 N93-13205

PROPELLERS

- On the maximum range of flying wings [AIAA PAPER 92-4223] p 504 A93-24492
Viscous flow computations of flow field around an advanced propeller [AIAA PAPER 93-0873] p 469 A93-24934
Theodorsen's ideal propeller performance with ambient pressure in the slipstream p 768 A93-37400
Propeller noise reduction by means of unsymmetrical blade-spacing p 1039 A93-46706
On the possibility of singularities in the acoustic field of supersonic sources when BEM is applied to a wave equation p 1039 A93-46805
The effect of a high thrust pusher propeller on the flow over a straight wing [AIAA PAPER 93-3436] p 978 A93-47228
Numerical simulation of incompressible viscous flow around a propeller [AIAA PAPER 93-3503] p 984 A93-47271
Modern propeller systems for advanced turboprop aircraft [AIAA PAPER 93-1846] p 1111 A93-49727
An approach to the calculation of the far acoustic field of a propeller p 1124 A93-51760
Aircraft accident report: Atlantic Southeast Airlines, Inc. Flight 2311, uncontrolled collision with terrain, an Embraer EMB-120, N270AS, Brunswick, Georgia, 5 April 1991 [PB92-910403] p 28 N93-11471
Unsteady propeller/wing aerodynamic interactions p 24 N93-12190
Estimation of rate of climb [ESDU-92019] p 164 N93-14541
Professor Wittenberg: His speciality and versatility [ISBN-90-6275-670-0] p 240 N93-19002
Propelling force and resistance p 298 N93-19003
Ship viscous flow: A report on the 1990 SSPA-IIHR Workshop p 840 N93-27466
Unsteady vortex loop/dipole theory applied to the work and acoustics of an ideal low speed propeller [AD-A264057] p 876 N93-29891
On the verification of a theory for sculling propulsion [ETN-93-94040] p 1031 N93-31519

PROPORTIONAL CONTROL

- New results in optimal missile avoidance analysis p 369 A93-22937
Reduced order proportional integral observer with application p 1166 A93-49605
Genetic design of digital model-following flight-control systems [AIAA PAPER 93-3883] p 1135 A93-51468

PROPORTIONAL COUNTERS

- The microstrip proportional counter p 549 A93-29485

PROPOSALS

- NASA SBIR abstracts of 1991 phase 1 projects [NASA-TM-108240] p 945 N93-29323

PROPULSION

- Integrated flight propulsion control research results using the NASA F-15 HIDEF Flight Research Facility [AIAA PAPER 92-4106] p 38 A93-11276
Some contributions to propulsion theory - Non-isentropic duct flow and the general drag wake traverse p 874 A93-43688
Integrated flight/propulsion control - Subsystem specifications for performance [AIAA PAPER 93-3808] p 1132 A93-51400
A comparative study of multivariable robustness analysis methods as applied to integrated flight and propulsion control [AIAA PAPER 93-3809] p 1102 A93-51401
A parameter optimization approach to controller partitioning for integrated flight/propulsion control application p 1206 A93-54268
Aeronautical technologies for the twenty-first century [NASA-CR-190918] p 4 N93-10647
The PEP Symposium on CFD Techniques for Propulsion Applications p 214 N93-13210
National Aero-Space Plane: Key issues facing the program. Testimony before the Subcommittee on Technology and Competitiveness, Committee on Science, Space, and Technology, House of Representatives [GAO/T-NSIAD-92-26] p 161 N93-13253
Electro-optic architecture for servicing sensors and actuators in advanced aircraft propulsion systems [NASA-CR-182269] p 232 N93-13762

PROPULSION SYSTEM CONFIGURATIONS

- Integrated flight propulsion control research results using the NASA F-15 HIDEF Flight Research Facility [AIAA PAPER 92-4106] p 38 A93-11276
Feasibility study on single bypass variable cycle engine with ejector [AIAA PAPER 92-4268] p 55 A93-13366

- Advancements in aircraft gas turbine engines - Past and future p 170 A93-14153
The new challenge of computational aerospace p 112 A93-14169

Over wing propeller aerodynamics

- p 113 A93-14189
Flight-determined benefits of integrated flight-propulsion control systems p 183 A93-14370
Design of digital multiple model-following integrated flight/propulsion control systems p 183 A93-14371
Analysis and development of a total energy control system for a large transport aircraft p 183 A93-14372
The Aircraft/Propulsion Integrated Assessment System p 226 A93-14396
Propulsion of a supersonic transport: What are the challenges? II - Achievements p 174 A93-16852
The ramjet engine in high speed propulsion p 174 A93-16853
Ramjet NOx emission - Use of a 3D CFD method for the combustor design of a super/hyper-sonic transport propulsion system [ASME PAPER 92-GT-255] p 353 A93-19464
A scoping study for hypersonic transport propulsion systems [ASME PAPER 92-GT-409] p 356 A93-19558
A graphical user-interface for propulsion system analysis [AIAA PAPER 93-0223] p 440 A93-23699
Aerodynamic performance of scramjet inlet models with a single strut [AIAA PAPER 93-0741] p 466 A93-24831
Some contributions to propulsion theory - Fuel consumption formulae and general range equation p 713 A93-34850

Hypersonic propulsion - Breaking the thermal barrier

- p 897 A93-40437
Prediction of static performance for single expansion ramp nozzles [AIAA PAPER 93-2571] p 898 A93-41047
CFD for hypersonic propulsion p 865 A93-42585
Propulsion system simulator with propfan for tests on a large scale model of IL-114 airplane in a full-size wind tunnel of TsAGI p 1013 A93-46933
Aerodynamic characteristics of the MMPT ATD vehicle at high angles of attack [AIAA PAPER 93-3493] p 982 A93-47265
Analysis of a high bypass ratio engine installation using the chimera domain decomposition technique [AIAA PAPER 93-1808] p 1100 A93-49697
Initial test results of 40,000 horsepower fan drive gear system for advanced ducted propulsion systems [AIAA PAPER 93-2146] p 1154 A93-49963
Robust control of hypersonic vehicles considering propulsive and aeroelastic effects [AIAA PAPER 93-3762] p 1131 A93-51357
New developments with the V2500 engine [ISABE 93-7085] p 1202 A93-54061
Evaluation of turbofanjet exhaust systems from scale model test data [ISABE 93-7109] p 1204 A93-54085
Compact heat exchanger fitted to engines of the inverted type [ISABE 93-7120] p 1221 A93-54095
NASA Langley's Aircraft Landing Dynamics Facility p 1250 A93-54400

Ultra-high temperature materials in the research and development of super/hypersonic transport propulsion system

- p 1252 A93-54712
LV software for supersonic flow analysis [NASA-CR-190911] p 16 N93-10069
Overview of high performance aircraft propulsion research [NASA-TM-105839] p 59 N93-11530
AFOSR Contractors Meeting in Propulsion [AD-A254484] p 195 N93-12575
Aerodynamic Engine/Airframe Integration for High Performance Aircraft and Missiles [AGARD-CP-498] p 213 N93-13199
Euler analysis of turbofan/superfan integration for a transport aircraft p 214 N93-13206
Propulsion integration results of the STOL and Maneuver Technology Demonstrator p 161 N93-13228
Integration of turbo-ramjet engines for hypersonic aircraft p 175 N93-13230
SR-SCARLET 1: Peregrin [NASA-CR-192048] p 337 N93-18155
Investigation of advanced counterrotation blade configuration concepts for high speed turboprop systems. Task 5: Unsteady counterrotation ducted propfan analysis [NASA-CR-187126] p 521 N93-20773
Aerodynamic design and synthesis of the oblique flying wing supersonic transport p 713 N93-24768
Development and testing of the Perseus proof-of-concept aircraft [DE93-010121] p 806 N93-28586

- Fatigue in single crystal nickel superalloys
[AD-A265451] p 1019 N93-31795
- PROPULSION SYSTEM PERFORMANCE**
- Turbine engine developers explore ways to lower NO(x) emission levels p 52 A93-10732
- A design approach to high Mach number scramjet performance
[AIAA PAPER 92-4248] p 55 A93-13360
- Design of propulsion systems for low operating costs p 55 A93-13405
- Advancements in aircraft gas turbine engines - Past and future p 170 A93-14153
- The application of human factors engineering at General Electric Aircraft Engines
[SAE PAPER 921039] p 108 A93-14659
- The control of aircraft engines in the 1990's p 173 A93-15042
- Concurrent optimization of airframe and engine design parameters
[AIAA PAPER 92-4713] p 323 A93-20281
- Multidisciplinary propulsion simulation using NPSS
[AIAA PAPER 92-4709] p 435 A93-20318
- Structural Tailoring/Analysis for Hypersonic Components - A computational simulation
[AIAA PAPER 92-4722] p 325 A93-20324
- Wake ingestion propulsion benefit p 411 A93-21660
- Aerothermodynamic analysis of combined-cycle propulsion systems p 359 A93-21671
- Aero-space plane figures of merit
[AIAA PAPER 92-5058] p 385 A93-22328
- Techniques for the measurement of scramjet inlet performance at hypersonic speeds
[AIAA PAPER 92-5104] p 274 A93-22374
- A graphical user-interface for propulsion system analysis
[AIAA PAPER 93-0223] p 440 A93-23699
- Propulsion/airframe integration issues for waverider aircraft
[AIAA PAPER 93-0506] p 505 A93-25533
- High-performance aircraft propulsion research p 529 A93-27904
- Impact of aeroelasticity on propulsion and longitudinal flight dynamics of an air-breathing hypersonic vehicle
[AIAA PAPER 93-1367] p 733 A93-33934
- Using a full potential solver for propulsion system exhaust simulation p 689 A93-34487
- AHS, Annual Forum, 48th, Washington, June 3-5, 1992, Proceedings, Vols. 1 & 2 p 763 A93-35901
- An advanced method for predicting the performance of helicopter propulsion system ejectors p 809 A93-35933
- Modeling of linear isentropic flow systems p 828 A93-37046
- Materials problems connected with the propulsion of supersonic air carriers
[ONERA, TP NO. 1992-157] p 824 A93-38736
- Hover testing a demonstrated and cost-effective risk reduction tool
[AIAA PAPER 93-2677] p 913 A93-42234
- CFD for hypersonic propulsion p 865 A93-42585
- A propulsion device driven by reflected shock waves p 1001 A93-45550
- Design optimization study for F-15 propulsion/forward fairing compatibility
[AIAA PAPER 93-3484] p 1003 A93-47291
- Screening studies of advanced control concepts for airbreathing engines
[AIAA PAPER 92-3320] p 1108 A93-49329
- Methodology for commercial engine/aircraft optimization
[AIAA PAPER 93-1807] p 1166 A93-49696
- Numerical study of the performance of swept, curved compression surface scramjet inlets
[AIAA PAPER 93-1837] p 1074 A93-49721
- CFD applications in an aeropropulsion test environment
[AIAA PAPER 93-1924] p 1112 A93-49790
- Boundary condition procedures for CFD analyses of propulsion systems - The multi-zone problem
[AIAA PAPER 93-1971] p 1077 A93-49819
- Future technology aim of the National Aerospace Plane Program
[AIAA PAPER 93-1988] p 1141 A93-49833
- Rapid computer simulation of ramjet performance
[AIAA PAPER 93-2049] p 1113 A93-49862
- Advanced instrumentation for next-generation aerospace propulsion control systems
[AIAA PAPER 93-2079] p 1154 A93-49906
- Development and use of hydrogen-air torches in an altitude facility
[AIAA PAPER 93-2176] p 1137 A93-49988
- Boron particle ignition in high-speed flow
[AIAA PAPER 93-2202] p 1145 A93-50014
- Engine testing at simulated altitude conditions
[AIAA PAPER 93-2452] p 1120 A93-50201

- An upgraded data acquisition and processing system for the Aeropropulsion Systems Test Facility at Arnold Engineering Development Center
[AIAA PAPER 93-2466] p 1138 A93-50213
- Implementation of an infrared thermal imaging system to measure temperature in a gas turbine engine
[AIAA PAPER 93-2469] p 1120 A93-50215
- Fusion-electric propulsion for hypersonic flight
[AIAA PAPER 93-2611] p 1142 A93-50318
- Dynamics of hypersonic flight vehicles exhibiting significant aeroelastic and aeropropulsive interactions
[AIAA PAPER 93-3763] p 1131 A93-51358
- Complementary role of ground testing, flight testing, and computations in aerospace plane propulsion development
[ISABE 93-7034] p 1197 A93-54010
- Performance and configuration analysis of jet-engine off-design behavior
[ISABE 93-7087] p 1202 A93-54063
- Thermodynamic and neutral network computer modelling of implanted component faults in a gas turbine engine
[ISABE 93-7089] p 1202 A93-54065
- Experimental analysis of turbine rotor flow at design and off-design conditions
[ISABE 93-7092] p 1186 A93-54068
- Effect of nozzle design on the performance of a highly loaded turbine stage
[ISABE 93-7096] p 1203 A93-54072
- An updated data acquisition and processing system for turbine engine testing p 1250 A93-54389
- The Eurojet EJ200 engine p 1246 A93-54839
- Turbofan propulsion simulator p 1247 A93-55493
- Performance analysis of a turbofan as a part of an airbreathing propulsion system for space shuttles p 1252 A93-56039
- LV software for supersonic flow analysis
[NASA-CR-190911] p 16 N93-10069
- An interactive preprocessor for the NASA engine performance program
[NASA-TM-105786] p 56 N93-10983
- Overview of high performance aircraft propulsion research
[NASA-TM-105839] p 59 N93-11530
- Concurrent optimization of airframe and engine design parameters
[NASA-TM-105908] p 60 N93-12402
- Subsonic flight test evaluation of a propulsion system parameter estimation process for the F100 engine
[NASA-TM-4426] p 175 N93-13155
- The influence of intake swirl distortion on the steady-state performance of a low bypass, twin-spool engine p 214 N93-13211
- Some aspects of intake design, performance and integration with the airframe p 161 N93-13219
- Hypersonic propulsion system force accounting p 175 N93-13229
- Propulsion system performance resulting from an integrated flight/propulsion control design
[NASA-TM-105874] p 180 N93-15525
- Upgrade and extension of the data acquisition system for propulsion and gas dynamic laboratories
[AD-A256836] p 235 N93-15637
- Experimental analysis of combustion oscillations with reference to ramjet propulsion p 392 N93-17614
- Preliminary analysis of the J-52 aircraft engine component improvement program
[AD-A257640] p 363 N93-17686
- Stall and surge in axial flow compressors p 423 N93-18724
- Experimental investigation of rotating stall in a mismatched three stage axial flow compressor p 423 N93-18727
- Nozzle/cowl optimization for a hypersonic vehicle on a typical trajectory
[AD-A258627] p 341 N93-19089
- Investigation of advanced counterrotation blade configuration concepts for high speed turboprop systems. Task 5: Unsteady counterrotation ducted propfan analysis
[NASA-CR-187126] p 521 N93-20773
- Screening studies of advanced control concepts for airbreathing engines
[NASA-TM-106042] p 721 N93-25079
- A modified approach to controller partitioning
[NASA-TM-106167] p 848 N93-28051
- Development and testing of the Perseus proof-of-concept aircraft
[DE93-010121] p 806 N93-28586
- Fatigue in single crystal nickel superalloys
[AD-A265451] p 1019 N93-31795
- PROPULSION EFFICIENCY**
- Aerodynamic analysis of flapping wing propulsion
[AIAA PAPER 93-0484] p 286 A93-23386
- The development of an efficient ornithopter wing p 873 A93-43685

- Zero-thrust glide testing for drag and propulsive efficiency of propeller aircraft p 995 A93-45143
- Thrust loss due to supersonic mixing
[AIAA PAPER 93-2140] p 1114 A93-49958
- Hypersonic inlet efficiency revisited p 16 N93-10012
- Design of high speed propellers using multiobjective optimization techniques p 336 N93-18065
- Optimum design of high speed prop rotors including the coupling of performance, aeroelastic stability and structures p 337 N93-18066
- PROTECTION**
- Correlations between engineering, medical and behavioural aspects in fire-related aircraft accidents p 494 N93-19693
- PROTECTIVE COATINGS**
- An electrostatic probe for determining particle characteristics in disperse flow p 76 A93-10178
- Microstructural study of aluminide surface coatings on single crystal nickel base superalloy substrates p 70 A93-12771
- Higher velocity thermal spray processes produce better aircraft engine coatings
[SAE PAPER 920947] p 202 A93-14090
- Data analysis techniques for pressure- and temperature-sensitive paint
[AIAA PAPER 93-0176] p 414 A93-22605
- Selection of protective coatings for parts in a computer-aided design system p 746 A93-35290
- Robotic aircraft painting with SAFARI
[SME PAPER AD92-198] p 855 A93-40662
- The effects of high-pressure water on the material integrity of selected aircraft coatings and substrates
[SME PAPER AD92-207] p 855 A93-40668
- 'No VOC' water-borne corrosion resistant primers for aerospace bonding applications p 1211 A93-53419
- Surface protection in the aircraft industry
[MBB-Z-0432-92-PUB] p 72 N93-11027
- Development of advanced carbon-carbon annular flameholders for gas turbines p 58 N93-11106
- Small particle impact damage in carbon-carbon composites
[PNR-90948] p 73 N93-11107
- Erosion predictions and measurements of high-temperature coatings and superalloys used in turbomachines p 74 N93-12189
- Current research in oxidation-resistant carbon-carbon composites at NASA, Langley Research Center p 74 N93-12456
- Waterborne polyurethane binder resins for compliant aircraft coatings
[AD-A256246] p 199 N93-14573
- F-14 wing lug coating investigation
[AD-A257384] p 328 N93-15858
- Field evaluation of six protective coatings applied to T-56 turbine blades after 2000 hours of engine use
[AD-A261112] p 522 N93-21316
- Platinum-modified diffusion aluminide coatings on nickel-base superalloys
[AD-A263597] p 917 N93-29981
- PROTOCOL (COMPUTERS)**
- The engine design engine. A clustered computer platform for the aerodynamic inverse design and analysis of a full engine
[NASA-TM-105838] p 21 N93-11223
- PROTOTYPES**
- Rapid prototyping via automatic software code generation from formal specifications - A case study p 227 A93-14685
- A rapid prototyping system for inflight simulation using the Calspan Learjet 25
[AIAA PAPER 93-3606] p 1191 A93-52691
- The changing nature of design
[PNR-91011] p 48 N93-11334
- A neural network prototype for predicting F-14B strains at the B.L. 10 longeron
[AD-A255272] p 165 N93-15004
- An investigation of a prototype OASYS effectiveness in maneuvering flight
[AD-A257901] p 338 N93-18339
- YF-22A prototype advanced tactical fighter demonstration/validation flight test program overview p 511 N93-19906
- YF-22A prototype advanced tactical fighter demonstration/validation flight test program overview p 805 N93-27173
- The design of a robust autopilot for the Archytas prototype via linear quadratic synthesis
[AD-A262151] p 820 N93-27546
- PROVING**
- Low-cost approaches to proving of high-risk fast VTOL designs
[SAE PAPER 920989] p 157 A93-14636

SUBJECT INDEX

- Rapid prototyping via automatic software code generation from formal specifications - A case study p 227 A93-14685
- The 'Rolls-Royce' way of validating fan integrity [AIAA PAPER 93-2602] p 1122 A93-50311
- Advanced Turbine Technology Applications Project (ATTAP) p 455 N93-18762
- [NASA-CR-189228] p 455 N93-18762
- ERS-1 directional wave spectra validation with the airborne SAR PHARS [BCRS-92-18] p 937 N93-31010
- PROXIMITY**
- Analysis of a 2-D airfoil motion flying in-proximity-to a wavy-wall surface: Finite difference method p 300 N93-19282
- Fundamentals of adaptive anticipation techniques for the detection of threatening air traffic conflicts: Investigation of the horizontal proximity situation in the case of expected heading changes [DLR-MITT-91-21] p 503 N93-21004
- UK airmisses involving commercial air transport, September - December 1991 [ETN-93-93930] p 992 N93-32409
- PSYCHOLOGICAL EFFECTS**
- Effects on health of noise disturbances due to air traffic p 1035 N93-31929
- PSYCHOLOGICAL TESTS**
- Performance-based testing and success in Naval advanced flight training [AD-A260838] p 717 N93-25933
- PUBLIC HEALTH**
- The airborne boundary concept for airport noise management p 564 A93-28482
- Final results from a study of community response to aircraft noise around Oslo Airport Fornebu p 558 A93-28486
- Air Traffic and Environment [GSF-BAND-8] p 1034 N93-31925
- Effects on health of noise disturbances due to air traffic p 1035 N93-31929
- Effects of commercial flight pollution on human health p 1035 N93-31931
- PUBLIC RELATIONS**
- Index to NASA news releases and speeches, 1991 [NASA-TM-108004] p 104 N93-10815
- Index to NASA news releases and speeches, 1990 [NASA-TM-108003] p 104 N93-10872
- PULLING**
- Fiber pulling apparatus modification [NASA-CR-184498] p 220 N93-14763
- PULSE COMPRESSION**
- Digital pulse compression with low range sidelobes p 929 A93-43463
- ACTA Aeronautica et Astronautica Sinica (selected articles) [AD-A255070] p 110 N93-13946
- PULSE DOPPLER RADAR**
- Acquisition and use of Orlando, Florida and Continental Airbus radar flight test data p 489 N93-19603
- PULSE DURATION MODULATION**
- Using numerical control algorithms in stabilization systems with digital correction p 941 A93-43113
- Dynamic compensator design in nonlinear aerospace systems p 1036 A93-44150
- Development and testing of the digital control system for the Archytas unmanned air vehicle [AD-A261656] p 729 N93-26196
- PULSE RADAR**
- Robust method for estimating the parameters of a linear FM waveform p 1147 A93-47650
- PULSE REPETITION RATE**
- Real time PRF control system for SAR p 884 A93-43464
- Aerodynamic phenomena in high pulse repetition rate XeCl laser p 1150 A93-48806
- PULSED JET ENGINES**
- The pioneers of thermopulsive nozzles p 235 A93-16854
- A propulsion device driven by reflected shock waves p 1001 A93-45550
- PULSED LASERS**
- Automated Laser Paint Stripping (ALPS) [SME PAPER AD92-206] p 855 A93-40667
- Multiparticle imaging technique for two-phase fluid flows using pulsed laser speckle velocimetry [DE93-011734] p 935 N93-30489
- PULSEJET ENGINES**
- Development of a pulse ramjet based on twin valveless pulse combustors coupled to operate in antiphase p 814 N93-27186
- PUMP IMPELLERS**
- Some unsteady fluid forces on pump impellers p 413 A93-22265
- The numerical simulation of the hydrodynamic field from the pump impellers zone by means of the finite element method p 476 A93-26905

PUMPS

- Analysis of the pump station of an aircraft hydraulic system as a subject of diagnosis p 321 A93-18374

PURSUIT TRACKING

- Application of the receding horizon strategy to singularly perturbed pursuit-evasion problems p 369 A93-22980

PUSHBROOM SENSOR MODES

- PBMR observations of surface soil moisture in Monsoon 90 p 1162 A93-47676

PYLON MOUNTING

- Effects of pylon yaw and lateral stiffness on the flutter of a delta wing with external store p 800 A93-36330
- Experimental study of pylon cross sections for a subsonic transport airplane p 1103 A93-52440
- Effect of pylon cross-sectional geometries on propulsion integration for a low-wing transport [NASA-TP-3333] p 788 N93-28070

PYLONS

- Effects of the pylon pitching stiffness on wing-store flutter p 41 A93-11820
- Juncture flow improvement for wing/pylon configurations by using CFD methodology [AIAA PAPER 93-0522] p 283 A93-23264
- Investigation of interference phenomena of modern wing-mounted high-bypass-ratio engines by the solution of the Euler-equations p 213 N93-13204
- Euler analysis of turbofan/superfan integration for a transport aircraft p 214 N93-13206
- Recent developments in low-speed TPS-testing for engine integration drag and installed thrust reverser simulation p 160 N93-13207
- Pressure distribution for the wing of the YAV-8B airplane; with and without pylons [NASA-TM-4429] p 136 N93-14451
- Effect of pylon cross-sectional geometries on propulsion integration for a low-wing transport [NASA-TP-3333] p 788 N93-28070

PYROLYSIS

- Polyethylene pyrolysis model for combustion calculations in solid fuel ramjets p 520 A93-27739

PYROMETERS

- Pyrometer for turbine applications in the presence of reflection and combustion [AIAA PAPER 93-2374] p 1156 A93-50143
- A passive infrared ice detection technique for helicopter applications [NASA-CR-193187] p 880 N93-29152

Q

Q FACTORS

- Quality of the surface layer and operating properties of aircraft engine components p 834 A93-39061
- Consumer interest in the air safety data of the airline quality rating. Testimony to the US House of Representatives, Committee on Government Operations, Government Activities and Transportation Subcommittee [NIAR-92-4] p 495 N93-19941

QUADRATIC PROGRAMMING

- Issues in large-scale optimization with expensive functions p 437 A93-20708
- Helicopter flight control system design using the linear quadratic regulator for robust eigenstructure assignment [AD-A258904] p 373 N93-19351
- Adjoint methods for aerodynamic wing design [NASA-CR-193086] p 805 N93-27089

QUADRUPOLES

- The influence of quadrupole sources in the boundary layer and wake of a blade on helicopter rotor noise p 566 A93-29410

QUALITATIVE ANALYSIS

- Applying commercial style acquisition practices to the procurement of commercially available aircraft [AD-A258143] p 455 N93-18087

QUALITY

- Consumer interest in the air safety data of the airline quality rating. Testimony to the US House of Representatives, Committee on Government Operations, Government Activities and Transportation Subcommittee [NIAR-92-4] p 495 N93-19941
- Satisfying the customer's requirements [PNR-90988] p 521 N93-20735

QUALITY CONTROL

- Statistical validation for GPS integrity test p 34 A93-11297
- Methodology in the development of avionics p 166 A93-15043
- Managing mistakes --- quality assurance in aircraft maintenance p 109 A93-17100
- Statistical quality control for kinematic GPS positioning p 314 A93-21162
- Ensuring the reliability and service life of flight vehicle structures by engineering methods p 745 A93-35276
- Valisys - A new quality assurance tool p 845 A93-36007

RADAR CLUTTER MAPS

- Aircraft monitoring of the planeness of the existing and new runways p 991 A93-45668
- Improved data validation and quality assurance in turbine engine test facilities [AIAA PAPER 93-2178] p 1137 A93-49990

- Advantages of a one-part resin system for processing aerospace parts by Resin Transfer Molding (RTM) [SME PAPER EM93-112] p 1159 A93-51729

- Integrated Blade Inspection System (IBIS) upgrade study [AD-A258912] p 365 N93-19356

- Nondestructive inspection of in-service aircraft [ETN-93-93059] p 496 N93-20928

QUANTUM MECHANICS

- The problem of two Coulomb centers and its applications in physical aerodynamics p 776 A93-39132
- Summer research program (1992). High School Apprenticeship Program (HSAP) reports. Volume 16: Arnold Engineering Development Center Civil Engineering Laboratory [AD-A262024] p 945 N93-29396

QUANTUM THEORY

- Turbulence and chaos in classical and quantum systems p 232 N93-14144

QUANTUM WELLS

- Sources and detectors for fiber communications; Proceedings of the Meeting, Boston, MA, Sept. 8, 9, 1992 [SPIE-1788] p 1151 A93-49455
- Compact high reliability fiber coupled laser diodes for avionics and related applications p 1152 A93-49470

QUASI-STEADY STATES

- Steady and quasisteady resonant lock-in of finned projectiles p 61 A93-12012

QUENCHING

- Effects of thermal history and jet fuel absorption on the properties of APC-2 p 534 A93-25252

R

RADAR ANTENNAS

- A proposed multi-modal FM/CW aircraft radar for use during ground operations p 206 A93-14678
- Update on the NASA ER-2 Doppler radar system (EDOP) p 807 A93-37737
- The PAVE PACE integrated RF architecture for next generation avionics p 896 A93-42784
- Radar 92: Proceedings of the International Conference, Brighton, United Kingdom, Oct. 12, 13, 1992 [ISBN 0-85296-533-2] p 929 A93-43376
- Experimental results on RIAS digital beamforming radar p 929 A93-43392
- A dual polarised active phased array antenna with low cross polarisation for a polarimetric airborne SAR p 883 A93-43401
- Dual band tuned radomes for radar applications p 929 A93-43405

- A Mode S implementation - Experiments about data-link and interconnected Mode S sensors p 883 A93-43409

- The PHARUS project, first results of the realization phase --- Phased Array Universal SAR p 884 A93-43454

- Adaptive waveform selection with a neural network p 942 A93-43470

- Inflight antenna diagram determination of spaceborne and airborne SAR-systems p 1161 A93-47583

RADAR APPROACH CONTROL

- Using TRACON as a teaching tool p 571 A93-27166
- Airport radar systems (2nd revised and enlarged edition) --- Russian book [ISBN 5-277-00610-9] p 992 A93-44505
- Terminal area forecasts FY 1992 - 2005 [AD-A255797] p 149 N93-15390
- Airspace Design Expert System (ADES), a 2D/3D mapping and modelling tool incorporating an expert system for use in instrument approach design p 888 N93-30357

RADAR BEACONS

- A description of the Mode Select beacon system (Mode S) and its associated benefits to the National Airspace System (NAS) [DOT/FAA/SE-92/6] p 35 N93-10738

RADAR BEAMS

- A technique to correct airborne Doppler data for coordinate transformation errors using surface clutter p 807 A93-37699

- Experimental results on RIAS digital beamforming radar p 929 A93-43392

RADAR CLUTTER MAPS

- Radar 92: Proceedings of the International Conference, Brighton, United Kingdom, Oct. 12, 13, 1992 [ISBN 0-85296-533-2] p 929 A93-43376
- Ground clutter measurements using an aerostat surveillance radar p 929 A93-43381

RADAR CROSS SECTIONS

- Adaptive clutter suppression for airborne array radars using clutter subspace approximation p 883 A93-43411
- Adaptive array processing for airborne radar p 883 A93-43412

RADAR CROSS SECTIONS

- Fundamentals of low radar cross-sectional aircraft design p 802 A93-37376
- Analysis of the effects of blade pitch on the radar return signal from rotating aircraft blades p 885 A93-43476
- Shape optimization for aerodynamic efficiency and low observability p 1062 A93-48285
- Receiving and scattering characteristics of an imaged monopole beneath a lossy sheet p 1158 A93-50543
- Ultra wide band 3-D cross section (RCS) holography [DE92-019133] p 89 N93-11802
- Ground clutter measurements using the NASA airborne doppler radar: Description of clutter at the Denver and Philadelphia airports p 490 N93-19608
- RCS of fundamental scatterers in the HF band by wire-grid modelling p 933 N93-30320

RADAR DATA

- Ground clutter measurements using an aerostat surveillance radar p 929 A93-43381
- Measurements of SSR bearing errors due to site obstructions — Secondary Surveillance Radar p 883 A93-43407
- NODE-air traffic management systems p 884 A93-43428
- Grazing angle dependency of SAR imagery p 884 A93-43455
- Motion compensation in a time domain SAR processor p 885 A93-43466
- Airport radar systems (2nd revised and enlarged edition) — Russian book p 992 A93-44505
- [ISBN 5-277-00610-9]
- Pilot weather advisor p 318 N93-16692
- [NASA-CR-189723]
- Air/ground wind shear information integration: Flight test results p 488 N93-19594
- Doppler radar results p 488 N93-19595
- Acquisition and use of Orlando, Florida and Continental Airbus radar flight test data p 489 N93-19603
- Comparison of simulated and actual wind shear radar data products p 490 N93-19610
- Classification of radar clutter in an air traffic control environment p 886 N93-30299

RADAR DETECTION

- Microbursts detection with airborne Doppler lidar p 433 A93-22201
- Evaluation of clear-air radar PROUST and Doppler radar RONSARD for airport low level-wind shear detection p 433 A93-22202
- Adaptive array processing for airborne radar p 883 A93-43412
- Space-time processing for AEW radar p 884 A93-43444
- Grazing angle dependency of SAR imagery p 884 A93-43455
- Digital pulse compression with low range sidelobes p 929 A93-43463
- Radar signals analysis oriented to target characterization applied to civilian ATC radar p 885 A93-43475
- Birds mimicking microbursts on 2 June 1990 in Orlando, Florida p 143 N93-14024
- [AD-A255703]
- Flight test operations p 488 N93-19592
- Discrete range clustering using Monte Carlo methods [NASA-TM-104004] p 706 N93-24914
- Future directions in aviation security p 880 N93-30274

RADAR ECHOES

- An integrated weather channel designed for an up-to-date ATC radar system p 929 A93-43434
- Radar signals analysis oriented to target characterization applied to civilian ATC radar p 885 A93-43475

RADAR EQUIPMENT

- A proposed multi-modal FM/CW aircraft radar for use during ground operations p 206 A93-14678
- Aureole lidar - Instrument design, data analysis, and comparison with aircraft spectrometer measurements p 1160 A93-52419
- Acquisition and use of Orlando, Florida and Continental Airbus radar flight test data p 489 N93-19603
- Installations and methods for measurement of aircraft radio components and systems p 1031 N93-31284

RADAR FILTERS

- Digital pulse compression with low range sidelobes p 929 A93-43463

RADAR IMAGERY

- Volume-imaging lidar observations of the convective structure surrounding the flight path of a flux-measuring aircraft p 425 A93-20579
- Superresolution radar imaging with linear prediction data extrapolation p 342 A93-20851

- The Meteorologist Weather Processor for U.S. National Weather Service units at Federal Aviation Administration sites p 428 A93-22130

- Results from a VHF impulse synthetic-aperture radar p 501 A93-28219
- Engineering a visual system for seeing through fog [SAE PAPER 921130] p 895 A93-41318
- Studies of superresolution range-Doppler imaging p 928 A93-43344

- Radar 92: Proceedings of the International Conference, Brighton, United Kingdom, Oct. 12, 13, 1992 [ISBN 0-85296-533-2] p 929 A93-43376
- Grazing angle dependency of SAR imagery p 884 A93-43455

- A refined procedure to generate calibrated imagery from airborne synthetic aperture radar data p 1162 A93-47657

- Automated extraction of aircraft runway patterns from radar imagery [AD-A254258] p 68 N93-11751
- Ultra wide band 3-D cross section (RCS) holography [DE92-019133] p 89 N93-11802

RADAR MAPS

- Topographic mapping using a Ku-band airborne elevation interferometer p 896 A93-42786
- Comparison of simulated and actual wind shear radar data products p 490 N93-19610

RADAR MEASUREMENT

- Maximum hail concentration that can be met by an aircraft in stormy precipitations p 430 A93-22152
- A technique to correct airborne Doppler data for coordinate transformation errors using surface clutter p 807 A93-37699
- Hydrometeor identification using cross polar radar measurements and aircraft verification p 844 A93-37719

- Ground clutter measurements using an aerostat surveillance radar p 929 A93-43381
- A multisensor-multitarget data association algorithm for heterogeneous sensors p 1020 A93-44168
- Program overview: 1991 flight test objectives p 488 N93-19591

- Doppler radar results p 488 N93-19595
- Three-dimensional numerical simulation of the 20 June 1991, Orlando microburst p 488 N93-19598
- Airborne doppler radar research at Rockwell International p 489 N93-19602
- Vertical wind estimation from horizontal wind measurements p 489 N93-19604
- Microburst characteristics determined from 1988-1991 TDWR testbed measurements p 490 N93-19605
- Ground clutter measurements using the NASA airborne doppler radar: Description of clutter at the Denver and Philadelphia airports p 490 N93-19608
- NASA airborne radar wind shear detection algorithm and the detection of wet microbursts in the vicinity of Orlando, Florida p 490 N93-19611

RADAR NAVIGATION

- Discrete range clustering using Monte Carlo methods [NASA-TM-104004] p 706 N93-24914

RADAR NETWORKS

- Embedded training capabilities for the LAMPS MK 3 system [AD-A250697] p 49 N93-11838

RADAR RANGE

- Correlation filters for aircraft identification from radar range profiles p 1097 A93-50636
- Discrete range clustering using Monte Carlo methods [NASA-TM-104004] p 706 N93-24914

RADAR RESOLUTION

- Prospective application of neural networks in superresolution radars p 211 A93-16849
- Results from a VHF impulse synthetic-aperture radar p 501 A93-28219

RADAR SCATTERING

- Dual band tuned radomes for radar applications p 929 A93-43405
- Birds mimicking microbursts on 2 June 1990 in Orlando, Florida p 143 N93-14024
- [AD-A255703]
- Systems issues in airborne Doppler radar/LIDAR certification p 145 N93-14855
- RCS of fundamental scatterers in the HF band by wire-grid modelling p 933 N93-30320

RADAR SIGNATURES

- Birds mimicking microbursts on 2 June 1990 in Orlando, Florida p 143 N93-14024

RADAR TARGETS

- A proposed multi-modal FM/CW aircraft radar for use during ground operations p 206 A93-14678
- Radar 92: Proceedings of the International Conference, Brighton, United Kingdom, Oct. 12, 13, 1992 [ISBN 0-85296-533-2] p 929 A93-43376
- Improvements in code validation algorithms for secondary surveillance radar p 883 A93-43408

SUBJECT INDEX

- An integrated weather channel designed for an up-to-date ATC radar system p 929 A93-43434
- Space-time processing for AEW radar p 884 A93-43444

- Radar signals analysis oriented to target characterization applied to civilian ATC radar p 885 A93-43475
- Motion errors and compensation possibilities p 212 N93-13052

- The real aperture antenna of SAR, a key element for performance p 213 N93-13053

RADAR TRACKING

- The dynamics of microbursts as revealed by Doppler radar observations and numerical simulations p 432 A93-22196

- Doppler radar observation of tornado and microburst around Chitose Airport p 432 A93-22199
- Track moving emitters with Kalman processing p 317 A93-22275

- Signal processing of jet noise from flyover test data [AIAA PAPER 93-0736] p 563 A93-24826

- Radar 92: Proceedings of the International Conference, Brighton, United Kingdom, Oct. 12, 13, 1992 [ISBN 0-85296-533-2] p 929 A93-43376

- Measurements of SSR bearing errors due to site obstructions — Secondary Surveillance Radar p 883 A93-43407

- NODE-air traffic management systems p 884 A93-43428

- Flight safety in Europe p 1227 A93-53726
- The effect of clock, media, and station location errors on Doppler measurement accuracy p 885 N93-29588

- Evolution of radar data processing in the French air traffic control system p 886 N93-30325

RADAR TRANSMISSION

- Airport radar systems (2nd revised and enlarged edition) — Russian book p 992 A93-44505

- [ISBN 5-277-00610-9]

RADAR TRANSMITTERS

- Adaptive waveform selection with a neural network p 942 A93-43470

RADARSCOPES

- Doppler radar results p 488 N93-19595

RADIAL DISTRIBUTION

- Analysis of high speed multistage compressor throughflow using spanwise mixing [ASME PAPER 92-GT-13] p 347 A93-19285

RADIAL FLOW

- Axial length influence on the performance of centrifugal impellers p 205 A93-14517

- Experimental and theoretical analysis of the flow in a centrifugal compressor volute [ASME PAPER 92-GT-30] p 400 A93-19290

- Aerodynamic design of turbomachinery blading in three-dimensional flow - An application to radial inflow turbines [ASME PAPER 92-GT-74] p 248 A93-19324

- Experimental analysis of transonic flow through the variable nozzle of a radial inflow turbine [ASME PAPER 92-GT-90] p 248 A93-19336

- Influence of blade aerodynamic loading on efficiency of radial-inflow turbines [ASME PAPER 92-GT-91] p 249 A93-19337

- The effects of blade loading in radial and mixed flow turbines [ASME PAPER 92-GT-92] p 349 A93-19338

- The design and evaluation of a high pressure ratio radial turbine [ASME PAPER 92-GT-93] p 349 A93-19339

- Aerodynamic design of pivotable nozzle vanes for radial-inflow turbines [ASME PAPER 92-GT-94] p 349 A93-19340

- Influence of surface heating condition on local heat transfer in a rotating square channel with smooth walls and radial outward flow [ASME PAPER 92-GT-188] p 402 A93-19413

- Investigations on a radial compressor tandem-rotor stage with adjustable geometry [ASME PAPER 92-GT-218] p 404 A93-19440

- Development and industrial application of the 'all-over-controlled vortex distribution method' for designing radial and mixed flow impellers [ASME PAPER 92-GT-262] p 405 A93-19466

- Rotor cavity flow and heat transfer with inlet swirl and radial outflow of cooling air [ASME PAPER 92-GT-378] p 406 A93-19536

- A laminar flow rotor for a radial inflow turbine [AIAA PAPER 93-1796] p 1074 A93-49686

- The combined effect of clearances and peripheral overlaps on the efficiency of microturbines with shrouded rotors p 1193 A93-52963

- Performance parameters and assessment p 81 N93-10052

- Aerodynamic investigation of radial turbines using computational methods p 81 N93-10056

- The integration of geometric modeling into an inverse design method and application of a PC-based inverse design method and comparison with test results p 81 N93-10058
- Partial admission and unsteady flow in radial turbines p 81 N93-10059
- Radial turbine cooling p 82 N93-10061
- Design and performance of nozzle-less volute casings for inward flow radial turbines p 722 N93-25471
- RADIAL VELOCITY**
- Investigation of compressor rotor wake structure at peak pressure rise coefficient and effects of loading [ASME PAPER 92-GT-32] p 246 A93-19292
- Radial transport and momentum exchange in an axial compressor [ASME PAPER 92-GT-364] p 257 A93-19528
- A simple, approximate model of parachute inflation [AIAA PAPER 93-1206] p 702 A93-35157
- Selection of the principal initial parameters for an axial-flow birotary turbine p 837 A93-39198
- Experimental study of the flow field inside a whirling annular seal p 85 N93-10892
- RADIANCE**
- Variability of geophysical parameters from aircraft radiance measurements for FIFE p 426 A93-20622
- Infrared detection of high altitude clear air turbulence [AIAA PAPER 93-0852] p 557 A93-24916
- Investigation of the radiance from the leading edge of a wing [AIAA PAPER 93-2728] p 1039 A93-46482
- RADIANT COOLING**
- Heat loads as key problem of hypersonic flight p 1222 A93-54276
- Heat loads as key problem of hypersonic flight [MBB-FE-202-S-PUB-0486] p 484 A93-21054
- RADIANT FLUX DENSITY**
- Prediction of the radiation characteristic of a helicopter exhaust jet p 172 A93-14494
- Spectral measurements of shock layer radiation in an arc-jet wind tunnel p 1251 A93-54409
- RADIANT HEATING**
- Iterative temperature calculation method for rectangular sandwich panel fins p 76 A93-10667
- Experimental simulation of the aerodynamic heating of bodies in a molecular region p 1090 A93-51871
- RADIATION DETECTORS**
- The GRAD Supernova Observer - First Flight of a very large balloon over Antarctica p 27 A93-11367
- RADIATION DISTRIBUTION**
- Calculation of sound field radiated by oscillating cascade p 231 A93-14269
- A study of optical distortions arising in radiation transmission through cavities with gas flow around them p 1225 A93-52945
- RADIATION DOSAGE**
- Radiation exposure in aircraft p 1035 N93-31928
- RADIATION EFFECTS**
- A monitor for the laboratory evaluation of control integrity in digital control systems operating in harsh electromagnetic environments [NASA-TM-4402] p 65 N93-12304
- Radiation exposure in aircraft p 1035 N93-31928
- RADIATION MEASUREMENT**
- Radiation safety in aircraft operations p 141 A93-14221
- Variability of geophysical parameters from aircraft radiance measurements for FIFE p 426 A93-20622
- RADIATION PROTECTION**
- Radiation safety in aircraft operations p 141 A93-14221
- RADIATION SOURCES**
- Propagation of high frequency jet noise using geometric acoustics [AIAA PAPER 93-0147] p 452 A93-23241
- Propagation of high frequency jet noise using geometric acoustics [NASA-TM-106013] p 233 N93-15575
- RADIATION TOLERANCE**
- Radiation exposure in aircraft p 1035 N93-31928
- RADIATIVE HEAT TRANSFER**
- Iterative temperature calculation method for rectangular sandwich panel fins p 76 A93-10667
- Prediction of engine casing temperature of fighter aircraft for infrared signature studies [SAE PAPER 920961] p 206 A93-14627
- Numerical study on atom-molecule radiation flowfield around a hypersonic blunt body p 770 A93-38434
- A convective and radiative heat transfer analysis for the FIRE II forebody [AIAA PAPER 93-3194] p 1021 A93-44231
- Radiative heat transfer from non-equilibrium high-enthalpy shock layers p 1024 A93-45515
- Monte Carlo simulation of radiating reentry flows [AIAA PAPER 93-2809] p 964 A93-46548
- Numerical calculation of polars and heat transfer for supersonic three-dimensional flow past wings with allowance for radiation p 1068 A93-48905
- Comparison of methodologies for describing relaxation in nonequilibrium gaseous systems p 419 N93-16786
- RADIATIVE TRANSFER**
- Numerical solution of radiative flowfield on the nose region of blunt bodies p 120 A93-14359
- Calculation of radiant energy transfer in hypersonic flow past blunt bodies using the P1 and P2 approximations of the spherical harmonic method p 124 A93-15209
- Computation of nonequilibrium radiating shock layers [AIAA PAPER 93-0144] p 414 A93-22588
- RADICALS**
- Employment of radicals and excited state species for supersonic combustion photochemical ignition of premixed hydrogen/oxygen mixtures with ArF laser p 73 N93-11135
- RADIO ALTIMETERS**
- GPS autoland considerations p 792 A93-38203
- Airborne gravimetry, altimetry, and GPS navigation errors p 1240 A93-55975
- Appraisal of digital terrain elevation data for low-altitude flight [NASA-TM-103896] p 35 N93-10745
- Integration of radar altimeter, precision navigation, and digital terrain data for low-altitude flight [NASA-TM-103958] p 36 N93-12320
- RADIO ANTENNAS**
- Models for performance assessment of HF antennas on the CH-135/Twin Huey helicopter p 933 N93-30291
- RADIO BEACONS**
- Decision making for a public differential GPS service p 314 A93-21165
- RADIO COMMUNICATION**
- European navigation into the 21st century - Frequency considerations p 311 A93-17754
- Applications of space techniques to civil aviation operations p 312 A93-20007
- A context-based introduction to aircraft radio communications p 570 A93-27164
- Three-dimensional cellular systems for aeronautical mobile radio communications p 502 A93-29639
- Airship/U.S. naval vessels UHF communications relay demonstration [AIAA PAPER 93-4032] p 1240 A93-54604
- Defence electronics industry profile, 1990-1991 [CTN-92-60515] p 84 N93-10653
- Summary of findings from the PIREP-based analyses conducted during the 1988 to 1990 evaluations of TDWR-based and TDWR/LLWAS-based alert services provided to landing/departing pilots [AD-A253859] p 93 N93-11144
- Embedded training capabilities for the LAMPS MK 3 system [AD-A250697] p 49 N93-11838
- Design issues and initial performance of an adaptive air/ground/air HF communication system p 934 N93-30342
- RADIO CONTROL**
- Flight test and wind-tunnel study of a scaled unmanned air vehicle [AIAA PAPER 92-4075] p 37 A93-11260
- A stability augmentation system for student designed remotely-piloted vehicles [AIAA PAPER 92-4261] p 63 A93-13365
- Operational and research aspects of a radio-controlled model flight test program [AIAA PAPER 93-0625] p 504 A93-24742
- Estimation of the service periods for complex systems in the case of a priori indeterminacy of system reliability data --- for radio electronic equipment of onboard navigation and landing p 856 A93-43109
- Increasing the reliability of an air traffic control radio system p 882 A93-43110
- Operational and research aspects of a radio-controlled model flight test program [NASA-TM-104266] p 339 N93-18616
- RADIO DIRECTION FINDERS**
- Discrete range clustering using Monte Carlo methods [NASA-TM-104004] p 706 N93-24914
- RADIO ELECTRONICS**
- Automated design and fabrication of radio-electronic circuits p 1151 A93-49000
- RADIO EQUIPMENT**
- Proposed revisions to RTCM SC-104 recommended standards for differential NAVSTAR/GPS service for carrier phase applications [AD-A255276] p 152 N93-15005
- Installations and methods for measurement of aircraft radio components and systems p 1031 N93-31284
- RADIO FREQUENCIES**
- European navigation into the 21st century - Frequency considerations p 311 A93-17754
- Integrated Soviet VLF/Omega Receiver design p 316 A93-21198
- RADIO FREQUENCY INTERFERENCE**
- Effect of skywave interference on the coverage of Loran-C p 33 A93-11095
- An optimal detection algorithm for harmonic interference signals in Loran-C p 993 A93-46889
- Carrier wave signals interfering with Loran-C [ETN-92-92528] p 318 N93-17584
- RADIO METEOROLOGY**
- Contributions to the American Meteorological Society's 26th International Conference on Radar Meteorology [AD-A263385] p 936 N93-29257
- RADIO NAVIGATION**
- European navigation into the 21st century - Frequency considerations p 311 A93-17754
- Flight management systems p 311 A93-17757
- The GPS system - Satellite radio-navigation p 312 A93-20008
- Institute of Navigation, National Technical Meeting, San Diego, CA, Jan. 27-29, 1992, Proceedings p 315 A93-21176
- Differential GPS and its applications in the aeronautical realm p 500 A93-28195
- Satcom Pacific Ocean trials p 501 A93-28198
- Relative sensitivity of Loran-C phase tracking and cycle selection to CWI p 792 A93-36502
- Half-scale modeling experience in the testing of radio navigation and landing systems p 882 A93-43112
- Integrated DGPS/IMU systems for airborne navigation in Poland p 1241 A93-56049
- Navstar global positioning system: Introduction and status [NLR-TP-91008-U] p 318 N93-17559
- On-board derived flight-path measurement as demonstrated by an ILS measurement system p 994 N93-31282
- RADIO RECEIVERS**
- Design, capabilities, and performance of the miniaturized airborne GPS receiver p 32 A93-11014
- Achieving modularity with tightly-coupled GPS/INS p 33 A93-11032
- The GPS system - Satellite radio-navigation p 312 A93-20008
- Description and capabilities of the Navcore-V GPS receiver engine p 312 A93-21127
- Digital hopping GPS/GLONASS receiver p 312 A93-21128
- GPS/GLONASS flight test, lab test and coverage analysis tests p 313 A93-21143
- Performance analysis of a miniaturized airborne GPS receiver p 313 A93-21147
- A new algorithm of Receiver Autonomous Integrity Monitoring (RAIM) for GPS navigation p 314 A93-21161
- Integrated Soviet VLF/Omega Receiver design p 316 A93-21198
- Analysis of a high-performance C/A-code GPS receiver in kinematic mode p 317 A93-21822
- A baseline GPS RAIM scheme and a note on the equivalence of three RAIM methods p 317 A93-21823
- New algorithms for hyperbolic radionavigation p 881 A93-40359
- Time delay measurements of current primary FAA air/ground transmitters and receivers [DOT/FAA/CT-TN93/14] p 842 N93-28555
- Embedded GPS: The Canadian Marconi approach p 886 N93-30330
- Experiences with two GPS receivers in northern Europe [NLR-TP-91168-U] p 993 N93-31120
- RADIO TRANSMITTERS**
- Time delay measurements of current primary FAA air/ground transmitters and receivers [DOT/FAA/CT-TN93/14] p 842 N93-28555
- RADIO WAVES**
- A computer simulation of the production of an artificially ionized layer using the Arecibo facility [DE93-010817] p 937 N93-30487
- RADIOISOTOPE BATTERIES**
- Overview of technical challenges of reentry analysis of radioisotope heat sources [AIAA PAPER 93-0379] p 386 A93-23059
- RADIOLOGY**
- The role of the radiologist in the medicolegal procedure after an aviation accident p 853 A93-39701
- RADIOMETERS**
- Coherent systems in the terahertz frequency range: Elements, operation, and examples p 841 N93-27727
- RADOME MATERIALS**
- Dual band tuned radomes for radar applications p 929 A93-43405
- RADOMES**
- 1992 - The year of the radome? p 209 A93-15525

RAIL TRANSPORTATION

A comparison between the impact of noise from aircraft, road traffic and trains on long-term recall and recognition of a text in children aged 12-14 years

p 1163 A93-49552

Aerodynamic forces on maglev vehicles
[PB93-154813]

p 782 N93-27413

RAIN

The Air Force Flight Test Center artificial icing and rain testing capability upgrade program

p 376 A93-22695

Verification of rain-flow reconstructions of a variable amplitude load history

p 91 N93-12411

Development of the Advance Warning Airborne System(AWAS)

p 144 N93-14849

Development of a large-scale, outdoor, ground-based test capability for evaluating the effect of rain on aircraft lift

p 779 N93-26899

RAINDROPS

Tracking of raindrops in flow over an airfoil
[AIAA PAPER 93-0168]

p 275 A93-22602

A laboratory investigation of raindrop oscillations

p 224 N93-13790

RAINSTORMS

Structure of downbursts associated with heavy rainfall observed in Tokyo

p 433 A93-22200

RAMAN SPECTRA

Coherent anti-Stokes Raman scattering (CARS) thermometry in a model gas turbine can combustor

p 387 A93-19366

Progress in laser spectroscopic techniques for aerodynamic measurements - An overview

p 549 A93-29308

CARS studies in hypersonic flows
[AIAA PAPER 93-3047]

p 1144 A93-48227

Thermometry inside a swirling turbulent flame - CARS advantages and limitations

p 1146 A93-51634

CARS temperature measurements in combustion
[ONERA, TP NO. 1993-78]

p 1212 A93-53599

RAMAN SPECTROSCOPY

Nonintrusive spectroscopic techniques for supersonic/hypersonic aerodynamics and combustion diagnostics

p 203 A93-14245

CARS thermometry in a liquid fueled model combustor
[AIAA PAPER 93-0366]

p 390 A93-23047

Rotational CARS measurements in a rotating cavity with axial throughflow of cooling air: Oxygen concentration measurements

p 72 N93-11035

RAMJET ENGINES

An experimental investigation on the combustor with bypass flow in integral liquid fuel ramjet

p 174 A93-16235

The ramjet engine in high speed propulsion

p 174 A93-16853

The pioneers of thermopulsive nozzles

p 235 A93-16854

Theoretical investigation of combustion characteristics in ram-jet dump combustor with side-inlet

p 346 A93-19121

Integration of turbo-expander- and turbo-ramjet-engines in hypersonic vehicles

p 353 A93-19428

Balance of moments for hypersonic vehicles
[ASME PAPER 92-GT-204]

p 253 A93-19460

Overview of the Japanese National Project for Super/Hyper-Sonic Transport propulsion system

p 239 A93-19461

Ramjet NOx emission - Use of a 3D CFD method for the combustor design of a super/hyper-sonic transport propulsion system

p 353 A93-19464

Some topics of research on hypersonic airbreathing engines at National Aerospace Laboratory

p 353 A93-19465

A scoping study for hypersonic transport propulsion systems

p 356 A93-19558

Combustion study on methane-fuel Laboratory Scaled Ram Combustor

p 356 A93-19561

An aerospace plane as a detonation wave ramjet/airframe integrated waverider

p 272 A93-22298

Test results on air turbo ramjet for a futurespace plane

p 359 A93-22325

Experimental results of shock trains in rectangular ducts

p 274 A93-22373

Some issues concerning active control of combustion instability in a ramjet

p 360 A93-22566

An estimate of the 'doomed propellant fraction' for a Superdetonative Ram Accelerator

[AIAA PAPER 93-0359]

p 385 A93-23042

Polyethylene pyrolysis model for combustion calculations in solid fuel ramjets

p 520 A93-27739

Studies of fuel-rich magnesium propellants in a small solid fuel ramjet combustor

p 535 A93-27759

Study of mixing flow field of a jet in a supersonic cross flow. I - Experimental facilities and preliminary experiments

p 857 A93-40430

Hugoniot analysis of the ram accelerator

p 1023 A93-45500

Initiation of combustion in the thermally choked ram accelerator

p 1016 A93-45501

Chemical-kinetics characteristics of combustion in a supersonic turbulent flow

p 1018 A93-47512

Slush hydrogen quantity gaging and mixing for the National Aerospace Plane

p 1150 A93-48635

Effects of side-inlet angle in a three-dimensional side-dump combustor

p 1109 A93-49610

CFD analysis and testing on a twin inlet ramjet

p 1075 A93-49723

Aerothermal ablative characterization of selected external insulator candidates

p 1145 A93-49735

Real gas simulation of air Blow-Down Facilities

p 1137 A93-49859

Rapid computer simulation of ramjet performance

p 1113 A93-49882

Boron particle ignition in high-speed flow

p 1145 A93-50014

Standing normal detonations and oblique detonations for propulsion

p 1116 A93-50105

Investigation of a combustion zone behind a wedge

p 1146 A93-51631

High temperature heat exchangers for gas turbines and future hypersonic air breathing propulsion

p 1218 A93-53596

CFD for ramjet and scramjet powered vehicles

p 1197 A93-54011

Hypersonic shock-induced combustion ramjet performance analysis

p 1197 A93-54013

Study of a pulse ramjet based on twin valveless combustors coupled to operate in antiphase

p 1197 A93-54014

The combustion performance of methane-fueled ram combustor

p 1201 A93-54055

Studies on methane-fuel ram combustor for HST combined cycle engine

p 1201 A93-54056

Test results of the hydrogen fueled model combustor for the air turbo ramjet engine

p 1201 A93-54058

Numerical simulation of ramjet and scramjet combustion using two-dimensional Euler equations with finite rate chemistry

p 1202 A93-54059

Numerical study of nitric oxide formation in a hypersonic ramjet engine

p 1204 A93-54100

Results of sea-level static tests on air turbo ramjet for a future space plane

p 1247 A93-55817

The combustion time lag and its role in ramjet combustion instability

p 73 N93-11137

Active control of combustion instability in a ramjet using large-eddy simulations

p 175 N93-14111

Control of asymmetric jet

p 219 N93-14400

Combustion instabilities in a side-dump model ramjet combustor

p 362 N93-17613

Experimental analysis of combustion oscillations with reference to ramjet propulsion

p 392 N93-17614

Prediction of the performances in combustion of ramjets and stato-rockets by isothermal experiments and modeling

p 363 N93-17622

What is the progress in propulsion?

p 298 N93-19006

Regression rate mechanism in a solid fuel ramjet

p 814 N93-27185

Flight mechanical model for performance calculations and interactions between flight vehicle and ramjet in regard to the flight orbit

p 893 N93-29464

[ESA-TT-1267]

RAMJET MISSILES

The ramjet engine in high speed propulsion

p 174 A93-16853

RAMP FUNCTIONS

Unsteady Navier-Stokes simulation of the canard-wing-body ramp motion

p 1058 A93-48235

[AIAA PAPER 93-3058]

RAMPS

Experiments on shock-wave/boundary-layer interactions produced by two-dimensional ramps and three-dimensional obstacles

p 865 A93-42589

An experimental contribution to the flat plate 2D compression ramp, shock/boundary layer interaction problem at Mach 14 - Test case 3.7

p 865 A93-42590

Viscous, 2-D, laminar hypersonic flows over compression ramps

p 866 A93-42591

Application of the Galerkin/least-squares formulation to the analysis of hypersonic flows. I - Flow over a two-dimensional ramp

p 866 A93-42593

Computation of flows over 2D ramps

p 866 A93-42595

Hypersonic viscous flow over two-dimensional ramps

p 866 A93-42596

Grid-refinement study of hypersonic laminar flow over a 2-D ramp

p 866 A93-42597

Computational results for flows over compression ramps

p 866 A93-42599

Implicit upwind finite-difference simulation of laminar hypersonic flow over a 2D ramp

p 867 A93-42600

A synthesis of results on the calculation of flow over a 2D ramp and a 3D obstacle - Antibes test cases 3 and 4

p 867 A93-42601

Control of low-speed turbulent separated flow over a backward-facing ramp

p 219 N93-14475

RAMPS (STRUCTURES)

Hypersonic single expansion ramp nozzle simulations

p 777 A93-39254

RANDOM ACCESS

Considerations for space and naval aviation applications of ferroelectric memory

p 759 N93-26294

RANDOM ACCESS MEMORY

Neutron-induced single event upsets in static RAMs observed at 10 KM flight altitude

p 1158 A93-50561

Single event upset in avionics

p 1158 A93-50566

RANDOM ERRORS

Analysis of random components during measurements in the computerized diagnostic system Analiz-86

p 321 A93-18344

RANDOM LOADS

A review of crack propagation under unsteady loading

p 399 A93-19207

A method and a software for constructing F-by-F random load spectrum

p 506 A93-27375

Estimation of the life of aircraft structures under stochastic steady state loading

p 545 A93-27620

Review of crack propagation under unsteady loading

p 837 A93-39416

Response of B-2 aircraft to nonuniform spanwise turbulence

p 1135 A93-52437

Fatigue life under random load history derived from exceedance curves using different algorithms

p 1260 A93-56544

RANDOM NOISE

Measurement technique for Loran-C pulse wave distortion measures and performance in an environment of noise

p 29 A93-10988

Optimal structure of discrete algorithms of finite-dimensional continuous-discrete filtering in the presence of Markov noise

p 1169 A93-51065

Detection performance of digital polarity sampled phase reversal code pulse compressors

p 842 N93-28289

RANDOM PROCESSES

Equivalent deterministic inputs for atmospheric turbulence

p 183 A93-14351

RANDOM VARIABLES

Comparison of neural network and Markov random field image segmentation techniques

p 397 A93-18652

Probabilistic assessment of composite structures

p 825 N93-27092

RANDOM VIBRATION

Finite element nonlinear random response of beams to acoustic and thermal loads applied simultaneously

p 740 A93-33978

RANGE ERRORS

Receiver autonomous integrity monitoring (RAIM) capability for sole-means GPS navigation in the oceanic phase of flight

p 33 A93-11035

The effects of ionospheric errors on single-frequency GPS users

p 313 A93-21141

RANGE FINDERS

Passive range sensor refinement using texture and segmentation

p 544 A93-27044

A fast algorithm for image-based ranging

p 544 A93-27045

RANGEFINDING

DME/P critical area determination on message passing processors

p 31 A93-11010

Receiver autonomous integrity monitoring (RAIM) capability for sole-means GPS navigation in the oceanic phase of flight

p 33 A93-11035

- Vision-based range estimation using helicopter flight data p 151 A93-17501
- Vision-based range estimation using helicopter flight data p 317 A93-21525
- New slant visual range measuring device promises improved airport operations p 529 A93-27395
- Passive range estimation for rotorcraft low-altitude flight p 948 A93-46608
- Vision based obstacle detection and grouping for helicopter guidance [AIAA PAPER 93-3871] p 1098 A93-51457
- Passive range estimation for rotorcraft low-altitude flight p 1190 A93-52881
- Discrete range clustering using Monte Carlo methods [NASA-TM-104004] p 706 N93-24914
- Image-based ranging and guidance for rotorcraft [NASA-CR-177608] p 708 N93-26549
- Neural networks application to divergence-based passive ranging [NASA-TM-103981] p 885 N93-29653
- Expansion-based passive ranging [NASA-TM-104025] p 994 N93-32348
- RANGES (FACILITIES)**
- A combined facility of ballistic range and shock tunnel using a fast action valve p 1012 A93-45532
- RANKINE CYCLE**
- Compound cycle engine for helicopter application [NASA-CR-180824] p 55 N93-10348
- RANKINE-HUGONIOT RELATION**
- A split-matrix Runge-Kutta type space marching procedure p 8 A93-11921
- RANKING**
- Trans-cockpit authority gradient in Navy/Marine aircraft mishaps p 146 N93-15016
- RAPID QUENCHING (METALLURGY)**
- FNAS modify matrix and transparent experiments [NASA-CR-184442] p 198 N93-13311
- RAPID TRANSIT SYSTEMS**
- TGV tunnel entry simulations using a finite element code with automatic remeshing [AIAA PAPER 93-0890] p 471 A93-24950
- Proposal and preliminary design for a high speed civil transport aircraft. Swift: A high speed civil transport for the year 2000 p 335 N93-18049
- HST mission analysis of waverider designs [NASA-CR-192193] p 515 N93-21646
- Aerodynamic forces on maglev vehicles [PB93-154813] p 782 N93-27413
- RAREFIED GAS DYNAMICS**
- Calculation of flow of a rarefied gas past a sphere for an arbitrary Knudsen number p 124 A93-15146
- Experiments on rarefied supersonic free jets using impact probes p 461 A93-24091
- Comparison of continuum and particle simulations of expanding rarefied flows [AIAA PAPER 93-0728] p 466 A93-24818
- Numerical simulation of hypersonic rarefied gas flow over blunt bodies p 687 A93-34356
- Hypersonic limiting flows of a relaxing gas with pressure changes in the main approximation p 776 A93-39135
- Stabilization of the Burnett equations and application to hypersonic flows p 778 A93-39410
- Rarefied-flow shuttle aerodynamics flight model [AIAA PAPER 93-3441] p 859 A93-41057
- Problem 6.4.1 - Rarefied flow around a double ellipse p 869 A93-42630
- The hypersonic double ellipse in rarefied flow p 869 A93-42631
- Experimental density flowfields over a delta wing located in rarefied hypersonic flows p 870 A93-42637
- Experiments on the heat transfer and on the aerodynamic coefficients of a delta wing in rarefied hypersonic flows p 870 A93-42638
- Rarefied gas flow around a 3D-deltawing p 870 A93-42639
- Appraisal of the rarefied flow computations (problems 6.4.1 and 7.2.1) p 871 A93-42640
- Formation of the shock reflection on a wedge p 1023 A93-45476
- Flow resolution and domain of influence in rarefied hypersonic blunt-body flows [AIAA PAPER 93-2806] p 964 A93-46546
- On numerical solutions of Burnett equations for hypersonic flow past 2-D circular blunt leading edges in continuum transition regime [AIAA PAPER 93-3092] p 1060 A93-48266
- DSMC simulation of ionized rarefied flows [AIAA PAPER 93-3095] p 1061 A93-48269
- DSMC numerical investigation of rarefied compression corner flow [AIAA PAPER 93-3096] p 1061 A93-48270
- A study of turbulence in rarefied gases [AIAA PAPER 93-3097] p 1061 A93-48271
- Development and application of the Monte Carlo method for solving the Boltzmann equation and its models p 1173 A93-51867
- Modeling the flow around a body via the solution of the relaxational kinetic equation p 1089 A93-51868
- Approximate calculation of the aerodynamic characteristics of simple bodies in hypersonic rarefied-gas flow p 1090 A93-51869
- Calculation of the aerodynamic characteristics of bodies with meshlike surfaces in hypersonic rarefied-gas flow p 1090 A93-51870
- Effect of Reynolds number on the aerodynamic characteristics of a semicone with a wing in the case of hypersonic flow velocities p 1090 A93-51878
- Quantitative Knudsen-number dependences of density disturbances in front of obstructions in supersonic divergent flows p 1239 A93-56220
- Application of a vectorized particle simulation to the study of plates and wedges in high-speed rarefied flow p 133 N93-13746
- Rarefied gas numerical wind tunnel. Part 7: OREX p 382 N93-19280
- Rarefied-flow Shuttle aerodynamics model [NASA-TM-107698] p 458 N93-19976
- Hypersonic panel flutter in a rarefied atmosphere [NASA-CR-4514] p 780 N93-27084
- RATINGS**
- The airline quality report, 1992 [NIAR-92-11] p 310 N93-18036
- Consumer interest in the air safety data of the airline quality rating. Testimony to the US House of Representatives, Committee on Government Operations, Government Activities and Transportation Subcommittee [NIAR-92-4] p 495 N93-19941
- RATIONAL FUNCTIONS**
- Multiple pole rational-function approximations for unsteady aerodynamics p 769 A93-37404
- RAY TRACING**
- Propagation of high frequency jet noise using geometric acoustics [AIAA PAPER 93-0147] p 452 A93-23241
- Design of an optimal single reflective holographic helmet display element p 517 A93-26886
- Propagation of high frequency jet noise using geometric acoustics [NASA-TM-106013] p 233 N93-15575
- RAYLEIGH EQUATIONS**
- Lord Rayleigh and hydrodynamic similarity p 211 A93-17408
- RAYLEIGH SCATTERING**
- Shock enhancement and control of hypersonic combustion [AD-A254295] p 72 N93-10843
- RAYLEIGH-RITZ METHOD**
- Nonlinear aeroelasticity of composite structures [AD-A254285] p 47 N93-10842
- A Rayleigh-Ritz analysis methodology for cutouts in composite structures p 923 N93-30889
- REACTING FLOW**
- Numerical simulation of a low-emission gas turbine combustor using KIVA-II p 170 A93-14077
- Numerical simulation of turbulent reacting flows in combustion chambers p 171 A93-14271
- A numerical study of slit V-gutter flows p 171 A93-14273
- Unstable branches of a hypersonic, chemically reacting boundary layer p 128 A93-17262
- Direct numerical simulation of nitric oxide evolution in underexpanded jets [ASME PAPER 92-GT-372] p 355 A93-19534
- Numerical simulation of shock-induced combustion/detonation p 410 A93-20719
- CFD analysis of hypersonic chemically reacting flowfields around a generic shape [AIAA PAPER 93-0323] p 281 A93-23015
- Development of a robust pressure-based numerical scheme for spray combustion applications [AIAA PAPER 93-0902] p 560 A93-24960
- Calculation of optical and electric characteristics from hypersonic blunt-body wakes p 680 A93-33729
- Reacting gas and surface coupling in high temperature air flows p 686 A93-34353
- Reactive and dissipative hypersonic flow in a wind tunnel nozzle p 687 A93-34358
- Hypersonic chemically reacting flow of a reentry body p 769 A93-38147
- Numerical analysis for chemically non-equilibrium flow p 770 A93-38148
- Kinetic theory of nonequilibrium flows of gas and disperse media with internal degrees of freedom and chemical reactions p 851 A93-39127
- Modeling of the physicochemical processes of nonequilibrium heat transfer in the subsonic jets of an induction plasmatron p 836 A93-39147
- Computation of hypersonic flow over a sphere using kinetic flux vector splitting scheme with equilibrium chemistry p 861 A93-42260
- Simulation of nonequilibrium hypersonic flows p 863 A93-42443
- Equilibrium and nonequilibrium modeling of hypersonic inviscid flows p 864 A93-42448
- Reactive and inert inviscid flow solutions by quasi-linear formulations and shock fitting p 927 A93-42625
- Contribution to Problem 6 using an upwind Euler solver with unstructured meshes p 869 A93-42627
- Three-dimensional calculation of a hydrogen jet injection into a supersonic air flow p 950 A93-44374
- Compressibility, exothermicity, and three dimensionality in spatially evolving reactive shear flows p 950 A93-44375
- Progress in local preconditioning of the Euler and Navier-Stokes equations [AIAA PAPER 93-3328] p 952 A93-45022
- Numerical simulation of supersonic flows with chemical reactions p 959 A93-45325
- A review of chemically reactive turbulent flow mixing mechanisms and a new design for a low NO(x) combustor p 1109 A93-49508
- The computation over unstructured grids of inviscid hypersonic reactive flow by upwind finite-volume schemes p 1073 A93-49532
- Swirling flows in a contoured-wall combustion chamber [AIAA PAPER 93-1765] p 1073 A93-49661
- CFD validation for scramjet combustor and nozzle flows. I [AIAA PAPER 93-1840] p 1111 A93-49724
- Summary of the GASP code application and evaluation effort for scramjet combustor flowfields [AIAA PAPER 93-1973] p 1077 A93-49820
- Mixing enhancement and combustion of gaseous fuel in a supersonic combustor [AIAA PAPER 93-2143] p 1114 A93-49960
- Modeling of turbulent supersonic H₂-air combustion with a multivariate beta PDF [AIAA PAPER 93-2198] p 1155 A93-50010
- Some supersonic and hypersonic research at GASL in the 1960s and 70s [AIAA PAPER 93-2327] p 1145 A93-50107
- Particulates and aerosols characterized in real time for harsh environments using the UMR mobile aerosol sampling system (MASS) [AIAA PAPER 93-2344] p 1156 A93-50118
- An extended insight into hypersonic flow phenomena using numerical methods p 1093 A93-51999
- Stagnation point computations of nonequilibrium inviscid blunt body flow p 1093 A93-52005
- Comparison of gasdynamic models in hypersonic flow p 1179 A93-53315
- Direct simulation of reacting fuel gas flows in a supersonic mixing layer [ISABE 93-7072] p 1201 A93-54048
- Numerical study of nitric oxide formation in a hypersonic ramjet engine [ISABE 93-7125] p 1204 A93-54100
- Computation of nonequilibrium hypersonic flowfields around hemisphere cylinders p 1229 A93-54469
- Effects of reacting flows with turbulence and shock waves on efficiency of scramjet combustors p 69 N93-11133
- Velocity and temperature measurements in a non-premixed reacting flow behind a backward facing step p 132 N93-13632
- Investigation of the aerothermodynamics of hypervelocity reacting flows in the ram accelerator [NASA-CR-191715] p 140 N93-15588
- Mixing and reaction in the subsonic 2-D turbulent free shear layer p 289 N93-16508
- Combustion instabilities in a side-dump model ramjet combustor p 362 N93-17613
- A new LU-SGS flow solver for calculating reentry flows p 698 N93-25759
- Visualization of a Mach 2 reacting flow using Planar Laser-Induced Fluorescence (PLIF) p 731 N93-26006
- Turbulence interacting with chemical kinetics in airbreathing combustion of ducted rockets p 734 N93-26012
- Comparison of reacting and non-reacting shear layers at a high subsonic Mach number [NASA-TM-106198] p 814 N93-27610
- Turbulence characteristics of an axisymmetric reacting flow [NASA-CR-4110] p 877 N93-30373
- Turbulence measurement in a reacting and non-reacting shear layer at a high subsonic Mach number [NASA-TM-106186] p 989 N93-31839
- REACTION CONTROL**
- Determination of YAV-8B Reaction Control System bleed flow usage [AIAA PAPER 92-4232] p 54 A93-13330

REACTION KINETICS

- Numerical analysis of reacting flow using finite rate chemistry models p 389 A93-21666
- Simplified jet fuel reaction mechanism for lean burn combustion application [AIAA PAPER 93-0021] p 390 A93-23238
- Combustion and reaction kinetics; Proceedings of the 22nd International Annual Conference of ICT, Karlsruhe, Germany, July 2-5, 1991 p 535 A93-27726
- Simulation of nonequilibrium hypersonic flows p 863 A93-42443
- Equilibrium and nonequilibrium modeling of hypersonic inviscid flows p 864 A93-42448
- Review of chemical-kinetic problems of future NASA missions. I - Earth entries p 872 A93-42899
- Chemical-kinetics characteristics of combustion in a supersonic turbulent flow p 1018 A93-47512
- Some supersonic and hypersonic research at GASL in the 1960s and 70s [AIAA PAPER 93-2327] p 1145 A93-50107
- Investigation of the structure of a multicomponent viscous shock layer p 1090 A93-51879
- Numerical simulation of ramjet and scramjet combustion using two-dimensional Euler equations with finite rate chemistry [ISABE 93-7083] p 1202 A93-54059
- Finite-rate H₂/air combustion effects in CRJ for hypersonic launchers p 1202 A93-54060
- [ISABE 93-7084] p 1202 A93-54060
- Influence of chemical kinetics effects in nozzles shape design [ISABE 93-7112] p 1188 A93-54087
- A finite element code for gas turbine combustor flow with Stretched Laminar Flamelet modelling [ISABE 93-7127] p 1204 A93-54102
- The effects of reaction rate constants and catalytic wall on the hypersonic flow field over blunt bodies p 1230 A93-54586
- Kinetic scheme selection in describing detonation in an H₂-air mixture behind shock waves p 1253 A93-55032
- Simplified jet-A kinetic mechanism for combustor application [NASA-TM-105940] p 200 N93-15504
- Chemical kinetic and aerodynamic structures of flames [AD-A256015] p 391 N93-15931
- Mixing and reaction in the subsonic 2-D turbulent free shear layer p 289 N93-16508
- A critical analysis of the accuracy of several numerical techniques for combustion kinetic rate equations [NASA-TP-3315] p 362 N93-16941
- Prediction of the performances in combustion of ramjets and stato-rockets by isothermal experiments and modeling p 363 N93-17622
- Projectile base bleed technology. Part 2: User's guide CMINT computer code, version 5.04-BRL [AD-A258630] p 551 N93-19999
- Turbulence interacting with chemical kinetics in airbreathing combustion of ducted rockets p 734 N93-26012
- Regression rate mechanism in a solid fuel ramjet p 814 N93-27185
- Studies of hydrogen-air diffusion flames and of compressibility effects related to high-speed propulsion p 917 N93-29125
- Generation of carbon monoxide in compartment fires [PB93-146702] p 880 N93-29211
- Kinetics and energy transfer in nonequilibrium fluid flows [AD-A263612] p 875 N93-29284
- Evaluation of candidate working fluid formulations for the electrothermal-chemical wind tunnel [NASA-CR-193366] p 1015 N93-31848
- REACTION PRODUCTS**
- A condensed phase test cell assembly for the System for Thermal Diagnostic Studies (STDS) [AD-A258463] p 393 N93-18242
- REACTION TIME**
- Two simulation studies of precision runway monitoring of independent approaches to closely spaced parallel runways [AD-A263433] p 911 N93-29815
- READOUT**
- Indian experience in flight data readout and analysis p 168 N93-15161
- Czechoslovak development and experience in flight data recorder readout and analysis p 168 N93-15162
- Solid state flight data recorder with rapid data access p 221 N93-15167
- REAL GASES**
- A comparison of upwind schemes for computation of three-dimensional hypersonic real-gas flows [AIAA PAPER 92-4350] p 15 A93-13306

- Accuracy and efficiency assessments for a weak statement CFD algorithm for high-speed aerodynamics [ASME PAPER 92-GT-433] p 435 A93-19576
- Real gas effects for compressible nozzle flows p 682 A93-33757
- Solution of the Euler equations around a double ellipsoidal shape using unstructured meshes and including real gas effects p 867 A93-42604
- On the accuracy and efficiency of CFD methods in real gas hypersonics p 871 A93-42869
- An overview of Ames experimental aerothermodynamics p 1011 A93-45496
- Real gas effects in two- and three-dimensional hypersonic, laminar boundary layers p 1073 A93-49530
- Real gas simulation of air Blow-Down Facilities [AIAA PAPER 93-2022] p 1137 A93-49859
- Calculation of real-gas effects on airfoil aerodynamic characteristics p 1229 A93-54477
- Hypersonic vehicle research by using a large shock tunnel [AAS PAPER 91-607] p 1250 A93-55841
- Computational study of real gas effects in high speed high temperature flow, volume 2 [AERO-REPT-9203-VOL-2] p 289 N93-16470
- Issues and approach to develop validated analysis tools for hypersonic flows: One perspective [NASA-TM-103937] p 305 N93-19379
- Hypersonic lateral and directional stability characteristics of aeroassist flight experiment configuration in air and CF4 [NASA-TM-4435] p 875 N93-29166
- REAL TIME OPERATION**
- Advanced real time integrated processors --- for Lockheed F-22 advanced tactical fighter p 50 A93-11000
- Real time DGPS service for precise positioning - Activities in the Federal Republic of Germany p 1 A93-11027
- Real-time capture, archiving, retrieval, processing, and presentation of large quantities of flight test/research information [AIAA PAPER 92-4073] p 95 A93-11258
- The development of an airborne information management system for flight test [AIAA PAPER 92-4113] p 51 A93-11281
- The Tenth Conference on Air Navigation - A landmark in the history of civil aviation p 34 A93-12559
- Development of generic helicopter performance methodology for real time mission analyses p 152 A93-14185
- Variable structure controller design and its real-time analysis for microprocessor-based flight control systems p 181 A93-14229
- Interactive hypersonic waverider design and optimization p 119 A93-14348
- An investigation of real-time diagnostic technique on aeroengine p 174 A93-16844
- Assessment of flight data in real time p 341 A93-18364
- FAA weather processor programs - Real-time dissemination of weather information to aviation end-users p 428 A93-22131
- Discrete-time LTR synthesis of delayed control systems p 439 A93-22855
- Anti-icing failure detection instrumentation using realtime optical measurement of anti-icing fluid properties [AIAA PAPER 93-0748] p 540 A93-24836
- Real-time optical measurement of alkali species in air for jet engine corrosion testing [AIAA PAPER 93-0791] p 541 A93-24870
- Advanced airborne 3D computer image generation systems technologies for the year 2000 p 518 A93-28176
- Optimal open multistep discretization formulas for real-time simulation p 757 A93-34539
- Automatic guidance and control laws for helicopter obstacle avoidance p 728 A93-35518
- A parametric study of real time mathematical modeling incorporating dynamic wake and elastic blades p 798 A93-35986
- A data system for the observation of flow conditions on an aircraft wing p 808 A93-37882
- Expert system for redundancy and reconfiguration management p 938 A93-42785
- Functionally Integrated Resource Manager for real-time avionics data p 940 A93-42832
- Real time PRF control system for SAR p 884 A93-43464
- Real-time parameter identification applied to flight simulation p 1006 A93-44142
- Use of Convex supercomputers for flight simulation at NASA Langley p 1013 A93-46806
- Simplified mathematical model and digital simulation of aeroengine p 1106 A93-48511

- Real-time simulation of maneuverable aircraft flight conditions on altitude test cell [AIAA PAPER 93-1845] p 1137 A93-49726
- Application of analog computing to real-time simulation of stall and surge dynamics [AIAA PAPER 93-2231] p 1080 A93-50037
- Particulates and aerosols characterized in real time for harsh environments using the UMR mobile aerosol sampling system (MASS) [AIAA PAPER 93-2344] p 1156 A93-50118
- Multiple radial basis function networks in modeling and control [AIAA PAPER 93-3731] p 1170 A93-51330
- The application of intelligent search strategies to robust flight control for hypersonic vehicles [AIAA PAPER 93-3732] p 1143 A93-51331
- A parallel implementation of a multisensor feature-based range-estimation method p 1099 A93-51967
- A high fidelity video delivery system for real-time flight simulation research [AIAA PAPER 93-3558] p 1214 A93-52659
- Terrain modeling for real-time photo-texture based visual simulation [AIAA PAPER 93-3607] p 1214 A93-52667
- Development and operation of a real-time simulation at the NASA Ames Vertical Motion Simulator [AIAA PAPER 93-3575] p 1208 A93-52671
- Enhancing real-time flight simulation execution by intercepting Run-Time Library calls [AIAA PAPER 93-3591] p 1224 A93-52684
- Development of a real time dynamic engine simulation model of a turbo fan engine [ISABE 93-7132] p 1205 A93-54107
- Improved flow measurement with simultaneous period/frequency recording --- in turbojet engines p 1254 A93-54381
- An updated data acquisition and processing system for turbine engine testing p 1250 A93-54389
- Research requirements for a real-time flight measurements and data analysis system for subsonic transport high-lift research p 1244 A93-54391
- A data acquisition system for high-speed rotor balancing p 1261 A93-54396
- Requirements analysis notebook for the flight data systems definition in the Real-Time Systems Engineering Laboratory (RSEL) [NASA-CR-185698] p 69 N93-10960
- Summary: Experimental validation of real-time fault-tolerant systems [NASA-CR-190985] p 175 N93-13697
- Wind shear related research at Princeton University p 145 N93-14854
- Real-time in-flight engine performance and health monitoring techniques for flight research application p 169 N93-15169
- Realization of real time graphics in vehicles with high dynamic motion [ETN-93-92739] p 443 N93-18630
- IOPS advisor: Research in progress on knowledge-intensive methods for irregular operations airline scheduling p 443 N93-18686
- Acquisition and use of Orlando, Florida and Continental Airbus radar flight test data p 489 N93-19603
- Aid in investigation by figure animation p 491 N93-19659
- Development of a realtime DGPS system [DLR-MITT-92-06] p 503 N93-20749
- Use of high performance networks and supercomputers for real-time flight simulation p 731 N93-25574
- A real-time, hardware-in-the-loop simulation of an unmanned aerial research vehicle [AD-A262477] p 893 N93-29409
- Two simulation studies of precision runway monitoring of independent approaches to closely spaced parallel runways [AD-A263433] p 911 N93-29815
- Three-dimensional graphical representation of objects according to movement data in realtime [ESA-TT-1258] p 942 N93-30104
- Issues of ATC conflict resolution under real-time constraints p 887 N93-30350
- REATTACHED FLOW**
- Transonic shock oscillations calculated with a new interactive boundary layer coupling method [AIAA PAPER 93-0777] p 269 A93-21119
- Prediction of fluctuating pressure in attached and separated compressible flow [AIAA PAPER 93-0286] p 279 A93-22687
- Control of pressure fluctuations in the reattachment region of a supersonic free shear layer [AIAA PAPER 93-0385] p 282 A93-23064
- Aerodynamic heating in the vicinity of hypersonic, axisymmetric, shock-wave boundary-layer interactions [AIAA PAPER 93-2766] p 963 A93-46512
- Control of a supersonic reattaching shear layer [AIAA PAPER 93-3248] p 966 A93-46793

SUBJECT INDEX

- Surface hot-film method for the measurement of transition, separation and reattachment points
[AIAA PAPER 93-2918] p 1148 A93-48120
- The effect of large scale unsteady motion on turbulent reattaching shear layer - Application to the supersonic compression ramp
[AIAA PAPER 93-3100] p 1061 A93-48273
- An experimental investigation of the separating/reattaching flow over a backstep
[NASA-CR-192105] p 298 A93-18781
- RECEIVERS**
- Guidelines for NAVSTAR GPS embedded receiver applications p 315 A93-21184
- Multipath effects in a Global Positioning Satellite system receiver p 318 A93-17311
- Attitude determination using GPS: Development of an all solid-state guidance, navigation, and control sensor for air and space vehicles based on the global positioning system p 888 A93-30605
- RECIRCULATIVE FLUID FLOW**
- A numerical study of slit V-gutter flows p 171 A93-14273
- Effects of back-pressure in a lean blowout research combustor
[ASME PAPER 92-GT-81] p 387 A93-19330
- Flow measurements behind V-gutter under non-combusting condition
[AIAA PAPER 93-0020] p 408 A93-20139
- Flow visualization and flow field measurements of a 1/12 scale tilt rotor aircraft in hover p 482 A93-29441
- Operation of a cross-flow heat exchanger with partial recirculation of one of the coolants p 833 A93-39051
- Modelling three-dimensional gas-turbine-combustor model flow using second-moment closure
[AIAA PAPER 93-3104] p 1149 A93-48277
- High lift airfoil flow simulation using a wall-corrected Algebraic Stress Model
[AIAA PAPER 93-3109] p 1061 A93-48280
- Experimental study of the flow field inside a whirling annular seal p 85 A93-10892
- RECOMBINATION REACTIONS**
- Determination of the $N_2(+) + e$ recombination rate constant from ballistic experiments p 1234 A93-55026
- RECONNAISSANCE**
- Testing of an experimental system for image reconnaissance p 1040 A93-31283
- RECONNAISSANCE AIRCRAFT**
- USCG HU-25A/GPS integration p 313 A93-21130
- Comanche airframe design - The PDT approach p 744 A93-34469
- Development status of the RAH-66 Comanche p 803 A93-38838
- Reconnaissance capable F/A-18D optical and infrared window antifog systems
[SAE PAPER 92-1182] p 890 A93-41361
- Testing of an energy efficient environmental control system for a patrol-type aircraft
[SAE PAPER 92-1225] p 890 A93-41399
- National airborne surveillance system - An engineering student study
[AIAA PAPER 93-4031] p 1242 A93-54603
- Airship: The 'Look Out' - A versatile surveillance platform
[AIAA PAPER 93-4033] p 1229 A93-54605
- The development progress of the U.S. Army's SASS LITE, unmanned robot airship
[AIAA PAPER 93-4047] p 1243 A93-54614
- Hypersonic reconnaissance aircraft
[NASA-CR-192049] p 333 A93-17804
- A manned hypersonic reconnaissance vehicle which does not require airborne fueling p 333 A93-17888
- Advanced hypersonic aircraft design
[NASA-CR-192046] p 334 A93-18037
- SR-SCARLET 1: Peregrin p 337 A93-18155
- [NASA-CR-192048] p 337 A93-18155
- High-altitude reconnaissance aircraft p 894 A93-29713
- RECOVERY PARACHUTES**
- Recent advances in the numerical analysis of ram air wings - The three dimensional simulation code 'PARA3D'
[AIAA PAPER 93-1203] p 702 A93-35154
- Development testing of large ram air inflated wings
[AIAA PAPER 93-1204] p 702 A93-35155
- Design of a recovery system for a reentry vehicle
[AIAA PAPER 93-1224] p 733 A93-35171
- RECTANGULAR PANELS**
- Iterative temperature calculation method for rectangular sandwich panel fins p 76 A93-10667
- Damage progression in stiffened composite panels
[AIAA PAPER 93-1345] p 738 A93-33915
- The free vibration of cylindrically-curved rectangular panels p 1022 A93-45113
- Flutter analysis of composite panels on many supports p 1022 A93-45119

- A Rayleigh-Ritz analysis methodology for cutouts in composite structures p 923 A93-30869
- RECTANGULAR PLANFORMS**
- Experimental unsteady pressures at flutter on the Supercritical Wing Benchmark Model
[AIAA PAPER 93-1592] p 683 A93-34123
- RECTANGULAR PLATES**
- A plate loaded by a transverse impulse force and in-plane forces p 828 A93-36799
- Nonlinear aeroelasticity of composite structures
[AD-A254285] p 47 A93-10842
- Uniform roughness studies
[WL-TR-92-3041] p 751 A93-25951
- RECTANGULAR WINGS**
- Flow past a finite-span wing in the presence of external acoustic loading p 127 A93-16707
- Dynamic stall on a three-dimensional rectangular wing
[AIAA PAPER 93-0637] p 463 A93-24753
- Interaction of a streamwise vortex with a free surface
[AIAA PAPER 93-0556] p 543 A93-25539
- Wave resistance of swept wings with supersonic edges p 478 A93-27624
- Extension of a nonlinear systems theory to general-frequency unsteady transonic aerodynamic responses
[AIAA PAPER 93-1590] p 683 A93-34122
- The three-dimensional representation of the lift and pitching moment coefficients on wedged rectangular wings in supersonic flow p 973 A93-46990
- An exploratory wind tunnel study of supersonic tip vortices
[AIAA PAPER 93-2923] p 1045 A93-48124
- Turbulent structure of a wingtip vortex in the near field
[AIAA PAPER 93-3011] p 1054 A93-48201
- Supersonic flow past a rectangular wing of finite thickness p 1086 A93-50972
- A summary of further measurements of steady and oscillatory pressures on a rectangular wing p 1096 A93-52594
- Unsteady aerodynamic characteristics of three rectangular wings of different aspect ratios p 1180 A93-53575
- An investigation of the dynamic response of lifting surfaces with concentrated structural nonlinearities p 162 A93-13807
- An experimental investigation of interacting wing-tip vortex pairs
[AD-A258471] p 295 A93-18272
- An experimental investigation of a finite circulation control wing
[AD-A259044] p 340 A93-18896
- Unsteady transition measurements on a pitching three-dimensional wing p 820 A93-27450
- RECTIFIERS**
- High temperature rectifiers and MOS devices in 6H-silicon carbide
[AD-A254725] p 90 A93-12340
- RECURSIVE FUNCTIONS**
- Vision-based recursive estimation of rotorcraft obstacle locations p 343 A93-22851
- REDUCED ORDER FILTERS**
- Design of reduced-order observers with precise loop transfer recovery p 184 A93-14587
- On the order reduction of LQG designed controllers
[AIAA PAPER 93-1420] p 756 A93-33973
- Augmentation of a navigation reference system with differential global positioning system pseudorange measurements p 881 A93-42798
- A three-dimensional pressure flux-split RNS application to sub/supersonic flow in inlets and ducts
[AIAA PAPER 93-3063] p 1058 A93-48239
- Reduced order proportional integral observer with application p 1166 A93-49605
- REDUNDANCY**
- Hetero-redundant architecture with Kalman filter for input processing in flight control system p 182 A93-14293
- Cross channel dependency requirements of the multi-path redundant avionics suite p 928 A93-42782
- Expert system for redundancy and reconfiguration management p 938 A93-42785
- Reliability assessment for self-repairing flight control systems p 907 A93-42804
- URV flight test of an Ada implemented self-repairing flight control system
[AD-A259205] p 527 A93-20551
- REELS**
- US Army helicopter inertia reel locking failures p 493 A93-19689
- REENTRY**
- Hybrid guidance for maneuvering flight vehicles
[AD-A254110] p 69 A93-11798
- REENTRY EFFECTS**
- One type of automatically adjusted difference scheme with artificial viscosity to calculate ablated exterior shapes
[AD-A254108] p 19 A93-10856

REFLECTED WAVES

- REENTRY PHYSICS**
- Taking into account surface roughness in computing hypersonic re-entry body p 686 A93-34354
- Hypersonic flows for reentry problems. Vols. 1 & 2 [ISBN 0-387-54428-3] p 864 A93-42576
- Gas-kinetic and Navier-Stokes simulations of reentry flows p 865 A93-42582
- REENTRY TRAJECTORIES**
- Payload vehicle aerodynamic re-entry analysis p 69 A93-12004
- REENTRY VEHICLES**
- A split-matrix Runge-Kutta type space marching procedure p 8 A93-11921
- High angle-of-attack inviscid Shuttle Orbiter computation p 9 A93-12020
- Atmospheric reentry flight test of winged space vehicle
[AIAA PAPER 92-5053] p 385 A93-22324
- Numerical simulation of flow past the X24C reentry vehicle
[AIAA PAPER 93-0319] p 280 A93-23011
- Taking into account surface roughness in computing hypersonic re-entry body p 686 A93-34354
- Design of a recovery system for a reentry vehicle
[AIAA PAPER 93-1224] p 733 A93-35171
- Energetics of gas-surface interactions in transitional flows at entry velocities p 778 A93-39259
- Workshop on hypersonic flows for reentry problems January 22-25th 1990 (Antibes) - Inaugural address p 856 A93-42577
- Experimental study of the longitudinal hypersonic corner flow field - HERMES-R&D research program, problem no. 5 p 867 A93-42602
- Hypersonic flows over a double or simple ellipse p 868 A93-42614
- Contribution to Problem 6 using an upwind Euler solver with unstructured meshes p 869 A93-42627
- Inviscid hypersonic flow over a delta wing p 870 A93-42634
- Two-layer convective heating prediction procedures and sensitivities for blunt body reentry vehicles
[AIAA PAPER 93-2763] p 963 A93-46509
- Survey of nonequilibrium re-entry heating for entry flight conditions
[AIAA PAPER 93-3230] p 1039 A93-46682
- Effects of wall conditions on chemically nonequilibrium shock-layer flow over hypersonic reentry bodies p 970 A93-46908
- Reentry control to a drag vs. energy profile
[AIAA PAPER 93-3790] p 1143 A93-51385
- Guidance and control law for automatic landing flight experiment of reentry space vehicle
[AIAA PAPER 93-3818] p 1143 A93-51409
- Numerical simulation of shock/shock and shock-wave/boundary-layer interactions in hypersonic flows p 1093 A93-52000
- Numerical solution of N-S equations for hypersonic flow over capsule-type vehicles p 1182 A93-53858
- Hybrid guidance for maneuvering flight vehicles
[AD-A254110] p 69 A93-11798
- Increase of stagnation pressure and enthalpy in shock tunnels p 295 A93-18086
- The role of computational fluid dynamics in aeronautical engineering. 9: Analysis of hypersonic equilibrium air flow p 301 A93-19294
- Computation of re-entry flows with two-temperature model p 301 A93-19295
- Combined LAURA-UPS hypersonic solution procedure
[NASA-TM-107682] p 747 A93-25176
- A new LU-SGS flow solver for calculating reentry flows p 698 A93-25759
- The infrared measurement for the reentry-body-translation
[AD-A263100] p 914 A93-29134
- Kinetics and energy transfer in nonequilibrium fluid flows
[AD-A263612] p 875 A93-29284
- REFINING**
- Midhani alloys in aeronautical service p 70 A93-12368
- REFLECTANCE**
- Improvement in gust front algorithm detection capability using reflectivity thin lines versus azimuthal shears p 427 A93-22120
- Case study of a low-reflectivity pulsating microburst - Numerical simulation of the Denver, 8 July 1989, storm p 1222 A93-52898
- REFLECTED WAVES**
- System and method for cancelling expansion waves in a wave rotor
[NASA-CASE-LEW-15218-1] p 86 A93-11172
- In situ material characterization for pavement evaluation by the Spectral-Analysis-of-Surface-Waves (SASW) method
[AD-A255660] p 194 A93-14128

REFRACTION

- Wing vortex refraction effects from BAC 1-11 flight tests p 450 A93-19226

REFRACTORY COATINGS

- Current Technology for Thermal Protection Systems [NASA-CP-3157] p 69 N93-12447

REFRACTORY MATERIALS

- Oxidation-resistant high-temperature materials p 915 A93-40362
International Symposium on Ultra-High Temperature Materials, Tajimi, Japan, Dec. 5, 6, 1991, Proceedings p 1252 A93-54708
Ultra-high temperature materials in the research and development of super/hypersonic transport propulsion system p 1252 A93-54712
Current Technology for Thermal Protection Systems [NASA-CP-3157] p 69 N93-12447
Thermostructural applications of heat pipes for cooling leading edges of high-speed aerospace vehicles p 91 N93-12460

REFRIGERATING MACHINERY

- The optimum design of air cycle refrigeration system with high pressure water separation p 202 A93-14180

REFRIGERATORS

- Test results of an orifice pulse tube refrigerator p 1149 A93-48612
Three-stage sorption type cryogenic refrigeration systems and methods employing heat regeneration [NASA-CASE-NPO-18366-1-CU] p 216 N93-13422

REFUELING

- Robotic aircraft refueling - A concept demonstration p 846 A93-37041
Aircraft and refueler bonding and grounding study [AD-A262027] p 911 N93-29398

REGENERATIVE COOLING

- A compact, intercooled and regenerated gas turbine for HALE applications [ASME PAPER 92-GT-401] p 355 A93-19550
Analytical investigation of a regeneratively cooled scramjet engine p 519 A93-24829
Test results of an orifice pulse tube refrigerator p 1149 A93-48612
Effect of film cooling/regenerative cooling on scramjet engine performances [ISABE 93-7036] p 1197 A93-54012
Three-stage sorption type cryogenic refrigeration systems and methods employing heat regeneration [NASA-CASE-NPO-18366-1-CU] p 216 N93-13422

REGRESSION ANALYSIS

- On engine parameter estimation with flight test data p 1107 A93-48520
Multiple radial basis function networks in modeling and control [AIAA PAPER 93-3731] p 1170 A93-51330
Aircraft trajectory tracking and prediction [AD-A259039] p 340 N93-18999
Review of initial experiments using the Hawk model, dynamic rig facility, and the CED 1401 digital data acquisition equipment [CRANFIELD-AERO-9017] p 531 N93-21406

REGRESSION COEFFICIENTS

- Example of statistical techniques applied to analysis of landing ground roll distance measurements (linear regression, correlation coefficient and F-test) [ESDU-92021] p 330 N93-16635
Example of statistical techniques applied to analysis of measurements of the landing airborne manoeuvre. (Multiple linear regression with two independent variables and one dependent variable.) [ESDU-92022] p 330 N93-16636

REGULATIONS

- New lamps for old - Safety regulation through structural airworthiness standards p 28 A93-13630
Introduction to regulatory problems for supersonic transports p 234 A93-15032
Airlines, airports and antitrust - A proposed strategy for enhanced competition p 760 A93-34821
Tobacco smoking in aircraft - A log of legal rhetoric? p 944 A93-40474
The probable cause - aircraft accidents p 1240 A93-56417

REINFORCED PLASTICS

- Mass loaded composite rotor for vibro-acoustic application [AD-D015604] p 535 N93-20016

REINFORCED PLATES

- Video holography and laser vibrometry...The dynamic duo p 210 A93-16611
Response of laminated composite plates to low-speed impact by airgun-propelled and dropped-weight impactors [AIAA PAPER 93-1402] p 739 A93-33962

Stiffness, thermal expansion, and thermal bending formulation of stiffened, fiber-reinforced composite panels

- [AIAA PAPER 93-1569] p 741 A93-34102
Shape sensitivities and approximations of modal response of laminated skew plates p 829 A93-37403
Stringer peeling effects at stiffened composite panels in the postbuckling range p 1160 A93-52453
Calculation of sandwich plates with polymer composite skins under conditions of high humidity p 1215 A93-52968
An experimental study of reinforced panels of composite materials p 1215 A93-52975
Flutter analysis of stiffened laminated composite plates and shells in supersonic flow p 1216 A93-53224
Reinforcement of the F-111 wing pivot fitting with a boron/epoxy doubler system - Materials engineering aspects p 1214 A93-54241
The effect of temperature on the natural frequencies and acoustically induced strains in CFRP plates p 1260 A93-56331

REINFORCED SHELLS

- Efficiency of using longitudinal and circumferential bands in the structures of an airtight fuselage p 801 A93-36795
Optimal design of honeycomb sandwich shell aircraft structures of composite materials p 828 A93-36800
A finite element for modeling skins of composite materials p 1215 A93-52979
Flutter analysis of stiffened laminated composite plates and shells in supersonic flow p 1216 A93-53224

REINFORCEMENT (STRUCTURES)

- Effect of stiffness characteristics on the response of composite grid-stiffened structures p 1022 A93-45148
An experimental study of reinforced panels of composite materials p 1215 A93-52975
Development of stitching reinforcement for transport wing panels p 921 N93-30852

REINFORCING FIBERS

- Beyond steel - TMCs for lighter landing gear p 1100 A93-49337

REINFORCING MATERIALS

- Machining cost comparison of silicon carbide discontinuously reinforced aluminum, unreinforced aluminum, and titanium [ISME PAPER EM92-252] p 925 A93-40656

REISSNER THEORY

- Nonlinear flutter of orthotropic composite panel under aerodynamic heating p 1025 A93-45740

RELAXATION METHOD (MATHEMATICS)

- A flow calculation and aerodynamic design method for turbomachine cascades p 12 A93-12764
A technique for accelerated convergence in transonic flow p 685 A93-34347
An upwind relaxation method for hypersonic viscous flows over a double-ellipsoidal body p 867 A93-42606
A coarse-grid correction/nonlinear relaxation algorithm for the three-dimensional, compressible Navier-Stokes equations [AIAA PAPER 93-3317] p 951 A93-45013
Multigrid convergence of an implicit symmetric relaxation scheme [AIAA PAPER 93-3357] p 954 A93-45051
Line relaxation methods for the solution of 2D and 3D compressible flows [AIAA PAPER 93-3366] p 955 A93-45059
Upwind-biased, point-implicit relaxation strategies for hypersonic flowfield simulations on supercomputers p 1175 A93-52770

RELIABILITY

- Update on GPS integrity requirements of the RTCA MOPS p 314 A93-21155
Work performed in the United Kingdom to establish the feasibility of RAIM in a GPS receiver in flight p 314 A93-21157
GPS continuity - Initial findings p 314 A93-21167
On the basis of experience: Built in product reliability [PNR-90932] p 85 N93-11034
Civil aircraft engines: The next generation [PNR-90962] p 58 N93-11085
Satisfying the customer's requirements [PNR-90988] p 521 N93-20735
Follow-on operational test and evaluation of the NAVSTAR global positioning system air integration/installation program [AD-A263067] p 793 N93-27925
Reliability assessment at airline inspection facilities. Volume 2: Protocol for an eddy current inspection reliability experiment [DOT/FAA/CT-92/12-VOL-2] p 842 N93-28685
- RELIABILITY ANALYSIS**
Advanced three-shaft engines - Configured for reliability, efficiency and growth p 53 A93-12236
A method for estimating the technico-economic efficiency of measures increasing the reliability of gas turbine engines in service p 54 A93-12822

Rotorcraft reliability and maintainability: Future design requirements; Proceedings of the Conference, London, United Kingdom, Mar. 20, 1991 [ISBN 0-903409-88-7]

- p 45 A93-13401
The military operator's experience of reliability and maintainability characteristics p 80 A93-13403
Aircraft designer's viewpoint of reliability and maintainability p 45 A93-13404
Reliability testing of the EH101 p 45 A93-13406
Rotorcraft reliability and maintainability - A CAA view of future trends p 45 A93-13407
Aircraft fatigue failures and tasks of structural reliability analysis p 210 A93-16246
Accuracy of nonparametric reliability estimates under varying operation conditions p 396 A93-18343
Diagnostics of the hydraulic system of Tu-204 aircraft p 396 A93-18360
Analysis of the pump station of an aircraft hydraulic system as a subject of diagnosis p 321 A93-18374
Aero-engine reliability - A GE view p 345 A93-18782
Engine reliability from an independent overhaul shops perspective p 239 A93-18788
Reliability considerations for weather hazard warning radar p 431 A93-22187
Method for assessing the electric power system reliability of multiple-engined aircraft p 810 A93-37398
Reliability assessment for self-repairing flight control systems p 907 A93-42804
Increasing the reliability of an air traffic control radio system p 882 A93-43110
Reliability and durability problems p 1150 A93-48825
The civil scene - The authorities re-appraisal of ageing aircraft p 1229 A93-54895
Assessment of NDT reliability p 1258 A93-54900
Theoretical and experimental investigations concerning the structural integrity of aeroengine compressor discs p 56 N93-10539
On the basis of experience: Built in product reliability [PNR-90932] p 85 N93-11034
Advanced three-shaft engines: Configured for reliability, efficiency, and growth [PNR-90986] p 58 N93-11068
Requirements for soldered electrical connections [NHB-5300.4(3A-2)] p 212 N93-12674
Using software metrics and software reliability models to attain acceptable quality software for flight and ground support software for avionic systems p 442 N93-17305
Application of a neural network as a potential aid in predicting NTF pump failure [NASA-TM-107667] p 442 N93-18332
Aircraft Accidents: Trends in Aerospace Medical Investigation Techniques [AGARD-CP-532] p 490 N93-19653
Estimating characteristic life and reliability of an aircraft engine component improvement in the early stages of the implementation process [AD-A262118] p 815 N93-28184
- RELIABILITY ENGINEERING**
Methodology in the development of avionics p 166 A93-15043
Finding fault with avionics p 410 A93-21629
CFD development and a future high speed computer p 847 A93-38128
Requirements for soldered electrical connections [NHB-5300.4(3A-2)] p 212 N93-12674
Reliability assessment at airline inspection facilities. Volume 1: A generic protocol for inspection reliability experiments [DOT/FAA/CT-92/12-VOL-1] p 704 N93-25110
- RELIEF MAPS**
Mapping new and old worlds with laser altimetry p 1034 A93-45699
- REMOTE CONTROL**
Differential GPS control of Starcar 2 p 317 A93-21201
Development and testing of the Perseus proof-of-concept aircraft [DE93-010121] p 806 N93-28586
- REMOTE SENSING**
Using ultralight flight vehicles for large-scale aerial photography p 92 A93-10098
Study on aircraft microwave remote sensing of sea-water surface salinity p 92 A93-12407
Assessing spatial and seasonal variations in grasslands with spectral reflectances from a helicopter platform p 426 A93-20621
Variability of geophysical parameters from aircraft radiance measurements for FIFE p 426 A93-20622
Canonical correlation relationships among spectral and phytometric variables for twenty winter wheat fields p 433 A93-22992
New concepts in remote sensing and geolocation p 556 A93-24173

- Remote sensing of volcanic ash hazards to aircraft
p 556 A93-24213
- Radar 92; Proceedings of the International Conference,
Brighton, United Kingdom, Oct. 12, 13, 1992
[ISBN 0-85296-533-2] p 929 A93-43376
- Remote sensing cloud properties from high spectral
resolution infrared observations p 1034 A93-46780
- Preliminary results of the ISM campaign - The Landes,
South West France p 1161 A93-47553
- Above the sky --- high altitude flight in ER-2 aircraft
p 1044 A93-52614
- Meeting review: Third NCAR Research Aircraft Fleet
Workshop
[PB92-222710] p 223 N93-12818
- Definition study PHARUS
[AD-A256560] p 221 N93-14805
- Solid-state coherent laser radar wind shear measuring
systems p 144 N93-14848
- Dual-band infrared imaging applications: Locating buried
minifields, mapping sea ice, and inspecting aging
aircraft
[DE93-000516] p 453 N93-17225
- Coherent systems in the terahertz frequency range:
Elements, operation, and examples p 841 N93-27727
- Optical technologies for UV remote sensing
instruments p 853 N93-28788
- REMOTE SENSORS**
- Volume-imaging lidar observations of the convective
structure surrounding the flight path of a flux-measuring
aircraft p 425 A93-20579
- Liquid water profiling using remote sensor
observations p 429 A93-22150
- A horizontal atmospheric temperature sounder -
Applications to remote sensing of atmospheric hazards
p 929 A93-43502
- NASA/LMSC coherent LIDAR airborne shear sensor:
System capabilities and flight test plans
p 144 N93-14847
- Development of the Advance Warning Airborne
System(AWAS) p 144 N93-14849
- REMOTELY PILOTED VEHICLES**
- Flight test and wind-tunnel study of a scaled unmanned
air vehicle
[AIAA PAPER 92-4075] p 37 A93-11260
- Phase I flight test of MIAG advanced development
model
[AIAA PAPER 92-4076] p 95 A93-11261
- Flying qualities of a remotely piloted vehicle
[AIAA PAPER 92-4083] p 61 A93-11266
- A stability augmentation system for student designed
remotely-piloted vehicles
[AIAA PAPER 92-4261] p 63 A93-13365
- Automatic guidance and control for recovery of remotely
piloted vehicles p 181 A93-14188
- An adaptive algorithm for estimation of a state vector
in the system of remotely-piloted aircraft control using
Kalman filter p 181 A93-14232
- An unmanned aircraft for dropwindsone deployment
and hurricane reconnaissance p 677 A93-34587
- Decentralized autonomous attitude determination using
an inertially stabilized payload
[AIAA PAPER 93-3857] p 1134 A93-51444
- Experimental and analytical investigation of the vibration
characteristics of a remotely piloted helicopter
[AD-A256131] p 163 N93-14248
- RPH preliminary design, trend analysis and initial
analysis of the NPS hummingbird
[AD-A257854] p 338 N93-18304
- JEFF: Air transport system design simulation
[NASA-CR-192069] p 338 N93-18350
- Report to the Chairman, Legislation, and National
Security Subcommittee, Committee on Government
Operations, House of Representatives. Unmanned aerial
vehicles: More testing needed before production of
short-range system
[AD-A259473] p 513 N93-20245
- Advanced Unmanned Search System (AUSS)
supervisory command, control and navigation
[AD-A263171] p 793 N93-28990
- A real-time, hardware-in-the-loop simulation of an
unmanned aerial research vehicle
[AD-A262477] p 893 N93-29409
- Design study to simulate the development of a
commercial transportation system p 894 N93-29718
- Solar powered multipurpose remotely powered aircraft
p 895 N93-29722
- Preliminary development of a VTOL unmanned air
vehicle for the close-range mission
[AD-A263514] p 933 N93-29969
- Testing of an experimental system for image
reconnaissance p 1040 N93-31283
- REMOVAL**
- Starch media blasting for aerospace finishing
applications
[SAE PAPER 920948] p 107 A93-14091

RENORMALIZATION GROUP METHODS

- Numerical solution of viscous compressible flows using
algebraic turbulence models p 770 A93-38162
- Prediction of turbine cascade flows with a
quasi-three-dimensional rotor viscous code and the
extension of the algebraic turbulence model
[AD-A256831] p 223 N93-15635

REPLACING

- Bearing servicing tool
[NASA-CASE-MSC-21881-1] p 221 N93-14871
- AEW aircraft design
[AD-A261800] p 718 N93-26444

REPORTS

- DLR, Annual report 1991/92 p 383 A93-18717
- Summaries of the 1991 publications of DLR research
reports and DLR communications
[ETN-93-92588] p 572 N93-21022
- UK airmisses involving commercial air transport,
September - December 1991
[ETN-93-93930] p 992 N93-32409

REPRODUCTION (COPYING)

- A database approach to aircraft carrier airplan
production
[AD-A257737] p 240 N93-17666

REQUIREMENTS

- Design and test of a small two stage counter-rotating
turbine for rocket engine application
[AIAA PAPER 93-2136] p 1142 A93-49954
- Rotorcraft en route ATC route standards
[AD-A249129] p 35 N93-10323
- Advanced materials in gas turbine engines: An
assessment
[PNR-90946] p 58 N93-11105
- Engine technologies for future spaceplanes
[ETN-92-92732] p 177 N93-15143
- Satisfying the customer's requirements
[PNR-90988] p 521 N93-20735

RESCUE OPERATIONS

- Red-hot simulation p 1209 A93-53774
- Operating helicopters in a demanding environment -
Mountain flying/high evaluations p 1190 A93-54289

RESEARCH AIRCRAFT

- Flight testing of an electric powered vehicle
[AIAA PAPER 92-4077] p 37 A93-11262
- Nonlinear multi-point modelling and parameter
estimation of the DO 28 research aircraft
p 41 A93-12727
- Flight test operations using an F-106B research airplane
modified with a wing leading-edge vortex flap
[AIAA PAPER 92-4094] p 42 A93-13261
- Test pilot's notes on flying the Low Altitude/Airspeed
Unmanned Research Aircraft (LAURA)
[AIAA PAPER 92-4078] p 42 A93-13269
- Digital fly-by-wire system for BK117 FBW research
helicopter p 181 A93-14209
- Limit cycle in the longitudinal motion of the USB STOL
ASKA - Control system functional mockup and actual
aircraft
[SAE PAPER 921040] p 185 A93-14660
- Breaking the stall barrier p 159 A93-17502
- Numerical simulation of flow past the X24C reentry
vehicle
[AIAA PAPER 93-0319] p 280 A93-23011
- Icing effects on aircraft stability and control determined
from flight data - Preliminary results
[AIAA PAPER 93-0398] p 370 A93-23073
- An unmanned aircraft for dropwindsone deployment
and hurricane reconnaissance p 677 A93-34587
- The development of an efficient orniptopter wing
p 873 A93-43685
- Actuated forebody strake controls for the F-18 high alpha
research vehicle
[AIAA PAPER 93-3675] p 1006 A93-44233
- Nonlinear aerodynamic modeling using multivariate
orthogonal functions
[AIAA PAPER 93-3636] p 1065 A93-48321
- Results and lessons learned from two Wright Laboratory
flight research programs
[AIAA PAPER 93-3661] p 1099 A93-48341
- Dynamic model testing of the X-31 configuration for
high-angle-of-attack flight dynamics research
[AIAA PAPER 93-3674] p 1129 A93-48351
- Liquid rocket propulsion applied to manned aircraft -
In historical perspective p 1174 A93-51497
- Identification of actuation system and aerodynamic
effects of direct-lift-control flaps p 1103 A93-52435
- Flight test progress of the STOL research aircraft
ASKA
[NAL-TM-643] p 49 N93-12354
- Determination of the stability and control derivatives of
the F/A-18 HARV from flight data using the maximum
likelihood method
[NASA-CR-191216] p 186 N93-12903
- NASA aeronautics: Research and technology program
highlights
[NASA-NP-159] p 109 N93-13110

- Icing effects on aircraft stability and control determined
from flight data: Preliminary results
[NASA-TM-105977] p 188 N93-14831
- The F-18 systems research aircraft facility
[NASA-TM-4433] p 381 N93-16753
- X-31A high angle of attack and initial post stall flight
testing p 511 N93-19911
- System identification for X-31A project support: Lessons
learned so far p 512 N93-19914
- In-flight structural mode excitation system for flutter
testing p 526 N93-19915
- Development and flight testing of a surface pressure
measurement installation on the EAP demonstrator
aircraft p 550 N93-19927
- International aviation (Selected articles)
[AD-A262566] p 765 N93-28576
- Development and testing of the Perseus
proof-of-concept aircraft
[DE93-010121] p 806 N93-28586
- The DLR test aircraft in the FZ-BS, -VFW 614/ATTAS,
Dornier DO 228-101, MBB BO105 S-3
p 1018 N93-31272
- The basic measurement equipment of the DLR test
aircraft p 1000 N93-31273
- Instigation and processing of flight tests in DLR
p 998 N93-31275
- Pallet for helicopter test instrumentation
p 1000 N93-31279

RESEARCH AND DEVELOPMENT

- Status of the NASA Balloon Program
p 1 A93-11365
- Advanced technology constant challenge and
evolutionary process p 109 A93-15054
- Engineering aspects of laminar flow research at Handley
Page p 235 A93-17275
- Development of a prototype of an expert system for
the design of comprehensive scientific-technical
development programs for civil aviation
p 434 A93-18373
- DLR, Annual report 1991/92 p 383 A93-18717
- Development of ultra-hypersonic shock tunnel for
aerodynamics test p 376 A93-21900
- German university research in hypersonics
[AIAA PAPER 92-5033] p 239 A93-22307
- A historical perspective on hypersonic research at the
NACA/NASA Langley Research Center (1944-1984)
[AIAA PAPER 92-5034] p 456 A93-22308
- Hypervelocity scramjet capabilities of the T5 Free-Piston
Tunnel at Caltech
[AIAA PAPER 92-5037] p 376 A93-22311
- Development of the NASA-Ames low disturbance
supersonic wind tunnel for transition research up to Mach
2.5
[AIAA PAPER 92-3909] p 462 A93-24488
- NASA's hypersonic flight research program
[AIAA PAPER 93-0308] p 457 A93-25516
- Ongoing and planned R&D efforts in airway facilities
maintenance p 458 A93-27134
- The history and development of coated Contrast
Enhancement Filters for cockpit displays
p 564 A93-28180
- The rebirth of the tiltrotor - The 1992 Alexander A.
Nikolsky Lecture p 712 A93-34256
- Spaceplanes - Back to the future p 733 A93-34265
- Comanche airframe design - The PDT approach
p 744 A93-34469
- Management miscues, delays snarl C-17 program
p 760 A93-34944
- Design developments for advanced general aviation
aircraft I p 801 A93-37174
- Russians completing new ground-effect vehicle
p 853 A93-38535
- Development status of the RAH-66 Comanche
p 803 A93-38838
- Materials development for light design - A suppliers
view p 915 A93-40777
- Flight research on natural laminar flow applications
p 890 A93-41779
- ARPA starts push for joint-service ASTOVL
p 856 A93-43625
- Cryogenic wind tunnels p 1010 A93-44886
- A perspective on a quarter century of CFD research
[AIAA PAPER 93-3291] p 1021 A93-44995
- Will aerospace plane development go international?
p 1043 A93-49331
- Evolutionary NASA - Inventors to bureaucrats
p 1174 A93-50330
- International aerospace STI p 1227 A93-53826
- Research and development of aircraft engine in Japan
- Historical review
[ISABE 93-7000] p 1227 A93-53977
- Japan's research and development program for
airbreathing engine technologies
[ISABE 93-7005] p 1194 A93-53981

- Development study on Air Turbo Ramjet engine for a future space plane
[ISABE 93-7016] p 1195 A93-53992
- Research and development of a turbo-accelerator for super/hypersonic transport
[ISABE 93-7066] p 1200 A93-54042
- Ultra-high temperature materials in the research and development of super/hypersonic transport propulsion system
p 1252 A93-54712
- Status of R&D of high-performance materials for severe environments (Composite materials)
p 1253 A93-54728
- Research activity at the shock tube facility at NASA Ames
p 1252 A93-54804
- From RB211 to Trent: An ongoing development strategy
[PNR-90938] p 56 N93-11038
- NSF Science and Technology Centers
[NSF-92-104] p 193 N93-13712
- Technical needs and research opportunities provided by projected aeronautical and space systems
[NASA-CR-192124] p 386 N93-16629
- 1991 research and technology
[NASA-TM-103924] p 456 N93-16652
- The NASA High-Speed Research Program
p 330 N93-16761
- National Aeronautics and Space Administration
p 454 N93-17091
- Modern helicopter technologies at MBB and the application in future programmes
[MBB-UD-0599-91-PUB] p 331 N93-17566
- Dr. Alexander H. Flax: Technologist of aeronautics
[AD-A258441] p 456 N93-17890
- National aero-space plane: Restructuring future research and development efforts
[AD-A258799] p 340 N93-18981
- The National Aero-Space Plane program: A revolutionary concept
p 511 N93-19908
- The 1992 Research/Technology report
[NASA-TM-105924] p 459 N93-20902
- Summaries of the 1991 publications of DLR research reports and DLR communications
[ETN-93-92588] p 572 N93-21022
- Current research activities: Applied and numerical mathematics, fluid mechanics, experiments in transition and turbulence and aerodynamics, and computer science
[NASA-CR-191408] p 758 N93-25084
- Applied aerodynamics: Challenges and expectations
[NASA-TM-103963] p 694 N93-25091
- JPRS report: Science and technology. Japan. 30th National Aerospace Laboratory Conference
[JPRS-JST-93-009] p 761 N93-25418
- JPRS report: Science and technology. Central Eurasia: Engineering and equipment
[JPRS-UEQ-92-003] p 749 N93-25427
- JPRS report: Science and technology. Central Eurasia: Engineering and equipment
[JPRS-UEQ-92-007] p 842 N93-28635
- JPRS report: Science and technology. Central Eurasia: Engineering and equipment
[JPRS-UEQ-92-006] p 842 N93-28636
- JPRS report: Science and technology. Central Eurasia: Engineering and equipment
[JPRS-UEQ-92-010] p 842 N93-28674
- JPRS report: Science and technology. Central Eurasia: Engineering and equipment
[JPRS-UEQ-92-008] p 842 N93-28675
- JPRS report: Science and technology. Central Eurasia: Engineering and equipment
[JPRS-UEQ-93-003] p 842 N93-28691
- JPRS report: Science and technology. Central Eurasia: Engineering and equipment
[JPRS-UEQ-93-004] p 930 N93-29090
- NASA SBIR abstracts of 1991 phase 1 projects
[NASA-TM-108240] p 945 N93-29323
- Research and technology objectives and plans: Summary fiscal year 1991
[NASA-TM-103086] p 946 N93-29452
- Rotorcraft master plan
p 857 N93-30677
- Technology transfer: Potential of BMFT concept for hypersonics
[MBB-LME-202-S-PUB-0505] p 1041 N93-31045
- RESEARCH FACILITIES**
- Integrated flight propulsion control research results using the NASA F-15 HIDEFC Flight Research Facility
[AIAA PAPER 92-4106] p 38 A93-11276
- Seeding materials for use in laser anemometry
[AIAA PAPER 93-0006] p 389 A93-20129
- German university research in hypersonics
[AIAA PAPER 92-5033] p 239 A93-22307
- A historical perspective on hypersonic research at the NACA/NASA Langley Research Center (1944-1984)
[AIAA PAPER 92-5034] p 456 A93-22308
- Hypervelocity scramjet capabilities of the T5 Free-Piston Tunnel at Caltech
[AIAA PAPER 92-5037] p 376 A93-22311
- The development of SIMONA - A simulator facility for advanced research into simulation techniques, motion system control and navigation systems technologies
[AIAA PAPER 93-3574] p 1208 A93-52670
- Scientific and engineering research facilities at universities and colleges: 1992
[NSF-92-325] p 192 N93-13407
- NSF Science and Technology Centers
[NSF-92-104] p 193 N93-13712
- Real-time in-flight engine performance and health monitoring techniques for flight research application
p 169 N93-15169
- The Goldstein Aeronautical Engineering Research Laboratory
[AERO-REPT-9109] p 240 N93-16465
- The F-18 systems research aircraft facility
[NASA-TM-4433] p 381 N93-16753
- Flight and wind-tunnel calibrations of a flush airdata sensor at high angles of attack and sideslip and at supersonic Mach numbers
[NASA-TM-104265] p 344 N93-19110
- Overview of the NASA Dryden Flight Research Facility aeronautical flight projects testing
p 512 N93-19916
- Structural dynamics branch research and accomplishments to FY 1992
[NASA-TM-105824] p 552 N93-20368
- Wright Laboratory research and development facilities handbook
[AD-A258746] p 572 N93-20403
- A laboratory study of subjective response to sonic booms measured at White Sands Missile Range
[NASA-TM-107746] p 852 N93-27272
- International aviation (Selected articles)
[AD-A262566] p 765 N93-28576
- Flight test of avionic and air-traffic control systems
[ESA-TT-1279] p 993 N93-31271
- Ground installations for preparation and evaluation of flight tests
p 1014 N93-31274
- Instigation and processing of flight tests in DLR
p 998 N93-31275
- Hypersonic engine component experiments in high heat flux, supersonic flow environment
[NASA-TM-106273] p 1032 N93-31860
- RESEARCH MANAGEMENT**
- Wright Laboratory research and development facilities handbook
[AD-A258746] p 572 N93-20403
- Research and technology objectives and plans: Summary fiscal year 1991
[NASA-TM-103086] p 946 N93-29452
- RESEARCH PROJECTS**
- Ceramic Technology Project
[DE92-018748] p 73 N93-11442
- The 1992 Research/Technology report
[NASA-TM-105924] p 459 N93-20902
- NASA SBIR abstracts of 1990 phase 1 projects
[NASA-TM-108145] p 572 N93-21794
- The Center of Excellence for Hypersonics Training and Research at the University of Texas at Austin
[NASA-CR-193070] p 781 N93-27126
- High-altitude reconnaissance aircraft
p 894 N93-29713
- Design of a turbofan powered regional transport aircraft
p 894 N93-29721
- Solar powered multipurpose remotely powered aircraft
p 895 N93-29722
- RESEARCH VEHICLES**
- The F-18 High Alpha Research Vehicle - A high-angle-of-attack testbed aircraft
[AIAA PAPER 92-4121] p 42 A93-13273
- Analysis of a hypersonic waverider research vehicle with a hydrocarbon scramjet engine
[AIAA PAPER 93-0509] p 386 A93-23256
- The effects of hypersonic flight test requirements on research vehicle design
[AIAA PAPER 93-0511] p 386 A93-23258
- A summary of the forebody high-angle-of-attack aerodynamics research on the F-18 and the X-29A aircraft
[NASA-TM-104261] p 25 N93-12353
- Flight and wind-tunnel calibrations of a flush airdata sensor at high angles of attack and sideslip and at supersonic Mach numbers
[NASA-TM-104265] p 344 N93-19110
- Overview of the NASA Dryden Flight Research Facility aeronautical flight projects testing
p 512 N93-19916
- Advanced Transport Operating System (ATOPS) Flight Management/Flight Controls (FM/FC) software description
[NASA-CR-191457] p 808 N93-28621
- A real-time, hardware-in-the-loop simulation of an unmanned aerial research vehicle
[AD-A262477] p 893 N93-29409
- Flight control system design factors for applying automated testing techniques
[NASA-TM-4242] p 910 N93-30764
- Design and implementation of fuzzy logic controllers
[NASA-CR-193268] p 1038 N93-31649
- RESIDUAL STRENGTH**
- Allowable compression strength for CFRP-components of fighter aircraft determined by CAI-test
p 537 N93-21531
- Numerical determination of the residual strength of battle damaged composite plates
p 537 N93-21533
- RESIDUAL STRESS**
- Study of the method for determining residual stress induced by machining in airplane canopies made of PMMA
p 534 A93-27366
- A study of the origin of residual stresses and strains in the transparencies of supersonic aircraft
p 801 A93-36784
- Automated measurement of residual stresses in the surface layer of parts
p 834 A93-39081
- Effect of the technological process structure on residual stress distribution in the blade foil of gas turbine engines
p 836 A93-39106
- Neutron diffraction residual stress studies for aero-engine component applications
[PNR-90908] p 85 N93-11014
- Development of the neutron diffraction technique for the determination of near surface residual stresses in critical gas turbine components
[PNR-90984] p 58 N93-11112
- F100 second stage fan disk bolthole crack propagation ferris wheel test
p 177 N93-14897
- RESIDUES**
- Interferometric JFTOT tube deposit measuring device
[AD-D015599] p 536 N93-20247
- RESIN MATRIX COMPOSITES**
- Novel approaches to complex geometry structure
p 546 A93-27969
- Development and fabrication of an autoclave molded PES/Quartz sandwich radome
p 547 A93-28279
- Buckling of open-section bead-stiffened composite panels
p 1157 A93-50420
- Thermoplastic composite parts manufacture at Du Pont
[SME PAPER EM93-106] p 1159 A93-51728
- Polymer infiltration studies
[NASA-CR-191652] p 200 N93-15431
- RESIN TRANSFER MOLDING**
- Development and fabrication of an autoclave molded PES/Quartz sandwich radome
p 547 A93-28279
- Advantages of a one-part resin system for processing aerospace parts by Resin Transfer Molding (RTM)
[SME PAPER EM93-112] p 1159 A93-51729
- Design for manufacture by resin transfer molding of composite parts for rotorcraft
[SME PAPER EM93-103] p 1159 A93-51733
- RESINS**
- Resin transfer molding for advanced composite primary aircraft structures
p 919 N93-30438
- Effects of intra- and inter-laminar resin content on the mechanical properties of toughened composite materials
p 921 N93-30845
- Development of stitching reinforcement for transport wing panels
p 921 N93-30852
- Development of resins for composites by resin transfer molding
p 921 N93-30853
- Advanced fiber/matrix material systems
p 921 N93-30854
- Mechanical and analytical screening of braided composites for transport fuselage applications
p 922 N93-30855
- RESISTANCE HEATING**
- Efficient finite element method for aircraft deicing problems
p 1103 A93-52443
- RESISTANCE THERMOMETERS**
- Heat flux microsensor measurements
[AIAA PAPER 92-5038] p 413 A93-22312
- RESISTOJET ENGINES**
- Gravity sensitivity of a resistojets water vaporizer
[AIAA PAPER 93-2402] p 1156 A93-50167
- Gravity sensitivity of a resistojets water vaporizer
[NASA-TM-106220] p 914 N93-29194
- RESONANCE TESTING**
- Turbine blade vibration monitoring system
[ASME PAPER 92-GT-159] p 402 A93-19386
- RESONANT FREQUENCIES**
- Resonance frequencies of a gondola submitted to a forced rotation under a stratospheric balloon
p 27 A93-11384
- Steady and quasisteady resonant lock-in of finned projectiles
p 61 A93-12012
- Dynamic analysis of a pre-and-post ice impacted blade
[AIAA PAPER 92-4273] p 54 A93-13333

A design study on the effect of support and system parameters on the natural frequencies of rotor systems p 210 A93-16374

An analysis system for blade forced response [ASME PAPER 92-GT-172] p 352 A93-19398

Flutter of grouped turbine blades [ASME PAPER 92-GT-227] p 404 A93-19444

Double mode behaviour of bladed disk assemblies in the resonance frequency range, visualized by means of holographic interferometry [ASME PAPER 92-GT-438] p 357 A93-19580

Enhancements to modal testing using finite elements p 548 A93-29258

Shape sensitivities and approximations of modal response of laminated skew plates p 829 A93-37403

Comparison of some direct multi-point force approximation methods p 928 A93-43338

The free vibration of cylindrically-curved rectangular panels p 1022 A93-45113

Dynamic analysis of a gear drive system in aeroengine p 1149 A93-48514

Determination of the natural vibrations of an acoustic medium in the cabin of a passenger aircraft by the finite element method p 1102 A93-51752

Spectral analysis of unsteady surface pressure on a pusher propeller p 1232 A93-54646

The use of beam-like modal data for stiffness profile estimation by the EBS method. I - Justification and implementation --- Equivalent Beam Stiffness p 1257 A93-54649

The effect of temperature on the natural frequencies and acoustically induced strains in CFRP plates p 1260 A93-56331

Dynamic analysis of a pre-and-post ice impacted blade [NASA-TM-105829] p 90 A93-12197

Resonant response analysis of a high speed gear p 553 A93-20662

Analysis of the static and dynamic response of a T-38 wing and comparison with experimental data [AD-A262363] p 806 A93-27692

RESONANT VIBRATION

On dynamic behavior of cracked rotors p 208 A93-15401

Turbine blade vibration monitoring system [ASME PAPER 92-GT-159] p 402 A93-19386

Investigation of helicopter air resonance in hover by complex coordinates and mutual excitation analysis p 893 A93-43777

Passive damping technology p 1259 A93-55866

Add-on damping treatment for the F-15 upper-outer wing skin [AD-A258470] p 337 A93-18248

RESOURCES MANAGEMENT

Trans-cockpit authority gradient in Navy/Marine aircraft mishaps p 146 A93-15016

Enhanced Aeronautical Resource Management training alternatives p 147 A93-15019

Taxonomy of flight variables p 147 A93-15022

Cockpit resource management proficiency as a factor of primary flight training [AD-A256995] p 328 A93-16262

RESPONSE TIME (COMPUTERS)

Dynamic simulation fidelity improvement using transfer function state extrapolation [AIAA PAPER 93-3552] p 1222 A93-52656

REUSABLE LAUNCH VEHICLES

Near-term two-stage-to-orbit, fully reusable, horizontal take-off/landing launch vehicle p 1015 A93-45441

REUSABLE ROCKET ENGINES

Ceramic matrix composites for rocket engine turbine applications [ASME PAPER 92-GT-394] p 388 A93-19547

REVERSE ENGINEERING

Design recovery for software library population [AD-A259292] p 572 A93-20611

REVERSED FLOW

A wide-range axial-flow compressor stage performance model [ASME PAPER 92-GT-58] p 348 A93-19308

Excitation of blade vibration due to surge of centrifugal compressors [ASME PAPER 92-GT-149] p 351 A93-19377

Effects of flow-path variations on internal reversing flow in a tailpipe offtake configuration for ASTOVL aircraft [AIAA PAPER 93-2438] p 1118 A93-50190

Effects of flow-path variations on internal reversing flow in a tailpipe offtake configuration for ASTOVL aircraft [NASA-TM-106149] p 900 A93-29065

REVERSING

Propulsion integration results of the STOL and Maneuver Technology Demonstrator p 161 A93-13228

REVIEWING

Accidents and errors: A review of recent UK Army Air Corps accidents p 495 A93-19701

REVOLVING

Navier-Stokes computations for kinetic energy projectiles in steady coning motion: A predictive capability for pitch damping [AD-A264111] p 1033 A93-32028

REYNOLDS EQUATION

A study on stability and response analysis of a nonlinear rotor system with mass unbalance and side load [ASME PAPER 92-GT-7] p 400 A93-19280

Evaluation of a CFD code for analysis of normal-shock trains [AIAA PAPER 93-0292] p 279 A93-22692

A numerical study of advanced rotor blades p 481 A93-29436

Calculation of optimum airfoils using direct solutions of the Navier-Stokes equations [AIAA PAPER 93-3323] p 952 A93-45017

Navier-Stokes prediction of a delta wing in roll with vortex breakdown [AIAA PAPER 93-3495] p 983 A93-47267

Some practical turbulence modeling options for Reynolds-averaged full Navier-Stokes calculations of three-dimensional flows [AIAA PAPER 93-2964] p 1048 A93-48158

REYNOLDS NUMBER

Effect of the Reynolds number on the aerodynamic characteristics of a body of revolution over a wide range of angles of attack p 242 A93-18384

Studies of jet thermal stability in a flowing system [ASME PAPER 92-GT-106] p 401 A93-19344

Viscous and inviscid instabilities of a trailing vortex p 268 A93-21042

The effect of Reynolds number and turbulence on airfoil aerodynamics at -90 degrees incidence [AIAA PAPER 93-0206] p 277 A93-22624

Measurements in the near-field of a turbulent wingtip vortex [AIAA PAPER 93-0551] p 285 A93-23290

Unit-Reynolds-number effects on boundary-layer transition p 288 A93-23560

The effect of Reynold's number on a natural low frequency flow oscillation over an airfoil near stall [AIAA PAPER 92-4040] p 463 A93-24489

Hysteresis effects on wind tunnel measurements of a two-element airfoil [AIAA PAPER 93-0646] p 464 A93-24761

An experimental parametric study of geometric, Reynolds number, and ratio of specific heats effects in three-dimensional sidewall compression scramjet inlets at Mach 6 [AIAA PAPER 93-0740] p 466 A93-24830

The effect of Reynolds number on vortex asymmetry about slender bodies p 475 A93-26176

A method for calculating the characteristics of plane compressor cascades for different values of the Reynolds criterion p 545 A93-27616

Cryogenic wind tunnels p 1010 A93-44886

Progress in local preconditioning of the Euler and Navier-Stokes equations [AIAA PAPER 93-3328] p 952 A93-45022

Numerical vorticity capturing for vortex-solid body interaction problems [AIAA PAPER 93-3343] p 954 A93-45037

Reynolds number effects on supersonic asymmetrical flows over a cone p 958 A93-45141

The effect of Reynolds number on control of forebody asymmetry by suction and bleed [AIAA PAPER 93-3265] p 968 A93-46831

The cryogenic wind tunnel p 1013 A93-46915

Instability of three-dimensional supersonic boundary layer p 973 A93-46987

On dynamics of the juncture vortex [AIAA PAPER 93-3473] p 980 A93-47252

Hypersonic flow past open cavities [AIAA PAPER 93-2969] p 1049 A93-48163

Effect of Reynolds number on the aerodynamic characteristics of a semicone with a wing in the case of hypersonic flow velocities p 1090 A93-51878

Multielement airfoil performance due to Reynolds and Mach number variations p 1095 A93-52442

Reynolds number dependence of the drag coefficient for laminar flow through fine-scale photoetched screens p 1218 A93-53815

Heat transfer in a five-pass irregular channel with and without pin-fins p 1256 A93-54633

The hemisphere-cylinder at an angle of attack p 21 A93-11250

Leading edge film cooling heat transfer including the effect of mainstream turbulence p 23 A93-11886

Comparative performance tests of a pitot-inlet in several European wind-tunnels at subsonic and supersonic speeds p 130 A93-13221

Parametric study of air sampling cyclones p 135 A93-14173

User manual for NASA Lewis 10 by 10 foot supersonic wind tunnel [NASA-TM-105626] p 194 A93-15498

Mixing and reaction in the subsonic 2-D turbulent free shear layer p 289 A93-16508

Effect of Reynolds number on the standards of a simplified anemoclinometric probe [IMFL-91-31] p 293 A93-17542

Lift and drag forces on droplets and particles in wall-bounded shear flows [DE93-002678] p 419 A93-17761

Numerical analysis of the flow in a tubulated rectangular duct simulating the cooling passages in a turbine blade [AD-A257855] p 420 A93-18305

Parabolized Navier-Stokes methods for hypersonic flows p 421 A93-18565

An experimental investigation of a finite circulation control wing [AD-A259044] p 340 A93-18896

Assessment of a flow-through balance for hypersonic wind tunnel models with scramjet exhaust flow simulation [NASA-TM-4441] p 779 A93-27005

Reynolds and Mach number effects on multielement airfoils p 785 A93-27446

Flow prediction over a transport multi-element high-lift system and comparison with flight measurements p 785 A93-27448

An experimental study of flow over a 6 to 1 prolate spheroid at incidence p 874 A93-29124

Determination of surface heat transfer and film cooling effectiveness in unsteady wake flow conditions p 902 A93-29933

Measurement of turbulent spots and intermittency modelling at gas-turbine conditions p 902 A93-29934

Turbulence characteristics of an axisymmetric reacting flow [NASA-CR-4110] p 877 A93-30373

Effects of buoyancy on gas jet diffusion flames [NASA-CR-191109] p 935 A93-31031

Reynolds number influences in aeronautics [NASA-TM-107730] p 989 A93-31732

Effects of an aft facing step on the surface of a laminar flow glider wing [NASA-CR-193302] p 990 A93-31855

REYNOLDS STRESS

Large-eddy simulation of turbulent flow above and within a forest p 92 A93-11404

Turbulence modelling requirements for the prediction of viscous transonic aerofoil flows p 115 A93-14249

Compressible turbulence measurements in a high-speed high Reynolds number mixing layer [AIAA PAPER 93-0660] p 465 A93-24773

Calculation of the flow around a high-lift airfoil using an explicit code and an algebraic Reynolds stress model p 685 A93-34344

Navier-Stokes stall predictions using an algebraic Reynolds-stress model p 778 A93-39260

Strong vortex/boundary layer interactions. I - Vortices high p 930 A93-43539

Strong vortex/boundary layer interactions. II - Vortices low p 965 A93-46744

Reynolds stress transport modelling of shock/boundary-layer interaction [AIAA PAPER 93-2936] p 1046 A93-48134

High lift airfoil flow simulation using a wall-corrected Algebraic Stress Model [AIAA PAPER 93-3109] p 1061 A93-48280

Reynolds stress profiles in the near wake of an oscillating airfoil p 1236 A93-55380

Explicit Navier-Stokes computation of turbomachinery flows p 83 A93-10370

A realizable Reynolds stress algebraic equation model [NASA-TM-105993] p 290 A93-16596

Turbulence: The chief outstanding difficulty of our subject p 783 A93-27428

RHODIUM ALLOYS

Field evaluation of six protective coatings applied to T-56 turbine blades after 2000 hours of engine use [AD-A261112] p 522 A93-21316

RIBBONS

Polymer infiltration studies [NASA-CR-191652] p 200 A93-15431

RIBLETS

Effect of longitudinal microribbing on the drag of a body of revolution p 5 A93-10147

A comparison of the drag-reducing benefits of riblets in internal and external flows p 395 A93-18054

The prediction of riblet behaviour with a low-Reynolds number k-epsilon model p 270 A93-21720

A study of the effect of surface riblets on the evolution of a solitary wave packet (lambda vortex) in a laminar boundary layer p 1067 A93-48827

Drag characteristics of extra-thin-fin-riblets in an air flow conduit p 1151 A93-49240

- The reduction of skin friction by riblets under the influence of an adverse pressure gradient
p 1218 A93-53810
- Fluid flow and heat convection studies for actively cooled airframes
[NASA-CR-190956] p 216 N93-13406
- Flow control of low heat load turbine airfoils
[AD-A260941] p 724 N93-26219
- Turbulent drag reduction: Studies of feedback control and flow over riblets
p 878 N93-30645
- RIBS (SUPPORTS)**
- Heat transfer performance comparisons of five different rectangular channels with parallel angled ribs
p 397 A93-18752
- Active rib experiment for shape control of an adaptive wing
[AIAA PAPER 93-1700] p 712 A93-34222
- Local heat transfer distribution in a rotating serpentine rib-roughened flow passage
p 1259 A93-55459
- The aerodynamic characteristics of the Gottingen 797 and Wortmann FX63-137 aerofoil sections at very low Reynolds numbers
[ETN-93-92999] p 295 N93-18128
- RICCATI EQUATION**
- Order reduction of aeroelastic models through LK transformation and Riccati iteration
[AIAA PAPER 93-3795] p 1159 A93-51388
- RIDING QUALITY**
- The Ultra Light Aircraft Testing
[NASA-CR-193043] p 895 N93-29774
- RIGGING**
- A study of the effects of tolerances on rigging screws, turnbuckles, and associated components in BS4429: 1987
[NPL-DMM(A)-53] p 86 N93-11326
- RIGID ROTOR HELICOPTERS**
- The cusp catastrophe and the stability problem of helicopter ground resonance
p 1099 A93-48059
- RIGID ROTORS**
- A study on stability and response analysis of a nonlinear rotor system with mass unbalance and side load
[ASME PAPER 92-GT-7] p 400 A93-19280
- Development of a structural optimization capability for the aeroelastic tailoring of composite rotor blades with straight and swept tips
[AIAA PAPER 92-4779] p 326 A93-20370
- Frequency-domain identification of BO 105 derivative models with rotor degrees of freedom
p 712 A93-34263
- Effects of dynamic stall and structural modeling on aeroelastic stability of elastic bending and torsion of hingeless rotor blades with experimental correlation
p 794 A93-35902
- Dynamic stall effects on hingeless rotor stability with experimental correlation
p 129 N93-13010
- Stability of elastically tailored rotor blades
p 164 N93-14828
- RIGID STRUCTURES**
- A method for calculating the aerodynamic and mass characteristics of coaxial rotors with rigid blade fastening (the ABC system)
p 1071 A93-49323
- Near-optimal, asymptotic tracking in control problems involving state-variable inequality constraints
[AIAA PAPER 93-3748] p 1170 A93-51344
- A simulation study on take-off and landing dynamics of fly-by-wire control system aircraft
p 1249 A93-55590
- Rigid body mode identification of the PAH-2 helicopter using the eigensystem realization algorithm
[NASA-TM-107690] p 88 N93-11544
- Numerical study of advanced rotor blades
p 23 N93-11899
- An investigation of the dynamic response of lifting surfaces with concentrated structural nonlinearities
p 162 N93-13807
- State of the art of airport pavement analysis and design
p 378 N93-16310
- A simulation study on take-off and landing dynamics of the aircraft of a fly-by-wire control system
[AD-A259286] p 510 N93-19849
- Dynamic simulation of flexible body systems by the vector solution method
p 553 N93-20666
- Development of a non-linear simulation for generic hypersonic vehicles - ASUHS1
[NASA-CR-192710] p 516 N93-22003
- Conical Euler analysis and active roll suppression for unsteady vortical flows about rolling delta wings
[NASA-TP-3259] p 701 N93-26134
- RIGID WINGS**
- Preliminary efforts toward development of data handling and analysis software for unsteady flow measurements: An application for aeroelastic transonic flow configurations
p 291 N93-16768
- Analytical and experimental investigation of flutter suppression by piezoelectric actuation
[NASA-TP-3241] p 513 N93-20584
- RIMS**
- Effective sealing of a disk cavity using a double-toothed rim seal
[ASME PAPER 92-GT-379] p 406 A93-19537
- RING LASERS**
- The ring laser gyro and its applications
p 927 A93-42657
- RING STRUCTURES**
- Application of artificial neural networks to the design optimization of aerospace structural components
[NASA-TM-4389] p 555 N93-21831
- RING WINGS**
- Towards an analytical treatment of the aerolastic problem of a circular wing
p 781 N93-27214
- RISK**
- Hover testing a demonstrated and cost-effective risk reduction tool
[AIAA PAPER 93-2677] p 913 A93-42234
- Being an engineer - A risky occupation? Proceedings of the Conference, London, United Kingdom, June 8, 1993
[ISBN 1-85768-120-7] p 945 A93-43869
- Risk analysis for aging aircraft fleets
p 1025 A93-45775
- National Aerospace Plane Integrated
Fuselage/Cryotank Risk Reduction program
[AIAA PAPER 93-2564] p 1142 A93-50284
- Aviation accidents, incidents, and violations: Psychological predictors among US pilots
p 144 N93-14693
- Measuring risk in single-engine and twin-engine helicopters
p 148 N93-15025
- Pre-flight risk assessment in Emergency Medical Service (EMS) helicopters
p 494 N93-19692
- A procedure for defining lightning risk to air vehicles
p 703 N93-24885
- RIVETED JOINTS**
- The fretting damage and effect of temperature in typical joint of aircraft construction
p 203 A93-14196
- Contact analysis for riveted and bolted joints of composite laminates
p 204 A93-14384
- High-strength combination fasteners for joint assembly in aircraft structures
p 745 A93-35283
- Selecting a method for sealing riveted joints in fuel compartments
p 746 A93-35295
- A laboratory study of fracture in the presence of lap splice multiple site damage
p 1027 A93-45790
- Test facility for evaluation of structural integrity of stiffened and jointed aircraft curved panels
p 1012 A93-45794
- RIVETING**
- Stress-strain state of the elements of a single-stringer riveted panel
p 746 A93-35288
- RIVETS**
- High-strength combination fasteners for joint assembly in aircraft structures
p 745 A93-35283
- Selecting a method for sealing riveted joints in fuel compartments
p 746 A93-35295
- ROADS**
- The use of digital road data by a navigation system
p 993 N93-31269
- ROBOT CONTROL**
- Application of concurrent engineering methods to the design of an autonomous aerial robot
[AD-A254968] p 212 N93-12555
- Using fuzzy behaviors for the outdoor navigation of a car with low-resolution sensors
[DE93-002428] p 706 N93-25120
- ROBOT SENSORS**
- RACE pulls for shared control --- telerobotics and automation technology for aircraft maintenance and inspection
p 458 A93-29130
- Using fuzzy behaviors for the outdoor navigation of a car with low-resolution sensors
[DE93-002428] p 706 N93-25120
- ROBOTICS**
- Robotic aircraft refueling - A concept demonstration
p 846 A93-37041
- Sensor-adaptive control for aircraft paint stripping
[SME PAPER AD92-200] p 855 A93-40663
- Robotic inspection and refurbishment of aircraft canopy transparencies
[SME PAPER AD92-203] p 855 A93-40665
- Intelligent robotics; Proceedings of the International Symposium, Bangalore, India, Jan. 2-5, 1991
[SPIE-1571] p 1166 A93-49350
- Various applications of robots in aircraft engine overhaul
[ISABE 93-7129] p 1175 A93-54104
- The development progress of the U.S. Army's SASS LITE, unmanned robot airship
[AIAA PAPER 93-4047] p 1243 A93-54614
- ROBOTS**
- Various applications of robots in aircraft engine overhaul
[ISABE 93-7129] p 1175 A93-54104
- Computational nonlinear control
[AD-A253547] p 98 N93-12258
- Application of concurrent engineering methods to the design of an autonomous aerial robot
[AD-A254968] p 212 N93-12555
- ROBUSTNESS (MATHEMATICS)**
- A robust direct-integration method for rotorcraft maneuver and periodic response
p 61 A93-10919
- The application of optimal robust control in control system design of flying vehicles
p 95 A93-11791
- Design of an adaptive flight control system with uncertainties
p 95 A93-12322
- Adaptive control of aircraft in windshear
p 62 A93-13126
- Control design for robust eigenstructure assignment in linear uncertain systems
p 97 A93-13241
- Design and robustness issues for highly augmented helicopter controls
p 185 A93-14594
- Stochastic measures of performance robustness in aircraft control systems
p 185 A93-14595
- Robust fault detection of jet engine sensor systems using eigenstructure assignment
p 173 A93-14608
- Synthesis of robust motion stabilization laws for flight vehicles
p 227 A93-16777
- Robust control of the separation of hypersonic lifting vehicles
p 385 A93-22289
- [AIAA PAPER 92-5013] p 385 A93-22289
- Robust stabilization based on topological connectedness
p 438 A93-22830
- Discrete-time LTR synthesis of delayed control systems
p 439 A93-22855
- Parameter optimization for an H2 problem with multivariable gain and phase margin constraints
p 439 A93-22971
- Development of a robust pressure-based numerical scheme for spray combustion applications
[AIAA PAPER 93-0902] p 560 A93-24960
- Robust integrated flight/propulsion control design for a STOVL aircraft using H-infinity control design techniques
p 524 A93-26432
- Robustness evaluation of a flexible aircraft control system
p 727 A93-34540
- Zero-gravity atmospheric flight by robust nonlinear inverse dynamics
p 728 A93-34550
- Design and evaluation of a robust dynamic neurocontroller for a multivariable aircraft control problem
p 817 A93-37004
- Robust stabilization of an aero-elastic system
p 817 A93-37044
- Robust sampled data eigenstructure assignment using the delta operator --- in relation to autopilot design
p 906 A93-41889
- A nonlinear control strategy for robust sliding mode performance in the presence of unmatched uncertainty
p 938 A93-42556
- Design of robust digital model-following flight control systems
p 907 A93-42810
- Field by field hybrid upwind splitting methods
[AIAA PAPER 93-3302] p 950 A93-45000
- Robust method for estimating the parameters of a linear FM waveform
p 1147 A93-47650
- A new approach to robust fault detection and identification
p 1166 A93-50631
- The application of intelligent search strategies to robust flight control for hypersonic vehicles
[AIAA PAPER 93-3732] p 1143 A93-51331
- Robust control of hypersonic vehicles considering propulsive and aerodynamic effects
[AIAA PAPER 93-3762] p 1131 A93-51357
- Design of a controller for a high performance fighter aircraft using Robust Inverse Dynamics Estimation (RIDE)
[AIAA PAPER 93-3779] p 1132 A93-51374
- Integrated flight/propulsion control - Subsystem specifications for performance
[AIAA PAPER 93-3808] p 1132 A93-51400
- A comparative study of multivariable robustness analysis methods as applied to integrated flight and propulsion control
[AIAA PAPER 93-3809] p 1102 A93-51401
- Guidance and control law for automatic landing flight experiment of reentry space vehicle
[AIAA PAPER 93-3818] p 1143 A93-51409
- Design, test, and evaluation of three active flutter suppression controllers
[NASA-TM-4338] p 63 N93-10070
- A problem formulation for glideslope tracking in wind shear using advanced robust control techniques
[NASA-TM-104164] p 64 N93-11176
- Design of robust suboptimal controllers for a generalized quadratic criterion
[AD-A257746] p 372 N93-17670
- Helicopter flight control system design using the linear quadratic regulator for robust eigenstructure assignment
[AD-A258904] p 373 N93-19351

SUBJECT INDEX

- Robust nonlinear control of vectored thrust aircraft
[NASA-CR-192727] p 728 N93-25199
- Robustness enhancement of neurocontroller and state estimator
[NASA-TM-106028] p 819 N93-26907
- ### ROCKET ENGINE DESIGN
- Integrated air separation and propulsion system for aerospace plane with atmospheric oxygen collection
[SAE PAPER 920974] p 195 A93-14633
- MAKS - Eastern promise? - multi-purpose aerospace system
p 733 A93-34266
- An analysis of air-turbo-rocket performance
[AIAA PAPER 93-1982] p 1141 A93-49829
- Future technology aim of the National Aerospace Plane Program
[AIAA PAPER 93-1988] p 1141 A93-49833
- Design and test of a small two stage counter-rotating turbine for rocket engine application
[AIAA PAPER 93-2136] p 1142 A93-49954
- CFD analysis on control of secondary losses in STME LOX turbines with endwall fences
p 419 N93-17289
- ### ROCKET ENGINES
- Philosophical approach to the basic understanding of the mechanics of jet propulsion
[SAE PAPER 920960] p 173 A93-14626
- Development of a model-based monitoring system for turbine and rocket engines
p 195 A93-16412
- Numerical analysis of high aspect ratio cooling passage flow and heat transfer
[AIAA PAPER 93-1829] p 1153 A93-49714
- Advanced instrumentation for next-generation aerospace propulsion control systems
[AIAA PAPER 93-2079] p 1154 A93-49906
- Development and use of hydrogen-air torches in an altitude facility
[AIAA PAPER 93-2176] p 1137 A93-49988
- Aeroelastic stability of supersonic nozzles with separated flow
[AIAA PAPER 93-2588] p 1142 A93-50300
- Characteristics of the flame air heater of a hypersonic wind tunnel
p 1140 A93-51884
- What is the progress in propulsion?
p 298 N93-19006
- Collection of papers of the 31st Israel Annual Conference on Aviation and Astronautics
(ITN-93-85187) p 764 N93-27166
- ### ROCKET EXHAUST
- A numerical inversion method for determining aerodynamic effects on particulate exhaust plumes from onboard irradiance data
p 823 A93-37482
- Some supersonic and hypersonic research at GASL in the 1960s and 70s
[AIAA PAPER 93-2327] p 1145 A93-50107
- Generic hypersonic vehicle performance model
[NASA-CR-192953] p 714 N93-25162
- An experimental study of under-expanded jets
p 696 N93-25467
- Kinetics and energy transfer in nonequilibrium fluid flows
[AD-A263612] p 875 N93-29284
- ### ROCKET PLANES
- Liquid rocket propulsion applied to manned aircraft - In historical perspective
p 1174 A93-51497
- ### ROCKS
- Crack models for a transversely isotropic medium
p 557 A93-24566
- ### ROLL
- Further analysis of high-rate rolling experiments of a 65 deg delta wing
[AIAA PAPER 93-0620] p 523 A93-24737
- Investigation of the aircraft spin via sensitivity analysis
p 524 A93-27300
- Results from a conical Euler methodology developed for unsteady vortical flows
p 692 A93-35612
- Application of leading-edge vortex manipulations to reduce wing rock amplitudes
p 1007 A93-45152
- Computation of delta-wing roll maneuvers
[AIAA PAPER 93-2975] p 1050 A93-48169
- Investigation of roll requirements for carrier approach
[AIAA PAPER 93-3649] p 1128 A93-48332
- Flow physics of critical states for rolling delta wings
[AIAA PAPER 93-3683] p 1129 A93-48355
- An experimental and computational investigation of slender wings undergoing wing rock
p 187 N93-13915
- Example of statistical techniques applied to analysis of landing ground roll distance measurements (linear regression, correlation coefficient and F-test)
[ESDU-92021] p 330 N93-16635
- Generation of helicopter roll axis bandwidth data through ground-based and in-flight simulation
p 511 N93-19909
- Conical Euler analysis and active roll suppression for unsteady vortical flows about rolling delta wings
[NASA-TP-3259] p 701 N93-26134

- An aerodynamic model for one and two degree of freedom wing rock of slender delta wings
[NASA-CR-193130] p 781 N93-27150
- Effect of vortex behavior on loads acting on a 65 deg delta wing oscillating in roll at high incidence
p 782 N93-27220
- Evaluation of four advanced nozzle concepts for short takeoff and landing performance
[NASA-TP-3314] p 875 N93-29165
- Computation of a delta-wing roll-and-hold maneuver
[AD-A264704] p 909 N93-30498
- ### ROLLER BEARINGS
- Dynamics of a high-rpm compressor
p 75 A93-10009
- On the fatigue life of M50 NiL rolling bearings
p 78 A93-11346
- Optimal design of centered squeeze film dampers
p 831 A93-38629
- ### ROLLING CONTACT LOADS
- On the fatigue life of M50 NiL rolling bearings
p 78 A93-11346
- ### ROLLING MOMENTS
- Wing rock of lifting systems
p 118 A93-14330
- Prediction and control of slender-wing rock
p 182 A93-14331
- Static roll moment characteristics of asymmetric tangential leading edge blowing on a delta wing at high angles of attack
[AIAA PAPER 93-0052] p 261 A93-20165
- Active control of wing rock of a delta wing at post-stall using tangential leading edge blowing
[AIAA PAPER 93-0056] p 367 A93-20169
- Numerical simulation of delta-wing roll
[AIAA PAPER 93-0554] p 285 A93-23293
- Body-axis rolling motion critical states of a 65-degree delta wing
[AIAA PAPER 93-0621] p 523 A93-24738
- Navier-Stokes prediction of a delta wing in roll with vortex breakdown
[AIAA PAPER 93-3495] p 983 A93-47267
- Measurements in 80- by 120-foot wind tunnel of hazard posed by lift-generated wakes
[AIAA PAPER 93-3518] p 1014 A93-47281
- Wake-vortex structure from lift and torque induced on a following wing
[AIAA PAPER 93-3013] p 1054 A93-48202
- Kinematics and aerodynamics of the velocity vector roll
[AIAA PAPER 93-3625] p 1126 A93-48310
- Analysis of missile configurations with wrap-around fins using computational fluid dynamics
[AIAA PAPER 93-3631] p 1064 A93-48316
- Program for calculation of aileron rolling moment and yawing moment coefficients at subsonic speeds
[ESDU-88040] p 136 N93-14514
- Experiments in the control of wing rock at high angle of attack using tangential leading edge blowing
p 1009 N93-31068
- ### ROTARY ENGINES
- A study of a direct-injection stratified-charge rotary engine for motor vehicle application
[SAE PAPER 930677] p 1158 A93-50524
- ### ROTARY GYROSCOPES
- Optimal vibration control for a flexible rotor with gyroscopic effects
p 98 A93-13420
- ### ROTARY STABILITY
- A study on stability and response analysis of a nonlinear rotor system with mass unbalance and side load
[ASME PAPER 92-GT-7] p 400 A93-19280
- Aeroelastic optimization of a composite helicopter rotor
[AIAA PAPER 92-4780] p 323 A93-20287
- On the effect of pitch/mast-bending coupling on whirl-mode stability
p 794 A93-35906
- Experimental analysis of rotary derivatives on a modern aircraft configuration
[AIAA PAPER 93-3514] p 985 A93-47278
- AM-X high angle of attack flight test experience (single and two seat versions)
p 511 N93-19910
- Design and application of Active Magnetic Bearings (AMB) for vibration control
p 1033 N93-32279
- ### ROTARY WING AIRCRAFT
- Ship airwake measurement and flow visualization
[AIAA PAPER 92-4088] p 7 A93-11267
- Preliminary design features of the RASCAL - A NASA/Army rotorcraft in-flight simulator
[AIAA PAPER 92-4175] p 42 A93-13311
- Fixed and rotary wing all weather operations; Proceedings of the Conference, London, United Kingdom, Apr. 23, 24, 1991
[ISBN 0-903409-90-9] p 142 A93-17301
- Vision-based recursive estimation of rotorcraft obstacle locations
p 343 A93-22851
- Refined H-infinity controller design for rotorcraft flight control
p 368 A93-22882

ROTARY WING AIRCRAFT

- An overview of shed ice impact studies in the NASA Lewis Icing Research Tunnel
[AIAA PAPER 93-0301] p 283 A93-23247
- Conceptual assessment of two high-speed rotorcraft
p 508 A93-28612
- Flutter calculations for fixed and rotating wings with state-space inflow dynamics
[AIAA PAPER 93-1300] p 709 A93-33877
- Aeromechanical stability of rotorcraft with advanced geometry blades
[AIAA PAPER 93-1304] p 725 A93-33880
- Aeromechanical stability of a bearingless composite rotor in forward flight
[AIAA PAPER 93-1305] p 726 A93-33881
- Effect of modeling techniques in the coupled rotor-body vibration analysis
[AIAA PAPER 93-1360] p 710 A93-33928
- Active control of vibratory airloads induced by helicopter rotor-fuselage interactions
[AIAA PAPER 93-1363] p 726 A93-33930
- AHS Annual Forum, 48th, Washington, June 3-5, 1992, Proceedings, Vols. 1 & 2
p 763 A93-35901
- The development of the coupled rotor-fuselage model (CRFM)
p 794 A93-35903
- Introduction of the M-85 high-speed rotorcraft concept
p 797 A93-35980
- Validation of R85/METAR on the Puma RAE flight tests
[ONERA, TP NO. 1992-123] p 802 A93-38597
- Passive range estimation for rotorcraft low-altitude flight
p 948 A93-46608
- The three-dimensional boundary layer flow due to a rotor-tip vortex
[AIAA PAPER 93-3081] p 1060 A93-48255
- Flow field characteristics of a complex blade tip at high angles of attack
[AIAA PAPER 93-3083] p 1060 A93-48257
- Summary of the interaction of a rotor wake with a circular cylinder
[AIAA PAPER 93-3084] p 1060 A93-48258
- An advanced parallel rotorcraft flight simulation model - Stability characteristics and handling qualities
[AIAA PAPER 93-3618] p 1125 A93-48305
- Engineering science research issues in high power density transmission dynamics for aerospace applications - rotorcraft geared rotors
[AIAA PAPER 93-2299] p 1155 A93-50084
- Passive range estimation for rotorcraft low-altitude flight
p 1190 A93-52881
- Rotorcraft en route ATC route standards
[AD-A249129] p 35 N93-10323
- Rotorcraft health and usage monitoring systems: A literature survey
[DOT/FAA/RD-91/6] p 48 N93-11461
- A theory for the analysis of rotorcraft operating in atmospheric turbulence
p 48 N93-11725
- The Fourth Workshop on Dynamics and Aeroelastic Stability Modeling of Rotorcraft Systems
[AD-A255065] p 50 N93-12485
- A simulation model of atmospheric turbulence for rotorcraft applications
p 224 N93-14588
- An overview of shed ice impact in the NASA Lewis Icing Research Tunnel
[NASA-TM-105969] p 139 N93-15404
- The Application of CFD to rotary wing flow problems
[NASA-TM-102803] p 139 N93-15483
- Ground based simulation evaluation of the effects of time delays and motion on rotorcraft handling qualities
[AD-A256921] p 328 N93-16186
- Developing a control system for ARES 2
p 371 N93-16769
- Trade-offs arising from mixture of color cueing and monocular, binocular, and stereoscopic cueing information for simulated rotorcraft flight
[NASA-TP-3268] p 338 N93-18333
- Basic research on design analysis methods for rotorcraft vibrations
[NASA-CR-191917] p 422 N93-18576
- Numerical investigation of performance degradation of wings and rotors due to icing
[NASA-CR-192233] p 339 N93-18783
- Flexible rotorcraft system dynamics with time-variant contact conditions
p 340 N93-19034
- A Government/Industry Summary of the Design Analysis Methods for Vibrations (DAMVIBS) Program
[NASA-CP-10114] p 514 N93-21310
- The NASA/Industry Design Analysis Methods for Vibrations (DAMVIBS) program: A government overview
p 514 N93-21311
- An aeroelastic model structure investigation for a manned real-time rotorcraft simulation
p 693 N93-24756
- Design and analysis of curved composite components for rotorcraft fuselage frames
p 716 N93-25701
- Image-based ranging and guidance for rotorcraft
[NASA-CR-177608] p 708 N93-26549

Robust crossfeed design for hovering rotorcraft
[NASA-CR-193107] p 805 A93-27241

Chaos in mechanical systems with especial reference to rotorcraft and missiles
[AD-A263703] p 943 A93-29384

Rotorcraft master plan
p 857 A93-30677

Determining the transferability of flight simulator data
p 913 A93-30685

Frequency-response techniques for documentation and improvement of rotorcraft simulators
p 913 A93-30689

Bandwidth and SIMDUCE as simulator fidelity criteria
p 913 A93-30690

Methodology development for evaluation of selective-fidelity rotorcraft simulation
p 913 A93-30691

ROTARY WINGS

Multiple input/multiple output (MIMO) analysis procedures with applications to flight data
p 60 A93-10777

ONERA makes progress in rotor aerodynamics, aeroelasticity, and acoustics
p 2 A93-11621

Boundary integral equation methods for aerodynamics
p 9 A93-12158

Reaction drive rotors - Lessons learned (Hero had a good idea - But) - jet helicopter performance
[AIAA PAPER 92-4279] p 55 A93-13352

Using aerodynamic analysis codes to assist in structural design and optimization of ducted rotor/wing blades
[AIAA PAPER 92-4280] p 44 A93-13353

Fatigue qualification of high thickness composite rotor components
p 81 A93-13646

Experimental and theoretical studies of helicopter rotor-fuselage interaction
[ONERA, TP NO. 1992-142] p 120 A93-14356

Experimental study of rotor wake/body interactions in hover
p 124 A93-14782

The rotor blade flap bending problem - An analytical test case
p 158 A93-14783

Choice of materials for military helicopters
p 158 A93-15028

Fixed and rotary wing all weather operations system requirements
p 142 A93-17303

The smart structures technology in the vibration control of helicopter blades in forward flight
p 386 A93-17721

Experience with boundary element methods to calculate the aerodynamic characteristics of aircraft
p 243 A93-19130

Aeroelastic optimization of a composite helicopter rotor
[AIAA PAPER 92-4780] p 323 A93-20287

Multidisciplinary optimization of helicopter rotor blades including design variable sensitivity
[AIAA PAPER 92-4783] p 323 A93-20289

Aerodynamic performance optimization of a rotor blade using a neural network as the analysis
[AIAA PAPER 92-4837] p 324 A93-20295

Multidisciplinary analysis and sensitivity derivatives for isolated helicopter rotors in hover
[AIAA PAPER 92-4696] p 324 A93-20308

Development of a structural optimization capability for the aeroelastic tailoring of composite rotor blades with straight and swept tips
[AIAA PAPER 92-4779] p 326 A93-20370

Fifty years of tandem rotor helicopter engineering
p 504 A93-25250

A generic harmonic rotor model for helicopter flight simulation
p 506 A93-27480

A retrospective of 3600 composite blades
p 507 A93-27963

Coupled composite rotor blades under bending and torsional loads
p 546 A93-27970

Continuous judgment of helicopter noise - On the validity of Leq and Zwicker's method (ISO 532B)
p 558 A93-28478

AHS and Royal Aeronautical Society, Technical Specialists' Meeting on Rotorcraft Acoustics/Fluid Dynamics, Philadelphia, PA, Oct. 15-17, 1991, Proceedings
p 565 A93-29401

High-speed helicopter rotor noise - Shock waves as a potent source of sound
p 565 A93-29403

Sensitivity of acoustic predictions to variation of input parameters
p 565 A93-29404

HHC study in the DNW to reduce BVI noise - An analysis
p 565 A93-29405

The role of blade elasticity in the prediction of blade-vortex interaction noise
p 566 A93-29406

Theoretical modelling of rotor noise radiation
p 566 A93-29407

Noise reduction for transonic blade-vortex interactions
p 566 A93-29408

The development of a prediction method for the calculation of blade-vortex interaction noise based on measured airloads
p 566 A93-29409

The influence of quadrupole sources in the boundary layer and wake of a blade on helicopter rotor noise
p 566 A93-29410

Shock waves and the Ffowcs Williams-Hawkins equation
p 480 A93-29411

Validation of high frequency airload calculations using full scale flight test acoustic data
p 567 A93-29417

NOTAR system - A quiet character
p 567 A93-29418

Acoustic characteristics of advanced model rotor systems
p 567 A93-29419

Recent developments in rotor wake modeling for helicopter noise prediction
p 481 A93-29437

Correlation of airloads on a two-bladed helicopter rotor
p 481 A93-29438

An overview on practical application of helicopter noise certification rules
p 487 A93-29442

Prediction of helicopter component loads using neural networks
[AIAA PAPER 93-1301] p 756 A93-33878

Sources of helicopter rotor hub inplane shears
[AIAA PAPER 93-1358] p 709 A93-33927

Efficient sensitivity analysis for rotary-wing aeromechanical problems
[AIAA PAPER 93-1648] p 711 A93-34173

Modal sensors and actuators for individual blade control
[AIAA PAPER 93-1703] p 712 A93-34225

Dynamic analysis of rotor flexbeams based on nonlinear anisotropic shell models
p 743 A93-34261

A modal-based procedure for efficiently predicting low vibration rotor designs
p 712 A93-34262

Frequency-domain identification of BO 105 derivative models with rotor degrees of freedom
p 712 A93-34263

Nonlinear large amplitude vibration of composite helicopter blade at large static deflection
p 713 A93-35630

URNS - A free-wake Euler/Navier-Stokes numerical method for helicopter rotors
p 692 A93-35634

A finite-volume Euler solver for computing rotary-wing aerodynamics on unstructured meshes
p 765 A93-35935

Digital resolver for helicopter model blade motion analysis
p 830 A93-37878

Unsteady analysis of helicopter rotor
p 770 A93-38193

A numerical procedure for aerodynamic optimization of helicopter rotor blades
[ONERA, TP NO. 1992-121] p 771 A93-38595

Study of soft-in-torsion blades - ROSOH operation
[ONERA, TP NO. 1992-124] p 803 A93-38598

Application of European CFD methods for helicopter rotors in forward flight
[ONERA, TP NO. 1992-125] p 772 A93-38599

Numerical calculation of helicopter rotor equations and comparison with experiment
[ONERA, TP NO. 1992-128] p 772 A93-38602

Laser velocimetry around helicopter blades in the DNW wind tunnel of the NLR
[ONERA, TP NO. 1992-143] p 831 A93-38613

Definition and evaluation of new helicopter rotor blade tips
[ONERA, TP NO. 1992-179] p 773 A93-38741

Toward the silent helicopter
[ONERA, TP NO. 1992-229] p 851 A93-38774

Effect of the aerodynamic interference of the rotor and the fuselage on the power requirements for the horizontal flight of a helicopter
p 819 A93-39179

Performance of higher harmonic control algorithms for helicopter vibration reduction
p 890 A93-41904

Results from a set of low speed blade-vortex interaction experiments
p 872 A93-43540

A multibody formulation for helicopter structural dynamic analysis
p 892 A93-43776

Tip vortex geometry of a hovering helicopter rotor in ground effect
p 893 A93-43779

Efficient free wake calculations using analytical/numerical matching
p 874 A93-43780

A finite-volume Euler solver for computing rotary-wing aerodynamics on unstructured meshes
p 874 A93-43782

An efficient method to calculate rotor flow in hover and forward flight
[AIAA PAPER 93-3336] p 953 A93-45030

Wake structure of a helicopter rotor in forward flight
p 958 A93-45138

Optimization of the blade angle of the AV-2 propeller for improving the flight performance characteristics of An-2 aircraft
p 996 A93-45663

Application of the shadowgraph flow visualization technique to a full-scale helicopter rotor in hover and forward flight
[AIAA PAPER 93-3411] p 1030 A93-47208

A critical assessment of UH-60 main rotor blade airfoil data
[AIAA PAPER 93-3413] p 975 A93-47210

Performance results from a test of an S-76 rotor in the NASA Ames 80- by 120-foot wind tunnel
[AIAA PAPER 93-3414] p 975 A93-47211

Characteristics of deformable leading edge for high performance helicopter rotor
[AIAA PAPER 93-3526] p 986 A93-47285

Helicopter external noise prediction and reduction
[ONERA, TP NO. 1993-48] p 1039 A93-47450

Free-wake computation of helicopter rotor flowfields in forward flight
[AIAA PAPER 93-3079] p 1059 A93-48253

Euler calculations of unsteady interaction of advancing rotor with a line vortex
p 1071 A93-49016

Finite state aeroelastic model for use in rotor design optimization
p 1104 A93-52454

Calculation of the position of the flow separation line in an analog model of flow past a body
p 1176 A93-52958

Optimization of large scale systems in elasticity
p 1255 A93-54544

ONERA calculation model of dynamic flow separation on an airfoil section
p 1238 A93-56212

Numerical study of advanced rotor blades
p 23 A93-11899

Studies of a flat wake rotor theory
[NASA-CR-190936] p 25 A93-12343

Dynamic stall effects on hingeless rotor stability with experimental correlation
p 129 A93-13010

The effect of wake dynamics on rotor eigenvalues in forward flight
p 137 A93-14595

Stability of elastically tailored rotor blades
p 184 A93-14828

Finite-state inflow applied to aeroelastic flutter of fixed and rotating wings
p 188 A93-14830

Helicopter installations: From motor to rotor
[LR-675] p 329 A93-16345

RPH preliminary design, trend analysis and initial analysis of the NPS hummingbird
[AD-A257854] p 338 A93-18304

Damage tolerance of a helicopter rotor high-strength steel
p 555 A93-21322

An aeroelastic model structure investigation for a manned real-time rotorcraft simulation
p 693 A93-24756

Rotor design optimization using a free wake analysis
[NASA-CR-177612] p 693 A93-25075

Application of finite-state inflow to flap-lag-torsion damping in hover
p 714 A93-25486

Aeroelastic response and aeromechanical stability of helicopters with elastically coupled composite rotor blades
p 715 A93-25530

An integrated finite-state model for rotor deformation, nonlinear airloads, inflow, and trim
p 715 A93-25538

Structural dynamic analysis of bearingless rotor blade
p 717 A93-25719

Unsteady airfoil flow solutions on moving zonal grids
[AD-A261925] p 701 A93-26198

Helicopter forced response vibration analysis method RTVIB20
[AD-A261809] p 730 A93-26260

Unsteady transition measurements on a pitching three-dimensional wing
p 820 A93-27450

A passive infrared ice detection technique for helicopter applications
[NASA-CR-193187] p 880 A93-29152

Flow visualization on helicopter blades using acenaphthen
[ESA-TT-1255] p 931 A93-29273

Aerodynamic characteristics of a rotorcraft airfoil designed for the tip region of a main rotor blade
[NASA-TM-4264] p 876 A93-29450

Computation of far-field helicopter rotor tone noise
[ONERA-P-1990-5] p 943 A93-30110

ROTATING BODIES

Calculation of turbulent flow for an enclosed rotating cone
[ASME PAPER 92-GT-70] p 400 A93-19320

Experimental study on the characteristics of the near wake of a rotating flat plate, III - Influence of the shape near the trailing edge on periodic-velocity-fluctuation phenomena
p 451 A93-21727

Hydrodynamics and heat transfer near the stagnation point in an arbitrary axisymmetric nonswirling flow incident on a rotating obstacle
p 691 A93-35270

A theoretical study on the ETHYLENE system - A fuzzy diagnostic expert system for large rotating machinery
p 846 A93-36327

Analysis of the effects of blade pitch on the radar return signal from rotating aircraft blades
p 885 A93-43476

Navier-Stokes calculations of rotating BERP planform blade flowfields
[AIAA PAPER 93-3527] p 986 A93-47286

- Active control of asymmetric conical flow using spinning and rotatory oscillations
[AIAA PAPER 93-2958] p 1048 A93-48152
- Turbine Engine Diagnostics (TED) system
[AIAA PAPER 93-1818] p 1110 A93-49706
- Rotating machinery - Transport phenomena; Proceedings of the 3rd International Symposium on Transport Phenomena and Dynamics of Rotating Machinery (ISROMAC-3), Honolulu, HI, Apr. 1-4, 1990 [ISBN 1-56032-147-4] p 1256 A93-54626
- Local heat transfer distribution in a rotating serpentine rib-roughened flow passage p 1259 A93-55459
- ROTATING CYLINDERS**
- Optimal control of lift/drag ratios on a rotating cylinder p 76 A93-10275
- In-flight investigation of a rotating cylinder-based structural excitation system for flutter testing
[AIAA PAPER 93-1537] p 711 A93-34074
- Moving wall effects in transverse subsonic flow past a rotating cylinder p 1179 A93-53573
- Development of the wake behind a circular cylinder impulsively started into rotatory and rectilinear motion p 1236 A93-55736
- Experimental investigation of the aerodynamics of independently rotating cylindrical shells
[AD-A258917] p 305 N93-19340
- ROTATING DISKS**
- Computation of laminar flow and heat transfer over an enclosed rotating disk with and without jet impingement p 201 A93-13982
- On the cross-flow instability near a rotating disk p 128 A93-17264
- Double mode behaviour of bladed disk assemblies in the resonance frequency range, visualized by means of holographic interferometry
[ASME PAPER 92-GT-438] p 357 A93-19580
- Linear stability of three-dimensional boundary layers - Effects of curvature and non-parallelism
[AIAA PAPER 93-0079] p 263 A93-20191
- Numerical study of mixed convection between two corotating symmetrically heated disks p 416 A93-23491
- Two dimensional incompressible flow through a vibrating bladed disc - Theoretical model p 973 A93-46991
- Prediction of rotating disc flow and heat transfer in gas turbine engines p 1256 A93-54634
- Theoretical and experimental investigations concerning the structural integrity of aeroengine compressor discs p 56 N93-10539
- Rotational CARS measurements in a rotating cavity with axial throughflow of cooling air: Oxygen concentration measurements
[PNR-90935] p 72 N93-11035
- Heat Transfer and Cooling in Gas Turbines
[AGARD-CP-527] p 901 N93-29926
- Flow and heat transfer between gas-turbine discs p 903 N93-29950
- ROTATING FLUIDS**
- A study of heat transfer from a disk in a rotating cavity with axial and radial-axial flow of a liquid p 54 A93-12812
- Influence of surface heating condition on local heat transfer in a rotating square channel with smooth walls and radial outward flow
[ASME PAPER 92-GT-188] p 402 A93-19413
- Heat transfer in serpentine flow passages with rotation
[ASME PAPER 92-GT-190] p 403 A93-19415
- Visualization and analysis of supersonic flow in rotating turbine stage. II - Analysis of the flow into the moving blades and their exit flow p 476 A93-27442
- Numerical analysis of the three-dimensional boundary layer on a turbomachinery rotor blade p 685 A93-34341
- The interaction between a steady jet flow and a supersonic blade tip p 688 A93-34415
- Stability of the vapour phase in a rotating two-phase fluid system subjected to different gravitational intensities p 926 A93-41714
- Inverse problem using S2-S1 approach for the design of the turbomachine with splitter blades p 971 A93-46929
- Instability of three-dimensional supersonic boundary layer p 973 A93-46987
- Design of axisymmetric channels with rotational flow
[AIAA PAPER 93-3117] p 1062 A93-48287
- Effect of rotation on heat transfer and hydraulic resistance in the radial cooling channels of turbine rotor blades p 1215 A93-52950
- Design of air intakes and nozzles for transonic rotational flows
[ISABE 93-7102] p 1187 A93-54078
- Prediction of rotating disc flow and heat transfer in gas turbine engines p 1256 A93-54634
- Analysis of unsteady wave processes in a rotating channel
[NASA-CR-191154] p 816 N93-28617

ROTATING GENERATORS

- The integral starter/generator development progress
[SAE PAPER 920967] p 173 A93-14629

ROTATING SHAFTS

- Damage tolerance evaluation of new manufacturing techniques for composite helicopter drive shafts
[AIAA PAPER 93-1400] p 739 A93-33960
- Fluid-film foil bearings control engine heat p 924 A93-39949
- Experimental study of the flow field inside a whirling annular seal p 85 N93-10892
- Optimal output feedback vibration control of rotor-bearing systems p 86 N93-11220
- Transient thermal behaviour of a compressor rotor with axial cooling air flow and co-rotating or contra-rotating shaft p 903 N93-29946
- Design and application of Active Magnetic Bearings (AMB) for vibration control p 1033 N93-32279

ROTATING STALLS

- Prediction of the inception of rotating stall for multistage axial flow compressors p 12 A93-12731
- A study of dynamic characteristics of axial compression systems by heat addition p 202 A93-14168
- Pressure fluctuation on casing wall of isolated axial compressor rotors at low flow rate
[ASME PAPER 92-GT-33] p 246 A93-19293
- Recess vane passive stall control
[ASME PAPER 92-GT-36] p 246 A93-19296
- An investigation of post stall transients and recoverability of axial compression systems. I - A simplified method
[ASME PAPER 92-GT-55] p 347 A93-19305
- An investigation of post stall transients and recoverability of axial compression systems. II - Numerical simulations
[ASME PAPER 92-GT-56] p 347 A93-19306
- Stability of fully developed rotating stall
[ASME PAPER 92-GT-57] p 348 A93-19307
- Modified surge in an axial flow compressor
[ASME PAPER 92-GT-59] p 247 A93-19309
- The vortex behaviour of the rotating-stall cell of a centrifugal compressor with vaned diffuser
[ASME PAPER 92-GT-66] p 400 A93-19316
- A study of stall in a low hub/tip ratio fan
[ASME PAPER 92-GT-85] p 248 A93-19334
- Blade excitation by circumferentially asymmetric rotating stall in centrifugal compressors
[ASME PAPER 92-GT-148] p 351 A93-19376
- Excitation of blade vibration due to surge of centrifugal compressors
[ASME PAPER 92-GT-149] p 351 A93-19377
- A unified model for rotating stall and surge p 259 A93-20119
- Prediction of active control of subsonic centrifugal compressor rotating stall
[AIAA PAPER 93-0153] p 274 A93-22591
- Solution schemes for stage-by-stage dynamic compression system modeling
[AIAA PAPER 93-0154] p 275 A93-22592
- A simplified approach for control of rotating stall. I - Theoretical development
[AIAA PAPER 93-2229] p 1080 A93-50035
- Local nonlinear control of stall inception in axial flow compressors
[AIAA PAPER 93-2230] p 1080 A93-50036
- A simplified approach for control of rotating stall. II - Experimental results
[AIAA PAPER 93-2234] p 1080 A93-50038
- A model for the selective amplification of spatially coherent waves in a centrifugal compressor on the verge of rotating stall
[AIAA PAPER 93-2236] p 1080 A93-50039
- Spatial domain characterization of abrupt rotating stall initiation in an axial flow compressor
[AIAA PAPER 93-2238] p 1081 A93-50040
- Study on surge and rotating stall in axial compressors. III - Numerical model for multiblade-row compressors p 1181 A93-53799
- Numerical study on inception of stall cells in rotating stall
[ISABE 93-7007] p 1183 A93-53983
- Some measurements of stall in an axial impeller
[ISABE 93-7008] p 1183 A93-53984
- The leading edge vortex of a rotating stall cell
[ISABE 93-7009] p 1183 A93-53985
- The energy dissipation in a rotating stall cell
[ISABE 93-7010] p 1183 A93-53986
- Review of stall, surge and active control in axial compressors
[ISABE 93-7011] p 1184 A93-53987
- An investigation of post stall transients and recoverability of axial compression systems
[ISABE 93-7012] p 1184 A93-53988
- Rotating stall inception in fans of low hub-tip ratio p 136 N93-14479
- Stall in axial flow aero engine compressors p 422 N93-18723

- Stall and surge in axial flow compressors p 423 N93-18724
- Experimental investigation of rotating stall in a mismatched three stage axial flow compressor p 423 N93-18727
- Application of recess vane casing treatment to axial flow fans p 423 N93-18728
- Axial Flow Compressors, volume 2
[VKI-LS-1992-02-VOL-2] p 423 N93-18731
- Rotating stall: Modeling-measurement techniques; unsteady loss-unsteady flow field p 424 N93-18732
- Rotating stall cell and Von Karman vortex street: A meteorological theory p 424 N93-18734
- Characterization of stall inception in high-speed single-stage compressors
[AD-A258973] p 365 N93-19093
- Combined experiment, phase 1
[DE93-000012] p 485 N93-21766
- Active stabilization of aeromechanical systems
[AD-A261366] p 725 N93-26335
- ROTATION**
- Acoustic mode measurements in the inlet of a model turbofan using a continuously rotating rake - Data collection/analysis techniques
[AIAA PAPER 93-0599] p 361 A93-23324
- The prediction of convective heat transfer in rotating square ducts
[PNR-90929] p 85 N93-11025
- Acoustic mode measurements in the inlet of a model turbofan using a continuously rotating rake: Data collection/analysis techniques
[NASA-TM-105936] p 179 N93-15403
- Rotating rake design for unique measurement of fan-generated spinning acoustic modes
[NASA-TM-105946] p 724 N93-26161
- Some recent applications of Navier-Stokes codes to rotorcraft p 786 N93-27452
- Navier-Stokes simulation of viscous, separated, supersonic flow over a projectile rotating band
[AD-A263073] p 788 N93-27955
- The effect of orthogonal-mode rotation on forced convection in a circular-sectioned tube fitted with full circumferential transverse ribs p 932 N93-29937
- Turbulent flow and heat transfer in idealized blade cooling passages p 902 N93-29938
- Local heat transfer measurement with liquid crystals on rotating surfaces including non-axisymmetric cases p 902 N93-29943
- Heat transfer and leakage in high-speed rotating stepped labyrinth seals p 903 N93-29951
- ROTOR AERODYNAMICS**
- On the use of the method of matched asymptotic expansions in propeller aerodynamics and acoustics p 8 A93-11553
- ONERA makes progress in rotor aerodynamics, aeroelasticity, and acoustics p 2 A93-11621
- An analysis of helicopter dynamic response to turbulence using fuselage and blade element atmospheric sampling techniques
[AIAA PAPER 92-4148] p 43 A93-13314
- Computer aided aerodynamic design of high pressure axial flow fan blade element p 16 A93-13649
- An interactive numerical procedure for rotor aeroelastic stability analysis using elastic lifting surface p 155 A93-14313
- Modified sparse time domain technique for rotor stability testing p 157 A93-14593
- Experimental study of dynamic fluid forces and moments for a long annular seal p 209 A93-15684
- Toward an integration of aerodynamics and aeroacoustics of rotors p 243 A93-19127
- Effects of a trailing edge flap on the aerodynamics and acoustics of rotor blade-vortex interactions p 244 A93-19144
- Numerical analysis of acoustic effect of rotor wakes in rotor-stator interaction p 447 A93-19182
- A numerical method for the prediction of quadrupole shock wave noise p 448 A93-19201
- Lifting surface theory for steady aerodynamic analysis of ducted counter rotation propfan
[ASME PAPER 92-GT-14] p 347 A93-19286
- Recess vane passive stall control
[ASME PAPER 92-GT-36] p 246 A93-19296
- Calculation of turbulent flow for an enclosed rotating cone
[ASME PAPER 92-GT-70] p 400 A93-19320
- Design and rotor performance of a 5:1 mixed-flow supersonic compressor
[ASME PAPER 92-GT-73] p 348 A93-19323
- Aerodynamic design of turbomachinery blading in three-dimensional flow - An application to radial inflow turbines
[ASME PAPER 92-GT-74] p 248 A93-19324
- Hot streaks and phantom cooling in a turbine rotor passage. II - Combined effects and analytical modelling
[ASME PAPER 92-GT-76] p 401 A93-19326

A study of stall in a low hub/tip ratio fan
[ASME PAPER 92-GT-85] p 248 A93-19334

Viscous interaction upstream and downstream of a turbine stator cascade with a periodic wake field
[ASME PAPER 92-GT-162] p 250 A93-19388

The use of interferometry in the study of rotorcraft aerodynamics p 407 A93-19914

Aerodynamic performance optimization of a rotor blade using a neural network as the analysis
[AIAA PAPER 92-4837] p 324 A93-20295

Multidisciplinary analysis and sensitivity derivatives for isolated helicopter rotors in hover
[AIAA PAPER 92-4696] p 324 A93-20308

Recent advances in integrated multidisciplinary optimization of rotorcraft
[AIAA PAPER 92-4777] p 325 A93-20369

An approach to tiltrotor wing aeroservoelastic optimization through increased productivity
[AIAA PAPER 92-4781] p 326 A93-20371

Vibration reduction for helicopter airframes - An application of the general-purpose structural optimization program STARS
[AIAA PAPER 92-4782] p 326 A93-20372

Analytical formulation of optimum rotor interdisciplinary design with a three-dimensional wake
[AIAA PAPER 92-4778] p 265 A93-20416

Investigation of the dynamic inflow's influence on rotor control derivatives p 266 A93-20802

Prediction of rotor dynamic destabilizing forces in axial flow compressors p 272 A93-22263

Direct boundary value solution of wave rotor flow fields
[AIAA PAPER 93-0483] p 415 A93-23385

Measurement of shed vorticity and circulation from rotating aerofoil by particle image velocimetry p 538 A93-23804

Experimental investigation of rotor/lifting surface interactions
[AIAA PAPER 93-0871] p 469 A93-24932

A new method for improved rotor free-wake convergence
[AIAA PAPER 93-0872] p 469 A93-24933

Eurofan rotor aerodynamic tests
[ONERA, TP NO. 1992-173] p 475 A93-26880

Surging limits of multistage axial-flow compressors p 476 A93-27443

Euler solutions to nonlinear acoustics of non-lifting rotor blades p 568 A93-29433

On the effect of pitch/mast-bending coupling on whirl-mode stability p 794 A93-35906

A finite-volume Euler solver for computing rotary-wing aerodynamics on unstructured meshes p 765 A93-35935

Numerical simulation of a hovering rotor using embedded grids p 765 A93-35936

Helicopter aerodynamics research techniques and rotor-fuselage interaction analysis p 765 A93-35938

Vortex methods for the computational analysis of rotor/body interaction p 765 A93-35939

Interactional aerodynamic effects on rotor performance in hover and forward flight p 766 A93-35941

A study of the rotor wake of a small-scale rotor model in forward flight using laser light sheet flow visualization with comparisons to analytical models p 766 A93-35957

An analysis on high speed impulsive noise of transonic helicopter rotor p 849 A93-35965

Prediction of BVI noise patterns and correlation with wake interaction locations p 849 A93-35966

Optimum design of high speed prop-rotors using a multidisciplinary approach p 798 A93-35985

Rotor blade airfoil design by numerical optimization and unsteady calculations
[ONERA, TP NO. 1992-65] p 766 A93-35993

A 2-D numerical model for predicting the aerodynamic performance of the NOTAR system tailboom p 766 A93-35994

Dynamic stall of sinusoidally oscillating three-dimensional swept and unswept wings in compressible flow p 766 A93-35995

Shadowgraph flow visualization of isolated tiltrotor and rotor/wing wakes p 767 A93-35996

Hover performance analysis of advanced rotor blades p 767 A93-35998

Theodorsen's ideal propeller performance with ambient pressure in the slipstream p 768 A93-37400

Aerodynamic rotor loads prediction method with free wake for low speed descent flights
[ONERA, TP NO. 1992-122] p 772 A93-38596

Blade-vortex interaction noise - Prediction and comparison with flight and wind tunnel tests
[ONERA, TP NO. 1992-126] p 851 A93-38600

Definition and evaluation of new helicopter rotor blade tips
[ONERA, TP NO. 1992-179] p 773 A93-38741

Effect of the aerodynamic interference of the rotor and the fuselage on the power requirements for the horizontal flight of a helicopter p 819 A93-39179

Direct periodic solutions of rotor free wake calculations p 874 A93-43781

A finite-volume Euler solver for computing rotary-wing aerodynamics on unstructured meshes p 874 A93-43782

Application of two chaos methods to Higher Harmonic Control data --- for suppression of helicopter vibration p 909 A93-43783

An adaptive finite element method for turbulent free shear flow past a propeller
[AIAA PAPER 93-3388] p 956 A93-45079

Nonlinear large amplitude aeroelastic behavior of composite rotor blades p 997 A93-45741

AIAA Applied Aerodynamics Conference, 11th, Monterey, CA, Aug. 9-11, 1993, Technical Papers. Pts. 1 & 2 p 974 A93-47201

Application of the shadowgraph flow visualization technique to a full-scale helicopter rotor in hover and forward flight
[AIAA PAPER 93-3411] p 1030 A93-47208

Flow visualization of mast-mounted-sight/main rotor aerodynamic interactions
[AIAA PAPER 93-3517] p 1009 A93-47280

Three-dimensional analysis of turbine rotor flow including tip clearance
[ASME PAPER 93-GT-111] p 987 A93-47446

SCV measurements in the wake of a rotor in hover and forward flight
[AIAA PAPER 93-3080] p 1059 A93-48254

The three-dimensional boundary layer flow due to a rotor-tip vortex
[AIAA PAPER 93-3081] p 1060 A93-48255

An aerodynamic design program for contra-rotating turbine cascades p 1067 A93-48521

Improving the design of the main fuel pump of Turbo-Jet 7 p 1107 A93-48555

Formulas for determining the induced velocity in the direct and inverse rotor problems p 1071 A93-49324

The effect of unsteady blade loading on the aeroacoustics of a pusher propeller
[AIAA PAPER 93-1805] p 1173 A93-49694

Flow investigation of a low-speed-operated centrifugal compressor over a flow range including zero flow
[AIAA PAPER 93-2240] p 1155 A93-50042

Analytic methods for design of wave cycles for wave rotor core engines
[AIAA PAPER 93-2523] p 1121 A93-50253

The combined effect of clearances and peripheral overlaps on the efficiency of microturbines with shroudless rotors p 1193 A93-52963

The flow lag angle in the rotor of a centrifugal compressor with allowance for viscosity effects p 1179 A93-53555

Laser velocimeter measurements of the flow field generated by a forward-swept propfan during flutter
[AIAA PAPER 93-2919] p 1180 A93-53591

Numerical study on inception of stall cells in rotating stall
[ISABE 93-7007] p 1183 A93-53983

Effects of blade geometry and mode shape on fan flutter
[ISABE 93-7028] p 1196 A93-54004

Investigation of the flow field through a variable pitch fan rotor with an inlet total pressure distortion
[ISABE 93-7029] p 1184 A93-54005

Navier-Stokes computation of the three dimensional flow fields through a transonic fan blade
[ISABE 93-7030] p 1184 A93-54006

Spectral analysis of unsteady surface pressure on a pusher propeller p 1232 A93-54646

Rotor/stator flow coupling in turbomachines p 1232 A93-54647

Helicopter noise reduction programme - AGUSTA achievements p 1262 A93-54721

Review of helicopter noise research in Europe p 1263 A93-54725

Radial turbine cooling p 82 A93-10061

Explicit Navier-Stokes computation of turbomachinery flows p 83 A93-10370

Tilt rotor hover aeroacoustics
[NASA-CR-177598] p 99 A93-10458

Harmonic analysis of the aerodynamic forces on a Darrieus rotor p 18 A93-10551

LDV Measurements of unsteady flow fields in radial turbine
[AD-A253592] p 19 A93-10648

Recent advances in multidisciplinary optimization of rotorcraft
[NASA-TM-107665] p 47 A93-10968

Dynamic stall effects on hingeless rotor stability with experimental correlation p 129 A93-13010

Overview on test cases for computation of internal flows in turbomachines p 214 A93-13209

Unsteady three-dimensional thin-layer Navier-Stokes solutions for turbomachinery in transonic flow p 218 A93-14025

Rotating stall inception in fans of low hub-tip ratio p 136 A93-14479

The effect of wake dynamics on rotor eigenvalues in forward flight p 137 A93-14595

Finite-state inflow applied to aeroelastic flutter of fixed and rotating wings p 188 A93-14830

Static pressure measurements of the shock-boundary layer interaction in a simulated fan passage
[AD-A256724] p 361 A93-15979

Developing a control system for ARES 2 p 371 A93-16769

Mean flow interactions of a counter-rotating propeller p 552 A93-20289

Rotor design optimization using a free wake analysis
[NASA-CR-177612] p 693 A93-25075

Far field rotor noise
[AD-A260703] p 759 A93-25651

Flow control of low heat load turbine airfoils
[AD-A260941] p 724 A93-26219

The blade curving effects in a turbine stator cascade with low aspect ratio p 725 A93-26239

Dynamic System Coupler Program (DYSCO 4.1). Volume 1: Theoretical manual p 848 A93-27531

Unsteady vortex loop/dipole theory applied to the work and acoustics of an ideal low speed propeller
[AD-A264057] p 876 A93-29891

Three-dimensional fiber-optic LDV measurements in the endwall region of a linear cascade of controlled-diffusion stator blades
[AD-A263513] p 933 A93-29968

Localization of aeroelastic modes in mistuned high-energy turbines p 1032 A93-31586

ROTOR BLADES

Dynamic analysis of a pre-and-post ice impacted blade
[AIAA PAPER 92-4273] p 54 A93-13333

Using aerodynamic analysis codes to assist in structural design and optimization of ducted rotor/wing blades
[AIAA PAPER 92-4280] p 44 A93-13353

Nonlinear rotor-fuselage coupled response to generic periodic control modes using advanced computation techniques p 153 A93-14226

An interactive numerical procedure for rotor aeroelastic stability analysis using elastic lifting surface p 155 A93-14313

Rapid fabrication of flight worthy composite parts p 209 A93-15792

Structural optimization of a cantilevered rotating beam p 210 A93-16248

The smart structures technology in the vibration control of helicopter blades in forward flight p 366 A93-17721

Acoustic flight test experience with the XV-15 Tiltrotor aircraft with the Advanced Technology Blade (ATB) p 445 A93-19143

Transmission of sound through a rotor p 447 A93-19183

Low aspect ratio transonic rotors. II - Influence of location of maximum thickness on transonic compressor performance
[ASME PAPER 92-GT-186] p 352 A93-19411

Calculation of three-dimensional boundary layers on rotor blades using integral methods
[ASME PAPER 92-GT-210] p 252 A93-19433

Investigations on a radial compressor tandem-rotor stage with adjustable geometry
[ASME PAPER 92-GT-218] p 404 A93-19440

Double mode behaviour of bladed disk assemblies in the resonance frequency range, visualized by means of holographic interferometry
[ASME PAPER 92-GT-438] p 357 A93-19580

Aerodynamic performance optimization of a rotor blade using a neural network as the analysis
[AIAA PAPER 92-4837] p 324 A93-20295

Structural tailoring of aircraft engine blade subject to ice impact constraints
[AIAA PAPER 92-4710] p 358 A93-20319

Recent advances in integrated multidisciplinary optimization of rotorcraft
[AIAA PAPER 92-4777] p 325 A93-20369

Development of a structural optimization capability for the aeroelastic tailoring of composite rotor blades with straight and swept tips
[AIAA PAPER 92-4779] p 326 A93-20370

Dynamic analysis of pretwisted elastically-coupled rotor blades p 326 A93-21125

A study of aerodynamic performance of a contra-rotating axial compressor stage p 463 A93-24524

Rotor blade unsteady aerodynamic gust response to inlet guide vane wakes
[ASME PAPER 91-GT-129] p 475 A93-26897

A comparative analysis of XV-15 tiltrotor hover test data and WOPWOP predictions incorporating the fountain effect p 509 A93-29414

Tiltrotor ground noise reduction from rotor parametric changes as predicted by ROTONET p 567 A93-29415

Blade-vortex interaction data obtained from a pressure-instrumented model rotor at the DNW p 568 A93-29430

A numerical study of advanced rotor blades p 481 A93-29436

Correlation of airloads on a two-bladed helicopter rotor p 481 A93-29438

Unsteady wake effect on rotor vibratory airloadings p 509 A93-29439

Vibration and flutter of stiff-inplane elastically tailored composite rotor blades p 725 A93-33879

[AIAA PAPER 93-1302]

Aeromechanical stability of rotorcraft with advanced geometry blades p 725 A93-33880

[AIAA PAPER 93-1304]

Full-scale wind tunnel investigation of a helicopter individual blade control system p 726 A93-33929

[AIAA PAPER 93-1361]

A new sensitivity analysis for structural optimization of composite rotor blades p 742 A93-34169

[AIAA PAPER 93-1644]

A modal-based procedure for efficiently predicting low vibration rotor designs p 712 A93-34262

Atmospheric turbulence simulation for rotorcraft applications p 757 A93-34264

Numerical analysis of the three-dimensional boundary layer on a turbomachinery rotor blade p 685 A93-34341

Advanced Technology Blade testing on the XV-15 Tilt Rotor Research Aircraft p 799 A93-36020

Blade twist-design of experiment p 800 A93-36025

Validation of R85/METAR on the Puma RAE flight tests p 802 A93-38597

[ONERA, TP NO. 1992-123]

Study of soft-in-torsion blades - ROSOH operation p 803 A93-38598

[ONERA, TP NO. 1992-124]

The measurement of blade deflections - A new implementation of the strain pattern analysis p 831 A93-38601

[ONERA, TP NO. 1992-127]

Definition and evaluation of new helicopter rotor blade tips p 773 A93-38741

[ONERA, TP NO. 1992-179]

A multibody formulation for helicopter structural dynamic analysis p 892 A93-43776

Investigation of helicopter air resonance in hover by complex coordinates and mutual excitation analysis p 893 A93-43777

Optimization of the blade angle of the AV-2 propeller for improving the flight performance characteristics of An-2 aircraft p 996 A93-45663

Characteristics of deformable leading edge for high performance helicopter rotor p 986 A93-47285

[AIAA PAPER 93-3526]

Navier-Stokes calculations of rotating BERP platform blade flowfields p 986 A93-47286

[AIAA PAPER 93-3527]

Correlation of unsteady pressure and inflow velocity fields of a pitching rotor blade p 1060 A93-48256

[AIAA PAPER 93-3082]

Flow field characteristics of a complex blade tip at high angles of attack p 1060 A93-48257

[AIAA PAPER 93-3083]

Summary of the interaction of a rotor wake with a circular cylinder p 1060 A93-48258

[AIAA PAPER 93-3084]

A method for calculating the aerodynamic and mass characteristics of coaxial rotors with rigid blade fastening (the ABC system) p 1071 A93-49323

Formulas for determining the induced velocity in the direct and inverse rotor problems p 1071 A93-49324

Rotor-rotor interaction for counter-rotating fans. I - Three dimensional flowfield measurements p 1075 A93-49729

[AIAA PAPER 93-1848]

Tip shock structures in transonic compressor rotors p 1075 A93-49744

[AIAA PAPER 93-1869]

An iterative multidisciplinary analysis for rotor blade shape determination p 1114 A93-49912

[AIAA PAPER 93-2085]

Compressor unsteady aerodynamic response to rotating stall and surge excitations p 1079 A93-49914

[AIAA PAPER 93-2087]

Spatial domain characterization of abrupt rotating stall initiation in an axial flow compressor p 1081 A93-50040

[AIAA PAPER 93-2238]

3-dimensional interactions in the rotor of an axial turbine p 1081 A93-50053

[AIAA PAPER 93-2255]

Stator relative, rotor blade-to-blade near wall flow in a multistage axial compressor with tip clearance variation p 1083 A93-50154

[AIAA PAPER 93-2389]

A comparison between numerically modelled and experimentally measured loss mechanisms in wave rotors p 1120 A93-50252

[AIAA PAPER 93-2522]

New approximate method of stress analysis for bladed rotating discs p 1219 A93-54035

[ISABE 93-7059]

Blade loss dynamics of a magnetically supported rotor p 1257 A93-54653

Recent advances in multidisciplinary optimization of rotorcraft p 47 A93-10968

[NASA-TM-107665]

Numerical study of advanced rotor blades p 23 A93-11899

Radial turbine cooling p 130 A93-13292

[NASA-TM-105658]

Influence of cross section variations on the structural behaviour of composite rotor blades p 332 A93-17569

[MBB-UD-0602-91-PUB]

Optimum Design of High Speed Prop-Rotors p 336 A93-18064

[NASA-CR-190915]

Design of high speed propellers using multiobjective optimization techniques p 336 A93-18065

Optimum design of high speed prop rotors including the coupling of performance, aeroelastic stability and structures p 337 A93-18066

An integrated optimum design approach for high speed prop-rotors including acoustic constraints p 893 A93-29153

[NASA-CR-193222]

ROTOR BLADES (TURBOMACHINERY)

Use of NASA LS (1) general aviation airfoil for a small wind turbine - An experience in Denmark p 92 A93-12364

Slicing model for foreign soft-body objects impacting on blade rows p 28 A93-12372

Investigation of compressor rotor wake structure at peak pressure rise coefficient and effects of loading p 246 A93-19292

[ASME PAPER 92-GT-32]

Aerodynamic design of turbomachinery blading in three-dimensional flow - An application to radial inflow turbines p 248 A93-19324

[ASME PAPER 92-GT-74]

Influence of blade aerodynamic loading on efficiency of radial-inflow turbines p 249 A93-19337

[ASME PAPER 92-GT-91]

Unsteady pressure measurements in a rotating centrifugal impeller p 402 A93-19379

[ASME PAPER 92-GT-152]

Computational techniques for probabilistic analysis of turbomachinery p 351 A93-19393

[ASME PAPER 92-GT-167]

An analysis system for blade forced response p 352 A93-19398

[ASME PAPER 92-GT-172]

Heat transfer in rotating serpentine passages with trips skewed to the flow p 403 A93-19416

[ASME PAPER 92-GT-191]

Investigation of rotor blade roughness effects on turbine performance p 354 A93-19487

[ASME PAPER 92-GT-297]

Ingestion into the upstream wheel-space of an axial turbine stage p 354 A93-19493

[ASME PAPER 92-GT-303]

Grid generation for three-dimensional turbomachinery geometries including tip clearance p 270 A93-21658

An interaction noise between vortex and airfoil p 562 A93-24726

[AIAA PAPER 93-0600]

The numerical simulation of the hydrodynamic field from the pump impellers zone by means of the finite element method p 476 A93-26905

Linearized Euler predictions of unsteady aerodynamic loads in cascades p 480 A93-29318

Euler solutions to nonlinear acoustics of non-lifting rotor blades p 568 A93-29433

Dynamics of rotating multicomponent turbomachinery systems p 742 A93-34157

[AIAA PAPER 93-1629]

Optimal open multistep discretization formulas for real-time simulation p 757 A93-34539

Effects of dynamic stall and structural modeling on aeroelastic stability of elastic bending and torsion of hingeless rotor blades with experimental correlation p 794 A93-35902

Aeromechanical stability of helicopters with composite rotor blades in forward flight p 794 A93-35904

Numerical simulation of a hovering rotor using embedded grids p 765 A93-35936

An investigation of helicopter rotor blade flap vibratory loads p 796 A93-35975

Aeroelastic behavior of composite rotor blades with swept tips p 827 A93-35978

Design and manufacturing concepts of Eurofar Model No. 2 blades p 798 A93-35983

A parametric study of real time mathematical modeling incorporating dynamic wake and elastic blades p 798 A93-35986

Helicopter response to atmospheric turbulence p 817 A93-35987

Helicopter rotor disk and Blade Element comparison p 799 A93-35991

Rotor blade airfoil design by numerical optimization and unsteady calculations p 766 A93-35993

[ONERA, TP NO. 1992-65]

A 2-D numerical model for predicting the aerodynamic performance of the NOTAR system tailboom p 766 A93-35994

Hover performance analysis of advanced rotor blades p 767 A93-35998

Nonlinear analysis of composite thin-walled helicopter blades p 827 A93-36006

Experimental and theoretical study for nonlinear aeroelastic behavior of a flexible rotor blade p 837 A93-39422

Aeroelastic response, loads, and stability of a composite rotor in forward flight p 906 A93-41919

Supersonic turbomachine rotor flutter control by aerodynamic detuning p 899 A93-42884

Blade row interaction effects on compressor measurements p 900 A93-42885

Nonlinear large amplitude aeroelastic behavior of composite rotor blades p 997 A93-45741

Analysis of turbine engine rotor containment and shielding structures p 1110 A93-49705

[AIAA PAPER 93-1817]

Some measurements of stall in an axial impeller p 1183 A93-53984

[ISABE 93-7008]

Tip clearance effects on the flow field of an axial turbine rotor blade cascade p 1185 A93-54033

[ISABE 93-7057]

Prediction of viscous flows in rotating machinery using Navier-Stokes techniques p 1232 A93-54639

Rotor/stator flow coupling in turbomachines p 1232 A93-54647

Dynamic analysis of annular cascade structures p 1259 A93-55586

An experimental and analytical study of TIP clearance effects in axial flow compressors p 179 A93-15337

[AD-A256434]

Dynamics of rotating multi-component turbomachinery systems p 421 A93-18426

[NASA-TM-105997]

Endwall flows and blading design for axial flow compressors p 423 A93-18730

Axial Flow Compressors, volume 2 p 423 A93-18731

[VKI-LS-1992-02-VOL-2]

Performance of controlled diffusion blades p 424 A93-18735

Analytic formulation of unsteady profile aerodynamics and its application to simulation of rotors p 485 A93-21659

[ESA-TT-1244]

Unsteady vortex loop/dipole theory applied to the work and acoustics of an ideal low speed propeller p 876 A93-29891

[AD-A264057]

Structural dynamic characteristics of individual blades p 1005 A93-32272

Structural dynamic characteristics of bladed assemblies p 1005 A93-32273

Vibration analysis in turbomachines p 1005 A93-32274

Transmission of sound through a rotor p 1006 A93-32386

[NLR-TP-92014-U]

ROTOR BODY INTERACTIONS

The influence of main design parameters on helicopter air resonance and its source of instability p 154 A93-14261

Experimental and theoretical studies of helicopter rotor-fuselage interaction p 120 A93-14356

[ONERA, TP NO. 1992-142]

The influence of rotor and fuselage wakes on rotorcraft stability and control p 183 A93-14373

Modified sparse time domain technique for rotor stability testing p 157 A93-14593

Experimental study of rotor wake/body interactions in hover p 124 A93-14782

Forcing function effects on unsteady aerodynamic gust response. I - Forcing functions p 251 A93-19400

[ASME PAPER 92-GT-174]

An approach for multi-stage calculations incorporating unsteadiness p 253 A93-19474

[ASME PAPER 92-GT-282]

Euler computations of rotor-stator interaction in turbomachinery cascades using adaptive triangular meshes p 282 A93-23065

[AIAA PAPER 93-0386]

An interaction noise between vortex and airfoil p 562 A93-24726

[AIAA PAPER 93-0600]

Experimental investigation of rotor/lifting surface interactions p 469 A93-24932

[AIAA PAPER 93-0871]

Investigation of methods for modeling propeller-induced flow fields p 469 A93-24935

[AIAA PAPER 93-0874]

- Effect of modeling techniques in the coupled rotor-body vibration analysis
[AIAA PAPER 93-1360] p 710 A93-33928
- Active control of vibratory airloads induced by helicopter rotor-fuselage interactions
[AIAA PAPER 93-1363] p 726 A93-33930
- Multipass three-dimensional Navier-Stokes simulation of turbine rotor-stator interaction
p 688 A93-34484
- The development of the coupled rotor-fuselage model (CRFM)
p 794 A93-35903
- Vortex methods for the computational analysis of rotor/body interaction
p 765 A93-35939
- Three-dimensional calculations of rotor-airframe interaction in forward flight
p 795 A93-35940
- Interaction aerodynamic effects on rotor performance in hover and forward flight
p 766 A93-35941
- Frequency-domain identification of coupled rotor/body models of an advanced attack helicopter
p 816 A93-35960
- Spectral analysis of unsteady surface pressure on a pusher propeller
p 1232 A93-54646
- An experimental and a theoretical investigation of rotor pitch damping using a model rotor
p 47 A93-10322
- Contributions to the experimental investigation of rotor/body aerodynamic interactions
p 20 A93-10877
- Developing a control system for ARES 2
p 371 A93-16769
- Aeroelastic response and aeromechanical stability of helicopters with elastically coupled composite rotor blades
p 715 A93-25530
- ROTOR DYNAMICS**
- Dynamics of a high-rpm compressor
p 75 A93-10009
- A method for optimizing the meridional passage in a centrifugal compressor
p 204 A93-14483
- Optimum balancing of flexible rotor
p 205 A93-14489
- Hybrid real-time simulation of a two-rotor engine
p 172 A93-14497
- A minimum-time acceleration control strategy for a two-rotor aeroengine
p 172 A93-14499
- A design study on the effect of support and system parameters on the natural frequencies of rotor systems
p 210 A93-16374
- A study on stability and response analysis of a nonlinear rotor system with mass unbalance and side load
[ASME PAPER 92-GT-7] p 400 A93-19280
- Computational techniques for probabilistic analysis of turbomachinery
[ASME PAPER 92-GT-167] p 351 A93-19393
- Recent advances in integrated multidisciplinary optimization of rotorcraft
[AIAA PAPER 92-4777] p 325 A93-20369
- A generic harmonic rotor model for helicopter flight simulation
p 506 A93-27480
- Dynamics of rotating multicomponent turbomachinery systems
[AIAA PAPER 93-1629] p 742 A93-34157
- Dynamics of a high speed impeller - Analysis and experimental verification
[AIAA PAPER 93-1362] p 743 A93-34239
- The development of the coupled rotor-fuselage model (CRFM)
p 794 A93-35903
- Overview of Tiger dynamics validation program
p 794 A93-35907
- Effects on load distribution in a helicopter rotor support structure associated with various boundary configurations
p 796 A93-35951
- Evaluation of tilt rotor aircraft design utilizing a realtime interactive simulation
p 798 A93-35989
- Helicopter rotor disk and Blade Element comparison
p 799 A93-35991
- Environmental conditions for certification testing of helicopter advanced composite main rotor components
p 824 A93-36003
- Digital resolver for helicopter model blade motion analysis
p 830 A93-37878
- Numerical calculation of helicopter rotor equations and comparison with experiment
[ONERA, TP NO. 1992-128] p 772 A93-38602
- Optimal design of centered squeeze film dampers
p 831 A93-38629
- Linear quadratic Gaussian/loop transfer recovery design for a helicopter in low-speed flight
p 906 A93-41896
- Influence of stator-rotor gap on axial-turbine unsteady forcing functions
p 899 A93-41918
- A multibody formulation for helicopter structural dynamic analysis
p 892 A93-43776
- Two-dimensional CFD modeling of wave rotor flow dynamics
[AIAA PAPER 93-3318] p 952 A93-45014
- Frontally tapered squared trench casing treatment for improvement of compressor performance
p 1108 A93-49202

- Rotor wake/stator interaction noise - Predictions vs data
p 1174 A93-52447
- The effects of fixed rotor tilt on the rotordynamic coefficients of incompressible flow annular seals
p 1161 A93-52601
- Rotating machinery - Dynamics; Proceedings of the 3rd International Symposium on Transport Phenomena and Dynamics of Rotating Machinery (ISROMAC-3), Honolulu, HI, Apr. 1-4, 1990
[ISBN 1-56032-147-4] p 1257 A93-54651
- Blade loss dynamics of a magnetically supported rotor
p 1257 A93-54653
- Effects of foundation excitation on multiple rub interactions in turbomachinery
p 1260 A93-55996
- An experimental and a theoretical investigation of rotor pitch damping using a model rotor
p 47 A93-10322
- Compressible and incompressible fluid seals: Influence on rotordynamic response and stability
[NASA-CR-190746] p 85 A93-10891
- Recent advances in multidisciplinary optimization of rotorcraft
[NASA-TM-107665] p 47 A93-10968
- Optimal output feedback vibration control of rotor-bearing systems
p 86 A93-11220
- New rotor trim and balance system for helicopter usage monitoring
p 169 A93-15180
- Optimum Design of High Speed Prop-Rotors
[NASA-CR-190915] p 336 A93-18064
- Dynamics of rotating multi-component turbomachinery systems
[NASA-TM-105997] p 421 A93-18426
- Analytic formulation of unsteady profile aerodynamics and its application to simulation of rotors
[ESA-TT-1244] p 485 A93-21659
- Application of finite-state inflow to flap-lag-torsion damping in hover
p 714 A93-25486
- Active magnetic bearings applied to industrial compressors
p 841 A93-27570
- The influence of variable flow velocity on unsteady airfoil behavior
[DLR-FB-92-22] p 988 A93-31320
- Structural dynamic characteristics of individual blades
p 1005 A93-32272
- Structural dynamic characteristics of bladed assemblies
p 1005 A93-32273
- Vibration analysis in turbomachines
p 1005 A93-32274
- ROTOR LIFT**
- Aerodynamic characteristics of a rotorcraft airfoil designed for the tip region of a main rotor blade
[NASA-TM-4264] p 876 A93-29450
- Definition of an airfoil family for the EUROFAIR rotor
[DLR-FB-92-04] p 998 A93-31197
- ROTOR SPEED**
- Brush seal leakage performance with gaseous working fluids at static and low rotor speed conditions
[ASME PAPER 92-GT-304] p 405 A93-19494
- Far-field hover acoustic characteristics of the XV-15 tiltrotor aircraft with Advanced Technology Blades
p 566 A93-29412
- Formulas for determining the induced velocity in the direct and inverse rotor problems
p 1071 A93-49324
- Benefits of variable rotor speed in integrated helicopter/engine control
[AIAA PAPER 93-3851] p 1134 A93-51438
- Blade loss dynamics of a magnetically supported rotor
p 1257 A93-54653
- An experimental and a theoretical investigation of rotor pitch damping using a model rotor
p 47 A93-10322
- An exploratory investigation of the flight dynamics effects of rotor rpm variations and rotor state feedback in hover
[NASA-TM-103968] p 373 A93-19380
- ROTORCRAFT AIRCRAFT**
- A robust direct-integration method for rotorcraft maneuver and periodic response
p 61 A93-10919
- Advanced technology Tilt Wing study
[AIAA PAPER 92-4237] p 44 A93-13359
- Rotorcraft reliability and maintainability: Future design requirements; Proceedings of the Conference, London, United Kingdom, Mar. 20, 1991
[ISBN 0-903409-88-7] p 45 A93-13401
- The military operator's experience of reliability and maintainability characteristics
p 80 A93-13403
- Rotorcraft reliability and maintainability - A CAA view of future trends
p 45 A93-13407
- The influence of rotor and fuselage wakes on rotorcraft stability and control
p 183 A93-14373
- Tailoring concepts for improved structural performance of rotorcraft flexbeams
p 207 A93-14811
- The use of interferometry in the study of rotorcraft aerodynamics
p 407 A93-19914
- Recent advances in integrated multidisciplinary optimization of rotorcraft
[AIAA PAPER 92-4777] p 325 A93-20369
- Flight simulator fidelity assessment in a rotorcraft lateral translation maneuver
p 378 A93-23510

- Time-variant analysis of rotorcraft systems dynamics - An exploitation of vector processors
p 416 A93-23512
- Parallel rotorcraft flight simulation
[AIAA PAPER 93-0623] p 524 A93-24740
- CST and rotorcraft - Expanding the view
p 560 A93-25085
- A fast algorithm for image-based ranging
p 544 A93-27045
- AHS National Technical Specialists' Meeting on Rotorcraft Structures, Williamsburg, VA, Oct. 29-31, 1991, Proceedings
p 506 A93-27951
- Application of a two-point exponential approximation method in optimizing rotorcraft airframe structures
p 507 A93-27956
- The development and evaluation of advanced Kevlar sandwich structure for application to rotorcraft airframes
p 546 A93-27965
- Conceptual assessment of two high-speed rotorcraft
p 508 A93-28612
- ADDRAS - An integrated systems approach
p 562 A93-29423
- Experimental study of a single strong vortex-airfoil interaction
p 481 A93-29432
- An overview on practical application of helicopter noise certification rules
p 487 A93-29442
- Atmospheric turbulence simulation for rotorcraft applications
p 757 A93-34264
- New European regulations for rotorcraft; Proceedings of the Conference, London, United Kingdom, Mar. 16, 1993
[ISBN 1-85768-085-5] p 701 A93-34616
- The criticalness of spares effectivity checks for aircraft configuration control
p 763 A93-35923
- A Taguchi analysis of helicopter maneuverability and agility
p 763 A93-35944
- On design and optimization of curved composite beams
p 826 A93-35953
- Handling qualities testing using the mission oriented requirements of ADS-33C
p 817 A93-35961
- Predicting rotorcraft transmission noise
p 850 A93-35968
- Coupled rotor fuselage mode shapes - A tool in understanding helicopter response
p 797 A93-35977
- Flap-lag damping in hover and forward flight with a three-dimensional wake
p 797 A93-35979
- Evaluation of thermoplastic stiffened panels for application to rotorcraft airframes
p 827 A93-36000
- Technologies for automating rotorcraft nap-of-the-earth flight
p 885 A93-43784
- Low-speed wind tunnel test results of the Canard Rotor/Wing concept
[AIAA PAPER 93-3412] p 975 A93-47209
- Vision based techniques for rotorcraft low altitude flight
p 1097 A93-49351
- Desirable characteristics for rotorcraft optical components
p 1172 A93-49468
- Electro-optical navigation for aircraft
p 1097 A93-50643
- Clustering methods for removing outliers from vision-based range estimates
p 1171 A93-51648
- Design for manufacture by resin transfer molding of composite parts for rotorcraft
[SME PAPER EM93-103] p 1159 A93-51733
- An advanced rotorcraft flight simulation model - Parallel implementation and performance analysis
[AIAA PAPER 93-3550] p 1222 A93-52654
- Removing the risk from rotorcraft testing
p 1192 A93-53772
- Recent advances in multidisciplinary optimization of rotorcraft
[NASA-TM-107665] p 47 A93-10968
- Robust crossfeed design for hovering rotorcraft
[NASA-CR-193107] p 805 A93-27241
- An integrated optimum design approach for high speed prop-rotors including acoustic constraints
[NASA-CR-193222] p 893 A93-29153
- Design and implementation of fuzzy logic controllers
[NASA-CR-193268] p 1038 A93-31649
- ROTORS**
- Vibration control algorithms for flexible rotors
p 95 A93-10741
- Optimal vibration control for a flexible rotor with gyroscopic effects
p 98 A93-13420
- On dynamic behavior of cracked rotors
p 208 A93-15401
- A design study on the effect of support and system parameters on the natural frequencies of rotor systems
p 210 A93-16374
- Acoustic performance of low pressure axial fan rotors with different blade chord length and radial load distribution
p 449 A93-19212
- Low aspect ratio transonic rotors. I - Baseline design and performance
[ASME PAPER 92-GT-185] p 352 A93-19410

Optimum design of rotor-bearing systems with eigenvalue constraints
[ASME PAPER 92-GT-307] p 405 A93-19497

An improved numerical model for wave rotor design and analysis
[AIAA PAPER 93-0482] p 361 A93-23384

The effectiveness of porous squeeze film dampers for suppressing nonsynchronous motions
p 545 A93-27316

Introduction of the M-85 high-speed rotorcraft concept
p 797 A93-35980

Modal analysis of multistage gear systems coupled with gearbox vibrations
p 827 A93-36588

Experimental evaluation of a cooled radial-inflow turbine
p 1110 A93-49685

Three-dimensional numerical simulation of gradual opening in a wave rotor passage
[AIAA PAPER 93-2526] p 1156 A93-50254

Brush seal low surface speed hard-rub characteristics
[AIAA PAPER 93-2534] p 1156 A93-50261

Identification of nonlinear mechanical systems using combined state and parameter evaluation
p 1224 A93-52732

Initial results from the NASA Lewis wave rotor experiment
[AIAA PAPER 93-2521] p 1193 A93-53589

Rotor fatigue monitoring data acquisition system
p 1261 A93-54353

A data acquisition system for high-speed rotor balancing
p 1261 A93-54396

The use of beam-like modal data for stiffness profile estimation by the EBS method. I - Justification and implementation --- Equivalent Beam Stiffness
p 1257 A93-54649

A study upon structural optimization of elastic rotors for mechanical systems
[INPE-5376-TDI/471] p 83 A93-10310

An experimental and a theoretical investigation of rotor pitch damping using a model rotor
p 47 A93-10322

Experimental heat transfer results in turbine stators and rotors and a comparison with theory
[PNR-90945] p 57 A93-11055

System and method for cancelling expansion waves in a wave rotor
[NASA-CASE-LEW-15218-1] p 86 A93-11172

Optimal output feedback vibration control of rotor-bearing systems
p 86 A93-11220

Stochastic sensitivity measure for mistuned high-performance turbines
p 90 A93-12277

[NASA-TM-105821] p 90 A93-12277

An improved numerical model for wave rotor design and analysis
[NASA-TM-105915] p 60 A93-12418

Investigation of hot streak migration and film cooling effects on heat transfer in rotor/stator interacting flows, report 1
[AD-A250688] p 102 A93-12490

User's Guide for the NREL Teetering Rotor Analysis Program (STRAP)
[DE92-010580] p 216 A93-13525

Online vibration control of a flexible rotor-bearing system
p 219 A93-14468

Rotating stall inception in fans of low hub-tip ratio
p 136 A93-14479

Onboard System Evaluation of Rotors Vibration, Engines (OBSERVE) monitoring system
[AD-A255366] p 165 A93-15227

An experimental and analytical study of TIP clearance effects in axial flow compressors
[AD-A256434] p 179 A93-15337

Prediction of turbine cascade flows with a quasi-three-dimensional rotor viscous code and the extension of the algebraic turbulence model
[AD-A256831] p 223 A93-15635

Brush seal bristle flexure and hard-rub characteristics
[NASA-TM-105864] p 421 A93-18321

A discussion of the results of the rainfall counting of a wide range of dynamics associated with the simultaneous operation of adjacent wind turbines
[DE93-000016] p 434 A93-18705

Mass loaded composite rotor for vibro-acoustic application
[AD-D015604] p 535 A93-20016

Stochastic finite element analysis for high speed rotors
p 554 A93-20696

The influence of the rotor test facilities ROTEST and ROTOS on the rotor inflow
[DLR-MITT-91-16] p 522 A93-21173

Variable-speed generators with flux weakening
p 750 A93-25599

Far field rotor noise
[AD-A260703] p 759 A93-25651

Radial inflow turbine study
[AD-A260767] p 724 A93-25917

Helicopter forced response vibration analysis method RTVIB20
[AD-A261809] p 730 A93-26260

Brush seal low surface speed hard-rub characteristics
[NASA-TM-106169] p 838 A93-27132

Experimental evaluation of a cooled radial-inflow turbine
[NASA-TM-106230] p 816 A93-28697

Use of local x ray computerized tomography for high-resolution, region-of-interest inspection of large ceramic components for engines
[DE93-005564] p 843 A93-28943

Three-dimensional numerical simulation of gradual opening in a wave rotor passage
[NASA-CR-191157] p 900 A93-29072

Robust control of intelligent rotor
[AD-A263707] p 909 A93-29985

Some implications of a differential turbomachinery equation with viscous correction
[AD-A264693] p 935 A93-30571

Penn State axial flow turbine facility: Performance and nozzle flow field
p 1032 A93-31588

Initial results from the NASA-Lewis wave rotor experiment
[NASA-TM-106148] p 1005 A93-32368

ROUGHNESS
Aerodynamic degradation due to distributed roughness on high lift configuration
[AIAA PAPER 93-0028] p 260 A93-20146

ROUTES
Scheduling of an aircraft fleet
p 443 A93-18665

An investigation of discovery-based learning in the route planning domain
[AD-A259141] p 513 A93-20560

Effect of personal and situational variables on noise annoyance: With special reference to implications for en route noise
[NASA-CR-189676] p 569 A93-21317

An analysis of en route controller-pilot voice communications
[AD-A264784] p 935 A93-30611

RUBBER
Method and apparatus for cleaning rubber deposits from airport runways and roadways
[NASA-CASE-LAR-14483-1] p 556 A93-22035

RUDDERS
Rudder and elevator effects on the incipient spin characteristics of a typical general aviation training aircraft
[AIAA PAPER 93-0016] p 367 A93-20138

The Boeing 747-400 upper rudder control system with triple tandem valve
[SAE PAPER 912133] p 327 A93-21843

RULES
Magnetic variation - A primitive concept and its hold on contemporary navigation
p 32 A93-11021

RUN TIME (COMPUTERS)
Accuracy and efficiency assessments for a weak statement CFD algorithm for high-speed aerodynamics
[ASME PAPER 92-GT-433] p 435 A93-19576

Enhancing real-time flight simulation execution by intercepting Run-Time Library calls
[AIAA PAPER 93-3591] p 1224 A93-52684

A model for determining task set schedulability in the presence of system effects
[AD-A258915] p 443 A93-19338

RUNGE-KUTTA METHOD
A split-matrix Runge-Kutta type space marching procedure
p 8 A93-11921

Accuracy and efficiency assessments for a weak statement CFD algorithm for high-speed aerodynamics
[ASME PAPER 92-GT-433] p 435 A93-19576

Accurate solution of the 2D Euler equations with an efficient cell-vertex upwind scheme
[AIAA PAPER 93-0071] p 262 A93-20183

Application of high-order accurate essentially nonoscillatory schemes to two-dimensional compressible viscous flows
[AIAA PAPER 93-0879] p 470 A93-24940

Adaptive mesh embedding for reentry flow problems
p 869 A93-42619

A multiblock, multigrid solution procedure for multielement airfoils
p 967 A93-46812

Computation of passively controlled transonic wing
[AIAA PAPER 93-3474] p 981 A93-47253

Analysis of wing-body junction flowfields using the incompressible Navier-Stokes equations, volumes 1 and 2
p 17 A93-10320

Nonlinear aeroelasticity of composite structures
[AD-A254285] p 47 A93-10842

Investigation of advanced counterrotation blade configuration concepts for high speed turboprop systems. Task 5: Unsteady counterrotation ducted propfan analysis. Computer program user's manual
[NASA-CR-187125] p 521 A93-20583

Investigation of advanced counterrotation blade configuration concepts for high speed turboprop systems. Task 5: Unsteady counterrotation ducted propfan analysis
[NASA-CR-187126] p 521 A93-20773

Development of an unstructured solution adaptive method for the quasi-three-dimensional Euler and Navier-Stokes equations
[NASA-CR-193241] p 930 A93-29213

Solution of Euler equations for forebody-inlet ensemble of aircraft at high angle of attack
[AD-A263905] p 876 A93-29862

The application of concentric vortex simulation to calculating the aerodynamic characteristics of bodies of revolution at high angles of attack
[AD-A263879] p 876 A93-29919

RUNWAY CONDITIONS
The state-of-the-art of nondestructive evaluation of military runways
p 375 A93-19659

Integrated runway meteorological observation system (IRMOS/SIOMA)
p 428 A93-22128

Ice prediction systems for runways
p 376 A93-22174

Some aspects of the design of combination landing gear --- for stable aircraft motion on runways
p 891 A93-42374

Determination of the vertical velocity component of aircraft landing on an airfield with a longitudinally sloping runway
p 1007 A93-45664

Characteristics of the detection of overloads in the center of mass of Il-76 and An-12 aircraft due to runway irregularities by a standard on-board recorder
p 1008 A93-45666

Operating an aircraft during the landing on an airfield with a substantial longitudinal macroslope of the runway
p 1008 A93-45667

Aircraft monitoring of the planeness of the existing and new runways
p 991 A93-45668

Using spectral analysis for estimating the effect of runway irregularities on the loading of transport aircraft structures
p 996 A93-45669

Effect of wet snow on the null-reference ILS system
p 1097 A93-50660

NASA Langley's Aircraft Landing Dynamics Facility
p 1250 A93-54400

RUNWAY LIGHTS
Ground visual aids - Recent research at RAE Bedford
p 191 A93-17311

The application of automatic surface lights to improve airport safety
p 821 A93-37069

RUNWAYS
Fracture of highway and airport pavements
p 547 A93-28290

Noise-induced reaction in a work community adjacent to aircraft runways - The Royal Australian Airforce
p 559 A93-28496

Upgrade Precision Runway Monitor (PRM) Operational Test and Evaluation (OT/E) test plan
[DOT/FAA/CT-TN92/13] p 67 A93-11616

Automated extraction of aircraft runway patterns from radar imagery
[AD-A254258] p 68 A93-11751

Limited production Precision Runway Monitor (PRM) master test plan
[DOT/FAA/CT-TN92/23] p 192 A93-12899

Prototype stop bar system evaluation at John F. Kennedy International Airport
[AD-A258667] p 192 A93-12902

A NASPAC-based analysis of the delay and cost effects of the Dallas/Fort Worth metroplex plan
[DOT/FAA/CT-TN92/21] p 193 A93-13447

Unified Airport Design and Analysis Concepts Workshop
[DOT/FAA/RD-92/17] p 378 A93-16309

State of the art of airport pavement analysis and design
p 378 A93-16310

Development of user guidelines for a three-dimensional finite element pavement model
p 379 A93-16311

Micro mechanical behavior of pavements
p 379 A93-16312

Federal Aviation Administration pavement modeling
p 379 A93-16315

An experimental examination of the thermal and acoustic environments on runway joint seals
[AD-A257965] p 382 A93-17734

ILS mathematical modeling study of an ILS glide slope proposed for runway 19L at the Meridian Naval Air Station, Mississippi
[DOT/FAA/CT-TN93/8] p 705 A93-24741

Runway Visual Range (RVR) Operational Test and Evaluation (OT&E) integration and OT&E operational test report
[DOT/FAA/CT-TN92/37] p 706 A93-25243

The dependent converging instrument approach procedure: An analysis of its safety and applicability
[DOE/FAA/RD-93/6] p 707 A93-25456

- Expedient repair of structural facilities
[AD-A260727] p 731 N93-25656
- Protection of taxiing traffic in airports through mode S secondary radar technology
[ETN-93-93455] p 791 N93-28206
- Two simulation studies of precision runway monitoring of independent approaches to closely spaced parallel runways
[AD-A263433] p 911 N93-29815
- Land subsidence and problems affecting land use at Edwards Air Force Base and vicinity, California, 1990
[PB93-182236] p 1036 N93-32191

S

S WAVES

- Jet mixer noise suppressor using acoustic feedback
[NASA-CASE-LEW-15170-1] p 853 N93-28953

SAAB AIRCRAFT

- Saab 2000 - An exercise in growth and commonality
p 505 A93-25357
- Speed, range boost Saab 2000's appeal
p 505 A93-25495
- The SAAB 2000 initial flight test - Status report
p 804 A93-38847
- Modal measurements and propeller field excitation on acoustic full scale mockup of SAAB 340 aircraft
[FFA-TN-1992-08] p 1039 N93-31051

SABOT PROJECTILES

- Analysis and demonstration of a Scramaccelerator system
[AIAA PAPER 93-2183] p 1142 A93-49995

SACCADIC EYE MOVEMENTS

- Air traffic control visual scanning
[DOT/FAA/CT-TN92/16] p 35 N93-10459

SAFETY

- A PC-based simulation of the National Transonic Facility's safety microprocessor
[NASA-TM-109003] p 1038 N93-32224

SAFETY DEVICES

- The methods of reducing impact loads on occupants in the civil aircraft crash condition p 140 A93-14220
- An approach to evaluating reactive airborne wind shear systems p 489 N93-19600
- RDR-4B doppler weather radar with forward looking wind shear detection capability p 489 N93-19601
- The 1992 International Aerospace and Ground Conference on Lightning and Static Electricity: Addendum
[DOT/FAA/CT-92/20-ADD-1] p 753 N93-24875
- Zoning of aircraft: A review of the definitions
p 703 N93-24880
- Comparison of the damage for various types of fibre reinforced composites due to different lightning test standards (MIL-STD-1757A, German military VG-standard 96903) p 736 N93-24891
- A single-point warning system for thunderstorms and electric fields p 747 N93-24900

SAFETY FACTORS

- Vision based techniques for rotorcraft low altitude flight p 1097 A93-49351
- The dependent converging instrument approach procedure: An analysis of its safety and applicability
[DOE/FAA/RD-93/6] p 707 N93-25456

SAFETY MANAGEMENT

- Maintaining the safety of an aging fleet of aircraft
p 3 A93-13632
- Progress and taboos in air safety orientations of research in human factors in air transport p 141 A93-14374
- Aero engine reliability, integrity and safety; Proceedings of the Conference, Bristol, United Kingdom, Oct. 17, 18, 1991
[ISBN 0-903409-70-4] p 345 A93-18778
- Safety through integrity and reliability --- for passenger and military aircraft p 239 A93-18779
- Reliability and safety considerations in engine management systems design p 346 A93-18786
- Hand-held cabin fire extinguishers - Transport aircraft
[SAE ARP 4712] p 1096 A93-52168
- The probable cause --- aircraft accidents
p 1240 A93-56417
- Introduction to the Rolls-Royce design process
[PNR-90939] p 57 N93-11039
- Aviation safety research at the National Institute for Aviation Research Wichita State University: A report to the FAA Technical Center
[NIAR-92-2] p 310 N93-16455
- Special investigation report: Flight attendant training and performance during emergency situations
[PB92-917006] p 310 N93-16834

SAGNAC EFFECT

- The LN-200 fiber gyro based tactical grade IMU
[AIAA PAPER 93-3798] p 1106 A93-51391

SAILS

- A sensitivity analysis of the stability of a tug-rope-sailplane system p 184 A93-14400

SALINITY

- Study on aircraft microwave remote sensing of sea-water surface salinity p 92 A93-12407

SALT SPRAY TESTS

- Accelerated and real-time corrosion testing of aluminum-lithium alloys
[NLR-TP-91203-U] p 1020 N93-32385

SAMPLING

- Development and testing of the digital control system for the Archytas unmanned air vehicle
[AD-A261656] p 729 N93-26196

SAND CASTING

- X-ray computed tomography for casting development
[AD-A261786] p 752 N93-26526

SANDS

- The chemistry of Saudi Arabian sand - A deposition problem on helicopter turbine airfoils p 1216 A93-53468
- Environmental effects of operations during Desert Shield/Desert Storm p 1190 A93-54291
- The T700 ... from salt spray to sand blast p 1205 A93-54292
- Physical effects of vegetation on wind-blown sand in the coastal environments of Florida
[PB92-188424] p 93 N93-11702

SANDWICH STRUCTURES

- Iterative temperature calculation method for rectangular sandwich panel fins p 76 A93-10667
- Choice of materials for military helicopters p 158 A93-15028
- Sandwich construction in the Starship p 159 A93-15737
- Computer-aided cure optimization p 209 A93-15804
- Photoelastic stress analysis of skewed cutout in a sandwich skew plate subjected to inplane and transverse eccentric load p 210 A93-16604
- The development and evaluation of advanced Kevlar sandwich structure for application to rotorcraft airframes p 546 A93-27965
- Development and fabrication of an autoclave molded PES/Quartz sandwich radome p 547 A93-28279
- Optimal design of honeycomb sandwich shell aircraft structures of composite materials p 828 A93-36800
- Calculation of sandwich plates with polymer composite skins under conditions of high humidity p 1215 A93-52968
- Optimization of sandwich structures with respect to local instabilities with MBB-LAGRANGE p 1255 A93-54540
- Stress calculations on the window section of an all-composite aircraft fuselage
[LR-688] p 328 N93-16215
- Optimization of composite sandwich cover panels subjected to compressive loadings p 922 N93-30862

SATELLITE ANTENNAS

- New concepts in remote sensing and geolocation
p 556 A93-24173

SATELLITE COMMUNICATION

- Capacity as a consideration for providing aeronautical mobile satellite air traffic services in the U.S. domestic airspace p 30 A93-11007
- The Tenth Conference on Air Navigation - A landmark in the history of civil aviation p 34 A93-12559
- Applications of space techniques to civil aviation operations p 312 A93-20007
- Decision making for a public differential GPS service p 314 A93-21165
- Communication satellites for commercial aircraft operations p 499 A93-25493
- Propagation results of aeronautical satellite communication experiments using INMARSAT satellite p 533 A93-29607
- Pilot weather advisor
[NASA-CR-189723] p 318 N93-16692
- A simulation study of the effects of communication delay on air traffic control
[AD-A258593] p 502 N93-19966
- Satellite communications for aeronautical and navigation service p 838 N93-26648
- Engineering management consideration for an integrated aeronautical mobile satellite service p 933 N93-30337

SATELLITE DESIGN

- New concepts in remote sensing and geolocation
p 556 A93-24173
- International aviation (Selected articles)
[AD-A262566] p 765 N93-28576

SATELLITE DRAG

- The representation of the aerodynamic torque in simulations of a spacecraft rotary motion p 1141 A93-48835
- Aeronomy coexperiments on drag-free satellites with proportional thrusters: GP-B and STEP p 195 N93-13922

SATELLITE IMAGERY

- Distribution of aviation weather graphics via airline communications networks p 426 A93-22113
- Remote sensing of volcanic ash hazards to aircraft p 556 A93-24213

SATELLITE INSTRUMENTS

- Satellite navigation in traffic management p 914 A93-43549
- Analytical study on the separation dynamics of LUNAR-A/penetrator p 1265 A93-56272

SATELLITE LIFETIME

- Progress towards joint civil use of GPS and GLONASS p 29 A93-10977

SATELLITE NAVIGATION SYSTEMS

- Precision navigation with an integrated navigation system p 29 A93-10782
- Progress towards joint civil use of GPS and GLONASS p 29 A93-10977
- Civil standardization of the Global Positioning System for the aviation community p 29 A93-10981
- Automatic dependant surveillance focus of civil avionics integration p 30 A93-10998
- Real time DGPS service for precise positioning - Activities in the Federal Republic of Germany p 1 A93-11027
- Receiver autonomous integrity monitoring (RAIM) capability for sole-means GPS navigation in the oceanic phase of flight p 33 A93-11035
- LOCSTAR - A satellite radiodetermination system for Europe p 150 A93-15037
- The applications, benefits, and issues of employing GPS and Glonass with Automatic Dependent Surveillance p 316 A93-21188
- Automatic Dependent Surveillance capacity of a geostationary satellite system in the U.S. domestic airspace p 316 A93-21192
- Data communication for airborne differential GPS/GLONASS application p 499 A93-27910
- The high accuracy applications of the GPS system to static positioning p 500 A93-28193
- GNSS - A global system of satellite-aided navigation p 500 A93-28194
- The use of satellites for aeronautical communications, navigation and surveillance p 881 A93-40436
- Navstar global positioning system: Introduction and status p 318 N93-17559
- A model of Global Positioning System (GPS) Master Control Station (MCS) operations
[AD-A258846] p 320 N93-19067
- An experimental health monitoring unit for GPS and GLONASS p 706 N93-25018
- Aerial cartography using SICAD NAV-AIR p 1034 N93-31258

SATELLITE NETWORKS

- GNSS - A global system of satellite-aided navigation p 500 A93-28194

SATELLITE OBSERVATION

- Spatial and temporal variations of the fluxes of carbon dioxide and sensible and latent heat over the FIFE site p 425 A93-20586
- A comparison of wind speed measured by the Special Sensor Microwave Imager (SSM/I) and the Geosat altimeter p 1033 A93-44862
- Calibration results for NOAA-11 AVHRR channels 1 and 2 from congruent path aircraft observations p 1143 A93-51237
- Proceedings of the National Weather Service Aviation Workshop: Postprint volume
[PB92-176148] p 94 N93-11803

SATELLITE ORBITS

- The representation of the aerodynamic torque in simulations of a spacecraft rotary motion p 1141 A93-48835

SATELLITE ROTATION

- The representation of the aerodynamic torque in simulations of a spacecraft rotary motion p 1141 A93-48835

SATELLITE TRACKING

- GPS integrity monitoring and system improvement with ground station and multistationary satellite support p 33 A93-11044
- The use of satellite geometry for prevention of cycle slips in a GPS processor p 34 A93-11298
- The application of phase tracking GPS for flight test trajectory determination
[NLR-TP-91349-U] p 994 N93-32337

SATELLITE TRANSMISSION

- Satcom Pacific Ocean trials p 501 A93-28198
- Fiber optics for aircraft entertainment systems p 1172 A93-49478

SATELLITE-BORNE INSTRUMENTS

- Bistatic radar using satellite-borne illuminators of opportunity p 914 A93-43437

SUBJECT INDEX

- Calibration results for NOAA-11 AVHRR channels 1 and 2 from congruent path aircraft observations
p 1143 A93-51237
- SAUDI ARABIA**
The chemistry of Saudi Arabian sand - A deposition problem on helicopter turbine airfoils
p 1216 A93-53468
- SCALARS**
A multi-dimensional upwind scheme for the Euler equations on structured grids
p 862 A93-42430
- SCALE (RATIO)**
Using ultralight flight vehicles for large-scale aerial photography
p 92 A93-10098
- SCALE EFFECT**
Scaling of the two-phase flow downstream of a gas turbine combustor swirl cup - Mean quantities
[ASME PAPER 92-GT-207] p 404 A93-19431
- SCALE MODELS**
Hemispherical and spherical flow parameter detectors
p 75 A93-10044
Investigation of leading edge ice accretion with cyclical pneumatic boot inflation
[AIAA PAPER 93-0007] p 306 A93-20130
Potential aircraft hazards in the vicinity of convective clouds - A review from the perspective of a scale-model study
p 427 A93-22116
Construction of a one-third scale model of the NASP
[AIAA PAPER 93-0427] p 386 A93-23345
Measured acoustic characteristics of ducted supersonic jets at different model scales
[AIAA PAPER 93-0731] p 563 A93-24821
A wind tunnel investigation of the pressure distribution on an F/A-18 wing
[AIAA PAPER 93-3468] p 980 A93-47249
Experimental study of 3-D separation on a large scale model
[AIAA PAPER 93-3007] p 1053 A93-48197
Simulation of hypersonic flight - A concerted European effort
p 1136 A93-49301
Low speed test results of subsonic, turbofan scarf inlets
[AIAA PAPER 93-2301] p 1082 A93-50086
Scale model test results for several spherical/two-dimensional nozzle concepts
[AIAA PAPER 93-2430] p 1117 A93-50186
Semi-full-scale dynamic simulation complex on the basis of centrifuge
[AIAA PAPER 93-3577] p 1208 A93-52673
Instrumentation and telemetry systems for free-flight drop model testing
p 1209 A93-52754
Evaluation of turbofanjet exhaust systems from scale model test data
[ISABE 93-7109] p 1204 A93-54085
Observation of fluctuation of 2D-nozzle flows
[ISABE 93-7110] p 1204 A93-54086
Aerodynamic characteristics of a semibuoyant station in the shape of a torus
[AIAA PAPER 93-4034] p 1231 A93-54615
Low-speed longitudinal and lateral-directional aerodynamic characteristics of the X-31 configuration
[NASA-TM-4351] p 22 A93-11622
ASTOVL model engine simulators for wind tunnel research
p 192 A93-13213
An investigation of jet engine test cell aerodynamics by means of scale model test studies with comparisons to full-scale test results
p 193 A93-14060
Investigations of detail design issues for the high speed acoustic wind tunnel using a 60th scale model tunnel. Part 1: Tests with open circuits
[NASA-CR-191671] p 137 A93-14737
Investigations of detail design issues for the high speed acoustic wind tunnel using a 60th scale model tunnel. Part 2: Tests with the closed circuit
[NASA-CR-191672] p 137 A93-14738
Prediction of the performances in combustion of ramjets and stato-rockets by isothermal experiments and modeling
p 363 A93-17622
Operational and research aspects of a radio-controlled model flight test program
[NASA-TM-104266] p 339 A93-18616
Improved ceramic slip casting technique --- application to aircraft model fabrication
[NASA-CASE-LAR-14471-1] p 536 A93-20041
A model study of the aircraft cabin environment resulting from in-flight fires
[DOT/FAA/CT-90/22] p 496 A93-21557
Construction, wind tunnel testing and data analysis for a 1/5 scale ultra-light wing model
p 876 A93-29778
- SCALING LAWS**
Scaling of incipient separation in high speed laminar flows
[AIAA PAPER 93-3435] p 978 A93-47227
Some aspects of the aeroacoustics of high-speed jets
[NASA-CR-191458] p 843 A93-28975

SCANDINAVIA

- Experiences with two GPS receivers in northern Europe
[NLR-TP-91168-U] p 993 A93-31120

SCANNERS

- Large-area aircraft scanner
p 407 A93-19693
Scanning Laser Aircraft Surveillance System for carrier flight operations
p 500 A93-26157
Wind tunnel operator aimed comparison between two electronic pressure scanner systems
p 830 A93-37876
Wind tunnel operator aimed comparison between two electronic pressure scanner systems
[DLAS-EST-TR-040] p 67 A93-11225

SCANNING

- Introduction of electronic pressure scanning at the Royal Aerospace Establishment
[RAE-TM-AERO-2222] p 23 A93-11882

SCANNING ELECTRON MICROSCOPY

- Material characterization and fractographic examination of Ti-17 fatigue crack growth specimens for SMP SC33
p 1004 A93-31744

SCARFING

- High speed test results of subsonic, turbofan scarf inlets
[AIAA PAPER 93-2302] p 1082 A93-50087

SCENE ANALYSIS

- Visual augmentation for night flight over featureless terrain
p 806 A93-35921
Image-based ranging and guidance for rotorcraft
[NASA-CR-177608] p 708 A93-26549

SCHEDULES

- IOPS advisor: Research in progress on knowledge-intensive methods for irregular operations airline scheduling
p 443 A93-18686
National aero-space plane: Restructuring future research and development efforts
[AD-A258799] p 340 A93-18981

SCHEDULING

- The application of scheduled H-infinity controllers to a VTOL aircraft
p 1135 A93-52249
Noise studies for environmental impact assessment of an outdoor engine test facility
p 99 A93-10672
Scheduling of an aircraft fleet
p 443 A93-18665
IOPS advisor: Research in progress on knowledge-intensive methods for irregular operations airline scheduling
p 443 A93-18686
A model for determining task set schedulability in the presence of system effects
[AD-A258915] p 443 A93-19338
Analytical foundations of gain scheduling
[AD-A264682] p 909 A93-30550

SCHLIEREN PHOTOGRAPHY

- Schlieren studies of compressibility effects on dynamic stall of transiently pitching airfoils
p 480 A93-28608
Schlieren device and holographic interferometer for hypersonic flow visualization
[ONERA, TP NO. 1992-160] p 832 A93-38739
Aerodynamic investigation with focusing schlieren in a cryogenic wind tunnel
[AIAA PAPER 93-3485] p 910 A93-41059

SCHOOLS

- Flight testing in the 90's
[AIAA PAPER 92-4123] p 102 A93-11256

SCIENCE

- Scientific and engineering research facilities at universities and colleges: 1992
[NSF-92-325] p 192 A93-13407

SCIENTIFIC VISUALIZATION

- Visualization and view simulation based on transputers
p 1037 A93-45150
Scientific visualization using the Flow Analysis Software Toolkit (FAST)
p 758 A93-25600

SCREWS

- A study of the effects of tolerances on rigging screws, turnbuckles, and associated components in BS4429: 1987
[NPL-DMM(A)-53] p 86 A93-11326

SEA ICE

- Dual-band infrared imaging applications: Locating buried minefields, mapping sea ice, and inspecting aging aircraft
[DE93-000516] p 453 A93-17225

SEA LEVEL

- Calculation of safe altitudes
p 991 A93-45675
Engine testing at simulated altitude conditions
[AIAA PAPER 93-2452] p 1120 A93-50201
Results of sea-level static tests on air turbo ramjet for a future space plane
[AAS PAPER 91-640] p 1247 A93-55817

SEA WATER

- Study on aircraft microwave remote sensing of sea-water surface salinity
p 92 A93-12407

SEALERS

- Ultrasonic NDE of adhesive and sealant bonded aluminum lap-splices
p 407 A93-19595

SECONDARY FLOW

SEALING

- State-of-the-art survey of flexible pavement crack sealing procedures in the United States
[AD-A258050] p 382 A93-17708

SEALS (STOPPERS)

- Experimental study of dynamic fluid forces and moments for a long annular seal
p 209 A93-15684
Low leakage fiber metal seals
[ASME PAPER 92-GT-141] p 402 A93-19373
Rim seal experiments and analysis of a rotor-stator system with nonaxisymmetric main flow
[ASME PAPER 92-GT-160] p 402 A93-19387
Ingestion into the upstream wheel-space of an axial turbine stage
[ASME PAPER 92-GT-303] p 354 A93-19493
Effective sealing of a disk cavity using a double-toothed rim seal
[ASME PAPER 92-GT-379] p 406 A93-19537
A hot dynamic seal rig for measuring hypersonic engine seal durability and flow performance
[AIAA PAPER 93-1346] p 738 A93-33916
Hysteresis and bristle stiffening effects of conventional brush seals
[AIAA PAPER 93-1996] p 1153 A93-49839
Testing of a high performance compressor discharge seal
[AIAA PAPER 93-1997] p 1153 A93-49840
The effects of fixed rotor tilt on the rotordynamic coefficients of incompressible flow annular seals
p 1161 A93-52601
Compressible and incompressible fluid seals: Influence on rotordynamic response and stability
[NASA-CR-190746] p 85 A93-10891
Experimental study of the flow field inside a whirling annular seal
p 85 A93-10892
An experimental examination of the thermal and acoustic environments on runway joint seals
[AD-A257965] p 382 A93-17734
Advanced bristle seals for gas turbine engines
[AD-A261296] p 752 A93-26564

SEAMS (JOINTS)

- High efficiency, low weight and volume energy absorbent seam
[AD-D015531] p 554 A93-20765

SEARCHING

- An information-search system in cybernetics
p 1168 A93-50957

SEATS

- Effects of seating configuration and number of type 3 exits on emergency aircraft evacuation
[AD-A256616] p 143 A93-14277
AM-X high angle of attack flight test experience (single and two seat versions)
p 511 A93-19910
Crashworthiness of composite seats for civil aircraft
p 703 A93-24773

SECONDARY FLOW

- A simple spanwise mixing model for turbulent diffusion and secondary flows in multistage axial-flow compressors
p 204 A93-14482
A high-frequency, secondary instability of crossflow vortices that leads to transition
p 128 A93-17253
Turbulence evaluation within the secondary flow region of a turbine cascade
[ASME PAPER 92-GT-60] p 247 A93-19310
Secondary flows in a transonic cascade - Validation of a 3-D Navier-Stokes code
[ASME PAPER 92-GT-62] p 247 A93-19312
An investigation of spanwise mixing in multistage axial flow compressors
[ASME PAPER 92-GT-64] p 247 A93-19314
Aeroloids and secondary flows in a transonic mixed flow turbine stage
[ASME PAPER 92-GT-72] p 248 A93-19322
Experimental and computational investigation of flow in catalytic monolith channels
[ASME PAPER 92-GT-118] p 387 A93-19354
Incidence angle and pitch-chord effects on secondary flows downstream of a turbine cascade
[ASME PAPER 92-GT-184] p 251 A93-19409
An experimental study of heat transfer in a large-scale turbine rotor passage
[ASME PAPER 92-GT-195] p 403 A93-19420
Heat transfer and aerodynamics of a high rim speed turbine nozzle guide vane with profiled end walls
[ASME PAPER 92-GT-243] p 253 A93-19452
Prediction of secondary losses in axial compressors
[ASME PAPER 92-GT-288] p 254 A93-19479
A simple method for estimating secondary losses in turbines at the preliminary design stage
[ASME PAPER 92-GT-294] p 254 A93-19484
Radial transport and momentum exchange in an axial compressor
[ASME PAPER 92-GT-364] p 257 A93-19528
Streamwise variation of mean velocity field for the turbulent boundary layer interacting with controlled longitudinal vortex arrays
p 267 A93-20933

- The coherent structure in a corner turbulent boundary layer p 548 A93-28575
- A study on two-dimensional and three-dimensional secondary jet interactions with a supersonic flow p 683 A93-34273
- Study on vortex generator flow control for the management of inlet distortion p 689 A93-34488
- Evolution of a three-dimensional nonequilibrium boundary layer in a dihedral angle behind a perturbation source p 872 A93-43013
- Secondary flow control on slender, sharp-edged configurations p 980 A93-47250
- [AIAA PAPER 93-3470]
- A calculation of secondary flows and deviation angles in multistage axial-flow compressors p 1066 A93-48509
- Secondary instability mechanisms in compressible axisymmetric boundary layers p 1070 A93-49009
- Secondary flow computation by means of an inviscid multigrid Finite Volume Lambda Formulation [AIAA PAPER 93-1974] p 1077 A93-49821
- Initial development of the two-dimensional ejector shear layer - Experimental results p 1118 A93-50192
- [AIAA PAPER 93-2440]
- 3D PARC Navier-Stokes analysis of an HSCST suppressor nozzle secondary inlet lip and duct p 1084 A93-50286
- [AIAA PAPER 93-2568]
- Verification of the TOTLOS method for calculating aerodynamic loss in film-cooled turbine cascade p 1087 A93-51191
- The combined effect of clearances and peripheral overlaps on the efficiency of microturbines with shrouded rotors p 1193 A93-52963
- The effects of end-bend regulations of compressor blade on the outlet flow field p 1185 A93-54009
- [ISABE 93-7033]
- Performance improvement by forward-skewed blading of axial fan moving blades p 1185 A93-54031
- [ISABE 93-7055]
- Effects of wake interaction of two turbine cascades on secondary/tip-leakage flows and losses p 1185 A93-54034
- [ISABE 93-7058]
- Air ejector experiments using the two-dimensional supersonic cascade tunnel: Relationship between ejector performance and throat area ratio, part 1 [NAL-TM-642-PT-1] p 25 N93-12352
- Investigation of hot streak migration and film cooling effects on heat transfer in rotor/stator interacting flows, report 1 p 102 N93-12490
- [AD-A250688]
- Analysis of thrust modulation of ram-rockets by a vortex valve p 814 N93-27187
- SECONDARY RADAR**
- An SSR/IFF Environment Model --- Secondary Surveillance Radar p 883 A93-43406
- Measurements of SSR bearing errors due to site obstructions --- Secondary Surveillance Radar p 883 A93-43407
- Improvements in code validation algorithms for secondary surveillance radar p 883 A93-43408
- A Mode S implementation - Experiments about data-link and interconnected Mode S sensors p 883 A93-43409
- The development of a prototype aircraft height monitoring unit utilizing an SSR-based difference in time of arrival technique p 884 A93-43432
- The effect of TCAS interrogations on the Chicago O'Hare ATCRBS system [DOT/FAA/CT-92/22] p 318 N93-16498
- SECURITY**
- Proceedings of the First International Symposium on Explosive Detection Technology [DOT/FAA/CT-92/11] p 496 N93-21856
- The UK perspective on aviation security p 496 N93-21858
- SEGMENTS**
- Passive range sensor refinement using texture and segmentation p 544 A93-27044
- SELF ADAPTIVE CONTROL SYSTEMS**
- Self-tuning guidance applied to aeroassisted plane change problems [AIAA PAPER 93-3791] p 1143 A93-51386
- SELF CONSISTENT FIELDS**
- Skin friction and velocity profile family for compressible turbulent boundary layers p 1070 A93-49008
- Theoretical characterization of the reaction $\text{NH}_2 + \text{O}$ yields products p 1263 A93-55666
- SELF EXCITATION**
- Self-excitation of intense oscillations in flow inside a wind tunnel with an open test section p 1091 A93-51883
- Enhanced mixing of a rectangular supersonic jet by natural and induced screech [NASA-TM-106245] p 989 N93-31672

SELF INDUCED VIBRATION

- The use of subscale models to predict self-induced oscillations of flight vehicles [AIAA PAPER 93-0093] p 264 A93-20199
- SELF OSCILLATION**
- Self-excited oscillations at supersonic off-design jet outflow p 6 A93-10402
- A study of the stability of the acceleration control of the hydromechanical automatic control system of an aviation gas turbine engine p 810 A93-39028
- Time-accurate simulation of a self-excited oscillatory supersonic external flow with a multi-block solution-adaptive mesh algorithm [AIAA PAPER 93-3387] p 956 A93-45078
- Effect of the size of a plane obstacle on self-oscillations generated in an underexpanded supersonic jet p 1068 A93-48849

SEMICONDUCTOR DEVICES

- The static-memory crash recorders p 167 A93-15048
- Developments in silicon carbide for aircraft propulsion system applications [AIAA PAPER 93-2581] p 1157 A93-50295

SEMICONDUCTOR LASERS

- Diffraction limited collimating optics for high aspect ratio laser diode arrays p 1172 A93-48411
- Compact high reliability fiber coupled laser diodes for avionics and related applications p 1152 A93-49470

SEMIEMPIRICAL EQUATIONS

- Prediction of 2D viscous transonic flow in compressor cascades using a semi-empirical shock/boundary-layer interaction method [ASME PAPER 92-GT-277] p 253 A93-19470

SENSITIVITY

- A sensitivity analysis of the stability of a tug-ropes-sailplane system p 184 A93-14400
- Investigation of the aircraft spin via sensitivity analysis p 524 A93-27300
- A new sensitivity analysis for structural optimization of composite rotor blades [AIAA PAPER 93-1644] p 742 A93-34169
- Efficient sensitivity analysis for rotary-wing aeromechanical problems [AIAA PAPER 93-1648] p 711 A93-34173
- Design of a low sensitivity and norm multivariable controller using eigenstructure assignment and the method of inequalities [AIAA PAPER 93-3802] p 1170 A93-51394
- Optimization of large scale systems in elasticity p 1255 A93-54544
- A computational aerodynamic design optimization method using sensitivity analysis p 716 N93-25552
- Sensitivity calculations for a 2D, inviscid, supersonic forebody problem [NASA-CR-191444] p 779 N93-27004

SENSORS

- Electro-optic architecture for servicing sensors and actuators in advanced aircraft propulsion systems [NASA-CR-182269] p 232 N93-13762
- NASA wind shear flight test in situ results p 488 N93-19593
- Digitization of analog data from in-flight lightning strikes p 753 N93-24884
- A single-point warning system for thunderstorms and electric fields p 747 N93-24900

SEPARATED FLOW

- An asymptotic model of a closed separation region in supersonic flow p 4 A93-10139
- A study of the effect of nonstationary perturbations on flow in the front separation region p 5 A93-10150
- Review of the normal force fluctuations of aerofoils with separated flow p 10 A93-12317
- A method for calculating flow past an arbitrary airfoil profile in the presence of flow separation p 13 A93-12807
- Nonstationary flow of a viscous incompressible fluid past an airfoil p 79 A93-12922
- Effect of the drag of the front body on the restructuring of flow between two bodies in the path of supersonic flow, with one body located in the wake of the other p 14 A93-12973
- Calculation of separated axisymmetric flow past bodies by solving Euler equations in the inner vortex region p 14 A93-12975
- Flow characteristics of an S-shaped inlet at high incidence p 114 A93-14213
- Calculation of 3-D unsteady subsonic flow with separation bubble using singularity method p 115 A93-14251
- An adaptive region method for computation of vortex sheet behind wing in compressible flow p 116 A93-14262
- A prediction of the stalling for wings with rear separation p 116 A93-14264
- Separation control and lift enhancement on airfoil using unsteady excitations p 118 A93-14305

- Subsonic separated flow past slender delta wings p 124 A93-15109
- A flat plate wing standing on a wall covered with a thick boundary layer. II - Wing characteristics under the effects of side wall boundary layer and wing tip vortex p 125 A93-15446
- Flow past a finite-span wing in the presence of external acoustic loading p 127 A93-16707
- Applications of laser techniques in fluid mechanics p 395 A93-17765
- Separated flow in a low speed two-dimensional cascade. I - Flow visualization and time-mean velocity measurements [ASME PAPER 92-GT-356] p 257 A93-19521
- Separated flow in a low speed two-dimensional cascade. II - Cascade performance [ASME PAPER 92-GT-357] p 257 A93-19522
- Prescribed-curvature-distribution airfoils for the preliminary geometric design of axial-turbomachinery cascades [ASME PAPER 92-GT-366] p 257 A93-19530
- Investigation of the characteristics of 3-dimensional separated flow in an annular compressor blade row with large angles of attack p 259 A93-20116
- A unified model for rotating stall and surge p 259 A93-20119
- Static roll moment characteristics of asymmetric tangential leading edge blowing on a delta wing at high angles of attack [AIAA PAPER 93-0052] p 261 A93-20165
- Calculations of separated vortex flows at low speed for low-aspect-ratio wings p 264 A93-20300
- A comparison of the predictive capabilities of several turbulence models using upwind and central-difference computer codes [AIAA PAPER 93-0192] p 268 A93-21102
- Transonic shock oscillations calculated with a new interactive boundary layer coupling method [AIAA PAPER 93-0777] p 269 A93-21119
- Forcing function generator fluid dynamic effects on compressor blade gust response [AIAA PAPER 93-0157] p 275 A93-22594
- Unsteady laminar separation on low-Reynolds-number airfoils [AIAA PAPER 93-0209] p 278 A93-22627
- The three-dimensional separated flow structure in a variable aspect ratio sudden expansion duct [AIAA PAPER 93-0213] p 278 A93-22630
- Prediction of fluctuating pressure in attached and separated compressible flow [AIAA PAPER 93-0286] p 279 A93-22687
- Unsteady vortex dynamics and surface pressure topologies on a pitching wing [AIAA PAPER 93-0435] p 286 A93-23349
- A study of flow separation on an oscillating flap at Mach number 2.4 [AIAA PAPER 93-0436] p 286 A93-23350
- Investigation on bi-flat jet separated flow in a rectangular combustor p 459 A93-23778
- Numerical modeling of leading edge separated flow at incompressible speeds p 460 A93-24079
- A Navier-Stokes simulation of vortex shedding from square cylinder in unconfined domain p 538 A93-24084
- The analysis of unsteady, three-dimensional flow separation [AIAA PAPER 93-0642] p 540 A93-24757
- Investigation of three-dimensional separation at wing/body junctions in supersonic flows using TVD McCormack's scheme [AIAA PAPER 93-0884] p 471 A93-24945
- Effect of a rotating propeller on the separation angle of attack [AIAA PAPER 93-0017] p 472 A93-24978
- Numerical investigation of flow field in a turbine volute [AIAA PAPER 93-0155] p 542 A93-25505
- Correlation of interaction sweepback effects on unsteady shock-induced turbulent separation [AIAA PAPER 93-0776] p 475 A93-25550
- Current status of computational methods for transonic unsteady aerodynamics and aeroelastic applications p 480 A93-29175
- Aeroelastic system identification of advanced technology aircraft through higher order signal processing p 525 A93-29297
- Application of particle image velocimetry in high-speed separated flows p 549 A93-29304
- Viscous-inviscid interaction coupled calculation of three-dimensional turbulent separated flow over dents p 681 A93-33748
- Parametrical investigation of the interaction between turbulent wall shear layers and normal shock waves, including separation p 681 A93-33752
- Hammerhead aeroelastic stability revisited [AIAA PAPER 93-1477] p 740 A93-34022

- Numerical methods in laminar and turbulent flow; Proceedings of the 7th International Conference, Stanford Univ., CA, July 15-19, 1991. Vol. 7, pts. 1 & 2 [ISBN 0-906674-77-8] p 743 A93-34301
- Computation of supersonic crossflow separation using a new parabolized Navier-Stokes code p 687 A93-34355
- A study of flow structure and heat transfer intensity in the vicinity of an expanding step on a plate p 691 A93-35268
- Study of supersonic intersection flowfield at modified wing-body junctions p 692 A93-35621
- Numerical calculation of separated flows around wing section in unsteady motion by using incompressible Navier-Stokes equations p 770 A93-38158
- A viscous-inviscid solver for high-lift incompressible flows over multi-element airfoils at deep separation conditions p 774 A93-38745
- [ONERA, TP NO. 1992-183] p 774 A93-38745
- Viscous-inviscid calculation of high-lift separated compressible flows over airfoils and wings p 774 A93-38746
- [ONERA, TP NO. 1992-184] p 774 A93-38746
- Aerodynamic heating in the vicinity of hypersonic, axisymmetric, shock-wave boundary-layer interactions [AIAA PAPER 93-2766] p 963 A93-46512
- Active forcing of an axisymmetric leading-edge turbulent separation bubble p 966 A93-46790
- [AIAA PAPER 93-3245] p 966 A93-46790
- Separated flowfield and lift on an airfoil with an oscillating leading-edge flap p 976 A93-47217
- [AIAA PAPER 93-3422] p 976 A93-47217
- Neural network prediction of three-dimensional unsteady separated flow fields p 977 A93-47221
- [AIAA PAPER 93-3426] p 977 A93-47221
- A wind tunnel investigation of the pressure distribution on an F/A-18 wing p 980 A93-47249
- [AIAA PAPER 93-3468] p 980 A93-47249
- On the modelling of separated flows about airfoils p 981 A93-47257
- [AIAA PAPER 93-3479] p 981 A93-47257
- Surface hot-film method for the measurement of transition, separation and reattachment points [AIAA PAPER 93-2918] p 1148 A93-48120
- Tip vortex, stall vortex, and separation observations on pitching three-dimensional wings p 1049 A93-48166
- [AIAA PAPER 93-2972] p 1049 A93-48166
- Three-dimensional unsteady separating flows around an oscillatory forward-swept wing p 1050 A93-48170
- [AIAA PAPER 93-2976] p 1050 A93-48170
- Vortex developments over steady and accelerated airfoils incorporating a trailing edge jet p 1054 A93-48198
- [AIAA PAPER 93-3008] p 1054 A93-48198
- Flow field characteristics of a complex blade tip at high angles of attack p 1060 A93-48257
- [AIAA PAPER 93-3083] p 1060 A93-48257
- A two layer k-epsilon computation of transonic viscous flow including separation over the DLR-F5 wing p 1061 A93-48281
- [AIAA PAPER 93-3110] p 1061 A93-48281
- Numerical simulation of unsteady flow in a transonic cascade p 1066 A93-48502
- Control of separation by dynamic air jets p 1066 A93-48504
- Experimental study on heat transfer of separated impingement jets in short distance p 1149 A93-48518
- Calculation of the parameters of instability waves in the preseparation region p 1067 A93-48826
- Effects of external excitation on the leading-edge separation flowfield p 1071 A93-49198
- Investigation of nacelle upper cowl flow separation using on- and off-body flow visualization techniques p 1072 A93-49507
- 3-D viscous flow CFD analysis of the propeller effect on an advanced ducted propeller subsonic inlet [AIAA PAPER 93-1847] p 1075 A93-49728
- A comparative study of Full Navier-Stokes and Reduced Navier-Stokes analyses for separating flows within a diffusing inlet S-duct p 1079 A93-49970
- [AIAA PAPER 93-2154] p 1079 A93-49970
- Spatial domain characterization of abrupt rotating stall initiation in an axial flow compressor p 1081 A93-50040
- [AIAA PAPER 93-2238] p 1081 A93-50040
- Ground facility interference on aircraft configurations with separated flow p 1140 A93-52441
- Calculation of the position of the flow separation line in an analog model of flow past a body p 1176 A93-52958
- Moving wall effects in transverse subsonic flow past a rotating cylinder p 1179 A93-53573
- A preliminary investigation of the control of separated flow by means of excitation p 1182 A93-53859
- Three-dimensional separated flow over a prolate spheroid p 1235 A93-55379
- An improved multiple line-vortex method for simulation of separated vortices of slender wings p 1236 A93-55412
- Free streamline-boundary layer analysis for separated flow over an airfoil p 1239 A93-56327
- Effect of passive flow-control devices on turbulent low-speed base flow p 82 N93-10304
- Forced unsteady separated flows on a 45 degree delta wing p 82 N93-10305
- Characteristics of separated flows including cavitation effects p 84 N93-10874
- An investigation of the effects of aft blowing on a 3.0 caliber tangent ogive body at high angles of attack [NASA-CR-190934] p 24 N93-12004
- Numerical investigations into the base drag of various wedges using the base flow model developed by Mauri Tanner p 26 N93-12414
- [REPT-B-36] p 26 N93-12414
- In-flight flow visualization results from the X-29A aircraft at high angles of attack p 131 N93-13322
- [NASA-TM-4430] p 131 N93-13322
- Overall effects of separation on thin aerofoils [ISBN-0-315-67464-4] p 135 N93-13930
- Control of low-speed turbulent separated flow over a backward-facing ramp p 219 N93-14475
- Investigations of detail design issues for the high speed acoustic wind tunnel using a 60th scale model tunnel. Part 1: Tests with open circuits p 137 N93-14737
- [NASA-CR-191671] p 137 N93-14737
- A realizable Reynolds stress algebraic equation model [NASA-TM-105993] p 290 N93-16596
- Effect of a rotating propeller on the separation angle of attack and distortion in ducted propeller inlets [NASA-TM-105935] p 290 N93-16625
- Hypersonic flows as related to the national aerospace plane p 296 N93-18378
- [NASA-CR-191980] p 296 N93-18378
- An experimental investigation of the separating/reattaching flow over a backstep p 298 N93-18781
- [NASA-CR-192105] p 298 N93-18781
- Stall departure resistance enhancer p 344 N93-19023
- [NASA-CASE-LAR-14221-1] p 344 N93-19023
- Numerical calculations of separating flows around oscillating airfoil p 300 N93-19284
- Numerical simulation of unsteady large scale separated flow around oscillating airfoil p 300 N93-19285
- Three dimensional calculation of flow inside supersonic inlet p 303 N93-19313
- Experimental investigations on wing-body combinations and their components at high angles of attack in the subsonic and transonic speed range p 516 N93-21762
- [DLR-FB-91-43] p 516 N93-21762
- Unsteady Navier-Stokes method for accelerated moving airfoils with separation p 485 N93-21763
- [DLR-FB-92-03] p 485 N93-21763
- Surface and flow field measurements in a symmetric crossing shock wave/turbulent boundary-layer interaction p 693 N93-24911
- [NASA-TM-106086] p 693 N93-24911
- An aerodynamic model for one and two degree of freedom wing rock of slender delta wings p 781 N93-27150
- [NASA-CR-193130] p 781 N93-27150
- Flow prediction over a transport multi-element high-lift system and comparison with flight measurements p 785 N93-27448
- Investigation of forced unsteady separated flows using velocity-vorticity form of Navier-Stokes equations p 840 N93-27451
- Some recent applications of Navier-Stokes codes to rotorcraft p 786 N93-27452
- Dynamic airfoil stall investigations p 786 N93-27453
- Calculation of fully three-dimensional separated flow with an unsteady viscous-inviscid interaction method p 786 N93-27455
- Plume effects on the flow around a blunted cone at hypersonic speeds p 787 N93-27460
- Navier-Stokes simulation of viscous, separated, supersonic flow over a projectile rotating band [AD-A263073] p 788 N93-27955
- Modification and calibration of the Naval Postgraduate School Academic Wind Tunnel p 823 N93-28189
- [AD-A262092] p 823 N93-28189
- An experimental study of flow over a 6 to 1 prolate spheroid at incidence p 874 N93-29124
- The 3-D viscous flow CFD analysis of the propeller effect on an advanced ducted propeller subsonic inlet [NASA-TM-106240] p 900 N93-29162
- A theoretical and computational study on active wake control p 878 N93-30892
- SEQUENTIAL ANALYSIS**
- An automated mode tracking strategy --- dynamic structural analysis of helicopter structures [AIAA PAPER 93-1414] p 739 A93-33970
- SERVICE LIFE**
- Reassessment of the C-141 structural life p 46 A93-13631
- Fleet fatigue cracking threshold prediction p 3 A93-13633
- A review of aging aircraft technology - An I.A.I. perspective p 3 A93-13634
- Aging review of the YS-11 aircraft p 46 A93-13635
- Analysis of multiple crack propagation in stiffened sheet p 81 A93-13638
- Damage severity of monitored fatigue load spectra p 154 A93-14253
- Engine Health Monitoring p 346 A93-18787
- The evolution of thermal barrier coatings in gas turbine engine applications p 388 A93-19427
- [ASME PAPER 92-GT-203] p 388 A93-19427
- Life assessment of gas turbine bucket coating based on degradation analysis p 533 A93-24464
- A damage tolerance/life processor for structural integrity and force management p 507 A93-27962
- Probabilistic turbine blade tip durability analysis [AIAA PAPER 93-1383] p 719 A93-33946
- Optimization of endurance performance --- of aircraft p 713 A93-34400
- Ways of increasing the service life and reliability of bolted joints p 745 A93-35281
- Effect of overloads on the service life of the structural elements of aircraft p 746 A93-35289
- Aging jet transport structural evaluation programs p 947 A93-45781
- How likely is multiple site damage? p 1027 A93-45791
- Experience in specifying/prolonging the airframe time limits p 948 A93-45797
- Repairs to damage tolerant aircraft p 948 A93-45799
- Reliability and durability problems p 1150 A93-48825
- Initial test results of 40,000 horsepower fan drive gear system for advanced ducted propulsion systems [AIAA PAPER 93-2146] p 1154 A93-49963
- Pyrometer for turbine applications in the presence of reflection and combustion p 1156 A93-50143
- [AIAA PAPER 93-2374] p 1156 A93-50143
- The 'Rolls-Royce' way of validating fan integrity [AIAA PAPER 93-2602] p 1122 A93-50311
- Monitoring load experience of individual aircraft p 1103 A93-52450
- Durability properties for adhesively bonded structural aerospace applications p 1217 A93-53515
- Selection of a method for protecting aircraft gas turbine engines against damage by foreign objects (Mathematical models) p 1193 A93-53554
- An evaluation of a method of reconstituting fatigue loading from Rainflow counting [RAE-TR-89057] p 82 N93-10198
- Verification of rain-flow reconstructions of a variable amplitude load history p 91 N93-12411
- [NASA-CR-189670] p 91 N93-12411
- Structural fatigue aspects of the P-3 Orion p 161 N93-13256
- [ARL-STRUC-TM-558] p 161 N93-13256
- Proceedings of the USAF Structural Integrity Program [AD-A255379] p 110 N93-14549
- TBD(exp 3) p 335 N93-18054
- [NASA-CR-192075] p 335 N93-18054
- Estimating characteristic life and reliability of an aircraft engine component improvement in the early stages of the implementation process p 815 N93-28184
- [AD-A262118] p 815 N93-28184
- Damage severity of monitored fatigue load spectra [NLR-TP-92009-U] p 999 N93-32205
- SERVICES**
- An investigation of ground access mode choice for departing passengers [TT-9201] p 67 N93-11224
- SERVOCONTROL**
- The Boeing 747-400 upper rudder control system with triple tandem valve [SAE PAPER 912133] p 327 A93-21843
- Simultaneous structure/control design optimization of a wing structure with a gust load alleviation system p 525 A93-28616
- Extension of a nonlinear systems theory to general-frequency unsteady transonic aerodynamic responses [AIAA PAPER 93-1590] p 683 A93-34122
- Robotic aircraft refueling - A concept demonstration p 846 A93-37041
- Actuator and aerodynamic modeling for high-angle-of-attack aeroservoelasticity [AIAA PAPER 93-1419] p 818 A93-37433
- Application of nonlinear systems theory to transonic unsteady aerodynamic responses p 1095 A93-52438
- SERVO MOTORS**
- Development and testing of the digital control system for the Archytas unmanned air vehicle [AD-A261656] p 729 N93-26196
- SET THEORY**
- An application of fuzzy logic and Dempster-Shafer theory to failure detection and identification p 96 A93-13079
- SEWING**
- Development of stitching reinforcement for transport wing panels p 921 N93-30852

SHADOWGRAPH PHOTOGRAPHY

- Shadowgraph flow visualization of isolated tiltrotor and rotor/wing wakes p 767 A93-35996
Application of the shadowgraph flow visualization technique to a full-scale helicopter rotor in hover and forward flight [AIAA PAPER 93-3411] p 1030 A93-47208

SHAFTS (MACHINE ELEMENTS)

- A High Deflection Diaphragm concept (HDD) for power transmission shafting p 826 A93-35931
Rotating machinery - Dynamics; Proceedings of the 3rd International Symposium on Transport Phenomena and Dynamics of Rotating Machinery (ISROMAC-3), Honolulu, HI, Apr. 1-4, 1990 [ISBN 1-56032-147-4] p 1257 A93-54651
Engine life assessment test case TF41 LP compressor shaft torsional fatigue p 177 N93-14896
Experimental investigation of the aerodynamics of independently rotating cylindrical shells [AD-A258917] p 305 N93-19340

SHALLOW SHELLS

- Supersonic panel flutter analysis of shallow shells p 927 A93-41935

SHALLOW WATER

- Sea fog and stratus - A major aviation hazard in the northern Gulf of Mexico p 429 A93-22141

SHAPE CONTROL

- Adaptive/conformal wing design for future aircraft p 320 A93-17728
Development of a Shape-controlled airfoil by use of SMA --- Shape Memory Alloys p 411 A93-21739
Active rib experiment for shape control of an adaptive wing [AIAA PAPER 93-1700] p 712 A93-34222
Hypersonic stagnation line merged layer flow on blunt axisymmetric bodies of arbitrary shape [AIAA PAPER 93-2723] p 962 A93-46478
Nonslender waveriders p 982 A93-47261
Automatic pulse shaping with the AN/FPN-42 and AN/FPN-44A Loran-C transmitters [AD-A257860] p 319 N93-18309

SHAPE FUNCTIONS

- Analysis of complicated plates by a nine-node spline plate element p 206 A93-14616
Airfoil shape optimization using sensitivity analysis on viscous flow equations p 682 A93-33755
Flight research on natural laminar flow applications p 890 A93-41779
Aerodynamic shape optimization using preconditioned conjugate gradient methods [AIAA PAPER 93-3322] p 952 A93-45016
A 3D Navier-Stokes analysis of a generic ground vehicle shape [AIAA PAPER 93-3521] p 985 A93-47283
Improvement of transonic wing buffet by geometric modifications [AIAA PAPER 93-3024] p 1055 A93-48209
Shape optimization for aerodynamic efficiency and low observability [AIAA PAPER 93-3115] p 1062 A93-48285
Analysis on space shape and tension distribution of towed flexible cables p 1043 A93-48554

SHAPE MEMORY ALLOYS

- Development of a Shape-controlled airfoil by use of SMA --- Shape Memory Alloys p 411 A93-21739
Articulated control surface [AD-D015464] p 371 N93-16463
Nonlinear analyses of composite aerospace structures in sonic fatigue [NASA-CR-193124] p 930 N93-29154
Articulated fin/wing control system [AD-D015712] p 909 N93-29278

SHAPES

- Optimized/adapted finite elements for structural shape optimization p 77 A93-10971
Exact-gradient shape optimization of a 2-D Euler flow p 462 A93-24308
Mesh generation for the computation of flowfields over complex aerodynamic shapes p 995 A93-44888
An iterative multidisciplinary analysis for rotor blade shape determination [AIAA PAPER 93-2085] p 1114 A93-49912
One type of automatically adjusted difference scheme with artificial viscosity to calculate ablated exterior shapes [AD-A254108] p 19 N93-10856
A laboratory investigation of raindrop oscillations p 224 N93-13790
Computational analysis of hypersonic flows past elliptic-cone waveriders [NASA-CR-191304] p 138 N93-14767
Category A F-16 accidents in the Belgian Air Force p 492 N93-19675
A composite structured/unstructured-mesh Euler method for complex airfoil shapes p 784 N93-27439

- Experimental and computational ice shapes and resulting drag increase for a NACA 0012 airfoil p 784 N93-27440

- Recent progress in the analysis of iced airfoils and wings p 784 N93-27441
An interactive boundary-layer approach to multielement airfoils at high lift p 785 N93-27445

SHARP LEADING EDGES

- Regimes of supersonic flow past the windward side of V-shaped wings p 5 A93-10144
Numerical simulations of high-speed flows about waveriders with sharp leading edges p 9 A93-12007
Experimental investigations of asymmetric vortex flows behind elliptic cones at incidence p 757 A93-35637
Nonequilibrium limiting hypersonic flow of a gas past three-dimensional tapered bodies with a separated shock p 776 A93-39133
Developing a data base for the calibration and validation of hypersonic CFD codes - Sharp cones [AIAA PAPER 93-3044] p 1057 A93-48224
A study of pressure fluctuations on the surface of a delta wing near the sharp leading edge p 1091 A93-51882
Pressure field and drag of a single cavity with rounded and sharp edges p 1258 A93-55018
Further buffeting tests in a cryogenic wind tunnel [NASA-TM-107621] p 22 N93-11610
Application of an Euler-equation method to a sharp-edged delta wing configuration with vortex flow [NLR-TP-91306] p 294 N93-17809
Conical Euler analysis and active roll suppression for unsteady vortical flows about rolling delta wings [NASA-TP-3259] p 701 N93-26134

SHEAR FLOW

- Boundary conditions for direct computation of aerodynamic sound generation p 447 A93-19176
Dynamics of the behavior of nematic films in gasdynamic flows p 746 A93-35345
Vortex-induced energy separation in shear flows p 837 A93-39427
Evolution of a three-dimensional nonequilibrium boundary layer in a dihedral angle behind a perturbation source p 872 A93-43013
Compressibility, exothermicity, and three dimensionality in spatially evolving reactive shear flows p 950 A93-44375
An adaptive finite element method for turbulent free shear flow past a propeller [AIAA PAPER 93-3388] p 956 A93-45079
On the steady subsonic shear flow past a slender body of revolution p 970 A93-46907
Boundary conditions for direct computation of aerodynamic sound generation p 1172 A93-49005
Direct simulation of reacting fuel gas flows in a supersonic mixing layer [ISABE 93-7072] p 1201 A93-54048
Lift and drag forces on droplets and particles in wall-bounded shear flows [DE93-002678] p 419 N93-17761
An analysis of lift forces on aerosols in a wall bounded turbulent shear flow [DE93-003362] p 747 N93-24963
Numerical simulation of free shear flows: Towards a predictive computational aeroacoustics capability [NASA-CR-191015] p 781 N93-27097
GARTEUR 3D shear layer experiment [FFA-TN-1992-26] p 987 N93-31052

SHEAR LAYERS

- On the measurements of the skin friction in 3-D flows - Application to a complete 3-D shear layer flow p 118 A93-14329
Streamline curvature in supersonic shear layers p 244 A93-19194
Transition prediction in attached and separated shear layers using an integral method [ASME PAPER 92-GT-281] p 253 A93-19473
An experimental investigation of twin fin buffeting and suppression [AIAA PAPER 93-0054] p 261 A93-20167
Total-pressure loss in supersonic parallel mixing [AIAA PAPER 93-0216] p 278 A93-22632
Vortical and turbulent structure of a lobed mixer free-shear layer [AIAA PAPER 93-0219] p 415 A93-22635
Control of pressure fluctuations in the reattachment region of a supersonic free shear layer: [AIAA PAPER 93-0385] p 282 A93-23064
Active control of the shear layer on a static airfoil [AIAA PAPER 93-0442] p 286 A93-23353
Parametrical investigation of the interaction between turbulent wall shear layers and normal shock waves, including separation p 681 A93-33752
Evaluation of an RNG-based algebraic turbulence model p 863 A93-42436
Vortex-induced disturbance field in a compressible shear layer p 873 A93-43628

- A numerical study of wave propagation in a confined mixing layer by eigenfunction expansions p 873 A93-43629

- Further study of high speed single free jets p 873 A93-43687
Organized structure in a compressible turbulent shear layer p 961 A93-45730
Free shear layer control and its application to fan noise [AIAA PAPER 93-3242] p 965 A93-46787
Enhanced mixing via geometric manipulation of a splitter plate [AIAA PAPER 93-3244] p 966 A93-46789
Control of a supersonic reattaching shear layer [AIAA PAPER 93-3248] p 966 A93-46793
The countercurrent mixing layer - Strategies for shear-layer control [AIAA PAPER 93-3260] p 968 A93-46826
Audio post-processing for shear layer calculations [AIAA PAPER 93-3075] p 1059 A93-48250
The effect of large scale unsteady motion on turbulent reattaching shear layer - Application to the supersonic compression ramp [AIAA PAPER 93-3100] p 1061 A93-48273
Model for entropy production and pressure variation in confined turbulent mixing p 1071 A93-49014
Thrust loss due to supersonic mixing [AIAA PAPER 93-2140] p 1114 A93-49958
Initial development of the two-dimensional ejector shear layer - Experimental results [AIAA PAPER 93-2440] p 1118 A93-50192
Comparison of the initial development of shear layers in two-dimensional and axisymmetric ejector configurations [AIAA PAPER 93-2441] p 1119 A93-50193
Flowfield simulation about the stratospheric observatory for infrared astronomy p 1095 A93-52446
Enhanced fuel-air mixing in hypersonic engines [ISABE 93-7115] p 1221 A93-54090
Comparison of confined, compressible, spatially developing mixing layers with temporal mixing layers p 1234 A93-55352
Shock enhancement and control of hypersonic combustion [AD-A254295] p 72 N93-10843
Special publication of National Aerospace Laboratory [DE93-716176] p 239 N93-15946
Mixing and reaction in the subsonic 2-D turbulent free shear layer p 289 N93-16508
Advanced adaptive computational methods for Navier-Stokes simulations in rotorcraft aerodynamics [NASA-CR-192282] p 483 N93-20256
Studies in air/air supersonic mixing layers p 700 N93-26007
Discrete-vortex simulation of pulsating flow on a turbulent leading-edge separation bubble p 787 N93-27457
Comparison of reacting and non-reacting shear layers at a high subsonic Mach number [NASA-TM-106198] p 814 N93-27610
A theoretical and computational study on active wake control p 878 N93-30892
GARTEUR 3D shear layer experiment [FFA-TN-1992-26] p 987 N93-31052
Enhanced mixing of a rectangular supersonic jet by natural and induced screech [NASA-TM-106245] p 989 N93-31672
Reynolds number influences in aeronautics [NASA-TM-107730] p 989 N93-31732
Turbulence measurement in a reacting and non-reacting shear layer at a high subsonic Mach number [NASA-TM-106186] p 989 N93-31839
Calculations on unsteady type 4 interaction at Mach 8 [AD-A265214] p 990 N93-32004
- SHEAR PROPERTIES**
Shock enhancement and control of hypersonic combustion [AD-A254295] p 72 N93-10843
- SHEAR STRAIN**
Dynamic analysis of pretwisted elastically-coupled rotor blades p 326 A93-21125
Propagation of transverse anti-plane waves in orthotropic layers p 412 A93-21878
- SHEAR STRENGTH**
Correlation of X-ray CT measurements to shear strength in pultruded composite materials p 396 A93-18618
- SHEAR STRESS**
Design sensitivity and optimization of composite cylinders p 71 A93-12781
Unsteady turbulent skin-friction measurement in an adverse pressure gradient p 206 A93-14545
Impact ice interface shear stresses caused by blade bending and twisting [AIAA PAPER 93-0030] p 307 A93-20147
A study of the flexural properties of carbon-epoxy composites in certain environments p 390 A93-21999

- Experimental investigations of the time and flow-direction responses of shear-stress-sensitive liquid crystal coatings
[AIAA PAPER 93-0181] p 542 A93-25508
- Recent developments in equivalent plate modeling for wing shape optimization
[AIAA PAPER 93-1647] p 742 A93-34172
- Use of shear-stress-sensitive, temperature-insensitive liquid crystals for boundary layer transition detection in hypersonic flows
[AIAA PAPER 93-3070] p 1059 A93-48245
- Laser Interferometer Skin-Friction measurements of crossing-shock wave/turbulent boundary-layer interactions
[AIAA PAPER 93-3072] p 1148 A93-48247
- Measurement of aerodynamic shear stress using side chain liquid crystal polymers
[AD-A254312] p 72 N93-10770
- Turbulence: The chief outstanding difficulty of our subject
p 783 N93-27428
- Surface shear stress estimates from geostrophic winds for use in sensible and latent heat flux formulations
p 936 N93-30044
- Compressible turbulence in a high-speed high Reynolds number mixing layer
p 878 N93-30583
- Structural response of bead-stiffened thermoplastic shear webs
p 923 N93-30873
- SHEARING**
Relationship between mechanical-property and energy-absorption trends for composite tubes
[NASA-TP-3284] p 392 N93-16537
- SHEARS**
Sources of helicopter rotor hub inplane shears
[AIAA PAPER 93-1358] p 709 A93-33927
- SHELL STABILITY**
Determination of the membrane and flexural shell deformations from the readings of a two-sided rosette-type strain gage
p 75 A93-10047
- A procedure for the thermal and strength testing of radiotransparent shells
p 1209 A93-52976
- SHELL THEORY**
Nonlinear deformation mechanics of multilayer transparency elements - General theory relations
p 79 A93-12800
- Thermomechanical postbuckling analysis of laminated composite shells
[AIAA PAPER 93-1337] p 738 A93-33907
- Fluid-structural interactions using Navier-Stokes flow equations coupled with shell finite element structures
[AIAA PAPER 93-3087] p 1099 A93-48261
- SHELLS (STRUCTURAL FORMS)**
Mode interaction in stiffened composite shells under combined mechanical and thermal loadings
p 419 N93-16793
- SHIP HULLS**
A fast multigrid method for solving incompressible hydrodynamic problems with free surfaces
[AIAA PAPER 93-0767] p 540 A93-24851
- SHIPS**
Ship airwake measurement and flow visualization
[AIAA PAPER 92-4088] p 7 A93-11267
- Simulation of DD-963 ship airwake by Navier-Stokes method
[AIAA PAPER 93-3002] p 1053 A93-48192
- Ship viscous flow: A report on the 1990 SSPA-IIHR Workshop
p 840 N93-27466
- SHOCK ABSORBERS**
Some dynamic problems in design of aircraft landing gear
p 155 A93-14321
- Optimization of oleo-pneumatic shock absorber of aircraft
p 1243 A93-55415
- SHOCK DISCONTINUITY**
Shock waves and the Ffowcs Williams-Hawkins equation
p 480 A93-29411
- SHOCK LAYERS**
Approximate methods for heat flows toward the surface of three-dimensional bodies
p 4 A93-10080
- Numerical solution of a free-boundary problem in hypersonic flow theory - Nonequilibrium viscous shock layers
p 8 A93-11920
- Viscous shock-layer numerical calculations of three dimensional nonequilibrium flows over hypersonic blunt bodies at high angle of attack
p 12 A93-12651
- Breakdown of steady state axisymmetric flow in a shock layer formed as a result of the impingement of a supersonic underexpanded jet on a perpendicular plane obstacle
p 241 A93-18230
- Nonequilibrium excitation of internal molecular degrees of freedom in the shock layer during hypersonic flight
p 412 A93-21922
- Computation of nonequilibrium radiating shock layers
[AIAA PAPER 93-0144] p 414 A93-22588
- The stagnation line solution of the equilibrium flow with radiation and mass injection
p 680 A93-33733
- Unsteady supersonic flow around a blunt body in thermal inhomogeneities in turbulent shock layer flows
p 691 A93-35266
- VSL analysis of nonequilibrium flows around a hypersonic body
p 769 A93-38146
- A numerical investigation of supersonic flow of a viscous gas over long blunt cones, taking into account equilibrium physicochemical transformations
p 775 A93-39124
- Nonequilibrium limiting hypersonic flow of a gas past three-dimensional tapered bodies with a separated shock
p 776 A93-39133
- Nonequilibrium heat transfer near the critical point of blunt bodies
p 777 A93-39145
- An experimental study of the three-dimensional interaction of a transverse jet with hypersonic flow
p 777 A93-39150
- An existence theorem for a free boundary problem of hypersonic flow theory
p 857 A93-40405
- Higher-order viscous shock-layer solutions for high altitude flows
[AIAA PAPER 93-2724] p 858 A93-41050
- Spectral solution of the viscous blunt-body problem
p 860 A93-41915
- Radiative heat transfer from non-equilibrium high-enthalpy shock layers
p 1024 A93-45515
- Enhancements to viscous-shock-layer technique
p 962 A93-46408
- A viscous shock-layer analysis of 2-D and axisymmetric flows
[AIAA PAPER 93-2751] p 963 A93-46500
- Effects of wall conditions on chemically nonequilibrium shock-layer flow over hypersonic reentry bodies
p 970 A93-46908
- Engineering method for calculating inlet face property profiles on high speed vehicle forebodies
[AIAA PAPER 93-3113] p 1062 A93-48283
- The problem of viscous hypersonic flow past blunt bodies in the spreading plane
p 1086 A93-50969
- Optimal wing shapes in a hypersonic nonequilibrium flow
p 1088 A93-51770
- A study of turbulent flow in a viscous shock layer in the case of gas flow past oblong blunt bodies
p 1089 A93-51820
- Investigation of the effect of physical processes on heat transfer to blunt bodies at low Reynolds numbers
p 1090 A93-51877
- Investigation of the structure of a multicomponent viscous shock layer
p 1090 A93-51879
- An economical difference factorization algorithm for the numerical calculation of the system of equations for a thin viscous shock layer
p 1091 A93-51880
- Numerical simulation of shock/shock and shock-wave/boundary-layer interactions in hypersonic flows
p 1093 A93-52000
- Application of the small parameter method to the problem of three-dimensional flow of a viscous gas past bodies
p 1178 A93-53314
- Comparison of gasdynamic models in hypersonic flow
p 1179 A93-53315
- Spectral measurements of shock layer radiation in an arc-jet wind tunnel
p 1251 A93-54409
- The effects of reaction rate constants and catalytic wall on the hypersonic flow field over blunt bodies
p 1230 A93-54586
- Nonequilibrium shock layer radiation in a simulated Titan atmosphere
p 1233 A93-54805
- Hypersonic flow of a gas past wing with heat transfer
p 1234 A93-55030
- AGARD WG13 aerodynamics of high speed air intakes: Assessment of CFD results
p 215 N93-13220
- Static pressure measurements of the shock-boundary layer interaction in a simulated fan passage
[AD-A256724] p 361 N93-15979
- Experimental investigation of Nozzle/Plume Aerodynamics at Hypersonic Speeds
[NASA-CR-191368] p 386 N93-18085
- An experimental study of under-expanded jets
p 696 N93-25467
- Calculation of fully three-dimensional separated flow with an unsteady viscous-inviscid interaction method
p 786 N93-27455
- SHOCK LOADS**
Shock-dependent, optimum thrust wings in supersonic flow
p 483 N93-20169
- SHOCK RESISTANCE**
Longitudinal acceleration test of overhead luggage bins in a transport airframe section
[DOT/FAA/CT-92/9] p 991 N93-31652
- SHOCK SIMULATORS**
Subjective response to simulated sonic booms with ground reflections
[NASA-TM-107764] p 852 N93-28692
- SHOCK TUBES**
Comparison of limiters in flux-split algorithms for Euler equations
[AIAA PAPER 93-0068] p 262 A93-20181
- Numerical prediction of instabilities in transonic internal flows using an Euler TVD code
[AIAA PAPER 93-0072] p 262 A93-20184
- Development of ultra-hypersonic shock tunnel for aerodynamics test
p 376 A93-21900
- Uniform high-order spectral methods for one- and two-dimensional Euler equations
p 476 A93-27068
- Modeling of flow in a pulsed shock tunnel
p 777 A93-39152
- Shock waves; Proceedings of the 18th International Symposium, Sendai, Japan, July 21-26, 1991. Vols. 1 & 2
[ISBN 0-387-55686-9] p 1023 A93-45451
- Shock tube application - High enthalpy European wind tunnels
p 1011 A93-45452
- Performance considerations in the operation of free-piston driven hypersonic test facilities
p 1011 A93-45497
- Shock tube validation experiments for the simulation of ram-accelerator-related combustion and gasdynamic problems
p 1016 A93-45499
- A laser induced fluorescence system for the high enthalpy shock tunnel (HEG) in Goettingen
p 1024 A93-45506
- Free piston facilities with air driver gas
p 1011 A93-45528
- Double diaphragm driven free piston expansion tube
p 1016 A93-45533
- A singularities tracking conservation law scheme for compressible duct flows
p 960 A93-45542
- Some measurements on dependence of rectangular cylinder drag on elevation
p 1025 A93-45745
- An investigation on the use of a heavy gas to improve the performance of the equilibrium interface technique in shock tube flows
[AIAA PAPER 93-2017] p 1078 A93-49855
- Research activity at the shock tube facility at NASA Ames
p 1252 A93-54804
- Shock enhancement and control of hypersonic combustion
[AD-A254295] p 72 N93-10843
- Computation of re-entry flows with two-temperature model
p 301 N93-19295
- SHOCK TUNNELS**
Experiments on Space Shuttle Orbiter models in a free piston shock tunnel
p 7 A93-11497
- Free piston shock tunnels - Developments and capabilities
p 66 A93-12316
- Development of ultra-hypersonic shock tunnel for aerodynamics test
p 376 A93-21900
- Hypervelocity scramjet capabilities of the T5 Free-Piston Tunnel at Caltech
[AIAA PAPER 92-5037] p 376 A93-22311
- Data analysis of the parametric scramjet combustor experiments conducted in the Calspan 96 inch shock tunnel - 4th entry
[AIAA PAPER 92-5098] p 359 A93-22368
- Transition on a sharp cone at high enthalpy - New measurements in the shock tunnel T5 at GALCIT
[AIAA PAPER 93-0343] p 281 A93-23030
- Increase in stagnation pressure and enthalpy in shock tunnels
[AIAA PAPER 93-0350] p 377 A93-23035
- Characterization of the performance of shock-tube wind tunnels
[AIAA PAPER 93-0351] p 377 A93-23036
- Quasi-one-dimensional modelling of free-piston shock tunnels
[AIAA PAPER 93-0352] p 377 A93-23037
- An optical comparison of wall and axial injection for high enthalpy reacting scramjet flows
[AIAA PAPER 93-0357] p 377 A93-23040
- Numerical study of the flow establishment time in hypersonic shock tunnels
p 480 A93-29153
- Numerical simulation of starting process in a hypersonic nozzle
p 684 A93-34275
- High-temperature supersonic combustion testing with optical diagnostics
p 730 A93-34498
- Development update for the NASA Ames 16-inch Shock Tunnel Facility
p 822 A93-37873
- Millisecond aerodynamic force measurement with side-jet model in the ISL shock tunnel
p 822 A93-39414
- Performance considerations in the operation of free-piston driven hypersonic test facilities
p 1011 A93-45497
- Performance data of the new free-piston shock tunnel T5 at GALCIT
p 1011 A93-45498
- A laser induced fluorescence system for the high enthalpy shock tunnel (HEG) in Goettingen
p 1024 A93-45506
- Shock tunnel studies of external combustion in high supersonic air flows
p 1017 A93-45517
- Free piston facilities with air driver gas
p 1011 A93-45528

- A combined facility of ballistic range and shock tunnel using a fast action valve p 1012 A93-45532
- Computational fluid dynamics code validation using a free piston hypervelocity shock tunnel p 960 A93-45545
- On the compression process in a free-piston shock-tunnel p 1136 A93-48041
- Absolute intensity measurements of impurity emissions in a shock tunnel and their consequences for laser-induced fluorescence experiments p 1147 A93-48044
- Shock tunnel experiments and approximate methods on hypervelocity side-jet control effectiveness [AIAA PAPER 93-1929] p 1077 A93-49794
- An investigation on the use of a heavy gas to improve the performance of the equilibrium interface technique in shock tube flows [AIAA PAPER 93-2017] p 1078 A93-49855
- Numerical study of the transient flow in the driven tube and the nozzle section of a shock tunnel [AIAA PAPER 93-2018] p 1078 A93-49856
- Hypersonic vehicle research by using a large shock tunnel [AAS PAPER 91-607] p 1250 A93-55841
- Experimental studies in the Aachen hypersonic shock tunnel p 1251 A93-56032
- Experimental Investigation of Nozzle/Plume Aerodynamics at Hypersonic Speeds [NASA-CR-191368] p 386 A93-18085
- Increase of stagnation pressure and enthalpy in shock tunnels p 295 A93-18086
- Numerical simulation of hypersonic flow around H-2 Orbiting Plane (HOPE), part 3 p 301 A93-19297
- Aerodynamic heating analysis for axisymmetric bodies in supersonic flow p 303 A93-19312
- Numerical simulation of the flow in a 1:57-scale axisymmetric model of a large blast simulator [AD-A265551] p 1015 A93-31916
- SHOCK WAVE ATTENUATION**
- Effect of the body shape on head shock attenuation at a large distance from the axis p 127 A93-16708
- SHOCK WAVE GENERATORS**
- Expanding the waverider design space using general supersonic and hypersonic generating flows [AIAA PAPER 93-0505] p 283 A93-23253
- Oblique shock formation in impulsively started wedge flows p 692 A93-35636
- SHOCK WAVE INTERACTION**
- Calculation of the three-dimensional interaction of a shock wave with a boundary layer on a cylinder p 12 A93-12766
- Shock wave interference on a wing with a partition at hypersonic velocities p 13 A93-12839
- An experimental study for interaction flow between shock wave and turbulent boundary layer p 120 A93-14355
- Supersonic wing/body interference p 121 A93-14391
- Euler solutions simulating strong shock waves and vortex phenomena over 3D wings p 121 A93-14392
- Hypersonic flow separation in shock wave boundary layer interactions [ASME PAPER 92-GT-205] p 251 A93-19429
- Prediction of 2D viscous transonic flow in compressor cascades using a semi-empirical shock/boundary-layer interaction method [ASME PAPER 92-GT-277] p 253 A93-19470
- Numerical simulation of shock-induced combustion/detonation p 410 A93-20719
- Computational analysis of hypersonic shock wave/wall jet interaction [AIAA PAPER 93-0604] p 269 A93-21113
- Holographic interferometric investigation of shock wave interaction with a ramp p 271 A93-21921
- Numerical simulation of unsteady transonic nozzle flows p 272 A93-22230
- Study of flow phenomena in high speed intakes [AIAA PAPER 92-5029] p 272 A93-22304
- A study of hypersonic swept shock wave/turbulent boundary layer interactions using a conical Navier-Stokes code [AIAA PAPER 92-5050] p 273 A93-22322
- Hypersonic turbulent expansion-corner flow with shock impingement [AIAA PAPER 92-5101] p 274 A93-22371
- Evaluation of a CFD code for analysis of normal-shock trains [AIAA PAPER 93-0292] p 279 A93-22692
- A parametric study of bleed in shock boundary layer interactions [AIAA PAPER 93-0294] p 280 A93-22694
- Wall pressure fluctuations beneath swept shock wave/boundary layer interactions [AIAA PAPER 93-0384] p 282 A93-23063
- Three-dimensional hypersonic shock wave/turbulent boundary-layer interactions p 287 A93-23533

- Shock/boundary-layer interaction control with vortex generators and passive cavity p 287 A93-23546
- Mean flowfield structure of a three-dimensional supersonic turbulent boundary layer [AIAA PAPER 93-0661] p 465 A93-24774
- The effect of shock motion on entropy production [AIAA PAPER 93-0665] p 465 A93-24777
- Multigrid techniques for hypersonic viscous flows [AIAA PAPER 93-0771] p 467 A93-24855
- On high speed turbulence modeling of shock-wave boundary-layer interaction [AIAA PAPER 93-0778] p 541 A93-24860
- Numerical simulation of crossing/turbulent boundary layer interaction at Mach 8.3 comparison of zero and two-equation turbulence models [AIAA PAPER 93-0779] p 467 A93-24861
- Interaction strength and model geometry effects on the structure of crossing-shock wave/turbulent boundary-layer interactions [AIAA PAPER 93-0780] p 467 A93-24862
- Hypersonic shock-wave/turbulent-boundary-layer interactions [AIAA PAPER 93-0781] p 467 A93-24863
- High-speed helicopter rotor noise - Shock waves as a potent source of sound p 565 A93-29403
- Shock waves and the Flowcs Williams-Hawkins equation p 480 A93-29411
- Interaction of compression waves with an elastic spherical dome p 550 A93-29718
- Numerical simulation of passive control of shock-boundary layer interaction for transonic airfoil p 680 A93-33719
- Parametrical investigation of the interaction between turbulent wall shear layers and normal shock waves, including separation p 681 A93-33752
- A unified hypersonic/supersonic method for aeroelastic applications including shock-unsteady wave interaction [AIAA PAPER 93-1317] p 738 A93-33892
- A study on two-dimensional and three-dimensional secondary jet interactions with a supersonic flow p 683 A93-34273
- A study on three-dimensional shock wave/turbulent boundary layer interaction induced by sweptback sharp fins at supersonic flow p 684 A93-34274
- Computations and experiments for a multiple normal shock/boundary-layer interaction p 688 A93-34486
- Calculation of the irregular interaction of shock waves p 691 A93-35339
- Applications of shock-induced mixing to supersonic combustion p 735 A93-35618
- Correlation of conical interactions induced by sharp fins and semicones p 692 A93-35635
- Experiments on shock wave-boundary layer interaction at high Mach number with entropy layer effect [ONERA, TP NO. 1992-101] p 771 A93-38581
- Analysis of turbulence in supersonic flows by means of laser velocimetry [ONERA, TP NO. 1992-148] p 773 A93-38729
- Shock/boundary layer interaction in a hypersonic flow in the presence of an entropy layer [ONERA, TP NO. 1992-181] p 773 A93-38743
- Shock wave/boundary layer interaction in a two-dimensional laminar hypersonic flow [ONERA, TP NO. 1992-182] p 773 A93-38744
- Theoretical and experimental study of the behavior of particles passing through a shock wave [ONERA, TP NO. 1992-233] p 774 A93-38777
- Asymptotic structure of a limiting hypersonic flow in a shock wave p 776 A93-39131
- An approximate method for calculating nonequilibrium flows near blunt bodies p 776 A93-39134
- Calculation of the effect of the shock wave of a delta wing on a second wing at supersonic velocities p 776 A93-39141
- Shock interference prediction using direct simulation Monte Carlo p 778 A93-39258
- The experimental study of the effect of sweptback angles and the front shape of the fin on reduction of shock wave/turbulent boundary layer interaction region p 858 A93-40431
- Passive control of a shock wave/turbulent boundary layer interaction in a transonic flow p 858 A93-40444
- High-speed turbulence modeling of shock-wave/boundary-layer interaction p 927 A93-41910
- Experiments on shock-wave/boundary-layer interactions produced by two-dimensional ramps and three-dimensional obstacles p 865 A93-42589
- An experimental contribution to the flat plate 2D compression ramp, shock/boundary layer interaction problem at Mach 14 - Test case 3.7 p 865 A93-42590
- Transonic shockwave/turbulent boundary layer interactions on a porous surface p 873 A93-43686
- Further study of high speed single free jets p 873 A93-43687

- Two-dimensional CFD modeling of wave rotor flow dynamics [AIAA PAPER 93-3318] p 952 A93-45014
- Shock waves; Proceedings of the 18th International Symposium, Sendai, Japan, July 21-26, 1991. Vols. 1 & 2 [ISBN 0-387-55686-9] p 1023 A93-45451
- Oscillations of circular shock waves with upstream disturbance p 1023 A93-45463
- Formation of the shock reflection on a wedge p 1023 A93-45476
- Aerodynamic heating phenomenon in three dimensional shock wave/turbulent boundary layer interaction induced by sweptback fins in hypersonic flows p 960 A93-45507
- Computation of unsteady nozzle flows p 960 A93-45543
- A propulsion device driven by reflected shock waves p 1001 A93-45550
- Viscous hypersonic shock-shock interaction on a blunt body at high altitude [AIAA PAPER 93-2722] p 962 A93-46477
- Aerodynamic heating in the vicinity of hypersonic, axisymmetric, shock-wave boundary-layer interactions [AIAA PAPER 93-2766] p 963 A93-46512
- Passive control of shock wave/boundary layer interaction at hypersonic speed [AIAA PAPER 93-3249] p 966 A93-46794
- Effects of bleed-hole geometry and plenum pressure on three-dimensional shock-wave/boundary-layer/bleed interactions [AIAA PAPER 93-3259] p 967 A93-46800
- Control of unsteady shock-induced turbulent boundary layer separation upstream of blunt fins [AIAA PAPER 93-3281] p 969 A93-46839
- Experiments on shock wave/boundary layer interaction in hypersonic flow p 970 A93-46888
- Calculations on a double-fin turbulent interaction at high speed [AIAA PAPER 93-3432] p 977 A93-47224
- Flow field measurements in a crossing shockwave turbulent boundary layer interaction at Mach 3 [AIAA PAPER 93-3434] p 977 A93-47226
- Scaling of incipient separation in high speed laminar flows [AIAA PAPER 93-3435] p 978 A93-47227
- Normal shock wave oscillations in supersonic diffusers p 1044 A93-48042
- Investigation of a hypersonic crossing shock wave/turbulent boundary layer interaction p 1044 A93-48043
- Effects of junction modifications on sharp-fin-induced shock wave/boundary layer interaction [AIAA PAPER 93-2935] p 1046 A93-48133
- Reynolds stress transport modelling of shock/boundary-layer interaction [AIAA PAPER 93-2936] p 1046 A93-48134
- Shock-wave/boundary layer interactions at hypersonic speeds by an implicit Navier-Stokes solver [AIAA PAPER 93-2938] p 1046 A93-48136
- Intense studies on unsteady secondary separations and oscillating shock waves in three-dimensional shock waves/turbulent boundary layer interaction regions induced by sharp and blunt fins [AIAA PAPER 93-2939] p 1046 A93-48137
- Improvement of conical similarity rule in swept shock wave/boundary layer interaction [AIAA PAPER 93-2941] p 1046 A93-48139
- Interaction of the sonic boom with atmospheric turbulence [AIAA PAPER 93-2943] p 1171 A93-48140
- Shock-vortex interaction over a 65-degree delta wing in transonic flow [AIAA PAPER 93-2973] p 1049 A93-48167
- Experimental study of shock wave and hypersonic boundary layer interactions near a convex corner [AIAA PAPER 93-2980] p 1051 A93-48173
- Effects of boundary layer bleed on swept-shock/boundary layer interaction [AIAA PAPER 93-2989] p 1052 A93-48182
- An investigation of shock wave turbulent boundary layer interaction with bleed through slanted slots [AIAA PAPER 93-2992] p 1052 A93-48184
- Laser interferometer Skin-Friction measurements of crossing-shock wave/turbulent boundary-layer interactions [AIAA PAPER 93-3072] p 1148 A93-48247
- Numerical simulation of a shock wave/turbulent boundary layer interaction in a duct [AIAA PAPER 93-3127] p 1063 A93-48293
- Experimental study of transitional axisymmetric shock-boundary layer interactions at Mach 5 [AIAA PAPER 93-3131] p 1063 A93-48296
- Exploratory study of shock reflection near an expansion corner [AIAA PAPER 93-3132] p 1063 A93-48297

Flowfield dynamics in blunt fin-induced shock wave/turbulent boundary layer interactions
[AIAA PAPER 93-3133] p 1063 A93-48298

Aerothermodynamic heating due to shock wave/laminar boundary-layer interactions in high-enthalpy hypersonic flow
[AIAA PAPER 93-3135] p 1064 A93-48299

A study of the interaction of a nonstationary shock wave with a boundary layer on a plate in the transition regime
p 1150 A93-48850

Multigrid techniques for hypersonic viscous flows
p 1071 A93-49027

Simulation of shock-boundary layer interaction in a fan blade passage
[AIAA PAPER 93-1980] p 1078 A93-49827

A numerical study of the unsteady processes associated with the type IV shock interaction
[AIAA PAPER 93-2479] p 1083 A93-50221

A study of incipient separation limits for shock-induced boundary layer separation for Mach 6 high Reynolds flow
[AIAA PAPER 93-2481] p 1084 A93-50222

Numerical simulation of shock/shock and shock-wave/boundary-layer interactions in hypersonic flows
p 1093 A93-52000

A time-accurate high-resolution TVD scheme for solving the Navier-Stokes equations
p 1093 A93-52006

Analysis of unstated supersonic flutter in cascade by semiactuator disk theory
p 1181 A93-53841

A study of the stability of vortical structures in supersonic inlets
[ISABE 93-7103] p 1187 A93-54079

Correlative behaviours of shock/boundary layer interaction induced by sharp fin and semicone
p 1230 A93-54581

Development of separation due to interaction between a shock wave and a turbulent boundary layer perturbed by rarefaction waves
p 1233 A93-55019

Effects of sweep on the physics of unsteady shock-induced turbulent separated flows
[AD-A247035] p 22 N93-11742

AGARD WG13 aerodynamics of high speed air intakes: Assessment of CFD results
p 215 N93-13220

Time dependent heat transfer rates in high Reynolds number hypersonic flowfields
p 216 N93-13664

Static pressure measurements of the shock-boundary layer interaction in a simulated fan passage
[AD-A256724] p 361 N93-15979

The effects of viscosity on a conically derived waverider
[AD-A259019] p 424 N93-19101

An experimental study of the sources of fluctuating pressure loads beneath swept shock/boundary-layer interactions
[NASA-CR-192918] p 749 N93-25266

Navier-Stokes simulations of unsteady transonic flow phenomena
p 697 N93-25542

Heat transfer measurements in swept shock wave/turbulent boundary-layer interactions
p 750 N93-25705

Parametric studies of shock wave/boundary layer interactions over 2D compression corners at Mach 6
[VKI-TN-181] p 988 N93-31538

Calculations on unsteady type 4 interaction at Mach 8
[AD-A265214] p 990 N93-32004

SHOCK WAVE PROFILES

Shock wave ahead of a liquid jet in supersonic cross flow
p 477 A93-27605

Analytic methods for design of wave cycles for wave rotor core engines
[AIAA PAPER 93-2523] p 1121 A93-50253

Shock shapes around slender diamond cones traveling at hypersonic speed
p 1181 A93-53840

Sonic boom minimization - Myth or reality?
p 1264 A93-55859

Two problems reducing the data accuracy in Transonic Wind Tunnel testing
p 304 N93-19321

SHOCK WAVE PROPAGATION

Viscous instability of hypersonic flow past a wedge
p 4 A93-10137

Analysis of structural dynamic response for aircraft operating in the environment of nuclear explosion shock waves
p 78 A93-11810

Oscillation of circular shock waves with upstream nonuniformity
p 208 A93-15496

Experimental results of shock trains in rectangular ducts
[AIAA PAPER 92-5103] p 274 A93-22373

Shock oscillation in two-dimensional, inviscid, unsteady channel flow
p 288 A93-23563

Reaction zone structure for strong, weak overdriven, and weak underdriven oblique detonations
p 746 A93-35492

Experimental investigation of slot injection into supersonic flow with an adverse pressure gradient
[AIAA PAPER 93-2442] p 1119 A93-50194

Surface and flow field measurements in a symmetric crossing shock wave/turbulent boundary-layer interaction
[NASA-TM-106086] p 693 N93-24911

Some aspects of the aeroacoustics of high-speed jets
[NASA-CR-191458] p 843 N93-28975

SHOCK WAVES

Numerical computations of turbomachinery cascade turbulent flows with shocks by using multigrid scheme
p 112 A93-14167

Turbulence modelling requirements for the prediction of viscous transonic aeroflow flows
p 115 A93-14249

Experimental investigations of the separation behavior in 3D shock wave/turbulent boundary-layer interactions
p 119 A93-14345

Visualization and analysis of supersonic flow in rotating turbine stage. I - Influence of shock wave between stationary and moving blades
p 126 A93-15449

Study on unsymmetrical supersonic nozzle flows
p 127 A93-16933

Effect of airfoil porosity on the shock wave position and intensity at transonic velocities
p 241 A93-18222

A numerical method for the prediction of quadrupole shock wave noise
p 448 A93-19201

Recent advances in simulating unsteady flow phenomena brought about by passage of shock waves in a linear turbine cascade
[ASME PAPER 92-GT-4] p 245 A93-19277

Blade loading and shock wave in a transonic circular cascade diffuser
[ASME PAPER 92-GT-34] p 246 A93-19294

Design and rotor performance of a 5:1 mixed-flow supersonic compressor
[ASME PAPER 92-GT-73] p 348 A93-19323

Transonic shock oscillations calculated with a new interactive boundary layer coupling method
[AIAA PAPER 93-0777] p 269 A93-21119

The Burnett shock structures in low density hypersonic flows
[AIAA PAPER 92-5048] p 273 A93-22320

Waverider design for generalized shock geometries
[AIAA PAPER 93-0774] p 467 A93-24858

Correlation of interaction sweepback effects on unsteady shock-induced turbulent separation
[AIAA PAPER 93-0776] p 475 A93-25550

The role of Kutta waves on oscillatory shock motion on an airfoil experiencing heavy buffeting
[AIAA PAPER 93-1589] p 682 A93-34121

Application of Oswatitsch's theorem to supercritical airfoil drag calculation
p 768 A93-37399

Engineering method for calculating surface pressures and heating rates on vehicles with embedded shocks
p 777 A93-39255

Mach disk of dual coaxial axisymmetric jets
p 861 A93-41932

Numerical experiments with nonoscillatory schemes using Eulerian and new Lagrangian formulations
p 862 A93-42432

Thermo-chemical models for hypersonic flows
p 863 A93-42433

Reactive and inert inviscid flow solutions by quasi-linear formulations and shock fitting
p 927 A93-42625

Review of chemical-kinetic problems of future NASA missions. I - Earth entries
p 872 A93-42899

Shock waves; Proceedings of the 18th International Symposium, Sendai, Japan, July 21-26, 1991. Vols. 1 & 2
[ISBN 0-387-55686-9] p 1023 A93-45451

Formation of shock waves in transient base flow
p 1023 A93-45460

Oscillations of circular shock waves with upstream disturbance
p 1023 A93-45463

Computation of crossing shock/turbulent boundary layer interaction at Mach 8.3
p 961 A93-45726

Non-equilibrium thermal radiation from air shock layers modelled with the Direct Simulation Monte Carlo method
[AIAA PAPER 93-2805] p 1028 A93-46544

On the shock-fitting scheme of Hall-Crawley for time-linearized time-harmonic flows using Euler equations
p 972 A93-46946

Clebsch variable model for unsteady inviscid transonic flow with strong shock waves
[AIAA PAPER 93-3025] p 1055 A93-48210

Numerical simulation of a blast inside a Boeing 747
[AIAA PAPER 93-3091] p 1099 A93-48265

Tip shock structures in transonic compressor rotors
[AIAA PAPER 93-1869] p 1075 A93-49744

A time-accurate high-resolution TVD scheme for solving the Navier-Stokes equations
p 1093 A93-52006

Results about the structure of the shock wave reflection process for strong incoming shock waves
p 1233 A93-54810

Numerical studies of Mach reflection with air chemistry
p 1233 A93-54815

Chemical nonequilibrium effects of Mach reflection
p 1233 A93-54816

Algebraic determination of the shock wave shape in axisymmetric flow over a circular cylinder
p 1237 A93-56030

Experimental investigations of hypersonic shock-boundary layer interaction
p 1238 A93-56037

Effects of reacting flows with turbulence and shock waves on efficiency of scramjet combustors
p 69 N93-11133

A preliminary study associated with the experimental measurement of the aero-optic characteristics of hypersonic configurations
[AD-A253792] p 24 N93-12063

Mach 4 testing of scramjet inlet models
[NAL-TR-1137] p 26 N93-12369

Effect of the flow non-uniformity on the mixing layer at the interface of parallel supersonic flows
[ISAS-RN-646] p 128 N93-12716

A preliminary study of the effect of equivalence ratio on a low emissions gas turbine combustor using KIVA-2
[DE92-018616] p 215 N93-13321

An experimental/computational study of heat transfer in sharp fin induced shock wave/turbulent boundary layer interactions at low hypersonic Mach numbers
p 217 N93-13826

Computational analysis of hypersonic flows past elliptic-cone waveriders
[NASA-CR-191304] p 138 N93-14767

Time-dependent predictions and analysis of turbine cascade data in the transonic flow region
[PNR-90957] p 139 N93-15489

Two- and three-dimensional blade vortex interactions
[NASA-CR-177567] p 293 N93-16942

Computation of internal flows using unstructured triangular meshes
p 299 N93-19276

Analytical and numerical study on steady Mach reflection
p 302 N93-19309

Numerical study on transverse hydrogen injection into a supersonic flowfield
p 302 N93-19311

Three dimensional calculation of flow inside supersonic inlet
p 303 N93-19313

Development and application of computational aerothermodynamics flowfield computer codes
[NASA-CR-192940] p 692 N93-24736

Fuel Injector: Air swirl characterization aerothermal modeling, phase 2, volume 2
[NASA-CR-189193-VOL-2] p 721 N93-25106

Computation of transonic flow over a porous surface projectile
p 696 N93-25409

Turbulence interacting with chemical kinetics in airbreathing combustion of ducted rockets
p 734 N93-26012

Adjoint methods for aerodynamic wing design
[NASA-CR-193086] p 805 N93-27089

Godunov-type schemes applied to detonation flows
[NASA-CR-191447] p 780 N93-27090

International aviation (Selected articles)
[AD-A262566] p 765 N93-28576

Analysis of unsteady wave processes in a rotating channel
[NASA-CR-191154] p 816 N93-28617

Kinetics and energy transfer in nonequilibrium fluid flows
[AD-A263612] p 875 N93-29284

Contribution to the study of the interaction between acoustic waves and coherent structures induced by a prismatic cylinder in a rectangular cavity
[ONERA-NT-1990-10] p 918 N93-30203

Calculations on unsteady type 4 interaction at Mach 8
[AD-A265214] p 990 N93-32004

SHORT CRACKS

Fatigue propagation behaviour of short cracks in titanium alloys
[ESDU-92023] p 392 N93-16637

Fatigue propagation behaviour of short cracks in aluminum alloys
[ESDU-92030] p 392 N93-16641

SHORT HAUL AIRCRAFT

A short range passenger/freighter canard - Some problems of a preliminary aerodynamic concept
[SAE PAPER 921012] p 157 A93-14642

Designed for work --- British Aerospace Jetstream 41 regional aircraft
p 506 A93-27276

Modern propeller systems for advanced turboprop aircraft
[AIAA PAPER 93-1846] p 1111 A93-49727

Aeronautical technologies for the twenty-first century
[NASA-CR-190918] p 4 N93-10647

SHORT TAKEOFF AIRCRAFT

Numerical simulation of STOL operations using thrust-vectoring
[AIAA PAPER 92-4254] p 15 A93-13342

A study of the effect of a moving ground belt on the vortex created by a jet impinging on the ground in a cross flow
[AIAA PAPER 92-4250] p 15 A93-13361

- Design of reduced-order observers with precise loop transfer recovery p 184 A93-14587
Limit cycle in the longitudinal motion of the USB STOL ASKA - Control system functional mockup and actual aircraft p 185 A93-14660
[SAE PAPER 921040]
HUD Guidance for the ASKA Experimental STOL Aircraft using Radar Position Information p 150 A93-14661
[SAE PAPER 921041]
Some aspects of variable geometry gas turbine operation p 356 A93-19556
[ASME PAPER 92-GT-407]
Zen and the art of airplane sizing p 504 A93-25174
Optimal takeoff procedures for a transport category tiltrotor p 802 A93-37377
AIAA Applied Aerodynamics Conference, 11th, Monterey, CA, Aug. 9-11, 1993, Technical Papers, Pts. 1 & 2 p 974 A93-47201
Results and lessons learned from two Wright Laboratory flight research programs p 1099 A93-48341
[AIAA PAPER 93-3661]
A method of wind shear detection for powered-lift STOL aircraft p 1104 A93-48345
[AIAA PAPER 93-3667]
Wind-shear endurance capability for powered-lift aircraft p 1129 A93-48348
[AIAA PAPER 93-3670]
Wind tunnel results for an advanced fighter configuration employing transverse thrust for enhanced STOL capability p 1100 A93-49796
[AIAA PAPER 93-1933]
A wind tunnel investigation to determine buffet countermeasures for STOL aircraft alpha-sweep flight testing p 65 N93-12362
[NAL-TR-1129]
Propulsion integration results of the STOL and Maneuver Technology Demonstrator p 161 N93-13228
High-speed aerodynamics of upper surface blowing aircraft configurations p 132 N93-13729
An investigation of two-propeller tilt wing V-STOL aircraft flight characteristics p 332 N93-17694
[AD-A257751]
An experimental investigation of a finite circulation control wing p 340 N93-18896
[AD-A259044]
Evaluation of four advanced nozzle concepts for short takeoff and landing performance p 875 N93-29165
[NASA-TP-3314]
- SHOT PEENING**
Development of the neutron diffraction technique for the determination of near surface residual stresses in critical gas turbine components p 58 N93-11112
[PNR-90984]
- SHROUDED PROPELLERS**
Aeroacoustic wind tunnel testing of a counterrotating shrouded propfan-model p 449 A93-19213
Forward rotor vortex effects on counter rotating propeller noise p 245 A93-19221
Rim seal experiments and analysis of a rotor-stator system with nonaxisymmetric main flow p 402 A93-19387
[ASME PAPER 92-GT-160]
Acoustic mode measurements in the inlet of a model turbofan using a continuously rotating rake - Data collection/analysis techniques p 361 A93-23324
[AIAA PAPER 93-0599]
Acoustic mode measurements in the inlet of a model turbofan using a continuously rotating rake p 563 A93-24783
[AIAA PAPER 93-0598]
Effect of a rotating propeller on the separation angle of attack p 472 A93-24978
[AIAA PAPER 93-0017]
3-D viscous flow CFD analysis of the propeller effect on an advanced ducted propeller subsonic inlet p 1075 A93-49728
[AIAA PAPER 93-1847]
Rotor wake/stator interaction noise - Predictions vs data p 1174 A93-52447
Comparison of radiated noise from shrouded and unshrouded propellers p 1264 A93-55861
Acoustic mode measurements in the inlet of a model turbofan using a continuously rotating rake: Data collection/analysis techniques p 179 N93-15403
[NASA-TM-105936]
Effect of a rotating propeller on the separation angle of attack and distortion in ducted propeller inlets p 290 N93-16625
[NASA-TM-105935]
Acoustic mode measurements in the inlet of a model turbofan using a continuously rotating rake p 362 N93-16705
[NASA-TM-105989]
Rotating rake design for unique measurement of fan-generated spinning acoustic modes p 724 N93-26161
[NASA-TM-105946]
The 3-D viscous flow CFD analysis of the propeller effect on an advanced ducted propeller subsonic inlet p 900 N93-29162
[NASA-TM-106240]
- SHROUDED TURBINES**
Tip clearance effect on heat transfer and leakage flows on the shroud-wall surface in an axial flow turbine [ASME PAPER 92-GT-200] p 403 A93-19425
Dynamic analysis of annular cascade structures p 1259 A93-55586
- SHROUDS**
Integrity testing of brush seal in shroud ring of T-700 engine p 421 N93-18380
[NASA-TM-105863]
- SHUTDOWNS**
Approach of modeling continuous turbine engine operation from startup to shutdown p 721 A93-34495
Modelling the engine temperature distribution between shut down and restart for life usage monitoring p 169 N93-15177
- SIDE INLETS**
An experimental study of the effects of bodyside compression on forward swept sidewall compression inlets ingesting a turbulent boundary layer p 1072 A93-49515
[AIAA PAPER 93-3125]
- SIDELobe REDUCTION**
Digital pulse compression with low range sidelobes p 929 A93-43463
[AD-A255070]
ACTA Aeronautica et Astronautica Sinica (selected articles) p 110 N93-13946
- SIDELobES**
ACTA Aeronautica et Astronautica Sinica (selected articles) p 110 N93-13946
[AD-A255070]
- SIDESLIP**
The aerodynamic effects of sideslip on double delta wings p 261 A93-20166
[AIAA PAPER 93-0053]
Aerodynamic forces and moments on a dihedral swept wing in a translation with attack and side-slip angle p 476 A93-26903
Mathematical phenomenology for thrust-vectoring-induced agility comparisons p 525 A93-28613
Installed F/A-18 inlet flow calculations at 60 deg angle-of-attack and 10 deg side slip p 1074 A93-49695
[AIAA PAPER 93-1806]
Contribution of ventral fins to sideforce and yawing moment derivatives due to sideslip at low angle of attack p 291 N93-16638
[ESDU-92029]
- SIERRA NEVADA MOUNTAINS (CA)**
Natural and augmented snowfall growth processes and their interactions with the natural and modified aerosol [PB93-153096] p 755 N93-25874
- SIGNAL ANALYSIS**
New algorithms for hyperbolic radionavigation p 881 A93-40359
Development of a system for transition characterization --- for aerodynamic simulations p 1030 A93-47246
[AIAA PAPER 93-3465]
Time-frequency domain analysis of vibration signals for machinery diagnostics. 3: The present power spectral density p 89 N93-11707
[QUEL-1911/92]
Classification of radar clutter in an air traffic control environment p 886 N93-30299
- SIGNAL DETECTION**
Detection and classification of acoustic signals from fixed-wing aircraft p 850 A93-37032
- SIGNAL DISTORTION**
Measurement technique for Loran-C pulse wave distortion measures and performance in an environment of noise p 29 A93-10988
- SIGNAL ENCODING**
An optimal detection algorithm for harmonic interference signals in Loran-C p 993 A93-46889
- SIGNAL FADING**
Multipath effects on GPS code phase measurements p 34 A93-11295
- SIGNAL PROCESSING**
Design, capabilities, and performance of the miniaturized airborne GPS receiver p 32 A93-11014
The use of satellite geometry for prevention of cycle slips in a GPS processor p 34 A93-11298
Analysis of a high-performance C/A-code GPS receiver in kinematic mode p 317 A93-21822
Signal processing of jet noise from flyover test data [AIAA PAPER 93-0736] p 563 A93-24826
Signal processing and system identification techniques for flutter test data analysis p 529 A93-29282
Some limitations on the effectiveness of airborne adaptive radar p 501 A93-29596
Digital resolver for helicopter model blade motion analysis p 830 A93-37878
Topographic mapping using a Ku-band airborne elevation interferometer p 896 A93-42786
- Radar 92: Proceedings of the International Conference, Brighton, United Kingdom, Oct. 12, 13, 1992 [ISBN 0-85296-533-2] p 929 A93-43376
Radar signals analysis oriented to target characterization applied to civilian ATC radar p 885 A93-43475
Robust method for estimating the parameters of a linear FM waveform p 1147 A93-47650
A novel-high-performance system for recording and analysing instantaneous total pressure distortion in air intakes p 214 N93-13215
ACTA Aeronautica et Astronautica Sinica (selected articles) p 110 N93-13946
[AD-A255070]
Signal processing for airborne doppler radar detection of hazardous wind shear as applied to NASA 1991 radar flight experiment data p 490 N93-19612
RAMSES: Multi-spectral experimental radar station installed on board the Transall p 550 N93-19925
Design, fabrication, and testing of a three-dimensional acoustic orientation instrument (3-D AOI): Drawings, engineering and associated lists (conceptual and development design) p 760 N93-25915
[AD-A260934]
Detection performance of digital polarity sampled phase reversal code pulse compressors p 842 N93-28289
[AD-A262930]
- SIGNAL RECEPTION**
Measurement technique for Loran-C pulse wave distortion measures and performance in an environment of noise p 29 A93-10988
Analysis of Loran-C performance in the Pemberton area, B.C. p 311 A93-17797
- SIGNAL TO NOISE RATIOS**
Calculation of the passive noise power for onboard single-pulse automatic direction tracking systems p 882 A93-43111
Digital pulse compression with low range sidelobes p 929 A93-43463
Detection performance of digital polarity sampled phase reversal code pulse compressors p 842 N93-28289
[AD-A262930]
The HYDICE instrument design and its application to planetary instruments p 842 N93-28766
- SIGNAL TRANSMISSION**
Development and flight testing of a fault-tolerant fly-by-light yaw control system p 1010 N93-31280
- SIGNATURE ANALYSIS**
A wall interference assessment/correction system [NASA-CR-190617] p 68 N93-11910
- SIGNATURES**
Wright Laboratory research and development facilities handbook [AD-A258746] p 572 N93-20403
Principles of nuclear-based explosive detection systems p 497 N93-21861
Subjective response to simulated sonic booms with ground reflections [NASA-TM-107764] p 852 N93-28692
- SIGNS AND SYMPTOMS**
Spurious symptom reduction in fault monitoring [NASA-CR-191453] p 942 N93-29192
- SIKORSKY AIRCRAFT**
Measurement of the dynamic undercarriage response of a Sikorsky S-70B-2 helicopter: Instrumentation and test methods: Flight mechanics technical memorandum [AD-A256319] p 329 N93-16404
The NASA/industry Design Analysis Methods for Vibrations (DAMVIBS) program: Sikorsky Aircraft: Advances toward interacting with the airframe design process p 515 N93-21315
- SILENCE**
Inter-noise '91: Proceedings of the 20th International Conference on Noise Control Engineering, Sydney, Australia, Dec. 2-4, 1991. Vols. 1 & 2 [ISBN 0-909882-12-6] p 557 A93-28476
- SILENCERS**
New design concepts for silencing aeroacoustic wind tunnels p 445 A93-19147
- SILICON**
Silicon differential pressure transducer line pressure effects and compensation p 830 A93-37890
- SILICON CARBIDES**
Machining cost comparison of silicon carbide discontinuously reinforced aluminum, unreinforced aluminum, and titanium [SME PAPER EM92-252] p 925 A93-40656
Carbon/silicon carbide composite materials in advanced unmanned gas turbine engine combustors [AIAA PAPER 93-1761] p 1144 A93-49658
Developments in silicon carbide for aircraft propulsion system applications [AIAA PAPER 93-2581] p 1157 A93-50295
Origin of the carbon rich sliding interface in alkali containing matrix-SiC nicalon fibre composites [ONERA, TP NO. 1993-77] p 1212 A93-53598

- High temperature rectifiers and MOS devices in 6H-silicon carbide
[AD-A254725] p 90 N93-12340
- FNAS modify matric and transparent experiments
[NASA-CR-184442] p 198 N93-13311
- Process optimization of Hexoloy SX-SiC towards improved mechanical properties
[DE93-007913] p 826 N93-28564
- SILICON NITRIDES**
- High temperature fracture mechanism of gas-pressure sintered silicon nitride p 825 A93-38893
- Improved silicon nitride for advanced heat engines
[NASA-CR-182193] p 917 N93-29451
- Microwave processing of silicon nitride for advanced gas turbine applications
[DE93-007910] p 917 N93-29767
- SILICON POLYMERS**
- Video luminescent barometry - The induction period
[AIAA PAPER 93-0179] p 414 A93-22607
- SILICONES**
- Oxidation-resistant high-temperature materials p 915 A93-40362
- Innovative bagging techniques on a composite P-51 Mustang replica p 1191 A93-53405
- SILVER IODIDES**
- Natural and augmented snowfall growth processes and their interactions with the natural and modified aerosol
[PB93-153096] p 755 N93-25874
- SIMD (COMPUTERS)**
- Numerical Wind Tunnel hardware p 383 N93-19289
- SIMILARITY THEOREM**
- Lord Rayleigh and hydrodynamic similarity p 211 A93-17408
- SIMPLE HARMONIC MOTION**
- A low-speed aerodynamic model for harmonically oscillating aircraft configurations p 8 A93-11500
- SIMULATED ANNEALING**
- Fast design of circular-harmonic filters using simulated annealing p 1038 A93-45556
- Optimization of blade arrangement in a randomly mistuned cascade using simulated annealing
[AIAA PAPER 93-2254] p 1115 A93-50052
- Discrete range clustering using Monte Carlo methods
[NASA-TM-104004] p 706 N93-24914
- Structural design using neural networks p 942 N93-31029
- SIMULATION**
- A wall interference assessment/correction system
[NASA-CR-190617] p 68 N93-11910
- ASTOVL model engine simulators for wind tunnel research p 192 N93-13213
- A simulation model of atmospheric turbulence for rotorcraft applications p 224 N93-14588
- Finite-difference solution for laminar or turbulent boundary layer flow over axisymmetric bodies with ideal gas, CF₄, or equilibrium air chemistry
[NASA-TP-3271] p 222 N93-15434
- Hermes CX-7: Air transport system design simulation
[NASA-CR-192082] p 335 N93-18056
- Arrow 227: Air transport system design simulation
[NASA-CR-192053] p 336 N93-18063
- The S.T.o.R.M. (tm): Air transport system design simulation
[NASA-CR-192070] p 338 N93-18349
- A simulation study of the effects of communication delay on air traffic control
[AD-A258593] p 502 N93-19966
- A model study of the aircraft cabin environment resulting from in-flight fires
[DOT/FAA/CT-90/22] p 496 N93-21557
- Studies in air/air supersonic mixing layers p 700 N93-26007
- Discrete-vortex simulation of pulsating flow on a turbulent leading-edge separation bubble p 787 N93-27457
- SIMULATORS**
- Turbofan propulsion simulator p 1247 A93-55493
- ASTOVL model engine simulators for wind tunnel research p 192 N93-13213
- Simulator evaluation of displays for a revised takeoff performance monitoring system
[NASA-TP-3270] p 189 N93-15366
- Loudness and annoyance response to simulated outdoor and indoor sonic booms
[NASA-TM-107756] p 852 N93-27271
- A laboratory study of subjective response to sonic booms measured at White Sands Missile Range
[NASA-TM-107746] p 852 N93-27272
- Development of a concept formulation process aid for analyzing training requirements and developing training devices
[AD-A263579] p 912 N93-29972
- Numerical simulation of the flow in a 1:57-scale axisymmetric model of a large blast simulator
[AD-A265551] p 1015 N93-31916
- SINGLE CRYSTALS**
- Microstructural study of aluminide surface coatings on single crystal nickel base superalloy substrates p 70 A93-12771
- Markov fatigue in single crystal airfoils
[ASME PAPER 92-GT-95] p 387 A93-19341
- Infrared thermography of plastic instabilities in a single crystal superalloy
[ONERA, TP NO. 1993-18] p 916 A93-41031
- Measurements of dynamic Young's modulus and damping in single crystals of a nickel-based superalloy as a function of temperature p 1147 A93-52513
- Fatigue in single crystal nickel superalloys
[AD-A254603] p 74 N93-12237
- Fatigue in single crystal nickel superalloys
[AD-A254704] p 198 N93-12746
- In-service considerations affecting component life p 177 N93-14898
- Fatigue in single crystal nickel superalloys
[AD-A258038] p 393 N93-17704
- Fatigue in single crystal nickel superalloys
[AD-A259191] p 536 N93-20275
- Fatigue in single crystal nickel superalloys
[AD-A260709] p 736 N93-25843
- Fatigue in single crystal nickel superalloys
[AD-A261742] p 737 N93-26282
- NDE of PWA 1480 single crystal turbine blade material
[NASA-TM-106140] p 815 N93-27640
- Fatigue in single crystal nickel superalloys
[AD-A265451] p 1019 N93-31795
- SINGLE EVENT UPSETS**
- Neutron-induced single event upsets in static RAMs observed at 10 KM flight altitude p 1158 A93-50561
- Single event upset in avionics p 1158 A93-50566
- SINGLE STAGE TO ORBIT VEHICLES**
- The United States in the conquest of the hypersonic p 109 A93-15056
- Aero-space plane figures of merit
[AIAA PAPER 92-5058] p 385 A93-22328
- An overview of aeroelasticity studies for the National Aero-Space Plane p 732 A93-33889
- [AIAA PAPER 93-1313] p 732 A93-33889
- MAKS - Eastern promise? --- multi-purpose aerospace system p 733 A93-34266
- Engineering method for calculating inlet face property profiles on high speed vehicle forebodies
[AIAA PAPER 93-3113] p 1062 A93-48283
- Hypersonic aerodynamic characteristics for Langley Test Technique Demonstrator
[AIAA PAPER 93-3443] p 1072 A93-49516
- Numerical simulations of a pulsed detonation wave augmentation device
[AIAA PAPER 93-1985] p 1112 A93-49832
- On stability and control of SSTO spaceplane in super- and hypersonic ascending phase
[NAL-TR-1128T] p 65 N93-12361
- Air-breathing hypersonic vehicle guidance and control studies: An integrated trajectory/control analysis methodology, phase 2
[NASA-CR-189703] p 65 N93-12413
- Robust nonlinear feedback guidance for an aerospace plane: A geometric approach p 189 N93-14835
- Aerospace-plane flights and stratospheric ozone: Review and preliminary assessment of the National Aerospace Plane (NASP) operations
[RAND/N-3464-AF] p 755 N93-26327
- SINGULAR INTEGRAL EQUATIONS**
- Numerical solution of the integral equations of the aerodynamics of porous surfaces p 13 A93-12768
- Integral equations in the problem of flow past an airfoil p 395 A93-18243
- Study on the numerical problem of the boundary element method in analysis of flow around a three-dimensional wing-body p 268 A93-20934
- Calculation of supersonic flow past a body of revolution with a piecewise linear distribution of singularities at its axis p 1092 A93-51910
- SINGULARITY (MATHEMATICS)**
- Calculation of 3-D unsteady subsonic flow with separation bubble using singularity method p 115 A93-14251
- A study of singularity formation in vortex-sheet motion by a spectrally accurate vortex method p 127 A93-16666
- Solving problems with singularities using conformal mappings p 397 A93-18978
- On the possibility of singularities in the acoustic field of supersonic sources when BEM is applied to a wave equation p 1039 A93-46805
- Optimal thrust magnitude on a singular arc in atmospheric flight p 758 N93-25410
- Analysis of wing wake roll-up using a vortex-in-cell method p 697 N93-25706
- SINTERING**
- High temperature fracture mechanism of gas-pressure sintered silicon nitride p 825 A93-38893
- Process optimization of Hexoloy SX-SiC towards improved mechanical properties
[DE93-007913] p 826 N93-28564
- SISO (CONTROL SYSTEMS)**
- The smart structures technology in the vibration control of helicopter blades in forward flight p 366 A93-17721
- An overview of possible and not-possible tasks for active control of sound and vibration p 568 A93-29429
- Applying variations of the quantitative feedback technique (QFT) to unstable, non-minimum phase aircraft dynamics models p 939 A93-42797
- Application of nonlinear systems theory to transonic unsteady aerodynamic responses p 1095 A93-52438
- Applications of active adaptive noise control to jet engines
[NASA-CR-192277] p 522 N93-21210
- SITE SELECTION**
- Adverse weather test site selection study
[AD-A259012] p 339 N93-18895
- SITTING POSITION**
- Experimental working position simulator to analyse, develop and optimize concepts for computer-aided Air Traffic Management p 191 A93-14412
- SIZE (DIMENSIONS)**
- Calculation of a collector-type annular plate heat exchanger p 833 A93-39045
- Modeling of the multiparameter assembly of engineering products for a specified priority of output geometrical parameters p 836 A93-39109
- Optimal conditions for flow turbulence reduction by a set of grids p 836 A93-39122
- Selection of the turbofan engine size p 899 A93-42379
- SIZE DISTRIBUTION**
- Atomization of JP-10/B4C gelled slurry fuel
[AD-A256827] p 391 N93-15686
- Particulate emissions from gas turbine engines
[AD-A261374] p 725 N93-26339
- SIZING (SURFACE TREATMENT)**
- Increasing the efficiency of the electrochemical dimensional machining of gas turbine engine blades of EP718VD alloy p 835 A93-39095
- Effect of the technological process structure on residual stress distribution in the blade foil of gas turbine engines p 836 A93-39106
- SKETCHING**
- Performance improvement by forward-skewed blading of axial fan moving blades
[ISABE 93-7055] p 1185 A93-54031
- SKIN (STRUCTURAL MEMBER)**
- Dynamics of skin-stringer panels using modified wave methods p 206 A93-14561
- The design development of the monolithic CFRP centre fuselage skin of the European fighter aircraft p 159 A93-15782
- The production of a monolithic CFRP fuselage skin for the European Fighter Aircraft p 109 A93-15810
- Geometrically nonlinear local flutter analysis of supersonic airplane skin plates in the potential supersonic flow
[ISBN 83-01-10939-4] p 394 A93-17569
- Assessment of aircraft structural integrity by detecting disbands through ultrasonic scanning p 406 A93-19587
- A wideband, embedded/conformal, antenna subsystem concept p 327 A93-22002
- Noise transmission of skin-stringer panels using a decaying wave method p 943 A93-41929
- Fuselage longitudinal splice design p 997 A93-45784
- Representation and probability issues in the simulation of multi-site damage p 1026 A93-45785
- Design and manufacture for producibility of carbon fiber/epoxy composite aircraft skins
[SME PAPER EM93-104] p 1043 A93-51732
- A finite element for modeling skins of composite materials p 1215 A93-52979
- Enhancement of conventional NDT methods for corrosion detection in layered skins p 1258 A93-54898
- Human engineering issues for data link systems p 1260 A93-55874
- Add-on damping treatment for the F-15 upper-outer wing skin
[AD-A258470] p 337 N93-18248
- Fabrication of the V-22 composite AFT fuselage using automated fiber placement p 920 N93-30443
- SKIN FRICTION**
- On the measurements of the skin friction in 3-D flows - Application to a complete 3-D shear layer flow p 118 A93-14329

- Unsteady turbulent skin-friction measurement in an adverse pressure gradient p 206 A93-14545
- Direct measurements of skin friction in supersonic combustion flow fields [ASME PAPER 92-GT-320] p 405 A93-19506
- Conventional skin friction measurement techniques for strongly perturbed supersonic turbulent boundary layers p 271 A93-21863
- Two-directional skin friction measurement utilizing a compact internally mounted thin-liquid-film skin friction meter [AIAA PAPER 93-0180] p 414 A93-22608
- Recent developments in international laminar flow research programs for transport aircraft [ONERA, TP NO. 1992-163] p 457 A93-26878
- Reduction of aerodynamic skin-friction drag p 871 A93-42656
- Development of a skin friction gauge for use in an impulse facility p 1024 A93-45526
- Laser Interferometer Skin-Friction measurements of crossing-shock wave/turbulent boundary-layer interactions [AIAA PAPER 93-3072] p 1148 A93-48247
- Skin friction and velocity profile family for compressible turbulent boundary layers p 1070 A93-49008
- Direct measurements of skin friction in a scramjet combustor [AIAA PAPER 93-2443] p 1119 A93-50195
- Low-Reynolds-number k-epsilon model for unsteady turbulent boundary-layer flows p 1177 A93-53208
- Skin-friction topology over a surface mounted semi-ellipsoidal wing at incidence p 1178 A93-53216
- The reduction of skin friction by riblets under the influence of an adverse pressure gradient p 1218 A93-53810
- Computational investigations of a NACA 0012 airfoil in low Reynolds number flows [AD-A257300] p 288 A93-15920
- Reflection type skin friction meter [NASA-CASE-LAR-14520-1-SB] p 296 A93-18275
- Analysis and evaluation of an integrated laminar flow control propulsion system [NASA-CR-192162] p 551 A93-20268
- Uniform roughness studies [WL-TR-92-3041] p 751 A93-25951
- Direct measurements of skin friction in supersonic combustion flow fields [AD-A262878] p 825 A93-28226
- SKIRTS**
- Canadian experience with air cushion vehicle skirts p 837 A93-39722
- SKY WAVES**
- Effect of skywave interference on the coverage of Loran-C p 33 A93-11095
- SLABS**
- Fracture of highway and airport pavements p 547 A93-28290
- SLEEP**
- The influence of nocturnal aircraft noise on sleep and on catecholamine secretion p 1163 A93-49554
- SLEEP DEPRIVATION**
- Night aircraft noise index and sleep research results p 558 A93-28485
- SLENDER BODIES**
- Calculation of transonic flow over bodies of varying complexity using Singular Perturbation Method p 116 A93-14265
- Analytical solutions for hypersonic flow past slender power-law bodies at small angle of attack p 122 A93-14550
- Air/helium ground-test simulation pertinent to the definition of slender body hypersonic aerodynamics [AIAA PAPER 93-0318] p 268 A93-21106
- The effect of Reynolds number on vortex asymmetry about slender bodies p 475 A93-26176
- Prediction of asymmetric vortical flows around slender bodies using Navier-Stokes equations p 478 A93-27925
- Analysis of slender bodies of revolution with an angle of attack in extreme ground effect p 679 A93-33716
- Numerical simulation of inviscid transonic flow over two-dimensional slender bodies p 686 A93-34348
- Experimental investigations of asymmetric vortex flows behind elliptic cones at incidence p 757 A93-35637
- Higher-order viscous shock-layer solutions for high altitude flows [AIAA PAPER 93-2724] p 858 A93-41050
- Application of an engineering inviscid-boundary layer method to slender three-dimensional vehicle forebodies [AIAA PAPER 93-2793] p 963 A93-46534
- On the steady subsonic shear flow past a slender body of revolution p 970 A93-46907
- Secondary flow control on slender, sharp-edged configurations [AIAA PAPER 93-3470] p 980 A93-47250

- Non slender waveriders [AIAA PAPER 93-3487] p 982 A93-47261
- Numerical simulation of upstream disturbance on flows around a slender body [AIAA PAPER 93-2956] p 1047 A93-48150
- Thoughts on conical flow asymmetry p 1070 A93-49003
- Investigation of vortex development on a pitching slender body of revolution p 1095 A93-52445
- Study on flow field around slender diamond cone traveling at hypersonic speed p 1189 A93-54314
- Steady-state supersonic flow of a vibrationally excited gas past a slender body of revolution at a small angle of attack p 1233 A93-55014
- The addition of algebraic turbulence modeling to program LAURA [NASA-TM-107758] p 840 A93-27250
- SLENDER CONES**
- High Mach number dynamic stability of blunt slender cones at angle of attack p 271 A93-21721
- Shock shapes around slender diamond cones traveling at hypersonic speed p 1181 A93-53840
- Modeling variable blowing on a slender cone in hypersonic flow p 138 A93-14836
- Transition induced normal forces and their effects on the aerodynamic characteristics of slender sharp cones [AD-A256802] p 288 A93-15889
- Combined LAURA-UPS hypersonic solution procedure [NASA-TM-107682] p 747 A93-25176
- SLENDER WINGS**
- Numerical modeling of supersonic flows past wings of different aspect ratios over a wide range of angles of attack within the framework of the plane section law p 5 A93-10141
- Transonic flutter/divergence characteristics of aeroelastically tailored and non-tailored high-aspect-ratio forward-swept wings p 10 A93-12273
- Prediction and control of slender-wing rock p 182 A93-14331
- Subsonic separated flow past slender delta wings p 124 A93-15109
- Slender wing rock revisited p 768 A93-37386
- Aerodynamics of maneuvering slender wings with leading-edge separation p 778 A93-39401
- Supersonic flow past energy release regions p 1069 A93-48973
- Effect of leading-edge geometry on delta wing unsteady aerodynamics p 1095 A93-52457
- Hypersonic flow of a gas past wing with heat transfer p 1234 A93-55030
- An improved multiple line-vortex method for simulation of separated vortices of slender wings p 1236 A93-55412
- Further buffeting tests in a cryogenic wind tunnel [NASA-TM-107621] p 22 A93-11610
- An experimental and computational investigation of slender wings undergoing wing rock p 187 A93-13915
- An aerodynamic model for one and two degree of freedom wing rock of slender delta wings [NASA-CR-193130] p 781 A93-27150
- SLICING**
- Slicing model for foreign soft-body objects impacting on blade rows p 28 A93-12372
- SLIDING**
- Origin of the carbon rich sliding interface in alkali containing matrix-SiC nicalon fibre composites [ONERA, TP NO. 1993-77] p 1212 A93-53598
- SLIDING FRICTION**
- Some physico-chemical characteristics of lubricating oil used in gas turbines p 70 A93-12202
- Characteristics of friction and wear in flight vehicle engine components p 811 A93-39075
- SLIP CASTING**
- Improved ceramic slip casting technique --- application to aircraft model fabrication [NASA-CASE-LAR-14471-1] p 536 A93-20041
- SLIPSTREAMS**
- Theodorsen's ideal propeller performance with ambient pressure in the slipstream p 768 A93-37400
- SLOTS**
- Effect of forebody tangential slot blowing on flow about a full aircraft geometry [AIAA PAPER 93-2962] p 1048 A93-48156
- An investigation of shock wave turbulent boundary layer interaction with bleed through normal and slanted slots [AIAA PAPER 93-2155] p 1079 A93-49971
- RB 199 high pressure compressor stage 3 spin pit tests p 176 A93-14893
- CF6-6 high pressure compressor stage 5 locking slot crack propagation spin pit test p 176 A93-14894
- A three-dimensional algebraic grid generation scheme for gas turbine combustors with inclined slots [NASA-CR-191095] p 746 A93-24759

- SLOTTED WIND TUNNELS**
- A semi-empirical theory of the noise in slotted tunnels caused by diffuser suction p 231 A93-14353
- Performance data of the new free-piston shock tunnel T5 at GALCIT p 1011 A93-45498
- Further noise measurements in a slotted cryogenic wind tunnel [RAE-TM-AERO-2201] p 101 A93-10805
- SLURRIES**
- Ultrasonic polishing p 750 A93-25580
- SLUSH**
- Slush hydrogen quantity gaging and mixing for the National Aerospace Plane p 1150 A93-48635
- SMALL PERTURBATION FLOW**
- Deforming grid variational principle for unsteady small disturbance flows in cascades p 692 A93-35623
- Waveriders with finlets [AIAA PAPER 93-3442] p 978 A93-47231
- Multiple solutions of the transonic perturbation equation p 987 A93-47331
- Aeroelastic computation for a flexible airfoil using the small perturbation method comparison with wind-tunnel results [ONERA, TP NO. 1993-43] p 987 A93-47448
- Interaction of the sonic boom with atmospheric turbulence [AIAA PAPER 93-2943] p 1171 A93-48140
- Steady transonic weakly perturbed flows in a vibrationally relaxing gas p 1088 A93-51768
- SMART STRUCTURES**
- Technological challenges with smart structures in German aircraft industry p 320 A93-17714
- The smart structures technology in the vibration control of helicopter blades in forward flight p 366 A93-17721
- Actuation strain decoupling through enhanced directional attachment in plates and aerodynamic surfaces p 394 A93-17727
- Adaptive/conformal wing design for future aircraft p 320 A93-17728
- Embedded fiber optic sensors in large structures p 410 A93-21085
- Application issues of fiber optic sensors in aircraft structures p 410 A93-21094
- A wideband, embedded/conformal, antenna subsystem concept p 327 A93-22002
- Damage detection in smart structures using neural networks and finite-element analyses p 438 A93-22540
- Optically smart surfaces for aerodynamic measurements [AIAA PAPER 92-3895] p 539 A93-24484
- Probabilistically configured adaptive composite structures [AIAA PAPER 93-1679] p 743 A93-34191
- Smart structures stabilized unstable control surfaces [AIAA PAPER 93-1701] p 712 A93-34223
- Embedded Bragg grating fiber optic sensor for composite flexbeams p 828 A93-37350
- Intelligent systems of flight-vehicle control p 1167 A93-50951
- Behavior of the particular quality characteristics of an intelligent flight vehicle control system in a multicriteria formulation p 1168 A93-50952
- Multilevel control systems and optimization of their structures p 1168 A93-50954
- Multilevel intelligent control systems for flight vehicles p 1168 A93-50955
- Acoustic emission technology for smart structures p 1263 A93-55331
- Robust control of intelligent rotor [AD-A263707] p 909 A93-29985
- SMOKE**
- Tobacco smoking in aircraft - A fog of legal rhetoric? p 944 A93-40474
- Test results of the effects of air ionization on cigarette smoke particulate levels within a commercial airplane [SAE PAPER 921183] p 855 A93-41362
- Smoke measurements inside a gas turbine combustor [AIAA PAPER 93-2070] p 1113 A93-49902
- Ventilation effects on smoke and temperature in an aircraft cabin quarter-scale model [DOT/FAA/CT-89/25] p 791 A93-28055
- Preliminary design of an intermittent smoke flow visualization system [NASA-CR-186027] p 806 A93-28693
- SNOW**
- Effect of wet snow on the null-reference ILS system p 1097 A93-50660
- Natural and augmented snowfall growth processes and their interactions with the natural and modified aerosol [PB93-153096] p 755 A93-25874
- SOCIAL FACTORS**
- Astronautics and society p 383 A93-18391
- The community response to aircraft noise around six Spanish airports p 1264 A93-55845

SODIUM SULFATES

Advanced turbine design for coal-fueled engines
[DE93-000224] p 554 N93-21254

SOFIA (AIRBORNE OBSERVATORY)

Flowfield simulation about the stratospheric observatory for infrared astronomy p 1095 A93-52446
Effect of jet engine exhaust on SOFIA stratospheric performance --- Stratospheric Observatory For Infrared Astronomy p 1263 A93-55178
Navier-Stokes simulations of unsteady transonic flow phenomena [NASA-TM-103962] p 129 N93-12721

SOFTWARE ENGINEERING

A control technology of integrated system of engineering supported by software engineering environments p 226 A93-14415
Cost control of the A320 software - The aircraft manufacturer's point of view p 227 A93-15044
Representation and presentation of requirements knowledge p 228 A93-17389
A method and a software for constructing F-by-F random load spectrum p 506 A93-27375
The importance of configuration management - An overview with test program sets p 853 A93-35926
Software - Design for maintenance p 847 A93-39537

Complexity metrics for avionics software

p 939 A93-42829
Evaluating the IOBIDS specification using gate-level system simulation p 940 A93-42851
Getting a handle on designing for avionics software supportability and maintainability p 941 A93-42862
Initial development of a research flight simulator software [AIAA PAPER 93-3590] p 1223 A93-52683
Requirements analysis notebook for the flight data systems definition in the Real-Time Systems Engineering Laboratory (RSEL) p 69 N93-10960
Software flexibility and configuration control for the A340/A330 Aircraft Condition Monitoring System (ACMS) p 167 N93-15154
A philosophy for integrated monitoring system design p 178 N93-15174

Data collection procedures for the Software Engineering Laboratory (SEL) database [NASA-TM-108579] p 230 N93-15579
Functional requirements of an advanced instructional design advisor: Simulation authoring, Volume 3 [AD-A256650] p 440 N93-16500

Domain specific software design for decision aiding p 442 N93-17517
A domain-specific design architecture for composite material design and aircraft part redesign p 442 N93-17522

Joint Integrated Avionics Working Group (JIAWG) object-oriented domain analysis method (JODA), version 3.1 [AD-A258468] p 344 N93-18270

Software design document for the generic avionics data bus tool kit [AD-A259329] p 519 N93-21259

SOFTWARE RELIABILITY

Avionics software performance p 939 A93-42822
Getting a handle on designing for avionics software supportability and maintainability p 941 A93-42862
Using software metrics and software reliability models to attain acceptable quality software for flight and ground support software for avionic systems p 442 N93-17305

Domain engineering validation case study: Synthesis for the air traffic display/collision warning monitor domain version 01.00.03 [AD-A259407] p 503 N93-21671

SOFTWARE REUSE

Reusable Ada avionics software packages library system p 944 A93-42828
Reusable code for helicopter simulation [AIAA PAPER 93-3594] p 1224 A93-52686
Domain specific software design for decision aiding p 442 N93-17517

Joint Integrated Avionics Working Group (JIAWG) object-oriented domain analysis method (JODA), version 3.1 [AD-A258468] p 344 N93-18270

Design recovery for software library population [AD-A259292] p 572 N93-20611

Domain engineering validation case study: Synthesis for the air traffic display/collision warning monitor domain version 01.00.03 [AD-A259407] p 503 N93-21671

Toward reusable graphics components in Ada [AD-A262568] p 849 N93-28577

SOFTWARE TOOLS

Software for the control of measurement data acquisition, processing, and monitoring during strength testings p 94 A93-10042
Rapid prototyping via automatic software code generation from formal specifications - A case study p 227 A93-14685

Stability and transition on swept wings [AIAA PAPER 93-0078] p 263 A93-20190
Issues in large-scale optimization with expensive functions p 437 A93-20708
Multidisciplinary computational aerodynamics p 437 A93-20711

MESH3D - A tool for the construction of three-dimensional meshes [ONERA, TP NO. 1992-164] p 561 A93-25339

Design of a recovery system for a reentry vehicle [AIAA PAPER 93-1224] p 733 A93-35171
Development and validation of a comprehensive real time AH-64 Apache simulation model p 799 A93-35992

Valisys - A new quality assurance tool p 845 A93-36007

An application of knowledge-based engineering to composite tooling design p 846 A93-36010
Software - Design for maintenance p 847 A93-39537

Computerized synthesis of three-dimensional kinematic landing gear schemes with a single turning axis p 891 A93-42376

Pave Pillar in-house research final report p 927 A93-42781

Software support for a computerized air situation documentation system p 941 A93-43115

An evaluation of software tools for the design and development of cockpit displays [AIAA PAPER 93-3593] p 1224 A93-52685

Future development and application of general structural analysis softwares in the aviation industry in China p 1262 A93-54420

Requirements analysis notebook for the flight data systems definition in the Real-Time Systems Engineering Laboratory (RSEL) [NASA-CR-185698] p 69 N93-10960

Intelligent diagnostics systems p 98 N93-11931
Flight dynamics system software development environment (FDS/SDE) tutorial [NASA-TM-108580] p 230 N93-15502

Development of a computer assisted toolbox for aerodynamic design of aircraft at subcritical conditions with application to three-surface and canard aircraft [ISBN-90-6275-768-5] p 441 N93-16567

Software Engineering Laboratory Ada performance study: Results and implications p 441 N93-17172

Practical architecture of design optimisation software for aircraft structures taking the MBB-LAGRANGE code as an example [MBB-FE-251-S-PUB-479] p 331 N93-17565

Design and implementation of a Global Positioning System (GPS) supported area navigation system with electronic aircraft [ILR-MITT-275(1992)] p 889 N93-30671

Multi-parameter optimization tool for low-cost commercial fuselage crown designs p 922 N93-30858
The HSCT mission analysis of waverider designs [NASA-CR-193467] p 879 N93-31037

SOHO MISSION

Optical technologies for UV remote sensing instruments p 853 N93-28788

SOIL MAPPING

PBMR observations of surface soil moisture in Monsoon 90 p 1162 A93-47676

SOIL MOISTURE

PBMR observations of surface soil moisture in Monsoon 90 p 1162 A93-47676

Mathematical model of frost heave and thaw settlement in pavements [CRRLE-REPT-93-2] p 912 N93-30103

SOIL SCIENCE

Mathematical model of frost heave and thaw settlement in pavements [CRRLE-REPT-93-2] p 912 N93-30103

SOILS

In-situ bioventing: Two US EPA and Air Force sponsored field studies [PB93-194231] p 1035 N93-32089

SOLAR CELLS

Computational and experimental investigation of a solar energy system for an atmospheric flight vehicle p 521 A93-29655

NASA advanced design program: Analysis, design, and construction of a solar powered aircraft [NASA-CR-192040] p 332 N93-17802

SOLAR COLLECTORS

Thermal effects testing at the National Solar Thermal Test Facility p 1255 A93-54402

Wind load design methods for ground-based heliostats and parabolic dish collectors [DE93-002737] p 433 N93-15839

SOLAR CYCLES

Radiation safety in aircraft operations p 141 A93-14221

SOLAR DYNAMIC POWER SYSTEMS

BIPS Turboalternator-Compressor characteristics and application to the NASA Solar Dynamic Ground Demonstration Program p 532 A93-25965

SOLAR POWERED AIRCRAFT

NASA advanced design program: Analysis, design, and construction of a solar powered aircraft [NASA-CR-192040] p 332 N93-17802

Solar powered multipurpose remotely powered aircraft p 895 N93-29722

SOLAR RADIATION

Recent refinements and increased capabilities in balloon vertical performance analysis p 40 A93-11361

Environmental effects of operations during Desert Shield/Desert Storm p 1190 A93-54291

SOLDERING

Requirements for soldered electrical connections [NHB-5300.4(3A-2)] p 212 N93-12674

Performance of thermal adhesives in forced convection p 924 N93-30974

SOLDERS

Requirements for soldered electrical connections [NHB-5300.4(3A-2)] p 212 N93-12674

SOLID MECHANICS

Development of computational solid mechanics and its application in aerospace engineering p 1255 A93-54419

Development of user guidelines for a three-dimensional finite element pavement model p 379 N93-16311

Micro mechanical behavior of pavements p 379 N93-16312

SOLID PROPELLANT COMBUSTION

Studies of fuel-rich magnesium propellants in a small solid fuel ramjet combustor p 535 A93-27759

SOLID PROPELLANT IGNITION

Ignition of boron particles coated by a thin titanium film [AIAA PAPER 93-2201] p 1145 A93-50013

SOLID PROPELLANT ROCKET ENGINES

Computational flow predictions for hypersonic drag devices p 777 A93-39257

National Aeronautics and Space Administration p 454 N93-17091

SOLID PROPELLANTS

Studies of fuel-rich magnesium propellants in a small solid fuel ramjet combustor p 535 A93-27759

SOLID STATE DEVICES

Solid state flight data recorders and their application in the flight operation analysis p 166 A93-14200

Solid state flight data recorder with rapid data access p 221 N93-15167

SOLID STATE LASERS

Thermal control of a lidar laser system using a non-conventional ram air heat exchanger p 1028 A93-46821

Sources and detectors for fiber communications; Proceedings of the Meeting, Boston, MA, Sept. 8, 9, 1992 [SPIE-1788] p 1151 A93-49455

Solid-state coherent laser radar wind shear measuring systems p 144 A93-14848

SOLID SURFACES

Effect of the drag of the front body on the restructuring of flow between two bodies in the path of supersonic flow, with one body located in the wake of the other p 14 A93-12973

Scattering kernels for gas-surface interaction p 943 A93-42580

Surface boundary conditions for the numerical solution of the Euler equations [AIAA PAPER 93-3334] p 953 A93-45028

CFD study of the flowfield due to a supersonic jet exiting into a hypersonic stream from a conical surface. II [AIAA PAPER 93-2926] p 1045 A93-48127

SOLID-SOLID INTERFACES

Determination of tire-wheel interface pressure distribution for aircraft wheels [AIAA PAPER 93-1343] p 709 A93-33913

Origin of the carbon rich sliding interface in alkali containing matrix-SiC nicalon fibre composites [ONERA, TP NO. 1993-77] p 1212 A93-53598

SOLIDS FLOW

Experimental investigation on effect of solid particles on blade pressure distribution in compressor cascade flow p 1066 A93-48513

SOLITARY WAVES

Buoyancy wave hazards to aviation p 430 A93-22151

SONAR

Bearings-only and Doppler-bearing tracking using instrumental variables p 501 A93-29600

SONIC ANEMOMETERS

A fine structure of the gust front observed with sonic anemometer p 430 A93-22158

SONIC BOOMS

Assessment and design of low boom configurations for supersonic transport aircraft p 446 A93-19163

Sonic boom spectra of Space Shuttle Columbia landing 10 December 1990 p 533 A93-28488

Sound exposure spectrum levels of sonic booms p 564 A93-28489

Limitations of linear theory for sonic boom calculations p 850 A93-37380

Unstructured grids for sonic-boom analysis [AIAA PAPER 93-2929] p 949 A93-44229

Interaction of the sonic boom with atmospheric turbulence p 1171 A93-48140

Euler/experiment correlations of sonic boom pressure signatures p 1095 A93-52439

A general introduction to aeroacoustics and atmospheric sound p 1264 A93-55852

Sonic boom minimization - Myth or reality? p 1264 A93-55859

Laboratory study of effects of sonic boom shaping on subjective loudness and acceptability [NASA-TP-3269] p 102 N93-11620

A general introduction to aeroacoustics and atmospheric sound p 102 N93-12021

Effect of sonic boom asymmetry on subjective loudness [NASA-TM-107708] p 453 N93-16755

Loudness and annoyance response to simulated outdoor and indoor sonic booms [NASA-TM-107756] p 852 N93-27271

A laboratory study of subjective response to sonic booms measured at White Sands Missile Range [NASA-TM-107746] p 852 N93-27272

Subjective response to simulated sonic booms with ground reflections [NASA-TM-107764] p 852 N93-28692

Sonic boom problem for future highspeed aircraft [ONERA-NT-1990-3] p 876 N93-30020

SONOBUOYS

Embedded training capabilities for the LAMPS MK 3 system [AD-A250697] p 49 N93-11838

SORPTION

Three-stage sorption type cryogenic refrigeration systems and methods employing heat regeneration [NASA-CASE-NPO-18366-1-CU] p 216 N93-13422

SOUND FIELDS

A new technique for aerodynamic noise calculation p 447 A93-19177

Effect of nozzle design on near acoustic field of supersonic circular and rectangular jets p 448 A93-19203

Experimental determination of the main noise sources in a profan model by analysis of the acoustic spinning modes in the exit plane p 449 A93-19214

An overview of possible and not-so-possible tasks for active control of sound and vibration p 568 A93-29429

Acoustic experiments of two scaled-model propellers on the ground p 1172 A93-48507

An approach to the calculation of the far acoustic field of a propeller p 1124 A93-51760

SOUND GENERATORS

Boundary conditions for direct computation of aerodynamic sound generation p 447 A93-19176

Radiation mechanism for the aerodynamic sound of gears - An explanation for the radiation process by air flow observation p 451 A93-21859

De-Dopplerization of aircraft acoustic signals [AIAA PAPER 93-0737] p 563 A93-24827

Sound generation by rotating stall in centrifugal turbomachines p 1039 A93-46701

A study on aerodynamic sound generated by interaction of jet and plate [AIAA PAPER 93-3118] p 1171 A93-48288

Boundary conditions for direct computation of aerodynamic sound generation p 1172 A93-49005

SOUND INTENSITY

Acoustic intensity of nonisothermal coaxial jets with an inverted velocity profile p 1124 A93-51759

Acoustic noise generation at the air/ocean boundary [DREA-CR-90-445] p 99 N93-10642

SOUND PRESSURE

Effect of nozzle design on near acoustic field of supersonic circular and rectangular jets p 448 A93-19203

Prediction of jet mixing noise in high-speed flight p 450 A93-19216

Acoustic mode measurements in the inlet of a model turbofan using a continuously rotating rake - Data collection/analysis techniques p 361 A93-23324

[AIAA PAPER 93-0599] p 361 A93-23324

Approximation methods for control of structural acoustics models with piezoceramic actuators p 452 A93-23744

Takeoff/approach noise for a model counterrotation propeller with a forward-swept upstream rotor [AIAA PAPER 93-0596] p 519 A93-24782

Introduction of small velocity and pressure variation into a stationary compressible fluid p 473 A93-25060

Far-field hover acoustic characteristics of the XV-15 tiltrotor aircraft with Advanced Technology Blades p 566 A93-29412

An experimental system for studying the vibrations and acoustic emission of cylindrical shells and panels in a field of turbulent pressure pulsations p 1140 A93-51754

Euler/experiment correlations of sonic boom pressure signatures p 1095 A93-52439

Prediction of jet mixing noise for high subsonic flight speeds p 100 N93-10685

Acoustic mode measurements in the inlet of a model turbofan using a continuously rotating rake: Data collection/analysis techniques p 179 N93-15403

Takeoff/approach noise for a model counterrotation propeller with a forward-swept upstream rotor [NASA-TM-105936] p 179 N93-15403

[NASA-TM-105979] p 362 N93-16715

SOUND PROPAGATION

An aeroacoustic stand for evaluating the efficiency of sound-absorbing structures under conditions of acoustic wave propagation in a moving medium p 1140 A93-51762

A general introduction to aeroacoustics and atmospheric sound p 1264 A93-55852

Noise studies for environmental impact assessment of an outdoor engine test facility p 99 N93-10672

A general introduction to aeroacoustics and atmospheric sound [NASA-CR-189717] p 102 N93-12021

Consecutive plate acoustic suppressor apparatus and methods [NASA-CASE-LEW-15430-1] p 453 N93-17051

Effects on health of noise disturbances due to air traffic p 1035 N93-31929

SOUND TRANSDUCERS

Instrumentation for in-flight acoustic measurements in an engine inlet duct of a Fokker 100 aircraft [NLR-TP-92100-U] p 1001 N93-32332

SOUND TRANSMISSION

Effect of flight conditions on the sound insulation of the aircraft passenger compartment p 42 A93-12978

Sound transmission through stiffened double-panel structures lined with elastic porous materials p 444 A93-19139

On sound attenuation in boundary layers p 446 A93-19164

Transmission of sound through a rotor p 447 A93-19183

Active control of sound transmission through stiff lightweight composite fuselage constructions p 447 A93-19187

High speed flight effects on transmission of sound through a nonflexible vibrating panel due to flow structural interaction in the ambience p 451 A93-20316

Acoustical properties of sound absorbing structures at high temperature p 1172 A93-48522

European research into helicopter internal noise p 1243 A93-54724

Structural-acoustic coupling in aircraft fuselage structures p 1243 A93-55856

Comparison of methodologies for describing relaxation in nonequilibrium gaseous systems p 419 N93-16786

Transmission of sound through a rotor [NLR-TP-92014-U] p 1006 N93-32386

SOUND WAVES

Calculation of sound field radiated by oscillating cascade p 231 A93-14269

On the coupling between a supersonic boundary layer and a flexible surface p 243 A93-19132

Technical prospects for computational aeroacoustics p 244 A93-19150

Nonlinear vibration and radiation from a panel with transition to chaos induced by acoustic waves p 398 A93-19173

Radiation mechanism for the aerodynamic sound of gears - An explanation for the radiation process by air flow observation p 451 A93-21859

Some issues concerning active control of combustion instability in a ramjet [AIAA PAPER 93-0116] p 360 A93-22566

Numerical prediction of aerodynamic noise radiated from low Mach number turbulent wake [AIAA PAPER 93-0145] p 452 A93-22589

Theoretical modelling of rotor noise radiation p 566 A93-29407

Theoretical studies of the active control of propeller induced cabin noise using secondary force inputs p 995 A93-45124

Transonic flutter suppression using active acoustic excitations [AIAA PAPER 93-3285] p 969 A93-46841

Aerodynamic phenomena in high pulse repetition rate XeCl laser p 1150 A93-48806

Blade row interaction effects on flutter and forced response [AIAA PAPER 93-2084] p 1114 A93-49911

Determination of the natural vibrations of an acoustic medium in the cabin of a passenger aircraft by the finite element method p 1102 A93-51752

Acoustic-wave propagation in ducts and free-field radiation [ONERA, TP NO. 1993-103] p 1226 A93-53616

Low-frequency combustion oscillations in a model afterburner p 1193 A93-53702

Passive damping technology p 1259 A93-55866

Numerical study for the study of medium speed internal noise problems [DILC-EST-TN-200] p 101 N93-11156

Ice prevention by ultrasonic nucleation of supercooled water droplets in front of subsonic aircraft [AD-A258212] p 142 N93-12816

Turbulence and chaos in classical and quantum systems p 232 N93-14144

Far field rotor noise [AD-A260703] p 759 N93-25651

Roughness-induced generation of crossflow vortices in three-dimensional boundary layers [NASA-CR-4505] p 780 N93-27096

Jet mixer noise suppressor using acoustic feedback [NASA-CASE-LEW-15170-1] p 853 N93-28953

SOUTH AMERICA

South American latest developments in the air law and air policy fields p 103 A93-12719

SPACE BASED RADAR

Antenna design for adaptive airborne MTI p 884 A93-43440

SPACE COMMERCIALIZATION

Space policy 2000 p 1174 A93-50333

SPACE COMMUNICATION

Satellite navigation in traffic management p 914 A93-43549

Ongoing GPS experiments demonstrate potential of satellite navigation technology p 1097 A93-49278

SPACE ENVIRONMENT SIMULATION

Thermal response and ablation characteristics of light weight ceramic ablators [AIAA PAPER 93-2790] p 1018 A93-46532

SPACE EXPLORATION

Space policy 2000 p 1174 A93-50333

Technical needs and research opportunities provided by projected aeronautical and space systems [NASA-CR-192124] p 386 N93-16629

SPACE FLIGHT

The start of the laboratory - The beginnings of the MIT Instrumentation Laboratory p 235 A93-17326

The 1992 Research/Technology report [NASA-TM-105924] p 459 N93-20902

Summaries of the 1991 publications of DLR research reports and DLR communications [ETN-93-92588] p 572 N93-21022

SPACE NAVIGATION

Application of advanced guidance and navigation systems to flight control of aircraft and future space vehicles p 500 A93-28153

Research on combined HOPE navigation technology p 533 N93-20428

Reference equations of motion for automatic rendezvous and capture [NASA-CR-185676] p 914 N93-29652

Attitude determination using GPS: Development of an all solid-state guidance, navigation, and control sensor for air and space vehicles based on the global positioning system p 888 N93-30605

SPACE PERCEPTION

A fast algorithm for obtaining dense depth maps for high speed navigation p 435 A93-19080

An automated system for the measurement of slant visual range p 413 A93-22176

SPACE PLATFORMS

The real aperture antenna of SAR, a key element for performance p 213 N93-13053

Vibration isolation technology: An executive summary of systems development and demonstration [NASA-TM-105937] p 110 N93-15573

SPACE PROCESSING

Materials processing in low gravity [NASA-CR-184421] p 91 N93-12401

SPACE PROGRAMS

Astronautics and society p 383 A93-18391

SUBJECT INDEX

Aeronautics and space report of the President: Fiscal year 1992 activities p 854 N93-27041

SPACE SHUTTLE MAIN ENGINE
Investigation of rotor blade roughness effects on turbine performance [ASME PAPER 92-GT-297] p 354 A93-19487
Subscale hot-fire testing of a formed platelet liner [AIAA PAPER 93-1827] p 1141 A93-49713
High Reynolds number and turbulence effects on aerodynamics and heat transfer in a turbine cascade [AIAA PAPER 93-2252] p 1155 A93-50050
CFD analysis on control of secondary losses in STME LOX turbines with endwall fences p 419 N93-17289
High Reynolds number and turbulence effects on aerodynamics and heat transfer in a turbine cascade [NASA-TM-106187] p 930 N93-29157
Overview of aerothermodynamic loads definition study p 1016 N93-31583
Three-dimensional analysis of the Pratt and Whitney alternate design SSME fuel turbine p 1031 N93-31584
Three-dimensional flow calculations inside SSME GGGT first stage blade rows p 1017 N93-31585
Localization of aeroelastic modes in mistuned high-energy turbines p 1032 N93-31586

SPACE SHUTTLE ORBITERS
Experiments on Space Shuttle Orbiter models in a free piston shock tunnel p 7 A93-11497
High angle-of-attack inviscid Shuttle Orbiter computation p 9 A93-12020
Flowfield computations over the Space Shuttle Orbiter with a proposed canard at a Mach number of 5.8 and 50 degrees angle of attack [AIAA PAPER 93-0322] p 281 A93-23014
Solution strategy for three-dimensional configurations at hypersonic speeds p 962 A93-46406
Navier-Stokes simulations of the Shuttle Orbiter aerodynamic characteristics with emphasis on pitch trim and body flap [AIAA PAPER 93-2814] p 965 A93-46552
Aerodynamics of Shuttle Orbiter at high altitudes [AIAA PAPER 93-2815] p 965 A93-46553
Flowfield computations over the Space Shuttle orbiter with a proposed canard at a Mach number of 5.8 and 50 deg angle of attack [AD-A258058] p 293 N93-17756
Rarefied-flow Shuttle aerodynamics model [NASA-TM-107698] p 458 N93-19976

SPACE SHUTTLES
SIR technology helps ensure safe landings for NASA --- Subsurface Interface Radar p 384 A93-21765
A comparison of hypersonic flight and prediction results [AIAA PAPER 93-0311] p 280 A93-23006
Sonic boom spectra of Space Shuttle Columbia landing 10 December 1990 p 533 A93-28488
Sound exposure spectrum levels of sonic booms p 564 A93-28489
Rarefied-flow shuttle aerodynamics flight model [AIAA PAPER 93-3441] p 859 A93-41057
Hypersonic stagnation line merged layer flow on blunt axisymmetric bodies of arbitrary shape [AIAA PAPER 93-2723] p 962 A93-46478
Performance analysis of a turbopump as a part of an airbreathing propulsion system for space shuttles p 1252 A93-56039
Current Technology for Thermal Protection Systems [NASA-CP-3157] p 69 N93-12447
A simple grid generation technique for hypersonic flow around complex configuration p 299 N93-19275
Numerical computations using multi-domain technique p 299 N93-19277
The role of computational fluid dynamics in aeronautical engineering. 9: Analysis of hypersonic equilibrium air flow p 301 N93-19294
Computation of re-entry flows with two-temperature model p 301 N93-19295
Numerical calculation of hypersonic non-equilibrium flow around OREX p 301 N93-19296
Numerical simulation of hypersonic flow around H-2 Orbiting Plane (HOPE), part 3 p 301 N93-19297

SPACE STATION FREEDOM
BIPS Turboalternator-Compressor characteristics and application to the NASA Solar Dynamic Ground Demonstration Program p 532 A93-25965
National Aeronautics and Space Administration p 454 N93-17091
The 1992 Research/Technology report [NASA-TM-105924] p 459 N93-20902

SPACE SURVEILLANCE (SPACEBORNE)
Automatic dependent surveillance (ADS) Pacific engineering trials (PET) p 30 A93-10999

SPACE TRANSPORTATION
The Hermes Carrier Aircraft (HCA) p 195 A93-14347

HL-20 operations and support requirements for the Personnel Launch System mission p 1210 A93-53745
Conceptual design of a Mars transportation system [NASA-CR-192039] p 420 N93-18047

SPACE TRANSPORTATION SYSTEM
How to enhance safety for future space transportation systems p 1015 A93-45444
An extended insight into hypersonic flow phenomena using numerical methods p 1093 A93-51999
Technical needs and research opportunities provided by projected aeronautical and space systems [NASA-CR-192124] p 386 N93-16629
CFD analysis on control of secondary losses in STME LOX turbines with endwall fences p 419 N93-17289
Technology transfer: Potential of BMFT concept for hypersonics [MBB-LME-202-S-PUB-0505] p 1041 N93-31045

SPACE-TIME FUNCTIONS
Space-time processing for AEW radar p 884 A93-43444

SPACEBORNE EXPERIMENTS
A convective and radiative heat transfer analysis for the FIRE II forebody [AIAA PAPER 93-3194] p 1021 A93-44231

SPACECRAFT ANTENNAS
Inflight antenna diagram determination of spaceborne and airborne SAR-systems p 1161 A93-47583

SPACECRAFT CHARGING
Intrusive and nonintrusive measurements of flow properties in arc jets p 943 A93-42584

SPACECRAFT CONFIGURATIONS
A parametric approach to preliminary design for aircraft and spacecraft configuration p 225 A93-14201
Constrained optimization of three-dimensional hypersonic vehicle configurations [AIAA PAPER 93-0039] p 260 A93-20152
Computational aerothermodynamics for 2D and 3D space vehicles p 1073 A93-49533
A configuration development strategy for the NASP p 46 N93-10011

SPACECRAFT CONSTRUCTION MATERIALS
Potential aerospace applications for metal matrix composites p 389 A93-21678
Potential and prospects of intermetallic materials for applications in the aerospace industry [ONERA, TP NO. 1992-99] p 824 A93-38580
Selection criteria for metallic high temperature structural materials in hypersonic flying equipment [MBB-LME-221-HYPAC-PUB-2-A] p 515 N93-21479

SPACECRAFT CONTROL
Guidance and control law for automatic landing flight experiment of reentry space vehicle [AIAA PAPER 93-3818] p 1143 A93-51409
Computation of optimal low- and medium-thrust orbit transfers [AIAA PAPER 93-3855] p 1144 A93-51442
Six-degree-of-freedom guidance and control-entry analysis of the HL-20 p 1210 A93-53737
Guidance and control of HOPE (H-II orbiting plane) [AAS PAPER 91-653] p 1252 A93-55825
Air-breathing hypersonic vehicle guidance and control studies: An integrated trajectory/control analysis methodology, phase 2 [NASA-CR-189703] p 65 N93-12413
Robust nonlinear feedback guidance for an aerospace plane: A geometric approach p 189 N93-14835
Research on combined HOPE navigation technology p 533 N93-20428
Collection of papers of the 31st Israel Annual Conference on Aviation and Astronautics [ITN-93-85187] p 764 N93-27166
Reference equations of motion for automatic rendezvous and capture [NASA-CR-185676] p 914 N93-29652

SPACECRAFT DESIGN
A parametric approach to preliminary design for aircraft and spacecraft configuration p 225 A93-14201
Survey - Applications of structural optimization methods to fixed wing aircraft and spacecraft [AIAA PAPER 92-4726] p 325 A93-20328
Aero-space plane figures of merit [AIAA PAPER 92-5058] p 385 A93-22328
Flying qualities of the Hermes spaceplane and the shape definition process p 532 A93-28437
Aerospace plane design challenge - Credible computations p 1015 A93-45145
The European Data Base - A new CFD validation tool for the design of space vehicles [AIAA PAPER 93-3045] p 1057 A93-48225
HL-20 operations and support requirements for the Personnel Launch System mission p 1210 A93-53745
HOPE and its thermal protection systems p 1252 A93-54711

SPACECRAFT MODELS

Air-breathing hypersonic vehicle guidance and control studies: An integrated trajectory/control analysis methodology, phase 2 [NASA-CR-189703] p 65 N93-12413
Multidisciplinary design optimization using response surface analysis p 330 N93-16796
Flowfield computations over the Space Shuttle orbiter with a proposed canard at a Mach number of 5.8 and 50 deg angle of attack [AD-A258058] p 293 N93-17756
Conceptual design of a Mars transportation system [NASA-CR-192039] p 420 N93-18047
Numerical methods for aerothermodynamic design of hypersonic space transport vehicles [MBB-FE-211-S-PUB-0481] p 514 N93-21056
Application of artificial neural networks to the design optimization of aerospace structural components [NASA-TM-4389] p 555 N93-21831
Applications of structural optimization methods to fixed-wing aircraft and spacecraft in the 1980s [NASA-TM-103939] p 1033 N93-32212

SPACECRAFT DOCKING
Reference equations of motion for automatic rendezvous and capture [NASA-CR-185676] p 914 N93-29652

SPACECRAFT ELECTRONIC EQUIPMENT
Enhanced heat transport in environmental systems using microencapsulated phase change materials [SAE PAPER 921224] p 926 A93-41398
Requirements analysis notebook for the flight data systems definition in the Real-Time Systems Engineering Laboratory (RSEL) [NASA-CR-185698] p 69 N93-10960

SPACECRAFT EQUIPMENT
Zvezda - The Russian pioneer in the field of life-support and escape systems for aeronautics and space p 195 A93-16878
Test results of an orifice pulse tube refrigerator p 1149 A93-48612

SPACECRAFT GUIDANCE
Autonomous guidance, navigation and control bridging program plan p 532 A93-27046
Trajectory control for a low-lift re-entry vehicle p 1141 A93-49592
Guidance and control law for automatic landing flight experiment of reentry space vehicle [AIAA PAPER 93-3818] p 1143 A93-51409
Six-degree-of-freedom guidance and control-entry analysis of the HL-20 p 1210 A93-53737
Guidance and control of HOPE (H-II orbiting plane) [AAS PAPER 91-653] p 1252 A93-55825
Air-breathing hypersonic vehicle guidance and control studies: An integrated trajectory/control analysis methodology, phase 2 [NASA-CR-189703] p 65 N93-12413
Research on combined HOPE navigation technology p 533 N93-20428
Trajectory optimization for the National aerospace plane [NASA-CR-192954] p 716 N93-25670
Reference equations of motion for automatic rendezvous and capture [NASA-CR-185676] p 914 N93-29652

SPACECRAFT INSTRUMENTS
Dual control vibration tests of flight hardware p 545 A93-27782

SPACECRAFT LANDING
Autonomous guidance, navigation and control bridging program plan p 532 A93-27046
Sonic boom spectra of Space Shuttle Columbia landing 10 December 1990 p 533 A93-28488
Sound exposure spectrum levels of sonic booms p 564 A93-28489
Effect of lift-to-drag ratio in pilot rating of the HL-20 landing task p 1210 A93-53738

SPACECRAFT LAUNCHING
Natural environment application for NASP-X-30 design and mission planning [AIAA PAPER 93-0851] p 531 A93-24915
Autonomous guidance, navigation and control bridging program plan p 532 A93-27046
The 1992 International Aerospace and Ground Conference on Lightning and Static Electricity: Addendum [DOT/FAA/CT-92/20-ADD-1] p 753 N93-24875
Development of models for predicting the triggering of lightning by launch vehicles p 734 N93-24899

SPACECRAFT MAINTENANCE
Intelligent diagnostics systems p 98 N93-11931

SPACECRAFT MANEUVERS
Optimal impulsive interorbital transfers with aerodynamic maneuvers p 1141 A93-48838

SPACECRAFT MODELS
Rarefied-flow Shuttle aerodynamics model [NASA-TM-107698] p 458 N93-19976

SPACECRAFT MOTION

Reentry control to a drag vs. energy profile
[AIAA PAPER 93-3790] p 1143 A93-51385

SPACECRAFT PROPULSION

Numerical analysis of reacting flow using finite rate chemistry models p 389 A93-21666
Numerical simulations of a pulsed detonation wave augmentation device p 1112 A93-49832
[AIAA PAPER 93-1985]
LV software for supersonic flow analysis
[NASA-CR-190911] p 16 A93-10069
Aeronomy coexperiments on drag-free satellites with proportional thrusters: GP-B and STEP p 195 A93-13922
Engine technologies for future spaceplanes
[ETN-92-92732] p 177 A93-15143
Collection of papers of the 31st Israel Annual Conference on Aviation and Astronautics
[ITN-93-85187] p 764 A93-27166
Studies of hydrogen-air diffusion flames and of compressibility effects related to high-speed propulsion p 917 A93-29125

SPACECRAFT RADIATORS

Joining carbon composite fins to metal heat pipes using ion beam techniques p 543 A93-25979

SPACECRAFT REENTRY

Payload vehicle aerodynamic re-entry analysis
p 69 A93-12004
Nuclear thermal rocket entry heating and thermal response preliminary analysis
[AIAA PAPER 93-0378] p 385 A93-23058
Overview of technical challenges of reentry analysis of radioisotope heat sources
[AIAA PAPER 93-0379] p 386 A93-23059
Rarefied-flow shuttle aerodynamics flight model
[AIAA PAPER 93-3441] p 859 A93-41057
Simulation of ablation in Earth atmospheric entry
[AIAA PAPER 93-2789] p 1027 A93-46531
A hybrid multigrid technique for computing steady-state solutions to supersonic flows p 700 A93-26078

SPACECRAFT STRUCTURES

Nonlinear response and sonic fatigue of high speed aircraft p 399 A93-19211
Evaluation of water-borne adhesive bonding primers for use on the advanced aircraft material aluminum-lithium p 1211 A93-53420
Selection criteria for metallic high temperature structural materials in hypersonic flying equipment
[MBB-LME-221-HYPAC-PUB-2-A] p 515 A93-21479

SPACECRAFT TRACKING

A dynamic inversion control approach for high-Mach trajectory tracking p 385 A93-22870
The effect of clock, media, and station location errors on Doppler measurement accuracy p 885 A93-29588

SPACECRAFT TRAJECTORIES

Air-breathing hypersonic vehicle guidance and control studies: An integrated trajectory/control analysis methodology, phase 2
[NASA-CR-189703] p 65 A93-12413

SPACERS

In-service considerations affecting component life p 177 A93-14898

SPACING

Blade row interaction effects on compressor measurements p 900 A93-42885
Propeller noise reduction by means of unsymmetrical blade-spacing p 1039 A93-46706
The challenges of simulating wake vortex encounters and assessing separation criteria
[AIAA PAPER 93-3568] p 1096 A93-49518

SPANWISE BLOWING

The suppression of single-fin buffeting using tangential leading edge blowing on a delta wing p 270 A93-21677
A visual study of recessed angled spanwise blowing method on a delta wing
[AIAA PAPER 93-3246] p 966 A93-46791
Response of B-2 aircraft to nonuniform spanwise turbulence p 1135 A93-52437
Assessment of potential aerodynamic benefits from spanwise blowing at the wing tip p 134 A93-13822
Experiments in the control of wing rock at high angle of attack using tangential leading edge blowing p 1009 A93-31068

SPATIAL DISTRIBUTION

A multisensor-multitarget data association algorithm for heterogeneous sensors p 1020 A93-44168
Implementing system simulation of C3 systems using autonomous objects
[NASA-CR-190845] p 89 A93-11716

SPATIAL MARCHING

A split-matrix Runge-Kutta type space marching procedure p 8 A93-11921
Application of space-marching methods to hypersonic forebody flow fields
[AIAA PAPER 92-5030] p 272 A93-22305

PNS predictions of axisymmetric hypersonic blunt-body and afterbody flowfields

[AIAA PAPER 93-2725] p 962 A93-46479
Space marching calculations about hypersonic configurations using a solution-adaptive mesh algorithm p 1177 A93-53212

SPATIAL RESOLUTION

Motion errors and compensation possibilities p 212 A93-13052

SPECIFIC HEAT

Evaporation and specific heats of motor fuels p 71 A93-12823
An experimental parametric study of geometric, Reynolds number, and ratio of specific heats effects in three-dimensional sidewall compression scramjet inlets at Mach 6
[AIAA PAPER 93-0740] p 466 A93-24830

SPECIFIC IMPULSE

Analytical investigation of a regeneratively cooled scramjet engine
[AIAA PAPER 93-0739] p 519 A93-24829
An analysis of air-turborocket performance
[AIAA PAPER 93-1982] p 1141 A93-49829
Hypersonic ignition and thrust production in a scramjet
[AIAA PAPER 93-2444] p 1119 A93-50196
Energy management --- aircraft propulsion system performance
[ISABE 93-7019] p 1195 A93-53995
Experiments and analysis concerning the use of external burning to reduce aerospace vehicle transonic drag p 70 A93-12537

SPECIFICATIONS

A study of the effects of tolerances on rigging screws, turnbuckles, and associated components in BS4429:1987 p 86 A93-11326
Specification of adaptive aiding systems
[AD-A254537] p 159 A93-12602
Aircraft performance in practice p 340 A93-19004
Nondestructive inspection of in-service aircraft
[ETN-93-93059] p 496 A93-20928

SPECIMEN GEOMETRY

Effects of aft geometry on vortex behavior and force production by a tangential jet on a body at high alpha
[AIAA PAPER 93-2961] p 1048 A93-48155

SPECKLE PATTERNS

Multiparticle imaging technique for two-phase fluid flows using pulsed laser speckle velocimetry
[DE93-011734] p 935 A93-30489

SPECTRA

Study of statistical variations of load spectra and material properties on aircraft fatigue life
[AD-A257961] p 339 A93-18451
Research support for the Laboratory for Lightwave Technology
[AD-A261488] p 760 A93-26343

SPECTRAL BANDS

Signal processing of jet noise from flyover test data
[AIAA PAPER 93-0736] p 563 A93-24826

SPECTRAL ENERGY DISTRIBUTION

Time-frequency domain analysis of vibration signals for machinery diagnostics. 3: The present power spectral density
[OUEL-1911/92] p 89 A93-11707

SPECTRAL METHODS

Effects of substrate anisotropy on coupled bilateral finlines p 208 A93-15409
Uniform high-order spectral methods for one- and two-dimensional Euler equations p 476 A93-27068
On the accurate prediction of the wall-normal velocity in compressible boundary-layer flow p 477 A93-27474
Spectral solution of the viscous blunt-body problem p 860 A93-41915
Spectral measurements of shock layer radiation in an arc-jet wind tunnel p 1251 A93-54409
Solution of compressible Navier-Stokes equations using spectral methods on arbitrary two-dimensional domains p 218 A93-14041
LES turbulence modeling using DNS data base p 299 A93-19274

SPECTRAL REFLECTANCE

Assessing spatial and seasonal variations in grasslands with spectral reflectances from a helicopter platform p 426 A93-20621
Canonical correlation relationships among spectral and phytometric variables for twenty winter wheat fields p 433 A93-22992

SPECTRAL RESOLUTION

The HYDICE instrument design and its application to planetary instruments p 842 A93-28766

SPECTROMETERS

Aureole lidar - Instrument design, data analysis, and comparison with aircraft spectrometer measurements p 1160 A93-52419
The HYDICE instrument design and its application to planetary instruments p 842 A93-28766

Summer research program (1992). High School Apprenticeship Program (HSAP) reports. Volume 16: Arnold Engineering Development Center Civil Engineering Laboratory
[AD-A262024] p 945 A93-29396

SPECTROSCOPY

Coherent systems in the terahertz frequency range: Elements, operation, and examples p 841 A93-27727

SPECTRUM ANALYSIS

Three-dimensional vortex method for parachutes p 872 A93-42874
Scale-up of the spectra of aerodynamic pressure pulsations with narrowband maxima p 1088 A93-51756
A data acquisition system for high-speed rotor balancing p 1261 A93-54396
ERS-1 directional wave spectra validation with the airborne SAR PHARS
[BCRS-92-18] p 937 A93-31010

SPEECH BASEBAND COMPRESSION

Advances in speech processing p 550 A93-19771

SPEECH RECOGNITION

Influence of aircraft noise on speech intelligibility p 558 A93-28483
The development of the speaker independent ARM continuous speech recognition system
[RSRE-MEMO-4473] p 87 A93-11383
Preliminary results on the use of linear discriminant analysis in the ARM continuous speech recognition system
[RSRE-MEMO-4511] p 87 A93-11384
The use of linear discriminant analysis in the ARM continuous speech recognition system
[RSRE-MEMO-4512] p 87 A93-11385
Advances in speech processing p 550 A93-19771
Fly-by voice, a technology demonstration p 526 A93-19918

SPEED CONTROL

Application of model reference adaptive control to speed control system in an aeroengine p 172 A93-14498

SPEED INDICATORS

Effect of Reynolds number on the standards of a simplified anemoclinometric probe
[IMFL-91-31] p 293 A93-17542

SPHERES

Three-dimensional flow over two spheres placed side by side p 539 A93-24412
Experimental investigation of spherical-convergent-flap thrust-vectoring two-dimensional plug nozzles
[AIAA PAPER 93-2431] p 898 A93-41045
Computation of hypersonic flow over a sphere using kinetic flux vector splitting scheme with equilibrium chemistry p 861 A93-42260
Scale model test results for several spherical/two-dimensional nozzle concepts
[AIAA PAPER 93-2430] p 1117 A93-50186

SPHERICAL COORDINATES

Transonic profile design in curvilinear coordinates using an approximate factorization algorithm p 7 A93-10778

SPHERICAL SHELLS

Interaction of compression waves with an elastic spherical dome p 550 A93-29718

SPIKES (AERODYNAMIC CONFIGURATIONS)

Numerical investigation of supersonic flows around a spiked blunt-body
[AIAA PAPER 93-0887] p 471 A93-24947

SPIN DYNAMICS

Unsteady aerodynamics in airplane stall-spin departure
[AIAA PAPER 93-0622] p 523 A93-24739
Computations of aerodynamic drag for turbulent transonic projectiles with and without spin
[AIAA PAPER 93-3416] p 975 A93-47212
A study of the rotary balance technique for predicting pitch damping
[AIAA PAPER 93-3619] p 1125 A93-48306

SPIN STABILIZATION

Investigation of the aircraft spin via sensitivity analysis p 524 A93-27300
Measurements of aerodynamic rotary stability derivatives using a whirling arm facility p 525 A93-28603
Free-spin damping measurement techniques
[AIAA PAPER 93-3457] p 1014 A93-47240

SPIN TESTS

Measurements of aerodynamic rotary stability derivatives using a whirling arm facility p 525 A93-28603
Recent experiences with implementing a video based six degree of freedom measurement system for airplane models in a 20 foot diameter vertical spin tunnel p 821 A93-37763
LARZAC HP turbine disk crack initiation and propagation spin pit test p 176 A93-14892
RB 199 high pressure compressor stage 3 spin pit tests p 176 A93-14893

- CF6-6 high pressure compressor stage 5 locking slot crack propagation spin pit test p 176 N93-14894
RB211-524B disc and drive cones hot cyclic spinning test p 177 N93-14895
- SPINE**
Evaluation of CKU-5/A ejection seat catapults under varied acceleration levels [AD-A248021] p 29 N93-12489
- SPLASHING**
Tracking of raindrops in flow over an airfoil [AIAA PAPER 93-0168] p 275 A93-22602
- SPLICING**
Fuselage longitudinal splice design p 997 A93-45784
A laboratory study of fracture in the presence of lap splice multiple site damage p 1027 A93-45790
Investigation of corrosion in aluminum/adhesive lap-splices using pulse-echo ultrasonic techniques [DE93-008074] p 749 N93-25518
- SPLINE FUNCTIONS**
Extracting dimensional geometric parameters from B-spline surface models of aircraft [AIAA PAPER 92-4283] p 43 A93-13340
Solving problems with singularities using conformal mappings p 397 A93-18978
Grid and aerodynamic sensitivity analyses of airplane components [AIAA PAPER 93-3475] p 981 A93-47254
Calculation of subsonic flow of a gas past an airfoil p 1068 A93-48908
Spline-collocation solution of a Fredholm equation of the second kind in the problem of flow past an airfoil p 1092 A93-51904
- SPLITTING**
A new flux splitting scheme p 973 A93-47189
- SPOILERS**
Turbulence/gust alleviation using spoiler control p 369 A93-22886
Calculation of the flowfield around an airfoil with spoiler [AIAA PAPER 93-0527] p 284 A93-23268
Spoiler actuator - A problem investigation p 801 A93-37175
Unsteady flow computations for a three-dimensional cavity with and without an acoustic suppression device [AIAA PAPER 93-3402] p 974 A93-47204
- SPRAY CHARACTERISTICS**
Ignition and exhaust emission characteristics of spray combustion in a pre-chamber type vortex combustor [ASME PAPER 92-GT-119] p 350 A93-19355
Influences on the sprays formed by high-shear fuel nozzle/swirler assemblies p 411 A93-21653
Dual-spray airblast fuel nozzle for advanced small gas turbine combustors [AIAA PAPER 93-2336] p 1116 A93-50113
- SPRAY NOZZLES**
Narrow-body aircraft water spray optimization study [DOT/FAA/CT-TN93/3] p 705 N93-25224
- SPRAYED COATINGS**
Higher velocity thermal spray processes produce better aircraft engine coatings [SAE PAPER 920947] p 202 A93-14090
The evolution of thermal barrier coatings in gas turbine engine applications [ASME PAPER 92-GT-203] p 388 A93-19427
- SPRAYERS**
A Eulerian/Lagrangian modelling to calculate the evolution of a water droplets spray [ISABE 93-7121] p 1221 A93-54096
Fuel injector: Air swirl characterization aerothermal modelling, phase 2, volume 1 [NASA-CR-189193-VOL-1] p 721 N93-24754
Fundamental studies of droplet interactions in dense sprays [AD-A261165] p 737 N93-25948
Velocity and drop size measurements in a swirl-stabilized, combustor spray [NASA-TM-106130] p 813 N93-27130
- SPRAYING**
A coupled multi-block solution procedure for spray combustion in complex geometries [AIAA PAPER 93-0108] p 539 A93-24230
- SPREAD SPECTRUM TRANSMISSION**
Lessons learned during testing of the Enhanced Position Location Reporting System (EPLRS) p 77 A93-10996
- SPRINGS (ELASTIC)**
Radii effect on the translation spring constant of force transducer beams p 829 A93-37867
- SQUARE WAVES**
Practical input optimization for aircraft parameter estimation experiments [NASA-CR-191462] p 820 N93-27264
- SQUEEZE FILMS**
The effectiveness of porous squeeze film dampers for suppressing nonsynchronous motions p 545 A93-27316
- Optimal design of centered squeeze film dampers p 831 A93-38629
- SR-71 AIRCRAFT**
The development of aircraft in the Lockheed Skunk Works from 1954 to 1991 p 805 N93-27168
- STABILITY**
Euler solutions to nonlinear acoustics of non-lifting rotor blades p 568 A93-29433
High-order cyclo-difference techniques: An alternative to finite differences [NASA-TM-107745] p 693 N93-25074
The transition prediction toolkit: LST, SIT, PSE, DNS, and LES p 783 N93-27429
- STABILITY AUGMENTATION**
A stability augmentation system for student designed remotely-piloted vehicles [AIAA PAPER 92-4261] p 63 A93-13365
Control augmentation system (CAS) synthesis via adaptation and learning [AIAA PAPER 93-3728] p 1170 A93-51328
Nonlinear command augmentation system for a high performance aircraft [AIAA PAPER 93-3777] p 1132 A93-51372
- STABILITY DERIVATIVES**
Experimental study of dynamic fluid forces and moments for a long annular seal p 209 A93-15684
Experimental investigation on aircraft dynamic stability parameters p 905 A93-40328
An experimental study of the relationship between forces and moments and vortex breakdown on a pitching delta wing p 49 N93-12206
Determination of the stability and control derivatives of the F/A-18 HARV from flight data using the maximum likelihood method [NASA-CR-191216] p 186 N93-12903
An examination of wing rock for the F-15 [AD-A256613] p 188 N93-14252
Advanced aircraft with thrust vector control [MBB-FE-1-S-PUB-0504] p 998 N93-31043
- STABILITY TESTS**
Modified sparse time domain technique for rotor stability testing p 157 A93-14593
Analysis of stability characteristics of a high performance aircraft [AIAA PAPER 93-3616] p 1125 A93-48303
Liquid hydrogen foil-bearing turbopump [AIAA PAPER 93-2537] p 1156 A93-50264
The role of turbomachinery testing for stability in distorted flow [PNR-90943] p 57 N93-11040
BLSTA: A boundary layer code for stability analysis [NASA-CR-4481] p 220 N93-14797
Multiple model adaptive estimation applied to the VISTA F-16 with actuator and sensor failures, volume 2 [AD-A256569] p 371 N93-16165
Aeroelastic response and aeromechanical stability of helicopters with elastically coupled composite rotor blades p 715 N93-25530
Stability investigations of airfoil flow by global analysis p 783 N93-27436
The onset of vortex turbulence p 788 N93-28251
- STABILIZATION**
Active stabilization of compressor instability and surge in a working engine [ASME PAPER 92-GT-88] p 348 A93-19335
Controlling common mode stabilization errors in airborne gravity gradiometry p 1245 A93-55978
Active stabilization to prevent surge in centrifugal compression systems [NASA-CR-191625] p 424 N93-18862
- STABILIZERS**
The investigation on vibration characteristics of all-movable stabilizer of an aircraft p 41 A93-11821
Investigation of flame stabilizers in the form of perforated grids p 1003 A93-47513
- STABILIZERS (FLUID DYNAMICS)**
Apparatus and method for improving spin recovery on aircraft [NASA-CASE-LAR-14747-1] p 526 N93-20039
The influence of structural optimization on the aeroelastic properties of a vertical tail [AD-A259140] p 513 N93-20575
- STAGE SEPARATION**
Robust control of the separation of hypersonic lifting vehicles [AIAA PAPER 92-5013] p 385 A93-22289
- STAGNATION FLOW**
In-flight detection of flow separation, stagnation, and transition p 166 A93-14326
The stagnation line solution of the equilibrium flow with radiation and mass injection p 680 A93-33733
Effects of a rear stagnation jet on the wake behind a cylinder p 1151 A93-49026
Flow over a leading edge with distributed roughness p 18 N93-10549
- STAGNATION POINT**
Measurement of attachment-line location in a wind-tunnel and in supersonic flight [AIAA PAPER 92-4089] p 39 A93-11285
Flight evaluation of a stagnation detection hot-film sensor [AIAA PAPER 92-4085] p 51 A93-13263
An investigation of the effects of a rear stagnation jet on the wake behind a cylinder [AIAA PAPER 93-3274] p 969 A93-46835
Analysis of the stability characteristics of hypersonic flow of a detonable gas mixture in the stagnation region of a blunt body [AIAA PAPER 93-1918] p 1076 A93-49784
Stagnation point computations of nonequilibrium inviscid blunt body flow p 1093 A93-52005
Performance and control of ascending trajectories to minimize heat load for transatmospheric aero-space planes p 133 N93-13745
- STAGNATION PRESSURE**
Evaluation of 2D scramjet nozzle performance p 52 A93-11209
Analysis of high speed multistage compressor throughflow using spanwise mixing [ASME PAPER 92-GT-13] p 347 A93-19285
Increase in stagnation pressure and enthalpy in shock tunnels [AIAA PAPER 93-0350] p 377 A93-23035
Performance considerations in the operation of free-piston driven hypersonic test facilities p 1011 A93-45497
Initial results from the NASA Lewis wave rotor experiment [AIAA PAPER 93-2521] p 1193 A93-53589
Increase of stagnation pressure and enthalpy in shock tunnels p 295 N93-18086
An experimental study of under-expanded jets p 696 N93-25467
Initial results from the NASA-Lewis wave rotor experiment [NASA-TM-106148] p 1005 N93-32368
- STAGNATION TEMPERATURE**
Experimental investigation of an axisymmetric hypersonic scramjet inlet for laser propulsion p 122 A93-14515
Analysis of high speed multistage compressor throughflow using spanwise mixing [ASME PAPER 92-GT-13] p 347 A93-19285
Investigation of a two-dimensional scramjet inlet, freestream M = 8-18 and Tsub 0 = 4100 K p 270 A93-21669
A finite element and symbolic method for studying laminar boundary layers of real gases in equilibrium at Mach numbers to 30 [AIAA PAPER 93-2986] p 1052 A93-48179
- STAINLESS STEELS**
Application of a sulphur-doped alkane system to the study of thermal oxidation of jet fuels [ASME PAPER 92-GT-122] p 387 A93-19356
Damage tolerance of a helicopter rotor high-strength steel p 555 N93-21322
External stress-corrosion cracking of a 1.22-m-diameter type 316 stainless steel air valve [NASA-TP-3190] p 737 N93-26201
- STALLING**
The F-18 High Alpha Research Vehicle - A high-angle-of-attack testbed aircraft [AIAA PAPER 92-4121] p 42 A93-13273
- STANDARD DEVIATION**
The development of swirl five-hole probe p 987 A93-47341
Study of statistical variations of load spectra and material properties on aircraft fatigue life [AD-A257961] p 339 N93-18451
General aviation aircraft: Normal acceleration data analysis and collection project [DOT/FAA/CT-91/20] p 713 N93-24739
Use of titanium castings without a casting factor [AD-A264414] p 1018 N93-31192
- STANDARDIZATION**
Civil standardization of the Global Positioning System for the aviation community p 29 A93-10981
International standards for the qualification of airplane flight simulators; Conference, London, United Kingdom, Jan. 16, 17, 1992, Document Approved [ISBN 1-85768-040-5] p 1140 A93-51934
Standardization of precipitation static test methods and equipment for the Navy [AD-A257025] p 165 N93-15361
Standardization of automatic test equipment in the US Air force [AD-A262076] p 809 N93-29004
- STANDARDS**
A transfer standard of an air flow rate unit VET 150-2-87 p 66 A93-10049

- Magnetic variation - A primitive concept and its hold on contemporary navigation p 32 A93-11021
Progress towards common standards for flight simulator qualification p 374 A93-18774
Mil-Prime specification for parachutes p 677 A93-35184
[AIAA PAPER 93-1247]
The technical background to standards for shackles [NPL-DMM(A)-51] p 86 A93-11325
The technical background to standards for eyebolts [NPL-DMM(A)-52] p 87 A93-11327
Proposed revisions to RTCM SC-104 recommended standards for differential NAVSTAR/GPS service for carrier phase applications p 152 A93-15005
[AD-A255276]
Zoning of aircraft: A review of the definitions p 703 A93-24880
NASA/FAA helicopter simulator workshop [NASA-CP-3156] p 857 A93-30673
Part 1: Executive summary p 857 A93-30674
- STANDING WAVES**
Hypersonic stagnation line merged layer flow on blunt axisymmetric bodies of arbitrary shape [AIAA PAPER 93-2723] p 962 A93-46478
- STARCHES**
Starch media blasting for aerospace finishing applications [SAE PAPER 920948] p 107 A93-14091
- STATE ESTIMATION**
Extended linear quadratic Gaussian control under randomly varying distributed delays p 439 A93-22854
A U-D factorization-based adaptive extended Kalman filter and its application to flight state estimation p 1169 A93-51198
Fault tolerant navigation for aircraft landing p 1191 A93-53866
On-line aircraft state and parameter estimation p 512 A93-19929
- STATE VECTORS**
An adaptive algorithm for estimation of a state vector in the system of remotely-piloted aircraft control using Kalman filter p 181 A93-14232
Testing concept of a taxiing control system, summary p 1010 A93-31278
- STATIC AERODYNAMIC CHARACTERISTICS**
Low velocity impact in a graphite/PEEK [AIAA PAPER 93-1403] p 734 A93-33963
Experimental and algorithmic means of identifying mathematical models of flight vehicle p 909 A93-43103
Low-speed longitudinal and lateral-directional aerodynamic characteristics of the X-31 configuration [NASA-TM-4351] p 22 A93-11622
- STATIC CHARACTERISTICS**
On the static stability of forward swept propfans [AIAA PAPER 93-1634] p 720 A93-34162
Improved static and dynamic performance of helicopter powerplant p 809 A93-35928
Static and dynamic errors in heat flux measurements p 1254 A93-54366
- STATIC DEFORMATION**
Nonlinear large amplitude aeroelastic behavior of composite rotor blades p 997 A93-45741
- STATIC ELECTRICITY**
Standardization of precipitation static test methods and equipment for the Navy [AD-A257025] p 165 A93-15361
The 1992 International Aerospace and Ground Conference on Lightning and Static Electricity: Addendum [DOT/FAA/CT-92/20-ADD-1] p 753 A93-24875
- STATIC LOADS**
An experimental study of the relationship between forces and moments and vortex breakdown on a pitching delta wing p 49 A93-12206
Load test set-up for the Airmass Sunburst Ultra-Light Aircraft p 895 A93-29776
Development of nose structure of a reconnaissance container for a supersonic jet aircraft [MBB-LME-242-S-PUB-0451] p 998 A93-31046
- STATIC PRESSURE**
A method for optimizing the meridional passage of the rotor in centrifugal compressors p 119 A93-14344
Experimental and theoretical analysis of the flow in a centrifugal compressor volute [ASME PAPER 92-GT-30] p 400 A93-19290
Investigation of compressor rotor wake structure at peak pressure rise coefficient and effects of loading [ASME PAPER 92-GT-32] p 246 A93-19292
Effects of back-pressure in a lean blowout research combustor [ASME PAPER 92-GT-81] p 387 A93-19330
Determination of gas flow rate in a duct from measured static pressures p 520 A93-27625
Comment on 'in-flight measurement of static pressures' p 807 A93-37407
- Prediction of static performance for single expansion ramp nozzles [AIAA PAPER 93-2571] p 898 A93-41047
The hemisphere-cylinder at an angle of attack p 21 A93-11250
Static pressure measurements of the shock-boundary layer interaction in a simulated fan passage [AD-A256724] p 361 A93-15979
A multi-faceted engineering study of aerodynamic errors of the Service Aircraft Instrumentation Package (SAIP) [AD-A258059] p 293 A93-17677
Surface and flow field measurements in a symmetric crossing shock wave/turbulent boundary-layer interaction [NASA-TM-106086] p 693 A93-24911
The transient development of vortices over delta wings p 695 A93-25269
Model fan passage flow simulation [AD-A261613] p 752 A93-26167
Analysis of fluctuating static pressure measurements in a large high Reynolds number transonic cryogenic wind tunnel [NASA-TM-108722] p 823 A93-27142
Modification and calibration of the Naval Postgraduate School Academic Wind Tunnel [AD-A262092] p 823 A93-28189
Performance characteristics of two multiaxis thrust-vectoring nozzles at Mach numbers up to 1.28 [NASA-TP-3313] p 874 A93-29160
- STATIC STABILITY**
On the static stability of forward swept propfans [AIAA PAPER 93-1634] p 720 A93-34162
Static aeroelastic control of an adaptive lifting surface p 995 A93-45147
Effect of geometry, static stability, and mass distribution on the tumbling characteristics of generic flying-wing models [AIAA PAPER 93-3615] p 1125 A93-48302
Estimation of neutral and maneuver points of aircraft by dynamic maneuvers [AIAA PAPER 93-3620] p 1126 A93-48307
Aerodynamic characteristics and static stability margin of conical star-shaped bodies at supersonic velocities p 1067 A93-48848
- STATIC TESTS**
Software for the control of measurement data acquisition, processing, and monitoring during strength testings p 94 A93-10042
Vortex breakdown study on a 65-deg delta wing tested in static and dynamic conditions p 121 A93-14407
Static tests of jet fuel thermal and oxidative stability p 389 A93-21651
Active control of the shear layer on a static airfoil [AIAA PAPER 93-0442] p 286 A93-23353
Methodology for studying the fracture of aircraft structures in static tests p 801 A93-36785
A study of the effect of the static aeroelasticity of a swept wing on its weight response p 801 A93-36798
Hysteresis and bristle stiffening effects of conventional brush seals [AIAA PAPER 93-1996] p 1153 A93-49839
Static internal performance tests of single expansion ramp nozzle concepts designed with LO considerations [AIAA PAPER 93-2429] p 1117 A93-50185
Results of sea-level static tests on air turbo ramjet for a future space plane [AAS PAPER 91-640] p 1247 A93-55817
Standardization of precipitation static test methods and equipment for the Navy [AD-A257025] p 165 A93-15361
- STATIC THRUST**
Performance characteristics of two multiaxis thrust-vectoring nozzles at Mach numbers up to 1.28 [NASA-TP-3313] p 874 A93-29160
- STATISTICAL ANALYSIS**
Statistical validation for GPS integrity test p 34 A93-11297
Accuracy of nonparametric reliability estimates under varying operation conditions p 396 A93-18343
A statistical approach to the experimental evaluation of transonic turbine airfoils in a linear cascade [ASME PAPER 92-GT-5] p 245 A93-19278
Estimation of the maximum values of instantaneous distortion index DC sub theta --- of fluid flow p 266 A93-20806
Aircraft collision avoidance using statistical decision theory p 500 A93-28155
An optimization method for statistical ascertainment of the most probable peak temperature at combustor exit p 1108 A93-49195
Statistical techniques for traffic flow management [AIAA PAPER 93-3834] p 1098 A93-51423
An improved method for determining force balance calibration accuracy p 1254 A93-54369
- Three-dimensional simulations of compressible mixing layers - Visualizations and statistical analysis p 1235 A93-55360
Response variability observed in reverberant acoustic test of a model aerospace structure p 1264 A93-55857
Numerical study for the study of medium speed internal noise problems [DILC-EST-TN-200] p 101 A93-11156
Example of statistical techniques applied to analysis of landing ground roll distance measurements (linear regression, correlation coefficient and F-test) [ESDU-92021] p 330 A93-16635
Example of statistical techniques applied to analysis of measurements of the landing airborne manoeuvre. (Multiple linear regression with two independent variables and one dependent variable.) [ESDU-92022] p 330 A93-16636
Effect of sonic boom asymmetry on subjective loudness [NASA-TM-107708] p 453 A93-16755
Statistical fatigue analysis of the SH-60B servo beam rail component [AD-A257474] p 332 A93-17660
Methodology for sensitivity analysis, approximate analysis, and design optimization in CFD for multidisciplinary applications [NASA-CR-192172] p 552 A93-20297
Load experience variability of fighter aircraft [NLR-TP-89172-U] p 514 A93-20742
Annual review of aircraft accident data: US general aviation calendar year 1989 [PB93-160687] p 790 A93-27033
Loudness and annoyance response to simulated outdoor and indoor sonic booms [NASA-TM-107756] p 852 A93-27271
A laboratory study of subjective response to sonic booms measured at White Sands Missile Range [NASA-TM-107746] p 852 A93-27272
Low cycle fatigue behaviour of titanium disc alloys p 1004 A93-31745
- STATISTICAL MECHANICS**
Adaptivity-fluids-localization. The challenge to computational mechanics p 553 A93-20618
- STATISTICAL TESTS**
Assessment of helicopter component statistical reliability computations [AD-A258931] p 510 A93-19447
- STATISTICAL WEATHER FORECASTING**
Terminal forecast amendments - A 'cloudy' issue --- valid for up to 24 hours for airport areas p 431 A93-22167
- STATOR BLADES**
Analytical method for subsonic cascade profile p 12 A93-12730
Forcing function effects on unsteady aerodynamic gust response. II - Low solidity airfoil row response [ASME PAPER 92-GT-175] p 251 A93-19401
Euler computations of rotor-stator interaction in turbomachinery cascades using adaptive triangular meshes [AIAA PAPER 93-0386] p 282 A93-23065
Navier-Stokes flow simulation in a 2D high pressure turbine cascade with a cooled slot trailing edge p 972 A93-46941
The blade curving effects in a turbine stator cascade with low aspect ratio [AD-A261063] p 725 A93-26239
Three-dimensional fiber-optic LDV measurements in the endwall region of a linear cascade of controlled-diffusion stator blades [AD-A263513] p 933 A93-29968
- STATORS**
Calculation of turbulent flow for an enclosed rotating cone [ASME PAPER 92-GT-70] p 400 A93-19320
Viscous interaction upstream and downstream of a turbine stator cascade with a periodic wake field [ASME PAPER 92-GT-162] p 250 A93-19388
An approach for multi-stage calculations incorporating unsteadiness [ASME PAPER 92-GT-282] p 253 A93-19474
Influence of stator-rotor gap on axial-turbine unsteady forcing functions p 899 A93-41918
Blade row interaction effects on compressor measurements p 900 A93-42885
Stator relative, rotor blade-to-blade near wall flow in a multistage axial compressor with tip clearance variation [AIAA PAPER 93-2389] p 1083 A93-50154
A transfer matrix method for calculation of support stiffness of aeroengine stator p 1122 A93-51193
Rotor wake/stator interaction noise - Predictions vs data p 1174 A93-52447
Characterisation of conventional and controlled diffusion stator blades in a transonic compressor stage [ISABE 93-7124] p 1189 A93-54099

- Experimental heat transfer results in turbine stators and rotors and a comparison with theory [PNR-90945] p 57 N93-11055
- Investigation of hot streak migration and film cooling effects on heat transfer in rotor/stator interacting flows, report 1 [AD-A250688] p 102 N93-12490
- The blade curving effects in a turbine stator cascade with low aspect ratio [AD-A261063] p 725 N93-26239
- STEADY FLOW**
- A flux-difference finite volume method for steady Euler equations on adaptive unstructured grids p 116 A93-14277
- A new Lagrangian method for steady supersonic flow computation. II - Slip-line resolution. III - Strong shocks p 243 A93-18855
- An investigation on the artificial viscosity in the transonic stream function formulation [ASME PAPER 92-GT-49] p 246 A93-19302
- Analysis of steady and unsteady turbine cascade flows by a locally implicit hybrid algorithm [ASME PAPER 92-GT-127] p 249 A93-19361
- Nonlinear relaxation/quasi-Newton algorithm for the compressible Navier-Stokes equations p 287 A93-23541
- Engineering approach to the prediction of shock patterns in bounded high-speed flows p 287 A93-23545
- Computing 3-D steady supersonic flow via a new Lagrangian approach [AIAA PAPER 93-0891] p 471 A93-24951
- The interaction between a steady jet flow and a supersonic blade tip p 688 A93-34415
- Higher-order-accurate upwind schemes for solving the compressible Euler and Navier-Stokes equations p 863 A93-42441
- Computational results for flows over compression ramps p 866 A93-42599
- Viscous and inviscid hypersonic flow about a double ellipsoid p 868 A93-42616
- Hypervelocity flows of argon produced in a free piston driven expansion tube p 1012 A93-45530
- Active flow control with neural networks [AIAA PAPER 93-3273] p 1037 A93-46834
- On the steady subsonic shear flow past a slender body of revolution p 970 A93-46907
- Intensive industrial use of 3D Euler numerical methods for axial flow turbine analysis and design p 1002 A93-46943
- Numerical solution of steady and unsteady Euler equations p 973 A93-46988
- Trajectory mapping of quasi-periodic structures in a vortex flow [AIAA PAPER 93-2914] p 1044 A93-48116
- Vortex developments over steady and accelerated airfoils incorporating a trailing edge jet [AIAA PAPER 93-3008] p 1054 A93-48198
- Averaging techniques for steady and unsteady calculations of a transonic fan stage [AIAA PAPER 93-3065] p 1059 A93-48241
- Effect of steady-state circumferential pressure and temperature distortions on compressor stability p 1106 A93-48503
- Efficient multigrid computation of steady hypersonic flows p 1152 A93-49527
- Steady transonic weakly perturbed flows in a vibrationally relaxing gas p 1088 A93-51768
- Steady state supersonic flows of a vibrationally excited gas past thin bodies p 1089 A93-51818
- Three-dimensional flow analysis inside turbomachinery stages with steady and unsteady Navier-Stokes method [ISABE 93-7095] p 1186 A93-54071
- Recent advances in steady compressible aerodynamic sensitivity analysis p 1236 A93-55400
- Vibration excitation in laminar hypersonic boundary layers p 1237 A93-56028
- Experimental studies in the Aachen hypersonic shock tunnel p 1251 A93-56032
- Free streamline-boundary layer analysis for separated flow over an airfoil p 1239 A93-56327
- Mathematical problems in inviscid hypersonic flow p 131 N93-13451
- An integral equation solution for multistage turbomachinery design calculations [NASA-TM-105970] p 179 N93-15521
- Computational investigations of a NACA 0012 airfoil in low Reynolds number flows [AD-A257300] p 288 N93-15920
- Development of a boundary element method program for numerical analysis of supersonic unsteady flow p 300 N93-19283
- Calculations of aerodynamic forces on a wing with thrust using BEM p 300 N93-19286
- Increased heat transfer to elliptical leading edges due to spanwise variations in the freestream momentum: Numerical and experimental results [NASA-TM-106150] p 838 N93-27020
- Stability investigations of airfoil flow by global analysis p 783 N93-27436
- STEADY STATE**
- Steady and quasisteady resonant lock-in of finned projectiles p 61 A93-12012
- Steady state model for the thermal regimes of shells of airships and hot air balloons p 207 A93-15072
- Breakdown of steady state axisymmetric flow in a shock layer formed as a result of the impingement of a supersonic underexpanded jet on a perpendicular plane obstacle p 241 A93-18230
- The influence of intake swirl distortion on the steady-state performance of a low bypass, twin-spool engine p 214 N93-13211
- Estimation of rate of climb [ESDU-92019] p 164 N93-14541
- Some experiments and ideas on GPA before reaching steady state of engine p 178 N93-15175
- A hybrid multigrid technique for computing steady-state solutions to supersonic flows p 700 N93-26078
- STEAM FLOW**
- Performance improvement of gas turbine with steam injection p 1107 A93-48523
- STEAM TURBINES**
- Visualization and analysis of supersonic flow in rotating turbine stage. II - Analysis of the flow into the moving blades and their exit flow p 476 A93-27442
- Prediction of three-dimensional low frequency unsteady transonic flow and forced vibration in axial turbine stages p 971 A93-46934
- STEELS**
- Fatigue crack growth in AerMet 100 steel [AD-A249068] p 74 N93-12248
- Stress corrosion susceptibility of ultra-high strength steels for Naval aircraft applications [AD-A256126] p 199 N93-15189
- Hydrogen-induced stress corrosion cracking susceptibility analysis of pitch links from the AH-64 Apache helicopter [AD-A260692] p 736 N93-25895
- STEEPEST DESCENT METHOD**
- Automatic pulse shaping with the AN/FPN-42 and AN/FPN-44A Loran-C transmitters [AD-A257860] p 319 N93-18309
- STEEPERABLE ANTENNAS**
- A self-steering array for the SHARP microwave-powered aircraft p 792 A93-37090
- Adaptive waveform selection with a neural network p 942 A93-43470
- STEERING**
- Braking, steering, and wear performance of radial-belted and bias-ply aircraft tires [SAE PAPER 921036] p 158 A93-14656
- The evolution of a nose-wheel steering system p 995 A93-44852
- Steering system of a vehicle, such as a snow removing machine for airfields [CA-PATENT-APPL-SN-1293201] p 83 N93-10367
- STEPS**
- Fluid flow and heat convection studies for actively cooled airframes [NASA-CR-190956] p 216 N93-13406
- STEREOSCOPIC VISION**
- A fast algorithm for obtaining dense depth maps for high speed navigation p 435 A93-19080
- Trade-offs arising from mixture of color cueing and monocular, binocular, and stereoscopic cueing information for simulated rotorcraft flight [NASA-TP-3268] p 338 N93-18333
- STIFFENING**
- Damage progression in stiffened composite panels [AIAA PAPER 93-1345] p 738 A93-33915
- Evaluation of thermoplastic stiffened panels for application to rotorcraft airframes p 827 A93-36000
- Test facility for evaluation of structural integrity of stiffened and jointed aircraft curved panels p 1012 A93-45794
- Hysteresis and bristle stiffening effects of conventional brush seals [AIAA PAPER 93-1996] p 1153 A93-49839
- Interlaminar stress analysis at the skin/stiffener interface of a grid-stiffened composite panel [NASA-CR-192177] p 393 N93-17920
- Design and analysis of grid stiffened concepts for aircraft composite primary structural applications p 922 N93-30861
- Structural response of bead-stiffened thermoplastic shear webs p 923 N93-30873
- STIFFNESS**
- Effects of the pylon pitching stiffness on wing-store flutter p 41 A93-11820
- Stiffness design method of symmetric laminates using lamination parameters p 206 A93-14569
- An inverse method for computation of structural stiffness distributions of aeroelastically optimized wings [AIAA PAPER 93-1540] p 741 A93-34077
- Stiffness, thermal expansion, and thermal bending formulation of stiffened, fiber-reinforced composite panels [AIAA PAPER 93-1569] p 741 A93-34102
- Effects of pylon yaw and lateral stiffness on the flutter of a delta wing with external store p 800 A93-36330
- Optimization of the stiffness and mass characteristics of lifting surface structures modeled by an elastic beam p 827 A93-36789
- The use of beam-like modal data for stiffness profile estimation by the EBS method. I - Justification and implementation --- Equivalent Beam Stiffness p 1257 A93-54649
- Multidisciplinary optimization of aeroservoelastic systems [NASA-CR-191255] p 220 N93-14766
- Relationship between mechanical property and energy-absorption trends for composite tubes [NASA-TP-3284] p 392 N93-16537
- STIFFNESS MATRIX**
- A transfer matrix method for calculation of support stiffness of aeroengine stator p 1122 A93-51193
- STIRLING CYCLE**
- Free-piston Stirling coolers for intermediate lift temperatures p 543 A93-26062
- Linear motor driven Stirling coolers for military and commercial applications p 543 A93-26064
- Flight data for the Cryogenic Heat Pipe (CRYOHP) Experiment [AIAA PAPER 93-2735] p 1027 A93-46488
- STIRLING ENGINES**
- Stirling engine - Available tools for long-life assessment --- for space propulsion p 195 A93-13824
- STOCHASTIC PROCESSES**
- Stochastic computational mechanics for aerospace structures p 78 A93-12157
- Stochastic modeling and adaptive control algorithm of brake bending p 227 A93-14417
- Stochastic measures of performance robustness in aircraft control systems p 185 A93-14595
- Modeling of human operator actions in the stochastic trajectory tracking problem for a dynamic plant p 228 A93-16783
- Optimization of a multistage axial compressor stochastic approach [ASME PAPER 92-GT-163] p 351 A93-19389
- Performance prediction of the interacting multiple model algorithm p 439 A93-22926
- A coupled multi-block solution procedure for spray combustion in complex geometries [AIAA PAPER 93-0108] p 539 A93-24230
- Numerical simulation of homogeneous non-Gaussian random vector fields p 561 A93-27584
- Further studies using matched filter theory and stochastic simulation for gust loads prediction [AIAA PAPER 93-1365] p 726 A93-33932
- An effective Mixed Annealing/Heuristic Algorithm for problems in kinematic mechanical design [AIAA PAPER 93-1581] p 741 A93-34113
- Statistical methods in flight vehicle control theory p 1165 A93-49306
- A theory for the analysis of rotorcraft operating in atmospheric turbulence p 48 N93-11725
- Stochastic sensitivity measure for mistuned high-performance turbines [NASA-TM-105821] p 90 N93-12277
- A stochastic optimal feedforward and feedback control methodology for superagility [NASA-CR-4471] p 229 N93-13370
- A simulation model of atmospheric turbulence for rotorcraft applications p 224 A93-14588
- Stochastic finite element analysis for high speed rotors p 554 N93-20696
- Fuel injector: Air swirl characterization aerothermal modeling, phase 2, volume 1 [NASA-CR-189193-VOL-1] p 721 N93-24754
- Fuel injector: Air swirl characterization aerothermal modeling, phase 2, volume 2 [NASA-CR-189193-VOL-2] p 721 N93-25106
- Control of complex dynamic systems by neural networks p 758 N93-25611
- STOCKPILING**
- Desert store --- of mothballed commercial jet aircraft p 1229 A93-54866
- STOICHIOMETRY**
- Modification of combustor stoichiometry distribution for reduced NO(x) emission from aircraft engines [ASME PAPER 92-GT-108] p 349 A93-19346

STORAGE STABILITY

The degradation of parachutes: Age and mechanical wear
[AD-A252243] p 24 N93-12179

STORAGE TANKS

National Aerospace Plane Integrated
Fuselage/Cryotank Risk Reduction program
[AIAA PAPER 93-2564] p 1142 A93-50284

STORMS (METEOROLOGY)

Natural and augmented snowfall growth processes and their interactions with the natural and modified aerosol
[PB93-153096] p 755 N93-25874

STOVL AIRCRAFT

Piloted simulation evaluation of pitch control designs for highly augmented STOVL aircraft
[AIAA PAPER 92-4234] p 63 A93-13328

Small scale jet effects and hot gas ingestion investigations at NASA Ames
[AIAA PAPER 92-4252] p 67 A93-13339

Developing control strategies for ASTOVL aircraft
p 366 A93-18777

Robust integrated flight/propulsion control design for a STOVL aircraft using H-infinity control design techniques
p 524 A93-26432

High-performance aircraft propulsion research
p 529 A93-27904

An initial comparison of CFD with experiment for a geometrically simplified STOVL model
[AIAA PAPER 93-3059] p 1058 A93-48236

Application of controller partitioning optimization procedure to integrated flight/propulsion control design for a STOVL aircraft
[AIAA PAPER 93-3766] p 1131 A93-51361

Overview of high performance aircraft propulsion research
[NASA-TM-105839] p 59 N93-11530

Propulsion system performance resulting from an integrated flight/propulsion control design
[NASA-TM-105874] p 180 N93-15525

Controller partitioning for integrated flight/propulsion control implementation
[NASA-TM-105804] p 527 N93-21197

Jet-induced ground effects on a parametric flat-plate model in hover
[NASA-TM-104001] p 700 N93-26099

STRAIN DISTRIBUTION

Actuation strain decoupling through enhanced directional attachment in plates and aerodynamic surfaces
p 394 A93-17727

A study of the origin of residual stresses and strains in the transparencies of supersonic aircraft
p 801 A93-36784

Effect of the wing planform on the optimal deformation of the middle surface
p 1150 A93-48909

Reliability of stiffened structural panels: Two examples
[NASA-TM-107687] p 219 N93-14483

Smart materials
p 536 N93-20624

STRAIN ENERGY METHODS

Parametric aeroelastic analysis of composite wing-boxes with active strain-energy tuning
p 156 A93-14361

Optimum balancing of flexible rotor
p 205 A93-14489

STRAIN GAGE BALANCES

Measurement of aerodynamic forces at high temperatures
p 75 A93-10030

Development of a six component flexured two shell internal strain gage balance
[AIAA PAPER 93-0793] p 541 A93-24872

Strain-gauge balance performance and internal temperature gradients measured in a cryogenic environment
[RAE-TM-AERO-2232] p 68 N93-11906

STRAIN GAGES

Determination of the membrane and flexural shell deformations from the readings of a two-sided rosette-type strain gage
p 75 A93-10047

A preliminary investigation of a method to calibrate strain gauge balances by means of a reference balance
p 210 A93-16845

High temperature thin film strain gauges
[ONERA, TP NO. 1992-171] p 542 A93-25346

Radi effect on the translation spring constant of force transducer beams
p 829 A93-37867

The measurement of blade deflections - A new implementation of the strain pattern analysis
[ONERA, TP NO. 1992-127] p 831 A93-38601

Aero-engine component damping estimation from full-scale aeromechanical test data
[AIAA PAPER 93-1873] p 1112 A93-49748

Development of a tethered satellite force transducer
p 1251 A93-54368

An improved method for determining force balance calibration accuracy
p 1254 A93-54369

Instrumentation and data acquisition for full-scale aircraft crash testing
p 1250 A93-54399

A method of testing two-dimensional airfoils
[AD-A253210] p 17 N93-10375

High-temperature strain measurement techniques: Current developments and challenges
p 217 N93-13669

Determination of stresses on laminated aircraft transparencies by the strain gage-hole drilling and sectioning method
[AD-A255548] p 164 N93-14571

STRAIN MEASUREMENT

Modeling and strain gauging of eddy current repulsion deicing systems
[AIAA PAPER 93-0296] p 327 A93-22696

Determination of tire-wheel interface pressure distribution for aircraft wheels
[AIAA PAPER 93-1343] p 709 A93-33913

The measurement of blade deflections - A new implementation of the strain pattern analysis
[ONERA, TP NO. 1992-127] p 831 A93-38601

Testing experience with unheated strain-gage balances in the NTF --- National Transonic Facility
p 1013 A93-47021

High-temperature strain measurement techniques: Current developments and challenges
p 217 N93-13669

A neural network prototype for predicting F-14B strains at the B.L. 10 longeron
[AD-A255272] p 165 N93-15004

Smart materials
p 536 N93-20624

STRAKES

Experimental study on the mechanism of favourable interferences of body strakes
p 121 A93-14405

Numerical analysis of a chined forebody with asymmetric strakes
[AIAA PAPER 93-0051] p 260 A93-20164

The aerodynamic effects of sideslip on double delta wings
[AIAA PAPER 93-0053] p 261 A93-20166

The strake - A simple means for directional control improvement
p 802 A93-37997

Actuated forebody strake controls for the F-18 high alpha research vehicle
[AIAA PAPER 93-3675] p 1006 A93-44233

Forebody vortex control on an F/A-18 using small, rotatable 'tip-strakes'
[AIAA PAPER 93-3450] p 1009 A93-47236

Euler analysis of forebody-strake vortex flows at supersonic speeds
p 1094 A93-52429

Effects of forebody strakes and Mach number on overall aerodynamic characteristics of configuration with 55 deg cropped delta wing
[NASA-TP-3253] p 131 N93-13353

Quantitative-force measurements of pneumatic control on a wing/strake model
[AD-A257343] p 289 N93-16157

Helicopter low-speed yaw control
[NASA-CASE-LAR-14219-1] p 729 N93-25998

STRATEGY

Human factors causes and management strategies in US Air Force F-16 mishaps 1984-present
p 492 N93-19673

STRATOSPHERE

The Superpressure Stratospheric Vehicle
p 39 A93-11357

Long-duration balloon flights in the middle stratosphere
p 40 A93-11369

Concept for an open-neck stratospheric balloon with long-duration flight capability
p 40 A93-11371

Polar Patrol Balloon Experiment in Antarctica
p 27 A93-11373

Stratospheric turbulence measurements and models for aerospace plane design
[AIAA PAPER 92-5072] p 433 A93-22342

Infrared detection of high altitude clear air turbulence
[AIAA PAPER 93-0852] p 557 A93-24916

Short-term atmospheric effects of high-altitude aircraft emissions
p 559 A93-28865

Implications of three-dimensional tracer studies for two-dimensional assessments of the impact of supersonic aircraft on stratospheric ozone
p 936 A93-41269

Plume and wake dynamics, mixing, and chemistry behind a high speed civil transport aircraft
p 1034 A93-45139

Computation of wake/exhaust mixing downstream of advanced transport aircraft
[AIAA PAPER 93-2944] p 1162 A93-48141

Predicted aircraft effects on stratospheric ozone
p 93 N93-11096

Stratospheric aircraft: Impact on the stratosphere?
[DE92-016997] p 94 N93-12104

Stratospheric aircraft exhaust plume and wake chemistry studies
[NASA-CR-189688] p 94 N93-12299

Stratospheric turbulence measurements and models for aerospace plane design
[NASA-TM-104262] p 223 N93-13288

The atmospheric effects of stratospheric aircraft. Report of the 1992 Models and Measurements Workshop. Volume 1: Workshop objectives and summary
[NASA-RP-1292-VOL-1] p 754 N93-25157

The atmospheric effects of stratospheric aircraft. Report of the 1992 Models and Measurements Workshop. Volume 2: Comparisons with global atmospheric measurements
[NASA-RP-1292-VOL-2] p 754 N93-25158

The atmospheric effects of stratospheric aircraft. Report of the 1992 Models and Measurements Workshop. Volume 3: Special diagnostic studies
[NASA-RP-1292-VOL-3] p 754 N93-25159

STRATUS CLOUDS

Sea fog and stratus - A major aviation hazard in the northern Gulf of Mexico
p 429 A93-22141

Seasonal weather hazards
p 431 A93-22180

Sea fog and stratus - A major aviation and marine hazard in the northern Gulf of Mexico
p 844 A93-39762

STREAK PHOTOGRAPHY

Effects of flow-path variations on internal reversing flow in a tailpipe offtake configuration for ASTOVL aircraft
[AIAA PAPER 93-2438] p 1118 A93-50190

Effects of flow-path variations on internal reversing flow in a tailpipe offtake configuration for ASTOVL aircraft
[NASA-TM-106149] p 900 N93-29065

STREAM FUNCTIONS (FLUIDS)

Three-dimensional flow calculations in turbomachinery using the stream function formulation
p 11 A93-12453

Streamline curvature in supersonic shear layers
p 244 A93-19194

An investigation on the artificial viscosity in the transonic stream function formulation
[ASME PAPER 92-GT-49] p 246 A93-19302

Prediction of rotor dynamic destabilizing forces in axial flow compressors
p 272 A93-22263

The numerical simulation of the hydrodynamic field from the pump impellers zone by means of the finite element method
p 476 A93-26905

Some contributions to propulsion theory - The Stream Force Theorem and applications to propulsion
p 924 A93-40472

Comparison of coordinate-invariant and coordinate-aligned upwinding for the Euler equations
[AIAA PAPER 93-3306] p 858 A93-41053

The use of streamwise vorticity to enhance ejector performance
[AIAA PAPER 93-3247] p 966 A93-46792

A visualizing method of streamlines around hypersonic vehicles
[AIAA PAPER 93-3440] p 1014 A93-47230

The streamline throughflow method of axial turbomachinery flow analysis
[ISABE 93-7031] p 1184 A93-54007

A new method for resolving transonic nozzle flows using orthogonal stream-lines coordinate system
p 1230 A93-54584

Two problems applied to the rheographical transformation of axisymmetric flow
p 1231 A93-54599

STREAMLINED BODIES

Preliminary design estimates of high-speed streamlines on arbitrary shaped vehicles defined by quadrilateral elements
[AIAA PAPER 93-3491] p 982 A93-47263

STRESS ANALYSIS

Nonlinear deformation mechanics of multilayer transparency elements - General theory relations
p 79 A93-12800

Analysis of the NASA Hypersonic Wing Test Structure
[AIAA PAPER 92-4724] p 409 A93-20326

Crack models for a transversely isotropic medium
p 557 A93-24566

Fracture of highway and airport pavements
p 547 A93-28290

Global/local interlaminar stress analysis of a grid-stiffened composite panel
p 548 A93-28543

On design and optimization of curved composite beams
p 826 A93-35953

Stress-strain analysis and optimal design of aircraft structures
p 827 A93-36782

Crack analysis using discontinuous boundary elements
p 925 A93-40775

Life prediction - Thermal fatigue from isothermal data
p 916 A93-40807

Simplified finite element representation of fuselage frames with flexible castellations
p 892 A93-43570

Optical methods of stress analysis applied to cracked components
p 1027 A93-45798

New approximate method of stress analysis for bladed rotating discs
[ISABE 93-7059] p 1219 A93-54035

The technical background to standards for shackles
[NPL-DMM(A)-51] p 86 N93-11325

Verification of rain-flow reconstructions of a variable amplitude load history
[NASA-CR-189670] p 91 N93-12411

- A domain decomposition method for parallel transient response calculations p 187 N93-13827
- Determination of stresses on laminated aircraft transparencies by the strain gage-hole drilling and sectioning method [AD-A255548] p 164 N93-14571
- RB 199 high pressure compressor stage 3 spin pit tests p 176 N93-14893
- CF6-6 high pressure compressor stage 5 locking slot crack propagation spin pit test p 176 N93-14894
- RB211-524B disc and drive cones hot cyclic spinning test p 177 N93-14895
- Analysis of in-flight structural failures of P-3C wing leading edge segments [AD-A256212] p 165 N93-15238
- Thermoviscoelastic analysis of pavements p 379 N93-16313
- Unified airport pavement design procedure p 380 N93-16318
- Three-dimensional stress analysis of multilayered airport pavements: Integral transform approach p 381 N93-16319
- A realizable Reynolds stress algebraic equation model [NASA-TM-105993] p 290 N93-16596
- Interlaminar stress analysis at the skin/stiffener interface of a grid-stiffened composite panel [NASA-CR-192177] p 393 N93-17920
- Study of statistical variations of load spectra and material properties on aircraft fatigue life [AD-A257961] p 339 N93-18451
- Structural Tailoring of Advanced Turboprops (STAT). Theoretical manual [NASA-CR-191017] p 556 N93-22005
- Stress calculation for the Sandia 34-meter wind turbine using the local circulation method and turbulent wind [DE93-004480] p 560 N93-22045
- Computational gearing mechanics [NASA-CR-191127] p 751 N93-25884
- External stress-corrosion cracking of a 1.22-m-diameter type 316 stainless steel air valve [NASA-TP-3190] p 737 N93-26201
- A Rayleigh-Ritz analysis methodology for cutouts in composite structures p 923 N93-30869
- STRESS CONCENTRATION**
- Bonded repair of multi-site damage p 947 A93-45786
- Optimization of large scale systems in elasticity p 1255 A93-54544
- RB 199 high pressure compressor stage 3 spin pit tests p 176 N93-14893
- Probabilistic assessment of composite structures [NASA-TP-106024] p 825 N93-27092
- STRESS CORROSION**
- Stress corrosion susceptibility of ultra-high strength steels for Naval aircraft applications [AD-A256126] p 199 N93-15189
- STRESS CORROSION CRACKING**
- Aspects of aging aircraft - A transatlantic view p 1026 A93-45776
- The effect of exfoliation corrosion on the fatigue behavior of structural aluminum alloys p 1017 A93-45778
- Results of review of Fokker F 28 'Fellowship' maintenance program p 948 A93-45793
- Stress corrosion susceptibility of ultra-high strength steels for Naval aircraft applications [AD-A256126] p 199 N93-15189
- Hydrogen-induced stress corrosion cracking susceptibility analysis of pitch links from the AH-64 Apache helicopter [AD-A260692] p 736 N93-25895
- External stress-corrosion cracking of a 1.22-m-diameter type 316 stainless steel air valve [NASA-TP-3190] p 737 N93-26201
- NASA-UVA Light Aerospace Alloy and Structures Technology Program (LA2ST) p 1019 N93-31739
- Accelerated and real-time corrosion testing of aluminum-lithium alloys [NLR-TP-91203-U] p 1020 N93-32385
- STRESS CYCLES**
- The minimal multiplier method in calculations of the stability, limiting vibration cycles, and limiting states of nonlinearly deformed structures p 836 A93-39176
- STRESS DISTRIBUTION**
- Influence of modelling loading on stress distribution in turbomachinery blade fastening in case of FEM p 520 A93-27296
- Increasing the durability of gas turbine engine compressor blades by using a combined hardening/finishing treatment to control the stressed state of the surface layer p 835 A93-39099
- Effect of the technological process structure on residual stress distribution in the blade foil of gas turbine engines p 836 A93-39106
- Theoretical and experimental investigations concerning the structural integrity of aeroengine compressor discs p 56 N93-10539
- Flow over a leading edge with distributed roughness p 18 N93-10549
- FAA unified pavement analysis 3-D finite element method p 379 N93-16314
- Design and analysis of curved composite components for rotorcraft fuselage frames p 716 N93-25701
- Structural dynamic analysis of bearingless rotor blade p 717 N93-25719
- Penn State axial flow turbine facility: Performance and nozzle flow field p 1032 N93-31588
- STRESS FUNCTIONS**
- Numerical solution of transonic full-potential-equivalent equations in von Mises co-ordinates p 111 A93-14080
- Root damage analysis of aircraft engine blade subject to ice impact [NASA-TM-105779] p 222 N93-15343
- Stress calculations on the window section of an all-composite aircraft fuselage [LR-688] p 328 N93-16215
- STRESS INTENSITY FACTORS**
- Mixed mode stress intensity-factors in transversely loaded plates p 200 A93-13943
- Experimental measurement of structural intensity on an aircraft fuselage p 544 A93-26999
- Fracture of highway and airport pavements p 547 A93-28290
- Application of a p-version finite element code to analysis of cracks [AIAA PAPER 93-1450] p 740 A93-33999
- Axial crack propagation and arrest in pressurized fuselage p 1026 A93-45788
- Optical methods of stress analysis applied to cracked components p 1027 A93-45798
- Fatigue crack growth in AerMet 100 steel [AD-A249068] p 74 N93-12248
- Fatigue propagation behaviour of short cracks in titanium alloys [ESDU-92023] p 392 N93-16637
- Fatigue propagation behaviour of short cracks in aluminum alloys [ESDU-92030] p 392 N93-16641
- STRESS MEASUREMENT**
- Automated measurement of residual stresses in the surface layer of parts p 834 A93-39081
- Measurement of aerodynamic shear stress using side chain liquid crystal polymers [AD-A254312] p 72 N93-10770
- Development of the neutron diffraction technique for the determination of near surface residual stresses in critical gas turbine components [PNR-90984] p 58 N93-11112
- STRESS RATIO**
- Estimation of the life of aircraft structures under stochastic steady state loading p 545 A93-27620
- Fatigue crack growth in AerMet 100 steel [AD-A249068] p 74 N93-12248
- Fatigue propagation behaviour of short cracks in titanium alloys [ESDU-92023] p 392 N93-16637
- STRESS RELAXATION**
- A study of the origin of residual stresses and strains in the transparencies of supersonic aircraft p 801 A93-36784
- Stress relaxation of low pressure plasma-sprayed NiCrAlY alloys p 1211 A93-52870
- STRESS-STRAIN DIAGRAMS**
- Low cycle fatigue behaviour of titanium disc alloys [NLR-TP-91346-U] p 1006 N93-32372
- STRESS-STRAIN RELATIONSHIPS**
- Determination of the membrane and flexural shell deformations from the readings of a two-sided rosette-type strain gage p 75 A93-10047
- Stirling engine - Available tools for long-life assessment ... for space propulsion p 195 A93-13824
- Computation of aeroelastic characteristics and stress-strained state of parachutes [AIAA PAPER 93-1237] p 744 A93-35178
- Stress-strain analysis and optimal design of aircraft structures p 827 A93-36782
- Efficiency of using longitudinal and circumferential bands in the structures of an airtight fuselage p 801 A93-36795
- Coupling conditions for substructures with varying idealization p 1029 A93-47078
- A study of the effect of the support fastening compliance on the stress-strain state of aircraft transparencies p 997 A93-47079
- An analytical-experimental method for studying the strength and stability of thin-walled structures p 1029 A93-47084
- Nonlinear deformation mechanics of multilayer transparency elements - Some calculation results ... for aircraft portholes p 1191 A93-52937
- Calculation of sandwich plates with polymer composite skins under conditions of high humidity p 1215 A93-52968
- Verification of rain-flow reconstructions of a variable amplitude load history [NASA-CR-189670] p 91 N93-12411
- STRESS-STRAIN-TIME RELATIONS**
- Thermoviscoelastic analysis of pavements p 379 N93-16313
- STRIATION**
- Trailing vortex/free-surface interaction [AD-A261654] p 701 N93-26195
- STRIPPING**
- Starch media blasting for aerospace finishing applications [SAE PAPER 920948] p 107 A93-14091
- STROUHAL NUMBER**
- Unsteady aerodynamic characteristics of three rectangular wings of different aspect ratios p 1180 A93-53575
- Determination of surface heat transfer and film cooling effectiveness in unsteady wake flow conditions p 902 N93-29933
- Vortex shedding by blunt/bluff bodies at high Reynolds numbers. Volume 4: Rectangles [AD-A264154] p 877 N93-30151
- STRUCTURAL ANALYSIS**
- MPC75 as the forerunner of a new regional aircraft family p 37 A93-10776
- Optimized/adapted finite elements for structural shape optimization p 77 A93-10971
- A very efficient tool for the structural analysis of hypersonic vehicles under high temperature aspects p 203 A93-14194
- Engineering optimization of aeronautical structures p 154 A93-14227
- Stiffness design method of symmetric laminates using lamination parameters p 206 A93-14569
- Fourier analysis of clamped moderately thick arbitrarily laminated plates p 206 A93-14571
- Structural optimization of a cantilevered rotating beam p 210 A93-16248
- Coupled multi-disciplinary simulation of composite engine structures in propulsion environment [ASME PAPER 92-GT-6] p 346 A93-19279
- Structural Tailoring/Analysis for Hypersonic Components - A computational simulation [AIAA PAPER 92-4722] p 325 A93-20324
- Thermal/structural analysis and aircraft design p 409 A93-20420
- Flexure-torsion behavior of prismatic beams. I - Section properties via power series p 417 A93-23557
- Europe adapts CST to its needs ... computational structures technology for aerospace industry p 560 A93-25088
- An accurate nonlinear finite element analysis and test correlation of a stiffened composite wing panel p 546 A93-27968
- Coupled composite rotor blades under bending and torsional loads p 546 A93-27970
- Sensitivity-based scaling for approximating structural response p 548 A93-28618
- Acoustical analysis of gear housing vibration p 567 A93-29420
- X-31A flight flutter test excitation by control surfaces [AIAA PAPER 93-1538] p 727 A93-34075
- Calculation of numerical boundary measure for wavelet-Galerkin approximations in aeroelasticity [AIAA PAPER 93-1539] p 741 A93-34076
- An inverse method for computation of structural stiffness distributions of aeroelastically optimized wings [AIAA PAPER 93-1540] p 741 A93-34077
- Stiffness, thermal expansion, and thermal bending formulation of stiffened, fiber-reinforced composite panels [AIAA PAPER 93-1569] p 741 A93-34102
- An effective Mixed Annealing/Heuristic Algorithm for problems in kinematic mechanical design [AIAA PAPER 93-1581] p 741 A93-34113
- Probabilistically configured adaptive composite structures [AIAA PAPER 93-1679] p 743 A93-34191
- On the effect of pitch/mast-bending coupling on whirl-mode stability p 794 A93-35906
- Crack growth/damage tolerance analysis methods as applied to V-22 fuselage and empennage p 795 A93-35948
- Application of generalized force determination to a full scale low cycle fatigue test of the SH-2G helicopter p 795 A93-35949
- Evaluation of thermoplastic stiffened panels for application to rotorcraft airframes p 827 A93-36000

Environmental conditions for certification testing of helicopter advanced composite main rotor components
p 824 A93-36003

A nonlinear analysis methodology for the design of skid landing gears
p 799 A93-36004
Nonlinear analysis of composite thin-walled helicopter blades
p 827 A93-36006

Efficiency of using longitudinal and circumferential bands in the structures of an airtight fuselage
p 801 A93-36795

A thermal/structural analysis process incorporating concurrent engineering
[SAE PAPER 921185]
p 938 A93-41364

Simplified finite element representation of fuselage frames with flexible castellations
p 892 A93-43570
Coupling conditions for substructures with varying idealization
p 1029 A93-47078

Aircraft safety evaluation
p 1043 A93-50486
Structural integrity validation of limited-life engines
[ISABE 93-7131]
p 1205 A93-54106

Future development and application of general structural analysis softwares in the aviation industry in China
p 1262 A93-54420

Zeppelin NT - A new concept in airship technology, based on rigid airship principles
[AIAA PAPER 93-4045]
p 1242 A93-54612

NDT for corrosion in aerospace structures; Proceedings of the Conference, London, United Kingdom, Feb. 12, 1992
[ISBN 0-903409-99-2]
p 1257 A93-54894

Fatigue life under random load history derived from exceedance curves using different algorithms
p 1260 A93-56544

The integration of geometric modeling into an inverse design method and application of a PC-based inverse design method and comparison with test results
p 81 A93-10058

Radial turbine cooling
p 82 A93-10061
Probabilistic evaluation of fuselage-type composite structures
[NASA-TM-105881]
p 212 A93-12735

Aircraft accident report: Britt Airways, Inc., d/b/a, Continental Express Flight 2574, in-flight structural breakup, EMB-120RT, N33701, Eagle Lake, Texas, September 11, 1991
[PB92-910405]
p 143 A93-13426

A domain decomposition method for parallel transient response calculations
p 187 A93-13827
Proceedings of the USAF Structural Integrity Program [AD-A25379]
p 110 A93-14549

SAPNEW: Parallel finite element code for thin shell structures on the Alliant FX-80
[NASA-CR-189212]
p 220 A93-14799

Propulsion and Energetics Panel Working Group 20 on Test Cases for Engine Life Assessment Technology [AGARD-AR-308]
p 176 A93-14890

Introduction to test cases for engine life assessment technology
p 176 A93-14891

Aeroplane crashes on the runway: Validation and final evaluation of the method of modeling an airframe structure
[IMFL-91-32]
p 165 A93-15126

Review of aeronautical fatigue investigation activities developed in Alenia-GAT during the period May 1990 - March 1991
[ETN-92-92884]
p 329 A93-16287

FAA unified pavement analysis 3-D finite element method
p 379 A93-16314

Federal Aviation Administration pavement modeling
p 379 A93-16315

Development of a unified airport pavement analysis and design system
p 380 A93-16317

Influence of cross section variations on the structural behaviour of composite rotor blades
[MBB-UD-0602-91-PUB]
p 332 A93-17569

Multidisciplinary tailoring of hot composite structures [NASA-TM-106027]
p 550 A93-19971

The influence of structural optimization on the aeroelastic properties of a vertical tail
[AD-A259140]
p 513 A93-20575

YIDOUYU and its application to aircraft design
[AD-A259262]
p 513 A93-20605

Fluid/structures interactions. Aircraft considerations
p 527 A93-20628

MSC/NASTRAN structure optimization test module version 67 (preliminary)
[REPT-5-191025]
p 554 A93-20907

Integrated aerodynamic-structural wing design optimization
p 714 A93-25279

Probabilistic assessment of composite structures [NASA-TM-106024]
p 825 A93-27092

Face-gear drives: Design, analysis, and testing for helicopter transmission applications
[NASA-TM-106101]
p 839 A93-27133

Testing a wheeled landing gear system for the TH-57 helicopter
[AD-A262152]
p 806 A93-27547

Nonlinear analyses of composite aerospace structures in sonic fatigue
[NASA-CR-193124]
p 930 A93-29154

The Ultra Light Aircraft Testing
[NASA-CR-193043]
p 895 A93-29774

Structural evaluation of curved stiffened composite panels fabricated using a THERM-Xsm process
p 919 A93-30435

Multiple methods integration for structural mechanics analysis and design
p 923 A93-30867

Structural response of bead-stiffened thermoplastic shear webs
p 923 A93-30873

Optimal design and imperfection sensitivity of nonlinear shell structures
[FFA-TN-1992-30]
p 1030 A93-31123

STRUCTURAL DESIGN
Multidisciplinary design of composite aircraft structures by Lagrange
p 76 A93-10273

Current developments in structural technology
p 77 A93-10780

Optimized/adapted finite elements for structural shape optimization
p 77 A93-10971

Stochastic computational mechanics for aerospace structures
p 78 A93-12157

Aging review of the YS-11 aircraft
p 46 A93-13635

The role of fatigue testing in the design, development and certification of the ATR 42/72
p 46 A93-13637

Advanced technologies airships
p 108 A93-14183

Inlet design using a blend of experimental and computational techniques
p 114 A93-14210

Engineering optimization of aeronautical structures
p 154 A93-14227

The use of a deep honeycomb to achieve high flow quality in the ARA 9 ft x 8 ft Transonic Wind Tunnel
p 190 A93-14276

An engineering method with artificial intelligence characteristics used for structural layout of wings
p 225 A93-14290

The aerodynamic and structural design of a variable camber wing (VCW)
p 117 A93-14291

Structural optimization in preliminary aircraft design - A finite-element approach
p 226 A93-14340

Rapid wind tunnel prototype using stereolithography and equivalent technologies
p 191 A93-14365

Case studies in composite material structural design, manufacture and testing
p 157 A93-14385

Optimum balancing of flexible rotor
p 205 A93-14489

Study on fracture failure of turbine blades in a series of turbojets
p 205 A93-14493

Stiffness design method of symmetric laminates using lamination parameters
p 206 A93-14569

Study of a Mach 2 supersonic transport aircraft
p 124 A93-15034

Improving anti-fatigue optimum design through AI-search strategy
p 208 A93-15342

Low aspect ratio transonic rotors. II - Influence of location of maximum thickness on transonic compressor performance
[ASME PAPER 92-GT-186]
p 352 A93-19411

Development and industrial application of the 'all-over-controlled vortex distribution method' for designing radial and mixed flow impellers
[ASME PAPER 92-GT-262]
p 405 A93-19466

Variable-complexity aerodynamic-structural design of a high-speed civil transport wing
[AIAA PAPER 92-4695]
p 323 A93-20279

Multidisciplinary optimization of helicopter rotor blades including design variable sensitivity
[AIAA PAPER 92-4783]
p 323 A93-20289

Optimization of anisotropic structures considering strength, stiffness and aeroelastic constraints
[AIAA PAPER 92-4796]
p 408 A93-20291

Structural optimization with frequency constraints - A review
[AIAA PAPER 92-4813]
p 408 A93-20293

Multidisciplinary design integration system for a supersonic transport aircraft
[AIAA PAPER 92-4841]
p 324 A93-20296

Structural optimization for joined-wing synthesis
[AIAA PAPER 92-4761]
p 325 A93-20356

Flutter optimization of large transport aircraft
[AIAA PAPER 92-4795]
p 326 A93-20381

Examples of dynamic response optimization using MSC/NASTRAN
[AIAA PAPER 92-4814]
p 436 A93-20394

Design vector parallelization to speedup the structural optimization process
[AIAA PAPER 92-4834]
p 436 A93-20411

Analytical formulation of optimum rotor interdisciplinary design with a three-dimensional wake
[AIAA PAPER 92-4778]
p 265 A93-20416

Thermal/structural analysis and aircraft design
p 409 A93-20420

Advanced direct-design procedure for centrifugal impellers
p 411 A93-21659

Development of a Shape-controlled airfoil by use of SMA --- Shape Memory Alloys
p 411 A93-21739

Expanding the waverider design space using general supersonic and hypersonic generating flows
[AIAA PAPER 93-0505]
p 283 A93-23253

Modeling, analysis, and prediction of flutter at transonic speeds
p 416 A93-23553

Aerodynamically efficient wing design with structural considerations
p 460 A93-24081

Development of highly loaded root end attachments for composite material high speed flying surfaces
p 539 A93-24122

Supercritical wing design, a three dimensional hodograph approach
[AIAA PAPER 92-2657]
p 472 A93-24986

CST gives aircraft industry a lift --- computational structures technology
p 560 A93-25086

Design of advanced beams considering elasto-plastic behaviour of material
p 544 A93-26904

Novel approaches to complex geometry structure
p 546 A93-27969

Euler study on porous transonic airfoils with a view toward multipoint design
p 479 A93-28604

Utilization of CAD/CAE for concurrent design of structural aircraft components
[AIAA PAPER 93-1466]
p 710 A93-34014

The use of artificial intelligence for buffet environments
[AIAA PAPER 93-1534]
p 727 A93-34071

A refined structural model of composite aircraft wings for the enhancement of vibrational and aeroelastic response characteristics
[AIAA PAPER 93-1536]
p 740 A93-34073

In-flight investigation of a rotating cylinder-based structural excitation system for flutter testing
[AIAA PAPER 93-1537]
p 711 A93-34074

An inverse method for computation of structural stiffness distributions of aeroelastically optimized wings
[AIAA PAPER 93-1540]
p 741 A93-34077

Probabilistically configured adaptive composite structures
[AIAA PAPER 93-1679]
p 743 A93-34191

Integrated structural tailoring and adaptive control of advanced flight vehicle structural vibration
[AIAA PAPER 93-1697]
p 757 A93-34219

Active constrained layer viscoelastic damping
[AIAA PAPER 93-1702]
p 743 A93-34224

A High Deflection Diaphragm concept (HDD) for power transmission shafting
p 826 A93-35931

Effects on load distribution in a helicopter rotor support structure associated with various boundary configurations
p 796 A93-35951

On design and optimization of curved composite beams
p 826 A93-35953

A nonlinear analysis methodology for the design of skid landing gears
p 799 A93-36004

Flight Deflection Measurement System
p 808 A93-37885

Materials development for light design - A suppliers view
p 915 A93-40777

Recent advances of time domain approach for nonlinear response and sonic fatigue
p 1022 A93-45106

Optimization using fuzzy set theory
p 1037 A93-45431

Applications to fixed-wing aircraft and spacecraft
p 996 A93-45432

Composite airframe structures. Practical design information and data --- Book
[ISBN 962-7128-06-6]
p 1100 A93-49105

Axial flow compressors - Mechanical design trends [ISABE 93-7061]
p 1199 A93-54037

Structural integrity validation of limited-life engines [ISABE 93-7131]
p 1205 A93-54106

Optimization of sandwich structures with respect to local instabilities with MBB-LAGRANGE
p 1255 A93-54540

An inverse method with regularity condition for transonic airfoil design
p 1230 A93-54583

Current research in oxidation-resistant carbon-carbon composites at NASA. Langley Research Center
p 74 A93-12456

Analysis and design of planar and non-planar wings for induced drag minimization
[NASA-CR-191274]
p 131 A93-13463

A90 project: Design of a composite fin
[ETN-92-92773]
p 329 A93-16562

Mathematical optimization: A powerful tool for aircraft design
[MBB-FE-2-S-PUB-478]
p 331 A93-17564

Influence of cross section variations on the structural behaviour of composite rotor blades
[MBB-UD-0602-91-PUB]
p 332 A93-17569

- Exodus: Prime Mover
[NASA-CR-192051] p 332 N93-17803
- CFD-based approximation concepts for aerodynamic design optimization with application to a 2-D scramjet vehicle
[AD-A258084] p 333 N93-17893
- Optimum Design of High Speed Prop-Rotors
[NASA-CR-190915] p 336 N93-18064
- Design of high speed propellers using multiobjective optimization techniques p 336 N93-18065
- Optimum design of high speed prop rotors including the coupling of performance, aeroelastic stability and structures p 337 N93-18066
- Study of statistical variations of load spectra and material properties on aircraft fatigue life
[AD-A257961] p 339 N93-18451
- The influence of structural optimization on the aeroelastic properties of a vertical tail
[AD-A259140] p 513 N93-20575
- Application of artificial neural networks to the design optimization of aerospace structural components
[NASA-TM-4389] p 555 N93-21831
- Grid sensitivity for aerodynamic optimization and flow analysis
[NASA-CR-192980] p 694 N93-25117
- Integrated aerodynamic-structural wing design optimization p 714 N93-25279
- Design and analysis of curved composite components for rotorcraft fuselage frames p 716 N93-25701
- Structural tailoring of aircraft engine blade subject to ice impact constraints p 838 N93-26999
- A demonstration of simple airfoils: Structural design and materials choices
[DE93-007882] p 789 N93-28662
- Report on the test set-up for the structural testing of the Airmass Sunburst Ultralight Aircraft p 895 N93-29775
- Effect of design selection on response surface performance
[NASA-CR-4520] p 895 N93-29885
- Multi-parameter optimization tool for low-cost commercial fuselage crown designs p 922 N93-30858
- A comparison of classical mechanics models and finite element simulation of elastically tailored wing boxes p 922 N93-30863
- Multiple methods integration for structural mechanics analysis and design p 923 N93-30867
- Tailored composite wings with elastically produced chordwise camber p 923 N93-30876
- Construction and testing of simple airfoils to demonstrate structural design, materials choice, and composite concepts p 879 N93-30979
- Structural design using neural networks p 942 N93-31029
- Development of nose structure of a reconnaissance container for a supersonic jet aircraft
[MBB-LME-242-S-PUB-0451] p 998 N93-31046
- GARTEUR 3D shear layer experiment
[FFA-TN-1992-26] p 987 N93-31052
- Optimal design and imperfection sensitivity of nonlinear shell structures
[FFA-TN-1992-30] p 1030 N93-31123
- Integrated structural design, vibration control, and aeroelastic tailoring by multiobjective optimization p 1030 N93-31137
- Applications of structural optimization methods to fixed-wing aircraft and spacecraft in the 1980s
[NASA-TM-103939] p 1033 N93-32212
- STRUCTURAL DESIGN CRITERIA**
- Design sensitivity and optimization of composite cylinders p 71 A93-12781
- Structural and aerodynamic considerations for an oblique all-wing aircraft
[AIAA PAPER 92-4220] p 43 A93-13336
- Using aerodynamic analysis codes to assist in structural design and optimization of ducted rotor/wing blades
[AIAA PAPER 92-4280] p 44 A93-13353
- Influence of sweep on structural optimization of a fighter wing
[AIAA PAPER 92-4794] p 323 A93-20290
- Survey - Applications of structural optimization methods to fixed wing aircraft and spacecraft
[AIAA PAPER 92-4726] p 325 A93-20328
- Aeroelastic model design using structural optimization
[AIAA PAPER 92-4730] p 409 A93-20329
- On alternative problem formulations for multidisciplinary design optimization p 436 A93-20350
- [AIAA PAPER 92-4752] p 436 A93-20350
- Observations on computational methodologies for use in large-scale, gradient-based, multidisciplinary design
[AIAA PAPER 92-4753] p 436 A93-20351
- Structural optimization using Newton Modified Barrier Method
[AIAA PAPER 92-4756] p 409 A93-20352
- Grid and design variables sensitivity analyses for NACA four-digit wing-sections
[AIAA PAPER 93-0195] p 276 A93-22616
- Global/local interlaminar stress analysis of a grid-stiffened composite panel p 548 A93-28543
- Sensitivity-based scaling for approximating structural response p 548 A93-28618
- Energy-absorbing-beam design for composite aircraft subfloors
[AIAA PAPER 93-1339] p 709 A93-33909
- Damage progression in stiffened composite panels
[AIAA PAPER 93-1345] p 738 A93-33915
- Effect of a combination of design and process-related factors on the fatigue strength of bolted joints in acoustically loaded aircraft structures p 745 A93-35278
- Stress-strain analysis and optimal design of aircraft structures p 827 A93-36782
- A study of the strength of a closed system of wings p 828 A93-36792
- A method for the optimum design of a large-aspect-ratio wing p 828 A93-36793
- Optimal design of honeycomb sandwich shell aircraft structures of composite materials p 828 A93-36800
- Development of a process for fabricating a plate heat exchanger for the heat recovery system of gas turbine engines p 834 A93-39053
- Selection of the scheme and optimal parameters of the turbine of a high-temperature bypass engine with a low bypass ratio p 811 A93-39180
- Hierarchical development of three direct-design methods for two-dimensional axial-turbomachinery cascades p 812 A93-39271
- Design and cost viability of composites in commercial aircraft p 915 A93-39963
- A software for optimum design of an aircraft structure p 938 A93-40495
- Flight research on natural laminar flow applications p 890 A93-41779
- Subsonic natural-laminar-flow airfoils p 860 A93-41780
- Supersonic laminar flow control p 860 A93-41782
- Characteristics of data processing during the development of a data base for a CAD system for aircraft design p 892 A93-42381
- Big time doorstep delivery p 892 A93-42995
- Airport surveillance radar design for increased air traffic p 883 A93-43410
- Fuselage longitudinal splice design p 997 A93-45784
- Experience in specifying/prolonging the airframe time limits p 948 A93-45797
- A computational method for inverse design of transonic airfoil and wing
[AIAA PAPER 93-3482] p 982 A93-47260
- Preliminary design estimates of high-speed streamlines on arbitrary shaped vehicles defined by quadrilateral elements
[AIAA PAPER 93-3491] p 982 A93-47263
- Structural design and analysis of a Mach zero to five turbo-ramjet system
[AIAA PAPER 93-1983] p 1112 A93-49830
- On design methods for bolted joints in composite aircraft structures p 1158 A93-50430
- Development of computational solid mechanics and its application in aerospace engineering p 1255 A93-54419
- Design problems of three-dimensional contractions --- in incompressible flow p 1236 A93-55584
- Interlaminar stress analysis at the skin/stiffener interface of a grid-stiffened composite panel
[NASA-CR-192177] p 393 N93-17920
- STRUCTURAL ENGINEERING**
- Aeronautical fatigue: Key to safety and structural integrity: Proceedings of the 16th ICAF Symposium, Tokyo, Japan, May 22-24, 1991
[ISBN 4-9900181-1-7] p 80 A93-13626
- Structural integrity challenges p 3 A93-13627
- An engineering method with artificial intelligence characteristics used for structural layout of wings p 225 A93-14290
- Vibration reduction for helicopter airframes - An application of the general-purpose structural optimization program STARS
[AIAA PAPER 92-4782] p 326 A93-20372
- Reliability and durability problems p 1150 A93-48825
- Structural integrity validation of limited-life engines
[ISABE 93-7131] p 1205 A93-54106
- STRUCTURAL FAILURE**
- Maintaining the safety of an aging fleet of aircraft p 3 A93-13632
- Analysis of multiple crack propagation in stiffened sheet p 81 A93-13638
- An Acoustic Emission Pre-failure Warning System for composite structural tests p 1161 A93-52560
- Reliability of stiffened structural panels: Two examples
[NASA-TM-107687] p 219 N93-14483
- Analysis of in-flight structural failures of P-3C wing leading edge segments
[AD-A256212] p 165 N93-15238
- Crash experience of the US Army Black Hawk helicopter p 493 N93-19688
- Thermally induced stresses in a composite exposed to fire
[AD-A261714] p 737 N93-26371
- STRUCTURAL MEMBERS**
- A new method to study the forming process of complicated sheetmetal aero-parts p 204 A93-14363
- Flow measurements behind V-gutter under non-combusting condition
[AIAA PAPER 93-0020] p 408 A93-20139
- Utilization of CAD/CAE for concurrent design of structural aircraft components
[AIAA PAPER 93-1466] p 710 A93-34014
- Problems of the organization of the mass testing of large structural elements of aircraft using testing machines p 821 A93-36791
- The influence of structural optimization on the aeroelastic properties of a vertical tail
[AD-A259140] p 513 N93-20575
- STRUCTURAL RELIABILITY**
- New lamps for old - Safety regulation through structural airworthiness standards p 28 A93-13630
- A review of aging aircraft technology - An I.A.I. perspective p 3 A93-13634
- Fatigue qualification of high thickness composite rotor components p 81 A93-13646
- A synthesized method in durability analysis p 203 A93-14286
- Aircraft fatigue failures and tasks of structural reliability analysis p 210 A93-16246
- A new method for determining the number of flight vehicle prototypes subject to full-scale testing p 434 A93-18316
- Selection of the time scale for preventive measures under service conditions p 237 A93-18375
- A structural reliability evaluation of fail-safe helicopter dynamic components p 506 A93-27952
- A damage tolerance/life processor for structural integrity and force management p 507 A93-27962
- A method for estimating the survivability of bodies of revolution p 745 A93-35287
- Effect of overloads on the service life of the structural elements of aircraft p 746 A93-35289
- Damage tolerance assessment of the fighter aircraft 37 Viggen main wing attachment p 802 A93-37390
- Concurrent field service and laboratory testing as a means of improving reliability in creep-rupture applications p 916 A93-40814
- The T700 ... from salt spray to sand blast p 1205 A93-54292
- Theoretical and experimental investigations concerning the structural integrity of aeroengine compressor discs p 56 A93-10539
- A domain decomposition method for parallel transient response calculations p 187 A93-13827
- Reliability of stiffened structural panels: Two examples
[NASA-TM-107687] p 219 N93-14483
- Damage tolerance assessment and usage variation analysis for C-130 aircraft in the Israeli Air Force p 839 A93-27210
- Ageing aircraft research in the Netherlands
[NLR-TP-91443-U] p 999 N93-32203
- STRUCTURAL STABILITY**
- Collection of works on measuring and computing systems for research on the aerodynamics, dynamics, and strength of flight vehicles p 75 A93-10026
- Software for the control of measurement data acquisition, processing, and monitoring during strength testings p 94 A93-10042
- Aeroelastic stability characteristics of composite cylindrical shells by the finite element method p 203 A93-14312
- An interactive numerical procedure for rotor aeroelastic stability analysis using elastic lifting surface p 155 A93-14313
- Instability of the periodic deflection of a panel surface in a turbulent boundary layer p 208 A93-15188
- Nonlinear vibration and radiation from a panel with transition to chaos induced by acoustic waves p 398 A93-19173
- Crack growth and repair of multi-site damage of fuselage lap joints p 547 A93-28291
- Aeromechanical stability of rotorcraft with advanced geometry blades
[AIAA PAPER 93-1304] p 725 A93-33880
- Aeromechanical stability of a bearingless composite rotor in forward flight
[AIAA PAPER 93-1305] p 726 A93-33881

- Supersonic aeroelastic instability results for a NASP-like wing model
[AIAA PAPER 93-1369] p 682 A93-33935
- Low velocity impact in a graphite/PEEK
[AIAA PAPER 93-1403] p 734 A93-33963
- An analysis of the post-instability behaviour of a two-dimensional airfoil with a structural nonlinearity
[AIAA PAPER 93-1474] p 726 A93-34020
- Hammerhead aeroelastic stability revisited
[AIAA PAPER 93-1477] p 740 A93-34022
- Application of differential quadrature to the analysis of static aeroelastic phenomena
[AIAA PAPER 93-1505] p 711 A93-34044
- A new sensitivity analysis for structural optimization of composite rotor blades
[AIAA PAPER 93-1644] p 742 A93-34169
- Post-critical behaviour of a tapered cantilever column subjected to a uniformly distributed tangential follower force
p 831 A93-38431
- The minimal multiplier method in calculations of the stability, limiting vibration cycles, and limiting states of nonlinearly deformed structures
p 836 A93-39176
- Estimation of wing stability in flow from the characteristics of the transient process
p 836 A93-39177
- Effects of floor location on response of composite fuselage frames
p 997 A93-46809
- Problems of the strength and fatigue of the elements of aircraft structures
p 1029 A93-47076
- An analytical-experimental method for studying the strength and stability of thin-walled structures
p 1029 A93-47084
- Stability of fluttered panels subjected to in-plane harmonic forces
p 1151 A93-49017
- Aeroelastic stability of supersonic nozzles with separated flow
[AIAA PAPER 93-2588] p 1142 A93-50300
- An experimental study of reinforced panels of composite materials
p 1215 A93-52975
- A study of damage tolerance of the landing gear structure
p 1219 A93-53881
- Optimization of sandwich structures with respect to local instabilities with MBB-LAGRANGE
p 1255 A93-54540
- DYNAC: A computer program for analyzing the dynamical stability of aircraft
[REPT-B-31] p 66 N93-12415
- Proceedings of the USAF Structural Integrity Program
[AD-A255379] p 110 N93-14549
- Aeroelastic stability and response of rotating structures
[NASA-CR-191803] p 371 N93-16560
- Optimum Design of High Speed Prop-Rotors
[NASA-CR-190915] p 336 N93-18064
- Repair, evaluation, maintenance, and rehabilitation research program. Continuous Deformation Monitoring System (CDMS)
[AD-A261833] p 708 N93-26274
- STRUCTURAL STRAIN**
- High-temperature strain measurement techniques: Current developments and challenges
p 217 N93-13669
- Low cycle fatigue behaviour of titanium disc alloys
[NLR-TP-9346-U] p 1006 N93-32372
- STRUCTURAL VIBRATION**
- The investigation on vibration characteristics of all-movable stabilizer of an aircraft
p 41 A93-11821
- Nonlinear problems of aeroelasticity
p 78 A93-12153
- Vibration monitoring and fault diagnosis of inflight aircraft engines
p 170 A93-14176
- Calculation of sound field radiated by oscillating cascade
p 231 A93-14269
- On the configuration buffet of a transport aircraft
p 117 A93-14298
- Nonlinear vibration and radiation from a panel with transition to chaos
p 205 A93-14543
- Modal analysis of unsteady aerodynamic response of subsonic annular cascade with steady loading under elastic vibration
p 126 A93-15495
- Misalignments of airborne laser beams due to mechanical vibrations
p 394 A93-17762
- Turbomachine blade vibration — Book
[ISBN 0-470-21764-2] p 344 A93-17899
- Matrix difference equation analysis of coupled structural-acoustic models for aircraft fuselage vibration and interior noise reduction
p 446 A93-19172
- Nonlinear vibration and radiation from a panel with transition to chaos induced by acoustic waves
p 398 A93-19173
- Sonic fatigue analysis of an aircraft wing flap by the matrix difference equation method
p 399 A93-19208
- Nonlinear response and sonic fatigue of high speed aircraft
p 399 A93-19211
- Vibro-acoustic analysis of propeller aircraft, integrating advanced experimental modeling with in-flight data analysis
p 451 A93-19230
- Advanced Ducted Engines - Impact of unsteady aerodynamics on fan vibration properties
[ASME PAPER 92-GT-228] p 252 A93-19445
- An efficient constraint to account for mistuning effects in the optimal design of engine rotors
[AIAA PAPER 92-4711] p 358 A93-20280
- Structural optimization with frequency constraints - A review
[AIAA PAPER 92-4813] p 408 A93-20293
- High speed flight effects on transmission of sound through a nonflexible vibrating panel due to flow structural interaction in the ambience
[AIAA PAPER 92-4708] p 451 A93-20316
- A method of finite element dynamic model optimization
p 367 A93-20812
- An overview of the evolution of vibrating beam accelerometer technology
p 412 A93-21934
- Comprehensive analysis of bearingless rotors - Model development and experimental correlation of modes, response, trim and stability
[AIAA PAPER 93-0624] p 504 A93-24741
- The vibration and flutter of composite material laminate
p 543 A93-26617
- Experimental measurement of structural intensity on an aircraft fuselage
p 544 A93-26999
- The NASA/industry design analysis methods for vibrations (DAMVIBS) program - Accomplishments and contributions
p 508 A93-27971
- Signal processing and system identification techniques for flutter test data analysis
p 529 A93-29282
- Thermoelastic vibration test techniques
p 549 A93-29293
- Aeroelastic system identification of advanced technology aircraft through higher order signal processing
p 525 A93-29297
- Vibration and flutter of stiff-inplane elastically tailored composite rotor blades
[AIAA PAPER 93-1302] p 725 A93-33879
- Composite 'Exoskin' doubler extends F-15 Vertical Tail fatigue life
[AIAA PAPER 93-1341] p 709 A93-33911
- Dynamic analysis of multiple row fuselage stiffened structures
[AIAA PAPER 93-1438] p 710 A93-33987
- A refined structural model of composite aircraft wings for the enhancement of vibrational and aeroelastic response characteristics
[AIAA PAPER 93-1536] p 740 A93-34073
- The investigation of limit cycle amplitude of nonlinear nose gear
p 800 A93-36342
- A plate loaded by a transverse impulse force and in-plane forces
p 828 A93-36799
- The minimal multiplier method in calculations of the stability, limiting vibration cycles, and limiting states of nonlinearly deformed structures
p 836 A93-39176
- Performance of higher harmonic control algorithms for helicopter vibration reduction
p 890 A93-41904
- A frequency domain theory for structural identification
p 930 A93-43778
- Vibration analysis of composite wing with tip mass using finite elements
p 1023 A93-45175
- Two dimensional incompressible flow through a vibrating bladed disc - Theoretical model
p 973 A93-46891
- Analysis of aeroelastic and resonance responses of a wind tunnel model support system
p 1013 A93-47022
- An experimental system for studying the vibrations and acoustic emission of cylindrical shells and panels in a field of turbulent pressure pulsations
p 1140 A93-51754
- Finite element analysis of natural vibrations of an aeroplane with asymmetric variable wing geometry
p 1218 A93-53778
- A dynamic stiffness/boundary element method for the prediction of interior noise levels
p 1226 A93-53817
- Forcing function modeling for flow induced vibration
[ISABE 93-7027] p 1196 A93-54003
- The use of beam-like modal data for stiffness profile estimation by the EBS method. I - Justification and implementation — Equivalent Beam Stiffness
p 1257 A93-54649
- Blade loss dynamics of a magnetically supported rotor
p 1257 A93-54653
- International Congress on Recent Developments in Air- and Structure-Borne Sound and Vibration, 2nd, Auburn Univ., AL, Mar. 4-6, 1992, Proceedings, Vols. 1-3
p 1259 A93-55851
- Effects of foundation excitation on multiple rub interactions in turbomachinery
p 1260 A93-55996
- Design and implementation of digital filters for analysis of F/A-18 flight test data
[AD-A253447] p 17 N93-10342
- Characteristics of separated flows including cavitation effects
p 84 N93-10874
- Rigid body mode identification of the PAH-2 helicopter using the eigensystem realization algorithm
[NASA-TM-107690] p 88 N93-11544
- Basic research on design analysis methods for rotorcraft vibrations
[NASA-CR-191917] p 422 N93-18576
- Multidisciplinary tailoring of hot composite structures
[NASA-TM-106027] p 550 N93-19971
- Dynamic simulation of flexible body systems by the vector solution method
p 553 N93-20666
- Computational gearing mechanics
[NASA-CR-191127] p 751 N93-25884
- A transfer matrix approach to vibration localization in mistuned blade assemblies
[NASA-TM-106112] p 838 N93-27088
- The natural excitation technique (NExT) for modal parameter extraction from operating wind turbines
[DE93-010611] p 845 N93-28603
- STRUCTURAL WEIGHT**
- Improving the lift to drag characteristics of low boom configuration
[AIAA PAPER 92-4218] p 16 A93-13380
- Air transportation system for shipping outsized cargoes
p 141 A93-14394
- Embedded fiber optic sensors in large structures
p 410 A93-21085
- Zen and the art of airplane sizing
p 504 A93-25174
- Optimization of the stiffness and mass characteristics of lifting surface structures modeled by an elastic beam
p 627 A93-36789
- A study of the strength of a closed system of wings
p 828 A93-36792
- A study of the effect of the static aeroelasticity of a swept wing on its weight response
p 801 A93-36798
- Materials development for light design - A suppliers view
p 915 A93-40777
- Aircraft braking systems
p 995 A93-44850
- Lightweight aircraft turbine protection
[AIAA PAPER 93-1815] p 1110 A93-49703
- An investigation of dynamic stress reduction of multi-body aircraft using active gust control
p 187 N93-13916
- Construction and testing of simple airfoils to demonstrate structural design, materials choice, and composite concepts
p 879 N93-30979
- STRUTS**
- Aerodynamic performance of scramjet inlet models with a single strut
[AIAA PAPER 93-0741] p 466 A93-24831
- Nonreflecting boundary conditions of three-dimensional Euler equation calculations for strut cascades
p 689 A93-34491
- A numerical investigation of supersonic strut/endpoint interactions in annular flow with varying strut thickness
[AIAA PAPER 93-2927] p 1045 A93-48128
- Navier-Stokes calculations for transport wing-body configurations with nacelles and struts
[AIAA PAPER 93-2945] p 1047 A93-48142
- Investigation of a strut/endpoint interaction in supersonic annular flow
[AIAA PAPER 93-1925] p 1076 A93-49791
- The 3D Navier-Stokes calculation of flow about scramjet inlet with strut
p 301 N93-19298
- STUDENTS**
- A context-based introduction to aircraft radio communications
p 570 A93-27164
- Use of full flight simulator technology enhances classroom training sessions
p 1136 A93-49277
- T-38 forward windshield development and performance demonstration report
[AD-A259240] p 513 N93-20579
- Preliminary studies of planning and flight strip use as air traffic controller memory aids
[DOT/FAA/CT-TN92/22] p 503 N93-21759
- Performance-based testing and success in Naval advanced flight training
[AD-A260838] p 717 N93-25933
- STYROFOAM (TRADEMARK)**
- Nonlinear aeroelasticity of composite structures
[AD-A254285] p 47 N93-10842
- SUBCRITICAL FLOW**
- The design of optimized airfoils in subcritical flow
[AIAA PAPER 93-0532] p 285 A93-23273
- SUBJECTS**
- USA aviation digest index, 1989, volume 11
[AD-A258673] p 571 N93-20388
- Index to USA aviation digest, 1990
[AD-A258678] p 572 N93-20389
- Index to USA aviation digest, 1991
[AD-A258679] p 572 N93-20390
- SUBLIMATION**
- Natural laminar flow test in-flight visualization
p 482 N93-19921
- Vortex structure and mass transfer near the base of a cylinder and a turbine blade
p 901 N93-29929
- SUBMARINES**
- Motion simulation of underwater vehicles
[VTT-PUBS-97] p 443 N93-18698

SUBROUTINES

Adaptive EAGLE dynamic solution adaptation and grid quality enhancement p 788 N93-27464

SUBSIDENCE

Land subsidence and problems affecting land use at Edwards Air Force Base and vicinity, California, 1990 [PB93-182236] p 1036 N93-32191

SUBSONIC AIRCRAFT

Effect of longitudinal microribbing on the drag of a body of revolution p 5 A93-10147

In-flight surface-flow measurements on a subsonic transport high-lift flap system p 166 A93-14327

Advanced technology constant challenge and evolutionary process p 109 A93-15054

Development of circulation control technology for application to advanced subsonic transport aircraft [AIAA PAPER 93-0644] p 464 A93-24759

Zero-gravity atmospheric flight by robust nonlinear inverse dynamics p 728 A93-34550

A CFD-based design strategy for advanced transonic wing concepts with practical ramifications for subsonic transports p 1047 A93-48143

Atmospheric aerosols due to aircraft and ecological problems p 1162 A93-48846

Interference between a high-lift sweptforward wing and the horizontal nose plane at subsonic velocities p 1135 A93-51906

Estimation of the effect of the longitudinal moment due to the engine thrust on the mass of a subsonic passenger aircraft p 1191 A93-52954

Research requirements for a real-time flight measurements and data analysis system for subsonic transport high-lift research p 1244 A93-54391

NO(y) from sub-sonic aircraft emissions - A global three-dimensional model study p 1261 A93-56236

Computational method in optimal bending-twisting comprehensive design of wings of subsonic and supersonic aircraft [AD-A262374] p 806 N93-27694

SUBSONIC FLOW

Dynamic stability of bodies of revolution in compressible flow p 12 A93-12558

Monotonicity characteristics of some plane vortex flows of incompressible fluids and subsonic gas flows p 13 A93-12932

An experimental study of dc discharges in supersonic and subsonic air flows p 14 A93-12980

Calculation of 3-D unsteady subsonic flow with separation bubble using singularity method p 115 A93-14251

Lateral aerodynamics characteristics of forebodies at high angle of attack in subsonic and transonic flows p 118 A93-14302

Generalized vortex lattice method for oscillating lifting surfaces in subsonic flow p 123 A93-14555

Subsonic separated flow past slender delta wings p 124 A93-15109

Oblique wave evolution in a plane subsonic boundary layer p 124 A93-15178

Assessment of a 3-D Euler code for subsonic turbine vane flows and study of the non radial blade stacking [ASME PAPER 92-GT-63] p 247 A93-19313

Numerical solutions for unsteady subsonic vortical flows around loaded cascades [ASME PAPER 92-GT-173] p 250 A93-19399

Prediction of active control of subsonic centrifugal compressor rotating stall p 274 A93-22591

Passive control of pre-entry shock in supersonic intakes [AIAA PAPER 93-0291] p 279 A93-22691

The influence of the boundary layer on the subsonic near-wake of a family of bluff bodies p 284 A93-23266

Aerodynamically efficient wing design with structural considerations p 460 A93-24081

Fundamental issues in subsonic/transonic expansion corner aerodynamics [AIAA PAPER 93-0649] p 465 A93-24764

A numerical investigation of a subsonic jet in a crossflow [AIAA PAPER 93-0870] p 469 A93-24931

Subsonic potential flow and the transonic controversy p 479 A93-28544

Nonlinear aeroelastic response of panels [AIAA PAPER 93-1599] p 741 A93-34130

Unsteady aerodynamics and flutter of propfans using a three-dimensional Full-Potential Solver [AIAA PAPER 93-1633] p 720 A93-34161

Comparison of several convection discretization schemes for all Mach number arbitrary 2D flows p 685 A93-34345

Calculation of the irregular interaction of shock waves p 691 A93-35339

Indicial lift approximations for two-dimensional subsonic flow as obtained from oscillatory measurements p 768 A93-37385

Underexpanded boundary jet in a wake flow p 775 A93-39123

Modeling of the physicochemical processes of nonequilibrium heat transfer in the subsonic jets of an induction plasmatron p 836 A93-39147

Subsonic natural-laminar-flow airfoils p 860 A93-41780

An extended Lagrangian method [AIAA PAPER 93-3305] p 951 A93-45003

Numerical investigation of subsonic and supersonic asymmetric vortical flow p 961 A93-45727

On the construction and calculation of optimal nonlifting critical airfoils p 969 A93-46857

On the steady subsonic shear flow past a slender body of revolution p 970 A93-46907

Unsteady aerodynamic response of two-dimensional subsonic and supersonic oscillating cascades with chordwise displacement and flexible deformation p 971 A93-46922

Three dimensional aero-thermal characteristics of a high pressure turbine nozzle guide vane p 1002 A93-46942

On the shock-fitting scheme of Hall-Crawley for time-linearized time-harmonic flows using Euler equations p 972 A93-46946

Solution of the Euler equations for airfoils using asymptotic methods [AIAA PAPER 93-2931] p 1045 A93-48130

An overview of recent subsonic laminar flow control flight experiments [AIAA PAPER 93-2987] p 1052 A93-48180

Study of the near-wake structure of a subsonic base cavity flowfield using PIV [AIAA PAPER 93-3040] p 1056 A93-48221

A three-dimensional pressure flux-split RNS application to sub/supersonic flow in inlets and ducts [AIAA PAPER 93-3063] p 1058 A93-48239

A study of turbulence in rarefied gases [AIAA PAPER 93-3097] p 1061 A93-48271

Aerodynamic characteristics of a sweptforward-wing aircraft model in unsteady motion at large angles of attack in subsonic flow p 1068 A93-48902

Calculation of subsonic flow of a gas past an airfoil p 1068 A93-48908

3-D viscous flow CFD analysis of the propeller effect on an advanced ducted propeller subsonic inlet [AIAA PAPER 93-1847] p 1075 A93-49728

Unsteady aerodynamics and flutter based on the potential equation [AIAA PAPER 93-2086] p 1079 A93-49913

C-2 subsonic freejet development and demonstration [AIAA PAPER 93-2180] p 1138 A93-49992

Numerical and experimental investigation of turbine tip gap flow [AIAA PAPER 93-2253] p 1081 A93-50051

Nontraditional methods of controlling the stability of a laminar subsonic boundary layer p 1085 A93-50962

Flux-vector splitting for compressible low Mach number flow p 1093 A93-52001

Transition correlation in subsonic flow over a flat plate p 1178 A93-53231

Moving wall effects in transverse subsonic flow past a rotating cylinder p 1179 A93-53573

Aerodynamic characteristics of conical triangular-planform wings of low aspect ratio in subsonic stalled flow p 1180 A93-53574

Characteristics of heat exchanger in supersonic/subsonic flows [ISABE 93-7119] p 1221 A93-54094

Mixing of multiple jets with a confined subsonic crossflow p 1189 A93-54324

Developing numerical techniques for solving low Mach number fluid-acoustic problems p 1235 A93-55353

Improved numerical simulation of Euler equations p 83 N93-10309

Mechanisms of sound generation in subsonic jets p 101 N93-10688

Experimental investigation of the effects of aft blowing with various nozzle exit geometries on a 3.0 caliber tangent ogive at high angles of attack: Forebody pressure distributions [NASA-CR-190935] p 22 N93-11605

An experimental investigation of the flow in a diffusing S-duct [NASA-TM-105809] p 60 N93-12077

Application of subsonic first-order panel methods for prediction of inlet and nozzle aerodynamic interactions with airframe p 130 N93-13223

Assessment of potential aerodynamic benefits from spanwise blowing at the wing tip p 134 N93-13822

Control of asymmetric jet [AD-A255967] p 219 N93-14400

A compilation of the mathematics leading to the doublet lattice method [AD-A256304] p 136 N93-14441

Prediction of turbine cascade flows with a quasi-three-dimensional rotor viscous code and the extension of the algebraic turbulence model [AD-A256831] p 223 N93-15635

Mixing and reaction in the subsonic 2-D turbulent free shear layer p 289 N93-16508

Analytical and numerical study on steady Mach reflection p 302 N93-19309

Uniform roughness studies [WL-TR-92-3041] p 751 N93-25951

Unsteady airfoil flow solutions on moving zonal grids [AD-A261925] p 701 N93-26198

Assessment of computational issues associated with analysis of high-lift systems p 785 N93-27449

Comparison of reacting and non-reacting shear layers at a high subsonic Mach number [NASA-TM-106198] p 814 N93-27610

The numerical solution of low Mach number flow in confined regions by Richardson extrapolation [TRITA-NA-9207] p 789 N93-29005

The 3-D viscous flow CFD analysis of the propeller effect on an advanced ducted propeller subsonic inlet [NASA-TM-106240] p 900 N93-29162

Experimental study of heat transfer close to a plane wall heated in the presence of multiple injections (subsonic flow) p 901 N93-29931

SUBSONIC FLUTTER

An experimental and analytical study of a lifting-body wind-tunnel model exhibiting body-freedom flutter [AIAA PAPER 93-1316] p 732 A93-33891

SUBSONIC SPEED

Review of the normal force fluctuations of aerofoils with separated flow p 10 A93-12317

Assessment and correction of tunnel wall interference by Navier-Stokes solutions p 116 A93-14275

Modal analysis of unsteady aerodynamic response of subsonic annular cascade with steady loading under elastic vibration p 126 A93-15495

Prediction of jet mixing noise in high-speed flight p 450 A93-19216

Subsonic static and dynamic stability characteristics of the test technique demonstrator NASP configuration [AIAA PAPER 93-0519] p 268 A93-21111

Acoustic mode measurements in the inlet of a model turbofan using a continuously rotating rake - Data collection/analysis techniques [AIAA PAPER 93-0599] p 361 A93-23324

Effect of a rotating propeller on the separation angle of attack [AIAA PAPER 93-0017] p 472 A93-24978

Vortex features of F-106B aircraft at subsonic speeds [AIAA PAPER 93-3471] p 859 A93-41058

Identification of a full subsonic envelope nonlinear aerodynamic model of the F-14 aircraft [AIAA PAPER 93-3634] p 1065 A93-48319

Testing of a high performance compressor discharge seal [AIAA PAPER 93-1997] p 1153 A93-49840

Applying and validating the RANS-3D flow-solver for evaluating a subsonic serpentine diffuser geometry [AIAA PAPER 93-2157] p 1079 A93-49973

Non-propulsive aerodynamic noise p 99 N93-10673

Prediction of jet mixing noise for high subsonic flight speeds p 100 N93-10685

A concept for a counterrotating fan with reduced tone noise [NASA-TM-105736] p 101 N93-11370

Formal representation of the requirements for an Advanced Subsonic Civil Transport (ASCT) flight control system [NASA-CR-189699] p 98 N93-12346

Comparative performance tests of a pitot-inlet in several European wind-tunnels at subsonic and supersonic speeds p 130 N93-13221

Acoustic mode measurements in the inlet of a model turbofan using a continuously rotating rake: Data collection/analysis techniques [NASA-TM-105936] p 179 N93-15403

Effect of a rotating propeller on the separation angle of attack and distortion in ducted propeller inlets [NASA-TM-105935] p 290 N93-16625

Drag due to gaps round undeflected trailing-edge controls and flaps at subsonic speeds [ESDU-92039] p 290 N93-16634

Contribution of ventral fins to sideforce and yawing moment derivatives due to sideslip at low angle of attack [ESDU-92029] p 291 N93-16638

Boundary-layer measurements on a high Reynolds number three-element airfoil p 292 N93-16787

- Experimental investigations on wing-body combinations and their components at high angles of attack in the subsonic and transonic speed range [DLR-FB-91-43] p 516 N93-21762
- Effect of underwing frost on transport aircraft takeoff performance [DOT/FAA/CT-TN93/9] p 791 N93-27252
- High-lift aerodynamics: Prospects and plans p 784 N93-27442
- Flow prediction over a transport multi-element high-lift system and comparison with flight measurements p 785 N93-27448
- Assessment of computational issues associated with analysis of high-lift systems p 785 N93-27449
- Unsteady transition measurements on a pitching three-dimensional wing p 820 N93-27450
- SUBSONIC WIND TUNNELS**
- Experimental and theoretical studies of helicopter rotor-fuselage interaction [ONERA, TP NO. 1992-142] p 120 A93-14356
- Fine control of Mach number in subsonic wind tunnel p 375 A93-20808
- Effect of sidewall suction on flow in two-dimensional wind tunnels p 287 A93-23538
- Interaction of Tollmien-Schlichting waves with localized disturbances p 545 A93-27637
- Evolution of a three-dimensional nonequilibrium boundary layer in a dihedral angle behind a perturbation source p 872 A93-43013
- High speed test results of subsonic, turbofan scarf inlets [AIAA PAPER 93-2302] p 1082 A93-50087
- Further noise measurements in a slotted cryogenic wind tunnel [RAE-TM-AERO-2201] p 101 N93-10805
- The measurement of the velocity field induced by a gust generator in a closed-circuit subsonic wind-tunnel [RAE-TM-MAT/STR-1102] p 67 N93-11435
- Experimental investigation of an ejector-powered free-jet facility [NASA-TM-105868] p 291 N93-16704
- Transition aerodynamics for 20-percent-scale VTOL unmanned aerial vehicle [NASA-TM-4419] p 779 N93-27032
- Aerodynamics of a finite wing with simulated ice p 784 N93-27437
- SUBSTRUCTURES**
- An overview of the crash dynamics failure behavior of metal and composite aircraft structures p 923 N93-30875
- SUCTION**
- Effect of sidewall suction on flow in two-dimensional wind tunnels p 287 A93-23538
- Surging limits of multistage axial-flow compressors p 476 A93-27443
- Temperature and suction effects on the instability of an infinite swept attachment line p 691 A93-35486
- Hypersonic stability and transition p 864 A93-42579
- The effect of Reynolds number on control of forebody asymmetry by suction and bleed [AIAA PAPER 93-3265] p 968 A93-46831
- Control of the dynamic-stall vortex over a pitching airfoil by leading-edge suction p 969 A93-46832
- Effect of boundary layer suction on the thrust and aerodynamic efficiency of a hypersonic flight vehicle p 1176 A93-52959
- Dynamical effects of suction/heating on turbulent boundary layers [AD-A248459] p 87 N93-11416
- Two problems reducing the data accuracy in Transonic Wind Tunnel testing p 304 N93-19321
- Analysis and evaluation of an integrated laminar flow control propulsion system [NASA-CR-192162] p 551 N93-20268
- The effect of surface suction near the leading edge of a swept-back wing [AERO-REPT-9205] p 484 N93-20807
- The generation of side force by distributed suction [NASA-CR-193129] p 839 N93-27151
- SULFIDATION**
- Advanced turbine design for coal-fueled engines [DE93-000224] p 554 N93-21254
- SULFIDES**
- Application of a sulphur-doped alkane system to the study of thermal oxidation of jet fuels [ASME PAPER 92-GT-122] p 387 A93-19356
- SULFUR**
- X-ray diffraction and electron microscope studies of Yttria Stabilized Zirconia (YSZ) ceramic coatings exposed to vanadia [AD-A258055] p 392 N93-17676

SULFUR FLUORIDES

- Modeling and control study of the NASA 0.3-meter transonic cryogenic tunnel for use with sulfur hexafluoride medium [NASA-CR-189737] p 418 N93-16379
- Modifications to Langley 0.3-m TCT adaptive wall software for heavy gas test medium, phase 1 studies [NASA-CR-189736] p 291 N93-16710

SULFURIC ACID

- Corrosion of ceramic matrix composites [ONERA, TP NO. 1993-82] p 1213 A93-53602

SUPERCHARGERS

- Performance simulation of a combustion engine charged by a variable geometry turbocharger. I - Prerequisites, boundary conditions and model development. II - Simulation algorithm, computed results p 1256 A93-54648

- Engine driven chiller and thermal storage integration (Large tonnage engine driven chiller development) [PB92-227891] p 555 N93-21465

- Radial inflow turbine study [AD-A260767] p 724 N93-25917

- Improved silicon nitride for advanced heat engines [NASA-CR-182193] p 917 N93-29451

SUPERCOMPUTERS

- Large-scale simulation of the three-dimensional Navier-Stokes equations p 437 A93-20739
- Use of Convex supercomputers for flight simulation at NASA Langley p 1013 A93-46806
- Upwind-biased, point-implicit relaxation strategies for hypersonic flowfield simulations on supercomputers p 1175 A93-52770

- The engine design engine. A clustered computer platform for the aerodynamic inverse design and analysis of a full engine [NASA-TM-105838] p 21 N93-11223

- Use of high performance networks and supercomputers for real-time flight simulation p 731 N93-25574

SUPERCONDUCTING MAGNETS

- The benefits of Maglev technology [AIAA PAPER 93-2949] p 1174 A93-48145
- Operating experience using venturi flow meters at liquid helium temperature [DE92-014693] p 90 N93-12140

SUPERCOOLING

- The FAA aircraft icing Forecasting Improvement Program - Validation of aircraft icing forecasts in the Denver area [AIAA PAPER 93-0393] p 309 A93-23069
- Icing prevention by ultrasonic nucleation of supercooled water droplets in front of subsonic aircraft [AD-A258212] p 142 N93-12816

SUPERCritical AIRFOILS

- Turbulence model evaluation for the prediction of flows over a supercritical airfoil with deflected aileron at high Reynolds number [AIAA PAPER 93-0191] p 276 A93-22615
- Application of Oswatitsch's theorem to supercritical airfoil drag calculation p 768 A93-37399
- Experience in the design of supercritical cascades for the flow straightener of a transonic fan p 777 A93-39196

- Multielement airfoil performance due to Reynolds and Mach number variations p 1095 A93-52442
- Characterisation of conventional and controlled diffusion stator blades in a transonic compressor stage [ISABE 93-7124] p 1189 A93-54099

- Numerical minimization of the moment coefficient of a supercritical airfoil section p 1238 A93-56214

SUPERCritical FLOW

- Numerical solution of transonic full-potential-equivalent equations in von Mises co-ordinates p 111 A93-14080
- Numerical simulation of flows in a supersonic air intake p 303 N93-19314

- Influence of supercritical conditions on pre-combustion chemistry and transport behavior of jet fuels [AD-A261813] p 737 N93-26268

SUPERCritical FLUIDS

- Measurement of diffusion in supercritical fluid systems - A review [AIAA PAPER 93-0809] p 534 A93-24884

- Design of a hydrogen test facility p 532 A93-25993
- A condensed phase test cell assembly for the System for Thermal Diagnostic Studies (STDS) [AD-A258463] p 393 N93-18242

SUPERCritical PRESSURES

- Fundamental studies of droplet interactions in dense sprays [AD-A261165] p 737 N93-25948

SUPERCritical WINGS

- Supercritical wing design, a three dimensional hodograph approach [AIAA PAPER 92-2657] p 472 A93-24986

- A numerical study of aerodynamic wing design for supercritical conditions of an advanced training and military aircraft p 1238 A93-56213

- Flight test results from a supercritical mission adaptive wing with smooth variable camber [NASA-TM-4415] p 49 N93-11663

- Pressure distribution for the wing of the YAV-8B airplane; with and without pylons [NASA-TM-4429] p 136 N93-14451

SUPERPLASTICITY

- Mechanical testing analyses of new aluminium alloy SPF typical-parts in aircraft p 196 A93-14174

SUPERPRESSURE BALLOONS

- The Superpressure Stratospheric Vehicle p 39 A93-11357

SUPERSONIC AIRCRAFT

- Transonic profile design in curvilinear coordinates using an approximate factorization algorithm p 7 A93-10778
- Passive boundary-layer bleed for supersonic intakes p 114 A93-14212

- Design of manoeuvrable simple and complex planform transonic wings with attained thrust, panel- and Euler-methods p 117 A93-14301

- Supersonic wing/body interference p 121 A93-14391

- Geometrically nonlinear local flutter analysis of supersonic airplane skin plates in the potential supersonic flow [ISBN 83-01-10939-4] p 394 A93-17569

- Method and results of studies of flow past supersonic flight vehicles at moderate and large angles of attack p 242 A93-18377

- Numerical simulation of the flow field around supersonic air-intakes [ASME PAPER 92-GT-206] p 251 A93-19430

- Parallel computation of 3-D Navier-Stokes flowfields for supersonic vehicles [AIAA PAPER 93-0064] p 261 A93-20177

- Starting and test rhombus characteristics of two-dimensional supersonic free-jet nozzle/generic supersonic aircraft inlet configurations [AIAA PAPER 92-5091] p 273 A93-22361

- Passive control of pre-entry shock in supersonic intakes [AIAA PAPER 93-0291] p 279 A93-22691

- The structure and material testing facility needed for future SST/HST development [AIAA PAPER 92-3887] p 528 A93-24481

- Some effects of wing and body geometry on the aerodynamic characteristics of configurations designed for high supersonic Mach numbers [AIAA PAPER 92-4246] p 463 A93-24493

- Development and fabrication of an autoclave molded PES/Quartz sandwich radome p 547 A93-28279

- Aeroelastic system identification of advanced technology aircraft through higher order signal processing p 525 A93-29297

- An analysis on high speed impulsive noise of transonic helicopter rotor p 849 A93-35965

- A study of the origin of residual stresses and strains in the transparencies of supersonic aircraft p 801 A93-36784

- Materials problems connected with the propulsion of supersonic air carriers [ONERA, TP NO. 1992-157] p 824 A93-38736

- Implications of three-dimensional tracer studies for two-dimensional assessments of the impact of supersonic aircraft on stratospheric ozone p 936 A93-41269

- It's time to go supersonic p 949 A93-44099

- Plume and wake dynamics, mixing, and chemistry behind a high speed civil transport aircraft p 1034 A93-45139

- Supersonic/hypersonic aerodynamic methods for aircraft design and analysis p 967 A93-46816

- Optimum poststall turning and supersonic turning [AIAA PAPER 93-3659] p 1128 A93-48339

- Determination of the aerodynamic balance efficiency of aircraft p 1130 A93-48903

- Near-optimal, asymptotic tracking in control problems involving state-variable inequality constraints [AIAA PAPER 93-3748] p 1170 A93-51344

- Wet layup materials for repair of bismaleimide composites p 1212 A93-53451

- LV software for supersonic flow analysis [NASA-CR-190911] p 16 N93-10069

- Predicted aircraft effects on stratospheric ozone p 93 N93-11096

- Overview of high performance aircraft propulsion research [NASA-TM-105839] p 59 N93-11530

- Minimum-time flight paths of supersonic aircraft p 160 N93-13140

- The PEP Symposium on CFD Techniques for Propulsion Applications p 214 N93-13210

- The influence of intake swirl distortion on the steady-state performance of a low bypass, twin-spool engine p 214 N93-13211

- Ideal aircraft handling quality models: Longitudinal axis [NAL-PD-FC-9203] p 187 N93-13566
- Impact of supersonic and subsonic aircraft on ozone: Including heterogeneous chemical reaction mechanisms [DE92-019619] p 224 N93-13655
- Definition of the 2005 flight deck environment [NASA-CR-4479] p 343 N93-16693
- Direct numerical simulation of combustion in turbulent supersonic flow [DS-2138] p 393 N93-17746
- High speed civil transport [NASA-CR-192041] p 337 N93-18161
- RTJ-303: Variable geometry, oblique wing supersonic aircraft [NASA-CR-192054] p 337 N93-18166
- The 3D Navier-Stokes calculation of flow about scramjet inlet with strut p 301 N93-19298
- Supersonic transport: Which material for the engine [DS-2023] p 522 N93-21459
- Experimental performance of a ventral nozzle with pitch and yaw vectoring capability for SSTOVL aircraft [NASA-TM-106054] p 722 N93-25129
- YF-22A prototype advanced tactical fighter demonstration/validation flight test program overview p 805 N93-27173
- Computational method in optimal bending-twisting comprehensive design of wings of subsonic and supersonic aircraft [AD-A262374] p 806 N93-27694
- Sonic boom problem for future highspeed aircraft [ONERA-NT-1990-3] p 876 N93-30020
- SUPERSONIC AIRFOILS**
- Numerical simulation of passive control of shock-boundary layer interaction for transonic airfoil p 580 N93-33719
- SUPERSONIC BOUNDARY LAYERS**
- Effect of wall heating on a supersonic turbulent boundary layer p 11 A93-12429
- Recent supersonic transition studies with emphasis on the swept cylinder case p 127 A93-17252
- On the coupling between a supersonic boundary layer and a flexible surface p 243 A93-19132
- Stability and transition on swept wings [AIAA PAPER 93-0078] p 263 A93-20190
- Conventional skin friction measurement techniques for strongly perturbed supersonic turbulent boundary layers p 271 A93-21863
- Instability and transition in three-dimensional supersonic boundary layers [AIAA PAPER 92-5049] p 273 A93-22321
- Mean flowfield structure of a three-dimensional supersonic turbulent boundary layer [AIAA PAPER 93-0661] p 465 A93-24774
- A new model for super/hypersonic turbulent boundary layers [AIAA PAPER 93-0897] p 472 A93-24957
- Boundary-layer transition extent measurements on a cone and flat plate at Mach 3.5 [AIAA PAPER 93-0342] p 474 A93-25517
- Experience with the use of liquid crystals in conjunction with the filament method is studying the structure of supersonic flow downstream of a plane step p 478 A93-27639
- Intermode exchange in a supersonic boundary layer p 691 A93-35346
- Analysis of thermal ignition in supersonic flat-plate boundary layers p 769 A93-37933
- Modeling supersonic inlet boundary-layer bleed roughness p 872 A93-42891
- Control of a supersonic reattaching shear layer [AIAA PAPER 93-3248] p 966 A93-46793
- Instability of three-dimensional supersonic boundary layer p 973 A93-46987
- Some stability characteristics of the boundary layer on a yawed cone [AIAA PAPER 93-3048] p 1057 A93-48228
- A time-accurate high-resolution TVD scheme for solving the Navier-Stokes equations p 1093 A93-52006
- Observations of liquid jets injected into a highly accelerated supersonic boundary layer p 1177 A93-53214
- Overview of supersonic laminar flow control research on the F-16XL ships 1 and 2 [NASA-TM-104257] p 20 N93-11221
- Application of a solution adaptive grid to flow over an embedded cavity p 130 N93-13141
- Two problems reducing the data accuracy in Transonic Wind Tunnel testing p 304 N93-19321
- On the disturbances development in the supersonic boundary layer p 484 N93-20686
- SUPERSONIC COMBUSTION**
- An experimental investigation of hydrogen-fueled supersonic combustor p 53 A93-12733
- Comment on 'Experimental study on autoignition in a scramjet combustor' p 172 A93-14525
- Direct measurements of skin friction in supersonic combustion flow fields [ASME PAPER 92-GT-320] p 405 A93-19506
- Planar imaging of OH density distributions in a supersonic combustion tunnel [AIAA PAPER 93-0042] p 389 A93-20155
- Effects of compression and expansion ramp fuel injector configuration on scramjet combustion and heat transfer [AIAA PAPER 93-0609] p 358 A93-21114
- Numerical analysis of reacting flow using finite rate chemistry models p 389 A93-21666
- Hypervelocity scramjet capabilities of the T5 Free-Piston Tunnel at Caltech [AIAA PAPER 92-5037] p 376 A93-22311
- Numerical and experimental investigation of mixing enhancement in scramjets [AIAA PAPER 92-5063] p 414 A93-22333
- Remote sensing of O₂ in a supersonic combustor using diode lasers and fiber optics [AIAA PAPER 92-5090] p 414 A93-22360
- Pdf prediction of supersonic hydrogen flames [AIAA PAPER 93-0448] p 391 A93-23358
- Finite element analysis of the Scramaccelerator with finite rate chemistry [AIAA PAPER 93-0745] p 540 A93-24833
- Development of a robust pressure-based numerical scheme for spray combustion applications [AIAA PAPER 93-0902] p 560 A93-24960
- Stability of oblique detonations in RAM accelerators [AIAA PAPER 92-0089] p 541 A93-24979
- Effect of combustion on the interaction of an underexpanded wall hydrogen jet with supersonic flow in a plane duct p 534 A93-27658
- Ignition and spread of combustion within a supersonic boundary layer p 535 A93-27732
- Ignition process of fuel droplet arrays in a supersonic flowfield p 535 A93-27766
- Laser selection criteria for OH fluorescence measurements in supersonic combustion test facilities p 549 A93-29315
- Experimental supersonic hydrogen combustion employing staged injection behind a rearward-facing step p 744 A93-34496
- Applications of shock-induced mixing to supersonic combustion p 735 A93-35618
- Ignition analysis of unpremixed reactants with chain mechanism in a supersonic mixing layer p 735 A93-35619
- Oxidation-resistant high-temperature materials p 915 A93-40362
- Study of mixing flow field of a jet in a supersonic cross flow. I - Experimental facilities and preliminary experiments p 857 A93-40430
- Shock tunnel studies of external combustion in high supersonic air flows p 1017 A93-45517
- Effects of external control circuit on coal-fired supersonic diagonal-type MHD generator p 1173 A93-49619
- Molecular mixing of jets in supersonic flow [AIAA PAPER 93-2021] p 1078 A93-49858
- Nonintrusive, multipoint velocity measurements in high-pressure combustion flows [AIAA PAPER 93-2032] p 1145 A93-49867
- Comparison of NO and OH PLIF temperature measurements in a scramjet model flowfield [AIAA PAPER 93-2035] p 1113 A93-49870
- Mixing enhancement and combustion of gaseous fuel in a supersonic combustor [AIAA PAPER 93-2143] p 1114 A93-49960
- Vortex generation and mixing in three-dimensional supersonic combustors [AIAA PAPER 93-2144] p 1115 A93-49961
- Analysis and demonstration of a Scramaccelerator system [AIAA PAPER 93-2183] p 1142 A93-49995
- A k-omega multivariate beta PDF for supersonic turbulent combustion [AIAA PAPER 93-2197] p 1154 A93-50009
- Modeling of turbulent supersonic H₂-air combustion with a multivariate beta PDF [AIAA PAPER 93-2198] p 1155 A93-50010
- Boron particle ignition in high-speed flow [AIAA PAPER 93-2202] p 1145 A93-50014
- Standing normal detonations and oblique detonations for propulsion [AIAA PAPER 93-2325] p 1116 A93-50105
- A review of supersonic combustion research at AEDC with hypersonic application [AIAA PAPER 93-2326] p 1116 A93-50106
- Determination of heat transfer to flow in a duct with a pseudodiscontinuity p 1179 A93-53365
- A study of self-ignition of methane-hydrogen mixture fuel injected into high enthalpy supersonic airstreams [ISABE 93-7049] p 1213 A93-54025
- Tandem transverse hydrogen gas injection into a supersonic airflow [ISABE 93-7069] p 1201 A93-54045
- Employment of radicals and excited state species for supersonic combustion photochemical ignition of premixed hydrogen/oxygen mixtures with ArF laser p 73 N93-11135
- Combustion in supersonic flows p 199 N93-14627
- Aerothermodynamic flow phenomena of the airframe-integrated supersonic combustion ramjet [NASA-TM-4376] p 196 N93-15528
- Investigation of the aerothermodynamics of hypervelocity reacting flows in the ram accelerator [NASA-CR-191715] p 140 N93-15588
- Chemical kinetic and aerodynamic structures of flames [AD-A256015] p 391 N93-15931
- Modeling of turbulent supersonic H₂-air combustion with an improved joint beta PDF [NASA-CR-191929] p 391 N93-16389
- Numerical calculation of flow field in supersonic combustion chamber p 304 N93-19317
- Computation of H₂/air reacting flowfields in drag-reduction external combustion [NASA-CR-191071] p 536 N93-20237
- A k-omega-multivariate beta PDF for supersonic combustion [NASA-CR-191930] p 537 N93-21749
- Turbulence interacting with chemical kinetics in airbreathing combustion of ducted rockets p 734 N93-26012
- Direct measurements of skin friction in supersonic combustion flow fields [AD-A262878] p 825 N93-28226
- Studies of hydrogen-air diffusion flames and of compressibility effects related to high-speed propulsion p 917 N93-29125
- SUPERSONIC COMBUSTION RAMJET ENGINES**
- Evaluation of 2D scramjet nozzle performance p 52 A93-11209
- A design approach to high Mach number scramjet performance [AIAA PAPER 92-4248] p 55 A93-13360
- Taking the measure of aerodynamic testing p 16 A93-13434
- Supersonic combustion and gasdynamic of scramjet p 170 A93-14242
- Scramjet combustor and nozzle computations p 171 A93-14243
- Experimental investigation of hydrogen burning and heat transfer in annular duct at supersonic velocity p 171 A93-14247
- Experimental investigation of an axisymmetric hypersonic scramjet inlet for laser propulsion p 122 A93-14515
- Comment on 'Experimental study on autoignition in a scramjet combustor' p 172 A93-14525
- Effects of vitiated air on the results of ground tests of scramjet combustor p 173 A93-16234
- Direct measurements of skin friction in supersonic combustion flow fields [ASME PAPER 92-GT-320] p 405 A93-19506
- Unsteady loads measurements in a generic high speed engine model by means of recessed transducers [AIAA PAPER 93-0287] p 342 A93-21104
- Effects of compression and expansion ramp fuel injector configuration on scramjet combustion and heat transfer [AIAA PAPER 93-0609] p 358 A93-21114
- Evaluation of scramjet nozzle configurations and film cooling for reduction of wall heating [AIAA PAPER 93-0744] p 358 A93-21118
- Scramjet fuel-air mixing establishment in a pulse facility p 359 A93-21667
- Investigation of a two-dimensional scramjet inlet, freestream M = 8-18 and Tsub 0 = 4100 K p 270 A93-21669
- Effects of injector geometry on scramjet combustor performance p 359 A93-21670
- Dual transverse injection of H₂ gas into Mach 1.8 flows at University Komaba wind tunnel p 376 A93-21833
- Data analysis of the parametric scramjet combustor experiments conducted in the Calspan 96 inch shock tunnel - 4th entry [AIAA PAPER 92-5098] p 359 A93-22368
- Study on steady and unsteady unstart phenomena due to compound choking and/or fluctuations in combustor of scramjet engines [AIAA PAPER 92-5102] p 359 A93-22372
- Techniques for the measurement of scramjet inlet performance at hypersonic speeds [AIAA PAPER 92-5104] p 274 A93-22374
- The effect of entrance radius and film injection on wall heating in scramjet nozzles p 360 A93-22505
- Total-pressure loss in supersonic parallel mixing [AIAA PAPER 93-0216] p 278 A93-22632
- An optical comparison of wall and axial injection for high enthalpy reacting scramjet flows [AIAA PAPER 93-0357] p 377 A93-23040

Isolator-combustor interaction in a dual-mode scramjet engine
[AIAA PAPER 93-0358] p 360 A93-23041
Analysis of a hypersonic waverider research vehicle with a hydrocarbon scramjet engine
[AIAA PAPER 93-0509] p 386 A93-23256
Analytical investigation of a regeneratively cooled scramjet engine
[AIAA PAPER 93-0739] p 519 A93-24829
An experimental parametric study of geometric, Reynolds number, and ratio of specific heats effects in three-dimensional sidewall compression scramjet inlets at Mach 6
[AIAA PAPER 93-0740] p 466 A93-24830
Aerodynamic performance of scramjet inlet models with a single strut
[AIAA PAPER 93-0741] p 466 A93-24831
A numerical study of mixing in supersonic combustors with hypermixing injectors
[AIAA PAPER 93-0215] p 520 A93-27801
Issues associated with long-duration high-enthalpy scramjet combustor testing
p 721 A93-34497
High-temperature supersonic combustion testing with optical diagnostics
p 730 A93-34498
A numerical simulation of a scram jet combustor flow
p 810 A93-38181
Investigation of a contoured wall injector for hypervelocity mixing augmentation
p 837 A93-39407
Thermal analysis of a shower-head burner
[SAE PAPER 92-1226] p 898 A93-41400
Research on supersonic combustion
p 899 A93-42877
Demonstration of mode transition in a scramjet combustor
p 899 A93-42878
Scramjet nozzle experiment with hypersonic external flow
p 899 A93-42879
A computational investigation of fuel mixing in a hypersonic scramjet
[AIAA PAPER 93-2994] p 1001 A93-44230
Development and operation of new arc heater technology for a large-scale scramjet propulsion test facility
[AIAA PAPER 93-2786] p 1016 A93-46528
Visual observations of supersonic transverse jets
p 965 A93-46750
Drag measurements on blunted cones and a scramjet vehicle in hypervelocity flow
[AIAA PAPER 93-2979] p 1050 A93-48172
Slush hydrogen quantity gaging and mixing for the National Aerospace Plane
p 1150 A93-48635
Validation studies of scramjet nozzle performance
p 1109 A93-49616
Calculation of scramjet inlet with thick boundary-layer ingestion
[AIAA PAPER 93-1836] p 1074 A93-49720
Numerical study of the performance of swept, curved compression surface scramjet inlets
[AIAA PAPER 93-1837] p 1074 A93-49721
CFD validation for scramjet combustor and nozzle flows.
[AIAA PAPER 93-1840] p 1111 A93-49724
Summary of the GASP code application and evaluation effort for scramjet combustor flowfields
[AIAA PAPER 93-1973] p 1077 A93-49820
Comparison of NO and OH PLIF temperature measurements in a scramjet model flowfield
[AIAA PAPER 93-2035] p 1113 A93-49870
Scramjet fuel mixing enhancement by cross-stream pressure gradients
[AIAA PAPER 93-2139] p 1114 A93-49957
Vortex generation and mixing in three-dimensional supersonic combustors
[AIAA PAPER 93-2144] p 1115 A93-49961
Gasdynamics of hydrogen-fueled scramjet combustors
[AIAA PAPER 93-2145] p 1115 A93-49962
Review of NASA's Hypersonic Research Engine Project
[AIAA PAPER 93-2323] p 1116 A93-50103
A review of supersonic combustion research at AEDC with hypersonic application
[AIAA PAPER 93-2326] p 1116 A93-50106
An approach to in-situ analysis of scramjet combustor behavior
[AIAA PAPER 93-2328] p 1116 A93-50108
Direct measurements of skin friction in a scramjet combustor
[AIAA PAPER 93-2443] p 1119 A93-50195
Hypersonic ignition and thrust production in a scramjet
[AIAA PAPER 93-2444] p 1119 A93-50196
Experimental studies of aerodynamic performances of hypersonic scramjet in impulse hot-shot tunnel
[AIAA PAPER 93-2446] p 1120 A93-50198
Design and investigation of the stand and flying scramjet models - Conceptions and results of experiments
[AIAA PAPER 93-2447] p 1120 A93-50199

Computational effects of inlet representation on powered hypersonic, airbreathing models
p 1094 A93-52427
CFD for ramjet and scramjet powered vehicles
[ISABE 93-7035] p 1197 A93-54011
Effect of film cooling/regenerative cooling on scramjet engine performances
[ISABE 93-7036] p 1197 A93-54012
Ignition and combustion performance of a scramjet combustor with a fuel injection strut
[ISABE 93-7050] p 1199 A93-54026
Study on unstart and its propagation along modules due to compound choking and/or fluctuations in combustor of scramjet engines
[ISABE 93-7052] p 1199 A93-54028
Application of functionally gradient materials to scramjet engines
[ISABE 93-7063] p 1200 A93-54039
Numerical simulation of ramjet and scramjet combustion using two-dimensional Euler equations with finite rate chemistry
[ISABE 93-7083] p 1202 A93-54059
Starting characteristics of scramjet inlets
[ISABE 93-7105] p 1203 A93-54081
Numerical simulation of a two-dimensional supersonic mixed-compression inlet
[ISABE 93-7107] p 1188 A93-54083
Off-design performance of scramjet nozzles
[ISABE 93-7108] p 1203 A93-54084
Thermal barrier design of gamma-TiAl functionally gradient materials (FGMs) for scramjet engine applications
p 1246 A93-54556
Preliminary design of experimental sub-scale scramjet engine
[AAS PAPER 91-639] p 1247 A93-55816
A configuration development strategy for the NASP
p 46 N93-10011
Hypersonic inlet efficiency revisited
p 16 N93-10012
Effects of reacting flows with turbulence and shock waves on efficiency of scramjet combustors
p 69 N93-11133
Hypervelocity scramjet combustor-nozzle analysis and design
[NASA-CR-190965] p 60 N93-12214
Mach 4 testing of scramjet inlet models
[NAL-TR-1137] p 26 N93-12369
Aerothermodynamic flow phenomena of the airframe-integrated supersonic combustion ramjet
[NASA-TM-4376] p 196 N93-15528
A numerical study of mixing in supersonic combustors with hypermixing injectors
[NASA-CR-191027] p 294 N93-17884
Nozzle/cowl optimization for a hypersonic vehicle on a typical trajectory
[AD-A258827] p 341 N93-19089
Generation of longitudinal vortices in supersonic flow
p 301 N93-19292
The 3D Navier-Stokes calculation of flow about scramjet inlet with strut
p 301 N93-19298
Numerical simulation of flow for a scramjet nozzle
p 302 N93-19299
A numerical investigation of 3D transverse injection into the supersonic flow behind rearward facing step
p 303 N93-19316
Numerical calculation of flow field in supersonic combustion chamber
p 304 N93-19317
A numerical simulations of inner flow of scramjet
p 304 N93-19318
Research in robust control for hypersonic vehicles
[NASA-CR-192127] p 527 N93-20296
Computational parametric study of sidewall-compression scramjet inlet performance at Mach 10
[NASA-TM-4411] p 552 N93-20299
Generic hypersonic vehicle performance model
[NASA-CR-192953] p 714 N93-25162
Optimized scramjet engine integration on a waverider airframe
p 722 N93-25480
Workshop Report: A validation study of Navier-Stokes codes for transverse injection into a Mach 2 flow
p 751 N93-26008
Assessment of a flow-through balance for hypersonic wind tunnel models with scramjet exhaust flow simulation
[NASA-TM-4441] p 779 N93-27005
Direct measurements of skin friction in supersonic combustion flow fields
[AD-A262878] p 825 N93-28226
Analytical and experimental investigations of the oblique detonation wave engine concept
[NASA-TM-102839] p 1006 N93-32374
SUPERSONIC COMMERCIAL AIR TRANSPORT
The impact of air traffic on the atmospheric environment
p 936 A93-42659

Engine technology challenges for a 21st Century High-Speed Civil Transport
[ISABE 93-7064] p 1200 A93-54040
HSCT mission analysis of waverider designs
[NASA-CR-192193] p 515 N93-21646
Engine technology challenges for a 21st Century High-Speed Civil Transport
[NASA-TM-106216] p 1004 N93-31671
SUPERSONIC COMPRESSORS
Design and rotor performance of a 5:1 mixed-flow supersonic compressor
[ASME PAPER 92-GT-73] p 348 A93-19323
Analysis of three-dimensional viscous flow in a supersonic axial flow compressor rotor with emphasis on tip leakage flow
[ASME PAPER 92-GT-388] p 257 A93-19543
Supersonic through flow compressors - A preliminary study: COVAXS
p 1001 A93-46930
Explicit Navier-Stokes computation of turbomachinery flows
p 83 N93-10370
SUPERSONIC CRUISE AIRCRAFT RESEARCH
Elements of NASA's high-speed research program
[AIAA PAPER 93-2942] p 947 A93-45155
HSCT mission analysis of waverider designs
[NASA-CR-192193] p 515 N93-21646
SUPERSONIC DIFFUSERS
Isolator-combustor interaction in a dual-mode scramjet engine
[AIAA PAPER 93-0358] p 360 A93-23041
A time dependent method in finite volume for transonic diffuser turbulent flows
p 476 A93-27368
Normal shock wave oscillations in supersonic diffusers
p 1044 A93-48042
Numerical simulations of the unstart phenomenon in a supersonic inlet/diffuser
[AIAA PAPER 93-2239] p 1081 A93-50041
SUPERSONIC DRAG
Methods and results of theoretical investigations for high-speed parachute systems
[AIAA PAPER 93-1227] p 690 A93-35173
Effect of anomalous aerodynamic heating during the descent of a parachute along a trajectory
p 1069 A93-48924
SUPERSONIC FLIGHT
Measurement of attachment-line location in a wind-tunnel and in supersonic flight
[AIAA PAPER 92-4089] p 39 A93-11285
Noninvasive spectroscopic techniques for supersonic/hypersonic aerodynamics and combustion diagnostics
p 203 A93-14245
Pulsed detonation engine experimental and theoretical review
[AIAA PAPER 92-3168] p 531 A93-24478
Consideration of the completeness of combustion and dissociation and recombination processes in mathematical models of jet engines for high supersonic flight velocities
p 520 A93-27627
Euler solution for wing-body combination at supersonic speeds
p 680 A93-33722
Unstructured grids for sonic-boom analysis
[AIAA PAPER 93-2929] p 949 A93-44229
Formation of shock waves in transient base flow
p 1023 A93-45460
On the possibility of singularities in the acoustic field of supersonic sources when BEM is applied to a wave equation
p 1039 A93-46805
Approximate method for the aerodynamic design of flight vehicles for high supersonic flight speeds
p 1069 A93-48966
Concorde propulsion: Did we get it right? The Rolls-Royce/SNECMA Olympus 593 engine reviewed
[PNR-90970] p 57 N93-11061
Overview of high performance aircraft propulsion research
[NASA-TM-105839] p 59 N93-11530
On stability and control of SSTO spaceplane in super- and hypersonic ascending phase
[NAL-TR-1128T] p 65 N93-12361
TBD(exp 3)
[NASA-CR-192075] p 335 N93-18054
SUPERSONIC FLOW
An asymptotic model of a closed separation region in supersonic flow
p 4 A93-10139
Numerical modeling of supersonic flows past wings of different aspect ratios over a wide range of angles of attack within the framework of the plane section law
p 5 A93-10141
Regimes of supersonic flow past the windward side of V-shaped wings
p 5 A93-10144
A study of the effect of nonstationary perturbations on flow in the front separation region
p 5 A93-10150
Self-excited oscillations at supersonic off-design jet outflow
p 6 A93-10402
Measurement of attachment-line location in a wind-tunnel and in supersonic flight
[AIAA PAPER 92-4089] p 39 A93-11285

- Nonlinear aeroelasticity and chaos p 79 A93-12165
Three-dimensional boundary-layer transition on a cone at Mach 3.5 p 9 A93-12177
Experimental analysis of turbulence within supersonic mixing layers p 11 A93-12428
Effect of the drag of the front body on the restructuring of flow between two bodies in the path of supersonic flow, with one body located in the wake of the other p 14 A93-12973
A study of the laminar-turbulent transition in a boundary layer and separation on cones at supersonic velocities p 14 A93-12974
An experimental study of dc discharges in supersonic and subsonic air flows p 14 A93-12980
A method for calculating supersonic three-dimensional flows in pyramidal nozzles p 125 A93-15216
Visualization and analysis of supersonic flow in rotating turbine stage. I - Influence of shock wave between stationary and moving blades p 126 A93-15449
Effect of the body shape on head shock attenuation at a large distance from the axis p 127 A93-16708
A new Lagrangian method for steady supersonic flow computation. II - Slip-line resolution. III - Strong shocks p 243 A93-18855
On space correlation of pressure pulsations on the streamlined surface before a step p 244 A93-19135
Streamline curvature in supersonic shear layers p 244 A93-19194
Shock formation in overexpanded tip leakage flow [ASME PAPER 92-GT-1] p 245 A93-19276
Performance analysis of supersonic through-flow fan by the lifting surface theory. I - Disturbance flow field and determination of blade loadings p 267 A93-20929
Workshop report - A validation study of Navier-Stokes codes for transverse injection into a Mach 2 flow p 270 A93-21330
High Mach number dynamic stability of blunt slender cones at angle of attack p 271 A93-21721
Experimental studies of the turbulent structure of supersonic mixing layers p 278 A93-22633 [AIAA PAPER 93-0217]
Passive control of pre-entry shock in supersonic intakes p 279 A93-22691 [AIAA PAPER 93-0291]
Shock-dependent, thrust wings for supersonic flow [AIAA PAPER 93-0321] p 280 A93-23013
Control of pressure fluctuations in the reattachment region of a supersonic free shear layer p 282 A93-23064 [AIAA PAPER 93-0385]
Expanding the waverider design space using general supersonic and hypersonic generating flows p 283 A93-23253 [AIAA PAPER 93-0505]
Three-dimensional supersonic vortex breakdown p 284 A93-23267 [AIAA PAPER 93-0526]
Numerical simulation of three-dimensional supersonic flows using Euler and boundary layer solvers p 284 A93-23272 [AIAA PAPER 93-0531]
Finite element nonlinear panel flutter with arbitrary temperatures in supersonic flow p 417 A93-23555
Compressible turbulence measurements in a high-speed high Reynolds number mixing layer p 465 A93-24773 [AIAA PAPER 93-0660]
Vortical solutions in supersonic corner flows p 466 A93-24845 [AIAA PAPER 93-0760]
Vortex distortion during vortex-surface interaction in a Mach 3 stream p 467 A93-24846 [AIAA PAPER 93-0761]
A numerical study of unsteady supersonic compression ramp flows p 470 A93-24943 [AIAA PAPER 93-0883]
Investigation of three-dimensional separation at wing/body junctions in supersonic flows using TVD McCormack's scheme p 471 A93-24945 [AIAA PAPER 93-0884]
Numerical simulation of supersonic flow around space plane for airframe-engine integration p 471 A93-24946 [AIAA PAPER 93-0886]
Numerical investigation of supersonic flows around a spiked blunt-body p 471 A93-24947 [AIAA PAPER 93-0887]
Computing 3-D steady supersonic flow via a new Lagrangian approach p 471 A93-24951 [AIAA PAPER 93-0891]
Stability of oblique detonations in RAM accelerators p 541 A93-24979 [AIAA PAPER 92-0089]
Visualization and analysis of supersonic flow in rotating turbine stage. II - Analysis of the flow into the moving blades and their exit flow p 476 A93-27442
Shock wave ahead of a liquid jet in supersonic cross flow p 477 A93-27605
Calculation of three-dimensional supersonic flow past lifting surfaces p 477 A93-27607
Wave resistance of swept wings with supersonic edges p 478 A93-27624
A numerical study of mixing in supersonic combustors with hypermixing injectors p 520 A93-27801 [AIAA PAPER 93-0215]
Numerical study on the interaction of supersonic flow past a wedge and free jet p 479 A93-28574
On the favorable interference in the supersonic flow p 679 A93-33713
Nonplanar Doublet-Point method for supersonic unsteady aerodynamics p 682 A93-34120 [AIAA PAPER 93-1588]
Nonlinear aeroelastic response of panels p 741 A93-34130 [AIAA PAPER 93-1599]
A study on two-dimensional and three-dimensional secondary jet interactions with a supersonic flow p 683 A93-34273
A study on three-dimensional shock wave/turbulent boundary layer interaction induced by sweptback sharp fins at supersonic flow p 684 A93-34274
Comparison of several convection discretization schemes for all Mach number arbitrary 2D flows p 685 A93-34345
Computation of supersonic crossflow separation using a new parabolized Navier-Stokes code p 687 A93-34355
Numerical simulation of two-dimensional compressible flows p 687 A93-34357
Unsteady supersonic flow around a blunt body in thermal inhomogeneities in turbulent shock layer flows p 691 A93-35266
A study of flow structure and heat transfer intensity in the vicinity of an expanding step on a plate p 691 A93-35268
A study of the temperature of bodies in the flow-around regime in the case of surface gas injection p 691 A93-35344
Study of supersonic intersection flowfield at modified wing-body junctions p 692 A93-35621
Oblique shock formation in impulsively started wedge flows p 692 A93-35636
An implicit finite-difference algorithm for the numerical simulation of supersonic flow over blunt bodies p 770 A93-38325
Supersonic vortical flows around an ogive-cylinder - Laminar and turbulent computations p 771 A93-38588 [ONERA, TP NO. 1992-111]
Transonic and supersonic flow calculations around aircrafts using a multidomain Euler code p 772 A93-38610 [ONERA, TP NO. 1992-137]
Some special purpose preconditioners for conjugate gradient-like methods applied to CFD p 772 A93-38638
Analysis of turbulence in supersonic flows by means of laser velocimetry p 773 A93-38729 [ONERA, TP NO. 1992-148]
Aerodynamic resistance of three-dimensional bodies with a starlike cross section at supersonic velocities, and problems of its calculation p 774 A93-39116
Supersonic flow of a gas over a semiinfinite plate with small-scale harmonic spanwise oscillations p 775 A93-39118
A numerical investigation of supersonic flow of a viscous gas over long blunt cones, taking into account equilibrium physicochemical transformations p 775 A93-39124
Calculation of the effect of the shock wave of a delta wing on a second wing at supersonic velocities p 776 A93-39141
Lifting line theory for supersonic flow applications p 778 A93-39402
Study of mixing flow field of a jet in a supersonic cross flow. I - Experimental facilities and preliminary experiments p 857 A93-40430
The numerical model of supersonic air flow field with hydrogen transverse injection p 859 A93-41736
Spectral solution of the viscous blunt-body problem p 860 A93-41915
A numerical study of the flutter of conical shells p 927 A93-42405
Numerical experiments with nonoscillatory schemes using Eulerian and new Lagrangian formulations p 862 A93-42432
Solution of three-dimensional supersonic flowfields via adapting unstructured meshes p 863 A93-42442
Computational results for 2-D and 3-D ramp flows with an upwind Navier-Stokes solver p 866 A93-42592
Supersonic turbomachine rotor flutter control by aerodynamic detuning p 899 A93-42884
Microsensors for high heat flux measurements p 928 A93-42920
Three-dimensional calculation of a hydrogen jet injection into a supersonic air flow p 950 A93-44374
An extended Lagrangian method p 951 A93-45003 [AIAA PAPER 93-3305]
An accuracy assessment of Cartesian-mesh approaches for the Euler equations p 953 A93-45029 [AIAA PAPER 93-3335]
Time-accurate simulation of a self-excited oscillatory supersonic external flow with a multi-block solution-adaptive mesh algorithm p 956 A93-45078 [AIAA PAPER 93-3387]
Reynolds number effects on supersonic asymmetrical flows over a cone p 958 A93-45141
Numerical simulation of supersonic flows with chemical reactions p 959 A93-45325
Shock tunnel studies of external combustion in high supersonic air flows p 1017 A93-45517
Numerical investigation of subsonic and supersonic asymmetric vortical flow p 961 A93-45727
Organized structure in a compressible turbulent shear layer p 961 A93-45730
Transition in supersonic flow past axisymmetric bodies p 967 A93-46817
The countercurving mixing layer - Strategies for shear-layer control p 968 A93-46826 [AIAA PAPER 93-3260]
3D/quasi-3D trans- and supersonic flow calculation in advanced centrifugal/axial compressor stages p 972 A93-46936
Heat transfer on blunt cones in nonuniform supersonic flow in the presence of gas injection from the surface p 972 A93-46975
The determination of hybrid analytical-numerical solutions for the three-dimensional compressible boundary layer p 1029 A93-46979
The three-dimensional representation of the pressure distribution on wedged delta wings with supersonic leading edges in supersonic-hypersonic flow p 973 A93-46989
The three-dimensional representation of the lift and pitching moment coefficients on wedged rectangular wings in supersonic flow p 973 A93-46990
Near-field supersonic flow predictions by an adaptive unstructured tetrahedral grid solver p 977 A93-47223 [AIAA PAPER 93-3430]
Flow field measurements in a crossing shockwave turbulent boundary layer interaction at Mach 3 p 977 A93-47226 [AIAA PAPER 93-3434]
Supersonic vortex breakdown over a delta wing in transonic flow p 980 A93-47251 [AIAA PAPER 93-3472]
Laser holographic interferometric measurements of the flow behind a rearward facing step p 985 A93-47279 [AIAA PAPER 93-3515]
Chemical-kinetics characteristics of combustion in a supersonic turbulent flow p 1018 A93-47512
An exploratory wind tunnel study of supersonic tip vortices p 1045 A93-48124 [AIAA PAPER 93-2923]
Supersonic base flow experiments in the near-wake of a cylindrical afterbody p 1045 A93-48125 [AIAA PAPER 93-2924]
A numerical investigation of supersonic strut/endwall interactions in annular flow with varying strut thickness p 1045 A93-48128 [AIAA PAPER 93-2927]
Asymmetric vortical solutions in supersonic corners - Steady 3D space-marching versus time-dependent conical results p 1047 A93-48151 [AIAA PAPER 93-2957]
Behaviour of the Johnson-King turbulence model in axis-symmetric supersonic flows p 1056 A93-48214 [AIAA PAPER 93-3032]
A three-dimensional pressure flux-split RNS application to sub/supersonic flow in inlets and ducts p 1058 A93-48239 [AIAA PAPER 93-3063]
The effect of large scale unsteady motion on turbulent reattaching shear layer - Application to the supersonic compression ramp p 1061 A93-48273 [AIAA PAPER 93-3100]
Experimental and numerical investigation of supersonic turbulent flow in an annular duct p 1063 A93-48291 [AIAA PAPER 93-3123]
Aerodynamic characteristics and static stability margin of conical star-shaped bodies at supersonic velocities p 1067 A93-48848
The use of triangular elements in panel methods for calculating flow past flight vehicles p 1068 A93-48904
Numerical calculation of polars and heat transfer for supersonic three-dimensional flow past wings with allowance for radiation p 1068 A93-48905
Supersonic flow past energy release regions p 1069 A93-48973
Vortical solutions in supersonic corner flows p 1071 A93-49015
CFD validation for scramjet combustor and nozzle flows. I p 1111 A93-49724 [AIAA PAPER 93-1840]
An adaptive grid/Navier-Stokes methodology for the calculation of nozzle afterbody base flows with a supersonic freestream p 1076 A93-49788 [AIAA PAPER 93-1922]

Investigation of a strut/endwall interaction in supersonic annular flow p 1076 A93-49791
 [AIAA PAPER 93-1925] p 1076 A93-49791
 Molecular mixing of jets in supersonic flow p 1078 A93-49858
 [AIAA PAPER 93-2021] p 1078 A93-49858
 Mixing enhancement and combustion of gaseous fuel in a supersonic combustor p 1114 A93-49960
 [AIAA PAPER 93-2143] p 1114 A93-49960
 Numerical and experimental investigation of turbine tip gap flow p 1081 A93-50051
 [AIAA PAPER 93-2253] p 1081 A93-50051
 A numerical analysis of supersonic flow over an axisymmetric afterbody p 1083 A93-50121
 [AIAA PAPER 93-2347] p 1083 A93-50121
 Experimental investigation of slot injection into supersonic flow with an adverse pressure gradient p 1119 A93-50194
 [AIAA PAPER 93-2442] p 1119 A93-50194
 Direct measurements of skin friction in a scramjet combustor p 1119 A93-50195
 [AIAA PAPER 93-2443] p 1119 A93-50195
 Experimental and numerical study of swept ramp injection into a supersonic flowfield p 1119 A93-50197
 [AIAA PAPER 93-2445] p 1119 A93-50197
 Substitution of oriented differences for central differences in a program for calculating smooth supersonic flows p 1085 A93-50966
 [AIAA PAPER 93-2445] p 1085 A93-50966
 Supersonic flow past a rectangular wing of finite thickness p 1086 A93-50972
 New derivation of relationship between Mach angle and Mach number p 1086 A93-51190
 Spectra of pressure pulsations on the surface of a cone in the transition region at supersonic flow velocities p 1088 A93-51755
 [AIAA PAPER 93-2445] p 1088 A93-51755
 Supersonic flow past a cone with heat transfer near its tip p 1089 A93-51780
 [AIAA PAPER 93-2445] p 1089 A93-51780
 Experimental studies of supersonic flow past wedges with longitudinal slots on the windward side p 1089 A93-51786
 [AIAA PAPER 93-2445] p 1089 A93-51786
 Steady state supersonic flows of a vibrationally excited gas past thin bodies p 1089 A93-51818
 Calculation of supersonic flow past a body of revolution with a piecewise linear distribution of singularities at its axis p 1092 A93-51910
 [AIAA PAPER 93-2445] p 1092 A93-51910
 Euler analysis of forebody-strake vortex flows at supersonic speeds p 1094 A93-52429
 [AIAA PAPER 93-2445] p 1094 A93-52429
 Flutter analysis of stiffened laminated composite plates and shells in supersonic flow p 1216 A93-53224
 Tandem transverse hydrogen gas injection into a supersonic airflow p 1201 A93-54045
 [ISABE 93-7069] p 1201 A93-54045
 Direct simulation of reacting fuel gas flows in a supersonic mixing layer p 1201 A93-54048
 [ISABE 93-7072] p 1201 A93-54048
 A study of the stability of vortical structures in supersonic inlets p 1187 A93-54079
 [ISABE 93-7103] p 1187 A93-54079
 Boundary conditions for unsteady supersonic inlet analyses p 1187 A93-54080
 [ISABE 93-7104] p 1187 A93-54080
 Two-dimensional and three-dimensional mixing flow structures with injected through slotted nozzle and circular nozzle into supersonic flows p 1221 A93-54092
 [ISABE 93-7117] p 1221 A93-54092
 Numerical and experimental study on two- and three-dimensional supersonic flow field with hydrogen injection p 1188 A93-54093
 [ISABE 93-7118] p 1188 A93-54093
 Characteristics of heat exchanger in supersonic/subsonic flows p 1221 A93-54094
 [ISABE 93-7119] p 1221 A93-54094
 Design of shockless supersonic region in the axisymmetric transonic flow p 1230 A93-54587
 Steady-state supersonic flow of a vibrationally excited gas past a slender body of revolution at a small angle of attack p 1233 A93-55014
 Instability of a supersonic vortex sheet inside a circular duct p 1234 A93-55142
 Control of supersonic throughflow turbomachines discrete frequency noise generation by aerodynamic detuning p 1248 A93-55860
 Algebraic determination of the shock wave shape in axisymmetric flow over a circular cylinder p 1237 A93-56030
 [AIAA PAPER 93-2445] p 1237 A93-56030
 Supersonic and hypersonic flow computations for the research configuration ELAC I and comparison to experimental data p 1237 A93-56034
 Quantitative Knudsen-number dependences of density disturbances in front of obstructions in supersonic divergent flows p 1239 A93-56220
 LV software for supersonic flow analysis p 16 A93-10069
 [NASA-CR-190911] p 16 A93-10069
 A finite element method for nonlinear panel flutter p 84 A93-10472
 Overview of supersonic laminar flow control research on the F-16XL ships 1 and 2 p 20 A93-11221
 [NASA-TM-104257] p 20 A93-11221

Boundary layer relaminarization device [NASA-CASE-LAR-14470-1] p 23 A93-11876
 Air ejector experiments using the two-dimensional supersonic cascade tunnel: Relationship between ejector performance and throat area ratio, part 1 [NAL-TM-642-PT-1] p 25 A93-12352
 Effect of the flow non-uniformity on the mixing layer at the interface of parallel supersonic flows p 128 A93-12716
 [ISAS-RN-646] p 128 A93-12716
 Numerical simulation of the acoustic instability in the spatially developing, confined, supersonic mixing layer p 132 A93-13521
 Planar measurement of flow field parameters in nonreacting supersonic flows with laser-induced iodine fluorescence p 133 A93-13801
 A plume-induced boundary layer separation experiment [AD-A255397] p 220 A93-14677
 Passive control of supersonic asymmetric vortical flows around cones p 220 A93-14692
 Direct numerical simulation of combustion in turbulent supersonic flow p 393 A93-17746
 [DS-2138] p 393 A93-17746
 A numerical study of mixing in supersonic combustors with hypermixing injectors p 294 A93-17884
 [NASA-CR-191027] p 294 A93-17884
 Proceedings of the Ninth NAL Symposium on Aircraft Computational Aerodynamics p 299 A93-19273
 [NAL-SP-16] p 299 A93-19273
 Development of a boundary element method program for numerical analysis of supersonic unsteady flow p 300 A93-19283
 Generation of longitudinal vortices in supersonic flow p 301 A93-19292
 Numerical simulation of flow for a scramjet nozzle p 302 A93-19299
 Numerical simulations of supersonic flow by a fourth-order compact MUSCL TVD scheme p 302 A93-19308
 Analytical and numerical study on steady Mach reflection p 302 A93-19309
 Numerical study on transverse hydrogen injection into a supersonic flowfield p 302 A93-19311
 Aerodynamic heating analysis for axisymmetric bodies in supersonic flow p 303 A93-19312
 Three dimensional calculation of flow inside supersonic inlet p 303 A93-19313
 Numerical simulation of flows in a supersonic air intake p 303 A93-19314
 A numerical investigation for supersonic inlet p 303 A93-19315
 A numerical investigation of 3D transverse injection into the supersonic flow behind rearward facing step p 303 A93-19316
 Shock-dependent, optimum thrust wings in supersonic flow p 483 A93-20169
 A k-omega-multivariate beta PDF for supersonic combustion [NASA-CR-191930] p 537 A93-21749
 Surface and flow field measurements in a symmetric crossing shock wave/turbulent boundary-layer interaction p 693 A93-24911
 [NASA-TM-106086] p 693 A93-24911
 A contribution to the great Riemann solver debate [NASA-CR-191409] p 694 A93-25083
 An investigation of laser velocimetry measurements within high speed, complex flows p 748 A93-25237
 Supersonic shock wave/vortex interaction [NASA-CR-192917] p 695 A93-25249
 Experimental and computational investigation of helium injection into air at supersonic and hypersonic speeds p 696 A93-25487
 Studies in air/air supersonic mixing layers p 700 A93-26007
 Workshop Report: A validation study of Navier-Stokes codes for transverse injection into a Mach 2 flow p 751 A93-26008
 A hybrid multigrid technique for computing steady-state solutions to supersonic flows p 700 A93-26078
 Sensitivity calculations for a 2D, inviscid, supersonic forebody problem [NASA-CR-191444] p 779 A93-27004
 Navier-Stokes simulation of viscous, separated, supersonic flow over a projectile rotating band [AD-A263073] p 789 A93-27955
 Hypersonic engine component experiments in high heat flux, supersonic flow environment [NASA-TM-106273] p 1032 A93-31860
SUPERSONIC FLUTTER
 Geometrically nonlinear local flutter analysis of supersonic airplane skin plates in the potential supersonic flow [ISBN 83-01-10939-4] p 394 A93-17569
 Finite element nonlinear panel flutter with arbitrary temperatures in supersonic flow p 417 A93-23555

Supersonic flutter analysis of composite plates and shells p 837 A93-39419
 Supersonic panel flutter analysis of shallow shells p 927 A93-41935
 A numerical study of the flutter of conical shells p 927 A93-42405
 Analysis of unstarted supersonic flutter in cascade by semiactuator disk theory p 1181 A93-53841
 The unsteady flow past a supersonic splitter plate [ISABE 93-7047] p 1185 A93-54023
SUPERSONIC HEAT TRANSFER
 Heat transfer measurements in swept shock wave/turbulent boundary-layer interactions p 750 A93-25705
SUPERSONIC INLETS
 Evaluation and application of the Baldwin-Lomax turbulence model in two-dimensional, unsteady, compressible boundary layers with and without separation in engine inlets p 111 A93-14118
 [AIAA PAPER 92-3676] p 111 A93-14118
 Experimental investigation of an axisymmetric hypersonic scramjet inlet for laser propulsion p 122 A93-14515
 Accuracy issues in the prediction of supersonic inlet flows p 258 A93-19549
 [ASME PAPER 92-GT-400] p 258 A93-19549
 Evaluation and application of the Baldwin-Lomax turbulence model in two-dimensional, unsteady, compressible boundary layers with and without separation in engine inlets p 414 A93-22509
 [AIAA PAPER 92-3676] p 414 A93-22509
 Experimental and numerical investigation of Mach 2.5 supersonic mixed compression inlet p 279 A93-22689
 [AIAA PAPER 93-0289] p 279 A93-22689
 Flow stability issues in supersonic inlet flow analyses [AIAA PAPER 93-0290] p 279 A93-22690
 Passive control of pre-entry shock in supersonic intakes p 279 A93-22691
 [AIAA PAPER 93-0291] p 279 A93-22691
 Aerodynamic performance of scramjet inlet models with a single strut p 466 A93-24831
 [AIAA PAPER 93-0741] p 466 A93-24831
 Modeling of linear isentropic flow systems p 828 A93-37046
 Supersonic through flow compressors - A preliminary study: COVAXS p 1001 A93-46930
 An experimental study of the effects of bodyside compression on forward swept sidewall compression inlets ingesting a turbulent boundary layer p 1072 A93-49515
 [AIAA PAPER 93-3125] p 1072 A93-49515
 CFD analysis and testing on a twin inlet ramjet [AIAA PAPER 93-1839] p 1075 A93-49723
 Numerical simulations of the unstart phenomenon in a supersonic inlet/diffuser p 1081 A93-50041
 [AIAA PAPER 93-2239] p 1081 A93-50041
 An experimental study of supersonic air-intake with 5-shock system at Mach 3 p 1082 A93-50089
 [AIAA PAPER 93-2305] p 1082 A93-50089
 A study of the stability of vortical structures in supersonic inlets p 1187 A93-54079
 [ISABE 93-7103] p 1187 A93-54079
 Boundary conditions for unsteady supersonic inlet analyses p 1187 A93-54080
 [ISABE 93-7104] p 1187 A93-54080
 A study on Mach 3 two-dimensional mixed compression air-intakes p 1188 A93-54082
 [ISABE 93-7106] p 1188 A93-54082
 Numerical simulation of a two-dimensional supersonic mixed-compression inlet p 1188 A93-54083
 [ISABE 93-7107] p 1188 A93-54083
 Off-design performance of scramjet nozzles [ISABE 93-7108] p 1203 A93-54084
 Evaluation and application of the Baldwin-Lomax turbulence model in two-dimensional, unsteady, compressible boundary layers with and without separation in engine inlets p 82 A93-10087
 [NASA-TM-105810] p 82 A93-10087
 Three dimensional calculation of flow inside supersonic inlet p 303 A93-19313
 A numerical investigation for supersonic inlet p 303 A93-19315
SUPERSONIC JET FLOW
 Breakdown of steady state axisymmetric flow in a shock layer formed as a result of the impingement of a supersonic underexpanded jet on a perpendicular plane obstacle p 241 A93-18230
 The noise from supersonic elliptic jets p 445 A93-19156
 The effects of temperature on supersonic jet noise emission p 446 A93-19159
 Acoustic properties of supersonic helium/air jets at low Reynolds numbers p 446 A93-19160
 The critical role of turbulence modeling in the prediction of supersonic jet structure for acoustic applications p 398 A93-19193

Effect of nozzle design on near acoustic field of supersonic circular and rectangular jets p 448 A93-19203

Combined noise and flow control of supersonic jets using swirl p 398 A93-19204

Penetration and mixing of bubbling liquid jets from multiple injectors normal to a supersonic air stream [AIAA PAPER 92-5060] p 413 A93-22330

A Laser Doppler Anemometry study of a supersonic jet in a low speed cross-flow p 459 A93-23807

Experiments on rarefied supersonic free jets using impact probes p 461 A93-24091

Measured acoustic characteristics of ducted supersonic jets at different model scales p 563 A93-24821 [AIAA PAPER 93-0731]

Computation of supersonic jet noise under imperfectly expanded conditions p 563 A93-24825 [AIAA PAPER 93-0735]

Induced Mach wave-flame interactions in laminar supersonic fuel jets p 475 A93-26183

The interaction between a steady jet flow and a supersonic blade tip p 688 A93-34415

A one-dimensional theory for supersonic gas jets above the critical pressure p 774 A93-39115

Flip-flop jet nozzle extended to supersonic flows p 778 A93-39409

Supersonic jet control via point disturbances inside the nozzle p 861 A93-41930

Mach disk of dual coaxial axisymmetric jets p 861 A93-41932

Visual observations of supersonic transverse jets p 965 A93-46750

Passive control of coherent vortices in compressible mixing layers p 968 A93-46828 [AIAA PAPER 93-3262]

CFD study of the flowfield due to a supersonic jet exiting into a hypersonic stream from a conical surface. II [AIAA PAPER 93-2926] p 1045 A93-48127

A study on aerodynamic sound generated by interaction of jet and plate p 1171 A93-48288 [AIAA PAPER 93-3118]

Effect of the size of a plane obstacle on self-oscillations generated in an underexpanded supersonic jet p 1068 A93-48849

An experimental study of a compound supersonic jet p 1069 A93-48914

Development of resonance perturbations in a supersonic jet p 1088 A93-51772

Calculation of a plane supersonic jet simulating the exhaust jet of a hypersonic flight vehicle engine p 1103 A93-51912

An experimental study of the dynamic effect of a supersonic underexpanded jet on a plane surface parallel to the nozzle axis p 1092 A93-51913

Numerical simulation and physical aspects of supersonic vortex breakdown p 1093 A93-52011

Streamwise vorticity generation and mixing enhancement in free jets by 'delta-tabs' [AIAA PAPER 93-3253] p 1180 A93-53592

Numerical study of supersonic flow over a backward step with transverse injection p 1182 A93-53853

Noise reduction of supersonic heated jet with jet mixing enhancement by tabs p 1198 A93-54022 [ISABE 93-7046]

Enhancement of mixing in high-speed heated jets using a counterflowing nozzle p 1235 A93-55359

Nozzle installation effects on the noise from supersonic exhaust plumes p 100 N93-10681

The prediction of noise radiation from supersonic elliptic jets p 100 N93-10684

Combustion in supersonic flows p 199 N93-14627

Computation of supersonic jet noise under imperfectly expanded conditions p 233 N93-15430 [NASA-TM-105961]

Streamwise vorticity generation and mixing enhancement in free jets by delta-tabs [NASA-TM-106235] p 988 N93-31648

Enhanced mixing of a rectangular supersonic jet by natural and induced screech p 989 N93-31672 [NASA-TM-106245]

Calculations on unsteady type 4 interaction at Mach 8 [AD-A265214] p 990 N93-32004

Control of jet noise p 1040 N93-32221 [NASA-CR-193552]

SUPERSONIC NOZZLES

Variational problem of the profiling of the side walls of the supersonic section of a narrow three-dimensional nozzle p 4 A93-10140

Evaluation of 2D scramjet nozzle performance p 52 A93-11209

Study on unsymmetrical supersonic nozzle flows p 127 A93-16933

Starting and test rhombus characteristics of two-dimensional supersonic free-jet nozzle/generic supersonic aircraft inlet configurations [AIAA PAPER 92-5091] p 273 A93-22361

Validation studies of scramjet nozzle performance p 1109 A93-49616

CFD applications in an aeropropulsion test environment p 1112 A93-49790 [AIAA PAPER 93-1924]

3D PARC Navier-Stokes analysis of an HSCST suppressor nozzle secondary inlet lip and duct [AIAA PAPER 93-2568] p 1084 A93-50286

Aeroelastic stability of supersonic nozzles with separated flow p 1142 A93-50300 [AIAA PAPER 93-2588]

Investigation of supersonic shaped nozzles in a low-pressure wind tunnel p 1091 A93-51881

Influence of chemical kinetics effects in nozzles shape design [ISABE 93-7112] p 1188 A93-54087

Design of a nozzle for a hypersonic wind tunnel [AERO-REPT-9113] p 381 N93-16468

Nozzle/cowl optimization for a hypersonic vehicle on a typical trajectory [AD-A258827] p 341 N93-19089

SUPERSONIC SPEED

Effects of turbine cooling assumptions on performance and sizing of high-speed civil transport p 55 A93-13383 [AIAA PAPER 92-4217]

Numerical study of jet interaction at super- and hypersonic speeds for flight vehicle control p 184 A93-14379

Civil aircraft challenges in engine/airframe integration [ASME PAPER 92-GT-45] p 322 A93-19299

A unified hypersonic/supersonic method for aeroelastic applications including shock-unsteady wave interaction [AIAA PAPER 93-1317] p 738 A93-33892

Supersonic aeroelastic instability results for a NASP-like wing model p 682 A93-33935 [AIAA PAPER 93-1369]

Methods and results of theoretical investigations for high-speed parachute systems p 690 A93-35173 [AIAA PAPER 93-1227]

Supersonic laminar flow control p 860 A93-41782

Flutter analysis of composite panels on many supports p 1022 A93-45119

Computational study of a conical wing having unit aspect ratio at supersonic speeds p 984 A93-47272 [AIAA PAPER 93-3505]

The numerical calculation on the flowfields of transverse jet interaction in the base of vehicle at supersonic speeds p 1077 A93-49795 [AIAA PAPER 93-1931]

Pressure measurements at supersonic speeds on the research configuration ELAC I p 1237 A93-56033

Control of panel flutter at high supersonic speed p 47 N93-10900

Comparative performance tests of a pitot-inlet in several European wind-tunnels at subsonic and supersonic speeds p 130 N93-13221

Performance and control of ascending trajectories to minimize heat load for transatmospheric aero-space planes p 133 N93-13745

Contribution of ventral fins to sideforce and yawing moment derivatives due to sideslip at low angle of attack [ESDU-92029] p 291 N93-16638

High speed civil transport [NASA-CR-192041] p 337 N93-18161

Flight and wind-tunnel calibrations of a flush airdata sensor at high angles of attack and sideslip and at supersonic Mach numbers p 344 N93-19110 [NASA-TM-104265]

Visualization of a Mach 2 reacting flow using Planar Laser-Induced Fluorescence (PLIF) p 731 N93-26006

Experimental effects of wing location on wing-body pressures at supersonic speeds p 700 N93-26085 [NASA-TM-4434]

Supersonic aeroelastic instability results for a NASP-like wing model p 718 N93-26553 [NASA-TM-107739]

Optically smart surfaces survivability testing at Mach 3 [AD-A261785] p 760 N93-26566

Calculation of fully three-dimensional separated flow with an unsteady viscous-inviscid interaction method p 786 N93-27455

Topology and grid adaption for high-speed flow computations p 934 N93-30375 [NASA-CR-4216]

SUPERSONIC TRANSPORTS

Oblique wing supersonic transport concepts [AIAA PAPER 92-4230] p 43 A93-13337

The conceptual study of supersonic transport structure [AIAA PAPER 92-4219] p 43 A93-13348

HSCST high-lift aerodynamic technology requirements [AIAA PAPER 92-4228] p 44 A93-13355

Aerodynamic characteristics of a next generation high-speed civil transport [AIAA PAPER 92-4229] p 15 A93-13356

Prospects for a second generation supersonic transport p 108 A93-14154

Introduction to regulatory problems for supersonic transports p 234 A93-15032

The opportunities and risks of the supersonic transport market - The Lufthansa point of view p 234 A93-15033

Study of a Mach 2 supersonic transport aircraft p 124 A93-15034

Propulsion of a supersonic transport: What are the challenges? II - Achievements p 174 A93-16852

Assessment and design of low boom configurations for supersonic transport aircraft p 446 A93-19163

Flowfield measurements for a supersonic mixer ejector in forward flight p 399 A93-19217

Overview of the Japanese National Project for Super/Hyper-Sonic Transport propulsion system [ASME PAPER 92-GT-252] p 239 A93-19461

Ramjet NOx emission - Use of a 3D CFD method for the combustor design of a super/hyper-sonic transport propulsion system [ASME PAPER 92-GT-255] p 353 A93-19464

Some topics of research on hypersonic airbreathing engines at National Aerospace Laboratory [ASME PAPER 92-GT-256] p 353 A93-19465

Aerodynamic optimization of an HSCST configuration using variable-complexity modeling [AIAA PAPER 93-0101] p 322 A93-19806

Variable-complexity aerodynamic-structural design of a high-speed civil transport wing [AIAA PAPER 92-4695] p 323 A93-20279

Multidisciplinary design integration system for a supersonic transport aircraft [AIAA PAPER 92-4841] p 324 A93-20296

Preliminary wing design of a high speed civil transport aircraft by multilevel decomposition techniques [AIAA PAPER 92-4721] p 325 A93-20323

Geometric requirements for multidisciplinary analysis of aerospace-vehicle design [AIAA PAPER 92-4773] p 436 A93-20366

The rebirth of supersonic transport p 457 A93-25325

Future supersonic transport studies at Aerospace p 505 A93-25491

Lessons from application of equivalent plate structural modeling to an HSCST wing [AIAA PAPER 93-1413] p 739 A93-33969

Acoustics due to flow-structural interaction and its transmission through a double-panel in high-speed cruising flight [AIAA PAPER 93-1431] p 710 A93-33981

Aeroelastic challenges for a High Speed Civil Transport [AIAA PAPER 93-1478] p 712 A93-34240

A French look at the future supersonic transport [ONERA, TP NO. 1992-209] p 803 A93-38763

Toward the second-generation supersonic transport [ONERA, TP NO. 1993-26] p 890 A93-41038

It's time to go supersonic p 949 A93-44099

Application of natural laminar flow to a supersonic transport concept [AIAA PAPER 93-3467] p 997 A93-47248

Application of a parabolized Navier-Stokes code to an HSCST configuration and comparison to wind tunnel test data [AIAA PAPER 93-3537] p 986 A93-47288

A detailed study of mean-flow solutions for stability analysis of transitional flows [AIAA PAPER 93-3052] p 1057 A93-48232

Screening studies of advanced control concepts for airbreathing engines [AIAA PAPER 92-3320] p 1108 A93-49329

Matching engine and aircraft lapse rates for the HSCST [AIAA PAPER 93-1809] p 1100 A93-49698

Advanced SST auxiliary air intakes design and analysis [AIAA PAPER 93-2304] p 1082 A93-50088

3D PARC Navier-Stokes analysis of an HSCST suppressor nozzle secondary inlet lip and duct [AIAA PAPER 93-2568] p 1084 A93-50286

Euler/experiment correlations of sonic boom pressure signatures p 1095 A93-52439

Research and development of a turbo-accelerator for super/hypersonic transport [ISABE 93-7066] p 1200 A93-54042

Material requirements for the High Speed Civil Transport [ISABE 93-7067] p 1200 A93-54043

Research and development of high pressure compressor for SST and HST engine [ISABE 93-7068] p 1186 A93-54044

Studies on methane-fuel ram combustor for HST combined cycle engine [ISABE 93-7080] p 1201 A93-54056

- A study on Mach 3 two-dimensional mixed compression air-intakes
[ISABE 93-7106] p 1188 A93-54082
- Sonic boom minimization - Myth or reality?
p 1264 A93-55859
- Overview of supersonic laminar flow control research on the F-16XL ships 1 and 2
[NASA-TM-104257] p 20 N93-11221
- Stratospheric aircraft: Impact on the stratosphere?
[DE92-016997] p 94 N93-12104
- Stratospheric aircraft exhaust plume and wake chemistry studies
[NASA-CR-189688] p 94 N93-12299
- Current Technology for Thermal Protection Systems
[NASA-CP-3157] p 69 N93-12447
- Technology benefits and ground test facilities for high-speed civil transport development
[NASA-TM-107670] p 378 N93-15790
- The NASA High-Speed Research Program
p 330 N93-16761
- The 1990 high-speed civil transport studies
[NASA-CR-189618] p 330 N93-16947
- The 1990 high-speed civil transport studies. Summary report
[NASA-CR-189619] p 330 N93-16999
- MM-122: High speed civil transport
[NASA-CR-192011] p 334 N93-17974
- Phoenix: Preliminary design of a high speed civil transport
[NASA-CR-192024] p 334 N93-17976
- Tesseract: Supersonic business transport
[NASA-CR-192072] p 334 N93-17977
- Proposal and preliminary design for a high speed civil transport aircraft. Swift: A high speed civil transport for the year 2000
[NASA-CR-192023] p 335 N93-18049
- TBD(Exp 3)
[NASA-CR-192075] p 335 N93-18054
- The Edge supersonic transport
[NASA-CR-192074] p 335 N93-18055
- A second-generation high speed civil transport: Stingray
[NASA-CR-192022] p 336 N93-18059
- The Trojan --- supersonic transport
[NASA-CR-192013] p 336 N93-18060
- Preliminary design of a high speed civil transport: The Opus 0-001
[NASA-CR-192018] p 336 N93-18061
- High speed civil transport
[NASA-CR-192041] p 337 N93-18161
- RTJ-303: Variable geometry, oblique wing supersonic aircraft
[NASA-CR-192054] p 337 N93-18166
- Aerodynamic design and synthesis of the oblique flying wing supersonic transport
p 713 N93-24768
- Screening studies of advanced control concepts for airbreathing engines
[NASA-TM-106042] p 721 N93-25079
- Bibliography on propulsion airframe integration technologies for high-speed civil transport applications, 1980-1991
[NASA-TM-105602] p 678 N93-26136
- The HST mission analysis of waverider designs
[NASA-CR-193467] p 879 N93-31037
- NASA-UVa light aerospace alloy and structure technology program supplement: Aluminum-based materials for high speed aircraft
[NASA-CR-4517] p 1019 N93-31643
- SUPERSONIC TURBINES**
- A statistical approach to the experimental evaluation of transonic turbine airfoils in a linear cascade
[ASME PAPER 92-GT-5] p 245 A93-19278
- Secondary flows in a transonic cascade - Validation of a 3-D Navier-Stokes code
[ASME PAPER 92-GT-62] p 247 A93-19312
- An analysis system for blade forced response
[ASME PAPER 92-GT-172] p 352 A93-19398
- An investigation of turbulence modelling in transonic fans including a novel implementation of an implicit k-epsilon turbulence model
[ASME PAPER 92-GT-308] p 256 A93-19498
- Three-dimensional Navier-Stokes computations of transonic fan flow using an explicit flow solver and an implicit k-epsilon solver
[ASME PAPER 92-GT-309] p 256 A93-19499
- Experimental study of mixed compression air-intake for hypersonic airbreathing engines
[ASME PAPER 92-GT-349] p 355 A93-19519
- Heat transfer and aerodynamics of a high rim speed turbine nozzle guide vane with profiled end walls
[AD-A258346] p 295 N93-17991
- The influence of non-uniform spanwise inlet temperature on turbine rotor heat transfer
p 901 N93-29932

- SUPERSONIC WAKES**
- Implicit Euler calculation of supersonic vortex wake/engine plume interaction
[AIAA PAPER 93-0656] p 540 A93-24769
- SUPERSONIC WIND TUNNELS**
- Dual transverse injection of H2 gas into Mach 1.8 flows at University Komaba wind tunnel
p 376 A93-21833
- Supersonic dynamic stability characteristics of the test technique demonstrator NASP configuration
[AIAA PAPER 92-5009] p 367 A93-22285
- Comparison of predictions with measurements for a quiet supersonic tunnel
[AIAA PAPER 93-0344] p 376 A93-23031
- Flow quality improvement in a high speed blowdown wind tunnel
[AIAA PAPER 93-0353] p 377 A93-23038
- Development of the NASA-Ames low disturbance supersonic wind tunnel for transition research up to Mach 2.5
[AIAA PAPER 92-3909] p 462 A93-24488
- Development of Polytechnic University's supersonic wind tunnel facility
[AIAA PAPER 93-0798] p 528 A93-24876
- Three-dimensional flow past an ogival-cylindrical body in combination with a delta wing
p 478 A93-27636
- Testing techniques for straight transonic and supersonic cascades
[ONERA, TP NO. 1992-155] p 773 A93-38734
- Free-spin damping measurement techniques
[AIAA PAPER 93-3457] p 1014 A93-47240
- Effects of junction modifications on sharp-fin-induced shock wave/boundary layer interaction
[AIAA PAPER 93-2935] p 1046 A93-48133
- An experimental study of supersonic air-intake with 5-shock system at Mach 3
[AIAA PAPER 93-2305] p 1082 A93-50089
- Air ejector experiments using the two-dimensional supersonic cascade tunnel: Relationship between ejector performance and throat area ratio, part 1
[NAL-TM-642-PT-1] p 25 N93-12352
- A plume-induced boundary layer separation experiment
[AD-A255397] p 220 N93-14677
- User manual for NASA Lewis 10 by 10 foot supersonic wind tunnel
[NASA-TM-105626] p 194 N93-15498
- Wind tunnel wall interference correction at subsonic speeds
p 304 N93-19320
- NASA Lewis 8- by 6-foot supersonic wind tunnel user manual
[NASA-TM-105771] p 730 N93-25080
- SUPERSONICS**
- Effect of planform and body on supersonic aerodynamics of multibody configurations
[NASA-TP-3212] p 19 N93-10824
- New acceleration potential method for supersonic unsteady aerodynamics of lifting surfaces, further extension of the nonplanar supersonic doublet point method, and nonlinear, nongradient optimized rational function approximations for supersonic, transient response unsteady aerodynamics
p 25 N93-12344
- SUPPORT SYSTEMS**
- A transfer matrix method for calculation of support stiffness of aeroengine stator
p 1122 A93-51193
- SUPPORTS**
- Effects on load distribution in a helicopter rotor support structure associated with various boundary configurations
p 796 A93-35951
- Flutter analysis of composite panels on many supports
p 1022 A93-45119
- SUPPRESSORS**
- Design verification of ground run-up noise suppressors for afterburning engines
p 910 A93-42892
- SURFACE CRACKS**
- Load-bearing capacity of an aircraft wing based on the condition of compressed surface fracture
p 801 A93-36794
- SURFACE DISTORTION**
- Supersonic flow of a gas over a semiinfinite plate with small-scale harmonic spanwise oscillations
p 775 A93-39118
- SURFACE EMITTING LASERS**
- Surface emitting lasers for avionics applications
p 1259 A93-55756
- SURFACE FINISHING**
- Effect of the proximity of the machined surface on the discharge coefficients of laser cutter nozzles
p 79 A93-12809
- Sensor-adaptive control for aircraft paint stripping
[SME PAPER AD92-200] p 855 A93-40663
- Evaluation of water-borne adhesive bonding primers for use on the advanced aircraft material aluminum-lithium
p 1211 A93-53420
- Surface protection in the aircraft industry
[MBB-Z-0432-92-PUB] p 72 N93-11027
- Ultrasonic polishing
p 750 N93-25580

- SURFACE GEOMETRY**
- A method for determining the aerodynamic coefficients of asymmetric bodies with allowance for nonlinear influence factors of the body shape
p 5 A93-10142
- A mathematical model of the vibrational impact hardening of parts
p 837 A93-39185
- Development of a transonic Euler method for complete aircraft configurations
p 779 A93-39721
- Experimental study of the effect of external turbulence and the shape of the surface on the characteristics of laminar and transition boundary layers
p 987 A93-47522
- Calculation of the aerodynamic characteristics of bodies with meshlike surfaces in hypersonic rarefied-gas flow
p 1090 A93-51870
- On machine capacitance dimensional and surface profile measurement system
p 750 N93-25579
- Computational gearing mechanics
[NASA-CR-191127] p 751 N93-25884
- SURFACE LAYERS**
- The composite shape and structure of coherent eddies in the convective boundary layer
p 93 A93-12643
- Automated measurement of residual stresses in the surface layer of parts
p 834 A93-39081
- Effect of the technological process structure on residual stress distribution in the blade foil of gas turbine engines
p 836 A93-39106
- SURFACE NAVIGATION**
- Real time DGPS service for precise positioning - Activities in the Federal Republic of Germany
p 1 A93-11027
- Errors in long distance kinematic GPS
p 314 A93-21154
- Differential GPS control of Starcar 2
p 317 A93-21201
- Using fuzzy behaviors for the outdoor navigation of a car with low-resolution sensors
[DE93-002428] p 706 N93-25120
- SURFACE PROPERTIES**
- Data analysis techniques for pressure- and temperature-sensitive paint
[AIAA PAPER 93-0176] p 414 A93-22605
- Quality of the surface layer and operating properties of aircraft engine components
p 834 A93-39061
- Characteristics of friction and wear in flight vehicle engine components
p 811 A93-39075
- Transonic shockwave/turbulent boundary layer interactions on a porous surface
p 873 A93-43686
- In situ material characterization for pavement evaluation by the Spectral-Analysis-of-Surface-Waves (SASW) method
[AD-A255660] p 194 N93-14128
- Microburst characteristics determined from 1988-1991 TDWR tested measurements
p 490 N93-19605
- SURFACE REACTIONS**
- Reacting gas and surface coupling in high temperature air flows
p 686 A93-34353
- NO(x) scavenging on carbonaceous aerosol surfaces in aircraft exhaust plumes. I
[AIAA PAPER 93-2343] p 1164 A93-50117
- SURFACE ROUGHNESS**
- Performance degradation due to hoar frost on lifting surfaces
p 305 A93-17798
- Erosion resistant titanium nitride coating for turbine compressor applications
[ASME PAPER 92-GT-417] p 388 A93-19565
- Close-up analysis of aircraft ice accretion
[AIAA PAPER 93-0029] p 309 A93-23239
- Surface roughness due to residual ice in the use of low power deicing systems
[AIAA PAPER 93-0031] p 282 A93-23240
- Flow past three-dimensional irregularities in a hypersonic boundary layer on a cooled body
p 775 A93-39119
- Modeling supersonic inlet boundary-layer bleed roughness
p 872 A93-42891
- Aircraft monitoring of the planeness of the existing and new runways
p 991 A93-45668
- Using spectral analysis for estimating the effect of runway irregularities on the loading of transport aircraft structures
p 996 A93-45669
- A lag model for turbulent boundary layers developing over rough bleed surfaces
[AIAA PAPER 93-2988] p 1052 A93-48181
- Local heat transfer distribution in a rotating serpentine rib-roughened flow passage
p 1259 A93-55459
- Flow over a leading edge with distributed roughness
p 18 N93-10549
- Surface roughness due to residual ice in the use of low power deicing systems
[NASA-TM-105971] p 139 N93-15338
- Close-up analysis of aircraft ice accretion
[NASA-TM-105952] p 148 N93-15360
- Uniform roughness studies
[WL-TR-92-3041] p 751 N93-25951

- Roughness-induced generation of crossflow vortices in three-dimensional boundary layers
[NASA-CR-4505] p 780 N93-27096
- Aerodynamics of a finite wing with simulated ice
p 784 N93-27437

SURFACE ROUGHNESS EFFECTS

- The effects of crushing surface roughness on the crushing characteristics of composite tubes
p 77 A93-10918
- Drag and drag partition on rough surfaces
p 79 A93-12460
- Investigation of rotor blade roughness effects on turbine performance
[ASME PAPER 92-GT-297] p 354 A93-19487
- Spatial simulation of boundary layer instability - Effects of surface roughness
[AIAA PAPER 93-0075] p 262 A93-20187
- Effect of micron-sized roughness on transition in swept-wing flows
[AIAA PAPER 93-0076] p 262 A93-20188
- Taking into account surface roughness in computing hypersonic re-entry body
p 686 A93-34354
- Characteristics of the detection of overloads in the center of mass of IL-76 and An-12 aircraft due to runway irregularities by a standard on-board recorder
p 1008 A93-45666

SURFACE TEMPERATURE

- Approximate methods for heat flows toward the surface of three-dimensional bodies
p 4 A93-10080
- Hot streaks and phantom cooling in a turbine rotor passage. I - Separate effects
[ASME PAPER 92-GT-75] p 401 A93-19325
- Hot streaks and phantom cooling in a turbine rotor passage. II - Combined effects and analytical modelling
[ASME PAPER 92-GT-76] p 401 A93-19326
- Near wake structure for a generic ASTV configuration
[AIAA PAPER 93-0271] p 268 A93-21103
- A study of the temperature of bodies in the flow-around regime in the case of surface gas injection
p 691 A93-35344
- Investigation of the radiance from the leading edge of a wing
[AIAA PAPER 93-2728] p 1039 A93-46482
- A preliminary investigation of the Helmholtz resonator concept for heat flux reduction
[AIAA PAPER 93-2742] p 963 A93-46493
- Thermal analysis of an arc heater electrode with a rotating arc foot
[AIAA PAPER 93-2855] p 1028 A93-46590
- Evaluation of 2D ceramic matrix composites in aeroconvective environments
p 1212 A93-53459
- Study of optical techniques for the Ames unitary wind tunnel. Part 5: Infrared imagery
[NASA-CR-191385] p 194 N93-14809
- IR imaging for combustion characteristics and optical properties of boron/boron oxide
[AD-A257747] p 393 N93-17693
- Local heat transfer measurement with liquid crystals on rotating surfaces including non-axisymmetric cases
p 902 N93-29943
- Transient thermal behaviour of a compressor rotor with axial cooling air flow and co-rotating or contra-rotating shaft
p 903 N93-29946

SURFACE TREATMENT

- Improvement of rotating brushes for surface cleaning
p 396 A93-18371
- A set of application programs for the smoothing of curves and surfaces by the method of monoidal transformations in the geometric module of a CAD system for the design of flight vehicles
p 561 A93-27629
- Prediction and control of the service-related properties of parts at the technological preparation stage and during the manufacture process ... of aircraft engine components
p 834 A93-39062
- Enhancing the performance of aircraft engine blades by surface hardening
p 811 A93-39072
- Increasing the durability of gas turbine engine compressor blades by using a combined hardening/finishing treatment to control the stressed state of the surface layer
p 835 A93-39099
- Hardening/finishing treatment of compressor blades using a machine with planetary container motion
p 835 A93-39102
- A mathematical model of the vibrational impact hardening of parts
p 837 A93-39185
- Application of a dynamic compression system model to a low aspect ratio fan - Casing treatment and distortion
[AIAA PAPER 93-1871] p 1111 A93-49746

SURFACE VEHICLES

- Simulator motion
[AD-A257683] p 381 N93-17687
- Airport landside planning and operations
[PB93-167880] p 822 N93-26636

SURFACE WAVES

- In situ material characterization for pavement evaluation by the Spectral-Analysis-of-Surface-Waves (SASW) method
[AD-A255660] p 194 N93-14128

SURGES

- An investigation of post stall transients and recoverability of axial compression systems. I - A simplified method
[ASME PAPER 92-GT-55] p 347 A93-19305
- An investigation of post stall transients and recoverability of axial compression systems. II - Numerical simulations
[ASME PAPER 92-GT-56] p 347 A93-19306
- Modified surge in an axial flow compressor
[ASME PAPER 92-GT-59] p 247 A93-19309
- Active stabilization of compressor instability and surge in a working engine
[ASME PAPER 92-GT-88] p 348 A93-19335
- Evaluation of approaches to active compressor surge stabilization
[ASME PAPER 92-GT-182] p 352 A93-19407
- Compressor surge and stall --- Book
[ISBN 0-933283-05-9] p 482 A93-29780
- Surge recovery and compressor working line control using compressor exit Mach number measurement
p 897 A93-40435
- Compressor unsteady aerodynamic response to rotating stall and surge excitations
[AIAA PAPER 93-2087] p 1079 A93-49914
- Application of analog computing to real-time simulation of stall and surge dynamics
[AIAA PAPER 93-2231] p 1080 A93-50037
- Stall in axial flow aero engine compressors
p 422 N93-18723
- Stall and surge in axial flow compressors
p 423 N93-18724
- Active control of stall and surge
p 423 N93-18725
- Stall transients including effects of inlet distortion and intake geometry
p 423 N93-18726
- Experimental investigation of rotating stall in a mismatched three stage axial flow compressor
p 423 N93-18727
- Active stabilization to prevent surge in centrifugal compression systems
[NASA-CR-191625] p 424 N93-18862
- Applications of stress envelope concepts to aircraft EMP and lightning survivability
p 704 N93-24898
- Active stabilization of aeromechanical systems
[AD-A261366] p 725 N93-26335

SURVEILLANCE

- Airport navigation and surveillance using GPS and ADS
p 313 A93-21145
- The use of satellites for aeronautical communications, navigation and surveillance
p 881 A93-40436
- AIAA Lighter-Than-Air Systems Technology Conference, 10th, Scottsdale, AZ, Sept. 14-16, 1993, Technical Papers
p 1229 A93-54601
- National airborne surveillance system - An engineering student study
[AIAA PAPER 93-4031] p 1242 A93-54603
- Airship/U.S. naval vessels UHF communications relay demonstration
[AIAA PAPER 93-4032] p 1240 A93-54604
- Airship: The 'Look Out' - A versatile surveillance platform
[AIAA PAPER 93-4033] p 1229 A93-54605
- The development progress of the U.S. Army's SASS LITE, unmanned robot airship
[AIAA PAPER 93-4047] p 1243 A93-54614

SURVEILLANCE RADAR

- The SSR mode-S data-link
p 312 A93-18553
- Track moving emitters with Kalman processing
p 317 A93-22275
- An SSR/IFF Environment Model --- Secondary Surveillance Radar
p 883 A93-43406
- Measurements of SSR bearing errors due to site obstructions --- Secondary Surveillance Radar
p 883 A93-43407
- Improvements in code validation algorithms for secondary surveillance radar
p 883 A93-43408
- A Mode S implementation - Experiments about data-link and interconnected Mode S sensors
p 883 A93-43409
- Airport surveillance radar design for increased air traffic
p 883 A93-43410
- The development of a prototype aircraft height monitoring unit utilising an SSR-based difference in time of arrival technique
p 884 A93-43432
- Bistatic radar using satellite-borne illuminators of opportunity
p 914 A93-43437
- A multisensor-multitarget data association algorithm for heterogeneous sensors
p 1020 A93-44168
- A description of the Mode Select beacon system (Mode S) and its associated benefits to the National Airspace System (NAS)
[DOT/FAA/SE-92/6] p 35 N93-10738

- The effect of TCAS interrogations on the Chicago O'Hare ATCRBS system
[DOT/FAA/CT-92/22] p 318 N93-16498
- The ATC evaluation of the prototype Airport Surveillance Radar Wind Shear Processor (ASR-WSP) at Orlando International Airport
[DOT/FAA/CT-TN92/48] p 748 N93-25210
- Protection of taxiing traffic in airports through mode S secondary radar technology
[ETN-93-93455] p 791 N93-28206

SURVEYS

- Survey on techniques used in aerodynamic nozzle/airframe integration
p 161 N93-13224
- Scientific and engineering research facilities at universities and colleges: 1992
[NSF-92-325] p 192 N93-13407
- Aviation accidents, incidents, and violations: Psychological predictors among US pilots
p 144 N93-14693
- Industry survey of space system cost benefits from New Ways Of Doing Business
p 454 N93-17325
- State-of-the-art survey of flexible pavement crack sealing procedures in the United States
[AD-A258050] p 382 N93-17708
- Canadian Forces helicopter ditchings: 1952-1990
p 493 N93-19685
- US Army's aviation life support equipment retrieval program real world design successes from proactive investigation
p 494 N93-19690
- Lessons learned from an historical look at flight testing
p 511 N93-19904
- Aircraft electrical and environmental systems, AFSCs 452x5, 454x5, and 454x6
[AD-A261213] p 717 N93-25733
- Quantitative three-dimensional low-speed wake surveys
p 785 N93-27447
- Reaction to aircraft noise near general aviation airfields
[DORA-8203] p 1040 N93-32377

SURVIVAL

- 737-400 at Kegworth, 8 January 1989: The AAIB investigation
p 491 N93-19661
- Canadian Forces helicopter ditchings: 1952-1990
p 493 N93-19685
- US Army's aviation life support equipment retrieval program real world design successes from proactive investigation
p 494 N93-19690
- Correlations between engineering, medical and behavioural aspects in fire-related aircraft accidents
p 494 N93-19693

SUSPENDING (HANGING)

- Scientific ballooning payload termination loads
p 27 A93-11383
- Optimal control of the rocking and damping of swings
p 1263 A93-54998

SUSPENDING (MIXING)

- Calculation of a gas-dispersion laminar boundary layer on a plate with allowance for liquid film formation
p 76 A93-10148

- Particle dynamics simulations in inlet separator with an experimentally based bounce model
[AIAA PAPER 93-2156] p 1115 A93-49972

SUSPENSION SYSTEMS (VEHICLES)

- The benefits of Maglev technology
[AIAA PAPER 93-2949] p 1174 A93-48145

SUSPENSIONS

- The degradation of parachutes: Age and mechanical wear
[AD-A252243] p 24 N93-12179

SWATH WIDTH

- The real aperture antenna of SAR, a key element for performance
p 213 N93-13053

SWEEP COOLING

- Numerical dissipation in F3D thin-layer Navier-Stokes solution for flows with wall transpiration
p 9 A93-12010

- A preliminary study associated with the experimental measurement of the aero-optic characteristics of hypersonic configurations
[AD-A253792] p 24 N93-12063

SWEEP ANGLE

- Experimental study on the aerodynamic effects of a forward-sweep angle
p 1094 A93-52434
- Effects of sweep on the physics of unsteady shock-induced turbulent separated flows
[AD-A247035] p 22 N93-11742
- Computational parametric study of sidewall-compression scramjet inlet performance at Mach 10
[NASA-TM-4411] p 552 N93-20299
- Unsteady transition measurements on a pitching three-dimensional wing
p 820 N93-27450

SWEEP EFFECT

- On the static stability of forward swept propfans
[AIAA PAPER 93-1634] p 720 A93-34162

Maximum lift of wings with leading-edge devices and trailing-edge flaps deployed
[ESDU-92031] p 290 N93-16522

SWEEPBACK

Correlation of interaction sweepback effects on unsteady shock-induced turbulent separation
[AIAA PAPER 93-0776] p 475 A93-25550
The experimental study of the effect of sweepback angles and the front shape of the fin on reduction of shock wave/turbulent boundary layer interaction region
p 858 A93-40431

SWEPT FORWARD WINGS

Transonic flutter/divergence characteristics of aerodynamically tailored and non-tailored high-aspect-ratio forward-swept wings
p 10 A93-12273
Application of differential quadrature to the analysis of static aeroelastic phenomena
[AIAA PAPER 93-1505] p 711 A93-34044
Three-dimensional unsteady separating flows around an oscillatory forward-swept wing
[AIAA PAPER 93-2976] p 1050 A93-48170
Aerodynamic characteristics of a sweptforward-wing aircraft model in unsteady motion at large angles of attack in subsonic flow
p 1068 A93-48902
An experimental study of the effects of bodyside compression on forward swept sidewall compression inlets ingesting a turbulent boundary layer
[AIAA PAPER 93-3125] p 1072 A93-49515
Interference between a high-lift sweptforward wing and the horizontal nose plane at subsonic velocities
p 1135 A93-51906
Experimental study on the aerodynamic effects of a forward-sweep angle
p 1094 A93-52434
Effect of canard wing positions on aerodynamic characteristics of swept-forward wing
[AD-A262373] p 789 N93-28493
Flight control system design factors for applying automated testing techniques
[NASA-TM-4242] p 910 N93-30764
Integrated structural design, vibration control, and aeroelastic tailoring by multiobjective optimization
p 1030 N93-31137

SWEPT WINGS

Breakdown analysis on delta wing vortices
p 7 A93-10779
Measurement of attachment-line location in a wind-tunnel and in supersonic flight
[AIAA PAPER 92-4089] p 39 A93-11285
Compressible laminar and turbulent boundary layer computation for the three-dimensional wing
p 12 A93-12735
Annual Paul E. Hemke Lecture in aerospace engineering
p 107 A93-14067
Experimental study of crossflow instability and laminar-turbulent transition on a swept wing
p 115 A93-14250
A prediction of the stalling for wings with rear separation
p 116 A93-14264
In-flight surface-flow measurements on a subsonic transport high-lift flap system
p 166 A93-14327
On the static aeroelastic tailoring of composite aircraft swept wings modelled as thin-walled beam structures
p 158 A93-14820
Recent supersonic transition studies with emphasis on the swept cylinder case
p 127 A93-17252
A high-frequency, secondary instability of crossflow vortices that leads to transition
p 128 A93-17253
Effect of micron-sized roughness on transition in swept-wing flows
[AIAA PAPER 93-0076] p 262 A93-20188
Transition studies for swept wing flows using PSE --- parabolized stability equations
[AIAA PAPER 93-0077] p 263 A93-20189
Stability and transition on swept wings
[AIAA PAPER 93-0078] p 263 A93-20190
Influence of sweep on structural optimization of a fighter wing
[AIAA PAPER 92-4794] p 323 A93-20290
Integrated aerodynamic-structural-control wing design
[AIAA PAPER 92-4694] p 324 A93-20307
Structural non-linearity effects on flutter of a swept wing in transonic flows
p 410 A93-20714
LDV flowfield measurements on a straight and swept wing with a simulated ice accretion
[AIAA PAPER 93-0300] p 280 A93-23001
Shock-dependent, thrust wings for supersonic flow
[AIAA PAPER 93-0321] p 280 A93-23013
Numerical simulation of delta-wing roll
[AIAA PAPER 93-0554] p 285 A93-23293
Body-axis rolling motion critical states of a 65-degree delta wing
[AIAA PAPER 93-0621] p 523 A93-24738
A calculation method for the three-dimensional boundary-layer equations in integral form
[AIAA PAPER 93-0786] p 541 A93-24868

Aerodynamic forces and moments on a dihedral swept wing in a translation with attack and side-slip angle
p 476 A93-26903

Wave resistance of swept wings with supersonic edges
p 478 A93-27624

Prandtl theory applied to paraglider aerodynamics
[AIAA PAPER 93-1220] p 690 A93-35169
Temperature and suction effects on the instability of an infinite swept attachment line
p 691 A93-35486
Results from a conical Euler methodology developed for unsteady vortical flows
p 692 A93-35612
Dynamic stall of sinusoidally oscillating three-dimensional swept and unswept wings in compressible flow
p 766 A93-35995
A study of the effect of the static aeroelasticity of a swept wing on its weight response
p 801 A93-36798
Shape sensitivities and approximations of modal response of laminated skew plates
p 829 A93-37403
A data system for the observation of flow conditions on an aircraft wing
p 808 A93-37882
Wave interaction theory and LFC
p 860 A93-41781
Supersonic laminar flow control
p 860 A93-41782
Static aeroelastic control of an adaptive lifting surface
p 995 A93-45147

Leading-edge transition and relaminarization phenomena on a subsonic high-lift system
[AIAA PAPER 93-3140] p 959 A93-45154

Vortex flap flight test operations, a safe approach
p 995 A93-45168
Backfire unveiled
p 997 A93-46024
A three dimensional view of velocity using lasers
p 1028 A93-46822

Numerical simulation of transition in two- and three-dimensional boundary layers
p 973 A93-46980
Boundary layer effects on the flow of a leading edge vortex
[AIAA PAPER 93-3463] p 980 A93-47245

Improvement of conical similarity rule in swept shock wave/boundary layer interaction
[AIAA PAPER 93-2941] p 1046 A93-48139
Computation of delta-wing roll maneuvers
[AIAA PAPER 93-2975] p 1050 A93-48169
Effects of boundary layer bleed on swept-shock/boundary layer interaction
[AIAA PAPER 93-2989] p 1052 A93-48182
Effect of curvature on stationary crossflow instability of a three-dimensional boundary layer
p 1070 A93-49010

Calculation of a compressible three-dimensional boundary layer on a swept wing
p 1179 A93-53551
Calculation of flow fields near a lifting wing
p 1179 A93-53552

Effect of planform and body on supersonic aerodynamics of multibody configurations
[NASA-TP-3212] p 19 N93-10824

Overview of supersonic laminar flow control research on the F-16XL ships 1 and 2
[NASA-TM-104257] p 20 N93-11221

Boundary layer relaminarization device
[NASA-CASE-LAR-14470-1] p 23 N93-11876

Assessment of potential aerodynamic benefits from spanwise blowing at the wing tip
p 134 N93-13822

The unsteady aerodynamics of a delta wing undergoing large-amplitude pitching motions
p 134 N93-13929
BLSTA: A boundary layer code for stability analysis
[NASA-CR-4481] p 220 N93-14797

Navier-Stokes calculation of transonic flow past the NTF 65-deg delta wing
p 292 N93-16797

Crossflow stability and transition experiments in a swept-wing flow
[NASA-TM-108650] p 555 N93-21819

Swept wing attachment line contamination fence
[NASA-CASE-LAR-13400-1] p 485 N93-22015

Stationary crossflow instability on an infinite swept wing
p 699 N93-25865

Conical Euler analysis and active roll suppression for unsteady vortical flows about rolling delta wings
[NASA-TP-3259] p 701 N93-26134

Supersonic aeroelastic instability results for a NASP-like wing model
[NASA-TM-107739] p 718 N93-26553

The experimental study of transition and leading edge contamination of swept wings
[LIB-TRANS-2197] p 782 N93-27274

Three-dimensional compressible stability-transition calculations using the spatial theory
p 783 N93-27431

Recent progress in the analysis of iced airfoils and wings
p 784 N93-27441

Computation of a delta-wing roll-and-hold maneuver
[AD-A264704] p 909 N93-30498
GARTEUR 3D shear layer experiment
[FFA-TN-1992-26] p 987 N93-31052

SWEPTBACK WINGS

The numerical calculation and application of compressible boundary layers on laminar-flow-control and natural-laminar-flow wings
p 680 A93-33727

Curvature and leading edge sweep back effects on grid fin aerodynamic characteristics
[AIAA PAPER 93-3480] p 981 A93-47258

Shock-vortex interaction over a 65-degree delta wing in transonic flow
[AIAA PAPER 93-2973] p 1049 A93-48167

Mach 4 testing of scramjet inlet models
[NAL-TR-1137] p 26 N93-12369

Three dimensional boundary-layer transition on a swept wing
p 419 N93-16818

Experiments on swept-wing boundary-layer transition
p 419 N93-16829

The effect of surface suction near the leading edge of a swept-back wing
[AERO-REPT-9205] p 484 N93-20807

SWIRLING

Combined noise and flow control of supersonic jets using swirl
p 398 A93-19204

Experimental and theoretical analysis of the flow in a centrifugal compressor volute
[ASME PAPER 92-GT-30] p 400 A93-19290

Emissions reduction by varying the swirler airflow split in advanced gas turbine combustors
[ASME PAPER 92-GT-110] p 349 A93-19347

Three component LDV velocity measurements in a can type research combustor for CFD validation. I - Isothermal
[ASME PAPER 92-GT-138] p 350 A93-19370

Scaling of the two-phase flow downstream of a gas turbine combustor swirl cup - Mean quantities
[ASME PAPER 92-GT-207] p 404 A93-19431

Rotor cavity flow and heat transfer with inlet swirl and radial outflow of cooling air
[ASME PAPER 92-GT-378] p 406 A93-19536

Flow field characteristics of an axisymmetric sudden-expansion pipe flow with different initial swirl distribution
p 411 A93-21688

Inlet velocity profile effects on turbulent swirling flow predictions
[AIAA PAPER 93-0133] p 274 A93-22580

Eduction of swirling structure using the velocity gradient tensor
p 416 A93-23547

Parameter effects on turbulent swirling flames in combustors
p 534 A93-25911

Cruise noise of an advanced propeller with swirl recovery vanes
p 564 A93-28609

Effect of nonaxisymmetric forcing on a swirling jet with vortex breakdown
[AIAA PAPER 93-3251] p 1028 A93-46796

The development of swirl five-hole probe
p 987 A93-47341

Modelling three-dimensional gas-turbine-combustor model flow using second-moment closure
[AIAA PAPER 93-3104] p 1149 A93-48277

Swirling flows in a contoured-wall combustion chamber
[AIAA PAPER 93-1765] p 1073 A93-49661

The effects of turbulence modeling on the numerical simulation of confined swirling flows
[AIAA PAPER 93-1976] p 1078 A93-49823

Experimental determination of the bulk swirl attenuation between two axial stations in the LM2500 inlet bellmouth
[AIAA PAPER 93-2203] p 1155 A93-50015

The influence of swirl generator characteristics on flow and combustion in turbulent diffusion flames
p 1159 A93-51632

Thermometry inside a swirling turbulent flame - CARS advantages and limitations
p 1146 A93-51634

Low NO(x) combustor development using aerodynamic staging
[ISABE 93-7021] p 1195 A93-53997

Active control of vortex breakdown by a spinning wave generator
[ISABE 93-7045] p 1219 A93-54021

An experimental investigation of the effects of swirling flow on the performance of nozzles
p 1247 A93-54859

Fuel Injector: Air swirl characterization aerothermal modeling, phase 2, volume 2
[NASA-CR-189193-VOL-2] p 721 N93-25106

SYMBOLIC PROGRAMMING

A primer on polynomial resultants
[AD-A246883] p 98 N93-11463

SYMBOLS

Design of instrument approach procedure charts: Comprehension speed of missed approach instructions coded in text or icons
[PB92-205673] p 36 N93-11252

On the typography of flight-deck documentation
[NASA-CR-177605] p 571 N93-19970

SYMMETRICAL BODIES

Improved numerical simulation of Euler equations
p 63 N93-10309

SYNCHRONISM

A model for determining task set schedulability in the presence of system effects
[AD-A258915] p 443 N93-19338

SYNCHROTRON RADIATION

Poster session: Fifth Users Meeting for the Advanced Photon Source
[DE93-006019] p 732 N93-26498

SYNOPTIC METEOROLOGY

Nowcasts of thunderstorm initiation and evolution
p 752 A93-33773
Studies of atmospheric eddy dynamics and energetics and climate problems
[ISBN 5-286-00610-8] p 753 A93-35689
An observational study of the dryline
p 844 A93-36034

SYNTHESIZERS

Design, fabrication, and testing of a three-dimensional acoustic orientation instrument (3-D AOI): Drawings, engineering and associated lists (conceptual and development design)
[AD-A260934] p 760 N93-25915

SYNTHETIC APERTURE RADAR

Research on ISAR motion compensation and imaging by modeling electromagnetic data p 342 A93-20852
The ISAR image-formation results of Boeing-727 p 342 A93-20857
Results from a VHF impulse synthetic-aperture radar p 501 A93-28219
ISAR motion compensation and superresolution imaging of aircraft p 928 A93-42793
Radar 92: Proceedings of the International Conference, Brighton, United Kingdom, Oct. 12, 13, 1992 [ISBN 0-85296-533-2] p 929 A93-43376
A dual polarised active phased array antenna with low cross polarisation for a polarimetric airborne SAR p 883 A93-43401
Antenna design for adaptive airborne MTI p 884 A93-43440
The PHARUS project, first results of the realization phase --- Phased Array Universal SAR p 884 A93-43454
Grazing angle dependency of SAR imagery p 884 A93-43455
Real time PRF control system for SAR p 884 A93-43464
Motion compensation in a time domain SAR processor p 885 A93-43466
Inflight antenna diagram determination of spaceborne and airborne SAR-systems p 1161 A93-47583
A refined procedure to generate calibrated imagery from airborne synthetic aperture radar data p 1162 A93-47657
The realization phase of the PHARUS project --- Phased Array Universal SAR p 1162 A93-47658
JPL AIRSAR processing activities and developments p 1162 A93-47865
Motion errors and compensation possibilities p 212 N93-13052
Definition study PHARUS [AD-A256560] p 221 N93-14805
Comparison of simulated and actual wind shear radar data products p 490 N93-19610
ERS-1 directional wave spectra validation with the airborne SAR PHARS [BCRS-92-18] p 937 N93-31010

SYNTHETIC APERTURES
The real aperture antenna of SAR, a key element for performance p 213 N93-13053

SYNTHETIC ARRAYS
Experimental results on RIAS digital beamforming radar p 929 A93-43392

SYSTEM EFFECTIVENESS
Prototype stop bar system evaluation at John F. Kennedy International Airport [AD-A258667] p 192 N93-12902
National Airspace System: Air traffic control and airspace management operational concept NAS-SR-132 [DOT/FAA/SE-92/5] p 502 N93-20164

SYSTEM FAILURES
Multilevel control of dynamical systems using neural networks p 96 A93-13011
An application of fuzzy logic and Dempster-Shafer theory to failure detection and identification p 96 A93-13079
Neural-network-based catastrophe avoidance control systems p 97 A93-13233
Electronics show their age p 80 A93-13447
Failure-accommodating neural network flight control [AIAA PAPER 92-4394] p 523 A93-24495
Autonomous guidance, navigation and control bridging program plan p 532 A93-27046
Development of advanced approach and departure procedures [AIAA PAPER 93-3833] p 1098 A93-51422
Summary: Experimental validation of real-time fault-tolerant systems [NASA-CR-190985] p 175 N93-13697

Multiple model adaptive estimation applied to the ViSTA F-16 with actuator and sensor failures
[AD-A256444] p 188 N93-14608

Detection of technical states with aircraft p 168 N93-15159
Failure diagnostic with MAINTEx based on AIMS at Swissair p 110 N93-15181
Application of a neural network as a potential aid in predicting NTF pump failure p 442 N93-18332
Detection of spoofing, jamming, or failure of a Global Positioning System (GPS) [AD-A259023] p 319 N93-18951
URV flight test of an Ada implemented self-repairing flight control system [AD-A259205] p 527 N93-20551
A simulator study into low speed longitudinal handling qualities of ACT transport aircraft [NLR-TP-89387-U] p 527 N93-20743
Design, analysis, and control of large transport aircraft utilizing engine thrust as a backup system for the primary flight controls [NASA-CR-192938] p 820 N93-27308

SYSTEM IDENTIFICATION

Multilevel control of dynamical systems using neural networks p 96 A93-13011
Identification of weakly nonlinear dynamic systems by means of random excitations p 227 A93-16472
An overview of the system identification procedure with applications to the X-31 drop model [AIAA PAPER 93-0010] p 366 A93-20132
Using system identification to improve the performance of a low-cost flight simulator p 369 A93-22885
On closed-loop identification of a certain aeroengine under flight conditions p 519 A93-24026
Pilot control identification using Minimum Model Error estimation [AIAA PAPER 92-4421] p 523 A93-24497
An identification method for dynamic systems with delay p 562 A93-27689
Signal processing and system identification techniques for flutter test data analysis p 529 A93-29282
Frequency-domain identification of BO 105 derivative models with rotor degrees of freedom p 712 A93-34263
Identification of the open loop dynamics of the T700 turbohaft engine p 809 A93-35934
Frequency-domain identification of coupled rotor/body models of an advanced attack helicopter p 816 A93-35960
A frequency domain theory for structural identification p 930 A93-43778
Identification of a full subsonic envelope nonlinear aerodynamic model of the F-14 aircraft [AIAA PAPER 93-3634] p 1065 A93-48319
Stall inception in a multi-stage high speed axial compressor [AIAA PAPER 93-2386] p 1117 A93-50153
System identification of unstable manipulators using ERA methods --- Eigensystem Realization Algorithm [AIAA PAPER 93-3842] p 1170 A93-51431
Identification of nonlinear mechanical systems using combined state and parameter evaluation p 1224 A93-52732
System identification for X-31A project support: Lessons learned so far p 512 N93-19914
On-line aircraft state and parameter estimation p 512 N93-19929
Robust nonlinear control of vectored thrust aircraft [NASA-CR-192727] p 728 N93-25199
Parameter identification for nonlinear aerodynamic systems [NASA-CR-193072] p 782 N93-27282

SYSTEMS ANALYSIS
MPC75 as the forerunner of a new regional aircraft family p 37 A93-10776
Aircraft optimization by a system approach - Achievements and trends p 153 A93-14205
Application of vibration-and-flutter integration analysis system for a trainer p 226 A93-14311
Analysis, modelling and simulation of the large-angle magnetic suspension test fixture p 375 A93-20297
AIAA/USAF/NASA/OAI Symposium on Multidisciplinary Analysis and Optimization, 4th, Cleveland, OH, Sept. 21-23, 1992, Technical Papers, Pts. 1 & 2 p 435 A93-20301
The Boeing 747-400 upper rudder control system with triple tandem valve [SAE PAPER 912133] p 327 A93-21843
Simulation in aeronautics p 437 A93-21868
A graphical user-interface for propulsion system analysis [AIAA PAPER 93-0223] p 440 A93-23699
Problems in the optimization of complex engineering systems p 1165 A93-49307

A comparative study of multivariable robustness analysis methods as applied to integrated flight and propulsion control [AIAA PAPER 93-3809] p 1102 A93-51401
Document for 270 Voltage Direct Current (270 V dc) System [SAE ARP 4729] p 1160 A93-52170
Summary: Experimental validation of real-time fault-tolerant systems [NASA-CR-190985] p 175 N93-13697
Information systems for airport operations [TT-9202] p 152 N93-14729
Results of in-service evaluation of wind shear systems p 146 N93-14856
Advanced technology wind shear prediction system evaluation p 146 N93-14858
Czechoslovak development and experience in flight data recorder readout and analysis p 168 N93-15162
Integrated Blade Inspection System (IBIS) upgrade study [AD-A258912] p 365 N93-19356
Assessment of computational issues associated with analysis of high-lift systems p 785 N93-27449
System analysis for a kinematic positioning system based on the global positioning system [AD-A262830] p 885 N93-29468

SYSTEMS ENGINEERING

Design and implementation of a flight simulation system --- Book p 66 A93-12216
Pilot/Vehicle display development from simulation to flight [AIAA PAPER 92-4174] p 51 A93-13310
Why simulators don't fly like the airplane: Data - An update with examples from the C-141B program [AIAA PAPER 92-4161] p 66 A93-13312
Flight simulator development in China p 191 A93-14410
Design philosophies of the Basic Research Simulator p 191 A93-14414
A control technology of integrated system of engineering supported by software engineering environments p 226 A93-14415
Advanced cooling for high power electric actuators [SAE PAPER 921022] p 158 A93-14649
Control of the pilot-system interface p 166 A93-15040
Optimization of pneumatic subsystems for transport aircraft p 159 A93-15049
Future systems for air traffic control p 150 A93-15052
A design study on the effect of support and system parameters on the natural frequencies of rotor systems p 210 A93-16374
Demonstration of an integrated, active 4 x 4 photonic crossbar p 211 A93-17392
An integrated knowledge system for wind tunnel testing - Project Engineers' Intelligent Assistant [AIAA PAPER 93-0560] p 377 A93-23297
High voltage quick-disconnect harness system for helmet-mounted displays p 516 A93-25922
Instrument systems of flight vehicles and their design --- Russian book [ISBN 5-217-00793-1] p 718 A93-35678
MIDAS technology transfer p 845 A93-35920
Logistic Support Analysis - An integrated approach to configuration management p 763 A93-35924
Software - Design for maintenance p 847 A93-39537
Robotic inspection and refurbishment of aircraft canopy transparencies [SME PAPER AD92-203] p 855 A93-40665
Database management for integrated avionics system p 939 A93-42831
Evaluating the IOBIDS specification using gate-level system simulation p 940 A93-42851
Development methodology for contemporary avionics systems [SAE PAPER 931591] p 1104 A93-49340
Changing the utility subsystem paradigm [SAE PAPER 931598] p 1165 A93-49347
Transport delay compensation - An inexpensive alternative to increasing image generator update rate [AIAA PAPER 93-3563] p 1223 A93-52663
Characterization of the faulted behavior of digital computers and fault tolerant systems p 1224 A93-52762
On definition and use of systems engineering processes, methods and tools p 1225 A93-53642
Developments towards versatility in digital engine control units [ISABE 93-7088] p 1202 A93-54064
An optical flameout detection system for NASA Langley's 8-Foot High Temperature Tunnel p 1254 A93-54372

- Requirements analysis notebook for the flight data systems definition in the Real-Time Systems Engineering Laboratory (RSEL) p 69 N93-10960
- Introduction to the Rolls-Royce design process [PNR-90939] p 57 N93-11039
- The application of manufacturing systems engineering for aero engine gears [PNR-90944] p 86 N93-11054
- Artificial intelligence and CFD: Expert systems for the design of airfoils and for grid generation [DIGE-EST-TN-016] p 48 N93-11161
- Flight simulation leaves the ground p 194 N93-14616
- Proceedings of the 16th Symposium on Aircraft Integrated Monitoring Systems [DLR-MITT-92-01] p 167 N93-15152
- The Teledyne controls aircraft condition monitoring system p 168 N93-15155
- Ground Support Equipment (GSE) for Aircraft Condition Monitoring System (ACMS) p 110 N93-15158
- Rewritable optical disk: Application to flight recording p 221 N93-15160
- Royal Air Force experience of the Harrier information management system p 234 N93-15170
- Helicopter flight data recorder and health and usage monitoring system p 169 N93-15178
- Helicopter health monitoring: Current practice and future trends p 169 N93-15179
- New rotor trim and balance system for helicopter usage monitoring p 169 N93-15180
- Failure diagnostic with MAINTEx based on AIMS at Swissair p 110 N93-15181
- Fly-by voice, a technology demonstration p 526 N93-19918
- Optimization and sensitivity computations for the conception of internal ventilation system in the aircraft engine [ETN-93-93375] p 521 N93-20913
- Multidisciplinary design optimization: An emerging new engineering discipline [NASA-TM-107761] p 806 N93-27258
- Flight evaluation of a computer aided low-altitude helicopter flight guidance system p 820 N93-28869
- Adapting system engineering principles to the Canadian Airspace System p 887 N93-30338
- Flight test of avionics and air-traffic control systems [ESA-TT-1279] p 993 N93-31271
- ATTAS experimental-cockpit and ATMOS for component and system investigations in flight guidance p 1014 N93-31276
- Testing of an experimental FMS p 998 N93-31277
- Pallet for helicopter test instrumentation p 1000 N93-31279
- Ground- and satellite-derived flight-path measurements as demonstrated in the AFES Avionics Flight Evaluation System (AFES) p 993 N93-31281
- ### SYSTEMS INTEGRATION
- Precision navigation with an integrated navigation system p 29 A93-10782
- Development of a TRN/INS/GPS integrated navigation system p 30 A93-11004
- Requirements for integrated flight and traffic management during final approach p 31 A93-11009
- Integration of full scale development aircraft GPS user equipment (AN/ARN-151) with Doppler radar systems p 31 A93-11012
- GPS integrity monitoring and system improvement with ground station and multistationary satellite support p 33 A93-11044
- Systems integration test laboratory - Application and experiences p 190 A93-13910
- Integration of flight control and carrier landing aid system [ONERA, TP NO. 1993-6] p 181 A93-14187
- Integration of aircraft design and manufacture using artificial intelligence paradigms p 225 A93-14202
- Integrated utilities management system for aircraft p 153 A93-14208
- Integrated control law synthesis of gust load alleviation and flutter margin augmentation for a transport aircraft p 182 A93-14281
- Application of vibration-and-flutter integration analysis system for a trainer p 226 A93-14311
- Flight-determined benefits of integrated flight-propulsion control systems p 183 A93-14370
- Design of digital multiple model-following integrated flight/propulsion control systems p 183 A93-14371
- Analysis and development of a total energy control system for a large transport aircraft p 183 A93-14372
- The Aircraft/Propulsion Integrated Assessment System p 226 A93-14396
- The integrated actuation package approach to primary flight control [SAE PAPER 920968] p 185 A93-14630
- Future systems for air traffic control p 150 A93-15052
- Multidisciplinary design integration system for a supersonic transport aircraft [AIAA PAPER 92-4841] p 324 A93-20296
- Integrated Terminal Weather System (ITWS) p 428 A93-22127
- Integrated runway meteorological observation system (IRMOS/SIOMA) p 428 A93-22128
- An integrated knowledge system for wind tunnel testing - Project Engineers' Intelligent Assistant [AIAA PAPER 93-0560] p 377 A93-23297
- Helmet Mounted Sight and display testing p 517 A93-26883
- Integration of a course and position reference system with GPS p 499 A93-27911
- DLR research program overview on airport surface movement guidance and control p 499 A93-27912
- Ground Movement and Control System (GMCS) p 499 A93-27913
- ADDRAS - An integrated systems approach p 562 A93-29423
- SAFEbus p 828 A93-37072
- A data reduction system for processing instrumented flight test data p 847 A93-37866
- Integrating controls and avionics on commercial aircraft p 892 A93-42778
- Cross channel dependency requirements of the multi-path redundant avionics suite p 928 A93-42782
- Reconfigurable photonic data networks for military aircraft p 928 A93-42783
- The PAVE PACE integrated RF architecture for next generation avionics p 896 A93-42784
- An integrated weather channel designed for an up-to-date ATC radar system p 929 A93-43434
- Problems in the optimization of complex engineering systems p 1165 A93-49307
- Changing the utility subsystem paradigm [SAE PAPER 931598] p 1165 A93-49347
- National Aerospace Plane Integrated Fuselage/Cryotank Risk Reduction program [AIAA PAPER 93-2564] p 1142 A93-50284
- Application of controller partitioning optimization procedure to integrated flight/propulsion control design for a STOLV aircraft [AIAA PAPER 93-3766] p 1131 A93-51361
- Integrated flight/propulsion control - Subsystem specifications for performance [AIAA PAPER 93-3808] p 1132 A93-51400
- A comparison of two multi-variable integrator windup protection schemes [AIAA PAPER 93-3812] p 1123 A93-51404
- Benefits of variable rotor speed in integrated helicopter/engine control [AIAA PAPER 93-3851] p 1134 A93-51438
- Finite state aeroelastic model for use in rotor design optimization p 1104 A93-52454
- Methodology for integration of digital control loaders in aircraft simulators [AIAA PAPER 93-3551] p 1207 A93-52655
- Digital flight recorded data - A method of estimating down draft from digital flight recorded data p 1241 A93-54559
- Integration of an integrated helmet system for PAH 2 p 1244 A93-55298
- Integrated DGPS/IMU systems for airborne navigation in Poland p 1241 A93-56049
- Terminal Doppler Weather Radar (TDWR) Operational Test and Evaluation (OT/E) integration test plan [DOT/FAA/CT-TN92/6] p 151 N93-13377
- Multiplexing electro-optic architectures for advanced aircraft integrated flight control systems [NASA-CR-182268] p 187 N93-13735
- Terminal Doppler weather radar/low-level wind shear alert system integration algorithm specification, version 1.1 [AD-A255319] p 224 N93-14547
- Proceedings of the 16th Symposium on Aircraft Integrated Monitoring Systems [DLR-MITT-92-01] p 167 N93-15152
- Detection of technical states with aircraft p 168 N93-15159
- Integrated engine control and monitoring with experiences derived from OLMOS p 178 N93-15168
- A philosophy for integrated monitoring system design p 178 N93-15174
- Personal computer based test- and emulation equipment for maintenance and ground support p 110 N93-15185
- Airbus Industrie TCAS experience p 152 N93-15186
- Test and integration concept for complex helicopter avionics systems [MBB-UD-0605-91-PUB] p 343 N93-17547
- The integrated design and manufacturing of composite structures for aircraft using an advanced tape layering technology [MBB-LME-251-S-PUB-0491-A] p 515 N93-21401
- Runway Visual Range (RVR) Operational Test and Evaluation (OT&E) integration and OT&E operational test report [DOT/FAA/CT-TN92/37] p 706 N93-25243
- Piloted simulation of an air-ground profile negotiation process in a time-based Air Traffic Control environment [NASA-TM-107748] p 707 N93-26087
- Bibliography on propulsion airframe integration technologies for high-speed civil transport applications, 1980-1991 [NASA-TM-105602] p 678 N93-26136
- Methodology investigation: Global Positioning System integration (GPS) [AD-A261054] p 708 N93-26237
- Improved selective catalytic NOx control technology for compressor station reciprocating engines [PB93-158566] p 755 N93-26529
- Status of the Fiber Optic Control System Integration (FOCSI) program [NASA-TM-106151] p 841 N93-28053
- Testing of an experimental FMS p 998 N93-31277
- ### SYSTEMS MANAGEMENT
- Changing role of telecommunications management in air traffic control in the FAA p 888 N93-30354
- ### SYSTEMS SIMULATION
- Design and implementation of a flight simulation system --- Book p 66 A93-12216
- Robust fault detection of jet engine sensor systems using eigenstructure assignment p 173 A93-14608
- Analysis, modelling and simulation of the large-angle magnetic suspension test fixture p 375 A93-20297
- Multidisciplinary propulsion simulation using NPSS [AIAA PAPER 92-4709] p 435 A93-20318
- Some questions of scale in simulation, and a few answers p 939 A93-42830
- Evaluating the IOBIDS specification using gate-level system simulation p 940 A93-42851
- Propulsion system simulator with proptan for tests on a large scale model of IL-114 airplane in a full-size wind tunnel of TsAGI p 1013 A93-46933
- Pseudo Aircraft Systems - A multi-aircraft simulation system for air traffic control research [AIAA PAPER 93-3585] p 1209 A93-52679
- Integrated fire control simulation systems p 1192 A93-53876
- The F-92 RELIANT: Air transport system design simulation [NASA-CR-192050] p 339 N93-18386
- Testing of an experimental FMS p 998 N93-31277
- ### SYSTEMS STABILITY
- Robust control of an aeroelastic system modeled by a singular integro-differential equation p 97 A93-13197
- H(infinity) optimal controllers for a distributed model of an unstable aircraft p 62 A93-13247
- A sensitivity analysis of the stability of a tug-rope-sailplane system p 184 A93-14400
- Analysis of airframe and engine control interactions and integrated flight/propulsion control p 185 A93-14596
- Robust stabilization of an aero-elastic system p 817 A93-37044
- SR-SCARLET 1: Peregrin [NASA-CR-192048] p 337 N93-18155
- ## T
- ### T-38 AIRCRAFT
- T-38 forward windshield development and performance demonstration report [AD-A259240] p 513 N93-20579
- Analysis of the static and dynamic response of a T-38 wing and comparison with experimental data [AD-A262363] p 806 N93-27692
- ### T-56 ENGINE
- Field evaluation of six protective coatings applied to T-56 turbine blades after 2000 hours of engine use [AD-A261112] p 522 N93-21316
- ### TABS (CONTROL SURFACES)
- Design of a full time wing leveler system using tab driven aileron controls [AIAA PAPER 92-4193] p 63 A93-13345
- Streamwise vorticity generation and mixing enhancement in free jets by 'delta-tabs' [AIAA PAPER 93-3253] p 1180 A93-53592
- Streamwise vorticity generation and mixing enhancement in free jets by delta-tabs [NASA-TM-106235] p 988 N93-31648
- ### TACTICS
- Implementation of expert systems within an interactive tactical environment [AIAA PAPER 93-3583] p 1223 A93-52678

- Design for tactical situation awareness display
[AD-A256194] p 170 N93-15235
- A high-fidelity, six-degree-of-freedom batch simulation environment for tactical guidance research and evaluation
[NASA-TM-4440] p 1010 N93-32380
- TAIL ASSEMBLIES**
- An investigation of mode shift flutter suppression scheme for empennages p 182 A93-14288
- Composite 'Exoskin' doubler extends F-15 Vertical Tail fatigue life p 709 A93-33911
- [AIAA PAPER 93-1341] p 711 A93-34137
- [AIAA PAPER 93-1607] p 711 A93-34137
- A computational and experimental investigation of a delta wing with vertical tails p 1054 A93-48199
- [AIAA PAPER 93-3009] p 1054 A93-48199
- Simulation of tail buffet using delta wing-vertical tail configuration p 1065 A93-48357
- [AIAA PAPER 93-3688] p 1065 A93-48357
- Unsteady pressure and load measurements on an F/A-18 vertical fin p 1095 A93-52451
- Design and implementation of digital filters for analysis of F/A-18 flight test data p 17 N93-10342
- [AD-A253447] p 17 N93-10342
- Apparatus and method for improving spin recovery on aircraft p 526 N93-20039
- [NASA-CASE-LAR-14747-1] p 526 N93-20039
- The influence of structural optimization on the aeroelastic properties of a vertical tail p 513 N93-20575
- [AD-A259140] p 513 N93-20575
- TAIL ROTORS**
- Helicopter main rotor/tail rotor noise radiation characteristics from scaled model rotor experiments in the DNW p 445 A93-19142
- Development and validation of 'quiet tail rotor' technology p 567 A93-29416
- Side-by-side hover performance comparison of MDHC 500 NOTAR and tail rotor anti-torque systems p 796 A93-35956
- TAIL SURFACES**
- In-flight tailload measurements p 155 A93-14285
- Characteristics of fatigue crack growth under the service-spectrum loading of the tail boom of a helicopter p 321 A93-18339
- Experimental investigation of vortex-fin interaction [AIAA PAPER 93-0050] p 260 A93-20163
- Development of an engineering level prediction method for high angle of attack aerodynamics [AIAA PAPER 93-0208] p 278 A93-22626
- Repair materials and processes for the MD-11 Composite Tailcone p 1216 A93-53452
- TAILLESS AIRCRAFT**
- Integrated aerodynamics and control system design for tailless aircraft p 42 A93-13284
- [AIAA PAPER 92-4604] p 42 A93-13284
- Optimization of the parameters of the lift-augmentation devices of the wing of a maneuverable aircraft equipped with an active load-reduction system p 804 A93-39189
- Effect of geometry, static stability, and mass distribution on the tumbling characteristics of generic flying-wing models [AIAA PAPER 93-3615] p 1125 A93-48302
- Aerodynamic effects on the B-2 maneuver response [AIAA PAPER 93-3664] p 1128 A93-48344
- A new flying qualities criterion for flying wings [AIAA PAPER 93-3668] p 1128 A93-48346
- Mathematical optimization: A powerful tool for aircraft design [MBB-FE-2-S-PUB-478] p 331 N93-17564
- TAKEOFF**
- The development of an efficient take-off performance monitor (TOPM) p 180 A93-14186
- Expanding the operation scope of aircraft through the use of air-cushion landing gear p 321 A93-18354
- Graph-theory studies of the possibility of occurrence of flight accidents and incidents during the take-off under special operating conditions p 306 A93-18365
- Aircraft take-off laboratory simulation for de/anti-icing study p 528 A93-23840
- Navier-Stokes computations and experimental comparisons for multi-element airfoil configurations [AIAA PAPER 93-0645] p 464 A93-24760
- Takeoff/approach noise for a model counterrotation propeller with a forward-swept upstream rotor [AIAA PAPER 93-0596] p 519 A93-24782
- Unsteady blade pressures on a propfan at takeoff - Euler analysis and flight data p 810 A93-37389
- Determination of the takeoff characteristics of jet engines during the preliminary design of aircraft p 892 A93-42378
- Takeoff and landing analysis methodology for an airbreathing space booster p 914 A93-42927
- The evolution of a nose-wheel steering system p 995 A93-44852
- Effects of flow-path variations on internal reversing flow in a tailpipe offtake configuration for ASTOVL aircraft [AIAA PAPER 93-2438] p 1118 A93-50190
- Control of takeoff of a hypersonic aircraft using neural networks p 1167 A93-50744
- Development of advanced approach and departure procedures [AIAA PAPER 93-3833] p 1098 A93-51422
- A simulation study on take-off and landing dynamics of fly-by-wire control system aircraft p 1249 A93-55590
- Summary of findings from the PIREP-based analyses conducted during the 1988 to 1990 evaluations of TDWR-based and TDWR/LLWAS-based alert services provided to landing/departing pilots [AD-A253859] p 93 N93-11144
- Simulator evaluation of displays for a revised takeoff performance monitoring system [NASA-TP-3270] p 189 N93-15366
- Takeoff/approach noise for a model counterrotation propeller with a forward-swept upstream rotor [NASA-TM-105979] p 362 N93-16715
- A simulation study on take-off and landing dynamics of the aircraft of a fly-by-wire control system [AD-A259286] p 510 N93-19849
- Analysis of aircraft noise levels in the vicinity of start-of-takeoff roll at Baltimore-Washington International Airport [PB92-221605] p 559 N93-21501
- Effect of underwing frost on transport aircraft takeoff performance [DOT/FAA/CT-TN93/9] p 791 N93-27252
- Efficient simulation of incompressible viscous flow over multi-element airfoils p 784 N93-27443
- Effects of flow-path variations on internal reversing flow in a tailpipe offtake configuration for ASTOVL aircraft [NASA-TM-106149] p 900 N93-29065
- TAKEOFF RUNS**
- Alternative approach routes to runway 24 at Oslo Airport, Fornebu p 487 A93-28481
- TANDEM ROTOR HELICOPTERS**
- Fifty years of tandem rotor helicopter engineering p 504 A93-25250
- TANKER AIRCRAFT**
- A review of aging aircraft technology - An I.A.I. perspective p 3 A93-13634
- The Air Force Flight Test Center artificial icing and rain testing capability upgrade program [AIAA PAPER 93-0295] p 376 A93-22695
- Lateral aerodynamic interference between tanker and receiver in air-to-air refueling p 1136 A93-52444
- The testing of fixed wing tanker and receiver aircraft to establish their air-to-air refueling capabilities, volume 11 [AGARD-AG-300-VOL-11] p 514 N93-21305
- TAPERED COLUMNS**
- Post-critical behaviour of a tapered cantilever column subjected to a uniformly distributed tangential follower force p 831 A93-38431
- TAPERING**
- Tapered geometries for improved crashworthiness under side loads p 743 A93-34259
- TARGET ACQUISITION**
- Sequential smoothing and filtering for maneuvering target tracking p 440 A93-22978
- A multisensor-multitarget data association algorithm for heterogeneous sensors p 1020 A93-44168
- Exact closed-form solution of generalized proportional navigation p 1130 A93-49598
- TARGET RECOGNITION**
- Space-time processing for AEW radar p 884 A93-43444
- Grazing angle dependency of SAR imagery p 884 A93-43455
- Radar signals analysis oriented to target characterization applied to civilian ATC radar p 885 A93-43475
- LONGBOW - Force multiplier for continuous operations p 1175 A93-54295
- TARGET SIMULATORS**
- Research on ISAR motion compensation and imaging by modeling electromagnetic data p 342 A93-20852
- TASK COMPLEXITY**
- A context-based introduction to aircraft radio communications p 570 A93-27164
- Performance-based testing and success in Naval advanced flight training [AD-A260838] p 717 N93-25933
- TASKS**
- Adaptive automation and human performance: Multi-task performance characteristics [AD-A254596] p 186 N93-12578
- Performance of color-dependent tasks of air traffic control specialists as a function of type and degree of color vision deficiency [AD-A256614] p 151 N93-14275
- Identifying ability requirements for operators of future automated air traffic control systems [AD-A256615] p 152 N93-14276
- Conversion of the CTA, Inc., en route operations concepts database into a formal sentence outline job task taxonomy [AD-A261410] p 708 N93-26447
- TAXIING**
- Optimization of oleo-pneumatic shock absorber of aircraft p 1243 A93-55415
- Aircraft landing gear shimmy p 340 N93-19029
- Protection of taxiing traffic in airports through mode S secondary radar technology [ETN-93-93455] p 791 N93-28206
- Testing concept of a taxiing control system, summary p 1010 N93-31278
- TAXONOMY**
- Taxonomy of flight variables p 147 N93-15022
- TAYLOR INSTABILITY**
- Experience with the use of liquid crystals in conjunction with the filament method is studying the structure of supersonic flow downstream of a plane step p 478 A93-27639
- TAYLOR SERIES**
- Fast three-dimensional vortex method for unsteady wake calculations p 1178 A93-53233
- TECHNOLOGICAL FORECASTING**
- Aerodynamic characteristics of a next generation high-speed civil transport [AIAA PAPER 92-4229] p 15 A93-13356
- MP-C75 - The evolution of a new regional airliner for the late nineties p 155 A93-14289
- Advanced technology constant challenge and evolutionary process p 109 A93-15054
- Saab 2000 - An exercise in growth and commonality p 505 A93-25357
- Future supersonic transport studies at Aerospatiale p 505 A93-25491
- Future availability of aircraft maintenance personnel p 570 A93-27133
- The role of flight management in future air traffic control p 499 A93-27909
- Application of advanced guidance and navigation systems to flight control of aircraft and future space vehicles p 500 A93-28153
- Advanced airborne 3D computer image generation systems technologies for the year 2000 p 518 A93-28176
- Managing the world's air traffic p 501 A93-28392
- Spaceplanes - Back to the future p 733 A93-34265
- Thrust vectoring nozzles give pilots an edge p 720 A93-34375
- A French look at the future supersonic transport [ONERA, TP NO. 1992-209] p 803 A93-38763
- Antennas now and future p 764 A93-39540
- The NASA Computational Fluid Dynamics (CFD) program - Building technology to solve future challenges [AIAA PAPER 93-3292] p 1041 A93-44996
- How to enhance safety for future space transportation systems p 1015 A93-45444
- The all-electric aircraft - In your future? p 997 A93-46824
- Future technology aim of the National Aerospace Plane Program [AIAA PAPER 93-1988] p 1141 A93-49833
- An investigation of the fuel-optimal periodic trajectories of a hypersonic vehicle [AIAA PAPER 93-3753] p 1101 A93-51349
- ADP - Engine concept of the future p 1246 A93-54842
- Future trends in IR sensors p 1258 A93-55295
- Small gas turbines in the 21st century p 1247 A93-55494
- JPRS report: Science and technology. Central Eurasia: Engineering and equipment [JPRS-UEQ-92-006] p 842 N93-28636
- JPRS report: Science and technology. Central Eurasia: Engineering and equipment [JPRS-UEQ-92-010] p 842 N93-28674
- JPRS report: Science and technology. Central Eurasia: Engineering and equipment [JPRS-UEQ-92-008] p 842 N93-28675
- JPRS report: Science and technology. Central Eurasia: Engineering and equipment [JPRS-UEQ-93-003] p 842 N93-28691
- TECHNOLOGIES**
- National Aero-Space Plane: Key issues facing the program. Testimony before the Subcommittee on Technology and Competitiveness, Committee on Science, Space, and Technology, House of Representatives [GAO/T-NSIAD-92-26] p 161 N93-13253
- NSF Science and Technology Centers [NSF-92-104] p 193 N93-13712
- JPRS report: Science and technology. Central Eurasia: Engineering and equipment [JPRS-UEQ-92-003] p 749 N93-25427

TECHNOLOGY ASSESSMENT

- Architectures and GPS/INS integration - Impact on mission accomplishment* p 31 A93-11013
The 21st century navigation station p 34 A93-12123
Free piston shock tunnels - Developments and capabilities p 66 A93-12316
Advanced cockpit technology in the real world p 2 A93-13409
Trends in advanced avionics --- Book [ISBN 0-8138-0749-2] p 341 A93-17574
Technological challenges with smart structures in German aircraft industry p 320 A93-17714
Progress towards common standards for flight simulator qualification p 374 A93-18774
Aerospace '92 - The year in review p 455 A93-19976
A historical perspective on hypersonic research at the NACA/NASA Langley Research Center (1944-1984) [AIAA PAPER 92-5034] p 456 A93-22308
The rebirth of supersonic transport p 457 A93-25325
NASP - Waveriders in a hypersonic sky. II p 532 A93-25359
Current technologies for waverider aircraft [AIAA PAPER 93-0400] p 505 A93-25521
Airport technology international 1993 p 532 A93-26920
East Europe's aircraft builders look West p 458 A93-28396
Miniature display technologies for integrated helmet systems p 718 A93-34819
Advanced Technology Blade testing on the XV-15 Tilt Rotor Research Aircraft p 799 A93-36020
The finite element method in the 1990's [ISBN 0-387-54930-7] p 925 A93-40823
IHPTET exhaust nozzle technology demonstrator --- integrated high performance turbine energy technology [AIAA PAPER 93-2569] p 1121 A93-50287
Advanced generating technologies - Motivation and selection process in electric utilities p 1164 A93-50950
The challenge of IHPTET --- Integrated High Performance Turbine Engine Technology [ISABE 93-7001] p 1194 A93-53978
Design and technology for engine manufacture --- for Rolls-Royce aerospace business [ISABE 93-7002] p 1194 A93-53979
Propulsion technology challenges for turn-of-the-century commercial aircraft p 1194 A93-53980
Japan's research and development program for airbreathing engine technologies [ISABE 93-7005] p 1194 A93-53981
Complementary role of ground testing, flight testing, and computations in aerospace plane propulsion development [ISABE 93-7034] p 1197 A93-54010
Presence and future of the electro-chemical processes in aero-engine production p 1257 A93-54840
Passive damping technology p 1259 A93-55866
Rolls-Royce civil engine technology [PNR-90936] p 56 A93-11036
The Trent: Towards greater thrust [PNR-90937] p 56 A93-11037
Introduction to the Rolls-Royce design process [PNR-90939] p 57 A93-11039
Development of advanced carbon-carbon annular flameholders for gas turbines [PNR-90947] p 58 A93-11106
The technical background to standards for eyebolts [NPL-DMM(A)-52] p 87 A93-11327
Future regional transport aircraft market, constraints, and technology stimuli [NASA-TM-107669] p 109 A93-13025
The V-22 Osprey: A case analysis [AD-A256445] p 164 A93-14601
Flight simulation leaves the ground p 194 A93-14616
Engine technologies for future spaceplanes [ETN-92-92732] p 177 A93-15143
Terminal area traffic management [LR-684] p 317 A93-16213
Technical needs and research opportunities provided by projected aeronautical and space systems [NASA-CR-192124] p 386 A93-16629
Navstar global positioning system: Introduction and status [NLR-TP-91008-U] p 318 A93-17559
Modern helicopter technologies at MBB and the application in future programmes [MBB-UD-0599-91-PUB] p 331 A93-17566
The technological evolution of high thrust turbine engines [DS-1881] p 364 A93-17882

- Airborne Wind Shear Detection and Warning Systems: Fourth Combined Manufacturers' and Technologists' Conference, part 1 [NASA-CP-10105-PT-1] p 488 A93-19590
Handling and using information systems with new technology [PNR-90910] p 572 A93-20734
Test techniques for evaluating flight displays [NASA-TM-103947] p 516 A93-21810
Small satellites and RPA's in global-change research [AD-A260762] p 755 A93-25837
In-flight near- and far-field acoustic data measured on the Propan Test Assessment (PTA) testbed and with an adjacent aircraft [NASA-TM-103719] p 852 A93-27058
Reliability assessment at airline inspection facilities. Volume 2: Protocol for an eddy current inspection reliability experiment [DOT/FAA/CT-92/12-VOL-2] p 842 A93-28685
Propulsion technology challenges for turn-of-the-century commercial aircraft [NASA-TM-106192] p 1005 A93-32351

TECHNOLOGY TRANSFER

- Will aerospace plane development go international? p 1043 A93-49331
NSF Science and Technology Centers [NSF-92-104] p 193 A93-13712
Reliability assessment at airline inspection facilities. Volume 2: Protocol for an eddy current inspection reliability experiment [DOT/FAA/CT-92/12-VOL-2] p 842 A93-28685

TECHNOLOGY UTILIZATION

- Evolution of helicopters and the status of technology in India p 2 A93-12234
Achieving manufacturing excellence for gas turbine components through focused implementation of technology [ASME PAPER 92-GT-139] p 401 A93-19371
Hypervelocity scramjet capabilities of the T5 Free-Piston Tunnel at Caltech [AIAA PAPER 92-5037] p 376 A93-22311
Nickel hydrogen batteries for terrestrial applications p 557 A93-26005
Applications of IR imagery to thermal evaluations [SAE PAPER 921223] p 926 A93-41397
Component and Engine Structural Assessment Research (CAESAR) [AIAA PAPER 93-2609] p 1122 A93-50316
Fiber-optic technology for transport aircraft p 1173 A93-50488
Airship: The 'Look Out' - A versatile surveillance platform [AIAA PAPER 93-4033] p 1229 A93-54605
Advanced technologies for enhancement of airships [AIAA PAPER 93-4040] p 1242 A93-54610
Technology benefits and ground test facilities for high-speed civil transport development [NASA-TM-107670] p 378 A93-15790
Dr. Alexander H. Flax: Technologist of aeronautics [AD-A258441] p 456 A93-17890
Advanced Turbine Technology Applications Project (ATTAP) [NASA-CR-189228] p 455 A93-18762
NASA SBIR abstracts of 1990 phase 1 projects [NASA-TM-108145] p 572 A93-21794
JPRS report: Science and technology. Central Eurasia: Engineering and equipment [JPRS-UEQ-92-007] p 842 A93-28635
JPRS report: Science and technology. Central Eurasia: Engineering and equipment [JPRS-UEQ-93-003] p 842 A93-28691
Aircraft structures in 2000: A technological challenge? [MBB-LME-202-S-PUB-0485] p 998 A93-31058

TEETERING

- User's Guide for the NREL Teetering Rotor Analysis Program (STRAP) [DE92-010580] p 216 A93-13525

TEFLON (TRADEMARK)

- COF2 radiation from an air-teflon wake p 12 A93-12659

TELECOMMUNICATION

- The Meteorological Data Collection and Reporting System - Status and future directions p 428 A93-22133
Communication satellites for commercial aircraft operations p 499 A93-25493
Implementing system simulation of C3 systems using autonomous objects [NASA-CR-190845] p 89 A93-11716
Future FAA telecommunications plan [AD-A249133] p 89 A93-11760
Multipath effects in a Global Positioning Satellite system receiver p 318 A93-17311
A simulation study of the effects of communication delay on air traffic control [AD-A258593] p 502 A93-19966

TELEMETRY

- A data reduction system for processing instrumented flight test data p 847 A93-37866
Instrumentation and telemetry systems for free-flight drop model testing p 1209 A93-52754
Ground installations for preparation and evaluation of flight tests p 1014 A93-31274

TELEOPERATORS

- Visual field information in Nap-of-the-Earth flight by teleoperated Helmet-Mounted displays p 517 A93-26884

TELEROBOTICS

- RACE pulls for shared control --- telerobotics and automation technology for aircraft maintenance and inspection p 458 A93-29130
Robotic aircraft painting with SAFARI [SME PAPER AD92-198] p 855 A93-40662

TELEVISION CAMERAS

- Recent experiences with implementing a video based six degree of freedom measurement system for airplane models in a 20 foot diameter vertical spin tunnel p 821 A93-37763

TELEVISION RECEIVERS

- HELITRAK: A helicopter-tracking receiver system for television outside broadcast links [BBC-RD-1992/5] p 552 A93-20573

TELEVISION SYSTEMS

- Fiber optics for aircraft entertainment systems p 1172 A93-49478
HELITRAK: A helicopter-tracking receiver system for television outside broadcast links [BBC-RD-1992/5] p 552 A93-20573

TEMPERATURE COMPENSATION

- Optical temperature compensation schemes of spectral modulation sensors for aircraft engine control p 1105 A93-49471

TEMPERATURE CONTROL

- A thermal analysis of an F/A-18 wing section for actuator thermal management [SAE PAPER 921023] p 158 A93-14650
The comparison of different simplified mathematical models of the gas turbine combustion chamber as an object of temperature and pressure control [ASME PAPER 92-GT-347] p 354 A93-19518
Study on dynamic characteristics of heat exchanger p 924 A93-40492
Thermal control of a lidar laser system using a non-conventional ram air heat exchanger p 1028 A93-46821
A procedure for the thermal and strength testing of radiotransparent shells p 1209 A93-52976
Current Technology for Thermal Protection Systems [NASA-CP-3157] p 69 A93-12447
Thermal control/oxidation resistant coatings for titanium-based alloys p 74 A93-12457

TEMPERATURE DEPENDENCE

- Measurements of dynamic Young's modulus and damping in single crystals of a nickel-based superalloy as a function of temperature p 1147 A93-52513

TEMPERATURE DISTRIBUTION

- Steady state model for the thermal regimes of shells of airships and hot air balloons p 207 A93-15072
Hot streaks and phantom cooling in a turbine rotor passage. I - Separate effects [ASME PAPER 92-GT-75] p 401 A93-19325
Effect of steady-state circumferential pressure and temperature distortions on compressor stability p 1106 A93-48503
Experimental research on a semiwater-gas-fired gas-turbine p 1107 A93-48524
Determination of the N2(+) + e recombination rate constant from ballistic experiments p 1234 A93-55026
Method of remotely characterizing thermal properties of a sample [NASA-CASE-LAR-13508-3-CU] p 67 A93-11057
A preliminary study of the effect of equivalence ratio on a low emissions gas turbine combustor using KIVA-2 [DE92-018616] p 215 A93-13321
Fluid flow and heat convection studies for actively cooled airframes [NASA-CR-190956] p 216 A93-13406
Modelling the engine temperature distribution between shut down and restart for life usage monitoring p 169 A93-15177
An experimental investigation of a round turbulent jet in a cross-flow p 553 A93-20689
A new LU-SGS flow solver for calculating reentry flows p 698 A93-25759
Experimental study of heat transfer close to a plane wall heated in the presence of multiple injections (subsonic flow) p 901 A93-29931
Local heat transfer measurement with liquid crystals on rotating surfaces including non-axisymmetric cases p 902 A93-29943

- Cooling predictions in turbofan engine components p 905 N93-29964
- TEMPERATURE EFFECTS**
- The fretting damage and effect of temperature in typical joint of aircraft construction p 203 A93-14196
- Finite element nonlinear panel flutter with arbitrary temperatures in supersonic flow p 417 A93-23555
- Thermoelastic vibration test techniques p 549 A93-29293
- An optical fiber based position sensor with immunity to temperature variation p 743 A93-34287
- Temperature and suction effects on the instability of an infinite swept attachment line p 691 A93-35486
- Effect of temperature on nonlinear two-dimensional panel flutter using finite elements p 1022 A93-45133
- Thermal effects testing at the National Solar Thermal Test Facility p 1255 A93-54402
- The effect of temperature on the natural frequencies and acoustically induced strains in CFRP plates p 1260 A93-56331
- Design of a high-temperature experiment for evaluating advanced structural materials (NASA-TM-105833) p 88 N93-11624
- Deformation mechanisms of NiAl cyclicly deformed near the brittle-to-ductile transformation temperature (NASA-CR-191649) p 391 N93-15830
- Mode interaction in stiffened composite shells under combined mechanical and thermal loadings p 419 N93-16793
- Thermally induced stresses in a composite exposed to fire (AD-A261714) p 737 N93-26371
- Ventilation effects on smoke and temperature in an aircraft cabin quarter-scale model (DOT/FAA/CT-89/25) p 791 N93-28055
- Thermal effects of a coolant film along the suction side of a high pressure turbine nozzle guide vane p 901 N93-29930
- TEMPERATURE GRADIENTS**
- Calculation of safe altitudes p 991 A93-45675
- Testing experience with unheated strain-gage balances in the NTF — National Transonic Facility p 1013 A93-47021
- Design of a high-temperature experiment for evaluating advanced structural materials (NASA-TM-105833) p 88 N93-11624
- Fluid flow and heat convection studies for actively cooled airframes (NASA-CR-190956) p 216 N93-13406
- TEMPERATURE MEASUREMENT**
- Estimation of maximal local temperature at exit of annular combustor p 172 A93-14496
- Coherent anti-Stokes Raman scattering (CARS) thermometry in a model gas turbine can combustor (ASME PAPER 92-GT-134) p 387 A93-19366
- Behaviors of the laterally injected jet in film cooling - Measurements of surface temperature and velocity/temperature field within the jet (AIAA PAPER 92-GT-180) p 402 A93-19405
- Remote sensing of O₂ in a supersonic combustor using diode lasers and fiber optics (AIAA PAPER 92-5090) p 414 A93-22360
- Data analysis techniques for pressure- and temperature-sensitive paint (AIAA PAPER 93-0176) p 414 A93-22605
- CARS thermometry in a liquid fueled model combustor (AIAA PAPER 93-0366) p 390 A93-23047
- USAF supercritical hydrocarbon fuels interests (AIAA PAPER 93-0807) p 533 A93-24883
- Applications of IR imagery to thermal evaluations (SAE PAPER 92-1223) p 926 A93-41397
- A horizontal atmospheric temperature sounder - Applications to remote sensing of atmospheric hazards p 929 A93-43502
- Comparison of NO and OH PLIF temperature measurements in a scramjet model flowfield (AIAA PAPER 93-2035) p 1113 A93-49870
- Implementation of an infrared thermal imaging system to measure temperature in a gas turbine engine (AIAA PAPER 93-2469) p 1120 A93-50215
- Thermometry inside a swirling turbulent flame - CARS advantages and limitations p 1146 A93-51634
- CARS temperature measurements in combustion (ONERA, TP NO. 1993-78) p 1212 A93-53599
- Experimental heat transfer results in turbine stators and rotors and a comparison with theory (PNR-90945) p 57 N93-11055
- Method of remotely characterizing thermal properties of a sample (NASA-CASE-LAR-13508-3-CU) p 67 N93-11057
- Operating experience using venturi flow meters at liquid helium temperature (DE92-014693) p 90 N93-12140
- Time dependent heat transfer rates in high Reynolds number hypersonic flowfields p 216 N93-13664

- Planar measurement of flow field parameters in nonreacting supersonic flows with laser-induced iodine fluorescence p 133 N93-13801
- Study of optical techniques for the Ames unitary wind tunnel. Part 5: Infrared imagery (NASA-CR-191385) p 194 N93-14809
- Electron beam probing of blow-down hypersonic flows (ONERA-NT-1992-7) p 298 N93-18701
- Research support for the Laboratory for Lightwave Technology (AD-A261488) p 760 N93-26343
- A passive infrared ice detection technique for helicopter applications (NASA-CR-193187) p 880 N93-29152
- Cooling predictions in turbofan engine components p 905 N93-29964
- TEMPERATURE MEASURING INSTRUMENTS**
- Correction of the frequency characteristic of the waveguide circuit of an acoustic-jet temperature transducer p 832 A93-39036
- Flight testing of a fiber optic temperature sensor p 1105 A93-49476
- TEMPERATURE PROFILES**
- Non-self-similarity of a boundary layer flow of a high-temperature gas in a Laval nozzle p 1176 A93-52946
- Strain-gauge balance performance and internal temperature gradients measured in a cryogenic environment (RAE-TM-AERO-2232) p 68 N93-11906
- SAC contrail formation study (AD-A254410) p 159 N93-12605
- A passive infrared ice detection technique for helicopter applications (NASA-CR-193187) p 880 N93-29152
- TEMPERATURE RATIO**
- Investigation of the flowfield around an isolated bypass engine with fan and core jet p 215 N93-13227
- Heat transfer and aerodynamics of a high rim speed turbine nozzle guide vane with profiled end walls (AD-A258346) p 295 N93-17991
- TEMPERATURE SENSORS**
- Fast-response aircraft temperature sensors p 167 A93-17095
- Heat flux microsensor measurements (AIAA PAPER 92-5038) p 413 A93-22312
- TEMPORAL RESOLUTION**
- CARS temperature measurements in combustion (ONERA, TP NO. 1993-78) p 1212 A93-53599
- TENSILE DEFORMATION**
- Inelasticity effect in a unidirectional boron/aluminum composite under uniaxial tension p 825 A93-39024
- Dynamic analysis of a compound elastic surface p 1030 A93-47086
- TENSILE STRENGTH**
- A study of the effect of the support fastening compliance on the stress-strain state of aircraft transparencies p 997 A93-47079
- Origin of the carbon rich sliding interface in alkali containing matrix-SiC nicalon fibre composites (ONERA, TP NO. 1993-77) p 1212 A93-53598
- Thermal design and analysis of an exhaust diffuser unit in a ceramic composite (ISABE 93-7060) p 1220 A93-54036
- The beta-CEZ, a new high performance titanium alloy for aerospace engines (DS-2022) p 393 N93-17852
- TENSILE TESTS**
- Infrared thermography of plastic instabilities in a single crystal superalloy (ONERA, TP NO. 1993-18) p 916 A93-41031
- Design and fabrication of panels with cutouts p 1215 A93-52973
- The application of diffusion bonding in the manufacture of aeroengine components p 1217 A93-53514
- Material characterization and fractographic examination of Ti-17 fatigue crack growth specimens for SMP SC33 p 1004 N93-31744
- Fatigue crack growth results for Ti-6Al-4V, IMI 685, and Ti-17 p 1004 N93-31746
- TENSOMETERS**
- Measurement of aerodynamic forces at high temperatures p 75 A93-10030
- SENSOR ANALYSIS**
- An analytical-experimental method for studying the strength and stability of thin-walled structures p 1029 A93-47084
- TERCOM**
- Information-based criteria of terrain navigability. Part 1: Data-base analysis p 793 N93-27178
- TERMINAL FACILITIES**
- Spatial orientation and wayfinding in airport passenger terminals - Implications for environmental design p 487 A93-27168

TERMINAL GUIDANCE

- Flight test evaluation of precision-code differential GPS for terminal approach and landing p 33 A93-11294
- Weather information requirements for Terminal Air Traffic Control Automation p 429 A93-22146
- Terminal forecast amendments - A 'cloudy' issue --- valid for up to 24 hours for airport areas p 431 A93-22167
- Status of the Terminal Doppler Weather Radar one year before deployment p 431 A93-22184
- Reliability considerations for weather hazard warning radar p 431 A93-22187
- Terminal Doppler Weather Radar program at Denver's Stapleton International Airport during 1989 and 1990 p 432 A93-22188
- Performance results and potential operational uses for the prototype TDWR microburst prediction product p 432 A93-22190
- An improved gust front detection algorithm for the TDWR p 432 A93-22191
- The detection and warning of low-level wind shear based on terminal single Doppler radar p 432 A93-22195
- Controller evaluation of initial data link terminal air traffic control services: Mini study 2, volume 1 (DOT/FAA/CT-92/2-VOL-1) p 36 N93-11704
- Controller evaluation of initial data link terminal air traffic control services: Mini study 2, volume 2 (DOT/FAA/CT-92/2-VOL-2) p 36 N93-11705
- The effect of TCAS interrogations on the Chicago O'Hare ATCRBS system (DOT/FAA/CT-92/22) p 318 N93-16498
- TERRAIN**
- The use of digital map data to provide enhanced navigation and displays for poor weather penetration and recovery p 992 A93-45165
- Advanced terrain displays to transport category aircraft (PB92-197136) p 35 N93-10065
- Automated extraction of aircraft runway patterns from radar imagery (AD-A254258) p 68 N93-11751
- Integration of radar altimeter, precision navigation, and digital terrain data for low-altitude flight (NASA-TM-103958) p 36 N93-12320
- Taxonomy of flight variables p 147 N93-15022
- ILS mathematical modeling study of an ILS glide slope proposed for runway 19L at the Meridian Naval Air Station, Mississippi (DOT/FAA/CT-TN93/8) p 705 N93-24741
- TERRAIN ANALYSIS**
- Accuracy analysis on image matching guidance systems p 62 A93-12653
- BUAA inertial terrain-aided navigation (BITAN) algorithm p 149 A93-14235
- Automatic guidance and control laws for helicopter obstacle avoidance p 728 A93-35518
- Visual augmentation for night flight over featureless terrain p 806 A93-35921
- Topographic mapping using a Ku-band airborne elevation interferometer p 896 A93-42786
- Efforts to reduce CFIT accidents should address failures of the aviation system itself p 1096 A93-49280
- Terrain modeling for real-time photo-texture based visual simulation (AIAA PAPER 93-3607) p 1214 A93-52667
- LONGBOW - Force multiplier for continuous operations p 1175 A93-54295
- Testing of an automatic, low altitude, all terrain ground collision avoidance system p 502 N93-19924
- Information-based criteria of terrain navigability. Part 1: Data-base analysis p 793 N93-27178
- TERRAIN FOLLOWING AIRCRAFT**
- AFTI/F-16 night close air support system testing p 808 A93-38841
- Prediction and planning of a flight vehicle route in the presence of motion inhibiting factors p 1130 A93-50961
- Multirate and event-driven Kalman filters for helicopter flight p 1245 A93-55760
- Appraisal of digital terrain elevation data for low-altitude flight (NASA-TM-103896) p 35 N93-10745
- Integration of radar altimeter, precision navigation, and digital terrain data for low-altitude flight (NASA-TM-103958) p 36 N93-12320
- Optimal trajectories for aircraft terrain following and terrain avoidance: A literature review update (AD-A264075) p 910 N93-30604
- TEST CHAMBERS**
- Development of the Boeing Low Speed Aeroacoustic Facility (LSAF) p 374 A93-19148
- The design of test-section inserts for higher speed aeroacoustic testing in the Ames 80- by 120-Foot Wind Tunnel p 374 A93-19149
- Liquid flow reactor and method of using (AD-D015392) p 222 N93-15232

TEST EQUIPMENT

A feasibility study of using Langley 0.3-m transonic cryogenic tunnel sidewall boundary-layer removal system for heavy gas testing
[NASA-CR-191438] p 747 N93-25087

Mathematical modeling and control law development for the atmospheric monitoring and control system of the Controlled Environment Research Chamber (CERC) at NASA Ames Research Center
[AD-A261978] p 911 N93-29436

TEST EQUIPMENT

A data reduction system for processing instrumented flight test data p 647 A93-37866
An evaluation of the pressure proof test concept for 2024-T3 aluminium alloy sheet p 1026 A93-45780
Parametric study of air sampling cyclones p 135 N93-14173

The USAF Advanced Turbine Aerothermal Research Rig (ATAARR) p 911 N93-29945

TEST FACILITIES

Design and utilization of a Flight Test Engineering Database Management System at the NASA Dryden Flight Research Facility p 97 A93-13264

Electronic Counter Countermeasures/Advanced Radar Test Bed (ECCM/ARTB) p 34 A93-13267

Systems integration test laboratory - Application and experiences p 190 A93-13910
Five years operational experiences with Indonesian Low Speed Tunnel (ILST) p 191 A93-14403

Testing for integrity --- of aircraft gas turbine engines p 346 A93-18785

The acoustic response of altitude test facility exhaust systems to axisymmetric and two-dimensional turbine engine exhaust plumes p 449 A93-19209

The dynamic characteristics of a high pressure turbine stage in a transient wind tunnel p 375 A93-19392

Arc jet testing in NASA Ames Research Center thermophysics facilities p 385 A93-22315

Icing testing of a large full-scale inlet at the Arnold Engineering Development Center p 376 A93-22697

Development of Polytechnic University's supersonic wind tunnel facility p 528 A93-24876

Design of a hydrogen test facility p 532 A93-25993
Advances in the design of jet engine test facilities for military aircraft in Australia p 529 A93-28491

Development and validation of 'quiet tail rotor' technology p 567 A93-29416

Data acquisition and analysis on a Macintosh p 562 A93-29422

High-temperature supersonic combustion testing with optical diagnostics p 730 A93-34498

AEDC expanded flow arc facility (HEAT-H2) description and calibration p 821 A93-37872

Development update for the NASA Ames 16-Inch Shock Tunnel Facility p 822 A93-37873

GE90 program moves into high gear p 810 A93-38701

Test facility for evaluation of structural integrity of stiffened and jointed aircraft curved panels p 1012 A93-45794

AEDC H2 Facility - New test capabilities for hypersonic air-breathing vehicles p 1012 A93-46525

Development and operation of new arc heater technology for a large-scale scramjet propulsion test facility p 1016 A93-46528

A report on the status of MHD hypersonic ground test technology in Russia p 1012 A93-46656

Langley proposed advanced hypervelocity aerophysics facility - A status report p 1013 A93-47015

Harvesting nitrous oxide for elevation of temperature and pressure in piston facilities p 1137 A93-49854

Ground test simulation fidelity of turbine engine airstarts p 1137 A93-49986

Improved data validation and quality assurance in turbine engine test facilities p 1137 A93-49990

Unique development testing at Allison Gas Turbine p 1138 A93-50200

An upgraded data acquisition and processing system for the Aeropropulsion Systems Test Facility at Arnold Engineering Development Center p 1138 A93-50213

Liquid hydrogen foil-bearing turbopump p 1156 A93-50264

Recent successes in modifying several existing jet engine test cells to accommodate large, high-bypass turbofan engines p 1139 A93-50266

The development of a large annular facility for testing gas turbine combustor diffuser systems p 1139 A93-50269

A test bench for rotorcraft hover control p 1140 A93-51440

NASA Langley's Aircraft Landing Dynamics Facility p 1250 A93-54400

Thermal effects testing at the National Solar Thermal Test Facility p 1255 A93-54402

Hypersonic vehicle research by using a large shock tunnel p 1250 A93-55841

Noise studies for environmental impact assessment of an outdoor engine test facility p 99 N93-10672

Testing for integrity p 56 N93-11024

A test facility for the thermofluid-dynamics of gas bearing lubrication films p 72 N93-11032

Rotational CARS measurements in a rotating cavity with axial throughflow of cooling air: Oxygen concentration measurements p 72 N93-11035

Developments in icing test techniques for aerospace applications in the RAE Pyestock (England) altitude test facility p 48 N93-11485

An investigation of jet engine test cell aerodynamics by means of scale model test studies with comparisons to full-scale test results p 193 N93-14060

Personal computer based test- and emulation equipment for maintenance and ground support p 110 N93-15185

Technology benefits and ground test facilities for high-speed civil transport development p 378 N93-15790

Experimental investigation of an ejector-powered free-jet facility p 291 N93-16704

[NASA-TM-105868] p 291 N93-16704

Flight Testing p 510 N93-19901

Evaluation of candidate working fluid formulations for the electrothermal - chemical wind tunnel p 530 N93-20312

The influence of the rotor test facilities ROTEST and ROTOS on the rotor inflow p 522 N93-21173

Development of a large-scale, outdoor, ground-based test capability for evaluating the effect of rain on airfoil lift p 779 N93-26899

[NASA-TM-4420] p 779 N93-26899

A laboratory study of subjective response to sonic booms measured at White Sands Missile Range p 852 N93-27272

[NASA-TM-107746] p 852 N93-27272

Modification and calibration of the Naval Postgraduate School Academic Wind Tunnel p 823 N93-28189

[AD-A262092] p 823 N93-28189

Flight test of avionic and air-traffic control systems p 993 N93-31271

[ESA-TT-1279] p 993 N93-31271

The DLR test aircraft in the FZ-BS, -VFW 614/ATTAS, Dornier DO 228-101, MBB BO105 S-3 p 1018 N93-31272

The basic measurement equipment of the DLR test aircraft p 1000 N93-31273

Instigation and processing of flight tests in DLR p 998 N93-31275

ATTAS experimental-cockpit and ATMOS for component and system investigations in flight guidance p 1014 N93-31276

Testing of an experimental FMS p 998 N93-31277

Pallet for helicopter test instrumentation p 1000 N93-31279

TEST FIRING

Development and operation of new arc heater technology for a large-scale scramjet propulsion test facility p 1016 A93-46528

[AIAA PAPER 93-2786] p 1016 A93-46528

Subscale hot-fire testing of a formed platelet liner p 1141 A93-49713

[AIAA PAPER 93-1827] p 1141 A93-49713

TEST STANDS

Helicopter in-flight simulator ATTHes - A multipurpose tested and its utilization p 43 A93-13315

[AIAA PAPER 92-4173] p 43 A93-13315

Effect of geometry, bleed rates and flow splits on pressure recovery of a canted hybrid vortex-controlled diffuser p 1109 A93-49659

[AIAA PAPER 93-1762] p 1109 A93-49659

Measured data for the Sandia 34-meter vertical axis wind turbine p 94 N93-12075

[DE92-019807] p 94 N93-12075

Microburst characteristics determined from 1988-1991 TDWR tested measurements p 490 N93-19605

A large hemi-anechoic enclosure for community-compatible aeroacoustic testing of aircraft propulsion systems p 760 N93-26551

[NASA-TM-106015] p 760 N93-26551

Load test set-up for the Airmass Sunburst Ultra-Light Aircraft p 895 N93-29776

The USAF Advanced Turbine Aerothermal Research Rig (ATAARR) p 911 N93-29945

TEST VEHICLES

INS/DGPS integration for trajectory determination of a test vehicle p 315 A93-21178

TETHERED BALLOONS

A joint Soviet-Bulgarian scientific program for free-flight and tethered aerostat observations p 2 A93-11374

TETHERED SATELLITES

Development of a tethered satellite force transducer p 1251 A93-54368

Effect of the atmosphere density gradient on aerodynamic stabilization p 1252 A93-55034

TETHERLINES

The stability and aerodynamic performances of clusters of small cruciform parachutes p 690 A93-35181

[AIAA PAPER 93-1242] p 690 A93-35181

TETRAHEDRONS

Geometry based Delaunay tetrahedralization and mesh movement strategies for multi-body CFD p 15 A93-13309

A new procedure for dynamic adaption of three-dimensional unstructured grids p 560 A93-24780

[AIAA PAPER 93-0672] p 560 A93-24780

Generation of unstructured tetrahedral meshes by advancing front technique p 1021 A93-44206

TEXTILES

The characterization and development of materials for advanced textile composites p 1211 A93-53434

Advanced fiber/matrix material systems p 921 N93-30854

TEXTURES

Passive range sensor refinement using texture and segmentation p 544 A93-27044

Terrain modeling for real-time photo-texture based visual simulation p 1214 A93-52667

[AIAA PAPER 93-3607] p 1214 A93-52667

Texture as a visual cueing element in computer image generation. I - Representation of the sea surface p 1214 A93-52695

[AIAA PAPER 93-3560] p 1214 A93-52695

THEODORSEN TRANSFORMATION

Theodorsen's ideal propeller performance with ambient pressure in the slipstream p 768 A93-37400

THEOREMS

Determination of the zone of the stall cell by means of the baroclinic wave theory p 424 N93-18733

Rotating stall cell and Von Karman vortex street: A meteorological theory p 424 N93-18734

THEORIES

Elements of a theory of natural decision making p 147 N93-15021

THEOREMS

Determination of the zone of the stall cell by means of the baroclinic wave theory p 424 N93-18733

Rotating stall cell and Von Karman vortex street: A meteorological theory p 424 N93-18734

THEORIES

Elements of a theory of natural decision making p 147 N93-15021

THEOREMS

Determination of the zone of the stall cell by means of the baroclinic wave theory p 424 N93-18733

Rotating stall cell and Von Karman vortex street: A meteorological theory p 424 N93-18734

THEORIES

Elements of a theory of natural decision making p 147 N93-15021

THEOREMS

Determination of the zone of the stall cell by means of the baroclinic wave theory p 424 N93-18733

Rotating stall cell and Von Karman vortex street: A meteorological theory p 424 N93-18734

THEORIES

Elements of a theory of natural decision making p 147 N93-15021

THEOREMS

Determination of the zone of the stall cell by means of the baroclinic wave theory p 424 N93-18733

Rotating stall cell and Von Karman vortex street: A meteorological theory p 424 N93-18734

THEORIES

Elements of a theory of natural decision making p 147 N93-15021

THEOREMS

Determination of the zone of the stall cell by means of the baroclinic wave theory p 424 N93-18733

Rotating stall cell and Von Karman vortex street: A meteorological theory p 424 N93-18734

THEORIES

Elements of a theory of natural decision making p 147 N93-15021

THEOREMS

Determination of the zone of the stall cell by means of the baroclinic wave theory p 424 N93-18733

Rotating stall cell and Von Karman vortex street: A meteorological theory p 424 N93-18734

THEORIES

Elements of a theory of natural decision making p 147 N93-15021

THEOREMS

Determination of the zone of the stall cell by means of the baroclinic wave theory p 424 N93-18733

Rotating stall cell and Von Karman vortex street: A meteorological theory p 424 N93-18734

THEORIES

Elements of a theory of natural decision making p 147 N93-15021

THEOREMS

Determination of the zone of the stall cell by means of the baroclinic wave theory p 424 N93-18733

Rotating stall cell and Von Karman vortex street: A meteorological theory p 424 N93-18734

THEORIES

Elements of a theory of natural decision making p 147 N93-15021

THEOREMS

Determination of the zone of the stall cell by means of the baroclinic wave theory p 424 N93-18733

Rotating stall cell and Von Karman vortex street: A meteorological theory p 424 N93-18734

THEORIES

Elements of a theory of natural decision making p 147 N93-15021

THEOREMS

Determination of the zone of the stall cell by means of the baroclinic wave theory p 424 N93-18733

Rotating stall cell and Von Karman vortex street: A meteorological theory p 424 N93-18734

THEORIES

Elements of a theory of natural decision making p 147 N93-15021

THEOREMS

Determination of the zone of the stall cell by means of the baroclinic wave theory p 424 N93-18733

Rotating stall cell and Von Karman vortex street: A meteorological theory p 424 N93-18734

THEORIES

Elements of a theory of natural decision making p 147 N93-15021

THEOREMS

Determination of the zone of the stall cell by means of the baroclinic wave theory p 424 N93-18733

Rotating stall cell and Von Karman vortex street: A meteorological theory p 424 N93-18734

THEORIES

Elements of a theory of natural decision making p 147 N93-15021

THEOREMS

Determination of the zone of the stall cell by means of the baroclinic wave theory p 424 N93-18733

Rotating stall cell and Von Karman vortex street: A meteorological theory p 424 N93-18734

THEORIES

Elements of a theory of natural decision making p 147 N93-15021

THEOREMS

Determination of the zone of the stall cell by means of the baroclinic wave theory p 424 N93-18733

Rotating stall cell and Von Karman vortex street: A meteorological theory p 424 N93-18734

THEORIES

Elements of a theory of natural decision making p 147 N93-15021

THEOREMS

Determination of the zone of the stall cell by means of the baroclinic wave theory p 424 N93-18733

Rotating stall cell and Von Karman vortex street: A meteorological theory p 424 N93-18734

THEORIES

Elements of a theory of natural decision making p 147 N93-15021

THEOREMS

Determination of the zone of the stall cell by means of the baroclinic wave theory p 424 N93-18733

Rotating stall cell and Von Karman vortex street: A meteorological theory p 424 N93-18734

THEORIES

Elements of a theory of natural decision making p 147 N93-15021

THEOREMS

Determination of the zone of the stall cell by means of the baroclinic wave theory p 424 N93-18733

Rotating stall cell and Von Karman vortex street: A meteorological theory p 424 N93-18734

THEORIES

Elements of a theory of natural decision making p 147 N93-15021

THEOREMS

Determination of the zone of the stall cell by means of the baroclinic wave theory p 424 N93-18733

Rotating stall cell and Von Karman vortex street: A meteorological theory p 424 N93-18734

THEORIES

Elements of a theory of natural decision making p 147 N93-15021

THEOREMS

THERMAL BUCKLING

Thermomechanical postbuckling analysis of laminated composite shells
[AIAA PAPER 93-1337] p 738 A93-33907

THERMAL CONTROL COATINGS

Technical note - Plasma-sprayed ceramic thermal barrier coatings for smooth intermetallic alloys
p 209 A93-15702

Influence of a thermal barrier coating on the performance of a turboprop engine
[ASME PAPER 92-GT-38] p 347 A93-19297

The evolution of thermal barrier coatings in gas turbine engine applications
[ASME PAPER 92-GT-203] p 388 A93-19427

Microstructure of yttria stabilized zirconia-hafnia plasma sprayed thermal barrier coatings
[ONERA, TP NO. 1993-54] p 1146 A93-51936

Stress relaxation of low pressure plasma-sprayed NiCrAlY alloys
p 1211 A93-52870

Calculation of sandwich plates with polymer composite skins under conditions of high humidity
p 1215 A93-52968

Thermal barrier design of gamma-TiAl Functionally Gradient Materials (FGMs) for scramjet engine applications
p 1246 A93-54556

Thermal control/oxidation resistant coatings for titanium-based alloys
p 74 A93-12457

Thermal barrier coating life prediction model development, phase 2
[NASA-CR-189111] p 198 A93-12589

X ray diffraction and electron microscope studies of Yttria Stabilized Zirconia (YSZ) ceramic coatings exposed to vanadia
[AD-A258055] p 392 A93-17676

THERMAL DECOMPOSITION

Results of high temperature JP-7 cracking assessment
[AIAA PAPER 93-0806] p 533 A93-24882

Measurement of diffusion in supercritical fluid systems - A review
[AIAA PAPER 93-0809] p 534 A93-24884

THERMAL DEGRADATION

Evaluation of metallurgical degradation on gas turbine components
p 915 A93-40804

Implementation of an infrared thermal imaging system to measure temperature in a gas turbine engine
[AIAA PAPER 93-2469] p 1120 A93-50215

Numerical method for simulating fluid-dynamic and heat-transfer changes in jet-engine injector feed-arm due to fouling
p 1245 A93-54467

THERMAL DISSOCIATION

Planar imaging of OH density distributions in a supersonic combustion tunnel
[AIAA PAPER 93-0042] p 389 A93-20155

THERMAL ENVIRONMENTS

An experimental examination of the thermal and acoustic environments on runway joint seals
[AD-A257965] p 382 A93-17734

THERMAL EXPANSION

INCOLOY 908, a low coefficient of expansion alloy for high-strength cryogenic applications. I - Physical metallurgy
p 534 A93-25686

Stiffness, thermal expansion, and thermal bending formulation of stiffened, fiber-reinforced composite panels
[AIAA PAPER 93-1569] p 741 A93-34102

THERMAL FATIGUE

Markov fatigue in single crystal airfoils
[ASME PAPER 92-GT-95] p 387 A93-19341

Life prediction - Thermal fatigue from isothermal data
p 916 A93-40807

Thermal fatigue life assessment of a convection-cooled gas turbine blade
[ISABE 93-7062] p 1199 A93-54038

Mechanisms and modelling of environment-dependent fatigue crack growth in a nickel based superalloy
[AD-A253967] p 71 A93-10717

Short fatigue crack growth in a nickel-base superalloy at room and elevated temperature
[PNR-90892] p 72 A93-11031

Fatigue in single crystal nickel superalloys
[AD-A254704] p 198 A93-12746

Creep fatigue life prediction for engine hot section materials (isotropic)
[NASA-CR-189221] p 364 A93-18578

Fatigue in single crystal nickel superalloys
[AD-A259191] p 536 A93-20275

Fatigue in single crystal nickel superalloys
[AD-A261742] p 737 A93-26282

Fatigue in single crystal nickel superalloys
[AD-A265451] p 1019 A93-31795

THERMAL INSTABILITY

Raising the high temperature limit of the nickel-iron-base superalloy
p 70 A93-12114

THERMAL INSULATION

Thermal response and ablation characteristics of light weight ceramic ablators
[AIAA PAPER 93-2790] p 1018 A93-46532

Current Technology for Thermal Protection Systems
[NASA-CP-3157] p 69 A93-12447

THERMAL MAPPING

Infrared thermography characterization of Goertler vortex type patterns in hypersonic flows
[ONERA, TP NO. 1993-13] p 925 A93-41029

Study of optical techniques for the Ames unitary wind tunnel. Part 5: Infrared imagery
[NASA-CR-191385] p 194 A93-14809

Dual-band infrared imaging applications: Locating buried minefields, mapping sea ice, and inspecting aging aircraft
[DE93-000516] p 453 A93-17225

Photoluminescent thermography in hypersonic blowdown wind tunnel: Feasibility study with pinpoint measurement
[ONERA-NT-1992-8] p 297 A93-18617

THERMAL NEUTRONS

A pulsed fast-thermal neutron interrogation system
p 497 A93-21866

Explosive detection system based on Electronic Neutron Generator (ENG)
p 497 A93-21870

THERMAL PROTECTION

Measurement of aerodynamic forces at high temperatures
p 75 A93-10030

High angle-of-attack inviscid Shuttle Orbiter computation
p 9 A93-12020

Hypersonic design
p 156 A93-14346

Arc jet testing in NASA Ames thermophysics facilities
[AIAA PAPER 92-5041] p 385 A93-22315

Non-equilibrium flow in an arc heated wind tunnel
p 910 A93-42642

Applications of infrared measurement technique in hypersonic facilities
p 1024 A93-45505

Evaluation of decomposition kinetic coefficients for a fiber-reinforced intumescent-epoxy
[AIAA PAPER 93-1856] p 1144 A93-49734

Aerodynamic heating environment definition/thermal protection system selection for the HL-20
p 1181 A93-53739

HOPE and its thermal protection systems
p 1252 A93-54711

Current Technology for Thermal Protection Systems
[NASA-CP-3157] p 69 A93-12447

Current research in oxidation-resistant carbon-carbon composites at NASA Langley Research Center
p 74 A93-12456

Active cooling from the sixties to NASP
p 49 A93-12458

SR-SCARLET 1: Peregrin
[NASA-CR-192048] p 337 A93-18155

THERMAL RADIATION

Recent developments in compressor-based Joule-Thomson cooling --- of thermal imaging equipment in ground and helicopter-borne applications
p 547 A93-28244

Measurement and analysis of nitric oxide radiation in an arc-jet flow
[AIAA PAPER 93-2800] p 1016 A93-46540

Non-equilibrium thermal radiation from air shock layers modelled with the Direct Simulation Monte Carlo method
[AIAA PAPER 93-2805] p 1028 A93-46544

THERMAL RESISTANCE

A procedure for the thermal and strength testing of radiotransparent shells
p 1209 A93-52976

Application of functionally gradient materials to scramjet engines
[ISABE 93-7063] p 1200 A93-54039

THERMAL SIMULATION

Prediction of engine casing temperature of fighter aircraft for infrared signature studies
[SAE PAPER 920961] p 206 A93-14627

THERMAL STABILITY

Experimental techniques for the assessment of fuel thermal stability
p 197 A93-14504

Studies of jet thermal stability in a flowing system
[ASME PAPER 92-GT-106] p 401 A93-19344

Ceramics for aero-engine applications
[ASME PAPER 92-GT-439] p 388 A93-19581

Advanced diagnostics for in situ measurement of particle formation and deposition in thermally stressed jet fuels
[AIAA PAPER 93-0363] p 390 A93-23045

High-temperature materials warm up for debut
p 535 A93-28393

Analysis of jet fuel thermal oxidation deposits by spectral fluorometric technique
p 1253 A93-55697

Thermal control/oxidation resistant coatings for titanium-based alloys
p 74 A93-12457

A condensed phase test cell assembly for the System for Thermal Diagnostic Studies (STDS)
[AD-A258463] p 393 A93-18242

Interferometric JFTOT tube deposit measuring device
[AD-D015599] p 536 A93-20247

Effect of a metal deactivator fuel additive on fuel deposition in fuel atomizers at high temperature
[AD-A260915] p 736 A93-25914

Advanced thermally-stable, coal-derived, jet fuels program: Experiment system and model development
[AD-A262747] p 917 A93-29402

THERMAL STRESSES

Thermal shock capabilities of infrared dome materials
p 70 A93-11454

The conceptual study of supersonic transport structure
[AIAA PAPER 92-4219] p 43 A93-13348

Analysis of the NASA Hypersonic Wing Test Structure
[AIAA PAPER 92-4724] p 409 A93-20326

Static tests of jet fuel thermal and oxidative stability
p 389 A93-21651

Advanced diagnostics for in situ measurement of particle formation and deposition in thermally stressed jet fuels
[AIAA PAPER 93-0363] p 390 A93-23045

Thermomechanical postbuckling analysis of laminated composite shells
[AIAA PAPER 93-1337] p 738 A93-33907

Aerothermoelastic analysis of a NASP demonstrator model
[AIAA PAPER 93-1366] p 733 A93-33933

Finite element nonlinear random response of beams to acoustic and thermal loads applied simultaneously
[AIAA PAPER 93-1427] p 740 A93-33978

Optimization of composite engine structures for mechanical and thermal loads
[AIAA PAPER 93-1583] p 719 A93-34115

High temperature fracture mechanism of gas-pressure sintered silicon nitride
p 825 A93-38893

Effect of temperature on nonlinear two-dimensional panel flutter using finite elements
p 1022 A93-45133

Application of functionally gradient materials to scramjet engines
[ISABE 93-7063] p 1200 A93-54039

Heat loads as key problem of hypersonic flight
p 1222 A93-54276

Design of a high-temperature experiment for evaluating advanced structural materials
[NASA-TM-105833] p 88 A93-11624

Thermoviscoelastic analysis of pavements
p 379 A93-16313

Advanced thermally-stable, coal-derived, jet fuels program: Experiment system and model development
[AD-A262747] p 917 A93-29402

THERMIONIC EMITTERS

Choice of the heating system for high-temperature generators using chemical fuel
p 559 A93-29660

THERMOCHEMICAL PROPERTIES

Application of program LAURA to thermochemical nonequilibrium flow through a nozzle
p 871 A93-42644

Calculation of real-gas effects on airfoil aerodynamic characteristics
p 1229 A93-54477

Development and application of computational aerothermodynamics flowfield computer codes
[NASA-CR-192940] p 692 A93-24736

THERMOCHEMISTRY

Theoretical study of the bond dissociation energies of propyne (C₃H₄)
p 230 A93-14099

Thermo-chemical models for hypersonic flows
p 863 A93-42433

Computation of thermochemical nonequilibrium flows around a simple and a double ellipse
p 869 A93-42629

Review of chemical-kinetic problems of future NASA missions. I - Earth entries
p 872 A93-42899

Development and application of computational aerothermodynamics flowfield computer codes
[NASA-CR-192940] p 692 A93-24736

THERMOCHROMATIC MATERIALS

The application and analysis of liquid crystal thermographs in short duration hypersonic flow
[AIAA PAPER 93-0182] p 542 A93-25509

THERMOCLINES

Modelling of interfacial and thermocline waves
[AERO-REPT-9209] p 420 A93-18103

THERMOCOUPLES

Optimal circumferential placement of cylindrical thermocouple probes for reduction of excitation forces
[ASME PAPER 92-GT-423] p 406 A93-19571

Heat flux microsensor measurements
[AIAA PAPER 92-5038] p 413 A93-22312

Determination of surface heat transfer and film cooling effectiveness in unsteady wake flow conditions
p 902 A93-29933

THERMODYNAMIC CYCLES

An optimisation-matching procedure for variable cycle jet engines
[ASME PAPER 92-GT-406] p 356 A93-19555

- Some aspects of variable geometry gas turbine operation
[ASME PAPER 92-GT-407] p 356 A93-19556
- THERMODYNAMIC EFFICIENCY**
Axial length influence on the performance of centrifugal impellers p 205 A93-14517
A compact, intercooled and regenerated gas turbine for HALE applications
[ASME PAPER 92-GT-401] p 355 A93-19550
High pressure ratio intercooled turbo-prop study
[ASME PAPER 92-GT-405] p 356 A93-19554
The tilt wing advantage - for high-speed VSTOL aircraft p 506 A93-27903
Choice of the heating system for high-temperature generators using chemical fuel p 559 A93-29660
Variable cycle engine concept
[ISABE 93-7065] p 1200 A93-54041
By-passing of heat exchangers in gas turbines p 814 A93-27189
- THERMODYNAMIC EQUILIBRIUM**
Viscous equilibrium computations using program LAURA p 8 A93-12002
Hypersonic inviscid and viscous flow computations with a new optimized thermodynamic equilibrium model
[AIAA PAPER 93-0893] p 471 A93-24953
- THERMODYNAMIC PROPERTIES**
Parametric diagnostics of the steady states of gas turbine engines p 54 A93-12815
Evaporation and specific heats of motor fuels p 71 A93-12823
Probability analysis of a method for diagnosing gas turbine engines on the basis of thermogasdynamic parameters p 345 A93-18337
Potential and prospects of intermetallic materials for applications in the aerospace industry
[ONERA, TP NO. 1992-99] p 824 A93-38580
Diffusion controlled evaporation of a multicomponent droplet - Theoretical studies on the importance of variable liquid properties p 1021 A93-44224
Hugoniot analysis of the ram accelerator p 1023 A93-45500
Characteristics of the flame air heater of a hypersonic wind tunnel p 1140 A93-51884
Method of remotely characterizing thermal properties of a sample
[NASA-CASE-LAR-13508-3-CU] p 67 A93-11057
A condensed phase test cell assembly for the System for Thermal Diagnostic Studies (STDS)
[AD-A258463] p 393 A93-18242
Microburst characteristics determined from 1988-1991 TDWR testbed measurements p 490 A93-19605
- THERMODYNAMICS**
Compound cycle engine for helicopter application
[NASA-CR-180824] p 55 A93-10348
Computer program for calculating and fitting thermodynamic functions p 231 A93-12967
[NASA-RP-1271] p 231 A93-12967
Creep fatigue life prediction for engine hot section materials (isotropic) p 364 A93-18578
[NASA-CR-189221] p 364 A93-18578
Compatibility of potential reinforcing ceramics with Ni and Fe aluminides p 394 A93-18784
[NASA-CR-192232] p 394 A93-18784
Measurements and computations of external heat transfer and film cooling in turbines
[RAE-TM-P-1223] p 722 A93-25455
Development of a pulse ramjet based on twin valveless pulse combustors coupled to operate in antiphase p 814 A93-27186
- THERMOELASTICITY**
Nonlinear deformation mechanics of multilayer transparency elements - General theory relations p 79 A93-12800
On the coupled thermomechanical analysis of hypersonic flight vehicle structures
[AIAA PAPER 92-5018] p 413 A93-22294
Thermoelastic vibration test techniques p 549 A93-29293
Active control of aerothermoelastic effects for a conceptual hypersonic aircraft p 1007 A93-45137
- THERMOGRAPHY**
Photoluminescent thermography - Feasibility study with pointwise measurements p 211 A93-16861
Comparison of heating protocols for detection of disbands in lap joints p 396 A93-18627
Automation of disbond detection in aircraft fuselage through thermal image processing p 407 A93-19598
The application and analysis of liquid crystal thermographs in short duration hypersonic flow
[AIAA PAPER 93-0182] p 542 A93-25509
Infrared thermography for hot-shot wind tunnel
[ONERA, TP NO. 1992-103] p 831 A93-38583
Infrared thermography characterization of Goertler vortex type patterns in hypersonic flows
[ONERA, TP NO. 1993-13] p 925 A93-41029
- Infrared thermography of plastic instabilities in a single crystal superalloy
[ONERA, TP NO. 1993-18] p 916 A93-41031
Applications of liquid crystal surface thermography to hypersonic flow p 1023 A93-45504
The inspection of aeronautical structures using transient thermography p 1258 A93-54899
Study of optical techniques for the Ames unitary wind tunnel. Part 5: Infrared imagery
[NASA-CR-191385] p 194 A93-14809
Photoluminescent thermography in hypersonic blowdown wind tunnel: Feasibility study with pinpoint measurement
[ONERA-NT-1992-8] p 297 A93-18617
- THERMOGRAVIMETRY**
Evaluation of decomposition kinetic coefficients for a fiber-reinforced intumescent-epoxy
[AIAA PAPER 93-1856] p 1144 A93-49734
Thermal control/oxidation resistant coatings for titanium-based alloys p 74 A93-12457
- THERMOELECTRIC TREATMENT**
Total quality management of forged products through finite element simulation p 1217 A93-53493
The beta-CEZ, a new high performance titanium alloy for aerospace engines
[DS-2022] p 393 A93-17852
- THERMOPLASTIC RESINS**
Thermoplastic and thermosetting matrix composite structures - Comparison of mechanical properties p 197 A93-15029
Development and fabrication of an autoclave molded PES/Quartz sandwich radome p 547 A93-28279
Evaluation of thermoplastic stiffened panels for application to rotorcraft airframes p 827 A93-36000
Evaluation of the fatigue behavior of discontinuous and continuous fiber thermoplastic composite laminates p 824 A93-36005
Thermoplastic composite parts manufacture at Du Pont
[SME PAPER EM93-106] p 1159 A93-51728
Structural applications of Avimid K3B LDF thermoplastic composites --- for advanced aircraft p 1216 A93-53429
Design and manufacturing concepts for thermoplastic structures p 919 A93-30434
F-15 composite engine access door p 920 A93-30442
Structural response of bead-stiffened thermoplastic shear webs p 923 A93-30873
- THERMOPLASTICITY**
Thermoplastic applications in helicopter components p 796 A93-35952
A finite element model for analysis of thermoviscoplastic behavior of hypersonic leading edge structures subject to intense aerothermal heating p 137 A93-14631
- THERMOSETTING RESINS**
Thermoplastic and thermosetting matrix composite structures - Comparison of mechanical properties p 197 A93-15029
Model multilayer structured composites p 533 A93-24509
'No VOC' water-borne corrosion resistant primers for aerospace bonding applications p 1211 A93-53419
Performance of thermal adhesives in forced convection p 924 A93-30974
- THERMOVISCOELASTICITY**
Thermoviscoelastic analysis of pavements p 379 A93-16313
- THICK PLATES**
Fourier analysis of clamped moderately thick arbitrarily laminated plates p 206 A93-14571
- THICKNESS**
Ultrasonic thickness measurement using the angle technique p 542 A93-25353
Effect of pylon cross-sectional geometries on propulsion integration for a low-wing transport
[NASA-TP-3333] p 788 A93-28070
- THICKNESS RATIO**
A numerical investigation of supersonic strut/endwall interactions in annular flow with varying strut thickness
[AIAA PAPER 93-2927] p 1045 A93-48128
Multi-point inverse design of isolated airfoils and airfoils in cascade in incompressible flow p 163 A93-14462
- THIN AIRFOILS**
Unsteady effects of camber on the aerodynamic characteristics of a thin airfoil moving near the ground p 270 A93-21719
Calculation of the flowfield around an airfoil with spoiler
[AIAA PAPER 93-0527] p 284 A93-23268
Passive drag reduction of a helicopter airfoil in an unsteady transonic flow p 482 A93-29440
Adaptive wall wind tunnel with two measured interfaces - Theory and experiment p 679 A93-33717
Transonic flow around the leading edge of a thin airfoil with a parabolic nose p 688 A93-34405
- Thrust imparted to an airfoil by passage through a sinusoidal upwash field p 1178 A93-53219
A discussion of the results of the rainfall counting of a wide range of dynamics associated with the simultaneous operation of adjacent wind turbines
[DE93-000016] p 434 A93-18705
Analysis of a 2-D airfoil motion flying in-proximity to a wavy-wall surface: Lifting-surface-method p 300 A93-19281
- THIN BODIES**
Steady state supersonic flows of a vibrationally excited gas past thin bodies p 1089 A93-51818
Determination of the aerodynamic characteristics of thin bodies of revolution with an arbitrary number of cantilever surfaces in inhomogeneous flow p 1092 A93-51911
- THIN FILMS**
Partially exposed polymer dispersed liquid crystals for boundary layer investigations p 399 A93-19250
High temperature thin film strain gauges
[ONERA, TP NO. 1992-171] p 542 A93-25346
An ac thin film electroluminescent (TFEL) display unit for cockpit control display unit application p 518 A93-28179
Thin gradient heat fluxmeters developed at ONERA
[ONERA, TP NO. 1992-87] p 831 A93-38571
Ignition of boron particles coated by a thin titanium film
[AIAA PAPER 93-2201] p 1145 A93-50013
Thermal effects of a coolant film along the suction side of a high pressure turbine nozzle guide vane p 901 A93-29930
Measurement of turbulent spots and intermittency modelling at gas-turbine conditions p 902 A93-29934
- THIN PLATES**
Nonlinear aeroelasticity and chaos p 79 A93-12165
Mixed mode stress intensity-factors in transversely loaded plates p 200 A93-13943
Analysis of complicated plates by a nine-node spline plate element p 206 A93-14616
Design and fabrication of panels with cutouts p 1215 A93-52973
- THIN WALLED SHELLS**
Determination of the membrane and flexural shell deformations from the readings of a two-sided rosette-type strain gage p 75 A93-10047
On the static aeroelastic tailoring of composite aircraft swept wings modelled as thin-walled beam structures p 158 A93-14820
Supersonic flutter analysis of composite plates and shells p 837 A93-39419
An analytical-experimental method for studying the strength and stability of thin-walled structures p 1029 A93-47084
SAPNEW: Parallel finite element code for thin shell structures on the Alliant FX/80
[NASA-CR-190663] p 84 A93-10372
SAPNEW: Parallel finite element code for thin shell structures on the Alliant FX-80
[NASA-CR-189212] p 220 A93-14799
Probabilistic assessment of composite structures
[NASA-TM-106024] p 825 A93-27092
Optimal design and imperfection sensitivity of nonlinear shell structures
[FFA-TN-1992-30] p 1030 A93-31123
- THIN WALLS**
Nonlinear analysis of composite thin-walled helicopter blades p 827 A93-36006
Problems of the organization of the mass testing of large structural elements of aircraft using testing machines p 821 A93-36791
Axial crack propagation and arrest in pressurized fuselage p 1026 A93-45788
- THIN WINGS**
An aerodynamic model of multiple lifting surfaces including wake deformation and tip effect p 10 A93-12366
A viscous flow based membrane wing model
[AIAA PAPER 93-2955] p 1047 A93-48149
Three-dimensional hypersonic flow of a gas past wings p 1069 A93-48971
Towards an analytical treatment of the aerodynamic problem of a circular wing p 781 A93-27214
Leading edge vortices in a chordwise periodic flow p 782 A93-27218
- THREADS**
A study of the effects of tolerances on rigging screws, turnbuckles, and associated components in BS4429: 1987 p 86 A93-11326
[NPL-DMM(A)-53] p 86 A93-11326
Single screw interrupted thread positive displacement mechanism
[AD-D015596] p 554 A93-20790
Development of stitching reinforcement for transport wing panels p 921 A93-30852

THREE DIMENSIONAL BODIES

Extreme value heat transfer problems for three-dimensional bodies moving at hypersonic velocities p 4 A93-10079

Approximate methods for heat flows toward the surface of three-dimensional bodies p 4 A93-10080

Variational problem of the profiling of the side walls of the supersonic section of a narrow three-dimensional nozzle p 4 A93-10140

A method for determining the aerodynamic coefficients of asymmetric bodies with allowance for nonlinear influence factors of the body shape p 5 A93-10142

Euler solutions simulating strong shock waves and vortex phenomena over 3D wings p 121 A93-14392

Incompressible potential flow calculation about harmonically oscillating three-dimensional configurations p 461 A93-24089

Hybrid prismatic/tetrahedral grid generation for complex 3-D geometries [AIAA PAPER 93-0669] p 465 A93-24778

Hypersonic chemically reacting flow of a reentry body p 769 A93-38147

Aerodynamic resistance of three-dimensional bodies with a starlike cross section at supersonic velocities, and problems of its calculation p 774 A93-39116

Experiments on shock-wave/boundary-layer interactions produced by two-dimensional ramps and three-dimensional obstacles p 865 A93-42589

A synthesis of results on the calculation of flow over a 2D ramp and a 3D obstacle - Antibes test cases 3 and 4 p 867 A93-42601

Rarefied gas flow around a 3D-delta-wing p 870 A93-42639

Mesh generation for the computation of flowfields over complex aerodynamic shapes p 995 A93-44888

Sensitivity analysis of a wing aeroelastic response p 958 A93-45142

Navier-Stokes analysis of three-dimensional S-ducts p 959 A93-45146

Application of an engineering inviscid-boundary layer method to slender three-dimensional vehicle forebodies [AIAA PAPER 93-2793] p 963 A93-46534

On the legitimacy and accuracy of downwash computations by panel methods on 3D wings p 970 A93-46885

Tip vortex, stall vortex, and separation observations on pitching three-dimensional wings [AIAA PAPER 93-2972] p 1049 A93-48166

Computational aerothermodynamics for 2D and 3D space vehicles p 1073 A93-49533

Approximate calculation of the aerodynamic characteristics of simple bodies in hypersonic rarefied-gas flow p 1090 A93-51869

Two and three-dimensional prediffuser combustor studies with air-water mixture [ISABE 93-7025] p 1213 A93-54001

THREE DIMENSIONAL BOUNDARY LAYER

Calculation of a three-dimensional boundary layer at the lee side of a finite-span delta wing in the case of viscous interaction with hypersonic flow p 5 A93-10143

Three-dimensional boundary-layer transition on a cone at Mach 3.5 p 9 A93-12177

Grid-characteristic method for calculating a three-dimensional boundary layer on the bounding surfaces of the blade passage of a turbomachine p 13 A93-12808

An algebraic turbulence model with memory for the computation of three dimensional turbulent boundary layers p 115 A93-14248

On the measurements of the skin friction in 3-D flows - Application to a complete 3-D shear layer flow p 118 A93-14329

A high-frequency, secondary instability of crossflow vortices that leads to transition p 128 A93-17253

On the cross-flow instability near a rotating disk p 128 A93-17264

Calculation of three-dimensional boundary layers on rotor blades using integral methods [ASME PAPER 92-GT-210] p 252 A93-19433

Receptivity of three-dimensional boundary layers [AIAA PAPER 93-0074] p 262 A93-20186

Stability and transition on swept wings [AIAA PAPER 93-0078] p 263 A93-20190

Linear stability of three-dimensional boundary layers - Effects of curvature and non-parallelism [AIAA PAPER 93-0079] p 263 A93-20191

Instability and transition in three-dimensional supersonic boundary layers [AIAA PAPER 92-5049] p 273 A93-22321

Prediction of fluctuating pressure in attached and separated compressible flow [AIAA PAPER 93-0286] p 279 A93-22687

Mean flowfield structure of a three-dimensional supersonic turbulent boundary layer [AIAA PAPER 93-0661] p 465 A93-24774

Stability theory and transition prediction applied to a general aviation fuselage p 479 A93-28601

Numerical analysis of the three-dimensional boundary layer on a turbomachinery rotor blade p 685 A93-34341

Inviscid instability of a skewed compressible mixing layer p 769 A93-37941

Evolution of a three-dimensional nonequilibrium boundary layer in a dihedral angle behind a perturbation source p 872 A93-43013

Passive control of shock wave/boundary layer interaction at hypersonic speed [AIAA PAPER 93-3249] p 966 A93-46794

Method of characteristics for computing three-dimensional boundary layers p 970 A93-46886

The determination of hybrid analytical-numerical solutions for the three-dimensional compressible boundary layer p 1029 A93-46979

Numerical simulation of transition in two- and three-dimensional boundary layers p 973 A93-46980

Instability of three-dimensional supersonic boundary layer p 973 A93-46987

Numerical simulation of linear interference wave development in three-dimensional boundary layers p 1029 A93-46993

The hemisphere-cylinder in dynamic pitch-up motions [AIAA PAPER 93-2963] p 1048 A93-48157

Experimental study of 3-D separation on a large scale model [AIAA PAPER 93-3007] p 1053 A93-48197

Transition for three-dimensional boundary layers on wings in the transonic regime [AIAA PAPER 93-3049] p 1057 A93-48229

Bypass transition in two- and three-dimensional boundary layers [AIAA PAPER 93-3050] p 1057 A93-48230

The three-dimensional boundary layer flow due to a rotor-tip vortex [AIAA PAPER 93-3081] p 1060 A93-48255

Effect of curvature on stationary crossflow instability of a three-dimensional boundary layer p 1070 A93-49010

Real gas effects in two- and three-dimensional hypersonic, laminar boundary layers p 1073 A93-49530

Numerical simulation of shock/shock and shock-wave/boundary-layer interactions in hypersonic flows p 1093 A93-52000

Calculation of a compressible three-dimensional boundary layer on a swept wing p 1179 A93-53551

Special publication of National Aerospace Laboratory [DE93-716176] p 239 A93-15946

Three dimensional boundary-layer transition on a swept wing p 419 A93-16818

Experiments on swept-wing boundary-layer transition p 419 A93-16829

Roughness-induced generation of crossflow vortices in three-dimensional boundary layers [NASA-CR-4505] p 780 A93-27096

Unsteady transition measurements on a pitching three-dimensional wing p 820 A93-27450

THREE DIMENSIONAL COMPOSITES

Automatic Through-the-Thickness braiding p 209 A93-15789

THREE DIMENSIONAL FLOW

A data processing and measuring system with a traversing probe for studying flow in the rotating impeller of an axial-flow fan p 75 A93-10032

Hemispherical and spherical flow parameter detectors p 75 A93-10044

Variational problem of the profiling of the side walls of the supersonic section of a narrow three-dimensional nozzle p 4 A93-10140

Three-dimensional flow of viscous gas in the blade passage of a straight compressor cascade p 5 A93-10187

Three-dimensional flow calculations in turbomachinery using the stream function formulation p 11 A93-12453

Viscous shock-layer numerical calculations of three dimensional nonequilibrium flows over hypersonic blunt bodies at high angle of attack p 12 A93-12651

The numerical study of 3-D flow past control surfaces [AIAA PAPER 92-4650] p 14 A93-13305

A comparison of upwind schemes for computation of three-dimensional hypersonic real-gas flows [AIAA PAPER 92-4350] p 15 A93-13306

Numerical analysis of three-dimensional viscous flows around an advanced counterrotating propeller p 112 A93-14165

Numerical solution of 3-D turbulent flows inside of new concept nozzles p 114 A93-14211

MELINA - A multi-block, multi-grid 3D Euler code with sub block technique for local mesh refinement p 115 A93-14217

THREE DIMENSIONAL FLOW

Calculation of 3-D unsteady subsonic flow with separation bubble using singularity method p 115 A93-14251

Numerical analysis of the 3-D turbulent flow in an S-shaped diffuser p 116 A93-14252

On the measurements of the skin friction in 3-D flows - Application to a complete 3-D shear layer flow p 118 A93-14329

Analytical solutions for hypersonic flow past slender power-law bodies at small angle of attack p 122 A93-14550

A fast method for calculating three-dimensional transonic potential flows in turbomachine blade rows p 125 A93-15215

A method for calculating supersonic three-dimensional flows in pyramidal nozzles p 125 A93-15216

Adaptive remeshing for three-dimensional compressible flow computations p 242 A93-18851

Experimental and theoretical analysis of the flow in a centrifugal compressor volute [ASME PAPER 92-GT-30] p 400 A93-19290

Aerodynamic performance of a transonic low aspect ratio turbine nozzle [ASME PAPER 92-GT-31] p 245 A93-19291

Three dimensional transonic flow measurements in an axial turbine with conical walls [ASME PAPER 92-GT-61] p 247 A93-19311

Aerodynamic design of turbomachinery blading in three-dimensional flow - An application to radial inflow turbines [ASME PAPER 92-GT-74] p 248 A93-19324

Calculation of three-dimensional unsteady flows in turbomachinery using the linearized harmonic Euler equations [ASME PAPER 92-GT-136] p 249 A93-19368

Three-dimensional flow phenomena in a transonic, high-through-flow, axial-flow compressor stage [ASME PAPER 92-GT-169] p 250 A93-19395

Advances in the numerical integration of the 3-D Euler equations in vibrating cascades [ASME PAPER 92-GT-170] p 351 A93-19396

Coupled 3-D aeroelastic stability analysis of bladed disks [ASME PAPER 92-GT-171] p 351 A93-19397

Numerical solutions for unsteady subsonic vortical flows around loaded cascades [ASME PAPER 92-GT-173] p 250 A93-19399

Incidence angle and pitch-chord effects on secondary flows downstream of a turbine cascade [ASME PAPER 92-GT-184] p 251 A93-19409

An experimental study of heat transfer in a large-scale turbine rotor passage [ASME PAPER 92-GT-195] p 403 A93-19420

A fully three-dimensional inverse method for turbomachinery blading in transonic flows [ASME PAPER 92-GT-209] p 251 A93-19432

Measurement of the three-dimensional tip region flowfield in an axial compressor [ASME PAPER 92-GT-211] p 252 A93-19434

A three-dimensional numerical method for turbomachinery blading [ASME PAPER 92-GT-291] p 254 A93-19482

Three-dimensional Navier-Stokes computations of transonic fan flow using an explicit flow solver and an implicit k-epsilon solver [ASME PAPER 92-GT-309] p 256 A93-19499

Radial transport and momentum exchange in an axial compressor [ASME PAPER 92-GT-364] p 257 A93-19528

Analysis of three-dimensional viscous flow in a supersonic axial flow compressor rotor with emphasis on tip leakage flow [ASME PAPER 92-GT-388] p 257 A93-19543

Experimental study on the three dimensional flow within a compressor cascade with tip clearance. I - Velocity and pressure fields [ASME PAPER 92-GT-215] p 258 A93-19574

Experimental study on the three dimensional flow within a compressor cascade with tip clearance. II - The tip leakage vortex [ASME PAPER 92-GT-432] p 258 A93-19575

Investigation of the characteristics of 3-dimensional separated flow in an annular compressor blade row with large angles of attack p 259 A93-20116

A theoretical approach for describing secondary instability features in three-dimensional boundary-layer flows [AIAA PAPER 93-0080] p 263 A93-20192

Study on the numerical problem of the boundary element method in analysis of flow around a three-dimensional wing-body p 268 A93-20934

The modelling of aerodynamic flows by solution of the Euler equations on mixed polyhedral grids p 269 A93-21218

- An algebraic turbulence model for three-dimensional viscous flows p 274 A93-22552
[AIAA PAPER 93-0083]
- A three-dimensional inviscid flow solver in Chimera flow simulation p 276 A93-22614
[AIAA PAPER 93-0190]
- The three-dimensional separated flow structure in a variable aspect ratio sudden expansion duct p 278 A93-22630
[AIAA PAPER 93-0213]
- Evaluation of a CFD code for analysis of normal-shock trains p 279 A93-22692
[AIAA PAPER 93-0292]
- Validation of a Navier-Stokes code using a (k, ϵ) turbulence model applied to a three-dimensional transonic channel p 279 A93-22693
[AIAA PAPER 93-0293]
- 3D Euler flow solutions using unstructured Cartesian and prismatic grids p 281 A93-23022
[AIAA PAPER 93-0331]
- Three-dimensional supersonic vortex breakdown p 284 A93-23267
[AIAA PAPER 93-0526]
- Numerical simulation of three-dimensional supersonic flows using Euler and boundary layer solvers p 284 A93-23272
[AIAA PAPER 93-0531]
- Measurements in a pressure-driven three-dimensional turbulent boundary layer during development and decay p 415 A93-23283
[AIAA PAPER 93-0543]
- Three-dimensional flow structure on delta wings at high angle-of-attack - Experimental concepts and issues p 285 A93-23289
[AIAA PAPER 93-0550]
- Three-dimensional hypersonic shock wave/turbulent boundary-layer interactions p 287 A93-23533
[AIAA PAPER 93-0550]
- Eduction of swirling structure using the velocity gradient tensor p 416 A93-23547
[AIAA PAPER 93-0550]
- On experimental study of 3-D flow in self-correcting wind tunnel p 528 A93-24033
[AIAA PAPER 93-0550]
- Three-dimensional flow simulation over axisymmetric bodies using Navier-Stokes equations at hypersonic Mach numbers p 461 A93-24090
[AIAA PAPER 93-0550]
- Three-dimensional unstructured grid Euler method applied to turbine blades p 461 A93-24233
[AIAA PAPER 93-0196]
- Driven cavity simulation of turbomachine blade flows with vortex control p 461 A93-24238
[AIAA PAPER 93-0390]
- Three-dimensional Navier-Stokes calculations using solution-adapted grids p 462 A93-24240
[AIAA PAPER 93-0431]
- Doppler global velocimetry - The next generation? p 539 A93-24486
[AIAA PAPER 92-3897]
- Dynamic stall on a three-dimensional rectangular wing p 463 A93-24753
[AIAA PAPER 93-0637]
- Unsteady panel method for flows with multiple bodies moving along various paths p 539 A93-24755
[AIAA PAPER 93-0640]
- The analysis of unsteady, three-dimensional flow separation p 540 A93-24757
[AIAA PAPER 93-0642]
- A new procedure for dynamic adaption of three-dimensional unstructured grids p 560 A93-24780
[AIAA PAPER 93-0672]
- A concurrent hybrid Navier-Stokes/Euler approach to fluid dynamic computations p 468 A93-24865
[AIAA PAPER 93-0789]
- A calculation method for the three-dimensional boundary-layer equations in integral form p 541 A93-24868
[AIAA PAPER 93-0786]
- A comparison of 'new' and 'old' flux-splitting schemes for the Euler equations p 470 A93-24937
[AIAA PAPER 93-0876]
- Computing 3-D steady supersonic flow via a new Lagrangian approach p 471 A93-24951
[AIAA PAPER 93-0891]
- Computational analysis of methods for reduction of induced drag p 474 A93-25536
[AIAA PAPER 93-0524]
- Nonreflecting boundary conditions for linearized unsteady aerodynamic calculations p 475 A93-25553
[AIAA PAPER 93-0882]
- Calculation of three-dimensional supersonic flow past lifting surfaces p 477 A93-27607
[AIAA PAPER 93-0882]
- Three-dimensional flow past an ogival-cylindrical body in combination with a delta wing p 478 A93-27636
[AIAA PAPER 93-0882]
- A numerical study of mixing in supersonic combustors with hypermixing injectors p 520 A93-27801
[AIAA PAPER 93-0215]
- Flowfield analysis of modern helicopter rotors in hover by Navier-Stokes method p 481 A93-29435
[AIAA PAPER 93-0882]
- Finite-volume-TVD scheme for 3-D Euler transonic flow computations in rotating curvilinear coordinates p 679 A93-33709
[AIAA PAPER 93-0882]
- The analysis and computation of viscous-inviscid interactive problem for three dimensional transonic flow p 681 A93-33741
[AIAA PAPER 93-0882]
- Viscous-inviscid interaction coupled calculation of three-dimensional turbulent separated flow over dents p 681 A93-33748
[AIAA PAPER 93-0882]
- A study on three-dimensional shock wave/turbulent boundary layer interaction induced by sweptback sharp fins at supersonic flow p 684 A93-34274
[AIAA PAPER 93-0882]
- Nonreflecting boundary conditions of three-dimensional Euler equation calculations for strut cascades p 689 A93-34491
[AIAA PAPER 93-0882]
- Hydrodynamics and heat transfer near the stagnation point in an arbitrary axisymmetric nonswirling flow incident on a rotating obstacle p 691 A93-35270
[AIAA PAPER 93-0882]
- Transonic and supersonic flow calculations around aircrafts using a multidomain Euler code p 772 A93-38610
[ONERA, TP NO. 1992-137]
- Flow past three-dimensional irregularities in a hypersonic boundary layer on a cooled body p 775 A93-39119
[AIAA PAPER 93-0882]
- An experimental study of the three-dimensional interaction of a transverse jet with hypersonic flow p 777 A93-39150
[AIAA PAPER 93-0882]
- The Langley 8-ft transonic pressure tunnel laminar-flow-control experiment p 910 A93-41783
[AIAA PAPER 93-0882]
- Measurements in a pressure-driven three-dimensional turbulent boundary layer during development and decay p 927 A93-41911
[AIAA PAPER 93-0882]
- Solution of three-dimensional supersonic flowfields via adapting unstructured meshes p 863 A93-42442
[AIAA PAPER 93-0882]
- CFD for hypersonic propulsion p 865 A93-42585
[AIAA PAPER 93-0882]
- Navier-Stokes calculations over a double ellipse and a double ellipsoid by an implicit non-centered method p 867 A93-42607
[AIAA PAPER 93-0882]
- Computation of the hypersonic flow over a double ellipsoid p 868 A93-42610
[AIAA PAPER 93-0882]
- Numerical simulation of laminar hypersonic flow past a double-ellipsoid p 868 A93-42612
[AIAA PAPER 93-0882]
- Finite volume 3DNS and PNS solutions of hypersonic viscous flow around a delta wing using Osher's flux difference splitting p 870 A93-42633
[AIAA PAPER 93-0882]
- Three-dimensional vortex method for parachutes p 872 A93-42874
[AIAA PAPER 93-0882]
- Multigrid calculation of three-dimensional viscous cascade flows p 872 A93-42889
[AIAA PAPER 93-0882]
- Visualisation and analysis of three dimensional transonic flows by holographic interferometry p 1020 A93-44194
[AIAA PAPER 93-0882]
- Adaptive-prismatic-grid method for external viscous flow computations p 951 A93-45010
[AIAA PAPER 93-3314]
- A coarse-grid correction/nonlinear relaxation algorithm for the three-dimensional, compressible Navier-Stokes equations p 951 A93-45013
[AIAA PAPER 93-3317]
- An efficient method to calculate rotor flow in hover and forward flight p 953 A93-45030
[AIAA PAPER 93-3336]
- Three-dimensional unstructured grid Euler computations using a fully-implicit, upwind method p 953 A93-45031
[AIAA PAPER 93-3337]
- A 3D unstructured adaptive multigrid scheme for the Euler equations p 954 A93-45033
[AIAA PAPER 93-3339]
- Multigrid convergence of an implicit symmetric relaxation scheme p 954 A93-45051
[AIAA PAPER 93-3357]
- Line relaxation methods for the solution of 2D and 3D compressible flows p 955 A93-45059
[AIAA PAPER 93-3366]
- 3D automatic Cartesian grid generation for Euler flows p 956 A93-45077
[AIAA PAPER 93-3386]
- Direct and iterative algorithms for the three-dimensional Euler equations p 957 A93-45102
[AIAA PAPER 93-3378]
- Hypersonic flow calculations using a multidomain MUSCL Euler solver p 960 A93-45547
[AIAA PAPER 93-3378]
- Low-to-high altitude predictions of three-dimensional ablative re-entry flowfields p 1027 A93-46407
[AIAA PAPER 93-3378]
- On the legitimacy and accuracy of downwash computations by panel methods on 3D wings p 970 A93-46885
[AIAA PAPER 93-3378]
- Societe Francaise des Mecaniciens, SNECMA, and ONERA, Symposium on Recent Advances in Compressor and Turbine Aerothermodynamics, Courbevoie, France, Nov. 24, 25, 1992, Reports p 1001 A93-46926
[AIAA PAPER 93-3378]
- The three dimensional flow in a compressor cascade at design and off-design conditions p 971 A93-46927
[AIAA PAPER 93-3378]
- Prediction of three-dimensional low frequency unsteady transonic flow and forced vibration in axial turbine stages p 971 A93-46934
[AIAA PAPER 93-3378]
- 3D/quasi-3D trans- and supersonic flow calculation in advanced centrifugal/axial compressor stages p 972 A93-46936
[AIAA PAPER 93-3378]
- Direct and inverse problems of calculating the axisymmetric and 3D flow in axial compressor blade rows p 972 A93-46938
[AIAA PAPER 93-3378]
- 3D viscous flow analysis in axial turbine including tip leakage phenomena p 972 A93-46940
[AIAA PAPER 93-3378]
- Three dimensional aero-thermal characteristics of a high pressure turbine nozzle guide vane p 1002 A93-46942
[AIAA PAPER 93-3378]
- Intensive industrial use of 3D Euler numerical methods for axial flow turbine analysis and design p 1002 A93-46943
[AIAA PAPER 93-3378]
- Multigrid methods for calculating 3D flows in complex geometries p 973 A93-46984
[AIAA PAPER 93-3378]
- The three-dimensional representation of the pressure distribution on wedged delta wings with supersonic leading edges in supersonic-hypersonic flow p 973 A93-46989
[AIAA PAPER 93-3378]
- Finite element solution of the 3D compressible Navier-Stokes equations by a velocity-vorticity method p 974 A93-47196
[AIAA PAPER 93-3378]
- Neural network prediction of three-dimensional unsteady separated flow fields p 977 A93-47221
[AIAA PAPER 93-3426]
- A zonal CFD method for three-dimensional wing simulations p 977 A93-47225
[AIAA PAPER 93-3433]
- Flow field measurements in a crossing shockwave turbulent boundary layer interaction at Mach 3 p 977 A93-47226
[AIAA PAPER 93-3434]
- A 3D Navier-Stokes analysis of a generic ground vehicle shape p 985 A93-47283
[AIAA PAPER 93-3521]
- The development of swirl five-hole probe p 987 A93-47341
[AIAA PAPER 93-3521]
- Three-dimensional analysis of turbine rotor flow including tip clearance p 987 A93-47446
[ASME PAPER 93-GT-111]
- Asymmetric vortical solutions in supersonic corners - Steady 3D space-marching versus time-dependent conical results p 1047 A93-48151
[AIAA PAPER 93-2957]
- Some practical turbulence modeling options for Reynolds-averaged full Navier-Stokes calculations of three-dimensional flows p 1048 A93-48158
[AIAA PAPER 93-2964]
- A numerical study of the effect of geometry variation, turbulence models, and dissipation on the flow past control surfaces p 1048 A93-48161
[AIAA PAPER 93-2967]
- Three-dimensional unsteady separating flows around an oscillatory forward-swept wing p 1050 A93-48170
[AIAA PAPER 93-2976]
- Multi-block calculations for flows in local chemical equilibrium p 1053 A93-48189
[AIAA PAPER 93-2999]
- A three-dimensional pressure flux-split RNS application to sub/supersonic flow in inlets and ducts p 1058 A93-48239
[AIAA PAPER 93-3063]
- Numerical calculation of polars and heat transfer for supersonic three-dimensional flow past wings with allowance for radiation p 1068 A93-48905
[AIAA PAPER 93-3063]
- Three-dimensional hypersonic flow of a gas past wings p 1069 A93-48971
[AIAA PAPER 93-3063]
- A computer program for meridional flows in multistage axial flow compressors with turbulence and multi-effects of 3-D flows p 1165 A93-49186
[AIAA PAPER 93-3063]
- Swirling flows in a contoured-wall combustion chamber p 1073 A93-49661
[AIAA PAPER 93-1765]
- Numerical analysis of high aspect ratio cooling passage flow and heat transfer p 1153 A93-49714
[AIAA PAPER 93-1829]
- 3-D viscous flow CFD analysis of the propeller effect on an advanced ducted propeller subsonic inlet p 1075 A93-49728
[AIAA PAPER 93-1847]
- Rotor-rotor interaction for counter-rotating fans. I - Three dimensional flowfield measurements p 1075 A93-49729
[AIAA PAPER 93-1848]
- Unsteady aerodynamic flow phenomena in a transonic compressor stage p 1075 A93-49743
[AIAA PAPER 93-1868]
- An unstructured grid flow solver for turbomachinery flows p 1076 A93-49780
[AIAA PAPER 93-1913]
- Turbofan flowfield simulation using Euler equations with body forces p 1078 A93-49825
[AIAA PAPER 93-1978]
- Unsteady, three-dimensional, Navier-Stokes simulations of multistage turbomachinery flows p 1153 A93-49826
[AIAA PAPER 93-1979]
- Computation of the flow field in an annular gas turbine combustor p 1113 A93-49903
[AIAA PAPER 93-2074]
- A comparative study of Full Navier-Stokes and Reduced Navier-Stokes analyses for separating flows within a diffusing inlet S-duct p 1079 A93-49970
[AIAA PAPER 93-2154]
- 3-dimensional interactions in the rotor of an axial turbine p 1081 A93-50053
[AIAA PAPER 93-2255]

Multistage turbomachinery flow solutions using three-dimensional implicit Euler method [AIAA PAPER 93-2382] p 1083 A93-50150

Three-dimensional flow field in a turbine nozzle passage [AIAA PAPER 93-2556] p 1084 A93-50278

3-D turbomachinery Euler and Navier-Stokes calculations with a multidomain cell-centered approach [AIAA PAPER 93-2576] p 1085 A93-50292

Substitution of oriented differences for central differences in a program for calculating smooth supersonic flows p 1085 A93-50966

On boundary-layer transition in transonic flow p 1087 A93-51280

Numerical model for predictions of reverse flow combustor aerothermal characteristics p 1123 A93-51645

New calculation methods contribution on turbomachinery design and development [ONERA, TP NO. 1993-60] p 1092 A93-51940

Progress towards understanding and predicting heat transfer in the turbine gas path p 1215 A93-52751

Numerical study of a delta planform with multiple jets in ground effect [SAE PAPER 892283] p 1176 A93-53200

Effective treatment of the singular line boundary problem for three-dimensional grids p 1177 A93-53204

Multigrid Navier-Stokes calculations for three-dimensional cascades p 1177 A93-53209

Space marching calculations about hypersonic configurations using a solution-adaptive mesh algorithm p 1177 A93-53212

Skin-friction topology over a surface mounted semi-ellipsoidal wing at incidence p 1178 A93-53216

Prismatic grid generation for three-dimensional complex geometries p 1178 A93-53217

Three-dimensional Navier-Stokes/full-potential coupled analysis for viscous transonic flow p 1178 A93-53218

Fast three-dimensional vortex method for unsteady wake calculations p 1178 A93-53233

3D laminar and 2D turbulent computations with the Navier-Stokes solver FLU3M [ONERA, TP NO. 1993-105] p 1180 A93-53618

Reynolds number dependence of the drag coefficient for laminar flow through fine-scale photoetched screens p 1218 A93-53815

Three-dimensional viscous flow analysis of compressor cascade channels p 1181 A93-53837

Navier-Stokes computation of the three dimensional flow fields through a transonic fan blade [ISABE 93-7030] p 1184 A93-54006

Isothermal flow characteristics behind V-shape gutter with and without injection p 1198 A93-54016

3D and 2.5D viscous flow computations for axial flow turbine blades [ISABE 93-7093] p 1186 A93-54069

Recent developments performed at ONERA for the simulation of 3D inviscid and viscous flows in turbomachinery by the solution of Euler and Navier-Stokes equations [ISABE 93-7094] p 1186 A93-54070

Three-dimensional flow analysis inside turbomachinery stages with steady and unsteady Navier-Stokes method [ISABE 93-7095] p 1186 A93-54071

A comparative assessment of two present generation turbine analysis codes [ISABE 93-7097] p 1203 A93-54073

LIF visualization of 3-dimensional hypersonic mixing [ISABE 93-7114] p 1221 A93-54089

Two-dimensional and three-dimensional mixing flow structures with injected through slotted nozzle and circular nozzle into supersonic flows [ISABE 93-7117] p 1221 A93-54092

Numerical and experimental study on two- and three-dimensional supersonic flow field with hydrogen injection [ISABE 93-7118] p 1188 A93-54093

Mixing of multiple jets with a confined subsonic crossflow p 1189 A93-54324

Prediction of viscous flows in rotating machinery using Navier-Stokes techniques p 1232 A93-54639

Three-dimensional flow analysis of a four-stage transonic axial compressor with inlet guide vanes p 1232 A93-54643

Rotor/stator flow coupling in turbomachines p 1232 A93-54647

Three-dimensional simulations of compressible mixing layers - Visualizations and statistical analysis p 1235 A93-55360

Three-dimensional separated flow over a prolate spheroid p 1235 A93-55379

Supersonic and hypersonic flow computations for the research configuration ELAC I and comparison to experimental data p 1237 A93-56034

Analysis of wing-body junction flowfields using the incompressible Navier-Stokes equations, volumes 1 and 2 p 17 N93-10320

Unsteady three-dimensional thin-layer Navier-Stokes solutions for turbomachinery in transonic flow p 218 N93-14025

An algebraic turbulence model for three-dimensional viscous flows [NASA-TM-105931] p 110 N93-14102

The 3D Navier-Stokes flow analysis for shared and distributed memory MIMD computers [AD-A256038] p 221 N93-15187

User's manual for Interactive Data Display System (IDDS) [NASA-TM-105572] p 441 N93-16613

Interferometric reconstruction of three-dimensional high-speed aerodynamic flows p 291 N93-16765

Direct numerical simulation of combustion in turbulent supersonic flow [DS-2138] p 393 N93-17746

A numerical study of mixing in supersonic combustors with hypermixing injectors [NASA-CR-191027] p 294 N93-17884

Validation of central and upwind 3D compressible flow solvers p 421 N93-18564

Endwall flows and blading design for axial flow compressors p 423 N93-18730

Proceedings of the Ninth NAL Symposium on Aircraft Computational Aerodynamics [NAL-SP-16] p 299 N93-19273

Rarefied gas numerical wind tunnel. Part 7: OREX p 382 N93-19280

Numerical calculation of hypersonic non-equilibrium flow around OREX p 301 N93-19296

Numerical simulation of hypersonic flow around H-2 Orbiting Plane (HOPE), part 3 p 301 N93-19297

The 3D Navier-Stokes calculation of flow about scramjet inlet with strut p 301 N93-19298

Three dimensional calculation of flow inside supersonic inlet p 303 N93-19313

A numerical investigation of 3D transverse injection into the supersonic flow behind rearward facing step p 303 N93-19316

Experimental investigations on wing-body combinations and their components at high angles of attack in the subsonic and transonic speed range [DLR-FB-91-43] p 516 N93-21762

Three-dimensional flow in radial turbomachinery and its impact on design [NASA-CR-192957] p 723 N93-25668

The addition of algebraic turbulence modeling to program LAURA [NASA-TM-107758] p 840 N93-27250

The transition prediction toolkit: LST, SIT, PSE, DNS, and LES p 783 N93-27429

Three-dimensional compressible stability-transition calculations using the spatial theory p 783 N93-27431

Calculation of fully three-dimensional separated flow with an unsteady viscous-inviscid interaction method p 786 N93-27455

An experimental study of flow over a 6 to 1 prolate spheroid at incidence p 874 N93-29124

The 3-D viscous flow CFD analysis of the propeller effect on an advanced ducted propeller subsonic inlet [NASA-TM-106240] p 900 N93-29162

Navier-Stokes analysis of three-dimensional flow and heat transfer inside turbine blade rows p 905 N93-29963

Three-dimensional fiber-optic LDV measurements in the endwall region of a linear cascade of controlled-diffusion stator blades [AD-A263513] p 933 N93-29968

Overview of aerothermodynamic loads definition study p 1016 N93-31583

Three-dimensional analysis of the Pratt and Whitney alternate design SSME fuel turbine p 1031 N93-31584

Three-dimensional flow calculations inside SSME GGGT first stage blade rows p 1017 N93-31585

THREE DIMENSIONAL MODELS

Numerical dissipation in F3D thin-layer Navier-Stokes solution for flows with wall transpiration p 9 A93-12010

Application of CAD system in geometric modeling for helicopter preliminary design p 153 A93-14203

Numerical simulation of a three-dimensional wave packet in a growing flat plate boundary layer p 128 A93-17265

Coupled multi-disciplinary simulation of composite engine structures in propulsion environment [ASME PAPER 92-GT-6] p 346 A93-19279

Assessment of a 3-D Euler code for subsonic turbine vane flows and study of the non radial blade stacking [ASME PAPER 92-GT-63] p 247 A93-19313

Three-dimensional gas turbine combustor emissions modeling [ASME PAPER 92-GT-129] p 350 A93-19363

Experimental and computational investigation of the NASA Low-Speed Centrifugal Compressor flow field [ASME PAPER 92-GT-213] p 252 A93-19436

Unsteady two- and three-dimensional Navier-Stokes simulations of multistage turbomachinery flows p 266 A93-20721

Large-scale simulation of the three-dimensional Navier-Stokes equations p 437 A93-20739

Improvement of the ONERA 3D icing code, comparison with 3D experimental shapes [AIAA PAPER 93-0169] p 275 A93-22603

Three-dimensional NOx modeling for rich/lean combustor [AIAA PAPER 93-0251] p 360 A93-22660

Experimental and numerical investigation of Mach 2.5 supersonic mixed compression inlet [AIAA PAPER 93-0289] p 279 A93-22689

3-D adaptive grid-embedding Euler technique [AIAA PAPER 93-0330] p 415 A93-23021

Three-dimensional Navier-Stokes analysis of the tip clearance flow in linear turbine cascades [AIAA PAPER 93-0391] p 282 A93-23068

Three-dimensional modeling and control of a twin-lift helicopter system p 370 A93-23511

Unstructured 3D Delaunay mesh generation applied to planes, trains and automobiles [AIAA PAPER 93-0673] p 560 A93-24781

An experimental parametric study of geometric, Reynolds number, and ratio of specific heats effects in three-dimensional sidewall compression scramjet inlets at Mach 6 [AIAA PAPER 93-0740] p 466 A93-24830

MESH3D - A tool for the construction of three-dimensional meshes [ONERA, TP NO. 1992-164] p 561 A93-25339

Experimental study of three-dimensional separation on a large-size model [ONERA, TP NO. 1992-174] p 473 A93-25348

Analysis of interlaminar stresses in symmetric and unsymmetric laminates under various loadings [AIAA PAPER 93-1511] p 740 A93-34050

Three-dimensional calculations of rotor-airframe interaction in forward flight p 795 A93-35940

Application of a full potential code to the definition of a transonic test section [ONERA, TP NO. 1992-84] p 822 A93-38569

Implications of three-dimensional tracer studies for two-dimensional assessments of the impact of supersonic aircraft on stratospheric ozone p 936 A93-41269

An approximate method for calculating heating rates on three-dimensional vehicles [AIAA PAPER 93-2881] p 949 A93-44228

Three-dimensional calculation of a hydrogen jet injection into a supersonic air flow p 950 A93-44374

Compressibility, exothermicity, and three dimensionality in spatially evolving reactive shear flows p 950 A93-44375

A three-dimensional Delaunay unstructured grid generator and flow solver for bodies in relative motion [AIAA PAPER 93-3349] p 954 A93-45043

Visual grid quality assessment for 3D unstructured meshes [AIAA PAPER 93-3352] p 1036 A93-45046

3D automatic Cartesian grid generation for Euler flows [AIAA PAPER 93-3386] p 956 A93-45077

A 3-D finite-volume scheme for the Euler equations on adaptive tetrahedral grids p 956 A93-45083

Preconditioned domain decomposition scheme for three-dimensional aerodynamic sensitivity analysis p 957 A93-45096

Single block three-dimensional volume grids about complex aerodynamic vehicles p 957 A93-45099

Advancing-layers method for generation of unstructured viscous grids p 957 A93-45101

Direct and iterative algorithms for the three-dimensional Euler equations [AIAA PAPER 93-3378] p 957 A93-45102

Adaptation of a 3-D pressure correction Navier-Stokes solver for the accurate modelling of tip clearance flows p 971 A93-46932

The three-dimensional representation of the lift and pitching moment coefficients on wedged rectangular wings in supersonic flow p 973 A93-46990

Unsteady flow computations for a three-dimensional cavity with and without an acoustic suppression device [AIAA PAPER 93-3402] p 974 A93-47204

A zonal CFD method for three-dimensional wing simulations [AIAA PAPER 93-3433] p 977 A93-47225

Unstructured grid generation using interactive three-dimensional boundary and efficient three-dimensional volume methods [AIAA PAPER 93-3452] p 1037 A93-47237

- Investigation of a hypersonic crossing shock wave/turbulent boundary layer interaction p 1044 A93-48043
- A numerical investigation of supersonic strut/andwall interactions in annular flow with varying strut thickness [AIAA PAPER 93-2927] p 1045 A93-48128
- The prediction of viscous nonequilibrium hypersonic flows about ablating configurations using an upwind parabolized Navier-Stokes code p 1053 A93-48188
- CFD code calibration and inlet-fairing effects on a 3D hypersonic powered-simulation model [AIAA PAPER 93-3041] p 1056 A93-48222
- Modelling three-dimensional gas-turbine-combustor model flow using second-moment closure [AIAA PAPER 93-3104] p 1149 A93-48277
- Integrated CFD modeling of gas turbine combustors [AIAA PAPER 93-2196] p 1115 A93-50008
- 3-D Euler simulation of vane-blade interaction in a transonic turbine [AIAA PAPER 93-2256] p 1081 A93-50054
- Three-dimensional emission modeling for diffusion flame, rich/lean, and lean gas turbine combustors [AIAA PAPER 93-2338] p 1117 A93-50115
- Three-dimensional prediffuser combustor studies with air-water mixture p 1120 A93-50217
- Three-dimensional numerical simulation of gradual opening in a wave rotor passage [AIAA PAPER 93-2526] p 1156 A93-50254
- 3D PARC Navier-Stokes analysis of an HSCT suppressor nozzle secondary inlet tip and duct [AIAA PAPER 93-2568] p 1084 A93-50286
- Numerical simulations of flows in centrifugal turbomachinery p 1085 A93-50293
- Aerodynamic calculation of complex three-dimensional configurations p 1094 A93-52426
- Mathematical modeling of the three-dimensional temperature fields of turbine blades p 1216 A93-53329
- Design of high-load aviation turbomachines using modern 3D computational methods [ISABE 93-7032] p 1196 A93-54008
- Three-dimensional Navier-Stokes analysis of tip clearance flow in linear turbine cascades p 1235 A93-55364
- NO(y) from sub-sonic aircraft emissions - A global three-dimensional model study p 1261 A93-56236
- Three-dimensional mesh embedding for the Navier-Stokes equations using upwind control volumes p 1239 A93-56402
- Transonic aeroelastic analysis of systems with structural nonlinearities p 217 N93-13769
- FAA unified pavement analysis 3-D finite element method p 379 N93-16314
- Three-dimensional stress analysis of multilayered airport pavements: Integral transform approach p 381 N93-16319
- Aerodynamic design and analysis of fans using 3D computational codes [DS-2140] p 294 N93-17880
- Wind tunnel wall interference correction at subsonic speeds p 304 N93-19320
- Three-dimensional numerical simulation of the 20 June 1991, Orlando microburst p 488 N93-19598
- Multidisciplinary tailoring of hot composite structures [NASA-TM-106027] p 550 N93-19971
- Merging sparse optical flow and edge connectivity between image features: A representation scheme for 2-D display of scene depth p 845 N93-27179
- Calculation of fully three-dimensional separated flow with an unsteady viscous-inviscid interaction method p 786 N93-27455
- Three-dimensional numerical simulation of gradual opening in a wave rotor passage [NASA-CR-191157] p 900 N93-29072
- NASTRAN analysis for the Airmass Sunburst model 'C' Ultralight Aircraft p 931 N93-29777
- Three-dimensional graphical representation of objects according to movement data in realtime [ESA-TT-1258] p 942 N93-30104
- THREE DIMENSIONAL MOTION**
- Kinematics of aeroinertial aircraft rotation p 819 A93-39192
- Nonlocal vs. local instability of compressible flows including body metric, flow divergence and 3D-wave propagation [AIAA PAPER 93-2982] p 1051 A93-48175
- THROTTLING**
- Flight testing and simulation of an F-15 airplane using throttles for flight control [AIAA PAPER 92-4109] p 39 A93-11278

- A unified approach to the construction of the throttle characteristics of postrepair turbojet engines, with the NK8-2U engine used as an example p 345 A93-18372
- Low bandwidth robust controllers for flight [NASA-CR-193085] p 819 N93-27156
- THRUST**
- Effects of thrust line offset on neutral point determination in stability flight testing [AIAA PAPER 92-4082] p 61 A93-11265
- The multi-heat addition turbine engine [AIAA PAPER 92-4272] p 54 A93-13334
- Measured thrust losses associated with secondary air injection through nozzle walls p 270 A93-21656
- Shock-dependent, thrust wings for supersonic flow [AIAA PAPER 93-0321] p 280 A93-23013
- Impulse guided Samara decelerator [AIAA PAPER 93-1234] p 690 A93-35175
- Rapid computer simulation of ramjet performance [AIAA PAPER 93-2049] p 1113 A93-49882
- Thrust loss due to supersonic mixing [AIAA PAPER 93-2140] p 1114 A93-49958
- Computation of optimal low- and medium-thrust orbit transfers [AIAA PAPER 93-3855] p 1144 A93-51442
- Thrust imparted to an airfoil by passage through a sinusoidal upwash field p 1178 A93-53219
- Introduction to the Rolls-Royce design process [PNR-90939] p 57 N93-11039
- Civil aircraft engines: The next generation [PNR-90962] p 58 N93-11085
- A computational and experimental investigation of the propulsive and lifting characteristics of oscillating airfoils and airfoil combinations in incompressible flow [AD-A258019] p 294 N93-17819
- Nozzle/cowl optimization for a hypersonic vehicle on a typical trajectory [AD-A258827] p 341 N93-19089
- Shock-dependent, optimum thrust wings in supersonic flow p 483 N93-20169
- Thrust augmentation system for low-cost-expendable turbojet engine [AD-A263727] p 905 N93-30877
- THRUST AUGMENTATION**
- Study of a circular cross section thrust augmenting ejector [AIAA PAPER 93-2439] p 1118 A93-50191
- Low bandwidth robust controllers for flight [NASA-CR-191774] p 372 N93-17800
- Thrust augmentation system for low-cost-expendable turbojet engine [AD-A263727] p 905 N93-30877
- Advanced aircraft with thrust vector control [MBB-FE-1-S-PUB-0504] p 998 N93-31043
- THRUST BEARINGS**
- An externally pressurized air bearing system, journals and thrust, for application to small turbomachinery [ASME PAPER 92-GT-382] p 406 A93-19539
- A test facility for the thermofluid-dynamics of gas bearing lubrication films [PNR-90897] p 72 N93-11032
- THRUST CONTROL**
- Flight-determined benefits of integrated flight-propulsion control systems p 183 A93-14370
- The control of aircraft engines in the 1990's p 173 A93-15042
- Preliminary flight test results of a fly-by-throttle emergency flight control system on an F-15 airplane [AIAA PAPER 93-1820] p 1100 A93-49708
- Engine testing at simulated altitude conditions [AIAA PAPER 93-2452] p 1120 A93-50201
- Optimal finite-thrust time-bounded direct-ascent interception p 734 N93-25272
- Analysis of thrust modulation of ram-rockets by a vortex valve p 814 N93-27187
- Design, analysis, and control of large transport aircraft utilizing engine thrust as a backup system for the primary flight controls [NASA-CR-192938] p 820 N93-27308
- THRUST LOADS**
- Transient/structural analysis of a combustor under explosive loads [NASA-TM-107660] p 420 N93-17779
- THRUST MEASUREMENT**
- Drag/thrust estimation via aircraft performance flight testing p 156 A93-14322
- AEDC H2 Facility - New test capabilities for hypersonic air-breathing vehicles [AIAA PAPER 93-2781] p 1012 A93-46525
- An experimental study of the thrust and aerodynamic characteristics of an operating ramjet engine in a blowdown wind tunnel p 1107 A93-48828
- F405 engine in-flight thrust methodology development for the T-45A flight test program [AIAA PAPER 93-2544] p 1121 A93-50268

- Effect of boundary layer suction on the thrust and aerodynamic efficiency of a hypersonic flight vehicle p 1176 A93-52959
- THRUST REVERSAL**
- Navier-Stokes computation on a pivoting doors thrust reverser and comparison with tests [ASME PAPER 92-GT-254] p 353 A93-19463
- An experimental study of thrust reverser models --- of axisymmetric exhaust systems of aerjet engines p 812 A93-39195
- Recent developments in low-speed TPS-testing for engine integration drag and installed thrust reverser simulation p 160 N93-13207
- Aerodynamic integration of thrust reversers on the Fokker 100 p 160 N93-13208
- THRUST VECTOR CONTROL**
- The F-18 High Alpha Research Vehicle - A high-angle-of-attack tested aircraft [AIAA PAPER 92-4121] p 42 A93-13273
- Numerical simulation of STOL operations using thrust-vectoring [AIAA PAPER 92-4254] p 15 A93-13342
- Advanced technology Tilt Wing study [AIAA PAPER 92-4237] p 44 A93-13359
- Design of digital multiple model-following integrated flight/propulsion control systems p 183 A93-14371
- Confined jet thrust vector control nozzle studies p 172 A93-14516
- Thrust vectoring - Theory, laboratory, and flight tests p 367 A93-21657
- Mathematical phenomenology for thrust-vectoring-induced agility comparisons p 525 A93-28613
- Thrust vectoring nozzles give pilots an edge p 720 A93-34375
- Experimental investigation of spherical-convergent-flap thrust-vectoring two-dimensional plug nozzles [AIAA PAPER 93-2431] p 898 A93-41045
- Internal performance characteristics of vectored axisymmetric ejector nozzles [AIAA PAPER 93-2432] p 898 A93-41046
- Prediction of static performance for single expansion ramp nozzles [AIAA PAPER 93-2571] p 898 A93-41047
- Singular arcs for blunt endoatmospheric vehicles p 1015 A93-44380
- The countercurrent mixing layer - Strategies for shear-layer control [AIAA PAPER 93-3260] p 968 A93-46826
- Thrust vectoring control from underexpanded asymmetric nozzles [AIAA PAPER 93-3261] p 968 A93-46827
- Fluidic scale model multi-plane thrust vector control test results [AIAA PAPER 93-2433] p 1117 A93-50187
- Quasi-optimal steady state and transient maneuvers with and without thrust vectoring [AIAA PAPER 93-3778] p 1132 A93-51373
- TVC control for the AIAA design challenge airplane [AIAA PAPER 93-3810] p 1122 A93-51402
- Novel nozzle p 1245 A93-54450
- Vectored thrust and two-dimensional nozzle p 1247 A93-54863
- Propulsion integration results of the STOL and Maneuver Technology Demonstrator p 161 N93-13228
- Longitudinal-control design approach for high-angle-of-attack aircraft [NASA-TP-3302] p 373 N93-19108
- Robust nonlinear control of vectored thrust aircraft [NASA-CR-192727] p 728 N93-25199
- YF-22A prototype advanced tactical fighter demonstration/validation flight test program overview p 805 N93-27173
- Performance characteristics of two multiaxis thrust-vectoring nozzles at Mach numbers up to 1.28 [NASA-TP-3313] p 874 N93-29160
- Advanced aircraft with thrust vector control [MBB-FE-1-S-PUB-0504] p 998 N93-31043
- THRUST-WEIGHT RATIO**
- Using advanced technology to achieve reliability as well as high performance p 346 A93-18790
- Optimum poststall turning and supersonic turning [AIAA PAPER 93-3659] p 1128 A93-48339
- Estimation of the effect of the longitudinal moment due to the engine thrust on the mass of a subsonic passenger aircraft p 1191 A93-52954
- Aero engine ceramics: The vision, the reality, and the progress [PNR-90983] p 72 N93-11066
- THUNDERSTORMS**
- Nowcasts of thunderstorm initiation and evolution p 752 A93-33773
- Comparison of airborne dual-Doppler and airborne/ground-based dual-Doppler analyses of North Dakota thunderstorms p 844 A93-37694

- Behavior of precipitating water drops under the influence of electrical and aerodynamic forces p 1034 A93-45176
- Three-dimensional simulation of the Denver 11 July 1988 microburst-producing storm p 1164 A93-50373
- The modelling of turbulence and downbursts for flight simulators p 193 N93-13542
- The 1992 International Aerospace and Ground Conference on Lightning and Static Electricity: Addendum [DOT/FAA/CT-92/20-ADD-1] p 753 N93-24875
- A single-point warning system for thunderstorms and electric fields p 747 N93-24900
- TIGHTNESS**
- Single-impact calibrated electromagnetic tightening of long-life bolted joints in aviation structures p 745 A93-35277
- TILT ROTOR AIRCRAFT**
- Navier-Stokes computation of wing/rotor interaction for a tilt rotor in hover p 122 A93-14537
- Advances in tilt rotor noise prediction p 447 A93-19184
- An approach to tiltrotor wing aeroservoelastic optimization through increased productivity [AIAA PAPER 92-4781] p 326 A93-20371
- Eurofar rotor aerodynamic tests [ONERA, TP NO. 1992-173] p 475 A93-26880
- A study of blade-vortex interaction sound generation and directionality p 565 A93-29402
- Active control of helicopter transmission noise p 568 A93-29428
- The development of a CFD potential method for the analysis of tilt-rotors p 481 A93-29434
- Flow visualization and flow field measurements of a 1/12 scale tilt rotor aircraft in hover p 482 A93-29441
- The rebirth of the tiltrotor - The 1992 Alexander A. Nikolsky Lecture p 712 A93-34256
- Civil tiltrotor noise impact prediction methodology p 850 A93-35967
- Advancing tiltrotor state-of-the-art with variable diameter rotors p 797 A93-35982
- Design and manufacturing concepts of Eurofar Model No. 2 blades p 798 A93-35983
- Evaluation of tilt rotor aircraft design utilizing a realtime interactive simulation p 798 A93-35989
- Shadowgraph flow visualization of isolated tiltrotor and rotor/wing wakes p 767 A93-35996
- V-22 tiltrotor Flight Test Development p 800 A93-36021
- Piloted simulator investigations of a civil tilt-rotor aircraft on steep instrument approaches p 800 A93-36023
- Optimal takeoff procedures for a transport category tiltrotor p 802 A93-37377
- Screening studies of advanced control concepts for airbreathing engines [AIAA PAPER 92-3320] p 1108 A93-49329
- Tilt rotor hover aeroacoustics [NASA-CR-177598] p 99 N93-10458
- Design of an air traffic computer simulation system to support investigation of civil tiltrotor aircraft operations [NASA-CR-190811] p 36 N93-11139
- The Fourth Workshop on Dynamics and Aeroelastic Stability Modeling of Rotorcraft Systems [AD-A255065] p 50 N93-12485
- Navier-Stokes flowfield computation of wing/rotor interaction for a tilt rotor aircraft in hover p 135 N93-14035
- Tiltrotor aircraft noise: A summary of the presentations and discussions at the 1991 FAA/Georgia Tech Workshop [DOT/FAA/RD-91/23] p 232 N93-14912
- Open airscrew VTOL concepts [NASA-CR-177603] p 240 N93-17883
- Screening studies of advanced control concepts for airbreathing engines [NASA-TM-106042] p 721 N93-25079
- Rotorcraft master plan p 857 N93-30677
- Definition of an airfoil family for the EUROFAR rotor [DLR-FB-92-04] p 998 N93-31197
- Civil tiltrotor transport point design: Model 940A [NASA-CR-191446] p 1019 N93-32234
- TILT ROTOR RESEARCH AIRCRAFT PROGRAM**
- Acoustic flight test experience with the XV-15 Tiltrotor aircraft with the Advanced Technology Blade (ATB) p 445 A93-19143
- Advanced Technology Blade testing on the XV-15 Tilt Rotor Research Aircraft p 799 A93-36020
- TILT WING AIRCRAFT**
- Piloted simulation study of two tilt-wing control concepts [AIAA PAPER 92-4236] p 63 A93-13338
- Advanced technology Tilt Wing study [AIAA PAPER 92-4237] p 44 A93-13359
- Phase II simulation evaluation of the flying qualities of two tilt-wing flap control concepts [SAE PAPER 920988] p 185 A93-14635
- The tilt wing advantage - for high-speed VSTOL aircraft p 506 A93-27903
- Conceptual assessment of two high-speed rotorcraft p 508 A93-28612
- Initial piloted simulation study of geared flap control for tilt-wing V/STOL aircraft [NASA-TM-103872] p 64 N93-10741
- An investigation of two-propeller tilt wing V/STOL aircraft flight characteristics [AD-A257751] p 332 N93-17694
- Open airscrew VTOL concepts [NASA-CR-177603] p 240 N93-17883
- TILTING ROTORS**
- Navier-Stokes computation of wing/rotor interaction for a tilt rotor in hover p 122 A93-14537
- Eurofar rotor aerodynamic tests [ONERA, TP NO. 1992-173] p 475 A93-26880
- The effects of fixed rotor tilt on the rotordynamic coefficients of incompressible flow annular seals p 1161 A93-52601
- Definition of an airfoil family for the EUROFAR rotor [DLR-FB-92-04] p 998 N93-31197
- TIME DEPENDENCE**
- Selection of the time scale for preventive measures under service conditions p 237 A93-18375
- Modified surge in an axial flow compressor [ASME PAPER 92-GT-59] p 247 A93-19309
- Unsteady panel method for flows with multiple bodies moving along various paths [AIAA PAPER 93-0640] p 539 A93-24755
- Time dependent heat transfer rates in high Reynolds number hypersonic flowfields p 216 N93-13664
- Time-dependent predictions and analysis of turbine cascade data in the transonic flow region [PNR-90957] p 139 N93-15489
- Volume 2: Explicit, multistage upwind schemes for Euler and Navier-Stokes equations [NASA-CR-191647] p 418 N93-16558
- Two- and three-dimensional blade vortex interactions [NASA-CR-177567] p 293 N93-16942
- The WINCOF-1 code: Detailed description [NASA-CR-190779] p 677 N93-24760
- TIME DIVISION MULTIPLE ACCESS**
- Lessons learned during testing of the Enhanced Position Location Reporting System (EPLRS) p 77 A93-10996
- TIME DIVISION MULTIPLEXING**
- Position sensor with two wavelength time domain multiplexing for civil aircraft application p 1104 A93-49432
- Optical sensors and multiplexing for aircraft engine control p 1105 A93-49474
- Data Multiplexing Network (DMN). Phase 3: Equipment Operational Test and Evaluation (OT/E) integration test report [DOT/FAA/CT-TN92/49] p 503 N93-20612
- The Data Multiplexing Network (DMN) phase 3 Extended Distance Data Cable (EDDC) test and evaluation [DOT/FAA/CT-TN93/11] p 752 N93-26160
- Data Multiplexing Network (DMN) equipment Operational Test and Evaluation (OT/E) integration test report [AD-A263172] p 942 N93-29490
- TIME LAG**
- Influence of pitch-lag coupling on damping requirements to stabilize 'ground/air resonance' p 158 A93-14784
- Discrete-time LTR synthesis of delayed control systems p 439 A93-22855
- Further analysis of high-rate rolling experiments of a 65 deg delta wing [AIAA PAPER 93-0620] p 523 A93-24737
- An identification method for dynamic systems with delay p 562 A93-27689
- Numerical computation and approximations of H(infinity) optimal controllers for a 2-parameter distributed model of an unstable aircraft p 817 A93-37040
- Extraction of inherent aerodynamic lag poles for the time domain representation of modal unsteady airloads [AIAA PAPER 93-1591] p 829 A93-37443
- Estimation of aerodynamic characteristics from flight-test data. V - Effects of gust and its time lag p 1230 A93-54560
- The combustion time lag and its role in ramjet combustion instability p 73 N93-11137
- Time delay measurements of current primary FAA air/ground transmitters and receivers [DOT/FAA/CT-TN93/14] p 842 N93-28555
- TIME MARCHING**
- Viscous flows in centrifugal compressor diffusers at transonic Mach numbers [ASME PAPER 92-GT-48] p 246 A93-19301
- The modelling of aerodynamic flows by solution of the Euler equations on mixed polyhedral grids p 269 A93-21218
- A time dependent method in finite volume for transonic diffuser turbulent flows p 476 A93-27368
- Numerical solution of non-isentropic transonic cascade flow by time-marching method p 679 A93-33715
- An efficient procedure for cascade aeroelastic stability determination using nonlinear, time-marching aerodynamic solvers [AIAA PAPER 93-1631] p 719 A93-34159
- Domain splitting explicit time marching scheme for simulation of unsteady high Reynolds number flow p 830 A93-38140
- An implicit time-marching procedure for high speed flow [AIAA PAPER 93-3315] p 951 A93-45011
- A simple multigrid procedure for explicit time-marching on unstructured grids p 956 A93-45087
- An acceleration technique for time accurate calculations - of unsteady flow around pitching delta wings p 957 A93-45092
- Numerical solution of steady and unsteady Euler equations p 973 A93-46988
- Three-dimensional time-marching aeroelastic analyses using an unstructured-grid Euler method p 1100 A93-49012
- 3-D viscous flow CFD analysis of the propeller effect on an advanced ducted propeller subsonic inlet [AIAA PAPER 93-1847] p 1075 A93-49728
- Volume 2: Explicit, multistage upwind schemes for Euler and Navier-Stokes equations [NASA-CR-191647] p 418 N93-16558
- Investigation of advanced counterrotation blade configuration concepts for high speed turboprop systems. Task 5: Unsteady counterrotation ducted propfan analysis [NASA-CR-187126] p 521 N93-20773
- Further development of the CANAERO computer code to include a time-stepping capability [DREA-CR-91-478] p 562 N93-21820
- The 3-D viscous flow CFD analysis of the propeller effect on an advanced ducted propeller subsonic inlet [NASA-TM-106240] p 900 N93-29162
- Measurement of turbulent spots and intermittency modelling at gas-turbine conditions p 902 N93-29934
- TIME OPTIMAL CONTROL**
- Flight path optimization and suboptimal control laws synthesis for transport mission of maneuverable aircraft p 180 A93-14160
- Optimality-based control laws for real-time aircraft control via parameter optimization p 180 A93-14161
- Application of the receding horizon strategy to singularly perturbed pursuit-evasion problems p 369 A93-22980
- Application of feedback linearization method in a digital restructurable flight control system p 370 A93-23514
- Generalized guidance law for collision courses p 727 A93-34533
- Optimal discrete-time dynamic output-feedback design - A w-domain approach p 757 A93-34536
- Optimal symmetric trajectories over a fixed-time domain [AIAA PAPER 93-3848] p 1133 A93-51435
- Benefits of variable rotor speed in integrated helicopter/engine control [AIAA PAPER 93-3851] p 1134 A93-51438
- Computation of optimal low- and medium-thrust orbit transfers [AIAA PAPER 93-3855] p 1144 A93-51442
- TIME RESPONSE**
- Experimental investigations of the time and flow-direction responses of shear-stress-sensitive liquid crystal coatings [AIAA PAPER 93-0181] p 542 A93-25508
- TIME SERIES ANALYSIS**
- Nonlinear time-series-based adaptive control applications p 97 A93-13230
- TIME TEMPERATURE PARAMETER**
- Resource conservation and improvement of the service characteristics of castings of high-temperature nickel alloys through a high-temperature melt treatment p 824 A93-36718
- Concurrent field service and laboratory testing as a means of improving reliability in creep-rupture applications p 916 A93-40814
- An evaluation of thermal energy storage options for precooled gas turbine inlet air [DE93-005980] p 754 N93-24975
- TIP DRIVEN ROTORS**
- Reaction drive rotors - Lessons learned (Hero had a good idea - But) - jet helicopter performance [AIAA PAPER 92-4279] p 55 A93-13352
- TIP SPEED**
- Experimental study of controlled tip disturbance effect on flow asymmetry p 211 A93-17417
- A concept for a counterrotating fan with reduced tone noise [NASA-TM-105736] p 101 N93-11370

TIRES

- Method and apparatus for cleaning rubber deposits from airport runways and roadways
[NASA-CASE-LAR-14483-1] p 556 N93-22035

TITAN

- Nonequilibrium shock layer radiation in a simulated Titan atmosphere p 1233 A93-54805

TITANIUM

- Joining carbon composite fins to titanium heat pipes [AD-A261970] p 825 N93-27667

TITANIUM ALLOYS

- The development of titanium alloys for gas turbines p 197 A93-15031
- High-temperature materials warm up for debut p 535 A93-28393
- Isothermal oxidation behavior of alpha-2 titanium aluminide alloys p 535 A93-29563
- Birth of the betas p 824 A93-38200
- Structural stability of 'beta-CEZ' alloy [ONERA, TP NO. 1992-106] p 824 A93-38586
- Materials problems connected with the propulsion of supersonic air carriers [ONERA, TP NO. 1992-157] p 824 A93-38736
- Machining cost comparison of silicon carbide discontinuously reinforced aluminum, unreinforced aluminum, and titanium [SME PAPER EM92-252] p 925 A93-40656
- Structure of martensite in titanium alloy Ti-6Al-1.6Zr-3.3Mo-0.3Si p 916 A93-43616
- Boeing 777 gets a boost from titanium p 1018 A93-45987
- Beyond steel - TMCs for lighter landing gear p 1100 A93-49337
- Ignition of boron particles coated by a thin titanium film [AIAA PAPER 93-2201] p 1145 A93-50013
- Friction surfacing and linear friction welding p 1217 A93-53499
- Ongoing challenges for titanium alloy cleanliness improvement in aircraft engine disk materials p 1212 A93-53506
- Thermal barrier design of gamma-TiAl Functionally Graded Materials (FGMs) for scramjet engine applications p 1246 A93-54556
- Status of R&D of high-performance materials for severe environments (Composite materials) p 1253 A93-54728
- Thermal control/oxidation resistant coatings for titanium-based alloys p 74 N93-12457
- HIP consolidation of aluminum-rich intermetallic alloys and their composites p 199 N93-14726
- Fatigue propagation behaviour of short cracks in titanium alloys [ESDU-92023] p 392 N93-16637
- The beta-CEZ, a new high performance titanium alloy for aerospace engines [DS-2022] p 393 N93-17852
- Selection criteria for metallic high temperature structural materials in hypersonic flying equipment [M8B-LME-221-HYPAC-PUB-2-A] p 515 N93-21479
- Use of titanium castings without a casting factor [AD-A264414] p 1018 N93-31192
- AGARD Engine Disc Cooperative Test Programme [AGARD-R-766-ADD] p 1004 N93-31741
- Fractographic investigation of IMI 685 crack propagation specimens for SMP SC33 p 1004 N93-31743
- Material characterization and fractographic examination of Ti-17 fatigue crack growth specimens for SMP SC33 p 1004 N93-31744
- Low cycle fatigue behaviour of titanium disc alloys p 1004 N93-31745
- Fatigue crack growth results for Ti-6Al-4V, IMI 685, and Ti-17 p 1004 N93-31746
- Low cycle fatigue behaviour of titanium disc alloys [NLR-TP-91346-U] p 1006 N93-32372
- TITANIUM BORIDES**
- Chemical stability of titanium diboride reinforcement in nickel aluminide matrices p 1147 A93-52473
- TITANIUM NITRIDES**
- Erosion resistant titanium nitride coating for turbine compressor applications [ASME PAPER 92-GT-417] p 388 A93-19565
- TOBACCO**
- Tobacco smoking in aircraft - A fog of legal rhetoric? p 944 A93-40474
- Test results of the effects of air ionization on cigarette smoke particulate levels within a commercial airplane [SAE PAPER 921183] p 855 A93-41362
- TOKAMAK DEVICES**
- Diagnostics systems for the TBR-E tokamak [INPE-5428-RPQ/662] p 232 N93-13257
- TOLERANCES (MECHANICALS)**
- An overview of shed ice impact studies in the NASA Lewis Icing Research Tunnel [AIAA PAPER 93-0301] p 283 A93-23247

- A study of the effects of tolerances on rigging screws, turnbuckles, and associated components in BS4429: 1987 [NPL-DMM(A)-53] p 86 N93-11326
- Using NDT techniques in the maintenance of aeronautical products [REPT-921-430-102] p 88 N93-11587
- An overview of shed ice impact in the NASA Lewis Icing Research Tunnel [NASA-TM-105969] p 139 N93-15404
- Damage tolerance assessment of boron/epoxy repairs to fuselage lap joints [AD-A258383] p 338 N93-18257
- Ultrasonic polishing p 750 N93-25580
- Damage tolerance assessment and usage variation analysis for C-130 aircraft in the Israeli Air Force p 839 N93-27210
- Developments in impact damage modeling for laminated composite structures p 922 N93-30857
- TOLMIEN-SCHLICHTING WAVES**
- On the coupling between a supersonic boundary layer and a flexible surface p 243 A93-19132
- Interaction of Tollmien-Schlichting waves with localized disturbances p 545 A93-27637
- Laminarization of the boundary layer on a vibrating wing p 1089 A93-51776
- Numerical simulation of leading-edge receptivity to freestream vorticity p 696 N93-25388
- TOOLING**
- A tooling trend at BCA - What and why [SME PAPER EM92-111] p 202 A93-14114
- Innovative bagging techniques on a composite P-51 Mustang replica p 1191 A93-53405
- Special tooling disposition for aircraft entering post production support [AD-A261614] p 678 N93-26168
- TOOLS**
- Single-impact calibrated electromagnetic tightening of long-life bolted joints in aviation structures p 745 A93-35277
- Bearing servicing tool [NASA-CASE-MSC-21881-1] p 221 N93-14871
- TOPOGRAPHY**
- Application of new GPS aircraft control/display system to topographic mapping of the Greenland ice cap p 499 A93-28152
- Mapping new and old worlds with laser altimetry p 1034 A93-45699
- TOPOLOGY**
- Robust stabilization based on topological connectedness p 438 A93-22830
- Unsteady vortex dynamics and surface pressure topologies on a pitching wing [AIAA PAPER 93-0435] p 286 A93-23349
- Validation of electromagnetic-topology concepts on a complex structure [ONERA, TP NO. 1992-63] p 542 A93-25327
- Instantaneous topology of the unsteady leading-edge vortex at high angle of attack p 961 A93-45728
- A solution-adaptive hybrid-grid method for the unsteady analysis of turbomachinery [AIAA PAPER 93-3015] p 1148 A93-48204
- Topological approach for the study of electromagnetic coupling [ONERA-P-1992-2] p 551 N93-20230
- TORCHES**
- Development and use of hydrogen-air torches in an altitude facility [AIAA PAPER 93-2176] p 1137 A93-49988
- TORNADOES**
- Doppler radar observation of tornado and microburst around Chitose Airport p 432 A93-22199
- TOROIDAL PLASMAS**
- Beta-limiting phenomena in high-aspect-ratio toroidal helical plasmas [NIFS-188] p 569 N93-20546
- TORQUE**
- Antitorque safety and the RAH-66 Fantail p 795 A93-35912
- T55 engine - The challenge of torque measurement p 809 A93-35929
- Side-by-side hover performance comparison of MDHC 500 NOTAR and tail rotor anti-torque systems p 796 A93-35956
- The representation of the aerodynamic torque in simulations of a spacecraft rotary motion p 1141 A93-48835
- Split torque transmission load sharing [NASA-TM-105884] p 212 N93-12736
- A discussion of the results of the rainfall counting of a wide range of dynamics associated with the simultaneous operation of adjacent wind turbines [DE93-000016] p 434 N93-18705
- Sikorsky Aircraft Advanced Rotorcraft Transmission (ART) program [NASA-CR-191079] p 840 N93-27268

TORSION

- Flexure-torsion behavior of prismatic beams. I - Section properties via power series p 417 A93-23557
- Nonlinear stall flutter of wings with bending-torsion coupling [AD-A254323] p 186 N93-12959
- Engine life assessment test case TF41 LP compressor shaft torsional fatigue p 177 N93-14896
- TORSIONAL STRESS**
- Coupled composite rotor blades under bending and torsional loads p 548 A93-27970
- Study of soft-in-torsion blades - ROSOH operation [ONERA, TP NO. 1992-124] p 803 A93-38598
- TORSIONAL VIBRATION**
- Bending-torsion flutter of linear viscoelastic wings including structural damping [AIAA PAPER 93-1475] p 711 A93-34021
- The investigation of limit cycle amplitude of nonlinear nose gear p 800 A93-36342
- Study of soft-in-torsion blades - ROSOH operation [ONERA, TP NO. 1992-124] p 803 A93-38598
- Optimization of an aeroelastic system using the dynamic stability condition p 1029 A93-47085
- Effect of flexural and rotational wing oscillations on the prevention of flow separation p 1150 A93-48911
- TOTAL QUALITY MANAGEMENT**
- Methodology in the development of avionics p 166 A93-15043
- Total Quality Management in curriculum development [AIAA PAPER 93-0326] p 454 A93-23018
- R&M 2000 field data requirements for a SPO operation p 856 A93-42853
- Total quality management of forged products through finite element simulation p 1217 A93-53493
- On definition and use of systems engineering processes, methods and tools p 1225 A93-53642
- The application of manufacturing systems engineering for aero engine gears [PNR-90944] p 86 N93-11054
- TOUCHDOWN**
- Example of statistical techniques applied to analysis of measurements of the landing airborne manoeuvre. (Multiple linear regression with two independent variables and one dependent variable.) [ESDU-92022] p 330 N93-16636
- TOUGHNESS**
- Automatic Through-the-Thickness braiding p 209 A93-15789
- Effects of intra- and inter-laminar resin content on the mechanical properties of toughened composite materials p 921 N93-30845
- TOWED BODIES**
- Longitudinal dynamics of a towed sailplane p 1130 A93-49577
- Modeling and control of a trailing wire antenna towed by an orbiting aircraft [AD-A256450] p 219 N93-14610
- Experimental study of the effect of helical grooves on an infinite cylinder [AD-A260890] p 751 N93-25912
- TOWING**
- Loads at the nose landing gears of civil transport aircraft during towbarless towing operations p 45 A93-13629
- The development of a parachute system for aerial delivery from high speed cargo aircraft [AIAA PAPER 93-1232] p 703 A93-35174
- Analysis on space shape and tension distribution of towed flexible cables p 1043 A93-48554
- TOXICITY**
- Comparison of toxicity rankings of six aircraft cabin polymers by lethality and by incapacitation in rats p 26 A93-10328
- TRACE CONTAMINANTS**
- A novel aircraft-based tandem mass spectrometer for atmospheric ion and trace gas measurements p 925 A93-40672
- Implications of three-dimensional tracer studies for two-dimensional assessments of the impact of supersonic aircraft on stratospheric ozone p 936 A93-41269
- TRACKING (POSITION)**
- Digital hopping GPS/GLONASS receiver p 312 A93-21128
- Tracking flow features using overset grids [AIAA PAPER 93-0197] p 276 A93-22617
- Performance prediction of the interacting multiple model algorithm p 439 A93-22926
- Output tracking control of nonlinear systems with weakly non-minimum phase p 439 A93-22968
- Relative sensitivity of Loran-C phase tracking and cycle selection to CWI p 792 A93-36502
- A survey of position trackers p 1151 A93-49396
- A problem formulation for glideslope tracking in wind shear using advanced robust control techniques [NASA-TM-104164] p 64 N93-11176
- Aircraft trajectory tracking and prediction [AD-A259039] p 340 N93-18999

HELITRAK: A helicopter-tracking receiver system for television outside broadcast links
[BBC-RD-1992/5] p 552 N93-20573

TRACKING FILTERS

Comparison of nonlinear tracking controllers for a compressible flow process p 66 A93-12224
Sequential smoothing and filtering for maneuvering target tracking p 440 A93-22978
Correlation filters for aircraft identification from radar range profiles p 1097 A93-50636

TRACKING PROBLEM

Output feedback control for output tracking of nonlinear uncertain systems p 96 A93-13177
Application of the receding horizon strategy to singularly perturbed pursuit-evasion problems p 369 A93-22980
Bearings-only and Doppler-bearing tracking using instrumental variables p 501 A93-29600
Performance prediction of the interacting multiple model algorithm p 1167 A93-50638
Linear quadratic tracking problems in Hilbert space - Application to optimal active noise suppression p 1224 A93-52763

TRACTORS

Transmission system for a transfer device gripping a double wheel
[CA-PATENT-APPL-SN-204585] p 731 N93-25178

TRADEOFFS

Future aero engine design trade offs p 1246 A93-54836

TRAFFIC

Airport landside planning and operations
[PB93-167880] p 822 N93-26636

TRAFFIC CONTROL

Future FAA telecommunications plan
[AD-A249133] p 89 N93-11760

TRAILING EDGE FLAPS

Effects of a trailing edge flap on the aerodynamics and acoustics of rotor blade-vortex interactions p 244 A93-19144
Active aerodynamic control of wake-airfoil interaction noise - Theory p 445 A93-19154
Lift enhancement of an airfoil using a Gurney flap and vortex generators p 464 A93-24762
Flowfield measurements about a multi-element airfoil at high Reynolds numbers p 1064 A93-48300
Drag due to gaps round undeflected trailing-edge controls and flaps at subsonic speeds p 290 N93-16634
Effect of underwing frost on transport aircraft takeoff performance
[DOT/FAA/CT-TN93/9] p 791 N93-27252

TRAILING EDGES

Review of the normal force fluctuations of aerofoils with separated flow p 10 A93-12317
Influence of trailing-edge grid structure on Navier-Stokes computation of turbomachinery cascade flow p 111 A93-14078
On the configuration buffet of a transport aircraft p 117 A93-14298
Effect of trailing-edge ejection on local heat (mass) transfer in pin fin cooling channels in turbine blades
[ASME PAPER 92-GT-178] p 352 A93-19404
Streamwise variation of mean velocity field for the turbulent boundary layer interacting with controlled longitudinal vortex arrays p 267 A93-20933
Viscous and inviscid instabilities of a trailing vortex p 268 A93-21042
Vortex breakdown over delta wings in unsteady free stream
[AIAA PAPER 93-0555] p 285 A93-23294
Pilot test of a low Reynolds number DTE-airfoil
[AIAA PAPER 93-0643] p 464 A93-24758
The role of Kutta waves on oscillatory shock motion on an airfoil experiencing heavy buffeting
[AIAA PAPER 93-1589] p 682 A93-34121
Analytical study on plate edge noise (Noise generation from tandemly situated trailing and leading edges) p 1038 A93-45561
Comment on 'Flow near the trailing edge of an airfoil' p 961 A93-45754
Enhanced mixing via geometric manipulation of a splitter plate
[AIAA PAPER 93-3244] p 966 A93-46789
Navier-Stokes flow simulation in a 2D high pressure turbine cascade with a cooled slot trailing edge p 972 A93-46941
A method for the prediction of induced drag for planar and nonplanar wings
[AIAA PAPER 93-3420] p 976 A93-47216
Waveriders with finlets p 978 A93-47231
Lift enhancement due to unsteady aerodynamics
[AIAA PAPER 93-3538] p 986 A93-47289

Vortex developments over steady and accelerated airfoils incorporating a trailing edge jet

[AIAA PAPER 93-3008] p 1054 A93-48198
Flow physics of critical states for rolling delta wings
[AIAA PAPER 93-3683] p 1129 A93-48355
A wake singularity potential flow model for airfoils experiencing trailing-edge stall p 1067 A93-48544
Viscous analysis of high pressure turbine inlet guide vane flow including cooling injections
[AIAA PAPER 93-1798] p 1074 A93-49687
Navier-Stokes investigation of blunt trailing-edge airfoils using O grids p 1095 A93-52459
Numerical study of a delta planform with multiple jets in ground effect
[SAE PAPER 892283] p 1176 A93-53200
Aerodynamics of turbine blades with trailing-edge damage - Measurements and computations
[ISABE 93-7130] p 1189 A93-54105
Effect of passive flow-control devices on turbulent low-speed base flow p 82 N93-10304
Flight test results from a supercritical mission adaptive wing with smooth variable camber
[NASA-TM-4415] p 49 N93-11863
Direct prediction of a separation boundary for aerofoils using a viscous-coupled calculation method
[ESDU-92008] p 136 N93-14516
An experimental study of a turbulent boundary layer in the trailing edge region of a circulation-control airfoil
[NASA-CR-191262] p 295 N93-17934
Experimental analysis of the aeroacoustics of cascaded airfoils
[AD-A257945] p 420 N93-18121
Articulated fin/wing control system
[AD-D015712] p 909 N93-29278
Topology and grid adaption for high-speed flow computations
[NASA-CR-4216] p 934 N93-30375

TRAINING AIRCRAFT

Application of vibration-and-flutter integration analysis system for a trainer p 226 A93-14311
Rudder and elevator effects on the incipient spin characteristics of a typical general aviation training aircraft
[AIAA PAPER 93-0016] p 367 A93-20138
Results from a GPS Shuttle Training Aircraft flight test p 384 A93-21148
Two leading-edge droop modifications for tailoring stall characteristics of a general aviation trainer configuration p 1008 A93-46807
Combat and training aircraft class A mishaps in the Belgian Air Force 1970-1990 p 492 N93-19677
Simulators for corporate pilot training and evaluation p 912 N93-30678

TRAINING ANALYSIS

Investigation of advanced technology for airway facilities maintenance training
[DOT/FAA/CT-TN92/24] p 994 N93-32336

TRAINING DEVICES

Use of full flight simulator technology enhances classroom training sessions p 1136 A93-49277
An aerodynamic model for the longitudinal motion of flight training devices p 1207 A93-54278
Water tunnel studies of inlet/airframe interference phenomena p 215 N93-13216
Simulator motion
[AD-A257683] p 381 N93-17687
Helicopter crash survival at sea: United States Navy/Marine Corps experience 1977-1990 p 493 N93-19687
Measurement of modulation transfer functions of simulator displays
[AD-A259401] p 530 N93-21268
Development of a concept formulation process aid for analyzing training requirements and developing training devices
[AD-A263579] p 912 N93-29972
Virtual reality flight control display with six-degree-of-freedom controller and spherical orientation overlay
[NASA-CASE-NPO-18733-1-CU] p 897 N93-30416

TRAINING EVALUATION

Use of full flight simulator technology enhances classroom training sessions p 1136 A93-49277
User-friendly codes for the training on gas turbine engines
[AIAA PAPER 93-2051] p 1166 A93-49884
Helicopter training simulators: Key market factors p 912 N93-30683
Determining the transferability of flight simulator data p 913 N93-30685
Progress through precedent: Going where no helicopter simulator has gone before p 913 N93-30686
Transfer of training and simulator qualification or myth and folklore in helicopter simulation p 913 N93-30687

TRAINING SIMULATORS

Why simulators don't fly like the airplane: Data - An update with examples from the C-141B program
[AIAA PAPER 92-4161] p 66 A93-13312
Experimental working position simulator to analyse, develop and optimize concepts for computer-aided Air Traffic Management p 191 A93-14412
A simulator solution for the parachute canopy control and guidance training problem
[SAE PAPER 920984] p 191 A93-14634
The benefits of ground maintenance simulators p 238 A93-18757
Parachute canopy control and guidance training requirements and methodology
[AIAA PAPER 93-1255] p 703 A93-35188
AIAA Flight Simulation Technologies Conference, Monterey, CA, Aug. 9-11, 1993, Technical Papers p 1207 A93-52651
Evolution of flight simulation
[AIAA PAPER 93-3545] p 1207 A93-52652
Implementation of expert systems within an interactive tactical environment
[AIAA PAPER 93-3583] p 1223 A93-52678
Flight update of aerodynamic math model
[AIAA PAPER 93-3596] p 1224 A93-52687
How to consider simulation fidelity and validity for an engineering simulator
[AIAA PAPER 93-3598] p 1209 A93-52688
Flight simulation - An overview p 1209 A93-53768
Red-hot simulation p 1209 A93-53774
NASA/FAA helicopter simulator workshop
[NASA-CP-3156] p 857 N93-30673
Part 1: Executive summary p 857 N93-30674
Helicopter simulator standards p 912 N93-30675
Simulators for corporate pilot training and evaluation p 912 N93-30678

TRAJECTORIES

Hybrid guidance for maneuvering flight vehicles
[AD-A254110] p 69 N93-11798
Preliminary design of an intermittent smoke flow visualization system
[NASA-CR-186027] p 806 N93-28693

TRAJECTORY ANALYSIS

Wind identification along a flight trajectory. I - 3D-kinematic approach p 223 A93-16324
A dynamic inversion control approach for high-Mach trajectory tracking p 385 A93-22870
Flight performance of hypersonic minor circle turning maneuvers
[AIAA PAPER 93-0627] p 531 A93-24744
The development of a parachute system for aerial delivery from high speed cargo aircraft
[AIAA PAPER 93-1232] p 703 A93-35174
Approximation of a flight vehicle trajectory using Walsh functions p 909 A93-43106
Operating an aircraft during the landing on an airfield with a substantial longitudinal macroslope of the runway p 1008 A93-45667
Trajectory mapping of quasi-periodic structures in a vortex flow
[AIAA PAPER 93-2914] p 1044 A93-48116
Effect of anomalous aerodynamic heating during the descent of a parachute along a trajectory p 1069 A93-48924
Analytical solutions to constrained hypersonic flight trajectories p 1141 A93-49596
The numerical errors in inverse simulation
[AIAA PAPER 93-3588] p 1223 A93-52681
CTS for a low speed wind tunnel - Captive Trajectory System p 1251 A93-56278
Air-breathing hypersonic vehicle guidance and control studies: An integrated trajectory/control analysis methodology, phase 2
[NASA-CR-189703] p 65 N93-12413
Analytical solutions to constrained hypersonic flight trajectories
[NASA-CR-191987] p 297 N93-18602

TRAJECTORY CONTROL

Limit of sampling periods for nonlinear flight trajectory controller of aircraft p 61 A93-11207
Modeling of human operator actions in the stochastic trajectory tracking problem for a dynamic plant p 228 A93-16783
Evaluation of some significant issues affecting trajectory and control management for air-breathing hypersonic vehicles
[AIAA PAPER 92-5011] p 384 A93-22287
Flying qualities of the Hermes spaceplane and the shape definition process p 532 A93-28437
Modeling and control design of a wind tunnel model support p 529 A93-29281
Trajectory control for a low-lift re-entry vehicle p 1141 A93-49592
Reentry control to a drag vs. energy profile
[AIAA PAPER 93-3790] p 1143 A93-51385

TRAJECTORY MEASUREMENT

Air-breathing hypersonic vehicle guidance and control studies: An integrated trajectory/control analysis methodology, phase 2
[NASA-CR-189703] p 65 N93-12413
Control and optimization of aircraft trajectories p 729 N93-25543

TRAJECTORY MEASUREMENT

INS/DGPS integration for trajectory determination of a test vehicle p 315 A93-21178
Aircraft trajectory tracking and prediction [AD-A259039] p 340 N93-18999
Ground- and satellite-derived flight-path measurements as demonstrated in the AFES Avionics Flight Evaluation System (AFES) p 993 N93-31281
On-board derived flight-path measurement as demonstrated by an ILS measurement system p 994 N93-31282

TRAJECTORY OPTIMIZATION

Near-optimal energy transitions for energy-state trajectories of hypersonic aircraft p 69 A93-13276
[AIAA PAPER 92-4300] p 69 A93-13276
Flight path optimization and suboptimal control laws synthesis for transport mission of maneuverable aircraft p 180 A93-14160
Optimality-based control laws for real-time aircraft control via parameter optimization p 180 A93-14161
Investigation on air refueling scheduling p 108 A93-14315

Solution of trajectory optimization methods using the Pontryagin maximum principle p 366 A93-18378
Evaluation of some significant issues affecting trajectory and control management for air-breathing hypersonic vehicles p 384 A93-22287
[AIAA PAPER 92-5011] p 384 A93-22287

Closed form solutions of constrained trajectories - Application in optimal ascent of aerospace plane [AIAA PAPER 92-5012] p 385 A93-22288
Determination of the vertical velocity component of aircraft landing on an airfield with a longitudinally sloping runway p 1007 A93-45664
AIAA Atmospheric Flight Mechanics Conference, Monterey, CA, Aug. 9-11, 1993, Technical Papers p 1125 A93-48301

Nonsmooth trajectory optimization - An approach using continuous simulated annealing p 1099 A93-48337
[AIAA PAPER 93-3657] p 1099 A93-48337
Optimal impulsive interorbital transfers with aerodynamic maneuvers p 1141 A93-48838

Analytical solutions to constrained hypersonic flight trajectories p 1141 A93-49596
Hodograph analysis in aircraft trajectory optimization [AIAA PAPER 93-3742] p 1101 A93-51338
The Generalized Legendre-Clebsch Condition on state/control constrained arcs p 1170 A93-51342
[AIAA PAPER 93-3746] p 1170 A93-51342

An investigation of the fuel-optimal periodic trajectories of a hypersonic vehicle p 1101 A93-51349
[AIAA PAPER 93-3753] p 1101 A93-51349
Optimal symmetric trajectories over a fixed-time domain p 1133 A93-51435
[AIAA PAPER 93-3848] p 1133 A93-51435

Computation of optimal low- and medium-thrust orbit transfers p 1144 A93-51442
[AIAA PAPER 93-3855] p 1144 A93-51442
Optimal performance of airplanes flying through windshear p 1102 A93-51480
[AIAA PAPER 93-3846] p 1102 A93-51480

Analysis of a turning point problem in flight trajectory optimization p 1210 A93-52885
[AIAA PAPER 93-3753] p 1210 A93-52885
Optimal trajectories for hypersonic launch vehicles p 1251 A93-54563
[AIAA PAPER 93-3846] p 1251 A93-54563

A simplified numerical procedure to compute the optimal trajectory of an aircraft p 48 N93-11719
Terminal area traffic management [LR-684] p 317 N93-16213
Combining direct and indirect methods in optimal control: Range maximization of a hang glider [REPT-313] p 371 N93-16618

Analytical solutions to constrained hypersonic flight trajectories p 297 N93-18602
[NASA-CR-191987] p 297 N93-18602
Optimal finite-thrust time-bounded direct-ascent interception p 734 N93-25272
[AIAA PAPER 93-3846] p 734 N93-25272

Optimal thrust magnitude on a singular arc in atmospheric flight p 758 N93-25410
[AIAA PAPER 93-3846] p 758 N93-25410
Control and optimization of aircraft trajectories p 729 N93-25543
[AIAA PAPER 93-3846] p 729 N93-25543

Trajectory optimization for the National aerospace plane [NASA-CR-192954] p 716 N93-25670
Optimal trajectories for aircraft terrain following and terrain avoidance: A literature review update [AD-A264075] p 910 N93-30604
[AIAA PAPER 93-3846] p 910 N93-30604

TRAJECTORY PLANNING

Investigation on air refueling scheduling p 108 A93-14315

Technologies for automating rotorcraft nap-of-the-earth flight p 885 A93-43784

Numerical experiment of the flight trajectory simulation by fluid dynamics and flight dynamics coupling [AIAA PAPER 93-3324] p 952 A93-45018

Development of a system for transition characterization - for aerodynamic simulations [AIAA PAPER 93-3465] p 1030 A93-47246

A simplified numerical procedure to compute the optimal trajectory of an aircraft p 48 N93-11719

Flight evaluation of a computer aided low-altitude helicopter flight guidance system [NASA-TM-103998] p 994 N93-32225

TRANSATMOSPHERIC VEHICLES

Application of an engineering inviscid-boundary layer method to slender three-dimensional vehicle forebodies [AIAA PAPER 93-2793] p 963 A93-46534

Hypersonic aerodynamic characteristics for Langley Test Technique Demonstrator [AIAA PAPER 93-3443] p 1072 A93-49516

Performance and control of ascending trajectories to minimize heat load for transatmospheric aero-space planes p 133 N93-13745

Information requirements analyses for transatmospheric vehicles [AD-A261189] p 718 N93-25949

TRANSducers

Unsteady loads measurements in a generic high speed engine model by means of recessed transducers [AIAA PAPER 93-0287] p 342 A93-21104

Thin gradient heat fluxmeters developed at ONERA [ONERA, TP NO. 1992-87] p 831 A93-38571

TRANSFER FUNCTIONS

Analysis and feedback control of aircraft flight in wind shear p 183 A93-14349

Dynamic simulation fidelity improvement using transfer function state extrapolation [AIAA PAPER 93-3552] p 1222 A93-52656

A contribution to the dynamic feedforward open loop control of multivariable systems and to the optimal design of command functions [DLR-FB-92-05] p 441 N93-16515

Improvements to LOGI/LTR methodology for plants with lightly damped or low frequency poles [AD-A258841] p 443 N93-19112

A transfer matrix approach to vibration localization in mistuned blade assemblies [NASA-TM-106112] p 838 N93-27088

TRANSFER OF TRAINING

Simulator motion [AD-A257683] p 381 N93-17687

Summer research program (1992). High School Apprenticeship Program (HSAP) reports. Volume 16: Arnold Engineering Development Center Civil Engineering Laboratory [AD-A262024] p 945 N93-29396

Transfer of training and simulator qualification or myth and folklore in helicopter simulation p 913 N93-30687

TRANSFER ORBITS

Optimal impulsive interorbital transfers with aerodynamic maneuvers p 1141 A93-48838

Self-tuning guidance applied to aerossisted plane change problems [AIAA PAPER 93-3791] p 1143 A93-51386

Computation of optimal low- and medium-thrust orbit transfers [AIAA PAPER 93-3855] p 1144 A93-51442

TRANSFORMERS

Extended surface heat sinks for electronic components: A computer optimization [AD-A256134] p 218 N93-14254

TRANSIENT LOADS

Estimation of wing stability in flow from the characteristics of the transient process p 836 A93-39177

Stability analysis of dynamic meshes for transient aeroleastic computations [AIAA PAPER 93-3325] p 1022 A93-45019

Transient/structural analysis of a combustor under explosive loads [NASA-TM-107660] p 420 N93-17779

TRANSIENT RESPONSE

Unsteady pressure measurements on the rotor of a model turbine stage in a transient flow facility [ASME PAPER 92-GT-156] p 250 A93-19383

Simulation of propulsion system's transient response to planar wave inlet distortion and the effect of compressor wear [AIAA PAPER 93-2384] p 1117 A93-50152

New acceleration potential method for supersonic unsteady aerodynamics of lifting surfaces, further extension of the nonplanar supersonic doublet point method, and nonlinear, nongradient optimized rational function approximations for supersonic, transient response unsteady aerodynamics p 25 N93-12344

A domain decomposition method for parallel transient response calculations p 187 N93-13827

Applications of stress envelope concepts to aircraft EMP and lightning survivability p 704 N93-24898

TRANSITION FLIGHT

Development and testing of the digital control system for the Archytas unmanned air vehicle [AD-A261656] p 729 N93-26196

TRANSITION FLOW

Weighted average method for evaluating the aerodynamic properties of transition flow p 8 A93-11872

Numerical simulation of compressible mixing zones p 10 A93-12427

Experimental study of crossflow instability and laminar-turbulent transition on a swept wing p 115 A93-14250

Unsteady boundary-layer transition in flow periodically disturbed by wakes [ASME PAPER 92-GT-283] p 254 A93-19475

The role of laminar-turbulent transition in gas turbine engines - A discussion [ASME PAPER 92-GT-301] p 255 A93-19491

Transition studies for swept wing flows using PSE - parabolized stability equations [AIAA PAPER 93-0077] p 263 A93-20189

Design of a wing shape for study of hypersonic crossflow transition in flight p 265 A93-20713

Transitional characteristics of vortices issued from a body which creates asymmetric flow field - In a case of thin symmetrical airfoil with angle of attack under rotational oscillation of small amplitude p 267 A93-20923

Multigrid techniques for hypersonic viscous flows [AIAA PAPER 93-0771] p 467 A93-24855

Interaction of Tollmien-Schlichting waves with localized disturbances p 545 A93-27637

Energetics of gas-surface interactions in transitional flows at entry velocities p 778 A93-39259

Hypersonic stability and transition p 864 A93-42579

Hypersonic cone flow predictions using an implicit upwind space-marching code p 865 A93-42568

Reduction of aerodynamic skin-friction drag p 871 A93-42656

Method of characteristics for computing three-dimensional boundary layers p 970 A93-46886

The effect of a high thrust pusher propeller on the flow over a straight wing [AIAA PAPER 93-3436] p 978 A93-47228

Surface hot-film method for the measurement of transition, separation and reattachment points [AIAA PAPER 93-2918] p 1148 A93-48120

A detailed study of mean-flow solutions for stability analysis of transitional flows [AIAA PAPER 93-3052] p 1057 A93-48232

On numerical solutions of Burnett equations for hypersonic flow past 2-D circular blunt leading edges in continuum transition regime [AIAA PAPER 93-3092] p 1060 A93-48266

Multigrid techniques for hypersonic viscous flows p 1071 A93-49027

Transition correlation in subsonic flow over a flat plate p 1178 A93-53231

Flow over a leading edge with distributed roughness p 18 N93-10549

Numerical simulation of the acoustic instability in the spatially developing, confined, supersonic mixing layer p 132 N93-13521

Modeling the transition region [NASA-CR-4492] p 298 N93-19015

Numerical simulations of hypersonic rarefied transition regime flows: DSMC method and Navier-Stokes computation p 299 N93-19278

Spurious frequencies as a result of numerical boundary treatments p 839 N93-27170

Keynote address: Unsteady, multimode transition in gas turbine engines p 901 N93-29927

Measurement of turbulent spots and intermittency modelling at gas-turbine conditions p 902 N93-29934

Reynolds number influences in aeronautics [NASA-TM-107730] p 989 N93-31732

Effects of an aft facing step on the surface of a laminar flow glider wing [NASA-CR-193302] p 990 N93-31855

TRANSMISSION EFFICIENCY 1992 - The year of the radome? p 209 A93-15525

TRANSMISSION LINES The SSR mode-S data-link p 312 A93-18553

Validation of electromagnetic-topology concepts on a complex structure [ONERA, TP NO. 1992-63] p 542 A93-25327

TRANSMISSIONS (MACHINE ELEMENTS) Time-variant analysis of rotorcraft systems dynamics - An exploitation of vector processors p 416 A93-23512

Parametric study of the gear blank structure in helicopter transmission design p 546 A93-27973

- Acoustical analysis of gear housing vibration
p 567 A93-29420
- Transmission error and load distribution analysis of spur and double helical gear pairs used in a split path helicopter transmission design
p 549 A93-29426
- Active control of helicopter transmission noise
p 568 A93-29428
- Low-noise, high-strength, spiral-bevel gears for helicopter transmissions
[AIAA PAPER 93-2149] p 1154 A93-49966
- Engineering science research issues in high power density transmission dynamics for aerospace applications
--- rotorcraft geared rotors
[AIAA PAPER 93-2299] p 1155 A93-50084
- Split torque transmission load sharing
[NASA-TM-105884] p 212 N93-12736
- Conditioned based machinery maintenance (helicopter fault detection)
[AD-A255796] p 329 N93-16396
- Transmission system for a transfer device gripping a double wheel
[CA-PATENT-APPL-SN-2024585] p 731 N93-25178
- Computational gearing mechanics
[NASA-CR-191127] p 751 N93-25884
- Fault detection of helicopter gearboxes using the multi-valued influence matrix method
[NASA-TM-106100] p 838 N93-27069
- Face-gear drives: Design, analysis, and testing for helicopter transmission applications
[NASA-TM-106101] p 839 N93-27133
- Sikorsky Aircraft Advanced Rotorcraft Transmission (ART) program
[NASA-CR-191079] p 840 N93-27268
- TRANSMITTER RECEIVERS**
- The PAVE PACE integrated RF architecture for next generation avionics
p 896 A93-42784
- Ongoing GPS experiments demonstrate potential of satellite navigation technology
p 1097 A93-49278
- Receiving and scattering characteristics of an imaged monopole beneath a lossy sheet
p 1158 A93-50543
- Uplink laser propagation measurements through the sea surface, haze and clouds
[AD-A264687] p 935 N93-30553
- TRANSMITTERS**
- Automatic pulse shaping with the AN/FPN-42 and AN/FPN-44A Loran-C transmitters
[AD-A257860] p 319 N93-18309
- TRANSOCEANIC FLIGHT**
- Receiver autonomous integrity monitoring (RAIM) capability for sole-means GPS navigation in the oceanic phase of flight
p 33 A93-11035
- Trans-oceanic, polar patrol balloons and future prospects
p 26 A93-11366
- Review and prospect of Chinese scientific balloon activities
p 1 A93-11368
- Trans-oceanic balloon flight over east China sea
p 27 A93-11372
- ETOPS across the Atlantic --- extended range operation of twin-engined transport aircraft
p 306 A93-18780
- The value of GNSS to aircraft operators
p 498 A93-25172
- Aspects of aging aircraft - A transatlantic view
p 1026 A93-45776
- TRANSONIC COMPRESSORS**
- Low aspect ratio transonic rotors. I - Baseline design and performance
[ASME PAPER 92-GT-185] p 352 A93-19410
- Low aspect ratio transonic rotors. II - Influence of location of maximum thickness on transonic compressor performance
[ASME PAPER 92-GT-186] p 352 A93-19411
- Calculation of three-dimensional boundary layers on rotor blades using integral methods
[ASME PAPER 92-GT-210] p 252 A93-19433
- The extension of a solution-adaptive 3D Navier-Stokes solver towards geometries of arbitrary complexity
[ASME PAPER 92-GT-363] p 257 A93-19527
- Blade loading of transonic circular cascade diffuser
p 267 A93-20919
- Unsteady aerodynamic flow phenomena in a transonic compressor stage
[AIAA PAPER 93-1868] p 1075 A93-49743
- Tip shock structures in transonic compressor rotors
[AIAA PAPER 93-1869] p 1075 A93-49744
- Stall inception in single stage, high-speed compressors with straight and swept leading edges
[AIAA PAPER 93-1870] p 1076 A93-49745
- Characterisation of conventional and controlled diffusion stator blades in a transonic compressor stage
[ISABE 93-7124] p 1189 A93-54099
- Three-dimensional flow analysis of a four-stage transonic axial compressor with inlet guide vanes
p 1232 A93-54643
- Characterization of stall inception in high-speed single-stage compressors
[AD-A258973] p 365 N93-19093

TRANSONIC FLIGHT

- Application of a full potential code to the definition of a transonic test section
[ONERA, TP NO. 1992-84] p 822 A93-38569
- Transonic shockwave/turbulent boundary layer interactions on a porous surface
p 873 A93-43686
- Computations of aerodynamic drag for turbulent transonic projectiles with and without spin
[AIAA PAPER 93-3416] p 975 A93-47212
- Development of the F/A-18 E/F air induction system
[AIAA PAPER 93-2152] p 1101 A93-49969
- Pressure distribution for the wing of the YAV-8B airplane; with and without pylons
[NASA-TM-4429] p 136 N93-14451
- TRANSONIC FLOW**
- Multi-point design of transonic airfoils using optimization
[AIAA PAPER 92-4225] p 16 A93-13382
- Adaptive multigrid for the steady Euler equations
p 201 A93-13988
- Numerical solution of transonic full-potential-equivalent equations in von Mises co-ordinates
p 111 A93-14080
- Numerical computations of turbomachinery cascade turbulent flows with shocks by using multigrid scheme
p 112 A93-14167
- Nozzle flow computations using the Euler equations
p 112 A93-14170
- Calculation of transonic viscous flow around a delta wing
p 113 A93-14191
- Multizone Navier-Stokes computations for a transonic projectile using MacCormack finite difference method
p 113 A93-14192
- Accelerated method of the Euler equation solution in transonic airfoil flow problem
p 113 A93-14193
- Turbulence modelling requirements for the prediction of viscous transonic aeroflow flows
p 115 A93-14249
- Calculation of transonic flow over bodies of varying complexity using Singular Perturbation Method
p 116 A93-14265
- Lateral aerodynamics characteristics of forebodies at high angle of attack in subsonic and transonic flows
p 118 A93-14302
- Digital simulation of transonic flow fields in a planar nozzle
p 122 A93-14479
- A fast method for calculating three-dimensional transonic potential flows in turbomachine blade rows
p 125 A93-15215
- An AF3 algorithm for the calculation of transonic nonconservative full potential flows over wings or wing/body combinations
p 125 A93-15341
- Unsteady transonic aerodynamic loadings on the airfoil caused by heaving, pitching oscillations and control surface
p 126 A93-15627
- Unsteady transonic flow past a quarter-plane
p 127 A93-16664
- Effect of airfoil porosity on the shock wave position and intensity at transonic velocities
p 241 A93-18222
- Experience with boundary element methods to calculate the aerodynamic characteristics of aircraft
p 243 A93-19130
- Blade loading and shock wave in a transonic circular cascade diffuser
[ASME PAPER 92-GT-34] p 246 A93-19294
- Viscous flows in centrifugal compressor diffusers at transonic Mach numbers
[ASME PAPER 92-GT-48] p 246 A93-19301
- An investigation on the artificial viscosity in the transonic stream function formulation
[ASME PAPER 92-GT-49] p 246 A93-19302
- Three dimensional transonic flow measurements in an axial turbine with conical walls
[ASME PAPER 92-GT-61] p 247 A93-19311
- Aeroloids and secondary flows in a transonic mixed flow turbine stage
[ASME PAPER 92-GT-72] p 248 A93-19322
- Experimental analysis of transonic flow through the variable nozzle of a radial inflow turbine
[ASME PAPER 92-GT-90] p 248 A93-19336
- Analysis of steady and unsteady turbine cascade flows by a locally implicit hybrid algorithm
[ASME PAPER 92-GT-127] p 249 A93-19361
- Boundary layer effects on the transonic flow in a straight turbine cascade
[ASME PAPER 92-GT-155] p 249 A93-19382
- Techniques for aerodynamic loss measurement of transonic turbine cascades with trailing-edge region coolant ejection
[ASME PAPER 92-GT-157] p 250 A93-19384
- Transonic flow through turbine cascades with nonuniform pitch
[ASME PAPER 92-GT-158] p 250 A93-19385
- Three-dimensional flow phenomena in a transonic, high-through-flow, axial-flow compressor stage
[ASME PAPER 92-GT-169] p 250 A93-19395

- A fully three-dimensional inverse method for turbomachinery blading in transonic flows
[ASME PAPER 92-GT-209] p 251 A93-19432
- Prediction of 2D viscous transonic flow in compressor cascades using a semi-empirical shock/boundary-layer interaction method
[ASME PAPER 92-GT-277] p 253 A93-19470
- Inverse design of compressor and turbine blades at transonic flow conditions
[ASME PAPER 92-GT-430] p 357 A93-19573
- A CAD computer system for centrifugal compressor impeller with transonic inflow
p 259 A93-20118
- Accurate solution of the 2D Euler equations with an efficient cell-vertex upwind scheme
[AIAA PAPER 93-0071] p 262 A93-20183
- Numerical prediction of instabilities in transonic internal flows using an Euler TVD code
[AIAA PAPER 93-0072] p 262 A93-20184
- A multi-point optimization for transonic airfoil design
[AIAA PAPER 92-4681] p 264 A93-20303
- An approximately factored incremental strategy for calculating consistent discrete aerodynamic sensitivity derivatives
[AIAA PAPER 92-4746] p 265 A93-20344
- Structural non-linearity effects on flutter of a swept wing in transonic flows
p 410 A93-20714
- Two-dimensional cascade tests of MCA blades in the high transonic Mach number region. V - Effect of space/chord ratio on the parameters of cascade performance
p 267 A93-20930
- A comparison of the predictive capabilities of several turbulence models using upwind and central-difference computer codes
[AIAA PAPER 93-0192] p 268 A93-21102
- Transonic shock oscillations calculated with a new interactive boundary layer coupling method
[AIAA PAPER 93-0777] p 269 A93-21119
- Numerical simulation of unsteady transonic nozzle flows
p 272 A93-22230
- Validation of a Navier-Stokes code using a (ϵ , epsilon) turbulence model applied to a three-dimensional transonic channel
[AIAA PAPER 93-0293] p 279 A93-22693
- High accuracy computation of fluid-structure interaction in transonic cascades
[AIAA PAPER 93-0485] p 287 A93-23387
- Direct solution of two-dimensional Navier-Stokes equations for static aeroelasticity problems
p 417 A93-23554
- Airfoil design using the Navier-Stokes equations
[AIAA PAPER 93-0648] p 464 A93-24763
- Fundamental issues in subsonic/transonic expansion corner aerodynamics
[AIAA PAPER 93-0649] p 465 A93-24764
- Supercritical wing design, a three dimensional hodograph approach
[AIAA PAPER 92-2657] p 472 A93-24986
- Euler study on porous transonic airfoils with a view toward multipoint design
p 479 A93-28604
- Current status of computational methods for transonic unsteady aerodynamics and aeroelastic applications
p 480 A93-29175
- Aeroelastic system identification of advanced technology aircraft through higher order signal processing
p 525 A93-29297
- Flowfield measurements of a two-element airfoil with large separation
p 480 A93-29307
- Noise reduction for transonic blade-vortex interactions
p 566 A93-29408
- Passive drag reduction of a helicopter airfoil in an unsteady transonic flow
p 482 A93-29443
- Finite-volume-TVD scheme for 3-D Euler transonic flow computations in rotating curvilinear coordinates
p 679 A93-33709
- Numerical solution of non-isentropic transonic cascade flow by time-marching method
p 679 A93-33715
- Numerical simulation of passive control of shock-boundary layer interaction for transonic airfoil
p 680 A93-33719
- The analysis and computation of viscous-inviscid interactive problem for three dimensional transonic flow
p 681 A93-33741
- The role of Kutta waves on oscillatory shock motion on an airfoil experiencing heavy buffeting
[AIAA PAPER 93-1589] p 682 A93-34121
- Unsteady transonic potential flow over a flexible fuselage
[AIAA PAPER 93-1593] p 683 A93-34124
- Experimental investigation of counter-rotating propfan flutter at cruise conditions
[AIAA PAPER 93-1632] p 720 A93-34160
- Sensitivity analysis of flutter response of a typical section and a wing in transonic flow
[AIAA PAPER 93-1646] p 742 A93-34171

- Comparison of several convection discretization schemes for all Mach number arbitrary 2D flows p 685 A93-34345
- A cell-vertex TVD scheme for transonic viscous flow p 685 A93-34346
- A technique for accelerated convergence in transonic flow p 685 A93-34347
- Numerical simulation of inviscid transonic flow over two-dimensional slender bodies p 686 A93-34348
- Implicit numerical solution of transonic flows using adaptive triangular grids p 686 A93-34349
- Computation of viscous transonic aerofoil flows using eddy-viscosity based turbulence models p 687 A93-34360
- Transonic flow around the leading edge of a thin airfoil with a parabolic nose p 688 A93-34405
- Implicit upwind solution algorithms for three-dimensional unstructured meshes p 691 A93-35607
- Application of Oswatitsch's theorem to supercritical airfoil drag calculation p 768 A93-37399
- Permeable airfoils in incompressible flow p 768 A93-37401
- Comment on 'In-flight measurement of static pressures' p 807 A93-37407
- Nonclassical aileron buzz in transonic flow [AIAA PAPER 93-1479] p 829 A93-37439
- Numerical solution of viscous compressible flows using algebraic turbulence models p 770 A93-38162
- Transonic and supersonic flow calculations around aircrafts using a multidomain Euler code [ONERA, TP NO. 1992-137] p 772 A93-38610
- Some special purpose preconditioners for conjugate gradient-like methods applied to CFD p 772 A93-38638
- Viscous-inviscid calculation of high-lift separated compressible flows over airfoils and wings [ONERA, TP NO. 1992-184] p 774 A93-38746
- Experience in the design of supercritical cascades for the flow straightener of a transonic fan p 777 A93-39196
- Unsteady transonic two-dimensional Euler solutions using finite elements p 778 A93-39412
- Development of a transonic Euler method for complete aircraft configurations p 779 A93-39721
- Passive control of a shock wave/turbulent boundary layer interaction in a transonic flow p 858 A93-40444
- The Langley 8-ft transonic pressure tunnel laminar-flow-control experiment p 910 A93-41783
- Subsonic/transonic cascade flutter using a full-potential solver p 861 A93-41934
- Transonic aerodynamics including strong effects from heat addition p 862 A93-42428
- Comparison of numerical methods in transonic aerodynamics p 864 A93-42446
- Treatment of vortex sheets for the transonic full-potential equation p 871 A93-42870
- Inviscid finite-volume lambda formulation p 872 A93-42888
- Stability conditions for a transonic decelerating flow in a duct p 872 A93-43027
- Visualisation and analysis of three dimensional transonic flows by holographic interferometry p 1020 A93-44194
- Unsteady flow simulation on a parallel computer p 1022 A93-45089
- Adaptive refinement-coarsening scheme for three-dimensional unstructured meshes p 961 A93-45735
- Kinematic domain decomposition for boundary-motion-induced flow simulations p 1028 A93-46811
- On the construction and calculation of optimal nonlifting critical airfoils p 969 A93-46857
- The cryogenic wind tunnel p 1013 A93-46915
- Prediction of three-dimensional low frequency unsteady transonic flow and forced vibration in axial turbine stages p 971 A93-46934
- 3D/quasi-3D trans- and supersonic flow calculation in advanced centrifugal/axial compressor stages p 972 A93-46936
- Three dimensional aero-thermal characteristics of a high pressure turbine nozzle guide vane p 1002 A93-46942
- On the shock-fitting scheme of Hall-Crawley for time-linearized time-harmonic flows using Euler equations p 972 A93-46946
- Numerical solution of steady and unsteady Euler equations p 973 A93-46988
- AIAA Applied Aerodynamics Conference, 11th, Monterey, CA, Aug. 9-11, 1993, Technical Papers, Pts. 1 & 2 p 974 A93-47201
- Computational analysis of drag reduction and buffet alleviation in viscous transonic flow over porous airfoils [AIAA PAPER 93-3419] p 976 A93-47215
- Supersonic vortex breakdown over a delta wing in transonic flow [AIAA PAPER 93-3472] p 980 A93-47251
- Computation of passively controlled transonic wing [AIAA PAPER 93-3474] p 981 A93-47253
- Application of computational fluid dynamics in transonic aerodynamic design [AIAA PAPER 93-3481] p 982 A93-47259
- A computational method for inverse design of transonic airfoil and wing [AIAA PAPER 93-3482] p 982 A93-47260
- The application of an Euler method and a Navier Stokes method to the vortical flow about a delta wing [AIAA PAPER 93-3510] p 984 A93-47276
- Multiple solutions of the transonic perturbation equation p 987 A93-47331
- Reynolds stress transport modelling of shock/boundary-layer interaction [AIAA PAPER 93-2936] p 1046 A93-48134
- A CFD-based design strategy for advanced transonic wing concepts with practical ramifications for subsonic transports [AIAA PAPER 93-2946] p 1047 A93-48143
- Multi-zonal Navier-Stokes code with the LU-SGS scheme [AIAA PAPER 93-2965] p 1148 A93-48159
- Shock-vortex interaction over a 65-degree delta wing in transonic flow [AIAA PAPER 93-2973] p 1049 A93-48167
- Computations of transonic wind tunnel flows about a fully configured model of aircraft by using multi-domain technique [AIAA PAPER 93-3022] p 1055 A93-48207
- Transonic mutual interference of wing-pylon-multiple body configurations using an overlapping grid scheme [AIAA PAPER 93-3023] p 1055 A93-48208
- Improvement of transonic wing buffet by geometric modifications [AIAA PAPER 93-3024] p 1055 A93-48209
- Clebsch variable model for unsteady inviscid transonic flow with strong shock waves [AIAA PAPER 93-3025] p 1055 A93-48210
- A fast robust viscous-inviscid interaction solver for transonic flow about wing/body configurations on the basis of full potential theory [AIAA PAPER 93-3026] p 1056 A93-48211
- Code validation for high speed flow simulation over the VLS launcher fairing --- Brazilian satellite launch vehicles [AIAA PAPER 93-3046] p 1057 A93-48226
- Transition for three-dimensional boundary layers on wings in the transonic regime [AIAA PAPER 93-3049] p 1057 A93-48229
- Navier-Stokes simulation of external/internal transonic flow on the forebody/inlet of the AV-8B Harrier II [AIAA PAPER 93-3057] p 1058 A93-48234
- Experimental and numerical study of transonic turbine cascade flow [AIAA PAPER 93-3064] p 1059 A93-48240
- Averaging techniques for steady and unsteady calculations of a transonic fan stage [AIAA PAPER 93-3065] p 1059 A93-48241
- A two layer k-epsilon computation of transonic viscous flow including separation over the DLR-F5 wing [AIAA PAPER 93-3110] p 1061 A93-48281
- Design efficiency evaluation for transonic airfoil optimization - A case for Navier-Stokes design [AIAA PAPER 93-3112] p 1062 A93-48282
- Demonstration of multipoint design procedures for transonic airfoils [AIAA PAPER 93-3114] p 1062 A93-48284
- Calculation of transonic longitudinal and lateral-directional characteristics of aircraft by the small disturbance theory [AIAA PAPER 93-3617] p 1125 A93-48304
- Numerical simulation of unsteady flow in a transonic cascade p 1066 A93-48502
- Viscous analysis of high pressure turbine inlet guide vane flow including cooling injections [AIAA PAPER 93-1798] p 1074 A93-49687
- 3-D Euler simulation of vane-blade interaction in a transonic turbine [AIAA PAPER 93-2256] p 1081 A93-50054
- Using a diagonal implicit algorithm to calculate transonic nozzle flow [AIAA PAPER 93-2345] p 1082 A93-50119
- Calibration of a transonic 5-hole probe for a multi-element airfoil cascade facility [AIAA PAPER 93-2471] p 1138 A93-50216
- Minimizing the wall effects in wind tunnels with a sectional pressure chamber p 1085 A93-50965
- On boundary-layer transition in transonic flow p 1087 A93-51280
- Steady transonic weakly perturbed flows in a vibrationally relaxing gas p 1088 A93-51768
- A finite difference study of the aerodynamic characteristics of wing profiles at transonic velocities p 1091 A93-51903
- Computation of subsonic viscous and transonic viscous-inviscid unsteady flow p 1094 A93-52012
- Transonic Navier-Stokes flow computations over wing-fuselage geometries p 1095 A93-52456
- Low aspect ratio wing code validation experiment p 1176 A93-53202
- Three-dimensional Navier-Stokes/full-potential coupled analysis for viscous transonic flow p 1178 A93-53218
- Calculation of flow fields near a lifting wing p 1179 A93-53552
- An implicit difference scheme of Euler equation for unsteady transonic flow p 1182 A93-53852
- Transonic area rule about lifting configurations p 1183 A93-53868
- Navier-Stokes computation of the three dimensional flow fields through a transonic fan blade [ISABE 93-7030] p 1184 A93-54006
- Transonic discharge flows around diffuser vanes from a centrifugal impeller [ISABE 93-7053] p 1185 A93-54029
- Navier-Stokes analysis of turbine flowfield and external heat transfer [ISABE 93-7075] p 1186 A93-54051
- Design of air intakes and nozzles for transonic rotational flows [ISABE 93-7102] p 1187 A93-54078
- Design of shockless supersonic region in the axisymmetric transonic flow p 1230 A93-54587
- Two-dimensional transonic flow around VKI turbine cascade p 1232 A93-54640
- Three-dimensional flow analysis of a four-stage transonic axial compressor with inlet guide vanes p 1232 A93-54643
- An airfoil in transonic flow in the presence of wind gusts and weak shock waves p 1233 A93-55015
- Measurement of turbulent boundary layer in transonic flow p 1236 A93-55411
- Determination of the transonic flow field around an airfoil section for a given lift force coefficient p 1239 A93-56215
- Interactive grid generation program for CAP-TSD [NASA-TM-102705] p 17 N93-10349
- A field panel method for transonic flows p 18 N93-10547
- Navier-Stokes simulations of unsteady transonic flow phenomena [NASA-TM-103962] p 129 N93-12721
- Transonic aeroelastic analysis of systems with structural nonlinearities p 217 N93-13769
- Unsteady three-dimensional thin-layer Navier-Stokes solutions for turbomachinery in transonic flow p 218 N93-14025
- Pressure drag and lift contributions for blunted forebodies of fineness ratio 2.0 in transonic flow (M infinity less than or equal to 1.4) [ESDU-89033] p 136 N93-14515
- Direct prediction of a separation boundary for aeroflows using a viscous-coupled calculation method [ESDU-92008] p 136 N93-14516
- Time-dependent predictions and analysis of turbine cascade data in the transonic flow region [PNR-90957] p 139 N93-15489
- Static pressure measurements of the shock-boundary layer interaction in a simulated fan passage [AD-A256724] p 361 N93-15979
- Navier-Stokes calculation of transonic flow past the NTF 65-deg delta wing p 292 N93-16797
- Application of an Euler-equation method to a sharp-edged delta wing configuration with vortex flow [NLR-TP-91306] p 294 N93-17809
- Numerical investigation of swirl-airfoil interactions in transonic area [MPIS-8/1991] p 297 N93-18627
- Transonic flow calculation around NACA-0012 p 302 N93-19301
- Wind tunnel wall interference correction at subsonic speeds p 304 N93-19320
- Advanced adaptive computational methods for Navier-Stokes simulations in rotorcraft aerodynamics [NASA-CR-192282] p 483 N93-20256
- Prediction of unsteady flows in turbomachinery using the linearized Euler equations on deforming grids [NASA-CR-192919] p 747 N93-25109
- Computation of transonic flow over a porous surface projectile p 696 N93-25409
- Navier-Stokes simulations of unsteady transonic flow phenomena p 697 N93-25542
- Model fan passage flow simulation [AD-A261613] p 752 N93-26167
- Unsteady airfoil flow solutions on moving zonal grids [AD-A261925] p 701 N93-26198
- Three-dimensional compressible stability-transition calculations using the spatial theory p 783 N93-27431

- Some recent applications of Navier-Stokes codes to rotorcraft p 786 N93-27452
- Calculation of fully three-dimensional separated flow with an unsteady viscous-inviscid interaction method p 786 N93-27455
- Transonic flows on an oscillating airfoil and their effect on the flutter-boundary [DLR-FB-92-08] p 790 N93-29006
- A Navier-Stokes solver with different turbulence models applied to film-cooled turbine cascades p 904 N93-29962
- TDLM: A Transonic Doublet Lattice Method for 3D potential unsteady transonic flow calculation [DLR-FB-92-25] p 988 N93-31171
- Development of a method to predict transonic limit cycle oscillation characteristics of fighter aircraft [NLR-TP-91359-U] p 999 N93-32338
- NLR inviscid transonic unsteady loads prediction methods in aeroelasticity [NLR-TP-91410-U] p 990 N93-32358
- ### TRANSONIC FLUTTER
- Transonic flutter/divergence characteristics of aerelastically tailored and non-tailored high-aspect-ratio forward-swept wings p 10 A93-12273
- Modeling, analysis, and prediction of flutter at transonic speeds p 416 A93-23553
- Current status of computational methods for transonic unsteady aerodynamics and aeroelastic applications p 480 A93-29175
- An experimental and analytical study of a lifting-body wind-tunnel model exhibiting body-freedom flutter [AIAA PAPER 93-1316] p 732 A93-33891
- Experimental investigation of counter-rotating propfan flutter at cruise conditions [AIAA PAPER 93-1632] p 720 A93-34160
- Transonic panel flutter [AIAA PAPER 93-1476] p 829 A93-37438
- Nonclassical aileron buzz in transonic flow [AIAA PAPER 93-1479] p 829 A93-37439
- Transonic flutter suppression using active acoustic excitations [AIAA PAPER 93-3285] p 969 A93-46841
- Numerical simulation of unsteady flow in a transonic cascade p 1066 A93-48502
- Nonlinear aspects of transonic aeroelasticity p 1096 A93-52642
- Transonic flows on an oscillating airfoil and their effect on the flutter-boundary [DLR-FB-92-08] p 790 N93-29006
- ### TRANSONIC NOZZLES
- Aerodynamic performance of a transonic low aspect ratio turbine nozzle [ASME PAPER 92-GT-31] p 245 A93-19291
- Heat transfer and aerodynamics of a high rim speed turbine nozzle guide vane with profiled end walls [ASME PAPER 92-GT-243] p 253 A93-19452
- Using a diagonal implicit algorithm to calculate transonic nozzle flow [AIAA PAPER 93-2345] p 1082 A93-50119
- A new method for resolving transonic nozzle flows using orthogonal stream-lines coordinate system p 1230 A93-54584
- Direct solutions of the Navier-Stokes equations with application to static aeroelasticity p 748 N93-25259
- ### TRANSONIC SPEED
- An analysis on high speed impulsive noise of transonic helicopter rotor p 849 A93-35965
- An inverse method with regularity condition for transonic airfoil design p 1230 A93-54583
- Computation of H₂/air reacting flowfields in drag-reduction external combustion [NASA-CR-191071] p 536 N93-20237
- Application of the Euler method EUFLEX to a fighter-type airplane configuration at transonic speed [MBB-FE-211-S-PUB-0489-A] p 484 N93-21059
- Experimental investigations on wing-body combinations and their components at high angles of attack in the subsonic and transonic speed range p 516 N93-21762
- [DLR-FB-91-43] p 516 N93-21762
- A feasibility study of using Langley 0.3-m transonic cryogenic tunnel sidewall boundary-layer removal system for heavy gas testing [NASA-CR-191438] p 747 N93-25087
- Visualization of a Mach 2 reacting flow using Planar Laser-Induced Fluorescence (PLIF) p 731 N93-26006
- ### TRANSONIC WIND TUNNELS
- The use of a deep honeycomb to achieve high flow quality in the ARA 9 ft x 8 ft Transonic Wind Tunnel p 190 A93-14276
- The cryogenic approach to simulating hot jet in transonic wind-tunnel testing p 117 A93-14297
- Generation of flow disturbances in transonic wind tunnels p 119 A93-14354
- The VKI compression tube annular cascade facility CT3 [ASME PAPER 92-GT-336] p 375 A93-19511
- Flow visualization studies on sidewall effects in two dimensional transonic airfoil testing [AIAA PAPER 93-0090] p 263 A93-20196
- Numerical prediction of flap losses in a transonic wind tunnel p 288 A93-23552
- Asymptotic methods for the prediction of transonic wind-tunnel wall interference p 730 A93-35625
- Application of a full potential code to the definition of a transonic test section [ONERA, TP NO. 1992-84] p 822 A93-38569
- Infrared thermography for hot-shot wind tunnel [ONERA, TP NO. 1992-103] p 831 A93-38583
- Testing techniques for straight transonic and supersonic cascades [ONERA, TP NO. 1992-155] p 773 A93-38734
- Aerodynamic investigation with focusing schlieren in a cryogenic wind tunnel [AIAA PAPER 93-3485] p 910 A93-41059
- The adaptive wall test section for the NASA Langley 0.3-m Transonic Cryogenic Tunnel p 1013 A93-46825
- Computations of transonic wind tunnel flows about a fully configured model of aircraft by using multi-domain technique [AIAA PAPER 93-3022] p 1055 A93-48207
- Advanced SST auxiliary air intakes design and analysis [AIAA PAPER 93-2304] p 1082 A93-50088
- Fluidic scale model multi-plane thrust vector control test results [AIAA PAPER 93-2433] p 1117 A93-50187
- Internal performance of Highly Integrated Deployable Exhaust Nozzles [AIAA PAPER 93-2570] p 1084 A93-50288
- Experimental study of pylon cross sections for a subsonic transport airplane p 1103 A93-52440
- Some acoustic features of perforated test section walls with splitter plates p 1226 A93-53222
- Wind of change p 1209 A93-53625
- Europe's new windtunnel p 1210 A93-54275
- Instrumentation and data acquisition system for the C.I.R.A. Transonic Pilot Tunnel p 1250 A93-54395
- Further noise measurements in a slotted cryogenic wind tunnel [RAE-TM-AERO-2201] p 101 N93-10805
- The design and commissioning of an acoustic liner for propeller noise testing in the ARA transonic wind tunnel [PNR-90880] p 101 N93-11204
- Modeling and control study of the NASA 0.3-meter transonic cryogenic tunnel for use with sulfur hexafluoride medium [NASA-CR-189737] p 418 N93-16379
- Modifications to Langley 0.3-m TCT adaptive wall software for heavy gas test medium, phase 1 studies [NASA-CR-189736] p 291 N93-16710
- Application of a neural network as a potential aid in predicting NTF pump failure [NASA-TM-107667] p 442 N93-18332
- Wind tunnel test and CFD in Kawasaki Heavy Industries, Gifu p 304 N93-19324
- NASA Lewis 8- by 6-foot supersonic wind tunnel user manual [NASA-TM-105771] p 730 N93-25080
- A feasibility study of using Langley 0.3-m transonic cryogenic tunnel sidewall boundary-layer removal system for heavy gas testing [NASA-CR-191438] p 747 N93-25087
- Performance characteristics of two multiaxis thrust-vectoring nozzles at Mach numbers up to 1.28 [NASA-TP-3313] p 874 N93-29160
- A break-down of sting interference effects [NLR-TP-91220-U] p 1014 N93-31042
- A PC-based simulation of the National Transonic Facility's safety microprocessor [NASA-TM-109003] p 1038 N93-32224
- ### TRANSPARENCY
- New model of bird impact response analysis and its engineering solution p 156 A93-14336
- Determination of stresses on laminated aircraft transparencies by the strain gage-hole drilling and sectioning method [AD-A255548] p 164 N93-14571
- ### TRANSPONDERS
- The Airborne Collision Avoidance System (ACAS) p 883 A93-43370
- ### TRANSPORT AIRCRAFT
- Transport resurrection p 41 A93-12434
- Effects of turbine cooling assumptions on performance and sizing of high-speed civil transport [AIAA PAPER 92-4217] p 55 A93-13383
- Advanced cockpit technology in the real world p 2 A93-13409
- Civil spin-off from military aircraft cockpit research p 45 A93-13415
- Loads at the nose landing gears of civil transport aircraft during towbarless towing operations p 45 A93-13629
- Aerodynamic characteristics of transport airplanes in low speed configuration p 113 A93-14172
- Inlet design using a blend of experimental and computational techniques p 114 A93-14210
- Integrated control law synthesis of gust load alleviation and flutter margin augmentation for a transport aircraft p 182 A93-14281
- The aerodynamic and structural design of a variable camber wing (VCW) p 117 A93-14291
- On the configuration buffet of a transport aircraft p 117 A93-14298
- In-flight surface-flow measurements on a subsonic transport high-lift flap system p 166 A93-14327
- Cost - The challenge for advanced materials and structures p 233 A93-14338
- Analysis and development of a total energy control system for a large transport aircraft p 183 A93-14372
- Hybrid laminar flow control applied to advanced turbofan engine nacelles [SAE PAPER 920962] p 123 A93-14628
- Optimization of pneumatic subsystems for transport aircraft p 159 A93-15049
- Using helicopters for transporting large and heavy loads p 306 A93-18350
- Concept of closed-circuit TV system for transport aircraft under examination p 306 A93-18542
- A scoping study for hypersonic transport propulsion systems [ASME PAPER 92-GT-409] p 356 A93-19558
- Flutter optimization of large transport aircraft [AIAA PAPER 92-4795] p 326 A93-20381
- Ice accretion prediction for a typical commercial transport aircraft [AIAA PAPER 93-0174] p 310 A93-23245
- Development of circulation control technology for application to advanced subsonic transport aircraft [AIAA PAPER 93-0644] p 464 A93-24759
- The FAA/NASA flight loads monitoring program - The prototype system and its benefits for the aviation community p 486 A93-25125
- Comparison of all-electric secondary power systems for civil transport p 519 A93-25997
- Recent developments in international laminar flow research programs for transport aircraft [ONERA, TP NO. 1992-163] p 457 A93-26878
- Noise reduction programs for in-service jet transports p 521 A93-28479
- Laminar-flow instrumentation for wind-tunnel and flight experiments p 479 A93-28605
- ISAC - A tool for aeroservoelastic modeling and analysis --- Interaction of Structures, Aerodynamics, and Control [AIAA PAPER 93-1421] p 726 A93-33974
- Using a full potential solver for propulsion system exhaust simulation p 689 A93-34487
- C-17 - High-tech 'lifter from Long Beach' p 713 A93-34519
- Machinery arrangements for small VTOL transport aircraft p 713 A93-34848
- Management miscues, delays snarl C-17 program p 760 A93-34944
- Optimal takeoff procedures for a transport category tiltrotor p 802 A93-37377
- C-17 should fulfill USAF airlift mission p 805 A93-39599
- Versatility, automation key to C-17 cargo operations p 805 A93-39600
- Effect of structural uncertainties on flutter analysis p 924 A93-40445
- Reduction of aerodynamic skin-friction drag p 871 A93-42656
- The ring laser gyro and its applications p 927 A93-42657
- Integrating controls and avionics on commercial aircraft p 892 A93-42778
- Big time doorstep delivery p 892 A93-42995
- Leading-edge transition and relaminarization phenomena on a subsonic high-lift system [AIAA PAPER 93-3140] p 959 A93-45154
- Classification of the principal fuel saving methods in flight operations p 996 A93-45660
- Using spectral analysis for estimating the effect of runway irregularities on the loading of transport aircraft structures p 996 A93-45669
- Aging jet transport structural evaluation programs p 947 A93-45781
- NASA airframe structural integrity program p 1026 A93-45782
- A study of the influence of the data acquisition system sampling rate on the accuracy of measured acceleration loads for transport aircraft p 1000 A93-46808
- CFD drag predictions for a wide body transport fuselage with flight test verification [AIAA PAPER 93-3418] p 976 A93-47214
- Computation of wake/exhaust mixing downstream of advanced transport aircraft [AIAA PAPER 93-2944] p 1162 A93-48141

- Navier-Stokes calculations for transport wing-body configurations with nacelles and struts
[AIAA PAPER 93-2945] p 1047 A93-48142
- Two-dimensional computational analysis of a transport high-lift system and a comparison with flight-test results
[AIAA PAPER 93-3533] p 1072 A93-49517
- NO(x) scavenging on carbonaceous aerosol surfaces in aircraft exhaust plumes. I
[AIAA PAPER 93-2343] p 1164 A93-50117
- Fiber-optic technology for transport aircraft
p 1173 A93-50488
- Longitudinal and lateral-directional flying qualities investigation of high-order characteristics for advanced-technology transports
[AIAA PAPER 93-3815] p 1133 A93-51406
- Initial results of an in-flight investigation of longitudinal flying qualities for augmented, large transports in approach and landing
[AIAA PAPER 93-3816] p 1133 A93-51407
- Hand-held cabin fire extinguishers - Transport aircraft
[SAE ARP 4712] p 1096 A93-52168
- Experimental study of pylon cross sections for a subsonic transport airplane
p 1103 A93-52440
- Multielement airfoil performance due to Reynolds and Mach number variations
p 1095 A93-52442
- The properties of newly developed highly damage tolerant and easy handleable carbon fiber/modified bismaleimide prepreg system
p 1212 A93-53448
- Wind of change
p 1209 A93-53625
- Propulsion technology challenges for turn-of-the-century commercial aircraft
[ISABE 93-7003] p 1194 A93-53980
- Conceptual design study on combined-cycle engine for hypersonic transport
[ISABE 93-7018] p 1195 A93-53994
- Noise reduction of supersonic heated jet with jet mixing enhancement by tabs
[ISABE 93-7046] p 1198 A93-54022
- Russian survivor - Tu-334 aircraft
p 1243 A93-54867
- Enhancement of conventional NDT methods for corrosion detection in layered skins
p 1258 A93-54898
- Advanced terrain displays to transport category aircraft
[PB92-197136] p 35 A93-10065
- Comparison of all-electric secondary power systems for civil subsonic transports
[NASA-TM-105852] p 55 A93-10456
- Aeronautical technologies for the twenty-first century
[NASA-CR-190918] p 4 A93-10647
- Initial piloted simulation study of geared flap control for tilt-wing V/STOL aircraft
[NASA-TM-103872] p 64 A93-10741
- Formal representation of the requirements for an Advanced Subsonic Civil Transport (ASCT) flight control system
[NASA-CR-189699] p 98 A93-12346
- Future regional transport aircraft market, constraints, and technology stimuli
[NASA-TM-107669] p 109 A93-13025
- Detailed analysis of wing-nacelle interaction for commercial transport aircraft
p 213 A93-13203
- Euler analysis of turbofan/superfan integration for a transport aircraft
p 214 A93-13206
- Aerodynamic integration of thrust reversers on the Fokker 100
p 160 A93-13208
- Ice accretion prediction for a typical commercial transport aircraft
[NASA-TM-105976] p 149 A93-15522
- Technology benefits and ground test facilities for high-speed civil transport development
[NASA-TM-107670] p 378 A93-15790
- Definition of the 2005 flight deck environment
[NASA-CR-4479] p 343 A93-16693
- The design of a long range megatransport aircraft
[NASA-CR-192077] p 332 A93-17711
- Improving military transport aircraft through highly integrated engine-wing design
[DS-1607] p 333 A93-17850
- Flight simulation evaluation of the flyability of curved MLS approaches with wide-body aircraft
[NLR-TP-90238-U] p 382 A93-17875
- Design of the advanced regional aircraft, the DART-75
[NASA-CR-192044] p 333 A93-17972
- Eagle RTS: A design for a regional transport aircraft
[NASA-CR-192032] p 334 A93-18017
- Proposal and preliminary design for a high speed civil transport aircraft. Swift: A high speed civil transport for the year 2000
[NASA-CR-192023] p 335 A93-18049
- Flight tests of the transport aircraft viewed from the industrial standpoint
p 510 A93-19903
- Analysis and evaluation of an integrated laminar flow control propulsion system
[NASA-CR-192162] p 551 A93-20268
- A simulator study into low speed longitudinal handling qualities of ACT transport aircraft
[NLR-TP-89387-U] p 527 A93-20743
- An approach to configuration design synthesis of subsonic transport aircraft using artificial intelligence techniques
p 716 A93-25692
- Effect of underwing frost on transport aircraft takeoff performance
[DOT/FAA/CT-TN93/9] p 791 A93-27252
- Design, analysis, and control of large transport aircraft utilizing engine thrust as a backup system for the primary flight controls
[NASA-CR-192938] p 820 A93-27308
- World jet airplane inventory at year-end 1992
[PB93-174324] p 765 A93-27405
- High-lift aerodynamics: Prospects and plans
p 784 A93-27442
- Quantitative three-dimensional low-speed wake surveys
p 785 A93-27447
- Flow prediction over a transport multi-element high-lift system and comparison with flight measurements
p 785 A93-27448
- The development of a parachute system for aerial delivery from high speed cargo aircraft
[DB93-008339] p 790 A93-29035
- Vortex wake characteristics of B757-200 and B767-200 aircraft using the tower fly-by technique
[PB93-180263] p 878 A93-30388
- Composites technology for transport primary structure
p 918 A93-30431
- Advanced technology commercial fuselage structure
p 918 A93-30432
- Design, analysis, and fabrication of the technology integration box beam
p 919 A93-30433
- Mechanical and analytical screening of braided composites for transport fuselage applications
p 922 A93-30855
- Optimization of composite sandwich cover panels subjected to compressive loadings
p 922 A93-30862
- Advanced fiber placement of composite fuselage structures
p 923 A93-30864
- Longitudinal acceleration test of overhead luggage bins in a transport airframe section
[DOT/FAA/CT-92/9] p 991 A93-31652
- Engine exhaust characteristics evaluation in support of aircraft acoustic testing
[NASA-TM-104263] p 1005 A93-32220
- Propulsion technology challenges for turn-of-the-century commercial aircraft
[NASA-TM-106192] p 1005 A93-32351
- UK airmisses involving commercial air transport, September - December 1991
[ETN-93-93930] p 992 A93-32409
- TRANSPORT PROPERTIES**
Transport processes in hypersonic flows
p 7 A93-11302
- Radial transport and momentum exchange in an axial compressor
[ASME PAPER 92-GT-364] p 257 A93-19528
- Flight data for the Cryogenic Heat Pipe (CRYOHP) Experiment
[AIAA PAPER 93-2735] p 1027 A93-46488
- Rotating machinery - Transport phenomena: Proceedings of the 3rd International Symposium on Transport Phenomena and Dynamics of Rotating Machinery (ISROMAC-3), Honolulu, HI, Apr. 1-4, 1990
[ISBN 1-56032-147-4] p 1256 A93-54626
- NO(y) from sub-sonic aircraft emissions - A global three-dimensional model study
p 1261 A93-56236
- Influence of the physical modelling of viscous terms on hypersonic flow computations
[INRIA-RR-1493] p 297 A93-18652
- TRANSPORT VEHICLES**
Integration of turbo-ramjet engines for hypersonic aircraft
p 175 A93-13230
- TRANSPORTATION**
An investigation of ground access mode choice for departing passengers
[TT-9201] p 67 A93-11224
- Airport landside planning and operations
[PB93-167880] p 822 A93-26636
- TRANSPUTERS**
Visualization and view simulation based on transputers
p 1037 A93-45150
- TRANSVERSE ACCELERATION**
Cancellation control law for lateral-directional dynamics of a supermaneuverable aircraft
[AIAA PAPER 93-3775] p 1131 A93-51370
- TRANSVERSE LOADS**
Photoelastic stress analysis of skewed cutout in a sandwich skew plate subjected to inplane and transverse eccentric load
p 210 A93-16604
- Thermomechanical postbuckling analysis of laminated composite shells
[AIAA PAPER 93-1337] p 738 A93-33907
- A plate loaded by a transverse impulse force and in-plane forces
p 828 A93-36799
- Effect of boundary conditions and panel geometry on the response of laminated panels subjected to transverse pressure loads
p 1259 A93-55674
- TRANSVERSE OSCILLATION**
Simulation analysis of a cable-mount system used for dynamic wind tunnel tests
[NAL-TR-1127] p 68 A93-12359
- TRANSVERSE WAVES**
Propagation of transverse anti-plane waves in orthotropic layers
p 412 A93-21878
- Numerical study of supersonic flow over a backward step with transverse injection
p 1182 A93-53853
- TRAPPED VORTICES**
Vortex capture by a two-dimensional airfoil with a small oscillating leading-edge flap
[AIAA PAPER 93-3266] p 968 A93-46830
- TRAVELING WAVES**
Shock shapes around slender diamond cones traveling at hypersonic speed
p 1181 A93-53840
- TRENDS**
From RB211 to Trent: An ongoing development strategy
[PNR-90938] p 56 A93-11038
- Aircraft Accidents: Trends in Aerospace Medical Investigation Techniques
[AGARD-CP-532] p 490 A93-19653
- TRIANGULATION**
Geometry based Delaunay tetrahedralization and mesh movement strategies for multi-body CFD
[AIAA PAPER 92-4575] p 15 A93-13309
- A frontal approach for internal node generation in Delaunay triangulations
p 1262 A93-56403
- TRISONIC WIND TUNNELS**
Some acoustic features of perforated test section walls with splitter plates
p 1226 A93-53222
- TROPICAL METEOROLOGY**
Microburst observations in tropical Australia
p 432 A93-22198
- TROPICAL STORMS**
Seasonal weather hazards
p 431 A93-22180
- TROPOSPHERE**
Infrared detection of high altitude clear air turbulence
[AIAA PAPER 93-0852] p 557 A93-24916
- An aircraft instrument design for in situ tropospheric OH measurements by laser induced fluorescence at low pressures
p 1159 A93-51528
- Predicted aircraft effects on stratospheric ozone
p 93 A93-11096
- TRUCKS**
LOCSTAR - A satellite radiodetermination system for Europe
p 150 A93-15037
- Aircraft and refueler bonding and grounding study
[AD-A262027] p 911 A93-29398
- TU-154 AIRCRAFT**
Calculation of fuel economy for the Tu-154 aircraft in relation to the washing of the NK-8-2U engine at civil aviation maintenance facilities
p 345 A93-18356
- Results of operational testing of a system for computing optimal flight regimes - of aircraft flight
p 996 A93-45665
- TUBE HEAT EXCHANGERS**
Test results of an orifice pulse tube refrigerator
p 1149 A93-48612
- TUBES**
Relationship between mechanical-property and energy-absorption trends for composite tubes
[NASA-TP-3284] p 392 A93-16537
- TUMBLING MOTION**
Effect of geometry, static stability, and mass distribution on the tumbling characteristics of generic flying-wing models
[AIAA PAPER 93-3615] p 1125 A93-48302
- TUNABLE LASERS**
Nonintrusive spectroscopic techniques for supersonic/hypersonic aerodynamics and combustion diagnostics
p 203 A93-14245
- Laser selection criteria for OH fluorescence measurements in supersonic combustion test facilities
p 549 A93-29315
- TUNING**
A transfer matrix approach to vibration localization in mistuned blade assemblies
[NASA-TM-106112] p 838 A93-27088
- Localization of aeroelastic modes in mistuned high-energy turbines
p 1032 A93-31586
- TUPOLEV AIRCRAFT**
Diagnostics of the hydraulic system of Tu-204 aircraft
p 396 A93-18360
- Backfire unveiled
p 997 A93-46024
- Russian survivor - Tu-334 aircraft
p 1243 A93-54867
- Bear facts - Soviet Tu-95 aircraft
p 1229 A93-55175

TURBINE BLADES

- Effect of a large-scale inhomogeneity of the incoming flow on flow in a plane turbine cascade p 6 A93-10189
- Turbine blade cascade flows p 10 A93-12361
- Grid-characteristic method for calculating a three-dimensional boundary layer on the bounding surfaces of the blade passage of a turbomachine p 13 A93-12808
- Navier-Stokes analysis of turbine blade heat transfer and performance p 201 A93-13978
- Comparison of heat transfer measurements with computations for turbulent flow around a 180 deg bend p 201 A93-13980
- Influence of surface heat flux ratio on heat transfer augmentation in square channels with parallel, crossed, and V-shaped angled ribs p 201 A93-13981
- Study on fracture failure of turbine blades in a series of turbojets p 205 A93-14493
- A fast method for calculating three-dimensional transonic potential flows in turbomachine blade rows p 125 A93-15215
- A conformal-integral method for solving the direct problem in turbomachine cascade aerodynamics p 125 A93-15217
- Turbomachine blade vibration --- Book [ISBN 0-470-21764-2] p 344 A93-17899
- Aspects of turbine blade design for integrity p 345 A93-18784
- Electromechanical measurement of turbomachinery blade tip-to-casing running clearance [ASME PAPER 92-GT-50] p 400 A93-19303
- Assessment of a 3-D Euler code for subsonic turbine vane flows and study of the non radial blade stacking [ASME PAPER 92-GT-63] p 247 A93-19313
- Aeroloids and secondary flows in a transonic mixed flow turbine stage p 248 A93-19322
- [ASME PAPER 92-GT-72] p 248 A93-19322
- Surface-curvature-distribution effects on turbine-cascade performance p 248 A93-19333
- [ASME PAPER 92-GT-84] p 248 A93-19333
- Analysis of steady and unsteady turbine cascade flows by a locally implicit hybrid algorithm [ASME PAPER 92-GT-127] p 249 A93-19361
- Evaluation of simple aluminate and platinum modified aluminate coatings on high pressure turbine blades after factory engine testing - Round II [ASME PAPER 92-GT-140] p 388 A93-19372
- Boundary layer effects on the transonic flow in a straight turbine cascade [ASME PAPER 92-GT-155] p 249 A93-19382
- Unsteady pressure measurements on the rotor of a model turbine stage in a transient flow facility [ASME PAPER 92-GT-156] p 250 A93-19383
- Turbine blade vibration monitoring system [ASME PAPER 92-GT-159] p 402 A93-19386
- An analysis system for blade forced response [ASME PAPER 92-GT-172] p 352 A93-19398
- Effect of trailing-edge ejection on local heat (mass) transfer in pin fin cooling channels in turbine blades [ASME PAPER 92-GT-178] p 352 A93-19404
- Incidence angle and pitch-chord effects on secondary flows downstream of a turbine cascade [ASME PAPER 92-GT-184] p 251 A93-19409
- Heat transfer and turbulence in a turbulated blade cooling circuit [ASME PAPER 92-GT-187] p 402 A93-19412
- Discharge coefficients of holes angled to the flow direction [ASME PAPER 92-GT-192] p 403 A93-19417
- Flutter of grouped turbine blades [ASME PAPER 92-GT-227] p 404 A93-19444
- Internal cooling passage heat transfer near the entrance to a film cooling hole - Experimental and computational results [ASME PAPER 92-GT-241] p 404 A93-19450
- An experimental investigation of convective heat transfer at the leading edge of a gas turbine airfoil [ASME PAPER 92-GT-248] p 405 A93-19457
- Measurement of unsteady flow and heat transfer in a linear turbine cascade [ASME PAPER 92-GT-323] p 256 A93-19507
- An automated flow line for gas turbine blade repair [ASME PAPER 92-GT-367] p 375 A93-19531
- Unsteady aerodynamics and gust response in compressors and turbines [ASME PAPER 92-GT-422] p 258 A93-19570
- Inverse design of compressor and turbine blades at transonic flow conditions [ASME PAPER 92-GT-430] p 357 A93-19573
- Double mode behaviour of bladed disk assemblies in the resonance frequency range, visualized by means of holographic interferometry [ASME PAPER 92-GT-438] p 357 A93-19580
- A fool-proof aerodynamic design code for turbine cascades p 259 A93-20117
- Life cycle assessment of an impingement-cooled gas turbine blade [AIAA PAPER 92-4716] p 358 A93-20321
- A rapid procedure for obtaining time-average interferograms of vibrating bodies p 412 A93-21857
- Three-dimensional Navier-Stokes analysis of the tip clearance flow in linear turbine cascades [AIAA PAPER 93-0391] p 282 A93-23068
- Three-dimensional unstructured grid Euler method applied to turbine blades [AIAA PAPER 93-0196] p 461 A93-24233
- Calculating the cutting depth during the milling of large gas turbine engine blades p 545 A93-27628
- Probabilistic turbine blade tip durability analysis [AIAA PAPER 93-1383] p 719 A93-33946
- Gas dynamics of cooled turbines --- Russian book [ISBN 5-217-00809-1] p 721 A93-35685
- Thin gradient heat fluxmeters developed at ONERA [ONERA, TP NO. 1992-87] p 831 A93-38571
- Enhancing the performance of aircraft engine blades by surface hardening p 811 A93-39072
- Effect of ion treatments on the fatigue strength of blades p 811 A93-39073
- Increasing the efficiency of the electrochemical dimensional machining of gas turbine engine blades of EP718VD alloy p 835 A93-39095
- Modeling of the multiparameter assembly of engineering products for a specified priority of output geometrical parameters p 836 A93-39109
- Selection of the principal initial parameters for an axial-flow birotary turbine p 837 A93-39198
- Life prediction - Thermal fatigue from isothermal data p 916 A93-40807
- Unsteady aerodynamic response of two-dimensional subsonic and supersonic oscillating cascades with chordwise displacement and flexible deformation p 971 A93-46922
- Turbine blade forces due to partial admission p 1029 A93-46928
- 3D viscous flow analysis in axial turbine including tip leakage phenomena p 972 A93-46940
- Intensive industrial use of 3D Euler numerical methods for axial flow turbine analysis and design p 1002 A93-46943
- Dynamic analysis of a compound elastic surface p 1030 A93-47086
- Mechanical anisotropy in directionally solidified turbine blade p 1018 A93-47356
- Experimental and numerical study of transonic turbine cascade flow [AIAA PAPER 93-3064] p 1059 A93-48240
- A calculation of secondary flows and deviation angles in multistage axial-flow compressors p 1066 A93-48509
- Experimental study on heat transfer of separated impingement jets in short distance p 1149 A93-48518
- An aerodynamic design program for contra-rotating turbine cascades p 1067 A93-48521
- An experimental study on blade negative curving in a turbine cascade with a large turning angle p 1071 A93-49185
- A laminar flow rotor for a radial inflow turbine [AIAA PAPER 93-1796] p 1074 A93-49686
- Computational analysis of nonlinear aeroelastic phenomena during stall flutter of cascaded airfoils [AIAA PAPER 93-2082] p 1079 A93-49909
- Blade row interaction effects on flutter and forced response [AIAA PAPER 93-2084] p 1114 A93-49911
- Optimization of blade arrangement in a randomly mistuned cascade using simulated annealing [AIAA PAPER 93-2254] p 1115 A93-50052
- 3-D Euler simulation of vane-blade interaction in a transonic turbine [AIAA PAPER 93-2256] p 1081 A93-50054
- Pyrometer for turbine applications in the presence of reflection and combustion [AIAA PAPER 93-2374] p 1156 A93-50143
- Chimera grids in the simulation of three-dimensional flowfields in turbine-blade-coolant passages [AIAA PAPER 93-2559] p 1157 A93-50280
- Numerical simulations of flows in centrifugal turbomachinery [AIAA PAPER 93-2578] p 1085 A93-50293
- Verification of the TOTLOS method for calculating aerodynamic loss in film-cooled turbine cascade p 1087 A93-51191
- Effect of rotation on heat transfer and hydraulic resistance in the radial cooling channels of turbine rotor blades p 1215 A93-52950
- Experimental investigation into the mechanism of discrete frequency noise (DFN) generation from a NACA 0012 blade p 1225 A93-53194
- Mathematical modeling of the three-dimensional temperature fields of turbine blades p 1216 A93-53329
- Measurements and computational analysis of heat transfer and flow in a simulated turbine blade internal cooling passage [AIAA PAPER 93-1797] p 1218 A93-53585
- Forcing function modeling for flow induced vibration [ISABE 93-7027] p 1196 A93-54003
- Effects of wake interaction of two turbine cascades on secondary/tip-leakage flows and losses [ISABE 93-7058] p 1185 A93-54034
- Heat transfer and material temperature conditions in the leading edge area of impingement-cooled turbine vanes [ISABE 93-7076] p 1220 A93-54052
- 3D and 2.5D viscous flow computations for axial flow turbine blades [ISABE 93-7093] p 1186 A93-54069
- Aerodynamics of turbine blades with trailing-edge damage - Measurements and computations [ISABE 93-7130] p 1189 A93-54105
- Two-dimensional transonic flow around VKI turbine cascade p 1232 A93-54640
- Three-dimensional Navier-Stokes analysis of tip clearance flow in linear turbine cascades p 1235 A93-55364
- Effect of blade leaning on the development of passage vortices and losses in the passage of turbine cascade with a great turning angle p 1236 A93-55397
- Analytical and experimental investigation of flow through a turbine vane cascade p 1248 A93-56348
- Erosion predictions and measurements of high-temperature coatings and superalloys used in turbomachines p 74 A93-12189
- Stochastic sensitivity measure for mistuned high-performance turbines [NASA-TM-105821] p 90 A93-12277
- Fatigue in single crystal nickel superalloys [AD-A254704] p 198 A93-12746
- Overview on test cases for computation of internal flows in turbomachines p 214 A93-13209
- Radial turbine cooling [NASA-TM-105658] p 130 A93-13292
- User's Guide for the NREL Force and Loads Analysis Program [DE92-010579] p 216 A93-13524
- Multi-point inverse design of isolated airfoils and airfoils in cascade in incompressible flow p 163 A93-14462
- SAPNEW: Parallel finite element code for thin shell structures on the Alliant FX-80 [NASA-CR-189212] p 220 A93-14799
- In-service considerations affecting component life p 177 A93-14898
- Prediction of turbine cascade flows with a quasi-three-dimensional rotor viscous code and the extension of the algebraic turbulence model [AD-A256831] p 223 A93-15635
- Bypass transition in compressible boundary layers p 417 A93-15801
- Deformation mechanisms of NiAl cyclically deformed near the brittle-to-ductile transformation temperature [NASA-CR-191649] p 391 A93-15830
- Hydrodynamic effects on heat transfer for film-cooled turbine blades [AD-A257291] p 361 A93-16080
- X ray diffraction and electron microscope studies of Yttria Stabilized Zirconia (YSZ) ceramic coatings exposed to vanadia [AD-A258055] p 392 A93-17676
- SNECMA M88 engine development status [ASME-90-GT-118] p 363 A93-17849
- Fatigue of turboengine discs [DS-2136] p 364 A93-18149
- Numerical analysis of the flow in a turbulated rectangular duct simulating the cooling passages in a turbine blade [AD-A257855] p 420 A93-18305
- Integrated Blade Inspection System (IBIS) upgrade study [AD-A258912] p 365 A93-19356
- Fatigue in single crystal nickel superalloys [AD-A259191] p 536 A93-20275
- Advanced turbine design for coal-fueled engines [DE93-000224] p 554 A93-21254
- Field evaluation of six protective coatings applied to T-56 turbine blades after 2000 hours of engine use [AD-A261112] p 522 A93-21316
- Stress calculation for the Sandia 34-meter wind turbine using the local circulation method and turbulent wind [DE93-004480] p 560 A93-22045
- Three-dimensional flow in radial turbomachinery and its impact on design [NASA-CR-192957] p 723 A93-25668
- Flow control of low heat load turbine airfoils [AD-A260941] p 724 A93-26219
- The blade curving effects in a turbine stator cascade with low aspect ratio [AD-A261063] p 725 A93-26239

- NDE of PWA 1480 single crystal turbine blade material
[NASA-TM-106140] p 815 N93-27640
- The natural excitation technique (NEXt) for modal parameter extraction from operating wind turbines
[DE93-010611] p 845 N93-28603
- Heat Transfer and Cooling in Gas Turbines
[AGARD-CP-527] p 901 N93-29926
- Vortex structure and mass transfer near the base of a cylinder and a turbine blade
p 901 N93-29929
- The influence of non-uniform spanwise inlet temperature on turbine rotor heat transfer
p 901 N93-29932
- Heat transfer in high turbulence flows: A 2-D planar wall jet
p 932 N93-29935
- The effect of orthogonal-mode rotation on forced convection in a circular-sectioned tube fitted with full circumferential transverse ribs
p 932 N93-29937
- Cooling geometry optimization using liquid crystal technique
p 902 N93-29939
- Prediction of jet impingement cooling scheme characteristics (airfoil leading edge application)
p 932 N93-29941
- Impingement/effusion cooling
p 932 N93-29954
- The aerodynamic effect of coolant ejection in the leading edge region of a film-cooled turbine blade
p 904 N93-29958
- Modeling of a turbulent flow in the presence of discrete parietal cooling jets
p 904 N93-29960
- Coupling of 3D-Navier-Stokes external flow calculations and internal 3D-heat conduction calculations for cooled turbine blades
p 904 N93-29961
- A Navier-Stokes solver with different turbulence models applied to film-cooled turbine cascades
p 904 N93-29962
- Navier-Stokes analysis of three-dimensional flow and heat transfer inside turbine blade rows
p 905 N93-29963
- Optical blade vibration measurement
[ETN-93-93454] p 905 N93-29999
- Three-dimensional flow calculations inside SSME GGGT first stage blade rows
p 1017 N93-31585
- Localization of aeroelastic modes in mistuned high-energy turbines
p 1032 N93-31586
- Measurements and computational analysis of heat transfer and flow in a simulated turbine blade internal cooling passage
[NASA-TM-106189] p 1032 N93-31647
- TURBINE ENGINES**
- Advanced three-shaft engines - Configured for reliability, efficiency and growth
p 53 A93-12236
- Effect of the powerplant configuration on the air flow rate of the jet shield
p 54 A93-12820
- The multi-heat addition turbine engine
[AIAA PAPER 92-4272] p 54 A93-13334
- Numerical simulation of a low-emission gas turbine combustor using KIVA-II
p 170 A93-14077
- A model-based monitoring system for turbine engines
[SAE PAPER 921006] p 206 A93-14639
- Development of a model-based monitoring system for turbine and rocket engines
p 195 A93-16412
- The acoustic response of altitude test facility exhaust systems to axisymmetric and two-dimensional turbine engine exhaust plumes
p 449 A93-19209
- Unsteady pressure measurements on the rotor of a model turbine stage in a transient flow facility
[ASME PAPER 92-GT-156] p 250 A93-19383
- Integration of turbo-expander- and turbo-ramjet-engines in hypersonic vehicles
[ASME PAPER 92-GT-204] p 353 A93-19428
- Aircraft turbine engine NOx emission limits - Status and trends
[ASME PAPER 92-GT-415] p 357 A93-19563
- Numerical investigation of flow field in a turbine volute
[AIAA PAPER 93-0155] p 542 A93-25505
- A comparison between numerical models and measurements in a Kaplan turbine guide vanes
p 685 A93-34339
- Developing the MD Explorer
p 744 A93-34472
- Approach of modeling continuous turbine engine operation from startup to shutdown
p 721 A93-34495
- Use of PCs in controlling simulated altitude environmental test conditions in support of turbine engine testing
p 846 A93-37856
- Turbine blade forces due to partial admission
p 1029 A93-46928
- Lightweight aircraft turbine protection
[AIAA PAPER 93-1815] p 1110 A93-49703
- Synchronous X-ray Sinography for nondestructive imaging of turbine engines under load
[AIAA PAPER 93-1819] p 1153 A93-49707
- Ground test simulation fidelity of turbine engine airstarts
[AIAA PAPER 93-2173] p 1137 A93-49986
- Improved data validation and quality assurance in turbine engine test facilities
[AIAA PAPER 93-2178] p 1137 A93-49990

- An upgraded data acquisition and processing system for the Aeropropulsion Systems Test Facility at Arnold Engineering Development Center
[AIAA PAPER 93-2466] p 1138 A93-50213
- Navier-Stokes analysis of radial turbine rotor performance
[AIAA PAPER 93-2555] p 1121 A93-50277
- Component and Engine Structural Assessment Research (CAESAR)
[AIAA PAPER 93-2609] p 1122 A93-50316
- The chemistry of Saudi Arabian sand - A deposition problem on helicopter turbine airfoils
p 1216 A93-53468
- CARS temperature measurements in combustion
[ONERA, TP NO. 1993-78] p 1212 A93-53599
- The challenge of IHPDET - Integrated High Performance Turbine Engine Technology
[ISABE 93-7001] p 1194 A93-53978
- Research and development of a turbo-accelerator for super/hypersonic transport
[ISABE 93-7066] p 1200 A93-54042
- Navier-Stokes analysis of turbine flowfield and external heat transfer
[ISABE 93-7075] p 1186 A93-54051
- Effect of nozzle design on the performance of a highly loaded turbine stage
[ISABE 93-7096] p 1203 A93-54072
- Development of a dynamic pressure response calibrator
p 1254 A93-54362
- New digital capacitive measurement system for blade clearances
p 1254 A93-54376
- An updated data acquisition and processing system for turbine engine testing
p 1250 A93-54389
- Control of supersonic throughflow turbomachines discrete frequency noise generation by aerodynamic detuning
p 1248 A93-55860
- Deformation mechanisms of NiAl cyclically deformed near the brittle-to-ductile transformation temperature
[NASA-CR-191849] p 391 N93-15830
- Turbomachinery and potential computations
[DS-2026] p 363 N93-17740
- Turbine engine combustor design at SNECMA
[DS-2129] p 363 N93-17851
- The technological evolution of high thrust turbine engines
[DS-1881] p 364 N93-17882
- Integrity testing of brush seal in shroud ring of T-700 engine
[NASA-TM-105863] p 421 N93-18380
- Multi-heat addition turbine engine
[NASA-CASE-LEW-15094-1] p 522 N93-22034
- Measurements and computations of external heat transfer and film cooling in turbines
[RAE-TM-P-1223] p 722 N93-25455
- Design and performance of nozzle-less volute casings for inward flow radial turbines
p 722 N93-25471
- Effect of a metal deactivator fuel additive on fuel deposition in fuel atomizers at high temperature
[AD-A260915] p 736 N93-25914
- Experimental investigation of turbine disk cavity aerodynamics and heat transfer
[NASA-CR-193831] p 812 N93-27115
- Navier-Stokes analysis of radial turbine rotor performance
[NASA-CR-191153] p 815 N93-28609
- Aero-thermal design of a cooled transonic NGV and comparison with experimental results
p 904 N93-29957
- TURBINE PUMPS**
- Investigation of rotor blade roughness effects on turbine performance
[ASME PAPER 92-GT-297] p 354 A93-19487
- Ceramic matrix composites for rocket engine turbine applications
[ASME PAPER 92-GT-394] p 388 A93-19547
- Inverse problem using S2-S1 approach for the design of the turbomachine with splitter blades
p 971 A93-46929
- Design and test of a small two stage counter-rotating turbine for rocket engine application
[AIAA PAPER 93-2136] p 1142 A93-49954
- High Reynolds number and turbulence effects on aerodynamics and heat transfer in a turbine cascade
[AIAA PAPER 93-2252] p 1155 A93-50050
- Liquid hydrogen foil-bearing turbopump
[AIAA PAPER 93-2537] p 1156 A93-50264
- Stochastic sensitivity measure for mistuned high-performance turbines
[NASA-TM-105821] p 90 N93-12277
- Experimental investigation of turbine disk cavity aerodynamics and heat transfer
[NASA-CR-193831] p 812 N93-27115
- High Reynolds number and turbulence effects on aerodynamics and heat transfer in a turbine cascade
[NASA-TM-106187] p 930 N93-29157

- Three-dimensional analysis of the Pratt and Whitney alternate design SSME fuel turbine
p 1031 N93-31584
- Three-dimensional flow calculations inside SSME GGGT first stage blade rows
p 1017 N93-31585
- Localization of aeroelastic modes in mistuned high-energy turbines
p 1032 N93-31586
- TURBINE WHEELS**
- Hot end cleaning - Corrosion pitting of turbine discs
[SAE PAPER 920930] p 202 A93-14081
- Aerodynamic design of turbomachinery blading in three-dimensional flow - An application to radial inflow turbines
[ASME PAPER 92-GT-74] p 248 A93-19324
- Hot streaks and phantom cooling in a turbine rotor passage. I - Separate effects
[ASME PAPER 92-GT-75] p 401 A93-19325
- The combined closed form-perturbation approach to the analysis of mistuned bladed disks
[ASME PAPER 92-GT-125] p 350 A93-19359
- An experimental study of heat transfer in a large-scale turbine rotor passage
[ASME PAPER 92-GT-195] p 403 A93-19420
- Flutter of grouped turbine blades
[ASME PAPER 92-GT-227] p 404 A93-19444
- Research and development of ceramic turbine wheels
[ASME PAPER 92-GT-295] p 354 A93-19485
- Rotor cavity flow and heat transfer with inlet swirl and radial outflow of cooling air
[ASME PAPER 92-GT-378] p 406 A93-19536
- Effect of environment on creep-fatigue crack propagation in turbine disc superalloys
[ONERA, TP NO. 1993-5] p 916 A93-41023
- Three-dimensional analysis of turbine rotor flow including tip clearance
[ASME PAPER 93-GT-111] p 987 A93-47446
- Vibration characteristics of mistuned bladed disk
p 1108 A93-49190
- Lightweight aircraft turbine protection
[AIAA PAPER 93-1815] p 1110 A93-49703
- Propulsion and Energetics Panel Working Group 20 on Test Cases for Engine Life Assessment Technology
[AGARD-AR-308] p 176 N93-14890
- Introduction to test cases for engine life assessment technology
p 176 N93-14891
- LARZAC HP turbine disk crack initiation and propagation spin pit test
p 176 N93-14892
- RB211-524B disc and drive cones hot cyclic spinning test
p 177 N93-14895
- F100 second stage fan disk bolthole crack propagation ferris wheel test
p 177 N93-14897
- Improved silicon nitride for advanced heat engines
[NASA-CR-182193] p 917 N93-29451
- TURBINES**
- Effects of turbine cooling assumptions on performance and sizing of high-speed civil transport
[AIAA PAPER 92-4217] p 55 A93-13383
- Recent advances in simulating unsteady flow phenomena brought about by passage of shock waves in a linear turbine cascade
[ASME PAPER 92-GT-4] p 245 A93-19277
- The effects of blade loading in radial and mixed flow turbines
[ASME PAPER 92-GT-92] p 349 A93-19338
- Profile losses of an annular turbine cascade in unsteady periodic flow
[ASME PAPER 92-GT-153] p 249 A93-19380
- The measurement and prediction of the tip clearance flow in linear turbine cascades
[ASME PAPER 92-GT-214] p 252 A93-19437
- The optimum value of the nozzle outlet angle of turbine stages
[ASME PAPER 92-GT-224] p 404 A93-19442
- Calculation of wake-induced unsteady flow in a turbine cascade
[ASME PAPER 92-GT-306] p 255 A93-19496
- Societe Francaise des Mecaniciens, SNECMA, and ONERA, Symposium on Recent Advances in Compressor and Turbine Aerothermodynamics, Courbevoie, France, Nov. 24, 25, 1992, Reports
p 1001 A93-46926
- Experimental evaluation of a cooled radial-inflow turbine
[AIAA PAPER 93-1795] p 1110 A93-49685
- A comparative assessment of two present generation turbine analysis codes
[ISABE 93-7097] p 1203 A93-54073
- Performance parameters and assessment
p 81 N93-10052
- Aerodynamic investigation of radial turbines using computational methods
p 81 N93-10056
- The integration of geometric modeling into an inverse design method and application of a PC-based inverse design method and comparison with test results
p 81 N93-10058
- Partial admission and unsteady flow in radial turbines
p 81 N93-10059

- Radial turbine cooling p 82 N93-10061
LDV Measurements of unsteady flow fields in radial turbine
[AD-A253592] p 19 N93-10648
Experimental heat transfer results in turbine stators and rotors and a comparison with theory
[PNR-90945] p 57 N93-11055
The use of simultaneous engineering for the design and manufacture of the low pressure turbine for the Rolls-Royce Trent engine
[PNR-90887] p 59 N93-11206
ASTOVL model engine simulators for wind tunnel research p 192 N93-13213
Radial turbine cooling
[NASA-TM-105658] p 130 N93-13292
L.D.V. measurements of unsteady flow fields in radial turbine
[AD-A255728] p 221 N93-15065
Prediction of turbine cascade flows with a quasi-three-dimensional rotor viscous code and the extension of the algebraic turbulence model
[AD-A256831] p 223 N93-15635
Estimating turbine limit load
[NASA-CR-191105] p 699 N93-25883
Development of a method to determine the autooxidation of turbine fuels
[AD-A260578] p 736 N93-25902
Radial inflow turbine study
[AD-A260767] p 724 N93-25917
Experimental evaluation of a cooled radial-inflow turbine
[NASA-TM-106230] p 816 N93-28697
Aerothermic calculations of flows in interdisc cavities of turbines p 903 N93-29947
- TURBOCOMPRESSORS**
Analytical method for subsonic cascade profile p 12 A93-12730
Prediction of the inception of rotating stall for multistage axial flow compressors p 12 A93-12731
Effect of hub treatment on performance of an axial flow compressor p 53 A93-12736
Computational studies of the characteristics of axial compressor cascades and stages in unsteady incoming flow p 13 A93-12805
A study of dynamic characteristics of axial compression systems by heat addition p 202 A93-14168
A simple spanwise mixing model for turbulent diffusion and secondary flows in multistage axial-flow compressors p 204 A93-14482
Experimental investigation of tip clearance noise in axial flow machines p 445 A93-19155
Analysis of high speed multistage compressor throughflow using spanwise mixing
[ASME PAPER 92-GT-13] p 347 A93-19285
Design features of the GTD 8000 and GTD 15000 marine gas turbine engines
[ASME PAPER 92-GT-15] p 400 A93-19287
Pressure fluctuation on casing wall of isolated axial compressor rotors at low flow rate
[ASME PAPER 92-GT-33] p 246 A93-19293
An investigation of post stall transients and recoverability of axial compression systems. I - A simplified method
[ASME PAPER 92-GT-55] p 347 A93-19305
An investigation of post stall transients and recoverability of axial compression systems. II - Numerical simulations
[ASME PAPER 92-GT-56] p 347 A93-19306
Stability of fully developed rotating stall
[ASME PAPER 92-GT-57] p 348 A93-19307
A wide-range axial-flow compressor stage performance model
[ASME PAPER 92-GT-58] p 348 A93-19308
Modified surge in an axial flow compressor
[ASME PAPER 92-GT-59] p 247 A93-19309
An investigation of spanwise mixing in multistage axial flow compressors
[ASME PAPER 92-GT-64] p 247 A93-19314
Optimization of a multistage axial compressor stochastic approach
[ASME PAPER 92-GT-163] p 351 A93-19389
Three-dimensional flow phenomena in a transonic, high-through-flow, axial-flow compressor stage
[ASME PAPER 92-GT-169] p 250 A93-19395
Low aspect ratio transonic rotors. I - Baseline design and performance
[ASME PAPER 92-GT-185] p 352 A93-19410
Measurement of the three-dimensional tip region flowfield in an axial compressor
[ASME PAPER 92-GT-211] p 252 A93-19434
Design of multi-stage turbomachinery blading by the circulation method - Actuator duct limit
[ASME PAPER 92-GT-286] p 254 A93-19477
Prediction of secondary losses in axial compressors
[ASME PAPER 92-GT-288] p 254 A93-19479
A viscous axisymmetric throughflow prediction method for multi-stage compressors
[ASME PAPER 92-GT-293] p 254 A93-19483
Investigation of tip clearance phenomena in an axial compressor cascade using Euler and Navier-Stokes procedures
[ASME PAPER 92-GT-299] p 255 A93-19489
Numerical simulation of compressor endwall and casing treatment flow phenomena
[ASME PAPER 92-GT-300] p 255 A93-19490
Viscous throughflow modelling for multi-stage compressor design
[ASME PAPER 92-GT-302] p 255 A93-19492
Effect of manufacturing deviations on performance of axial flow compressor blading
[ASME PAPER 92-GT-326] p 257 A93-19510
Separated flow in a low speed two-dimensional cascade. I - Flow visualization and time-mean velocity measurements
[ASME PAPER 92-GT-356] p 257 A93-19521
Performance of gas turbine compressor cleaners
[ASME PAPER 92-GT-360] p 355 A93-19524
Radial transport and momentum exchange in an axial compressor
[ASME PAPER 92-GT-364] p 257 A93-19528
Using contra-rotating rotors for decreasing sizes and component number in small GTE
[ASME PAPER 92-GT-414] p 356 A93-19562
Erosion resistant titanium nitride coating for turbine compressor applications
[ASME PAPER 92-GT-417] p 388 A93-19565
A novel approach to high resolution compressible cascade flow analysis using the Navier-Stokes equations
[ASME PAPER 92-GT-419] p 258 A93-19567
Optimization of a multistage axial compressor in a gas turbine engine system
[ASME PAPER 92-GT-424] p 357 A93-19572
Unsteady two- and three-dimensional Navier-Stokes simulations of multistage turbomachinery flows p 266 A93-20721
Blade loading of transonic circular cascade diffuser p 267 A93-20919
Prediction of rotor dynamic destabilizing forces in axial flow compressors p 272 A93-22263
A study of aerodynamic performance of a contra-rotating axial compressor stage p 463 A93-24524
Surging limits of multistage axial-flow compressors p 476 A93-27443
Recent developments in compressor-based Joule-Thomson cooling --- of thermal imaging equipment in ground and helicopter-borne applications p 547 A93-28244
The analysis of viscous wakes noise in axial flow compressor p 759 A93-33710
A theoretical study on the ETHYLENE system - A fuzzy diagnostic expert system for large rotating machinery p 846 A93-36327
Selection of the principal initial parameters for an axial-flow birotary turbine p 837 A93-39198
Supersonic through flow compressors - A preliminary study: COVAXS p 1001 A93-46930
3D/quasi-3D trans- and supersonic flow calculation in advanced centrifugal/axial compressor stages p 972 A93-46936
Direct and inverse problems of calculating the axisymmetric and 3D flow in axial compressor blade rows p 972 A93-46938
The prediction and the active control of surge in multi-stage axial-flow compressors p 1002 A93-46945
A calculation of secondary flows and deviation angles in multistage axial-flow compressors p 1066 A93-48509
Magnetic bearings for cryogenic turbomachines p 1149 A93-48601
A computer program for meridional flows in multistage axial flow compressors with turbulence and multi-effects of 3-D flows p 1165 A93-49186
A blade element method for predicting the off-design performance of compressors p 1107 A93-49187
Frontally tapered squared trench casing treatment for improvement of compressor performance p 1108 A93-49202
Vane optimization for maximum efficiency using design of experiments
[AIAA PAPER 93-1867] p 1111 A93-49742
Application of a dynamic compression system model to a low aspect ratio fan - Casing treatment and distortion
[AIAA PAPER 93-1871] p 1111 A93-49746
An approach to the stall monitoring in a single stage axial compressor
[AIAA PAPER 93-1872] p 1112 A93-49747
Unsteady, three-dimensional, Navier-Stokes simulations of multistage turbomachinery flows
[AIAA PAPER 93-1979] p 1153 A93-49826
Compressor unsteady aerodynamic response to rotating stall and surge excitations
[AIAA PAPER 93-2087] p 1079 A93-49914
A simplified approach for control of rotating stall. I - Theoretical development
[AIAA PAPER 93-2229] p 1080 A93-50035
Local nonlinear control of stall inception in axial flow compressors
[AIAA PAPER 93-2230] p 1080 A93-50036
A simplified approach for control of rotating stall. II - Experimental results
[AIAA PAPER 93-2234] p 1080 A93-50038
Spatial domain characterization of abrupt rotating stall initiation in an axial flow compressor
[AIAA PAPER 93-2238] p 1081 A93-50040
Simulation of propulsion system's transient response to planar wave inlet distortion and the effect of compressor wear
[AIAA PAPER 93-2384] p 1117 A93-50152
Stall inception in a multi-stage high speed axial compressor
[AIAA PAPER 93-2386] p 1117 A93-50153
Stator relative, rotor blade-to-blade near wall flow in a multistage axial compressor with tip clearance variation
[AIAA PAPER 93-2389] p 1083 A93-50154
Analysis of wake-induced unsteady flow in axial compressors - Radial variations of wake excitation forces estimated by strip theory p 1086 A93-51123
Estimation of the change of axial-flow compressor characteristics during long-term service p 1193 A93-52949
The combined effect of clearances and peripheral overlaps on the efficiency of microturbines with shrouded rotors p 1193 A93-52963
The acoustics of axial compressors
[ONERA, TP NO. 1993-102] p 1226 A93-53615
Study on surge and rotating stall in axial compressors. III - Numerical model for multiblade-row compressors p 1181 A93-53799
The energy dissipation in a rotating stall cell
[ISABE 93-7010] p 1183 A93-53986
Review of stall, surge and active control in axial compressors
[ISABE 93-7011] p 1184 A93-53987
An investigation of post stall transients and recoverability of axial compression systems
[ISABE 93-7012] p 1184 A93-53988
The streamline throughflow method of axial turbomachinery flow analysis
[ISABE 93-7031] p 1184 A93-54007
Performance improvement by forward-skewed blading of axial fan moving blades
[ISABE 93-7055] p 1185 A93-54031
Tip clearance effects on the flow field of an axial turbine rotor blade cascade
[ISABE 93-7057] p 1185 A93-54033
New approximate method of stress analysis for bladed rotating discs
[ISABE 93-7059] p 1219 A93-54035
Axial flow compressors - Mechanical design trends
[ISABE 93-7061] p 1199 A93-54037
Boundary conditions for unsteady supersonic inlet analyses
[ISABE 93-7104] p 1187 A93-54080
Performance simulation of a combustion engine charged by a variable geometry turbocharger. I - Prerequisites, boundary conditions and model development. II - Simulation algorithm, computed results p 1256 A93-54648
Dynamic analysis of annular cascade structures
p 1259 A93-55586
A new method for predicting the end wall boundary layers and the blade force defects inside the passage of axial compressor cascades p 1236 A93-55589
Alternative systems for fuel gas boosters for small gas turbine engines
[PB92-223049] p 212 N93-12977
Overview on test cases for computation of internal flows in turbomachines p 214 N93-13209
An experimental and analytical study of TIP clearance effects in axial flow compressors
[AD-A256434] p 179 N93-15337
Fatigue of turboengine discs
[DS-2136] p 364 N93-18149
Axial Flow Compressors, volume 1
[VKI-LS-1992-02-VOL-1] p 422 N93-18721
The effect of aircraft inlets on the behaviour of aero engine axial flow compressors p 422 N93-18722
Stall in axial flow aero engine compressors p 422 N93-18723
Stall and surge in axial flow compressors p 423 N93-18724
Active control of stall and surge p 423 N93-18725
Experimental investigation of rotating stall in a mismatched three stage axial flow compressor p 423 N93-18727
Application of recess vaned casing treatment to axial flow fans p 423 N93-18728

- A study of stall in a low hub/tip ratio fan p 423 N93-18729
- Endwall flows and blading design for axial flow compressors p 423 N93-18730
- Axial Flow Compressors, volume 2 [VKI-LS-1992-02-VOL-2] p 423 N93-18731
- Rotating stall: Modeling-measurement techniques; unsteady loss-unsteady flow field p 424 N93-18732
- Determination of the zone of the stall cell by means of the baroclinic wave theory p 424 N93-18733
- Characterization of stall inception in high-speed single-stage compressors [AD-A258973] p 365 N93-19093
- Engine driven chiller and thermal storage integration (Large tonnage engine driven chiller development) [PB92-227891] p 555 N93-21465
- The effects of reaction on axial compressor performance p 724 N93-25882
- Radial inflow turbine study [AD-A260767] p 724 N93-25917
- Active stabilization of aeromechanical systems [AD-A261366] p 725 N93-26335
- Flow phenomena in turbomachines [AD-A263049] p 930 N93-29141
- Improved silicon nitride for advanced heat engines [NASA-CR-182193] p 917 N93-29451

TURBOFAN AIRCRAFT

- Extended range operations of two and three turbofan engines p 802 N93-37391
- In-flight near- and far-field acoustic data measured on the Propan Test Assessment (PTA) testbed and with an adjacent aircraft [NASA-TM-103719] p 852 N93-27058
- Design of a turbofan powered regional transport aircraft p 894 N93-29721

TURBOFAN ENGINES

- An experimental study of a method for reducing the jet noise of bypass engines using mechanical flow mixers p 53 A93-12810
- Allowing for the effect of flow nonisothermality on total pressure losses in the afterburner diffusers of augmented turbofan engines p 53 A93-12811
- Numerical investigation of the unsteady flow through a counter-rotating fan p 112 A93-14166
- The Aircraft/Propulsion Integrated Assessment System p 226 A93-14396
- Hybrid laminar flow control applied to advanced turbofan engine nacelles [SAE PAPER 920962] p 123 A93-14628
- ETOPS across the Atlantic --- extended range operation of twin-engine transport aircraft p 306 A93-18780
- Transmission of sound through a rotor p 447 A93-19183
- Radiated noise of ducted fans p 450 A93-19215
- A numerical investigation into the nozzle flow of high by-pass turbofans [ASME PAPER 92-GT-10] p 346 A93-19283
- Conceptual design of turbo-accelerator for HST combined cycle engine [ASME PAPER 92-GT-253] p 353 A93-19462
- Optimization of a multistage axial compressor in a gas turbine engine system [ASME PAPER 92-GT-424] p 357 A93-19572
- Experimental investigation of exhaust system mixers for a high bypass turbofan engine [AIAA PAPER 93-0022] p 357 A93-20140
- Robust digital control of a high-performance engine --- F-100 turbofan p 359 A93-21792
- Active control of fan noise from a turbofan engine [AIAA PAPER 93-0597] p 452 A93-23323
- Integration of high bypass ratio engines on modern transonic wings for regional aircraft p 506 A93-27479
- Commercial turbofan engine exhaust nozzle flow analyses p 689 A93-34489
- Advanced Tupolev twinjet combines Russian and Western technologies p 802 A93-38565
- GE90 program moves into high gear p 810 A93-38701
- Selection of the turbofan engine size p 899 A93-42379
- Free shear layer control and its application to fan noise [AIAA PAPER 93-3242] p 965 A93-46787
- Localization of noise sources in the exhaust jet of a turbofan engine p 1003 A93-47509
- On the estimation algorithm for adaptive performance optimization of turbofan engines [AIAA PAPER 93-1823] p 1111 A93-49710
- Turbofan flowfield simulation using Euler equations with body forces [AIAA PAPER 93-1978] p 1078 A93-49825
- Simulation of shock-boundary layer interaction in a fan blade passage [AIAA PAPER 93-1980] p 1078 A93-49827

- Initial test results of 40,000 horsepower fan drive gear system for advanced ducted propulsion systems [AIAA PAPER 93-2146] p 1154 A93-49963
- Studies into the hail ingestion characteristics of turbofan engines [AIAA PAPER 93-2174] p 1115 A93-49987
- Low speed test results of subsonic, turbofan scarf inlets [AIAA PAPER 93-2301] p 1082 A93-50086
- High speed test results of subsonic, turbofan scarf inlets [AIAA PAPER 93-2302] p 1082 A93-50087
- Development of an advanced exhaust mixer for a high bypass ratio turbofan engine [AIAA PAPER 93-2435] p 1118 A93-50188
- Engine testing at simulated altitude conditions [AIAA PAPER 93-2452] p 1120 A93-50201
- Recent successes in modifying several existing jet engine test cells to accommodate large, high-bypass turbofan engines [AIAA PAPER 93-2542] p 1139 A93-50266
- F405 engine in-flight thrust methodology development for the T-45A flight test program [AIAA PAPER 93-2544] p 1121 A93-50268
- Nonlinear dynamic simulation of single- and multi-spool core engines [AIAA PAPER 93-2580] p 1122 A93-50294
- The "Rolls-Royce" way of validating fan integrity [AIAA PAPER 93-2602] p 1122 A93-50311
- A study on 3-D velocity distribution of isothermal flows behind an afterburner flame stabilizer [ISABE 93-7039] p 1197 A93-54015
- Axial flow compressors - Mechanical design trends [ISABE 93-7061] p 1199 A93-54037
- Design of limit-tracking systems incorporating a turbofan engine with constant disturbances [ISABE 93-7090] p 1203 A93-54066
- Neural network fault diagnosis of a turbofan engine [ISABE 93-7091] p 1203 A93-54067
- Development of a real time dynamic engine simulation model of a turbo fan engine [ISABE 93-7132] p 1205 A93-54107
- Expert Systems for the simulation of turbofan engines [ISABE 93-7133] p 1225 A93-54108
- Uncertainty assessments for engine thrust derived from two methods p 1254 A93-54392
- Turbofan propulsion simulator p 1247 A93-55493
- Performance analysis of a turbofan as a part of an airbreathing propulsion system for space shuttles p 1252 A93-56039
- Engine for change p 1248 A93-56350
- SAPNEW: Parallel finite element code for thin shell structures on the Alliant FX/80 [NASA-CR-190663] p 84 N93-10372
- From RB211 to Trent: An ongoing development strategy [PNR-90938] p 56 N93-11038
- Subsonic flight test evaluation of a propulsion system parameter estimation process for the F100 engine [NASA-TM-4426] p 175 N93-13155
- Tests of models equipped with TPS in low speed ONERA F1 pressurized wind tunnel p 213 N93-13201
- Euler analysis of turbofan/superfan integration for a transport aircraft p 214 N93-13206
- The influence of intake swirl distortion on the steady-state performance of a low bypass, twin-spool engine p 214 N93-13211
- The jet behaviour of an actual high-bypass engine as determined by LDA-measurements in ground tests p 175 N93-13218
- Investigation of the flowfield around an isolated bypass engine with fan and core jet p 215 N93-13227
- An investigation of jet engine test cell aerodynamics by means of scale model test studies with comparisons to full-scale test results p 193 N93-14060
- SAPNEW: Parallel finite element code for thin shell structures on the Alliant FX-80 [NASA-CR-189212] p 220 N93-14799
- SNCGMA M88 engine development status [ASME-90-GT-118] p 363 N93-17849
- MM-122: High speed civil transport [NASA-CR-192011] p 334 N93-17974
- Experimental and numerical examinations of the influence of inlet distortion perturbations on the working behavior of turbofan compressors [ETN-93-92733] p 364 N93-18628
- Investigation of advanced counterrotation blade configuration concepts for high speed turboprop systems. Task 4: Advanced fan section aerodynamic analysis computer program user's manual [NASA-CR-187127] p 364 N93-18702
- Applications of active adaptive noise control to jet engines [NASA-CR-192277] p 522 N93-21210
- Supersonic transport: Which material for the engine [DS-2023] p 522 N93-21459

- The WINCOF-I code: Detailed description [NASA-CR-190779] p 677 N93-24760
- Transient performance of fan engine with water ingestion [NASA-CR-190778] p 677 N93-25134
- Model fan passage flow simulation [AD-A261613] p 752 N93-26167
- Cooling predictions in turbofan engine components p 905 N93-29964

TURBOFANS

- Evolving noise issue could persist into the next century p 99 A93-10731
- A comparison of the measured and predicted flowfield in a modern fan-bypass configuration [ASME PAPER 92-GT-298] p 254 A93-19488
- An investigation of turbulence modelling in transonic fans including a novel implementation of an implicit k-epsilon turbulence model [ASME PAPER 92-GT-308] p 256 A93-19498
- Three-dimensional Navier-Stokes computations of transonic fan flow using an explicit flow solver and an implicit k-epsilon solver [ASME PAPER 92-GT-309] p 256 A93-19499
- Acoustic mode measurements in the inlet of a model turbofan using a continuously rotating rake - Data collection/analysis techniques [AIAA PAPER 93-0599] p 361 A93-23324
- Experience in the design of supercritical cascades for the flow straightener of a transonic fan p 777 A93-39196
- Life analysis of a gas turbine fan disc p 897 A93-40803
- Averaging techniques for steady and unsteady calculations of a transonic fan stage [AIAA PAPER 93-3065] p 1059 A93-48241
- Propulsion technology challenges for turn-of-the-century commercial aircraft [ISABE 93-7003] p 1194 A93-53980
- A prediction model for the vortex shedding noise from the wake of an airfoil or axial flow fan blades p 1265 A93-55995
- Investigations of detail design issues for the high speed acoustic wind tunnel using a 60th scale model tunnel. Part 2: Tests with the closed circuit [NASA-CR-191672] p 137 N93-14738
- Acoustic mode measurements in the inlet of a model turbofan using a continuously rotating rake: Data collection/analysis techniques [NASA-TM-105936] p 179 N93-15403
- Improving military transport aircraft through highly integrated engine-wing design [DS-1607] p 333 N93-17850
- Application of recess vane casing treatment to axial flow fans p 423 N93-18728
- A study of stall in a low hub/tip ratio fan p 423 N93-18729
- Propulsion technology challenges for turn-of-the-century commercial aircraft [NASA-TM-106192] p 1005 N93-32351

TURBOGENERATORS

- A systems dynamics approach to modeling gas turbine combustor wear [ASME PAPER 92-GT-47] p 347 A93-19300

TURBOJET ENGINE CONTROL

- Application of controller partitioning optimization procedure to integrated flight/propulsion control design for a STOVL aircraft [AIAA PAPER 93-3766] p 1131 A93-51361

TURBOJET ENGINES

- A study of a pulsed electrical field near the jet of a turbojet engine p 52 A93-10179
- Research of starting test of the small turbojet in simulated altitude condition p 53 A93-11870
- A numerical study of slit V-gutter flows p 171 A93-14273
- The Aircraft/Propulsion Integrated Assessment System p 226 A93-14396
- Elimination of overtemperature in turbojet p 172 A93-14481
- Study on fracture failure of turbine blades in a series of turbojets p 205 A93-14493
- Generic developmental turbojet fuel control p 172 A93-14519
- Low aspect ratio transonic rotors. I - Baseline design and performance [ASME PAPER 92-GT-185] p 352 A93-19410
- Overview of the Japanese National Project for Super/Hyper-Sonic Transport propulsion system [ASME PAPER 92-GT-252] p 239 A93-19461
- Experimental study of mixed compression air-intake for hypersonic airbreathing engines [ASME PAPER 92-GT-349] p 355 A93-19519
- Models for predicting the performance of Brayton-cycle engines [ASME PAPER 92-GT-361] p 355 A93-19525

- Wind tunnel investigation with an operational turbojet engine
[AIAA PAPER 93-0036] p 322 A93-20150
Test results on air turbo ramjet for a futurespace plane
[AIAA PAPER 92-5054] p 359 A93-22325
A hot dynamic seal rig for measuring hypersonic engine seal durability and flow performance
[AIAA PAPER 93-1346] p 738 A93-33916
An experimental study of thrust reverser models --- of axisymmetric exhaust systems of aerojet engines
p 812 A93-39195
Toward the second-generation supersonic transport [ONERA, TP NO. 1993-26] p 890 A93-41038
Experimental investigation on starting of a turbojet engine in flight p 898 A93-41740
The experimental investigation of combination effect by using injection effect of aeroengine jet exhaust
p 898 A93-41742
Processing integral impeller 4-coordinate numerically controlled milling machine p 926 A93-41749
Supersonic through flow compressors - A preliminary study: COVAXS p 1001 A93-46930
An acoustic suppressor for the jet noise of a turbojet engine p 1003 A93-47510
Effect of steady-state circumferential pressure and temperature distortions on compressor stability
p 1106 A93-48503
Experimental investigation on patterned blades of compressor p 1066 A93-48515
Improving the design of the main fuel pump of Turbo-Jet 7 p 1107 A93-48555
Application of analog computing to real-time simulation of stall and surge dynamics
[AIAA PAPER 93-2231] p 1080 A93-50037
Simulation of propulsion system's transient response to planar wave inlet distortion and the effect of compressor wear
[AIAA PAPER 93-2384] p 1117 A93-50152
A study of surge control by using pulse cut-off for dual spool turbo-jet engine p 1194 A93-53862
Measurement and prediction of flow in a gas turbine engine exhaust plume
[ISABE 93-7113] p 1204 A93-54088
Structural integrity validation of limited-life engines
[ISABE 93-7131] p 1205 A93-54106
Improved flow measurement with simultaneous period/frequency recording --- in turbojet engines
p 1254 A93-54381
Potential use of alternative fuels in aviation
p 1243 A93-54838
The Eurojet EJ200 engine p 1246 A93-54839
A preliminary sizing method for unmanned aircraft using multi-variate optimisation p 714 A93-25408
Thrust augmentation system for low-cost-expendable turbojet engine
[AD-A263727] p 905 A93-30877
- TURBOMACHINE BLADES**
A flow calculation and aerodynamic design method for turbomachine cascades p 12 A93-12764
Experimental study on the unsteady aerodynamic response of a three dimensional cascade with oscillating blades p 242 A93-18499
Coupled 3-D aeroelastic stability analysis of bladed disks
[ASME PAPER 92-GT-171] p 351 A93-19397
A fully three-dimensional inverse method for turbomachinery blading in transonic flows
[ASME PAPER 92-GT-209] p 251 A93-19432
Transition prediction in attached and separated shear layers using an integral method
[ASME PAPER 92-GT-281] p 253 A93-19473
An approach for multi-stage calculations incorporating unsteadiness
[ASME PAPER 92-GT-282] p 253 A93-19474
Unsteady boundary-layer transition in flow periodically disturbed by wakes
[ASME PAPER 92-GT-283] p 254 A93-19475
Design of multi-stage turbomachinery blading by the circulation method - Actuator duct limit
[ASME PAPER 92-GT-286] p 254 A93-19477
A three-dimensional numerical method for turbomachinery blading
[ASME PAPER 92-GT-291] p 254 A93-19482
Prescribed-curvature-distribution airfoils for the preliminary geometric design of axial-turbomachinery cascades
[ASME PAPER 92-GT-366] p 257 A93-19530
Blade loading of transonic circular cascade diffuser
p 267 A93-20919
Euler computations of rotor-stator interaction in turbomachinery cascades using adaptive triangular meshes
[AIAA PAPER 93-0386] p 282 A93-23065
- Driven cavity simulation of turbomachine blade flows with vortex control
[AIAA PAPER 93-0390] p 461 A93-24238
Life assessment of gas turbine bucket coating based on degradation analysis p 533 A93-24464
Modelling of the flow in the blade-ring design process of turbomachinery p 520 A93-27291
Influence of modelling loading on stress distribution in turbomachinery blade fastening in case of FEM
p 520 A93-27296
Visualization and analysis of supersonic flow in rotating turbine stage. II - Analysis of the flow into the moving blades and their exit flow p 476 A93-27442
Dynamics of a high speed impeller - Analysis and experimental verification
[AIAA PAPER 93-1362] p 743 A93-34239
Hierarchical development of three direct-design methods for two-dimensional axial-turbomachinery cascades p 812 A93-39271
Inverse problem using S2-S1 approach for the design of the turbomachine with splitter blades
p 971 A93-46929
Adaptation of a 3-D pressure correction Navier-Stokes solver for the accurate modelling of tip clearance flows
p 971 A93-46932
High resolution numerical simulation of the linearized Euler equations in conservation law form
[AIAA PAPER 93-2934] p 1148 A93-48132
Unsteady, three-dimensional, Navier-Stokes simulations of multistage turbomachinery flows
[AIAA PAPER 93-1979] p 1153 A93-49826
A comparative assessment of two present generation turbine analysis codes
[ISABE 93-7097] p 1203 A93-54073
Characterisation of conventional and controlled diffusion stator blades in a transonic compressor stage
[ISABE 93-7124] p 1189 A93-54099
Experimental investigation of effect of particles on blade pressure distribution in impulse cascade flow
p 1236 A93-55398
A new method for predicting the end wall boundary layers and the blade force defects inside the passage of axial compressor cascades p 1236 A93-55589
Time-dependent predictions and analysis of turbine cascade data in the transonic flow region
[PNR-90957] p 139 A93-15489
Prediction of unsteady flows in turbomachinery using the linearized Euler equations on deforming grids
[NASA-CR-192919] p 747 A93-25109
Three-dimensional flow in radial turbomachinery and its impact on design
[NASA-CR-192957] p 723 A93-25668
- TURBOMACHINERY**
Numerical simulation for aeroelasticity in turbomachines with vortex method. I - Theory and method
p 53 A93-12452
Three-dimensional flow calculations in turbomachinery using the stream function formulation p 11 A93-12453
Influence of trailing-edge grid structure on Navier-Stokes computation of turbomachinery cascade flow
p 111 A93-14078
Method of simulating unsteady turbomachinery flows with multiple perturbations p 123 A93-14556
Calculation of three-dimensional unsteady flows in turbomachinery using the linearized harmonic Euler equations
[ASME PAPER 92-GT-136] p 249 A93-19368
Computational techniques for probabilistic analysis of turbomachinery
[ASME PAPER 92-GT-167] p 351 A93-19393
On the conservation of rothalpy in turbomachines
[ASME PAPER 92-GT-217] p 252 A93-19439
Use of advanced CFD codes in the turbomachinery design process
[ASME PAPER 92-GT-324] p 256 A93-19508
Meridional flow calculation using advanced CFD techniques
[ASME PAPER 92-GT-325] p 256 A93-19509
An externally pressurized air bearing system, journals and thrust, for application to small turbomachinery
[ASME PAPER 92-GT-382] p 406 A93-19539
Navier-Stokes calculations for the unsteady flowfield of turbomachinery
[AIAA PAPER 93-0676] p 465 A93-24786
Dynamics of rotating multicomponent turbomachinery systems
[AIAA PAPER 93-1629] p 742 A93-34157
Machinery arrangements for small VTOL transport aircraft p 713 A93-34848
The application of CFD to turbomachine design - Past and future p 769 A93-38130
Sound generation by rotating stall in centrifugal turbomachines p 1039 A93-46701
The practical application of solution-adaption to the numerical simulation of complex turbomachinery problems p 970 A93-46916
- Societe Francaise des Mecaniciens, SNECMA, and ONERA, Symposium on Recent Advances in Compressor and Turbine Aerothermodynamics, Courbevoie, France, Nov. 24, 25, 1992, Reports p 1001 A93-46926
Adaptation of a 3-D pressure correction Navier-Stokes solver for the accurate modelling of tip clearance flows
p 971 A93-46932
A solution-adaptive hybrid-grid method for the unsteady analysis of turbomachinery
[AIAA PAPER 93-3015] p 1148 A93-48204
A nonperiodic boundary approach for computation of compressible viscous flows in advanced turbine cascades
[AIAA PAPER 93-1799] p 1074 A93-49688
An unstructured grid flow solver for turbomachinery flows
[AIAA PAPER 93-1913] p 1076 A93-49780
An unstructured adaptive quadrilateral mesh-based scheme for viscous turbomachinery flow calculations
[AIAA PAPER 93-1975] p 1077 A93-49822
Multistage turbomachinery flow solutions using three-dimensional implicit Euler method
[AIAA PAPER 93-2382] p 1083 A93-50150
Computer aided design of turbo-machinery components p 1166 A93-50489
New calculation methods contribution on turbomachinery design and development
[ONERA, TP NO. 1993-60] p 1092 A93-51940
Aerodynamic inverse design and analysis for a full engine
[ISABE 93-7086] p 1186 A93-54062
Recent developments performed at ONERA for the simulation of 3D inviscid and viscous flows in turbomachinery by the solution of Euler and Navier-Stokes equations
[ISABE 93-7094] p 1186 A93-54070
Three-dimensional flow analysis inside turbomachinery stages with steady and unsteady Navier-Stokes method
[ISABE 93-7095] p 1186 A93-54071
Analysis of high Reynolds number inviscid/viscid interactions in cascades p 1234 A93-55351
Effects of foundation excitation on multiple rub interactions in turbomachinery p 1260 A93-55996
Compound cycle engine for helicopter application
[NASA-CR-180824] p 55 A93-10348
Explicit Navier-Stokes computation of turbomachinery flows p 83 A93-10370
SAPNEW: Parallel finite element code for thin shell structures on the Alliant FX/80
[NASA-CR-190663] p 84 A93-10372
The role of turbomachinery testing for stability in distorted flow
[PNR-90943] p 57 A93-11040
Active control of aeroacoustic couplings by means of adaptive systems
[ECL-91-18] p 64 A93-11576
Erosion predictions and measurements of high-temperature coatings and superalloys used in turbomachines p 74 A93-12189
Stochastic sensitivity measure for mistuned high-performance turbines
[NASA-TM-105821] p 90 A93-12277
Turbomachinery CFD on parallel computers
[NASA-TM-105932] p 228 A93-13154
Unsteady three-dimensional thin-layer Navier-Stokes solutions for turbomachinery in transonic flow
p 218 A93-14025
SAPNEW: Parallel finite element code for thin shell structures on the Alliant FX-80
[NASA-CR-189212] p 220 A93-14799
User's manual for Interactive Data Display System (IDDS)
[NASA-TM-105572] p 441 A93-16613
Dynamics of rotating multi-component turbomachinery systems
[NASA-TM-105997] p 421 A93-18426
Performance of controlled diffusion blades
p 424 A93-18735
Investigation of advanced counterrotation blade configuration concepts for high speed turbo-prop systems. Task 5: Unsteady counterrotation ducted propfan analysis
[NASA-CR-187126] p 521 A93-20773
Three-dimensional flow in radial turbomachinery and its impact on design
[NASA-CR-192957] p 723 A93-25668
Numerical modelling of viscous turbomachinery flows with a pressure correction method p 723 A93-25702
Unsteady vortex loop/dipole theory applied to the work and acoustics of an ideal low speed propeller
[AD-A264057] p 876 A93-29891
Modelling thermal behaviour of turbomachinery discs and casings p 903 A93-29949
Some implications of a differential turbomachinery equation with viscous correction
[AD-A264693] p 935 A93-30571

TURBOPROP AIRCRAFT

- Comparison of advanced turboprop interior noise control ground and flight test data p 444 A93-19136
- Takeoff/approach noise for a model counterrotation propeller with a forward-swept upstream rotor [AIAA PAPER 93-0596] p 519 A93-24782
- Zen and the art of airplane sizing p 504 A93-25174
- Big time doorstep delivery p 892 A93-42995
- Artificial transition - A tool for high Reynolds number simulation? p 967 A93-46799
- Modern propeller systems for advanced turboprop aircraft p 1111 A93-49727
- Bear facts --- Soviet Tu-95 aircraft p 1229 A93-55175
- Takeoff/approach noise for a model counterrotation propeller with a forward-swept upstream rotor [NASA-TM-105979] p 382 N93-16715
- Eagle RTS: A design for a regional transport aircraft [NASA-CR-192032] p 334 N93-18017
- User's manual for UCAP: Unified Counter-Rotation Aero-Acoustics Program [NASA-CR-191034] p 852 N93-27148
- TURBOPROP ENGINES**
- Dynamic characteristics of two new vibration modes of the disk-shell shaped gear p 204 A93-14484
- Comparison of advanced turboprop interior noise control ground and flight test data p 444 A93-19136
- Influence of a thermal barrier coating on the performance of a turboprop engine p 347 A93-19297
- [ASME PAPER 92-GT-38] p 351 A93-19375
- An update on the development of the T407/GLC38 modern technology gas turbine engine [ASME PAPER 92-GT-147] p 351 A93-19375
- High pressure ratio intercooled turboprop study [ASME PAPER 92-GT-405] p 356 A93-19554
- The effect of unsteady blade loading on the aeroacoustics of a pusher propeller [AIAA PAPER 93-1805] p 1173 A93-49694
- The T700 ... from salt spray to sand blast p 1205 A93-54292
- Investigation of advanced counterrotation blade configuration concepts for high speed turboprop systems. Task 4: Advanced fan section aerodynamic analysis [NASA-CR-187128] p 174 N93-12695
- Investigation of advanced counterrotation blade configuration concepts for high speed turboprop systems. Task 5: Unsteady counterrotation ducted propfan analysis p 521 N93-20773
- [NASA-CR-187126] p 521 N93-20773
- Structural Tailoring of Advanced Turboprops (STAT). Theoretical manual [NASA-CR-191017] p 556 N93-22005
- TURBORAMJET ENGINES**
- Combined engines for hypersonic flight p 171 A93-14244
- Conceptual design of turbo-accelerator for HST combined cycle engine [ASME PAPER 92-GT-253] p 353 A93-19462
- Experimental study of mixed compression air-intake for hypersonic airbreathing engines [ASME PAPER 92-GT-349] p 355 A93-19519
- Structural design and analysis of a Mach zero to five turbo-ramjet system [AIAA PAPER 93-1983] p 1112 A93-49830
- The study of experimental turboramjets - Heat state and cooling problems [AIAA PAPER 93-1989] p 1112 A93-49834
- Mach 5 turboramjet requirements and design approach [ISABE 93-7015] p 1194 A93-53991
- Development study on Air Turbo Ramjet engine for a future space plane [ISABE 93-7016] p 1195 A93-53992
- Evaluation of turboramjet exhaust systems from scale model test data [ISABE 93-7109] p 1204 A93-54085
- Characteristics of heat exchanger in supersonic/subsonic flows [ISABE 93-7119] p 1221 A93-54094
- Integration of turbo-ramjet engines for hypersonic aircraft p 175 N93-13230
- TURBOROCKET ENGINES**
- An analysis of air-turborocket performance [AIAA PAPER 93-1982] p 1141 A93-49829
- TURBOSHAPTS**
- Reaction drive rotors - Lessons learned (Hero had a good idea - But) --- jet helicopter performance [AIAA PAPER 92-4279] p 555 A93-13352
- Experimental study of the acoustic spinning modes generated by a helicopter turboshaft engine [ONERA, TP NO. 1992-141] p 230 A93-14266
- The effect of compressor rotor tip crops on turboshaft engine performance [ASME PAPER 92-GT-83] p 348 A93-19332

- An update on the development of the T407/GLC38 modern technology gas turbine engine [ASME PAPER 92-GT-147] p 351 A93-19375
- MTR390 - Engine for the future [ASME PAPER 92-GT-250] p 353 A93-19459
- Identification of the open loop dynamics of the T700 turboshaft engine p 809 A93-35934
- Combustor development for advanced helicopter engines p 1246 A93-54841
- Advanced three-shaft engines: Configured for reliability, efficiency, and growth [PNR-90986] p 58 N93-11068
- Experimental analysis of steady-state and dynamic monitoring of power shaft turbines p 178 N93-15176
- Analysis of consolidation of intermediate level maintenance for Atlantic Fleet T700-GE-401 engines [AD-A257754] p 363 N93-17695
- TURBULENCE**
- Measurements of the effect of free-stream turbulence length scale on heat transfer [ASME PAPER 92-GT-244] p 405 A93-19453
- The effect of shock motion on entropy production [AIAA PAPER 93-0665] p 465 A93-24777
- Turbulence and stall in plane diffusers - Computational study p 744 A93-34311
- Experimental study of the flow field inside a whirling annular seal p 85 N93-10892
- Effects of reacting flows with turbulence and shock waves on efficiency of scramjet combustors p 69 N93-11133
- An experimental study of flow patterns and endwall heat transfer upstream of a surface-mounted rectangular obstruction in a turbulent boundary layer p 89 N93-11698
- Motion errors and compensation possibilities p 212 N93-13052
- Turbulence and chaos in classical and quantum systems p 232 N93-14144
- L.D.V. measurements of unsteady flow fields in radial turbine [AD-A255728] p 221 N93-15065
- Numerical analysis of the flow in a turbulent rectangular duct simulating the cooling passages in a turbine blade [AD-A257855] p 420 N93-18305
- A k-omega-multivariate beta PDF for supersonic combustion [NASA-CR-191930] p 537 N93-21749
- Flow visualizations of perpendicular blade vortex interactions [NASA-CR-192725] p 748 N93-25208
- Studies in air/air supersonic mixing layers p 700 N93-26007
- Turbulence interacting with chemical kinetics in airbreathing combustion of ducted rockets p 734 N93-26012
- Increased heat transfer to elliptical leading edges due to spanwise variations in the freestream momentum: Numerical and experimental results [NASA-TM-106150] p 838 N93-27020
- Spurious frequencies as a result of numerical boundary treatments p 839 N93-27170
- Turbulence: The chief outstanding difficulty of our subject p 783 N93-27428
- Discrete-vortex simulation of pulsating flow on a turbulent leading-edge separation bubble p 787 N93-27457
- Comparison of reacting and non-reacting shear layers at a high subsonic Mach number [NASA-TM-106198] p 814 N93-27610
- The onset of vortex turbulence p 788 N93-28251
- Chaos in mechanical systems with special reference to rotorcraft and missiles [AD-A263703] p 943 N93-29384
- Keynote address: Unsteady, multimode transition in gas turbine engines p 901 N93-29927
- Measurement of turbulent spots and intermittency modelling at gas-turbine conditions p 902 N93-29934
- Heat transfer in high turbulence flows: A 2-D planar wall jet p 932 N93-29935
- Heat transfer with moderate free stream turbulence p 932 N93-29936
- Cooling geometry optimization using liquid crystal technique p 902 N93-29939
- Turbulence characteristics of an axisymmetric reacting flow [NASA-CR-4110] p 877 N93-30373
- TURBULENCE EFFECTS**
- Jet streams and associated turbulence and their effects on air transport flight operations p 154 A93-14231
- Heat transfer performance comparisons of five different rectangular channels with parallel angled ribs p 397 A93-18752
- The effects of incident turbulence and moving wakes on laminar heat transfer in gas turbines [ASME PAPER 92-GT-377] p 406 A93-19535

- Experimental study of the effect of external turbulence and the shape of the surface on the characteristics of laminar and transition boundary layers p 987 A93-47522
- A computer program for meridional flows in multistage axial flow compressors with turbulence and multi-effects of 3-D flows p 1165 A93-49186
- High Reynolds number and turbulence effects on aerodynamics and heat transfer in a turbine cascade [AIAA PAPER 93-2252] p 1155 A93-50050
- A general introduction to aeroacoustics and atmospheric sound p 1264 A93-55852
- Leading edge film cooling heat transfer including the effect of mainstream turbulence p 23 N93-11886
- A general introduction to aeroacoustics and atmospheric sound [NASA-CR-189717] p 102 N93-12021
- A simulation model of atmospheric turbulence for rotorcraft applications p 224 N93-14588
- Bypass transition in compressible boundary layers p 417 N93-15801
- Hydrodynamic effects on heat transfer for film-cooled turbine blades [AD-A257291] p 361 N93-16080
- Numerical modelling of viscous turbomachinery flows with a pressure correction method p 723 N93-25702
- The ground vortex flow field associated with a jet in a cross flow impinging on a ground plane for uniform and annular turbulent axisymmetric jets [NASA-CR-4513] p 789 N93-28449
- High Reynolds number and turbulence effects on aerodynamics and heat transfer in a turbine cascade [NASA-TM-106187] p 930 N93-29157
- TURBULENCE METERS**
- Turbulent structure of a wingtip vortex in the near field [AIAA PAPER 93-3011] p 1054 A93-48201
- TURBULENCE MODELS**
- Taking the measure of aerodynamic testing p 16 A93-13434
- Evaluation and application of the Baldwin-Lomax turbulence model in two-dimensional, unsteady, compressible boundary layers with and without separation in engine inlets [AIAA PAPER 92-3676] p 111 A93-14118
- Navier-Stokes calculations of the flow about wing-flap combinations p 112 A93-14171
- An algebraic turbulence model with memory for the computation of three dimensional turbulent boundary layers p 115 A93-14248
- Turbulence modelling requirements for the prediction of viscous transonic aeroflow flows p 115 A93-14249
- Correlation of mean velocity measurements downstream of a swept backward-facing step p 123 A93-14552
- Comparison of algebraic turbulence models for afterbody flows with jet exhaust p 123 A93-14554
- The critical role of turbulence modeling in the prediction of supersonic jet structure for acoustic applications p 398 A93-19193
- An investigation of turbulence modelling in transonic fans including a novel implementation of an implicit k-epsilon turbulence model [ASME PAPER 92-GT-308] p 256 A93-19498
- A comparison of the predictive capabilities of several turbulence models using upwind and central-difference computer codes [AIAA PAPER 93-0192] p 268 A93-21102
- Evaluation and application of the Baldwin-Lomax turbulence model in two-dimensional, unsteady, compressible boundary layers with and without separation in engine inlets [AIAA PAPER 92-3676] p 414 A93-22509
- An algebraic turbulence model for three-dimensional viscous flows [AIAA PAPER 93-0083] p 274 A93-22552
- Turbulence model evaluation for the prediction of flows over a supercritical airfoil with deflected aileron at high Reynolds number [AIAA PAPER 93-0191] p 276 A93-22615
- Turbulence modeling for complex hypersonic flows [AIAA PAPER 93-0200] p 277 A93-22620
- The computation of the post-stall behavior of a circulation controlled airfoil [AIAA PAPER 93-0207] p 277 A93-22625
- Calculation of the flowfield around an airfoil with spoiler [AIAA PAPER 93-0527] p 284 A93-23268
- Measurements in a pressure-driven three-dimensional turbulent boundary layer during development and decay [AIAA PAPER 93-0543] p 415 A93-23283
- A study of compressible turbulence [AIAA PAPER 93-0659] p 465 A93-24772
- Compressible turbulence measurements in a high-speed high Reynolds number mixing layer [AIAA PAPER 93-0660] p 465 A93-24773

- Two-dimensional Navier-Stokes analysis of high-lift multi-element airfoils using the q -omega turbulence model
[AIAA PAPER 93-0679] p 466 A93-24787
- On high speed turbulence modeling of shock-wave boundary-layer interaction
[AIAA PAPER 93-0778] p 541 A93-24860
- A numerical investigation of a subsonic jet in a crossflow
[AIAA PAPER 93-0870] p 469 A93-24931
- A new model for super/hypersonic turbulent boundary layers
[AIAA PAPER 93-0897] p 472 A93-24957
- Progress in high-lift aerodynamic calculations
[AIAA PAPER 93-0194] p 474 A93-25512
- Numerical simulation of the turbulent drag reduction by plate manipulators
p 681 A93-33736
- Evaluation of RNG algebraic turbulence models for boundary layers
p 684 A93-34331
- Vortex initiation during dynamic stall of an airfoil
p 684 A93-34335
- An implicit treatment of two equations turbulence models for high speed flow computations
p 686 A93-34350
- Computation of viscous transonic aeroflow flows using eddy-viscosity based turbulence models
p 687 A93-34360
- Nonequilibrium turbulence modeling study on light dynamic stall of a NACA0012 airfoil
p 768 A93-37379
- Comparison of two Navier-Stokes codes for simulating high-incidence vortical flow
p 768 A93-37387
- Numerical solution of viscous compressible flows using algebraic turbulence models
p 770 A93-38162
- A numerical simulation of a scram jet combustor flow
p 810 A93-38181
- High-speed turbulence modeling of shock-wave/boundary-layer interaction
p 927 A93-41910
- Measurements in a pressure-driven three-dimensional turbulent boundary layer during development and decay
p 927 A93-41911
- Evaluation of an RNG-based algebraic turbulence model
p 863 A93-42436
- Modeling supersonic inlet boundary-layer bleed roughness
p 872 A93-42891
- Calculation of optimum airfoils using direct solutions of the Navier-Stokes equations
[AIAA PAPER 93-3323] p 952 A93-45017
- Method of characteristics for computing three-dimensional boundary layers
p 970 A93-46886
- Calculations on a double-fin turbulent interaction at high speed
[AIAA PAPER 93-3432] p 977 A93-47224
- Aerodynamic flow simulation using a pressure-based method and a two-equation turbulence model
[AIAA PAPER 93-2902] p 1147 A93-48111
- A numerical study of the effect of geometry variation, turbulence models, and dissipation on the flow past control surfaces
[AIAA PAPER 93-2967] p 1048 A93-48161
- A computational study of wingtip vortex flowfield
[AIAA PAPER 93-3010] p 1054 A93-48200
- Application of a two-equation turbulence model for high speed compressible flows using unstructured grids
[AIAA PAPER 93-3029] p 1056 A93-48213
- Behaviour of the Johnson-King turbulence model in axis-symmetric supersonic flows
[AIAA PAPER 93-3032] p 1056 A93-48214
- Effects of side-inlet angle in a three-dimensional side-dump combustor
p 1109 A93-49610
- Viscous analysis of high pressure turbine inlet guide vane flow including cooling injections
[AIAA PAPER 93-1798] p 1074 A93-49687
- Unsteady aerodynamic flow phenomena in a transonic compressor stage
[AIAA PAPER 93-1868] p 1075 A93-49743
- The effects of turbulence modeling on the numerical simulation of confined swirling flows
[AIAA PAPER 93-1976] p 1078 A93-49823
- Particle dynamics simulations in inlet separator with an experimentally based bounce model
p 1115 A93-49972
- [AIAA PAPER 93-2156] p 1115 A93-49972
- A k -omega multivariate beta PDF for supersonic turbulent combustion
[AIAA PAPER 93-2197] p 1154 A93-50009
- Modeling of turbulent supersonic H₂-air combustion with a multivariate beta PDF
[AIAA PAPER 93-2198] p 1155 A93-50010
- Navier-Stokes investigation of blunt trailing-edge airfoils using O grids
p 1095 A93-52459
- Analytical expression of dissipation integral for kinetic energy integral equation --- calculation of turbulent compressible boundary layer in aerodynamics
p 1183 A93-53860
- Numerical study on inception of stall cells in rotating stall
[ISABE 93-7007] p 1183 A93-53983
- 3D and 2.5D viscous flow computations for axial flow turbine blades
[ISABE 93-7093] p 1186 A93-54069
- Recent developments performed at ONERA for the simulation of 3D inviscid and viscous flows in turbomachinery by the solution of Euler and Navier-Stokes equations
[ISABE 93-7094] p 1186 A93-54070
- Three-dimensional flow analysis inside turbomachinery stages with steady and unsteady Navier-Stokes method
[ISABE 93-7095] p 1186 A93-54071
- A Eulerian/Lagrangian modelling to calculate the evolution of a water droplets spray
[ISABE 93-7121] p 1221 A93-54096
- Numerical study of nitric oxide formation in a hypersonic ramjet engine
[ISABE 93-7125] p 1204 A93-54100
- Evaluation and application of the Baldwin-Lomax turbulence model in two-dimensional, unsteady, compressible boundary layers with and without separation in engine inlets
[NASA-TM-105810] p 82 A93-10087
- The prediction of convective heat transfer in rotating square ducts
[PNR-90929] p 85 A93-11025
- A problem formulation for glideslope tracking in wind shear using advanced robust control techniques
[NASA-TM-104164] p 64 A93-11176
- Physical effects of vegetation on wind-blown sand in the coastal environments of Florida
[PB92-188424] p 93 A93-11702
- A theory for the analysis of rotorcraft operating in atmospheric turbulence
p 48 A93-11725
- The modelling of turbulence and downbursts for flight simulators
p 193 A93-13542
- An algebraic turbulence model for three-dimensional viscous flows
[NASA-TM-105931] p 110 A93-14102
- Prediction of turbine cascade flows with a quasi-three-dimensional rotor viscous code and the extension of the algebraic turbulence model
[AD-A256831] p 223 A93-15635
- Modeling of turbulent supersonic H₂-air combustion with an improved joint beta PDF
[NASA-CR-191929] p 391 A93-16389
- Parabolized Navier-Stokes methods for hypersonic flows
p 421 A93-18565
- Modeling the transition region
[NASA-CR-4492] p 298 A93-19015
- Numerical simulation of unsteady large scale separated flow around oscillating airfoil
p 300 A93-19285
- The role of computational fluid dynamics in aeronautical engineering. 9: Analysis of hypersonic equilibrium air flow
p 301 A93-19294
- Transonic flow calculation around NACA-0012
p 302 A93-19301
- Numerical study on transverse hydrogen injection into a supersonic flowfield
p 302 A93-19311
- Numerical calculation of flow field in supersonic combustion chamber
p 304 A93-19317
- Projectile base bleed technology. Part 2: User's guide CMINT computer code, version 5.04-BRL
[AD-A256830] p 551 A93-19999
- Turbulence modeling for hypersonic flight
[NASA-CR-192288] p 483 A93-20235
- A k -omega-multivariate beta PDF for supersonic combustion
[NASA-CR-191930] p 537 A93-21749
- The addition of algebraic turbulence modeling to program LAURA
[NASA-TM-107758] p 840 A93-27250
- The remarkable ability of turbulence model equations to describe transition
p 783 A93-27432
- Efficient simulation of incompressible viscous flow over multi-element airfoils
p 784 A93-27443
- Unstructured mesh algorithms for aerodynamic calculations
p 785 A93-27444
- Development of an unstructured solution adaptive method for the quasi-three-dimensional Euler and Navier-Stokes equations
[NASA-CR-193241] p 930 A93-29213
- A Navier-Stokes solver with different turbulence models applied to film-cooled turbine cascades
p 904 A93-29962
- Navier-Stokes analysis of three-dimensional flow and heat transfer inside turbine blade rows
p 905 A93-29963
- Overview of aerothermodynamic loads definition study
p 1016 A93-31583
- TURBULENT BOUNDARY LAYER**
- Numerical simulation of compressible mixing zones
p 10 A93-12427
- Compressible laminar and turbulent boundary layer computation for the three-dimensional wing
p 12 A93-12735
- Calculation of the three-dimensional interaction of a shock wave with a boundary layer on a cylinder
p 12 A93-12766
- Grid-characteristic method for calculating a three-dimensional boundary layer on the bounding surfaces of the blade passage of a turbomachine
p 13 A93-12808
- A study of the laminar-turbulent transition in a boundary layer and separation on cones at supersonic velocities
p 14 A93-12974
- An algebraic turbulence model with memory for the computation of three dimensional turbulent boundary layers
p 115 A93-14248
- Experimental study of crossflow instability and laminar-turbulent transition on a swept wing
p 115 A93-14250
- Experimental investigations of the separation behavior in 3D shock wave/turbulent boundary-layer interactions
p 119 A93-14345
- An experimental study for interaction flow between shock wave and turbulent boundary layer
p 120 A93-14355
- Supersonic wing/body interference
p 121 A93-14391
- Instability of the periodic deflection of a panel surface in a turbulent boundary layer
p 208 A93-15188
- Experimental investigation of laminar to turbulent boundary layer transition with separation bubbles at low Reynolds number
p 128 A93-17277
- Boundary-layer induced noise in aircraft
p 444 A93-19137
- Boundary layer effects on the transonic flow in a straight turbine cascade
[ASME PAPER 92-GT-155] p 249 A93-19382
- Hypersonic flow separation in shock wave boundary layer interactions
[ASME PAPER 92-GT-205] p 251 A93-19429
- Measurements of the effect of free-stream turbulence length scale on heat transfer
[ASME PAPER 92-GT-244] p 405 A93-19453
- Prediction of 2D viscous transonic flow in compressor cascades using a semi-empirical shock/boundary-layer interaction method
[ASME PAPER 92-GT-277] p 253 A93-19470
- Streamwise variation of mean velocity field for the turbulent boundary layer interacting with controlled longitudinal vortex arrays
p 267 A93-20933
- Conventional skin friction measurement techniques for strongly perturbed supersonic turbulent boundary layers
p 271 A93-21863
- A study of hypersonic swept shock wave/turbulent boundary layer interactions using a conical Navier-Stokes code
[AIAA PAPER 92-5050] p 273 A93-22322
- Vortical and turbulent structure of a lobed mixer free-shear layer
[AIAA PAPER 93-0219] p 415 A93-22635
- A parametric study of bleed in shock boundary layer interactions
[AIAA PAPER 93-0294] p 280 A93-22694
- Transition on a sharp cone at high enthalpy - New measurements in the shock tunnel T5 at GALCIT
[AIAA PAPER 93-0343] p 281 A93-23030
- Wall pressure fluctuations beneath swept shock wave/boundary layer interactions
[AIAA PAPER 93-0384] p 282 A93-23063
- Measurements in a pressure-driven three-dimensional turbulent boundary layer during development and decay
[AIAA PAPER 93-0543] p 415 A93-23283
- A study of flow separation on an oscillating flap at Mach number 2.4
[AIAA PAPER 93-0436] p 286 A93-23350
- Three-dimensional hypersonic shock wave/turbulent boundary-layer interactions
p 287 A93-23533
- Shock/boundary-layer interaction control with vortex generators and passive cavity
p 287 A93-23546
- Mean flowfield structure of a three-dimensional supersonic turbulent boundary layer
[AIAA PAPER 93-0661] p 465 A93-24774
- On high speed turbulence modeling of shock-wave boundary-layer interaction
[AIAA PAPER 93-0778] p 541 A93-24860
- Numerical simulation of crossing/turbulent boundary layer interaction at Mach 8.3 comparison of zero and two-equation turbulence models
[AIAA PAPER 93-0779] p 467 A93-24861
- Interaction strength and model geometry effects on the structure of crossing-shock wave/turbulent boundary-layer interactions
[AIAA PAPER 93-0780] p 467 A93-24862
- Hypersonic crossing shock-wave/turbulent-boundary-layer interactions
[AIAA PAPER 93-0781] p 467 A93-24863
- On the breakdown of a hypersonic laminar boundary layer
[AIAA PAPER 93-0896] p 472 A93-24956

- A new model for super/hypersonic turbulent boundary layers
[AIAA PAPER 93-0897] p 472 A93-24957
- The coherent structure in a corner turbulent boundary layer
p 548 A93-28575
- Numerical simulation of the turbulent drag reduction by plate manipulators
p 681 A93-33736
- Parametrical investigation of the interaction between turbulent wall shear layers and normal shock waves, including separation
p 681 A93-33752
- A study on two-dimensional and three-dimensional secondary jet interactions with a supersonic flow
p 683 A93-34273
- A study on three-dimensional shock wave/turbulent boundary layer interaction induced by sweptback sharp fins at supersonic flow
p 684 A93-34274
- Evaluation of RNG algebraic turbulence models for boundary layers
p 684 A93-34331
- Computations and experiments for a multiple normal shock/boundary-layer interaction
p 688 A93-34486
- Correlation of conical interactions induced by sharp fins and semicones
p 692 A93-35635
- The experimental study of the effect of sweptback angles and the front shape of the fin on reduction of shock wave/turbulent boundary layer interaction region
p 858 A93-40431
- Passive control of a shock wave/turbulent boundary layer interaction in a transonic flow
p 858 A93-40444
- High-speed turbulence modeling of shock-wave/boundary-layer interaction
p 927 A93-41910
- Measurements in a pressure-driven three-dimensional turbulent boundary layer during development and decay
p 927 A93-41911
- Evaluation of an RNG-based algebraic turbulence model
p 863 A93-42436
- Computation of hypersonic turbulent flow over a rearward facing step
p 865 A93-42587
- Reduction of aerodynamic skin-friction drag
p 871 A93-42656
- Strong vortex/boundary layer interactions. I - Vortices high
p 930 A93-43539
- Transonic shockwave/turbulent boundary layer interactions on a porous surface
p 873 A93-43686
- Aerodynamic heating phenomenon in three dimensional shock wave/turbulent boundary layer interaction induced by sweptback fins in hypersonic flows
p 960 A93-45507
- Computation of crossing shock/turbulent boundary layer interaction at Mach 8.3
p 961 A93-45726
- Strong vortex/boundary layer interactions. II - Vortices low
p 965 A93-46744
- Control of unsteady shock-induced turbulent boundary layer separation upstream of blunt fins
[AIAA PAPER 93-3281] p 969 A93-46839
- Calculations on a double-fin turbulent interaction at high speed
[AIAA PAPER 93-3432] p 977 A93-47224
- Flow field measurements in a crossing shockwave turbulent boundary layer interaction at Mach 3
[AIAA PAPER 93-3434] p 977 A93-47226
- Normal shock wave oscillations in supersonic diffusers
p 1044 A93-48042
- Investigation of a hypersonic crossing shock wave/turbulent boundary layer interaction
p 1044 A93-48043
- Effects of junction modifications on sharp-fin-induced shock wave/boundary layer interaction
[AIAA PAPER 93-2935] p 1046 A93-48133
- Reynolds stress transport modelling of shock/boundary-layer interaction
[AIAA PAPER 93-2936] p 1046 A93-48134
- Intense studies on unsteady secondary separations and oscillating shock waves in three-dimensional shock waves/turbulent boundary layer interaction regions induced by sharp and blunt fins
[AIAA PAPER 93-2939] p 1046 A93-48137
- Hypersonic, turbulent viscous interaction past an expansion corner
[AIAA PAPER 93-2985] p 1051 A93-48178
- A lag model for turbulent boundary layers developing over rough bleed surfaces
[AIAA PAPER 93-2988] p 1052 A93-48181
- Effects of boundary layer bleed on swept-shock/boundary layer interaction
[AIAA PAPER 93-2989] p 1052 A93-48182
- The effect of expansion on the large scale structure of a compressible turbulent boundary layer
[AIAA PAPER 93-2991] p 1052 A93-48183
- An investigation of shock wave turbulent boundary layer interaction with bleed through slanted slots
[AIAA PAPER 93-2992] p 1052 A93-48184
- Laser Interferometer Skin-Friction measurements of crossing-shock wave/turbulent boundary-layer interactions
[AIAA PAPER 93-3072] p 1148 A93-48247
- Numerical simulation of a shock wave/turbulent boundary layer interaction in a duct
[AIAA PAPER 93-3127] p 1063 A93-48293
- Flowfield dynamics in blunt fin-induced shock wave/turbulent boundary layer interactions
[AIAA PAPER 93-3133] p 1063 A93-48298
- A study of the effect of surface riblets on the evolution of a solitary wave packet (lambda vortex) in a laminar boundary layer
p 1067 A93-48827
- A study of the interaction of a nonstationary shock wave with a boundary layer on a plate in the transition regime
p 1150 A93-48850
- Flow and heat transfer in a turbulent boundary layer through skewed and pitched jets
p 1151 A93-49007
- Skin friction and velocity profile family for compressible turbulent boundary layers
p 1070 A93-49008
- An experimental study of the effects of body-side compression on forward swept sidewall compression inlets ingesting a turbulent boundary layer
[AIAA PAPER 93-3125] p 1072 A93-49515
- An investigation of shock wave turbulent boundary layer interaction with bleed through normal and slanted slots
[AIAA PAPER 93-2155] p 1079 A93-49971
- A study of incipient separation limits for shock-induced boundary layer separation for Mach 6 high Reynolds flows
[AIAA PAPER 93-2481] p 1084 A93-50222
- Low-Reynolds-number k-epsilon model for unsteady turbulent boundary-layer flows
p 1177 A93-53208
- Analytical expression of dissipation integral for kinetic energy integral equation --- calculation of turbulent compressible boundary layer in aerodynamics
p 1183 A93-53860
- Correlative behaviours of shock/boundary layer interaction induced by sharp fin and semicone
p 1230 A93-54581
- Development of separation due to interaction between a shock wave and a turbulent boundary layer perturbed by rarefaction waves
p 1233 A93-55019
- Measurement of turbulent boundary layer in transonic flow
p 1236 A93-55411
- Dynamical effects of suction/heating on turbulent boundary layers
[AD-A248459] p 87 N93-11416
- An experimental study of flow patterns and endwall heat transfer upstream of a surface-mounted rectangular obstruction in a turbulent boundary layer
p 89 N93-11698
- Laminar boundary-layer breakdown
[AD-A254489] p 90 N93-12162
- Flow prediction for three-dimensional intakes and ducts using viscous-inviscid interaction methods
p 218 N93-13953
- Modeling variable blowing on a slender cone in hypersonic flow
p 138 N93-14836
- Finite-difference solution for laminar or turbulent boundary layer flow over axisymmetric bodies with ideal gas, CF₄, or equilibrium air chemistry
[NASA-TP-32711] p 222 N93-15434
- Hydrodynamic effects on heat transfer for film-cooled turbine blades
[AD-A257291] p 361 N93-16080
- An experimental study of a turbulent boundary layer in the trailing edge region of a circulation-control airfoil
[NASA-CR-191262] p 295 N93-17934
- Experimental analysis of the aeroacoustics of cascaded airfoils
[AD-A257945] p 420 N93-18121
- An experimental investigation of the separating/reattaching flow over a backstep
[NASA-CR-192105] p 298 N93-18781
- Modeling the transition region
[NASA-CR-4492] p 298 N93-19015
- Transonic flow calculation around NACA-0012
p 302 N93-19301
- Swept wing attachment line contamination fence
[NASA-CASE-LAR-13400-1] p 485 N93-22015
- Surface and flow field measurements in a symmetric crossing shock wave/turbulent boundary-layer interaction
[NASA-TM-106086] p 693 N93-24911
- An experimental study of the sources of fluctuating pressure loads beneath swept shock/boundary-layer interactions
[NASA-CR-192918] p 749 N93-25266
- Heat transfer measurements in swept shock wave/turbulent boundary-layer interactions
p 750 N93-25705
- Large-eddy simulation of temporally developing boundary layers with embedded streamwise vortices
p 750 N93-25753
- Uniform roughness studies
[WL-TR-92-3041] p 751 N93-25951
- Direct measurements of skin friction in supersonic combustion flow fields
[AD-A262878] p 825 N93-28226
- Keynote address: Unsteady, multimode transition in gas turbine engines
p 901 N93-29927
- Heat transfer in high turbulence flows: A 2-D planar wall jet
p 932 N93-29935
- Heat transfer with moderate free stream turbulence
p 932 N93-29936
- Turbulent drag reduction: Studies of feedback control and flow over riblets
p 878 N93-30645
- TURBULENT COMBUSTION**
- A coupled multi-block solution procedure for spray combustion in complex geometries
[AIAA PAPER 93-0108] p 539 A93-24230
- Parameter effects on turbulent swirling flames in combustors
p 534 A93-25911
- Chemical-kinetics characteristics of combustion in a supersonic turbulent flow
p 1018 A93-47512
- Intake flow modeling in a four stroke diesel using KIVA3
[AIAA PAPER 93-2952] p 1148 A93-48146
- A review of chemically reactive turbulent flow mixing mechanisms and a new design for a low NO(x) combustor
p 1109 A93-49508
- A k-omega multivariate beta PDF for supersonic turbulent combustion
[AIAA PAPER 93-2197] p 1154 A93-50009
- Modeling of turbulent supersonic H₂-air combustion with a multivariate beta PDF
[AIAA PAPER 93-2198] p 1155 A93-50010
- Investigation of a combustion zone behind a wedge
p 1146 A93-51631
- The influence of swirl generator characteristics on flow and combustion in turbulent diffusion flames
p 1159 A93-51632
- Thermometry inside a swirling turbulent flame - CARs advantages and limitations
p 1146 A93-51634
- Blowout of turbulent disc/pilot stabilized jet diffusion flames
[ISABE 93-7026] p 1213 A93-54002
- Large eddy simulation of turbulent combustion behind flame holders
[ISABE 93-7042] p 1198 A93-54018
- Numerical simulation of gas turbine combustors with complex geometries
[ISABE 93-7128] p 1204 A93-54103
- Chemical kinetic and aerodynamic structures of flames
[AD-A256015] p 391 N93-15931
- Modeling of turbulent supersonic H₂-air combustion with an improved joint beta PDF
[NASA-CR-191929] p 391 N93-16389
- Turbulence measurement in a reacting and non-reacting shear layer at a high subsonic Mach number
[NASA-TM-106186] p 989 N93-31839
- TURBULENT DIFFUSION**
- A simple spanwise mixing model for turbulent diffusion and secondary flows in multistage axial-flow compressors
p 204 A93-14482
- An investigation of spanwise mixing in multistage axial flow compressors
[ASME PAPER 92-GT-64] p 247 A93-19314
- The coherent structure in a corner turbulent boundary layer
p 548 A93-28575
- Vortex generation and mixing in three-dimensional supersonic combustors
[AIAA PAPER 93-2144] p 1115 A93-49961
- Large eddy simulation of turbulent combustion behind flame holders
[ISABE 93-7042] p 1198 A93-54018
- TURBULENT FLOW**
- Turbulent jet flows with condensation and electrophysical effects --- Russian book
p 76 A93-10176
- Experimental study of condensation vapor-air jets
p 76 A93-10180
- Large-eddy simulation of turbulent flow above and within a forest
p 92 A93-11404
- Experimental analysis of turbulence within supersonic mixing layers
p 11 A93-12428
- Effect of wall heating on a supersonic turbulent boundary layer
p 11 A93-12429
- Comparison of heat transfer measurements with computations for turbulent flow around a 180 deg bend
p 201 A93-13980
- Numerical computations of turbomachinery cascade turbulent flows with shocks by using multigrid scheme
p 112 A93-14167
- Numerical solution of 3-D turbulent flows inside of new concept nozzles
p 114 A93-14211
- Numerical analysis of the 3-D turbulent flow in an S-shaped diffuser
p 116 A93-14252
- Numerical simulation of turbulent reacting flows in combustion chambers
p 171 A93-14271
- A multi-zonal local solution methodology for the accelerated solution of the turbulent Navier-Stokes equations
p 117 A93-14279

- Viscous flow field prediction in axisymmetric passages p 204 A93-14478
- Numerical analysis of two-dimensional turbulent flows through an oscillating cascade p 126 A93-15494
- On space correlation of pressure pulsations on the streamlined surface before a step p 244 A93-19135
- On the acoustic radiation nature of a turbulent vortex ring p 446 A93-19167
- Turbulence evaluation within the secondary flow region of a turbine cascade [ASME PAPER 92-GT-60] p 247 A93-19310
- Calculation of turbulent flow for an enclosed rotating cone [ASME PAPER 92-GT-70] p 400 A93-19320
- An approximately factored incremental strategy for calculating consistent discrete aerodynamic sensitivity derivatives [AIAA PAPER 92-4746] p 265 A93-20344
- Hypersonic turbulent expansion-corner flow with shock impingement [AIAA PAPER 92-5101] p 274 A93-22371
- Inlet velocity profile effects on turbulent swirling flow predictions [AIAA PAPER 93-0133] p 274 A93-22580
- Direct numerical simulation of turbulent flow in a square duct [AIAA PAPER 93-0198] p 277 A93-22618
- Numerical simulation of the turbulent flow in round jets [AIAA PAPER 93-0199] p 277 A93-22619
- The three-dimensional separated flow structure in a variable aspect ratio sudden expansion duct [AIAA PAPER 93-0213] p 278 A93-22630
- Experimental studies of the turbulent structure of supersonic mixing layers [AIAA PAPER 93-0217] p 278 A93-22633
- Measurements in the near-field of a turbulent wingtip vortex [AIAA PAPER 93-0551] p 285 A93-23290
- Effects of free-stream turbulence on boundary-layer transition [AIAA PAPER 93-0488] p 416 A93-23390
- Analytical comparison of convective heat transfer correlations in supercritical hydrogen p 416 A93-23477
- A study of compressible turbulence [AIAA PAPER 93-0659] p 465 A93-24772
- Experimental study of three-dimensional separation on a large-size model [ONERA, TP NO. 1992-174] p 473 A93-25348
- Artificial viscosity models for the Navier-Stokes equations and their effect in drag prediction [AIAA PAPER 93-0193] p 473 A93-25511
- Progress in high-lift aerodynamic calculations [AIAA PAPER 93-0194] p 474 A93-25512
- Correlation of interaction sweepback effects on unsteady shock-induced turbulent separation [AIAA PAPER 93-0776] p 475 A93-25550
- A time dependent method in finite volume for transonic diffuser turbulent flows p 476 A93-27368
- Pressure fluctuations on the surface of two circular cylinders in tandem arrangements at high Reynolds numbers p 679 A93-33718
- Numerical simulation of the turbulent drag reduction by plate manipulators p 681 A93-33736
- Viscous-inviscid interaction coupled calculation of three-dimensional turbulent separated flow over dents p 681 A93-33748
- Numerical methods in laminar and turbulent flow; Proceedings of the 7th International Conference, Stanford Univ., CA, July 15-19, 1991. Vol. 7, pts. 1 & 2 [ISBN 0-906674-77-8] p 743 A93-34301
- A comparison between numerical models and measurements in a Kaplan turbine guide vanes p 685 A93-34339
- Computation of turbulent compressible flows on a DLR wing and a blade to blade passage using an upwind scheme p 687 A93-34359
- Inlet turbulence distortion and viscous flow development in a controlled-diffusion compressor cascade at very high incidence p 688 A93-34485
- Unsteady supersonic flow around a blunt body in thermal inhomogeneities in turbulent shock layer flows p 691 A93-35266
- Study of supersonic intersection flowfield at modified wing-body junctions p 692 A93-35621
- Numerical prediction of aerodynamic sound using large eddy simulation p 850 A93-38150
- Turbulent flow simulation around the aerofoil with pseudo-compressibility p 830 A93-38155
- Supersonic vortical flows around an ogive-cylinder - Laminar and turbulent computations [ONERA, TP NO. 1992-111] p 771 A93-38588
- Analysis of turbulence in supersonic flows by means of laser velocimetry [ONERA, TP NO. 1992-148] p 773 A93-38729
- Optimal conditions for flow turbulence reduction by a set of grids p 836 A93-39122
- Laminar flow flight experiments - A review p 890 A93-41778
- Damping of surface pressure fluctuations in hypersonic turbulent flow past expansion corners p 860 A93-41914
- Implicit multigrid techniques for compressible flows p 862 A93-42429
- Computation of hypersonic turbulent flow over a rearward facing step p 865 A93-42587
- Three-dimensional vortex method for parachutes p 872 A93-42874
- Evolution of a three-dimensional nonequilibrium boundary layer in a dihedral angle behind a perturbation source p 872 A93-43013
- Results from a set of low speed blade-vortex interaction experiments p 872 A93-43540
- An experimental study of a turbulent wing-body junction and wake flow p 873 A93-43541
- An adaptive finite element method for turbulent free shear flow past a propeller [AIAA PAPER 93-3388] p 956 A93-45079
- An upwind multigrid algorithm for calculating flows on unstructured grids p 957 A93-45088
- Organized structure in a compressible turbulent shear layer p 961 A93-45730
- Active forcing of an axisymmetric leading-edge turbulent separation bubble [AIAA PAPER 93-3245] p 966 A93-46790
- Method of characteristics for computing three-dimensional boundary layers p 970 A93-46886
- Computations of aerodynamic drag for turbulent transonic projectiles with and without spin [AIAA PAPER 93-3416] p 975 A93-47212
- Mathematical model for the effect of turbulent velocity pulsations on the stability of a powerplant p 1003 A93-47508
- Chemical-kinetics characteristics of combustion in a supersonic turbulent flow p 1018 A93-47512
- Reynolds stress transport modelling of shock/boundary-layer interaction [AIAA PAPER 93-2936] p 1046 A93-48134
- Multi-zonal Navier-Stokes code with the LU-SGS scheme [AIAA PAPER 93-2965] p 1148 A93-48159
- A study of turbulence in rarefied gases [AIAA PAPER 93-3097] p 1061 A93-48271
- The effect of large scale unsteady motion on turbulent reattaching shear layer - Application to the supersonic compression ramp [AIAA PAPER 93-3100] p 1061 A93-48273
- High lift airfoil flow simulation using a wall-corrected Algebraic Stress Model [AIAA PAPER 93-3109] p 1061 A93-48280
- Experimental and numerical investigation of supersonic turbulent flow in an annular duct [AIAA PAPER 93-3123] p 1063 A93-48291
- Experimental study on turbulent two-phase flow in a dual-inlet side dump combustor p 1106 A93-48506
- Calculation of the parameters of instability waves in the preseparation region p 1067 A93-48826
- Effects of external excitation on the leading-edge separation flowfield p 1071 A93-49198
- Drag characteristics of extra-thin-fin-riblets in an air flow conduit p 1151 A93-49240
- An unstructured grid flow solver for turbomachinery flows [AIAA PAPER 93-1913] p 1076 A93-49780
- High Reynolds number and turbulence effects on aerodynamics and heat transfer in a turbine cascade [AIAA PAPER 93-2252] p 1155 A93-50050
- Some supersonic and hypersonic research at GASL in the 1960s and 70s [AIAA PAPER 93-2327] p 1145 A93-50107
- Experimental and numerical study of swept ramp injection into a supersonic flowfield [AIAA PAPER 93-2445] p 1119 A93-50197
- Some key problems in the design of the NPU open-circuit low-turbulence wind tunnel p 1139 A93-51188
- A study of turbulent flow in a viscous shock layer in the case of gas flow past oblong blunt bodies p 1089 A93-51820
- Efficient simulation of incompressible viscous flow over single and multi-element airfoils p 1095 A93-52448
- Non-self-similarity of a boundary layer flow of a high-temperature gas in a Laval nozzle p 1176 A93-52946
- Numerical analysis of flow within cascade with tip clearance p 1176 A93-53192
- Zonal-local solution method for the turbulent Navier-Stokes equations p 1177 A93-53205
- Multigrid Navier-Stokes calculations for three-dimensional cascades p 1177 A93-53209
- 3D laminar and 2D turbulent computations with the Navier-Stokes solver FLU3M [ONERA, TP NO. 1993-105] p 1180 A93-53618
- A Eulerian/Lagrangian modelling to calculate the evolution of a water droplets spray [ISABE 93-7121] p 1221 A93-54096
- Experimental investigation of boundary layer transition on a flat plate with C4 leading edge [ISABE 93-7123] p 1222 A93-54098
- Rotor/stator flow coupling in turbomachines p 1232 A93-54647
- Three-dimensional mesh embedding for the Navier-Stokes equations using upwind control volumes p 1239 A93-56402
- LV software for supersonic flow analysis [NASA-CR-190911] p 16 N93-10069
- Effect of passive flow-control devices on turbulent low-speed base flow p 82 N93-10304
- Explicit Navier-Stokes computation of turbomachinery flows p 83 N93-10370
- Effects of sweep on the physics of unsteady shock-induced turbulent separated flows [AD-A257035] p 22 N93-11742
- Velocity and temperature measurements in a non-premixed reacting flow behind a backward facing step p 132 N93-13632
- Control of asymmetric jet [AD-A255967] p 219 N93-14400
- Control of low-speed turbulent separated flow over a backward-facing ramp p 219 N93-14475
- Finite-difference solution for laminar or turbulent boundary layer flow over axisymmetric bodies with ideal gas, CF₄, or equilibrium air chemistry [NASA-TP-3271] p 222 N93-15434
- Transition induced normal forces and their effects on the aerodynamic characteristics of slender sharp cones [AD-A256802] p 288 N93-15889
- Special publication of National Aerospace Laboratory [DE93-716176] p 239 N93-15946
- Hydrodynamic effects on heat transfer for film-cooled turbine blades [AD-A257291] p 361 N93-16080
- A realizable Reynolds stress algebraic equation model [NASA-TM-105993] p 290 N93-16596
- Direct numerical simulation of combustion in turbulent supersonic flow [DS-2138] p 393 N93-17746
- Lift and drag forces on droplets and particles in wall-bounded shear flows [DE93-002678] p 419 N93-17761
- Modeling the transition region [NASA-CR-4492] p 298 N93-19015
- LES turbulence modeling using DNS data base p 299 N93-19274
- Aerodynamic heating analysis for axisymmetric bodies in supersonic flow p 303 N93-19312
- Analysis and evaluation of an integrated laminar flow control propulsion system [NASA-CR-192162] p 551 N93-20268
- Methodology for sensitivity analysis, approximate analysis, and design optimization in CFD for multidisciplinary applications [NASA-CR-192172] p 552 N93-20297
- An experimental investigation of a round turbulent jet in a cross-flow p 553 N93-20689
- An analysis of lift forces on aerosols in a wall bounded turbulent shear flow [DE93-003362] p 747 N93-24963
- Visualization of a Mach 2 reacting flow using Planar Laser-Induced Fluorescence (PLIF) p 731 N93-26006
- Trailing vortex/tree-surface interaction [AD-A261654] p 701 N93-26195
- The generation of side force by distributed suction [NASA-CR-193129] p 839 N93-27151
- Airfoil stability in turbulent flow p 781 N93-27212
- The addition of algebraic turbulence modeling to program LAURA [NASA-TM-107758] p 840 N93-27250
- The remarkable ability of turbulence model equations to describe transition p 783 N93-27432
- Calculation of fully three-dimensional separated flow with an unsteady viscous-inviscid interaction method p 786 N93-27455
- Prediction of airfoil stall using Navier-Stokes equations in streamline coordinates p 787 N93-27456
- Discrete-vortex simulation of pulsating flow on a turbulent leading-edge separation bubble p 787 N93-27457
- Ship viscous flow: A report on the 1990 SSPA-IIHR Workshop p 840 N93-27466
- An assessment of inlet total-pressure distortion requirements for the Compressor Research Facility (CFR) [AD-A262299] p 815 N93-27679

- Navier-Stokes simulation of viscous, separated, supersonic flow over a projectile rotating band
[AD-A23073] p 788 N93-27955
- Modification and calibration of the Naval Postgraduate School Academic Wind Tunnel
[AD-A262092] p 823 N93-28189
- Studies of origin of three-dimensionality in laminar wakes
[AD-A262281] p 841 N93-28242
- High Reynolds number and turbulence effects on aerodynamics and heat transfer in a turbine cascade
[NASA-TM-106187] p 930 N93-29157
- Development of an unstructured solution adaptive method for the quasi-three-dimensional Euler and Navier-Stokes equations
[NASA-CR-193241] p 930 N93-29213
- Heat Transfer and Cooling in Gas Turbines
[AGARD-CP-527] p 901 N93-29926
- Keynote address: Unsteady, multimode transition in gas turbine engines
p 901 N93-29927
- Heat transfer in high turbulence flows: A 2-D planar wall jet
p 932 N93-29935
- Turbulent flow and heat transfer in idealized blade cooling passages
p 902 N93-29938
- Modeling of a turbulent flow in the presence of discrete parietal cooling jets
p 904 N93-29960
- Turbulence characteristics of an axisymmetric reacting flow
[NASA-CR-4110] p 877 N93-30373
- GARTEUR 3D shear layer experiment
[FFA-TN-1992-26] p 987 N93-31052
- Turbulence measurement in a reacting and non-reacting shear layer at a high subsonic Mach number
[NASA-TM-106186] p 989 N93-31839
- Numerical simulation of the flow in a 1:57-scale axisymmetric model of a large blast simulator
[AD-A265551] p 1015 N93-31916
- The prediction of noise from co-axial jets
[ISVR-TR-215] p 1040 N93-32339
- TURBULENT HEAT TRANSFER**
- Influence of high mainstream turbulence on leading edge film cooling heat transfer - Effect of film hole spacing
p 207 A93-15068
- Heat transfer and turbulence in a turbulated blade cooling circuit
[ASME PAPER 92-GT-187] p 402 A93-19412
- Augmentation of turbulent heat transfer with a vortex generator attached to a LEBU plate
p 411 A93-21729
- Time-resolved surface heat flux measurements in the wing/body junction vortex
[AIAA PAPER 93-0918] p 472 A93-24972
- Effects of longitudinal vortex generators on heat transfer and flow loss in turbulent channel flows
p 1021 A93-44222
- Leading edge film cooling heat transfer including the effect of mainstream turbulence
p 23 N93-11886
- Turbulent flow and heat transfer in idealized blade cooling passages
p 902 N93-29938
- Compressible turbulence in a high-speed high Reynolds number mixing layer
p 878 N93-30583
- TURBULENT JETS**
- Turbulent jet flows with condensation and electrophysical effects --- Russian book
p 76 A93-10176
- Calculation of three-dimensional turbulent jets propagating behind nozzles of rectangular cross section
p 6 A93-10192
- Flow field measurements in a turbulent free jet issuing from a sharp-edged square slot
p 244 A93-19158
- Control of coherent structures and aero-acoustic characteristics of subsonic and supersonic turbulent jets
p 448 A93-19196
- Experimental investigations and efficiency prediction of jet noise reduction techniques
p 449 A93-19206
- Experimental and numerical investigations of the vortex-flame interactions in a driven jet diffusion flame
[AIAA PAPER 93-0455] p 534 A93-25532
- Numerical study of an axisymmetric turbulent jet-impingement flow
[AIAA PAPER 93-0652] p 543 A93-25545
- Characteristics of three-dimensional turbulent jets in crossflow
p 772 A93-38695
- An acoustic suppressor for the jet noise of a turbojet engine
p 1003 A93-47510
- The influence of swirl generator characteristics on flow and combustion in turbulent diffusion flames
p 1159 A93-51632
- On the analysis of an impinging jet on ground effects
p 1260 A93-56339
- Mechanisms of sound generation in subsonic jets
p 101 N93-10688
- An experimental study of under-expanded jets
p 696 N93-25467
- Oxides of nitrogen emissions from turbulent hydrocarbon/air jet diffusion flames, phase 2
[PB93-152478] p 756 N93-26533
- The ground vortex flow field associated with a jet in a cross flow impinging on a ground plane for uniform and annular turbulent axisymmetric jets
[NASA-CR-4513] p 789 N93-28449
- TURBULENT MIXING**
- A simple spanwise mixing model for turbulent diffusion and secondary flows in multistage axial-flow compressors
p 204 A93-14482
- Control of coherent structures and aero-acoustic characteristics of subsonic and supersonic turbulent jets
p 448 A93-19196
- An investigation of spanwise mixing in multistage axial flow compressors
[ASME PAPER 92-GT-64] p 247 A93-19314
- Streamwise vortex meander in a plane mixing layer
[AIAA PAPER 93-0553] p 285 A93-23292
- Compressible turbulence measurements in a high-speed high Reynolds number mixing layer
[AIAA PAPER 93-0660] p 465 A93-24773
- Computation of supersonic jet noise under imperfectly expanded conditions
[AIAA PAPER 93-0735] p 563 A93-24825
- Applications of shock-induced mixing to supersonic combustion
p 735 A93-35618
- A computational investigation of fuel mixing in a hypersonic scramjet
[AIAA PAPER 93-2994] p 1001 A93-44230
- Model for entropy production and pressure variation in confined turbulent mixing
p 1071 A93-49014
- A review of chemically reactive turbulent flow mixing mechanisms and a new design for a low NO(x) combustor
p 1109 A93-49508
- Mixing in the dome region of a staged gas turbine combustor
p 1109 A93-49612
- Summary of the GASP code application and evaluation effort for scramjet combustor flowfields
[AIAA PAPER 93-1973] p 1077 A93-49820
- Molecular mixing of jets in supersonic flow
[AIAA PAPER 93-2021] p 1078 A93-49858
- Scramjet fuel mixing enhancement by cross-stream pressure gradients
[AIAA PAPER 93-2139] p 1114 A93-49957
- Thrust loss due to supersonic mixing
[AIAA PAPER 93-2140] p 1114 A93-49958
- A k-omega multivariate beta PDF for supersonic turbulent combustion
[AIAA PAPER 93-2197] p 1154 A93-50009
- Experimental investigation of slot injection into supersonic flow with an adverse pressure gradient
[AIAA PAPER 93-2442] p 1119 A93-50194
- The turbulence and mixing characteristics of the complex flow in a simulated augmentor
p 1123 A93-51642
- Computation of supersonic jet noise under imperfectly expanded conditions
[NASA-TM-105961] p 233 N93-15430
- An experimental study of under-expanded jets
p 696 N93-25467
- TURBULENT WAKES**
- Intensification of flow mixing behind an oblique shock wave
p 4 A93-10138
- 'Wingwake' - A computational model for preliminary assessment of wake vortex attenuation schemes
[AIAA PAPER 92-4209] p 15 A93-13377
- Turbulent structure in a vortex wake shed from an inclined circular cylinder
p 125 A93-15443
- Unsteady boundary-layer transition in flow periodically disturbed by wakes
[ASME PAPER 92-GT-283] p 254 A93-19475
- The effects of incident turbulence and moving wakes on laminar heat transfer in gas turbines
[ASME PAPER 92-GT-377] p 406 A93-19535
- Analysis of jet/wake mixing in a vaneless diffuser
[ASME PAPER 92-GT-418] p 258 A93-19566
- Numerical prediction of aerodynamic noise radiated from low Mach number turbulent wake
[AIAA PAPER 93-0145] p 452 A93-22589
- Calculation of laminar and turbulent asymmetric wakes
p 684 A93-34318
- Numerical computation of aerodynamic noise radiation by the large eddy simulation
p 850 A93-38151
- Phenomenology and simplified modeling of a vortex wake generated by a transverse jet
[ONERA, TP NO. 1992-194] p 774 A93-38755
- Underexpanded boundary jet in a wake flow
p 775 A93-39123
- Strong vortex/boundary layer interactions. I - Vortices
p 930 A93-43539
- An experimental study of a turbulent wing-body junction and wake flow
p 873 A93-43541
- Wake structure of a helicopter rotor in forward flight
p 958 A93-45138
- Turbulent structure of a wingtip vortex in the near field
[AIAA PAPER 93-3011] p 1054 A93-48201
- Wake-vortex structure from lift and torque induced on a following wing
[AIAA PAPER 93-3013] p 1054 A93-48202
- Laser velocimeter measurements of the flow field generated by a forward-swept propfan during flutter
[AIAA PAPER 93-2919] p 1180 A93-53591
- An experimental investigation of base bleed effect on the wake turbulent structure behind a two-dimensional blunt model
[MPIS-9/1991] p 139 N93-15131
- Numerical investigation of swirl-airfoil interactions in transonic area
[MPIS-8/1991] p 297 N93-18627
- Heat Transfer and Cooling in Gas Turbines
[AGARD-CP-527] p 901 N93-29926
- Determination of surface heat transfer and film cooling effectiveness in unsteady wake flow conditions
p 902 N93-29933
- TURNING FLIGHT**
- Flight performance of hypersonic minor circle turning maneuvers
[AIAA PAPER 93-0627] p 531 A93-24744
- Parafoli steady turn response to control input
[AIAA PAPER 93-1241] p 728 A93-35180
- Wind tunnel investigation of wind shear effect on turning flight
[AIAA PAPER 93-3641] p 1127 A93-48326
- Optimum poststall turning and supersonic turning
[AIAA PAPER 93-3659] p 1128 A93-48339
- Analysis of a turning point problem in flight trajectory optimization
p 1210 A93-52885
- Minimum time turn of a helicopter
p 1248 A93-54554
- Flight simulation evaluation of the flyability of curved MLS approaches with wide-body aircraft
[NLR-TP-90238-U] p 382 N93-17875
- Aircraft turns into and down wind
[AERO-REPT-9201] p 337 N93-18131
- TVD SCHEMES**
- Numerical investigation of the unsteady flow through a counter-rotating fan
p 112 A93-14166
- Numerical prediction of instabilities in transonic internal flows using an Euler TVD code
[AIAA PAPER 93-0072] p 262 A93-20184
- Numerical simulation of unsteady transonic nozzle flows
p 272 A93-22230
- Pressure-based high-order TVD methodology for dynamic stall simulation
[AIAA PAPER 93-0680] p 466 A93-24788
- Computation of inviscid flowfield around 3-D aerospace vehicles and comparison with experimental and flight data
[AIAA PAPER 93-0885] p 470 A93-24944
- Investigation of three-dimensional separation at wing/body junctions in supersonic flows using TVD MacCormack's scheme
[AIAA PAPER 93-0884] p 471 A93-24945
- Artificial viscosity models for the Navier-Stokes equations and their effect in drag prediction
[AIAA PAPER 93-0193] p 473 A93-25511
- Numerical study of the flow establishment time in hypersonic shock tunnels
p 480 A93-29153
- Finite-volume-TVD scheme for 3-D Euler transonic flow computations in rotating curvilinear coordinates
p 679 A93-33709
- Numerical simulation of starting process in a hypersonic nozzle
p 684 A93-34275
- A cell-vertex TVD scheme for transonic viscous flow
p 685 A93-34346
- An integrated flow simulation system on a parallel computer. I - Basic concept. II - The flow solver
p 688 A93-34370
- Numerical experiments with nonoscillatory schemes using Eulerian and new Lagrangian formulations
p 862 A93-42432
- A multidimensional generalization of Roe's flux difference splitter for the Euler equations
p 863 A93-42437
- Higher-order-accurate upwind schemes for solving the compressible Euler and Navier-Stokes equations
p 863 A93-42441
- Hypersonic flows over a double or simple ellipse
p 868 A93-42614
- New upwind dissipation models with a multidimensional approach
[AIAA PAPER 93-3304] p 950 A93-45002
- An implicit time-marching procedure for high speed flow
[AIAA PAPER 93-3315] p 951 A93-45011
- Implicit multigrid Euler solutions with symmetric Total-Variation-Diminishing dissipation
[AIAA PAPER 93-3358] p 955 A93-45052
- A multigrid nonoscillatory method for computing high speed flows
[AIAA PAPER 93-3319] p 958 A93-45103
- Numerical simulation of supersonic flows with chemical reactions
p 959 A93-45325

- Comparison of ENO and TVD schemes for the parabolized Navier-Stokes equations
[AIAA PAPER 93-2970] p 1049 A93-48164
- Two-dimensional numerical simulation for Mach-3 multishock air-intake with bleed systems
[AIAA PAPER 93-2306] p 1082 A93-50090
- A numerical study of the unsteady processes associated with the type IV shock interaction
[AIAA PAPER 93-2479] p 1083 A93-50221
- A fourth-order MUSCL finite-difference scheme for solving the unsteady compressible Euler equations
p 1086 A93-51121
- A time-accurate high-resolution TVD scheme for solving the Navier-Stokes equations
p 1093 A93-52006
- Three-dimensional viscous flow analysis of compressor cascade channels
p 1181 A93-53837
- Numerical solution of N-S equations for hypersonic flow over capsule-type vehicles
p 1182 A93-53858
- A 2-D compressible N-S simulation of starting- and stalling-flows in a compressor cascades system
[ISABE 93-7006] p 1183 A93-53982
- Locally implicit total variation diminishing schemes on mixed quadrilateral-triangular meshes
p 1235 A93-55356
- Hypersonic flows including real gas effects
[AERO-REPT-9112] p 289 A93-16467
- Numerical simulations of hypersonic rarefied transition regime flows: DSMC method and Navier-Stokes computation
p 299 A93-19278
- TWISTING**
- Impact ice interface shear stresses caused by blade bending and twisting
[AIAA PAPER 93-0030] p 307 A93-20147
- Computational method in optimal bending-twisting comprehensive design of wings of subsonic and supersonic aircraft
[AD-A262374] p 806 A93-27694
- TWO DIMENSIONAL BODIES**
- Transition of flutter mode of two-dimensional wing with external store
p 41 A93-11818
- An analysis of the post-instability behaviour of a two-dimensional airfoil with a structural nonlinearity
[AIAA PAPER 93-1474] p 726 A93-34020
- Nonlinear aeroelastic response of panels
[AIAA PAPER 93-1599] p 741 A93-34130
- Numerical simulation of inviscid transonic flow over two-dimensional slender bodies
p 886 A93-34348
- Hierarchical development of three direct-design methods for two-dimensional axial-turbomachinery cascades
p 812 A93-39271
- Experimental investigation of spherical-convergent-flap thrust-vectoring two-dimensional plug nozzles
[AIAA PAPER 93-2431] p 898 A93-41045
- An experimental contribution to the flat plate 2D compression ramp, shock/boundary layer interaction problem at Mach 14 - Test case 3.7
p 865 A93-42590
- Application of the Galerkin/least-squares formulation to the analysis of hypersonic flows. I - Flow over a two-dimensional ramp
p 866 A93-42593
- Hypersonic viscous flow over two-dimensional ramps
p 866 A93-42596
- Grid-refinement study of hypersonic laminar flow over a 2-D ramp
p 866 A93-42597
- Implicit upwind finite-difference simulation of laminar hypersonic flow over a 2D ramp
p 867 A93-42600
- A synthesis of results on the calculation of flow over a 2D ramp and a 3D obstacle - Antibes test cases 3 and 4
p 867 A93-42601
- Appraisal of the rarefied flow computations (problems 6.4.1 and 7.2.1)
p 871 A93-42640
- Effect of temperature on nonlinear two-dimensional panel flutter using finite elements
p 1022 A93-45133
- Computational aerothermodynamics for 2D and 3D space vehicles
p 1073 A93-49533
- Scale model test results for several spherical/two-dimensional nozzle concepts
[AIAA PAPER 93-2430] p 1117 A93-50186
- Wake similarity and vortex formation for two-dimensional bluff bodies
p 138 A93-15101
- Analysis of a 2-D airfoil motion flying in-proximity-to a wavy-wall surface: Lifting-surface-method
p 300 A93-19281
- Analysis of a 2-D airfoil motion flying in-proximity-to a wavy-wall surface: Finite difference method
p 300 A93-19282
- TWO DIMENSIONAL BOUNDARY LAYER**
- Boundary layer separation in a corner formed by two planes
p 6 A93-10188
- Evaluation and application of the Baldwin-Lomax turbulence model in two-dimensional, unsteady, compressible boundary layers with and without separation in engine inlets
[AIAA PAPER 92-3676] p 111 A93-14118
- On the coupling between a supersonic boundary layer and a flexible surface
p 243 A93-19132
- Evaluation and application of the Baldwin-Lomax turbulence model in two-dimensional, unsteady, compressible boundary layers with and without separation in engine inlets
[AIAA PAPER 92-3676] p 414 A93-22509
- Prediction of fluctuating pressure in attached and separated compressible flow
[AIAA PAPER 93-0286] p 279 A93-22687
- Shock wave/boundary layer interaction in a two-dimensional laminar hypersonic flow
[ONERA, TP NO. 1992-182] p 773 A93-38744
- Numerical simulation of transition in two- and three-dimensional boundary layers
p 973 A93-46980
- Bypass transition in two- and three-dimensional boundary layers
[AIAA PAPER 93-3050] p 1057 A93-48230
- Real gas effects in two- and three-dimensional hypersonic, laminar boundary layers
p 1073 A93-49530
- Verification of the TOTLOS method for calculating aerodynamic loss in film-cooled turbine cascade
p 1087 A93-51191
- Evaluation and application of the Baldwin-Lomax turbulence model in two-dimensional, unsteady, compressible boundary layers with and without separation in engine inlets
[NASA-TM-105810] p 82 A93-10087
- TWO DIMENSIONAL FLOW**
- Optimal control of lift/drag ratios on a rotating cylinder
p 76 A93-10275
- Finite memory approximations for a singular neutral system arising in aeroelasticity
p 97 A93-13246
- Parallel implementation of the feature associated mesh embedding method for the 2D-Euler equations (FAME2D)
p 225 A93-14278
- Experimental and numerical study on the basic performance of a two-dimensional right-angled intake flow
p 208 A93-15486
- Numerical analysis of two-dimensional turbulent flows through an oscillating cascade
p 126 A93-15494
- Strong coupling between inviscid fluid and boundary layer for airfoils with a sharp edge. II - 2D unsteady case for isolated airfoil and straight blade cascade
p 126 A93-16473
- A novel approach to high resolution compressible cascade flow analysis using the Navier-Stokes equations
[ASME PAPER 92-GT-419] p 258 A93-19567
- The role of noise in two-dimensional vortex merging
p 408 A93-19967
- A new rotated upwind difference scheme for the Euler equations
[AIAA PAPER 93-0066] p 261 A93-20179
- Air flow dynamics around an airfoil by the stabilized finite difference method
p 266 A93-20741
- Numerical analysis of two-dimensional flows around elliptic wings above a flat plate
p 267 A93-20924
- Two-dimensional cascade tests of MCA blades in the high transonic Mach number region. V - Effect of space/chord ratio on the parameters of cascade performance
p 267 A93-20930
- Measured thrust losses associated with secondary air injection through nozzle walls
p 270 A93-21656
- Investigation of a two-dimensional scramjet inlet, freestream $M = 8-18$ and $T_{sub} 0 = 4100$ K
p 270 A93-21669
- Turbulence modeling for complex hypersonic flows
[AIAA PAPER 93-0200] p 277 A93-22620
- Discontinuous Galerkin finite element method for two dimensional conservation laws
[AIAA PAPER 93-0337] p 281 A93-23026
- A hybrid structured-unstructured grid method for unsteady turbomachinery flow computations
[AIAA PAPER 93-0387] p 282 A93-23066
- Effect of sidewall suction on flow in two-dimensional wind tunnels
p 287 A93-23538
- Nonlinear relaxation/quasi-Newton algorithm for the compressible Navier-Stokes equations
p 287 A93-23541
- Eduction of swirling structure using the velocity gradient tensor
p 416 A93-23547
- Shock oscillation in two-dimensional, inviscid, unsteady channel flow
p 288 A93-23563
- Exact-gradient shape optimization of a 2-D Euler flow
p 462 A93-24308
- Three-dimensional flow over two spheres placed side by side
p 539 A93-24412
- Comparison of PMARC and analytic results for two-dimensional unsteady airfoils
[AIAA PAPER 93-0636] p 463 A93-24752
- A physically guided zonal approach for two-dimensional airfoil flows
[AIAA PAPER 93-0790] p 468 A93-24869
- Numerical simulation of vortex generation and capture above an airfoil
[AIAA PAPER 93-0864] p 468 A93-24926
- Numerical experiments on the stability of leading edge boundary layer flow - A two-dimensional linear study
p 477 A93-27475
- Subsonic potential flow and the transonic controversy
p 479 A93-28544
- Compressible flow in a hovercraft air cushion
p 480 A93-29316
- Structure-attached corotational fluid grid for transient aeroelastic computations
p 480 A93-29326
- Comparison of several convection discretization schemes for all Mach number arbitrary 2D flows
p 685 A93-34345
- Numerical simulation of two-dimensional compressible flows
p 687 A93-34357
- Convenient method to convert two-dimensional CFD codes into axisymmetric ones
p 689 A93-34499
- Applications of shock-induced mixing to supersonic combustion
p 735 A93-35618
- Ignition analysis of unpremixed reactants with chain mechanism in a supersonic mixing layer
p 735 A93-35619
- Influence of coupling incidence and velocity variations on the airfoil dynamic stall
p 767 A93-35999
- Vortex generators used to control laminar separation bubbles
p 768 A93-37381
- Indicial lift approximations for two-dimensional subsonic flow as obtained from oscillatory measurements
p 768 A93-37385
- A new adaptive test section at ONERA Chalais-Meudon
[ONERA, TP NO. 1992-117] p 822 A93-38592
- Unsteady transonic two-dimensional Euler solutions using finite elements
p 778 A93-39412
- Numerical experiments with nonoscillatory schemes using Eulerian and new Lagrangian formulations
p 862 A93-42432
- Thermo-chemical models for hypersonic flows
p 863 A93-42433
- Higher-order-accurate upwind schemes for solving the compressible Euler and Navier-Stokes equations
p 863 A93-42441
- Viscous, 2-D, laminar hypersonic flows over compression ramps
p 866 A93-42591
- Computation of flows over 2D ramps
p 866 A93-42595
- Navier-Stokes calculations over a double ellipse and a double ellipsoid by an implicit non-centered method
p 867 A93-42607
- 2D hypersonic viscous flow past a double ellipse geometry
p 868 A93-42613
- Two-dimensional CFD modeling of wave rotor flow dynamics
[AIAA PAPER 93-3318] p 952 A93-45014
- Line relaxation methods for the solution of 2D and 3D compressible flows
[AIAA PAPER 93-3366] p 955 A93-45059
- A simulation technique for 2-D unsteady inviscid flows around arbitrarily moving and deforming bodies of arbitrary geometry
[AIAA PAPER 93-3391] p 956 A93-45082
- Numerical simulation of two-dimensional and axisymmetric compressible flows
p 960 A93-45546
- Flow resolution and domain of influence in rarefied hypersonic blunt-body flows
[AIAA PAPER 93-2806] p 964 A93-46546
- Vortex capture by a two-dimensional airfoil with a small oscillating leading-edge flap
[AIAA PAPER 93-3266] p 968 A93-46830
- Two dimensional incompressible flow through a vibrating bladed disc - Theoretical model
p 973 A93-46991
- Multiple solutions of the transonic perturbation equation
p 987 A93-47331
- Solution of the Euler equations for airfoils using asymptotic methods
[AIAA PAPER 93-2931] p 1045 A93-48130
- A solution-adaptive hybrid-grid method for the unsteady analysis of turbomachinery
[AIAA PAPER 93-3015] p 1148 A93-48204
- A viscous-inviscid interaction method for 2-D unsteady, compressible flows
[AIAA PAPER 93-3019] p 1055 A93-48206
- Behaviour of the Johnson-King turbulence model in axis-symmetric supersonic flows
[AIAA PAPER 93-3032] p 1056 A93-48214
- A nonperiodic boundary approach for computation of compressible viscous flows in advanced turbine cascades
[AIAA PAPER 93-1799] p 1074 A93-49688
- Secondary flow computation by means of an inviscid multigrid Finite Volume Lambda Formulation
[AIAA PAPER 93-1974] p 1077 A93-49821
- Numerical and experimental investigation of turbine tip gap flow
[AIAA PAPER 93-2253] p 1081 A93-50051

- Establishing two-dimensional flow in a large-scale cascade of controlled-diffusion compressor blades
[AIAA PAPER 93-2383] p 1083 A93-50151
- Initial development of the two-dimensional ejector shear layer - Experimental results
[AIAA PAPER 93-2440] p 1118 A93-50192
- Comparison of the initial development of shear layers in two-dimensional and axisymmetric ejector configurations
[AIAA PAPER 93-2441] p 1119 A93-50193
- Numerical aspects of a block structured compressible flow solver
p 1169 A93-51279
- A collocated finite volume method for predicting flows at all speeds
p 1087 A93-51736
- Transition correlation in subsonic flow over a flat plate
p 1178 A93-53231
- 3D laminar and 2D turbulent computations with the Navier-Stokes solver FLU3M
[ONERA, TP NO. 1993-105] p 1180 A93-53618
- On the numerical simulation of the two-dimensional flow field around a hypersonic air-intake-compressibility effects
[ISABE 93-7100] p 1187 A93-54076
- A study on Mach 3 two-dimensional mixed compression air-intakes
[ISABE 93-7106] p 1188 A93-54082
- Observation of fluctuation of 2D-nozzle flows
[ISABE 93-7110] p 1204 A93-54086
- Two-dimensional and three-dimensional mixing flow structures with injected through slotted nozzle and circular nozzle into supersonic flows
[ISABE 93-7117] p 1221 A93-54092
- Numerical and experimental study on two- and three-dimensional supersonic flow field with hydrogen injection
[ISABE 93-7118] p 1188 A93-54093
- Prediction of viscous flows in rotating machinery using Navier-Stokes techniques
p 1232 A93-54639
- Two-dimensional transonic flow around VKI turbine cascade
p 1232 A93-54640
- Vectoring thrust and two-dimensional nozzle
p 1247 A93-54863
- Discontinuous Galerkin finite element method for Euler and Navier-Stokes equations
p 1235 A93-55357
- Vibration excitation in laminar hypersonic boundary layers
p 1237 A93-56028
- Improved numerical simulation of Euler equations
p 83 N93-10309
- A method of testing two-dimensional airfoils
[AD-A253210] p 17 N93-10375
- A field panel method for transonic flows
p 18 N93-10547
- Characteristics of separated flows including cavitation effects
p 84 N93-10874
- Air ejector experiments using the two-dimensional supersonic cascade tunnel: Relationship between ejector performance and throat area ratio, part 1
[NAL-TM-642-PT-1] p 25 N93-12352
- Mathematical problems in inviscid hypersonic flow
p 131 N93-13451
- Overall effects of separation on thin aerofoils
[ISBN-0-315-67464-4] p 135 N93-13930
- BLSTA: A boundary layer code for stability analysis
[NASA-CR-4481] p 220 N93-14797
- Supersonic investigation of two dimensional hypersonic exhaust nozzles
[NASA-TM-105687] p 179 N93-15342
- Mixing and reaction in the subsonic 2-D turbulent free shear layer
p 289 N93-16508
- Maximum lift of wings with leading-edge devices and trailing-edge flaps deployed
[ESDU-92031] p 290 N93-16522
- On flutter behavior of a 2-D compressor cascade in incompressible flow
[DLR-FB-91-26] p 418 N93-16543
- Exact-gradient shape optimization of a 2D Euler flow
[INRIA-RR-1540] p 422 N93-18623
- Analysis of a 2-D airfoil motion flying in-proximity-to a wavy-wall surface: Lifting-surface-method
p 300 N93-19281
- Numerical calculations of separating flows around oscillating airfoil
p 300 N93-19284
- Numerical simulation of flow for a scramjet nozzle
p 302 N93-19299
- Numerical simulations of supersonic flow by a fourth-order compact MUSCL TVD scheme
p 302 N93-19308
- A numerical investigation for supersonic inlet
p 303 N93-19315
- A numerical simulations of inner flow of scramjet
p 304 N93-19318
- Two problems reducing the data accuracy in Transonic Wind Tunnel testing
p 304 N93-19321
- Heat transfer in high turbulence flows: A 2-D planar wall jet
p 932 N93-29935

- A theoretical and computational study on active wake control
p 878 N93-30892
- TWO DIMENSIONAL JETS**
- Computations of a twin-jet impingement on a flat surface
p 271 A93-22227
- Phenomenology and simplified modeling of a vortex wake generated by a transverse jet
[ONERA, TP NO. 1992-194] p 774 A93-38755
- The numerical calculation on the flowfields of transverse jet interaction in the base of vehicle at supersonic speeds
[AIAA PAPER 93-1931] p 1077 A93-49795
- TWO DIMENSIONAL MODELS**
- Application of laminar flow to aero engine nacelles
p 128 A93-17256
- Unsteady two- and three-dimensional Navier-Stokes simulations of multistage turbomachinery flows
p 266 A93-20721
- Workshop report - A validation study of Navier-Stokes codes for transverse injection into a Mach 2 flow
p 270 A93-21330
- NOZ2D - A two dimensional explicit inviscid upwind code for convergent divergent nozzles
p 460 A93-24080
- A two-dimensional elliptic grid generator for a wing-body section involving grid control functions
p 460 A93-24083
- An implicit finite difference algorithm for two dimensional Euler equation
p 461 A93-24085
- Two-dimensional Navier-Stokes analysis of high-lift multi-element airfoils using the q-omega turbulence model
[AIAA PAPER 93-0679] p 466 A93-24787
- Wind identification along a flight trajectory. II - 2D-kinematic approach
p 524 A93-28469
- Structural modeling of low-aspect ratio composite wings
[AIAA PAPER 93-1371] p 739 A93-33937
- A 2-D numerical model for predicting the aerodynamic performance of the NOTAR system tailboom
p 766 A93-35994
- Implications of three-dimensional tracer studies for two-dimensional assessments of the impact of supersonic aircraft on stratospheric ozone
p 936 A93-41269
- Subsonic/transonic cascade flutter using a full-potential solver
p 861 A93-41934
- Numerical solution of axisymmetric heat conduction problems using finite control volume technique
p 928 A93-42909
- Wind identification along a flight trajectory. III - 2D dynamic approach
p 1007 A93-45401
- A viscous shock-layer analysis of 2-D and axisymmetric flows
[AIAA PAPER 93-2751] p 963 A93-46500
- A lag model for turbulent boundary layers developing over rough bleed surfaces
[AIAA PAPER 93-2988] p 1052 A93-48181
- 2-D theoretical analysis of circumferential grooved casing treatment
p 1066 A93-48501
- Two-dimensional computational analysis of a transport high-lift system and a comparison with flight-test results
[AIAA PAPER 93-3533] p 1072 A93-49517
- A two-dimensional analysis of multiple matrix cracking in a laminated composite close to its characteristic damage state
p 1157 A93-50405
- Optimal symmetric trajectories over a fixed-time domain
[AIAA PAPER 93-3848] p 1133 A93-51435
- Atmospheric disturbances over mountains and the flight safety
p 1164 A93-51856
- Estimation of the change of axial-flow compressor characteristics during long-term service
p 1193 A93-52949
- A 2-D compressible N-S simulation of starting- and stalling-flows in a compressor cascades system
[ISABE 93-7006] p 1183 A93-53982
- New approximate method of stress analysis for bladed rotating discs
[ISABE 93-7059] p 1219 A93-54035
- The combustion performance of methane-fueled ram combustor
[ISABE 93-7079] p 1201 A93-54055
- Numerical simulation of a two-dimensional supersonic mixed-compression inlet
[ISABE 93-7107] p 1188 A93-54083
- Application of laminar flow to aero engine nacelles
[PNR-90916] p 20 N93-11020
- Transonic aeroelastic analysis of systems with structural nonlinearities
p 217 N93-13769
- An experimental investigation of base bleed effect on the wake turbulent structure behind a two-dimensional blunt model
[MPIS-9/1991] p 139 N93-15131
- Numerical simulation of the flow through non-uniform airfoil cascade
p 302 N93-19310

- Workshop Report: A validation study of Navier-Stokes codes for transverse injection into a Mach 2 flow
p 751 N93-26008
- Model fan passage flow simulation
[AD-A261613] p 752 N93-26167
- Merging sparse optical flow and edge connectivity between image features: A representation scheme for 2-D display of scene depth
p 845 N93-27179
- TWO FLUID MODELS**
- Initial development of the two-dimensional ejector shear layer - Experimental results
[AIAA PAPER 93-2440] p 1118 A93-50192
- Comparison of the initial development of shear layers in two-dimensional and axisymmetric ejector configurations
[AIAA PAPER 93-2441] p 1119 A93-50193
- Three-dimensional prediffuser combustor studies with air-water mixture
[AIAA PAPER 93-2474] p 1120 A93-50217
- TWO PHASE FLOW**
- An electrostatic probe for determining particle characteristics in disperse flow
p 76 A93-10178
- Two-phase injection from the front surface of a blunt body in hypersonic flow
p 241 A93-18233
- Simulation of the secondary air system of aero engines
[ASME PAPER 92-GT-68] p 348 A93-19318
- Experimental and theoretical investigation of a research atomizer/combustion chamber configuration
[ASME PAPER 92-GT-137] p 401 A93-19369
- Scaling of the two-phase flow downstream of a gas turbine combustor swirl cup - Mean quantities
[ASME PAPER 92-GT-207] p 404 A93-19431
- Penetration and mixing of bubbling liquid jets from multiple injectors normal to a supersonic air stream
[AIAA PAPER 92-5060] p 413 A93-22330
- Theoretical and experimental study of the behavior of particles passing through a shock wave
[ONERA, TP NO. 1992-233] p 774 A93-38777
- Flow density distribution in a two-phase submerged jet
p 836 A93-39144
- Enhanced heat transport in environmental systems using microencapsulated phase change materials
[SAE PAPER 921224] p 926 A93-41398
- Stability of the vapour phase in a rotating two-phase fluid system subjected to different gravitational intensities
p 926 A93-41714
- Transonic aerodynamics including strong effects from heat addition
p 862 A93-42428
- Experimental study on turbulent two-phase flow in a dual-inlet side dump combustor
p 1106 A93-48506
- Experimental investigation on effect of solid particles on blade pressure distribution in compressor cascade flow
p 1066 A93-48513
- A comparison between centered and upwind schemes for two-phase compressible flows
[AIAA PAPER 93-2346] p 1083 A93-50120
- Experimental investigation of effect of particles on blade pressure distribution in impulse cascade flow
p 1236 A93-55398
- Current Technology for Thermal Protection Systems
[NASA-CP-3157] p 69 N93-12447
- Fuel Injector: Air swirl characterization aerothermal modeling, phase 2, volume 2
[NASA-CR-189193-VOL-2] p 721 N93-25106
- Flow visualizations of perpendicular blade vortex interactions
[NASA-CR-192725] p 748 N93-25208
- Multiparticle imaging technique for two-phase fluid flows using pulsed laser speckle velocimetry
[DE93-011734] p 935 N93-30489
- TWO STAGE TURBINES**
- Selection of the scheme and optimal parameters of the turbine of a high-temperature bypass engine with a low bypass ratio
p 811 A93-39180
- Estimating turbine limit load
[NASA-CR-191105] p 699 N93-25883
- Three-dimensional analysis of the Pratt and Whitney alternate design SSME fuel turbine
p 1031 N93-31584
- U**
- U.S.S.R.**
- JPRS report: Central Eurasia. Aviation and cosmonautics, no. 9, September 1992
[JPRS-UAC-93-003] p 678 N93-26325
- U-2 AIRCRAFT**
- Above the sky -- high altitude flight in ER-2 aircraft
p 1044 A93-52614
- The development of aircraft in the Lockheed Skunk Works from 1954 to 1991
p 605 N93-27168

UH-60A HELICOPTER

- Preliminary design features of the RASCAL - A NASA/Army rotorcraft in-flight simulator [AIAA PAPER 92-4175] p 42 A93-13311
- A treatment to flight controller nonlinearity effects - An adaptive compensator approach p 524 A93-26948
- Synthesis and evaluation of an H2 control law for a hovering helicopter p 728 A93-34542
- Aerodynamic and wake methodology evaluation using model UH-60A experimental data p 767 A93-35997
- A simulation model of atmospheric turbulence for rotorcraft applications p 224 A93-14588
- Crash experience of the US Army Black Hawk helicopter p 493 A93-19688
- Techniques for designing rotorcraft control systems [NASA-CR-192960] p 729 A93-26046
- Helicopter forced response vibration analysis method RTVIB20 [AD-A261809] p 730 A93-26260
- Helicopter approach capability using the differential global positioning system [NASA-CR-193183] p 793 A93-28936

ULTRAHIGH FREQUENCIES

- Lessons learned during testing of the Enhanced Position Location Reporting System (EPLRS) p 77 A93-10996
- Airship/U.S. naval vessels UHF communications relay demonstration [AIAA PAPER 93-4032] p 1240 A93-54604

ULTRAHIGH VACUUM

- Undulator Spectromicroscopy Facility at the Advanced Light Source [DE93-007964] p 823 A93-28490

ULTRALIGHT AIRCRAFT

- An ultralight freewheeling aircraft design study [AIAA PAPER 92-4194] p 44 A93-13371
- Cabin noise source-path identification for AD-200 ultralight aircraft p 444 A93-19138
- Helicopter noise standards - Requirements, compliance, and improvements p 569 A93-29443
- The Ultra Light Aircraft Testing [NASA-CR-193043] p 895 A93-29774
- Report on the test set-up for the structural testing of the Airmass Sunburst Ultralight Aircraft p 895 A93-29775
- Load test set-up for the Airmass Sunburst Ultra-Light Aircraft p 895 A93-29776
- NASTRAN analysis for the Airmass Sunburst model 'C' Ultralight Aircraft p 931 A93-29777
- Construction, wind tunnel testing and data analysis for a 1/5 scale ultra-light wing model p 876 A93-29778

ULTRASONIC CLEANING

- Ultrasonic polishing p 750 A93-25580

ULTRASONIC FLAW DETECTION

- Selection of methods and equipment for monitoring the technical condition of booster system components --- of aircraft hydraulic systems p 395 A93-18329
- Elastic constants for unidirectional boron-epoxy composites p 387 A93-18636
- Comparison of neural network and Markov random field image segmentation techniques p 397 A93-18652
- Assessment of aircraft structural integrity by detecting disbands through ultrasonic scanning p 406 A93-19587
- Ultrasonic NDE of adhesive and sealant bonded aluminum lap-splices p 407 A93-19595
- p-version finite element modeling for NDE p 407 A93-19699
- Ultrasonic thickness measurement using the angle technique p 542 A93-25353

ULTRASONIC MACHINING

- Ultrasonic polishing p 750 A93-25580

ULTRASONIC RADIATION

- Icing prevention by ultrasonic nucleation of supercooled water droplets in front of subsonic aircraft [AD-A258212] p 142 A93-12816

ULTRASONIC SCANNERS

- Damage detection by Acousto-Ultrasonic Location (AUL) p 555 A93-21529

ULTRASONIC TESTS

- Investigation of corrosion in aluminum/adhesive lap-splices using pulse-echo ultrasonic techniques [DE93-008074] p 749 A93-25518

ULTRASONIC WELDING

- Performance of thermal adhesives in forced convection p 924 A93-30974

ULTRAVIOLET EMISSION

- Kinetics and energy transfer in nonequilibrium fluid flows [AD-A263612] p 875 A93-29284

ULTRAVIOLET SPECTRA

- Optical technologies for UV remote sensing instruments p 853 A93-28788

ULTRAVIOLET SPECTROMETERS

- Optical technologies for UV remote sensing instruments p 853 A93-28788

UNDERCARRIAGES

- Measurement of the dynamic undercarriage response of a Sikorsky S-70B-2 helicopter: Instrumentation and test methods: Flight mechanics technical memorandum [AD-A256319] p 329 A93-16404

UNDERWATER VEHICLES

- Correction of inertial measurements using GPS updates for underwater navigation [AD-A257329] p 317 A93-15988
- Motion simulation of underwater vehicles [VTT-PUBS-97] p 443 A93-18698
- Simultaneous mapping of the unsteady flow fields by Particle Displacement Velocimetry (PDV) p 786 A93-27454
- Advanced Unmanned Search System (AUSS) supervisory command, control and navigation [AD-A263171] p 793 A93-28990

UNIFORM FLOW

- Dynamic characteristics of an airfoil at high speed change of pitch angle p 10 A93-12324
- The use of a deep honeycomb to achieve high flow quality in the ARA 9 ft x 8 ft Transonic Wind Tunnel p 190 A93-14276
- Turbulent structure in a vortex wake shed from an inclined circular cylinder p 125 A93-15443
- Oscillation of circular shock waves with upstream nonuniformity p 208 A93-15496
- Advancing the state of the art hypersonic testing - HYTEST/MTMI [AIAA PAPER 93-2023] p 1113 A93-49860
- Investigation of supersonic shaped nozzles in a low-pressure wind tunnel p 1091 A93-51881
- Experiments on smooth cantilevered circular cylinders in a low-turbulence uniform flow. Part 2: Fluctuating loads on a cantilever of aspect ratio 30 [PB93-110500] p 555 A93-21382
- Experiments on smooth cantilevered circular cylinders in low-turbulence uniform flow. Part 1: Mean loading with aspect ratios in the range 4 to 30 [PB93-111763] p 555 A93-21383

UNITED KINGDOM

- UK airmisses involving commercial air transport, May-August 1991 [ETN-92-92260] p 28 A93-11357
- UK airmisses involving commercial air transport, January-April-1991 [ETN-92-92261] p 87 A93-11358
- The UK perspective on aviation security p 496 A93-21858
- Reportable accidents to UK registered aircraft, and to foreign registered aircraft in UK airspace, 1990 [CAP-600] p 991 A93-31730

UNITED STATES

- Insights into US domestic aviation p 496 A93-21859
- Aeronautics and space report of the President: Fiscal year 1992 activities p 854 A93-27041
- International aircraft operator information system [DOT/FAA/CT-93/4] p 949 A93-32232
- UNIVERSITIES**
- Specific educational aspects of airport engineering in Spain and the Hispanic world p 103 A93-12560
- German university research in hypersonics [AIAA PAPER 92-5033] p 239 A93-22307
- AIAA's role in aerospace education [AIAA PAPER 93-0324] p 454 A93-23016
- Reform of the aeronautics and astronautics curriculum at MIT [AIAA PAPER-93-0325] p 454 A93-23017
- Total Quality Management in curriculum development [AIAA PAPER 93-0326] p 454 A93-23018
- Scientific and engineering research facilities at universities and colleges: 1992 [NSF-92-325] p 192 A93-13407

UNIVERSITY PROGRAM

- The design of a senior-level CAD course with emphasis on fluid/thermal systems [AIAA PAPER 93-0426] p 454 A93-23344
- The development of a mature external Master's degree program in aeronautical engineering - A university/industry partnership [AIAA PAPER 92-4256] p 570 A93-24296
- The design of a long range megatransport aircraft [NASA-CR-192077] p 332 A93-17711
- Phoenix: Preliminary design of a high speed civil transport [NASA-CR-192024] p 334 A93-17976
- Tesseract: Supersonic business transport [NASA-CR-192072] p 334 A93-17977
- Eagle RTS: A design for a regional transport aircraft [NASA-CR-192032] p 334 A93-18017
- Advanced hypersonic aircraft design [NASA-CR-192046] p 334 A93-18037
- Conceptual design of a Mars transportation system [NASA-CR-192039] p 420 A93-18047

- Proposal and preliminary design for a high speed civil transport aircraft. Swift: A high speed civil transport for the year 2000 [NASA-CR-192023] p 335 A93-18049

- TBD(exp 3) [NASA-CR-192075] p 335 A93-18054

- The Edge supersonic transport [NASA-CR-192074] p 335 A93-18055
- Hermes CX-7: Air transport system design simulation [NASA-CR-192082] p 335 A93-18056

- A second-generation high speed civil transport: Stingray [NASA-CR-192022] p 336 A93-18059

- The Trojan --- supersonic transport [NASA-CR-192013] p 336 A93-18060

- Preliminary design of a high speed civil transport: The Opus 0-001 [NASA-CR-192018] p 336 A93-18061

- Arrow 227: Air transport system design simulation [NASA-CR-192053] p 336 A93-18063

- SR-SCARLET 1: Peregrin [NASA-CR-192048] p 337 A93-18155

- RTJ-303: Variable geometry, oblique wing supersonic aircraft [NASA-CR-192054] p 337 A93-18166

- High-altitude reconnaissance aircraft p 894 A93-29713

- Project ARES 2: High-altitude battery-powered aircraft p 894 A93-29715

- Preliminary design studies of an advanced general aviation aircraft p 894 A93-29717

- Design of a turbofan powered regional transport aircraft p 894 A93-29721

- Solar powered multipurpose remotely powered aircraft p 895 A93-29722

UNIX (OPERATING SYSTEM)

- The operating system for Numerical Wind Tunnel p 383 A93-19290

UNMANNED SPACECRAFT

- HOPE and its thermal protection systems p 1252 A93-54711
- Guidance and control of HOPE (H-I) orbiting plane) [AAS PAPER 91-653] p 1252 A93-55825
- Transition aerodynamics for 20-percent-scale VTOL unmanned aerial vehicle [NASA-TM-4419] p 779 A93-27032
- Project ARES 2: High-altitude battery-powered aircraft p 894 A93-29715

UNSTEADY AERODYNAMICS

- Viscous instability of hypersonic flow past a wedge p 4 A93-10137
- Effect of a large-scale inhomogeneity of the incoming flow on flow in a plane turbine cascade p 6 A93-10189
- A low-speed aerodynamic model for harmonically oscillating aircraft configurations p 8 A93-11500
- Numerical simulation for aeroelasticity in turbomachines with vortex method. I - Theory and method p 53 A93-12452
- Aeroservoelastic analysis of an aircraft model incorporating the minimum state method for approximating unsteady aerodynamics p 154 A93-14258
- Calculation of sound field radiated by oscillating cascade p 231 A93-14269
- Dynamic stability, coupling and active control of elastic vehicles with unsteady aerodynamic forces modeling p 182 A93-14282
- Analytic continuation of Pade approximations to the unsteady kernel functions to obtain a better understanding of the analytic continuation of Pade approximations to unsteady parameters in general p 117 A93-14283
- An investigation of mode shift flutter suppression scheme for empennages p 182 A93-14288
- Extending the useful frequency of 'rigid' wind tunnel models with active control p 190 A93-14299
- The effect of wind tunnel constraint on unsteady aerodynamics experiments p 190 A93-14300
- Separation control and lift enhancement on airfoil using unsteady excitations p 118 A93-14305
- Cobra maneuver considerations p 182 A93-14306
- Modelling for aileron induced unsteady aerodynamic effects for parameter estimation p 118 A93-14323
- Prediction and control of slender-wing rock p 182 A93-14331
- Flow structures around a constant-rate pitching airfoil and mechanism of dynamic stall p 118 A93-14332
- Generalized vortex lattice method for oscillating lifting surfaces in subsonic flow p 123 A93-14555
- Method of simulating unsteady turbomachinery flows with multiple perturbations p 123 A93-14556
- Concurrent processing adaptation of aeroelastic analysis of propfans p 173 A93-14624
- Oblique wave evolution in a plane subsonic boundary layer p 124 A93-15178

- Modal analysis of unsteady aerodynamic response of subsonic annular cascade with steady loading under elastic vibration p 126 A93-15495
- A finite element study of incompressible flows past oscillating cylinders and aerofoils p 241 A93-17750
- Periodic Euler and Navier-Stokes solutions about oscillating airfoils p 241 A93-17799
- Experimental study on the unsteady aerodynamic response of a three dimensional cascade with oscillating blades p 242 A93-18499
- On space correlation of pressure pulsations on the streamlined surface before a step p 244 A93-19135
- Transmission of sound through a rotor p 447 A93-19183
- Nonlinear response and sonic fatigue of high speed aircraft p 399 A93-19211
- The dynamic characteristics of a high pressure turbine stage in a transient wind tunnel [ASME PAPER 92-GT-166] p 375 A93-19392
- Advances in the numerical integration of the 3-D Euler equations in vibrating cascades [ASME PAPER 92-GT-170] p 351 A93-19396
- An analysis system for blade forced response [ASME PAPER 92-GT-172] p 352 A93-19398
- Numerical solutions for unsteady subsonic vortical flows around loaded cascades [ASME PAPER 92-GT-173] p 250 A93-19399
- Forcing function effects on unsteady aerodynamic gust response. I - Forcing functions [ASME PAPER 92-GT-174] p 251 A93-19400
- Forcing function effects on unsteady aerodynamic gust response. II - Low solidity airfoil row response [ASME PAPER 92-GT-175] p 251 A93-19401
- Advanced Ducted Engines - Impact of unsteady aerodynamics on fan vibration properties [ASME PAPER 92-GT-228] p 252 A93-19445
- Unsteady aerodynamics and gust response in compressors and turbines [ASME PAPER 92-GT-422] p 258 A93-19570
- Some asymptotic aspects of the nonstationary aerofoil theory p 259 A93-19966
- Unsteady two- and three-dimensional Navier-Stokes simulations of multistage turbomachinery flows p 266 A93-20721
- Investigation of the dynamic inflow's influence on rotor control derivatives p 266 A93-20802
- A new technique for analysis of unsteady aerodynamic responses of cascade airfoils with blunt leading edge. I - Theory p 267 A93-20909
- Spatial adaptation procedures on tetrahedral meshes for unsteady aerodynamic flow calculations [AIAA PAPER 93-0670] p 269 A93-21116
- Unsteady effects of camber on the aerodynamic characteristics of a thin aerofoil moving near the ground p 270 A93-21719
- Conventional skin friction measurement techniques for strongly perturbed supersonic turbulent boundary layers p 271 A93-21863
- Numerical simulation of unsteady transonic nozzle flows p 272 A93-22230
- Study on steady and unsteady unstart phenomena due to compound choking and/or fluctuations in combustor of scramjet engines [AIAA PAPER 92-5102] p 359 A93-22372
- Numerical prediction of aerodynamic noise radiated from low Mach number turbulent wake [AIAA PAPER 93-0145] p 452 A93-22589
- What makes the Cobra maneuver possible? [AIAA PAPER 93-0183] p 367 A93-22609
- Aerodynamic foundations for use of unsteady aerodynamic effects in flight control [AIAA PAPER 93-0188] p 276 A93-22613
- Development of an engineering level prediction method for high angle of attack aerodynamics [AIAA PAPER 93-0208] p 278 A93-22626
- Unsteady compressible airfoil aerodynamics using an adaptive time-discontinuous GLS finite element method [AIAA PAPER 93-0339] p 281 A93-23027
- A hybrid structured-unstructured grid method for unsteady turbomachinery flow computations [AIAA PAPER 93-0387] p 282 A93-23066
- Single passage Euler analysis of oscillating cascade unsteady aerodynamics for arbitrary interblade phase angle [AIAA PAPER 93-0389] p 282 A93-23067
- Unsteady vortex dynamics and surface pressure topologies on a pitching wing [AIAA PAPER 93-0435] p 286 A93-23349
- Estimation of unsteady lift on a pitching airfoil from wake velocity surveys [AIAA PAPER 93-0437] p 286 A93-23351
- Adaptive finite volume upwind approach on mixed quadrilateral-triangular meshes p 287 A93-23542
- Modeling, analysis, and prediction of flutter at transonic speeds p 416 A93-23553
- NOZZD - A two dimensional explicit inviscid upwind code for convergent divergent nozzles p 460 A93-24080
- Incompressible potential flow calculation about harmonically oscillating three-dimensional configurations p 461 A93-24089
- Unsteady aerodynamics in airplane stall-spin departure [AIAA PAPER 93-0622] p 523 A93-24739
- Numerical investigations on airfoil performance subjected to aerodynamic interference from an upstream airfoil [AIAA PAPER 93-0639] p 463 A93-24754
- Experimental investigation of rotor/lifting surface interactions [AIAA PAPER 93-0871] p 469 A93-24932
- TGV tunnel entry simulations using a finite element code with automatic remeshing [AIAA PAPER 93-0890] p 471 A93-24950
- Computational analysis of methods for reduction of induced drag [AIAA PAPER 93-0524] p 474 A93-25536
- Nonreflecting boundary conditions for linearized unsteady aerodynamic calculations [AIAA PAPER 93-0882] p 475 A93-25553
- Determination of nonstationary aerodynamic loading on cascade blades in the case of dynamic changes of the angle of attack p 544 A93-26817
- Rotor blade unsteady aerodynamic gust response to inlet guide vane wakes [ASME PAPER 91-GT-129] p 475 A93-26897
- Calculation of three-dimensional supersonic flow past lifting surfaces p 477 A93-27607
- Physics of forced unsteady flow for a NACA 0015 airfoil undergoing constant-rate pitch-up motion p 478 A93-27922
- Current status of computational methods for transonic unsteady aerodynamics and aeroelastic applications p 480 A93-29175
- Linearized Euler predictions of unsteady aerodynamic loads in cascades p 480 A93-29318
- Unsteady wake effect on rotor vibratory airloadings p 509 A93-29439
- Passive drag reduction of a helicopter airfoil in an unsteady transonic flow p 482 A93-29440
- Numerical solution of non-isentropic transonic cascade flow by time-marching method p 679 A93-33715
- Real gas effects for compressible nozzle flows p 682 A93-33757
- An overview of aeroelasticity studies for the National Aero-Space Plane [AIAA PAPER 93-1313] p 732 A93-33889
- ISAC - A tool for aeroservoelastic modeling and analysis --- Interaction of Structures, Aerodynamics, and Control [AIAA PAPER 93-1421] p 726 A93-33974
- Wing flutter boundary prediction using unsteady Euler aerodynamic method [AIAA PAPER 93-1422] p 739 A93-33975
- Nonplanar Doublet-Point method for supersonic unsteady aerodynamics [AIAA PAPER 93-1588] p 682 A93-34120
- Extension of a nonlinear systems theory to general-frequency unsteady transonic aerodynamic responses [AIAA PAPER 93-1590] p 683 A93-34122
- Unsteady aerodynamics and flutter of propfans using a three-dimensional Full-Potential Solver [AIAA PAPER 93-1633] p 720 A93-34161
- Effect of an unsteady three-dimensional wake on elastic blade-flapping eigenvalues in hover p 683 A93-34260
- Vortex initiation during dynamic stall of an airfoil p 684 A93-34335
- Efficient hybrid scheme for the analysis of counter-rotating propellers p 688 A93-34483
- TURNS - A free-wake Euler/Navier-Stokes numerical method for helicopter rotors p 692 A93-35634
- Rotor blade airfoil design by numerical optimization and unsteady calculations [ONERA, TP NO. 1992-65] p 766 A93-35993
- Dynamic stall of sinusoidally oscillating three-dimensional swept and unswept wings in compressible flow p 766 A93-35995
- Aerodynamic and wake methodology evaluation using model UH-60A experimental data p 767 A93-35997
- Influence of coupling incidence and velocity variations on the airfoil dynamic stall p 767 A93-35999
- Transonic blade-vortex interactions - Noise reduction p 850 A93-37396
- Multiple pole rational-function approximations for unsteady aerodynamics p 769 A93-37404
- Comment on 'In-flight measurement of static pressures' p 807 A93-37407
- Extraction of inherent aerodynamic lag poles for the time domain representation of modal unsteady airfoils [AIAA PAPER 93-1591] p 829 A93-37443
- Validation of R85/METAR on the Puma RAE flight tests [ONERA, TP NO. 1992-123] p 802 A93-38597
- Application of European CFD methods for helicopter rotors in forward flight [ONERA, TP NO. 1992-125] p 772 A93-38599
- Aerodynamics of maneuvering slender wings with leading-edge separation p 778 A93-39401
- Unsteady transonic two-dimensional Euler solutions using finite elements p 778 A93-39412
- Vortex-induced energy separation in shear flows p 837 A93-39427
- Research in unsteady aerodynamics and computational aeroelasticity at the NASA Langley Research Center p 804 A93-39498
- Influence of stator-rotor gap on axial-turbine unsteady forcing functions p 899 A93-41918
- Subsonic/transonic cascade flutter using a full-potential solver p 861 A93-41934
- Numerical simulation of vortex shedding past triangular cylinders at high Reynolds number using a k-epsilon turbulence model p 871 A93-42873
- Supersonic turbomachine rotor flutter control by aerodynamic detuning p 899 A93-42884
- Newtonian and hypersonic flows over oscillating bodies of revolution. II - Parabolic bodies p 872 A93-42931
- Virtual zone Navier-Stokes computations for oscillating control surfaces [AIAA PAPER 93-3363] p 955 A93-45056
- An acceleration technique for time accurate calculations --- of unsteady flow around pitching delta wings p 957 A93-45092
- S-plane aerodynamics of nonplanar lifting surfaces p 958 A93-45134
- Time domain panel method for wings p 958 A93-45135
- Aileron and sideslip-induced unsteady aerodynamic modeling for lateral parameter estimation p 1007 A93-45144
- Control of unsteady shock-induced turbulent boundary layer separation upstream of blunt fins [AIAA PAPER 93-3281] p 969 A93-46839
- Unsteady aerodynamic response of two-dimensional subsonic and supersonic oscillating cascades with chordwise displacement and flexible deformation p 971 A93-46922
- AIAA Applied Aerodynamics Conference, 11th, Monterey, CA, Aug. 9-11, 1993, Technical Papers. Pts. 1 & 2 p 974 A93-47201
- Numerical simulation of wing-wall juncture flow for a pitching wing [AIAA PAPER 93-3401] p 974 A93-47203
- Unsteady ground effects on aerodynamic coefficients of finite wings with camber [AIAA PAPER 93-3423] p 976 A93-47218
- The moving wall effect vis-a-vis other dynamic stall flow mechanisms [AIAA PAPER 93-3424] p 1008 A93-47219
- Neural network prediction of three-dimensional unsteady separated flow fields [AIAA PAPER 93-3426] p 977 A93-47221
- Calculating crossflow separation using boundary layer computations coupled with an inviscid method [AIAA PAPER 93-3459] p 979 A93-47242
- Lift enhancement due to unsteady aerodynamics [AIAA PAPER 93-3538] p 986 A93-47289
- Three-dimensional analysis of turbine rotor flow including tip clearance [ASME PAPER 93-GT-111] p 987 A93-47446
- Intense studies on unsteady secondary separations and oscillating shock waves in three-dimensional shock waves/turbulent boundary layer interaction regions induced by sharp and blunt fins [AIAA PAPER 93-2939] p 1046 A93-48137
- Precise pitching airfoil computations by use of dynamic unstructured meshes [AIAA PAPER 93-2971] p 1049 A93-48165
- Experimental study of 3-D separation on a large scale model [AIAA PAPER 93-3007] p 1053 A93-48197
- Study of the near-wake structure of a subsonic base cavity flowfield using PIV [AIAA PAPER 93-3040] p 1056 A93-48221
- Unsteady Navier-Stokes simulation of the canard-wing-body ramp motion [AIAA PAPER 93-3058] p 1058 A93-48235
- Averaging techniques for steady and unsteady calculations of a transonic fan stage [AIAA PAPER 93-3065] p 1059 A93-48241
- Audio post-processing for shear layer calculations [AIAA PAPER 93-3075] p 1059 A93-48250
- Correlation of unsteady pressure and inflow velocity fields of a pitching rotor blade [AIAA PAPER 93-3082] p 1060 A93-48256

The effect of large scale unsteady motion on turbulent reattaching shear layer - Application to the supersonic compression ramp

[AIAA PAPER 93-3100] p 1061 A93-48273

AIAA Atmospheric Flight Mechanics Conference, Monterey, CA, Aug. 9-11, 1993, Technical Papers p 1125 A93-48301

Unsteady aerodynamic models for maneuvering aircraft

[AIAA PAPER 93-3626] p 1126 A93-48311

Numerical simulation of unsteady flow in a transonic cascade p 1066 A93-48502

Aerodynamic characteristics of a sweptforward-wing aircraft model in unsteady motion at large angles of attack in subsonic flow p 1068 A93-48902

Euler calculations of unsteady interaction of advancing rotor with a line vortex p 1071 A93-49016

The effect of unsteady blade loading on the aeroacoustics of a pusher propeller [AIAA PAPER 93-1805] p 1173 A93-49694

Blade row interaction effects on flutter and forced response p 1114 A93-49911

[AIAA PAPER 93-2084] p 1114 A93-49911

Unsteady aerodynamics and flutter based on the potential equation p 1079 A93-49913

[AIAA PAPER 93-2086] p 1079 A93-49913

Compressor unsteady aerodynamic response to rotating stall and surge excitations p 1079 A93-49914

[AIAA PAPER 93-2087] p 1079 A93-49914

Using a diagonal implicit algorithm to calculate transonic nozzle flow p 1082 A93-50119

[AIAA PAPER 93-2345] p 1082 A93-50119

A numerical study of the unsteady processes associated with the type IV shock interaction p 1083 A93-50221

[AIAA PAPER 93-2479] p 1083 A93-50221

Analytic methods for design of wave cycles for wave rotor core engines p 1121 A93-50253

[AIAA PAPER 93-2523] p 1121 A93-50253

A fourth-order MUSCL finite-difference scheme for solving the unsteady compressible Euler equations p 1086 A93-51121

A new technique for analysis of unsteady aerodynamic responses of cascade airfoils with blunt leading edge - Unsteady aerodynamic responses of the cascade in incompressible flow p 1086 A93-51122

Analysis of wake-induced unsteady flow in axial compressors - Radial variations of wake excitation forces estimated by strip theory p 1086 A93-51123

Implicit schemes for unsteady Euler equations on unstructured meshes p 1171 A93-51944

[ONERA, TP NO. 1993-64] p 1171 A93-51944

Unsteady aerodynamic behavior of an airfoil with and without a slot p 1093 A93-52007

Computation of subsonic viscous and transonic viscous-inviscid unsteady flow p 1094 A93-52012

Application of nonlinear systems theory to transonic unsteady aerodynamic responses p 1095 A93-52438

Effect of leading-edge geometry on delta wing unsteady aerodynamics p 1095 A93-52457

Boundary layer and pressure measurements on a cylinder with unsteady circulation control p 1177 A93-53207

Fast three-dimensional vortex method for unsteady wake calculations p 1178 A93-53233

Unsteady aerodynamic characteristics of three rectangular wings of different aspect ratios p 1180 A93-53575

Analysis of unstarted supersonic flutter in cascade by semiactuator disk theory p 1181 A93-53841

Numerical analysis of the flow through a centrifugal impeller by vortex distribution model of a boundary layer. I - Theoretical analysis p 1182 A93-53843

An implicit difference scheme of Euler equation for unsteady transonic flow p 1182 A93-53852

Forcing function modeling for flow induced vibration [ISABE 93-7027] p 1196 A93-54003

The unsteady flow past a supersonic splitter plate [ISABE 93-7047] p 1185 A93-54023

The forms of unsteady concentrated vortex-breakdown and its reactions to disturbance p 1231 A93-54594

Reynolds stress profiles in the near wake of an oscillating airfoil p 1236 A93-55380

ONERA calculation model of dynamic flow separation on an airfoil section p 1238 A93-56212

Forced unsteady separated flows on a 45 degree delta wing p 82 A93-10305

Control of lift and drag in unsteady flows [AD-A253146] p 17 N93-10340

Further noise measurements in a slotted cryogenic wind tunnel [RAE-TM-AERO-2201] p 101 N93-10805

Unsteady propeller/wing aerodynamic interactions p 24 N93-12190

New acceleration potential method for supersonic unsteady aerodynamics of lifting surfaces, further extension of the nonplanar supersonic doublet point method, and nonlinear, nongradient optimized rational function approximations for supersonic, transient response unsteady aerodynamics p 25 N93-12344

An investigation of the dynamic response of lifting surfaces with concentrated structural nonlinearities p 162 N93-13807

The unsteady aerodynamics of a delta wing undergoing large-amplitude pitching motions p 134 N93-13929

A compilation of the mathematics leading to the doublet lattice method [AD-A256304] p 136 N93-14441

The effect of wake dynamics on rotor eigenvalues in forward flight p 137 N93-14595

Multi-disciplinary optimization of aeroservoelastic systems [NASA-CR-191255] p 220 N93-14766

Estimation of unsteady lift on a pitching airfoil from wake velocity surveys [NASA-TM-105947] p 138 N93-14791

On flutter behavior of a 2-D compressor cascade in incompressible flow [DLR-FB-91-26] p 418 N93-16543

Beyond the frequency limits of time-linearized methods [NLR-TP-91216-U] p 295 N93-17929

Introduction to Flutter of Winged Aircraft, volume 1 [VKI-LS-1992-01] p 372 N93-18142

The unified method of aeroelasticity p 372 N93-18143

Computational Fluid Dynamics, volume 2 [VKI-LS-1992-04-VOL-2] p 421 N93-18563

Algorithm development with applications to aerodynamics and aeroelasticity p 422 N93-18566

Analytic formulation of unsteady profile aerodynamics and its application to simulation of rotors [ESA-TT-1244] p 485 N93-21659

Aerodynamic foundations for use of unsteady aerodynamic effects in flight control p 695 N93-25274

Application of finite-state inflow to flap-lag-torsion damping in hover p 714 N93-25486

An aerodynamic model for one and two degree of freedom wing rock of slender delta wings [NASA-CR-193130] p 781 N93-27150

Leading edge vortices in a chordwise periodic flow p 782 N93-27218

Transonic flows on an oscillating airfoil and their effect on the flutter-boundary [DLR-FB-92-08] p 790 N93-29006

Unsteady vortex loop/dipole theory applied to the work and acoustics of an ideal low speed propeller [AD-A264057] p 876 N93-29891

The influence of variable flow velocity on unsteady airfoil behavior [DLR-FB-92-22] p 988 N93-31320

UNSTEADY FLOW

Numerical simulation of compressible mixing zones p 10 A93-12427

Computational studies of the characteristics of axial compressor cascades and stages in unsteady incoming flow p 13 A93-12805

Nonstationary flow of a viscous incompressible fluid past an airfoil p 79 A93-12922

Finite memory approximations for a singular neutral system arising in aeroelasticity p 97 A93-13246

Numerical investigation of the unsteady flow through a counter-rotating fan p 112 A93-14166

Flow characteristics of an S-shaped inlet at high incidence p 114 A93-14213

Calculation of 3-D unsteady subsonic flow with separation bubble using singularity method p 115 A93-14251

Separation control and lift enhancement on airfoil using unsteady excitations p 118 A93-14305

Development of a system for aerodynamic fast-response probe measurements p 203 A93-14325

Generation of flow disturbances in transonic wind tunnels p 119 A93-14354

Unsteady turbulent skin-friction measurement in an adverse pressure gradient p 206 A93-14545

Hybrid grid approach to study dynamic stall p 122 A93-14548

Unsteady transonic aerodynamic loadings on the airfoil caused by heaving, pitching oscillations and control surface p 126 A93-15627

Unsteady transonic flow past a quarter-plane p 127 A93-16664

Study on unsymmetrical supersonic nozzle flows p 127 A93-16933

Unsteady pressures under impinging jets in crossflows p 399 A93-19220

Recent advances in simulating unsteady flow phenomena brought about by passage of shock waves in a linear turbine cascade [ASME PAPER 92-GT-4] p 245 A93-19277

Modified surge in an axial flow compressor [ASME PAPER 92-GT-59] p 247 A93-19309

Analysis of steady and unsteady turbine cascade flows by a locally implicit hybrid algorithm [ASME PAPER 92-GT-127] p 249 A93-19361

An inviscid-viscous interaction approach to the calculation of dynamic stall initiation on airfoils [ASME PAPER 92-GT-128] p 249 A93-19362

Calculation of three-dimensional unsteady flows in turbomachinery using the linearized harmonic Euler equations [ASME PAPER 92-GT-136] p 249 A93-19368

Unsteady pressure measurements in a rotating centrifugal impeller [ASME PAPER 92-GT-152] p 402 A93-19379

Profile losses of an annular turbine cascade in unsteady periodic flow [ASME PAPER 92-GT-153] p 249 A93-19380

Unsteady pressure measurements on the rotor of a model turbine stage in a transient flow facility [ASME PAPER 92-GT-156] p 250 A93-19383

On the conservation of rothalpy in turbomachines [ASME PAPER 92-GT-217] p 252 A93-19439

An approach for multi-stage calculations incorporating unsteadiness [ASME PAPER 92-GT-282] p 253 A93-19474

Calculation of wake-induced unsteady flow in a turbine cascade [ASME PAPER 92-GT-306] p 255 A93-19496

Measurement of unsteady flow and heat transfer in a linear turbine cascade [ASME PAPER 92-GT-323] p 256 A93-19507

Analysis of jet/wake mixing in a vaneless diffuser [ASME PAPER 92-GT-418] p 258 A93-19566

Spatial adaptation procedures on tetrahedral meshes for unsteady aerodynamic flow calculations [AIAA PAPER 93-0670] p 269 A93-21116

Some unsteady fluid forces on pump impellers p 413 A93-22265

Direct numerical simulation of turbulent flow in a square duct [AIAA PAPER 93-0198] p 277 A93-22618

Calculation of the flowfield around an airfoil with spoiler [AIAA PAPER 93-0527] p 284 A93-23268

An improved numerical model for wave rotor design and analysis [AIAA PAPER 93-0482] p 361 A93-23384

Shock oscillation in two-dimensional, inviscid, unsteady channel flow p 288 A93-23563

Comparison of PMARC and analytic results for two-dimensional unsteady airfoils [AIAA PAPER 93-0636] p 463 A93-24752

A moving mesh system for the calculation of unsteady flows [AIAA PAPER 93-0641] p 464 A93-24756

The analysis of unsteady, three-dimensional flow separation [AIAA PAPER 93-0642] p 540 A93-24757

Navier-Stokes calculations for the unsteady flowfield of turbomachinery [AIAA PAPER 93-0676] p 465 A93-24786

A numerical study of unsteady supersonic compression ramp flows [AIAA PAPER 93-0883] p 470 A93-24943

Physics of forced unsteady flow for a NACA 0015 airfoil undergoing constant-rate pitch-up motion p 478 A93-27522

Prediction of asymmetric vortical flows around slender bodies using Navier-Stokes equations p 478 A93-27925

Nonsteady, one-dimensional, internal, compressible flows - Theory and applications --- Book [ISBN 0-19-507358-4] p 548 A93-28749

Linearized Euler predictions of unsteady aerodynamic loads in cascades p 480 A93-29318

Structure-attached corotational fluid grid for transient aeroelastic computations p 480 A93-29326

A numerical method of unsteady separating flow over delta wings p 681 A93-33746

Studies of the dynamic stall problem on airfoils p 681 A93-33747

A unified hypersonic/supersonic method for aeroelastic applications including shock-unsteady wave interaction [AIAA PAPER 93-1317] p 738 A93-33892

Unsteady transonic potential flow over a flexible fuselage [AIAA PAPER 93-1593] p 683 A93-34124

An integrated flow simulation system on a parallel computer. I - Basic concept. II - The flow solver p 688 A93-34370

Unsteady supersonic flow around a blunt body in thermal inhomogeneities in turbulent shock layer flows p 691 A93-35266

Results from a conical Euler methodology developed for unsteady vortical flows p 692 A93-35612

Deforming grid variational principle for unsteady small disturbance flows in cascades p 692 A93-35623

Unsteady blade pressures on a propfan at takeoff - Euler analysis and flight data p 810 A93-37389

Domain splitting explicit time marching scheme for simulation of unsteady high Reynolds number flow p 830 A93-38140

Contribution of visualization to the study of unsteady aspects of vortex breakdown [ONERA, TP NO. 1992-93] p 771 A93-38576

Vortex-induced energy separation in shear flows p 837 A93-39427

Newtonian and hypersonic flows over oscillating bodies of revolution. I - Circular cones p 857 A93-39942

Higher-order-accurate upwind schemes for solving the compressible Euler and Navier-Stokes equations p 863 A93-42441

Dynamic overset grid communication on distributed memory parallel processors [AIAA PAPER 93-3311] p 1036 A93-45007

Two-dimensional CFD modeling of wave rotor flow dynamics [AIAA PAPER 93-3318] p 952 A93-45014

Virtual zone Navier-Stokes computations for oscillating control surfaces [AIAA PAPER 93-3363] p 955 A93-45056

Time-accurate simulation of a self-excited oscillatory supersonic external flow with a multi-block solution-adaptive mesh algorithm [AIAA PAPER 93-3387] p 956 A93-45078

A simulation technique for 2-D unsteady inviscid flows around arbitrarily moving and deforming bodies of arbitrary geometry [AIAA PAPER 93-3391] p 956 A93-45082

Unsteady flow simulation on a parallel computer p 1022 A93-45089

Computation of shock diffraction in external and internal flows p 1024 A93-45537

Computation of unsteady nozzle flows p 960 A93-45543

Instantaneous topology of the unsteady leading-edge vortex at high angle of attack p 961 A93-45728

Visual observations of supersonic transverse jets p 965 A93-46750

Turbine blade forces due to partial admission p 1029 A93-46928

Prediction of three-dimensional low frequency unsteady transonic flow and forced vibration in axial turbine stages p 971 A93-46934

Numerical analysis of airfoil cascades subjected to unsteady flow p 972 A93-46944

Numerical solution of steady and unsteady Euler equations p 973 A93-46988

Unsteady flow computations for a three-dimensional cavity with and without an acoustic suppression device [AIAA PAPER 93-3402] p 974 A93-47204

Neural network prediction of three-dimensional unsteady separated flow fields [AIAA PAPER 93-3426] p 977 A93-47221

High resolution numerical simulation of the linearized Euler equations in conservation law form [AIAA PAPER 93-2934] p 1148 A93-48132

Three-dimensional unsteady separating flows around an oscillatory forward-swept wing [AIAA PAPER 93-2976] p 1050 A93-48170

A high-order streamline Godunov scheme for steady hypersonic equilibrium flows [AIAA PAPER 93-2997] p 1053 A93-48187

A solution-adaptive hybrid-grid method for the unsteady analysis of turbomachinery [AIAA PAPER 93-3015] p 1148 A93-48204

Dynamic-overlapped-grid simulation of aerodynamically determined relative motion [AIAA PAPER 93-3018] p 1055 A93-48205

A viscous-inviscid interaction method for 2-D unsteady, compressible flows [AIAA PAPER 93-3019] p 1055 A93-48206

Clebsch variable model for unsteady inviscid transonic flow with strong shock waves [AIAA PAPER 93-3025] p 1055 A93-48210

Unsteady aerodynamic flow phenomena in a transonic compressor stage [AIAA PAPER 93-1868] p 1075 A93-49743

Unsteady, three-dimensional, Navier-Stokes simulations of multistage turbomachinery flows [AIAA PAPER 93-1979] p 1153 A93-49826

Spatial domain characterization of abrupt rotating stall initiation in an axial flow compressor [AIAA PAPER 93-2238] p 1081 A93-50040

Analysis of wake-induced unsteady flow in axial compressors - Radial variations of wake excitation forces estimated by strip theory p 1086 A93-51123

On boundary-layer transition in transonic flow p 1087 A93-51280

New calculation methods contribution on turbomachinery design and development [ONERA, TP NO. 1993-60] p 1092 A93-51940

Numerical simulation of unsteady flow induced by a flat plate moving near ground p 1094 A93-52432

Investigation of vortex development on a pitching slender body of revolution p 1095 A93-52445

Flowfield simulation about the stratospheric observatory for infrared astronomy p 1095 A93-52446

Experimental investigation into the mechanism of discrete frequency noise (DFN) generation from a NACA 0012 blade p 1225 A93-53194

Low-Reynolds-number k-epsilon model for unsteady turbulent boundary-layer flows p 1177 A93-53208

A 2-D compressible N-S simulation of starting- and stalling-flows in a compressor cascades system [ISABE 93-7006] p 1183 A93-53982

Three-dimensional flow analysis inside turbomachinery stages with steady and unsteady Navier-Stokes method [ISABE 93-7095] p 1186 A93-54071

Boundary conditions for unsteady supersonic inlet analyses [ISABE 93-7104] p 1187 A93-54080

Study on flow field around slender diamond cone traveling at hypersonic speed p 1189 A93-54314

Partial admission and unsteady flow in radial turbines p 81 A93-10059

Forced unsteady separated flows on a 45 degree delta wing p 82 A93-10305

Control of lift and drag in unsteady flows [AD-A253146] p 17 A93-10340

Interactive grid generation program for CAP-TSD [NASA-TM-102705] p 17 A93-10349

LDV Measurements of unsteady flow fields in radial turbine [AD-A253592] p 19 A93-10648

System and method for cancelling expansion waves in a wave rotor [NASA-CASE-LEW-15218-1] p 86 A93-11172

Effects of sweep on the physics of unsteady shock-induced turbulent separated flows [AD-A247035] p 22 A93-11742

Unsteady propeller/wing aerodynamic interactions p 24 A93-12190

An improved numerical model for wave rotor design and analysis [NASA-TM-105915] p 60 A93-12418

Investigation of hot streak migration and film cooling effects on heat transfer in rotor/stator interacting flows, report 1 [AD-A250688] p 102 A93-12490

Navier-Stokes simulations of unsteady transonic flow phenomena [NASA-TM-103962] p 129 A93-12721

Mathematical problems in inviscid hypersonic flow p 131 A93-13451

L.D.V. measurements of unsteady flow fields in radial turbine [AD-A255728] p 221 A93-15065

Preliminary efforts toward development of data handling and analysis software for unsteady flow measurements: An application for aeroelastic transonic flow configurations p 291 A93-16768

Experimental Investigation of Nozzle/Plume Aerodynamics at Hypersonic Speeds [NASA-CR-191368] p 386 A93-18085

Simulation of unsteady rotational flow over propfan configuration [NASA-CR-192234] p 296 A93-18585

Rotating stall: Modeling-measurement techniques; unsteady loss-unsteady flow field p 424 A93-18732

Development of a boundary element method program for numerical analysis of supersonic unsteady flow p 300 A93-19283

Unsteady Navier-Stokes method for accelerated moving airfoils with separation [DLR-FB-92-03] p 485 A93-21763

Further development of the CANAERO computer code to include a time-stepping capability [DREA-CR-91-478] p 562 A93-21820

Prediction of unsteady flows in turbomachinery using the linearized Euler equations on deforming grids [NASA-CR-192919] p 747 A93-25109

A simple, approximate model of parachute inflation [DE93-002465] p 694 A93-25121

Navier-Stokes simulations of unsteady transonic flow phenomena p 697 A93-25542

Conical Euler analysis and active roll suppression for unsteady vortical flows about rolling delta wings [NASA-TP-3259] p 701 A93-26134

Unsteady airfoil flow solutions on moving zonal grids [AD-A261925] p 701 A93-26198

An aerodynamic model for one and two degree of freedom wing rock of slender delta wings [NASA-CR-193130] p 781 A93-27150

Leading edge vortices in a chordwise periodic flow p 782 A93-27218

Investigation of forced unsteady separated flows using velocity-vorticity form of Navier-Stokes equations p 840 A93-27451

Dynamic airfoil stall investigations p 786 A93-27453

Simultaneous mapping of the unsteady flow fields by Particle Displacement Velocimetry (PDV) p 786 A93-27454

Discrete-vortex simulation of pulsating flow on a turbulent leading-edge separation bubble p 787 A93-27457

Prediction of vortex breakdown on a delta wing p 787 A93-27459

Analysis of unsteady wave processes in a rotating channel [NASA-CR-191154] p 816 A93-28617

Stabilized space-time finite element formulations for unsteady incompressible flows involving fluid-body interactions p 843 A93-29040

Flow phenomena in turbomachines [AD-A263049] p 930 A93-29141

Keynote address: Unsteady, multimode transition in gas turbine engines p 901 A93-29927

Determination of surface heat transfer and film cooling effectiveness in unsteady wake flow conditions p 902 A93-29933

Simulation, characterization and control of forced unsteady viscous flows using Navier-Stokes equations [AD-A264333] p 934 A93-30369

Computation of a delta-wing roll-and-hold maneuver [AD-A264704] p 909 A93-30498

A theoretical and computational study on active wake control p 878 A93-30892

TOLM: A Transonic Doublet Lattice Method for 3D potential unsteady transonic flow calculation [DLR-FB-92-25] p 988 A93-31171

Calculations on unsteady type 4 interaction at Mach 8 [AD-A265214] p 990 A93-32004

NLR inviscid transonic unsteady loads prediction methods in aerolasticity [NLR-TP-91410-U] p 990 A93-32358

UNSWEEP WINGS

LDV flowfield measurements on a straight and swept wing with a simulated ice accretion [AIAA PAPER 93-0300] p 280 A93-23001

Application of a flush airdata sensing system to a wing leading edge (LE-FADS) [AIAA PAPER 93-0634] p 516 A93-24750

Application of a flush airdata sensing system to a wing leading edge (LE-FADS) [NASA-TM-104267] p 518 A93-20163

Integrated structural design, vibration control, and aeroelastic tailoring by multiobjective optimization p 1030 A93-31137

UPLINKING

Uplink laser propagation measurements through the sea surface, haze and clouds [AD-A264687] p 935 A93-30553

UPPER ATMOSPHERE

A joint Soviet-Bulgarian scientific program for free-flight and tethered aerostat observations p 2 A93-11374

Effect of the formation of excited oxygen molecules on the kinetics of exchange reactions and the heat flux during braking in the upper layers of the atmosphere p 1070 A93-48975

Development of a tethered satellite force transducer p 1251 A93-54368

UPPER SURFACE BLOWING

Static roll moment characteristics of asymmetric tangential leading edge blowing on a delta wing at high angles of attack [AIAA PAPER 93-0052] p 261 A93-20165

A wind tunnel investigation to determine buffet countermeasures for STOL aircraft alpha-sweep flight testing [NAL-TR-1129] p 65 A93-12362

Wind tunnel investigation of a twin-engine jet transport semi-span model with upper surface blown jet flap [NAL-TR-1134] p 26 A93-12503

High-speed aerodynamics of upper surface blowing aircraft configurations p 132 A93-13729

UPSTREAM

Viscous interaction upstream and downstream of a turbine stator cascade with a periodic wake field [ASME PAPER 92-GT-162] p 250 A93-19388

Numerical simulation of upstream disturbance on flows around a slender body [AIAA PAPER 93-2956] p 1047 A93-48150

Calculation of perturbation propagation upstream in a hypersonic laminar boundary layer p 1086 A93-50968
 Volume 2: Explicit, multistage upwind schemes for Euler and Navier-Stokes equations
 [NASA-CR-191647] p 418 N93-16558

UPWASH
 Thrust imparted to an airfoil by passage through a sinusoidal upwash field p 1178 A93-53219

UPWIND SCHEMES (MATHEMATICS)
 Viscous equilibrium computations using program LAURA p 8 A93-12002
 Computation of viscous compressible flows using an upwind algorithm and unstructured meshes p 9 A93-12163
 A comparison of upwind schemes for computation of three-dimensional hypersonic real-gas flows
 [AIAA PAPER 92-4350] p 15 A93-13306
 A new rotated upwind difference scheme for the Euler equations p 261 A93-20179
 [AIAA PAPER 93-0066] p 261 A93-20179
 Flux limiters in a rotated upwind scheme for the Euler equations p 262 A93-20180
 [AIAA PAPER 93-0067] p 262 A93-20180
 Comparison of limiters in flux-split algorithms for Euler equations p 262 A93-20181
 [AIAA PAPER 93-0068] p 262 A93-20181
 Accurate solution of the 2D Euler equations with an efficient cell-vertex upwind scheme p 262 A93-20183
 [AIAA PAPER 93-0071] p 262 A93-20183
 A comparison of the predictive capabilities of several turbulence models using upwind and central-difference computer codes p 268 A93-21102
 [AIAA PAPER 93-0192] p 268 A93-21102
 Adaptive finite volume upwind approach on mixed quadrilateral-triangular meshes p 287 A93-23542
 NO22D - A two dimensional explicit inviscid upwind code for convergent divergent nozzles p 460 A93-24080
 An upwind formulation for the solution of thin-layer Navier-Stokes equations p 461 A93-24088
 An upwind, kinetic flux-vector splitting method for flows in chemical and thermal non-equilibrium p 472 A93-24954
 [AIAA PAPER 93-0894] p 472 A93-24954
 A third order upwind scheme for aero-acoustic applications p 564 A93-25504
 [AIAA PAPER 93-0149] p 564 A93-25504
 Recent developments in high order K-exact reconstruction on unstructured meshes p 475 A93-25546
 [AIAA PAPER 93-0668] p 475 A93-25546
 A kind of improved flux-split method for solving the Euler equations p 681 A93-33739
 Real gas effects for compressible nozzle flows p 682 A93-33757
 Comparison of several convection discretization schemes for all Mach number arbitrary 2D flows p 685 A93-34345
 Computation of turbulent compressible flows on a DLR wing and a blade to blade passage using an upwind scheme p 687 A93-34359
 Application of the multigrid solution technique to hypersonic entry vehicles p 858 A93-41049
 [AIAA PAPER 93-2721] p 858 A93-41049
 Comparison of coordinate-invariant and coordinate-aligned upwinding for the Euler equations [AIAA PAPER 93-3306] p 858 A93-41053
 International Symposium on Computational Fluid Dynamics, 4th, Univ. of California, Davis, Sept. 9-12, 1991, Selected Papers p 862 A93-42426
 A multi-dimensional upwind scheme for the Euler equations on structured grids p 862 A93-42430
 FUM - An efficient MmB solver for steady inviscid flows p 862 A93-42431
 Higher-order-accurate upwind schemes for solving the compressible Euler and Navier-Stokes equations p 863 A93-42441
 Hypersonic cone flow predictions using an implicit upwind space-marching code p 865 A93-42588
 The application of an adaptive upwind unstructured grid solution algorithm to the simulation of compressible laminar viscous flows over compression corners p 866 A93-42594
 Implicit upwind finite-difference simulation of laminar hypersonic flow over a 2D ramp p 867 A93-42600
 An upwind relaxation method for hypersonic viscous flows over a double-ellipsoidal body p 867 A93-42606
 Contribution to Problem 6 using an upwind Euler solver with unstructured meshes p 869 A93-42627
 Application of program LAURA to thermochemical nonequilibrium flow through a nozzle p 871 A93-42644
 On the accuracy and efficiency of CFD methods in real gas hypersonics p 871 A93-42869
 Computations of inviscid compressible flows using fluctuation-splitting on triangular meshes p 950 A93-44999
 [AIAA PAPER 93-3301] p 950 A93-44999
 Field by field hybrid upwind splitting methods [AIAA PAPER 93-3302] p 950 A93-45000

A multi-dimensional kinetic-based upwind solver for the Euler equations p 950 A93-45001
 [AIAA PAPER 93-3303] p 950 A93-45001
 New upwind dissipation models with a multidimensional approach p 950 A93-45002
 [AIAA PAPER 93-3304] p 950 A93-45002
 An extended Lagrangian method p 951 A93-45003
 [AIAA PAPER 93-3305] p 951 A93-45003
 Three-dimensional unstructured grid Euler computations using a fully-implicit, upwind method p 953 A93-45031
 [AIAA PAPER 93-3337] p 953 A93-45031
 An upwind multigrid algorithm for calculating flows on unstructured grids p 957 A93-45088
 Numerical solution of Navier-Stokes equations and k-omega turbulence model equations using a staggered upwind method p 1049 A93-48162
 [AIAA PAPER 93-2968] p 1049 A93-48162
 The prediction of viscous nonequilibrium hypersonic flows about ablating configurations using an upwind parabolized Navier-Stokes code p 1053 A93-48188
 [AIAA PAPER 93-2998] p 1053 A93-48188
 A detailed study of mean-flow solutions for stability analysis of transitional flows p 1057 A93-48232
 [AIAA PAPER 93-3052] p 1057 A93-48232
 Upwind finite-volume Navier-Stokes computations on unstructured triangular meshes p 1070 A93-49011
 The computation over unstructured grids of inviscid hypersonic reactive flow by upwind finite-volume schemes p 1073 A93-49532
 A comparison between centered and upwind schemes for two-phase compressible flows p 1083 A93-50120
 [AIAA PAPER 93-2346] p 1083 A93-50120
 A second-order upwind finite-volume method for the Euler solution on unstructured triangular meshes p 1087 A93-51738
 Upwind-biased, point-implicit relaxation strategies for hypersonic flowfield simulations on supercomputers p 1175 A93-52770
 Three-dimensional mesh embedding for the Navier-Stokes equations using upwind control volumes p 1239 A93-56402
 Navier-Stokes simulations of unsteady transonic flow phenomena p 697 N93-25542

USER MANUALS (COMPUTER PROGRAMS)
 An interactive preprocessor for the NASA engine performance program p 56 N93-10983
 [NASA-TM-105786] p 56 N93-10983
 BLSTA: A boundary layer code for stability analysis [NASA-CR-4481] p 220 N93-14797
 User's manual for Interactive Data Display System (IDDS) p 441 N93-16613
 [NASA-TM-105572] p 441 N93-16613
 Investigation of advanced counterrotation blade configuration concepts for high speed turboprop systems. Task 4: Advanced fan section aerodynamic analysis computer program user's manual p 364 N93-18702
 [NASA-CR-187127] p 364 N93-18702
 Management of Automatic Data Processing (ADP) system documentation in the Department of Defense [AD-A258507] p 571 N93-20048
 User's manual for UCAP: Unified Counter-Rotation Aero-Acoustics Program p 852 N93-27148
 [NASA-CR-191034] p 852 N93-27148
 Dynamic System Coupler Program (DYSCO 4.1). Volume 2: User's manual p 848 N93-27589
 [AD-B131157L] p 848 N93-27589
 Dynamic System Coupler Program (DYSCO 4.1). Volume 3: User's manual supplement p 848 N93-27590
 [AD-B131158L] p 848 N93-27590
 Operation of the helicopter antenna radiation prediction code p 1030 N93-31110
 [NASA-CR-193259] p 1030 N93-31110
 WBNFLOW: Multi-grid/multi-block potential solver for compressible flow. User's guide p 1031 N93-31146
 [FFA-TN-1992-43] p 1031 N93-31146

USER REQUIREMENTS
 Environmental definition of a multi-platform avionics system p 896 A93-42855
 Formal representation of the requirements for an Advanced Subsonic Civil Transport (ASCT) flight control system p 98 N93-12346
 [NASA-CR-189699] p 98 N93-12346
 Coordinating Council. Sixth Meeting: Who Are Our Key Users? p 234 N93-12672
 [NASA-TM-108021] p 234 N93-12672

UTILITY AIRCRAFT
 Results of testing of models of joint-wing utility class aircraft p 157 A93-14643
 [SAE PAPER 921013] p 157 A93-14643

V-22 AIRCRAFT
 V-22 program overview p 457 A93-24299
 [AIAA PAPER 92-4277] p 457 A93-24299
 The effects of composite material on the configuration and design of the V-22 wing p 507 A93-27964
 Crack growth/damage tolerance analysis methods as applied to V-22 fuselage and empennage p 795 A93-35948
 Civil tiltrotor noise impact prediction methodology p 850 A93-35967
 Cost/weight savings for the V-22 wing stow p 797 A93-35981
 Fail safety aspects of the V-22 pylon conversion actuator p 798 A93-35984
 V-22 tiltrotor Flight Test Development p 800 A93-36021
 Blade twist-design of experiment p 800 A93-36025
 The V-22 for SOF p 800 A93-36026
 V-22 nacelle conversion actuator p 889 A93-40438
 Moving body overset grid methods for complete aircraft tiltrotor simulations p 954 A93-45044
 [AIAA PAPER 93-3350] p 954 A93-45044
 The V-22 Osprey: A case analysis p 164 N93-14601
 [AD-A256445] p 164 N93-14601
 Tiltrotor aircraft noise: A summary of the presentations and discussions at the 1991 FAA/Georgia Tech Workshop p 232 N93-14912
 [DOT/FAA/RD-91/23] p 232 N93-14912
 Fabrication of the V-22 composite AFT fuselage using automated fiber placement p 920 N93-30443

V/STOL AIRCRAFT
 Transport resurrection p 41 A93-12434
 Determination of YAV-8B Reaction Control System bleed flow usage p 54 A93-13330
 [AIAA PAPER 92-4232] p 54 A93-13330
 Infrared flow visualization of V/STOL aircraft p 80 A93-13343
 [AIAA PAPER 92-4253] p 80 A93-13343
 Ground vortex formation for uniform and nonuniform jets impinging on a ground plane p 80 A93-13362
 [AIAA PAPER 92-4251] p 80 A93-13362
 Aeroacoustic environment of an advanced short takeoff and vertical landing aircraft in hover p 231 A93-14539
 Some aspects of variable geometry gas turbine operation p 356 A93-19556
 [ASME PAPER 92-GT-407] p 356 A93-19556
 The tilt wing advantage - for high-speed VSTOL aircraft p 506 A93-27903
 Optimal takeoff of a helicopter for category A V/STOL operations p 525 A93-28611
 Calculation of V/STOL aircraft aerodynamics with deflected jets in ground effect p 986 A93-47287
 [AIAA PAPER 93-3530] p 986 A93-47287
 Performance characteristics of a variable-area vane nozzle for vectoring an ASTOVL exhaust jet up to 45 deg p 1118 A93-50189
 [AIAA PAPER 93-2437] p 1118 A93-50189
 Effects of flow-path variations on internal reversing flow in a tailpipe offtake configuration for ASTOVL aircraft [AIAA PAPER 93-2438] p 1118 A93-50190
 Study of a circular cross section thrust augmenting ejector p 1118 A93-50191
 [AIAA PAPER 93-2439] p 1118 A93-50191
 Internal performance of Highly Integrated Deployable Exhaust Nozzles p 1084 A93-50288
 [AIAA PAPER 93-2570] p 1084 A93-50288
 The application of scheduled H-infinity controllers to a VSTOL aircraft p 1135 A93-52249
 Advanced aerodynamic airframe/nozzle integration [ISABE 93-7099] p 1187 A93-54075
 Initial piloted simulation study of geared flap control for tilt-wing V/STOL aircraft p 64 N93-10741
 [NASA-TM-103872] p 64 N93-10741
 ASTOVL model engine simulators for wind tunnel research p 192 N93-13213
 Experimental performance of a ventral nozzle with pitch and yaw vectoring capability for SSTOVL aircraft [NASA-TM-106054] p 722 N93-25129
 ASTOVL combat aircraft design synthesis and optimization p 717 N93-25704
 Jet-induced ground effects on a parametric flat-plate model in hover p 700 N93-26099
 [NASA-TM-104001] p 700 N93-26099
 Performance characteristics of a variable-area vane nozzle for vectoring an ASTOVL exhaust jet up to 45 deg p 813 N93-27131
 [NASA-TM-106114] p 813 N93-27131
 The ground vortex flow field associated with a jet in a cross flow impinging on a ground plane for uniform and annular turbulent axisymmetric jets p 789 N93-28449
 [NASA-CR-4513] p 789 N93-28449
 Effects of flow-path variations on internal reversing flow in a tailpipe offtake configuration for ASTOVL aircraft [NASA-TM-106149] p 900 N93-29065

VACUUM
 LARZAC HP turbine disk crack initiation and propagation spin pit test p 176 N93-14892

VACUUM CHAMBERS

Development of ultra-hypersonic shock tunnel for aerodynamics test p 376 A93-21900

VACUUM MELTING

INCOLOY 908, a low coefficient of expansion alloy for high-strength cryogenic applications. I - Physical metallurgy p 534 A93-25686

VALLEYS

Land subsidence and problems affecting land use at Edwards Air Force Base and vicinity, California, 1990 [PB93-182236] p 1036 A93-32191

VALUE ENGINEERING

On the basis of experience: Built in product reliability [PNR-90932] p 85 A93-11034

VALVES

External stress-corrosion cracking of a 1.22-m-diameter type 316 stainless steel air valve [NASA-TP-3190] p 737 A93-26201
Preliminary design of an intermittent smoke flow visualization system [NASA-CR-186027] p 806 A93-28693

VANADIUM

X-ray diffraction and electron microscope studies of Ytria Stabilized Zirconia (YSZ) ceramic coatings exposed to vanadia [AD-A258055] p 392 A93-17676

VANADIUM COMPOUNDS

Application of vanadium hydride compressors for Joule-Thomson cryocoolers p 1149 A93-48616

VANELESS DIFFUSERS

Experimental research for the discharge flow of a centrifugal impeller and the flowfield in the vaneless diffuser p 11 A93-12454
Analysis of jet/wake mixing in a vaneless diffuser [ASME PAPER 92-GT-418] p 258 A93-19566

VANES

The vortex behaviour of the rotating-stall cell of a centrifugal compressor with vane diffuser [ASME PAPER 92-GT-66] p 400 A93-19316
Analysis of the friction and wear mechanisms of multilayered plasma-sprayed ceramic coatings p 548 A93-28567
Cruise noise of an advanced propeller with swirl recovery vanes p 564 A93-28609
Vane optimization for maximum efficiency using design of experiments p 1111 A93-49742
3-D Euler simulation of vane-blade interaction in a transonic turbine [AIAA PAPER 93-2256] p 1081 A93-50054
Application of recess vane casing treatment to axial flow fans p 423 A93-18728
Three-dimensional flow in radial turbomachinery and its impact on design [NASA-CR-192957] p 723 A93-25668
Advanced aircraft with thrust vector control [MBB-FE-1-S-PUB-0504] p 998 A93-31043
Penn State axial flow turbine facility: Performance and nozzle flow field p 1032 A93-31588

VAPOR DEPOSITION

Evaluation of simple aluminate and platinum modified aluminate coatings on high pressure turbine blades after factory engine testing - Round II [ASME PAPER 92-GT-140] p 388 A93-19372
Thermal barrier coating life prediction model development, phase 2 [NASA-CR-189111] p 198 A93-12589

VAPOR JETS

Experimental study of condensation vapor-air jets p 76 A93-10180

VAPOR PHASES

Stability of the vapour phase in a rotating two-phase fluid system subjected to different gravitational intensities p 926 A93-41714
Correlation of droplet behavior with gas-phase structures in a gas turbine combustor [AIAA PAPER 93-1767] p 1152 A93-49663
A condensed phase test cell assembly for the System for Thermal Diagnostic Studies (STDS) [AD-A258463] p 393 A93-18242
The WINCOF-I code: Detailed description [NASA-CR-190779] p 677 A93-24760

VAPORIZERS

Vaporizer performance p 79 A93-12784
Gravity sensitivity of a resistojet water vaporizer [AIAA PAPER 93-2402] p 1156 A93-50167
Gravity sensitivity of a resistojet water vaporizer [NASA-TM-106220] p 914 A93-29194

VAPORIZING

Diffusion controlled evaporation of a multicomponent droplet - Theoretical studies on the importance of variable liquid properties p 1021 A93-44224
Fundamental studies of droplet interactions in dense sprays [AD-A261165] p 737 A93-25948

VARIABILITY

Use of titanium castings without a casting factor [AD-A264414] p 1018 A93-31192

VARIABLE

The role of under-determined approximations in engineering and science application p 441 A93-16763

VARIABLE CYCLE ENGINES

Feasibility study on single bypass variable cycle engine with ejector [AIAA PAPER 92-4268] p 55 A93-13366
Effects of turbine cooling assumptions on performance and sizing of high-speed civil transport [AIAA PAPER 92-4217] p 55 A93-13383
Propulsion of a supersonic transport: What are the challenges? II - Achievements p 174 A93-16852
Conceptual design of turbo-accelerator for HST combined cycle engine [ASME PAPER 92-GT-253] p 353 A93-19462
Some topics of research on hypersonic airbreathing engines at National Aerospace Laboratory [ASME PAPER 92-GT-256] p 353 A93-19465
Toward the second-generation supersonic transport [ONERA, TP NO. 1993-26] p 890 A93-41038
Evaluation of a nonlinear PSC algorithm on a variable cycle engine [AIAA PAPER 93-2077] p 1114 A93-49904
A simplified representation of the off-design characteristics of high speed, high pressure ratio axial turbomachinery stages [AIAA PAPER 93-2257] p 1081 A93-50055
Advanced SST auxiliary air intakes design and analysis [AIAA PAPER 93-2304] p 1082 A93-50088
Variable cycle engine concept [ISABE 93-7065] p 1200 A93-54041
MM-122: High speed civil transport [NASA-CR-192011] p 334 A93-17974

VARIABLE GEOMETRY STRUCTURES

Some aspects of variable geometry gas turbine operation [ASME PAPER 92-GT-407] p 356 A93-19556
Control of contaminants in gas turbines with variable-flow combustion chambers and hydrogen addition p 520 A93-27478
Hypersonic stagnation line merged layer flow on blunt axisymmetric bodies of arbitrary shape [AIAA PAPER 93-2723] p 962 A93-46478
A numerical study of the effect of geometry variation, turbulence models, and dissipation on the flow past control surfaces [AIAA PAPER 93-2967] p 1048 A93-48161

VARIABLE PITCH PROPELLERS

Design of the variable pitch fan for the McDonnell Douglas MD 520N helicopter equipped with the NOTAR system p 794 A93-35908

VARIABLE THRUST

Performance and control of ascending trajectories to minimize heat load for transatmospheric aero-space planes p 133 A93-13745

VARIATIONAL PRINCIPLES

Variational problem of the profiling of the side walls of the supersonic section of a narrow three-dimensional nozzle p 4 A93-10140
Deforming grid variational principle for unsteady small disturbance flows in cascades p 692 A93-35623
Coupling conditions for substructures with varying idealization p 1029 A93-47078
Optimal wing shapes in a hypersonic nonequilibrium flow p 1088 A93-51770
Numerical optimization methods for variational inverse boundary value problems of aerodynamics p 1088 A93-51771

VECTOR ANALYSIS

Numerical simulation of homogeneous non-Gaussian random vector fields p 561 A93-27584
A graphically interactive approach to structured and unstructured surface grid quality analysis [AIAA PAPER 93-3351] p 954 A93-45045
Kinematics and aerodynamics of the velocity vector roll [AIAA PAPER 93-3625] p 1126 A93-48310
Equations of the steady motion of aircraft in spin and spiral dive p 1248 A93-54969

VECTOR PROCESSING (COMPUTERS)

Time-variant analysis of rotorcraft systems dynamics - An exploitation of vector processors p 416 A93-23512
A new parallel-vector finite element analysis software on distributed-memory computers [AIAA PAPER 93-1307] p 756 A93-33883
SAPNEW: Parallel finite element code for thin shell structures on the Alliant FX/80 [NASA-CR-190663] p 84 A93-10372
Numerical Wind Tunnel: Requirements and the outline p 383 A93-19288

Numerical Wind Tunnel hardware p 383 A93-19289
The language processor system for the Numerical Wind Tunnel p 383 A93-19291

VEGETATION

Physical effects of vegetation on wind-blown sand in the coastal environments of Florida [PB92-188424] p 93 A93-11702

VEHICLE WHEELS

Wheel shimmy analysis for main landing gear of aircraft p 41 A93-11809
Improved lubricating greases for aircraft wheel bearings [SAE PAPER 921038] p 197 A93-14658
Determination of tire-wheel interface pressure distribution for aircraft wheels [AIAA PAPER 93-1343] p 709 A93-33913
Wheel and brake design and test requirements for military aircraft [SAE ARP 1493] p 1103 A93-52165

VELOCITY DISTRIBUTION

Surface-curvature-distribution effects on turbine-cascade performance [ASME PAPER 92-GT-84] p 248 A93-19333
Streamwise variation of mean velocity field for the turbulent boundary layer interacting with controlled longitudinal vortex arrays p 267 A93-20933
3-D LDV measurements over a delta wing in pitch-up motion [AIAA PAPER 93-0185] p 275 A93-22610
Seed particle response and size characterization in high speed flows p 459 A93-23811
Flow visualization and flow field measurements of a 1/12 scale tilt rotor aircraft in hover p 482 A93-29441
Influence of coupling incidence and velocity variations on the airfoil dynamic stall p 767 A93-35999
Instantaneous structure of vortex breakdown on a delta wing via particle image velocimetry p 779 A93-39428
Experimental investigation of leading edge vortices using LDA p 861 A93-42254
Stability conditions for a transonic decelerating flow in a duct p 872 A93-43027
Determination of the shape of a wing profile in boundary layer flow with a given velocity diagram p 1067 A93-48844
Skin friction and velocity profile family for compressible turbulent boundary layers p 1070 A93-49008
Rotor-rotor interaction for counter-rotating fans. I - Three dimensional flowfield measurements [AIAA PAPER 93-1848] p 1075 A93-49729
The effects of fixed rotor tilt on the rotorodynamic coefficients of incompressible flow annular seals p 1161 A93-52601
Velocity fluctuation based on the difference in the flow pattern in the channels of a centrifugal impeller p 1182 A93-53842
A study on 3-D velocity distribution of isothermal flows behind an afterburner flame stabilizer [ISABE 93-7039] p 1197 A93-54015
Analytical and experimental investigation of flow through a turbine vane cascade p 1248 A93-56348
Experimental study of the flow field inside a whirling annular seal p 85 A93-10892
The measurement of the velocity field induced by a gust generator in a closed-circuit subsonic wind-tunnel [RAE-TM-MAT/STR-1102] p 67 A93-11435
A theory for the analysis of rotorcraft operating in atmospheric turbulence p 48 A93-11725
The jet behaviour of an actual high-bypass engine as determined by LDA-measurements in ground tests p 175 A93-13218
Velocity and temperature measurements in a non-premixed reacting flow behind a backward facing step p 132 A93-13632
Dynamics of vortex rings in cross-flow p 134 A93-13917
Multi-point inverse design of isolated airfoils and airfoils in cascade in incompressible flow p 163 A93-14462
Boundary-layer measurements on a high Reynolds number three-element airfoil p 292 A93-16787
Effect of Reynolds number on the standards of a simplified anemodimetric probe [IMFL-91-31] p 293 A93-17542
Monte Carlo simulation of normal shock wave, Part 1: Lennard-Jones potential p 300 A93-19279
Application of the program profile for the design of low-speed, low-observable configuration airfoils [AD-A258842] p 305 A93-19364
The transient development of vortices over delta wings p 695 A93-25269
The ground vortex flow field associated with a jet in a cross flow impinging on a ground plane for uniform and annular turbulent axisymmetric jets [NASA-CR-4513] p 789 A93-28449

VELOCITY ERRORS

- Adaptive filtering of Doppler velocimeter errors due to the characteristics of the reflecting surface p 992 A93-45650

VELOCITY MEASUREMENT

- Vaporizer performance p 79 A93-12784
Correlation of mean velocity measurements downstream of a swept backward-facing step p 123 A93-14552
Measurement of a one-dimensional mobility using a laser-Doppler velocimeter p 210 A93-16647
Applications of laser techniques in fluid mechanics p 395 A93-17765
Three component LDV velocity measurements in a can type research combustor for CFD validation. I - Isothermal [ASME PAPER 92-GT-138] p 350 A93-19370
Measurement of the three-dimensional tip region flowfield in an axial compressor [ASME PAPER 92-GT-211] p 252 A93-19434
Experimental and computational investigation of the NASA Low-Speed Centrifugal Compressor flow field [ASME PAPER 92-GT-213] p 252 A93-19436
Separated flow in a low speed two-dimensional cascade. I - Flow visualization and time-mean velocity measurements [ASME PAPER 92-GT-356] p 257 A93-19521
Separated flow in a low speed two-dimensional cascade. II - Cascade performance [ASME PAPER 92-GT-357] p 257 A93-19522
Vortical and turbulent structure of a lobed mixer free-shear layer [AIAA PAPER 93-0219] p 415 A93-22635
Measurement of shed vorticity and circulation from rotating aerofoil by particle image velocimetry p 538 A93-23804
A Laser Doppler Anemometry study of a supersonic jet in a low speed cross-flow p 459 A93-23807
Experimental investigation of a 2D parallel vortex/airfoil interaction p 538 A93-23808
Determination of gas flow rate in a duct from measured static pressures p 520 A93-27625
Application of particle image velocimetry in high-speed separated flows p 549 A93-29304
Laser velocimetry around helicopter blades in the DNW wind tunnel of the NLR [ONERA, TP NO. 1992-143] p 831 A93-38613
Two-dimensional laser velocimetry for the study of dual-flow jets with flight effect in the CEPRA 19 anechoic wind tunnel [ONERA, TP NO. 1992-144] p 831 A93-38614
Laser-velocimeter study of vortex breakdown on a 70-deg swept delta wing in incompressible flow [ONERA, TP NO. 1992-147] p 773 A93-38728
Analysis of turbulence in supersonic flows by means of laser velocimetry [ONERA, TP NO. 1992-148] p 773 A93-38729
Surge recovery and compressor working line control using compressor exit Mach number measurement p 897 A93-40435
Determination of the vertical velocity component of aircraft landing on an airfield with a longitudinally sloping runway p 1007 A93-45664
Damping of a gyro horizon-compass with arbitrary displacement of the suspension point p 1025 A93-45684
Observations of large-scale structures in wakes behind axisymmetric bodies p 965 A93-46748
SCV measurements in the wake of a rotor in hover and forward flight [AIAA PAPER 93-3080] p 1059 A93-48254
Formulas for determining the induced velocity in the direct and inverse rotor problems p 1071 A93-49324
Nonintrusive, multipoint velocity measurements in high-pressure combustion flows [AIAA PAPER 93-2032] p 1145 A93-49867
An experimental study of flow patterns and endwall heat transfer upstream of a surface-mounted rectangular obstruction in a turbulent boundary layer p 89 A93-11698
The jet behaviour of an actual high-bypass engine as determined by LDA-measurements in ground tests p 175 A93-13218
Planar measurement of flow field parameters in nonreacting supersonic flows with laser-induced iodine fluorescence p 133 A93-13801
Airfoil-vortex interaction and the wake of an oscillating airfoil p 134 A93-13803
Wind tunnel seeding particles for laser velocimeter p 292 A93-16770
Digital data acquisition and preliminary instrumentation study for the F-16 laminar flow control vehicle p 292 A93-16784
An experimental investigation of interacting wing-tip vortex pairs [AD-A258471] p 295 A93-18272

- Electron beam probing of blow-down hypersonic flows [ONERA-NT-1992-7] p 298 A93-18701
An investigation of laser velocimetry measurements within high speed, complex flows p 748 A93-25237
The transient development of vortices over delta wings p 695 A93-25269
An investigation on planar velocimetry by spatial cross-correlation p 697 A93-25664
An investigation of photothermal velocimetry for application to transient, high-speed gas flows p 698 A93-25720
System for calibrating a gyro navigator [AD-D015668] p 708 A93-26093
Trailing vortex/free-surface interaction [AD-A261654] p 701 A93-26195
Velocity and drop size measurements in a swirl-stabilized, combustor spray [NASA-TM-106130] p 813 A93-27130
Simultaneous mapping of the unsteady flow fields by Particle Displacement Velocimetry (PDV) p 786 A93-27454
Turbulence characteristics of an axisymmetric reacting flow [NASA-CR-4110] p 877 A93-30373
Multiparticle imaging technique for two-phase fluid flows using pulsed laser speckle velocimetry [DE93-011734] p 935 A93-30489
Turbulence measurement in a reacting and non-reacting shear layer at a high subsonic Mach number [NASA-TM-106186] p 989 A93-31839
VENTILATION
Optimization and sensitivity computations for the conception of internal ventilation system in the aircraft engine [ETN-93-93375] p 521 A93-20913
A model study of the aircraft cabin environment resulting from in-flight fires [DOT/FAA/CT-90/22] p 496 A93-21557
Ventilation effects on smoke and temperature in an aircraft cabin quarter-scale model [DOT/FAA/CT-89/25] p 791 A93-28055
VENTILATION FANS
A data processing and measuring system with a traversing probe for studying flow in the rotating impeller of an axial-flow fan p 75 A93-10032
VENTING
In-situ bioventing: Two US EPA and Air Force sponsored field studies [PB93-194231] p 1035 A93-32089
VENTURI TUBES
Operating experience using venturi flow meters at liquid helium temperature [DE92-014693] p 90 A93-12140
VERBAL COMMUNICATION
Comparison of performance on the Shipley Institute of Living Scale, Air Traffic Control Specialist Selection Test, and FAA Academy Screen [AD-A259249] p 502 A93-20582
VERTICAL DISTRIBUTION
Large-eddy simulation of turbulent flow above and within a forest p 92 A93-11404
Microburst characteristics determined from 1988-1991 TDWR testbed measurements p 490 A93-19605
VERTICAL FLIGHT
Dynamical variable structure control of a helicopter in vertical flight p 369 A93-22887
Rotorcraft master plan p 857 A93-30677
VERTICAL LANDING
Determination of YAV-8B Reaction Control System bleed flow usage [AIAA PAPER 92-4232] p 54 A93-13330
Stable cross type parachute with inflation aid [AIAA PAPER 93-1201] p 702 A93-35152
ARPA starts push for joint-service ASTOVL p 856 A93-43625
Determination of the takeoff and landing characteristics of aircraft by using a conditional polar p 1007 A93-45662
Determination of the vertical velocity component of aircraft landing on an airfield with a longitudinally sloping runway p 1007 A93-45664
Effects of flow-path variations on internal reversing flow in a tailpipe offtake configuration for ASTOVL aircraft [AIAA PAPER 93-2438] p 1118 A93-50190
Effects of flow-path variations on internal reversing flow in a tailpipe offtake configuration for ASTOVL aircraft [NASA-TM-106149] p 900 A93-29065
VERTICAL MOTION
Recent refinements and increased capabilities in balloon vertical performance analysis p 40 A93-11361
Determination of balloon gas mass and revised estimates of drag and virtual mass coefficients p 7 A93-11362
SAC contrail formation study [AD-A254410] p 159 A93-12605

VERTICAL MOTION SIMULATORS

- Synthesis and evaluation of an H2 control law for a hovering helicopter p 728 A93-34542
A high fidelity video delivery system for real-time flight simulation research [AIAA PAPER 93-3558] p 1214 A93-52659
Development and operation of a real-time simulation at the NASA Ames Vertical Motion Simulator [AIAA PAPER 93-3575] p 1208 A93-52671
Simulation motion effect on single axis compensatory tracking [AIAA PAPER 93-3579] p 1208 A93-52675
Initial piloted simulation study of geared flap control for tilt-wing V/STOL aircraft [NASA-TM-103872] p 64 A93-10741
Ground based simulation evaluation of the effects of time delays and motion on rotorcraft handling qualities [AD-A256921] p 328 A93-16186
Generation of helicopter roll axis bandwidth data through ground-based and in-flight simulation p 511 A93-19909
Frequency-response techniques for documentation and improvement of rotorcraft simulators p 913 A93-30689
VERTICAL TAKEOFF
Determination of the takeoff and landing characteristics of aircraft by using a conditional polar p 1007 A93-45662
VERTICAL TAKEOFF AIRCRAFT
Unorthodoxy rising --- VTOL p 1 A93-11250
Reaction drive rotors - Lessons learned (Hero had a good idea - But) --- jet helicopter performance [AIAA PAPER 92-4279] p 55 A93-13352
Low-cost approaches to proving of high-risk fast VTOL designs [SAE PAPER 920989] p 157 A93-14636
Computations of a twin-jet impingement on a flat surface p 271 A93-22227
Zen and the art of airplane sizing p 504 A93-25174
Optimal takeoff of a helicopter for category A V/STOL operations p 525 A93-28611
Machinery arrangements for small VTOL transport aircraft p 713 A93-34848
Advancing tiltrotor state-of-the-art with variable diameter rotors p 797 A93-35982
The UTA autonomous aerial vehicle - Automatic control and navigation p 908 A93-42813
Flight test progress of the STOL research aircraft ASKA [NAL-TM-643] p 49 A93-12354
Open aircrew VTOL concepts [NASA-CR-177603] p 240 A93-17883
Reduction in size and unsteadiness of a VTOL ground vortex by ground fences [NASA-CR-192997] p 700 A93-26049
Transition aerodynamics for 20-percent-scale VTOL unmanned aerial vehicle [NASA-TM-4419] p 779 A93-27032
The design of a robust autopilot for the Archytas prototype via linear quadratic synthesis [AD-A262151] p 820 A93-27546
Preliminary development of a VTOL unmanned air vehicle for the close-range mission [AD-A263514] p 933 A93-29969
VERY HIGH FREQUENCIES
A localizer design to improve missed approach guidance p 992 A93-44143
Development of a realtime DGPS system [DLR-MITT-92-06] p 503 A93-20749
VERY HIGH FREQUENCY RADIO EQUIPMENT
Lessons learned during testing of the Enhanced Position Location Reporting System (EPLRS) p 77 A93-10996
VERY LARGE SCALE INTEGRATION
A large flat panel multifunction display for military and space applications p 77 A93-10963
Analysis of fault-tolerant neurocontrol architectures [NASA-TM-105898] p 65 A93-12305
VERY LOW FREQUENCIES
Integrated Soviet VLF/Omega Receiver design p 316 A93-21198
ELF, VLF and LF radiation from a very large loop antenna with a mountain core p 924 A93-40334
VHF OMNIRANGE NAVIGATION
Merger and acquisition - Enhancing Loran propagation technology with artificial intelligence p 29 A93-10987
VHSIC (CIRCUITS)
Pave Pillar in-house research final report p 927 A93-42781
Design of an Ada expert system shell for the VHSIC avionics modular flight processor p 98 A93-11947
VIBRATION
Dynamics of rotating multicomponent turbomachinery systems [AIAA PAPER 93-1629] p 742 A93-34157
Modal analysis of multistage gear systems coupled with gearbox vibrations p 827 A93-36588

- Dynamics of rotating multi-component turbomachinery systems
[NASA-TM-105997] p 421 N93-18426
- A Government/Industry Summary of the Design Analysis Methods for Vibrations (DAMVIBS) Program
[NASA-CP-10114] p 514 N93-21310
- The NASA/Industry Design Analysis Methods for Vibrations (DAMVIBS) program: A government overview
p 514 N93-21311
- The NASA/industry Design Analysis Methods for Vibrations (DAMVIBS) program: Bell Helicopter Textron accomplishments
p 514 N93-21312
- The NASA/industry Design Analysis Methods for Vibrations (DAMVIBS) program: Boeing Helicopters airframe finite element modeling
p 515 N93-21313
- The NASA/industry Design Analysis Methods for Vibrations (DAMVIBS) program: McDonnell-Douglas Helicopter Company achievements
p 515 N93-21314
- The NASA/industry Design Analysis Methods for Vibrations (DAMVIBS) program: Sikorsky Aircraft: Advances toward interacting with the airframe design process
p 515 N93-21315
- Vibration analysis in turbomachines
p 1005 N93-32274

VIBRATION DAMPING

- Vibration control algorithms for flexible rotors
p 95 A93-10741
- Resonance frequencies of a gondola submitted to a forced rotation under a stratospheric balloon
p 27 A93-11384
- The investigation on vibration characteristics of all-movable stabilizer of an aircraft
p 41 A93-11821
- Finite memory approximations for a singular neutral system arising in aeroelasticity
p 97 A93-13246
- Optimal vibration control for a flexible rotor with gyroscopic effects
p 98 A93-13420
- Modified sparse time domain technique for rotor stability testing
p 157 A93-14593
- The smart structures technology in the vibration control of helicopter blades in forward flight
p 366 A93-17721
- Actuation strain decoupling through enhanced directional attachment in plates and aerodynamic surfaces
p 394 A93-17727
- Vibrational monitoring and diagnostics of the technical condition of gas turbine engines at civil aviation repair facilities
p 374 A93-18362
- Improving the service characteristics of an aircraft through the gyroscopic damping of its structure
p 366 A93-18363
- Measurement of the center-of-gravity using X-ray computed tomography
p 396 A93-18619
- Boundary-layer induced noise in aircraft
p 444 A93-19137
- Optimal circumferential placement of cylindrical thermocouple probes for reduction of excitation forces
[ASME PAPER 92-GT-423] p 406 A93-19571
- Multidisciplinary optimization of helicopter rotor blades including design variable sensitivity
[AIAA PAPER 92-4783] p 323 A93-20289
- Influence of sweep on structural optimization of a fighter wing
[AIAA PAPER 92-4794] p 323 A93-20290
- Structural optimization with frequency constraints - A review
[AIAA PAPER 92-4813] p 408 A93-20293
- High speed flight effects on transmission of sound through a nonflexible vibrating panel due to flow structural interaction in the ambience
[AIAA PAPER 92-4708] p 451 A93-20316
- Aeroservoelasticity in HISAIR --- High Speed Airframe Integration Research
[AIAA PAPER 92-4719] p 324 A93-20322
- Exact solution sensitivities for boundary element aerodynamics codes
[AIAA PAPER 92-4745] p 436 A93-20343
- Vibration reduction for helicopter airframes - An application of the general-purpose structural optimization program STARS
[AIAA PAPER 92-4782] p 326 A93-20372
- Optimal control law synthesis for flutter suppression using active acoustic excitations
p 370 A93-23516
- Dual control vibration tests of flight hardware
p 545 A93-27782
- Progress in the application of a non-linear programming methodology to the design of a low-vibration airframe
p 507 A93-27959
- Experiences at Langley Research Center in the application of optimization techniques to helicopter airframes for vibration reduction
p 508 A93-27972
- An overview of possible and not-so-possible tasks for active control of sound and vibration
p 568 A93-29429
- Sources of helicopter rotor hub inplane shears
[AIAA PAPER 93-1358] p 709 A93-33927

- Active control of vibratory airloads induced by helicopter rotor-fuselage interactions
[AIAA PAPER 93-1363] p 726 A93-33930
- Integrated structural tailoring and adaptive control of advanced flight vehicle structural vibration
[AIAA PAPER 93-1697] p 757 A93-34219
- Active constrained layer viscoelastic damping
[AIAA PAPER 93-1702] p 743 A93-34224
- Modal sensors and actuators for individual blade control
[AIAA PAPER 93-1703] p 712 A93-34225
- A modal-based procedure for efficiently predicting low vibration rotor designs
p 712 A93-34262
- Evaluation and extension of the flutter-margin method for flight flutter prediction
p 828 A93-37393
- Dynamic processes in the powerplants and power-generating equipment of flight vehicles
p 832 A93-39027
- The required damping and control process quality in a fuel pressure regulator
p 810 A93-39034
- Correction of the frequency characteristic of the waveguide circuit of an acoustic-jet temperature transducer
p 832 A93-39036
- A study of the effect of the working medium on the start-up characteristic of an aviation gas turbine engine
p 811 A93-39037
- Aeroelastic response, loads, and stability of a composite rotor in forward flight
p 906 A93-41919
- Application of two chaos methods to Higher Harmonic Control data --- for suppression of helicopter vibration
p 909 A93-43783
- Transonic flutter suppression using active acoustic excitations
[AIAA PAPER 93-3285] p 969 A93-46841
- Aero-engine component damping estimation from full-scale aeromechanical test data
[AIAA PAPER 93-1873] p 1112 A93-49748
- Engineering science research issues in high power density transmission dynamics for aerospace applications --- rotorcraft geared rotors
[AIAA PAPER 93-2299] p 1155 A93-50084
- Blade loss dynamics of a magnetically supported rotor
p 1257 A93-54653
- International Congress on Recent Developments in Air- and Structure-Borne Sound and Vibration, 2nd, Auburn Univ., AL, Mar. 4-6, 1992, Proceedings. Vols. 1-3
p 1259 A93-55851
- Noise and vibration analysis in propeller aircraft by advanced experimental modeling techniques
p 1264 A93-55862
- Vibration isolation of aviation power plants taking into account real dynamic characteristics of engine and aircraft
p 1244 A93-55863
- Passive damping technology
p 1259 A93-55866
- Damping in aerospace composite materials
p 1260 A93-55869
- Damped advanced composite parts
p 1253 A93-55871
- Human engineering issues for data link systems
p 1260 A93-55874
- Design, test, and evaluation of three active flutter suppression controllers
[NASA-TM-4338] p 63 N93-10070
- Control of panel flutter at high supersonic speed
p 47 N93-10900
- Optimal output feedback vibration control of rotor-bearing systems
p 86 N93-11220
- Active flutter suppression using dipole filters
[NASA-TM-107594] p 186 N93-13367
- An examination of wing rock for the F-15
[AD-A256613] p 188 N93-14252
- Online vibration control of a flexible rotor/bearing system
p 219 N93-14468
- Onboard System Evaluation of Rotors Vibration, Engines (OBSERVE) monitoring system
p 165 N93-15227
- Add-on damping treatment for the F-15 upper-outer wing skin
[AD-A258470] p 337 N93-18248
- Mass loaded composite rotor for vibro-acoustic application
[AD-D015604] p 535 N93-20016
- Structural dynamics branch research and accomplishments to FY 1992
[NASA-TM-105824] p 552 N93-20368
- Analytical and experimental investigation of flutter suppression by piezoelectric actuation
[NASA-TP-3241] p 513 N93-20584
- Apparatus for reduction of vibration in liquid-injected gas compressor system
[AD-D015607] p 554 N93-20772
- The NASA/industry Design Analysis Methods for Vibrations (DAMVIBS) program: Bell Helicopter Textron accomplishments
p 514 N93-21312

- The natural excitation technique (NExT) for modal parameter extraction from operating wind turbines
[DE93-010611] p 845 N93-28603
- Modal survey of a full-scale F-18 wind tunnel model
[AD-A262482] p 875 N93-29410
- Integrated structural design, vibration control, and aeroelastic tailoring by multiobjective optimization
p 1030 N93-31137
- Design and application of Active Magnetic Bearings (AMB) for vibration control
p 1033 N93-32279
- VIBRATION EFFECTS**
Electronics show their age
p 80 A93-13447
- VIBRATION ISOLATORS**
The effectiveness of porous squeeze film dampers for suppressing nonsynchronous motions
p 545 A93-27316
- Active control of interior noise in a large scale cylinder using piezoelectric actuators
p 568 A93-29425
- Optimal design of centered squeeze film dampers
p 831 A93-38629
- Vibration isolation of aviation power plants taking into account real dynamic characteristics of engine and aircraft
p 1244 A93-55863
- Vibration isolation technology: An executive summary of systems development and demonstration
[NASA-TM-105937] p 110 N93-15573
- VIBRATION MEASUREMENT**
Vibration monitoring and fault diagnosis of inflight aircraft engines
p 170 A93-14176
- Turbine blade vibration monitoring system
[ASME PAPER 92-GT-159] p 402 A93-19386
- A rapid procedure for obtaining time-average interferograms of vibrating bodies
p 412 A93-21857
- High temperature thin film strain gauges
[ONERA, TP NO. 1992-171] p 542 A93-25346
- A vibration monitoring acquisition and diagnostic system for helicopter drive train bench tests
p 826 A93-35930
- A data acquisition system for high-speed rotor balancing
p 1261 A93-54396
- New rotor trim and balance system for helicopter usage monitoring
p 169 N93-15180
- Fault detection of helicopter gearboxes using the multi-valued influence matrix method
[NASA-TM-106100] p 838 N93-27069
- Optical blade vibration measurement
[ETN-93-93454] p 905 N93-29999
- Efficient fault diagnosis of helicopter gearboxes
[NASA-TM-106253] p 1032 N93-31846
- VIBRATION METERS**
Video holography and laser vibrometry...The dynamic duo
p 210 A93-16611
- VIBRATION MODE**
Transition of flutter mode of two-dimensional wing with external store
p 41 A93-11818
- Dynamic analysis of a pre-and-post ice impacted blade
[AIAA PAPER 92-4273] p 54 A93-13333
- Dynamic characteristics of two new vibration modes of the disk-shell shaped gear
p 204 A93-14484
- Turbomachine blade vibration --- Book
[ISBN 0-470-21764-2] p 344 A93-17899
- Experimental determination of the main noise sources in a profan model by analysis of the acoustic spinning modes in the exit plane
p 449 A93-19214
- Double mode behaviour of bladed disk assemblies in the resonance frequency range, visualized by means of holographic interferometry
[ASME PAPER 92-GT-438] p 357 A93-19580
- A rapid procedure for obtaining time-average interferograms of vibrating bodies
p 412 A93-21857
- Expanding test mode shapes for better visualization
p 549 A93-29264
- Thermoelastic vibration test techniques
p 549 A93-29293
- Acoustical analysis of gear housing vibration
p 567 A93-29420
- An automated mode tracking strategy --- dynamic structural analysis of helicopter structures
[AIAA PAPER 93-1414] p 739 A93-33970
- Shape sensitivities and approximations of modal response of laminated skew plates
p 829 A93-37403
- Effect of structural uncertainties on flutter analysis
p 924 A93-40445
- Investigation of helicopter air resonance in hover by complex coordinates and mutual excitation analysis
p 893 A93-43777
- Vibration analysis of composite wing with tip mass using finite elements
p 1023 A93-45175
- Vibration characteristics of mistuned bladed disk
p 1108 A93-49190
- Finite element analysis of natural vibrations of an aeroplane with asymmetric variable wing geometry
p 1218 A93-53776
- A dynamic stiffness/boundary element method for the prediction of interior noise levels
p 1226 A93-53817

- Effects of blade geometry and mode shape on fan flutter
[ISABE 93-7028] p 1196 A93-54004
- The use of beam-like modal data for stiffness profile estimation by the EBS method. I - Justification and implementation --- Equivalent Beam Stiffness p 1257 A93-54649
- Noise and vibration analysis in propeller aircraft by advanced experimental modeling techniques p 1264 A93-55862
- A study upon structural optimization of elastic rotors for mechanical systems
[INPE-5376-TDI/471] p 83 N93-10310
- Nonlinear aeroelasticity of composite structures
[AD-A254285] p 47 N93-10842
- Rigid body mode identification of the PAH-2 helicopter using the eigensystem realization algorithm
[NASA-TM-107690] p 88 N93-11544
- Dynamic analysis of a pre-and-post ice impacted blade
[NASA-TM-105829] p 90 N93-12197
- Add-on damping treatment for the F-15 upper-outer wing skin
[AD-A258470] p 337 N93-18248
- Modal survey of a full-scale F-18 wind tunnel model
[AD-A262482] p 875 N93-29410
- Localization of aeroelastic modes in mistuned high-energy turbines p 1032 N93-31586
- Structural dynamic characteristics of bladed assemblies p 1005 N93-32273
- Design and application of Active Magnetic Bearings (AMB) for vibration control p 1033 N93-32279
- VIBRATION TESTS**
- Application of vibration-and-flutter integration analysis system for a trainer p 226 A93-14311
- Misalignments of airborne laser beams due to mechanical vibrations p 394 A93-17762
- Testing for integrity --- of aircraft gas turbine engines p 346 A93-18785
- Blade excitation by circumferentially asymmetric rotating stall in centrifugal compressors
[ASME PAPER 92-GT-148] p 351 A93-19376
- Excitation of blade vibration due to surge of centrifugal compressors
[ASME PAPER 92-GT-149] p 351 A93-19377
- Flutter calculations for a system with interacting nonlinearities
[AIAA PAPER 92-4682] p 409 A93-20304
- Dual control vibration tests of flight hardware p 545 A93-27782
- Ground vibration test on Piaggio P. 180 aircraft - Comparison between two modal test methods p 509 A93-29246
- Application of FEM model correlation and updating techniques on an aircraft using test data of a ground vibration survey p 509 A93-29267
- Signal processing and system identification techniques for flutter test data analysis p 529 A93-29282
- Thermoelastic vibration test techniques p 549 A93-29293
- Effect of modeling techniques in the coupled rotor-body vibration analysis
[AIAA PAPER 93-1360] p 710 A93-33928
- Comparison of some direct multi-point force appropriation methods p 928 A93-43338
- Unsteady aerodynamic models for maneuvering aircraft
[AIAA PAPER 93-3626] p 1126 A93-48311
- Low-noise, high-strength, spiral-bevel gears for helicopter transmissions
[AIAA PAPER 93-2149] p 1154 A93-49966
- Response variability observed in reverberant acoustic test of a model aerospace structure p 1264 A93-55857
- Testing for integrity
[PNR-90927] p 56 N93-11024
- A knowledge-based blackboard system to interpret graphical data from vibration tests of gas turbines
[PNR-90993] p 59 N93-11114
- Experimental and analytical investigation of the vibration characteristics of a remotely piloted helicopter
[AD-A256131] p 163 N93-14248
- Experimental and analytical investigation of dynamic characteristics of extension-twist-coupled composite tubular spars
[NASA-TP-3225] p 553 N93-20585
- Modal survey of a full-scale F-18 wind tunnel model
[AD-A262482] p 875 N93-29410
- VIBRATIONAL SPECTRA**
- CARS studies in hypersonic flows
[AIAA PAPER 93-3047] p 1144 A93-48227
- Time-frequency domain analysis of vibration signals for machinery diagnostics. 3: The present power spectral density
[OUEL-1911/92] p 89 N93-11707

VIBRATIONAL STRESS

- Unsteady wake effect on rotor vibratory airloadings p 509 A93-29439
- Dynamic analysis of a gear drive system in aeroengine p 1149 A93-48514
- The effect of temperature on the natural frequencies and acoustically induced strains in CFRP plates p 1260 A93-56331
- VIBRATORY LOADS**
- Multidisciplinary optimization of helicopter rotor blades including design variable sensitivity
[AIAA PAPER 92-4783] p 323 A93-20289
- Active control of vibratory airloads induced by helicopter rotor-fuselage interactions p 726 A93-33930
- [AIAA PAPER 93-1363] p 796 A93-35975
- An investigation of helicopter rotor blade flap vibratory loads p 797 A93-35980
- Introduction of the M-85 high-speed rotorcraft concept p 837 A93-39185
- A mathematical model of the vibrational impact hardening of parts p 906 A93-41919
- Aeroelastic response, loads, and stability of a composite rotor in forward flight p 1260 A93-55874
- Human engineering issues for data link systems

VIDEO DATA

- Aircraft lightning initiation and interception from in situ electric measurements and fast video observations p 140 A93-14064
- A high fidelity video delivery system for real-time flight simulation research
[AIAA PAPER 93-3558] p 1214 A93-52659

VIDEO EQUIPMENT

- Fiber optics for aircraft entertainment systems p 1172 A93-49478
- A passive infrared ice detection technique for helicopter applications
[NASA-CR-193187] p 880 N93-29152

VIRTUAL MEMORY SYSTEMS

- The language processor system for the Numerical Wind Tunnel p 383 N93-19291

VIRTUAL REALITY

- Simulation in aeronautics p 437 A93-21868
- A survey of position trackers p 1151 A93-49396
- A synthetic environment flight simulator: The AFIT virtual cockpit
[AD-A259220] p 530 N93-20576
- Virtual reality flight control display with six-degree-of-freedom controller and spherical orientation overlay
[NASA-CASE-NPO-18733-1-CU] p 897 N93-30416

VISCOELASTIC DAMPING

- Bending-torsion flutter of linear viscoelastic wings including structural damping
[AIAA PAPER 93-1475] p 711 A93-34021
- Active constrained layer viscoelastic damping
[AIAA PAPER 93-1702] p 743 A93-34224
- Add-on damping treatment for the F-15 upper-outer wing skin
[AD-A258470] p 337 N93-18248

VISCOPLASTICITY

- On the coupled thermomechanical analysis of hypersonic flight vehicle structures
[AIAA PAPER 92-5018] p 413 A93-22294
- A finite element model for analysis of thermoviscoplastic behavior of hypersonic leading edge structures subject to intense aerothermal heating p 137 N93-14631

VISCOSITY

- Viscosity of aviation fuel components (n-alkanes) p 71 A93-12824
- An investigation on the artificial viscosity in the transonic stream function formulation
[ASME PAPER 92-GT-49] p 246 A93-19302
- Prediction of the ice accretion with viscous effects on aircraft wings
[AIAA PAPER 93-0027] p 307 A93-20145
- Viscosity of aviation fuel components - Aromatic hydrocarbons (alkyl benzenes) p 1211 A93-52961
- One type of automatically adjusted difference scheme with artificial viscosity to calculate ablated exterior shapes
[AD-A254108] p 19 N93-10856
- The effects of viscosity on a conically derived waverider
[AD-A259019] p 424 N93-19101

VISCOUS DAMPING

- Numerical wave propagation and steady state solutions. II - Bulk Viscosity Damping
[AIAA PAPER 93-3331] p 953 A93-45025
- Optimal control of the rocking and damping of swings p 1263 A93-54998
- An experimental and a theoretical investigation of rotor pitch damping using a model rotor p 47 N93-10322

VISCOUS DRAG

- Artificial viscosity models for the Navier-Stokes equations and their effect in drag prediction
[AIAA PAPER 93-0193] p 473 A93-25511
- Development of a skin friction gauge for use in an impulse facility p 1024 A93-45526
- Active flow control with neural networks
[AIAA PAPER 93-3273] p 1037 A93-46834

VISCOUS FLOW

- Viscous instability of hypersonic flow past a wedge p 4 A93-10137
- Three-dimensional flow of viscous gas in the blade passage of a straight compressor cascade p 5 A93-10187
- Optimal control of lift/drag ratios on a rotating cylinder p 76 A93-10275
- Numerical solution of a free-boundary problem in hypersonic flow theory - Nonequilibrium viscous shock layers p 8 A93-11920
- Viscous equilibrium computations using program LAURA p 8 A93-12002
- Computation of viscous compressible flows using an upwind algorithm and unstructured meshes p 9 A93-12163
- Viscous shock-layer numerical calculations of three dimensional nonequilibrium flows over hypersonic blunt bodies at high angle of attack p 12 A93-12651
- Nonstationary flow of a viscous incompressible fluid past an airfoil p 79 A93-12922
- Numerical analysis of three-dimensional viscous flows around an advanced counterrotating propeller p 112 A93-14165
- Calculation of transonic viscous flow around a delta wing p 113 A93-14191
- Turbulence modelling requirements for the prediction of viscous transonic aeroflow flows p 115 A93-14249
- Viscous flow field prediction in axisymmetric passages p 204 A93-14478
- Marching grid generation for external viscous flow problems p 228 A93-16979
- Unstable branches of a hypersonic, chemically reacting boundary layer p 128 A93-17262
- Viscous flows in centrifugal compressor diffusers at transonic Mach numbers
[ASME PAPER 92-GT-48] p 246 A93-19301
- Aeroloads and secondary flows in a transonic mixed flow turbine stage
[ASME PAPER 92-GT-72] p 248 A93-19322
- Viscous interaction upstream and downstream of a turbine stator cascade with a periodic wake field
[ASME PAPER 92-GT-162] p 250 A93-19388
- Prediction of 2D viscous transonic flow in compressor cascades using a semi-empirical shock/boundary-layer interaction method
[ASME PAPER 92-GT-277] p 253 A93-19470
- A viscous axisymmetric throughflow prediction method for multi-stage compressors
[ASME PAPER 92-GT-293] p 254 A93-19483
- Viscous throughflow modelling for multi-stage compressor design
[ASME PAPER 92-GT-302] p 255 A93-19492
- Analysis of three-dimensional viscous flow in a supersonic axial flow compressor rotor with emphasis on tip leakage flow
[ASME PAPER 92-GT-388] p 257 A93-19543
- Newton-like methods for fast high resolution simulation of hypersonic viscous flows p 437 A93-20740
- Viscous and inviscid instabilities of a trailing vortex p 268 A93-21042
- Grid generation for three-dimensional turbomachinery geometries including tip clearance p 270 A93-21658
- An algebraic turbulence model for three-dimensional viscous flows
[AIAA PAPER 93-0083] p 274 A93-22552
- The effect of Reynolds number and turbulence on airfoil aerodynamics at -90 degrees incidence
[AIAA PAPER 93-0206] p 277 A93-22624
- Numerical computation of viscous hypersonic flow around spherically blunted cones at angle of attack p 460 A93-24082
- An upwind formulation for the solution of thin-layer Navier-Stokes equations p 461 A93-24088
- Multigrid techniques for hypersonic viscous flows
[AIAA PAPER 93-0771] p 467 A93-24855
- Viscous flow computations of flow field around an advanced propeller
[AIAA PAPER 93-0873] p 469 A93-24934
- Application of high-order accurate essentially nonoscillatory schemes to two-dimensional compressible viscous flows
[AIAA PAPER 93-0879] p 470 A93-24940
- Hypersonic inviscid and viscous flow computations with a new optimized thermodynamic equilibrium model
[AIAA PAPER 93-0893] p 471 A93-24953
- Numerical investigation of flow field in a turbine volute
[AIAA PAPER 93-0155] p 542 A93-25505

Hypersonic viscous flow simulations p 478 A93-27926

Current status of computational methods for transonic unsteady aerodynamics and aeroelastic applications p 480 A93-29175

Flowfield analysis of modern helicopter rotors in hover by Navier-Stokes method p 481 A93-29435

The analysis of viscous wakes noise in axial flow compressor p 759 A93-33710

The stagnation line solution of the equilibrium flow with radiation and mass injection p 680 A93-33733

The analysis and computation of viscous-inviscid interactive problem for three dimensional transonic flow p 681 A93-33741

Viscous-inviscid interaction coupled calculation of three-dimensional turbulent separated flow over dents p 681 A93-33748

Airfoil shape optimization using sensitivity analysis on viscous flow equations p 682 A93-33755

Numerical analysis of the three-dimensional boundary layer on a turbomachinery rotor blade p 685 A93-34341

A cell-vertex TVD scheme for transonic viscous flow p 685 A93-34346

Computation of viscous transonic aerofoil flows using eddy-viscosity based turbulence models p 687 A93-34360

Inlet turbulence distortion and viscous flow development in a controlled-diffusion compressor cascade at very high incidence p 688 A93-34485

VSL analysis of nonequilibrium flows around a hypersonic body p 769 A93-38146

Numerical solution of viscous compressible flows using algebraic turbulence models p 770 A93-38162

Viscous nonequilibrium flow calculations [ONERA, TP NO. 1992-89] p 771 A93-38573

Calculations of viscous nonequilibrium flows in nozzles [ONERA, TP NO. 1992-91] p 771 A93-38574

A viscous-inviscid solver for high-lift incompressible flows over multi-element airfoils at deep separation conditions [ONERA, TP NO. 1992-183] p 774 A93-38745

Viscous-inviscid calculation of high-lift separated compressible flows over airfoils and wings [ONERA, TP NO. 1992-184] p 774 A93-38746

A numerical investigation of supersonic flow of a viscous gas over long blunt cones, taking into account equilibrium physicochemical transformations p 775 A93-39124

Kinetic theory of hypersonic flows of a viscous gas p 775 A93-39130

Accuracy of flux-split algorithms in high-speed viscous flows p 860 A93-41912

Spectral solution of the viscous blunt-body problem p 860 A93-41915

International Symposium on Computational Fluid Dynamics, 4th, Univ. of California, Davis, Sept. 9-12, 1991, Selected Papers p 862 A93-42426

Implicit multigrid techniques for compressible flows p 862 A93-42429

Enhanced numerical inviscid and viscous fluxes for cell centered finite volume schemes p 864 A93-42444

CFD for hypersonic propulsion p 865 A93-42585

Viscous, 2-D, laminar hypersonic flows over compression ramps p 866 A93-42591

The application of an adaptive upwind unstructured grid solution algorithm to the simulation of compressible laminar viscous flows over compression corners p 866 A93-42594

Hypersonic viscous flow over two-dimensional ramps p 866 A93-42596

Computational results for flows over compression ramps p 866 A93-42599

An upwind relaxation method for hypersonic viscous flows over a double-ellipsoidal body p 867 A93-42606

2D hypersonic viscous flow past a double ellipse geometry p 868 A93-42613

Viscous and inviscid hypersonic flow about a double ellipsoid p 868 A93-42616

Hypersonic viscous flow past double ellipse and past double ellipsoid - Numerical results p 868 A93-42618

Computation of thermochemical nonequilibrium flows around a simple and a double ellipse p 869 A93-42629

Finite volume 3DNS and PNS solutions of hypersonic viscous flow around a delta wing using Osher's flux difference splitting p 870 A93-42633

Multigrid calculation of three-dimensional viscous cascade flows p 872 A93-42889

The status of CFD - An Air Force perspective [AIAA PAPER 93-3293] p 1021 A93-44997

Adaptive-prismatic-grid method for external viscous flow computations [AIAA PAPER 93-3314] p 951 A93-45010

Pseudo-compressibility methods for the incompressible flow equations [AIAA PAPER 93-3329] p 952 A93-45023

Numerical simulation of two-dimensional and axis-symmetric compressible flows p 960 A93-45546

Comment on 'Flow near the trailing edge of an airfoil' p 961 A93-45754

Solution strategy for three-dimensional configurations at hypersonic speeds p 962 A93-46406

Enhancements to viscous-shock-layer technique p 962 A93-46408

A viscous shock-layer analysis of 2-D and axisymmetric flows [AIAA PAPER 93-2751] p 963 A93-46500

3D viscous flow analysis in axial turbine including tip leakage phenomena p 972 A93-46940

Computational analysis of drag reduction and buffet alleviation in viscous transonic flow over porous airfoils [AIAA PAPER 93-3419] p 976 A93-47215

A Laplace interaction law for the computation of viscous airfoil flow in low and high speed aerodynamics [AIAA PAPER 93-3462] p 979 A93-47244

Numerical simulation of incompressible viscous flow around a propeller p 984 A93-47271

Shock-wave/boundary layer interactions at hypersonic speeds by an implicit Navier-Stokes solver [AIAA PAPER 93-2938] p 1046 A93-48136

A viscous flow based membrane wing model [AIAA PAPER 93-2955] p 1047 A93-48149

A numerical study of the effect of geometry variation, turbulence models, and dissipation on the flow past control surfaces [AIAA PAPER 93-2967] p 1048 A93-48161

The prediction of viscous nonequilibrium hypersonic flows about ablating configurations using an upwind parabolized Navier-Stokes code [AIAA PAPER 93-2998] p 1053 A93-48188

A viscous-inviscid interaction method for 2-D unsteady, compressible flows [AIAA PAPER 93-3019] p 1055 A93-48206

A fast robust viscous-inviscid interaction solver for transonic flow about wing/body configurations on the basis of full potential theory [AIAA PAPER 93-3026] p 1056 A93-48211

Investigation of the flowfield over parallel-arranged launch vehicles [AIAA PAPER 93-3060] p 1058 A93-48237

A two layer k-epsilon computation of transonic viscous flow including separation over the DLR-F5 wing [AIAA PAPER 93-3110] p 1061 A93-48281

Multigrid techniques for hypersonic viscous flows p 1071 A93-49027

Computational methods for viscous hypersonic flows p 1152 A93-49523

A nonperiodic boundary approach for computation of compressible viscous flows in advanced turbine cascades [AIAA PAPER 93-1799] p 1074 A93-49688

3-D viscous flow CFD analysis of the propeller effect on an advanced ducted propeller subsonic inlet [AIAA PAPER 93-1847] p 1075 A93-49728

An unstructured grid flow solver for turbomachinery flows [AIAA PAPER 93-1913] p 1076 A93-49780

An unstructured adaptive quadrilateral mesh-based scheme for viscous turbomachinery flow calculations [AIAA PAPER 93-1975] p 1077 A93-49822

Numerical study of the transient flow in the driven tube and the nozzle section of a shock tunnel [AIAA PAPER 93-2018] p 1078 A93-49856

Applying and validating the RANS-3D flow-solver for evaluating a subsonic serpentine diffuser geometry [AIAA PAPER 93-2157] p 1079 A93-49973

A comparison between numerically modelled and experimentally measured loss mechanisms in wave rotors [AIAA PAPER 93-2522] p 1120 A93-50252

Numerical modeling of flow in a hypersonic laminar boundary layer p 1086 A93-50967

The problem of viscous hypersonic flow past blunt bodies in the spreading plane p 1086 A93-50969

A study of turbulent flow in a viscous shock layer in the case of gas flow past oblong blunt bodies p 1089 A93-51820

Investigation of the structure of a multicomponent viscous shock layer p 1090 A93-51879

An economical difference factorization algorithm for the numerical calculation of the system of equations for a thin viscous shock layer p 1091 A93-51880

Efficient simulation of incompressible viscous flow over single and multi-element airfoils p 1095 A93-52448

Prismatic grid generation for three-dimensional complex geometries p 1178 A93-53217

Three-dimensional Navier-Stokes/full-potential coupled analysis for viscous transonic flow p 1178 A93-53218

Application of the small parameter method to the problem of three-dimensional flow of a viscous gas past bodies p 1178 A93-53314

The flow lag angle in the rotor of a centrifugal compressor with allowance for viscosity effects p 1179 A93-53555

3D and 2.5D viscous flow computations for axial flow turbine blades [ISABE 93-7093] p 1186 A93-54069

Recent developments performed at ONERA for the simulation of 3D inviscid and viscous flows in turbomachinery by the solution of Euler and Navier-Stokes equations [ISABE 93-7094] p 1186 A93-54070

Prediction of viscous flows in rotating machinery using Navier-Stokes techniques p 1232 A93-54639

Analysis of high Reynolds number inviscid/viscid interactions in cascades p 1234 A93-55351

Computation of viscous hypersonic non-equilibrium blunt body flow p 1238 A93-56038

Numerical study of slightly compressible Navier-Stokes simulation of blade-vortex interaction p 1239 A93-56216

Development and computation of continuum higher order constitutive relations for high-altitude hypersonic flow p 132 A93-13578

Application of a vectorized particle simulation to the study of plates and wedges in high-speed rarefied flow p 133 A93-13746

Unsteady three-dimensional thin-layer Navier-Stokes solutions for turbomachinery in transonic flow p 218 A93-14025

An algebraic turbulence model for three-dimensional viscous flows [NASA-TM-105931] p 110 A93-14102

A study of viscous interaction effects on hypersonic waveriders p 135 A93-14160

Prediction of turbine cascade flows with a quasi-three-dimensional rotor viscous code and the extension of the algebraic turbulence model [AD-A256831] p 223 A93-15635

Navier-Stokes calculation of transonic flow past the NTF 65-deg delta wing p 292 A93-16797

H-P adaptive methods for finite element analysis of aerothermal loads in high-speed flows [NASA-CR-189739] p 420 A93-18093

A Blottner type numerical model for nonequilibrium viscous hypersonic flows in upwind finite elements [INRIA-RR-1476] p 297 A93-18648

Influence of the physical modelling of viscous terms on hypersonic flow computations [INRIA-RR-1493] p 297 A93-18652

Numerical investigation of performance degradation of wings and rotors due to icing [NASA-CR-192233] p 339 A93-18783

The effects of viscosity on a conically derived waverider [AD-A259019] p 424 A93-19101

Numerical simulations of supersonic flow by a fourth-order compact MUSCL TVD scheme p 302 A93-19308

The semi-discrete Galerkin finite element modelling of compressible viscous flow past an airfoil [NASA-CR-192161] p 483 A93-20018

Advanced adaptive computational methods for Navier-Stokes simulations in rotorcraft aerodynamics [NASA-CR-192282] p 483 A93-20256

Prediction of forces and moments for hypersonic flight vehicle control effectors [NASA-CR-193033] p 728 A93-24762

An analysis of lift forces on aerosols in a wall bounded turbulent shear flow [DE93-003362] p 747 A93-24963

Numerical modelling of viscous turbomachinery flows with a pressure correction method p 723 A93-25702

Model fan passage flow simulation [AD-A261613] p 752 A93-26167

The generation of side force by distributed suction [NASA-CR-193129] p 839 A93-27151

Efficient simulation of incompressible viscous flow over multi-element airfoils p 784 A93-27443

Ship viscous flow: A report on the 1990 SSPA-IIHR Workshop p 840 A93-27466

Navier-Stokes simulation of viscous, separated, supersonic flow over a projectile rotating band [AD-A263073] p 788 A93-27955

Axisymmetric vortex sheet roll-up p 788 A93-28078

The 3-D viscous flow CFD analysis of the propeller effect on an advanced ducted propeller subsonic inlet [NASA-TM-106240] p 900 A93-29162

Simulation, characterization and control of forced unsteady viscous flows using Navier-Stokes equations [AD-A264333] p 934 A93-30369

Some implications of a differential turbomachinery equation with viscous correction [AD-A264693] p 935 A93-30571

Three-dimensional analysis of the Pratt and Whitney alternate design SSME fuel turbine p 1031 A93-31584

Reynolds number influences in aeronautics
[NASA-TM-107730] p 989 N93-31732

Numerical simulation of the flow in a 1:57-scale
axisymmetric model of a large blast simulator
[AD-A265551] p 1015 N93-31916

Calculations on unsteady type 4 interaction at Mach 8
[AD-A265214] p 990 N93-32004

VISCOUS FLUIDS

On the conservation of rothalpy in turbomachines
[ASME PAPER 92-GT-217] p 252 A93-19439

Free streamline-boundary layer analysis for separated
flow over an airfoil p 1239 A93-56327

VISIBILITY

Development of laser conducting landing system
p 150 A93-14320

An automated system for the measurement of slant
visual range p 413 A93-22176

New slant visual range measuring device promises
improved airport operations p 529 A93-27395

Evaluation of alternatives for increasing A-7D rearward
visibility p 50 N93-12488

[AD-A255071] p 50 N93-12488

Runway Visual Range (RVR) Operational Test and
Evaluation (OT&E) integration and OT&E operational test
report p 706 N93-25243

[DOT/FAA/CT-TN92/37] p 706 N93-25243

Preliminary evaluation of aviation-impact variables
derived from numerical models p 1034 N93-31202

[PB93-190197] p 1034 N93-31202

VISION

Engineering a visual system for seeing through fog
[SAE PAPER 921130] p 895 A93-41318

VISUAL ACUITY

Realization of real time graphics in vehicles with high
dynamic motion p 443 N93-18630

[ETN-93-92739] p 443 N93-18630

VISUAL AIDS

Ground visual aids - Recent research at RAE Bedford
p 191 A93-17311

A history of visual approach guidance indicator systems
in Australia p 498 A93-25171

AIAA Flight Simulation Technologies Conference,
Monterey, CA, Aug. 9-11, 1993, Technical Papers
p 1207 A93-52651

VISUAL FIELDS

Visual field information in Nap-of-the-Earth flight by
teleoperated Helmet-Mounted displays p 517 A93-26884

VISUAL FLIGHT

Airborne trials of Loran-C p 311 A93-17756

Weather forecasts for aviation in Canada (FACN and
FTCN) - The way they are taught and how they can be
made more suitable to the needs of pilots p 454 A93-22108

An automated system for the measurement of slant
visual range p 413 A93-22176

Visual augmentation for night flight over featureless
terrain p 806 A93-35921

Visual approach data collection at St. Louis Lambert
Field (STL) p 706 N93-24948

[DOT/FAA/CT-TN93/2] p 706 N93-24948

VISUAL FLIGHT RULES

Maps and charts for visual air navigation p 498 A93-25170

Unusual attitudes - Helicopters and instrument flight
p 1240 A93-54550

Rotorcraft en route ATC route standards
[AD-A249129] p 35 N93-10323

VISUAL OBSERVATION

Vision-based range estimation using helicopter flight
data p 151 A93-17501

Vision-based range estimation using helicopter flight
data p 317 A93-21525

VISUAL PERCEPTION

Survey of helmet tracking technologies p 517 A93-26882

Helmet Mounted Sight and display testing p 517 A93-26883

Some considerations on indication means for helicopter
pilot vision systems p 807 A93-36018

VISUAL SIGNALS

Texture as a visual cueing element in computer image
generation. I - Representation of the sea surface
[AIAA PAPER 93-3560] p 1214 A93-52695

VISUAL TASKS

Vision-based recursive estimation of rotorcraft obstacle
locations p 343 A93-22851

VOICE COMMUNICATION

The development of the speaker independent ARM
continuous speech recognition system p 87 N93-11383

[RSRE-MEMO-4473] p 87 N93-11383

Preliminary results on the use of linear discriminant
analysis in the ARM continuous speech recognition
system p 87 N93-11384

[RSRE-MEMO-4511] p 87 N93-11384

The use of linear discriminant analysis in the ARM
continuous speech recognition system p 87 N93-11385

[RSRE-MEMO-4512] p 87 N93-11385

Advances in speech processing p 550 N93-19771

A simulation study of the effects of communication delay
on air traffic control p 502 N93-19966

[AD-A258593] p 502 N93-19966

An analysis of en route controller-pilot voice
communications p 935 N93-30611

[AD-A264784] p 935 N93-30611

VOICE CONTROL

Fly-by voice, a technology demonstration p 526 N93-19918

A simulation study of the effects of communication delay
on air traffic control p 502 N93-19966

[AD-A258593] p 502 N93-19966

VOICE DATA PROCESSING

Preliminary results on the use of linear discriminant
analysis in the ARM continuous speech recognition
system p 87 N93-11384

[RSRE-MEMO-4511] p 87 N93-11384

High Capacity Voice Recorder (HCVR) Operational Test
and Evaluation (OT/E) integration test report p 88 N93-11460

[DOT/FAA/CT-TN92/30] p 88 N93-11460

Advances in speech processing p 550 N93-19771

VOIDS

NDE of PWA 1480 single crystal turbine blade
material p 815 N93-27640

[NASA-TM-106140] p 815 N93-27640

VOLCANOES

The aeronautical volcanic ash problem p 309 A93-22156

Volcanic ash and aircraft operations p 309 A93-22181

Aviation safety can benefit from simulation of the
dispersion of hazardous material p 487 A93-27393

Volcanic clouds --- aircraft hazards p 487 A93-28196

VOLTERRA EQUATIONS

Extension of a nonlinear systems theory to
general-frequency unsteady transonic aerodynamic
responses p 683 A93-34122

[AIAA PAPER 93-1590] p 683 A93-34122

Application of nonlinear systems theory to transonic
unsteady aerodynamic responses p 1095 A93-52438

VON KARMAN EQUATION

Digital simulation of atmospheric turbulence for Dryden
and von Karman models p 416 A93-23517

VORTEX ALLEVIATION

'Wingwake' - A computational model for preliminary
assessment of wake vortex attenuation schemes p 15 A93-13377

[AIAA PAPER 92-4209] p 15 A93-13377

Experimental investigation of flows behind different
Large-Eddy Breakup (LEBU) devices in thick boundary
layers p 18 N93-10550

Aerodynamic surface tip vortex attenuation system
[AD-D015606] p 483 N93-20017

VORTEX AVOIDANCE

A low-speed wind tunnel study of vortex interaction
control techniques on a chine-forebody/delta-wing
configuration p 122 A93-14409

Turbulence avoidance p 309 A93-22160

Proceedings of the Aircraft Wake Vortices conference,
volume 1 p 485 N93-21796

[PB93-126449] p 485 N93-21796

Proceedings of the Aircraft Wake Vortices conference,
volume 2 p 559 N93-21799

[PB93-127728] p 559 N93-21799

VORTEX BREAKDOWN

Breakdown analysis on delta wing vortices p 7 A93-10779

Vortex breakdown study on a 65-deg delta wing tested
in static and dynamic conditions p 121 A93-14407

Three-dimensional supersonic vortex breakdown
[AIAA PAPER 93-0526] p 284 A93-23267

Streamwise vortex meander in a plane mixing layer
[AIAA PAPER 93-0553] p 285 A93-23292

Vortex breakdown over delta wings in unsteady free
stream p 285 A93-23294

[AIAA PAPER 93-0555] p 285 A93-23294

Further analysis of high-rate rolling experiments of a
65 deg delta wing p 523 A93-24737

A simple criterion for vortex breakdown p 469 A93-24928

[AIAA PAPER 93-0866] p 469 A93-24928

Structure of vortex breakdown on a pitching delta wing
[AIAA PAPER 93-0434] p 474 A93-25528

Investigation of vortex breakdown on delta wings using
Navier-Stokes equations p 478 A93-27924

Experimental and nonlinear vortex lattice method results
for various wing-canard configurations p 479 A93-28607

Instantaneous structure of vortex breakdown on a delta
wing via particle image velocimetry p 779 A93-39428

Experimental investigation of leading edge vortices using
LDA p 861 A93-42254

An acceleration technique for time accurate calculations
--- of unsteady flow around pitching delta wings p 957 A93-45092

Effect of nonaxisymmetric forcing on a swirling jet with
vortex breakdown p 1028 A93-46796

[AIAA PAPER 93-3251] p 1028 A93-46796

Adaptive computations of flow around a delta wing with
vortex breakdown p 974 A93-47202

[AIAA PAPER 93-3400] p 974 A93-47202

A visualization study of the vortical flow over a
double-delta wing in dynamic motion p 976 A93-47220

[AIAA PAPER 93-3425] p 976 A93-47220

Supersonic vortex breakdown over a delta wing in
transonic flow p 980 A93-47251

[AIAA PAPER 93-3472] p 980 A93-47251

Flow control over delta wings at high angles of attack
[AIAA PAPER 93-3494] p 983 A93-47266

Navier-Stokes prediction of a delta wing in roll with vortex
breakdown p 983 A93-47267

[AIAA PAPER 93-3495] p 983 A93-47267

Experimental and computational investigations of the
flowfield around the F117A p 984 A93-47274

[AIAA PAPER 93-3508] p 984 A93-47274

Side force augmentation at high angle of attack from
pneumatic vortex flow control p 1124 A93-48153

[AIAA PAPER 93-2959] p 1124 A93-48153

Shock-vortex interaction over a 65-degree delta wing
in transonic flow p 1049 A93-48167

[AIAA PAPER 93-2973] p 1049 A93-48167

Computational study of vortex breakdown on a pitching
delta wing p 1050 A93-48168

[AIAA PAPER 93-2974] p 1050 A93-48168

Lateral control at high angles of attack using pneumatic
blowing through a chined forebody p 1126 A93-48309

[AIAA PAPER 93-3624] p 1126 A93-48309

Flow physics of critical states for rolling delta wings
[AIAA PAPER 93-3683] p 1129 A93-48355

Simulation of tail buffet using delta wing-vertical tail
configuration p 1065 A93-48357

[AIAA PAPER 93-3688] p 1065 A93-48357

Pressure pulsations on a delta wing in incompressible
flow p 1069 A93-48912

Numerical simulation and physical aspects of supersonic
vortex breakdown p 1093 A93-52011

Active control of vortex breakdown by a spinning wave
generator p 1219 A93-54021

[ISABE 93-7045] p 1219 A93-54021

The forms of unsteady concentrated vortex-breakdown
and its reactions to disturbance p 1231 A93-54594

Control of lift and drag in unsteady flows
[AD-A253146] p 17 N93-10340

Vortex breakdown incipience: Theoretical
considerations p 290 N93-16627

[NASA-CR-189734] p 290 N93-16627

Supersonic shock wave/vortex interaction
[NASA-CR-192917] p 695 N93-25249

Simulation of vortex bursting p 699 N93-25881

Effect of vortex behavior on loads acting on a 65 deg
delta wing oscillating in roll at high incidence p 782 N93-27220

Prediction of vortex breakdown on a delta wing
p 787 N93-27459

VORTEX FILAMENTS

The vortex behaviour of the rotating-stall cell of a
centrifugal compressor with vaned diffuser p 400 A93-19316

[ASME PAPER 92-GT-66] p 400 A93-19316

Experimental study on the three dimensional flow within
a compressor cascade with tip clearance. I - Velocity and
pressure fields p 258 A93-19574

[ASME PAPER 92-GT-215] p 258 A93-19574

Vortex/surface interaction p 468 A93-24925

[AIAA PAPER 93-0863] p 468 A93-24925

Efficient free wake calculations using
analytical/numerical matching p 874 A93-43780

VORTEX FLAPS

Flight test operations using an F-106B research airplane
modified with a wing leading-edge vortex flap p 42 A93-13261

[AIAA PAPER 92-4094] p 42 A93-13261

Experimental studies of vortex flaps and vortex plates
p 121 A93-14406

Experiments on a 60 deg delta wing with vortex flaps
and vortex plates p 477 A93-27482

Vortex flap flight test operations, a safe approach
p 995 A93-45168

VORTEX GENERATORS

Effect of the drag of the front body on the restructuring
of flow between two bodies in the path of supersonic flow,
with one body located in the wake of the other p 14 A93-12973

Calculation of separated axisymmetric flow past bodies
by solving Euler equations in the inner vortex region p 14 A93-12975

The effect of wind tunnel constraint on unsteady
aerodynamics experiments p 190 A93-14300

Detection of Goertler vortices in hypersonic flow
p 120 A93-14382

- Study on vortex flow control of inlet distortion
p 122 A93-14520
- Longitudinal vortex control - Techniques and applications (The 32nd Lanchester Lecture)
p 242 A93-18526
- Unsteady boundary-layer transition in flow periodically disturbed by wakes
[ASME PAPER 92-GT-283] p 254 A93-19475
- Experimental investigation of vortex-fin interaction
[AIAA PAPER 93-0050] p 260 A93-20163
- Augmentation of turbulent heat transfer with a vortex generator attached to a LEBU plate
p 411 A93-21729
- Shock/boundary-layer interaction control with vortex generators and passive cavity
p 287 A93-23546
- Lift enhancement of an airfoil using a Gurney flap and vortex generators
[AIAA PAPER 93-0647] p 464 A93-24762
- Vortex distortion during vortex-surface interaction in a Mach 3 stream
[AIAA PAPER 93-0761] p 467 A93-24846
- Numerical simulation of vortex generation and capture above an airfoil
[AIAA PAPER 93-0864] p 468 A93-24926
- An examination of vortex convection effects during blade-vortex interaction
p 473 A93-25360
- Study on vortex generator flow control for the management of inlet distortion
p 689 A93-34488
- Vortex generators used to control laminar separation bubbles
p 768 A93-37381
- Contribution of visualization to the study of unsteady aspects of vortex breakdown
[ONERA, TP NO. 1992-93] p 771 A93-38576
- Laser-velocimeter study of vortex breakdown on a 70-deg swept delta wing in incompressible flow
[ONERA, TP NO. 1992-147] p 773 A93-38728
- Results from a set of low speed blade-vortex interaction experiments
p 872 A93-43540
- Effects of longitudinal vortex generators on heat transfer and flow loss in turbulent channel flows
p 1021 A93-44222
- Numerical investigation of subsonic and supersonic asymmetric vortical flow
p 961 A93-45727
- On the aerodynamics and performance of active vortex generators
[AIAA PAPER 93-3447] p 979 A93-47234
- Measurements in 80- by 120-foot wind tunnel of hazard posed by lift-generated wakes
[AIAA PAPER 93-3518] p 1014 A93-47281
- Forebody vortex control - A progress review
[AIAA PAPER 93-3540] p 986 A93-47292
- Effects of aft geometry on vortex behavior and force production by a tangential jet on a body at high alpha
[AIAA PAPER 93-2961] p 1048 A93-48155
- Turbulent structure of a wingtip vortex in the near field
[AIAA PAPER 93-3011] p 1054 A93-48201
- Vortex generation and mixing in three-dimensional supersonic combustors
[AIAA PAPER 93-2144] p 1115 A93-49961
- An experimental study of supersonic air-intake with 5-shock system at Mach 3
[AIAA PAPER 93-2305] p 1082 A93-50089
- Streamwise vorticity generation and mixing enhancement in free jets by 'delta-tabs'
[AIAA PAPER 93-3253] p 1180 A93-53592
- Effect of blade leaning on the development of passage vortices and losses in the passage of turbine cascade with a great turning angle
p 1236 A93-55397
- Effect of passive flow-control devices on turbulent low-speed base flow
p 82 A93-10304
- Static pressure measurements of the shock-boundary layer interaction in a simulated fan passage
[AD-A256724] p 361 A93-15979
- Streamwise vorticity generation and mixing enhancement in free jets by delta-tabs
[NASA-TM-106235] p 988 A93-31648
- VORTEX IN CELL TECHNIQUE**
- Computation of wake roll-up for complete aircraft configurations
[AIAA PAPER 93-3509] p 984 A93-47275
- VORTEX INJECTORS**
- Attenuation of airplane wake vortices by excitation of far-field instability
[AIAA PAPER 93-3511] p 984 A93-47277
- VORTEX LATTICE METHOD**
- An aerodynamic model of multiple lifting surfaces including wake deformation and tip effect
p 10 A93-12366
- Generalized vortex lattice method for oscillating lifting surfaces in subsonic flow
p 123 A93-14555
- Experience with boundary element methods to calculate the aerodynamic characteristics of aircraft
p 243 A93-19130
- Experimental and nonlinear vortex lattice method results for various wing-canard configurations
p 479 A93-28607
- Unsteady wake effect on rotor vibratory airloadings
p 509 A93-29439
- Experimental validation of a discrete vortex method for inviscid axisymmetric flow around parachute canopies
[AIAA PAPER 93-1216] p 689 A93-35165
- Prandtl theory applied to paraglider aerodynamics
[AIAA PAPER 93-1220] p 690 A93-35169
- A study of the rotary balance technique for predicting pitch damping
[AIAA PAPER 93-3619] p 1125 A93-48306
- Lateral aerodynamic interference between tanker and receiver in air-to-air refueling
p 1136 A93-52444
- VORTEX RINGS**
- On the acoustic radiation nature of a turbulent vortex ring
p 446 A93-19167
- A wind shear hazard window useful in studying the effect of wind shear on the airplane during the landing approach
[AIAA PAPER 93-3643] p 1127 A93-48327
- Dynamics of vortex rings in cross-flow
p 134 A93-13917
- Axisymmetric vortex sheet roll-up
p 788 A93-28078
- VORTEX SHEDDING**
- The frequency of incipient vortex-shedding from a circular cylinder in a laminar boundary layer (The effect of the gap ratio on the vortex shedding frequency)
p 126 A93-15488
- Viscous and inviscid instabilities of a trailing vortex
p 268 A93-21042
- Numerical simulation of dynamic lift enhancement using oscillatory leading edge flaps
[AIAA PAPER 93-0186] p 276 A93-22611
- Unsteady laminar separation on low-Reynolds-number airfoils
[AIAA PAPER 93-0209] p 278 A93-22627
- Measurement of shed vorticity and circulation from rotating aerofoil by particle image velocimetry
p 538 A93-23804
- A Navier-Stokes simulation of vortex shedding from square cylinder in unconfined domain
p 538 A93-24084
- An interaction noise between vortex and airfoil
[AIAA PAPER 93-0600] p 562 A93-24726
- The interaction between a steady jet flow and a supersonic blade tip
p 688 A93-34415
- Numerical simulation of vortex shedding past triangular cylinders at high Reynolds number using a k-epsilon turbulence model
p 871 A93-42873
- Observations of large-scale structures in wakes behind axisymmetric bodies
p 965 A93-46748
- The hemisphere-cylinder in dynamic pitch-up motions
[AIAA PAPER 93-2963] p 1048 A93-48157
- Study of the near-wake structure of a subsonic base cavity flowfield using PIV
[AIAA PAPER 93-3040] p 1056 A93-48221
- Minimization of the induced drag of nonplanar lifting systems
p 1068 A93-48910
- Periodic vortex shedding over delta wings
p 1070 A93-49002
- Thoughts on conical flow asymmetry
p 1070 A93-49003
- Effect of rounding side corners on vortices shedding and downwash from square cylinder of finite length placed on a ground plane
p 1160 A93-51893
- Euler analysis of forebody-strake vortex flows at supersonic speeds
p 1094 A93-52429
- Numerical analysis of the flow through a centrifugal impeller by vortex distribution model of a boundary layer. I - Theoretical analysis
p 1182 A93-53843
- The unsteady flow past a supersonic splitter plate
[ISABE 93-7047] p 1185 A93-54023
- Development of the wake behind a circular cylinder impulsively started into rotatory and rectilinear motion
p 1236 A93-55736
- A prediction model for the vortex shedding noise from the wake of an airfoil or axial flow fan blades
p 1265 A93-55995
- An investigation of the effects of aft blowing on a 3.0 caliber tangent ogive body at high angles of attack
[NASA-CR-190934] p 24 A93-12004
- Wake similarity and vortex formation for two-dimensional bluff bodies
p 138 A93-15101
- Experiments on smooth cantilevered circular cylinders in low-turbulence uniform flow. Part 1: Mean loading with aspect ratios in the range 4 to 30
[PB93-111763] p 555 A93-21383
- The transient development of vortices over delta wings
p 695 A93-25269
- Spurious frequencies as a result of numerical boundary treatments
p 839 A93-27170
- Studies of origin of three-dimensionality in laminar wakes
[AD-A262281] p 841 A93-28242
- Vortex shedding by blunt/bluff bodies at high Reynolds numbers. Volume 4: Rectangles
[AD-A264154] p 877 A93-30151
- Vortex shedding by blunt/bluff bodies at high Reynolds numbers. Volume 1: Data analysis
[AD-A264151] p 877 A93-30171
- Vortex shedding by Blunt/Bluff bodies at high Reynolds numbers. Volume 2: Cylinders, octagon, hexagon
[AD-A264152] p 877 A93-30172
- Vortex shedding by blunt/bluff bodies at high Reynolds numbers. Volume 3: Cubes
[AD-A264153] p 877 A93-30173
- A theoretical and computational study on active wake control
p 878 A93-30892
- VORTEX SHEETS**
- An adaptive region method for computation of vortex sheet behind wing in compressible flow
p 116 A93-14262
- The influence of the fuselage on high alpha vortical flows and the subsequent effect on fin buffeting
p 116 A93-14263
- A study of singularity formation in vortex-sheet motion by a spectrally accurate vortex method
p 127 A93-16666
- Instability of rectangular jets
p 398 A93-19157
- Three dimensional near field behavior of a tip vortex developing on an elliptic foil
[AIAA PAPER 93-0865] p 468 A93-24927
- Instability of rectangular jets
p 720 A93-34410
- Treatment of vortex sheets for the transonic full-potential equation
p 871 A93-42870
- Effect of ground and ceiling planes on shape of energized wakes
[AIAA PAPER 93-3410] p 974 A93-47207
- Three-dimensional numerical simulation of gradual opening in a wave rotor passage
[AIAA PAPER 93-2526] p 1156 A93-50254
- Thrust imparted to an airfoil by passage through a sinusoidal upwash field
p 1178 A93-53219
- A method for aerodynamic calculation by placing linear vari-strength vortex panels on airfoil contour
p 1231 A93-54597
- Instability of a supersonic vortex sheet inside a circular duct
p 1234 A93-55142
- Analysis of wing wake roll-up using a vortex-in-cell method
p 697 A93-25706
- Axisymmetric vortex sheet roll-up
p 788 A93-28078
- Three-dimensional numerical simulation of gradual opening in a wave rotor passage
[NASA-CR-191157] p 900 A93-29072
- VORTEX STREETS**
- Further studies on the asymmetrical flow past yawed cylinders
p 118 A93-14304
- Studies of origin of three-dimensionality in laminar wakes
[AD-A262281] p 841 A93-28242
- Contribution to the study of the interaction between acoustic waves and coherent structures induced by a prismatic cylinder in a rectangular cavity
[ONERA-NT-1990-10] p 918 A93-30203
- VORTICES**
- Rotation and cavitation of a marginal vortex
p 11 A93-12433
- The composite shape and structure of coherent eddies in the convective boundary layer
p 93 A93-12643
- Monotonicity characteristics of some plane vortex flows of incompressible fluids and subsonic gas flows
p 13 A93-12932
- A study of the effect of a moving ground belt on the vortex created by a jet impinging on the ground in a cross flow
[AIAA PAPER 92-4250] p 15 A93-13361
- Ground vortex formation for uniform and nonuniform jets impinging on a ground plane
[AIAA PAPER 92-4251] p 80 A93-13362
- Vortex control technology
p 111 A93-14152
- Modelling for airfoil induced unsteady aerodynamic effects for parameter estimation
p 118 A93-14323
- Leading edge vortices in a chordwise periodic flow
p 119 A93-14333
- Experimental study on the mechanism of favourable interferences of body strakes
p 121 A93-14405
- A vortex control technique for the attenuation of fin buffet
p 121 A93-14408
- A low-speed wind tunnel study of vortex interaction control techniques on a chine-forebody/delta-wing configuration
p 122 A93-14409
- Study on vortex flow control of inlet distortion
p 122 A93-14520
- Determination of vortex burst location on delta wings from surface pressure measurements
p 123 A93-14557
- Coriolis effects on Goertler vortices in the boundary-layer flow on concave wall
p 123 A93-14564
- Acoustic control of flow separation on a straight and a yawed wing
p 125 A93-15256
- On the cross-flow instability near a rotating disk
p 128 A93-17264

The use of the Polhamus and discrete vortex methods for calculating the nonlinear characteristics of delta wings and wings with a strake p 242 A93-18379

Motion and decay of trailing vortices within the atmospheric surface layer p 425 A93-18548

Flow field measurements in a turbulent free jet issuing from a sharp-edged square slot p 244 A93-19158

Boundary conditions for direct computation of aerodynamic sound generation p 447 A93-19176

Forward rotor vortex effects on counter rotating propeller noise p 245 A93-19221

An assessment of wake structure behind forward swept and aft swept propfans at high loading p 245 A93-19222

Numerical solutions for unsteady subsonic vortical flows around loaded cascades [ASME PAPER 92-GT-173] p 250 A93-19399

The role of noise in two-dimensional vortex merging p 408 A93-19967

A sensitivity study for pneumatic vortex control on a chined forebody [AIAA PAPER 93-0049] p 260 A93-20162

Numerical analysis of a chined forebody with asymmetric strakes [AIAA PAPER 93-0051] p 260 A93-20164

Static roll moment characteristics of asymmetric tangential leading edge blowing on a delta wing at high angles of attack [AIAA PAPER 93-0052] p 261 A93-20165

Calculations of separated vortex flows at low speed for low-aspect-ratio wings p 264 A93-20300

Transitional characteristics of vortices issued from a body which creates asymmetric flow field - In a case of thin symmetrical airfoil with angle of attack under rotational oscillation of small amplitude p 267 A93-20923

Streamwise variation of mean velocity field for the turbulent boundary layer interacting with controlled longitudinal vortex arrays p 267 A93-20933

Flow around two circular cylinders by the random-vortex method p 271 A93-21925

Experimental and numerical analysis of the wing rock characteristics of a 'wing-body-tail' configuration [AIAA PAPER 93-0187] p 368 A93-22612

Vortical and turbulent structure of a lobed mixer free-shear layer [AIAA PAPER 93-0219] p 415 A93-22635

Measurements of circulation and vorticity in the leading-edge vortex of a delta wing p 288 A93-23548

Experimental investigation of a 2D parallel vortex/airfoil interaction p 538 A93-23808

Driven cavity simulation of turbomachine blade flows with vortex control [AIAA PAPER 93-0390] p 461 A93-24238

Doppler global velocimetry - The next generation? [AIAA PAPER 92-3897] p 539 A93-24486

Pressure-based high-order TVD methodology for dynamic stall simulation [AIAA PAPER 93-0680] p 466 A93-24788

A concurrent hybrid Navier-Stokes/Euler approach to fluid dynamic computations [AIAA PAPER 93-0789] p 468 A93-24865

A new method for improved rotor free-wake convergence [AIAA PAPER 93-0872] p 469 A93-24933

Introduction of small velocity and pressure variation into a stationary compressible fluid p 473 A93-25060

Experimental and numerical investigations of the vortex-flame interactions in a driven jet diffusion flame [AIAA PAPER 93-0455] p 534 A93-25532

Interaction of a streamwise vortex with a free surface [AIAA PAPER 93-0556] p 543 A93-25539

The effect of Reynolds number on vortex asymmetry about slender bodies p 475 A93-26176

Uniform high-order spectral methods for one- and two-dimensional Euler equations p 476 A93-27068

Calculation of three-dimensional supersonic flow past lifting surfaces p 477 A93-27607

Experience with the use of liquid crystals in conjunction with the filament method is studying the structure of supersonic flow downstream of a plane step p 478 A93-27639

Prediction of asymmetric vortical flows around slender bodies using Navier-Stokes equations p 478 A93-27925

Potential hazard of aircraft wake vortices in ground effect with crosswind p 479 A93-28606

Role of leading-edge vortex flows in prop-fan interaction noise p 565 A93-28614

Current status of computational methods for transonic unsteady aerodynamics and aeroelastic applications p 480 A93-29175

Flowfield analysis of modern helicopter rotors in hover by Navier-Stokes method p 481 A93-29435

Vortex initiation during dynamic stall of an airfoil p 684 A93-34335

Prandtl theory applied to paraglider aerodynamics [AIAA PAPER 93-1220] p 690 A93-35169

Computation of aeroelastic characteristics and stress-strained state of parachutes [AIAA PAPER 93-1237] p 744 A93-35178

Results from a conical Euler methodology developed for unsteady vortical flows p 692 A93-35612

Applications of shock-induced mixing to supersonic combustion p 735 A93-35618

Vortex methods for the computational analysis of rotor/body interaction p 765 A93-35939

Numerical prediction of aerodynamic sound using large eddy simulation p 850 A93-38150

Numerical computation of aerodynamic noise radiation by the large eddy simulation p 850 A93-38151

Supersonic vortical flows around an ogive-cylinder - Laminar and turbulent computations [ONERA, TP NO. 1992-111] p 771 A93-38588

Phenomenology and simplified modeling of a vortex wake generated by a transverse jet [ONERA, TP NO. 1992-194] p 774 A93-38755

Vortex-induced energy separation in shear flows p 837 A93-39427

An aerodynamic model for flapping-wing flight p 858 A93-40470

A study of the interaction between a wake vortex and an encountering airplane [AIAA PAPER 93-3642] p 858 A93-40714

Infrared thermography characterization of Goertler vortex type patterns in hypersonic flows [ONERA, TP NO. 1993-13] p 925 A93-41029

Symmetry breaking in vortical flows over cones - Theory and numerical experiments [AIAA PAPER 93-3408] p 859 A93-41056

Vortex features of F-106B aircraft at subsonic speeds [AIAA PAPER 93-3471] p 859 A93-41058

Control of vortices on a delta wing by leading-edge injection p 860 A93-41906

Experimental investigation of leading edge vortices using LDA p 861 A93-42254

Strong vortex/boundary layer interactions. I - Vortices high p 930 A93-43539

Vortex-induced disturbance field in a compressible shear layer p 873 A93-43628

Effects of spatial order of accuracy on the computation of vortical flowfields [AIAA PAPER 93-3371] p 955 A93-45064

Plume and wake dynamics, mixing, and chemistry behind a high speed civil transport aircraft p 1034 A93-45139

Effects of wing-tip vortex flaps p 959 A93-45153

Instantaneous topology of the unsteady leading-edge vortex at high angle of attack p 961 A93-45728

Decay of aircraft vortices near the ground p 961 A93-45751

Strong vortex/boundary layer interactions. II - Vortices low p 965 A93-46744

A visual study of recessed angled spanwise blowing method on a delta wing [AIAA PAPER 93-3246] p 966 A93-46791

A three dimensional view of velocity using lasers p 1028 A93-46822

Passive control of coherent vortices in compressible mixing layers [AIAA PAPER 93-3262] p 968 A93-46828

Effect of canard oscillations on the vortical flowfield of a X-31A-like fighter model in dynamic motion [AIAA PAPER 93-3427] p 1008 A93-47222

Forebody vortex control with jet and slot blowing on an F/A-18 [AIAA PAPER 93-3449] p 1009 A93-47235

Forebody vortex control on an F/A-18 using small, rotatable 'tip-strakes' [AIAA PAPER 93-3450] p 1009 A93-47236

Boundary layer effects on the flow of a leading edge vortex [AIAA PAPER 93-3463] p 980 A93-47245

Trajectory mapping of quasi-periodic structures in a vortex flow [AIAA PAPER 93-2914] p 1044 A93-48116

An exploratory wind tunnel study of supersonic tip vortices [AIAA PAPER 93-2923] p 1045 A93-48124

Simulation of DD-963 ship airwake by Navier-Stokes method [AIAA PAPER 93-3002] p 1053 A93-48192

Vortex developments over steady and accelerated airfoils incorporating a trailing edge jet [AIAA PAPER 93-3008] p 1054 A93-48198

Wake-vortex structure from lift and torque induced on a following wing [AIAA PAPER 93-3013] p 1054 A93-48202

Control of separation by dynamic air jets p 1066 A93-48504

A calculation of secondary flows and deviation angles in multistage axial-flow compressors p 1066 A93-48509

A study of the effect of surface riblets on the evolution of a solitary wave packet (lambda vortex) in a laminar boundary layer p 1067 A93-48827

Boundary conditions for direct computation of aerodynamic sound generation p 1172 A93-49005

Flow and heat transfer in a turbulent boundary layer through skewed and pitched jets p 1151 A93-49007

The challenges of simulating wake vortex encounters and assessing separation criteria [AIAA PAPER 93-3568] p 1096 A93-49518

Effect of geometry, bleed rates and flow splits on pressure recovery of a canted hybrid vortex-controlled diffuser [AIAA PAPER 93-1762] p 1109 A93-49659

Rotor-rotor interaction for counter-rotating fans. I - Three dimensional flowfield measurements [AIAA PAPER 93-1848] p 1075 A93-49729

Scramjet fuel mixing enhancement by cross-stream pressure gradients [AIAA PAPER 93-2139] p 1114 A93-49957

Effects of flow-path variations on internal reversing flow in a tailpipe offtake configuration for ASTOVL aircraft [AIAA PAPER 93-2438] p 1118 A93-50190

Three-dimensional numerical simulation of gradual opening in a wave rotor passage [AIAA PAPER 93-2526] p 1156 A93-50254

Nonplanar wings with a minimum induced drag p 1089 A93-51779

A study of pressure fluctuations on the surface of a delta wing near the sharp leading edge p 1091 A93-51882

Investigation of vortex development on a pitching slender body of revolution p 1095 A93-52445

Construction of wakes in the discrete vortex method p 1179 A93-53333

Streamwise vorticity generation and mixing enhancement in free jets by 'delta-tabs' [AIAA PAPER 93-3253] p 1180 A93-53592

The development of a new air filtration system for the Alouette III helicopter [ISABE 93-7048] p 1199 A93-54024

A study of the stability of vortical structures in supersonic inlets [ISABE 93-7103] p 1187 A93-54079

An improved multiple line-vortex method for simulation of separated vortices of slender wings p 1236 A93-55412

Interaction of compressible vortices with a rigid plate p 1239 A93-56219

Navier-Stokes dynamics and aeroelastic computations for vortical flows, buffet and aeroelastic applications [NASA-CR-190692] p 17 N93-10098

Forced unsteady separated flows on a 45 degree delta wing p 82 N93-10305

Control of lift and drag in unsteady flows [AD-A253146] p 17 N93-10340

Shock enhancement and control of hypersonic combustion [AD-A254295] p 72 N93-10843

Contributions to the experimental investigation of rotor/body aerodynamic interactions p 20 N93-10877

Dynamical effects of suction/heating on turbulent boundary layers [AD-A248459] p 87 N93-11416

The convection speed of the dynamic stall vortex [AD-A247258] p 21 N93-11464

Experimental investigation of the effects of aft blowing with various nozzle exit geometries on a 3.0 caliber tangent ogive at high angles of attack: Forebody pressure distributions [NASA-CR-190935] p 22 N93-11605

An experimental study of flow patterns and endwall heat transfer upstream of a surface-mounted rectangular obstruction in a turbulent boundary layer p 89 N93-11698

An investigation of the effects of aft blowing on a 3.0 caliber tangent ogive body at high angles of attack [NASA-CR-190934] p 24 N93-12004

Unsteady propeller/wing aerodynamic interactions p 24 N93-12190

The influence of intake swirl distortion on the steady-state performance of a low bypass, twin-spool engine p 214 N93-13211

The jet behaviour of an actual high-bypass engine as determined by LDA-measurements in ground tests p 175 N93-13218

In-flight flow visualization results from the X-29A aircraft at high angles of attack [NASA-TM-4430] p 131 N93-13322

Chaotic vortical motion in the near region of a plane jet p 131 N93-13493

Airfoil-vortex interaction and the wake of an oscillating airfoil p 134 N93-13803

The unsteady aerodynamics of a delta wing undergoing large-amplitude pitching motions p 134 N93-13929

- Passive control of supersonic asymmetric vortical flows around cones p 220 N93-14692
- Wake similarity and vortex formation for two-dimensional bluff bodies p 239 N93-15101
- Flowfield study of a close-coupled canard configuration [AD-A256311] p 139 N93-15245
- Special publication of National Aerospace Laboratory [DE93-716176] p 239 N93-15946
- Experimental and numerical investigation of vortex flow over a 76/60-deg double-delta wing [LR-680] p 289 N93-16210
- Vortex breakdown incipience: Theoretical considerations [NASA-CR-189734] p 290 N93-16627
- Two- and three-dimensional blade vortex interactions [NASA-CR-177567] p 293 N93-16942
- Application of an Euler-equation method to a sharp-edged delta wing configuration with vortex flow [NLR-TP-91306] p 294 N93-17809
- Simulation of unsteady rotational flow over propfan configuration [NASA-CR-192234] p 296 N93-18585
- Experimental and numerical examinations of the influence of inlet distortion perturbations on the working behavior of turbofan compressors [ETN-93-92733] p 364 N93-18628
- The stability of a trailing-line vortex in compressible flow [NASA-CR-189738] p 298 N93-18771
- Proceedings of the Ninth NAL Symposium on Aircraft Computational Aerodynamics [NAL-SP-16] p 299 N93-19273
- Generation of longitudinal vortices in supersonic flow p 301 N93-19292
- Three dimensional calculation of flow inside supersonic inlet p 303 N93-19313
- Advanced adaptive computational methods for Navier-Stokes simulations in rotorcraft aerodynamics [NASA-CR-192282] p 483 N93-20256
- Proceedings of the Aircraft Wake Vortices conference, volume 1 [PB93-126449] p 485 N93-21796
- Proceedings of the Aircraft Wake Vortices conference, volume 2 [PB93-127728] p 559 N93-21799
- Crossflow stability and transition experiments in a swept-wing flow [NASA-TM-108650] p 555 N93-21819
- Computational study of the aerodynamics and control by blowing of asymmetric vortical flows over delta wings p 693 N93-24772
- Flow visualizations of perpendicular blade vortex interactions [NASA-CR-192725] p 748 N93-25208
- Supersonic shock wave/vortex interaction [NASA-CR-192917] p 695 N93-25249
- The transient development of vortices over delta wings p 695 N93-25269
- Tangential fuselage blowing on an ogive cylinder p 697 N93-25545
- Analysis of wing wake roll-up using a vortex-in-cell method p 697 N93-25706
- Initial streamwise vorticity formation in a two-stream mixing layer p 698 N93-25752
- Large-eddy simulation of temporally developing boundary layers with embedded streamwise vortices p 750 N93-25753
- Simulation of vortex bursting p 699 N93-25881
- Method of measuring cross-flow vortices by use of an array of hot-film sensors [NASA-CASE-LAR-14824-1-SB] p 751 N93-26000
- Reduction in size and unsteadiness of a VTOL ground vortex by ground fences [NASA-CR-192997] p 700 N93-26049
- Conical Euler analysis and active roll suppression for unsteady vortical flows about rolling delta wings [NASA-TP-3259] p 701 N93-26134
- Trailing vortex/free-surface interaction [AD-A261654] p 701 N93-26195
- Roughness-induced generation of crossflow vortices in three-dimensional boundary layers [NASA-CR-4505] p 780 N93-27096
- Leading edge vortices in a chordwise periodic flow p 782 N93-27218
- Turbulence: The chief outstanding difficulty of our subject p 783 N93-27428
- The transition prediction toolkit: LST, SIT, PSE, DNS, and LES p 783 N93-27429
- Investigation of forced unsteady separated flows using velocity-vorticity form of Navier-Stokes equations p 840 N93-27451
- Simultaneous mapping of the unsteady flow fields by Particle Displacement Velocimetry (PDV) p 786 N93-27454
- Prediction of vortex breakdown on a delta wing p 787 N93-27459
- Axisymmetric vortex sheet roll-up p 788 N93-28078
- Studies of origin of three-dimensionality in laminar wakes [AD-A262281] p 841 N93-28242
- The onset of vortex turbulence p 788 N93-28251
- The ground vortex flow field associated with a jet in a cross flow impinging on a ground plane for uniform and annular turbulent axisymmetric jets [NASA-CR-4513] p 789 N93-28449
- Effects of flow-path variations on internal reversing flow in a tailpipe offtake configuration for ASTOVL aircraft [NASA-TM-106149] p 900 N93-29065
- Three-dimensional numerical simulation of gradual opening in a wave rotor passage [NASA-CR-191157] p 900 N93-29072
- Unsteady vortex loop/dipole theory applied to the work and acoustics of an ideal low speed propeller [AD-A264057] p 876 N93-29891
- The application of concentric vortex simulation to calculating the aerodynamic characteristics of bodies of revolution at high angles of attack [AD-A263879] p 876 N93-29919
- Vortex structure and mass transfer near the base of a cylinder and a turbine blade p 901 N93-29929
- Three-dimensional fiber-optic LDV measurements in the endwall region of a linear cascade of controlled-diffusion stator blades [AD-A263513] p 933 N93-29968
- Vortex shedding by blunt/bluff bodies at high Reynolds numbers. Volume 4: Rectangles [AD-A264154] p 877 N93-30151
- Vortex wake characteristics of B757-200 and B767-200 aircraft using the tower fly-by technique [PB93-180255] p 878 N93-30387
- Vortex wake characteristics of B757-200 and B767-200 aircraft using the tower fly-by technique [PB93-180263] p 878 N93-30388
- Streamwise vorticity generation and mixing enhancement in free jets by delta-tabs [NASA-TM-106235] p 988 N93-31648
- VORTICITY**
- Vortex control technology p 111 A93-14152
- Flow structures around a constant-rate pitching airfoil and mechanism of dynamic stall p 118 A93-14332
- Study on vortex flow control of inlet distortion p 122 A93-14520
- Experimental study on the three dimensional flow within a compressor cascade with tip clearance. II - The tip leakage vortex [ASME PAPER 92-GT-432] p 258 A93-19575
- 3-D LDV measurements over a delta wing in pitch-up motion [AIAA PAPER 93-0185] p 275 A93-22610
- Visualization of vortical flows with yet another post-processor [AIAA PAPER 93-0222] p 415 A93-22638
- Vortical solutions in supersonic corner flows [AIAA PAPER 93-0760] p 466 A93-24845
- Experimental study of three-dimensional separation on a large-size model [ONERA, TP NO. 1992-174] p 473 A93-25348
- On the principle of sidewall effects on airfoil testing p 730 A93-33732
- A numerical method of unsteady separating flow over delta wings p 681 A93-33746
- Numerical methods in laminar and turbulent flow; Proceedings of the 7th International Conference, Stanford Univ., CA, July 15-19, 1991. Vol. 7, pts. 1 & 2 [ISBN 0-906674-77-8] p 743 A93-34301
- Study of supersonic intersection flowfield at modified wing-body junctions p 692 A93-35621
- Comparison of two Navier-Stokes codes for simulating high-incidence vortical flow p 768 A93-37387
- Transonic blade-vortex interactions - Noise reduction p 850 A93-37396
- Theodorsen's ideal propeller performance with ambient pressure in the slipstream p 768 A93-37400
- Characteristics of three-dimensional turbulent jets in crossflow p 772 A93-38695
- Instantaneous structure of vortex breakdown on a delta wing via particle image velocimetry p 779 A93-39428
- Effects of spatial order of accuracy on the computation of vortical flowfields [AIAA PAPER 93-3371] p 955 A93-45064
- Shock waves; Proceedings of the 18th International Symposium, Sendai, Japan, July 21-26, 1991. Vols. 1 & 2 [ISBN 0-387-55686-9] p 1023 A93-45451
- Strong vortex/boundary layer interactions. II - Vortices low p 965 A93-46744
- The use of streamwise vorticity to enhance ejector performance [AIAA PAPER 93-3247] p 966 A93-46792
- Vorticity dynamics in spatially developing rectangular jets [AIAA PAPER 93-3286] p 969 A93-46842
- Inverse problem using S2-S1 approach for the design of the turbomachine with splitter blades p 971 A93-46929
- AIAA Applied Aerodynamics Conference, 11th, Monterey, CA, Aug. 9-11, 1993, Technical Papers, Pts. 1 & 2 p 974 A93-47201
- Effect of ground and ceiling planes on shape of energized wakes [AIAA PAPER 93-3410] p 974 A93-47207
- Separated flowfield and lift on an airfoil with an oscillating leading-edge flap [AIAA PAPER 93-3422] p 976 A93-47217
- Vortical solutions in supersonic corner flows p 1071 A93-49015
- Vortex generation and mixing in three-dimensional supersonic combustors [AIAA PAPER 93-2144] p 1115 A93-49961
- Streaming vorticity flux from oscillating walls with finite amplitude p 1160 A93-52517
- Fast three-dimensional vortex method for unsteady wake calculations p 1178 A93-53233
- The Application of CFD to rotary wing flow problems [NASA-TM-102803] p 139 N93-15483
- The transient development of vortices over delta wings p 695 N93-25269
- Numerical simulation of leading-edge receptivity to freestream vorticity p 696 N93-25388
- Initial streamwise vorticity formation in a two-stream mixing layer p 698 N93-25752
- Investigation of forced unsteady separated flows using velocity-vorticity form of Navier-Stokes equations p 840 N93-27451
- Studies of origin of three-dimensionality in laminar wakes [AD-A262281] p 841 N93-28242
- VORTICITY EQUATIONS**
- Control of numerical diffusion in computational modeling of vortex flows p 9 A93-12156
- Integral equations in the problem of flow past an airfoil p 395 A93-18243
- Three-dimensional vortex method for parachutes p 872 A93-42874
- Numerical vorticity capturing for vortex-solid body interaction problems [AIAA PAPER 93-3343] p 954 A93-45037
- Finite element solution of the 3D compressible Navier-Stokes equations by a velocity-vorticity method p 974 A93-47196
- Asymmetric vortical solutions in supersonic corners - Steady 3D space-marching versus time-dependent conical results [AIAA PAPER 93-2957] p 1047 A93-48151
- VULNERABILITY**
- Insights into US domestic aviation p 496 N93-21859
- W**
- WAKES**
- Ship airwake measurement and flow visualization [AIAA PAPER 92-4088] p 7 A93-11267
- An assessment of wake structure behind forward swept and aft swept propfans at high loading p 245 A93-19222
- Investigation of compressor rotor wake structure at peak pressure rise coefficient and effects of loading [ASME PAPER 92-GT-32] p 246 A93-19292
- Viscous interaction upstream and downstream of a turbine stator cascade with a periodic wake field [ASME PAPER 92-GT-162] p 250 A93-19388
- Calculation of wake-induced unsteady flow in a turbine cascade [ASME PAPER 92-GT-306] p 255 A93-19496
- Analytical formulation of optimum rotor interdisciplinary design with a three-dimensional wake [AIAA PAPER 92-4778] p 265 A93-20416
- Subharmonic and harmonic forced response of the wake of a circular cylinder p 288 A93-23565
- The analysis of viscous wakes noise in axial flow compressor p 759 A93-33710
- A study of the rotor wake of a small-scale rotor model in forward flight using laser light sheet flow visualization with comparisons to analytical models p 766 A93-35957
- Prediction of BVI noise patterns and correlation with wake interaction locations p 849 A93-35966
- Flap-lag damping in hover and forward flight with a three-dimensional wake p 797 A93-35979
- A parametric study of real time mathematical modeling incorporating dynamic wake and elastic blades p 798 A93-35986

Shadowgraph flow visualization of isolated tiltrotor and rotor/wing wakes p 767 A93-35996

Aerodynamic and wake methodology evaluation using model UH-60A experimental data p 767 A93-35997

An aerodynamic model for flapping-wing flight p 858 A93-40470

Oscillations of circular shock waves with upstream disturbance p 1023 A93-45463

Observations of large-scale structures in wakes behind axisymmetric bodies p 965 A93-46748

Effect of ground and ceiling planes on shape of energized wakes p 974 A93-47207

[AIAA PAPER 93-3410]

SCV measurements in the wake of a rotor in hover and forward flight p 1059 A93-48254

[AIAA PAPER 93-3080]

Analysis of wake-induced unsteady flow in axial compressors - Radial variations of wake excitation forces estimated by strip theory p 1086 A93-51123

Development of the wake behind a circular cylinder impulsively started into rotatory and rectilinear motion p 1236 A93-55736

Contributions to the experimental investigation of rotor/body aerodynamic interactions p 20 N93-10877

Stratospheric aircraft exhaust plume and wake chemistry studies p 94 N93-12299

[NASA-CR-189688]

Airfoil-vortex interaction and the wake of an oscillating airfoil p 134 N93-13803

The effect of wake dynamics on rotor eigenvalues in forward flight p 137 N93-14595

Wake similarity and vortex formation for two-dimensional bluff bodies p 138 N93-15101

An experimental study of a turbulent boundary layer in the trailing edge region of a circulation-control airfoil [NASA-CR-191262] p 295 N93-17934

Application of finite-state inflow to flap-lag-torsion damping in hover p 714 N93-25486

Analysis of wing wake roll-up using a vortex-in-cell method p 697 N93-25706

Quantitative three-dimensional low-speed wake surveys p 785 N93-27447

Some recent applications of Navier-Stokes codes to rotorcraft p 786 N93-27452

A theoretical and computational study on active wake control p 878 N93-30892

Penn State axial flow turbine facility: Performance and nozzle flow field p 1032 N93-31588

WALL FLOW

Variational problem of the profiling of the side walls of the supersonic section of a narrow three-dimensional nozzle p 4 A93-10140

Numerical dissipation in F3D thin-layer Navier-Stokes solution for flows with wall transpiration p 9 A93-12010

Effect of wall heating on a supersonic turbulent boundary layer p 11 A93-12429

Influence of surface heat flux ratio on heat transfer augmentation in square channels with parallel, crossed, and V-shaped angled ribs p 201 A93-13981

Further studies on the asymmetrical flow past yawed cylinders p 118 A93-14304

On the measurements of the skin friction in 3-D flows - Application to a complete 3-D shear layer flow p 118 A93-14329

Coriolis effects on Goertler vortices in the boundary-layer flow on concave wall p 123 A93-14564

Three dimensional transonic flow measurements in an axial turbine with conical walls p 247 A93-19311

[ASME PAPER 92-GT-61]

Numerical simulation of compressor endwall and casing treatment flow phenomena p 255 A93-19490

[ASME PAPER 92-GT-300]

Viscous throughflow modelling for multi-stage compressor design p 255 A93-19492

[ASME PAPER 92-GT-302]

Comparison of predictions with measurements for a quiet supersonic tunnel p 376 A93-23031

[AIAA PAPER 93-0344]

An optical comparison of wall and axial injection for high enthalpy reacting scramjet flows p 377 A93-23040

[AIAA PAPER 93-0357]

The influence of wall friction on sidewall interference p 680 A93-33723

On the principle of sidewall effects on airfoil testing p 730 A93-33732

Parametrical investigation of the interaction between turbulent wall shear layers and normal shock waves, including separation p 681 A93-33752

Asymptotic methods for the prediction of transonic wind-tunnel wall interference p 730 A93-35625

A new adaptive test section at ONERA Chalais-Meudon [ONERA, TP NO. 1992-117] p 822 A93-38592

On model for predicting blade force defect in end wall boundary layer inside axial compressor cascade p 862 A93-42271

Surface boundary conditions for the numerical solution of the Euler equations p 953 A93-45028

[AIAA PAPER 93-3334]

Effects of wall conditions on chemically nonequilibrium shock-layer flow over hypersonic reentry bodies p 970 A93-46908

A pointwise version of the Baldwin-Barth turbulence model p 985 A93-47284

[AIAA PAPER 93-3523]

High lift airfoil flow simulation using a wall-corrected Algebraic Stress Model p 1061 A93-48280

[AIAA PAPER 93-3109]

An experimental investigation of endwall flow control in a compressor plane cascade wind tunnel p 1066 A93-48512

A blade element method for predicting the off-design performance of compressors p 1107 A93-49187

Investigation of a strut/endwall interaction in supersonic annular flow p 1076 A93-49791

[AIAA PAPER 93-1925]

Unsteady, three-dimensional, Navier-Stokes simulations of multistage turbomachinery flows p 1153 A93-49826

[AIAA PAPER 93-1979]

Stator relative, rotor blade-to-blade near wall flow in a multistage axial compressor with tip clearance variation p 1083 A93-50154

[AIAA PAPER 93-2389]

Minimizing the wall effects in wind tunnels with a sectional pressure chamber p 1085 A93-50965

Streaming vorticity flux from oscillating walls with finite amplitude p 1160 A93-52517

Skin-friction topology over a surface mounted semi-ellipsoidal wing at incidence p 1178 A93-53216

The effects of reaction rate constants and catalytic wall on the hypersonic flow field over blunt bodies p 1230 A93-54586

A new method for predicting the end wall boundary layers and the blade force defects inside the passage of axial compressor cascades p 1236 A93-55589

Characteristics of separated flows including cavitation effects p 84 N93-10874

Application of a solution adaptive grid to flow over an embedded cavity p 130 N93-13141

An experimental and analytical study of TIP clearance effects in axial flow compressors p 179 N93-15337

[AD-A256434]

A wall interference assessment/correction system p 296 N93-18384

[NASA-CR-191889]

Numerical simulations of hypersonic rarefied transition regime flows: DSMC method and Navier-Stokes computation p 299 N93-19278

An analysis of lift forces on aerosols in a wall bounded turbulent shear flow p 747 N93-24963

[DE93-003362]

Turbulence: The chief outstanding difficulty of our subject p 783 N93-27428

An interactive boundary-layer approach to multielement airfoils at high lift p 785 N93-27445

Investigations on entropy layer along hypersonic hypoboloids using a defect boundary layer p 787 N93-27462

Experimental study of heat transfer close to a plane wall heated in the presence of multiple injections (subsonic flow) p 901 N93-29931

WALL JETS

Computational analysis of hypersonic shock wave/wall jet interaction p 269 A93-21113

[AIAA PAPER 93-0604]

Effect of combustion on the interaction of an underexpanded wall hydrogen jet with supersonic flow in a plane duct p 534 A93-27658

Wall jets created by single and twin high pressure jet impingement p 744 A93-34847

Investigation of a contoured wall injector for hypervelocity mixing augmentation p 837 A93-39407

Reduction in size and unsteadiness of a VTOL ground vortex by ground fences p 700 N93-26049

[NASA-CR-192997]

Heat transfer in high turbulence flows: A 2-D planar wall jet p 932 N93-29935

WALL PRESSURE

Wall pressure fluctuations beneath swept shock wave/boundary layer interactions p 282 A93-23063

[AIAA PAPER 93-0384]

A study of flow separation on an oscillating flap at Mach number 2.4 p 286 A93-23350

[AIAA PAPER 93-0436]

Two important improvements upon wall pressure signature correction method of low-speed wind tunnel p 730 A93-33704

Underexpanded boundary jet in a wake flow p 775 A93-39123

The experimental study of the effect of sweptback angles and the front shape of the fin on reduction of shock wave/turbulent boundary layer interaction region p 858 A93-40431

Experimental study of the flow around a double ellipsoid configuration p 867 A93-42603

A study of pressure fluctuations on the surface of a delta wing near the sharp leading edge p 1091 A93-51882

A wall interference assessment/correction system [NASA-CR-191889] p 296 N93-18384

An experimental study of the sources of fluctuating pressure loads beneath swept shock/boundary-layer interactions [NASA-CR-192918] p 749 N93-25266

WALL TEMPERATURE

Effects of back-pressure in a lean blowout research combustor p 387 A93-19330

[ASME PAPER 92-GT-81]

Evaluation of scramjet nozzle configurations and film cooling for reduction of wall heating p 358 A93-21118

[AIAA PAPER 93-0744]

Experiments on shock wave/boundary layer interaction in hypersonic flow p 970 A93-46888

Subscale hot-fire testing of a formed platelet liner [AIAA PAPER 93-1827] p 1141 A93-49713

Separation phenomenon in a hypersonic flow with strong wall cooling - Subcritical regime p 1189 A93-54266

Investigation of hot streak migration and film cooling effects on heat transfer in rotor/stator interacting flows, report 1 p 102 N93-12490

[AD-A250688]

Hot experimental technique: A new requirement of aerothermodynamics p 293 N93-17543

[MBB-FE-202-S-PUB-480]

Three-dimensional compressible stability-transition calculations using the spatial theory p 783 N93-27431

WALLS

Initial results from the NASA Lewis wave rotor experiment p 1193 A93-53589

[AIAA PAPER 93-2521]

Heat transfer and aerodynamics of a high rim speed turbine nozzle guide vane with profiled end walls p 295 N93-17991

[AD-A258346]

An analysis of lift forces on aerosols in a wall bounded turbulent shear flow p 747 N93-24963

[DE93-003362]

Direct measurements of skin friction in supersonic combustion flow fields p 825 N93-28226

[AD-A262878]

Experimental study of heat transfer close to a plane wall heated in the presence of multiple injections (subsonic flow) p 901 N93-29931

Initial results from the NASA-Lewis wave rotor experiment p 1005 N93-32368

[NASA-TM-106148]

WALSH FUNCTION

Approximation of a flight vehicle trajectory using Walsh functions p 909 A93-43106

WARNING SYSTEMS

The hazard and alarm of windshear p 141 A93-14317

Lidar windshear detection for commercial aircraft p 341 A93-17864

An experimental cockpit display for TDWR wind shear alerts p 343 A93-22111

Hazard assessment and cockpit presentation issues for microburst alerting systems p 308 A93-22112

A 'new age' in aviation weather forecasting p 427 A93-22123

Anemometer siting criteria for low level wind shear alert system p 413 A93-22178

The redesigned Low Level Wind Shear Alert System p 431 A93-22179

Reliability considerations for weather hazard warning radar p 431 A93-22187

The detection and warning of low-level wind shear based on terminal single Doppler radar p 432 A93-22195

The problem of avoiding aircraft collisions during group flights p 819 A93-39191

First moves towards an 'intelligent' GPWS p 896 A93-43624

A method of wind shear detection for powered-lift STOL aircraft p 1104 A93-48345

[AIAA PAPER 93-3667]

An Acoustic Emission Pre-failure Warning System for composite structural tests p 1161 A93-52560

Advanced terrain displays to transport category aircraft p 35 N93-10065

[PB92-197136]

Summary of findings from the PIREP-based analyses conducted during the 1988 to 1990 evaluations of TDWR-based and TDWR/LLWAS-based alert services provided to landing/departing pilots p 93 N93-11144

[AD-A253859]

- Terminal Doppler weather radar/low-level wind shear alert system integration algorithm specification, version 1.1
[AD-A255319] p 224 N93-14547
Airborne Wind Shear Detection and Warning Systems. Fourth Combined Manufacturers' and Technologists' Conference, part 2
[NASA-CP-10105-PT-2] p 144 N93-14844
Development of the Advance Warning Airborne System(AWAS) p 144 N93-14849
A millimeter-wave radiometer for detecting microbursts p 145 N93-14850
Experimental evaluation of candidate graphical microburst alert displays p 145 N93-14853
Wind shear related research at Princeton University p 145 N93-14854
In-service evaluation of wind shear systems p 146 N93-14857
Advanced technology wind shear prediction system evaluation p 146 N93-14858
Proceedings of the 16th Symposium on Aircraft Integrated Monitoring Systems
[DLR-MITT-92-01] p 167 N93-15152
The effect of TCAS interrogations on the Chicago O'Hare ATRCBS system
[DOT/FAA/CT-92/22] p 318 N93-16498
Results of DATAS investigation of illegal mode S ID's at JFK Airport
[DOT/FAA/CT-92/26] p 318 N93-16841
Airborne Wind Shear Detection and Warning Systems: Fourth Combined Manufacturers' and Technologists' Conference, part 1
[NASA-CP-10105-PT-1] p 488 N93-19590
Program overview: 1991 flight test objectives p 488 N93-19591
Three-dimensional numerical simulation of the 20 June 1991, Orlando microburst p 488 N93-19598
An approach to evaluating reactive airborne wind shear systems p 489 N93-19600
RDR-4B doppler weather radar with forward looking wind shear detection capability p 489 N93-19601
Airborne doppler radar research at Rockwell International p 489 N93-19602
Acquisition and use of Orlando, Florida and Continental Airbus radar flight test data p 489 N93-19603
Vertical wind estimation from horizontal wind measurements p 489 N93-19604
NASA airborne radar wind shear detection algorithm and the detection of wet microbursts in the vicinity of Orlando, Florida p 490 N93-19611
Signal processing for airborne doppler radar detection of hazardous wind shear as applied to NASA 1991 radar flight experiment data p 490 N93-19612
Aviation safety: Users differ in views of collision avoidance system and cite problems. Report to the Chairman, Subcommittee on Investigations and Oversight, Committee on Science, Space, and Technology, House of Representatives
[GAO/RCED-92-113] p 502 N93-19843
A single-point warning system for thunderstorms and electric fields p 747 N93-24900
PROAV Cable Warning System (CWS) - U.S. Army aircraft integration assessment and OCONUS field evaluation
[AD-A261233] p 705 N93-26263
Detection performance of digital polarity sampled phase reversal code pulse compressors
[AD-A262930] p 842 N93-28289
Results of DATAS investigation of ATRCBS environment at the Los Angeles International Airport
[DOT/FAA/CT-93/6] p 793 N93-28625
Future directions in aviation security p 880 N93-30274
Explosives detection systems for airport security gas chromatographic based devices p 881 N93-30276
Airborne derivation of microburst alerts from ground-based Terminal Doppler Weather Radar information: A flight evaluation
[NASA-TM-108990] p 1000 N93-32223
- WASHERS (CLEANERS)**
Calculation of fuel economy for the Tu-154 aircraft in relation to the washing of the NK-8-2U engine at civil aviation maintenance facilities p 345 A93-18356
A system for washing the combustion chamber nozzles and flow path components of the NK-8-2U engine during service p 373 A93-18357
Improvement of rotating brushes for surface cleaning p 396 A93-18371
Performance of gas turbine compressor cleaners
[NLR-TP-91237-U] p 1003 N93-31111
- WASHING**
Method and apparatus for cleaning rubber deposits from airport runways and roadways
[NASA-CASE-LAR-14483-1] p 556 N93-22035
- WASPALOV**
Short fatigue crack growth in a nickel-base superalloy at room and elevated temperature
[PNR-90892] p 72 N93-11031
- WASTE DISPOSAL**
The ecological balance of Swissair: An example of waste management p 1035 N93-31930
- WATER**
Liquid water profiling using remote sensor observations p 429 A93-22150
The effects of high-pressure water on the material integrity of selected aircraft coatings and substrates
[SME PAPER AD92-207] p 855 A93-40668
A Eulerian/Lagrangian modelling to calculate the evolution of a water droplets spray
[ISABE 93-7121] p 1221 A93-54096
Preliminary design of experimental sub-scale scramjet engine
[AAS PAPER 91-639] p 1247 A93-55816
Royal Naval helicopter ditching experience p 492 N93-19684
Helicopter accidents over water in the national navy: Epidemiological study over the period 1980-1991 p 493 N93-19686
Helicopter crash survival at sea: United States Navy/Marine Corps experience 1977-1990 p 493 N93-19687
Method and apparatus for cleaning rubber deposits from airport runways and roadways
[NASA-CASE-LAR-14483-1] p 556 N93-22035
The WINCOF-I code: Detailed description
[NASA-CR-190779] p 677 N93-24760
Narrow-body aircraft water spray optimization study
[DOT/FAA/CT-TN93/3] p 705 N93-25224
- WATER COLOR**
The Airborne Ocean Color Imager - System description and image processing p 1157 A93-50369
- WATER INJECTION**
The possibility of reducing the emission of benzo(a)pyrene with the exhaust gases of aviation gas turbine engines by water injection into the combustion chamber p 812 A93-39201
Two and three-dimensional predifuser combustor studies with air-water mixture
[ISABE 93-7025] p 1213 A93-54001
- WATER PRESSURE**
Ultra-high pressure water jet technology - An overview of a new process for aerospace paint stripping
[SME PAPER AD92-196] p 855 A93-40661
- WATER TAKEOFF AND LANDING AIRCRAFT**
Ground effect on the take-off characteristics of sea-based aircraft p 679 A93-33706
- WATER TUNNEL TESTS**
Vortex breakdown over delta wings in unsteady free stream
[AIAA PAPER 93-0555] p 285 A93-23294
Experimental investigation of a 2D parallel vortex/airfoil interaction p 538 A93-23808
Pressure measurements on a pitching airfoil in a water channel
[AIAA PAPER 93-0184] p 473 A93-25510
Interaction of a streamwise vortex with a free surface
[AIAA PAPER 93-0556] p 543 A93-25539
Contribution of visualization to the study of unsteady aspects of vortex breakdown
[ONERA, TP NO. 1992-93] p 771 A93-38576
A visualization study of the vortical flow over a double-delta wing in dynamic motion
[AIAA PAPER 93-3425] p 976 A93-47220
Experiments on low aspect ratio hydroplanes to measure lift under static and dynamic conditions
[ARE-TM(UHR)-90306] p 21 N93-11365
Lift coefficient of a randomly oscillating hydroplane
[DRA/MAR-TM(MTH)-91320] p 21 N93-11377
Water tunnel studies of inlet/airframe interference phenomena p 215 N93-13216
Control of low-speed turbulent separated flow over a backward-facing ramp p 219 N93-14475
- WATER VAPOR**
The optimum design of air cycle refrigeration system with high pressure water separation p 202 A93-14180
Gravity sensitivity of a resistojet water vaporizer
[AIAA PAPER 93-2402] p 1156 A93-50167
The WINCOF-I code: Detailed description
[NASA-CR-190779] p 677 N93-24760
Gravity sensitivity of a resistojet water vaporizer
[NASA-TM-106220] p 914 N93-29194
- WAVE DIFFRACTION**
Computation of shock diffraction in external and internal flows p 1024 A93-45537
- WAVE DISPERSION**
Dispersion-relation-preserving schemes for computational aeroacoustics p 244 A93-19151
Numerical simulation of free shear flows: Towards a predictive computational aeroacoustics capability
[NASA-CR-191015] p 781 N93-27097
- WAVE DRAG**
Constrained optimization of three-dimensional hypersonic vehicle configurations
[AIAA PAPER 93-0039] p 260 A93-20152
Demonstration of multipoint design procedures for transonic airfoils
[AIAA PAPER 93-3114] p 1062 A93-48284
- WAVE EQUATIONS**
On the possibility of singularities in the acoustic field of supersonic sources when BEM is applied to a wave equation p 1039 A93-46805
Acoustic-wave propagation in ducts and free-field radiation
[ONERA, TP NO. 1993-103] p 1226 A93-53616
- WAVE FRONT RECONSTRUCTION**
Interferometric reconstruction of three-dimensional high-speed aerodynamic flows p 291 N93-16765
- WAVE FRONTS**
Linear stability of three-dimensional boundary layers - Effects of curvature and non-parallelism
[AIAA PAPER 93-0079] p 263 A93-20191
The role of Kutta waves on oscillatory shock motion on an airfoil experiencing heavy buffeting
[AIAA PAPER 93-1589] p 682 A93-34121
- WAVE GENERATION**
Formation of shock waves in transient base flow p 1023 A93-45460
Kelvin-Helmholtz wave generation beneath hovercraft skirts p 1219 A93-53820
Active control of vortex breakdown by a spinning wave generator
[ISABE 93-7045] p 1219 A93-54021
- WAVE INTERACTION**
Induced Mach wave-flame interactions in laminar supersonic fuel jets p 475 A93-26183
Wave interaction theory and LFC p 860 A93-41781
FUM - An efficient MMB solver for steady inviscid flows p 862 A93-42431
Development of resonance perturbations in a supersonic jet p 1088 A93-51772
Modelling of interfacial and thermocline waves
[AERO-REPT-9209] p 420 N93-18103
- WAVE PACKETS**
Numerical simulation of a three-dimensional wave packet in a growing flat plate boundary layer p 128 A93-17265
Calculation of the parameters of instability waves in the preseparation region p 1067 A93-48826
A study of the effect of surface riblets on the evolution of a solitary wave packet (lambda vortex) in a laminar boundary layer p 1067 A93-48827
- WAVE PROPAGATION**
Dynamics of skin-stringer panels using modified wave methods p 206 A93-14561
Dispersion-relation-preserving schemes for computational aeroacoustics p 244 A93-19151
Instability of rectangular jets p 398 A93-19157
Propagation of transverse anti-plane waves in orthotropic layers p 412 A93-21878
The role of Kutta waves on oscillatory shock motion on an airfoil experiencing heavy buffeting
[AIAA PAPER 93-1589] p 682 A93-34121
A numerical study of wave propagation in a confined mixing layer by eigenfunction expansions p 873 A93-43629
Nonlocal vs. local instability of compressible flows including body metric, flow divergence and 3D-wave propagation
[AIAA PAPER 93-2982] p 1051 A93-48175
Blade row interaction effects on flutter and forced response
[AIAA PAPER 93-2084] p 1114 A93-49911
A model for the selective amplification of spatially coherent waves in a centrifugal compressor on the verge of rotating stall
[AIAA PAPER 93-2236] p 1080 A93-50039
Three-dimensional numerical simulation of gradual opening in a wave rotor passage
[AIAA PAPER 93-2526] p 1156 A93-50254
High-frequency acoustic radiation from a curved duct of circular cross section
[ONERA, TP NO. 1993-55] p 1173 A93-51937
Acoustic-wave propagation in ducts and free-field radiation
[ONERA, TP NO. 1993-103] p 1226 A93-53616
In situ material characterization for pavement evaluation by the Spectral-Analysis-of-Surface-Waves (SASW) method
[AD-A255660] p 194 A93-14128
Three-dimensional numerical simulation of gradual opening in a wave rotor passage
[NASA-CR-191157] p 900 N93-29072
- WAVE REFLECTION**
Formation of the shock reflection on a wedge p 1023 A93-45476

- A propulsion device driven by reflected shock waves
p 1001 A93-45550
- Exploratory study of shock reflection near an expansion corner
[AIAA PAPER 93-3132] p 1063 A93-48297
- WAVE RESISTANCE**
Wave resistance of swept wings with supersonic edges
p 478 A93-27624
- WAVE SCATTERING**
Topological approach for the study of electromagnetic coupling
[ONERA-P-1992-2] p 551 N93-20230
- WAVEFORMS**
Adaptive waveform selection with a neural network
p 942 A93-43470
Robust method for estimating the parameters of a linear FM waveform
p 1147 A93-47650
- WAVEGUIDE FILTERS**
Photoelectrochemical etching of high aspect ratio submillimeter waveguide filters from n(+)-GaAs wafers
p 409 A93-20644
- WAVEGUIDES**
Effects of substrate anisotropy on coupled bilateral finlines
p 208 A93-15409
Demonstration of an integrated, active 4 x 4 photonic crossbar
p 211 A93-17392
- WAVERIDERS**
Numerical simulations of high-speed flows about waveriders with sharp leading edges
p 9 A93-12007
Practical considerations in waverider applications
[AIAA PAPER 92-4247] p 43 A93-13326
Interactive hypersonic waverider design and optimization
p 119 A93-14348
Air-breathing hypersonic cruise - Prospects for Mach 4-7 waverider aircraft
[ASME PAPER 92-GT-437] p 384 A93-19579
Design of a hypersonic waverider-derived airplane
[AIAA PAPER 93-0401] p 384 A93-21108
An aerospace plane as a detonation wave ramjet/airframe integrated waverider
[AIAA PAPER 92-5022] p 272 A93-22298
Numerical solution of inviscid hypersonic flow around a conically-derived waverider
[AIAA PAPER 93-0320] p 280 A93-23012
Expanding the waverider design space using general supersonic and hypersonic generating flows
[AIAA PAPER 93-0505] p 283 A93-23253
Engine/airframe integration for waverider cruise vehicles
[AIAA PAPER 93-0507] p 283 A93-23254
Stability and control of hypersonic waveriders
[AIAA PAPER 93-0508] p 370 A93-23255
Analysis of a hypersonic waverider research vehicle with a hydrocarbon scramjet engine
[AIAA PAPER 93-0509] p 386 A93-23256
Experiences in fabrication of a waverider model for wind tunnel testing
[AIAA PAPER 93-0510] p 328 A93-23257
A re-evaluation of the waverider design process
[AIAA PAPER 93-0404] p 440 A93-23326
Waverider design for generalized shock geometries
[AIAA PAPER 93-0774] p 467 A93-24858
NASP - Waveriders in a hypersonic sky. I
p 532 A93-25355
NASP - Waveriders in a hypersonic sky. II
p 532 A93-25359
Hypersonic waveriders - Where do we stand?
[AIAA PAPER 93-0399] p 474 A93-25520
Current technologies for waverider aircraft
[AIAA PAPER 93-0400] p 505 A93-25521
A hypersonic waverider research vehicle
[AIAA PAPER 93-0402] p 505 A93-25522
Propulsion/airframe integration issues for waverider aircraft
[AIAA PAPER 93-0506] p 505 A93-25533
Waveriders with finlets
[AIAA PAPER 93-3442] p 978 A93-47231
Nonslender waveriders
[AIAA PAPER 93-3487] p 982 A93-47261
Computational analysis of off-design waveriders
[AIAA PAPER 93-3488] p 982 A93-47262
Interpretation of waverider performance data using computational fluid dynamics
p 1044 A93-48122
Experimental studies of supersonic flow past wedges with longitudinal slots on the windward side
p 1089 A93-51786
A study of viscous interaction effects on hypersonic waveriders
p 135 A93-14160
Computational analysis of hypersonic flows past elliptic-cone waveriders
[NASA-CR-191304] p 138 A93-14767
Hypersonic reconnaissance aircraft
[NASA-CR-192049] p 333 A93-17804
- The effects of viscosity on a conically derived waverider
[AD-A259019] p 424 N93-19101
Computational analysis of hypersonic flows past generalized cone-derived waveriders
p 483 N93-20288
HSCT mission analysis of waverider designs
[NASA-CR-192913] p 515 N93-21646
Optimized scramjet engine integration on a waverider airframe
p 722 N93-25480
Aerodynamic analysis of hypersonic waverider aircraft
[NASA-CR-192981] p 780 N93-27093
The HSCT mission analysis of waverider designs
[NASA-CR-193467] p 879 N93-31037
- WEAPON SYSTEMS**
Backfire unveiled
p 997 A93-46024
Development of the F/A-18 E/F air induction system
[AIAA PAPER 93-2152] p 1101 A93-49969
AQUS: A PC-based air quality and permit information system
[DE92-040092] p 434 N93-18587
- WEAPONS DELIVERY**
YF-22A prototype advanced tactical fighter demonstration/validation flight test program overview
p 805 N93-27173
- WEAPONS DEVELOPMENT**
Additional developments in embedded computer performance measurement
p 940 A93-42833
- WEAR**
Braking, steering, and wear performance of radial-belted and bias-ply aircraft tires
[SAE PAPER 921036] p 158 A93-14656
A systems dynamics approach to modeling gas turbine combustor wear
[ASME PAPER 92-GT-47] p 347 A93-19300
Evaluation of brush seals for limited-life engines
p 411 A93-21665
Measurements of wear and acoustic emission from fuel-wetted surfaces
p 744 A93-34925
The degradation of parachutes: Age and mechanical wear
[AD-A252243] p 24 N93-12179
Advanced bristle seals for gas turbine engines
[AD-A261296] p 752 N93-26564
- WEAR RESISTANCE**
Coking characteristics of polyphenyl ether lubricants using a Static Coker and a Micro Carbon Residue Tester
p 77 A93-11341
Ceramic coatings enhance material performance
p 71 A93-13648
Characteristics of friction and wear in flight vehicle engine components
p 811 A93-39075
Estimation of the change of axial-flow compressor characteristics during long-term service
p 1193 A93-52949
F-14 wing lug coating investigation
[AD-A257384] p 328 N93-15858
- WEAR TESTS**
Analysis of the friction and wear mechanisms of multilayered plasma-sprayed ceramic coatings
p 548 A93-28567
Ferrographic analysis of polyphenyl ether fluids
p 735 A93-34561
Brush seal low surface speed hard-rub characteristics
[AIAA PAPER 93-2534] p 1156 A93-50261
Brush seal bristle flexure and hard-rub characteristics
[NASA-TM-105864] p 421 N93-18321
Integrity testing of brush seal in shroud ring of T-700 engine
[NASA-TM-105863] p 421 N93-18380
Brush seal low surface speed hard-rub characteristics
[NASA-TM-106169] p 838 N93-27132
- WEATHER**
Visual weather simulation using meteorological databases
[AIAA PAPER 93-3566] p 1207 A93-52665
Proceedings of the National Weather Service Aviation Workshop: Postprint volume
[PB92-176148] p 94 N93-11803
Pilot weather advisor
[NASA-CR-189723] p 318 N93-16692
Adverse weather test site selection study
[AD-A259012] p 339 N93-18895
Contributions to the American Meteorological Society's 26th International Conference on Radar Meteorology
[AD-A263385] p 936 N93-29257
- WEATHER FORECASTING**
International Conference on Aviation Weather Systems, 4th, Paris, France, June 24-28, 1991, Preprints
p 426 A93-22101
Low-level wind-shear terminology
p 426 A93-22104
An index of resource materials for aviation meteorology education and training
p 453 A93-22105
- Weather forecasts for aviation in Canada (FACN and FTCN) - The way they are taught and how they can be made more suitable to the needs of pilots
p 454 A93-22108
Distribution of aviation weather graphics via airline communications networks
p 426 A93-22113
The Federal Aviation Administration (FAA) and the National Weather Service (NWS) modernization programs - Catalysts for change in weather services
p 427 A93-22114
The importance of proper aviation weather dissemination to pilots - An airline captain's perspective
p 308 A93-22115
Preliminary results of the detection of clear air turbulence by the Wind Profiler Demonstration Network
p 427 A93-22119
A 'new age' in aviation weather forecasting
p 427 A93-22123
Developing the Aviation Gridded Forecast System
p 427 A93-22124
The Aviation Weather Products Generator
p 428 A93-22125
Integrated Terminal Weather System (ITWS)
p 428 A93-22127
The Meteorologist Weather Processor for U.S. National Weather Service units at Federal Aviation Administration sites
p 428 A93-22130
FAA weather processor programs - Real-time dissemination of weather information to aviation end-users
p 428 A93-22131
MIST - A remote briefing system
p 437 A93-22132
The Meteorological Data Collection and Reporting System - Status and future directions
p 428 A93-22133
Automated Weather Distribution System (AWDS) for support of global aviation
p 428 A93-22134
A proposed icing severity index based upon meteorology
p 429 A93-22136
Impact of weather on aviation - A global view
p 308 A93-22143
Improved efficiency of air transportation through aviation weather system modernization
p 308 A93-22144
Operational aviation weather service requirements
p 429 A93-22145
An evaluation of aircraft icing forecasts for the continental United States
p 429 A93-22149
Diagnostic studies of clear air turbulence in isentropic coordinates
p 430 A93-22154
Validation of aviation weather products for the Advanced Traffic Management System
p 430 A93-22161
The role of national meteorological services in aviation servicing under the final phase of the World Area Forecast System
p 431 A93-22162
Short range forecasts for air traffic control using high resolution aircraft data
p 431 A93-22164
Ice prediction systems for runways
p 376 A93-22174
The FAA aircraft Icing Forecasting Improvement Program - Validation of aircraft icing forecasts in the Denver area
[AIAA PAPER 93-0393] p 309 A93-23069
Atmospheric turbulence aloft - A review of possible methods for detection, warning, and validation of prediction models
[AIAA PAPER 93-0847] p 557 A93-24914
A comparison of wind speed measured by the Special Sensor Microwave Imager (SSM/I) and the Geosat altimeter
p 1033 A93-44862
Summary of findings from the PIREP-based analyses conducted during the 1988 to 1990 evaluations of TDWR-based and TDWR/LLWAS-based alert services provided to landing/departing pilots
[AD-A253859] p 93 N93-11144
SAC contrail formation study
[AD-A254410] p 159 N93-12605
Terminal Doppler Weather Radar (TDWR) Operational Test and Evaluation (OT/E) integration test plan
[DOT/FAA/CT-TN92/6] p 151 N93-13377
Pilot weather advisor
[NASA-CR-189723] p 318 N93-16692
A single-point warning system for thunderstorms and electric fields
p 747 N93-24900
The ATC evaluation of the prototype Airport Surveillance Radar Wind Shear Processor (ASR-WSP) at Orlando International Airport
[DOT/FAA/CT-TN92/48] p 748 N93-25210
Aircraft guidance for wind shear avoidance: Decision-making under uncertainty
p 889 N93-31005
- WEAVING**
Advanced fiber/matrix material systems
p 921 N93-30854
Mechanical and analytical screening of braided composites for transport fuselage applications
p 922 N93-30855

WEBBING

Structural response of bead-stiffened thermoplastic shear webs p 923 N93-30873

WEDGE FLOW

Viscous instability of hypersonic flow past a wedge p 4 A93-10137

A study of the effect of nonstationary perturbations on flow in the front separation region p 5 A93-10150

A numerical study of unsteady supersonic compression ramp flows p 470 A93-24943

[AIAA PAPER 93-0883] p 470 A93-24943

Oblique shock formation in impulsively started wedge flows p 692 A93-35636

The three-dimensional representation of the pressure distribution on wedged delta wings with supersonic leading edges in supersonic-hypersonic flow p 973 A93-46989

The three-dimensional representation of the lift and pitching moment coefficients on wedged rectangular wings in supersonic flow p 973 A93-46990

Effects of boundary layer bleed on swept-shock/boundary layer interaction p 1052 A93-48182

[AIAA PAPER 93-2989] p 1052 A93-48182

Supersonic flow past a cone with heat transfer near its tip p 1089 A93-51780

Results about the structure of the shock wave reflection process for strong incoming shock waves p 1233 A93-54810

Investigation of a combustion zone behind a wedge p 1146 A93-51631

Numerical investigations into the base drag of various wedges using the base flow model developed by Mauri Tanner p 26 N93-12414

[REPT-B-36] p 26 N93-12414

Application of a vectorized particle simulation to the study of plates and wedges in high-speed rarefied flow p 133 N93-13746

Combined LAURA-UPS hypersonic solution procedure [NASA-TM-107682] p 747 N93-25176

WEDGES

Investigation of a combustion zone behind a wedge p 1146 A93-51631

Numerical investigations into the base drag of various wedges using the base flow model developed by Mauri Tanner p 26 N93-12414

[REPT-B-36] p 26 N93-12414

Application of a vectorized particle simulation to the study of plates and wedges in high-speed rarefied flow p 133 N93-13746

Combined LAURA-UPS hypersonic solution procedure [NASA-TM-107682] p 747 N93-25176

WEDGES

Investigation of a combustion zone behind a wedge p 1146 A93-51631

Numerical investigations into the base drag of various wedges using the base flow model developed by Mauri Tanner p 26 N93-12414

[REPT-B-36] p 26 N93-12414

Application of a vectorized particle simulation to the study of plates and wedges in high-speed rarefied flow p 133 N93-13746

Combined LAURA-UPS hypersonic solution procedure [NASA-TM-107682] p 747 N93-25176

WEDGES

Investigation of a combustion zone behind a wedge p 1146 A93-51631

Numerical investigations into the base drag of various wedges using the base flow model developed by Mauri Tanner p 26 N93-12414

[REPT-B-36] p 26 N93-12414

Application of a vectorized particle simulation to the study of plates and wedges in high-speed rarefied flow p 133 N93-13746

Combined LAURA-UPS hypersonic solution procedure [NASA-TM-107682] p 747 N93-25176

WEDGES

Investigation of a combustion zone behind a wedge p 1146 A93-51631

Numerical investigations into the base drag of various wedges using the base flow model developed by Mauri Tanner p 26 N93-12414

[REPT-B-36] p 26 N93-12414

Application of a vectorized particle simulation to the study of plates and wedges in high-speed rarefied flow p 133 N93-13746

Combined LAURA-UPS hypersonic solution procedure [NASA-TM-107682] p 747 N93-25176

WEDGES

Investigation of a combustion zone behind a wedge p 1146 A93-51631

Numerical investigations into the base drag of various wedges using the base flow model developed by Mauri Tanner p 26 N93-12414

[REPT-B-36] p 26 N93-12414

Application of a vectorized particle simulation to the study of plates and wedges in high-speed rarefied flow p 133 N93-13746

Combined LAURA-UPS hypersonic solution procedure [NASA-TM-107682] p 747 N93-25176

WEDGES

Investigation of a combustion zone behind a wedge p 1146 A93-51631

Numerical investigations into the base drag of various wedges using the base flow model developed by Mauri Tanner p 26 N93-12414

[REPT-B-36] p 26 N93-12414

Application of a vectorized particle simulation to the study of plates and wedges in high-speed rarefied flow p 133 N93-13746

Combined LAURA-UPS hypersonic solution procedure [NASA-TM-107682] p 747 N93-25176

Zeppelin NT - A new concept in airship technology, based on rigid airship principles p 1242 A93-54612

[AIAA PAPER 93-4045] p 1242 A93-54612

An investigation of dynamic stress reduction of multi-body aircraft using active gust control p 187 N93-13916

Sikorsky Aircraft Advanced Rotorcraft Transmission (ART) program p 840 N93-27268

[NASA-CR-191079] p 840 N93-27268

Advanced composite structural concepts and material technologies for primary aircraft structures p 918 N93-30430

Composites technology for transport primary structure p 918 N93-30431

Advanced technology commercial fuselage structure p 918 N93-30432

Cost studies for commercial fuselage crown designs p 920 N93-30440

Aircraft structures in 2000: A technological challenge? [MBB-LME-202-S-PUB-0485] p 998 N93-31058

WEIGHTING FUNCTIONS

Weighted average method for evaluating the aerodynamic properties of transition flow p 8 A93-11872

Prediction and planning of a flight vehicle route in the presence of motion inhibiting factors p 1130 A93-50961

WEIGHTLESSNESS

Numerical study of cavity natural convection flow with augmenting and counteracting effects by projection finite element method p 749 N93-25540

Effects of buoyancy on gas jet diffusion flames [NASA-CR-191109] p 935 N93-31031

WELDABILITY

Selection criteria for metallic high temperature structural materials in hypersonic flying equipment [MBB-LME-221-HYPAC-PUB-2-A] p 515 N93-21479

WELDED JOINTS

A fuel-oil matrix heat exchanger p 833 A93-39052

External stress-corrosion cracking of a 1.22-m-diameter type 316 stainless steel air valve p 737 N93-26201

[NASA-TP-3190] p 737 N93-26201

WELDED STRUCTURES

Main directions of improving the quality of aluminum-lithium alloys for welded aircraft structures p 1146 A93-51104

WELDING

Welding wire selection critical to jet engine repair work p 208 A93-15375

An automated flow line for gas turbine blade repair [ASME PAPER 92-GT-367] p 375 A93-19531

WENTZEL-KRAMER-BRILLOUIN METHOD

An analytical description of hypersonic boundary layer stability [AIAA PAPER 93-2981] p 1051 A93-48174

WHEAT

Canonical correlation relationships among spectral and phytometric variables for twenty winter wheat fields p 433 A93-22992

WHEELCHAIRS

Cabin accommodations for passengers with ambulatory disabilities - Transport category aircraft [SAE ARP 4387] p 1103 A93-52166

WHEELS

Reanalysis of multiple-wheel landing gear traffic tests [AD-A256593] p 194 A93-14238

WHISKER COMPOSITES

Erosion characteristics of ceramic particulate and whisker reinforced aluminum composites [ASME PAPER 92-GT-369] p 388 A93-19532

Improved silicon nitride for advanced heat engines [NASA-CR-182193] p 917 N93-29451

WHITE NOISE

The HYDICE instrument design and its application to planetary instruments p 842 N93-28766

WIDE ANGLE LENSES

Optical design of a wide-angle simulator probe p 211 A93-17140

WIDEBAND COMMUNICATION

A wideband, embedded/conformal, antenna subsystem concept p 327 A93-22002

WIGGLER MAGNETS

Undulator Spectromicroscopy Facility at the Advanced Light Source [DE93-007964] p 823 N93-28490

WINCHES

Modeling and analysis of the winch launch of a glider p 528 A93-27294

WIND (METEOROLOGY)

Worst-case wind modeling and its influence on capturing of aircraft penetration trajectory p 1248 A93-54857

Physical effects of vegetation on wind-blown sand in the coastal environments of Florida [PB92-188424] p 93 N93-11702

WIND DIRECTION

Simulation of DD-963 ship airwake by Navier-Stokes method [AIAA PAPER 93-3002] p 1053 A93-48192

Aircraft turns into and down wind [AERO-REPT-9201] p 337 N93-18131

WIND EFFECTS

Trans-oceanic, polar patrol balloons and future prospects p 26 A93-11366

Drag and drag partition on rough surfaces p 79 A93-12460

Wind lifting of aerosol particles p 223 A93-15079

Expanding the operation scope of aircraft through the use of air-cushion landing gear p 321 A93-18354

Estimation of the external loading of airships in flight p 366 A93-18383

Wind tunnel investigation of wind shear effect on turning flight [AIAA PAPER 93-3641] p 1127 A93-48326

Digital flight recorded data - A method of estimating down draft from digital flight recorded data p 1241 A93-54559

An airfoil in transonic flow in the presence of wind gusts and weak shock waves p 1233 A93-55015

Physical effects of vegetation on wind-blown sand in the coastal environments of Florida [PB92-188424] p 93 N93-11702

User's Guide for the NREL Force and Loads Analysis Program [DE92-010579] p 216 N93-13524

User's Guide for the NREL Teetering Rotor Analysis Program (STRAP) [DE92-010580] p 216 N93-13525

Aircraft turns into and down wind [AERO-REPT-9201] p 337 N93-18131

WIND MEASUREMENT

Lidar windshear detection for commercial aircraft p 341 A93-17864

Recent experiment focuses on operational impact of jet stream forecast errors p 487 A93-27394

Comparison of three methods to deduce three-dimensional wind fields in a hurricane with airborne Doppler radar p 844 A93-37691

Solid-state coherent laser radar wind shear measuring systems p 144 A93-14848

Airborne Wind Shear Detection and Warning Systems: Fourth Combined Manufacturers' and Technologists' Conference, part 1 [NASA-CP-10105-PT-1] p 488 N93-19590

Program overview: 1991 flight test objectives p 488 N93-19591

Flight test operations p 488 N93-19592

NASA wind shear flight test in situ results p 488 N93-19593

Three-dimensional numerical simulation of the 20 June 1991, Orlando microburst p 488 N93-19598

RDR-4B doppler weather radar with forward looking wind shear detection capability p 489 N93-19601

Airborne doppler radar research at Rockwell International p 489 N93-19602

Vertical wind estimation from horizontal wind measurements p 489 N93-19604

Microburst characteristics determined from 1988-1991 TDWR testbed measurements p 490 N93-19605

NASA airborne radar wind shear detection algorithm and the detection of wet microbursts in the vicinity of Orlando, Florida p 490 N93-19611

WIND PRESSURE

Wind load design methods for ground-based heliostats and parabolic dish collectors [DE93-002737] p 433 N93-15839

WIND PROFILES

Ship airwake measurement and flow visualization [AIAA PAPER 92-4088] p 7 A93-11267

Sensing a change in the wind p 307 A93-21627

Preliminary results of the detection of clear air turbulence by the Wind Profiler Demonstration Network p 427 A93-22119

Improved efficiency of air transportation through aviation weather system modernization p 308 A93-22144

Short range forecasts for air traffic control using high resolution aircraft data p 431 A93-22164

Wind identification along a flight trajectory. II - 2D-kinematic approach p 524 A93-28469

A comparison of wind speed measured by the Special Sensor Microwave Imager (SSM/I) and the Geosat altimeter p 1033 A93-44862

Wind identification along a flight trajectory. III - 2D dynamic approach p 1007 A93-45401

Alternative solution to optimum gliding velocity in a steady head wind or tail wind p 1136 A93-52458

Case study of a low-reflectivity pulsating microburst - Numerical simulation of the Denver, 8 July 1989, storm p 1222 A93-52898

WIND SHEAR

- Design and conduct of a windshear detection flight experiment
[AIAA PAPER 92-4092] p 38 A93-11268
- Adaptive control of aircraft in windshear p 62 A93-13126
- The hazard and alarm of windshear p 141 A93-14317
- Analysis and feedback control of aircraft flight in wind shear p 183 A93-14349
- Lidar windshear detection for commercial aircraft p 341 A93-17864
- Sensing a change in the wind p 307 A93-21627
- Low-level wind-shear terminology p 426 A93-22104
- An experimental cockpit display for TDWR wind shear alerts p 343 A93-22111
- Hazard assessment and cockpit presentation issues for microburst alerting systems p 308 A93-22112
- Potential aircraft hazards in the vicinity of convective clouds - A review from the perspective of a scale-model study p 427 A93-22116
- Detection of microburst-related gust fronts using Doppler radar p 427 A93-22118
- A 'new age' in aviation weather forecasting p 427 A93-22123
- The Aviation Weather Products Generator p 428 A93-22125
- Improved efficiency of air transportation through aviation weather system modernization p 308 A93-22144
- Extremely low level jet in the evening in Kanto Plain p 430 A93-22159
- A quantitative method to estimate the microburst wind shear hazard to aircraft p 309 A93-22172
- Elevated array detection and measurement of microbursts using Theta(E) p 412 A93-22173
- SAAW - Italy's answer to the windshear challenge p 431 A93-22175
- Anemometer siting criteria for low level wind shear alert system p 413 A93-22178
- The redesigned Low Level Wind Shear Alert System p 431 A93-22179
- Status of the Terminal Doppler Weather Radar one year before deployment p 431 A93-22184
- Terminal Doppler Weather Radar program at Denver's Stapleton International Airport during 1989 and 1990 p 432 A93-22188
- Performance results and potential operational uses for the prototype TDWR microburst prediction product p 432 A93-22190
- An improved gust front detection algorithm for the TDWR p 432 A93-22191
- The detection and warning of low-level wind shear based on terminal single Doppler radar p 432 A93-22195
- Microburst observations in tropical Australia p 432 A93-22198
- Doppler radar observation of tornado and microburst around Chitose Airport p 432 A93-22199
- Evaluation of clear-air radar PROUST and Doppler radar RONSARD for airport low level-wind shear detection p 433 A93-22202
- Wind shear alert system brings safety improvements to major U.S. airports p 529 A93-27396
- A data processing and control system for counteracting wind shear p 524 A93-27604
- Wind identification along a flight trajectory. II - 2D-kinematic approach p 524 A93-28469
- Flight safety in a perturbed atmosphere --- Russian book p 487 A93-29431
- [ISBN 5-277-00815-2] p 487 A93-29431
- A horizontal atmospheric temperature sounder - Applications to remote sensing of atmospheric hazards p 929 A93-43502
- Microburst avoidance crew procedures for forward-look sensor equipped aircraft p 1007 A93-44234
- [AIAA PAPER 93-3942] p 1007 A93-44234
- Wind identification along a flight trajectory. III - 2D dynamic approach p 1007 A93-45401
- AIAA Atmospheric Flight Mechanics Conference, Monterey, CA, Aug. 9-11, 1993, Technical Papers p 1125 A93-48301
- Wind tunnel investigation of wind shear effect on turning flight p 1127 A93-48326
- [AIAA PAPER 93-3641] p 1127 A93-48326
- A wind shear hazard window useful in studying the effect of wind shear on the airplane during the landing approach p 1127 A93-48327
- [AIAA PAPER 93-3643] p 1127 A93-48327
- A method of wind shear detection for powered-lift STOL aircraft p 1104 A93-48345
- [AIAA PAPER 93-3667] p 1104 A93-48345
- Wind-shear endurance capability for powered-lift aircraft p 1129 A93-48348
- [AIAA PAPER 93-3670] p 1129 A93-48348
- Fuzzy logic control algorithm for suppressing E-6A Long Trailing Wire Antenna wind shear induced oscillations [AIAA PAPER 93-3868] p 1171 A93-51454

- Optimal performance of airplanes flying through windshear p 1102 A93-51480
- [AIAA PAPER 93-3846] p 1102 A93-51480
- Case study of a low-reflectivity pulsating microburst - Numerical simulation of the Denver, 8 July 1989, storm p 1222 A93-52898
- Identification of the phase characteristics and wind-induced perturbations of an aircraft from flight test results p 1206 A93-52943
- A study on low level windshear hazard index p 1240 A93-55414
- Summary of findings from the PIREP-based analyses conducted during the 1988 to 1990 evaluations of TDWR-based and TDWR/LLWAS-based alert services provided to landing/departing pilots p 93 A93-11144
- [AD-A253859] p 93 A93-11144
- A problem formulation for glideslope tracking in wind shear using advanced robust control techniques p 64 A93-11176
- [NASA-TM-104164] p 64 A93-11176
- Terminal Doppler weather radar/low-level wind shear alert system integration algorithm specification, version 1.1 p 224 A93-14547
- [AD-A255319] p 224 A93-14547
- Airborne Wind Shear Detection and Warning Systems. Fourth Combined Manufacturers' and Technologists' Conference, part 2 p 144 A93-14844
- [NASA-CP-10105-PT-2] p 144 A93-14844
- NASA/LLMSC coherent LIDAR airborne shear sensor: System capabilities and flight test plans p 144 A93-14847
- Solid-state coherent laser radar wind shear measuring systems p 144 A93-14848
- Development of the Advance Warning Airborne System(AWAS) p 144 A93-14849
- A millimeter-wave radiometer for detecting microbursts p 145 A93-14850
- The Orlando TDWR testbed and airborne wind shear date comparison results p 145 A93-14851
- TDWR 1991 Program Review p 145 A93-14852
- Wind shear related research at Princeton University p 145 A93-14854
- Results of in-service evaluation of wind shear systems p 146 A93-14856
- In-service evaluation of wind shear systems p 146 A93-14857
- Advanced technology wind shear prediction system evaluation p 146 A93-14858
- Airborne Wind Shear Detection and Warning Systems. Fourth Combined Manufacturers' and Technologists' Conference, part 1 p 488 A93-19590
- [NASA-CP-10105-PT-1] p 488 A93-19590
- Program overview: 1991 flight test objectives p 488 A93-19591
- Flight test operations p 488 A93-19592
- NASA wind shear flight test in situ results p 488 A93-19593
- Air/ground wind shear information integration: Flight test results p 488 A93-19594
- Doppler radar results p 488 A93-19595
- Wind shear hazard determination p 488 A93-19597
- Three-dimensional numerical simulation of the 20 June 1991, Orlando microburst p 488 A93-19598
- An approach to evaluating reactive airborne wind shear systems p 489 A93-19600
- RDR-4B doppler weather radar with forward looking wind shear detection capability p 489 A93-19601
- Airborne doppler radar research at Rockwell International p 489 A93-19602
- Acquisition and use of Orlando, Florida and Continental Airbus radar flight test data p 489 A93-19603
- Vertical wind estimation from horizontal wind measurements p 489 A93-19604
- Microburst characteristics determined from 1988-1991 TDWR testbed measurements p 490 A93-19605
- Ground clutter measurements using the NASA airborne doppler radar: Description of clutter at the Denver and Philadelphia airports p 490 A93-19608
- Comparison of simulated and actual wind shear radar data products p 490 A93-19610
- NASA airborne radar wind shear detection algorithm and the detection of wet microbursts in the vicinity of Orlando, Florida p 490 A93-19611
- Signal processing for airborne doppler radar detection of hazardous wind shear as applied to NASA 1991 radar flight experiment data p 490 A93-19612
- The ATC evaluation of the prototype Airport Surveillance Radar Wind Shear Processor (ASR-WSP) at Orlando International Airport p 748 A93-25210
- [DOT/FAA/CT-TN92/48] p 748 A93-25210
- Setting values for TDWR/LLWAS 3 integration parameters p 755 A93-25645
- [AD-A260740] p 755 A93-25645
- A statistical characterization of Denver-area microbursts p 845 A93-27675
- [AD-A262127] p 845 A93-27675

- Aircraft guidance for wind shear avoidance: Decision-making under uncertainty p 889 A93-31005
- Airborne derivation of microburst alerts from ground-based Terminal Doppler Weather Radar information: A flight evaluation [NASA-TM-108990] p 1000 A93-32223
- WIND TUNNEL APPARATUS**
- A preliminary investigation of a method to calibrate strain gauge balances by means of a reference balance p 210 A93-16845
- The design of test-section inserts for higher speed aerodynamic testing in the Ames 80- by 120-Foot Wind Tunnel p 374 A93-19149
- Development of the NASA-Ames low disturbance supersonic wind tunnel for transition research up to Mach 2.5 p 462 A93-24488
- [AIAA PAPER 92-3909] p 462 A93-24488
- Development of a six component flexured two shell internal strain gage balance p 541 A93-24872
- [AIAA PAPER 93-0793] p 541 A93-24872
- Modeling and control design of a wind tunnel model support p 529 A93-29281
- Design philosophy for wind tunnel model positioning control systems p 822 A93-37877
- A laser induced fluorescence system for the high enthalpy shock tunnel (HEG) in Goettingen p 1024 A93-45506
- Icing Research Tunnel rotating bar calibration measurement system p 1255 A93-54398
- CTS for a low speed wind tunnel --- Captive Trajectory System p 1251 A93-56278
- Design philosophy for wind tunnel model positioning systems p 192 A93-12552
- [AD-A254958] p 192 A93-12552
- Transient/structural analysis of a combustor under explosive loads p 420 A93-17779
- [NASA-TM-107660] p 420 A93-17779
- Application of a neural network as a potential aid in predicting NTF pump failure p 442 A93-18332
- [NASA-TM-107667] p 442 A93-18332
- Study of optical techniques for the Ames unitary wind tunnel, part 7 p 382 A93-18520
- [NASA-CR-192165] p 382 A93-18520
- Review of initial experiments using the Hawk model, dynamic rig facility, and the CED 1401 digital data acquisition equipment p 531 A93-21406
- [CRANFIELD-AERO-9017] p 531 A93-21406
- NASA Lewis 8- by 6-foot supersonic wind tunnel user manual p 730 A93-25080
- [NASA-TM-105771] p 730 A93-25080
- Nozzle diffuser for use with an open test section of a wind tunnel p 731 A93-25996
- [NASA-CASE-LAR-14424-1-SB] p 731 A93-25996
- WIND TUNNEL CALIBRATION**
- Performance results from a test of an S-76 rotor in the NASA Ames 80- by 120-foot wind tunnel p 975 A93-47211
- [AIAA PAPER 93-3414] p 975 A93-47211
- Flight and wind-tunnel calibrations of a flush airdata sensor at high angles of attack and sideslip and at supersonic Mach numbers p 344 A93-19110
- [NASA-TM-104265] p 344 A93-19110
- Modification and calibration of the Naval Postgraduate School Academic Wind Tunnel p 823 A93-28189
- [AD-A262092] p 823 A93-28189
- A break-down of sting interference effects [NLR-TP-91220-U] p 1014 A93-31042
- WIND TUNNEL DRIVES**
- Power generation source for an electrothermal hypersonic wind tunnel p 376 A93-22317
- [AIAA PAPER 92-5045] p 376 A93-22317
- Performance considerations in the operation of free-piston driven hypersonic test facilities p 1011 A93-45497
- Production of oscillatory flow in wind tunnels p 1218 A93-53812
- WIND TUNNEL MODELS**
- Experiments on Space Shuttle Orbiter models in a free piston shock tunnel p 7 A93-11497
- Transonic flutter/divergence characteristics of aeroelastically tailored and non-tailored high-aspect-ratio forward-swept wings p 10 A93-12273
- Hybrid grid approach to study dynamic stall p 122 A93-14548
- Forcing function effects on unsteady aerodynamic gust response. I - Forcing functions p 251 A93-19400
- [ASME PAPER 92-GT-174] p 251 A93-19400
- Forcing function effects on unsteady aerodynamic gust response. II - Low solidity airfoil row response p 251 A93-19401
- [ASME PAPER 92-GT-175] p 251 A93-19401
- Experimental study of mixed compression air-intake for hypersonic airbreathing engines p 355 A93-19519
- [ASME PAPER 92-GT-349] p 355 A93-19519
- An experimental investigation of twin fin buffeting and suppression [AIAA PAPER 93-0054] p 261 A93-20167

- Aeroelastic model design using structural optimization [AIAA PAPER 92-4730] p 409 A93-20329
- Experimental study of three-dimensional separation on a large-size model [ONERA, TP NO. 1992-174] p 473 A93-25348
- Modeling and control design of a wind tunnel model support p 529 A93-29281
- Blade-vortex interaction data obtained from a pressure-instrumented model rotor at the DNW p 568 A93-29430
- Dynamic stability derivatives evaluation in a low-speed wind tunnel p 821 A93-37402
- Design philosophy for wind tunnel model positioning control systems p 822 A93-37877
- Activities of the GARTEUR high lift research program [ONERA, TP NO. 1992-152] p 803 A93-38731
- Modeling of flow in a pulsed shock tunnel p 777 A93-39152
- Experimental and algorithmic means of identifying mathematical models of flight vehicle p 909 A93-43103
- Propulsion system simulator with propfan for tests on a large scale model of IL-114 airplane in a full-size wind tunnel of TsAGI p 1013 A93-46933
- Analysis of aeroelastic and resonance responses of a wind tunnel model support system p 1013 A93-47022
- Aerodynamic design of a hypersonic body with a constant favorable pressure gradient [AIAA PAPER 93-3444] p 978 A93-47232
- A study of the effect of the shape of a parasail on its lift-drag ratio p 1069 A93-48913
- High-pressure hypervelocity electrothermal wind-tunnel performance study and subscale tests p 1137 A93-49617
- Aerothermodynamics of the high-altitude flight p 1089 A93-51783
- An improved calibration technique for wind tunnel model attitude sensors p 1253 A93-54356
- An improved method for determining force balance calibration accuracy p 1254 A93-54369
- Design, test, and evaluation of three active flutter suppression controllers [NASA-TM-4338] p 63 A93-10070
- Arguments concerning wind tunnel test studies of the trim characteristics of objects with small asymmetries [AD-A254111] p 19 A93-10858
- Study of optical techniques for the Ames unitary wind tunnels. Part 4: Model deformation [NASA-CR-190980] p 68 A93-12349
- Mach 4 testing of scramjet inlet models [NAL-TR-1137] p 26 A93-12369
- Design philosophy for wind tunnel model positioning systems [AD-A254958] p 192 A93-12552
- Aerodynamic integration of thrust reversers on the Fokker 100 p 160 A93-13208
- A novel-high-performance system for recording and analysing instantaneous total pressure distortion in air intakes p 214 A93-13215
- Multiple-function multi-input/multi-output digital control and on-line analysis [NASA-TM-107697] p 162 A93-13565
- Rarefied gas numerical wind tunnel. Part 7: OREX p 382 A93-19280
- Numerical Wind Tunnel: Requirements and the outline p 383 A93-19288
- Numerical Wind Tunnel hardware p 383 A93-19289
- The operating system for Numerical Wind Tunnel p 383 A93-19290
- The language processor system for the Numerical Wind Tunnel p 383 A93-19291
- Numerical simulation of hypersonic flow around H-2 Orbiting Plane (HOPE), part 3 p 301 A93-19297
- Role of wind tunnel tests and CFD analysis for the development of aero-engines in IHI p 365 A93-19326
- Improved ceramic slip casting technique -- application to aircraft model fabrication [NASA-CASE-LAR-14471-1] p 536 A93-20041
- Review of initial experiments using the Hawk model, dynamic rig facility, and the CED 1401 digital data acquisition equipment [CRANFIELD-AERO-9017] p 531 A93-21406
- Combined experiment, phase 1 [DE93-000012] p 485 A93-21766
- Fabrication of composite propfan blades for a cruise missile wind tunnel model [NASA-TM-105270] p 752 A93-26202
- Optically smart surfaces survivability testing at Mach 3 [AD-A261785] p 760 A93-26566
- Modal survey of a full-scale F-18 wind tunnel model [AD-A262482] p 875 A93-29410
- Supersonic aerodynamic characteristics of an advanced F-16 derivative aircraft configuration [NASA-TP-3355] p 989 A93-31733

WIND TUNNEL NOZZLES

- Aerodynamic design of axisymmetric hypersonic wind-tunnel nozzles using a least-squares/parabolized Navier-Stokes procedure p 9 A93-12011
- Goertler instability and hypersonic quiet nozzle design p 480 A93-29155
- Reactive and dissipative hypersonic flow in a wind tunnel nozzle p 687 A93-34358
- Testing techniques for straight transonic and supersonic cascades [ONERA, TP NO. 1992-155] p 773 A93-38734
- Design of a nozzle for a hypersonic wind tunnel [AERO-REPT-9113] p 381 A93-16468
- WIND TUNNEL STABILITY TESTS**
- Wind tunnel investigation with an operational turbojet engine [AIAA PAPER 93-0036] p 322 A93-20150
- TGV tunnel entry simulations using a finite element code with automatic remeshing [AIAA PAPER 93-0890] p 471 A93-24950
- Experimental investigation on aircraft dynamic stability parameters p 905 A93-40328
- Review of initial experiments using the Hawk model, dynamic rig facility, and the CED 1401 digital data acquisition equipment [CRANFIELD-AERO-9017] p 531 A93-21406
- WIND TUNNEL TESTS**
- A transfer standard of an air flow rate unit VET 150-2-87 p 66 A93-10049
- A study of the effect of nonstationary perturbations on flow in the front separation region p 5 A93-10150
- On improving adequacy of modeling in wind tunnel problems p 6 A93-10404
- MPC75 as the forerunner of a new regional aircraft family p 37 A93-10776
- Breakdown analysis on delta wing vortices p 7 A93-10779
- Flight test and wind-tunnel study of a scaled unmanned air vehicle [AIAA PAPER 92-4075] p 37 A93-11260
- Measurement of attachment-line location in a wind-tunnel and in supersonic flight [AIAA PAPER 92-4089] p 39 A93-11285
- A method of calculating elastic curve of semiflexible plate nozzle p 66 A93-12097
- Subharmonic bifurcation analysis of wing with store flutter p 78 A93-12098
- Three-dimensional boundary-layer transition on a cone at Mach 3.5 p 9 A93-12177
- Experimental analysis of turbulence within supersonic mixing layers p 11 A93-12428
- A study of the effect of a moving ground belt on the vortex created by a jet impinging on the ground in a cross flow [AIAA PAPER 92-4250] p 15 A93-13361
- An ultralight freewind aircraft design study [AIAA PAPER 92-4194] p 44 A93-13371
- Heat transfer, adiabatic effectiveness, and injectant distributions downstream of a single row and two staggered rows of compound angle film-cooling holes p 201 A93-13976
- Over wing propeller aerodynamics p 113 A93-14189
- DNW test highlights related to aircraft environment p 190 A93-14274
- An investigation of mode shift flutter suppression scheme for empennages p 182 A93-14288
- The cryogenic approach to simulating hotjet in transonic wind-tunnel testing p 117 A93-14297
- Extending the useful frequency of 'rigid' wind tunnel models with active control p 190 A93-14299
- The effect of wind tunnel constraint on unsteady aerodynamics experiments p 190 A93-14300
- A low speed wind-tunnel with extreme flow quality - Design and tests p 190 A93-14352
- A semi-empirical theory of the noise in slotted tunnels caused by diffuser suction p 231 A93-14353
- Five years operational experiences with Indonesian Low Speed Tunnel (ILST) p 191 A93-14403
- Vortex breakdown study on a 65-deg delta wing tested in static and dynamic conditions p 121 A93-14407
- A low-speed wind tunnel study of vortex interaction control techniques on a chine-forebody/delta-wing configuration p 122 A93-14409
- Correlation of mean velocity measurements downstream of a swept backward-facing step p 123 A93-14552
- Development of a hydrogen external burning flight test experiment on the NASA Dryden SR-71A aircraft [SAE PAPER 920997] p 157 A93-14638
- Toulouse - Flight tests of the Airbus A340 p 159 A93-16859
- Estimation of aerodynamic characteristics from flight test data. II - Analysis methods under in-flight wind tunnel test concept p 191 A93-16934
- Application of laminar flow to aero engine nacelles p 128 A93-17256

- On space correlation of pressure pulsations on the streamlined surface before a step p 244 A93-19135
- Helicopter main rotor/tail rotor noise radiation characteristics from scaled model rotor experiments in the DNW p 445 A93-19142
- New design concepts for silencing aeroacoustic wind tunnels p 445 A93-19147
- Aeroacoustic wind tunnel testing of a counterrotating shrouded propfan-model p 449 A93-19213
- Recent advances in simulating unsteady flow phenomena brought about by passage of shock waves in a linear turbine cascade [ASME PAPER 92-GT-4] p 245 A93-19277
- Boundary layer effects on the transonic flow in a straight turbine cascade [ASME PAPER 92-GT-155] p 249 A93-19382
- On aerodynamic loading of linear compressor cascades [ASME PAPER 92-GT-275] p 253 A93-19468
- The VKI compression tube annular cascade facility CT3 [ASME PAPER 92-GT-336] p 375 A93-19511
- A new semiempirical method for computing nonlinear angle-of-attack aerodynamics on wing-body-tail configurations [AIAA PAPER 93-0034] p 260 A93-20148
- Flow visualization studies on sidewall effects in two dimensional transonic airfoil testing [AIAA PAPER 93-0090] p 263 A93-20196
- The problem of dynamic stall simulation revisited [AIAA PAPER 93-0091] p 264 A93-20197
- The use of subscale models to predict self-induced oscillations of flight vehicles [AIAA PAPER 93-0093] p 264 A93-20199
- Circulation control wing model study [AIAA PAPER 93-0094] p 264 A93-20200
- Fiber optic-based laser vapor screen flow visualization systems for aerodynamic research in larger-scale subsonic and transonic wind tunnels p 408 A93-20298
- Wall-signature methods for high speed wind tunnel wall interference corrections p 375 A93-20803
- Air/helium ground-test simulation pertinent to the definition of slender body hypersonic aerodynamics [AIAA PAPER 93-0318] p 268 A93-21106
- Lift enhancement of ground-effect wing. II - Experimental investigation of the power augmented ram wing in ground effect through the wind tunnel p 271 A93-21738
- Supersonic dynamic stability characteristics of the test technique demonstrator NASP configuration [AIAA PAPER 92-5009] p 367 A93-22285
- Some aspects of the aerodynamic methodology in hypersonic vehicle concept studies [AIAA PAPER 92-5027] p 272 A93-22303
- CFD comparisons with wind tunnel and flight data for the X-15 [AIAA PAPER 92-5047] p 273 A93-22319
- Data analysis of the parametric scramjet combustor experiments conducted in the Calspan 96 inch inch combustor tunnel - 4th entry [AIAA PAPER 92-5098] p 359 A93-22368
- Hypersonic turbulent expansion-corner flow with shock impingement [AIAA PAPER 92-5101] p 274 A93-22371
- Experimental results of shock trains in rectangular ducts [AIAA PAPER 92-5103] p 274 A93-22373
- Results of Low Power Deicer tests on a swept inlet component in the NASA Lewis Icing Research Tunnel [AIAA PAPER 93-0032] p 327 A93-22551
- Numerical simulation of dynamic lift enhancement using oscillatory leading edge flaps [AIAA PAPER 93-0186] p 276 A93-22611
- Experimental and numerical analysis of the wing rock characteristics of a 'wing-body-tail' configuration [AIAA PAPER 93-0187] p 368 A93-22612
- Experimental studies of the turbulent structure of supersonic mixing layers [AIAA PAPER 93-0217] p 278 A93-22633
- Experimental and numerical investigation of Mach 2.5 supersonic mixed compression inlet [AIAA PAPER 93-0289] p 279 A93-22689
- Icing testing of a large full-scale inlet at the Arnold Engineering Development Center [AIAA PAPER 93-0299] p 376 A93-22697
- LDV flowfield measurements on a straight and swept wing with a simulated ice accretion [AIAA PAPER 93-0300] p 280 A93-23001
- An optical comparison of wall and axial injection for high enthalpy reacting scramjet flows [AIAA PAPER 93-0357] p 377 A93-23040
- An overview of shed ice impact studies in the NASA Lewis Icing Research Tunnel [AIAA PAPER 93-0301] p 283 A93-23247
- Experiences in fabrication of a waverider model for wind tunnel testing [AIAA PAPER 93-0510] p 328 A93-23257

- Streamwise vortex meander in a plane mixing layer
[AIAA PAPER 93-0553] p 285 A93-23292
- An integrated knowledge system for wind tunnel testing
- Project Engineers' Intelligent Assistant
[AIAA PAPER 93-0560] p 377 A93-23297
- Unit-Reynolds-number effects on boundary-layer transition
[AIAA PAPER 93-0560] p 288 A93-23560
- On experimental study of 3-D flow in self-correcting wind tunnel
[AIAA PAPER 93-0560] p 528 A93-24033
- Development of the NASA-Ames low disturbance supersonic wind tunnel for transition research up to Mach 2.5
[AIAA PAPER 92-3909] p 462 A93-24488
- The effect of Reynold's number on a natural low frequency flow oscillation over an airfoil near stall
[AIAA PAPER 92-4040] p 463 A93-24489
- Body-axis rolling motion critical states of a 65-degree delta wing
[AIAA PAPER 93-0621] p 523 A93-24738
- Wind tunnel test techniques for UAV separation investigations
[AIAA PAPER 93-0626] p 524 A93-24743
- Application of a flush airdata sensing system to a wing leading edge (LE-FADS)
[AIAA PAPER 93-0634] p 516 A93-24750
- Hysteresis effects on wind tunnel measurements of a two-element airfoil
[AIAA PAPER 93-0646] p 464 A93-24761
- Lift enhancement of an airfoil using a Gurney flap and vortex generators
[AIAA PAPER 93-0647] p 464 A93-24762
- Takeoff/approach noise for a model counterrotation propeller with a forward-swept upstream rotor
[AIAA PAPER 93-0596] p 519 A93-24782
- Development of a six component flexured two shell internal strain gage balance
[AIAA PAPER 93-0793] p 541 A93-24872
- On the breakdown of a hypersonic laminar boundary layer
[AIAA PAPER 93-0896] p 472 A93-24956
- Experimental and numerical delta wing study at high angles of attack and sideslip
[AIAA PAPER 92-2713] p 473 A93-24990
- Oscillatory blowing, a tool to delay boundary layer separation
[AIAA PAPER 93-0440] p 474 A93-25529
- Correlation of interaction sweepback effects on unsteady shock-induced turbulent separation
[AIAA PAPER 93-0776] p 475 A93-25550
- Determination of nonstationary aerodynamic loading on cascade blades in the case of dynamic changes of the angle of attack
[AIAA PAPER 93-0776] p 544 A93-26817
- High-performance aircraft propulsion research
[AIAA PAPER 93-0776] p 529 A93-27904
- Laminar-flow instrumentation for wind-tunnel and flight experiments
[AIAA PAPER 93-0776] p 479 A93-28605
- Modeling and control design of a wind tunnel model support
[AIAA PAPER 93-0776] p 529 A93-29281
- Aerodynamic applications of pressure sensitive paint
[AIAA PAPER 93-0776] p 549 A93-29301
- Two important improvements upon wall pressure signature correction method of low-speed wind tunnel
[AIAA PAPER 93-0776] p 730 A93-33704
- Adaptive wall wind tunnel with two measured interfaces - Theory and experiment
[AIAA PAPER 93-0776] p 679 A93-33717
- The influence of wall friction on sidewall interference
[AIAA PAPER 93-0776] p 680 A93-33723
- On the principle of sidewall effects on airfoil testing
[AIAA PAPER 93-0776] p 730 A93-33732
- An experimental and analytical study of a lifting-body wind-tunnel model exhibiting body-freedom flutter
[AIAA PAPER 93-1316] p 732 A93-33891
- Full-scale wind tunnel investigation of a helicopter individual blade control system
[AIAA PAPER 93-1361] p 726 A93-33929
- Experimental unsteady pressures at flutter on the Supercritical Wing Benchmark Model
[AIAA PAPER 93-1592] p 683 A93-34123
- Experimental investigation of counter-rotating propeller flutter at cruise conditions
[AIAA PAPER 93-1632] p 720 A93-34160
- A simple, approximate model of parachute inflation
[AIAA PAPER 93-1206] p 702 A93-35157
- Comparison of electrostatic and aerodynamic forces during parachute opening
[AIAA PAPER 93-1210] p 689 A93-35160
- Experimental validation of a discrete vortex method for inviscid axisymmetric flow around parachute canopies
[AIAA PAPER 93-1216] p 689 A93-35165
- Design of a recovery system for a reentry vehicle
[AIAA PAPER 93-1224] p 733 A93-35171
- Impulse guided Samara decelerator
[AIAA PAPER 93-1234] p 690 A93-35175
- The stability and aerodynamic performances of clusters of small cruciform parachutes
[AIAA PAPER 93-1242] p 690 A93-35181
- Navier-Stokes correlations to fuselage wind tunnel test data
[AIAA PAPER 93-35937] p 765 A93-35937
- Investigation of subharmonic response of limit cycle flutter of wing-store system
[AIAA PAPER 93-36339] p 800 A93-36339
- Vortex generators used to control laminar separation bubbles
[AIAA PAPER 93-37381] p 768 A93-37381
- Dynamic stability derivatives evaluation in a low-speed wind tunnel
[AIAA PAPER 93-37402] p 821 A93-37402
- Recent experiences with implementing a video based six degree of freedom measurement system for airplane models in a 20 foot diameter vertical spin tunnel
[AIAA PAPER 93-37763] p 821 A93-37763
- Gas analysis system for the Eight Foot High Temperature Tunnel
[AIAA PAPER 93-37875] p 822 A93-37875
- Digital resolver for helicopter model blade motion analysis
[AIAA PAPER 93-37878] p 830 A93-37878
- Experiments on shock wave-boundary layer interaction at high Mach number with entropy layer effect
[ONERA, TP NO. 1992-101] p 771 A93-38581
- A new adaptive test section at ONERA Chalais-Meudon
[ONERA, TP NO. 1992-117] p 822 A93-38592
- Study of soft-in-torsion blades - ROSOH operation
[ONERA, TP NO. 1992-124] p 803 A93-38598
- Blade-vortex interaction noise - Prediction and comparison with flight and wind tunnel tests
[ONERA, TP NO. 1992-126] p 851 A93-38600
- Numerical calculation of helicopter rotor equations and comparison with experiment
[ONERA, TP NO. 1992-128] p 772 A93-38602
- Laser velocimetry around helicopter blades in the DNW wind tunnel of the NLR
[ONERA, TP NO. 1992-143] p 831 A93-38613
- Activities of the GARTEUR high lift research program
[ONERA, TP NO. 1992-152] p 803 A93-38731
- Testing techniques for straight transonic and supersonic cascades
[ONERA, TP NO. 1992-155] p 773 A93-38734
- Schlieren device and holographic interferometer for hypersonic flow visualization
[ONERA, TP NO. 1992-160] p 832 A93-38739
- A study of the interaction between a wake vortex and an encountering airplane
[AIAA PAPER 93-3642] p 858 A93-40714
- The Langley 8-ft transonic pressure tunnel laminar-flow-control experiment
[AIAA PAPER 93-3642] p 910 A93-41783
- Non-equilibrium flow in an arc heated wind tunnel
[AIAA PAPER 93-3642] p 910 A93-42642
- DeAs - A programming system for data processing and system control: New software developments for wind tunnel operation
[AIAA PAPER 93-44452] p 1036 A93-44452
- Wake structure of a helicopter rotor in forward flight
[AIAA PAPER 93-45138] p 958 A93-45138
- Shock tube application - High enthalpy European wind tunnels
[AIAA PAPER 93-45452] p 1011 A93-45452
- Formation of shock waves in transient base flow
[AIAA PAPER 93-45460] p 1023 A93-45460
- Applications of infrared measurement technique in hypersonic facilities
[AIAA PAPER 93-45505] p 1024 A93-45505
- Computation of unsteady nozzle flows
[AIAA PAPER 93-45543] p 960 A93-45543
- Burnett solutions along the stagnation line of a cooled cylinder in low-density hypersonic flows
[AIAA PAPER 93-2726] p 962 A93-46480
- Measurement and analysis of nitric oxide radiation in an arc-jet flow
[AIAA PAPER 93-2800] p 1016 A93-46540
- A report on the status of MHD hypersonic ground test technology in Russia
[AIAA PAPER 93-3193] p 1012 A93-46656
- Artificial transition - A tool for high Reynolds number simulation?
[AIAA PAPER 93-3258] p 967 A93-46799
- Comparative wind tunnel tests at high Reynolds numbers of NACA 64 621 airfoils with two alleron configurations
[AIAA PAPER 93-46823] p 967 A93-46823
- The adaptive wall test section for the NASA Langley 0.3-m Transonic Cryogenic Tunnel
[AIAA PAPER 93-46825] p 1013 A93-46825
- The cryogenic wind tunnel
[AIAA PAPER 93-46915] p 1013 A93-46915
- Propulsion system simulator with propan for tests on a large scale model of IL-114 airplane in a full-size wind tunnel of TsAGI
[AIAA PAPER 93-46933] p 1013 A93-46933
- Low-speed wind tunnel test results of the Canard Rotor/Wing concept
[AIAA PAPER 93-3412] p 975 A93-47209
- A critical assessment of UH-60 main rotor blade airfoil data
[AIAA PAPER 93-3413] p 975 A93-47210
- Performance results from a test of an S-76 rotor in the NASA Ames 80- by 120-foot wind tunnel
[AIAA PAPER 93-3414] p 975 A93-47211
- Aerodynamic design of a hypersonic body with a constant favorable pressure gradient
[AIAA PAPER 93-3444] p 978 A93-47232
- Forebody vortex control with jet and slot blowing on an F/A-18
[AIAA PAPER 93-3449] p 1009 A93-47235
- Wind-tunnel tests of an inclined cylinder having helical grooves
[AIAA PAPER 93-3456] p 979 A93-47239
- Free-spin damping measurement techniques
[AIAA PAPER 93-3457] p 1014 A93-47240
- Boundary layer effects on the flow of a leading edge vortex
[AIAA PAPER 93-3463] p 980 A93-47245
- A wind tunnel investigation of the pressure distribution on an F/A-18 wing
[AIAA PAPER 93-3468] p 980 A93-47249
- Effect of leeward flow dividers on the wing rock of a delta wing
[AIAA PAPER 93-3492] p 982 A93-47264
- A flowfield study of a close-coupled canard configuration
[AIAA PAPER 93-3499] p 983 A93-47269
- Measurements in 80- by 120-foot wind tunnel of hazard posed by lift-generated wakes
[AIAA PAPER 93-3518] p 1014 A93-47281
- Application of a parabolized Navier-Stokes code to an HSCAT configuration and comparison to wind tunnel test data
[AIAA PAPER 93-3537] p 986 A93-47288
- Lift enhancement due to unsteady aerodynamics
[AIAA PAPER 93-3538] p 986 A93-47289
- The development of swirl five-hole probe
[AIAA PAPER 93-3537] p 987 A93-47341
- Aeroelastic computation for a flexible airfoil using the small perturbation method comparison with wind-tunnel results
[ONERA, TP NO. 1993-43] p 987 A93-47448
- Interpretation of waverider performance data using computational fluid dynamics
[AIAA PAPER 93-2921] p 1044 A93-48122
- An exploratory wind tunnel study of supersonic tip vortices
[AIAA PAPER 93-2923] p 1045 A93-48124
- CFD study of the flowfield due to a supersonic jet exiting into a hypersonic stream from a conical surface. II
[AIAA PAPER 93-2926] p 1045 A93-48127
- Application of parabolized Navier-Stokes technique for high-L/D, hypersonic vehicle design
[AIAA PAPER 93-2948] p 1047 A93-48144
- Effect of forebody tangential slot blowing on flow about a full aircraft geometry
[AIAA PAPER 93-2962] p 1048 A93-48156
- An overview of recent subsonic laminar flow control flight experiments
[AIAA PAPER 93-2987] p 1052 A93-48180
- Flowfield measurements about a multi-element airfoil at high Reynolds numbers
[AIAA PAPER 93-3137] p 1064 A93-48300
- Analysis of stability characteristics of a high performance aircraft
[AIAA PAPER 93-3616] p 1125 A93-48303
- A study of the rotary balance technique for predicting pitch damping
[AIAA PAPER 93-3619] p 1125 A93-48306
- A qualitative assessment of control effectors on an advanced fighter configuration
[AIAA PAPER 93-3627] p 1127 A93-48312
- Base drag prediction on missile configurations
[AIAA PAPER 93-3629] p 1064 A93-48314
- Wind tunnel investigation of wind shear effect on turning flight
[AIAA PAPER 93-3641] p 1127 A93-48326
- An experimental study of the thrust and aerodynamic characteristics of an operating ramjet engine in a blowdown wind tunnel
[AIAA PAPER 93-3641] p 1107 A93-48828
- Simulation of hypersonic flight - A concerted European effort
[AIAA PAPER 93-3641] p 1136 A93-49301
- Wind tunnel results for an advanced fighter configuration employing transverse thrust for enhanced STOL capability
[AIAA PAPER 93-1933] p 1100 A93-49796
- Simulation of shock-boundary layer interaction in a fan blade passage
[AIAA PAPER 93-1980] p 1078 A93-49827
- Development of the F/A-18 E/F air induction system
[AIAA PAPER 93-2152] p 1101 A93-49969
- Subscale validation of a freejet inlet-engine test capability
[AIAA PAPER 93-2179] p 1138 A93-49991
- High speed test results of subsonic, turbofan scarf inlets
[AIAA PAPER 93-2302] p 1082 A93-50087
- Fluidic scale model multi-plane thrust vector control test results
[AIAA PAPER 93-2433] p 1117 A93-50187
- Internal performance of Highly Integrated Deployable Exhaust Nozzles
[AIAA PAPER 93-2570] p 1084 A93-50288

- Minimizing the wall effects in wind tunnels with a sectional pressure chamber p 1085 A93-50965
Investigation of the effect of physical processes on heat transfer to blunt bodies at low Reynolds numbers p 1090 A93-51877
Investigation of supersonic shaped nozzles in a low-pressure wind tunnel p 1091 A93-51881
Self-excitation of intense oscillations in flow inside a wind tunnel with an open test section p 1091 A93-51883
Interference between a high-lift sweptforward wing and the horizontal nose plane at subsonic velocities p 1135 A93-51906
A study of the aerodynamics of a wing with end slots p 1092 A93-51907
Aerodynamic characteristics of airship models of different shapes p 1092 A93-51909
Experimental study of pylon cross sections for a subsonic transport airplane p 1103 A93-52440
Ground facility interference on aircraft configurations with separated flow p 1140 A93-52441
Lateral aerodynamic interference between tanker and receiver in air-to-air refueling p 1136 A93-52444
A summary of further measurements of steady and oscillatory pressures on a rectangular wing p 1096 A93-52594
Some acoustic features of perforated test section walls with splitter plates p 1226 A93-53222
Aerodynamic characteristics of the HL-20 p 1181 A93-53736
Tandem transverse hydrogen gas injection into a supersonic airflow [ISABE 93-7069] p 1201 A93-54045
A comparative assessment of two present generation turbine analysis codes [ISABE 93-7097] p 1203 A93-54073
Wind tunnel tests of the model of intake-airframe integration [ISABE 93-7101] p 1192 A93-54077
Starting characteristics of scramjet inlets [ISABE 93-7105] p 1203 A93-54081
A study on Mach 3 two-dimensional mixed compression air-intakes [ISABE 93-7106] p 1188 A93-54082
Europe's new windtunnel p 1210 A93-54275
Rotor fatigue monitoring data acquisition system p 1261 A93-54353
An improved calibration technique for wind tunnel model attitude sensors p 1253 A93-54356
An optical flameout detection system for NASA Langley's 8-Foot High Temperature Tunnel p 1254 A93-54372
Data acquisition for aeroelastic testing at the NASA Langley Transonic Dynamics Facility p 1250 A93-54397
Spectral measurements of shock layer radiation in an arc-jet wind tunnel p 1251 A93-54409
The experimental evaluation of annular ejector system under concurrent mixing and diffusion p 1250 A93-54593
Oscillatory blowing - A tool to delay boundary-layer separation p 1235 A93-55362
Pressure measurements at supersonic speeds on the research configuration ELAC I p 1237 A93-56033
Low-speed aerodynamics of the hypersonic research configuration ELAC I p 1237 A93-56035
Thermodynamic aspects of model testing in cryogenic wind tunnels p 1251 A93-56222
CTS for a low speed wind tunnel ... Captive Trajectory System p 1251 A93-56278
Design, test, and evaluation of three active flutter suppression controllers [NASA-TM-4338] p 63 N93-10070
Effect of passive flow-control devices on turbulent low-speed base flow p 82 N93-10304
A method of testing two-dimensional airfoils [AD-A253210] p 17 N93-10375
Experimental investigation of flows behind different Large-Eddy Breakup (LEBU) devices in thick boundary layers p 18 N93-10550
Wind tunnel spin data reduction to obtain aerodynamic spin damping coefficients by using nonlinear equation of motion [AD-A253880] p 19 N93-10811
Effect of planform and body on supersonic aerodynamics of multibody configurations [NASA-TP-3212] p 19 N93-10824
Shock enhancement and control of hypersonic combustion [AD-A254295] p 72 N93-10843
Arguments concerning wind tunnel test studies of the trim characteristics of objects with small asymmetries [AD-A254111] p 19 N93-10858
Application of laminar flow to aero engine nacelles [PNR-90916] p 20 N93-11020
An experimental evaluation of prediction methods for contrafans [PNR-90924] p 56 N93-11023
Method of remotely characterizing thermal properties of a sample [NASA-CASE-LAR-13508-3-CU] p 67 N93-11057
The measurement of the velocity field induced by a gust generator in a closed-circuit subsonic wind-tunnel [RAE-TM-MAT/STR-1102] p 67 N93-11435
The convection speed of the dynamic stall vortex [AD-A247258] p 21 N93-11464
Experimental investigation of the effects of aft blowing with various nozzle exit geometries on a 3.0 caliber tangent ogive at high angles of attack: Forebody pressure distributions [NASA-CR-190935] p 22 N93-11605
Further buffeting tests in a cryogenic wind tunnel [NASA-TM-107621] p 22 N93-11610
Low-speed longitudinal and lateral-directional aerodynamic characteristics of the X-31 configuration [NASA-TM-4351] p 22 N93-11622
Introduction of electronic pressure scanning at the Royal Aerospace Establishment [RAE-TM-AERO-2222] p 23 N93-11882
The 13 ft by 9 ft low speed wind tunnel facility at DRA (Aerospace Division) Bedford (England) [RAE-TM-AERO-2228] p 23 N93-11883
Strain-gauge balance performance and internal temperature gradients measured in a cryogenic environment [RAE-TM-AERO-2232] p 68 N93-11906
A wall interference assessment/correction system [NASA-CR-190617] p 68 N93-11910
An investigation of the effects of aft blowing on a 3.0 caliber tangent ogive body at high angles of attack [NASA-CR-190934] p 24 N93-12004
A preliminary study associated with the experimental measurement of the aero-optic characteristics of hypersonic configurations [AD-A253792] p 24 N93-12063
An experimental study of the relationship between forces and moments and vortex breakdown on a pitching delta wing p 49 N93-12206
Solution of nonlinear flow equations for complex aerodynamic shapes [NASA-CR-190979] p 90 N93-12329
Study of optical techniques for the Ames unitary wind tunnels. Part 4: Model deformation [NASA-CR-190980] p 68 N93-12349
Simulation analysis of a cable-mount system used for dynamic wind tunnel tests [NAL-TR-1127] p 68 N93-12359
A wind tunnel investigation to determine buffet countermeasures for STOL aircraft alpha-sweep flight testing [NAL-TR-1129] p 65 N93-12362
Mach 4 testing of scramjet inlet models [NAL-TR-1137] p 26 N93-12369
Wind tunnel investigation of a twin-engine jet transport semi-span model with upper surface blown jet flap [NAL-TR-1134] p 26 N93-12503
Icing prevention by ultrasonic nucleation of supercooled water droplets in front of subsonic aircraft [AD-A258212] p 142 N93-12816
Test techniques for engine/airframe integration p 213 N93-13200
Tests of models equipped with TPS in low speed ONERA F1 pressurized wind tunnel p 213 N93-13201
Detailed analysis of wing-nacelle interaction for commercial transport aircraft p 213 N93-13203
Recent developments in low-speed TPS-testing for engine integration drag and installed thrust reversal simulation p 160 N93-13207
Aerodynamic integration of thrust reversers on the Fokker 100 p 160 N93-13208
Flight analysis of air intake/engine compatibility p 161 N93-13212
ASTOVL model engine simulators for wind tunnel research p 192 N93-13213
A novel-high-performance system for recording and analysing instantaneous total pressure distortion in air intakes p 214 N93-13215
Comparative performance tests of a pilot-inlet in several European wind-tunnels at subsonic and supersonic speeds p 130 N93-13221
Effects of forebody strakes and Mach number on overall aerodynamic characteristics of configuration with 55 deg cropped delta wing [NASA-TP-3253] p 131 N93-13353
Time dependent heat transfer rates in high Reynolds number hypersonic flowfields p 216 N93-13664
High-speed aerodynamics of upper surface blowing aircraft configurations p 132 N93-13729
The unsteady aerodynamics of a delta wing undergoing large-amplitude pitching motions p 134 N93-13929
Control of low-speed turbulent separated flow over a backward-facing ramp p 219 N93-14475
Facilities and capabilities catalog for landing and escape systems [NASA-RP-1282] p 196 N93-14495
Investigations of detail design issues for the high speed acoustic wind tunnel using a 60th scale model tunnel. Part 1: Tests with open circuits [NASA-CR-191671] p 137 N93-14737
Investigations of detail design issues for the high speed acoustic wind tunnel using a 60th scale model tunnel. Part 2: Tests with the closed circuit [NASA-CR-191672] p 137 N93-14738
Results of low power deicer tests on a swept inlet component in the NASA Lewis icing research tunnel [NASA-TM-105968] p 138 N93-14911
Wake similarity and vortex formation for two-dimensional bluff bodies p 138 N93-15101
An overview of shed ice impact in the NASA Lewis Icing Research Tunnel [NASA-TM-105969] p 139 N93-15404
User manual for NASA Lewis 10 by 10 foot supersonic wind tunnel [NASA-TM-105626] p 194 N93-15498
Upgrade and extension of the data acquisition system for propulsion and gas dynamic laboratories [AD-A256836] p 235 N93-15637
Transition induced normal forces and their effects on the aerodynamic characteristics of slender sharp cones [AD-A256802] p 288 N93-15889
Quantitative-force measurements of pneumatic control on a wing/strike model [AD-A257343] p 289 N93-16157
Experimental and numerical investigation of vortex flow over a 76/60-deg double-delta wing [LR-680] p 289 N93-16210
On flutter behavior of a 2-D compressor cascade in incompressible flow [DLR-FB-91-26] p 418 N93-16543
Takeoff/approach noise for a model counterrotation propeller with a forward-swept upstream rotor [NASA-TM-105979] p 362 N93-16715
Wind tunnel seeding particles for laser velocimeter p 292 N93-16770
Three dimensional boundary-layer transition on a swept wing p 419 N93-16818
Experiments on swept-wing boundary-layer transition p 419 N93-16829
A multi-faceted engineering study of aerodynamic errors of the Service Aircraft Instrumentation Package (SAIP) [AD-A258059] p 293 N93-17677
A computational and experimental investigation of the propulsive and lifting characteristics of oscillating airfoils and airfoil combinations in incompressible flow [AD-A258019] p 294 N93-17819
The aerodynamic characteristics of the Gottingen 797 and Wortmann FX63-137 aerofoil sections at very low Reynolds numbers [ETN-93-92999] p 295 N93-18128
An experimental investigation of the separating/reattaching flow over a backstep [NASA-CR-192105] p 298 N93-18781
An experimental investigation of a finite circulation control wing [AD-A259044] p 340 N93-18896
Propelling force and resistance p 298 N93-19003
Flight and wind-tunnel calibrations of a flush airdata sensor at high angles of attack and sideslip and at supersonic Mach numbers [NASA-TM-104265] p 344 N93-19110
Aerodynamic heating analysis for axisymmetric bodies in supersonic flow p 303 N93-19312
Two problems reducing the data accuracy in Transonic Wind Tunnel testing p 304 N93-19321
On the roles of wind tunnel testing and computational fluid dynamics in the aircraft development p 341 N93-19322
Wind tunnel tests and CFD in Fuji Heavy Industries p 304 N93-19323
Wind tunnel test and CFD in Kawasaki Heavy Industries, Gifu p 304 N93-19324
Wind tunnel testing and CFD simulation in Mitsubishi Heavy Industries p 305 N93-19325
Experimental investigation of the aerodynamics of independently rotating cylindrical shells [AD-A258917] p 305 N93-19340
AM-X high angle of attack flight test experience (single and two seat versions) p 511 N93-19910
System identification for X-31A project support: Lessons learned so far p 512 N93-19914
Natural laminar flow test in-flight visualization p 482 N93-19921
Development and flight testing of a surface pressure measurement installation on the EAP demonstrator aircraft p 550 N93-19927

Application of a flush airdata sensing system to a wing leading edge (LE-FADS)
[NASA-TM-104267] p 518 N93-20163

The influence of the rotor test facilities ROTEST and ROTOS on the rotor inflow
[DLR-MITT-91-16] p 522 N93-21173

Program of research in flight dynamics in the JIAFS at NASA-Langley Research Center
[NASA-CR-191885] p 484 N93-21562

Combined experiment, phase 1
[DE93-000012] p 485 N93-21766

Crossflow stability and transition experiments in a swept-wing flow
[NASA-TM-108650] p 555 N93-21819

A simple, approximate model of parachute inflation
[DE93-002465] p 694 N93-25121

Experimental study of the effect of helical grooves on an infinite cylinder
[AD-A260890] p 751 N93-25912

Fabrication of composite propan blades for a cruise missile wind tunnel model
[NASA-TM-105270] p 752 N93-26202

Supersonic aeroelastic instability results for a NASP-like wing model
[NASA-TM-107739] p 718 N93-26553

Assessment of a flow-through balance for hypersonic wind tunnel models with scramjet exhaust flow simulation
[NASA-TM-4441] p 779 N93-27005

Transition aerodynamics for 20-percent-scale VTOL unmanned aerial vehicle
[NASA-TM-4419] p 779 N93-27032

Aerodynamics of a finite wing with simulated ice
p 784 N93-27437

Comparison of reacting and non-reacting shear layers at a high subsonic Mach number
[NASA-TM-106198] p 814 N93-27610

Studies of origin of three-dimensionality in laminar wakes
[AD-A262281] p 841 N93-28242

International aviation (Selected articles)
[AD-A262566] p 765 N93-28576

Modal survey of a full-scale F-18 wind tunnel model
[AD-A262482] p 875 N93-29410

High-Reynolds-number test of a 5-percent-thick low-aspect-ratio semispan wing in the Langley 0.3-meter transonic cryogenic tunnel: Wing pressure distributions
[NASA-TM-4227] p 875 N93-29449

Aerodynamic characteristics of a rotorcraft airfoil designed for the tip region of a main rotor blade
[NASA-TM-4264] p 876 N93-29450

The Ultra Light Aircraft Testing
[NASA-CR-193043] p 895 N93-29774

Construction, wind tunnel testing and data analysis for a 1/5 scale ultra-light wing model
p 876 N93-29778

Vortex shedding by blunt/bluff bodies at high Reynolds numbers. Volume 1: Data analysis
[AD-A264151] p 877 N93-30171

Vortex shedding by Blunt/Bluff bodies at high Reynolds numbers. Volume 2: Cylinders, octagon, hexagon
[AD-A264152] p 877 N93-30172

Vortex shedding by blunt/bluff bodies at high Reynolds numbers. Volume 3: Cubes
[AD-A264153] p 877 N93-30173

Experiments in the control of wing rock at high angle of attack using tangential leading edge blowing
p 1009 N93-31068

Low-speed wind tunnel study of the direct side-force characteristics of a joined-wing airplane with an upper fin
[DE93-767966] p 988 N93-31189

Definition of an airfoil family for the EUROFAIR rotor
[DLR-FB-92-04] p 998 N93-31197

Parametric studies of shock wave/boundary layer interactions over 2D compression corners at Mach 6
[VKI-TN-181] p 988 N93-31538

Supersonic aerodynamic characteristics of an advanced F-16 derivative aircraft configuration
[NASA-TP-3355] p 989 N93-31733

Evaluation of candidate working fluid formulations for the electrothermal-chemical wind tunnel
[NASA-CR-193366] p 1015 N93-31848

Analytical and experimental investigations of the oblique detonation wave engine concept
[NASA-TM-102839] p 1006 N93-32374

WIND TUNNEL WALLS

Assessment and correction of tunnel wall interference by Navier-Stokes solutions
p 116 N93-14275

Generation of flow disturbances in transonic wind tunnels
p 119 N93-14354

Flow visualization studies on sidewall effects in two dimensional transonic airfoil testing
[AIAA PAPER 93-0090] p 263 N93-20196

Wall-signature methods for high speed wind tunnel wall interference corrections
p 375 N93-20803

Comparison of predictions with measurements for a quiet supersonic tunnel
[AIAA PAPER 93-0344] p 376 N93-23031

Preliminary assessment of tunnel wall interference in the NDA cryogenic wind tunnel
[AIAA PAPER 93-0421] p 285 N93-23340

On experimental study of 3-D flow in self-correcting wind tunnel
p 528 N93-24033

Adaptive wall wind tunnel with two measured interfaces - Theory and experiment
p 679 N93-33717

The influence of wall friction on sidewall interference
p 680 N93-33723

A new adaptive test section at ONERA
Chalais-Meudon
[ONERA, TP NO. 1992-117] p 822 N93-38592

The adaptive wall test section for the NASA Langley 0.3-m Transonic Cryogenic Tunnel
p 1013 N93-46825

Effects of junction modifications on sharp-fin-induced shock wave/boundary layer interaction
[AIAA PAPER 93-2935] p 1046 N93-48133

Minimizing the wall effects in wind tunnels with a sectional pressure chamber
p 1085 N93-50965

Dynamical effects of suction/heating on turbulent boundary layers
[AD-A248459] p 87 N93-11416

A wall interference assessment/correction system
[NASA-CR-190617] p 68 N93-11910

Modifications to Langley 0.3-m TCT adaptive wall software for heavy gas test medium, phase 1 studies
[NASA-CR-189736] p 291 N93-16710

A wall interference assessment/correction system
[NASA-CR-191889] p 296 N93-18384

Wind tunnel wall interference correction at subsonic speeds
p 304 N93-19320

Two problems reducing the data accuracy in Transonic Wind Tunnel testing
p 304 N93-19321

Wind tunnel tests and CFD in Fuji Heavy Industries
p 304 N93-19323

WIND TUNNELS

Rapid wind tunnel prototype using stereolithography and equivalent technologies
p 191 N93-14365

Excitation of velocity fluctuations and noise in a wind tunnel
p 444 N93-18242

The design of test-section inserts for higher speed aeroacoustic testing in the Ames 80- by 120-Foot Wind Tunnel
p 374 N93-19149

Close-up analysis of aircraft ice accretion
[AIAA PAPER 93-0029] p 309 N93-23239

Suggestions for development of three-phase 60 Hz arc heated wind tunnels
[AIAA PAPER 93-0795] p 528 N93-24874

Design philosophy for wind tunnel model positioning control systems
p 822 N93-37877

Numerical computation of aerodynamic noise radiation by the large eddy simulation
p 850 N93-38151

Optimal conditions for flow turbulence reduction by a set of grids
p 836 N93-39122

Cryogenic wind tunnels
p 1010 N93-44886

AIAA Applied Aerodynamics Conference, 11th, Monterey, CA, Aug. 9-11, 1993, Technical Papers. Pts. 1 & 2
p 974 N93-47201

Effect of ground and ceiling planes on shape of energized wakes
[AIAA PAPER 93-3410] p 974 N93-47207

Some key problems in the design of the NPU open-circuit low-turbulence wind tunnel
p 1139 N93-51188

Production of oscillatory flow in wind tunnels
p 1218 N93-53812

Icing Research Tunnel rotating bar calibration measurement system
p 1255 N93-54398

Design problems of three-dimensional contractions --- in incompressible flow
p 1236 N93-55584

Non-propulsive aerodynamic noise
p 99 N93-10673

Winds of change: Expanding the frontiers of flight. Langley Research Center's 75 years of accomplishment, 1917-1992
[NASA-NP-130] p 104 N93-11100

An experimental study of flow patterns and endwall heat transfer upstream of a surface-mounted rectangular obstruction in a turbulent boundary layer
p 89 N93-11698

A wall interference assessment/correction system
[NASA-CR-190617] p 68 N93-11910

Design philosophy for wind tunnel model positioning systems
[AD-A254958] p 192 N93-12552

Subsonic aerodynamic research laboratory
[AD-A256060] p 137 N93-14661

Close-up analysis of aircraft ice accretion
[NASA-TM-105952] p 148 N93-15360

Upgrade and extension of the data acquisition system for propulsion and gas dynamic laboratories
[AD-A256836] p 235 N93-15637

Transient/structural analysis of a combustor under explosive loads
[NASA-TM-107660] p 420 N93-17779

A wall interference assessment/correction system
[NASA-CR-191889] p 296 N93-18384

Study of optical techniques for the Ames unitary wind tunnel: Digital image processing, part 6
[NASA-CR-192164] p 382 N93-18766

Flight and wind-tunnel calibrations of a flush airdata sensor at high angles of attack and sideslip and at supersonic Mach numbers
[NASA-TM-104265] p 344 N93-19110

Evaluation of candidate working fluid formulations for the electrothermal - chemical wind tunnel
[NASA-CR-192196] p 530 N93-20312

Nozzle diffuser for use with an open test section of a wind tunnel
[NASA-CASE-LAR-14424-1-SB] p 731 N93-25996

Modification and calibration of the Naval Postgraduate School Academic Wind Tunnel
[AD-A262092] p 823 N93-28189

Summer research program (1992). High School Apprenticeship Program (HSAP) reports. Volume 16: Arnold Engineering Development Center Civil Engineering Laboratory
[AD-A262024] p 945 N93-29396

WIND TURBINES

Use of NASA LS (1) general aviation airfoil for a small wind turbine - An experience in Denmark
p 92 N93-12364

Measurement of shed vorticity and circulation from rotating airfoil by particle image velocimetry
p 538 N93-23804

Numerical calculation of helicopter rotor equations and comparison with experiment
[ONERA, TP NO. 1992-128] p 772 N93-38602

Measured data for the Sandia 34-meter vertical axis wind turbine
[DE92-019807] p 94 N93-12075

User's Guide for the NREL Force and Loads Analysis Program
[DE92-010579] p 216 N93-13524

User's Guide for the NREL Teetering Rotor Analysis Program (STRAP)
[DE92-010580] p 216 N93-13525

Aeroelastic stability and response of rotating structures
[NASA-CR-191803] p 371 N93-16560

A discussion of the results of the rainfall counting of a wide range of dynamics associated with the simultaneous operation of adjacent wind turbines
[DE93-000016] p 434 N93-18705

Combined experiment, phase 1
[DE93-000012] p 485 N93-21766

The natural excitation technique (NEXT) for modal parameter extraction from operating wind turbines
[DE93-010611] p 845 N93-28603

WIND VELOCITY

Large-eddy simulation of turbulent flow above and within a forest
p 92 N93-11404

Wind identification along a flight trajectory. I - 3D-kinematic approach
p 223 N93-16324

A fine structure of the gust front observed with sonic anemometer
p 430 N93-22158

A microcomputer program for estimating low altitude wind and turbulence fields
p 438 N93-22163

Evaluation of clear-air radar PROUST and Doppler radar RONSARD for airport low level-wind shear detection
p 433 N93-22202

Recent experiment focuses on operational impact of jet stream forecast errors
p 487 N93-27394

A comparison of wind speed measured by the Special Sensor Microwave Imager (SSM/I) and the Geosat altimeter
p 1033 N93-44862

Wind identification along a flight trajectory. III - 2D dynamic approach
p 1007 N93-45401

A study on low level windshear hazard index
p 1240 N93-55414

Acoustic noise generation at the air/ocean boundary
[DREA-CR-90-445] p 99 N93-10612

Aircraft turns into and down wind
[AERO-REPT-9201] p 337 N93-18131

Surface shear stress estimates from geostrophic winds for use in sensible and latent heat flux formulations
p 936 N93-30044

Vortex shedding by blunt/bluff bodies at high Reynolds numbers. Volume 4: Rectangles
[AD-A264154] p 877 N93-30151

WIND VELOCITY MEASUREMENT

Detection and parameter estimation of atmospheric turbulence by ground-based and airborne CO2 Doppler lidars
p 395 N93-17862

Stratospheric turbulence measurements and models for aerospace plane design
[AIAA PAPER 92-5072] p 433 N93-22342

Stratospheric turbulence measurements and models for aerospace plane design
[NASA-TM-104262] p 223 N93-13288

WINDOWS (APERTURES)

- IR window damage measured by reflective scatter p 851 A93-39544
- Nonlinear deformation mechanics of multilayer transparency elements - Some calculation results --- for aircraft portholes p 1191 A93-52937
- Stress calculations on the window section of an all-composite aircraft fuselage [LR-688] p 328 N93-16215

WINDS ALOFT

- Atmospheric turbulence aloft - A review of possible methods for detection, warning, and validation of prediction models [AIAA PAPER 93-0847] p 557 A93-24914

WINDSHIELDS

- Bird impact dynamic response analysis for aircraft arc windshield p 41 A93-11815
- New model of bird impact response analysis and its engineering solution p 156 A93-14336
- An impact dynamics investigation on some problems in bird strike on windshields of high speed aircraft p 197 A93-15346

- T-38 forward windshield development and performance demonstration report [AD-A259240] p 513 N93-20579

WING CAMBER

- Flight test results from a supercritical mission adaptive wing with smooth variable camber [NASA-TM-4415] p 49 N93-11863
- Tailored composite wings with elastically produced chordwise camber p 923 N93-30876

WING FLAPS

- Navier-Stokes calculations of the flow about wing-flap combinations p 112 A93-14171
- Navier-Stokes computation of wing/rotor interaction for a tilt rotor in hover p 122 A93-14537
- Sonic fatigue analysis of an aircraft wing flap by the matrix difference equation method p 399 A93-19208
- Icing effects on aircraft stability and control determined from flight data - Preliminary results [AIAA PAPER 93-0398] p 370 A93-23073
- Application of leading-edge vortex manipulations to reduce wing rock amplitudes p 1007 A93-45152
- Effects of wing-tip vortex flaps p 959 A93-45153
- Icing effects on aircraft stability and control determined from flight data: Preliminary results [NASA-TM-105977] p 188 N93-14831

WING LOADING

- Wing pressure loads in canard configurations - A comparison between numerical results and experimental data p 7 A93-11499
- Design sensitivity and optimization of composite cylinders p 71 A93-12781
- Modeling of interfaces in problems of flow of a ponderable fluid past a wing profile p 124 A93-15189
- Refinement of algorithms for calculating the remaining life from magnetic recording instrument data --- for IL-86 aircraft wing p 320 A93-18330
- Analysis of the NASA Hypersonic Wing Test Structure [AIAA PAPER 92-4724] p 409 A93-20326
- Stability of the vertical autorotation of a single-winged samara p 274 A93-22443
- An analytically designed subcomponent test to reproduce the failure of a composite wing box beam [AIAA PAPER 93-1344] p 709 A93-33914
- Development testing of large ram air inflated wings [AIAA PAPER 93-1204] p 702 A93-35155
- Impulse guided Samara decelerator [AIAA PAPER 93-1234] p 690 A93-35175
- Apparent mass effects on parafoil dynamics [AIAA PAPER 93-1236] p 690 A93-35177
- A study of the strength of a closed system of wings p 828 A93-36792
- Load-bearing capacity of an aircraft wing based on the condition of compressed surface fracture p 801 A93-36794
- Optimization of the parameters of the lift-augmentation devices of the wing of a maneuverable aircraft equipped with an active load-reduction system p 804 A93-39189
- Dependence of the service life of a wing on its strength uniformity and landing gear location p 891 A93-42377
- Time domain panel method for wings p 958 A93-45135
- Load rating for a delta wing box based on a reliability criterion p 1030 A93-47093
- Calculation of aerodynamic loads on the wing of rigid and elastic aircraft with allowance for load correction from experimental data p 1103 A93-51905
- Monitoring load experience of individual aircraft p 1103 A93-52450
- Calculation of flow fields near a lifting wing p 1179 A93-53552

- An experimental study of the relationship between forces and moments and vortex breakdown on a pitching delta wing p 49 N93-12206

- Towards an analytical treatment of the aerolastic problem of a circular wing p 781 N93-27214
- Effect of vortex behavior on loads acting on a 65 deg delta wing oscillating in roll at high incidence p 782 N93-27220
- High-Reynolds-number test of a 5-percent-thick low-aspect-ratio semispan wing in the Langley 0.3-meter transonic cryogenic tunnel: Wing pressure distributions [NASA-TM-4227] p 875 N93-29449

WING NACELLE CONFIGURATIONS

- Juncture flow improvement for wing/pylon configurations by using CFD methodology [AIAA PAPER 93-0522] p 283 A93-23264
- Navier-Stokes calculations for transport wing-body configurations with nacelles and struts [AIAA PAPER 93-2945] p 1047 A93-48142
- Analysis of a high bypass ratio engine installation using the chimera domain decomposition technique [AIAA PAPER 93-1808] p 1100 A93-49697
- Detailed analysis of wing-nacelle interaction for commercial transport aircraft p 213 N93-13203
- Aerodynamic analysis of slipstream/wing/nacelle interference for preliminary design of aircraft configurations p 130 N93-13205
- Euler analysis of turbofan/superfan integration for a transport aircraft p 214 N93-13206
- Recent developments in low-speed TPS-testing for engine integration drag and installed thrust reversal simulation p 160 N93-13207
- Application of subsonic first-order panel methods for prediction of inlet and nozzle aerodynamic interactions with airframe p 130 N93-13223
- High-speed aerodynamics of upper surface blowing aircraft configurations p 132 N93-13729
- Improving military transport aircraft through highly integrated engine-wing design [DS-1607] p 333 N93-17850
- WBNFLOW: Multi-grid/multi-block potential solver for compressible flow. User's guide [FFA-TN-1992-43] p 1031 N93-31146

WING OSCILLATIONS

- Effects of the pylon pitching stiffness on wing-store flutter p 41 A93-11820
- An ultralight freewing aircraft design study [AIAA PAPER 92-4194] p 44 A93-13371
- Extending the useful frequency of 'rigid' wind tunnel models with active control p 190 A93-14299
- Generalized vortex lattice method for oscillating lifting surfaces in subsonic flow p 123 A93-14555
- Acoustic control of flow separation on a straight and a yawed wing p 125 A93-15256
- Experimental study on the unsteady aerodynamic response of a three dimensional cascade with oscillating blades p 242 A93-18499
- Active control of wing rock of a delta wing at post-stall using tangential leading edge blowing [AIAA PAPER 93-0056] p 367 A93-20169
- Experimental and numerical analysis of the wing rock characteristics of a 'wing-body-tail' configuration [AIAA PAPER 93-0187] p 368 A93-22612
- Aerodynamic analysis of flapping wing propulsion [AIAA PAPER 93-0484] p 286 A93-23386
- Incompressible potential flow calculation about harmonically oscillating three-dimensional configurations p 461 A93-24089
- Elementary stall flutter of an aircraft wing p 545 A93-27289

- Wing flutter boundary prediction using unsteady Euler aerodynamic method [AIAA PAPER 93-1422] p 739 A93-33975
- Experimental unsteady pressures at flutter on the Supercritical Wing Benchmark Model [AIAA PAPER 93-1592] p 683 A93-34123
- Dynamic stall of sinusoidally oscillating three-dimensional swept and unswept wings in compressible flow p 766 A93-35995
- Investigation of subharmonic response of limit cycle flutter of wing-store system p 800 A93-36339
- Slender wing rock revisited p 768 A93-37386
- Numerical calculation of separated flows around wing section in unsteady motion by using incompressible Navier-Stokes equations p 770 A93-38158
- Estimation of wing stability in flow from the characteristics of the transient process p 836 A93-39177
- Spanwise aileron oscillations p 819 A93-39190
- Application of leading-edge vortex manipulations to reduce wing rock amplitudes p 1007 A93-45152
- Lift enhancement due to unsteady aerodynamics [AIAA PAPER 93-3538] p 986 A93-47289
- Three-dimensional unsteady separating flows around an oscillatory forward-swept wing [AIAA PAPER 93-2976] p 1050 A93-48170
- Navier-Stokes computations on full-span wing-body configuration with oscillating control surfaces [AIAA PAPER 93-3687] p 1065 A93-48356

- Effect of flexural and rotational wing oscillations on the prevention of flow separation p 1150 A93-48911
- Laminarization of the boundary layer on a vibrating wing p 1089 A93-51776
- The forms of unsteady concentrated vortex-breakdown and its reactions to disturbance p 1231 A93-54594
- Airfoil-vortex interaction and the wake of an oscillating airfoil p 134 A93-13803
- An experimental and computational investigation of slender wings undergoing wing rock p 187 N93-13915
- An examination of wing rock for the F-15 [AD-A256613] p 188 N93-14252
- Lift enhancement using a close-coupled oscillating canard [AD-A257877] p 296 N93-18336
- Airfoil stability in turbulent flow p 781 N93-27212
- Effect of vortex behavior on loads acting on a 65 deg delta wing oscillating in roll at high incidence p 782 N93-27220

WING PANELS

- Design of a full time wing leveler system using tab driven aileron controls [AIAA PAPER 92-4193] p 63 A93-13345
- Compression after impact (CAI) properties of CF/PEEK (APC-2) and conventional CF/epoxy stiffened panels p 196 A93-14307
- Composite wing results of Deutsche Airbus technology program p 109 A93-15808
- An accurate nonlinear finite element analysis and test correlation of a stiffened composite wing panel p 546 A93-27968
- Global/local interlaminar stress analysis of a grid-stiffened composite panel p 548 A93-28543
- Lessons from application of equivalent plate structural modeling to an HSCT wing [AIAA PAPER 93-1413] p 739 A93-33969
- Human engineering issues for data link systems p 1260 A93-55874
- Reliability of stiffened structural panels: Two examples [NASA-TM-107687] p 219 N93-14483
- Design, analysis, and fabrication of the technology integration box beam p 919 A93-30433
- Development of stitching reinforcement for transport wing panels p 921 N93-30852

WING PLANFORMS

- Improving the lift to drag characteristics of low boom configuration [AIAA PAPER 92-4218] p 16 A93-13380
- Effect of wing planforms on induced drag reduction p 127 A93-16932
- Variable-complexity aerodynamic-structural design of a high-speed civil transport wing [AIAA PAPER 92-4695] p 323 A93-20279
- Experimental and nonlinear vortex lattice method results for various wing-canard configurations p 479 A93-28607
- Sensitivity analysis of a wing aeroelastic response p 958 A93-45142
- Induced drag of a crescent wing planform p 1094 A93-52430
- Aerodynamic characteristics of conical triangular-planform wings of low aspect ratio in subsonic stalled flow p 1180 A93-53574
- Effect of planform and body on supersonic aerodynamics of multibody configurations [NASA-TP-3212] p 19 N93-10824
- Review of aerodynamic design in the Netherlands [NLR-TP-91260-U] p 999 N93-31840

WING PROFILES

- Numerical modeling of supersonic flows past wings of different aspect ratios over a wide range of angles of attack within the framework of the plane section law p 5 A93-10141
- Regimes of supersonic flow past the windward side of V-shaped wings p 5 A93-10144
- Transition of flutter mode of two-dimensional wing with external store p 41 A93-11818
- Maximizing the critical Mach number for lifting wing profiles p 13 A93-12841
- Increasing the lift-drag ratio of wings of small aspect ratio at hypersonic velocities p 13 A93-12933
- Advanced technology Tilt Wing study [AIAA PAPER 92-4237] p 44 A93-13359
- Over wing propeller aerodynamics p 113 A93-14189
- A study of propeller/wing interaction including the effect of ground proximity p 113 A93-14190
- An adaptive region method for computation of vortex sheet behind wing in compressible flow p 116 A93-14262
- An engineering method with artificial intelligence characteristics used for structural layout of wings p 225 A93-14290
- The aerodynamic and structural design of a variable camber wing (VCW) p 117 A93-14291

- Design of manoeuvrable simple and complex planform transonic wings with attained thrust-, panel- and Euler-methods p 117 A93-14301
- Parametric aeroelastic analysis of composite wing-boxes with active strain-energy tuning p 156 A93-14361
- Aeroelastic analysis of composite wing with control surface p 157 A93-14386
- Euler solutions simulating strong shock waves and vortex phenomena over 3D wings p 121 A93-14392
- Results of testing of models of joint-wing utility class aircraft [SAE PAPER 921013] p 157 A93-14643
- Adaptive aeroelastic composite wings - Control and optimization issues p 185 A93-14818
- Acoustic control of flow separation on a straight and a yawed wing p 125 A93-15256
- The Concorde wing - A useful model p 126 A93-16400
- Adaptive/conformal wing design for future aircraft p 320 A93-17728
- Effect of airfoil porosity on the shock wave position and intensity at transonic velocities p 241 A93-18222
- The use of the Polhamus and discrete vortex methods for calculating the nonlinear characteristics of delta wings and wings with a strake p 242 A93-18379
- Circulation control wing model study [AIAA PAPER 93-0094] p 264 A93-20200
- Preliminary wing design of a high speed civil transport aircraft by multilevel decomposition techniques [AIAA PAPER 92-4721] p 325 A93-20323
- Design of a wing shape for study of hypersonic crossflow transition in flight p 265 A93-20713
- Numerical analysis of two-dimensional flows around elliptic wings above a flat plate p 267 A93-20924
- Study on the numerical problem of the boundary element method in analysis of flow around a three-dimensional wing-body p 268 A93-20934
- Grid and design variables sensitivity analyses for NACA four-digit wing-sections [AIAA PAPER 93-0195] p 276 A93-22616
- Unsteady vortex dynamics and surface pressure topologies on a pitching wing [AIAA PAPER 93-0435] p 286 A93-23349
- Effects of free-stream turbulence on boundary-layer transition [AIAA PAPER 93-0488] p 416 A93-23390
- Supercritical wing design, a three dimensional hodograph approach [AIAA PAPER 92-2657] p 472 A93-24986
- Problems in the optimum design of a wing profile for nonseparated flow over a range of angles of attack p 477 A93-27614
- Simultaneous structure/control design optimization of a wing structure with a gust load alleviation system p 525 A93-28616
- Recent developments in equivalent plate modeling for wing shape optimization [AIAA PAPER 93-1647] p 742 A93-34172
- Recent advances in the numerical analysis of ram air wings - The three dimensional simulation code 'PARA3D' [AIAA PAPER 93-1203] p 702 A93-35154
- Development testing of large ram air inflated wings [AIAA PAPER 93-1204] p 702 A93-35155
- Prandtl theory applied to paraglider aerodynamics [AIAA PAPER 93-1220] p 690 A93-35169
- Impulse guided Samara decelerator [AIAA PAPER 93-1234] p 690 A93-35175
- A method for the optimum design of a large-aspect-ratio wing p 828 A93-36793
- Rarefied gas flow around a 3D-deltawing p 870 A93-42639
- Investigation of the radiance from the leading edge of a wing [AIAA PAPER 93-2728] p 1039 A93-46482
- On the legitimacy and accuracy of downwash computations by panel methods on 3D wings p 970 A93-46885
- On dynamics of the juncture vortex [AIAA PAPER 93-3473] p 980 A93-47252
- Computation of passively controlled transonic wing [AIAA PAPER 93-3474] p 981 A93-47253
- Calculation of AGARD Wing 445.6 flutter using Navier-Stokes aerodynamics [AIAA PAPER 93-3476] p 981 A93-47255
- A computational method for inverse design of transonic airfoil and wing [AIAA PAPER 93-3482] p 982 A93-47260
- Effect of leeward flow dividers on the wing rock of a delta wing [AIAA PAPER 93-3492] p 982 A93-47264
- Computational study of a conical wing having unit aspect ratio at supersonic speeds [AIAA PAPER 93-3505] p 984 A93-47272
- A CFD-based design strategy for advanced transonic wing concepts with practical ramifications for subsonic transports [AIAA PAPER 93-2946] p 1047 A93-48143
- Tip vortex, stall vortex, and separation observations on pitching three-dimensional wings [AIAA PAPER 93-2972] p 1049 A93-48166
- Improvement of transonic wing buffet by geometric modifications [AIAA PAPER 93-3024] p 1055 A93-48209
- Transition for three-dimensional boundary layers on wings in the transonic regime [AIAA PAPER 93-3049] p 1057 A93-48229
- A two layer k-epsilon computation of transonic viscous flow including separation over the DLR-F5 wing [AIAA PAPER 93-3110] p 1061 A93-48281
- Aircraft with single axis aerodynamically deployed wings [AIAA PAPER 93-3673] p 1129 A93-48350
- Calculation of the parameters of instability waves in the preseparation region p 1067 A93-48826
- Determination of the shape of a wing profile in boundary layer flow with a given velocity diagram p 1067 A93-48844
- Effect of the wing planform on the optimal deformation of the middle surface p 1150 A93-48909
- Minimization of the induced drag of nonplanar lifting systems p 1068 A93-48910
- A study of the effect of the shape of a parasail on its lift-drag ratio p 1069 A93-48913
- Supersonic flow past a rectangular wing of finite thickness p 1086 A93-50972
- Optimal wing shapes in a hypersonic nonequilibrium flow p 1088 A93-51770
- Numerical optimization methods for variational inverse boundary value problems of aerodynamics p 1088 A93-51771
- Heat transfer on tip fins in hypersonic flow p 1088 A93-51775
- Effect of Reynolds number on the aerodynamic characteristics of a semicone with a wing in the case of hypersonic flow velocities p 1090 A93-51878
- A finite difference study of the aerodynamic characteristics of wing profiles at transonic velocities p 1091 A93-51903
- A study of the aerodynamics of a wing with end slots p 1092 A93-51907
- A study of air intake parameters on the aerodynamic characteristics of a parasail p 1092 A93-51908
- Finite element analysis of natural vibrations of an aeroplane with asymmetric variable wing geometry p 1218 A93-53776
- Wind tunnel investigation of a twin-engine jet transport semi-span model with upper surface blown jet flap [NAL-TR-1134] p 26 N93-12503
- WING ROOTS**
- Stability of the vertical autorotation of a single-winged samara p 274 A93-22443
- Development of highly loaded root end attachments for composite material high speed flying surfaces p 539 A93-24122
- Supersonic aeroelastic instability results for a NASP-like wing model [AIAA PAPER 93-1369] p 682 A93-33935
- WING SLOTS**
- An investigation of shock wave turbulent boundary layer interaction with bleed through slanted slots [AIAA PAPER 93-2992] p 1052 A93-48184
- WING SPAN**
- Calculation of a three-dimensional boundary layer at the lee side of a finite-span delta wing in the case of viscous interaction with hypersonic flow p 5 A93-10143
- Numerical solution of the integral equations of the aerodynamics of porous surfaces p 13 A93-12768
- Structural and aerodynamic considerations for an oblique all-wing aircraft [AIAA PAPER 92-4220] p 43 A93-13336
- Spanwise aileron oscillations p 819 A93-39190
- Computation of induced drag for elliptical and crescent-shaped wings p 958 A93-45136
- An experimental study of droop leading edge modifications on high and low aspect ratio wings up to 50 deg angle of attack [AIAA PAPER 93-3496] p 983 A93-47268
- Attenuation of airplane wake vortices by excitation of far-field instability [AIAA PAPER 93-3511] p 984 A93-47277
- Lift enhancement due to unsteady aerodynamics [AIAA PAPER 93-3538] p 986 A93-47289
- Navier-Stokes computations on full-span wing-body configuration with oscillating control surfaces [AIAA PAPER 93-3687] p 1065 A93-48356
- Effect of the wing planform on the optimal deformation of the middle surface p 1150 A93-48909
- Nonplanar wings with a minimum induced drag p 1089 A93-51779
- Analysis of in-flight structural failures of P-3C wing leading edge segments [AD-A256212] p 165 N93-15238
- WING TANKS**
- Subharmonic bifurcation analysis of wing with store flutter p 78 A93-12098
- Aircraft wing compartment liner concept to reduce fuel spillage [DOT/FAA/CT-TN92/34] p 331 N93-17219
- WING TIP VORTICES**
- 'Wingwake' - A computational model for preliminary assessment of wake vortex attenuation schemes [AIAA PAPER 92-4209] p 15 A93-13377
- Euler solutions simulating strong shock waves and vortex phenomena over 3D wings p 121 A93-14392
- Experimental study of rotor wake/body interactions in hover p 124 A93-14782
- A flat plate wing standing on a wall covered with a thick boundary layer. II - Wing characteristics under the effects of side wall boundary layer and wing tip vortex p 125 A93-15446
- Wing vortex refraction effects from BAC 1-11 flight tests p 450 A93-19226
- Measurements in the near-field of a turbulent wingtip vortex [AIAA PAPER 93-0551] p 285 A93-23290
- Unsteady vortex dynamics and surface pressure topologies on a pitching wing [AIAA PAPER 93-0435] p 286 A93-23349
- Near-field behavior of a tip vortex p 288 A93-23549
- Three dimensional near field behavior of a tip vortex developing on an elliptic foil [AIAA PAPER 93-0865] p 468 A93-24927
- Computational analysis of methods for reduction of induced drag [AIAA PAPER 93-0524] p 474 A93-25536
- Experimental investigations of asymmetric vortex flows behind elliptic cones at incidence p 757 A93-35637
- Effects of blowing on delta wing vortices during dynamic pitching p 768 A93-37384
- Tip vortex geometry of a hovering helicopter rotor in ground effect p 893 A93-43779
- A flowfield study of a close-coupled canard configuration [AIAA PAPER 93-3499] p 983 A93-47269
- The application of an Euler method and a Navier Stokes method to the vortical flow about a delta wing [AIAA PAPER 93-3510] p 984 A93-47276
- Attenuation of airplane wake vortices by excitation of far-field instability [AIAA PAPER 93-3511] p 984 A93-47277
- Elliptic cross section tip effects on the vortex wake of an axisymmetric body at angle of attack [AIAA PAPER 93-2960] p 1124 A93-48154
- Tip vortex, stall vortex, and separation observations on pitching three-dimensional wings [AIAA PAPER 93-2972] p 1049 A93-48166
- A computational study of wingtip vortex flowfield [AIAA PAPER 93-3010] p 1054 A93-48200
- Turbulent structure of a wingtip vortex in the near field [AIAA PAPER 93-3011] p 1054 A93-48201
- Unsteady wing surface pressures in the wake of a propeller p 1095 A93-52436
- An experimental investigation of interacting wing-tip vortex pairs [AD-A258471] p 295 N93-18272
- WING TIPS**
- Interaction of a streamwise vortex with a free surface [AIAA PAPER 93-0556] p 543 A93-25539
- Effects of wing-tip vortex flaps p 959 A93-45153
- An experimental study of the effects of deformable tip on the performance of fins and finite wings [AIAA PAPER 93-3000] p 1053 A93-48190
- Heat transfer on tip fins in hypersonic flow p 1088 A93-51775
- A study of the aerodynamics of a wing with end slots p 1092 A93-51907
- WING-FUSELAGE STORES**
- Unstructured grid solutions to a wing/pylon/store configuration using VGRID3D/USM3D [AIAA PAPER 92-4572] p 14 A93-13303
- Investigation of subharmonic response of limit cycle flutter of wing-store system p 800 A93-36339
- Aircraft with single axis aerodynamically deployed wings [AIAA PAPER 93-3673] p 1129 A93-48350
- WINGED VEHICLES**
- High angle-of-attack inviscid Shuttle Orbiter computation p 9 A93-12020
- Structural and aerodynamic considerations for an oblique all-wing aircraft [AIAA PAPER 92-4220] p 43 A93-13336
- WINGS**
- Experimental study on the mechanism of favourable interferences of body strakes p 121 A93-14405

A flat plate wing standing on a wall covered with a thick boundary layer. II - Wing characteristics under the effects of side wall boundary layer and wing tip vortex p 125 A93-15446

Performance degradation due to hoar frost on lifting surfaces p 305 A93-17798

Aerodynamic degradation due to distributed roughness on high lift configuration p 260 A93-20146 [AIAA PAPER 93-0028]

Variable-complexity aerodynamic-structural design of a high-speed civil transport wing p 323 A93-20279 [AIAA PAPER 92-4695]

Static aeroelastic analysis of a maneuvering aircraft with damaged wing p 325 A93-20360 [AIAA PAPER 92-4765]

An approach to tiltrotor wing aeroservoelastic optimization through increased productivity p 326 A93-20371 [AIAA PAPER 92-4781]

Lift enhancement of ground-effect wing. I - Results of screening tests of various concepts p 271 A93-21737

Application of a Navier-Stokes aeroelastic method to improve fighter wing performance at maneuver flight conditions p 284 A93-23270 [AIAA PAPER 93-0529]

Aerodynamically efficient wing design with structural considerations p 460 A93-24081

A two-dimensional elliptic grid generator for a wing-body section involving grid control functions p 460 A93-24083

Direct multivariable adaptive controller with application to wing flutter p 524 A93-26946

Microchannel plate modal gain variations with temperature p 477 A93-27445

Dornier 228 experimental with laminar wing p 506 A93-27500

The effects of composite material on the configuration and design of the V-22 wing p 507 A93-27964

Structural analysis of box beams using symbolic manipulation technique p 548 A93-28615

Exact flutter solution of advanced anisotropic composite cantilevered wing structures p 727 A93-34072 [AIAA PAPER 93-1535]

A refined structural model of composite aircraft wings for the enhancement of vibrational and aeroelastic response characteristics p 740 A93-34073 [AIAA PAPER 93-1536]

An inverse method for computation of structural stiffness distributions of aeroelastically optimized wings p 741 A93-34077 [AIAA PAPER 93-1540]

Sensitivity analysis of aeroelastic response of a wing using piecewise pressure representation p 742 A93-34170 [AIAA PAPER 93-1645]

Sensitivity analysis of flutter response of a typical section and a wing in transonic flow p 742 A93-34171 [AIAA PAPER 93-1646]

Integrated structural tailoring and adaptive control of advanced flight vehicle structural vibration p 757 A93-34219 [AIAA PAPER 93-1697]

Active rib experiment for shape control of an adaptive wing p 712 A93-34222 [AIAA PAPER 93-1700]

Smart structures stabilized unstable control surfaces p 712 A93-34223 [AIAA PAPER 93-1701]

Cost/weight savings for the V-22 wing stow p 797 A93-35981

Activities of the GARTEUR high lift research program (ONERA, TP NO. 1992-152) p 803 A93-38731

An aerodynamic model for flapping-wing flight p 858 A93-40470

Lift and pitching moment measurements in vertical gusts p 906 A93-42259

Vibration analysis of composite wing with tip mass using finite elements p 1023 A93-45175

A method for the prediction of induced drag for planar and nonplanar wings p 976 A93-47216 [AIAA PAPER 93-3420]

A zonal CFD method for three-dimensional wing simulations p 977 A93-47225 [AIAA PAPER 93-3433]

Development of an innovative natural laminar flow wing concept for high-speed civil transports p 980 A93-47247 [AIAA PAPER 93-3466]

Application of natural laminar flow to a supersonic transport concept p 997 A93-47248 [AIAA PAPER 93-3467]

A wind tunnel investigation of the pressure distribution on an F/A-18 wing p 980 A93-47249 [AIAA PAPER 93-3468]

Design for cyclic loading endurance of composites p 1216 A93-53395

Reinforcement of the F-111 wing pivot fitting with a boron/epoxy doubler system - Materials engineering aspects p 1214 A93-54241

Control of lift and drag in unsteady flows p 17 A93-10340 [AD-A253146]

Nonlinear aeroelasticity of composite structures [AD-A254285] p 47 N93-10842

Unsteady propeller/wing aerodynamic interactions p 24 N93-12190

Nonlinear stall flutter of wings with bending-torsion coupling p 186 N93-12959 [AD-A254323]

Analysis and design of planar and non-planar wings for induced drag minimization p 131 N93-13463 [NASA-CR-191274]

Transonic aeroelastic analysis of systems with structural nonlinearities p 217 N93-13769

Navier-Stokes flowfield computation of wing/rotor interaction for a tilt rotor aircraft in hover p 135 N93-14035

Proceedings of the USAF Structural Integrity Program [AD-A255379] p 110 N93-14549

Analysis of in-flight structural failures of P-3C wing leading edge segments p 165 N93-15238 [AD-A256212]

F-14 wing lug coating investigation p 328 N93-15858 [AD-A257384]

Quantitative-force measurements of pneumatic control on a wing/strike model p 289 N93-16157 [AD-A257343]

Lanchester: The man p 456 N93-16464 [AERO-REPT-9111]

Maximum lift of wings with leading-edge devices and trailing-edge flaps deployed p 290 N93-16522 [ESDU-92031]

Pitching moment of low aspect ratio wing-body combinations up to high angles of attack at supersonic speeds p 333 N93-17958 [ESDU-92043]

Add-on damping treatment for the F-15 upper-outer wing skin p 337 N93-18248 [AD-A258470]

Lift enhancement using a close-coupled oscillating canard p 296 N93-18336 [AD-A257877]

Analysis of a 2-D airfoil motion flying in-proximity to a wavy-wall surface: Finite difference method p 300 N93-19282

Calculations of aerodynamic forces on a wing with thrust using BEM p 300 N93-19286

Shock-dependent, optimum thrust wings in supersonic flow p 483 N93-20169

Application of artificial neural networks to the design optimization of aerospace structural components p 555 N93-21831 [NASA-TM-4389]

General aviation aircraft: Normal acceleration data analysis and collection project p 713 N93-24739 [DOT/FAA/CT-91/20]

Analysis of wing wake roll-up using a vortex-in-cell method p 697 N93-25706

Adjoint methods for aerodynamic wing design p 805 N93-27089 [NASA-CR-193086]

Probabilistic assessment of composite structures p 825 N93-27092 [NASA-TM-106024]

Effect of underwing frost on transport aircraft takeoff performance p 791 N93-27252 [DOT/FAA/CT-TN93/9]

Aerodynamics of a finite wing with simulated ice p 784 N93-27437

Reynolds and Mach number effects on multielement airfoils p 785 N93-27446

Analysis of the static and dynamic response of a T-38 wing and comparison with experimental data p 806 N93-27692 [AD-A262363]

Computational method in optimal bending-twisting comprehensive design of wings of subsonic and supersonic aircraft p 806 N93-27694 [AD-A262374]

Effect of pylon cross-sectional geometries on propulsion integration for a low-wing transport p 788 N93-28070 [NASA-TP-3333]

A demonstration of simple airfoils: Structural design and materials choices p 789 N93-28662 [DE93-007882]

Articulated fin/wing control system p 909 N93-29278 [AD-D015712]

Construction, wind tunnel testing and data analysis for a 1/5 scale ultra-light wing model p 876 N93-29778

Topology and grid adaption for high-speed flow computations p 934 N93-30375 [NASA-CR-4216]

First NASA Advanced Composites Technology Conference, part 2 p 921 N93-30841 [NASA-CP-3104-PT-2]

Optimization of composite sandwich cover panels subjected to compressive loadings p 922 N93-30862

A comparison of classical mechanics models and finite element simulation of elastically tailored wing boxes p 922 N93-30863

Construction and testing of simple airfoils to demonstrate structural design, materials choice, and composite concepts p 879 N93-30979

Effects of an aft facing step on the surface of a laminar flow glider wing p 990 N93-31855 [NASA-CR-193302]

WIRE

New developments in organized wire systems p 764 A93-35973

Modeling and control of a trailing wire antenna towed by an orbiting aircraft p 219 N93-14610 [AD-A256450]

PROAV Cable Warning System (CWS) - U.S. Army aircraft integration assessment and OCONUS field evaluation p 705 N93-26263 [AD-A261233]

WIRE CLOTH

Reynolds number dependence of the drag coefficient for laminar flow through fine-scale photoetched screens p 1218 A93-53815

Reduction in size and unsteadiness of a VTOL ground vortex by ground fences p 700 N93-26049 [NASA-CR-192997]

WORK HARDENING

Selection criteria for metallic high temperature structural materials in hypersonic flying equipment p 515 N93-21479 [MBB-LME-221-HYPAC-PUB-2-A]

WORKING FLUIDS

Compressible flow pressure losses in wye-junctions [ASME PAPER 92-GT-71] p 248 A93-19321

A study of the effect of the working medium on the start-up characteristic of an aviation gas turbine engine p 811 A93-39037

Calculation of a collector-type annular plate heat exchanger p 833 A93-39045

A model for calculating the element of a high-temperature heat exchanger with spiral-wire fins p 833 A93-39046

Operation of a cross-flow heat exchanger with partial recirculation of one of the coolants p 833 A93-39051

A fuel-oil matrix heat exchanger p 833 A93-39052

Free piston facilities with air driver gas p 1011 A93-45528

System and method for cancelling expansion waves in a wave rotor p 86 N93-11172 [NASA-CASE-LEW-15218-1]

Evaluation of candidate working fluid formulations for the electrothermal - chemical wind tunnel p 530 N93-20312 [NASA-CR-192196]

Evaluation of candidate working fluid formulations for the electrothermal-chemical wind tunnel p 1015 N93-31848 [NASA-CR-193366]

WORKLOADS (PSYCHOPHYSIOLOGY)

A review of alternative philosophies --- methods for operating in ICAO category 3 weather conditions p 142 A93-17305

The development and implementation of a head-up guidance system (HGS) for manual CAT III landings p 151 A93-17306

Helicopter approaches in low visibility using RGPS and EFIS --- EFIS - Electronic Flight Instrumentation System p 142 A93-17309

Pilot task monitoring using neural networks p 940 A93-42846

Vision based techniques for rotorcraft low altitude flight p 1097 A93-49351

Adaptive automation and human performance: Multi-task performance characteristics p 186 N93-12578 [AD-A254596]

Theory and design of adaptive automation in aviation systems p 160 N93-12613 [AD-A254595]

Use of microprocessor-based simulator technology and MEG/EEG measurement techniques in pilot emergency-maneuver training p 530 N93-19706

WORKSTATIONS

Noise-induced reaction in a work community adjacent to aircraft runways - The Royal Australian Airforce p 559 A93-28496

Use of full flight simulator technology enhances classroom training sessions p 1136 A93-49277

An approach to the stall monitoring in a single stage axial compressor p 1112 A93-49747 [AIAA PAPER 93-1872]

The Canadian Automated Air Traffic System p 886 N93-30323

WOVEN COMPOSITES

Mechanical and analytical screening of braided composites for transport fuselage applications p 922 N93-30855

WRAP

Analysis of missile configurations with wrap-around fins using computational fluid dynamics p 1064 A93-48316 [AIAA PAPER 93-3631]

WROUGHT ALLOYS

Creep fatigue life prediction for engine hot section materials (isotropic)
[NASA-CR-189221] p 364 N93-18578

X

X RAY ANALYSIS

X-ray computed tomography for casting development
[AD-A261786] p 752 N93-26526
X-ray microscopy resource center at the Advanced Light Source
[DE93-010449] p 911 N93-29869

X RAY APPARATUS

Poster session: Fifth Users Meeting for the Advanced Photon Source
[DE93-006019] p 732 N93-26498

X RAY DETECTORS

A transportable luggage examination system based on neutron interrogation p 497 N93-21863

X RAY DIFFRACTION

X-ray diffraction and electron microscope studies of Yttria Stabilized Zirconia (YSZ) ceramic coatings exposed to vanadia
[AD-A258055] p 392 N93-17676

X RAY IMAGERY

Correlation of X-ray CT measurements to shear strength in pultruded composite materials p 396 A93-18618
Measurement of the center-of-gravity using X-ray computed tomography p 396 A93-18619
Synchronous X-ray Sinography for nondestructive imaging of turbine engines under load
[AIAA PAPER 93-1819] p 1153 A93-49707
X-ray microscopy resource center at the Advanced Light Source
[DE93-010449] p 911 N93-29869
Automatic detection of explosives using x ray imaging p 880 N93-30275

X RAY INSPECTION

Coherent X-ray imaging for corrosion evaluation - A preliminary assessment p 396 A93-18611
Use of local x ray computerized tomography for high-resolution, region-of-interest inspection of large ceramic components for engines
[DE93-005564] p 843 N93-28943
Automatic detection of explosives using x ray imaging p 880 N93-30275

X RAY SOURCES

X-ray microscopy resource center at the Advanced Light Source
[DE93-010449] p 911 N93-29869

X RAY SPECTROSCOPY

Undulator Spectromicroscopy Facility at the Advanced Light Source
[DE93-007964] p 823 N93-28490

X RAYS

Undulator Spectromicroscopy Facility at the Advanced Light Source
[DE93-007964] p 823 N93-28490
X-ray microscopy resource center at the Advanced Light Source
[DE93-010449] p 911 N93-29869

X-15 AIRCRAFT

CFD comparisons with wind tunnel and flight data for the X-15
[AIAA PAPER 92-5047] p 273 A93-22319
The X-15 airplane - Lessons learned p 456 A93-23005
[AIAA PAPER 93-0309] p 456 A93-23005
A comparison of hypersonic flight and prediction results
[AIAA PAPER 93-0311] p 280 A93-23006
Review of NASA's Hypersonic Research Engine Project
[AIAA PAPER 93-2323] p 1116 A93-50103
The X-15/HL-20 operations support comparison
[NASA-TM-4453] p 1017 N93-32379

X-29 AIRCRAFT

In-flight flow visualization results from the X-29 aircraft at high angles of attack
[AIAA PAPER 92-4102] p 38 A93-11272
Correlation of forebody pressures and aircraft yawing moments on the X-29 aircraft at high angles of attack
[AIAA PAPER 92-4105] p 38 A93-11273
Systems integration test laboratory - Application and experiences p 190 A93-13910
Breaking the stall barrier p 159 A93-17502
What makes the Cobra maneuver possible?
[AIAA PAPER 93-0183] p 367 A93-22609
Neural network controllers for the X29 aircraft p 817 A93-37005
X-29 vortex flow control tests p 804 A93-38846
CFD analysis of the X-29 inlet at high angle of attack p 958 A93-45140

Results and lessons learned from two Wright Laboratory flight research programs
[AIAA PAPER 93-3661] p 1099 A93-48341

X-29 high-angle-of-attack flight testing p 1101 A93-50487

Correlation of forebody pressures and aircraft yawing moments on the X-29 aircraft at high angles of attack
[NASA-TM-4417] p 22 N93-11532

A summary of the forebody high-angle-of-attack aerodynamics research on the F-18 and the X-29A aircraft
[NASA-TM-104261] p 25 N93-12353

X-29 linear aerodynamic perturbation model
[AD-A254810] p 160 N93-12752

NASA aeronautics: Research and technology program highlights
[NASA-NP-159] p 109 N93-13110

In-flight flow visualization results from the X-29A aircraft at high angles of attack
[NASA-TM-4430] p 131 N93-13322

Flight control system design factors for applying automated testing techniques
[NASA-TM-4242] p 910 N93-30764

X-30 VEHICLE

Natural environment application for NASP-X-30 design and mission planning
[AIAA PAPER 93-0851] p 531 A93-24915

Boundary-layer transition extent measurements on a cone and flat plate at Mach 3.5
[AIAA PAPER 93-0342] p 474 A93-25517

National Aero-Space Plane: Key issues facing the program. Testimony before the Subcommittee on Technology and Competitiveness, Committee on Science, Space, and Technology, House of Representatives
[GAO/T-NSIAD-92-26] p 161 N93-13253

Aerospace-plane flights and stratospheric ozone: Review and preliminary assessment of the National Aerospace Plane (NASP) operations
[RAND/N-3464-AF] p 755 N93-26327

XENON CHLORIDE LASERS

Aerodynamic phenomena in high pulse repetition rate XeCl laser p 1150 A93-48806

XV-15 AIRCRAFT

Tiltrotor Research Aircraft composite blade repairs - Lessons learned p 108 A93-14819
Acoustic flight test experience with the XV-15 Tiltrotor aircraft with the Advanced Technology Blade (ATB)
p 445 A93-19143

Far-field hover acoustic characteristics of the XV-15 tiltrotor aircraft with Advanced Technology Blades
p 566 A93-29412

A comparative analysis of XV-15 tiltrotor hover test data and WOPWOP predictions incorporating the fountain effect p 509 A93-29414

Tiltrotor ground noise reduction from rotor parametric changes as predicted by ROTONET p 567 A93-29415

Tiltrotor interior noise characteristics p 509 A93-29421

Advanced Technology Blade testing on the XV-15 Tilt Rotor Research Aircraft p 799 A93-36020

Tilt rotor hover aeroacoustics
[NASA-CR-177598] p 99 N93-10458

Tiltrotor aircraft noise: A summary of the presentations and discussions at the 1991 FAA/Georgia Tech Workshop
[DOT/FAA/RD-91/23] p 232 N93-14912

Y

YARNS

Advanced fiber/matrix material systems p 921 N93-30854

YAW

Effects of pylon yaw and lateral stiffness on the flutter of a delta wing with external store p 800 A93-36330

Detailed near surface flow about yawed, stranded cables
[AD-A257382] p 418 N93-15857

Application of recess vane casing treatment to axial flow fans p 423 N93-18728

Helicopter low-speed yaw control
[NASA-CASE-LAR-14219-1] p 729 N93-25998

Advanced aircraft with thrust vector control
[MBB-FE-1-S-PUB-0504] p 998 N93-31043

YAWING MOMENTS

In-flight flow visualization results from the X-29A aircraft at high angles of attack
[AIAA PAPER 92-4102] p 38 A93-11272

Correlation of forebody pressures and aircraft yawing moments on the X-29A aircraft at high angles of attack
[AIAA PAPER 92-4105] p 38 A93-11273

Steady and quasisteady resonant lock-in of finned projectiles p 61 A93-12012

A sensitivity study for pneumatic vortex control on a chined forebody
[AIAA PAPER 93-0049] p 260 A93-20162

Tangential Forebody Blowing-yaw control at high alpha
[AIAA PAPER 93-3406] p 1008 A93-47205

Some stability characteristics of the boundary layer on a yawed cone
[AIAA PAPER 93-3048] p 1057 A93-48228

Correlation of forebody pressures and aircraft yawing moments on the X-29A aircraft at high angles of attack
[NASA-TM-4417] p 22 N93-11532

Program for calculation of aileron rolling moment and yawing moment coefficients at subsonic speeds
[ESDU-88040] p 136 N93-14514

Contribution of ventral fins to sideforce and yawing moment derivatives due to sideslip at low angle of attack
[ESDU-92029] p 291 N93-16638

YF-12 AIRCRAFT

The development of aircraft in the Lockheed Skunk Works from 1954 to 1991 p 805 N93-27168

YF-16 AIRCRAFT

Human factors causes and management strategies in US Air Force F-16 mishaps 1984-present p 492 N93-19673

YIELD STRENGTH

Application of the cyclic J-integral to fatigue crack propagation p 839 N93-27182

YS-11 AIRCRAFT

Aging review of the YS-11 aircraft p 46 A93-13635

Damage tolerance assessment on the multisite cracks for the YS-11 aircraft p 46 A93-13642

YTTRIUM COMPOUNDS

Process optimization of Hexoloy SX-SiC towards improved mechanical properties
[DE93-007913] p 826 N93-28564

YTTRIUM OXIDES

Microstructure of yttria stabilized zirconia-hafnia plasma sprayed thermal barrier coatings
[ONERA, TP NO. 1993-54] p 1146 A93-51936

X-ray diffraction and electron microscope studies of Yttria Stabilized Zirconia (YSZ) ceramic coatings exposed to vanadia
[AD-A258055] p 392 N93-17676

Z

ZERO ANGLE OF ATTACK

Application of the small parameter method to the problem of three-dimensional flow of a viscous gas past bodies p 1178 A93-53314

Transonic flow calculation around NACA-0012 p 302 N93-19301

ZIRCONIUM COMPOUNDS

Preparation and characterization of continuous fiber reinforced zirconium diboride matrix composites for a leading edge material p 1211 A93-53445

ZIRCONIUM OXIDES

Microstructure of yttria stabilized zirconia-hafnia plasma sprayed thermal barrier coatings
[ONERA, TP NO. 1993-54] p 1146 A93-51936

Thermal barrier coating life prediction model development, phase 2
[NASA-CR-189111] p 198 N93-12589

X-ray diffraction and electron microscope studies of Yttria Stabilized Zirconia (YSZ) ceramic coatings exposed to vanadia
[AD-A258055] p 392 N93-17676

ZONAL FLOW (METEOROLOGY)

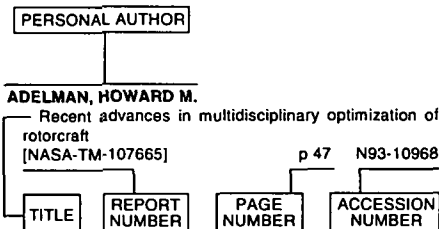
Nowcasts of thunderstorm initiation and evolution p 752 A93-33773

Axial Flow Compressors, volume 2
[VKI-LS-1992-02-VOL-2] p 423 N93-18731

Determination of the zone of the stall cell by means of the baroclinic wave theory p 424 N93-18733

Rotating stall cell and Von Karman vortex street: A meteorological theory p 424 N93-18734

Typical Personal Author Index Listing



Listings in this index are arranged alphabetically by personal author. The title of the document is used to provide a brief description of the subject matter. The report number helps to indicate the type of document (e.g., NASA report, translation, NASA contractor report). The page and accession numbers are located beneath and to the right of the title. Under any one author's name the accession numbers are arranged in sequence.

A

- ABALAKOV, G. V.**
Effect of the proximity of the machined surface on the discharge coefficients of laser cutter nozzles p 79 A93-12809
- ABARBANEL, S.**
Spurious frequencies as a result of numerical boundary treatments p 839 A93-27170
- ABATE, GREGG L.**
Analysis of missile configurations with wrap-around fins using computational fluid dynamics [AIAA PAPER 93-3631] p 1064 A93-48316
- ABBAS, G. L.**
Ladar fiber optic sensor system for aircraft applications p 1105 A93-49467
- ABBAS, JEHAD F.**
Nonlinear flutter of orthotropic composite panel under aerodynamic heating p 1025 A93-45740
- ABBERGER, STEVEN**
A tooling trend at BCA - What and why [SME PAPER EM92-111] p 202 A93-14114
- ABBITT, JOHN D.**
Molecular mixing of jets in supersonic flow [AIAA PAPER 93-2021] p 1078 A93-49858
- ABBITT, JOHN D., III**
Experimental supersonic hydrogen combustion employing staged injection behind a rearward-facing step p 744 A93-34496
- ABDEL-FATTAH, A. M.**
Design verification of ground run-up noise suppressors for afterburning engines p 910 A93-42892
- ABDELWAHAB, M.**
Measured acoustic characteristics of ducted supersonic jets at different model scales [AIAA PAPER 93-0731] p 563 A93-24821
- ABDI, FRANK**
CST gives aircraft industry a lift p 560 A93-25086
- ABDOL-HAMID, KHALED S.**
Comparison of algebraic turbulence models for afterbody flows with jet exhaust p 123 A93-14554
Commercial turbofan engine exhaust nozzle flow analyses p 689 A93-34489
Prediction of static performance for single expansion ramp nozzles [AIAA PAPER 93-2571] p 898 A93-41047

- ABDY, G.**
A numerical study of advanced rotor blades p 481 A93-29436
- ABDY, GHASEM L.**
Numerical study of advanced rotor blades p 23 N93-11899
- ABE, T.**
A combined facility of ballistic range and shock tunnel using a fast action valve p 1012 A93-45532
- ABE, TAKASHI**
Effects of wall conditions on chemically nonequilibrium shock-layer flow over hypersonic reentry bodies p 970 A93-46908
Effect of the flow non-uniformity on the mixing layer at the interface of parallel supersonic flows [ISAS-RN-646] p 128 N93-12716
- ABE, YOSHIYUKI**
Aircraft experiments on microgravity pool boiling - Vapor-liquid behaviour and heat transfer characteristics in boiling of n-pentane, CFC-113 and water p 410 A93-20920
- ABED, EYAD H.**
Local nonlinear control of stall inception in axial flow compressors [AIAA PAPER 93-2230] p 1080 A93-50036
- ABEDIN, M. N.**
Assessment of aircraft structural integrity by detecting disbands through ultrasonic scanning p 406 A93-19587
- ABEL, IRVING**
Research and applications in structural dynamics and aeroelasticity p 153 A93-14223
- ABEL, PETER**
Calibration results for NOAA-11 AVHRR channels 1 and 2 from congruent path aircraft observations p 1143 A93-51237
- ABERLE, JAMES T.**
Advanced electromagnetic methods for aerospace vehicles [NASA-CR-193468] p 936 N93-31036
- ABEYOUNIS, WILLIAM K.**
Comparison of algebraic turbulence models for afterbody flows with jet exhaust p 123 A93-14554
- ABEYRATNE, R. I. R.**
Tobacco smoking in aircraft - A fog of legal rhetoric? p 944 A93-40474
- ABGRALL, REMI**
The European Data Base - A new CFD validation tool for the design of space vehicles [AIAA PAPER 93-3045] p 1057 A93-48225
- ABIDAT, M.**
The effects of blade loading in radial and mixed flow turbines [ASME PAPER 92-GT-92] p 349 A93-19338
- ABIHANA, OSAMA A.**
Design and implementation of fuzzy logic controllers [NASA-CR-193268] p 1038 N93-31649
- ABO, EICHI**
Flight test progress of the STOL research aircraft ASKA [NAL-TM-643] p 49 N93-12354
- ABOLFADL, MOHAMED**
Numerical investigation of flow field in a turbine volute [AIAA PAPER 93-0155] p 542 A93-25505
- ABOLFADL, MOHAMED A.**
Experimental investigation of exhaust system mixers for a high bypass turbofan engine [AIAA PAPER 93-0022] p 357 A93-20140
- ABOLHASSANI, JAMSHID S.**
A graphically interactive approach to structured and unstructured surface grid quality analysis [AIAA PAPER 93-3351] p 954 A93-45045
Topology and grid adaption for high-speed flow computations [NASA-CR-4216] p 934 N93-30375
- ABOU-AMER, SEOUO AHMED**
Control of panel flutter at high supersonic speed p 47 N93-10900
- ABOU-HAIDAR, N. I.**
Compressible flow pressure losses in wye-junctions [ASME PAPER 92-GT-71] p 248 A93-19321

- ABOUELKHEIR, M.**
Nonlinear dynamic simulation of single- and multi-spool core engines [AIAA PAPER 93-2580] p 1122 A93-50294
- ABRAMOVSKAYA, M. G.**
Certain improved algorithms for calculating the aerodynamic characteristics of flight vehicles in free-molecular flow p 1090 A93-51872
- ABRAMOWITZ, ALLAN**
Ventilation effects on smoke and temperature in an aircraft cabin quarter-scale model [DOT/FAA/CT-89/25] p 791 N93-28055
- ABRAMS, RICHARD**
YF-22A prototype advanced tactical fighter demonstration/validation flight test program overview p 511 N93-19906
- ABREU, M. A.**
Misalignments of airborne laser beams due to mechanical vibrations p 394 A93-17762
- ABREVAYA, ADAM**
An improved gust front detection algorithm for the TDWR p 432 A93-22191
- ABU-SABA, ELIAS G.**
Lumped mass modelling for the dynamic analysis of aircraft structures p 510 N93-19460
- ABUAF, N.**
Heat transfer and turbulence in a turbulated blade cooling circuit [ASME PAPER 92-GT-187] p 402 A93-19412
- ABUMERI, G.**
Structural Tailoring/Analysis for Hypersonic Components - A computational simulation [AIAA PAPER 92-4722] p 325 A93-20324
- ABUMERI, G. H.**
Dynamic analysis of a pre-and-post ice impacted blade [AIAA PAPER 92-4273] p 54 A93-13333
Structural tailoring of aircraft engine blade subject to ice impact constraints [AIAA PAPER 92-4710] p 358 A93-20319
BLASIM - A computational tool to assess ice impact damage on engine blades [AIAA PAPER 93-1638] p 720 A93-34165
Dynamic analysis of a pre-and-post ice impacted blade [NASA-TM-105829] p 90 N93-12197
Root damage analysis of aircraft engine blade subject to ice impact [NASA-TM-105779] p 222 N93-15343
Structural tailoring of aircraft engine blade subject to ice impact constraints [NASA-TM-106033] p 838 N93-26999
Blasim: A computational tool to assess ice impact damage on engine blades [NASA-TM-106225] p 1031 N93-31193
- ABURATANI, Y.**
Evaluation of metallurgical degradation on gas turbine components p 915 A93-40804
- ACEE, HAP**
The integrated actuation package approach to primary flight control [SAE PAPER 920968] p 185 A93-14630
- ACHACHE, M.**
A closed loop controller for BVI impulsive noise reduction by Higher Harmonic Control p 849 A93-35963
- ACHAIBOU, A. K.**
Zero-gravity atmospheric flight by robust nonlinear inverse dynamics p 728 A93-34550
- ACHAR, NAGARI SHRIRANGA**
Trim analysis by shooting and finite elements and Floquet eigenanalysis by QR and subspace iterations in helicopter dynamics p 163 N93-13914
- ACHARYA, MUKUND**
Control of the dynamic-stall vortex over a pitching airfoil by leading-edge suction [AIAA PAPER 93-3267] p 969 A93-46832
- ACHARYA, SUMANTA**
Space marching calculations about hypersonic configurations using a solution-adaptive mesh algorithm p 1177 A93-53212

- ACHENBACH, J. D.**
Towards quantitative non-destructive evaluation of aging aircraft p 1025 A93-45773
- ACHESON, K. E.**
Design optimization study for F-15 propulsion/forward fairing compatibility [AIAA PAPER 93-3484] p 1003 A93-47291
- ACKERMAN, STEVEN A.**
Remote sensing cloud properties from high spectral resolution infrared observations p 1034 A93-46780
- ACKROYD, J. A. D.**
Lanchester: The man [AERO-REPT-9111] p 456 N93-16464
- ACOSTA, WALDO A.**
An efficient liner cooling scheme for advanced small gas turbine combustors [AIAA PAPER 93-1763] p 1109 A93-49660
- ADAM, EUGENE C.**
Tactical cockpits - The coming revolution p 505 A93-27238
- ADAM, PETER**
Presence and future of the electro-chemical processes in aero-engine production p 1257 A93-54840
Laser and skill enhance results p 1257 A93-54843
- ADAM, VOLKMAR**
Testing of an experimental FMS p 998 N93-31277
- ADAMCZYK, J. J.**
Numerical simulation of compressor endwall and casing treatment flow phenomena [ASME PAPER 92-GT-300] p 255 A93-19490
Three-dimensional analysis of the Pratt and Whitney alternate design SSME fuel turbine p 1031 N93-31584
- ADAMCZYK, JOHN J.**
Investigation of advanced counterrotation blade configuration concepts for high speed turboprop systems. Task 5: Unsteady counterrotation ducted propfan analysis. Computer program user's manual [NASA-CR-187125] p 521 N93-20583
- ADAMS, CATHERINE A.**
Workshop on Aeronautical Decision Making (ADM). Volume 2: Plenary Session With Presentations and Proposed Action Plan [DOT/FAA/RD-92/14-VOL-2] p 146 N93-15013
- ADAMS, D. O.**
A structural reliability evaluation of fail-safe helicopter dynamic components p 506 A93-27952
- ADAMS, DARRYL**
Cross channel dependency requirements of the multi-path redundant avionics suite p 928 A93-42782
- ADAMS, J. C.**
Fault detection, isolation, and reconfiguration for aircraft using neural networks [AIAA PAPER 93-3870] p 1135 A93-51456
- ADAMS, JOHN W.**
Comparison measurements of currents induced by radiation and injection p 926 A93-41575
- ADAMS, RICHARD J.**
Full envelope multivariable control law synthesis for a high-performance test aircraft p 1130 A93-49595
Robust, nonlinear, high angle-of-attack control design for a supermaneuverable vehicle [AIAA PAPER 93-3774] p 1131 A93-51369
Workshop on Aeronautical Decision Making (ADM). Volume 2: Plenary Session With Presentations and Proposed Action Plan [DOT/FAA/RD-92/14-VOL-2] p 146 N93-15013
How expert pilots think p 147 N93-15017
Enhanced Aeronautical Resource Management training alternatives p 147 N93-15019
Progress through precedent: Going where no helicopter simulator has gone before p 913 N93-30686
- ADAMS, WILLIAM M., JR.**
ISAC - A tool for aeroservoelastic modeling and analysis [AIAA PAPER 93-1421] p 726 A93-33974
Design, test, and evaluation of three active flutter suppression controllers [NASA-TM-4338] p 63 N93-10070
- ADAMSON, H. PATRICK**
Development of the Advance Warning Airborne System(AWAS) p 144 N93-14849
- ADELMAN, HENRY**
Numerical simulations of a pulsed detonation wave augmentation device [AIAA PAPER 93-1985] p 1112 A93-49832
- ADELMAN, HENRY G.**
NO(x) reduction additives for aircraft gas turbine engines [AIAA PAPER 93-2594] p 1122 A93-50306
Analytical and experimental investigations of the oblique detonation wave engine concept [NASA-TM-102839] p 1006 N93-32374
- ADELMAN, HOWARD M.**
Recent advances in integrated multidisciplinary optimization of rotorcraft [AIAA PAPER 92-4777] p 325 A93-20369
Recent advances in multidisciplinary optimization of rotorcraft [NASA-TM-107665] p 47 N93-10968
- ADEY, R. A.**
Crack analysis using discontinuous boundary elements p 925 A93-40775
- ADIBHATLA, SHRIDER**
Evaluation of a nonlinear PSC algorithm on a variable cycle engine [AIAA PAPER 93-2077] p 1114 A93-49904
- ADIBROTO, A.**
Five years operational experiences with Indonesian Low Speed Tunnel (ILST) p 191 A93-14403
- ADIGA, B. S.**
Indian experience in flight data readout and analysis p 168 N93-15161
- ADIKISSON, LORI**
Investigation of advanced technology for airway facilities maintenance training [DOT/FAA/CT-TN92/24] p 994 N93-32336
- ADOMAITIS, RAYMOND A.**
Local nonlinear control of stall inception in axial flow compressors [AIAA PAPER 93-2230] p 1080 A93-50036
- ADROV, V. M.**
Estimation of the life of aircraft structures under stochastic steady state loading p 545 A93-27620
- ADVANI, S. K.**
Design philosophies of the Basic Research Simulator p 191 A93-14414
The development of SIMONA - A simulator facility for advanced research into simulation techniques, motion system control and navigation systems technologies [AIAA PAPER 93-3574] p 1208 A93-52670
- ADYNOWSKI, JAKUB**
A numerical study of aerodynamic wing design for supercritical conditions of an advanced training and military aircraft p 1238 A93-56213
- AERNI, MIKE E.**
Results from a GPS Shuttle Training Aircraft flight test p 384 A93-21148
- AESCHLIMAN, D. P.**
Use of shear-stress-sensitive, temperature-insensitive liquid crystals for boundary layer transition detection in hypersonic flows [AIAA PAPER 93-3070] p 1059 A93-48245
- AFCHAIN, DIDIER**
Laser-velocimeter study of vortex breakdown on a 70-deg swept delta wing in incompressible flow [ONERA, TP NO. 1992-147] p 773 A93-38728
- AFFES, H.**
The three-dimensional boundary layer flow due to a rotor-tip vortex [AIAA PAPER 93-3081] p 1060 A93-48255
- AFOLABI, D.**
The cusp catastrophe and the stability problem of helicopter ground resonance p 1099 A93-48059
- AFONIN, K. A.**
Definition of the structure of expert preferences for the multicriterial analysis of control systems p 1168 A93-50953
- AFREMOV, V. G.**
Using ultralight flight vehicles for large-scale aerial photography p 92 A93-10098
- AFROSIMOVA, V. N.**
Fuel film formation in the fuel-air premixer of the combustion chamber p 812 A93-39193
- AGAPITOV, S. A.**
Using numerical control algorithms in stabilization systems with digital correction p 941 A93-43113
- AGARWAL, AVAL K.**
Method of measuring cross-flow vortices by use of an array of hot-film sensors [NASA-CASE-LAR-14824-1-SB] p 751 N93-26000
- AGARWAL, NAVAL K.**
Measurement of attachment-line location in a wind-tunnel and in supersonic flight [AIAA PAPER 92-4089] p 39 A93-11285
- AGARWAL, R. K.**
A comparison of upwind schemes for computation of three-dimensional hypersonic real-gas flows [AIAA PAPER 92-4350] p 15 A93-13306
A novel algorithm for the solution of compressible Euler equations in wave/particle split (WPS) form p 957 A93-45093
- AGEEV, VLADIMIR M.**
Instrument systems of flight vehicles and their design [ISBN 5-217-00793-1] p 718 A93-35678
- AGNELI, A.**
Damping in aerospace composite materials p 1260 A93-55869
- AGNES, GREGORY S.**
Active constrained layer viscoelastic damping [AIAA PAPER 93-1702] p 743 A93-34224
- AGOSTA, ROXANA**
The Edge supersonic transport [NASA-CR-192074] p 335 N93-18055
- AGRAWAL, S.**
Transonic Navier-Stokes flow computations over wing-fuselage geometries p 1095 A93-52456
Prediction of vortex breakdown on a delta wing p 787 A93-27459
- AGUILAR, JOSEPH**
Phoenix: Preliminary design of a high speed civil transport [NASA-CR-192024] p 334 N93-17976
- AH-FA, M.**
Optimization of afterbodies and engine nozzle by using CFD methods [ISABE 93-7098] p 1187 A93-54074
- AHLVIN, RICHARD G.**
Reanalysis of multiple-wheel landing gear traffic tests [AD-A256593] p 194 N93-14238
- AHMAD, I.**
Combustion of microemulsion sprays [AIAA PAPER 93-0131] p 390 A93-22578
- AHMAD, SHAHEEN**
Dynamical variable structure control of a helicopter in vertical flight p 369 A93-22887
- AHMADI, ALI R.**
The development of a mature external Master's degree program in aeronautical engineering - A university/industry partnership [AIAA PAPER 92-4256] p 570 A93-24296
- AHMED, A.**
On dynamics of the juncture vortex [AIAA PAPER 93-3473] p 980 A93-47252
- AHMED, ANWAR**
Subharmonic and harmonic forced response of the wake of a circular cylinder p 288 A93-23565
- AHMED, S.**
Schlieren studies of compressibility effects on dynamic stall of transiently pitching airfoils p 480 A93-28608
Velocity and vorticity distributions over an oscillating airfoil under compressible dynamic stall p 778 A93-39403
- AHMED, S. A.**
Flow field characteristics of an axisymmetric sudden-expansion pipe flow with different initial swirl distribution p 411 A93-21688
- AHMED, SAAD A.**
Three component LDV velocity measurements in a can type research combustor for CFD validation. I - Isothermal [ASME PAPER 92-GT-138] p 350 A93-19370
- AHN, SEUNGKI**
An experimental study of flow over a 6 to 1 prolate spheroid at incidence p 874 N93-29124
- AHUJA, J. K.**
Numerical simulation of shock-induced combustion/detonation p 410 A93-20719
- AHUJA, K. K.**
A review of crack propagation under unsteady loading p 399 A93-19207
Measured acoustic characteristics of ducted supersonic jets at different model scales [AIAA PAPER 93-0731] p 563 A93-24821
Review of crack propagation under unsteady loading p 837 A93-39416
Tiltrotor aircraft noise: A summary of the presentations and discussions at the 1991 FAA/Georgia Tech Workshop [DOT/FAA/RD-91/23] p 232 N93-14912
- AHUMADA, A.**
Engineering a visual system for seeing through fog [SAE PAPER 921130] p 895 A93-41318
- AIHARA, Y.**
Experimental investigation of aerothermal problems associated with hypersonic flight of HST p 120 A93-14380
- AIKEN, EDWIN W.**
Preliminary design features of the RASCAL - A NASA/Army rotorcraft in-flight simulator [AIAA PAPER 92-4175] p 42 A93-13311
- AINSWORTH, J. C.**
Airspace Design Expert System (ADES), a 2D/3D mapping and modelling tool incorporating an expert system for use in instrument approach design p 888 N93-30357
- AINSWORTH, R. W.**
Unsteady pressure measurements on the rotor of a model turbine stage in a transient flow facility [ASME PAPER 92-GT-156] p 250 A93-19383
The dynamic characteristics of a high pressure turbine stage in a transient wind tunnel [ASME PAPER 92-GT-166] p 375 A93-19392

- Experimental heat transfer results in turbine stators and rotors and a comparison with theory
[PNR-90945] p 57 N93-11055
- AIT-ALI-YAHIA, D.**
Implicit numerical solution of transonic flows using adaptive triangular grids p 686 A93-34349
- AITA, SAMIR**
TGV tunnel entry simulations using a finite element code with automatic remeshing
[AIAA PAPER 93-0890] p 471 A93-24950
- AITKEN, A. A.**
Handling and using information systems with new technology
[PNR-90910] p 572 N93-20734
- AITKEN, J. F.**
Canadian low-gravity research using parabolic aircraft p 384 A93-21908
- AKAGI, YUJI**
A study of a direct-injection stratified-charge rotary engine for motor vehicle application
[SAE PAPER 93-0677] p 1158 A93-50524
- AKEADA, KENJI**
Structure of downbursts associated with heavy rainfall observed in Tokyo p 433 A93-22200
- AKHMANOV, S. A.**
Detection and parameter estimation of atmospheric turbulence by ground-based and airborne CO2 Doppler lidars p 395 A93-17862
Study of artificial and natural turbulence in atmospheric boundary layer with a CW Doppler CO2 lidar p 1257 A93-54799
- AKIBA, MASASHI**
Visualization and analysis of supersonic flow in rotating turbine stage. I - Influence of shock wave between stationary and moving blades p 126 A93-15449
Visualization and analysis of supersonic flow in rotating turbine stage. II - Analysis of the flow into the moving blades and their exit flow p 476 A93-27442
- AKIBA, RYOJIRO**
Atmospheric reentry flight test of winged space vehicle
[AIAA PAPER 92-5053] p 385 A93-22324
- AKIMOV, A. N.**
An algorithm with prediction in a control problem with functional constraints p 757 A93-35307
- AKITA, KOICHI**
Effect of stress level of gust cycles on fatigue crack propagation behavior (Acceleration and retardation of crack propagation under simplified flight simulation loading) p 198 A93-17033
- AKIYAMA, H.**
The improvement of the static launch method in Japan p 26 A93-11364
Trans-oceanic balloon flight over east China sea p 27 A93-11372
- AKMANDOR, I. S.**
Numerical simulation of ramjet and scramjet combustion using two-dimensional Euler equations with finite rate chemistry
[ISABE 93-7083] p 1202 A93-54059
- AKYURTU, ATEŞ**
Evaluation of candidate working fluid formulations for the electrothermal - chemical wind tunnel
[NASA-CR-192196] p 530 N93-20312
Evaluation of candidate working fluid formulations for the electrothermal-chemical wind tunnel
[NASA-CR-193366] p 1015 N93-31848
- AKYURTU, JALE F.**
Evaluation of candidate working fluid formulations for the electrothermal - chemical wind tunnel
[NASA-CR-192196] p 530 N93-20312
Evaluation of candidate working fluid formulations for the electrothermal-chemical wind tunnel
[NASA-CR-193366] p 1015 N93-31848
- AL-ASMI, K.**
Production of oscillatory flow in wind tunnels p 1218 A93-53812
- AL-GARNI, AHMED ZAFER**
Performance and control of ascending trajectories to minimize heat load for transatmospheric aero-space planes p 133 N93-13745
- AL-KHALIL, KAMEL M.**
Numerical modeling of anti-icing systems and comparison to test results on a NACA 0012 airfoil
[AIAA PAPER 93-0170] p 327 A93-23242
Ice accretion and performance degradation calculations with LEWICE/NS
[AIAA PAPER 93-0173] p 310 A93-23244
Numerical modeling of anti-icing systems and comparison to test results on a NASA 0012 airfoil
[NASA-TM-105975] p 148 N93-15345
Ice accretion and performance degradation calculations with LEWICE/NS
[NASA-TM-105972] p 148 N93-15354
Numerical modeling of runback water on ice protected aircraft surfaces p 840 N93-27438
- AL-KHOVAITER, SOLIMAN H.**
Some physico-chemical characteristics of lubricating oil used in gas turbines p 70 A93-12202
- AL-SAGGAF, UBAID M.**
Robust digital control of a high-performance engine p 359 A93-21792
- AL-ZUBAIDY, S. N. J.**
Axial length influence on the performance of centrifugal impellers p 205 A93-14517
- AL-ZUBAIDY, SARUM N. J.**
Advanced direct-design procedure for centrifugal impellers p 411 A93-21659
- ALAG, SATNAM S.**
An effective Mixed Annealing/Heuristic Algorithm for problems in kinematic mechanical design
[AIAA PAPER 93-1581] p 741 A93-34113
- ALAKOZ, A. V.**
Characteristics of the detection of overloads in the center of mass of Il-76 and An-12 aircraft due to runway irregularities by a standard on-board recorder p 1008 A93-45666
- ALBEGOV, R. V.**
Experimental investigation of hydrogen burning and heat transfer in annular duct at supersonic velocity p 171 A93-14247
- ALBERS, S. C.**
The FAA aircraft Icing Forecasting Improvement Program - Validation of aircraft icing forecasts in the Denver area
[AIAA PAPER 93-0393] p 309 A93-23069
Preliminary evaluation of aviation-impact variables derived from numerical models
[PB93-190197] p 1034 N93-31202
- ALBERS, STEVE**
Validation of aviation weather products for the Advanced Traffic Management System p 430 A93-22161
- ALCAYDE, D.**
Preliminary results of the ISM campaign - The Landes, South West France p 1161 A93-47553
- ALCORN, CHARLES W.**
The influence of the boundary layer on the subsonic near-wake of a family of bluff bodies
[AIAA PAPER 93-0525] p 284 A93-23266
- ALDABAGH, A. M.**
Impingement/effusion cooling p 932 N93-29954
- ALDERFER, D. W.**
An optical flameout detection system for NASA Langley's 8-Foot High Temperature Tunnel p 1254 A93-54372
- ALEKSANDROV, V. YU.**
Approximate method for the aerodynamic design of flight vehicles for high supersonic flight speeds p 1069 A93-48966
- ALEKSANDROVA, I. I.**
Software for the control of measurement data acquisition, processing, and monitoring during strength testings p 94 A93-10042
- ALEKSEEV, A. R.**
A study of optical distortions arising in radiation transmission through cavities with gas flow around them p 1225 A93-52945
- ALEKSEEV, V. YU.**
Investigation of flame stabilizers in the form of perforated grids p 1003 A93-47513
- ALEM, NABIH M.**
The effectiveness of airbags in reducing the severity of head injury from gunshot strikes in attack helicopters p 494 N93-19691
- ALEXANDER, DON R.**
In situ material characterization for pavement evaluation by the Spectral-Analysis-of-Surface-Waves (SASW) method
[AD-A255660] p 194 N93-14128
- ALEXANDER, MICHAEL G.**
A qualitative assessment of control effectors on an advanced fighter configuration
[AIAA PAPER 93-3627] p 1127 A93-48312
- ALEXANDER, WILLIAM, JR.**
Thermal control of a lidar laser system using a non-conventional ram air heat exchanger p 1028 A93-46821
- ALEXIOU, K.**
Comparison of some direct multi-point force appropriation methods p 928 A93-43338
- ALEXOPOULOS, G. A.**
A k-omega multivariate beta PDF for supersonic turbulent combustion
[AIAA PAPER 93-2197] p 1154 A93-50009
A k-omega multivariate beta PDF for supersonic combustion
[NASA-CR-191930] p 537 N93-21749
- ALFEROV, VADIM**
A report on the status of MHD hypersonic ground test technology in Russia
[AIAA PAPER 93-3193] p 1012 A93-46656
- ALIGHANBARI, H.**
An analysis of the post-instability behaviour of a two-dimensional airfoil with a structural nonlinearity
[AIAA PAPER 93-1474] p 726 A93-34020
- ALKABIE, H. S.**
An ultra low NO(x) pilot combustor for staged low NO(x) combustion
[ISABE 93-7020] p 1195 A93-53996
- ALKOV, ROBERT A.**
Trans-cockpit authority gradient in Navy/Marine aircraft mishaps p 146 A93-15016
- ALLAN, T.**
New developments with the V2500 engine
[ISABE 93-7085] p 1202 A93-54061
- ALLAN, W. D. E.**
Experimental heat transfer results in turbine stators and rotors and a comparison with theory
[PNR-90945] p 57 N93-11055
- ALLEGRE, J.**
Experimental density flowfields over a delta wing located in rarefied hypersonic flows p 870 A93-42637
- ALLEN, CARL L.**
The design of a long range megatransport aircraft
[NASA-CR-192077] p 332 N93-17711
- ALLEN, CHRISTOPHER S.**
On the scaling of small-scale jet noise to large scale p 448 A93-19195
- ALLEN, JERRY M.**
Experimental effects of wing location on wing-body pressures at supersonic speeds
[NASA-TM-4434] p 700 N93-26085
- ALLEN, L. D.**
Evolution of flight simulation
[AIAA PAPER 93-3545] p 1207 A93-52652
- ALLEN, M.**
Nonintrusive, multipoint velocity measurements in high-pressure combustion flows
[AIAA PAPER 93-2032] p 1145 A93-49867
- ALLEN, M. G.**
An optical comparison of wall and axial injection for high enthalpy reacting scramjet flows
[AIAA PAPER 93-0357] p 377 A93-23040
High-temperature supersonic combustion testing with optical diagnostics p 730 A93-34498
- ALLEN, R. W.**
A simulator solution for the parachute canopy control and guidance training problem
[SAE PAPER 920984] p 191 A93-14634
Parachute canopy control and guidance training requirements and methodology
[AIAA PAPER 93-1255] p 703 A93-35188
- ALLEN, RICHARD M.**
Development of the Boeing Low Speed Aeroacoustic Facility (LSAF) p 374 A93-19148
- ALLEN, S. J.**
Photoelectrochemical etching of high aspect ratio submillimeter waveguide filters from n(+) GaAs wafers p 409 A93-20644
- ALLIOT, JEAN-CLAUDE**
Aircraft lightning initiation and interception in situ electric measurements and fast video observations p 140 A93-14064
- ALLISON, BRYAN H.**
Development of a model-based monitoring system for turbine and rocket engines p 195 A93-16412
- ALLMAN, D. J.**
GARTEUR damage mechanics for composite materials: Analytical/experimental research on delaminations p 537 N93-21513
- ALLWOOD, R. J.**
A knowledge-based blackboard system to interpret graphical data from vibration tests of gas turbines
[PNR-90993] p 59 N93-11114
- ALLWRIGHT, D. J.**
Active stabilization of compressor instability and surge in a working engine
[ASME PAPER 92-GT-88] p 348 A93-19335
- ALLWRIGHT, J. C.**
Turbulence/gust alleviation using spoiler control p 369 A93-22886
- ALMOSNINO, D.**
Experimental and nonlinear vortex lattice method results for various wing-canard configurations p 479 A93-28607
- ALMOSNINO, DAN**
Calculating crossflow separation using boundary layer computations coupled with an inviscid method
[AIAA PAPER 93-3459] p 979 A93-47242
- ALPERINE, S.**
Microstructure of yttria stabilized zirconia-hafnia plasma sprayed thermal barrier coatings
[ONERA, TP NO. 1993-54] p 1146 A93-51936
- ALSALIHI, ZUHEYR**
Viscous, 2-D, laminar hypersonic flows over compression ramps p 866 A93-42591

- ALSPAUGH, THOMAS A.**
Software requirements for the A-7E aircraft
[AD-A255746] p 229 N93-15052
- ALTER, K. W.**
Definition of the 2005 flight deck environment
[NASA-CR-4479] p 343 N93-16693
- ALTER, STEPHEN J.**
Single block three-dimensional volume grids about complex aerodynamic vehicles p 957 A93-45099
- ALTHOFF, S.**
Recent developments in rotor wake modeling for helicopter noise prediction p 481 A93-29437
- ALVAREZ, P.**
Analysis of turbine engine rotor containment and shielding structures
[AIAA PAPER 93-1817] p 1110 A93-49705
- ALVERMANN, KLAUS**
Visualization and view simulation based on transputers
p 1037 A93-45150
Three-dimensional graphical representation of objects according to movement data in realtime
[ESA-TT-1258] p 942 N93-30104
- ALZARI, T.**
Attempt to evaluate the computations for test case 6.1 - Cold hypersonic flow past ellipsoidal shapes
p 869 A93-42620
- AMANO, KANICHI**
Two-dimensional Navier-Stokes analysis of high-lift multi-element airfoils using the q-omega turbulence model
[AIAA PAPER 93-0679] p 466 A93-24787
- AMBUR, DAMODAR R.**
An analytically designed subcomponent test to reproduce the failure of a composite wing box beam
[AIAA PAPER 93-1344] p 709 A93-33914
Response of laminated composite plates to low-speed impact by airgun-propelled and dropped-weight impactors
[AIAA PAPER 93-1402] p 739 A93-33962
Effect of stiffness characteristics on the response of composite grid-stiffened structures p 1022 A93-45148
Design and analysis of grid stiffened concepts for aircraft composite primary structural applications
p 922 N93-30861
- AMENDOLA, A.**
An advanced graphics-interactive system for a multi-block structured grid generation within an industrial environment
[ETN-92-92885] p 440 N93-16288
- AMER, BRIAN**
Hermes CX-7: Air transport system design simulation
[NASA-CR-192082] p 335 N93-18056
- AMER, S.**
PBMR observations of surface soil moisture in Monsoon 90 p 1162 A93-47676
- AMERI, ALI**
High Reynolds number and turbulence effects on aerodynamics and heat transfer in a turbine cascade
[NASA-TM-106187] p 930 N93-29157
- AMINENI, N. K.**
Flow investigation of a low-speed-operated centrifugal compressor over a flow range including zero flow
[AIAA PAPER 93-2240] p 1155 A93-50042
- AMINI, A.**
A design study on the effect of support and system parameters on the natural frequencies of rotor systems
p 210 A93-16374
- AMINOV, N. M.**
A data processing and control system for counteracting wind shear p 524 A93-27604
- AMINPOUR, M. A.**
Multiple methods integration for structural mechanics analysis and design p 923 N93-30867
- AMIROUCHE, F. M. L.**
Time-variant analysis of rotorcraft systems dynamics - An exploitation of vector processors p 416 A93-23512
- AMITAY, M.**
Leading edge vortices in a chordwise periodic flow p 119 A93-14333
Leading edge vortices in a chordwise periodic flow p 782 N93-27218
- AMORIM, J. C.**
Numerical analysis of the three-dimensional boundary layer on a turbomachinery rotor blade p 685 A93-34341
- AMRAM, K.**
Theoretical and experimental study of the behavior of particles passing through a shock wave
[ONERA, TP NO. 1992-233] p 774 A93-38777
- AMUNDSEN, PETER C.**
BIPS Turboalternator-Compressor characteristics and application to the NASA Solar Dynamic Ground Demonstration Program p 532 A93-25965
- AN, C.-F.**
Numerical solution of transonic full-potential-equivalent equations in von Mises co-ordinates p 111 A93-14080
- AN, FU-QI**
A study of damage tolerance of the landing gear structure p 1219 A93-53881
- AN, JIGUANG**
A numerical method of unsteady separating flow over delta wings p 681 A93-33746
- AN, MICHAEL Y.**
Computation of inviscid flowfield around 3-D aerospace vehicles and comparison with experimental and flight data
[AIAA PAPER 93-0885] p 470 A93-24944
Two-layer convective heating prediction procedures and sensitivities for blunt body reentry vehicles
[AIAA PAPER 93-2763] p 963 A93-46509
- ANANTHKRISHNAN, N.**
Steady and quasisteady resonant lock-in of finned projectiles p 61 A93-12012
- ANDERS, KURT**
MM-122: High speed civil transport
[NASA-CR-192011] p 334 N93-17974
- ANDERSEN, C. A.**
Robotic aircraft refueling - A concept demonstration p 846 A93-37041
- ANDERSEN, G. W.**
A comparison of the drag-reducing benefits of riblets in internal and external flows p 395 A93-18054
- ANDERSEN, HARALD T.**
F-16 accidents: The Norwegian experience p 492 N93-19674
- ANDERSON, B. H.**
A comparative study of Full Navier-Stokes and Reduced Navier-Stokes analyses for separating flows within a diffusing inlet S-duct
[AIAA PAPER 93-2154] p 1079 A93-49970
- ANDERSON, BERNHARD H.**
Study on vortex flow control of inlet distortion p 122 A93-14520
Study on vortex generator flow control for the management of inlet distortion p 689 A93-34488
- ANDERSON, BIANCA T.**
Measurement of attachment-line location in a wind-tunnel and in supersonic flight
[AIAA PAPER 92-4089] p 39 A93-11285
Overview of supersonic laminar flow control research on the F-16XL ships 1 and 2
[NASA-TM-104257] p 20 N93-11221
- ANDERSON, C. N.**
Free piston facilities with air driver gas p 1011 A93-45528
- ANDERSON, CHARLES W.**
Future technology aim of the National Aerospace Plane Program
[AIAA PAPER 93-1988] p 1141 A93-49833
- ANDERSON, DAVID J.**
Bibliography on propulsion airframe integration technologies for high-speed civil transport applications, 1980-1991
[NASA-TM-105602] p 678 N93-26136
- ANDERSON, JOHN D., JR.**
Expanding the waverider design space using general supersonic and hypersonic generating flows
[AIAA PAPER 93-0505] p 283 A93-23253
Hypersonic waveriders - Where do we stand?
[AIAA PAPER 93-0399] p 474 A93-25520
- ANDERSON, LEONARD R.**
Order reduction of aeroelastic models through LK transformation and Riccati iteration
[AIAA PAPER 93-3795] p 1159 A93-51388
- ANDERSON, MARK**
The state-of-the-art of nondestructive evaluation of military runways p 375 A93-19659
- ANDERSON, MARK R.**
Robustness evaluation of a flexible aircraft control system p 727 A93-34540
Analytical development of an equivalent system mismatch function p 905 A93-41890
- ANDERSON, MILTON H.**
Processing of high temperature carbon fiber reinforced polymers
[SME PAPER EM92-215] p 925 A93-40654
- ANDERSON, R. E.**
The integral starter/generator development progress
[SAE PAPER 920967] p 173 A93-14629
- ANDERSON, ROBERT L.**
Advanced fiber placement of composite fuselage structures p 923 N93-30864
- ANDERSON, S. D.**
Results of high temperature JP-7 cracking assessment
[AIAA PAPER 93-0806] p 533 A93-24882
- ANDERSON, SETH B.**
Lessons learned from an historical look at flight testing p 511 N93-19904
- ANDERSON, STEVEN D.**
Static tests of jet fuel thermal and oxidative stability p 389 A93-21651
- ANDERSON, THOMAS E.**
Robo-line storage: Low latency, high capacity storage systems over geographically distributed networks
[NASA-CR-192910] p 758 N93-25130
- ANDERSON, W. K.**
Navier-Stokes computations and experimental comparisons for multielement airfoil configurations
[AIAA PAPER 93-0645] p 464 A93-24760
- ANDERSSON, PER**
Fatigue effects of noise among airplane mechanics p 558 A93-28495
- ANDES, ROBERT C.**
Specification of adaptive aiding systems
[AD-A254537] p 159 N93-12602
- ANDO, SHIGENORI**
Analysis of a 2-D airfoil motion flying in-proximity-to a wavy-wall surface: Lifting-surface-method p 300 N93-19281
Analysis of a 2-D airfoil motion flying in-proximity-to a wavy-wall surface: Finite difference method p 300 N93-19282
- ANDO, YASUNORI**
A study on two-dimensional and three-dimensional secondary jet interactions with a supersonic flow p 683 A93-34273
Two-dimensional and three-dimensional mixing flow structures with injected through slotted nozzle and circular nozzle into supersonic flows
[ISABE 93-7117] p 1221 A93-54092
A numerical investigation of 3D transverse injection into the supersonic flow behind rearward facing step p 303 N93-19316
- ANDO, YOUCHI**
Pressure fluctuation on casing wall of isolated axial compressor rotors at low flow rate
[ASME PAPER 92-GT-33] p 246 A93-19293
- ANDRE, ANTHONY D.**
Spatial orientation and wayfinding in airport passenger terminals - Implications for environmental design p 487 A93-27168
- ANDREEV, A. A.**
An experimental system for studying the vibrations and acoustic emission of cylindrical shells and panels in a field of turbulent pressure pulsations p 1140 A93-51754
An aeroacoustic stand for evaluating the efficiency of sound-absorbing structures under conditions of acoustic wave propagation in a moving medium p 1140 A93-51762
- ANDREEV, VASILII K.**
A practical course in aircraft maintenance. I - The powerplant p 811 A93-39175
- ANDREEV, YU. V.**
Interference between a high-lift sweptforward wing and the horizontal nose plane at subsonic velocities p 1135 A93-51906
- ANDREPOPOULOS, J.**
Wake structure of a helicopter rotor in forward flight p 958 A93-45138
- ANDREOTTI, ROBERT J.**
Promoting general aviation safety - A revision of pilot negligence law p 1265 A93-56540
- ANDRESEN, P.**
A laser induced fluorescence system for the high enthalpy shock tunnel (HEG) in Goettingen p 1024 A93-45506
- ANDREW, T. L.**
Low speed test results of subsonic, turbofan scari inlets
[AIAA PAPER 93-2301] p 1082 A93-50086
High speed test results of subsonic, turbofan scari inlets
[AIAA PAPER 93-2302] p 1082 A93-50087
- ANDREWS, EARL H.**
Review of NASA's Hypersonic Research Engine Project
[AIAA PAPER 93-2323] p 1116 A93-50103
- ANDREWS, G. E.**
An ultra low NO(x) pilot combustor for staged low NO(x) combustion
[ISABE 93-7020] p 1195 A93-53996
Impingement/effusion cooling p 932 N93-29954
- ANDREWS, JOHN**
Weather information requirements for Terminal Air Traffic Control Automation p 429 A93-22146

- ANDRIAMANALINA, D.**
Analytical solutions for hypersonic flow past slender power-law bodies at small angle of attack
p 122 A93-14550
- ANDRIANI, R.**
Performance and configuration analysis of jet-engine off-design behavior
[ISABE 93-7087] p 1202 A93-54063
- ANDRIENKO, V. M.**
An experimental study of thrust reverser models
p 812 A93-39195
An experimental study of reinforced panels of composite materials
p 1215 A93-52975
- ANDRONOV, A. M.**
A model of the maintenance of a fleet of TU-204 aircraft at a maintenance and repair center
p 237 A93-18327
- ANDRONOV, N. N.**
Behavior of the particular quality characteristics of an intelligent flight vehicle control system in a multicriterial formulation
p 1168 A93-50952
- ANFIMOV, N. A.**
Harnessing nitrous oxide for elevation of temperature and pressure in piston facilities
[AIAA PAPER 93-2016] p 1137 A93-49854
- ANG, HAISSONG**
Aeroelastic analysis of composite wing with control surface
p 157 A93-14386
- ANGRAND, F.**
Hypersonic flows over a double or simple ellipse
p 868 A93-42614
- ANGUS, JAMES P.**
Aero engine ceramics: The vision, the reality, and the progress
[PNR-90983] p 72 N93-11066
- ANISIMKIN, I. U. S.**
The required damping and control process quality in a fuel pressure regulator
p 810 A93-39034
- ANKUDINOV, A. L.**
The problem of viscous hypersonic flow past blunt bodies in the spreading plane
p 1086 A93-50969
- ANNIS, CHARLES**
Markov fatigue in single crystal airfoils
[ASME PAPER 92-GT-95] p 387 A93-19341
Fatigue in single crystal nickel superalloys
[AD-A254603] p 74 N93-12237
Fatigue in single crystal nickel superalloys
[AD-A258038] p 393 N93-17704
Fatigue in single crystal nickel superalloys
[AD-A259191] p 536 N93-20275
Fatigue in single crystal nickel superalloys
[AD-A260709] p 736 N93-25843
Fatigue in single crystal nickel superalloys
[AD-A265451] p 1019 N93-31795
- ANNIS, MARTIN**
Automatic detection of explosives using x ray imaging
p 880 N93-30275
- ANNUSHKINA, L. P.**
An experimental study of the air drying process in air coolers
p 834 A93-39059
- ANSART, D.**
Ramjet NOx emission - Use of a 3D CFD method for the combustor design of a super/hyper-sonic transport propulsion system
[ASME PAPER 92-GT-255] p 353 A93-19464
- ANTANI, D. L.**
HSCT high-lift aerodynamic technology requirements
[AIAA PAPER 92-4228] p 44 A93-13355
- ANTARAN, ALBERT**
RTJ-303: Variable geometry, oblique wing supersonic aircraft
[NASA-CR-192054] p 337 N93-18166
- ANTHONY, G. T.**
The technical background to standards for shackles
[NPL-DMM(A)-51] p 86 N93-11325
- ANTOLOVICH, STEPHEN D.**
Deformation mechanisms of NiAl cyclicly deformed near the brittle-to-ductile transformation temperature
[NASA-CR-191649] p 391 N93-15830
- ANTON, L. E.**
The numerical simulation of the hydrodynamic field from the pump impellers zone by means of the finite element method
p 476 A93-26905
- ANTONENKO, P.**
A history of visual approach guidance indicator systems in Australia
p 498 A93-25171
- ANTONIAK, Z. I.**
An evaluation of thermal energy storage options for precooling gas turbine inlet air
[DE93-005980] p 754 N93-24975
- ANTONOV, A. N.**
Determination of the dynamic characteristics of heat exchangers for the heat recovery system of gas turbine engines
p 834 A93-39054
- Solution of the problem of determining the dynamic characteristics of the cross-flow heat exchanger of the heat recovery system of gas turbine engines
p 834 A93-39055
- A method for calculating the dynamic characteristics of heat exchangers with single-phase cryogenic coolants
p 851 A93-39057
- ANTOSIEWICZ, MALGORZATA**
A numerical study of aerodynamic wing design for supercritical conditions of an advanced training and military aircraft
p 1238 A93-56213
- AOI, Y.**
Effects of wake interaction of two turbine cascades on secondary/tip-leakage flows and losses
[ISABE 93-7058] p 1185 A93-54034
- AOKI, SUNAO**
The application of CFD to turbomachine design - Past and future
p 769 A93-38130
- AOKI, T.**
Conceptual design of turbo-accelerator for HST combined cycle engine
[ASME PAPER 92-GT-253] p 353 A93-19462
A scoping study for hypersonic transport propulsion systems
[ASME PAPER 92-GT-409] p 356 A93-19558
Conceptual design study on combined-cycle engine for hypersonic transport
[ISABE 93-7018] p 1195 A93-53994
- AQUIDEF, AHMED**
Coriolis effects on Goertler vortices in the boundary-layer flow on concave wall
p 123 A93-14564
- AOYAMA, TAKASHI**
Unsteady analysis of helicopter rotor
p 770 A93-38193
- APARICIO, J. P.**
Validation of electromagnetic-topology concepts on a complex structure
[ONERA, TP NO. 1992-63] p 542 A93-25327
- APATHY, ISTVAN**
DAR-2: On-board data acquisition system for aircraft engines
p 169 N93-15166
- APATHY, J.**
Solid state flight data recorders and their application in the flight operation analysis
p 166 A93-14200
Application of flight data for diagnostic purposes
p 166 A93-14295
- APPLEWHITE, HUGH L.**
A survey of position trackers
p 1151 A93-49396
- ARABSHAH, ABDOLLAH**
A study of CFD algorithms applied to complete aircraft configurations
[AIAA PAPER 93-0784] p 468 A93-24864
Multi-block calculations for flows in local chemical equilibrium
[AIAA PAPER 93-2999] p 1053 A93-48189
Turbulent flowfield simulation using Euler equations with body forces
[AIAA PAPER 93-1978] p 1078 A93-49825
- ARAI, MASATAKA**
Characteristics of liquid jet atomization across a high-speed airstream. I - Experiment on shape of spray, spatial distribution of injected liquid and Sauter mean diameter
p 411 A93-21743
Characteristics of liquid jet atomization across a high-speed airstream. II - Calculation of spatial distribution of liquid, variation of drop diameter and drop trajectory
p 412 A93-21744
- ARAI, TAKAKAGE**
Penetration and mixing of bubbling liquid jets from multiple injectors normal to a supersonic air stream
[AIAA PAPER 92-5060] p 413 A93-22330
- ARAKAWA, C.**
A numerical simulation of a scram jet combustor flow
p 810 A93-38181
- ARAKAWA, CHUICHI**
Turbulent flow simulation around the aerofoil with pseudo-compressibility
p 830 A93-38155
- ARALOV, G. D.**
Dependence of the service life of a wing on its strength uniformity and landing gear location
p 891 A93-42377
- ARANA, CARLOS**
Carbon/silicon carbide composite materials in advanced unmanned gas turbine engine combustors
[AIAA PAPER 93-1761] p 1144 A93-49658
Effect of geometry, bleed rates and flow splits on pressure recovery of a canted hybrid vortex-controlled diffuser
[AIAA PAPER 93-1762] p 1109 A93-49659
- ARATA, WINFIELD H., JR.**
Advanced technologies airships
p 108 A93-14183
Advanced technologies for enhancement of airships
[AIAA PAPER 93-4040] p 1242 A93-54610
- ARATANI, T.**
Air flow dynamics around an aerofoil by the stabilized finite difference method
p 266 A93-20741
- ARCARA, P. C., JR.**
Hybrid laminar flow control applied to advanced turbofan engine nacelles
[SAE PAPER 920962] p 123 A93-14628
- ARCHER, FRANCES A.**
The chemistry of Saudi Arabian sand - A deposition problem on helicopter turbine airfoils
p 1216 A93-53468
- ARDEMA, M. D.**
Near-optimal energy transitions for energy-state trajectories of hypersonic aircraft
[AIAA PAPER 92-4300] p 69 A93-13276
Structural and aerodynamic considerations for an oblique all-wing aircraft
[AIAA PAPER 92-4220] p 43 A93-13336
- ARDEMA, MARK D.**
Optimal trajectories for hypersonic launch vehicles
p 1251 A93-54563
- ARENA, A. S., JR.**
The use of subscale models to predict self-induced oscillations of flight vehicles
[AIAA PAPER 93-0093] p 264 A93-20199
Lateral control at high angles of attack using pneumatic blowing through a chined forebody
[AIAA PAPER 93-3624] p 1126 A93-48309
- ARENA, ANDREW SALVATORE, JR.**
An experimental and computational investigation of slender wings undergoing wing rock
p 187 N93-13915
- ARENDSEN, P.**
Structural optimization in preliminary aircraft design - A finite-element approach
p 226 A93-14340
- ARENDTS, F. J.**
Current developments in structural technology
p 77 A93-10780
- ARENT, LAUREN**
757 fly-by-wire demonstrator flight test
[AIAA PAPER 92-4099] p 38 A93-11271
- ARES, AURORA A.**
The Foreign Sovereign Immunities Act of 1976 - Misjoinder, nonjoinder, and collusive joinder
p 944 A93-42998
- ARGUCHINTSEVA, M. A.**
Extreme value heat transfer problems for three-dimensional bodies moving at hypersonic velocities
p 4 A93-10079
- ARGYRIS, J.**
Hypersonic viscous flow past double ellipse and past double ellipsoid - Numerical results
p 868 A93-42618
- ARIELI, R.**
Lateral aerodynamics characteristics of forebodies at high angle of attack in subsonic and transonic flows
p 118 A93-14302
- ARIGA, HIRONOBU**
Effect of the flow non-uniformity on the mixing layer at the interface of parallel supersonic flows
[ISAS-RN-646] p 128 N93-12716
- ARKUN, UGUR**
Numerical simulation of ramjet and scramjet combustion using two-dimensional Euler equations with finite rate chemistry
[ISABE 93-7083] p 1202 A93-54059
- ARMEN, HARRY**
CST gives aircraft industry a lift
p 560 A93-25086
- ARMSTRONG, JEFFREY**
Carbon/silicon carbide composite materials in advanced unmanned gas turbine engine combustors
[AIAA PAPER 93-1761] p 1144 A93-49658
- ARNAL, D.**
Recent supersonic transition studies with emphasis on the swept cylinder case
p 127 A93-17232
The experimental study of transition and leading edge contamination of swept wings
[LIB-TRANS-2197] p 782 N93-27274
Three-dimensional compressible stability-transition calculations using the spatial theory
p 783 N93-27431
- ARNAL, DANIEL**
Reduction of aerodynamic skin-friction drag
p 871 A93-42656
- ARNAUD, ALAIN**
The United States in the conquest of the hypersonic
p 109 A93-15056
- ARNAUD, G.**
Validation of R85/METAR on the Puma RAE flight tests
[ONERA, TP NO. 1992-123] p 802 A93-38597
- ARNETTE, STEPHEN A.**
The effect of expansion on the large scale structure of a compressible turbulent boundary layer
[AIAA PAPER 93-2991] p 1052 A93-48183
- ARNOLD, F.**
Measurements of jet aircraft emissions at cruise altitude. I - The odd-nitrogen gases NO, NO₂, HNO₂ and HNO₃
p 556 A93-24391

- A novel aircraft-based tandem mass spectrometer for atmospheric ion and trace gas measurements
p 925 A93-40672
- A Laplace interaction law for the computation of viscous airfoil flow in low and high speed aerodynamics
[AIAA PAPER 93-3462] p 979 A93-47244
- ARNOLD, RICHARD P.**
The Microwave Landing System - A precision approach for the future p 32 A93-11023
- ARNONE, A.**
Multigrid calculation of three-dimensional viscous cascade flows p 872 A93-42889
Pseudo-compressibility methods for the incompressible flow equations
[AIAA PAPER 93-3329] p 952 A93-45023
- ARNONE, ANDREA**
Investigation of advanced counterrotation blade configuration concepts for high speed turboprop systems. Task 5: Unsteady counterrotation ducted propfan analysis. Computer program user's manual
[NASA-CR-187125] p 521 N93-20583
- ARORA, N. L.**
Numerical modeling of leading edge separated flow at incompressible speeds p 460 A93-24079
- ARREDONDO, P.**
Aerodynamics design of convergent-divergent nozzles
[AIAA PAPER 93-2574] p 1085 A93-50290
- ARTAMONOV, N. I.**
Choice of the heating system for high-temperature generators using chemical fuel p 559 A93-29660
- ARTHEY, R. P.**
Civil aircraft engines: The next generation
[PNR-90962] p 58 N93-11085
- ARTHUR, TREY**
A comparison using APPL and PVM for a parallel implementation of an unstructured grid generation program
[NASA-CR-191425] p 757 N93-25073
- ARTS, T.**
The VKI compression tube annular cascade facility CT3
[ASME PAPER 92-GT-336] p 375 A93-19511
Three dimensional aero-thermal characteristics of a high pressure turbine nozzle guide vane p 1002 A93-46942
Thermal effects of a coolant film along the suction side of a high pressure turbine nozzle guide vane p 901 N93-29930
- ARTZ, TIMOTHY J.**
Onboard Connectivity Network for command and control aircraft p 1166 A93-49481
- ARZHANENKO, A. YU.**
Statistical methods in flight vehicle control theory p 1165 A93-49306
- ASAI, KEISUKE**
The cryogenic approach to simulating hot jet in transonic wind-tunnel testing p 117 A93-14297
- ASBURY, MICHAEL J. A.**
Work performed in the United Kingdom to establish the feasibility of RAIM in a GPS receiver in flight p 314 A93-21157
- ASBURY, SCOTT C.**
Internal performance of Highly Integrated Deployable Exhaust Nozzles
[AIAA PAPER 93-2570] p 1084 A93-50288
- ASCOUGH, T. H.**
Testing of an automatic, low altitude, all terrain ground collision avoidance system p 502 N93-19924
- ASEEV, B. E.**
A new method for determining the number of flight vehicle prototypes subject to full-scale testing p 434 A93-18316
- ASERE, A. A.**
Impingement/effusion cooling p 932 N93-29954
- ASH, ROBERT L.**
Volume 2: Explicit, multistage upwind schemes for Euler and Navier-Stokes equations
[NASA-CR-191647] p 418 N93-16558
- ASHBY, DALE L.**
Unsteady panel method for flows with multiple bodies moving along various paths
[AIAA PAPER 93-0640] p 539 A93-24755
- ASHCRAFT, JANE**
State-of-the-art survey of flexible pavement crack sealing procedures in the United States
[AD-A258050] p 382 N93-17708
- ASHENDEN, RUSSELL A.**
The Air Force Flight Test Center artificial icing and rain testing capability upgrade program
[AIAA PAPER 93-0295] p 376 A93-22695
- ASHFORD, N. J.**
Airport stand assignment model
[TT-9104] p 67 N93-11728
Information systems for airport operations
[TT-9202] p 152 N93-14729
- ASHFORD, NORMAN**
An investigation of ground access mode choice for departing passengers
[TT-9201] p 67 N93-11224
- ASHLEY, HOLT**
Active control for fin buffet alleviation
[AIAA PAPER 93-3817] p 1133 A93-51408
- ASHLEY, PATRICK A.**
Investigation of high-alpha lateral-directional control power requirements for high-performance aircraft
[AIAA PAPER 93-3647] p 1130 A93-49519
- ASHLEY, STEVEN**
Boeing 777 gets a boost from titanium p 1018 A93-45987
- ASHPOLE, RON**
Software - Design for maintenance p 847 A93-39537
- ASHRAFIUON, H.**
Optimal design of centered squeeze film dampers p 831 A93-38629
- ASHWILL, T. D.**
Measured data for the Sandia 34-meter vertical axis wind turbine
[DE92-019807] p 94 N93-12075
- ASKIN, RON W.**
Crack growth/damage tolerance analysis methods as applied to V-22 fuselage and empennage p 795 A93-35948
- ASKINS, P. A.**
Measurements in 80- by 120-foot wind tunnel of hazard posed by lift-generated wakes
[AIAA PAPER 93-3518] p 1014 A93-47281
- ASO, S.**
Aerodynamic heating phenomenon in three dimensional shock wave/turbulent boundary layer interaction induced by sweptback fins in hypersonic flows p 960 A93-45507
- ASO, SHIGERU**
A study on two-dimensional and three-dimensional secondary jet interactions with a supersonic flow p 683 A93-34273
A study on three-dimensional shock wave/turbulent boundary layer interaction induced by sweptback sharp fins at supersonic flow p 684 A93-34274
Numerical calculation of separated flows around wing section in unsteady motion by using incompressible Navier-Stokes equations p 770 A93-38158
The experimental study of the effect of sweptback angles and the front shape of the fin on reduction of shock wave/turbulent boundary layer interaction region p 858 A93-40431
Intense studies on unsteady secondary separations and oscillating shock waves in three-dimensional shock waves/turbulent boundary layer interaction regions induced by sharp and blunt fins
[AIAA PAPER 93-2939] p 1046 A93-48137
Aerodynamic heating with boundary layer transition and heat protection with mass addition on blunt body in hypersonic flows
[AIAA PAPER 93-2984] p 1051 A93-48177
Two-dimensional and three-dimensional mixing flow structures with injected through slotted nozzle and circular nozzle into supersonic flows
[ISABE 93-7117] p 1221 A93-54092
Numerical calculations of separating flows around oscillating airfoil p 300 N93-19284
Aerodynamic heating analysis for axisymmetric bodies in supersonic flow p 303 N93-19312
- ASO, Y.**
Diagnostics systems for the TBR-E tokamak
[INRE-5428-RPQ/662] p 232 N93-13257
- ASSMANN, G.**
Air Traffic and Environment
[GSF-BAND-8] p 1034 N93-31925
- ASTILLERO, RICARDO**
Upgrade Precision Runway Monitor (PRM) Operational Test and Evaluation (OT/E) test plan
[DOT/FAA/CT-TN92/13] p 67 N93-11616
- ASTON, J. A. G.**
Theoretical modelling of rotor noise radiation p 566 A93-29407
- ATAMANCHUK, TARAS M.**
An aerospace plane as a detonation wave ramjet/airframe integrated waverider
[AIAA PAPER 92-5022] p 272 A93-22298
- ATASSI, H. M.**
Numerical solutions for unsteady subsonic vortical flows around loaded cascades
[ASME PAPER 92-GT-173] p 250 A93-19399
- ATCLIFFE, P.**
Plume effects at hypersonic speeds p 959 A93-45494
Plume effects on the flow around a blunted cone at hypersonic speeds p 787 N93-27460
- ATENCIO, A., JR.**
Flight simulator fidelity assessment in a rotorcraft lateral translation maneuver p 378 A93-23510
- ATENCIO, ADOLPH, JR.**
Ground based simulation evaluation of the effects of time delays and motion on rotorcraft handling qualities
[AD-A256921] p 328 N93-16186
- ATHAVALE, M. M.**
Driven cavity simulation of turbomachine blade flows with vortex control
[AIAA PAPER 93-0390] p 461 A93-24238
- ATKINSON, MICHAEL L.**
Advanced composite helicopter MISERS GOLD test/analysis p 508 A93-27974
- ATKINSON, ROBERT J.**
Variability of geophysical parameters from aircraft radiance measurements for FIFE p 426 A93-20622
- ATLER, DOUG**
Development and operation of new arc heater technology for a large-scale scramjet propulsion test facility
[AIAA PAPER 93-2786] p 1016 A93-46528
- ATLURI, SATYA N.**
Computational nonlinear mechanics in aerospace engineering
[ISBN 1-56347-044-6] p 78 A93-12151
Structural integrity of aging airplanes
[ISBN 0-540-53461-X] p 947 A93-45772
Computational schemes for integrity analyses of fuselage panels in aging airplanes p 1025 A93-45774
- ATSUCHI, S.**
A study on aerodynamic sound generated by interaction of jet and plate
[AIAA PAPER 93-3118] p 1171 A93-48288
- ATTANASIO, G.**
MSC/NASTRAN structure optimization test module version 67 (preliminary)
[REPT-5-191025] p 554 N93-20907
- ATTWOOD, D.**
X ray microscopy resource center at the Advanced Light Source
[DE93-010449] p 911 N93-29869
- ATWOOD, C. A.**
Navier-Stokes simulations of unsteady transonic flow phenomena
[NASA-TM-103962] p 129 N93-12721
- ATWOOD, CHRISTOPHER A.**
Flowfield simulation about the stratospheric observatory for infrared astronomy p 1095 A93-52446
- ATWOOD, CHRISTOPHER ALEXANDER**
Navier-Stokes simulations of unsteady transonic flow phenomena p 697 N93-25542
- AU, ROBERT H.**
Spreadsheet microcomputer numerical method for the compressible laminar wake flow p 684 A93-34308
- AUDIFFREN, N.**
Effect of wall heating on a supersonic turbulent boundary layer p 11 A93-12429
- AUER, PETER**
Development of cure cycles: From laboratory analysis and testing to production of large scale composites
[MBB-Z-0442-92-PUB] p 536 N93-20845
- AULD, DOUGLASS J.**
Experimental investigation of laminar to turbulent boundary layer transition with separation bubbles at low Reynolds number p 128 A93-17277
- AULDS, J. M.**
High voltage quick-disconnect harness system for helmet-mounted displays p 516 A93-25922
- AULT, DARRELL**
Longitudinal acceleration test of overhead luggage bins in a transport airframe section
[DOT/FAA/CT-92/9] p 991 N93-31652
- AUMAN, LAMAR M.**
Wind tunnel investigation with an operational turbojet engine
[AIAA PAPER 93-0036] p 322 A93-20150
- AUPOIX, B.**
Second-order effects in hypersonic laminar boundary layers p 1073 A93-49529
Real gas effects in two- and three-dimensional hypersonic, laminar boundary layers p 1073 A93-49530
Investigations on entropy layer along hypersonic hyperboloids using a defect boundary layer p 787 N93-27462
- AURENCHÉ, Y.**
Microbursts detection with airborne Doppler lidar p 433 A93-22201
- AURIOL, ANDRE**
Sonic boom problem for future highspeed aircraft
[ONERA-NT-1990-3] p 876 N93-30020
- AUSLENDER, AARON H.**
Numerical study of the performance of swept, curved compression surface scramjet inlets
[AIAA PAPER 93-1837] p 1074 A93-49721

B

- AUSTIN, ERIC M.**
Passive damping technology p 1259 A93-55866
- AUSTIN, F.**
Adaptive/conformal wing design for future aircraft p 320 A93-17728
Active rib experiment for shape control of an adaptive wing [AIAA PAPER 93-1700] p 712 A93-34222
- AUSTIN, JOHN B.**
A general framework for analyzing choice-of-law problems in air crash litigation p 1265 A93-56537
- AUWETER-KURTZ, M.**
Non-equilibrium flow in an arc heated wind tunnel p 910 A93-42642
- AVDEEV-FEDOSEEV, ARTUR N.**
A practical course in aircraft maintenance. I - The powerplant p 811 A93-39175
- AVDOSHIN, A. P.**
Autonomous mobile laser complex p 395 A93-17767
- AVDUEVSKII, V. S.**
Astronautics and society p 383 A93-18391
- AVDYUKHINA, T. M.**
Some aspects of the design of combination landing gear p 891 A93-42374
- AVELINE, SERGE**
Two-dimensional laser velocimetry for the study of dual-flow jets with flight effect in the CEPRA 19 anechoic wind tunnel [ONERA, TP NO. 1992-144] p 831 A93-38614
- AVERILL, R. C.**
Thermomechanical postbuckling analysis of laminated composite shells [AIAA PAPER 93-1337] p 738 A93-33907
- AVERY, WILLIAM B.**
Effects of intra- and inter-laminar resin content on the mechanical properties of toughened composite materials p 921 A93-30845
Developments in impact damage modeling for laminated composite structures p 922 A93-30857
- AVITAL, GAVRIEL**
Analysis of wind-tunnel data for elliptic cross-sectioned forebodies at Mach numbers 0.4 to 5.0 p 782 A93-27221
- AVKHADIEV, F. G.**
Maximizing the critical Mach number for lifting wing profiles p 13 A93-12841
- AVKHMIOVICH, BORIS M.**
Fundamentals of flight vehicle design [ISBN 5-217-01299-4] p 893 A93-43831
- AVRAN, PATRICK**
High temperature heat exchangers for gas turbines and future hypersonic air breathing propulsion [ONERA, TP NO. 1993-75] p 1218 A93-53596
- AWAJI, H.**
High temperature fracture mechanism of gas-pressure sintered silicon nitride p 825 A93-38893
- AWFORD, IAN**
Handling the legal consequences of aviation disasters - Passenger compensation [ISBN 3-452-22293-4] p 103 A93-11411
- AYDER, E.**
Experimental and theoretical analysis of the flow in a centrifugal compressor volute [ASME PAPER 92-GT-30] p 400 A93-19290
- AYER, T. C.**
Analysis of high Reynolds number inviscid/viscid interactions in cascades p 1234 A93-55351
- AYMER, D.**
Experimental study of the flow around a double ellipsoid configuration p 867 A93-42603
- AZEVEDO, D.**
A study of incipient separation limits for shock-induced boundary layer separation for Mach 6 high Reynolds flow [AIAA PAPER 93-2481] p 1084 A93-50222
- AZEVEDO, D. J.**
Engineering approach to the prediction of shock patterns in bounded high-speed flows p 287 A93-23545
- AZEVEDO, DAVID**
Measured thrust losses associated with secondary air injection through nozzle walls p 270 A93-21656
- AZEVEDO, J. L. F.**
Transonic profile design in curvilinear coordinates using an approximate factorization algorithm p 7 A93-10778
Code validation for high speed flow simulation over the VLS launcher fairing [AIAA PAPER 93-3046] p 1057 A93-48226
- AZEVEDO, JOAO L. F.**
Nozzle flow computations using the Euler equations p 112 A93-14170
- AZIMIAN, A. R.**
Application of recess vaned casing treatment to axial flow fans p 423 A93-18728
- BAARS, PUL, M.**
Design philosophies of the Basic Research Simulator p 191 A93-14414
A 'low-cost' full flight simulator for basic IFR training p 374 A93-18776
- BAART, DOUGLAS**
A NASPAC-based analysis of the delay and cost effects of the Dallas/Fort Worth metroplex plan [DOT/FAA/CT-TN92/21] p 193 A93-13447
- BABA, SHIGERU**
A wind tunnel investigation to determine buffet countermeasures for STOL aircraft alpha-sweep flight testing [NAL-TR-1129] p 65 A93-12362
- BABA, YORIAKI**
Limit of sampling periods for nonlinear flight trajectory controller of aircraft p 61 A93-11207
Generalized guidance law for collision courses p 727 A93-34533
- BABICH, O. V.**
Experimental study of crossflow instability and laminar-turbulent transition on a swept wing p 115 A93-14250
- BABIKIAN, DIKRAN S.**
Measurement and analysis of nitric oxide radiation in an arc-jet flow [AIAA PAPER 93-2800] p 1016 A93-46540
- BABILON, J.**
Engine testing at simulated altitude conditions [AIAA PAPER 93-2452] p 1120 A93-50201
- BABINSKY, H.**
The application and analysis of liquid crystal thermographs in short duration hypersonic flow [AIAA PAPER 93-0182] p 542 A93-25509
- BABUSHKIN, ANATOLII I.**
Modeling and optimization of aircraft assembly [ISBN 5-217-00808-3] p 677 A93-35677
- BACH, R. E.**
A summary of investigations of severe turbulence incidents using airline flight records p 308 A93-22153
- BACHALO, E. J.**
Liquid water content measurements using the Phase Doppler Particle Analyzer in the NASA Lewis Icing Research Tunnel [AIAA PAPER 93-0298] p 378 A93-23698
- BACHALO, W. D.**
Liquid water content measurements using the Phase Doppler Particle Analyzer in the NASA Lewis Icing Research Tunnel [AIAA PAPER 93-0298] p 378 A93-23698
- BACHALO, WILLIAM D.**
Seed particle response and size characterization in high speed flows p 459 A93-23811
- BACHAR, T.**
Oscillatory blowing, a tool to delay boundary layer separation [AIAA PAPER 93-0440] p 474 A93-25529
Oscillatory blowing - A tool to delay boundary-layer separation p 1235 A93-55362
- BACHELET, E.**
Fatigue of turboengine discs [DS-2136] p 364 A93-18149
- BACHMANOVA, N. S.**
Hypersonic flow past a low-aspect-ratio triangular plate at large angles of attack p 1069 A93-48974
- BACHNER, STEPHEN D.**
Identification of a full subsonic envelope nonlinear aerodynamic model of the F-14 aircraft [AIAA PAPER 93-3634] p 1065 A93-48319
- BADER, ANTON**
Personal computer based test- and emulation equipment for maintenance and ground support p 110 A93-15185
- BADER, R. M.**
Structural integrity challenges p 3 A93-13627
- BADESHA, S.**
Aerodynamics of the TCOM 71M aerostat [AIAA PAPER 93-4036] p 1231 A93-54607
- BADMUS, O. O.**
A simplified approach for control of rotating stall. I - Theoretical development [AIAA PAPER 93-2229] p 1080 A93-50035
A simplified approach for control of rotating stall. II - Experimental results [AIAA PAPER 93-2234] p 1080 A93-50038
- BADURKA, WILLIAM**
The applications, benefits, and issues of employing GPS and Glonass with Automatic Dependent Surveillance p 316 A93-21188
- BAEDER, J. D.**
Euler solutions to nonlinear acoustics of non-lifting rotor blades p 568 A93-29433
TURNS - A free-wake Euler/Navier-Stokes numerical method for helicopter rotors p 692 A93-35634
- BAEK, J. H.**
Two-dimensional transonic flow around VKI turbine cascade p 1232 A93-54640
- BAEK, JE-HYUN**
Influence of trailing-edge grid structure on Navier-Stokes computation of turbomachinery cascade flow p 111 A93-14078
- BAEUMKER, M.**
Integration of a course and position reference system with GPS p 499 A93-27911
- BAGAI, A.**
Experimental study of rotor wake/body interactions in hover p 124 A93-14782
- BAGEPALLI, B.**
A systems dynamics approach to modeling gas turbine combustor wear [ASME PAPER 92-GT-47] p 347 A93-19300
- BAGNALL, S. M.**
Aspects of turbine blade design for integrity p 345 A93-18784
- BAHADORI, M. YOUSEF**
Effects of buoyancy on gas jet diffusion flames [NASA-CR-191109] p 935 A93-31031
- BAHR, D. W.**
Turbine engine developers explore ways to lower NO(x) emission levels p 52 A93-10732
Aircraft turbine engine NOx emission limits - Status and trends [ASME PAPER 92-GT-415] p 357 A93-19563
- BAHRI, TOUFIK**
Adaptive automation and human performance: Multi-task performance characteristics [AD-A254596] p 186 A93-12578
Theory and design of adaptive automation in aviation systems [AD-A254595] p 160 A93-12613
- BAI, CUNRU**
Some key problems in the design of the NPU open-circuit low-turbulence wind tunnel p 1139 A93-51188
- BAI, J. J.**
Researches on sonic fatigue of the air-inlet duct of XX aircraft p 154 A93-14256
- BAI, KUI**
The stagnation line solution of the equilibrium flow with radiation and mass injection p 680 A93-33733
- BAI, L.**
Multigrid methods for calculating 3D flows in complex geometries p 973 A93-46984
- BAI, TIEJUN**
Aero-engine component damping estimation from full-scale aeromechanical test data [AIAA PAPER 93-1873] p 1112 A93-49748
- BAI, X. S.**
Numerical simulation of turbulent reacting flows in combustion chambers p 171 A93-14271
- BAILEY, E. D.**
Flight management systems p 311 A93-17757
- BAILEY, F. R.**
The new challenge of computational aerospace p 112 A93-14169
- BAILEY, MELVIN L.**
Effect of lift-to-drag ratio in pilot rating of the HL-20 landing task p 1210 A93-53738
- BAILEY, RANDALL E.**
Pilot control identification using Minimum Model Error estimation [AIAA PAPER 92-4421] p 523 A93-24497
Initial results of an in-flight investigation of longitudinal flying qualities for augmented, large transports in approach and landing [AIAA PAPER 93-3816] p 1133 A93-51407
- BAILLEUL, GILLES**
New digital capacitive measurement system for blade clearances p 1254 A93-54376
- BAILLEUX, P.**
Effect of Reynolds number on the standards of a simplified anemoclinometric probe [IMFL-91-31] p 293 A93-17542
- BAILLIE, STEWART W.**
The flight test and data analysis program for the development of a Boeing/De Havilland Dash 8 simulator model p 512 A93-19930
- BAIN, D. B.**
CFD mixing analysis of axially opposed rows of jets injected into confined crossflow [NASA-TM-106179] p 813 A93-27128
- BAIN, J. G.**
Measurement and prediction of flow in a gas turbine engine exhaust plume [ISABE 93-7113] p 1204 A93-54088
- BAINES, N. C.**
The effects of blade loading in radial and mixed flow turbines [ASME PAPER 92-GT-92] p 349 A93-19338

- The design and evaluation of a high pressure ratio radial turbine
[ASME PAPER 92-GT-93] p 349 A93-19339
Performance parameters and assessment p 81 N93-10052
Partial admission and unsteady flow in radial turbines p 81 N93-10059
- BAIRD, JAMES C.**
Strategies for optimal control design of normal acceleration command following on the F-16
[AD-A258975] p 373 N93-19095
- BAKER, A. A.**
Reinforcement of the F-111 wing pivot fitting with a boron/epoxy doubler system - Materials engineering aspects p 1214 A93-54241
- BAKER, A. J.**
Accuracy and efficiency assessments for a weak statement CFD algorithm for high-speed aerodynamics
[ASME PAPER 92-GT-433] p 435 A93-19576
- BAKER, BRADLEY**
A technique for the measurement of cloud structure on centimeter scales p 1158 A93-51243
- BAKER, C. J.**
Bistatic radar using satellite-borne illuminators of opportunity p 914 A93-43437
Grazing angle dependency of SAR imagery p 884 A93-43455
- BAKER, DAVID**
NASP - Waveriders in a hypersonic sky. I p 532 A93-25355
NASP - Waveriders in a hypersonic sky. II p 532 A93-25359
- BAKER, N. R.**
Effects of compression and expansion ramp fuel injector configuration on scramjet combustion and heat transfer
[AIAA PAPER 93-0609] p 358 A93-21114
Evaluation of scramjet nozzle configurations and film cooling for reduction of wall heating
[AIAA PAPER 93-0744] p 358 A93-21118
The effect of entrance radius and film injection on wall heating in scramjet nozzles p 360 A93-22505
- BAKER, SUSAN P.**
Human factors in crashes of commuter airplanes p 486 A93-24048
- BAKER, TIMOTHY**
Mesh generation for the computation of flowfields over complex aerodynamic shapes p 995 A93-44888
- BAKER, TIMOTHY J.**
Solution of three-dimensional supersonic flowfields via adapting unstructured meshes p 863 A93-42442
- BAKER, WALTER L.**
Control augmentation system (CAS) synthesis via adaptation and learning
[AIAA PAPER 93-3728] p 1170 A93-51328
- BAKHLE, MILIND A.**
APPLE - An aeroelastic analysis system for turbomachines and propfans
[AIAA PAPER 92-4712] p 358 A93-20320
An efficient procedure for cascade aeroelastic stability determination using nonlinear, time-marching aerodynamic solvers
[AIAA PAPER 93-1631] p 719 A93-34159
Unsteady aerodynamics and flutter of propfans using a three-dimensional Full-Potential Solver
[AIAA PAPER 93-1633] p 720 A93-34161
Subsonic/transonic cascade flutter using a full-potential solver p 861 A93-41934
Unsteady aerodynamics and flutter based on the potential equation
[AIAA PAPER 93-2086] p 1079 A93-49913
- BAKLANOV, V. S.**
Vibration isolation of aviation power plants taking into account real dynamic characteristics of engine and aircraft p 1244 A93-55863
- BAKOS, R.**
Mixing and combustion studies using discrete orifice injection at hypervelocity flight conditions p 205 A93-14523
- BAKULEV, V. I.**
Consideration of the completeness of combustion and dissociation and recombination processes in mathematical models of jet engines for high supersonic flight velocities p 520 A93-27627
- BALACHANDAR, RAMASWAMI**
Characteristics of separated flows including cavitation effects p 84 N93-10874
- BALAGEAS, D.**
Infrared thermography characterization of Goertler vortex type patterns in hypersonic flows
[ONERA, TP NO. 1993-13] p 925 A93-41029
Infrared thermography of plastic instabilities in a single crystal superalloy
[ONERA, TP NO. 1993-18] p 916 A93-41031
- BALAKRISHNA, S.**
Modeling and control study of the NASA 0.3-meter transonic cryogenic tunnel for use with sulfur hexafluoride medium
[NASA-CR-189737] p 418 N93-16379
A feasibility study of using Langley 0.3-m transonic cryogenic tunnel sidewall boundary-layer removal system for heavy gas testing
[NASA-CR-191438] p 747 N93-25087
A PC-based simulation of the National Transonic Facility's safety microprocessor
[NASA-TM-109003] p 1038 N93-32224
- BALAKRISHNAN, GANESHAN**
Studies of hydrogen-air diffusion flames and of compressibility effects related to high-speed propulsion p 917 N93-29125
- BALAKRISHNAN, N.**
Acoustic flux vector splitting scheme for Euler equations p 460 A93-24078
- BALAKRISHNAN, S. N.**
Self-tuning guidance applied to aeroassisted plane change problems
[AIAA PAPER 93-3791] p 1143 A93-51386
- BALAKUMAR, P.**
Linear stability of three-dimensional boundary layers - Effects of curvature and non-parallelism
[AIAA PAPER 93-0079] p 263 A93-20191
Instability and transition in three-dimensional supersonic boundary layers
[AIAA PAPER 92-5049] p 273 A93-22321
- BALALAEV, V. A.**
Determination of nonstationary aerodynamic loading on cascade blades in the case of dynamic changes of the angle of attack p 544 A93-26817
- BALANIS, CONSTANTINE A.**
Advanced electromagnetic methods for aerospace vehicles
[NASA-CR-193468] p 936 N93-31036
- BALAS, GARY J.**
Design of a flight control system for a highly maneuverable aircraft using mu synthesis
[AIAA PAPER 93-3776] p 1132 A93-51371
- BALASHOV, BORIS**
ICAO analyses trends in fuel consumption by world's airlines p 1 A93-10733
- BALASUBRAMANIAM, KRISHNAN**
p-version finite element modeling for NDE p 407 A93-19699
- BALASUBRAMANIAM, R.**
Assessment of computational issues associated with analysis of high-lift systems p 785 N93-27449
- BALBONI, JOHN**
Development and operation of new arc heater technology for a large-scale scramjet propulsion test facility
[AIAA PAPER 93-2786] p 1016 A93-46528
- BALDAN, AHMET**
Effects of grain size and carbides on the creep resistance and rupture properties of a conventionally cast nickel-base superalloy p 389 A93-21699
- BALDOCCHI, ROBERT L.**
Modification and calibration of the Naval Postgraduate School Academic Wind Tunnel
[AD-A262092] p 823 N93-28189
- BALDWIN, R. E.**
Alternative equipment test procedures for simultaneous current injection on multiple cable bundles p 747 N93-24903
- BALDWIN, RUSTY O.**
A model for determining task set schedulability in the presence of system effects
[AD-A258915] p 443 N93-19338
- BALEPIN, V. V.**
Integrated air separation and propulsion system for aerospace plane with atmospheric oxygen collection
[SAE PAPER 920974] p 195 A93-14633
- BALESTRA, C. L.**
Demonstration of an integrated, active 4 x 4 photonic crossbar p 211 A93-17392
- BALIS CREMA, L.**
Damping in aerospace composite materials p 1260 A93-55869
- BALL, CALVIN L.**
Propulsion technology challenges for turn-of-the-century commercial aircraft
[ISABE 93-7003] p 1194 A93-53980
Propulsion technology challenges for turn-of-the-century commercial aircraft
[NASA-TM-106192] p 1005 N93-32351
- BALL, JOHN W., SR.**
System Status - The diagnostic edge of the pilot's associate p 808 A93-37853
- BALLA, R. JEFFREY**
Visualization of a Mach 2 reacting flow using Planar Laser-Induced Fluorescence (PLIF) p 731 N93-26006
- BALLAL, D. R.**
Effects of back-pressure in a lean blowout research combustor
[ASME PAPER 92-GT-81] p 387 A93-19330
Studies of jet thermal stability in a flowing system
[ASME PAPER 92-GT-106] p 401 A93-19344
- BALLER, C. R.**
An experimental study of the effects of deformable tip on the performance of fins and finite wings
[AIAA PAPER 93-3000] p 1053 A93-48190
- BALLESTEROS CASAL, JOSE L.**
The Tenth Conference on Air Navigation - A landmark in the history of civil aviation p 34 A93-12559
- BALLINGER, R. G.**
INCOLOY 908, a low coefficient of expansion alloy for high-strength cryogenic applications. I - Physical metallurgy p 534 A93-25686
- BALLMANN, J.**
Flow computation for the hypersonic configuration ELAC I at low speeds and large incidence p 1238 A93-56036
Computation of viscous hypersonic non-equilibrium blunt body flow p 1238 A93-56038
- BALOEY, A. A.**
Control synthesis with incomplete, complete, and supercomplete measurements p 561 A93-27603
- BALSTER, W. J.**
Application of a sulphur-doped alkane system to the study of thermal oxidation of jet fuels
[ASME PAPER 92-GT-122] p 387 A93-19356
- BALTER-PETERSON, ALIZA**
Arc jet testing in NASA Ames Research Center thermophysics facilities
[AIAA PAPER 92-5041] p 385 A93-22315
Evaluation of 2D ceramic matrix composites in aeroconvective environments p 1212 A93-53459
- BAM-ZELIKOVICH, G. M.**
Boundary layer separation in a corner formed by two planes p 6 A93-10188
- BAMFORD, DOUGLAS L.**
Enhancing availability, performance, and flexibility of air traffic control air-ground services p 887 N93-30353
- BANBAN, B. F.**
A system for washing the combustion chamber nozzles and flow path components of the NK-8-2U engine during service p 373 A93-18357
- BANBAN, V. F.**
Effect of design and service-related factors on the formation of combustion residues in the fuel nozzles of gas turbine engines p 345 A93-18342
Calculation of fuel economy for the Tu-154 aircraft in relation to the washing of the NK-8-2U engine at civil aviation maintenance facilities p 345 A93-18356
- BANCROFT, GORDON V.**
Scientific visualization using the Flow Analysis Software Toolkit (FAST) p 758 N93-25600
- BANDA, SIVA**
Application of structured singular value synthesis to a fighter aircraft p 368 A93-22865
- BANDA, SIVA S.**
Application of structured singular value synthesis to a fighter aircraft p 1130 A93-49594
Full envelope multivariable control law synthesis for a high-performance test aircraft p 1130 A93-49595
Robust, nonlinear, high angle-of-attack control design for a supermaneuverable vehicle
[AIAA PAPER 93-3774] p 1131 A93-51369
- BANDARU, R. V.**
Oxides of nitrogen emissions from turbulent hydrocarbon/air jet diffusion flames, phase 2
[PB93-152478] p 756 N93-26533
- BANDO, TOSHIO**
A method of wind shear detection for powered-lift STOL aircraft
[AIAA PAPER 93-3667] p 1104 A93-48345
Wind-shear endurance capability for powered-lift aircraft
[AIAA PAPER 93-3670] p 1129 A93-48348
- BANDYOPADHYAY, G.**
A Navier-Stokes simulation of vortex shedding from square cylinder in unconfined domain p 538 A93-24084
- BANDYOPADHYAY, PROMODE R.**
Reflection type skin friction meter
[NASA-CASE-LAR-14520-1-SB] p 296 N93-18275
- BANDYOPADHYAY, S.**
A study of the flexural properties of carbon-epoxy composites in certain environments p 390 A93-21999
- BANFORD, MICHAEL P.**
Modal survey of a full-scale F-18 wind tunnel model
[AD-A262482] p 875 N93-29410
- BANGALORE, A.**
Effects of icing on the aerodynamic performance of high lift airfoils
[AIAA PAPER 93-0026] p 259 A93-20144

- BANIEGHBAI, M. R.**
3-dimensional interactions in the rotor of an axial turbine
[AIAA PAPER 93-2255] p 1081 A93-50053
- BANKS-SILLS, LESLIE**
Application of the cyclic J-integral to fatigue crack propagation p 839 N93-27182
- BANKS, DANIEL W.**
Low-speed longitudinal and lateral-directional aerodynamic characteristics of the X-31 configuration [NASA-TM-4351] p 22 N93-11622
- BANKS, DAVID W.**
Tracking flow features using overset grids [AIAA PAPER 93-0197] p 276 A93-22617
- BANKS, H. T.**
Approximation methods for control of structural acoustics models with piezoceramic actuators p 452 A93-23744
Linear quadratic tracking problems in Hilbert space - Application to optimal active noise suppression p 1224 A93-52763
- BANKS, JAMES R.**
Definitional mission for civil aviation master plan for Poland [PB92-213974] p 459 N93-21713
- BANKS, P.**
Small satellites and RPA's in global-change research [AD-A260762] p 755 N93-25837
- BANKSTON, NATHANIEL G.**
Zoning of aircraft: A review of the definitions p 703 N93-24880
- BANUELOS, AEROBEL**
Proposal and preliminary design for a high speed civil transport aircraft. Swift: A high speed civil transport for the year 2000 [NASA-CR-192023] p 335 N93-18049
- BAO, HE-SHENG**
An impact dynamics investigation on some problems in bird strike on windshields of high speed aircraft p 197 A93-15346
- BAO, JINSONG**
Investigation of the dynamic inflow's influence on rotor control derivatives p 266 A93-20802
- BAPU, P. T.**
High voltage quick-disconnect harness system for helmet-mounted displays p 516 A93-25922
- BAR-ITZHACK, ITZHACK Y.**
Observability analysis of piece-wise constant systems. I - Theory p 501 A93-29599
- BAR-NIR, I. M.**
Experience with explosive detection systems in airports p 498 N93-21895
- BAR-SHALOM, YAAKOV**
A multisensor-multitarget data association algorithm for heterogeneous sensors p 439 A93-22899
Performance prediction of the interacting multiple model algorithm p 439 A93-22926
A multisensor-multitarget data association algorithm for heterogeneous sensors p 1020 A93-44168
Performance prediction of the interacting multiple model algorithm p 1167 A93-50638
- BAR, DORON**
A rapid procedure for obtaining time-average interferograms of vibrating bodies p 412 A93-21857
- BARANOV, IU. F.**
Heat exchangers of gas turbine engines p 833 A93-39044
The use of aviation gas-liquid heat exchangers employing heat pipes p 833 A93-39050
- BARANOVSKII, B. V.**
Evaluation of the efficiency of the direct search method in solving the problem of numerical calculation of the complex hydraulic cooling systems of aviation gas turbine engines p 54 A93-12818
- BARANOVSKII, S. I.**
Shock wave ahead of a liquid jet in supersonic cross flow p 477 A93-27605
- BARANOVSKIY, S. I.**
Chemical-kinetics characteristics of combustion in a supersonic turbulent flow p 1018 A93-47512
- BARATA, J. M. M.**
On the analysis of an impinging jet on ground effects p 1260 A93-56339
- BARBE, S.**
Infrared thermography for hot-shot wind tunnel [ONERA, TP NO. 1992-103] p 831 A93-38583
- BARBER, T. J.**
Role of hydrogen/air chemistry in nozzle performance for a hypersonic propulsion system p 359 A93-21668
- BARBERIS, D.**
Experimental study of three-dimensional separation on a large-size model [ONERA, TP NO. 1992-174] p 473 A93-25348
Experimental study of 3-D separation on a large scale model [AIAA PAPER 93-3007] p 1053 A93-48197
- BARBIER, PIERRE**
Using NDT techniques in the maintenance of aeronautical products [REPT-921-430-102] p 88 N93-11587
- BARD, STEVEN**
Three-stage sorption type cryogenic refrigeration systems and methods employing heat regeneration [NASA-CASE-NPO-18366-1-CU] p 216 N93-13422
- BARDAGI, THIERRY**
Advanced SST auxiliary air intakes design and analysis [AIAA PAPER 93-2304] p 1082 A93-50088
- BARDELL, N. S.**
The free vibration of cylindrically-curved rectangular panels p 1022 A93-45113
- BARDINA, JORGE E.**
Turbulence modeling for hypersonic flight [NASA-CR-192288] p 483 N93-20235
- BARDON, M. F.**
Experimental and computational investigation of flow in catalytic monolith channels [ASME PAPER 92-GT-118] p 387 A93-19354
- BARENES, R.**
Investigation of the flow field through a variable pitch fan rotor with an inlet total pressure distortion [ISABE 93-7029] p 1184 A93-54005
- BARILE, EDWARD C.**
Some limitations on the effectiveness of airborne adaptive radar p 501 A93-29596
- BARKAI, S. M.**
Nonlinear rotor-fuselage coupled response to generic periodic control modes using advanced computation techniques p 153 A93-14226
- BARKER, C. O.**
Helicopter crash survival at sea: United States Navy/Marine Corps experience 1977-1990 p 493 N93-19687
- BARKER, DAVID R.**
The dependent converging instrument approach procedure: An analysis of its safety and applicability [DOE/FAA/RD-93/6] p 707 N93-25456
- BARKER, MICHAEL J.**
'No VOC' water-borne corrosion resistant primers for aerospace bonding applications p 1211 A93-53419
- BARKHOUDARIAN, S.**
Advanced instrumentation for next-generation aerospace propulsion control systems [AIAA PAPER 93-2079] p 1154 A93-49906
- BARLOW, JEWEL**
Techniques for designing rotorcraft control systems [NASA-CR-192960] p 729 N93-26046
- BARLOW, JEWEL B.**
An ultralight freeewing aircraft design study [AIAA PAPER 92-4194] p 44 A93-13371
Design of reduced-order observers with precise loop transfer recovery p 184 A93-14587
- BARNA, P. STEPHEN**
Investigations of detail design issues for the high speed acoustic wind tunnel using a 60th scale model tunnel. Part 1: Tests with open circuits [NASA-CR-191671] p 137 N93-14737
Investigations of detail design issues for the high speed acoustic wind tunnel using a 60th scale model tunnel. Part 2: Tests with the closed circuit [NASA-CR-191672] p 137 N93-14738
Nozzle diffuser for use with an open test section of a wind tunnel [NASA-CASE-LAR-14424-1-SB] p 731 N93-25996
- BARNARD, GEORGE A.**
The effect of extreme altitude on parachute filling distance [AIAA PAPER 93-1207] p 702 A93-35158
- BARNES, J.**
A systems dynamics approach to modeling gas turbine combustor wear [ASME PAPER 92-GT-47] p 347 A93-19300
- BARNES, MICHAEL**
Theory and design of adaptive automation in aviation systems [AD-A254595] p 160 N93-12613
- BARNETT, M.**
Analysis of high Reynolds number inviscid/viscid interactions in cascades p 1234 A93-55351
- BARNETT, MARK**
Low-Reynolds-number k-epsilon model for unsteady turbulent boundary-layer flows p 1177 A93-53208
- BARNETT, R. M.**
Prediction of vortex breakdown on a delta wing p 787 N93-27459
- BARNETT, W. M.**
NO(x) scavenging on carbonaceous aerosol surfaces in aircraft exhaust plumes. I [AIAA PAPER 93-2343] p 1164 A93-50117
- BARNHART, D. S.**
Expert system for redundancy and reconfiguration management p 938 A93-42785
- BARNIV, YAIR**
Neural networks application to divergence-based passive ranging [NASA-TM-103981] p 885 N93-29653
Expansion-based passive ranging [NASA-TM-104025] p 994 N93-32348
- BARNWELL, R. W.**
Natural laminar flow and laminar flow control [ISBN 0-387-97737-6] p 859 A93-41776
- BARNWELL, RICHARD W.**
Effect of sidewall suction on flow in two-dimensional wind tunnels p 287 A93-23538
- BARONE, PHILIP A.**
Automated Laser Paint Stripping (ALPS) [SME PAPER AD92-206] p 855 A93-40667
- BARONETS, P. N.**
Modeling of the physicochemical processes of nonequilibrium heat transfer in the subsonic jets of an induction plasmatron p 836 A93-39147
- BAROTH, THOMAS G.**
Cost/weight savings for the V-22 wing stow p 797 A93-35981
- BARQUET, H.**
The development of a crashworthy composite fuselage and landing gear p 799 A93-36001
- BARR, R.**
ELF, VLF and LF radiation from a very large loop antenna with a mountain core p 924 A93-40334
- BARRERE, M.**
Energy management [ISABE 93-7019] p 1195 A93-53995
- BARRETT, DAVID J.**
Damped advanced composite parts p 1253 A93-55871
- BARRETT, DAVID M.**
Current research in oxidation-resistant carbon-carbon composites at NASA. Langley Research Center p 74 N93-12456
- BARRETT, RON**
Actuation strain decoupling through enhanced directional attachment in plates and aerodynamic surfaces p 394 A93-17727
On the aerodynamics and performance of active vortex generators [AIAA PAPER 93-3447] p 979 A93-47234
- BARRIE, DOUGLAS**
Hovering decisions p 46 A93-13700
Advancing helicopters p 327 A93-21836
Fighting for air p 1243 A93-54650
- BARRON, R. M.**
Numerical solution of transonic full-potential-equivalent equations in von Mises co-ordinates p 111 A93-14080
- BARRON, W. D.**
Acoustic properties of supersonic helium/air jets at low Reynolds numbers p 446 A93-19160
- BARROW, PETER**
Getting it together p 78 A93-11682
- BARROWS, T.**
Aerodynamic forces on maglev vehicles [PB93-154813] p 782 N93-27413
- BARRY, JOHN W.**
Decay of aircraft vortices near the ground p 961 A93-45751
- BARSCHDORFF, DIETER**
Neural network based condition monitoring p 230 N93-15183
- BARSON, JOHN V.**
The effectiveness of airbags in reducing the severity of head injury from gunsight strikes in attack helicopters p 494 N93-19691
- BARSZCZ, ERIC**
Dynamic overset grid communication on distributed memory parallel processors [AIAA PAPER 93-3311] p 1036 A93-45007
- BARTA, A. B.**
Development of an advanced exhaust mixer for a high bypass ratio turbofan engine [AIAA PAPER 93-2435] p 1118 A93-50188
- BARTEL, TIMOTHY J.**
DSMC simulation of ionized rarefied flows [AIAA PAPER 93-3095] p 1061 A93-48269
- BARTELOS, G.**
Ageing aircraft research in the Netherlands [NLR-TP-91443-U] p 999 N93-32203
- BARTER, JOHN**
Hermes CX-7: Air transport system design simulation [NASA-CR-192082] p 335 N93-18056
- BARTER, S. A.**
Aspects of fatigue affecting the design and maintenance of modern military aircraft p 1043 A93-52548
- BARTH, G.-J.**
Ground installations for preparation and evaluation of flight tests p 1014 N93-31274

BARTH, TIMOTHY J.

- A solution scheme for the Euler equations based on a multi-dimensional wave model
[AIAA PAPER 93-0065] p 261 A93-20178
- Recent developments in high order K-exact reconstruction on unstructured meshes
[AIAA PAPER 93-0668] p 475 A93-25546
- A finite-volume Euler solver for computing rotary-wing aerodynamics on unstructured meshes
p 765 A93-35935
- A finite-volume Euler solver for computing rotary-wing aerodynamics on unstructured meshes
p 874 A93-43782

BARTHELEMY, J.-F. M.

- Multidisciplinary design integration system for a supersonic transport aircraft
[AIAA PAPER 92-4841] p 324 A93-20296

BARTHELEMY, JEAN-FRANCOIS M.

- Sensitivity analysis of aeroelastic response of a wing using piecewise pressure representation
[AIAA PAPER 93-1645] p 742 A93-34170
- Sensitivity analysis of flutter response of a typical section and a wing in transonic flow
[AIAA PAPER 93-1646] p 742 A93-34171
- Sensitivity analysis of a wing aeroelastic response
p 958 A93-45142

BARTHELEMY, ROBERT R.

- The National Aero-Space Plane program: A revolutionary concept
p 511 N93-19908

BARTHOLOMEW, P.

- Vibration reduction for helicopter airframes - An application of the general-purpose structural optimization program STARS
[AIAA PAPER 92-4782] p 326 A93-20372

BARTHOLOMEW, REDGE

- Design, capabilities, and performance of the miniaturized airborne GPS receiver
p 32 A93-11014

BARTHOLOMEW, REDGE G.

- Performance analysis of a miniaturized airborne GPS receiver
p 313 A93-21147

BARTKO, J.

- A review of the development of a luggage explosive detection system
p 497 N93-21862

BARTLER, TOMASZ

- Elementary stall flutter of an aircraft wing
p 545 A93-27289
- ONERA calculation model of dynamic flow separation on an airfoil section
p 1238 A93-56212
- A numerical study of aerodynamic wing design for supercritical conditions of an advanced training and military aircraft
p 1238 A93-56213
- Numerical minimization of the moment coefficient of a supercritical airfoil section
p 1238 A93-56214

BARTLETT, C. S.

- Icing testing of a large full-scale inlet at the Arnold Engineering Development Center
[AIAA PAPER 93-0299] p 376 A93-22697

BARTLETT, C. T.

- Displaying the night
p 1244 A93-55297

BARTLETT, D. W.

- Laminar flow flight experiments - A review
p 890 A93-41778

BARTOLOTTA, PAUL A.

- Stirling engine - Available tools for long-life assessment
p 195 A93-13824

BARTON, P.

- Royal Naval helicopter ditching experience
p 492 N93-19684

BARUZZI, G.

- Some special purpose preconditioners for conjugate gradient-like methods applied to CFD
p 772 A93-38638

BARWEY, DINESH

- Effects of dynamic stall and structural modeling on aeroelastic stability of elastic bending and torsion of hingeless rotor blades with experimental correlation
p 794 A93-35902
- Dynamic stall effects on hingeless rotor stability with experimental correlation
p 129 N93-13010

BARYSHEV, E. E.

- Resource conservation and improvement of the service characteristics of castings of high-temperature nickel alloys through a high-temperature melt treatment
p 824 A93-36718

BARYSHEV, E. S.

- Improvement of rotating brushes for surface cleaning
p 396 A93-18371

BARYSHEV, EVGENII S.

- Maintenance of the liquid and gas systems of the Il-76 aircraft
p 804 A93-39203

BASCOM, WILLARD D.

- Effects of intra- and inter-laminar resin content on the mechanical properties of toughened composite materials
p 921 N93-30845

BASEDOW, R.

- The HYDICE instrument design and its application to planetary instruments
p 842 N93-28766

BASELEY, H. M.

- Advanced three-shaft engines - Configured for reliability, efficiency and growth
p 53 A93-12236
- Advanced three-shaft engines: Configured for reliability, efficiency, and growth
[PNR-90986] p 58 N93-11068

BASHARIN, S. V.

- Evaporation and specific heats of motor fuels
p 71 A93-12823

BASHFORD, P. J.

- The civil scene - The authorities re-appraisal of ageing aircraft
p 1229 A93-54895

BASHKIN, V. A.

- Supersonic flow of a gas over a semi-infinite plate with small-scale harmonic spanwise oscillations
p 775 A93-39118

BASHKIRTSEV, A. V.

- Calculating the cutting depth during the milling of large gas turbine engine blades
p 545 A93-27628

BASILE, M.

- An integrated weather channel designed for an up-to-date ATC radar system
p 929 A93-43434

BASS, J. M.

- H-P adaptive methods for finite element analysis of aerothermal loads in high-speed flows
[NASA-CR-189739] p 420 N93-18093
- Advanced adaptive computational methods for Navier-Stokes simulations in rotorcraft aerodynamics
[NASA-CR-192282] p 483 N93-20256

BASS, STEVEN M.

- Using aerodynamic analysis codes to assist in structural design and optimization of ducted rotor/wing blades
[AIAA PAPER 92-4280] p 44 A93-13353
- Advanced technology Tilt Wing study
[AIAA PAPER 92-4237] p 44 A93-13359
- Low-speed wind tunnel test results of the Canard Rotor/Wing concept
[AIAA PAPER 93-3412] p 975 A93-47209

BASS, V. P.

- Certain improved algorithms for calculating the aerodynamic characteristics of flight vehicles in free-molecular flow
p 1090 A93-51872

BASSANINI, PIERO

- Free streamline-boundary layer analysis for separated flow over an airfoil
p 1239 A93-56327

BASSEZ, PASCAL

- Eurofar rotor aerodynamic tests
[ONERA, TP NO. 1992-173] p 475 A93-26880

BASSI, F.

- Secondary flows in a transonic cascade - Validation of a 3-D Navier-Stokes code
[ASME PAPER 92-GT-62] p 247 A93-19312
- A Navier-Stokes solver with different turbulence models applied to film-cooled turbine cascades
p 904 N93-29962

BASSON, A. H.

- Investigation of tip clearance phenomena in an axial compressor cascade using Euler and Navier-Stokes procedures
[ASME PAPER 92-GT-299] p 255 A93-19489

BASSON, ANTON H.

- Grid generation for three-dimensional turbomachinery geometries including tip clearance
p 270 A93-21658

BASTART, J.

- Optimization and sensitivity computations for the conception of internal ventilation system in the aircraft engine
[ETN-93-93375] p 521 N93-20913

BASU, AMIT J.

- The role of noise in two-dimensional vortex merging
p 408 A93-19967

BASU, P.

- Hysteresis and bristle stiffening effects of conventional brush seals
[AIAA PAPER 93-1996] p 1153 A93-49839

BASU, S.

- Flow studies in ducted twin-rotor contra-rotating axial flow fans
[ASME PAPER 92-GT-390] p 258 A93-19545

BATES, BRENT L.

- Multiblock Navier-Stokes solutions about the F/A-18 wing-LEX-fuselage configuration
p 767 A93-37378

BATES, L. B.

- Starting and test rhombus characteristics of two-dimensional supersonic free-jet nozzle/generic supersonic aircraft inlet configurations
[AIAA PAPER 92-5091] p 273 A93-22361

BATES, PRESTON R.

- A damage tolerance/life processor for structural integrity and force management
p 507 A93-27962

BATILL, S. M.

- Detailed near surface flow about yawed, stranded cables
[AD-A257382] p 418 N93-15857

BATINA, JOHN T.

- A gridless Euler/Navier-Stokes solution algorithm for complex-aircraft applications
[AIAA PAPER 93-0333] p 268 A93-21107
- Spatial adaptation procedures on tetrahedral meshes for unsteady aerodynamic flow calculations
[AIAA PAPER 93-0670] p 269 A93-21116
- Wing flutter boundary prediction using unsteady Euler aerodynamic method
[AIAA PAPER 93-1422] p 739 A93-33975
- Implicit upwind solution algorithms for three-dimensional unstructured meshes
p 691 A93-35607
- Results from a conical Euler methodology developed for unsteady vortical flows
p 692 A93-35612
- Calculation of AGARD Wing 445.6 flutter using Navier-Stokes aerodynamics
[AIAA PAPER 93-3476] p 981 A93-47255
- Three-dimensional time-marching aerodynamic analyses using an unstructured-grid Euler method
p 1100 A93-49012

- Conical Euler analysis and active roll suppression for unsteady vortical flows about rolling delta wings
[NASA-TP-3259] p 701 A93-26134
- Reynolds number influences in aeronautics
[NASA-TM-107730] p 989 N93-31732

BATT, R. G.

- Some measurements on dependence of rectangular cylinder drag on elevation
p 1025 A93-45745

BATTS, G. W.

- Natural environment application for NASP-X-30 design and mission planning
[AIAA PAPER 93-0851] p 531 A93-24915

BAUCHAU, O. A.

- On design and optimization of curved composite beams
p 826 A93-35953
- A multibody formulation for helicopter structural dynamic analysis
p 892 A93-43776

BAUCHAU, OLIVIER A.

- Dynamic analysis of rotor flexbeams based on nonlinear anisotropic shell models
p 743 A93-34261

BAUCOM, ROBERT M.

- Experimental and analytical investigation of dynamic characteristics of extension-twist-coupled composite tubular spars
[NASA-TP-3225] p 553 N93-20585

BAUDOIN, C.

- Ramjet NOx emission - Use of a 3D CFD method for the combustor design of a super/hyper-sonic transport propulsion system
[ASME PAPER 92-GT-255] p 353 A93-19464

BAUDOIN, CHRISTOPHE

- Direct numerical simulation of nitric oxide evolution in underexpanded jets
[ASME PAPER 92-GT-372] p 355 A93-19534

BAUDOUY, B.

- Infrared thermography characterization of Goertler vortex type patterns in hypersonic flows
[ONERA, TP NO. 1993-13] p 925 A93-41029

BAUDRY, Y.

- Optimization and sensitivity computations for the conception of internal ventilation system in the aircraft engine
[ETN-93-93375] p 521 N93-20913

BAUER, ANDREW B.

- Zero-thrust glide testing for drag and propulsive efficiency of propeller aircraft
p 995 A93-45143

BAUER, J.

- Allowable compression strength for CFRP-components of fighter aircraft determined by CAI-test
[MBB-FE-221-S-PUB-0483] p 537 N93-21462
- Allowable compression strength for CFRP-components of fighter aircraft determined by CAI-test
p 537 N93-21531

- Consideration of impact damages by dimensioning CFC (Carbon Fiber Reinforced Composites) components
[MBB-FE-221-S-PUB-0501] p 1018 N93-31044

BAUER, NIKKOL

- Exodus: Prime Mover
[NASA-CR-192051] p 332 N93-17803

BAUER, R. C.

- A review of supersonic combustion research at AEDC with hypersonic application
[AIAA PAPER 93-2326] p 1116 A93-50106

BAUER, STEVEN X. S.

- Effect of planform and body on supersonic aerodynamics of multibody configurations
[NASA-TP-3212] p 19 N93-10824

BAUGHAN, JIM

- TBD(exp 3)
[NASA-CR-192075] p 335 N93-18054

- BAULD, N. R., JR.**
Global/local interlaminar stress analysis of a grid-stiffened composite panel p 548 A93-28543
Interlaminar stress analysis at the skin/stiffener interface of a grid-stiffened composite panel [NASA-CR-192177] p 393 N93-17920
- BAUM, B. A.**
Resource conservation and improvement of the service characteristics of castings of high-temperature nickel alloys through a high-temperature melt treatment p 824 A93-36718
- BAUM, JOSEPH D.**
Numerical solution of the Euler equations for complex aerodynamic configurations using an edge-based finite element scheme [AIAA PAPER 93-2933] p 1046 A93-48131
Numerical simulation of a blast inside a Boeing 747 [AIAA PAPER 93-3091] p 1099 A93-48265
- BAUMAN, A. V.**
Pressure pulsations on a delta wing in incompressible flow p 1069 A93-48912
- BAUMANN, DANIEL D.**
Mathematical phenomenology for thrust-vectoring-induced agility comparisons p 525 A93-28613
- BAUMANN, JEFFREY ALLEN**
Aircraft landing gear shimmy p 340 N93-19029
- BAUMANN, PIERRE**
Photoluminescent thermography - Feasibility study with pointwise measurements p 211 A93-16861
Photoluminescent thermography in hypersonic blowdown wind tunnel: Feasibility study with pinpoint measurement [ONERA-NT-1992-8] p 297 N93-18617
- BAUMBICK, ROBERT J.**
Status of the Fiber Optic Control System Integration (FOCSI) program [NASA-TM-106151] p 841 N93-28053
- BAUMGARDNER, DARREL**
A technique for the measurement of cloud structure on centimeter scales p 1158 A93-51243
- BAUMINGER, S.**
Pilot test of a low Reynolds number DTE-airfoil [AIAA PAPER 93-0643] p 464 A93-24758
- BAURLE, R. A.**
A k-omega multivariate beta PDF for supersonic turbulent combustion [AIAA PAPER 93-2197] p 1154 A93-50009
Modeling of turbulent supersonic H2-air combustion with a multivariate beta PDF [AIAA PAPER 93-2198] p 1155 A93-50010
Modeling of turbulent supersonic H2-air combustion with an improved joint beta PDF [NASA-CR-191929] p 391 N93-16389
A k-omega-multivariate beta PDF for supersonic combustion [NASA-CR-191930] p 537 N93-21749
- BAUSCHLICHER, CHARLES W., JR.**
Theoretical study of the bond dissociation energies of propyne (C3H4) p 230 A93-14099
- BAVENDIEK, KLAUS**
Realization of real time graphics in vehicles with high dynamic motion [ETN-93-92739] p 443 N93-18630
- BAVUSO, SALVATORE J.**
Characterization of the faulted behavior of digital computers and fault tolerant systems p 1224 A93-52762
- BAWCOM, D. W.**
Status of the NASA Balloon Program p 1 A93-11365
- BAXA, ERNEST G., JR.**
Signal processing for airborne doppler radar detection of hazardous wind shear as applied to NASA 1991 radar flight experiment data p 490 N93-19612
- BAXENDALE, A. J.**
The use of a deep honeycomb to achieve high flow quality in the ARA 9 ft x 8 ft Transonic Wind Tunnel p 190 A93-14276
- BAYLISS, ALVIN**
On the coupling between a supersonic boundary layer and a flexible surface p 243 A93-19132
- BAYLISS, E.**
Integrated use of GPS and GLONASS in civil aviation navigation. II - Experience with GLONASS p 313 A93-21142
Receiver Autonomous Integrity Monitoring (RAIM) of GPS and GLONASS p 993 A93-46891
- BAYSAL, O.**
Flow analysis and design optimization methods for nozzle-afterbody of a hypersonic vehicle p 1073 A93-49531
- BAYSAL, OKTAY**
Improving the efficiency of aerodynamic shape optimization procedures [AIAA PAPER 92-4697] p 264 A93-20309
- Aerodynamic shape optimization via sensitivity analysis on decomposed computational domains [AIAA PAPER 92-4698] p 265 A93-20310
Airfoil shape optimization using sensitivity analysis on viscous flow equations p 682 A93-33755
Aerodynamic shape optimization using preconditioned conjugate gradient methods [AIAA PAPER 93-3322] p 952 A93-45016
Preconditioned domain decomposition scheme for three-dimensional aerodynamic sensitivity analysis p 957 A93-45096
Kinematic domain decomposition for boundary-motion-induced flow simulations p 1028 A93-46811
Dynamic-overlapped-grid simulation of aerodynamically determined relative motion [AIAA PAPER 93-3018] p 1055 A93-48205
- BAYYUK, SAMI A.**
A simulation technique for 2-D unsteady inviscid flows around arbitrarily moving and deforming bodies of arbitrary geometry [AIAA PAPER 93-3391] p 956 A93-45082
- BAZZIDI-TEHRANI, F.**
Impingement/effusion cooling p 932 N93-29954
- BEACH, T. A.**
Aeroloading and secondary flows in a transonic mixed flow turbine stage [ASME PAPER 92-GT-72] p 248 A93-19322
Three-dimensional analysis of the Pratt and Whitney alternate design SSME fuel turbine p 1031 N93-31584
- BEAL, ERNA J.**
Liquid flow reactor and method of using [AD-D015392] p 222 N93-15232
- BEAL, T. R.**
Digital simulation of atmospheric turbulence for Dryden and von Karman models p 416 A93-23517
- BEALE, D. K.**
Subscale validation of a freejet inlet-engine test capability [AIAA PAPER 93-2179] p 1138 A93-49991
- BEAM, JERRY E.**
Design of a hydrogen test facility p 532 A93-25993
- BEAM, SHERILEE F.**
The NASA High-Speed Research Program p 330 N93-16761
- BEAMAN, J. J.**
Comparison of nonlinear tracking controllers for a compressible flow process p 66 A93-12224
- BEAN, D. E.**
The suppression of single-fin buffeting using tangential leading edge blowing on a delta wing p 270 A93-21677
- BEAN, DAVID E.**
A vortex control technique for the attenuation of fin buffet p 121 A93-14408
An experimental investigation of twin fin buffeting and suppression [AIAA PAPER 93-0054] p 261 A93-20167
- BEARDEN, HILLMAN E.**
Unusual attitudes - Helicopters and instrument flight p 1240 A93-54550
- BEATTY, JOHN**
Hydrogen-induced stress corrosion cracking susceptibility analysis of pitch links from the AH-64 Apache helicopter [AD-A260692] p 736 N93-25895
- BEAUCHAMP, CHARLES H.**
Articulated fin/wing control system [AD-D015712] p 909 N93-29278
- BEAUMIER, P.**
Validation of R85/METAR on the Puma RAE flight tests [ONERA, TP NO. 1992-123] p 802 A93-38597
Study of soft-in-torsion blades - ROSOH operation [ONERA, TP NO. 1992-124] p 803 A93-38598
- BECHER, P. E.**
Neutron-induced single event upsets in static RAMs observed at 10 KM flight altitude p 1158 A93-50561
- BECHTEL, G. S.**
Probabilistic turbine blade tip durability analysis [AIAA PAPER 93-1383] p 719 A93-33946
- BECHTOLD, J. K.**
Analysis of thermal ignition in supersonic flat-plate boundary layers p 769 A93-37933
- BECK, CORIN P.**
An analysis of helicopter dynamic response to turbulence using fuselage and blade element atmospheric sampling techniques [AIAA PAPER 92-4148] p 43 A93-13314
- BECK, JEFFREY A.**
Agility potential [SAE PAPER 921016] p 185 A93-14645
- BECK, W. H.**
A laser induced fluorescence system for the high enthalpy shock tunnel (HEG) in Goettingen p 1024 A93-45506
- BECKER, A.**
DLR research program overview on airport surface movement guidance and control p 499 A93-27912
Testing concept of a taxiing control system, summary p 1010 N93-31278
- BECKER, K.**
MELINA - A multi-block, multi-grid 3D Euler code with sub block technique for local mesh refinement p 115 A93-14217
Integration of high bypass ratio engines on modern transonic wings for regional aircraft p 506 A93-27479
- BECKER, LAWRENCE E.**
ADDRAS - An integrated systems approach p 562 A93-29423
- BECKETT, NEVILLE**
Backfire unveiled p 997 A93-46024
- BECKMAN, BRIAN C.**
Virtual reality flight control display with six-degree-of-freedom controller and spherical orientation overlay [NASA-CASE-1973-1-CU] p 897 N93-30416
- BECKMANN, MARTIN**
Carrier wave signals interfering with Loran-C [ETN-92-92528] p 318 N93-17584
- BECKWITH, IVAN E.**
Goertler instability and hypersonic quiet nozzle design p 480 A93-29155
- BECKLE, J. P.**
Recent developments in low-speed TPS-testing for engine integration drag and installed thrust reverser simulation p 160 N93-13207
- BECS, GEORGES A.**
Optimization of blade arrangement in a randomly mistuned cascade using simulated annealing [AIAA PAPER 93-2254] p 1115 A93-50052
- BEDARD, A. J., JR.**
Atmospheric turbulence aloft - A review of possible methods for detection, warning, and validation of prediction models [AIAA PAPER 93-0847] p 557 A93-24914
- BEDARD, ALFRED J., JR.**
Potential aircraft hazards in the vicinity of convective clouds - A review from the perspective of a scale-model study p 427 A93-22116
- BEECK, A.**
The aerodynamic effect of coolant ejection in the leading edge region of a film-cooled turbine blade p 904 N93-29958
- BEEMAN, DAVID**
A procedure for defining lightning risk to air vehicles p 703 N93-24885
- BEEVERS, C. J.**
Short fatigue crack growth in a nickel-base superalloy at room and elevated temperature [PNR-90892] p 72 N93-11031
- BEGGS, ROBERT M.**
MIDAS technology transfer p 845 A93-35920
- BEGUIRISTAIN, R.**
X ray microscopy resource center at the Advanced Light Source [DE93-010449] p 911 N93-29869
- BEHR, V. L.**
The development of a parachute system for aerial delivery from high speed cargo aircraft [DE93-008339] p 790 N93-29035
- BEHR, VANCE L.**
The development of a parachute system for aerial delivery from high speed cargo aircraft [AIAA PAPER 93-1232] p 703 A93-35174
- BEIN, T.**
Hypersonic flutter of a curved shallow panel with aerodynamic heating [AIAA PAPER 93-1318] p 829 A93-37428
Rotor/stator flow coupling in turbomachines p 1232 A93-54647
- BEKEBREDE, GERARD**
Technical solutions to reduce and to control the noise load in the Netherlands p 564 A93-28492
- BEKER, BENJAMIN**
Effects of substrate anisotropy on coupled bilateral finlines p 208 A93-15409
- BEKHMET'EV, V. I.**
Single-impact calibrated electromagnetic tightening of long-life bolted joints in aviation structures p 745 A93-35277
Effect of a combination of design and process-related factors on the fatigue strength of bolted joints in acoustically loaded aircraft structures p 745 A93-35278

- BEKKI, S.**
Potential impact of combined NO(x) and SO(x) emissions from future High Speed Civil Transport aircraft on stratospheric aerosols and ozone p 753 A93-35372
- BELANGER, J.**
Performance data of the new free-piston shock tunnel T5 at GALTIT p 1011 A93-45498
- BELCASTRO, CELESTE M.**
A monitor for the laboratory evaluation of control integrity in digital control systems operating in harsh electromagnetic environments [NASA-TM-4402] p 65 N93-12304
- BELCASTRO, CHRISTINE M.**
A problem formulation for glideslope tracking in wind shear using advanced robust control techniques [NASA-TM-104164] p 64 N93-11176
- BELCHER, JOHN M.**
Engineering management consideration for an integrated aeronautical mobile satellite service p 933 N93-30337
- BELCHER, P. J.**
Takeoff and landing analysis methodology for an airbreathing space booster p 914 A93-42927
- BELDERRAIN, JOSE L. R.**
Optimal performance of airplanes flying through wind shear [AIAA PAPER 93-3846] p 1102 A93-51480
- BELETE, HAILU**
RTJ-303: Variable geometry, oblique wing supersonic aircraft [NASA-CR-192054] p 337 N93-18166
- BELETSKIY, V. V.**
Effect of the atmosphere density gradient on aerodynamic stabilization p 1252 A93-55034
- BELGER, L.**
Ground Movement and Control System (GMCS) p 499 A93-27913
- BELIK, V. V.**
Grid-characteristic method for calculating a three-dimensional boundary layer on the bounding surfaces of the blade passage of a turbomachine p 13 A93-12808
- BELK, D. M.**
Numerical investigation of subsonic and supersonic asymmetric vortical flow p 961 A93-45727
- BELK, DAVY M.**
Visualization of vortical flows with yet another post-processor [AIAA PAPER 93-0222] p 415 A93-22638
- BELL, JOHN B.**
Adaptive Cartesian grid methods for representing geometry in inviscid compressible flow [AIAA PAPER 93-3385] p 955 A93-45076
- BELL, R. E.**
Airborne gravimetry from a light aircraft p 1245 A93-55972
- BELL, WAYNE**
High Capacity Voice Recorder (HCVR) Operational Test and Evaluation (OT/E) integration test report [DOT/FAA/CT-TN92/30] p 88 N93-11460
- BELL, WAYNE E.**
Data Multiplexing Network (DMN). Phase 3: Equipment Operational Test and Evaluation (OT/E) integration test report [DOT/FAA/CT-TN92/49] p 503 N93-20612
The Data Multiplexing Network (DMN) phase 3 Extended Distance Data Cable (EDDC) test and evaluation [DOT/FAA/CT-TN93/11] p 752 N93-26160
Data Multiplexing Network (DMN) equipment Operational Test and Evaluation (OT/E) integration test report [AD-A263172] p 942 N93-29490
- BELL, WILLIAM A.**
Investigation of the radiance from the leading edge of a wing [AIAA PAPER 93-2728] p 1039 A93-46482
LV software for supersonic flow analysis [NASA-CR-190911] p 16 N93-10069
- BELLAICHE, PASCALE**
Thermometry inside a swirling turbulent flame - CARS advantages and limitations p 1146 A93-51634
- BELLEUDY, JACQUES**
Influence of coupling incidence and velocity variations on the airfoil dynamic stall p 767 A93-35999
- BELO, E. M.**
Initial development of a research flight simulator software [AIAA PAPER 93-3590] p 1223 A93-52683
- BELOGLAZKIN, A. N.**
Effect of airfoil porosity on the shock wave position and intensity at transonic velocities p 241 A93-18222
- BELOTSERKOVETS, I. S.**
Calculation of the irregular interaction of shock waves p 691 A93-35339
- BELOUS, V. A.**
A study of the effect of the static aeroelasticity of a swept wing on its weight response p 801 A93-36798
- BELOZEROV, L. G.**
Problems of the organization of the mass testing of large structural elements of aircraft using testing machines p 821 A93-36791
A procedure for the thermal and strength testing of radiotransparent shells p 1209 A93-52976
- BELYAEV, D. V.**
Estimation of the change of axial-flow compressor characteristics during long-term service p 1193 A93-52949
- BELYTSCHKO, T.**
Stochastic computational mechanics for aerospace structures p 78 A93-12157
- BEN-NETICHA, Z.**
Analysis of flight flutter test data p 523 A93-23839
- BENCHERIF, L.**
Inverse problem using S2-S1 approach for the design of the turbomachine with splitter blades p 971 A93-46929
- BENDAHAN, JOSEPH**
Explosive detection system based on Electronic Neutron Generator (ENG) p 497 A93-21870
- BENDER, K.**
Development and flight testing of a fault-tolerant fly-by-light yaw control system p 1010 N93-31280
- BENDIKSEN, ODDVAR O.**
Transonic panel flutter [AIAA PAPER 93-1476] p 829 A93-37438
Nonclassical aileron buzz in transonic flow [AIAA PAPER 93-1479] p 829 A93-37439
Unsteady transonic two-dimensional Euler solutions using finite elements p 778 A93-39412
- BENEDEK, K. R.**
Improved selective catalytic NOx control technology for compressor station reciprocating engines [PB93-158566] p 755 N93-26529
- BENGELINK, R. L.**
The value of a computational/experimental partnership in aerodynamic design p 114 A93-14215
- BENJAMIN, M. A.**
Initial development of the two-dimensional ejector shear layer - Experimental results [AIAA PAPER 93-2440] p 1118 A93-50192
Comparison of the initial development of shear layers in two-dimensional and axisymmetric ejector configurations [AIAA PAPER 93-2441] p 1119 A93-50193
- BENNE, M. E.**
Data analysis techniques for pressure- and temperature-sensitive paint [AIAA PAPER 93-0176] p 414 A93-22605
- BENNETT, A. G.**
Construction of a one-third scale model of the NASP [AIAA PAPER 93-0427] p 386 A93-23345
- BENNETT, J. C., JR.**
Vortical and turbulent structure of a lobed mixer free-shear layer [AIAA PAPER 93-0219] p 415 A93-22635
- BENNETT, PETER J.**
The use of digital map data to provide enhanced navigation and displays for poor weather penetration and recovery p 992 A93-45165
- BENNETT, R. A.**
Robotic aircraft refueling - A concept demonstration p 846 A93-37041
- BENNETT, ROBERT M.**
Experimental unsteady pressures at flutter on the Supercritical Wing Benchmark Model [AIAA PAPER 93-1592] p 683 A93-34123
Analysis of aeroelastic and resonance responses of a wind tunnel model support system p 1013 A93-47022
- BENNEY, RICHARD J.**
A computational model that couples aerodynamic and structural dynamic behavior of parachutes during the opening process [AD-A264115] p 877 N93-30119
- BENSI, G.**
New developments with the V2500 engine [ISABE 93-7085] p 1202 A93-54061
- BENSON, C. E.**
Improved selective catalytic NOx control technology for compressor station reciprocating engines [PB93-158566] p 755 N93-26529
- BENSON, PAUL**
Recent developments in compressor-based Joule-Thomson cooling p 547 A93-28244
- BENSON, RICHARD**
SIR technology helps ensure safe landings for NASA p 384 A93-21765
- BENSON, RUSTY A.**
Time-accurate simulation of a self-excited oscillatory supersonic external flow with a multi-block solution-adaptive mesh algorithm [AIAA PAPER 93-3387] p 956 A93-45078
Numerical simulations of the unstart phenomenon in a supersonic inlet/diffuser [AIAA PAPER 93-2239] p 1081 A93-50041
- BENSON, T. J.**
AGARD WG13 aerodynamics of high speed air intakes: Assessment of CFD results p 215 N93-13220
- BENTO COELHO, J. L.**
Air traffic noise monitoring in and around Lisbon Airport p 564 A93-28494
- BENTZ, JOHN C.**
Fuel cell powered electric propulsion for HALE aircraft [ASME PAPER 92-GT-404] p 356 A93-19553
- BENZ, E.**
The aerodynamic effect of coolant ejection in the leading edge region of a film-cooled turbine blade p 904 N93-29958
- BERCHOWITZ, DAVID M.**
Free-piston Stirling coolers for intermediate lift temperatures p 543 A93-26062
- BERCHTOLD, G.**
The integrated design and manufacturing of composite structures for aircraft using an advanced tape layering technology [MBB-LME-251-S-PUB-0491-A] p 515 N93-21401
- BERDAHL, C. H.**
Eduction of swirling structure using the velocity gradient tensor p 416 A93-23547
- BERDNIKOV, V. V.**
Dynamic processes in the powerplants and power-generating equipment of flight vehicles p 832 A93-39027
- BERENS, A. P.**
Risk analysis for aging aircraft fleets p 1025 A93-45775
- BERESLAVSKIY, EH. N.**
Some Fuchs-type equations in fluid mechanics p 1165 A93-48967
- BEREZIN, CHARLES R.**
Aerodynamic and wake methodology evaluation using model UH-60A experimental data p 767 A93-35997
- BERG, H. P.**
Heat transfer and material temperature conditions in the leading edge area of impingement-cooled turbine vanes [ISABE 93-7076] p 1220 A93-54052
- BERG, MARTIN C.**
Optimal discrete-time dynamic output-feedback design - A w-domain approach p 757 A93-34536
- BERG, RICHARD L.**
Mathematical model of frost heave and thaw settlement in pavements [CRREL-REPT-93-2] p 912 N93-30103
- BERGAMINI, LORENZO**
A comparison of 'new' and 'old' flux-splitting schemes for the Euler equations [AIAA PAPER 93-0876] p 470 A93-24937
- BERGEN, W. R.**
Automated Weather Distribution System (AWDS) for support of global aviation p 428 A93-22134
- BERGER, MARSHA J.**
3D automatic Cartesian grid generation for Euler flows [AIAA PAPER 93-3386] p 956 A93-45077
- BERGER, STANLEY A.**
Vortex breakdown incipience: Theoretical considerations [NASA-CR-189734] p 290 N93-16627
- BERGIN, A. L.**
Application of laminar flow to aero engine nacelles p 128 A93-17256
Application of laminar flow to aero engine nacelles [PNR-90916] p 20 N93-11020
- BERGMAN, MAGNUS**
A family of multiblock codes for computational aerothermodynamics - Application to complete vehicle hypersonic flows [AIAA PAPER 93-3042] p 1056 A93-48223
- BERKCAN, E.**
Optical temperature compensation schemes of spectral modulation sensors for aircraft engine control p 1105 A93-49471
Optical sensors and multiplexing for aircraft engine control p 1105 A93-49474
Sensors with centroid based common sensing scheme and their multiplexing p 1192 A93-52994
- BERKE, ANTHONY**
The Orlando TDWR testbed and airborne wind shear date comparison results p 145 N93-14851
- BERKE, LASZLO**
Application of artificial neural networks to the design optimization of aerospace structural components [NASA-TM-4389] p 555 N93-21831

- BERKUT, V. D.**
Effect of the formation of excited oxygen molecules on the kinetics of exchange reactions and the heat flux during braking in the upper layers of the atmosphere
p 1070 A93-48975
- BERLIN, BRETT R.**
Machining cost comparison of silicon carbide discontinuously reinforced aluminum, unreinforced aluminum, and titanium
[SME PAPER EM92-252] p 925 A93-40656
- BERMAN, ALEX**
Dynamic System Coupler Program (DYSCO 4.1). Volume 1: Theoretical manual
[AD-B131156L] p 848 N93-27531
Dynamic System Coupler Program (DYSCO 4.1). Volume 2: User's manual
[AD-B131157L] p 848 N93-27589
Dynamic System Coupler Program (DYSCO 4.1). Volume 3: User's manual supplement
[AD-B131158L] p 848 N93-27590
- BERNARD, PIERRE**
High temperature heat exchangers for gas turbines and future hypersonic air breathing propulsion
[ONERA, TP NO. 1993-75] p 1218 A93-53596
- BERNHARDT, J. E.**
The effect of Reynolds number on vortex asymmetry about slender bodies
p 475 A93-26176
- BERNHARDT, JOHN**
The effect of Reynolds number on control of forebody asymmetry by suction and bleed
[AIAA PAPER 93-3265] p 968 A93-46831
- BERNT, MARVIN**
IR window damage measured by reflective scatter
p 851 A93-39544
- BEROUL, FREDERIC**
Eurofar rotor aerodynamic tests
[ONERA, TP NO. 1992-173] p 475 A93-26880
- BERRY, B. F.**
A prediction model for noise from low-altitude military aircraft
[AD-A262494] p 852 N93-27662
- BERRY, C. M.**
Geometry based Delaunay tetrahedralization and mesh movement strategies for multi-body CFD
[AIAA PAPER 92-4575] p 15 A93-13309
- BERRY, CURTIS**
Experiences in fabrication of a waverider model for wind tunnel testing
[AIAA PAPER 93-0510] p 328 A93-23257
- BERRY, HENRY K.**
Robotic aircraft painting with SAFARI
[SME PAPER AD92-198] p 855 A93-40662
- BERRY, J. D.**
Digital resolver for helicopter model blade motion analysis
p 830 A93-37878
- BERRY, ROBERT**
Linear motor driven Stirling coolers for military and commercial applications
p 543 A93-26064
- BERRY, W.**
Computational aerothermodynamics for 2D and 3D space vehicles
p 1073 A93-49533
- BERSHDER, D.**
Nonequilibrium shock layer radiation in a simulated Titan atmosphere
p 1233 A93-54805
- BERTELROD, A.**
Design of a wing shape for study of hypersonic crossflow transition in flight
p 265 A93-20713
- BERTELROD, ARILD**
Development of a system for transition characterization
[AIAA PAPER 93-3465] p 1030 A93-47246
- BERTIN, F.**
Evaluation of clear-air radar PROUST and Doppler radar RONSARD for airport low level-wind shear detection
p 433 A93-22202
- BERTIN, JOHN J.**
Developing a data base for the calibration and validation of hypersonic CFD codes - Sharp cones
[AIAA PAPER 93-3044] p 1057 A93-48224
- BERTON, E.**
Study of soft-in-torsion blades - ROSOH operation
[ONERA, TP NO. 1992-124] p 803 A93-38598
- BERTON, JEFFREY J.**
An interactive preprocessor for the NASA engine performance program
[NASA-TM-105786] p 56 N93-10983
- BERTRAND, DENIS J. S. R.**
Neural network controllers for the X29 aircraft
p 817 A93-37005
- BESER, ERIC**
Reusable Ada avionics software packages library system
p 944 A93-42828
- BESER, JACQUES**
On the selection of a GPS validity indicator for aircraft navigation in the National Airspace System (NAS)
p 316 A93-21186
- BESSERMAN, D. L.**
Comparison of heat transfer measurements with computations for turbulent flow around a 180 deg bend
p 201 A93-13980
- BESSONE, J.**
Numerical calculation of helicopter rotor equations and comparison with experiment
[ONERA, TP NO. 1992-128] p 772 A93-38602
- BEST, DANA**
Hypersonic design
p 156 A93-14346
- BESTEK, HORST**
Numerical simulation of linear interference wave development in three-dimensional boundary layers
p 1029 A93-46993
- BETTELLE, ROGER**
Airbus or the revival of European civil aviation
p 856 A93-42655
- BETHEA, J. W.**
Position reporting using GPS/OMEGA and INS
p 498 A93-25173
- BETTOUN, M.**
Drag/thrust estimation via aircraft performance flight testing
p 156 A93-14322
- BETTS, A. K.**
FIFE atmospheric boundary layer budget methods
p 426 A93-20591
- BETTS, C.**
The experimental study of transition and leading edge contamination of swept wings
[LIB-TRANS-2197] p 782 N93-27274
- BETTSCHEART, N.**
Experimental and theoretical studies of helicopter rotor-fuselage interaction
[ONERA, TP NO. 1992-142] p 120 A93-14356
- BEUX, FRANCOIS**
Exact-gradient shape optimization of a 2-D Euler flow
[INRIA-RR-1540] p 462 A93-24308
Exact-gradient shape optimization of a 2D Euler flow
p 422 N93-18623
- BEVER, GLENN**
The development of an airborne information management system for flight test
[AIAA PAPER 92-4113] p 51 A93-11281
- BEWICK, CLARE**
Comparison of experimental ground testing and computational fluid dynamics for the re-engined 727-100 center engine inlet
[AIAA PAPER 92-3920] p 462 A93-24294
- BEYER, RALF**
ATTAS experimental-cockpit and ATMOS for component and system investigations in flight guidance
p 1014 N93-31276
- BEYER, TODD B.**
Evaluation of piezoceramic actuators for control of aircraft interior noise
p 447 A93-19186
Noise transmission properties and control strategies for composite structures
p 919 N93-30436
- BEYERS, M. E.**
Ground facility interference on aircraft configurations with separated flow
p 1140 A93-52441
- BEZ'IAZYCHNYI, V. F.**
Quality of the surface layer and operating properties of aircraft engine components
p 834 A93-39061
Prediction and control of the service-related properties of parts at the technological preparation stage and during the manufacture process
p 834 A93-39062
- BEZARD, HERVE**
Rotor blade airfoil design by numerical optimization and unsteady calculations
[ONERA, TP NO. 1992-65] p 766 A93-35993
- BEZDEK, WILLIAM J.**
Dynamic simulation fidelity improvement using transfer function state extrapolation
[AIAA PAPER 93-3552] p 1222 A93-52656
- BEZMENOV, V. IA.**
Modeling of flow in a pulsed shock tunnel
p 777 A93-39152
- BEZOS, GAUDY M.**
Development of a large-scale, outdoor, ground-based test capability for evaluating the effect of rain on airfoil lift
[NASA-TM-4420] p 779 N93-26899
- BHALWANKAR, ROHINI V.**
The onset of disintegration and corona in water drops falling at terminal velocity in horizontal electric fields
p 1163 A93-49130
- BHANUMATHI, V.**
Composites: A catalogue of books and conference proceedings available in the NAL library
[NAL-SP-IC-9201] p 234 N93-13368
- BHARADVAJ, BALA K.**
Three-dimensional Navier-Stokes/full-potential coupled analysis for viscous transonic flow
p 1178 A93-53218
- BHARGAVA REDDY, G.**
Development of a real time dynamic engine simulation model of a turbo fan engine
[ISABE 93-7132] p 1205 A93-54107
- BHAT, M. K.**
A low-speed wind tunnel study of vortex interaction control techniques on a chine-forebody/delta-wing configuration
p 122 A93-14409
- BHAT, THONSE R. S.**
The noise from supersonic elliptic jets
p 445 A93-19156
The prediction of noise radiation from supersonic elliptic jets
p 100 N93-10684
- BHATIA, KUMAR G.**
Lessons from application of equivalent plate structural modeling to an HSCT wing
[AIAA PAPER 93-1413] p 739 A93-33969
Aeroelastic challenges for a High Speed Civil Transport
[AIAA PAPER 93-1478] p 712 A93-34240
- BHATTACHARYA, A. K.**
Numerical modeling of leading edge separated flow at incompressible speeds
p 460 A93-24079
- BHATTACHARYA, S.**
A low-speed aerodynamic model for harmonically oscillating aircraft configurations
p 8 A93-11500
- BHAVARAJU, MURTY P.**
Advanced generating technologies - Motivation and selection process in electric utilities
p 1164 A93-50950
- BHAVNANI, S. H.**
Effective sealing of a disk cavity using a double-toothed rim seal
[ASME PAPER 92-GT-379] p 406 A93-19537
- BHUTTA, BILAL A.**
Low-to-high altitude predictions of three-dimensional ablative re-entry flowfields
p 1027 A93-46407
PNS predictions of axisymmetric hypersonic blunt-body and afterbody flowfields
[AIAA PAPER 93-2725] p 962 A93-46479
Application of parabolized Navier-Stokes technique for high-L/D, hypersonic vehicle design
[AIAA PAPER 93-2948] p 1047 A93-48144
- BI, NAI-PEI**
Experimental investigation of rotor/lifting surface interactions
[AIAA PAPER 93-0871] p 469 A93-24932
- BI, NAIPEI**
Contributions to the experimental investigation of rotor/body aerodynamic interactions
p 20 N93-10877
- BIAGIOLI, F.**
Finite-rate H2/air combustion effects in CRJ for hypersonic launchers
[ISABE 93-7084] p 1202 A93-54060
- BIAN, Y.**
Relative sensitivity of Loran-C phase tracking and cycle selection to CWI
p 792 A93-36502
- BIAN, YINGUI**
Finite-volume-TVD scheme for 3-D Euler transonic flow computations in rotating curvilinear coordinates
p 679 A93-33709
- BIANCO, JEAN**
Nitric oxide formation in a lean, premixed-prevaporized jet A/air flame tube: An experimental and analytical study
[NASA-TM-105722] p 844 N93-27012
- BIBER, KASIM**
Hysteresis effects on wind tunnel measurements of a two-element airfoil
[AIAA PAPER 93-0646] p 464 A93-24761
Flowfield measurements of a two-element airfoil with large separation
p 480 A93-29307
- BIBKO, V. N.**
Spectra of pressure pulsations on the surface of a cone in the transition region at supersonic flow velocities
p 1088 A93-51755
Scale-up of the spectra of aerodynamic pressure pulsations with narrowband maxima
p 1088 A93-51756
- BIDWELL, C. S.**
Ice accretion prediction for a typical commercial transport aircraft
[AIAA PAPER 93-0174] p 310 A93-23245
Ice accretion prediction for a typical commercial transport aircraft
[NASA-TM-105976] p 149 N93-15522
- BIEDRON, ROBERT T.**
Multiblock Navier-Stokes solutions about the F/A-18 wing-LEX-fuselage configuration
p 767 A93-37378
- BIESEMANS, I.**
Combat and training aircraft class A mishaps in the Belgian Air Force 1970-1990
p 492 N93-19677
- BIESIADNY, THOMAS J.**
Overview of high performance aircraft propulsion research
[NASA-TM-105839] p 59 N93-11530

BIESINGER, TH.

Turbulence evaluation within the secondary flow region of a turbine cascade
[ASME PAPER 92-GT-60] p 247 A93-19310

BIETERMAN, MICHAEL B.

Using a full potential solver for propulsion system exhaust simulation p 689 A93-34487

BIEZAD, DANIEL

A pseudo-loop design strategy for the longitudinal control of hypersonic aircraft
[AIAA PAPER 93-3814] p 1132 A93-51405

BIEZAD, DANIEL J.

Pilot-in-the-loop analysis of propulsive-only flight control systems p 908 A93-42812
Real-time parameter identification applied to flight simulation p 1006 A93-44142
Low bandwidth robust controllers for flight [NASA-CR-191774] p 372 A93-17800
Low bandwidth robust controllers for flight [NASA-CR-193085] p 819 A93-27156

BIGBEE-HANSEN, WILLIAM J.

A compact, intercooled and regenerated gas turbine for HALE applications
[ASME PAPER 92-GT-401] p 355 A93-19550

BIGDELI, BEHZAD

Hypersonic, turbulent viscous interaction past an expansion corner
[AIAA PAPER 93-2985] p 1051 A93-48178

BIHARI, TOM

Design concepts for the development of cooperative problem-solving systems
[NASA-CR-192708] p 707 A93-25261

BIL, C.

Structural optimization in preliminary aircraft design - A finite-element approach p 226 A93-14340

BILANIN, ALAN J.

Decay of aircraft vortices near the ground p 961 A93-45751

Computation of wake/exhaust mixing downstream of advanced transport aircraft
[AIAA PAPER 93-2944] p 1162 A93-48141

BILBIA, DUSHAN

The Edge supersonic transport
[NASA-CR-192074] p 335 A93-18055

BILGEN, E.

Numerical solutions of Euler equations by using a new flux vector splitting scheme p 1087 A93-51740

BILL, ROBERT C.

Introduction to test cases for engine life assessment technology p 176 A93-14891
Integrity testing of brush seal in shroud ring of T-700 engine [NASA-TM-105863] p 421 A93-18380

BILLET, MICHAEL L.

Reduction in size and unsteadiness of a VTOL ground vortex by ground fences
[NASA-CR-192997] p 700 A93-26049

BILLIG, F. S.

Research on supersonic combustion p 899 A93-42877

BILLIG, FREDERICK S.

ISABE - International Symposium on Air Breathing Engines, 11th, Tokyo, Japan, Sept. 20-24, 1993. Proceedings. Vols. 1 & 2
[ISBN 1-56347-071-3] p 1194 A93-53976

BILLINGS, S. A.

Identification of system dynamics of a high incidence research model [RR-407] p 339 A93-18507

BILLONNET, G.

3D viscous flow analysis in axial turbine including tip leakage phenomena p 972 A93-46940
Three-dimensional analysis of turbine rotor flow including tip clearance [ASME PAPER 93-GT-111] p 987 A93-47446

BILLONNET, GILLES

3D and 2.5D viscous flow computations for axial flow turbine blades
[ISABE 93-7093] p 1186 A93-54069

BIN, L.

Review and prospect of Chinese scientific balloon activities p 1 A93-11368

BINNS, J. M.

Reliability and safety considerations in engine management systems design p 346 A93-18786

BINQIAN, ZHANG

Effect of canard wing positions on aerodynamic characteristics of swept-forward wing [AD-A262373] p 789 A93-28493

BIOCCA, FRANK A.

A survey of position trackers p 1151 A93-49396

BIR, GUNJIT S.

Aeromechanical stability of rotorcraft with advanced geometry blades
[AIAA PAPER 93-1304] p 725 A93-33880

BIRCH, I. D.

Airborne trials of Loran-C p 311 A93-17756

BIRCH, N. T.

A European collaborative NLF nacelle flight demonstrator [PNR-90992] p 20 A93-11113

BIRCKELBAW, LARRY D.

Infrared flow visualization of V/STOL aircraft
[AIAA PAPER 92-4253] p 80 A93-13343

BIRCKELBAW, LARRY DEAN

High-speed aerodynamics of upper surface blowing aircraft configurations p 132 A93-13729

BIRCKELBAW, LOURDES G.

Piloted simulation study of two tilt-wing control concepts
[AIAA PAPER 92-4236] p 63 A93-13338

Phase II simulation evaluation of the flying qualities of two tilt-wing flap control concepts
[SAE PAPER 920988] p 185 A93-14635

BIRD, F. J.

Measurement of the dynamic undercarriage response of a Sikorsky S-70B-2 helicopter: Instrumentation and test methods: Flight mechanics technical memorandum
[AD-A256319] p 329 A93-16404

BIRD, J. W.

Uncertainty assessments for engine thrust derived from two methods p 1254 A93-54392

BIRINGEN, S.

Direct numerical simulation of turbulent flow in a square duct
[AIAA PAPER 93-0198] p 277 A93-22618

BIRIUK, V. I.

A study of the effect of the static aeroelasticity of a swept wing on its weight response p 801 A93-36798

BIRK, FRANK T.

B-2 flight test update p 803 A93-38844

BIRKAN, M. A.

AFOSR Contractors Meeting in Propulsion
[AD-A254484] p 195 A93-12575

BIRKENHEUER, D. L.

Preliminary evaluation of aviation-impact variables derived from numerical models [PB93-190197] p 1034 A93-31202

BIRMAN, A.

A singularities tracking conservation law scheme for compressible duct flows p 960 A93-45542

BIRON, D. G.

A high resolution airborne multisensor system p 343 A93-21966

BIRON, PAUL J.

Microburst characteristics determined from 1988-1991 TDWR testbed measurements p 490 A93-19605

BIRT, E. A.

Imaging flaws in thin metal plates using a magneto-optic device p 397 A93-18670

BIRTCHEER, CRAIG R.

Advanced electromagnetic methods for aerospace vehicles
[NASA-CR-193468] p 936 A93-31036

BISBEE, L. S.

Measurements in 80- by 120-foot wind tunnel of hazard posed by lift-generated wakes
[AIAA PAPER 93-3518] p 1014 A93-47281

BISHOP, D. T.

Heat transfer, adiabatic effectiveness, and injectant distributions downstream of a single row and two staggered rows of compound angle film-cooling holes p 201 A93-13976

BISHOP, DAVID G.

A three-dimensional Delaunay unstructured grid generator and flow solver for bodies in relative motion
[AIAA PAPER 93-3349] p 954 A93-45043

BISMARCK-NASR, MAHER N.

Supersonic panel flutter analysis of shallow shells p 927 A93-41935

BISMES, F.

Prediction of the performances in combustion of ramjets and stato-rockets by isothermal experiments and modeling p 363 A93-17622

BISSINGER, N. C.

AGARD WG13 aerodynamics of high speed air intakes: Assessment of CFD results p 215 A93-13220

BISWAS, RUPAK

A new procedure for dynamic adaption of three-dimensional unstructured grids
[AIAA PAPER 93-0672] p 560 A93-24780

BITER, CLEON

Terminal Doppler Weather Radar program at Denver's Stapleton International Airport during 1989 and 1990 p 432 A93-22188

BITTNER, ROBERT D.

Summary of the GASP code application and evaluation effort for scramjet combustor flowfields
[AIAA PAPER 93-1973] p 1077 A93-49820

BIZE, D.

Schlieren device and holographic interferometer for hypersonic flow visualization [ONERA, TP NO. 1992-160] p 832 A93-38739

BJARKE, LISA J.

A summary of the forebody high-angle-of-attack aerodynamics research on the F-18 and the X-29A aircraft [NASA-TM-104261] p 25 A93-12353

BJORNSON, BRIAN M.

SAC control formation study [AD-A254410] p 159 A93-12605

BLAAS, ACHIM

Full-scale wind tunnel investigation of a helicopter individual blade control system
[AIAA PAPER 93-1361] p 726 A93-33929

BLACK, J.

Scanning Laser Aircraft Surveillance System for carrier flight operations p 500 A93-28157

BLACK, JOHN D.

Rotational CARS measurements in a rotating cavity with axial throughflow of cooling air: Oxygen concentration measurements [PNR-90935] p 72 A93-11035

BLACK, KLIFFTON M.

The UTA autonomous aerial vehicle - Automatic control and navigation p 908 A93-42813

BLACKBURN, ALBERT W.

A distributed, message-based, airspace environment p 313 A93-21144

BLACKWELDER, R. F.

Vortex generators used to control laminar separation bubbles p 768 A93-37381

BLACKWELDER, RON

Dynamical effects of suction/heating on turbulent boundary layers [AD-A248459] p 87 A93-11416

BLACKWELL, B. F.

Numerical solution of axisymmetric heat conduction problems using finite control volume technique p 928 A93-42909

BLACKWELL, R. J.

Ablation problems using a finite control volume technique [DE93-009861] p 942 A93-29187

BLACKWELL, R. J.

Demonstration of an integrated, active 4 x 4 photonic crossbar p 211 A93-17392

BLACKWOOD, M. I.

Progress towards common standards for flight simulator qualification p 374 A93-18774

BLAGODARNYJ, M. A.

Determination of the vertical velocity component of aircraft landing on an airfield with a longitudinally sloping runway p 1007 A93-45664

Operating an aircraft during the landing on an airfield with a substantial longitudinal macro slope of the runway p 1008 A93-45667

BLAGOSKLONOV, V. I.

Flow density distribution in a two-phase submerged jet p 836 A93-39144

BLAHA, F. A.

Application issues of fiber optic sensors in aircraft structures p 410 A93-21094

BLAIGNAN, VINCENT B.

Stiffness enhancement of flight control actuator p 1006 A93-44151

BLAIR, JESSE L.

Pave Pillar in-house research final report p 927 A93-42781

BLAIR, MAX

Time domain panel method for wings p 958 A93-45135

A compilation of the mathematics leading to the doublet lattice method [AD-A256304] p 136 A93-14441

BLAIR, MICHAEL F.

An experimental study of heat transfer in a large-scale turbine rotor passage [ASME PAPER 92-GT-195] p 403 A93-19420

BLAKE, DAVID

The effectiveness of hand-held fire extinguishers on cargo container fires [DOT/FAA/CT-TN92/42] p 496 A93-21821

BLAKE, KENNETH R.

Unstructured 3D Delaunay mesh generation applied to planes, trains and automobiles [AIAA PAPER 93-0673] p 560 A93-24781

BLAKE, MATTHEW W.

A concurrent hybrid Navier-Stokes/Euler approach to fluid dynamic computations [AIAA PAPER 93-0789] p 468 A93-24865

BLAKE, W. B.

A study of the effect of a moving ground belt on the vortex created by a jet impinging on the ground in a cross flow [AIAA PAPER 92-4250] p 15 A93-13361

- BLAKE, WILLIAM B.**
A study of the rotary balance technique for predicting pitch damping
[AIAA PAPER 93-3619] p 1125 A93-48306
- BLAKE, WILLIAM K.**
Mass loaded composite rotor for vibro-acoustic application
[AD-D015604] p 535 N93-20016
- BLANCHARD, ROBERT C.**
Rarefied-flow shuttle aerodynamics flight model
[AIAA PAPER 93-3441] p 859 A93-41057
Rarefied-flow Shuttle aerodynamics model
[NASA-TM-107698] p 458 N93-19976
- BLAND, SAMUEL R.**
Interactive grid generation program for CAP-TSD
[NASA-TM-102705] p 17 N93-10349
- BLAND, T. J.**
Advanced cooling for high power electric actuators
[SAE PAPER 921022] p 158 A93-14649
- BLANK, HANS-JOACHIM**
Advanced hypersonic aircraft design
[NASA-CR-192046] p 334 N93-18037
- BLANK, S. C.**
Supersonic wing/body interference
p 121 A93-14391
- BLANKEN, CHRIS L.**
Generation of helicopter roll axis bandwidth data through ground-based and in-flight simulation
p 511 N93-19909
- BLANKENSHIP, D. D.**
Airborne gravimetry from a light aircraft
p 1245 A93-55972
- BLANKSON, ISIAHAH**
NASA's hypersonic flight research program
[AIAA PAPER 93-0308] p 457 A93-25516
- BLANKSON, ISIAHAH M.**
Air-breathing hypersonic cruise - Prospects for Mach 4-7 waverider aircraft
[ASME PAPER 92-GT-437] p 384 A93-19579
Current technologies for waverider aircraft
[AIAA PAPER 93-0400] p 505 A93-25521
Propulsion/airframe integration issues for waverider aircraft
[AIAA PAPER 93-0506] p 505 A93-25533
- BLASZCZYK, J.**
Finite element analysis of natural vibrations of an aeroplane with asymmetric variable wing geometry
p 1218 A93-53776
- BLAZART, P.**
Investigation of a combustion zone behind a wedge
p 1146 A93-51631
- BLECH, RICHARD A.**
Turbomachinery CFD on parallel computers
[NASA-TM-105932] p 228 N93-13154
- BLECK, MAX E.**
Annual Paul E. Hemke Lecture in aerospace engineering
p 107 A93-14067
- BLESS, ROBERT R.**
Hodograph analysis in aircraft trajectory optimization
[AIAA PAPER 93-3742] p 1101 A93-51338
- BLEVINS, J. A.**
Engineering method for calculating inlet face property profiles on high speed vehicle forebodies
[AIAA PAPER 93-3113] p 1062 A93-48283
- BLIN, ELISABETH**
Analysis of turbulence in supersonic flows by means of laser velocimetry
[ONERA, TP NO. 1992-148] p 773 A93-38729
- BLISS, D. B.**
Vortex methods for the computational analysis of rotor/body interaction
p 765 A93-35939
- BLISS, DONALD B.**
Efficient free wake calculations using analytical/numerical matching
p 874 A93-43780
Direct periodic solutions of rotor free wake calculations
p 874 A93-43781
- BLOCH, GREGORY S.**
A wide-range axial-flow compressor stage performance model
[ASME PAPER 92-GT-58] p 348 A93-19308
An assessment of inlet total-pressure distortion requirements for the Compressor Research Facility (CRF)
[AD-A262299] p 815 N93-27679
- BLODGETT, JAMES C.**
Land subsidence and problems affecting land use at Edwards Air Force Base and vicinity, California, 1990
[PB93-182236] p 1036 N93-32191
- BLOM, ANDERS F.**
Damage tolerance assessment of the fighter aircraft 37 Viggen main wing attachment
p 802 A93-37390
- BLOM, G. A.**
Application of a parabolized Navier-Stokes code to an HSCAT configuration and comparison to wind tunnel test data
[AIAA PAPER 93-3537] p 986 A93-47288
- BLONDET, PASCAL**
Using NDT techniques in the maintenance of aeronautical products
[REPT-921-430-102] p 88 N93-11587
- BLOOM, S. H.**
Helicopter plume detection by using an ultranarrow-band noncoherent laser Doppler velocimeter
p 542 A93-25198
- BLOOMFIELD, D. P.**
Electropneumatic actuator, phase 1
[PB93-174951] p 1033 N93-31876
- BLOOMFIELD, JOHN R.**
Elements of a theory of natural decision making
p 147 N93-15021
Taxonomy of flight variables
p 147 N93-15022
- BLOSSER, MAX L.**
Active cooling from the sixties to NASP
p 49 N93-12458
- BLOWER, DAVID J.**
Performance-based testing and success in Naval advanced flight training
[AD-A260838] p 717 N93-25933
- BLOY, A. W.**
Lateral aerodynamic interference between tanker and receiver in air-to-air refueling
p 1136 A93-52444
Aircraft turns into and down wind
[AERO-REPT-9201] p 337 N93-18131
- BLUEMCKE, E.**
Experimental and theoretical investigation of a research atomizer/combustion chamber configuration
[ASME PAPER 92-GT-137] p 401 A93-19369
- BLUYER, JOHN E.**
A data reduction system for processing instrumented flight test data
p 847 A93-37866
- BLYTHER, A. A.**
Engineering aspects of laminar flow research at Handley Page
p 235 A93-17275
- BO, T.**
The prediction of convective heat transfer in rotating square ducts
[PNR-90929] p 85 N93-11025
Turbulent flow and heat transfer in idealized blade cooling passages
p 902 N93-29938
- BOALBEY, R. E.**
A sensitivity study for pneumatic vortex control on a chined forebody
[AIAA PAPER 93-0049] p 260 A93-20162
- BOBBITT, PERCY J.**
The Langley 8-ft transonic pressure tunnel laminar-flow-control experiment
p 910 A93-41783
- BOBKOVA, A. N.**
Optimal impulsive interorbital transfers with aerodynamic maneuvers
p 1141 A93-48838
- BOBLITT, WAYNE W.**
Single screw interrupted thread positive displacement mechanism
[AD-D015596] p 554 N93-20790
- BOBO, STEPHEN N.**
Magneto-optic imaging inspection of selected corrosion specimens
[DOT/FAA/CT-TN92/20] p 88 N93-11617
- BOBRONNIKOV, V. T.**
Problems in the optimization of complex engineering systems
p 1165 A93-49307
- BOBSKILL, GLENN J.**
Summary of the GASP code application and evaluation effort for scramjet combustor flowfields
[AIAA PAPER 93-1973] p 1077 A93-49820
- BOBULA, GEORGE B.**
Integrity testing of brush seal in shroud ring of T-700 engine
[NASA-TM-105863] p 421 N93-18380
- BOCCACCIO, E.**
Reactive and dissipative hypersonic flow in a wind tunnel nozzle
p 687 A93-34358
- BOCCICCHIO, RICHARD L.**
Applications of IR imagery to thermal evaluations
[SAE PAPER 921223] p 926 A93-41397
- BOCKELIE, MICHAEL J.**
A comparison using APPL and PVM for a parallel implementation of an unstructured grid generation program
[NASA-CR-191425] p 757 N93-25073
- BODSTEIN, G. C. R.**
Vortex/surface interaction
[AIAA PAPER 93-0863] p 468 A93-24925
- BODZEK, RICHARD S.**
Logistic Support Analysis - An integrated approach to configuration management
p 763 A93-35924
- BOEHM, H.-D. V.**
Helmet Mounted Sight and display testing
p 517 A93-26883
Integration of an integrated helmet system for PAH 2
p 1244 A93-55298
- BOEHM, HANS-DIETER**
Integrated helmet system testing for a nightflying helicopter
[MBB-UD-0604-91-PUB] p 343 N93-17570
- BOELCS, A.**
Time-dependent predictions and analysis of turbine cascade data in the transonic flow region
[PNR-90957] p 139 N93-15489
- BOER, J. F.**
Helicopter installations: From motor to rotor
[LR-675] p 329 N93-16345
- BOER, J. N.**
Aerodynamic degradation due to distributed roughness on high lift configuration
[AIAA PAPER 93-0028] p 260 A93-20146
- BOETTCHER, CAROLYN**
Functionally Integrated Resource Manager for real-time avionics data
p 940 A93-42832
- BOETTCHER, J.**
Aeroacoustic wind tunnel testing of a counterrotating shrouded propfan-model
p 449 A93-19213
- BOETTCHER, JAN**
Prediction of jet mixing noise in high-speed flight
p 450 A93-19216
The noise of jet aircraft flying with high speeds at low altitudes
p 450 A93-19218
Comparison of flyover noise data from aircraft at high subsonic speeds with prediction
p 100 N93-10674
Prediction of jet mixing noise for high subsonic flight speeds
p 100 N93-10685
Calculation of noise emission caused by jet aircraft during takeoff, approach and horizontal flyover
[DLR-MITT-91-15] p 569 N93-21368
- BOEX, TONY**
Follow-on operational test and evaluation of the NAVSTAR global positioning system air integration/installation program
[AD-A263067] p 793 N93-27925
- BOGARD, DAVID G.**
Hydrodynamic effects on heat transfer for film-cooled turbine blades
[AD-A257291] p 361 N93-16080
- BOGDANOFF, D. W.**
Initiation of combustion in the thermally choked ram accelerator
p 1016 A93-45501
- BOGDANOFF, DAVID W.**
Increase in stagnation pressure and enthalpy in shock tunnels
[AIAA PAPER 93-0350] p 377 A93-23035
Experimental Investigation of Nozzle/Plume Aerodynamics at Hypersonic Speeds
[NASA-CR-191368] p 386 N93-18085
Increase of stagnation pressure and enthalpy in shock tunnels
p 295 N93-18086
- BOGDANOV, A. N.**
Steady transonic weakly perturbed flows in a vibrationally relaxing gas
p 1088 A93-51768
Steady state supersonic flows of a vibrationally excited gas past thin bodies
p 1089 A93-51818
Steady-state supersonic flow of a vibrationally excited gas past a slender body of revolution at a small angle of attack
p 1233 A93-55014
- BOGDONOFF, SEYMOUR M.**
Comments on experiments for computational validation for fluid dynamic predictions
p 927 A93-42578
Hypersonics revisited
p 781 N93-27167
- BOGNER, S.**
Experimental analysis of steady-state and dynamic monitoring of power shaft turbines
p 178 N93-15176
- BOGOD, A. B.**
Direct and inverse problems of calculating the axisymmetric and 3D flow in axial compressor blade rows
p 972 A93-46938
- BOGOLYUBOV, A. A.**
Multilevel control systems and optimization of their structures
p 1168 A93-50954
- BOGOMOLOV, A. I.**
Stabilization of the dynamic characteristics of the automatic control systems of a flight vehicle
p 62 A93-12802
Stabilization of the dynamic characteristics of the two-channel automatic control system of aircraft
p 1205 A93-52941
- BOGOMOLOV, M. K.**
A model of the maintenance of a fleet of TU-204 aircraft at a maintenance and repair center
p 237 A93-18327
- BOGOSLOVSKI, S. V.**
Experimental and algorithmic means of identifying mathematical models of flight vehicle
p 909 A93-43103
- BOGUE, RODNEY K.**
Recent flight-test results of optical airdata techniques
[AIAA PAPER 92-4086] p 51 A93-13265
Taking the measure of aerodynamic testing
p 16 A93-13434

BOHN-MEYER, MARTA

Overview of supersonic laminar flow control research on the F-16XL ships 1 and 2
[NASA-TM-104257] p 20 N93-11221

BOHN, HANS E.

Alternative approach routes to rwy 24 at Oslo Airport, Fornebu p 487 A93-28481

BOHON, HERMAN L.

First NASA Advanced Composites Technology Conference, part 2
[NASA-CP-3104-PT-2] p 921 N93-30841

BOIKO, A. V.

Instability of local separated flows with respect to small-amplitude perturbations p 125 A93-15254

BOIKO, L. G.

Experience in the design of supercritical cascades for the flow straightener of a transonic fan p 777 A93-39196

BOITNOTT, R. L.

An experimental and analytical investigation on the response of GR/EP composite I-frames p 546 A93-27975

BOITNOTT, RICHARD L.

An overview of the crash dynamics failure behavior of metal and composite aircraft structures p 923 N93-30875

BOITSOV, B. V.

Effect of overloads on the service life of the structural elements of aircraft p 746 A93-35289

BOITSOV, V. B.

A method for estimating the survivability of bodies of revolution p 745 A93-35287

BOITSOV, B. V.

Reliability and durability problems p 1150 A93-48825

BOLAND, JOSEPH R.

Aircraft control requirements and achievable dynamics prediction
[AIAA PAPER 93-3648] p 1128 A93-48331

BOLDMAN, D. R.

Effect of a rotating propeller on the separation angle of attack
[AIAA PAPER 93-0017] p 472 A93-24978
Effect of a rotating propeller on the separation angle of attack and distortion in ducted propeller inlets
[NASA-TM-105935] p 290 N93-16625

BOLDMAN, DONALD R.

3-D viscous flow CFD analysis of the propeller effect on an advanced ducted propeller subsonic inlet
[AIAA PAPER 93-1847] p 1075 A93-49728
The 3-D viscous flow CFD analysis of the propeller effect on an advanced ducted propeller subsonic inlet
[NASA-TM-106240] p 900 N93-29162

BOLDVICH, JOHN A.

Simulator motion
[AD-A257683] p 381 N93-17687

BOLLAND, SARA LOUISE

An investigation of ground access mode choice for departing passengers
[TT-9201] p 67 N93-11224

BOLLER, CHR.

Technological challenges with smart structures in German aircraft industry p 320 A93-17714

BOLTON, J. S.

Sound transmission through stiffened double-panel structures lined with elastic porous materials p 444 A93-19139

BOLUKBASI, AKIF O.

Test and analysis of an advanced technology landing gear p 37 A93-10917

A nonlinear analysis methodology for the design of skid landing gears p 799 A93-36004

BOMAN, BRET L.

Engineering method for calculating surface pressures and heating rates on vehicles with embedded shocks p 777 A93-39255

BOMAN, PER-OLOF

Damage tolerance assessment of the fighter aircraft 37 Viggen main wing attachment p 802 A93-37390

BONAPARTE, MICHAEL J.

Nozzle/cowl optimization for a hypersonic vehicle on a typical trajectory
[AD-A258827] p 341 N93-19089

BOND, J.

Application of analog computing to real-time simulation of stall and surge dynamics
[AIAA PAPER 93-2231] p 1080 A93-50037

BOND, THOMAS H.

Results of Low Power Deicer tests on a swept inlet component in the NASA Lewis Icing Research Tunnel
[AIAA PAPER 93-0032] p 327 A93-22551
Surface roughness due to residual ice in the use of low power deicing systems
[AIAA PAPER 93-0031] p 282 A93-23240

An overview of shed ice impact studies in the NASA Lewis Icing Research Tunnel

[AIAA PAPER 93-0301] p 283 A93-23247

Results of a low power ice protection system test and a new method of imaging data analysis p 795 A93-35932

Results of low power deicer tests on a swept inlet component in the NASA Lewis icing research tunnel

[NASA-TM-105968] p 138 N93-14911

Surface roughness due to residual ice in the use of low power deicing systems

[NASA-TM-105971] p 139 N93-15338

An overview of shed ice impact in the NASA Lewis Icing Research Tunnel

[NASA-TM-105969] p 139 N93-15404

Experimental and computational ice shapes and resulting drag increase for a NACA 0012 airfoil

p 784 N93-27440

BOND, W.

A domain-specific design architecture for composite material design and aircraft part redesign p 442 N93-17522

BONDAREV, E. N.

An experimental study of a compound supersonic jet p 1069 A93-48914

An experimental study of the dynamic effect of a supersonic underexpanded jet on a plane surface parallel to the nozzle axis p 1092 A93-51913

BONESS, R. J.

Measurements of wear and acoustic emission from fuel-wetted surfaces p 744 A93-34925

BONEV, B.

A joint Soviet-Bulgarian scientific program for free-flight and tethered aerostat observations p 2 A93-11374

BONHAUS, DARYL L.

Navier-Stokes computations and experimental comparisons for multielement airfoil configurations
[AIAA PAPER 93-0645] p 464 A93-24760

An upwind multigrid algorithm for calculating flows on unstructured grids p 957 A93-45088

BONNAR, GERARD R.

Repair materials and processes for the MD-11 Composite Tailcone p 1216 A93-53452

BONNET, J. P.

Experimental analysis of turbulence within supersonic mixing layers p 11 A93-12428

Experimental studies of the turbulent structure of supersonic mixing layers

[AIAA PAPER 93-0217] p 278 A93-22633

BONNIN, A.

The role of the radiologist in the medicolegal procedure after an aviation accident p 853 A93-39701

BONTEMPI, MICHAEL

Arrow 227: Air transport system design simulation
[NASA-CR-192053] p 336 N93-18063

BOOHER, M. E.

Development of an advanced exhaust mixer for a high bypass ratio turbofan engine

[AIAA PAPER 93-2435] p 1118 A93-50188

BOOKER, A. J.

Inlet design using a blend of experimental and computational techniques p 114 A93-14210

BOOKHAM, R. P.

Royal Air Force experience of the Harrier information management system p 234 N93-15170

BOOKOUT, GREG

Texture as a visual cueing element in computer image generation. I - Representation of the sea surface

[AIAA PAPER 93-3560] p 1214 A93-52695

BOORLA, RAGHUPATI

Load variability of a two-bladed helicopter p 507 A93-27954

BOOTH, EARL R., JR.

HHC study in the DNW to reduce BVI noise - An analysis p 565 A93-29405

BOOTH, ERIC W.

Software Engineering Laboratory Ada performance study: Results and implications p 441 N93-17172

BOOTH, PAMELA F.

Curvature and leading edge sweep back effects on grid fin aerodynamic characteristics

[AIAA PAPER 93-3480] p 981 A93-47258

BOOTHE, EDWARD M.

Helicopter simulator standards p 912 N93-30675

BOQUIST, CAY-R.

Effective 406-MHz ELT demonstrates the potential to save more lives p 311 A93-18543

BORCHARDT, HEINRICH

New slant visual range measuring device promises improved airport operations p 529 A93-27395

BORCHERS, PAUL F.

Determination of YAV-8B Reaction Control System bleed flow usage

[AIAA PAPER 92-4232] p 54 A93-13330

BORE, C. L.

Some contributions to propulsion theory - Fuel consumption formulae and general range equation

p 713 A93-34850

Some contributions to propulsion theory - The Stream Force Theorem and applications to propulsion

p 924 A93-40472

Some contributions to propulsion theory - Non-isentropic duct flow and the general drag wake traverse

p 874 A93-43688

BORG, RONALD

CFD analysis and testing on a twin inlet ramjet
[AIAA PAPER 93-1839] p 1075 A93-49723

BORG, S. E.

An optical flameout detection system for NASA Langley's 8-Foot High Temperature Tunnel

p 1254 A93-54372

BORGGAARD, JEFF

Sensitivity calculations for a 2D, inviscid, supersonic forebody problem
[NASA-CR-191444] p 779 N93-27004

BORGONOVI, GIANCARLO

Reliability assessment at airline inspection facilities. Volume 1: A generic protocol for inspection reliability experiments

[DOT/FAA/CT-92/12-VOL-1] p 704 N93-25110

Reliability assessment at airline inspection facilities. Volume 2: Protocol for an eddy current inspection reliability experiment

[DOT/FAA/CT-92/12-VOL-2] p 842 N93-28685

BORISOV, V. M.

Calculation of radiant energy transfer in hypersonic flow past blunt bodies using the P1 and P2 approximations of the spherical harmonic method

p 124 A93-15209

BORNSTEIN, N. S.

Advanced turbine design for coal-fueled engines
[DE93-000224] p 554 A93-21254

BOROVJOV, V. YA.

Heat transfer on tip fins in hypersonic flow p 1088 A93-51775

BOROWSKY, M. S.

Helicopter crash survival at sea: United States Navy/Marine Corps experience 1977-1990

p 493 N93-19687

BOROWSKY, MICHAEL S.

Trans-cockpit authority gradient in Navy/Marine aircraft mishaps p 146 N93-15016

BORREL, M.

Supersonic vortical flows around an ogive-cylinder - Laminar and turbulent computations

[ONERA, TP NO. 1992-111] p 771 A93-38588

Hypersonic flow calculations using a multidomain MUSCL Euler solver

p 960 A93-45547

BORRELLI, SALVATORE

A contribution to the prediction of hypersonic non-equilibrium flows p 869 A93-42624

BORSE, JOHN E.

IOPS advisor: Research in progress on knowledge-intensive methods for irregular operations

airline scheduling p 443 N93-18686

BORSI, M.

Comparison of solution of various Euler solvers and one Navier-Stokes solver for the flow about a sharp-edged

cropped delta wing

[NLR-TP-90340-U] p 418 N93-16411

BORST, ROBERT G.

Fuzzy logic control algorithm for suppressing E-6A Long Trailing Wire Antenna wind shear induced oscillations

[AIAA PAPER 93-3868] p 1171 A93-51454

BORTOLUS, MARCOS V.

Generalized vortex lattice method for oscillating lifting surfaces in subsonic flow p 123 A93-14555

BOSCHER, D.

Infrared thermography for hot-shot wind tunnel
[ONERA, TP NO. 1992-103] p 831 A93-38583

Infrared thermography characterization of Goertler vortex type patterns in hypersonic flows

[ONERA, TP NO. 1993-13] p 925 A93-41029

BOSCHITSCH, ALEXANDER

High accuracy computation of fluid-structure interaction in transonic cascades

[AIAA PAPER 93-0485] p 287 A93-23387

BOSCHITSCH, ALEXANDER H.

Rotor design optimization using a free wake analysis
[NASA-CR-177612] p 693 N93-25075

BOSCHMA, JAMES H.

The development progress of the U.S. Army's SASS LITE, unmanned robot airship

[AIAA PAPER 93-4047] p 1243 A93-54614

BOSE, DAVE

Arrow 227: Air transport system design simulation
[NASA-CR-192053] p 336 N93-18063

BOSIN, P. A.

Definition of the structure of expert preferences for the multicriterial analysis of control systems

p 1168 A93-50953

- BOSLEY, GARY S.**
Commercial airplane primary structure
[SME PAPER EM92-115] p 107 A93-14112
- BOSSE, S.**
The application of an Euler method and a Navier Stokes method to the vortical flow about a delta wing
[AIAA PAPER 93-3510] p 984 A93-47276
- BOSSI, JOSEPH A.**
Development and application of a nonlinear fin mixer
p 368 A93-22869
- BOSSI, R.**
Correlation of X-ray CT measurements to shear strength in pultruded composite materials p 396 A93-18618
Measurement of the center-of-gravity using X-ray computed tomography p 396 A93-18619
- BOSSI, R. H.**
Computed tomography of advanced materials and processes p 832 A93-38975
- BOSSI, RICHARD H.**
X-ray computed tomography for casting development
[AD-A261786] p 752 N93-26526
- BOSSLER, R. B., JR.**
Face-gear drives: Design, analysis, and testing for helicopter transmission applications
[NASA-TM-106101] p 839 N93-27133
- BOTA, KOFI**
Aero-engine component damping estimation from full-scale aeromechanical test data
[AIAA PAPER 93-1873] p 1112 A93-49748
- BOTEZ, R.**
A comparative study of semi-empirical dynamic stall models p 18 N93-10544
- BOTHE, HELMUT**
Flight test of avionic and air-traffic control systems
[ESA-TT-1279] p 993 N93-31271
The basic measurement equipment of the DLR test aircraft p 1000 N93-31273
Instigation and processing of flight tests in DLR p 998 N93-31275
- BOTIN, A. V.**
Interference of an oblique shock with a shock layer on a blunt edge for small Reynolds numbers p 775 A93-39120
Investigation of the effect of physical processes on heat transfer to blunt bodies at low Reynolds numbers p 1090 A93-51877
- BOTT, JULIAN**
Integrated engine control and monitoring with experiences derived from OLMOS p 178 N93-15168
- BOUCARUT, R. A.**
Optical technologies for UV remote sensing instruments p 853 N93-28788
- BOUCHARD, G.**
Experimental evaluation of flat plate boundary layer growth over an anti-icing fluid film p 1140 A93-52645
- BOUCHARD, GILLES**
Aircraft take-off laboratory simulation for de/anti-icing study p 528 A93-23840
- BOUCHARD, MICHAEL P.**
Advanced transparency development for USAF aircraft
[AIAA PAPER 93-1391] p 710 A93-33954
- BOUCHARDY, P.**
CARS studies in hypersonic flows
[AIAA PAPER 93-3047] p 1144 A93-48227
CARS temperature measurements in combustion
[ONERA, TP NO. 1993-78] p 1212 A93-53599
- BOUDREAU, A. H.**
Trends in international aerospace ground test facilities
[AIAA PAPER 93-0348] p 528 A93-25518
Complementary role of ground testing, flight testing, and computations in aerospace plane propulsion development
[ISABE 93-7034] p 1197 A93-54010
- BOUILLET, ROGER**
The technological evolution of high thrust turbine engines
[DS-1881] p 364 N93-17882
- BOUISSET, JEAN-FRANCOIS**
Tomorrow's security p 141 A93-15058
- BOULAY, J. L.**
Electrostatic discharges
[ONERA, TP NO. 1992-82] p 844 A93-38567
- BOULBIN, F.**
Turbine blade forces due to partial admission p 1029 A93-46928
- BOURDAIS, P.**
Method for developing the RAFALE flight control system p 512 N93-19912
- BOUSGARBIES, J.-L.**
Experimental study of heat transfer close to a plane wall heated in the presence of multiple injections (subsonic flow) p 901 N93-29931
- BOUSLOG, STANLEY A.**
Two-layer convective heating prediction procedures and sensitivities for blunt body reentry vehicles
[AIAA PAPER 93-2763] p 963 A93-46509
- BOUSMAN, WILLIAM G.**
An investigation of helicopter rotor blade flap vibratory loads p 796 A93-35975
- BOUSQUET, J. M.**
Computational methods applied to the aerodynamics of spaceplanes and launchers
[ONERA, TP NO. 1992-140] p 114 A93-14216
- BOUTIER, ALAIN**
Laser velocimetry around helicopter blades in the DNW wind tunnel of the NLR
[ONERA, TP NO. 1992-143] p 831 A93-38613
- BOUTRY, J. M.**
RAMSES: Multi-spectral experimental radar station installed on board the Transall p 550 N93-19925
- BOUVIER, F.**
A new adaptive test section at ONERA
Chalais-Meudon
[ONERA, TP NO. 1992-117] p 822 A93-38592
- BOUVER, GERD**
Helicopter in-flight simulator ATThES - A multipurpose testbed and its utilization p 43 A93-13315
ATThES - A helicopter in-flight simulator with high bandwidth capability p 821 A93-35988
- BOWEN, BRENT D.**
The airline quality report, 1992 p 310 N93-18036
Consumer interest in the air safety data of the airline quality rating. Testimony to the US House of Representatives, Committee on Government Operations, Government Activities and Transportation Subcommittee
[NIAR-92-4] p 495 N93-19941
- BOWER, DANIEL R.**
An analytical description of hypersonic boundary layer stability
[AIAA PAPER 93-2981] p 1051 A93-48174
- BOWERS, C. P.**
Repair of delaminations and impact damage in composite aircraft structures p 457 A93-24107
- BOWERS, DOUGLAS L.**
Advanced aerodynamic airframe/nozzle integration
[ISABE 93-7099] p 1187 A93-54075
Survey on techniques used in aerodynamic nozzle/airframe integration p 161 N93-13224
- BOWERS, M. W.**
Parallel implementation of the feature associated mesh embedding method for the 2D-Euler equations (FAME2D) p 225 A93-14278
- BOWERSOX, RODNEY D. W.**
Compressible turbulence measurements in a high-speed high Reynolds number mixing layer
[AIAA PAPER 93-0660] p 465 A93-24773
- BOWERSOX, RODNEY DALE WELCH**
Compressible turbulence in a high-speed high Reynolds number mixing layer p 878 N93-30583
- BOWLES, J. V.**
Near-optimal energy transitions for energy-state trajectories of hypersonic aircraft
[AIAA PAPER 92-4300] p 69 A93-13276
- BOWLES, JEFFREY V.**
Analysis of a hypersonic waverider research vehicle with a hydrocarbon scramjet engine
[AIAA PAPER 93-0509] p 386 A93-23256
Optimal trajectories for hypersonic launch vehicles p 1251 A93-54563
- BOWLES, R. I.**
On boundary-layer transition in transonic flow p 1087 A93-51280
- BOWLES, R. L.**
Three-dimensional simulation of the Denver 11 July 1988 microburst-producing storm p 1164 A93-50373
- BOWLES, ROLAND L.**
Lidar windshear detection for commercial aircraft p 341 A93-17864
Airborne Wind Shear Detection and Warning Systems. Fourth Combined Manufacturers' and Technologists' Conference, part 2
[NASA-CP-10105-PT-2] p 144 A93-14844
Airborne Wind Shear Detection and Warning Systems: Fourth Combined Manufacturers' and Technologists' Conference, part 1
[NASA-CP-10105-PT-1] p 488 N93-19590
Program overview: 1991 flight test objectives p 488 N93-19591
- BOWMAN, H. L.**
Effect of nozzle design on near acoustic field of supersonic circular and rectangular jets p 448 A93-19203
- BOWMAN, R. C., JR.**
Application of vanadium hydride compressors for Joule-Thomson cryocoolers p 1149 A93-48616
- BOYCE, R. R.**
Computational fluid dynamics code validation using a free piston hypervelocity shock tunnel p 960 A93-45545
- BOYCE, REX A.**
Bearing servicing tool
[NASA-CASE-MSC-21881-1] p 221 N93-14871
- BOYD, D. D., JR.**
HHC study in the DNW to reduce BVI noise - An analysis p 565 A93-29405
- BOYD, IAIN D.**
Comparison of continuum and particle simulations of expanding rarefied flows
[AIAA PAPER 93-0728] p 466 A93-24818
Relaxation of discrete rotational energy distributions using a Monte Carlo method p 1234 A93-55146
- BOYDEN, R. P.**
Further buffeting tests in a cryogenic wind tunnel
[NASA-TM-107621] p 22 N93-11610
- BOYDEN, RICHMOND P.**
Subsonic static and dynamic stability characteristics of the test technique demonstrator NASP configuration
[AIAA PAPER 93-0519] p 268 A93-21111
Supersonic dynamic stability characteristics of the test technique demonstrator NASP configuration
[AIAA PAPER 92-5009] p 367 A93-22285
- BOYER, K. M.**
Stall inception in single stage, high-speed compressors with straight and swept leading edges
[AIAA PAPER 93-1870] p 1076 A93-49745
- BOYER, KEITH M.**
Characterization of stall inception in high-speed single-stage compressors
[AD-A258973] p 365 N93-19093
- BOYLE, R. J.**
Heat transfer performance comparisons of five different rectangular channels with parallel angled ribs p 397 A93-18752
An algebraic turbulence model for three-dimensional viscous flows
[AIAA PAPER 93-0083] p 274 A93-22552
An algebraic turbulence model for three-dimensional viscous flows
[NASA-TM-105931] p 110 N93-14102
- BOYNTON, J. L.**
Investigation of rotor blade roughness effects on turbine performance
[ASME PAPER 92-GT-297] p 354 A93-19487
- BOZZOLA, RICCARDO**
Three-dimensional Navier-Stokes analysis of the tip clearance flow in linear turbine cascades
[AIAA PAPER 93-0391] p 282 A93-23068
Three-dimensional Navier-Stokes analysis of tip clearance flow in linear turbine cascades p 1235 A93-55364
- BRAASCH, MICHAEL S.**
Guidance accuracy considerations for realtime GPS interferometry p 342 A93-21146
- BRABBS, THEODORE A.**
Multi-heat addition turbine engine
[NASA-CASE-LEW-15094-1] p 522 N93-22034
- BRACALENTE, EMEGIO M.**
Doppler radar results p 488 N93-19595
NASA airborne radar wind shear detection algorithm and the detection of wet microbursts in the vicinity of Orlando, Florida p 490 N93-19611
- BRACKNEY, LARRY**
Applications of active adaptive noise control to jet engines
[NASA-CR-192277] p 522 N93-21210
- BRADEN, KEVIN W.**
Application of advanced guidance and navigation systems to flight control of aircraft and future space vehicles p 500 A93-28153
- BRADLEY, CURTISS**
Compound cycle engine for helicopter application
[NASA-CR-180824] p 55 N93-10348
- BRADLEY, DAVID E.**
Application of a neural network as a potential aid in predicting NTF pump failure
[NASA-TM-107667] p 442 N93-18332
- BRADLEY, JOHN**
The testing of fixed wing tanker and receiver aircraft to establish their air-to-air refuelling capabilities, volume 11
[AGARD-AG-300-VOL-11] p 514 N93-21305
- BRADLEY, R. G., JR.**
AGARD WG13 aerodynamics of high speed air intakes: Assessment of CFD results p 215 N93-13220
- BRADSHAW, P.**
Strong vortex/boundary layer interactions. I - Vortices high p 930 A93-43539
Strong vortex/boundary layer interactions. II - Vortices low p 965 A93-46744
Skin friction and velocity profile family for compressible turbulent boundary layers p 1070 A93-49008
- BRADSHAW, PETER**
Measurements in a pressure-driven three-dimensional turbulent boundary layer during development and decay
[AIAA PAPER 93-0543] p 415 A93-23283

BRADY, R. A.

- Measurements in the near-field of a turbulent wingtip vortex
[AIAA PAPER 93-0551] p 285 A93-23290
- Measurements in a pressure-driven three-dimensional turbulent boundary layer during development and decay
p 927 A93-41911
- Turbulent structure of a wingtip vortex in the near field
[AIAA PAPER 93-3011] p 1054 A93-48201
- Turbulence: The chief outstanding difficulty of our subject
p 783 N93-27428

BRADY, R. A.

- Mixing in the dome region of a staged gas turbine combustor
p 1109 A93-49612

BRAEDEN, E. W.

- Operation of the helicopter antenna radiation prediction code
[NASA-CR-193259] p 1030 N93-31110

BRAGG, M. B.

- LDV flowfield measurements on a straight and swept wing with a simulated ice accretion
[AIAA PAPER 93-0300] p 280 A93-23001
- Aerodynamics of a finite wing with simulated ice
p 784 N93-27437

BRAGG, MICHAEL B.

- Low-frequency flow oscillation over airfoils near stall
p 861 A93-41931

- Effect of underwing frost on transport aircraft takeoff performance
[DOT/FAA/CT-TN93/9] p 791 N93-27252

BRAHIMI, M. T.

- Prediction of the ice accretion with viscous effects on aircraft wings
[AIAA PAPER 93-0027] p 307 A93-20145

BRAILKO, L. G.

- Aircraft monitoring of the planeness of the existing and new runways
p 991 A93-45668

BRAISTED, W. R.

- Foreign object impact assessment of a high-Mach engine inlet
[AIAA PAPER 93-1630] p 711 A93-34158

BRAMSKI, STEFAN

- Laboratory for modelling of prospective board equipment systems for aircraft
p 374 A93-18529

BRAND, A. G.

- Navier-Stokes correlations to fuselage wind tunnel test data
p 765 A93-35937

BRANDEIS, J.

- Numerical study of jet interaction at super- and hypersonic speeds for flight vehicle control
p 184 A93-14379

BRANDON, JAY

- Vortex features of F-106B aircraft at subsonic speeds
[AIAA PAPER 93-3471] p 859 A93-41058
- Unsteady aerodynamic models for maneuvering aircraft
[AIAA PAPER 93-3626] p 1126 A93-48311

BRANDSMA, F. J.

- The application of an Euler method and a Navier Stokes method to the vortical flow about a delta wing
[AIAA PAPER 93-3510] p 984 A93-47276

BRANDT, M.

- Experimental and theoretical investigation of a research atomizer/combustion chamber configuration
[ASME PAPER 92-GT-137] p 401 A93-19369

BRANDT, MADS H.

- Flight data and flight safety in SAS
p 168 N93-15156

BRANGIER, FRANCIS

- The SSR mode-S data-link
p 312 A93-18553

BRANNON, CYPRIAN P.

- Aeroelastic character of a National Aerospace Plane demonstrator concept
[AIAA PAPER 93-1314] p 732 A93-33890

BRANSCOME, CAROL W.

- Improved efficiency of air transportation through aviation weather system modernization
p 308 A93-22144

BRANSTROM, B. R.

- Design and test of a small two stage counter-rotating turbine for rocket engine application
[AIAA PAPER 93-2136] p 1142 A93-49954

BRASLOW, A. L.

- Laminar flow flight experiments - A review
p 890 A93-41778

BRASWELL, DOROTHY O.

- Some effects of wing and body geometry on the aerodynamic characteristics of configurations designed for high supersonic Mach numbers
[AIAA PAPER 92-4246] p 463 A93-24493

BRASZ, J. J.

- Experimental and theoretical analysis of the flow in a centrifugal compressor volute
[ASME PAPER 92-GT-30] p 400 A93-19290

BRASZ, JOOST J.

- Analysis of jet/wake mixing in a vaneless diffuser
[ASME PAPER 92-GT-418] p 256 A93-19566

BRATTON, THOMAS

- Upgrade Precision Runway Monitor (PRM) Operational Test and Evaluation (OT/E) test plan
[DOT/FAA/CT-TN92/13] p 67 N93-11616
- Limited production Precision Runway Monitor (PRM) master test plan
[DOT/FAA/CT-TN92/23] p 192 N93-12899

BRATUKHIN, A. G.

- Main directions of improving the quality of aluminum-lithium alloys for welded aircraft structures
p 1146 A93-51104

BRAUN, DIETER

- Mission oriented investigation of handling qualities through simulation
[MBB-UD-0600-91-PUB] p 332 N93-17567

BRAUNSTINGL, R.

- An aerodynamic model for the longitudinal motion of flight training devices
p 1207 A93-54278

BRAY, D.

- Unsteady pressures under impinging jets in crossflows
p 399 A93-19220

BRAY, RICHARD S.

- NASA/FAA helicopter simulator workshop
[NASA-CP-3156] p 857 N93-30673
- Part 1: Executive summary
p 857 N93-30674

BRAY, ROBERT M.

- Flight test and wind-tunnel study of a scaled unmanned air vehicle
[AIAA PAPER 92-4075] p 37 A93-11260

BRAZIER, J. P.

- Investigations on entropy layer along hypersonic hyperboloids using a defect boundary layer
p 787 N93-27462

BRAZIER, J. PH.

- Second-order effects in hypersonic laminar boundary layers
p 1073 A93-49529

BRAZIER, MICHAEL E.

- Variable cycle engine concept
[ISABE 93-7065] p 1200 A93-54041

BREAULT, ROBERT P.

- Stray radiation in optical systems II; Proceedings of the Meeting, San Diego, CA, July 20-22, 1992
[SPIE-1753] p 1263 A93-55176

BREER, MARLIN D.

- Three-dimensional water droplet trajectory code validation using an ECS inlet geometry
[NASA-CR-191097] p 791 N93-27267

BREGGER, RANDALL E.

- Side-by-side hover performance comparison of MDHC 500 NOTAR and tail rotor anti-torque systems
p 796 A93-35956

BREINDEL, DOUGLAS S.

- A data acquisition system for high-speed rotor balancing
p 1261 A93-54396

BREINL, S.

- The influence of nocturnal aircraft noise on sleep and on catecholamine secretion
p 1163 A93-49554

BREITBACH, ELMAR

- The smart structures technology in the vibration control of helicopter blades in forward flight
p 366 A93-17721

BRENEMAN, KEVIN

- Flying qualities of a remotely piloted vehicle
[AIAA PAPER 92-4083] p 61 A93-11266

BRENNAN, PATRICK J.

- Flight data for the Cryogenic Heat Pipe (CRYOHP) Experiment
[AIAA PAPER 93-2735] p 1027 A93-46488

BRENNER, ALFRED

- Numerical methods for aerothermodynamic design of hypersonic space transport vehicles
[MBB-FE-211-S-PUB-0481] p 514 N93-21056

BRENNEN, C. E.

- Some unsteady fluid forces on pump impellers
p 413 A93-22265

BRENNER, G.

- CFD analysis of hypersonic chemically reacting flowfields around a generic shape
[AIAA PAPER 93-0323] p 281 A93-23015

BRENNER, G.

- Hypersonic viscous flow simulations
p 478 A93-27926

- Numerical simulation of shock/shock and shock-wave/boundary-layer interactions in hypersonic flows
p 1093 A93-52000

BRENNER, MARTIN J.

- Actuator and aerodynamic modeling for high-angle-of-attack aeroservoelasticity
[AIAA PAPER 93-1419] p 818 A93-37433

BRENNER, MATS A.

- GPS/GLONASS flight test, lab test and coverage analysis tests
p 313 A93-21143

BRENNER, R. C.

- In-situ bioventing: Two US EPA and Air Force sponsored field studies
[PB93-194231] p 1035 N93-32089

BRENNER, WILLIAM E.

- Runway Visual Range (RVR) Operational Test and Evaluation (OT&E) integration and OT&E operational test report
[DOT/FAA/CT-TN92/37] p 706 N93-25243

BRENTNER, KENNETH S.

- Helicopter noise prediction - The current status and future direction
p 448 A93-19202
- Sensitivity of acoustic predictions to variation of input parameters
p 565 A93-29404
- The influence of quadrupole sources in the boundary layer and wake of a blade on helicopter rotor noise
p 566 A93-29410

BRESCHIA, JOSEPH A.

- Evaluation of water-borne adhesive bonding primers for use on the advanced aircraft material aluminum-lithium
p 1211 A93-53420

BRETZ, P. L.

- Raising the high temperature limit of the nickel-iron-base superalloy
p 70 A93-12114

BREUER, KENNETH S.

- Close-up analysis of aircraft ice accretion
[AIAA PAPER 93-0029] p 309 A93-23239
- Bypass transition in two- and three-dimensional boundary layers
[AIAA PAPER 93-3050] p 1057 A93-48230

BREUER, KENNETH S.

- Close-up analysis of aircraft ice accretion
[NASA-TM-105952] p 148 N93-15360

BREUGELMANS, F. A. E.

- The leading edge vortex of a rotating stall cell
[ISABE 93-7009] p 1183 A93-53985

BREUGELMANS, F. A. E.

- The energy dissipation in a rotating stall cell
[ISABE 93-7010] p 1183 A93-53986

BREUGELMANS, FRANS A. E.

- Rotating stall: Modeling-measurement techniques; unsteady loss-unsteady flow field
p 424 A93-18732

BRIASSULIS, G.

- Wake structure of a helicopter rotor in forward flight
p 958 A93-45138

BRICE, JOHN L.

- Analysis of jet fuel thermal oxidation deposits by spectral fluorometric technique
p 1253 A93-55697

BRIDGEFORD, N.

- Bonded repair of multi-site damage
p 947 A93-45786

BRIDGEMAN, JOHN O.

- The development of a CFD potential method for the analysis of tilt-rotors
p 481 A93-29434

BRIDGES, ALAN L.

- Advanced airborne 3D computer image generation systems technologies for the year 2000
p 518 A93-28176

- An ac thin film electroluminescent (TFEL) display unit for cockpit control display unit application
p 518 A93-28179

BRIDGES, DAVID H.

- Elliptic cross section tip effects on the vortex wake of an axisymmetric body at angle of attack
[AIAA PAPER 93-2960] p 1124 A93-48154

BRIDGES, PHILIP D.

- Alternative solution to optimum gliding velocity in a steady head wind or tail wind
p 1136 A93-52458

BRILEY, W. R.

- Two- and three-dimensional blade vortex interactions
[NASA-CR-177567] p 293 N93-16942

BRILL, J.

- Comparative performance tests of a pitot-inlet in several European wind-tunnels at subsonic and supersonic speeds
p 130 N93-13221

BRINDLEY, W. J.

- Stress relaxation of low pressure plasma-sprayed NiCrAlY alloys
p 1211 A93-52870

BRINGEN, S.

- Spatial simulation of boundary layer instability - Effects of surface roughness
[AIAA PAPER 93-0075] p 262 A93-20187

BRINK-SPALINK, JAN

- Multiple pole rational-function approximations for unsteady aerodynamics
p 769 A93-37404

BRINKLEY, JAMES W.

- Evaluation of CKU-5/A ejection seat catapults under varied acceleration levels
[AD-A248021] p 29 N93-12489

BRIOTTET, X.

- Digital image processing applied to heat transfer measurement in hypersonic wind tunnel
[ONERA, TP NO. 1992-118] p 831 A93-38593

BRISTOW, J. W.

- The effect of exfoliation corrosion on the fatigue behavior of structural aluminum alloys
p 1017 A93-45778

BRISTOW, JOHN W.

- Aspects of aging aircraft - A transatlantic view
p 1026 A93-45776

BRITCHER, COLIN P.

- Analysis, modelling and simulation of the large-angle magnetic suspension test fixture
p 375 A93-20297

- The influence of the boundary layer on the subsonic near-wake of a family of bluff bodies
[AIAA PAPER 93-0525] p 284 A93-23266
- A magnetic suspension system with a large angular range
p 1139 A93-51295
- Approaches to control of the large angle magnetic suspension test fixture
[NASA-CR-191890] p 381 N93-16695
- Large angle magnetic suspension test fixture
[NASA-CR-193123] p 1015 N93-31836
- BRITT, CHARLES L.**
Comparison of simulated and actual wind shear radar data products p 490 N93-19610
- NASA airborne radar wind shear detection algorithm and the detection of wet microbursts in the vicinity of Orlando, Florida p 490 N93-19611
- BRITT, R. T.**
Aeroelastic effects on the B-2 maneuver response
[AIAA PAPER 93-3664] p 1128 A93-48344
- BRITT, ROBERT T.**
Response of B-2 aircraft to nonuniform spanwise turbulence p 1135 A93-52437
- BRITTON, KATHRYN H.**
Software requirements for the A-7E aircraft
[AD-A255746] p 229 N93-15052
- BRITTON, RANDALL K.**
An overview of shed ice impact studies in the NASA Lewis Icing Research Tunnel
[AIAA PAPER 93-0301] p 283 A93-23247
- An overview of shed ice impact in the NASA Lewis Icing Research Tunnel
[NASA-TM-105969] p 139 N93-15404
- BRITTON, THOMAS C.**
Analysis, modelling and simulation of the large-angle magnetic suspension test fixture p 375 A93-20297
- BROACH, DANA**
Identifying ability requirements for operators of future automated air traffic control systems
[AD-A256615] p 152 N93-14276
- BROCKHAUS, R.**
Nonlinear multi-point modelling and parameter estimation of the DO 28 research aircraft p 41 A93-12727
- Sensor fault detection using nonlinear observer and polynomial classifier p 170 N93-15182
- BROCKMAN, R. A.**
Foreign object impact assessment of a high-Mach engine inlet
[AIAA PAPER 93-1630] p 711 A93-34158
- BRODA, J.-C.**
Standing normal detonations and oblique detonations for propulsion
[AIAA PAPER 93-2325] p 1116 A93-50105
- BROEDE, JURGEN**
RB 199 high pressure compressor stage 3 spin pit tests p 176 N93-14893
- BROEK, D.**
Estimation of requirements of inspection intervals for panels susceptible to Multiple Site Damage p 948 A93-45795
- BROEK, DAVID**
The civil Damage Tolerance Requirements in theory and practice p 1026 A93-45777
- BROERS, C. A. M.**
An experimental study of the effects of deformable tip on the performance of fins and finite wings
[AIAA PAPER 93-3000] p 1053 A93-48190
- BROICHHAUSEN, K. D.**
Prediction of 2D viscous transonic flow in compressor cascades using a semi-empirical shock/boundary-layer interaction method
[ASME PAPER 92-GT-277] p 253 A93-19470
- BRONNIMANN, CH.**
A 'low-cost' full flight simulator for basic IFR training p 374 A93-18776
- BRONSON, RICHARD**
Flight test evaluation of precision-code differential GPS for terminal approach and landing p 33 A93-11294
- BROOKE, M.**
Application of analog computing to real-time simulation of stall and surge dynamics
[AIAA PAPER 93-2231] p 1080 A93-50037
- BROOKS, C. J.**
Canadian Forces helicopter ditchings: 1952-1990 p 493 N93-19685
- BROOKS, CUYLER W., JR.**
The Langley 8-ft transonic pressure tunnel laminar-flow-control experiment p 910 A93-41783
- BROOKS, DON**
Engineering simulators enhance 777 development p 1192 A93-53771
- BROOKS, THOMAS F.**
HHC study in the DNW to reduce BVI noise - An analysis p 565 A93-29405
- BROOKSBY, G.**
Sensors with centroid based common sensing scheme and their multiplexing p 1192 A93-52994
- BROPHY, GEORGEANN**
Arrow 227: Air transport system design simulation
[NASA-CR-192053] p 336 N93-18063
- BROSAN, M. J.**
X-31A flight flutter test excitation by control surfaces
[AIAA PAPER 93-1538] p 727 A93-34075
- BROT, A.**
A review of aging aircraft technology - An I.A.I. perspective p 3 A93-13634
- BROUGHTON, T.**
Design and technology for engine manufacture
[ISABE 93-7002] p 1194 A93-53979
- Innovation in engineering
[PNR-90889] p 59 N93-11207
- Simultaneous engineering in aero gas turbine design and manufacture
[PNR-90890] p 59 N93-11208
- BROUILLETTE, M.**
Performance data of the new free-piston shock tunnel T5 at GALCIT p 1011 A93-45498
- BROUWER, H. H.**
On the use of the method of matched asymptotic expansions in propeller aerodynamics and acoustics p 8 A93-11553
- BROWN, ALAN C.**
Fundamentals of low radar cross-sectional aircraft design p 802 A93-37376
- BROWN, ALAN S.**
Electronics show their age p 80 A93-13447
- Finding fault with avionics p 410 A93-21629
- High-temperature materials warm up for debut p 535 A93-28393
- Birth of the betas p 824 A93-38200
- What can Japan teach the U.S. about composites? p 1144 A93-49336
- BROWN, ALISON**
Differential GPS autonomous failure detection p 314 A93-21152
- BROWN, C.**
Helicopter approaches in low visibility using RGPS and EFIS p 142 A93-17309
- BROWN, CHAD**
SR-SCARLET 1: Peregrin
[NASA-CR-192048] p 337 N93-18155
- BROWN, D. R.**
An evaluation of thermal energy storage options for precooled gas turbine inlet air
[DE93-005980] p 754 N93-24975
- BROWN, DONALD E.**
Nonlinear vibration and radiation from a panel with transition to chaos p 205 A93-14543
- Nonlinear vibration and radiation from a panel with transition to chaos induced by acoustic waves p 398 A93-19173
- BROWN, GLEN J.**
Apparent mass effects on parafoil dynamics
[AIAA PAPER 93-1236] p 690 A93-35177
- Parafoil steady turn response to control input
[AIAA PAPER 93-1241] p 728 A93-35180
- BROWN, JAMES M.**
Embedded GPS: The Canadian Marconi approach p 886 N93-30330
- BROWN, JEFF**
An experimental study of a turbulent boundary layer in the trailing edge region of a circulation-control airfoil
[NASA-CR-191262] p 295 N93-17934
- BROWN, JEFFREY J.**
3D PARC Navier-Stokes analysis of an HSCT suppressor nozzle secondary inlet lip and duct
[AIAA PAPER 93-2568] p 1084 A93-50286
- BROWN, JON**
Wind shear alert system brings safety improvements to major U.S. airports p 529 A93-27396
- BROWN, K. W.**
Structural Tailoring of Advanced Turboprops (STAT). Theoretical manual
[NASA-CR-191017] p 556 N93-22005
- BROWN, MARK E.**
Lessons learned during testing of the Enhanced Position Location Reporting System (EPLRS) p 77 A93-10996
- BROWN, PHILIP W.**
Flight test operations using an F-106B research airplane modified with a wing leading-edge vortex flap
[AIAA PAPER 92-4094] p 42 A93-13261
- BROWN, R. C.**
Plume and wake dynamics, mixing, and chemistry behind a high speed civil transport aircraft p 1034 A93-45139
- Stratospheric aircraft exhaust plume and wake chemistry studies
[NASA-CR-189688] p 94 N93-12299
- BROWN, R. G.**
Update on GPS integrity requirements of the RTCA MOPS p 314 A93-21155
- A baseline GPS RAIM scheme and a note on the equivalence of three RAIM methods p 317 A93-21823
- BROWN, RICHARD**
Hydrogen-induced stress corrosion cracking susceptibility analysis of pitch links from the AH-64 Apache helicopter
[AD-A260692] p 736 N93-25895
- BROWN, RICHARD T.**
Automatic Through-the-Thickness braiding p 209 A93-15789
- BROWN, RODGER A.**
Comparison of airborne dual-Doppler and airborne/ground-based dual-Doppler analyses of North Dakota thunderstorms p 844 A93-37694
- BROWN, S. C.**
Natural environment application for NASP-X-30 design and mission planning
[AIAA PAPER 93-0851] p 531 A93-24915
- BROWN, S. W.**
Construction of a one-third scale model of the NASP
[AIAA PAPER 93-0427] p 386 A93-23345
- BROWNING, CLINT C.**
Application of advanced guidance and navigation systems to flight control of aircraft and future space vehicles p 500 A93-28153
- BROZENA, J. M.**
Airborne gravimetry from a light aircraft p 1245 A93-55972
- Multiple receiver, zero-length baseline kinematic GPS positioning techniques for airborne gravity measurement p 1240 A93-55974
- BRUCE, DAVID A.**
NDT for corrosion in aerospace structures - A review of NDT techniques p 1258 A93-54897
- BRUCKART, JAMES E.**
Radiated electric field measurements in U.S. Army helicopters p 209 A93-16163
- BRUCKER, DAVID**
Improved numerical simulation of Euler equations p 83 N93-10309
- BRUCKNER, A. P.**
Hugoniot analysis of the ram accelerator p 1023 A93-45500
- Initiation of combustion in the thermally choked ram accelerator p 1016 A93-45501
- Investigation of the aerothermodynamics of hypervelocity reacting flows in the ram accelerator
[NASA-CR-191715] p 140 N93-15588
- BRUCKNER, DEAN C.**
Automatic pulse shaping with the AN/FPN-42 and AN/FPN-44A Loran-C transmitters
[AD-A257860] p 319 N93-18309
- BRUEL, P.**
Investigation of a combustion zone behind a wedge p 1146 A93-51631
- BRUEL, PER V.**
Noise evaluation of light propeller-driven aircraft p 398 A93-19189
- BRUESKE, KURT F.**
Implications of three-dimensional tracer studies for two-dimensional assessments of the impact of supersonic aircraft on stratospheric ozone p 936 A93-41269
- BRUGHMANS, M.**
Application of FEM model correlation and updating techniques on an aircraft using test data of a ground vibration survey p 509 A93-29267
- BRUHIS, OFER**
Helicopter rotor disk and Blade Element comparison p 799 A93-35991
- BRUN, R.**
Flow problems posed by reentry in planetary atmospheres p 11 A93-12432
- BRUNE, G. W.**
Quantitative three-dimensional low-speed wake surveys p 785 N93-27447
- BRUNE, WILLIAM H.**
An aircraft instrument design for in situ tropospheric OH measurements by laser induced fluorescence at low pressures p 1159 A93-51528
- BRUNO, C.**
Reacting gas and surface coupling in high temperature air flows p 686 A93-34353
- Finite-rate H₂/air combustion effects in CRJ for hypersonic launchers
[ISABE 93-7084] p 1202 A93-54060
- BRUNO, THOMAS J.**
Measurement of diffusion in supercritical fluid systems - A review
[AIAA PAPER 93-0809] p 534 A93-24884
- BRUNS, J. E.**
Navier-Stokes analysis of three-dimensional S-ducts p 959 A93-45146

BRUSILOVSKII, I. V.

A data processing and measuring system with a traversing probe for studying flow in the rotating impeller of an axial-flow fan p 75 A93-10032

BRUSNIAK, L.

Flowfield dynamics in blunt fin-induced shock wave/turbulent boundary layer interactions [AIAA PAPER 93-3133] p 1063 A93-48298

BRUSOV, V. S.

Problems in the optimization of complex engineering systems p 1165 A93-49307

BRUST, F. W.

Accelerated corrosion fatigue test methods for aging aircraft p 198 A93-16623

BRYAN, E. C.

Using advanced technology to achieve reliability as well as high performance p 346 A93-18790

BRYAN, H. H.

A review of crack propagation under unsteady loading p 399 A93-19207

Review of crack propagation under unsteady loading p 837 A93-39416

BRYANSTON-CROSS, P. J.

Visualisation and analysis of three dimensional transonic flows by holographic interferometry p 1020 A93-44194

Particle imaging techniques and applications p 1020 A93-44195

BRYANT, CHARLES S.

Data acquisition for aeroelastic testing at the NASA Langley Transonic Dynamics Facility p 1250 A93-54397

BRYANT, Y. G.

Enhanced heat transport in environmental systems using microencapsulated phase change materials [SAE PAPER 921224] p 926 A93-41398

BRYCE, W. D.

Wing vortex refraction effects from BAC 1-11 flight tests p 450 A93-19226

BRYER, PAUL

Eagle RTS: A design for a regional transport aircraft [NASA-CR-192032] p 334 A93-18017

BRYKINA, I. G.

Approximate methods for heat flows toward the surface of three-dimensional bodies p 4 A93-10080

BSCHORR, O.

Reduction of propeller noise by active noise control p 450 A93-19224

Reduction of propeller noise by active noise control p 101 A93-10692

BUACHIDZE, G. L.

Ways of increasing the service life and reliability of bolted joints p 745 A93-35281

BUBLIKOV, I. I.

Oblique wave evolution in a plane subsonic boundary layer p 124 A93-15178

BUCHHOLZ, J. J.

Sensor fault detection using nonlinear observer and polynomial classifier p 170 A93-15182

BUCK, FRANK

FAA Technical Center Aeronautical Data Link Research Plan [DOT/FAA/CT-92/23] p 417 A93-15698

BUCK, GREGORY M.

Improved ceramic slip casting technique [NASA-CASE-LAR-14471-1] p 536 A93-20041

BUCKLES, JON

Eagle RTS: A design for a regional transport aircraft [NASA-CR-192032] p 334 A93-18017

BUCKLEY, D. J.

Spatial and temporal variations of the fluxes of carbon dioxide and sensible and latent heat over the FIFE site p 425 A93-20586

BUCKLEY, JAMES A.

Ribless ram air parachute [AD-D015351] p 20 A93-11050

High efficiency, low weight and volume energy absorbent seam [AD-D015531] p 554 A93-20765

BUCKLEY, JAMES E.

Investigation of roll requirements for carrier approach [AIAA PAPER 93-3649] p 1128 A93-48332

BUCKLEY, PAUL

Hydrogen-induced stress corrosion cracking susceptibility analysis of pitch links from the AH-64 Apache helicopter [AIAA-260692] p 736 A93-25895

BUCKLEY, W. R.

Modal analysis in the certification of a commercial aircraft p 509 A93-29241

BUDA, LASZLO I.

Reconnaissance capable F/A-18D optical and infrared window antifog systems [SAE PAPER 921182] p 890 A93-41361

BUDD, GERALD D.

Operational and research aspects of a radio-controlled model flight test program [AIAA PAPER 93-0625] p 504 A93-24742

Operational and research aspects of a radio-controlled model flight test program [NASA-TM-104266] p 339 A93-18616

BUELL, JOHN

Flight dynamics system software development environment (FDS/SDE) tutorial [NASA-TM-108580] p 230 A93-15502

BUETEFISCH, K. A.

Time-dependent 3-component laser-Doppler-anemometer and simultaneous position measurements in the flow of an aircraft engine p 538 A93-23809

The jet behaviour of an actual high-bypass engine as determined by LDA-measurements in ground tests p 175 A93-13218

BUETHE, S. A.

A rapid prototyping system for inflight simulation using the Calspan Learjet 25 [AIAA PAPER 93-3606] p 1191 A93-52691

BUFFINGTON, JAMES M.

Robust, nonlinear, high angle-of-attack control design for a supermaneuverable vehicle [AIAA PAPER 93-3774] p 1131 A93-51369

BUFFUM, DANIEL H.

Blade row interaction effects on flutter and forced response [AIAA PAPER 93-2084] p 1114 A93-49911

BUGGE, JENS-JORGEN

Preliminary results from a study of community response to noise from military aircraft exercise p 558 A93-28484

BUGGELN, R. C.

Two- and three-dimensional blade vortex interactions [NASA-CR-177567] p 293 A93-16942

BUGGELN, RICHARD C.

Projectile base bleed technology. Part 2: User's guide CMINT computer code, version 5.04-BRL [AD-A258630] p 551 A93-19999

BUI, TRONG T.

Some practical turbulence modeling options for Reynolds-averaged full Navier-Stokes calculations of three-dimensional flows [AIAA PAPER 93-2964] p 1048 A93-48158

BUIKOV, M. V.

Wind lifting of aerosol particles p 223 A93-15079

BUKOV, V. N.

An algorithm with prediction in a control problem with functional constraints p 757 A93-35307

BULIRSCH, R.

Combining direct and indirect methods in optimal control: Range maximization of a hang glider [REPT-313] p 371 A93-16618

BULK, TIM

Hypersonic reconnaissance aircraft [NASA-CR-192049] p 333 A93-17804

BULLEN, R. B.

Noise-induced reaction in a work community adjacent to aircraft runways - The Royal Australian Airforce p 559 A93-28496

BULLOCK, DANIEL

Embedded Bragg grating fiber optic sensor for composite flexbeams p 828 A93-37350

BULLOCK, ELLEN P.

Supersonic aeroelastic instability results for a NASP-like wing model [AIAA PAPER 93-1369] p 682 A93-33935

A flutter investigation of all-moveable NASP-like wings at hypersonic speeds [AIAA PAPER 93-1315] p 769 A93-37427

Supersonic aeroelastic instability results for a NASP-like wing model [NASA-TM-107739] p 718 A93-26553

BULMAN, M. J.

Advancing the state of the art hypersonic testing - HYTEST/MTMI [AIAA PAPER 93-2023] p 1113 A93-49860

BULZAN, DANIEL L.

Velocity and drop size measurements in a swirl-stabilized, combustor spray [NASA-TM-106130] p 813 A93-27130

BUNING, PIETER G.

Flowfield computations over the Space Shuttle Orbiter with a proposed canard at a Mach number of 5.8 and 50 degrees angle of attack [AIAA PAPER 93-0322] p 281 A93-23014

BUNNELL, L. ROY

A demonstration of simple airfoils: Structural design and materials choices [DE93-007882] p 789 A93-28662

Construction and testing of simple airfoils to demonstrate structural design, materials choice, and composite concepts p 879 A93-30979

BUR, R.

Passive control of a shock wave/turbulent boundary layer interaction in a transonic flow p 858 A93-40444

BURAYLEV, S. I.

Estimation of the service periods for complex systems in the case of a priori indeterminacy of system reliability data p 856 A93-43109

BURCHAM, FRANK W., JR.

Flight testing and simulation of an F-15 airplane using throttles for flight control [AIAA PAPER 92-4109] p 39 A93-11278

Flight-determined benefits of integrated flight-propulsion control systems p 183 A93-14370

Preliminary flight test results of a fly-by-throttle emergency flight control system on an F-15 airplane [AIAA PAPER 93-1820] p 1100 A93-49708

Flight-determined engine exhaust characteristics of an F404 engine in an F-18 airplane [AIAA PAPER 93-2543] p 1121 A93-50267

BURCHAM, KAREN L.

Complementary MLS and GNSS operations p 384 A93-21160

Planning for complementary MLS/GPS operations p 315 A93-21180

BURDISO, R. A.

Preliminary experiments on active control of fan noise from a turbofan engine p 759 A93-34957

BURDISO, RICARDO A.

Active control of fan noise from a turbofan engine [AIAA PAPER 93-0597] p 452 A93-23323

BURESTI, G.

Wing pressure loads in canard configurations - A comparison between numerical results and experimental data p 7 A93-11499

BURGE, LEGAND L.

Dr. Alexander H. Flax: Technologist of aeronautics [AD-A258441] p 456 A93-17890

BURGESS, D. H.

Noise-induced reaction in a work community adjacent to aircraft runways - The Royal Australian Airforce p 559 A93-28496

BURGESS, K. S.

Use of PCs in controlling simulated altitude environmental test conditions in support of turbine engine testing p 846 A93-37856

BURGESS, MALCOM A.

Synthetic vision - A view in the fog p 792 A93-37068

BURGGRAF, U.

Vibration excitation in laminar hypersonic boundary layers p 1237 A93-56028

BURGREEN, GREG W.

Improving the efficiency of aerodynamic shape optimization procedures [AIAA PAPER 92-4697] p 264 A93-20309

Aerodynamic shape optimization using preconditioned conjugate gradient methods [AIAA PAPER 93-3322] p 952 A93-45016

BURGSMUELLER, W.

Recent developments in low-speed TPS-testing for engine integration drag and installed thrust reverser simulation p 160 A93-13207

BURKE, M. J.

Active control of helicopter transmission noise p 568 A93-29428

BURKET, KEVIN

Receiving and scattering characteristics of an imaged monopole beneath a lossy sheet p 1158 A93-50543

BURKHARD, ALAN

Changing the utility subsystem paradigm [SAE PAPER 931598] p 1165 A93-49347

BURKHARD, NEIL

Domain engineering validation case study: Synthesis for the air traffic display/collision warning monitor domain version 01.00.03 [AD-A259407] p 503 A93-21671

BURKHARDT, C.

Transient thermal behaviour of a compressor rotor with axial cooling air flow and co-rotating or contra-rotating shaft p 903 A93-29946

BURKHARDT, LEO

Design of a hypersonic waverider-derived airplane [AIAA PAPER 93-0401] p 384 A93-21108

BURLEY, CASEY L.

Sensitivity of acoustic predictions to variation of input parameters p 565 A93-29404

BURLEY, JAMES R., II

Pilot/Vehicle display development from simulation to flight [AIAA PAPER 92-4174] p 51 A93-13310

BURNETT, DAVID

Experiences in fabrication of a waverider model for wind tunnel testing [AIAA PAPER 93-0510] p 328 A93-23257

- BURNETT, DAVID W.**
A re-evaluation of the waverider design process
[AIAA PAPER 93-0404] p 440 A93-23326
- BURNETT, JACK C.**
Liquid flow reactor and method of using
[AD-D015392] p 222 N93-15232
- BURNHAM, E. A.**
Initiation of combustion in the thermally choked ram accelerator
p 1016 A93-45501
- BURNLEY, V.**
Combustion noise and combustion instabilities in propulsion systems
p 100 N93-10682
- BURNS, J. G.**
Risk analysis for aging aircraft fleets
p 1025 A93-45775
- BURNS, JOHN A.**
Optimal control of lift/drag ratios on a rotating cylinder
p 76 A93-10275
Sensitivity calculations for a 2D, inviscid, supersonic forebody problem
[NASA-CR-191444] p 779 N93-27004
- BURNS, KEITH A.**
Development of an accuracy criteria for body-on-fin carryover interference
[AIAA PAPER 93-3633] p 1065 A93-48318
- BURNSIDE, O. H.**
Applications of advanced fracture mechanics to fuselage
p 1026 A93-45787
- BURPO, STEVEN J.**
Design and manufacturing concepts for thermoplastic structures
p 919 N93-30434
- BURR, R. F.**
Three-dimensional simulations of compressible mixing layers - Visualizations and statistical analysis
p 1235 A93-55360
- BURROS, RAYMOND H.**
Track moving emitters with Kalman processing
p 317 A93-22275
- BURROWS, S. P.**
Design of insensitive multirate aircraft control using optimized eigenstructure assignment
p 370 A93-23515
- BURSTEIN, P.**
Synchronous X-ray Sinography for nondestructive imaging of turbine engines under load
[AIAA PAPER 93-1819] p 1153 A93-49707
- BURTON, C. D.**
Measurements and computations of external heat transfer and film cooling in turbines
[RAE-TM-P-1223] p 722 N93-25455
- BURTON, RODNEY L.**
High-pressure hypervelocity electrothermal wind-tunnel performance study and subscale tests
p 1137 A93-49617
- BURTSCHELL, Y.**
On the compression process in a free-piston shock-tunnel
p 1136 A93-48041
- BUSCHEK, H.**
Research in robust control for hypersonic vehicles
[NASA-CR-192127] p 527 N93-20296
- BUSCHEK, HARALD**
Robust control of hypersonic vehicles considering propulsive and aeroelastic effects
[AIAA PAPER 93-3762] p 1131 A93-51357
- BUSH, R. H.**
Boundary condition procedures for CFD analyses of propulsion systems - The multi-zone problem
[AIAA PAPER 93-1971] p 1077 A93-49819
- BUSHNELL, D. M.**
Longitudinal vortex control - Techniques and applications (The 32nd Lanchester Lecture)
p 242 A93-18526
Supersonic laminar flow control
p 860 A93-41782
- BUSHNELL, DENNIS M.**
Reynolds number influences in aeronautics
[NASA-TM-107730] p 989 N93-31732
- BUSSARD, R. W.**
Fusion-electric propulsion for hypersonic flight
[AIAA PAPER 93-2611] p 1142 A93-50318
- BUSSI, GIUSEPPE**
An analysis of air-turborocket performance
[AIAA PAPER 93-1982] p 1141 A93-49829
Nozzle effects on linear stability behaviour of combustors
[ISABE 93-7044] p 1198 A93-54020
- BUSSOLETTI, JOHN E.**
Using a full potential solver for propulsion system exhaust simulation
p 689 A93-34487
- BUT, A. S.**
Calculation of the position of the flow separation line in an analog model of flow past a body
p 1176 A93-52958
- BUTCHER, M. C.**
The use of simultaneous engineering for the design and manufacture of the low pressure turbine for the Rolls-Royce Trent engine
[PNR-90887] p 59 N93-11206
- BUTER, THOMAS ALAN**
Numerical simulation of leading-edge receptivity to freestream vorticity
p 696 N93-25388
- BUTLER, R. G.**
Design philosophy for wind tunnel model positioning systems
[AD-A254958] p 192 N93-12552
- BUTLER, RANDALL S.**
Preliminary analysis of the J-52 aircraft engine component improvement program
p 363 N93-17686
- BUTLER, ROY G.**
Design philosophy for wind tunnel model positioning control systems
p 822 A93-37877
- BUTLER, STEWART E.**
Estimating the regional economic significance of airports
[AD-A257658] p 382 N93-17793
- BUTOV, A. M.**
Using current numerical methods in a mathematical model of flight vehicle synthesis
p 804 A93-39188
- BUTROS, I. B.**
Graph-theory studies of the possibility of occurrence of flight accidents and incidents during the take-off under special operating conditions
p 306 A93-18365
- BUTTERFIELD, C. P.**
Combined experiment, phase 1
[DE93-00012] p 485 N93-21766
- BUTTERWORTH-HAYES, PHILIP**
East Europe's aircraft builders look West
p 458 A93-28396
- BUTTRILL, CAREY S.**
Modeling and model simplification of aeroelastic vehicles: An overview
[NASA-TM-107691] p 64 N93-12216
- BUTTSCHARDT, W.**
Performance simulation of a combustion engine charged by a variable geometry turbocharger. I - Prerequisites, boundary conditions and model development. II - Simulation algorithm, computed results
p 1256 A93-54648
- BUXBAUM, O.**
Loads at the nose landing gears of civil transport aircraft during towbarless towing operations
p 45 A93-13629
- BUYUKATAMAN, K.**
High speed, heavily loaded and precision aircraft type epicyclic gear system dynamic analysis overview and special considerations
[AIAA PAPER 93-2151] p 1154 A93-49968
- BUZENKOV, V. V.**
Diagnostics of the hydraulic system of Tu-204 aircraft
p 396 A93-18360
Monitoring the purity of the working fluids of aircraft hydraulic systems during service
p 321 A93-18367
- BUZOGANY, L. E.**
Automated control of aircraft in formation flight
[AIAA PAPER 93-3852] p 1134 A93-51439
- BYCHKOV, YU. L.**
Determination of the takeoff and landing characteristics of aircraft by using a conditional polar
p 1007 A93-45662
- BYERLEY, A. R.**
Internal cooling passage heat transfer near the entrance to a film cooling hole - Experimental and computational results
[ASME PAPER 92-GT-241] p 404 A93-19450
- BYKOV, S. N.**
Using numerical control algorithms in stabilization systems with digital correction
p 941 A93-43113
- BYRD, GREGORY P.**
A quantitative method to estimate the microburst wind shear hazard to aircraft
p 309 A93-22172
- BYRD, RITA J.**
Coking characteristics of polyphenyl ether lubricants using a Static Coker and a Micro Carbon Residue Tester
p 77 A93-11341
- BYROM, TED GARY**
A finite element model for analysis of thermoviscoplastic behavior of hypersonic leading edge structures subject to intense aerothermal heating
p 137 N93-14631
- BYUN, CHANSUP**
Fluid-structural interactions using Navier-Stokes flow equations coupled with shell finite element structures
[AIAA PAPER 93-3087] p 1099 A93-48261
- BYVALTSEV, P. M.**
A flow calculation and aerodynamic design method for turbomachine cascades
p 12 A93-12764
A fast method for calculating three-dimensional transonic potential flows in turbomachine blade rows
p 125 A93-15215
- BYZOV, YA. B.**
Selection of the powerplant for a thermoplane
p 899 A93-42380

C

- CABALLERO, MARIA L.**
Proposal and preliminary design for a high speed civil transport aircraft. Swift: A high speed civil transport for the year 2000
[NASA-CR-192023] p 335 N93-18049
- CABE, J. L.**
Research and development of a turbo-accelerator for super/hypersonic transport
[ISABE 93-7066] p 1200 A93-54042
- CABE, JERRY L.**
Advanced bristle seals for gas turbine engines
[AD-A261296] p 752 N93-26564
- CABELL, R. H.**
The prediction of nonlinear dynamic loads on helicopters from flight variables using artificial neural networks
p 322 A93-19231
- CABLE, A. J.**
Upgrade of ballistic range facilities at AEDC - Two-thirds complete
[AIAA PAPER 93-0349] p 377 A93-23034
- CADA, GUENTHER**
Aerial cartography using SICAD NAV-AIR
p 1034 N93-31258
- CAHEN, CLAUDE**
Thermometry inside a swirling turbulent flame - CARS advantages and limitations
p 1146 A93-51634
- CAHEN, JULIETTE**
Validation of a Navier-Stokes code using a (k,epsilon) turbulence model applied to a three-dimensional transonic channel
[AIAA PAPER 93-0293] p 279 A93-22693
- CAI, HANLONG**
An experimental study for interaction flow between shock wave and turbulent boundary layer
p 120 A93-14355
- CAI, LUJING**
Adaptive array processing for airborne radar
p 883 A93-43412
- CAI, RUIXIAN**
A fool-proof aerodynamic design code for turbine cascades
p 259 A93-20117
An aerodynamic design program for contra-rotating turbine cascades
p 1067 A93-48521
- CAI, TIMIN**
Using a diagonal implicit algorithm to calculate transonic nozzle flow
[AIAA PAPER 93-2345] p 1082 A93-50119
- CAI, WEI**
Uniform high-order spectral methods for one- and two-dimensional Euler equations
p 476 A93-27068
- CAIN, A. B.**
An efficient approach to optimal aerodynamic design. I - Analytic geometry and aerodynamic sensitivities
[AIAA PAPER 93-0099] p 264 A93-20204
An efficient approach to optimal aerodynamic design. II - Implementation and evaluation
[AIAA PAPER 93-0100] p 264 A93-20205
- CAIN, TERENCE M.**
An experimental study of under-expanded jets
p 696 N93-25467
- CAIRNS, M. M.**
Preliminary evaluation of aviation-impact variables derived from numerical models
[PB93-190197] p 1034 N93-31202
- CALABRESE, P. R.**
Flight testing of a fiber optic temperature sensor
p 1105 A93-49476
- CALDWELL, DONALD**
Design and robustness issues for highly augmented helicopter controls
p 185 A93-14594
- CALDWELL, KEVIN M.**
TCAS II testing conflicts and resolutions
p 165 A93-14158
- CALDWELL, RONALD G.**
HL-20 operations and support requirements for the Personnel Launch System mission
p 1210 A93-53745
- CALEFFI, T.**
Initial development of a research flight simulator software
[AIAA PAPER 93-3590] p 1223 A93-52683
- CALI, PHILIP**
Implicit Euler calculation of supersonic vortex wake/engine plume interaction
[AIAA PAPER 93-0656] p 540 A93-24769
- CALISE, A. J.**
Near-optimal, asymptotic tracking in control problems involving state-variable inequality constraints
[AIAA PAPER 93-3748] p 1170 A93-51344

- Guidance and flight control law development for hypersonic vehicles
[NASA-CR-192102] p 526 N93-19960
- Research in robust control for hypersonic vehicles
[NASA-CR-192127] p 527 N93-20296
- CALISE, ANTHONY J.**
Optimal open multistep discretization formulas for real-time simulation p 757 A93-34539
Matched asymptotic expansion of the Hamilton-Jacobi-Bellman equation for aeroassisted plane-change maneuvers
[AIAA PAPER 93-3752] p 1143 A93-51348
Robust control of hypersonic vehicles considering propulsive and aerodynamic effects
[AIAA PAPER 93-3762] p 1131 A93-51357
- CALLIS, JAMES B.**
Video luminescent barometry - The induction period
[AIAA PAPER 93-0179] p 414 A93-22607
- CALMON, JEAN**
Propulsion of a supersonic transport: What are the challenges? II - Achievements p 174 A93-16852
- CALTA, DAVID**
TBD(exp 3)
[NASA-CR-192075] p 335 N93-18054
- CAMARDA, CHARLES J.**
Thermostructural applications of heat pipes for cooling leading edges of high-speed aerospace vehicles
p 91 N93-12460
- CAMBIER, JEAN-LUC**
Increase in stagnation pressure and enthalpy in shock tunnels
[AIAA PAPER 93-0350] p 377 A93-23035
Numerical simulations of a pulsed detonation wave augmentation device
[AIAA PAPER 93-1985] p 1112 A93-49832
Numerical study of the transient flow in the driven tube and the nozzle section of a shock tunnel
[AIAA PAPER 93-2018] p 1078 A93-49856
NO(x) reduction additives for aircraft gas turbine engines
[AIAA PAPER 93-2594] p 1122 A93-50306
Experimental investigation of Nozzle/Plume Aerodynamics at Hypersonic Speeds
[NASA-CR-191368] p 386 N93-18085
Increase of stagnation pressure and enthalpy in shock tunnels p 295 N93-18086
Analytical and experimental investigations of the oblique detonation wave engine concept
[NASA-TM-102839] p 1006 N93-32374
- CAMBY, D.**
A two-dimensional analysis of multiple matrix cracking in a laminated composite close to its characteristic damage state p 1157 A93-50405
- CAMCI, C.**
Fluid dynamics and convective heat transfer in impinging jets through implementation of a high resolution liquid crystal technique
[ISABE 93-7077] p 1220 A93-54053
- CAMERON, CHRISTOPHER P.**
Thermal effects testing at the National Solar Thermal Test Facility p 1255 A93-54402
- CAMERON, MURDO**
Innovative bagging techniques on a composite P-51 Mustang replica p 1191 A93-53405
- CAMPANA, J. P.**
The role of the radiologist in the medicolegal procedure after an aviation accident p 853 A93-39701
- CAMPBELL, BRYAN A.**
Development of a large-scale, outdoor, ground-based test capability for evaluating the effect of rain on airfoil lift
[NASA-TM-4420] p 779 N93-26899
- CAMPBELL, GLEN S.**
Canadian low-gravity research using parabolic aircraft p 384 A93-21908
- CAMPBELL, GRADY**
Domain engineering validation case study: Synthesis for the air traffic display/collision warning monitor domain version 01.00.03
[AD-A259407] p 503 N93-21671
- CAMPBELL, RICHARD L.**
Demonstration of multipoint design procedures for transonic airfoils
[AIAA PAPER 93-3114] p 1062 A93-48284
An approach to constrained aerodynamic design with application to airfoils
[NASA-TP-3260] p 24 N93-12321
- CAMPBELL, ROGER L.**
Hypervelocity scramjet capabilities of the T5 Free-Piston Tunnel at Caltech
[AIAA PAPER 92-5037] p 376 A93-22311
- CAMPBELL, STEVEN**
The Orlando TDWR testbed and airborne wind shear date comparison results p 145 N93-14851
- CAMPBELL, STEVEN D.**
An experimental cockpit display for TDWR wind shear alerts p 343 A93-22111
Performance results and potential operational uses for the prototype TDWR microburst prediction product p 432 A93-22190
- CAMPBELL, TAMMY P.**
Management of Automatic Data Processing (ADP) system documentation in the Department of Defense
[AD-A258507] p 571 N93-20048
- CAMPOS, E.**
Mechanisms of sound generation in subsonic jets p 101 N93-10688
- CAMPOS, L. M. B. C.**
On sound attenuation in boundary layers p 446 A93-19164
On automated analysis of flight test data p 512 N93-19913
- CANDEL, S.**
Low-frequency combustion instability mechanisms in a side-dump combustor p 1247 A93-55220
Combustion instabilities in a side-dump model ramjet combustor p 362 N93-17613
- CANDEL, SEBASTIEN**
Numerical solution of a free-boundary problem in hypersonic flow theory - Nonequilibrium viscous shock layers p 8 A93-11920
- CANDLER, G. V.**
Analysis of hypersonic nozzles including vibrational nonequilibrium and intermolecular force effects p 861 A93-41916
- CANDLER, GRAHAM V.**
Direct boundary value solution of wave rotor flow fields
[AIAA PAPER 93-0483] p 415 A93-23385
Simulation of ablation in Earth atmospheric entry
[AIAA PAPER 93-2789] p 1027 A93-46531
- CANFIELD, DENNIS V.**
Postmortem alcohol production in fatal aircraft accidents
[AD-A255766] p 143 N93-14026
- CANFIELD, ROBERT ARTHUR**
Integrated structural design, vibration control, and aeroelastic tailoring by multiobjective optimization p 1030 N93-31137
- CANNON, JOHN R.**
The analysis of expert performance in the redesign of the en route air traffic control curriculum p 571 A93-27189
- CANNON, M. E.**
Maintaining high accuracy GPS positioning 'on the fly' p 92 A93-11028
Analysis of a high-performance C/A-code GPS receiver in kinematic mode p 317 A93-21822
- CANNON, S.**
Observations of large-scale structures in wakes behind axisymmetric bodies p 965 A93-46748
- CANTIN, JEAN-GUY**
Weather forecasts for aviation in Canada (FACN and FTCN) - The way they are taught and how they can be made more suitable to the needs of pilots p 454 A93-22108
- CANUPP, P. W.**
Analysis of hypersonic nozzles including vibrational nonequilibrium and intermolecular force effects p 861 A93-41916
- CAO, CHUAN-JUN**
Calculation of sound field radiated by oscillating cascade p 231 A93-14269
- CAO, JIANFA**
The body-fitted coordinates generation for multi-element airfoils p 1231 A93-54598
- CAO, QIPENG**
Numerical simulation of the turbulent drag reduction by plate manipulators p 681 A93-33736
- CAO, Y.**
Conjugate modeling of high-temperature nose cap and wing leading edge heat pipes p 1259 A93-55465
- CAO, Y. H.**
A new method for calculation of helicopter maneuvering flight p 184 A93-14401
- CAPDEVILLE, G.**
Computation of turbulent compressible flows on a DLR wing and a blade to blade passage using an upwind scheme p 687 A93-34359
- CAPLOT, MICHEL**
Computation of far-field helicopter rotor tone noise
[ONERA-P-1990-5] p 943 N93-30110
- CAPONE, FRANCIS J.**
Performance characteristics of two multiaxis thrust-vectoring nozzles at Mach numbers up to 1.28
[NASA-TP-3313] p 874 N93-29160
- CAPORICCI, L.**
GPS integrity monitoring and system improvement with ground station and multistationary satellite support p 33 A93-11044
- CAPRIOTTI, D. P.**
Effects of compression and expansion ramp fuel injector configuration on scramjet combustion and heat transfer
[AIAA PAPER 93-0609] p 358 A93-21114
Evaluation of scramjet nozzle configurations and film cooling for reduction of wall heating
[AIAA PAPER 93-0744] p 358 A93-21118
The effect of entrance radius and film injection on wall heating in scramjet nozzles p 360 A93-22505
- CARADONNA, F. X.**
Free-wake computation of helicopter rotor flowfields in forward flight
[AIAA PAPER 93-3079] p 1059 A93-48253
The Application of CFD to rotary wing flow problems
[NASA-TM-102803] p 139 N93-15483
- CARADONNA, FRANCIS X.**
The development of a CFD potential method for the analysis of tilt-rotors p 481 A93-29434
- CARAM, JOSE M.**
Two-layer convective heating prediction procedures and sensitivities for blunt body reentry vehicles
[AIAA PAPER 93-2763] p 963 A93-46509
- CARAMASCHI, VITTORIO**
Design and manufacturing concepts of Eurofar Model No. 2 blades p 798 A93-35983
- CARANDE, R.**
JPL AIRSAR processing activities and developments p 1162 A93-47865
- CARBONE, D.**
Aero-thermal design of a cooled transonic NGV and comparison with experimental results p 904 N93-29957
- CARBONI, JEANNE D.**
Supersonic investigation of two dimensional hypersonic exhaust nozzles
[NASA-TM-105687] p 179 N93-15342
- CARDEN, HUEY D.**
Energy-absorbing-beam design for composite aircraft subfloors
[AIAA PAPER 93-1339] p 709 A93-33909
Effects of floor location on response of composite fuselage frames p 997 A93-46809
An overview of the crash dynamics failure behavior of metal and composite aircraft structures p 923 N93-30875
- CARDENAS, MANUEL**
Carbon/silicon carbide composite materials in advanced unmanned gas turbine engine combustors
[AIAA PAPER 93-1761] p 1144 A93-49658
Effect of geometry, bleed rates and flow splits on pressure recovery of a canted hybrid vortex-controlled diffuser
[AIAA PAPER 93-1762] p 1109 A93-49659
- CARDONE, G.**
Detection of Goertler vortices in hypersonic flow p 120 A93-14382
- CARDOSI, KIM M.**
An analysis of en route controller-pilot voice communications
[AD-A264784] p 935 N93-30611
- CARDOSO, A. DA S.**
Case studies in composite material structural design, manufacture and testing p 157 A93-14385
- CARDOSO, A. M. G.**
On automated analysis of flight test data p 512 N93-19913
- CARDULLO, FRANK M.**
Transport delay compensation - An inexpensive alternative to increasing image generator update rate
[AIAA PAPER 93-3563] p 1223 A93-52663
- CAREL, OLIVIER**
Applications of space techniques to civil aviation operations p 312 A93-20007
- CAREY, G. F.**
A performance comparison of massively parallel Parabolized Navier-Stokes solutions
[AIAA PAPER 93-0059] p 435 A93-20172
- CARGILL, A.**
Time-dependent predictions and analysis of turbine cascade data in the transonic flow region
[PNR-90957] p 139 N93-15489
- CARGILL, A. M.**
The low frequency aeroacoustics of buried nozzle systems p 1205 A93-54244
- CARICO, DEAN**
Simulation of DD-963 ship airwake by Navier-Stokes method
[AIAA PAPER 93-3002] p 1053 A93-48192
- CARIOU, R.**
Numerical simulation of three-dimensional supersonic flows using Euler and boundary layer solvers
[AIAA PAPER 93-0531] p 284 A93-23272
- CARLE, MARK**
The Airborne Ocean Color Imager - System description and image processing p 1157 A93-50369

- CARLETTI, M. J.**
The use of streamwise vorticity to enhance ejector performance
[AIAA PAPER 93-3247] p 966 A93-46792
- CARLIER, THIERRY M.**
GPS continuity - Initial findings p 314 A93-21167
- CARLILE, JULIE A.**
Brush seal leakage performance with gaseous working fluids at static and low rotor speed conditions
[ASME PAPER 92-GT-304] p 405 A93-19494
Brush seal low surface speed hard-rub characteristics
[AIAA PAPER 93-2534] p 1156 A93-50261
Brush seal bristle flexure and hard-rub characteristics
[NASA-TM-105864] p 421 A93-18321
Brush seal low surface speed hard-rub characteristics
[NASA-TM-106169] p 838 A93-27132
- CARLIN, P. W.**
Variable-speed generators with flux weakening
p 750 N93-25599
- CARLOMAGNO, G.**
Experimental study of the flow around a double ellipsoid configuration p 867 A93-42603
- CARLOMAGNO, G. M.**
Detection of Goertler vortices in hypersonic flow p 120 A93-14382
- CARLSON, ANN B.**
Shock interference prediction using direct simulation Monte Carlo p 778 A93-39258
Monte Carlo simulation of radiating reentry flows
[AIAA PAPER 93-2809] p 964 A93-46548
- CARLSON, JOHN R.**
Commercial turbofan engine exhaust nozzle flow analyses p 689 A93-34489
Prediction of static performance for single expansion ramp nozzles
[AIAA PAPER 93-2571] p 898 A93-41047
- CARLSON, LELAND A.**
Survey of nonequilibrium re-entry heating for entry flight conditions
[AIAA PAPER 93-3230] p 1039 A93-46682
- CARLTON, JOHN**
The benefits of ground maintenance simulators p 238 A93-18757
- CARMICHAEL, R. F., III**
Unified airport pavement design procedure p 380 N93-16318
- CARNE, THOMAS G.**
The natural excitation technique (NEXT) for modal parameter extraction from operating wind turbines
[DE93-010611] p 845 N93-28603
- CARNEY, TERRANCE**
Control of takeoff of a hypersonic aircraft using neural networks p 1167 A93-50744
- CAROLUS, THOMAS**
Acoustic performance of low pressure axial fan rotors with different blade chord length and radial load distribution p 449 A93-19212
- CARON, P.**
Infrared thermography of plastic instabilities in a single crystal superalloy
[ONERA, TP NO. 1993-18] p 916 A93-41031
- CARPARELLI, DONATO**
CWAS - Clean wing advisory system: A new approach to ice detection
[AIAA PAPER 93-0747] p 516 A93-24835
- CARPENTER, M. H.**
Numerical simulation of shock-induced combustion/detonation p 410 A93-20719
- CARPENTER, MARK H.**
High-order cyclo-difference techniques: An alternative to finite differences
[NASA-TM-107745] p 693 N93-25074
- CARPENTER, WILLIAM C.**
The role of under-determined approximations in engineering and science application p 441 N93-16763
Effect of design selection on response surface performance
[NASA-CR-4520] p 895 N93-29885
- CARPENTIER, J.**
Workshop on hypersonic flows for reentry problems January 22-25th 1990 (Antibes) - Inaugural address p 856 A93-42577
- CARPENTIER, JEAN**
The impact of air traffic on the atmospheric environment p 936 A93-42659
- CARR, L. W.**
Interferometric investigations of compressible dynamic stall over a transiently pitching airfoil
[AIAA PAPER 93-0211] p 278 A93-22628
Corrections to fringe distortion due to flow density gradients in optical interferometry
[AIAA PAPER 93-0631] p 539 A93-24748
Schlieren studies of compressibility effects on dynamic stall of transiently pitching airfoils p 480 A93-28608
- Prediction of stall and post-stall behavior of airfoils at low and high Reynolds numbers
[AIAA PAPER 93-3502] p 983 A93-47270
Transition effects on compressible dynamic stall of transiently pitching airfoils
[AIAA PAPER 93-2978] p 1050 A93-48171
Dynamic airfoil stall investigations p 786 N93-27453
- CARR, LAWRENCE W.**
The use of interferometry in the study of rotorcraft aerodynamics p 407 A93-19914
- CARRASCO, ARMANDO**
Spectral measurements of shock layer radiation in an arc-jet wind tunnel p 1251 A93-54409
- CARRAU, A.**
Taking into account surface roughness in computing hypersonic re-entry body p 686 A93-34354
- CARRELLI, DAVID J.**
The FAA/NASA flight loads monitoring program - The prototype system and its benefits for the aviation community p 486 A93-25125
- CARRERE, A.**
Investigation of the flow field through a variable pitch fan rotor with an inlet total pressure distortion
[ISABE 93-7029] p 1184 A93-54005
- CARROLL, B. F.**
Computations and experiments for a multiple normal shock/boundary-layer interaction p 688 A93-34486
- CARROLL, BRUCE F.**
Molecular mixing of jets in supersonic flow
[AIAA PAPER 93-2021] p 1078 A93-49858
- CARROLL, DAVID P.**
Selecting locations for avionics antennas - A structured approach p 892 A93-42794
- CARROTTE, J. F.**
The development of a large annular facility for testing gas turbine combustor diffuser systems
[AIAA PAPER 93-2546] p 1139 A93-50269
- CARSALLEN, W. E.**
Aerodynamic performance of a transonic low aspect ratio turbine nozzle
[ASME PAPER 92-GT-31] p 245 A93-19291
- CARTA, FRANKLIN O.**
Unsteady transition measurements on a pitching three-dimensional wing p 820 N93-27450
- CARTE, I. N.**
The numerical simulation of the hydrodynamic field from the pump impellers zone by means of the finite element method p 476 A93-26905
- CARTER, C.**
Electronic Counter Countermeasures/Advanced Radar Test Bed (ECCM/ARTB)
[AIAA PAPER 92-4098] p 34 A93-13267
- CARTER, C. H., JR.**
High temperature rectifiers and MOS devices in 6H-silicon carbide
[AD-A254725] p 90 N93-12340
- CARTER, MIKE**
Development of an expert system for cockpit emergency procedures p 845 A93-35915
- CARTER, NELSON DAVID**
A numerical study of hypersonic flow with strong surface blowing p 129 N93-13128
- CARTER, R. D. G.**
737-400 at Kegworth, 8 January 1989: The AAIB investigation p 491 N93-19661
- CARTY, THOMAS C.**
Runway Visual Range (RVR) Operational Test and Evaluation (OT&E) integration and OT&E operational test report
[DOT/FAA/CT-TN92/37] p 706 N93-25243
- CARUSO, STEVEN C.**
LEWICE droplet trajectory calculations on a parallel computer
[AIAA PAPER 93-0172] p 438 A93-22604
- CARVALHO, FERNANDO D.**
Misalignments of airborne laser beams due to mechanical vibrations p 394 A93-17762
- CARVER, D. B.**
AEDC expanded flow arc facility (HEAT-H2) description and calibration p 821 A93-37872
Flow calibration of two hypersonic nozzles in the AEDC HEAT-H2 high-enthalpy arc-heated wind tunnel
[AIAA PAPER 93-2782] p 1012 A93-46526
- CASALINI, FRANCESCO**
Inviscid finite-volume lambda formulation p 872 A93-42888
Secondary flow computation by means of an inviscid multigrid Finite Volume Lambda Formulation
[AIAA PAPER 93-1974] p 1077 A93-49821
- CASEY, W. L.**
Design considerations for air-to-air laser communications p 312 A93-18932
- CASHIN, TIMOTHY**
Arrow 227: Air transport system design simulation
[NASA-CR-192053] p 336 N93-18063
- CASSADAY, W. L.**
Ground clutter measurements using an aerostat surveillance radar p 929 A93-43381
- CASSELL, RICK**
Evaluation of category 3 MLS designs p 888 N93-30358
- CASSETTI, M.**
Finite-rate H₂/air combustion effects in CRJ for hypersonic launchers
[ISABE 93-7084] p 1202 A93-54060
- CASSIDAY, B. K.**
RACE pulls for shared control p 458 A93-29130
- CASTAN, C.**
Recent developments in low-speed TPS-testing for engine integration drag and installed thrust reverser simulation p 160 N93-13207
- CASTELBOU, CLAUDE**
Evolution of European air space toward precision navigation (P/RNAV) p 882 A93-43369
- CASTELLANI, A.**
Damping in aerospace composite materials p 1260 A93-55869
- CASTELLI, MICHAEL G.**
An overview of elevated temperature damage mechanisms and fatigue behavior of a unidirectional SCS-6/Ti-15-3 composite
[NASA-TM-106131] p 825 N93-26702
- CASTELLINO, R. C.**
Aerodynamic forces on maglev vehicles
[PB93-154813] p 782 N93-27413
- CASTLEDINE, C.**
Explosives detection systems for airport security gas chromatographic based devices p 881 N93-30276
- CASTOR, JERE**
Compound cycle engine for helicopter application
[NASA-CR-180824] p 55 N93-10348
- CASTRO-CEDEÑO, MARIO**
Design of a high-temperature experiment for evaluating advanced structural materials
[NASA-TM-105833] p 88 N93-11624
- CASTRO, I. P.**
Production of oscillatory flow in wind tunnels p 1218 A93-53812
- CATALANO, F. M.**
The effect of a high thrust pusher propeller on the flow over a straight wing
[AIAA PAPER 93-3436] p 978 A93-47228
- CATAPANG, DAVID R.**
Robust crossfeed design for hovering rotorcraft
[NASA-CR-193107] p 805 N93-27241
- CATT, JEFFREY A.**
Decreasing F-16 nozzle drag using computational fluid dynamics
[AIAA PAPER 93-2572] p 1084 A93-50289
- CATT, TYRONE**
The simulation of aircraft landing gear dynamics p 155 N93-14318
- CATTAFESTA, L.**
Supersonic shock wave/vortex interaction
[NASA-CR-192917] p 695 N93-25249
- CATTANI, LUIS C.**
Aircraft trajectory tracking and prediction
[AD-A259039] p 340 N93-18999
- CATTOLICA, ROBERT J.**
Characterization of electron beam propagation for hypersonic flight research applications
[AIAA PAPER 92-5087] p 452 A93-22357
- CAUGHEY, DAVID A.**
Implicit multigrid techniques for compressible flows p 862 A93-42429
Implicit multigrid Euler solutions with symmetric Total-Variation-Diminishing dissipation
[AIAA PAPER 93-3358] p 955 A93-45052
- CAVAGE, WILLIAM M.**
Ground vortex formation for uniform and nonuniform jets impinging on a ground plane
[AIAA PAPER 92-4251] p 80 A93-13362
The ground vortex flow field associated with a jet in a cross flow impinging on a ground plane for uniform and annular turbulent axisymmetric jets
[NASA-CR-4513] p 789 N93-28449
- CAVATORTA, ENRICO**
Study on vortex flow control of inlet distortion p 122 A93-14520
- CAVE, CHRIS**
Computational analysis of methods for reduction of induced drag
[AIAA PAPER 93-0524] p 474 A93-25536
- CAVONE, ANGELO A.**
Doppler global velocimetry measurements of the vortical flow above an F/A-18
[AIAA PAPER 93-0414] p 415 A93-23333
- CAZES, R. J.**
Aircraft tracking optimization of parameters selection p 3 A93-13628

CEBECI, T.

- An inviscid-viscous interaction approach to the calculation of dynamic stall initiation on airfoils [ASME PAPER 92-GT-128] p 249 A93-19362
 Prediction of stall and post-stall behavior of airfoils at low and high Reynolds numbers [AIAA PAPER 93-3502] p 983 A93-47270
 Three-dimensional compressible stability-transition calculations using the spatial theory p 783 A93-27431
- CEBECI, TUNCER**
 Recent progress in the analysis of iced airfoils and wings p 784 A93-27441
 An interactive boundary-layer approach to multielement airfoils at high lift p 785 A93-27445
- CEGAR, RICHARD D.**
 Analysis of a high bypass ratio engine installation using the chimera domain decomposition technique [AIAA PAPER 93-1808] p 1100 A93-49697
- CELENK, M.**
 DME/IP critical area determination on message passing processors p 31 A93-11010
- CELENK, MEHMET**
 Implementation of BMLS computer model on hypercube systems p 32 A93-11024
- CELL, ROBERTO**
 Efficient sensitivity analysis for rotary-wing aeromechanical problems [AIAA PAPER 93-1648] p 711 A93-34173
 Effects of higher order dynamics on helicopter flight control law design p 816 A93-35959
- CENTER, K. B.**
 Interactive hypersonic waverider design and optimization p 119 A93-14348
- CERCIGNANI, CARLO**
 Scattering kernels for gas-surface interaction p 943 A93-42580
- CERNIGLIA, MARK C.**
 Implications of three-dimensional tracer studies for two-dimensional assessments of the impact of supersonic aircraft on stratospheric ozone p 936 A93-41269
- CERRUTTI, P.**
 Rotation and cavitation of a marginal vortex p 11 A93-12433
- CERVISI, R. T.**
 The effects of hypersonic flight test requirements on research vehicle design [AIAA PAPER 93-0511] p 386 A93-23258
 A hypersonic waverider research vehicle [AIAA PAPER 93-0402] p 505 A93-25522
- CETINICH, MICHAEL R.**
 Distribution of aviation weather graphics via airline communications networks p 426 A93-22113
- CHA, SOYOUNG STEPHEN**
 Interferometric reconstruction of three-dimensional high-speed aerodynamic flows p 291 A93-16765
- CHADERJIAN, N. M.**
 Algorithm development with applications to aerodynamics and aeroelasticity p 422 A93-18566
- CHADERJIAN, NEAL M.**
 Comparison of two Navier-Stokes codes for simulating high-incidence vortical flow p 768 A93-37387
 Navier-Stokes prediction of a delta wing in roll with vortex breakdown [AIAA PAPER 93-3495] p 983 A93-47267
- CHADWICK, K. M.**
 Direct measurements of skin friction in supersonic combustion flow fields [ASME PAPER 92-GT-320] p 405 A93-19506
 Direct measurements of skin friction in supersonic combustion flow fields [AD-A262878] p 825 A93-28226
- CHAI, X. J.**
 Development and industrial application of the 'all-over-controlled vortex distribution method' for designing radial and mixed flow impellers [ASME PAPER 92-GT-262] p 405 A93-19466
- CHAIMOVICH, M.**
 A generic harmonic rotor model for helicopter flight simulation p 506 A93-27480
 Investigation of the flight mechanics simulation of a hovering helicopter p 798 A93-35990
- CHAJEC, WOJCIECH**
 Consideration of mass elements of the control system in a flutter analysis p 1249 A93-56217
- CHALLIS, L. A.**
 Design verification of ground run-up noise suppressors for afterburning engines p 910 A93-42892
- CHALLIS, LOUIS A.**
 Advances in the design of jet engine test facilities for military aircraft in Australia p 529 A93-28491
- CHALOT, F.**
 Application of the Galerkin/least-squares formulation to the analysis of hypersonic flows. I - Flow over a two-dimensional ramp p 866 A93-42593

- Application of the Galerkin/least-squares formulation to the analysis of hypersonic flows. II - Flow past a double ellipse p 868 A93-42608
- CHAMBERLIN, ERIC**
 Integrated Soviet VLF/Omega Receiver design p 316 A93-21198
- CHAMBERS, JOHN G.**
 Maintainability of large gas turbine aero engines [PNR-90987] p 58 A93-11069
- CHAMBRES, O.**
 Experimental studies of the turbulent structure of supersonic mixing layers [AIAA PAPER 93-0217] p 278 A93-22633
- CHAMIS, C. C.**
 Dynamic analysis of a pre-and-post ice impacted blade [AIAA PAPER 92-4273] p 54 A93-13333
 Structural tailoring of aircraft engine blade subject to ice impact constraints [AIAA PAPER 92-4710] p 358 A93-20319
 BLASIM - A computational tool to assess ice impact damage on engine blades [AIAA PAPER 93-1638] p 720 A93-34165
 Dynamic analysis of a pre-and-post ice impacted blade [NASA-TM-105829] p 90 A93-12197
 Root damage analysis of aircraft engine blade subject to ice impact [NASA-TM-105779] p 222 A93-15343
 Structural tailoring of aircraft engine blade subject to ice impact constraints [NASA-TM-106033] p 838 A93-26999
 Probabilistic assessment of composite structures [NASA-TM-106024] p 825 A93-27092
 Blasim: A computational tool to assess ice impact damage on engine blades [NASA-TM-106225] p 1031 A93-31193
- CHAMIS, CHRISTOS C.**
 Coupled multi-disciplinary simulation of composite engine structures in propulsion environment [ASME PAPER 92-GT-6] p 346 A93-19279
 Structural Tailoring/Analysis for Hypersonic Components - A computational simulation [AIAA PAPER 92-4722] p 325 A93-20324
 Damage progression in stiffened composite panels [AIAA PAPER 93-1345] p 738 A93-33915
 Quantification of uncertainties in composites [AIAA PAPER 93-1440] p 734 A93-33989
 Probabilistically configured adaptive composite structures [AIAA PAPER 93-1679] p 743 A93-34191
 Probabilistic evaluation of fuselage-type composite structures [NASA-TM-105881] p 212 A93-12735
 Multidisciplinary tailoring of hot composite structures [NASA-TM-106027] p 550 A93-19971
- CHAMITOFF, GREGORY E.**
 The application of intelligent search strategies to robust flight control for hypersonic vehicles [AIAA PAPER 93-3732] p 1143 A93-51331
- CHAMPAGNE, F.**
 Observations of large-scale structures in wakes behind axisymmetric bodies p 965 A93-46748
- CHAMPAGNE, GEORGE**
 A scoping study for hypersonic transport propulsion systems [ASME PAPER 92-GT-409] p 356 A93-19558
- CHAMPIN, B.**
 The beta-CEZ, a new high performance titanium alloy for aerospace engines [DS-2022] p 393 A93-17852
- CHAMPION, M.**
 Investigation of a combustion zone behind a wedge p 1146 A93-51631
 Combustion in supersonic flows p 199 A93-14627
- CHAMPION, MICHEL**
 Ignition and spread of combustion within a supersonic boundary layer p 535 A93-27732
- CHAN, AGNES**
 NASA advanced design program: Analysis, design, and construction of a solar powered aircraft [NASA-CR-192040] p 332 A93-17802
- CHAN, DANIEL C.**
 Development of a robust pressure-based numerical scheme for spray combustion applications [AIAA PAPER 93-0902] p 560 A93-24960
- CHAN, S. C.**
 CFD study of the flowfield due to a supersonic jet exiting into a hypersonic stream from a conical surface. II [AIAA PAPER 93-2926] p 1045 A93-48127
- CHAN, W. K.**
 Applications of laser techniques in fluid mechanics p 395 A93-17765

CHAN, W. S.

- Analysis of interlaminar stresses in symmetric and unsymmetric laminates under various loadings [AIAA PAPER 93-1511] p 740 A93-34050
- CHAN, Y. T.**
 Bearings-only and Doppler-bearing tracking using instrumental variables p 501 A93-29600
- CHANA, K. S.**
 Heat transfer and aerodynamics of a high rim speed turbine nozzle guide vane with profiled end walls [ASME PAPER 92-GT-243] p 253 A93-19452
 Heat transfer and aerodynamics of a high rim speed turbine nozzle guide vane with profiled end walls [AD-A258346] p 295 A93-17991
 Measurements and computations of external heat transfer and film cooling in turbines [RAE-TM-P-1223] p 722 A93-25455
 Heat transfer and aerodynamics of a 3D design nozzle guide vane tested in the Pyestock Isentropic Light Piston Facility p 901 A93-29928
- CHANAT, STEPHANIE**
 Preparation and characterization of continuous fiber reinforced zirconium diboride matrix composites for a leading edge material p 1211 A93-53445
- CHANDA, B. N.**
 Computer aided aerodynamic design of high pressure axial flow fan blade element p 16 A93-13649
- CHANDLER, FRANK O.**
 Aircraft cryogenic fuel system design issues [AIAA PAPER 93-2567] p 1121 A93-50285
- CHANDLER, P. R.**
 A Hopfield neural network for adaptive control [AIAA PAPER 93-3729] p 1130 A93-51329
- CHANDLER, PHILLIP R.**
 Symposium proceedings on Quantitative Feedback Theory [AD-A255527] p 187 A93-13872
- CHANDLER, T.**
 F405 engine in-flight thrust methodology development for the T-45A flight test program [AIAA PAPER 93-2544] p 1121 A93-50268
- CHANDRA, RAMESH**
 Coupled composite rotor blades under bending and torsional loads p 546 A93-27970
- CHANDRA, U.**
 Total quality management of forged products through finite element simulation p 1217 A93-53493
- CHANDRASEKHARA, M. S.**
 Interferometric investigations of compressible dynamic stall over a transiently pitching airfoil [AIAA PAPER 93-0211] p 278 A93-22628
 Corrections to fringe distortion due to flow density gradients in optical interferometry [AIAA PAPER 93-0631] p 539 A93-24748
 Schlieren studies of compressibility effects on dynamic stall of transiently pitching airfoils p 480 A93-28608
 Velocity and vorticity distributions over an oscillating airfoil under compressible dynamic stall p 778 A93-39403
 Transition effects on compressible dynamic stall of transiently pitching airfoils [AIAA PAPER 93-2978] p 1050 A93-48171
 Dynamic airfoil stall investigations p 786 A93-27453
- CHANDRASEKHARAN, S.**
 Total quality management of forged products through finite element simulation p 1217 A93-53493
- CHANETZ, B.**
 Shock/boundary layer interaction in a hypersonic flow in the presence of an entropy layer [ONERA, TP NO. 1992-181] p 773 A93-38743
 Shock wave/boundary layer interaction in a two-dimensional laminar hypersonic flow [ONERA, TP NO. 1992-182] p 773 A93-38744
- CHANETZ, BRUNO**
 Experiments on shock wave-boundary layer interaction at high Mach number with entropy layer effect [ONERA, TP NO. 1992-101] p 771 A93-38581
 Experiments on shock wave/boundary layer interaction in hypersonic flow p 970 A93-46888
- CHANEY, KENNETH**
 Active control for fin buffet alleviation [AIAA PAPER 93-3817] p 1133 A93-51408
- CHANEY, M. J.**
 Comparison of nonlinear tracking controllers for a compressible flow process p 66 A93-12224
- CHANEZ, P.**
 Navier-Stokes flow simulation in a 2D high pressure turbine cascade with a cooled slot trailing edge p 972 A93-46941
- CHANEZ, PHILIPPE**
 Viscous analysis of high pressure turbine inlet guide vane flow including cooling injections [AIAA PAPER 93-1798] p 1074 A93-49687

- CHANG, B.-C.**
A problem formulation for glideslope tracking in wind shear using advanced robust control techniques
[NASA-TM-104164] p 64 N93-11176
- CHANG, C. T.**
Comparison of reacting and non-reacting shear layers at a high subsonic Mach number
[NASA-TM-106198] p 814 N93-27610
Turbulence measurement in a reacting and non-reacting shear layer at a high subsonic Mach number
[NASA-TM-106186] p 989 N93-31839
- CHANG, CHAU-LYAN**
The transition prediction toolkit: LST, SIT, PSE, DNS, and LES p 783 N93-27429
- CHANG, CHIEN-CHENG**
Instability of a supersonic vortex sheet inside a circular duct p 1234 A93-55142
- CHANG, H. J.**
H-P adaptive methods for finite element analysis of aerothermal loads in high-speed flows
[NASA-CR-189739] p 420 N93-18093
- CHANG, JING-TANG**
Flutter analysis of composite panels on many supports p 1022 A93-45119
- CHANG, JINHWA**
A study of viscous interaction effects on hypersonic waveriders p 135 N93-14160
- CHANG, JOHN**
An investigation of dynamic stress reduction of multi-body aircraft using active gust control p 187 N93-13916
- CHANG, K. T.**
Holographic interferometric investigation of shock wave interaction with a ramp p 271 A93-21921
- CHANG, KWAN J.**
Sensitivity-based scaling for approximating structural response p 548 A93-28618
- CHANG, LEON**
Multigrid convergence of an implicit symmetric relaxation scheme
[AIAA PAPER 93-3357] p 954 A93-45051
- CHANG, RYA C.**
Improvement of high-AOA airfoil stalling performance by internal acoustic excitation p 243 A93-19134
- CHANG, STEPHEN**
A comparison of classical mechanics models and finite element simulation of elastically tailored wing boxes p 922 N93-30863
Tailored composite wings with elastically produced chordwise camber p 923 N93-30876
- CHANG, X.**
Radiative heat transfer from non-equilibrium high-enthalpy shock layers p 1024 A93-45515
- CHANG, XIN-YU**
Numerical study on atom-molecule radiation flowfield around a hypersonic blunt body p 770 A93-38434
- CHANG, Y. L.**
A three-dimensional algebraic grid generation scheme for gas turbine combustors with inclined slots
[NASA-CR-191095] p 746 N93-24759
- CHANG, YOUNG KEUN**
Dynamics of vortex rings in cross-flow p 134 N93-13917
- CHANG, YUAN B.**
A study on stability and response analysis of a nonlinear rotor system with mass unbalance and side load
[ASME PAPER 92-GT-7] p 400 A93-19280
- CHANGYOU, HUANG**
Computational method in optimal bending-twisting comprehensive design of wings of subsonic and supersonic aircraft
[AD-A262374] p 806 N93-27694
- CHAO, Y. C.**
The turbulence and mixing characteristics of the complex flow in a simulated augmentor p 1123 A93-51642
- CHAPLEO, A. Q.**
Over wing propeller aerodynamics p 113 A93-14189
- CHAPMAN, B.**
JPL AIRSAR processing activities and developments p 1162 A93-47865
- CHAPMAN, DEAN R.**
Stabilization of the Burnett equations and application to hypersonic flows p 778 A93-39410
Viscous hypersonic shock-shock interaction on a blunt body at high altitude
[AIAA PAPER 93-2722] p 962 A93-46477
- CHAPMAN, GARY T.**
Nonlinear aerodynamic parameter estimation and model structure identification
[AIAA PAPER 92-4502] p 15 A93-13308
A study of flow separation on an oscillating flap at Mach number 2.4
[AIAA PAPER 93-0436] p 286 A93-23350
- CHAPPEL, SHERRY**
Design of a cooperative problem-solving system for enroute flight planning: An empirical study of its use by airline dispatchers
[NASA-CR-192709] p 707 N93-25330
- CHAPPELL, M. A.**
Approach of modeling continuous turbine engine operation from startup to shutdown p 721 A93-34495
- CHAR, JIR-MING**
Ignition process of fuel droplet arrays in a supersonic flowfield p 535 A93-27766
- CHARLES, B. D.**
Effects of a trailing edge flap on the aerodynamics and acoustics of rotor blade-vortex interactions p 244 A93-19144
- CHARLES, D.**
Potential aerospace applications for metal matrix composites p 389 A93-21678
- CHARLTON, M. T.**
Flight test and analysis procedures for new handling criteria
[RAE-TM-FM-26] p 47 N93-10803
- CHASE, NED A.**
Test and analysis of an advanced technology landing gear p 37 A93-10917
- CHATTERJEE, A.**
Experimental investigation of leading edge vortices using LDA p 861 A93-42254
- CHATTERJEE, ANIMESH**
Computational analysis of methods for reduction of induced drag
[AIAA PAPER 93-0524] p 474 A93-25536
- CHATTERJEE, D.**
Coupling gain computation between antennas on circular cylinders at SHF/EHF frequencies p 933 N93-30309
- CHATTERJI, G. B.**
A fast algorithm for image-based ranging p 544 A93-27045
Discrete range clustering using Monte Carlo methods
[NASA-TM-104004] p 706 N93-24914
- CHATTERJI, GANO**
Passive range sensor refinement using texture and segmentation p 544 A93-27044
Vision based obstacle detection and grouping for helicopter guidance
[AIAA PAPER 93-3871] p 1098 A93-51457
- CHATTERJI, GANO B.**
Electro-optical navigation for aircraft p 1097 A93-50643
- CHATTOPADHYAY, ADITI**
Design sensitivity and optimization of composite cylinders p 71 A93-12781
Multidisciplinary optimization of helicopter rotor blades including design variable sensitivity
[AIAA PAPER 92-4783] p 323 A93-20289
Optimum design of high speed prop-rotors using a multidisciplinary approach p 798 A93-35985
Optimum Design of High Speed Prop-Rotors
[NASA-CR-190915] p 336 N93-18064
Design of high speed propellers using multiobjective optimization techniques p 336 N93-18065
Optimum design of high speed prop rotors including the coupling of performance, aeroelastic stability and structures p 337 N93-18066
An integrated optimum design approach for high speed prop-rotors including acoustic constraints
[NASA-CR-193222] p 893 N93-29153
- CHATURVEDI, ARVIND K.**
Comparison of toxicity rankings of six aircraft cabin polymers by lethality and by incapacitation in rats p 26 A93-10328
- CHATURVEDI, SUSHIL K.**
Langley 8-foot high-temperature tunnel oxygen measurement system p 1010 A93-44892
- CHATZIKONSTANTINOU, T.**
Recent advances in the numerical analysis of ram air wings - The three dimensional simulation code 'PARA3D'
[AIAA PAPER 93-1203] p 702 A93-35154
- CHAUDHURI, REAZ A.**
Fourier analysis of clamped moderately thick arbitrarily laminated plates p 206 A93-14571
- CHAUSSEE, DENNY S.**
The numerical study of 3-D flow past control surfaces
[AIAA PAPER 92-4650] p 14 A93-13305
A numerical study of the effect of geometry variation, turbulence models, and dissipation on the flow past control surfaces
[AIAA PAPER 93-2967] p 1048 A93-48161
- CHAUVIN, J.**
Supersonic through flow compressors - A preliminary study: COVAXS p 1001 A93-46930
- CHAUZY, SERGE**
Behavior of precipitating water drops under the influence of electrical and aerodynamical forces p 1034 A93-45176
- CHAVEZ, F. R.**
A unified hypersonic/supersonic method for aeroelastic applications including shock-unsteady wave interaction
[AIAA PAPER 93-1317] p 738 A93-33692
- CHAVEZ, FRANK R.**
Dynamics of hypersonic flight vehicles exhibiting significant aeroelastic and aeropropulsive interactions
[AIAA PAPER 93-3763] p 1131 A93-51358
Generic hypersonic vehicle performance model
[NASA-CR-192953] p 714 N93-25162
- CHAVIAROPOULOS, P.**
Meridional flow calculation using advanced CFD techniques
[ASME PAPER 92-GT-325] p 256 A93-19509
Design of axisymmetric channels with rotational flow
[AIAA PAPER 93-1117] p 1062 A93-48287
- CHAWLA, K.**
Numerical study of a delta planform with multiple jets in ground effect
[SAE PAPER 892283] p 1176 A93-53200
- CHAWLA, KALPANA**
Numerical simulation of STOL operations using thrust-vectoring
[AIAA PAPER 92-4254] p 15 A93-13342
Tracking flow features using overset grids
[AIAA PAPER 93-0197] p 276 A93-22617
- CHAWLA, M. D.**
Determination of tire-wheel interface pressure distribution for aircraft wheels
[AIAA PAPER 93-1343] p 709 A93-33913
- CHEATWOOD, F. MCNEIL**
The addition of algebraic turbulence modeling to program LAURA
[NASA-TM-107758] p 840 N93-27250
- CHEDIK, V. V.**
Optimization of the stiffness and mass characteristics of lifting surface structures modeled by an elastic beam p 827 A93-36789
- CHEE, SONNY H. S.**
Optical actuators for fly-by-light applications p 1172 A93-49475
- CHEGODAIEV, D. E.**
Control of the quality of dynamic processes in the valves of power-generating equipment p 832 A93-39030
- CHEKHOVSKII, V. F.**
Flow density distribution in a two-phase submerged jet p 836 A93-39144
- CHEN, BINGYONG**
Numerical simulation of passive control of shock-boundary layer interaction for transonic airfoil p 680 A93-33719
Second generation low order panel method and its application for a case of nacelle p 1231 A93-54595
- CHEN, CHING I.**
Aircraft failure detection and identification using neural networks
[AIAA PAPER 93-3869] p 1171 A93-51455
- CHEN, D.**
Bulging of fatigue cracks in a pressurized aircraft fuselage p 81 A93-13639
- CHEN, F. Y.**
Stability of fluttered panels subjected to in-plane harmonic forces p 1151 A93-49017
- CHEN, FANG**
A new aircraft integrated positioning and communication system based on satellite p 150 A93-14236
- CHEN, FANG-JENQ**
Boundary-layer transition extent measurements on a cone and flat plate at Mach 3.5
[AIAA PAPER 93-0342] p 474 A93-25517
Goertler instability and hypersonic quiet nozzle design p 480 A93-29155
- CHEN, FUQUAN**
A new method for predicting the end wall boundary layers and the blade force defects inside the passage of axial compressor cascades p 1236 A93-55589
- CHEN, FUQUAN**
A digital simulation and its experimental investigation for the response of gas-turbine engines to intake flow distortion p 120 A93-14366
On model for predicting blade force defect in end wall boundary layer inside axial compressor cascade p 862 A93-42271
Effect of steady-state circumferential pressure and temperature distortions on compressor stability p 1106 A93-48503
- CHEN, G.**
Numerical and experimental investigation of turbine tip gap flow
[AIAA PAPER 93-2253] p 1081 A93-50051
- CHEN, GANG**
A simulation study on take-off and landing dynamics of fly-by-wire control system aircraft p 1249 A93-55590

CHEN, GUIBIN

A simulation study on take-off and landing dynamics of the aircraft of a fly-by-wire control system
[AD-A259286] p 510 N93-19849

CHEN, GUIBIN

The vibration and flutter of composite material laminate p 543 A93-26617

CHEN, H.

The effects of blade loading in radial and mixed flow turbines
[ASME PAPER 92-GT-92] p 349 A93-19338
Performance parameters and assessment p 81 N93-10052

CHEN, H. C.

An installed nacelle design method using multiblock Euler solver
[AIAA PAPER 93-0528] p 284 A93-23269
Euler analysis of turbofan/supercan integration for a transport aircraft p 214 N93-13206

CHEN, H. H.

An inviscid-viscous interaction approach to the calculation of dynamic stall initiation on airfoils
[ASME PAPER 92-GT-128] p 249 A93-19362
Three-dimensional compressible stability-transition calculations using the spatial theory p 783 N93-27431

CHEN, HONG-QUAN

An AF3 algorithm for the calculation of transonic nonconservative full potential flows over wings or wing/body combinations p 125 A93-15341

CHEN, HSUN H.

Recent progress in the analysis of iced airfoils and wings p 784 N93-27441

CHEN, J.

Robust fault detection of jet engine sensor systems using eigenstructure assignment p 173 A93-14608
Design of a low sensitivity and norm multivariable controller using eigenstructure assignment and the method of inequalities
[AIAA PAPER 93-3802] p 1170 A93-51394

CHEN, J. B.

X-31A flight flutter test excitation by control surfaces
[AIAA PAPER 93-1538] p 727 A93-34075

CHEN, J. L.

A constrained flight route monitor system in terminal control area for air traffic control p 882 A93-42816

CHEN, J. S.

Variable structure controller design and its real-time analysis for microprocessor-based flight control systems p 181 A93-14229

CHEN, JEN P.

Navier-Stokes calculations for the unsteady flowfield of turbomachinery
[AIAA PAPER 93-0676] p 465 A93-24786

CHEN, JEN PING

Unsteady three-dimensional thin-layer Navier-Stokes solutions for turbomachinery in transonic flow p 218 N93-14025

CHEN, K. L.

A constrained flight route monitor system in terminal control area for air traffic control p 882 A93-42816

CHEN, K. M.

Receiving and scattering characteristics of an imaged monopole beneath a lossy sheet p 1158 A93-50543

CHEN, KEMING

Recent advances in jet simulation techniques for flight vehicles p 66 A93-12656

CHEN, KUILIN

Application of vibration-and-flutter integration analysis system for a trainer p 226 A93-14311

CHEN, KUO-HUEY

A coupled multi-block solution procedure for spray combustion in complex geometries
[AIAA PAPER 93-0108] p 539 A93-24230

CHEN, L.

Development of an optical sensor for active control of a gas turbine combustor
[AIAA PAPER 93-0118] p 360 A93-22568

CHEN, L. D.

Experimental and numerical investigations of the vortex-flame interactions in a driven jet diffusion flame
[AIAA PAPER 93-0455] p 534 A93-25532

CHEN, L. T.

A composite structured/unstructured-mesh Euler method for complex airfoil shapes p 784 N93-27439

CHEN, LIDE

Exhaust system model test and research p 1107 A93-48525

CHEN, M.-Z.

An investigation of spanwise mixing in multistage axial flow compressors
[ASME PAPER 92-GT-64] p 247 A93-19314

CHEN, MAOZHANG

A simple spanwise mixing model for turbulent diffusion and secondary flows in multistage axial-flow compressors p 204 A93-14482

A calculation of secondary flows and deviation angles in multistage axial-flow compressors p 1066 A93-48509

A computer program for meridional flows in multistage axial flow compressors with turbulence and multi-effects of 3-D flows p 1165 A93-49186

CHEN, MING-HUA

Theoretical investigation of combustion characteristics in ram-jet dump combustor with side-inlet p 346 A93-19121

Computations of a twin-jet impingement on a flat surface p 271 A93-22227

CHEN, MULAN

A method of finite element dynamic model optimization p 367 A93-20812

A software for optimum design of an aircraft structure p 938 A93-40495

CHEN, NAIXING

Numerical computations of turbomachinery cascade turbulent flows with shocks by using multigrid scheme p 112 A93-14167

CHEN, PEI-REN

Development of laser conducting landing system p 150 A93-14320

CHEN, PI-FUAY

Automated extraction of aircraft runway patterns from radar imagery
[AD-A254258] p 68 N93-11751

CHEN, QUAN

An experimental study of flow patterns and endwall heat transfer upstream of a surface-mounted rectangular obstruction in a turbulent boundary layer p 89 N93-11698

CHEN, R.

Numerical simulation of a low-emission gas turbine combustor using KIVA-II p 170 A93-14077

A preliminary study of the effect of equivalence ratio on a low emissions gas turbine combustor using KIVA-2 [DE92-018616] p 215 N93-13321

A three-dimensional algebraic grid generation scheme for gas turbine combustors with inclined slots [NASA-CR-191095] p 746 N93-24759

CHEN, ROBERT T. N.

An exploratory investigation of the flight dynamics effects of rotor rpm variations and rotor state feedback in hover [NASA-TM-103968] p 373 N93-19380

CHEN, RUIXI

Finite element nonlinear random response of beams to acoustic and thermal loads applied simultaneously [AIAA PAPER 93-1427] p 740 A93-33978

CHEN, S.

An optical fiber based position sensor with immunity to temperature variation p 743 A93-34287

CHEN, SHIH H.

Multistage turbomachinery flow solutions using three-dimensional implicit Euler method
[AIAA PAPER 93-2382] p 1083 A93-50150

CHEN, SHILU

Dynamic stability, coupling and active control of elastic vehicles with unsteady aerodynamic forces modeling p 182 A93-14282

Coupling characteristics analysis of elastic vehicle p 1169 A93-51189

CHEN, SHYI-YAUNG

Application of component mode synthesis to modeling the dynamic response of Bearingless Main Rotors p 796 A93-35976

CHEN, SHYI-YUANG

Dynamic System Coupler Program (DYSCO 4.1). Volume 1: Theoretical manual [AD-B131156L] p 848 N93-27531

Dynamic System Coupler Program (DYSCO 4.1). Volume 2: User's manual [AD-B131157L] p 848 N93-27589

Dynamic System Coupler Program (DYSCO 4.1). Volume 3: User's manual supplement [AD-B131158L] p 848 N93-27590

CHEN, SONG-TSUEN

Optimal vibration control for a flexible rotor with gyroscopic effects p 98 A93-13420

CHEN, T.

Computational analysis of nonlinear aeroelastic phenomena during stall flutter of cascaded airfoils [AIAA PAPER 93-2082] p 1079 A93-49909

CHEN, T. L. C.

An automated mode tracking strategy [AIAA PAPER 93-1414] p 739 A93-33970

CHEN, TIJIAN

Reliability assessment for self-repairing flight control systems p 907 A93-42804

CHEN, TING-YU

Optimum design of rotor-bearing systems with eigenvalue constraints [ASME PAPER 92-GT-307] p 405 A93-19497

CHEN, TONY D.

Langley 8-foot high-temperature tunnel oxygen measurement system p 1010 A93-44892

CHEN, TZU-CHANG

Multizone Navier-Stokes computations for a transonic projectile using MacCormack finite difference method p 113 A93-14192

CHEN, VICTOR

Composites technology for transport primary structure p 918 N93-30431

CHEN, WANCHUN

Euler solution for wing-body combination at supersonic speeds p 680 A93-33722

CHEN, WANNONG

Application of model reference adaptive control to speed control system in an aeroengine p 172 A93-14498

CHEN, WEI

Slicing model for foreign soft-body objects impacting on blade rows p 28 A93-12372

CHEN, WEIPIG

An ultralight freewheeling aircraft design study [AIAA PAPER 92-4194] p 44 A93-13371

CHEN, WENPU

YIDOUYU and its application to aircraft design [AD-A259262] p 513 N93-20605

CHEN, WON-ZON

Parameter optimization for an H2 problem with multivariable gain and phase margin constraints p 439 A93-22971

CHEN, XI

The computation of internal flow fields in centrifugal compressor impellers p 259 A93-20120

CHEN, XIANG-JUN

Dynamic analysis of annular cascade structures p 1259 A93-55586

CHEN, XIAOXING

Elimination of overtemperature in turbojet p 172 A93-14481

CHEN, XINHAI

Nonlinear multi-point modelling and parameter estimation of the DO 28 research aircraft p 41 A93-12727

CHEN, Y. K.

Convective heat-transfer rate distributions over a 140 deg blunt cone at hypersonic speeds in different gas environments [AIAA PAPER 93-2787] p 1027 A93-46529

CHEN, Y. N.

The vortex behaviour of the rotating-stall cell of a centrifugal compressor with vaned diffuser [ASME PAPER 92-GT-66] p 400 A93-19316

Determination of the zone of the stall cell by means of the baroclinic wave theory p 424 N93-18733

Rotating stall cell and Von Karman vortex street: A meteorological theory p 424 N93-18734

CHEN, Y.-J. D.

Face-gear drives: Design, analysis, and testing for helicopter transmission applications [NASA-TM-106101] p 839 N93-27133

CHEN, YANGQING

The body-fitted coordinates generation for multi-element airfoils p 1231 A93-54598

CHEN, YEN-MING

Development of the wake behind a circular cylinder impulsively started into rotatory and rectilinear motion p 1236 A93-55736

CHEN, YEN-SEN

Calculation of V/STOL aircraft aerodynamics with deflected jets in ground effect [AIAA PAPER 93-3530] p 986 A93-47287

CHEN, YIH-JEN D.

Parametric study of the gear blank structure in helicopter transmission design p 546 A93-27973

CHEN, Z.

BUAA inertial terrain-aided navigation (BITAN) algorithm p 149 A93-14235

CHEN, ZHI-WEI

A method and a software for constructing F-by-F random load spectrum p 506 A93-27375

CHEN, ZHIWEI

The method for developing F-by-F load spectra of fighter aircraft based on manoeuvres p 154 A93-14254

CHEN, ZUOBIN

The analysis and computation of viscous-inviscid interactive problem for three dimensional transonic flow p 681 A93-33741

CHENG, BIN

Air carriers' liability for passenger injury or death - The Japanese Initiative and Response to the recent EC Consultation Paper p 1226 A93-52930

CHENG, C. H.

Crack models for a transversely isotropic medium p 557 A93-24566

CHENG, CHIU-PIN

A new flight control design scheme using optimal dynamic output feedback p 368 A93-22883

- CHENG, H.**
Takeoff and landing analysis methodology for an airbreathing space booster p 914 A93-42927
- CHENG, J.**
An application of fuzzy logic and Dempster-Shafer theory to failure detection and identification p 96 A93-13079
- CHENG, JEN-CHIEH**
Upwind finite-volume Navier-Stokes computations on unstructured triangular meshes p 1070 A93-49011
A second-order upwind finite-volume method for the Euler solution on unstructured triangular meshes p 1087 A93-51738
- CHENG, KEMING**
The influence of wall friction on sidewall interference p 680 A93-33723
Simulation for hot jet by cryogenic wind tunnels p 730 A93-33750
- CHENG, LIANJUN**
The economic effectiveness analysis of technological progress in aviation industry p 1265 A93-54854
- CHENG, RONGHUI**
Investigation of flows in a controlled diffusion airfoil cascade passage p 1071 A93-49188
- CHENG, VICTOR H. L.**
Automatic guidance and control laws for helicopter obstacle avoidance p 728 A93-35518
Technologies for automating rotorcraft nap-of-the-earth flight p 885 A93-43784
- CHENG, WEI-MIN**
Three-dimensional flow analysis of a four-stage transonic axial compressor with inlet guide vanes p 1232 A93-54643
- CHENG, WEILI**
Accuracy analysis on image matching guidance systems p 62 A93-12653
- CHENG, YANQIU**
The forms of unsteady concentrated vortex-breakdown and its reactions to disturbance p 1231 A93-54594
- CHERENKOV, A. S.**
Diagnostics of the hydraulic system of Tu-204 aircraft p 396 A93-18360
- CHERNIKOVA, L. G.**
Investigation of the effect of physical processes on heat transfer to blunt bodies at low Reynolds numbers p 1090 A93-51877
- CHERNYKH, V. I.**
Effect of gasdynamic parameters on the specific weight of gas-turbine aircraft engines p 899 A93-42372
- CHERUKAT, P.**
An analysis of lift forces on aerosols in a wall bounded turbulent shear flow [DE93-003362] p 747 N93-24963
- CHESTER, R. J.**
Reinforcement of the F-111 wing pivot fitting with a boron/epoxy doubler system - Materials engineering aspects p 1214 A93-54241
- CHETELAT, MONIQUE**
Development and operation of a real-time simulation at the NASA Ames Vertical Motion Simulator [AIAA PAPER 93-3575] p 1208 A93-52671
- CHETTY, SHYAM**
Ideal aircraft handling quality models: Longitudinal axis [NAL-PD-FC-9203] p 187 N93-13566
- CHEU, TSU-CHIEN**
Optimal circumferential placement of cylindrical thermocouple probes for reduction of excitation forces [ASME PAPER 92-GT-423] p 406 A93-19571
- CHEUNG, F. B.**
Numerical study of an axisymmetric turbulent jet-impingement flow [AIAA PAPER 93-0652] p 543 A93-25545
- CHEUNG, K.**
A simple criterion for vortex breakdown [AIAA PAPER 93-0866] p 469 A93-24928
- CHEUNG, KWOK-HUNG**
NASA advanced design program: Analysis, design, and construction of a solar powered aircraft [NASA-CR-192040] p 332 N93-17802
- CHEW, J. W.**
Calculation of turbulent flow for an enclosed rotating cone [ASME PAPER 92-GT-70] p 400 A93-19320
Modelling thermal behaviour of turbomachinery discs and casings p 903 N93-29949
- CHEW, JOHN W.**
Prediction of rotating disc flow and heat transfer in gas turbine engines p 1256 A93-54634
- CHIANG, C. H.**
Fundamental studies of droplet interactions in dense sprays [AD-A261165] p 737 N93-25948
- CHIANG, HSIAO-WEI D.**
An analysis system for blade forced response [ASME PAPER 92-GT-172] p 352 A93-19398
- CHIANG, WUYING**
Dynamic analysis of rotor flexbeams based on nonlinear anisotropic shell models p 743 A93-34261
Structural dynamic analysis of bearingless rotor blade p 717 N93-25719
- CHIAO, SHING**
Aeroelastic analysis of composite wing with control surface p 157 A93-14386
- CHIAPPA, THIERRY**
Assessment of a 3-D Euler code for subsonic turbine vane flows and study of the non radial blade stacking [ASME PAPER 92-GT-63] p 247 A93-19313
- CHIARELLI, CHARLES**
Fluidic scale model multi-plane thrust vector control test results [AIAA PAPER 93-2433] p 1117 A93-50187
- CHIARINI, DAVID**
Hypersonic reconnaissance aircraft [NASA-CR-192049] p 333 N93-17804
- CHIARLONE, PAOLO**
Ground vibration test on Piaggio P. 180 aircraft - Comparison between two modal test methods p 509 A93-29246
- CHIBA, K.**
Research and development of high pressure compressor for SST and HST engine [ISABE 93-7068] p 1186 A93-54044
- CHIBA, KAORU**
A 2-D compressible N-S simulation of starting- and stalling-flows in a compressor cascades system [ISABE 93-7006] p 1183 A93-53982
- CHIENG, CHING-CHANG**
Multizone Navier-Stokes computations for a transonic projectile using MacCormack finite difference method p 113 A93-14192
Variant bi-conjugate gradient methods for the compressible Navier-Stokes solver with a two-equation model of turbulence [AIAA PAPER 93-3316] p 951 A93-45012
- CHILDERS, BROOKS A.**
Recent experiences with implementing a video based six degree of freedom measurement system for airplane models in a 20 foot diameter vertical spin tunnel p 821 A93-37763
Computer-aided light sheet flow visualization [AIAA PAPER 93-2915] p 1147 A93-48117
- CHILDRESS, OTIS, JR.**
Development and validation of 'quiet tail rotor' technology p 567 A93-29416
- CHILDS, ROBERT E.**
A study of compressible turbulence [AIAA PAPER 93-0659] p 465 A93-24772
- CHIMA, R. V.**
An algebraic turbulence model for three-dimensional viscous flows [AIAA PAPER 93-0083] p 274 A93-22552
Averaging techniques for steady and unsteady calculations of a transonic fan stage [AIAA PAPER 93-3065] p 1059 A93-48241
An algebraic turbulence model for three-dimensional viscous flows [NASA-TM-105931] p 110 N93-14102
- CHIMA, RODRICK V.**
Two-dimensional CFD modeling of wave rotor flow dynamics [AIAA PAPER 93-3318] p 952 A93-45014
- CHIMENTI, DALE E.**
Review of progress in quantitative nondestructive evaluation. Vol. 11B; Proceedings of the 18th Annual Review, Brunswick, ME, July 28-Aug. 2, 1991 Vol. 11B [ISBN 0-306-44206-X] p 406 A93-19582
- CHIMONAS, GEORGE**
Surface drag instabilities in the atmospheric boundary layer p 1163 A93-49069
- CHIN, GERALD Y.**
Update on GPS integrity requirements of the RTCA MOPS p 314 A93-21155
- CHIN, H.**
Efficient fault diagnosis of helicopter gearboxes [NASA-TM-106253] p 1032 N93-31846
- CHIN, HSINYUNG**
Fault detection of helicopter gearboxes using the multi-valued influence matrix method [NASA-TM-106100] p 838 N93-27069
- CHIN, J. H.**
Numerical methods in laminar and turbulent flow; Proceedings of the 7th International Conference, Stanford Univ., CA, July 15-19, 1991. Vol. 7, pts. 1 & 2 [ISBN 0-906674-77-8] p 743 A93-34301
- CHIN, J. S.**
Experimental techniques for the assessment of fuel thermal stability p 197 A93-14504
- CHIN, SUEI**
Development of nonlinear aerodynamic models for unsteady responses p 19 N93-10845
- CHIN, VINCENT D.**
Flowfield measurements about a multi-element airfoil at high Reynolds numbers [AIAA PAPER 93-3137] p 1064 A93-48300
- CHIN, YAN-SHIN**
Discontinuous Galerkin finite element method for two dimensional conservation laws [AIAA PAPER 93-0337] p 281 A93-23026
Discontinuous Galerkin finite element method for Euler and Navier-Stokes equations p 1235 A93-55357
- CHINITZ, W.**
Mixing and combustion studies using discrete orifice injection at hypervelocity flight conditions p 205 A93-14523
- CHINITZ, WALLACE**
High-pressure hypervelocity electrothermal wind-tunnel performance study and subscale tests p 1137 A93-49617
Some supersonic and hypersonic research at GASL in the 1960s and 70s [AIAA PAPER 93-2327] p 1145 A93-50107
- CHINZEI, NOBUO**
Effects of injector geometry on scramjet combustor performance p 359 A93-21670
Preliminary design of experimental sub-scale scramjet engine [AAS PAPER 91-639] p 1247 A93-55816
Mach 4 testing of scramjet inlet models [NAL-TR-1137] p 26 N93-12369
- CHIOU, J.**
Local heat transfer distribution in a rotating serpentine rib-roughened flow passage p 1259 A93-55459
- CHIRIKHIN, A. V.**
Numerical study of spontaneous nitrogen condensation in the axisymmetric hypersonic nozzles of wind tunnels p 777 A93-39143
- CHISHOLM, J.**
F405 engine in-flight thrust methodology development for the T-45A flight test program [AIAA PAPER 93-2544] p 1121 A93-50268
- CHITTUM, CHARLES B.**
Effects of seating configuration and number of type 3 exits on emergency aircraft evacuation [AD-A256616] p 143 N93-14277
- CHIU, ING-TSAU**
Navier-Stokes computations on full-span wing-body configuration with oscillating control surfaces [AIAA PAPER 93-3687] p 1065 A93-48356
- CHIU, STEPHEN H.**
A numerical investigation of a subsonic jet in a crossflow [AIAA PAPER 93-0870] p 469 A93-24931
- CHIU, T. W.**
An experimental study of the effects of deformable tip on the performance of fins and finite wings [AIAA PAPER 93-3000] p 1053 A93-48190
- CHIVANOV, S. V.**
Determination of the dynamic characteristics of heat exchangers for the heat recovery system of gas turbine engines p 834 A93-39054
Solution of the problem of determining the dynamic characteristics of the cross-flow heat exchanger of the heat recovery system of gas turbine engines p 834 A93-39055
A method for calculating the dynamic characteristics of heat exchangers with single-phase cryogenic coolants p 851 A93-39057
- CHIZHOV, V. V.**
Selection of the principal initial parameters for an axial-flow birotary turbine p 837 A93-39198
- CHMIELNIAK, TADEUSZ**
Modelling of the flow in the blade-ring design process of turbomachinery p 520 A93-27291
- CHO, DONG**
General aviation turbine markets - An economic overview [AIAA PAPER 92-4191] p 103 A93-13369
- CHO, JINSOO**
S-plane aerodynamics of nonplanar lifting surfaces p 958 A93-45134
- CHO, N.-H.**
Calculation of wake-induced unsteady flow in a turbine cascade [ASME PAPER 92-GT-306] p 255 A93-19496
- CHO, Y. C.**
Corrections to fringe distortion due to flow density gradients in optical interferometry [AIAA PAPER 93-0631] p 539 A93-24748
Fiber-optic interferometric sensors for measurements of pressure fluctuations - Experimental evaluation [AIAA PAPER 93-0738] p 540 A93-24828
- CHOI, D. H.**
Prediction of airfoil stall using Navier-Stokes equations in streamline coordinates p 787 N93-27456

CHOI, G. S.

Summary: Experimental validation of real-time fault-tolerant systems
[NASA-CR-190985] p 175 N93-13697

CHOI, HAECHEON

Turbulent drag reduction: Studies of feedback control and flow over riblets p 878 N93-30645

CHOI, JAI J.

Spurious symptom reduction in fault monitoring
[NASA-CR-191453] p 942 N93-29192

CHOI, K.

Helicopter plume detection by using an ultranarrow-band noncoherent laser Doppler velocimeter p 542 A93-25198

CHOI, K. Y.

Organized structure in a compressible turbulent shear layer p 961 A93-45730

CHOJNACKI, K. T.

Engineering method for calculating inlet face property profiles on high speed vehicle forebodies
[AIAA PAPER 93-3113] p 1062 A93-48283

CHOKANI, N.

Transonic shockwave/turbulent boundary layer interactions on a porous surface p 873 A93-43686

CHOKANI, NDAONA

Flow field measurements in a crossing shockwave turbulent boundary layer interaction at Mach 3
[AIAA PAPER 93-3434] p 977 A93-47226

Laser holographic interferometric measurements of the flow behind a rearward facing step

[AIAA PAPER 93-3515] p 985 A93-47279

Hypersonic flow past open cavities
[AIAA PAPER 93-2969] p 1049 A93-48163

Experimental investigation of the effects of aft blowing with various nozzle exit geometries on a 3.0 caliber tangent ogive at high angles of attack: Forebody pressure distributions

[NASA-CR-190935] p 22 N93-11605

CHOLLET, J. P.

Direct numerical simulation of combustion in turbulent supersonic flow
[DS-2138] p 393 N93-17746

CHOLLET, JEAN-PIERRE

Direct numerical simulation of nitric oxide evolution in underexpanded jets
[ASME PAPER 92-GT-372] p 355 A93-19534

CHONG, DIANNE

Use of titanium castings without a casting factor
[AD-A264414] p 1018 N93-31192

CHOO, Y. K.

Three-dimensional Navier-Stokes calculations using solution-adapted grids
[AIAA PAPER 93-0431] p 462 A93-24240

CHOPRA, INDERJIT

Modified sparse time domain technique for rotor stability testing p 157 A93-14593

Aeroelastic optimization of a composite helicopter rotor
[AIAA PAPER 92-4780] p 323 A93-20287

Coupled composite rotor blades under bending and torsional loads p 546 A93-27970

Aeromechanical stability of rotorcraft with advanced geometry blades

[AIAA PAPER 93-1304] p 725 A93-33880

Aeromechanical stability of a bearingless composite rotor in forward flight

[AIAA PAPER 93-1305] p 726 A93-33881

Effect of modeling techniques in the coupled rotor-body vibration analysis

[AIAA PAPER 93-1360] p 710 A93-33928

Aeromechanical stability of helicopters with composite rotor blades in forward flight p 794 A93-35904

Aeroelastic response, loads, and stability of a composite rotor in forward flight p 906 A93-41919

The Fourth Workshop on Dynamics and Aeroelastic Stability Modeling of Rotorcraft Systems

[AD-A255065] p 50 N93-12485

CHOU, HWEI-LAN

Pilot-in-the-loop analysis of propulsive-only flight control systems p 908 A93-42812

Low bandwidth robust controllers for flight
[NASA-CR-191774] p 372 N93-17800

Low bandwidth robust controllers for flight
[NASA-CR-193085] p 819 N93-27156

CHOU, JACK C.

Structural evaluation of curved stiffened composite panels fabricated using a THERM-Xsm process p 919 N93-30435

CHOU, L. C.

Burnett solutions along the stagnation line of a cooled cylinder in low-density hypersonic flows
[AIAA PAPER 93-2726] p 962 A93-46480

CHOU, LYNN C.

The Burnett shock structures in low density hypersonic flows
[AIAA PAPER 92-5048] p 273 A93-22320

CHOUDHARI, MEELAN

Roughness-induced generation of crossflow vortices in three-dimensional boundary layers
[NASA-CR-4505] p 780 N93-27096

CHOW, CHUEN-YEN

Juncture flow improvement for wing/pylon configurations by using CFD methodology
[AIAA PAPER 93-0522] p 283 A93-23264

Improvement of transonic wing buffet by geometric modifications

[AIAA PAPER 93-3024] p 1055 A93-48209

Navier-Stokes simulation of external/internal transonic flow on the forebody/inlet of the AV-8B Harrier II

[AIAA PAPER 93-3057] p 1058 A93-48234

CHOW, JIM

A computational study of wingtip vortex flowfield
[AIAA PAPER 93-3010] p 1054 A93-48200

CHOW, JIM S.

Measurements in the near-field of a turbulent wingtip vortex

[AIAA PAPER 93-0551] p 285 A93-23290

Turbulent structure of a wingtip vortex in the near field

[AIAA PAPER 93-3011] p 1054 A93-48201

CHOW, LOUIS C.

Design of a hydrogen test facility p 532 A93-25993

CHOW, S. K.

Scalar characteristics in a liquid-fuelled combustor with curved exit nozzle p 1123 A93-51643

CHOWDHURY, S.

A simplified approach for control of rotating stall. I - Theoretical development

[AIAA PAPER 93-2229] p 1080 A93-50035

A simplified approach for control of rotating stall. II - Experimental results

[AIAA PAPER 93-2234] p 1080 A93-50038

CHOY, F. K.

Modal analysis of multistage gear systems coupled with gearbox vibrations p 827 A93-36588

Effects of foundation excitation on multiple rub interactions in turbomachinery p 1260 A93-55996

CHPOUN, A.

DSMC numerical investigation of rarefied compression corner flow

[AIAA PAPER 93-3096] p 1061 A93-48270

Experimental study of transitional axisymmetric shock-boundary layer interactions at Mach 5

[AIAA PAPER 93-3131] p 1063 A93-48296

CHRISS, R. M.

Experimental and computational investigation of the NASA Low-Speed Centrifugal Compressor flow field

[ASME PAPER 92-GT-213] p 252 A93-19436

CHRISTHILF, DAVID M.

Design, test, and evaluation of three active flutter suppression controllers

[NASA-TM-4338] p 63 N93-10070

CHRISTIAN, N. L.

Optical interconnection and packaging technologies for advanced avionics systems p 77 A93-10960

CHRISTIE, D. R.

Buoyancy wave hazards to aviation p 430 A93-22151

CHRISTMAN, T. K.

Accelerated corrosion fatigue test methods for aging aircraft p 198 A93-16623

CHRISTY, STEVEN R.

Adverse weather test site selection study
[AD-A259012] p 339 N93-18895

CHU, JULIO

High-Reynolds-number test of a 5-percent-thick low-aspect-ratio semispan wing in the Langley 0.3-meter transonic cryogenic tunnel: Wing pressure distributions

[NASA-TM-4227] p 875 N93-29449

CHU, M. L.

Impact ice interface shear stresses caused by blade bending and twisting

[AIAA PAPER 93-0030] p 307 A93-20147

CHU, YUNFENG

Designing to aircraft system effectiveness/cost/time with VERT - The system analysis method for aircraft

[AIAA PAPER 93-3855] p 1144 A93-51442

CHUA, KIAT

Fast three-dimensional vortex method for unsteady wake calculations p 1178 A93-53233

Rotor design optimization using a free wake analysis

[NASA-CR-177612] p 693 N93-25075

CHUANG, C.-H.

Computation of optimal low- and medium-thrust orbit transfers

[AIAA PAPER 93-3855] p 1144 A93-51442

CHUANG, SHU-HAO

Theoretical investigation of combustion characteristics in ram-jet dump combustor with side-inlet

p 346 A93-19121

Computations of a twin-jet impingement on a flat surface p 271 A93-22227

CHUBAN, V. D.

RISK - interactive multidisciplinary system for designing airframes p 226 A93-14337

CHUBB, J. P.

The effect of exfoliation corrosion on the fatigue behavior of structural aluminum alloys p 1017 A93-45778

CHUN, CH.-H.

Experiments on the heat transfer and on the aerodynamic coefficients of a delta wing in rarefied hypersonic flows p 870 A93-42638

CHUN, KUE

A review of chemically reactive turbulent flow mixing mechanisms and a new design for a low NO(x) combustor p 1109 A93-49508

CHUNG, H. T.

Two-dimensional transonic flow around VKI turbine cascade p 1232 A93-54640

CHUNG, HEE-TAEG

Influence of trailing-edge grid structure on Navier-Stokes computation of turbomachinery cascade flow

p 111 A93-14078

CHUNG, JIN-DEOG

Mean flow interactions of a counter-rotating propeller p 552 A93-20289

CHUNG, KUNG-MING

Hypersonic turbulent expansion-corner flow with shock impingement

[AIAA PAPER 92-5101] p 274 A93-22371

Damping of surface pressure fluctuations in hypersonic turbulent flow past expansion corners

p 860 A93-41914

Exploratory study of shock reflection near an expansion corner

[AIAA PAPER 93-3132] p 1063 A93-48297

CHUNG, M. K.

A prediction model for the vortex shedding noise from the wake of an airfoil or axial flow fan blades

p 1265 A93-55995

CHUNG, T. J.

Effects of reacting flows with turbulence and shock waves on efficiency of scramjet combustors

p 69 N93-11133

Turbulence interacting with chemical kinetics in airbreathing combustion of ducted rockets

p 734 N93-26012

CHUNG, VINCENT

Carbon/silicon carbide composite materials in advanced unmanned gas turbine engine combustors

[AIAA PAPER 93-1761] p 1144 A93-49658

CHUNG, Y. M.

A numerical study of unsteady supersonic compression ramp flows

[AIAA PAPER 93-0883] p 470 A93-24943

CHUPP, RAYMOND E.

Evaluation of brush seals for limited-life engines p 411 A93-21665

CHURSANOV, S. A.

Computerized synthesis of three-dimensional kinematic landing gear schemes with a single turning axis

p 891 A93-42376

CHURSHIN, V. A.

Localization of noise sources in the exhaust jet of a turbofan engine p 1003 A93-47509

CHYZEWSKI, THOMAS S.

Solution of the Euler and Navier Stokes equations on parallel processors using a transposed/Thomas ADI Algorithm

[AIAA PAPER 93-3310] p 1036 A93-45006

CHYU, MINGKING K.

CFD analysis on control of secondary losses in STME LOX turbines with endwall fences p 419 N93-17289

CHYU, WEI J.

Juncture flow improvement for wing/pylon configurations by using CFD methodology

[AIAA PAPER 93-0522] p 283 A93-23264

Effects of bleed-hole geometry and plenum pressure on three-dimensional shock-wave/boundary-layer/bleed interactions

[AIAA PAPER 93-3259] p 967 A93-43800

Navier-Stokes simulation of external/internal transonic flow on the forebody/inlet of the AV-8B Harrier II

[AIAA PAPER 93-3057] p 1058 A93-48234

CICCOLI, MARIE-CLAUDE

Homenthalpic-flow approach for hypersonic inviscid non-equilibrium flows

[INRIA-RR-1652] p 788 N93-28440

CIMBALA, JOHN M.

Reduction in size and unsteadiness of a VTOL ground vortex by ground fences

[NASA-CR-192997] p 700 N93-26049

CINCOTTA, MANUEL

Articulated control surface

[AD-D015464] p 371 N93-16463

CINCOTTA, MANUEL, JR.

Articulated fin/wing control system

[AD-D015712] p 909 N93-29278

CINNELLA, PASQUALE

A comparison of 'new' and 'old' flux-splitting schemes for the Euler equations
[AIAA PAPER 93-0876] p 470 A93-24937

Multi-block calculations for flows in local chemical equilibrium
[AIAA PAPER 93-2999] p 1053 A93-48189

CINQUE, G.

Numerical model for predictions of reverse flow combustor aerothermal characteristics
p 1123 A93-51645

Numerical simulation of gas turbine combustors with complex geometries
[ISABE 93-7128] p 1204 A93-54103

CINQUETTI, P.

Natural laminar flow test in-flight visualization
p 482 N93-19921

CIRIELLO, S.

Heat transfer, adiabatic effectiveness, and injectant distributions downstream of a single row and two staggered rows of compound angle film-cooling holes
p 201 A93-13976

CITAVY, JAN

On aerodynamic loading of linear compressor cascades
[ASME PAPER 92-GT-275] p 253 A93-19468

CITURS, KEVIN D.

Development of flying qualities and agility evaluation maneuvers
[AIAA PAPER 93-3645] p 1127 A93-48329

Aircraft control requirements and achievable dynamics prediction
[AIAA PAPER 93-3648] p 1128 A93-48331

Investigation of roll requirements for carrier approach
[AIAA PAPER 93-3649] p 1128 A93-48332

CIVINSKAS, K. C.

Chimera grids in the simulation of three-dimensional flowfields in turbine-blade-coolant passages
[AIAA PAPER 93-2559] p 1157 A93-50280

CLAPP, LEONARD H.

Characterization of electron beam propagation for hypersonic flight research applications
[AIAA PAPER 92-5087] p 452 A93-22357

CLARK, B. A. J.

A history of visual approach guidance indicator systems in Australia
p 498 A93-25171

CLARK, DAVID

Weather information requirements for Terminal Air Traffic Control Automation
p 429 A93-22146

CLARK, G.

Aspects of fatigue affecting the design and maintenance of modern military aircraft
p 1043 A93-52548

CLARK, J. P.

Measurement of turbulent spots and intermittency modelling at gas-turbine conditions
p 902 N93-29934

CLARK, RAYMOND

Flight evaluation of a computer aided low-altitude helicopter flight guidance system
p 820 N93-28869

Flight evaluation of a computer aided low-altitude helicopter flight guidance system
[NASA-TM-103998] p 994 N93-32225

CLARK, ROBERT M.

Description and capabilities of the Navcore-V GPS receiver engine
p 312 A93-21127

CLARK, RONALD K.

Thermal control/oxidation resistant coatings for titanium-based alloys
p 74 N93-12457

CLARK, ROSS D.

The V-22 for SOF
p 800 A93-36026

CLARK, WILLIAM A. T.

Compatibility of potential reinforcing ceramics with Ni and Fe aluminides
[NASA-CR-192232] p 394 N93-18784

CLARK, WILLIAM S.

Nonreflecting boundary conditions for linearized unsteady aerodynamic calculations
[AIAA PAPER 93-0882] p 475 A93-25553

Linearized Euler predictions of unsteady aerodynamic loads in cascades
p 480 A93-29318

Prediction of unsteady-flows in turbomachinery using the linearized Euler equations on deforming grids
[NASA-CR-192919] p 747 N93-25109

CLARKE, JERRY

A study of CFD algorithms applied to complete aircraft configurations
[AIAA PAPER 93-0784] p 468 A93-24854

CLAUS, RUSSELL W.

Multidisciplinary propulsion simulation using NPSS
[AIAA PAPER 92-4709] p 435 A93-20318

CLAWSON, K. L.

Vortex wake characteristics of B757-200 and B767-200 aircraft using the tower fly-by technique
[PB93-180255] p 878 N93-30387

Vortex wake characteristics of B757-200 and B767-200 aircraft using the tower fly-by technique
[PB93-180263] p 878 N93-30388

CLAY, K.

Neutron diffraction residual stress studies for aero-engine component applications
[PNR-90908] p 85 N93-11014

CLAYTON, J. Q.

Aspects of fatigue affecting the design and maintenance of modern military aircraft
p 1043 A93-52548

CLEMENTS, SHAUN

Online vibration control of a flexible rotor/bearing system
p 219 N93-14468

CLEMMONS, MICHAEL G.

Antitorque safety and the RAH-66 Fantail
p 795 A93-35912

CLEMMONS, PAUL

Optimal open multistep discretization formulas for real-time simulation
p 757 A93-34539

CLER, DANIEL L.

Experimental investigation of spherical-convergent-flap thrust-vectoring two-dimensional plug nozzles
[AIAA PAPER 93-2431] p 898 A93-41045

CLERE, J. M.

Air accidents in the French Air Force
p 492 N93-19676

CLEVELAND, JEFF I., II

Use of Convex supercomputers for flight simulation at NASA Langley
p 1013 A93-46806

Use of high performance networks and supercomputers for real-time flight simulation
p 731 N93-25574

CLIFF, E. M.

Finite memory approximations for a singular neutral system arising in aeroelasticity
p 97 A93-13246

CLIFF, EUGENE

Sensitivity calculations for a 2D, inviscid, supersonic forebody problem
[NASA-CR-191444] p 779 N93-27004

CLIFF, EUGENE M.

Hodograph analysis in aircraft trajectory optimization
[AIAA PAPER 93-3742] p 1101 A93-51338

The Generalized Legendre-Clebsch Condition on state/control constrained arcs
[AIAA PAPER 93-3746] p 1170 A93-51342

CLIFF, SUSAN E.

Euler/experiment correlations of sonic boom pressure signatures
p 1095 A93-52439

CLIFTON, JAMES M.

Wind-tunnel tests of an inclined cylinder having helical grooves
[AIAA PAPER 93-3456] p 979 A93-47239

Modeling and control of a trailing wire antenna towed by an orbiting aircraft
[AD-A256450] p 219 N93-14610

CLIMIE, B. R.

Automatic dependant surveillance focus of civil avionics integration
p 30 A93-10998

CLINE, D. D.

A performance comparison of massively parallel Parabolized Navier-Stokes solutions
[AIAA PAPER 93-0059] p 435 A93-20172

Large-scale simulation of the three-dimensional Navier-Stokes equations
p 437 A93-20739

CLINE, M. C.

Numerical simulation of a low-emission gas turbine combustor using KIVA-II
p 170 A93-14077

A preliminary study of the effect of equivalence ratio on a low emissions gas turbine combustor using KIVA-2
[DE92-018616] p 215 N93-13321

A three-dimensional algebraic grid generation scheme for gas turbine combustors with inclined slots
[NASA-CR-191095] p 746 N93-24759

CLINE, MICHAEL C.

Emissions reduction by varying the swirler airflow split in advanced gas turbine combustors
[ASME PAPER 92-GT-110] p 349 A93-19347

Computation of the flow field in an annular gas turbine combustor
[AIAA PAPER 93-2074] p 1113 A93-49903

Numerical analysis of the flow fields in a RQL gas turbine combustor
[DE92-017509] p 89 N93-11767

CLINEDINST, WINSTON C.

Advanced Transport Operating System (ATOPS) Flight Management/Flight Controls (FM/FC) software description
[NASA-CR-191457] p 808 N93-28621

Advanced Transport Operating System (ATOPS) utility library software description
[NASA-CR-191469] p 1000 N93-32218

CLOTHIAUX, JOHN D.

Verification of rain-flow reconstructions of a variable amplitude load history
[NASA-CR-189670] p 91 N93-12411

CLOUSER, S.

Innovative high temperature aircraft engine fuel nozzle design
[ASME PAPER 92-GT-132] p 350 A93-19365

Determination of surface heat transfer and film cooling effectiveness in unsteady wake flow conditions
p 902 N93-29933

CLOUTIER, JAMES R.

Control design for robust eigenstructure assignment in linear uncertain systems
p 97 A93-13241

Sequential smoothing and filtering for maneuvering target tracking
p 440 A93-22978

COAKLEY, B. J.

Airborne gravimetry from a light aircraft
p 1245 A93-55972

COAKLEY, T. J.

Turbulence modeling for complex hypersonic flows
[AIAA PAPER 93-0200] p 277 A93-22620

Skin friction and velocity profile family for compressible turbulent boundary layers
p 1070 A93-49008

COBB, EBEN C.

Optimal circumferential placement of cylindrical thermocouple probes for reduction of excitation forces
[ASME PAPER 92-GT-423] p 406 A93-19571

COCHRAN, ROLAND

Wet layup materials for repair of bismaleimide composites
p 1212 A93-53451

COCKRELL, CHARLES E., JR.

Interpretation of waverider performance data using computational fluid dynamics
[AIAA PAPER 93-2921] p 1044 A93-48122

COCKRELL, DAVID J.

Influence of the canopy-payload coupling on the dynamic stability in pitch of a parachute system
[AIAA PAPER 93-1248] p 690 A93-35185

COEN, P. G.

Multidisciplinary design integration system for a supersonic transport aircraft
[AIAA PAPER 92-4841] p 324 A93-20296

COET, M.-C.

Shock/boundary layer interaction in a hypersonic flow in the presence of an entropy layer
[ONERA, TP NO. 1992-181] p 773 A93-38743

Shock wave/boundary layer interaction in a two-dimensional laminar hypersonic flow
[ONERA, TP NO. 1992-182] p 773 A93-38744

Infrared thermography characterization of Goertler vortex type patterns in hypersonic flows
[ONERA, TP NO. 1993-13] p 925 A93-41029

Experiments on shock-wave/boundary-layer interactions produced by two-dimensional ramps and three-dimensional obstacles
p 865 A93-42589

COET, MARIE-CLAIRE

Experiments on shock wave-boundary layer interaction at high Mach number with entropy layer effect
[ONERA, TP NO. 1992-101] p 771 A93-38581

Experiments on shock wave/boundary layer interaction in hypersonic flow
p 970 A93-46888

COFFEN, C. D.

Advances in tilt rotor noise prediction
p 447 A93-19184

COFFEN, CHARLES D.

A comparative analysis of XV-15 tiltrotor hover test data and WOPWOP predictions incorporating the fountain effect
p 509 A93-29414

Flow visualization and flow field measurements of a 1/12 scale tilt rotor aircraft in hover
p 482 A93-29441

COFFEN, CHARLES DAVID

Tilt rotor hover aeroacoustics
[NASA-CR-177598] p 99 N93-10458

COHEN, CLARK EMERSON

Attitude determination using GPS: Development of an all solid-state guidance, navigation, and control sensor for air and space vehicles based on the global positioning system
p 888 N93-30605

COHEN, GERALD C.

Formal representation of the requirements for an Advanced Subsonic Civil Transport (ASCT) flight control system
[NASA-CR-189699] p 98 N93-12346

Formal design specification of a Processor Interface Unit
[NASA-CR-189698] p 99 N93-12538

COHEN, J. M.

Influences on the sprays formed by high-shear fuel nozzle/swirler assemblies
p 411 A93-21653

COHEN, L.

DSMC numerical investigation of rarefied compression corner flow
[AIAA PAPER 93-3096] p 1061 A93-48270

COHN, MARC

An introduction to the onboard LAN (OLAN)
p 1166 A93-49480

COIRIER, WILLIAM J.

An accuracy assessment of Cartesian-mesh approaches for the Euler equations
[AIAA PAPER 93-3335] p 953 A93-45029

COLANTUONI, S.

Aerodesign and performance analysis of a radial transonic impeller for a 9:1 pressure ratio compressor
[ASME PAPER 92-GT-183] p 352 A93-19408
Aero-thermal design of a cooled transonic NGV and comparison with experimental results p 904 N93-29957

A Navier-Stokes solver with different turbulence models applied to film-cooled turbine cascades p 904 N93-29962

COLASURDO, GUIDO

An analysis of air-turborocket performance
[AIAA PAPER 93-1982] p 1141 A93-49829
Nozzle effects on linear stability behaviour of combustors
[ISABE 93-7044] p 1198 A93-54020

COLDING-JORGENSEN, J.

Prediction of rotor dynamic destabilizing forces in axial flow compressors p 272 A93-22263

COLE, J. D.

Asymptotic methods for the prediction of transonic wind-tunnel wall interference p 730 A93-35625
On the construction and calculation of optimal nonlifting critical airfoils p 969 A93-46857
Interaction of the sonic boom with atmospheric turbulence
[AIAA PAPER 93-2943] p 1171 A93-48140

COLE, RODNEY E.

Terminal Doppler weather radar/low-level wind shear alert system integration algorithm specification, version 1.1
[AD-A255319] p 224 A93-14547
Setting values for TDWR/LLWAS 3 integration parameters
[AD-A260740] p 755 A93-25645

COLE, RUSSELL L.

Experience with explosive detection systems in airports p 498 A93-21895

COLE, STANLEY R.

Supersonic aeroelastic instability results for a NASP-like wing model
[AIAA PAPER 93-1369] p 682 A93-33935
Supersonic aeroelastic instability results for a NASP-like wing model
[NASA-TM-107739] p 718 A93-26553

COLELLA, A.

Aerodesign and performance analysis of a radial transonic impeller for a 9:1 pressure ratio compressor
[ASME PAPER 92-GT-183] p 352 A93-19408
Aero-thermal design of a cooled transonic NGV and comparison with experimental results p 904 N93-29957

COLELLA, PHILLIP

Adaptive Cartesian grid methods for representing geometry in inviscid compressible flow
[AIAA PAPER 93-3385] p 955 A93-45076

COLEMAN, MONTE

A study of CFD algorithms applied to complete aircraft configurations
[AIAA PAPER 93-0784] p 468 A93-24864

COLEMAN, R. M.

Numerical simulation of vortex generation and capture above an airfoil
[AIAA PAPER 93-0864] p 468 A93-24926

COLLARD, DUDLEY

Study of a Mach 2 supersonic transport aircraft p 124 A93-15034
Future supersonic transport studies at Aerospatiale p 505 A93-25491

COLLERCANDY, R.

Computational methods applied to the aerodynamics of spaceplanes and launchers
[ONERA, TP NO. 1992-140] p 114 A93-14216

COLLIE, J. C.

Recent advances in simulating unsteady flow phenomena brought about by passage of shock waves in a linear turbine cascade
[ASME PAPER 92-GT-4] p 245 A93-19277

COLLIER, CRAIG S.

Stiffness, thermal expansion, and thermal bending formulation of stiffened, fiber-reinforced composite panels
[AIAA PAPER 93-1569] p 741 A93-34102

COLLIER, F. S., JR.

Hybrid laminar flow control applied to advanced turbofan engine nacelles
[SAE PAPER 920962] p 123 A93-14628
Laminar flow flight experiments - A review p 890 A93-41778

An overview of recent subsonic laminar flow control flight experiments
[AIAA PAPER 93-2987] p 1052 A93-48180

COLLIER, J. P.

Raising the high temperature limit of the nickel-iron-base superalloy p 70 A93-12114

COLLIN, G.

CARS temperature measurements in combustion
[ONERA, TP NO. 1993-78] p 1212 A93-53599

COLLINS, C. C.

Simulation of shock-boundary layer interaction in a fan blade passage
[AIAA PAPER 93-1804] p 1078 A93-49827

COLLINS, CHRIS R.

An investigation of the influence of advanced aircraft diagnostics on the technological sophistication of maintenance personnel
[AD-A258988] p 240 A93-18887

COLLINS, DANIEL J.

Neural network controllers for the X29 aircraft p 817 A93-37005

COLLINS, H. D.

Ultra wide band 3-D cross section (RCS) holography
[DE92-019133] p 89 A93-11802

COLLINS, M.

Engine Health Monitoring p 346 A93-18787

COLLINS, MICHAEL W.

Flow and heat transfer in a turbulent boundary layer through skewed and pitched jets p 1151 A93-49007

COLLINS, MIKE

A manned hypersonic reconnaissance vehicle which does not require airborne fueling p 333 A93-17888

COLLINS, WILLIAM E.

A review of civil aviation propeller-to-person accidents: 1980-1989
[AD-A260695] p 705 A93-25896

COLOMBAN, PH.

Origin of the carbon rich sliding interface in alkali containing matrix-SiC nicalon fibre composites
[ONERA, TP NO. 1993-77] p 1212 A93-53598
Corrosion of ceramic matrix composites
[ONERA, TP NO. 1993-82] p 1213 A93-53602

COLOMBO, O.

Requirements for airborne vector gravimetry p 1241 A93-55976

COLOMBO, OSCAR L.

Errors in long distance kinematic GPS p 314 A93-21154
Airborne gravimetry, altimetry, and GPS navigation errors p 1240 A93-55975

COLON, ANDY

High Capacity Voice Recorder (HCVR) Operational Test and Evaluation (OT/E) integration test report
[DOT/FAA/CT-TN92/30] p 88 A93-11460

COLONIUS, TIM

Boundary conditions for direct computation of aerodynamic sound generation p 447 A93-19176
Boundary conditions for direct computation of aerodynamic sound generation p 1172 A93-49005

COLUCCI, JAY

Hermes CX-7: Air transport system design simulation
[NASA-CR-192082] p 335 A93-18056

COLVIN, B. J.

Composite 'Exoskin' doubler extends F-15 Vertical Tail fatigue life
[AIAA PAPER 93-1341] p 709 A93-33911

COLVIN, D. P.

Enhanced heat transport in environmental systems using microencapsulated phase change materials
[SAE PAPER 921224] p 926 A93-41398

COMBS, S. R.

Flight management system on the F-117A p 908 A93-42815

COMEAX, KEITH A.

Viscous hypersonic shock-shock interaction on a blunt body at high altitude
[AIAA PAPER 93-2722] p 962 A93-46477

COMOGGIO, RONALD L.

Adverse weather test site selection study
[AD-A259012] p 339 A93-18895

COMPERE, M. D.

Measurements of dynamic Young's modulus and damping in single crystals of a nickel-based superalloy as a function of temperature p 1147 A93-52513

COMPTON, WILLIAM B., III

Comparison of algebraic turbulence models for afterbody flows with jet exhaust p 123 A93-14554

COMTE, P.

Numerical simulation of compressible mixing zones p 10 A93-12427

CONGER, RAND N.

Pressure measurements on a pitching airfoil in a water channel
[AIAA PAPER 93-0184] p 473 A93-25510

CONIEN, C.

A 'low-cost' full flight simulator for basic IFR training p 374 A93-18776

CONLEY, KRISTIN

NASA advanced design program: Analysis, design, and construction of a solar powered aircraft
[NASA-CR-192040] p 332 A93-17802

CONLEY, RALPH R.

Analytical and experimental investigation of annular propulsive nozzles
[AD-A262685] p 815 A93-28391

CONLISK, A. T.

The three-dimensional boundary layer flow due to a rotor-tip vortex
[AIAA PAPER 93-3081] p 1060 A93-48255

CONNELL, LEONARD W.

Nuclear thermal rocket entry heating and thermal response preliminary analysis
[AIAA PAPER 93-0378] p 385 A93-23058

CONNELL, STUART D.

A 3D unstructured adaptive multigrid scheme for the Euler equations
[AIAA PAPER 93-3339] p 954 A93-45033
Visual grid quality assessment for 3D unstructured meshes
[AIAA PAPER 93-3352] p 1036 A93-45046

CONNELLY, J. M.

An optical flameout detection system for NASA Langley's 8-Foot High Temperature Tunnel p 1254 A93-54372

CONNER, DAVID A.

Acoustic flight test experience with the XV-15 Tiltrotor aircraft with the Advanced Technology Blade (ATB) p 445 A93-19143
Far-field hover acoustic characteristics of the XV-15 tiltrotor aircraft with Advanced Technology Blades p 566 A93-29412

CONNOR, JEFFREY A.

Evaluation of simple aluminide and platinum modified aluminide coatings on high pressure turbine blades after factory engine testing - Round II
[ASME PAPER 92-GT-140] p 388 A93-19372

CONRAD, G. R.

Recent refinements and increased capabilities in balloon vertical performance analysis p 40 A93-11361

CONSTANTINESCU, V. N.

Lifting line theory for supersonic flow applications p 778 A93-39402

CONTENT, D. A.

Optical technologies for UV remote sensing instruments p 853 A93-28788

CONWAY, J.

Further development of the CANAERO computer code to include a time-stepping capability
[DREA-CR-91-478] p 562 A93-21820

CONWAY, PETER C.

Investigation of nacelle upper cowl flow separation using on- and off-body flow visualization techniques p 1072 A93-49507

CONWELL, PETE

Exodus: Prime Mover
[NASA-CR-192051] p 332 A93-17803

COOK, A. B.

The prediction of nonlinear dynamic loads on helicopters from flight variables using artificial neural networks p 322 A93-19231

COOK, JEFFREY S.

Analysis of consolidation of intermediate level maintenance for Atlantic Fleet T700-GE-401 engines
[AD-A257754] p 363 A93-17695

COOK, M. V.

Review of initial experiments using the Hawk model, dynamic rig facility, and the CED 1401 digital data acquisition equipment
[CRANFIELD-AERO-9017] p 531 A93-21406

COOK, T. S.

Probabilistic turbine blade tip durability analysis
[AIAA PAPER 93-1383] p 719 A93-33946

COOK, THERESA

Analysis of missile configurations with wrap-around fins using computational fluid dynamics
[AIAA PAPER 93-3631] p 1064 A93-48316

COOKSON, ROY A.

New approximate method of stress analysis for bladed rotating discs
[ISABE 93-7059] p 1219 A93-54035

COOLEY, DUANE

The Meteorologist Weather Processor for U.S. National Weather Service units at Federal Aviation Administration sites p 428 A93-22130

COON, MICHAEL D.

A study of flow separation on an oscillating flap at Mach number 2.4
[AIAA PAPER 93-0436] p 286 A93-23350

COOPER, BARRY

Taxonomy of flight variables p 147 A93-15022

COOPER, BETH A.

A large hemi-anechoic enclosure for community-compatible aeroacoustic testing of aircraft propulsion systems
[NASA-TM-106015] p 760 A93-26551

- COOPER, E. E.**
An experimental examination of the thermal and acoustic environments on runway joint seals
[AD-A257965] p 382 N93-17734
- COOPER, GEOFFREY**
Battle damage repairs p 239 A93-22698
- COOPER, J. E.**
Envelope function - A tool for analyzing flutter data p 1136 A93-52455
- COOPER, JOHN C.**
Hermetic sealing and EMI shielding gasket
[AD-D015359] p 199 N93-13414
- COOPER, JOHN W.**
Calibration results for NOAA-11 AVHRR channels 1 and 2 from congruent path aircraft observations p 1143 A93-51237
- COOPER, R. K.**
Over wing propeller aerodynamics p 113 A93-14189
Parallel implementation of the feature associated mesh embedding method for the 2D-Euler equations (FAME2D) p 225 A93-14278
- COOPER, T. P.**
Development of highly loaded root end attachments for composite material high speed flying surfaces p 539 A93-24122
- COOPER, THOMAS D.**
Proceedings of the USAF Structural Integrity Program [AD-A255379] p 110 N93-14549
- COPENHAVER, W. W.**
Unsteady aerodynamic flow phenomena in a transonic compressor stage p 1075 A93-49743
[AIAA PAPER 93-1868]
Three-dimensional flow analysis inside turbomachinery stages with steady and unsteady Navier-Stokes method [ISABE 93-7095] p 1186 A93-54071
- COPENHAVER, WILLIAM W.**
Three-dimensional flow phenomena in a transonic, high-through-flow, axial-flow compressor stage [ASME PAPER 92-GT-169] p 250 A93-19395
Tip shock structures in transonic compressor rotors [AIAA PAPER 93-1869] p 1075 A93-49744
Stall inception in single stage, high-speed compressors with straight and swept leading edges [AIAA PAPER 93-1870] p 1076 A93-49745
- COQUEL, F.**
Viscous nonequilibrium flow calculations [ONERA, TP NO. 1992-89] p 771 A93-38573
Calculations of viscous nonequilibrium flows in nozzles [ONERA, TP NO. 1992-91] p 771 A93-38574
Navier-Stokes calculations over a double ellipse and a double ellipsoid by an implicit non-centered method p 867 A93-42607
- COQUEL, FREDERIC**
Field by field hybrid upwind splitting methods [AIAA PAPER 93-3302] p 950 A93-45000
- COQUILLAT, SYLVAIN**
Behavior of precipitating water drops under the influence of electrical and aerodynamical forces p 1034 A93-45176
- CORCORAN, TRICIA**
A manned hypersonic reconnaissance vehicle which does not require airborne fueling p 333 N93-17888
- CORD, THOMAS J.**
Agility potential [SAE PAPER 921016] p 185 A93-14645
Development of flying qualities and agility evaluation maneuvers [AIAA PAPER 93-3645] p 1127 A93-48329
- CORDE, J. C.**
SNECMA M88 engine development status [ASME-90-GT-118] p 363 N93-17849
- CORDE, JEAN C.**
Aircraft engine integration for the M88-Rafale couple [ASME PAPER 92-GT-403] p 322 A93-19552
- CORDERLEY, G.**
Case studies in composite material structural design, manufacture and testing p 157 A93-14385
- CORGAT, ANTHONY M.**
Low-cost approaches to proving of high-risk fast VTOL designs [SAE PAPER 920989] p 157 A93-14636
- CORJON, A.**
Method of characteristics for computing three-dimensional boundary layers p 970 A93-46886
- CORKER, KEVIN**
Design of a cooperative problem-solving system for enroute flight planning: An empirical study of its use by airline dispatchers [NASA-CR-192709] p 707 N93-25330
- CORLISS, LLOYD D.**
Piloted simulation study of two tilt-wing control concepts [AIAA PAPER 92-4236] p 63 A93-13338
- Phase II simulation evaluation of the flying qualities of two tilt-wing flap control concepts [SAE PAPER 920988] p 185 A93-14635
Initial piloted simulation study of geared flap control for tilt-wing V/STOL aircraft [NASA-TM-103872] p 64 N93-10741
- CORNELISON, CHARLES J.**
Development update for the NASA Ames 16-Inch Shock Tunnel Facility p 822 A93-37873
- CORNELIUS, KENNETH C.**
Thrust vectoring control from underexpanded asymmetric nozzles [AIAA PAPER 93-3261] p 968 A93-46827
Side force augmentation at high angle of attack from pneumatic vortex flow control [AIAA PAPER 93-2959] p 1124 A93-48153
- CORNMAN, LARRY**
Terminal Doppler Weather Radar program at Denver's Stapleton International Airport during 1989 and 1990 p 432 A93-22188
- CORNIAULT, CHRISTIAN**
Europe adapts CST to its needs p 560 A93-25088
- CORNWALL, BRYAN**
Material characterization and fractographic examination of Ti-17 fatigue crack growth specimens for SMP SC33 p 1004 N93-31744
- CORNWALL, J.**
Small satellites and RPA's in global-change research [AD-A260762] p 755 N93-25837
- CORNWELL, PHILLIP J.**
Trajectory control for a low-lift re-entry vehicle p 1141 A93-49592
- CORR, ROBERT A.**
NO(x) sensitivities for gas turbine engines operated on lean-premixed combustion and conventional diffusion flames [ASME PAPER 92-GT-115] p 349 A93-19351
- CORREA, SANJAY M.**
Carbon monoxide emissions in lean premixed combustion p 197 A93-14503
- CORTELEZZI, LUCA**
A theoretical and computational study on active wake control p 878 N93-30892
- CORTES, V.**
Nondestructive inspection of in-service aircraft [ETN-93-93059] p 496 N93-20928
- COSENTINO, GARY B.**
Applying and validating the RANS-3D flow-solver for evaluating a subsonic serpentine diffuser geometry [AIAA PAPER 93-2157] p 1079 A93-49973
- COSTA, P.**
Materials problems connected with the propulsion of supersonic air carriers [ONERA, TP NO. 1992-157] p 824 A93-38736
- COSTELLO, MARK FRANCIS**
A theory for the analysis of rotorcraft operating in atmospheric turbulence p 48 N93-11725
- COSTES, M.**
A numerical procedure for aerodynamic optimization of helicopter rotor blades [ONERA, TP NO. 1992-121] p 771 A93-38595
Aerodynamic rotor loads prediction method with free wake for low speed descent flights [ONERA, TP NO. 1992-122] p 772 A93-38596
Application of European CFD methods for helicopter rotors in forward flight [ONERA, TP NO. 1992-125] p 772 A93-38599
- COSTIN, DANIEL PATRICK**
Optimum design of aircraft structures with manufacturing and buckling constraints p 162 N93-13815
- COTTI, B.**
Optical interconnection and packaging technologies for advanced avionics systems p 77 A93-10960
- COTTON, WILLIAM B.**
TCAS display issues [AIAA PAPER 92-4242] p 51 A93-13351
- COTUGNO, ELOISE**
No rescue in sight for Warsaw plaintiffs from either courts or legislature - Montreal Protocol 3 drowns in committee p 945 A93-42999
- COUAILLIER, V.**
Transonic and supersonic flow calculations around aircrafts using a multidomain Euler code [ONERA, TP NO. 1992-137] p 772 A93-38610
3D viscous flow analysis in axial turbine including tip leakage phenomena p 972 A93-46940
Three-dimensional analysis of turbine rotor flow including tip clearance [ASME PAPER 93-GT-111] p 987 A93-47446
3-D turbomachinery Euler and Navier-Stokes calculations with a multidomain cell-centered approach [AIAA PAPER 93-2576] p 1085 A93-50292
- Recent developments performed at ONERA for the simulation of 3D inviscid and viscous flows in turbomachinery by the solution of Euler and Navier-Stokes equations [ISABE 93-7094] p 1186 A93-54070
- COUAILLIER, VINCENT**
Validation of a Navier-Stokes code using a (k,epsilon) turbulence model applied to a three-dimensional transonic channel [AIAA PAPER 93-0293] p 279 A93-22693
- COULLIETTE, C.**
Environmental conditions for certification testing of helicopter advanced composite main rotor components p 824 A93-36003
- COULTER, P. R.**
The stability and aerodynamic performances of clusters of small cruciform parachutes [AIAA PAPER 93-1242] p 690 A93-35181
- COUPIER, ALAIN**
Methodology in the development of avionics p 166 A93-15043
- COURCOUX, PIERRE**
Helicopter accidents over water in the national navy: Epidemiological study over the period 1980-1991 p 493 N93-19686
- COUREAU, JEAN**
Aid in investigation by figure animation p 491 N93-19659
- COURTRIGHT, E. L.**
Ultrahigh temperature assessment study: Ceramic matrix composites [AD-A262740] p 826 N93-28592
- COUSINS, D.**
A numerical inversion method for determining aerodynamic effects on particulate exhaust plumes from onboard irradiance data p 823 A93-37482
- COUSSEMENT, GREGORY**
Structured grid variational adaption - Reaching the limit? [ONERA, TP NO. 1992-114] p 771 A93-38590
- COUSTEIX, J.**
Second-order effects in hypersonic laminar boundary layers p 1073 A93-49529
Real gas effects in two- and three-dimensional hypersonic, laminar boundary layers p 1073 A93-49530
Investigations on entropy layer along hypersonic hyperboloids using a defect boundary layer p 787 N93-27462
- COUSTEIX, JEAN**
Reduction of aerodynamic skin-friction drag p 871 A93-42656
- COUSTOLS, ERIC**
Reduction of aerodynamic skin-friction drag p 871 A93-42656
- COUTERET, J.**
Preliminary results of the ISM campaign - The Landes, South West France p 1161 A93-47553
- COUTTS, R. S. P.**
A study of the flexural properties of carbon-epoxy composites in certain environments p 390 A93-21999
- COVERT, EUGENE E.**
Unsteady turbulent skin-friction measurement in an adverse pressure gradient p 206 A93-14545
- COVEY, JIM H.**
Lightning protection of composite structure p 141 A93-15801
- COWIE, W. D.**
A damage tolerance approach for management of aging gas turbine engines p 1001 A93-45779
- COWINGS, PATRICIA S.**
Autogenic-feedback training improves pilot performance during emergency flying conditions [NASA-TM-104005] p 790 N93-27076
- COWLEY, IVOR G.**
New cabin electronics p 804 A93-39542
- COWLING, DAVID**
The simulation of aircraft landing gear dynamics p 155 A93-14318
- COWLING, J. E.**
An experimental study of a turbulent wing-body junction and wake flow p 873 A93-43541
- COX, CAREY F.**
Multi-block calculations for flows in local chemical equilibrium [AIAA PAPER 93-2999] p 1053 A93-48189
- COX, CHADWICK J.**
Control of takeoff of a hypersonic aircraft using neural networks p 1167 A93-50744
- COX, CHARLES**
Helicopter noise standards - Requirements, compliance, and improvements p 569 A93-29443
- COX, CRAIG**
Advanced hypersonic aircraft design [NASA-CR-192046] p 334 N93-18037

- COX, J. W. R.**
Corroboration of a moment-method calculation of the maximum mutual coupling between two HF antennas mounted on a helicopter p 881 A93-40332
- COX, M. E.**
European studies to investigate the feasibility of using 1000 ft vertical separation minima above FL(290). III - Further results and overall conclusions p 992 A93-45166
- COX, R. A.**
Waveriders with finlets [AIAA PAPER 93-3442] p 978 A93-47231
- COYLE, EDWARD J.**
Thermoplastic composite parts manufacture at Du Pont [SME PAPER EM93-106] p 1159 A93-51728
- COYNE, FRANCIS J.**
Merger and acquisition - Enhancing Loran propagation technology with artificial intelligence p 29 A93-10987
- CRABB, C. A.**
Issues of ATC conflict resolution under real-time constraints p 887 N93-30350
- CRABILL, N. L.**
Pilot weather advisor [NASA-CR-189723] p 318 N93-16692
- CRABILL, NORMAN L.**
The FAA/NASA flight loads monitoring program - The prototype system and its benefits for the aviation community p 486 A93-25125
- CRADDOCK, W.**
NASA Long Duration Balloon capability development project p 2 A93-11370
- CRAGO, RICHARD D.**
Surface shear stress estimates from geostrophic winds for use in sensible and latent heat flux formulations p 936 N93-30044
- CRAIG, ANDREW**
Unsteady aerodynamics in airplane stall-spin departure [AIAA PAPER 93-0622] p 523 A93-24739
- CRAIG, KENNETH JOHN**
Computational study of the aerodynamics and control by blowing of asymmetric vortical flows over delta wings p 693 N93-24772
- CRAIG, ROGER**
Spectral measurements of shock layer radiation in an arc-jet wind tunnel p 1251 A93-54409
- CRAMER, EVIN J.**
On alternative problem formulations for multidisciplinary design optimization [AIAA PAPER 92-4752] p 436 A93-20350
- CRANER, MICHAEL**
Update on the NASA ER-2 Doppler radar system (EDOP) p 807 A93-37737
- CRASSIDIS, JOHN L.**
Automatic carrier landing system utilizing aircraft sensors p 1097 A93-49590
- CRATCH, PRESTON**
FAA Technical Center Aeronautical Data Link Research Plan [DOT/FAA/CT-92/23] p 417 N93-15698
- CRAWFORD, MICHAEL E.**
Hydrodynamic effects on heat transfer for film-cooled turbine blades [AD-A257291] p 361 N93-16080
- CRAWLEY, E. F.**
Reform of the aeronautics and astronautics curriculum at MIT [AIAA PAPER 93-0325] p 454 A93-23017
- CREAMER, PAUL N.**
GPS availability and reliability for aircraft precision approach p 315 A93-21182
- CRÉE, W. C.**
Meteorological information for aviation: A systems approach p 937 N93-30298
- CREEL, THEODORE R.**
Boundary layer relaminarization device [NASA-CASE-LAR-14470-1] p 23 N93-11876
- CREISMEAS, PAUL**
A Eulerian/Lagrangian modelling to calculate the evolution of a water droplets spray [ISABE 93-7121] p 1221 A93-54096
- CREITZER, E. M.**
Flow phenomena in turbomachines [AD-A263049] p 930 N93-29141
- CRESCI, ROBERT J.**
Development of Polytechnic University's supersonic wind tunnel facility [AIAA PAPER 93-0798] p 528 A93-24876
- CRESWELL, ROLAND**
The Boeing 747-400 upper rudder control system with triple tandem valve [SAE PAPER 912133] p 327 A93-21843
- CREWS, A.**
Measurement of the center-of-gravity using X-ray computed tomography p 396 A93-18619
- CREWS, ALAN R.**
X-ray computed tomography for casting development [AD-A261786] p 752 N93-26526
- CREWS, B. S.**
Comparison of heating protocols for detection of disbands in lap joints p 396 A93-18627
- CRICELLI, ANTONIO M.**
Unsteady airflow flow solutions on moving zonal grids [AD-A261925] p 701 N93-26198
- CRIGHTON, D. G.**
The unsteady flow past a supersonic splitter plate [ISABE 93-7047] p 1185 A93-54023
- CRISPIN, YECHEL**
The low frequency aeroacoustics of buried nozzle systems p 1205 A93-54244
- CRIMALDI, JOHN P.**
Response of B-2 aircraft to nonuniform spanwise turbulence p 1135 A93-52437
- CRIPPS, M. N.**
The 13 ft by 9 ft low speed wind tunnel facility at DRA (Aerospace Division) Bedford (England) [RAE-TM-AERO-2228] p 23 N93-11883
- CRISTION, JOHN A.**
Adaptive optimization of general aviation aircraft [AIAA PAPER 92-4195] p 44 A93-13372
- CRISTION, JOHN A.**
Control of complex dynamic systems by neural networks p 758 N93-25611
- CRITES, R. C.**
Data analysis techniques for pressure- and temperature-sensitive paint [AIAA PAPER 93-0176] p 414 A93-22605
- CRITTENDEN, LUCILLE H.**
Aerodynamic applications of pressure sensitive paint p 549 A93-29301
- CRITTENDEN, LUCILLE H.**
Comparison of simulated and actual wind shear radar data products p 490 N93-18610
- CRIVELLI, PAUL M.**
NASA advanced design program: Analysis, design, and construction of a solar powered aircraft [NASA-CR-192040] p 332 N93-17802
- CROCKER, D. S.**
Dual-spray airblast fuel nozzle for advanced small gas turbine combustors [AIAA PAPER 93-2336] p 1116 A93-50113
- CROCKER, MALCOLM J.**
International Congress on Recent Developments in Air- and Structure-Borne Sound and Vibration, 2nd, Auburn Univ., AL, Mar. 4-6, 1992, Proceedings. Vols. 1-3 p 1259 A93-55851
- CROLL, R. H.**
Use of shear-stress-sensitive, temperature-insensitive liquid crystals for boundary layer transition detection in hypersonic flows [AIAA PAPER 93-3070] p 1059 A93-48245
- CROMAN, ROBERT**
Evaluation of the fatigue behavior of discontinuous and continuous fiber thermoplastic composite laminates p 824 A93-36005
- CRONKHITE, JAMES**
CST and rotorcraft - Expanding the view p 560 A93-25085
- CRONKHITE, JAMES D.**
The NASA/industry Design Analysis Methods for Vibrations (DAMVIBS) program: Bell Helicopter Textron accomplishments p 514 N93-21312
- CROOK, A. J.**
Numerical simulation of compressor endwall and casing treatment flow phenomena [ASME PAPER 92-GT-300] p 255 A93-19490
- CROOK, ANDREW J.**
Investigation of advanced counterrotation blade configuration concepts for high speed turboprop systems. Task 4: Advanced fan section aerodynamic analysis [NASA-CR-187128] p 174 N93-12695
- CROOK, ANDREW J.**
Investigation of advanced counterrotation blade configuration concepts for high speed turboprop systems. Task 4: Advanced fan section aerodynamic analysis computer program user's manual [NASA-CR-187127] p 364 N93-18702
- CROOKS, RICHARD S.**
Probing questions for aerodynamic testing p 80 A93-13437
- CROOM, MARK A.**
Dynamic model testing of the X-31 configuration for high-angle-of-attack flight dynamics research [AIAA PAPER 93-3674] p 1129 A93-48351
- CROSKY, A. G.**
A study of the flexural properties of carbon-epoxy composites in certain environments p 390 A93-21999
- CROSLLEY, DAVID R.**
Kinetics and energy transfer in nonequilibrium fluid flows [AD-A263612] p 875 N93-29284
- CROSS, ALVIN**
Flight testing of an electric powered vehicle [AIAA PAPER 92-4077] p 37 A93-11262
- CROSS, G. S.**
Advanced instrumentation for next-generation aerospace propulsion control systems [AIAA PAPER 93-2079] p 1154 A93-49906
- CROSS, M. A.**
Ground test simulation fidelity of turbine engine airstarts [AIAA PAPER 93-2173] p 1137 A93-49986
- CROSS, VICTOR**
TBD(exp 3) [NASA-CR-192075] p 335 N93-18054
- CROSSLEY, WILLIAM A.**
Using aerodynamic analysis codes to assist in structural design and optimization of ducted rotor/wing blades [AIAA PAPER 92-4280] p 44 A93-13353
- CROUCH, J. D.**
Receptivity of three-dimensional boundary layers [AIAA PAPER 93-0074] p 262 A93-20186
- CROUSE, D.**
A 3D Navier-Stokes analysis of a generic ground vehicle shape [AIAA PAPER 93-3521] p 985 A93-47283
- CROUSE, G. L., JR.**
A new method for improved rotor free-wake convergence [AIAA PAPER 93-0872] p 469 A93-24933
- CROUSE, G. L., JR.**
Active control of vibratory airloads induced by helicopter rotor-fuselage interactions [AIAA PAPER 93-1363] p 726 A93-33930
- CROW, EDDIE C., JR.**
Interactional aerodynamic effects on rotor performance in hover and forward flight p 766 A93-35941
- CROW, EDDIE C., JR.**
Automatic Through-the-Thickness braiding p 209 A93-15789
- CROW, S. E.**
RB211-524B disc and drive cones hot cyclic spinning test p 177 N93-14895
- CROW, STEVEN C.**
Differential GPS control of Starcar 2 p 317 A93-21201
- CROWDER, JAMES P.**
Probing questions for aerodynamic testing p 80 A93-13437
- CROWE, W. M.**
Optical correlator field test results p 1038 A93-44458
- CROWELL, CYNTHIA A.**
Helicopter low-speed yaw control [NASA-CASE-LAR-14219-1] p 729 N93-25998
- CROWLEY, STEVEN M.**
Expanding test mode shapes for better visualization p 549 A93-29264
- CROWTHER, W. J.**
Tangential Forebody Blowing-yaw control at high alpha [AIAA PAPER 93-3406] p 1008 A93-47205
- CRUCE, ANDREW C.**
Development methodology for contemporary avionics systems [SAE PAPER 931591] p 1104 A93-49340
- CRUM, T. S.**
Low speed test results of subsonic, turbofan scarf inlets [AIAA PAPER 93-2301] p 1082 A93-50086
- CRUTCHFIELD, WILLIAM Y.**
High speed test results of subsonic, turbofan scarf inlets [AIAA PAPER 93-2302] p 1082 A93-50087
- CRUTCHFIELD, WILLIAM Y.**
Adaptive Cartesian grid methods for representing geometry in inviscid compressible flow [AIAA PAPER 93-3385] p 955 A93-45076
- CRUZ, C. I.**
Hypersonic aerodynamic characteristics for Langley Test Technique Demonstrator [AIAA PAPER 93-3443] p 1072 A93-49516
- CRUZ, CHRISTOPHER I.**
Subsonic static and dynamic stability characteristics of the test technique demonstrator NASP configuration [AIAA PAPER 93-0519] p 268 A93-21111
- CRUZ, CHRISTOPHER I.**
Supersonic dynamic stability characteristics of the test technique demonstrator NASP configuration [AIAA PAPER 92-5009] p 367 A93-22285
- CRUZ, JOSE**
Aerodynamic characteristics of the HL-20 p 1181 A93-53736
- CRUZ, JOSE**
Comparison measurements of currents induced by radiation and injection p 926 A93-41575
- CRUZ, JUAN R.**
Optimization of composite sandwich cover panels subjected to compressive loadings p 922 N93-30862
- CRUAN, SCOTT P.**
Results from a GPS Shuttle Training Aircraft flight test p 384 A93-21148
- CUI, E. J.**
Separation control and lift enhancement on airfoil using unsteady excitations p 118 A93-14305

- CUI, PINGYUAN**
Comment on 'Equation decoupling - A new approach to the aerodynamic identification of unstable aircraft'
p 818 A93-37406
- CULBERT, JAMES**
An improved gust front detection algorithm for the TDWR
p 432 A93-22191
- CULICK, F. E. C.**
Combustion noise and combustion instabilities in propulsion systems
p 100 N93-10682
- CULL, RAY**
Innovative bagging techniques on a composite P-51 Mustang replica
p 1191 A93-53405
- CULLERS, CHERYL**
Deformation mechanisms of NiAl cyclicly deformed near the brittle-to-ductile transformation temperature
[NASA-CR-191649] p 391 N93-15830
- CULVER, E. M.**
User's manual for UCAP: Unified Counter-Rotation Aero-Acoustics Program
[NASA-CR-191034] p 852 N93-27148
- CUMMING, A. C. D.**
The user friendly airliner (The 37th Roy Chadwick Lecture)
p 307 A93-21718
- CUMMINGS, E.**
Transition on a sharp cone at high enthalpy - New measurements in the shock tunnel T5 at GALTIT
[AIAA PAPER 93-0343] p 281 A93-23030
- CUMMINS, K. L.**
A single-point warning system for thunderstorms and electric fields
p 747 N93-24900
- CUNNINGHAM, A. M., JR.**
Development of a method to predict transonic limit cycle oscillation characteristics of fighter aircraft
[NLR-TP-91359-U] p 999 N93-32338
- CUNNINGHAM, WILLIAM**
Potential aircraft hazards in the vicinity of convective clouds - A review from the perspective of a scale-model study
p 427 A93-22116
- CUNNINGTON, GEORGE R.**
Thermal control/oxidation resistant coatings for titanium-based alloys
p 74 N93-12457
- CUNY, J. J.**
Loads at the nose landing gears of civil transport aircraft during towbarless towing operations
p 45 A93-13629
- CUOMO, S.**
Radar signals analysis oriented to target characterization applied to civilian ATC radar
p 885 A93-43475
- CURCHITSER, ENRIQUE N.**
Solution of the Euler and Navier Stokes equations on parallel processors using a transposed/Thomas ADI Algorithm
[AIAA PAPER 93-3310] p 1036 A93-45006
- CURIO, I.**
Results of a low-altitude flight noise study in Germany - Acute extraural effects
p 1163 A93-49557
- CURLETT, BRIAN P.**
A graphical user-interface for propulsion system analysis
[AIAA PAPER 93-0223] p 440 A93-23699
- CURLISS, DAVID B.**
Effects of thermal history and jet fuel absorption on the properties of APC-2
p 534 A93-25252
- CURRAN, JIM**
Trends in advanced avionics
[ISBN 0-8138-0749-2] p 341 A93-17574
- CURRIE, T. C.**
A simple multigrid procedure for explicit time-marching on unstructured grids
p 956 A93-45087
- CURRIER, JEFFREY M.**
NOTAR system - A quiet character
p 567 A93-29418
- Noise characteristics of helicopters with the NOTAR anti-torque system
p 1262 A93-54722
- CURTISS, H. C.**
Evaluation of tilt rotor aircraft design utilizing a realtime interactive simulation
p 798 A93-35989
- CURTISS, H. C., JR.**
Studies of a flat wake rotor theory
[NASA-CR-190936] p 25 N93-12343
- CURWEN, PETER**
Test results of an orifice pulse tube refrigerator
p 1149 A93-48612
- CUSCHIERI, J. M.**
Experimental measurement of structural intensity on an aircraft fuselage
p 544 A93-26999
- CUTBIRTH, JAMES W.**
Chaotic vortical motion in the near region of a plane jet
p 131 N93-13493
- CUTLER, A. D.**
Strong vortex/boundary layer interactions. I - Vortices high
p 930 A93-43539
- Strong vortex/boundary layer interactions. II - Vortices low
p 965 A93-46744
- CYRUS, VACLAV**
Prediction of secondary losses in axial compressors
[ASME PAPER 92-GT-288] p 254 A93-19479
- CZEKAJSKI, C.**
GARTEUR damage mechanics for composite materials: Analytical/experimental research on delaminations
p 537 N93-21513
- CZERNIEJEWSKI, MARK W.**
Application of a flush airdata sensing system to a wing leading edge (LE-FADS)
[AIAA PAPER 93-0634] p 516 A93-24750
- Application of a flush airdata sensing system to a wing leading edge (LE-FADS)
[NASA-TM-104267] p 518 N93-20163
- D**
- D'ADDIO, E.**
An integrated weather channel designed for an up-to-date ATC radar system
p 929 A93-43434
- D'AMBRA, F.**
An overview on practical application of helicopter noise certification rules
p 487 A93-29442
- D'AZZO, J. J.**
Automated control of aircraft in formation flight
[AIAA PAPER 93-3852] p 1134 A93-51439
- D'ESPINEY, P.**
Supersonic vortical flows around an ogive-cylinder - Laminar and turbulent computations
[ONERA, TP NO. 1992-111] p 771 A93-38588
- 3D laminar and 2D turbulent computations with the Navier-Stokes solver FLU3M
[ONERA, TP NO. 1993-105] p 1180 A93-53618
- D'HERVILLY, GUY**
STANAG 3910 - The data bus for the next generation of European avionics systems
[SAE PAPER 931595] p 1104 A93-49344
- DA COSTA, J. L.**
Hypersonic flow calculations using a multidomain MUSCL Euler solver
p 960 A93-45547
- DA SILVA, LUIS F. F.**
Ignition and spread of combustion within a supersonic boundary layer
p 535 A93-27732
- DABORA, E. K.**
Standing normal detonations and oblique detonations for propulsion
[AIAA PAPER 93-2325] p 1116 A93-50105
- DACLES-MARIANI, JENNIFER**
A computational study of wingtip vortex flowfield
[AIAA PAPER 93-3010] p 1054 A93-48200
- Turbulent structure of a wingtip vortex in the near field
[AIAA PAPER 93-3011] p 1054 A93-48201
- DADD, G. J.**
Surge recovery and compressor working line control using compressor exit Mach number measurement
p 897 A93-40435
- DADONE, A.**
Surface boundary conditions for the numerical solution of the Euler equations
[AIAA PAPER 93-3334] p 953 A93-45028
- DADONE, ANDREA**
Inviscid finite-volume lambda formulation
p 872 A93-42888
- Secondary flow computation by means of an inviscid multigrid Finite Volume Lambda Formulation
[AIAA PAPER 93-1974] p 1077 A93-49821
- DADONE, L.**
Recent developments in rotor wake modeling for helicopter noise prediction
p 481 A93-29437
- DAFAALLA, ABDUL S. A.**
Some physico-chemical characteristics of lubricating oil used in gas turbines
p 70 A93-12202
- DAGENHART, JOHN RAY**
Crossflow stability and transition experiments in a swept-wing flow
[NASA-TM-108650] p 555 N93-21819
- DAHL, C.**
An experimental examination of the thermal and acoustic environments on runway joint seals
[AD-A257965] p 382 N93-17734
- DAHLKILD, A. A.**
Some stability characteristics of the boundary layer on a yawed cone
[AIAA PAPER 93-3048] p 1057 A93-48228
- DAHLSTROM, M.**
A simplified representation of the off-design characteristics of high speed, high pressure ratio axial turbomachinery stages
[AIAA PAPER 93-2257] p 1081 A93-50055
- DAI, GUAN-ZHONG**
Integrated fire control simulation systems
p 1192 A93-53876
- DAI, GUANZHONG**
A U-D factorization-based adaptive extended Kalman filter and its application to flight state estimation
p 1169 A93-51198
- DAIGUJI, H.**
Higher-order-accurate upwind schemes for solving the compressible Euler and Navier-Stokes equations
p 863 A93-42441
- DAIGUJI, HISAOKI**
A fourth-order MUSCL finite-difference scheme for solving the unsteady compressible Euler equations
p 1086 A93-51121
- Numerical simulations of supersonic flow by a fourth-order compact MUSCL TVD scheme
p 302 N93-19308
- DAILEY, G. M.**
3-dimensional interactions in the rotor of an axial turbine
[AIAA PAPER 93-2255] p 1081 A93-50053
- DALA, L.**
Computational methods applied to the aerodynamics of spaceplanes and launchers
[ONERA, TP NO. 1992-140] p 114 A93-14216
- DALL, HANS J.**
Wind tunnel results for an advanced fighter configuration employing transverse thrust for enhanced STOL capability
[AIAA PAPER 93-1933] p 1100 A93-49796
- DALLDORFF, LOTHAR**
A new flying qualities criterion for flying wings
[AIAA PAPER 93-3668] p 1128 A93-48346
- DALLMANN, U.**
A theoretical approach for describing secondary instability features in three-dimensional boundary-layer flows
[AIAA PAPER 93-0080] p 263 A93-20192
- Flow over a leading edge with distributed roughness
p 18 N93-10549
- DALLMANN, UWE**
Nonlocal vs. local instability of compressible flows including body metric, flow divergence and 3D-wave propagation
[AIAA PAPER 93-2982] p 1051 A93-48175
- Instability of hypersonic flow past blunt cones - Effects of mean flow variations
[AIAA PAPER 93-2983] p 1051 A93-48176
- DALY, KIERAN**
Advancing helicopters
p 327 A93-21836
- DALY, P.**
Progress towards joint civil use of GPS and GLONASS
p 29 A93-10977
- DALY, PETER M.**
An experimental cockpit display for TDWR wind shear alerts
p 343 A93-22111
- DAMODARAN, K. A.**
Mach disk of dual coaxial axisymmetric jets
p 861 A93-41932
- Analytical and experimental investigation of flow through a turbine vane cascade
p 1248 A93-56348
- DANA, WILLIAM H.**
The X-15 airplane - Lessons learned
[AIAA PAPER 93-0309] p 456 A93-23005
- DANABASOGLU, G.**
Spatial simulation of boundary layer instability - Effects of surface roughness
[AIAA PAPER 93-0075] p 262 A93-20187
- DANAHER, JAMES**
Digital hopping GPS/GLONASS receiver
p 312 A93-21128
- DANAI, K.**
Efficient fault diagnosis of helicopter gearboxes
[NASA-TM-106253] p 1032 N93-31846
- DANAI, KOUROSH**
Fault detection of helicopter gearboxes using the multi-valued influence matrix method
[NASA-TM-106100] p 838 N93-27069
- DANBERG, JAMES E.**
Correlation of mean velocity measurements downstream of a swept backward-facing step
p 123 A93-14552
- Navier-Stokes simulation of viscous, separated, supersonic flow over a projectile rotating band
[AD-A263073] p 788 N93-27955
- DANEK, GEORGE L.**
Pseudo Aircraft Systems - A multi-aircraft simulation system for air traffic control research
[AIAA PAPER 93-3585] p 1209 A93-52679
- DANG, T. Q.**
A fully three-dimensional inverse method for turbomachinery blading in transonic flows
[ASME PAPER 92-GT-209] p 251 A93-19432
- Design of multi-stage turbomachinery blading by the circulation method - Actuator duct limit
[ASME PAPER 92-GT-286] p 254 A93-19477
- Treatment of vortex sheets for the transonic full-potential equation
p 871 A93-42870

DANIEL, D. C.

DANIEL, D. C.

Trends in international aerospace ground test facilities
[AIAA PAPER 93-0348] p 528 A93-25518

DANIEL, DAVID R.

Compact high reliability fiber coupled laser diodes for
avionics and related applications p 1152 A93-49470

DANIEL, E.

A comparison between centered and upwind schemes
for two-phase compressible flows
[AIAA PAPER 93-2346] p 1083 A93-50120

DANIEL, L.

The high accuracy applications of the GPS system to
static positioning p 500 A93-28193

DANIEL, TIM

Application and integration of diverse technology in an
aviation system: The National Aeronautical Information
Processing System p 887 A93-30339

DANIELS, GRAHAME

Helicopter flight data recorder and health and usage
monitoring system p 169 A93-15178

DANIELS, T. S.

Digital resolver for helicopter model blade motion
analysis p 830 A93-37878

DANIELS, W. A.

Experimental investigation of turbine disk cavity
aerodynamics and heat transfer
[NASA-CR-193831] p 812 A93-27115

DANILIN, M. IU.

Short-term atmospheric effects of high-altitude aircraft
emissions p 559 A93-28865

DANILOV, YU. P.

Calculation of the passive noise power for onboard
single-pulse automatic direction tracking systems
p 882 A93-43111

DANKERT, CARL

Condensation of nitrogen in hypersonic flows -
Measurements confirm a theoretical model
p 111 A93-13945

DANKS, M.

The aerodynamic performance of laser drilled sheets
[AERO-REPT-9204] p 484 A93-20806
The effect of surface suction near the leading edge of
a swept-back wing
[AERO-REPT-9205] p 484 A93-20807

DANNENHOFFER, JOHN F., III

3-D adaptive grid-embedding Euler technique
[AIAA PAPER 93-0330] p 415 A93-23021
Techniques for the visual evaluation of computational
grids
[AIAA PAPER 93-3353] p 1037 A93-45047

DANSBERRY, BRYAN E.

Experimental unsteady pressures at flutter on the
Supercritical Wing Benchmark Model
[AIAA PAPER 93-1592] p 683 A93-34123

DAOUD, YOUNIS SHARIF

Control and optimization of aircraft trajectories
p 729 A93-25543

DARABY, A.

The effects of forced oscillations on the performance
of airfoils
[AIAA PAPER 93-3264] p 968 A93-46829

DARDEN, CHRISTINE M.

Assessment and design of low boom configurations for
supersonic transport aircraft p 446 A93-19163
Limitations of linear theory for sonic boom calculations
p 850 A93-37380
Elements of NASA's high-speed research program
[AIAA PAPER 93-2942] p 947 A93-45155

DARE, ALAN R.

Pilot/Vehicle display development from simulation to
flight
[AIAA PAPER 92-4174] p 51 A93-13310

DARLING, DAVID

A radar altitude and line of sight attachment
[AIAA PAPER 93-3587] p 1223 A93-52680

DARLING, DOUGLAS

Evaluation and application of the Baldwin-Lomax
turbulence model in two-dimensional, unsteady,
compressible boundary layers with and without separation
in engine inlets
[AIAA PAPER 92-3676] p 111 A93-14118
Evaluation and application of the Baldwin-Lomax
turbulence model in two-dimensional, unsteady,
compressible boundary layers with and without separation
in engine inlets
[AIAA PAPER 92-3676] p 414 A93-22509
Evaluation and application of the Baldwin-Lomax
turbulence model in two-dimensional, unsteady,
compressible boundary layers with and without separation
in engine inlets
[NASA-TM-105810] p 82 A93-10087

DARLOW, M. S.

The use of beam-like modal data for stiffness profile
estimation by the EBS method. I - Justification and
implementation p 1257 A93-54649

DARTER, M. I.

Development of a unified airport pavement analysis and
design system p 380 A93-16317

DASGUPTA, A.

Computations of spray, fuel-air mixing, and combustion
in a lean-premixed-prevaporized combustor
[AIAA PAPER 93-2069] p 1153 A93-49901

DASH, R.

High speed flight effects on transmission of sound
through a nonflexible vibrating panel due to flow structural
interaction in the ambience
[AIAA PAPER 92-4708] p 451 A93-20316
Acoustics due to flow-structural interaction and its
transmission through a double-panel in high-speed cruising
flight
[AIAA PAPER 93-1431] p 710 A93-33981

DASH, S. M.

The critical role of turbulence modeling in the prediction
of supersonic jet structure for acoustic applications
p 398 A93-19193

DASHEVSKIY, A. G.

Determination of the natural vibrations of an acoustic
medium in the cabin of a passenger aircraft by the finite
element method p 1102 A93-51752

DATTA, A.

Hysteresis and bristle stiffening effects of conventional
brush seals
[AIAA PAPER 93-1996] p 1153 A93-49839

DAUTOV, E. A.

A nomographic model for multicriterial optimization
during the design of a flight vehicle powerplant
p 95 A93-12821

DAUTOV, N. G.

Kinetic scheme selection in describing detonation in an
H₂-air mixture behind shock waves p 1253 A93-55032

DAVENPORT, WILLIAM J.

Flow visualizations of perpendicular blade vortex
interactions
[NASA-CR-192725] p 748 A93-25208

DAVID, E.

Ramjet NO_x emission - Use of a 3D CFD method for
the combustor design of a super/hyper-sonic transport
propulsion system
[ASME PAPER 92-GT-255] p 353 A93-19464

DAVID, J. F.

The human factor problem in the Canadian Forces
aviation p 491 A93-19657

DAVIDENKO, D. M.

Shock wave ahead of a liquid jet in supersonic cross
flow p 477 A93-27605

DAVIDSON, D. P.

ASTOVL model engine simulators for wind tunnel
research p 192 A93-13213

DAVIDSON, L.

Calculation of the flow around a high-lift airfoil using
an explicit code and an algebraic Reynolds stress model
p 685 A93-34344

DAVIDSON, LARS

Navier-Stokes stall predictions using an algebraic
Reynolds-stress model p 778 A93-39260
Numerical simulation of vortex shedding past triangular
cylinders at high Reynolds number using a k-epsilon
turbulence model p 871 A93-42873
Reynolds stress transport modelling of
shock/boundary-layer interaction
[AIAA PAPER 93-2936] p 1046 A93-48134

DAVIES, A. J.

The effect of surface suction near the leading edge of
a swept-back wing
[AERO-REPT-9205] p 484 A93-20807

DAVIES, PETER

Air transport and the environment - Regulating aircraft
noise p 1226 A93-52931

DAVIES, R.

A nonlinear control strategy for robust sliding mode
performance in the presence of unmatched uncertainty
p 938 A93-42556

DAVIES, S. J.

An externally pressurized air bearing system, journals
and thrust, for application to small turbomachinery
[ASME PAPER 92-GT-382] p 406 A93-19539

DAVIN, J.

Test facility for evaluation of structural integrity of
stiffened and jointed aircraft curved panels
p 1012 A93-45794

DAVIS, D. D., JR.

An accurate nonlinear finite element analysis and test
correlation of a stiffened composite wing panel
p 546 A93-27968

An analytically designed subcomponent test to
reproduce the failure of a composite wing box beam
[AIAA PAPER 93-1344] p 709 A93-33914

DAVIS, D. DALE, JR.

Reliability of stiffened structural panels: Two examples
[NASA-TM-107687] p 219 A93-14483

DAVIS, D. L.

Scramjet fuel mixing enhancement by cross-stream
pressure gradients
[AIAA PAPER 93-2139] p 1114 A93-49957

DAVIS, D. O.

Surface and flow field measurements in a symmetric
crossing shock wave/turbulent boundary-layer
interaction
[NASA-TM-106086] p 693 A93-24911

DAVIS, GARY A.

Transonic panel flutter
[AIAA PAPER 93-1476] p 829 A93-37438
Unsteady transonic two-dimensional Euler solutions
using finite elements p 778 A93-39412

DAVIS, GUY D.

Durability properties for adhesively bonded structural
aerospace applications p 1217 A93-53515

DAVIS, J. A.

A design approach to high Mach number scramjet
performance
[AIAA PAPER 92-4248] p 55 A93-13360
Hypersonic inlet efficiency revisited
p 16 A93-10012

DAVIS, JAMES A.

Hypervelocity scramjet capabilities of the T5 Free-Piston
Tunnel at Caltech
[AIAA PAPER 92-5037] p 376 A93-22311

DAVIS, JOHN G., JR.

Cost - The challenge for advanced materials and
structures p 233 A93-14338
First NASA Advanced Composites Technology
Conference, part 2
[NASA-CP-3104-PT-2] p 921 A93-30841

DAVIS, JOSEPH P.

The design of a robust autopilot for the Archytas
prototype via linear quadratic synthesis
[AD-A262151] p 820 A93-27546

DAVIS, L. M.

AEDC expanded flow arc facility (HEAT-H2) description
and calibration p 821 A93-37872

DAVIS, M. J.

Reinforcement of the F-111 wing pivot fitting with a
boron/epoxy doubler system - Materials engineering
aspects p 1214 A93-54241

DAVIS, M. W., JR.

Application of a dynamic compression system model
to a low aspect ratio fan - Casing treatment and
distortion
[AIAA PAPER 93-1871] p 1111 A93-49746

DAVIS, MARK W.

A modal-based procedure for efficiently predicting low
vibration rotor designs p 712 A93-34262

DAVIS, PAMELA A.

Braking, steering, and wear performance of radial-belted
and bias-ply aircraft tires
[SAE PAPER 921036] p 158 A93-14656
NASA Langley's Aircraft Landing Dynamics Facility
p 1250 A93-54400

DAVIS, PATRICIA P.

Gas analysis system for the Eight Foot High Temperature
Tunnel p 822 A93-37875

DAVIS, R. L.

Navier-Stokes analysis of turbine blade heat transfer
and performance p 201 A93-13978

DAVIS, RANDALL C.

An analytically designed subcomponent test to
reproduce the failure of a composite wing box beam
[AIAA PAPER 93-1344] p 709 A93-33914

DAVIS, ROGER L.

3-D adaptive grid-embedding Euler technique
[AIAA PAPER 93-0330] p 415 A93-23021
Numerical simulation of turbine 'hot spot' alleviation
using film cooling p 744 A93-34476

Numerical simulations of flows in centrifugal
turbomachinery
[AIAA PAPER 93-2578] p 1085 A93-50293

Prediction of viscous flows in rotating machinery using
Navier-Stokes techniques p 1232 A93-54639

Investigation of hot streak migration and film cooling
effects on heat transfer in rotor/stator interacting flows,
report 1
[AD-A250688] p 102 A93-12490

DAVIS, S.

Nonintrusive, multipoint velocity measurements in
high-pressure combustion flows
[AIAA PAPER 93-2032] p 1145 A93-49867

DAVIS, STEVEN

Phoenix: Preliminary design of a high speed civil
transport
[NASA-CR-192024] p 334 A93-17976

DAVIS, WARREN H.

High lift multiple element airfoil analysis with unstructured
grids
[AIAA PAPER 93-3478] p 981 A93-47256

- DAVISON, MICHAEL T.**
An examination of wing rock for the F-15
[AD-A256613] p 188 N93-14252
- DAVISSON, JOSEPH C.**
Advanced transparency development for USAF aircraft
[AIAA PAPER 93-1391] p 710 A93-33954
- DAYOUDZADEH, F.**
Two- and three-dimensional blade vortex interactions
[NASA-CR-177567] p 293 N93-16942
- DAYDOV, V. G.**
Main directions of improving the quality of aluminum-lithium alloys for welded aircraft structures
p 1146 A93-51104
- DAYDOV, YU. M.**
Effect of anomalous aerodynamic heating during the descent of a parachute along a trajectory
p 1069 A93-48924
- DAWES, W. N.**
A comparison of the measured and predicted flowfield in a modern fan-bypass configuration
[ASME PAPER 92-GT-298] p 254 A93-19488
The extension of a solution-adaptive 3D Navier-Stokes solver towards geometries of arbitrary complexity
[ASME PAPER 92-GT-363] p 257 A93-19527
Analysis of three-dimensional viscous flow in a supersonic axial flow compressor rotor with emphasis on tip leakage flow
[ASME PAPER 92-GT-388] p 257 A93-19543
A novel approach to high resolution compressible cascade flow analysis using the Navier-Stokes equations
[ASME PAPER 92-GT-419] p 258 A93-19567
The practical application of solution-adaptation to the numerical simulation of complex turbomachinery problems
p 970 A93-46916
Numerical and experimental investigation of turbine tip gap flow
[AIAA PAPER 93-2253] p 1081 A93-50051
- DAWICKE, D. S.**
An evaluation of the pressure proof test concept for 2024-T3 aluminum alloy sheet
p 1026 A93-45780
- DAWSON, SETH**
Side-by-side hover performance comparison of MDHC 500 NOTAR and tail rotor anti-torque systems
p 796 A93-35956
- DAY, BRAD A.**
Semi-discrete Galerkin solution of the compressible boundary-layer equations with viscous-inviscid interaction
[AIAA PAPER 93-3520] p 985 A93-47282
- DAY, C. R.**
Options for control and navigation of unmanned aircraft
p 34 A93-12124
- DAY, I. J.**
Review of stall, surge and active control in axial compressors
[ISABE 93-7011] p 1184 A93-53987
- DAY, IVOR J.**
Stall and surge in axial flow compressors
p 423 N93-18724
Active control of stall and surge
p 423 N93-18725
- DAYTON, K. E.**
National Aerospace Plane Integrated Fuselage/Cryotank Risk Reduction program
[AIAA PAPER 93-2564] p 1142 A93-50284
- DAYWITT, JAMES E.**
Application of parabolized Navier-Stokes technique for high-L/D, hypersonic vehicle design
[AIAA PAPER 93-2948] p 1047 A93-48144
- DE BERNARDIS, E.**
On the possibility of singularities in the acoustic field of supersonic sources when BEM is applied to a wave equation
p 1039 A93-46805
- DE GUZMAN, E.**
Spanish-Indonesian cooperation in the development, production, certification and marketing of CN-235 commuter aircraft
p 108 A93-14156
- DE HOFF, RONALD L.**
Turbine Engine Diagnostics (TED) system
[AIAA PAPER 93-1818] p 1110 A93-49706
- DE JONG, R. G.**
Review - Extra-aural health effects of aircraft noise
p 1164 A93-49559
- DE JONGE, J. B.**
Damage severity of monitored fatigue load spectra
p 154 A93-14253
Monitoring load experience of individual aircraft
p 1103 A93-52450
- DE LA CHAPELLE, M.**
Ladar fiber optic sensor system for aircraft applications
p 1105 A93-49467
- DE LUCA, DANIEL P.**
Markov fatigue in single crystal airfoils
[ASME PAPER 92-GT-95] p 387 A93-19341
- DE LUCA, L.**
Detection of Goertler vortices in hypersonic flow
p 120 A93-14382
- Experimental study of the flow around a double ellipsoid configuration
p 867 A93-42603
- DE MATTEIS, GUIDO**
A sensitivity analysis of the stability of a tug-rope-sailplane system
p 184 A93-14400
Longitudinal dynamics of a towed sailplane
p 1130 A93-49577
- DE MATTEIS, P.**
On the modelling of separated flows about airfoils
[AIAA PAPER 93-3479] p 981 A93-47257
- DE MATOS, B. S.**
Transonic profile design in curvilinear coordinates using an approximate factorization algorithm
p 7 A93-10778
- DE MONTALK, J. P. P.**
On-board maintenance aids
p 764 A93-39538
- DE PIOLENC, F. M.**
The largest freight airship that can fit in Moffett hangar no. 1
[AIAA PAPER 93-4046] p 1242 A93-54613
- DE PONTE, S.**
On the measurements of the skin friction in 3-D flows - Application to a complete 3-D shear layer flow
p 118 A93-14329
- DE PONTE, SERGIO**
Further studies on the asymmetrical flow past yawed cylinders
p 118 A93-14304
- DE RESENDE, OTTO C.**
Computation of wake roll-up for complete aircraft configurations
[AIAA PAPER 93-3509] p 984 A93-47275
- DE SOCIO, LUCIANO M.**
A sensitivity analysis of the stability of a tug-rope-sailplane system
p 184 A93-14400
- DE WILDE, J. P.**
Polyethylene pyrolysis model for combustion calculations in solid fuel ramjets
p 520 A93-27739
- DE WITT, KENNETH J.**
Investigation of an electrothermal de-icer pad using a three-dimensional finite element simulation
[AIAA PAPER 93-0397] p 327 A93-23072
Efficient finite element method for aircraft deicing problems
p 1103 A93-52443
- DEANDRADE, DONIZETI**
Application of finite-state inflow to flap-lag-torsion damping in hover
p 714 A93-25486
- DEARMON, JAMES S.**
Statistical techniques for traffic flow management
[AIAA PAPER 93-3834] p 1098 A93-51423
- DEARMON, JOHN M.**
Icing Research Tunnel rotating bar calibration measurement system
p 1255 A93-54398
- DEATON, JERRY W.**
Structural evaluation of curved stiffened composite panels fabricated using a THERM-Xsm process
p 919 A93-30435
- DEATON, JOHN E.**
Theory and design of adaptive automation in aviation systems
[AD-A254595] p 160 N93-12613
- DEB, SOMNATH**
A multisensor-multitarget data association algorithm for heterogeneous sensors
p 439 A93-22899
A multisensor-multitarget data association algorithm for heterogeneous sensors
p 1020 A93-44168
- DEBIEVE, J. F.**
Effect of wall heating on a supersonic turbulent boundary layer
p 11 A93-12429
- DEBISSCHOP, J. R.**
Experimental analysis of turbulence within supersonic mixing layers
p 11 A93-12428
Experimental studies of the turbulent structure of supersonic mixing layers
[AIAA PAPER 93-0217] p 278 A93-22633
- DEBOER, W. P.**
A simulator study into low speed longitudinal handling qualities of ACT transport aircraft
[NLR-TP-89387-U] p 527 N93-20743
- DEBONIS, J. R.**
Navier-Stokes analysis of three-dimensional S-ducts
p 959 A93-45146
- DECAMPS, B.**
Measurements of dynamic Young's modulus and damping in single crystals of a nickel-based superalloy as a function of temperature
p 1147 A93-52513
- DECHER, RUDOLF**
Aerospace '92 - The year in review
p 455 A93-19976
- DECKER, F.**
Low-speed aerodynamics of the hypersonic research configuration ELAC I
p 1237 A93-56035
- DECKER, JERALD**
The aeronautical volcanic ash problem
p 309 A93-22156
- DECKER, RAND**
Tracking of raindrops in flow over an airfoil
[AIAA PAPER 93-0168] p 275 A93-22602
- DECKER, WILLIAM A.**
Piloted simulator investigations of a civil tilt-rotor aircraft on steep instrument approaches
p 800 A93-36023
- DECKERT, JAMES A.**
Integrating TCAS into the airspace management system
p 30 A93-11005
- DECONINCK, H.**
A multidimensional generalization of Roe's flux difference splitter for the Euler equations
p 863 A93-42437
Computations of inviscid compressible flows using fluctuation-splitting on triangular meshes
[AIAA PAPER 93-3301] p 950 A93-44999
A frontal approach for internal node generation in Delaunay triangulations
p 1262 A93-56403
- DECONINCK, HERMAN**
Viscous, 2-D, laminar hypersonic flows over compression ramps
p 866 A93-42591
- DEDDEN, A.**
Automatic guidance and control for recovery of remotely piloted vehicles
p 181 A93-14188
- DEDEKIND, MANFRED O.**
Life cycle assessment of an impingement-cooled gas turbine blade
[AIAA PAPER 92-4716] p 358 A93-20321
- DEDEKIND, MANFRED O.**
Thermal fatigue life assessment of a convection-cooled gas turbine blade
[ISABE 93-7062] p 1199 A93-54038
- DEDOES, DIRK**
On the selection of a GPS validity indicator for aircraft navigation in the National Airspace System (NAS)
p 316 A93-21186
A statistical comparison of differential GPS and laser generated time, space positioning information for aircraft flight testing
p 316 A93-21199
- DEDOUSSIS, V.**
Design of axisymmetric channels with rotational flow
[AIAA PAPER 93-3117] p 1062 A93-48287
- DEEB, JOSEPH M.**
Flight simulator for hypersonic vehicle and a study of NASP handling qualities
p 530 A93-19456
- DEFER, G.**
Flight tests of the transport aircraft viewed from the industrial standpoint
p 510 A93-19903
- DEFIGUEIREDO, RUI J. P.**
Neural-network-based catastrophe avoidance control systems
p 97 A93-13233
- DEFLORE, THOMAS**
General aviation aircraft: Normal acceleration data analysis and collection project
[DOT/FAA/CT-91/20] p 713 A93-24739
- DEFOSSE, P.**
Aircraft tracking optimization of parameters selection
p 3 A93-13628
- DEFRESNE, G.**
A numerical procedure for aerodynamic optimization of helicopter rotor blades
[ONERA, TP NO. 1992-121] p 771 A93-38595
- DEFRUTOS, Y.**
Nondestructive inspection of in-service aircraft
[ETN-93-03059] p 496 A93-20928
- DEGANI, ASAF**
On the topography of flight-deck documentation
[NASA-CR-177605] p 571 N93-19970
- DEGANI, DAVID**
Experimental study of controlled tip disturbance effect on flow asymmetry
p 211 A93-17417
Numerical simulation of upstream disturbance on flows around a slender body
[AIAA PAPER 93-2956] p 1047 A93-48150
- DEGOZZALI, SALLY**
Statistical fatigue analysis of the SH-60B servo beam rail component
[AD-A257474] p 332 A93-17660
- DEGREZ, G.**
Asymmetric vortical solutions in supersonic corners - Steady 3D space-marching versus time-dependent conical results
[AIAA PAPER 93-2957] p 1047 A93-48151
- DEHOFF, RONALD L.**
Intelligent diagnostics systems
p 98 A93-11931
- DEHUA, LIU**
Computational method in optimal bending-twisting comprehensive design of wings of subsonic and supersonic aircraft
[AD-A262374] p 806 A93-27694
- DEIWERT, GEORGE S.**
Issues and approach to develop validated analysis tools for hypersonic flows: One perspective
[NASA-TM-103937] p 305 A93-19379
- DEJARNETTE, FRED R.**
Engineering method for calculating surface pressures and heating rates on vehicles with embedded shocks
p 777 A93-39255

- An approximate method for calculating heating rates on three-dimensional vehicles
[AIAA PAPER 93-2881] p 949 A93-44228
- DEJESUS, RAFAEL O.**
Aeroelastic character of a National Aerospace Plane demonstrator concept
[AIAA PAPER 93-1314] p 732 A93-33890
- DEJONG, T.**
Stress calculations on the window section of an all-composite aircraft fuselage
[LR-688] p 328 N93-16215
- DEJONGE, J. B.**
Review of aeronautical fatigue investigations in the Netherlands during the period March 1989 - March 1991
[NLR-TP-91092-U] p 331 N93-17535
Load experience variability of fighter aircraft
[NLR-TP-89172-U] p 514 N93-20742
Ageing aircraft research in the Netherlands
[NLR-TP-91443-U] p 999 N93-32203
Damage severity of monitored fatigue load spectra
[NLR-TP-92009-U] p 999 N93-32205
- DEKOK, R. E.**
The Airbus floor beam: Towards a cost-effective composite design and manufacture research project sponsored by Airbus industry
[LR-677] p 329 N93-16283
- DEL BALZO, JOSEPH**
Airspace redesign - Making the GRADE
p 317 A93-21630
- DEL FRATE, JOHN H.**
In-flight flow visualization results from the X-29A aircraft at high angles of attack
[AIAA PAPER 92-4102] p 38 A93-11272
- DEL MAR, ANTHONY**
Use of full flight simulator technology enhances classroom training sessions p 1136 A93-49277
- DELAHARPE, V.**
Three-dimensional compressible stability-transition calculations using the spatial theory p 783 N93-27431
- DELANEY, R. A.**
3-D Euler simulation of vane-blade interaction in a transonic turbine
[AIAA PAPER 93-2256] p 1081 A93-50054
- DELANEY, ROBERT A.**
Investigation of advanced counterrotation blade configuration concepts for high speed turboprop systems. Task 4: Advanced fan section aerodynamic analysis
[NASA-CR-187128] p 174 N93-12695
Investigation of advanced counterrotation blade configuration concepts for high speed turboprop systems. Task 4: Advanced fan section aerodynamic analysis computer program user's manual
[NASA-CR-187127] p 364 N93-18702
Investigation of advanced counterrotation blade configuration concepts for high speed turboprop systems. Task 5: Unsteady counterrotation ducted propfan analysis. Computer program user's manual
[NASA-CR-187125] p 521 N93-20583
Investigation of advanced counterrotation blade configuration concepts for high speed turboprop systems. Task 5: Unsteady counterrotation ducted propfan analysis
[NASA-CR-187126] p 521 N93-20773
- DELAORTE, PH. C.**
Aerodynamic phenomena in high pulse repetition rate XeCl laser p 1150 A93-48806
- DELAURIER, J. D.**
An aerodynamic model for flapping-wing flight
p 858 A93-40470
The development of an efficient ornithopter wing
p 873 A93-43685
- DELAUZUN, FREDERIC**
Liquid crystal displays replacing the CRT and CLE of future cockpits p 518 N93-19783
- DELEEUW, JAAP**
The flight test and data analysis program for the development of a Boeing/De Havilland Dash 8 simulator model p 512 N93-19930
- DELERY, J.**
Shock/boundary layer interaction in a hypersonic flow in the presence of an entropy layer
[ONERA, TP NO. 1992-181] p 773 A93-38743
Infrared thermography characterization of Goertler vortex type patterns in hypersonic flows
[ONERA, TP NO. 1993-13] p 925 A93-41029
Experiments on shock-wave/boundary-layer interactions produced by two-dimensional ramps and three-dimensional obstacles p 865 A93-42589
- DELERY, JEAN**
Validation of a Navier-Stokes code using a (k,epsilon) turbulence model applied to a three-dimensional transonic channel
[AIAA PAPER 93-0293] p 279 A93-22693
Experiments on shock wave-boundary layer interaction at high Mach number with entropy layer effect
[ONERA, TP NO. 1992-101] p 771 A93-38581
- DELETOMBE, E.**
Aeroplane crashes on the runway: Validation and final evaluation of the method of modeling an airframe structure
[IMFL-91-32] p 165 N93-15126
- DELFRATE, JOHN H.**
A summary of the forebody high-angle-of-attack aerodynamics research on the F-18 and the X-29A aircraft
[NASA-TM-104261] p 25 N93-12353
In-flight flow visualization results from the X-29A aircraft at high angles of attack
[NASA-TM-4430] p 131 N93-13322
Pressure distribution for the wing of the YAV-8B airplane; with and without pylons
[NASA-TM-4429] p 136 N93-14451
- DELGADO, A.**
Experimental investigation of the management of large-sized drops and the onset of Marangoni-convection p 926 A93-41700
Calibration of thermal anemometer at very low Reynolds numbers under microgravity p 926 A93-41729
- DELGRANDE, N. K.**
Dual-band infrared imaging applications: Locating buried minefields, mapping sea ice, and inspecting aging aircraft
[DE93-000516] p 453 N93-17225
- DELHAYE, R.**
Category A F-16 accidents in the Belgian Air Force p 492 N93-19675
- DELIANIDES, THEODORE PHILIP**
An investigation of photothermal velocimetry for application to transient, high-speed gas flows p 698 N93-25720
- DELIBERATO, TONY J.**
Integrated Blade Inspection System (IBIS) upgrade study
[AD-A258912] p 365 N93-19356
- DELISI, DONALD P.**
Potential hazard of aircraft wake vortices in ground effect with crosswind p 479 A93-28606
- DELLAROCCHO, PAMELA S.**
Comparison of performance on the Shipley Institute of Living Scale, Air Traffic Control Specialist Selection Test, and FAA Academy Screen
[AD-A259249] p 502 N93-20582
- DELNORE, VICTOR E.**
Ground clutter measurements using the NASA airborne doppler radar: Description of clutter at the Denver and Philadelphia airports p 490 N93-19608
- DELUCA, DANIEL P.**
Fatigue in single crystal nickel superalloys
[AD-A254603] p 74 N93-12237
Fatigue in single crystal nickel superalloys
[AD-A254704] p 198 N93-12746
Fatigue in single crystal nickel superalloys
[AD-A260709] p 736 N93-25843
Fatigue in single crystal nickel superalloys
[AD-A261742] p 737 N93-26282
Fatigue in single crystal nickel superalloys
[AD-A265451] p 1019 N93-31795
- DELUCA, J. J.**
Lightweight aircraft turbine protection
[AIAA PAPER 93-1815] p 1110 A93-49703
- DEMANDANTE, CARLO G.**
Measurement of aerodynamic shear stress using side chain liquid crystal polymers
[AD-A254312] p 72 N93-10770
- DEMAREST, BILL**
MM-122: High speed civil transport
[NASA-CR-192011] p 334 N93-17974
- DEMARGNE, A.**
Computational methods applied to the aerodynamics of spaceplanes and launchers
[ONERA, TP NO. 1992-140] p 114 A93-14216
- DEMEIS, RICHARD**
Red-hot simulation p 1209 A93-53774
- DEMETRIADES, ANTHONY**
Comparison of predictions with measurements for a quiet supersonic tunnel
[AIAA PAPER 93-0344] p 376 A93-23031
- DEMIDOVICH, I. S.**
Effect of ion treatments on the fatigue strength of blades p 811 A93-39073
- DEMILLO, ROBERT J.**
An experimental cockpit display for TDWR wind shear alerts p 343 A93-22111
- DEMIN, A. E.**
Experience in the design of supercritical cascades for the flow straightener of a transonic fan p 777 A93-39196
- DEMIN, M. V.**
Increasing the efficiency of the electrochemical dimensional machining of gas turbine engine blades of EP718VD alloy p 835 A93-39095
- DEMIRDZIC, I.**
A collocated finite volume method for predicting flows at all speeds p 1087 A93-51736
- DEMISTRY, PETER F.**
AFTI/F-16 night close air support system testing p 808 A93-38841
- DEMPSEY, PAUL S.**
Airlines, airports and antitrust - A proposed strategy for enhanced competition p 760 A93-34821
- DEMUREN, A. O.**
Turbulence and stall in plane diffusers - Computational study p 744 A93-34311
Characteristics of three-dimensional turbulent jets in crossflow p 772 A93-38695
- DEMUTS, E.**
Low velocity impact in a graphite/PEEK
[AIAA PAPER 93-1403] p 734 A93-33963
- DENBRAVEN, W.**
NARSIM and EFMS: Tools for research on integrated ATM
[NLR-TP-89336-U] p 319 N93-17954
- DENG, CONG**
Classification of radar clutter in an air traffic control environment p 886 A93-30299
- DENG, X. F.**
Investigation of precise approach and landing of civil aircraft using integrated system based on GPS p 180 A93-14159
- DENG, XUE-YING**
Experimental investigations of the separation behavior in 3D shock wave/turbulent boundary-layer interactions p 119 A93-14345
Correlation of conical interactions induced by sharp fins and semicones p 692 A93-35635
- DENG, XUEYING**
Improvement of conical similarity rule in swept shock wave/boundary layer interaction
[AIAA PAPER 93-2941] p 1046 A93-48139
Correlative behaviours of shock/boundary layer interaction induced by sharp fin and semicone p 1230 A93-54581
Vectoring jet effects on the flow and aerodynamic behaviors of fighter model p 1241 A93-54590
- DENG, ZHENG-TAO**
The Burnett shock structures in low density hypersonic flows
[AIAA PAPER 92-5048] p 273 A93-22320
- DENHARD, WILLIAM G.**
The start of the laboratory - The beginnings of the MIT Instrumentation Laboratory p 235 A93-17326
- DENIBOIRE, P.**
Experimental study of heat transfer close to a plane wall heated in the presence of multiple injections (subsonic flow) p 901 N93-29931
- DENISOV, V.**
Use of alternative fuels for aviation p 196 A93-14292
- DENISOV, V. E.**
Air transportation system for shipping outsized cargoes p 141 A93-14394
- DENKE, P. H.**
Matrix difference equation analysis of coupled structural-acoustic models for aircraft fuselage vibration and interior noise reduction p 446 A93-19172
Sonic fatigue analysis of an aircraft wing flap by the matrix difference equation method p 399 A93-19208
- DENNIS, J. E., JR.**
On alternative problem formulations for multidisciplinary design optimization
[AIAA PAPER 92-4752] p 436 A93-20350
- DEOM, A.**
Infrared thermography characterization of Goertler vortex type patterns in hypersonic flows
[ONERA, TP NO. 1993-13] p 925 A93-41029
Infrared thermography of plastic instabilities in a single crystal superalloy
[ONERA, TP NO. 1993-18] p 916 A93-41031
- DEOTTE, ROBERT E., JR.**
Experimental study of the flow field inside a whirling annular seal p 85 N93-10892
- DEPPE, P. R.**
A rapid prototyping system for inflight simulation using the Calspan Learjet 25
[AIAA PAPER 93-3606] p 1191 A93-52691
- DERBUNOVICH, G. I.**
Optimal conditions for flow turbulence reduction by a set of grids p 836 A93-39122
- DERHAM, ROBERT C.**
The role of blade elasticity in the prediction of blade-vortex interaction noise p 566 A93-29406
- DERICKSON, R. G.**
Wind load design methods for ground-based heliostats and parabolic dish collectors
[DE93-002737] p 433 N93-15839

- DERMOTT, WILLIAM**
Strategic avionics technology definition studies. Subtask 3-1A: Electrical Actuation (ELA) systems
[NASA-CR-193237] p 914 N93-29215
- DEROBERT, D.**
Microbursts detection with airborne Doppler lidar
p 433 A93-22201
- DEROSA, S.**
Numerical study for the study of medium speed internal noise problems
[DILC-EST-TN-200] p 101 N93-11156
- DESHOWITZ, ADAM L.**
A passive infrared ice detection technique for helicopter applications
[NASA-CR-193187] p 880 N93-29152
- DERVIEUX, ALAIN**
Exact-gradient shape optimization of a 2-D Euler flow
p 462 A93-24308
Evaluation of contributions for test case 7.1.1 and 7.1.2
p 870 A93-42636
Exact-gradient shape optimization of a 2D Euler flow
[INRIA-RR-1540] p 422 N93-18623
- DESAI, ATUL**
Durability properties for adhesively bonded structural aerospace applications
p 1217 A93-53515
- DESAULTY, M.**
Turbine engine combustor design at SNECMA
[DS-2129] p 363 N93-17851
- DESCAMPS, A.**
Contribution to Problem 6 using an upwind Euler solver with unstructured meshes
p 869 A93-42627
- DESCHAMPS, J.**
Infrared thermography for hot-shot wind tunnel
[ONERA, TP NO. 1992-103] p 831 A93-38583
- DESHAIES, B.**
Investigation of a combustion zone behind a wedge
p 1146 A93-51631
Combustion in supersonic flows
p 199 N93-14627
- DESHAIES, BRUNO**
Ignition and spread of combustion within a supersonic boundary layer
p 535 A93-27732
- DESHPANDE, S. M.**
Acoustic flux vector splitting scheme for Euler equations
p 460 A93-24078
Computation of hypersonic flow over a sphere using kinetic flux vector splitting scheme with equilibrium chemistry
p 861 A93-42260
- DESIDERI, J.-A.**
The computation over unstructured grids of inviscid hypersonic reactive flow by upwind finite-volume schemes
p 1073 A93-49532
- DESIDERI, JEAN-ANTOINE**
Hypersonic flows for reentry problems. Vols. 1 & 2
[ISBN 0-387-54428-3] p 864 A93-42576
The European Data Base - A new CFD validation tool for the design of space vehicles
[AIAA PAPER 93-3045] p 1057 A93-48225
Homothermal-flow approach for hypersonic inviscid non-equilibrium flows
[INRIA-RR-1652] p 788 N93-28440
- DESIPIO, RICHARD G.**
Airship: The 'Look Out' - A versatile surveillance platform
[AIAA PAPER 93-4033] p 1229 A93-54605
- DESJARDINS, R. L.**
Spatial and temporal variations of the fluxes of carbon dioxide and sensible and latent heat over the FIFE site
p 425 A93-20586
- DESMOND, JOHN**
The development and implementation of a head-up guidance system (HGS) for manual CAT III landings
p 151 A93-17306
- DESOPPER, A.**
Experimental and theoretical studies of helicopter rotor-fuselage interaction
[ONERA, TP NO. 1992-142] p 120 A93-14356
Aerodynamic rotor loads prediction method with free wake for low speed descent flights
[ONERA, TP NO. 1992-122] p 772 A93-38596
- DESROCHERS, G.**
A discussion of the results of the rainfall counting of a wide range of dynamics associated with the simultaneous operation of adjacent wind turbines
[DE93-000016] p 434 N93-18705
- DESTARAC, G.**
Flight tests of the transport aircraft viewed from the industrial standpoint
p 510 N93-19903
- DETERS, K. J.**
Preliminary design estimates of high-speed streamlines on arbitrary shaped vehicles defined by quadrilateral elements
[AIAA PAPER 93-3491] p 982 A93-47263
- DETLEFSEN, WOLFGANG**
Protection of taxiing traffic in airports through mode S secondary radar technology
[ETN-93-93455] p 791 N93-28206
- DETURRIS, D. J.**
Direct measurements of skin friction in supersonic combustion flow fields
[ASME PAPER 92-GT-320] p 405 A93-19506
Direct measurements of skin friction in supersonic combustion flow fields
[AD-A262878] p 825 N93-28226
- DEUR, J. M.**
Computations of spray, fuel-air mixing, and combustion in a lean-premixed-prevaporized combustor
[AIAA PAPER 93-2069] p 1153 A93-49901
- DEUR, JOHN M.**
The effects of turbulence modeling on the numerical simulation of confined swirling flows
[AIAA PAPER 93-1976] p 1078 A93-49823
Computation of the flow field in an annular gas turbine combustor
[AIAA PAPER 93-2074] p 1113 A93-49903
Nitric oxide formation in a lean, premixed-prevaporized jet A/air flame tube: An experimental and analytical study
[NASA-TM-105722] p 844 N93-27012
- DEUTCHMAN, ARNOLD H.**
Joining carbon composite fins to metal heat pipes using ion beam techniques
p 543 A93-25979
Joining carbon composite fins to titanium heat pipes
[AD-A261970] p 825 N93-27667
- DEUTSCH, MARC**
The Edge supersonic transport
[NASA-CR-192074] p 335 N93-18055
- DEVADIGA, SADASHIVA**
A model-based approach for detection of objects in low resolution passive millimeter wave images
[NASA-CR-193161] p 808 N93-28418
- DEVAN, L.**
A new semiempirical method for computing nonlinear angle-of-attack aerodynamics on wing-body-tail configurations
[AIAA PAPER 93-0034] p 260 A93-20148
- DEVARAJAN, VENKAT**
Terrain modeling for real-time photo-texture based visual simulation
[AIAA PAPER 93-3607] p 1214 A93-52667
- DEVAUX, N.**
Flying qualities of the Hermes spaceplane and the shape definition process
p 532 A93-28437
- DEVENPORT, W. J.**
An experimental study of a turbulent wing-body junction and wake flow
p 873 A93-43541
An experimental investigation of interacting wing-tip vortex pairs
[AD-A258471] p 295 N93-18272
- DEVLIN, B. T.**
MD-11 Automatic Flight System
p 818 A93-37075
- DEVOS, J. P.**
Numerical prediction of instabilities in transonic internal flows using an Euler TVD code
[AIAA PAPER 93-0072] p 262 A93-20184
- DEVRIES, W. R.**
Design for manufacture by resin transfer molding of composite parts for rotorcraft
[SME PAPER EM93-103] p 1159 A93-51733
- DEWELL, LARRY D.**
An investigation of the fuel-optimal periodic trajectories of a hypersonic vehicle
[AIAA PAPER 93-3753] p 1101 A93-51349
- DEWITT, KENNETH J.**
Experimental assessment of airframe damage due to impacting ice
[AIAA PAPER 93-0751] p 504 A93-24838
Analysis and evaluation of an integrated laminar flow control propulsion system
[NASA-CR-192162] p 551 N93-20268
Numerical modeling of runback water on ice protected aircraft surfaces
p 840 N93-27438
- DEWOLF, W. B.**
Propelling force and resistance
p 298 N93-19003
- DHANAK, MANHAR R.**
Instability of flow in a streamwise corner
[NASA-CR-191410] p 694 N93-25153
- DHONDT, G.**
Modelling the engine temperature distribution between shut down and restart for life usage monitoring
p 169 N93-15177
- DI FRANCESCANTONIO, PAOLO**
A numerical method for the prediction of quadrupole shock wave noise
p 448 A93-19201
- DI LAZZARO, M.**
An integrated weather channel designed for an up-to-date ATC radar system
p 929 A93-43434
- DI MARTINO, P.**
Numerical model for predictions of reverse flow combustor aerothermal characteristics
p 1123 A93-51645
- Numerical simulation of gas turbine combustors with complex geometries
[ISABE 93-7128] p 1204 A93-54103
- DIAB, HASSAN**
Design and implementation of a flight simulation system
p 66 A93-12216
- DIAMOND, JOHN**
Development of a system for transition characterization
[AIAA PAPER 93-3465] p 1030 A93-47246
- DIBENEDETTO, M.**
DME/P critical area determination on message passing processors
p 31 A93-11010
- DICARLO, DANIEL J.**
Flight test operations using an F-106B research airplane modified with a wing leading-edge vortex flap
[AIAA PAPER 92-4094] p 42 A93-13261
Actuated forebody strake controls for the F-18 high alpha research vehicle
[AIAA PAPER 93-3675] p 1006 A93-44233
Vortex flap flight test operations, a safe approach
p 995 A93-45168
- DICICCO, L. D.**
Experimental evaluation of a cooled radial-inflow turbine
[AIAA PAPER 93-1795] p 1110 A93-49685
- DICICCO, L. DANIELLE**
Experimental evaluation of a cooled radial-inflow turbine
[NASA-TM-106230] p 816 N93-28697
- DICK, ERIK**
A flux-difference finite volume method for steady Euler equations on adaptive unstructured grids
p 1116 A93-14277
- DICKERSON, LEROY**
The effectiveness of hand-held fire extinguishers on cargo container fires
[DOT/FAA/CT-TN92/42] p 496 N93-21821
- DICKINSON, J.**
Experimental investigation of flows behind different Large-Eddy Breakup (LEBU) devices in thick boundary layers
p 18 N93-10550
- DICKINSON, PHILIP J.**
The airnoise boundary concept for airport noise management
p 564 A93-28482
- DICKOPP, CH.**
Computation of viscous hypersonic non-equilibrium blunt body flow
p 1238 A93-56038
- DICKSON, RICHARD W.**
Advanced Transport Operating System (ATOPS) Flight Management/Flight Controls (FM/FC) software description
[NASA-CR-191457] p 808 N93-28621
Advanced Transport Operating System (ATOPS) utility library software description
[NASA-CR-191469] p 1000 N93-32218
- DIEGAN, WANG**
WBNFLOW: Multi-grid/multi-block potential solver for compressible flow. User's guide
[FFA-TN-1992-43] p 1031 N93-31146
- DIEHL, ALAN E.**
Does cockpit management training reduce aircrew error?
p 146 N93-15014
Cockpit decision making
p 146 N93-15015
- DIEHL, L. W.**
Meteorological information for aviation: A systems approach
p 937 N93-30298
- DIEKMANN, ANDREAS**
On stability and control of SSTO spaceplane in super- and hypersonic ascending phase
[NAL-TR-11287] p 65 N93-12361
- DIERKS, MICHAEL W.**
Linear and nonlinear aircraft flight control for the AIAA Controls Design Challenge
[AIAA PAPER 92-4628] p 62 A93-13286
TVC control for the AIAA design challenge airplane
[AIAA PAPER 93-3810] p 1122 A93-51402
- DIETL, LOTHAR**
Test and integration concept for complex helicopter avionic systems
[MBB-UD-0605-91-PUB] p 343 N93-17547
- DIETZ, A. J.**
Unsteady pressure measurements on the rotor of a model turbine stage in a transient flow facility
[ASME PAPER 92-GT-156] p 250 A93-19383
The dynamic characteristics of a high pressure turbine stage in a transient wind tunnel
[ASME PAPER 92-GT-166] p 375 A93-19392
- DIGUMARTI, RAMARAO**
Active control for fin buffet alleviation
[AIAA PAPER 93-3817] p 1133 A93-51408
- DILIGENSKII, S. N.**
Synthesis of robust motion stabilization laws for flight vehicles
p 227 A93-16777

- DILLER, T. E.**
Heat flux microsensor measurements
[AIAA PAPER 92-5038] p 413 A93-22312
Time-resolved surface heat flux measurements in the wing/body junction vortex
[AIAA PAPER 93-0918] p 472 A93-24972
Microsensors for high heat flux measurements
p 928 A93-42920
- DILLEY, ARTHUR D.**
CFD comparisons with wind tunnel and flight data for the X-15
[AIAA PAPER 92-5047] p 273 A93-22319
Application of CFD to a generic hypersonic flight research study
[AIAA PAPER 93-0312] p 280 A93-23007
- DILLMANN, ANDREAS**
Condensation of nitrogen in hypersonic flows - Measurements confirm a theoretical model
p 111 A93-13945
- DIMA, C.**
On the modelling of separated flows about airfoils
[AIAA PAPER 93-3479] p 981 A93-47257
- DIMARCO, JOHN S.**
Investigation of the radiance from the leading edge of a wing
[AIAA PAPER 93-2728] p 1039 A93-46482
- DMITRIADIS, K. P.**
A cell-vertex TVD scheme for transonic viscous flow
p 685 A93-34346
- DINC, S.**
A systems dynamics approach to modeling gas turbine combustor wear
[ASME PAPER 92-GT-47] p 347 A93-19300
- DINDAR, MUSTAFA**
Nonequilibrium turbulence modeling study on light dynamic stall of a NACA0012 airfoil
p 768 A93-37379
- DING, HUILIANG**
Engineering optimization of aeronautical structures
p 154 A93-14227
- DING, JI-PING**
A study of aircraft global dynamic stability in rapid rolling maneuver
p 1206 A93-53869
- DING, YISHENG**
An optimization method for statistical ascertainment of the most probable peak temperature at combustor exit
p 1108 A93-49195
- DINGUIRARD, M.**
Digital image processing applied to heat transfer measurement in hypersonic wind tunnel
[ONERA, TP NO. 1992-118] p 831 A93-38593
- DINI, SAID**
Investigation of nacelle upper cowl flow separation using on- and off-body flow visualization techniques
p 1072 A93-49507
- DINICOLA, ALBERT J.**
Structural evaluation of curved stiffened composite panels fabricated using a THERM-Xsm process
p 919 A93-30435
- DINOLA, L.**
Aero-thermal design of a cooled transonic NGV and comparison with experimental results
p 904 A93-29957
- DIOT, C.**
Microstructure of yttria stabilized zirconia-hafnia plasma sprayed thermal barrier coatings
[ONERA, TP NO. 1993-54] p 1146 A93-51936
- DIRESKENELI, HALDUN**
A stochastic optimal feedforward and feedback control methodology for superagility
[NASA-CR-4471] p 229 A93-13370
- DIRLING, R.**
Development of advanced carbon-carbon annular flameholders for gas turbines
[PNR-90947] p 58 A93-11106
- DISARIO, ROBERT**
A simulation study of the effects of communication delay on air traffic control
[AD-A258593] p 502 A93-19966
- DITKIN, V. V.**
A numerical study of the flutter of conical shells
p 927 A93-42405
- DITTMAR, JAMES H.**
Cruise noise of an advanced propeller with swirl recovery vanes
p 564 A93-28609
A concept for a counterrotating fan with reduced tone noise
[NASA-TM-105736] p 101 A93-11370
- DIUZHNEV, V. I.**
A heat transfer element of a high-temperature heat exchanger
p 833 A93-39047
- DIXON, CHARLES S.**
Work performed in the United Kingdom to establish the feasibility of RAIM in a GPS receiver in flight
p 314 A93-21157
- DIXON, S. L.**
Compressible flow pressure losses in wye-junctions
[ASME PAPER 92-GT-71] p 248 A93-19321
- DJERASSI, SHLOMO**
Aircraft with single axis aerodynamically deployed wings
[AIAA PAPER 93-3673] p 1129 A93-48350
- DJILALI, N.**
Development of a transonic Euler method for complete aircraft configurations
p 779 A93-39721
- DJOJODIHARDJO, HARIJONO**
Calculation of 3-D unsteady subsonic flow with separation bubble using singularity method
p 115 A93-14251
- DJOMEHRI, M. J.**
A concurrent hybrid Navier-Stokes/Euler approach to fluid dynamic computations
[AIAA PAPER 93-0789] p 468 A93-24865
Near-field supersonic flow predictions by an adaptive unstructured tetrahedral grid solver
[AIAA PAPER 93-3430] p 977 A93-47223
- DJOMEHRI, M. JAHED**
Solution of nonlinear flow equations for complex aerodynamic shapes
[NASA-CR-190979] p 90 A93-12329
- DMITRENKO, A. V.**
Non-self-similarity of a boundary layer flow of a high-temperature gas in a Laval nozzle
p 1176 A93-52946
- DNEPROV, IGOR' V.**
Computation of aeroelastic characteristics and stress-strained state of parachutes
[AIAA PAPER 93-1237] p 744 A93-35178
- DOANE, DOUGLAS H.**
Preliminary design features of the RASCAL - A NASA/Army rotorcraft in-flight simulator
[AIAA PAPER 92-4175] p 42 A93-13311
- DOANE, K. B.**
Autonomous guidance, navigation and control bridging program plan
p 532 A93-27046
- DOBBS, S. K.**
X-31A flight flutter test excitation by control surfaces
[AIAA PAPER 93-1538] p 727 A93-34075
- DOBER, D.**
Establishing two-dimensional flow in a large-scale cascade of controlled-diffusion compressor blades
[AIAA PAPER 93-2383] p 1083 A93-50151
- DOBER, DAVID M.**
Three-dimensional fiber-optic LDV measurements in the endwall region of a linear cascade of controlled-diffusion stator blades
[AD-A263513] p 933 A93-29968
- DOBLER, W.**
Optimization of sandwich structures with respect to local instabilities with MBB-LAGRANGE
p 1255 A93-54540
- DOBROVOL'SKII, A. S.**
Fuel film formation in the fuel-air premix of the combustion chamber
p 612 A93-39193
- DOBRYNSKI, W.**
Aeroacoustic wind tunnel testing of a counterrotating shrouded propfan-model
p 449 A93-19213
Propeller noise reduction by means of unsymmetrical blade-spacing
p 1039 A93-46706
- DOCKER, STEVE**
Advanced expert systems increase aircraft maintenance efficiency - An overview
p 238 A93-18767
- DOD, LOUIS R.**
Update on the NASA ER-2 Doppler radar system (EDOP)
p 807 A93-37737
- DODBELE, SIMHA S.**
Design optimization of natural laminar flow bodies in compressible flow
[NASA-CR-4478] p 292 A93-16940
- DODD, A. G.**
The use of simultaneous engineering for the design and manufacture of the low pressure turbine for the Rolls-Royce Trent engine
[PNR-90887] p 59 A93-11206
- DODD, ROBERT S.**
Human factors in crashes of commuter airplanes
p 486 A93-24048
Public-sector aviation issues: Graduate research award papers, 1990 - 1991
[PB92-222629] p 143 A93-13787
- DODDS, R. H.**
Development of a unified airport pavement analysis and design system
p 380 A93-16317
- DODDS, W. J.**
Innovative high temperature aircraft engine fuel nozzle design
[ASME PAPER 92-GT-132] p 350 A93-19365
- DOEL, DAVID L.**
TEMPER - A gas-path analysis tool for commercial jet engines
[ASME PAPER 92-GT-315] p 354 A93-19501
- A philosophy for integrated monitoring system design
p 178 A93-15174
- DOERNBACH, JAY D.**
A scoping study for hypersonic transport propulsion systems
[ASME PAPER 92-GT-409] p 556 A93-19558
- DOGGETT, ROBERT V., JR.**
Data acquisition for aeroelastic testing at the NASA Langley Transonic Dynamics Facility
p 1250 A93-54397
- DOGRA, V. K.**
Energetics of gas-surface interactions in transitional flows at entry velocities
p 778 A93-39259
- DOGRA, VIRENDRA K.**
Near wake structure for a generic ASTV configuration
[AIAA PAPER 93-0271] p 268 A93-21103
Zonally-decoupled DSMC solutions of hypersonic blunt body wake flows
[AIAA PAPER 93-2808] p 949 A93-44227
Hypersonic blunt body wake computations using DSMC and Navier-Stokes solvers
[AIAA PAPER 93-2807] p 964 A93-46547
- DOHERR, KARL-FRIEDRICH**
Stable cross type parachute with inflation aid
[AIAA PAPER 93-1201] p 702 A93-35152
- DOHME, JACK**
Transfer of training and simulator qualification or myth and folklore in helicopter simulation
p 913 A93-30687
- DOI, HIROFUMI**
Analysis of unstarted supersonic flutter in cascade by semiactuator disk theory
p 1181 A93-53841
- DOLFI, A.**
Microbursts detection with airborne Doppler lidar
p 433 A93-22201
- DOLL, DAVID B.**
An automated flow line for gas turbine blade repair
[ASME PAPER 92-GT-367] p 375 A93-19531
- DOLL, KENNETH A.**
Investigation of roll requirements for carrier approach
[AIAA PAPER 93-3649] p 1128 A93-48332
- DOLLING, D. S.**
Correlation of interaction sweepback effects on unsteady shock-induced turbulent separation
[AIAA PAPER 93-0776] p 475 A93-25550
Organized structure in a compressible turbulent shear layer
p 961 A93-45730
A preliminary investigation of the Helmholtz resonator concept for heat flux reduction
[AIAA PAPER 93-2742] p 963 A93-46493
Control of unsteady shock-induced turbulent boundary layer separation upstream of blunt fins
[AIAA PAPER 93-3281] p 969 A93-46839
Flowfield dynamics in blunt fin-induced shock wave/turbulent boundary layer interactions
[AIAA PAPER 93-3133] p 1063 A93-48298
- DOLLING, DAVID S.**
A study of hypersonic swept shock wave/turbulent boundary layer interactions using a conical Navier-Stokes code
[AIAA PAPER 92-5050] p 273 A93-22322
Effects of sweep on the physics of unsteady shock-induced turbulent separated flows
[AD-A247035] p 22 A93-11742
The Center of Excellence for Hypersonics Training and Research at the University of Texas at Austin
[NASA-CR-193070] p 781 A93-27126
- DOLTSINIS, I. ST.**
Hypersonic viscous flow past double ellipse and past double ellipsoid - Numerical results
p 868 A93-42618
- DOMACK, CHRISTOPHER S.**
Reynolds number influences in aeronautics
[NASA-TM-107730] p 989 A93-31732
- DOMAS, PAUL A.**
CF6-6 high pressure compressor stage 5 locking slot crack propagation spin pit test
p 176 A93-14894
- DOMINIK, CHET J.**
Multielement airfoil performance due to Reynolds and Mach number variations
p 1095 A93-52442
Reynolds and Mach number effects on multielement airfoils
p 785 A93-27446
- DOMINY, W. T., JR.**
Cost effective process selection for composite structure
[SME PAPER EM93-100] p 1043 A93-51727
- DOMOTENKO, NIKOLAI T.**
Maintenance of the liquid and gas systems of the Il-76 aircraft
p 804 A93-39203
- DONER, J. P.**
Improved lubricating greases for aircraft wheel bearings
[SAE PAPER 921038] p 197 A93-14658
- DOONES, F.**
Ladar fiber optic sensor system for aircraft applications
p 1105 A93-49467

- DONEY, RICHARD H.**
The UK perspective on aviation security p 496 N93-21858
- DONG, MINGCHUN**
Inlet velocity profile effects on turbulent swirling flow predictions [AIAA PAPER 93-0133] p 274 A93-22580
Parameter effects on turbulent swirling flames in combustors p 534 A93-25911
- DONG, SONGYE**
Multiple solutions of the transonic perturbation equation p 987 A93-47331
- DONNA, JAMES I.**
The effects of ionospheric errors on single-frequency GPS users p 313 A93-21141
- DONNELLAN, MARY E.**
HIP consolidation of aluminum-rich intermetallic alloys and their composites [NAWCADWAR-92003-60] p 199 N93-14726
- DONNELLY, CHRISTOPHER F.**
Evaluating the IOBIDS specification using gate-level system simulation p 940 A93-42851
- DONNELLY, J. P.**
Development of user guidelines for a three-dimensional finite element pavement model p 379 N93-16311
- DONNERHACK, STEFAN**
Combustor development for advanced helicopter engines p 1246 A93-54841
- DONNET, G.**
Numerical modelling of induced effects of lightning strike on an all composite helicopter p 703 N93-24879
- DONOHUE, JAMES M.**
Experimental and numerical study of swept ramp injection into a supersonic flowfield [AIAA PAPER 93-2445] p 1119 A93-50197
- DONOVAN, J. F.**
Conventional skin friction measurement techniques for strongly perturbed supersonic turbulent boundary layers p 271 A93-21863
Data analysis techniques for pressure- and temperature-sensitive paint [AIAA PAPER 93-0176] p 414 A93-22605
Aerodynamic applications of pressure sensitive paint p 549 A93-29301
- DONZAC, J. M.**
Fiber reinforced composites: A new class of glass and glass ceramic materials for thermomechanical applications [REPT-921-430-104] p 200 N93-15490
- DOOG, DANIEL A.**
Experimental assessment of airframe damage due to impacting ice [AIAA PAPER 93-0751] p 504 A93-24838
- DOOTSON, P. A.**
Reliability and safety considerations in engine management systems design p 346 A93-18786
- DORFMAN, GERALD A.**
The dependent converging instrument approach procedure: An analysis of its safety and applicability [DOE/FAA/RD-93/6] p 707 N93-25456
- DORIGNAC, E.**
Experimental study of heat transfer close to a plane wall heated in the presence of multiple injections (subsonic flow) p 901 N93-29931
- DORNEY, D. J.**
Navier-Stokes analysis of turbine blade heat transfer and performance p 201 A93-13978
- DORNEY, DANIEL J.**
Numerical simulation of turbine 'hot spot' alleviation using film cooling p 744 A93-34476
Numerical simulations of flows in centrifugal turbomachinery [AIAA PAPER 93-2578] p 1085 A93-50293
Investigation of hot streak migration and film cooling effects on heat transfer in rotor/stator interacting flows, report 1 [AD-A250688] p 102 N93-12490
- DORNHEIM, MICHAEL A.**
Versatility, automation key to C-17 cargo operations p 805 A93-39600
- DOROSHENKO, V. M.**
Nonequilibrium excitation of internal molecular degrees of freedom in the shock layer during hypersonic flight p 412 A93-21922
- DORSEY, J.**
Application of analog computing to real-time simulation of stall and surge dynamics [AIAA PAPER 93-2231] p 1080 A93-50037
- DORTMANN, KLAUS**
Viscous and inviscid hypersonic flow about a double ellipsoid p 868 A93-42616
- DOSSENA, V.**
Incidence angle and pitch-chord effects on secondary flows downstream of a turbine cascade [ASME PAPER 92-GT-184] p 251 A93-19409
- DOST, E. F.**
Experimental investigations into composite fuselage impact damage resistance and post-impact compression behavior p 159 A93-15812
- DOST, ERNEST F.**
Developments in impact damage modeling for laminated composite structures p 922 N93-30857
- DOU, HUA-SHU**
Experimental investigations of the separation behavior in 3D shock wave/turbulent boundary-layer interactions p 119 A93-14345
- DOUGHERTY, F. C.**
Numerical simulations of high-speed flows about waveriders with sharp leading edges p 9 A93-12007
Interactive hypersonic waverider design and optimization p 119 A93-14348
Waverider design for generalized shock geometries [AIAA PAPER 93-0774] p 467 A93-24858
- DOUGHTY, G. R.**
Design considerations for air-to-air laser communications p 312 A93-18932
- DOUGHTY, R. L.**
A statistical approach to the experimental evaluation of transonic turbine airfoils in a linear cascade [ASME PAPER 92-GT-5] p 245 A93-19278
- DOUGLASS, ANNE R.**
Implications of three-dimensional tracer studies for two-dimensional assessments of the impact of supersonic aircraft on stratospheric ozone p 936 A93-41269
- DOUSIS, DIMITRI A.**
A vibration monitoring acquisition and diagnostic system for helicopter drive train bench tests p 826 A93-35930
- DOVGAL', A. V.**
Instability of local separated flows with respect to small-amplitude perturbations p 125 A93-15254
- DOVI, A. R.**
Multidisciplinary design integration system for a supersonic transport aircraft [AIAA PAPER 92-4841] p 324 A93-20296
- DOVIANK, R. J.**
Buoyancy wave hazards to aviation p 430 A93-22151
- DOVZHAK, S. V.**
Localization of noise sources in the exhaust jet of a turbofan engine p 1003 A93-47509
- DOW, MARVIN B.**
Development of stitching reinforcement for transport wing panels p 921 N93-30852
- DOWELL, E. H.**
Experimental and theoretical study for nonlinear aeroelastic behavior of a flexible rotor blade p 837 A93-39422
- DOWELL, EARL H.**
Nonlinear aeroelasticity and chaos p 79 A93-12165
Nonlinear aeroelastic response of panels [AIAA PAPER 93-1599] p 741 A93-34130
An efficient procedure for cascade aeroelastic stability determination using nonlinear, time-marching aerodynamic solvers [AIAA PAPER 93-1631] p 719 A93-34159
Chaos in mechanical systems with especial reference to rotorcraft and missiles [AD-A263703] p 943 N93-29384
- DOWLING, A. P.**
Active boundary-layer control in diffusers [AIAA PAPER 93-3255] p 966 A93-46798
Low-frequency combustion oscillations in a model afterburner p 1193 A93-53702
- DOWLING, NORMAN E.**
Verification of rain-flow reconstructions of a variable amplitude load history [NASA-CR-189670] p 91 N93-12411
- DOWNES, M.**
Helicopter approaches in low visibility using RGPS and EFIS p 142 A93-17309
- DOWNNEY, JAMES REAGLE**
Optimal finite-thrust time-bounded direct-ascent interception p 734 N93-25272
- DOYCHAK, J.**
Technical note - Plasma-sprayed ceramic thermal barrier coatings for smooth intermetallic alloys p 209 A93-15702
- DOYCHAK, JOSEPH**
Consecutive plate acoustic suppressor apparatus and methods [NASA-CASE-LEW-15430-1] p 453 N93-17051
- DOYLE, JOHN C.**
Robust nonlinear control of vectored thrust aircraft [NASA-CR-192727] p 728 N93-25199
- DOYLE, P. A.**
Elastic constants for unidirectional boron-epoxy composites p 387 A93-18636
- DRAKE, R. G. T.**
Developments in icing test techniques for aerospace applications in the RAE Pyestock (England) altitude test facility [RAE-TM-P-1214] p 48 N93-11485
- DRAKE, AARON**
Selected experiments in laminar flow: An annotated bibliography [NASA-TM-103989] p 990 N93-32226
- DRECHSLER, GENA K.**
Conversion of the CTA, Inc., en route operations concepts database into a formal sentence outline job task taxonomy [AD-A261410] p 708 N93-26447
- DREGALIN, A. F.**
Viscosity of aviation fuel components (n-alkanes) p 71 A93-12824
Viscosity of aviation fuel components - Aromatic hydrocarbons (alkyl benzenes) p 1211 A93-52961
- DREIBACH, RODNEY**
CST gives aircraft industry a lift p 560 A93-25086
- DRELA, MARK**
Implicit Euler calculation of supersonic vortex wake/engine plume interaction [AIAA PAPER 93-0656] p 540 A93-24769
A calculation method for the three-dimensional boundary-layer equations in integral form [AIAA PAPER 93-0786] p 541 A93-24868
- DRENNAN, S. A.**
Emission characteristics of a model gas turbine combustor at practical conditions [ISABE 93-7023] p 1196 A93-53999
- DRESHFIELD, ROBERT L.**
NDE of PWA 1480 single crystal turbine blade material [NASA-TM-106140] p 815 N93-27640
- DRESS, DAVID A.**
Subsonic static and dynamic stability characteristics of the test technique demonstrator NASP configuration [AIAA PAPER 93-0519] p 268 A93-21111
Supersonic dynamic stability characteristics of the test technique demonstrator NASP configuration [AIAA PAPER 92-5009] p 367 A93-22285
- DRIKAKIS, D.**
A multi-zonal local solution methodology for the accelerated solution of the turbulent Navier-Stokes equations p 117 A93-14279
Real gas effects for compressible nozzle flows p 682 A93-33757
On the accuracy and efficiency of CFD methods in real gas hypersonics p 871 A93-42869
Zonal-local solution method for the turbulent Navier-Stokes equations p 1177 A93-53205
- DRING, ROBERT P.**
Hot streaks and phantom cooling in a turbine rotor passage. I - Separate effects [ASME PAPER 92-GT-75] p 401 A93-19325
Hot streaks and phantom cooling in a turbine rotor passage. II - Combined effects and analytical modelling [ASME PAPER 92-GT-76] p 401 A93-19326
Radial transport and momentum exchange in an axial compressor [ASME PAPER 92-GT-364] p 257 A93-19528
- DRISCOLL, KEVIN**
SAFEbus p 828 A93-37072
- DROLLINGER, MICHAEL T.**
Public-sector aviation issues: Graduate research award papers, 1990 - 1991 [PB92-222629] p 143 N93-13787
- DROR, SHAHAR**
Identification and control of non-linear time-varying dynamical systems using artificial neural networks [AD-A257595] p 372 N93-18193
- DROST, M. K.**
An evaluation of thermal energy storage options for precooling gas turbine inlet air [DE93-005980] p 754 A93-24975
- DROUET, C.**
Fiber reinforced composites: A new class of glass and glass ceramic materials for thermomechanical applications [REPT-921-430-104] p 200 N93-15490
- DROZDOV, R. V.**
Half-scale modeling experience in the testing of radio navigation and landing systems p 882 A93-43112
- DRUMMOND, COLIN K.**
Gas turbine system simulation: An object-oriented approach [NASA-TM-106044] p 723 N93-25673
- DRYZMKOWSKI, MARK**
RTJ-303: Variable geometry, oblique wing supersonic aircraft [NASA-CR-192054] p 337 N93-18166

- DU PLESSIS, L. J. H.**
The development of a new air filtration system for the Alouette III helicopter [ISABE 93-7048] p 1199 A93-54024
- DU VAL, RONALD W.**
Helicopter rotor disk and Blade Element comparison p 799 A93-35991
- DU, CHENGLIN**
Improving the design of the main fuel pump of Turbo-Jet 7 p 1107 A93-48555
- DU, J. Y.**
An investigation on the artificial viscosity in the transonic stream function formulation [ASME PAPER 92-GT-49] p 246 A93-19302
A three-dimensional numerical method for turbomachinery blading [ASME PAPER 92-GT-291] p 254 A93-19482
- DU, ZHAOHUI**
Effect of hub treatment on performance of an axial flow compressor p 53 A93-12736
2-D theoretical analysis of circumferential grooved casing treatment p 1066 A93-48501
Frontally tapered squared trench casing treatment for improvement of compressor performance p 1108 A93-49202
- DUBOIS, FRANCOIS**
Solution of the Euler equations around a double ellipsoidal shape using unstructured meshes and including real gas effects p 867 A93-42604
- DUBOIS, ISABELLE**
Toward the second-generation supersonic transport [ONERA, TP NO. 1993-26] p 890 A93-41038
- DUBOUE, J. M.**
Three-dimensional analysis of turbine rotor flow including tip clearance [ASME PAPER 93-GT-111] p 987 A93-47446
- DUBOV, B. S.**
A transfer standard of an air flow rate unit VET 150-2-87 p 66 A93-10049
- DUBREUIL, X. H.**
Experimental density flowfields over a delta wing located in rarefied hypersonic flows p 870 A93-42637
- DUBROCA, B.**
Hypersonic flows over a double or simple ellipse p 668 A93-42614
- DUBROW, ALAN**
T55 engine - The challenge of torque measurement p 809 A93-35929
- DOCARTERON, J. P.**
Resonance frequencies of a gondola submitted to a forced rotation under a stratospheric balloon p 27 A93-11384
- DUCK, PETER W.**
The stability of a trailing-line vortex in compressible flow [NASA-CR-189738] p 298 A93-18771
- DUCOS, J. S.**
MTR390 - Engine for the future [ASME PAPER 92-GT-250] p 353 A93-19459
- DUDA, U.**
Experimental investigation of the management of large-sized drops and the onset of Marangoni-convection p 926 A93-41700
- ODAS, CHARLES**
Upgrade Precision Runway Monitor (PRM) Operational Test and Evaluation (OT/E) test plan [DOT/FAA/CT-TN92/13] p 67 A93-11616
- DUCHENKO, A. A.**
Design and fabrication of panels with cutouts p 1215 A93-52973
- DUDEBOUT, RUDOLPH**
An aerospace plane as a detonation wave ramjet/airframe integrated waverider [AIAA PAPER 92-5022] p 272 A93-22298
Hypersonic shock-induced combustion ramjet performance analysis [ISABE 93-7037] p 1197 A93-54013
- DUDEK, HEINZ-LEO**
Increased safety through knowledge-based pilot assistance p 518 A93-27499
- DUDIN, G. N.**
Calculation of a three-dimensional boundary layer at the lee side of a finite-span delta wing in the case of viscous interaction with hypersonic flow p 5 A93-10143
- DUKIN, V. P.**
Effect of overloads on the service life of the structural elements of aircraft p 746 A93-35289
- DUERR, T. E.**
Effect of terrain masking on GPS position dilution of precision p 317 A93-21824
- DUFFLOCQ, M.**
Initial development of the two-dimensional ejector shear layer - Experimental results [AIAA PAPER 93-2440] p 1118 A93-50192
- Comparison of the initial development of shear layers in two-dimensional and axisymmetric ejector configurations [AIAA PAPER 93-2441] p 1119 A93-50193
- DUFFY, PAUL**
Russian survivor p 1243 A93-54867
- DUGGE, PEGGY**
Aerospace '92 - The year in review p 455 A93-19976
- DUGGINS, R. K.**
Aeronautical engineering education for the armed forces p 453 A93-21681
- DUGUE, C.**
Rotation and cavitation of a marginal vortex p 11 A93-12433
- DUGUNDJI, JOHN**
Nonlinear problems of aeroelasticity p 78 A93-12153
Nonlinear large amplitude vibration of composite helicopter blade at large static deflection p 713 A93-35630
Nonlinear large amplitude aeroelastic behavior of composite rotor blades p 997 A93-45741
Nonlinear aeroelasticity of composite structures [AD-A254285] p 47 A93-10842
Nonlinear stall flutter of wings with bending-torsion coupling [AD-A254323] p 186 A93-12959
- DUNPHY, JAMES**
Embedded Bragg grating fiber optic sensor for composite flexbeams p 828 A93-37350
- DUPARCO, J.-L.**
Design of an advanced nacelle for a very high bypass ratio engine p 505 A93-25362
- DUPLANTIER, S.**
Investigation of a combustion zone behind a wedge p 1146 A93-51631
- DUPONT, P.**
Effect of wall heating on a supersonic turbulent boundary layer p 11 A93-12429
- DUQUE, E. P. N.**
Flowfield analysis of modern helicopter rotors in hover by Navier-Stokes method p 481 A93-29435
- DUQUE, EARL-PETER N.**
Numerical simulation of a hovering rotor using embedded grids p 765 A93-35936
- DURAND, JEAN M.**
GPS continuity - Initial findings p 314 A93-21167
- DURAND, JEAN-MARIE**
GNSS - A global system of satellite-aided navigation p 500 A93-28194
- DURAND, R. L.**
Method for developing the RAFALE flight control system p 512 A93-19912
- DURAO, D. F. G.**
On the analysis of an impinging jet on ground effects p 1260 A93-56339
- DURBIN, P. F.**
Dual-band infrared imaging applications: Locating buried minefields, mapping sea ice, and inspecting aging aircraft [DE93-000516] p 453 A93-17225
- DURHAM, MICHAEL H.**
Experimental unsteady pressures at flutter on the Supercritical Wing Benchmark Model [AIAA PAPER 93-1592] p 683 A93-34123
- DURHAM, W. C.**
Development of lateral-directional departure criteria [AIAA PAPER 93-3650] p 1128 A93-48333
- DURHAM, WAYNE C.**
Constrained control allocation p 938 A93-41891
Kinematics and aerodynamics of the velocity vector roll [AIAA PAPER 93-3625] p 1126 A93-48310
- DUSA, D. J.**
Evaluation of turbofanjet exhaust systems from scale model test data [ISABE 93-7109] p 1204 A93-54085
- DUSING, DOUGLAS W.**
On computing vortex asymmetries about cones at angle of attack using the conical Navier-Stokes equations [AIAA PAPER 93-3628] p 1064 A93-48313
- DUSSAC, M.**
A new methodology for helicopter internal noise reduction application to the AS332 L2 p 1243 A93-54723
- DUTOYA, D.**
Aerothermic calculations of flows in interdisc cavities of turbines p 903 A93-29947
- DUTTON, J. C.**
Application of particle image velocimetry in high-speed separated flows p 549 A93-29304
Computations and experiments for a multiple normal shock/boundary-layer interaction p 688 A93-34486
Supersonic base flow experiments in the near-wake of a cylindrical afterbody [AIAA PAPER 93-2924] p 1045 A93-48125
Study of the near-wake structure of a subsonic base cavity flowfield using PIV [AIAA PAPER 93-3040] p 1056 A93-48221
Three-dimensional simulations of compressible mixing layers - Visualizations and statistical analysis p 1235 A93-55360
A plume-induced boundary layer separation experiment [AD-A255397] p 220 A93-14677
- DUVAL, RONALD**
Validation and upgrading of physically based mathematical models p 942 A93-30688
- DUVAUT, GEORGES**
Modelisation and computation of composite materials p 537 A93-21518
- DUYAR, AHMET**
Identification of the open loop dynamics of the T700 turboshaft engine p 809 A93-35934

DWOYER, DOUGLAS L.

- The new challenge of computational aeroseience
p 112 A93-14169
- Computational fluid dynamics for hypersonic airbreathing aircraft
p 865 A93-42581
- The NASA Computational Fluid Dynamics (CFD) program - Building technology to solve future challenges [AIAA PAPER 93-3292]
p 1041 A93-44996
- Requirements for facilities and measurement techniques to support CFD development for hypersonic aircraft
p 1014 A93-47024

DWYER, HARRY A.

- International Symposium on Computational Fluid Dynamics, 4th, Univ. of California, Davis, Sept. 9-12, 1991. Selected Papers
p 862 A93-42426
- Shape optimization for aerodynamic efficiency and low observability
[AIAA PAPER 93-3115]
p 1062 A93-48285

DWYER, M. E.

- Quasi-optimal steady state and transient maneuvers with and without thrust vectoring
[AIAA PAPER 93-3778]
p 1132 A93-51373

DWYER, W. P.

- A 3D Navier-Stokes analysis of a generic ground vehicle shape
[AIAA PAPER 93-3521]
p 985 A93-47283

DYKES, B. C.

- An Acoustic Emission Pre-failure Warning System for composite structural tests
p 1161 A93-52560

DYNE, BARRY R.

- Finite element analysis of the Scramaccelerator with finite rate chemistry
[AIAA PAPER 93-0745]
p 540 A93-24833

DYNNIK, K. P.

- Automation of aircraft service testing tasks using the automatic control system Bezopasnost'-3
p 306 A93-18345
- Development of a prototype of an expert system for the design of comprehensive scientific-technical development programs for civil aviation
p 434 A93-18373

DYSON, B. F.

- Recent evolution of gas turbine materials and the development of models for life prediction
p 915 A93-40802

DYSON, F.

- Small satellites and RPA's in global-change research [AD-A260762]
p 755 A93-25837

DZHAICHEKOV, N. ZH.

- Calculation of flow of a rarefied gas past a sphere for an arbitrary Knudsen number
p 124 A93-15146

DZIDA, MAREK

- The comparison of different simplified mathematical models of the gas turbine combustion chamber as an object of temperature and pressure control
[ASME PAPER 92-GT-347]
p 354 A93-19518

DZIEDZIC, WILLIAM M.

- Design of a hypersonic waverider-derived airplane
[AIAA PAPER 93-0401]
p 384 A93-21108
- Analytical comparison of convective heat transfer correlations in supercritical hydrogen
p 416 A93-23477

DZIURA, T. G.

- Surface emitting lasers for avionics applications
p 1259 A93-55756

DZYGDLO, Z.

- Analysis of spatial motion dynamics of a helicopter for various models of the induced velocity field
p 1191 A93-53721

E**E, QIN**

- Compressible laminar and turbulent boundary layer computation for the three-dimensional wing
p 12 A93-12735

EAGLE, PAUL J.

- Aircraft trajectory tracking and prediction
[AD-A259039]
p 340 A93-18999

EAMES, DAVID J. H.

- Determination of YAV-8B Reaction Control System bleed flow usage
[AIAA PAPER 92-4232]
p 54 A93-13330

EAST, R. A.

- Applications of liquid crystal surface thermography to hypersonic flow
p 1023 A93-45504

EAST, THOMAS W. R.

- A self-steering array for the SHARP microwave-powered aircraft
p 792 A93-37090

EASTEP, F. E.

- Aeroelastic model design using structural optimization
[AIAA PAPER 92-4730]
p 409 A93-20329

EASTERBROOK, CALVIN C.

- Development of models for predicting the triggering of lightning by launch vehicles
p 734 A93-24899

EATON, ROBERT A.

- State-of-the-art survey of flexible pavement crack sealing procedures in the United States
[AD-A258050]
p 382 A93-17708

EBEL, A.

- Short-term atmospheric effects of high-altitude aircraft emissions
p 559 A93-28865

EBERHARDT, D. S.

- Calculation of the flowfield around an airfoil with spoiler
[AIAA PAPER 93-0527]
p 284 A93-23268
- Comparison of confined, compressible, spatially developing mixing layers with temporal mixing layers
p 1234 A93-55352

EBERHARDT, SCOTT

- Audio post-processing for shear layer calculations
[AIAA PAPER 93-3075]
p 1059 A93-48250

EBERLE, ALBRECHT

- Enhanced numerical inviscid and viscous fluxes for cell centered finite volume schemes
p 864 A93-42444
- Numerical methods for aerothermodynamic design of hypersonic space transport vehicles
[MBB-FE-211-S-PUB-0481]
p 514 A93-21056
- Application of the Euler method EULFLEX to a fighter-type airplane configuration at transonic speed
[MBB-FE-211-S-PUB-0489-A]
p 484 A93-21059

EBERT, LEE G.

- Special tooling disposition for aircraft entering post production support
[AD-A261614]
p 678 A93-26168

EBRAHIMI, HOUSHANG B.

- Numerical analysis of reacting flow using finite rate chemistry models
p 389 A93-21666
- CFD validation for scramjet combustor and nozzle flows.
[AIAA PAPER 93-1840]
p 1111 A93-49724

ECCLLES, DAVID A.

- Computer-controlled alignment for a 2000-line color monitor
p 886 A93-30324

ECCLLES, PETER J.

- Elevated array detection and measurement of microbursts using Theta(E)
p 412 A93-22173

ECHIN, A. I.

- Protective properties of aviation oils
p 735 A93-35299

ECKARDT, DIETRICH

- Future aero engine design trade offs
p 1246 A93-54836

ECKBRETH, ALAN C.

- Shedding new light on gas dynamics
p 80 A93-13435

ECKEL, ANDREW J.

- Ceramic matrix composites for rocket engine turbine applications
[ASME PAPER 92-GT-394]
p 388 A93-19547

ECKELMANN, H.

- An experimental investigation of base bleed effect on the wake turbulent structure behind a two-dimensional blunt model
[MPIS-9/1991]
p 139 A93-15131

ECKERLE, W. A.

- Heat transfer in high turbulence flows: A 2-D planar wall jet
p 932 A93-29935

ECKERT, E.

- Optimization aspects of an ejector type hypersonic thrust nozzle
[ASME PAPER 92-GT-402]
p 355 A93-19551

ECKOLDT, D.

- New design concepts for silencing aeroacoustic wind tunnels
p 445 A93-19147

EDELMAN, RAYMOND B.

- Effects of buoyancy on gas jet diffusion flames
[NASA-CR-191109]
p 935 A93-31031

EDENS, ELEANA

- Taxonomy of flight variables
p 147 A93-15022

EDINGTON, JEFF W.

- Materials development for light design - A suppliers view
p 915 A93-40777

EDMOND, J. A.

- High temperature rectifiers and MOS devices in 6H-silicon carbide
[AD-A254725]
p 90 A93-12340

EDWARDS, DAVID E.

- Investigation of hot streak migration and film cooling effects on heat transfer in rotor/stator interacting flows, report 1
[AD-A250688]
p 102 A93-12490

EDWARDS, J. A.

- The application and analysis of liquid crystal thermographs in short duration hypersonic flow
[AIAA PAPER 93-0182]
p 542 A93-25509

EDWARDS, J. W.

- Current status of computational methods for transonic unsteady aerodynamics and aeroelastic applications
p 480 A93-29175

EDWARDS, JACK R.

- Nonlinear relaxation/quasi-Newton algorithm for the compressible Navier-Stokes equations
p 287 A93-23541

- A coarse-grid correction/nonlinear relaxation algorithm for the three-dimensional, compressible Navier-Stokes equations
[AIAA PAPER 93-3317]
p 951 A93-45013

EDWARDS, JOHN W.

- Transonic shock oscillations calculated with a new interactive boundary layer coupling method
[AIAA PAPER 93-0777]
p 269 A93-21119

EDWARDS, MARK B.

- En route air traffic controllers use of flight progress strips: A graph-theoretic analysis
[AD-A259062]
p 319 A93-18927

EDWARDS, OLIVER J.

- Performance considerations for high-definition head-mounted displays
p 518 A93-27242

EDWARDS, T.

- Results of high temperature JP-7 cracking assessment
[AIAA PAPER 93-0806]
p 533 A93-24882

EDWARDS, THOMAS A.

- Fluid/chemistry modeling for hypersonic flight analysis
p 111 A93-14120

EDWARDS, TIM

- USAF supercritical hydrocarbon fuels interests
[AIAA PAPER 93-0807]
p 533 A93-24883

EDY, J. L.

- Digital image processing applied to heat transfer measurement in hypersonic wind tunnel
[ONERA, TP NO. 1992-118]
p 831 A93-38593

EERTINK, O.

- The energy dissipation in a rotating stall cell
[ISABE 93-7010]
p 1183 A93-53986

EFIMOV, O. E.

- Flight path optimization and suboptimal control laws synthesis for transport mission of maneuverable aircraft
p 180 A93-14160

EFIMTSOV, B. M.

- An experimental system for studying the vibrations and acoustic emission of cylindrical shells and panels in a field of turbulent pressure pulsations
p 1140 A93-51754
- Spectra of pressure pulsations on the surface of a cone in the transition region at supersonic flow velocities
p 1088 A93-51755

EFIMTSOV, BORIS M.

- On space correlation of pressure pulsations on the streamlined surface before a step
p 244 A93-19135

EFREMOV, A. IU.

- Synthesis of robust motion stabilization laws for flight vehicles
p 227 A93-16777

EGAMI, KOICHI

- Two-dimensional Navier-Stokes analysis of high-lift multi-element airfoils using the q-omega turbulence model
[AIAA PAPER 93-0679]
p 466 A93-24787

EGGERS, H.

- GARTEUR damage mechanics for composite materials: Analytical/experimental research on delaminations
p 537 A93-21513

EGOAVIL, MARCO A.

- Thermal analysis of a shower-head burner
[SAE PAPER 921226]
p 898 A93-41400

EGOLF, T. A.

- Prediction of BVI noise patterns and correlation with wake interaction locations
p 849 A93-35966

EGOROV, A. B.

- Aerodynamic characteristics of airship models of different shapes
p 1092 A93-51909

EGOROV, I. N.

- Optimization of a multistage axial compressor stochastic approach
[ASME PAPER 92-GT-163]
p 351 A93-19389

- Optimization of a multistage axial compressor in a gas turbine engine system
[ASME PAPER 92-GT-424]
p 357 A93-19572

EGOROV, I. V.

- Effect of real air properties on integral aerodynamic characteristics
p 242 A93-18241
- Nonequilibrium heat transfer near the critical point of blunt bodies
p 777 A93-39145

EGOROV, Z. M.

- An experimental study of dc discharges in supersonic and subsonic air flows
p 14 A93-12980

EHERNBERGER, L. J.

- Stratospheric turbulence measurements and models for aerospace plane design
[AIAA PAPER 92-5072]
p 433 A93-22342

- Stratospheric turbulence measurements and models for aerospace plane design
[NASA-TM-104262]
p 223 A93-13288

EHLERS, S. M.

- Static aeroelastic control of an adaptive lifting surface
p 995 A93-45147

- EHLERS, STEVEN M.**
Adaptive aeroelastic composite wings - Control and optimization issues p 185 A93-14818
- EHRENFRIED, KLAUS**
Numerical investigation of swirl-airfoil interactions in transonic area [MPIS-8/1991] p 297 N93-18627
- EHRESMAN, C. M.**
Two and three-dimensional prediffuser combustor studies with air-water mixture [AIAA PAPER 93-0240] p 390 A93-22652
Three-dimensional prediffuser combustor studies with air-water mixture [AIAA PAPER 93-2474] p 1120 A93-50217
Liquid rocket propulsion applied to manned aircraft - In historical perspective p 1174 A93-51497
- EICH, T.**
Measurement of shed vorticity and circulation from rotating aerofoil by particle image velocimetry p 538 A93-23804
- EICHSTEDT, DAVID**
Operational and research aspects of a radio-controlled model flight test program [AIAA PAPER 93-0625] p 504 A93-24742
Operational and research aspects of a radio-controlled model flight test program [NASA-TM-104266] p 339 N93-18616
- EICKOFF, H.**
Experimental and theoretical investigation of a research atomizer/combustion chamber configuration [ASME PAPER 92-GT-137] p 401 A93-19369
- EIDE, MICHAEL C.**
Acquisition and use of Orlando, Florida and Continental Airbus radar flight test data p 489 N93-19603
- EIDEBERG, KENNETH**
Ongoing GPS experiments demonstrate potential of satellite navigation technology p 1097 A93-49278
- EIDELMAN, S.**
A propulsion device driven by reflected shock waves p 1001 A93-45550
- EIDELMAN, SHMUEL**
Pulsed detonation engine experimental and theoretical review [AIAA PAPER 92-3168] p 531 A93-24478
- EIFLER, P.**
Pdf prediction of supersonic hydrogen flames [AIAA PAPER 93-0448] p 391 A93-23358
- EIKMANN, THOMAS**
Effects of commercial flight pollution on human health p 1035 N93-31931
- EILBERT, JAMES**
Failure-accommodating neural network flight control [AIAA PAPER 92-4394] p 523 A93-24495
- EILTS, MICHAEL D.**
An improved gust front detection algorithm for the TDWR p 432 A93-22191
- EISSFELLER, B.**
An experimental health monitoring unit for GPS and GLONASS p 706 N93-25018
- EITELBERG, G.**
A laser induced fluorescence system for the high enthalpy shock tunnel (HEG) in Goettingen p 1024 A93-45506
Simulation of hypersonic flight - A concerted European effort p 1136 A93-49301
- EJIRI, M.**
Polar Patrol Balloon Experiment in Antarctica p 27 A93-11373
- EKATERINARIS, J. A.**
Effects of spatial order of accuracy on the computation of vortical flowfields [AIAA PAPER 93-3371] p 955 A93-45064
Dynamic airfoil stall investigations p 786 N93-27453
- EKATERINARIS, JOHN A.**
A viscous-inviscid interaction method for 2-D unsteady, compressible flows [AIAA PAPER 93-3019] p 1055 A93-48206
- EKLUND, DEAN R.**
Workshop report - A validation study of Navier-Stokes codes for transverse injection into a Mach 2 flow p 270 A93-21330
Workshop Report: A validation study of Navier-Stokes codes for transverse injection into a Mach 2 flow p 751 N93-26008
- EKLUND, T. I.**
A model study of the aircraft cabin environment resulting from in-flight fires [DOT/FAA/CT-90/22] p 496 N93-21557
- EL-BANHAWY, Y. H.**
Blowout of turbulent disc/pilot stabilized jet diffusion flames [ISABE 93-7026] p 1213 A93-54002
- EL-EHWANY, A. A.**
Blowout of turbulent disc/pilot stabilized jet diffusion flames [ISABE 93-7026] p 1213 A93-54002
- EL-SEOUD, S. A.**
An implicit finite-difference algorithm for the numerical simulation of supersonic flow over blunt bodies p 770 A93-38325
- EL-SHARAWY, EL-BUDAWY**
Advanced electromagnetic methods for aerospace vehicles [NASA-CR-193468] p 936 N93-31036
- ELAM, SANDRA K.**
Subscale hot-fire testing of a formed platelet liner [AIAA PAPER 93-1827] p 1141 A93-49713
- ELANDS, P. J. M.**
Polyethylene pyrolysis model for combustion calculations in solid fuel ramjets p 520 A93-27739
- ELCRAT, ALAN**
Free streamline-boundary layer analysis for separated flow over an airfoil p 1239 A93-56327
- ELDER, R. L.**
Recess vane passive stall control [ASME PAPER 92-GT-36] p 246 A93-19296
A study of stall in a low hub/tip ratio fan [ASME PAPER 92-GT-85] p 248 A93-19334
Adaptation of a 3-D pressure correction Navier-Stokes solver for the accurate modelling of tip clearance flows p 971 A93-46932
The prediction and the active control of surge in multi-stage axial-flow compressors p 1002 A93-46945
Experimental investigation of boundary layer transition on a flat plate with C4 leading edge [ISABE 93-7123] p 1222 A93-54098
Experimental investigation of rotating stall in a mismatched three stage axial flow compressor p 423 N93-18727
Application of recess vane casing treatment to axial flow fans p 423 N93-18728
A study of stall in a low hub/tip ratio fan p 423 N93-18729
Radial inflow turbine study [AD-A260767] p 724 N93-25917
- ELDRED, LLOYD B.**
Sensitivity analysis of aeroelastic response of a wing using piecewise pressure representation [AIAA PAPER 93-1645] p 742 A93-34170
Sensitivity analysis of a wing aeroelastic response p 958 A93-45142
- ELENA, M.**
Effect of wall heating on a supersonic turbulent boundary layer p 11 A93-12429
- ELESHAKY, MOHAMED E.**
Improving the efficiency of aerodynamic shape optimization procedures [AIAA PAPER 92-4697] p 264 A93-20309
Aerodynamic shape optimization via sensitivity analysis on decomposed computational domains [AIAA PAPER 92-4698] p 265 A93-20310
Airfoil shape optimization using sensitivity analysis on viscous flow equations p 682 A93-33755
- ELESHAKY, MOHAMED EL-AMIN**
A computational aerodynamic design optimization method using sensitivity analysis p 716 N93-25552
- ELESHAKY, MOHAMMED E.**
Preconditioned domain decomposition scheme for three-dimensional aerodynamic sensitivity analysis p 957 A93-45096
- ELGHOBASHI, S. E.**
Fundamental studies of droplet interactions in dense sprays [AD-A261165] p 737 N93-25948
- ELGHOBASHI, SAID**
Three-dimensional flow over two spheres placed side by side p 539 A93-24412
- ELIASSEN, PETER**
Hypersonic leeside delta-wing-flow computations using centered schemes p 870 A93-42635
Implementation of a multidomain Navier-Stokes code on the Intel iPSC2 hypercube [FFA-TN-1992-37] p 843 N93-28994
- ELISHAKOFF, ISAAC**
Reliability of stiffened structural panels: Two examples [NASA-TM-107687] p 219 N93-14483
- ELIZAROV, A. M.**
Maximizing the critical Mach number for lifting wing profiles p 13 A93-12841
Numerical optimization methods for variational inverse boundary value problems of aerodynamics p 1088 A93-51771
- ELKS, CARL R.**
A performance assessment of a byzantine resilient fault-tolerant computer [AIAA PAPER 89-3064] p 938 A93-41296
- ELLINGSON, W. A.**
Use of local x ray computerized tomography for high-resolution, region-of-interest inspection of large ceramic components for engines [DE93-005564] p 843 N93-28943
- ELLIOTT, D. W.**
Matching engine and aircraft lapse rates for the HSCT [AIAA PAPER 93-1809] p 1100 A93-49698
- ELLIOTT, GREGORY S.**
The effect of expansion on the large scale structure of a compressible turbulent boundary layer [AIAA PAPER 93-2991] p 1052 A93-48183
- ELLIOTT, JAMES R.**
Vortex flap flight test operations, a safe approach p 995 A93-45168
Digitization of analog data from in-flight lightning strikes p 753 N93-24884
- ELLIOTT, JOE W.**
A study of the rotor wake of a small-scale rotor model in forward flight using laser light sheet flow visualization with comparisons to analytical models p 766 A93-35957
- ELLIOTT, S. J.**
Active control of sound transmission through stiff lightweight composite fuselage constructions p 447 A93-19187
Theoretical studies of the active control of propeller induced cabin noise using secondary force inputs p 995 A93-45124
- ELLIOTT, SIMON**
Managing mistakes p 109 A93-17100
Advancing helicopters p 327 A93-21836
Wind of change p 1209 A93-53625
- ELLIOTT, STEVE**
Design of the advanced regional aircraft, the DART-75 [NASA-CR-192044] p 333 N93-17972
- ELLIS, DAVID R.**
Aviation safety research at the National Institute for Aviation Research Wichita State University: A report to the FAA Technical Center [NIAR-92-2] p 310 N93-16455
- ELLIS, JOHN M.**
International aircraft operator information system [DOT/FAA/CT-93/4] p 949 N93-32232
- ELLIS, THOMAS D., JR.**
An evaluation of software tools for the design and development of cockpit displays [AIAA PAPER 93-3593] p 1224 A93-52685
- ELLISON, K. A.**
Powder metallurgy repair of turbine components [ASME PAPER 92-GT-312] p 354 A93-19500
- ELMENDORF, W.**
Design and rotor performance of a 5:1 mixed-flow supersonic compressor [ASME PAPER 92-GT-73] p 348 A93-19323
- ELMILIGUI, ALAA**
Volume 2: Explicit, multistage upwind schemes for Euler and Navier-Stokes equations [NASA-CR-191647] p 418 N93-16558
- ELMORE, KIM**
TDWR 1991 Program Review p 145 N93-14852
- ELMORE, KIMBERLY L.**
A statistical characterization of Denver-area microbursts [AD-A262127] p 845 N93-27675
- ELMQUIST, A. R.**
Evaluation of a CFD code for analysis of normal-shock trains [AIAA PAPER 93-0292] p 279 A93-22692
- ELNOUBI, SAID M.**
Three-dimensional cellular systems for aeronautical mobile radio communications p 502 A93-29639
- ELORANTA, EDWIN W.**
Volume-imaging lidar observations of the convective structure surrounding the flight path of a flux-measuring aircraft p 425 A93-20579
- ELORANTA, JORMA**
CWAS - Clean wing advisory system: A new approach to ice detection [AIAA PAPER 93-0747] p 516 A93-24835
- ELSENAAR, A.**
A break-down of sting interference effects [NLR-TP-91220-U] p 1014 N93-31042
- ELSTON, SIDNEY B., III**
Aero-engine reliability - A GE view p 345 A93-18782
- ELWARD, KEVIN M.**
Shock formation in overexpanded tip leakage flow [ASME PAPER 92-GT-1] p 245 A93-19276
- ELY, W. L.**
A sensitivity study for pneumatic vortex control on a chined forebody [AIAA PAPER 93-0049] p 260 A93-20162
The aerodynamic effects of sideslip on double delta wings [AIAA PAPER 93-0053] p 261 A93-20166

- ELZEIN, A.**
Crack analysis using discontinuous boundary elements
p 925 A93-40775
- EMANUEL, G.**
Nonlinear waveriders
[AIAA PAPER 93-3487] p 982 A93-47261
- EMANUEL, KERRY A.**
An unmanned aircraft for dropwindsonde deployment and hurricane reconnaissance p 677 A93-34587
- EMBORG, URBAN**
Vibro-acoustic analysis of propeller aircraft, integrating advanced experimental modeling with in-flight data analysis p 451 A93-19230
- EMERSON, KAREN**
The testing of fixed wing tanker and receiver aircraft to establish their air-to-air refuelling capabilities, volume 11
[AGARD-AG-300-VOL-11] p 514 N93-21305
- EMERY, J. H.**
Development of an expert system for cockpit emergency procedures p 845 A93-35915
- EMILE, EDDY**
Guidelines for NAVSTAR GPS embedded receiver applications p 315 A93-21184
- EMIN, O. N.**
Selection of the scheme and optimal parameters of the turbine of a high-temperature bypass engine with a low bypass ratio p 811 A93-39180
- EMMERSON, A. J.**
New lamps for old - Safety regulation through structural airworthiness standards p 28 A93-13630
- EMMETT, P. R.**
Envelope function - A tool for analyzing flutter data p 1136 A93-52455
- ENDE, H.**
Millisecond aerodynamic force measurement with side-jet model in the ISL shock tunnel p 822 A93-39414
Shock tunnel experiments and approximative methods on hypervelocity side-jet control effectiveness
[AIAA PAPER 93-1929] p 1077 A93-49794
- ENDECOTT, BOYD R.**
Comparison of toxicity rankings of six aircraft cabin polymers by lethality and by incapacitation in rats p 26 A93-10328
- ENDOH, TSUYOSHI**
Numerical analysis of two-dimensional flows around elliptic wings above a flat plate p 267 A93-20924
- ENGDAHL, SEAN**
A second-generation high speed civil transport: Stingray
[NASA-CR-192022] p 336 N93-18059
- ENGEDA, A.**
Flow investigation of a low-speed-operated centrifugal compressor over a flow range including zero flow
[AIAA PAPER 93-2240] p 1155 A93-50042
- ENGEL, K.**
Numerical investigation of the unsteady flow through a counter-rotating fan p 112 A93-14166
An integrated flow simulation system on a parallel computer. I - Basic concept. II - The flow solver p 688 A93-34370
Unsteady flow simulation on a parallel computer p 1022 A93-45089
- ENGEL, STEVE**
Failure-accommodating neural network flight control
[AIAA PAPER 92-4394] p 523 A93-24495
- ENGELHART, M.**
Integration of full scale development aircraft GPS user equipment (AN/ARN-151) with Doppler radar systems p 31 A93-11012
- ENGELLAND, JAMES D.**
Avionics systems architectures p 808 N93-27169
- ENGELLAND, S. A.**
Piloted simulation evaluation of pitch control designs for highly augmented STOVL aircraft
[AIAA PAPER 92-4234] p 63 A93-13328
- ENGELUND, WALTER C.**
Aerothermoelastic analysis of a NASP demonstrator model
[AIAA PAPER 93-1366] p 733 A93-33933
- ENGLAND, HARVEY M., JR.**
Inward contaminant leakage tests of the S-Tron Corporation emergency escape breathing device. Phase 1: Tests of the original design. Phase 2: Tests with the redesigned neck seal
[DOT/FAA/AM-92/18] p 704 N93-25205
- ENGLANDER, B.**
Drag/thrust estimation via aircraft performance flight testing p 156 A93-14322
- ENGLAR, ROBERT J.**
Development of circulation control technology for application to advanced subsonic transport aircraft
[AIAA PAPER 93-0644] p 464 A93-24759
- ENNIX, KIMBERLY A.**
Flight-determined engine exhaust characteristics of an F404 engine in an F-18 airplane
[AIAA PAPER 93-2543] p 1121 A93-50267
Engine exhaust characteristics evaluation in support of aircraft acoustic testing
[NASA-TM-104263] p 1005 N93-32220
- ENNS, DALE**
H(infinity) optimal controllers for a distributed model of an unstable aircraft p 62 A93-13247
Numerical computation and approximations of H(infinity) optimal controllers for a 2-parameter distributed model of an unstable aircraft p 817 A93-37040
- ENNS, DALE F.**
Nonlinear feedback control of highly manoeuvrable aircraft p 40 A93-11654
- ENOMOTO, FRANCIS Y.**
3D automatic Cartesian grid generation for Euler flows
[AIAA PAPER 93-3386] p 956 A93-45077
- EPIFANOV, V. M.**
Mathematical modeling of the three-dimensional temperature fields of turbine blades p 1216 A93-53329
- EPPARD, W. M.**
An upwind, kinetic flux-vector splitting method for flows in chemical and thermal non-equilibrium
[AIAA PAPER 93-0894] p 472 A93-24954
A multi-dimensional kinetic-based upwind solver for the Euler equations
[AIAA PAPER 93-3303] p 950 A93-45001
- EPSTEIN, A. H.**
Evaluation of approaches to active compressor surge stabilization
[ASME PAPER 92-GT-182] p 352 A93-19407
Blade row interaction effects on compressor measurements p 900 A93-42885
Flow control of low heat load turbine airfoils
[AD-A260941] p 724 N93-26219
Flow phenomena in turbomachines p 930 N93-29141
The influence of non-uniform spanwise inlet temperature on turbine rotor heat transfer p 901 N93-29932
- EPSTEIN, ALAN H.**
Active stabilization to prevent surge in centrifugal compression systems
[NASA-CR-191625] p 424 N93-18862
Active stabilization of aeromechanical systems
[AD-A261366] p 725 N93-26335
- EPTON, MICHAEL A.**
Exact solution sensitivities for boundary element aerodynamics codes
[AIAA PAPER 92-4745] p 436 A93-20343
- ER-AL, J.**
Leading edge vortices in a chordwise periodic flow p 782 N93-27218
- ER-EL, J.**
Leading edge vortices in a chordwise periodic flow p 119 A93-14333
- ERBLAND, PETER J.**
Taking the measure of aerodynamic testing p 16 A93-13434
- ERDOS, J. I.**
Mixing and combustion studies using discrete orifice injection at hypervelocity flight conditions p 205 A93-14523
- EREJEJTSEV, I. G.**
A study of turbulent flow in a viscous shock layer in the case of gas flow past oblong blunt bodies p 1089 A93-51820
- ERIC, PERRAUD**
New concepts for fiber optic position sensors p 1106 A93-49477
- ERICKSEN, L.**
Engine driven chiller and thermal storage integration (Large tonnage engine driven chiller development)
[PB92-227891] p 555 N93-21465
- ERICKSON, GARY E.**
Fiber optic-based laser vapor screen flow visualization systems for aerodynamic research in larger-scale subsonic and transonic wind tunnels p 408 A93-20298
Effects of forebody strakes and Mach number on overall aerodynamic characteristics of configuration with 55 deg cropped delta wing
[NASA-TP-3253] p 131 N93-13353
- ERICKSON, LARRY L.**
A concurrent hybrid Navier-Stokes/Euler approach to fluid dynamic computations
[AIAA PAPER 93-0789] p 468 A93-24865
Near-field supersonic flow predictions by an adaptive unstructured tetrahedral grid solver
[AIAA PAPER 93-3430] p 977 A93-47223
- ERICKSON, W. D.**
Analysis of hypersonic nozzles including vibrational nonequilibrium and intermolecular force effects p 861 A93-41916
- ERICSSON, K. ANDERS**
Methodology for studying and training expertise p 147 N93-15018
- ERICSSON, L. E.**
Hammerhead aeroelastic stability revisited
[AIAA PAPER 93-1477] p 740 A93-34022
Thoughts on conical flow asymmetry p 1070 A93-49003
Ground facility interference on aircraft configurations with separated flow p 1140 A93-52441
Effect of leading-edge geometry on delta wing unsteady aerodynamics p 1095 A93-52457
- ERICSSON, LARS E.**
Cobra maneuver considerations p 182 A93-14306
The problem of dynamic stall simulation revisited
[AIAA PAPER 93-0091] p 264 A93-20197
What makes the Cobra maneuver possible?
[AIAA PAPER 93-0183] p 367 A93-22609
Further analysis of high-rate rolling experiments of a 65 deg delta wing
[AIAA PAPER 93-0620] p 523 A93-24737
Slender wing rock revisited p 768 A93-37386
The moving wall effect vis-a-vis other dynamic stall flow mechanisms
[AIAA PAPER 93-3424] p 1008 A93-47219
Flow physics of critical states for rolling delta wings
[AIAA PAPER 93-3683] p 1129 A93-48355
- ERIKSSON, L.-E.**
Large eddy simulation of turbulent combustion behind flame holders
[ISABE 93-7042] p 1198 A93-54018
- ERIKSSON, LARS-ERIK**
CFD analysis and testing on a twin inlet ramjet
[AIAA PAPER 93-1839] p 1075 A93-49723
- ERKELENS, L. J. J.**
Flight simulation evaluation of the flyability of curved MLS approaches with wide-body aircraft
[NLR-TP-90238-U] p 382 N93-17875
- ERKELENS, LOUIS J. J.**
Flight simulator research into advanced MLS approach and departure procedures p 149 A93-14234
Development of advanced approach and departure procedures
[AIAA PAPER 93-3833] p 1098 A93-51422
Evaluation of the flyability of MLS curved approaches for wide-body aircraft
[NLR-TP-91396-U] p 999 N93-32416
- ERL, P.**
Optimization of sandwich structures with respect to local instabilities with MBB-LAGRANGE p 1255 A93-54540
- ERLEBACHER, GORDON**
Vortex breakdown incipience: Theoretical considerations
[NASA-CR-189734] p 290 N93-16627
- ERCHKIN, M. P.**
Development of a process for fabricating a plate heat exchanger for the heat recovery system of gas turbine engines p 834 A93-39053
- ERSHOV, V. N.**
Experience in the design of supercritical cascades for the flow straightener of a transonic fan p 777 A93-39196
- ESCHENAUER, H. A.**
Multidisciplinary design of composite aircraft structures by Lagrange p 76 A93-10273
- ESCURET, J. F.**
The prediction and the active control of surge in multi-stage axial-flow compressors p 1002 A93-46945
- ESFAHANI, LILI**
Thermal response and ablation characteristics of light weight ceramic ablaters
[AIAA PAPER 93-2790] p 1018 A93-46532
- ESFAHANIAN, V.**
Effects of free-stream turbulence on boundary-layer transition
[AIAA PAPER 93-0488] p 416 A93-23390
- ESFAHANIAN, VAHID**
Stability and transition on swept wings
[AIAA PAPER 93-0078] p 263 A93-20190
- ESFANDIARI, SHAHRAM**
Models for performance assessment of HF antennas on the CH-135/Twin Huey helicopter p 933 N93-30291
- ESHOW, MICHELLE M.**
Preliminary design features of the RASCAL - A NASA/Army rotorcraft in-flight simulator
[AIAA PAPER 92-4175] p 42 A93-13311
Improvements in hover display dynamics for a combat helicopter p 727 A93-34257
- ESKELINEN, PEKKA**
Effects of equipment calibration, test flight procedures and analysing methods on the accuracy of ILS glide path measurements p 881 A93-41600

ESKER, BARBARA S.

- Performance characteristics of a variable-area vane nozzle for vectoring an ASTOVL exhaust jet up to 45 deg
[AIAA PAPER 93-2437] p 1118 A93-50189
- Effects of flow-path variations on internal reversing flow in a tailpipe offtake configuration for ASTOVL aircraft
[AIAA PAPER 93-2438] p 1118 A93-50190
- Experimental performance of a ventral nozzle with pitch and yaw vectoring capability for SSTOVL aircraft
[NASA-TM-106054] p 722 N93-25129
- Performance characteristics of a variable-area vane nozzle for vectoring an ASTOVL exhaust jet up to 45 deg
[NASA-TM-106114] p 813 N93-27131
- Effects of flow-path variations on internal reversing flow in a tailpipe offtake configuration for ASTOVL aircraft
[NASA-TM-106149] p 900 N93-29065
- ESMAILI, HOSSEIN**
- Large-eddy simulation of temporally developing boundary layers with embedded streamwise vortices
p 750 N93-25753

ESPANA, MARTIN D.

- On the estimation algorithm for adaptive performance optimization of turbofan engines
[AIAA PAPER 93-1823] p 1111 A93-49710

ESPINOSA, PAUL S.

- Tiltrotor Research Aircraft composite blade repairs - Lessons learned p 108 A93-14819

ESSERS, U.

- New design concepts for silencing aeroacoustic wind tunnels p 445 A93-19147

ESTIVAL

- An overview on practical application of helicopter noise certification rules p 487 A93-29442

EUSSEN, B. J. G.

- Beyond the frequency limits of time-linearized methods
[NLR-TP-91216-U] p 295 N93-17929

EUSTACE, RICHARD

- Neural network fault diagnosis of a turbofan engine
[ISABE 93-7091] p 1203 A93-54067

EUSTACE, RICHARD W.

- Fault signatures obtained from fault implant tests on an F404 engine
[ASME PAPER 92-GT-82] p 348 A93-19331

EVANS, AUSTIN L.

- Multidisciplinary propulsion simulation using NPSS
[AIAA PAPER 92-4709] p 435 A93-20318

EVANS, B. F.

- Computational techniques for probabilistic analysis of turbomachinery
[ASME PAPER 92-GT-167] p 351 A93-19393

EVANS, D. H.

- Flutter of grouped turbine blades
[ASME PAPER 92-GT-227] p 404 A93-19444

EVANS, JAMES

- Systems issues in airborne Doppler radar/LIDAR certification p 145 N93-14855

EVANS, JAMES E.

- Integrated Terminal Weather System (ITWS)
p 428 A93-22127
- Status of the Terminal Doppler Weather Radar one year before deployment p 431 A93-22184

EVDOKIMOV, A. I.

- A method for estimating the technico-economic efficiency of measures increasing the reliability of gas turbine engines in service p 54 A93-12822

EVEKER, K. M.

- A simplified approach for control of rotating stall. I - Theoretical development
[AIAA PAPER 93-2229] p 1080 A93-50035
- A simplified approach for control of rotating stall. II - Experimental results
[AIAA PAPER 93-2234] p 1080 A93-50038

EVERS, W.

- Viscous flows in centrifugal compressor diffusers at transonic Mach numbers
[ASME PAPER 92-GT-48] p 246 A93-19301

EVERSMAN, WALTER

- Radiated noise of ducted fans p 450 A93-19215
- Comparison of radiated noise from shrouded and unshrouded propellers p 1264 A93-55861

EWINS, D. J.

- Structural dynamic characteristics of individual blades p 1005 N93-32272
- Structural dynamic characteristics of bladed assemblies p 1005 N93-32273

EXTON, R. J.

- Nonintrusive spectroscopic techniques for supersonic/hypersonic aerodynamics and combustion diagnostics p 203 A93-14245

EYI, S.

- Multi-point design of transonic airfoils using optimization
[AIAA PAPER 92-4225] p 16 A93-13382

- A multi-point optimization for transonic airfoil design
[AIAA PAPER 92-4681] p 264 A93-20303

- Airfoil design using the Navier-Stokes equations
[AIAA PAPER 93-0648] p 464 A93-24763

- Design efficiency evaluation for transonic airfoil optimization - A case for Navier-Stokes design
[AIAA PAPER 93-3112] p 1062 A93-48282

EYRAUD, J. L.

- Flight analysis of air intake/engine compatibility p 161 N93-13212

EYTH, JACOB, JR.

- Recent improvements on the Dynamic Flight Simulator p 1011 A93-45167

EZEILO, A. N.

- Development of the neutron diffraction technique for the determination of near surface residual stresses in critical gas turbine components
[PNR-90984] p 58 N93-11112

F

FABIAN, PETER

- Climatic effects of turbofan emissions in the stratosphere and the higher troposphere p 1035 N93-31927

FABRY, E.

- The leading edge vortex of a rotating stall cell
[ISABE 93-7009] p 1183 A93-53985

FABUNMI, JAMES A.

- Aero-engine component damping estimation from full-scale aeromechanical test data
[AIAA PAPER 93-1873] p 1112 A93-49748

FACEIRE, JEFF

- Domain engineering validation case study: Synthesis for the air traffic display/collision warning monitor domain version 01.00.03
[AD-A259407] p 503 N93-21671

FADEEV, I. V.

- Effect of longitudinal microribbing on the drag of a body of revolution p 5 A93-10147

FADEEV, V. T.

- An analytical-experimental method for studying the strength and stability of thin-walled structures p 1029 A93-47084

FADEEVA, I. P.

- Search strategies for a sequence of baseline indices for building sections of a flight-safety automatic control system in the interactive mode p 306 A93-18346

FADEL, GEORGES M.

- Application of a two-point exponential approximation method in optimizing rotorcraft airframe structures p 507 A93-27956

FADEN, M.

- Numerical investigation of the unsteady flow through a counter-rotating fan p 112 A93-14166
- An integrated flow simulation system on a parallel computer. I - Basic concept. II - The flow solver p 688 A93-34370

- Unsteady flow simulation on a parallel computer p 1022 A93-45089

FAGHRI, A.

- Conjugate modeling of high-temperature nose cap and wing leading edge heat pipes p 1259 A93-55465

FAIBISH, S.

- Information-based criteria of terrain navigability. Part 1: Data-base analysis p 793 N93-27178

FAIRLIE, GREGORY W.

- Effects of seating configuration and number of type 3 exits on emergency aircraft evacuation
[AD-A256616] p 143 N93-14277

FAKHRUTDINOV, I. KH.

- Autonomous mobile laser complex p 395 A93-17767

FALATKO, JAY

- 757 fly-by-wire demonstrator flight test
[AIAA PAPER 92-4099] p 38 A93-11271

FALCO, MICHAEL

- Systems integration test laboratory - Application and experiences p 190 A93-13910

FALCONI, D.

- On high speed turbulence modeling of shock-wave boundary-layer interaction
[AIAA PAPER 93-0778] p 541 A93-24860

- High-speed turbulence modeling of shock-wave/boundary-layer interaction p 927 A93-41910

FALCOVITZ, J.

- Oblique shock formation in impulsively started wedge flows p 692 A93-35636
- A singularities tracking conservation law scheme for compressible duct flows p 960 A93-45542

FALETTI, MATTHEW J.

- Cockpit resource management proficiency as a factor of primary flight training
[AD-A256995] p 328 N93-16262

FALEV, V. A.

- Using numerical control algorithms in stabilization systems with digital correction p 941 A93-43113

FALLER, WILLIAM E.

- Neural network prediction of three-dimensional unsteady separated flow fields
[AIAA PAPER 93-3426] p 977 A93-47221

FAN, GUANGWU WILLIAM

- Optimal output feedback vibration control of rotor-bearing systems p 86 N93-11220

FAN, MENG

- Euler solutions simulating strong shock waves and vortex phenomena over 3D wings p 121 A93-14392

FAN, S. C.

- Analysis of complicated plates by a nine-node spline plate element p 206 A93-14616

FAN, SIOI

- On closed-loop identification of a certain aeroengine under flight conditions p 519 A93-24026

- On engine parameter estimation with flight test data p 1107 A93-48520

FAN, SIXIN

- Low-Reynolds-number k-epsilon model for unsteady turbulent boundary-layer flows p 1177 A93-53208

FAN, WEIHONG

- Numerical analysis of aerodynamic losses in film-cooled vane cascade p 1066 A93-48517

- Verification of the TOTLOS method for calculating aerodynamic loss in film-cooled turbine cascade p 1087 A93-51191

FAN, XUETONG

- Active flow control with neural networks
[AIAA PAPER 93-3273] p 1037 A93-46834

FAN, ZUO-MIN

- Fewest-fault integral optimization algorithm for engine fault diagnosis p 173 A93-15343

FANG, HO T.

- Improved silicon nitride for advanced heat engines
[NASA-CR-182193] p 917 N93-29451

FANG, J.

- Numerical solutions for unsteady subsonic vortical flows around loaded cascades
[ASME PAPER 92-GT-173] p 250 A93-19399

FANG, JIUNN

- Sweeping algorithm for unstructured-grid generation on two-dimensional non-convex domains p 1262 A93-56413

FANG, PING

- The analysis of viscous wakes noise in axial flow compressor p 759 A93-33710

FANG, W.

- Approximation methods for control of structural acoustics models with piezoceramic actuators p 452 A93-23744

FANN, FRANKLIN

- Ventilation effects on smoke and temperature in an aircraft cabin quarter-scale model
[DOT/FAA/CT-89/25] p 791 N93-28055

FANN, S.

- Local heat transfer distribution in a rotating serpentine rib-roughened flow passage p 1259 A93-55459

FANNING, F. JESSE

- Design of an Ada expert system shell for the VHSIC avionic modular flight processor p 98 N93-11947

FANTE, RONALD L.

- Some limitations on the effectiveness of airborne adaptive radar p 501 A93-29596

FARAMAZIAN, V. V.

- A study of a pulsed electrical field near the jet of a turbojet engine p 52 A93-10179

FARASSAT, F.

- Helicopter noise prediction - The current status and future direction p 448 A93-19202

- High-speed helicopter rotor noise - Shock waves as a potent source of sound p 565 A93-29403

- The influence of quadrupole sources in the boundary layer and wake of a blade on helicopter rotor noise p 566 A93-29410

- High speed propeller acoustics and aerodynamics - A boundary element approach p 967 A93-46804

- On the possibility of singularities in the acoustic field of supersonic sources when BEM is applied to a wave equation p 1039 A93-46805

FARDOUN, A. A.

- Variable-speed generators with flux weakening p 750 N93-25599

FARHAT, C.

- Structure-attached corotational fluid grid for transient aeroelastic computations p 480 A93-29326

- Stability analysis of dynamic meshes for transient aeroelastic computations
[AIAA PAPER 93-3325] p 1022 A93-45019

FARIDUZZAMAN

- Five years operational experiences with Indonesian Low Speed Tunnel (ILST) p 191 A93-14403

- FARINA, A.**
Space-time processing for AEW radar p 884 A93-43444
- FARINEAU, JACQUES**
A longitudinal control law integrating flight controls and engine controls p 186 A93-15046
- FARKAS, JANOS**
DAR-2: On-board data acquisition system for aircraft engines p 169 N93-15166
- FARKAS, T.**
Solid state flight data recorders and their application in the flight operation analysis p 166 A93-14200
Application of flight data for diagnostic purposes p 166 A93-14295
- FARLEY, GARY**
Rapid detection and quantification of impact damage in composite structures p 547 A93-27978
- FARLEY, GARY L.**
The effects of crushing surface roughness on the crushing characteristics of composite tubes p 77 A93-10918
An analytically designed subcomponent test to reproduce the failure of a composite wing box beam [AIAA PAPER 93-1344] p 709 A93-33914
Relationship between mechanical-property and energy-absorption trends for composite tubes [NASA-TP-3284] p 392 N93-16537
- FARMALIDES, C. D.**
The effects of reaction on axial compressor performance p 724 N93-25882
- FARMER, J.**
A fast multigrid method for solving incompressible hydrodynamic problems with free surfaces [AIAA PAPER 93-0767] p 540 A93-24851
- FARMER, THOMAS E.**
F100 second stage fan disk bolt hole crack propagation ferris wheel test p 177 N93-14897
- FARNWORTH, R. G.**
Effect of skywave interference on the coverage of Loran-C p 33 A93-11095
- FAROKHI, S.**
Computational study of advanced exhaust system transition ducts with experimental validation p 689 A93-34490
- FAROKHI, SAEED**
Separated flowfield and lift on an airfoil with an oscillating leading-edge flap [AIAA PAPER 93-3422] p 976 A93-47217
Aerodynamic characteristics of a delta wing with a body-hinged leading-edge extension [AIAA PAPER 93-3446] p 978 A93-47233
On the aerodynamics and performance of active vortex generators [AIAA PAPER 93-3447] p 979 A93-47234
The effect of unsteady blade loading on the aeroacoustics of a pusher propeller [AIAA PAPER 93-1805] p 1173 A93-49694
Spectral analysis of unsteady surface pressure on a pusher propeller p 1232 A93-54646
- FARQUHAR, B. W.**
Inlet design using a blend of experimental and computational techniques p 114 A93-14210
- FARRELL, JAMES L.**
Statistical validation for GPS integrity test p 34 A93-11297
- FASANELLA, EDWIN L.**
Effects of floor location on response of composite fuselage frames p 997 A93-46809
Instrumentation and data acquisition for full-scale aircraft crash testing p 1250 A93-54399
An overview of the crash dynamics failure behavior of metal and composite aircraft structures p 923 N93-30875
- FASEL, H.**
Numerical simulation of a three-dimensional wave packet in a growing flat plate boundary layer p 128 A93-17265
- FASTL, HUGO**
Loudness versus level of aircraft noise p 557 A93-28477
- FATHAUER, BRETT W.**
A computational investigation of fuel mixing in a hypersonic scramjet [AIAA PAPER 93-2994] p 1001 A93-44230
- FAULK, STUART R.**
Software requirements for the A-7E aircraft [AD-A255746] p 229 N93-15052
- FAULKNER, HENRY B.**
Alternative systems for fuel gas boosters for small gas turbine engines [PB92-223049] p 212 N93-12977
- FAUS, L. J.**
The community response to aircraft noise around six Spanish airports p 1264 A93-55845
- FAVIER, DANIEL**
Influence of coupling incidence and velocity variations on the airfoil dynamic stall p 767 A93-35999
- FAVINI, B.**
Equilibrium and nonequilibrium modeling of hypersonic inviscid flows p 864 A93-42448
Reactive and inert inviscid flow solutions by quasi-linear formulations and shock fitting p 927 A93-42625
Influence of chemical kinetics effects in nozzles shape design [ISABE 93-7112] p 1188 A93-54087
- FAWCETT, P. A.**
SCV measurements in the wake of a rotor in hover and forward flight [AIAA PAPER 93-3080] p 1059 A93-48254
- FAWCETT, PHILIP ANDREW**
An investigation on planar velocimetry by spatial cross-correlation p 697 N93-25664
- FAXLANGER, EDWARD A., JR.**
Thermally induced stresses in a composite exposed to fire [AD-A261714] p 737 N93-26371
- FAY, RUSSELL**
The development and evaluation of advanced Kevlar sandwich structure for application to rotorcraft airframes p 546 A93-27965
- FEATHER, MARTIN S.**
Representation and presentation of requirements knowledge p 228 A93-17389
- FEDOROV, A. V.**
Intermode exchange in a supersonic boundary layer p 691 A93-35346
- FEDOROV, E. V.**
Problems in the optimum design of a wing profile for nonseparated flow over a range of angles of attack p 477 A93-27614
Numerical optimization methods for variational inverse boundary value problems of aerodynamics p 1088 A93-51771
- FEDOROV, R. M.**
Computational studies of the characteristics of axial compressor cascades and stages in unsteady incoming flow p 13 A93-12805
- FEDOT'EV, V. A.**
Vibrational monitoring and diagnostics of the technical condition of gas turbine engines at civil aviation repair facilities p 374 A93-18362
- FEDRO, MARK J.**
Mechanical and analytical screening of braided composites for transport fuselage applications p 922 N93-30855
- FEI, BIN-JUN**
The crack initiation approach for durability analysis p 1259 A93-55585
- FEIEREISEN, WILLIAM J.**
The hypersonic double ellipse in rarefied flow p 869 A93-42631
- FEINGOLD, A. D.**
Passive drag reduction of a helicopter airfoil in an unsteady transonic flow p 482 A93-29440
- FEJTEK, IAN**
Navier-Stokes computation of wing/rotor interaction for a tilt rotor in hover p 122 A93-14537
- FEJTEK, IAN GEORGE**
Navier-Stokes flowfield computation of wing/rotor interaction for a tilt rotor aircraft in hover p 135 N93-14035
- FELDERMAN, E. J.**
AEDC expanded flow arc facility (HEAT-H2) description and calibration p 821 A93-37872
- FELKER, FORT F.**
Direct solution of two-dimensional Navier-Stokes equations for static aeroelasticity problems p 417 A93-23554
Calculation of optimum airfoils using direct solutions of the Navier-Stokes equations [AIAA PAPER 93-3323] p 952 A93-45017
- FELKER, FORT FRASER**
Direct solutions of the Navier-Stokes equations with application to static aeroelasticity p 748 N93-25259
- FELLMAN, LYNN**
National Airspace System Performance Analysis Capability (NASPAC) simulation model p 887 N93-30351
- FENBERT, J. A.**
Fundamentals of composite repair [SME PAPER EM92-100] p 196 A93-14101
- FENBERT, JAMES W.**
Reynolds number influences in aeronautics [NASA-TM-107730] p 989 N93-31732
- FENG, JINZHANG**
An interaction noise between vortex and airfoil [AIAA PAPER 93-0600] p 562 A93-24726
- FENG, MINGXI**
Arguments concerning wind tunnel test studies of the trim characteristics of objects with small asymmetries [AD-A254111] p 19 N93-10858
- FENG, QI**
Numerical research on flows in nonuniform cascades [ASME PAPER 92-GT-276] p 253 A93-19469
- FENG, QIN**
Flight simulator development in China p 191 A93-14410
- FENG, YA-CHANG**
A simulation study on take-off and landing dynamics of fly-by-wire control system aircraft p 1249 A93-55590
- FENG, YACHANG**
Longitudinal closed-loop pilot/vehicle analysis of DFBW aircraft during approach and landing p 1206 A93-54277
A simulation study on take-off and landing dynamics of the aircraft of a fly-by-wire control system [AD-A259286] p 510 N93-19849
- FENG, YANAN**
Experimental study on the mechanism of favourable interferences of body strakes p 121 A93-14405
The effect of outboard leading-edge bluntness of double-delta wing on its aerodynamic characteristics p 1230 A93-54589
- FENNER, THOMAS**
SIR technology helps ensure safe landings for NASA p 384 A93-21765
- FENTON, B. C.**
Lightweight aircraft turbine protection [AIAA PAPER 93-1815] p 1110 A93-49703
- FERBER, JACQUES**
A reactive approach for distributed air traffic control [ONERA, TP NO. 1993-83] p 1190 A93-53603
CRAASH - A coordinated collision avoidance system [ONERA, TP NO. 1993-84] p 1191 A93-53604
- FERBER, M. K.**
Process optimization of Hexoloy SX-SiC towards improved mechanical properties [DE93-007913] p 826 N93-28564
- FEREBEE, I. C.**
The use of satellites for aeronautical communications, navigation and surveillance p 881 A93-40436
- FERGIONE, JOHN**
F-16 Digital Flight Control System improvements p 818 A93-38843
- FERGUSON, DAVID L.**
YF-22A prototype advanced tactical fighter demonstration/validation flight test program overview p 805 N93-27173
- FERGUSON, FREDERICK**
Expanding the waverider design space using general supersonic and hypersonic generating flows [AIAA PAPER 93-0505] p 283 A93-23253
- FERGUSON, S.**
Accuracy of GPS-derived acceleration from moving platform tests p 1240 A93-55973
- FERMAN, MARTY A.**
Experimental investigation of vortex-fin interaction [AIAA PAPER 93-0050] p 260 A93-20163
Composite 'Exoskin' doubler extends F-15 Vertical Tail fatigue life [AIAA PAPER 93-1341] p 709 A93-33911
- FERNANDES, S. T.**
Autonomous guidance, navigation and control bridging program plan p 532 A93-27046
- FERNANDEZ, F.**
Nondestructive inspection of in-service aircraft [ETN-93-83059] p 496 N93-20928
- FERNANDO, E. M.**
Conventional skin friction measurement techniques for strongly perturbed supersonic turbulent boundary layers p 271 A93-21863
- FERNHOLZ, H. H.**
Vortex capture by a two-dimensional airfoil with a small oscillating leading-edge flap [AIAA PAPER 93-3266] p 968 A93-46830
- FERRANTI, MICHAEL**
Removing the risk from rotorcraft testing p 1192 A93-53772
- FERRARA, GUS**
Proceedings of the AIAA/FAA Joint Symposium on General Aviation Systems [AD-A257780] p 240 N93-17732
- FERRARO, PETER J.**
Aeroacoustic environment of an advanced short takeoff and vertical landing aircraft in hover p 231 A93-14539
- FERRARO, PIETRO**
Evaluation by holographic interferometry of impact damage in composite aeronautical structures p 1020 A93-44193
- FERREIRA, ANTONIO**
Air traffic noise monitoring in and around Lisbon Airport p 564 A93-28494

- FERREIRA, J. G.**
Diagnostics systems for the TBR-E tokamak
[INPE-5428-RPQ/662] p 232 N93-13257
- FERREIRA, J. L.**
Diagnostics systems for the TBR-E tokamak
[INPE-5428-RPQ/662] p 232 N93-13257
- FERREIRA, JAY**
Design sensitivity and optimization of composite cylinders p 71 A93-12781
- FERRI DEGLI ANTONI, L.**
Performance and configuration analysis of jet-engine off-design behavior
[ISABE 93-7087] p 1202 A93-54063
- FERRIN, FRANK J.**
Survey of helmet tracking technologies p 517 A93-26882
- FERRIS, ALICE T.**
Testing experience with unheated stain-gage balances in the NTF p 1013 A93-47021
An improved method for determining force balance calibration accuracy p 1254 A93-54369
- FERRIS, KENNETH D.**
An internetworking brouter for avionics applications p 1097 A93-49479
- FEUERSTEIN, DAVID N.**
Results from a GPS Shuttle Training Aircraft flight test p 384 A93-21148
- FEY, M.**
Stagnation point computations of nonequilibrium inviscid blunt body flow p 1093 A93-52005
- FEYOCK, STEFAN**
The use of multiple models in case-based diagnosis p 759 N93-25969
- FICKEISEN, F. C.**
Interrelationships between commercial airplane design and operational requirements and procedures p 153 A93-14219
- FICKLIN, ROBERT W.**
Results from a VHF impulse synthetic-aperture radar p 501 A93-28219
- FICO, NIDE G. C. R., JR.**
Nozzle flow computations using the Euler equations p 112 A93-14170
Numerical prediction of flap losses in a transonic wind tunnel p 288 A93-23552
- FIDDES, S. P.**
A moving mesh system for the calculation of unsteady flows
[AIAA PAPER 93-0641] p 464 A93-24756
Theoretical modelling of rotor noise radiation p 566 A93-29407
- FIEBIG, M.**
Effects of longitudinal vortex generators on heat transfer and flow loss in turbulent channel flows p 1021 A93-44222
Multigrid methods for calculating 3D flows in complex geometries p 973 A93-46984
- FIEDLER, K.**
Some experiments and ideas on GPA before reaching steady state of engine p 178 N93-15175
- FIELDING, J. P.**
The aerodynamic and structural design of a variable camber wing (VCW) p 117 A93-14291
- FIELDS, JAMES M.**
Effect of personal and situational variables on noise annoyance: With special reference to implications for en route noise
[NASA-CR-189676] p 569 N93-21317
- FIELDS, RICHARD S., JR.**
Proposal and preliminary design for a high speed civil transport aircraft. Swift: A high speed civil transport for the year 2000
[NASA-CR-19023] p 335 N93-18049
- FIGAROL, D.**
Evolution of radar data processing in the French air traffic control system p 886 N93-30325
- FIGUEROA, LUIS**
Specialty fiber optic systems for mobile platforms and plastic optical fibers; *Proceedings of the Meeting, Boston, MA, Sept. 9-11, 1992*
[SPIE-1799] p 1105 A93-49462
- FILATOV, GENNADI A.**
Flight safety in a perturbed atmosphere
[ISBN 5-277-00815-2] p 487 A93-29431
- FILIPPOV, L.**
A joint Soviet-Bulgarian scientific program for free-flight and tethered aerostat observations p 2 A93-11374
- FILIPPOV, IU. N.**
A heat transfer element of a high-temperature heat exchanger p 833 A93-39047
- FILIPPOV, S. I.**
Modeling of interfaces in problems of flow of a ponderable fluid past a wing profile p 124 A93-15189
- FILIPPOV, V. P.**
Characteristics of the detection of overloads in the center of mass of Il-76 and An-12 aircraft due to runway irregularities by a standard on-board recorder p 1008 A93-45666
- FILLATRE, O.**
Identification of weakly nonlinear dynamic systems by means of random excitations p 227 A93-16472
- FINAISH, F.**
Vortex developments over steady and accelerated airfoils incorporating a trailing edge jet
[AIAA PAPER 93-3008] p 1054 A93-48198
- FINAISH, FATHI**
Preliminary efforts toward development of data handling and analysis software for unsteady flow measurements: An application for aeroelastic transonic flow configurations p 291 N93-16768
- FINK, L.**
Near-term two-stage-to-orbit, fully reusable, horizontal take-off/landing launch vehicle p 1015 A93-45441
- FINKE, A. K.**
Design and test of a small two stage counter-rotating turbine for rocket engine application
[AIAA PAPER 93-2136] p 1142 A93-49954
- FINLEY, TOM D.**
An improved calibration technique for wind tunnel model attitude sensors p 1253 A93-54356
- FINN, S. R.**
Experimental investigations into composite fuselage impact damage resistance and post-impact compression behavior p 159 A93-15812
- FINNEY, M. J.**
Flight testing of a fiber optic temperature sensor p 1105 A93-49476
- FIRSOV, V. A.**
Nonlinear deformation mechanics of multilayer transparency elements - General theory relations p 79 A93-12800
Single-impact calibrated electromagnetic tightening of long-life bolted joints in aviation structures p 745 A93-35277
A study of the effect of the support fastening compliance on the stress-strain state of aircraft transparencies p 997 A93-47079
Nonlinear deformation mechanics of multilayer transparency elements - Some calculation results p 1191 A93-52937
- FIRTH, M. R.**
The effects of blade loading in radial and mixed flow turbines
[ASME PAPER 92-GT-92] p 349 A93-19338
- FISCHER, BERTRAM**
MPC75 - The evolution of a new regional airliner for the late nineties p 155 A93-14289
- FISCHER, M.**
Predevelopment of a flight control system for a small civil aircraft p 1249 A93-56031
- FISCHER, T. M.**
A theoretical approach for describing secondary instability features in three-dimensional boundary-layer flows
[AIAA PAPER 93-0080] p 263 A93-20192
- FISCHER, TERENCE**
FAA Technical Center Aeronautical Data Link Research Plan
[DOT/FAA/CT-92/23] p 417 N93-15698
- FISCHL, ROBERT**
A problem formulation for glideslope tracking in wind shear using advanced robust control techniques
[NASA-TM-104164] p 64 N93-11176
A monitor for the laboratory evaluation of control integrity in digital control systems operating in harsh electromagnetic environments
[NASA-TM-4402] p 65 N93-12304
- FISH, JOHN C.**
Tailoring concepts for improved structural performance of rotorcraft flexbeams p 207 A93-14811
- FISHER, A.**
Autoland, the developing need p 142 A93-17302
- FISHER, A. J.**
New algorithms for hyperbolic radionavigation p 881 A93-40359
- FISHER, BRUCE D.**
Joint NASA/USAF Airborne Field Mill Program - Operation and safety considerations during flights of a Lear 28 airplane in adverse weather
[AIAA PAPER 92-4093] p 93 A93-13262
- FISHER, DAVID F.**
Correlation of forebody pressures and aircraft yawing moments on the X-29A aircraft at high angles of attack
[AIAA PAPER 92-4105] p 38 A93-11273
Correlation of forebody pressures and aircraft yawing moments on the X-29A aircraft at high angles of attack
[NASA-TM-4417] p 22 N93-11532
- A summary of the forebody high-angle-of-attack aerodynamics research on the F-18 and the X-29A aircraft
[NASA-TM-104261] p 25 N93-12353
- FISHER, GENE**
Formal representation of the requirements for an Advanced Subsonic Civil Transport (ASCT) flight control system
[NASA-CR-189699] p 98 N93-12346
- FISHER, JERRY F.**
Avionic systems in support of covert helicopter operations p 1193 A93-54294
- FISHER, M. J.**
Experiments on the active control of boundary layer transition p 243 A93-19133
The prediction of noise from co-axial jets
[ISVR-TR-215] p 1040 N93-32339
- FISHER, MICHAEL C.**
Measurement of attachment-line location in a wind-tunnel and in supersonic flight
[AIAA PAPER 92-4089] p 39 A93-11285
- FISHER, P.**
Generic developmental turbojet fuel control p 172 A93-14519
- FISHER, S. A.**
Design verification of ground run-up noise suppressors for afterburning engines p 910 A93-42892
- FISKE, MICHAEL R.**
Aerospace '92 - The year in review p 455 A93-19976
- FITCH, C. E.**
Experimental investigations into composite fuselage impact damage resistance and post-impact compression behavior p 159 A93-15812
- FITE, E. BRIAN**
Fabrication of composite propfan blades for a cruise missile wind tunnel model
[NASA-TM-105270] p 752 N93-26202
- FITZPATRICK, DANIEL T.**
Underlying causes of human error in US Army rotary wind accidents p 492 N93-19678
- FITZPATRICK, J. A.**
The application of diffusion bonding in the manufacture of aeroengine components p 1217 A93-53514
- FITZPATRICK, K.**
A visual study of recessed angled spanwise blowing method on a delta wing
[AIAA PAPER 93-3246] p 966 A93-46791
- FITZSIMONS, BERNARD**
First moves towards an 'intelligent' GPWS p 896 A93-43624
- FITZSIMONS, PHILIP M.**
Developing a control system for ARES 2 p 371 N93-16769
- FLAHERTY, J. E.**
Unsteady compressible airfoil aerodynamics using an adaptive time-discontinuous GLS finite element method
[AIAA PAPER 93-0339] p 281 A93-23027
- FLAHERTY, JOSEPH E.**
A finite element and symbolic method for studying laminar boundary layers of real gases in equilibrium at Mach numbers to 30
[AIAA PAPER 93-2986] p 1052 A93-48179
- FLAMENT, C.**
Viscous nonequilibrium flow calculations
[ONERA, TP NO. 1992-89] p 771 A93-38573
- FLANAGAN, M. J., JR.**
Aerodynamic heating in the vicinity of hypersonic, axisymmetric, shock-wave boundary-layer interactions
[AIAA PAPER 93-2766] p 963 A93-46512
Calibration of a transonic 5-hole probe for a multi-element airfoil cascade facility
[AIAA PAPER 93-2471] p 1138 A93-50216
- FLANAGAN, MICHAEL J.**
Time dependent heat transfer rates in high Reynolds number hypersonic flowfields p 216 N93-13664
- FLAX, BENNETT**
A minimum rate of position reporting in the future oceanic air traffic control system p 30 A93-11006
- FLEETER, S.**
Rotor blade unsteady aerodynamic gust response to inlet guide vane wakes
[ASME PAPER 91-GT-129] p 475 A93-26897
- FLEETER, SANFORD**
Forcing function effects on unsteady aerodynamic gust response. I - Forcing functions
[ASME PAPER 92-GT-174] p 251 A93-19400
Forcing function effects on unsteady aerodynamic gust response. II - Low solidity airfoil row response
[ASME PAPER 92-GT-175] p 251 A93-19401
Prediction of active control of subsonic centrifugal compressor rotating stall
[AIAA PAPER 93-0153] p 274 A93-22591
Forcing function generator fluid dynamic effects on compressor blade gust response
[AIAA PAPER 93-0157] p 275 A93-22594

- Single passage Euler analysis of oscillating cascade unsteady aerodynamics for arbitrary interblade phase angle
[AIAA PAPER 93-0389] p 282 A93-23067
- Supersonic turbomachine rotor flutter control by aerodynamic detuning p 899 A93-42884
- Compressor unsteady aerodynamic response to rotating stall and surge excitations
[AIAA PAPER 93-2087] p 1079 A93-49914
- A model for the selective amplification of spatially coherent waves in a centrifugal compressor on the verge of rotating stall
[AIAA PAPER 93-2236] p 1080 A93-50039
- Spatial domain characterization of abrupt rotating stall initiation in an axial flow compressor
[AIAA PAPER 93-2238] p 1081 A93-50040
- Forcing function modeling for flow induced vibration [ISABE 93-7027] p 1196 A93-54003
- Control of supersonic throughflow turbomachines discrete frequency noise generation by aerodynamic detuning p 1248 A93-55860
- FLEETWOOD, C. M.**
Optical technologies for UV remote sensing instruments p 853 A93-28788
- FLEMING, D. B. A.**
Critical dispatch - A pilot's view p 790 A93-39541
- FLEMING, DAVID C.**
Tapered geometries for improved crashworthiness under side loads p 743 A93-34259
- FLEMING, J. L.**
An experimental study of a turbulent wing-body junction and wake flow p 873 A93-43541
- FLETCHER, MICHAEL J.**
Applying and validating the RANS-3D flow-solver for evaluating a subsonic serpentine diffuser geometry [AIAA PAPER 93-2157] p 1079 A93-49973
- FLETCHER, P. N.**
Blade twist-design of experiment p 800 A93-36025
- FLEURY, ANDRE**
Can one do without the magnetic reference? p 501 A93-28197
- FLITTER, LANCE**
Prediction of helicopter component loads using neural networks [AIAA PAPER 93-1301] p 756 A93-33878
- FLITTIE, KIRK J.**
Unsteady turbulent skin-friction measurement in an adverse pressure gradient p 206 A93-14545
- FLORANCE, JAMES R.**
Supersonic aeroelastic instability results for a NASP-like wing model [AIAA PAPER 93-1369] p 682 A93-33935
- Supersonic aeroelastic instability results for a NASP-like wing model [NASA-TM-107739] p 718 A93-26553
- FLORENTINE, ROBERT A.**
3-D braided preforms; cost to manufacture: Magnawave. I - Identifying cost factors p 1226 A93-53423
- FLORYAN, J. M.**
Flow over a leading edge with distributed roughness p 18 A93-10549
- FLOWERS, DIANE**
SR-SCARLET 1: Peregrin [NASA-CR-192048] p 337 A93-18155
- FLYNN, MICHAEL J.**
Center for Aeronautics and Space Information Sciences [NASA-CR-193140] p 848 A93-27289
- FLYNN, WILLIAM**
F-16 Digital Flight Control System improvements p 818 A93-38843
- FOCH, RICHARD J.**
Test pilot's notes on flying the Low Altitude/Airspeed Unmanned Research Aircraft (LAURA) [AIAA PAPER 92-4078] p 42 A93-13269
- FODALE, ROBERT**
Flight Deflection Measurement System p 808 A93-37885
- FODOR, GEORGE E.**
Development of a method to determine the autooxidation of turbine fuels [AD-A260578] p 736 A93-25902
- FOGARTY, JAMES W.**
The development of an Altitude Awareness Program - An integrated approach p 486 A93-27136
- FOKIN, D. A.**
Maximizing the critical Mach number for lifting wing profiles p 13 A93-12841
- FOLEN, RAYMOND A.**
Autogenic-feedback training improves pilot performance during emergency flying conditions [NASA-TM-104005] p 790 A93-27076
- FOLEY, CARYN**
Hermes CX-7: Air transport system design simulation [NASA-CR-192082] p 335 A93-18056
- FOLK, EARL W.**
Effects of seating configuration and number of type 3 exits on emergency aircraft evacuation [AD-A256616] p 143 A93-14277
- FOLKMAN, CACHE C.**
An advanced method for predicting the performance of helicopter propulsion system ejectors p 809 A93-35933
- FOLLEN, GREGORY J.**
Multidisciplinary propulsion simulation using NPSS [AIAA PAPER 92-4709] p 435 A93-20318
- Gas turbine system simulation: An object-oriented approach [NASA-TM-106044] p 723 A93-25673
- FOMICHEV, V. M.**
Oblique wave evolution in a plane subsonic boundary layer p 124 A93-15178
- FOMIN, V. P.**
Methodology for studying the fracture of aircraft structures in static tests p 801 A93-36785
- A method for the optimum design of a large-aspect-ratio wing p 828 A93-36793
- FONAREV, A. S.**
An airfoil in transonic flow in the presence of wind gusts and weak shock waves p 1233 A93-55015
- FONG, C. VANESSA**
Procedural development prototype in Automated En Route Air Traffic Control p 887 A93-30352
- FONSECA, A. A.**
On automated analysis of flight test data p 512 A93-19913
- FONT, G. I.**
Effects of aft geometry on vortex behavior and force production by a tangential jet on a body at high alpha [AIAA PAPER 93-2961] p 1048 A93-48155
- FONT, GABRIEL IVAN**
Tangential fuselage blowing on an ogive cylinder p 697 A93-25545
- FONTAINE, B. L.**
Aerodynamic phenomena in high pulse repetition rate XeCl laser p 1150 A93-48806
- FONTANARI, J.**
Preliminary results of the ISM campaign - The Landes, South West France p 1161 A93-47553
- FORAN, D. A.**
In-flight evaluation of noise levels and assessment of active noise reduction systems in the Seahawk S-70B-2 helicopter [AD-A260689] p 759 A93-25649
- FORD, D. A.**
The changing nature of design [PNR-91011] p 48 A93-11334
- FOREMAN, BRENT**
Future regional transport aircraft market, constraints, and technology stimuli [NASA-TM-107669] p 109 A93-13025
- FORESTIER, B. M.**
Aerodynamic phenomena in high pulse repetition rate XeCl laser p 1150 A93-48806
- FORMAGGIA, L.**
Inviscid calculations by an upwind finite element method of hypersonic flows over a double (single) ellipse p 869 A93-42626
- FORMAL'SKI, A. M.**
Optimal control of the rocking and damping of swings p 1263 A93-54998
- FORNASIER, LUCIANO**
Application of the Euler method EUFLEX to a fighter-type airplane configuration at transonic speed [MBB-FE-211-S-PUB-0489-A] p 484 A93-21059
- FORREST, DANA K.**
Supersonic aerodynamic characteristics of an advanced F-16 derivative aircraft configuration [NASA-TP-3355] p 989 A93-31733
- FORREST, DANIEL K.**
Volume-imaging lidar observations of the convective structure surrounding the flight path of a flux-measuring aircraft p 425 A93-20579
- FORSYTHE, R. A.**
Royal Air Force support helicopters - Night operations p 1190 A93-54293
- FORT, IVAN**
Velocity vector LDA measurement inside a pitched blade impeller p 924 A93-40390
- FORT, J.**
Numerical solution of steady and unsteady Euler equations p 973 A93-46988
- FORTE, T.**
Federal Aviation Administration pavement modeling p 379 A93-16315
- FORTIN, M.**
Some special purpose preconditioners for conjugate gradient-like methods applied to CFD p 772 A93-38638
- FORTSON, N.**
Small satellites and RPA's in global-change research [AD-A260762] p 755 A93-25837
- FORWARD, BERNIE**
Concept of closed-circuit TV system for transport aircraft under examination p 306 A93-18542
- FOSS, FREDERICK J.**
Operational aviation weather service requirements p 429 A93-22145
- FOSS, J. F.**
Enhanced mixing via geometric manipulation of a splitter plate [AIAA PAPER 93-3244] p 966 A93-46789
- FOSSARD, A. J.**
Helicopter control law based on sliding mode with model following p 907 A93-42559
- FOSTER, JOHN V.**
Status of the validation of high-angle-of-attack nose-down pitch control margin design guidelines [AIAA PAPER 93-3623] p 1126 A93-48308
- Investigation of high-alpha lateral-directional control power requirements for high-performance aircraft [AIAA PAPER 93-3647] p 1130 A93-49519
- FOTTNER, L.**
The aerodynamic effect of coolant ejection in the leading edge region of a film-cooled turbine blade p 904 A93-29958
- FOTTNER, LEONHARD**
Overview on test cases for computation of internal flows in turbomachines p 214 A93-13209
- The influence of intake swirl distortion on the steady-state performance of a low bypass, twin-spool engine p 214 A93-13211
- FOUCAULT, E.**
Experimental study of heat transfer close to a plane wall heated in the presence of multiple injections (subsonic flow) p 901 A93-29931
- FOUILLET, Y.**
Numerical simulation of compressible mixing zones p 10 A93-12427
- FOULADI, KAMRAN**
Unstructured grids for sonic-boom analysis [AIAA PAPER 93-2929] p 949 A93-44229
- FOURMAUX, ANTOINE**
3D and 2.5D viscous flow computations for axial flow turbine blades [ISABE 93-7093] p 1186 A93-54069
- FOUTCH, DAVID W.**
Using a full potential solver for propulsion system exhaust simulation p 689 A93-34487
- FOUTTER, R. R.**
An optical comparison of wall and axial injection for high enthalpy reacting scramjet flows [AIAA PAPER 93-0357] p 377 A93-23040
- High-temperature supersonic combustion testing with optical diagnostics p 730 A93-34498
- FOX, CHARLES H., JR.**
Subsonic static and dynamic stability characteristics of the test technique demonstrator NASP configuration [AIAA PAPER 93-0519] p 268 A93-21111
- FOX, MIKE C.**
Supersonic aerodynamic characteristics of an advanced F-16 derivative aircraft configuration [NASA-TP-3355] p 989 A93-31733
- FOX, ROY G.**
Embedded ADM reduces helicopter human error accidents p 147 A93-15024
- Measuring risk in single-engine and twin-engine helicopters p 148 A93-15025
- FOX, T. A.**
Experiments on smooth cantilevered circular cylinders in a low-turbulence uniform flow. Part 2: Fluctuating loads on a cantilever of aspect ratio 30 [PB93-110500] p 555 A93-21382
- Experiments on smooth cantilevered circular cylinders in low-turbulence uniform flow. Part 1: Mean loading with aspect ratios in the range 4 to 30 [PB93-111763] p 555 A93-21383
- FOX, U.**
Computation of hypersonic high-temperature nozzle flow p 1238 A93-56040
- FRABEL, P.**
Preliminary results of the ISM campaign - The Landes, South West France p 1161 A93-47553
- FRADENBURGH, EVAN A.**
Advancing tiltrotor state-of-the-art with variable diameter rotors p 797 A93-35982
- FRANCISCUS, LEO C.**
The multi-heat addition turbine engine [AIAA PAPER 92-4272] p 54 A93-13334
- Multi-heat addition turbine engine [NASA-CASE-LEW-15094-1] p 522 A93-22034
- FRANCOIS, G.**
Simulation of hypersonic flight - A concerted European effort p 1136 A93-49301

- FRANK-SUSICH, D.**
Computer-aided cure optimization p 209 A93-15804
- FRANK, G. J.**
Evaluation of alternatives for increasing A-7D rearward visibility
[AD-A255071] p 50 N93-12488
- FRANK, PAUL D.**
On alternative problem formulations for multidisciplinary design optimization
[AIAA PAPER 92-4752] p 436 A93-20350
- FRANKE, ERNEST A.**
Sensor-adaptive control for aircraft paint stripping
[SME PAPER AD92-200] p 855 A93-40663
Robotic inspection and refurbishment of aircraft canopy transparencies
[SME PAPER AD92-203] p 855 A93-40665
- FRANKE, M. E.**
Confined jet thrust vector control nozzle studies
p 172 A93-14516
Circulation control wing model study
[AIAA PAPER 93-0094] p 264 A93-20200
Study of a circular cross section thrust augmenting ejector
[AIAA PAPER 93-2439] p 1118 A93-50191
- FRANKLIN, J. A.**
Piloted simulation evaluation of pitch control designs for highly augmented STOV aircraft
[AIAA PAPER 92-4234] p 63 A93-13328
- FRANSSON, T.**
Time-dependent predictions and analysis of turbine cascade data in the transonic flow region
[PNR-90957] p 139 N93-15489
- FRANTZEN, CLAUDE**
Introduction to regulatory problems for supersonic transports p 234 A93-15032
- FRATELLO, DAVID J.**
Dynamic model testing of the X-31 configuration for high-angle-of-attack flight dynamics research
[AIAA PAPER 93-3674] p 1129 A93-48351
- FRAZIER, SAM**
Applications of stress envelope concepts to aircraft EMP and lightning survivability p 704 A93-24898
- FRAZIER, WILLIAM E.**
HIP consolidation of aluminum-rich intermetallic alloys and their composites
[NAWCADWAR-92003-60] p 199 N93-14726
- FREEBORN, PAUL**
Helicopter noise - Public perspective p 1261 A93-54719
- FREEDMAN, RICHARD S.**
The Airborne Ocean Color Imager - System description and image processing p 1157 A93-50369
- FREEMAN, B. D.**
Application of vanadium hydride compressors for Joule-Thomson cryocoolers p 1149 A93-48616
- FREEMAN, CHRISTOPHER J.**
The effect of aircraft inlets on the behaviour of aero engine axial flow compressors p 422 N93-18722
Stall in axial flow aero engine compressors p 422 N93-18723
- FREEMAN, W. TOM**
A unified approach for composite cost reporting and prediction in the ACT program p 920 N93-30441
- FREEMAN, WILLIAM T., JR.**
Cost - The challenge for advanced materials and structures p 233 A93-14338
- FREIDENBERG, ELIZABETH M.**
South American latest developments in the air law and air policy fields p 103 A93-12719
- FREISCHMIDT, G.**
A study of the flexural properties of carbon-epoxy composites in certain environments p 390 A93-21999
- FREITAS, J. C.**
Misalignments of airborne laser beams due to mechanical vibrations p 394 A93-17762
- FREMAUX, C. M.**
Effect of geometry, static stability, and mass distribution on the tumbling characteristics of generic flying-wing models
[AIAA PAPER 93-3615] p 1125 A93-48302
- FREMAUX, CHARLES M.**
Recent experiences with implementing a video based six degree of freedom measurement system for airplane models in a 20 foot diameter vertical spin tunnel p 821 A93-37763
- FRENCH, MARK**
Aeroelastic model design using structural optimization
[AIAA PAPER 92-4730] p 409 A93-20329
- FRENDI, ABDELKADER**
Nonlinear vibration and radiation from a panel with transition to chaos p 205 A93-14543
On the coupling between a supersonic boundary layer and a flexible surface p 243 A93-19132
Nonlinear vibration and radiation from a panel with transition to chaos induced by acoustic waves p 398 A93-19173
- FRENKEL, MARK A.**
Aerodynamic questions related to the safety and cost-effective utilization of airships p 818 A93-39125
- FRENSTER, JEFF**
Rotorcraft health and usage monitoring systems: A literature survey
[DOT/FAA/RD-91/6] p 48 N93-11461
- FRESKOS, G.**
Numerical simulation of the flow field around supersonic air-intakes
[ASME PAPER 92-GT-206] p 251 A93-19430
An implicit treatment of two equations turbulence models for high speed flow computations p 686 A93-34350
High lift airfoil flow simulation using a wall-corrected Algebraic Stress Model
[AIAA PAPER 93-3109] p 1061 A93-48280
On the numerical simulation of the two-dimensional flow field around a hypersonic air-intake-compressibility effects
[ISABE 93-7100] p 1187 A93-54076
- FREULER, R. J.**
Experimental determination of the bulk swirl attenuation between two axial stations in the LM2500 inlet bellmouth
[AIAA PAPER 93-2203] p 1155 A93-50015
Recent successes in modifying several existing jet engine test cells to accommodate large, high-bypass turbofan engines
[AIAA PAPER 93-2542] p 1139 A93-50266
- FREULER, RICHARD JEFFREY**
An investigation of jet engine test cell aerodynamics by means of scale model test studies with comparisons to full-scale test results p 193 N93-14060
- FREW, D.**
A study of incipient separation limits for shock-induced boundary layer separation for Mach 6 high Reynolds flow
[AIAA PAPER 93-2481] p 1084 A93-50222
- FRIAR, P. D.**
A90 project: Design of a composite fin
[ETN-92-92773] p 329 N93-16562
- FRICKE, M.**
Experimental working position simulator to analyse, develop and optimize concepts for computer-aided Air Traffic Management p 191 A93-14412
- FRIDDELL, J. H.**
Confined jet thrust vector control nozzle studies p 172 A93-14516
- FRIDLENDER, M. O.**
Influence of second-order boundary layer effects in hypersonic flow past blunt cones of large aspect ratio p 241 A93-18238
- FRIDLYANDER, I. N.**
Main directions of improving the quality of aluminum-lithium alloys for welded aircraft structures p 1146 A93-51104
- FRIEDMAN, D. M.**
CFD drag predictions for a wide body transport fuselage with flight test verification
[AIAA PAPER 93-3418] p 976 A93-47214
- FRIEDMAN, M. A.**
Issues associated with long-duration high-enthalpy scramjet combustor testing p 721 A93-34497
- FRIEDMANN, P.**
Hypersonic flutter of a curved shallow panel with aerodynamic heating
[AIAA PAPER 93-1318] p 829 A93-37428
- FRIEDMANN, P. P.**
Development of a structural optimization capability for the aeroelastic tailoring of composite rotor blades with straight and swept tips
[AIAA PAPER 92-4779] p 326 A93-20370
A new sensitivity analysis for structural optimization of composite rotor blades
[AIAA PAPER 93-1644] p 742 A93-34169
Integrated structure/control/aerodynamic synthesis of actively controlled composite wings p 818 A93-37392
- FRIEDMANN, PERETZ P.**
Aeroelastic behavior of composite rotor blades with swept tips p 827 A93-35978
- FRIEHE, CARL A.**
Fast-response aircraft temperature sensors p 167 A93-17095
- FRIELER, CLIFFORD EUGENE**
Mixing and reaction in the subsonic 2-D turbulent free shear layer p 289 A93-16508
- FRIEND, EDWARD L.**
Flight test results from a supercritical mission adaptive wing with smooth variable camber
[AIAA PAPER 92-4101] p 38 A93-11274
Flight test results from a supercritical mission adaptive wing with smooth variable camber
[NASA-TM-4415] p 49 N93-11863
- FRIES, JOSEPH**
Helicopter forced response vibration analysis method RTVIB20
[AD-A261809] p 730 N93-26260
- FRIGERIO, J.**
Vortex developments over steady and accelerated airfoils incorporating a trailing edge jet
[AIAA PAPER 93-3008] p 1054 A93-48198
- FRINCKE, DEBORAH**
Formal representation of the requirements for an Advanced Subsonic Civil Transport (ASCT) flight control system
[NASA-CR-189699] p 98 N93-12346
- FRINK, NEAL T.**
Unstructured grid solutions to a wing/pylon/store configuration using VGRID3D/USM3D
[AIAA PAPER 92-4572] p 14 A93-13303
- FRISCHBIER, JOERG**
All-composite fan blade for advanced ducted engines p 1246 A93-54837
- FRITH, PETER C.**
The effect of compressor rotor tip crops on turboshaft engine performance
[ASME PAPER 92-GT-83] p 348 A93-19332
- FRITSCHKE, BENT**
Condensation of nitrogen in hypersonic flows - Measurements confirm a theoretical model p 111 A93-13945
- FRITZEN, CLAUD-PETER**
Identification of nonlinear mechanical systems using combined state and parameter evaluation p 1224 A93-52732
- FRIZ, H.**
Hypersonic viscous flow past double ellipse and past double ellipsoid - Numerical results p 868 A93-42618
- FROLOV, V. A.**
The use of the Polhamus and discrete vortex methods for calculating the nonlinear characteristics of delta wings and wings with a strake p 242 A93-18379
- FROLOVA, A. A.**
Effect of heat supply on the gasdynamic parameters of gas flow in Laval nozzles p 12 A93-12760
- FRONEK, DENNIS**
Initial results from the NASA Lewis wave rotor experiment
[AIAA PAPER 93-2521] p 1193 A93-53589
Initial results from the NASA-Lewis wave rotor experiment
[NASA-TM-106148] p 1005 N93-32368
- FRONING, H. D., JR.**
Fusion-electric propulsion for hypersonic flight
[AIAA PAPER 93-2611] p 1142 A93-50318
- FROST, I. R.**
Hydrometeor identification using cross polar radar measurements and aircraft verification p 844 A93-37719
- FROSTIG, Y.**
Post buckling of laminated composite stiffened curved panels subjected to cyclic shear and compression p 204 A93-14334
- FRUCHT, Y.**
Experimental validation of a discrete vortex method for inviscid axisymmetric flow around parachute canopies
[AIAA PAPER 93-1216] p 689 A93-35165
- FRUMAN, D. H.**
Rotation and cavitation of a marginal vortex p 11 A93-12433
- FRY, DAVID J.**
Simultaneous mapping of the unsteady flow fields by Particle Displacement Velocimetry (PDV) p 786 N93-27454
- FRY, K.**
Visualisation and analysis of three dimensional transonic flows by holographic interferometry p 1020 A93-44194
- FRYLAND, ERIC**
Repair and maintenance of fiber optic data links on Navy aircraft p 1172 A93-48538
- FU, G. M.**
Separation control and lift enhancement on airfoil using unsteady excitations p 118 A93-14305
- FU, JAN-KAUNG**
Computations of aerodynamic drag for turbulent transonic projectiles with and without spin
[AIAA PAPER 93-3416] p 975 A93-47212
- FU, KUANG-HUA**
Frequency-domain identification of BO 105 derivative models with rotor degrees of freedom p 712 A93-34263
- FU, LI-CHEN**
Output tracking control of nonlinear systems with weakly non-minimum phase p 439 A93-22968
- FU, MINYUE**
Output feedback control for output tracking of nonlinear uncertain systems p 96 A93-13177
- FU, QIANG**
Calculation of transonic flow over bodies of varying complexity using Singular Perturbation Method p 116 A93-14265

- FU, T. C.**
Near-field behavior of a tip vortex p 288 A93-23549
- FU, THOMAS C.**
Simultaneous mapping of the unsteady flow fields by Particle Displacement Velocimetry (PDV) p 786 N93-27454
- FUCHS, E. F.**
Variable-speed generators with flux weakening p 750 N93-25599
- FUCHS, H. V.**
New design concepts for silencing aeroacoustic wind tunnels p 445 A93-19147
- FUCHS, J.**
Formation of the shock reflection on a wedge p 1023 A93-45476
- FUCHS, JUERGEN**
Results about the structure of the shock wave reflection process for strong incoming shock waves p 1233 A93-54810
- FUCHS, L.**
Numerical simulation of turbulent reacting flows in combustion chambers p 171 A93-14271
- FUCHS, S. P.**
High voltage quick-disconnect harness system for helmet-mounted displays p 516 A93-25922
- FUGLUM, KNUIT**
Alternative approach routes to rw 24 at Oslo Airport, Fornebu p 487 A93-28481
- FUHRMANN, HENRI D.**
Application of natural laminar flow to a supersonic transport concept [AIAA PAPER 93-3467] p 997 A93-47248
- FUJI, A.**
Creep crack growth and tail part behavior of low alloy steels and Ni based super alloy p 916 A93-40808
- FUJI, M.**
Trans-oceanic balloon flight over east China sea p 27 A93-11372
- FUJIEDA, H.**
Low-speed wind tunnel study of the direct side-force characteristics of a joined-wing airplane with an upper fin [DE93-767966] p 988 N93-31189
- FUJIEDA, HIROTOSHI**
Wind tunnel investigation of a twin-engine jet transport semi-span model with upper surface blown jet flap [NAL-TR-1134] p 26 N93-12503
- FUJII, K.**
Integrated control law synthesis of gust load alleviation and flutter margin augmentation for a transport aircraft p 182 A93-14281
A multi-dimensional upwind scheme for the Euler equations on structured grids p 862 A93-42430
- FUJII, KENJI**
Guidance and control law for automatic landing flight experiment of reentry space vehicle [AIAA PAPER 93-3818] p 1143 A93-51409
- FUJII, KOZO**
Numerical investigation of supersonic flows around a spiked blunt-body [AIAA PAPER 93-0887] p 471 A93-24947
Nonequilibrium turbulence modeling study on light dynamic stall of a NACA0012 airfoil p 768 A93-37379
Numerical experiment of the flight trajectory simulation by fluid dynamics and flight dynamics coupling [AIAA PAPER 93-3324] p 952 A93-45018
- FUJII, M.**
The improvement of the static launch method in Japan p 26 A93-11364
- FUJII, R.**
Polar Patrol Balloon Experiment in Antarctica p 27 A93-11373
- FUJIMORI, TOSHIRO**
A study on two-dimensional and three-dimensional secondary jet interactions with a supersonic flow p 683 A93-34273
A numerical investigation of 3D transverse injection into the supersonic flow behind rearward facing step p 303 N93-19316
- FUJIMOTO, AKIRA**
Experimental and numerical investigation of Mach 2.5 supersonic mixed compression inlet [AIAA PAPER 93-0289] p 279 A93-22689
Three dimensional calculation of flow inside supersonic inlet p 303 N93-19313
- FUJIOKA, JUNZO**
Thermal barrier design of gamma-TiAl Functionally Gradient Materials (FGMs) for scramjet engine applications p 1246 A93-54556
- FUJISAWA, NOBUYUKI**
Experimental and numerical study on the basic performance of a two-dimensional right-angled intake flow p 208 A93-15486
- FUJITA, H.**
Transonic discharge flows around diffuser vanes from a centrifugal impeller [ISABE 93-7053] p 1185 A93-54029
- FUJITA, HAJIME**
Numerical prediction of aerodynamic noise radiated from low Mach number turbulent wake [AIAA PAPER 93-0145] p 452 A93-22589
- FUJITA, M.**
Effects of external control circuit on coal-fired supersonic diagonal-type MHD generator p 1173 A93-49619
- FUJITA, T.**
Low-speed wind tunnel study of the direct side-force characteristics of a joined-wing airplane with an upper fin [DE93-767966] p 988 N93-31189
- FUJITA, TOSHIMI**
Wind tunnel investigation of a twin-engine jet transport semi-span model with upper surface blown jet flap [NAL-TR-1134] p 26 N93-12503
- FUJIWARA, GENKICHI**
Aircraft fatigue failures and tasks of structural reliability analysis p 210 A93-16246
- FUJIWARA, T.**
Radiative heat transfer from non-equilibrium high-enthalpy shock layers p 1024 A93-45515
- FUJIWARA, TOSHI**
Hypersonic chemically reacting flow of a reentry body p 769 A93-38147
Numerical study on atom-molecule radiation flowfield around a hypersonic blunt body p 770 A93-38434
LIF visualization of 3-dimensional hypersonic mixing [ISABE 93-7114] p 1221 A93-54089
Characteristics of heat exchanger in supersonic/subsonic flows [ISABE 93-7119] p 1221 A93-54094
- FUJIWARA, TOSHITAKA**
Microchannel plate modal gain variations with temperature p 477 A93-27445
- FUJIYAMA, K.**
Evaluation of metallurgical degradation on gas turbine components p 915 A93-40804
Crack simulation and life assessment of gas turbine nozzles p 915 A93-40805
- FUJIYAMA, KAZUNORI**
Life assessment of gas turbine bucket coating based on degradation analysis p 533 A93-24464
- FUKANO, TOHRU**
Experimental study on the characteristics of the near wake of a rotating flat plate. III - Influence of the shape near the trailing edge on periodic-velocity-fluctuation phenomena p 451 A93-21727
Experimental investigation into the mechanism of discrete frequency noise (DFN) generation from a NACA 0012 blade p 1225 A93-53194
- FUKUDA, HIDEO**
Computation of internal flows using unstructured triangular meshes p 299 N93-19276
- FUKUDA, K.**
Evaluation of metallurgical degradation on gas turbine components p 915 A93-40804
- FUKUDA, MASAHIRO**
Two-dimensional and three-dimensional mixing flow structures with injected through slotted nozzle and circular nozzle into supersonic flows [ISABE 93-7117] p 1221 A93-54092
The operating system for Numerical Wind Tunnel p 383 N93-19290
The language processor system for the Numerical Wind Tunnel p 383 N93-19291
A numerical investigation of 3D transverse injection into the supersonic flow behind rearward facing step p 303 N93-19316
- FUKUE, I.**
Investigation of combustion structure inside low NO(x) combustors for a 1500 C-class gas turbine [ASME PAPER 92-GT-123] p 350 A93-19357
- FUKUHARA, MINORU**
Experimental study on the characteristics of the near wake of a rotating flat plate. III - Influence of the shape near the trailing edge on periodic-velocity-fluctuation phenomena p 451 A93-21727
- FUKUMOTO, M.**
The properties of newly developed highly damage tolerant and easy handleable carbon fiber/modified bismaleimide prepreg system p 1212 A93-53448
- FUKUNAGA, HISAO**
Stiffness design method of symmetric laminates using lamination parameters p 206 A93-14569
- FUKUSHIMA, CHIHARU**
Streamwise variation of mean velocity field for the turbulent boundary layer interacting with controlled longitudinal vortex arrays p 267 A93-20933
- FUKUYAMA, A.**
Beta-limiting phenomena in high-aspect-ratio toroidal helical plasmas [NIFS-188] p 569 N93-20546
- FULGHAM, DAN D.**
Development of a flight instrument package [AD-A260830] p 719 N93-25783
- Inflight evaluation of an acoustic orientation instrument [AD-A260752] p 719 N93-25909
Design, fabrication, and testing of a three-dimensional acoustic orientation instrument (3-D AOI): Drawings, engineering and associated lists (conceptual and development design) [AD-A260934] p 760 N93-25915
- FULLER, C. R.**
Active control of interior noise in model aircraft fuselages using piezoceramic actuators p 231 A93-14540
The prediction of nonlinear dynamic loads on helicopters from flight variables using artificial neural networks p 322 A93-19231
Preliminary experiments on active control of fan noise from a turbofan engine p 759 A93-34957
- FULLER, CHRIS R.**
Evaluation of piezoceramic actuators for control of aircraft interior noise p 447 A93-19186
- FULLER, CHRISTOPHER R.**
Active control of fan noise from a turbofan engine [AIAA PAPER 93-0597] p 452 A93-23323
- FULLER, E. J.**
Integrated CFD modeling of gas turbine combustors [AIAA PAPER 93-2196] p 1115 A93-50008
- FULLER, ERIC J.**
Dual-spray airblast fuel nozzle for advanced small gas turbine combustors [AIAA PAPER 93-2336] p 1116 A93-50113
- FULLER, ERIC JAMES**
Experimental and computational investigation of helium injection into air at supersonic and hypersonic speeds p 696 N93-25487
- FULLERTON, C. G.**
Preliminary flight test results of a fly-by-throttle emergency flight control system on an F-15 airplane [AIAA PAPER 93-1820] p 1100 A93-49708
- FULLERTON, GORDON**
X-29 vortex flow control tests p 804 A93-38846
- FULTON, C. L.**
A guidance display system for single pilot operation [AIAA PAPER 92-4196] p 51 A93-13373
- FULTON, MARK VERNER**
Stability of elastically tailored rotor blades p 164 N93-14828
- FUNABIKI, K.**
A combined facility of ballistic range and shock tunnel using a fast action valve p 1012 A93-45532
- FUNABIKI, KATSUSHI**
Effect of the flow non-uniformity on the mixing layer at the interface of parallel supersonic flows [ISAS-RN-646] p 128 N93-12716
- FUNABIKI, KOHEI**
A method of wind shear detection for powered-lift STOL aircraft [AIAA PAPER 93-3667] p 1104 A93-48345
- FUNATANI, K.**
High temperature fracture mechanism of gas-pressure sintered silicon nitride p 825 A93-38893
- FUNAZAKI, KEN-ICHI**
A new technique for analysis of unsteady aerodynamic responses of cascade airfoils with blunt leading edge. I - Theory p 267 A93-20909
A new technique for analysis of unsteady aerodynamic responses of cascade airfoils with blunt leading edge - Unsteady aerodynamic responses of the cascade in incompressible flow p 1086 A93-51122
Analysis of wake-induced unsteady flow in axial compressors - Radial variations of wake excitation forces estimated by strip theory p 1086 A93-51123
- FUNG, K.-Y.**
Modeling, analysis, and prediction of flutter at transonic speeds p 416 A93-23553
- FUNK, JOHN D., JR.**
An analysis of helicopter dynamic response to turbulence using fuselage and blade element atmospheric sampling techniques [AIAA PAPER 92-4148] p 43 A93-13314
- FUNK, R. B.**
SCV measurements in the wake of a rotor in hover and forward flight [AIAA PAPER 93-3080] p 1059 A93-48254
- FUNKE, K. D.**
Advanced cooling for high power electric actuators [SAE PAPER 921022] p 158 A93-14649
- FUNKHOUSER, GORDON E.**
Effects of seating configuration and number of type 3 exits on emergency aircraft evacuation [AD-A256616] p 143 N93-14277
- FURA, DAVID A.**
Formal design specification of a Processor Interface Unit [NASA-CR-189698] p 99 N93-12538
- FUSCO, F.**
Wind tunnel operator aimed comparison between two electronic pressure scanner systems p 830 A93-37876

- Instrumentation and data acquisition system for the C.I.R.A. Transonic Pilot Tunnel p 1250 A93-54395
Wind tunnel operator aimed comparison between two electronic pressure scanner systems [DLAS-EST-TR-040] p 67 N93-11225
- FUSCO, FRANCESCO**
Experimental investigation on aircraft dynamic stability parameters p 905 A93-40328
- FUTAMURA, H.**
A scoping study for hypersonic transport propulsion systems [ASME PAPER 92-GT-409] p 356 A93-19558
- FUTATSUDERA, NAOKI**
Feasibility study on single bypass variable cycle engine with ejector [AIAA PAPER 92-4268] p 55 A93-13366
- FYNBO, P. B.**
Neutron-induced single event upsets in static RAMs observed at 10 KM flight altitude p 1158 A93-50561

G

- GABEL, M.**
Drag/thrust estimation via aircraft performance flight testing p 156 A93-14322
- GABEL, R.**
The NASA/industry Design Analysis Methods for Vibrations (DAMVIBS) program: Boeing Helicopters airframe finite element modeling p 515 N93-21313
- GABELMANN, JEFFREY**
Design, fabrication, and testing of a three-dimensional acoustic orientation instrument (3-D AOI): Drawings, engineering and associated lists (conceptual and development design) [AD-A260934] p 760 N93-25915
- GABRIEL, EDWARD A.**
General aviation aircraft: Normal acceleration data analysis and collection project [DOT/FAA/CT-91/20] p 713 N93-24739
- GAEDKE, M.**
GARTEUR damage mechanics for composite materials: Analytical/experimental research on delaminations p 537 N93-21513
- GAETA, R. J., JR.**
A design approach to high Mach number scramjet performance [AIAA PAPER 92-4248] p 55 A93-13360
Hypersonic inlet efficiency revisited p 16 N93-10012
- GAGE, P.**
Development of the quasi-procedural method for use in aircraft configuration optimization [AIAA PAPER 92-4693] p 322 A93-20278
- GAHURA, A.**
Simulation of propulsion system's transient response to planar wave inlet distortion and the effect of compressor wear [AIAA PAPER 93-2384] p 1117 A93-50152
- GAI, S. L.**
Free piston shock tunnels - Developments and capabilities p 66 A93-12316
- GAIBLE, F.**
Numerical simulation of three-dimensional supersonic flows using Euler and boundary layer solvers [AIAA PAPER 93-0531] p 284 A93-23272
- GAILLARD, HENRY**
Differential GPS and its applications in the aeronautical realm p 500 A93-28195
- GAILLARD, R.**
Testing techniques for straight transonic and supersonic cascades [ONERA, TP NO. 1992-155] p 773 A93-38734
- GAINES, MIKE**
Bear facts p 1229 A93-55175
- GAINUTDINOV, O. I.**
Improving the service characteristics of an aircraft through the gyroscopic damping of its structure p 366 A93-18363
- GAINUTDINOV, V. G.**
The minimal multiplier method in calculations of the stability, limiting vibration cycles, and limiting states of nonlinearly deformed structures p 836 A93-39176
- GAITONDE, ANN L.**
A moving mesh system for the calculation of unsteady flows [AIAA PAPER 93-0641] p 464 A93-24756
- GAITONDE, D.**
Numerical solution of inviscid hypersonic flow around a conically-derived waverider [AIAA PAPER 93-0320] p 280 A93-23012
- GAITONDE, DATTA**
Numerical simulation of flow past the X24C reentry vehicle [AIAA PAPER 93-0319] p 280 A93-23011

- Hypersonic nonequilibrium flow computations using the Roe flux-difference split scheme p 692 A93-35609
Accuracy of flux-split algorithms in high-speed viscous flows p 860 A93-41912
Calculations on a double-fin turbulent interaction at high speed [AIAA PAPER 93-3432] p 977 A93-47224
Calculations on unsteady type 4 interaction at Mach 8 [AD-A265214] p 990 N93-32004
- GAJENDRAN, F.**
New adaptive controllers for aircraft p 847 N93-27180
- GAJNUTDINOV, V. G.**
Dynamic analysis of a compound elastic surface p 1030 A93-47086
- GAL-OR, BENJAMIN**
Thrust vectoring - Theory, laboratory, and flight tests p 367 A93-21657
Mathematical phenomenology for thrust-vectoring-induced agility comparisons p 525 A93-28613
- GALTSEV, A. P.**
Study of artificial and natural turbulence in atmospheric boundary layer with a CW Doppler CO2 lidar p 1257 A93-54799
- GALASSI, L.**
A study of incipient separation limits for shock-induced boundary layer separation for Mach 6 high Reynolds flow [AIAA PAPER 93-2481] p 1084 A93-50222
- GALBRAITH, R. A.**
The convection speed of the dynamic stall vortex [AD-A247258] p 21 N93-11464
- GALBRAITH, R. A. MCD.**
The effect of wind tunnel constraint on unsteady aerodynamics experiments p 190 A93-14300
An examination of vortex convection effects during blade-vortex interaction p 473 A93-25360
Results from a set of low speed blade-vortex interaction experiments p 872 A93-43540
- GALE, W. F.**
Microstructural study of aluminide surface coatings on single crystal nickel base superalloy substrates p 70 A93-12771
- GALEA, S. C. P.**
The effect of temperature on the natural frequencies and acoustically induced strains in CFRP plates p 1260 A93-56331
- GALIMORE, REGINALD N.**
Calibration results for NOAA-11 AVHRR channels 1 and 2 from congruent path aircraft observations p 1143 A93-51237
- GALINSKI, CEZARY**
Results of testing of models of joint-wing utility class aircraft [SAE PAPER 921013] p 157 A93-14643
- GALKIN, V. F.**
Load-bearing capacity of an aircraft wing based on the condition of compressed surface fracture p 801 A93-36794
- GALKIN, V. M.**
Experimental study of crossflow instability and laminar-turbulent transition on a swept wing p 115 A93-14250
Calculation of the parameters of instability waves in the preseparation region p 1067 A93-48826
- GALKIN, V. S.**
Approximate method for the aerodynamic design of flight vehicles for high supersonic flight speeds p 1069 A93-48966
- GALLANT, DAVID**
The Edge supersonic transport [NASA-CR-192074] p 335 N93-18055
- GALLEITHNER, H.**
X-31A high angle of attack and initial post stall flight testing p 511 N93-19911
System identification for X-31A project support: Lessons learned so far p 512 N93-19914
- GALLERY, JEAN**
Video luminescent barometry - The induction period [AIAA PAPER 93-0179] p 414 A93-22607
- GALLGHER, T. F.**
Remote sensing of O2 in a supersonic combustor using diode lasers and fiber optics [AIAA PAPER 92-5090] p 414 A93-22360
- GALLICE, G.**
Taking into account surface roughness in computing hypersonic re-entry body p 686 A93-34354
- GALLIMORE, S. J.**
Viscous throughflow modelling for multi-stage compressor design [ASME PAPER 92-GT-302] p 255 A93-19492
- GALLIS, M. A.**
Non-equilibrium thermal radiation from air shock layers modelled with the Direct Simulation Monte Carlo method [AIAA PAPER 93-2805] p 1028 A93-46544

- GALLMAN, JOHN W.**
Structural optimization for joined-wing synthesis [AIAA PAPER 92-4761] p 325 A93-20356
- GALLMAN, JOHN WALDEMAR**
Structural and aerodynamic optimization of joined-wing aircraft p 715 N93-25526
- GALLMAN, JUDITH M.**
Acoustic characteristics of advanced model rotor systems p 567 A93-29419
- GALLON, MARC**
Contribution of visualization to the study of unsteady aspects of vortex breakdown [ONERA, TP NO. 1992-93] p 771 A93-38576
- GALLONE, S.**
Improvements in code validation algorithms for secondary surveillance radar p 883 A93-43408
- GALLOPS, G. W.**
On-board condition management for aircraft gas turbines [ASME PAPER 92-GT-416] p 357 A93-19564
- GALLOWAY, THOMAS**
Oblique wing supersonic transport concepts [AIAA PAPER 92-4230] p 43 A93-13337
- GALLUS, H. E.**
Design and rotor performance of a 5:1 mixed-flow supersonic compressor [ASME PAPER 92-GT-73] p 348 A93-19323
Experimental analysis of transonic flow through the variable nozzle of a radial inflow turbine [ASME PAPER 92-GT-90] p 248 A93-19336
Performance analysis of a turbofan as a part of an airbreathing propulsion system for space shuttles p 1252 A93-56039
- GALLY, THOMAS A.**
Survey of nonequilibrium re-entry heating for entry flight conditions [AIAA PAPER 93-3230] p 1039 A93-46682
- GALYUTIN, V. B.**
Multilevel control systems and optimization of their structures p 1168 A93-50954
- GAMACHE, JOHN F.**
Comparison of three methods to deduce three-dimensional wind fields in a hurricane with airborne Doppler radar p 844 A93-37691
- GAMMA, F.**
Performance and configuration analysis of jet-engine off-design behavior [ISABE 93-7087] p 1202 A93-54063
- GAMMEL, FRANZ JOSEF**
Surface protection in the aircraft industry [MBB-Z-0432-92-PUB] p 72 N93-11027
- GAN, SU**
An impact dynamics investigation on some problems in bird strike on windshields of high speed aircraft p 197 A93-15346
- GAN, X.**
Flow and heat transfer between gas-turbine discs p 903 N93-29950
- GAN'ZHA, D. KH.**
Influence of second-order boundary layer effects in hypersonic flow past blunt cones of large aspect ratio p 241 A93-18238
- GANDY, C.**
HELITRACK: A helicopter-tracking receiver system for television outside broadcast links [BBC-RD-1992/5] p 552 N93-20573
- GANESAN, P.**
Corrosion resistance of Inconel Alloy 617 in simulated gas turbine environments [ASME PAPER 92-GT-142] p 388 A93-19374
- GANESAN, R.**
Stochastic finite element analysis for high speed rotors p 554 A93-20696
- GANESAN, V.**
A study on 3-D velocity distribution of isothermal flows behind an afterburner flame stabilizer [ISABE 93-7039] p 1197 A93-54015
- GANG, CHEN**
Longitudinal closed-loop pilot/vehicle analysis of DFBW aircraft during approach and landing p 1206 A93-54277
- GANGLOFF, RICHARD P.**
NASA-UVA Light Aerospace Alloy and Structures Technology Program (LA2ST) [NASA-CR-193412] p 1019 N93-31739
- GANGULEE, D.**
Secondary flow control on slender, sharp-edged configurations [AIAA PAPER 93-3470] p 980 A93-47250
- GANGULI, RANJAN**
Aeroelastic optimization of a composite helicopter rotor [AIAA PAPER 92-4780] p 323 A93-20287
- GANJI, A. R.**
Aerothermodynamic analysis of combined-cycle propulsion systems p 359 A93-21671

- GANLEY, G. A.**
Concorde propulsion: Did we get it right? The Rolls-Royce/SNECMA Olympus 593 engine reviewed [PNR-90970] p 57 N93-11061
- GANY, ALON**
Ignition of boron particles coated by a thin titanium film [AIAA PAPER 93-2201] p 1145 A93-50013
Regression rate mechanism in a solid fuel ramjet p 814 N93-27185
Analysis of thrust modulation of ram-rockets by a vortex valve p 814 N93-27187
- GANZ, H.**
Airbus Industrie TCAS experience p 152 N93-15186
- GAO, C.**
Inverse simulation of large-amplitude aircraft maneuvers p 906 A93-41893
- GAO, DEPING**
Effect of bird impact load types on blade response p 174 A93-16846
- GAO, GE**
Experimental investigation on patterned blades of compressor p 1066 A93-48515
- GAO, HAO**
The influence of fighter agility on air combat effectiveness p 184 A93-14398
- GAO, HONG**
Numerical analysis of the flow through a centrifugal impeller by vortex distribution model of a boundary layer. I - Theoretical analysis p 1182 A93-53843
- GAO, JIANMIN**
On dynamic behavior of cracked rotors p 208 A93-15401
- GAO, JINGSHI**
Experimental investigation on effect of solid particles on blade pressure distribution in compressor cascade flow p 1066 A93-48513
- GAO, MINGYAN**
A multi-functional computer-aided aircraft exterior shape modelling prototype system p 504 A93-24032
- GAO, XIANGQUNG**
Dynamic characteristics of two new vibration modes of the disk-shell shaped gear p 204 A93-14484
- GAO, XIAO-GUANG**
The influence of fighter agility on air combat effectiveness p 184 A93-14398
- GAO, YANG**
A new algorithm of Receiver Autonomous Integrity Monitoring (RAIM) for GPS navigation p 314 A93-21161
- GAO, Z.**
A new method for calculation of helicopter maneuvering flight p 184 A93-14401
- GAO, ZHENG-HONG**
Unsteady transonic aerodynamic loadings on the airfoil caused by heaving, pitching oscillations and control surface p 126 A93-15627
An implicit difference scheme of Euler equation for unsteady transonic flow p 1182 A93-53852
- GAO, ZHENGHONG**
A kind of improved flux-split method for solving the Euler equations p 681 A93-33739
- GAONKAR, G. H.**
Atmospheric turbulence simulation for rotorcraft applications p 757 A93-34264
Helicopter response to atmospheric turbulence p 817 A93-35987
- GAONKAR, GOPAL H.**
Effects of dynamic stall and structural modeling on aeroelastic stability of elastic bending and torsion of hingeless rotor blades with experimental correlation p 794 A93-35902
Flap-lag damping in hover and forward flight with a three-dimensional wake p 797 A93-35979
- GAPONOV, S. A.**
On the disturbances development in the supersonic boundary layer p 484 N93-20686
- GARABEDIAN, P. R.**
Comparison of numerical methods in transonic aerodynamics p 864 A93-42446
- GARBINSKI, GARY**
Tesseract: Supersonic business transport [NASA-CR-192072] p 334 N93-17977
- GARCIA CRUZADO, MARCOS**
Specific educational aspects of airport engineering in Spain and the Hispanic world p 103 A93-12560
- GARCIA CRUZADO, MARCOS**
Aeronautical technologies and communications - Toward advanced technology passenger terminals p 529 A93-27477
- GARCIA JULIAN, G.**
Dynamic stability of bodies of revolution in compressible flow p 12 A93-12558
- GARCIA-FOGEDA, P.**
Dynamic stability of bodies of revolution in compressible flow p 12 A93-12558
- GARCIA, A.**
The community response to aircraft noise around six Spanish airports p 1264 A93-55845
- GARCIA, A. M.**
The community response to aircraft noise around six Spanish airports p 1264 A93-55845
- GARCON, F.**
Comparative performance tests of a pitot-inlet in several European wind-tunnels at subsonic and supersonic speeds p 130 N93-13221
- GARDAREIN, PATRICK**
Eurofar rotor aerodynamic tests [ONERA, TP NO. 1992-173] p 475 A93-26880
- GARDNER-BONNEAU, DARYLE J.**
Ongoing and planned R&D efforts in airway facilities maintenance p 458 A93-27134
- GARDNER, P.**
Options for control and navigation of unmanned aircraft p 34 A93-12124
- GARG, S.**
Wall pressure fluctuations beneath swept shock wave/boundary layer interactions [AIAA PAPER 93-0384] p 282 A93-23063
Design and evaluation of a robust dynamic neurocontroller for a multivariable aircraft control problem p 817 A93-37004
An experimental study of the sources of fluctuating pressure loads beneath swept shock/boundary-layer interactions [NASA-CR-192918] p 749 N93-25266
- GARG, SANJAY**
Robust integrated flight/propulsion control design for a STOVL aircraft using H-infinity control design techniques p 524 A93-26432
Neurocontrol design and analysis for a multivariable aircraft control problem p 906 A93-41894
Application of controller partitioning optimization procedure to integrated flight/propulsion control design for a STOVL aircraft [AIAA PAPER 93-3766] p 1131 A93-51361
A parameter optimization approach to controller partitioning for integrated flight/propulsion control application p 1206 A93-54268
Propulsion system performance resulting from an integrated flight/propulsion control design [NASA-TM-105874] p 180 N93-15525
Controller partitioning for integrated flight/propulsion control implementation [NASA-TM-105804] p 527 N93-21197
A modified approach to controller partitioning [NASA-TM-106167] p 848 N93-28051
- GARIFULLIN, M. F.**
Estimation of wing stability in flow from the characteristics of the transient process p 836 A93-39177
- GARIPOV, R. Z.**
Fuel film formation in the fuel-air premixer of the combustion chamber p 812 A93-39193
- GARLICK, RALPH G.**
The chemistry of Saudi Arabian sand - A deposition problem on helicopter turbine airfoils p 1216 A93-53468
- GARNER, H. D.**
Development of a microcomputer-based magnetic heading sensor p 1160 A93-52152
- GARNER, VAN H.**
The development of a mature external Master's degree program in aeronautical engineering - A university/industry partnership [AIAA PAPER 92-4256] p 570 A93-24296
- GARNERO, P.**
Some aspects of the aerodynamic methodology in hypersonic vehicle concept studies [AIAA PAPER 92-5027] p 272 A93-22303
CFD for ramjet and scramjet powered vehicles [ISABE 93-7035] p 1197 A93-54011
- GARNETT, A. J.**
Bistatic radar using satellite-borne illuminators of opportunity p 914 A93-43437
- GARNIER, FRANCOIS**
Contribution to the study of the interaction between acoustic waves and coherent structures induced by a prismatic cylinder in a rectangular cavity [ONERA-NT-1990-10] p 918 N93-30203
- GARNIER, VINCENT H.**
Active stabilization of aeromechanical systems [AD-A261366] p 725 N93-26335
- GARODZ, L. J.**
Vortex wake characteristics of B757-200 and B767-200 aircraft using the tower fly-by technique [PB93-180255] p 878 N93-30388
- Vortex wake characteristics of B757-200 and B767-200 aircraft using the tower fly-by technique [PB93-180263] p 878 N93-30388
- GARRARD, WILLIAM L.**
Nonlinear feedback control of highly manoeuvrable aircraft p 40 A93-11654
Design of flight control systems to meet rotorcraft handling qualities specifications p 370 A93-23509
Design of a recovery system for a reentry vehicle [AIAA PAPER 93-1224] p 733 A93-35171
Design of a flight control system for a highly manoeuvrable aircraft using mu synthesis [AIAA PAPER 93-3776] p 1132 A93-51371
Design of a helicopter control system to meet handling quality specifications using H(infinity) techniques [AIAA PAPER 93-3850] p 1134 A93-51437
- GARRATT, V. E. W.**
Developments in icing test techniques for aerospace applications in the RAE Pyestock (England) altitude test facility [RAE-TM-P-1214] p 48 N93-11485
- GARRETON, DANIELLE**
Thermometry inside a swirling turbulent flame - CARS advantages and limitations p 1146 A93-51634
- GARRISON, T. J.**
Interaction strength and model geometry effects on the structure of crossing-shock wave/turbulent boundary-layer interactions [AIAA PAPER 93-0780] p 467 A93-24862
Laser Interferometer Skin-Friction measurements of crossing-shock wave/turbulent boundary-layer interactions [AIAA PAPER 93-3072] p 1148 A93-48247
- GARROOD, STUART T.**
Pilot evaluations of augmented flight simulator motion [AIAA PAPER 93-3580] p 1208 A93-52676
- GARSIDE, T.**
Experimental heat transfer results in turbine stators and rotors and a comparison with theory [PNR-90945] p 57 N93-11055
- GARTENBERG, EHUD**
Aerodynamic investigation with focusing schlieren in a cryogenic wind tunnel [AIAA PAPER 93-3485] p 910 A93-41059
- GARVIN, JAMES B.**
Mapping new and old worlds with laser altimetry p 1034 A93-45699
- GARWIN, R.**
Small satellites and RPA's in global-change research [AD-A260762] p 755 N93-25837
- GASS, F. D.**
On-board condition management for aircraft gas turbines [ASME PAPER 92-GT-416] p 357 A93-19564
- GASS, J.**
Particle imaging techniques and applications p 1020 A93-44195
- GASTELLU-ETCHEGORRY, J. P.**
Preliminary results of the ISM campaign - The Landes, South West France p 1161 A93-47553
- GATARD, JACQUES**
Two-dimensional laser velocimetry for the study of dual-flow jets with flight effect in the CEPRA 19 anechoic wind tunnel [ONERA, TP NO. 1992-144] p 831 A93-38614
- GATENS, DENNIS R.**
An internetworking router for avionics applications p 1097 A93-49479
- GATHMANN, R. J.**
Direct numerical simulation of combustion in turbulent supersonic flow [DS-2138] p 393 N93-17746
- GATHMANN, RALF J.**
Direct numerical simulation of nitric oxide evolution in underexpanded jets [ASME PAPER 92-GT-372] p 355 A93-19534
- GATLIN, B.**
Adaptive EAGLE dynamic solution adaptation and grid quality enhancement p 788 N93-27464
- GATLIN, BOYD**
Solution-adaptive and quality-enhancing grid generation p 480 A93-28610
- GATLIN, DONALD**
The F-18 High Alpha Research Vehicle - A high-angle-of-attack testbed aircraft [AIAA PAPER 92-4121] p 42 A93-13273
- GATLIN, DONALD H.**
Flight-determined benefits of integrated flight-propulsion control systems p 183 A93-14370
- GATLIN, GREGORY M.**
Low-speed longitudinal and lateral-directional aerodynamic characteristics of the X-31 configuration [NASA-TM-4351] p 22 N93-11622

GATZKE, TIMOTHY D.

- GATZKE, TIMOTHY D.**
Unstructured grid generation using interactive three-dimensional boundary and efficient three-dimensional volume methods
[AIAA PAPER 93-3452] p 1037 A93-47237
- GAUFFRE, G.**
Infrared thermography for hot-shot wind tunnel
[ONERA, TP NO. 1992-103] p 831 A93-38583
- GAUGLER, RAYMOND E.**
Overview of aerothermodynamic loads definition study
p 1016 N93-31583
- GAUTHIER, BENOIT G.**
Articulated fin/wing control system
[AD-D015712] p 909 N93-29278
- GAUTHIER, D.**
Validation of electromagnetic-topology concepts on a complex structure
[ONERA, TP NO. 1992-63] p 542 A93-25327
- GAVALI, S.**
Multipassage three-dimensional Navier-Stokes simulation of turbine rotor-stator interaction
p 688 A93-34484
- GAWTHROP, P. J.**
Improving dynamic response of a single-spool gas turbine engine using a nonlinear controller
[ASME PAPER 92-GT-392] p 355 A93-19546
- GAYDA, JOHN**
An overview of elevated temperature damage mechanisms and fatigue behavior of a unidirectional SCS-6/Ti-15-3 composite
[NASA-TM-106131] p 825 N93-26702
- GAZAIX, M.**
Hypersonic inviscid and viscous flow computations with a new optimized thermodynamic equilibrium model
[AIAA PAPER 93-0893] p 471 A93-24953
- GE, M. C.**
An investigation on the artificial viscosity in the transonic stream function formulation
[ASME PAPER 92-GT-49] p 246 A93-19302
- GE, S.**
Researches on sonic fatigue of the air-inlet duct of XX aircraft
p 154 A93-14256
- GEA, LIE-MINE**
Juncture flow improvement for wing/pylon configurations by using CFD methodology
[AIAA PAPER 93-0522] p 283 A93-23264
- GEDDES, J. N.**
Meteorological information for aviation: A systems approach
p 937 N93-30298
- GEDDES, NORMAN D.**
Methods and principles for determining task dependent interface content
[NASA-CR-190837] p 36 N93-10961
- GEE, KEN**
Computational investigation of a pneumatic forebody flow control concept
p 768 A93-37383
Effect of forebody tangential slot blowing on flow about a full aircraft geometry
[AIAA PAPER 93-2962] p 1048 A93-48156
- GEENEN, ROBERT J.**
Measurement of attachment-line location in a wind-tunnel and in supersonic flight
[AIAA PAPER 92-4089] p 39 A93-11285
- GEERING, HANS P.**
A test bench for rotorcraft hover control
[AIAA PAPER 93-3853] p 1140 A93-51440
- GEHLHAR, B.**
Aeroacoustic wind tunnel testing of a counterrotating shrouded propfan-model
p 449 A93-19213
- GEHLUSCH, KLAUS**
Real gas simulation of air Blow-Down Facilities
[AIAA PAPER 93-2022] p 1137 A93-49859
- GEIDEL, H. A.**
Axial flow compressors - Mechanical design trends
[ISABE 93-7061] p 1199 A93-54037
- GEIER, F.**
The production of a monolithic CFRP fuselage skin for the European Fighter Aircraft
p 109 A93-15810
- GEIER, G. J.**
System analysis for a kinematic positioning system based on the global positioning system
[AD-A262830] p 885 N93-29468
- GEIGER, DAVID L. I.**
Static tests of jet fuel thermal and oxidative stability
p 389 A93-21651
- GEIGER, GREG**
Ceramic coatings enhance material performance
p 71 A93-13648
- GEISSLER, WOLFGANG**
Unsteady Navier-Stokes method for accelerated moving airfoils with separation
[DLR-FB-92-03] p 485 N93-21763
- GELBACH, HERMAN R.**
A data system for the observation of flow conditions on an aircraft wing
p 808 A93-37882

- GELHAUSEN, P.**
Extracting dimensional geometric parameters from B-spline surface models of aircraft
[AIAA PAPER 92-4283] p 43 A93-13340
- GELHAUSEN, PAUL**
Oblique wing supersonic transport concepts
[AIAA PAPER 92-4230] p 43 A93-13337
- GELLERT, R. I.**
Laser Centerline Localizer and Laser Glideslope Indicator for visual guidance on approach to landing
p 500 A93-28156
Scanning Laser Aircraft Surveillance System for carrier flight operations
p 500 A93-28157
- GENDRICH, C. P.**
Initial acceleration effects on the flow field development around rapidly pitching airfoils
[AIAA PAPER 93-0438] p 286 A93-23352
- GENDRON, S.**
An experimental investigation of convective heat transfer at the leading edge of a gas turbine airfoil
[ASME PAPER 92-GT-248] p 405 A93-19457
- GENERAZIO, EDWARD R.**
Nondestructive evaluation of ceramic and metal matrix composites for NASA's HITEMP and enabling propulsion materials programs
[NASA-TM-105807] p 85 N93-10963
- GENNARETTI, M.**
Toward an integration of aerodynamics and aeroacoustics of rotors
p 243 A93-19127
- GENNARETTI, MASSIMO**
Boundary integral equation methods for aerodynamics
p 9 A93-12158
- GENOV, P.**
A joint Soviet-Bulgarian scientific program for free-flight and tethered aerostat observations
p 2 A93-11374
- GENSURE, JOHN R.**
Extended surface heat sinks for electronic components: A computer optimization
[AD-A256134] p 218 N93-14254
- GENTRY, THOMAS A.**
X-29 linear aerodynamic perturbation model
[AD-A254810] p 160 N93-12752
- GEOFFROY, P.**
Aeroplane crashes on the runway: Validation and final evaluation of the method of modeling an airframe structure
[IMFL-91-32] p 165 N93-15126
- GEORGE, A.**
Millisecond aerodynamic force measurement with side-jet model in the ISL shock tunnel
p 822 A93-39414
Shock tube validation experiments for the simulation of ram-accelerator-related combustion and gasdynamic problems
p 1016 A93-45499
Shock tunnel experiments and approximative methods on hypervelocity side-jet control effectiveness
[AIAA PAPER 93-1929] p 1077 A93-49794
- GEORGE, A. R.**
Advances in tilt rotor noise prediction
p 447 A93-19184
Vortex/surface interaction
[AIAA PAPER 93-0863] p 468 A93-24925
- GEORGE, ALBERT R.**
A study of blade-vortex interaction sound generation and directionality
p 565 A93-29402
A comparative analysis of XV-15 tiltrotor hover test data and WOPWOP predictions incorporating the fountain effect
p 509 A93-29414
Flow visualization and flow field measurements of a 1/12 scale tilt rotor aircraft in hover
p 482 A93-29441
Effects of ingested atmospheric turbulence on measured tail rotor acoustics
p 849 A93-35964
- GEORGE, GARY**
Transport delay compensation - An inexpensive alternative to increasing image generator update rate
[AIAA PAPER 93-3563] p 1223 A93-52663
- GEORGESON, G.**
Correlation of X-ray CT measurements to shear strength in pultruded composite materials
p 396 A93-18618
- GEORGESON, G. E.**
Computed tomography of advanced materials and processes
p 832 A93-38975
- GEORGESON, GARY E.**
X-ray computed tomography for casting development
[AD-A261786] p 752 N93-26526
- GERACI, M.**
Low area ratio aircraft fuel jet-pump performances with and without cavitation
p 272 A93-22264
- GERADIN, MICHEL**
Europe adapts CST to its needs
p 560 A93-25088
Vibration analysis in turbomachines
p 1005 N93-32274
- GERASHCHENKO, N. P.**
A model for calculating the element of a high-temperature heat exchanger with spiral-wire fins
p 833 A93-39046

PERSONAL AUTHOR INDEX

- GERASIMOV, V. F.**
Increasing the efficiency of the electrochemical dimensional machining of gas turbine engine blades of EP718VD alloy
p 835 A93-39095
- GERBSCH, R. A.**
A comparison of upwind schemes for computation of three-dimensional hypersonic real-gas flows
[AIAA PAPER 92-4350] p 15 A93-13306
- GERHARDT, HEINZ A.**
Development of an innovative natural laminar flow wing concept for high-speed civil transports
[AIAA PAPER 93-3466] p 980 A93-47247
- GERHOLD, T.**
Numerical simulation of shock/shock and shock-wave/boundary-layer interactions in hypersonic flows
p 1093 A93-52000
- GERING, GREG**
Advanced technology wind shear prediction system evaluation
p 146 N93-14858
- GERLACH, RONALD R.**
Digital hopping GPS/GLONASS receiver
p 312 A93-21128
- GERLING, WILFRIED**
Fundamentals of adaptive anticipation techniques for the detection of threatening air traffic conflicts: Investigation of the horizontal proximity situation in the case of expected heading changes
[DLR-MITT-91-21] p 503 N93-21004
- GERMAIN, P.**
Transition on a sharp cone at high enthalpy - New measurements in the shock tunnel T5 at GALCIT
[AIAA PAPER 93-0343] p 281 A93-23030
- GERMANCHUK, F. K.**
Design characteristics of the functional systems of aircraft and prediction of their technical condition
p 320 A93-18334
- GERNERT, NELSON J.**
A thermal analysis of an F/A-18 wing section for actuator thermal management
[SAE PAPER 921023] p 158 A93-14650
- GEROLYMOS, G. A.**
On the shock-fitting scheme of Hall-Crawley for time-linearized time-harmonic flows using Euler equations
p 972 A93-46946
- GEROLYMOS, GEORG A.**
Advances in the numerical integration of the 3-D Euler equations in vibrating cascades
[ASME PAPER 92-GT-170] p 351 A93-19396
Coupled 3-D aeroelastic stability analysis of bladed disks
[ASME PAPER 92-GT-171] p 351 A93-19397
- GERREN, DONNA S.**
Design, analysis, and control of large transport aircraft utilizing engine thrust as a backup system for the primary flight controls
[NASA-CR-192938] p 820 N93-27308
- GERSFELD, JONATHAN**
Mass loaded composite rotor for vibro-acoustic application
[AD-D015604] p 535 N93-20016
- GESANG, WANG-JIE**
Receiving and scattering characteristics of an imaged monopole beneath a lossy sheet
p 1158 A93-50543
- GESSNER, F. B.**
A numerical investigation of supersonic strut/endwall interactions in annular flow with varying strut thickness
[AIAA PAPER 93-2927] p 1045 A93-48128
Experimental and numerical investigation of supersonic turbulent flow in an annular duct
[AIAA PAPER 93-3123] p 1063 A93-48291
Investigation of a strut/endwall interaction in supersonic annular flow
[AIAA PAPER 93-1925] p 1076 A93-49791
- GEURTS, B. J.**
Numerical aspects of a block structured compressible flow solver
p 1169 A93-51279
- GEYER, E. M.**
GPS availability and reliability for aircraft precision approach
p 315 A93-21182
- GHAFFARI, FARHAD**
Multiblock Navier-Stokes solutions about the F/A-18 wing-LEX-fuselage configuration
p 767 A93-37378
- GHANBARI, CHERYL M.**
Thermal effects testing at the National Solar Thermal Test Facility
p 1255 A93-54402
- GHARIB, MORTEZA**
Studies of origin of three-dimensionality in laminar wakes
[AD-A262281] p 841 N93-28242
- GHATTAS, O. N.**
Massively parallel aerodynamic shape optimization
p 266 A93-20729
- GHAZI, MOHAMMAD A.**
Wind tunnel investigation of wind shear effect on turning flight
[AIAA PAPER 93-3641] p 1127 A93-48326

- GHAZI, MUHAMMAD A.**
Effect of rotary atmospheric gusts on fighter airplane
[AIAA PAPER 93-3644] p 1127 A93-48328
- GHEE, TERENCE A.**
A study of the rotor wake of a small-scale rotor model in forward flight using laser light sheet flow visualization with comparisons to analytical models
p 766 A93-35957
Flow visualization of mast-mounted-sight/main rotor aerodynamic interactions
[AIAA PAPER 93-3517] p 1009 A93-47280
- GHEZZI, U.**
Performance and configuration analysis of jet-engine off-design behavior
[ISABE 93-7087] p 1202 A93-54063
- GHAIA, K. N.**
Physics of forced unsteady flow for a NACA 0015 airfoil undergoing constant-rate pitch-up motion
p 478 A93-27922
Investigation of forced unsteady separated flows using velocity-vorticity form of Navier-Stokes equations
p 840 A93-27451
Simulation, characterization and control of forced unsteady viscous flows using Navier-Stokes equations
[AD-A264333] p 934 A93-30369
- GHAIA, U.**
Physics of forced unsteady flow for a NACA 0015 airfoil undergoing constant-rate pitch-up motion
p 478 A93-27922
Investigation of forced unsteady separated flows using velocity-vorticity form of Navier-Stokes equations
p 840 A93-27451
Simulation, characterization and control of forced unsteady viscous flows using Navier-Stokes equations
[AD-A264333] p 934 A93-30369
- GHOFRANI, MEHRAN**
Analysis, modelling and simulation of the large-angle magnetic suspension test fixture
p 375 A93-20297
A magnetic suspension system with a large angular range
p 1139 A93-51295
Approaches to control of the large angle magnetic suspension test fixture
[NASA-CR-191890] p 381 A93-16695
- GHONEM, H.**
Mechanisms and modelling of environment-dependent fatigue crack growth in a nickel based superalloy
[AD-A253967] p 71 A93-10717
- GHORASHI, BAHMAN**
Simplified jet fuel reaction mechanism for lean burn combustion application
[AIAA PAPER 93-0021] p 390 A93-23238
A review of chemically reactive turbulent flow mixing mechanisms and a new design for a low NO(x) combustor
p 1109 A93-49508
Simplified jet-A kinetic mechanism for combustor application
[NASA-TM-105940] p 200 A93-15504
Nitric oxide formation in a lean, premixed-prevaporized jet A/air flame tube: An experimental and analytical study
[NASA-TM-105722] p 844 A93-27012
- GHORBANIAN, K.**
An estimate of the 'doomed propellant fraction' for a Superdetonative Ram Accelerator
[AIAA PAPER 93-0359] p 385 A93-23042
- GHORIESHI, ANTHONY**
Wind tunnel seeding particles for laser velocimeter
p 292 A93-16770
- GHOSH, A. K.**
Parameter estimates of an aeroelastic aircraft as affected by model simplifications
[AIAA PAPER 93-3640] p 1127 A93-48325
- GHOSH, AMIT K.**
Lift and pitching moment measurements in vertical gusts
p 906 A93-42259
- GHOSH, KUNAL**
Use of NASA LS (1) general aviation airfoil for a small wind turbine - An experience in Denmark
p 92 A93-12364
- GHOSH, R. N.**
Recent evolution of gas turbine materials and the development of models for life prediction
p 915 A93-40802
- GIANNAKOGLU, K.**
Adaptation of a 3-D pressure correction Navier-Stokes solver for the accurate modelling of tip clearance flows
p 971 A93-46932
- GIANNISSIS, G. L.**
Experimental investigation of rotating stall in a mismatched three stage axial flow compressor
p 423 A93-18727
- GIBB, JAMES**
Study on vortex generator flow control for the management of inlet distortion
p 689 A93-34488
- GIBBENS, PETER W.**
Output feedback control for output tracking of nonlinear uncertain systems
p 96 A93-13177
- GIBBONS, MICHAEL D.**
Aeroelastic character of a National Aerospace Plane demonstrator concept
[AIAA PAPER 93-1314] p 732 A93-33890
Unsteady transonic potential flow over a flexible fuselage
[AIAA PAPER 93-1593] p 683 A93-34124
- GIBBONS, STEPHENS**
Development of a concept formulation process aid for analyzing training requirements and developing training devices
[AD-A263579] p 912 A93-29972
- GIBELING, HOWARD J.**
Projectile base bleed technology. Part 2: User's guide CMINT computer code, version 5.04-BRL
[AD-A258630] p 551 A93-19999
- GIBERT, P.**
Optimization and sensitivity computations for the conception of internal ventilation system in the aircraft engine
[ETN-93-93375] p 521 A93-20913
- GIBSON, BERRY T.**
Development of an innovative natural laminar flow wing concept for high-speed civil transports
[AIAA PAPER 93-3466] p 980 A93-47247
- GIBSON, JOSEPH P., JR.**
An approach to evaluating reactive airborne wind shear systems
p 489 A93-19600
- GIBSON, RONALD F.**
Nonlinear flutter of orthotropic composite panel under aerodynamic heating
p 1025 A93-45740
- GIBSON, THERESA L.**
Icing Research Tunnel rotating bar calibration measurement system
p 1255 A93-54398
- GIEL, P. W.**
An algebraic turbulence model for three-dimensional viscous flows
[AIAA PAPER 93-0083] p 274 A93-22552
An algebraic turbulence model for three-dimensional viscous flows
[NASA-TM-105931] p 110 A93-14102
- GIESE, P.**
Solid state flight data recorders and their application in the flight operation analysis
p 166 A93-14200
The SIROM flight data recorder and evaluation system
p 168 A93-15165
- GILBERT, MICHAEL G.**
Active control of aerothermoelastic effects for a conceptual hypersonic aircraft
p 1007 A93-45137
- GILBRECH, RICHARD J.**
Liquid hydrogen foil-bearing turbopump
[AIAA PAPER 93-2537] p 1156 A93-50264
- GILE, BRENDA E.**
Effects of blowing on delta wing vortices during dynamic pitching
p 768 A93-37384
- GILSON, A. A.**
A study of optical distortions arising in radiation transmission through cavities with gas flow around them
p 1225 A93-52945
- GILES, GARY L.**
Sensitivity-based scaling for approximating structural response
p 548 A93-28618
- GILES, M. B.**
Blade row interaction effects on compressor measurements
p 900 A93-42885
Flow phenomena in turbomachines
[AD-A263049] p 930 A93-29141
- GILES, MICHAEL**
An approach for multi-stage calculations incorporating unsteadiness
[ASME PAPER 92-GT-282] p 253 A93-19474
- GILETTA, D.**
GARTEUR damage mechanics for composite materials: Analytical/experimental research on delaminations
p 537 A93-21513
- GILKEY, SAMUEL**
Engine technology challenges for a 21st Century High-Speed Civil Transport
[ISABE 93-7064] p 1200 A93-54040
Engine technology challenges for a 21st Century High-Speed Civil Transport
[NASA-TM-106216] p 1004 A93-31671
- GILLAN, MARK A.**
Computational analysis of drag reduction and buffet alleviation in viscous transonic flow over porous airfoils
[AIAA PAPER 93-3419] p 976 A93-47215
- GILLE, JENNIFER**
Performance considerations for high-definition head-mounted displays
p 518 A93-27242
- GILLINGWATER, D.**
Information systems for airport operations
[TT-9202] p 152 A93-14729
- GILLIS, JAMES R.**
Test results of the effects of air ionization on cigarette smoke particulate levels within a commercial airplane
[SAE PAPER 921183] p 855 A93-41362
- GILMAN, J. A.**
NASA SBIR abstracts of 1990 phase 1 projects
[NASA-TM-108145] p 572 A93-21794
The NASA SBIR product catalog
[NASA-TM-108242] p 945 A93-29322
NASA SBIR abstracts of 1991 phase 1 projects
[NASA-TM-108240] p 945 A93-29323
- GILMAN, RONALD L.**
Operational and research aspects of a radio-controlled model flight test program
[AIAA PAPER 93-0625] p 504 A93-24742
Operational and research aspects of a radio-controlled model flight test program
[NASA-TM-104266] p 339 A93-18616
- GILMORE, RANDY**
Ultrasonic polishing
p 750 A93-25580
- GILREATH, H. E.**
Numerical and experimental investigation of mixing enhancement in scramjets
[AIAA PAPER 92-5063] p 414 A93-22333
Enhanced fuel-air mixing in hypersonic engines
[ISABE 93-7115] p 1221 A93-54090
- GILYARD, GLENN B.**
Performance-seeking control - Program overview and future directions
[AIAA PAPER 93-3765] p 1102 A93-51360
Subsonic flight test evaluation of a propulsion system parameter estimation process for the F100 engine
[NASA-TM-4426] p 175 A93-13155
- GIMADIEV, A. G.**
Dynamic processes in the powerplants and power-generating equipment of flight vehicles
p 832 A93-39027
Correction of the frequency characteristic of the waveguide circuit of an acoustic-jet temperature transducer
p 832 A93-39036
A study of the effect of the working medium on the start-up characteristic of an aviation gas turbine engine
p 811 A93-39037
- GIMMESTAD, GARY G.**
An automated system for the measurement of slant visual range
p 413 A93-22176
- GINEVSKII, A. S.**
Control of coherent structures and aero-acoustic characteristics of subsonic and supersonic turbulent jets
p 448 A93-19196
- GINEVSKIY, A. S.**
An acoustic suppressor for the jet noise of a turbojet engine
p 1003 A93-47510
- GINTY, CAROL A.**
Overview of NASA's advanced high temperature engine materials technology program
p 1212 A93-53453
- GIORDANO, G.**
Preliminary results of the ISM campaign - The Landes, South West France
p 1161 A93-47553
- GIORI, KATHY L.**
Comparison of the electrical charging and discharging environments of multiple aircraft-borne electric-field measurement systems
p 704 A93-24887
- GIOVANGIGLI, VINCENT**
Numerical solution of a free-boundary problem in hypersonic flow theory - Nonequilibrium viscous shock layers
p 8 A93-11920
An existence theorem for a free boundary problem of hypersonic flow theory
p 857 A93-40405
- GIPPET, J.-M.**
Design of an advanced nacelle for a very high bypass ratio engine
p 505 A93-25562
- GIRARD, A.**
Infrared thermography for hot-shot wind tunnel
[ONERA, TP NO. 1992-103] p 831 A93-38583
- GIRARD, M.**
Digital image processing applied to heat transfer measurement in hypersonic wind tunnel
[ONERA, TP NO. 1992-118] p 831 A93-38593
- GIRARD, R.**
GARTEUR damage mechanics for composite materials: Analytical/experimental research on delaminations
p 537 A93-21513
- GIRGIS, S.**
Effect of nozzle design on the performance of a highly loaded turbine stage
[ISABE 93-7096] p 1203 A93-54072
- GIRKE, M.**
Numerical simulation of a two-dimensional supersonic mixed-compression inlet
[ISABE 93-7107] p 1188 A93-54083
- GIRODROUX-LAVIGNE, P.**
Calculation of fully three-dimensional separated flow with an unsteady viscous-inviscid interaction method
p 786 A93-27455

GIROTTI, JAY R.

Evolutionary NASA - Inventors to bureaucrats
p 1174 A93-50330

GIRTS, R. D.

MD-11 Automatic Flight System p 818 A93-37075

GIRY, PIERRE

Helicopter accidents over water in the national navy:
Epidemiological study over the period 1980-1991
p 493 N93-19686

GISLASON, JASON

Design of the advanced regional aircraft, the DART-75
[NASA-CR-192044] p 333 N93-17972

GISQUET, D.

Detailed analysis of wing-nacelle interaction for
commercial transport aircraft p 213 N93-13203

GITTNER, N. M.

Experimental investigation of the effects of aft blowing
with various nozzle exit geometries on a 3.0 caliber tangent
ogive at high angles of attack: Forebody pressure
distributions
[NASA-CR-190935] p 22 N93-11605

GITTNER, NATHAN M.

An investigation of the effects of aft blowing on a 3.0
caliber tangent ogive body at high angles of attack
[NASA-CR-190934] p 24 N93-12004

GIUSTINIANI, P.

Improvements in code validation algorithms for
secondary surveillance radar p 883 A93-43408

GJESTLAND, T.

Final results from a study of community response to
aircraft noise around Oslo Airport Fornebu
p 425 A93-19192

GJESTLAND, TRULS

Influence of aircraft noise on speech intelligibility
p 558 A93-28483
Preliminary results from a study of community response
to noise from military aircraft exercise
p 558 A93-28484

Final results from a study of community response to
aircraft noise around Oslo Airport Fornebu
p 558 A93-28486

GLADDEN, HERBERT J.

Design of a high-temperature experiment for evaluating
advanced structural materials
[NASA-TM-105833] p 88 N93-11624
Hypersonic engine component experiments in high heat
flux, supersonic flow environment
[NASA-TM-106273] p 1032 N93-31860

GLAESER, BERNHARD

Combustor development for advanced helicopter
engines p 1246 A93-54841

GLASHEEN, W. M.

Electro-optic architecture for servicing sensors and
actuators in advanced aircraft propulsion systems
[NASA-CR-182269] p 232 N93-13762

GLASS, DAVID E.

Thermostructural applications of heat pipes for cooling
leading edges of high-speed aerospace vehicles
p 91 N93-12460

GLASS, J. M.

Reliability considerations for weather hazard warning
radar p 431 A93-22187

GLASSER, SIDNEY P.

Aircraft cryogenic fuel system design issues
[AIAA PAPER 93-2567] p 1121 A93-50285

GLASSMAN, ARTHUR J.

Estimating turbine limit load
[NASA-CR-191105] p 699 N93-25883

GLAZNEV, V. N.

Self-excited oscillations at supersonic off-design jet
outflow p 6 A93-10402
Effect of the size of a plane obstacle on self-oscillations
generated in an underexpanded supersonic jet
p 1068 A93-48849

GLEESON, RONALD F.

A primer on polynomial resultants
[AD-A246883] p 98 N93-11463

GLESNER, M.

An approach to the stall monitoring in a single stage
axial compressor
[AIAA PAPER 93-1872] p 1112 A93-49747

GLEZER, A.

Observations of large-scale structures in wakes behind
axisymmetric bodies p 965 A93-46748

GLICKSTEIN, IRA

Database management for integrated avionics system
p 939 A93-42831

GLIKMAN, B. F.

Dynamic processes in the powerplants and
power-generating equipment of flight vehicles
p 832 A93-39027

GLINKSY, NATHALIE

A Blottner type numerical model for nonequilibrium
viscous hypersonic flows in upwind finite elements
[INRIA-RR-1476] p 297 N93-18648

GLIZER, V. Y.

Application of the receding horizon strategy to singularly
perturbed pursuit-evasion problems p 369 A93-22980

GLOCKER, B.

Non-equilibrium flow in an arc heated wind tunnel
p 910 A93-42642

GLOECKLER, FRED

Proposed revisions to RTCM SC-104 recommended
standards for differential NAVSTAR/GPS service for
carrier phase applications
[AD-A255276] p 152 N93-15005

GLOMB, W. L., JR.

Electro-optic architecture (EOA) for sensors and
actuators in aircraft propulsion systems
[NASA-CR-182270] p 233 N93-15116

GLOVER, KEITH

The application of scheduled H-infinity controllers to a
VSTOL aircraft p 1135 A93-52249

GLOWINSKI, ROLAND

Hypersonic flows for reentry problems. Vols. 1 & 2
[ISBN 0-387-54428-3] p 864 A93-42576

GLUKHOVSKII, G. I.

A fuel-oil matrix heat exchanger p 833 A93-39052

GLYNN, MICHAEL S.

Lightning data acquisition p 753 N93-24883

GNEDENKO, V. V.

Some recommendations concerning the prevention of
fuel boiling in the igniters of the combustion chambers of
gas turbine engines p 812 A93-39200

GNEMMI, P.

Experimental investigation of a 2D parallel vortex/airfoil
interaction p 538 A93-23808

GNOFFO, PETER A.

Application of program LAURA to thermochemical
nonequilibrium flow through a nozzle
p 871 A93-42644

Solution strategy for three-dimensional configurations
at hypersonic speeds p 962 A93-46406

Navier-Stokes simulations of the Shuttle Orbiter
aerodynamic characteristics with emphasis on pitch trim
and bodyflap
[AIAA PAPER 93-2814] p 965 A93-46552
Upwind-biased, point-implicit relaxation strategies for
hypersonic flowfield simulations on supercomputers
p 1175 A93-52770

GOBIN, V.

Validation of electromagnetic-topology concepts on a
complex structure
[ONERA, TP NO. 1992-63] p 542 A93-25327

GODARD, J. L.

Detailed analysis of wing-nacelle interaction for
commercial transport aircraft p 213 N93-13203

GODDARD, J. W. F.

Hydrometeor identification using cross polar radar
measurements and aircraft verification
p 844 A93-37719

GODEFROY, J. C.

High temperature thin film strain gauges
[ONERA, TP NO. 1992-171] p 542 A93-25346
Thin gradient heat fluxmeters developed at ONERA
[ONERA, TP NO. 1992-87] p 831 A93-38571

GODIL, A.

Design of a wing shape for study of hypersonic crossflow
transition in flight p 265 A93-20713

GOEHLER, DAVID J.

Jeppesen worldwide electronic NOTAM service
p 1 A93-11020

GOEING, M.

Optimization aspects of an ejector type hypersonic thrust
nozzle
[ASME PAPER 92-GT-402] p 355 A93-19551

GOELZ, T.

Non-equilibrium flow in an arc heated wind tunnel
p 910 A93-42642

GOELZENLEUCHTER, HORST

Test and integration concept for complex helicopter
avionic systems
[MBB-UD-0605-91-PUB] p 343 N93-17547

GOEPEL, CHRISTIAN

The influence of the rotor test facilities ROTEST and
ROTOS on the rotor inflow
[DLR-MITT-91-16] p 522 N93-21173

GOGEL, T.

Non-equilibrium flow in an arc heated wind tunnel
p 910 A93-42642

GOGOLIN, V. P.

Estimation of the effect of the longitudinal moment due
to the engine thrust on the mass of a subsonic passenger
aircraft p 1191 A93-52954

GOH, JEFFREY

Air transport and the environment - Regulating aircraft
noise p 1226 A93-52931

GOKCEN, TAHIR

Computation of nonequilibrium radiating shock layers
[AIAA PAPER 93-0144] p 414 A93-22588

Computation of thermochemical nonequilibrium flows
around a simple and a double ellipse p 869 A93-42629

GOKHALE, S. S.

Turbine blade cascade flows p 10 A93-12361

GOLDBERG, URIEL C.

A pointwise version of the Baldwin-Barth turbulence
model
[AIAA PAPER 93-3523] p 985 A93-47284

GOLDEN, W. L., JR.

Simulation of shock-boundary layer interaction in a fan
blade passage
[AIAA PAPER 93-1980] p 1078 A93-49827

GOLDEN, WILLIAM L., JR.

Static pressure measurements of the shock-boundary
layer interaction in a simulated fan passage
[AD-A256724] p 361 N93-15979

GOLDIEZ, BRIAN

Representation of vehicle location in networked
simulations
[AIAA PAPER 93-3582] p 1214 A93-52677

GOLDIEZ, BRIAN F.

Networks extend simulation's reach
p 1225 A93-53770

GOLDIN, DANIEL S.

It's time to go supersonic p 949 A93-44099

GOLDMAN, CLAUDIO

Analysis of thrust modulation of ram-rockets by a vortex
valve p 814 N93-27187

GOLDMAN, Y.

Boron particle ignition in high-speed flow
[AIAA PAPER 93-2202] p 1145 A93-50014

Study of a pulse ramjet based on twin valveless
combustors coupled to operate in antiphase
[ISABE 93-7038] p 1197 A93-54014

Development of a pulse ramjet based on twin valveless
pulse combustors coupled to operate in antiphase
p 814 N93-27186

GOLDSMITH, E. L.

Some aspects of intake design, performance and
integration with the airframe p 161 N93-13219
Comparative performance tests of a pilot-inlet in several
European wind-tunnels at subsonic and supersonic
speeds p 130 N93-13221

GOLDSMITH, PAUL F.

Coherent systems in the terahertz frequency range:
Elements, operation, and examples p 841 N93-27727

GOLDSTEIN, R. J.

Vortex structure and mass transfer near the base of a
cylinder and a turbine blade p 901 N93-29929

GOLINVAL, J. C.

Vibration analysis in turbomachines
p 1005 N93-32274

GOLLAHALLI, S. R.

Combustion of microemulsion sprays
[AIAA PAPER 93-0131] p 390 A93-22578

GOLOVACHEV, I. U. P.

Unsteady supersonic flow around a blunt body in thermal
inhomogeneities in turbulent shock layer flows
p 691 A93-35266

GOLOVIN, A. N.

Computational models of dampers for computer-aided
design p 832 A93-39032

GOLUB, ROBERT A.

Tiltrotor ground noise reduction from rotor parametric
changes as predicted by ROTONET p 567 A93-29415

ADDRAS - An integrated systems approach
p 562 A93-29423

GOLUBEV, V. A.

An experimental study of thrust reverser models
p 812 A93-39195

GOLUBKIN, V. N.

Shock wave interference on a wing with a partition at
hypersonic velocities p 13 A93-12839

Increasing the lift-drag ratio of wings of small aspect
ratio at hypersonic velocities p 13 A93-12933

Three-dimensional hypersonic flow of a gas past
wings p 1069 A93-48971

Optimal wing shapes in a hypersonic nonequilibrium
flow p 1088 A93-51770

Hypersonic flow of a gas past wing with heat transfer
p 1234 A93-55030

GOMA, WILLY S.

Seasonal weather hazards p 431 A93-22180

GOMES, WENDY M.

Waterborne polyurethane binder resins for compliant
aircraft coatings
[AD-A256246] p 199 N93-14573

GONCHARENKO, V. P.

Using current numerical methods in a mathematical
model of flight vehicle synthesis p 804 A93-39188

GONDOT, PASCAL

Numerical modelling of induced effects of lightning strike
on an all composite helicopter p 703 N93-24879

- GONG, BENQUAN**
An experimental investigation on the combustor with bypass flow in integral liquid fuel ramjet p 174 A93-16235
- GONG, YAO-NAN**
New model of bird impact response analysis and its engineering solution p 156 A93-14336
- GONG, YAONAN**
Development of computational solid mechanics and its application in aerospace engineering p 1255 A93-54419
- GONSALEZ, J. C.**
Correlation of interaction sweepback effects on unsteady shock-induced turbulent separation [AIAA PAPER 93-0776] p 475 A93-25550
- GONSALVES, PAUL G.**
Design for tactical situation awareness display [AD-A256194] p 170 N93-15235
- GONTHIER, KEITH A.**
Reaction zone structure for strong, weak overdriven, and weak underdriven oblique detonations p 746 A93-35492
- GONZALEZ, HUGO A.**
An experimental study of droop leading edge modifications on high and low aspect ratio wings up to 50 deg angle of attack [AIAA PAPER 93-3496] p 983 A93-47268
- GONZALEZ, M. A.**
Prandtl theory applied to paraglider aerodynamics [AIAA PAPER 93-1220] p 690 A93-35169
- GONZALEZ, OSCAR R.**
Design and implementation of fuzzy logic controllers [NASA-CR-193268] p 1038 N93-31649
- GONZALEZ, VICTOR H.**
Results from a VHF impulse synthetic-aperture radar p 501 A93-28219
- GOODLING, J. S.**
Effective sealing of a disk cavity using a double-toothed rim seal [ASME PAPER 92-GT-379] p 406 A93-19537
- GOODMAN, MARK P.**
Three-dimensional water droplet trajectory code validation using an ECS inlet geometry [NASA-CR-191097] p 791 N93-27267
- GOODRICH, D.**
PBM observations of surface soil moisture in Monsoon 90 p 1162 A93-47676
- GOODRICH, J. A.**
Onboard System Evaluation of Rotors Vibration, Engines (OBSERVE) monitoring system [AD-A255366] p 165 N93-15227
- GOODRICH, KENNETH H.**
A high-fidelity, six-degree-of-freedom batch simulation environment for tactical guidance research and evaluation [NASA-TM-4440] p 1010 N93-32380
- GOODRICH, MICHAEL S.**
Ground clutter measurements using the NASA airborne doppler radar: Description of clutter at the Denver and Philadelphia airports p 490 N93-19608
- GOODSON, TROY D.**
Computation of optimal low- and medium-thrust orbit transfers [AIAA PAPER 93-3855] p 1144 A93-51442
- GOODY, A. J.**
Integrating the maintenance requirement maintenance ground based data systems - The missing link? p 238 A93-18760
- GOODYER, M. J.**
The cryogenic wind tunnel p 1013 A93-46915
- GOORJIAN, P. M.**
Algorithm development with applications to aerodynamics and aeroelasticity p 422 N93-18566
- GOPALRATNAM, GIRIJA**
Estimation of neutral and maneuver points of aircraft by dynamic maneuvers [AIAA PAPER 93-3620] p 1126 A93-48307
- GOPALSWAMY, SWAMINATHAN**
Control of a high performance aircraft with unacceptable zero dynamics p 369 A93-22905
- GOPALSWAMY, SWAMINATHAN**
Adaptive control of nonlinear nonminimum phase systems p 229 N93-14470
- GOPAL, NIGEL K. J. M.**
Measurement and analysis of nitric oxide radiation in an arc-jet flow [AIAA PAPER 93-2800] p 1016 A93-46540
- GORANSON, ULF G.**
Aging jet transport structural evaluation programs p 947 A93-45781
- GORBACHEVSKI, S. K.**
Adaptive filtering of Doppler velocimeter errors due to the characteristics of the reflecting surface p 992 A93-45650
- GORDER, P. J.**
Quantitative feedback theory applied to the design of a rotorcraft flight control system p 906 A93-41895
- GORDIENKO, V. M.**
Detection and parameter estimation of atmospheric turbulence by ground-based and airborne CO2 Doppler lidars p 395 A93-17862
- GORDIENKO, V. M.**
Study of artificial and natural turbulence in atmospheric boundary layer with a CW Doppler CO2 lidar p 1257 A93-54799
- GORDIS, JOSHUA H.**
A frequency domain theory for structural identification p 930 A93-43778
- GORDNER, RAYMOND E.**
Numerical simulation of delta-wing roll [AIAA PAPER 93-0554] p 285 A93-23293
- GORDNER, RAYMOND E.**
Computation of delta-wing roll maneuvers [AIAA PAPER 93-2975] p 1050 A93-48169
- GORDNER, RAYMOND E.**
Computation of a delta-wing roll-and-hold maneuver [AD-A264704] p 909 N93-30498
- GORDON, LEONARD B.**
An analysis of the correlation between the J52 engine component improvement program and improved maintenance parameters [AD-A262062] p 816 N93-28984
- GORDON, NEIL**
The role of national meteorological services in aviation servicing under the final phase of the World Area Forecast System p 431 A93-22162
- GORDON, SANFORD**
Computer program for calculating and fitting thermodynamic functions [NASA-RP-1271] p 231 N93-12967
- GORELOV, D. N.**
Integral equations in the problem of flow past an airfoil p 395 A93-18243
- GORELOV, S. L.**
Development and application of the Monte Carlo method for solving the Boltzmann equation and its models p 1173 A93-51867
- GORENBUKH, P. I.**
Approximate calculation of the aerodynamic characteristics of simple bodies in hypersonic rarefied-gas flow p 1090 A93-51869
- GORENBUKH, P. I.**
Effect of Reynolds number on the aerodynamic characteristics of a semicone with a wing in the case of hypersonic flow velocities p 1090 A93-51878
- GORLEY, T. A. E.**
The technical background to standards for shackles [NPL-DMM(A)-51] p 86 N93-11325
- GORLEY, T. A. E.**
A study of the effects of tolerances on rigging screws, turnbuckles, and associated components in BS4429: 1987 [NPL-DMM(A)-53] p 86 N93-11326
- GORLEY, T. A. E.**
The technical background to standards for eyebolts [NPL-DMM(A)-52] p 87 N93-11327
- GOROSH, A. K.**
A comparison of wind speed measured by the Special Sensor Microwave Imager (SSM/I) and the Geosat altimeter p 1033 A93-44862
- GORRELL, S. E.**
Application of a dynamic compression system model to a low aspect ratio fan - Casing treatment and distortion [AIAA PAPER 93-1871] p 1111 A93-49746
- GORSHKOV, V. A.**
Helicopters - Handbook [ISBN 5-203-00804-3] p 458 A93-28874
- GORSKI, JAN**
Thermodynamic aspects of model testing in cryogenic wind tunnels p 1251 A93-56222
- GOSHEN-MESKIN, DRORA**
Observability analysis of piece-wise constant systems. I - Theory p 501 A93-29599
- GOSIEWSKI, Z.**
Vibration control algorithms for flexible rotors p 95 A93-10741
- GOSLIN, JOSEPH J.**
Runway Visual Range (RVR) Operational Test and Evaluation (OT&E) integration and OT&E operational test report [DOT/FAA/CT-TN92/37] p 706 N93-25243
- GOSS, L. P.**
Experimental and numerical investigations of the vortex-flame interactions in a driven jet diffusion flame [AIAA PAPER 93-0455] p 534 A93-25532
- GOSSWEILER, C.**
Development of a system for aerodynamic fast-response probe measurements p 203 A93-14325
- GOSWAMI, T.**
Life prediction - Thermal fatigue from isothermal data p 916 A93-40807
- GOSWAMI, TARUN**
Life analysis of a gas turbine fan disc p 897 A93-40803
- GOTO, MITSUSHIGE**
Performance improvement by forward-skewed blading of axial fan moving blades [ISABE 93-7055] p 1185 A93-54031
- GOTO, NOBORU**
Combustion performance of a hydrogen-fueled small combustor for a micro gas turbine p 389 A93-21731
- GOTO, NORIHIRO**
Pilots' control behavior including feedback structures identified by an improved method [AIAA PAPER 93-3669] p 1129 A93-48347
- GOTTLIEB, J. J.**
Experimental study of shock wave and hypersonic boundary layer interactions near a convex corner [AIAA PAPER 93-2980] p 1051 A93-48173
- GOTTSCHECH, JOSEPH M.**
Heat pipe turbine vane cooling p 519 A93-26114
- GOTTUK, DANIEL T.**
Generation of carbon monoxide in compartment fires [PB93-146702] p 880 N93-29211
- GOUCK, ROBERT F.**
The criticalness of spares effectivity checks for aircraft configuration control p 763 A93-35923
- GOUGHIN, PATRICK**
AIAA's role in aerospace education [AIAA PAPER 93-0324] p 454 A93-23016
- GOULD, DANA C.**
Analytical comparison of convective heat transfer correlations in supercritical hydrogen p 416 A93-23477
- GOULD, J.**
Theoretical modelling of rotor noise radiation p 566 A93-29407
- GOULD, RICHARD D.**
Turbulence characteristics of an axisymmetric reacting flow [NASA-CR-4110] p 877 N93-30373
- GOULETTE, M.**
Advanced materials in gas turbine engines: An assessment [PNR-90946] p 58 N93-11105
- GOUNET, H.**
Experimental study of the acoustic spinning modes generated by a helicopter turboshaft engine [ONERA, TP NO. 1992-141] p 230 A93-14266
- GOUTERMAN, MARTIN**
Video luminescent barometry - The induction period [AIAA PAPER 93-0179] p 414 A93-22607
- GOVARDHAN, M.**
Effect of radial distortion on the performance of a centrifugal compressor p 861 A93-42256
- GOVARDHAN, M.**
Tip clearance effects on the flow field of an axial turbine rotor blade cascade [ISABE 93-7057] p 1185 A93-54033
- GOYAL, R. K.**
A comparison of the measured and predicted flowfield in a modern fan-bypass configuration [ASME PAPER 92-GT-298] p 254 A93-19488
- GOZANI, TSAHI**
Principles of nuclear-based explosive detection systems p 497 N93-21861
- GOZANI, TSAHI**
PFNA technique for the detection of explosives p 497 N93-21865
- GOZANI, TSAHI**
Explosive detection system based on Electronic Neutron Generator (ENG) p 497 N93-21870
- GRABOWSKI, L.**
Short fatigue crack growth in a nickel-base superalloy at room and elevated temperature [PNR-90892] p 72 N93-11031
- GRACEY, C.**
Analysis of a turning point problem in flight trajectory optimization p 1210 A93-52885
- GRACHEV, L. P.**
An experimental study of dc discharges in supersonic and subsonic air flows p 14 A93-12980
- GRADY, DANIEL F.**
A data acquisition system for high-speed rotor balancing p 1261 A93-54396
- GRAESSER, DOUGLAS**
Multi-parameter optimization tool for low-cost commercial fuselage crown designs p 922 N93-30858
- GRAFFMAN, I.**
Pilot weather advisor [NASA-CR-189723] p 318 N93-16692
- GRAHAM, DANIEL O.**
Space policy 2000 p 1174 A93-50333
- GRAHAM, H. C.**
Ultrahigh temperature assessment study: Ceramic matrix composites [AD-A262740] p 826 N93-28592
- GRAHAM, R. L.**
A performance assessment of a byzantine resilient fault-tolerant computer [AIAA PAPER 89-3064] p 938 A93-41296
- GRAHAM, W. R.**
Boundary-layer induced noise in aircraft p 444 A93-19137
- GRAINGER, CEDRIC A.**
A comparison of several airborne measures of turbulence p 308 A93-22121

GRAMZOW, RICHARD H.

GRAMZOW, RICHARD H.

The redesigned Low Level Wind Shear Alert System
p 431 A93-22179

GRAN, RICHARD J.

The benefits of Maglev technology
[AIAA PAPER 93-2949] p 1174 A93-48145

GRANDA, THOMAS M.

The development of an Altitude Awareness Program -
An integrated approach p 486 A93-27136

GRANDAGE, J. M.

Structural fatigue aspects of the P-3 Orion
[ARL-STRUC-TM-558] p 161 N93-13256

GRANDE, DODD H.

Effects of intra- and inter-laminar resin content on the
mechanical properties of toughened composite materials
p 921 N93-30845

GRANDHI, R. V.

Structural optimization with frequency constraints - A
review p 408 A93-20293

[AIAA PAPER 92-4813] p 408 A93-20293
Takeoff and landing analysis methodology for an
airbreathing space booster p 914 A93-42927

GRANDLE, ROBERT E.

ADDRAS - An integrated systems approach
p 562 A93-29423

GRANGER, ROBERT A.

The unified method of aeroelasticity
p 372 N93-18143

GRANOIEN, I.

Final results from a study of community response to
aircraft noise around Oslo Airport Fornebu
p 425 A93-19192

GRANOIEN, IDAR

Preliminary results from a study of community response
to noise from military aircraft exercise
p 558 A93-28484

GRANOIEN, IDAR L. N.

Comparison of airport noise calculation models
p 564 A93-28480

Influence of aircraft noise on speech intelligibility
p 558 A93-28483

Final results from a study of community response to
aircraft noise around Oslo Airport Fornebu
p 558 A93-28486

GRANT, CARROLL G.

Advanced fiber placement of composite fuselage
structures p 923 N93-30864

GRANT, I.

Measurement of shed vorticity and circulation from
rotating aerofoil by particle image velocimetry
p 538 A93-23804

GRANTZ, A. C.

The effects of hypersonic flight test requirements on
research vehicle design
[AIAA PAPER 93-0511] p 386 A93-23258

A hypersonic waverider research vehicle
[AIAA PAPER 93-0402] p 505 A93-25522

GRAS'KIN, S. S.

Method and results of studies of flow past supersonic
flight vehicles at moderate and large angles of attack
p 242 A93-18377

Calculation of three-dimensional supersonic flow past
lifting surfaces p 477 A93-27607

GRASCHER, JEFFREY

Sea fog and stratus - A major aviation hazard in the
northern Gulf of Mexico p 429 A93-22141

Sea fog and stratus - A major aviation and marine hazard
in the northern Gulf of Mexico p 844 A93-39762

GRASLEY, STEVEN S.

RDR-4B doppler weather radar with forward looking wind
shear detection capability p 489 N93-19601

GRASS, ROLF-DIETER

Activities report of Lufthansa
[ETN-92-92100] p 28 N93-11319

GRASSO, F.

Numerical simulations of high speed inlet flows
p 115 A93-14246

Multigrid techniques for hypersonic viscous flows
[AIAA PAPER 93-0771] p 467 A93-24855

On high speed turbulence modeling of shock-wave
boundary-layer interaction p 541 A93-24860

[AIAA PAPER 93-0778] p 541 A93-24860

High-speed turbulence modeling of
shock-wave/boundary-layer interaction
p 927 A93-41910

Adaptive mesh embedding for reentry flow problems
p 869 A93-42619

Multigrid techniques for hypersonic viscous flows
p 1071 A93-49027

GRATTAN, K. T. V.

An optical fiber based position sensor with immunity to
temperature variation p 743 A93-34287

GRAU, J. Y.

Air accidents in the French Air Force
p 492 N93-19676

GRAUER-CARSTENSEN, H.

Time-dependent 3-component
laser-Doppler-anemometer and simultaneous position
measurements in the flow of an aircraft engine
p 538 A93-23809

GRAVELLE, ALAIN

Modal identification of aircraft structures - ONERA
methods p 802 A93-38570

[ONERA, TP NO. 1992-86]

GRAVES, SHARON

Development of a system for transition
characterization p 1030 A93-47246

[AIAA PAPER 93-3465]

GRAY, CARL E., JR.

Large-amplitude finite element flutter analysis of
composite panels in hypersonic flow p 837 A93-39417

Vector unsymmetric eigenequation solver for nonlinear
flutter analysis on high-performance computers
p 1160 A93-52449

A finite element method for nonlinear panel flutter
p 84 N93-10472

GRAY, HUGH R.

Overview of NASA's advanced high temperature engine
materials technology program p 1212 A93-53453

GRAY, R. E.

A simplified representation of the off-design
characteristics of high speed, high pressure ratio axial
turbomachinery stages p 1081 A93-50055

[AIAA PAPER 93-2257]

GRAY, RON

A statistical comparison of differential GPS and laser
generated time, space positioning information for aircraft
flight testing p 316 A93-21199

GREBENKIN, ALEKSANDR V.

Aerodynamic questions related to the safety and
cost-effective utilization of airships p 818 A93-39125

GREBER, ISAAC

Numerical simulation of a shock wave/turbulent
boundary layer interaction in a duct p 1063 A93-48293

[AIAA PAPER 93-3127]

GREBESHOV, EH. P.

Unsteady aerodynamic characteristics of three
rectangular wings of different aspect ratios p 1180 A93-53575

[AD-A247258]

GREEN, DAVID

Determining the transferability of flight simulator data
p 913 N93-30685

GREEN, J. E.

The use of a deep honeycomb to achieve high flow
quality in the ARA 9 ft x 8 ft Transonic Wind Tunnel
p 190 A93-14276

GREEN, MICHAEL J.

Application of CFD to a generic hypersonic flight
research study p 280 A93-23007

[AIAA PAPER 93-0312]

GREEN, R. B.

The effect of wind tunnel constraint on unsteady
aerodynamics experiments p 190 A93-14300

The convection speed of the dynamic stall vortex
[AD-A247258] p 21 N93-11464

GREEN, ROBERT S.

Total Quality Management in curriculum development
[AIAA PAPER 93-0326] p 454 A93-23018

GREEN, S. T.

Applications of advanced fracture mechanics to
fuselage p 1026 A93-45787

GREEN, STEVEN M.

Piloted simulation of an air-ground profile negotiation
process in a time-based Air Traffic Control environment
[NASA-TM-107748] p 707 N93-26087

GREEN, T.

Ingestion into the upstream wheel-space of an axial
turbine stage p 354 A93-19493

[ASME PAPER 92-GT-303]

GREENBLAT, DAVID

Life cycle assessment of an impingement-cooled gas
turbine blade p 358 A93-20321

[AIAA PAPER 92-4716]

GREENBLATT, DAVID

Thermal fatigue life assessment of a convection-cooled
gas turbine blade p 1199 A93-54038

[ISABE 93-7062]

GREENDYKE, ROBERT B.

A convective and radiative heat transfer analysis for the
FIRE II forebody p 1021 A93-44231

[AIAA PAPER 93-3194] p 1021 A93-44231

Finite-difference solution for laminar or turbulent
boundary layer flow over axisymmetric bodies with ideal
gas, CF₄, or equilibrium air chemistry p 222 N93-15434

[NASA-TP-3271]

GREENE, FRANCIS A.

Viscous equilibrium computations using program
LAURA p 8 A93-12002

[NASA-TP-3271]

PERSONAL AUTHOR INDEX

Application of the multigrid solution technique to
hypersonic entry vehicles p 858 A93-41049

[AIAA PAPER 93-2721] p 858 A93-41049

An approximate method for calculating heating rates on
three-dimensional vehicles p 949 A93-44228

[AIAA PAPER 93-2881] p 949 A93-44228

Navier-Stokes simulations of the Shuttle Orbiter
aerodynamic characteristics with emphasis on pitch trim
and bodyflap p 965 A93-46552

[AIAA PAPER 93-2814] p 965 A93-46552

HL-20 computational fluid dynamics analysis
p 1181 A93-53740

GREENE, TIMOTHY L.

The characterization and development of materials for
advanced textile composites p 1211 A93-53434

GREENHALGH, SAMUEL

Lift enhancement due to unsteady aerodynamics
[AIAA PAPER 93-3538] p 986 A93-47289

GREENHORNE, D.

Reliability testing of the EH101 p 45 A93-13406

GREENSPAN, RICHARD L.

The effects of ionospheric errors on single-frequency
GPS users p 313 A93-21141

GREENWELL, D. I.

Static roll moment characteristics of asymmetric
tangential leading edge blowing on a delta wing at high
angles of attack p 261 A93-20165

[AIAA PAPER 93-0052]

GREENWELL, DOUGLAS I.

A vortex control technique for the attenuation of fin
buffet p 121 A93-14408

Determination of vortex burst location on delta wings
from surface pressure measurements p 123 A93-14557

GREFF, E.

Integration of high bypass ratio engines on modern
transonic wings for regional aircraft p 506 A93-27479

GREGOREK, G. M.

Comparative wind tunnel tests at high Reynolds numbers
of NACA 64 621 airfoils with two aileron configurations
p 967 A93-48823

GREGORY-SMITH, D. G.

Turbulence evaluation within the secondary flow region
of a turbine cascade p 247 A93-19310

[ASME PAPER 92-GT-60]

A simple method for estimating secondary losses in
turbines at the preliminary design stage p 254 A93-19484

[ASME PAPER 92-GT-294]

GREGORY, B. A.

Recent advances in simulating unsteady flow
phenomena brought about by passage of shock waves
in a linear turbine cascade p 245 A93-19277

[ASME PAPER 92-GT-4]

A statistical approach to the experimental evaluation
of transonic turbine airfoils in a linear cascade
p 245 A93-19278

[ASME PAPER 92-GT-5]

GREGORY, DON A.

Optical correlator field test results
p 1038 A93-44458

GREGORY, PEYTON B.

Transient/structural analysis of a combustor under
explosive loads p 420 N93-17779

[NASA-TM-107660]

GREIDANUS, H.

ERS-1 directional wave spectra validation with the
airborne SAR PHARS p 937 N93-31010

[BCRS-92-18]

GREISZ, GLEN F.

Fuzzy logic control algorithm for suppressing E-6A Long
Trailing Wire Antenna wind shear induced oscillations
[AIAA PAPER 93-3868] p 1171 A93-51454

GREITZER, E. M.

Evaluation of approaches to active compressor surge
stabilization p 352 A93-19407

[ASME PAPER 92-GT-182]

Numerical simulation of compressor endwall and casing
treatment flow phenomena p 255 A93-19490

[ASME PAPER 92-GT-300]

Reform of the aeronautics and astronautics curriculum
at MIT p 454 A93-23017

[AIAA PAPER 93-0325]

GREITZER, EDWARD M.

Active stabilization to prevent surge in centrifugal
compression systems p 424 N93-18862

[NASA-CR-191625]

Active stabilization of aeromechanical systems
[AD-A261366] p 725 N93-26335

GREK, G. R.

Interaction of Tollmien-Schlichting waves with localized
disturbances p 545 A93-27637

A study of the effect of surface riblets on the evolution
of a solitary wave packet (lambda vortex) in a laminar
boundary layer p 1067 A93-48827

- GRENIER, T.**
Fiber reinforced composites: A new class of glass and glass ceramic materials for thermomechanical applications
[REPT-921-430-104] p 200 A93-15490
- GRENON, R.**
Transonic and supersonic flow calculations around aircraft using a multidomain Euler code
[ONERA, TP NO. 1992-137] p 772 A93-38610
- GRETH, RICKY L.**
Concept feasibility demonstration for the Army Cockpit Delethalization Program p 795 A93-35916
- GREVTSOV, N. M.**
Flight path optimization and suboptimal control laws synthesis for transport mission of maneuverable aircraft p 180 A93-14160
- GREY, JERRY**
Will aerospace plane development go international? p 1043 A93-49331
- GRIBBLE, JEREMY J.**
Linear quadratic Gaussian/loop transfer recovery design for a helicopter in low-speed flight p 906 A93-41896
- GRIEFAHN, BARBARA**
Effects on health of noise disturbances due to air traffic p 1035 A93-31929
- GRIFFIN, C. F.**
Design, analysis, and fabrication of the technology integration box beam p 919 A93-30433
- GRIFFIN, MICHAEL J.**
Incompressible flow computation of forces and moments on bodies of revolution at incidence
[AIAA PAPER 93-0787] p 541 A93-24867
- GRIFFIN, O. H., JR.**
An experimental and analytical investigation on the response of GR/EP composite I-frames p 546 A93-27975
- GRIFFIN, O. HAYDEN, JR.**
Static and dynamic large deflection flexural response of graphite-epoxy beams
[NASA-CR-4118] p 934 A93-30374
- GRIFFIN, THOMAS A.**
Integrity testing of brush seal in shroud ring of T-700 engine
[NASA-TM-105863] p 421 A93-18380
- GRIFFITHS, H. D.**
Bistatic radar using satellite-borne illuminators of opportunity p 914 A93-43437
- GRIFFITHS, ROBERT C.**
Investigation of leading edge ice accretion with cyclical pneumatic boot inflation
[AIAA PAPER 93-0007] p 306 A93-20130
- GRIGOREV, V. M.**
Prediction of fatigue crack growth kinetics in the plane structural elements of aircraft in the biaxial stress state p 1025 A93-45670
- GRIGORIU, M. D.**
Representation and probability issues in the simulation of multi-site damage p 1026 A93-45785
- GRIGORIU, MITCH M.**
Expert systems for maintenance engineering p 434 A93-18762
- GRIMES, CRAIG A.**
A proposed multi-modal FM/CW aircraft radar for use during ground operations p 206 A93-14678
- GRIMES, DALE M.**
A proposed multi-modal FM/CW aircraft radar for use during ground operations p 206 A93-14678
- GRIMM, R.**
The influence of nocturnal aircraft noise on sleep and on catecholamine secretion p 1163 A93-49554
- GRINSTEIN, F. F.**
Compressibility, exothermicity, and three dimensionality in spatially evolving reactive shear flows p 950 A93-44375
- GRINSTEIN, FERNANDO F.**
Vorticity dynamics in spatially developing rectangular jets
[AIAA PAPER 93-3286] p 969 A93-46842
- GRISCH, F.**
CARS studies in hypersonic flows
[AIAA PAPER 93-3047] p 1144 A93-48227
- GRISHANINA, T. V.**
Optimization of an aeroelastic system using the dynamic stability condition p 1029 A93-47085
- GRISHIN, A. P.**
Problems in the optimization of complex engineering systems p 1165 A93-49307
- GRISMER, D. S.**
The aerodynamic effects of sideslip on double delta wings
[AIAA PAPER 93-0053] p 261 A93-20166
- GRITSAL, S. D.**
Selection of the scheme and optimal parameters of the turbine of a high-temperature bypass engine with a low bypass ratio p 811 A93-39180
- GRITSOV, N. N.**
An experimental study of dc discharges in supersonic and subsonic air flows p 14 A93-12980
- GROCCOTT, D. F. H.**
The 21st century navigation station p 34 A93-12123
- GRODSINSKY, CARLOS M.**
Vibration isolation technology: An executive summary of systems development and demonstration
[NASA-TM-105937] p 110 A93-15573
- GROENIG, H.**
Shock tube application - High enthalpy European wind tunnels p 1011 A93-45452
Experimental studies in the Aachen hypersonic shock tunnel p 1251 A93-56032
- GROEPLER, DAVID R.**
Tiltrotor Research Aircraft composite blade repairs - Lessons learned p 108 A93-14819
- GROKHOL'SKII, S. V.**
Analysis of the pump station of an aircraft hydraulic system as a subject of diagnosis p 321 A93-18374
- GROMASHEV, A. G.**
Mathematical statement of the problem of optimizing the design of an airframe for ease of manufacture p 745 A93-35286
- GROMELSKI, STAN**
Preliminary studies of planning and flight strip use as air traffic controller memory aids
[DOT/FAA/CT-TN92/22] p 503 A93-21759
- GROMOV, V. F.**
High-strength combination fasteners for joint assembly in aircraft structures p 745 A93-35283
Stress-strain state of the elements of a single-stringer riveted panel p 746 A93-35288
- GROEMMEYER, STEVEN A.**
Description and capabilities of the Navcore-V GPS receiver engine p 312 A93-21127
- GROPENGIESSER, F.**
Rarefied gas flow around a 3D-deltawing p 870 A93-42639
- GROSCHE, C. E.**
Induced Mach wave-flame interactions in laminar supersonic fuel jets p 475 A93-26183
- GROSS, KEITH**
Integrated Soviet VLF/Omega Receiver design p 316 A93-21198
- GROSSMAN, B.**
Aerodynamic optimization of an HSCT configuration using variable-complexity modeling
[AIAA PAPER 93-0101] p 322 A93-19806
Variable-complexity aerodynamic-structural design of a high-speed civil transport wing
[AIAA PAPER 92-4695] p 323 A93-20279
Integrated aerodynamic-structural-control wing design
[AIAA PAPER 92-4694] p 324 A93-20307
Structural non-linearity effects on flutter of a swept wing in transonic flows p 410 A93-20714
An upwind, kinetic flux-vector splitting method for flows in chemical and thermal non-equilibrium
[AIAA PAPER 93-0894] p 472 A93-24954
A multi-dimensional kinetic-based upwind solver for the Euler equations
[AIAA PAPER 93-3303] p 950 A93-45001
Surface boundary conditions for the numerical solution of the Euler equations
[AIAA PAPER 93-3334] p 953 A93-45028
- GROSSMAN, BERNARD**
Adjoint methods for aerodynamic wing design
[NASA-CR-193086] p 805 A93-27089
- GROSSMANN, W.**
A propulsion device driven by reflected shock waves p 1001 A93-45550
- GROSSMANN, WILLIAM**
Pulsed detonation engine experimental and theoretical review
[AIAA PAPER 92-3168] p 531 A93-24478
- GRUBIN, S. E.**
The asymptotic theory of hypersonic boundary-layer stability p 462 A93-24409
The long-wave limit in the asymptotic theory of hypersonic boundary-layer stability p 462 A93-24410
- GRUNDMANN, R.**
Introduction to the physical aspects of hypersonic aerodynamics p 1072 A93-49522
Vibration excitation in laminar hypersonic boundary layers p 1237 A93-56028
- GRUNWALD, ARTHUR J.**
Visual field information in Nap-of-the-Earth flight by teleoperated Helmet-Mounted displays p 517 A93-26884
- GSCHWENDER, LOIS**
Development of MIL-H-53119, -54 C to 175 C high-temperature nonflammable hydraulic fluid for Air Force systems p 1214 A93-54250
- GU, ALSTON**
Liquid hydrogen foil-bearing turbopump
[AIAA PAPER 93-2537] p 1156 A93-50264
- GU, C. W.**
Three-dimensional flow calculations in turbomachinery using the stream function formulation p 11 A93-12453
A three-dimensional numerical method for turbomachinery blading
[ASME PAPER 92-GT-291] p 254 A93-19482
- GU, CHANGYAO**
Designing to aircraft system effectiveness/cost/time with VERT - The system analysis method for aircraft p 153 A93-14204
- GU, JIALIU**
Vibration characteristics of mistuned bladed disk p 1108 A93-49190
- GU, JIALU**
A transfer matrix method for calculation of support stiffness of aeroengine stator p 1122 A93-51193
- GU, W.**
Control of vortices on a delta wing by leading-edge injection p 860 A93-41906
- GU, WEIZAO**
Heat transfer in a five-pass irregular channel with and without pin-fins p 1256 A93-54633
- GU, ZHEN**
Identification of the open loop dynamics of the T700 turboshaft engine p 809 A93-35934
- GU, ZHIFU**
Pressure fluctuations on the surface of two circular cylinders in tandem arrangements at high Reynolds numbers p 679 A93-33718
- GUAN, JIAN-CHENG**
A study on the marginal analysis method for the airline yield management p 487 A93-27370
- GUAN, SHIYI**
Accuracy analysis on image matching guidance systems p 62 A93-12653
- GUAN, YUPING**
A new approach to robust fault detection and identification p 1166 A93-50631
- GUARINO, C. R.**
Robust method for estimating the parameters of a linear FM waveform p 1147 A93-47650
- GUARINO, L.**
Reacting gas and surface coupling in high temperature air flows p 686 A93-34353
- GUEDOU, J.-Y.**
Fatigue of turboengine discs
[DS-2136] p 364 A93-18149
- GUENETTE, G. R.**
Flow control of low heat load turbine airfoils
[AD-A260941] p 724 A93-26219
The influence of non-uniform spanwise inlet temperature on turbine rotor heat transfer p 901 A93-29932
- GUENTHER, B.**
Calibration results for NOAA-11 AVHRR channels 1 and 2 from congruent path aircraft observations p 1143 A93-51237
- GUENTHER, G.**
Allowable compression strength for CFRP-components of fighter aircraft determined by CAI-test p 537 A93-21531
- GUENTHER, GEORG**
Allowable compression strength for CFRP-components of fighter aircraft determined by CAI-test
[MBB-FE-221-S-PUB-0483] p 537 A93-21462
- GUERRERO, LOURDES M.**
Initial piloted simulation study of geared flap control for tilt-wing V/STOL aircraft
[NASA-TM-103872] p 64 A93-10741
- GUEVREMONT, G.**
Finite element solution of the 3D compressible Navier-Stokes equations by a velocity-vorticity method p 974 A93-47196
- GUFFOND, D.**
Improvement of the ONERA 3D icing code, comparison with 3D experimental shapes
[AIAA PAPER 93-0169] p 275 A93-22603
- GUGLIELMI, JOHN D.**
Atomization of JP-10/B4C gelled slurry fuel
[AD-A256827] p 391 A93-15686
- GUGLIERI, G.**
Breakdown analysis on delta wing vortices p 7 A93-10779
Vortex breakdown study on a 65-deg delta wing tested in static and dynamic conditions p 121 A93-14407
Dynamic stability derivatives evaluation in a low-speed wind tunnel p 821 A93-37402
Analysis of stability characteristics of a high performance aircraft
[AIAA PAPER 93-3616] p 1125 A93-48303
- GUGLIERI, G. R.**
Experimental analysis of rotary derivatives on a modern aircraft configuration
[AIAA PAPER 93-3514] p 985 A93-47278

GUGLIERI, GIORGIO

Experimental investigation on aircraft dynamic stability parameters p 905 A93-40328

GUICHETEAU, PH.

Nonlinear analysis and flight dynamics [ONERA, TP NO. 1992-83] p 818 A93-38568

Stability analysis through bifurcation theory. I, II [ONERA, TP NO. 1993-108] p 1225 A93-53620

Non-linear flight dynamics [ONERA, TP NO. 1993-109] p 1206 A93-53621

GUIDONE, J. A.

Engine testing at simulated altitude conditions [AIAA PAPER 93-2452] p 1120 A93-50201

GUIDOS, BERNARD J.

Navier-Stokes simulation of viscous, separated, supersonic flow over a projectile rotating band [AD-A263073] p 788 N93-27955

GUILLEN, PH.

Hypersonic flow calculations using a multidomain MUSCL Euler solver p 960 A93-45547

GUILLOT, MARTIN J.

The effect of large scale unsteady motion on turbulent reattaching shear layer - Application to the supersonic compression ramp [AIAA PAPER 93-3100] p 1061 A93-48273

GUILMETTE, NEAL

Prediction of forces and moments for hypersonic flight vehicle control effectors [NASA-CR-193033] p 728 N93-24762

GUIMBAL, BRUNO

The Cabri two-seat helicopter - Design and first flights p 799 A93-36019

GULATI, SURESH K.

Employment of radicals and excited state species for supersonic combustion photochemical ignition of premixed hydrogen/oxygen mixtures with ArF laser p 73 N93-11135

GUM, J. S.

Optical technologies for UV remote sensing instruments p 853 N93-28788

GUN'KO, YU. P.

Effect of boundary layer suction on the thrust and aerodynamic efficiency of a hypersonic flight vehicle p 1176 A93-52959

GUNDY-BURLET, K. L.

Unsteady two- and three-dimensional Navier-Stokes simulations of multistage turbomachinery flows p 266 A93-20721

GUNDY-BURLET, KAREN L.

Unsteady, three-dimensional, Navier-Stokes simulations of multistage turbomachinery flows [AIAA PAPER 93-1979] p 1153 A93-49826

GUNJI, YOSHIHISA

Ignition and exhaust emission characteristics of spray combustion in a pre-chamber type vortex combustor [ASME PAPER 92-GT-119] p 350 A93-19355

GUNSALLUS, C. T.

AH-64A rotating load usage monitoring from fixed system information p 507 A93-27953

GUNTHER, CHRISTIAN

Mechanical and analytical screening of braided composites for transport fuselage applications p 922 N93-30855

GUNZBURGER, MAX

Sensitivity calculations for a 2D, inviscid, supersonic forebody problem [NASA-CR-191444] p 779 N93-27004

GUO, D. W.

Researches on sonic fatigue of the air-inlet duct of XX aircraft p 154 A93-14256

GUO, JIE

A unified model for rotating stall and surge p 259 A93-20119

GUO, K. L.

Burnett solutions along the stagnation line of a cooled cylinder in low-density hypersonic flows [AIAA PAPER 93-2726] p 962 A93-46480

GUO, R. W.

Flow characteristics of an S-shaped inlet at high incidence p 114 A93-14213

Numerical analysis of the 3-D turbulent flow in an S-shaped diffuser p 116 A93-14252

GUO, SUOFENG

Analysis and development of a total energy control system for a large transport aircraft p 183 A93-14372

GUO, WEN-HAI

An improved multiple line-vortex method for simulation of separated vortices of slender wings p 1236 A93-55412

GUO, XIANMIN

Parameter selection of electro-impulse de-icing systems p 889 A93-40493

GUPTA, ASHWANI K.

Low NO(x) combustor development using aerodynamic staging [ISABE 93-7021] p 1195 A93-53997

GUPTA, B.

Midhani alloys in aeronautical service p 70 A93-12368

GUPTA, DINESH K.

The evolution of thermal barrier coatings in gas turbine engine applications [ASME PAPER 92-GT-203] p 388 A93-19427

GUPTA, K. K.

On some recent advances in multidisciplinary analysis of hypersonic vehicles [AIAA PAPER 92-5026] p 438 A93-22302

GUPTA, ROOP N.

Viscous equilibrium computations using program LAURA p 8 A93-12002

Higher-order viscous shock-layer solutions for high altitude flows [AIAA PAPER 93-2724] p 858 A93-41050

Enhancements to viscous-shock-layer technique p 962 A93-46408

A viscous shock-layer analysis of 2-D and axisymmetric flows [AIAA PAPER 93-2751] p 963 A93-46500

GUPTA, S.

Advanced materials in gas turbine engines: An assessment [PNR-90946] p 58 N93-11105

Development of advanced carbon-carbon annular flameholders for gas turbines [PNR-90947] p 58 N93-11106

Small particle impact damage in carbon-carbon composites [PNR-90948] p 73 N93-11107

GUPTA, S. C.

Stability considerations for enhanced manoeuvrability - An overview p 184 A93-14397

Aerodynamically efficient wing design with structural considerations p 460 A93-24081

GUPTA, SURESH

Erosion characteristics of ceramic particulate and whisker reinforced aluminum composites [ASME PAPER 92-GT-369] p 388 A93-19532

GURBACH, J. J.

Application of a p-version finite element code to analysis of cracks [AIAA PAPER 93-1450] p 740 A93-33999

GURETSKII, V. V.

Ways of increasing the service life and reliability of bolted joints p 745 A93-35281

GUREVICH, I. U. G.

Three-dimensional flow of viscous gas in the blade passage of a straight compressor cascade p 5 A93-10187

Effect of a large-scale inhomogeneity of the incoming flow on flow in a plane turbine cascade p 6 A93-10189

GURNAK, V. S.

Spectra of pressure pulsations on the surface of a cone in the transition region at supersonic flow velocities p 1088 A93-51755

GURSUL, ISMET

Vortex breakdown over delta wings in unsteady free stream [AIAA PAPER 93-0555] p 285 A93-23294

Effect of nonaxisymmetric forcing on a swirling jet with vortex breakdown [AIAA PAPER 93-3251] p 1028 A93-46796

GURUPRASAD, G.

Reusable code for helicopter simulation [AIAA PAPER 93-3594] p 1224 A93-52686

GURUPRASAD, S. A.

Characterisation of conventional and controlled diffusion stator blades in a transonic compressor stage [ISABE 93-7124] p 1189 A93-54099

GURUSWAMY, G. P.

Algorithm development with applications to aerodynamics and aeroelasticity p 422 N93-18566

GURUSWAMY, GURU P.

Coupled finite-difference/finite-element approach for wing-body aeroelasticity [AIAA PAPER 92-4680] p 409 A93-20302

Unsteady Navier-Stokes simulation of the canard-wing-body ramp motion [AIAA PAPER 93-3058] p 1058 A93-48235

Fluid-structural interactions using Navier-Stokes flow equations coupled with shell finite element structures [AIAA PAPER 93-3087] p 1099 A93-48261

Navier-Stokes computations on full-span wing-body configuration with oscillating control surfaces [AIAA PAPER 93-3687] p 1065 A93-48356

GUSAROV, S. A.

The combined effect of clearances and peripheral overlaps on the efficiency of microturbines with shroudless rotors p 1193 A93-52963

GUSEV, A. A.

Control synthesis with incomplete, complete, and supercomplete measurements p 561 A93-27603

GUSEV, V. N.

Simulation of a hypersonic flow over vehicles at low Reynolds numbers p 120 A93-14381

Aerothermodynamics of the high-altitude flight p 1089 A93-51783

Investigation of the effect of physical processes on heat transfer to blunt bodies at low Reynolds numbers p 1090 A93-51877

GUSNIN, S. I. U.

A design concept for a flight vehicle computer system with artificial intelligence elements p 757 A93-35663

GUSTAVSON, BRUCE

Dynamic System Coupler Program (DYSCO 4.1). Volume 1: Theoretical manual p 848 N93-27531

Dynamic System Coupler Program (DYSCO 4.1). Volume 2: User's manual [AD-B131157L] p 848 N93-27589

Dynamic System Coupler Program (DYSCO 4.1). Volume 3: User's manual supplement [AD-B131158L] p 848 N93-27590

GUSTAVSSON, LARS

Modal measurements and propeller field excitation on acoustic full scale mockup of SAAB 340 aircraft [FFA-TN-1992-08] p 1039 N93-31051

GUSTAVSSON, MATS

Vibro-acoustic analysis of propeller aircraft, integrating advanced experimental modeling with in-flight data analysis p 451 A93-19230

GUTHLEIN, PETER

Terminal Doppler Weather Radar (TDWR) Operational Test and Evaluation (OT/E) integration test plan [DOT/FAA/CT-TN92/6] p 151 N93-13377

GUTHRIE, ANN R.

Experimental investigation of spherical-convergent-flap thrust-vectoring two-dimensional plug nozzles [AIAA PAPER 93-2431] p 898 A93-41045

GUTKNECHT, PETER

The ecological balance of Swissair: An example of waste management p 1035 N93-31930

GUTMAN, GEORGES

Zvezda - The Russian pioneer in the field of life-support and escape systems for aeronautics and space p 195 A93-16878

GUTMARK, E.

Effect of nozzle design on near acoustic field of supersonic circular and rectangular jets p 448 A93-19203

Combustion characteristics and passive control of an annular dump combustor [AIAA PAPER 93-1772] p 1110 A93-49668

Periodic chemical energy release for active combustion control [ISABE 93-7043] p 1198 A93-54019

GUTMARK, EFFIE

Passive control of coherent vortices in compressible mixing layers [AIAA PAPER 93-3262] p 968 A93-46828

GUTTMANN, A. J.

Subsonic potential flow and the transonic controversy p 479 A93-28544

GUYMON, GARY L.

Mathematical model of frost heave and thaw settlement in pavements [CRREL-REPT-93-2] p 912 N93-30103

GUYON, P.

Optimization and sensitivity computations for the conception of internal ventilation system in the aircraft engine [ETN-93-93375] p 521 N93-20913

GUZIAK, ROBERT

Silicon differential pressure transducer line pressure effects and compensation p 830 A93-37890

GYSLING, DANIEL L.

Active stabilization of aeromechanical systems [AD-A261366] p 725 N93-26335

H

HA, CHEOLKEUN

Optimal discrete-time dynamic output-feedback design - A w-domain approach p 757 A93-34536

HAAGENSEN, P. L.

The FAA aircraft icing Forecasting Improvement Program - Validation of aircraft icing forecasts in the Denver area [AIAA PAPER 93-0393] p 309 A93-23069

HAAKER, T. I.

On the dynamics of aeroelastic oscillators with one degree of freedom [REPT-92-96] p 1040 N93-31653

HAAS, BRIAN L.

Flow resolution and domain of influence in rarefied hypersonic blunt-body flows [AIAA PAPER 93-2806] p 964 A93-46546

- HAAS, DAVID J.**
Prediction of helicopter component loads using neural networks
[AIAA PAPER 93-1301] p 756 A93-33878
- HAASE, WERNER**
Computational results for flows over compression ramps p 866 A93-42599
- HAAYASOJA, T.**
Ice prediction systems for runways p 376 A93-22174
- HABASHI, MOZHI**
TBD(exp 3)
[NASA-CR-192075] p 335 N93-18054
- HABASHI, W.**
Some special purpose preconditioners for conjugate gradient-like methods applied to CFD p 772 A93-38638
- HABASHI, W. G.**
Finite element solution of the 3D compressible Navier-Stokes equations by a velocity-vorticity method p 974 A93-47196
- HABIBIE, B. J.**
Spanish-Indonesian cooperation in the development, production, certification and marketing of CN-235 commuter aircraft p 108 A93-14156
- HACHEMIN, J.-V.**
CFD analysis of hypersonic chemically reacting flowfields around a generic shape
[AIAA PAPER 93-0323] p 281 A93-23015
- HACHENBERG, D.**
Stringer peeling effects at stiffened composite panels in the postbuckling range p 1160 A93-52453
- HACKER, J. M.**
The composite shape and structure of coherent eddies in the convective boundary layer p 93 A93-12643
- HACKETT, CHARLES M.**
Aerothermodynamic heating due to shock wave/laminar boundary-layer interactions in high-enthalpy hypersonic flow
[AIAA PAPER 93-3135] p 1064 A93-48299
- HADAR, ILAN**
Regression rate mechanism in a solid fuel ramjet p 814 N93-27185
- HADDEN, J.**
Federal Aviation Administration pavement modeling p 379 N93-16315
- HADFIELD, C.**
Pitch control margin at high angle of attack - Quantitative requirements (flight test correlation with simulation predictions)
[AIAA PAPER 92-4107] p 39 A93-11277
- HAENLEIN, GEORG**
Pallet for helicopter test instrumentation p 1000 N93-31279
- HAENEL, D.**
An upwind relaxation method for hypersonic viscous flows over a double-ellipsoidal body p 867 A93-42606
Computational methods for viscous hypersonic flows p 1152 A93-49523
Supersonic and hypersonic flow computations for the research configuration ELAC I and comparison to experimental data p 1237 A93-56034
- HAERI, MITCHELL BEHJAN**
Turbulence and chaos in classical and quantum systems p 232 N93-14144
- HAERTIG, J.**
Experimental investigation of a 2D parallel vortex/airfoil interaction p 538 A93-23808
- HAUSER, J.**
Computational aerothermodynamics for 2D and 3D space vehicles p 1073 A93-49533
- HAFEZ, M.**
Euler solutions for blunt bodies using triangular meshes - Artificial viscosity forms and numerical boundary conditions
[AIAA PAPER 93-3333] p 953 A93-45027
- HAFEZ, M. M.**
Finite element solution of the 3D compressible Navier-Stokes equations by a velocity-vorticity method p 974 A93-47196
- HAFTKA, R. T.**
Aerodynamic optimization of an HSCT configuration using variable-complexity modeling
[AIAA PAPER 93-0101] p 322 A93-19806
Variable-complexity aerodynamic-structural design of a high-speed civil transport wing
[AIAA PAPER 92-4695] p 323 A93-20279
Integrated aerodynamic-structural-control wing design
[AIAA PAPER 92-4694] p 324 A93-20307
- HAFTKA, RAPHAEL T.**
Sensitivity-based scaling for approximating structural response p 548 A93-28618
- HAGABHUSHANAM, J.**
Flap-lag damping in hover and forward flight with a three-dimensional wake p 797 A93-35979
- HAGAR, H. D.**
Design philosophy for wind tunnel model positioning control systems p 822 A93-37877
Design philosophy for wind tunnel model positioning systems
[AD-A254958] p 192 N93-12552
- HAGEMEYER, D. A.**
Aeroelastic effects on the B-2 maneuver response
[AIAA PAPER 93-3664] p 1128 A93-48344
- HAGEN, DONALD E.**
NO(x) scavenging on carbonaceous aerosol surfaces in aircraft exhaust plumes. I
[AIAA PAPER 93-2343] p 1164 A93-50117
Particulates and aerosols characterized in real time for harsh environments using the UMR mobile aerosol sampling system (MASS)
[AIAA PAPER 93-2344] p 1156 A93-50118
- HAGEN, MARTIN J.**
Effects of ingested atmospheric turbulence on measured tail rotor acoustics p 849 A93-35964
- HAGENLOCHER, KLAUS**
Zeppelin NT - A new concept in airship technology, based on rigid airship principles
[AIAA PAPER 93-4045] p 1242 A93-54612
- HAGER, J. M.**
Heat flux microsensor measurements
[AIAA PAPER 92-5038] p 413 A93-22312
Microsensors for high heat flux measurements p 928 A93-42920
- HAGER, J. O.**
Multi-point design of transonic airfoils using optimization
[AIAA PAPER 92-4225] p 16 A93-13382
A multi-point optimization for transonic airfoil design
[AIAA PAPER 92-4681] p 264 A93-20303
Airfoil design using the Navier-Stokes equations
[AIAA PAPER 93-0648] p 464 A93-24763
Design efficiency evaluation for transonic airfoil optimization - A case for Navier-Stokes design
[AIAA PAPER 93-3112] p 1062 A93-48282
- HAGIWARA, YOSHIMICHI**
Augmentation of turbulent heat transfer with a vortex generator attached to a LEBU plate p 411 A93-21729
- HAGSETH, PAUL**
Propulsion/airframe integration issues for waverider aircraft
[AIAA PAPER 93-0506] p 505 A93-25533
- HAGSETH, PAUL E.**
Current technologies for waverider aircraft
[AIAA PAPER 93-0400] p 505 A93-25521
- HAH, C.**
Unsteady aerodynamic flow phenomena in a transonic compressor stage
[AIAA PAPER 93-1868] p 1075 A93-49743
Three-dimensional flow analysis inside turbomachinery stages with steady and unsteady Navier-Stokes method [ISABE 93-7095] p 1186 A93-54071
Navier-Stokes analysis of three-dimensional flow and heat transfer inside turbine blade rows p 905 N93-29963
- HAH, CHUNILL**
Three-dimensional flow phenomena in a transonic, high-through-flow, axial-flow compressor stage
[ASME PAPER 92-GT-169] p 250 A93-19395
Three-dimensional unstructured grid Euler method applied to turbine blades
[AIAA PAPER 93-0196] p 461 A93-24233
Three-dimensional flow calculations inside SSME GGGT first stage blade rows p 1017 N93-31585
- HAHN, O. J.**
Design of a hydrogen test facility p 532 A93-25993
- HAIDAR, N. I. A.**
Influence of the canopy-payload coupling on the dynamic stability in pitch of a parachute system
[AIAA PAPER 93-1248] p 690 A93-35185
- HAIGH, STEPHEN J.**
Parameters influencing the hot-spot ignition of aviation fuel/air and ethylene/air mixtures p 704 N93-24886
Alternative equipment test procedures for simultaneous current injection on multiple cable bundles p 747 N93-24903
- HAILYE, MICHAEL**
Flip-flop jet nozzle extended to supersonic flows p 778 A93-39409
- HAIMES, ROBERT**
Visual grid quality assessment for 3D unstructured meshes
[AIAA PAPER 93-3352] p 1036 A93-45046
- HAJ-HARIRI, HOSSEIN**
Experimental and numerical study of swept ramp injection into a supersonic flowfield
[AIAA PAPER 93-2445] p 1119 A93-50197
- HALDEMAN, C. W., JR.**
The USAF Advanced Turbine Aerothermal Research Rig (ATARR) p 911 N93-29945
- HALFORD, GARY R.**
Stirling engine - Available tools for long-life assessment p 195 A93-13824
- HALL, BEVERLY M.**
USA aviation digest index, 1989, volume 11
[AD-A258673] p 571 N93-20388
Index to USA aviation digest, 1990
[AD-A258678] p 572 N93-20389
Index to USA aviation digest, 1991
[AD-A258679] p 572 N93-20390
- HALL, CHARLES E., JR.**
A stability augmentation system for student designed remotely-piloted vehicles
[AIAA PAPER 92-4261] p 63 A93-13365
- HALL, DAVID G.**
Acoustic mode measurements in the inlet of a model turbofan using a continuously rotating rake - Data collection/analysis techniques
[AIAA PAPER 93-0599] p 361 A93-23324
Takeoff/approach noise for a model counterrotation propeller with a forward-swept upstream rotor
[AIAA PAPER 93-0596] p 519 A93-24782
Acoustic mode measurements in the inlet of a model turbofan using a continuously rotating rake
[AIAA PAPER 93-0598] p 563 A93-24783
Cruise noise of an advanced propeller with swirl recovery vanes p 564 A93-28609
Acoustic mode measurements in the inlet of a model turbofan using a continuously rotating rake: Data collection/analysis techniques
[NASA-TM-105936] p 179 N93-15403
Acoustic mode measurements in the inlet of a model turbofan using a continuously rotating rake
[NASA-TM-105989] p 362 N93-16705
Takeoff/approach noise for a model counterrotation propeller with a forward-swept upstream rotor
[NASA-TM-105979] p 362 N93-16715
- HALL, EDWARD J.**
Investigation of advanced counterrotation blade configuration concepts for high speed turboprop systems. Task 5: Unsteady counterrotation ducted propfan analysis. Computer program user's manual
[NASA-CR-187125] p 521 N93-20583
Investigation of advanced counterrotation blade configuration concepts for high speed turboprop systems. Task 5: Unsteady counterrotation ducted propfan analysis
[NASA-CR-187126] p 521 N93-20773
- HALL, G. R.**
Development of the F/A-18 E/F air induction system
[AIAA PAPER 93-2152] p 1101 A93-49969
- HALL, I. M.**
Hypersonic flows including real gas effects
[AERO-REPT-9112] p 289 N93-16467
Design of a nozzle for a hypersonic wind tunnel
[AERO-REPT-9113] p 381 N93-16468
Computational study of real gas effects in high speed high temperature flow, volume 2
[AERO-REPT-9203-VOL-2] p 289 N93-16470
- HALL, JIM W., JR.**
Reanalysis of multiple-wheel landing gear traffic tests
[AD-A255893] p 194 N93-14238
- HALL, K. R.**
Construction of a one-third scale model of the NASP
[AIAA PAPER 93-0427] p 386 A93-23345
- HALL, KENNETH C.**
Calculation of three-dimensional unsteady flows in turbomachinery using the linearized harmonic Euler equations
[ASME PAPER 92-GT-136] p 249 A93-19368
Nonreflecting boundary conditions for linearized unsteady aerodynamic calculations
[AIAA PAPER 93-0882] p 475 A93-25553
Linearized Euler predictions of unsteady aerodynamic loads in cascades p 480 A93-29318
Deforming grid variational principle for unsteady small disturbance flows in cascades p 692 A93-35623
Prediction of unsteady flows in turbomachinery using the linearized Euler equations on deforming grids
[NASA-CR-192919] p 747 N93-25109
- HALL, L. E.**
Multidisciplinary design integration system for a supersonic transport aircraft
[AIAA PAPER 92-4841] p 324 A93-20296
- HALL, P. D.**
ETOPS across the Atlantic p 306 A93-18780
- HALL, PHILIP**
Wave interaction theory and LFC p 860 A93-41781
- HALL, S. R.**
Reform of the aeronautics and astronautics curriculum at MIT
[AIAA PAPER 93-0325] p 454 A93-23017
- HALL, STEVEN R.**
Performance of higher harmonic control algorithms for helicopter vibration reduction p 890 A93-41904

- HALL, T. E.**
Ultra wide band 3-D cross section (RCS) holography
[DE92-019133] p 89 N93-11802
- HALL, U.**
Effects of blade geometry and mode shape on fan flutter
[ISABE 93-7028] p 1196 A93-54004
- HALLISY, JAMES B.**
Flight test operations using an F-106B research airplane modified with a wing leading-edge vortex flap
[AIAA PAPER 92-4094] p 42 A93-13261
- HALLOCK, J. N.**
Proceedings of the Aircraft Wake Vortices conference, volume 1
[PB93-126449] p 485 N93-21796
Proceedings of the Aircraft Wake Vortices conference, volume 2
[PB93-127728] p 559 N93-21799
- HALPAIN, N. D.**
Position reporting using GPS/OMEGA and INS
p 498 A93-25173
- HALPERN, M. E.**
Optimal trajectories for aircraft terrain following and terrain avoidance: A literature review update
[AD-A264075] p 910 N93-30604
- HALT, D. W.**
A novel algorithm for the solution of compressible Euler equations in wave/particle split (WPS) form
p 957 A93-45093
- HALYO, NESIM**
A stochastic optimal feedforward and feedback control methodology for supergility
[NASA-CR-4471] p 229 N93-13370
- HAM, JOHNNIE A.**
Handling qualities flight test techniques and analyses used with the proposed MIL-H-8501B
[AIAA PAPER 92-4081] p 61 A93-11264
Handling qualities testing using the mission oriented requirements of ADS-33C
p 817 A93-35961
- HAMABE, K.**
Rim seal experiments and analysis of a rotor-stator system with nonaxisymmetric main flow
[ASME PAPER 92-GT-160] p 402 A93-19387
- HAMADA, SEIICHI**
An evaluation system for impact damage and erosion of ceramic gas turbine components
p 79 A93-12229
- HAMED, A.**
Hypersonic flow separation in shock wave boundary layer interactions
[ASME PAPER 92-GT-205] p 251 A93-19429
A parametric study of bleed in shock boundary layer interactions
[AIAA PAPER 93-0294] p 280 A93-22694
An investigation of shock wave turbulent boundary layer interaction with bleed through slanted slots
[AIAA PAPER 93-2992] p 1052 A93-48184
An investigation of shock wave turbulent boundary layer interaction with bleed through normal and slanted slots
[AIAA PAPER 93-2155] p 1079 A93-49971
Particle dynamics simulations in inlet separator with an experimentally based bounce model
[AIAA PAPER 93-2156] p 1115 A93-49972
Simulation of propulsion system's transient response to planar wave inlet distortion and the effect of compressor wear
[AIAA PAPER 93-2384] p 1117 A93-50152
- HAMID, S.**
Radial inflow turbine study
[AD-A260767] p 724 N93-25917
- HAMILTON, GORDON L.**
Civil aircraft challenges in engine/airframe integration
[ASME PAPER 92-GT-45] p 322 A93-19299
- HAMILTON, H. H., II**
An approximate method for calculating heating rates on three-dimensional vehicles
[AIAA PAPER 93-2881] p 949 A93-44228
- HAMILTON, H. HARRIS, II**
Finite-difference solution for laminar or turbulent boundary layer flow over axisymmetric bodies with ideal gas, CF₄, or equilibrium air chemistry
[NASA-TP-3271] p 222 N93-15434
- HAMILTON, TODD A.**
Dynamic attitude measurement system
[AIAA PAPER 93-3801] p 1139 A93-51393
- HAMM, DAVE**
Hypersonic design
p 156 A93-14346
- HAMMETT, ROBERT**
Computer-aided design of avionics diagnostics algorithms
p 941 A93-42863
- HAMMOND, J.**
Rapid wind tunnel prototype using stereolithography and equivalent technologies
p 191 A93-14365
- HAMMOND, JAMES H.**
Embedded training capabilities for the LAMPS MK 3 system
[AD-A250697] p 49 N93-11838
- HAMORY, PHILIP J.**
Flight experience with lightweight, low-power miniaturized instrumentation systems
[AIAA PAPER 92-4111] p 39 A93-11280
- HAMPSON, BRIAN**
Helicopter simulator qualification
p 912 N93-30681
- HAMPTON, HERBERT**
Flight Deflection Measurement System
p 808 A93-37885
- HAMSTAD, M. A.**
Acoustic emission technology for smart structures
p 1263 A93-55331
- HAN, ARRIS**
An integrated optimum design approach for high speed prop-rotors including acoustic constraints
[NASA-CR-193222] p 893 N93-29153
- HAN, BUZHANG**
A preliminary investigation of a method to calibrate strain gauge balances by means of a reference balance
p 210 A93-16845
- HAN, CHAO**
Analysis and feedback control of aircraft flight in wind shear
p 183 A93-14349
- HAN, J. C.**
Influence of surface heat flux ratio on heat transfer augmentation in square channels with parallel, crossed, and V-shaped angled ribs
p 201 A93-13981
Influence of high mainstream turbulence on leading edge film cooling heat transfer - Effect of film hole spacing
p 207 A93-15068
Heat transfer performance comparisons of five different rectangular channels with parallel angled ribs
p 397 A93-18752
Influence of surface heating condition on local heat transfer in a rotating square channel with smooth walls and radial outward flow
[ASME PAPER 92-GT-188] p 402 A93-19413
Heat transfer in a five-pass irregular channel with and without pin-fins
p 1256 A93-54633
Determination of surface heat transfer and film cooling effectiveness in unsteady wake flow conditions
p 902 A93-29933
- HAN, S. O. T. H.**
A break-down of sting interference effects
[NLR-TP-91220-U] p 1014 N93-31042
- HAN, SEUNGJUK**
Wind tunnel spin data reduction to obtain aerodynamic spin damping coefficients by using nonlinear equation of motion
[AD-A253880] p 19 N93-10811
- HAN, WANJIN**
An experimental study on blade negative curving in a turbine cascade with a large turning angle
p 1071 A93-49185
Effect of blade leaning on the development of passage vortices and losses in the passage of turbine cascade with a great turning angle
p 1236 A93-55397
- HANADA, TOSHIYA**
Performance analysis of supersonic through-flow fan by the lifting surface theory. I - Disturbance flow field and determination of blade loadings
p 267 A93-20929
- HANAGUD, S.**
Basic research on design analysis methods for rotorcraft vibrations
[NASA-CR-191917] p 422 N93-18576
- HANAMITSU, A.**
Numerical studies of Mach reflection with air chemistry
p 1233 A93-54815
- HANAMITSU, AKIRA**
The role of computational fluid dynamics in aeronautical engineering. 9: Analysis of hypersonic equilibrium air flow
p 301 N93-19294
- HANAWA, KIRK**
Development of ultra-hypersonic shock tunnel for aerodynamics test
p 376 A93-21900
- HANCOCK, J. W.**
Thermal design and analysis of an exhaust diffuser unit in a ceramic composite
[ISABE 93-7060] p 1220 A93-54036
- HANCOCK, REGIS**
X-29 vortex flow control tests
p 804 A93-38846
- HANDSCHUH, ROBERT F.**
Low-noise, high-strength, spiral-bevel gears for helicopter transmissions
[AIAA PAPER 93-2149] p 1154 A93-49966
- HANE, CARL E.**
An observational study of the dryline
p 844 A93-36034
- HANEY, J. W.**
The effects of hypersonic flight test requirements on research vehicle design
[AIAA PAPER 93-0511] p 386 A93-23258
A hypersonic waverider research vehicle
[AIAA PAPER 93-0402] p 505 A93-25522
- HANFF, E. S.**
Effect of vortex behavior on loads acting on a 65 deg delta wing oscillating in roll at high incidence
p 782 N93-27220
- HANFF, ERNEST S.**
Further analysis of high-rate rolling experiments of a 65 deg delta wing
[AIAA PAPER 93-0620] p 523 A93-24737
Body-axis rolling motion critical states of a 65-degree delta wing
[AIAA PAPER 93-0621] p 523 A93-24738
- HANGE, C. E.**
Small scale jet effects and hot gas ingestion investigations at NASA Ames
[AIAA PAPER 92-4252] p 67 A93-13339
- HANGE, CRAIG E.**
Jet-induced ground effects on a parametric flat-plate model in hover
[NASA-TM-104001] p 700 N93-26099
- HANIFI, A.**
Some stability characteristics of the boundary layer on a yawed cone
[AIAA PAPER 93-3048] p 1057 A93-48228
- HANIU, HIROYUKI**
Transitional characteristics of vortices issued from a body which creates asymmetric flow field - In a case of thin symmetrical airfoil with angle of attack under rotational oscillation of small amplitude
p 267 A93-20923
- HANKEY, W. L.**
Takeoff and landing analysis methodology for an airbreathing space booster
p 914 A93-42927
- HANKS, LYNN**
Handling qualities flight test techniques and analyses used with the proposed MIL-H-8501B
[AIAA PAPER 92-4081] p 61 A93-11264
- HANLON, PETER D.**
Failure identification using multiple model adaptive estimation for the LAMBDA flight vehicle
[AD-A259137] p 527 N93-20596
- HANNEMANN, K.**
Numerical simulation of shock/shock and shock-wave/boundary-layer interactions in hypersonic flows
p 1093 A93-52000
Numerical simulation of a two-dimensional supersonic mixed-compression inlet
[ISABE 93-7107] p 1188 A93-54083
- HANNEMANN, V.**
Numerical simulation of a two-dimensional supersonic mixed-compression inlet
[ISABE 93-7107] p 1188 A93-54083
- HANOTEL, R.**
Experimental and theoretical studies of helicopter rotor-fuselage interaction
[ONERA, TP NO. 1992-142] p 120 A93-14356
- HANSEN, ARTHUR L.**
A 'new age' in aviation weather forecasting
p 427 A93-22123
- HANSEN, C. H.**
Active control of interior noise in model aircraft fuselages using piezoceramic actuators
p 231 A93-14540
- HANSEN, ROBERT J.**
Recent progress in the implementation of active combustion control
p 171 A93-14272
- HANSEN, WILLIAM P., JR.**
Receiving and scattering characteristics of an imaged monopole beneath a lossy sheet
p 1158 A93-50543
- HANSFORD, ROBERT E.**
The development of the coupled rotor-fuselage model (CRFM)
p 794 A93-35903
- HANSMAN, J. R.**
Reform of the aeronautics and astronautics curriculum at MIT
[AIAA PAPER 93-0325] p 454 A93-23017
- HANSMAN, R. H., JR.**
Hazard assessment and cockpit presentation issues for microburst alerting systems
p 308 A93-22112
- HANSMAN, R. J.**
Advanced terrain displays to transport category aircraft
[PB92-197136] p 35 N93-10065
- HANSMAN, R. J., JR.**
Close-up analysis of aircraft ice accretion
[AIAA PAPER 93-0029] p 309 A93-23239
- HANSMAN, R. JOHN**
Experimental evaluation of candidate graphical microburst alert displays
p 145 N93-14853
Close-up analysis of aircraft ice accretion
[NASA-TM-105952] p 148 N93-15360
- HANSMAN, R. JOHN, JR.**
A passive infrared ice detection technique for helicopter applications
[NASA-CR-193187] p 880 N93-29152
- HANSON, JOHN**
Computation of optimal low- and medium-thrust orbit transfers
[AIAA PAPER 93-3855] p 1144 A93-51442

- HANSON, R. K.**
Comparison of NO and OH PLIF temperature measurements in a scramjet model flowfield [AIAA PAPER 93-2035] p 1113 A93-49870
- HANSON, RONALD K.**
Shedding new light on gas dynamics p 80 A93-13435
- HAO, QING**
Experimental investigation of effect of particles on blade pressure distribution in impulse cascade flow p 1236 A93-55398
- HARASGAMA, S. P.**
Measurements and computations of external heat transfer and film cooling in turbines [RAE-TM-P-1223] p 722 N93-25455
- HARBAUGH, DARCY J.**
The effects of high-pressure water on the material integrity of selected aircraft coatings and substrates [SME PAPER AD92-207] p 855 A93-40668
- HARDAWAY, ROBERT M.**
Airlines, airports and antitrust - A proposed strategy for enhanced competition p 760 A93-34821
- HARDERSEN, C. P.**
A retrospective of 3600 composite blades p 507 A93-27963
- HARDESTY, MARK**
NOTAR system - A quiet character p 567 A93-29418
- HARDIN, J. C.**
A new technique for aerodynamic noise calculation p 447 A93-19177
- HARDIN, J. D.**
Flow prediction over a transport multi-element high-lift system and comparison with flight measurements p 785 A93-27448
- HARDIN, JAY C.**
Reynolds number influences in aeronautics [NASA-TM-107730] p 989 N93-31732
- HARDIN, JAY D.**
Subsonic high-lift flight research on the NASA Transport System Research Vehicle (TSRV) [AIAA PAPER 92-4103] p 38 A93-11275
In-flight surface-flow measurements on a subsonic transport high-lift flap system p 166 A93-14327
Two-dimensional computational analysis of a transport high-lift system and a comparison with flight-test results [AIAA PAPER 93-3533] p 1072 A93-49517
- HARDING, JEFFREY W.**
Frequency-domain identification of coupled rotor/body models of an advanced attack helicopter p 816 A93-35960
- HARDINGE, HAL**
Flow visualization and flow field measurements of a 1/12 scale tilt rotor aircraft in hover p 482 A93-29441
- HARDRATH, W. T.**
An Acoustic Emission Pre-failure Warning System for composite structural tests p 1161 A93-52560
- HARDWICK, C. JOHN**
Parameters influencing the hot-spot ignition of aviation fuel/air and ethylene/air mixtures p 704 N93-24886
A computational approach to predicting the extent of arc root damage in CFC panels p 735 N93-24890
Zoning of aircraft by electric field modelling p 704 N93-24894
Alternative equipment test procedures for simultaneous current injection on multiple cable bundles p 747 N93-24903
- HARDY, DENNIS R.**
Liquid flow reactor and method of using [AD-D015392] p 222 N93-15232
- HARDY, G. H.**
Piloted simulation evaluation of pitch control designs for highly augmented STOV aircraft [AIAA PAPER 92-4234] p 63 A93-13328
- HARDY, GORDON H.**
HUD Guidance for the ASKA Experimental STOL Aircraft using Radar Position Information [SAE PAPER 921041] p 150 A93-14661
A method of wind shear detection for powered-lift STOL aircraft [AIAA PAPER 93-3667] p 1104 A93-48345
Wind-shear endurance capability for powered-lift aircraft [AIAA PAPER 93-3670] p 1129 A93-48348
- HARIHARAN, NATHAN**
A third order upwind scheme for aero-acoustic applications [AIAA PAPER 93-0149] p 564 A93-25504
- HARIZOPOULOS, IOANNIS**
Experimental and computational investigations of the flowfield around the F117A [AIAA PAPER 93-3508] p 984 A93-47274
- HARLOFF, G. J.**
Navier-Stokes analysis of three-dimensional S-ducts p 959 A93-45146
- A numerical investigation of supersonic strut/endwall interactions in annular flow with varying strut thickness [AIAA PAPER 93-2927] p 1045 A93-48128
Experimental and numerical investigation of supersonic turbulent flow in an annular duct [AIAA PAPER 93-3123] p 1063 A93-48291
Investigation of a strut/endwall interaction in supersonic annular flow [AIAA PAPER 93-1925] p 1076 A93-49791
- HARMAN, TODD B.**
Reduction in size and unsteadiness of a VTOL ground vortex by ground fences [NASA-CR-192997] p 700 N93-26049
- HARPER, M. F. L.**
Active stabilization of compressor instability and surge in a working engine [ASME PAPER 92-GT-88] p 348 A93-19335
- HARPER, MICHAEL R.**
The effects of turbulence modeling on the numerical simulation of confined swirling flows [AIAA PAPER 93-1976] p 1078 A93-49823
Computation of the flow field in an annular gas turbine combustor [AIAA PAPER 93-2074] p 1113 A93-49903
- HARPER, S. E.**
An optical flameout detection system for NASA Langley's 8-Foot High Temperature Tunnel p 1254 A93-54372
- HARPER, WILLIAM B., JR.**
BIPS Turboalternator-Compressor characteristics and application to the NASA Solar Dynamic Ground Demonstration Program p 532 A93-25965
- HARRAH, STEVEN D.**
Ground clutter measurements using the NASA airborne doppler radar: Description of clutter at the Denver and Philadelphia airports p 490 N93-19608
- HARRIS, A. E.**
Visualisation and analysis of three dimensional transonic flows by holographic interferometry p 1020 A93-44194
Test techniques for engine/airframe integration p 213 N93-13200
ASTOVL model engine simulators for wind tunnel research p 192 N93-13213
- HARRIS, A. P.**
A study of propeller/wing interaction including the effect of ground proximity p 113 A93-14190
- HARRIS, C. E.**
An evaluation of the pressure proof test concept for 2024-T3 aluminium alloy sheet p 1026 A93-45780
- HARRIS, CHARLES D.**
The Langley 8-ft transonic pressure tunnel laminar-flow-control experiment p 910 A93-41783
- HARRIS, CHARLES E.**
NASA airframe structural integrity program p 1026 A93-45782
- HARRIS, DAVID R.**
Representation and presentation of requirements knowledge p 228 A93-17389
- HARRIS, FRANKLIN D.**
The rotor blade flap bending problem - An analytical test case p 158 A93-14783
- HARRIS, FRANKLIN K.**
Research requirements for a real-time flight measurements and data analysis system for subsonic transport high-lift research p 1244 A93-54391
- HARRIS, PHILIP S.**
Recent developments in aviation case law p 569 A93-23870
- HARRIS, T. A.**
On the fatigue life of M50 NiL rolling bearings p 78 A93-11346
- HARRISON, D.**
European studies to investigate the feasibility of using 1000 ft vertical separation minima above FL(290). III - Further results and overall conclusions p 992 A93-45166
- HARRISON, G. F.**
Lifting philosophies for aero engine fracture critical parts p 345 A93-18783
- HARRISON, LAURIE**
International aerospace STI p 1227 A93-53826
- HART, RONALD E.**
B-2 flight test program - An update [AIAA PAPER 92-4118] p 42 A93-13266
- HARTFIELD, AMY**
Phase I flight test of MIAG advanced development model [AIAA PAPER 92-4076] p 95 A93-11261
- HARTFIELD, ROY J., JR.**
Experimental investigation of slot injection into supersonic flow with an adverse pressure gradient [AIAA PAPER 93-2442] p 1119 A93-50194
- HARTFIELD, ROY JAMES, JR.**
Planar measurement of flow field parameters in nonreacting supersonic flows with laser-induced iodine fluorescence p 133 N93-13801
- HARTLE, MICHAEL S.**
Optimization of composite engine structures for mechanical and thermal loads [AIAA PAPER 93-1583] p 719 A93-34115
- HARTLEY, TOM T.**
Modeling of linear isentropic flow systems p 828 A93-37046
- HARTMAN, RANDOLPH G.**
GPS/GLONASS flight test, lab test and coverage analysis tests p 313 A93-21143
- HARTMANN, KLAUS**
Experimental investigations on wing-body combinations and their components at high angles of attack in the subsonic and transonic speed range [DLR-FB-91-43] p 516 N93-21762
- HARTNESS, J. T.**
The characterization and development of materials for advanced textile composites p 1211 A93-53434
- HARTNESS, J. TIMOTHY**
Advanced fiber/matrix material systems p 921 N93-30854
- HARTUNG, LIN C.**
A convective and radiative heat transfer analysis for the FIRE II forebody [AIAA PAPER 93-3194] p 1021 A93-44231
- HARTWICH, PETER M.**
Euler study on porous transonic airfoils with a view toward multipoint design p 479 A93-28604
Comparison of coordinate-invariant and coordinate-aligned upwinding for the Euler equations [AIAA PAPER 93-3306] p 858 A93-41053
Symmetry breaking in vortical flows over cones - Theory and numerical experiments [AIAA PAPER 93-3408] p 859 A93-41056
- HARTZHEIM, W.**
Multidisciplinary design of composite aircraft structures by Lagrange p 76 A93-10273
- HARVEY, ALBERT D.**
Space marching calculations about hypersonic configurations using a solution-adaptive mesh algorithm p 1177 A93-53212
- HARVEY, GREG**
Advanced hypersonic aircraft design [NASA-CR-192046] p 334 N93-18037
- HARVEY, J. K.**
Appraisal of the rarefied flow computations (problems 6.4.1 and 7.2.1) p 871 A93-42640
Non-equilibrium thermal radiation from air shock layers modelled with the Direct Simulation Monte Carlo method [AIAA PAPER 93-2805] p 1028 A93-46544
- HARVEY, N. W.**
Experimental heat transfer results in turbine stators and rotors and a comparison with theory [PNR-90945] p 57 N93-11055
- HARVEY, P. R.**
Creep fatigue life prediction for engine hot section materials (isotropic) [NASA-CR-189221] p 364 N93-18578
- HARVEY, W. DON**
Future regional transport aircraft market, constraints, and technology stimuli [NASA-TM-107669] p 109 N93-13025
- HARVEY, WILLIAM D.**
The Langley 8-ft transonic pressure tunnel laminar-flow-control experiment p 910 A93-41783
- HASE, JACK E.**
Flux limiters in a rotated upwind scheme for the Euler equations [AIAA PAPER 93-0067] p 262 A93-20180
- HASEMANN, H.**
Blade excitation by circumferentially asymmetric rotating stall in centrifugal compressors [ASME PAPER 92-GT-148] p 351 A93-19376
Excitation of blade vibration due to surge of centrifugal compressors [ASME PAPER 92-GT-149] p 351 A93-19377
- HASEN, G. A.**
Numerical solution of inviscid hypersonic flow around a conically-derived waverider [AIAA PAPER 93-0320] p 280 A93-23012
- HASHEMI-KIA, MOSTAFA**
The NASA/industry Design Analysis Methods for Vibrations (DAMVIBS) program: McDonnell-Douglas Helicopter Company achievements p 515 N93-21314
- HASHIBA, Y.**
Formation of shock waves in transient base flow p 1023 A93-45460
- HASHIDATE, MASATAKA**
A wind tunnel investigation to determine buffet countermeasures for STOL aircraft alpha-sweep flight testing [NAL-TR-1129] p 65 N93-12362

- HASSA, C.**
Experimental and theoretical investigation of a research atomizer/compression chamber configuration
[ASME PAPER 92-GT-137] p 401 A93-19369
- HASSAN, A. A.**
Effects of a trailing edge flap on the aerodynamics and acoustics of rotor blade-vortex interactions
p 244 A93-19144
- HASSAN, AHMED**
A 2-D numerical model for predicting the aerodynamic performance of the NOTAR system tailboom
p 766 A93-35994
- HASSAN, H. A.**
Monte Carlo simulation of radiating reentry flows
[AIAA PAPER 93-2809] p 964 A93-46548
Comparisons between DSMC and the Navier-Stokes equations for reentry flows
[AIAA PAPER 93-2810] p 964 A93-46549
A k-omega multivariate beta PDF for supersonic turbulent combustion
[AIAA PAPER 93-2197] p 1154 A93-50009
Modeling of turbulent supersonic H₂-air combustion with a multivariate beta PDF
[AIAA PAPER 93-2198] p 1155 A93-50010
Modeling of turbulent supersonic H₂-air combustion with an improved joint beta PDF
[NASA-CR-191929] p 391 N93-16389
A k-omega-multivariate beta PDF for supersonic combustion
[NASA-CR-191930] p 537 N93-21749
- HASSAN, O.**
The application of an adaptive unstructured grid method to the solution of hypersonic flows past double ellipse and double ellipsoid configurations
p 868 A93-42609
Line relaxation methods for the solution of 2D and 3D compressible flows
[AIAA PAPER 93-3366] p 955 A93-45059
Adaptive inviscid flow solutions for aerospace geometries on efficiently generated unstructured tetrahedral meshes
[AIAA PAPER 93-3390] p 956 A93-45081
- HASSAN, OSSAMA M.**
Flexible manufacturing of aircraft engine parts
[ASME PAPER 92-GT-229] p 404 A93-19446
- HASSAN, T. A.**
Multiparticle imaging technique for two-phase fluid flows using pulsed laser speckle velocimetry
[DE93-011734] p 935 N93-30489
- HATCH, RONALD R.**
Proposed revisions to RTCM SC-104 recommended standards for differential NAVSTAR/GPS service for carrier phase applications
[AD-A255276] p 152 N93-15005
- HATCHER, DARRIN**
Multi-parameter optimization tool for low-cost commercial fuselage crown designs
p 922 N93-30858
- HATHAWAY, M. D.**
Experimental and computational investigation of the NASA Low-Speed Centrifugal Compressor flow field
[ASME PAPER 92-GT-213] p 252 A93-19436
- HATHAWAY, R.**
HIRF and lightning
p 764 A93-39539
- HATTINGH, H. V.**
The design and development of an afterburner
[ISABE 93-7041] p 1198 A93-54017
- HATTIS, PHILIP D.**
Evaluation of some significant issues affecting trajectory and control management for air-breathing hypersonic vehicles
[AIAA PAPER 92-5011] p 384 A93-22287
Air-breathing hypersonic vehicle guidance and control studies: An integrated trajectory/control analysis methodology, phase 2
[NASA-CR-189703] p 65 N93-12413
- HATTORI, HIROSHI**
Mechanical anisotropy in directionally solidified turbine blade
p 1018 A93-47356
- HAUNSCHILD, M.**
An experimental health monitoring unit for GPS and GLONASS
p 706 N93-25018
- HAUPRICH, WILLIAM A.**
The whale with a tail
p 803 A93-38837
- HAUPT, M.**
A very efficient tool for the structural analysis of hypersonic vehicles under high temperature aspects
p 203 A93-14194
- HAUPT, U.**
The vortex behaviour of the rotating-stall cell of a centrifugal compressor with vaned diffuser
[ASME PAPER 92-GT-66] p 400 A93-19316
Blade excitation by circumferentially asymmetric rotating stall in centrifugal compressors
[ASME PAPER 92-GT-148] p 351 A93-19376
Excitation of blade vibration due to surge of centrifugal compressors
[ASME PAPER 92-GT-149] p 351 A93-19377

- Determination of the zone of the stall cell by means of the baroclinic wave theory
p 424 N93-18733
Rotating stall cell and Von Karman vortex street: A meteorological theory
p 424 N93-18734
- HAUPTMAN, A.**
Towards an analytical treatment of the aerodynamic problem of a circular wing
p 781 N93-27214
- HAURY, H.-J.**
Air Traffic and Environment
[GSF-BAND-8] p 1034 N93-31925
- HAUSER, AMBROSE A.**
Aero-engine reliability - A GE view
p 345 A93-18782
- HAUSER, ROBERT G.**
Adverse weather test site selection study
[AD-A259012] p 339 N93-18895
- HAUSMANN, CLIFFORD R.**
Rotating rake design for unique measurement of fan-generated spinning acoustic modes
[NASA-TM-105946] p 724 N93-26161
- HAVENER, GEORGE**
Aero-optical phase measurements using Fourier transform holographic interferometry
p 549 A93-29302
- HAVERLAND, MANFRED**
Data communication for airborne differential GPS/GLONASS application
p 499 A93-27910
- HAWBOLDT, R. J.**
Experimental study of shock wave and hypersonic boundary layer interactions near a convex corner
[AIAA PAPER 93-2980] p 1051 A93-48173
- HAWKES, TIM M.**
IHPET exhaust nozzle technology demonstrator
[AIAA PAPER 93-2569] p 1121 A93-50287
- HAWKINS, RICHARD W.**
CFD comparisons with wind tunnel and flight data for the X-15
[AIAA PAPER 92-5047] p 273 A93-22319
Application of CFD to a generic hypersonic flight research study
[AIAA PAPER 93-0312] p 280 A93-23007
- HAWLEY, ARTHUR**
Composites technology for transport primary structure
p 918 N93-30431
- HAWORTH, LORAN A.**
Test techniques for evaluating flight displays
[NASA-TM-103947] p 516 N93-21810
- HAWTHORNE, W. R.**
Aerodynamic design of turbomachinery blading in three-dimensional flow - An application to radial inflow turbines
[ASME PAPER 92-GT-74] p 248 A93-19324
- HAWTHORNE, WILLIAM**
Three-dimensional flow in radial turbomachinery and its impact on design
[NASA-CR-192957] p 723 N93-25668
- HAY, N.**
Discharge coefficients of holes angled to the flow direction
[ASME PAPER 92-GT-192] p 403 A93-19417
- HAYAMI, H.**
Blade loading and shock wave in a transonic circular cascade diffuser
[ASME PAPER 92-GT-34] p 246 A93-19294
- HAYAMI, HIROSHI**
Blade loading of transonic circular cascade diffuser
p 267 A93-20919
- HAYASHI, A. K.**
Three-dimensional calculation of a hydrogen jet injection into a supersonic air flow
p 950 A93-44374
- HAYASHI, HIDECHITO**
Experimental study on the characteristics of the near wake of a rotating flat plate. III - Influence of the shape near the trailing edge on periodic-velocity-fluctuation phenomena
p 451 A93-21727
Experimental investigation into the mechanism of discrete frequency noise (DFN) generation from a NACA 0012 blade
p 1225 A93-53194
- HAYASHI, M.**
Aerodynamic heating phenomenon in three dimensional shock wave/turbulent boundary layer interaction induced by sweptback fins in hypersonic flows
p 960 A93-45507
- HAYASHI, MASANORI**
Numerical calculation of separated flows around wing section in unsteady motion by using incompressible Navier-Stokes equations
p 770 A93-38158
- HAYASHI, S.**
The properties of newly developed highly damage tolerant and easy handleable carbon fiber/modified bismaleimide prepreg system
p 1212 A93-53448
- HAYASHI, TSUTOMU**
Turbulent structure in a vortex wake shed from an inclined circular cylinder
p 125 A93-15443

- HAYASHI, YOICHI**
Compression after impact (CAI) properties of CF/PEEK (APC-2) and conventional CF/epoxy stiffened panels
p 196 A93-14307
- HAYASHI, YOSHIO**
A wind tunnel investigation to determine buffet countermeasures for STOL aircraft alpha-sweep flight testing
[NAL-TR-1129] p 65 N93-12362
- HAYDER, M. E.**
Numerical simulations of a high Mach number jet flow
[AIAA PAPER 93-0653] p 540 A93-24766
- HAYDER, M. EHTESHAM**
Numerical simulation of a high Mach number jet flow
[NASA-TM-105985] p 551 N93-20057
- HAYES, ROBERT D.**
Synthetic vision - A view in the fog
p 792 A93-37068
- HAYES, T. W.**
Use of PCs in controlling simulated altitude environmental test conditions in support of turbine engine testing
p 846 A93-37856
- HAYES, WILLIAM A.**
Subscale hot-fire testing of a formed platelet liner
[AIAA PAPER 93-1827] p 1141 A93-49713
- HAYKIN, SIMON**
Classification of radar clutter in an air traffic control environment
p 886 N93-30299
- HAYNER, CHESTER**
Achieving manufacturing excellence for gas turbine components through focused implementation of technology
[ASME PAPER 92-GT-139] p 401 A93-19371
- HAYS, ANTHONY P.**
Zen and the art of airplane sizing
p 504 A93-25174
- HAZAN, DIDIER**
Close-up analysis of aircraft ice accretion
[AIAA PAPER 93-0029] p 309 A93-23239
Close-up analysis of aircraft ice accretion
[NASA-TM-105952] p 148 N93-15360
- HAZAN, N.**
Experimental validation of a discrete vortex method for inviscid axisymmetric flow around parachute canopies
[AIAA PAPER 93-1216] p 689 A93-35165
- HAZERBROUCQ, V.**
The role of the radiologist in the medicolegal procedure after an aviation accident
p 853 A93-39701
- HE, CHENGJIAN**
Analytical formulation of optimum rotor interdisciplinary design with a three-dimensional wake
[AIAA PAPER 92-4778] p 265 A93-20416
A parametric study of real time mathematical modeling incorporating dynamic wake and elastic blades
p 798 A93-35986
Finite state aeroelastic model for use in rotor design optimization
p 1104 A93-52454
- HE, DEXIN**
Pressure fluctuations on the surface of two circular cylinders in tandem arrangements at high Reynolds numbers
p 679 A93-33718
- HE, HONGQING**
Using a diagonal implicit algorithm to calculate transonic nozzle flow
[AIAA PAPER 93-2345] p 1082 A93-50119
- HE, JIAJU**
On experimental study of 3-D flow in self-correcting wind tunnel
p 528 A93-24033
- HE, JIANLIANG**
Forces on a magnet moving past figure-eight coils
[DE93-009965] p 943 N93-29189
- HE, KEMIN**
Some key problems in the design of the NPU open-circuit low-turbulence wind tunnel
p 1139 A93-51188
- HE, LI**
Method of simulating unsteady turbomachinery flows with multiple perturbations
p 123 A93-14556
- HE, LINSHU**
An engineering method with artificial intelligence characteristics used for structural layout of wings
p 225 A93-14290
- HE, LONG-DE**
Analytical expression of dissipation integral for kinetic energy integral equation
p 1183 A93-53860
- HE, QING-ZHI**
Optimization of oleo-pneumatic shock absorber of aircraft
p 1243 A93-55415
- HE, X.**
Waveriders with finlets
[AIAA PAPER 93-3442] p 978 A93-47231
Nonlender waveriders
[AIAA PAPER 93-3467] p 982 A93-47261
Computational analysis of off-design waveriders
[AIAA PAPER 93-3488] p 982 A93-47262

- HE, XIAOHAI**
Computational analysis of hypersonic flows past generalized cone-derived waveriders p 483 N93-20288
- HE, XIAOYI**
The analysis and computation of viscous-inviscid interactive problem for three dimensional transonic flow p 681 A93-33741
- HE, YONGMEI**
A fool-proof aerodynamic design code for turbine cascades p 259 A93-20117
An aerodynamic design program for contra-rotating turbine cascades p 1067 A93-48521
- HE, ZHIDAI**
Ground effect on the take-off characteristics of sea-based aircraft p 679 A93-33706
- HEAD, ROBERT E.**
Reaction drive rotors - Lessons learned (Hero had a good idea - But) [AIAA PAPER 92-4279] p 55 A93-13352
- HEADLEY, DEAN E.**
The airline quality report, 1992 [NIAR-92-11] p 310 N93-18036
Consumer interest in the air safety data of the airline quality rating. Testimony to the US House of Representatives, Committee on Government Operations, Government Activities and Transportation Subcommittee [NIAR-92-4] p 495 N93-19941
- HEALY, J. C.**
Short fatigue crack growth in a nickel-base superalloy at room and elevated temperature [PNR-90892] p 72 N93-11031
- HEATH, D. MICHELE**
Method of remotely characterizing thermal properties of a sample [NASA-CASE-LAR-13508-3-CU] p 67 N93-11057
- HEATH, G.**
Face-gear drives: Design, analysis, and testing for helicopter transmission applications [NASA-TM-106101] p 839 N93-27133
- HEBBAR, S. K.**
Aerodynamic characteristics of the MMPT ATD vehicle at high angles of attack [AIAA PAPER 93-3493] p 982 A93-47265
- HEBBAR, SHESHAGIRI K.**
A visualization study of the vortical flow over a double-delta wing in dynamic motion [AIAA PAPER 93-3425] p 976 A93-47220
Effect of canard oscillations on the vortical flowfield of a X-31A-like fighter model in dynamic motion [AIAA PAPER 93-3427] p 1008 A93-47222
- HEBRARD, P.**
Prediction of the performances in combustion of ramjets and stato-rockets by isothermal experiments and modeling p 363 N93-17622
- HECHT, HERBERT**
Avionics software performability p 939 A93-42822
- HECHT, MYRON**
Complexity metrics for avionics software p 939 A93-42829
- HECHT, RALPH J.**
Material requirements for the High Speed Civil Transport [ISABE 93-7067] p 1200 A93-54043
- HECKMAN, NANCY L.**
Testing a wheeled landing gear system for the TH-57 helicopter [AD-A262152] p 806 N93-27547
- HED, ZEEV**
Icing prevention by ultrasonic nucleation of supercooled water droplets in front of subsonic aircraft [AD-A258212] p 142 N93-12816
- HEDDE, T.**
Improvement of the ONERA 3D icing code, comparison with 3D experimental shapes [AIAA PAPER 93-0169] p 275 A93-22603
- HEDGECOCK, C. E.**
The use of artificial intelligence for buffet environments [AIAA PAPER 93-1534] p 727 A93-34071
- HEDGES, LINDA SIGALLA**
Numerical simulation of the acoustic instability in the spatially developing, confined, supersonic mixing layer p 132 N93-13521
- HEDRICK, J. K.**
Control of a high performance aircraft with unacceptable zero dynamics p 369 A93-22905
- HEEG, JENNIFER**
Aerothermoelastic analysis of a NASP demonstrator model [AIAA PAPER 93-1366] p 733 A93-33933
Active control of aerothermoelastic effects for a conceptual hypersonic aircraft p 1007 A93-45137
Analytical and experimental investigation of flutter suppression by piezoelectric actuation [NASA-TP-3241] p 513 N93-20584
- HEERSCHAP, M. E.**
Simplified finite element representation of fuselage frames with flexible castellations p 892 A93-43570
- HEFAZI, H.**
A composite structured/unstructured-mesh Euler method for complex airfoil shapes p 784 N93-27439
- HEFFNER, K. S.**
DSMC numerical investigation of rarefied compression corner flow [AIAA PAPER 93-3096] p 1061 A93-48270
Experimental study of transitional axisymmetric shock-boundary layer interactions at Mach 5 [AIAA PAPER 93-3131] p 1063 A93-48296
- HEFFNER, PEGGY L.**
Recent improvements on the Dynamic Flight Simulator p 1011 A93-45167
- HEFNER, JERRY N.**
Laminar flow control - Introduction and overview p 859 A93-41777
- HEGARTY, DANIEL M.**
Flight test evaluation of precision-code differential GPS for terminal approach and landing p 33 A93-11294
- HEGEDUS, CHARLES R.**
F-14 wing lug coating investigation [AD-A257384] p 328 N93-15858
- HEGWOOD, JULIE ANNE YATES**
Public-sector aviation issues: Graduate research award papers, 1990 - 1991 [PB92-222629] p 143 N93-13787
- HEID, G.**
Prediction of the performances in combustion of ramjets and stato-rockets by isothermal experiments and modeling p 363 N93-17622
- HEIDARI-MIANDOAB, FARID**
Effect of passive flow-control devices on turbulent low-speed base flow p 82 N93-10304
- HEIDELBERG, LAURENCE**
Acoustic mode measurements in the inlet of a model turbofan using a continuously rotating rake - Data collection/analysis techniques [AIAA PAPER 93-0599] p 361 A93-23324
Acoustic mode measurements in the inlet of a model turbofan using a continuously rotating rake: Data collection/analysis techniques [NASA-TM-105936] p 179 N93-15403
- HEIDELBERG, LAURENCE J.**
Acoustic mode measurements in the inlet of a model turbofan using a continuously rotating rake [AIAA PAPER 93-0598] p 563 A93-24783
Acoustic mode measurements in the inlet of a model turbofan using a continuously rotating rake [NASA-TM-105989] p 362 N93-16705
- HEIDER, R.**
3D viscous flow analysis in axial turbine including tip leakage phenomena p 972 A93-46940
Three-dimensional analysis of turbine rotor flow including tip clearance [ASME PAPER 93-GT-111] p 987 A93-47446
- HEIDNER, SUSAN J.**
Public-sector aviation issues: Graduate research award papers, 1990 - 1991 [PB92-222629] p 143 N93-13787
- HEIGL, JOHN C.**
Rapid fabrication of flight worthy composite parts p 209 A93-15792
- HEIKKINEN, BONNIE D.**
CFD applications in an aeropropulsion test environment [AIAA PAPER 93-1924] p 1112 A93-49790
- HEIMBERG, F.**
Development of a realtime DGPS system [DLR-MITT-92-06] p 503 N93-20749
- HEIN, G.**
Requirements for airborne vector gravimetry p 1241 A93-55976
- HEIN, S.**
A theoretical approach for describing secondary instability features in three-dimensional boundary-layer flows [AIAA PAPER 93-0080] p 263 A93-20192
- HEINECK, JAMES T.**
Experimental investigations of the time and flow-direction responses of shear-stress-sensitive liquid crystal coatings [AIAA PAPER 93-0181] p 542 A93-25508
- HEINEMANN, K.**
An experimental study of a turbulent boundary layer in the trailing edge region of a circulation-control airfoil [NASA-CR-191262] p 295 N93-17934
Experimental Investigation of Nozzle/Plume Aerodynamics at Hypersonic Speeds [NASA-CR-191368] p 386 N93-18085
- HEINRICH, D. C.**
The effect of Reynold's number on a natural low frequency flow oscillation over an airfoil near stall [AIAA PAPER 92-4040] p 463 A93-24489
- HEINRICH, DOUGLAS C.**
Low-frequency flow oscillation over airfoils near stall p 861 A93-41931
Effect of underwing frost on transport aircraft takeoff performance [DOT/FAA/CT-TN93/9] p 791 N93-27252
- HEINRICH, G.**
SIPOET DEPCOS and SIPOET ARRCOS - More than an electronic airstrip replacement p 499 A93-27914
- HEINRICH, JUAN C.**
Finite element analysis of the Scramaccelerator with finite rate chemistry [AIAA PAPER 93-0745] p 540 A93-24833
- HEINRICH, W.**
Radiation exposure in aircraft p 1035 N93-31928
- HEISER, WILLIAM H.**
Isolator-combustor interaction in a dual-mode scramjet engine [AIAA PAPER 93-0358] p 360 A93-23041
- HEISS, STEFAN**
Enhanced numerical inviscid and viscous fluxes for cell centered finite volume schemes p 864 A93-42444
Numerical methods for aerothermodynamic design of hypersonic space transport vehicles [MBB-FE-211-S-PUB-0481] p 514 N93-21056
Application of the Euler method EUFLEX to a fighter-type airplane configuration at transonic speed [MBB-FE-211-S-PUB-0489-A] p 484 N93-21059
- HEITOR, M. V.**
On the analysis of an impinging jet on ground effects p 1260 A93-56339
- HELD, DANIEL N.**
Topographic mapping using a Ku-band airborne elevation interferometer p 896 A93-42786
- HELIN, HANK E.**
Unsteady vortex dynamics and surface pressure topologies on a pitching wing [AIAA PAPER 93-0435] p 286 A93-23349
- HELLBAUM, R. F.**
Direct measurements of skin friction in supersonic combustion flow fields [AD-A262878] p 825 N93-28226
- HELLBOM, KURT**
On design methods for bolted joints in composite aircraft structures p 1158 A93-50430
- HELLER, GERARD**
Data collection procedures for the Software Engineering Laboratory (SEL) database [NASA-TM-108579] p 230 N93-15579
- HEMDAN, HANDI T.**
Newtonian and hypersonic flows over oscillating bodies of revolution. I - Circular cones p 857 A93-39942
Newtonian and hypersonic flows over oscillating bodies of revolution. II - Parabolic bodies p 872 A93-42931
- HENKNER, P. W.**
Efficient multigrid computation of steady hypersonic flows p 1152 A93-49527
- HEMPSELL, MARK**
MAKS - Eastern promise? p 733 A93-34266
- HENAFF, GILBERT**
Damage tolerance of a helicopter rotor high-strength steel p 555 N93-21322
- HENBEST, S. M.**
Measurement and prediction of flow in a gas turbine engine exhaust plume [ISABE 93-7113] p 1204 A93-54088
- HENCKELS, A.**
Experimental study of the longitudinal hypersonic corner flow field - HERMES-R&D research program, problem no. 5 p 867 A93-42602
Applications of infrared measurement technique in hypersonic facilities p 1024 A93-455C5
Experimental investigations of hypersonic shock-boundary layer interaction p 1238 A93-56037
- HENDERSON, DAVID M.**
Reference equations of motion for automatic rendezvous and capture [NASA-CR-185676] p 914 N93-29652
- HENDERSON, DOUGLAS A.**
Modal survey of a full-scale F-18 wind tunnel model [AD-A262482] p 875 N93-29410
- HENDERSON, GREGORY H.**
Forcing function effects on unsteady aerodynamic gust response. I - Forcing functions [ASME PAPER 92-GT-174] p 251 A93-19400
Forcing function effects on unsteady aerodynamic gust response. II - Low solidity airfoil row response [ASME PAPER 92-GT-175] p 251 A93-19401
- HENDERSON, T. L.**
Three-dimensional Navier-Stokes calculations using solution-adapted grids [AIAA PAPER 93-0431] p 462 A93-24240
- HENDGES, ALOIS**
Aerial cartography using SICAD NAV-AIR p 1034 N93-31258

HENDREN, SCOTT

HENDREN, SCOTT

Test results of the effects of air ionization on cigarette smoke particulate levels within a commercial airplane [SAE PAPER 921183] p 855 A93-41362

HENDRICKS, E. W.

A comparison of the drag-reducing benefits of riblets in internal and external flows p 395 A93-18054

HENDRICKS, ERIC W.

Recent progress in the implementation of active combustion control p 171 A93-14272

HENDRICKS, R. C.

Driven cavity simulation of turbomachine blade flows with vortex control [AIAA PAPER 93-0390] p 461 A93-24238

HENDRICKS, ROBERT C.

Brush seal leakage performance with gaseous working fluids at static and low rotor speed conditions [ASME PAPER 92-GT-304] p 405 A93-19494

Brush seal low surface speed hard-rub characteristics [AIAA PAPER 93-2534] p 1156 A93-50261

Brush seal bristle flexure and hard-rub characteristics [NASA-TM-105864] p 421 N93-18321

Integrity testing of brush seal in shroud ring of T-700 engine [NASA-TM-105863] p 421 N93-18380

Brush seal low surface speed hard-rub characteristics [NASA-TM-106169] p 838 N93-27132

HENDRICKS, WILLIAM R.

The Aloha Airlines accident - A new era for aging aircraft p 991 A93-45783

HENDRIX, B. C.

Raising the high temperature limit of the nickel-iron-base superalloy p 70 A93-12114

HENEGHAN, S. P.

Effects of back-pressure in a lean blowout research combustor [ASME PAPER 92-GT-81] p 387 A93-19330

Studies of jet thermal stability in a flowing system [ASME PAPER 92-GT-106] p 401 A93-19344

HENEGHAN, SHAWN P.

Static tests of jet fuel thermal and oxidative stability p 389 A93-21651

HENK, R. W.

The analysis of unsteady, three-dimensional flow separation [AIAA PAPER 93-0642] p 540 A93-24757

HENKE, H.

Computation of subsonic viscous and transonic viscous-inviscid unsteady flow p 1094 A93-50212

HENKE, R.

The jet behaviour of an actual high-bypass engine as determined by LDA-measurements in ground tests p 175 N93-13218

HENNECKE, D. K.

An approach to the stall monitoring in a single stage axial compressor [AIAA PAPER 93-1872] p 1112 A93-49747

Heat transfer and material temperature conditions in the leading edge area of impingement-cooled turbine vanes [ISABE 93-7076] p 1220 A93-54052

The effect of main stream flow angle on flame tube film cooling p 932 N93-29953

HENNESSY, ROBERT T.

Visual augmentation for night flight over featureless terrain p 806 A93-35921

HENNINGS, ELSA J.

High efficiency, low weight and volume energy absorbent seam [AD-D015531] p 554 N93-20765

HENRI, AGNES

Structural stability of 'beta-CEZ' alloy [ONERA, TP NO. 1992-106] p 824 A93-38586

HENRY, R.

Structural dynamic characteristics of individual blades p 1005 N93-32272

HENRY, ZACHARY S.

Low-noise, high-strength, spiral-bevel gears for helicopter transmissions [AIAA PAPER 93-2149] p 1154 A93-49966

HENSHALL, S. E.

Discharge coefficients of holes angled to the flow direction [ASME PAPER 92-GT-192] p 403 A93-19417

HENSHAW, DAVID GEOFFREY

An experimental evaluation of prediction methods for contrails [PNR-90924] p 56 N93-11023

HENZE, A.

Supersonic and hypersonic flow computations for the research configuration ELAC I and comparison to experimental data p 1237 A93-56034

HERBELL, THOMAS P.

Ceramic matrix composites for rocket engine turbine applications [ASME PAPER 92-GT-394] p 388 A93-19547

HERBERT, TH.

Effects of free-stream turbulence on boundary-layer transition [AIAA PAPER 93-0468] p 416 A93-23390

HERBERT, THORWALD

Stability and transition on swept wings [AIAA PAPER 93-0078] p 263 A93-20190

Active flow control with neural networks [AIAA PAPER 93-3273] p 1037 A93-46834

HERDMAN, TERRY L.

Finite memory approximations for a singular neutral system arising in aeroelasticity p 97 A93-13246

HERMES, LAURIE G.

Detection of microburst-related gust fronts using Doppler radar p 427 A93-22118

An improved gust front detection algorithm for the TDWR p 432 A93-22191

HERMES, PHILLIP

R&M 2000 field data requirements for a SPO operation p 856 A93-42853

HERNANDEZ, FRANCISCO

Correlation of airloads on a two-bladed helicopter rotor p 481 A93-29438

HERON, K. H.

European research into helicopter internal noise p 1243 A93-54724

HERON, RUTH M.

Use of microprocessor-based simulator technology and MEG/EEG measurement techniques in pilot emergency-maneuver training p 530 N93-19706

HERRIN, J. L.

Supersonic base flow experiments in the near-wake of a cylindrical afterbody [AIAA PAPER 93-2924] p 1045 A93-48125

HERRING, PAUL G. C.

Flow quality improvement in a high speed blowdown wind tunnel [AIAA PAPER 93-0353] p 377 A93-23038

HERRMANN, O.

Integration of turbo-expander- and turbo-ramjet-engines in hypersonic vehicles [ASME PAPER 92-GT-204] p 353 A93-19428

Integration of turbo-ramjet engines for hypersonic aircraft p 175 N93-13230

HERRMANN, U.

Computation of flows over 2D ramps p 866 A93-42595

Computation of the hypersonic flow over a double ellipsoid p 868 A93-42610

HERSCH, PHILIP L.

General aviation turbine markets - An economic overview [AIAA PAPER 92-4191] p 103 A93-13369

HERSEE, STEPHEN D.

Sources and detectors for fiber communications; Proceedings of the Meeting, Boston, MA, Sept. 8, 9, 1992 [SPIE-1788] p 1151 A93-49455

HERTZBERG, A.

Initiation of combustion in the thermally choked ram accelerator p 1016 A93-45501

Investigation of the aerothermodynamics of hypervelocity reacting flows in the ram accelerator [NASA-CR-191715] p 140 N93-15588

HERZING, WOLFGANG

The costs of noise at the new Munich airport p 558 A93-28493

HESELHAUS, A.

Coupling of 3D-Navier-Stokes external flow calculations and internal 3D-heat conduction calculations for cooled turbine blades p 904 N93-29961

HESLEHURST, RIKARD B.

Accuracy of a simple hole damage analysis method in composite structures p 197 A93-15748

HESS, CECIL F.

Optical microphone for the detection of hidden helicopters p 205 A93-14542

HESS, ERIC

Terminal Doppler Weather Radar (TDWR) Operational Test and Evaluation (OT/E) integration test plan [DOT/FAA/CT-TN92/6] p 151 N93-13377

HESS, R. A.

Flight simulator fidelity assessment in a rotorcraft lateral translation maneuver p 378 A93-23510

Inverse simulation of large-amplitude aircraft maneuvers p 906 A93-41893

Quantitative feedback theory applied to the design of a rotorcraft flight control system p 906 A93-41895

HESS, ROBERT A.

On the use of back propagation with feed-forward neural networks for the aerodynamic estimation problem [AIAA PAPER 93-3638] p 1165 A93-48323

HESEL, R. P.

Intake flow modeling in a four stroke diesel using KIVA3 [AIAA PAPER 93-2952] p 1148 A93-48146

HETU, JEAN-FRANCOIS

An adaptive finite element method for turbulent free shear flow past a propeller [AIAA PAPER 93-3388] p 956 A93-45079

HETYEI, JOSEPH

Airborne MLS equipment p 312 A93-18555

HEULER, PAUL

Fractographic investigation of IMI 685 crack propagation specimens for SMP SC33 p 1004 N93-31743

Crack growth prediction models p 1004 N93-31747

HEVENOR, RICHARD A.

Automated extraction of aircraft runway patterns from radar imagery [AD-A254258] p 68 N93-11751

HEWITT, JOHN

T55 engine - The challenge of torque measurement p 809 A93-35929

HEYES, F. J. G.

The measurement and prediction of the tip clearance flow in linear turbine cascades [ASME PAPER 92-GT-214] p 252 A93-19437

HEYMAN, JOSEPH S.

Method of remotely characterizing thermal properties of a sample [NASA-CASE-LAR-13508-3-CU] p 67 N93-11057

HEYMSFIELD, GERALD M.

Update on the NASA ER-2 Doppler radar system (EDOP) p 807 A93-37737

HICKEY, P. K.

A design approach to high Mach number scramjet performance [AIAA PAPER 92-4248] p 55 A93-13360

HICKS, D. L.

Genetic design of digital model-following flight-control systems [AIAA PAPER 93-3883] p 1135 A93-51468

HICKS, DUANE

Fail safety aspects of the V-22 pylon conversion actuator p 798 A93-35984

HICKS, JOHN W.

Development of a hydrogen external burning flight test experiment on the NASA Dryden SR-71A aircraft [SAE PAPER 920997] p 157 A93-14638

Real-time in-flight engine performance and health monitoring techniques for flight research application p 169 N93-15169

HIGASHINO, FUMIO

Study on unsymmetrical supersonic nozzle flows p 127 A93-16933

Numerical investigation of supersonic flows around a spiked blunt-body [AIAA PAPER 93-0887] p 471 A93-24947

Numerical simulation of flow for a scramjet nozzle p 302 N93-19299

HIGASHINO, KAZUYUKI

Results of sea-level static tests on air turbo ramjet for a future space plane [AAS PAPER 91-640] p 1247 A93-55817

HIGGINS, JAMES

RTJ-303: Variable geometry, oblique wing supersonic aircraft [NASA-CR-192054] p 337 N93-18166

HIGGINS, T. M.

Experimental determination of the bulk swirl attenuation between two axial stations in the LM2500 inlet bellmouth [AIAA PAPER 93-2203] p 1155 A93-50015

HIGGINS, TIMOTHY

A manned hypersonic reconnaissance vehicle which does not require airborne fueling p 333 N93-17888

HILBY, D. L.

The development of the Boeing Human Model p 561 A93-27150

HILDEBRAND, PETER H.

A technique to correct airborne Doppler data for coordinate transformation errors using surface clutter p 807 A93-37639

HILGENSTOCK, ACHIM

The ViB-code to simulate 3-D stator/rotor flow in axial turbines [DLR-FB-92-19] p 1003 N93-31170

HILL, A. J.

Aircraft designer's viewpoint of reliability and maintainability p 45 A93-13404

HILL, C. K.

Natural environment application for NASP-X-30 design and mission planning [AIAA PAPER 93-0851] p 531 A93-24915

HILL, DALLAS

Test results of an orifice pulse tube refrigerator p 1149 A93-48612

HILL, JAMES D.

Mach 5 turboramjet requirements and design approach [ISABE 93-7015] p 1194 A93-53991

- HILL, JEFFREY S.**
Application of a neural network as a potential aid in predicting NTF pump failure
[NASA-TM-107667] p 442 N93-18332
- HILL, KEVIN**
Hypersonic reconnaissance aircraft
[NASA-CR-192049] p 333 N93-17804
- HILL, R. J.**
Simultaneous engineering in the design of aero engines
[PNR-90973] p 57 N93-11062
The Trent family of engines
[PNR-90974] p 58 N93-11063
- HILL, RICHARD J.**
The challenge of IHPTET
[ISABE 93-7001] p 1194 A93-53978
- HILL, S. H.**
The design and evaluation of a high pressure ratio radial turbine
[ASME PAPER 92-GT-93] p 349 A93-19339
- HILL, W. G., JR.**
CFD analysis of the X-29 inlet at high angle of attack
p 958 A93-45140
- HILLGERT, R.**
GARTEUR damage mechanics for composite materials: Analytical/experimental research on delaminations
p 537 N93-21513
- HILLIER, R.**
Computation of unsteady nozzle flows
p 960 A93-45543
- HILLSTROEM, LARS**
Optical blade vibration measurement
[ETN-93-93454] p 905 N93-29999
- HILTNER, D. W.**
Calibration of a transonic 5-hole probe for a multi-element airfoil cascade facility
[AIAA PAPER 93-2471] p 1138 A93-50216
- HILTON, HARRY H.**
Bending-torsion flutter of linear viscoelastic wings including structural damping
[AIAA PAPER 93-1475] p 711 A93-34021
- HILTON, P. D.**
Development of a unified airport pavement analysis and design system
p 380 N93-16317
- HINADA, MOTOKI**
Atmospheric reentry flight test of winged space vehicle
[AIAA PAPER 92-5053] p 385 A93-22324
Analytical study on the separation dynamics of LUNAR-A/penetrator
p 1265 A93-56272
- HINCHEE, R. E.**
In-situ bioventing: Two US EPA and Air Force sponsored field studies
[PB93-194231] p 1035 N93-32089
- HINCHEY, M. J.**
On hovercraft overwater heave stability
p 1219 A93-53819
Kelvin-Helmholtz wave generation beneath hovercraft skirts
p 1219 A93-53820
- HINDS, H. A.**
Review of initial experiments using the Hawk model, dynamic rig facility, and the CED 1401 digital data acquisition equipment
[CRANFIELD-AERO-9017] p 531 N93-21406
- HINDS, J. M.**
A computer simulation of the production of an artificially ionized layer using the Arecibo facility
[DE93-010817] p 937 N93-30487
- HINDSON, WILLIAM S.**
Preliminary design features of the RASCAL - A NASA/Army rotorcraft in-flight simulator
[AIAA PAPER 92-4175] p 42 A93-13311
- HINES, RICHARD**
Engine technology challenges for a 21st Century High-Speed Civil Transport
[ISABE 93-7064] p 1200 A93-54040
Engine technology challenges for a 21st Century High-Speed Civil Transport
[NASA-TM-106216] p 1004 N93-31671
- HINGORANI, S. S.**
Optimization of a highly-loaded axial splittor rotor design
p 1002 A93-46931
- HINGST, W. R.**
Surface and flow field measurements in a symmetric crossing shock wave/turbulent boundary-layer interaction
[NASA-TM-106086] p 693 N93-24911
- HINKELMAN, JOHN**
Preliminary results of the detection of clear air turbulence by the Wind Profiler Demonstration Network
p 427 A93-22119
- HINKELMAN, JOHN W., JR.**
Operational aviation weather service requirements
p 429 A93-22145
- HINNANT, HOWARD E.**
Dynamic analysis of pretwisted elastically-coupled rotor blades
p 326 A93-21125
- HINTON, DAVID A.**
Microburst avoidance crew procedures for forward-look sensor equipped aircraft
[AIAA PAPER 93-3942] p 1007 A93-44234
Air/ground wind shear information integration: Flight test results
p 488 N93-19594
Airborne derivation of microburst alerts from ground-based Terminal Doppler Weather Radar information: A flight evaluation
[NASA-TM-108990] p 1000 N93-32223
- HINZ, B.**
Design and fabrication of a composite transmission housing for a helicopter tail rotor
p 156 A93-14339
- HIPPENSTEELE, STEVEN A.**
High Reynolds number and turbulence effects on aerodynamics and heat transfer in a turbine cascade
[AIAA PAPER 93-2252] p 1155 A93-50050
Measurements and computational analysis of heat transfer and flow in a simulated turbine blade internal cooling passage
[AIAA PAPER 93-1797] p 1218 A93-53585
High Reynolds number and turbulence effects on aerodynamics and heat transfer in a turbine cascade
[NASA-TM-106187] p 930 N93-29157
Measurements and computational analysis of heat transfer and flow in a simulated turbine blade internal cooling passage
[NASA-TM-106189] p 1032 N93-31647
- HIPPLER, H.**
A laser induced fluorescence system for the high enthalpy shock tunnel (HEG) in Goettingen
p 1024 A93-45506
- HIRAIWA, TETSUO**
Evaluation of 2D scramjet nozzle performance
p 52 A93-11209
Off-design performance of scramjet nozzles
[ISABE 93-7108] p 1203 A93-54084
- HIRAMOTO, T.**
The conceptual study of supersonic transport structure
[AIAA PAPER 92-4219] p 43 A93-13348
- HIRANO, K.**
Active control of vortex breakdown by a spinning wave generator
[ISABE 93-7045] p 1219 A93-54021
- HIRAOKA, KATSUMI**
Effect of the flow non-uniformity on the mixing layer at the interface of parallel supersonic flows
[ISAS-RN-646] p 128 N93-12716
- HIRASAWA, KAZUYUKI**
Numerical simulation of flows in a supersonic air intake
p 303 N93-19314
- HIRASAWA, T.**
Polar Patrol Balloon Experiment in Antarctica
p 27 A93-11373
- HIRATA, MASARU**
Dual transverse injection of H2 gas into Mach 1.8 flows at University Komaba wind tunnel
p 376 A93-21833
- HIRATA, SHINGO**
Research on combined HOPE navigation technology
p 533 N93-20428
- HIROKAWA, JUNICHI**
Feasibility study on single bypass variable cycle engine with ejector
[AIAA PAPER 92-4268] p 55 A93-13366
- HIROKAWA, YASUO**
Experimental study on the characteristics of the near wake of a rotating flat plate. III - Influence of the shape near the trailing edge on periodic-velocity-fluctuation phenomena
p 451 A93-21727
- HIROSAWA, H.**
The improvement of the static launch method in Japan
p 26 A93-11364
Trans-oceanic balloon flight over east China sea
p 27 A93-11372
- HIROSE, HIDEHIRO**
Wind tunnel tests and CFD in Fuji Heavy Industries
p 304 N93-19323
- HIROSE, KOJI**
A flat plate wing standing on a wall covered with a thick boundary layer. II - Wing characteristics under the effects of side wall boundary layer and wing tip vortex
p 125 A93-15446
- HIROYASU, HIROYUKI**
Characteristics of liquid jet atomization across a high-speed airstream. I - Experiment on shape of spray, spatial distribution of injected liquid and Sauter mean diameter
p 411 A93-21743
Characteristics of liquid jet atomization across a high-speed airstream. II - Calculation of spatial distribution of liquid, variation of drop diameter and drop trajectory
p 412 A93-21744
- HIRSCH, CH.**
Experimental study on the three dimensional flow within a compressor cascade with tip clearance. I - Velocity and pressure fields
[ASME PAPER 92-GT-215] p 258 A93-19574
Experimental study on the three dimensional flow within a compressor cascade with tip clearance. II - The tip leakage vortex
[ASME PAPER 92-GT-432] p 258 A93-19575
New upwind dissipation models with a multidimensional approach
[AIAA PAPER 93-3304] p 950 A93-45002
The three dimensional flow in a compressor cascade at design and off-design conditions
p 971 A93-46927
The PEP Symposium on CFD Techniques for Propulsion Applications
p 214 N93-13210
- HIRSCHFEL, E. H.**
Heat loads as key problem of hypersonic flight
p 1222 A93-54276
Hot experimental technique: A new requirement of aerothermodynamics
[MBB-FE-202-S-PUB-480] p 293 N93-17543
Heat loads as key problem of hypersonic flight
[MBB-FE-202-S-PUB-0486] p 484 N93-21054
Technology transfer: Potential of BMFT concept for hypersonics
[MBB-LME-202-S-PUB-0505] p 1041 N93-31045
- HIRSINGER, FRANCIS**
Toward the second-generation supersonic transport
[ONERA, TP NO. 1993-26] p 890 A93-41038
- HIRST, DONALD J.**
F-14 wing lug coating investigation
[AD-A257384] p 328 N93-15858
- HISERT, GLEN L.**
Autogenic-feedback training improves pilot performance during emergency flying conditions
[NASA-TM-104005] p 790 N93-27076
- HITZEL, STEPHAN M.**
Inviscid hypersonic flow over a delta wing
p 870 A93-42634
- HO, CHIEN-KO**
Numerical simulation of unsteady transonic nozzle flows
p 272 A93-22230
- HO, CHIH-MING**
Vortex breakdown over delta wings in unsteady free stream
[AIAA PAPER 93-0555] p 285 A93-23294
Free shear layer control and its application to fan noise
[AIAA PAPER 93-3242] p 965 A93-46787
Control of lift and drag in unsteady flows
[AD-A253146] p 17 N93-10340
Control of asymmetric jet
[AD-A255967] p 219 N93-14400
- HO, THINH Q.**
Effects of substrate anisotropy on coupled bilateral finlines
p 208 A93-15409
- HOAD, DANNY R.**
Acoustic flight test experience with the XV-15 Tiltrotor aircraft with the Advanced Technology Blade (ATB)
p 445 A93-19143
- HOADLEY, D.**
Test facility for evaluation of structural integrity of stiffened and jointed aircraft curved panels
p 1012 A93-45794
- HOADLEY, SHERWOOD T.**
ISAC - A tool for aeroservoelastic modeling and analysis
[AIAA PAPER 93-1421] p 726 A93-33974
Multiple-function multi-input/multi-output digital control and on-line analysis
[NASA-TM-107697] p 162 N93-13565
- HOANG, N. T.**
3-D LDV measurements over a delta wing in pitch-up motion
[AIAA PAPER 93-0185] p 275 A93-22610
- HOANG, NGOC THAI**
The hemisphere-cylinder at an angle of attack
p 21 N93-11250
- HOANG, PHILLIP P.**
Data Multiplexing Network (DMN). Phase 3: Equipment Operational Test and Evaluation (OT/E) integration test report
[DOT/FAA/CT-TN92/49] p 503 N93-20612
The Data Multiplexing Network (DMN) phase 3 Extended Distance Data Cable (EDDC) test and evaluation
[DOT/FAA/CT-TN93/11] p 752 N93-26160
Data Multiplexing Network (DMN) equipment Operational Test and Evaluation (OT/E) integration test report
[AD-A263172] p 942 N93-29490
- HOARD, M. A.**
Reconfigurable photonic data networks for military aircraft
p 928 A93-42783

HOBBS, CHRIS

The inspection of aeronautical structures using transient thermography p 1258 A93-54899

HOBSON, G. V.

Inlet turbulence distortion and viscous flow development in a controlled-diffusion compressor cascade at very high incidence p 688 A93-34485

Establishing two-dimensional flow in a large-scale cascade of controlled-diffusion compressor blades [AIAA PAPER 93-2383] p 1083 A93-50151

HOBSON, GARTH V.

Flowfield computations over the Space Shuttle Orbiter with a proposed canard at a Mach number of 5.8 and 50 degrees angle of attack p 281 A93-23014 [AIAA PAPER 93-0322]

HOCHEMANN, DAVID

Transmission error and load distribution analysis of spur and double helical gear pairs used in a split path helicopter transmission design p 549 A93-29426

HOCKENHULL, B. S.

The effect of exfoliation corrosion on the fatigue behavior of structural aluminum alloys p 1017 A93-45778

HODGE, JEFFREY S.

A flutter investigation of all-moveable NASP-like wings at hypersonic speeds p 769 A93-37427 [AIAA PAPER 93-1315]

HODGE, S. M.

Airborne gravimetry from a light aircraft p 1245 A93-55972

HODGES, DEWEY H.

An interactive numerical procedure for rotor aeroelastic stability analysis using elastic lifting surface p 155 A93-14313

HODGKINS, P. DOUGLAS

A description of the Mode Select beacon system (Mode S) and its associated benefits to the National Airspace System (NAS) [DOT/FAA/SE-92/6] p 35 A93-10738

HODGKINSON, JOHN

Aerospace '92 - The year in review p 455 A93-19976

Longitudinal and lateral-directional flying qualities investigation of high-order characteristics for advanced-technology transports p 1133 A93-51406 [AIAA PAPER 93-3815]

Initial results of an in-flight investigation of longitudinal flying qualities for augmented, large transports in approach and landing p 1133 A93-51407 [AIAA PAPER 93-3816]

HODSON, C. H.

X-31A flight flutter test excitation by control surfaces p 727 A93-34075 [AIAA PAPER 93-1538]

HODSON, H. P.

The measurement and prediction of the tip clearance flow in linear turbine cascades p 252 A93-19437 [ASME PAPER 92-GT-214]

A laminar flow rotor for a radial inflow turbine p 1074 A93-49686 [AIAA PAPER 93-1796]

Numerical and experimental investigation of turbine tip gap flow p 1081 A93-50051 [AIAA PAPER 93-2253]

3-dimensional interactions in the rotor of an axial turbine p 1081 A93-50053 [AIAA PAPER 93-2255]

HOEFLE, E.

Propulsion system simulator with propan for tests on a large scale model of IL-114 airplane in a full-size wind tunnel of TsAGI p 1013 A93-46933

HOEGER, M.

Prediction of 2D viscous transonic flow in compressor cascades using a semi-empirical shock/boundary-layer interaction method p 253 A93-19470 [ASME PAPER 92-GT-277]

HOEIJMAKERS, H. W. M.

The application of an Euler method and a Navier Stokes method to the vortical flow about a delta wing p 984 A93-47276 [AIAA PAPER 93-3510]

Comparison of solution of various Euler solvers and one Navier-Stokes solver for the flow about a sharp-edged cropped delta wing p 418 A93-16411 [NLR-TP-90340-U]

Application of an Euler-equation method to a sharp-edged delta wing configuration with vortex flow p 294 A93-17809 [NLR-TP-91306]

Panel methods for aerodynamic analysis and design p 990 A93-32357 [NLR-TP-91404-U]

HOENLINGER, H.

Technological challenges with smart structures in German aircraft industry p 320 A93-17714

HOEY, ROBERT G.

Research on the stability and control of soaring birds p 61 A93-11284 [AIAA PAPER 92-4122]

Why simulators don't fly like the airplane: Data - An update with examples from the C-141B program p 66 A93-13312 [AIAA PAPER 92-4161]

HOFFMAN, JAY

Optimal circumferential placement of cylindrical thermocouple probes for reduction of excitation forces [ASME PAPER 92-GT-423] p 406 A93-19571

HOFFMAN, JOE D.

Hypervelocity scramjet combustor-nozzle analysis and design p 60 A93-12214 [NASA-CR-190965]

Analytical and experimental investigation of annular propulsive nozzles p 815 A93-28391 [AD-A262685]

HOFFMAN, JONATHAN M.

Recent developments in aviation case law p 569 A93-23870

HOFFMAN, MARGERY E.

A neural network prototype for predicting F-14B strains at the B.L. 10 longeron p 165 A93-15004 [AD-A255272]

HOFFMANN, B.

Investigations on a radial compressor tandem-rotor stage with adjustable geometry p 404 A93-19440 [ASME PAPER 92-GT-218]

HOFFMANN, HANS-EBERHARD

Identification of icing water clouds by NOAA AVHRR satellite data p 434 A93-16477 [DLR-FB-92-11]

HOFFMANN, LORENZ

Active flow control with neural networks p 1037 A93-46834 [AIAA PAPER 93-3273]

HOGABOOM, R.

Integrated use of GPS and GLONASS in civil aviation navigation. II - Experience with GLONASS p 313 A93-21142

HOGAN, R. E.

Numerical solution of axisymmetric heat conduction problems using finite control volume technique p 928 A93-42909

Ablation problems using a finite control volume technique p 942 A93-29187 [DE93-009861]

HOGG, S. I.

A test facility for the thermofluid-dynamics of gas bearing lubrication films p 72 A93-11032 [PNR-90897]

HOGGARD, A. W.

Maintaining the safety of an aging fleet of aircraft p 3 A93-13632

HOGGARD, AMOS W.

Fuselage longitudinal splice design p 997 A93-45784

HOGUE, JEFFREY R.

A simulator solution for the parachute canopy control and guidance training problem p 191 A93-14634 [SAE PAPER 920984]

Parachute canopy control and guidance training requirements and methodology p 703 A93-35188 [AIAA PAPER 93-1255]

HOH, ROGER

The development and implementation of a head-up guidance system (HGS) for manual CAT III landings p 151 A93-17306

HOH, ROGER H.

Handling qualities testing using the mission oriented requirements of ADS-33C p 817 A93-35961

Ground based simulation evaluation of the effects of time delays and motion on rotorcraft handling qualities p 328 A93-16186 [AD-A256921]

HOHEISEL, H.

Time-dependent 3-component laser-Doppler-anemometer and simultaneous position measurements in the flow of an aircraft engine p 538 A93-23809

The jet behaviour of an actual high-bypass engine as determined by LDA-measurements in ground tests p 175 A93-13218

Investigation of the flowfield around an isolated bypass engine with fan and core jet p 215 A93-13227

HOISINGTON, M. A.

Model multilayer structured composites p 533 A93-24509

HOKARI, TAKASHI

Numerical simulation of the flow through non-uniform airfoil cascade p 302 A93-19310

HOLDEMAN, J. D.

Optimization of circular orifice jets mixing into a heated crossflow in a cylindrical duct p 361 A93-23246 [AIAA PAPER 93-0249]

An analytical study of dilution jet mixing in a cylindrical duct p 1113 A93-49876 [AIAA PAPER 93-2043]

Optimization of circular orifice jets mixing into a heated cross flow in a cylindrical duct p 179 A93-15359 [NASA-TM-105984]

Experimental investigation of crossflow jet mixing in a rectangular duct p 812 A93-27026 [NASA-TM-106152]

CFD mixing analysis of axially opposed rows of jets injected into confined crossflow p 813 A93-27128 [NASA-TM-106179]

An analytical study of dilution jet mixing in a cylindrical duct p 814 A93-27160 [NASA-TM-106181]

HOLDEMAN, JAMES D.

Mixing of multiple jets with a confined subsonic crossflow p 1189 A93-54324

HOLDEN, MICHAEL S.

A preliminary study associated with the experimental measurement of the aero-optic characteristics of hypersonic configurations p 24 A93-12063 [AD-A253792]

HOLIBAUGH, ROBERT

Joint Integrated Avionics Working Group (JIAWG) object-oriented domain analysis method (JODA), version 3.1 p 344 A93-18270 [AD-A258468]

HOLL, MICHAEL

A comparison of classical mechanics models and finite element simulation of elastically tailored wing boxes p 922 A93-30863

HOLL, MICHAEL W.

Tailored composite wings with elastically produced chordwise camber p 923 A93-30876

HOLLAND, ANNE D.

Transient/structural analysis of a combustor under explosive loads p 420 A93-17779 [NASA-TM-107660]

HOLLAND, RAINER

Helicopter in-flight simulator ATTHS - A multipurpose testbed and its utilization p 43 A93-13315 [AIAA PAPER 92-4173]

HOLLAND, SCOTT D.

An experimental parametric study of geometric, Reynolds number, and ratio of specific heats effects in three-dimensional sidewall compression scramjet inlets at Mach 6 p 466 A93-24830 [AIAA PAPER 93-0740]

Computational parametric study of sidewall-compression scramjet inlet performance at Mach 10 p 552 A93-20299 [NASA-TM-4411]

HOLLANDERS, H.

Some aspects of the aerodynamic methodology in hypersonic vehicle concept studies p 272 A93-22303 [AIAA PAPER 92-5027]

Navier-Stokes calculations over a double ellipse and a double ellipsoid by an implicit non-centered method p 867 A93-42607

HOLLENBACK, D. M.

Application of a parabolized Navier-Stokes code to an HST configuration and comparison to wind tunnel test data p 986 A93-47288 [AIAA PAPER 93-3537]

HOLLEY, C. D.

Development of an expert system for cockpit emergency procedures p 845 A93-35915

HOLLINGS, ERNEST F.

National Aeronautics and Space Administration Authorization Act, fiscal year 1993 p 234 A93-13798 [S-REPT-102-364]

HOLLIS, JEANETTE

New developments in organized wire systems p 764 A93-35973

HOLLMAN, EDWARD J.

Controlling hazardous configurations in helicopter systems p 763 A93-35927

HOLLOWAY, D. A.

Use of local x ray computerized tomography for high-resolution, region-of-interest inspection of large ceramic components for engines p 843 A93-28943 [DE93-005564]

HOLMES, BRUCE J.

Flight research on natural laminar flow applications p 890 A93-41779

Swept wing attachment line contamination fence p 485 A93-22015 [NASA-CASE-LAR-13400-1]

HOLMES, D. G.

A 3D unstructured adaptive multigrid scheme for the Euler equations p 954 A93-45033 [AIAA PAPER 93-3339]

HOLMES, J. W.

Introduction of electronic pressure scanning at the Royal Aerospace Establishment p 23 A93-11882 [RAE-TM-AERO-2222]

HOLOWECKY, BRIAN R.

A parameter optimization approach to controller partitioning for integrated flight/propulsion control application p 1206 A93-54268

HOLSTE, F.

Experimental determination of the main noise sources in a profan model by analysis of the acoustic spinning modes in the exit plane p 449 A93-19214

- HOLT, DANIEL J.**
Aircraft braking systems p 995 A93-44850
- HOLT, M.**
Flight vehicle aerodynamics calculated by a Galerkin finite element/finite difference method p 266 A93-20738
- HOLTZCLAW, K. W.**
Real-time optical measurement of alkali species in air for jet engine corrosion testing [AIAA PAPER 93-0791] p 541 A93-24870
- HOLZ, R.**
High-speed helicopter rotor noise - Shock waves as a potent source of sound p 565 A93-29403
- HOLZ, RICHARD**
A 2-D numerical model for predicting the aerodynamic performance of the NOTAR system tailboom p 766 A93-35994
- HOLZHAUSER, T. B.**
The development of the Boeing Human Model p 561 A93-27150
- HOMMA, NAOKI**
LIF visualization of 3-dimensional hypersonic mixing [ISABE 93-7114] p 1221 A93-54089
- HOMSY, G. M.**
Numerical methods in laminar and turbulent flow; Proceedings of the 7th International Conference, Stanford Univ., CA, July 15-19, 1991. Vol. 7, pts. 1 & 2 [ISBN 0-906674-77-8] p 743 A93-34301
- HONAMI, SHINJI**
Behaviors of the laterally injected jet in film cooling - Measurements of surface temperature and velocity/temperature field within the jet [ASME PAPER 92-GT-180] p 402 A93-19405
Experimental study of mixed compression air-intake for hypersonic airbreathing engines [ASME PAPER 92-GT-349] p 355 A93-19519
Effects of boundary layer bleed on swept-shock/boundary layer interaction [AIAA PAPER 93-2989] p 1052 A93-48182
An experimental study of supersonic air-intake with 5-shock system at Mach 3 [AIAA PAPER 93-2305] p 1082 A93-50089
Two-dimensional numerical simulation for Mach-3 multishock air-intake with bleed systems [AIAA PAPER 93-2306] p 1082 A93-50090
A study on Mach 3 two-dimensional mixed compression air-intakes [ISABE 93-7106] p 1188 A93-54082
- HONDL, KURT**
An improved gust front detection algorithm for the TDWR p 432 A93-22191
- HONER, A.**
Wind tunnel test techniques for UAV separation investigations [AIAA PAPER 93-0626] p 524 A93-24743
- HONERMANN, ANDREAS**
The three-dimensional representation of the pressure distribution on wedged delta wings with supersonic leading edges in supersonic-hypersonic flow p 973 A93-46989
- HONG, C.-S.**
Integrated optoelectronics for communication and processing; Proceedings of the Meeting, Boston, MA, Sept. 3, 4, 1991 [SPIE-1582] p 1158 A93-51250
- HONG, CHIH-CHIANG**
Discontinuous Galerkin finite element method for two dimensional conservation laws [AIAA PAPER 93-0337] p 281 A93-23026
- HONG, GUANXIN**
Investigation on air refueling scheduling p 108 A93-14315
- HONG, JOHN**
An aerodynamic model for one and two degree of freedom wing rock of slender delta wings [NASA-CR-193130] p 781 A93-27150
The generation of side force by distributed suction [NASA-CR-193129] p 839 A93-27151
- HONG, LIU**
Design problems of three-dimensional contractions p 1236 A93-55584
- HONGTIAN, LOU**
Transition induced normal forces and their effects on the aerodynamic characteristics of slender sharp cones [AD-A256802] p 288 A93-15689
- HONNORAT, Y.**
The beta-CEZ, a new high performance titanium alloy for aerospace engines [DS-2022] p 393 A93-17852
- HONNORAT, YVES**
The modeling of forging and precision-casting forming processes p 207 A93-15030
- HONORS, O. P.**
F-14D flight director development, test, and evaluation p 803 A93-38840
- HOOGBOOM, P.**
Definition study PHARUS [AD-A256560] p 221 N93-14805
- HOOGBOOM, P. J.**
DME-derived positions compared with MLS- and ILS-derived positions [NLR-TP-90119-U] p 318 A93-16343
- HOOGBOOM, PETER**
A dual polarised active phased array antenna with low cross polarisation for a polarimetric airborne SAR p 883 A93-43401
The PHARUS project, first results of the realization phase p 884 A93-43454
The realization phase of the PHARUS project p 1162 A93-47658
- HOOPER, W. E.**
Fifty years of tandem rotor helicopter engineering p 504 A93-25250
- HOOPER, WILLIAM P.**
Aureole lidar - Instrument design, data analysis, and comparison with aircraft spectrometer measurements p 1160 A93-52419
- HOORELBEKE, J.**
Testing techniques for straight transonic and supersonic cascades [ONERA, TP NO. 1992-155] p 773 A93-38734
- HOOS, JON A.**
A high-frequency, secondary instability of crossflow vortices that leads to transition p 128 A93-17253
- HOOPER, BRIAN D.**
Human response to helicopter noise - A test of A-weighting p 567 A93-29424
- HOOPER, GREGORY A.**
Aircraft ice detectors and related technologies for onground and inflight applications [DOT/FAA/CT-92/27] p 791 N93-27269
- HOPKINS, DALE A.**
Structural Tailoring/Analysis for Hypersonic Components - A computational simulation [AIAA PAPER 92-4722] p 325 A93-20324
- HOPKINS, HARRY**
Designed for work p 506 A93-27276
Big time doorstep delivery p 892 A93-42995
West powers East p 1244 A93-56349
- HORAK, DAN T.**
A model-based monitoring system for turbine engines [SAE PAPER 921006] p 206 A93-14639
Development of a model-based monitoring system for turbine and rocket engines p 195 A93-16412
- HORENSTEIN, M.**
Comparison of electrostatic and aerodynamic forces during parachute opening [AIAA PAPER 93-1210] p 689 A93-35160
- HORIUTI, KIYOSHI**
LES turbulence modeling using DNS data base p 299 A93-19274
- HORMANN, F.**
Technology transfer: Potential of BMFT concept for hypersonics [MBB-LME-202-S-PUB-0505] p 1041 A93-31045
- HORMANN, FRITZ**
The Hermes Carrier Aircraft (HCA) p 195 A93-14347
- HORN, D. D.**
AEDC expanded flow arc facility (HEAT-H2) description and calibration p 821 A93-37872
- HORN, RALF**
A refined procedure to generate calibrated imagery from airborne synthetic aperture radar data p 1162 A93-47657
- HORNBLLOWER, C.**
Rolls-Royce civil engine technology [PNR-90936] p 56 A93-11036
The Trent: Towards greater thrust [PNR-90937] p 56 A93-11037
From RB211 to Trent: An ongoing development strategy [PNR-90938] p 56 A93-11038
- HORNE, A. M.**
Grazing angle dependency of SAR imagery p 884 A93-43455
- HORNER, M. B.**
An examination of vortex convection effects during blade-vortex interaction p 473 A93-25360
Results from a set of low speed blade-vortex interaction experiments p 872 A93-43540
- HORNUNG, H.**
Transition on a sharp cone at high enthalpy - New measurements in the shock tunnel T5 at GARCIT [AIAA PAPER 93-0343] p 281 A93-23030
Performance data of the new free-piston shock tunnel T5 at GARCIT p 1011 A93-45498
- HORNUNG, HANS G.**
Hypervelocity scramjet capabilities of the T5 Free-Piston Tunnel at Caltech [AIAA PAPER 92-5037] p 376 A93-22311
- Two-directional skin friction measurement utilizing a compact internally mounted thin-liquid-film skin friction meter [AIAA PAPER 93-0180] p 414 A93-22608
Elliptic cross section tip effects on the vortex wake of an axisymmetric body at angle of attack [AIAA PAPER 93-2960] p 1124 A93-48154
- HORONJEFF, RICHARD D.**
Analysis of aircraft noise levels in the vicinity of start-of-takeoff roll at Baltimore-Washington International Airport [PB92-221605] p 559 N93-21501
- HORSLEY, J.**
Testing for integrity p 346 A93-18785
The 'Rolls-Royce' way of validating fan integrity [AIAA PAPER 93-2602] p 1122 A93-50311
Testing for integrity [PNR-90927] p 56 N93-11024
- HORSTMAN, C. C.**
Numerical simulation of crossing/turbulent boundary layer interaction at Mach 8.3 comparison of zero and two-equation turbulence models [AIAA PAPER 93-0779] p 467 A93-24861
Hypersonic crossing shock-wave/turbulent-boundary-layer interactions [AIAA PAPER 93-0781] p 467 A93-24863
Computation of crossing shock/turbulent boundary layer interaction at Mach 8.3 p 961 A93-45726
Investigation of a hypersonic crossing shock wave/turbulent boundary layer interaction p 1044 A93-48043
Development of separation due to interaction between a shock wave and a turbulent boundary layer perturbed by rarefaction waves p 1233 A93-55019
- HORSTMAN, K. C.**
Three-dimensional hypersonic shock wave/turbulent boundary-layer interactions p 287 A93-23533
Hypersonic crossing shock-wave/turbulent-boundary-layer interactions [AIAA PAPER 93-0781] p 467 A93-24863
- HORSTMANN, K. H.**
A European collaborative NLF nacelle flight demonstrator [PNR-90992] p 20 N93-11113
- HORSTMANN, KARL-HEIZ**
Dornier 228 experimental with laminar wing p 506 A93-27500
- HORVATH, THOMAS J.**
Reynolds number influences in aeronautics [NASA-TM-107730] p 989 A93-31732
- HOSAKA, YASUSHI**
Numerical simulation of flow for a scramjet nozzle p 302 N93-19299
- HOSHINO, HIDEO**
A wind tunnel investigation to determine buffet countermeasures for STOL aircraft alpha-sweep flight testing [NAL-TR-1129] p 65 N93-12362
- HOSOKAWA, SHIGEO**
Flow measurements behind V-gutter under non-combusting condition [AIAA PAPER 93-0020] p 408 A93-20139
Isothermal flow characteristics behind V-shape gutter with and without injection [ISABE 93-7040] p 1198 A93-54016
- HOUE, G. J.-W.**
An approximately factored incremental strategy for calculating consistent discrete aerodynamic sensitivity derivatives [AIAA PAPER 92-4746] p 265 A93-20344
Observations on computational methodologies for use in large-scale, gradient-based, multidisciplinary design [AIAA PAPER 92-4753] p 436 A93-20351
- HOUE, GENE J.-W.**
Recent advances in steady compressible aerodynamic sensitivity analysis p 1236 A93-55400
- HOUE, GENE W.**
Multidisciplinary analysis and sensitivity derivatives for isolated helicopter rotors in hover [AIAA PAPER 92-4696] p 324 A93-20308
Methodology for sensitivity analysis, approximate analysis, and design optimization in CFD for multidisciplinary applications [NASA-CR-192172] p 552 A93-20297
- HOUE, XIAO**
Using a diagonal implicit algorithm to calculate transonic nozzle flow [AIAA PAPER 93-2345] p 1082 A93-50119
- HOUEAS, L.**
On the compression process in a free-piston shock-tunnel p 1136 A93-48041
- HOUEVILLE, R.**
Numerical simulation of three-dimensional supersonic flows using Euler and boundary layer solvers [AIAA PAPER 93-0531] p 284 A93-23272

- Method of characteristics for computing three-dimensional boundary layers p 970 A93-46886
- HOUGHTON, RONALD C. C.**
Jet streams and associated turbulence and their effects on air transport flight operations p 154 A93-14231
- HOUJOH, HARUO**
Radiation mechanism for the aerodynamic sound of gears - An explanation for the radiation process by air flow observation p 451 A93-21859
- HOUNAM, DAVID**
Motion errors and compensation possibilities p 212 N93-13052
- HOUNJET, M. H. L.**
Clebsch variable model for unsteady inviscid transonic flow with strong shock waves [AIAA PAPER 93-3025] p 1055 A93-48210
Beyond the frequency limits of time-linearized methods [NLR-TP-91216-U] p 295 N93-17929
NLR inviscid transonic unsteady loads prediction methods in aeroelasticity [NLR-TP-91410-U] p 990 N93-32358
- HOUPIS, CONSTANTINE H.**
Symposium proceedings on Quantitative Feedback Theory [AD-A255527] p 187 N93-13872
- HOURIGAN, D. T.**
Measurement of the dynamic undercarriage response of a Sikorsky S-70B-2 helicopter: Instrumentation and test methods: Flight mechanics technical memorandum [AD-A256319] p 329 N93-16404
- HOUSER, DONALD R.**
Transmission error and load distribution analysis of spur and double helical gear pairs used in a split path helicopter transmission design p 549 A93-29426
Engineering science research issues in high power density transmission dynamics for aerospace applications [AIAA PAPER 93-2299] p 1155 A93-50084
- HOUSNER, J. M.**
Multiple methods integration for structural mechanics analysis and design p 923 N93-30867
- HOUSTON, S. S.**
Flight test and analysis procedures for new handling criteria [RAE-TM-FM-26] p 47 N93-10803
- HOUTZ, JOHN**
URV flight test of an Ada implemented self-repairing flight control system [AD-A259205] p 527 N93-20551
- HOUWING, A. F. P.**
Absolute intensity measurements of impurity emissions in a shock tunnel and their consequences for laser-induced fluorescence experiments p 1147 A93-48044
- HOUWINK, R.**
Application of European CFD methods for helicopter rotors in forward flight [ONERA, TP NO. 1992-125] p 772 A93-38599
- HOWARD, J. H.**
Raising the high temperature limit of the nickel-iron-base superalloy p 70 A93-12114
- HOWARD, M. A.**
Viscous throughflow modelling for multi-stage compressor design [ASME PAPER 92-GT-302] p 255 A93-19492
- HOWARD, RICHARD M.**
Flight test and wind-tunnel study of a scaled unmanned air vehicle [AIAA PAPER 92-4075] p 37 A93-11260
A flowfield study of a close-coupled canard configuration [AIAA PAPER 93-3499] p 983 A93-47269
- HOWARD, RONALD W.**
Breaking through the 10 exp 6 barrier p 27 A93-11498
- HOWE, DAVID A.**
Modeling and control design of a wind tunnel model support p 529 A93-29281
- HOWE, HAROLD W.**
Integrity testing of brush seal in shroud ring of T-700 engine [NASA-TM-105863] p 421 N93-18380
- HOWE, ROBERT M.**
Generalized guidance law for collision courses p 727 A93-34533
- HOWELL, DOROTHY T.**
Effect of planform and body on supersonic aerodynamics of multibody configurations [NASA-TP-3212] p 19 N93-10824
- HOWELL, P. A.**
Comparison of heating protocols for detection of disbands in lap joints p 396 A93-18627
- HOWERTON, WALTER C.**
Experimental investigation of the aerodynamics of independently rotating cylindrical shells [AD-A258917] p 305 N93-19340
- HOWIE, PHILIP V.**
Developing the MD Explorer p 744 A93-34472
- HOYING, DONALD A.**
Stall inception in a multi-stage high speed axial compressor [AIAA PAPER 93-2386] p 1117 A93-50153
- HOYME, KENNETH**
SAFEbus p 828 A93-37072
- HOYT, W. A.**
An integrated knowledge system for wind tunnel testing - Project Engineers' Intelligent Assistant [AIAA PAPER 93-0560] p 377 A93-23297
- HOZUMI, K.**
Experimental investigation of aerothermal problems associated with hypersonic flight of HST p 120 A93-14380
- HROMADKA, THEODORE V.**
Mathematical model of frost heave and thaw settlement in pavements [CRREL-REPT-93-2] p 912 N93-30103
- HRZYCKO, G.**
Application of FEM model correlation and updating techniques on an aircraft using test data of a ground vibration survey p 509 A93-29267
- HSIAO, FEI-BIN**
Improvement of high-AOA airfoil stalling performance by internal acoustic excitation p 243 A93-19134
- HSIAO, K.-L.**
Noncoaxial mixing in a rectangular duct p 205 A93-14518
- HSING, C. A.**
Assessment and correction of tunnel wall interference by Navier-Stokes solutions p 116 A93-14275
- HSING, T. D.**
An algebraic turbulence model with memory for the computation of three dimensional turbulent boundary layers p 115 A93-14248
- HSIUNG, JIH-LAN**
Computation of transonic flow over a porous surface projectile p 696 N93-25409
- HSU, C. A.**
Computation of shock diffraction in external and internal flows p 1024 A93-45537
A high-order streamline Godunov scheme for steady hypersonic equilibrium flows [AIAA PAPER 93-2997] p 1053 A93-48187
- HSU, C.-H.**
Calculations of separated vortex flows at low speed for low-aspect-ratio wings p 264 A93-20300
Investigation of vortex breakdown on delta wings using Navier-Stokes equations p 478 A93-27924
- HSU, CHIANG-AN**
Numerical experiments with nonoscillatory schemes using Eulerian and new Lagrangian formulations p 862 A93-42432
- HSU, D. K.**
Investigation of corrosion in aluminum/adhesive lap-splices using pulse-echo ultrasonic techniques [DE93-008074] p 749 N93-25518
- HSU, DAVID K.**
Ultrasonic NDE of adhesive and sealant bonded aluminum lap-splices p 407 A93-19595
- HSU, K. Y.**
Experimental and numerical investigations of the vortex-flame interactions in a driven jet diffusion flame [AIAA PAPER 93-0455] p 534 A93-25532
- HSU, SHIH-CHE**
Exact closed-form solution of generalized proportional navigation p 1130 A93-49598
- HU, ANREN**
System identification of unstable manipulators using ERA methods [AIAA PAPER 93-3842] p 1170 A93-51431
- HU, C. Q.**
FUM - An efficient MMB solver for steady inviscid flows p 862 A93-42431
- HU, CHIEN-CHUNG**
Unsteady aerodynamic models for maneuvering aircraft [AIAA PAPER 93-3626] p 1126 A93-48311
- HU, E. L.**
Photoelectrochemical etching of high aspect ratio submillimeter waveguide filters from n(+) GaAs wafers p 409 A93-20644
- HU, F. Q.**
Induced Mach wave-flame interactions in laminar supersonic fuel jets p 475 A93-26183
Temperature and suction effects on the instability of an infinite swept attachment line p 691 A93-35486
- HU, FANG Q.**
A numerical study of wave propagation in a confined mixing layer by eigenfunction expansions p 873 A93-43629
- HU, J.**
A study of dynamic characteristics of axial compression systems by heat addition p 202 A93-14168
- An investigation of post stall transients and recoverability of axial compression systems [ISABE 93-7012] p 1184 A93-53988
- HU, JUN**
An investigation of post stall transients and recoverability of axial compression systems. I - A simplified method [ASME PAPER 92-GT-55] p 347 A93-19305
An investigation of post stall transients and recoverability of axial compression systems. II - Numerical simulations [ASME PAPER 92-GT-56] p 347 A93-19306
- HU, LUXING**
Future development and application of general structural analysis softwares in the aviation industry in China p 1262 A93-54420
- HU, S. G.**
A new method to study the forming process of complicated sheetmetal aero-parts p 204 A93-14363
- HU, SI-MING**
A study of surge control by using pulse cut-off for dual spool turbo-jet engine p 1194 A93-53862
- HU, XIN-HONG**
Development of laser conducting landing system p 150 A93-14320
- HU, XINPING**
Processing integral impeller 4-coordinate numerically controlled milling machine p 926 A93-41749
- HU, ZHANGWEI**
Cabin noise source-path identification for AD-200 ultralight aircraft p 444 A93-19138
- HU, ZHAOFENG**
Worst-case wind modeling and its influence on capturing of aircraft penetration trajectory p 1248 A93-54857
Vectoring thrust and two-dimensional nozzle p 1247 A93-54863
- HU, ZONG'AN**
Acoustic experiments of two scaled-model propellers on the ground p 1172 A93-48507
- HUA, XIANMING**
Experimental study of dynamic stall on an oscillating airfoil p 266 A93-20804
- HUA, YAONAN**
Viscous flow field prediction in axisymmetric passages p 204 A93-14478
- HUAN, FUMING**
Dynamic stability, coupling and active control of elastic vehicles with unsteady aerodynamic forces modeling p 182 A93-14282
- HUANG, CHANGHUA**
Multilevel solution of the elastohydrodynamic lubrication of concentrated contacts in spiroid gears p 1161 A93-52606
- HUANG, CHIEN**
Optimization-based linear and nonlinear design methodologies for aircraft control. II - Final simulations [AIAA PAPER 92-4627] p 62 A93-13285
Failure-accommodating neural network flight control [AIAA PAPER 92-4394] p 523 A93-24495
- HUANG, J. C.**
A high-order streamline Godunov scheme for steady hypersonic equilibrium flows [AIAA PAPER 93-2997] p 1053 A93-48187
- HUANG, J. R.**
Investigation of an electrothermal de-icer pad using a three-dimensional finite element simulation [AIAA PAPER 93-0397] p 327 A93-23072
Efficient finite element method for aircraft deicing problems p 1103 A93-52443
- HUANG, JINQUAN**
Adaptive engine stall margin control p 1108 A93-49200
- HUANG, LI-JENG**
Optimal control law synthesis for flutter suppression using active acoustic excitations p 370 A93-23516
- HUANG, MING-KE**
An AF3 algorithm for the calculation of transonic nonconservative full potential flows over wings or wing/body combinations p 125 A93-15341
- HUANG, P. G.**
Turbulence modeling for complex hypersonic flows [AIAA PAPER 93-0200] p 277 A93-22620
Skin friction and velocity profile family for compressible turbulent boundary layers p 1070 A93-49008
Hypersonic flows as related to the national aerospace plane [NASA-CR-191980] p 296 N93-18378
- HUANG, PAO S.**
Study on vortex flow control of inlet distortion p 122 A93-14520
Comparison of experimental ground testing and computational fluid dynamics for the re-engined 727-100 center engine inlet [AIAA PAPER 92-3920] p 462 A93-24294
- HUANG, PING**
Multilevel solution of the elastohydrodynamic lubrication of concentrated contacts in spiroid gears p 1161 A93-52606

- HUANG, T. T.**
Near-field behavior of a tip vortex p 288 A93-23549
Three dimensional near field behavior of a tip vortex developing on an elliptic foil
[AIAA PAPER 93-0865] p 468 A93-24927
- HUANG, THOMAS T.**
Incompressible flow computation of forces and moments on bodies of revolution at incidence
[AIAA PAPER 93-0787] p 541 A93-24867
Simultaneous mapping of the unsteady flow fields by Particle Displacement Velocimetry (PDV)
p 786 N93-27454
- HUANG, W.**
Three-dimensional Navier-Stokes calculations using solution-adapted grids
[AIAA PAPER 93-0431] p 462 A93-24240
- HUANG, WEN-CHAO**
Investigation of cabin noise reduction in the Y12
p 41 A93-11816
Investigation of cabin noise reduction in the Y12
p 506 A93-27371
- HUANG, WENHU**
A theoretical study on the ETHYLENE system - A fuzzy diagnostic expert system for large rotating machinery
p 846 A93-36327
- HUANG, X.**
Variable-complexity aerodynamic-structural design of a high-speed civil transport wing
[AIAA PAPER 92-4695] p 323 A93-20279
- HUANG, X. Z.**
Effect of vortex behavior on loads acting on a 65 deg delta wing oscillating in roll at high incidence
p 782 N93-27220
- HUANG, XI-CHENG**
Three-dimensional flow analysis of a four-stage transonic axial compressor with inlet guide vanes
p 1232 A93-54643
- HUANG, XI-JUN**
A time dependent method in finite volume for transonic diffuser turbulent flows
p 476 A93-27368
- HUANG, XUEQIAO**
A dual-Euler method for solving all-attitude angles of the aircraft
[AIAA PAPER 93-3589] p 1223 A93-52682
- HUANG, Y.**
Heat transfer performance comparisons of five different rectangular channels with parallel angled ribs
p 397 A93-18752
- HUANG, YIYI**
The influence of wall friction on sidewall interference
p 680 A93-33723
- HUANG, Z.**
An experimental investigation of a round turbulent jet in a cross-flow
p 553 N93-20689
- HUANG, ZHI-TAO**
A new method for predicting the end wall boundary layers and the blade force defects inside the passage of axial compressor cascades
p 1236 A93-55589
- HUANG, ZHICHENG**
On the favorable interference in the supersonic flow
p 679 A93-33713
- HUANG, ZHITAO**
On model for predicting blade force defect in end wall boundary layer inside axial compressor cascade
p 862 A93-42271
- HUBBARD, D. G.**
Visual observations of supersonic transverse jets
p 965 A93-46750
- HUBER, C. C.**
AQUIS: A PC-based air quality and permit information system
[DE92-040092] p 434 N93-18587
- HUBER, F. W.**
Design and test of a small two stage counter-rotating turbine for rocket engine application
[AIAA PAPER 93-2136] p 1142 A93-49954
- HUBER, GARY T.**
Development and use of hydrogen-air torches in an altitude facility
[AIAA PAPER 93-2176] p 1137 A93-49988
- HUBER, GREG**
The onset of vortex turbulence
p 788 N93-28251
- HUBER, P.**
X-31A high angle of attack and initial post stall flight testing
p 511 N93-19911
- HUBIN, WILBERT N.**
The science of flight - Pilot-oriented aerodynamics
[ISBN 0-8138-0398-5] p 240 A93-17526
- HUBLER, D.**
The engine design engine. A clustered computer platform for the aerodynamic inverse design and analysis of a full engine
[NASA-TM-105838] p 21 N93-11223
- HUBNER, J. P.**
Trajectory mapping of quasi-periodic structures in a vortex flow
[AIAA PAPER 93-2914] p 1044 A93-48116
- HUCHER, MICHEL**
The ring laser gyro and its applications
p 927 A93-42657
- HUDDLE, J. R.**
Airborne vector gravimetry with an aided inertial survey system
p 1241 A93-55977
- HUDDLESTON, DAVID H.**
A study of CFD algorithms applied to complete aircraft configurations
[AIAA PAPER 93-0784] p 468 A93-24864
- HUDSON, S. T.**
Investigation of rotor blade roughness effects on turbine performance
[ASME PAPER 92-GT-297] p 354 A93-19487
- HUDSON, SCOTT**
Correlation filters for aircraft identification from radar range profiles
p 1097 A93-50636
- HUDSON, T. D.**
Optical correlator field test results
p 1038 A93-44458
- HUEBNER, L. D.**
Development and application of GASP 2.0
[AIAA PAPER 92-5067] p 438 A93-22337
- HUEBNER, LAWRENCE D.**
CFD code calibration and inlet-fairing effects on a 3D hypersonic powered-simulation model
[AIAA PAPER 93-3041] p 1056 A93-48222
Computational effects of inlet representation on powered hypersonic, airbreathing models
p 1094 A93-52427
Assessment of a flow-through balance for hypersonic wind tunnel models with scramjet exhaust flow simulation
[NASA-TM-4441] p 779 N93-27005
- HUESCHEN, RICHARD M.**
Analysis of DGPS/INS and MLS/INS final approach navigation errors and control performance data
p 315 A93-21183
- HUFF, DENNIS L.**
High resolution numerical simulation of the linearized Euler equations in conservation law form
[AIAA PAPER 93-2934] p 1148 A93-48132
- HUFF, R. W.**
F-14D flight director development, test, and evaluation
p 803 A93-38840
- HUFFAKER, R. MILTON**
Solid-state coherent laser radar wind shear measuring systems
p 144 N93-14848
- HUFFINE, EDWIN F.**
Postmortem alcohol production in fatal aircraft accidents
[AD-A255766] p 143 N93-14026
- HUFFMAN, JARRETT K.**
Subsonic static and dynamic stability characteristics of the test technique demonstrator NASP configuration
[AIAA PAPER 93-0519] p 268 A93-21111
- HUFFMAN, M. F.**
Component and Engine Structural Assessment Research (CAESAR)
[AIAA PAPER 93-2609] p 1122 A93-50316
- HUFFSTETLER, MARK**
Design of the advanced regional aircraft, the DART-75
[NASA-CR-192044] p 333 N93-17972
- HUFSTETLER, GERARD**
Embedded Bragg grating fiber optic sensor for composite flexbeams
p 828 A93-37350
- HUGHES, S. J.**
A test facility for the thermofluid-dynamics of gas bearing lubrication films
[PNR-90897] p 72 N93-11032
- HUGHES, T. J. R.**
Application of the Galerkin/least-squares formulation to the analysis of hypersonic flows. I - Flow over a two-dimensional ramp
p 866 A93-42593
Application of the Galerkin/least-squares formulation to the analysis of hypersonic flows. II - Flow past a double ellipse
p 868 A93-42608
- HUGUES, E. C.**
CFD analysis of hypersonic chemically reacting flowfields around a generic shape
[AIAA PAPER 93-0323] p 281 A93-23015
- HUI, C. Y.**
Vortex/surface interaction
[AIAA PAPER 93-0863] p 468 A93-24925
- HUI, KEN**
The flight test and data analysis program for the development of a Boeing/De Havilland Dash 8 simulator model
p 512 N93-19930
- HUI, W. H.**
A new Lagrangian method for steady supersonic flow computation. II - Slip-line resolution. III - Strong shocks
p 243 A93-18855
- HUILI, SHEN**
Solution of Euler equations for forebody-inlet ensemble of aircraft at high angle of attack
[AD-A263905] p 876 N93-29862
- HUIZING, A. G.**
Adaptive waveform selection with a neural network
p 942 A93-43470
- HULL, DAVID G.**
Guidance law based on piecewise constant control for hypersonic gliders
[AIAA PAPER 93-3888] p 1144 A93-51472
- HUMERICK, DOUGLAS W.**
Applying commercial style acquisition practices to the procurement of commercially available aircraft
[AD-A258143] p 455 N93-18087
- HUMI, MAYER**
Three-dimensional vortex method for parachutes
p 872 A93-42874
- HUMM, H.**
Development of a system for aerodynamic fast-response probe measurements
p 203 A93-14325
- HUMPHREY, JOSEPH W.**
Finite element analysis of the Scramaccelerator with finite rate chemistry
[AIAA PAPER 93-0745] p 540 A93-24833
Analysis and demonstration of a Scramaccelerator system
[AIAA PAPER 93-2183] p 1142 A93-49995
- HUMPHREYS, B. E.**
The aerodynamic performance of laser drilled sheets
[AERO-REPT-9204] p 484 N93-20806
- HUMPHRIES, R. G.**
Meteorological information for aviation: A systems approach
p 937 N93-30298
- HUNT, JAMES L.**
Design of a hypersonic waverider-derived airplane
[AIAA PAPER 93-0401] p 384 A93-21108
Aero-space plane figures of merit
[AIAA PAPER 92-5058] p 385 A93-22328
- HUNT, JOHN D.**
Structural analysis of the light weight hard nose of the 71M aerostat
[AIAA PAPER 93-4037] p 1255 A93-54608
- HUNT, MALCOLM**
Computer-based modelling of aircraft noise impact
p 559 A93-28497
- HUNTER, C. G.**
Requirements for integrated flight and traffic management during final approach
p 31 A93-11009
- HUNTINGTON, D. E.**
Dynamic analysis of multiple row fuselage stiffened structures
[AIAA PAPER 93-1438] p 710 A93-33987
- HUNTINGTON, DONALD E.**
Dynamics of skin-stringer panels using modified wave methods
p 206 A93-14561
Noise transmission of skin-stringer panels using a decaying wave method
p 943 A93-41929
- HUNTLEY, M. STEPHEN**
Design of instrument approach procedure charts: Comprehension speed of missed approach instructions coded in text or icons
[PB92-205673] p 36 N93-11252
- HUNTSMAN, I.**
A laminar flow rotor for a radial inflow turbine
[AIAA PAPER 93-1796] p 1074 A93-49686
- HURLEY, C. D.**
Smoke measurements inside a gas turbine combustor
[AIAA PAPER 93-2070] p 1113 A93-49902
- HURLEY, FRANK**
Low-cost approaches to proving of high-risk fast VTOL designs
[SAE PAPER 920989] p 157 A93-14636
- HURRASS, KARLHEINZ**
Ground- and satellite-derived flight-path measurements as demonstrated in the AFES Avionics Flight Evaluation System (AFES)
p 993 N93-31281
On-board derived flight-path measurement as demonstrated by an ILS measurement system
p 994 N93-31282
- HURST, D. W.**
A study of propeller/wing interaction including the effect of ground proximity
p 113 A93-14190
- HURST, DAVID W.**
A Laser Doppler Anemometry study of a supersonic jet in a low speed cross-flow
p 459 A93-23807
- HURST, PATRICIA**
Dynamic System Coupler Program (DYSCO 4.1). Volume 1: Theoretical manual
[AD-B131156L] p 848 N93-27531
Dynamic System Coupler Program (DYSCO 4.1). Volume 2: User's manual
[AD-B131157L] p 848 N93-27589
Dynamic System Coupler Program (DYSCO 4.1). Volume 3: User's manual supplement
[AD-B131158L] p 848 N93-27590

HURWITZ, W. M.

Development of the F/A-18 E/F air induction system
[AIAA PAPER 93-2152] p 1101 A93-49969

HUSER, A.

Direct numerical simulation of turbulent flow in a square duct
[AIAA PAPER 93-0198] p 277 A93-22618

HUSSAINI, M. Y.

Natural laminar flow and laminar flow control
[ISBN 0-387-97737-6] p 859 A93-41776

HUSSEIN, BASSAM

Vision-based range estimation using helicopter flight data
p 151 A93-17501

HUSSIEN, B.

Passive range estimation for rotorcraft low-altitude flight
p 948 A93-46608
Clustering methods for removing outliers from vision-based range estimates
p 1171 A93-51648
Passive range estimation for rotorcraft low-altitude flight
p 1190 A93-52881

HUSSIEN, BASSAM

Multirate and event-driven Kalman filters for helicopter flight
p 1245 A93-55760

HUSSIEN, BASSAM

Vision-based range estimation using helicopter flight data
p 317 A93-21525

HUSSON, D.

Maximum hail concentration that can be met by an aircraft in stormy precipitations
p 430 A93-22152

HUSTAK, J. F.

Active magnetic bearings applied to industrial compressors
p 841 A93-27570

HUSTON, RONALD L.

Computational gearing mechanics
[NASA-CR-191127] p 751 A93-25884

HUTCHERSON, S.

Vortex generators used to control laminar separation bubbles
p 768 A93-37381

HUTCHINS, JOANNE G.

Thermoplastic applications in helicopter components
p 796 A93-35952

HUTCHINSON, JOHN J.

Aviation safety research at the National Institute for Aviation Research Wichita State University: A report to the FAA Technical Center
[NIAR-92-2] p 310 A93-16455
International aircraft operator information system
[DOT/FAA/CT-93/4] p 949 A93-32232

HUTCHISON, M. G.

Aerodynamic optimization of an HSCT configuration using variable-complexity modeling
[AIAA PAPER 93-0101] p 322 A93-19806
Variable-complexity aerodynamic-structural design of a high-speed civil transport wing
[AIAA PAPER 92-4695] p 323 A93-20279

HUTTSSELL, LAWRENCE J.

An overview of aeroelasticity studies for the National Aero-Space Plane
[AIAA PAPER 93-1313] p 732 A93-33889

HUYER, STEPHEN ALBERT

Forced unsteady separated flows on a 45 degree delta wing
p 82 A93-10305

HUYNH, H. T.

A simulator study into low speed longitudinal handling qualities of ACT transport aircraft
[NLR-TP-89387-U] p 527 A93-20743

HUYNH, LOC C.

Analysis of a hypersonic waverider research vehicle with a hydrocarbon scramjet engine
[AIAA PAPER 93-0509] p 386 A93-23256

HWANG, C. J.

Analysis of steady and unsteady turbine cascade flows by a locally implicit hybrid algorithm
[ASME PAPER 92-GT-127] p 249 A93-19361
Adaptive finite volume upwind approach on mixed quadrilateral-triangular meshes
p 287 A93-23542
Locally implicit total variation diminishing schemes on mixed quadrilateral-triangular meshes
p 1235 A93-55356

HWANG, D. P.

Effect of a rotating propeller on the separation angle of attack
[AIAA PAPER 93-0017] p 472 A93-24978
Effect of a rotating propeller on the separation angle of attack and distortion in ducted propeller inlets
[NASA-TM-105935] p 290 A93-16625

HWANG, I. S.

INCOLOY 908, a low coefficient of expansion alloy for high-strength cryogenic applications. I - Physical metallurgy
p 534 A93-25886

HWANG, JON L.

A study on stability and response analysis of a nonlinear rotor system with mass unbalance and side load
[ASME PAPER 92-GT-7] p 400 A93-19280

HWOSCHINSKY, PETER V.

Rotorcraft master plan
p 857 A93-30677

HYDE, CHARLES R.

Instrumentation and telemetry systems for free-flight drop model testing
p 1209 A93-52754

HYDE, RICHARD A.

The application of scheduled H-infinity controllers to a VSTOL aircraft
p 1135 A93-52249

HYMER, T.

A new semiempirical method for computing nonlinear angle-of-attack aerodynamics on wing-body-tail configurations
[AIAA PAPER 93-0034] p 260 A93-20148
Base drag prediction on missile configurations
[AIAA PAPER 93-3629] p 1064 A93-48314

HYNES, CHARLES S.

A method of wind shear detection for powered-lift STOL aircraft
[AIAA PAPER 93-3667] p 1104 A93-48345
Wind-shear endurance capability for powered-lift aircraft
[AIAA PAPER 93-3670] p 1129 A93-48348

HYNES, R. H.

Reliability considerations for weather hazard warning radar
p 431 A93-22187

HYNES, T. P.

The role of turbomachinery testing for stability in distorted flow
[PNR-80943] p 57 A93-11040

HYGGE, S.

A comparison between the impact of noise from aircraft, road traffic and trains on long-term recall and recognition of a text in children aged 12-14 years
p 1163 A93-49552

IABLONSKII, EVGENII V.

Some considerations on indication means for helicopter pilot vision systems
p 807 A93-36018

IACOVIDES, H.

The prediction of convective heat transfer in rotating square ducts
[PNR-80929] p 85 A93-11025

IAKIMENKO, O. IA.

Solution of trajectory optimization methods using the Pontryagin maximum principle
p 366 A93-18378

IAKIMOV, A. S.

A study of the temperature of bodies in the flow-around regime in the case of surface gas injection
p 691 A93-35344

IAKUNIN, V. I.

A set of application programs for the smoothing of curves and surfaces by the method of monoidal transformations in the geometric module of a CAD system for the design of flight vehicles
p 561 A93-27629

IAKUSHIN, M. I.

Modeling of the physicochemical processes of nonequilibrium heat transfer in the subsonic jets of an induction plasmatron
p 836 A93-39147

IANCU, G.

Optimization of large scale systems in elasticity
p 1255 A93-54544

IANKOV, V. P.

An experimental study of dc discharges in supersonic and subsonic air flows
p 14 A93-12980

IANNELLI, G. S.

Accuracy and efficiency assessments for a weak statement CFD algorithm for high-speed aerodynamics
[ASME PAPER 92-GT-433] p 435 A93-19576

IANNELLO, VICTOR

Magnetic bearings for cryogenic turbomachines
p 1149 A93-48601

IARKOVETS, A. I.

Ensuring the reliability and service life of flight vehicle structures by engineering methods
p 745 A93-35276
Stress-strain state of the elements of a single-stringer riveted panel
p 746 A93-35288

IAROSHEVSKII, V. A.

Estimation of the probability of large flight parameters deviations
p 184 A93-14399

IASTREBOV, V. M.

Some characteristics of the design of heads for the cutting of bevel gears with negative curvature of the circular-arc tooth line
p 835 A93-39093

IATSKIV, I. V.

Probability analysis of a method for diagnosing gas turbine engines on the basis of thermogasdynamic parameters
p 345 A93-18337

IBEGAZENE, H.

Microstructure of yttria stabilized zirconia-hafnia plasma sprayed thermal barrier coatings
[ONERA, TP NO. 1993-54] p 1146 A93-51936

IBOSHI, NAOHIRO

Structural optimization of a cantilevered rotating beam
p 210 A93-16248

IBRAHIM, MOUNIR

3-D viscous flow CFD analysis of the propeller effect on an advanced ducted propeller subsonic inlet
[AIAA PAPER 93-1847] p 1075 A93-49728
The 3-D viscous flow CFD analysis of the propeller effect on an advanced ducted propeller subsonic inlet
[NASA-TM-106240] p 900 A93-29162

IBRAHIM, R. A.

Nonlinear flutter of orthotropic composite panel under aerodynamic heating
p 1025 A93-45740

ICHIMARU, OSAMU

Overview of the Japanese National Project for Super/Hyper-Sonic Transport propulsion system
[ASME PAPER 92-GT-252] p 239 A93-19461

IDDINGS, FRANK A.

Large-area aircraft scanner
p 407 A93-19693
Emerging technology for large-area scanning of aging aircraft
[SME PAPER AD92-205] p 925 A93-40666

IDE, TOSHIYUKI

Propagation results of aeronautical satellite communication experiments using INMARSAT satellite
p 533 A93-29607

IDO, Y.

Active forcing of an axisymmetric leading-edge turbulent separation bubble
[AIAA PAPER 93-3245] p 966 A93-46790

IDOTA, YOSHINORI

Ignition and exhaust emission characteristics of spray combustion in a pre-chamber type vortex combustor
[ASME PAPER 92-GT-119] p 350 A93-19355

IEK, C.

Effect of a rotating propeller on the separation angle of attack
[AIAA PAPER 93-0017] p 472 A93-24978
Effect of a rotating propeller on the separation angle of attack and distortion in ducted propeller inlets
[NASA-TM-105935] p 290 A93-16625

IEK, CHANTHY

3-D viscous flow CFD analysis of the propeller effect on an advanced ducted propeller subsonic inlet
[AIAA PAPER 93-1847] p 1075 A93-49728
The 3-D viscous flow CFD analysis of the propeller effect on an advanced ducted propeller subsonic inlet
[NASA-TM-106240] p 900 A93-29162

IERUSALIMSKII, K. M.

Methodology for studying the fracture of aircraft structures in static tests
p 801 A93-36785

IGARASHI, SABURO

Problem 6.4.1 - Rarefied flow around a double ellipse
p 869 A93-42630

IGNAT'EV, S. G.

A comparative analysis of algorithms for solving systems of high-order linear algebraic equations
p 96 A93-12977
Calculation of flow fields near a lifting wing
p 1179 A93-53552

IGO, KENICHI

Hypersonic vehicle research by using a large shock tunnel
[AAS PAPER 91-607] p 1250 A93-55841

IGOE, WILLIAM B.

Analysis of fluctuating static pressure measurements in a large high Reynolds number transonic cryogenic wind tunnel
[NASA-TM-108722] p 823 A93-27142

IIDA, AKIYISHI

Numerical computation of aerodynamic noise radiation by the large eddy simulation
p 850 A93-38151

IIDA, AKIYOSHI

Numerical prediction of aerodynamic noise radiated from low Mach number turbulent wake
[AIAA PAPER 93-0145] p 452 A93-22589

IINUMA, H.

Turbine blade vibration monitoring system
[ASME PAPER 92-GT-159] p 402 A93-19386

IITSUKA, TORU

Microchannel plate modal gain variations with temperature
p 477 A93-27445

IKEDA, MASAYUKI

Numerical Wind Tunnel hardware
p 383 A93-19289

IKEDA, YUJI

Flow measurements behind V-gutter under non-combusting condition
[AIAA PAPER 93-0020] p 408 A93-20139
Isothermal flow characteristics behind V-shape gutter with and without injection
[ISABE 93-7040] p 1198 A93-54016

IKEGAWA, MASASHIRO

Numerical prediction of aerodynamic noise radiated from low Mach number turbulent wake
[AIAA PAPER 93-0145] p 452 A93-22589

Numerical computation of aerodynamic noise radiation by the large eddy simulation
p 850 A93-38151

- IKUHARA, Y.**
High temperature fracture mechanism of gas-pressure sintered silicon nitride p 825 A93-38893
- IL'INSKI, N. B.**
Determination of the shape of a wing profile in boundary layer flow with a given velocity diagram p 1067 A93-48844
- ILCEWICZ, L. B.**
Advanced technology commercial fuselage structure p 918 N93-30432
- ILCEWICZ, LARRY**
Multi-parameter optimization tool for low-cost commercial fuselage crown designs p 922 N93-30858
- ILCEWICZ, LARRY B.**
Advanced technology composite aircraft structures [NASA-CR-190420] p 894 N93-29498
Effects of intra- and inter-laminar resin content on the mechanical properties of toughened composite materials p 921 N93-30845
- ILIFF, KENNETH W.**
A comparison of hypersonic flight and prediction results [AIAA PAPER 93-0311] p 280 A93-23006
- ILINCA, FLORIN**
An adaptive finite element method for turbulent free shear flow past a propeller [AIAA PAPER 93-3388] p 956 A93-45079
- ILLARIONOV, V. F.**
Effect of flight conditions on the sound insulation of the aircraft passenger compartment p 42 A93-12978
- ILLINGWORTH, A. J.**
Hydrometeor identification using cross polar radar measurements and aircraft verification p 844 A93-37719
- ILVES, G. J.**
State of the art review of rutting and cracking in pavements p 380 N93-16316
- IM, H. G.**
Analysis of thermal ignition in supersonic flat-plate boundary layers p 769 A93-37933
- IMAM, I.**
A systems dynamics approach to modeling gas turbine combustor wear [ASME PAPER 92-GT-47] p 347 A93-19300
- IMANARI, K.**
Nonreflecting boundary conditions of three-dimensional Euler equation calculations for strut cascades p 689 A93-34491
- IMBERT, M.**
Reactive and dissipative hypersonic flow in a wind tunnel nozzle p 687 A93-34358
- IMBESI, DOMINICK J.**
The Pave Pace integrated core processor p 941 A93-42856
- IMLAY, SCOTT T.**
The 3D Navier-Stokes flow analysis for shared and distributed memory MIMD computers [AD-A256038] p 221 N93-15187
- IMMARIGEON, J. P.**
An experimental investigation of convective heat transfer at the leading edge of a gas turbine airfoil [ASME PAPER 92-GT-248] p 405 A93-19457
- INABA, K.**
The conceptual study of supersonic transport structure [AIAA PAPER 92-4219] p 43 A93-13348
- INABA, KENJI**
Damage tolerance assessment on the multisite cracks for the YS-11 aircraft p 46 A93-13642
- INADA, M.**
Investigation of combustion structure inside low NO(x) combustors for a 1500 C-class gas turbine [ASME PAPER 92-GT-123] p 350 A93-19357
- INAKA, KYOJI**
Augmentation of turbulent heat transfer with a vortex generator attached to a LEBU plate p 411 A93-21729
- INATANI, YOSHIFUMI**
Atmospheric reentry flight test of winged space vehicle [AIAA PAPER 92-5053] p 385 A93-22324
- INCE, A. NEJAT**
Advances in speech processing p 550 N93-19771
- INENAGA, ANDREW S.**
Fiber optic-based laser vapor screen flow visualization systems for aerodynamic research in larger-scale subsonic and transonic wind tunnels p 408 A93-20298
- INFELD, D.**
Measurement of shed vorticity and circulation from rotating aerofoil by particle image velocimetry p 538 A93-23804
- ING, DAN N.**
A study of single jet impingement ground effect lift loss [AIAA PAPER 93-0869] p 469 A93-24930
- INGALLS, STEPHEN A.**
Application of concurrent engineering methods to the design of an autonomous aerial robot [AD-A254968] p 212 N93-12555
- INGER, G. R.**
Application of Oswatitsch's theorem to supercritical airfoil drag calculation p 768 A93-37399
- INGER, GEORGE R.**
Scaling of incipient separation in high speed laminar flows [AIAA PAPER 93-3435] p 978 A93-47227
- INGHAM, D. B.**
Fluid flows around cascades p 479 A93-28518
- INGLE, STEVEN J.**
Effects of higher order dynamics on helicopter flight control law design p 816 A93-35959
- INGRAFFEA, A. R.**
Representation and probability issues in the simulation of multi-site damage p 1026 A93-45785
- INGRALDI, ANTHONY M.**
Experimental study of pylon cross sections for a subsonic transport airplane p 1103 A93-52440
Effect of pylon cross-sectional geometries on propulsion integration for a low-wing transport [NASA-TP-3333] p 788 N93-28070
- INGRAM, CLINT L.**
Time-accurate simulation of a self-excited oscillatory supersonic external flow with a multi-block solution-adaptive mesh algorithm [AIAA PAPER 93-3387] p 956 A93-45078
- INOKUCHI, YUZO**
Study of mixing flow field of a jet in a supersonic cross flow. I - Experimental facilities and preliminary experiments p 857 A93-40430
- INOUE, MASAHIRO**
Pressure fluctuation on casing wall of isolated axial compressor rotors at low flow rate [ASME PAPER 92-GT-33] p 246 A93-19293
- INOUE, MASATO**
Effect of rounding side corners on vortices shedding and downwash from square cylinder of finite length placed on a ground plane p 1160 A93-51893
- INOUE, OSAMU**
Domain splitting explicit time marching scheme for simulation of unsteady high Reynolds number flow p 830 A93-38140
- INOUE, TAKASHI**
A wind tunnel investigation to determine buffet countermeasures for STOL aircraft alpha-sweep flight testing [NAL-TR-1129] p 65 N93-12362
- IOANNIDES, A. M.**
Development of user guidelines for a three-dimensional finite element pavement model p 379 N93-16311
- IONOV, A. A.**
An experimental study of reinforced panels of composite materials p 1215 A93-52975
- IONTA, P.**
A finite element code for gas turbine combustor flow with Stretched Laminar Flamelet modelling [ISABE 93-7127] p 1204 A93-54102
- IRELAND, P. T.**
Internal cooling passage heat transfer near the entrance to a film cooling hole - Experimental and computational results [ASME PAPER 92-GT-241] p 404 A93-19450
- IRELAND, W.**
ELF, VLF and LF radiation from a very large loop antenna with a mountain core p 924 A93-40334
- IREMAN, TOMAS**
On design methods for bolted joints in composite aircraft structures p 1158 A93-50430
- IRONS, GARY**
Higher velocity thermal spray processes produce better aircraft engine coatings [SAE PAPER 920947] p 202 A93-14090
- IRWIN, A. N.**
Design features influencing the distribution of fuel within the spray from an air blast fuel injector [ASME PAPER 92-GT-235] p 353 A93-19448
- ISAACS, D.**
Aerodynamics of turbine blades with trailing-edge damage - Measurements and computations [ISABE 93-7130] p 1189 A93-54105
- ISAIUK-SAEVSKAIA, A. R.**
Dynamics of a high-rpm compressor p 75 A93-10009
- ISAKOW, MICHAEL**
Decentralized autonomous attitude determination using an inertially stabilized payload [AIAA PAPER 93-3857] p 1134 A93-51444
- ISAMINGER, M. A.**
Birds mimicking microbursts on 2 June 1990 in Orlando, Florida [AD-A255703] p 143 N93-14024
- ISAMINGER, MARK A.**
Microburst characteristics determined from 1988-1991 TDWR tested measurements p 490 N93-19605
- ISHAL, V. A.**
Correction of the frequency characteristic of the waveguide circuit of an acoustic-jet temperature transducer p 832 A93-39036
- ISHAQUE, K.**
Signal processing and system identification techniques for flutter test data analysis p 529 A93-29282
- ISHIDA, K.**
Rim seal experiments and analysis of a rotor-stator system with nonaxisymmetric main flow [ASME PAPER 92-GT-160] p 402 A93-19387
- ISHIGURO, TOMIKO**
Numerical computations using multi-domain technique p 299 N93-19277
The 3D Navier-Stokes calculation of flow about scramjet inlet with strut p 301 N93-19298
- ISHIHARA, MASAHIITO**
Structure of downbursts associated with heavy rainfall observed in Tokyo p 433 A93-22200
- ISHII, HIROSHI**
Study on surge and rotating stall in axial compressors. III - Numerical model for multiblade-row compressors p 1181 A93-53799
- ISHII, RYUJI**
Generation of longitudinal vortices in supersonic flow p 301 N93-19292
- ISHIKAWA, KAZUTOSHI**
Guidance and control law for automatic landing flight experiment of reentry space vehicle [AIAA PAPER 93-3818] p 1143 A93-51409
- ISHIKAWA, M.**
Effects of external control circuit on coal-fired supersonic diagonal-type MHD generator p 1173 A93-49619
- ISHIKAWA, MUNENORI**
Digital fly-by-wire system for BK117 FBW research helicopter p 181 A93-14209
- ISHIKAWA, TAKASHI**
Compression after impact (CAI) properties of CF/PEEK (APC-2) and conventional CF/epoxy stiffened panels p 196 A93-14307
- ISHIZAKA, KOICHI**
A fourth-order MUSCL finite-difference scheme for solving the unsteady compressible Euler equations p 1086 A93-51121
- ISHIZAWA, K.**
New developments with the V2500 engine [ISABE 93-7085] p 1202 A93-54061
- ISHIZUKA, MAKOTO**
Overview of the Japanese National Project for Super/Hyper-Sonic Transport propulsion system [ASME PAPER 92-GT-252] p 239 A93-19461
- ISING, H.**
The influence of nocturnal aircraft noise on sleep and on catecholamine secretion p 1163 A93-49554
- ISKAKOV, K. M.**
Effect of rotation on heat transfer and hydraulic resistance in the radial cooling channels of turbine rotor blades p 1215 A93-52950
- ISMAIL, IBRAHIM H.**
Simulation of aircraft gas turbine engine p 723 N93-25751
- ISMAIL, SHAIK**
Ideal aircraft handling quality models: Longitudinal axis [NAL-PD-FC-9203] p 187 N93-13566
- ISOBE, HIROSHI**
Experimental study on the characteristics of the near wake of a rotating flat plate. III - Influence of the shape near the trailing edge on periodic-velocity-fluctuation phenomena p 451 A93-21727
- ISOGAI, K.**
Transonic flutter/divergence characteristics of aeroelastically tailored and non-tailored high-aspect-ratio forward-swept wings p 10 A93-12273
- ISOGAI, KOJI**
Numerical simulation of unsteady large scale separated flow around oscillating airfoil p 300 N93-19285
- ISOM, MORRIS P.**
Shock waves and the Ffowcs Williams-Hawkins equation p 480 A93-29411
- ISPAS, I.**
Experimental analysis of transonic flow through the variable nozzle of a radial inflow turbine [ASME PAPER 92-GT-90] p 248 A93-19336
- ISSA, CAMILLE A.**
p-version finite element modeling for NDE p 407 A93-19699
- ISSAC, F.**
Validation of electromagnetic-topology concepts on a complex structure [ONERA, TP NO. 1992-63] p 542 A93-25327

ISSAC, JASON C.

- Sensitivity analysis of flutter response of a typical section and a wing in transonic flow
[AIAA PAPER 93-1646] p 742 A93-34171

ITAHARA, H.

- Conceptual design of turbo-accelerator for HST combined cycle engine
[ASME PAPER 92-GT-253] p 353 A93-19462

- Research and development of a turbo-accelerator for super/hypersonic transport
[ISABE 93-7066] p 1200 A93-54042

ITO, TAKESHI

- Wind tunnel tests of the model of intake-airframe integration
[ISABE 93-7101] p 1192 A93-54077

ITOH, H.

- Tandem transverse hydrogen gas injection into a supersonic airflow
[ISABE 93-7069] p 1201 A93-54045

ITOH, K.

- Beta-limiting phenomena in high-aspect-ratio toroidal helical plasmas
[NIFS-188] p 569 N93-20546

ITOH, KATSUHIRO

- Aerodynamic performance of scramjet inlet models with a single strut
[AIAA PAPER 93-0741] p 466 A93-24831

- Analytical and numerical study on steady Mach reflection
p 302 N93-19309

ITOH, S.

- Penn State axial flow turbine facility: Performance and nozzle flow field
p 1032 N93-31588

ITOH, S.-I.

- Beta-limiting phenomena in high-aspect-ratio toroidal helical plasmas
[NIFS-188] p 569 N93-20546

ITTY, I. P.

- Vortex initiation during dynamic stall of an airfoil
p 684 A93-34335

JUNGKIND, I. V.

- Using helicopters for transporting large and heavy loads
p 306 A93-18350

IUROV, V. M.

- A method for determining the aerodynamic coefficients of asymmetric bodies with allowance for nonlinear influence factors of the body shape
p 5 A93-10142

IUSO, G.

- On the measurements of the skin friction in 3-D flows - Application to a complete 3-D shear layer flow
p 118 A93-14329

IVANKOV, A. A.

- Calculation of radiant energy transfer in hypersonic flow past blunt bodies using the P1 and P2 approximations of the spherical harmonic method
p 124 A93-15209

IVANOV, A. M.

- Characteristics of data processing during the development of a data base for a CAD system for aircraft design
p 892 A93-42381

IVANOV, M. IA.

- Calculation of the three-dimensional interaction of a shock wave with a boundary layer on a cylinder
p 12 A93-12766

- A fast method for calculating three-dimensional transonic potential flows in turbomachine blade rows
p 125 A93-15215

IVANOV, M. J.

- Design of high-load aviation turbomachines using modern 3D computational methods
[ISABE 93-7032] p 1196 A93-54008

IVANOV, M. YA.

- Numerical simulation of aerothermodynamics processes in gas turbine engine components
p 1002 A93-46939

IVANOV, V. E.

- Choice of the heating system for high-temperature generators using chemical fuel
p 559 A93-29660

IVANOVA, N. M.

- A data processing and measuring system with a traversing probe for studying flow in the rotating impeller of an axial-flow fan
p 75 A93-10032

IVANTEEV, V. I.

- RISK - Interactive multidisciplinary system for designing airframes
p 226 A93-14337

IVERSON, DONALD G.

- A compact, intercooled and regenerated gas turbine for HALE applications
[ASME PAPER 92-GT-401] p 355 A93-19550

IWAMURA, YOSHIO

- Visualization and analysis of supersonic flow in rotating turbine stage. II - Analysis of the flow into the moving blades and their exit flow
p 476 A93-27442

IWASAKI, A.

- Low-speed wind tunnel study of the direct side-force characteristics of a joined-wing airplane with an upper fin
[DE93-767966] p 988 N93-31189

IWASAKI, AKIHITO

- Wind tunnel investigation of a twin-engine jet transport semi-span model with upper surface blown jet flap
[NAL-TR-1134] p 26 N93-12503

IWASAWA, YOSHIKI

- The structure and material testing facility needed for future SST/HST development
[AIAA PAPER 92-3887] p 528 A93-24481

IWATA, SATOSHI

- Tip clearance effect on heat transfer and leakage flows on the shroud-wall surface in an axial flow turbine
[ASME PAPER 92-GT-200] p 403 A93-19425

IWATA, TAKANORI

- Benefits of variable rotor speed in integrated helicopter/engine control
[AIAA PAPER 93-3851] p 1134 A93-51438

IWATSUBO, TAKUZO

- Experimental study of dynamic fluid forces and moments for a long annular seal
p 209 A93-15684

IYER, R. K.

- Summary: Experimental validation of real-time fault-tolerant systems
[NASA-CR-190985] p 175 N93-13697

IZADPANAH, AMIR P.

- Experimental and analytical investigation of dynamic characteristics of extension-twist-coupled composite tubular spars
[NASA-TP-3225] p 553 N93-20585

IZADPANAH, K.

- Examples of dynamic response optimization using MSC/NASTRAN
[AIAA PAPER 92-4814] p 436 A93-20394

J

JABBARI, M. Y.

- Vortex structure and mass transfer near the base of a cylinder and a turbine blade
p 901 N93-29929

JACKLIN, STEPHEN A.

- Full-scale wind tunnel investigation of a helicopter individual blade control system
[AIAA PAPER 93-1361] p 726 A93-33929

JACKSON, A. J. B.

- Introduction to the Rolls-Royce design process
[PNR-90939] p 57 N93-11039

JACKSON, A. S.

- Machinery arrangements for small VTOL transport aircraft
p 713 A93-34848

JACKSON, ANTHONY

- Advanced composite structural concepts and material technologies for primary aircraft structures
p 918 N93-30430

JACKSON, E. B.

- Effect of lift-to-drag ratio in pilot rating of the HL-20 landing task
p 1210 A93-53738

JACKSON, FRED

- New developments in a PI-Bus specification by the JIAWG and SAE
p 940 A93-42852

JACKSON, JOSEPH

- Investigation of advanced technology for airway facilities maintenance training
[DOT/FAA/CT-TN92/24] p 994 N93-32336

JACKSON, ROBERT L.

- Low-level wind-shear terminology
p 426 A93-22104

JACKSON, T. J.

- PBMR observations of surface soil moisture in Monsoon 90
p 1162 A93-47676

JACKSON, T. L.

- Induced Mach wave-flame interactions in laminar supersonic fuel jets
p 475 A93-26183

JACOBS, J. H.

- The use of artificial intelligence for buffet environments
[AIAA PAPER 93-1534] p 727 A93-34071

JACOBS, P. A.

- Quasi-one-dimensional modelling of free-piston shock tunnels
[AIAA PAPER 93-0352] p 377 A93-23037

JACOBS, PETER F.

- Testing experience with unheated stain-gage balances in the NTF
p 1013 A93-47021

JACOBSEN, ROBERT A.

- Preliminary design features of the RASCAL - A NASA/Army rotorcraft in-flight simulator
[AIAA PAPER 92-4175] p 42 A93-13311

JACQUET, J.-M.

- Methodology for commercial engine/aircraft optimization
[AIAA PAPER 93-1807] p 1166 A93-49696

JACQUIN, L.

- Phenomenology and simplified modeling of a vortex wake generated by a transverse jet
[ONERA, TP NO. 1992-194] p 774 A93-38755

JACQUIN, LAURENT

- Analysis of turbulence in supersonic flows by means of laser velocimetry
[ONERA, TP NO. 1992-148] p 773 A93-38729

JACQUOT, F.

- Hypersonic flow calculations using a multidomain MUSCL Euler solver
p 960 A93-45547

JACQUOTTE, O. P.

- MESH3D - A tool for the construction of three-dimensional meshes
[ONERA, TP NO. 1992-164] p 561 A93-25339

JACQUOTTE, O.-P.

- Detailed analysis of wing-nacelle interaction for commercial transport aircraft
p 213 N93-13203

JACQUOTTE, OLIVIER-PIERRE

- Structured grid variational adaption - Reaching the limit?
[ONERA, TP NO. 1992-114] p 771 A93-38590

JADIC, I.

- Lifting line theory for supersonic flow applications
p 778 A93-39402

JAENSCH, PETER

- Pallet for helicopter test instrumentation
p 1000 N93-31279

JAFJE, RICHARD

- Employment of radicals and excited state species for supersonic combustion photochemical ignition of premixed hydrogen/oxygen mixtures with ArF laser
p 73 N93-11135

JAFROUDI, H.

- Asymptotic methods for the prediction of transonic wind-tunnel wall interference
p 730 A93-35625

JAFRY, YUSUF R.

- Aeronomy coexperiments on drag-free satellites with proportional thrusters: GP-B and STEP
p 195 N93-13922

JAGANATHAN, C.

- A mathematical model to determine the health of components based on SOAP data
p 53 A93-12238

JAHNS, THOMAS M.

- A new resonant link aircraft power generating system
p 809 A93-36268

JAIN, AMOLAK S.

- Hypersonic stagnation line merged layer flow on blunt axisymmetric bodies of arbitrary shape
[AIAA PAPER 93-2723] p 962 A93-46478

JAIN, GIAN P.

- Enhancing availability, performance, and flexibility of air traffic control air-ground services
p 887 N93-30353

JAIN, RAMESH

- A fast algorithm for obtaining dense depth maps for high speed navigation
p 435 A93-19080

JAKOBS, ROGER

- The three-dimensional representation of the lift and pitching moment coefficients on wedged rectangular wings in supersonic flow
p 973 A93-46990

JAMBUNATHAN, V.

- Comprehensive analysis of bearingless rotors - Model development and experimental correlation of modes, response, trim and stability
[AIAA PAPER 93-0624] p 504 A93-24741

JAMES, GEORGE H., III

- The natural excitation technique (NExT) for modal parameter extraction from operating wind turbines
[DE93-010611] p 845 N93-28603

JAMES, GREGORY D.

- A transportable luggage examination system based on neutron interrogation
p 497 N93-21863

JAMES, KEVIN D.

- Forebody vortex control with jet and slot blowing on an F/A-18
[AIAA PAPER 93-3449] p 1009 A93-47235

JAMES, MICHAEL D.

- Construction, wind tunnel testing and data analysis for a 1/5 scale ultra-light wing model
p 876 N93-29778

JAMES, P. W.

- Calculation of turbulent flow for an enclosed rotating cone
[ASME PAPER 92-GT-70] p 400 A93-19320

JAMESON, A.

- A fast multigrid method for solving incompressible hydrodynamic problems with free surfaces
[AIAA PAPER 93-0767] p 540 A93-24851

JAMESON, ANTONY

- Cascade flow calculations by a multigrid Euler method
p 270 A93-21662

- Solution of three-dimensional supersonic flowfields via adapting unstructured meshes
p 863 A93-42442

JAMIESON, R.

- Rapid wind tunnel prototype using stereolithography and equivalent technologies
p 191 A93-14365

- JAMISON, B. D.**
Preliminary evaluation of aviation-impact variables derived from numerical models
[PB93-190197] p 1034 N93-31202
- JAN, JIN-FA**
Theoretical investigation of combustion characteristics in ram-jet dump combustor with side-inlet
p 346 A93-19121
- JANAKIRAM, RAM D.**
Noise characteristics of helicopters with the NOTAR anti-torque system p 1262 A93-54722
- JANECKI, D.**
Vibration control algorithms for flexible rotors
p 95 A93-10741
- JANETZKE, D. C.**
Concurrent processing adaptation of aeroelastic analysis of proflaps p 173 A93-14624
- JANG, CORY S.**
Lift enhancement of an airfoil using a Gurney flap and vortex generators
[AIAA PAPER 93-0647] p 464 A93-24762
- JANG, H. M.**
An inviscid-viscous interaction approach to the calculation of dynamic stall initiation on airfoils
[ASME PAPER 92-GT-128] p 249 A93-19362
- JANG, KYUNG-SOO**
Supercritical wing design, a three dimensional hodograph approach
[AIAA PAPER 92-2657] p 472 A93-24986
- JANG, SHYH-DING**
Ignition process of fuel droplet arrays in a supersonic flowfield p 535 A93-27766
- JANSCHKE, A.**
An experimental health monitoring unit for GPS and GLONASS p 706 N93-25018
- JANSEN, BERNARD J.**
The effects of temperature on supersonic jet noise emission p 446 A93-19159
- JANSSEN, ADRIAN P.**
Compact high reliability fiber coupled laser diodes for avionics and related applications p 1152 A93-49470
- JANUS, J. M.**
Computational analysis of methods for reduction of induced drag
[AIAA PAPER 93-0524] p 474 A93-25536
- JANY, ERIC**
Crack growth prediction models p 1004 N93-31747
- JANZEN, DOYLE**
F-16 Digital Flight Control System improvements p 818 A93-38843
- JARRABET, G. P.**
Low leakage fiber metal seals
[ASME PAPER 92-GT-141] p 402 A93-19373
- JARRETT, D. N.**
Civil spin-off from military aircraft cockpit research p 45 A93-13415
- JARVIS, A. F.**
Development of advanced carbon-carbon annular flameholders for gas turbines
[PNR-90947] p 58 N93-11106
- JARVIS, BRIAN**
Enhancements to modal testing using finite elements p 548 A93-29258
- JATEGAONKAR, R. V.**
Identification of actuation system and aerodynamic effects of direct-lift-control flaps p 1103 A93-52435
- JAVORSKI, CHRISTIAN T.**
NASA advanced design program: Analysis, design, and construction of a solar powered aircraft
[NASA-CR-192040] p 332 N93-17802
- JAYARAM, U.**
Extracting dimensional geometric parameters from B-spline surface models of aircraft
[AIAA PAPER 92-4283] p 43 A93-13340
- JEAL, R. H.**
The development of titanium alloys for gas turbines p 197 A93-15031
- JEDLOVEC, GARY J.**
Variability of geophysical parameters from aircraft radiance measurements for FIFE p 426 A93-20622
- JEERAGE, MAHESH**
The Texas Instruments/Honeywell GPS Guidance Package p 32 A93-11015
- JEGLEY, DAWN C.**
Effect of boundary conditions and panel geometry on the response of laminated panels subjected to transverse pressure loads p 1259 A93-55674
- JEHL, JEAN-FRANCOIS**
The GPS system - Satellite radio-navigation p 312 A93-20008
- JELETIC, KELLYANN**
Software Management Environment (SME) installation guide
[NASA-TM-108578] p 230 N93-15578
- JELTSCH, R.**
Stagnation point computations of nonequilibrium inviscid blunt body flow p 1093 A93-52005
Computation of viscous hypersonic non-equilibrium blunt body flow p 1238 A93-56038
- JEN-CHENG, YANG**
IR imaging for combustion characteristics and optical properties of boron/boron oxide
[AD-A257747] p 393 N93-17693
- JENG, YIH N.**
Two modified versions of Hsu-Lee's elliptic solver of grid generation p 95 A93-11085
- JENKINS, D. M.**
Performance considerations in the operation of free-piston driven hypersonic test facilities p 1011 A93-45497
- JENKINS, DOUGLAS M.**
Flexible manufacturing of aircraft engine parts
[ASME PAPER 92-GT-229] p 404 A93-19446
- JENKINS, JERRY E.**
Body-axis rolling motion critical states of a 65-degree delta wing
[AIAA PAPER 93-0621] p 523 A93-24738
- JENKINS, LAWRENCE M.**
RB211-524B disc and drive cones hot cyclic spinning test p 177 N93-14895
- JENKINS, LUTHER N.**
Experimental investigation of vortex-fin interaction
[AIAA PAPER 93-0050] p 260 A93-20163
- JENKINS, M.**
Performance data of the new free-piston shock tunnel T5 at GALCIT p 1011 A93-45498
- JENKINS, M. G.**
Process optimization of Hexoloy SX-SiC towards improved mechanical properties
[DE93-007913] p 826 N93-28564
- JENKINSON, LLOYD R.**
Regional fanjet aircraft optimization studies p 508 A93-28602
- JENNINGS, NICHOLAS**
A computational approach to predicting the extent of arc root damage in CFC panels p 735 N93-24890
- JENNIONS, I. K.**
Three-dimensional Navier-Stokes computations of transonic fan flow using an explicit flow solver and an implicit k-epsilon solver
[ASME PAPER 92-GT-309] p 256 A93-19499
- JENNIONS, IAN K.**
An investigation of turbulence modelling in transonic fans including a novel implementation of an implicit k-epsilon turbulence model
[ASME PAPER 92-GT-308] p 256 A93-19498
- JENNISON, MICHAEL B.**
Bilateral transfers of safety oversight will prove beneficial to all states p 1174 A93-49279
- JEPSEN, KAREN R.**
Comparison of neural network and Markov random field image segmentation techniques p 397 A93-18652
- JERACKI, ROBERT J.**
Takeoff/approach noise for a model counterrotation propeller with a forward-swept upstream rotor
[AIAA PAPER 93-0596] p 519 A93-24782
Takeoff/approach noise for a model counterrotation propeller with a forward-swept upstream rotor
[NASA-TM-105979] p 362 N93-16715
- JESSEN, C.**
Experimental studies in the Aachen hypersonic shock tunnel p 1251 A93-56032
- JESUROGA, RICHARD**
Preliminary results of the detection of clear air turbulence by the Wind Profiler Demonstration Network p 427 A93-22119
- JESUROGA, RICHARD T.**
Validation of aviation weather products for the Advanced Traffic Management System p 430 A93-22161
- JETT, BRIAN**
Phoenix: Preliminary design of a high speed civil transport
[NASA-CR-192024] p 334 N93-17976
- Ji, CHUQUIN**
Euler solution for wing-body combination at supersonic speeds p 680 A93-33722
- Ji, MINGGANG**
Solution of Euler equations for complex forebody-inlet combinations p 680 A93-33730
- Ji, SHAN-HONG**
Numerical simulation of hypersonic rarefied gas flow over blunt bodies p 687 A93-34356
- JIANG, C. T.**
Computation of shock diffraction in external and internal flows p 1024 A93-45537
- JIANG, C. W.**
Rotor/stator flow coupling in turbomachines p 1232 A93-54647
- JIANG, CAI-HONG**
A study of surge control by using pulse cut-off for dual spool turbo-jet engine p 1194 A93-53862
- JIANG, DACHUN**
Hypersonic viscous flow over two-dimensional ramps p 866 A93-42596
- JIANG, GUIQING**
Two important improvements upon wall pressure signature correction method of low-speed wind tunnel p 730 A93-33704
- JIANG, H.**
The role of Kutta waves on oscillatory shock motion on an airfoil experiencing heavy buffeting
[AIAA PAPER 93-1589] p 682 A93-34121
- JIANG, LIPING**
Aeroelastic analysis of composite wing with control surface p 157 A93-14386
- JIANG, MING**
A study of aircraft global dynamic stability in rapid rolling maneuver p 1206 A93-53869
- JIANG, TAO**
Numerical analysis of aerodynamic losses in film-cooled vane cascade p 1066 A93-48517
Verification of the TOTLOS method for calculating aerodynamic loss in film-cooled turbine cascade p 1087 A93-51191
- JIANG, XIAOMIN**
Numerical solution of non-isentropic transonic cascade flow by time-marching method p 679 A93-33715
- JIANG, YI-TSANN**
Development of an unstructured solution adaptive method for the quasi-three-dimensional Euler and Navier-Stokes equations
[NASA-CR-193241] p 930 N93-29213
- JIANG, YIHE**
Experimental investigation on starting of a turbojet engine in flight p 898 A93-41740
- JIANG, YUNXIANG**
Improvement in application of eigenstructure assignment to flight control system design p 227 A93-15406
- JIN, C. J.**
The hazard and alarm of windshear p 141 A93-14317
- JIN, CHANG-JIANG**
A study on low level windshear hazard index p 1240 A93-55414
- JIN, D.**
Blade excitation by circumferentially asymmetric rotating stall in centrifugal compressors
[ASME PAPER 92-GT-148] p 351 A93-19376
Excitation of blade vibration due to surge of centrifugal compressors
[ASME PAPER 92-GT-149] p 351 A93-19377
- JIN, H.**
Generation of unstructured tetrahedral meshes by advancing front technique p 1021 A93-44206
- JIN, HUI**
Numerical solution of 3-D turbulent flows inside of new concept nozzles p 114 A93-14211
- JIN, NING**
Fine control of Mach number in subsonic wind tunnel p 375 A93-20808
- JINGLI, MAO**
An analysis of the reliability and maintainability of the Jian 6 and Jian 7 aircraft and ways to improve them
[AD-A261060] p 678 N93-26238
- JIRSA, J. O.**
Expedient repair of structural facilities
[AD-A260727] p 731 N93-25656
- JOB, R. F. S.**
Noise-induced reaction in a work community adjacent to aircraft runways - The Royal Australian Airforce p 559 A93-28496
- JOHAN, Z.**
Application of the Galerkin/least-squares formulation to the analysis of hypersonic flows. I - Flow over a two-dimensional ramp p 866 A93-42593
Application of the Galerkin/least-squares formulation to the analysis of hypersonic flows. II - Flow past a double ellipse p 868 A93-42608
- JOHANNESSEN, ROLF**
Work performed in the United Kingdom to establish the feasibility of RAIM in a GPS receiver in flight p 314 A93-21157
- JOHANSSON, ARNE V.**
A low speed wind-tunnel with extreme flow quality - Design and tests p 190 A93-14352
- JOHANSSON, B. CHRISTER V.**
The numerical solution of low Mach number flow in confined regions by Richardson extrapolation
[TRITA-NA-9207] p 789 N93-29005
- JOHANSSON, STEFAN H.**
Numerical simulation of vortex shedding past triangular cylinders at high Reynolds number using a k-epsilon turbulence model p 871 A93-42873

JOHANSSON, ULF

JOHANSSON, ULF

CFD analysis and testing on a twin inlet ramjet
[AIAA PAPER 93-1839] p 1075 A93-49723

JOHARI, H.

A visual study of recessed angled spanwise blowing
method on a delta wing
[AIAA PAPER 93-3246] p 966 A93-46791

JOHE, C.

Experimental investigation of a 2D parallel vortex/airfoil
interaction p 538 A93-23808

JOHNSON, RAYMOND K.

Fluidic scale model multi-plane thrust vector control test
results [AIAA PAPER 93-2433] p 1117 A93-50187

JOHNSON, A. F.

Design and fabrication of a composite transmission
housing for a helicopter tail rotor p 156 A93-14339

JOHNSON, ANDREW M.

Material requirements for the High Speed Civil
Transport [ISABE 93-7067] p 1200 A93-54043

JOHNSON, ARTHUR W.

Observations of liquid jets injected into a highly
accelerated supersonic boundary layer p 1177 A93-53214

JOHNSON, B. C.

Demonstration of an integrated, active 4 x 4 photonic
crossbar p 211 A93-17392

JOHNSON, B. V.

Heat transfer in rotating serpentine passages with trips
skewed to the flow [ASME PAPER 92-GT-191] p 403 A93-19416
Experimental investigation of turbine disk cavity
aerodynamics and heat transfer [NASA-CR-193831] p 812 A93-27115

JOHNSON, COLIN

Predicted aircraft effects on stratospheric ozone
p 93 A93-11096

JOHNSON, CONOR D.

Passive damping technology p 1259 A93-55866

JOHNSON, D. L.

Natural environment application for NASP-X-30 design
and mission planning [AIAA PAPER 93-0851] p 531 A93-24915

JOHNSON, D. T.

Flight performance of hypersonic minor circle turning
maneuvers [AIAA PAPER 93-0627] p 531 A93-24744

JOHNSON, DANIEL P.

False alarm probability determination for the Honeywell
Hexad Fault-Tolerant INS p 342 A93-21193

JOHNSON, DERECK F.

External stress-corrosion cracking of a 1.22-m-diameter
type 316 stainless steel air valve [NASA-TP-3190] p 737 A93-26201

JOHNSON, E. H.

Examples of dynamic response optimization using
MSC/NASTRAN [AIAA PAPER 92-4814] p 436 A93-20394

JOHNSON, ERIC R.

Static and dynamic large deflection flexural response
of graphite-epoxy beams [NASA-CR-4118] p 934 A93-30374

JOHNSON, FORRESTER T.

Using a full potential solver for propulsion system
exhaust simulation p 689 A93-34487

JOHNSON, G. A.

Sea fog and stratus - A major aviation hazard in the
northern Gulf of Mexico p 429 A93-22141
Sea fog and stratus - A major aviation and marine hazard
in the northern Gulf of Mexico p 844 A93-39762

JOHNSON, G. I.

A preliminary investigation of a method to calibrate strain
gauge balances by means of a reference balance p 210 A93-16845

JOHNSON, JAMES

SR-SCARLET 1: Peregrin [NASA-CR-192048] p 337 A93-18155

JOHNSON, JOSEPH

Test results of an orifice pulse tube refrigerator
p 1149 A93-48612

JOHNSON, JOSEPH L., JR.

Stall departure resistance enhancer
[NASA-CASE-LAR-14221-1] p 344 A93-19023

JOHNSON, KARLA L.

Evaluation of a nonlinear PSC algorithm on a variable
cycle engine [AIAA PAPER 93-2077] p 1114 A93-49904

JOHNSON, MARTIN

Advanced Tupolev twinjet combines Russian and
Western technologies p 802 A93-38565

JOHNSON, MATT

Exodus: Prime Mover [NASA-CR-192051] p 332 A93-17803

JOHNSON, P. D.

Design and test of a small two stage counter-rotating
turbine for rocket engine application [AIAA PAPER 93-2136] p 1142 A93-49954

JOHNSON, R.

Hysteresis and bristle stiffening effects of conventional
brush seals [AIAA PAPER 93-1996] p 1153 A93-49839

JOHNSON, R. W.

Advanced technology commercial fuselage structure
p 918 A93-30432

JOHNSON, SPENCER T.

Ultra-high pressure water jet technology - An overview
of a new process for aerospace paint stripping [SME PAPER AD92-196] p 855 A93-40661

JOHNSON, THOMAS D., JR.

Vortex features of F-106B aircraft at subsonic speeds
[AIAA PAPER 93-3471] p 859 A93-41058

JOHNSON, TIMOTHY A.

Skin-friction topology over a surface mounted
semi-ellipsoidal wing at incidence p 1178 A93-53216

JOHNSON, W. G., JR.

Further buffeting tests in a cryogenic wind tunnel
[NASA-TM-107621] p 22 A93-11610

JOHNSON, W. L.

Representation and presentation of requirements
knowledge p 228 A93-17389

JOHNSON, WALTER A.

A simulator solution for the parachute canopy control
and guidance training problem [SAE PAPER 920984] p 191 A93-14634
Parachute canopy control and guidance training
requirements and methodology [AIAA PAPER 93-1255] p 703 A93-35188

JOHNSON, WALTER W.

Visual augmentation for night flight over featureless
terrain p 806 A93-35921

JOHNSON, WAYNE

Correlation of airloads on a two-bladed helicopter
rotor p 481 A93-29438
Performance results from a test of an S-76 rotor in the
NASA Ames 80- by 120-foot wind tunnel [AIAA PAPER 93-3414] p 975 A93-47211

JOHNSON, WILLIAM B.

The National Plan for Aviation Human Factors -
Maintenance research issues p 457 A93-27132

JOHNSTON, G. W.

Nonlinear aspects of transonic aeroelasticity
p 1096 A93-52642

JOHNSTON, H.

Stratospheric aircraft: Impact on the stratosphere?
[DE92-016997] p 94 A93-12104

JOHNSTON, L. J.

Computation of viscous transonic aerofoil flows using
eddy-viscosity based turbulence models p 687 A93-34360

JOHNSTON, LESLIE J.

Turbulence modelling requirements for the prediction
of viscous transonic aerofoil flows p 115 A93-14249
Compressible flow calculations using a two-equation
turbulence model and unstructured grids p 686 A93-34351

JOHNSTON, R. P.

Royal Naval helicopter ditching experience
p 492 A93-19684

JOHNSTON, R. T.

Unsteady wing surface pressures in the wake of a
propeller p 1095 A93-52436

JOHNSTON, ROBERT THOMAS

Unsteady propeller/wing aerodynamic interactions
p 24 A93-12190

JOLY, V.

Viscous nonequilibrium flow calculations
[ONERA, TP NO. 1992-89] p 771 A93-38573
Calculations of viscous nonequilibrium flows in nozzles
[ONERA, TP NO. 1992-91] p 771 A93-38574

JONES, D.

Canadian experience with air cushion vehicle skirts
p 837 A93-39722

JONES, D. J.

Navier-Stokes investigation of blunt trailing-edge airfoils
using O grids p 1095 A93-52459

JONES, E. G.

Application of a sulphur-doped alkane system to the
study of thermal oxidation of jet fuels [ASME PAPER 92-GT-122] p 387 A93-19356

JONES, G. N.

Identification of system dynamics of a high incidence
research model [RR-407] p 339 A93-18507

JONES, H. E.

An approximately factored incremental strategy for
calculating consistent discrete aerodynamic sensitivity
derivatives [AIAA PAPER 92-4746] p 265 A93-20344

JONES, HENRY E.

Multidisciplinary analysis and sensitivity derivatives for
isolated helicopter rotors in hover [AIAA PAPER 92-4696] p 324 A93-20308

Recent advances in steady compressible aerodynamic
sensitivity analysis p 1236 A93-55400

JONES, HOWARD

Test results of an orifice pulse tube refrigerator
p 1149 A93-48612

JONES, J. E.

Observations on computational methodologies for use
in large-scale, gradient-based, multidisciplinary design
[AIAA PAPER 92-4753] p 436 A93-20351

JONES, JACK A.

Three-stage sorption type cryogenic refrigeration
systems and methods employing heat regeneration
[NASA-CASE-NPO-18366-1-CU] p 216 A93-13422

JONES, JUDI P.

En route air traffic controllers use of flight progress strips:
A graph-theoretic analysis [AD-A259062] p 319 A93-18927

JONES, JULIE

Investigation of advanced technology for airway facilities
maintenance training [DOT/FAA/CT-TN92/24] p 994 A93-32336

JONES, K. D.

Interactive hypersonic waverider design and
optimization p 119 A93-14348
Waverider design for generalized shock geometries
[AIAA PAPER 93-0774] p 467 A93-24858

JONES, KENNETH M.

Assessment of computational issues associated with
analysis of high-lift systems p 785 A93-27449

JONES, KENNETH R.

Nickel hydrogen batteries for terrestrial applications
p 557 A93-26005

JONES, KEVIN D.

Numerical simulations of high-speed flows about
waveriders with sharp leading edges p 9 A93-12007

JONES, LISA E.

Effects of floor location on response of composite
fuselage frames p 997 A93-46809
Instrumentation and data acquisition for full-scale aircraft
crash testing p 1250 A93-54399

An overview of the crash dynamics failure behavior of
metal and composite aircraft structures p 923 A93-30875

JONES, MARK K.

Functional requirements of an advanced instructional
design advisor: Simulation authoring, Volume 3
[AD-A256650] p 440 A93-16500

JONES, MICHAEL G.

Unsteady loads measurements in a generic high speed
engine model by means of recessed transducers
[AIAA PAPER 93-0287] p 342 A93-21104

JONES, R.

Crack growth and repair of multi-site damage of fuselage
lap joints p 547 A93-28291

Bonded repair of multi-site damage p 947 A93-45786

Damage tolerance assessment of boron/epoxy repairs
to fuselage lap joints [AD-A258383] p 338 A93-18257

JONES, R. A.

Experimental investigation of an axisymmetric
hypersonic scramjet inlet for laser propulsion p 122 A93-14515

Comparison of reacting and non-reacting shear layers
at a high subsonic Mach number [NASA-TM-106198] p 814 A93-27610

Turbulence measurement in a reacting and non-reacting
shear layer at a high subsonic Mach number [NASA-TM-106186] p 989 A93-31839

JONES, R. MCC.

The military operator's experience of reliability and
maintainability characteristics p 80 A93-13403

JONES, R. R., III

The acoustic response of altitude test facility exhaust
systems to axisymmetric and two-dimensional turbine
engine exhaust plumes p 449 A93-19209

Measured acoustic characteristics of ducted supersonic
jets at different model scales [AIAA PAPER 93-0731] p 563 A93-24821

JONES, R. T.

The measurement of the velocity field induced by a gust
generator in a closed-circuit subsonic wind-tunnel
[RAE-TM-MAT/STR-1102] p 67 A93-11435

JONES, RAYMOND D.

Flight evaluation of a computer aided low-altitude
helicopter flight guidance system p 820 A93-28869

Flight evaluation of a computer aided low-altitude
helicopter flight guidance system [NASA-TM-103998] p 994 A93-32225

JONES, RICHARD D.

Development and application of a nonlinear fin mixer
p 368 A93-22869

- JONES, ROLLIE, JR.**
Configuration management impacts on customer support and satisfaction p 853 A93-35922
- JONES, S. P.**
Aerodynamics of the TCOM 71M aerostat [AIAA PAPER 93-4036] p 1231 A93-54607
- JONES, STEPHEN B.**
Recent experiences with implementing a video based six degree of freedom measurement system for airplane models in a 20 foot diameter vertical spin tunnel p 821 A93-37763
- JONES, STUART C.**
Analytical comparison of convective heat transfer correlations in supercritical hydrogen p 416 A93-23477
- JONES, T. V.**
Internal cooling passage heat transfer near the entrance to a film cooling hole - Experimental and computational results [ASME PAPER 92-GT-241] p 404 A93-19450
A test facility for the thermofluid-dynamics of gas bearing lubrication films [PNR-90897] p 72 N93-11032
Experimental heat transfer results in turbine stators and rotors and a comparison with theory [PNR-90945] p 57 N93-11055
Measurement of turbulent spots and intermittency modelling at gas-turbine conditions p 902 N93-29934
- JONES, W. P.**
Measurements of gas composition and temperature inside a can type model combustor p 1123 A93-51644
- JONGEBREUR, A. A.**
Results of review of Fokker F 28 'Fellowship' maintenance program p 948 A93-45793
- JOOS, FRANZ**
Combustor development for advanced helicopter engines p 1246 A93-54841
- JORDAN, FRANK L., JR.**
Flight and wind-tunnel calibrations of a flush airdata sensor at high angles of attack and sideslip and at supersonic Mach numbers [NASA-TM-104265] p 344 N93-19110
- JOSHI, MAHENDRA C.**
Aerospace '92 - The year in review p 455 A93-19976
- JOST, DRAGICA**
A comparison between numerical models and measurements in a Kaplan turbine guide vanes p 685 A93-34339
- JOSUHN-KADNER, B.**
Investigations on a radial compressor tandem-rotor stage with adjustable geometry [ASME PAPER 92-GT-218] p 404 A93-19440
- JOSYULA, ESWAR**
Hypersonic nonequilibrium flow computations using the Roe flux-difference split scheme p 692 A93-35609
Computation of hypersonic flow past blunt body for nonequilibrium weakly ionized air [AIAA PAPER 93-2995] p 1053 A93-48185
Computation of nonequilibrium hypersonic flowfields around hemisphere cylinders p 1229 A93-54469
- JOUBERT, H.**
Flight analysis of air intake/engine compatibility p 161 N93-13212
- JOUET, C.**
Supersonic vortical flows around an ogive-cylinder - Laminar and turbulent computations [ONERA, TP NO. 1992-111] p 771 A93-38588
3D laminar and 2D turbulent computations with the Navier-Stokes solver FLU3M [ONERA, TP NO. 1993-105] p 1180 A93-53618
- JOUIN, PIERRE**
An application of knowledge-based engineering to composite tooling design p 846 A93-36010
- JOUIN, PIERRE H.**
Rapid fabrication of flight worthy composite parts p 209 A93-15792
- JOUMA'A, M.**
Lateral aerodynamic interference between tanker and receiver in air-to-air refueling p 1136 A93-52444
- JOURDREN, C.**
Navier-Stokes flow simulation in a 2D high pressure turbine cascade with a cooled slot trailing edge p 972 A93-46941
- JOURDREN, CHRISTINE**
Viscous analysis of high pressure turbine inlet guide vane flow including cooling injections [AIAA PAPER 93-1798] p 1074 A93-49687
- JOVENOT, CLAUDE**
Onboard maintenance monitoring systems in modern aircraft p 167 A93-15047
- JOVANOVIC, J.**
Drag characteristics of extra-thin-fin-riblets in an air flow conduit p 1151 A93-49240
- JOVIC, SRBOLJUB**
An experimental investigation of the separating/reattaching flow over a backstep [NASA-CR-192105] p 298 N93-18781
- JOYCE, RICHARD K.**
A method of testing two-dimensional airfoils [AD-A253210] p 17 N93-10375
- JU, AN-CHI**
Improvements to LQGI/LTR methodology for plants with lightly damped or low frequency poles [AD-A258841] p 443 N93-19112
- JU, Y.**
Ignition analysis of unpremixed reactants with chain mechanism in a supersonic mixing layer p 735 A93-35619
- JUANG, JYH-CHING**
Estimation of aerodynamic coefficients using neural networks [AIAA PAPER 93-3639] p 1165 A93-48324
Multiple radial basis function networks in modeling and control [AIAA PAPER 93-3731] p 1170 A93-51330
- JUDGE, T. R.**
Particle imaging techniques and applications p 1020 A93-44195
- JUE, TSWEN-CHYUAN**
Numerical study of cavity natural convection flow with augmenting and counteracting effects by projection finite element method p 749 N93-25540
- JUGGINS, PHILIP T. W.**
Coupled rotor fuselage mode shapes - A tool in understanding helicopter response p 797 A93-35977
- JUILLEN, J. C.**
The experimental study of contamination and leading edge contamination of swept wings [LIB-TRANS-2197] p 782 N93-27274
- JULA, A.**
A numerical investigation into the nozzle flow of high by-pass turbofans [ASME PAPER 92-GT-10] p 346 A93-19283
- JUMPER, E. J.**
A simple criterion for vortex breakdown [AIAA PAPER 93-0866] p 469 A93-24928
Attenuation of airplane wake vortices by excitation of far-field instability [AIAA PAPER 93-3511] p 984 A93-47277
- JUMPER, ERIC J.**
'Wingwake' - A computational model for preliminary assessment of wake vortex attenuation schemes [AIAA PAPER 92-4209] p 15 A93-13377
- JUMPER, STEPHEN J.**
Tiltrotor ground noise reduction from rotor parametric changes as predicted by ROTONET p 567 A93-29415
- JUN, Y. D.**
Particle dynamics simulations in inlet separator with an experimentally based bounce model [AIAA PAPER 93-2156] p 1115 A93-49972
- JUNDI, KHALED**
Real-time monitoring for software development and testing p 939 A93-42824
- JUNG, W. G.**
Adaptive/conformal wing design for future aircraft p 320 A93-17728
- JUNQUA, I.**
Validation of electromagnetic-topology concepts on a complex structure [ONERA, TP NO. 1992-63] p 542 A93-25327
- JUSSILA, MATTI**
Interaction between ice and propeller [VTI-TIED-1281] p 841 N93-27832
- JUSTIZ, CHARLES R.**
DSMC simulation of ionized rarefied flows [AIAA PAPER 93-3095] p 1061 A93-48269
- K**
- KABANOV, S. A.**
Solution of the terminal guidance problem for a flight vehicle using analytical mechanics methods p 228 A93-16778
- KABIR, HUMAYUN R. H.**
Fourier analysis of clamped moderately thick arbitrarily laminated plates p 206 A93-14571
- KABIS, HANEE Z.**
Design of a hypersonic waverider-derived airplane [AIAA PAPER 93-0401] p 384 A93-21108
- KACHANOV, B. O.**
An identification method for dynamic systems with delay p 562 A93-27689
A method for the spectral-time identification of the longitudinal and lateral motions of an aircraft p 1205 A93-52942
- KACIREK, JEFF**
Design, capabilities, and performance of the miniaturized airborne GPS receiver p 32 A93-11014
- KACPRZYNSKI, J. J.**
An experimental investigation of convective heat transfer at the leading edge of a gas turbine airfoil [ASME PAPER 92-GT-248] p 405 A93-19457
- KADOKURA, A.**
Polar Patrol Balloon Experiment in Antarctica p 27 A93-11373
- KADYARDUSOV, P. A.**
The study of experimental turboramjets - Heat state and cooling problems [AIAA PAPER 93-1989] p 1112 A93-49834
- KAERCHER, BRANDON W.**
SAE Aero Design '92 [SAE PAPER 921009] p 157 A93-14641
- KAFYEKE, F.**
Multi-block grid generation for complete aircraft configurations p 460 A93-23838
Development of a transonic Euler method for complete aircraft configurations p 779 A93-39721
- KAGAN, E.**
Feasibility study of an active aeroelastic control system for the F-16 aircraft p 181 A93-14224
- KAGAWA, RYOJI**
A study of a direct-injection stratified-charge rotary engine for motor vehicle application [SAE PAPER 930677] p 1158 A93-50524
- KAGERBAUER, G.**
The design development of the monolithic CFRP centre fuselage skin of the European fighter aircraft p 159 A93-15782
- KAHN, WILLIAM C.**
Utilization of CAD/CAE for concurrent design of structural aircraft components [AIAA PAPER 93-1466] p 710 A93-34014
- KAILASANATH, K.**
Stability of oblique detonations in RAM accelerators [AIAA PAPER 92-0089] p 541 A93-24979
Compressibility, exothermicity, and three dimensionality in spatially evolving reactive shear flows p 950 A93-44375
- KAISER, MARY K.**
Visual augmentation for night flight over featureless terrain p 806 A93-35921
- KAISER, STEFAN A.**
The legal status of ekranoplanes p 453 A93-20900
Stumbling blocks for airport construction in the new German federal states p 1227 A93-53727
- KAIZOJI, ALLYNE**
Effects on load distribution in a helicopter rotor support structure associated with various boundary configurations p 796 A93-35951
- KAJI, SHOJIRO**
Study on steady and unsteady unstart phenomena due to compound choking and/or fluctuations in combustor of scramjet engines [AIAA PAPER 92-5102] p 359 A93-22372
Analytical study on plate edge noise (Noise generation from tandemly situated trailing and leading edges) p 1038 A93-45561
Analysis of unstarted supersonic flutter in cascade by semiactuator disk theory p 1181 A93-53841
Study on unstart and its propagation along modules due to compound choking and/or fluctuations in combustor of scramjet engines [ISABE 93-7052] p 1199 A93-54028
Numerical and experimental study on two- and three-dimensional supersonic flow field with hydrogen injection [ISABE 93-7118] p 1188 A93-54093
Numerical study on transverse hydrogen injection into a supersonic flowfield p 302 N93-19311
- KAKHOVSKII, K. V.**
An experimental study of a method for reducing the jet noise of bypass engines using mechanical flow mixers p 53 A93-12810
- KAKUDATE, SATOSHI**
A new technique for analysis of unsteady aerodynamic responses of cascade airfoils with blunt leading edge. I - Theory p 267 A93-20909
- KALASHNIKOV, A. I.**
Nonlinear deformation mechanics of multilayer transparency elements - General theory relations p 79 A93-12800
Nonlinear deformation mechanics of multilayer transparency elements - Some calculation results p 1191 A93-52937
- KALBE, HELMUT**
Software flexibility and configuration control for the A340/A330 Aircraft Condition Monitoring System (ACMS) p 167 N93-15154

- KALDELLIS, J. K.**
Parametrical investigation of the interaction between turbulent wall shear layers and normal shock waves, including separation p 681 A93-33752
- KALETKA, JUERGEN**
Frequency-domain identification of BO 105 derivative models with rotor degrees of freedom p 712 A93-34263
- KALFAS, A. I.**
Experimental investigation of boundary layer transition on a flat plate with C4 leading edge [ISABE 93-7123] p 1222 A93-54098
- KALFON, J. P.**
Nonlinear analysis of composite thin-walled helicopter blades p 827 A93-36006
- KALIAMIN, D. V.**
Experience in the design of supercritical cascades for the flow straightener of a transonic fan p 777 A93-39196
- KALININA, S. V.**
Pressure field and drag of a single cavity with rounded and sharp edges p 1258 A93-55018
- KALKHORAN, IRAJ M.**
Vortex distortion during vortex-surface interaction in a Mach 3 stream [AIAA PAPER 93-0761] p 467 A93-24846
Development of Polytechnic University's supersonic wind tunnel facility [AIAA PAPER 93-0798] p 528 A93-24876
- KALKWARF, MIKE**
MM-122: High speed civil transport [NASA-CR-192011] p 334 A93-17974
- KALLERGIS, M.**
Experimental results on propeller noise attenuation using an 'active noise control' technique p 450 A93-19223
- KALLINDERIS, Y.**
Hybrid prismatic/tetrahedral grid generation for complex 3-D geometries [AIAA PAPER 93-0669] p 465 A93-24778
A 3-D finite-volume scheme for the Euler equations on adaptive tetrahedral grids p 956 A93-45083
Adaptive refinement-coarsening scheme for three-dimensional unstructured meshes p 961 A93-45735
Prismatic grid generation for three-dimensional complex geometries p 1178 A93-53217
- KALSKE, SEPPO**
Motion simulation of underwater vehicles [VTI-PUBS-97] p 443 A93-18698
- KAM, MOSHE**
A monitor for the laboratory evaluation of control integrity in digital control systems operating in harsh electromagnetic environments [NASA-TM-4402] p 65 A93-12304
- KAMAL, A. K.**
Airport surveillance radar design for increased air traffic p 883 A93-43410
- KAMARSU, SRIGOURI**
Self-tuning guidance applied to aeroassisted plane change problems [AIAA PAPER 93-3791] p 1143 A93-51386
- KAMAT, MANOHAR P.**
SAPNEW: Parallel finite element code for thin shell structures on the Alliant FX/80 [NASA-CR-190663] p 84 A93-10372
SAPNEW: Parallel finite element code for thin shell structures on the Alliant FX-80 [NASA-CR-189212] p 220 A93-14799
- KAMATH, PRADEEP S.**
Scramjet combustor and nozzle computations p 171 A93-14243
- KAMELER, F.**
Experimental investigation of tip clearance noise in axial flow machines p 445 A93-19155
- KAMEMOTO, KYOJI**
Numerical analysis of the flow through a centrifugal impeller by vortex distribution model of a boundary layer. I - Theoretical analysis p 1182 A93-53843
- KAMINER, A. A.**
Determination of nonstationary aerodynamic loading on cascade blades in the case of dynamic changes of the angle of attack p 544 A93-26817
- KAMINSKI, WITOLD ST.**
Experimental study of a single strong vortex-airfoil interaction p 481 A93-29432
- KAMMEYER, MARK**
Experiences in fabrication of a waverider model for wind tunnel testing [AIAA PAPER 93-0510] p 328 A93-23257
- KAMPA, KONSTANTIN**
Mission oriented investigation of handling qualities through simulation [MBB-UD-0600-91-PUB] p 332 A93-17567
- KAMRA, A. K.**
The onset of disintegration and corona in water drops falling at terminal velocity in horizontal electric fields p 1163 A93-49130
- KANAI, KIMIO**
Design of an adaptive flight control system with uncertainties p 95 A93-12322
A new way of pole placement in LQR and its application to flight control [AIAA PAPER 93-3845] p 1133 A93-51433
- KANARIOS, MICHAEL**
Arrow 227: Air transport system design simulation [NASA-CR-192053] p 336 A93-18063
- KANDA, HIROSHI**
Flow visualization studies on sidewall effects in two dimensional transonic airfoil testing [AIAA PAPER 93-0090] p 263 A93-20196
- KANDA, TAKESHI**
Analytical investigation of a regeneratively cooled scramjet engine [AIAA PAPER 93-0739] p 519 A93-24829
Aerodynamic performance of scramjet inlet models with a single strut [AIAA PAPER 93-0741] p 466 A93-24831
Effect of film cooling/regenerative cooling on scramjet engine performances [ISABE 93-7036] p 1197 A93-54012
Starting characteristics of scramjet inlets [ISABE 93-7105] p 1203 A93-54081
Mach 4 testing of scramjet inlet models [NAL-TR-1137] p 26 A93-12369
- KANDARPA, S.**
Determination of tire-wheel interface pressure distribution for aircraft wheels [AIAA PAPER 93-1343] p 709 A93-33913
- KANDEBO, STANLEY W.**
GE90 program moves into high gear p 810 A93-38701
- KANDIL, H. A.**
Numerical simulation and physical aspects of supersonic vortex breakdown p 1093 A93-52011
- KANDIL, HAMDY A.**
Three-dimensional supersonic vortex breakdown [AIAA PAPER 93-0526] p 284 A93-23267
Supersonic vortex breakdown over a delta wing in transonic flow [AIAA PAPER 93-3472] p 980 A93-47251
Shock-vortex interaction over a 65-degree delta wing in transonic flow [AIAA PAPER 93-2973] p 1049 A93-48167
Simulation of tail buffet using delta wing-vertical tail configuration [AIAA PAPER 93-3688] p 1065 A93-48357
- KANDIL, O. A.**
Numerical simulation and physical aspects of supersonic vortex breakdown p 1093 A93-52011
- KANDIL, OSAMA A.**
Prediction and control of slender-wing rock p 182 A93-14331
Three-dimensional supersonic vortex breakdown [AIAA PAPER 93-0526] p 284 A93-23267
Prediction of asymmetric vortical flows around slender bodies using Navier-Stokes equations p 478 A93-27925
Supersonic vortex breakdown over a delta wing in transonic flow [AIAA PAPER 93-3472] p 980 A93-47251
Active control of asymmetric conical flow using spinning and rotary oscillations [AIAA PAPER 93-2958] p 1048 A93-48152
Shock-vortex interaction over a 65-degree delta wing in transonic flow [AIAA PAPER 93-2973] p 1049 A93-48167
Simulation of tail buffet using delta wing-vertical tail configuration [AIAA PAPER 93-3688] p 1065 A93-48357
Navier-Stokes dynamics and aeroelastic computations for vortical flows, buffet and aeroelastic applications [NASA-CR-190692] p 17 A93-10098
Passive control of supersonic asymmetric vortical flows around cones p 220 A93-14692
- KANDULA, M.**
Numerical dissipation in F3D thin-layer Navier-Stokes solution for flows with wall transpiration p 9 A93-12010
- KANEHIRA, NORIYUKI**
Numerical calculations of separating flows around oscillating airfoil p 300 A93-19284
- KANEMORI, YUJI**
Experimental study of dynamic fluid forces and moments for a long annular seal p 209 A93-15684
- KANG, DELI**
Study on fracture failure of turbine blades in a series of turbojets p 205 A93-14493
- KANG, H.**
An application of fuzzy logic and Dempster-Shafer theory to failure detection and identification p 96 A93-13079
- KANG, HYUNG SUK**
Two-dimensional fin analysis p 750 A93-25737
- KANG, N. K.**
A multibody formulation for helicopter structural dynamic analysis p 892 A93-43776
- KANG, S.**
The three dimensional flow in a compressor cascade at design and off-design conditions p 971 A93-46927
- KANG, SHUN**
Experimental study on the three dimensional flow within a compressor cascade with tip clearance. I - Velocity and pressure fields [ASME PAPER 92-GT-215] p 258 A93-19574
Experimental study on the three dimensional flow within a compressor cascade with tip clearance. II - The tip leakage vortex [ASME PAPER 92-GT-432] p 258 A93-19575
- KANG, YING**
Experimental study on heat transfer of separated impingement jets in short distance p 1149 A93-48518
- KANIA, WOJCIECH**
A numerical study of aerodynamic wing design for supercritical conditions of an advanced training and military aircraft p 1238 A93-56213
Numerical minimization of the moment coefficient of a supercritical airfoil section p 1238 A93-56214
- KANNAPELL, F.**
The role of the radiologist in the medicolegal procedure after an aviation accident p 853 A93-39701
- KANNINEN, M. F.**
Applications of advanced fracture mechanics to fuselage p 1026 A93-45787
- KANT, NAGU M.**
GPS/GLONASS flight test, lab test and coverage analysis tests p 313 A93-21143
- KAO, PI-JEN**
Sensitivity-based scaling for approximating structural response p 548 A93-28618
- KAO, T. J.**
Navier-Stokes calculations for transport wing-body configurations with nacelles and struts [AIAA PAPER 93-2945] p 1047 A93-48142
Euler analysis of turbofan/superfan integration for a transport aircraft p 214 A93-13206
- KAPANIA, R. K.**
Structural non-linearity effects on flutter of a swept wing in transonic flows p 410 A93-20714
- KAPANIA, RAKESH K.**
Sensitivity analysis of aeroelastic response of a wing using piecewise pressure representation [AIAA PAPER 93-1645] p 742 A93-34170
Sensitivity analysis of flutter response of a typical section and a wing in transonic flow [AIAA PAPER 93-1646] p 742 A93-34171
Shape sensitivities and approximations of modal response of laminated skew plates p 829 A93-37403
Sensitivity analysis of a wing aeroelastic response p 958 A93-45142
- KAPLOW, WESLEY K.**
The Pave Pace integrated core processor p 941 A93-42856
- KAPOOR, K.**
A comparative study of Full Navier-Stokes and Reduced Navier-Stokes analyses for separating flows within a diffusing inlet S-duct [AIAA PAPER 93-2154] p 1079 A93-49970
- KAPPLER, G.**
Experimental analysis of steady-state and dynamic monitoring of power shaft turbines p 178 A93-15176
- KARADIMAS, GEORGE**
Aerodynamic design and analysis of fans using 3D computational codes [DS-2140] p 294 A93-17880
- KARAEV, K. Z.**
Using spectral analysis for estimating the effect of runway irregularities on the loading of transport aircraft structures p 996 A93-45669
Prediction of fatigue crack growth kinetics in the plane structural elements of aircraft in the biaxial stress state p 1025 A93-45670
- KARAMOUZIS, STAMOS T.**
The use of multiple models in case-based diagnosis p 759 A93-25969
- KARANIK, A. N.**
Damage detection by Acousto-Ultrasonic Location (AUL) p 555 A93-21529
- KARAPETIAN, GURGEN R.**
Mi-26 autorotational landings p 816 A93-35955
- KARAS, O. V.**
Calculation of flow fields near a lifting wing p 1179 A93-53552

KARASHIMA, KEIICHI

Intense studies on unsteady secondary separations and oscillating shock waves in three-dimensional shock waves/turbulent boundary layer interaction regions induced by sharp and blunt fins
[AIAA PAPER 93-2939] p 1046 A93-48137

KARAVAEV, E. A.

Wing rock of lifting systems p 118 A93-14330

KARAVOSOV, R. K.

An acoustic suppressor for the jet noise of a turbojet engine p 1003 A93-47510

A study of pressure fluctuations on the surface of a delta wing near the sharp leading edge p 1091 A93-51882

Self-excitation of intense oscillations in flow inside a wind tunnel with an open test section p 1091 A93-51883

KARIM, M. A.

Control of the dynamic-stall vortex over a pitching airfoil by leading-edge suction [AIAA PAPER 93-3267] p 969 A93-46832

KARIMIPANAH, M. T.

Calculation of three-dimensional boundary layers on rotor blades using integral methods [ASME PAPER 92-GT-210] p 252 A93-19433

KARITA, TAKESHI

Reflection and numerical study on steady Mach reflection p 302 A93-19309

KARPEL, MARDECHAY

Multi-disciplinary optimization of aeroservoelastic systems [NASA-CR-191255] p 220 A93-14766

KARPOUZIAN, G.

Exact flutter solution of advanced anisotropic composite cantilevered wing structures [AIAA PAPER 93-1535] p 727 A93-34072

KARR, C. L.

The use of genetic algorithms in the design of fuzzy logic controllers p 1167 A93-50779

KARTASHEV, I. V.

Problems of the organization of the mass testing of large structural elements of aircraft using testing machines p 821 A93-36791

KARULIN, E. I.

A data processing and measuring system with a traversing probe for studying flow in the rotating impeller of an axial-flow fan p 75 A93-10032

KARWIN, M.

Integration of high bypass ratio engines on modern transonic wings for regional aircraft p 506 A93-27479

KASHANI, REZA

Robust control of intelligent rotor [AD-A263707] p 909 A93-29985

KASHIN, A. G.

Synthesis of a data processing and measuring system for flight vehicle control systems p 908 A93-43102

KASHIWABARA, YASUSHIGE

Study on surge and rotating stall in axial compressors. III - Numerical model for multiblade-row compressors p 1181 A93-53799

KASHIWAGI, TAKESHI

Test results of the hydrogen fueled model combustor for the air turbo ramjet engine [ISABE 93-7082] p 1201 A93-54058

Results of sea-level static tests on air turbo ramjet for a future space plane [AAS PAPER 91-640] p 1247 A93-55817

KASIBHATLA, PRASAD S.

NO(y) from sub-sonic aircraft emissions - A global three-dimensional model study p 1261 A93-56236

KASSAPOGLOU, CHRISTOS

Structural evaluation of curved stiffened composite panels fabricated using a THERM-Xsm process p 919 A93-30435

KASTURI, RANGACHAR

A model-based approach for detection of objects in low resolution passive millimeter wave images [NASA-CR-193161] p 808 A93-28418

KATAEV, A. G.

A study of the temperature of bodies in the flow-around regime in the case of surface gas injection p 691 A93-35344

KATAYAMA, MASAYUKI

Aerodynamic heating with boundary layer transition and heat protection with mass addition on blunt body in hypersonic flows [AIAA PAPER 93-2984] p 1051 A93-48177
Aerodynamic heating analysis for axisymmetric bodies in supersonic flow p 303 A93-19312

KATHEDER, K.

A numerical investigation into the nozzle flow of high by-pass turbofans [ASME PAPER 92-GT-10] p 346 A93-19283

KATO, CHISACHI

Numerical prediction of aerodynamic noise radiated from low Mach number turbulent wake [AIAA PAPER 93-0145] p 452 A93-22589

Numerical computation of aerodynamic noise radiation by the large eddy simulation p 850 A93-38151

KATO, DAI

A 2-D compressible N-S simulation of starting- and stalling-flows in a compressor cascades system [ISABE 93-7006] p 1183 A93-53982

KATO, HIROYUKI

Numerical solution of viscous compressible flows using algebraic turbulence models p 770 A93-38162

KATO, KANICHIRO

Analysis of approach paths of a single aircraft p 367 A93-20823
Digital flight recorded data - A method of estimating down draft from digital flight recorded data p 1241 A93-54559

KATS, E. L.

New corrosion resistant nickel-base super-alloys and technological processes of casting gas turbines parts with directional single crystal and regulable equiaxial minimized microporosity structure p 916 A93-40811

KATTA, V. R.

Experimental and numerical investigations of the vortex-flame interactions in a driven jet diffusion flame [AIAA PAPER 93-0455] p 534 A93-25532

Numerical method for simulating fluid-dynamic and heat-transfer changes in jet-engine injector feed-arm due to fouling p 1245 A93-54467

KATZ, A.

Vortex methods for the computational analysis of rotor/body interaction p 765 A93-35939

KATZ, A. P.

Ultrahigh temperature assessment study: Ceramic matrix composites [AD-A262740] p 826 A93-28592

KATZ, AMNON

Methodology for integration of digital control loaders in aircraft simulators [AIAA PAPER 93-3551] p 1207 A93-52655

KATZ, ERIC S.

Prototype stop bar system evaluation at John F. Kennedy International Airport [AD-A258667] p 192 A93-12902

KATZ, J.

Near-field behavior of a tip vortex p 288 A93-23549
Three dimensional near field behavior of a tip vortex developing on an elliptic foil [AIAA PAPER 93-0865] p 468 A93-24927

KATZ, JOSEPH

Unsteady panel method for flows with multiple bodies moving along various paths [AIAA PAPER 93-0640] p 539 A93-24755
Application of leading-edge vortex manipulations to reduce wing rock amplitudes p 1007 A93-45152
Simultaneous mapping of the unsteady flow fields by Particle Displacement Velocimetry (PDV) p 786 A93-27454

KATZ, RANDY H.

Robo-line storage: Low latency, high capacity storage systems over geographically distributed networks [NASA-CR-192910] p 758 A93-25130

KAUFMAN, ALBERT

Design of a high-temperature experiment for evaluating advanced structural materials [NASA-TM-105833] p 88 A93-11624

KAUFMANN, DAVID N.

Helicopter approach capability using the differential global positioning system [NASA-CR-193183] p 793 A93-28936

KAUPS, KALLE

Recent progress in the analysis of iced airfoils and wings p 784 A93-27441

KAURINKOSKI, PETRI

Calculation of transonic viscous flow around a delta wing p 113 A93-14191

KAVALLIERATOS, P.

Nonlinear response and sonic fatigue of high speed aircraft p 399 A93-19211

KAWACHI, KEIJI

Optimal takeoff of a helicopter for category A V/STOL operations p 525 A93-28611
Optimal takeoff procedures for a transport category tiltrotor p 802 A93-37377

Unsteady analysis of helicopter rotor p 770 A93-38193

KAWAGUCHI, N.

Blade loading and shock wave in a transonic circular cascade diffuser [ASME PAPER 92-GT-34] p 246 A93-19294

KAWAGUCHI, NOBUMASA

Blade loading of transonic circular cascade diffuser p 267 A93-20919

KAWAHARA, HIROYASU

Flight simulator evaluation of D-size liquid crystal flat panel displays [NAL-TR-1136] p 52 A93-12367

Liquid crystal flat panel display evaluation tests using a flight simulator [NAL-TR-1122] p 52 A93-12383

KAWAI, MASAFUMI

A numerical investigation of 3D transverse injection into the supersonic flow behind rearward facing step p 303 A93-19316

KAWALL, J. G.

An experimental investigation of a round turbulent jet in a cross-flow p 553 A93-20689

KAWAMOTO, IWAO

Two problems reducing the data accuracy in Transonic Wind Tunnel testing p 304 A93-19321

KAWAMURA, TETSUYA

Turbulent structure in a vortex wake shed from an inclined circular cylinder p 125 A93-15443

KAWANO, ISAO

Research on combined HOPE navigation technology p 533 A93-20428

KAWASHIMA, EIJI

Aerodynamic characteristics of a next generation high-speed civil transport [AIAA PAPER 92-4229] p 15 A93-13356

KAWASHIMA, T.

Turbine blade vibration monitoring system [ASME PAPER 92-GT-159] p 402 A93-19386

KAWASHIMA, TAKASHI

Three-dimensional viscous flow analysis of compressor cascade channels p 1181 A93-53837

KAWASHIMA, TOSHIHIRO

The structure and material testing facility needed for future SST/HST development [AIAA PAPER 92-3887] p 528 A93-24481

KAWAZOE, H.

A study on aerodynamic sound generated by interaction of jet and plate [AIAA PAPER 93-3118] p 1171 A93-48288

KAY, BRUCE F.

Comanche airframe design - The PDT approach p 744 A93-34469
PDT approach for developing RAH-66 Comanche airframe systems p 795 A93-35909

KAYA, T.

Investigation of the flow field through a variable pitch fan rotor with an inlet total pressure distortion [ISABE 93-7029] p 1184 A93-54005

KAYABA, SHIGEO

A wind tunnel investigation to determine buffet countermeasures for STOL aircraft alpha-sweep flight testing [NAL-TR-1129] p 65 A93-12362

KAYE, G. T.

Uplink laser propagation measurements through the sea surface, haze and clouds [AD-A264687] p 935 A93-30553

KAYE, R. H.

Development of a menu driven materials data base for use on personal computers: Aircraft structures technical memorandum [AD-A256317] p 392 A93-16403

KAYNAK, UNVER

Nonequilibrium turbulence modeling study on light dynamic stall of a NACA0012 airfoil p 768 A93-37379

KAYSER, P.

High temperature thin film strain gauges [ONERA, TP NO. 1992-171] p 542 A93-25346

Thin gradient heat fluxmeters developed at ONERA [ONERA, TP NO. 1992-87] p 831 A93-38571

KAZAKOV, A. V.

Nontraditional methods of controlling the stability of a laminar subsonic boundary layer p 1085 A93-50962

KAZANTSEV, A. YU.

The fuel/timing problem in a computer-aided flight preparation system for civil aircraft p 996 A93-45672

General concepts related to the determination of the individual flight performance characteristics of aircraft for establishing fuel consumption standards and optimal flight regimes p 996 A93-45673

KAZARIAN, DAVE

A manned hypersonic reconnaissance vehicle which does not require airborne fueling p 333 A93-17888

KAZEROUNIAN, K.

High speed, heavily loaded and precision aircraft type epicyclic gear system dynamic analysis overview and special considerations [AIAA PAPER 93-2151] p 1154 A93-49968

KAZIMIROV, I. V.

A finite element for modeling skins of composite materials p 1215 A93-52979

KEARSEY, P. R.

Helicopter noise certification p 1262 A93-54720

KEARY, P. E.

Application of generalized force determination to a full scale low cycle fatigue test of the SH-2G helicopter
p 795 A93-35949

An improved method of structural dynamic test design for ground flying and its application to the SH-2F and SH-2G helicopters
p 512 N93-19928

KEAVENEY, S.

Bistatic radar using satellite-borne illuminators of opportunity
p 914 A93-43437

KEDROV, A. V.

Effect of flight conditions on the sound insulation of the aircraft passenger compartment
p 42 A93-12978

KEEFE, LAURENCE R.

A study of compressible turbulence
[AIAA PAPER 93-0659] p 465 A93-24772

KEELING, S. L.

Linear quadratic tracking problems in Hilbert space - Application to optimal active noise suppression
p 1224 A93-52763

KEELING, STEPHEN L.

A strategy for the optimal design of nozzle contours
[AIAA PAPER 93-2720] p 962 A93-46476

KEENAN, JAMES A.

Simulation of ablation in Earth atmospheric entry
[AIAA PAPER 93-2789] p 1027 A93-46531

KEENAN, R.

Advancing the state of the art hypersonic testing - HYTEST/MTM
[AIAA PAPER 93-2023] p 1113 A93-49860

KEENER, EARL R.

Hypersonic single expansion ramp nozzle simulations
p 777 A93-39254

KEFFER, J. F.

An experimental investigation of a round turbulent jet in a cross-flow
p 553 N93-20689

KEGELMAN, J. T.

Aerodynamic applications of pressure sensitive paint
p 549 A93-29301

KEHAYAS, N.

ASTOVL combat aircraft design synthesis and optimization
p 717 N93-25704

KEHAYIAS, J.

A pulsed fast-thermal neutron interrogation system
p 497 N93-21866

KEHOE, MICHAEL W.

Thermoelastic vibration test techniques
p 549 A93-29293

KEIL, H.

Testing of an experimental system for image reconnaissance
p 1040 N93-31283

KEIR, JIM

The well made engine
p 1122 A93-50352

KEITH, B. D.

Commercial turbofan engine exhaust nozzle flow analyses
p 689 A93-34489

KEITH, THEO G., JR.

Investigation of an electrothermal de-icer pad using a three-dimensional finite element simulation
[AIAA PAPER 93-0397] p 327 A93-23072

Subsonic/transonic cascade flutter using a full-potential solver
p 861 A93-41934

Unsteady aerodynamics and flutter based on the potential equation
[AIAA PAPER 93-2086] p 1079 A93-49913

Efficient finite element method for aircraft deicing problems
p 1103 A93-52443

Aeroplastic stability and response of rotating structures
[NASA-CR-191803] p 371 N93-16560

Analysis and evaluation of an integrated laminar flow control propulsion system
[NASA-CR-192162] p 551 N93-20268

Numerical modeling of runback water on ice protected aircraft surfaces
p 840 N93-27438

KEITZ, EDWIN L.

Improved efficiency of air transportation through aviation weather system modernization
p 308 A93-22144

KEIZER, W. P.

Definition study PHARUS
[AD-A256560] p 221 N93-14805

KELZON, A. S.

Dynamics of a high-rpm compressor
p 75 A93-10009

KELAITA, PAUL G.

Scientific visualization using the Flow Analysis Software Toolkit (FAST)
p 758 N93-25600

KELLACKEY, C. J.

Impact ice interface shear stresses caused by blade bending and twisting
[AIAA PAPER 93-0030] p 307 A93-20147

KELLAR, MICHAEL A.

Autogenic-feedback training improves pilot performance during emergency flying conditions
[NASA-TM-104005] p 790 N93-27076

KELLAS, SOTIRIS

Energy-absorbing-beam design for composite aircraft subfloors
[AIAA PAPER 93-1339] p 709 A93-33909

KELLER, K. J.

A domain-specific design architecture for composite material design and aircraft part redesign
p 442 N93-17522

KELLER, KIRBY

Domain specific software design for decision aiding
p 442 N93-17517

KELLER, KIRBY J.

Pilot task monitoring using neural networks
p 940 A93-42846

KELLERER, R.

Double mode behaviour of bladed disk assemblies in the resonance frequency range, visualized by means of holographic interferometry
[ASME PAPER 92-GT-438] p 357 A93-19580

KELLEY, HENRY L.

The strake - A simple means for directional control improvement
p 802 A93-37997

Flow visualization of mast-mounted-sight/main rotor aerodynamic interactions
[AIAA PAPER 93-3517] p 1009 A93-47280

Helicopter low-speed yaw control
[NASA-CASE-LAR-14219-1] p 729 N93-25998

KELLEY, N.

A discussion of the results of the rainflow counting of a wide range of dynamics associated with the simultaneous operation of adjacent wind turbines
[DE93-000016] p 434 N93-18705

KELLEY, SEAN M.

Development of circulation control technology for application to advanced subsonic transport aircraft
[AIAA PAPER 93-0644] p 464 A93-24759

KELLY, G. M.

Development of a skin friction gauge for use in an impulse facility
p 1024 A93-45526

KELLY, GEORGE R.

Measurement of modulation transfer functions of simulator displays
[AD-A259401] p 530 N93-21268

KELLY, H. N.

Actively cooled panel testing perils, problems, and pitfalls
p 1028 A93-46802

KELLY, H. NEALE

Active cooling from the sixties to NASP
p 49 N93-12458

KELLY, JEFFREY J.

Signal processing of jet noise from flyover test data
[AIAA PAPER 93-0736] p 563 A93-24826

De-Dopplerization of aircraft acoustic signals
[AIAA PAPER 93-0737] p 563 A93-24827

KELLY, P. G.

Subscale validation of a freejet inlet-engine test capability
[AIAA PAPER 93-2179] p 1138 A93-49991

KEMMERLY, GUY T.

Evaluation of four advanced nozzle concepts for short takeoff and landing performance
[NASA-TP-3314] p 875 N93-29165

KEMPEL, ROBERT

The F-18 High Alpha Research Vehicle - A high-angle-of-attack testbed aircraft
[AIAA PAPER 92-4121] p 42 A93-13273

KENDER, JOHN R.

A formalization and implementation of topological visual navigation in two dimensions
p 435 A93-19101

KENNEDY, DEIRDRE D.

USA aviation digest index, 1989, volume 11
[AD-A258673] p 571 N93-20388

Index to USA aviation digest, 1990
[AD-A258678] p 572 N93-20389

Index to USA aviation digest, 1991
[AD-A258679] p 572 N93-20390

KENNEDY, J.

Federal Aviation Administration pavement modeling
p 379 N93-16315

KENNEDY, JOHN M.

The effects of crushing surface roughness on the crushing characteristics of composite tubes
p 77 A93-10918

KENNEDY, M. H.

On-board condition management for aircraft gas turbines
[ASME PAPER 92-GT-416] p 357 A93-19564

KENNEDY, THOMAS A.

Sensor alignment Kalman filters for inertial stabilization systems
p 50 A93-11018

KENNEL, ELLIOT B.

Joining carbon composite fins to metal heat pipes using ion beam techniques
p 543 A93-25979

Joining carbon composite fins to titanium heat pipes
[AD-A261970] p 825 N93-27667

KENNELLY, ROBERT A., JR.

Selected experiments in laminar flow: An annotated bibliography
[NASA-TM-103989] p 990 N93-32226

KENNON, S. R.

Geometry based Delaunay tetrahedralization and mesh movement strategies for multi-body CFD
[AIAA PAPER 92-4575] p 15 A93-13309

KENNON, STEPHEN R.

Sweeping algorithm for unstructured-grid generation on two-dimensional non-convex domains
p 1262 A93-56413

KENTFIELD, JOHN A. C.

Nonsteady, one-dimensional, internal, compressible flows - Theory and applications
[ISBN 0-19-507358-4] p 548 A93-28749

KENYON, M. W.

European navigation into the 21st century - Frequency considerations
p 311 A93-17754

KENZAKOWSKI, D. C.

The critical role of turbulence modeling in the prediction of supersonic jet structure for acoustic applications
p 398 A93-19193

KERANS, R. J.

Ultrahigh temperature assessment study: Ceramic matrix composites
[AD-A262740] p 826 N93-28592

KERCHER, D. M.

Heat transfer and turbulence in a turbulated blade cooling circuit
[ASME PAPER 92-GT-167] p 402 A93-19412

KERHO, M.

Vortex generators used to control laminar separation bubbles
p 768 A93-37381

Aerodynamics of a finite wing with simulated ice
p 784 N93-27437

KERHO, M. F.

LDV flowfield measurements on a straight and swept wing with a simulated ice accretion
[AIAA PAPER 93-0300] p 280 A93-23001

KERKEMEYER, BRUCE

Linear and nonlinear aircraft flight control for the AIAA Controls Design Challenge
[AIAA PAPER 92-4628] p 62 A93-13286

KERMAREC, J.

Turbine blade forces due to partial admission
p 1029 A93-46928

KERN, ALEXANDER W.

Comparison of the damage for various types of fibre reinforced composites due to different lightning test standards (MIL-STD-1757A, German military VG-standard 96903)
p 736 N93-24891

KERNEY, PAUL T.

Vane optimization for maximum efficiency using design of experiments
[AIAA PAPER 93-1867] p 1111 A93-49742

KERR, PATIRCA A.

Geometric requirements for multidisciplinary analysis of aerospace-vehicle design
[AIAA PAPER 92-4773] p 436 A93-20366

KERSCHEN, EDWARD J.

Active aerodynamic control of wake-airfoil interaction noise - Theory
p 445 A93-19154

KESKI-KUHA, R. A. M.

Optical technologies for UV remote sensing instruments
p 853 N93-28788

KESSLER, G. K.

F-14D flight director development, test, and evaluation
p 803 A93-38840

KESSLER, W.

Nonintrusive, multipoint velocity measurements in high-pressure combustion flows
[AIAA PAPER 93-2032] p 1145 A93-49867

KESTER, JAMES E.

Some questions of scale in simulation, and a few answers
p 939 A93-42830

KEY, DAVID

Bandwidth and SIMDUCE as simulator fidelity criteria
p 913 N93-30690

KEY, DAVID L.

Ground based simulation evaluation of the effects of time delays and motion on rotorcraft handling qualities
[AD-A256921] p 328 N93-16186

KHABIBULLIN, M. G.

Effect of the powerplant configuration on the air flow rate of the jet shield
p 54 A93-12820

KHADEM, M.

Aerothermodynamic analysis of combined-cycle propulsion systems
p 359 A93-21671

KHALFALLAH, K.

Analysis of implicit treatments for a centred Euler solver
p 864 A93-42449

KHALID, M.

High Mach number dynamic stability of blunt slender cones at angle of attack
p 271 A93-21721

- Navier-Stokes investigation of blunt trailing-edge airfoils using O grids p 1095 A93-52459
- KHALIL, GAMAL**
Video luminescent barometry - The induction period [AIAA PAPER 93-0179] p 414 A93-22607
- KHALIL, S. E.**
Blowout of turbulent disc/pilot stabilized jet diffusion flames [ISABE 93-7026] p 1213 A93-54002
- KHALILI, PAYMAN**
A fast algorithm for obtaining dense depth maps for high speed navigation p 435 A93-19080
- KHALIMULIN, R. M.**
A mathematical model of the vibrational impact hardening of parts p 837 A93-39185
- KHAN, M. A.**
Nonsmooth trajectory optimization - An approach using continuous simulated annealing [AIAA PAPER 93-3657] p 1099 A93-48337
A new technique for nonlinear control of aircraft [AIAA PAPER 93-3881] p 1135 A93-51466
- KHAN, M. J.**
On dynamics of the juncture vortex [AIAA PAPER 93-3473] p 980 A93-47252
- KHAN, MOHAMMAD J.**
Subharmonic and harmonic forced response of the wake of a circular cylinder p 288 A93-23565
- KHAN, SIRAJ M.**
Proceedings of the First International Symposium on Explosive Detection Technology [DOT/FAA/CT-92/11] p 496 N93-21856
- KHAN, TASADDUQ**
Potential and prospects of intermetallic materials for applications in the aerospace industry [ONERA, TP NO. 1992-99] p 824 A93-38580
Designing new multi-phase intermetallic materials based on phase compatibility considerations [ONERA, TP NO. 1992-131] p 772 A93-38605
- KHANANOV, R. I.**
The use of aviation gas-liquid heat exchangers employing heat pipes p 833 A93-39050
- KHANDANI, S. M. H.**
Aerothermodynamic analysis of combined-cycle propulsion systems p 359 A93-21671
- KHARCHENKO, A. G.**
Software for the control of measurement data acquisition, processing, and monitoring during strength testings p 94 A93-10042
- KHAIR, R.**
Photoelectrochemical etching of high aspect ratio submillimeter waveguide filters from n(+) GaAs wafers p 409 A93-20644
- KHARITONOV, A. M.**
On improving adequacy of modeling in wind tunnel problems p 6 A93-10404
Three-dimensional flow past an ogival-cylindrical body in combination with a delta wing p 478 A93-27636
- KHATWA, R.**
The development of an efficient take-off performance monitor (TOPM) p 180 A93-14186
- KHAVERAN, A.**
Propagation of high frequency jet noise using geometric acoustics [AIAA PAPER 93-0147] p 452 A93-23241
Propagation of high frequency jet noise using geometric acoustics [NASA-TM-106013] p 233 N93-15575
- KHAVERAN, ABBAS**
Computation of supersonic jet noise under imperfectly expanded conditions [AIAA PAPER 93-0735] p 563 A93-24825
Computation of supersonic jet noise under imperfectly expanded conditions [NASA-TM-105961] p 233 N93-15430
- KHAZANOV, KH. S.**
Problems of the strength and fatigue of the elements of aircraft structures p 1029 A93-47076
A nonlinear finite element of an arbitrary beam p 1215 A93-52939
- KHEIFETS, D. V.**
A study of a pulsed electrical field near the jet of a turbojet engine p 52 A93-10179
- KHELIF, DJAMAL**
Fast-response aircraft temperature sensors p 167 A93-17095
- KHILNANI, V. I.**
Effective sealing of a disk cavity using a double-toothed rim seal [ASME PAPER 92-GT-379] p 406 A93-19537
- KHLEBNIKOV, V. S.**
A study of the effect of nonstationary perturbations on flow in the front separation region p 5 A93-10150
A study of the interaction of a nonstationary shock wave with a boundary layer on a plate in the transition regime p 1150 A93-48850
- KHLOPKOV, YU. I.**
Development and application of the Monte Carlo method for solving the Boltzmann equation and its models p 1173 A93-51867
Modeling the flow around a body via the solution of the relaxational kinetic equation p 1089 A93-51868
- KHODADADI, J. M.**
Effective sealing of a disk cavity using a double-toothed rim seal [ASME PAPER 92-GT-379] p 406 A93-19537
- KHODADOUST, A.**
LDV flowfield measurements on a straight and swept wing with a simulated ice accretion [AIAA PAPER 93-0300] p 280 A93-23001
Aerodynamics of a finite wing with simulated ice p 784 N93-27437
- KHODADOUST, ABDOLLAH**
Low-frequency flow oscillation over airfoils near stall p 861 A93-41931
- KHODATAEV, K. V.**
An experimental study of dc discharges in supersonic and subsonic air flows p 14 A93-12980
- KHODORKOVSKIY, A. M.**
Determination of the vertical velocity component of aircraft landing on an airfield with a longitudinally sloping runway p 1007 A93-45664
Operating an aircraft during the landing on an airfield with a substantial longitudinal macroslope of the runway p 1008 A93-45667
- KHOKHLENKOV, S. M.**
Optimal design of honeycomb sandwich shell aircraft structures of composite materials p 828 A93-36800
- KHOKHLOV, A. P.**
Intermode exchange in a supersonic boundary layer p 691 A93-35346
- KHOLA, H. S.**
Review of human error accidents in civil aviation p 27 A93-12367
- KHOSID, S.**
On the stability of the process of formation of combustion generated particles by coagulation and simultaneous shrinkage due to particle oxidation [AIAA PAPER 93-2478] p 1146 A93-50220
- KHOSLA, P. K.**
A three-dimensional pressure flux-split RNS application to sub/supersonic flow in inlets and ducts [AIAA PAPER 93-3063] p 1058 A93-48239
- KHOT, N. S.**
Structural optimization using Newton Modified Barrier Method [AIAA PAPER 92-4756] p 409 A93-20352
- KHROMOVA, M. A.**
Measurement of aerodynamic forces at high temperatures p 75 A93-10030
- KHRISTOV, A.**
A joint Soviet-Bulgarian scientific program for free-flight and tethered aerostat observations p 2 A93-11374
- KHROLOVICH, K. B.**
An identification method for dynamic systems with delay p 562 A93-27689
A method for the spectral-time identification of the longitudinal and lateral motions of an aircraft p 1205 A93-52942
- KHUDIYAKOV, A. I.**
Calculation of a collector-type annular plate heat exchanger p 833 A93-39045
Development of a process for fabricating a plate heat exchanger for the heat recovery system of gas turbine engines p 834 A93-39053
- KHVOROSTUKHIN, L. A.**
Effect of ion treatments on the fatigue strength of blades p 811 A93-39073
- KIBENS, V.**
Streamline curvature in supersonic shear layers p 244 A93-19194
- KIDIDIS, ANDREW S.**
Mil-Prime specification for parachutes [AIAA PAPER 93-1247] p 677 A93-35184
- KIELB, ROBERT E.**
An analysis system for blade forced response [ASME PAPER 92-GT-172] p 352 A93-19398
- KIENHOLZ, DAVID A.**
Development of a dynamic pressure response calibrator p 1254 A93-54362
- KIENITZ, KARL H.**
Controller design using fuzzy logic - A case study p 756 A93-33793
- KIERNAN, LAURENCE J.**
Estimating the regional economic significance of airports [AD-A257658] p 382 N93-17793
- KIGGANS, J. O.**
Microwave processing of silicon nitride for advanced gas turbine applications [DE93-007910] p 917 N93-29767
- KIL, KAZUO**
Computer-controlled alignment for a 2000-line color monitor p 886 N93-30324
- KIKUCHI, H.**
New approximate method of stress analysis for bladed rotating discs [ISABE 93-7059] p 1219 A93-54035
- KIKUCHI, K.**
Navier-Stokes computation of the three dimensional flow fields through a transonic fan blade [ISABE 93-7030] p 1184 A93-54006
- KIKUCHI, KAZUO**
Numerical simulation of the flow through non-uniform airfoil cascade p 302 N93-19310
- KIKUCHI, M.**
Active control of vortex breakdown by a spinning wave generator [ISABE 93-7045] p 1219 A93-54021
- KIKUKAWA, HIROSHIGE**
The structure and material testing facility needed for future SST/HST development [AIAA PAPER 92-3887] p 528 A93-24481
- KILGORE, ROBERT A.**
Cryogenic wind tunnels p 1010 A93-44886
- KILGORE, W. A.**
Pilot weather advisor [NASA-CR-189723] p 318 N93-16692
A PC-based simulation of the National Transonic Facility's safety microprocessor [NASA-TM-109003] p 1038 N93-32224
- KILGORE, W. ALLEN**
Modeling and control study of the NASA 0.3-meter transonic cryogenic tunnel for use with sulfur hexafluoride medium [NASA-CR-189737] p 418 N93-16379
A feasibility study of using Langley 0.3-m transonic cryogenic tunnel sidewall boundary-layer removal system for heavy gas testing [NASA-CR-191438] p 747 N93-25087
- KILIAN, MIKE**
SR-SCARLET 1: Peregrin [NASA-CR-192048] p 337 N93-18155
- KILIC, M.**
Flow and heat transfer between gas-turbine discs p 903 N93-29950
- KILL, N.**
Vibration analysis in turbomachines p 1005 N93-32274
- KILLEY, KEVIN G.**
A comparative assessment of two present generation turbine analysis codes [ISABE 93-7097] p 1203 A93-54073
- KILLOUGH, BRIAN D.**
Thermal control of a lidar laser system using a non-conventional ram air heat exchanger p 1028 A93-46821
- KILPATRICK, FREEMAN A., JR.**
An investigation of discovery-based learning in the route planning domain [AD-A259141] p 513 N93-20560
- KIM, CHAN M.**
Computation of supersonic jet noise under imperfectly expanded conditions [AIAA PAPER 93-0735] p 563 A93-24825
Computation of supersonic jet noise under imperfectly expanded conditions [NASA-TM-105961] p 233 N93-15430
- KIM, DANIEL B.**
Jacobian update strategies for quadratic and near-quadratic convergence of Newton and Newton-like implicit schemes [AIAA PAPER 93-0878] p 470 A93-24909
- KIM, FREDERICK DONG**
Formulation and validation of high-order mathematical models of helicopter flight dynamics p 162 N93-13821
- KIM, G. M.**
Platinum-modified diffusion aluminide coatings on nickel-base superalloys [AD-A263597] p 917 N93-29981
- KIM, GUN-IN**
Multi-parameter optimization tool for low-cost commercial fuselage crown designs p 922 N93-30858
- KIM, H. J.**
Adaptive EAGLE dynamic solution adaptation and grid quality enhancement p 788 N93-27464
- KIM, H.-D.**
Normal shock wave oscillations in supersonic diffusers p 1044 A93-48042
- KIM, HYUN D.**
A time-accurate high-resolution TVD scheme for solving the Navier-Stokes equations p 1093 A93-52006
- KIM, I.**
An application of fuzzy logic and Dempster-Shafer theory to failure detection and identification p 96 A93-13079

- Computation of passively controlled transonic wing
[AIAA PAPER 93-3474] p 981 A93-47253
Fundamental studies of droplet interactions in dense sprays
[AD-A261165] p 737 N93-25948
- KIM, INCHUL**
Three-dimensional flow over two spheres placed side by side
p 539 A93-24412
- KIM, J. H.**
Rotating machinery - Transport phenomena; Proceedings of the 3rd International Symposium on Transport Phenomena and Dynamics of Rotating Machinery (ISROMAC-3), Honolulu, HI, Apr. 1-4, 1990 [ISBN 1-56032-147-4] p 1256 A93-54626
Rotating machinery - Dynamics; Proceedings of the 3rd International Symposium on Transport Phenomena and Dynamics of Rotating Machinery (ISROMAC-3), Honolulu, HI, Apr. 1-4, 1990 [ISBN 1-56032-147-4] p 1257 A93-54651
- KIM, J. M.**
The three-dimensional boundary layer flow due to a rotor-tip vortex
[AIAA PAPER 93-3081] p 1060 A93-48255
Summary of the interaction of a rotor wake with a circular cylinder
[AIAA PAPER 93-3084] p 1060 A93-48258
- KIM, JUNG H.**
Flight simulator for hypersonic vehicle and a study of NASP handling qualities p 530 N93-19456
- KIM, K.**
Fluid dynamics and convective heat transfer in impinging jets through implementation of a high resolution liquid crystal technique
[ISABE 93-7077] p 1220 A93-54053
- KIM, KUK H.**
Forcing function generator fluid dynamic effects on compressor blade gust response
[AIAA PAPER 93-0157] p 275 A93-22594
Compressor unsteady aerodynamic response to rotating stall and surge excitations
[AIAA PAPER 93-2087] p 1079 A93-49914
- KIM, KUK K.**
Spatial domain characterization of abrupt rotating stall initiation in an axial flow compressor
[AIAA PAPER 93-2238] p 1081 A93-50040
- KIM, M. N.**
An ultra low NO(x) pilot combustor for staged low NO(x) combustion
[ISABE 93-7020] p 1195 A93-53996
- KIM, S.**
Heat transfer and leakage in high-speed rotating stepped labyrinth seals p 903 N93-29951
- KIM, S. C.**
Calculation of scramjet inlet with thick boundary-layer ingestion
[AIAA PAPER 93-1836] p 1074 A93-49720
- KIM, S. E.**
Silicon differential pressure transducer line pressure effects and compensation p 830 A93-37890
- KIM, SEONG-HWAN**
An efficient method to calculate rotor flow in hover and forward flight
[AIAA PAPER 93-3336] p 953 A93-45030
- KIM, TAEHYOUN**
Nonlinear large amplitude vibration of composite helicopter blade at large static deflection p 713 A93-35630
Nonlinear large amplitude aeroelastic behavior of composite rotor blades p 997 A93-45741
- KIM, Y. K.**
Local heat transfer measurement with liquid crystals on rotating surfaces including non-axisymmetric cases p 902 N93-29943
- KIM, Y.-H.**
A prediction model for the vortex shedding noise from the wake of an airfoil or axial flow fan blades p 1265 A93-55995
- KIM, YONG S.**
An analysis on high speed impulsive noise of transonic helicopter rotor p 849 A93-35965
- KIM, YOUNG I.**
Nonlinear flutter of composite plates with damage evolution
[AIAA PAPER 93-1546] p 829 A93-37441
- KIMASOV, YU. I.**
Direct and inverse problems of calculating the axisymmetric and 3D flow in axial compressor blade rows p 972 A93-46938
- KIMBERLIN, RALPH D.**
Airspeed calibration using GPS
[AIAA PAPER 92-4090] p 51 A93-13272
- KIMLIK, N. M.**
Refinement of algorithms for calculating the remaining life from magnetic recording instrument data p 320 A93-18330
- KIMMEL, ROGER L.**
Unit-Reynolds-number effects on boundary-layer transition p 288 A93-23560
On the breakdown of a hypersonic laminar boundary layer
[AIAA PAPER 93-0896] p 472 A93-24956
- KIMURA, C. Y.**
World commercial aircraft accidents
[DE93-010892] p 791 N93-28571
- KIMURA, K.**
Crack simulation and life assessment of gas turbine nozzles p 915 A93-40805
- KINARD, T. A.**
Transonic Navier-Stokes flow computations over wing-fuselage geometries p 1095 A93-52456
- KIND, R. J.**
Performance degradation due to hoar frost on lifting surfaces p 305 A93-17798
- KINELEV, V. G.**
Control of the quality of dynamic processes in the valves of power-generating equipment p 832 A93-39030
- KING, H. H.**
Effect of leading-edge geometry on delta wing unsteady aerodynamics p 1095 A93-52457
- KING, J. E.**
Microstructural study of aluminate surface coatings on single crystal nickel base superalloy substrates p 70 A93-12771
- KING, JANET**
Differential GPS autonomous failure detection p 314 A93-21152
- KING, LYNDALL S.**
Comparison of predictions with measurements for a quiet supersonic tunnel
[AIAA PAPER 93-0344] p 376 A93-23031
Development of the NASA-Ames low disturbance supersonic wind tunnel for transition research up to Mach 2.5
[AIAA PAPER 92-3909] p 462 A93-24488
- KING, P. I.**
Stall inception in single stage, high-speed compressors with straight and swept leading edges
[AIAA PAPER 93-1870] p 1076 A93-49745
- KING, R. A.**
Three-dimensional boundary-layer transition on a cone at Mach 3.5 p 9 A93-12177
- KING, R. B.**
In-flight evaluation of noise levels and assessment of active noise reduction systems in the Seahawk S-70B-2 helicopter
[AD-A260689] p 759 N93-25649
- KING, S. P.**
A knowledge-based blackboard system to interpret graphical data from vibration tests of gas turbines
[PNR-90993] p 59 N93-11114
- KING, T.**
Electronic Counter Countermeasures/Advanced Radar Test Bed (ECCM/ARTB)
[AIAA PAPER 92-4098] p 34 A93-13267
- KINGCOMBE, R. C.**
Experimental heat transfer results in turbine stators and rotors and a comparison with theory
[PNR-90945] p 57 N93-11055
- KINNISON, D. E.**
Impact of supersonic and subsonic aircraft on ozone: Including heterogeneous chemical reaction mechanisms
[DE92-019619] p 224 N93-13655
- KINOSHITA, Y.**
Combustion study on methane-fuel Laboratory Scaled Ram Combustor
[ASME PAPER 92-GT-413] p 356 A93-19561
Studies on methane-fuel ram combustor for HST combined cycle engine
[ISABE 93-7080] p 1201 A93-54056
- KIOUSIS, P.**
Meridional flow calculation using advanced CFD techniques
[ASME PAPER 92-GT-325] p 256 A93-19509
- KIR'YANOV, A. L.**
Aerodynamic characteristics of a sweptforward-wing aircraft model in unsteady motion at large angles of attack in subsonic flow p 1068 A93-48902
Interference between a high-lift sweptforward wing and the horizontal nose plane at subsonic velocities p 1135 A93-51906
- KIRBY, DENISE**
Aero-optical phase measurements using Fourier transform holographic interferometry p 549 A93-29302
- KIRCHNER, T.**
Synchronous X-ray Sinography for nondestructive imaging of turbine engines under load
[AIAA PAPER 93-1819] p 1153 A93-49707
- KIREEV, A. IU.**
Numerical modeling of ionization in nonequilibrium nitrogen flows in hypersonic nozzles p 836 A93-39137
- KIREEV, V. A.**
Problems of the organization of the mass testing of large structural elements of aircraft using testing machines p 821 A93-36791
A procedure for the thermal and strength testing of radiotransparent shells p 1209 A93-52976
- KIREICHIKOV, V. A.**
Precision increasing and integrity monitoring of navigation data for GPS/inertial hybrid solution p 149 A93-14157
- KIRILLIN, A. N.**
Aerodynamic characteristics of airship models of different shapes p 1092 A93-51909
- KIRK, R. G.**
Active magnetic bearings applied to industrial compressors p 841 N93-27570
- KIRKNER, D. J.**
Determination of tire-wheel interface pressure distribution for aircraft wheels
[AIAA PAPER 93-1343] p 709 A93-33913
- KIRPICHNIKOV, S. N.**
Optimal impulsive interorbital transfers with aerodynamic maneuvers p 1141 A93-48838
- KIRSCH, JAMES C.**
Optical correlator field test results p 1038 A93-44458
- KIRSTEN, TREVOR J.**
Life cycle assessment of an impingement-cooled gas turbine blade
[AIAA PAPER 92-4716] p 358 A93-20321
Thermal fatigue life assessment of a convection-cooled gas turbine blade
[ISABE 93-7062] p 1199 A93-54038
- KIRTLEY, K. R.**
Aeroloids and secondary flows in a transonic mixed flow turbine stage
[ASME PAPER 92-GT-72] p 248 A93-19322
Three-dimensional analysis of the Pratt and Whitney alternate design SSME fuel turbine p 1031 N93-31584
- KISELEV, A. P.**
Investigation of flame stabilizers in the form of perforated grids p 1003 A93-47513
- KISELEV, E. V.**
Automated measurement of residual stresses in the surface layer of parts p 834 A93-39081
- KISELEV, N. M.**
Mathematical statement of the problem of optimizing the design of an airframe for ease of manufacture p 745 A93-35286
Selection of protective coatings for parts in a computer-aided design system p 746 A93-35290
- KISH, J. G.**
Split torque transmission load sharing
[NASA-TM-105884] p 212 N93-12736
- KISH, JULES G.**
Sikorsky Aircraft Advanced Rotorcraft Transmission (ART) program
[NASA-CR-191079] p 840 N93-27268
- KISHIMOTO, TAKUJI**
The role of computational fluid dynamics in aeronautical engineering. 9: Analysis of hypersonic equilibrium air flow p 301 N93-19294
- KISLITZIN, KATHERINE T.**
A concurrent hybrid Navier-Stokes/Euler approach to fluid dynamic computations
[AIAA PAPER 93-0789] p 468 A93-24865
- KISLYKH, V. V.**
Harnessing nitrous oxide for elevation of temperature and pressure in piston facilities
[AIAA PAPER 93-2016] p 1137 A93-49854
- KISS, LASZLO I.**
Static and dynamic errors in heat flux measurements p 1254 A93-54366
- KISS, T.**
A statistical approach to the experimental evaluation of transonic turbine airfoils in a linear cascade
[ASME PAPER 92-GT-5] p 245 A93-19278
- KISS, TIBOR**
Experimental and numerical study of transonic turbine cascade flow
[AIAA PAPER 93-3064] p 1059 A93-48240
- KISTLER, DAVID**
Software Management Environment (SME) installation guide
[NASA-TM-108578] p 230 N93-15578
- KITA, YOSHINORI**
A flat plate wing standing on a wall covered with a thick boundary layer. II - Wing characteristics under the effects of side wall boundary layer and wing tip vortex p 125 A93-15446

- KITAGAWA, M.**
Creep crack growth and tail part behavior of low alloy steels and Ni based super alloy p 916 A93-40808
- KITAJIMA, J.**
Combustion study on methane-fuel Laboratory Scaled Ram Combustor [ASME PAPER 92-GT-413] p 356 A93-19561
Studies on methane-fuel ram combustor for HST combined cycle engine [ISABE 93-7080] p 1201 A93-54056
- KITAZAWA, MOTOTAKA**
Specialty fiber optic systems for mobile platforms and plastic optical fibers; Proceedings of the Meeting, Boston, MA, Sept. 9-11, 1992 [SPIE-1799] p 1105 A93-49462
- KITHCART, M.**
Uniform roughness studies [WL-TR-92-3041] p 751 N93-25951
- KITSON, S. T.**
Aerodynamic investigation of radial turbines using computational methods p 81 N93-10056
- KIVITY, V.**
Oblique shock formation in impulsively started wedge flows p 692 A93-35636
- KIYA, M.**
Active forcing of an axisymmetric leading-edge turbulent separation bubble [AIAA PAPER 93-3245] p 966 A93-46790
- KIYA, MASARU**
Discrete-vortex simulation of pulsating flow on a turbulent leading-edge separation bubble p 787 N93-27457
- KIYOTO, SHIN-ICHIRO**
Application of functionally gradient materials to scramjet engines [ISABE 93-7063] p 1200 A93-54039
- KJELLBERG, ANDERS**
Fatigue effects of noise among airplane mechanics p 558 A93-28495
- KJERSTAD, KEVIN J.**
Transition aerodynamics for 20-percent-scale VTOL unmanned aerial vehicle [NASA-TM-4419] p 779 N93-27032
- KLAETSCHKE, H.**
Loads at the nose landing gears of civil transport aircraft during towbarless towing operations p 45 A93-13629
- KLAVENESS, SUZANNE**
F-16 accidents: The Norwegian experience p 492 N93-19674
- KLAVETTER, E. A.**
Advanced diagnostics for in situ measurement of particle formation and deposition in thermally stressed jet fuels [AIAA PAPER 93-0363] p 390 A93-23045
- KLAVETTER, ELMER**
Advanced thermally-stable, coal-derived, jet fuels program: Experiment system and model development [AD-A262747] p 917 N93-29402
- KLEB, WILLIAM L.**
High angle-of-attack inviscid Shuttle Orbiter computation p 9 A93-12020
- KLEIFGES, K.**
Control of unsteady shock-induced turbulent boundary layer separation upstream of blunt fins [AIAA PAPER 93-3281] p 969 A93-46839
- KLEIJWEG, J. C. M.**
ERS-1 directional wave spectra validation with the airborne SAR PHARS [BCRS-92-18] p 937 N93-31010
- KLEIMAN, S.**
Integrated utilities management system for aircraft p 153 A93-14208
- KLEIN, GARY A.**
A cognitive model for training decision making in aircrews p 147 N93-15020
- KLEIN, W. A.**
Aerodynamics of turbine blades with trailing-edge damage - Measurements and computations [ISABE 93-7130] p 1189 A93-54105
- KLEISER, L.**
Numerical simulation of transition in two- and three-dimensional boundary layers p 973 A93-46980
- KLEMM, R.**
Antenna design for adaptive airborne MTI p 884 A93-43440
- KLENK, ALAN**
RTJ-303: Variable geometry, oblique wing supersonic aircraft [NASA-CR-192054] p 337 N93-18166
- KLENNER, J.**
The production of a monolithic CFRP fuselage skin for the European Fighter Aircraft p 109 A93-15810
The integrated design and manufacturing of composite structures for aircraft using an advanced tape layering technology [MBB-LME-251-S-PUB-0491-A] p 515 N93-21401
- KLEPIN, K. M.**
Onboard System Evaluation of Rotors Vibration, Engines (OBSERVE) monitoring system [AD-A255366] p 165 N93-15227
- KLETT, D. E.**
Uniform roughness studies [WL-TR-92-3041] p 751 N93-25951
- KLEUSBERG, ALFRED**
System analysis for a kinematic positioning system based on the global positioning system [AD-A262830] p 885 N93-29468
- KLEVENOW, F. T.**
Operation of the helicopter antenna radiation prediction code [NASA-CR-193259] p 1030 N93-31110
- KLEY, DIETER**
Predicted aircraft effects on stratospheric ozone p 93 N93-11096
- KLIJN, J. M.**
Instrumentation for in-flight acoustic measurements in an engine inlet duct of a Fokker 100 aircraft [NLR-TP-91200-U] p 1001 N93-32332
- KLIMA, STANLEY J.**
NDE of PWA 1480 single crystal turbine blade material [NASA-TM-106140] p 815 N93-27640
- KLIMENKO, G. V.**
A finite difference study of the aerodynamic characteristics of wing profiles at transonic velocities p 1091 A93-51903
- KLIMENKO, R. V.**
Calculation of subsonic flow of a gas past an airfoil p 1068 A93-48908
- KLINE-SCHODER, ROBERT J.**
Fault detection, isolation, and reconfiguration for aircraft using neural networks [AIAA PAPER 93-3870] p 1135 A93-51456
- KLINGER, H.**
The effect of main stream flow angle on flame tube film cooling p 932 N93-29953
- KLINGLE-WILSON, DIANA**
Improvement in gust front algorithm detection capability using reflectivity thin lines versus azimuthal shears p 427 A93-22120
An improved gust front detection algorithm for the TDWR p 432 A93-22191
- KLOBUCHAR, JOHN A.**
The effects of ionospheric errors on single-frequency GPS users p 313 A93-21141
- KLOEPEL, VALENTIN**
Review of helicopter noise research in Europe p 1263 A93-54725
- KLOOSTER, STEVEN A.**
The Airborne Ocean Color Imager - System description and image processing p 1157 A93-50369
- KLOPFER, G. H.**
Virtual zone Navier-Stokes computations for oscillating control surfaces [AIAA PAPER 93-3363] p 955 A93-45056
Multi-zonal Navier-Stokes code with the LU-SGS scheme [AIAA PAPER 93-2965] p 1148 A93-48159
- KLOPFER, GOETZ H.**
The numerical study of 3-D flow past control surfaces [AIAA PAPER 92-4650] p 14 A93-13305
- KLOSE, ARNO H.**
Advanced Ducted Engines - Impact of unsteady aerodynamics on fan vibration properties [ASME PAPER 92-GT-228] p 252 A93-19445
- KLOTZSCHE, MAX**
Composites technology for transport primary structure p 918 N93-30431
- KLUTE, SANDRA M.**
Flow control over delta wings at high angles of attack [AIAA PAPER 93-3494] p 983 A93-47266
- KNAUB, CLETE W.**
An investigation of the influence of advanced aircraft diagnostics on the technological sophistication of maintenance personnel [AD-A258988] p 240 N93-18887
- KNEELING, W. D.**
Modeling supersonic inlet boundary-layer bleed roughness p 872 A93-42891
- KNEER, R.**
Diffusion controlled evaporation of a multicomponent droplet - Theoretical studies on the importance of variable liquid properties p 1021 A93-44224
- KNICKMEYER, E. T.**
Requirements for airborne vector gravimetry p 1241 A93-55976
- KNIGHT, D.**
Mean flowfield structure of a three-dimensional supersonic turbulent boundary layer [AIAA PAPER 93-0661] p 465 A93-24774
- KNIGHT, D. D.**
Numerical simulation of crossing/turbulent boundary layer interaction at Mach 8.3 comparison of zero and two-equation turbulence models [AIAA PAPER 93-0779] p 467 A93-24861
Computation of crossing shock/turbulent boundary layer interaction at Mach 8.3 p 961 A93-45726
Investigation of a hypersonic crossing shock wave/turbulent boundary layer interaction p 1044 A93-48043
- KNIGHT, DONALD T.**
Achieving modularity with tightly-coupled GPS/INS p 33 A93-11032
- KNIGHT, DOYLE D.**
A fully implicit Navier-Stokes algorithm using an unstructured grid and flux difference splitting [AIAA PAPER 93-0875] p 470 A93-24936
- KNIGHTON, DONNA L.**
Design and utilization of a Flight Test Engineering Database Management System at the NASA Dryden Flight Research Facility [AIAA PAPER 92-4072] p 97 A93-13264
- KNISKERN, MARC W.**
Nuclear thermal rocket entry heating and thermal response preliminary analysis [AIAA PAPER 93-0378] p 385 A93-23058
Assessment of a flow-through balance for hypersonic wind tunnel models with scramjet exhaust flow simulation [NASA-TM-4441] p 779 N93-27005
- KNOBLAUCH, RANDAL C.**
Reconnaissance capable F/A-18D optical and infrared window antifog systems [SAE PAPER 921182] p 890 A93-41361
- KNOWLEN, C.**
Hugoniot analysis of the ram accelerator p 1023 A93-45500
Initiation of combustion in the thermally choked ram accelerator p 1016 A93-45501
Investigation of the aerothermodynamics of hypervelocity reacting flows in the ram accelerator [NASA-CR-191715] p 140 N93-15588
- KNOWLES, G. J.**
Adaptive/conformal wing design for future aircraft p 320 A93-17728
- KNOWLES, K.**
Combined noise and flow control of supersonic jets using swirl p 398 A93-19204
Unsteady pressures under impinging jets in crossflows p 399 A93-19220
- KNOX, CHARLES E.**
Manual flying of curved precision approaches to landing with electromechanical instrumentation. A piloted simulation study [NASA-TP-3255] p 344 N93-18408
- KNUTESON, R. O.**
Remote sensing cloud properties from high spectral resolution infrared observations p 1034 A93-46780
- KO, CHIH-HSIN**
Discontinuous Galerkin finite element method for two dimensional conservation laws [AIAA PAPER 93-0337] p 281 A93-23026
- KO, FRANK K.**
Mechanical and analytical screening of braided composites for transport fuselage applications p 922 N93-30855
- KO, JEONGHWAN**
Calculation of numerical boundary measure for wavelet-Galerkin approximations in aeroelasticity [AIAA PAPER 93-1539] p 741 A93-34076
- KO, M. K. W.**
Stratospheric aircraft exhaust plume and wake chemistry studies [NASA-CR-189688] p 94 N93-12299
- KO, MALCOLM K. W.**
Predicted aircraft effects on stratospheric ozone p 93 N93-11096
- KO, TZU-HSIANG**
Effects of side-inlet angle in a three-dimensional side-dump combustor p 1109 A93-49610
- KOBAYAKAWA, MAKOTO**
Adaptive grid generation using optimal control theory p 770 A93-38187
- KOBAYASHI, A. S.**
Axial crack propagation and arrest in pressurized fuselage p 1026 A93-45788
- KOBAYASHI, AKIRA**
Aeronautical fatigue: Key to safety and structural integrity; Proceedings of the 16th ICAF Symposium, Tokyo, Japan, May 22-24, 1991 [ISBN 4-9900181-1-7] p 80 A93-13626
- KOBAYASHI, H.**
Noise reduction of supersonic heated jet with jet mixing enhancement by tabs [ISABE 93-7046] p 1198 A93-54022

- KOBAYASHI, ICHIZO**
Digital map display technology p 77 A93-11206
- KOBAYASHI, K.**
Research and development of high pressure compressor for SST and HST engine [ISABE 93-7068] p 1186 A93-54044
- KOBAYASHI, M. H.**
Comparison of several convection discretization schemes for all Mach number arbitrary 2D flows p 685 A93-34345
- KOBAYASHI, OSAMU**
Estimation of aerodynamic characteristics from flight test data. II - Analysis methods under in-flight wind tunnel test concept p 191 A93-16934
Estimation of aerodynamic characteristics from flight-test data. IV - Principal component analysis and perpendicular error method p 1241 A93-54551
Estimation of aerodynamic characteristics from flight-test data. V - Effects of gust and its time lag p 1230 A93-54560
- KOBAYASHI, TOSHIO**
Numerical prediction of aerodynamic sound using large eddy simulation p 850 A93-38150
- KOBISH, T. R.**
Innovative high temperature aircraft engine fuel nozzle design [ASME PAPER 92-GT-132] p 350 A93-19365
- KOCHERSBERGER, K.**
Measurement of a one-dimensional mobility using a laser-Doppler velocimeter p 210 A93-16647
- KOCHINA, P. YA.**
Some Fuchs-type equations in fluid mechanics p 1165 A93-48967
- KOCK AM BRINK, B.**
Enhanced mixing via geometric manipulation of a splitter plate [AIAA PAPER 93-3244] p 966 A93-46789
- KOCKLER, JAMES**
Hermes CX-7: Air transport system design simulation [NASA-CR-192082] p 335 A93-18056
- KODAMA, H.**
Nonreflecting boundary conditions of three-dimensional Euler equation calculations for strut cascades p 689 A93-34491
- KODAMA, HIDEKAZU**
Lifting surface theory for steady aerodynamic analysis of ducted counter rotation propfan [ASME PAPER 92-GT-14] p 347 A93-19286
- KODAMA, YOSHIO**
Experimental investigation into the mechanism of discrete frequency noise (DFN) generation from a NACA 0012 blade p 1225 A93-53194
- KODIALAM, SRINIVAS**
Optimized/adapted finite elements for structural shape optimization p 77 A93-10971
Optimization of composite engine structures for mechanical and thermal loads [AIAA PAPER 93-1583] p 719 A93-34115
- KOEHAN, FRANCIS L.**
Waterborne polyurethane binder resins for compliant aircraft coatings [AD-A256246] p 199 A93-14573
- KOENIG, A.**
An approach to the stall monitoring in a single stage axial compressor [AIAA PAPER 93-1872] p 1112 A93-49747
- KOENIG, MARK A.**
Control augmentation system (CAS) synthesis via adaptation and learning [AIAA PAPER 93-3728] p 1170 A93-51328
- KOGAN, A.**
Navier-Stokes calculations of the flow about wing-flap combinations p 112 A93-14171
- KOGAN, M. N.**
Nontraditional methods of controlling the stability of a laminar subsonic boundary layer p 1085 A93-50962
- KOGINOV, M. V.**
A control algorithm for a navigation-landing system in the case of a priori indeterminacy of failure data p 882 A93-43108
- KOHALMI, DIANE**
Additional developments in embedded computer performance measurement p 940 A93-42833
- KOHAMA, YASUAKI**
A high-frequency, secondary instability of crossflow vortices that leads to transition p 128 A93-17253
Three dimensional boundary-layer transition on a swept wing p 419 A93-16818
- KOHARA, S.**
Research and development of a turbo-accelerator for super/hypersonic transport [ISABE 93-7066] p 1200 A93-54042
- KOHLER, N.**
High temperature fracture mechanism of gas-pressure sintered silicon nitride p 825 A93-38893
- KOHLI, DALIP K.**
Development of polyimide adhesives for 371 C (700 F) structural performance for aerospace bonding applications - FM 680 system p 198 A93-15757
- KOHN, S.**
Visual field information in Nap-of-the-Earth flight by teleoperated Helmet-Mounted displays p 517 A93-26884
- KOIDE, S.**
Effects of junction modifications on sharp-fin-induced shock wave/boundary layer interaction [AIAA PAPER 93-2935] p 1046 A93-48133
- KOIKE, M.**
X ray microscopy resource center at the Advanced Light Source [DE93-010449] p 911 A93-29869
- KOKKALIS, A.**
Application of European CFD methods for helicopter rotors in forward flight [ONERA, TP NO. 1992-125] p 772 A93-38599
Results from a set of low speed blade-vortex interaction experiments p 872 A93-43540
- KOKKINS, S. J.**
FAA unified pavement analysis 3-D finite element method p 379 A93-16314
- KOKOREV, G. D.**
Algorithms and automated techniques for the design of control systems for moving objects p 562 A93-29690
Selection of transducer measuring ranges in flight vehicle control systems p 526 A93-29691
- KOKOTOFF, DAVID**
Advanced electromagnetic methods for aerospace vehicles [NASA-CR-193468] p 936 A93-31036
- KOKUBUN, S.**
Polar Patrol Balloon Experiment in Antarctica p 27 A93-11373
- KOLAR, RAMESH**
Application of two chaos methods to Higher Harmonic Control data p 909 A93-43783
- KOLAX, MICHAEL W.**
Composite wing results of Deutsche Airbus technology program p 109 A93-15808
- KOLB, C. E.**
Plume and wake dynamics, mixing, and chemistry behind a high speed civil transport aircraft p 1034 A93-45139
Stratospheric aircraft exhaust plume and wake chemistry studies [NASA-CR-189688] p 94 A93-12299
- KOLBAEV, A. N.**
A pressure distribution measuring system with pneumatic switches and automatic band selection p 75 A93-10029
- KOLDEN, JENNIFER J.**
A compact, intercooled and regenerated gas turbine for HALE applications [ASME PAPER 92-GT-401] p 355 A93-19550
- KOLDORKINA, V. A.**
Modeling of the multiparameter assembly of engineering products for a specified priority of output geometrical parameters p 836 A93-39109
- KOLESHNIKOV, A. F.**
Modeling of the physicochemical processes of nonequilibrium heat transfer in the subsonic jets of an induction plasmatron p 836 A93-39147
- KOLESHNIKOV, E. V.**
A method for estimating the survivability of bodies of revolution p 745 A93-35287
- KOLESHNIKOV, O. M.**
Supersonic combustion and gasdynamic of scramjet p 170 A93-14242
Effect of combustion on the interaction of an underexpanded wall hydrogen jet with supersonic flow in a plane duct p 534 A93-27658
- KOLGANOV, N. A.**
A pressure distribution measuring system with pneumatic switches and automatic band selection p 75 A93-10029
- KOLKMAN, H. J.**
Performance of gas turbine compressor cleaners [ASME PAPER 92-GT-360] p 355 A93-19524
Performance of gas turbine compressor cleaners [NLR-TP-91237-U] p 1003 A93-31111
- KOLLER, U.**
Air Traffic and Environment [GSF-BAND-8] p 1034 A93-31925
- KOLLMANN, W.**
Numerical simulation of the turbulent flow in round jets [AIAA PAPER 93-0199] p 277 A93-22619
Pdf prediction of supersonic hydrogen flames [AIAA PAPER 93-0448] p 391 A93-23358
- KOLOBANOV, V. IU.**
Effect of design and service-related factors on the formation of combustion residues in the fuel nozzles of gas turbine engines p 345 A93-18342
- Calculation of fuel economy for the Tu-154 aircraft in relation to the washing of the NK-8-2U engine at civil aviation maintenance facilities p 345 A93-18356
Vibrational monitoring and diagnostics of the technical condition of gas turbine engines at civil aviation repair facilities p 374 A93-18362
- KOLOBKOV, A. N.**
Minimization of the induced drag of nonplanar lifting systems p 1068 A93-48910
Interference between a high-lift sweptforward wing and the horizontal nose plane at subsonic velocities p 1135 A93-51906
- KOLOCHINSKI, YU. YU.**
Experimental simulation of the aerodynamic heating of bodies in a molecular region p 1090 A93-51871
- KOLOMIETS, V. P.**
Determination of the membrane and flexural shell deformations from the readings of a two-sided rosette-type strain gage p 75 A93-10047
- KOLOTUKHIN, E. V.**
Resource conservation and improvement of the service characteristics of castings of high-temperature nickel alloys through a high-temperature melt treatment p 824 A93-36718
- KOMAROV, M. M.**
The representation of the aerodynamic torque in simulations of a spacecraft rotary motion p 1141 A93-48835
- KOMERATH, N. M.**
Trajectory mapping of quasi-periodic structures in a vortex flow [AIAA PAPER 93-2914] p 1044 A93-48116
SCV measurements in the wake of a rotor in hover and forward flight [AIAA PAPER 93-3080] p 1059 A93-48254
The three-dimensional boundary layer flow due to a rotor-tip vortex [AIAA PAPER 93-3081] p 1060 A93-48255
Correlation of unsteady pressure and inflow velocity fields of a pitching rotor blade [AIAA PAPER 93-3082] p 1060 A93-48256
Flow field characteristics of a complex blade tip at high angles of attack [AIAA PAPER 93-3083] p 1060 A93-48257
Summary of the interaction of a rotor wake with a circular cylinder [AIAA PAPER 93-3084] p 1060 A93-48258
- KOMIYAMA, FUMIO**
Effects of boundary layer bleed on swept-shock/boundary layer interaction [AIAA PAPER 93-2989] p 1052 A93-48182
- KOMURO, TOMOYUKI**
Effects of injector geometry on scramjet combustor performance p 359 A93-21670
Aerodynamic performance of scramjet inlet models with a single strut [AIAA PAPER 93-0741] p 466 A93-24831
Ignition and combustion performance of a scramjet combustor with a fuel injection strut [ISABE 93-7050] p 1199 A93-54026
Mach 4 testing of scramjet inlet models [NAL-TR-1137] p 26 A93-12369
- KONDO, KIMIO**
Propagation results of aeronautical satellite communication experiments using INMARSAT satellite p 533 A93-29607
- KONDO, NOBUYUKI**
Aerodynamic heating with boundary layer transition and heat protection with mass addition on blunt body in hypersonic flows [AIAA PAPER 93-2984] p 1051 A93-48177
- KONDOS, KOSTANDINOS G.**
X ray diffraction and electron microscope studies of Ytria Stabilized Zirconia (YSZ) ceramic coatings exposed to vanadia [AD-A258055] p 392 A93-17676
- KONDRASHOV, V. Z.**
Selecting a method for sealing riveted joints in fuel compartments p 746 A93-35295
Reliability and durability problems p 1150 A93-48825
- KONDRATEV, A. A.**
Crack growth under conditions of service loading p 396 A93-18370
- KONNO, KEVIN**
Acoustic mode measurements in the inlet of a model turbofan using a continuously rotating rake - Data collection/analysis techniques [AIAA PAPER 93-0599] p 361 A93-23324
Acoustic mode measurements in the inlet of a model turbofan using a continuously rotating rake: Data collection/analysis techniques [NASA-TM-105936] p 179 A93-15403

- KONNO, KEVIN E.**
Rotating rake design for unique measurement of fan-generated spinning acoustic modes [NASA-TM-105946] p 724 N93-26161
- KONO, M.**
A study of self-ignition of methane-hydrogen mixture fuel injected into high enthalpy supersonic airstreams [ISABE 93-7049] p 1213 A93-54025
- KONO, MICHIKATA**
Dual transverse injection of H₂ gas into Mach 1.8 flows at University Komaba wind tunnel p 376 A93-21833
- KONONOV, V. K.**
High-efficiency machining methods for aviation materials [ISBN 5-230-16902-8] p 835 A93-39084
- KONOPKA, PIOTR**
Modeling and analysis of the winch launch of a glider p 528 A93-27294
- KONOSHENKO, M. P.**
A study of the possibility of the parallel execution of a program for calculating the aerodynamic characteristics of flight vehicles using an improved panel method p 95 A93-10045
- KONOTOP, T. V.**
Flow past three-dimensional irregularities in a hypersonic boundary layer on a cooled body p 775 A93-39119
- KONOVALOV, S. F.**
Effect of longitudinal microribbing on the drag of a body of revolution p 5 A93-10147
- KONRAD, W.**
Mean flowfield structure of a three-dimensional supersonic turbulent boundary layer [AIAA PAPER 93-0661] p 465 A93-24774
- KONSTANTINOVSKI, O. N.**
Mathematical model for the effect of turbulent velocity pulsations on the stability of a powerplant p 1003 A93-47508
- KONTER, M. L.**
New corrosion resistant nickel-base super-alloys and technological processes of casting gas turbines parts with directional single crystal and regulable equiaxial minimized microporosity structure p 916 A93-40811
- KONZELMANN, U.**
Numerical simulation of a three-dimensional wave packet in a growing flat plate boundary layer p 128 A93-17265
- KOOCHESFAHANI, M. M.**
Initial acceleration effects on the flow field development around rapidly pitching airfoils [AIAA PAPER 93-0438] p 286 A93-23352
- KOOCHESFAHANI, MANOOCHHEHR M.**
Initial acceleration effects on flow evolution around airfoils pitching to high angles of attack p 961 A93-45750
- KOOI, J. W.**
Recent developments in low-speed TPS-testing for engine integration drag and installed thrust reverser simulation p 160 N93-13207
- KOONEN, P. J.**
Definition study PHARUS [AD-A256560] p 221 N93-14805
- KOONEN, PETER J.**
A dual polarised active phased array antenna with low cross polarisation for a polarimetric airborne SAR p 883 A93-43401
The PHARUS project, first results of the realization phase p 884 A93-43454
The realization phase of the PHARUS project p 1162 A93-47658
- KOOMULLIL, GEORGE PAULOSE**
Solution of compressible Navier-Stokes equations using spectral methods on arbitrary two-dimensional domains p 218 N93-14041
- KOONCE, JEFFERSON M.**
Spatial orientation and wayfinding in airport passenger terminals - Implications for environmental design p 487 A93-27168
- KOPEV, VIKTOR F.**
On the acoustic radiation nature of a turbulent vortex ring p 446 A93-19167
- KOPEIKIN, A. G.**
Evaporation and specific heats of motor fuels p 71 A93-12823
- KOPRIYA, DAVID A.**
Spectral solution of the viscous blunt-body problem p 860 A93-41915
- KOPYLOVA, L. V.**
An experimental study of reinforced panels of composite materials p 1215 A93-52975
- KOPYTOV, R. A.**
Analysis of random components during measurements in the computerized diagnostic system Analiz-86 p 321 A93-18344
Assessment of flight data in real time p 341 A93-18364
- KORAKIANITIS, T.**
Hierarchical development of three direct-design methods for two-dimensional axial-turbomachinery cascades p 812 A93-39271
- KORAKIANITIS, THEODOSIOS**
Surface-curvature-distribution effects on turbine-cascade performance [ASME PAPER 92-GT-84] p 248 A93-19333
Models for predicting the performance of Brayton-cycle engines [ASME PAPER 92-GT-361] p 355 A93-19525
Prescribed-curvature-distribution airfoils for the preliminary geometric design of axial-turbomachinery cascades [ASME PAPER 92-GT-366] p 257 A93-19530
Influence of stator-rotor gap on axial-turbine unsteady forcing functions p 899 A93-41918
- KORDULLA, W.**
Hypersonic viscous flow simulations p 478 A93-27926
Attempt to evaluate the computations for test case 6.1 - Cold hypersonic flow past ellipsoidal shapes p 869 A93-42620
Comparison of solution of various Euler solvers and one Navier-Stokes solver for the flow about a sharp-edged cropped delta wing [NLR-TP-90340-U] p 418 N93-16411
- KOREN, B.**
Efficient multigrid computation of steady hypersonic flows p 1152 A93-49527
- KOREN, S.**
Lateral aerodynamics characteristics of forebodies at high angle of attack in subsonic and transonic flows p 118 A93-14302
- KOREVAAR, ERIC**
Helicopter plume detection by using an ultranarrow-band noncoherent laser Doppler velocimeter p 542 A93-25198
- KORIVI, MOHAN**
Multidisciplinary analysis and sensitivity derivatives for isolated helicopter rotors in hover [AIAA PAPER 92-4696] p 324 A93-20308
- KORIVI, V. M.**
An approximately factored incremental strategy for calculating consistent discrete aerodynamic sensitivity derivatives [AIAA PAPER 92-4746] p 265 A93-20344
Observations on computational methodologies for use in large-scale, gradient-based, multidisciplinary design [AIAA PAPER 92-4753] p 436 A93-20351
- KORN, C.**
An experimental investigation of convective heat transfer at the leading edge of a gas turbine airfoil [ASME PAPER 92-GT-248] p 405 A93-19457
- KORNGOLD, J. C.**
Design for manufacture by resin transfer molding of composite parts for rotorcraft [SME PAPER EM93-103] p 1159 A93-51733
- KORNILOV, V. I.**
Evolution of a three-dimensional nonequilibrium boundary layer in a dihedral angle behind a perturbation source p 872 A93-43013
- KOROBOV, R. M.**
Canonical correlation relationships among spectral and phytometric variables for twenty winter wheat fields p 433 A93-22992
- KOROLEV, A. S.**
An experimental study of the three-dimensional interaction of a transverse jet with hypersonic flow p 777 A93-39150
- KORONOV, M. Z.**
Prediction of fatigue crack growth kinetics in the plane structural elements of aircraft in the biaxial stress state p 1025 A93-45670
- KOROVIN, E. M.**
Calculating the cutting depth during the milling of large gas turbine engine blades p 545 A93-27628
- KORTE, JOHN J.**
Aerodynamic design of axisymmetric hypersonic wind-tunnel nozzles using a least-squares/parabolized Navier-Stokes procedure p 9 A93-12011
Numerical study of the performance of swept, curved compression surface scramjet inlets [AIAA PAPER 93-1837] p 1074 A93-49721
- KORTING, P. A. O. G.**
What is the progress in propulsion? p 298 N93-19006
- KOSAI, M.**
Axial crack propagation and arrest in pressurized fuselage p 1026 A93-45788
- KOSCHEL, W.**
Computation of hypersonic high-temperature nozzle flow p 1238 A93-56040
- KOSCHEL, W. W.**
Study of flow phenomena in high speed intakes [AIAA PAPER 92-5029] p 272 A93-22304
- KOSHIOKA, YASUHIRO**
Wind tunnel tests and CFD in Fuji Heavy Industries p 304 N93-19323
- KOSMATKA, J. B.**
Flexure-torsion behavior of prismatic beams. I - Section properties via power series p 417 A93-23557
- KOSOVSKII, L. A.**
Detection and parameter estimation of atmospheric turbulence by ground-based and airborne CO₂ Doppler lidars p 395 A93-17862
- KOSOVSKI, L. A.**
Study of artificial and natural turbulence in atmospheric boundary layer with a CW Doppler CO₂ lidar p 1257 A93-54799
- KOSOWSKI, KRZYSZTOF**
The optimum value of the nozzle outlet angle of turbine stages [ASME PAPER 92-GT-224] p 404 A93-19442
- KOSS, D.**
Pilot test of a low Reynolds number DTE-airfoil [AIAA PAPER 93-0643] p 464 A93-24758
Oscillatory blowing, a tool to delay boundary layer separation [AIAA PAPER 93-0440] p 474 A93-25529
Oscillatory blowing - A tool to delay boundary-layer separation p 1235 A93-55362
- KOSSIRA, H.**
A very efficient tool for the structural analysis of hypersonic vehicles under high temperature aspects p 203 A93-14194
Stringer peeling effects at stiffened composite panels in the postbuckling range p 1160 A93-52453
- KOST, A.**
Multigrid methods for calculating 3D flows in complex geometries p 973 A93-46984
- KOST, F.**
Three dimensional transonic flow measurements in an axial turbine with conical walls [ASME PAPER 92-GT-61] p 247 A93-19311
- KOSTEJE, V. K.**
Design of high-load aviation turbomachines using modern 3D computational methods [ISABE 93-7032] p 1196 A93-54008
- KOSTEN, SUE E.**
FNAS modify matric and transparent experiments [NASA-CR-184442] p 198 N93-13311
- KOSTER, DAVID N.**
A model of Global Positioning System (GPS) Master Control Station (MCS) operations [AD-A258846] p 320 N93-19067
- KOSTEZH, V. K.**
Numerical simulation of aerothermodynamics processes in gas turbine engine components p 1002 A93-46939
- KOSYKH, A. P.**
Numerical calculation of polars and heat transfer for supersonic three-dimensional flow past wings with allowance for radiation p 1068 A93-48905
- KOTAKE, MUTSUO**
Development of ultra-hypersonic shock tunnel for aerodynamics test p 376 A93-21900
Pressure distribution measurement around hypersonic delta winged semicone - Measurement by means of magnet tape p 1176 A93-53193
Shock shapes around slender diamond cones traveling at hypersonic speed p 1181 A93-53840
Study on flow field around slender diamond cone traveling at hypersonic speed p 1189 A93-54314
- KOTANI, Y.**
Tandem transverse hydrogen gas injection into a supersonic airflow [ISABE 93-7069] p 1201 A93-54045
- KOTIUGA, P. L.**
Finite element solution of the 3D compressible Navier-Stokes equations by a velocity-vorticity method p 974 A93-47196
- KOTOLEVSKII, I. U. M.**
A method for evaluating the technical condition of hydraulic control boosters without their disassembly p 395 A93-18335
- KOTOV, YU. V.**
New corrosion resistant nickel-base super-alloys and technological processes of casting gas turbines parts with directional single crystal and regulable equiaxial minimized microporosity structure p 916 A93-40811
- KOTOVICH, A. V.**
An experimental study of thrust reverser models p 812 A93-39195
- KOTOVSKII, V. N.**
Computational studies of the characteristics of axial compressor cascades and stages in unsteady incoming flow p 13 A93-12805
- KOTTAPALLI, SESI**
Sources of helicopter rotor hub inplane shears [AIAA PAPER 93-1358] p 709 A93-33927

- KOTZEV, SHMUEL**
Aircraft with single axis aerodynamically deployed wings
[AIAA PAPER 93-3673] p 1129 A93-48350
- KOUGUCHI, NOBUYOSHI**
Measurement technique for Loran-C pulse wave distortion measures and performance in an environment of noise p 29 A93-10988
- KOUMANDAKIS, M.**
Design of axisymmetric channels with rotational flow
[AIAA PAPER 93-3117] p 1062 A93-48287
- KOUMOTO, HIROAKI**
A flat plate wing standing on a wall covered with a thick boundary layer. II - Wing characteristics under the effects of side wall boundary layer and wing tip vortex p 125 A93-15446
- KOUNTZ, JOHN**
Effect of leeward flow dividers on the wing rock of a delta wing
[AIAA PAPER 93-3492] p 982 A93-47264
- KOURA, KATSUHISA**
Numerical simulations of hypersonic rarefied transition regime flows: DSMC method and Navier-Stokes computation p 299 A93-19278
Monte Carlo simulation of normal shock wave. Part 1: Lennard-Jones potential p 300 A93-19279
Rarefied gas numerical wind tunnel. Part 7: OREX p 382 A93-19280
- KOVAL', I. A.**
Efficiency of using longitudinal and circumferential bands in the structures of an airtight fuselage p 801 A93-36795
- KOVALENKO, A. A.**
Numerical modeling of flow in a hypersonic laminar boundary layer p 1086 A93-50967
Calculation of perturbation propagation upstream in a hypersonic laminar boundary layer p 1086 A93-50968
- KOVALENKO, L. V.**
Resource conservation and improvement of the service characteristics of castings of high-temperature nickel alloys through a high-temperature melt treatment p 824 A93-36718
- KOVALEV, V. E.**
Calculation of a compressible three-dimensional boundary layer on a swept wing p 1179 A93-53551
- KOVRIZHNIKIN, O. G.**
Solution of the boundary value problem in flight dynamics by the opposite motion method p 1206 A93-52944
- KOVZAN, L. A.**
Behavior of the particular quality characteristics of an intelligent flight vehicle control system in a multicriterial formulation p 1168 A93-50952
- KOWALECZKO, G.**
Analysis of spatial motion dynamics of a helicopter for various models of the induced velocity field p 1191 A93-53721
- KOZAK, J.**
Czechoslovak development and experience in flight data recorder readout and analysis p 168 A93-15162
- KOZEL, KAREL**
Numerical solution of steady and unsteady Euler equations p 973 A93-46988
- KOZHEVNIKOV, I. V.**
Parametric diagnostics of the steady states of gas turbine engines p 54 A93-12815
- KOZHEVNIKOV, V. N.**
Atmospheric disturbances over mountains and the flight safety p 1164 A93-51856
- KOZHEVNIKOV, YU. V.**
Identification of the phase characteristics and wind-induced perturbations of an aircraft from flight test results p 1206 A93-52943
- KOZHINA, T. D.**
Automated measurement of residual stresses in the surface layer of parts p 834 A93-39081
- KOZLIKOV, V. V.**
Consideration of the completeness of combustion and dissociation and recombination processes in mathematical models of jet engines for high supersonic flight velocities p 520 A93-27627
- KOZLOV, A. I.**
Correction of the frequency characteristic of the waveguide circuit of an acoustic-jet temperature transducer p 832 A93-39036
- KOZLOV, V. A.**
Design and fabrication of panels with cutouts p 1215 A93-52973
- KOZLOV, V. P.**
Moving wall effects in transverse subsonic flow past a rotating cylinder p 1179 A93-53573
- KOZLOV, V. V.**
Acoustic control of flow separation on a straight and a yawed wing p 125 A93-15256
Estimation of the external loading of airships in flight p 366 A93-18383
- Interaction of Tollmien-Schlichting waves with localized disturbances p 545 A93-27637
A study of the effect of surface riblets on the evolution of a solitary wave packet (lambda vortex) in a laminar boundary layer p 1067 A93-48827
- KOZOL, JOSEPH**
Stress corrosion susceptibility of ultra-high strength steels for Naval aircraft applications
[AD-A256126] p 199 A93-15189
- KRACHT, M.**
A very efficient tool for the structural analysis of hypersonic vehicles under high temperature aspects p 203 A93-14194
- KRAEMER, JOHN H.**
Update on GPS integrity requirements of the RTCA MOPS p 314 A93-21155
- KRAFFT, R.**
Turbomachinery and potential computations
[DS-2026] p 363 A93-17740
- KRAFFT, ROLAND**
LARZAC HP turbine disk crack initiation and propagation spin pit test p 176 A93-14892
- KRAFT, ECKARD**
ADP - Engine concept of the future p 1246 A93-54842
- KRAIKO, A. N.**
Variational problem of the profiling of the side walls of the supersonic section of a narrow three-dimensional nozzle p 4 A93-10140
- KRAIN, H.**
A CAD computer system for centrifugal compressor impeller with transonic inflow p 259 A93-20118
Coupling of 3D-Navier-Stokes external flow calculations and internal 3D-heat conduction calculations for cooled turbine blades p 904 A93-29961
- KRAJKO, A. N.**
3D/quasi-3D trans- and supersonic flow calculation in advanced centrifugal/axial compressor stages p 972 A93-46936
- KRAJNOV, V. A.**
Calculation of compressible gas flow on optimal difference grids p 1091 A93-51902
- KRAJZMAN, V. E.**
Multilevel intelligent control systems for flight vehicles p 1168 A93-50955
- KRAL, STEPHEN F.**
Test results of an orifice pulse tube refrigerator p 1149 A93-48612
- KRAMARENKO, E. A.**
Solution of the boundary value problem in flight dynamics by the opposite motion method p 1206 A93-52944
- KRAMER, BRIAN R.**
Forebody vortex control with jet and slot blowing on an F/A-18 p 1009 A93-47235
[AIAA PAPER 93-3449] p 1009 A93-47235
Forebody vortex control on an F/A-18 using small, rotatable 'tip-strakes' p 1009 A93-47236
[AIAA PAPER 93-3450] p 1009 A93-47236
- KRAMMER, J.**
Practical architecture of design optimisation software for aircraft structures taking the MBB-LAGRANGE code as an example
[MBB-FE-251-S-PUB-479] p 331 A93-17565
- KRAMMER, P.**
Engine technologies for future spaceplanes
[ETN-92-92732] p 177 A93-15143
Technology transfer: Potential of BMFT concept for hypersonics
[MBB-LME-202-S-PUB-0505] p 1041 A93-31045
- KRANTZ, T. L.**
Split torque transmission load sharing
[NASA-TM-105884] p 212 A93-12736
- KRAPIVNOJ, K. V.**
Harnessing nitrous oxide for elevation of temperature and pressure in piston facilities
[AIAA PAPER 93-2016] p 1137 A93-49854
- KRASHAKOV, I. U. F.**
Optimal design of honeycomb sandwich shell aircraft structures of composite materials p 828 A93-36800
- KRASHENINNIKOV, S. I.**
Calculation of three-dimensional turbulent jets propagating behind nozzles of rectangular cross section p 6 A93-10192
- KRASHENINNIKOV, S. YU.**
Localization of noise sources in the exhaust jet of a turbofan engine p 1003 A93-47509
- KRATOCHVIL, GARY**
SIR technology helps ensure safe landings for NASA p 384 A93-21765
- KRAUSE, E.**
German university research in hypersonics
[AIAA PAPER 92-5033] p 239 A93-22307
Supersonic and hypersonic flow computations for the research configuration ELAC I and comparison to experimental data p 1237 A93-56034
- KRAUSS, R. H.**
Planar imaging of OH density distributions in a supersonic combustion tunnel
[AIAA PAPER 93-0042] p 389 A93-20155
Laser selection criteria for OH fluorescence measurements in supersonic combustion test facilities p 549 A93-29315
- KRAUSS, ROLAND H.**
Experimental supersonic hydrogen combustion employing staged injection behind a rearward-facing step p 744 A93-34496
- KRAVCHENKO, S. A.**
Calculation of separated axisymmetric flow past bodies by solving Euler equations in the inner vortex region p 14 A93-12975
- KRAVETS, M. B.**
Three-dimensional flow of viscous gas in the blade passage of a straight compressor cascade p 5 A93-10187
- KRAVTSOVA, M. A.**
A numerical solution of the asymptotic problem of boundary layer separation in an incompressible liquid upstream of the corner point of a body p 965 A93-46699
- KREINS, A. F.**
Applications of infrared measurement technique in hypersonic facilities p 1024 A93-45505
Experimental investigations of hypersonic shock-boundary layer interaction p 1238 A93-56037
- KREJNIN, V. G.**
A procedure for the thermal and strength testing of radiotransparent shells p 1209 A93-52976
- KREJSA, E. A.**
Propagation of high frequency jet noise using geometric acoustics
[AIAA PAPER 93-0147] p 452 A93-23241
Propagation of high frequency jet noise using geometric acoustics
[NASA-TM-106013] p 233 A93-15575
- KREJSA, EUGENE A.**
Computation of supersonic jet noise under imperfectly expanded conditions p 563 A93-24825
[AIAA PAPER 93-0735] p 563 A93-24825
Computation of supersonic jet noise under imperfectly expanded conditions
[NASA-TM-105961] p 233 A93-15430
- KREK, R. M.**
Experiments on Space Shuttle Orbiter models in a free piston shock tunnel p 7 A93-11497
- KREMER, FRANS G. J.**
Balance of moments for hypersonic vehicles
[ASME PAPER 92-GT-251] p 253 A93-19460
Flight mechanical model for performance calculations and interactions between flight vehicle and ramjet in regard to the flight orbit
[ESA-TT-1267] p 893 A93-29464
- KREMER, H.**
The influence of swirl generator characteristics on flow and combustion in turbulent diffusion flames p 1159 A93-51632
- KREMER, R.**
Helicopter plume detection by using an ultranarrow-band noncoherent laser Doppler velocimeter p 542 A93-25198
- KREN, LAWRENCE A.**
A hot dynamic seal rig for measuring hypersonic engine seal durability and flow performance
[AIAA PAPER 93-1346] p 738 A93-33916
- KRENER, A. J.**
Computational nonlinear control
[AD-A253547] p 98 A93-12258
- KRESS, GREGORY A.**
Preliminary development of a VTOL unmanned air vehicle for the close-range mission
[AD-A263514] p 933 A93-29969
- KRETSCHMER, D.**
The combustion of droplets within gas turbine combustors - Some recent observations on combustor efficiency
[ASME PAPER 92-GT-135] p 388 A93-19367
The prediction of thermal NO(x) in gas turbine exhausts
[ISABE 93-7022] p 1195 A93-53998
- KRIDER, E. PHILIP**
A single-point warning system for thunderstorms and electric fields p 747 A93-24900
- KRIEBEL, KARL-THEODOR**
Identification of icing water clouds by NOAA AVHRR satellite data
[DLR-FB-92-11] p 434 A93-16477
- KRIEGELSTEIN, H.**
The production of a monolithic CFRP fuselage skin for the European Fighter Aircraft p 109 A93-15810
- KRINER, B.**
Evolution of radar data processing in the French air traffic control system p 886 A93-30325

- KRISHNA PRASAD, K.**
The reduction of skin friction by riblets under the influence of an adverse pressure gradient p 1218 A93-53810
- KRISHNA, K. M.**
An implicit finite difference algorithm for two dimensional Euler equation p 461 A93-24085
- KRISHNAMURTHY, R.**
A two-dimensional elliptic grid generator for a wing-body section involving grid control functions p 460 A93-24083
- KRISHNAMURTHY, T.**
An accurate nonlinear finite element analysis and test correlation of a stiffened composite wing panel p 546 A93-27968
- KRISHNAMURTHY, THIAGARAJA**
Reliability of stiffened structural panels: Two examples [NASA-TM-107687] p 219 N93-14483
- KRISHNAN, ANANTHA**
Influence of supercritical conditions on pre-combustion chemistry and transport behavior of jet fuels [AD-A261813] p 737 N93-26268
- KRISHNAN, M. R.**
Development of an advanced exhaust mixer for a high bypass ratio turbofan engine [AIAA PAPER 93-2435] p 1118 A93-50188
- KRISHNAPPA, G.**
Noise studies for environmental impact assessment of an outdoor engine test facility p 99 N93-10672
- KRIST, SHERRIE L.**
A computational and experimental investigation of a delta wing with vertical tails [AIAA PAPER 93-3009] p 1054 A93-48199
- KRIUCHKOV, A. N.**
A study of the stability of the acceleration circuit of the hydromechanical automatic control system of an aviation gas turbine engine p 810 A93-39028
- KROENKE, I. M.**
Slush hydrogen quantity gaging and mixing for the National Aerospace Plane p 1150 A93-48635
- KROLL, J. T.**
Optimization of circular orifice jets mixing into a heated crossflow in a cylindrical duct [AIAA PAPER 93-0249] p 361 A93-23246
Optimization of circular orifice jets mixing into a heated cross flow in a cylindrical duct [NASA-TM-105984] p 179 N93-15359
- KROO, I.**
Structural and aerodynamic considerations for an oblique all-wing aircraft [AIAA PAPER 92-4220] p 43 A93-13336
Development of the quasi-procedural method for use in aircraft configuration optimization [AIAA PAPER 92-4693] p 322 A93-20278
- KROO, ILAN**
Comparison of PMARC and analytic results for two-dimensional unsteady airfoils [AIAA PAPER 93-0636] p 463 A93-24752
Aerodynamic analyses for design and education [AIAA PAPER 92-2664] p 473 A93-24988
- KROO, ILAN M.**
Structural optimization for joined-wing synthesis [AIAA PAPER 92-4761] p 325 A93-20356
Computation of induced drag for elliptical and crescent-shaped wings p 958 A93-45136
- KROPFLI, ROBERT A.**
The dynamics of microbursts as revealed by Doppler radar observations and numerical simulations p 432 A93-22196
- KROPINSKI, M. C. A.**
On the construction and calculation of optimal nonlifting critical airfoils p 969 A93-46857
- KROTHAPALLI, A.**
Supersonic jet control via point disturbances inside the nozzle p 861 A93-41930
The countercurrent mixing layer - Strategies for shear-layer control [AIAA PAPER 93-3260] p 968 A93-46826
Enhancement of mixing in high-speed heated jets using a counterflowing nozzle p 1235 A93-55359
- KRUCZYNSKI, D. L.**
New experiments in a 120-mm ram accelerator at high pressures [AIAA PAPER 93-2589] p 1142 A93-50301
- KRUEDENER, MATTHIAS**
Software for flight recorder data evaluation developed by Lufthansa p 230 N93-15163
- KRUEGER, B. C.**
Short-term atmospheric effects of high-altitude aircraft emissions p 559 A93-28865
- KRUG, DANIEL W.**
Load test set-up for the Airmass Sunburst Ultra-Light Aircraft p 895 N93-29776
- KRUICHKOV, A. N.**
A study of the effect of the working medium on the start-up characteristic of an aviation gas turbine engine p 811 A93-39037
- KRUMENACKER, JOSEPH L.**
Results and lessons learned from two Wright Laboratory flight research programs [AIAA PAPER 93-3661] p 1099 A93-48341
- KRUPA, V. G.**
Calculation of the three-dimensional interaction of a shock wave with a boundary layer on a cylinder p 12 A93-12766
Numerical simulation of aerothermodynamics processes in gas turbine engine components p 1002 A93-46939
Design of high-load aviation turbomachines using modern 3D computational methods [ISABE 93-7032] p 1196 A93-54008
- KRUPAR, MARTIN J.**
Laser velocimeter measurements of the flow field generated by a forward-swept propfan during flutter [AIAA PAPER 93-2919] p 1180 A93-53591
- KRUT'KO, P. D.**
Active algorithms for controlling the rotational motion of flight vehicles p 908 A93-43079
- KRYLOV, B. A.**
The combined effect of clearances and peripheral overlaps on the efficiency of microturbines with shrouded rotors p 1193 A93-52963
- KRYSINSKI, TOMASZ**
Overview of Tiger dynamics validation program p 794 A93-35907
- KUBANKE, D.**
Reduction of propeller noise by active noise control p 101 N93-10692
- KUBASEK, JOE**
A manned hypersonic reconnaissance vehicle which does not require airborne fueling p 333 N93-17888
- KUBE, R.**
A closed loop controller for BVI impulsive noise reduction by Higher Harmonic Control p 849 A93-35963
- KUBE, ROLAND**
HHC study in the DNW to reduce BVI noise - An analysis p 565 A93-29405
- KUBESH, RODNEY JOSEPH**
A laboratory investigation of raindrop oscillations p 224 N93-13790
- KUBIN, L.**
Infrared thermography of plastic instabilities in a single crystal superalloy [ONERA, TP NO. 1993-18] p 916 A93-41031
- KUBINA, S. J.**
Coupling gain computation between antennas on circular cylinders at SHF/EHF frequencies p 933 N93-30309
RCS of fundamental scatterers in the HF band by wire-grid modelling p 933 N93-30320
- KUBINA, STANLEY J.**
Models for performance assessment of HF antennas on the CH-135/Twin Huey helicopter p 933 N93-30291
- KUBOTA, HIROTOSHI**
Thermo-chemical models for hypersonic flows p 863 A93-42433
- KUBOTA, TOSHI**
Applications of shock-induced mixing to supersonic combustion p 735 A93-35618
- KUBYSHINA, T. V.**
Heat transfer on tip fins in hypersonic flow p 1088 A93-51775
- KUCHAR, J. K.**
Advanced terrain displays to transport category aircraft [PB92-197136] p 35 N93-10065
- KUDINOV, A. A.**
Some recommendations concerning the prevention of fuel boiling in the igniters of the combustion chambers of gas turbine engines p 812 A93-39200
- KUDINOV, V. A.**
Some recommendations concerning the prevention of fuel boiling in the igniters of the combustion chambers of gas turbine engines p 812 A93-39200
- KUDO, KENJI**
Mach 4 testing of scramjet inlet models [NAL-TR-1137] p 26 N93-12369
- KUDOU, KENJI**
Effects of injector geometry on scramjet combustor performance p 359 A93-21670
Aerodynamic performance of scramjet inlet models with a single strut [AIAA PAPER 93-0741] p 466 A93-24831
- KUDRIAVTSEV, N. N.**
Nonequilibrium excitation of internal molecular degrees of freedom in the shock layer during hypersonic flight p 412 A93-29122
- KUDRYAVTSEV, P. S.**
Generation of a plant description dictionary based on expert survey data p 1168 A93-50956
- KUDYA, J. N.**
Damage detection in smart structures using neural networks and finite-element analyses p 438 A93-22540
- KUEHL, W.**
Performance analysis of a turbofan as a part of an airbreathing propulsion system for space shuttles p 1252 A93-56039
- KUENY, J. L.**
Numerical analysis of the three-dimensional boundary layer on a turbomachinery rotor blade p 685 A93-34341
- KUERTEN, H.**
Numerical aspects of a block structured compressible flow solver p 1169 A93-51279
- KUFNER, EWALD**
Instability of hypersonic flow past blunt cones - Effects of mean flow variations [AIAA PAPER 93-2983] p 1051 A93-48176
- KUHLMAN, JOHN M.**
Ground vortex formation for uniform and nonuniform jets impinging on a ground plane [AIAA PAPER 92-4251] p 80 A93-13362
The ground vortex flow field associated with a jet in a cross flow impinging on a ground plane for uniform and annular turbulent axisymmetric jets [NASA-CR-4513] p 789 N93-28449
- KUHN, PETER M.**
Infrared detection of high altitude clear air turbulence [AIAA PAPER 93-0852] p 557 A93-24916
- KUHN, RICHARD E.**
Jet-induced ground effects on a parametric flat-plate model in hover [NASA-TM-104001] p 700 N93-26099
- KUIMOV, S. V.**
A study of the interaction of a nonstationary shock wave with a boundary layer on a plate in the transition regime p 1150 A93-48850
- KUIVINEN, DAVID E.**
External stress-corrosion cracking of a 1.22-m-diameter type 316 stainless steel air valve [NASA-TP-3190] p 737 N93-26201
- KULESHOV, N. S.**
A unified approach to the construction of the throttle characteristics of postrepair turbojet engines, with the NK8-2U engine used as an example p 345 A93-18372
- KULESHOVA, E. A.**
Resource conservation and improvement of the service characteristics of castings of high-temperature nickel alloys through a high-temperature melt treatment p 824 A93-36718
- KULICKI, PIOTR**
A short range passenger/freighter canard - Some problems of a preliminary aerodynamic concept [SAE PAPER 921012] p 157 A93-14642
- KULIKOVA, T. I.**
Synthesis of the optimal control of flight vehicle braking with allowance for the discrete nature of control action generation p 1169 A93-51063
- KULIKOVSKI, V. A.**
Steady transonic weakly perturbed flows in a vibrationally relaxing gas p 1088 A93-51768
Steady state supersonic flows of a vibrationally excited gas past thin bodies p 1089 A93-51818
Steady-state supersonic flow of a vibrationally excited gas past a slender body of revolution at a small angle of attack p 1233 A93-55014
- KULISA, P.**
Modeling of a turbulent flow in the presence of discrete parietal cooling jets p 904 N93-29960
- KULTYSHEV, I. D.**
Estimation of the service periods for complex systems in the case of a priori indeterminacy of system reliability data p 856 A93-43109
- KULYAPIN, A. N.**
Investigation of flame stabilizers in the form of perforated grids p 1003 A93-47513
- KUMADA, H.**
Aging review of the YS-11 aircraft p 46 A93-13635
- KUMADA, MASAYA**
Tip clearance effect on heat transfer and leakage flows on the shroud-wall surface in an axial flow turbine [ASME PAPER 92-GT-200] p 403 A93-19425
- KUMAGAI, T.**
A new cooling system for ultra high temperature turbines [ISABE 93-7073] p 1201 A93-54049
- KUMAMOTO, YUICHI**
Aerodynamic heating with boundary layer transition and heat protection with mass addition on blunt body in hypersonic flows [AIAA PAPER 93-2984] p 1051 A93-48177

KUMAR LAHA, MANAS

An aerodynamic model of multiple lifting surfaces including wake deformation and tip effect p 10 A93-12366

KUMAR, A.

A detailed study of mean-flow solutions for stability analysis of transitional flows [AIAA PAPER 93-3052] p 1057 A93-48232

KUMAR, AJAY

Hypersonic flow separation in shock wave boundary layer interactions [ASME PAPER 92-GT-205] p 251 A93-19429
Computational fluid dynamics for hypersonic airbreathing aircraft p 865 A93-42581
Grid-refinement study of hypersonic laminar flow over a 2-D ramp p 866 A93-42597
Numerical study of the performance of swept, curved compression surface scramjet inlets [AIAA PAPER 93-1837] p 1074 A93-49721

KUMAR, D.

Plume effects on the flow around a blunted cone at hypersonic speeds p 787 A93-27460

KUMAR, K. K.

The use of genetic algorithms in the design of fuzzy logic controllers p 1167 A93-50779

KUMAR, PRASHANT

Delaminations of barely visible impact damage in CFRP laminates p 737 A93-33798

KUMAR, R. R.

Effect of radial distortion on the performance of a centrifugal compressor p 861 A93-42256

KUMAR, V. K.

Numerical computation of viscous hypersonic flow around spherically blunted cones at angle of attack p 460 A93-24082

KUMASAKA, KAZUHIRO

Aerodynamic heating analysis for axisymmetric bodies in supersonic flow p 303 A93-19312

KUNAI, TAKASHI

The operating system for Numerical Wind Tunnel p 383 A93-19290

KUNDU, K.

Computations of spray, fuel-air mixing, and combustion in a lean-premixed-prevaporized combustor [AIAA PAPER 93-2069] p 1153 A93-49901

KUNDU, KRISHNA

Simplified jet fuel reaction mechanism for lean burn combustion application [AIAA PAPER 93-0021] p 390 A93-23238
Simplified jet-A kinetic mechanism for combustor application [NASA-TM-105940] p 200 A93-15504

KUNDU, KRISHNA P.

Computation of the flow field in an annular gas turbine combustor [AIAA PAPER 93-2074] p 1113 A93-49903

KUNDU, NIKHIL K.

Performance of thermal adhesives in forced convection p 924 A93-30974

KUNST, BOB

Hypersonic reconnaissance aircraft [NASA-CR-192049] p 333 A93-17804

KUNZ, DONALD L.

On the effect of pitch/mast-bending coupling on whirl-mode stability p 794 A93-35906

KUNZ, R. F.

Investigation of tip clearance phenomena in an axial compressor cascade using Euler and Navier-Stokes procedures [ASME PAPER 92-GT-299] p 255 A93-19489

KUNZ, ROBERT F.

Grid generation for three-dimensional turbomachinery geometries including tip clearance p 270 A93-21658

KUNZ, ROBERT FRANCIS

Explicit Navier-Stokes computation of turbomachinery flows p 83 A93-10370

KUO, CHIH-YU

Instability of a supersonic vortex sheet inside a circular duct p 1234 A93-55142

KUO, KENNETH K.

Numerical study of an axisymmetric turbulent jet-impingement flow [AIAA PAPER 93-0652] p 543 A93-25545

KUO, SIMION C.

A scoping study for hypersonic transport propulsion systems [ASME PAPER 92-GT-409] p 356 A93-19558

KUPAREV, V. A.

Calculation of the parameters of instability waves in the preseparation region p 1067 A93-48826
Nontraditional methods of controlling the stability of a laminar subsonic boundary layer p 1085 A93-50962

KUPERMAN, GILBERT G.

Information requirements analyses for transatmospheric vehicles [AD-A261189] p 718 A93-25949

KUPFERSCHMIED, P.

Development of a system for aerodynamic fast-response probe measurements p 203 A93-14325

KUPEC, THOMAS C.

Postmortem alcohol production in fatal aircraft accidents [AD-A255766] p 143 A93-14026

KUPPA, S.

In-flight detection of flow separation, stagnation, and transition p 166 A93-14326

KURAISHI, TAKEO

Bypass transition in two- and three-dimensional boundary layers [AIAA PAPER 93-3050] p 1057 A93-48230

KURDILA, ANDREW J.

Calculation of numerical boundary measure for wavelet-Galerkin approximations in aeroelasticity [AIAA PAPER 93-1539] p 741 A93-34076

Nonlinear flutter of composite plates with damage evolution [AIAA PAPER 93-1546] p 829 A93-37441

KURE, FUMIO

Lift enhancement of ground-effect wing. I - Results of screening tests of various concepts p 271 A93-21737

Lift enhancement of ground-effect wing. II - Experimental investigation of the power augmented ram wing in ground effect through the wind tunnel p 271 A93-21738

Microchannel plate modal gain variations with temperature p 477 A93-27445

KURKOV, ANATOLE P.

Experimental investigation of counter-rotating propfan flutter at cruise conditions [AIAA PAPER 93-1632] p 720 A93-34160

KUROCHKIN, I. V.

Modeling of human operator actions in the stochastic trajectory tracking problem for a dynamic plant p 228 A93-16783

KUROCHKIN, N. N.

Detection and parameter estimation of atmospheric turbulence by ground-based and airborne CO₂ Doppler lidars p 395 A93-17862

Study of artificial and natural turbulence in atmospheric boundary layer with a CW Doppler CO₂ lidar p 1257 A93-54799

KURODA, SHIGEAKI

Numerical analysis of a flat plate in a pitching motion. II - Effect on the flow of the position of the pivot, etc p 1181 A93-53798

KURODA, SHINICHI

Numerical simulation of supersonic flow around space plane for airframe-engine integration [AIAA PAPER 93-0886] p 471 A93-24946

KUROSAKA, M.

Vortex-induced energy separation in shear flows p 837 A93-39427

Active control of vortex breakdown by a spinning wave generator [ISABE 93-7045] p 1219 A93-54021

KUROSAKI, RYUJIRO

Aerodynamic heating with boundary layer transition and heat protection with mass addition on blunt body in hypersonic flows [AIAA PAPER 93-2984] p 1051 A93-48177

Aerodynamic heating analysis for axisymmetric bodies in supersonic flow p 303 A93-19312

KUROUMARU, MOTOO

Pressure fluctuation on casing wall of isolated axial compressor rotors at low flow rate [ASME PAPER 92-GT-33] p 246 A93-19293

KURTZ, RICK V.

The PAVE PACE integrated RF architecture for next generation avionics p 896 A93-42784

KURYACHIJ, A. P.

Nontraditional methods of controlling the stability of a laminar subsonic boundary layer p 1085 A93-50962

KURZ, R.

Transonic flow through turbine cascades with nonuniform pitch [ASME PAPER 92-GT-158] p 250 A93-19385

KUSHIDA, TAKEHIRO

The coherent structure in a corner turbulent boundary layer p 548 A93-28575

KUSHPATOVA, V. L.

Effect of the atmosphere density gradient on aerodynamic stabilization p 1252 A93-55034

KUSSOY, M. I.

Three-dimensional hypersonic shock wave/turbulent boundary-layer interactions p 287 A93-23533
Hypersonic shock-wave/turbulent-boundary-layer interactions [AIAA PAPER 93-0781] p 467 A93-24863

KUSSOY, MARVIN

Hypersonic flows as related to the national aerospace plane [NASA-CR-191980] p 296 A93-18378

KUT'INOV, V. F.

Methodology for studying the fracture of aircraft structures in static tests p 801 A93-36785
Design and fabrication of panels with cutouts p 1215 A93-52973

KUTLER, P.

Multidisciplinary computational aerosciences p 437 A93-20711

KUTLER, PAUL

The NASA Computational Fluid Dynamics (CFD) program - Building technology to solve future challenges [AIAA PAPER 93-3292] p 1041 A93-44996

KUTNEY, JOHN T., SR.

A new and working automatic calibration machine for wind tunnel internal force balances [AIAA PAPER 93-2467] p 1138 A93-50214

KUTSCHENREUTER, P. H.

A design approach to high Mach number scramjet performance [AIAA PAPER 92-4248] p 55 A93-13360

KUTSCHENREUTER, PAUL H.

Hypersonic inlet efficiency revisited p 16 A93-10012

KUTZ, K. J.

Simulation of the secondary air system of aero engines [ASME PAPER 92-GT-68] p 348 A93-19318

KUWAHARA, K.

Two-dimensional transonic flow around VKI turbine cascade p 1232 A93-54640

KUWAHARA, TAKUO

Preliminary design of experimental sub-scale scramjet engine [AAS PAPER 91-639] p 1247 A93-55816

KUWANO, SONOKO

Continuous judgment of helicopter noise - On the validity of Leq and Zwicker's method (ISO 532B) p 558 A93-28478

KUZ'MICHEV, V. S.

Expert evaluation of the technological level of aviation gas turbine engine designs p 811 A93-39187

KUZ'MIN, A. G.

Stability conditions for a transonic decelerating flow in a duct p 872 A93-43027

KUZMIN, V. P.

Estimation of the probability of large flight parameters deviations p 184 A93-14399

KUZNETSOV, A. V.

Spline-collocation solution of a Fredholm equation of the second kind in the problem of flow past an airfoil p 1092 A93-51904

KUZNETSOV, I. U. E.

An experimental study of dc discharges in supersonic and subsonic air flows p 14 A93-12980

KUZNETSOV, M. M.

Kinetic theory of hypersonic flows of a viscous gas p 775 A93-39130

Asymptotic structure of a limiting hypersonic flow in a shock wave p 776 A93-39131

Nonequilibrium limiting hypersonic flow of a gas past three-dimensional tapered bodies with a separated shock p 776 A93-39133

Hypersonic limiting flows of a relaxing gas with pressure changes in the main approximation p 776 A93-39135

Nonequilibrium heat transfer near the critical point of blunt bodies p 777 A93-39145

KUZNETSOV, N. C.

Calculation of fuel economy for the Tu-154 aircraft in relation to the washing of the NK-8-2U engine at civil aviation maintenance facilities p 345 A93-18356

KUZNETSOV, N. D.

Propan engines [AIAA PAPER 93-1981] p 1112 A93-49828

KUZNETSOV, N. P.

Selection of methods and equipment for monitoring the technical condition of booster system components p 395 A93-18329

Diagnostics of the hydraulic system of Tu-204 aircraft p 396 A93-18360

KUZNETSOV, S. P.

A study of the effect of the support fastening compliance on the stress-strain state of aircraft transparencies p 997 A93-47079

KUZNETSOV, V. G.

Protective properties of aviation oils p 735 A93-35299

KUZNETSOV, V. I.

Selection of the scheme and optimal parameters of the turbine of a high-temperature bypass engine with a low bypass ratio p 811 A93-39180

KUZNETSOV, V. M.

Problems in physical gas dynamics p 775 A93-39126

Kinetic theory of nonequilibrium flows of gas and disperse media with internal degrees of freedom and chemical reactions p 851 A93-39127

- Acoustic intensity of nonisothermal coaxial jets with an inverted velocity profile p 1124 A93-51759
- KUZNETSOV, VLADIMIR M.**
Experimental investigations and efficiency prediction of jet noise reduction techniques p 449 A93-19206
- KUZNICKI, THOMAS**
Terrorism and air-specific perils and the liability of air freight carriers under Article 17 of the Warsaw Agreement p 570 A93-24252
- KVATERNIK, RAYMOND G.**
The NASA/industry design analysis methods for vibrations (DAMVIBS) program - Accomplishments and contributions p 508 A93-27971
Experiences at Langley Research Center in the application of optimization techniques to helicopter airframes for vibration reduction p 508 A93-27972
A Government/Industry Summary of the Design Analysis Methods for Vibrations (DAMVIBS) Program [NASA-CP-10114] p 514 A93-21310
The NASA/industry Design Analysis Methods for Vibrations (DAMVIBS) program: A government overview p 514 A93-21311
- KWAK, DOCHAN**
Implicit Navier-Stokes solver for three-dimensional compressible flows p 122 A93-14546
Multigrid convergence of an implicit relaxation scheme [AIAA PAPER 93-3357] p 954 A93-45051
A computational study of wingtip vortex flowfield [AIAA PAPER 93-3010] p 1054 A93-48200
Efficient simulation of incompressible viscous flow over single and multi-element airfoils p 1095 A93-52448
Efficient simulation of incompressible viscous flow over multi-element airfoils p 784 A93-27443
- KWON, OH J.**
Three-dimensional unstructured grid Euler method applied to turbine blades [AIAA PAPER 93-0196] p 461 A93-24233
Numerical investigation of performance degradation of wings and rotors due to icing [NASA-CR-192233] p 339 A93-18783
- KWON, OKEY**
Development of an advanced exhaust mixer for a high bypass ratio turbofan engine [AIAA PAPER 93-2435] p 1118 A93-50188
- KWONG, A. H. M.**
Active boundary-layer control in diffusers [AIAA PAPER 93-3255] p 966 A93-46798
- L**
- LA DUE, JAMES C.**
Anti-icing failure detection instrumentation using realtime optical measurement of anti-icing fluid properties [AIAA PAPER 93-0748] p 540 A93-24836
- LA VALLE, LODOVICO**
SAAW - Italy's answer to the windshear challenge p 431 A93-22175
- LAANANEN, D.**
Computer-aided cure optimization p 209 A93-15804
- LAANANEN, D. H.**
Buckling of open-section bead-stiffened composite panels p 1157 A93-50420
- LABAN, M.**
On-line aircraft state and parameter estimation p 512 A93-19929
- LABENDIK, V. P.**
Calculation of fuel economy for the Tu-154 aircraft in relation to the washing of the NK-8-2U engine at civil aviation maintenance facilities p 345 A93-18356
- LABOUDIGUE, BRUNO**
Numerical solution of a free-boundary problem in hypersonic flow theory - Nonequilibrium viscous shock layers p 8 A93-11920
- LABRACHERIE, L.**
On the compression process in a free-piston shock-tunnel p 1136 A93-48041
- LABRUJERE, T. E.**
Computational methods for aerodynamic design of aircraft components [NLR-TP-92072-4] p 987 A93-31148
Review of aerodynamic design in the Netherlands [NLR-TP-91260-U] p 999 A93-31840
- LABURTHE, F.**
Recent supersonic transition studies with emphasis on the swept cylinder case p 127 A93-17252
- LACASSE, J. E. P.**
Subscale validation of a freejet inlet-engine test capability [AIAA PAPER 93-2179] p 1138 A93-49991
- LACH, ALAN**
Development of an engine/airframe performance matching scheme for jet engine retrofit [AD-A258822] p 365 A93-18997
- LACHAPELLE, G.**
Analysis of Loran-C performance in the Pemberton area, B.C. p 311 A93-17797
Analysis of a high-performance C/A-code GPS receiver in kinematic mode p 317 A93-21822
- LACHOWICZ, JASON T.**
Flow field measurements in a crossing shockwave turbulent boundary layer interaction at Mach 3 [AIAA PAPER 93-3434] p 977 A93-47226
- LACKEY, J.**
Pitch control margin at high angle of attack - Quantitative requirements (flight test correlation with simulation predictions) [AIAA PAPER 92-4107] p 39 A93-11277
F/A-18 departure recovery improvement evaluation [AIAA PAPER 93-3671] p 1129 A93-48349
- LACKEY, JAMES B.**
F/A-18 controls released departure recovery - Flight test evaluation p 803 A93-38839
Status of the validation of high-angle-of-attack nose-down pitch control margin design guidelines [AIAA PAPER 93-3623] p 1126 A93-48308
F/A-18 controls released departure recovery flight test evaluation [AD-A256522] p 189 A93-15396
- LACOMBE, G.**
Analysis of implicit treatments for a centred Euler solver p 864 A93-42449
- LADENDE, FOLUSO**
The design of a senior-level CAD course with emphasis on fluid/thermal systems [AIAA PAPER 93-0426] p 454 A93-23344
- LAFLAMME, J. C. G.**
Influence of a thermal barrier coating on the performance of a turboprop engine [ASME PAPER 92-GT-38] p 347 A93-19297
- LAFLAUR, R. S.**
Example of the Couette iceform design model - Flat plate iceformation p 207 A93-15070
- LAFON, A.**
Comparison of ENO and TVD schemes for the parabolized Navier-Stokes equations [AIAA PAPER 93-2970] p 1049 A93-48164
- LAFON, P.**
Numerical prediction of instabilities in transonic internal flows using an Euler TVD code [AIAA PAPER 93-0072] p 262 A93-20184
- LAFORTE, J. L.**
Experimental evaluation of flat plate boundary layer growth over an anti-icing fluid film p 1140 A93-52645
- LAFORTE, JEAN-LOUIS**
Aircraft take-off laboratory simulation for de/anti-icing study p 528 A93-23840
- LAFREY, R.**
Integrated use of GPS and GLONASS in civil aviation navigation. II - Experience with GLONASS p 313 A93-21142
Receiver Autonomous Integrity Monitoring (RAIM) of GPS and GLONASS p 993 A93-46891
- LAGANELLI, A. L.**
Prediction of fluctuating pressure in attached and separated compressible flow [AIAA PAPER 93-0286] p 279 A93-22687
- LAGEN, NICHOLAS T.**
The effects of temperature on supersonic jet noise emission p 446 A93-19159
- LAGRAFF, J. E.**
Measurement of turbulent spots and intermittency modelling at gas-turbine conditions p 902 A93-29934
- LAGRANGE, J. P.**
Three dimensional aero-thermal characteristics of a high pressure turbine nozzle guide vane p 1002 A93-46942
- LAHA, MANAS K.**
Lift and pitching moment measurements in vertical gusts p 906 A93-42259
- LAHR, THOMAS**
International aerospace STI p 1227 A93-53826
- LAI, CHUANXIN**
Numerical solution of 3-D turbulent flows inside of new concept nozzles p 114 A93-14211
- LAI, H. T.**
Calculation of scramjet inlet with thick boundary-layer ingestion [AIAA PAPER 93-1836] p 1074 A93-49720
Computation of H₂/air reacting flowfields in drag-reduction external combustion [NASA-CR-191071] p 536 A93-20237
- LAI, JENKIN**
NO(x) sensitivities for gas turbine engines operated on lean-premixed combustion and conventional diffusion flames [ASME PAPER 92-GT-115] p 349 A93-19351
- LAI, Y. G. J.**
Aerodynamic flow simulation using a pressure-based method and a two-equation turbulence model [AIAA PAPER 93-2902] p 1147 A93-48111
- LAINE, SEPPO**
Calculation of transonic viscous flow around a delta wing p 113 A93-14191
Numerical investigations into the base drag of various wedges using the base flow model developed by Mauri Tanner [REPT-B-36] p 26 A93-12414
- LAING, P.**
Three-dimensional prediffuser combustor studies with air-water mixture [AIAA PAPER 93-2474] p 1120 A93-50217
Two and three-dimensional prediffuser combustor studies with air-water mixture [ISABE 93-7025] p 1213 A93-54001
- LAING, PETER**
Two and three-dimensional prediffuser combustor studies with air-water mixture [AIAA PAPER 93-0240] p 390 A93-22652
- LAKE, RENEE C.**
Experimental and analytical investigation of dynamic characteristics of extension-twist-coupled composite tubular spars [NASA-TP-3225] p 553 A93-20585
- LAKSHMANAN, B.**
Investigation of three-dimensional separation at wing/body junctions in supersonic flows using TVD MacCormack's scheme [AIAA PAPER 93-0884] p 471 A93-24945
Study of supersonic intersection flowfield at modified wing-body junctions p 692 A93-35621
- LAKSHMANAN, B. K.**
Numerical solution of dynamic equations arising in a jet engine simulation p 53 A93-12237
Development of a real time dynamic engine simulation model of a turbo fan engine [ISABE 93-7132] p 1205 A93-54107
- LAKSHMINARAYANA, B.**
Investigation of compressor rotor wake structure at peak pressure rise coefficient and effects of loading [ASME PAPER 92-GT-32] p 246 A93-19292
Investigation of tip clearance phenomena in an axial compressor cascade using Euler and Navier-Stokes procedures [ASME PAPER 92-GT-299] p 255 A93-19489
Three-dimensional flow field in a turbine nozzle passage [AIAA PAPER 93-2556] p 1084 A93-50278
Navier-Stokes analysis of turbine flowfield and external heat transfer [ISABE 93-7075] p 1186 A93-54051
Penn State axial flow turbine facility: Performance and nozzle flow field p 1032 A93-31588
- LAKSHMINARAYANA, BUDUGUR**
Grid generation for three-dimensional turbomachinery geometries including tip clearance p 270 A93-21658
Low-Reynolds-number k-epsilon model for unsteady turbulent boundary-layer flows p 1177 A93-53208
- LAL, MIHIR K.**
Correlation of unsteady pressure and inflow velocity fields of a pitching rotor blade [AIAA PAPER 93-3082] p 1060 A93-48256
- LAM, C.-M. G.**
Vortex methods for the computational analysis of rotor/body interaction p 765 A93-35939
- LAM, F.**
Induced drag of a crescent wing planform p 1094 A93-52430
- LAM, L.**
Airspace Design Expert System (ADES), a 2D/3D mapping and modelling tool incorporating an expert system for use in instrument approach design p 888 A93-30357
- LAM, QUANG M.**
A treatment to flight controller nonlinearity effects - An adaptive compensator approach p 524 A93-26948
- LAM, T.**
Automatic guidance and control laws for helicopter obstacle avoidance p 728 A93-35518
- LAMAR, JOHN E.**
Vortex features of F-106B aircraft at subsonic speeds [AIAA PAPER 93-3471] p 859 A93-41058
- LAMARCHE, L.**
A field panel method for transonic flows p 18 A93-10547
- LAMARSH, WILLIAM J., II**
Aerodynamic performance optimization of a rotor blade using a neural network as the analysis [AIAA PAPER 92-4837] p 324 A93-20295
Application of a neural network as a potential aid in predicting NTF pump failure [NASA-TM-107667] p 442 A93-18332

- LAMB, MARGARET W.**
Human factors in crashes of commuter airplanes
p 486 A93-24048
- LAMB, MILTON**
Internal performance characteristics of vectored axisymmetric ejector nozzles
[AIAA PAPER 93-2432] p 898 A93-41046
Internal performance of Highly Integrated Deployable Exhaust Nozzles
[AIAA PAPER 93-2570] p 1084 A93-50288
Supersonic investigation of two dimensional hypersonic exhaust nozzles
[NASA-TM-105687] p 179 N93-15342
- LAMBERT, B.**
Proceedings of the National Weather Service Aviation Workshop: Postprint volume
[PB92-176148] p 94 N93-11803
- LAMBERTON, H. M.**
Future trends in IR sensors p 1258 A93-55295
- LAMBETH, BENJAMIN S.**
Trends in air power - New systems, old platforms?
p 856 A93-43650
- LAMERIS, J.**
GARTEUR damage mechanics for composite materials: Analytical/experimental research on delaminations
p 537 N93-21513
- LAMKA, JAROMIR**
Velocity vector LDA measurement inside a pitched blade impeller
p 924 A93-40390
- LAMY, PERRY**
Measuring flight test progress on large scale development programs
[AIAA PAPER 92-4070] p 37 A93-11257
- LAM, C. E.**
Assessment and correction of tunnel-wall interference by Navier-Stokes solutions p 116 A93-14275
Calculation of V/STOL aircraft aerodynamics with deflected jets in ground effect
[AIAA PAPER 93-3530] p 986 A93-47287
Calculation of transonic longitudinal and lateral-directional characteristics of aircraft by the small disturbance theory
[AIAA PAPER 93-3617] p 1125 A93-48304
Unsteady aerodynamic models for maneuvering aircraft
[AIAA PAPER 93-3626] p 1126 A93-48311
- LANCIOTTI, A.**
The role of fatigue testing in the design, development and certification of the ATR 42/72 p 46 A93-13637
- LAND, JAMES E.**
Helicopter flight data recorder and health and usage monitoring system p 169 N93-15178
- LANDAHL, M.**
Reform of the aeronautics and astronautics curriculum at MIT
[AIAA PAPER 93-0325] p 454 A93-23017
- LANDERS, STEPHEN**
Correlation of forebody pressures and aircraft yawing moments on the X-29A aircraft at high angles of attack
[AIAA PAPER 92-4105] p 38 A93-11273
Correlation of forebody pressures and aircraft yawing moments on the X-29A aircraft at high angles of attack
[NASA-TM-4417] p 22 N93-11532
- LANDRUM, D. B.**
Engineering method for calculating surface pressures and heating rates on vehicles with embedded shocks
p 777 A93-39255
Engineering method for calculating inlet face property profiles on high speed vehicle forebodies
[AIAA PAPER 93-3113] p 1062 A93-48283
- LANDSBERG, ALEXANDRA**
Control of numerical diffusion in computational modeling of vortex flows p 9 A93-12156
- LANEVILLE, ANDRE**
Harmonic analysis of the aerodynamic forces on a Darrieus rotor p 18 N93-10551
- LANG, P.**
The NASA/industry Design Analysis Methods for Vibrations (DAMVIBS) program: Boeing Helicopters airframe finite element modeling p 515 N93-21313
- LANG, PHILLIP**
CST and rotorcraft - Expanding the view
p 560 A93-25085
- LANG, R.**
Selection criteria for metallic high temperature structural materials in hypersonic flying equipment
[MBB-LME-221-HYPAC-PUB-2-A] p 515 N93-21479
- LANGE, DIETER G.**
European merger control in the air transport industry - Comments on the Delta Air Lines/Pan Am decision of the European Commission
[ISBN 3-452-22293-4] p 103 A93-11412
- LANGFORD, JOHN S.**
An unmanned aircraft for dropwindsonde deployment and hurricane reconnaissance p 677 A93-34587
- Development and testing of the Perseus proof-of-concept aircraft
[DE93-010121] p 806 N93-28586
- LANGHOFF, STEPHEN R.**
Theoretical study of the bond dissociation energies of propyne (C3H4) p 230 A93-14099
- LANGLEY, L. W.**
Microsensors for high heat flux measurements
p 928 A93-42920
- LANGLEY, R. S.**
A dynamic stiffness/boundary element method for the prediction of interior noise levels p 1226 A93-53817
- LANIGAN, CARL A.**
Repair, evaluation, maintenance, and rehabilitation research program. Continuous Deformation Monitoring System (CDMS)
[AD-A261833] p 708 N93-26274
- LAPIDUS, I.**
Thermal effects of a coolant film along the suction side of a high pressure turbine nozzle guide vane
p 901 N93-29930
- LAPIN, I. A.**
Damping of a gyro horizon-compass with arbitrary displacement of the suspension point
p 1025 A93-45684
- LAPISKA, CARL**
Flight simulation - An overview p 1209 A93-53768
- LAPWORTH, B. L.**
Three-dimensional mesh embedding for the Navier-Stokes equations using upwind control volumes
p 1239 A93-56402
- LAPYGIN, V. I.**
Hypersonic flow past a low-aspect-ratio triangular plate at large angles of attack p 1069 A93-48974
- LARACH, EDWARD**
Experiences in fabrication of a waverider model for wind tunnel testing
[AIAA PAPER 93-0510] p 328 A93-23257
- LARDELLIER, A.**
Improving military transport aircraft through highly integrated engine-wing design
[DS-1607] p 333 N93-17850
- LARGUIER, R.**
Experimental and theoretical studies of helicopter rotor-fuselage interaction
[ONERA, TP NO. 1992-142] p 120 A93-14356
Aerodynamic calculation of complex three-dimensional configurations p 1094 A93-52426
- LARIMER, J.**
Engineering a visual system for seeing through fog
[SAE PAPER 921130] p 895 A93-41318
- LARIMER, JAMES**
Performance considerations for high-definition head-mounted displays p 518 A93-27242
- LARINI, M.**
A comparison between centered and upwind schemes for two-phase compressible flows
[AIAA PAPER 93-2346] p 1083 A93-50120
- LARIONOV, V. N.**
Resource conservation and improvement of the service characteristics of castings of high-temperature nickel alloys through a high-temperature melt treatment
p 824 A93-36718
- LARKIN, M.**
Effect of a rotating propeller on the separation angle of attack
[AIAA PAPER 93-0017] p 472 A93-24978
Effect of a rotating propeller on the separation angle of attack and distortion in ducted propeller inlets
[NASA-TM-105935] p 290 N93-16625
- LARMAN, KEVIN T.**
Rarefied-flow shuttle aerodynamics flight model
[AIAA PAPER 93-3441] p 859 A93-41057
Rarefied-flow Shuttle aerodynamics model
[NASA-TM-107698] p 458 N93-19976
- LARNAC, G.**
Fiber reinforced composites: A new class of glass and glass ceramic materials for thermomechanical applications
[REPT-921-430-104] p 200 N93-15490
- LAROCCA, FRANCESCO**
Design of air intakes and nozzles for transonic rotational flows
[ISABE 93-7102] p 1187 A93-54078
- LAROSILIERE, L. M.**
Navier-Stokes analysis of radial turbine rotor performance
[AIAA PAPER 93-2555] p 1121 A93-50277
Navier-Stokes analysis of radial turbine rotor performance
[NASA-CR-191153] p 815 N93-28609
Analysis of unsteady wave processes in a rotating channel
[NASA-CR-191154] p 816 N93-28617
- LAROSILIERE, LOUIS M.**
Three-dimensional numerical simulation of gradual opening in a wave rotor passage
[AIAA PAPER 93-2526] p 1156 A93-50254
Three-dimensional numerical simulation of gradual opening in a wave rotor passage
[NASA-CR-191157] p 900 N93-29072
- LARRAMENDY, PANXIKA**
A longitudinal control law integrating flight controls and engine controls p 186 A93-15046
- LARSEN, WILLIAM E.**
NASA/FAA helicopter simulator workshop
[NASA-CP-3156] p 857 N93-30673
Part 1: Executive summary p 857 N93-30674
- LARSON, D. E.**
Design for manufacture by resin transfer molding of composite parts for rotorcraft
[SME PAPER EM93-103] p 1159 A93-51733
- LARSON, VICTOR**
Detection and classification of acoustic signals from fixed-wing aircraft p 850 A93-37032
- LARSSON, LARS**
Ship viscous flow: A report on the 1990 SSPA-IIHR Workshop p 840 N93-27466
- LARVOR, J. P.**
Digital pulse compression with low range sidelobes
p 929 A93-43463
- LASALMONIE, A.**
Materials problems connected with the propulsion of supersonic air carriers
[ONERA, TP NO. 1992-157] p 824 A93-38736
Supersonic transport: Which material for the engine
[DS-2023] p 522 N93-21459
- LASALMONIE, ALAIN**
The modeling of forging and precision-casting forming processes p 207 A93-15030
- LASCHKA, B.**
Effect of canard wing positions on aerodynamic characteristics of swept-forward wing
[AD-A262373] p 789 N93-28493
- LASEK, MACIEJ**
A short range passenger/freighter canard - Some problems of a preliminary aerodynamic concept
[SAE PAPER 921012] p 157 A93-14642
- LASHCHEV, A. YA.**
An information-search system in cybernetics
p 1168 A93-50957
- LASHKOV, IU. A.**
Effect of longitudinal microribbing on the drag of a body of revolution p 5 A93-10147
- LASSEIGNE, D. G.**
Induced Mach wave-flame interactions in laminar supersonic fuel jets p 475 A93-26183
Temperature and suction effects on the instability of an infinite swept attachment line p 691 A93-35486
- LAST, D.**
Relative sensitivity of Loran-C phase tracking and cycle selection to CWI p 792 A93-36502
- LAST, J. D.**
Effect of skywave interference on the coverage of Loran-C p 33 A93-11095
- LATAPY, M. O.**
High speed test results of subsonic, turbofan scarf inlets
[AIAA PAPER 93-2302] p 1082 A93-50087
- LATTERMAN, DONALD**
Guidelines for NAVSTAR GPS embedded receiver applications p 315 A93-21184
- LATYPOVA, E. I.**
A method for calculating flow past an arbitrary airfoil profile in the presence of flow separation
p 13 A93-12807
- LATYSHEV, A. L.**
Pressure pulsations on a delta wing in incompressible flow p 1069 A93-48912
- LAU, S. C.**
Effect of trailing-edge ejection on local heat (mass) transfer in pin fin cooling channels in turbine blades
[ASME PAPER 92-GT-178] p 352 A93-19404
- LAU, S. K.**
Process optimization of Hexoloy SX-SiC towards improved mechanical properties
[DE93-007913] p 826 N93-28564
- LAUB, JAMES A.**
Development of the NASA-Ames low disturbance supersonic wind tunnel for transition research up to Mach 2.5
[AIAA PAPER 92-3909] p 462 A93-24488
- LAUCHLE, G. C.**
Experimental analysis of the aeroacoustics of cascaded airfoils
[AD-A257945] p 420 N93-18121
- LAUFER, G.**
Planar imaging of OH density distributions in a supersonic combustion tunnel
[AIAA PAPER 93-0042] p 389 A93-20155

- Laser selection criteria for OH fluorescence measurements in supersonic combustion test facilities p 549 A93-29315
- LAUFFER, JAMES P.**
The natural excitation technique (NEXt) for modal parameter extraction from operating wind turbines [DE93-010611] p 845 N93-28603
- LAUGHREY, J. A.**
Propulsion integration results of the STOL and Maneuver Technology Demonstrator p 161 N93-13228
- LAUGHREY, JAMES A.**
Survey on techniques used in aerodynamic nozzle/airframe integration p 161 N93-13224
- LAUNDER, B. E.**
The prediction of riblet behaviour with a low-Reynolds number k-epsilon model p 270 A93-21720
The prediction of convective heat transfer in rotating square ducts [PNR-90929] p 85 N93-11025
Turbulent flow and heat transfer in idealized blade cooling passages p 902 N93-29938
- LAUR, MICHELE**
Forward rotor vortex effects on counter rotating propeller noise p 245 A93-19221
- LAURIE, KURT B.**
Separated flowfield and lift on an airfoil with an oscillating leading-edge flap [AIAA PAPER 93-3422] p 976 A93-47217
- LAVAL, G.**
Some aspects of the aerodynamic methodology in hypersonic vehicle concept studies [AIAA PAPER 92-5027] p 272 A93-22303
- LAVALLE, THOMAS M.**
Concurrent optimization of airframe and engine design parameters [AIAA PAPER 92-4713] p 323 A93-20281
Concurrent optimization of airframe and engine design parameters [NASA-TM-105908] p 60 N93-12402
- LAVERGNE, G.**
Prediction of the performances in combustion of ramjets and stato-rockets by isothermal experiments and modeling p 363 N93-17622
- LAVID, MOSHE**
Employment of radicals and excited state species for supersonic combustion photochemical ignition of premixed hydrogen/oxygen mixtures with ArF laser p 73 N93-11135
- LAVRICH, P.**
An assessment of wake structure behind forward swept and aft swept propfans at high loading p 245 A93-19222
Active aerodynamic control of wake-airfoil interaction noise - Experiment p 1225 A93-53206
- LAVRICH, P. L.**
Active aerodynamic control of wake-airfoil interaction noise - Experiment p 445 A93-19153
Role of leading-edge vortex flows in prop-fan interaction noise p 565 A93-28614
- LAVROV, P. P.**
Choice of the heating system for high-temperature generators using chemical fuel p 559 A93-29660
- LAVROVSKI, EH. K.**
Optimal control of the rocking and damping of swings p 1263 A93-54998
- LAW, C. H.**
Low aspect ratio transonic rotors. I - Baseline design and performance [ASME PAPER 92-GT-185] p 352 A93-19410
Low aspect ratio transonic rotors. II - Influence of location of maximum thickness on transonic compressor performance [ASME PAPER 92-GT-186] p 352 A93-19411
- LAW, C. K.**
On the structure and response of aerodynamically-strained planar premixed flames [AIAA PAPER 93-0246] p 390 A93-22657
Analysis of thermal ignition in supersonic flat-plate boundary layers p 769 A93-37933
Chemical kinetic and aerodynamic structures of flames [AD-A256015] p 391 N93-15931
- LAW, DANIEL**
Preliminary results of the detection of clear air turbulence by the Wind Profiler Demonstration Network p 427 A93-22119
- LAW, R. D.**
Strain-gauge balance performance and internal temperature gradients measured in a cryogenic environment [RAE-TM-AERO-2232] p 68 N93-11906
- LAWER, ALAN**
A statistical comparison of differential GPS and laser generated time, space positioning information for aircraft flight testing p 316 A93-21199
- LAWHEAD, PAUL**
Electro-modulated control of supply pressure in hydraulic systems [SAE PAPER 912119] p 412 A93-21842
- LAWING, PIERCE L.**
High-Reynolds-number test of a 5-percent-thick low-aspect-ratio semispan wing in the Langley 0.3-meter transonic cryogenic tunnel: Wing pressure distributions [NASA-TM-4227] p 875 N93-29449
Reynolds number influences in aeronautics [NASA-TM-107730] p 989 N93-31732
- LAWLESS, PATRICK B.**
Prediction of active control of subsonic centrifugal compressor rotating stall [AIAA PAPER 93-0153] p 274 A93-22591
A model for the selective amplification of spatially coherent waves in a centrifugal compressor on the verge of rotating stall [AIAA PAPER 93-2236] p 1080 A93-50039
Spatial domain characterization of abrupt rotating stall initiation in an axial flow compressor [AIAA PAPER 93-2238] p 1081 A93-50040
- LAWRENCE, ANITA**
Inter-noise '91: Proceedings of the 20th International Conference on Noise Control Engineering, Sydney, Australia, Dec. 2-4, 1991. Vols. 1 & 2 [ISBN 0-909882-12-6] p 557 A93-28476
- LAWRENCE, CHARLES**
Dynamics of rotating multicomponent turbomachinery systems [AIAA PAPER 93-1629] p 742 A93-34157
Dynamics of rotating multi-component turbomachinery systems [NASA-TM-105997] p 421 N93-18426
Structural dynamics branch research and accomplishments to FY 1992 [NASA-TM-105824] p 552 N93-20368
- LAWRENCE, R. M.**
An optical flameout detection system for NASA Langley's 8-Foot High Temperature Tunnel p 1254 A93-54372
- LAWRENCE, S. L.**
Parabolized Navier-Stokes methods for hypersonic flows p 421 N93-18565
- LAWRENCE, SCOTT L.**
Application of space-marching methods to hypersonic forebody flow fields [AIAA PAPER 92-5030] p 272 A93-22305
Application of CFD to a generic hypersonic flight research study [AIAA PAPER 93-0312] p 280 A93-23007
Hypersonic cone flow predictions using an implicit upwind space-marching code p 865 A93-42588
Space marching calculations about hypersonic configurations using a solution-adaptive mesh algorithm p 1177 A93-53212
- LAWRENCE, STELLA**
Using software metrics and software reliability models to attain acceptable quality software for flight and ground support software systems p 442 N93-17305
- LAWRYSYN, M. A.**
Performance degradation due to hoar frost on lifting surfaces p 305 A93-17798
- LAWSON, C. L.**
On some recent advances in multidisciplinary analysis of hypersonic vehicles [AIAA PAPER 92-5026] p 438 A93-22302
- LAWSON, LARRY**
Coherent X-ray imaging for corrosion evaluation - A preliminary assessment p 396 A93-18611
- LAYTON, CHARLES**
Design of a cooperative problem-solving system for enroute flight planning: An empirical study of its use by airline dispatchers [NASA-CR-192709] p 707 N93-25330
- LAYTON, CHUCK**
Design concepts for the development of cooperative problem-solving systems [NASA-CR-192708] p 707 N93-25261
- LAZALIER, G. R.**
The acoustic response of altitude test facility exhaust systems to axisymmetric and two-dimensional turbine engine exhaust plumes p 449 A93-19209
- LAZAREV, L. IA.**
Selection of the principal initial parameters for an axial-flow birotary turbine p 837 A93-39198
- LAZZERI, L.**
The role of fatigue testing in the design, development and certification of the ATR 42/72 p 46 A93-13637
- LE BALLEUR, J. C.**
A viscous-inviscid solver for high-lift incompressible flows over multi-element airfoils at deep separation conditions [ONERA, TP NO. 1992-183] p 774 A93-38745
- Viscous-inviscid calculation of high-lift separated compressible flows over airfoils and wings [ONERA, TP NO. 1992-184] p 774 A93-38746
- LE BEAU, G. J.**
Finite element computation of compressible flows with the SUPG formulation p 482 A93-29774
- LE BEL, ALICE A.**
The development of a mature external Master's degree program in aeronautical engineering - A university/industry partnership [AIAA PAPER 92-4256] p 570 A93-24296
- LE GATH, JOSEPH S.**
Aerospace '92 - The year in review p 455 A93-19976
- LE MOING, T.**
Integration of flight control and carrier landing aid system [ONERA, TP NO. 1993-6] p 181 A93-14187
- LE SANT, Y.**
A new adaptive test section at ONERA Chalais-Meudon [ONERA, TP NO. 1992-117] p 822 A93-38592
- LE, DZU K.**
Robust stabilization based on topological connectedness p 438 A93-22830
- LEA, K. A.**
Lateral aerodynamic interference between tanker and receiver in air-to-air refueling p 1136 A93-52444
Aircraft turns into and down wind [AERO-REPT-9201] p 337 N93-18131
- LEACH, MARK P.**
Results from a GPS Shuttle Training Aircraft flight test p 384 A93-21148
- LEAHY, M. B., JR.**
RACE pulls for shared control p 458 A93-29130
Robotic aircraft refueling - A concept demonstration p 846 A93-37041
- LEAR, WILLIAM E., JR.**
Direct boundary value solution of wave rotor flow fields [AIAA PAPER 93-0483] p 415 A93-23385
- LEARMOUNT, DAVID**
A330 - Completing the family p 40 A93-11418
Advancing helicopters p 327 A93-21836
- LEARY, NEILL**
Maps and charts for visual air navigation p 498 A93-25170
- LEATHERWOOD, J. D.**
Subjective response to simulated sonic booms with ground reflections [NASA-TM-107764] p 852 N93-28692
- LEATHERWOOD, JACK D.**
Laboratory study of effects of sonic boom shaping on subjective loudness and acceptability [NASA-TP-3269] p 102 N93-11620
Effect of sonic boom asymmetry on subjective loudness [NASA-TM-107708] p 453 N93-16755
Loudness and annoyance response to simulated outdoor and indoor sonic booms [NASA-TM-107756] p 852 N93-27271
A laboratory study of subjective response to sonic booms measured at White Sands Missile Range [NASA-TM-107746] p 852 N93-27272
- LEAVITT, LAURENCE D.**
Supersonic investigation of two dimensional hypersonic exhaust nozzles [NASA-TM-105687] p 179 N93-15342
- LEBAIL, F.**
Numerical analysis of high aspect ratio cooling passage flow and heat transfer [AIAA PAPER 93-1829] p 1153 A93-49714
- LEBALLEUR, J. C.**
Calculation of fully three-dimensional separated flow with an unsteady viscous-inviscid interaction method p 786 N93-27455
- LEBEDENKO, V. V.**
An experimental study of dc discharges in supersonic and subsonic air flows p 14 A93-12980
- LEBEDEV, A. A.**
Problems in the optimization of complex engineering systems p 1165 A93-49307
- LEBEDEV, G. N.**
Behavior of the particular quality characteristics of an intelligent flight vehicle control system in a multicriterial formulation p 1168 A93-50952
- LEBLANC, D. J.**
Vision-based recursive estimation of rotorcraft obstacle locations p 343 A93-22851
- LEBOEUF, F.**
Analysis of three-dimensional viscous flow in a supersonic axial flow compressor rotor with emphasis on tip leakage flow [ASME PAPER 92-GT-388] p 257 A93-19543
Modeling of a turbulent flow in the presence of discrete parietal cooling jets p 904 A93-29960

LEBOEUF, RICHARD L.

Streamwise vortex meander in a plane mixing layer
[AIAA PAPER 93-0553] p 285 A93-23292

LECA, L.

High temperature thin film strain gauges
[ONERA, TP NO. 1992-171] p 542 A93-25346

LECCE, L.

Numerical study for the study of medium speed internal noise problems
[DILC-EST-TN-200] p 101 N93-11156

LECHNER, WOLFGANG

Real time DGPS service for precise positioning - Activities in the Federal Republic of Germany
p 1 A93-11027

LECK, CHET L.

A new rotated upwind difference scheme for the Euler equations
[AIAA PAPER 93-0066] p 261 A93-20179

LECLERCQ, M. P.

Characteristic multigrid method application to solve the Euler equations with unstructured and unstructured grids
p 476 A93-27065

LECOMTE, CLAUDE

Sonic boom problem for future highspeed aircraft
[ONERA-NT-1990-3] p 876 N93-30020

LECOMTE, D.

The role of the radiologist in the medicolegal procedure after an aviation accident
p 853 A93-39701

LECOMTE, PIERRE

Flight safety and human errors
p 141 A93-16860

LECORDIX, J.-L.

Design of an advanced nacelle for a very high bypass ratio engine
p 505 A93-25362

LECORDIX, JEAN-LOIC

Advanced SST auxiliary air intakes design and analysis
[AIAA PAPER 93-2304] p 1082 A93-50088

LECOZ, D.

RAMSES: Multi-spectral experimental radar station installed on board the Transall
p 550 N93-19925

LEDESMA, MARTHA E.

Proposal and preliminary design for a high speed civil transport aircraft. Swift: A high speed civil transport for the year 2000
[NASA-CR-192023] p 335 N93-18049

LEDNICER, D. A.

CFD zonal modeling of leading-edge ice effects for a complete aircraft
[AIAA PAPER 93-0167] p 275 A93-22601

LEE-RAUSCH, ELIZABETH M.

Wing flutter boundary prediction using unsteady Euler aerodynamic method
[AIAA PAPER 93-1422] p 739 A93-33975

Calculation of AGARD Wing 445.6 flutter using Navier-Stokes aerodynamics
[AIAA PAPER 93-3476] p 981 A93-47255

Conical Euler analysis and active roll suppression for unsteady vortical flows about rolling delta wings
[NASA-TP-3259] p 701 N93-26134

LEE, ALBERT W.

Control of nonlinear systems under input constraints with applications to flight control
p 729 N93-25353

LEE, AN-CHEN

Optimal vibration control for a flexible rotor with gyroscopic effects
p 98 A93-13420

LEE, ANDREW J.

High speed databus evaluation - Further work
[SAE PAPER 931597] p 1151 A93-49346

LEE, B. H. K.

Analysis of flight flutter test data
p 523 A93-23839
An analysis of the post-instability behaviour of a two-dimensional airfoil with a structural nonlinearity
[AIAA PAPER 93-1474] p 726 A93-34020

The role of Kutta waves on oscillatory shock motion on an airfoil experiencing heavy buffeting
[AIAA PAPER 93-1589] p 682 A93-34121

Evaluation and extension of the flutter-margin method for flight flutter prediction
p 828 A93-37393

A wind tunnel investigation of the pressure distribution on an F/A-18 wing
[AIAA PAPER 93-3468] p 980 A93-47249

Unsteady pressure and load measurements on an F/A-18 vertical fin
p 1095 A93-52451

Fluid/structures interactions. Aircraft considerations
p 527 N93-20628

LEE, BOO I.

Reynolds stress profiles in the near wake of an oscillating airfoil
p 1236 A93-55380

LEE, C.

A prediction model for the vortex shedding noise from the wake of an airfoil or axial flow fan blades
p 1265 A93-55995

LEE, C. C.

A study of the flexural properties of carbon-epoxy composites in certain environments
p 390 A93-21999

LEE, C. P.

Influence of surface heat flux ratio on heat transfer augmentation in square channels with parallel, crossed, and V-shaped angled ribs
p 201 A93-13981

Influence of surface heating condition on local heat transfer in a rotating square channel with smooth walls and radial outward flow
[ASME PAPER 92-GT-188] p 402 A93-19413

LEE, CALVIN K.

Radial reefing method for accelerated and controlled parachute opening
[AIAA PAPER 93-1209] p 702 A93-35159

LEE, CHI-MING

Simplified jet fuel reaction mechanism for lean burn combustion application
[AIAA PAPER 93-0021] p 390 A93-23238

Simplified jet-A kinetic mechanism for combustor application
[NASA-TM-105940] p 200 N93-15504

Nitric oxide formation in a lean, premixed-prevaporized jet A/air flame tube: An experimental and analytical study
[NASA-TM-105722] p 844 N93-27012

LEE, CHUNHIAN

The forms of unsteady concentrated vortex-breakdown and its reactions to disturbance
p 1231 A93-54594

LEE, CYNTHIA C.

Flight evaluation of a stagnation detection hot-film sensor
[AIAA PAPER 92-4085] p 51 A93-13263

LEE, D.

A numerical study of slit V-gutter flows
p 171 A93-14273

Swirling flows in a contoured-wall combustion chamber
[AIAA PAPER 93-1765] p 1073 A93-49661

LEE, DOHYUNG

Progress in local preconditioning of the Euler and Navier-Stokes equations
[AIAA PAPER 93-3328] p 952 A93-45022

LEE, DONG-HO

An efficient method to calculate rotor flow in hover and forward flight
[AIAA PAPER 93-3336] p 953 A93-45030

LEE, DONGHO

Navier-Stokes calculations of rotating BERP planform blade flowfields
[AIAA PAPER 93-3527] p 986 A93-47286

LEE, EDWIN E., JR.

Aerodynamic investigation with focusing schlieren in a cryogenic wind tunnel
[AIAA PAPER 93-3485] p 910 A93-41059

LEE, ELIZABETH M.

Results from a conical Euler methodology developed for unsteady vortical flows
p 692 A93-35612

LEE, EUN U.

Fatigue crack growth in AerMet 100 steel
[AD-A249068] p 74 N93-12248

LEE, GEORGE

Study of optical techniques for the Ames unitary wind tunnels. Part 4: Model deformation
[NASA-CR-190980] p 68 N93-12349

Study of optical techniques for the Ames unitary wind tunnel. Part 5: Infrared imagery
[NASA-CR-191385] p 194 N93-14809

Study of optical techniques for the Ames unitary wind tunnel, part 7
[NASA-CR-192165] p 382 N93-18520

Study of optical techniques for the Ames unitary wind tunnel: Digital image processing, part 6
[NASA-CR-192164] p 382 N93-18766

LEE, HSING-JUIN

Method for assessing the electric power system reliability of multiple-engined aircraft
p 810 A93-37399

LEE, HSING-WEI

Method for assessing the electric power system reliability of multiple-engined aircraft
p 810 A93-37398

LEE, IN

Vibration analysis of composite wing with tip mass using finite elements
p 1023 A93-45175

LEE, J.

A numerical study of mixing in supersonic combustors with hypermixing injectors
[AIAA PAPER 93-0215] p 520 A93-27801

A lag model for turbulent boundary layers developing over rough bleed surfaces
[AIAA PAPER 93-2988] p 1052 A93-48181

A numerical study of mixing in supersonic combustors with hypermixing injectors
[NASA-CR-191027] p 294 N93-17884

LEE, J. Y.

Numerical study of the flow establishment time in hypersonic shock tunnels
p 480 A93-29153

LEE, JEAN

Resonant response analysis of a high speed gear
p 553 N93-20662

LEE, JOSEPH W.

Doppler global velocimetry measurements of the vortical flow above an F/A-18
[AIAA PAPER 93-0414] p 415 A93-23333

LEE, JUNG-JIN

Vibration analysis of composite wing with tip mass using finite elements
p 1023 A93-45175

LEE, K. D.

Multi-point design of transonic airfoils using optimization
[AIAA PAPER 92-4225] p 16 A93-13382

A multi-point optimization for transonic airfoil design
[AIAA PAPER 92-4681] p 264 A93-20303

Three-dimensional Navier-Stokes calculations using solution-adapted grids
[AIAA PAPER 93-0431] p 462 A93-24240

Airfoil design using the Navier-Stokes equations
[AIAA PAPER 93-0648] p 464 A93-24763

Application of computational fluid dynamics in transonic aerodynamic design
[AIAA PAPER 93-3481] p 982 A93-47259

Design efficiency evaluation for transonic airfoil optimization - A case for Navier-Stokes design
[AIAA PAPER 93-3112] p 1062 A93-48282

LEE, KAM-FUI

Higher-order viscous shock-layer solutions for high altitude flows
[AIAA PAPER 93-2724] p 858 A93-41050

Enhancements to viscous-shock-layer technique
p 962 A93-46408

A viscous shock-layer analysis of 2-D and axisymmetric flows
[AIAA PAPER 93-2751] p 963 A93-46500

LEE, KUOK-MING

Aircraft grid generation using interactive environment
[AIAA PAPER 93-0224] p 438 A93-22639

LEE, MIN-GYOO

Numerical simulation of starting process in a hypersonic nozzle
p 684 A93-43275

LEE, RICHARD S. L.

Aerothermodynamics in combustors; IUTAM Symposium, National Taiwan Univ., Taipei, June 3-5, 1991, Selected Papers
[ISBN 0-387-55404-1] p 1146 A93-51626

LEE, ROBERT A.

Comparison of airport noise calculation models
p 564 A93-28480

LEE, SOOGAB

Effect of leading-edge porosity on blade-vortex interaction noise
[AIAA PAPER 93-0601] p 563 A93-24727

Characteristics of deformable leading edge for high performance helicopter rotor
[AIAA PAPER 93-3526] p 986 A93-47285

Strong parallel blade-vortex interaction and noise propagation in helicopter flight
p 944 N93-30980

LEE, WILLIS

Explosive detection system based on Electronic Neutron Generator (ENG)
p 497 N93-21870

LEE, Y.-T.

Rotor/stator flow coupling in turbomachines
p 1232 A93-54647

LEE, YEOL

Heat transfer measurements in swept shock wave/turbulent boundary-layer interactions
p 750 N93-25705

LEE, YOUNG C.

Receiver autonomous integrity monitoring (RAIM) capability for sole-means GPS navigation in the oceanic phase of flight
p 33 A93-11035

LEE, YU-TAI

An interaction noise between vortex and airfoil
[AIAA PAPER 93-0600] p 562 A93-24726

LEE, YUNG-JANG

High-speed helicopter rotor noise - Shock waves as a potent source of sound
p 565 A93-29403

LEEP, L. J.

Three-dimensional simulations of compressible mixing layers - Visualizations and statistical analysis
p 1235 A93-55360

LEFEBVRE, A. H.

Experimental techniques for the assessment of fuel thermal stability
p 197 A93-14504

LEFEBVRE, SYLVIE

Evaluation of piezoceramic actuators for control of aircraft interior noise
p 447 A93-19186

LEFEVRE, JEAN

Laser velocimetry around helicopter blades in the DNW wind tunnel of the NLR
[ONERA, TP NO. 1992-143] p 831 A93-38613

LEFEVRE, RANDY J.

Adverse weather test site selection study
[AD-A259012] p 339 N93-18895

LEGENDRE, ROBERT G.

The Concorde wing - A useful model
p 126 A93-16400

- LEGER, C. A.**
Analysis of interlaminar stresses in symmetric and unsymmetric laminates under various loadings
[AIAA PAPER 93-1511] p 740 A93-34050
- LEGGETT, DAVE B.**
Initial results of an in-flight investigation of longitudinal flying qualities for augmented, large transports in approach and landing
[AIAA PAPER 93-3816] p 1133 A93-51407
- LEGNER, H.**
Nonintrusive, multipoint velocity measurements in high-pressure combustion flows
[AIAA PAPER 93-2032] p 1145 A93-49867
- LEGNER, H. H.**
High-temperature supersonic combustion testing with optical diagnostics p 730 A93-34498
- LEGRADY, O.**
Explosives detection systems for airport security gas chromatographic based devices p 881 N93-30276
- LEGRAS, M.**
Navier-Stokes computation on a pivoting doors thrust reverser and comparison with tests
[ASME PAPER 92-GT-254] p 353 A93-19463
- LEHMAN, S. E.**
Design optimization study for F-15 propulsion/forward fairing compatibility
[AIAA PAPER 93-3484] p 1003 A93-47291
- LEHMANN, B.**
The jet behaviour of an actual high-bypass engine as determined by LDA-measurements in ground tests p 175 N93-13218
- LEHRKE, H.-P.**
Analysis of multiple crack propagation in stiffened sheet p 81 A93-13638
- LEI, ZHENDONG**
Study on aircraft microwave remote sensing of sea-water surface salinity p 92 A93-12407
- LEIGHTY, BRADLEY D.**
Gas analysis system for the Eight Foot High Temperature Tunnel p 822 A93-37875
- LEJDENS, H.**
The reduction of skin friction by riblets under the influence of an adverse pressure gradient p 1218 A93-53810
- LEINGANG, J. L.**
Rapid computer simulation of ramjet performance
[AIAA PAPER 93-2049] p 1113 A93-49882
- LEISHMAN, J. G.**
Experimental study of rotor wake/body interactions in hover p 124 A93-14782
Experimental investigation of rotor/lifting surface interactions
[AIAA PAPER 93-0871] p 469 A93-24932
A new method for improved rotor free-wake convergence
[AIAA PAPER 93-0872] p 469 A93-24933
Interactional aerodynamic effects on rotor performance in hover and aerodynamic p 766 A93-35941
Initial lift approximations for two-dimensional subsonic flow as obtained from oscillatory measurements p 768 A93-37385
Boundary layer and pressure measurements on a cylinder with unsteady circulation control p 1177 A93-53207
- LEITH, J. R.**
Vortex initiation during dynamic stall of an airfoil p 684 A93-34335
- LEITMANN, GEORGE**
Adaptive control of aircraft in windshear p 62 A93-13126
- LEJBOV, V. G.**
Experience in specifying/prolonging the airframe time limits p 948 A93-45797
- LELE, SANJIVA K.**
Boundary conditions for direct computation of aerodynamic sound generation p 447 A93-19176
Inviscid instability of a skewed compressible mixing layer p 769 A93-37941
Vortex-induced disturbance field in a compressible shear layer p 873 A93-43628
Boundary conditions for direct computation of aerodynamic sound generation p 1172 A93-49005
- LEMCOE, M. M.**
High-temperature strain measurement techniques: Current developments and challenges p 217 N93-13669
- LEMKE, PAUL**
Eagle RTS: A design for a regional transport aircraft
[NASA-CR-192032] p 334 A93-18017
- LEMMER, L.**
The design development of the monolithic CFRP centre fuselage skin of the European fighter aircraft p 159 A93-15782
- LENGRAND, J. C.**
DSMC numerical investigation of rarefied compression corner flow
[AIAA PAPER 93-3096] p 1061 A93-48270
Experimental study of transitional axisymmetric shock-boundary layer interactions at Mach 5
[AIAA PAPER 93-3131] p 1063 A93-48296
- LENOROVITZ, JEFFREY M.**
Russians completing new ground-effect vehicle p 853 A93-38535
- LENSEIGNE, CLAUDE**
Toward the second-generation supersonic transport
[ONERA, TP NO. 1993-26] p 890 A93-41038
- LENTINI, D.**
A finite element code for gas turbine combustor flow with Stretched Laminar Flamelet modelling
[ISABE 93-127] p 1204 A93-54102
- LENTZ, JOHN C.**
Testing of an energy efficient environmental control system for a patrol-type aircraft
[SAE PAPER 92-1225] p 890 A93-41399
- LEONARD, J.**
Advancing the state of the art hypersonic testing - HYTEST/MTMI
[AIAA PAPER 93-2023] p 1113 A93-49860
- LEONARD, O.**
Inverse design of compressor and turbine blades at transonic flow conditions
[ASME PAPER 92-GT-430] p 357 A93-19573
- LEONARD, RACHEL**
Laser holographic interferometric measurements of the flow behind a rearward facing step
[AIAA PAPER 93-3515] p 985 A93-47279
- LEONI, PETER B.**
Improved Airframe Manufacturing Technology p 763 A93-35971
- LEONOV, GERMAN N.**
Improved static and dynamic performance of helicopter powerplant p 809 A93-35928
- LEOUTSAKOS, G.**
Transition prediction in attached and separated shear layers using an integral method
[ASME PAPER 92-GT-281] p 253 A93-19473
- LERAT, A.**
Analysis of implicit treatments for a centred Euler solver p 864 A93-42449
- LEROUGE, DANIEL**
Control of the pilot-system interface p 166 A93-15040
- LEROUX, C.**
Evaluation of clear-air radar PROUST and Doppler radar RONSARD for airport low level-wind shear detection p 433 A93-22202
- LEROY, MICHEL**
Integrated runway meteorological observation system (IRMOS/SIOMA) p 428 A93-22128
- LESCH, KLAUS**
Periodic maximum range cruise with singular control p 890 A93-41903
- LESCHZINER, M. A.**
A cell-vertex TVD scheme for transonic viscous flow p 685 A93-34346
- LESIEUR, M.**
Numerical simulation of compressible mixing zones p 10 A93-12427
- LESKOV, L. V.**
Astronautics and society p 383 A93-18391
- LESMERISES, A. L.**
Effects of back-pressure in a lean blowout research combustor
[ASME PAPER 92-GT-81] p 387 A93-19330
- LESOINNE, M.**
Stability analysis of dynamic meshes for transient aeroelastic computations
[AIAA PAPER 93-3325] p 1022 A93-45019
- LESPEDE, P.**
Fiber reinforced composites: A new class of glass and glass ceramic materials for thermomechanical applications
[REPT-921-430-104] p 200 N93-15490
- LESTER, H. C.**
Active control of interior noise in a large scale cylinder using piezoelectric actuators p 568 A93-29425
- LESTER, HAROLD C.**
Noise transmission properties and control strategies for composite structures p 919 N93-30436
- LESTER, P. F.**
A summary of investigations of severe turbulence incidents using airline flight records p 308 A93-22153
- LESTER, PETER**
A microcomputer program for estimating low altitude wind and turbulence fields p 438 A93-22163
- LETALLEC, P.**
Taking into account surface roughness in computing hypersonic re-entry body p 686 A93-34354
- LETNIKOV, VIKTOR B.**
Helicopter aerodynamics research techniques and rotor-fuselage interaction analysis p 765 A93-35938
- LEU, J. H.**
The turbulence and mixing characteristics of the complex flow in a simulated augmentor p 1123 A93-51642
- LEU, TZONG-SHYNG**
Free shear layer control and its application to fan noise
[AIAA PAPER 93-3242] p 965 A93-46787
- LEUCHTER, O.**
Theoretical and experimental study of the behavior of particles passing through a shock wave
[ONERA, TP NO. 1992-233] p 774 A93-38777
- LEUNG, C. P.**
Applications of advanced fracture mechanics to fuselage p 1026 A93-45787
- LEURIDAN, J.**
Application of FEM model correlation and updating techniques on an aircraft using test data of a ground vibration survey p 509 A93-29267
Signal processing and system identification techniques for flutter test data analysis p 529 A93-29282
- LEVAN, G. W.**
Creep fatigue life prediction for engine hot section materials (isotropic)
[NASA-CR-189221] p 364 N93-18578
- LEVASHOV, P. D.**
Coupling conditions for substructures with varying idealization p 1029 A93-47078
- LEVERTON, JOHN W.**
Lynx: High performance - Low noise p 322 A93-19185
- LEVESQUE, P.**
Infrared thermography of plastic instabilities in a single crystal superalloy
[ONERA, TP NO. 1993-18] p 916 A93-41031
- LEVIN, D.**
Experimental validation of a discrete vortex method for inviscid axisymmetric flow around parachute canopies
[AIAA PAPER 93-1216] p 689 A93-35165
- LEVIN, KERRY M.**
Developing automation for terminal air traffic control: Case study of the imaging aid p 888 N93-30356
- LEVIN, KLAS**
Characterization of delamination and fiber fractures in carbon fiber reinforced plastics induced from impact p 915 A93-40787
- LEVIN, M. P.**
A method for calculating supersonic three-dimensional flows in pyramidal nozzles p 125 A93-15216
- LEVIN, STEPHEN D.**
Development and fabrication of an autoclave molded PES/Quartz sandwich radome p 547 A93-28279
- LEVIN, V. A.**
Supersonic flow past a cone with heat transfer near its tip p 1089 A93-51780
- LEVINE, WILLIAM S.**
Techniques for designing rotorcraft control systems
[NASA-CR-192960] p 729 N93-26046
- LEVIONNOIS, A.**
Ground Support Equipment (GSE) for Aircraft Condition Monitoring System (ACMS) p 110 N93-15158
- LEVISON, LIBBY**
Action composition for the animation of natural language instructions
[AD-A254963] p 228 N93-12554
- LEVITAN, LEE**
Taxonomy of flight variables p 147 N93-15022
- LEVITON, D. B.**
Optical technologies for UV remote sensing instruments p 853 N93-28788
- LEVITSKII, N. P.**
Measurement of aerodynamic forces at high temperatures p 75 A93-10030
- LEVRAEA, VINCENT**
Add-on damping treatment for the F-15 upper-outer wing skin
[AD-A258470] p 337 N93-18248
- LEVRAEA, VINCENT J.**
Human engineering issues for data link systems p 1260 A93-55874
Modal survey of a full-scale F-18 wind tunnel model
[AD-A262482] p 875 N93-29410
- LEVSHIRBANOV, S. R.**
A method for calculating flow past an arbitrary airfoil profile in the presence of flow separation p 13 A93-12807
- LEVY, DAVID W.**
Design of a full time wing leveler system using tab driven aileron controls
[AIAA PAPER 92-4193] p 63 A93-13345

LEVY, MILTON

LEVY, MILTON

Hydrogen-induced stress corrosion cracking susceptibility analysis of pitch links from the AH-64 Apache helicopter
[AD-A260692] p 736 N93-25895

LEVY, R. L.

Aerodynamic applications of pressure sensitive paint p 549 A93-29301

LEVY, RICHARD A.

A method for investigating human factor aspects of military aircraft accidents p 491 N93-19656

LEW, T. M.

The Supersonic Stratospheric Vehicle p 39 A93-11357

LEWANDOWSKI, J. J.

Chemical stability of titanium diboride reinforcement in nickel aluminide matrices p 1147 A93-52473

LEWANTOWICZ, ZDZISLAW H.

Architectures and GPS/INS integration - Impact on mission accomplishment p 31 A93-11013

LEWENDON, DAVE

Looking and seeing - A practical problem p 238 A93-18758

LEWICKI, D. G.

Face-gear drives: Design, analysis, and testing for helicopter transmission applications
[NASA-TM-106101] p 839 N93-27133

Efficient fault diagnosis of helicopter gearboxes
[NASA-TM-106253] p 1032 N93-31846

LEWICKI, DAVID G.

Low-noise, high-strength, spiral-bevel gears for helicopter transmissions
[AIAA PAPER 93-2149] p 1154 A93-49966

Fault detection of helicopter gearboxes using the multi-valued influence matrix method
[NASA-TM-106100] p 838 N93-27069

LEWIS, CLARK H.

Low-to-high altitude predictions of three-dimensional ablative re-entry flowfields p 1027 A93-46407

PNS predictions of axisymmetric hypersonic blunt-body and afterbody flowfields
[AIAA PAPER 93-2725] p 962 A93-46479

Application of parabolized Navier-Stokes technique for high-L/D, hypersonic vehicle design
[AIAA PAPER 93-2948] p 1047 A93-48144

LEWIS, D. J.

Time-resolved surface heat flux measurements in the wing/body junction vortex
[AIAA PAPER 93-0918] p 472 A93-24972

LEWIS, F. L.

Output feedback eigenstructure assignment using two Sylvester equations p 847 A93-38214

LEWIS, M. J.

Numerical study of the flow establishment time in hypersonic shock tunnels p 480 A93-29153

LEWIS, MARK J.

Engine/airframe integration for waverider cruise vehicles
[AIAA PAPER 93-0507] p 283 A93-23254

Stability and control of hypersonic waveriders
[AIAA PAPER 93-0508] p 370 A93-23255

A re-evaluation of the waverider design process
[AIAA PAPER 93-0404] p 440 A93-23326

Hypersonic waveriders - Where do we stand?
[AIAA PAPER 93-0399] p 474 A93-25520

A numerical study of the unsteady processes associated with the type IV shock interaction
[AIAA PAPER 93-2479] p 1083 A93-50221

LEWIS, MICHAEL S.

Design and conduct of a windshear detection flight experiment
[AIAA PAPER 92-4092] p 38 A93-11268

Sensing a change in the wind p 307 A93-21627

Flight test operations p 488 N93-19592

Wind shear hazard determination p 488 N93-19597

LEWIS, MIKE

A manned hypersonic reconnaissance vehicle which does not require airborne fueling p 333 N93-17888

LEWIS, NORRIS E.

Specialty fiber optic systems for mobile platforms and plastic optical fibers: Proceedings of the Meeting, Boston, MA, Sept. 9-11, 1992
[SPIE-1799] p 1105 A93-49462

LEWIS, R. G.

Adapting system engineering principles to the Canadian Airspace System p 887 N93-30338

LEWIS, S. J.

The approach to airworthiness clearance with the introduction of advanced materials and manufacturing technologies into the design of aerospace structures p 2 A93-12235

LEWIS, SHARON

An application of knowledge-based engineering to composite tooling design p 846 A93-36010

LEWIS, WILLIAM D.

A parametric study of real time mathematical modeling incorporating dynamic wake and elastic blades p 798 A93-35986

Development and validation of a comprehensive real time AH-64 Apache simulation model p 799 A93-35992

Methodology development for evaluation of selective-fidelity rotorcraft simulation p 913 N93-30691

LEWIS, WILLIAM DEAN

An aeroelastic model structure investigation for a manned real-time rotorcraft simulation p 693 N93-24756

LEWY, S.

Experimental study of the acoustic spinning modes generated by a helicopter turboshaft engine
[ONERA, TP NO. 1992-141] p 230 A93-14266

High-frequency acoustic radiation from a curved duct of circular cross section
[ONERA, TP NO. 1993-55] p 1173 A93-51937

LEWY, SERGE

Toward the silent helicopter
[ONERA, TP NO. 1992-229] p 851 A93-38774

Helicopter external noise prediction and reduction
[ONERA, TP NO. 1993-48] p 1039 A93-47450

The acoustics of axial compressors
[ONERA, TP NO. 1993-102] p 1226 A93-53615

Acoustic-wave propagation in ducts and free-field radiation
[ONERA, TP NO. 1993-103] p 1226 A93-53616

LEYENDECKER, HAGEN

A contribution to the dynamic feedforward open loop control of multivariable systems and to the optimal design of command functions
[DLR-FB-92-05] p 441 N93-16515

LEYLAND, JANE A.

Full-scale wind tunnel investigation of a helicopter individual blade control system
[AIAA PAPER 93-1361] p 726 A93-33929

LEYLAND, P.

2D hypersonic viscous flow past a double ellipse geometry p 868 A93-42613

LEYLAND, PENELOPE

Shock-wave/boundary layer interactions at hypersonic speeds by an implicit Navier-Stokes solver
[AIAA PAPER 93-2938] p 1046 A93-48136

Precise pitching airfoil computations by use of dynamic unstructured meshes
[AIAA PAPER 93-2971] p 1049 A93-48165

A family of multiblock codes for computational aerothermodynamics - Application to complete vehicle hypersonic flows
[AIAA PAPER 93-3042] p 1056 A93-48223

LEYNAERT, J.

Tests of models equipped with TPS in low speed ONERA F1 pressurized wind tunnel p 213 N93-13201

Comparative performance tests of a pilot-inlet in several European wind-tunnels at subsonic and supersonic speeds p 130 N93-13221

LEZBERG, ERWIN A.

In-stream measurements of combustion during Mach 5 to 7 tests of the Hypersonic Research Engine (HRE)
[AIAA PAPER 93-2324] p 1116 A93-50104

LI, C.

Stability of oblique detonations in RAM accelerators
[AIAA PAPER 92-0089] p 541 A93-24979

LI, C. P.

A multigrid nonoscillatory method for computing high speed flows
[AIAA PAPER 93-3319] p 958 A93-45103

LI, CHUNXUAN

A new method for resolving transonic nozzle flows using orthogonal stream-lines coordinate system p 1230 A93-54584

LI, DUJUAN

Experimental research for the discharge flow of a centrifugal impeller and the flowfield in the vaneless diffuser p 11 A93-12454

LI, F.

Transition studies for swept wing flows using PSE
[AIAA PAPER 93-0077] p 263 A93-20189

LI, FENG-HSI

A visualization study of the vortical flow over a double-delta wing in dynamic motion
[AIAA PAPER 93-3425] p 976 A93-47220

LI, FENGWEI

Compressible laminar and turbulent boundary layer computation for the three-dimensional wing p 12 A93-12735

LI, GUANSHENG

Engineering optimization of aeronautical structures p 154 A93-14227

LI, GUOHUA

Human factors in crashes of commuter airplanes p 486 A93-24048

LI, HONGJUN

A nonperiodic boundary approach for computation of compressible viscous flows in advanced turbine cascades
[AIAA PAPER 93-1799] p 1074 A93-49688

LI, HUAITI

Performance improvement of gas turbine with steam injection p 1107 A93-48523

LI, HUAXING

On experimental study of 3-D flow in self-correcting wind tunnel p 528 A93-24033

LI, JIAN

A method and a software for constructing F-by-F random load spectrum p 506 A93-27375

LI, JING P.

A method for optimizing the meridional passage of the rotor in centrifugal compressors p 119 A93-14344

LI, JINGPING

A method for optimizing the meridional passage in a centrifugal compressor p 204 A93-14483

LI, LEXIN

Study on fracture failure of turbine blades in a series of turbojets p 205 A93-14493

LI, LIGUO

Prediction of the radiation characteristic of a helicopter exhaust jet p 172 A93-14494

A numerical study on the radiation characteristic of an elliptical exhaust jet p 174 A93-16236

Impingement cooling with film coolant extraction in the airfoil leading edge regions
[ISABE 93-7078] p 1220 A93-54054

LI, LIJUN

A unified model for rotating stall and surge p 259 A93-20119

LI, LING

Effects of pylon yaw and lateral stiffness on the flutter of a delta wing with external store p 800 A93-36330

LI, MING-XING

Bird impact dynamic response analysis for aircraft arc windshield p 41 A93-11815

LI, NAIHONG

Comment on 'Equation decoupling - A new approach to the aerodynamic identification of unstable aircraft' p 818 A93-37406

LI, PEI-QIONG

A simulation study on take-off and landing dynamics of fly-by-wire control system aircraft p 1249 A93-55590

LI, PEIQIONG

A simulation study on take-off and landing dynamics of the aircraft of a fly-by-wire control system
[AD-A259286] p 510 N93-19849

LI, QIHAN

The effectiveness of porous squeeze film dampers for suppressing nonsynchronous motions p 545 A93-27316

LI, S.-M.

An investigation of spanwise mixing in multistage axial flow compressors
[ASME PAPER 92-GT-64] p 247 A93-19314

LI, S.-P.

The prediction of riblet behaviour with a low-Reynolds number k-epsilon model p 270 A93-21720

LI, SHENGJIN

Fully automatic FEM data pre-processing for aeronautical electrical machine p 538 A93-24030

LI, SHIMING

A simple spanwise mixing model for turbulent diffusion and secondary flows in multistage axial-flow compressors p 204 A93-14482

A calculation of secondary flows and deviation angles in multistage axial-flow compressors p 1066 A93-48509

A computer program for meridional flows in multistage axial flow compressors with turbulence and multi-effects of 3-D flows p 1165 A93-49186

LI, SHUREN

On closed-loop identification of a certain aeroengine under flight conditions p 519 A93-24026

On engine parameter estimation with flight test data p 1107 A93-48520

LI, SUXUN

An experimental study for interaction flow between shock wave and turbulent boundary layer p 120 A93-14355

Passive control of shock wave/boundary layer interaction at hypersonic speed
[AIAA PAPER 93-3249] p 966 A93-46794

LI, TZUEN R.

Analysis of the friction and wear mechanisms of multilayered plasma-sprayed ceramic coatings p 548 A93-28567

LI, TZU-HSENG S.

A new flight control design scheme using optimal dynamic output feedback p 368 A93-22883

- LI, WEI**
Contact analysis for riveted and bolted joints of composite laminates p 204 A93-14384
- LI, WEIYE**
An investigation of real-time diagnostic technique on aeroengine p 174 A93-16844
Simplified mathematical model and digital simulation of aeroengine p 1106 A93-48511
- LI, WENLAN**
The numerical calculation of aircraft propeller noise p 174 A93-16239
- LI, X. J.**
A study of dynamic characteristics of axial compression systems by heat addition p 202 A93-14168
- LI, X. R.**
Performance prediction of the interacting multiple model algorithm p 439 A93-22926
- LI, XIAO R.**
Performance prediction of the interacting multiple model algorithm p 1167 A93-50638
- LI, XIAODONG**
Acoustic experiments of two scaled-model propellers on the ground p 1172 A93-48507
- LI, XIHONG**
An experimental investigation of endwall flow control in a compressor plane cascade wind tunnel p 1066 A93-48512
- LI, XIMING**
Future development and application of general structural analysis softwares in the aviation industry in China p 1262 A93-54420
- LI, XUEREN**
A fuzzy dynamic analysis method for aeromaintenance system p 225 A93-14177
- LI, YAN-SHENG**
Three-dimensional flow analysis of a four-stage transonic axial compressor with inlet guide vanes p 1232 A93-54643
- LI, YUAN**
A parametric approach to preliminary design for aircraft and spacecraft configuration p 225 A93-14201
- LI, YUHONG**
Investigation of the characteristics of 3-dimensional separated flow in an annular compressor blade row with large angles of attack p 259 A93-20116
- LI, Z.**
Computations of spray, fuel-air mixing, and combustion in a lean-premixed-prevaporized combustor [AIAA PAPER 93-2069] p 1153 A93-49901
- LI, Z. N.**
A synthesized method in durability analysis p 203 A93-14286
- LI, ZHAOHUI**
Impingement cooling with film coolant extraction in the airfoil leading edge regions [ISABE 93-7078] p 1220 A93-54054
- LI, ZHONGMING**
Fully automatic FEM data pre-processing for aeronautical electrical machine p 538 A93-24030
- LI, ZHONGQING**
Processing integral impeller 4-coordinate numerically controlled milling machine p 926 A93-41749
- LIAKHOVENKO, I. A.**
Stress-strain analysis and optimal design of aircraft structures p 827 A93-36782
- LIAMIS, N.**
Transonic and supersonic flow calculations around aircrafts using a multidomain Euler code [ONERA, TP NO. 1992-137] p 772 A93-38610
Three-dimensional analysis of turbine rotor flow including tip clearance [ASME PAPER 93-GT-111] p 987 A93-47446
3-D turbomachinery Euler and Navier-Stokes calculations with a multidomain cell-centered approach [AIAA PAPER 93-2576] p 1085 A93-50292
- LIAN, KUANG-YOW**
Output tracking control of nonlinear systems with weakly non-minimum phase p 439 A93-22968
- LIAN, Q. X.**
Flow structures around a constant-rate pitching airfoil and mechanism of dynamic stall p 118 A93-14332
- LIAN, QIXIANG**
An experimental investigation on laminar boundary layer separation over a backward-facing step p 1230 A93-54588
- LIAN, XIAOCHUN**
Effect of steady-state circumferential pressure and temperature distortions on compressor stability p 1106 A93-48503
- LIANG, ANITA D.**
Brush seal low surface speed hard-rub characteristics [AIAA PAPER 93-2534] p 1156 A93-50261
Brush seal bristle flexure and hard-rub characteristics [NASA-TM-105864] p 421 A93-18321
Brush seal low surface speed hard-rub characteristics [NASA-TM-106169] p 838 A93-27132
- LIANG, DEWANG**
Estimation of the maximum values of instantaneous distortion index DC sub theta p 266 A93-20806
- LIANG, PAK-YAN**
Development of a robust pressure-based numerical scheme for spray combustion applications [AIAA PAPER 93-0902] p 560 A93-24960
- LIANG, SHEN-MIN**
Numerical simulation of unsteady transonic nozzle flows p 272 A93-22230
Shock oscillation in two-dimensional, inviscid, unsteady channel flow p 288 A93-23563
Computations of aerodynamic drag for turbulent transonic projectiles with and without spin [AIAA PAPER 93-3416] p 975 A93-47212
- LIAO, C. W.**
Swirling flows in a contoured-wall combustion chamber [AIAA PAPER 93-1765] p 1073 A93-49661
- LIAO, CHANGMING**
Experimental study on turbulent two-phase flow in a dual-inlet side dump combustor p 1106 A93-48506
- LIAO, CHUNG-LI**
Flutter analysis of stiffened laminated composite plates and shells in supersonic flow p 1216 A93-53224
- LIAO, JIN HUA**
Correlation of conical interactions induced by sharp fins and semicones p 692 A93-35635
- LIAO, JINHUA**
Improvement of conical similarity rule in swept shock wave/boundary layer interaction [AIAA PAPER 93-2941] p 1046 A93-48139
Correlative behaviours of shock/boundary layer interaction induced by sharp fin and semicone p 1230 A93-54581
- LIAO, K.**
Characterization of ceramic composite materials for gas turbine applications [DE93-009719] p 905 A93-30168
- LIAO, LIANCHANG**
Study on aircraft microwave remote sensing of sea-water surface salinity p 92 A93-12407
- LIAO, TEH-LU**
Output tracking control of nonlinear systems with weakly non-minimum phase p 439 A93-22968
- LIAPUNOV, M. L.**
High-strength combination fasteners for joint assembly in aircraft structures p 745 A93-35283
Stress-strain state of the elements of a single-stringer riveted panel p 746 A93-35288
- LIAPUNOV, S. V.**
Accelerated method of the Euler equation solution in transonic airfoil flow problem p 113 A93-14193
- LIASJO, K. H.**
Final results from a study of community response to aircraft noise around Oslo Airport Fornebu p 425 A93-19192
- LIASJO, KARE**
Preliminary results from a study of community response to noise from military aircraft exercise p 558 A93-28484
- LIASJO, KARE H.**
Comparison of airport noise calculation models p 564 A93-28480
Influence of aircraft noise on speech intelligibility p 558 A93-28483
Final results from a study of community response to aircraft noise around Oslo Airport Fornebu p 558 A93-28486
- LIAW, D. G.**
Quantification of uncertainties in composites [AIAA PAPER 93-1440] p 734 A93-33989
- LIAW, G. S.**
Burnett solutions along the stagnation line of a cooled cylinder in low-density hypersonic flows [AIAA PAPER 93-2726] p 962 A93-46480
- LIAW, GOANG-SHIN**
The Burnett shock structures in low density hypersonic flows [AIAA PAPER 92-5048] p 273 A93-22320
- LIAW, PAUL C.**
Calculation of V/STOL aircraft aerodynamics with deflected jets in ground effect [AIAA PAPER 93-3530] p 986 A93-47287
- LIBIS, N.**
Study of a pulse ramjet based on twin valveless combustors coupled to operate in antiphase [ISABE 93-7038] p 1197 A93-54014
Development of a pulse ramjet based on twin valveless pulse combustors coupled to operate in antiphase p 814 A93-27186
- LIBRESCU, L.**
Exact flutter solution of advanced anisotropic composite cantilevered wing structures [AIAA PAPER 93-1535] p 727 A93-34072
- A refined structural model of composite aircraft wings for the enhancement of vibrational and aeroelastic response characteristics [AIAA PAPER 93-1536] p 740 A93-34073
Integrated structural tailoring and adaptive control of advanced flight vehicle structural vibration [AIAA PAPER 93-1697] p 757 A93-34219
- LIBRESCU, LIVIU**
On the static aeroelastic tailoring of composite aircraft swept wings modelled as thin-walled beam structures p 158 A93-14820
- LIBURDI, J.**
Powder metallurgy repair of turbine components [ASME PAPER 92-GT-312] p 354 A93-19500
Erosion resistant titanium nitride coating for turbine compressor applications [ASME PAPER 92-GT-417] p 388 A93-19565
- LICHTENWALNER, P. F.**
The use of artificial intelligence for buffet environments [AIAA PAPER 93-1534] p 727 A93-34071
- LICHTENWALNER, PETER F.**
Comparison of neural network and Markov random field image segmentation techniques p 397 A93-18652
- LICINA, JOSEPH R.**
US Army's aviation life support equipment retrieval program real world design successes from proactive investigation p 494 A93-19690
- LIEBECK, R. H.**
Vortex generators used to control laminar separation bubbles p 768 A93-37381
- LIEBST, BRAD S.**
A simplified wing rock prediction method [AIAA PAPER 93-3662] p 1128 A93-48342
- LIENAU, J. J.**
Numerical simulation of the turbulent flow in round jets [AIAA PAPER 93-0199] p 277 A93-22619
- LIERMAN, BRUCE C.**
The analysis of expert performance in the redesign of the en route air traffic control curriculum p 571 A93-27189
- LIFANOV, I. K.**
Construction of wakes in the discrete vortex method p 1179 A93-53333
- LIFANOVA, T. A.**
Effect of aqueous solutions of water-crystallization inhibiting fluids on Thiokol-based sealants p 1017 A93-45689
- LIGHT, JEFFREY S.**
Shadowgraph flow visualization of isolated tiltrotor and rotor/wing wakes p 767 A93-35996
Tip vortex geometry of a hovering helicopter rotor in ground effect p 893 A93-43779
- LIGHTHILL, JAMES**
A general introduction to aeroacoustics and atmospheric sound p 1264 A93-55852
A general introduction to aeroacoustics and atmospheric sound [NASA-CR-189717] p 102 A93-12021
Report on the final panel discussion on computational aeroacoustics [NASA-CR-189718] p 231 A93-12986
Some aspects of the aeroacoustics of high-speed jets [NASA-CR-191458] p 843 A93-28975
- LIGLER, GEORGE T.**
The Meteorological Data Collection and Reporting System - Status and future directions p 428 A93-22133
- LIGRANI, P. M.**
Heat transfer, adiabatic effectiveness, and injectant distributions downstream of a single row and two staggered rows of compound angle film-cooling holes p 201 A93-13976
- LIGUORE, SALVATORE L.**
Composite 'Exoskin' doubler extends F-15 Vertical Tail fatigue life [AIAA PAPER 93-1341] p 709 A93-33911
- LIJEWSKI, LAWRENCE E.**
Transonic mutual interference of wing-pylon-multiple body configurations using an overlapping grid scheme [AIAA PAPER 93-3023] p 1055 A93-48208
- LIKHTER, V. A.**
A study of a pulsed electrical field near the jet of a turbojet engine p 52 A93-10179
Experimental study of condensation vapor-air jets p 76 A93-10180
- LIKHTEROVA, N. M.**
Effect of aqueous solutions of water-crystallization inhibiting fluids on Thiokol-based sealants p 1017 A93-45689
- LILEK, Z.**
A collocated finite volume method for predicting flows at all speeds p 1087 A93-51736

LILENFELD, HARVEY V.

- NO(x) scavenging on carbonaceous aerosol surfaces in aircraft exhaust plumes. I
[AIAA PAPER 93-2343] p 1164 A93-50117
- Particulates and aerosols characterized in real time for harsh environments using the UMR mobile aerosol sampling system (MASS)
[AIAA PAPER 93-2344] p 1156 A93-50118

LILLEY, DAVID G.

- Inlet velocity profile effects on turbulent swirling flow predictions
[AIAA PAPER 93-0133] p 274 A93-22580
- Parameter effects on turbulent swirling flames in combustors p 534 A93-25911

LILLEY, J. S.

- Generic developmental turbojet fuel control
p 172 A93-14519

LILLEY, K. G.

- Fixed and rotary wing all weather operations system requirements p 142 A93-17303

LILLY, J. E.

- A comparison of wind speed measured by the Special Sensor Microwave Imager (SSM/I) and the Geosat altimeter p 1033 A93-44862

LIM, DENNIS

- An adaptive grid/Navier-Stokes methodology for the calculation of nozzle afterbody base flows with a supersonic freestream
[AIAA PAPER 93-1922] p 1076 A93-49788

LIM, SAM-KYU

- Toward reusable graphics components in Ada
[AD-A262568] p 849 A93-28577

LIM, T. B.

- Viscous flow computations of flow field around an advanced propeller
[AIAA PAPER 93-0873] p 469 A93-24934

LIMBERG, W.

- Pressure measurements at supersonic speeds on the research configuration ELAC I p 1237 A93-56033

LIN, C. A.

- Modelling three-dimensional gas-turbine-combustor model flow using second-moment closure
[AIAA PAPER 93-3104] p 1149 A93-48277

LIN, C. E.

- A constrained flight route monitor system in terminal control area for air traffic control p 882 A93-42816

LIN, C. K.

- The turbulence and mixing characteristics of the complex flow in a simulated augmentor p 1123 A93-51642

LIN, CHAO-QIANG

- Design problems of three-dimensional contractions p 1236 A93-55584

LIN, CHIN E.

- Refined H-infinity controller design for rotorcraft flight control p 368 A93-22882

LIN, CHING-FANG

- A new flight control design scheme using optimal dynamic output feedback p 368 A93-22883
- Sequential smoothing and filtering for maneuvering target tracking p 440 A93-22978

LIN, CHUNG-CHIH

- The combined closed form-perturbation approach to the analysis of mistuned bladed disks
[ASME PAPER 92-GT-125] p 350 A93-19359

LIN, F.

- Specification of a class of discrete event processes and their controllers p 96 A93-13078

LIN, GUOFENG

- Ground effect on the take-off characteristics of sea-based aircraft p 679 A93-33706

LIN, HERNG

- Variant bi-conjugate gradient methods for the compressible Navier-Stokes solver with a two-equation model of turbulence
[AIAA PAPER 93-3316] p 951 A93-45012

LIN, HSUN-CHENG

- Theoretical investigation of combustion characteristics in ram-jet dump combustor with side-inlet p 346 A93-19121

LIN, J. C. M.

- Unsteady laminar separation on low-Reynolds-number airfoils
[AIAA PAPER 93-0209] p 278 A93-22627

LIN, JEFFREY S.

- Thermal shock capabilities of infrared dome materials p 70 A93-11454

LIN, JEN F.

- Analysis of the friction and wear mechanisms of multilayered plasma-sprayed ceramic coatings p 548 A93-28567

LIN, JOHN C.

- Surface hot-film method for the measurement of transition, separation and reattachment points
[AIAA PAPER 93-2918] p 1148 A93-48120
- Reynolds number influences in aeronautics
[NASA-TM-107730] p 989 A93-31732

LIN, JOHN CHING-NIEN

- Control of low-speed turbulent separated flow over a backward-facing ramp p 219 A93-14475

LIN, JUANG-LU

- Receiving and scattering characteristics of an imaged monopole beneath a lossy sheet p 1158 A93-50543

LIN, K. C.

- The numerical errors in inverse simulation
[AIAA PAPER 93-3588] p 1223 A93-52681

LIN, K. Y.

- Experimental investigations into composite fuselage impact damage resistance and post-impact compression behavior p 159 A93-15812

LIN, KUEN Y.

- Developments in impact damage modeling for laminated composite structures p 922 A93-30857

LIN, KUO-CHI

- Using system identification to improve the performance of a low-cost flight simulator p 369 A93-22885

- Representation of vehicle location in networked simulations
[AIAA PAPER 93-3582] p 1214 A93-52677

- Reusable code for helicopter simulation
[AIAA PAPER 93-3594] p 1224 A93-52686

LIN, Q.

- Flow characteristics of an S-shaped inlet at high incidence p 114 A93-14213

- Numerical analysis of the 3-D turbulent flow in an S-shaped diffuser p 116 A93-14252

LIN, RAY-SING

- Effect of curvature on stationary crossflow instability of a three-dimensional boundary layer p 1070 A93-49010

- Stationary crossflow instability on an infinite swept wing p 699 A93-25865

LIN, SAN-YIH

- Discontinuous Galerkin finite element method for two dimensional conservation laws
[AIAA PAPER 93-0337] p 281 A93-23026

- Numerical investigations on airfoil performance subjected to aerodynamic interference from an upstream airfoil
[AIAA PAPER 93-0639] p 463 A93-24754

- Discontinuous Galerkin finite element method for Euler and Navier-Stokes equations p 1235 A93-55357

LIN, SHIJIE

- Study on aircraft microwave remote sensing of sea-water surface salinity p 92 A93-12407

LIN, T. Y.

- Structure-attached corotational fluid grid for transient aeroelastic computations p 480 A93-29326

LIN, WANG Z.

- Longitudinal closed-loop pilot/vehicle analysis of DFBW aircraft during approach and landing p 1206 A93-54277

LIN, XIURONG

- An optimization method for statistical ascertainment of the most probable peak temperature at combustor exit p 1108 A93-49195

LIN, ZHAO-FU

- Fewest-fault integral optimization algorithm for engine fault diagnosis p 173 A93-15343

LIN, ZHUD

- Aircraft trajectory tracking and prediction
[AD-A259039] p 340 A93-18999

LINCOLN, JOHN W.

- Reassessment of the C-141 structural life p 46 A93-13631

- Proceedings of the USAF Structural Integrity Program
[AD-A255379] p 110 A93-14549

LIND, ANN MARIE T.

- Two simulation studies of precision runway monitoring of independent approaches to closely spaced parallel runways
[AD-A263433] p 911 A93-29815

LIND, CHARLES A.

- A numerical study of the unsteady processes associated with the type IV shock interaction
[AIAA PAPER 93-2479] p 1083 A93-50221

LIND, EDWARD

- High Capacity Voice Recorder (HCVR) Operational Test and Evaluation (OT/E) integration test report
[DOT/FAA/CT-TN92/30] p 88 A93-11460

LIND, EDWARD N.

- The Data Multiplexing Network (DMN) phase 3 Extended Distance Data Cable (EDDC) test and evaluation
[DOT/FAA/CT-TN93/11] p 752 A93-26160

LINDAU, J. W.

- Solution schemes for stage-by-stage dynamic compression system modeling
[AIAA PAPER 93-0154] p 275 A93-22592

LINDBERG, LENNART

- Fatigue effects of noise among airplane mechanics p 558 A93-28495

LINDBLAD, INGEMAR

- Implementation of a multidomain Navier-Stokes code on the Intel iPC2 hypercube
[FFA-TN-1992-37] p 843 A93-28994

LINDE, MAGNUS

- Leeside flow over delta wing at M = 7.15 - Experimental results for test case 7.1.2 p 870 A93-42632

- Evaluation of contributions for test case 7.1.1 and 7.1.2 p 870 A93-42636

LING, DEHAI

- Hybrid guidance for maneuvering flight vehicles
[AD-A254110] p 69 A93-11798

LING, YUNPEI

- The experimental evaluation of annular ejector system under concurrent mixing and diffusion p 1250 A93-54593

LING, ZHIGUANG

- Numerical solution of non-isentropic transonic cascade flow by time-marching method p 679 A93-33715

LINGAIAH, K.

- Photoelastic stress analysis of skewed cutout in a sandwich skew plate subjected to inplane and transverse eccentric load p 210 A93-16604

LINGNER, U.

- Experimental analysis of transonic flow through the variable nozzle of a radial inflow turbine
[ASME PAPER 92-GT-90] p 248 A93-19336

LINTON, SAMUEL W.

- The computation of the post-stall behavior of a circulation controlled airfoil
[AIAA PAPER 93-0207] p 277 A93-22625

LINTON, SAMUEL WITHERSPOON

- The numerical simulation of circulation controlled airfoil flowfields p 879 A93-30947

LIOR, DAVID

- By-passing of heat exchangers in gas turbines p 814 A93-27189

LIOU, LUEN-WOEI

- Extended linear quadratic Gaussian control under randomly varying distributed delays p 439 A93-22854

LIOU, M.-S.

- Computing 3-D steady supersonic flow via a new Lagrangian approach
[AIAA PAPER 93-0891] p 471 A93-24951

- Multigrid calculation of three-dimensional viscous cascade flows p 872 A93-42889

LIOU, MENG-SING

- Field by field hybrid upwind splitting methods
[AIAA PAPER 93-3302] p 950 A93-45000

An extended Lagrangian method

- [AIAA PAPER 93-3305] p 951 A93-45003

- A new flux splitting scheme p 973 A93-47189

LIOU, S. G.

- Correlation of unsteady pressure and inflow velocity fields of a pitching rotor blade
[AIAA PAPER 93-3082] p 1060 A93-48256

- Flow field characteristics of a complex blade tip at high angles of attack
[AIAA PAPER 93-3083] p 1060 A93-48257

LIOU, T.-M.

- Noncoaxial mixing in a rectangular duct p 205 A93-14518

LIOU, YUAN C.

- Two modified versions of Hsu-Lee's elliptic solver of grid generation p 95 A93-11085

LIPAJ, ANDREJ

- A comparison between numerical models and measurements in a Kaplan turbine guide vanes p 685 A93-34339

LIPIN, A. V.

- Investigation of supersonic shaped nozzles in a low-pressure wind tunnel p 1091 A93-51881

LIPIN, E. K.

- Optimization of the stiffness and mass characteristics of lifting surface structures modeled by an elastic beam p 827 A93-36789

LIPNITSKIY, YU. M.

- Hypersonic flow past a low-aspect-ratio triangular plate at large angles of attack p 1069 A93-48974

LIPP, A. M.

- Synthesis of a helicopter nonlinear flight controller using approximate model inversion
[AIAA PAPER 92-4468] p 62 A93-13280

LIPPERT, P.

- Rotating stall: Modeling-measurement techniques; unsteady loss-unsteady flow field p 424 A93-18732

LIPPKE, C.

- Nonlinear dynamic simulation of single- and multi-spool core engines
[AIAA PAPER 93-2580] p 1122 A93-50294

LISAL, M.

- Profile losses of an annular turbine cascade in unsteady periodic flow
[ASME PAPER 92-GT-153] p 249 A93-19380

- LISCHINSKY-ARENAS, PABLO**
Dynamic compensator design in nonlinear aerospace systems p 1036 A93-44150
- LISCHE, MICHAEL P.**
TEAMS - Technical expert aircraft maintenance system p 941 A93-42865
- LISCINSKY, D. S.**
Experimental investigation of crossflow jet mixing in a rectangular duct [NASA-TM-106152] p 812 N93-27026
Experimental study of cross flow mixing in cylindrical and rectangular ducts [NASA-CR-187141] p 815 N93-27680
- LISEJTSEV, N. K.**
Formalization of the problem of preliminary aircraft design p 891 A93-42375
- LISIECKI, B.**
Infrared thermography of plastic instabilities in a single crystal superalloy [ONERA, TP NO. 1993-18] p 916 A93-41031
- LISLE, CURTIS**
Reusable code for helicopter simulation [AIAA PAPER 93-3594] p 1224 A93-52686
- LISSAMAN, P. B. S.**
Apparent mass effects on parafoil dynamics [AIAA PAPER 93-1236] p 690 A93-35177
- LISZEWSKI, ANNA M.**
The T700 ... from salt spray to sand blast p 1205 A93-54292
- LITT, JONATHAN S.**
Identification of the open loop dynamics of the T700 turboshaft engine p 809 A93-35934
- LITTLE, THOMAS G.**
The PAVE PACE integrated RF architecture for next generation avionics p 896 A93-42784
- LITTLEJOHN, KENNETH**
Complexity metrics for avionics software p 939 A93-42829
- LITTLETON, ERIC C.**
PROAV Cable Warning System (CWS) - U.S. Army aircraft integration assessment and OCONUS field evaluation [AD-A261233] p 705 N93-26263
- LITVIN, F. L.**
Face-gear drives: Design, analysis, and testing for helicopter transmission applications [NASA-TM-106101] p 839 N93-27133
- LITVIN, FAYDOR L.**
Low-noise, high-strength, spiral-bevel gears for helicopter transmissions [AIAA PAPER 93-2149] p 1154 A93-49966
- LITZINGER, THOMAS A.**
Numerical study of an axisymmetric turbulent jet-impingement flow [AIAA PAPER 93-0652] p 543 A93-25545
- LIU, A.**
Measurement of shed vorticity and circulation from rotating aerofoil by particle image velocimetry p 538 A93-23804
- LIU, A. F.**
Application of a p-version finite element code to analysis of cracks [AIAA PAPER 93-1450] p 740 A93-33999
- LIU, ALEX B.**
Modeling the effects of drop drag and breakup on fuel sprays [AD-A263650] p 931 N93-29388
- LIU, BO**
Analytical method for subsonic cascade profile p 12 A93-12730
- LIU, C. H.**
Vaporizer performance p 79 A93-12784
Calculations of separated vortex flows at low speed for low-aspect-ratio wings p 264 A93-20300
Three-dimensional supersonic vortex breakdown [AIAA PAPER 93-0526] p 284 A93-23267
Investigation of vortex breakdown on delta wings using Navier-Stokes equations p 478 A93-27924
Prediction of asymmetric vortical flows around slender bodies using Navier-Stokes equations p 478 A93-27925
Supersonic vortex breakdown over a delta wing in transonic flow [AIAA PAPER 93-3472] p 980 A93-47251
Active control of asymmetric conical flow using spinning and rotatory oscillations [AIAA PAPER 93-2958] p 1048 A93-48152
Shock-vortex interaction over a 65-degree delta wing in transonic flow [AIAA PAPER 93-2973] p 1049 A93-48167
Numerical simulation and physical aspects of supersonic vortex breakdown p 1093 A93-52011
Passive control of supersonic asymmetric vortical flows around cones p 220 N93-14692
- LIU, C. Y.**
Applications of laser techniques in fluid mechanics p 395 A93-17765
- LIU, CHANG**
A study of aircraft global dynamic stability in rapid rolling maneuver p 1206 A93-53869
- LIU, CHING S.**
An analytical description of hypersonic boundary layer stability [AIAA PAPER 93-2981] p 1051 A93-48174
- LIU, CHING SHI**
Engineering approach to the prediction of shock patterns in bounded high-speed flows p 287 A93-23545
- LIU, D. D.**
A unified hypersonic/supersonic method for aeroelastic applications including shock-unsteady wave interaction [AIAA PAPER 93-1317] p 738 A93-33892
- LIU, DA-MING**
Effect of canard oscillations on the vortical flowfield of a X-31A-like fighter model in dynamic motion [AIAA PAPER 93-3427] p 1008 A93-47222
- LIU, DEZHANG**
The experimental investigation of combination effect by using injection effect of aeroengine jet exhaust p 898 A93-41742
- LIU, FENG**
Cascade flow calculations by a multigrid Euler method p 270 A93-21662
Numerical solution of Navier-Stokes equations and k-omega turbulence model equations using a staggered upwind method [AIAA PAPER 93-2968] p 1049 A93-48162
A staggered finite volume scheme for solving cascade flow with a two-equation model of turbulence [AIAA PAPER 93-1912] p 1076 A93-49779
Multigrid Navier-Stokes calculations for three-dimensional cascades p 1177 A93-53209
- LIU, G. P.**
Design of a low sensitivity and norm multivariable controller using eigenstructure assignment and the method of inequalities [AIAA PAPER 93-3802] p 1170 A93-51394
- LIU, HAN-LIEH**
Simultaneous mapping of the unsteady flow fields by Particle Displacement Velocimetry (PDV) p 786 N93-27454
- LIU, HANHUI**
A proposal concerning the dynamic analysis method of continuous gust design rules p 181 A93-14197
- LIU, HONGJUN**
Effects of pylon yaw and lateral stiffness on the flutter of a delta wing with external store p 800 A93-36330
- LIU, HUAIXUN**
Variable structure controller design and its real-time analysis for microprocessor-based flight control systems p 181 A93-14229
- LIU, J.**
A multilevel composite grid method for fluid flow computations [AIAA PAPER 93-0768] p 541 A93-24852
- LIU, J. L.**
Analysis of steady and unsteady turbine cascade flows by a locally implicit hybrid algorithm [ASME PAPER 92-GT-127] p 249 A93-19361
- LIU, JI-KE**
An investigation of mode shift flutter suppression scheme for empennages p 182 A93-14288
- LIU, JINGHUA**
An experimental investigation of hydrogen-fueled supersonic combustor p 53 A93-12733
The numerical model of supersonic air flow field with hydrogen transverse injection p 859 A93-41736
- LIU, JINHUA**
Effects of vitiated air on the results of ground tests of scramjet combustor p 173 A93-16234
- LIU, JONG-SHANG**
Three-dimensional Navier-Stokes analysis of the tip clearance flow in linear turbine cascades [AIAA PAPER 93-0391] p 282 A93-23068
Three-dimensional Navier-Stokes analysis of tip clearance flow in linear turbine cascades p 1235 A93-55364
- LIU, KEXING**
Optical actuators for fly-by-light applications p 1172 A93-49475
- LIU, LI**
Optimization of oleo-pneumatic shock absorber of aircraft p 1243 A93-55415
- LIU, LING**
An experimental investigation of hydrogen-fueled supersonic combustor p 53 A93-12733
Effects of vitiated air on the results of ground tests of scramjet combustor p 173 A93-16234
The numerical model of supersonic air flow field with hydrogen transverse injection p 859 A93-41736
- LIU, MINGJIA**
A method of calculating elastic curve of semiflexible plate nozzle p 66 A93-12097
- LIU, N.-S.**
Two- and three-dimensional blade vortex interactions [NASA-CR-177567] p 293 N93-16942
- LIU, NAN-SUEY**
A time-accurate high-resolution TVD scheme for solving the Navier-Stokes equations p 1093 A93-52006
- LIU, QIANGANG**
A kind of improved flux-split method for solving the Euler equations p 681 A93-33739
- LIU, QIANZHI**
2-D theoretical analysis of circumferential grooved casing treatment p 1066 A93-46501
- LIU, QIZHOU**
Optimum balancing of flexible rotor p 205 A93-14489
- LIU, RIZHI**
The effect of outboard leading-edge bluntness of double-delta wing on its aerodynamic characteristics p 1230 A93-54589
- LIU, S. K.**
Numerical simulation of hypersonic aerodynamics and the computational needs for the design of an aerospace plane [AD-A260681] p 699 N93-25894
Aerospace-plane flights and stratospheric ozone: Review and preliminary assessment of the National Aerospace Plane (NASP) operations [RAND/N-3464-AF] p 755 N93-26327
- LIU, S. X.**
Development and industrial application of the 'all-over-controlled vortex distribution method' for designing radial and mixed flow impellers [ASME PAPER 92-GT-262] p 405 A93-19466
- LIU, SANDY R.**
Acoustic characteristics of advanced model rotor systems p 567 A93-29419
- LIU, SHAIYIN**
Hybrid real-time simulation of a two-rotor engine p 172 A93-14497
A minimum-time acceleration control strategy for a two-rotor aeroengine p 172 A93-14499
- LIU, SONG-LING**
A new method for predicting the end wall boundary layers and the blade force defects inside the passage of axial compressor cascades p 1236 A93-55589
- LIU, SONGLING**
On model for predicting blade force defect in end wall boundary layer inside axial compressor cascade p 862 A93-42271
Numerical analysis of aerodynamic losses in film-cooled vane cascade p 1066 A93-48517
- LIU, SONLING**
Verification of the TOTLOS method for calculating aerodynamic loss in film-cooled turbine cascade p 1087 A93-51191
- LIU, W. K.**
Stochastic computational mechanics for aerospace structures p 78 A93-12157
- LIU, WEI**
Acoustical properties of sound absorbing structures at high temperature p 1172 A93-48522
- LIU, WEIGUO**
Fully automatic FEM data pre-processing for aeronautical electrical machine p 538 A93-24030
- LIU, WEN-TING**
The crack initiation approach for durability analysis p 1259 A93-55585
- LIU, X.**
Calculation of wake-induced unsteady flow in a turbine cascade [ASME PAPER 92-GT-306] p 255 A93-19496
Measurement of unsteady flow and heat transfer in a linear turbine cascade [ASME PAPER 92-GT-323] p 256 A93-19507
- LIU, XIAOFENG**
Experimental study on the mechanism of favourable interferences of body strakes p 121 A93-14405
- LIU, XIAOXIAN**
Experimental and numerical delta wing study at high angles of attack and sideslip [AIAA PAPER 92-2713] p 473 A93-24990
- LIU, XIN**
Aircraft trajectory tracking and prediction [AD-A259039] p 340 N93-18999
- LIU, XU**
A software for optimum design of an aircraft structure p 938 A93-40495
- LIU, YAN**
A digital simulation and its experimental investigation for the response of gas-turbine engines to intake flow distortion p 120 A93-14366

LIU, YONG

LIU, YONG

The experimental investigation of combination effect by using injection effect of aeroengine jet exhaust
p 898 A93-41742

LIU, ZHIMING

The effects of reaction rate constants and catalytic wall on the hypersonic flow field over blunt bodies
p 1230 A93-54586

LIU, ZHIWEI

Prediction of the inception of rotating stall for multistage axial flow compressors p 12 A93-12731
Effect of hub treatment on performance of an axial flow compressor p 53 A93-12736
2-D theoretical analysis of circumferential grooved casing treatment p 1066 A93-48501
Frontally tapered squared trench casing treatment for improvement of compressor performance p 1108 A93-49202

Vectoring jet effects on the flow and aerodynamic behaviors of fighter model p 1241 A93-54590

LIVINGS, JEFFREY

Upgrade Precision Runway Monitor (PRM) Operational Test and Evaluation (OT/E) test plan [DOT/FAA/CT-TN92/13] p 67 N93-11616

LIVNE, E.

Integrated structure/control/aerodynamic synthesis of actively controlled composite wings p 818 A93-37392

LIVNE, ELI

Lessons from application of equivalent plate structural modeling to an HSCT wing [AIAA PAPER 93-1413] p 739 A93-33969
Recent developments in equivalent plate modeling for wing shape optimization [AIAA PAPER 93-1647] p 742 A93-34172
Alternative approximations for integrated control/structure aeroservoelastic synthesis p 819 A93-39418

LIVNEH, R.

Direct multivariable adaptive controller with application to wing flutter p 524 A93-26946

LLANES-SANTIAGO, ORESTES

Dynamic compensator design in nonlinear aerospace systems p 1036 A93-44150

LLANOS, A. S.

Environmental conditions for certification testing of helicopter advanced composite main rotor components p 824 A93-36003

LLINCA, A.

Aircraft model for multicriterial analysis in decision making [AIAA PAPER 92-4192] p 44 A93-13370

LLORENTE, STEVEN

The development and evaluation of advanced Kevlar sandwich structure for application to rotorcraft airframes p 546 A93-27965

LLORENTE, STEVEN G.

Evaluation of thermoplastic stiffened panels for application to rotorcraft airframes p 827 A93-36000
Evaluation of the fatigue behavior of discontinuous and continuous fiber thermoplastic composite laminates p 824 A93-36005

LLOYD, A. R. J. M.

Experiments on low aspect ratio hydroplanes to measure lift under static and dynamic conditions [ARE-TM(UHR)-90306] p 21 N93-11365

LO, C. F.

Adaptive wall wind tunnel with two measured interfaces - Theory and experiment p 679 A93-33717

LO, CHING F.

An integrated knowledge system for wind tunnel testing - Project Engineers' Intelligent Assistant [AIAA PAPER 93-0560] p 377 A93-23297
A wall interference assessment/correction system [NASA-CR-190617] p 68 N93-11910
A wall interference assessment/correction system [NASA-CR-191889] p 296 N93-18384

LOBAO, D. C.

An implicit time-marching procedure for high speed flow [AIAA PAPER 93-3315] p 951 A93-45011

LOCKE, JAMES E.

General aviation aircraft: Normal acceleration data analysis and collection project [DOT/FAA/CT-91/20] p 713 N93-24739

LOCKLEAR, STACY L.

Static tests of jet fuel thermal and oxidative stability p 389 A93-21651

LODIGIANI, G.

Cooling geometry optimization using liquid crystal technique p 902 A93-29939

LOEFFLER, IRVIN J.

In-flight near- and far-field acoustic data measured on the Propan Test Assessment (PTA) testbed and with an adjacent aircraft [NASA-TM-103719] p 852 N93-27058

LOEHNER, RAINALD

TGV tunnel entry simulations using a finite element code with automatic remeshing [AIAA PAPER 93-0890] p 471 A93-24950

Simulation of flow past complex geometries using a parallel implicit incompressible flow solver p 957 A93-45095

Numerical solution of the Euler equations for complex aerodynamic configurations using an edge-based finite element scheme [AIAA PAPER 93-2933] p 1046 A93-48131

Numerical simulation of a blast inside a Boeing 747 [AIAA PAPER 93-3091] p 1099 A93-48265

LOETSCHER, TONY

Operating helicopters in a demanding environment - Mountain flying/high evaluations p 1190 A93-54289

LOEWENTHAL, R.

Hysteresis and bristle stiffening effects of conventional brush seals [AIAA PAPER 93-1996] p 1153 A93-49839

LOEWY, ROBERT G.

Influence of pitch-lag coupling on damping requirements to stabilize 'ground/air resonance' p 158 A93-14784
Smart structures stabilized unstable control surfaces [AIAA PAPER 93-1701] p 712 A93-34223

LOFTUS, P. J.

Improved selective catalytic NOx control technology for compressor station reciprocating engines [PB93-158566] p 755 N93-26529

LOGSDON, KIRK A.

Vibration isolation technology: An executive summary of systems development and demonstration [NASA-TM-105937] p 110 N93-15573

LOGVINOV, A. N.

Inelasticity effect in a unidirectional boron/aluminum composite under uniaxial tension p 825 A93-39024

LOH, C. Y.

A new Lagrangian method for steady supersonic flow computation. II - Slip-line resolution. III - Strong shocks p 243 A93-18655

Computing 3-D steady supersonic flow via a new Lagrangian approach [AIAA PAPER 93-0891] p 471 A93-24951

LOH, ROBERT

Overview of the FAA's differential GPS CAT III technical feasibility demonstration program [AIAA PAPER 93-3836] p 1098 A93-51425

LOHMANN, R. P.

Experimental study of cross flow mixing in cylindrical and rectangular ducts [NASA-CR-187141] p 815 N93-27680

LOHMUELLER, BRUNO L.

Aerospace '92 - The year in review p 455 A93-19976

LOHNER, RAINALD

A parallel implicit incompressible flow solver using unstructured meshes [AD-A263395] p 931 N93-29851

LOHRENTZ, MAURA C.

Digital map databases in support of avionics display systems p 544 A93-26888

LOKAI, N. V.

The use of aviation gas-liquid heat exchangers employing heat pipes p 833 A93-39050

LOKOS, WILLIAM A.

Flight test results from a supercritical mission adaptive wing with smooth variable camber [AIAA PAPER 92-4101] p 38 A93-11274

Flight test results from a supercritical mission adaptive wing with smooth variable camber [NASA-TM-4415] p 49 N93-11863

LOMBARDI, G.

Wing pressure loads in canard configurations - A comparison between numerical results and experimental data p 7 A93-11499

LOMBARDI, GIOVANNI

Experimental study on the aerodynamic effects of a forward-sweep angle p 1094 A93-52434

LONDENBERG, W. K.

Turbulence model evaluation for the prediction of flows over a supercritical airfoil with deflected aileron at high Reynolds number [AIAA PAPER 93-0191] p 276 A93-22615

LONDOT, RONNIE D.

The Meteorological Data Collection and Reporting System - Status and future directions p 428 A93-22133

LONG, CHRISTOPHER A.

Rotational CARS measurements in a rotating cavity with axial throughflow of cooling air: Oxygen concentration measurements [PNR-90935] p 72 N93-11035

LONG, L.

Validation of engineering methods for predicting hypersonic vehicle control forces and moments p 906 A93-41897

LONG, LYLE N.

Prediction of forces and moments for hypersonic flight vehicle control effectors [NASA-CR-193033] p 728 N93-24762

LONG, MARY JO

Experimental investigation of an ejector-powered free-jet facility [NASA-TM-105868] p 291 N93-16704

LONG, QIHAO

YIDOYU and its application to aircraft design [AD-A259262] p 513 N93-20605

LONGO, J. M. A.

Computation of flows over 2D ramps p 866 A93-42595
Computation of the hypersonic flow over a double ellipsoid p 868 A93-42610

LONGOBARDI, R.

EH 101 ship interface trials p 796 A93-35954

LONGVAL, J. R.

Experimental investigation of flows behind different Large-Eddy Breakup (LEBU) devices in thick boundary layers p 18 N93-10550

LOO, Y.-W.

Application of differential quadrature to the analysis of static aeroelastic phenomena [AIAA PAPER 93-1505] p 711 A93-34044

LOOIJ, C. E. W.

Fractographic and microstructural analysis of fatigue crack growth in Ti-6Al-4V fan disc forgings p 1004 N93-31742

Low cycle fatigue behaviour of titanium disc alloys p 1004 N93-31745

Low cycle fatigue behaviour of titanium disc alloys [NLR-TP-91346-U] p 1006 N93-32372

LOOMIS, PETER V.

System analysis for a kinematic positioning system based on the global positioning system [AD-A262830] p 885 N93-29468

LOPES, KEVIN

A second-generation high speed civil transport: Stingray [NASA-CR-192022] p 336 N93-18059

LOPEZ JUSTE, G.

Control of contaminants in gas turbines with variable-flow combustion chambers and hydrogen addition p 520 A93-27478

LOPEZ-FERNANDEZ, P. A.

Computations and experiments for a multiple normal shock/boundary-layer interaction p 688 A93-34486

LOPEZ, ALFRED R.

GPS autoland considerations p 792 A93-38203

LORAUD, J. C.

A comparison between centered and upwind schemes for two-phase compressible flows [AIAA PAPER 93-2346] p 1083 A93-50120

LORBER, PETER F.

Blade-vortex interaction data obtained from a pressure-instrumented model rotor at the DNW p 568 A93-29430

Prediction of BVI noise patterns and correlation with wake interaction locations p 849 A93-35966

Dynamic stall of sinusoidally oscillating three-dimensional swept and unswept wings in compressible flow p 766 A93-35995

Tip vortex, stall vortex, and separation observations on pitching three-dimensional wings [AIAA PAPER 93-2972] p 1049 A93-48166

Unsteady transition measurements on a pitching three-dimensional wing p 820 N93-27450

LOREN, J. R.

Design for global competition - The Boeing 777 [AIAA PAPER 92-4190] p 2 A93-13368

LORENCE, CHRISTOPHER B.

Calculation of three-dimensional unsteady flows in turbomachinery using the linearized harmonic Euler equations [ASME PAPER 92-GT-136] p 249 A93-19368

Nonreflecting boundary conditions for linearized unsteady aerodynamic calculations [AIAA PAPER 93-0882] p 475 A93-25553

LORENZO, CARL F.

Screening studies of advanced control concepts for airbreathing engines [AIAA PAPER 92-3320] p 1108 A93-49329

Advanced instrumentation for next-generation aerospace propulsion control systems [AIAA PAPER 93-2079] p 1154 A93-49906

Screening studies of advanced control concepts for airbreathing engines [NASA-TM-106042] p 721 N93-25079

LORSBACH, G.

Correlation of X-ray CT measurements to shear strength in pultruded composite materials p 396 A93-18618

LOSCHKE, R. C.

Flight management system on the F-117A p 908 A93-42815

- LOSFELD, G.**
Testing techniques for straight transonic and supersonic cascades
[ONERA, TP NO. 1992-155] p 773 A93-38734
- LOTFULLIN, M. V.**
Modeling of interfaces in problems of flow of a ponderable fluid past a wing profile p 124 A93-15189
Determination of the shape of a wing profile in boundary layer flow with a given velocity diagram p 1067 A93-48844
- LOTSMANOV, G. S.**
Justification for the linear recording of fatigue damage summation for aircraft structures under operating conditions p 320 A93-18331
- LOTT, DENNIS A.**
Analysis of in-flight structural failures of P-3C wing leading edge segments
[AD-A256212] p 165 N93-15238
- LOTTATI, I.**
A propulsion device driven by reflected shock waves p 1001 A93-45550
- LOTTER, K. W.**
A novel-high-performance system for recording and analysing instantaneous total pressure distortion in air intakes p 214 N93-13215
- LOTTE, P.**
Axial flow compressors - Mechanical design trends
[ISABE 93-7061] p 1199 A93-54037
- LOTTIG, ROY A.**
Development and use of hydrogen-air torches in an altitude facility
[AIAA PAPER 93-2176] p 1137 A93-49988
- LOTTS, CHRISTINE G.**
An analytically designed subcomponent test to reproduce the failure of a composite wing box beam
[AIAA PAPER 93-1344] p 709 A93-33914
- LOU, GENLIANG**
A new type of fuel control model p 1108 A93-49204
- LOU, Y.**
JPL AIRSAR processing activities and developments p 1162 A93-47865
- LOUCHEZ, P. R.**
Experimental evaluation of flat plate boundary layer growth over an anti-icing fluid film p 1140 A93-52645
- LOUCHEZ, PATRICK**
Aircraft take-off laboratory simulation for de/anti-icing study p 528 A93-23840
- LOUDIN, JEFFREY A.**
Optical correlator field test results p 1038 A93-44458
- LOUGHER, WAYNE**
Preparation and characterization of continuous fiber reinforced zirconium diboride matrix composites for a leading edge material p 1211 A93-53445
- LOUIE, KEN**
Mathematical problems in inviscid hypersonic flow p 131 N93-13451
- LOUNSBURY, RICHARD J.**
An unstructured grid flow solver for turbomachinery flows
[AIAA PAPER 93-1913] p 1076 A93-49780
- LOUW, WILLEN J.**
Life cycle assessment of an impingement-cooled gas turbine blade
[AIAA PAPER 92-4716] p 358 A93-20321
- LOVATO, J. A.**
Active control of the shear layer on a static airfoil
[AIAA PAPER 93-0442] p 286 A93-23353
- LOVE, WENDELL**
Arc jet testing in NASA Ames Research Center thermophysics facilities
[AIAA PAPER 92-5041] p 385 A93-22315
- LOVE, WENDELL L.**
Evaluation of 2D ceramic matrix composites in aeroconvective environments p 1212 A93-53459
- LOVELL, T. A.**
A comparative study of multivariable robustness analysis methods as applied to integrated flight and propulsion control
[AIAA PAPER 93-3809] p 1102 A93-51401
- LOVELL, T. ALAN**
Development of a non-linear simulation for generic hypersonic vehicles - ASUHS1
[NASA-CR-192710] p 516 N93-22003
- LOVENGUTH, MARC A.**
Conceptual assessment of two high-speed rotorcraft p 508 A93-28612
- LOVERN, MICHAEL**
Uplink laser propagation measurements through the sea surface, haze and clouds
[AD-A264687] p 935 N93-30553
- LOVIAGIN, ALEKSANDR F.**
A practical course in aircraft maintenance. I - The powerplant p 811 A93-39175
- LOW, EICHER**
Design of flight control systems to meet rotorcraft handling qualities specifications p 370 A93-23509
- LOWDEN, P.**
Powder metallurgy repair of turbine components
[ASME PAPER 92-GT-312] p 354 A93-19500
- LOWER, MARK**
Flying qualities of a remotely piloted vehicle
[AIAA PAPER 92-4083] p 61 A93-11266
- LOWSON, M. V.**
Theoretical modelling of rotor noise radiation p 566 A93-29407
- LOZANO, MARTIN E.**
Aircraft cryogenic fuel system design issues
[AIAA PAPER 93-2567] p 1121 A93-50285
- LU, BIAO**
Investigation of the characteristics of 3-dimensional separated flow in an annular compressor blade row with large angles of attack p 259 A93-20116
- LU, BOYING**
A new aircraft integrated positioning and communication system based on satellite p 150 A93-14236
- LU, C. M.**
Modelling three-dimensional gas-turbine-combustor model flow using second-moment closure
[AIAA PAPER 93-3104] p 1149 A93-48277
- LU, C. Q.**
Variable structure controller design and its real-time analysis for microprocessor-based flight control systems p 181 A93-14229
- LU, FRANK K.**
Hypersonic turbulent expansion-corner flow with shock impingement
[AIAA PAPER 92-5101] p 274 A93-22371
Damping of surface pressure fluctuations in hypersonic turbulent flow past expansion corners p 860 A93-41914
Hypersonic, turbulent viscous interaction past an expansion corner
[AIAA PAPER 93-2985] p 1051 A93-48178
Exploratory study of shock reflection near an expansion corner
[AIAA PAPER 93-3132] p 1063 A93-48297
- LU, GANG**
Statistical quality control for kinematic GPS positioning p 314 A93-21162
Fully automatic FEM data pre-processing for aeronautical electrical machine p 538 A93-24030
- LU, GANYU**
Inviscid instability of a skewed compressible mixing layer p 769 A93-37941
- LU, JIAN**
Fine control of Mach number in subsonic wind tunnel p 375 A93-20808
- LU, L.**
Low leakage fiber metal seals
[ASME PAPER 92-GT-141] p 402 A93-19373
- LU, P.**
The numerical errors in inverse simulation
[AIAA PAPER 93-3588] p 1223 A93-52681
- LU, PING**
Closed form solutions of constrained trajectories - Application in optimal ascent of aerospace plane
[AIAA PAPER 92-5012] p 385 A93-22288
Nonsmooth trajectory optimization - An approach using continuous simulated annealing
[AIAA PAPER 93-3657] p 1099 A93-48337
Analytical solutions to constrained hypersonic flight trajectories p 1141 A93-49596
A new technique for nonlinear control of aircraft
[AIAA PAPER 93-3881] p 1135 A93-51466
Analytical solutions to constrained hypersonic flight trajectories
[NASA-CR-191987] p 297 N93-18602
Trajectory optimization for the National aerospace plane
[NASA-CR-192954] p 716 N93-25670
- LU, PONG-JEU**
Optimal control law synthesis for flutter suppression using active acoustic excitations p 370 A93-23516
Transonic flutter suppression using active acoustic excitations
[AIAA PAPER 93-3285] p 969 A93-46841
- LU, SHUQUAN**
TDLM: A Transonic Doublet Lattice Method for 3D potential unsteady transonic flow calculation
[DLR-FB-92-25] p 988 N93-31171
- LU, T.**
Explosives detection systems for airport security gas chromatographic based devices p 881 N93-30276
- LU, WEN**
A multi-functional computer-aided aircraft exterior shape modelling prototype system p 504 A93-24032
- LU, Z. J.**
Application issues of fiber optic sensors in aircraft structures p 410 A93-21094
- LU, ZHIYONG**
The forms of unsteady concentrated vortex-breakdown and its reactions to disturbance p 1231 A93-54594
- LUA, Y. J.**
Stochastic computational mechanics for aerospace structures p 78 A93-12157
- LUAH, M. H.**
Analysis of complicated plates by a nine-node spline plate element p 206 A93-14616
- LUBENETS, V. P.**
New corrosion resistant nickel-base super-alloys and technological processes of casting gas turbines parts with directional single crystal and regulable equiaxed minimized microporosity structure p 916 A93-40811
- LUBNER, MAXINE ESTA**
Aviation accidents, incidents, and violations: Psychological predictors among US pilots p 144 N93-14693
- LUBOMSKI, JOSEPH F.**
Vibration isolation technology: An executive summary of systems development and demonstration
[NASA-TM-105937] p 110 N93-15573
- LUC, A.**
CFD analysis of hypersonic chemically reacting flowfields around a generic shape
[AIAA PAPER 93-0323] p 281 A93-23015
- LUCCHETTO, L. A.**
Environmental conditions for certification testing of helicopter advanced composite main rotor components p 824 A93-36003
- LUCE, ANNE-SOPHIE**
Experimental results on RIAS digital beamforming radar p 929 A93-43392
- LUCERO, E. F.**
Overview of technical challenges of reentry analysis of radioisotope heat sources
[AIAA PAPER 93-0379] p 386 A93-23059
- LUCHEV, OLEG A.**
Steady state model for the thermal regimes of shells of airships and hot air balloons p 207 A93-15072
- LUCHINI, P.**
Compressible flow in a hovercraft air cushion p 480 A93-29316
- LUCIUS, GERALD A.**
Thrust vectoring control from underexpanded asymmetric nozzles
[AIAA PAPER 93-3261] p 968 A93-46827
Side force augmentation at high angle of attack from pneumatic vortex flow control
[AIAA PAPER 93-2959] p 1124 A93-48153
- LUCJANEK, WIESLAW**
Problems in the modeling of helicopter flight p 506 A93-27293
- LUCKEMEYER, JAMES A.**
Robotic inspection and refurbishment of aircraft canopy transparencies
[SME PAPER AD92-203] p 855 A93-40665
- LUCKRING, JAMES M.**
Multiblock Navier-Stokes solutions about the F/A-18 wing-LEX-fuselage configuration p 767 A93-37378
- LUDWIG, DON E.**
The Canadian Automated Air Traffic System p 886 N93-30323
- LUDWIG, F. L.**
A microcomputer program for estimating low altitude wind and turbulence fields p 438 A93-22163
- LUECKING, P.**
A European collaborative NLF nacelle flight demonstrator
[PNR-90992] p 20 N93-11113
- LUEHMANN, W. A.**
Aerothermal ablative characterization of selected external insulator candidates
[AIAA PAPER 93-1857] p 1145 A93-49735
- LUHUA, J.**
Review and prospect of Chinese scientific balloon activities p 1 A93-11368
- LUK, W. S.**
Rapid prototyping via automatic software code generation from formal specifications - A case study p 227 A93-14685
- LUK'YANOV, V. V.**
Half-scale modeling experience in the testing of radio navigation and landing systems p 882 A93-43112
- LUKACHEV, S. V.**
The possibility of reducing the emission of benzo(a)pyrene with the exhaust gases of aviation gas turbine engines by water injection into the combustion chamber p 812 A93-39201
- LUKHTURA, F. I.**
A one-dimensional theory for supersonic gas jets above the critical pressure p 774 A93-39115
- LUKOWICZ, HENRYK**
Modelling of the flow in the blade-ring design process of turbomachinery p 520 A93-27291

- LUM, BEN T. F.**
Strategic avionics technology definition studies. Subtask 3-1A: Electrical Actuation (ELA) systems
[NASA-CR-193237] p 914 A93-29215
- LUMLEY, JOHN L.**
A realizable Reynolds stress algebraic equation model
[NASA-TM-105993] p 290 A93-16596
- LUMPKIN, FORREST E., III**
Comparison of continuum and particle simulations of expanding rarefied flows
[AIAA PAPER 93-0728] p 466 A93-24818
- LUMSDEN, R. B.**
A review of alternative philosophies
p 142 A93-17305
- LUNA, GUILHERME C.**
Nozzle flow computations using the Euler equations
p 112 A93-14170
- LUNDBERG, W. R.**
Evaluation of three models used for predicting noise propagated long distances overground
[AD-A255963] p 232 A93-14406
- LUNDER, JOSEPH**
FAA Technical Center Aeronautical Data Link Research Plan
[DOT/FAA/CT-92/23] p 417 A93-15698
- LUNDERSTADT, R.**
Some experiments and ideas on GPA before reaching steady state of engine
p 178 A93-15175
- LUNDGREN, ROGER**
Studies of fuel-rich magnesium propellants in a small solid fuel ramjet combustor
p 535 A93-27759
- LUNDQUIST, DAVID L.**
LONGBOW - Force multiplier for continuous operations
p 1175 A93-54295
- LUNEV, VLADIMIR V.**
Abnormal peaks of increased heat-transfer on the blunt delta wing in the hypersonic flow
[AIAA PAPER 93-3129] p 1063 A93-48294
- LUNN, KEN**
V-22 tiltrotor Flight Test Development
p 800 A93-36021
- LUNNON, R. W.**
Optimization of time saving in navigation through an area of variable flow
p 34 A93-12125
Numerical forecasting of liquid water content to assess airframe icing risk
p 429 A93-22147
Short range forecasts for air traffic control using high resolution aircraft data
p 431 A93-22164
- LUO, BIAO**
A study on low level windshear hazard index
p 1240 A93-55414
- LUO, CHUNRONG**
New derivation of relationship between Mach angle and Mach number
p 1086 A93-51190
- LUO, HONG**
Numerical solution of the Euler equations for complex aerodynamic configurations using an edge-based finite element scheme
[AIAA PAPER 93-2933] p 1046 A93-48131
Numerical simulation of a blast inside a Boeing 747
[AIAA PAPER 93-3091] p 1099 A93-48265
- LUO, J.**
Navier-Stokes analysis of turbine flowfield and external heat transfer
[ISABE 93-7075] p 1186 A93-54051
- LUONG, PHU V.**
Solution-adaptive and quality-enhancing grid generation
p 480 A93-28610
- LUONG, PHU VINH**
Adaptive EAGLE dynamic solution adaptation and grid quality enhancement
p 788 A93-27464
- LUPAL, A. M.**
Software support for a computerized air situation documentation system
p 941 A93-43115
- LUPASH, LAWRENCE**
On the selection of a GPS validity indicator for aircraft navigation in the National Airspace System (NAS)
p 316 A93-21186
- LURAU, ISABELLE**
Compact heat exchanger fitted to engines of the inverted type
[ISABE 93-7120] p 1221 A93-54095
- LUSCHER, A. F.**
Design for manufacture by resin transfer molding of composite parts for rotorcraft
[SME PAPER EM93-103] p 1159 A93-51733
- LUSHIN, V. N.**
Acoustic control of flow separation on a straight and a yawed wing
p 125 A93-15256
Flow past a finite-span wing in the presence of external acoustic loading
p 127 A93-16707
- LUTTER, G. L.**
Solving problems with singularities using conformal mappings
p 397 A93-18978
- LUTTGES, MARVIN W.**
Aerodynamic foundations for use of unsteady aerodynamic effects in flight control
[AIAA PAPER 93-0188] p 276 A93-22613
Neural network prediction of three-dimensional unsteady separated flow fields
[AIAA PAPER 93-3426] p 977 A93-47221
- LUTZE, F. H.**
Development of lateral-directional departure criteria
[AIAA PAPER 93-3650] p 1128 A93-48333
Quasi-optimal steady state and transient maneuvers with and without thrust vectoring
[AIAA PAPER 93-3778] p 1132 A93-51373
- LUTZE, FREDERICK H.**
Kinematics and aerodynamics of the velocity vector roll
[AIAA PAPER 93-3625] p 1126 A93-48310
- LUU, T. S.**
Inverse problem using S2-S1 approach for the design of the turbomachine with splitter blades
p 971 A93-46929
- LUX, PETER**
Increased safety through knowledge-based pilot assistance
p 518 A93-27499
- LY, UY-LOI**
Optimal discrete-time dynamic output-feedback design - A w-domain approach
p 757 A93-34536
- LYALL, ELIZABETH A.**
Taxonomy of flight variables
p 147 A93-15022
- LYAPUNOV, S. V.**
Nonplanar wings with a minimum induced drag
p 1089 A93-51779
- LYMAN, F. A.**
On the conservation of rothalpy in turbomachines
[ASME PAPER 92-GT-217] p 252 A93-19439
- LYMBERPOULOS, N.**
Adaptation of a 3-D pressure correction Navier-Stokes solver for the accurate modelling of tip clearance flows
p 971 A93-46932
- LYNCH, F. T.**
A CFD-based design strategy for advanced transonic wing concepts with practical ramifications for subsonic transports
[AIAA PAPER 93-2946] p 1047 A93-48143
- LYNN, ROBERT R.**
The rebirth of the tiltrotor - The 1992 Alexander A. Nikolsky Lecture
p 712 A93-34256
- LYON, ERVIN F.**
The application of automatic surface lights to improve airport safety
p 821 A93-37069
- LYON, J. F.**
Aerothermal ablative characterization of selected external insulator candidates
[AIAA PAPER 93-1857] p 1145 A93-49735
- LYRINTZIS, A. S.**
The design of optimized airfoils in subcritical flow
[AIAA PAPER 93-0532] p 285 A93-23273
Noise reduction for transonic blade-vortex interactions
p 566 A93-29408
Transonic blade-vortex interactions - Noise reduction
p 850 A93-37396
- LYRINTZIS, C. S.**
Dynamics of skin-stringer panels using modified wave methods
p 206 A93-14561
Dynamic analysis of multiple row fuselage stiffened structures
[AIAA PAPER 93-1438] p 710 A93-33987
- LYRINTZIS, CONSTANTINOS S.**
Noise transmission of skin-stringer panels using a decaying wave method
p 943 A93-41929
- LYTLE, CARROLL D.**
Research requirements for a real-time flight measurements and data analysis system for subsonic transport high-lift research
p 1244 A93-54391
- LYTTON, R.**
Micro mechanical behavior of pavements
p 379 A93-16312
- M**
- MA, CAIFEN**
Experimental investigation on effect of solid particles on blade pressure distribution in compressor cascade flow
p 1066 A93-48513
Experimental investigation of effect of particles on blade pressure distribution in impulse cascade flow
p 1236 A93-55398
- MA, H. Y.**
Vortex capture by a two-dimensional airfoil with a small oscillating leading-edge flap
[AIAA PAPER 93-3266] p 968 A93-46830
- MA, HAN-DONG**
Numerical study of supersonic flow over a backward step with transverse injection
p 1182 A93-53853
- MA, TIEYOU**
Euler solutions simulating strong shock waves and vortex phenomena over 3D wings
p 121 A93-14392
- MA, XIA**
Viscous-inviscid interaction coupled calculation of three-dimensional turbulent separated flow over dents
p 681 A93-33748
- MA, XIA L.**
Remote sensing cloud properties from high spectral resolution infrared observations
p 1034 A93-46780
- MA, XIAO-JUN**
Investigation of cabin noise reduction in the Y12
p 41 A93-11816
Investigation of cabin noise reduction in the Y12
p 506 A93-27371
- MA, YAN-WEN**
Numerical study of supersonic flow over a backward step with transverse injection
p 1182 A93-53853
- MA, Z. E.**
Stochastic modeling and adaptive control algorithm of brake bending
p 227 A93-14417
- MAAS, U.**
Simulation of nonequilibrium hypersonic flows
p 863 A93-42443
- MABEY, D. G.**
Review of the normal force fluctuations of aerofoils with separated flow
p 10 A93-12317
A semi-empirical theory of the noise in slotted tunnels caused by diffuser suction
p 231 A93-14353
The suppression of single-fin buffeting using tangential leading edge blowing on a delta wing
p 270 A93-21677
A summary of further measurements of steady and oscillatory pressures on a rectangular wing
p 1096 A93-52594
Further noise measurements in a slotted cryogenic wind tunnel
[RAE-TM-AERO-2201] p 101 A93-10805
Further buffeting tests in a cryogenic wind tunnel
[NASA-TM-107621] p 22 A93-11610
- MABEY, DENNIS G.**
Comment on 'In-flight measurement of static pressures'
p 807 A93-37407
- MACANDER, ALEKSANDER B.**
Mass loaded composite rotor for vibro-acoustic application
[AD-D015604] p 535 A93-20016
- MACARAEG, M. G.**
Transition in supersonic flow past axisymmetric bodies
p 967 A93-46817
- MACARTHUR, C. D.**
The USAF Advanced Turbine Aerothermal Research Rig (ATARR)
p 911 A93-29945
- MACCALLUM, N. R. L.**
Improving dynamic response of a single-spool gas turbine engine using a nonlinear controller
[ASME PAPER 92-GT-392] p 355 A93-19546
- MACCI, S. H. M.**
The aerodynamic and structural design of a variable camber wing (VCW)
p 117 A93-14291
- MACCORMAC, J. K. M.**
Automatic guidance and control for recovery of remotely piloted vehicles
p 181 A93-14188
- MACCORMACK, ROBERT W.**
Stabilization of the Burnett equations and application to hypersonic flows
p 778 A93-39410
A perspective on a quarter century of CFD research
[AIAA PAPER 93-3291] p 1021 A93-44995
Viscous hypersonic shock-shock interaction on a blunt body at high altitude
[AIAA PAPER 93-2722] p 962 A93-46477
- MACEY, I. D.**
Measurements of SSR bearing errors due to site obstructions
p 883 A93-43407
- MACHA, J. M.**
A simple, approximate model of parachute inflation
[AIAA PAPER 93-1206] p 702 A93-35157
A simple, approximate model of parachute inflation
[DE93-002465] p 694 A93-25121
- MACHIDA, SHIGERU**
The methods of reducing impact loads on occupants in the civil aircraft crash condition
p 140 A93-14220
- MACKALL, DALE A.**
Flight research simulation takes off
p 1192 A93-53769
- MACKENZIE, BEN**
1992 - The year of the radome?
p 209 A93-15525
- MACKENZIE, FRANKLIN D.**
Merger and acquisition - Enhancing Loran propagation technology with artificial intelligence
p 29 A93-10987
- MACKINNON, A. V.**
The aerodynamic and structural design of a variable camber wing (VCW)
p 117 A93-14291
- MACKINTOSH, G. B.**
Uncertainty assessments for engine thrust derived from two methods
p 1254 A93-54392

- MACKLEY, ERNEST A.**
Review of NASA's Hypersonic Research Engine Project
[AIAA PAPER 93-2323] p 1116 A93-50103
- MACKRODT, P.-A.**
Comparative performance tests of a pitot-inlet in several European wind-tunnels at subsonic and supersonic speeds p 130 N93-13221
- MACLEAN, DAVID N.**
Analog simulation as part of a power supply design analysis universal platform p 543 A93-25962
- MACLEAN, MALCOLM K.**
Static internal performance tests of single expansion ramp nozzle concepts designed with LO considerations [AIAA PAPER 93-2429] p 1117 A93-50185
Scale model test results for several spherical/two-dimensional nozzle concepts [AIAA PAPER 93-2430] p 1117 A93-50186
- MACLEOD, J. D.**
Influence of a thermal barrier coating on the performance of a turbo-prop engine [ASME PAPER 92-GT-38] p 347 A93-19297
Implementation of an infrared thermal imaging system to measure temperature in a gas turbine engine [AIAA PAPER 93-2469] p 1120 A93-50215
- MACLEOD, K. J.**
Impact of weather on aviation - A global view p 308 A93-22143
- MACPHAIL, D. C.**
Machinery arrangements for small VTOL transport aircraft p 713 A93-34848
- MACPHERSON, J. I.**
Spatial and temporal variations of the fluxes of carbon dioxide and sensible and latent heat over the FIFE site p 425 A93-20586
- MACQUISTEN, M. A.**
Low-frequency combustion oscillations in a model afterburner p 1193 A93-53702
- MADAVAN, N. K.**
Multipassage three-dimensional Navier-Stokes simulation of turbine rotor-stator interaction p 688 A93-34484
- MADAVAN, NATERI K.**
A hybrid structured-unstructured grid method for unsteady turbomachinery flow computations [AIAA PAPER 93-0387] p 282 A93-23066
A solution-adaptive hybrid-grid method for the unsteady analysis of turbomachinery [AIAA PAPER 93-3015] p 1148 A93-48204
Unsteady, three-dimensional, Navier-Stokes simulations of multistage turbomachinery flows [AIAA PAPER 93-1979] p 1153 A93-49826
- MADDALON, D. V.**
Laminar flow flight experiments - A review p 890 A93-41778
- MADDALON, DAL V.**
Method of measuring cross-flow vortices by use of an array of hot-film sensors [NASA-CASE-LAR-14824-1-SB] p 751 N93-26000
- MADSEN, JOHN F., III**
Optimum design of high speed prop rotors including the coupling of performance, aeroelastic stability and structures p 337 N93-18066
- MADSEN, T. J.**
Mixing enhancement and combustion of gaseous fuel in a supersonic combustor [AIAA PAPER 93-2143] p 1114 A93-49960
- MADDUX, GENE E.**
Video holography and laser vibrometry...The dynamic duo p 210 A93-16611
- MADER, G. L.**
Multiple receiver, zero-length baseline kinematic GPS positioning techniques for airborne gravity measurement p 1240 A93-55974
- MADHURANATH, PADMA**
Estimation of neutral and maneuver points of aircraft by dynamic maneuvers [AIAA PAPER 93-3620] p 1126 A93-48307
- MADISON, T. J.**
Optical technologies for UV remote sensing instruments p 853 N93-28788
- MADIWALE, APPA**
Weather information requirements for Terminal Air Traffic Control Automation p 429 A93-22146
- MADORE, A.**
Validation of electromagnetic-topology concepts on a complex structure [ONERA, TP NO. 1992-63] p 542 A93-25327
- MAEKAWA, S.**
Aerodynamic heating phenomenon in three dimensional shock wave/turbulent boundary layer interaction induced by sweptback fins in hypersonic flows p 960 A93-45507
- MAEKAWA, SHOJI**
The structure and material testing facility needed for future SST/HST development [AIAA PAPER 92-3887] p 528 A93-24481
- MAEKAWA, SHOZO**
Two-dimensional and three-dimensional mixing flow structures with injected through slotted nozzle and circular nozzle into supersonic flows [ISABE 93-7117] p 1221 A93-54092
- MAEKAWA, SYOZO**
A study on three-dimensional shock wave/turbulent boundary layer interaction induced by sweptback sharp fins at supersonic flow p 684 A93-34274
The experimental study of the effect of sweptback angles and the front shape of the fin on reduction of shock wave/turbulent boundary layer interaction region p 858 A93-40431
Intense studies on unsteady secondary separations and oscillating shock waves in three-dimensional shock waves/turbulent boundary layer interaction regions induced by sharp and blunt fins [AIAA PAPER 93-2939] p 1046 A93-48137
- MAESTRELLO, LUCIO**
Nonlinear vibration and radiation from a panel with transition to chaos p 205 A93-14543
On the coupling between a supersonic boundary layer and a flexible surface p 243 A93-19132
Nonlinear vibration and radiation from a panel with transition to chaos induced by acoustic waves p 398 A93-19173
- MAFFIOLI, GIANCARLO**
Design and manufacturing concepts of Eurofar Model No. 2 blades p 798 A93-35883
- MAGALDI, RICK**
Knowledge based systems and avionics equipment failure diagnosis p 238 A93-18765
- MAGARI, P. J.**
Measurement of turbulent spots and intermittency modelling at gas-turbine conditions p 902 N93-29934
- MAGERL, CHRISTIAN**
Effects of air traffic on nature and environment in the neighborhood of airports by example of the Munich 2 Airport (Germany) p 1035 N93-31932
- MAGGIO, R.**
Water tunnel studies of inlet/airframe interference phenomena p 215 N93-13216
- MAGILL, J.**
Application of analog computing to real-time simulation of stall and surge dynamics [AIAA PAPER 93-2231] p 1080 A93-50037
- MAGISO, A. H.**
Repair of a severely damaged composite fuel pod p 508 A93-27966
- MAGNESS, C.**
Instantaneous topology of the unsteady leading-edge vortex at high angle of attack p 961 A93-45728
- MAGNUSON, RONALD A.**
V-22 tiltrotor Flight Test Development p 800 A93-36021
- MAGRE, P.**
CARS temperature measurements in combustion [ONERA, TP NO. 1993-78] p 1212 A93-53599
- MAHABIR, WINSTON**
Methods of economic evaluation - Forecasting critique [AIAA PAPER 92-4285] p 570 A93-24300
- MAHAJAN, APARAJIT J.**
An efficient procedure for cascade aeroelastic stability determination using nonlinear, time-marching aerodynamic solvers [AIAA PAPER 93-1631] p 719 A93-34159
An iterative multidisciplinary analysis for rotor blade shape determination [AIAA PAPER 93-2085] p 1114 A93-49912
- MAHON, J.**
Consolidation of graphite thermoplastic textile preforms for primary aircraft structure p 919 N93-30439
- MAHOOD, DAVID B.**
Explosive detection system based on Electronic Neutron Generator (ENG) p 497 N93-21870
- MAHRENHOLZ, BOB G.**
Improved flow measurement with simultaneous period/frequency recording p 1254 A93-54381
- MAHULIKAR, SHRIPAD P.**
Philosophical approach to the basic understanding of the mechanics of jet propulsion [SAE PAPER 920960] p 173 A93-14626
Prediction of engine casing temperature of fighter aircraft for infrared signature studies [SAE PAPER 920961] p 206 A93-14627
- MAIER, LAUNA M.**
Joint NASA/USAF Airborne Field Mill Program - Operation and safety considerations during flights of a Lear 28 airplane in adverse weather [AIAA PAPER 92-4093] p 93 A93-13262
- MAIER, MATTHEW R.**
Standardization of precipitation static test methods and equipment for the Navy [AD-A257025] p 165 N93-15361
- MAIER, THOMAS H.**
An investigation of helicopter rotor blade flap vibratory loads p 796 A93-35975
- MAIGNAN, GEORGES**
Future systems for air traffic control p 150 A93-15052
- MAINE, TRINDEL**
Flight testing and simulation of an F-15 airplane using throttles for flight control [AIAA PAPER 92-4109] p 39 A93-11278
- MAINE, TRINDEL A.**
Preliminary flight test results of a fly-by-throttle emergency flight control system on an F-15 airplane [AIAA PAPER 93-1820] p 1100 A93-49708
- MAINGRE, E.**
Optimization of afterbodies and engine nozzle by using CFD methods [ISABE 93-7098] p 1187 A93-54074
- MAJIDZADEH, K.**
State of the art review of rutting and cracking in pavements p 380 N93-16316
- MAJIZADEH, K.**
Federal Aviation Administration pavement modeling p 379 N93-16315
- MAKAROV, L. N.**
Effect of the aerodynamic interference of the rotor and the fuselage on the power requirements for the horizontal flight of a helicopter p 819 A93-39179
Calculation of the position of the flow separation line in an analog model of flow past a body p 1176 A93-52958
- MAKEVET, E.**
Damage tolerance assessment and usage variation analysis for C-130 aircraft in the Israeli Air Force p 839 N93-27210
- MAKI, M. C.**
Future directions in aviation security p 880 N93-30274
- MAKLAKOV, D. V.**
Determination of the shape of a wing profile in boundary layer flow with a given velocity diagram p 1067 A93-48844
- MAKLASHKIN, S. V.**
Calculation of the parameters of a crane helicopter with one disabled engine p 366 A93-18381
- MAL'CHEVSKI, V. V.**
Structure of a knowledge base used in the computerized synthesis of aircraft layout p 891 A93-42373
- MALTSEV, A. A.**
Modeling of human operator actions in the stochastic trajectory tracking problem for a dynamic plant p 228 A93-16783
- MALATERRE, P.**
Long-duration balloon flights in the middle stratosphere p 40 A93-11369
- MALCHOW, HARVEY L.**
Evaluation of some significant issues affecting trajectory and control management for air-breathing hypersonic vehicles [AIAA PAPER 92-5011] p 384 A93-22287
Air-breathing hypersonic vehicle guidance and control studies: An integrated trajectory/control analysis methodology, phase 2 [NASA-CR-189703] p 65 N93-12413
- MALCOLM, GERALD N.**
Experimental and numerical analysis of the wing rock characteristics of a 'wing-body-tail' configuration [AIAA PAPER 93-0187] p 368 A93-22612
Forebody vortex control with jet and slot blowing on an F/A-18 [AIAA PAPER 93-3449] p 1009 A93-47235
Forebody vortex control on an F/A-18 using small, rotatable 'tip-strokes' [AIAA PAPER 93-3450] p 1009 A93-47236
Forebody vortex control - A progress review [AIAA PAPER 93-3540] p 986 A93-47292
- MALDONADO, MIGUEL A.**
A new resonant link aircraft power generating system p 809 A93-36268
- MALEEV, A. F.**
Dynamic processes in the powerplants and power-generating equipment of flight vehicles p 832 A93-39027
- MALIK, M. R.**
Transition studies for swept wing flows using PSE [AIAA PAPER 93-0077] p 263 A93-20189
Linear stability of three-dimensional boundary layers - Effects of curvature and non-parallelism [AIAA PAPER 93-0079] p 263 A93-20191
Instability and transition in three-dimensional supersonic boundary layers [AIAA PAPER 92-5049] p 273 A93-22321

- Transition in supersonic flow past axisymmetric bodies
p 967 A93-46817
- Transition correlation in subsonic flow over a flat plate
p 1178 A93-53231
- MALISKA, C. R.**
Code validation for high speed flow simulation over the VLS launcher fairing
[AIAA PAPER 93-3046] p 1057 A93-48226
- MALLEN, F.**
Mechanisms of sound generation in subsonic jets
p 101 N93-10688
- MALLET, M.**
A synthesis of results on the calculation of flow over a 2D ramp and a 3D obstacle - Antibes test cases 3 and 4
p 867 A93-42601
- Contribution to Problem 6 using an upwind Euler solver with unstructured meshes
p 869 A93-42627
- MALLET, MICHEL**
Validation of aerodynamic simulation methods for Hermes spaceplane and future hypersonic vehicles
[AIAA PAPER 92-5065] p 273 A93-22335
- The European Data Base - A new CFD validation tool for the design of space vehicles
[AIAA PAPER 93-3045] p 1057 A93-48225
- MALLOY, DONALD J.**
Improved data validation and quality assurance in turbine engine test facilities
[AIAA PAPER 93-2178] p 1137 A93-49990
- MALMBORG, ERIC W.**
Design vector parallelization to speedup the structural optimization process
[AIAA PAPER 92-4834] p 436 A93-20411
- MALMUTH, N. D.**
Asymptotic methods for the prediction of transonic wind-tunnel wall interference
p 730 A93-35625
- MALOBABIC, M.**
Performance simulation of a combustion engine charged by a variable geometry turbocharger. I - Prerequisites, boundary conditions and model development. II - Simulation algorithm, computed results
p 1256 A93-54648
- MALONE, BRETT**
Aircraft concept optimization using the global sensitivity approach and parametric multiobjective figures of merit
[AIAA PAPER 92-4221] p 45 A93-13381
- MALONE, J. B.**
Current status of computational methods for transonic unsteady aerodynamics and aeroelastic applications
p 480 A93-29175
- MALONE, M. B.**
A 3D Navier-Stokes analysis of a generic ground vehicle shape
[AIAA PAPER 93-3521] p 985 A93-47283
- MALONEY, P. F.**
A retrospective of 3600 composite blades
p 507 A93-27963
- MALSBURY, T.**
Flight simulator fidelity assessment in a rotorcraft lateral translation maneuver
p 378 A93-23510
- MALTBAEK, CHRISTINA**
Turbine Engine Diagnostics (TED) system
[AIAA PAPER 93-1818] p 1110 A93-49706
- MALTE, PHILIP C.**
NO(x) sensitivities for gas turbine engines operated on lean-premixed combustion and conventional diffusion flames
[ASME PAPER 92-GT-115] p 349 A93-19351
- MALY, JOSEPH R.**
Development of a dynamic pressure response calibrator
p 1254 A93-54362
- MALYSHEV, A. M.**
Algorithms for constructing models of the interaction of diagnostic systems with reserved aviation equipment
p 847 A93-39043
- MALYSHEV, V. V.**
Intelligent systems of flight-vehicle control
p 1167 A93-50951
- Optimization of algorithms for information processing and control
p 1169 A93-51062
- MANCHEC, JOHN**
MM-122: High speed civil transport
[NASA-CR-192011] p 334 N93-17974
- MANCUSO, B.**
Engine testing at simulated altitude conditions
[AIAA PAPER 93-2452] p 1120 A93-50201
- MANDAI, S.**
Investigation of combustion structure inside low NO(x) combustors for a 1500 C-class gas turbine
[ASME PAPER 92-GT-123] p 350 A93-19357
- MANGALAM, S. M.**
In-flight detection of flow separation, stagnation, and transition
p 166 A93-14326
- MANGALAM, SIVA M.**
Method of measuring cross-flow vortices by use of an array of hot-film sensors
[NASA-CASE-LAR-14824-1-SB] p 751 N93-26000
- MANI, SATISH V.**
Multidisciplinary analysis and sensitivity derivatives for isolated helicopter rotors in hover
[AIAA PAPER 92-4696] p 324 A93-20308
- MANJUNATH, A. R.**
Flap-lag damping in hover and forward flight with a three-dimensional wake
p 797 A93-35979
- MANKBADI, REDA R.**
Numerical simulations of a high Mach number jet flow
[AIAA PAPER 93-0653] p 540 A93-24766
- Numerical simulation of a high Mach number jet flow
[NASA-TM-105985] p 551 A93-20057
- MANN, JON**
Design of the advanced regional aircraft, the DART-75
[NASA-CR-192044] p 333 N93-17972
- MANN, RICHARD**
Classification of radar clutter in an air traffic control environment
p 886 A93-30299
- MANNA, M.**
Validation of central and upwind 3D compressible flow solvers
p 421 A93-18564
- MANNES, M. A.**
Aspects of multivariable flight control law design for helicopters using eigenstructure assignment
p 60 A93-10916
- MANNING, A.**
Discharge coefficients of holes angled to the flow direction
[ASME PAPER 92-GT-192] p 403 A93-19417
- MANNING, CAROL A.**
Identifying ability requirements for operators of future automated air traffic control systems
[AD-A256615] p 152 N93-14276
- En route air traffic controllers use of flight progress strips: A graph-theoretic analysis
[AD-A259062] p 319 N93-18927
- MANNING, FRANK L.**
Differential GPS control of Starcar 2
p 317 A93-21201
- MANNIS, C.**
Integration of full scale development aircraft GPS user equipment (AN/ARN-151) with Doppler radar systems
p 31 A93-11012
- MANNO, VINCENT P.**
Developing numerical techniques for solving low Mach number fluid-acoustic problems
p 1235 A93-55353
- MANOLESCU, S.**
Optimal symmetric trajectories over a fixed-time domain
[AIAA PAPER 93-3848] p 1133 A93-51435
- MANSFELD, G.**
Development and flight testing of a fault-tolerant fly-by-light yaw control system
p 1010 N93-31280
- MANSON, S. S.**
Concurrent field service and laboratory testing as a means of improving reliability in creep-rupture applications
p 916 A93-40814
- MANSUR, M. H.**
Investigation of the flight mechanics simulation of a hovering helicopter
p 798 A93-35990
- MANUJLOVICH, S. V.**
Laminarization of the boundary layer on a vibrating wing
p 1089 A93-51776
- MANUKHOV, I. I.**
Vibrational monitoring and diagnostics of the technical condition of gas turbine engines at civil aviation repair facilities
p 374 A93-18362
- MANWARING, S. R.**
Unsteady aerodynamics and gust response in compressors and turbines
[ASME PAPER 92-GT-422] p 258 A93-19570
- Rotor blade unsteady aerodynamic gust response to inlet guide vane wakes
[ASME PAPER 91-GT-129] p 475 A93-26897
- MANZO, F.**
Compressible flow in a hovercraft air cushion
p 480 A93-29316
- MAO, JIANGUO**
An investigation of real-time diagnostic technique on aeroengine
p 174 A93-16844
- MAPLE, RAYMOND C.**
Visualization of vortical flows with yet another post-processor
[AIAA PAPER 93-0222] p 415 A93-22638
- MAR, JAMES W.**
Structural integrity of aging airplanes - A perspective
p 948 A93-45789
- MARAWA, A.**
Airport stand assignment model
[TT-9104] p 67 N93-11728
- MARBLE, FRANK E.**
Investigation of a contoured wall injector for hypervelocity mixing augmentation
p 837 A93-39407
- Shock enhancement and control of hypersonic combustion
[AD-A254295] p 72 N93-10843
- MARCHAND, N. J.**
An experimental investigation of convective heat transfer at the leading edge of a gas turbine airfoil
[ASME PAPER 92-GT-248] p 405 A93-19457
- MARCHAND, O.**
A comparative study of semi-empirical dynamic stall models
p 18 N93-10544
- A field panel method for transonic flows
p 18 N93-10547
- MARCHANT, M. J.**
Adaptive inviscid flow solutions for aerospace geometries on efficiently generated unstructured tetrahedral meshes
[AIAA PAPER 93-3390] p 956 A93-45081
- The construction of nearly orthogonal multiblock grids for compressible flow simulation
p 1219 A93-53847
- MARCHELLO, JOSEPH M.**
Polymer infiltration studies
[NASA-CR-191652] p 200 N93-15431
- MARCHETTO, B.**
AM-X high angle of attack flight test experience (single and two seat versions)
p 511 N93-19910
- MARCHI, C. H.**
Code validation for high speed flow simulation over the VLS launcher fairing
[AIAA PAPER 93-3046] p 1057 A93-48226
- MARCHIONNE, DARRYL**
Development of a model to predict electric vehicle performance over a variety of driving conditions
p 570 A93-26011
- MARCHMAN, JAMES F., III**
AIAA's role in aerospace education
[AIAA PAPER 93-0324] p 454 A93-23016
- MARCHUKOV, E. I. U.**
The possibility of reducing the emission of benzo(a)pyrene with the exhaust gases of aviation gas turbine engines by water injection into the combustion chamber
p 812 A93-39201
- MARCOLINI, MICHAEL A.**
Sensitivity of acoustic predictions to variation of input parameters
p 565 A93-29404
- Prediction of BVI noise patterns and correlation with wake interaction locations
p 849 A93-35966
- MARCON, G.**
Effect of environment on creep-fatigue crack propagation in turbine disc superalloys
[ONERA, TP NO. 1993-5] p 916 A93-41023
- MARCONI, FRANK**
Solution of the Euler and Navier Stokes equations on parallel processors using a transposed/Thomas ADI Algorithm
[AIAA PAPER 93-3310] p 1036 A93-45006
- MARCOPOLI, VINCENT R.**
Antiwindup analysis and design approaches for MIMO systems
[AIAA PAPER 93-3811] p 1123 A93-51403
- MARCUM, D. L.**
Adaptive inviscid flow solutions for aerospace geometries on efficiently generated unstructured tetrahedral meshes
[AIAA PAPER 93-3390] p 956 A93-45081
- MARCUM, R. B.**
The PAVE PACE integrated RF architecture for next generation avionics
p 896 A93-42784
- MAREC, J.-P.**
Toward the second-generation supersonic transport
[ONERA, TP NO. 1993-26] p 890 A93-41038
- MAREK, C. J.**
Comparison of reacting and non-reacting shear layers at a high subsonic Mach number
[NASA-TM-106198] p 814 N93-27610
- Turbulence measurement in a reacting and non-reacting shear layer at a high subsonic Mach number
[NASA-TM-106186] p 989 N93-31839
- MARESCA, CHRISTIAN**
Influence of coupling incidence and velocity variations on the airfoil dynamic stall
p 767 A93-35999
- MARGASON, RICHARD J.**
A numerical investigation of a subsonic jet in a crossflow
[AIAA PAPER 93-0870] p 469 A93-24931
- MARGOT, X. M.**
A physically guided zonal approach for two-dimensional aeroflow flows
[AIAA PAPER 93-0790] p 468 A93-24869
- MARGUET, ROGER**
The ramjet engine in high speed propulsion
p 174 A93-16853
- MARIANI, U.**
Fatigue qualification of high thickness composite rotor components
p 81 A93-13646
- MARING, LISE D.**
Reliability of stiffened structural panels: Two examples
[NASA-TM-107687] p 219 N93-14483

- MARINI, M.**
Numerical simulations of high speed inlet flows p 115 A93-14246
Low area ratio aircraft fuel jet-pump performances with and without cavitation p 272 A93-22264
Multigrid techniques for hypersonic viscous flows [AIAA PAPER 93-0771] p 467 A93-24855
Multigrid techniques for hypersonic viscous flows p 1071 A93-49027
- MARINOV, NICK N.**
NO(x) sensitivities for gas turbine engines operated on lean-premixed combustion and conventional diffusion flames [ASME PAPER 92-GT-115] p 349 A93-19351
- MARIOLI-RIGA, Z. P.**
Damage detection by Acousto-Ultrasonic Location (AUL) p 555 A93-21529
- MARK, S.**
Aerodynamic forces on maglev vehicles [PB93-154813] p 782 A93-27413
- MARKER, TIMOTHY R.**
Narrow-body aircraft water spray optimization study [DOT/FAA/CT-TN93/3] p 705 A93-25224
- MARKIE, TRACY**
JIAWG compatible development boards for the i960 [SAE PAPER 931596] p 1104 A93-49345
- MARKIN, KELLY R.**
Evaluation of category 3 MLS designs p 888 A93-30358
- MARKL, ABERT**
Reentry control to a drag vs. energy profile [AIAA PAPER 93-3790] p 1143 A93-51385
- MARKLOW, A. D.**
Optimization of time saving in navigation through an area of variable flow p 34 A93-12125
- MARKMAN, STEVEN R.**
USAF in-flight simulation - A cost-effective operating approach [AIAA PAPER 93-3604] p 1175 A93-52690
- MARKOPOULOS, N.**
Near-optimal, asymptotic tracking in control problems involving state-variable inequality constraints [AIAA PAPER 93-3748] p 1170 A93-51344
Guidance and flight control law development for hypersonic vehicles [NASA-CR-192102] p 526 A93-19960
- MARKS, FRANK D., JR.**
Comparison of three methods to deduce three-dimensional wind fields in a hurricane with airborne Doppler radar p 844 A93-37691
- MARKUS, ALAN**
Composites technology for transport primary structure p 918 A93-30431
Resin transfer molding for advanced composite primary aircraft structures p 919 A93-30438
- MARMIGNON, C.**
Viscous nonequilibrium flow calculations [ONERA, TP NO. 1992-89] p 771 A93-38573
Calculations of viscous nonequilibrium flows in nozzles [ONERA, TP NO. 1992-91] p 771 A93-38574
Navier-Stokes calculations over a double ellipse and a double ellipsoid by an implicit non-centered method p 867 A93-42607
- MAROM, S.**
Navier-Stokes calculations of the flow about wing-flap combinations p 112 A93-14171
- MAROTTA, D.**
Aero-thermal design of a cooled transonic NGV and comparison with experimental results p 904 A93-29957
- MAROTTE, H.**
Air accidents in the French Air Force p 492 A93-19676
- MARQUART, E. J.**
Free-spin damping measurement techniques [AIAA PAPER 93-3457] p 1014 A93-47240
- MARR, ROGER L.**
V-22 tiltrotor Flight Test Development p 800 A93-36021
- MARRAFA, LIONEL**
Quasi monodimensional inviscid non equilibrium nozzle flow computation p 927 A93-42646
- MARROQUIN, ADRIAN**
Preliminary results of the detection of clear air turbulence by the Wind Profiler Demonstration Network p 427 A93-22119
Diagnostic studies of clear air turbulence in isentropic coordinates p 430 A93-22154
- MARSH, ALAN H.**
Noise reduction programs for in-service jet transports p 521 A93-28479
- MARSH, JOHN**
Database management for integrated avionics system p 939 A93-42831
Functionally Integrated Resource Manager for real-time avionics data p 940 A93-42832
- MARSHAKOV, A. V.**
Direct measurements of skin friction in a scramjet combustor [AIAA PAPER 93-2443] p 1119 A93-50195
- MARSHALL, IAN**
Optical design of a wide-angle simulator probe p 211 A93-17140
- MARSILIO, R.**
Vortical solutions in supersonic corner flows [AIAA PAPER 93-0760] p 466 A93-24845
Asymmetric vortical solutions in supersonic corners - Steady 3D space-marching versus time-dependent conical results [AIAA PAPER 93-2957] p 1047 A93-48151
Vortical solutions in supersonic corner flows p 1071 A93-49015
A study of the stability of vortical structures in supersonic inlets [ISABE 93-7103] p 1187 A93-54079
- MARSON, EZIO**
Effect of manufacturing deviations on performance of axial flow compressor blading [ASME PAPER 92-GT-326] p 257 A93-19510
- MARSTON, R. K.**
Design considerations for air-to-air laser communications p 312 A93-18932
- MARTEL, C. R.**
Studies of jet thermal stability in a flowing system [ASME PAPER 92-GT-106] p 401 A93-19344
- MARTELLI, F.**
Studies on coolant problems in aeronautical turbine cascades [ISABE 93-7074] p 1220 A93-54050
- MARTELLUCCI, ANTHONY**
Developing a data base for the calibration and validation of hypersonic CFD codes - Sharp cones [AIAA PAPER 93-3044] p 1057 A93-48224
- MARTENS, SCOTT L.**
Estimating characteristic life and reliability of an aircraft engine component improvement in the early stages of the implementation process [AD-A262118] p 815 A93-28184
- MARTIN, CHARLES E.**
Air piracy and terrorism directed against U.S. Air carriers [AD-A264120] p 880 A93-30194
- MARTIN, D. L.**
Ladar fiber optic sensor system for aircraft applications p 1105 A93-49467
- MARTIN, DANIEL M.**
Comparison of PMARC and analytic results for two-dimensional unsteady airfoils [AIAA PAPER 93-0636] p 463 A93-24752
- MARTIN, DARRELL**
System identification of unstable manipulators using ERA methods [AIAA PAPER 93-3842] p 1170 A93-51431
- MARTIN, F. W., JR.**
Numerical dissipation in F3D thin-layer Navier-Stokes solution for flows with wall transpiration p 9 A93-12010
- MARTIN, FRED**
Cross channel dependency requirements of the multi-path redundant avionics suite p 928 A93-42782
- MARTIN, J.**
Analysis of the effects of blade pitch on the radar return signal from rotating aircraft blades p 885 A93-43476
- MARTIN, JOHN**
Compound cycle engine for helicopter application [NASA-CR-180824] p 55 A93-10348
- MARTIN, JOHN G.**
Aero-space plane figures of merit [AIAA PAPER 92-5058] p 385 A93-22328
- MARTIN, LARRY K.**
Methodology investigation: Global Positioning System integration (GPS) [AD-A261054] p 708 A93-26237
- MARTIN, ROBERT A.**
Flow control over delta wings at high angles of attack [AIAA PAPER 93-3494] p 983 A93-47266
- MARTIN, RUTH M.**
Prediction of BVI noise patterns and correlation with wake interaction locations p 849 A93-35966
- MARTIN, S. J.**
Advanced diagnostics for in situ measurement of particle formation and deposition in thermally stressed jet fuels [AIAA PAPER 93-0363] p 390 A93-23045
- MARTIN, STANLEY, JR.**
The V-22 for SOF p 800 A93-36026
- MARTIN, STEVE**
Advanced thermally-stable, coal-derived, jet fuels program: Experiment system and model development [AD-A262747] p 917 A93-29402
- MARTINELLI, L.**
A fast multigrid method for solving incompressible hydrodynamic problems with free surfaces [AIAA PAPER 93-0767] p 540 A93-24851
- MARTINEZ-SANCHEZ, M.**
Plume and wake dynamics, mixing, and chemistry behind a high speed civil transport aircraft p 1034 A93-45139
Stratospheric aircraft exhaust plume and wake chemistry studies [NASA-CR-189688] p 94 A93-12299
- MARTINEZ-VAL, R.**
Aerodynamic characteristics of transport airplanes in low speed configuration p 113 A93-14172
- MARTINEZ-VAL, RODRIGO**
Extended range operations of two and three turbofan engines p 802 A93-37391
- MARTINEZ, OSCAR E.**
Control of takeoff of a hypersonic aircraft using neural networks p 1167 A93-50744
- MARTINEZ, RADAME**
The ATC evaluation of the prototype Airport Surveillance Radar Wind Shear Processor (ASR-WSP) at Orlando International Airport [DOT/FAA/CT-TN92/48] p 748 A93-25210
- MARTINI, S.**
Natural laminar flow test in-flight visualization p 482 A93-19921
- MARTINSON, VELORIA J.**
Braking, steering, and wear performance of radial-belted and bias-ply aircraft tires [SAE PAPER 921036] p 158 A93-14656
- MARTINUZZI, ROBERT**
Transition for three-dimensional boundary layers on wings in the transonic regime [AIAA PAPER 93-3049] p 1057 A93-48229
- MARTONE, M.**
Determination of balloon gas mass and revised estimates of drag and virtual mass coefficients p 7 A93-11362
- MARTY, G.**
Preliminary results of the ISM campaign - The Landes, South West France p 1161 A93-47553
- MARTY, M.**
Effect of environment on creep-fatigue crack propagation in turbine disc superalloys [ONERA, TP NO. 1993-5] p 916 A93-41023
- MARTYNEKO, S. I.**
A method for calculating the dynamic characteristics of heat exchangers with single-phase cryogenic coolants p 851 A93-39057
- MARULO, F.**
Numerical study for the study of medium speed internal noise problems [DILC-EST-TN-200] p 101 A93-11156
- MARUYAMA, YUICHI**
Development of a boundary element method program for numerical analysis of supersonic unsteady flow p 300 A93-19283
- MARYNIAK, JERZY**
Modeling and analysis of the winch launch of a glider p 528 A93-27294
- MARZE, HENRI-JAMES**
Toward the silent helicopter [ONERA, TP NO. 1992-229] p 851 A93-38774
- MASAD, J. A.**
Transition correlation in subsonic flow over a flat plate p 1178 A93-53231
- MASCARELL, J. P.**
Turbomachinery and potential computations [DS-2026] p 363 A93-17740
- MASCHKE, C.**
The influence of nocturnal aircraft noise on sleep and on catecholamine secretion p 1163 A93-49554
- MASELAND, J. E. J.**
Experimental and numerical investigation of vortex flow over a 76/60-deg double-delta wing [LR-680] p 289 A93-16210
- MASER, J.**
X ray microscopy resource center at the Advanced Light Source [DE93-010449] p 911 A93-29869
- MASIULANIEC, K. C.**
Experimental assessment of airframe damage due to impacting ice [AIAA PAPER 93-0751] p 504 A93-24838
- MASLENNIKOVA, G. E.**
Optimization of the blade angle of the AV-2 propeller for improving the flight performance characteristics of An-2 aircraft p 996 A93-45663
- MASLOV, I. V.**
High-strength combination fasteners for joint assembly in aircraft structures p 745 A93-35283
Stress-strain state of the elements of a single-stringer riveted panel p 746 A93-35288

MASLOV, V. G.

Expert evaluation of the technological level of aviation gas turbine engine designs p 811 A93-39187

MASON, J. G.

Inlet design using a blend of experimental and computational techniques p 114 A93-14210

MASON, KAREN

Proceedings of the AIAA/FAA Joint Symposium on General Aviation Systems [AD-A257780] p 240 N93-17732

MASON, MARY L.

Experimental investigation of spherical-convergent-flap thrust-vectoring two-dimensional plug nozzles [AIAA PAPER 93-2431] p 898 A93-41045
Internal performance of Highly Integrated Deployable Exhaust Nozzles [AIAA PAPER 93-2570] p 1084 A93-50288

MASON, W.

Kinematics and aerodynamics of the velocity vector roll [AIAA PAPER 93-3625] p 1126 A93-48310

MASON, W. H.

Aircraft concept optimization using the global sensitivity approach and parametric multiobjective figures of merit [AIAA PAPER 92-4221] p 45 A93-13381

Aerodynamic optimization of an HSCT configuration using variable-complexity modeling [AIAA PAPER 93-0101] p 322 A93-19806

Variable-complexity aerodynamic-structural design of a high-speed civil transport wing [AIAA PAPER 92-4695] p 323 A93-20279

Fundamental issues in subsonic/transonic expansion corner aerodynamics [AIAA PAPER 93-0649] p 465 A93-24764

Development of lateral-directional departure criteria [AIAA PAPER 93-3650] p 1128 A93-48333

MASSARDO, A.

Low area ratio aircraft fuel jet-pump performances with and without cavitation p 272 A93-22264

MASSE, B.

Stress calculation for the Sandia 34-meter wind turbine using the local circulation method and turbulent wind [DE93-004480] p 560 N93-22045

MASSEY, STEVEN J.

Simulation of tail buffet using delta wing-vertical tail configuration [AIAA PAPER 93-3688] p 1065 A93-48357

MASSIE, JEFFREY J.

Instrumentation and telemetry systems for free-flight drop model testing p 1209 A93-52754

MASSOGLIA, PETER L.

Automatic dependent surveillance (ADS) Pacific engineering trials (PET) p 30 A93-10999

MASSON, C.

A field panel method for transonic flows p 18 N93-10547

MASTIN, C. W.

Adaptive EAGLE dynamic solution adaptation and grid quality enhancement p 788 N93-27464

MASUDA, MASAOKI

Research and development of ceramic turbine wheels [ASME PAPER 92-GT-295] p 354 A93-19485

MASUDA, WATARU

Effects of nozzle contour on the aerodynamic characteristics of underexpanded annular impinging jets p 1024 A93-45563

MASUTANI, JYO

Performance improvement by forward-skewed blading of axial fan moving blades [ISABE 93-7055] p 1185 A93-54031

MASUYA, GORO

Effects of injector geometry on scramjet combustor performance p 359 A93-21670

Analytical investigation of a regeneratively cooled scramjet engine [AIAA PAPER 93-0739] p 519 A93-24829

Effect of film cooling/regenerative cooling on scramjet engine performances [ISABE 93-7036] p 1197 A93-54012

Ignition and combustion performance of a scramjet combustor with a fuel injection strut [ISABE 93-7050] p 1199 A93-54026

Mach 4 testing of scramjet inlet models [NAL-TR-1137] p 26 N93-12369

MASUYA, GOROU

Preliminary design of experimental sub-scale scramjet engine [AAS PAPER 91-639] p 1247 A93-55816

MATESANZ, A.

Aerodynamics design of convergent-divergent nozzles [AIAA PAPER 93-2574] p 1085 A93-50290

Cooling predictions in turbofan engine components p 905 N93-29964

MATHENY, NEIL

The F-18 High Alpha Research Vehicle - A high-angle-of-attack testbed aircraft [AIAA PAPER 92-4121] p 42 A93-13273

MATHER, DANIEL

Modeling the effects of drop drag and breakup on fuel sprays [AD-A263650] p 931 N93-29388

MATHER, JAMES H.

An aircraft instrument design for in situ tropospheric OH measurements by laser induced fluorescence at low pressures p 1159 A93-51528

MATHERS, BRUCE H.

Mathematical modeling and control law development for the atmospheric monitoring and control system of the Controlled Environment Research Chamber (CERC) at NASA Ames Research Center [AD-A261978] p 911 N93-29436

MATHEWS, BRUCE

Acquisition and use of Orlando, Florida and Continental Airbus radar flight test data p 489 N93-19603

MATHEWS, E. H.

Numerical simulation of inviscid transonic flow over two-dimensional slender bodies p 686 A93-34348

MATHEWS, JAMES

T55 engine - The challenge of torque measurement p 809 A93-35929

MATHIAS, D. W.

Optimization of anisotropic structures considering strength, stiffness and aeroelastic constraints [AIAA PAPER 92-4796] p 408 A93-20291

MATHIAS, DONOVAN

TBD(exp 3) [NASA-CR-192075] p 335 N93-18054

MATHIEU, G.

Millisecond aerodynamic force measurement with side-jet model in the ISL shock tunnel p 822 A93-39414

Shock tube validation experiments for the simulation of ram-accelerator-related combustion and gasdynamic problems p 1016 A93-45499

Shock tunnel experiments and approximative methods on hypervelocity side-jet control effectiveness [AIAA PAPER 93-1929] p 1077 A93-49794

MATHIS, J. A.

Analysis of turbine engine rotor containment and shielding structures [AIAA PAPER 93-1817] p 1110 A93-49705

MATHUR, GOPAL P.

Sound transmission through stiffened double-panel structures lined with elastic porous materials p 444 A93-19139

Experimental and analytical investigations of fuselage modal characteristics and structural-acoustic coupling p 451 A93-19229

Structural-acoustic coupling in aircraft fuselage structures p 1243 A93-55856

MATHUR, SANJAY R.

A hybrid structured-unstructured grid method for unsteady turbomachinery flow computations [AIAA PAPER 93-0387] p 282 A93-23066

Three-dimensional calculations of rotor-airframe interaction in forward flight p 795 A93-35940

A solution-adaptive hybrid-grid method for the unsteady analysis of turbomachinery [AIAA PAPER 93-3015] p 1148 A93-48204

MATSUBARA, TAKENORI

Lift enhancement of ground-effect wing. I - Results of screening tests of various concepts p 271 A93-21737

Lift enhancement of ground-effect wing. II - Experimental investigation of the power augmented ram wing in ground effect through the wind tunnel p 271 A93-21738

Microchannel plate modal gain variations with temperature p 477 A93-27445

MATSUHIRO, KEIJI

Research and development of ceramic turbine wheels [ASME PAPER 92-GT-295] p 354 A93-19485

MATSUI, MINORU

Research and development of ceramic turbine wheels [ASME PAPER 92-GT-295] p 354 A93-19485

MATSUKI, MASAKATSU

Research and development of aircraft engine in Japan - Historical review [ISABE 93-7000] p 1227 A93-53977

MATSUMOTO, ASAMI

Numerical analysis for chemically non-equilibrium flow p 770 A93-38148

MATSUMOTO, HIROAKI

Monte Carlo simulation of normal shock wave. Part 1: Lennard-Jones potential p 300 N93-19279

MATSUMOTO, JOY A.

Visual augmentation for night flight over featureless terrain p 806 A93-35921

MATSUMOTO, MASASHI

Evaluation of 2D scramjet nozzle performance p 52 A93-11209

Validation studies of scramjet nozzle performance p 1109 A93-49616

Off-design performance of scramjet nozzles [ISABE 93-7108] p 1203 A93-54084

MATSUMOTO, SHUICHI

Research on combined HOPE navigation technology p 533 N93-20428

MATSUNAGA, KOJI

Numerical simulation of the flow through non-uniform airfoil cascade p 302 N93-19310

MATSUNAGA, SHIGENORI

Development of a Shape-controlled airfoil by use of SMA p 411 A93-21739

MATSUNO, KENICHI

Flow visualization studies on sidewall effects in two dimensional transonic airfoil testing [AIAA PAPER 93-0090] p 263 A93-20196

MATSUO, K.

Normal shock wave oscillations in supersonic diffusers p 1044 A93-48042

MATSUO, SHIGERU

Study on unsymmetrical supersonic nozzle flows p 127 A93-16933

MATSUO, YUICHI

Numerical analysis of three-dimensional viscous flows around an advanced counterrotating propeller p 112 A93-14165

MATSUOKA, MIWA

Adaptive quadratic stabilization control with application to flight controller design [AIAA PAPER 93-3847] p 1133 A93-51434

MATSUSHIMA, HIDEYUKI

Dynamic characteristics of an airfoil at high speed change of pitch angle p 10 A93-12324

MATSUSHIMA, KOICHI

On stability and control of SSTO spaceplane in super- and hypersonic ascending phase [NAL-TR-11287] p 65 N93-12361

MATSUSHIMA, MASAMICHI

Compression after impact (CAI) properties of CF/PEEK (APC-2) and conventional CF/epoxy stiffened panels p 196 A93-14307

MATSUSHITA, H.

Integrated control law synthesis of gust load alleviation and flutter margin augmentation for a transport aircraft p 182 A93-14281

MATSUZAKA, Y.

The improvement of the static launch method in Japan p 26 A93-11364

Trans-oceanic balloon flight over east China sea p 27 A93-11372

MATSUZAKI, H.

Investigation of combustion structure inside low NO(x) combustors for a 1500 C-class gas turbine [ASME PAPER 92-GT-123] p 350 A93-19357

MATSUZAKI, YUJI

Thermal barrier design of gamma-TiAl Functionally Gradient Materials (FGMs) for scramjet engine applications p 1246 A93-54556

MATTERN, DUANE

A comparison of two multi-variable integrator windup protection schemes [AIAA PAPER 93-3812] p 1123 A93-51404

Propulsion system performance resulting from an integrated flight/propulsion control design [NASA-TM-105874] p 180 N93-15525

MATTHEWS, JOHN D.

Robotic aircraft painting with SAFARI [SME PAPER AD92-198] p 855 A93-40662

MATTHEWS, MICHAEL

The Orlando TDWR testbed and airborne wind shear date comparison results p 145 N93-14851

MATTHEWS, RAYMOND H.

Rotorcraft en route ATC route standards [AD-A249129] p 35 N93-10323

MATTHEWS, WILLIAM T.

Assessment of helicopter component statistical reliability computations [AD-A258931] p 510 N93-19447

MATTICK, A. T.

Investigation of the aerothermodynamics of hypervelocity reacting flows in the ram accelerator [NASA-CR-191715] p 140 N93-15588

MATTISSEK, A.

Integration of a course and position reference system with GPS p 499 A93-27911

MATUS, RICHARD J.

High lift multiple element airfoil analysis with unstructured grids [AIAA PAPER 93-3478] p 981 A93-47256

An unstructured grid flow solver for turbomachinery flows [AIAA PAPER 93-1913] p 1076 A93-49780

MATUSKA, DAVID G.

Advancing tiltrotor state-of-the-art with variable diameter rotors p 797 A93-35982

- MATVEENKO, A. M.**
Current methods of selecting the configurations and parameters of flight vehicles p 891 A93-42369
- MATVEEV, A. F.**
Numerical solution of the integral equations of the aerodynamics of porous surfaces p 13 A93-12768
- MATVEEV, A. I.**
A methodological approach to the development of service and technical specifications for an actively controlled multistrut landing gear p 321 A93-18349
Determination of the aerodynamic balance efficiency of aircraft p 1130 A93-48903
- MATVEEV, S. G.**
The possibility of reducing the emission of benzo(a)pyrene with the exhaust gases of aviation gas turbine engines by water injection into the combustion chamber p 812 A93-39201
- MATVEEV, S. K.**
Calculation of flow of a rarefied gas past a sphere for an arbitrary Knudsen number p 124 A93-15146
- MATVEEV, V. M.**
A model for calculating the element of a high-temperature heat exchanger with spiral-wire fins p 833 A93-39046
A heat transfer element of a high-temperature heat exchanger p 833 A93-39047
- MATVIENKO, A. S.**
Computational studies of the characteristics of axial compressor cascades and stages in unsteady incoming flow p 13 A93-12805
- MAUFFRET, T.**
Optimization of afterbodies and engine nozzle by using CFD methods [ISABE 93-7098] p 1187 A93-54074
- MAUGHMER, M.**
Validation of engineering methods for predicting hypersonic vehicle control forces and moments p 906 A93-41897
- MAUGHMER, MARK D.**
Generalized multipoint inverse airfoil design p 122 A93-14541
A method for the prediction of induced drag for planar and nonplanar wings [AIAA PAPER 93-3420] p 976 A93-47216
Analysis and design of planar and non-planar wings for induced drag minimization [NASA-CR-191274] p 131 A93-13463
Prediction of forces and moments for hypersonic flight vehicle control effectors [NASA-CR-193033] p 728 A93-24762
- MAUK, CLAY S.**
The effect of unsteady blade loading on the aeroacoustics of a pusher propeller [AIAA PAPER 93-1805] p 1173 A93-49694
- MAULL, D. J.**
Induced drag of a crescent wing planform p 1094 A93-52430
- MAURER, F.**
Experimental study of the longitudinal hypersonic corner flow field - HERMES-R&D research program, problem no. 5 p 867 A93-42602
Applications of infrared measurement technique in hypersonic facilities p 1024 A93-45505
Experimental investigations of hypersonic shock-boundary layer interaction p 1238 A93-56037
- MAURICE, J. M.**
Modeling of a turbulent flow in the presence of discrete parietal cooling jets p 904 A93-29960
- MAURICE, MARK S.**
Quantitative laser velocimetry measurements in the hypersonic regime by the integration of experimental and computational analysis [AIAA PAPER 93-0089] p 263 A93-20195
An investigation of laser velocimetry measurements within high speed, complex flows p 748 A93-25237
- MAURINO, DANIEL**
Efforts to reduce CFIT accidents should address failures of the aviation system itself p 1096 A93-49280
- MAVRILIS, D. J.**
Unstructured mesh algorithms for aerodynamic calculations p 785 A93-27444
- MAVRITSKII, V.**
Use of alternative fuels for aviation p 196 A93-14292
- MAVRITSKII, V. I.**
Air transportation system for shipping outsized cargoes p 141 A93-14394
Problems in the aerodynamics and dynamics of flight vehicles in the light of K.E. Tsiolkovsky's ideas; Lectures Devoted to K.E. Tsiolkovsky's Ideas, 25th, Kaluga, Russia, Sept. 11-14, 1990, Transactions p 237 A93-18376
- MAWID, M.**
Analysis of unsteady wave processes in a rotating channel [NASA-CR-191154] p 816 A93-28617
- MAY, M.**
Integration of full scale development aircraft GPS user equipment (AN/ARN-151) with Doppler radar systems p 31 A93-11012
- MAY, N. E.**
Calculation of turbulent flow for an enclosed rotating cone [ASME PAPER 92-GT-70] p 400 A93-19320
- MAYA, T.**
A new cooling system for ultra high temperature turbines [ISABE 93-7073] p 1201 A93-54049
- MAYANAGI, MITSUYOSHI**
An optical fiber multi-terminal data bus system for aircraft [NAL-TR-1125] p 52 A93-12370
- MAYBECK, PETER S.**
Multiple model adaptive estimation applied to the VISTA F-16 flight control system with actuator and sensor failures p 907 A93-42806
- MAYER, A.**
Transient thermal behaviour of a compressor rotor with axial cooling air flow and co-rotating or contra-rotating shaft p 903 A93-29946
- MAYER, DAVID W.**
Flow stability issues in supersonic inlet flow analyses [AIAA PAPER 93-0290] p 279 A93-22680
Boundary conditions for unsteady supersonic inlet analyses [ISABE 93-7104] p 1187 A93-54080
- MAYER, ERNST W.**
Viscous and inviscid instabilities of a trailing vortex p 268 A93-21042
- MAYER, J. F.**
Prediction of three-dimensional low frequency unsteady transonic flow and forced vibration in axial turbine stages p 971 A93-46934
- MAYLE, R. E.**
The effects of incident turbulence and moving wakes on laminar heat transfer in gas turbines [ASME PAPER 92-GT-377] p 406 A93-19535
- MAYLE, ROBERT E.**
Keynote address: Unsteady, multimode transition in gas turbine engines p 901 A93-29927
- MAYNARD, SHAWN J.**
Development of resins for composites by resin transfer molding p 921 A93-30853
- MAYVILLE, RONALD A.**
A laboratory study of fracture in the presence of lap splice multiple site damage p 1027 A93-45790
- MAYWALD, P. V.**
C-2 subsonic freejet development and demonstration [AIAA PAPER 93-2180] p 1138 A93-49992
- MAZAHERI, K.**
Numerical wave propagation and steady state solutions. II - Bulk Viscosity Damping [AIAA PAPER 93-3331] p 953 A93-45025
- MAZHUL, I. I.**
Effect of boundary layer suction on the thrust and aerodynamic efficiency of a hypersonic flight vehicle p 1176 A93-52959
- MAZIN, C.**
Method of characteristics for computing three-dimensional boundary layers p 970 A93-46886
- MAZOUZI, ABDELKRIM**
Harmonic analysis of the aerodynamic forces on a Darrieus rotor p 18 A93-10551
- MAZUR, JOHN J., JR.**
Valisys - A new quality assurance tool p 845 A93-36007
- MAZUR, VLADISLAV**
Aircraft lightning initiation and interception in situ electric measurements and fast video observations p 140 A93-14064
- MALISTER, K. W.**
Characteristics of deformable leading edge for high performance helicopter rotor [AIAA PAPER 93-3526] p 986 A93-47285
- MALISTER, KENNETH W.**
Unsteady aerodynamic behavior of an airfoil with and without a slat p 1093 A93-52007
- MARDLE, JACK G.**
Performance characteristics of a variable-area vane nozzle for vectoring an ASTOVL exhaust jet up to 45 deg [AIAA PAPER 93-2437] p 1118 A93-50189
Effects of flow-path variations on internal reversing flow in a tailpipe offtake configuration for ASTOVL aircraft [AIAA PAPER 93-2438] p 1118 A93-50190
Experimental performance of a ventral nozzle with pitch and yaw vectoring capability for SSTOVL aircraft [NASA-TM-106054] p 722 A93-25129
Performance characteristics of a variable-area vane nozzle for vectoring an ASTOVL exhaust jet up to 45 deg [NASA-TM-106114] p 813 A93-27131
- Effects of flow-path variations on internal reversing flow in a tailpipe offtake configuration for ASTOVL aircraft [NASA-TM-106149] p 900 A93-29065
- MARTHUR, DONALD E.**
Terrain modeling for real-time photo-texture based visual simulation [AIAA PAPER 93-3607] p 1214 A93-52667
- MCBEATH, GIORGIO**
A review of chemically reactive turbulent flow mixing mechanisms and a new design for a low NO(x) combustor p 1109 A93-49508
- MCBRIDE, BONNIE J.**
Computer program for calculating and fitting thermodynamic functions [NASA-RP-1271] p 231 A93-12967
- MCBRIDE, STUART L.**
Acoustic emission monitoring of aging aircraft structures p 407 A93-19697
- MCCABE, R. KEVIN**
Scientific visualization using the Flow Analysis Software Toolkit (FAST) p 758 A93-25600
- MCCAFFERTY, J. D.**
Thermal design and analysis of an exhaust diffuser unit in a ceramic composite [ISABE 93-7060] p 1220 A93-54036
- MCCAFFREY, B. J.**
A model study of the aircraft cabin environment resulting from in-flight fires [DOT/FAA/CT-90/22] p 496 A93-21557
- MCCANN, W. J.**
Over wing propeller aerodynamics p 113 A93-14189
- MCCARTHY, JOHN**
The Aviation Weather Products Generator p 428 A93-22125
A statistical characterization of Denver-area microbursts [AD-A262127] p 845 A93-27675
- MCCARTHY, THOMAS**
An integrated optimum design approach for high speed prop-rotors including acoustic constraints [NASA-CR-193222] p 893 A93-29153
- MCCARTHY, THOMAS R.**
Multidisciplinary optimization of helicopter rotor blades including design variable sensitivity [AIAA PAPER 92-4783] p 323 A93-20289
Design of high speed propellers using multiobjective optimization techniques p 336 A93-18065
Optimum design of high speed prop rotors including the coupling of performance, aeroelastic stability and structures p 337 A93-18066
- MCCARTY, J. E.**
Design and cost viability of composites in commercial aircraft p 915 A93-39963
- MCCARTY, JOHN E.**
Composites: A viable option p 918 A93-30429
- MCCARTY, P. E.**
An upgraded data acquisition and processing system for the Aeropropulsion Systems Test Facility at Arnold Engineering Development Center [AIAA PAPER 93-2466] p 1138 A93-50213
An updated data acquisition and processing system for turbine engine testing p 1250 A93-54389
- MCCARTY, W. D.**
Rendering the out-the-window view for the AFIT virtual cockpit [AD-A262599] p 823 A93-28467
- MCCAUGHAN, F. E.**
Stability of fully developed rotating stall [ASME PAPER 92-GT-57] p 348 A93-19307
- MCCLAMROCH, N. H.**
Vision-based recursive estimation of rotorcraft obstacle locations p 343 A93-22851
- MCCCLARY, CHARLES R.**
A fault-tolerant air data/inertial reference system p 50 A93-10982
- MCCLEARY, S. L.**
An accurate nonlinear finite element analysis and test correlation of a stiffened composite wing panel p 546 A93-27968
- MCCLELLIN, CHARLES R.**
Scramjet combustor and nozzle computations p 171 A93-14243
- MCCLEURE, DONALD H.**
The development of an Altitude Awareness Program - An integrated approach p 486 A93-27136
- MCCLEURE, MARK A.**
Applying variations of the quantitative feedback technique (QFT) to unstable, non-minimum phase aircraft dynamics models p 939 A93-42797
- MCCOLGAN, C. J.**
User's manual for UCAP: Unified Counter-Rotation Aero-Acoustics Program [NASA-CR-191034] p 852 A93-27148

MCCORMICK, D.

- MCCORMICK, D.**
An assessment of wake structure behind forward swept and aft swept propfans at high loading p 245 A93-19222
- MCCORMICK, D. C.**
Vortical and turbulent structure of a lobed mixer free-shear layer [AIAA PAPER 93-0219] p 415 A93-22635
Shock/boundary-layer interaction control with vortex generators and passive cavity p 287 A93-23546
Role of leading-edge vortex flows in prop-fan interaction noise p 565 A93-28614
- MCCORMICK, DAVE**
High voltage quick-disconnect harness system for helmet-mounted displays p 516 A93-25922
- MCCORMICK, DAVID M.**
New cathode-ray tube (CRT) gun interconnection assembly p 547 A93-28175
- MCCOY, C. ELAINE**
Design of a cooperative problem-solving system for enroute flight planning: An empirical study of its use by airline dispatchers [NASA-CR-192709] p 707 N93-25330
- MCCOY, ELAINE**
Design concepts for the development of cooperative problem-solving systems [NASA-CR-192708] p 707 N93-25261
- MCCRACKEN, H. B.**
Advanced Unmanned Search System (AUSS) supervisory command, control and navigation [AD-A263171] p 793 N93-28990
- MCCROSKEY, W. J.**
Euler calculations of unsteady interaction of advancing rotor with a line vortex p 1071 A93-49016
Some recent applications of Navier-Stokes codes to rotorcraft p 786 N93-27452
- MCCULLOUGH, B. F.**
Unified airport pavement design procedure p 380 N93-16318
- MCCULLUM, D.**
Aerodynamic forces on maglev vehicles [PB93-154813] p 782 N93-27413
- MCCUNE, J. E.**
Flow phenomena in turbomachines [AD-A263049] p 930 N93-29141
- MCCUNE, JAMES E.**
Aerodynamics of maneuvering slender wings with leading-edge separation p 778 A93-39401
- MCCUNE, M. E.**
Initial test results of 40,000 horsepower fan drive gear system for advanced ducted propulsion systems [AIAA PAPER 93-2146] p 1154 A93-49963
- MCDANIEL, J. C.**
Workshop report - A validation study of Navier-Stokes codes for transverse injection into a Mach 2 flow p 270 A93-21330
Workshop Report: A validation study of Navier-Stokes codes for transverse injection into a Mach 2 flow p 751 N93-26008
- MCDANIEL, J. C., JR.**
Planar imaging of OH density distributions in a supersonic combustion tunnel [AIAA PAPER 93-0042] p 389 A93-20155
Laser selection criteria for OH fluorescence measurements in supersonic combustion test facilities p 549 A93-29315
- MCDANIEL, JAMES C.**
Experimental supersonic hydrogen combustion employing staged injection behind a rearward-facing step p 744 A93-34496
- MCDANIEL, JAMES C., JR.**
Experimental and numerical study of swept ramp injection into a supersonic flowfield [AIAA PAPER 93-2445] p 1119 A93-50197
- MCDANIEL, MICHAEL L.**
Airship applications of modern flight test techniques [AIAA PAPER 93-4035] p 1242 A93-54606
- MCDONALD, GEORGE**
Optimization of pneumatic subsystems for transport aircraft p 159 A93-15049
- MCDONALD, KEITH D.**
Complementary MLS and GNSS operations p 384 A93-21160
The applications, benefits, and issues of employing GPS and Gionass with Automatic Dependent Surveillance p 316 A93-21188
- MCDONALD, MALCOLM W.**
Multipath effects in a Global Positioning Satellite system receiver p 318 N93-17311
- MCDONELL, V. G.**
Scaling of the two-phase flow downstream of a gas turbine combustor swirl cup - Mean quantities [ASME PAPER 92-GT-207] p 404 A93-19431
Development of an optical sensor for active control of a gas turbine combustor [AIAA PAPER 93-0118] p 360 A93-22568

- Fuel injector: Air swirl characterization aerothermal modeling, phase 2, volume 1 [NASA-CR-189193-VOL-1] p 721 N93-24754
Fuel injector: Air swirl characterization aerothermal modeling, phase 2, volume 2 [NASA-CR-189193-VOL-2] p 721 N93-25106
- MCDONNELL, V. G.**
Correlation of droplet behavior with gas-phase structures in a gas turbine combustor [AIAA PAPER 93-1767] p 1152 A93-49663
- MCDUGALL, GERALD**
General aviation turbine markets - An economic overview [AIAA PAPER 92-4191] p 103 A93-13369
- MCDOWALL, ROSEMARIE L.**
Lightning data acquisition p 753 N93-24883
- MCENTIRE, B. JOSEPH**
US Army helicopter inertia reel locking failures p 493 N93-19689
- MCFADDEN, P. D.**
Time-frequency domain analysis of vibration signals for machinery diagnostics. 3: The present power spectral density [OUEL-1911/92] p 89 N93-11707
- MC FARLAND, ERIC R.**
An integral equation solution for multistage turbomachinery design calculations [NASA-TM-105970] p 179 N93-15521
- MC FARLAND, RICHARD H.**
A localizer design to improve missed approach guidance p 992 A93-44143
- MC FARLAND, VERNON E.**
Viscous interaction upstream and downstream of a turbine stator cascade with a periodic wake field [ASME PAPER 92-GT-162] p 250 A93-19388
- MC GEACHY, J. D.**
Aerodynamic performance of a transonic low aspect ratio turbine nozzle [ASME PAPER 92-GT-31] p 245 A93-19291
- MC GHEE, ROBERT J.**
Flowfield measurements about a multi-element airfoil at high Reynolds numbers [AIAA PAPER 93-3137] p 1064 A93-48300
Multielement airfoil performance due to Reynolds and Mach number variations p 1095 A93-52442
Reynolds and Mach number effects on multielement airfoils p 785 N93-27446
- MC GINLEY, J. A.**
The FAA aircraft Icing Forecasting Improvement Program - Validation of aircraft icing forecasts in the Denver area [AIAA PAPER 93-0393] p 309 A93-23069
- MC GINLEY, WILLIAM M.**
Lumped mass modelling for the dynamic analysis of aircraft structures p 510 N93-19460
- MC GRATH, BRIAN E.**
Computational study of a conical wing having unit aspect ratio at supersonic speeds [AIAA PAPER 93-3505] p 984 A93-47272
- MC GRATH, JAMES M.**
Automatic carrier landing system utilizing aircraft sensors p 1097 A93-49590
- MC GRAW, SANDRA M.**
Multiple-function multi-input/multi-output digital control and on-line analysis [NASA-TM-107697] p 162 N93-13565
- MC GREGOR, I.**
Comparative performance tests of a pitot-inlet in several European wind-tunnels at subsonic and supersonic speeds p 130 N93-13221
- MC GREGOR, LLOYD F.**
The Airborne Ocean Color Imager - System description and image processing p 1157 A93-50369
- MC GRORY, W. D.**
Development and application of GASP 2.0 [AIAA PAPER 92-5067] p 438 A93-22337
- MC GUIRE, GWENDOLYN**
USA aviation digest index, 1989, volume 11 [AD-A258673] p 571 N93-20388
Index to USA aviation digest, 1990 [AD-A258678] p 572 N93-20389
Index to USA aviation digest, 1991 [AD-A258679] p 572 N93-20390
- MC GUIRK, J. J.**
A physically guided zonal approach for two-dimensional aeroflow flows [AIAA PAPER 93-0790] p 468 A93-24869
On the analysis of an impinging jet on ground effects p 1260 A93-56339
- MC HENRY, RONALD**
FAA weather processor programs - Real-time dissemination of weather information to aviation end-users p 428 A93-22131

PERSONAL AUTHOR INDEX

- MCHUGH, C. A.**
The use of a deep honeycomb to achieve high flow quality in the ARA 9 ft x 8 ft Transonic Wind Tunnel p 190 A93-14276
- MCILVEEN, M.**
Engine testing at simulated altitude conditions [AIAA PAPER 93-2452] p 1120 A93-50201
- MCINTOSH, JOHN**
Helicopter training simulators: Key market factors p 912 N93-30683
- MCINTYRE, T. J.**
A laser induced fluorescence system for the high enthalpy shock tunnel (HEG) in Goettingen p 1024 A93-45506
- MCKAY, ESTHER L.**
The aeronautical volcanic ash problem p 309 A93-22156
- MCKEE, MIKE**
Advanced hypersonic aircraft design [NASA-CR-192046] p 334 N93-18037
- MCKENZIE, A. B.**
Recess vane passive stall control [ASME PAPER 92-GT-36] p 246 A93-19296
Experimental investigation of rotating stall in a mismatched three stage axial flow compressor p 423 N93-18727
Application of recess vane casing treatment to axial flow fans p 423 N93-18728
- MCKENZIE, ROBERT L.**
Shedding new light on gas dynamics p 80 A93-13435
Progress in laser spectroscopic techniques for aerodynamic measurements - An overview p 549 A93-29308
- MCKILLIP, R. M., JR.**
Studies of a flat wake rotor theory [NASA-CR-190936] p 25 N93-12343
- MCKINNEL, R. J.**
Extending the useful frequency of 'rigid' wind tunnel models with active control p 190 A93-14299
- MCKINNEY, GEORGE C.**
A distributed, message-based, airspace environment p 313 A93-21144
- MCKINNEY, R.**
Modification of combustor stoichiometry distribution for reduced NO(x) emission from aircraft engines [ASME PAPER 92-GT-108] p 349 A93-19346
- MCKNIGHT, R. L.**
Probabilistic turbine blade tip durability analysis [AIAA PAPER 93-1383] p 719 A93-33946
- MCKNIGHT, RICHARD L.**
Optimization of composite engine structures for mechanical and thermal loads [AIAA PAPER 93-1583] p 719 A93-34115
- MCLACHLAN, D. G.**
Design issues and initial performance of an adaptive air/ground/air HF communication system p 934 N93-30342
- MCLACHLAN, R.**
Asymptotic methods for the prediction of transonic wind-tunnel wall interference p 730 A93-35625
- MCLAFFERTY, G. H.**
Experimental results of shock trains in rectangular ducts [AIAA PAPER 92-5103] p 274 A93-22373
- MCLAUGHLIN, ASTON**
Federal Aviation Administration pavement modeling p 379 N93-16315
- MCLAUGHLIN, D. K.**
Sound generation by rotating stall in centrifugal turbomachines p 1039 A93-46701
- MCLAUGHLIN, DENNIS K.**
Acoustic properties of supersonic helium/air jets at low Reynolds numbers p 446 A93-19160
Numerical simulations of flows in centrifugal turbomachinery [AIAA PAPER 93-2578] p 1085 A93-50293
- MCLAUGHLIN, J. B.**
Lift and drag forces on droplets and particles in wall-bounded shear flows [DE93-002678] p 419 N93-17761
An analysis of lift forces on aerosols in a wall bounded turbulent shear flow [DE93-003362] p 747 N93-24963
- MCLAUGHLIN, P. W.**
Approach of modeling continuous turbine engine operation from startup to shutdown p 721 A93-34495
- MCLAUGHLIN, THOMAS E.**
Aerodynamic foundations for use of unsteady aerodynamic effects in flight control [AIAA PAPER 93-0188] p 276 A93-22613
- MCLAUGHLIN, THOMAS EUGENE**
Aerodynamic foundations for use of unsteady aerodynamic effects in flight control p 695 N93-25274

MCLEAN, GARNET A.

Effects of seating configuration and number of type 3 exits on emergency aircraft evacuation
[AD-A256616] p 143 N93-14277

Inward contaminant leakage tests of the S-Tron Corporation emergency escape breathing device. Phase 1: Tests of the original design. Phase 2: Tests with the redesigned neck seal
[DOT/FAA/AM-92/18] p 704 N93-25205

MCLEAN, M.

Recent evolution of gas turbine materials and the development of models for life prediction p 915 A93-40802

MCLEES, R. E.

Formal representation of the requirements for an Advanced Subsonic Civil Transport (ASCT) flight control system
[NASA-CR-189699] p 98 N93-12346

MCLEOD, J. D.

Thermodynamic and neural network computer modelling of implanted component faults in a gas turbine engine
[ISABE 93-7089] p 1202 A93-54065

MCMANUS, H. L.

Reform of the aeronautics and astronautics curriculum at MIT
[AIAA PAPER 93-0325] p 454 A93-23017

MCMANUS, K.

Noninvasive, multipoint velocity measurements in high-pressure combustion flows
[AIAA PAPER 93-2032] p 1145 A93-49867

MCMANUS, RICH

Exodus: Prime Mover
[NASA-CR-192051] p 332 N93-17803

MC MILLAN, R. W.

A horizontal atmospheric temperature sounder - Applications to remote sensing of atmospheric hazards p 929 A93-43502

MC MILLAN, ROBERT

A millimeter-wave radiometer for detecting microbursts p 145 N93-14850

MC MILLIN, B. K.

Comparison of NO and OH PLIF temperature measurements in a scramjet model flowfield
[AIAA PAPER 93-2035] p 1113 A93-49870

MC MILLIN, R. D.

Effect of trailing-edge ejection on local heat (mass) transfer in pin fin cooling channels in turbine blades
[ASME PAPER 92-GT-178] p 352 A93-19404

MC MILLIN, S. NAOMI

Effect of planform and body on supersonic aerodynamics of multibody configurations
[NASA-TP-3212] p 19 N93-10824

MC MINN, JOHN D.

Impact of aeroelasticity on propulsion and longitudinal flight dynamics of an air-breathing hypersonic vehicle
[AIAA PAPER 93-1367] p 733 A93-33934

MC NALLY, B. D.

Flight test evaluation of precision-code differential GPS for terminal approach and landing p 33 A93-11294

MC NALLY, DAVID J.

The development of a mature external Master's degree program in aeronautical engineering - A university/industry partnership
[AIAA PAPER 92-4256] p 570 A93-24296

MC NAMARA, B.

F/A-18 departure recovery improvement evaluation
[AIAA PAPER 93-3671] p 1129 A93-48349

MC NAMARA, DAVID K.

Durability properties for adhesively bonded structural aerospace applications p 1217 A93-53515

MC NAMARA, JAMES E.

Testing of an energy efficient environmental control system for a patrol-type aircraft
[SAE PAPER 921225] p 890 A93-41399

MC QUADE, PETER D.

CFD-based approximation concepts for aerodynamic design optimization with application to a 2-D scramjet vehicle
[AD-A258084] p 333 N93-17893

MC QUEEN, M.

Airspace Design Expert System (ADES), a 2D/3D mapping and modelling tool incorporating an expert system for use in instrument approach design p 888 N93-30357

MC QUISTON, BARBARA

Rotorcraft health and usage monitoring systems: A literature survey
[DOT/FAA/RD-91/6] p 48 N93-11461

MC QUISTON, BARBARA M.

Intelligent diagnostics systems p 98 N93-11931

MC RAE, D. S.

Nonlinear relaxation/quasi-Newton algorithm for the compressible Navier-Stokes equations p 287 A93-23541

A coarse-grid correction/nonlinear relaxation algorithm for the three-dimensional, compressible Navier-Stokes equations

[AIAA PAPER 93-3317] p 951 A93-45013

Time-accurate simulation of a self-excited oscillatory supersonic external flow with a multi-block solution-adaptive mesh algorithm

[AIAA PAPER 93-3387] p 956 A93-45078

Numerical simulations of the unstart phenomenon in a supersonic inlet/diffuser
[AIAA PAPER 93-2239] p 1081 A93-50041

MCSWAIN, G. G.

Autonomous guidance, navigation and control bridging program plan p 532 A93-27046

MEADE, A. J., JR.

Flight vehicle aerodynamics calculated by a Galerkin finite element/finite difference method p 266 A93-20738

MEADE, ANDREW J., JR.

An application of artificial neural networks to experimental data approximation
[AIAA PAPER 93-0408] p 440 A93-23330

Calculation of compressible boundary layers by a hybrid finite element method p 692 A93-35613

Semi-discrete Galerkin solution of the compressible boundary-layer equations with viscous-inviscid interaction
[AIAA PAPER 93-3520] p 985 A93-47282

The semi-discrete Galerkin finite element modelling of compressible viscous flow past an airfoil
[NASA-CR-192161] p 483 N93-20018

MEADE, L. E.

Design, analysis, and fabrication of the technology integration box beam p 919 N93-30433

MEAKIN, ROBERT L.

Dynamic overset grid communication on distributed memory parallel processors
[AIAA PAPER 93-3311] p 1036 A93-45007

Moving body overset grid methods for complete aircraft tiltrotor simulations
[AIAA PAPER 93-3350] p 954 A93-45044

MEARS, M. J.

A Hopfield neural network for adaptive control
[AIAA PAPER 93-3729] p 1130 A93-51329

MEARS, MARK J.

URV flight test of an Ada implemented self-repairing flight control system
[AD-A259205] p 527 N93-20551

MEASURES, RAYMOND M.

Optical actuators for fly-by-light applications
Smart materials p 1172 A93-49475

[AIAA PAPER 93-3729] p 536 N93-20624

MEAUZE, GEORGES

Societe Generale des Mecaniciens, SNECMA, and ONERA, Symposium on Recent Advances in Compressor and Turbine Aerothermodynamics, Courbevoie, France, Nov. 24, 25, 1992, Reports p 1001 A93-46926

New calculation methods contribution on turbomachinery design and development
[ONERA, TP NO. 1993-60] p 1092 A93-51940

MECHERLE, G. S.

Diffraction limited collimating optics for high aspect ratio laser diode arrays p 1172 A93-48411

MEDEPALLI, SUDHAKAR

Optical thrust magnitude on a singular arc in atmospheric flight p 758 N93-25410

MEDINA, M.

Feasibility study of an active aeroelastic control system for the F-16 aircraft p 181 A93-14224

MEDLEY, JOHN A.

Hypervelocity scramjet capabilities of the T5 Free-Piston Tunnel at Caltech
[AIAA PAPER 92-5037] p 376 A93-22311

MEDVED, B. L.

Generation of flow disturbances in transonic wind tunnels p 119 A93-14354

MEDVED, BORIS L.

Some acoustic features of perforated test section walls with splitter plates p 1226 A93-53222

MEDVEDEV, V. V.

Allowing for the effect of flow nonisothermality on total pressure losses in the afterburner diffusers of augmented turbofan engines p 53 A93-12811

MEDWIN, STEVEN J.

Thermoplastic composite parts manufacture at Du Pont
[SME PAPER EM93-106] p 1159 A93-51728

MEDZORIAN, JOHN

High speed aircraft tire dynamics/issues
[SAE PAPER 921037] p 158 A93-14657

MEE, D. J.

Techniques for aerodynamic loss measurement of transonic turbine cascades with trailing-edge region coolant ejection
[ASME PAPER 92-GT-157] p 250 A93-19384

Drag measurements on blunted cones and a scramjet vehicle in hypervelocity flow
[AIAA PAPER 93-2979] p 1050 A93-48172

MEECHAM, W. C.

Increase in mortality rates due to aircraft noise p 1163 A93-49551

MEEDER, J. P.

Boundary layer effects on the flow of a leading edge vortex
[AIAA PAPER 93-3463] p 980 A93-47245

MEGGITT, B. T.

An optical fiber based position sensor with immunity to temperature variation p 743 A93-34287

MEGUID, S. A.

Theoretical and experimental investigations concerning the structural integrity of aeroengine compressor discs p 56 N93-10539

MEHENDALE, A. B.

Influence of high mainstream turbulence on leading edge film cooling heat transfer - Effect of film hole spacing p 207 A93-15068

MEHLHORN, RAINER

Enhancement of endurance performance by periodic optimal camber control p 727 A93-34541

MEHMED, O.

On the static stability of forward swept propfans
[AIAA PAPER 93-1634] p 720 A93-34162

MEHMED, ORAL

APPLE - An aeroelastic analysis system for turbomachines and propfans
[AIAA PAPER 92-4712] p 358 A93-20320

Experimental investigation of counter-rotating propfan flutter at cruise conditions
[AIAA PAPER 93-1632] p 720 A93-34160

MEHRKAM, PAUL

Wet layup materials for repair of bismaleimide composites p 1212 A93-53451

MEHTA, RABINDRA D.

Streamwise vortex meander in a plane mixing layer
[AIAA PAPER 93-0553] p 285 A93-23292

MEHTA, UNMEEL B.

Aerospace plane design challenge - Credible computations p 1015 A93-45145

MEI, CHUH

Finite element nonlinear panel flutter with arbitrary temperatures in supersonic flow p 417 A93-23555

Finite element nonlinear random response of beams to acoustic and thermal loads applied simultaneously
[AIAA PAPER 93-1427] p 740 A93-33978

Large-amplitude finite element flutter analysis of composite panels in hypersonic flow p 837 A93-39417

Effect of temperature on nonlinear two-dimensional panel flutter using finite elements p 1022 A93-45133

Vector unsymmetric eigenequation solver for nonlinear flutter analysis on high-performance computers p 1160 A93-52449

A finite element method for nonlinear panel flutter p 84 N93-10472

Nonlinear analyses of composite aerospace structures in sonic fatigue
[NASA-CR-193124] p 930 N93-29154

MEI, F.

Influence of sweep on structural optimization of a fighter wing
[AIAA PAPER 92-4794] p 323 A93-20290

MEIER, C.

Development of a realtime DGPS system
[DLR-MITT-92-06] p 503 N93-20749

MEIER, ERICH

A refined procedure to generate calibrated imagery from airborne synthetic aperture radar data p 1162 A93-47657

MEIER, G. E. A.

Interaction of compressible vortices with a rigid plate p 1239 A93-56219

MEIER, G. H.

Platinum-modified diffusion aluminide coatings on nickel-base superalloys
[AD-A263597] p 917 N93-29981

MEIER, H. U.

DNW test highlights related to aircraft environment p 190 A93-14274

MEIER, HANS-ULRICH

Artificial traction - A tool for high Reynolds number simulation?
[AIAA PAPER 93-3258] p 967 A93-46799

MEIER, SUSAN M.

The evolution of thermal barrier coatings in gas turbine engine applications
[ASME PAPER 92-GT-203] p 388 A93-19427

MEIER, SUSAN MANNING

Thermal barrier coating life prediction model development, phase 2
[NASA-CR-189111] p 198 N93-12589

- MEIER, ULRICH**
Critical considerations on European air transport politics p 103 A93-12718
- MEIJER, J. J.**
Development of a method to predict transonic limit cycle oscillation characteristics of fighter aircraft [NLR-TP-91359-U] p 999 N93-32338
- MEININGER, MATTHEW**
Heat pipe turbine vane cooling p 519 A93-26114
- MEIROVITCH, L.**
Structural modeling of low-aspect ratio composite wings [AIAA PAPER 93-1371] p 739 A93-33937
A refined structural model of composite aircraft wings for the enhancement of vibrational and aeroelastic response characteristics [AIAA PAPER 93-1536] p 740 A93-34073
Integrated structural tailoring and adaptive control of advanced flight vehicle structural vibration [AIAA PAPER 93-1697] p 757 A93-34219
- MEISL, CLAUD J.**
Rocket engine versus jet engine comparison [AIAA PAPER 92-3686] p 531 A93-24479
- MEITIN, JOSE G.**
Comparison of airborne dual-Doppler and airborne/ground-based dual-Doppler analyses of North Dakota thunderstorms p 844 A93-37694
- MEITIN, REBECCA J.**
Comparison of airborne dual-Doppler and airborne/ground-based dual-Doppler analyses of North Dakota thunderstorms p 844 A93-37694
- MEKKES, GREGORY L.**
Computational analysis of hypersonic shock wave/wall jet interaction [AIAA PAPER 93-0604] p 269 A93-21113
- MEKKES, L. T.**
Dual-spray airblast fuel nozzle for advanced small gas turbine combustors [AIAA PAPER 93-2336] p 1116 A93-50113
- MEL'NIKOV, A. N.**
A study of the aerodynamics of a wing with end slots p 1092 A93-51907
- MELAMA, H. J.**
Ice prediction systems for runways p 376 A93-22174
- MELAMED, B.**
Experimental and nonlinear vortex lattice method results for various wing-canard configurations p 479 A93-28607
- MELAMED, NAHUM**
Matched asymptotic expansion of the Hamilton-Jacobi-Bellman equation for aeroassisted plane-change maneuvers [AIAA PAPER 93-3752] p 1143 A93-51348
- MELIET, J. C.**
Design of propulsion systems for low operating costs p 55 A93-13405
- MELIS, MATTHEW E.**
Hypersonic engine component experiments in high heat flux, supersonic flow environment [NASA-TM-106273] p 1032 N93-31860
- MELQUIST, DEAN**
Comparison measurements of currents induced by radiation and injection p 926 A93-41575
- MELTON, JOHN E.**
3D Euler flow solutions using unstructured Cartesian and prismatic grids [AIAA PAPER 93-0331] p 281 A93-23022
3D automatic Cartesian grid generation for Euler flows [AIAA PAPER 93-3386] p 956 A93-45077
- MELTON, ROBERT G.**
Singular arcs for blunt endoatmospheric vehicles p 1015 A93-44380
- MELTTS, I. O.**
Flight path optimization and suboptimal control laws synthesis for transport mission of maneuverable aircraft p 180 A93-14160
- MELVIN, ROBIN G.**
Using a full potential solver for propulsion system exhaust simulation p 689 A93-34487
- MELVIN, W. W.**
Wind identification along a flight trajectory. I - 3D-kinematic approach p 223 A93-16324
Wind identification along a flight trajectory. II - 2D-kinematic approach p 524 A93-28469
Wind identification along a flight trajectory. III - 2D dynamic approach p 1007 A93-45401
- MEN'SHIKOV, V. A.**
Grid-characteristic method for calculating a three-dimensional boundary layer on the bounding surfaces of the blade passage of a turbomachine p 13 A93-12808
- MEN'SHIKOVA, V. L.**
Effect of the thermodynamic air model on the aerodynamic characteristics of profiles with bends p 776 A93-39136
- MEN'SHOV, A. L.**
Theory of the machining of polyhedral holes by plunge cutting p 835 A93-39091
- MENDELBOIM, T.**
Drag/thrust estimation via aircraft performance flight testing p 156 A93-14322
- MENEZ, J.**
Effect of environment on creep-fatigue crack propagation in turbine disc superalloys [ONERA, TP NO. 1993-5] p 916 A93-41023
- MENEZ, GENE P.**
Numerical simulations of a pulsed detonation wave augmentation device [AIAA PAPER 93-1985] p 1112 A93-49832
NO(x) reduction additives for aircraft gas turbine engines [AIAA PAPER 93-2594] p 1122 A93-50306
Analytical and experimental investigations of the oblique detonation wave engine concept [NASA-TM-102839] p 1006 N93-32374
- MENESSIER, E.**
Fiber reinforced composites: A new class of glass and glass ceramic materials for thermomechanical applications [REPT-921-430-104] p 200 N93-15490
- MENGERT, PETER**
A simulation study of the effects of communication delay on air traffic control [AD-A258593] p 502 N93-19966
- MENK, BRUCE**
Innovative bagging techniques on a composite P-51 Mustang replica p 1191 A93-53405
- MENKE, TIMOTHY E.**
Multiple model adaptive estimation applied to the VISTA F-16 flight control system with actuator and sensor failures p 907 A93-42806
Multiple model adaptive estimation applied to the VISTA F-16 with actuator and sensor failures [AD-A256444] p 188 N93-14608
Multiple model adaptive estimation applied to the VISTA F-16 with actuator and sensor failures, volume 2 [AD-A256569] p 371 N93-16165
- MENNA, R.**
Improvements in code validation algorithms for secondary surveillance radar p 883 A93-43408
- MENNE, S.**
An extended insight into hypersonic flow phenomena using numerical methods p 1093 A93-51999
- MENON, P. K. A.**
A fast algorithm for image-based ranging p 544 A93-27045
Electro-optical navigation for aircraft p 1097 A93-50643
Control theoretic approach to air traffic conflict resolution [AIAA PAPER 93-3832] p 1097 A93-51421
Image-based ranging and guidance for rotorcraft [NASA-CR-177608] p 708 N93-26549
- MENON, R. K. A.**
Nonlinear command augmentation system for a high performance aircraft [AIAA PAPER 93-3777] p 1132 A93-51372
- MENON, S.**
Active control of combustion instability in a ramjet using large-eddy simulations [AD-A255226] p 175 N93-14111
- MENON, SURESH**
Some issues concerning active control of combustion instability in a ramjet [AIAA PAPER 93-0116] p 360 A93-22566
- MENSO, G.**
AM-X high angle of attack flight test experience (single and two seat versions) p 511 N93-19910
- MENTE, LAWRENCE J.**
Advanced composite helicopter MISERS GOLD test/analysis p 508 A93-27974
- MENTER, F.**
Hypersonic flows as related to the national aerospace plane [NASA-CR-191980] p 296 N93-18378
- MERCADIE, YVES**
Integrated runway meteorological observation system (IRMOS/SIOMA) p 428 A93-22128
- MERCIER, J. F.**
The role of the radiologist in the medicolegal procedure after an aviation accident p 853 A93-39701
- MEREDITH, D. L.**
The use of genetic algorithms in the design of fuzzy logic controllers p 1167 A93-50779
- MERGLER, F.**
Investigation of the flowfield over parallel-arranged launch vehicles [AIAA PAPER 93-3060] p 1058 A93-48237
- MERHAV, S. J.**
Visual field information in Nap-of-the-Earth flight by teleoperated Helmet-Mounted displays p 517 A93-26884
Merging sparse optical flow and edge connectivity between image features: A representation scheme for 2-D display of scene depth p 845 N93-27179
- MERLENNE, M. C.**
Digital image processing applied to heat transfer measurement in hypersonic wind tunnel [ONERA, TP NO. 1992-118] p 831 A93-38593
- MERKLE, CHARLES L.**
An interaction noise between vortex and airfoil [AIAA PAPER 93-0600] p 562 A93-24726
- MERKUR'EV, A. V.**
A plate loaded by a transverse impulse force and in-plane forces p 828 A93-36799
- MERKUR'EV, V. I.**
A study of the origin of residual stresses and strains in the transparencies of supersonic aircraft p 801 A93-36784
- MERLEN, A.**
Analytical solutions for hypersonic flow past slender power-law bodies at small angle of attack p 122 A93-14550
- MERLENBACH, CHRIS**
The importance of configuration management - An overview with test program sets p 853 A93-35926
- MERRICK, VERNON K.**
Determination of YAV-8B Reaction Control System bleed flow usage [AIAA PAPER 92-4232] p 54 A93-13330
- MERRIFIELD, TERRY**
Evolution of the SIIIS-3 Ejection Seat into a Reduced Weight (RW) ejection seat p 1239 A93-54549
- MERRILL, B. R.**
Vortex shedding by blunt/bluff bodies at high Reynolds numbers. Volume 4: Rectangles [AD-A264154] p 877 N93-30151
Vortex shedding by blunt/bluff bodies at high Reynolds numbers. Volume 1: Data analysis [AD-A264151] p 877 N93-30171
Vortex shedding by Blunt/Bluff bodies at high Reynolds numbers. Volume 2: Cylinders, octagon, hexagon [AD-A264152] p 877 N93-30172
Vortex shedding by blunt/bluff bodies at high Reynolds numbers. Volume 3: Cubes [AD-A264153] p 877 N93-30173
- MERRILL, M. D.**
Functional requirements of an advanced instructional design advisor: Simulation authoring, Volume 3 [AD-A256650] p 440 N93-16500
- MERRILL, W.**
Design and evaluation of a robust dynamic neurocontroller for a multivariable aircraft control problem p 817 A93-37004
Analysis of fault-tolerant neurocontrol architectures [NASA-TM-105898] p 65 N93-12305
- MERRILL, WALTER**
Neurocontrol design and analysis for a multivariable aircraft control problem p 906 A93-41894
- MERRILL, WALTER C.**
Screening studies of advanced control concepts for airbreathing engines [AIAA PAPER 92-3320] p 1108 A93-49329
Screening studies of advanced control concepts for airbreathing engines [NASA-TM-106042] p 721 N93-25079
- MERRINGTON, GRAEME L.**
Fault signatures obtained from fault implant tests on an F404 engine [ASME PAPER 92-GT-82] p 348 A93-19331
- MERRITT, FERGUS J.**
Scientific visualization using the Flow Analysis Software Toolkit (FAST) p 758 N93-25600
- MERTENS, HENRY W.**
Performance of color-dependent tasks of air traffic control specialists as a function of type and degree of color vision deficiency [AD-A256614] p 151 N93-14275
Comparison of performance on the Shipley Institute of Living Scale, Air Traffic Control Specialist Selection Test, and FAA Academy Screen [AD-A259249] p 502 N93-20582
- MERZ, PAUL V.**
Development and testing of the digital control system for the Archytas unmanned air vehicle [AD-A261656] p 729 N93-26196
- MESANDER, GEERT A.**
Results of a low power ice protection system test and a new method of imaging data analysis p 795 A93-35932
- MESAROS, L. M.**
Computations of inviscid compressible flows using fluctuation-splitting on triangular meshes [AIAA PAPER 93-3301] p 950 A93-44999

- MESAROVIC, S.**
State of the art review of rutting and cracking
in pavements p 380 N93-16316
- MESHCHERIAKOV, E. A.**
Supersonic combustion and gasdynamic of scramjet
p 170 A93-14242
- MESHCHERYAKOV, E. A.**
Characteristics of the flame air heater of a hypersonic
wind tunnel p 1140 A93-51884
- MESNARD, G.**
Super Puma MK II - Rotor and gearbox fatigue
p 46 A93-13636
- MESSEH, W. ABDEL**
Prediction of jet impingement cooling scheme
characteristics (airfoil leading edge application)
p 932 N93-29941
- MESSERSCHMID, E.**
Non-equilibrium flow in an arc heated wind tunnel
p 910 A93-42642
- MESSERSCHMID, ERNST W.**
How to enhance safety for future space transportation
systems p 1015 A93-45444
- MESTREAU, ERIC**
TGV tunnel entry simulations using a finite element code
with automatic remeshing
[AIAA PAPER 93-0890] p 471 A93-24950
- METCALF, VERN L.**
Evaluation of piezoceramic actuators for control of
aircraft interior noise p 447 A93-19186
- METLOVA, A. EH.**
Architecture of multiprocessor data processing
machines and dispatching of the knowledge acquisition
process in flight control p 1168 A93-50958
- METSCHAN, S. L.**
Cost studies for commercial fuselage crown designs
p 920 N93-30440
- METSCHAN, STEPHEN**
Process and assembly plans for low cost commercial
fuselage structure p 923 N93-30865
- METWALLY, METWALLY ANWAR**
Erosion predictions and measurements of
high-temperature coatings and superalloys used in
turbomachines p 144 A93-12189
- METZGER, D. E.**
Computation of laminar flow and heat transfer over an
enclosed rotating disk with and without jet impingement
p 201 A93-13982
Effects of turn region treatments on pressure loss
through sharp 180-degree bends p 1256 A93-54636
Local heat transfer measurement with liquid crystals on
rotating surfaces including non-axisymmetric cases
p 902 N93-29943
- METZGER, MARK**
Handling qualities testing using the mission oriented
requirements of ADS-33C p 817 A93-35961
- METZLER, ALLEN J.**
In-stream measurements of combustion during Mach 5
to 7 tests of the Hypersonic Research Engine (HRE)
[AIAA PAPER 93-2324] p 1116 A93-50104
- MEUNIER, S.**
Ramjet NOx emission - Use of a 3D CFD method for
the combustor design of a super/hyper-sonic transport
propulsion system
[ASME PAPER 92-GT-255] p 353 A93-19464
- MEURZEC, J. L.**
Aeroelastic computation for a flexible airfoil using the
small perturbation method comparison with wind-tunnel
results
[ONERA, TP NO. 1993-43] p 987 A93-47448
- MEUSBERGER, YVES**
Satcom Pacific Ocean trials p 501 A93-28198
- MEYER-ILSE, W.**
X ray microscopy resource center at the Advanced Light
Source
[DE93-010449] p 911 N93-29869
- MEYER, BRADLEY J.**
Controlling hazardous configurations in helicopter
systems p 763 A93-35927
- MEYER, BRIAN E.**
Scale model test results for several
spherical/two-dimensional nozzle concepts
[AIAA PAPER 93-2430] p 1117 A93-50186
- MEYER, F.-W.**
The influence of rotor and fuselage wakes on rotorcraft
stability and control p 183 A93-14373
- MEYER, HANS-L.**
The DLR test aircraft in the FZ-BS, -VFW 614/ATTAS,
Dornier DO 228-101, MBB BO105 S-3
p 1018 N93-31272
- MEYER, KENNETH**
A survey of position trackers p 1151 A93-49396
- MEYER, KENNETH L.**
TEAMS - Technical expert aircraft maintenance
system p 941 A93-42865
- MEYER, ROBERT R., JR.**
Overview of the NASA Dryden Flight Research Facility
aeronautical flight projects testing p 512 N93-19916
- MEYER, W.**
The influence of intake swirl distortion on the
steady-state performance of a low bypass, twin-spool
engine p 214 N93-13211
- MEYERING, J. M.**
Geometry based Delaunay tetrahedralization and mesh
movement strategies for multi-body CFD
[AIAA PAPER 92-4575] p 15 A93-13309
- MEYERS, B. B.**
Analysis of Loran-C performance in the Pemberton area,
B.C. p 311 A93-17797
- MEYERS, JAMES F.**
Doppler global velocimetry measurements of the vortical
flow above an F/A-18
[AIAA PAPER 93-0414] p 415 A93-23333
Doppler global velocimetry - The next generation?
[AIAA PAPER 92-3897] p 539 A93-24486
A three dimensional view of velocity using lasers
p 1028 A93-46822
- MEYERSON, ROBERT E.**
Facilities and capabilities catalog for landing and escape
systems
[NASA-RP-1282] p 196 N93-14495
- MEYLER, KAREN L.**
Evaluation of water-borne adhesive bonding primers for
use on the advanced aircraft material aluminum-lithium
p 1211 A93-53420
- MEYRUEIS, PATRICK**
Design of an optimal single reflective holographic helmet
display element p 517 A93-26886
- MEZEIX, J. F.**
Maximum hail concentration that can be met by an
aircraft in stormy precipitations p 430 A93-22152
- MAILLIER, BERNARD**
The Airborne Collision Avoidance System (ACAS)
p 883 A93-43370
- MAKAE-LYE, R. C.**
Plume and wake dynamics, mixing, and chemistry behind
a high speed civil transport aircraft p 1034 A93-45139
Stratospheric aircraft exhaust plume and wake chemistry
studies
[NASA-CR-189688] p 94 N93-12299
- MAKAE-LYE, RICHARD**
Icing prevention by ultrasonic nucleation of supercooled
water droplets in front of subsonic aircraft
[AD-A258212] p 142 N93-12816
- MIAO, RUNTIAN**
Experimental investigation on patterned blades of
compressor p 1066 A93-48515
- MIAO, YONGMIAO**
The computation of internal flow fields in centrifugal
compressor impellers p 259 A93-20120
- MICHALAK, R.**
Results of a low-altitude flight noise study in Germany
- Acute extraaural effects p 1163 A93-49557
- MICALSKI, WIESLAW J.**
Active aircraft recovery from a spin
p 524 A93-27295
- MICHAUT, CHRISTIANE**
Toward the second-generation supersonic transport
[ONERA, TP NO. 1993-26] p 890 A93-41038
- MICHAUX, OLIVIER**
Solution of the Euler equations around a double
ellipsoidal shape using unstructured meshes and including
real gas effects p 867 A93-42604
- MICHEA, B.**
Aerodynamic rotor loads prediction method with free
wake for low speed descent flights
[ONERA, TP NO. 1992-122] p 772 A93-38596
Blade-vortex interaction noise - Prediction and
comparison with flight and wind tunnel tests
[ONERA, TP NO. 1992-126] p 851 A93-38600
- MICHEL, ULF**
Prediction of jet mixing noise in high-speed flight
p 450 A93-19216
The noise of jet aircraft flying with high speeds at low
altitudes p 450 A93-19218
Comparison of flyover noise data from aircraft at high
subsonic speeds with prediction p 100 N93-10674
Prediction of jet mixing noise for high subsonic flight
speeds p 100 N93-10685
Calculation of noise emission caused by jet aircraft
during takeoff, approach and horizontal flyover
[DLR-MITT-91-15] p 569 N93-21368
- MICHELASSI, V.**
Studies on coolant problems in aeronautical turbine
cascades
[ISABE 93-7074] p 1220 A93-54050
- MICHEL, FRANCIS**
Analysis of turbulence in supersonic flows by means
of laser velocimetry
[ONERA, TP NO. 1992-148] p 773 A93-38729
- MICKLOW, G. J.**
Numerical simulation of a low-emission gas turbine
combustor using KIVA-II p 170 A93-14077
- MICKLOW, GERALD J.**
Emissions reduction by varying the swirler airflow split
in advanced gas turbine combustors
[ASME PAPER 92-GT-110] p 349 A93-19347
A nonperiodic boundary approach for computation of
compressible viscous flows in advanced turbine
cascades
[AIAA PAPER 93-1799] p 1074 A93-49688
The effects of turbulence modeling on the numerical
simulation of confined swirling flows
[AIAA PAPER 93-1976] p 1078 A93-49823
Computation of the flow field in an annular gas turbine
combustor
[AIAA PAPER 93-2074] p 1113 A93-49903
Numerical analysis of the flow fields in a RQL gas turbine
combustor
[DE92-017509] p 89 N93-11767
- MICOL, JOHN R.**
Hypersonic lateral and directional stability characteristics
of aerobassist flight experiment configuration in air and
CF4
[NASA-TM-4435] p 875 N93-29166
- MIDDEL, JAN**
Development of a computer assisted toolbox for
aerodynamic design of aircraft at subcritical conditions with
application to three-surface and canard aircraft
[ISBN-90-6275-768-5] p 441 N93-16567
- MIDDLETON, DAVID B.**
Simulator evaluation of displays for a revised takeoff
performance monitoring system
[NASA-TP-3270] p 189 N93-15366
- MIDDLETON, ELIZABETH M.**
Assessing spatial and seasonal variations in grasslands
with spectral reflectances from a helicopter platform
p 426 A93-20621
- MIELE, A.**
Wind identification along a flight trajectory. I -
3D-kinematic approach p 223 A93-16324
Wind identification along a flight trajectory. II -
2D-kinematic approach p 524 A93-28469
Wind identification along a flight trajectory. III - 2D
dynamic approach p 1007 A93-45401
- MIFSUD, BRIAN**
Arc jet testing in NASA Ames Research Center
thermophysics facilities
[AIAA PAPER 92-5041] p 385 A93-22315
- MIGNOLET, MARC P.**
The combined closed form-perturbation approach to the
analysis of mistuned bladed disks
[ASME PAPER 92-GT-125] p 350 A93-19359
- MIJS, J.**
The leading edge vortex of a rotating stall cell
[ISABE 93-7009] p 1183 A93-53985
- MIKAMI, TADASHI**
Development of ultra-hypersonic shock tunnel for
aerodynamics test p 376 A93-21900
- MIKESELL, BRIAN G.**
Methods and principles for determining task dependent
interface content
[NASA-CR-190837] p 36 N93-10961
- MIKHAILOV, V. I.**
Shock wave interference on a wing with a partition at
hypersonic velocities p 13 A93-12839
- MIKHAILOV, V. V.**
Effect of longitudinal microribbing on the drag of a body
of revolution p 5 A93-10147
- MIKHAILOV, YU. YA.**
Substitution of oriented differences for central
differences in a program for calculating smooth supersonic
flows p 1085 A93-50966
- MIKHAIJLYUK, A. A.**
A study of the effect of the shape of a parasail on its
lift-drag ratio p 1069 A93-48913
A study of air intake parameters on the aerodynamic
characteristics of a parasail p 1092 A93-51908
- MIKITEEN, BRIAN**
Development of a flight instrument package
[AD-A260830] p 719 A93-25783
Inflight evaluation of an acoustic orientation instrument
[AD-A260752] p 719 N93-25909
- MIKULIN, E. I.**
A fuel-oil matrix heat exchanger p 833 A93-39052
- MILANO, JOEL**
Prediction of helicopter component loads using neural
networks
[AIAA PAPER 93-1301] p 756 A93-33878
- MILBANK, J.**
Measurement and prediction of flow in a gas turbine
engine exhaust plume
[ISABE 93-7113] p 1204 A93-54088

- MILBURN, NELDA**
Comparison of performance on the Shipley Institute of Living Scale, Air Traffic Control Specialist Selection Test, and FAA Academy Screen
[AD-A259249] p 502 N93-20582
- MILBURN, NELDA J.**
Performance of color-dependent tasks of air traffic control specialists as a function of type and degree of color vision deficiency
[AD-A256614] p 151 N93-14275
- MILESHIN, V. I.**
3D/quasi-3D trans- and supersonic flow calculation in advanced centrifugal/axial compressor stages
p 972 A93-46936
- MILEY, STAN J.**
Measurement of attachment-line location in a wind-tunnel and in supersonic flight
[AIAA PAPER 92-4089] p 39 A93-11285
- MILIKH, G. M.**
A computer simulation of the production of an artificially ionized layer using the Arecibo facility
[DE93-010817] p 937 N93-30487
- MILLARD, DOUG**
Spaceplanes - Back to the future p 733 A93-34265
- MILLER, CHRISTOPHER J.**
Investigation of advanced counterrotation blade configuration concepts for high speed turboprop systems. Task 5: Unsteady counterrotation ducted propfan analysis. Computer program user's manual
[NASA-CR-187125] p 521 N93-20583
- MILLER, DAVID G.**
The influence of structural optimization on the aeroelastic properties of a vertical tail
[AD-A259140] p 513 N93-20575
- MILLER, EDWARD**
Volcanic ash and aircraft operations
p 309 A93-22181
- MILLER, GLEN E.**
Fiber optic position sensors p 1105 A93-49465
- MILLER, J. K.**
The effect of clock, media, and station location errors on Doppler measurement accuracy p 885 N93-29588
- MILLER, JEFFREY H.**
A hot dynamic seal rig for measuring hypersonic engine seal durability and flow performance
[AIAA PAPER 93-1346] p 738 A93-33916
- MILLER, KURTIS B.**
Design of robust suboptimal controllers for a generalized quadratic criterion
[AD-A257746] p 372 N93-17670
- MILLER, L. E.**
Optimal cruise performance p 802 A93-37394
- MILLER, L. S.**
Effects of blowing on delta wing vortices during dynamic pitching p 768 A93-37384
- MILLER, LARRY**
Rotorcraft health and usage monitoring systems: A literature survey
[DOT/FAA/RD-91/6] p 48 N93-11461
- MILLER, LEE**
Update on the NASA ER-2 Doppler radar system (EDOP) p 807 A93-37737
- MILLER, MARK J.**
Silicon differential pressure transducer line pressure effects and compensation p 830 A93-37890
- MILLER, MARK S.**
Curvature and leading edge sweep back effects on grid fin aerodynamic characteristics
[AIAA PAPER 93-3480] p 981 A93-47258
- MILLER, MATTHEW**
Aging jet transport structural evaluation programs p 947 A93-45781
- MILLER, NORMAN**
Design of a recovery system for a reentry vehicle
[AIAA PAPER 93-1224] p 733 A93-35171
- MILLER, P.**
Wall jets created by single and twin high pressure jet impingement p 744 A93-34847
- MILLER, PAUL G.**
Royal Navy helicopter operations in the maritime environment p 1190 A93-54290
- MILLER, R. A.**
Technical note - Plasma-sprayed ceramic thermal barrier coatings for smooth intermetallic alloys p 209 A93-15702
- MILLER, R. J.**
Preliminary evaluation of aviation-impact variables derived from numerical models
[PB93-190197] p 1034 N93-31202
- MILLER, R. N.**
In-situ bioventing: Two US EPA and Air Force sponsored field studies
[PB93-194231] p 1035 N93-32089
- MILLER, ROGER**
Internally coherent system of innovation - The case of flight simulation
[AIAA PAPER 93-3548] p 1226 A93-52653
- MILLER, W. A.**
Variable speed rotary compressor and adjustable speed drive efficiencies measured in the laboratory
[DE92-040026] p 222 N93-15278
- MILLER, WAYNE O.**
Efficient free wake calculations using analytical/numerical matching p 874 A93-43780
Direct periodic solutions of rotor free wake calculations p 874 A93-43781
- MILLER, WILLIAM E.**
Method of remotely characterizing thermal properties of a sample
[NASA-CASE-LAR-13508-3-CU] p 67 N93-11057
- MILLINGTON, PETER J.**
Control augmentation system (CAS) synthesis via adaptation and learning
[AIAA PAPER 93-3728] p 1170 A93-51328
- MILLMAN, DANIEL R.**
Finite-difference solution for laminar or turbulent boundary layer flow over axisymmetric bodies with ideal gas, CF₄, or equilibrium air chemistry
[NASA-TP-3271] p 222 N93-15434
- MILLS, A. F.**
Fluid flow and heat convection studies for actively cooled airframes
[NASA-CR-190956] p 216 N93-13406
- MILLS, RAYMOND ARTHUR**
Robust controller and estimator design using minimax methods p 229 N93-13925
- MILLWATER, H. R.**
Computational techniques for probabilistic analysis of turbomachinery
[ASME PAPER 92-GT-167] p 351 A93-19393
- MILNER, EDWARD J.**
Turbomachinery CFD on parallel computers
[NASA-TM-105932] p 228 N93-13154
- MILOH, T.**
Towards an analytical treatment of the aerolastic problem of a circular wing p 781 N93-27214
- MILOS, FRANK S.**
Thermal analysis of an arc heater electrode with a rotating arc foot
[AIAA PAPER 93-2855] p 1028 A93-46590
- MILOTOV, YU. N.**
Calculation of the position of aircraft center of gravity on an IBM PC p 996 A93-45671
General concepts related to the determination of the individual flight performance characteristics of aircraft for establishing fuel consumption standards and optimal flight regimes p 996 A93-45673
- MILSTEIN, D.**
Integrated utilities management system for aircraft p 153 A93-14208
- MILTHORPE, J. F.**
Numerical simulation of two-dimensional compressible flows p 687 A93-34357
Numerical simulation of two-dimensional and axisymmetric compressible flows p 960 A93-45546
- MILTO, A. V.**
Selection of methods and equipment for monitoring the technical condition of booster system components p 395 A93-18329
Diagnostics of the hydraulic system of Tu-204 aircraft p 396 A93-18360
Characteristics of the diagnostics of booster system components p 321 A93-18361
- MIMURA, F.**
A new cooling system for ultra high temperature turbines
[ISABE 93-7073] p 1201 A93-54049
- MINAGAWA, N.**
Turbine blade vibration monitoring system
[ASME PAPER 92-GT-159] p 402 A93-19386
- MINAILOS, A. N.**
Calculation of the effect of the shock wave of a delta wing on a second wing at supersonic velocities p 776 A93-39141
Calculation of the effect of flow conicity in a hypersonic nozzle on the aerodynamics of a flight vehicle model p 776 A93-39142
- MINATO, MASASHI**
Flow measurements behind V-gutter under non-combusting condition
[AIAA PAPER 93-0020] p 408 A93-20139
Isothermal flow characteristics behind V-shape gutter with and without injection
[ISABE 93-7040] p 1198 A93-54016
- MINDICH, G. KH.**
Determination of nonstationary aerodynamic loading on cascade blades in the case of dynamic changes of the angle of attack p 544 A93-26817
- MINECK, RAYMOND E.**
The adaptive wall test section for the NASA Langley 0.3-m Transonic Cryogenic Tunnel p 1013 A93-46825
Demonstration of multipoint design procedures for transonic airfoils
[AIAA PAPER 93-3114] p 1062 A93-48284
- MINECK, RAYMOND EDWARD**
Assessment of potential aerodynamic benefits from spanwise blowing at the wing tip p 134 A93-13822
- MINIEV, B. I.**
Experimental study of the effect of external turbulence and the shape of the surface on the characteristics of laminar and transition boundary layers p 987 A93-47522
- MINEKAWA, HIDEOTO**
Characteristics of heat exchanger in supersonic/subsonic flows
[ISABE 93-7119] p 1221 A93-54094
- MINENO, HITOSHI**
Guidance and control of HOPE (H-II orbiting plane)
[AAS PAPER 91-653] p 1252 A93-55825
Research on combined HOPE navigation technology p 533 N93-20428
- MINER, PAUL S.**
Characterization of the faulted behavior of digital computers and fault tolerant systems p 1224 A93-52762
- MINER, TIMOTHY H.**
New initiatives for aviation meteorology training - 1989 through 1991 p 307 A93-22109
- MING, TANG**
An experimental investigation of hydrogen-fueled supersonic combustor p 53 A93-12733
- MINGUET, PIERRE**
The development and evaluation of advanced Kevlar sandwich structure for application to rotorcraft airframes p 546 A93-27965
- MINGUET, PIERRE J. A.**
Damage tolerance evaluation of new manufacturing techniques for composite helicopter drive shafts
[AIAA PAPER 93-1400] p 739 A93-33960
- MINH, H. H.**
High lift airfoil flow simulation using a wall-corrected Algebraic Stress Model
[AIAA PAPER 93-3109] p 1061 A93-48280
On the numerical simulation of the two-dimensional flow field around a hypersonic air-intake-compressibility effects
[ISABE 93-7100] p 1187 A93-54076
- MININ, I. I.**
Selection of methods and equipment for monitoring the technical condition of booster system components p 395 A93-18329
Characteristics of the diagnostics of booster system components p 321 A93-18361
Monitoring the purity of the working fluids of aircraft hydraulic systems during service p 321 A93-18367
Analysis of the pump station of an aircraft hydraulic system as a subject of diagnosis p 321 A93-18374
- MINNETYAN, LEVON**
Damage progression in stiffened composite panels
[AIAA PAPER 93-1345] p 738 A93-33915
- MINNICH, STEVEN H.**
Applying commercial style acquisition practices to the procurement of commercially available aircraft
[AD-A258143] p 455 N93-18087
- MINODA, M.**
Noise reduction of supersonic heated jet with jet mixing enhancement by tabs
[ISABE 93-7046] p 1198 A93-54022
- MINODA, MITSUHIRO**
Some topics of research on hypersonic airbreathing engines at National Aerospace Laboratory
[ASME PAPER 92-GT-256] p 353 A93-19465
- MINUCCI, M. A. S.**
Experimental investigation of an axisymmetric hypersonic scramjet inlet for laser propulsion p 122 A93-14515
Investigation of a two-dimensional scramjet inlet, freestream M = 8-18 and Tsub 0 = 4100 K p 270 A93-21669
- MINUCCI, MARCO A. S.**
An investigation on the use of a heavy gas to improve the performance of the equilibrium interface technique in shock tube flows
[AIAA PAPER 93-2017] p 1078 A93-49855
- MINUTO, A.**
The role of fatigue testing in the design, development and certification of the ATR 42/72 p 46 A93-13637
Review of aeronautical fatigue investigation activities developed in Alenia-GAT during the period May 1990 - March 1991
[ETN-92-92884] p 329 N93-16287
- MODUSHEVSKII, P. V.**
A new production technology for complex-shaped structural elements 'creep forming' p 202 A93-14175

- MIQUEL, J.**
Numerical simulation of hypersonic flow over a double ellipse using a Taylor-Galerkin finite element formulation with adaptive grids p 868 A93-42617
- MIRESSI, MICHAEL J.**
Magnetic variation - A primitive concept and its hold on contemporary navigation p 32 A93-11021
- MIRFAKHRAIE, ZOHREH**
Design of a helicopter control system to meet handling quality specifications using H(infinity) techniques [AIAA PAPER 93-3850] p 1134 A93-51437
- MIRKIN, V. A.**
Using ultralight flight vehicles for large-scale aerial photography p 92 A93-10098
- MIRONOV, A. K.**
Localization of noise sources in the exhaust jet of a turbofan engine p 1003 A93-47509
- MIRONOV, A. M.**
A pressure distribution measuring system with pneumatic switches and automatic band selection p 75 A93-10029
- MIRSAFIAN, S.**
A guidance display system for single pilot operation [AIAA PAPER 92-4196] p 51 A93-13373
- MIRSHAMS, MOHSEN**
Transition for three-dimensional boundary layers on wings in the transonic regime [AIAA PAPER 93-3049] p 1057 A93-48229
- MISAWA, HIROSHI**
Effect of stress level of gust cycles on fatigue crack propagation behavior (Acceleration and retardation of crack propagation under simplified flight simulation loading) p 198 A93-17033
- MISHCHENKO, A. A.**
An algorithm with prediction in a control problem with functional constraints p 757 A93-35307
- MISHCHENKOV, M. T.**
Development of a process for fabricating a plate heat exchanger for the heat recovery system of gas turbine engines p 834 A93-39053
- MISHIN, V. F.**
Effect of gasdynamic parameters on the specific weight of gas-turbine aircraft engines p 899 A93-42372
Determination of the takeoff characteristics of jet engines during the preliminary design of aircraft p 892 A93-42378
- MISHULIN, I. B.**
Calculation of sandwich plates with polymer composite skins under conditions of high humidity p 1215 A93-52968
- MISKOVISH, R. S.**
Some unsteady fluid forces on pump impellers p 413 A93-22265
- MISRA, P.**
Integrated use of GPS and GLONASS in civil aviation navigation. II - Experience with GLONASS p 313 A93-21142
Receiver Autonomous Integrity Monitoring (RAIM) of GPS and GLONASS p 993 A93-46891
- MITANI, TOHRU**
Evaluation of 2D scramjet nozzle performance p 52 A93-11209
Validation studies of scramjet nozzle performance p 1109 A93-49616
Off-design performance of scramjet nozzles [ISABE 93-7108] p 1203 A93-54084
- MITCHELL, A.**
Clean melting and the removal of defects from aero-engine materials p 1217 A93-53503
- MITCHELL, CLARK A.**
Conceptual assessment of two high-speed rotorcraft p 508 A93-28612
- MITCHELL, DAVID G.**
Ground based simulation evaluation of the effects of time delays and motion on rotorcraft handling qualities [AD-A256921] p 328 A93-16186
- MITCHELL, K.**
Miniature display technologies for integrated helmet systems p 718 A93-34819
- MITCHELL, L. D.**
Measurement of a one-dimensional mobility using a laser-Doppler velocimeter p 210 A93-16647
- MITCHELLE, ROBERT A.**
Zonally-decoupled DSMC solutions of hypersonic blunt body wake flows [AIAA PAPER 93-2808] p 949 A93-44227
Hypersonic blunt body wake computations using DSMC and Navier-Stokes solvers [AIAA PAPER 93-2807] p 964 A93-46547
- MITIAGIN, V. A.**
Protective properties of aviation oils p 735 A93-35299
- MITIN, B. M.**
Heat exchangers of gas turbine engines p 833 A93-39044
- MITON, H.**
Supersonic through flow compressors - A preliminary study: COVAXS p 1001 A93-46930
- MITRA, N. K.**
Effects of longitudinal vortex generators on heat transfer and flow loss in turbulent channel flows p 1021 A93-44222
Multigrid methods for calculating 3D flows in complex geometries p 973 A93-46984
- MITRIAEV, K. F.**
Increasing the durability of gas turbine engine compressor blades by using a combined hardening/finishing treatment to control the stressed state of the surface layer p 835 A93-39099
- MITROFANOV, A. A.**
A method for calculating the characteristics of plane compressor cascades for different values of the Reynolds criterion p 545 A93-27616
- MITROFIOVICH, V. V.**
A data processing and measuring system with a traversing probe for studying flow in the rotating impeller of an axial-flow fan p 75 A93-10032
- MITROKHIN, V. T.**
Direct and inverse problems of calculating the axisymmetric and 3D flow in axial compressor blade rows p 972 A93-46938
- MITTAL, MANOJ**
Three-dimensional modeling and control of a twin-lift helicopter system p 370 A93-23511
- MITTAL, S.**
A finite element study of incompressible flows past oscillating cylinders and aerofoils p 241 A93-17750
- MITTAL, SANJAY**
Stabilized space-time finite element formulations for unsteady incompressible flows involving fluid-body interactions p 843 A93-29040
- MITTY, TODD J.**
Solution of three-dimensional supersonic flowfields via adapting unstructured meshes p 863 A93-42442
- MIURA, HIROKAZU**
Survey - Applications of structural optimization methods to fixed wing aircraft and spacecraft p 325 A93-20328
Applications to fixed-wing aircraft and spacecraft [AIAA PAPER 92-4726] p 996 A93-45432
Applications of structural optimization methods to fixed-wing aircraft and spacecraft in the 1980s [NASA-TM-103939] p 1033 A93-32212
- MIYAGAWA, H.**
Conceptual design study on combined-cycle engine for hypersonic transport [ISABE 93-7018] p 1195 A93-53994
- MIYAGI, H.**
Conceptual design study on combined-cycle engine for hypersonic transport [ISABE 93-7018] p 1195 A93-53994
- MIYAJIMA, HIROSHI**
Evaluation of 2D scramjet nozzle performance p 52 A93-11209
Validation studies of scramjet nozzle performance p 1109 A93-49616
- MIYAKAWA, JUNICHI**
Wind tunnel testing and CFD simulation in Mitsubishi Heavy Industries p 305 A93-19325
- MIYAOKA, H.**
Polar Patrol Balloon Experiment in Antarctica p 27 A93-11373
- MIYATA, MASAFUMI**
The coherent structure in a corner turbulent boundary layer p 548 A93-28575
- MIYAZAWA, Y.**
Integrated control law synthesis of gust load alleviation and flutter margin augmentation for a transport aircraft p 182 A93-14281
- MIYAZAWA, YOSHIKAZU**
Guidance and control law for automatic landing flight experiment of reentry space vehicle [AIAA PAPER 93-3818] p 1143 A93-51409
- MIYOSHI, HAJIME**
CFD development and a future high speed computer p 847 A93-38128
Numerical Wind Tunnel: Requirements and the outline p 383 A93-19288
Numerical Wind Tunnel hardware p 383 A93-19289
- MIZUKAMI, MASASHI**
Bibliography on propulsion airframe integration technologies for high-speed civil transport applications, 1980-1991 [NASA-TM-105602] p 678 A93-26136
- MIZUKI, SHIMPEI**
Numerical analysis of flow within cascade with tip clearance p 1176 A93-53192
- MIZUTANI, TOMOAKI**
Results of sea-level static tests on air turbo ramjet for a future space plane [AAS PAPER 91-640] p 1247 A93-55817
- MKHITARIAN, S. L.**
Selection of the scheme and optimal parameters of the turbine of a high-temperature bypass engine with a low bypass ratio p 811 A93-39180
- MKPADI, M. C.**
Impingement/effusion cooling p 932 A93-29954
- MO, J.**
Effects of a rear stagnation jet on the wake behind a cylinder p 1151 A93-49026
- MO, J. D.**
An investigation of the effects of a rear stagnation jet on the wake behind a cylinder [AIAA PAPER 93-3274] p 969 A93-46835
- MO, JIA-DA**
The Burnett shock structures in low density hypersonic flows [AIAA PAPER 92-5048] p 273 A93-22320
- MOAS, E. JR.**
An experimental and analytical investigation on the response of GR/EP composite I-frames p 546 A93-27975
- MOATS, CHRISTINA D.**
Rarefied-flow shuttle aerodynamics flight model [AIAA PAPER 93-3441] p 859 A93-41057
Rarefied-flow Shuttle aerodynamics model [NASA-TM-107698] p 458 A93-19976
- MOBLEY, THOMAS**
'No VOC' water-borne corrosion resistant primers for aerospace bonding applications p 1211 A93-53419
- MOCHIZUKI, O.**
Active forcing of an axisymmetric leading-edge turbulent separation bubble [AIAA PAPER 93-3245] p 966 A93-46790
- MOCHIZUKI, S.**
Heat transfer in serpentine flow passages with rotation [ASME PAPER 92-GT-190] p 403 A93-19415
- MOCKLER, THEODORE T.**
Design of a high-temperature experiment for evaluating advanced structural materials [NASA-TM-105833] p 88 A93-11624
- MOCSARI, JEFFREY C.**
Analytic methods for design of wave cycles for wave rotor core engines [AIAA PAPER 93-2523] p 1121 A93-50253
- MODIANO, DAVID**
Experimental and computational investigations of the flowfield around the F117A [AIAA PAPER 93-3508] p 984 A93-47274
- MODIANO, DAVID L.**
An acceleration technique for time accurate calculations p 957 A93-45092
Adaptive computations of flow around a delta wing with vortex breakdown [AIAA PAPER 93-3400] p 974 A93-47202
- MOEHLKAMP, K.**
Increasing airport safety and capacity using automated maneuvering area control p 885 A93-43550
- MOEHLER, O.**
A novel aircraft-based tandem mass spectrometer for atmospheric ion and trace gas measurements p 925 A93-40672
- MOEHRES, W.**
Modelling the engine temperature distribution between shut down and restart for life usage monitoring p 169 A93-15177
- MOEK, G.**
European studies to investigate the feasibility of using 1000 ft vertical separation minima above FL(290). III - Further results and overall conclusions p 992 A93-45166
- MOEKEN, BERTUS**
Dornier 228 experimental with laminar wing p 506 A93-27500
- MOEN, VERLYN**
Design, capabilities, and performance of the miniaturized airborne GPS receiver p 32 A93-11014
- MOENICH, MARCEL**
New digital capacitive measurement system for blade clearances p 1254 A93-54376
- MOENIG, R.**
Design and rotor performance of a 5:1 mixed-flow supersonic compressor [ASME PAPER 92-GT-73] p 348 A93-19323
- MOENNICH, WULF**
A new flying qualities criterion for flying wings [AIAA PAPER 93-3668] p 1128 A93-48346
- MOERDER, DANIEL D.**
Optimal open multistep discretization formulas for real-time simulation p 757 A93-34539
- MOES, TIMOTHY R.**
Application of a flush airdata sensing system to a wing leading edge (LE-FADS) [AIAA PAPER 93-0634] p 516 A93-24750

- Flight and wind-tunnel calibrations of a flush airdata sensor at high angles of attack and sideslip and at supersonic Mach numbers
[NASA-TM-104265] p 344 A93-19110
- Application of a flush airdata sensing system to a wing leading edge (LE-FADS)
[NASA-TM-104267] p 518 A93-20163
- MOEWS, J.**
Numerical determination of the residual strength of battle damaged composite plates p 537 A93-21533
- MOFFITT, ROBERT C.**
Development and validation of 'quiet tail rotor' technology p 567 A93-29416
- MOHAMED, AJMAL KHAN**
Electron beam probing of blow-down hypersonic flows [ONERA-NT-1992-7] p 298 A93-18701
- MOHAMED, TENNICH**
Dynamic simulation of flexible body systems by the vector solution method p 553 A93-20666
- MOHAN, JAI**
A technique for accelerated convergence in transonic flow p 685 A93-34347
- MOHLEJI, SATISH C.**
Flight management systems information exchange with AERA to support future air traffic control concepts p 31 A93-11008
- MOHLER, R. R.**
Nonlinear time-series-based adaptive control applications p 97 A93-13230
- MOIN, PARVIZ**
Boundary conditions for direct computation of aerodynamic sound generation p 447 A93-19176
Boundary conditions for direct computation of aerodynamic sound generation p 1172 A93-49005
- MOKHOV, V. F.**
Methodology for studying the fracture of aircraft structures in static tests p 801 A93-36785
- MOKHTARIAN, F.**
Multi-block grid generation for complete aircraft configurations p 460 A93-23838
Development of a transonic Euler method for complete aircraft configurations p 779 A93-39721
- MOLE, P. J.**
Development of a six component flexured two shell internal strain gage balance [AIAA PAPER 93-0793] p 541 A93-24872
- MOLENT, L.**
Crack growth and repair of multi-site damage of fuselage lap joints p 547 A93-28291
Bonded repair of multi-site damage p 947 A93-45786
Damage tolerance assessment of boron/epoxy repairs to fuselage lap joints [AD-A258383] p 338 A93-18257
- MOLEZZI, M. J.**
Application of particle image velocimetry in high-speed separated flows p 549 A93-29304
Study of the near-wake structure of a subsonic base cavity flowfield using PIV [AIAA PAPER 93-3040] p 1056 A93-48221
- MOLIAKOV, N. M.**
Numerical solution of the integral equations of the aerodynamics of porous surfaces p 13 A93-12768
- MOLINA, HELENE**
Experimental results on RIAS digital beamforming radar p 929 A93-43392
- MOLLOY, ROBERT**
Adaptive automation and human performance: Multi-task performance characteristics [AD-A254596] p 186 A93-12578
- MOLNAR, DAVE**
Advanced hypersonic aircraft design [NASA-CR-192046] p 334 A93-18037
- MOLTON, P.**
Experimental study of 3-D separation on a large scale model [AIAA PAPER 93-3007] p 1053 A93-48197
- MOLTON, PASCAL**
Laser-velocimeter study of vortex breakdown on a 70-deg swept delta wing in incompressible flow [ONERA, TP NO. 1992-147] p 773 A93-38728
- MOLVIK, GREGORY A.**
Analysis of a hypersonic waverider research vehicle with a hydrocarbon scramjet engine [AIAA PAPER 93-0509] p 386 A93-23256
- MOMIGLIANO, ALBERTO**
Scheduling of an aircraft fleet p 443 A93-18665
- MONAHAN, P. L.**
Automated Weather Distribution System (AWDS) for support of global aviation p 428 A93-22134
- MONAHEMI, MOGHEN M.**
Design of reduced-order observers with precise loop transfer recovery p 184 A93-14587
- MONFORTE, E.**
AM-X high angle of attack flight test experience (single and two seat versions) p 511 A93-19910

- MONGEAU, L.**
Sound generation by rotating stall in centrifugal turbomachines p 1039 A93-46701
- MONGIA, H. C.**
Three-dimensional gas turbine combustor emissions modeling [ASME PAPER 92-GT-129] p 350 A93-19363
Three-dimensional NOx modeling for rich/lean combustor [AIAA PAPER 93-0251] p 360 A93-22660
An analytical study of dilution jet mixing in a cylindrical duct [AIAA PAPER 93-2043] p 1113 A93-49876
Three-dimensional emission modeling for diffusion flame, rich/lean, and lean gas turbine combustors [AIAA PAPER 93-2338] p 1117 A93-50115
Fuel injector: Air swirl characterization aerothermal modeling, phase 2, volume 1 [NASA-CR-189193-VOL-1] p 721 A93-24754
Fuel injector: Air swirl characterization aerothermal modeling, phase 2, volume 2 [NASA-CR-189193-VOL-2] p 721 A93-25106
An analytical study of dilution jet mixing in a cylindrical duct [NASA-TM-106181] p 814 A93-27160
- MONGIA, HUKAM C.**
An efficient liner cooling scheme for advanced small gas turbine combustors [AIAA PAPER 93-1763] p 1109 A93-49660
- MONICO, R. D.**
Modelling thermal behaviour of turbomachinery discs and casings p 903 A93-29949
- MONNOYER, F.**
Hypersonic configuration optimization with an Euler/boundary layer coupling technique [AIAA PAPER 93-3116] p 1062 A93-48286
- MONTA, WILLIAM J.**
Assessment of a flow-through balance for hypersonic wind tunnel models with scramjet exhaust flow simulation [NASA-TM-4441] p 779 A93-27005
- MONTAG, BRUCE**
Visual weather simulation using meteorological databases [AIAA PAPER 93-3566] p 1207 A93-52665
- MONTAGUE, TIMOTHY**
Integrated Soviet VLF/Omega Receiver design p 316 A93-21198
- MONTARDI, Y.**
Fiber reinforced composites: A new class of glass and glass ceramic materials for thermomechanical applications [REPT-921-430-104] p 200 A93-15490
- MONTEZ, MOISES N.**
Results from a GPS Shuttle Training Aircraft flight test p 384 A93-21148
- MONTGOMERY, RAYMOND C.**
Lumped mass modelling for the dynamic analysis of aircraft structures p 510 A93-19460
- MONTICONE, LEONE C.**
Enhancing availability, performance, and flexibility of air traffic control air-ground services p 887 A93-30353
- MONTIGNY-RANNOU, F.**
MESHD - A tool for the construction of three-dimensional meshes [ONERA, TP NO. 1992-164] p 561 A93-25339
- MOODY, LARRY A.**
Dynamic simulation fidelity improvement using transfer function state extrapolation [AIAA PAPER 93-3552] p 1222 A93-52656
- MOODY, R. E.**
Inlet design using a blend of experimental and computational techniques p 114 A93-14210
- MOON, H. A.**
Flight simulation leaves the ground p 194 A93-14616
- MOOK, D. J.**
Pilot control identification using Minimum Model Error estimation [AIAA PAPER 92-4421] p 523 A93-24497
Automatic carrier landing system utilizing aircraft sensors p 1097 A93-49590
Theoretical constraints in the design of multivariable control systems [NASA-CR-191900] p 442 A93-18372
- MOON, DON**
Real-time monitoring for software development and testing p 939 A93-42624
- MOORE, ALLAN S.**
External stress-corrosion cracking of a 1.22-m-diameter type 316 stainless steel air valve [NASA-TP-3190] p 737 A93-26201
- MOORE, E. S.**
Machinery arrangements for small VTOL transport aircraft p 713 A93-34848

- MOORE, F. G.**
A new semiempirical method for computing nonlinear angle-of-attack aerodynamics on wing-body-tail configurations [AIAA PAPER 93-0034] p 260 A93-20148
Base drag prediction on missile configurations [AIAA PAPER 93-3629] p 1064 A93-48314
- MOORE, F. K.**
Stall transients including effects of inlet distortion and intake geometry p 423 A93-18726
- MOORE, G. J.**
Examples of dynamic response optimization using MSC/NASTRAN [AIAA PAPER 92-4814] p 436 A93-20394
- MOORE, GARY**
Summer research program (1992). High School Apprenticeship Program (HSAP) reports. Volume 16: Arnold Engineering Development Center Civil Engineering Laboratory [AD-A262024] p 945 A93-29396
- MOORE, J.**
Real-time optical measurement of alkali species in air for jet engine corrosion testing [AIAA PAPER 93-0791] p 541 A93-24870
- MOORE, JAMES A.**
Terminal Doppler Weather Radar program at Denver's Stapleton International Airport during 1989 and 1990 p 432 A93-22188
- MOORE, JOHN**
Shock formation in overexpanded tip leakage flow [ASME PAPER 92-GT-1] p 245 A93-19276
- MOORE, L. F.**
Ground clutter measurements using an aerostat surveillance radar p 929 A93-43381
- MOORE, MARK**
Oblique wing supersonic transport concepts [AIAA PAPER 92-4230] p 43 A93-13337
- MOORE, MURRAY EDWARD**
Parametric study of air sampling cyclones p 135 A93-14173
- MOORE, P. E.**
British Airways ETOPs flight planning system p 990 A93-45164
- MOORE, THOMAS J.**
External stress-corrosion cracking of a 1.22-m-diameter type 316 stainless steel air valve [NASA-TP-3190] p 737 A93-26201
- MOORHOUSE, D. J.**
Propulsion integration results of the STOL and Maneuver Technology Demonstrator p 161 A93-13228
- MOORHOUSE, DAVID J.**
Results and lessons learned from two Wright Laboratory flight research programs [AIAA PAPER 93-3661] p 1099 A93-48341
- MOOSAKHANIAN, ALFRED**
FAA weather processor programs - Real-time dissemination of weather information to aviation end-users p 428 A93-22131
- MORA-CAMINO, F.**
Zero-gravity atmospheric flight by robust nonlinear inverse dynamics p 728 A93-34550
- MORAD, T. A.**
The effect of exfoliation corrosion on the fatigue behavior of structural aluminum alloys p 1017 A93-45778
- MORAES, AUGUSTO C. M.**
A finite element and symbolic method for studying laminar boundary layers of real gases in equilibrium at Mach numbers to 30 [AIAA PAPER 93-2986] p 1052 A93-48179
- MORAES, P. JR.**
Code validation for high speed flow simulation over the VLS launcher fairing [AIAA PAPER 93-3046] p 1057 A93-48226
- MORALEZ, ERNESTO, III**
Determination of YAV-8B Reaction Control System bleed flow usage [AIAA PAPER 92-4232] p 54 A93-13330
- MOREAU, JEAN-PATRICK**
Aircraft lightning initiation and interception from in situ electric measurements and fast video observations p 140 A93-14064
- MOREIRA, JOAO**
A refined procedure to generate calibrated imagery from airborne synthetic aperture radar data p 1162 A93-47657
- MOREIRA, JOAO R.**
Real time PRF control system for SAR p 884 A93-43464
- MORELLI, EUGENE A.**
Nonlinear aerodynamic modeling using multivariate orthogonal functions [AIAA PAPER 93-3636] p 1065 A93-48321
Practical input optimization for aircraft parameter estimation experiments [NASA-CR-191462] p 820 A93-27264

- MORETTI, G.**
Reactive and inert inviscid flow solutions by quasi-linear formulations and shock fitting p 927 A93-42625
- MORFORD, S.**
Modification of combustor stoichiometry distribution for reduced NO(x) emission from aircraft engines [ASME PAPER 92-GT-108] p 349 A93-19346
- MORGAN, J. MURRAY**
Fly-by voice, a technology demonstration p 526 N93-19918
- MORGAN, K.**
Computation of viscous compressible flows using an upwind algorithm and unstructured meshes p 9 A93-12163
Adaptive remeshing for three-dimensional compressible flow computations p 242 A93-18851
The application of an adaptive upwind unstructured grid solution algorithm to the simulation of compressible laminar viscous flows over compression corners p 866 A93-42594
The application of an adaptive unstructured grid method to the solution of hypersonic flows past double ellipse and double ellipsoid configurations p 868 A93-42609
Line relaxation methods for the solution of 2D and 3D compressible flows [AIAA PAPER 93-3366] p 955 A93-45059
- MORGAN, MICHAEL**
Flight data for the Cryogenic Heat Pipe (CRYOHP) Experiment [AIAA PAPER 93-2735] p 1027 A93-46488
- MORGAN, MICHAEL J.**
Design of a hydrogen test facility p 532 A93-25993
- MORGAN, R. G.**
Double diaphragm driven free piston expansion tube p 1016 A93-45533
- MORGENSTERN, ALAGACYR, JR.**
Hypersonic flow past open cavities [AIAA PAPER 93-2969] p 1049 A93-48163
- MORGENSTERN, J. M.**
HST high-lift aerodynamic technology requirements [AIAA PAPER 92-4228] p 44 A93-13355
- MORI, SHIGEHIO**
Research on combined HOPE navigation technology p 533 N93-20428
- MORI, YASUHIKO H.**
Aircraft experiments on microgravity pool boiling - Vapor-liquid behaviour and heat transfer characteristics in boiling of n-pentane, CFC-113 and water p 410 A93-20920
- MORINAGA, NORIHIKO**
Measurement technique for Loran-C pulse wave distortion measures and performance in an environment of noise p 29 A93-10988
- MORINAGA, TOMOAKI**
Dynamic characteristics of an airfoil at high speed change of pitch angle p 10 A93-12324
- MORINISHI, KOJI**
Numerical analysis for chemically non-equilibrium flow p 770 A93-38148
Numerical solution of viscous compressible flows using algebraic turbulence models p 770 A93-38162
- MORINO, L.**
Toward an integration of aerodynamics and aeroacoustics of rotors p 243 A93-19127
- MORINO, LUIGI**
Boundary integral equation methods for aerodynamics p 9 A93-12158
- MORINO, YOSHIKI**
HOPE and its thermal protection systems p 1252 A93-54711
- MORISHITA, E.**
Experimental investigation of aerothermal problems associated with hypersonic flight of HST p 120 A93-14380
- MORISSET, JACQUES**
Toulouse - Flight tests of the Airbus A340 p 159 A93-16859
- MORITA, M.**
Conceptual design of turbo-accelerator for HST combined cycle engine [ASME PAPER 92-GT-253] p 353 A93-19462
Conceptual design study on combined-cycle engine for hypersonic transport [ISABE 93-7018] p 1195 A93-53994
Research and development of a turbo-accelerator for super/hypersonic transport [ISABE 93-7066] p 1200 A93-54042
- MORITA, NAOMI**
A procedure for defining lightning risk to air vehicles p 703 N93-24885
- MORITA, YASUHIRO**
Analytical study on the separation dynamics of LUNAR-A/penetrator p 1265 A93-56272
- MORO, AKIO**
Analytical investigation of a regeneratively cooled scramjet engine [AIAA PAPER 93-0739] p 519 A93-24829
Effect of film cooling/regenerative cooling on scramjet engine performances [ISABE 93-7036] p 1197 A93-54012
- MORONEY, BRIAN W.**
Utilizing a microcomputer based flight simulation in teaching human factors in aviation p 570 A93-27165
- MORONEY, WILLIAM F.**
Utilizing a microcomputer based flight simulation in teaching human factors in aviation p 570 A93-27165
- MOROZOV, M. A.**
Expert evaluation of the technological level of aviation gas turbine engine designs p 811 A93-39187
- MORRA, M. M.**
INCOLOY 908, a low coefficient of expansion alloy for high-strength cryogenic applications. I - Physical metallurgy p 534 A93-25686
- MORREUW, J. P.**
Hypersonic flows over a double or simple ellipse p 868 A93-42614
- MORREN, W. E.**
Gravity sensitivity of a resistojet water vaporizer [AIAA PAPER 93-2402] p 1156 A93-50167
- MORREN, W. EARL**
Gravity sensitivity of a resistojet water vaporizer [NASA-TM-106220] p 914 N93-29194
- MORRIS, GLENN**
Analysis of the NASA Hypersonic Wing Test Structure [AIAA PAPER 92-4724] p 409 A93-20326
- MORRIS, JOHN**
Robust nonlinear control of vectored thrust aircraft [NASA-CR-192727] p 728 N93-25199
- MORRIS, M. J.**
Data analysis techniques for pressure- and temperature-sensitive paint [AIAA PAPER 93-0176] p 414 A93-22605
Aerodynamic applications of pressure sensitive paint p 549 A93-29301
- MORRIS, PHILIP J.**
The noise from supersonic elliptic jets p 445 A93-19156
The prediction of noise radiation from supersonic elliptic jets p 100 N93-10684
- MORRIS, ROBERT E.**
Interferometric JFTOT tube deposit measuring device [AD-D015599] p 536 N93-20247
- MORRIS, SHELBY J.**
Advanced cargo aircraft may offer a potential renaissance in freight transportation p 991 A93-47023
- MORRIS, SHELBY J., JR.**
Technology benefits and ground test facilities for high-speed civil transport development [NASA-TM-107670] p 378 N93-15790
- MORRIS, STEPHEN J.**
Integrated aerodynamics and control system design for tailless aircraft [AIAA PAPER 92-4604] p 42 A93-13284
- MORRIS, W. D.**
HL-20 operations and support requirements for the Personnel Launch System mission p 1210 A93-53745
The effect of orthogonal-mode rotation on forced convection in a circular-sectioned tube fitted with full circumferential transverse ribs p 932 N93-29937
- MORRIS, W. DOUGLAS**
The X-15/HL-20 operations support comparison [NASA-TM-4453] p 1017 N93-32379
- MORRISON, GERALD L.**
Experimental study of the flow field inside a whirling annular seal p 85 N93-10892
- MORRISON, JEFFREY G.**
Theory and design of adaptive automation in aviation systems [AD-A254595] p 160 N93-12613
- MORRISON, W. R. B.**
Performance considerations in the operation of free-piston driven hypersonic test facilities p 1011 A93-45497
- MORSE, T. F.**
Research support for the Laboratory for Lightwave Technology [AD-A261488] p 760 N93-26343
- MORTARA, KARL W.**
A method for the prediction of induced drag for planar and nonplanar wings [AIAA PAPER 93-3420] p 976 A93-47216
Analysis and design of planar and non-planar wings for induced drag minimization [NASA-CR-191274] p 131 N93-13463
- MORTAZAVIAN, H.**
Specification of a class of discrete event processes and their controllers p 96 A93-13078
- MORTCHELEWICZ, G. D.**
Implicit schemes for unsteady Euler equations on unstructured meshes [ONERA, TP NO. 1993-64] p 1171 A93-51944
- MORTON, BLAISE**
A dynamic inversion control approach for high-Mach trajectory tracking p 385 A93-22870
- MORTON, MARK H.**
Effects on load distribution in a helicopter rotor support structure associated with various boundary configurations p 796 A93-35951
- MORTON, W. K.**
An upgraded data acquisition and processing system for the Aeropropulsion Systems Test Facility at Arnold Engineering Development Center [AIAA PAPER 93-2466] p 1138 A93-50213
An updated data acquisition and processing system for turbine engine testing p 1250 A93-54389
- MORZYNSKI, MAREK**
Stability investigations of airfoil flow by global analysis p 783 A93-27436
- MOSCHETTA, J.-M.**
Comparison of ENO and TVD schemes for the parabolized Navier-Stokes equations [AIAA PAPER 93-2970] p 1049 A93-48164
- MOSCHETTA, JEAN-MARC**
Computation of supersonic crossflow separation using a new parabolized Navier-Stokes code p 687 A93-34355
- MOSEEV, IURII V.**
Methods and results of theoretical investigations for high-speed parachute systems [AIAA PAPER 93-1227] p 690 A93-35173
- MOSER, JEFFREY A.**
Compatibility of potential reinforcing ceramics with Ni and Fe aluminides [NASA-CR-192232] p 394 A93-18784
- MOSES, CLIFFORD A.**
Effect of a metal deactivator fuel additive on fuel deposition in fuel atomizers at high temperature [AD-A260915] p 736 N93-25914
- MOSES, H. L.**
Recent advances in simulating unsteady flow phenomena brought about by passage of shock waves in a linear turbine cascade [ASME PAPER 92-GT-4] p 245 A93-19277
A statistical approach to the experimental evaluation of transonic turbine airfoils in a linear cascade [ASME PAPER 92-GT-5] p 245 A93-19278
- MOSES, HAL L.**
Experimental and numerical study of transonic turbine cascade flow [AIAA PAPER 93-3064] p 1059 A93-48240
- MOSES, PAUL L.**
Design of a hypersonic waverider-derived airplane [AIAA PAPER 93-0401] p 384 A93-21108
Structural design and analysis of a Mach zero to five turbo-ramjet system [AIAA PAPER 93-1983] p 1112 A93-49830
- MOSHER, MARIANNE**
Effects of ingested atmospheric turbulence on measured tail rotor acoustics p 849 A93-35964
- MOSHIN, IU. N.**
Autonomous mobile laser complex p 395 A93-17767
- MOSKOVKO, IU. G.**
A data processing and measuring system with a traversing probe for studying flow in the rotating impeller of an axial-flow fan p 75 A93-10032
- MOSLEY, A.**
Miniature display technologies for integrated helmet systems p 718 A93-34819
- MOSLEY, R. F.**
GARTEUR damage mechanics for composite materials: Analytical/experimental research on delaminations p 537 N93-21513
- MOSPANOV, E. I.**
An experimental study of a compound supersonic jet p 1069 A93-48914
An experimental study of the dynamic effect of a supersonic underexpanded jet on a plane surface parallel to the nozzle axis p 1092 A93-51913
- MOSS, A. J.**
Repair of delaminations and impact damage in composite aircraft structures p 457 A93-24107
- MOSS, J. N.**
Energetics of gas-surface interactions in transitional flows at entry velocities p 778 A93-39259
- MOSS, JAMES N.**
Near wake structure for a generic ASTV configuration [AIAA PAPER 93-0271] p 268 A93-21103
Zonally-decoupled DSMC solutions of hypersonic blunt body wake flows [AIAA PAPER 93-2808] p 949 A93-44227

- Hypersonic blunt body wake computations using DSMC and Navier-Stokes solvers
[AIAA PAPER 93-2807] p 964 A93-46547
- MOSS, R. W.**
Measurements of the effect of free-stream turbulence length scale on heat transfer
[ASME PAPER 92-GT-244] p 405 A93-19453
- MOSSER, P. E.**
The beta-CEZ, a new high performance titanium alloy for aerospace engines
[DS-2022] p 393 N93-17852
- MOUCHON, E.**
Origin of the carbon rich sliding interface in alkali containing matrix-SiC nicalon fibre composites
[ONERA, TP NO. 1993-77] p 1212 A93-53598
- MOUGIN, E.**
Preliminary results of the ISM campaign - The Landes, South West France p 1161 A93-47553
- MOULTON, CAREY L.**
Air Force procedure for predicting noise around airbases: Noise exposure model (Noisemap)
[AD-A255769] p 224 N93-14655
- MOUNIR, H.**
Evaluation of clear-air radar PROUST and Doppler radar RONSARD for airport low level-wind shear detection
p 433 A93-22202
- MOUNTS, JON S.**
Analysis of jet/wake mixing in a vaneless diffuser
[ASME PAPER 92-GT-418] p 258 A93-19566
- MOUSSINE-POUCHKINE, N.**
A Mode S implementation - Experiments about data-link and interconnected Mode S sensors p 883 A93-43409
- MOUSTAFA, G. H.**
Further study of high speed single free jets p 873 A93-43687
- MOUSTAPHA, S. H.**
Aerodynamic performance of a transonic low aspect ratio turbine nozzle
[ASME PAPER 92-GT-31] p 245 A93-19291
Effect of nozzle design on the performance of a highly loaded turbine stage
[ISABE 93-7096] p 1203 A93-54072
- MOWAFY, LYN**
Visual augmentation for night flight over featureless terrain p 806 A93-35921
- MOXON, JULIAN**
Potent Trent p 53 A93-11419
- MOYER, S. A.**
Wind tunnel test techniques for UAV separation investigations
[AIAA PAPER 93-0626] p 524 A93-24743
- MOYLE, I. N.**
Stator relative, rotor blade-to-blade near wall flow in a multistage axial compressor with tip clearance variation
[AIAA PAPER 93-2389] p 1083 A93-50154
- MOYLE, IAN N.**
An experimental and analytical study of TIP clearance effects in axial flow compressors
[AD-A256434] p 179 N93-15337
- MOZGOVOJ, V. A.**
Effect of anomalous aerodynamic heating during the descent of a parachute along a trajectory p 1069 A93-48924
- MSHVIDOBADZE, YU. M.**
Pressure field and drag of a single cavity with rounded and sharp edges p 1258 A93-55018
- MU, JONG-SU**
Ignition process of fuel droplet arrays in a supersonic flowfield p 535 A93-27766
- MUCHNIK, R.**
Receiver Autonomous Integrity Monitoring (RAIM) of GPS and GLONASS p 993 A93-46891
- MUEHLEK, P.**
Numerical study of nitric oxide formation in a hypersonic ramjet engine
[ISABE 93-7125] p 1204 A93-54100
- MUELLER, B.**
Implicit upwind finite-difference simulation of laminar hypersonic flow over a 2D ramp p 867 A93-42600
Computation of shock diffraction in external and internal flows p 1024 A93-45537
- MUELLER, BERNHARD**
Flux-vector splitting for compressible low Mach number flow p 1093 A93-52001
- MUELLER, C. A.**
Flow computation for the hypersonic configuration ELAC I at low speeds and large incidence p 1238 A93-56036
- MUELLER, CYNTHIA K.**
Nowcasts of thunderstorm initiation and evolution p 752 A93-33773
- MUELLER, F. D.**
Dual Engine application of the Performance Seeking Control algorithm
[AIAA PAPER 93-1822] p 1110 A93-49709
- MUELLER, J.-D.**
Computations of inviscid compressible flows using fluctuation-splitting on triangular meshes
[AIAA PAPER 93-3301] p 950 A93-44999
A frontal approach for internal node generation in Delaunay triangulations p 1262 A93-56403
- MUELLER, S.**
Stagnation point computations of nonequilibrium inviscid blunt body flow p 1093 A93-52005
Computation of viscous hypersonic non-equilibrium blunt body flow p 1238 A93-56038
- MUELLER, T.**
Development of a realtime DGPS system
[DLR-MITT-92-06] p 503 N93-20749
- MUELLER, U. R.**
Computation of subsonic viscous and transonic viscous-inviscid unsteady flow p 1094 A93-52012
- MUELLER, WOLFGANG**
Numerical simulation of linear interference wave development in three-dimensional boundary layers p 1029 A93-46993
- MUENKEL, CHRISTOPH**
New slant visual range measuring device promises improved airport operations p 529 A93-27395
- MUGHAL, BILAL**
A calculation method for the three-dimensional boundary-layer equations in integral form
[AIAA PAPER 93-0786] p 541 A93-24868
- MUHOEN, J.**
Design considerations for air-to-air laser communications p 312 A93-18932
- MUIJTJENS, RUDOLF MATHIAS ROISALIE**
On the verification of a theory for sculling propulsion [ETN-93-94040] p 1031 N93-31519
- MUIR, E. A. M.**
Design of a controller for a high performance fighter aircraft using Robust Inverse Dynamics Estimation (RIDE)
[AIAA PAPER 93-3779] p 1132 A93-51374
- MUIR, HELEN C.**
Human factors of aircraft cabin safety p 140 A93-14218
- MUKHERJEE, S. K.**
A Navier-Stokes simulation of vortex shedding from square cylinder in unconfined domain p 538 A93-24084
- MUKHIN, VALERII N.**
A practical course in aircraft maintenance. I - The powerplant p 811 A93-39175
Maintenance of the liquid and gas systems of the II-76 aircraft p 804 A93-39203
- MUKHOPADHYAY, SNEHASIS**
Multilevel control of dynamical systems using neural networks p 96 A93-13011
- MUKHOPADHYAY, VIVEK**
Design, test, and evaluation of three active flutter suppression controllers
[NASA-TM-4338] p 63 N93-10070
- MUKVICH, O. V.**
Using helicopters for transporting large and heavy loads p 306 A93-18350
- MULCAHY, T. H.**
Forces on a magnet moving past figure-eight coils
[OE93-009965] p 943 N93-29189
- MULDER, J. A.**
Estimation of aircraft inertia characteristics from bifilar pendulum test data p 1249 A93-56029
Flight testing: Past, present, and future p 164 N93-14615
- MULGREW, B.**
Analysis of the effects of blade pitch on the radar return signal from rotating aircraft blades p 885 A93-43476
- MULHALL, P.**
Nonintrusive, multipoint velocity measurements in high-pressure combustion flows
[AIAA PAPER 93-2032] p 1145 A93-49867
- MULIUKIN, O. P.**
Control of the quality of dynamic processes in the valves of power-generating equipment p 832 A93-39030
- MULKENS, MARC J. M.**
Measurements of aerodynamic rotary stability derivatives using a whirling arm facility p 525 A93-28603
- MULLEN, R.**
Integration of full scale development aircraft GPS user equipment (AN/ARN-151) with Doppler radar systems p 31 A93-11012
- MULLENDER, A. J.**
Application of laminar flow to aero engine nacelles p 128 A93-17256
Application of laminar flow to aero engine nacelles [PNR-90916] p 20 N93-11020
A combined experimental and theoretical study of laminar flow control with particular relevance to aero engine nacelles [PNR-90991] p 20 N93-11070
- MULLER, DANIEL**
Experimental results on RIAS digital beamforming radar p 929 A93-43392
- MULLER, MICHAEL R.**
Anti-icing failure detection instrumentation using realtime optical measurement of anti-icing fluid properties
[AIAA PAPER 93-0748] p 540 A93-24836
Field studies of hold-over-times for type II anti-icing fluids - Results and insights
[AIAA PAPER 93-0749] p 486 A93-24837
- MULLICAN, A.**
The WINCOF-I code: Detailed description
[NASA-CR-190779] p 677 N93-24760
Transient performance of fan engine with water ingestion
[NASA-CR-190778] p 677 N93-25134
- MULLIGAN, J. C.**
Enhanced heat transport in environmental systems using microencapsulated phase change materials
[SAE PAPER 921224] p 926 A93-41398
- MULLIGAN, M. F.**
Uncertainty assessments for engine thrust derived from two methods p 1254 A93-54392
- MUNDELL, A. R. G.**
ASTOVL model engine simulators for wind tunnel research p 192 N93-13213
- MUNDRA, ANAND D.**
The dependent converging instrument approach procedure
[AIAA PAPER 93-3835] p 1098 A93-51424
The dependent converging instrument approach procedure: An analysis of its safety and applicability
[DOE/FAA/RD-93/6] p 707 N93-25456
Developing automation for terminal air traffic control: Case study of the imaging aid p 888 N93-30356
- MUNDT, CH.**
Computational fluid dynamics code validation using a free piston hypervelocity shock tunnel p 960 A93-45545
- MUNDUS, B.**
The influence of swirl generator characteristics on flow and combustion in turbulent diffusion flames p 1159 A93-51632
- MUNDY, JAMES A.**
The effects of viscosity on a conically derived waverider
[AD-A259019] p 424 N93-19101
- MUNGAL, M. G.**
Supersonic jet control via point disturbances inside the nozzle p 861 A93-41930
- MUNIN, A. G.**
An aeroacoustic stand for evaluating the efficiency of sound-absorbing structures under conditions of acoustic wave propagation in a moving medium p 1140 A93-51762
- MUNIR, N.**
Damage detection in smart structures using neural networks and finite-element analyses p 438 A93-22540
- MUNK, R.**
A diesel powerplant development program for airships
[AIAA PAPER 93-4038] p 1246 A93-54609
- MUNOZ, T.**
Aerodynamic characteristics of transport airplanes in low speed configuration p 113 A93-14172
- MUNSON, JOHN H.**
Testing of a high performance compressor discharge seal
[AIAA PAPER 93-1997] p 1153 A93-49840
- MURAGLIA, DIDIER**
Integrated runway meteorological observation system (IRMOS/SIOMA) p 428 A93-22128
- MURAKAMI, AKIRA**
Experimental study of mixed compression air-intake for hypersonic airbreathing engines
[ASME PAPER 92-GT-349] p 355 A93-19519
Effects of boundary layer bleed on swept-shock/boundary layer interaction
[AIAA PAPER 93-2989] p 1052 A93-48182
An experimental study of supersonic air-intake with 5-shock system at Mach 3
[AIAA PAPER 93-2305] p 1082 A93-50089
Two-dimensional numerical simulation for Mach-3 multishock air-intake with bleed systems
[AIAA PAPER 93-2306] p 1082 A93-50090
Wind tunnel tests of the model of intake-airframe integration
[ISABE 93-7101] p 1192 A93-54077
A study on Mach 3 two-dimensional mixed compression air-intakes
[ISABE 93-7106] p 1188 A93-54082
- MURAKAMI, ATSUO**
Effects of injector geometry on scramjet combustor performance p 359 A93-21670

- Aerodynamic performance of scramjet inlet models with a single strut
[AIAA PAPER 93-0741] p 466 A93-24831
- Ignition and combustion performance of a scramjet combustor with a fuel injection strut
[ISABE 93-7050] p 1199 A93-54026
- Mach 4 testing of scramjet inlet models
[NAL-TR-1137] p 26 N93-12369
- MURAKAMI, ITARU**
Life assessment of gas turbine bucket coating based on degradation analysis p 533 A93-24464
- MURAKAMI, KEI-ICHI**
Hypersonic chemically reacting flow of a reentry body p 769 A93-38147
- MURAKAMI, LYNNE A.**
Proposal and preliminary design for a high speed civil transport aircraft. Swift: A high speed civil transport for the year 2000
[NASA-CR-192023] p 335 N93-18049
- MURAKAMI, SATOSHI**
Effect of rounding side corners on vortices shedding and downwash from square cylinder of finite length placed on a ground plane p 1160 A93-51893
- MURALIDHAR, S. J.**
Indian experience in flight data readout and analysis p 168 N93-15161
- MURAMOTO, KENNETH K.**
The prediction of viscous nonequilibrium hypersonic flows about ablating configurations using an upwind parabolized Navier-Stokes code
[AIAA PAPER 93-2998] p 1053 A93-48188
- MURAO, R.**
Effects of wake interaction of two turbine cascades on secondary/tip-leakage flows and losses
[ISABE 93-7058] p 1185 A93-54034
- MURAOKA, KAZUO**
The frequency of incipient vortex-shedding from a circular cylinder in a laminar boundary layer (The effect of the gap ratio on the vortex shedding frequency) p 126 A93-15488
- MURASHIMA, KANJI**
Overview of the Japanese National Project for Super/Hyper-Sonic Transport propulsion system
[ASME PAPER 92-GT-252] p 239 A93-19461
- Ultra-high temperature materials in the research and development of super/hypersonic transport propulsion system p 1252 A93-54712
- MURATORE, JOSEPH J., JR.**
Experimental investigations of the time and flow-direction responses of shear-stress-sensitive liquid crystal coatings
[AIAA PAPER 93-0181] p 542 A93-25508
- MURAWSKI, C. G.**
The USAF Advanced Turbine Aerothermal Research Rig (ATARR) p 911 N93-29945
- MURAYAMA, MOTOHIDE**
Ignition and combustion performance of a scramjet combustor with a fuel injection strut
[ISABE 93-7050] p 1199 A93-54026
- MURAYAMA, T.**
Radiative heat transfer from non-equilibrium high-enthalpy shock layers p 1024 A93-45515
- MURGATROYD, R.**
Assessment of NDT reliability p 1258 A93-54900
- MURMAN, EARLL**
Control of numerical diffusion in computational modeling of vortex flows p 9 A93-12156
- Experimental and computational investigations of the flowfield around the F117A
[AIAA PAPER 93-3508] p 984 A93-47274
- MURMAN, EARLL M.**
An acceleration technique for time accurate calculations p 957 A93-45092
- Adaptive computations of flow around a delta wing with vortex breakdown
[AIAA PAPER 93-3400] p 974 A93-47202
- MUROTA, KAZUAKI**
Effect of rounding side corners on vortices shedding and downwash from square cylinder of finite length placed on a ground plane p 1160 A93-51893
- MURPHY, KELLY J.**
An experimental parametric study of geometric, Reynolds number, and ratio of specific heats effects in three-dimensional sidewall compression scramjet inlets at Mach 6
[AIAA PAPER 93-0740] p 466 A93-24830
- MURR, TODD**
Results of in-service evaluation of wind shear systems p 146 N93-14856
- MURRAY-SMITH, D. J.**
Aspects of multivariable flight control law design for helicopters using eigenstructure assignment p 60 A93-10916
- MURRAY, JAMES E.**
Flight experience with lightweight, low-power miniaturized instrumentation systems
[AIAA PAPER 92-4111] p 39 A93-11280
- MURRAY, RICHARD**
Robust nonlinear control of vectored thrust aircraft
[NASA-CR-192727] p 728 N93-25199
- MURRI, DANIEL G.**
Actuated forebody strake controls for the F-18 high alpha research vehicle
[AIAA PAPER 93-3675] p 1006 A93-44233
- MURTHY, A. V.**
Modifications to Langley 0.3-m TCT adaptive wall software for heavy gas test medium, phase 1 studies
[NASA-CR-189736] p 291 N93-16710
- A feasibility study of using Langley 0.3-m transonic cryogenic tunnel sidewall boundary-layer removal system for heavy gas testing
[NASA-CR-191438] p 747 N93-25087
- MURTHY, D. V.**
Concurrent processing adaptation of aeroelastic analysis of propfans p 173 A93-14624
- MURTHY, DURBHA V.**
An efficient constraint to account for mistuning effects in the optimal design of engine rotors
[AIAA PAPER 92-4711] p 358 A93-20280
- Aeroelastic dynamics of mistuned blade assemblies with closely spaced blade modes
[AIAA PAPER 93-1628] p 810 A93-37446
- Stochastic sensitivity measure for mistuned high-performance turbines
[NASA-TM-105821] p 90 N93-12277
- Localization of aeroelastic modes in mistuned high-energy turbines p 1032 N93-31586
- MURTHY, J. Y.**
Computation of laminar flow and heat transfer over an enclosed rotating disk with and without jet impingement p 201 A93-13982
- MURTHY, P. L. N.**
Dynamic analysis of a pre-and-post ice impacted blade
[AIAA PAPER 92-4273] p 54 A93-13333
- Structural tailoring of aircraft engine blade subject to ice impact constraints
[AIAA PAPER 92-4710] p 358 A93-20319
- Quantification of uncertainties in composites
[AIAA PAPER 93-1440] p 734 A93-33989
- Dynamic analysis of a pre-and-post ice impacted blade
[NASA-TM-105829] p 90 N93-12197
- Root damage analysis of aircraft engine blade subject to ice impact
[NASA-TM-105779] p 222 N93-15343
- Structural tailoring of aircraft engine blade subject to ice impact constraints
[NASA-TM-106033] p 838 N93-26999
- MURTHY, P. N.**
Flow studies in ducted twin-rotor contra-rotating axial flow fans
[ASME PAPER 92-GT-390] p 258 A93-19545
- MURTHY, PAPPU L. N.**
Damage progression in stiffened composite panels
[AIAA PAPER 93-1345] p 738 A93-33915
- Design for cyclic loading endurance of composites p 1216 A93-53395
- Application of artificial neural networks to the design optimization of aerospace structural components
[NASA-TM-4389] p 555 N93-21831
- MURTHY, S. N. B.**
Two-, three-, and four-poster jets in cross flow
[AIAA PAPER 93-0023] p 408 A93-20141
- Two and three-dimensional prediffuser combustor studies with air-water mixture
[AIAA PAPER 93-0240] p 390 A93-22652
- Three-dimensional prediffuser combustor studies with air-water mixture
[AIAA PAPER 93-2474] p 1120 A93-50217
- Two and three-dimensional prediffuser combustor studies with air-water mixture
[ISABE 93-7025] p 1213 A93-54001
- The WINCOF-I code: Detailed description
[NASA-CR-190779] p 677 N93-24760
- Transient performance of fan engine with water ingestion
[NASA-CR-190778] p 677 N93-25134
- Heat transfer with moderate free stream turbulence p 932 N93-29936
- MURTHY, S. T.**
Photoelastic stress analysis of skewed cutout in a sandwich skew plate subjected to inplane and transverse eccentric load p 210 A93-16604
- MURTHY, T. K. S.**
Computational methods in hypersonic aerodynamics [ISBN 0-7923-1673-8] p 1072 A93-49521
- MURTHY, V. R.**
Parallel rotorcraft flight simulation
[AIAA PAPER 93-0623] p 524 A93-24740
- Comprehensive analysis of bearingless rotors - Model development and experimental correlation of modes, response, trim and stability
[AIAA PAPER 93-0624] p 504 A93-24741
- An advanced parallel rotorcraft flight simulation model - Stability characteristics and handling qualities
[AIAA PAPER 93-3618] p 1125 A93-48305
- An advanced rotorcraft flight simulation model - Parallel implementation and performance analysis
[AIAA PAPER 93-3550] p 1222 A93-52654
- MURTY, H.**
The role of Kutta waves on oscillatory shock motion on an airfoil experiencing heavy buffeting
[AIAA PAPER 93-1589] p 682 A93-34121
- MURTY, H. S.**
Nonlinear aspects of transonic aeroelasticity p 1096 A93-52642
- MURUGESAN, K.**
Correlations for flow property variation at outlet of a centrifugal impeller
[ISABE 93-7054] p 1185 A93-54030
- MUSAT, VIRGIL M.**
Permeable airfoils in incompressible flow p 768 A93-37401
- MUSIAL, W. P.**
Combined experiment, phase 1
[DE93-000012] p 485 N93-21766
- MUSSER, D. E.**
F-14D flight director development, test, and evaluation p 803 A93-38840
- MUTABAZI, INNOCENT**
Coriolis effects on Goertler vortices in the boundary-layer flow on concave wall p 123 A93-14564
- MUYLAERT, J.**
Computational aerothermodynamics for 2D and 3D space vehicles p 1073 A93-49533
- MUYSHONDT, ARNOLD**
CFD calibration for three-dimensional nozzle/afterbody configurations p 215 N93-13226
- MUZZY, WILLIAM H., III**
The effectiveness of airbags in reducing the severity of head injury from gunsight strikes in attack helicopters p 494 N93-19691
- MYATT, JAMES H.**
Body-axis rolling motion critical states of a 65-degree delta wing
[AIAA PAPER 93-0621] p 523 A93-24738
- Preliminary design of an intermittent smoke flow visualization system
[NASA-CR-186027] p 806 N93-28693
- MYERS, GEOFF**
Effect of geometry, bleed rates and flow splits on pressure recovery of a canted hybrid vortex-controlled diffuser
[AIAA PAPER 93-1762] p 1109 A93-49659
- MYERS, JAMES W.**
T-38 forward windshield development and performance demonstration report
[AD-A259240] p 513 N93-20579
- MYERS, M. K.**
High speed propeller acoustics and aerodynamics - A boundary element approach p 967 A93-46804
- MYERS, PHILIP**
Flight dynamics system software development environment (FDS/SDE) tutorial
[NASA-TM-108580] p 230 N93-15502
- MYKLEBUST, ARVID**
Extracting dimensional geometric parameters from B-spline surface models of aircraft
[AIAA PAPER 92-4283] p 43 A93-13340
- MYLVAGANAM, MOHANAHARAN**
Implementation of BMLS computer model on hypercube systems p 32 A93-11024
- MYRABO, L. N.**
Experimental investigation of an axisymmetric hypersonic scramjet inlet for laser propulsion p 122 A93-14515
- MYRE, D. D.**
Simulation of shock-boundary layer interaction in a fan blade passage
[AIAA PAPER 93-1980] p 1078 A93-49827
- MYRE, DAVID D.**
Model fan passage flow simulation
[AD-A261613] p 752 N93-26167
- MYSKO, STEPHEN J.**
Navier-Stokes simulation of external/internal transonic flow on the forebody/inlet of the AV-8B Harrier II
[AIAA PAPER 93-3057] p 1058 A93-48234
- MYSOVA, V. M.**
Modeling of the physicochemical processes of nonequilibrium heat transfer in the subsonic jets of an induction plasmatron p 836 A93-39147

NACHSHON, YEHUDA

Employment of radicals and excited state species for supersonic combustion photochemical ignition of premixed hydrogen/oxygen mixtures with ArF laser p 73 N93-11135

NACSON, S.

Explosives detection systems for airport security gas chromatographic based devices p 881 N93-30276

NADEZHIN, A. D.

The problem of two Coulomb centers and its applications in physical aerodynamics p 776 N93-39132

NADLER, ERIC D.

A simulation study of the effects of communication delay on air traffic control [AD-A258593] p 502 N93-19966

NADOLINK, RICHARD H.

Articulated control surface [AD-D015464] p 371 N93-16463

NADVORSKI, A. S.

Chemical-kinetics characteristics of combustion in a supersonic turbulent flow p 1018 A93-47512

NAEGELI, DAVID W.

Development of a method to determine the autoxidation of turbine fuels [AD-A260578] p 736 N93-25902

NAGABHUSHANA, S.

Indian experience in flight data readout and analysis p 168 N93-15161

NAGAMATSU, F.

Discussion for the ideal AIMS p 167 N93-15153

NAGAMATSU, H. T.

Experimental investigation of an axisymmetric hypersonic scramjet inlet for laser propulsion p 122 A93-14515

Investigation of a two-dimensional scramjet inlet, freestream M = 8-18 and Tsub 0 = 4100 K p 270 A93-21669

Passive drag reduction of a helicopter airfoil in an unsteady transonic flow p 482 A93-29440

Calculation of scramjet inlet with thick boundary-layer ingestion [AIAA PAPER 93-1836] p 1074 A93-49720

NAGAMATSU, HENRY T.

A finite element and symbolic method for studying laminar boundary layers of real gases in equilibrium at Mach numbers to 30 [AIAA PAPER 93-2986] p 1052 A93-48179

An investigation on the use of a heavy gas to improve the performance of the equilibrium interface technique in shock tube flows [AIAA PAPER 93-2017] p 1078 A93-49855

NAGARAJA, SRINIVASA R.

Helicopter noise reduction programme - AGUSTA achievements p 1262 A93-54721

NAGARATHINAM, M.

A two-dimensional elliptic grid generator for a wing-body section involving grid control functions p 460 A93-24083

NAGASHIMA, AKIRA

Aircraft experiments on microgravity pool boiling - Vapor-liquid behaviour and heat transfer characteristics in boiling of n-pentane, CFC-113 and water p 410 A93-20920

NAGASHIMA, T.

Transonic discharge flows around diffuser vanes from a centrifugal impeller [ISABE 93-7053] p 1185 A93-54029

Tandem transverse hydrogen gas injection into a supersonic airflow [ISABE 93-7069] p 1201 A93-54045

Direct simulation of reacting fuel gas flows in a supersonic mixing layer [ISABE 93-7072] p 1201 A93-54048

NAGASHIMA, TOMOARI

Structural optimization of a cantilevered rotating beam p 210 A93-16248

Minimum time turn of a helicopter p 1248 A93-54554

NAGASHIMA, TOSHIO

Dual transverse injection of H2 gas into Mach 1.8 flows at University Komaba wind tunnel p 376 A93-21833

NAGATA, H.

A study of self-ignition of methane-hydrogen mixture fuel injected into high enthalpy supersonic airstreams [ISABE 93-7049] p 1213 A93-54025

NAGATI, M. G.

A guidance display system for single pilot operation [AIAA PAPER 92-4196] p 51 A93-13373

Approximate decoupling flight control system design with output feedback for nonlinear systems [AIAA PAPER 93-3880] p 1135 A93-51465

NAGATOMO, MAKOTO

Atmospheric reentry flight test of winged space vehicle [AIAA PAPER 92-5053] p 385 A93-22324

NAGAYASU, MASAHIKO

Simulation analysis of a cable-mount system used for dynamic wind tunnel tests [NAL-TR-1127] p 68 N93-12359

Accuracy improvement of linear estimated motion using differential type sensors [NAL-TR-1135] p 91 N93-12365

NAGEL, ROBERT T.

Forward rotor vortex effects on counter rotating propeller noise p 245 A93-19221

NAGENGAST, STEVE

Correction of inertial measurements using GPS updates for underwater navigation [AD-A257329] p 317 N93-15988

NAGESWARA RAO, B.

Post-critical behaviour of a tapered cantilever column subjected to a uniformly distributed tangential follower force p 831 A93-38431

NAGPURWALA, Q. H.

Characterisation of conventional and controlled diffusion stator blades in a transonic compressor stage [ISABE 93-7124] p 1189 A93-54099

NAGY, D. R.

Erosion resistant titanium nitride coating for turbine compressor applications [ASME PAPER 92-GT-417] p 388 A93-19565

NAGY, E. J.

Application of generalized force determination to a full scale low cycle fatigue test of the SH-2G helicopter p 795 A93-35949

An improved method of structural dynamic test design for ground flying and its application to the SH-2F and SH-2G helicopters p 512 N93-19928

NAGY, GREG

Advanced hypersonic aircraft design [NASA-CR-192046] p 334 A93-18037

NAH, SEUNG-HYEOG

DESAID (the development of an expert system for aircraft initial design) p 163 N93-14448

NAIDE, TOMOHIKO

Analytical study on the separation dynamics of LUNAR-A/penetrator p 1265 A93-56272

NAIK, D. A.

Euler analysis of turbofan/superfan integration for a transport aircraft p 214 A93-13206

NAIK, DINESH A.

Experimental study of pylon cross sections for a subsonic transport airplane p 1103 A93-52440

Effect of pylon cross-sectional geometries on propulsion integration for a low-wing transport [NASA-TP-3333] p 788 A93-28070

NAIR, C. G. K.

Evolution of helicopters and the status of technology in India p 2 A93-12234

NAKA, SHIGEHISA

Potential and prospects of intermetallic materials for applications in the aerospace industry [ONERA, TP NO. 1992-99] p 824 A93-38580

Designing new multi-phase intermetallic materials based on phase compatibility considerations [ONERA, TP NO. 1992-131] p 772 A93-38605

NAKAGAWA, Y. G.

Mechanical anisotropy in directionally solidified turbine blade p 1018 A93-47356

NAKAHASHI, KAZUHIRO

Marching grid generation for external viscous flow problems p 228 A93-16979

Adaptive-prismatic-grid method for external viscous flow computations [AIAA PAPER 93-3314] p 951 A93-45010

NAKAJIMA, KATSUHIKO

Iterative temperature calculation method for rectangular sandwich panel fins p 76 A93-10667

NAKAJIMA, TAKASHI

Analytical study on the separation dynamics of LUNAR-A/penetrator p 1265 A93-56272

NAKAJIMA, TSUYOSHI

Flow measurements behind V-gutter under non-combusting condition [AIAA PAPER 93-0020] p 408 A93-20139

Isothermal flow characteristics behind V-shape gutter with and without injection [ISABE 93-7040] p 1198 A93-54016

NAKAMURA, AKIHIRO

Ignition and combustion performance of a scramjet combustor with a fuel injection strut [ISABE 93-7050] p 1199 A93-54026

NAKAMURA, IKUO

The coherent structure in a corner turbulent boundary layer p 548 A93-28575

NAKAMURA, SHINGO

Two-dimensional Navier-Stokes analysis of high-lift multi-element airfoils using the q-omega turbulence model [AIAA PAPER 93-0679] p 466 A93-24787

NAKAMURA, SHUJI

Digital fly-by-wire system for BK117 FBW research helicopter p 181 A93-14209

NAKAMURA, SYUICHI

The language processor system for the Numerical Wind Tunnel p 383 N93-19291

NAKAMURA, T.

Blade loading and shock wave in a transonic circular cascade diffuser [ASME PAPER 92-GT-34] p 246 A93-19294

NAKAMURA, TAKANORI

Blade loading of transonic circular cascade diffuser p 267 A93-20919

NAKAMURA, TAKAO

Effects of nozzle contour on the aerodynamic characteristics of underexpanded annular impinging jets p 1024 A93-45563

NAKAMURA, TAKASHI

The language processor system for the Numerical Wind Tunnel p 302 N93-19291

NAKAMURA, TOMOYUKI

Observation of fluctuation of 2D-nozzle flows [ISABE 93-7110] p 1204 A93-54086

NAKAMURA, Y.

Some asymptotic aspects of the nonstationary aerofoil theory p 259 A93-19966

A study on aerodynamic sound generated by interaction of jet and plate [AIAA PAPER 93-3118] p 1171 A93-48288

NAKAMURA, YOSHIKI

Evaluation of an RNG-based algebraic turbulence model p 863 A93-42436

Transonic flow calculation around NACA-0012 p 302 N93-19301

NAKAMURA, YOSHIKO

Aerodynamic heating with boundary layer transition and heat protection with mass addition on blunt body in hypersonic flows [AIAA PAPER 93-2984] p 1051 A93-48177

Aerodynamic heating analysis for axisymmetric bodies in supersonic flow p 303 N93-19312

NAKANO, HIROSHI

Computer-controlled alignment for a 2000-line color monitor p 886 N93-30324

NAKAO, S.

Aerodynamic heating phenomenon in three dimensional shock wave/turbulent boundary layer interaction induced by sweptback fins in hypersonic flows p 960 A93-45507

NAKAO, SHIGEHIDE

A study on three-dimensional shock wave/turbulent boundary layer interaction induced by sweptback sharp fins at supersonic flow p 684 A93-34274

The experimental study of the effect of sweptback angles and the front shape of the fin on reduction of shock wave/turbulent boundary layer interaction region p 858 A93-40431

NAKATA, M.

Aging review of the YS-11 aircraft p 46 A93-13635

NAKATA, MASAHIKO

Damage tolerance assessment on the multisite cracks for the YS-11 aircraft p 46 A93-13642

NAKATA, Y.

Computation of laminar flow and heat transfer over an enclosed rotating disk with and without jet impingement p 201 A93-13982

NAKAYA, TERUOMI

A wind tunnel investigation to determine buffet countermeasures for STOL aircraft alpha-sweep flight testing [NAL-TR-1129] p 65 N93-12362

NAKAYAMA, AKIHIKO

Surface hot-film method for the measurement of transition, separation and reattachment points [AIAA PAPER 93-2918] p 1148 A93-48120

NALIM, M. R.

Analytic methods for design of wave cycles for wave rotor core engines [AIAA PAPER 93-2523] p 1121 A93-50253

NALLASAMY, M.

Unsteady blade pressures on a propfan at takeoff - Euler analysis and flight data p 810 A93-37389

NAM, CHANJIN

Navier-Stokes calculations of rotating BERP planform blade flowfields [AIAA PAPER 93-3527] p 986 A93-47286

NAMAN, R. A.

Feasibility study of an active aeroelastic control system for the F-16 aircraft p 181 A93-14224

- NAMBA, M.**
Unsteady aerodynamic response of two-dimensional subsonic and supersonic oscillating cascades with chordwise displacement and flexible deformation
p 971 A93-46922
- NAMBA, MASANOBU**
Experimental study on the unsteady aerodynamic response of a three dimensional cascade with oscillating blades
p 242 A93-18499
Lifting surface theory for steady aerodynamic analysis of ducted counter rotation propfan
[ASME PAPER 92-GT-14] p 347 A93-19286
Performance analysis of supersonic through-flow fan by the lifting surface theory. I - Disturbance flow field and determination of blade loadings p 267 A93-20929
Study of mixing flow field of a jet in a supersonic cross flow. I - Experimental facilities and preliminary experiments p 857 A93-40430
Numerical simulation of supersonic flows with chemical reactions p 959 A93-45325
- NAMBA, SEIICHIRO**
Continuous judgment of helicopter noise - On the validity of Leq and Zwicker's method (ISO 532B)
p 558 A93-28478
- NAMIKI, M.**
The improvement of the static launch method in Japan
p 26 A93-11364
Trans-oceanic balloon flight over east China sea
p 27 A93-11372
- NAMKUNG, M.**
Imaging flaws in thin metal plates using a magneto-optic device
p 397 A93-18670
- NAMURA, KIYOSHI**
Numerical analysis of two-dimensional turbulent flows through an oscillating cascade p 126 A93-15494
- NANBA, MASANOBU**
Modal analysis of unsteady aerodynamic response of subsonic annular cascade with steady loading under elastic vibration p 126 A93-15495
- NANBU, KENICHI**
Problem 6.4.1 - Rarefied flow around a double ellipse
p 869 A93-42630
- NANEVICZ, J. E.**
Comparison of the electrical charging and discharging environments of multiple aircraft-borne electric-field measurement systems p 704 A93-24887
- NANGIA, R. K.**
Design of manoeuvrable simple and complex planform transonic wings with attained thrust, panel- and Euler-methods p 117 A93-14301
Application of subsonic first-order panel methods for prediction of inlet and nozzle aerodynamic interactions with airframe p 130 A93-13223
- NAOR, M.**
Dual band tuned radomes for radar applications
p 929 A93-43405
- NAPFEL, HANS F.**
Solid state flight data recorder with rapid data access
p 221 A93-15167
- NAPOLITANO, KEVIN**
Active constrained layer viscoelastic damping
[AIAA PAPER 93-1702] p 743 A93-34224
- NAPOLITANO, MARCELLO R.**
Aircraft failure detection and identification using neural networks
[AIAA PAPER 93-3869] p 1171 A93-51455
Determination of the stability and control derivatives of the F/A-18 HARV from flight data using the maximum likelihood method
[NASA-CR-191216] p 186 A93-12903
- NARASIMHA, R.**
A civil aircraft industry for India p 2 A93-12233
- NARAYANAN, J. L.**
Calculation of laminar and turbulent asymmetric wakes
p 684 A93-34318
- NARAYAN, JOHNNY R.**
Optimum design of high speed prop-rotors using a multidisciplinary approach p 798 A93-35985
- NARAYANA MURTHY, R. V.**
Structural integrity validation of limited-life engines
[ISABE 93-7131] p 1205 A93-54106
- NARAYANA SWAMY, S.**
Structural integrity validation of limited-life engines
[ISABE 93-7131] p 1205 A93-54106
- NARAYANAN, ANIL K.**
Mach disk of dual coaxial axisymmetric jets
p 861 A93-41932
- NARAYANAN, G. V.**
Structural Tailoring/Analysis for Hypersonic Components - A computational simulation
[AIAA PAPER 92-4722] p 325 A93-20324
- NARAYANAN, VIMALA**
Analytical and experimental investigation of flow through a turbine vane cascade p 1248 A93-56348
- NARAYANSWAMI, N.**
Investigation of a hypersonic crossing shock wave/turbulent boundary layer interaction
p 1044 A93-48043
- NARAYANSWAMI, N.**
Numerical simulation of crossing/turbulent boundary layer interaction at Mach 8.3 comparison of zero and two-equation turbulence models
[AIAA PAPER 93-0779] p 467 A93-24861
Computation of crossing shock/turbulent boundary layer interaction at Mach 8.3 p 961 A93-45726
- NARCISO, E.**
Numerical model for predictions of reverse flow combustor aerothermal characteristics
p 1123 A93-51645
- NARENDRA, KUMPATI S.**
Multilevel control of dynamical systems using neural networks p 96 A93-13011
- NARKIEWICZ, JANUSZ**
Elementary stall flutter of an aircraft wing
p 545 A93-27289
ONERA calculation model of dynamic flow separation on an airfoil section p 1238 A93-56212
- NARRAMORE, J. C.**
Navier-Stokes correlations to fuselage wind tunnel test data p 765 A93-35937
- NARUO, YOSHIHIRO**
Test results on air turbo ramjet for a futurespace plane
[AIAA PAPER 92-5054] p 359 A93-22325
Development study on Air Turbo Ramjet engine for a future space plane
[ISABE 93-7016] p 1195 A93-53992
Test results of the hydrogen fueled model combustor for the air turbo ramjet engine
[ISABE 93-7082] p 1201 A93-54058
Results of sea-level static tests on air turbo ramjet for a future space plane
[AAS PAPER 91-640] p 1247 A93-55817
- NASCIMENTO, MARCO A. C.**
An investigation on the use of a heavy gas to improve the performance of the equilibrium interface technique in shock tube flows
[AIAA PAPER 93-2017] p 1078 A93-49855
- NASCIMENTO, MARCO A. R.**
An optimisation-matching procedure for variable cycle jet engines
[ASME PAPER 92-GT-406] p 356 A93-19555
- NASH, P. T.**
Expedient repair of structural facilities
[AD-A260727] p 731 A93-25656
- NASH, STEVEN**
Three-dimensional flow calculations inside SSME GGGT first stage blade rows p 1017 A93-31585
- NASIRAN, M. B.**
Five years operational experiences with Indonesian Low Speed Tunnel (ILST) p 191 A93-14403
- NASON, EARL R.**
Functional requirements of an advanced instructional design advisor: Simulation authoring, Volume 3
[AD-A256650] p 440 A93-16500
- NASTASE, ADRIANA**
The determination of hybrid analytical-numerical solutions for the three-dimensional compressible boundary layer p 1029 A93-46979
The three-dimensional representation of the pressure distribution on wedged delta wings with supersonic leading edges in supersonic-hypersonic flow p 973 A93-46989
The three-dimensional representation of the lift and pitching moment coefficients on wedged rectangular wings in supersonic flow p 973 A93-46990
- NASUTI, F.**
Reacting gas and surface coupling in high temperature air flows p 686 A93-34353
- NATAN, BENVENISTE**
Ignition of boron particles coated by a thin titanium film
[AIAA PAPER 93-2201] p 1145 A93-50013
- NATARAJ, C.**
Optimal design of centered squeeze film dampers
p 831 A93-38629
- NATHAN, A.**
A review of aging aircraft technology - An I.A.I. perspective p 3 A93-13634
- NATUSHKIN, V. F.**
Kinematics of aeroinertial aircraft rotation
p 819 A93-39192
- NAUMANN, K. W.**
Millisecond aerodynamic force measurement with side-jet model in the ISL shock tunnel
p 822 A93-39414
Shock tunnel experiments and approximative methods on hypervelocity side-jet control effectiveness
[AIAA PAPER 93-1929] p 1077 A93-49794
- NAUMENKO, S. V.**
Experience with the use of liquid crystals in conjunction with the filament method is studying the structure of supersonic flow downstream of a plane step
p 478 A93-27639
- NAUMENKO, Z. N.**
An aeroacoustic stand for evaluating the efficiency of sound-absorbing structures under conditions of acoustic wave propagation in a moving medium
p 1140 A93-51762
- NAUMOV, V. A.**
Calculation of a gas-dispersion laminar boundary layer on a plate with allowance for liquid film formation
p 76 A93-10148
- NAWROT, T.**
Experimental investigation of tip clearance noise in axial flow machines p 445 A93-19155
- NAYANI, SUDHEER N.**
Higher-order viscous shock-layer solutions for high altitude flows
[AIAA PAPER 93-2724] p 858 A93-41050
- NAYFEH, ALI H.**
Laminar boundary-layer breakdown
[AD-A254489] p 90 A93-12162
- NAYLOR, STEVE**
Aircraft failure detection and identification using neural networks
[AIAA PAPER 93-3869] p 1171 A93-51455
- NAZARI, A.**
Impingement/effusion cooling p 932 A93-29954
- NDOH, PATRICK N.**
An investigation of ground access mode choice for departing passengers
[TT-9201] p 67 A93-11224
- NEACE, KERRIN S.**
Aerodynamic analysis of flapping wing propulsion
[AIAA PAPER 93-0484] p 286 A93-23386
- NEACE, KERRY S.**
A computational and experimental investigation of the propulsive and lifting characteristics of oscillating airfoils and airfoil combinations in incompressible flow
[AD-A258019] p 294 A93-17819
- NEAL, DONALD M.**
Assessment of helicopter component statistical reliability computations
[AD-A258931] p 510 A93-19447
- NEALY, J. E.**
Radiation safety in aircraft operations
p 141 A93-14221
- NEBRES, J. V.**
Detailed near surface flow about yawed, stranded cables
[AD-A257382] p 418 A93-15857
- NEBRES, JOSE LUIS VILLAFRANCA**
Wake similarity and vortex formation for two-dimensional bluff bodies p 138 A93-15101
- NEEDHAM, C.**
Chemical nonequilibrium effects of Mach reflection
p 1233 A93-54816
- NEEDLEMAN, H. C.**
Status of the NASA Balloon Program
p 1 A93-11365
- NEELY, A. J.**
Hypervelocity flows of argon produced in a free piston driven expansion tube p 1012 A93-45530
- NEGAST, WILLIAM J.**
Augmentation of a navigation reference system with differential global positioning system pseudorange measurements p 881 A93-42798
- NEGODA, V. V.**
Increasing the lift-drag ratio of wings of small aspect ratio at hypersonic velocities p 13 A93-12933
Optimal wing shapes in a hypersonic nonequilibrium flow p 1088 A93-51770
- NEIGHBORS, W. K.**
Integrated flight/propulsion control - Subsystem specifications for performance
[AIAA PAPER 93-3808] p 1132 A93-51400
- NEILAND, V. IA.**
Problems in physical gas dynamics
p 775 A93-39126
Nonequilibrium heat transfer near the critical point of blunt bodies p 777 A93-39145
- NEILL, DOUGLAS J.**
Survey - Applications of structural optimization methods to fixed wing aircraft and spacecraft
[AIAA PAPER 92-4726] p 325 A93-20328
Applications to fixed-wing aircraft and spacecraft
p 896 A93-45432
Applications of structural optimization methods to fixed-wing aircraft and spacecraft in the 1980s
[NASA-TM-103939] p 1033 A93-32212
- NEISE, W.**
Experimental investigation of tip clearance noise in axial flow machines p 445 A93-19155

- Experimental determination of the main noise sources in a profan model by analysis of the acoustic spinning modes in the exit plane p 449 A93-19214
- NEJAD, A. S.**
Flow field characteristics of an axisymmetric sudden-expansion pipe flow with different initial swirl distribution p 411 A93-21688
- NEJAD, ABDOLLAH S.**
Three component LDV velocity measurements in a can type research combustor for CFD validation. I - Isothermal [ASME PAPER 92-GT-138] p 350 A93-19370
- NEJLAND, V. YA.**
Air dissociation effects on aerodynamic characteristics of an aerospace plane p 959 A93-45149
- NEKHIN, S. S.**
Using ultralight flight vehicles for large-scale aerial photography p 92 A93-10098
- NEKOHASHI, TOSHIFUMI**
Structural optimization of a cantilevered rotating beam p 210 A93-16248
Minimum time turn of a helicopter p 1248 A93-54554
- NELSON, ANDREW**
Civil standardization of the Global Positioning System for the aviation community p 29 A93-10981
The derivation of path following error and control motion noise filters for the reduction of Global Positioning System flight test data p 32 A93-11022
- NELSON, B. W.**
Development and demonstration of a new filter system to control emissions during jet engine testing [AD-A261203] p 755 A93-26243
- NELSON, C. C.**
The effects of fixed rotor tilt on the rotordynamic coefficients of incompressible flow annular seals p 1161 A93-52601
- NELSON, EDWARD L.**
Infrared flow visualization of V/STOL aircraft [AIAA PAPER 92-4253] p 80 A93-13343
- NELSON, GERALD**
Advanced thermally-stable, coal-derived, jet fuels program: Experiment system and model development [AD-A262747] p 917 A93-29402
- NELSON, HAROLD, JR.**
National Airspace System flight planning operational concept NAS-SR-131 [PB93-124659] p 310 A93-18031
National Airspace System: Air traffic control and airspace management operational concept NAS-SR-132 [DOT/FAA/SE-92/5] p 502 A93-20164
- NELSON, J.**
Correlation of X-ray CT measurements to shear strength in pultruded composite materials p 396 A93-18618
Measurement of the center-of-gravity using X-ray computed tomography p 396 A93-18619
- NELSON, P. A.**
Experiments on the active control of boundary layer transition p 243 A93-19133
Active control of sound transmission through stiff lightweight composite fuselage constructions p 447 A93-19187
Theoretical studies of the active control of propeller induced cabin noise using secondary force inputs p 995 A93-45124
- NELSON, PAUL**
Evaluation of brush seals for limited-life engines p 411 A93-21665
- NELSON, R. C.**
The aerodynamic effects of sideslip on double delta wings [AIAA PAPER 93-0053] p 261 A93-20166
The use of subscale models to predict self-induced oscillations of flight vehicles [AIAA PAPER 93-0093] p 264 A93-20199
Measurements of circulation and vorticity in the leading-edge vortex of a delta wing p 288 A93-23548
A simple criterion for vortex breakdown [AIAA PAPER 93-0866] p 469 A93-24928
Lateral control at high angles of attack using pneumatic blowing through a chined forebody [AIAA PAPER 93-3624] p 1126 A93-48309
- NELSON, R. S.**
Creep fatigue life prediction for engine hot section materials (isotropic) [NASA-CR-189221] p 364 A93-18578
- NELSON, ROBERT C.**
"Wingwake" - A computational model for preliminary assessment of wake vortex attenuation schemes [AIAA PAPER 92-4209] p 15 A93-13377
- NELSON, S. G.**
Development and demonstration of a new filter system to control emissions during jet engine testing [AD-A261203] p 755 A93-26243
- NERON, M.**
A viscous-inviscid solver for high-lift incompressible flows over multi-element airfoils at deep separation conditions [ONERA, TP NO. 1992-183] p 774 A93-38745
- NERSESOV, G. G.**
Approximate method for the aerodynamic design of flight vehicles for high supersonic flight speeds p 1069 A93-48966
Substitution of oriented differences for central differences in a program for calculating smooth supersonic flows p 1085 A93-50966
- NERZ, E.**
Combining direct and indirect methods in optimal control: Range maximization of a hang glider [REPT-313] p 371 A93-16618
- NESEL, MICHAEL C.**
Real-time capture, archiving, retrieval, processing, and presentation of large quantities of flight test/research information [AIAA PAPER 92-4073] p 95 A93-11258
- NESTERENKO, G. I.**
Experience in specifying/prolonging the airframe time limits p 948 A93-45797
- NETT, C. N.**
A simplified approach for control of rotating stall. I - Theoretical development [AIAA PAPER 93-2229] p 1080 A93-50035
A simplified approach for control of rotating stall. II - Experimental results [AIAA PAPER 93-2234] p 1080 A93-50038
- NETTEFIELD, M. P.**
Computation of hypersonic turbulent flow over a rearward facing step p 865 A93-42587
- NEU, CHARLES E.**
Stress corrosion susceptibility of ultra-high strength steels for Naval aircraft applications [AD-A256126] p 199 A93-15189
- NEUBERT, D.**
Interaction of a streamwise vortex with a free surface [AIAA PAPER 93-0556] p 543 A93-25539
- NEUBERT, DONALD E., JR.**
Trailing vortex/free-surface interaction [AD-A261654] p 701 A93-26195
- NEUHART, DAN H.**
Aerodynamic characteristics of a delta wing with a body-hinged leading-edge extension [AIAA PAPER 93-3446] p 978 A93-47233
- NEUHOFF, TOM, JR.**
Obstacles to increasing airspace - Jumping through environmental law hoops p 569 A93-23872
- NEUMAIER, RAINER**
Development of cure cycles: From laboratory analysis and testing to production of large scale composites [MBB-Z-0442-92-PUB] p 536 A93-20845
- NEUMAN, D. A.**
The design and commissioning of an acoustic liner for propeller noise testing in the ARA transonic wind tunnel [PNR-90880] p 101 A93-11204
- NEUMANN, RICHARD D.**
Developing a data base for the calibration and validation of hypersonic CFD codes - Sharp cones [AIAA PAPER 93-3044] p 1057 A93-48224
- NEUMANN, W. T.**
A single-point warning system for thunderstorms and electric fields p 747 A93-24900
- NEUMEIER, R.**
Allowable compression strength for CFRP-components of fighter aircraft determined by CAI-test [MBB-FE-221-S-PUB-0483] p 537 A93-21462
Allowable compression strength for CFRP-components of fighter aircraft determined by CAI-test p 537 A93-21531
- NEUMEISTER, KARL-HEINZ**
In the pursuit of a single European air traffic control system p 150 A93-15053
- NEUNZERT, H.**
Rarefied gas flow around a 3D-delta wing p 870 A93-42639
- NEUWERTH, G.**
Low-speed aerodynamics of the hypersonic research configuration ELAC I p 1237 A93-56035
- NEVILLE, KENDALL W.**
Flight update of aerodynamic math model [AIAA PAPER 93-3596] p 1224 A93-52687
- NEVZOROV, F. F.**
A conformal-integral method for solving the direct problem in turbomachine cascade aerodynamics p 125 A93-15217
- NEWBERRY, CONRAD F.**
The development of a mature external Master's degree program in aeronautical engineering - A university/industry partnership [AIAA PAPER 92-4256] p 570 A93-24296
- NEWMAN, E. H.**
Operation of the helicopter antenna radiation prediction code [NASA-CR-193259] p 1030 A93-31110
- NEWMAN, J. C.**
An evaluation of the pressure proof test concept for 2024-T3 aluminium alloy sheet p 1026 A93-45780
- NEWMAN, J. C., JR.**
Mixed mode stress intensity-factors in transversely loaded plates p 200 A93-13943
- NEWMAN, P. A.**
An approximately factored incremental strategy for calculating consistent discrete aerodynamic sensitivity derivatives [AIAA PAPER 92-4746] p 265 A93-20344
Observations on computational methodologies for use in large-scale, gradient-based, multidisciplinary design [AIAA PAPER 92-4753] p 436 A93-20351
- NEWMAN, PERRY A.**
Multidisciplinary analysis and sensitivity derivatives for isolated helicopter rotors in hover [AIAA PAPER 92-4696] p 324 A93-20308
Recent advances in steady compressible aerodynamic sensitivity analysis p 1236 A93-55400
- NEWMAN, RICHARD L.**
Test techniques for evaluating flight displays [NASA-TM-103947] p 516 A93-21810
- NEWMAN, ROBB W.**
Oxidation-resistant high-temperature materials p 915 A93-40362
- NEWPORT, JOHN**
Additional developments in embedded computer performance measurement p 940 A93-42833
- NEWSOME, RICHARD W.**
Numerical simulation of wing-wall juncture flow for a pitching wing [AIAA PAPER 93-3401] p 974 A93-47203
- NG, CHIU H.**
Wind tunnel spin data reduction to obtain aerodynamic spin damping coefficients by using nonlinear equation of motion [AD-A253880] p 19 A93-10811
- NG, E. Y.-K.**
A novel approach to high resolution compressible cascade flow analysis using the Navier-Stokes equations [ASME PAPER 92-GT-419] p 258 A93-19567
- NG, HUAT**
Representation of vehicle location in networked simulations [AIAA PAPER 93-3582] p 1214 A93-52677
- NG, LIAN L.**
Secondary instability mechanisms in compressible axisymmetric boundary layers p 1070 A93-49009
The transition prediction toolkit: LST, SIT, PSE, DNS, and LES p 783 A93-27429
- NG, T. T.**
Effect of leeward flow dividers on the wing rock of a delta wing [AIAA PAPER 93-3492] p 982 A93-47264
- NGAI, E. C.**
Dual band tuned radomes for radar applications p 929 A93-43405
- NGAN, ANGELEN**
A second-generation high speed civil transport: Stingray [NASA-CR-192022] p 336 A93-18059
- NGO, H.**
Dynamics of a high speed impeller - Analysis and experimental verification [AIAA PAPER 93-1362] p 743 A93-34239
- NGUYEN, DUC T.**
A new parallel-vector finite element analysis software on distributed-memory computers [AIAA PAPER 93-1307] p 756 A93-33883
- NGUYEN, H. L.**
Numerical simulation of a low-emission gas turbine combustor using KIVA-II p 170 A93-14077
Emissions reduction by varying the swirler airflow split in advanced gas turbine combustors [ASME PAPER 92-GT-110] p 349 A93-19347
Numerical analysis of the flow fields in a RQL gas turbine combustor [DE92-017509] p 89 A93-11767
- NGUYEN, SANG**
Fiber optics for aircraft entertainment systems p 1172 A93-49478
- NGUYEN, V. D.**
Experimental investigation of flows behind different Large-Eddy Breakup (LEBU) devices in thick boundary layers p 18 A93-10550
- NI, MAOLIN**
The application of optimal robust control in control system design of flying vehicles p 95 A93-11791
- NI, WEIDOU**
Hybrid real-time simulation of a two-rotor engine p 172 A93-14497

- A minimum-time acceleration control strategy for a two-rotor aeroengine p 172 A93-14499
- NIBBELINK, BRUCE D.**
Flutter calculations for fixed and rotating wings with state-space inflow dynamics [AIAA PAPER 93-1300] p 709 A93-33877
- NIBBELINK, BRUCE DAVID**
Finite-state inflow applied to aeroelastic flutter of fixed and rotating wings p 188 A93-14830
- NICHOLAS, E. D.**
Friction surfacing and linear friction welding p 1217 A93-53499
- NICHOLAS, O. P.**
A simulator study into low speed longitudinal handling qualities of ACT transport aircraft [NLR-TP-89387-U] p 527 N93-20743
- NICHOLS, DOUGLAS A.**
Application of a flush airdata sensing system to a wing leading edge (LE-FADS) [AIAA PAPER 93-0634] p 516 A93-24750
Application of a flush airdata sensing system to a wing leading edge (LE-FADS) [NASA-TM-104267] p 518 A93-20163
- NICHOLS, FRANK**
Arc jet testing in NASA Ames Research Center thermophysics facilities [AIAA PAPER 92-5041] p 385 A93-22315
- NICHOLS, LESTER D.**
The new challenge of computational aeroscience p 112 A93-14169
- NICOL, DAVID**
NO(x) sensitivities for gas turbine engines operated on lean-premixed combustion and conventional diffusion flames [ASME PAPER 92-GT-115] p 349 A93-19351
- NICOLAOU, D.**
Modelling of interfacial and thermocline waves [AERO-REPT-9209] p 420 N93-18103
- NICOLIC, VOJIN**
"Wingwake" - A computational model for preliminary assessment of wake vortex attenuation schemes [AIAA PAPER 92-4209] p 15 A93-13377
- NICOUT, D.**
Shock wave/boundary layer interaction in a two-dimensional laminar hypersonic flow [ONERA, TP NO. 1992-182] p 773 A93-38744
- NIEBANCK, CHARLES F.**
Progress in the application of a non-linear programming methodology to the design of a low-vibration airframe p 507 A93-27959
- NIEDORODA, A. W.**
Physical effects of vegetation on wind-blown sand in the coastal environments of Florida [PB92-188424] p 93 N93-11702
- NIEDRINGHAUS, WILLIAM P.**
Maneuver option manager - Automated simplification of complex air traffic control problems p 498 A93-25480
- NIEHUIS, REINHARD**
ADP - Engine concept of the future p 1246 A93-54842
- NIELSEN, HUGO L.**
Control measures used to reduce community noise from civil aviation in Denmark p 425 A93-19191
- NIES, ROGER**
Uplink laser propagation measurements through the sea surface, haze and clouds [AD-A264687] p 935 N93-30553
- NIESL, G.**
A closed loop controller for BVI impulsive noise reduction by Higher Harmonic Control p 849 A93-35963
- NIESL, GEORG H.**
HHC study in the DNW to reduce BVI noise - An analysis p 565 A93-29405
- NIETHAMMER, R.**
Three-dimensional compressible stability-transition calculations using the spatial theory p 783 N93-27431
- NIEUSMA, WILLIAM J., JR.**
An investigation of two-propeller tilt wing V/STOL aircraft flight characteristics [AD-A257751] p 332 N93-17694
- NIEUWLAND, ANDRE K.**
An optimal detection algorithm for harmonic interference signals in Loran-C p 993 A93-46689
- NIEUWSTADT, F. T. M.**
The reduction of skin friction by riblets under the influence of an adverse pressure gradient p 1218 A93-53810
- NIGHTINGALE, L. F.**
Unique development testing at Allison Gas Turbine [AIAA PAPER 93-2450] p 1138 A93-50200
- NIGMATULLIN, R. Z.**
Numerical simulation of aerothermodynamics processes in gas turbine engine components p 1002 A93-46939
Design of high-load aviation turbomachines using modern 3D computational methods [ISABE 93-7032] p 1196 A93-54008
- NIHEI, KOUICHI**
A new technique for analysis of unsteady aerodynamic responses of cascade airfoils with blunt leading edge - Unsteady aerodynamic responses of the cascade in incompressible flow p 1086 A93-51122
- NIINO, MASAYUKI**
Application of functionally gradient materials to scramjet engines [ISABE 93-7063] p 1200 A93-54039
Preliminary design of experimental sub-scale scramjet engine [AAS PAPER 91-639] p 1247 A93-55816
- NIIOKA, T.**
Ignition analysis of unpremixed reactants with chain mechanism in a supersonic mixing layer p 735 A93-35619
- NIKIFOROV, E. G.**
Studies of atmospheric eddy dynamics and energetics and climate problems [ISBN 5-286-00610-8] p 753 A93-35689
- NIKIFORUK, P. N.**
Adaptive quadratic stabilization control with application to flight controller design [AIAA PAPER 93-3847] p 1133 A93-51434
- NIKITIN, M. A.**
Theory of the machining of polyhedral holes by plunge cutting p 835 A93-39091
- NIKITIN, M. P.**
Estimation of the external loading of airships in flight p 366 A93-18383
- NIKITIN, V. E.**
A pressure distribution measuring system with pneumatic switches and automatic band selection p 75 A93-10029
- NIKJOOY, M.**
Fuel injector: Air swirl characterization aerothermal modeling, phase 2, volume 1 [NASA-CR-189193-VOL-1] p 721 N93-24754
Fuel injector: Air swirl characterization aerothermal modeling, phase 2, volume 2 [NASA-CR-189193-VOL-2] p 721 N93-25106
- NIKLASCH, N.**
An experimental health monitoring unit for GPS and GLONASS p 706 N93-25018
- NIKOL'SKII, V. S.**
Kinetic theory of hypersonic flows of a viscous gas p 775 A93-39130
Asymptotic structure of a limiting hypersonic flow in a shock wave p 776 A93-39131
- NIKOLAENKO, N. S.**
Optimization of the parameters of the lift-augmentation devices of the wing of a maneuverable aircraft equipped with an active load-reduction system p 804 A93-39189
- NIKOLAEV, K. V.**
Development and application of the Monte Carlo method for solving the Boltzmann equation and its models p 1173 A93-51867
- NIKOLAEV, M. I.**
Effect of the wing planform on the optimal deformation of the middle surface p 1150 A93-48909
Minimization of the induced drag of nonplanar lifting systems p 1068 A93-48910
- NIKOLAEV, V. S.**
Approximate method for the aerodynamic design of flight vehicles for high supersonic flight speeds p 1069 A93-48966
- NIKOLAEVA, M. G.**
A control algorithm for a navigation-landing system in the case of a priori indeterminacy of failure data p 882 A93-43108
- NIKOLAOU, I.**
Adaptation of a 3-D pressure correction Navier-Stokes solver for the accurate modelling of tip clearance flows p 971 A93-46932
- NIKOLAYEV, YURI**
Joining carbon composite fins to titanium heat pipes [AD-A261970] p 825 N93-27667
- NIKOLIC, V. R.**
Attenuation of airplane wake vortices by excitation of far-field instability [AIAA PAPER 93-3511] p 984 A93-47277
- NILSSON, JOHNNY**
Ongoing GPS experiments demonstrate potential of satellite navigation technology p 1097 A93-49278
- NIMIR, Y. L.**
An externally pressurized air bearing system, journals and thrust, for application to small turbomachinery [ASME PAPER 92-GT-382] p 406 A93-19539
- NINA, M. N. R.**
Experimental analysis of combustion oscillations with reference to ramjet propulsion p 392 N93-17614
- NING, YONG**
The economic effectiveness analysis of technological progress in aviation industry p 1265 A93-54854
- NINOMIYA, KAZUYOSHI**
Preliminary design of experimental sub-scale scramjet engine [AAS PAPER 91-639] p 1247 A93-55816
- NIRASAWA, HIROSHI**
A fine structure of the gust front observed with sonic anemometer p 430 A93-22158
- NISHIDA, KEIYA**
Characteristics of liquid jet atomization across a high-speed airstream. I - Experiment on shape of spray, spatial distribution of injected liquid and Sauter mean diameter p 411 A93-21743
Characteristics of liquid jet atomization across a high-speed airstream. II - Calculation of spatial distribution of liquid, variation of drop diameter and drop trajectory p 412 A93-21744
- NISHIDA, M.**
Numerical studies of Mach reflection with air chemistry p 1233 A93-54815
- NISHIDA, MICHIO**
Numerical simulation of starting process in a hypersonic nozzle p 684 A93-34275
VSL analysis of nonequilibrium flows around a hypersonic body p 769 A93-38146
- NISHIGUCHI, F.**
Influence of blade aerodynamic loading on efficiency of radial-inflow turbines [ASME PAPER 92-GT-91] p 249 A93-19337
- NISHIHARA, YOSHIMI**
Surging limits of multistage axial-flow compressors p 476 A93-27443
- NISHIMURA, J.**
The improvement of the static launch method in Japan p 26 A93-11364
Trans-oceanic, polar patrol balloons and future prospects p 26 A93-11366
Trans-oceanic balloon flight over east China sea p 27 A93-11372
Polar Patrol Balloon Experiment in Antarctica p 27 A93-11373
- NISHIMURA, TOSHIHIKO**
Damage tolerance assessment on the multisite cracks for the YS-11 aircraft p 46 A93-13642
- NISHINO, MASATOMI**
A visualizing method of streamlines around hypersonic vehicles [AIAA PAPER 93-3440] p 1014 A93-47230
- NISHIO, MASATOMI**
Pressure distribution measurement around hypersonic delta winged semicone - Measurement by means of magnet tape p 1176 A93-53193
Shock shapes around slender diamond cones traveling at hypersonic speed p 1181 A93-53840
Study on flow field around slender diamond cone traveling at hypersonic speed p 1189 A93-54314
- NISHIOKA, MICHIO**
Generation of longitudinal vortices in supersonic flow p 301 N93-19292
- NISHIUCHI, MAKOTO**
Numerical calculation of flow field in supersonic combustion chamber p 304 N93-19317
- NISHIZAWA, TOSHIO**
Numerical study on inception of stall cells in rotating stall [ISABE 93-7007] p 1183 A93-53983
- NISHRI, B.**
The effects of forced oscillations on the performance of airfoils [AIAA PAPER 93-3264] p 968 A93-46829
- NISSIM, E.**
On the order reduction of LQG designed controllers [AIAA PAPER 93-1420] p 756 A93-33973
- NISSLEY, DAVID M.**
Thermal barrier coating life prediction model development, phase 2 [NASA-CR-189111] p 198 N93-12589
- NITA, M. M.**
Aerodynamic forces and moments on a dihedral swept wing in a translation with attack and side-slip angle p 476 A93-26903
- NITSCHKE, MONIKA**
Axisymmetric vortex sheet roll-up p 788 N93-28078
- NITSCHKE, WOLFGANG**
Laminar-flow instrumentation for wind-tunnel and flight experiments p 479 A93-28605
- NITTA, KYOKO**
Analysis of a 2-D airfoil motion flying in-proximity-to a wavy-wall surface: Lifting-surface-method p 300 N93-19281
Analysis of a 2-D airfoil motion flying in-proximity-to a wavy-wall surface: Finite difference method p 300 N93-19282
- NITTI, F.**
Wind tunnel operator aimed comparison between two electronic pressure scanner systems p 830 A93-37876

- Instrumentation and data acquisition system for the C.I.R.A. Transonic Pilot Tunnel p 1250 A93-54395
Wind tunnel operator aimed comparison between two electronic pressure scanner systems [DLAS-EST-TR-040] p 67 N93-11225
- MITTINGER, K.**
The opportunities and risks of the supersonic transport market - The Lufthansa point of view p 234 A93-15033
- NITZSCHE, F.**
Modal sensors and actuators for individual blade control [AIAA PAPER 93-1703] p 712 A93-34225
- NITZSCHE, FRED**
The smart structures technology in the vibration control of helicopter blades in forward flight p 366 A93-17721
- NIU, MICHAEL C.-Y.**
Composite airframe structures. Practical design information and data [ISBN 962-7128-06-6] p 1100 A93-49105
- NIU, YANG-YAO**
Comparison of limiters in flux-split algorithms for Euler equations [AIAA PAPER 93-0068] p 262 A93-20181
- NIVEN, A. J.**
The convection speed of the dynamic stall vortex [AD-A247258] p 21 N93-11464
- NIWA, NOBUO**
Experimental and numerical investigation of Mach 2.5 supersonic mixed compression inlet [AIAA PAPER 93-0289] p 279 A93-22689
- NIXON, DAVID**
Development of an engineering level prediction method for high angle of attack aerodynamics [AIAA PAPER 93-0208] p 278 A93-22626
A study of compressible turbulence [AIAA PAPER 93-0659] p 465 A93-24772
The effect of shock motion on entropy production [AIAA PAPER 93-0665] p 465 A93-24777
A study of turbulence in rarefied gases [AIAA PAPER 93-3097] p 1061 A93-48271
- NIXON, MARK W.**
Dynamic analysis of pretwisted elastically-coupled rotor blades p 326 A93-21125
- NOACK, RALPH W.**
A three-dimensional Delaunay unstructured grid generator and flow solver for bodies in relative motion [AIAA PAPER 93-3349] p 954 A93-45043
- NOBBS, S. G.**
Dual Engine application of the Performance Seeking Control algorithm [AIAA PAPER 93-1822] p 1110 A93-49709
- NOCK, R. S.**
Status of the NASA Balloon Program p 1 A93-11365
- NODA, JUNNACHI**
Wind tunnel tests of the model of intake-airframe integration [ISABE 93-7101] p 1192 A93-54077
- NODERER, KEITH D.**
An overview of the system identification procedure with applications to the X-31 drop model [AIAA PAPER 93-0010] p 366 A93-20132
- NOEL, F.**
Some aspects of the aerodynamic methodology in hypersonic vehicle concept studies [AIAA PAPER 92-5027] p 272 A93-22303
- NOGUCHI, MASAYOSHI**
A wind tunnel investigation to determine buffet countermeasures for STOL aircraft alpha-sweep flight testing [NAL-TR-1129] p 65 N93-12362
- NOGUCHI, S.**
Tandem transverse hydrogen gas injection into a supersonic airflow [ISABE 93-7069] p 1201 A93-54045
- NOGUCHI, Y.**
Behaviour of the Johnson-King turbulence model in axisymmetric supersonic flows [AIAA PAPER 93-3032] p 1056 A93-48214
- NOGUE, JEAN-MICHEL**
Cost control of the A320 software - The aircraft manufacturer's point of view p 227 A93-15044
- NOLAN, ROBERT C.**
A simplified wing rock prediction method [AIAA PAPER 93-3662] p 1128 A93-48342
- NOLL, B.**
Diffusion controlled evaporation of a multicomponent droplet - Theoretical studies on the importance of variable liquid properties p 1021 A93-44224
- NOLL, THOMAS E.**
An overview of aeroelasticity studies for the National Aero-Space Plane [AIAA PAPER 93-1313] p 732 A93-33889

- NOMOTO, HIDEKI**
Wind tunnel testing and CFD simulation in Mitsubishi Heavy Industries p 305 N93-19325
- NOMURA, S.**
Experimental investigation of aerothermal problems associated with hypersonic flight of HST p 120 A93-14380
- NOMURA, TOSHIO**
Application of functionally gradient materials to scramjet engines [ISABE 93-7063] p 1200 A93-54039
- NOMURA, TOSHIYUKI**
Generation of longitudinal vortices in supersonic flow p 301 N93-19292
- NOMURA, YOSHIHIRO**
Ignition and exhaust emission characteristics of spray combustion in a pre-chamber type vortex combustor [ASME PAPER 92-GT-119] p 350 A93-19355
- NONAKA, ISAMU**
A wind tunnel investigation to determine buffet countermeasures for STOL aircraft alpha-sweep flight testing [NAL-TR-1129] p 65 N93-12362
- NOONAN, KEVIN W.**
Aerodynamic characteristics of a rotorcraft airfoil designed for the tip region of a main rotor blade [NASA-TM-4264] p 876 N93-29450
- NOOR, AHMED K.**
High-performance computing for flight vehicles; Proceedings of the Symposium, Washington, Dec. 7-9, 1992 p 437 A93-20701
Technical needs and research opportunities provided by projected aeronautical and space systems [NASA-CR-192124] p 386 N93-16629
- NORBY, W. P.**
Development of the F/A-18 E/F air induction system [AIAA PAPER 93-2152] p 1101 A93-49969
- NORLING, B. L.**
An overview of the evolution of vibrating beam accelerometer technology p 412 A93-21934
- NORMAND, E.**
Single event upset in avionics p 1158 A93-50566
- NORRIS, GUY**
The smart truck p 40 A93-11420
Breaking the stall barrier p 159 A93-17502
Advancing helicopters p 327 A93-21836
Desert store p 1229 A93-54866
- NORRIS, JACK**
Zero-thrust glide testing for drag and propulsive efficiency of propeller aircraft p 995 A93-45143
- NORTH, DAVID M.**
Speed, range boost Saab 2000's appeal p 505 A93-25495
C-17 should fulfill USAF airlift mission p 805 A93-39599
- NORTH, JIM**
Internation aircraft operator information system [DOT/FAA/CT-93/4] p 949 N93-32232
- NORTHAM, G. B.**
Effects of compression and expansion ramp fuel injector configuration on scramjet combustion and heat transfer [AIAA PAPER 93-0609] p 358 A93-21114
Evaluation of scramjet nozzle configurations and film cooling for reduction of wall heating [AIAA PAPER 93-0744] p 358 A93-21118
Workshop report - A validation study of Navier-Stokes codes for transverse injection into a Mach 2 flow p 270 A93-21330
The effect of entrance radius and film injection on wall heating in scramjet nozzles p 360 A93-22505
- NORTHAM, G. BURTON**
Workshop Report: A validation study of Navier-Stokes codes for transverse injection into a Mach 2 flow p 751 N93-26008
- NORTHROP, PATTI**
TBD(exp 3) [NASA-CR-192075] p 335 N93-18054
- NOURRY, G. R.**
Design issues and initial performance of an adaptive air/ground/air HF communication system p 934 N93-30342
- NOUSE, HIROYUKI**
Some topics of research on hypersonic airbreathing engines at National Aerospace Laboratory [ASME PAPER 92-GT-256] p 353 A93-19465
Japan's research and development program for airbreathing engine technologies [ISABE 93-7005] p 1194 A93-53981
- NOVAK, O.**
Use of advanced CFD codes in the turbomachinery design process [ASME PAPER 92-GT-324] p 256 A93-19508
- NOVIKOV, A. S.**
Development of a process for fabricating a plate heat exchanger for the heat recovery system of gas turbine engines p 834 A93-39053

- NOVIKOV, O. V.**
Expert evaluation of the technological level of aviation gas turbine engine designs p 811 A93-39187
- NOVIKOV, VLADIMIR N.**
Fundamentals of flight vehicle design [ISBN 5-217-01299-4] p 893 A93-43831
- NOWAK, LISA M.**
Computational investigations of a NACA 0012 airfoil in low Reynolds number flows [AD-A257300] p 288 N93-15920
- NOWLIN, BRENT C.**
Experimental evaluation of a cooled radial-inflow turbine [AIAA PAPER 93-1795] p 1110 A93-49685
Experimental evaluation of a cooled radial-inflow turbine [NASA-TM-106230] p 816 N93-28697
- NOZAKI, O.**
Navier-Stokes computation of the three dimensional flow fields through a transonic fan blade [ISABE 93-7030] p 1184 A93-54006
- NTUEN, CELESTINE A.**
Flight simulator for hypersonic vehicle and a study of NASP handling qualities p 530 N93-19456
- NUGMANOV, Z. KH.**
A method for calculating flow past an arbitrary airfoil profile in the presence of flow separation p 13 A93-12807
- NUHAIT, A. O.**
Unsteady effects of camber on the aerodynamic characteristics of a thin airfoil moving near the ground p 270 A93-21719
Unsteady ground effects on aerodynamic coefficients of finite wings with camber [AIAA PAPER 93-3423] p 976 A93-47218
Numerical simulation of unsteady flow induced by a flat plate moving near ground p 1094 A93-52432
- NUMBERS, K.**
Hypersonic propulsion system force accounting p 175 N93-13229
- NURICK, ALAN**
Effects of wing-tip vortex flaps p 959 A93-45153
- NURMAKHANOV, B. N.**
A set of application programs for the smoothing of curves and surfaces by the method of monoidal transformations in the geometric module of a CAD system for the design of flight vehicles p 561 A93-27629
- NUSSBAUM, JAMES**
The applications, benefits, and issues of employing GPS and Glonass with Automatic Dependent Surveillance p 316 A93-21188
- NUTAKOR, JOHN J.**
Supercritical wing design, a three dimensional hodograph approach [AIAA PAPER 92-2657] p 472 A93-24986
- NWOKAH, OSITA D. I.**
Robust stabilization based on topological connectedness p 438 A93-22830
Model reference control of a linear plant with feedthrough element p 846 A93-37034
- NYDICK, I.**
Hypersonic flutter of a curved shallow panel with aerodynamic heating [AIAA PAPER 93-1318] p 829 A93-37428
- NYE, EDWARD**
Computer-based modelling of aircraft noise impact p 559 A93-28497
- NYHUS, DANIEL**
Design of the variable pitch fan for the McDonnell Douglas MD 520N helicopter equipped with the NOTAR system p 794 A93-35908
- NYMAN, TONNY**
On design methods for bolted joints in composite aircraft structures p 1158 A93-50430
- NYSTUEN, J. A.**
A comparison of wind speed measured by the Special Sensor Microwave Imager (SSM/I) and the Geosat altimeter p 1033 A93-44862
- O'BRIEN, JAMES D.**
Topographic mapping using a Ku-band airborne elevation interferometer p 896 A93-42786
- O'BRIEN, W. F.**
The prediction of nonlinear dynamic loads on helicopters from flight variables using artificial neural networks p 322 A93-19231
Preliminary experiments on active control of fan noise from a turbofan engine p 759 A93-34957
- O'BRIEN, WALTER F.**
A wide-range axial-flow compressor stage performance model [ASME PAPER 92-GT-58] p 348 A93-19308

- Separated flow in a low speed two-dimensional cascade.
I - Flow visualization and time-mean velocity measurements
[ASME PAPER 92-GT-356] p 257 A93-19521
- Separated flow in a low speed two-dimensional cascade.
II - Cascade performance
[ASME PAPER 92-GT-357] p 257 A93-19522
- Solution schemes for stage-by-stage dynamic compression system modeling
[AIAA PAPER 93-0154] p 275 A93-22592
- Active control of fan noise from a turbofan engine
[AIAA PAPER 93-0597] p 452 A93-23323
- O'CALLAGHAN, J. J.**
Vortex-induced energy separation in shear flows
p 837 A93-39427
- O'CONNELL, JAMES M.**
NOTAR system - A quiet character
p 567 A93-29418
- O'CONNELL, JIM**
Predicting rotorcraft transmission noise
p 850 A93-35968
- O'CONNOR, LEO**
Fluid-film foil bearings control engine heat
p 924 A93-39949
- O'DELL, L.**
Correlation of X-ray CT measurements to shear strength in pultruded composite materials
p 396 A93-18618
- O'DONOGHUE, P. E.**
Applications of advanced fracture mechanics to fuselage
p 1026 A93-45787
- O'HERN, T. J.**
Advanced diagnostics for in situ measurement of particle formation and deposition in thermally stressed jet fuels
[AIAA PAPER 93-0363] p 390 A93-23045
- Reynolds number dependence of the drag coefficient for laminar flow through fine-scale photoetched screens
p 1218 A93-53815
- O'LEARY, DIANNE P.**
Design of reduced-order observers with precise loop transfer recovery
p 184 A93-14587
- O'LEARY, JOHN F.**
A flowfield study of a close-coupled canard configuration
[AIAA PAPER 93-3499] p 983 A93-47269
- O'ROURKE, MATTHEW J.**
Conceptual assessment of two high-speed rotorcraft
p 508 A93-28612
- Dynamic model testing of the X-31 configuration for high-angle-of-attack flight dynamics research
[AIAA PAPER 93-3674] p 1129 A93-48351
- OBARA, CLIFFORD J.**
Flight research on natural laminar flow applications
p 890 A93-41779
- OBATA, MASAKAZU**
Tip clearance effect on heat transfer and leakage flows on the shroud-wall surface in an axial flow turbine
[ASME PAPER 92-GT-200] p 403 A93-19425
- Test results of the hydrogen fueled model combustor for the air turbo ramjet engine
[ISABE 93-7082] p 1201 A93-54058
- Results of sea-level static tests on air turbo ramjet for a future space plane
[AAS PAPER 91-640] p 1247 A93-55817
- OBATA, S.**
Direct simulation of reacting fuel gas flows in a supersonic mixing layer
[ISABE 93-7072] p 1201 A93-54048
- OBATA, YOSHIHIRO**
Transitional characteristics of vortices issued from a body which creates asymmetric flow field - In a case of thin symmetrical airfoil with angle of attack under rotational oscillation of small amplitude
p 267 A93-20923
- OBAYASHI, S.**
Virtual zone Navier-Stokes computations for oscillating control surfaces
[AIAA PAPER 93-3363] p 955 A93-45056
- Algorithm development with applications to aerodynamics and aeroelasticity
p 422 A93-18566
- OBAYASHI, SHIGERU**
Unsteady Navier-Stokes simulation of the canard-wing-body ramp motion
[AIAA PAPER 93-3058] p 1058 A93-48235
- Navier-Stokes computations on full-span wing-body configuration with oscillating control surfaces
[AIAA PAPER 93-3687] p 1065 A93-48356
- OBBERDANK, KAZIMIR**
A comparison between numerical models and measurements in a Kaplan turbine guide vanes
p 685 A93-34339
- OBBERKAMPF, WILLIAM L.**
Application of CFD to a generic hypersonic flight research study
[AIAA PAPER 93-0312] p 280 A93-23007
- OBBERMEIER, F.**
Karman vortex street-airfoil interaction
p 678 A93-33703
- OBRIEN, MARK A.**
The V-22 Osprey: A case analysis
[AD-A256445] p 164 N93-14601
- OBYE, ROGER C.**
IHPTET exhaust nozzle technology demonstrator
[AIAA PAPER 93-2569] p 1121 A93-50287
- OCH, FRIEDRICH**
Choice of materials for military helicopters
p 158 A93-15028
- OCHI, NOBUO**
Recent aircraft accidents
p 307 A93-20819
- OCHI, YOSHIMASA**
Application of feedback linearization method in a digital restructurable flight control system
p 370 A93-23514
- A new way of pole placement in LQR and its application to flight control
[AIAA PAPER 93-3845] p 1133 A93-51433
- OCNNOR, JIM**
Domain engineering validation case study: Synthesis for the air traffic display/collision warning monitor domain version 01.00.03
[AD-A259407] p 503 N93-21671
- ODA, TETSUYA**
Characteristics of liquid jet atomization across a high-speed airstream. I - Experiment on shape of spray, spatial distribution of injected liquid and Sauter mean diameter
p 411 A93-21743
- Characteristics of liquid jet atomization across a high-speed airstream. II - Calculation of spatial distribution of liquid, variation of drop diameter and drop trajectory
p 412 A93-21744
- ODABAS, ONUR R.**
On the coupled thermomechanical analysis of hypersonic flight vehicle structures
[AIAA PAPER 92-5018] p 413 A93-22294
- ODEN, J. T.**
Geometry based Delaunay tetrahedralization and mesh movement strategies for multi-body CFD
[AIAA PAPER 92-4575] p 15 A93-13309
- H-P adaptive methods for finite element analysis of aerothermal loads in high-speed flows
[NASA-CR-189739] p 420 N93-18093
- Advanced adaptive computational methods for Navier-Stokes simulations in rotorcraft aerodynamics
[NASA-CR-192282] p 483 N93-20256
- ODGEN, CHRIS**
Hypersonic reconnaissance aircraft
[NASA-CR-192049] p 333 N93-17804
- ODGERS, J.**
The combustion of droplets within gas turbine combustors - Some recent observations on combustor efficiency
[ASME PAPER 92-GT-135] p 388 A93-19367
- The prediction of thermal NO(x) in gas turbine exhausts
[ISABE 93-7022] p 1195 A93-53998
- OECHSLE, V. L.**
An analytical study of dilution jet mixing in a cylindrical duct
[AIAA PAPER 93-2043] p 1113 A93-49876
- An analytical study of dilution jet mixing in a cylindrical duct
[NASA-TM-106181] p 814 N93-27160
- OELKERS, W.**
High capacity aircraft
p 157 A93-14395
- OERTEL, H., JR.**
Gas-kinetical and Navier-Stokes simulations of reentry flows
p 865 A93-42582
- OESTREICH, JOHN**
Starch media blasting for aerospace finishing applications
[SAE PAPER 920948] p 107 A93-14091
- OETTL, HERWIG**
The real aperture antenna of SAR, a key element for performance
p 213 N93-13053
- OGARKOV, VITALIJ N.**
Airport radar systems (2nd revised and enlarged edition)
[ISBN 5-277-00610-9] p 992 A93-44505
- OGAWA, SATORU**
Thermo-chemical models for hypersonic flows
p 863 A93-42433
- Computations of transonic wind tunnel flows about a fully configured model of aircraft by using multi-domain technique
[AIAA PAPER 93-3022] p 1055 A93-48207
- A simple grid generation technique for hypersonic flow around complex configuration
p 299 N93-19275
- Numerical computations using multi-domain technique
p 299 N93-19277
- The 3D Navier-Stokes calculation of flow about scramjet inlet with strut
p 301 N93-19298
- OGAWA, TOSHIO**
Limit cycle in the longitudinal motion of the USB STOL ASKA - Control system functional mockup and actual aircraft
[SAE PAPER 921040] p 185 A93-14660
- OGBURN, MARILYN E.**
Status of the validation of high-angle-of-attack nose-down pitch control margin design guidelines
[AIAA PAPER 93-3623] p 1126 A93-48308
- OGGIANO, M. S.**
On the measurements of the skin friction in 3-D flows - Application to a complete 3-D shear layer flow
p 118 A93-14329
- OGORODNIKOV, D. A.**
Real-time simulation of maneuverable aircraft flight conditions on altitude test cell
[AIAA PAPER 93-1845] p 1137 A93-49726
- OGOT, MADARA M.**
An effective Mixed Annealing/Heuristic Algorithm for problems in kinematic mechanical design
[AIAA PAPER 93-1581] p 741 A93-34113
- OGUCHI, H.**
A combined facility of ballistic range and shock tunnel using a fast action valve
p 1012 A93-45532
- OGUMA, MASATO**
Results of sea-level static tests on air turbo ramjet for a future space plane
[AAS PAPER 91-640] p 1247 A93-55817
- OH, BYUNG K.**
The role of blade elasticity in the prediction of blade-vortex interaction noise
p 566 A93-29406
- OH, C. S.**
Prediction of airfoil stall using Navier-Stokes equations in streamline coordinates
p 787 N93-27456
- OHBA, HIDEYUKI**
Numerical analysis of a flat plate in a pitching motion. II - Effect on the flow of the position of the pivot, etc
p 1181 A93-53798
- OHERN, TIM**
Advanced thermally-stable, coal-derived, jet fuels program: Experiment system and model development
[AD-A262747] p 917 N93-29402
- OHKITA, YUJI**
Test results of the hydrogen fueled model combustor for the air turbo ramjet engine
[ISABE 93-7082] p 1201 A93-54058
- OHKUBO, YUICHIROU**
Ignition and exhaust emission characteristics of spray combustion in a pre-chamber type vortex combustor
[ASME PAPER 92-GT-119] p 350 A93-19355
- OHLHORST, CRAIG W.**
Current research in oxidation-resistant carbon-carbon composites at NASA. Langley Research Center
p 74 N93-12456
- OHMIT, ERIC E.**
Initial results of an in-flight investigation of longitudinal flying qualities for augmented, large transports in approach and landing
[AIAA PAPER 93-3816] p 1133 A93-51407
- OHMORI, YASUNORI**
A numerical investigation of 3D transverse injection into the supersonic flow behind rearward facing step
p 303 N93-19316
- OHNO, HISAO**
A fine structure of the gust front observed with sonic anemometer
p 430 A93-22158
- Extremely low level jet in the evening in Kanto Plain
p 430 A93-22159
- OHTA, HIROBUMI**
Adaptive quadratic stabilization control with application to flight controller design
[AIAA PAPER 93-3847] p 1133 A93-51434
- OHTA, S.**
The improvement of the static launch method in Japan
p 26 A93-11364
- Trans-oceanic balloon flight over east China sea
p 27 A93-11372
- OHYA, YOSHIO**
Mechanical anisotropy in directionally solidified turbine blade
p 1018 A93-47356
- OHTMER, O.**
Solving problems with singularities using conformal mappings
p 397 A93-18978
- OHTSUKA, K.**
Case study and simulation of fatigue damages and DTE of aging aircraft - A review of researches in Japan
p 948 A93-45800
- OHWAKI, KATSURA**
Ignition and combustion performance of a scramjet combustor with a fuel injection strut
[ISABE 93-7050] p 1199 A93-54026
- OHWAKI, TOSHIKAZU**
Lift enhancement of ground-effect wing. I - Results of screening tests of various concepts
p 271 A93-21737

- Lift enhancement of ground-effect wing. II - Experimental investigation of the power augmented ram wing in ground effect through the wind tunnel p 271 A93-21738
- OINUMA, H.**
Noise reduction of supersonic heated jet with jet mixing enhancement by tabs [ISABE 93-7046] p 1198 A93-54022
- OJHA, S. K.**
Optimization of constant altitude-constant airspeed flight for piston-prop aircraft p 889 A93-40473
- OK, HONAM**
Calculation of the flowfield around an airfoil with spoiler [AIAA PAPER 93-0527] p 284 A93-23268
- OKA, TOSHIHARU**
Aircraft experiments on microgravity pool boiling - Vapor-liquid behaviour and heat transfer characteristics in boiling of *n*-pentane, CFC-113 and water p 410 A93-20920
- OKABE, N.**
Evaluation of metallurgical degradation on gas turbine components p 915 A93-40804
Crack simulation and life assessment of gas turbine nozzles p 915 A93-40805
- OKABE, NAGATOSHI**
Life assessment of gas turbine bucket coating based on degradation analysis p 533 A93-24464
- OKABE, Y.**
The improvement of the static launch method in Japan p 26 A93-11364
Trans-oceanic balloon flight over east China sea p 27 A93-11372
- OKADA, NORIYAKI**
Limit cycle in the longitudinal motion of the USB STOL ASKA - Control system functional mockup and actual aircraft [SAE PAPER 921040] p 185 A93-14660
- OKADA, SHIN**
The language processor system for the Numerical Wind Tunnel p 383 A93-19291
- OKAMOTO, SHIKI**
Effect of rounding side corners on vortices shedding and downwash from square cylinder of finite length placed on a ground plane p 1160 A93-51893
- OKAMOTO, YUKI**
Computer-controlled alignment for a 2000-line color monitor p 886 A93-30324
- OKAMURA, OKIYOSHI**
Air cell [CA-PATENT-APPL-SN-2001346] p 83 A93-10368
- OKAN, M. B.**
A simple method for estimating secondary losses in turbines at the preliminary design stage [ASME PAPER 92-GT-294] p 254 A93-19484
- OKAZAKI, SYUNKI**
A study of a direct-injection stratified-charge rotary engine for motor vehicle application [SAE PAPER 930677] p 1158 A93-50524
- OKHAPKIN, E. V.**
A heat transfer element of a high-temperature heat exchanger p 833 A93-39047
- OKIISHI, THEODORE H.**
An experimental investigation of the flow in a diffusing S-duct [NASA-TM-105809] p 60 A93-12077
- OKONG'O, N.**
Vortex developments over steady and accelerated airfoils incorporating a trailing edge jet [AIAA PAPER 93-3008] p 1054 A93-48198
- OKUNO, YOSHINORI**
Optimal takeoff of a helicopter for category A V/STOL operations p 525 A93-28611
Optimal takeoff procedures for a transport category tiltrotor p 802 A93-37377
- OKUNUKI, T.**
Experimental investigation of aerothermal problems associated with hypersonic flight of HST p 120 A93-14380
- OKUYAMA, SATOSHI**
A study on two-dimensional and three-dimensional secondary jet interactions with a supersonic flow p 683 A93-34273
Intense studies on unsteady secondary separations and oscillating shock waves in three-dimensional shock waves/turbulent boundary layer interaction regions induced by sharp and blunt fins [AIAA PAPER 93-2939] p 1046 A93-48137
Two-dimensional and three-dimensional mixing flow structures with injected through slotted nozzle and circular nozzle into supersonic flows [ISABE 93-7117] p 1221 A93-54092
- OLDENBURG, J. R.**
Liquid water content measurements using the Phase Doppler Particle Analyzer in the NASA Lewis Icing Research Tunnel [AIAA PAPER 93-0298] p 378 A93-23698
- OLDFIELD, M. L. G.**
Measurements of the effect of free-stream turbulence length scale on heat transfer [ASME PAPER 92-GT-244] p 405 A93-19453
- OLEARY, JOHN F.**
Flowfield study of a close-coupled canard configuration [AD-A256311] p 139 A93-15245
- OLEJNICZAK, J.**
The design of optimized airfoils in subcritical flow [AIAA PAPER 93-0532] p 285 A93-23273
- OLEJNIK, A.**
Geometrically nonlinear local flutter analysis of supersonic airplane skin plates in the potential supersonic flow [ISBN 83-01-10939-4] p 394 A93-17569
- OLEKSUK, L.**
Characterization of ceramic composite materials for gas turbine applications [DE93-009719] p 905 A93-30168
- OLINGER, D.**
A visual study of recessed angled spanwise blowing method on a delta wing [AIAA PAPER 93-3246] p 966 A93-46791
- OLIVER, M. L.**
Accelerated corrosion fatigue test methods for aging aircraft p 198 A93-16623
- OLIVO, KEVIN G.**
PAA-core aluminum honeycomb - An end user's evaluation p 209 A93-15738
- OLLEROS, F. X.**
Internally coherent system of innovation - The case of flight simulation [AIAA PAPER 93-3548] p 1226 A93-52653
- OLOVSSON, S.**
Large eddy simulation of turbulent combustion behind flame holders [ISABE 93-7042] p 1198 A93-54018
- OLSEN, J.**
Neutron-induced single event upsets in static RAMs observed at 10 KM flight altitude p 1158 A93-50561
- OLSEN, MICHAEL E.**
Low aspect ratio wing code validation experiment p 1176 A93-53202
- OLSON, ERIK D.**
Elements of NASA's high-speed research program [AIAA PAPER 93-2942] p 947 A93-45155
- OLSON, GERALDINE L.**
Optimization of an internally finned rotating heat pipe [AD-A256725] p 453 A93-15980
- OLSON, JOHN R.**
Reducing helicopter operating costs p 486 A93-25249
- OLSON, LARRY E.**
The design of test-section inserts for higher speed aerodynamic testing in the Ames 80- by 120-Foot Wind Tunnel p 374 A93-19149
- OLSON, LAWRENCE E.**
High-lift aerodynamics: Prospects and plans p 784 A93-27442
- OLSON, RON**
An evaluation of aircraft icing forecasts for the continental United States p 429 A93-22149
- OLSON, STEPHEN H.**
An improved gust front detection algorithm for the TOWR p 432 A93-22191
- OLSSON, E.**
Calculation of three-dimensional boundary layers on rotor blades using integral methods [ASME PAPER 92-GT-210] p 252 A93-19433
- OLSSON, ERIK**
Numerical simulation of vortex shedding past triangular cylinders at high Reynolds number using a k-epsilon turbulence model p 871 A93-42873
- OLSSON, MATS-OLOF**
Damage tolerance assessment of the fighter aircraft 37 Vigen main wing attachment p 802 A93-37390
- OLYNICK, DAVID R.**
Comparisons between DSMC and the Navier-Stokes equations for reentry flows [AIAA PAPER 93-2810] p 964 A93-46549
- OLYNICK, DAVID RAMOS**
A new LU-SGS flow solver for calculating reentry flows p 698 A93-25759
- OMELIK, A. I.**
Experimental simulation of the aerodynamic heating of bodies in a molecular region p 1090 A93-51871
- OMI, JUNSUKE**
An experimental study of supersonic air-intake with 5-shock system at Mach 3 [AIAA PAPER 93-2305] p 1082 A93-50089
Two-dimensional numerical simulation for Mach-3 multishock air-intake with bleed systems [AIAA PAPER 93-2306] p 1082 A93-50090
- ONATE, E.**
The finite element method in the 1990's [ISBN 0-387-54930-7] p 925 A93-40823
Numerical simulation of hypersonic flow over a double ellipse using a Taylor-Galerkin finite element formulation with adaptive grids p 868 A93-42617
- ONEILL, J.**
Pilot weather advisor [NASA-CR-189723] p 318 A93-16692
- ONEILL, MARY KAE LOCKWOOD**
Optimized scramjet engine integration on a waverider airframe p 722 A93-25480
- ONG, LIH-YENN**
Aircraft grid generation using interactive environment [AIAA PAPER 93-0224] p 438 A93-22639
- ONG, LISA**
International aircraft operator information system [DOT/FAA/CT-93/4] p 949 A93-32232
- ONG, SHAW Y.**
Optimality-based control laws for real-time aircraft control via parameter optimization p 180 A93-14161
- ONISHI, S.**
Heat flux microsensor measurements [AIAA PAPER 92-5038] p 413 A93-22312
Microsensors for high heat flux measurements p 928 A93-42920
- ONO, FUMIEI**
Effect of film cooling/regenerative cooling on scramjet engine performances [ISABE 93-7036] p 1197 A93-54012
- ONODERA, TAKUO**
Study on unstart and its propagation along modules due to compound choking and/or fluctuations in combustor of scramjet engines [ISABE 93-7052] p 1199 A93-54028
- ONOFRI, M.**
Equilibrium and nonequilibrium modeling of hypersonic inviscid flows p 864 A93-42448
Reactive and inert inviscid flow solutions by quasi-linear formulations and shock fitting p 927 A93-42625
Influence of chemical kinetics effects in nozzles shape design [ISABE 93-7112] p 1188 A93-54087
- ONORATO, M.**
Breakdown analysis on delta wing vortices p 7 A93-10779
Vortex breakdown study on a 65-deg delta wing tested in static and dynamic conditions p 121 A93-14407
- OPALKA, KLAUS O.**
Numerical simulation of the flow in a 1:57-scale axisymmetric model of a large blast simulator [AD-A265551] p 1015 A93-31916
- ORAN, E. S.**
Stability of oblique detonations in RAM accelerators [AIAA PAPER 92-0089] p 541 A93-24979
- ORANGE, THOMAS W.**
NDE of PWA 1480 single crystal turbine blade material [NASA-TM-106140] p 815 A93-27640
- ORASANU, JUDITH**
Shared mental models and crew decision making p 147 A93-15023
Design of a cooperative problem-solving system for enroute flight planning: An empirical study of its use by airline dispatchers [NASA-CR-192709] p 707 A93-25330
- OREKHOV, I. K.**
3D/quasi-3D trans- and supersonic flow calculation in advanced centrifugal/axial compressor stages p 972 A93-46936
- ORSHNIKOV, V. V.**
Development of a process for fabricating a plate heat exchanger for the heat recovery system of gas turbine engines p 834 A93-39053
- ORKISZEWSKI, CHARLES**
CST gives aircraft industry a lift p 560 A93-25086
- ORKWIS, PAUL D.**
Jacobian update strategies for quadratic and near-quadratic convergence of Newton and Newton-like implicit schemes [AIAA PAPER 93-0878] p 470 A93-24939
On computing vortex asymmetries about cones at angle of attack using the conical Navier-Stokes equations [AIAA PAPER 93-3628] p 1064 A93-48313
- ORLADY, HARRY W.**
Advanced cockpit technology in the real world p 2 A93-13409
- ORLOV, B. A.**
A numerical study of the flutter of conical shells p 927 A93-42405
- ORLOV, E. F.**
Prediction of fatigue crack growth kinetics in the plane structural elements of aircraft in the biaxial stress state p 1025 A93-45670

- ORLOV, KIM YA.**
Design of aircraft, helicopters, and aviation engines
[ISBN 5-277-01192-7] p 947 A93-44508
- ORLOV, V. N.**
Dynamic processes in the powerplants and power-generating equipment of flight vehicles p 832 A93-39027
- ORME, JOHN S.**
Performance-seeking control - Program overview and future directions p 1102 A93-51360
Subsonic flight test evaluation of a propulsion system parameter estimation process for the F100 engine [NASA-TM-4426] p 175 N93-13155
- ORMEROD, ALBERT O.**
Measurements of aerodynamic rotary stability derivatives using a whirling arm facility p 525 A93-28603
- OROZCO, C. E.**
Massively parallel aerodynamic shape optimization p 266 A93-20729
- ORR, JOHN L.**
Development of a flight instrument package [AD-A260830] p 719 N93-25783
Inflight evaluation of an acoustic orientation instrument [AD-A260752] p 719 N93-25909
- ORRINGER, OSCAR**
How likely is multiple site damage? p 1027 A93-45791
- ORTEGA, MARCOS A.**
Nozzle flow computations using the Euler equations p 112 A93-14170
Numerical prediction of flap losses in a transonic wind tunnel p 288 A93-23552
- ORTH, R. C.**
Data analysis of the parametric scramjet combustor experiments conducted in the Calspan 96 inch shock tunnel - 4th entry [AIAA PAPER 92-5098] p 359 A93-22368
- ORTH, U.**
Unsteady boundary-layer transition in flow periodically disturbed by wakes [ASME PAPER 92-GT-283] p 254 A93-19475
- OSAKA, HIDEO**
Streamwise variation of mean velocity field for the turbulent boundary layer interacting with controlled longitudinal vortex arrays p 267 A93-20933
- OSANTOWSKI, J. F.**
Optical technologies for UV remote sensing instruments p 853 N93-28788
- OSBORN, A. R.**
Developments in icing test techniques for aerospace applications in the RAE Pyestock (England) altitude test facility [RAE-TM-P-1214] p 48 N93-11485
- OSBORNE, DAVID W.**
Design of instrument approach procedure charts: Comprehension speed of missed approach instructions coded in text or icons [PB92-205673] p 36 N93-11252
- OSDER, STEPHEN**
Design and robustness issues for highly augmented helicopter controls p 185 A93-14594
- OSEGUERA, ROSA M.**
Microburst avoidance crew procedures for forward-look sensor equipped aircraft [AIAA PAPER 93-3942] p 1007 A93-44234
NASA wind shear flight test in situ results p 488 N93-19593
- OSHIMA, K.**
FUM - An efficient MmB solver for steady inviscid flows p 862 A93-42431
- OSHIMA, S.**
Oscillations of circular shock waves with upstream disturbance p 1023 A93-45463
- OSHIMA, SHUZO**
Oscillation of circular shock waves with upstream nonuniformity p 208 A93-15496
- OSHMAN, Y.**
Drag/thrust estimation via aircraft performance flight testing p 156 A93-14322
- OSHMAN, YAAKOV**
Decentralized autonomous attitude determination using an inertially stabilized payload [AIAA PAPER 93-3857] p 1134 A93-51444
- OSIPOV, V. V.**
Modeling of flow in a pulsed shock tunnel p 777 A93-39152
- OSIPTSOV, A. N.**
Two-phase injection from the front surface of a blunt body in hypersonic flow p 241 A93-18233
- OSKAM, B.**
Aerodynamic analysis of slipstream/wing/nacelle interference for preliminary design of aircraft configurations p 130 N93-13205
- OSKAM, BASTIAAN**
A synthesis of results on the calculation of flow over a 2D ramp and a 3D obstacle - Antibes test cases 3 and 4 p 867 A93-42601
- OSSARD, G.**
Air accidents in the French Air Force p 492 N93-19676
- OSWALD, G. A.**
Physics of forced unsteady flow for a NACA 0015 airfoil undergoing constant-rate pitch-up motion p 478 A93-27922
Investigation of forced unsteady separated flows using velocity-vorticity form of Navier-Stokes equations p 840 N93-27451
- OSTACHOWICZ, WIESLAW**
Influence of modelling loading on stress distribution in turbomachinery blade fastening in case of FEM p 520 A93-27296
- OSTAPENKO, N. A.**
Regimes of supersonic flow past the windward side of V-shaped wings p 5 A93-10144
Aerodynamic resistance of three-dimensional bodies with a starlike cross section at supersonic velocities, and problems of its calculation p 774 A93-39116
Aerodynamic characteristics and static stability margin of conical star-shaped bodies at supersonic velocities p 1067 A93-48848
- OSTOWARI, CYRUS**
Digital data acquisition and preliminary instrumentation study for the F-16 laminar flow control vehicle p 292 N93-16784
- OSTRANDER, MARK J.**
Analysis of a high bypass ratio engine installation using the chimera domain decomposition technique [AIAA PAPER 93-1808] p 1100 A93-49697
- OSTRAS, V. N.**
Gasdynamics of hydrogen-fueled scramjet combustors [AIAA PAPER 93-2145] p 1115 A93-49962
- OSTRAS, V. N.**
Supersonic combustion and gasdynamic of scramjet p 170 A93-14242
- OSTROFF, AARON J.**
Longitudinal-control design approach for high-angle-of-attack aircraft [NASA-TP-3302] p 373 N93-19108
- OSWALD, FRED B.**
Acoustical analysis of gear housing vibration p 567 A93-29420
- OSWALD, J.**
Computational methods applied to the aerodynamics of spaceplanes and launchers [ONERA, TP NO. 1992-140] p 114 A93-14216
- OTTARSON, GISLI**
A transfer matrix approach to vibration localization in mistuned blade assemblies [NASA-TM-106112] p 838 N93-27088
- OTTARSSON, GISLI**
An efficient constraint to account for mistuning effects in the optimal design of engine rotors [AIAA PAPER 92-4711] p 358 A93-20280
- OTTAVY, A.**
Effect of Reynolds number on the standards of a simplified anemoclinometric probe [IMFL-91-31] p 293 N93-17542
- OTTE, DIRK**
Vibro-acoustic analysis of propeller aircraft, integrating advanced experimental modeling with in-flight data analysis p 451 A93-19230
Noise and vibration analysis in propeller aircraft by advanced experimental modeling techniques p 1264 A93-55862
- OTTEN, M. P.**
Definition study PHARUS [AD-A256560] p 221 N93-14805
- OTTEN, MATERN P. G.**
Motion compensation in a time domain SAR processor p 885 A93-43466
- OTTIGER, R.**
Failure diagnostic with MAINTEx based on AIMS at Swissair p 110 N93-15181
- OTTO, J.**
A detailed study of mean-flow solutions for stability analysis of transitional flows [AIAA PAPER 93-3052] p 1057 A93-48232
- OTTO, JOHN C.**
High-order cyclo-difference techniques: An alternative to finite differences [NASA-TM-107745] p 693 N93-25074
- OTUGEN, M. V.**
The three-dimensional separated flow structure in a variable aspect ratio sudden expansion duct [AIAA PAPER 93-0213] p 278 A93-22630
- OU, S.**
Heat transfer performance comparisons of five different rectangular channels with parallel angled ribs p 397 A93-18752
- OU, SHICHUAN**
Leading edge film cooling heat transfer including the effect of mainstream turbulence p 23 N93-11886
- OU, YUH-ROUNG**
Optimal control of lift/drag ratios on a rotating cylinder p 76 A93-10275
Development of the wake behind a circular cylinder impulsively started into rotatory and rectilinear motion p 1236 A93-55736
- OUSSET, Y.**
The limit model of a thin strip exhibiting two delaminations [ONERA, TP NO. 1992-212] p 832 A93-38764
- OUSTERHOUT, JOHN K.**
Robo-line storage: Low latency, high capacity storage systems over geographically distributed networks [NASA-CR-192910] p 758 N93-25130
- OUTA, E.**
Noise reduction of supersonic heated jet with jet mixing enhancement by tabs [ISABE 93-7046] p 1198 A93-54022
- OUTA, EISUKE**
A 2-D compressible N-S simulation of starting- and stalling-flows in a compressor cascades system [ISABE 93-7006] p 1183 A93-53982
- OUZTS, PETER J.**
Screening studies of advanced control concepts for airbreathing engines [AIAA PAPER 92-3320] p 1108 A93-49329
Screening studies of advanced control concepts for airbreathing engines [NASA-TM-106042] p 721 N93-25079
- OVCHINNIKOV, V.**
Use of alternative fuels for aviation p 196 A93-14292
- OVCHINNIKOV, V. A.**
A method for calculating flow past an arbitrary airfoil profile in the presence of flow separation p 13 A93-12807
- OVERBY, GLENN**
A wall interference assessment/correction system [NASA-CR-191889] p 296 N93-18384
- OVERD, MICHAEL L.**
Carbon composite repairs of helicopter metallic primary structures p 1101 A93-50429
- OVERGAARD, DAN**
MM-122: High speed civil transport [NASA-CR-192011] p 334 N93-17974
- OVODENKO, A. A.**
Estimation of the service periods for complex systems in the case of a priori indeterminacy of system reliability data p 856 A93-43109
- OWARISH, HASSAM O.**
Design and performance of nozzle-less volute casings for inward flow radial turbines p 722 N93-25471
- OWEN, J. M.**
Flow and heat transfer between gas-turbine discs p 903 N93-29950
- OWENS, CHRISTOPHER C.**
IOPS advisor: Research in progress on knowledge-intensive methods for irregular operations airline scheduling p 443 N93-18686
- OWUSU-ANTWI, E.**
Development of a unified airport pavement analysis and design system p 380 N93-16317
- OXENDINE, CHARLES R.**
Selection and static calibration of the Marsh J1678 pressure gauge p 931 N93-29779
- OYIBO, GABRIEL**
Supercritical wing design, a three dimensional hodograph approach [AIAA PAPER 92-2657] p 472 A93-24986
- OZAWA, TADAO**
Research and development of ceramic turbine wheels [ASME PAPER 92-GT-295] p 354 A93-19485
- OZBAY, HITAY**
Robust control of an aeroelastic system modeled by a singular integro-differential equation p 97 A93-13197
H(infinity) optimal controllers for a distributed model of an unstable aircraft p 62 A93-13247
Numerical computation and approximations of H(infinity) optimal controllers for a 2-parameter distributed model of an unstable aircraft p 817 A93-37040
Robust stabilization of an aero-elastic system p 817 A93-37044
- OZEKI, T.**
Formation of shock waves in transient base flow p 1023 A93-45460
- OZORA, AKIRA**
The operating system for Numerical Wind Tunnel p 383 N93-19290
- OZOROSKI, L.**
Validation of engineering methods for predicting hypersonic vehicle control forces and moments p 906 A93-41897

P

- PACHTER, M.**
A Hopfield neural network for adaptive control
[AIAA PAPER 93-3729] p 1130 A93-51329
Automated control of aircraft in formation flight
[AIAA PAPER 93-3852] p 1134 A93-51439
- PACI, CORRADO**
Numerical investigation of flow field in a turbine volute
[AIAA PAPER 93-0155] p 542 A93-25505
- PACI, L.**
Cooling geometry optimization using liquid crystal technique
p 902 A93-29939
- PACIA, ARNEL**
Add-on damping treatment for the F-15 upper-outer wing skin
[AD-A258470] p 337 N93-18248
- PACIA, ARNEL P.**
Modal survey of a full-scale F-18 wind tunnel model
[AD-A262462] p 875 N93-29410
- PACIORRI, R.**
Influence of chemical kinetics effects in nozzles shape design
[ISABE 93-7112] p 1188 A93-54087
- PACK, WILLIAM D.**
In-stream measurements of combustion during Mach 5 to 7 tests of the Hypersonic Research Engine (HRE)
[AIAA PAPER 93-2324] p 1116 A93-50104
- PADGETT, MARY L.**
WN 92: Proceedings of the 3rd Workshop on Neural Networks: Academic/Industrial/NASA/Defense, Auburn Univ., AL, Feb. 10-12, 1992 and South Shore Harbour, TX, Nov. 4-6, 1992
[SPIE-1721] p 1167 A93-50726
- PADO, L. E.**
The use of artificial intelligence for buffet environments
[AIAA PAPER 93-1534] p 727 A93-34071
- PADOVAN, J.**
Effects of foundation excitation on multiple rub interactions in turbomachinery
p 1260 A93-55996
- PAETZOLD, H.**
Use of advanced CFD codes in the turbomachinery design process
[ASME PAPER 92-GT-324] p 256 A93-19508
- PAGANO, PETER**
Prediction of forces and moments for hypersonic flight vehicle control effectors
[NASA-CR-193033] p 728 N93-24762
- PAGANO, THOMAS**
The effect of TCAS interrogations on the Chicago O'Hare ATCRBS system
[DOT/FAA/CT-92/22] p 318 N93-16498
Results of DATAS investigation of illegal mode S ID's at JFK Airport
[DOT/FAA/CT-92/26] p 318 N93-16841
Results of DATAS investigation of ATCRBS environment at the Los Angeles International Airport
[DOT/FAA/CT-93/6] p 793 N93-28625
- PAGGI, B.**
EH 101 ship interface trials
p 796 A93-35954
- PAGLIONE, PEDRO**
Optimal performance of airplanes flying through wind shear
[AIAA PAPER 93-3846] p 1102 A93-51480
- PAHLE, JOSEPH W.**
Status of the validation of high-angle-of-attack nose-down pitch control margin design guidelines
[AIAA PAPER 93-3623] p 1126 A93-48308
- PAHLKE, K.**
Application of European CFD methods for helicopter rotors in forward flight
[ONERA, TP NO. 1992-125] p 772 A93-38599
- PAI, B. R.**
Characterisation of conventional and controlled diffusion stator blades in a transonic compressor stage
[ISABE 93-7124] p 1189 A93-54099
- PAIGE, J. B.**
NASA SBIR abstracts of 1990 phase 1 projects
[NASA-TM-108145] p 572 N93-21794
The NASA SBIR product catalog
[NASA-TM-108242] p 945 N93-29322
NASA SBIR abstracts of 1991 phase 1 projects
[NASA-TM-108240] p 945 N93-29323
- PAILLERE, H.**
Computations of inviscid compressible flows using fluctuation-splitting on triangular meshes
[AIAA PAPER 93-3301] p 950 A93-44999
- PAIMUSHIN, V. N.**
Nonlinear deformation mechanics of multilayer transparency elements - General theory relations
p 79 A93-12800
- PAIPETIS, S. A.**
Damage detection by Acousto-Ultrasonic Location (AUL)
p 555 N93-21529

- PAIS, MARTIN R.**
Design of a hydrogen test facility
p 532 A93-25993
- PAJMUSHIN, V. I.**
Nonlinear deformation mechanics of multilayer transparency elements - Some calculation results
p 1191 A93-52937
- PAKNYS, R.**
Coupling gain computation between antennas on circular cylinders at SHF/EHF frequencies
p 933 N93-30309
- PAL, A.**
Data analysis techniques for pressure- and temperature-sensitive paint
[AIAA PAPER 93-0176] p 414 A93-22605
- PALATKA, ROBERT M.**
Numerical analysis of the flow in a turbulated rectangular duct simulating the cooling passages in a turbine blade
[AD-A257855] p 420 N93-18305
- PALKIN, V. A.**
Combined engines for hypersonic flight
p 171 A93-14244
The study of experimental turboramjets - Heat state and cooling problems
[AIAA PAPER 93-1989] p 1112 A93-49834
- PALLEK, D.**
Time-dependent 3-component laser-Doppler-anemometer and simultaneous position measurements in the flow of an aircraft engine
p 538 A93-23809
- PALMA, P. C.**
Absolute intensity measurements of impurity emissions in a shock tunnel and their consequences for laser-induced fluorescence experiments
p 1147 A93-48044
- PALMBERG, BJORN**
Damage tolerance assessment of the fighter aircraft 37 Viggen main wing attachment
p 802 A93-37390
- PALMER, A. W.**
An optical fiber based position sensor with immunity to temperature variation
p 743 A93-34287
- PALMER, EV**
Design of a cooperative problem-solving system for enroute flight planning: An empirical study of its use by airline dispatchers
[NASA-CR-192709] p 707 N93-25330
- PALMER, GRANT**
Effective treatment of the singular line boundary problem for three-dimensional grids
p 1177 A93-53204
- PALMER, M. E.**
Application of subsonic first-order panel methods for prediction of inlet and nozzle aerodynamic interactions with airframe
p 130 N93-13223
- PALMER, RAY**
Composites technology for transport primary structure
p 918 N93-30431
Resin transfer molding for advanced composite primary aircraft structures
p 919 N93-30438
- PALMER, RAYMOND J.**
Development of stitching reinforcement for transport wing panels
p 921 N93-30852
- PALMOUR, J. W.**
High temperature rectifiers and MOS devices in 6H-silicon carbide
[AD-A254725] p 90 N93-12340
- PALSANE, SANJAY**
Numerical solution of dynamic equations arising in a jet engine simulation
p 53 A93-12237
Development of a real time dynamic engine simulation model of a turbo fan engine
[ISABE 93-7132] p 1205 A93-54107
- PALTRINIERI, MASSIMO**
Scheduling of an aircraft fleet
p 443 N93-18665
- PALUMBO, GIUSEPPE**
Spectral measurements of shock layer radiation in an arc-jet wind tunnel
p 1251 A93-54409
- PAMPREEN, RONALD C.**
Compressor surge and stall
[ISBN 0-933283-05-9] p 482 A93-29780
- PAN, BINGCHEN**
Engineering optimization of aeronautical structures
p 154 A93-14227
YIDOYU and its application to aircraft design
[AD-A259262] p 513 N93-20605
- PAN, DARTZI**
Upwind finite-volume Navier-Stokes computations on unstructured triangular meshes
p 1070 A93-49011
A second-order upwind finite-volume method for the Euler solution on unstructured triangular meshes
p 1087 A93-51738
- PAN, GUANGXI**
A software for optimum design of an aircraft structure
p 938 A93-40495
- PAN, H.**
Studies into the hail ingestion characteristics of turbofan engines
[AIAA PAPER 93-2174] p 1115 A93-49987

- PANAYAPPAN, RAMANATHAN**
Hermetic sealing and EMI shielding gasket
[AD-D015359] p 199 N93-13414
- PANDA, BRAHMANANDA**
A robust direct-integration method for rotorcraft maneuver and periodic response
p 61 A93-10919
- PANDA, J.**
Estimation of unsteady lift on a pitching airfoil from wake velocity surveys
[AIAA PAPER 93-0437] p 286 A93-23351
Estimation of unsteady lift on a pitching airfoil from wake velocity surveys
[NASA-TM-105947] p 138 N93-14791
- PANDA, K.**
Extraction of inherent aerodynamic lag poles for the time domain representation of modal unsteady airloads
[AIAA PAPER 93-1591] p 829 A93-37443
- PANDEY, SANDEEP**
Adaptive control of aircraft in windshear
p 62 A93-13126
- PANDOLFI, M.**
Asymmetric vortical solutions in supersonic corners - Steady 3D space-marching versus time-dependent conical results
[AIAA PAPER 93-2957] p 1047 A93-48151
- PANDOLFI, MAURIZIO**
A contribution to the prediction of hypersonic non-equilibrium flows
p 869 A93-42624
- PANDYA, SHISHIR A.**
3D Euler flow solutions using unstructured Cartesian and prismatic grids
[AIAA PAPER 93-0331] p 281 A93-23022
- PANEFIEU, BERNARD**
INS/DGPS integration for trajectory determination of a test vehicle
p 315 A93-21178
- PANENKA, J.**
Controlling common mode stabilization errors in airborne gravity gradiometry
p 1245 A93-55978
- PANG, CHUNG-KIANG**
Aerodynamic analysis of flapping wing propulsion
[AIAA PAPER 93-0484] p 286 A93-23386
- PANGBURN, DANIEL W.**
Impulse guided Samara decelerator
[AIAA PAPER 93-1234] p 690 A93-35175
- PANKAJAKSHAN, RAMESH**
Turbolam flowfield simulation using Euler equations with body forces
[AIAA PAPER 93-1978] p 1078 A93-49825
- PANKOV, S. V.**
Direct and inverse problems of calculating the axisymmetric and 3D flow in axial compressor blade rows
p 972 A93-46938
- PANKOV, V. A.**
An experimental system for studying the vibrations and acoustic emission of cylindrical shells and panels in a field of turbulent pressure pulsations
p 1140 A93-51754
- PANTELEEV, A. V.**
Synthesis of the optimal control of flight vehicle braking with allowance for the discrete nature of control action generation
p 1169 A93-51063
- PANTELEEV, I. M.**
Numerical modeling of supersonic flows past wings of different aspect ratios over a wide range of angles of attack within the framework of the plane section law
p 5 A93-10141
- PANTELIDES, RALPH**
An SSR/IFF Environment Model
p 883 A93-43406
- PANZER, E. C.**
The hemisphere-cylinder in dynamic pitch-up motions
[AIAA PAPER 93-2963] p 1048 A93-48157
- PAONESSA, A.**
Numerical study for the study of medium speed internal noise problems
[DILC-EST-TN-200] p 101 N93-11156
- PAONESSA, F. A.**
Modelling of interfacial and thermocline waves
[AERO-REPT-9209] p 420 N93-18103
- PAP, ROBERT M.**
Control of takeoff of a hypersonic aircraft using neural networks
p 1167 A93-50744
- PAPADAKIS, MICHAEL**
Experimental and numerical delta wing study at high angles of attack and sideslip
[AIAA PAPER 92-2713] p 473 A93-24990
Artificial viscosity models for the Navier-Stokes equations and their effect in drag prediction
[AIAA PAPER 93-0193] p 473 A93-25511
- PAPADOPOULOS, G.**
The three-dimensional separated flow structure in a variable aspect ratio sudden expansion duct
[AIAA PAPER 93-0213] p 278 A93-22630
- PAPAGIANNIDIS, PASCHALIS**
Surface-curvature-distribution effects on turbine-cascade performance
[ASME PAPER 92-GT-84] p 248 A93-19333

- PAPAGIORCOPULO, GEORGE**
Airport technology international 1993
p 532 A93-26920
- PAPAILIOU, K. D.**
Transition prediction in attached and separated shear layers using an integral method
[ASME PAPER 92-GT-281] p 253 A93-19473
Meridional flow calculation using advanced CFD techniques
[ASME PAPER 92-GT-325] p 256 A93-19509
Adaptation of a 3-D pressure correction Navier-Stokes solver for the accurate modelling of tip clearance flows
p 971 A93-46932
Design of axisymmetric channels with rotational flow
[AIAA PAPER 93-3117] p 1062 A93-48287
- PAPAMOSCHOU, D.**
Visual observations of supersonic supersonic jets
p 965 A93-46750
- PAPAMOSCHOU, DIMITRI**
Total-pressure loss in supersonic parallel mixing
[AIAA PAPER 93-0216] p 278 A93-22632
Vortex-induced disturbance field in a compressible shear layer
p 873 A93-43628
Model for entropy production and pressure variation in confined turbulent mixing
p 1071 A93-49014
Thrust loss due to supersonic mixing
[AIAA PAPER 93-2140] p 1114 A93-49958
- PAPANICOLAPOULOS, ALECK**
Advanced composite fiber/metal pressure vessels for aircraft applications
[AIAA PAPER 93-2246] p 1155 A93-50047
- PAPARIZOS, L.**
Combustion noise and combustion instabilities in propulsion systems
p 100 A93-10682
- PAPPA, RICHARD S.**
Rigid body mode identification of the PAH-2 helicopter using the eigensystem realization algorithm
[NASA-TM-107690] p 88 A93-11544
- PAPPAS, G.**
The influence of non-uniform spanwise inlet temperature on turbine rotor heat transfer
p 901 A93-29932
- PAPSHEV, D. D.**
Enhancing the performance of aircraft engine blades by surface hardening
p 811 A93-39072
- PAQUAY, M. H.**
Definition study PHARUS
[AD-A256560] p 221 A93-14805
- PAQUAY, MAURICE H.**
A dual polarised active phased array antenna with low cross polarisation for a polarimetric airborne SAR
p 883 A93-43401
- PARAMESWARAN, V. R.**
Erosion resistant titanium nitride coating for turbine compressor applications
[ASME PAPER 92-GT-417] p 388 A93-19565
- PARAMONOV, I. U. M.**
Refinement of algorithms for calculating the remaining life from magnetic recording instrument data
p 320 A93-18330
Characteristics of fatigue crack growth under the service-spectrum loading of the tail boom of a helicopter
p 321 A93-18339
- PARASCHIVOIU, I.**
Prediction of the ice accretion with viscous effects on aircraft wings
[AIAA PAPER 93-0027] p 307 A93-20145
A comparative study of semi-empirical dynamic stall models
p 18 A93-10544
A field panel method for transonic flows
p 18 A93-10547
- PARASCHIVOIU, ION**
Transition for three-dimensional boundary layers on wings in the transonic regime
[AIAA PAPER 93-3049] p 1057 A93-48229
- PARASCHIVOIU, M.**
Periodic Euler and Navier-Stokes solutions about oscillating airfoils
p 241 A93-17799
Euler computations of rotor-stator interaction in turbomachinery cascades using adaptive triangular meshes
[AIAA PAPER 93-0386] p 282 A93-23065
- PARASURAMAN, RAJA**
Adaptive automation and human performance: Multi-task performance characteristics
[AD-A254596] p 186 A93-12578
Theory and design of adaptive automation in aviation systems
[AD-A254595] p 160 A93-12613
- PARDINI, S.**
Radar signals analysis oriented to target characterization applied to civilian ATC radar
p 885 A93-43475
- PARDUHN, S. C.**
Analysis of turbine engine rotor containment and shielding structures
[AIAA PAPER 93-1817] p 1110 A93-49705
- PAREKH, D. E.**
The use of streamwise vorticity to enhance ejector performance
[AIAA PAPER 93-3247] p 966 A93-46792
- PARETZKE, H. G.**
Radiation exposure in aircraft
p 1035 A93-31928
- PARIKH, PARESH**
Unstructured grid solutions to a wing/pylon/store configuration using VGRID3D/USM3D
[AIAA PAPER 92-4572] p 14 A93-13303
- PARIN, MIKE**
Add-on damping treatment for the F-15 upper-outer wing skin
[AD-A258470] p 337 A93-18248
- PARK, C.**
An overview of Ames experimental aerothermodynamics
p 1011 A93-45496
- PARK, C. S.**
Nonequilibrium shock layer radiation in a simulated Titan atmosphere
p 1233 A93-54805
- PARK, CHUL**
Review of chemical-kinetic problems of future NASA missions. I - Earth entries
p 872 A93-42899
Measurement and analysis of nitric oxide radiation in an arc-jet flow
[AIAA PAPER 93-2800] p 1016 A93-46540
Calculation of real-gas effects on airfoil aerodynamic characteristics
p 1229 A93-54477
- PARK, EUI H.**
Flight simulator for hypersonic vehicle and a study of NASP handling qualities
p 530 A93-19456
- PARK, IL-PYUNG**
A formalization and implementation of topological visual navigation in two dimensions
p 435 A93-19101
- PARK, J. S.**
Heat transfer performance comparisons of five different rectangular channels with parallel angled ribs
p 397 A93-18752
- PARK, JONGHWA**
Concurrent field service and laboratory testing as a means of improving reliability in creep-rupture applications
p 916 A93-40814
- PARK, M. K.**
Oscillations of circular shock waves with upstream disturbance
p 1023 A93-45463
- PARK, MYEONG-KWAN**
Oscillation of circular shock waves with upstream nonuniformity
p 208 A93-15496
- PARK, S.**
Digital resolver for helicopter model blade motion analysis
p 830 A93-37878
Approximate decoupling flight control system design with output feedback for nonlinear systems
[AIAA PAPER 93-3880] p 1135 A93-51465
- PARK, S. O.**
A numerical study of unsteady supersonic compression ramp flows
[AIAA PAPER 93-0883] p 470 A93-24943
- PARK, SANG-YOUNG**
Calculation of numerical boundary measure for wavelet-Galerkin approximations in aerelasticity
[AIAA PAPER 93-1539] p 741 A93-34076
- PARK, SEUNG O.**
Reynolds stress profiles in the near wake of an oscillating airfoil
p 1236 A93-55380
- PARK, WARN-GYU**
Numerical simulation of incompressible viscous flow around a propeller
[AIAA PAPER 93-3503] p 984 A93-47271
- PARKER, JAMES F., JR.**
Future availability of aircraft maintenance personnel
p 570 A93-27133
- PARKER, NIGEL**
Differential GPS/inertial navigation approach/landing flight test results
p 32 A93-11019
- PARKER, R. A.**
Software requirements for the A-7E aircraft
[AD-A255746] p 229 A93-15052
- PARKER, T.**
Nonintrusive, multipoint velocity measurements in high-pressure combustion flows
[AIAA PAPER 93-2032] p 1145 A93-49867
- PARKER, T. E.**
An optical comparison of wall and axial injection for high enthalpy reacting scramjet flows
[AIAA PAPER 93-0357] p 377 A93-23040
High-temperature supersonic combustion testing with optical diagnostics
p 730 A93-34498
- PARKER, WILLIAM H.**
Engine life assessment test case TF41 LP compressor shaft torsional fatigue
p 177 A93-14896
- PARKHIMOVICH, VIKTOR A.**
Design of aircraft, helicopters, and aviation engines
[ISBN 5-277-01192-7] p 947 A93-44508
- PARKINSON, BOB**
MAKS - Eastern promise?
p 733 A93-34266
- PARKINSON, G. V.**
A wake singularity potential flow model for airfoils experiencing trailing-edge stall
p 1067 A93-48544
- PARLETTE, EDWARD B.**
Development of a flexible and efficient multigrid-based multiblock flow solver
[AIAA PAPER 93-0677] p 269 A93-21117
- PARLIER, M.**
Fiber reinforced composites: A new class of glass and glass ceramic materials for thermomechanical applications
[REPT-921-430-104] p 200 A93-15490
- PARMANTIER, J. P.**
Validation of electromagnetic-topology concepts on a complex structure
[ONERA, TP NO. 1992-63] p 542 A93-25327
- PARMANTIER, JEAN-PHILIPPE**
Topological approach for the study of electromagnetic coupling
[ONERA-P-1992-2] p 551 A93-20230
- PARMAR, DEVENDRA S.**
Partially exposed polymer dispersed liquid crystals for boundary layer investigations
p 399 A93-19250
- PARMEY, KELLY L.**
Techniques for the visual evaluation of computational grids
[AIAA PAPER 93-3353] p 1037 A93-45047
- PARNAS, DAVID L.**
Software requirements for the A-7E aircraft
[AD-A255746] p 229 A93-15052
- PARNIS, P.**
Flying qualities of the Hermes spaceplane and the shape definition process
p 532 A93-28437
- PARPIA, I. H.**
Sweeping algorithm for unstructured-grid generation on two-dimensional non-convex domains
p 1262 A93-56413
- PARPIA, IJAZ H.**
A solution scheme for the Euler equations based on a multi-dimensional wave model
[AIAA PAPER 93-0065] p 261 A93-20178
Flux limiters in a rotated upwind scheme for the Euler equations
[AIAA PAPER 93-0067] p 262 A93-20180
- PARRISH, RUSSELL V.**
Trade-offs arising from mixture of color cueing and monocular, binocular, and stereoscopic cueing information for simulated rotorcraft flight
[NASA-TP-3268] p 338 A93-18333
- PARROTT, TONY**
Consecutive plate acoustic suppressor apparatus and methods
[NASA-CASE-LEW-15430-1] p 453 A93-17051
- PARROTT, TONY L.**
Unsteady loads measurements in a generic high speed engine model by means of recessed transducers
[AIAA PAPER 93-0287] p 342 A93-21104
- PARSONS, DAVID B.**
The dynamics of microbursts as revealed by Doppler radar observations and numerical simulations
p 432 A93-22196
- PARTHASARATHY, V. N.**
Optimized/adapted finite elements for structural shape optimization
p 77 A93-10971
Optimization of composite engine structures for mechanical and thermal loads
[AIAA PAPER 93-1583] p 719 A93-34115
- PARTHASARATHY, VIJAYAN**
A 3-D finite-volume scheme for the Euler equations on adaptive tetrahedral grids
p 956 A93-45083
- PARTIDGE, MARY A.**
Advanced composite helicopter MISERS GOLD test/analysis
p 508 A93-27974
- PARTYKA, ROBERT L.**
Joining carbon composite fins to titanium heat pipes
[AD-A261970] p 825 A93-27667
- PARVU, P.**
Aerodynamic forces and moments on a dihedral swept wing in a translation with attack and side-slip angle
p 476 A93-26903
- PARZYCH, D.**
An assessment of wake structure behind forward swept and aft swept propfans at high loading
p 245 A93-19222
- PASARIBU, H. M.**
An approach to configuration design synthesis of subsonic transport aircraft using artificial intelligence techniques
p 716 A93-25692
- PASCHAL, A.**
Comparison of experimental ground testing and computational fluid dynamics for the re-engined 727-100 center engine inlet
[AIAA PAPER 92-3920] p 462 A93-24294
- PASCHAL, WILLIAM A.**
Study on vortex flow control of inlet distortion
p 122 A93-14520

- PASCHALL, RANDALL N.**
Applying variations of the quantitative feedback technique (QFT) to unstable, non-minimum phase aircraft dynamics models p 939 A93-42797
Augmentation of a navigation reference system with differential global positioning system pseudorange measurements p 881 A93-42798
- PASHA, S. G. A.**
Computer aided design of turbo-machinery components p 1166 A93-50489
- PASHCHENKO, O. B.**
Optimization of equipment layout in the fuselage of maneuverable aircraft p 891 A93-42370
- PASIN, M.**
LDV Measurements of unsteady flow fields in radial turbine [AD-A253592] p 19 N93-10648
LDV measurements of unsteady flow fields in radial turbine [AD-A255728] p 221 N93-15065
- PASINI, S.**
Performance and configuration analysis of jet-engine off-design behavior [ISABE 93-7087] p 1202 A93-54063
- PASKIN, MARC D.**
An efficient liner cooling scheme for advanced small gas turbine combustors [AIAA PAPER 93-1763] p 1109 A93-49660
- PASQUALI, L.**
An integrated weather channel designed for an up-to-date ATC radar system p 929 A93-43434
- PASSALACQUA, M.**
Adaptive mesh embedding for reentry flow problems p 869 A93-42619
- PASSALACQUA, MASSIMO**
Influence of the physical modelling of viscous terms on hypersonic flow computations [INRIA-RR-1493] p 297 N93-18652
- PASSMAN, ROBERT H.**
Airborne Wind Shear Detection and Warning Systems. Fourth Combined Manufacturers' and Technologists' Conference, part 2 [NASA-CP-10105-PT-2] p 144 N93-14844
Airborne Wind Shear Detection and Warning Systems: Fourth Combined Manufacturers' and Technologists' Conference, part 1 [NASA-CP-10105-PT-1] p 488 N93-19590
- PASTOREL, H.**
Stress calculation for the Sandia 34-meter wind turbine using the local circulation method and turbulent wind [DE93-004480] p 560 N93-22045
- PASTRONE, DARIO**
An analysis of air-turborocket performance [AIAA PAPER 93-1982] p 1141 A93-49829
Nozzle effects on linear stability behaviour of combustors [ISABE 93-7044] p 1198 A93-54020
- PATEL, K. S.**
The effects of hypersonic flight test requirements on research vehicle design [AIAA PAPER 93-0511] p 386 A93-23258
- PATEL, NISHEETH**
A study of CFD algorithms applied to complete aircraft configurations [AIAA PAPER 93-0784] p 468 A93-24864
- PATEL, VIRENDRA C.**
Skin-friction topology over a surface mounted semi-elliptical wing at incidence p 1178 A93-53216
Ship viscous flow: A report on the 1990 SSPA-IIHR Workshop p 840 N93-27466
- PATEL, Y.**
Design of insensitive multirate aircraft control using optimized eigenstructure assignment p 370 A93-23515
- PATIL, S. R.**
Experimental investigations on wing-body combinations and their components at high angles of attack in the subsonic and transonic speed range [DLR-FB-91-43] p 516 N93-21762
- PATNAIK, SURYA N.**
Application of artificial neural networks to the design optimization of aerospace structural components [NASA-TM-4389] p 555 N93-21831
- PATRICK, W.**
Flowfield measurements for a supersonic mixer ejector in forward flight p 399 A93-19217
- PATTERSON, DAVID A.**
Robo-line storage: Low latency, high capacity storage systems over geographically distributed networks [NASA-CR-192910] p 758 N93-25130
- PATTERSON, EDWARD M.**
An automated system for the measurement of slant visual range p 413 A93-22176
- PATTERSON, GRANT T.**
Ground test simulation fidelity of turbine engine airstarts [AIAA PAPER 93-2173] p 1137 A93-49986
- PATTERSON, WALTER W.**
Multiple function sensors for Enhanced Vision application p 807 A93-37071
- PATTIPATI, KRISHNA**
A multisensor-multitarget data association algorithm for heterogeneous sensors p 1020 A93-44168
- PATTIPATI, KRISHNA R.**
A multisensor-multitarget data association algorithm for heterogeneous sensors p 439 A93-22899
- PATTON, R. J.**
Robust fault detection of jet engine sensor systems using eigenstructure assignment p 173 A93-14608
Design of insensitive multirate aircraft control using optimized eigenstructure assignment p 370 A93-23515
Design of a low sensitivity and norm multivariable controller using eigenstructure assignment and the method of inequalities [AIAA PAPER 93-3802] p 1170 A93-51394
- PATTON, STEVEN L.**
Performance analysis of a miniaturized airborne GPS receiver p 313 A93-21147
- PATTON, T. C.**
Investigation of corrosion in aluminum/adhesive lap-splices using pulse-echo ultrasonic techniques [DE93-008074] p 749 N93-25518
- PATTON, THADD C.**
Ultrasonic NDE of adhesive and sealant bonded aluminum lap-splices p 407 A93-19595
- PATWA, PRANAV D.**
Multidisciplinary analysis and sensitivity derivatives for isolated helicopter rotors in hover [AIAA PAPER 92-4696] p 324 A93-20308
- PAUL, BERNARD P., JR.**
Analysis of wing-body junction flowfields using the incompressible Navier-Stokes equations, volumes 1 and 2 p 17 N93-10320
- PAUL, DIANE**
Additional developments in embedded computer performance measurement p 940 A93-42833
- PAUL, WOLFGANG**
Application of the Euler method EUFLEX to a fighter-type airplane configuration at transonic speed [MBB-FE-211-S-PUB-0489-A] p 484 N93-21059
- PAULAT, J. C.**
Some aspects of the aerodynamic methodology in hypersonic vehicle concept studies [AIAA PAPER 92-5027] p 272 A93-22303
- PAULEY, LAURA L.**
Unsteady laminar separation on low-Reynolds-number airfoils [AIAA PAPER 93-0209] p 278 A93-22627
- PAULI, ROBERT**
Lockheed adopts media blast dry stripping for the C-130 [SAE PAPER 920949] p 107 A93-14092
- PAULL, A.**
Development of a skin friction gauge for use in an impulse facility p 1024 A93-45526
Free piston facilities with air driver gas p 1011 A93-45528
Drag measurements on blunted cones and a scramjet vehicle in hypervelocity flow p 1050 A93-48172
Hypersonic ignition and thrust production in a scramjet [AIAA PAPER 93-2444] p 1119 A93-50196
- PAULSON, JOHN W., JR.**
Low-speed longitudinal and lateral-directional aerodynamic characteristics of the X-31 configuration [NASA-TM-4351] p 22 N93-11622
Transition aerodynamics for 20-percent-scale VTOL unmanned aerial vehicle [NASA-TM-4419] p 779 N93-27032
Evaluation of four advanced nozzle concepts for short takeoff and landing performance [NASA-TP-3314] p 875 N93-29165
- PAULSON, RANDY E.**
Variable cycle engine concept [ISABE 93-7065] p 1200 A93-54041
- PAUSDER, HEINZ-JUERGEN**
Helicopter in-flight simulator ATHeS - A multipurpose testbed and its utilization p 43 A93-13315
ATHeS - A helicopter in-flight simulator with high bandwidth capability p 821 A93-35988
Generation of helicopter roll axis bandwidth data through ground-based and in-flight simulation p 511 N93-19909
- PAVEL, M.**
Engineering a visual system for seeing through fog [SAE PAPER 921130] p 895 A93-41318
- PAVELKO, V. P.**
Crack growth under conditions of service loading p 396 A93-18370
- PAVLATH, GEORGE A.**
The LN-200 fiber gyro based tactical grade IMU [AIAA PAPER 93-3798] p 1106 A93-51391
- PAVLENKO, A. P.**
Atmospheric disturbances over mountains and the flight safety p 1164 A93-51856
- PAVLIKA, M.**
Optimizing the cruising fuel efficiency of commercial aircraft on the basis of flight manual data p 321 A93-18351
- PAVLINSKY, J.**
Hover testing a demonstrated and cost-effective risk reduction tool [AIAA PAPER 93-2677] p 913 A93-42234
- PAVLOV, A. S.**
A study of the effect of the shape of a parasail on its lift-drag ratio p 1069 A93-48913
A study of air intake parameters on the aerodynamic characteristics of a parasail p 1092 A93-51908
- PAVLOV, G. I.**
Software support for a computerized air situation documentation system p 941 A93-43115
- PAVLOV, V. A.**
Dynamic analysis of a compound elastic surface p 1030 A93-47086
- PAVLOVA, NATALIJA V.**
Instrument systems of flight vehicles and their design [ISBN 5-217-00793-1] p 718 A93-35678
- PAXSON, DANIEL E.**
An improved numerical model for wave rotor design and analysis [AIAA PAPER 93-0482] p 361 A93-23384
A comparison between numerically modelled and experimentally measured loss mechanisms in wave rotors [AIAA PAPER 93-2522] p 1120 A93-50252
System and method for cancelling expansion waves in a wave rotor [NASA-CASE-LEW-15218-1] p 86 N93-11172
An improved numerical model for wave rotor design and analysis [NASA-TM-105915] p 60 N93-12418
- PAYNE, BARRY**
Helicopter simulation: Making it work p 912 N93-30682
- PAYNTER, G. C.**
Accuracy issues in the prediction of supersonic inlet flows [ASME PAPER 92-GT-400] p 258 A93-19549
A lag model for turbulent boundary layers developing over rough bleed surfaces [AIAA PAPER 93-2988] p 1052 A93-48181
- PAYNTER, GERALD C.**
Flow stability issues in supersonic inlet flow analyses [AIAA PAPER 93-0290] p 279 A93-22690
Modeling supersonic inlet boundary-layer bleed roughness p 872 A93-42891
Boundary conditions for unsteady supersonic inlet analyses [ISABE 93-7104] p 1187 A93-54080
- PAZUR, W.**
The influence of intake swirl distortion on the steady-state performance of a low bypass, twin-spool engine p 214 N93-13211
- PAZUR, WOLFRAM**
Experimental and numerical examinations of the influence of inlet distortion perturbations on the working behavior of turbofan compressors [ETN-93-92733] p 364 N93-18628
- PEABODY, S. A., II**
Some measurements on dependence of rectangular cylinder drag on elevation p 1025 A93-45745
- PEACE, A. J.**
The modelling of aerodynamic flows by solution of the Euler equations on mixed polyhedral grids p 269 A93-21218
- PEAKE, KIRK**
Eagle RTS: A design for a regional transport aircraft [NASA-CR-192032] p 334 N93-18017
- PEAKE, N.**
Unsteady transonic flow past a quarter-plane p 127 A93-16664
The interaction between a steady jet flow and a supersonic blade tip p 688 A93-34415
The unsteady flow past a supersonic splitter plate [ISABE 93-7047] p 1185 A93-54023
- PEALAT, M.**
CARS studies in hypersonic flows [AIAA PAPER 93-3047] p 1144 A93-48227
CARS temperature measurements in combustion [ONERA, TP NO. 1993-78] p 1212 A93-53599

- PEARCE, G. F.**
The combustion of droplets within gas turbine combustors - Some recent observations on combustor efficiency [ASME PAPER 92-GT-135] p 388 A93-19367
The prediction of thermal NO(x) in gas turbine exhausts [ISABE 93-7022] p 1195 A93-53998
- PEARLSTEIN, ARNE J.**
Development of the wake behind a circular cylinder impulsively started into rotatory and rectilinear motion p 1236 A93-55736
- PEARSON, ALLAN E.**
Parameter identification for nonlinear aerodynamic systems [NASA-CR-193072] p 782 N93-27282
- PEARSON, L. G.**
The whale with a tail p 803 A93-38837
- PECHERITSA, A. V.**
An experimental study of a compound supersonic jet p 1069 A93-48914
An experimental study of the dynamic effect of a supersonic underexpanded jet on a plane surface parallel to the nozzle axis p 1092 A93-51913
- PECK, A. W.**
On design and optimization of curved composite beams p 826 A93-35953
- PECK, ANN W.**
Design and analysis of curved composite components for rotorcraft fuselage frames p 716 N93-25701
- PEELING, S. M.**
Preliminary results on the use of linear discriminant analysis in the ARM continuous speech recognition system [RSRE-MEMO-4511] p 87 N93-11384
The use of linear discriminant analysis in the ARM continuous speech recognition system [RSRE-MEMO-4512] p 87 N93-11385
- PEGG, ROBERT J.**
Design of a hypersonic waverider-derived airplane [AIAA PAPER 93-0401] p 384 A93-21108
- PEIRO, J.**
Adaptive remeshing for three-dimensional compressible flow computations p 242 A93-18851
The application of an adaptive unstructured grid method to the solution of hypersonic flows past double ellipse and double ellipsoid configurations p 868 A93-42609
- PEKKARI, L.-O.**
Aeroelastic stability of supersonic nozzles with separated flow [AIAA PAPER 93-2588] p 1142 A93-50300
- PELKMAN, R. A.**
A CFD-based design strategy for advanced transonic wing concepts with practical ramifications for subsonic transports [AIAA PAPER 93-2946] p 1047 A93-48143
- PELLEGRINI, P. F.**
Radar signals analysis oriented to target characterization applied to civilian ATC radar p 885 A93-43475
- PELLETIER, DOMINIQUE**
An adaptive finite element method for turbulent free shear flow past a propeller [AIAA PAPER 93-3388] p 956 A93-45079
- PELLETIER, M. E.**
Circulation control wing model study [AIAA PAPER 93-0094] p 264 A93-20200
- PELZ, RICHARD B.**
Solution of the Euler and Navier Stokes equations on parallel processors using a transposed/Thomas ADI Algorithm [AIAA PAPER 93-3310] p 1036 A93-45006
- PEMBER, RICHARD B.**
Adaptive Cartesian grid methods for representing geometry in inviscid compressible flow [AIAA PAPER 93-3385] p 955 A93-45076
- PENANHOAT, O.**
Numerical simulation of the flow field around supersonic air-intakes [ASME PAPER 92-GT-206] p 251 A93-19430
- PENDERGRAFT, ODIS C., JR.**
Experimental study of pylon cross sections for a subsonic transport airplane p 1103 A93-52440
Effect of pylon cross-sectional geometries on propulsion integration for a low-wing transport [NASA-TP-3333] p 788 N93-28070
- PENG, JIAN**
Advanced electromagnetic methods for aerospace vehicles [NASA-CR-193468] p 936 N93-31036
- PENG, SHIYI**
Estimation of maximal local temperature at exit of annular combustor p 172 A93-14496
- PENG, XIAO Y.**
Flight simulator development in China p 191 A93-14410
- PENG, ZEYAN**
An experimental investigation of endwall flow control in a compressor plane cascade wind tunnel p 1066 A93-48512
- PENGELLY, S. L.**
Generic developmental turbojet fuel control p 172 A93-14519
- PENNERON, N.**
Turbine blade forces due to partial admission p 1029 A93-46928
- PENNINGTON, I. P.**
The design and development of an afterburner [ISABE 93-7041] p 1198 A93-54017
- PEPIN, JOHN N.**
Fiber reinforced structures for turbine engine fragment containment [AIAA PAPER 93-1816] p 1110 A93-49704
- PEPLER, PHILIPP W.**
Advantages of using a projected head-up display in a flight simulator [AD-A255332] p 194 A93-14559
- PERAIRE, J.**
Computation of viscous compressible flows using an upwind algorithm and unstructured meshes p 9 A93-12163
Adaptive remeshing for three-dimensional compressible flow computations p 242 A93-18851
The application of an adaptive upwind unstructured grid solution algorithm to the simulation of compressible laminar viscous flows over compression corners p 866 A93-42594
The application of an adaptive unstructured grid method to the solution of hypersonic flows past double ellipse and double ellipsoid configurations p 868 A93-42609
Line relaxation methods for the solution of 2D and 3D compressible flows [AIAA PAPER 93-3366] p 955 A93-45059
- PERAIRE, JAIME**
Experimental and computational investigations of the flowfield around the F117A [AIAA PAPER 93-3508] p 984 A93-47274
- PERALA, RODNEY A.**
Development of models for predicting the triggering of lightning by launch vehicles p 734 A93-24899
- PERDICHIZZI, A.**
Incidence angle and pitch-chord effects on secondary flows downstream of a turbine cascade [ASME PAPER 92-GT-184] p 251 A93-19409
- PEREIRA, J. C. F.**
Comparison of several convection discretization schemes for all Mach number arbitrary 2D flows p 685 A93-34345
- PERES, P.**
Fiber reinforced composites: A new class of glass and glass ceramic materials for thermomechanical applications [REPT-921-430-104] p 200 N93-15490
- PEREVEZENTSEV, LEV T.**
Airport radar systems (2nd revised and enlarged edition) [ISBN 5-277-00610-9] p 992 A93-44505
- PEREZ-ORTIZ, B. M.**
Vaporizer performance p 79 A93-12784
- PEREZ, E.**
Aerodynamic characteristics of transport airplanes in low speed configuration p 113 A93-14172
- PEREZ, EMILIO**
Extended range operations of two and three turbofan engined airplanes p 802 A93-37391
- PEREZ, RONALD A.**
Robust stabilization based on topological connectedness p 438 A93-22830
Model reference control of a linear plant with feedthrough element p 846 A93-37034
- PERIAUX, J.**
The finite element method in the 1990's [ISBN 0-387-54930-7] p 925 A93-40823
Attempt to evaluate the computations for test case 6.1 - Cold hypersonic flow past ellipsoidal shapes p 869 A93-42620
Contribution to Problem 6 using an upwind Euler solver with unstructured meshes p 869 A93-42627
- PERIAUX, JACQUES**
Validation of aerodynamic simulation methods for Hermes spaceplane and future hypersonic vehicles [AIAA PAPER 92-5065] p 273 A93-22335
Hypersonic flows for reentry problems. Vols. 1 & 2 [ISBN 0-387-54428-3] p 864 A93-42576
The European Data Base - A new CFD validation tool for the design of space vehicles [AIAA PAPER 93-3045] p 1057 A93-48225
- PERIC, M.**
A collocated finite volume method for predicting flows at all speeds p 1087 A93-51736
- PERKINS, D. E.**
Dual-band infrared imaging applications: Locating buried minefields, mapping sea ice, and inspecting aging aircraft [DE93-000516] p 453 N93-17225
- PERKINS, J. N.**
Analysis of hypersonic nozzles including vibrational nonequilibrium and intermolecular force effects p 861 A93-41916
- PERKINS, JOHN N.**
Two leading-edge droop modifications for tailoring stall characteristics of a general aviation trainer configuration p 1008 A93-46807
- PERKINS, PORTER J.**
Aircraft icing problems - After 50 years [AIAA PAPER 93-0392] p 486 A93-24239
- PERKINS, STANLEY C., JR.**
A study of turbulence in rarefied gases [AIAA PAPER 93-3097] p 1061 A93-48271
- PERKINS, STEVEN W.**
Integrated Blade Inspection System (IBIS) upgrade study [AD-A258912] p 365 N93-19356
- PERMINOV, V. D.**
Certain improved algorithms for calculating the aerodynamic characteristics of flight vehicles in free-molecular flow p 1090 A93-51872
- PEROV, S. N.**
Load rating for a delta wing box based on a reliability criterion p 1030 A93-47093
- PERRAUD, ERIC**
Position sensor with two wavelength time domain multiplexing for civil aircraft application p 1104 A93-49432
- PERRELL, FRANCOISE**
A family of multiblock codes for computational aerothermodynamics - Application to complete vehicle hypersonic flows [AIAA PAPER 93-3042] p 1056 A93-48223
- PERRELLA, ANDREW P.**
Structural applications of Avimid K3B LDF thermoplastic composites p 1216 A93-53429
- PERRETT, B. H. E.**
An evaluation of a method of reconstituting fatigue loading from Rainflow counting [RAE-TR-89057] p 82 N93-10198
- PERRIER, PIERRE**
Simulation in aeronautics p 437 A93-21868
The European Data Base - A new CFD validation tool for the design of space vehicles [AIAA PAPER 93-3045] p 1057 A93-48225
- PERRIN, G.**
Analysis of three-dimensional viscous flow in a supersonic axial flow compressor rotor with emphasis on tip leakage flow [ASME PAPER 92-GT-388] p 257 A93-19543
- PERRIN, JOSEPH**
A second-generation high speed civil transport: Stingray [NASA-CR-192022] p 336 N93-18059
- PERRY, BERNARD**
The future of area navigation in Western Europe p 311 A93-17752
- PERRY, BOYD, III**
Further studies using matched filter theory and stochastic simulation for gust loads prediction [AIAA PAPER 93-1365] p 726 A93-33932
Computation of maximized gust loads for nonlinear aircraft using matched-filter-based schemes p 1136 A93-52452
- PERRY, L. A.**
Experimental analysis of the aeroacoustics of cascaded airfoils [AD-A257945] p 420 N93-18121
- PERRYMORE, L. G.**
Demonstration of an integrated, active 4 x 4 photonic crossbar p 211 A93-17392
- PERSHIN, I. S.**
Modeling of the physicochemical processes of nonequilibrium heat transfer in the subsonic jets of an induction plasmatron p 836 A93-39147
- PERSIANI, F.**
Parametric aeroelastic analysis of composite wing-boxes with active strain-energy tuning p 156 A93-14361
- PERSON, LEE H.**
Design and conduct of a windshear detection flight experiment [AIAA PAPER 92-4092] p 38 A93-11268
- PERSON, LEE H., JR.**
Simulator evaluation of displays for a revised takeoff performance monitoring system [NASA-TP-3270] p 189 N93-15366
- PESCH, H. J.**
Combining direct and indirect methods in optimal control: Range maximization of a hang glider [REPT-313] p 371 N93-16618

PESCHKE, WILLIAM T.

An approach to in-situ analysis of scramjet combustor behavior

[AIAA PAPER 93-2328] p 1116 A93-50108

PESSIN, DAVID N.

Aerodynamic analysis of hypersonic waverider aircraft [NASA-CR-192981] p 780 N93-27093

PETAGNA, P.

Wing pressure loads in canard configurations - A comparison between numerical results and experimental data p 7 A93-11499

PETERKA, J. A.

Wind load design methods for ground-based heliostats and parabolic dish collectors [DE93-002737] p 433 N93-15839

PETERKA, JON A.

Anemometer siting criteria for low level wind shear alert system p 413 A93-22178

PETERS, DAVID A.

An interactive numerical procedure for rotor aeroelastic stability analysis using elastic lifting surface p 155 A93-14313

Analytical formulation of optimum rotor interdisciplinary design with a three-dimensional wake [AIAA PAPER 92-4778] p 265 A93-20416

Flutter calculations for fixed and rotating wings with state-space inflow dynamics [AIAA PAPER 93-1300] p 709 A93-33877

Effect of an unsteady three-dimensional wake on elastic blade-flapping eigenvalues in hover p 683 A93-34260

Flap-lag damping in hover and forward flight with a three-dimensional wake p 797 A93-35979

Finite state aeroelastic model for use in rotor design optimization p 1104 A93-52454

PETERS, DAVID W.

Flowfield measurements about a multi-element airfoil at high Reynolds numbers [AIAA PAPER 93-3137] p 1064 A93-48300

PETERS, M. F.

Multiple receiver, zero-length baseline kinematic GPS positioning techniques for airborne gravity measurement p 1240 A93-55974

PETERS, MICHAEL A. G.

Development of a TRN/INS/GPS integrated navigation system p 30 A93-11004

PETERSEN, K. L.

On some recent advances in multidisciplinary analysis of hypersonic vehicles [AIAA PAPER 92-5026] p 438 A93-22302

PETERSEN, STEVE

Advanced hypersonic aircraft design [NASA-CR-192046] p 334 N93-18037

PETERSON, BENJAMIN

Integrated Soviet VLF/Omega Receiver design p 316 A93-21198

PETERSON, CARL W.

The fluid physics of parachute inflation p 1189 A93-54347

PETERSON, TIMOTHY

Arrow 227: Air transport system design simulation [NASA-CR-192053] p 336 N93-18063

PETERSON, VICTOR L.

Applied aerodynamics: Challenges and expectations [NASA-TM-103963] p 694 N93-25091

PETIT, JEAN

Damage tolerance of a helicopter rotor high-strength steel p 555 N93-21322

PETLEY, DENNIS H.

Design of a hypersonic waverider-derived airplane [AIAA PAPER 93-0401] p 384 A93-21108

Analytical comparison of convective heat transfer correlations in supercritical hydrogen p 416 A93-23477

PETOT, B.

Assessment of a 3-D Euler code for subsonic turbine vane flows and study of the non radial blade stacking [ASME PAPER 92-GT-63] p 247 A93-19313

Intensive industrial use of 3D Euler numerical methods for axial flow turbine analysis and design p 1002 A93-46943

Three-dimensional analysis of turbine rotor flow including tip clearance [ASME PAPER 93-GT-111] p 987 A93-47446

PETOT, BERTRAND

Viscous analysis of high pressure turbine inlet guide vane flow including cooling injections [AIAA PAPER 93-1798] p 1074 A93-49687

3D and 2.5D viscous flow computations for axial flow turbine blades [ISABE 93-7093] p 1186 A93-54069

PETOT, D.

Numerical calculation of helicopter rotor equations and comparison with experiment [ONERA, TP NO. 1992-128] p 772 A93-38602

PETRAKOV, V. V.

Experimental simulation of the aerodynamic heating of bodies in a molecular region p 1090 A93-51871

PETRIE, S. P.

Lightweight aircraft turbine protection [AIAA PAPER 93-1815] p 1110 A93-49703

PETRISHIN, S. F.

Supersonic flow past a rectangular wing of finite thickness p 1086 A93-50972

PETRO, JOHN

Time delay measurements of current primary FAA air/ground transmitters and receivers [DOT/FAA/CT-TN93/14] p 842 N93-28555

PETROSKI, M.

Flow field characteristics of a complex blade tip at high angles of attack [AIAA PAPER 93-3083] p 1060 A93-48257

PETROV, BORIS I.

Flight-vehicle drives (2nd revised and enlarged edition) [ISBN 5-217-00802-4] p 713 A93-35676

PETROV, M. D.

Experimental investigation of hydrogen burning and heat transfer in annular duct at supersonic velocity p 171 A93-14247

Direct measurements of skin friction in a scramjet combustor [AIAA PAPER 93-2443] p 1119 A93-50195

PETROV, V. I.

Theory of the machining of polyhedral holes by plunge cutting p 835 A93-39091

PETROV, V. YU.

The fuel/timing problem in a computer-aided flight preparation system for civil aircraft p 996 A93-45672

Calculation of safe altitudes p 991 A93-45675

PETTA, ARNO E.

The PAVE PACE integrated RF architecture for next generation avionics p 896 A93-42784

PETTERS, D. P.

Rapid computer simulation of ramjet performance [AIAA PAPER 93-2049] p 1113 A93-49882

PETERSSON, A.

Effects of blade geometry and mode shape on fan flutter [ISABE 93-7028] p 1196 A93-54004

PETTIT, F. S.

Platinum-modified diffusion aluminide coatings on nickel-base superalloys [AD-A263597] p 917 N93-29981

PETUKHOV, IU. V.

Effect of overloads on the service life of the structural elements of aircraft p 746 A93-35289

PETUNIN, A. N.

Hemispherical and spherical flow parameter detectors p 75 A93-10044

A transfer standard of an air flow rate unit VET 150-2-87 p 66 A93-10049

PEWSEY, STEPHEN M. S.

The application of manufacturing systems engineering for aero engine gears [PNR-90944] p 86 N93-11054

PEZZULLO, G.

Numerical study for the study of medium speed internal noise problems [DILC-EST-TN-200] p 101 N93-11156

PFAFF, K.

Heat transfer and material temperature conditions in the leading edge area of impingement-cooled turbine vanes [ISABE 93-7076] p 1220 A93-54052

PFAFFENBERGER, E. E.

High temperature corrosion resistant bearing steel development [AIAA PAPER 93-2000] p 1145 A93-49842

PFAHL, C. L.

Cost studies for commercial fuselage crown designs p 920 N93-30440

PFOERTNER, H.

RB199 engine oil system failure diagnostics by comparison of measured and calculated oil consumption using the OLMOS on-board monitoring system p 178 N93-15173

PHAENGSOOK, N.

Effects of icing on the aerodynamic performance of high lift airfoils [AIAA PAPER 93-0026] p 259 A93-20144

PHARES, WILLIAM J.

Icing testing of a large full-scale inlet at the Arnold Engineering Development Center [AIAA PAPER 93-0299] p 376 A93-22697

PHATAK, ANIL

Passive range sensor refinement using texture and segmentation p 544 A93-27044

PHELAN, PAUL

Advancing helicopters p 327 A93-21836

PHILBERT, M.

Schlieren device and holographic interferometer for hypersonic flow visualization [ONERA, TP NO. 1992-160] p 832 A93-38739

PHILIPPE, J. J.

Definition and evaluation of new helicopter rotor blade tips [ONERA, TP NO. 1992-179] p 773 A93-38741

PHILIPPE, JEAN-JACQUES

ONERA makes progress in rotor aerodynamics, aeroelasticity, and acoustics p 2 A93-11621

PHILPIDIS, T. P.

Damage detection by Acousto-Ultrasonic Location (AUL) p 555 N93-21529

PHILLIPS, J. R.

Application of vanadium hydride compressors for Joule-Thomson cryocoolers p 1149 A93-48616

PHILLIPS, MICHAEL R.

Joint NASA/USAF Airborne Field Mill Program - Operation and safety considerations during flights of a Lear 28 airplane in adverse weather [AIAA PAPER 92-4093] p 93 A93-13262

PHILLIPS, STEPHEN M.

Antiwindup analysis and design approaches for MIMO systems [AIAA PAPER 93-3811] p 1123 A93-51403

PHILLIPS, W. P.

Hypersonic aerodynamic characteristics for Langley Test Technique Demonstrator [AIAA PAPER 93-3443] p 1072 A93-49516

PHILLIS, DAVID L.

Experimental and numerical delta wing study at high angles of attack and sideslip [AIAA PAPER 92-2713] p 473 A93-24990

PHIPPS, MARCUS

A second-generation high speed civil transport: Stingray [NASA-CR-192022] p 336 N93-18059

PIATYSHEV, R. V.

Problems in the aerodynamics and dynamics of flight vehicles in the light of K.E. Tsiolkovsky's ideas; Lectures Devoted to K.E. Tsiolkovsky's Ideas, 25th, Kaluga, Russia, Sept. 11-14, 1990, Transactions p 237 A93-18376

PICHON, R.

Application of a full potential code to the definition of a transonic test section [ONERA, TP NO. 1992-84] p 822 A93-38569

PICKERELL, THOMAS

National Airspace System flight planning operational concept NAS-SR-131 [PB93-124659] p 310 N93-18031

National Airspace System: Air traffic control and airspace management operational concept NAS-SR-132 [DOT/FAA/SE-92/5] p 502 N93-20164

PICKERINE, JO A.

Reusable code for helicopter simulation [AIAA PAPER 93-3594] p 1224 A93-52686

PICKINGS, RICHARD D.

A comparison of classical mechanics models and finite element simulation of elastically tailored wing boxes p 922 N93-30863

Tailored composite wings with elastically produced chordwise camber p 923 N93-30876

PIDAPARTI, R. M. V.

Supersonic flutter analysis of composite plates and shells p 837 A93-39419

PIECHNA, J.

Numerical study of slightly compressible Navier-Stokes simulation of blade-vortex interaction p 1239 A93-56216

PIECHNA, J. R.

Interaction of compressible vortices with a rigid plate p 1239 A93-56219

PIEDELIEVRE, C.

The role of the radiologist in the medicolegal procedure after an aviation accident p 853 A93-39701

PIELLISCH, RICHARD

Composites roll sevens p 3 A93-13448

Beyond steel - TMCs for lighter landing gear p 1100 A93-49337

PIERCE, DAVE

Parachute canopy control and guidance training requirements and methodology [AIAA PAPER 93-1255] p 703 A93-35188

PIERCE, G. A.

Correlation of unsteady pressure and inflow velocity fields of a pitching rotor blade [AIAA PAPER 93-3082] p 1060 A93-48256

PIERRE, CHRISTOPHE

An efficient constraint to account for mistuning effects in the optimal design of engine rotors [AIAA PAPER 92-4711] p 358 A93-20280

Aeroelastic dynamics of mistuned blade assemblies with closely spaced blade modes [AIAA PAPER 93-1628] p 810 A93-37446

- Stochastic sensitivity measure for mistuned high-performance turbines
[NASA-TM-105821] p 90 N93-12277
- Localization of aeroelastic modes in mistuned high-energy turbines p 1032 N93-31586
- PIERRE, CHRISTOPHE**
A transfer matrix approach to vibration localization in mistuned blade assemblies
[NASA-TM-106112] p 838 N93-27088
- PIERS, W. J.**
Aerodynamic analysis of slipstream/wing/nacelle interference for preliminary design of aircraft configurations p 130 N93-13205
- PIERSON, BION L.**
Optimality-based control laws for real-time aircraft control via parameter optimization p 180 N93-14161
- PIETERSEN, O. B. M.**
Navstar global positioning system: Introduction and status
[NLR-TP-91008-U] p 318 N93-17559
Experiences with two GPS receivers in northern Europe
[NLR-TP-91168-U] p 993 N93-31120
- PIETRUSZKA, JANUSZ**
The whirl-flutter problem in aircraft construction p 1249 A93-56218
- PIIPPO, STEVE W.**
A demonstration of simple airfoils: Structural design and materials choices
[DE93-007882] p 789 N93-28662
- PIIPPO, STEVEN W.**
Construction and testing of simple airfoils to demonstrate structural design, materials choice, and composite concepts p 879 N93-30979
- PIKE, A. C.**
Validation of high frequency airload calculations using full scale flight test acoustic data p 567 A93-29417
- PIKE, TONY C.**
Lynx: High performance - Low noise p 322 A93-19185
- PIKULA, EH. R.**
Estimation of the change of axial-flow compressor characteristics during long-term service p 1193 A93-52949
- PILIDIS, PERICLES**
An optimisation-matching procedure for variable cycle jet engines
[ASME PAPER 92-GT-406] p 356 A93-19555
- PILUGIN, N. N.**
Extreme value heat transfer problems for three-dimensional bodies moving at hypersonic velocities p 4 A93-10079
- PILLASCH, DANIEL W.**
Impulse guided Samara decelerator
[AIAA PAPER 93-1234] p 690 A93-35175
- PILLEY, H. R.**
Airport navigation and surveillance using GPS and ADS p 313 A93-21145
Terminal area surveillance using GPS p 316 A93-21190
- PILLEY, LOIS V.**
Airport navigation and surveillance using GPS and ADS p 313 A93-21145
Terminal area surveillance using GPS p 316 A93-21190
- PILYUGIN, N. N.**
Heat transfer on blunt cones in nonuniform supersonic flow in the presence of gas injection from the surface p 972 A93-46975
A study of turbulent flow in a viscous shock layer in the case of gas flow past oblong blunt bodies p 1089 A93-51820
Determination of the $N_2(+) + e$ recombination rate constant from ballistic experiments p 1234 A93-55026
- PIMSHTAIN, V. G.**
Control of coherent structures and aero-acoustic characteristics of subsonic and supersonic turbulent jets p 448 A93-19196
- PIN, F. G.**
Using fuzzy behaviors for the outdoor navigation of a car with low-resolution sensors
[DE93-002428] p 706 N93-25120
- PINCKNEY, ROBERT L.**
Fabrication of the V-22 composite AFT fuselage using automated fiber placement p 920 N93-30443
- PINCKNEY, S. Z.**
Design of a hypersonic waverider-derived airplane
[AIAA PAPER 93-0401] p 384 A93-21108
- PINCKNEY, S. ZANE**
A configuration development strategy for the NASP p 46 N93-10011
- PINEIRO, LUIS A.**
Real-time parameter identification applied to flight simulation p 1006 A93-44142
- PINET, JEAN**
Progress and taboos in air safety orientations of research in human factors in air transport p 141 A93-14374
Progress and taboos in flight safety - Human-factors research in air transportation p 879 A93-42654
- PINNINGTON, R. J.**
Active control of sound transmission through stiff lightweight composite fuselage constructions p 447 A93-19187
- PIOU, JEAN E.**
Robust sampled data eigenstructure assignment using the delta operator p 906 A93-41889
- PIPERNI, P.**
Multi-block grid generation for complete aircraft configurations p 460 A93-23838
Development of a transonic Euler method for complete aircraft configurations p 779 A93-39721
- PIRRELLI, P.**
Cooling geometry optimization using liquid crystal technique p 902 N93-29939
- PIRZADEH, SHAHYAR**
Unstructured grid solutions to a wing/pylon/store configuration using VGRID3D/USM3D
[AIAA PAPER 92-4572] p 14 A93-13303
Advancing-layers method for generation of unstructured viscous grids p 957 A93-45101
Unstructured viscous grid generation by advancing-layers method
[AIAA PAPER 93-3453] p 979 A93-47238
Unstructured viscous grid generation by advancing-front method
[NASA-CR-191449] p 780 N93-27067
- PISANO, JOSEPH J.**
GPS availability and reliability for aircraft precision approach p 315 A93-21182
- PISCHEL, K.**
The engine design engine. A clustered computer platform for the aerodynamic inverse design and analysis of a full engine
[NASA-TM-105838] p 21 N93-11223
- PITA, G. P. A.**
Experimental analysis of combustion oscillations with reference to ramjet propulsion p 392 N93-17614
- PITARYS, MARC**
Avionics software performability p 939 A93-42822
- PITTMAN, JAMES L.**
Shock-dependent, thrust wings for supersonic flow
[AIAA PAPER 93-0321] p 280 A93-23013
Euler analysis of forebody-strake vortex flows at supersonic speeds p 1094 A93-52429
- PITTMAN, JAMES LEE**
Shock-dependent, optimum thrust wings in supersonic flow p 483 N93-20169
- PITTS, N. J.**
A knowledge-based blackboard system to interpret graphical data from vibration tests of gas turbines
[PNR-90993] p 59 N93-11114
- PIVOVAROV, V. V.**
A procedure for the thermal and strength testing of radiotransparent shells p 1209 A93-52976
- PLAETSCHKE, E.**
System identification for X-31A project support: Lessons learned so far p 512 N93-19914
- PLAFF, MARK S.**
Concept feasibility demonstration for the Army Cockpit Delethalization Program p 795 A93-35916
- PLAKHTIENKO, N. P.**
Spanwise aileron oscillations p 819 A93-39190
- PLANQUET, C.**
Materials problems connected with the propulsion of supersonic air carriers
[ONERA, TP NO. 1992-157] p 824 A93-38736
- PLATONOV, A. V.**
Effect of overloads on the service life of the structural elements of aircraft p 746 A93-35289
- PLATT, JEFFREY R.**
The creation of a Community cabotage area in the European Community and its implications for the US bilateral aviation system p 104 A93-13423
- PLATZER, M.**
Aerodynamic characteristics of the MMPT ATD vehicle at high angles of attack
[AIAA PAPER 93-3493] p 982 A93-47265
- PLATZER, M. F.**
An inviscid-viscous interaction approach to the calculation of dynamic stall initiation on airfoils
[ASME PAPER 92-GT-128] p 249 A93-19362
Dynamic airfoil stall investigations p 786 N93-27453
- PLATZER, MAX F.**
Aerodynamic analysis of flapping wing propulsion
[AIAA PAPER 93-0484] p 286 A93-23386
A visualization study of the vortical flow over a double-delta wing in dynamic motion
[AIAA PAPER 93-3425] p 976 A93-47220
- Effect of canard oscillations on the vortical flowfield of a X-31A-like fighter model in dynamic motion
[AIAA PAPER 93-3427] p 1008 A93-47222
A viscous-inviscid interaction method for 2-D unsteady, compressible flows
[AIAA PAPER 93-3019] p 1055 A93-48206
- PLEITNER, J.**
A very efficient tool for the structural analysis of hypersonic vehicles under high temperature aspects p 203 A93-14194
- PLENCNER, ROBERT M.**
Concurrent optimization of airframe and engine design parameters
[AIAA PAPER 92-4713] p 323 A93-20281
An interactive preprocessor for the NASA engine performance program
[NASA-TM-105786] p 56 N93-10983
Concurrent optimization of airframe and engine design parameters
[NASA-TM-105908] p 60 N93-12402
- PLESSEL, TODD C.**
Scientific visualization using the Flow Analysis Software Toolkit (FAST) p 758 N93-25600
- PLEVICH, C. W.**
Effects of turn region treatments on pressure loss through sharp 180-degree bends p 1256 A93-54636
- PLOTKIN, KENNETH J.**
Sonic boom minimization - Myth or reality? p 1264 A93-55859
- PLUMBRIDGE, W. J.**
Life prediction - Thermal fatigue from isothermal data p 916 A93-40807
- PLUMER, J. ANDERSON**
Lightning data acquisition p 753 N93-24883
Lightning phenomenology bases for full threat return stroke occurrence following extended leader sweep at flight altitudes p 754 N93-24895
- PLUVIOSE, M.**
Turbine blade forces due to partial admission p 1029 A93-46928
- PODAFEJ, V. V.**
Behavior of the particular quality characteristics of an intelligent flight vehicle control system in a multicriterial formulation p 1168 A93-50952
- PODBOLOTOVA, N. A.**
Calculation of aerodynamic loads on the wing of rigid and elastic aircraft with allowance for load correction from experimental data p 1103 A93-51905
- PODBOY, GARY G.**
Takeoff/approach noise for a model counterrotation propeller with a forward-swept upstream rotor
[AIAA PAPER 93-0596] p 519 A93-24782
Laser velocimeter measurements of the flow field generated by a forward-swept propfan during flutter
[AIAA PAPER 93-2919] p 1180 A93-53591
Takeoff/approach noise for a model counterrotation propeller with a forward-swept upstream rotor
[NASA-TM-105979] p 362 N93-16715
- PODLESKI, S. D.**
Installed F/A-18 inlet flow calculations at 60 deg angle-of-attack and 10 deg side slip
[AIAA PAPER 93-1806] p 1074 A93-49695
- POE, C. C., JR.**
An evaluation of the pressure proof test concept for 2024-T3 aluminum alloy sheet p 1026 A93-45780
- POELLOT, MICHAEL R.**
An index of resource materials for aviation meteorology education and training p 453 A93-22105
A comparison of several airborne measures of turbulence p 308 A93-22121
- POGGIE, J.**
Control of pressure fluctuations in the reattachment region of a supersonic free shear layer
[AIAA PAPER 93-0385] p 282 A93-23064
Control of a supersonic reattaching shear layer
[AIAA PAPER 93-3248] p 966 A93-46793
- POGOSEV, G. A.**
Detection and parameter estimation of atmospheric turbulence by ground-based and airborne CO2 Doppler lidars p 395 A93-17862
Study of artificial and natural turbulence in atmospheric boundary layer with a CW Doppler CO2 lidar p 1257 A93-54799
- POGOZELSKI, E. M.**
Three dimensional near field behavior of a tip vortex developing on an elliptic foil
[AIAA PAPER 93-0865] p 468 A93-24927
- POINSATTE, PHILIP E.**
Measurements and computational analysis of heat transfer and flow in a simulated turbine blade internal cooling passage
[AIAA PAPER 93-1797] p 1218 A93-53585
High Reynolds number and turbulence effects on aerodynamics and heat transfer in a turbine cascade
[NASA-TM-106187] p 930 N93-29157

- Measurements and computational analysis of heat transfer and flow in a simulated turbine blade internal cooling passage
[NASA-TM-106189] p 1032 N93-31647
- POINSOT, T.**
Low-frequency combustion instability mechanisms in a side-dump combustor p 1247 A93-55220
Combustion instabilities in a side-dump model ramjet combustor p 362 N93-17613
- POIRION, F.**
Numerical simulation of homogeneous non-Gaussian random vector fields p 561 A93-27584
Effect of structural uncertainties on flutter analysis p 924 A93-40445
- POISSON-QUINTON, PH.**
A French look at the future supersonic transport
[ONERA, TP NO. 1992-209] p 803 A93-38763
- POISSON-QUINTON, PHILIPPE**
The ramjet engine in high speed propulsion p 174 A93-16853
Toward the second-generation supersonic transport
[ONERA, TP NO. 1993-26] p 890 A93-41038
- POKORNY, S.**
Numerical investigation of the unsteady flow through a counter-rotating fan p 112 A93-14166
An integrated flow simulation system on a parallel computer. I - Basic concept. II - The flow solver p 688 A93-34370
Unsteady flow simulation on a parallel computer p 1022 A93-45089
- POLAND, J. B.**
Modal analysis in the certification of a commercial aircraft p 509 A93-29241
- POLANSKY, L.**
A new and working automatic calibration machine for wind tunnel internal force balances
[AIAA PAPER 93-2467] p 1138 A93-50214
- POLIAKOV, S. I.**
Estimation of the external loading of airships in flight p 366 A93-18383
- POLIAKOV, A. R.**
Variational problem of the profiling of the side walls of the supersonic section of a narrow three-dimensional nozzle p 4 A93-10140
- POLIAKOV, I. O.**
An approximate method for calculating nonequilibrium flows near blunt bodies p 776 A93-39134
Hypersonic limiting flows of a relaxing gas with pressure changes in the main approximation p 776 A93-39135
- POLLING, D.**
Recent developments in rotor wake modeling for helicopter noise prediction p 481 A93-29437
- POLITES, MICHAEL**
Aerospace '92 - The year in review p 455 A93-19976
- POLITOVICH, M. K.**
The FAA aircraft icing Forecasting Improvement Program - Validation of aircraft icing forecasts in the Denver area
[AIAA PAPER 93-0393] p 309 A93-23069
- POLITOVICH, MARCIA K.**
A proposed icing severity index based upon meteorology p 429 A93-22136
An evaluation of aircraft icing forecasts for the continental United States p 429 A93-22149
- POLKOVNIKOV, VITALII A.**
Flight-vehicle drives (2nd revised and enlarged edition)
[ISBN 5-217-00802-4] p 713 A93-35676
- POLL, D. I. A.**
Application of laminar flow to aero engine nacelles p 128 A93-17256
Application of laminar flow to aero engine nacelles
[PNR-90916] p 20 N93-11020
A combined experimental and theoretical study of laminar flow control with particular relevance to aero engine nacelles
[PNR-90991] p 20 N93-11070
Computational study of real gas effects in high speed high temperature flow, volume 2
[AERO-REPT-9203-VOL-2] p 289 N93-16470
The aerodynamic performance of laser drilled sheets
[AERO-REPT-9204] p 484 N93-20806
The effect of surface suction near the leading edge of a swept-back wing
[AERO-REPT-9205] p 484 N93-20807
- POLLACK, KRISTINA**
How do we investigate the human factor in aircraft accidents? p 491 N93-19655
- POLLARD, MICHAEL D.**
Acoustic emission monitoring of aging aircraft structures p 407 A93-19697
- POLOMSKI, PETER P.**
Anti-icing failure detection instrumentation using realtime optical measurement of anti-icing fluid properties
[AIAA PAPER 93-0748] p 540 A93-24836
- Field studies of hold-over-times for type II anti-icing fluids - Results and insights
[AIAA PAPER 93-0749] p 486 A93-24837
- POLTAVSKI, V. V.**
Autonomous mobile laser complex p 395 A93-17767
- POLUBOYAROV, V. M.**
Methods and equipment for data processing and acquisition in information management systems p 856 A93-43101
- POLYAK, R.**
Structural optimization using Newton Modified Barrier Method
[AIAA PAPER 92-4756] p 409 A93-20352
- POLZ, G.**
Current European rotorcraft research activities on development of advanced CFD methods for the design of rotor blades (BRITE/EURAM DACRO project)
[MBB-UD-0601-91-PUB] p 293 N93-17568
- POMERANTZ, ARTHUR**
A NASPAC-based analysis of the delay and cost effects of the Dallas/Fort Worth metroplex plan
[DOT/FAA/CT-TN92/21] p 193 N93-13447
- POMMELLET, PIERRE E.**
INS/DGPS integration for trajectory determination of a test vehicle p 315 A93-21178
- PONCELINDERACOURT, P.**
Aerothermic calculations of flows in interdisc cavities of turbines p 903 N93-29947
- POND, CHARLES**
Strategic avionics technology definition studies. Subtask 3-1A: Electrical Actuation (ELA) systems
[NASA-CR-193237] p 914 N93-29215
- PONOMAREV, B. A.**
Using contra-rotating rotors for decreasing sizes and component number in small GTE
[ASME PAPER 92-GT-414] p 356 A93-19562
- PONOMAREV, N. N.**
Allowing for the effect of flow nonisothermality on total pressure losses in the afterburner diffusers of augmented turbofan engines p 53 A93-12811
- PONTING, K. M.**
Preliminary results on the use of linear discriminant analysis in the ARM continuous speech recognition system
[RSRE-MEMO-4511] p 87 N93-11384
The use of linear discriminant analysis in the ARM continuous speech recognition system p 87 N93-11385
- PONTON, MICHAEL K.**
The effects of temperature on supersonic jet noise emission p 446 A93-19159
- POPE, D. S.**
A new technique for aerodynamic noise calculation p 447 A93-19177
- POPOV, BORIS N.**
Flight-vehicle drives (2nd revised and enlarged edition)
[ISBN 5-217-00802-4] p 713 A93-35676
- POPOV, M. P.**
An information-search system in cybernetics p 1168 A93-50957
- POPOV, O. S.**
Crack growth under conditions of service loading p 396 A93-18370
- POPOV, V. YU.**
Effect of the size of a plane obstacle on self-oscillations generated in an underexpanded supersonic jet p 1068 A93-48849
- POPOVYAN, A. G.**
Propulsion system simulator with propan for tests on a large scale model of IL-114 airplane in a full-size wind tunnel of TsAGI p 1013 A93-46933
- POPP, M.**
Numerical analysis of high aspect ratio cooling passage flow and heat transfer
[AIAA PAPER 93-1829] p 1153 A93-49714
- POPPE, M.**
Development of a realtime DGPS system
[DLR-MITT-92-06] p 503 N93-20749
- POPPEL, G. L.**
Electro-optic architecture for servicing sensors and actuators in advanced aircraft propulsion systems
[NASA-CR-182269] p 232 N93-13762
- POPYTALOV, S. A.**
Problems in the aerodynamics and dynamics of flight vehicles in the light of K.E. Tsiolkovsky's ideas; Lectures Devoted to K.E. Tsiolkovsky's Ideas, 25th, Kaluga, Russia, Sept. 11-14, 1990, Transactions p 237 A93-18376
Method and results of studies of flow past supersonic flight vehicles at moderate and large angles of attack p 242 A93-18377
- PORDAL, H. S.**
A three-dimensional pressure flux-split RNS application to sub/supersonic flow in inlets and ducts
[AIAA PAPER 93-3063] p 1058 A93-48239
- PORTER, B.**
Design of digital multiple model-following integrated flight/proposition control systems p 183 A93-14371
Design of robust digital model-following flight control systems p 907 A93-42810
Design of reconfigurable digital multiple model-following flight control systems p 908 A93-42811
Genetic design of digital model-following flight-control systems
[AIAA PAPER 93-3883] p 1135 A93-51468
- PORTER, BRIAN**
Design of limit-tracking systems incorporating a turbofan engine with constant disturbances
[ISABE 93-7090] p 1203 A93-54066
- PORTER, C. R.**
Ladar fiber optic sensor system for aircraft applications p 1105 A93-49467
- PORTER, L. M.**
Drag measurements on blunted cones and a scramjet vehicle in hypervelocity flow
[AIAA PAPER 93-2979] p 1050 A93-48172
- PORTER, M. J.**
Surge recovery and compressor working line control using compressor exit Mach number measurement p 897 A93-40435
- PORTER, TODD**
Starch media blasting for aerospace finishing applications
[SAE PAPER 920948] p 107 A93-14091
- PORTNEY, JOSEPH N.**
History of aerial polar navigation p 104 A93-11300
- POSTANS, P. J.**
Materials: Toward the non-metallic engine
[PNR-90915] p 56 N93-11019
- POSTLETHWAITE, I.**
Discrete time H(infinity) control laws for a high performance helicopter p 96 A93-13007
- POSTNOV, A. I.**
Measurement of aerodynamic forces at high temperatures p 75 A93-10030
- POSTNOV, A. N.**
Automated measurement of residual stresses in the surface layer of parts p 834 A93-39081
- POSTNOV, S. E.**
A study of the origin of residual stresses and strains in the transparencies of supersonic aircraft p 801 A93-36784
- POT, T.**
Shock wave/boundary layer interaction in a two-dimensional laminar hypersonic flow
[ONERA, TP NO. 1992-182] p 773 A93-38744
- POT, THIERRY**
Validation of a Navier-Stokes code using a (k,epsilon) turbulence model applied to a three-dimensional transonic channel
[AIAA PAPER 93-0293] p 279 A93-22693
- POTAPCZUK, MARK G.**
Numerical modeling of anti-icing systems and comparison to test results on a NACA 0012 airfoil
[AIAA PAPER 93-0170] p 327 A93-23242
Ice accretion and performance degradation calculations with LEWICE/NS
[AIAA PAPER 93-0173] p 310 A93-23244
Numerical modeling of anti-icing systems and comparison to test results on a NACA 0012 airfoil
[NASA-TM-105975] p 148 N93-15345
Ice accretion and performance degradation calculations with LEWICE/NS
[NASA-TM-105972] p 148 N93-15354
- POTAPOV, G. P.**
Estimation of the parameters of the electrodynamic system engine-exhaust jet p 1193 A93-52965
- POTAPOV, V. N.**
A fuel-oil matrix heat exchanger p 833 A93-39052
- POTASHEV, A. V.**
Determination of the shape of a wing profile in boundary layer flow with a given velocity diagram p 1067 A93-48844
- POTIER, E.**
A Mode S implementation - Experiments about data-link and interconnected Mode S sensors p 883 A93-43409
- POTKANSKI, WOJCIECH**
Flutter calculations for a system with interacting nonlinearities
[AIAA PAPER 92-4682] p 409 A93-20304
- POTOTZKY, ANTHONY S.**
A method of predicting quasi-steady aerodynamics for flutter analysis of high speed vehicles using steady CFD calculations
[AIAA PAPER 93-1364] p 682 A93-33931
Further studies using matched filter theory and stochastic simulation for gust loads prediction
[AIAA PAPER 93-1365] p 726 A93-33932

- Aerothermoelastic analysis of a NASP demonstrator model**
[AIAA PAPER 93-1366] p 733 A93-33933
Impact of aeroelasticity on propulsion and longitudinal flight dynamics of an air-breathing hypersonic vehicle [AIAA PAPER 93-1367] p 733 A93-33934
Active control of aerothermoelastic effects for a conceptual hypersonic aircraft p 1007 A93-45137
Computation of maximized gust loads for nonlinear aircraft using matched-filter-based schemes p 1136 A93-52452
- POTTER, DONALD L.**
Nuclear thermal rocket entry heating and thermal response preliminary analysis [AIAA PAPER 93-0378] p 385 A93-23058
- POTTER, KENNETH J.**
Helicopter automatic flight control systems for all weather operations - EH101 and beyond p 186 A93-17310
- POTTER, R. C.**
Leading-edge transition and relaminarization phenomena on a subsonic high-lift system [AIAA PAPER 93-3140] p 959 A93-45154
Two-dimensional computational analysis of a transport high-lift system and a comparison with flight-test results [AIAA PAPER 93-3533] p 1072 A93-49517
- POTTER, R. T.**
GARTEUR damage mechanics for composite materials: Analytical/experimental research on delaminations p 537 N93-21513
- POTTHOFF, J.**
New design concepts for silencing aeroacoustic wind tunnels p 445 A93-19147
- POTTS, RODNEY J.**
Microburst observations in tropical Australia p 432 A93-22198
- POUWELS, HENK**
A dual polarised active phased array antenna with low cross polarisation for a polarimetric airborne SAR p 883 A93-43401
The PHARUS project, first results of the realization phase p 884 A93-43454
The realization phase of the PHARUS project p 1162 A93-47658
- POVINELLI, L. A.**
Multigrid calculation of three-dimensional viscous cascade flows p 872 A93-42889
- POVINELLI, LOUIS A.**
CFD for hypersonic propulsion p 865 A93-42585
The NASA Computational Fluid Dynamics (CFD) program - Building technology to solve future challenges [AIAA PAPER 93-3292] p 1041 A93-44996
- POVITSKY, A.**
Boron particle ignition in high-speed flow [AIAA PAPER 93-2202] p 1145 A93-50014
- POWELL, ALISTAIR**
The benefits of ground maintenance simulators p 238 A93-18757
- POWELL, KENNETH G.**
A solution scheme for the Euler equations based on a multi-dimensional wave model [AIAA PAPER 93-0065] p 261 A93-20178
Viscous and inviscid instabilities of a trailing vortex p 268 A93-21042
An accuracy assessment of Cartesian-mesh approaches for the Euler equations [AIAA PAPER 93-3335] p 953 A93-45029
A simulation technique for 2-D unsteady inviscid flows around arbitrarily moving and deforming bodies of arbitrary geometry [AIAA PAPER 93-3391] p 956 A93-45082
- POWELL, RICHARD W.**
Six-degree-of-freedom guidance and control-entry analysis of the HL-20 p 1210 A93-53737
- POWELL, ROBERT E.**
Response variability observed in reverberant acoustic test of a model aerospace structure p 1264 A93-55857
- POWER, GREG D.**
CFD applications in an aeropropulsion test environment [AIAA PAPER 93-1924] p 1112 A93-49790
- POWERS, E. J.**
Aeroelastic system identification of advanced technology aircraft through higher order signal processing p 525 A93-29297
- POWERS, JOSEPH M.**
Reaction zone structure for strong, weak overdriven, and weak underdriven oblique detonations p 746 A93-35492
- POWERS, PHILIP**
Pave Pillar in-house research final report p 927 A93-42781
- POWERS, SHERYLL G.**
Flight test results from a supercritical mission adaptive wing with smooth variable camber [AIAA PAPER 92-4101] p 38 A93-11274
- POWERS, SHERYLL GOECKE**
Flight test results from a supercritical mission adaptive wing with smooth variable camber [NASA-TM-4415] p 49 N93-11863
- POZEFSKY, PETER**
Aeroelastic character of a National Aerospace Plane demonstrator concept [AIAA PAPER 93-1314] p 732 A93-33890
- POZZI, A.**
Compressible flow in a hovercraft air cushion p 480 A93-29316
- PRABHU, D. R.**
Imaging flaws in thin metal plates using a magneto-optic device p 397 A93-18670
Assessment of aircraft structural integrity by detecting disbands through ultrasonic scanning p 406 A93-19587
Automation of disbond detection in aircraft fuselage through thermal image processing p 407 A93-19598
- PRABHU, KIKRAM**
Changing role of telecommunications management in air traffic control in the FAA p 888 N93-30354
- PRABHU, RAMADAS K.**
Application of a two-equation turbulence model for high speed compressible flows using unstructured grids [AIAA PAPER 93-3029] p 1056 A93-48213
- PRAKASH, B. G.**
Extraction of inherent aerodynamic lag poles for the time domain representation of modal unsteady airloads [AIAA PAPER 93-1591] p 829 A93-37443
- PRAKASH, RAGHU V.**
Fatigue life under random load history derived from exceedance curves using different algorithms p 1260 A93-56544
- PRANANTA, BONIFACIUS**
Calculation of 3-D unsteady subsonic flow with separation bubble using singularity method p 115 A93-14251
- PRANDI, B.**
The beta-CEZ, a new high performance titanium alloy for aerospace engines [DS-2022] p 393 N93-17852
- PRASAD, CHUNCHU B.**
Response of laminated composite plates to low-speed impact by airgun-propelled and dropped-weight impactors [AIAA PAPER 93-1402] p 739 A93-33962
- PRASAD, J. V. R.**
Synthesis of a helicopter nonlinear flight controller using approximate model inversion [AIAA PAPER 92-4468] p 62 A93-13280
Three-dimensional modeling and control of a twin-lift helicopter system p 370 A93-23511
Atmospheric turbulence simulation for rotorcraft applications p 757 A93-34264
Helicopter response to atmospheric turbulence p 817 A93-35987
Development and validation of a comprehensive real time AH-64 Apache simulation model p 799 A93-35992
Methodology development for evaluation of selective-fidelity rotorcraft simulation p 913 N93-30691
- PRASANTH, RAVI K.**
Design of exhaust nozzles using GA optimized neural networks [AIAA PAPER 93-0410] p 361 A93-23331
- PRATER, DAVID L.**
F/A-18 controls released departure recovery - Flight test evaluation p 803 A93-38839
F/A-18 controls released departure recovery flight test evaluation [AD-A256522] p 189 N93-15396
- PRATHER, MICHAEL J.**
Predicted aircraft effects on stratospheric ozone p 93 N93-11096
The atmospheric effects of stratospheric aircraft. Report of the 1992 Models and Measurements Workshop. Volume 1: Workshop objectives and summary [NASA-RP-1292-VOL-1] p 754 N93-25157
The atmospheric effects of stratospheric aircraft. Report of the 1992 Models and Measurements Workshop. Volume 2: Comparisons with global atmospheric measurements [NASA-RP-1292-VOL-2] p 754 N93-25158
The atmospheric effects of stratospheric aircraft. Report of the 1992 Models and Measurements Workshop. Volume 3: Special diagnostic studies [NASA-RP-1292-VOL-3] p 754 N93-25159
- PRATO, J.**
Investigation of compressor rotor wake structure at peak pressure rise coefficient and effects of loading [ASME PAPER 92-GT-32] p 246 A93-19292
- PRATT, D. T.**
An estimate of the 'doomed propellant fraction' for a Superdetonative Ram Accelerator [AIAA PAPER 93-0359] p 385 A93-23042
- PRATT, DAVID T.**
NO(x) sensitivities for gas turbine engines operated on lean-premixed combustion and conventional diffusion flames [ASME PAPER 92-GT-115] p 349 A93-19351
Isolator-combustor interaction in a dual-mode scramjet engine [AIAA PAPER 93-0358] p 360 A93-23041
- PRATT, M.**
Integrated use of GPS and GLONASS in civil aviation navigation. II - Experience with GLONASS p 313 A93-21142
Receiver Autonomous Integrity Monitoring (RAIM) of GPS and GLONASS p 993 A93-46891
- PRATT, R. W.**
Developing control strategies for ASTOVL aircraft p 366 A93-18777
- PRAZDNICHNOV, YU. N.**
Calculation of the passive noise power for onboard single-pulse automatic direction tracking systems p 882 A93-43111
- PREIST, J.**
Recent developments in international laminar flow research programs for transport aircraft [ONERA, TP NO. 1992-163] p 457 A93-26878
- PREMONT, GUY**
Fast design of circular-harmonic filters using simulated annealing p 1038 A93-45556
- PREOBRAZHENSKII, N. G.**
Dynamics of the behavior of nematic films in gasdynamic flows p 746 A93-35345
- PRESTON, G. A.**
The prediction of noise from co-axial jets [ISVR-TR-215] p 1040 N93-32339
- PREVOST, JACQUES-ETIENNE**
The static-memory crash recorders p 167 A93-15048
- PREWO, K. M.**
Ceramics for aero-engine applications [ASME PAPER 92-GT-439] p 388 A93-19581
- PRICE, JOSEPH M.**
Near wake structure for a generic ASTV configuration [AIAA PAPER 93-0271] p 268 A93-21103
- PRICE, MARK L.**
Uncertainty of derived results on X-Y plots p 1261 A93-54382
- PRICE, S. J.**
An analysis of the post-instability behaviour of a two-dimensional airfoil with a structural nonlinearity [AIAA PAPER 93-1474] p 726 A93-34020
Evaluation and extension of the flutter-margin method for flight flutter prediction p 828 A93-37393
- PRICHARD, DEVON**
Tiltrotor ground noise reduction from rotor parametric changes as predicted by ROTONET p 567 A93-29415
The development of a CFD potential method for the analysis of tilt-rotors p 481 A93-29434
- PRIESSHEV, A. V.**
Detection and parameter estimation of atmospheric turbulence by ground-based and airborne CO2 Doppler lidars p 395 A93-17862
- PRIEST, J. A.**
Demonstration of an integrated, active 4 x 4 photonic crossbar p 211 A93-17392
- PRIEZZHEV, A. V.**
Study of artificial and natural turbulence in atmospheric boundary layer with a CW Doppler CO2 lidar p 1257 A93-54799
- PRINZ, U.**
Hypersonic viscous flow simulations p 478 A93-27926
- PRIOR, A. C.**
Passive IR surveillance for helicopter systems - The Sea Owl equipment p 1244 A93-55299
- PRISAZNUK, PAUL J.**
Integrated modular avionics p 896 A93-42777
- PRITCHARD, JOCELYN I.**
Recent advances in integrated multidisciplinary optimization of rotorcraft [AIAA PAPER 92-4777] p 325 A93-20369
Recent advances in multidisciplinary optimization of rotorcraft [NASA-TM-107665] p 47 N93-10968
- PROBERT, E. J.**
Line relaxation methods for the solution of 2D and 3D compressible flows [AIAA PAPER 93-3366] p 955 A93-45059
- PROBST, D. K.**
Demonstration of an integrated, active 4 x 4 photonic crossbar p 211 A93-17392

PROCTOR, F. H.

- PROCTOR, F. H.**
Three-dimensional simulation of the Denver 11 July 1988 microburst-producing storm p 1164 A93-50373
- PROCTOR, FRED H.**
Case study of a low-reflectivity pulsating microburst - Numerical simulation of the Denver, 8 July 1989, storm p 1222 A93-52898
Three-dimensional numerical simulation of the 20 June 1991, Orlando microburst p 488 N93-19598
- PRODROMOU, P.**
Computation of unsteady nozzle flows p 960 A93-45543
- PROFFITT, J. T.**
Very high reliability - Cost and consequences p 397 A93-18789
- PROFFITT, MELISSA S.**
Longitudinal-control design approach for high-angle-of-attack aircraft [NASA-TP-3302] p 373 N93-19108
- PROKOP'EV, A. N.**
Improving the service characteristics of an aircraft through the gyroscopic damping of its structure p 366 A93-18363
- PRONICHEV, N. D.**
Effect of the technological process structure on residual stress distribution in the blade foil of gas turbine engines p 836 A93-39106
- PRONIN, A. V.**
Determination of the $N_2(+) + e$ recombination rate constant from ballistic experiments p 1234 A93-55026
- PROSKAWETZ, K. O.**
Estimation of aircraft inertia characteristics from bifilar pendulum test data p 1249 A93-56029
- PROVOTOROV, V. P.**
Investigation of the effect of physical processes on heat transfer to blunt bodies at low Reynolds numbers p 1090 A93-51877
Investigation of the structure of a multicomponent viscous shock layer p 1090 A93-51879
An economical difference factorization algorithm for the numerical calculation of the system of equations for a thin viscous shock layer p 1091 A93-51880
- PROZOROV, A. G.**
Excitation of velocity fluctuations and noise in a wind tunnel p 444 A93-18242
A study of pressure fluctuations on the surface of a delta wing near the sharp leading edge p 1091 A93-51882
Self-excitation of intense oscillations in flow inside a wind tunnel with an open test section p 1091 A93-51883
- PRUDNIKOV, I. A.**
Wing rock of lifting systems p 118 A93-14330
- PRUEGER, GEORGE H.**
Multistage turbomachinery flow solutions using three-dimensional implicit Euler method [AIAA PAPER 93-2382] p 1083 A93-50150
- PRUETT, C. D.**
Direct numerical simulation of laminar breakdown in high-speed, axisymmetric boundary layers p 8 A93-11527
On the accurate prediction of the wall-normal velocity in compressible boundary-layer flow p 477 A93-27474
- PRUETT, STAN**
URV flight test of an Ada implemented self-repairing flight control system [AD-A259205] p 527 N93-20551
- PRUITT, D. W.**
Starting and test rhombus characteristics of two-dimensional supersonic free-jet nozzle/generic supersonic aircraft inlet configurations [AIAA PAPER 92-5091] p 273 A93-22361
- PRUITT, JAMES S.**
A large flat panel multifunction display for military and space applications p 77 A93-10963
- PRUTZER, S.**
A high resolution airborne multisensor system p 343 A93-21966
- PRZEKAS, A. J.**
Driven cavity simulation of turbomachine blade flows with vortex control [AIAA PAPER 93-0390] p 461 A93-24238
Dynamic stall on a three-dimensional rectangular wing [AIAA PAPER 93-0637] p 463 A93-24753
Pressure-based high-order TVD methodology for dynamic stall simulation [AIAA PAPER 93-0680] p 466 A93-24788
Aerodynamic flow simulation using a pressure-based method and a two-equation turbulence model [AIAA PAPER 93-2902] p 1147 A93-48111
Three-dimensional unsteady separating flows around an oscillatory forward-swept wing [AIAA PAPER 93-2976] p 1050 A93-48170

PERSONAL AUTHOR INDEX

- PRZYBYLKO, STEPHEN J.**
Developments in silicon carbide for aircraft propulsion system applications [AIAA PAPER 93-2581] p 1157 A93-50295
- PSALTIS, DEMETRI**
Correlation filters for aircraft identification from radar range profiles p 1097 A93-50636
- PSARUDAKIS, P.**
Numerical analysis of airfoil cascades subjected to unsteady flow p 972 A93-46944
- PSHENICHNOV, G. I.**
A numerical study of the flutter of conical shells p 927 A93-42405
- PTACNIK, MICHAL**
Velocity vector LDA measurement inside a pitched blade impeller p 924 A93-40390
- PUCKETT, LUKE**
In-service inspection of commercial aircraft composite structure [SME PAPER EM92-124] p 107 A93-14116
- PUCKETT, PAUL M.**
Development of resins for composites by resin transfer molding p 921 A93-30853
- PUDYKIEWICZ, J. A.**
Aviation safety can benefit from simulation of the dispersion of hazardous material p 487 A93-27393
- PUKITE, J.**
Expert system for redundancy and reconfiguration management p 938 A93-42785
- PUKITE, P. R.**
Expert system for redundancy and reconfiguration management p 938 A93-42785
- PULLEN, K. R.**
The design and evaluation of a high pressure ratio radial turbine [ASME PAPER 92-GT-93] p 349 A93-19339
- PUMINOVA, GALINA S.**
Flight safety in a perturbed atmosphere [ISBN 5-277-00815-2] p 487 A93-29431
- PUNCH, W. F., III**
A domain-specific design architecture for composite material design and aircraft part redesign p 442 N93-17522
- PUNDHIR, D. S.**
A study of aerodynamic performance of a contra-rotating axial compressor stage p 463 A93-24524
- PUNTUS, A. A.**
Statistical methods in flight vehicle control theory p 1165 A93-49306
- PURCELL, ANTHONY J.**
Acoustic noise generation at the air/ocean boundary [DREA-CR-90-445] p 99 N93-10642
- PURCELL, JANINE A.**
The analysis of expert performance in the redesign of the en route air traffic control curriculum p 571 A93-27189
- PURCELL, T. W.**
The value of a computational/experimental partnership in aerodynamic design p 114 A93-14215
- PURI, OM**
Aero-engine component damping estimation from full-scale aeromechanical test data [AIAA PAPER 93-1873] p 1112 A93-49748
- PURIFOY, DANA D.**
AFTI/F-16 night close air support system testing p 808 A93-38841
- PUST, LIBOR**
Modified surge in an axial flow compressor [ASME PAPER 92-GT-59] p 247 A93-19309
- PUSTER, RICHARD L.**
Gas analysis system for the Eight Foot High Temperature Tunnel p 822 A93-37875
- PUSTOVOJCHENKO, O. N.**
Scale-up of the spectra of aerodynamic pressure pulsations with narrowband maxima p 1088 A93-51756
- PATERBAUCH, S. L.**
Three-dimensional flow analysis inside turbomachinery stages with steady and unsteady Navier-Stokes method [ISABE 93-7095] p 1186 A93-54071
- PATERBAUGH, S. L.**
Unsteady aerodynamic flow phenomena in a transonic compressor stage [AIAA PAPER 93-1868] p 1075 A93-49743
- PATERBAUGH, STEVEN L.**
Three-dimensional flow phenomena in a transonic, high-through-flow, axial-flow compressor stage [ASME PAPER 92-GT-169] p 250 A93-19395
Tip shock structures in transonic compressor rotors [AIAA PAPER 93-1869] p 1075 A93-49744
- PUTNAM, PETER**
The human factors aspects of aircraft ground handling p 237 A93-18756

- PUTT, CHARLES W.**
Gas turbine system simulation: An object-oriented approach [NASA-TM-106044] p 723 N93-25673
- PUTTRE, MICHAEL**
Thrust vectoring nozzles give pilots an edge p 720 A93-34375
- PYLE, J. A.**
Potential impact of combined NO(x) and SO(x) emissions from future High Speed Civil Transport aircraft on stratospheric aerosols and ozone p 753 A93-35372
- PYLE, JON**
NASA's hypersonic flight research program [AIAA PAPER 93-0308] p 457 A93-25516
- PYNE, C. R.**
A summary of further measurements of steady and oscillatory pressures on a rectangular wing p 1096 A93-52594
- Q**
- QI, D. T.**
Development and industrial application of the 'all-over-controlled vortex distribution method' for designing radial and mixed flow impellers [ASME PAPER 92-GT-262] p 405 A93-19466
- QI, O. F.**
Improving dynamic response of a single-spool gas turbine engine using a nonlinear controller [ASME PAPER 92-GT-392] p 355 A93-19546
- QIAN, CATHY X.**
A wall interference assessment/correction system [NASA-CR-190617] p 68 N93-11910
A wall interference assessment/correction system [NASA-CR-191889] p 296 N93-18384
- QIAN, CHUN**
New model of bird impact response analysis and its engineering solution p 156 A93-14336
- QIAN, LING**
Numerical simulation of the turbulent drag reduction by plate manipulators p 681 A93-33736
- QIAN, LUHONG**
Experimental investigation on patterned blades of compressor p 1066 A93-48515
- QIAN, W.**
Effects of foundation excitation on multiple rub interactions in turbomachinery p 1260 A93-55996
- QIAN, YANSHENG**
Performance improvement of gas turbine with steam injection p 1107 A93-48523
- QIAN, YI**
Turbulent flow simulation around the aerofoil with pseudo-compressibility p 830 A93-38155
- QIAN, YIJI**
Design of shockless supersonic region in the axisymmetric transonic flow p 1230 A93-54587
Two problems applied to the rheographical transformation of axisymmetric flow p 1231 A93-54599
- QIAO, WEIYANG**
The numerical calculation of aircraft propeller noise p 174 A93-16239
A unified model for rotating stall and surge p 259 A93-20119
- QIAO, XIN**
The investigation of limit cycle amplitude of nonlinear nose gear p 800 A93-36342
A software for optimum design of an aircraft structure p 938 A93-40495
- QIAO, ZHIDE**
An adaptive region method for computation of vortex sheet behind wing in compressible flow p 116 A93-14262
- QIN, JIANGNING**
A new parallel-vector finite element analysis software on distributed-memory computers [AIAA PAPER 93-1307] p 756 A93-33883
Vector unsymmetric eigenequation solver for nonlinear flutter analysis on high-performance computers p 1160 A93-52449
- QIN, N.**
Newton-like methods for fast high resolution simulation of hypersonic viscous flows p 437 A93-20740
Finite volume 3DNS and PNS solutions of hypersonic viscous flow around a delta wing using Osher's flux difference splitting p 870 A93-42633
- QIU, SHIJUNG**
Dynamic characteristics of two new vibration modes of the disk-shell shaped gear p 204 A93-14484
- QIU, XIEGANG**
Parameter selection of electro-impulse de-icing systems p 889 A93-40493

R

QIU, XINYU

An experimental investigation on the combustor with bypass flow in integral liquid fuel ramjet p 174 A93-16235

QIU, XUGUANG

Experimental study on heat transfer of separated impingement jets in short distance p 1149 A93-48518

QU, ZHANG-HUA

Numerical solution of radiative flowfield on the nose region of blunt bodies p 120 A93-14359

QU, ZHANGHUA

The stagnation line solution of the equilibrium flow with radiation and mass injection p 680 A93-33733

QUACKENBUSH, T. R.

Vortex methods for the computational analysis of rotor/body interaction p 765 A93-35939

QUACKENBUSH, TODD

High accuracy computation of fluid-structure interaction in transonic cascades p 287 A93-23387

QUACKENBUSH, TODD R.

Computation of wake/exhaust mixing downstream of advanced transport aircraft p 1162 A93-48141

[AIAA PAPER 93-0485] p 1162 A93-48141

Fast three-dimensional vortex method for unsteady wake calculations p 1178 A93-53233

Rotor design optimization using a free wake analysis [NASA-CR-177612] p 693 A93-25075

QUAGLIARELLA, DOMENICO

Artificial intelligence and CFD: Expert systems for the design of airfoils and for grid generation p 48 A93-11161

QUAGLIAROLI, T. M.

Planar imaging of OH density distributions in a supersonic combustion tunnel p 389 A93-20155

Laser selection criteria for OH fluorescence measurements in supersonic combustion test facilities p 549 A93-29315

QUAGLIOTTI, F.

Breakdown analysis on delta wing vortices p 7 A93-10779

QUAGLIOTTI, F. B.

Vortex breakdown study on a 65-deg delta wing tested in static and dynamic conditions p 121 A93-14407

Dynamic stability derivatives evaluation in a low-speed wind tunnel p 821 A93-37402

Experimental analysis of rotary derivatives on a modern aircraft configuration p 985 A93-47278

[AIAA PAPER 93-3514] p 985 A93-47278

Analysis of stability characteristics of a high performance aircraft p 1125 A93-48303

[AIAA PAPER 93-3616] p 1125 A93-48303

QUANDT, EARL

Unsteady vortex loop/dipole theory applied to the work and acoustics of an ideal low speed propeller p 876 A93-29891

[AD-A264057] p 876 A93-29891

QUANG, SHUIWU

Viscous shock-layer numerical calculations of three dimensional nonequilibrium flows over hypersonic blunt bodies at high angle of attack p 12 A93-12651

QUEALY, ANGELA

Turbomachinery CFD on parallel computers p 228 A93-13154

[NASA-TM-105932] p 228 A93-13154

QUINN, W. R.

Flow field measurements in a turbulent free jet issuing from a sharp-edged square slot p 244 A93-19158

QUINTANA, F.

Numerical simulation of hypersonic flow over a double ellipse using a Taylor-Galerkin finite element formulation with adaptive grids p 868 A93-42617

QUINTARD, M.

Effect of environment on creep-fatigue crack propagation in turbine disc superalloys p 916 A93-41023

[ONERA, TP NO. 1993-5] p 916 A93-41023

QUINTO, P. FRANK

Evaluation of four advanced nozzle concepts for short takeoff and landing performance p 875 A93-29165

[NASA-TP-3314] p 875 A93-29165

QUIRK, JAMES J.

A contribution to the great Riemann solver debate p 694 A93-25083

[NASA-CR-191409] p 694 A93-25083

Godunov-type schemes applied to detonation flows p 780 A93-27090

[NASA-CR-191447] p 780 A93-27090

QUIST, T. M.

A high resolution airborne multisensor system p 343 A93-21966

QUMEI, IYAD KHALIL

An investigation of the dynamic response of lifting surfaces with concentrated structural nonlinearities p 162 A93-13807

QUYNN, ALLEN G.

Fuzzy logic control algorithm for suppressing E-6A Long Trailing Wire Antenna wind shear induced oscillations p 1171 A93-51454

[AIAA PAPER 93-3868] p 1171 A93-51454

RAABE, HERBERT P.

An MLS for the twenty-first century p 316 A93-21197

RAABY, P.

Neutron-induced single event upsets in static RAMs observed at 10 KM flight altitude p 1158 A93-50561

RACCA, EDDY L.

Aircrew integrated management p 141 A93-14376

RACHAKONDA, S.

Total quality management of forged products through finite element simulation p 1217 A93-53493

RADEMAKER, E. R.

Instrumentation for in-flight acoustic measurements in an engine inlet duct of a Fokker 100 aircraft p 1001 A93-32332

[NLR-TP-91200-U] p 1001 A93-32332

RADEMEYER, I. J.

The development of a new air filtration system for the Alouette III helicopter p 1199 A93-54024

[ISABE 93-7048] p 1199 A93-54024

RADESPIEL, R.

Computation of flows over 2D ramps p 866 A93-42595

Computation of the hypersonic flow over a double ellipsoid p 868 A93-42610

RADETSKY, RONALD H., JR.

Effect of micron-sized roughness on transition in swept-wing flows p 262 A93-20188

[AIAA PAPER 93-0076] p 262 A93-20188

RADHADRISHNAN, KRISHNAN

A critical analysis of the accuracy of several numerical techniques for combustion kinetic rate equations p 362 A93-16941

[NASA-TP-3315] p 362 A93-16941

RADKE, LAWRENCE F.

Meeting review: Third NCAR Research Aircraft Fleet Workshop p 223 A93-12818

[PB92-222710] p 223 A93-12818

RADTSIG, A. N.

Pressure pulsations on a delta wing in incompressible flow p 1069 A93-48912

RAEVSKAIA, G. A.

A new production technology for complex-shaped structural elements 'creep forming' p 202 A93-14175

RAFATI, HAMID

Helicopter rotor disk and Blade Element comparison p 799 A93-35991

RAFFA, ANTHONY V.

Articulated fin/wing control system p 909 A93-29278

[AD-D015712] p 909 A93-29278

RAFFAELE, ROBERT

Lockheed adopts media blast dry stripping for the C-130 p 107 A93-14092

[SAE PAPER 920949] p 107 A93-14092

RAFFIN, M.

Experimental density flowfields over a delta wing located in rarefied hypersonic flows p 870 A93-42637

RAGGI, M.

Fatigue qualification of high thickness composite rotor components p 81 A93-13646

RAGHAVAN, V.

Flowfield analysis of modern helicopter rotors in hover by Navier-Stokes method p 481 A93-29435

RAGHUNATHAN, S.

Passive boundary-layer bleed for supersonic intakes p 114 A93-14212

Passive control of pre-entry shock in supersonic intakes p 279 A93-22691

[AIAA PAPER 93-0291] p 279 A93-22691

RAHIER, G.

Blade-vortex interaction noise - Prediction and comparison with flight and wind tunnel tests p 851 A93-38600

[ONERA, TP NO. 1992-126] p 851 A93-38600

RAHMANI, S.

Rapid prototyping via automatic software code generation from formal specifications - A case study p 227 A93-14685

RAHMANI, SHAWN

On definition and use of systems engineering processes, methods and tools p 1225 A93-53642

RAI, BADRI

Delaminations of barely visible impact damage in CFRP laminates p 737 A93-33798

RAI, M. M.

Multipassage three-dimensional Navier-Stokes simulation of turbine rotor-stator interaction p 688 A93-34484

Unsteady, three-dimensional, Navier-Stokes simulations of multistage turbomachinery flows p 1153 A93-49826

[AIAA PAPER 93-1979] p 1153 A93-49826

RAIFORD, RICHARD R.

Wind tunnel results for an advanced fighter configuration employing transverse thrust for enhanced STOL capability p 1100 A93-49796

[AIAA PAPER 93-1933] p 1100 A93-49796

RAILIAN, V. IA.

Canonical correlation relationships among spectral and phytometric variables for twenty winter wheat fields p 433 A93-22992

RAILLON, E.

Flying qualities of the Hermes spaceplane and the shape definition process p 532 A93-28437

RAIS-ROHANI, M.

Integrated aerodynamic-structural-control wing design p 324 A93-20307

[AIAA PAPER 92-4694] p 324 A93-20307

Construction of a one-third scale model of the NASP p 386 A93-23345

RAISINGHANI, S. C.

Steady and quasisteady resonant lock-in of finned projectiles p 61 A93-12012

Modelling for aileron induced unsteady aerodynamic effects for parameter estimation p 118 A93-14323

Aileron and sideslip-induced unsteady aerodynamic modeling for lateral parameter estimation p 1007 A93-45144

Parameter estimates of an aeroelastic aircraft as affected by model simplifications p 1127 A93-48325

[AIAA PAPER 93-3640] p 1127 A93-48325

RAIZENNE, M. D.

Fatigue crack growth results for Ti-6Al-4V, IMI 685, and Ti-17 p 1004 A93-31746

RAJAGOPALAN, R. G.

A hybrid structured-unstructured grid method for unsteady turbomachinery flow computations p 282 A93-23066

[AIAA PAPER 93-0387] p 282 A93-23066

Three-dimensional calculations of rotor-airframe interaction in forward flight p 795 A93-35940

A solution-adaptive hybrid-grid method for the unsteady analysis of turbomachinery p 1148 A93-48204

RAJAN, P. A.

Some measurements of stall in an axial impeller p 1183 A93-53984

[ISABE 93-7008] p 1183 A93-53984

RAJASEKARAN, R.

Numerical solution of dynamic equations arising in a jet engine simulation p 53 A93-12237

RAJENDRAN, J.

DME/P critical area determination on message passing processors p 31 A93-11010

RAJKHER, V. L.

Experience in specifying/prolonging the airframe time limits p 948 A93-45797

RAJKOV, L. G.

Control problem for a plant with artificial intelligence p 1168 A93-50960

RAJKUMAR, V.

Nonlinear time-series-based adaptive control applications p 97 A93-13230

RAJU, A.

Flow studies in ducted twin-rotor contra-rotating axial flow fans p 258 A93-19545

[ASME PAPER 92-GT-390] p 258 A93-19545

RAJU, CHANNA

Experiments on rarefied supersonic free jets using impact probes p 461 A93-24091

RAJU, P. K.

International Congress on Recent Developments in Air and Structure-Borne Sound and Vibration, 2nd, Auburn Univ., AL, Mar. 4-6, 1992, Proceedings. Vols. 1-3 p 1259 A93-55851

RALPH, MARK E.

Thermal effects testing at the National Solar Thermal Test Facility p 1255 A93-54402

RAMACHANDRA, C.

Structure of martensite in titanium alloy p 916 A93-43616

Ti-6Al-1.6Zr-3.3Mo-0.3Si p 916 A93-43616

RAMACHANDRAN, K.

Hover performance analysis of advanced rotor blades p 767 A93-35998

Free-wake computation of helicopter rotor flowfields in forward flight p 1059 A93-48253

[AIAA PAPER 93-3079] p 1059 A93-48253

RAMAKRISHNAN, R.

A detailed study of mean-flow solutions for stability analysis of transitional flows p 1057 A93-48232

[AIAA PAPER 93-3052] p 1057 A93-48232

RAMAKRISHNAN, SEKARIPURAM V.

A pointwise version of the Baldwin-Barth turbulence model p 985 A93-47284

[AIAA PAPER 93-3523] p 985 A93-47284

RAMAMURTHY, S.

Correlations for flow property variation at outlet of a centrifugal impeller p 1185 A93-54030

[ISABE 93-7054] p 1185 A93-54030

RAMAMURTI, RAVI

Simulation of flow past complex geometries using a parallel implicit incompressible flow solver p 957 A93-45095

Flip-flop jet nozzle extended to supersonic flows p 778 A93-39409

- Enhanced mixing of a rectangular supersonic jet by natural and induced screech
[NASA-TM-106245] p 989 N93-31672
- RAMAPRIAN, B. R.**
Pressure measurements on a pitching airfoil in a water channel
[AIAA PAPER 93-0184] p 473 A93-25510
- RAMBONE, JAMES D.**
ILS mathematical modeling study of the effects of an ASR-9 structure at the Long Island MacArthur Airport, Islip, NY
[DOT/FAA/CT-TN92/25] p 192 N93-12668
ILS mathematical modeling study of an ILS glide slope proposed for runway 19L at the Meridian Naval Air Station, Mississippi
[DOT/FAA/CT-TN93/8] p 705 N93-24741
The ILS mathematical modeling study of the Runway 10 ILS Localizer at Luis Munoz Marin International Airport, San Juan, Puerto Rico
[DOT/FAA/CT-TN93/10] p 792 N93-27017
- RAMECKERS, FERDINAND H. J. I.**
Underlying causes of accidents: Casual networks
p 491 N93-19658
- RAMER, JAMES**
Validation of aviation weather products for the Advanced Traffic Management System
p 430 A93-22161
- RAMETTE, PHILIPPE**
Aircraft engine integration for the M88-Rafale couple
[ASME PAPER 92-GT-403] p 322 A93-19552
- RAMKUMAR, RAMASWAMY L.**
F-15 composite engine access door
p 920 N93-30442
- RAMOHALLI, GAUTHAM**
BITE vs human judgement - The aircraft side
p 238 A93-18759
- RAMSAMOOJ, D. V.**
Fracture of highway and airport pavements
p 547 A93-28290
- RAMSAY, R. B.**
In-flight structural mode excitation system for flutter testing
p 526 N93-19915
- RAMSDEN, J. M.**
Maintainable A330
p 107 A93-13957
- RAMSEY, B. D.**
The microstrip proportional counter
p 549 A93-29485
- RAMU, S. ANANTHA**
Stochastic finite element analysis for high speed rotors
p 554 N93-20896
- RANAHAH, W. L.**
Terminal forecast amendments - A 'cloudy' issue
p 431 A93-22167
- RANAUDO, R. J.**
Icing effects on aircraft stability and control determined from flight data - Preliminary results
[AIAA PAPER 93-0398] p 370 A93-23073
Icing effects on aircraft stability and control determined from flight data: Preliminary results
[NASA-TM-105977] p 188 N93-14831
- RAND, J. L.**
The Superspeed Stratospheric Vehicle
p 39 A93-11357
- RAND, O.**
Nonlinear rotor-fuselage coupled response to generic periodic control modes using advanced computation techniques
p 153 A93-14226
A generic harmonic rotor model for helicopter flight simulation
p 506 A93-27480
Investigation of the flight mechanics simulation of a hovering helicopter
p 798 A93-35990
Nonlinear analysis of composite thin-walled helicopter blades
p 827 A93-36006
- RANDAZZO, PHILIP**
Time delay measurements of current primary FAA air/ground transmitters and receivers
[DOT/FAA/CT-TN93/14] p 842 N93-28555
- RANDLE, ROBERT J., JR.**
NASA/FAA helicopter simulator workshop
[NASA-CP-3156] p 857 N93-30673
Part 1: Executive summary
p 857 N93-30674
- RANEY, DAVID L.**
Impact of aeroelasticity on propulsion and longitudinal flight dynamics of an air-breathing hypersonic vehicle
[AIAA PAPER 93-1367] p 733 A93-33934
- RANGANATHAN, NARAYAMASWAMI**
Damage tolerance of a helicopter rotor high-strength steel
p 555 N93-21322
- RANIAMURTI, RAVI**
A parallel implicit incompressible flow solver using unstructured meshes
[AD-A263395] p 931 N93-29851
- RANKIN, STEVE**
Design, capabilities, and performance of the miniaturized airborne GPS receiver
p 32 A93-11014
- RANTALAHTI, ESKO T.**
Steering system of a vehicle, such as a snow removing machine for airfields
[CA-PATENT-APPL-SN-1293201] p 83 N93-10367
- RAO, CARLO**
Design of the variable pitch fan for the McDonnell Douglas MD 520N helicopter equipped with the NOTAR system
p 794 A93-35908
- RAO, DHANVADA M.**
A low-speed wind tunnel study of vortex interaction control techniques on a chine-forebody/delta-wing configuration
p 122 A93-14409
Side-force control on a forebody of diamond cross-section at high angles of attack
[AIAA PAPER 93-3407] p 1008 A93-47206
- RAO, J. S.**
Turbomachine blade vibration
[ISBN 0-470-21764-2] p 344 A93-17899
- RAO, JIANG**
A method for optimizing the meridional passage of the rotor in centrifugal compressors
p 119 A93-14344
A method for optimizing the meridional passage in a centrifugal compressor
p 204 A93-14483
- RAO, K. V.**
3-D Euler simulation of vane-blade interaction in a transonic turbine
[AIAA PAPER 93-2256] p 1081 A93-50054
Numerical study of a delta planform with multiple jets in ground effect
[SAE PAPER 892283] p 1176 A93-53200
- RAO, M. N.**
New analytical solutions for proportional navigation
p 728 A93-34545
- RAO, S. S.**
Optimization using fuzzy set theory
p 1037 A93-45431
- RAPOPORT, ELIEZER**
A rapid procedure for obtaining time-average interferograms of vibrating bodies
p 412 A93-21857
- RAPP, DAVID**
Hermes CX-7: Air transport system design simulation
[NASA-CR-192082] p 335 N93-18056
- RAPP, H.**
Optimization of sandwich structures with respect to local instabilities with MBB-LAGRANGE
p 1255 A93-54540
- RAPP, HELMUT**
Influence of cross section variations on the structural behaviour of composite rotor blades
[MBB-UD-0602-91-PUB] p 332 N93-17569
- RAPPOPORT, W.**
The HYDICE instrument design and its application to planetary instruments
p 842 N93-28766
- RASHIDI, M.**
Split torque transmission load sharing
[NASA-TM-105884] p 212 N93-12736
- RASHIDIAN, BIJAN**
A simplified numerical procedure to compute the optimal trajectory of an aircraft
p 48 N93-11719
- RASKY, DANIEL J.**
Thermal response and ablation characteristics of light weight ceramic ablators
[AIAA PAPER 93-2790] p 1018 A93-46532
- RASMUSSEN, M. L.**
Waveriders with finlets
[AIAA PAPER 93-3442] p 978 A93-47231
Computational analysis of off-design waveriders
[AIAA PAPER 93-3488] p 982 A93-47262
- RASMUSSEN, MAURICE L.**
Computational analysis of hypersonic flows past elliptic-cone waveriders
[NASA-CR-191304] p 138 N93-14767
- RASMUSSEN, R. M.**
Liquid water profiling using remote sensor observations
p 429 A93-22150
The FAA aircraft icing Forecasting Improvement Program - Validation of aircraft icing forecasts in the Denver area
[AIAA PAPER 93-0393] p 309 A93-23069
- RASSKAZOV, S. P.**
Load rating for a delta wing box based on a reliability criterion
p 1030 A93-47093
- RASTRIGIN, V. L.**
Accuracy of nonparametric reliability estimates under varying operation conditions
p 396 A93-18343
Assessment of flight data in real time
p 341 A93-18364
- RATAF'EVA, L. S.**
Damping of a gyro horizon-compass with arbitrary displacement of the suspension point
p 1025 A93-45684
- RATER, LON M.**
Results from a GPS Shuttle Training Aircraft flight test
p 384 A93-21148
- RATH, H. J.**
Experimental investigation of the management of large-sized drops and the onset of Marangoni-convection
p 926 A93-41700
Calibration of thermal anemometer at very low Reynolds numbers under microgravity
p 926 A93-41729
- RATLIFF, EARL**
A survey of display technologies for military aircraft cockpit applications
p 517 A93-27239
- RATTAN, KULDIP S.**
Design of a rule-based fuzzy controller for the pitch axis of an unmanned research vehicle
p 907 A93-42807
- RATVASKY, T. P.**
Icing effects on aircraft stability and control determined from flight data - Preliminary results
[AIAA PAPER 93-0398] p 370 A93-23073
Icing effects on aircraft stability and control determined from flight data: Preliminary results
[NASA-TM-105977] p 188 N93-14831
- RAUCH, HERBERT E.**
Fault detection, isolation, and reconfiguration for aircraft using neural networks
[AIAA PAPER 93-3870] p 1135 A93-51456
- RAUL, R.**
Numerical and experimental investigation of mixing enhancement in scramjets
[AIAA PAPER 92-5063] p 414 A93-22333
Enhanced fuel-air mixing in hypersonic engines
[ISABE 93-7115] p 1221 A93-54090
- RAULT, DIDIER F. G.**
A systems approach to a DSMC calculation of a control jet interaction experiment
[AIAA PAPER 93-2798] p 964 A93-46538
Aerodynamics of Shuttle Orbiter at high altitudes
[AIAA PAPER 93-2815] p 965 A93-46553
- RAUPACH, M. R.**
Drag and drag partition on rough surfaces
p 79 A93-12460
- RAUSCH, RUSS D.**
Spatial adaptation procedures on tetrahedral meshes for unsteady aerodynamic flow calculations
[AIAA PAPER 93-0670] p 269 A93-21116
Three-dimensional time-marching aeroelastic analyses using an unstructured-grid Euler method
p 1100 A93-49012
- RAUTENBERG, M.**
The vortex behaviour of the rotating-stall cell of a centrifugal compressor with vaned diffuser
[ASME PAPER 92-GT-66] p 400 A93-19316
Blade excitation by circumferentially asymmetric rotating stall in centrifugal compressors
[ASME PAPER 92-GT-148] p 351 A93-19376
Excitation of blade vibration due to surge of centrifugal compressors
[ASME PAPER 92-GT-149] p 351 A93-19377
Performance simulation of a combustion engine charged by a variable geometry turbocharger. I - Prerequisites, boundary conditions and model development. II - Simulation algorithm, computed results
p 1256 A93-54648
Determination of the zone of the stall cell by means of the baroclinic wave theory
p 424 N93-18733
Rotating stall cell and Von Karman vortex street: A meteorological theory
p 424 N93-18734
- RAUTER, MICHAEL**
Development of nose structure of a reconnaissance container for a supersonic jet aircraft
[MBB-LMC-242-S-PUB-0451] p 998 N93-31046
- RAVIBABU, K.**
Flow studies in ducted twin-rotor contra-rotating axial flow fans
[ASME PAPER 92-GT-390] p 258 A93-19545
- RAVICHANDRAN, M.**
A study on 3-D velocity distribution of isothermal flows behind an afterburner flame stabilizer
[ISABE 93-7039] p 1197 A93-54015
- RAVINDRA, K.**
CFD drag predictions for a wide body transport fuselage with flight test verification
[AIAA PAPER 93-3418] p 976 A93-47214
- RAVIN, DANIEL**
A vision-based method for autonomous landing
p 1190 A93-53172
- RAWLINS, W. T.**
An optical comparison of wall and axial injection for high enthalpy reacting scramjet flows
[AIAA PAPER 93-0357] p 377 A93-23040
High-temperature supersonic combustion testing with optical diagnostics
p 730 A93-34498
- RAWNSLEY, BRIAN W.**
Helicopter automatic flight control systems for all weather operations - EH101 and beyond
p 186 A93-17310
- RAY, ASOK**
Extended linear quadratic Gaussian control under randomly varying distributed delays
p 439 A93-22854

- Discrete-time LTR synthesis of delayed control systems p 439 A93-22855
- RAY, JAMES A.**
Environmental effects of operations during Desert Shield/Desert Storm p 1190 A93-54291
- RAY, LAURA R.**
Stochastic measures of performance robustness in aircraft control systems p 185 A93-14595
- RAY, RONALD J.**
Real-time in-flight engine performance and health monitoring techniques for flight research application p 169 N93-15169
- RAYMER, DANIEL P.**
RDS - A PC-based aircraft design, sizing, and performance system [AIAA PAPER 92-4226] p 97 A93-13354
- REA, JON**
Boeing 777 high lift control system p 1249 A93-55753
- REARDON, FREDERICK H.**
Heat Transfer and Fluid Mechanics Institute, 33rd, California State Univ., Sacramento, June 3, 4, 1993, Proceedings p 1152 A93-49505
The combustion time lag and its role in ramjet combustion instability p 73 N93-11137
- REBAY, S.**
A Navier-Stokes solver with different turbulence models applied to film-cooled turbine cascades p 904 N93-29962
- REBIERE, J. L.**
A two-dimensional analysis of multiple matrix cracking in a laminated composite close to its characteristic damage state p 1157 A93-50405
- REBOLO, R.**
Aerodynamics design of convergent-divergent nozzles [AIAA PAPER 93-2574] p 1085 A93-50290
Cooling predictions in turbofan engine components p 905 N93-29964
- RECORDS, ROGER M.**
Spurious symptom reduction in fault monitoring [NASA-CR-191453] p 942 N93-29192
- REDA, DANIEL C.**
Development of the NASA-Ames low disturbance supersonic wind tunnel for transition research up to Mach 2.5 [AIAA PAPER 92-3909] p 462 A93-24488
Experimental investigations of the time and flow-direction responses of shear-stress-sensitive liquid crystal coatings [AIAA PAPER 93-0181] p 542 A93-25508
- REDDAN, MICHEL**
Volcanic clouds p 487 A93-28196
- REDDING, RICHARD E.**
The analysis of expert performance in the redesign of the en route air traffic control curriculum p 571 A93-27189
- REDDY, D. R.**
A comparative study of Full Navier-Stokes and Reduced Navier-Stokes analyses for separating flows within a diffusing inlet S-duct [AIAA PAPER 93-2154] p 1079 A93-49970
- REDDY, E. S.**
Dynamic analysis of a pre-and-post ice impacted blade [AIAA PAPER 92-4273] p 54 A93-13333
Structural tailoring of aircraft engine blade subject to ice impact constraints [AIAA PAPER 92-4710] p 358 A93-20319
Structural Tailoring/Analysis for Hypersonic Components - A computational simulation [AIAA PAPER 92-4722] p 325 A93-20324
BLASIM - A computational tool to assess ice impact damage on engine blades p 720 A93-34165 [AIAA PAPER 93-1638]
Dynamic analysis of a pre-and-post ice impacted blade [NASA-TM-105829] p 90 N93-12197
Root damage analysis of aircraft engine blade subject to ice impact [NASA-TM-105779] p 222 N93-15343
Structural tailoring of aircraft engine blade subject to ice impact constraints [NASA-TM-106033] p 838 N93-26999
Blasim: A computational tool to assess ice impact damage on engine blades p 1031 N93-31193 [NASA-TM-106225]
- REDDY, J. N.**
Thermomechanical postbuckling analysis of laminated composite shells [AIAA PAPER 93-1337] p 738 A93-33907
- REDDY, N. M.**
Three-dimensional flow simulation over axisymmetric bodies using Navier-Stokes equations at hypersonic Mach numbers p 461 A93-24090
- REDDY, N. N.**
A third order upwind scheme for aero-acoustic applications [AIAA PAPER 93-0149] p 564 A93-25504
- REDDY, S. K.**
Thermoviscoelastic analysis of pavements p 379 N93-16313
- REDDY, SURYAKUMAR**
Artificial viscosity models for the Navier-Stokes equations and their effect in drag prediction [AIAA PAPER 93-0193] p 473 A93-25511
- REDDY, T. S. R.**
APPLE - An aeroelastic analysis system for turbomachines and propfans p 358 A93-20320
Unsteady aerodynamics and flutter of propfans using a three-dimensional Full-Potential Solver [AIAA PAPER 93-1633] p 720 A93-34161
Subsonic/transonic cascade flutter using a full-potential solver p 861 A93-41934
- REDDY, WILLIAM D., JR.**
Ship airwake measurement and flow visualization [AIAA PAPER 92-4088] p 7 A93-11267
- REDING, J. P.**
Hammerhead aeroelastic stability revisited [AIAA PAPER 93-1477] p 740 A93-34022
- REDINIOTIS, O. K.**
3-D LDV measurements over a delta wing in pitch-up motion [AIAA PAPER 93-0185] p 275 A93-22610
The hemisphere-cylinder in dynamic pitch-up motions [AIAA PAPER 93-2963] p 1048 A93-48157
Periodic vortex shedding over delta wings p 1070 A93-49002
- REDINIOTIS, OTHON K.**
Flow control over delta wings at high angles of attack [AIAA PAPER 93-3494] p 983 A93-47266
- REDINIOTIS, OTHON KONS**
The transient development of vortices over delta wings p 695 N93-25269
- REDMAN, RICHARD**
Insights into US domestic aviation p 496 N93-21859
- REED, CHRISTOPHER L.**
CFD calibration for three-dimensional nozzle/afterbody configurations p 215 N93-13226
- REED, D.**
The NASA/industry Design Analysis Methods for Vibrations (DAMVIBS) program: Boeing Helicopters airframe finite element modeling p 515 N93-21313
- REED, DAVID H.**
Development of the Boeing Low Speed Aerodynamic Facility (LSAF) p 374 A93-19148
- REED, H. L.**
The analysis of unsteady, three-dimensional flow separation [AIAA PAPER 93-0642] p 540 A93-24757
- REED, HELEN**
A 2-D numerical model for predicting the aerodynamic performance of the NOTAR system tailboom p 766 A93-35994
- REED, HELEN L.**
Unstable branches of a hypersonic, chemically reacting boundary layer p 128 A93-17262
Effect of curvature on stationary crossflow instability of a three-dimensional boundary layer p 1070 A93-49010
- REEHORST, ANDREW**
Close-up analysis of aircraft ice accretion [AIAA PAPER 93-0029] p 309 A93-23239
Close-up analysis of aircraft ice accretion [NASA-TM-105952] p 148 N93-15360
- REES, D.**
Damage tolerance assessment of boron/epoxy repairs to fuselage lap joints [AD-A258383] p 338 N93-18257
- REES, W. D.**
Installation of electrical cable looms p 764 A93-39536
- REGAL, D. M.**
Definition of the 2005 flight deck environment [NASA-CR-4479] p 343 N93-16693
- REGENIE, VICTORIA**
The F-18 High Alpha Research Vehicle - A high-angle-of-attack testbed aircraft [AIAA PAPER 92-4121] p 42 A93-13273
- REGGIO, M.**
Periodic Euler and Navier-Stokes solutions about oscillating airfoils p 241 A93-17799
Euler computations of rotor-stator interaction in turbomachinery cascades using adaptive triangular meshes [AIAA PAPER 93-0386] p 282 A93-23065
Implicit numerical solution of transonic flows using adaptive triangular grids p 686 A93-34349
- REHFIELD, LAWRENCE W.**
Effect of stiffness characteristics on the response of composite grid-stiffened structures p 1022 A93-45148
A comparison of classical mechanics models and finite element simulation of elastically tailored wing boxes p 922 N93-30863
Tailored composite wings with elastically produced chordwise camber p 923 N93-30876
- REIBERT, MARK S.**
Effect of micron-sized roughness on transition in swept-wing flows [AIAA PAPER 93-0076] p 262 A93-20188
- REICHERT, BRUCE A.**
An experimental investigation of the flow in a diffusing S-duct [NASA-TM-105809] p 60 N93-12077
- REICHERT, G.**
The influence of rotor and fuselage wakes on rotorcraft stability and control p 183 A93-14373
- REID, G. W.**
Mechanical damage to aircraft structures from lightning strikes p 879 A93-40432
- REID, LLOYD D.**
Pilot evaluations of augmented flight simulator motion [AIAA PAPER 93-3580] p 1208 A93-52676
- REIDY, L. W.**
A comparison of the drag-reducing benefits of riblets in internal and external flows p 395 A93-18054
- REIFSNIDER, K.**
Characterization of ceramic composite materials for gas turbine applications [DE93-009719] p 905 N93-30168
- REILE, E.**
Transient thermal behaviour of a compressor rotor with axial cooling air flow and co-rotating or contra-rotating shaft p 903 N93-29946
- REIMANN, K.**
The production of a monolithic CFRP fuselage skin for the European Fighter Aircraft p 109 A93-15810
- REINBACHS, NAMEJS**
Enhancing real-time flight simulation execution by intercepting Run-Time Library calls [AIAA PAPER 93-3591] p 1224 A93-52684
- REINECKE, W. G.**
High-temperature supersonic combustion testing with optical diagnostics p 730 A93-34498
- REINELT, R.**
An Euler code with new energy equation and new enthalpy damping approach p 686 A93-34352
- REINER, JACOB**
Design of a flight control system for a highly maneuverable aircraft using mu synthesis [AIAA PAPER 93-3776] p 1132 A93-51371
- REINER, TH.**
A novel aircraft-based tandem mass spectrometer for atmospheric ion and trace gas measurements p 925 A93-40672
- REINHARD, HANS-DIETER**
Satellite navigation in traffic management p 914 A93-43549
- REINHARDT, M. E.**
Measurements of jet aircraft emissions at cruise altitude. I - The odd-nitrogen gases NO, NO₂, HNO₂ and HNO₃ p 556 A93-24391
- REINL, WERNER**
Modern helicopter technologies at MBB and the application in future programmes [MBB-UD-0599-91-PUB] p 331 N93-17566
- REISDORFER, D. A.**
Evolution of permanent composite repair designs p 508 A93-27967
- REISDORFER, DALE**
Civil tiltrotor transport point design: Model 940A [NASA-CR-191446] p 1019 N93-32234
- REISENTHAL, PATRICK H.**
Development of an engineering level prediction method for high angle of attack aerodynamics [AIAA PAPER 93-0208] p 278 A93-22626
A study of turbulence in rarefied gases [AIAA PAPER 93-3097] p 1061 A93-48271
- REISIGER, DENNIS**
Application of modular avionics to the EF-111A systems improvement program p 896 A93-42780
- REITSMA, SCOTT H.**
Developing numerical techniques for solving low Mach number fluid-acoustic problems p 1235 A93-55353
- REITZ, ROLF D.**
Modeling the effects of drop drag and breakup on fuel sprays [AD-A263650] p 931 N93-29388
- REJMAN, MICHAEL H.**
Towards an integrated approach to proactive monitoring and accident prevention p 495 N93-19700
Accidents and errors: A review of recent UK Army Air Corps accidents p 495 N93-19701

- Prediction of success from training p 495 N93-19702
- REMSBERG, ELLIS E.**
The atmospheric effects of stratospheric aircraft. Report of the 1992 Models and Measurements Workshop. Volume 2: Comparisons with global atmospheric measurements [NASA-RP-1292-VOL-2] p 754 N93-25158
The atmospheric effects of stratospheric aircraft. Report of the 1992 Models and Measurements Workshop. Volume 3: Special diagnostic studies [NASA-RP-1292-VOL-3] p 754 N93-25159
- REMSBURG, ELLIS E.**
The atmospheric effects of stratospheric aircraft. Report of the 1992 Models and Measurements Workshop. Volume 1: Workshop objectives and summary [NASA-RP-1292-VOL-1] p 754 N93-25157
- REN, BING**
Weighted average method for evaluating the aerodynamic properties of transition flow p 8 A93-11872
- REN, GUOPIN**
Control of separation by dynamic air jets p 1066 A93-48504
- REN, RUOEN**
The economic effectiveness analysis of technological progress in aviation industry p 1265 A93-54854
- REN, XINGMIN**
A transfer matrix method for calculation of support stiffness of aeroengine stator p 1122 A93-51193
- RENDER, P. M.**
The stability and aerodynamic performances of clusters of small cruciform parachutes [AIAA PAPER 93-1242] p 690 A93-35181
Studies into the hail ingestion characteristics of turbofan engines [AIAA PAPER 93-2174] p 1115 A93-49987
- RENEAUX, J.**
Recent developments in international laminar flow research programs for transport aircraft [ONERA, TP NO. 1992-163] p 457 A93-26878
- RENIERI, MICHAEL P.**
Design and manufacturing concepts for thermoplastic structures p 919 N93-30434
- RENKO, KARI**
DYNAC: A computer program for analyzing the dynamical stability of aircraft [REPT-B-31] p 66 N93-12415
- RENO, JEFFREY M.**
Decreasing F-16 nozzle drag using computational fluid dynamics [AIAA PAPER 93-2572] p 1084 A93-50289
- RENTALL, MICHAEL E.**
Airship insurance in London [AIAA PAPER 93-4043] p 1265 A93-54611
- RENTZ, DAVID D.**
Comparison of all-electric secondary power systems for civil transport p 519 A93-25997
Comparison of all-electric secondary power systems for civil subsonic transports [NASA-TM-105852] p 55 N93-10456
- RENZE, S. P.**
Buckling of open-section bead-stiffened composite panels p 1157 A93-50420
- REPIK, E. U.**
Optimal conditions for flow turbulence reduction by a set of grids p 836 A93-39122
- RESENDE, HUGO B.**
Hypersonic panel flutter in a rarefied atmosphere p 188 N93-13928
Hypersonic panel flutter in a rarefied atmosphere [NASA-CR-4514] p 780 N93-27084
- RESHETNIAK, E. P.**
A nonsearch adaptive control system with a reference model and derivative measurement p 561 A93-26838
- RESHOTKO, ELI**
Hypersonic stability and transition p 864 A93-42579
Tesseract: Supersonic business transport [NASA-CR-192072] p 334 N93-17977
- RESKA, RAYMOND S.**
Lessons learned during testing of the Enhanced Position Location Reporting System (EPLRS) p 77 A93-10996
- RESLER, EDWIN L., JR.**
Analytic methods for design of wave cycles for wave rotor core engines [AIAA PAPER 93-2523] p 1121 A93-50253
- RESNICK, RALPH**
On machine capacitance dimensional and surface profile measurement system p 750 N93-25579
- RESTER, A. C.**
The GRAD Supernova Observer - First Flight of a very large balloon over Antarctica p 27 A93-11367
- RESTIVO, JON**
Test results of an orifice pulse tube refrigerator p 1149 A93-48612
- RESWEBER, R.**
Shock tube validation experiments for the simulation of ram-accelerator-related combustion and gasdynamic problems p 1016 A93-45499
- RETCHEFORD, J. A.**
Reinforcement of the F-111 wing pivot fitting with a boron/epoxy doubler system - Materials engineering aspects p 1214 A93-54241
- REU, TAEKYU**
Hybrid grid approach to study dynamic stall p 122 A93-14548
- REUBUSH, DAVID E.**
A historical perspective on hypersonic research at the NACA/NASA Langley Research Center (1944-1984) [AIAA PAPER 92-5034] p 456 A93-22308
- REUTER, WILLIAM H.**
Flowfield computations over the Space Shuttle Orbiter with a proposed canard at a Mach number of 5.8 and 50 degrees angle of attack [AIAA PAPER 93-0322] p 281 A93-23014
Flowfield computations over the Space Shuttle orbiter with a proposed canard at a Mach number of 5.8 and 50 deg angle of attack [AD-A258058] p 293 N93-17756
- REUTOV, V. P.**
Instability of the periodic deflection of a panel surface in a turbulent boundary layer p 208 A93-15188
- REVERCOMB, H. E.**
Remote sensing cloud properties from high spectral resolution infrared observations p 1034 A93-46780
- REYES, JOE T.**
Proposal and preliminary design for a high speed civil transport aircraft. Swift: A high speed civil transport for the year 2000 [NASA-CR-192023] p 335 N93-18049
- REYNOLDS, D.**
Photoelectrochemical etching of high aspect ratio submillimeter waveguide filters from n(+) GaAs wafers p 409 A93-20644
- REYNOLDS, ROBERT R.**
Nonlinear aeroelastic response of panels [AIAA PAPER 93-1599] p 741 A93-34130
- REZNICHENKO, V. I.**
Design and fabrication of panels with cutouts p 1215 A93-52973
- REZNIKOV, M. S.**
Effect of the body shape on head shock attenuation at a large distance from the axis p 127 A93-16708
- RHEW, RAY D.**
Development of a tethered satellite force transducer p 1251 A93-54368
- RHIE, CHAE M.**
Numerical analysis of reacting flow using finite rate chemistry models p 389 A93-21666
- RHIM, JAE WOOK**
Discrete-vortex simulation of pulsating flow on a turbulent leading-edge separation bubble p 787 N93-27457
- RHO, OHYUN**
An analysis on high speed impulsive noise of transonic helicopter rotor p 849 A93-35965
- RHOADES, KENNETH**
On the selection of a GPS validity indicator for aircraft navigation in the National Airspace System (NAS) p 316 A93-21186
- RHODES, J. A.**
CFD drag predictions for a wide body transport fuselage with flight test verification [AIAA PAPER 93-3418] p 976 A93-47214
- RIABIKOV, P. V.**
Enhancing the performance of aircraft engine blades by surface hardening p 811 A93-39072
- RIABOV, N. A.**
An experimental study of thrust reverser models p 812 A93-39195
- RIADCHIKOV, V. E.**
A pressure distribution measuring system with pneumatic switches and automatic band selection p 75 A93-10029
- RIABI, A.**
Prediction of jet impingement cooling scheme characteristics (airfoil leading edge application) p 932 N93-29941
- RIAZ, J.**
Atmospheric turbulence simulation for rotorcraft applications p 757 A93-34264
Helicopter response to atmospheric turbulence p 817 A93-35987
- RIAZ, JAMSHED**
A simulation model of atmospheric turbulence for rotorcraft applications p 224 N93-14588
- RIBAUD, YVES**
Compact heat exchanger fitted to engines of the inverted type [ISABE 93-7120] p 1221 A93-54095
- RIBEIRO, RENATO S.**
Computation of wake roll-up for complete aircraft configurations [AIAA PAPER 93-3509] p 984 A93-47275
- RIBEIRO, RENATO SILVA**
Analysis of wing wake roll-up using a vortex-in-cell method p 697 N93-25706
- RIBNER, HERBERT S.**
Thrust imparted to an airfoil by passage through a sinusoidal upwash field p 1178 A93-53219
- RICCITIELLO, SALVATORE R.**
Evaluation of 2D ceramic matrix composites in aeroconvective environments p 1212 A93-53459
- RICCO, PHILIPPE**
The pioneers of thermopulsive nozzles p 235 A93-16854
- RICE, EDWARD J.**
Flip-flop jet nozzle extended to supersonic flows p 778 A93-39409
Jet mixer noise suppressor using acoustic feedback [NASA-CASE-LEW-15170-1] p 853 N93-28953
Enhanced mixing of a rectangular supersonic jet by natural and induced screech [NASA-TM-106245] p 989 N93-31672
- RICH, BEN R.**
The development of aircraft in the Lockheed Skunk Works from 1954 to 1991 p 805 N93-27168
- RICH, CHRIS**
Hot end cleaning - Corrosion pitting of turbine discs [SAE PAPER 920930] p 202 A93-14081
- RICHARD, MARC J.**
Dynamic simulation of flexible body systems by the vector solution method p 553 N93-20666
- RICHARDS, B. E.**
Newton-like methods for fast high resolution simulation of hypersonic viscous flows p 437 A93-20740
Hypersonic viscous flow over two-dimensional ramps p 866 A93-42596
Finite volume 3DNS and PNS solutions of hypersonic viscous flow around a delta wing using Osher's flux difference splitting p 870 A93-42633
- RICHARDS, E. J.**
Laminar flow research in the 1940-1950s - A personal recollection p 235 A93-17271
- RICHARDS, GORDON S.**
Compact high reliability fiber coupled laser diodes for avionics and related applications p 1152 A93-49470
- RICHARDS, JOHN C.**
The control of aircraft engines in the 1990's p 173 A93-15042
- RICHARDSON, J. D.**
An externally pressurized air bearing system, journals and thrust, for application to small turbomachinery [ASME PAPER 92-GT-382] p 406 A93-19539
- RICHARDSON, PAMELA F.**
The NASA Computational Fluid Dynamics (CFD) program - Building technology to solve future challenges [AIAA PAPER 93-3292] p 1041 A93-44996
- RICHARDSON, SCOTT M.**
An unstructured adaptive quadrilateral mesh-based scheme for viscous turbomachinery flow calculations [AIAA PAPER 93-1975] p 1077 A93-49822
- RICHASON, THOMAS F.**
Unsteady panel method for flows with multiple bodies moving along various paths [AIAA PAPER 93-0640] p 539 A93-24755
- RICHIE, JOSEPH M.**
A NASPAC-based analysis of the delay and cost effects of the Dallas/Fort Worth metroplex plan [DOT/FAA/CT-TN92/21] p 193 N93-13447
- RICHTER, ELKE**
The integral starter/generator development progress [SAE PAPER 920967] p 173 A93-14629
- RICHTER, ROLAND**
Precise pitching airfoil computations by use of dynamic unstructured meshes [AIAA PAPER 93-2971] p 1049 A93-48165
- RICHWINE, DAVID M.**
Correlation of forebody pressures and aircraft yawing moments on the X-29A aircraft at high angles of attack [AIAA PAPER 92-4105] p 38 A93-11273
Correlation of forebody pressures and aircraft yawing moments on the X-29A aircraft at high angles of attack [NASA-TM-4417] p 22 N93-11532
- RICK, H.**
Experimental analysis of steady-state and dynamic monitoring of power shaft turbines p 178 N93-15176
- RICK, W.**
Study of flow phenomena in high speed intakes [AIAA PAPER 92-5029] p 272 A93-22304
Computation of hypersonic high-temperature nozzle flow p 1238 A93-56040
- RICKARD, D. C.**
The development of a prototype aircraft height monitoring unit utilising an SSR-based difference in time of arrival technique p 884 A93-43432

- RICKETTS, RODNEY H.**
An overview of aerelasticity studies for the National Aero-Space Plane
[AIAA PAPER 93-1313] p 732 A93-33889
- RIEDEL, H.**
A European collaborative NLF nacelle flight demonstrator
[PNR-90992] p 20 N93-11113
- RIEDEL, U.**
Simulation of nonequilibrium hypersonic flows
p 863 A93-42443
- RIEDELBAUCH, S.**
Hypersonic viscous flow simulations
p 478 A93-27926
Numerical simulation of laminar hypersonic flow past a double-ellipsoid
p 868 A93-42612
- RIEDELBAUCH, STEFAN**
Aerothermodynamic properties of hypersonic flows over radiation-adiabatic surfaces
[DLR-FB-91-42] p 485 N93-21761
- RIEDL, A.**
A laser induced fluorescence system for the high enthalpy shock tunnel (HEG) in Goettingen
p 1024 A93-45506
- RIEKE, WILLIAM J.**
Aircraft icing problems - After 50 years
[AIAA PAPER 93-0392] p 486 A93-24239
- RIEMSLAGH, KRIS**
A flux-difference finite volume method for steady Euler equations on adaptive unstructured grids
p 116 A93-14277
- RIENECKER, LISA**
RTJ-303: Variable geometry, oblique wing supersonic aircraft
[NASA-CR-192054] p 337 N93-18166
- RIFE, MICHAEL C.**
Flow visualizations of perpendicular blade vortex interactions
[NASA-CR-192725] p 748 N93-25208
- RIGBY, D. L.**
Increased heat transfer to elliptical leading edges due to spanwise variations in the freestream momentum: Numerical and experimental results
[NASA-TM-106150] p 838 N93-27020
- RIGGINS, D. W.**
Vortex generation and mixing in three-dimensional supersonic combustors
[AIAA PAPER 93-2144] p 1115 A93-49961
- RIGNEY, J. D.**
Chemical stability of titanium diboride reinforcement in nickel aluminide matrices
p 1147 A93-52473
- RIGNEY, TOM**
Liquid hydrogen foil-bearing turbopump
[AIAA PAPER 93-2537] p 1156 A93-50264
- RILEY, CHRISTOPHER J.**
Application of an engineering inviscid-boundary layer method to slender three-dimensional vehicle forebodies
[AIAA PAPER 93-2793] p 963 A93-46534
- RILEY, DAVID R.**
Development of flying qualities and agility evaluation maneuvers
[AIAA PAPER 93-3645] p 1127 A93-48329
Aircraft control requirements and achievable dynamics prediction
[AIAA PAPER 93-3648] p 1128 A93-48331
- RILEY, RICHARD G., JR.**
Civil tiltrotor noise impact prediction methodology
p 850 A93-35967
- RILEY, S. J.**
Studies into the hail ingestion characteristics of turbofan engines
[AIAA PAPER 93-2174] p 1115 A93-49987
- RILL, S.**
MELINA - A multi-block, multi-grid 3D Euler code with sub block technique for local mesh refinement
p 115 A93-14217
Integration of high bypass ratio engines on modern transonic wings for regional aircraft
p 506 A93-27479
- RIMER, MELVYN**
Systems integration test laboratory - Application and experiences
p 190 A93-13910
- RIMLINGER, M. J.**
Chimera grids in the simulation of three-dimensional flowfields in turbine-blade-coolant passages
[AIAA PAPER 93-2559] p 1157 A93-50280
- RIMLINGER, MARK J.**
Effects of bleed-hole geometry and plenum pressure on three-dimensional shock-wave/boundary-layer/bleed interactions
[AIAA PAPER 93-3259] p 967 A93-46800
- RINGERTZ, ULF**
Optimal design and imperfection sensitivity of nonlinear shell structures
[FFA-TN-1992-30] p 1030 N93-31123
- RINGLER, T. D.**
Advances in tilt rotor noise prediction
p 447 A93-19184
- RINGLER, TODD D.**
A study of blade-vortex interaction sound generation and directionality
p 565 A93-29402
- RINGO, LESLIE**
Phoenix: Preliminary design of a high speed civil transport
[NASA-CR-192024] p 334 N93-17976
- RINKINEN, W. J.**
A model study of the aircraft cabin environment resulting from in-flight fires
[DOT/FAA/CT-90/22] p 496 N93-21557
- RINOIE, K.**
Experimental studies of vortex flaps and vortex plates
p 121 A93-14406
Experiments on a 60 deg delta wing with vortex flaps and vortex plates
p 477 A93-27482
- RIQUAL, J.-L.**
Experiments on the active control of boundary layer transition
p 243 A93-19133
- RISHA, D. J.**
Studies in air/air supersonic mixing layers
p 700 N93-26007
- RISHEL, H. L.**
The effects of hypersonic flight test requirements on research vehicle design
[AIAA PAPER 93-0511] p 386 A93-23258
- RISPOLI, F.**
A finite element code for gas turbine combustor flow with Stretched Laminar Flamelet modelling
[ISABE 93-7127] p 1204 A93-54102
- RISTIC, D.**
Three-dimensional flow field in a turbine nozzle passage
[AIAA PAPER 93-2556] p 1084 A93-50278
- RIVERA, C. J.**
A simplified approach for control of rotating stall. I - Theoretical development
[AIAA PAPER 93-2229] p 1080 A93-50035
A simplified approach for control of rotating stall. II - Experimental results
[AIAA PAPER 93-2234] p 1080 A93-50038
- RIVERA, JOSE A.**
Experimental unsteady pressures at flutter on the Supercritical Wing Benchmark Model
[AIAA PAPER 93-1592] p 683 A93-34123
- RIVERS, JAMES M.**
Damage progression in stiffened composite panels
[AIAA PAPER 93-1345] p 738 A93-33915
- RIVERS, ROBERT A.**
Effect of lift-to-drag ratio in pilot rating of the HL-20 landing task
p 1210 A93-53738
- RIVIR, R. B.**
Heat transfer in high turbulence flows: A 2-D planar wall jet
p 932 N93-29935
- RIXEY, JOSEPH W.**
A multi-faceted engineering study of aerodynamic errors of the Service Aircraft Instrumentation Package (SAIP)
[AD-A258059] p 293 N93-17677
- RIZK, N. K.**
Three-dimensional gas turbine combustor emissions modeling
[ASME PAPER 92-GT-129] p 350 A93-19363
Three-dimensional NOx modeling for rich/lean combustor
[AIAA PAPER 93-0251] p 360 A93-22660
Three-dimensional emission modeling for diffusion flame, rich/lean, and lean gas turbine combustors
[AIAA PAPER 93-2338] p 1117 A93-50115
- RIZK, YEHIA M.**
Effect of forebody tangential slot blowing on flow about a full aircraft geometry
[AIAA PAPER 93-2962] p 1048 A93-48156
- RIZKALLA, O.**
Mixing and combustion studies using discrete orifice injection at hypervelocity flight conditions
p 205 A93-14523
- RIZKALLA, O. F.**
Data analysis of the parametric scramjet combustor experiments conducted in the Calspan 96 inch shock tunnel - 4th entry
[AIAA PAPER 92-5098] p 359 A93-22368
- RIZKALLA, OUSSAMA F.**
High-pressure hypervelocity electrothermal wind-tunnel performance study and subscale tests
p 1137 A93-49617
- RIZZI, ARTHUR**
Navier-Stokes stall predictions using an algebraic Reynolds-stress model
p 778 A93-39260
Hypersonic leeside delta-wing-flow computations using centered schemes
p 870 A93-42635
Evaluation of contributions for test case 7.1.1 and 7.1.2
p 870 A93-42636
- ROACH, CARL C.**
A high fidelity video delivery system for real-time flight simulation research
[AIAA PAPER 93-3558] p 1214 A93-52659
- ROACH, DENNIS**
Reliability assessment at airline inspection facilities. Volume 1: A generic protocol for inspection reliability experiments
[DOT/FAA/CT-92/12-VOL-1] p 704 N93-25110
Reliability assessment at airline inspection facilities. Volume 2: Protocol for an eddy current inspection reliability experiment
[DOT/FAA/CT-92/12-VOL-2] p 842 N93-28685
- ROACH, ROBERT L.**
Evaluation and application of the Baldwin-Lomax turbulence model in two-dimensional, unsteady, compressible boundary layers with and without separation in engine inlets
[AIAA PAPER 92-3676] p 111 A93-14118
Evaluation and application of the Baldwin-Lomax turbulence model in two-dimensional, unsteady, compressible boundary layers with and without separation in engine inlets
[AIAA PAPER 92-3676] p 414 A93-22509
Evaluation and application of the Baldwin-Lomax turbulence model in two-dimensional, unsteady, compressible boundary layers with and without separation in engine inlets
[NASA-TM-105810] p 82 N93-10087
- ROAN, V. P.**
Initial development of the two-dimensional ejector shear layer - Experimental results
[AIAA PAPER 93-2440] p 1118 A93-50192
Comparison of the initial development of shear layers in two-dimensional and axisymmetric ejector configurations
[AIAA PAPER 93-2441] p 1119 A93-50193
- ROARK, CHUCK**
Additional developments in embedded computer performance measurement
p 940 A93-42833
New developments in a PI-Bus specification by the JIAWG and SAE
p 940 A93-42852
- ROBACK, RICHARD J.**
Hot streaks and phantom cooling in a turbine rotor passage. I - Separate effects
[ASME PAPER 92-GT-75] p 401 A93-19325
Hot streaks and phantom cooling in a turbine rotor passage. II - Combined effects and analytical modelling
[ASME PAPER 92-GT-76] p 401 A93-19326
- ROBBINS, E.**
Determination of balloon gas mass and revised estimates of drag and virtual mass coefficients
p 7 A93-11362
Scientific ballooning payload termination loads
p 27 A93-11383
- ROBEL, MICHAEL C.**
Results from a GPS Shuttle Training Aircraft flight test
p 384 A93-21148
- ROBERTS, C.**
Structural and aerodynamic considerations for an oblique all-wing aircraft
[AIAA PAPER 92-4220] p 43 A93-13336
- ROBERTS, J. D.**
Reinforcement of the F-111 wing pivot fitting with a boron/epoxy doubler system - Materials engineering aspects
p 1214 A93-54241
- ROBERTS, J. H.**
Engine testing at simulated altitude conditions
[AIAA PAPER 93-2452] p 1120 A93-50201
- ROBERTS, L.**
Active control of wing rock of a delta wing at post-stall using tangential leading edge blowing
[AIAA PAPER 93-0056] p 367 A93-20169
- ROBERTS, LEONARD**
Navier-Stokes computation of wing/rotor interaction for a tilt rotor in hover
p 122 A93-14537
The generation of side force by distributed suction
[NASA-CR-193129] p 839 N93-27151
- ROBERTS, N.**
Comparison of electrostatic and aerodynamic forces during parachute opening
[AIAA PAPER 93-1210] p 689 A93-35160
- ROBERTS, R. P.**
Aerosevostatic analysis of an aircraft model incorporating the minimum state method for approximating unsteady aerodynamics
p 154 A93-14258
- ROBERTS, RICHARD A.**
The UTA autonomous aerial vehicle - Automatic control and navigation
p 908 A93-42813
- ROBERTS, SEAN C.**
Flight testing in the 90's
[AIAA PAPER 92-4123] p 102 A93-11256
- ROBERTSON, ROY E.**
Airborne doppler radar research at Rockwell International
p 489 N93-19602

ROBERTSON, SCOTT

Phase I flight test of MIAG advanced development model

[AIAA PAPER 92-4076] p 95 A93-11261

ROBERTSON, SCOTT D.

A real-time, hardware-in-the-loop simulation of an unmanned aerial research vehicle

[AD-A262477] p 893 N93-29409

ROBESON, ERIC

AH-64A rotating load usage monitoring from fixed system information

p 507 A93-27953

ROBINS, ROBERT E.

Potential hazard of aircraft wake vortices in ground effect with crosswind

p 479 A93-28606

ROBINSON, A. M.

The aerodynamic characteristics of the Gottingen 797 and Wortmann FX63-137 aerofoil sections at very low Reynolds numbers

[ETN-93-92999] p 295 N93-18128

ROBINSON, B. A.

A sensitivity study for pneumatic vortex control on a chined forebody

[AIAA PAPER 93-0049] p 260 A93-20162

Prediction of vortex breakdown on a delta wing

p 787 N93-27459

ROBINSON, CHRISTOPHER J.

Endwall flows and blading design for axial flow compressors

p 423 N93-18730

ROBINSON, G. N.

Stratospheric aircraft exhaust plume and wake chemistry studies

[NASA-CR-189688] p 94 N93-12299

ROBINSON, MICHAEL C.

Aerodynamic foundations for use of unsteady aerodynamic effects in flight control

[AIAA PAPER 93-0188] p 276 A93-22613

ROBINSON, O.

Control of vortices on a delta wing by leading-edge injection

p 860 A93-41906

Instantaneous topology of the unsteady leading-edge vortex at high angle of attack

p 961 A93-45728

ROBINSON, PAUL

NASA/LMSC coherent LIDAR airborne shear sensor: System capabilities and flight test plans

p 144 N93-14847

ROBINSON, PAUL AARON

The modelling of turbulence and downbursts for flight simulators

p 193 N93-13542

ROBINSON, THOMAS H.

Advanced real time integrated processors

p 50 A93-11000

ROCHERY, V.

Computation of turbulent compressible flows on a DLR wing and a blade to blade passage using an upwind scheme

p 687 A93-34359

ROCK, S. M.

Active control of wing rock of a delta wing at post-stall using tangential leading edge blowing

[AIAA PAPER 93-0056] p 367 A93-20169

ROCK, STEPHEN M.

Integrated flight/propulsion control - Subsystem specifications for performance

[AIAA PAPER 93-3808] p 1132 A93-51400

Active control for fin buffet alleviation

[AIAA PAPER 93-3817] p 1133 A93-51408

Benefits of variable rotor speed in integrated helicopter/engine control

[AIAA PAPER 93-3851] p 1134 A93-51438

ROCKWELL, D.

Instantaneous structure of vortex breakdown on a delta wing via particle image velocimetry

p 779 A93-39428

Control of vortices on a delta wing by leading-edge injection

p 860 A93-41906

Instantaneous topology of the unsteady leading-edge vortex at high angle of attack

p 961 A93-45728

ROCKWELL, DONALD

Three-dimensional flow structure on delta wings at high angle-of-attack - Experimental concepts and issues

[AIAA PAPER 93-0550] p 285 A93-23289

ROCKWELL, R.

The HYDICE instrument design and its application to planetary instruments

p 842 N93-28766

RODDEN, W. P.

Aeroelastic effects on the B-2 maneuver response

[AIAA PAPER 93-3664] p 1128 A93-48344

RODDEN, WILLIAM P.

Response of B-2 aircraft to nonuniform spanwise turbulence

p 1135 A93-52437

RODGERS, C.

High pressure ratio intercooled turboprop study

[ASME PAPER 92-GT-405] p 356 A93-19554

RODGERS, MARK D.

Conversion of the CTA, Inc., en route operations concepts database into a formal sentence outline job task taxonomy

[AD-A261410] p 708 N93-26447

RODI, PATRICK E.

A study of hypersonic swept shock wave/turbulent boundary layer interactions using a conical Navier-Stokes code

[AIAA PAPER 92-5050] p 273 A93-22322

An experimental study of the effects of bodyside compression on forward swept sidewall compression inlets ingesting a turbulent boundary layer

[AIAA PAPER 93-3125] p 1072 A93-49515

RODI, PATRICK ELROY

An experimental/computational study of heat transfer in sharp fin induced shock wave/turbulent boundary layer interactions at low hypersonic Mach numbers

p 217 N93-13826

RODI, W.

Calculation of wake-induced unsteady flow in a turbine cascade

[ASME PAPER 92-GT-306] p 255 A93-19496

Measurement of unsteady flow and heat transfer in a linear turbine cascade

[ASME PAPER 92-GT-323] p 256 A93-19507

RODIN, ERVIN Y.

Artificial intelligence methodologies in flight related differential game, control and optimization problems

[AD-A262405] p 848 N93-28498

RODIONOV, I. N.

Effect of the aerodynamic interference of the rotor and the fuselage on the power requirements for the horizontal flight of a helicopter

p 819 A93-39179

Calculation of the position of the flow separation line in an analog model of flow past a body

p 1176 A93-52958

RODMAN, LAURA C.

Development of an engineering level prediction method for high angle of attack aerodynamics

[AIAA PAPER 93-0208] p 278 A93-22626

A study of compressible turbulence

[AIAA PAPER 93-0659] p 465 A93-24772

RODRIGUES, F. C.

Misalignments of airborne laser beams due to mechanical vibrations

p 394 A93-17762

RODRIGUES, M.

Thin gradient heat fluxmeters developed at ONERA [ONERA, TP NO. 1992-87]

p 831 A93-38571

RODRIGUES, ROGERIO LACOURT

A study upon structural optimization of elastic rotors for mechanical systems

[INPE-5376-TDI/471] p 83 N93-10310

RODRIGUEZ, ARMANDO A.

Vertical guidance for a Lockheed L1011-100 using optimal dynamic interpolation

p 369 A93-22884

RODRIGUEZ, J. M.

Stratospheric aircraft exhaust plume and wake chemistry studies

[NASA-CR-189688] p 94 N93-12299

RODRIGUEZ, JOSE L.

Teaching aircraft preliminary design - The first three years

[AIAA PAPER 92-4257] p 103 A93-13363

RODRIGUEZ, M.

Aerodynamics design of convergent-divergent nozzles

[AIAA PAPER 93-2574] p 1085 A93-50290

Cooling predictions in turbofan engine components

p 905 N93-29964

RODZEVICH, G. V.

Propulsion system simulator with propfan for tests on a large scale model of IL-114 airplane in a full-size wind tunnel of TsAGI

p 1013 A93-46933

ROE, P. L.

Technical prospects for computational aeroacoustics

p 244 A93-19150

A multidimensional generalization of Roe's flux difference splitter for the Euler equations

p 863 A93-42437

Computations of inviscid compressible flows using fluctuation-splitting on triangular meshes

[AIAA PAPER 93-3301] p 950 A93-44999

Numerical wave propagation and steady state solutions. II - Bulk Viscosity Damping

[AIAA PAPER 93-3331] p 953 A93-45025

A frontal approach for internal node generation in Delaunay triangulations

p 1262 A93-56403

ROEHLE, H.

Optimization of anisotropic structures considering strength, stiffness and aeroelastic constraints

[AIAA PAPER 92-4796] p 408 A93-20291

ROELKE, RICHARD J.

Radial turbine cooling

p 82 N93-10061

Radial turbine cooling

[NASA-TM-105658] p 130 N93-13292

ROENKE, AXEL J.

Trajectory control for a low-lift re-entry vehicle

p 1141 A93-49592

Reentry control to a drag vs. energy profile

[AIAA PAPER 93-3790] p 1143 A93-51385

ROGER, R. P.

CFD study of the flowfield due to a supersonic jet exiting into a hypersonic stream from a conical surface. II

[AIAA PAPER 93-2926] p 1045 A93-48127

ROGERS, C. B.

The use of streamwise vorticity to enhance ejector performance

[AIAA PAPER 93-3247] p 966 A93-46792

ROGERS, CHARLES

Civil tiltrotor transport point design: Model 940A

[NASA-CR-191446] p 1019 N93-32234

ROGERS, JAMES L.

Aerodynamic performance optimization of a rotor blade using a neural network as the analysis

[AIAA PAPER 92-4837] p 324 A93-20295

Application of a neural network as a potential aid in predicting NTF pump failure

[NASA-TM-107667] p 442 N93-18332

ROGERS, LAWRENCE W.

Effects of forebody strakes and Mach number on overall aerodynamic characteristics of configuration with 55 deg cropped delta wing

[NASA-TP-3253] p 131 N93-13353

ROGERS, LYNN

Add-on damping treatment for the F-15 upper-outer wing skin

[AD-A258470] p 337 N93-18248

ROGERS, LYNN C.

Human engineering issues for data link systems

p 1260 A93-55874

ROGERS, R. C.

Scramjet fuel-air mixing establishment in a pulse facility

p 359 A93-21667

A computational investigation of fuel mixing in a hypersonic scramjet

[AIAA PAPER 93-2994] p 1001 A93-44230

ROGERS, RALPH V.

Design of an air traffic computer simulation system to support investigation of civil tiltrotor aircraft operations

[NASA-CR-190811] p 36 N93-11139

Implementing system simulation of C3 systems using autonomous objects

[NASA-CR-190845] p 89 N93-11716

Design of an air traffic computer simulation system to support investigation of civil tiltrotor aircraft operations

[NASA-CR-192920] p 707 N93-26052

ROGERS, STUART

A computational study of wingtip vortex flowfield

[AIAA PAPER 93-3010] p 1054 A93-48200

ROGERS, STUART E.

Progress in high-lift aerodynamic calculations

[AIAA PAPER 93-0194] p 474 A93-25512

Efficient simulation of incompressible viscous flow over single and multielement airfoils

p 1095 A93-52448

Efficient simulation of incompressible viscous flow over multi-element airfoils

p 784 N93-27443

ROGERS, T. F.

Sales, not subsidies, are the sticking point

p 945 A93-43677

ROGGERO, F.

Aerodynamic calculation of complex three-dimensional configurations

p 1094 A93-52426

ROGO, CASS

Aerofoils and secondary flows in a transonic mixed flow turbine stage

[ASME PAPER 92-GT-72] p 248 A93-19322

ROHACS, J.

Solid state flight data recorders and their application in the flight operation analysis

p 166 A93-14200

Application of flight data for diagnostic purposes

p 166 A93-14295

Detection of technical states with aircraft

p 168 N93-15159

ROHARDT, CLAAS-HINRIK

Flow visualization on helicopter blades using acenaphthen

[ESA-TT-1255] p 931 N93-29273

ROHL, PETER J.

Preliminary wing design of a high speed civil transport aircraft by multilevel decomposition techniques

[AIAA PAPER 92-4721] p 325 A93-20323

ROHLF, D.

System identification for X-31A project support: Lessons learned so far

p 512 N93-19914

ROHR, J. J.

A comparison of the drag-reducing benefits of riblets in internal and external flows

p 395 A93-18054

ROJAS, R. G.

Operation of the helicopter antenna radiation prediction code

[NASA-CR-193259] p 1030 N93-31110

ROKHIMISTROV, O. V.

Wing rock of lifting systems

p 118 A93-14330

ROKHSAR, KAMRAN

Use of neural networks in control of high-alpha maneuvers

p 1130 A93-49593

- ROKNAIDIN, F.**
Prediction of stall and post-stall behavior of airfoils at low and high Reynolds numbers
[AIAA PAPER 93-3502] p 983 A93-47270
- ROKUTANDA, ITARU**
Test results on air turbo ramjet for a future space plane
[AIAA PAPER 92-5054] p 359 A93-22325
Development study on Air Turbo Ramjet engine for a future space plane
[ISABE 93-7016] p 1195 A93-53992
Results of sea-level static tests on air turbo ramjet for a future space plane
[AAS PAPER 91-640] p 1247 A93-55817
- ROLL, DEANNA**
A manned hypersonic reconnaissance vehicle which does not require airborne fueling p 333 N93-17888
- ROLL, R.**
Results of review of Fokker F 28 'Fellowship' maintenance program p 948 A93-45793
- ROLLIN, G.**
Optimization of afterbodies and engine nozzle by using CFD methods
[ISABE 93-7098] p 1187 A93-54074
- ROLSTON, S.**
Passive control of pre-entry shock in supersonic intakes
[AIAA PAPER 93-0291] p 279 A93-22691
- ROLSTON, S. C.**
Passive boundary-layer bleed for supersonic intakes p 114 A93-14212
- ROM, J.**
Lateral aerodynamics characteristics of forebodies at high angle of attack in subsonic and transonic flows p 118 A93-14302
Experimental and nonlinear vortex lattice method results for various wing-canard configurations p 479 A93-28607
- ROM, JOSEF**
Analysis of the stability characteristics of hypersonic flow of a detonable gas mixture in the stagnation region of a blunt body
[AIAA PAPER 93-1918] p 1076 A93-49784
- ROMALEWSKI, ROBERT S.**
Embedded training capabilities for the LAMPS MK 3 system
[AD-A250697] p 49 N93-11838
- ROMANI, DONALD C., JR.**
Unsteady aerodynamics in airplane stall-spin departure
[AIAA PAPER 93-0622] p 523 A93-24739
- ROMANKOV, O. N.**
Design and investigation of the stand and flying scramjet models - Conceptions and results of experiments
[AIAA PAPER 93-2447] p 1120 A93-50199
- ROMANOV, V. F.**
Studies of atmospheric eddy dynamics and energetics and climate problems
[ISBN 5-286-00610-8] p 753 A93-35689
- ROMANOV, VIKTOR I.**
Design features of the GTD 8000 and GTD 15000 marine gas turbine engines
[ASME PAPER 92-GT-15] p 400 A93-19287
- ROMASHKOVA, D. D.**
Chemical-kinetics characteristics of combustion in a supersonic turbulent flow p 1018 A93-47512
- ROMER, W. W.**
Boundary condition procedures for CFD analyses of propulsion systems - The multi-zone problem
[AIAA PAPER 93-1971] p 1077 A93-49819
- RONG, BAISEN**
Fine control of Mach number in subsonic wind tunnel p 375 A93-20808
- RONG, XIANGJUN**
On engine parameter estimation with flight test data p 1107 A93-48520
- RONZHEIMER, A.**
Investigation of the flowfield around an isolated bypass engine with fan and core jet p 215 N93-13227
- RONZHEIMER, A.**
Investigation of interference phenomena of modern wing-mounted high-bypass-ratio engines by the solution of the Euler-equations p 213 N93-13204
- ROOD, RICHARD B.**
Implications of three-dimensional tracer studies for two-dimensional assessments of the impact of supersonic aircraft on stratospheric ozone p 936 A93-41269
- ROONEY, ARTHUR J., JR.**
Standardization of automatic test equipment in the US Air force
[AD-A262076] p 809 N93-29004
- ROOS, T. H.**
The streamline throughflow method of axial turbomachinery flow analysis
[ISABE 93-7031] p 1184 A93-54007
- ROOZEN, NICOLAAS BERNARDUS**
Quiet by design: Numerical acousto-elastic analysis of aircraft structures
[ISBN-90-386-0042-9] p 893 N93-29268
- ROQUEMORE, W. M.**
Experimental and numerical investigations of the vortex-flame interactions in a driven jet diffusion flame
[AIAA PAPER 93-0455] p 534 A93-25532
Numerical method for simulating fluid-dynamic and heat-transfer changes in jet-engine injector feed-arm due to fouling p 1245 A93-54467
- ROSCHKE, HENRY, III**
Digital map databases in support of avionic display systems p 544 A93-26888
- ROSCHE, H. J.**
The jet behaviour of an actual high-bypass engine as determined by LDA-measurements in ground tests p 175 N93-13218
- ROSE, A.**
Automatic guidance and control for recovery of remotely piloted vehicles p 181 A93-14188
- ROSE, ALAN**
Three component LDV velocity measurements in a can type research combustor for CFD validation. I - Isothermal
[ASME PAPER 92-GT-138] p 350 A93-19370
- ROSE, DON**
The Edge supersonic transport
[NASA-CR-192074] p 335 N93-18055
- ROSE, O. J.**
Euler analysis of forebody-strake vortex flows at supersonic speeds p 1094 A93-52429
- ROSE, WILLIAM I.**
Remote sensing of volcanic ash hazards to aircraft p 556 A93-24213
- ROSEN, A.**
Stability of the vertical autorotation of a single-winged samara p 274 A93-22443
A generic harmonic rotor model for helicopter flight simulation p 506 A93-27480
Investigation of the flight mechanics simulation of a hovering helicopter p 798 A93-35990
- ROSEN, ROBERT**
The rebirth of supersonic transport p 457 A93-25325
- ROSENBAUD, VALERY**
Ignition of boron particles coated by a thin titanium film
[AIAA PAPER 93-2201] p 1145 A93-50013
- ROSENBERG, D.**
The HYDICE instrument design and its application to planetary instruments p 842 N93-28766
- ROSENSTEIN, LEO M.**
Environmental definition of a multi-platform avionics system p 896 A93-42855
- ROSENTHAL, DAVID M.**
Optically smart surfaces for aerodynamic measurements
[AIAA PAPER 92-3895] p 539 A93-24484
- ROSFJORD, T. J.**
Influences on the sprays formed by high-shear fuel nozzle/swirler assemblies p 411 A93-21653
- ROSKAM, JAN**
Out with the mechanical fasteners
[AIAA PAPER 92-4210] p 44 A93-13378
- ROSLIAKOV, A. D.**
Some recommendations concerning the prevention of fuel boiling in the igniters of the combustion chambers of gas turbine engines p 812 A93-39200
- ROSMAIT, RUSSELL L.**
Industry survey of space system cost benefits from New Ways Of Doing Business p 454 N93-17325
- ROSS, HANNES**
Advanced aircraft with thrust vector control
[MBB-FE-1-S-PUB-0504] p 998 N93-31043
- ROSS, HOLLY M.**
Two leading-edge droop modifications for tailoring stall characteristics of a general aviation trainer configuration p 1008 A93-46807
Investigation of high-alpha lateral-directional control power requirements for high-performance aircraft
[AIAA PAPER 93-3647] p 1130 A93-49519
Stall departure resistance enhancer
[NASA-CASE-LAR-14221-1] p 344 N93-19023
- ROSS, I. M.**
Singular arcs for blunt endoatmospheric vehicles p 1015 A93-44380
- ROSS, LARRY**
Flight simulation - An overview p 1209 A93-53768
- ROSSER, DAVID C., JR.**
Data acquisition for aeroelastic testing at the NASA Langley Transonic Dynamics Facility p 1250 A93-54397
- ROSSI, GLENN T.**
Novel approaches to complex geometry structure p 546 A93-27969
- ROSSI, M. J.**
Active rib experiment for shape control of an adaptive wing
[AIAA PAPER 93-1700] p 712 A93-34222
- ROSSING, T. D.**
Forces on a magnet moving past figure-eight coils
[DE93-009965] p 943 N93-29189
- ROSSITTO, KEN F.**
Longitudinal and lateral-directional flying qualities investigation of high-order characteristics for advanced-technology transports
[AIAA PAPER 93-3815] p 1133 A93-51406
Initial results of an in-flight investigation of longitudinal flying qualities for augmented, large transports in approach and landing
[AIAA PAPER 93-3816] p 1133 A93-51407
- ROSSO, RAYMOND**
LOCSTAR - A satellite radiodetermination system for Europe p 150 A93-15037
- ROSSONI, MIKE**
Liquid hydrogen foil-bearing turbopump
[AIAA PAPER 93-2537] p 1156 A93-50264
- ROSSOW, C.-C.**
Accurate solution of the 2D Euler equations with an efficient cell-vertex upwind scheme
[AIAA PAPER 93-0071] p 262 A93-20183
Investigation of interference phenomena of modern wing-mounted high-bypass-ratio engines by the solution of the Euler-equations p 213 N93-13204
Investigation of the flowfield around an isolated bypass engine with fan and core jet p 215 N93-13227
- ROSSOW, V. J.**
Measurements in 80- by 120-foot wind tunnel of hazard posed by lift-generated wakes
[AIAA PAPER 93-3518] p 1014 A93-47281
- ROSSOW, VERNON J.**
Effect of ground and ceiling planes on shape of energized wakes
[AIAA PAPER 93-3410] p 974 A93-47207
Wake-vortex structure from lift and torque induced on a following wing
[AIAA PAPER 93-3013] p 1054 A93-48202
- ROSTAND, PHILIPPE**
Validation of aerodynamic simulation methods for Hermes spaceplane and future hypersonic vehicles
[AIAA PAPER 92-5065] p 273 A93-22335
- ROTE, D. M.**
Forces on a magnet moving past figure-eight coils
[DE93-009965] p 943 N93-29189
- ROTENBERGER, KEVIN**
Load variability of a two-bladed helicopter p 507 A93-27954
- ROTH, G.**
Unsteady pressure measurements in a rotating centrifugal impeller
[ASME PAPER 92-GT-152] p 402 A93-19379
- ROTH, JAN-UWE**
Comparison of the damage for various types of fibre reinforced composites due to different lightning test standards (MIL-STD-1757A, German military VG-standard 96903) p 736 N93-24891
- ROTH, KARLIN R.**
A numerical investigation of a subsonic jet in a crossflow
[AIAA PAPER 93-0870] p 469 A93-24931
An initial comparison of CFD with experiment for a geometrically simplified STOVL model
[AIAA PAPER 93-3059] p 1058 A93-48236
- ROTH, MARTIN**
Material characterization and fractographic examination of Ti-17 fatigue crack growth specimens for SMP SC33 p 1004 N93-31744
- ROTHER, M.**
Numerical determination of the residual strength of battle damaged composite plates p 537 N93-21533
- ROTHWELL, A.**
Structural optimization in preliminary aircraft design - A finite-element approach p 226 A93-14340
- ROTHWELL, E.**
Receiving and scattering characteristics of an imaged monopole beneath a lossy sheet p 1158 A93-50543
- ROTT, N.**
Lord Rayleigh and hydrodynamic similarity p 211 A93-17408
- ROTTER, A. J.**
En route air traffic controllers use of flight progress strips: A graph-theoretic analysis
[AD-A259062] p 319 N93-18927
- ROTZ, CHRISTOPHER A.**
Damped advanced composite parts p 1253 A93-55871
- ROUDOLFF, F.**
The limit model of a thin strip exhibiting two delaminations
[ONERA, TP NO. 1992-212] p 832 A93-38764

ROUNDY, LANCE M.

ROUNDY, LANCE M.

Design and manufacturing concepts for thermoplastic structures p 919 N93-30434

ROURKE, R. D.

Implementation of expert systems within an interactive tactical environment [AIAA PAPER 93-3583] p 1223 A93-52678

ROUSE, MARSHALL

Structural response of bead-stiffened thermoplastic shear webs p 923 N93-30873

ROUSE, WILLIAM B.

Specification of adaptive aiding systems [AD-A254537] p 159 N93-12602

ROUSSEAU, P. G.

Numerical simulation of inviscid transonic flow over two-dimensional slender bodies p 686 A93-34348

ROUX, FRANK

Comparison of three methods to deduce three-dimensional wind fields in a hurricane with airborne Doppler radar p 844 A93-37691

ROUZAUD, J.

Preliminary results of the ISM campaign - The Landes, South West France p 1161 A93-47553

ROVER, RICHARD C., III

Development of circulation control technology for application to advanced subsonic transport aircraft [AIAA PAPER 93-0644] p 464 A93-24759

ROWEY, R. J.

Design and test of a small two stage counter-rotating turbine for rocket engine application [AIAA PAPER 93-2136] p 1142 A93-49954

ROY-AIKINS, J. E. A.

Some aspects of variable geometry gas turbine operation [ASME PAPER 92-GT-407] p 356 A93-19556

ROY, BHASKAR

Flow studies in ducted twin-rotor contra-rotating axial flow fans [ASME PAPER 92-GT-390] p 258 A93-19545

ROY, GABRIEL D.

High density strained hydrocarbon fuels for air breathing propulsion [ISABE 93-7081] p 1213 A93-54057

ROY, S.

Applications of advanced fracture mechanics to fuselage p 1026 A93-45787

ROYCHOUDHURY, SUBIR

Emissions reduction by varying the swirl air flow split in advanced gas turbine combustors [ASME PAPER 92-GT-110] p 349 A93-19347

RUAN, Y. F.

Modal analysis of multistage gear systems coupled with gearbox vibrations p 827 A93-36588

RUBERG, STEVE

Database management for integrated avionics system p 939 A93-42831

RUBERG, STEVEN

Functionally Integrated Resource Manager for real-time avionics data p 940 A93-42832

RUBEY, W. A.

A condensed phase test cell assembly for the System for Thermal Diagnostic Studies (STDS) [AD-A258463] p 393 N93-18242

RUBIN, A. M.

Common failure modes for composite aircraft structures due to secondary loads p 207 A93-14812

RUBIN, N.

The effects of fixed rotor tilt on the rotordynamic coefficients of incompressible flow annular seals p 1161 A93-52601

RUBIN, S. G.

A three-dimensional pressure flux-split RNS application to sub/supersonic flow in inlets and ducts [AIAA PAPER 93-3063] p 1058 A93-48239

RUBINS, P. M.

A review of supersonic combustion research at AEDC with hypersonic application [AIAA PAPER 93-2326] p 1116 A93-50106

RUDAKOV, A. I.

Effect of the body shape on head shock attenuation at a large distance from the axis p 127 A93-16708

RUDAKOV, A. YU.

A set of IBM PC software for processing helicopter flight tests data to determine the flight performance characteristics p 1037 A93-45661
Calculation of the position of aircraft center of gravity on an IBM PC p 996 A93-45671

RUDD, J. L.

Risk analysis for aging aircraft fleets p 1025 A93-45775

RUDDY, F. H.

A review of the development of a luggage explosive detection system p 497 N93-21862

RUDENKO, E. A.

Optimal structure of discrete algorithms of finite-dimensional continuous-discrete filtering in the presence of Markov noise p 1169 A93-51065

RUDLAND, R. S.

Slush hydrogen quantity gaging and mixing for the National Aerospace Plane p 1150 A93-48635

RUDNICKI, STEPHEN W.

Bearings-only and Doppler-bearing tracking using instrumental variables p 501 A93-29600

RUDNIK, R.

Investigation of the flowfield around an isolated bypass engine with fan and core jet p 215 N93-13227

RUDOFF, R. C.

Liquid water content measurements using the Phase Doppler Particle Analyzer in the NASA Lewis Icing Research Tunnel [AIAA PAPER 93-0298] p 378 A93-23698

RUDOFF, ROGER C.

Seed particle response and size characterization in high speed flows p 459 A93-23811

RUDOLPH, TERENCE H.

Development of models for predicting the triggering of lightning by launch vehicles p 734 N93-24899

RUDY, DAVID H.

Grid-refinement study of hypersonic laminar flow over a 2-D ramp p 866 A93-42597

RUEGGEBERG, T.

Study of flow phenomena in high speed intakes [AIAA PAPER 92-5029] p 272 A93-22304

RUES, D.

Numerical simulation of shock/shock and shock-wave/boundary-layer interactions in hypersonic flows p 1093 A93-52000

RUFFIN, STEPHEN M.

Hypersonic single expansion ramp nozzle simulations p 777 A93-39254

RUFFLES, P. C.

Safety through integrity and reliability p 239 A93-18779

RUFFNER, D.

Computer-aided cure optimization p 209 A93-15804

RUFIN, ANTONIO C.

Extending the fatigue life of aircraft engine components by hole cold expansion technology [ASME PAPER 92-GT-77] p 401 A93-19327

RUGH, WILSON J.

Analytical foundations of gain scheduling [AD-A264682] p 909 N93-30550

RULEV, I. K.

Modeling of the physicochemical processes of nonequilibrium heat transfer in the subsonic jets of an induction plasmatron p 836 A93-39147

RUMBERGER, WILLIAM E.

Cost/weight savings for the V-22 wing stow p 797 A93-35981

RUMSEY, C. L.

Estimation of unsteady lift on a pitching airfoil from wake velocity surveys [AIAA PAPER 93-0437] p 286 A93-23351

Estimation of unsteady lift on a pitching airfoil from wake velocity surveys [NASA-TM-105947] p 138 N93-14791

RUMSEY, CHRISTOPHER L.

A comparison of the predictive capabilities of several turbulence models using upwind and central-difference computer codes [AIAA PAPER 93-0192] p 268 A93-21102

RUNACRES, TONY A.

Fault signatures obtained from fault implant tests on an F404 engine [ASME PAPER 92-GT-82] p 348 A93-19331

RUOPS, J. A.

Dynamics of a high speed impeller - Analysis and experimental verification [AIAA PAPER 93-1362] p 743 A93-34239

RUSAK, Z.

Unsteady compressible airfoil aerodynamics using an adaptive time-discontinuous GLS finite element method [AIAA PAPER 93-0339] p 281 A93-23027

Transonic flow around the leading edge of a thin airfoil with a parabolic nose p 688 A93-34405

Interaction of the sonic boom with atmospheric turbulence [AIAA PAPER 93-2943] p 1171 A93-48140

RUSAKOV, V. V.

Approximate methods for heat flows toward the surface of three-dimensional bodies p 4 A93-10080

RUSHALO, A. M.

An electrostatic probe for determining particle characteristics in disperse flow p 76 A93-10178

RUSHBY, JOHN M.

Formal verification of algorithms for critical systems p 846 A93-37623

RUSSELL, A. J.

Repair of delaminations and impact damage in composite aircraft structures p 457 A93-24107

RUSSELL, A. L.

Engine reliability from an independent overhaul shops perspective p 239 A93-18788

RUSSELL, G. W.

Evaluation of decomposition kinetic coefficients for a fiber-reinforced intumescent-epoxy [AIAA PAPER 93-1856] p 1144 A93-49734

RUSSELL, JOHN D.

Effects of thermal history and jet fuel absorption on the properties of APC-2 p 534 A93-25252

RUSSELL, LOUIS M.

Measurements and computational analysis of heat transfer and flow in a simulated turbine blade internal cooling passage [AIAA PAPER 93-1797] p 1218 A93-53585

Measurements and computational analysis of heat transfer and flow in a simulated turbine blade internal cooling passage [NASA-TM-106189] p 1032 N93-31647

RUSSELL, M. J.

The development of the speaker independent ARM continuous speech recognition system [RSRE-MEMO-4473] p 87 N93-11383

RUSSELL, STEVEN G.

A Rayleigh-Ritz analysis methodology for cutouts in composite structures p 923 N93-30869

RUSSO, S. G.

Field evaluation of six protective coatings applied to T-56 turbine blades after 2000 hours of engine use [AD-A261112] p 522 N93-21316

RUSTERHOLZ, KENNETH P.

An update on the development of the T407/GLC38 modern technology gas turbine engine [ASME PAPER 92-GT-147] p 351 A93-19375

RUTHERFORD, JOHN W.

Advanced technology Tilt Wing study [AIAA PAPER 92-4237] p 44 A93-13359

Conceptual assessment of two high-speed rotorcraft p 508 A93-28612

Low-speed wind tunnel test results of the Canard Rotor/Wing concept [AIAA PAPER 93-3412] p 975 A93-47209

RUTKOVSKAIA, E. I.

Diagnostics of the hydraulic system of Tu-204 aircraft p 396 A93-18360

RUTKOVSKAIA, Z. I.

Selection of methods and equipment for monitoring the technical condition of booster system components p 395 A93-18329

Characteristics of the diagnostics of booster system components p 321 A93-18361

Monitoring the purity of the working fluids of aircraft hydraulic systems during service p 321 A93-18367

RUTLAND, C. J.

Intake flow modeling in a four stroke diesel using KIVA3 [AIAA PAPER 93-2952] p 1148 A93-48146

RUTLEDGE, CHARLES K.

Acoustic flight test experience with the XV-15 Tiltrotor aircraft with the Advanced Technology Blade (ATB) p 445 A93-19143

A comparative analysis of XV-15 tiltrotor hover test data and WOPWOP predictions incorporating the fountain effect p 509 A93-29414

ADDRAS - An integrated systems approach p 562 A93-29423

RUTOVSKIJ, V. B.

Investigation of flame stabilizers in the form of perforated grids p 1003 A93-47513

RYABOV, V. V.

Investigation of the effect of physical processes on heat transfer to blunt bodies at low Reynolds numbers p 1090 A93-51877

Investigation of the structure of a multicomponent viscous shock layer p 1090 A93-51879

RYALL, KATHLEEN

A graphical user-interface for propulsion system analysis [AIAA PAPER 93-0223] p 440 A93-23699

RYAN, EUGENE

Adaptive control of aircraft in windshear p 62 A93-13126

RYAN, J.

A numerical method for solving Navier-Stokes equations for low Mach number compressible flows p 463 A93-24672

RYAN, JAMES S.

Parallel computation of 3-D Navier-Stokes flowfields for supersonic vehicles [AIAA PAPER 93-0064] p 261 A93-20177

RYAN, STEVE

Arrow 227: Air transport system design simulation [NASA-CR-192053] p 336 N93-18063

- RYCKMAN, J. S., JR.**
AQUIS: A PC-based air quality and permit information system
[DE92-040092] p 434 N93-18587
- RYDAEV, A. I.**
A method for estimating the technico-economic efficiency of measures increasing the reliability of gas turbine engines in service p 54 A93-12822
- RYDEN, R.**
Large eddy simulation of turbulent combustion behind flame holders
[ISABE 93-7042] p 1198 A93-54018
- RYDER, JOAN M.**
The analysis of expert performance in the redesign of the en route air traffic control curriculum p 571 A93-27189
- RYE, J.**
The certification of head up displays for category 3 operation p 142 A93-17304
- RYGE, PETER**
Explosive detection system based on Electronic Neutron Generator (ENG) p 497 N93-21870
- RYL'KOV, V. D.**
A data processing and measuring system with a traversing probe for studying flow in the rotating impeller of an axial-flow fan p 75 A93-10032
- RYLOW, A. I.**
Monotonicity characteristics of some plane vortex flows of incompressible fluids and subsonic gas flows p 13 A93-12932
- RYNASKI, E. G.**
Theoretical constraints in the design of multivariable control systems
[NASA-CR-191900] p 442 N93-18372
- RYO, SHIKO**
Study on the numerical problem of the boundary element method in analysis of flow around a three-dimensional wing-body p 268 A93-20934
- RYZHOV, YU. A.**
Problems in the aerodynamics of flight vehicles and their parts p 1068 A93-48901
Problems in the aerodynamics of flight vehicles and their components p 1091 A93-51901
- RZADKOWSKI, R.**
Two dimensional incompressible flow through a vibrating bladed disc - Theoretical model p 973 A93-46991
- S**
- SAABAS, H. J.**
Prediction of jet impingement cooling scheme characteristics (airfoil leading edge application) p 932 A93-29941
- SABA, COSTANDY S.**
Coking characteristics of polyphenyl ether lubricants using a Static Coker and a Micro Carbon Residue Tester p 77 A93-11341
Ferrographic analysis of polyphenyl ether fluids p 735 A93-34561
- SABAEV, G. V.**
Development of a process for fabricating a plate heat exchanger for the heat recovery system of gas turbine engines p 834 A93-39053
- SABEL'NIKOV, V. A.**
Supersonic combustion and gasdynamic of scramjet p 170 A93-14242
Gasdynamics of hydrogen-fueled scramjet combustors
[AIAA PAPER 93-2145] p 1115 A93-49962
- SABETTA, F.**
Equilibrium and nonequilibrium modeling of hypersonic inviscid flows p 864 A93-42448
Reactive and inert inviscid flow solutions by quasi-linear formulations and shock fitting p 927 A93-42625
- SABHARWAL, DEEPAK**
Design of a rule-based fuzzy controller for the pitch axis of an unmanned research vehicle p 907 A93-42807
- SABROSKE, KELLY R.**
Seeding materials for use in laser anemometry
[AIAA PAPER 93-0006] p 389 A93-20129
- SABSAY, CATHERINE M.**
Pressure distribution for the wing of the YAV-8B airplane; with and without pylons
[NASA-TM-4429] p 136 N93-14451
- SACCO, G.**
Natural laminar flow test in-flight visualization p 482 A93-19921
- SACCO, J. N.**
Measurements in 80- by 120-foot wind tunnel of hazard posed by lift-generated wakes
[AIAA PAPER 93-3518] p 1014 A93-47281
- SACHER, P. W.**
Technology transfer: Potential of BMFT concept for hypersonics
[MBB-LME-202-S-PUB-0505] p 1041 N93-31045
- SACHS, GOTTFRIED**
Robust control of the separation of hypersonic lifting vehicles
[AIAA PAPER 92-5013] p 385 A93-22289
Optimization of endurance performance p 713 A93-34400
Enhancement of endurance performance by periodic optimal camber control p 727 A93-34541
Periodic maximum range cruise with singular control p 890 A93-41903
- SACHS, WERNER**
DeAs - A programming system for data processing and system control: New software developments for wind tunnel operation p 1036 A93-44452
On flutter behavior of a 2-D compressor cascade in incompressible flow [DLR-FB-91-26] p 418 N93-16543
- SADEKOVA, G. S.**
Aerodynamic characteristics of a sweptforward-wing aircraft model in unsteady motion at large angles of attack in subsonic flow p 1068 A93-48902
Interference between a high-lift sweptforward wing and the horizontal nose plane at subsonic velocities p 1135 A93-51906
- SADLER, G.**
The Royal Air Force experience of artificial intelligence aircraft maintenance p 435 A93-18764
- SADREHAGHIGHI, I.**
Grid sensitivity for aerodynamic optimization and flow analysis
[NASA-CR-192980] p 694 N93-25117
- SADREHAGHIGHI, IDEEN**
Grid and design variables sensitivity analyses for NACA four-digit wing-sections
[AIAA PAPER 93-0195] p 276 A93-22616
Grid and aerodynamic sensitivity analyses of airplane components
[AIAA PAPER 93-3475] p 981 A93-47254
- SAFARIK, P.**
Boundary layer effects on the transonic flow in a straight turbine cascade
[ASME PAPER 92-GT-155] p 249 A93-19382
- SAFRONOV, EH. D.**
Formulas for determining the induced velocity in the direct and inverse rotor problems p 1071 A93-49324
- SAGER, J.**
Innovative high temperature aircraft engine fuel nozzle design
[ASME PAPER 92-GT-132] p 350 A93-19365
- SAGGIANI, G. M.**
Parametric aeroelastic analysis of composite wing-boxes with active strain-energy tuning p 156 A93-14361
- SAGGU, J. S.**
Integration of aircraft design and manufacture using artificial intelligence paradigms p 225 A93-14202
- SAHA, T. T.**
Optical technologies for UV remote sensing instruments p 853 N93-28788
- SAIAPIN, G. N.**
Numerical modeling of ionization in nonequilibrium nitrogen flows in hypersonic nozzles p 836 A93-39137
- SAIDA, N.**
Formation of shock waves in transient base flow p 1023 A93-45460
- SAIF, MEHRDAD**
Reduced order proportional integral observer with application p 1166 A93-49605
A new approach to robust fault detection and identification p 1166 A93-50631
- SAIKI, NEAL**
Effects of an aft facing step on the surface of a laminar flow glider wing
[NASA-CR-193302] p 990 N93-31855
- SAILLOT, P.**
Supersonic transport: Which material for the engine [DS-2023] p 522 N93-21459
- SAITO, AKIRA**
LIF visualization of 3-dimensional hypersonic mixing
[ISABE 93-7114] p 1221 A93-54089
- SAITO, D.**
Evaluation of metallurgical degradation on gas turbine components p 915 A93-40804
- SAITO, DAIZO**
Life assessment of gas turbine bucket coating based on degradation analysis p 533 A93-24464
- SAITO, MASAKI**
Wind tunnel investigation of a twin-engine jet transport semi-span model with upper surface blown jet flap [NAL-TR-1134] p 26 N93-12503
- SAITO, SHIGERU**
Numerical analysis of three-dimensional viscous flows around an advanced counterrotating propeller p 112 A93-14165
Unsteady analysis of helicopter rotor p 770 A93-38193
- Numerical simulation of the flow through non-uniform airfoil cascade p 302 N93-19310
- SAITO, TERUO**
Preliminary assessment of tunnel wall interference in the NDA cryogenic wind tunnel
[AIAA PAPER 93-0421] p 285 A93-23340
- SAITO, TORU**
Application of functionally gradient materials to scramjet engines
[ISABE 93-7063] p 1200 A93-54039
- SAITO, TOSHIHITO**
Application of functionally gradient materials to scramjet engines
[ISABE 93-7063] p 1200 A93-54039
- SAITO, Y.**
Navy-Stokes computation of the three dimensional flow fields through a transonic fan blade
[ISABE 93-7030] p 1184 A93-54006
- SAJBEN, MIKLOS**
Uncertainty estimates for pressure sensitive paint measurements p 1258 A93-55369
- SAKAGAWA, KEIJI**
Three-dimensional viscous flow analysis of compressor cascade channels p 1181 A93-53837
- SAKAGUCHI, HAJIME**
Two-dimensional cascade tests of MCA blades in the high transonic Mach number region. V - Effect of space/chord ratio on the parameters of cascade performance p 267 A93-20930
Air ejector experiments using the two-dimensional supersonic cascade tunnel: Relationship between ejector performance and throat area ratio, part 1 [NAL-TM-642-PT-1] p 25 N93-12352
- SAKAI, KENJI**
Wind tunnel test and CFD in Kawasaki Heavy Industries, Gifu p 304 A93-19324
- SAKAI, TETSU**
Analysis of a 2-D airfoil motion flying in-proximity-to a wavy-wall surface: Lifting-surface-method p 300 N93-19281
Analysis of a 2-D airfoil motion flying in-proximity-to a wavy-wall surface: Finite difference method p 300 N93-19282
- SAKAKIBARA, HITOSHI**
Structure of downbursts associated with heavy rainfall observed in Tokyo p 433 A93-22200
- SAKAMOTO, AKIRA**
Status of R&D of high-performance materials for severe environments (Composite materials) p 1253 A93-54728
- SAKAMOTO, ATSUSHIRO**
Numerical calculation of separated flows around wing section in unsteady motion by using incompressible Navier-Stokes equations p 770 A93-38158
Numerical calculations of separating flows around oscillating airfoil p 300 N93-19284
- SAKAMOTO, HIROSHI**
Transitional characteristics of vortices issued from a body which creates asymmetric flow field - In a case of thin symmetrical airfoil with angle of attack under rotational oscillation of small amplitude p 267 A93-20923
- SAKAMOTO, KAZUYUKI**
An experimental study of supersonic air-intake with 5-shock system at Mach 3
[AIAA PAPER 93-2305] p 1082 A93-50089
- SAKAMOTO, YOSHINORI**
The operating system for Numerical Wind Tunnel p 383 N93-19290
- SAKAMURA, YOSHITAKA**
VSL analysis of nonequilibrium flows around a hypersonic body p 769 A93-38146
- SAKATA, KIMIO**
Some topics of research on hypersonic airbreathing engines at National Aerospace Laboratory
[ASME PAPER 92-GT-256] p 353 A93-19465
Experimental study of mixed compression air-intake for hypersonic airbreathing engines
[ASME PAPER 92-GT-349] p 355 A93-19519
Effects of boundary layer bleed on swept-shock/boundary layer interaction
[AIAA PAPER 93-2989] p 1052 A93-48182
An experimental study of supersonic air-intake with 5-shock system at Mach 3
[AIAA PAPER 93-2305] p 1082 A93-50089
Two-dimensional numerical simulation for Mach-3 multishock air-intake with bleed systems
[AIAA PAPER 93-2306] p 1082 A93-50090
Wind tunnel tests of the model of intake-airframe integration
[ISABE 93-7101] p 1192 A93-54077
A study on Mach 3 two-dimensional mixed compression air-intakes
[ISABE 93-7106] p 1188 A93-54082

SAKAUE, TADASHI

Preliminary assessment of tunnel wall interference in the NDA cryogenic wind tunnel
[AIAA PAPER 93-0421] p 285 A93-23340

SAKELL, LEONIDAS

The status of CFD - An Air Force perspective
[AIAA PAPER 93-3293] p 1021 A93-44997

SAKOWSKI, BARBARA

Evaluation and application of the Baldwin-Lomax turbulence model in two-dimensional, unsteady, compressible boundary layers with and without separation in engine inlets
[AIAA PAPER 92-3676] p 111 A93-14118

Evaluation and application of the Baldwin-Lomax turbulence model in two-dimensional, unsteady, compressible boundary layers with and without separation in engine inlets
[AIAA PAPER 92-3676] p 414 A93-22509

Evaluation and application of the Baldwin-Lomax turbulence model in two-dimensional, unsteady, compressible boundary layers with and without separation in engine inlets
[NASA-TM-105810] p 82 N93-10087

SAKURANAKA, NOBORU

Application of functionally gradient materials to scramjet engines
[ISABE 93-7063] p 1200 A93-54039

SAKYA, ANDI E.

Evaluation of an RNG-based algebraic turbulence model
p 863 A93-42436

SAKYA, ANDI EKA

Transonic flow calculation around NACA-0012
p 302 N93-19301

SALAS, JUAN

Development of a non-linear simulation for generic hypersonic vehicles - ASUHS1
[NASA-CR-192710] p 516 N93-22003

SALAY, C. R.

Matching engine and aircraft lapse rates for the HSCT
[AIAA PAPER 93-1809] p 1100 A93-49698

SALAZAR, LYDIA R.

Results from a GPS Shuttle Training Aircraft flight test
p 384 A93-21148

SALAZAR, MICHAEL E.

Aerodynamic characteristics of the MMPT ATD vehicle at high angles of attack
[AIAA PAPER 93-3493] p 982 A93-47265

SALEMI, R.

The effect of orthogonal-mode rotation on forced convection in a circular-sectioned tube fitted with full circumferential transverse ribs
p 932 N93-29937

SALIKUDDIN, M.

Unsteady pressures on exhaust nozzle interior surfaces - Empirical correlations for prediction
p 244 A93-19219

SALIVERO, E.

An examination of vortex convection effects during blade-vortex interaction
p 473 A93-25360

SALMAN, AHMED A.

Prediction and control of slender-wing rock
p 182 A93-14331

SALMINEN, ESA

Numerical investigations into the base drag of various wedges using the base flow model developed by Mauri Tanner
[REPT-B-36] p 26 N93-12414

SALMON, ROBERT F.

Aircraft wing compartment liner concept to reduce fuel spillage
[DOT/FAA/CT-TN92/34] p 331 N93-17219

SALOV, N. N.

A study of heat transfer from a disk in a rotating cavity with axial and radial-axial flow of a liquid
p 54 A93-12812

SALTAIS, E. A.

A fuel-oil matrix heat exchanger
p 833 A93-39052

SALTHOUSE, ROBERT W.

Making clean gasoline: The effect on jet fuels
[AD-A264302] p 1019 N93-32085

SALTZMAN, EDWIN J.

Pressure distribution for the wing of the YAV-8B airplane; with and without pylons
[NASA-TM-4429] p 136 N93-14451

SALTZMAN, JOHN A.

In-flight flow visualization results from the X-29A aircraft at high angles of attack
[AIAA PAPER 92-4102] p 38 A93-11272

In-flight flow visualization results from the X-29A aircraft at high angles of attack
[NASA-TM-4430] p 131 N93-13322

SALVA MONFORT, J. J.

Control of contaminants in gas turbines with variable-flow combustion chambers and hydrogen addition
p 520 A93-27478

SALVETTI, MARIA VITTORIA

Influence of the physical modelling of viscous terms on hypersonic flow computations
[INRIA-RR-1493] p 297 N93-18652

SALVINO, J. T.

Lightweight aircraft turbine protection
[AIAA PAPER 93-1815] p 1110 A93-49703

SAMANIEGO, J. M.

Low-frequency combustion instability mechanisms in a side-dump combustor
p 1247 A93-55220

Combustion instabilities in a side-dump model ramjet combustor
p 362 N93-17613

SAMAREH-ABOLHASSANI, JAMSHID

Unstructured grids on NURBS surfaces
[AIAA PAPER 93-3454] p 949 A93-44232

SAMARKINA, T. V.

Numerical simulation of aerothermodynamics processes in gas turbine engine components
p 1002 A93-46939

SAMAVEDAM, G.

Test facility for evaluation of structural integrity of stiffened and jointed aircraft curved panels
p 1012 A93-45794

Three-dimensional stress analysis of multilayered airport pavements: Integral transform approach
p 381 N93-16319

SAMEJIMA, M.

A numerical simulation of a scram jet combustor flow
p 810 A93-38181

SAMIMY, MO

The effect of expansion on the large scale structure of a compressible turbulent boundary layer
[AIAA PAPER 93-2991] p 1052 A93-48183

SAMOKHIN, V. F.

An approach to the calculation of the far acoustic field of a propeller
p 1124 A93-51760

SAMPATH, K. S.

Operation of the helicopter antenna radiation prediction code
[NASA-CR-193259] p 1030 N93-31110

SAMPATH, S.

Estimation of requirements of inspection intervals for panels susceptible to Multiple Site Damage
p 948 A93-45795

SAMPATH, SAM G.

Structural integrity of aging airplanes
[ISBN 0-540-53461-X] p 947 A93-45772

SAMSUNDAR, JOHN

Closed form solutions of constrained trajectories - Application in optimal ascent of aerospace plane
[AIAA PAPER 92-5012] p 385 A93-22288

SAMUELSEN, G. S.

Coherent anti-Stokes Raman scattering (CARS) thermometry in a model gas turbine can combustor
[ASME PAPER 92-GT-134] p 387 A93-19366

Scaling of the two-phase flow downstream of a gas turbine combustor swirl cup - Mean quantities
[ASME PAPER 92-GT-207] p 404 A93-19431

Development of an optical sensor for active control of a gas turbine combustor
[AIAA PAPER 93-0118] p 360 A93-22568

CARS thermometry in a liquid fueled model combustor
[AIAA PAPER 93-0366] p 390 A93-23047

Optimization of circular orifice jets mixing into a heated crossflow in a cylindrical duct
[AIAA PAPER 93-0249] p 361 A93-23246

Mixing in the dome region of a staged gas turbine combustor
p 1109 A93-49612

Correlation of droplet behavior with gas-phase structures in a gas turbine combustor
[AIAA PAPER 93-1767] p 1152 A93-49663

Emission characteristics of a model gas turbine combustor at practical conditions
[ISABE 93-7023] p 1196 A93-53999

Optimization of circular orifice jets mixing into a heated cross flow in a cylindrical duct
[NASA-TM-105984] p 179 N93-15359

Fuel injector: Air swirl characterization aerothermal modeling, phase 2, volume 1
[NASA-CR-189193-VOL-1] p 721 N93-24754

SAMUELSON, G. S.

Fuel Injector: Air swirl characterization aerothermal modeling, phase 2, volume 2
[NASA-CR-189193-VOL-2] p 721 N93-25106

SAMUELSSON, A.

The finite element method in the 1990's
[ISBN 0-387-54930-7] p 925 A93-40823

SAND, W. R.

The FAA aircraft icing Forecasting Improvement Program - Validation of aircraft icing forecasts in the Denver area
[AIAA PAPER 93-0393] p 309 A93-23069

SAND, WAYNE R.

A proposed icing severity index based upon meteorology
p 429 A93-22136

SANDEMAN, R. J.

Absolute intensity measurements of impurity emissions in a shock tunnel and their consequences for laser-induced fluorescence experiments
p 1147 A93-48044

SANDERS, DONALD C.

Comparison of toxicity rankings of six aircraft cabin polymers by lethality and by incapacitation in rats
p 26 A93-10328

SANDERS, RICHARD

A hybrid multigrid technique for computing steady-state solutions to supersonic flows
p 700 N93-26078

SANDERSON, S.

Performance data of the new free-piston shock tunnel T5 at GALTIT
p 1011 A93-45498

SANDLIN, DORAL R.

Aerodynamic analysis of hypersonic waverider aircraft
[NASA-CR-192981] p 780 N93-27093

Effects of an aft facing step on the surface of a laminar flow glider wing
[NASA-CR-193302] p 990 N93-31855

SANDSTROM, TIMOTHY A.

Scientific visualization using the Flow Analysis Software Toolkit (FAST)
p 758 N93-25600

SANETRIK, MARK D.

Development of a flexible and efficient multigrid-based multiblock flow solver
[AIAA PAPER 93-0677] p 269 A93-21117

A multiblock, multigrid solution procedure for multielement airfoils
p 967 A93-46812

SANGCHAT, S.

Results from a GPS Shuttle Training Aircraft flight test
p 384 A93-21148

SANGIOVANNI, J. J.

Role of hydrogen/air chemistry in nozzle performance for a hypersonic propulsion system
p 359 A93-21668

SANIEL, NADER

Investigation of nacelle upper cowl flow separation using on- and off-body flow visualization techniques
p 1072 A93-49507

SANKAR, L. N.

Effects of icing on the aerodynamic performance of high lift airfoils
[AIAA PAPER 93-0026] p 259 A93-20144

A third order upwind scheme for aero-acoustic applications
[AIAA PAPER 93-0149] p 564 A93-25504

Simulation of unsteady rotational flow over propfan configuration
[NASA-CR-192234] p 296 N93-18585

SANKAR, LAKSHMI N.

Numerical simulation of dynamic lift enhancement using oscillatory leading edge flaps
[AIAA PAPER 93-0186] p 276 A93-22611

Viscous flow computations of flow field around an advanced propeller
[AIAA PAPER 93-0873] p 469 A93-24934

Efficient hybrid scheme for the analysis of counter-rotating propellers
p 688 A93-34483

Numerical simulation of incompressible viscous flow around a propeller
[AIAA PAPER 93-3503] p 984 A93-47271

Three-dimensional Navier-Stokes/full-potential coupled analysis for viscous transonic flow
p 1178 A93-53218

Numerical investigation of performance degradation of wings and rotors due to icing
[NASA-CR-192233] p 339 N93-18783

SANKAR, T. S.

A design study on the effect of support and system parameters on the natural frequencies of rotor systems
p 210 A93-16374

Stochastic finite element analysis for high speed rotors
p 554 A93-20696

SANNIKOV, V. A.

Optimizing the cruising fuel efficiency of commercial aircraft on the basis of flight manual data
p 321 A93-18351

SANNIKOV, VLADIMIR A.

Aerodynamic questions related to the safety and cost-effective utilization of airships
p 818 A93-39125

SANO, MANABU

Dynamic characteristics of an airfoil at high speed change of pitch angle
p 10 A93-12324

SANSARTIER, GILLES

Weather forecasts for aviation in Canada (FACN and FTCN) - The way they are taught and how they can be made more suitable to the needs of pilots
p 454 A93-22108

SANSOM, RUSSELL

A radar altitude and line of sight attachment
[AIAA PAPER 93-3587] p 1223 A93-52680

SANTINI, P.

Parametric aeroelastic analysis of composite wing-boxes with active strain-energy tuning
p 156 A93-14361

SANTO-TOMAS, J.

Aerodynamic characteristics of transport airplanes in low speed configuration
p 113 A93-14172

- SANTORIello, G.**
A Navier-Stokes solver with different turbulence models applied to film-cooled turbine cascades p 904 N93-29962
- SANZ, J.**
The engine design engine. A clustered computer platform for the aerodynamic inverse design and analysis of a full engine [NASA-TM-105838] p 21 N93-11223
- SANZ, JOSE M.**
Aerodynamic inverse design and analysis for a full engine [ISABE 93-7086] p 1186 A93-54062
- SAPLIN, STEVEN K.**
Integrated Blade Inspection System (IBIS) upgrade study [AD-A258912] p 365 N93-19356
- SAPORITI, A.**
Application of European CFD methods for helicopter rotors in forward flight [ONERA, TP NO. 1992-125] p 772 A93-38599
- SARAF, C. L.**
State of the art review of rutting and cracking in pavements p 380 N93-16316
- SARANTOPOULOS, ATHAN D.**
Modeling of linear isentropic flow systems p 828 A93-37046
- SARATHY, S.**
Parallel rotorcraft flight simulation [AIAA PAPER 93-0623] p 524 A93-24740
An advanced parallel rotorcraft flight simulation model - Stability characteristics and handling qualities [AIAA PAPER 93-3618] p 1125 A93-48305
An advanced rotorcraft flight simulation model - Parallel implementation and performance analysis [AIAA PAPER 93-3550] p 1222 A93-52654
- SAREEN, ASHISH K.**
Application of a two-point exponential approximation method in optimizing rotorcraft airframe structures p 507 A93-27956
- SARIC, W. S.**
Experiments on swept-wing boundary-layer transition p 419 N93-16829
- SARIC, WILLIAM S.**
A high-frequency, secondary instability of crossflow vortices that leads to transition p 128 A93-17253
Effect of micron-sized roughness on transition in swept-wing flows [AIAA PAPER 93-0076] p 262 A93-20188
- SARIGUL-KLIJN, MARTI M.**
Application of two chaos methods to Higher Harmonic Control data p 909 A93-43783
- SARIGUL-KLIJN, NESRIN**
On the coupled thermomechanical analysis of hypersonic flight vehicle structures [AIAA PAPER 92-5018] p 413 A93-22294
- SARLIN, P.**
The development of a crashworthy composite fuselage and landing gear p 799 A93-36001
- SARPKAYA, T.**
Interaction of a streamwise vortex with a free surface [AIAA PAPER 93-0556] p 543 A93-25539
- SARRAF, DAVID B.**
A thermal analysis of an F/A-18 wing section for actuator thermal management [SAE PAPER 921023] p 158 A93-14650
- SASA, SHUICHI**
Simulation analysis of a cable-mount system used for dynamic wind tunnel tests [NAL-TR-1127] p 68 N93-12359
Accuracy improvement of linear estimated motion using differential type sensors [NAL-TR-1135] p 91 N93-12365
- SASAHARA, O.**
Various applications of robots in aircraft engine overhaul [ISABE 93-7129] p 1175 A93-54104
- SASAKI, ATSUSHI**
A new technique for analysis of unsteady aerodynamic responses of cascade airfoils with blunt leading edge - Unsteady aerodynamic responses of the cascade in incompressible flow p 1086 A93-51122
- SASAKI, SHIGERU**
Minimum time turn of a helicopter p 1248 A93-54554
- SASAKI, Y.**
Conceptual design of turbo-accelerator for HST combined cycle engine [ASME PAPER 92-GT-253] p 353 A93-19462
- SASOH, A.**
Radiative heat transfer from non-equilibrium high-enthalpy shock layers p 1024 A93-45515
- SASOH, AKIHIRO**
Numerical study on atom-molecule radiation flowfield around a hypersonic blunt body p 770 A93-38434
- SATAKE, MASATO**
Numerical prediction of aerodynamic sound using large eddy simulation p 850 A93-38150
- SATHE, A. B.**
The onset of disintegration and corona in water drops falling at terminal velocity in horizontal electric fields p 1163 A93-49130
- SATHYAMOORTHY, M.**
Structural analysis of box beams using symbolic manipulation technique p 548 A93-28615
- SATO, JUNZO**
Effect of wing planforms on induced drag reduction p 127 A93-16932
- SATO, KIYOSHI**
Intense studies on unsteady secondary separations and oscillating shock waves in three-dimensional shock waves/turbulent boundary layer interaction regions induced by sharp and blunt fins [AIAA PAPER 93-2939] p 1046 A93-48137
- SATO, MAMORU**
Flow visualization studies on sidewall effects in two dimensional transonic airfoil testing [AIAA PAPER 93-0090] p 263 A93-20196
- SATO, MASASHI**
Measurement technique for Loran-C pulse wave detection measures and performance in an environment of noise p 29 A93-10988
- SATO, N.**
Polar Patrol Balloon Experiment in Antarctica p 27 A93-11373
- SATO, SHIGERU**
Evaluation of 2D scramjet nozzle performance p 52 A93-11209
Validation studies of scramjet nozzle performance p 1109 A93-49616
Off-design performance of scramjet nozzles [ISABE 93-7108] p 1203 A93-54084
- SATO, TETSUYA**
Study on steady and unsteady unstart phenomena due to compound choking and/or fluctuations in combustor of scramjet engines [AIAA PAPER 92-5102] p 359 A93-22372
Development study on Air Turbo Ramjet engine for a future space plane [ISABE 93-7016] p 1195 A93-53992
Study on unstart and its propagation along modules due to compound choking and/or fluctuations in combustor of scramjet engines [ISABE 93-7052] p 1199 A93-54028
- SATOFUKA, NOBUYUKI**
Numerical analysis for chemically non-equilibrium flow p 770 A93-38148
Numerical solution of viscous compressible flows using algebraic turbulence models p 770 A93-38162
- SATONAKA, KAZUYA**
Limit of sampling periods for nonlinear flight trajectory controller of aircraft p 61 A93-11207
- SATTA, A.**
Low area ratio aircraft fuel jet-pump performances with and without cavitation p 272 A93-22264
- SATTERTHWAITE, CHARLES P.**
Getting a handle on designing for avionics software supportability and maintainability p 941 A93-42862
- SAUERLAND, K. H.**
Time-dependent 3-component laser-Doppler-anemometer and simultaneous position measurements in the flow of an aircraft engine p 538 A93-23809
- SAUNDERS, PENNY E.**
Results from a GPS Shuttle Training Aircraft flight test p 384 A93-21148
- SAUREL, R.**
A comparison between centered and upwind schemes for two-phase compressible flows [AIAA PAPER 93-2346] p 1083 A93-50120
- SAUTNER, M.**
Determination of surface heat transfer and film cooling effectiveness in unsteady wake flow conditions p 902 N93-29933
- SAVEL'EV, I. U. P.**
Hydrodynamics and heat transfer near the stagnation point in an arbitrary axisymmetric nonswirling flow incident on a rotating obstacle p 691 A93-35270
- SAVENKOV, I. V.**
Viscous instability of hypersonic flow past a wedge p 4 A93-10137
- SAVILLE, MARSHALL**
Liquid hydrogen foil-bearing turbopump [AIAA PAPER 93-2537] p 1156 A93-50264
- SAVIN, N. M.**
Direct and inverse problems of calculating the axisymmetric and 3D flow in axial compressor blade rows p 972 A93-46938
- SAVINI, M.**
Secondary flows in a transonic cascade - Validation of a 3-D Navier-Stokes code [ASME PAPER 92-GT-62] p 247 A93-19312
A Navier-Stokes solver with different turbulence models applied to film-cooled turbine cascades p 904 N93-29962
- SAVINOV, A. P.**
Some characteristics of the design of heads for the cutting of bevel gears with negative curvature of the circular-arc tooth line p 835 A93-39093
- SAWA, ZDZISLAW P.**
PFNA technique for the detection of explosives p 497 N93-21865
- SAWADA, F.**
The properties of newly developed highly damage tolerant and easy handleable carbon fiber/modified bismaleimide prepreg system p 1212 A93-53448
- SAWADA, HIDEO**
Wind tunnel wall interference correction at subsonic speeds p 304 N93-19320
- SAWADA, KEISUKE**
Domain splitting explicit time marching scheme for simulation of unsteady high Reynolds number flow p 830 A93-38140
Three dimensional calculation of flow inside supersonic inlet p 303 N93-19313
- SAWADA, TERUO**
Development of a boundary element method program for numerical analysis of supersonic unsteady flow p 300 N93-19283
- SAWAE, M.**
Blade loading and shock wave in a transonic circular cascade diffuser [ASME PAPER 92-GT-34] p 246 A93-19294
- SAWAE, MASAYUKI**
Blade loading of transonic circular cascade diffuser p 267 A93-20919
- SAWYER, BRIAN M.**
Rotorcraft on route ATC route standards [AD-A249129] p 35 N93-10323
- SAWYER, WALLACE C.**
Advanced cargo aircraft may offer a potential renaissance in freight transportation p 991 A93-47023
- SAXENA, ASHOK**
Deformation mechanisms of NiAl cyclicly deformed near the brittle-to-ductile transformation temperature [NASA-CR-191649] p 391 N93-15830
- SAXENA, S. K.**
An upwind formulation for the solution of thin-layer Navier-Stokes equations p 461 A93-24088
- SAYADYAN, K. G.**
Minimizing the wall effects in wind tunnels with a sectional pressure chamber p 1085 A93-50965
- SAYLES, G. D.**
In-situ bioventing: Two US EPA and Air Force sponsored field studies [PB93-194231] p 1035 N93-32089
- SAZONOV, M. B.**
Increasing the durability of gas turbine engine compressor blades by using a combined hardening/finishing treatment to control the stressed state of the surface layer p 835 A93-39099
- SAZONOV, V. V.**
The representation of the aerodynamic torque in simulations of a spacecraft rotary motion p 1141 A93-48835
- SCAFARO, S.**
The role of fatigue testing in the design, development and certification of the ATR 42/72 p 46 A93-13637
- SCALA, C. M.**
Elastic constants for unidirectional boron-epoxy composites p 387 A93-18636
- SCALLION, WILLIAM I.**
Langley proposed advanced hypervelocity aerophysics facility - A status report p 1013 A93-47015
- SCANLON, TIMOTHY J.**
The application of human factors engineering at General Electric Aircraft Engines [SAE PAPER 921039] p 108 A93-14659
- SCANU, T.**
Corrosion of ceramic matrix composites [ONERA, TP NO. 1993-82] p 1213 A93-53602
- SCARDELLO, MICHAEL A.**
Real-time capture, archiving, retrieval, processing, and presentation of large quantities of flight test/research information [AIAA PAPER 92-4073] p 95 A93-11258
- SCAVUZZO, R. J.**
Impact ice interface shear stresses caused by blade bending and twisting [AIAA PAPER 93-0030] p 307 A93-20147
- SCHABER, V.**
Prediction of three-dimensional low frequency unsteady transonic flow and forced vibration in axial turbine stages p 971 A93-46934

SCHACHT, NORMAN

SR-SCARLET 1: Peregrin
[NASA-CR-192048] p 337 N93-18155

SCHADOW, K. C.

Effect of nozzle design on near acoustic field of supersonic circular and rectangular jets p 448 A93-19203

Combustion characteristics and passive control of an annular dump combustor
[AIAA PAPER 93-1772] p 1110 A93-49668

Periodic chemical energy release for active combustion control
[ISABE 93-7043] p 1198 A93-54019

SCHADOW, KLAUS C.

Recent progress in the implementation of active combustion control p 171 A93-14272

Passive control of coherent vortices in compressible mixing layers
[AIAA PAPER 93-3262] p 968 A93-46828

SCHAEFER, O.

Use of advanced CFD codes in the turbomachinery design process
[ASME PAPER 92-GT-324] p 256 A93-19508

SCHAEFFER, J. C.

Isothermal oxidation behavior of alpha-2 titanium aluminide alloys p 535 A93-29563

SCHAFER, DAVID

Automatic detection of explosives using x ray imaging p 880 N93-30275

SCHAFFRANEK, D.

A simulator study into low speed longitudinal handling qualities of ACT transport aircraft
[NLR-TP-89387-U] p 527 N93-20743

SCHAMLE, MARC F.

Methodology for integration of digital control loaders in aircraft simulators
[AIAA PAPER 93-3551] p 1207 A93-52655

SCHARRER, J. K.

The effects of fixed rotor tilt on the rotordynamic coefficients of incompressible flow annular seals p 1161 A93-52601

SCHARTON, TERRY D.

Dual control vibration tests of flight hardware p 545 A93-27782

SCHAUB, U. W.

Effect of nozzle design on the performance of a highly loaded turbine stage
[ISABE 93-7096] p 1203 A93-54072

SCHERER, KLAUS J.

Responsibility and assignment of roles on overlong flights p 570 A93-24253

SCHIED, J.

Measurements of jet aircraft emissions at cruise altitude. I - The odd-nitrogen gases NO, NO₂, HNO₂ and HNO₃ p 556 A93-24391

SCHIEK, J. T.

Operation of the helicopter antenna radiation prediction code
[NASA-CR-193259] p 1030 N93-31110

SCHENK, AXEL

Rigid body mode identification of the PAH-2 helicopter using the eigensystem realization algorithm
[NASA-TM-107690] p 88 N93-11544

SCHERBAUM, R.-D.

A novel-high-performance system for recording and analysing instantaneous total pressure distortion in air intakes p 214 N93-13215

SCHERER, T.

Heat transfer and leakage in high-speed rotating stepped labyrinth seals p 903 N93-29951

SCHERGER, CHAD

A manned hypersonic reconnaissance vehicle which does not require airborne fueling p 333 N93-17888

SCHERR, STEPHEN

Implementation of an explicit Navier-Stokes algorithm on a distributed memory parallel computer
[AIAA PAPER 93-0063] p 261 A93-20176

SCHETZ, J. A.

Recent advances in simulating unsteady flow phenomena brought about by passage of shock waves in a linear turbine cascade
[ASME PAPER 92-GT-4] p 245 A93-19277

Direct measurements of skin friction in supersonic combustion flow fields
[ASME PAPER 92-GT-320] p 405 A93-19506

Direct measurements of skin friction in a scramjet combustor
[AIAA PAPER 93-2443] p 1119 A93-50195

Direct measurements of skin friction in supersonic combustion flow fields
[AD-A262878] p 825 N93-28226

SCHETZ, JOSEPH A.

Penetration and mixing of bubbling liquid jets from multiple injectors normal to a supersonic air stream
[AIAA PAPER 92-5060] p 413 A93-22330

Compressible turbulence measurements in a high-speed

high Reynolds number mixing layer
[AIAA PAPER 93-0660] p 465 A93-24773

Experimental and numerical study of transonic turbine cascade flow
[AIAA PAPER 93-3064] p 1059 A93-48240

SCHICKEL, KLAUS-PETER

Identification of icing water clouds by NOAA AVHRR satellite data
[DLR-FB-92-11] p 434 N93-16477

SCHIERENBECK, DETLEF

Aeroelastic investigations as applied to Airbus airplanes p 155 A93-14280

SCHIERMAN, JOHN D.

Analysis of airframe and engine control interactions and integrated flight/propulsion control p 185 A93-14596

A comparative study of multivariable robustness analysis methods as applied to integrated flight and propulsion control
[AIAA PAPER 93-3809] p 1102 A93-51401

SCHIFF, L. B.

Lateral control at high angles of attack using pneumatic blowing through a chined forebody
[AIAA PAPER 93-3624] p 1126 A93-48309

SCHIFF, LEWIS B.

Computational investigation of a pneumatic forebody flow control concept p 768 A93-37383

Navier-Stokes prediction of a delta wing in roll with vortex breakdown
[AIAA PAPER 93-3495] p 983 A93-47267

Effect of forebody tangential slot blowing on flow about a full aircraft geometry
[AIAA PAPER 93-2962] p 1048 A93-48156

SCHIJVE, J.

Bulging of fatigue cracks in a pressurized aircraft fuselage p 81 A93-13639

SCHILLING, LAWRENCE J.

Flight research simulation takes off p 1192 A93-53769

SCHILLING, V. K.

Motion and decay of trailing vortices within the atmospheric surface layer p 425 A93-18548

SCHIMKE, DIETER

Mission oriented investigation of handling qualities through simulation
[MBB-UD-0600-91-PUB] p 332 N93-17567

SCHIMKE, SUE

Recent progress in the analysis of iced airfoils and wings p 784 A93-27441

SCHINDEL, LEON H.

Characterization of the performance of shock-tube wind tunnels
[AIAA PAPER 93-0351] p 377 A93-23036

SCHIPHOLT, G. J.

Investigation of methods for modeling propeller-induced flow fields
[AIAA PAPER 93-0874] p 469 A93-24935

SCHIPPER, BRIAN

Differential GPS/inertial navigation approach/landing flight test results p 32 A93-11019

SCHKOLNIK, GERALD S.

Identification of integrated airframe-propulsion effects on an F-15 aircraft for application to drag minimization
[AIAA PAPER 93-3764] p 1101 A93-51359

SCHLAGER, H.

Measurements of jet aircraft emissions at cruise altitude. I - The odd-nitrogen gases NO, NO₂, HNO₂ and HNO₃ p 556 A93-24391

SCHLAM, ELLIOTT

High-resolution displays and projection systems; Proceedings of the Meeting, San Jose, CA, Feb. 11, 12, 1992
[SPIE-1664] p 544 A93-27237

SCHLECHTRIEM, S.

Free-wake computation of helicopter rotor flowfields in forward flight
[AIAA PAPER 93-3079] p 1059 A93-48253

SCHMID, RONALD

Air transport within the European single market - How will it look after 1992? A suggested view on the future p 104 A93-13424

SCHMID, SCOTT J.

Analysis of the effect of surface heating on boundary layer development over an NLS-0215 airfoil
[AIAA PAPER 93-3437] p 978 A93-47229

SCHMIDT, B.

Formation of the shock reflection on a wedge p 1023 A93-45476

SCHMIDT, BERND

Results about the structure of the shock wave reflection process for strong incoming shock waves p 1233 A93-54810

SCHMIDT, DAVID K.

Analysis of airframe and engine control interactions and integrated flight/propulsion control p 185 A93-14596

Dynamics of hypersonic flight vehicles exhibiting significant aeroelastic and aeropropulsive interactions
[AIAA PAPER 93-3763] p 1131 A93-51358

A comparative study of multivariable robustness analysis methods as applied to integrated flight and propulsion control
[AIAA PAPER 93-3809] p 1102 A93-51401

Modeling and model simplification of aeroelastic vehicles: An overview
[NASA-TM-107691] p 64 N93-12216

Development of a non-linear simulation for generic hypersonic vehicles - ASUHS1
[NASA-CR-192710] p 516 N93-22003

Generic hypersonic vehicle performance model
[NASA-CR-192953] p 714 N93-25162

SCHMIDT, DEAN C.

Lift enhancement using a close-coupled oscillating canard
[AD-A257877] p 296 N93-18336

SCHMIDT, H.-J.

Evaluation methodologies applied for pressurized fuselages of Airbus A/C p 948 A93-45796

SCHMIDT, K.-J.

Some experiments and ideas on GPA before reaching steady state of engine p 178 N93-15175

SCHMIDT, LOUIS V.

Wind-tunnel tests of an inclined cylinder having helical grooves
[AIAA PAPER 93-3456] p 979 A93-47239

SCHMIDT, MATTHIAS

Definition of an airfoil family for the EUROFAR rotor
[DLR-FB-92-04] p 998 N93-31197

SCHMIDT, PHILLIP H.

Application of controller partitioning optimization procedure to integrated flight/propulsion control design for a STOVL aircraft
[AIAA PAPER 93-3766] p 1131 A93-51361

A parameter optimization approach to controller partitioning for integrated flight/propulsion control application p 1206 A93-54268

SCHMIDT, VERN

Aerospace '92 - The year in review p 455 A93-19976

SCHMIDTKE, KLAUS

Development of cure cycles: From laboratory analysis and testing to production of large scale composites
[MBB-Z-0442-92-PUB] p 536 N93-20845

SCHMIT, L. A.

Integrated structure/control/aerodynamic synthesis of actively controlled composite wings p 818 A93-37392

SCHMITT, DIETER

Advanced technology constant challenge and evolutionary process p 109 A93-15054

SCHMOLL, W. J.

Heat transfer in high turbulence flows: A 2-D planar wall jet p 932 A93-29935

SCHMUGGE, T.

PBMR observations of surface soil moisture in Monsoon 90 p 1162 A93-47676

SCHMUHL, H. J.

Axial flow compressors - Mechanical design trends
[ISABE 93-7061] p 1199 A93-54037

SCHNACK, E.

Optimization of large scale systems in elasticity p 1255 A93-54544

SCHNEIDER, DAVID J.

Remote sensing of volcanic ash hazards to aircraft p 556 A93-24213

SCHNEIDER, M.

Diffusion controlled evaporation of a multicomponent droplet - Theoretical studies on the importance of variable liquid properties p 1021 A93-44224

SCHNEIDER, STEVEN P.

Hot film wall shear instrumentation for compressible boundary layer transition research
[NASA-CR-191360] p 294 N93-17855

SCHNEIDER, T.

Numerical determination of the residual strength of battle damaged composite plates p 537 A93-21533

SCHNERR, GUENTER H.

Transonic aerodynamics including strong effects from heat addition p 862 A93-42428

SCHNEUR, R.

Structural optimization using Newton Modified Barrier Method
[AIAA PAPER 92-4756] p 409 A93-20352

SCHOBELI, T.

One-dimensional methods for accurate prediction of off-design performance behavior of axial turbines
[ASME PAPER 92-GT-54] p 347 A93-19304

Nonlinear dynamic simulation of single- and multi-spool core engines
[AIAA PAPER 93-2580] p 1122 A93-50294

- SCHODER, WOLFGANG**
Robust control of the separation of hypersonic lifting vehicles
[AIAA PAPER 92-5013] p 385 A93-22289
- SCHOELCH, M.**
Aerodynamic design of pivotable nozzle vanes for radial-inflow turbines
[ASME PAPER 92-GT-94] p 349 A93-19340
- SCHOENECK, K. A.**
Active magnetic bearings applied to industrial compressors p 841 A93-27570
- SCHOENUNG, B.**
Calculation of wake-induced unsteady flow in a turbine cascade
[ASME PAPER 92-GT-306] p 255 A93-19496
Use of advanced CFD codes in the turbomachinery design process
[ASME PAPER 92-GT-324] p 256 A93-19508
- SCHOENUNG, JULIE M.**
The development of a mature external Master's degree program in aeronautical engineering - A university/industry partnership
[AIAA PAPER 92-4256] p 570 A93-24296
- SCHOEPPFEL, A.**
Analysis of multiple crack propagation in stiffened sheet p 81 A93-13638
- SCHOEVERS, H. W. C. L.**
Helicopters in action p 340 N93-19005
- SCHOFIELD, M. J.**
Envelope function - A tool for analyzing flutter data p 1136 A93-52455
- SCHOLTEALBERS, G. A. M.**
Stress calculations on the window section of an all-composite aircraft fuselage
[LR-688] p 328 N93-16215
- SCHOMER, PAUL D.**
Human response to helicopter noise - A test of A-weighting p 567 A93-29424
- SCHOOR, B.**
Airspace Design Expert System (ADES), a 2D/3D mapping and modelling tool incorporating an expert system for use in instrument approach design p 888 N93-30357
- SCHOUTEN, GERRIT**
Theodorsen's ideal propeller performance with ambient pressure in the slipstream p 768 A93-37400
- SCHRA, L.**
Flight simulation and constant amplitude fatigue crack growth in aluminum-lithium sheet and plate p 71 A93-13644
Flight simulation and constant amplitude fatigue crack growth in aluminum-lithium sheet and plate
[NLR-TP-91104-U] p 331 N93-17562
Accelerated and real-time corrosion testing of aluminum-lithium alloys
[NLR-TP-91203-U] p 1020 N93-32385
- SCHRADE, H. O.**
Non-equilibrium flow in an arc heated wind tunnel p 910 A93-42642
- SCHRAGE, D. P.**
Atmospheric turbulence simulation for rotorcraft applications p 757 A93-34264
Helicopter response to atmospheric turbulence p 817 A93-35987
Methodology development for evaluation of selective-fidelity rotorcraft simulation p 913 N93-30691
- SCHRAGE, DANIEL P.**
Preliminary wing design of a high speed civil transport aircraft by multilevel decomposition techniques
[AIAA PAPER 92-4721] p 325 A93-20323
An approach to tiltrotor wing aeroservoelastic optimization through increased productivity
[AIAA PAPER 92-4781] p 326 A93-20371
Application of a two-point exponential approximation method in optimizing rotorcraft airframe structures p 507 A93-27956
Development and validation of a comprehensive real time AH-64 Apache simulation model p 799 A93-35992
- SCHRRANNER, R. S.**
Helmet Mounted Sight and display testing p 517 A93-26883
- SCHRECK, SCOTT J.**
Unsteady vortex dynamics and surface pressure topologies on a pitching wing
[AIAA PAPER 93-0435] p 286 A93-23349
Neural network prediction of three-dimensional unsteady separated flow fields
[AIAA PAPER 93-3426] p 977 A93-47221
- SCHRECK, STEFAN**
Control of jet noise
[NASA-CR-193552] p 1040 N93-32221
- SCHREIBER, L.**
Navier-Stokes computation on a pivoting doors thrust reverser and comparison with tests
[ASME PAPER 92-GT-254] p 353 A93-19463
- SCHREIBER, WILLARD C.**
Comparison of methodologies for describing relaxation in nonequilibrium gaseous systems p 419 N93-16786
- SCHREYER, H.**
Helmet Mounted Sight and display testing p 517 A93-26883
Integration of an integrated helmet system for PAH 2 p 1244 A93-55298
- SCHREYER, HERBERT**
Integrated helmet system testing for a nightflying helicopter
[MBB-UD-0604-91-PUB] p 343 N93-17570
- SCHROEDER, J. A.**
Liquid water profiling using remote sensor observations p 429 A93-22150
- SCHROEDER, J. E.**
Optical interconnection and packaging technologies for advanced avionics systems p 77 A93-10960
- SCHROEDER, JEFFERY A.**
Simulation motion effect on single axis compensatory tracking
[AIAA PAPER 93-3579] p 1208 A93-52675
- SCHROEDER, JEFFREY A.**
Improvements in hover display dynamics for a combat helicopter p 727 A93-34257
- SCHROEDER, W.**
Investigation of the flowfield over parallel-arranged launch vehicles
[AIAA PAPER 93-3060] p 1058 A93-48237
An extended insight into hypersonic flow phenomena using numerical methods p 1093 A93-51999
- SCHUDT, E. E.**
Determination of tire-wheel interface pressure distribution for aircraft wheels
[AIAA PAPER 93-1343] p 709 A93-33913
- SCHUELER, DARYL J.**
Why simulators don't fly like the airplane: Data - An update with examples from the C-141B program
[AIAA PAPER 92-4161] p 66 A93-13312
- SCHUEPP, P. H.**
Spatial and temporal variations of the fluxes of carbon dioxide and sensible and latent heat over the FIFE site p 425 A93-20586
- SCHUETZ, H.**
Numerical study of nitric oxide formation in a hypersonic ramjet engine
[ISABE 93-7125] p 1204 A93-54100
- SCHUHMACHER, G.**
Multidisciplinary design of composite aircraft structures by Lagrange p 76 A93-10273
- SCHULTEN, J. B. H. M.**
Transmission of sound through a rotor p 447 A93-19183
Transmission of sound through a rotor
[NLR-TP-92014-U] p 1006 N93-32386
- SCHULTZ, F. J.**
A pulsed fast-thermal neutron interrogation system p 497 N93-21866
- SCHULTZ, J.**
Neutron-induced single event upsets in static RAMs observed at 10 KM flight altitude p 1158 A93-50561
- SCHULTZ, J. L.**
Ramjet NOx emission - Use of a 3D CFD method for the combustor design of a super/hyper-sonic transport propulsion system
[ASME PAPER 92-GT-255] p 353 A93-19464
- SCHULTZ, JAMES**
Winds of change: Expanding the frontiers of flight. Langley Research Center's 75 years of accomplishment, 1917-1992
[NASA-NP-130] p 104 N93-11100
- SCHULTZ, K.-J.**
Helicopter main rotor/tail rotor noise radiation characteristics from scaled model rotor experiments in the DNW p 445 A93-19142
- SCHULTZ, KLAUS -J.**
HHC study in the DNW to reduce BVI noise - An analysis p 565 A93-29405
- SCHULTZ, THOMAS A.**
Flight test evaluation of precision-code differential GPS for terminal approach and landing p 33 A93-11294
- SCHULZ, P.**
Testing of an experimental system for image reconnaissance p 1040 N93-31283
- SCHULZ, UWE**
Integrated engine control and monitoring with experiences derived from OLMOS p 178 N93-15168
- SCHULZ, WILLIAM D.**
Static tests of jet fuel thermal and oxidative stability p 389 A93-21651
- SCHUMANN, ULRICH**
Large-eddy simulation of turbulent flow above and within a forest p 92 A93-11404
- SCHUR, D.**
Damage tolerance assessment and usage variation analysis for C-130 aircraft in the Israeli Air Force p 839 N93-27210
- SCHURMAN, DON**
Reliability assessment at airline inspection facilities. Volume 1: A generic protocol for inspection reliability experiments
[DOT/FAA/CT-92/12-VOL-1] p 704 N93-25110
Reliability assessment at airline inspection facilities. Volume 2: Protocol for an eddy current inspection reliability experiment
[DOT/FAA/CT-92/12-VOL-2] p 842 N93-28685
- SCHUSTER, DAVID M.**
Application of a Navier-Stokes aeroelastic method to improve fighter wing performance at maneuver flight conditions
[AIAA PAPER 93-0529] p 284 A93-23270
An inverse method for computation of structural stiffness distributions of aeroelastically optimized wings
[AIAA PAPER 93-1540] p 741 A93-34077
- SCHUTT, J. A.**
Large-scale simulation of the three-dimensional Navier-Stokes equations p 437 A93-20739
- SCHWAB, R. R.**
Engine technologies for future spaceplanes
[ETN-92-92732] p 177 N93-15143
- SCHWAB, S. D.**
Aerodynamic applications of pressure sensitive paint p 549 A93-29301
- SCHWANE, R.**
An upwind relaxation method for hypersonic viscous flows over a double-ellipsoidal body p 867 A93-42606
- SCHWARTZ, DANIEL B.**
Transition to a seamless communications system requires much experimentation p 792 A93-38564
- SCHWARTZ, JASON**
Aeroelastic system identification of advanced technology aircraft through higher order signal processing p 525 A93-29297
- SCHWARZ-VAN MANEN, A.**
The reduction of skin friction by riblets under the influence of an adverse pressure gradient p 1218 A93-53810
- SCHWARZ, K. P.**
Maintaining high accuracy GPS positioning 'on the fly' p 92 A93-11028
Accuracy of GPS-derived acceleration from moving platform tests p 1240 A93-55973
Requirements for airborne vector gravimetry p 1241 A93-55976
Controlling common mode stabilization errors in airborne gravity gradiometry p 1245 A93-55978
- SCHWARZ, WALTER R.**
Measurements in a pressure-driven three-dimensional turbulent boundary layer during development and decay
[AIAA PAPER 93-0543] p 415 A93-23283
Measurements in a pressure-driven three-dimensional turbulent boundary layer during development and decay p 927 A93-41911
- SCHWEIGER, P.**
Effect of a rotating propeller on the separation angle of attack
[AIAA PAPER 93-0017] p 472 A93-24978
Effect of a rotating propeller on the separation angle of attack and distortion in ducted propeller inlets
[NASA-TM-105935] p 290 N93-16625
- SCHWEIKHARD, WILLIAM G.**
Why simulators don't fly like the airplane: Data - An update with examples from the C-141B program
[AIAA PAPER 92-4161] p 66 A93-13312
- SCHWEIKL, L.**
New developments with the V2500 engine
[ISABE 93-7085] p 1202 A93-54061
- SCHWEITZER, G.**
Blade loss dynamics of a magnetically supported rotor p 1257 A93-54653
- SCHWENDEMAN, D. W.**
On the construction and calculation of optimal nonlifting critical airfoils p 969 A93-46857
- SCHWENK, F. C.**
NASA SBIR abstracts of 1990 phase 1 projects
[NASA-TM-108145] p 572 N93-21794
- SCHWENK, F. CARL**
The NASA SBIR product catalog
[NASA-TM-108242] p 945 N93-29322
NASA SBIR abstracts of 1991 phase 1 projects
[NASA-TM-108240] p 945 N93-29323
- SCHWENK, RUEDIGER**
Flight safety in Europe p 1227 A93-53726
- SCHWENK, WALTER**
Flight safety in Europe p 1227 A93-53726

SCIALOM, G.

SCIALOM, G.

Evaluation of clear-air radar PROUST and Doppler radar RONSARD for airport low level-wind shear detection
p 433 A93-22202

SCOTT, C. E.

Radii effect on the translation spring constant of force transducer beams
p 829 A93-37867

SCOTT, CARL D.

Intrusive and nonintrusive measurements of flow properties in arc jets
p 943 A93-42584

SCOTT, CHARLES

On definition and use of systems engineering processes, methods and tools
p 1225 A93-53642

SCOTT, JAMES N.

Accuracy considerations in the computational analysis of jet noise
[AIAA PAPER 93-0146]
p 451 A93-19804

Comparison of limiters in flux-split algorithms for Euler equations
[AIAA PAPER 93-0068]
p 262 A93-20181

SCOTT, MICHAEL A.

Flight evaluation of a stagnation detection hot-film sensor
[AIAA PAPER 92-4085]
p 51 A93-13263

SCOTT, ROBERT C.

A method of predicting quasi-steady aerodynamics for flutter analysis of high speed vehicles using steady CFD calculations
[AIAA PAPER 93-1364]
p 682 A93-33931

Further studies using matched filter theory and stochastic simulation for gust loads prediction
[AIAA PAPER 93-1365]
p 726 A93-33932

Computation of maximized gust loads for nonlinear aircraft using matched-filter-based schemes
p 1136 A93-52452

SCOTT, STEPHEN J.

Current Technology for Thermal Protection Systems [NASA-CP-3157]
p 69 N93-12447

SCULLY, JOHN R.

NASA-UVA Light Aerospace Alloy and Structures Technology Program (LA2ST)
[NASA-CR-193412]
p 1019 N93-31739

SEAL, D. W.

Reconfigurable photonic data networks for military aircraft
p 928 A93-42783

Multiplexing electro-optic architectures for advanced aircraft integrated flight control systems
[NASA-CR-182268]
p 187 N93-13735

SEAMAN, L.

Unified airport pavement design procedure
p 380 N93-16318

SEAMSTER, THOMAS L.

The analysis of expert performance in the redesign of the en route air traffic control curriculum
p 571 A93-27189

SEARCY, P. A.

Helicopter plume detection by using an ultranarrow-band noncoherent laser Doppler velocimeter
p 542 A93-25198

SEARLE, M. D.

Effect of skywave interference on the coverage of Loran-C
p 33 A93-11095

SEASTONE, A. J.

New concepts in remote sensing and geolocation
p 556 A93-24173

SEBANI, MOHAMMED

Active control of aeroacoustic couplings by means of adaptive systems
[ECL-91-18]
p 64 N93-11576

SEDYAKIN, A. V.

Experimental and algorithmic means of identifying mathematical models of flight vehicle
p 909 A93-43103

SEEBASS, A. R.

Interactive hypersonic waverider design and optimization
p 119 A93-14348

Waverider design for generalized shock geometries [AIAA PAPER 93-0774]
p 467 A93-24858

SEEGERS, BRYAN J.

Thrust augmentation system for low-cost-expendable turbojet engine
[AD-A263727]
p 905 N93-30877

SEEGMILLER, H. L.

Low aspect ratio wing code validation experiment
p 1176 A93-53202

SEELEMAN, T.

A laser induced fluorescence system for the high enthalpy shock tunnel (HEG) in Goettingen
p 1024 A93-45506

SEELHORST, U.

Time-dependent 3-component laser-Doppler anemometer and simultaneous position measurements in the flow of an aircraft engine
p 538 A93-23809

The jet behaviour of an actual high-bypass engine as determined by LDA-measurements in ground tests
p 175 N93-13218

SEELY, L. G.

The Superpressure Stratospheric Vehicle
p 39 A93-11357

SEFERIS, J. C.

Fundamentals of composite repair [SME PAPER EM92-100]
p 196 A93-14101

Model multilayer structured composites
p 533 A93-24509

SEGAL, A.

Post buckling of laminated composite stiffened curved panels subjected to cyclic shear and compression
p 204 A93-14334

SEGAL, CORIN

Experimental supersonic hydrogen combustion employing staged injection behind a rearward-facing step
p 744 A93-34496

Molecular mixing of jets in supersonic flow [AIAA PAPER 93-2021]
p 1078 A93-49858

SEGARS, RONALD A.

The degradation of parachutes: Age and mechanical wear
[AD-A252243]
p 24 N93-12179

SEGINER, A.

Leading edge vortices in a chordwise periodic flow
p 119 A93-14333

Leading edge vortices in a chordwise periodic flow
p 782 N93-27218

SEGUIN, JEAN-MARIE

Guidance law based on piecewise constant control for hypersonic gliders
[AIAA PAPER 93-3888]
p 1144 A93-51472

SEHMBEY, MANINDER S.

Design of a hydrogen test facility
p 532 A93-25993

SEHRA, A. K.

Blade row interaction effects on compressor measurements
p 900 A93-42885

Optimization of a highly-loaded axial splittor rotor design
p 1002 A93-46931

SEHRA, ARUN

Numerical investigation of flow field in a turbine volute
[AIAA PAPER 93-0155]
p 542 A93-25505

SEHRA, ARUN K.

Experimental investigation of exhaust system mixers for a high bypass turbofan engine
[AIAA PAPER 93-0022]
p 357 A93-20140

SEIBOLD, S.

Identification of nonlinear mechanical systems using combined state and parameter evaluation
p 1224 A93-52732

SEIDEL, JONATHAN A.

Concurrent optimization of airframe and engine design parameters
[AIAA PAPER 92-4713]
p 323 A93-20281

Concurrent optimization of airframe and engine design parameters
[NASA-TM-105908]
p 60 N93-12402

SEIDEL, U.

The vortex behaviour of the rotating-stall cell of a centrifugal compressor with vane diffuser
[ASME PAPER 92-GT-66]
p 400 A93-19316

Determination of the zone of the stall cell by means of the baroclinic wave theory
p 424 N93-18733

Rotating stall cell and Von Karman vortex street: A meteorological theory
p 424 N93-18734

SEIFERT, A.

Pilot test of a low Reynolds number DTE-airfoil
[AIAA PAPER 93-0643]
p 464 A93-24758

Oscillatory blowing, a tool to delay boundary layer separation
[AIAA PAPER 93-0440]
p 474 A93-25529

The effects of forced oscillations on the performance of airfoils
[AIAA PAPER 93-3264]
p 968 A93-46829

Oscillatory blowing - A tool to delay boundary-layer separation
p 1235 A93-55362

SEIFERT, P.

Inflight antenna diagram determination of spaceborne and airborne SAR-systems
p 1161 A93-47583

SEILER, F.

Shock tube validation experiments for the simulation of ram-accelerator-related combustion and gasdynamic problems
p 1016 A93-45499

SEINER, JOHN M.

The effects of temperature on supersonic jet noise emission
p 446 A93-19159

SEITZ, GERHARD

Overview of Tiger dynamics validation program
p 794 A93-35907

SEITZ, T. J.

Structural modeling of low-aspect ratio composite wings
[AIAA PAPER 93-1371]
p 739 A93-33937

SEITZ, TIMOTHY J.

Formulation of a structural model for flutter analysis of low aspect ratio composite aircraft wings
p 372 N93-19019

SEITZMAN, J. M.

Comparison of NO and OH PLIF temperature measurements in a scramjet model flowfield
[AIAA PAPER 93-2035]
p 1113 A93-49870

SEIWEIT, D. L.

Methodology for commercial engine/aircraft optimization
[AIAA PAPER 93-1807]
p 1166 A93-49696

SEKAR, B.

Studies in air/air supersonic mixing layers
p 700 N93-26007

SEKAR, S.

A two-dimensional elliptic grid generator for a wing-body section involving grid control functions
p 460 A93-24083

SEKAR, WIDJAJA K.

Calculation of 3-D unsteady subsonic flow with separation bubble using singularity method
p 115 A93-14251

SEKI, Y.

Studies on methane-fuel ram combustor for HST combined cycle engine
[ISABE 93-7080]
p 1201 A93-54056

SEKIDO, T.

Conceptual design study on combined-cycle engine for hypersonic transport
[ISABE 93-7018]
p 1195 A93-53994

SEKIDO, TOSHINOBU

Feasibility study on single bypass variable cycle engine with ejector
[AIAA PAPER 92-4268]
p 55 A93-13366

SEKINE, HIDEKI

Stiffness design method of symmetric laminates using lamination parameters
p 206 A93-14569

SEKINO, NOBUHIRO

Numerical simulation of flows in a supersonic air intake
p 303 N93-19314

SEKUNDOV, A. N.

Experimental study of the effect of external turbulence and the shape of the surface on the characteristics of laminar and transition boundary layers
p 987 A93-47522

SELBERG, BRUCE P.

Analysis of the effect of surface heating on boundary layer development over an NLS-0215 airfoil
[AIAA PAPER 93-3437]
p 978 A93-47229

SELBY, GREGORY V.

Boundary-layer measurements on a high Reynolds number three-element airfoil
p 292 N93-16787

SELIG, MICHAEL S.

Generalized multipoint inverse airfoil design
p 122 A93-14541

SELIG, MICHAEL SCOTT

Multi-point inverse design of isolated airfoils and airfoils in cascade in incompressible flow
p 163 N93-14462

SELIKHOV, A. F.

Experience in specifying/prolonging the airframe time limits
p 948 A93-45797

SELLERS, WILLIAM L. III

Requirements for facilities and measurement techniques to support CFD development for hypersonic aircraft
p 1014 A93-47024

SELLIN, M. D.

Tip shock structures in transonic compressor rotors
[AIAA PAPER 93-1869]
p 1075 A93-49744

SELMIN, V.

Inviscid calculations by an upwind finite element method of hypersonic flows over a double (single) ellipse
p 869 A93-42626

SELS, ROBERT A.

Lessons from application of equivalent plate structural modeling to an HSCT wing
[AIAA PAPER 93-1413]
p 739 A93-33969

SEMENTOV, P. K.

Stabilization of the dynamic characteristics of the automatic control systems of a flight vehicle
p 62 A93-12802

Stabilization of the dynamic characteristics of the two-channel automatic control system of aircraft
p 1205 A93-52941

SEMENTOV, V. N.

A study of the strength of a closed system of wings
p 828 A93-36792

SEMENTOV, V. V.

Statistical methods in flight vehicle control theory
p 1165 A93-49306

SEN, JOYANTO K.

Test and analysis of an advanced technology landing gear
p 37 A93-10917

SEN, P. K.

Computer aided aerodynamic design of high pressure axial flow fan blade element
p 16 A93-13649

- SENARD, PASCAL**
Satcom Pacific Ocean trials p 501 A93-28198
- SENATORE, PAOLO**
Life cycle assessment of an impingement-cooled gas turbine blade
[AIAA PAPER 92-4716] p 358 A93-20321
- SENDECKY, G. P.**
Acoustic emission technology for smart structures p 1263 A93-55331
- SENCHAL, C. G.**
The value of GNSS to aircraft operators p 498 A93-25172
- SENFFNER, DAVID**
The use of satellite geometry for prevention of cycle slips in a GPS processor p 34 A93-11298
- SENICK, PAUL F.**
Effects of turbine cooling assumptions on performance and sizing of high-speed civil transport
[AIAA PAPER 92-4217] p 55 A93-13383
- SEMINA, O. A.**
Increasing the efficiency of the electrochemical dimensional machining of gas turbine engine blades of EP718VD alloy p 835 A93-39095
- SENIOR, C. L.**
Real-time optical measurement of alkali species in air for jet engine corrosion testing
[AIAA PAPER 93-0791] p 541 A93-24870
- SENN, E. E., JR.**
The effects of composite material on the configuration and design of the V-22 wing p 507 A93-27964
- SENNOTT, JAMES W.**
The use of satellite geometry for prevention of cycle slips in a GPS processor p 34 A93-11298
- SENS, A. S.**
Implicit schemes for unsteady Euler equations on unstructured meshes
[ONERA, TP NO. 1993-64] p 1171 A93-51944
- SENSBURG, O.**
Technological challenges with smart structures in German aircraft industry p 320 A93-17714
- SENSBURG, OTTO**
Mathematical optimization: A powerful tool for aircraft design
[MBB-FE-2-S-PUB-478] p 331 A93-17564
- SENSMEIER, MARK D.**
Static and dynamic large deflection flexural response of graphite-epoxy beams
[NASA-CR-4118] p 934 A93-30374
- SENTIS, M. L.**
Aerodynamic phenomena in high pulse repetition rate XeCl laser p 1150 A93-48806
- SERGEEV, A. V.**
Flight-vehicle drives (2nd revised and enlarged edition)
[ISBN 5-217-00802-4] p 713 A93-35676
- SERGEEV, V. B.**
Development of a process for fabricating a plate heat exchanger for the heat recovery system of gas turbine engines p 834 A93-39053
- SERGENT, DANIEL G.**
A concluding study of the altitude determination deficiencies of the Service Aircraft Instrumentation Package (SAIP)
[AD-A263515] p 897 A93-29971
- SERMANOV, V. N.**
Supersonic combustion and gasdynamic of scramjet p 170 A93-14242
Gasdynamics of hydrogen-fueled scramjet combustors
[AIAA PAPER 93-2145] p 1115 A93-49962
- SESTERHENN, JOERN**
Flux-vector splitting for compressible low Mach number flow p 1093 A93-52001
- SETER, D.**
Stability of the vertical autorotation of a single-winged samara p 274 A93-22443
- SETH, S.**
Pilot weather advisor
[NASA-CR-189723] p 318 A93-16692
- SETO, JEFFREY A.**
Two-directional skin friction measurement utilizing a compact internally mounted thin-liquid-film skin friction meter
[AIAA PAPER 93-0180] p 414 A93-22608
- SETTLES, G. S.**
Wall pressure fluctuations beneath swept shock wave/boundary layer interactions
[AIAA PAPER 93-0384] p 282 A93-23063
Interaction strength and model geometry effects on the structure of crossing-shock wave/turbulent boundary-layer interactions
[AIAA PAPER 93-0780] p 467 A93-24862
Laser Interferometer Skin-Friction measurements of crossing-shock wave/turbulent boundary-layer interactions
[AIAA PAPER 93-3072] p 1148 A93-48247
Supersonic shock wave/vortex interaction
[NASA-CR-192917] p 695 A93-25249
- An experimental study of the sources of fluctuating pressure loads beneath swept shock/boundary-layer interactions
[NASA-CR-192918] p 749 A93-25266
- SEVERANCE, KURT**
Computer-aided light sheet flow visualization
[AIAA PAPER 93-2915] p 1147 A93-48117
- SEVERT, CLARENCE**
The integral starter/generator development progress
[SAE PAPER 920967] p 173 A93-14629
- SEVICH, G. J.**
New developments with the V2500 engine
[ISABE 93-7085] p 1202 A93-54061
- SEYBERT, A. F.**
Acoustical analysis of gear housing vibration p 567 A93-29420
- SEYWALD, HANS**
Hodograph analysis in aircraft trajectory optimization
[AIAA PAPER 93-3742] p 1101 A93-51338
The Generalized Legendre-Clebsch Condition on state/control constrained arcs
[AIAA PAPER 93-3746] p 1170 A93-51342
- SFORZA, PASQUALE M.**
Development of Polytechnic University's supersonic wind tunnel facility
[AIAA PAPER 93-0798] p 528 A93-24876
An exploratory wind tunnel study of supersonic tip vortices
[AIAA PAPER 93-2923] p 1045 A93-48124
- SHA, ZHENGPING**
A control technology of integrated system of engineering supported by software engineering environments p 226 A93-14415
- SHABANOV, V. N.**
Supersonic flow of a gas over a semiinfinite plate with small-scale harmonic spanwise oscillations p 775 A93-39118
- SHABUROV, I. V.**
A study of the stability of the acceleration circuit of the hydromechanical automatic control system of an aviation gas turbine engine p 810 A93-39028
A study of the effect of the working medium on the start-up characteristic of an aviation gas turbine engine p 811 A93-39037
- SHADID, J. N.**
A performance comparison of massively parallel Parabolized Navier-Stokes solutions
[AIAA PAPER 93-0059] p 435 A93-20172
- SHADRINA, T. S.**
Problems in physical gas dynamics p 775 A93-39126
- SHAHER, MARY F.**
A comparison of hypersonic flight and prediction results
[AIAA PAPER 93-0311] p 280 A93-23006
- SHAFFER, D. K.**
Durability properties for adhesively bonded structural aerospace applications p 1217 A93-53515
- SHAH, GAUTAM H.**
Actuated forebody strake controls for the F-18 high alpha research vehicle
[AIAA PAPER 93-3675] p 1006 A93-44233
- SHAH, TUSHAR K.**
Durability properties for adhesively bonded structural aerospace applications p 1217 A93-53515
- SHAHPAR, S.**
Hypersonic flows including real gas effects
[AERO-REPT-9112] p 289 A93-16467
Computational study of real gas effects in high speed high temperature flow, volume 2
[AERO-REPT-9203-VOL-2] p 289 A93-16470
- SHAKARVENE, E. P.**
Unsteady aerodynamic characteristics of three rectangular wings of different aspect ratios p 1180 A93-53575
- SHAKHOVA, L. I.**
Collection of works on measuring and computing systems for research on the aerodynamics, dynamics, and strength of flight vehicles p 75 A93-10026
- SHAKIB, F.**
Application of the Galerkin/least-squares formulation to the analysis of hypersonic flows. I - Flow over a two-dimensional ramp p 866 A93-42593
Application of the Galerkin/least-squares formulation to the analysis of hypersonic flows. II - Flow past a double ellipse p 868 A93-42608
- SHAL'MAN, E. IU.**
Effect of a large-scale inhomogeneity of the incoming flow on flow in a plane turbine cascade p 6 A93-10189
- SHALEV, D.**
Post buckling of laminated composite stiffened curved panels subjected to cyclic shear and compression p 204 A93-14334
- SHALIN, VALERIE L.**
Methods and principles for determining task dependent interface content
[NASA-CR-190837] p 36 A93-10961
- SHALYGIN, A. S.**
Solution of the terminal guidance problem for a flight vehicle using analytical mechanics methods p 228 A93-16778
- SHAMANSKY, H. T.**
Operation of the helicopter antenna radiation prediction code
[NASA-CR-193259] p 1030 A93-31110
- SHAMBLE, CLIFFORD E.**
Ongoing challenges for titanium alloy cleanliness improvement in aircraft engine disk materials p 1212 A93-53506
- SHAMROTH, S. J.**
Two- and three-dimensional blade vortex interactions
[NASA-CR-177567] p 293 A93-16942
- SHAN'GIN, D. M.**
Solution of trajectory optimization methods using the Pontriagin maximum principle p 366 A93-18378
- SHANABARGER, MICKEY R.**
Gas phase hydrogen permeation in a Ni-Fe-Co superalloy p 735 A93-34510
- SHANAHAN, DENNIS F.**
Crash experience of the US Army Black Hawk helicopter p 493 A93-19688
The effectiveness of airbags in reducing the severity of head injury from gunsight strikes in attack helicopters p 494 A93-19691
- SHANG, J. S.**
Numerical simulation of flow past the X24C reentry vehicle
[AIAA PAPER 93-0319] p 280 A93-23011
Accuracy of flux-split algorithms in high-speed viscous flows p 860 A93-41912
Calculations on a double-fin turbulent interaction at high speed
[AIAA PAPER 93-3432] p 977 A93-47224
- SHANG, JOSEPH S.**
Hypersonic nonequilibrium flow computations using the Roe flux-difference split scheme p 692 A93-35609
Computation of nonequilibrium hypersonic flowfields around hemisphere cylinders p 1229 A93-54469
- SHANG, SHIYING**
Identification and conversion of foundation parameters for airport pavement p 538 A93-24035
- SHANG, T.**
Blade row interaction effects on compressor measurements p 900 A93-42885
- SHANG, YI**
Elimination of overtemperature in turbojet p 172 A93-14481
- SHANK, SUZANNA S.**
Tiltrotor interior noise characteristics p 509 A93-29421
- SHANTZ, ARTHUR**
The Federal Aviation Administration (FAA) and the National Weather Service (NWS) modernization programs - Catalysts for change in weather services p 427 A93-22114
- SHANYAVSKIY, A. A.**
Prediction of fatigue crack growth kinetics in the plane structural elements of aircraft in the biaxial stress state p 1025 A93-45670
- SHAO, CH.**
Researches on sonic fatigue of the air-inlet duct of XX aircraft p 154 A93-14256
- SHAO, RONG S.**
Harmonic oscillation in FBW system p 1206 A93-53877
- SHAODA, ZHU**
Detection performance of digital polarity sampled phase reversal code pulse compressors
[AD-A262930] p 842 A93-28289
- SHAPIRO, E. G.**
Two-phase injection from the front surface of a blunt body in hypersonic flow p 241 A93-18233
- SHAPOVALOV, G. K.**
A transfer standard of an air flow rate unit VET 150-2-87 p 66 A93-10049
Effect of longitudinal microribbing on the drag of a body of revolution p 5 A93-10147
Spectra of pressure pulsations on the surface of a cone in the transition region at supersonic flow velocities p 1088 A93-51755
- SHAPOVALOV, O. K.**
Experimental study of crossflow instability and laminar-turbulent transition on a swept wing p 115 A93-14250
- SHARAF EL-DIN, HAZEM H.**
Active control of asymmetric conical flow using spinning and rotatory oscillations
[AIAA PAPER 93-2958] p 1048 A93-48152

SHAREEF, N. H.

- Time-variant analysis of rotorcraft systems dynamics -
An exploitation of vector processors p 416 A93-23512

SHARMA, ANIL K.

- Flutter optimization of large transport aircraft
[AIAA PAPER 92-4795] p 326 A93-20381

SHARMA, GAUTAM

- Side-force control on a forebody of diamond
cross-section at high angles of attack
[AIAA PAPER 93-3407] p 1008 A93-47206

SHARMA, M. G.

- Thermoviscoelastic analysis of pavements
p 379 N93-16313
Development of a unified airport pavement analysis and
design system p 380 N93-16317

SHARMA, P. B.

- A study of aerodynamic performance of a contra-rotating
axial compressor stage p 463 A93-24524

SHARMA, SHASHI K.

- Development of MIL-H-53119, -54 C to 175 C
high-temperature nonflammable hydraulic fluid for Air
Force systems p 1214 A93-54250

SHARMA, SURENDRA P.

- Research activity at the shock tube facility at NASA
Ames p 1252 A93-54804

SHARP, GREGORY A.

- Application of the program profile for the design of
low-speed, low-observable configuration airfoils
[AD-A258842] p 305 N93-19364

SHASHIKALA, G.

- Composites: A catalogue of books and conference
proceedings available in the NAL library
[NAL-SP-IC-9201] p 234 N93-13368

SHASTRI, R. P.

- Three-dimensional prediffuser combustor studies with
air-water mixture
[AIAA PAPER 93-2474] p 1120 A93-50217

SHATALOV, YU. S.

- Effect of rotation on heat transfer and hydraulic
resistance in the radial cooling channels of turbine rotor
blades p 1215 A93-52950

SHATTUCK, COLMAN

- Modern propeller systems for advanced turboprop
aircraft
[AIAA PAPER 93-1846] p 1111 A93-49727

SHAU, Y. R.

- Organized structure in a compressible turbulent shear
layer p 961 A93-45730

SHAW, J. A.

- The modelling of aerodynamic flows by solution of the
Euler equations on mixed polyhedral grids p 269 A93-21218

SHAW, N. A.

- Increase in mortality rates due to aircraft noise
p 1163 A93-49551

SHAW, ROBERT J.

- Engine technology challenges for a 21st Century
High-Speed Civil Transport
[ISABE 93-7064] p 1200 A93-54040

- Engine technology challenges for a 21st Century
High-Speed Civil Transport
[NASA-TM-106216] p 1004 N93-31671

SHAW, ROGER H.

- Large-eddy simulation of turbulent flow above and within
a forest p 92 A93-11404

SHAW, RUSSELL J.

- A plume-induced boundary layer separation
experiment
[AD-A255397] p 220 N93-14677

SHAW, TONY B.

- Weather-related accidents in the Canadian aviation
industry - An analysis of the chief contributory factors
p 307 A93-22106

SHAW, W. J. D.

- Effects of prior fatigue damage on crack propagation
rates in 2024-T351 aluminum alloy p 71 A93-13640

SHAWLER, WENDELL H.

- Flight testing in the 90's
[AIAA PAPER 92-4123] p 102 A93-11256

SHCHAVINSKII, R. V.

- Using helicopters for transporting large and heavy
loads p 306 A93-18350

SHCHEKIN, G. A.

- Numerical calculation of polars and heat transfer for
supersonic three-dimensional flow past wings with
allowance for radiation p 1068 A93-48905

SHCHELIN, V. S.

- Comparison of gasdynamic models in hypersonic flow
p 1179 A93-53315

SHCHERBAK, V. G.

- Approximate methods for heat flows toward the surface
of three-dimensional bodies p 4 A93-10080
Comparison of gasdynamic models in hypersonic flow
p 1179 A93-53315

SHCHERBIK, D. V.

- Effect of boundary layer suction on the thrust and
aerodynamic efficiency of a hypersonic flight vehicle
p 1176 A93-52959

SHCHIPIN, S. K.

- 3D/quasi-3D trans- and supersonic flow calculation in
advanced centrifugal/axial compressor stages
p 972 A93-46936

SHCHUKIN, G. G.

- Principles of the design of automated meteorological
support systems for aviation
[ISBN 5-286-00342-7] p 151 A93-15224

SHE, ZHISHUN

- Prospective application of neural networks in
superresolution radars p 211 A93-16849
The ISAR image-formation results of Boeing-727
p 342 A93-20857

- ISAR motion compensation and superresolution imaging
of aircraft p 928 A93-42793
Studies of superresolution range-Doppler imaging
p 928 A93-43344

SHEA, J. F.

- Reform of the aeronautics and astronautics curriculum
at MIT
[AIAA PAPER 93-0325] p 454 A93-23017

SHEARD, A. G.

- Electromechanical measurement of turbomachinery
blade tip-to-casing running clearance
[ASME PAPER 92-GT-50] p 400 A93-19303

- The dynamic characteristics of a high pressure turbine
stage in a transient wind tunnel
[ASME PAPER 92-GT-166] p 375 A93-19392

SHEBEKO, S. V.

- Prediction and planning of a flight vehicle route in the
presence of motion inhibiting factors p 1130 A93-50961

SHEEDY, E. M.

- Adaptive/conformal wing design for future aircraft
p 320 A93-17728

SHEFFELS, MICHAEL L.

- A fault-tolerant Air Data/Inertial Reference Unit
p 807 A93-37074

SHEFFER, SCOTT G.

- Constrained optimization of three-dimensional
hypersonic vehicle configurations
[AIAA PAPER 93-0039] p 260 A93-20152

SHEFFLER, KEITH D.

- Thermal barrier coating life prediction model
development, phase 2
[NASA-CR-189111] p 198 N93-12589

SHEKARRIZ, A.

- Near-field behavior of a tip vortex p 288 A93-23549
Three dimensional near field behavior of a tip vortex
developing on an elliptic foil
[AIAA PAPER 93-0865] p 468 A93-24927

SHELDON, J. C.

- Dual-spray airblast fuel nozzle for advanced small gas
turbine combustors
[AIAA PAPER 93-2336] p 1116 A93-50113

SHELLEY, M. J.

- A study of singularity formation in vortex-sheet motion
by a spectrally accurate vortex method p 127 A93-16666

SHELTON, J.

- Information systems for airport operations
[TT-9202] p 152 N93-14729

SHELTON, M. L.

- A statistical approach to the experimental evaluation
of transonic turbine airfoils in a linear cascade
[ASME PAPER 92-GT-5] p 245 A93-19278

SHELUKHO, S. I.

- Fuel film formation in the fuel-air premix of the
combustion chamber p 812 A93-39193

SHEMWELL, D. M.

- Laser Centerline Localizer and Laser Glideslope
Indicator for visual guidance on approach to landing
p 500 A93-28156

- Scanning Laser Aircraft Surveillance System for carrier
flight operations p 500 A93-28157

SHEN, GUANOING

- Contact analysis for riveted and bolted joints of
composite laminates p 204 A93-14384

- A control technology of integrated system of engineering
supported by software engineering environments
p 226 A93-14415

SHEN, H.

- An investigation on the artificial viscosity in the transonic
stream function formulation
[ASME PAPER 92-GT-49] p 246 A93-19302

SHEN, HUI-LI

- Numerical simulation of hypersonic rarefied gas flow over
blunt bodies p 687 A93-34356

SHEN, HUILI

- Solution of Euler equations for complex forebody-inlet
combinations p 680 A93-33730

SHEN, JENNY H.

- Discrete-time LTR synthesis of delayed control
systems p 439 A93-22855

SHEN, JI YAO

- Lumped mass modelling for the dynamic analysis of
aircraft structures p 510 N93-19460

SHEN, JIAN-WEI

- Numerical solution of radiative flowfield on the nose
region of blunt bodies p 120 A93-14359

SHEN, JIANWEI

- The stagnation line solution of the equilibrium flow with
radiation and mass injection p 680 A93-33733

SHEN, M. M.

- Requirements for integrated flight and traffic
management during final approach p 31 A93-11009

SHEN, MENGSHAN

- Application of CAD system in geometric modeling for
helicopter preliminary design p 153 A93-14203

SHEN, XIONG

- Experimental study on turbulent two-phase flow in a
dual-inlet side dump combustor p 1106 A93-48506

SHEN, YONGZHANG

- Analysis and development of a total energy control
system for a large transport aircraft p 183 A93-14372

SHENG, CHUNHUA

- Numerical research on flows in nonuniform cascades
[ASME PAPER 92-GT-276] p 253 A93-19469

SHENG, YUANSHEG

- The numerical calculation for the coupling of multiple
propeller discrete noise and its interaction with the fuselage
boundary p 231 A93-14268

SHENG, YUNLONG

- Fast design of circular-harmonic filters using simulated
annealing p 1038 A93-45556

SHENK, IU. V.

- Numerical modeling of the impact of a bird against
aircraft transparencies p 801 A93-36797

SHENOY, RAJARAMA K.

- Development and validation of 'quiet tail rotor'
technology p 567 A93-29416

SHEPARD, CHARLES E.

- Thermal analysis of an arc heater electrode with a
rotating arc foot
[AIAA PAPER 93-2855] p 1028 A93-46590

SHEPETA, A. P.

- Calculation of the passive noise power for onboard
single-pulse automatic direction tracking systems
p 882 A93-43111

SHEPHERD, M. S.

- Unsteady compressible airfoil aerodynamics using an
adaptive time-discontinuous GLS finite element method
[AIAA PAPER 93-0339] p 281 A93-23027

SHEPHERD, ALAN

- The simulation of aircraft landing gear dynamics
p 155 A93-14318

SHEPHERD, D. P.

- Lifting philosophies for aero engine fracture critical
parts p 345 A93-18783

SHEPHERD, ERIC W.

- Towards an integrated approach to proactive monitoring
and accident prevention p 495 N93-19700
Prediction of success from training p 495 N93-19702

SHEPHERD, KEVIN P.

- Assessment and design of low boom configurations for
supersonic transport aircraft p 446 A93-19163

SHEPHERD, WILLIAM T.

- Future availability of aircraft maintenance personnel
p 570 A93-27133

SHEPPARD, D. M.

- Physical effects of vegetation on wind-blown sand in
the coastal environments of Florida
[PB92-188424] p 93 N93-11702

SHEPPARD, SHIRIN

- Development and operation of a real-time simulation at
the NASA Ames Vertical Motion Simulator
[AIAA PAPER 93-3575] p 1208 A93-52671

SHEPSHELOVICH, M.

- Pilot test of a low Reynolds number DTE-airfoil
[AIAA PAPER 93-0643] p 464 A93-24758
Oscillatory blowing, a tool to delay boundary layer
separation [AIAA PAPER 93-0440] p 474 A93-25529

- Oscillatory blowing - A tool to delay boundary-layer
separation p 1235 A93-55362

SHERBAUM, VALERY

- Thrust vectoring - Theory, laboratory, and flight tests
p 367 A93-21657

SHERRATT, S. R.

- Air Traffic Control ground movement control in low
visibility p 151 A93-17308

SHERRETZ, LYNN

- Developing the Aviation Gridded Forecast System
p 427 A93-22124

- SHERRY, D. J.**
The development of a prototype aircraft height monitoring unit utilizing an SSR-based difference in time of arrival technique p 884 A93-43432
- SHERWOOD, M.**
Studies into the hail ingestion characteristics of turbofan engines [AIAA PAPER 93-2174] p 1115 A93-49987
- SHESTAKOV, G. V.**
Computational models of dampers for computer-aided design p 832 A93-39032
- SHESTAKOV, V. Z.**
Using helicopters for transporting large and heavy loads p 306 A93-18350
Expanding the operation scope of aircraft through the use of air-cushion landing gear p 321 A93-18354
- SHEU, DONGLONG**
Minimum-time flight paths of supersonic aircraft p 160 A93-13140
- SHEVCHENKO, IA. D.**
Design characteristics of the functional systems of aircraft and prediction of their technical condition p 320 A93-18334
- SHEVCHENKO, O. A.**
An aeroacoustic stand for evaluating the efficiency of sound-absorbing structures under conditions of acoustic wave propagation in a moving medium p 1140 A93-51762
- SHEVICH, IU. A.**
A fuel-oil matrix heat exchanger p 833 A93-39052
- SHI, FASHU**
Multiple solutions of the transonic perturbation equation p 987 A93-47331
- SHI, GEORGE Z.**
An integrated knowledge system for wind tunnel testing - Project Engineers' Intelligent Assistant [AIAA PAPER 93-0560] p 377 A93-23297
- SHI, HONG**
Effect of blade leaning on the development of passage vortices and losses in the passage of turbine cascade with a great turning angle p 1236 A93-55397
- SHI, Y.**
Equivalent deterministic inputs for atmospheric turbulence p 183 A93-14351
- SHI, YUEDING**
An experimental study for interaction flow between shock wave and turbulent boundary layer p 120 A93-14355
Passive control of shock wave/boundary layer interaction at hypersonic speed [AIAA PAPER 93-3249] p 966 A93-46794
- SHI, YUZHONG**
Weighted average method for evaluating the aerodynamic properties of transition flow p 8 A93-11872
- SHI, ZHONGKE**
A maximum likelihood method for flight test data compatibility check p 95 A93-12732
- SHIA, R.-L.**
Stratospheric aircraft exhaust plume and wake chemistry studies [NASA-CR-189688] p 94 A93-12299
- SHIAO, MICHAEL C.**
Probabilistically configured adaptive composite structures [AIAA PAPER 93-1679] p 743 A93-34191
Design for cyclic loading endurance of composites p 1216 A93-53395
Probabilistic evaluation of fuselage-type composite structures [NASA-TM-105881] p 212 A93-12735
Probabilistic assessment of composite structures [NASA-TM-106024] p 825 A93-27092
- SHIAU, LE-CHUNG**
Flutter analysis of composite panels on many supports p 1022 A93-45119
- SHIAU, NAE-MING**
Sound transmission through stiffened double-panel structures lined with elastic porous materials p 444 A93-19139
- SHIAU, TING N.**
A study on stability and response analysis of a nonlinear rotor system with mass unbalance and side load [ASME PAPER 92-GT-7] p 400 A93-19280
- SHIBATA, MINORU**
Trends of the airborne cockpit display format p 50 A93-11203
- SHIEH, CHIH F.**
Fluidic scale model multi-plane thrust vector control test results [AIAA PAPER 93-2433] p 1117 A93-50187
- SHIEH, T. H.**
Modeling, analysis, and prediction of flutter at transonic speeds p 416 A93-23553
- A multigrid nonoscillatory method for computing high speed flows [AIAA PAPER 93-3319] p 958 A93-45103
- SHIELDS, ELWOOD M.**
Technology benefits and ground test facilities for high-speed civil transport development [NASA-TM-107670] p 378 A93-15790
- SHIELDS, ELWOOD W.**
Elements of NASA's high-speed research program [AIAA PAPER 93-2942] p 947 A93-45155
- SHIELDS, WENDY**
Exodus: Prime Mover [NASA-CR-192051] p 332 A93-17803
- SHIFRIN, B. M.**
Spanwise aileron oscillations p 819 A93-39190
- SHIGEMATSU, JUNJI**
Two-dimensional numerical simulation for Mach-3 multishock air-intake with bleed systems [AIAA PAPER 93-2306] p 1082 A93-50090
A numerical investigation for supersonic inlet p 303 A93-19315
- SHIH, S. H.**
A parametric study of bleed in shock boundary layer interactions [AIAA PAPER 93-0294] p 280 A93-22694
An investigation of shock wave turbulent boundary layer interaction with bleed through slanted slots [AIAA PAPER 93-2992] p 1052 A93-48184
An investigation of shock wave turbulent boundary layer interaction with bleed through normal and slanted slots [AIAA PAPER 93-2155] p 1079 A93-49971
- SHIH, SHAO-CHIU**
An impact dynamics investigation on some problems in bird strike on windshields of high speed aircraft p 197 A93-15346
- SHIH, T. I.-P.**
Computations of spray, fuel-air mixing, and combustion in a lean-premixed-prevaporized combustor [AIAA PAPER 93-2069] p 1153 A93-49901
Chimera grids in the simulation of three-dimensional flowfields in turbine-blade-coolant passages [AIAA PAPER 93-2559] p 1157 A93-50280
- SHIH, TOM I.-P.**
Effects of bleed-hole geometry and plenum pressure on three-dimensional shock-wave/boundary-layer/bleed interactions [AIAA PAPER 93-3259] p 967 A93-46800
- SHIH, TSAN-HSING**
A realizable Reynolds stress algebraic equation model [NASA-TM-105993] p 290 A93-16596
- SHIKANO, YOSHIO**
Numerical analysis of two-dimensional turbulent flows through an oscillating cascade p 126 A93-15494
- SHILEJN, EH. KH.**
Development of separation due to interaction between a shock wave and a turbulent boundary layer perturbed by rarefaction waves p 1233 A93-55019
- SHILOH, KLARA**
A rapid procedure for obtaining time-average interferograms of vibrating bodies p 412 A93-21857
- SHILOV, A. A.**
Equations of the steady motion of aircraft in spin and spiral dive p 1248 A93-54969
- SHILOV, S. V.**
Computer-aided study of flight regimes and fuel consumption for helicopter flight operations p 997 A93-45674
- SHILOV, V. T.**
Software for the control of measurement data acquisition, processing, and monitoring during strength testings p 94 A93-10042
- SHIMA, EIJI**
Two-dimensional Navier-Stokes analysis of high-lift multi-element airfoils using the q-omega turbulence model [AIAA PAPER 93-0679] p 466 A93-24787
- SHIMADA, TORU**
Numerical simulations of hypersonic rarefied transition regime flows: DSMC method and Navier-Stokes computation p 299 A93-19278
Numerical simulation of flows in a supersonic air intake p 303 A93-19314
- SHIMIZU, M.**
Active forcing of an axisymmetric leading-edge turbulent separation bubble [AIAA PAPER 93-3245] p 966 A93-46790
- SHIMIZU, YOSHIHISA**
The methods of reducing impact loads on occupants in the civil aircraft crash condition p 140 A93-14220
- SHIMODAIRA, K.**
The combustion performance of methane-fueled ram combustor [ISABE 93-7079] p 1201 A93-54055
- SHIMOMURA, TAKASHI**
Simulation analysis of a cable-mount system used for dynamic wind tunnel tests [NAL-TR-1127] p 68 A93-12359
Accuracy improvement of linear estimated motion using differential type sensors [NAL-TR-1135] p 91 A93-12365
- SHIMOMURA, Y.**
The conceptual study of supersonic transport structure [AIAA PAPER 92-4219] p 43 A93-13348
- SHIMSHI, JASON P.**
An investigation of aerodynamic heating to spherically blunted cones at angle of attack [AIAA PAPER 93-2764] p 963 A93-46510
- SHIN, HYOUN-WOO**
Rotor-rotor interaction for counter-rotating fans. I - Three dimensional flowfield measurements [AIAA PAPER 93-1848] p 1075 A93-49729
- SHIN, JAIWON**
Results of Low Power Deicer tests on a swept inlet component in the NASA Lewis Icing Research Tunnel [AIAA PAPER 93-0032] p 327 A93-22551
Surface roughness due to residual ice in the use of low power deicing systems [AIAA PAPER 93-0031] p 282 A93-23240
Results of a low power ice protection system test and a new method of imaging data analysis p 795 A93-35932
Results of low power deicer tests on a swept inlet component in the NASA Lewis icing research tunnel [NASA-TM-105968] p 138 A93-14911
Surface roughness due to residual ice in the use of low power deicing systems [NASA-TM-105971] p 139 A93-15338
Experimental and computational ice shapes and resulting drag increase for a NACA 0012 airfoil p 784 A93-27440
- SHINAR, J.**
New results in optimal missile avoidance analysis p 369 A93-22937
Application of the receding horizon strategy to singularly perturbed pursuit-evasion problems p 369 A93-22980
- SHINDO, SHIGEMI**
Experimental study of mixed compression air-intake for hypersonic airbreathing engines [ASME PAPER 92-GT-349] p 355 A93-19519
Effects of boundary layer bleed on swept-shock/boundary layer interaction [AIAA PAPER 93-2989] p 1052 A93-48182
An experimental study of supersonic air-intake with 5-shock system at Mach 3 [AIAA PAPER 93-2305] p 1082 A93-50089
Wind tunnel tests of the model of intake-airframe integration [ISABE 93-7101] p 1192 A93-54077
A study on Mach 3 two-dimensional mixed compression air-intakes [ISABE 93-7106] p 1188 A93-54082
- SHINGLEDECKER, CLARK**
FAA Technical Center Aeronautical Data Link Research Plan [DOT/FAA/CT-92/23] p 417 A93-15698
- SHINODA, PATRICK M.**
Performance results from a test of an S-76 rotor in the NASA Ames 80-by 120-foot wind tunnel [AIAA PAPER 93-3414] p 975 A93-47211
- SHINOZAKI, NOBORU**
Ignition and combustion performance of a scramjet combustor with a fuel injection strut [ISABE 93-7050] p 1199 A93-54026
Preliminary design of experimental sub-scale scramjet engine [AAS PAPER 91-639] p 1247 A93-55816
- SHIOHARA, T.**
Aging review of the YS-11 aircraft p 46 A93-13635
- SHIPLEY, P. P.**
A European collaborative NLF nacelle flight demonstrator [PNR-90992] p 20 A93-11113
- SHIPLEY, S. T.**
Pilot weather advisor [NASA-CR-189723] p 318 A93-16692
- SHIRAGA, TAKASHI**
Transitional characteristics of vortices issued from a body which creates asymmetric flow field - In a case of thin symmetrical airfoil with angle of attack under rotational oscillation of small amplitude p 267 A93-20923
- SHIRAHARA, M.**
Combustion study on methane-fuel Laboratory Scaled Ram Combustor [ASME PAPER 92-GT-413] p 356 A93-19561
- SHIRAISHI, KAZUO**
Effects of boundary layer bleed on swept-shock/boundary layer interaction [AIAA PAPER 93-2989] p 1052 A93-48182

- An experimental study of supersonic air-intake with 5-shock system at Mach 3
[AIAA PAPER 93-2305] p 1082 A93-50089
- Two-dimensional numerical simulation for Mach-3 multishock air-intake with bleed systems
[AIAA PAPER 93-2306] p 1082 A93-50090
- Wind tunnel tests of the model of intake-airframe integration
[ISABE 93-7101] p 1192 A93-54077
- A study on Mach 3 two-dimensional mixed compression air-intakes
[ISABE 93-7106] p 1188 A93-54082
- A numerical investigation for supersonic inlet
p 303 N93-19315

SHIRAISHI, KSAZUO

- Experimental study of mixed compression air-intake for hypersonic airbreathing engines
[ASME PAPER 92-GT-349] p 355 A93-19519

SHIRAKAWA, MASAKAZU

- Experimental and numerical study on the basic performance of a two-dimensional right-angled intake flow
p 208 A93-15486

SHIRATORI, T.

- Behaviour of the Johnson-King turbulence model in axisymmetric supersonic flows
[AIAA PAPER 93-3032] p 1056 A93-48214

SHIRCK, SAM

- In-service evaluation of wind shear systems
p 146 N93-14857

SHIROOKA, RYUICHI

- Doppler radar observation of tornado and microburst around Chitose Airport
p 432 A93-22199

SHIU, Y. C.

- Robotic aircraft refueling - A concept demonstration
p 846 A93-37041

SHIVAKUMAR, KUNIGAL N.

- Mixed mode stress intensity-factors in transversely loaded plates
p 200 A93-13943

SHIVARAMAN, KARTHIKEYAN

- A nonperiodic boundary approach for computation of compressible viscous flows in advanced turbine cascades
[AIAA PAPER 93-1799] p 1074 A93-49688

SHIVELY, CURTIS

- Overview of the FAA's differential GPS CAT III technical feasibility demonstration program
[AIAA PAPER 93-3836] p 1098 A93-51425

SHIVELY, CURTIS A.

- Capacity as a consideration for providing aeronautical mobile satellite air traffic services in the U.S. domestic airspace
p 30 A93-11007
- Automatic Dependent Surveillance capability of a geostationary satellite system in the U.S. domestic airspace
p 316 A93-21192

SHIVELY, R. J.

- Pre-flight risk assessment in Emergency Medical Service (EMS) helicopters
p 494 A93-19692

SHIVERS, WENDELL W.

- Configuration management impacts on customer support and satisfaction
p 853 A93-35922

SHIZAWA, TAKAOKI

- Behaviors of the laterally injected jet in film cooling - Measurements of surface temperature and velocity/temperature field within the jet
[ASME PAPER 92-GT-180] p 402 A93-19405

- Effects of boundary layer bleed on swept-shock/boundary layer interaction
[AIAA PAPER 93-2989] p 1052 A93-48182

- An experimental study of supersonic air-intake with 5-shock system at Mach 3
[AIAA PAPER 93-2305] p 1082 A93-50089

SHKADOV, L. M.

- Air transportation system for shipping outsized cargoes
p 141 A93-14394

SHKADOV, V. IA.

- Effect of airfoil porosity on the shock wave position and intensity at transonic velocities
p 241 A93-18222

SHKLYARCHUK, F. N.

- Optimization of an aeroelastic system using the dynamic stability condition
p 1029 A93-47085

SHMILOVICH, A.

- A CFD-based design strategy for advanced transonic wing concepts with practical ramifications for subsonic transports
[AIAA PAPER 93-2946] p 1047 A93-48143

SHOCKEY, D. A.

- Unified airport pavement design procedure
p 380 N93-16318

SHONTZ, WILLIAM D.

- Spurious symptom reduction in fault monitoring
[NASA-CR-191453] p 942 N93-29192

SHOPE, F. L.

- Aerodynamic design of a hypersonic body with a constant favorable pressure gradient
[AIAA PAPER 93-3444] p 978 A93-47232

SHOPE, W. B.

- Concept feasibility demonstration for the Army Cockpit Delethalization Program
p 795 A93-35916

SHORE, DREW

- The role of flight management in future air traffic control
p 499 A93-27909

SHORIN, V. P.

- Dynamic processes in the powerplants and power-generating equipment of flight vehicles
p 832 A93-39027

- A study of the effect of the working medium on the start-up characteristic of an aviation gas turbine engine
p 811 A93-39037

SHORT, ART

- Fail safety aspects of the V-22 pylon conversion actuator
p 798 A93-35984

SHORT, J.

- Hysteresis and bristle stiffening effects of conventional brush seals
[AIAA PAPER 93-1996] p 1153 A93-49839

SHOURESHI, RAHMAT

- Applications of active adaptive noise control to jet engines
[NASA-CR-192277] p 522 N93-21210

SHOUSE, D.

- Effects of back-pressure in a lean blowout research combustor
[ASME PAPER 92-GT-81] p 387 A93-19330

SHPATAKOVSKII, A. F.

- Hardening/finishing treatment of compressor blades using a machine with planetary container motion
p 835 A93-39102

SHRADER, B.

- Effects of a rear stagnation jet on the wake behind a cylinder
p 1151 A93-49026

SHREEVE, R. P.

- Inlet turbulence distortion and viscous flow development in a controlled-diffusion compressor cascade at very high incidence
p 688 A93-34485

- Simulation of shock-boundary layer interaction in a fan blade passage
[AIAA PAPER 93-1980] p 1078 A93-49827

- Stator relative, rotor blade-to-blade near wall flow in a multistage axial compressor with tip clearance variation
[AIAA PAPER 93-2389] p 1083 A93-50154

SHREEVE, RAYMOND P.

- A viscous axisymmetric throughflow prediction method for multi-stage compressors
[ASME PAPER 92-GT-293] p 254 A93-19483

SHREINER, DAVID G.

- Thrust augmentation system for low-cost-expendable turbojet engine
[AD-A263727] p 905 N93-30877

SHREVE, GENE

- The Edge supersonic transport
[NASA-CR-192074] p 335 N93-18055

SHRIVASTAVA, VINOD K.

- Definitional mission for civil aviation master plan for Poland
[PB92-213974] p 459 N93-21713

SHTREKALKIN, S. I.

- Experience with the use of liquid crystals in conjunction with the filament method is studying the structure of supersonic flow downstream of a plane step
p 478 A93-27639

- A study of flow structure and heat transfer intensity in the vicinity of an expanding step on a plate
p 691 A93-35268

SHU, CHI-WANG

- Uniform high-order spectral methods for one- and two-dimensional Euler equations
p 476 A93-27068

SHU, K.

- The HYDICE instrument design and its application to planetary instruments
p 842 N93-28766

SHUART, MARK J.

- An analytically designed subcomponent test to reproduce the failure of a composite wing box beam
[AIAA PAPER 93-1344] p 709 A93-33914

SHUBIN, E. B.

- Three-dimensional flow of viscous gas in the blade passage of a straight compressor cascade
p 5 A93-10187

SHUBIN, GREGORY R.

- On alternative problem formulations for multidisciplinary design optimization
[AIAA PAPER 92-4752] p 436 A93-20350

SHUDE, TU

- Detection performance of digital polarity sampled phase reversal code pulse compressors
[AD-A262930] p 842 N93-28289

SHUEN, JIAN-SHUN

- A coupled multi-block solution procedure for spray combustion in complex geometries
[AIAA PAPER 93-0108] p 539 A93-24230

SHUL'GIN, V. I.

- A study of a pulsed electrical field near the jet of a turbojet engine
p 52 A93-10179

- Experimental study of condensation vapor-air jets
p 76 A93-10180

SHUL'KIN, E. A.

- Assessment of flight data in real time
p 341 A93-18364

SHUL'KIN, Z. A.

- Accuracy of nonparametric reliability estimates under varying operation conditions
p 396 A93-18343

SHUL'ZHIK, S. V.

- A unified approach to the construction of the throttle characteristics of postrepair turbojet engines, with the NK8-2U engine used as an example
p 345 A93-18372

- Selection of the time scale for preventive measures under service conditions
p 237 A93-18375

SHUMILOV, I. S.

- Selection of methods and equipment for monitoring the technical condition of booster system components
p 395 A93-18329

- Characteristics of the diagnostics of booster system components
p 321 A93-18361

- Monitoring the purity of the working fluids of aircraft hydraulic systems during service
p 321 A93-18367

SHUMSKII, N. P.

- Absolute stability of an automatic control system for gas turbine engines
p 810 A93-39033

SHUSTOV, A. P.

- Study of artificial and natural turbulence in atmospheric boundary layer with a CW Doppler CO2 lidar
p 1257 A93-54799

SHUSTOV, V. V.

- Determination of the aerodynamic characteristics of thin bodies of revolution with an arbitrary number of cantilever surfaces in inhomogeneous flow
p 1092 A93-51911

SHUSTOVA, G. N.

- Measurement of aerodynamic forces at high temperatures
p 75 A93-10030

SHUSTOVA, L. I.

- A comparative analysis of algorithms for solving systems of high-order linear algebraic equations
p 96 A93-12977

SHVALEV, IU. G.

- A study of the laminar-turbulent transition in a boundary layer and separation on cones at supersonic velocities
p 14 A93-12974

SHVAROV, V. G.

- The flow lag angle in the rotor of a centrifugal compressor with allowance for viscosity effects
p 1179 A93-53555

SHVEDOV, A. V.

- Calculation of the aerodynamic characteristics of bodies with meshlike surfaces in hypersonic rarefied-gas flow
p 1090 A93-51870

- Certain improved algorithms for calculating the aerodynamic characteristics of flight vehicles in free-molecular flow
p 1090 A93-51872

SHVETS, A. I.

- Subsonic separated flow past slender delta wings
p 124 A93-15109

- Experimental studies of supersonic flow past wedges with longitudinal slots on the windward side
p 1089 A93-51786

- Aerodynamic characteristics of conical triangular-planform wings of low aspect ratio in subsonic stalled flow
p 1180 A93-53574

SHYNE, RICKEY J.

- Supersonic investigation of two dimensional hypersonic exhaust nozzles
[NASA-TM-105687] p 179 N93-15342

SHYU, RONG-NAN

- Improvement of high-AOA airfoil stalling performance by internal acoustic excitation
p 243 A93-19134

SHYY, W.

- A multilevel composite grid method for fluid flow computations
[AIAA PAPER 93-0768] p 541 A93-24852

SHYY, WEI

- A viscous flow based membrane wing model
[AIAA PAPER 93-2955] p 1047 A93-48149

- A numerical analysis of supersonic flow over an axisymmetric afterbody
[AIAA PAPER 93-2347] p 1083 A93-50121

SICKLES, W. L.

- A wall interference assessment/correction system
[NASA-CR-190617] p 68 N93-11910

- A wall interference assessment/correction system
[NASA-CR-191889] p 296 N93-18384

SIDDIQI, SHAHID

- Cost - The challenge for advanced materials and structures
p 233 A93-14338

- A unified approach for composite cost reporting and prediction in the ACT program
p 920 N93-30441

- SIDEN, L. D. G.**
Effects of blade geometry and mode shape on fan flutter
[ISABE 93-7028] p 1196 A93-54004
- SIDOROV, L. V.**
A method for calculating supersonic three-dimensional flows in pyramidal nozzles p 125 A93-15216
- SIDOROV, O. P.**
Wave resistance of swept wings with supersonic edges p 478 A93-27624
- SIDOROV, S. YU.**
An experimental system for studying the vibrations and acoustic emission of cylindrical shells and panels in a field of turbulent pressure pulsations p 1140 A93-51754
- SIEBOLD, JOACHIM**
The use of digital road data by a navigation system p 993 N93-31269
- SIEGEL, BRIAN K.**
Pilot task monitoring using neural networks p 940 A93-42846
- SIEGWART, ROLAND**
Design and application of Active Magnetic Bearings (AMB) for vibration control p 1033 N93-32279
- SEKMANN, J.**
Experimental investigation of the management of large-sized drops and the onset of Marangoni-convection p 926 A93-41700
- SIEVERDING, C. H.**
The VKI compression tube annular cascade facility CT3
[ASME PAPER 92-GT-336] p 375 A93-19511
- SIGAIEV, A. YU.**
Identification of the phase characteristics and wind-induced perturbations of an aircraft from flight test results p 1206 A93-52943
- SIGAL, ASHER**
Analysis of wind-tunnel data for elliptic cross-sectioned forebodies at Mach numbers 0.4 to 5.0 p 782 N93-27221
- SIGALLA HEDGES, LINDA**
Comparison of confined, compressible, spatially developing mixing layers with temporal mixing layers p 1234 A93-55352
- SIGNOR, DAVID B.**
Effects of ingested atmospheric turbulence on measured tail rotor acoustics p 849 A93-35964
- SIKONEN, TIMO**
Calculation of transonic viscous flow around a delta wing p 113 A93-14191
- SIKES, GREGORY D.**
Flutter optimization of large transport aircraft
[AIAA PAPER 92-4795] p 326 A93-20381
- SIKORA, TIMOTHY P.**
Actively cooled panel testing perils, problems, and pitfalls p 1028 A93-46802
- SIKORSKI, SIEGFRIED**
All-composite fan blade for advanced ducted engines p 1246 A93-54837
- SIKSIK, D. N.**
Implementation of expert systems within an interactive tactical environment
[AIAA PAPER 93-3583] p 1223 A93-52678
- SIL'VESTROV, PAVEL V.**
Flight safety in a perturbed atmosphere
[ISBN 5-277-00815-2] p 487 A93-29431
- SILAIEV, V. V.**
Calculation of a plane supersonic jet simulating the exhaust jet of a hypersonic flight vehicle engine p 1103 A93-51912
- SILCOX, R. J.**
Active control of interior noise in model aircraft fuselages using piezoceramic actuators p 231 A93-14540
Approximation methods for control of structural acoustics models with piezoceramic actuators p 452 A93-23744
Active control of interior noise in a large scale cylinder using piezoelectric actuators p 568 A93-29425
Linear quadratic tracking problems in Hilbert space - Application to optimal active noise suppression p 1224 A93-52763
- SILCOX, RICHARD J.**
Evaluation of piezoceramic actuators for control of aircraft interior noise p 447 A93-19186
Noise transmission properties and control strategies for composite structures p 919 N93-30436
- SILVA, A. F. C.**
Code validation for high speed flow simulation over the VLS launcher fairing
[AIAA PAPER 93-3046] p 1057 A93-48226
- SILVA, M. A. G.**
Propagation of transverse anti-plane waves in orthotropic layers p 412 A93-21878
- SILVA, WALTER A.**
Extension of a nonlinear systems theory to general-frequency unsteady transonic aerodynamic responses
[AIAA PAPER 93-1590] p 683 A93-34122
Experimental unsteady pressures at flutter on the Supercritical Wing Benchmark Model
[AIAA PAPER 93-1592] p 683 A93-34123
Application of nonlinear systems theory to transonic unsteady aerodynamic responses p 1095 A93-52438
- SILVANO, SILENZI**
The FAIR (Flight Animated and Interactive Reconstruction) tool p 148 N93-15164
- SILVERGLATE, P.**
The HYDICE instrument design and its application to planetary instruments p 842 N93-28766
- SILVERTHORN, L. J.**
Dynamics of a high speed impeller - Analysis and experimental verification
[AIAA PAPER 93-1362] p 743 A93-34239
- SIMEN, MARTIN**
Nonlocal vs. local instability of compressible flows including body metric, flow divergence and 3D-wave propagation
[AIAA PAPER 93-2982] p 1051 A93-48175
- SIMEONIDES, G.**
An experimental contribution to the flat plate 2D compression ramp, shock/boundary layer interaction problem at Mach 14 - Test case 3.7 p 865 A93-42590
Parametric studies of shock wave/boundary layer interactions over 2D compression corners at Mach 6 [VKI-TN-181] p 988 N93-31538
- SIMEONOV, A.**
Results of operational testing of a system for computing optimal flight regimes p 996 A93-45665
- SIMMONS, J. M.**
Development of a skin friction gauge for use in an impulse facility p 1024 A93-45526
Free piston facilities with air driver gas p 1011 A93-45528
- SIMMS, D. A.**
Combined experiment, phase 1
[DE93-000012] p 485 N93-21766
- SIMMS, SANDRA**
MOI - Magneto-optic/eddy current imaging p 927 A93-41751
- SIMON, BURKHARD**
Combustor development for advanced helicopter engines p 1246 A93-54841
- SIMON, FREDERICK F.**
Progress towards understanding and predicting heat transfer in the turbine gas path p 1215 A93-52751
- SIMON, J. S.**
Evaluation of approaches to active compressor surge stabilization
[ASME PAPER 92-GT-182] p 352 A93-19407
- SIMON, JON S.**
Active stabilization to prevent surge in centrifugal compression systems
[NASA-CR-191625] p 424 N93-18862
- SIMONEAU, ROBERT J.**
Progress towards understanding and predicting heat transfer in the turbine gas path p 1215 A93-52751
- SIMONICH, J.**
An assessment of wake structure behind forward swept and aft swept propfans at high loading p 245 A93-19222
Active aerodynamic control of wake-airfoil interaction noise - Experiment p 1225 A93-53206
- SIMONICH, J. C.**
Active aerodynamic control of wake-airfoil interaction noise - Experiment p 445 A93-19153
Role of leading-edge vortex flows in prop-fan interaction noise p 565 A93-28614
- SIMONS, J. W.**
Unified airport pavement design procedure p 380 N93-16318
- SIMONYI, PATRICIA S.**
Measurements and computational analysis of heat transfer and flow in a simulated turbine blade internal cooling passage
[AIAA PAPER 93-1797] p 1218 A93-53585
Measurements and computational analysis of heat transfer and flow in a simulated turbine blade internal cooling passage
[NASA-TM-106189] p 1032 N93-31647
- SIMPSON, MYLES A.**
Comparison of advanced turboprop interior noise control ground and flight test data p 444 A93-19136
Experimental and analytical investigations of fuselage modal characteristics and structural-acoustic coupling p 451 A93-19229
Structural-acoustic coupling in aircraft fuselage structures p 1243 A93-55856
- SIMPSON, R. L.**
Time-resolved surface heat flux measurements in the wing/body junction vortex
[AIAA PAPER 93-0918] p 472 A93-24972
An experimental study of a turbulent wing-body junction and wake flow p 873 A93-43541
- SIMPSON, THEODORE R.**
Managing the world's air traffic p 501 A93-28392
- SIMS, JOSEPH P.**
Airspeed calibration using GPS
[AIAA PAPER 92-4090] p 51 A93-13272
- SIMSON, JOHN**
Helicopter noise - Public perspective p 1261 A93-54719
- SINACORI, JOHN**
Texture as a visual cueing element in computer image generation. I - Representation of the sea surface
[AIAA PAPER 93-3560] p 1214 A93-52695
- SINCLAIR, PETER C.**
Infrared detection of high altitude clear air turbulence
[AIAA PAPER 93-0852] p 557 A93-24916
- SINENKO, A. V.**
Vibrational monitoring and diagnostics of the technical condition of gas turbine engines at civil aviation repair facilities p 374 A93-18362
- SINGER, BART A.**
Modeling the transition region
[NASA-CR-4492] p 298 N93-19015
- SINGER, GIDEON**
The SAAB 2000 initial flight test - Status report p 804 A93-38847
- SINGER, MICHAEL J.**
Development of a concept formulation process aid for analyzing training requirements and developing training devices
[AD-A263579] p 912 N93-29972
- SINGH, A. K.**
Structure of martensite in titanium alloy Ti-6Al-1.6Zr-3.3Mo-0.3Si p 916 A93-43616
- SINGH, D. J.**
Numerical simulation of shock-induced combustion/detonation p 410 A93-20719
Numerical study of the performance of swept, curved compression surface scramjet inlets
[AIAA PAPER 93-1837] p 1074 A93-49721
- SINGH, JAG J.**
Partially exposed polymer dispersed liquid crystals for boundary layer investigations p 399 A93-19250
- SINGH, JATINDER**
Modelling for aileron induced unsteady aerodynamic effects for parameter estimation p 118 A93-14323
Aileron and sideslip-induced unsteady aerodynamic modeling for lateral parameter estimation p 1007 A93-45144
- SINGH, N.**
A low-speed aerodynamic model for harmonically oscillating aircraft configurations p 8 A93-11500
Incompressible potential flow calculation about harmonically oscillating three-dimensional configurations p 461 A93-24089
- SINGH, RAJENDRA**
Engineering science research issues in high power density transmission dynamics for aerospace applications
[AIAA PAPER 93-2299] p 1155 A93-50084
- SINGH, SARABJEET**
Experimental assessment of airframe damage due to impacting ice
[AIAA PAPER 93-0751] p 504 A93-24838
- SINGH, V.**
Structure of martensite in titanium alloy Ti-6Al-1.6Zr-3.3Mo-0.3Si p 916 A93-43616
- SINGHAL, S. N.**
Quantification of uncertainties in composites
[AIAA PAPER 93-1440] p 734 A93-33989
- SINGHAL, SURENDRA N.**
Coupled multi-disciplinary simulation of composite engine structures in propulsion environment
[ASME PAPER 92-GT-6] p 346 A93-19279
Multidisciplinary tailoring of hot composite structures
[NASA-TM-106027] p 550 N93-19971
- SINGHVI, SARVESH**
Shape sensitivities and approximations of modal response of laminated skew plates p 829 A93-37403
- SINGSHINSUK, P.**
Development of the F/A-18 E/F air induction system
[AIAA PAPER 93-2152] p 1101 A93-49969
- SINHA, AGAM N.**
Improved efficiency of air transportation through aviation weather system modernization p 308 A93-22144
- SINHA, KAUSHIK**
An aerodynamic model of multiple lifting surfaces including wake deformation and tip effect p 10 A93-12366

SINHA, N.

The critical role of turbulence modeling in the prediction of supersonic jet structure for acoustic applications p 398 A93-19193

SINHA, P. K.

A two-dimensional elliptic grid generator for a wing-body section involving grid control functions p 460 A93-24083

SINHMAHAPATRA, K. P.

Incompressible potential flow calculation about harmonically oscillating three-dimensional configurations p 461 A93-24089

SINKKONEN, MATTI

Transmission system for a transfer device gripping a double wheel [CA-PATENT-APPL-SN-2024585] p 731 N93-25178

SIPPO, ARTHUR C.

US Army's aviation life support equipment retrieval program real world design successes from proactive investigation p 494 A93-19690

SIRA-RAMIREZ, HEBERTT

Dynamical variable structure control of a helicopter in vertical flight p 369 A93-22887
Dynamic compensator design in nonlinear aerospace systems p 1036 A93-44150

SIRAZH, I. A.

Effect of a deformed electric field on the precision of the electrochemical machining of gas turbine engine components p 835 A93-39094

SIRBAUGH, JAMES R.

An improved far field drag calculation method for nonlinear CFD codes [AIAA PAPER 93-3417] p 975 A93-47213

SIRIGIRI, RAVINDRA

Structural analysis of box beams using symbolic manipulation technique p 548 A93-28615

SIRIGNANO, W. A.

Fundamental studies of droplet interactions in dense sprays [AD-A261165] p 737 N93-25948

SIRIGNANO, WILLIAM A.

Three-dimensional flow over two spheres placed side by side p 539 A93-24412

SIROCKY, PAUL J.

A hot dynamic seal rig for measuring hypersonic engine seal durability and flow performance [AIAA PAPER 93-1346] p 738 A93-33916

SIROK, B.

Propulsion system simulator with propan for tests on a large scale model of IL-114 airplane in a full-size wind tunnel of TsAGI p 1013 A93-46933

SISLER, CLIFFORD E.

The history and development of coated Contrast Enhancement Filters for cockpit displays p 564 A93-28180

SISLIAN, JEAN P.

An aerospace plane as a detonation wave ramjet/airframe integrated waverider [AIAA PAPER 92-5022] p 272 A93-22298
Hypersonic shock-induced combustion ramjet performance analysis [ISABE 93-7037] p 1197 A93-54013

SISTO, F.

Numerical simulation for aeroelasticity in turbomachines with vortex method. I - Theory and method p 53 A93-12452

Computational analysis of nonlinear aeroelastic phenomena during stall flutter of cascaded airfoils [AIAA PAPER 93-2082] p 1079 A93-49909

SITARAM, N.

Effect of radial distortion on the performance of a centrifugal compressor p 861 A93-42256

SITZ, JOEL R.

The F-18 systems research aircraft facility [NASA-TM-4433] p 381 N93-16753
Flight control system design factors for applying automated testing techniques [NASA-TM-4242] p 910 N93-30764

SIU, T.

Explosives detection systems for airport security gas chromatographic based devices p 881 N93-30276

SIVERS, E. A.

Use of local x ray computerized tomography for high-resolution, region-of-interest inspection of large ceramic components for engines [DE93-005564] p 843 N93-28943

SIVES, C.

Integration of full scale development aircraft GPS user equipment (AN/ARN-151) with Doppler radar systems p 31 A93-11012

SIXSMITH, HERBERT

Magnetic bearings for cryogenic turbomachines p 1149 A93-48601

SIZEMORE, D. R.

Fleet fatigue cracking threshold prediction p 3 A93-13633

SJOLANDER, S. A.

Aerodynamics of turbine blades with trailing-edge damage - Measurements and computations [ISABE 93-7130] p 1189 A93-54105

SKAAR, TORE

Arctic environment - Helicopter operations in cold climates p 1189 A93-54288

SKAFF, TONY

Effect of leeward flow dividers on the wing rock of a delta wing [AIAA PAPER 93-3492] p 982 A93-47264

SKIBA, G. G.

A method for determining the aerodynamic coefficients of asymmetric bodies with allowance for nonlinear influence factors of the body shape p 5 A93-10142

SKILLER, JOHN

On the fatigue life of M50 NiL rolling bearings p 78 A93-11346

SKOE, IVAR HELGE

The integration of geometric modeling into an inverse design method and application of a PC-based inverse design method and comparison with test results p 81 N93-10058

SKOLDSTROM, BJORN

Fatigue effects of noise among airplane mechanics p 558 A93-28495

SKOMOROKHOV, V. I.

Viscosity of aviation fuel components (n-alkanes) p 71 A93-12824

Viscosity of aviation fuel components - Aromatic hydrocarbons (alkyl benzenes) p 1211 A93-52961

SKOOG, M. A.

Testing of an automatic, low altitude, all terrain ground collision avoidance system p 502 N93-19924

SKORMIN, VICTOR A.

Stiffness enhancement of flight control actuator p 1006 A93-44151

SKOVRTSOV, YU. V.

A nonlinear finite element of an arbitrary beam p 1215 A93-52939

SKRIPKA, M. L.

Refinement of algorithms for calculating the remaining life from magnetic recording instrument data p 320 A93-18330

Characteristics of fatigue crack growth under the service-spectrum loading of the tail boom of a helicopter p 321 A93-18339

SKRIPNICHENKO, S. YU.

Problems in the aerodynamics, strength, and flight operations of aircraft p 947 A93-45659

Classification of the principal fuel saving methods in flight operations p 996 A93-45660

Results of operational testing of a system for computing optimal flight regimes p 996 A93-45665

SKRUCH, HARRY J.

Apparatus for reduction of vibration in liquid-injected gas compressor system [AD-D015607] p 554 N93-20772

SKUJINS, MARGARET B.

Wright Laboratory research and development facilities handbook [AD-A258746] p 572 N93-20403

SKVORTSOV, V. V.

An experimental study of dc discharges in supersonic and subsonic air flows p 14 A93-12980

SLACK, D. C.

Development and application of GASP 2.0 [AIAA PAPER 92-5067] p 438 A93-22337

SLAOUTI, A.

Flow around two circular cylinders by the random-vortex method p 271 A93-21925

SLASKI, L.

Ground clutter measurements using an aerostat surveillance radar p 929 A93-43381

SLATER, ANDREW P.

Comparison of experimental ground testing and computational fluid dynamics for the re-engined 727-100 center engine inlet [AIAA PAPER 92-3920] p 462 A93-24294

SLATER, G. L.

Direct multivariable adaptive controller with application to wing flutter p 524 A93-26946

SLEZIONA, P. C.

Non-equilibrium flow in an arc heated wind tunnel p 910 A93-42642

SLOAN, M. L.

A lag model for turbulent boundary layers developing over rough bleed surfaces [AIAA PAPER 93-2988] p 1052 A93-48181

SLOCUM, C.

A systems dynamics approach to modeling gas turbine combustor wear [ASME PAPER 92-GT-47] p 347 A93-19300

SLOMINSKI, CHRISTOPHER J.

Advanced Transport Operating System (ATOPS) Flight Management/Flight Controls (FM/FC) software description [NASA-CR-191457] p 808 N93-28621

Advanced Transport Operating System (ATOPS) utility library software description [NASA-CR-191469] p 1000 N93-32218

SLOMSKI, J. F.

Numerical simulation of vortex generation and capture above an airfoil [AIAA PAPER 93-0864] p 468 A93-24926

SLOOFF, J. W.

Computational methods for aerodynamic design of aircraft components [NLR-TP-92072-4] p 987 N93-31148

SLUSARCZUK, MARKO M.

High-resolution displays and projection systems; Proceedings of the Meeting, San Jose, CA, Feb. 11, 12, 1992 [SPIE-1664] p 544 A93-27237

SLUZ, ANDREW

Federal Aviation Administration pavement modeling p 379 N93-16315

SLYE, ROBERT E.

The Airborne Ocean Color Imager - System description and image processing p 1157 A93-50369

SLYUSARENKO, A. S.

Algorithmic method for optimizing the precision characteristics of a fuel metering system p 999 A93-45681

SMALANSKAS, JOSEPH P.

A wideband, embedded/conformal, antenna subsystem concept p 327 A93-22002

SMALL, C.

Neutron diffraction residual stress studies for aero-engine component applications [PNR-90908] p 85 N93-11014

SMALLEY, A. J.

Computational techniques for probabilistic analysis of turbomachinery [ASME PAPER 92-GT-167] p 351 A93-19393

SMARIO, DAVID

The Edge supersonic transport [NASA-CR-192074] p 335 N93-18055

SMART, DON

Flight simulation - An overview p 1209 A93-53768

SMART, J. R.

The FAA aircraft icing Forecasting Improvement Program - Validation of aircraft icing forecasts in the Denver area [AIAA PAPER 93-0393] p 309 A93-23069

SMEETS, G.

Shock tube validation experiments for the simulation of ram-accelerator-related combustion and gasdynamic problems p 1016 A93-45499

Shock tunnel studies of external combustion in high supersonic air flows p 1017 A93-45517

SMELOV, V. V.

A model of the maintenance of a fleet of TU-204 aircraft at a maintenance and repair center p 237 A93-18327

SMETANIN, V. V.

Nonequilibrium excitation of internal molecular degrees of freedom in the shock layer during hypersonic flight p 412 A93-21922

SMIALEK, JAMES L.

The chemistry of Saudi Arabian sand - A deposition problem on helicopter turbine airfoils p 1216 A93-53468

SMIGIELSKI, PAUL

Progress in industrial holography in France p 1020 A93-44197

SMILJANOVSKI, VANCO

Initial acceleration effects on flow evolution around airfoils pitching to high angles of attack p 961 A93-45750

SMIRNOV, A. V.

Calculation of flow fields near a lifting wing p 1179 A93-53552

SMIRNOV, G. V.

Effect of the technological process structure on residual stress distribution in the blade foil of gas turbine engines p 836 A93-39106

SMITH, A. E.

AQUIS: A PC-based air quality and permit information system [DE92-040092] p 434 N93-18587

SMITH, A. J.

Ground visual aids - Recent research at RAE Bedford p 191 A93-17311

SMITH, ALEX E.

Evaluation of category 3 MLS designs p 888 N93-30358

SMITH, ALEXANDER E.

Complementary MLS and GNSS operations p 384 A93-21160

- SMITH, ANDREW**
ICAO analyses trends in fuel consumption by world's airlines p 1 A93-10733
- SMITH, ARTHUR P., III**
The dependent converging instrument approach procedure [AIAA PAPER 93-3835] p 1098 A93-51424
The dependent converging instrument approach procedure: An analysis of its safety and applicability [DOE/FAA/RD-93/6] p 707 N93-25456
- SMITH, B.**
A discussion of the results of the rainflow counting of a wide range of dynamics associated with the simultaneous operation of adjacent wind turbines [DE93-000016] p 434 N93-18705
- SMITH, BARRY T.**
Rapid detection and quantification of impact damage in composite structures p 547 A93-27978
- SMITH, BROOKE C.**
Experimental and numerical analysis of the wing rock characteristics of a 'wing-body-tail' configuration [AIAA PAPER 93-0187] p 368 A93-22612
- SMITH, BRUCE A.**
Quiet operations key to MD-90 success p 708 A93-33700
Management miscues, delays snarl C-17 program p 760 A93-34944
- SMITH, C. E.**
Integrated CFD modeling of gas turbine combustors [AIAA PAPER 93-2196] p 1115 A93-50008
CFD mixing analysis of axially opposed rows of jets injected into confined crossflow [NASA-TM-106179] p 813 N93-27128
- SMITH, C. F.**
Navier-Stokes analysis of three-dimensional S-ducts p 959 A93-45146
- SMITH, C. W.**
Optical methods of stress analysis applied to cracked components p 1027 A93-45798
- SMITH, CHARLES A.**
The evolution of a nose-wheel steering system p 995 A93-44852
Applied aerodynamics: Challenges and expectations [NASA-TM-103963] p 694 A93-25091
- SMITH, CHRIS M.**
Composite 'Exoskin' doubler extends F-15 Vertical Tail fatigue life [AIAA PAPER 93-1341] p 709 A93-33911
- SMITH, CLIFF**
Workshop report - A validation study of Navier-Stokes codes for transverse injection into a Mach 2 flow p 270 A93-21330
Workshop Report: A validation study of Navier-Stokes codes for transverse injection into a Mach 2 flow p 751 N93-26008
- SMITH, CLIFFORD E.**
Dual-spray airblast fuel nozzle for advanced small gas turbine combustors [AIAA PAPER 93-2336] p 1116 A93-50113
- SMITH, D. M.**
Flow calibration of two hypersonic nozzles in the AEDC HEAT-H2 high-enthalpy arc-heated wind tunnel [AIAA PAPER 93-2782] p 1012 A93-46526
- SMITH, D. R.**
Conventional skin friction measurement techniques for strongly perturbed supersonic turbulent boundary layers p 271 A93-21863
- SMITH, DONALD L.**
Development of stitching reinforcement for transport wing panels p 921 N93-30852
- SMITH, EDMUND H.**
Aerodynamic characteristics of the MMPT ATD vehicle at high angles of attack [AIAA PAPER 93-3493] p 982 A93-47265
- SMITH, EDWARD C.**
Vibration and flutter of stiff-inplane elastically tailored composite rotor blades [AIAA PAPER 93-1302] p 725 A93-33879
Aeromechanical stability of helicopters with composite rotor blades in forward flight p 794 A93-35904
Aeroelastic response, loads, and stability of a composite rotor in forward flight p 906 A93-41919
Aeroelastic response and aeromechanical stability of helicopters with elastically coupled composite rotor blades p 715 N93-25530
- SMITH, F. T.**
On boundary-layer transition in transonic flow p 1087 A93-51280
- SMITH, FRED G.**
Comparison of neural network and Markov random field image segmentation techniques p 397 A93-18652
- SMITH, G. D.**
Corrosion resistance of Inconel Alloy 617 in simulated gas turbine environments [ASME PAPER 92-GT-142] p 388 A93-19374
- SMITH, G. H.**
Measurement of shed vorticity and circulation from rotating aerofoil by particle image velocimetry p 538 A93-23804
- SMITH, GRAHAM**
A comparative assessment of two present generation turbine analysis codes [ISABE 93-7097] p 1203 A93-54073
- SMITH, GUY A.**
FNAS modify matric and transparent experiments [NASA-CR-184442] p 198 N93-13311
Fiber pulling apparatus modification [NASA-CR-184498] p 220 N93-14763
- SMITH, HOOVER A.**
Coking characteristics of polyphenyl ether lubricants using a Static Coker and a Micro Carbon Residue Tester p 77 A93-11341
Ferrogaphic analysis of polyphenyl ether fluids p 735 A93-34561
- SMITH, HOWARD W.**
General aviation aircraft: Normal acceleration data analysis and collection project [DOT/FAA/CT-91/20] p 713 N93-24739
The Ultra Light Aircraft Testing [NASA-CR-193043] p 895 N93-29774
Report on the test set-up for the structural testing of the Airmass Sunburst Ultralight Aircraft p 895 N93-29775
Load test set-up for the Airmass Sunburst Ultra-Light Aircraft p 895 N93-29776
NASTRAN analysis for the Airmass Sunburst model 'C' Ultralight Aircraft p 931 N93-29777
Construction, wind tunnel testing and data analysis for a 1/5 scale ultra-light wing model p 876 N93-29778
Selection and static calibration of the Marsh J1678 pressure gauge p 931 N93-29779
- SMITH, I. G.**
Issues of ATC conflict resolution under real-time constraints p 887 N93-30350
- SMITH, I. S., JR.**
NASA balloon design and flight - Philosophy and criteria p 40 A93-11363
- SMITH, JEFFREY O.**
The UTA autonomous aerial vehicle - Automatic control and navigation p 908 A93-42813
- SMITH, JOE A.**
Flow quality improvement in a high speed blowdown wind tunnel [AIAA PAPER 93-0353] p 377 A93-23038
- SMITH, KENNETH O.**
Engine testing of a prototype low NO(x) gas turbine combustor [ASME PAPER 92-GT-116] p 401 A93-19352
- SMITH, KENT F.**
Concept feasibility demonstration for the Army Cockpit Delethalization Program p 795 A93-35916
PROAV Cable Warning System (CWS) - U.S. Army aircraft Integration assessment and OCONUS field evaluation [AD-A261233] p 705 N93-26263
- SMITH, LEROY H., JR.**
Wake ingestion propulsion benefit p 411 A93-21660
- SMITH, LINDA G.**
Optically smart surfaces survivability testing at Mach 3 [AD-A261785] p 760 N93-26566
- SMITH, M.**
The numerical errors in inverse simulation [AIAA PAPER 93-3588] p 1223 A93-52681
- SMITH, M. J.**
ELF, VLF and LF radiation from a very large loop antenna with a mountain core p 924 A93-40334
Lift coefficient of a randomly oscillating hydroplane [DRA/MAR-TM(MTH)-91320] p 21 N93-11377
Comparison of reacting and non-reacting shear layers at a high subsonic Mach number [NASA-TM-106198] p 814 N93-27610
Turbulence measurement in a reacting and non-reacting shear layer at a high subsonic Mach number [NASA-TM-106186] p 989 N93-31839
- SMITH, M. J. T.**
Evolving noise issue could persist into the next century p 99 A93-10731
- SMITH, MAHLON C.**
National airborne surveillance system - An engineering student study [AIAA PAPER 93-4031] p 1242 A93-54603
- SMITH, MARILYN J.**
Development of circulation control technology for application to advanced subsonic transport aircraft [AIAA PAPER 93-0644] p 464 A93-24759
- SMITH, P. J.**
Advanced technology commercial fuselage structure p 918 N93-30432
Cost studies for commercial fuselage crown designs p 920 N93-30440
- SMITH, PHILIP**
Vision based techniques for rotorcraft low altitude flight p 1097 A93-49351
- SMITH, PHILIP J.**
Design concepts for the development of cooperative problem-solving systems [NASA-CR-192708] p 707 N93-25261
Design of a cooperative problem-solving system for enroute flight planning: An empirical study of its use by airline dispatchers [NASA-CR-192709] p 707 N93-25330
- SMITH, PHILLIP**
Multirate and event-driven Kalman filters for helicopter flight p 1245 A93-55760
- SMITH, PHILLIP N.**
Vision-based range estimation using helicopter flight data p 151 A93-17501
Vision-based range estimation using helicopter flight data p 317 A93-21525
- SMITH, PHILLIP RAYMOND**
Application of eigenstructure assignment to the control of powered lift combat aircraft p 64 N93-11871
- SMITH, R.**
A Hopfield neural network for adaptive control [AIAA PAPER 93-3729] p 1130 A93-51329
- SMITH, R. A.**
Combustion characteristics and passive control of an annular dump combustor [AIAA PAPER 93-1772] p 1110 A93-49668
Periodic chemical energy release for active combustion control [ISABE 93-7043] p 1198 A93-54019
- SMITH, R. C.**
Approximation methods for control of structural acoustics models with piezoceramic actuators p 452 A93-23744
- SMITH, R. L.**
Assessment of NDT reliability p 1258 A93-54900
- SMITH, R. R.**
Passive drag reduction of a helicopter airfoil in an unsteady transonic flow p 482 A93-29440
- SMITH, RANDALL F.**
Development of generic helicopter performance methodology for real time mission analyses p 152 A93-14185
- SMITH, RICHARD**
A viscous flow based membrane wing model [AIAA PAPER 93-2955] p 1047 A93-48149
Satellite communications for aeronautical and navigation service p 838 N93-26648
- SMITH, RITA A.**
ADDRAS - An integrated systems approach p 562 A93-29423
- SMITH, ROBERT A.**
Enhancement of conventional NDT methods for corrosion detection in layered skins p 1258 A93-54898
- SMITH, ROBERT E.**
Geometric requirements for multidisciplinary analysis of aerospace-vehicle design [AIAA PAPER 92-4773] p 436 A93-20366
Grid and design variables sensitivity analyses for NACA four-digit wing-sections [AIAA PAPER 93-0195] p 276 A93-22616
Grid and aerodynamic sensitivity analyses of airplane components [AIAA PAPER 93-3475] p 981 A93-47254
- SMITH, RON**
Reliability assessment at airline inspection facilities. Volume 1: A generic protocol for inspection reliability experiments [DOT/FAA/CT-92/12-VOL-1] p 704 N93-25110
Reliability assessment at airline inspection facilities. Volume 2: Protocol for an eddy current inspection reliability experiment [DOT/FAA/CT-92/12-VOL-2] p 842 N93-28685
- SMITH, S. G.**
Automatic navigation in the air and at sea p 1099 A93-52593
- SMITH, S. H.**
Accelerated corrosion fatigue test methods for aging aircraft p 198 A93-16623
- SMITH, S. M.**
Measurements in 80- by 120-foot wind tunnel of hazard posed by lift-generated wakes [AIAA PAPER 93-3518] p 1014 A93-47281
- SMITH, SAMUEL O.**
Modeling and strain gauging of eddy current repulsion deicing systems [AIAA PAPER 93-0296] p 327 A93-22696
- SMITH, SCOTT M.**
Rotor fatigue monitoring data acquisition system p 1261 A93-54353
- SMITH, STEPHEN C.**
Computation of induced drag for elliptical and crescent-shaped wings p 958 A93-45136

- SMITH, T. D.**
Design optimization study for F-15 propulsion/forward fairing compatibility
[AIAA PAPER 93-3484] p 1003 A93-47291
- SMITH, T. R.**
A hypersonic waverider research vehicle
[AIAA PAPER 93-0402] p 505 A93-25522
- SMITH, TODD E.**
Localization of aeroelastic modes in mistuned high-energy turbines p 1032 A93-31586
- SMITH, V. J.**
ASTOVL model engine simulators for wind tunnel research p 192 A93-13213
- SMITH, V. K. III**
Complementary role of ground testing, flight testing, and computations in aerospace plane propulsion development
[ISABE 93-7034] p 1197 A93-54010
- SMITH, WILLIAM L.**
Remote sensing cloud properties from high spectral resolution infrared observations p 1034 A93-46780
- SMITS, A. J.**
Conventional skin friction measurement techniques for strongly perturbed supersonic turbulent boundary layers p 271 A93-21863
Control of pressure fluctuations in the reattachment region of a supersonic free shear layer
[AIAA PAPER 93-0385] p 282 A93-23064
Mean flowfield structure of a three-dimensional supersonic turbulent boundary layer
[AIAA PAPER 93-0661] p 465 A93-24774
Control of a supersonic reattaching shear layer
[AIAA PAPER 93-3248] p 966 A93-46793
- SMOLENSKY, MARK W.**
Using TRACON as a teaching tool p 571 A93-27166
- SMOLSKI, A. P.**
Dual band tuned radomes for radar applications p 929 A93-43405
- SMORODIN, F. K.**
Effect of the proximity of the machined surface on the discharge coefficients of laser cutter nozzles p 79 A93-12809
- SNELL, ANTONY**
Cancellation control law for lateral-directional dynamics of a supermaneuverable aircraft
[AIAA PAPER 93-3775] p 1131 A93-51370
- SNELL, S. A.**
Nonlinear feedback control of highly manoeuvrable aircraft p 40 A93-11654
- SNIDER, KARL**
Application and integration of diverse technology in an aviation system: The National Aeronautical Information Processing System p 887 A93-30339
- SNOEIJ, PAUL**
A dual polarised active phased array antenna with low cross polarisation for a polarimetric airborne SAR p 883 A93-43401
The PHARUS project, first results of the realization phase p 884 A93-43454
The realization phase of the PHARUS project p 1162 A93-47658
- SNOW, WALTER L.**
Recent experiences with implementing a video based six degree of freedom measurement system for airplane models in a 20 foot diameter vertical spin tunnel p 821 A93-37763
- SNYDER, CARL E., JR.**
Development of MIL-H-53119, -54 C to 175 C high-temperature nonflammable hydraulic fluid for Air Force systems p 1214 A93-54250
- SNYDER, CURTIS D.**
A configuration development strategy for the NASP p 46 A93-10011
- SNYDER, H. T.**
Thermoelastic vibration test techniques p 549 A93-29293
- SNYDER, JOHN G.**
Integrated Blade Inspection System (IBIS) upgrade study
[AD-A258912] p 365 A93-19356
- SNYDER, S. D.**
Active control of interior noise in model aircraft fuselages using piezoceramic actuators p 231 A93-14540
- SNYDER, SCOTT**
Differential GPS/inertial navigation approach/landing flight test results p 32 A93-11019
- SO, R. M. C.**
Aerodynamic flow simulation using a pressure-based method and a two-equation turbulence model
[AIAA PAPER 93-2902] p 1147 A93-48111
- SOBEL, KENNETH M.**
Robust sampled data eigenstructure assignment using the delta operator p 906 A93-41889
- SOBIECZKY, H.**
Interactive hypersonic waverider design and optimization p 119 A93-14348
Waverider design for generalized shock geometries
[AIAA PAPER 93-0774] p 467 A93-24858
Design of shockless supersonic region in the axisymmetric transonic flow p 1230 A93-54587
Two problems applied to the rheographical transformation of axisymmetric flow p 1231 A93-54599
- SOBIESZCZANSKI-SOBIESKI, JAROSLAW**
Aircraft optimization by a system approach - Achievements and trends p 153 A93-14205
Multidisciplinary design optimization: An emerging new engineering discipline
[NASA-TM-107761] p 806 A93-27258
- SOBOLEV, A. F.**
Determination of fan noise in a lined duct with flow using the Green function method p 1124 A93-51761
- SOBOTA, THOMAS H.**
Analysis and demonstration of a Scramaccelerator system
[AIAA PAPER 93-2183] p 1142 A93-49995
- SOCH, P.**
Profile losses of an annular turbine cascade in unsteady periodic flow
[ASME PAPER 92-GT-153] p 249 A93-19380
- SODDU, C.**
GPS integrity monitoring and system improvement with ground station and multistationary satellite support p 33 A93-11044
- SODERMAN, P. T.**
Fiber-optic interferometric sensors for measurements of pressure fluctuations - Experimental evaluation
[AIAA PAPER 93-0738] p 540 A93-24828
- SODERMAN, PAUL T.**
The design of test-section inserts for higher speed aerodynamic testing in the Ames 80- by 120-Foot Wind Tunnel p 374 A93-19149
On the scaling of small-scale jet noise to large scale p 448 A93-19195
- SOEDER, RONALD H.**
User manual for NASA Lewis 10 by 10 foot supersonic wind tunnel
[NASA-TM-105626] p 194 A93-15498
NASA Lewis 8- by 6-foot supersonic wind tunnel user manual
[NASA-TM-105771] p 730 A93-25080
- SOETRISNO, MOELJO**
The 3D Navier-Stokes flow analysis for shared and distributed memory MIMD computers
[AD-A256038] p 221 A93-15187
- SOFRIN, T.**
Active aerodynamic control of wake-airfoil interaction noise - Experiment p 1225 A93-53206
- SOFRIN, T. G.**
Active aerodynamic control of wake-airfoil interaction noise - Experiment p 445 A93-19153
- SOFRONOV, V. D.**
Calculation of subsonic flow of a gas past an airfoil p 1068 A93-48908
Spline-collocation solution of a Fredholm equation of the second kind in the problem of flow past an airfoil p 1092 A93-51904
- SOGA, TAKEO**
Numerical study on the interaction of supersonic flow past a wedge and free jet p 479 A93-28574
- SOH, W. Y.**
Numerical simulation of free shear flows: Towards a predictive computational aeroacoustics capability
[NASA-CR-191015] p 781 A93-27097
- SOHN, C. H.**
Prediction of airfoil stall using Navier-Stokes equations in streamline coordinates p 787 A93-27456
- SOININEN, HARRI**
Interaction between ice and propeller
[VTT-TIED-1281] p 841 A93-27832
- SOISTMANN, DAVID L.**
Aeroelastic character of a National Aerospace Plane demonstrator concept
[AIAA PAPER 93-1314] p 732 A93-33890
An experimental and analytical study of a lifting-body wind-tunnel model exhibiting body-freedom flutter
[AIAA PAPER 93-1316] p 732 A93-33891
- SOIZE, C.**
Strong coupling between inviscid fluid and boundary layer for airfoils with a sharp edge. II - 2D unsteady case for isolated airfoil and straight blade cascade p 126 A93-16473
- SOLOLOV, E. I.**
Breakdown of steady state axisymmetric flow in a shock layer formed as a result of the impingement of a supersonic underexpanded jet on a perpendicular plane obstacle p 241 A93-18230
- SOLAN, MICHAEL**
Systems integration test laboratory - Application and experiences p 190 A93-13910
- SOLDATKIN, V. M.**
A data processing and control system for counteracting wind shear p 524 A93-27604
- SOLEY, PAUL**
Hot end cleaning - Corrosion pitting of turbine discs
[SAE PAPER 920930] p 202 A93-14081
- SOLIES, U. P.**
Effects of thrust line offset on neutral point determination in stability flight testing
[AIAA PAPER 92-4082] p 61 A93-11265
- SOLIGNAC, JEAN-LOUIS**
Contribution of visualization to the study of unsteady aspects of vortex breakdown
[ONERA, TP NO. 1992-93] p 771 A93-38576
- SOLNECHNYI, E. M.**
A study of the problem of developing a weakly invariant flight vehicle control system p 561 A93-27688
- SOLOMON, DEMPSEY D.**
Helicopter flight control system design using the linear quadratic regulator for robust eigenstructure assignment
[AD-A258904] p 373 A93-19351
- SOLOMON, W. C.**
Mixing enhancement and combustion of gaseous fuel in a supersonic combustor
[AIAA PAPER 93-2143] p 1114 A93-49960
- SOLONIN, V. I.**
The study of experimental turboramjets - Heat state and cooling problems
[AIAA PAPER 93-1989] p 1112 A93-49834
- SOLTANI, MOHAMMAD REZA**
An experimental study of the relationship between forces and moments and vortex breakdown on a pitching delta wing p 49 A93-12206
- SOMERS, DAN M.**
Subsonic natural-laminar-flow airfoils p 860 A93-41780
- SOMYO, NOBUHIRO**
A study of a direct-injection stratified-charge rotary engine for motor vehicle application
[SAE PAPER 930677] p 1158 A93-50524
- SONAR, TH.**
Numerical simulation of a two-dimensional supersonic mixed-compression inlet
[ISABE 93-7107] p 1188 A93-54083
- SONG, O.**
A refined structural model of composite aircraft wings for the enhancement of vibrational and aeroelastic response characteristics
[AIAA PAPER 93-1536] p 740 A93-34073
Integrated structural tailoring and adaptive control of advanced flight vehicle structural vibration
[AIAA PAPER 93-1697] p 757 A93-34219
- SONG, OHSEOP**
On the static aeroelastic tailoring of composite aircraft swept wings modelled as thin-walled beam structures p 158 A93-14820
- SONI, BHARAT K.**
A study of CFD algorithms applied to complete aircraft configurations
[AIAA PAPER 93-0784] p 468 A93-24864
- SONNENFROH, D.**
Nonintrusive, multipoint velocity measurements in high-pressure combustion flows
[AIAA PAPER 93-2032] p 1145 A93-49867
- SONNENFROH, D. M.**
An optical comparison of wall and axial injection for high enthalpy reacting scramjet flows
[AIAA PAPER 93-0357] p 377 A93-23040
- SOONG, C. Y.**
Numerical study of mixed convection between two corotating symmetrically heated disks p 416 A93-23491
- SOPHER, ROBERT**
Application of component mode synthesis to modeling the dynamic response of Bearingless Main Rotors p 796 A93-35976
- SOPULIS, IU. IU.**
A unified approach to the construction of the throttle characteristics of postrepair turbojet engines, with the NK8-2U engine used as an example p 345 A93-18372
- SORENSEN, J. A.**
Requirements for integrated flight and traffic management during final approach p 31 A93-11009
- SOROKIN, A. A.**
Atmospheric aerosols due to aircraft and ecological problems p 1162 A93-48846
- SOROKIN, YU. S.**
The use of triangular elements in panel methods for calculating flow past flight vehicles p 1068 A93-48904
Calculation of supersonic flow past a body of revolution with a piecewise linear distribution of singularities at its axis p 1092 A93-51910

- SOROKOPUD, V. A.**
Automated design and fabrication of radio-electronic circuits p 1151 A93-49000
- SOSEDKO, I. U. P.**
Optimal conditions for flow turbulence reduction by a set of grids p 836 A93-39122
- SOSNIN, O. V.**
A new production technology for complex-shaped structural elements 'creep forming' p 202 A93-14175
- SOSUNOV, V. A.**
The study of experimental turboramjets - Heat state and cooling problems [AIAA PAPER 93-1989] p 1112 A93-49834
- SOTIRIOU, CONSTANTINOS PANTELJ**
An experimental and a theoretical investigation of rotor pitch damping using a model rotor p 47 N93-10322
- SOTSENKO, I. U. V.**
Using contra-rotating rotors for decreasing sizes and component number in small GTE [ASME PAPER 92-GT-414] p 356 A93-19562
- SOUDRANAYAGAM, M.**
A study of stall in a low hub/tip ratio fan p 423 N93-18729
- SOULEVANT, DIDIER**
Laser velocimetry around helicopter blades in the DNW wind tunnel of the NLR [ONERA, TP NO. 1992-143] p 831 A93-38613
Two-dimensional laser velocimetry for the study of dual-flow jets with flight effect in the CEPRA 19 anechoic wind tunnel [ONERA, TP NO. 1992-144] p 831 A93-38614
- SOUDRANAYAGAM, M.**
A study of stall in a low hub/tip ratio fan [ASME PAPER 92-GT-85] p 248 A93-19334
Rotating stall inception in fans of low hub-tip ratio p 136 N93-14479
- SOUNDNARAYAGAM, S.**
Some measurements of stall in an axial impeller [ISABE 93-7008] p 1183 A93-53984
- SOUTHCORBE, G.**
The designs for safety p 321 A93-18755
- SOVIERO, PAULO A. O.**
Generalized vortex lattice method for oscillating lifting surfaces in subsonic flow p 123 A93-14555
- SOWA, W. A.**
Coherent anti-Stokes Raman scattering (CARS) thermometry in a model gas turbine can combustor [ASME PAPER 92-GT-134] p 387 A93-19366
Scaling of the two-phase flow downstream of a gas turbine combustor swirl cup - Mean quantities [ASME PAPER 92-GT-207] p 404 A93-19431
CARS thermometry in a liquid fueled model combustor [AIAA PAPER 93-0366] p 390 A93-23047
Optimization of circular orifice jets mixing into a heated crossflow in a cylindrical duct p 361 A93-23246
Mixing in the dome region of a staged gas turbine combustor p 1109 A93-49612
Emission characteristics of a model gas turbine combustor at practical conditions [ISABE 93-7023] p 1196 A93-53999
Optimization of circular orifice jets mixing into a heated cross flow in a cylindrical duct [NASA-TM-105984] p 179 N93-15359
- SPAGNUOLO, JOELLE M.**
Determination of the stability and control derivatives of the F/A-18 HARV from flight data using the maximum likelihood method [NASA-CR-191216] p 186 N93-12903
- SPAUD, FRANK W.**
Hypersonic single expansion ramp nozzle simulations p 777 A93-39254
Flowfield measurements about a multi-element airfoil at high Reynolds numbers [AIAA PAPER 93-3137] p 1064 A93-48300
- SPAIN, CHARLES V.**
Aeroelastic character of a National Aerospace Plane demonstrator concept [AIAA PAPER 93-1314] p 732 A93-33890
An experimental and analytical study of a lifting-body wind-tunnel model exhibiting body-freedom flutter [AIAA PAPER 93-1316] p 732 A93-33891
Aerothermoelastic analysis of a NASP demonstrator model [AIAA PAPER 93-1366] p 733 A93-33933
Supersonic aeroelastic instability results for a NASP-like wing model p 682 A93-33935
A flutter investigation of all-moveable NASP-like wings at hypersonic speeds p 769 A93-37427
Supersonic aeroelastic instability results for a NASP-like wing model [NASA-TM-107739] p 718 N93-26553
- SPALART, P. R.**
On the cross-flow instability near a rotating disk p 128 A93-17264
- SPALDING, JOSEPH**
Differential GPS autonomous failure detection p 314 A93-21152
- SPALL, JAMES C.**
Control of complex dynamic systems by neural networks p 758 N93-25611
- SPALL, R. E.**
Stability theory and transition prediction applied to a general aviation fuselage p 479 A93-28601
- SPANIER, GERARD**
A simulation study of the effects of communication delay on air traffic control [AD-A258593] p 502 N93-19966
- SPARA, KAREN M.**
Supersonic turbomachine rotor flutter control by aerodynamic detuning p 899 A93-42884
- SPARKS, ANDREW**
Application of structured singular value synthesis to a fighter aircraft p 368 A93-22865
Application of structured singular value synthesis to a fighter aircraft p 1130 A93-49594
Full envelope multivariable control law synthesis for a high-performance test aircraft p 1130 A93-49595
- SPAZZINI, P. G.**
Asymmetric vortical solutions in supersonic corners - Steady 3D space-marching versus time-dependent conical results [AIAA PAPER 93-2957] p 1047 A93-48151
- SPEAKMAN, J. D.**
A prediction model for noise from low-altitude military aircraft [AD-A262494] p 852 N93-27662
- SPEARMAN, M. L.**
Some effects of wing and body geometry on the aerodynamic characteristics of configurations designed for high supersonic Mach numbers [AIAA PAPER 92-4246] p 463 A93-24493
- SPEER, T. M.**
Simulation of the secondary air system of aero engines [ASME PAPER 92-GT-68] p 348 A93-19318
- SPENCE, ANNE-MARIE**
Efficient sensitivity analysis for rotary-wing aeromechanical problems [AIAA PAPER 93-1648] p 711 A93-34173
- SPENCER, B. F., JR.**
Determination of tire-wheel interface pressure distribution for aircraft wheels [AIAA PAPER 93-1343] p 709 A93-33913
- SPENCER, FLOYD**
Reliability assessment at airline inspection facilities. Volume 1: A generic protocol for inspection reliability experiments [DOT/FAA/CT-92/12-VOL-1] p 704 N93-25110
Reliability assessment at airline inspection facilities. Volume 2: Protocol for an eddy current inspection reliability experiment [DOT/FAA/CT-92/12-VOL-2] p 842 N93-28685
- SPENCER, M. A.**
The development of the Rolls-Royce Trent aero gas turbine [PNR-90949] p 58 N93-11108
- SPENCER, R. H.**
Active control of helicopter transmission noise p 568 A93-29428
- SPERANSKII, A. N.**
Flight-vehicle drives (2nd revised and enlarged edition) [ISBN 5-217-00802-4] p 713 A93-35676
- SPERINCK, N. P. B.**
Plume effects at hypersonic speeds p 959 A93-45494
- SPEYER, JASON L.**
An investigation of the fuel-optimal periodic trajectories of a hypersonic vehicle [AIAA PAPER 93-3753] p 1101 A93-51349
Game theoretic synthesis for robust aerospace controllers p 819 N93-27171
- SPIEGEL, P.**
Blade-vortex interaction noise - Prediction and comparison with flight and wind tunnel tests [ONERA, TP NO. 1992-126] p 851 A93-38600
- SPINDLER, BRIEUC**
Applications of space techniques to civil aviation operations p 312 A93-20007
- SPINETTI, R. L.**
Aerodynamic design of a hypersonic body with a constant favorable pressure gradient [AIAA PAPER 93-3444] p 978 A93-47232
- SPIRONOV, E. V.**
New corrosion resistant nickel-base super-alloys and technological processes of casting gas turbines parts with directional single crystal and regulable equiaxial minimized microporosity structure p 916 A93-40811
- SPIRKL, A.**
MTR390 - Engine for the future [ASME PAPER 92-GT-250] p 353 A93-19459
- SPITZER, CARY**
Differential GPS/inertial navigation approach/landing flight test results p 32 A93-11019
- SPITZER, CARY R.**
Digital avionics systems - Principles and practices (2nd revised and enlarged edition) [ISBN 0-07-060333-2] p 342 A93-19801
Analysis of DGPS/INS and MLS/INS final approach navigation errors and control performance data p 315 A93-21183
The all-electric aircraft - In your future? p 997 A93-46824
- SPITZER, RONALD F.**
On the fatigue life of M50 NiL rolling bearings p 78 A93-11346
- SPIVAK, V. I.**
Half-scale modeling experience in the testing of radio navigation and landing systems p 882 A93-43112
- SPLETTSTOESSER, W. R.**
Helicopter main rotor/tail rotor noise radiation characteristics from scaled model rotor experiments in the DNW p 445 A93-19142
A closed loop controller for BVI impulsive noise reduction by Higher Harmonic Control p 849 A93-35963
- SPLETTSTOESSER, WOLF R.**
HHC study in the DNW to reduce BVI noise - An analysis p 565 A93-29405
- SPOTH, KEVIN A.**
Design of a hypersonic waverider-derived airplane [AIAA PAPER 93-0401] p 384 A93-21108
Structural design and analysis of a Mach zero to five turbo-ramjet system [AIAA PAPER 93-1983] p 1112 A93-49830
- SPRAGLE, GREGORY S.**
Unstructured 3D Delaunay mesh generation applied to planes, trains and automobiles [AIAA PAPER 93-0673] p 560 A93-24781
- SPRENG, M.**
Specific features of military low-altitude flight noise - Criteria for risk of damage and physiological effects p 1164 A93-49558
- SPRINGER, TIMOTHY A.**
Testing of an energy efficient environmental control system for a patrol-type aircraft [SAE PAPER 921225] p 890 A93-41399
- SPRINKLE, C. H.**
Impact of weather on aviation - A global view p 308 A93-22143
- SPRINKLE, DANNY R.**
Langley 8-foot high-temperature tunnel oxygen measurement system p 1010 A93-44892
- SPRUETT, J. A.**
Adaptive waveform selection with a neural network p 942 A93-43470
- SPURGEON, S. K.**
A nonlinear control strategy for robust sliding mode performance in the presence of unmatched uncertainty p 938 A93-42556
- SPYERS-DURAN, PAUL**
Meeting review: Third NCAR Research Aircraft Fleet Workshop [PB92-222710] p 223 N93-12818
- SQUIRE, L. C.**
Transonic shockwave/turbulent boundary layer interactions on a porous surface p 873 A93-43686
- SQUIRES, BECKY**
Forward rotor vortex effects on counter rotating propeller noise p 245 A93-19221
- SRAHEK, L.**
Investigation of a combustion zone behind a wedge p 1146 A93-51631
- SREEKANTA MURTHY, T.**
Experiences at Langley Research Center in the application of optimization techniques to helicopter airframes for vibration reduction p 508 A93-27972
- SREEKANTH**
Three-dimensional flow simulation over axisymmetric bodies using Navier-Stokes equations at hypersonic Mach numbers p 461 A93-24090
- SREEKANTH, A. K.**
Numerical computation of viscous hypersonic flow around spherically blunted cones at angle of attack p 460 A93-24082
Experiments on rarefied supersonic free jets using impact probes p 461 A93-24091
- SREENIVAS, KIDAMBI**
High resolution numerical simulation of the linearized Euler equations in conservation law form [AIAA PAPER 93-2934] p 1148 A93-48132
- SREENIVASAN, K. R.**
Observations of liquid jets injected into a highly accelerated supersonic boundary layer p 1177 A93-53214

SRIDHAR, B.

- A fast algorithm for image-based ranging
p 544 A93-27045
- Passive range estimation for rotorcraft low-altitude flight
p 948 A93-46608
- Passive range estimation for rotorcraft low-altitude flight
p 1190 A93-52881
- Discrete range clustering using Monte Carlo methods [NASA-TM-104004]
p 706 A93-24914

SRIDHAR, BANAVAR

- Vision-based range estimation using helicopter flight data
p 151 A93-17501
- Validation of vision-based obstacle detection algorithms for low-altitude helicopter flight
p 374 A93-19077
- Vision-based range estimation using helicopter flight data
p 317 A93-21525
- Passive range sensor refinement using texture and segmentation
p 544 A93-27044
- Technologies for automating rotorcraft nap-of-the-earth flight
p 885 A93-43784
- Vision based techniques for rotorcraft low altitude flight
p 1097 A93-49351
- Electro-optical navigation for aircraft
p 1097 A93-50643

- Vision based obstacle detection and grouping for helicopter guidance
[AIAA PAPER 93-3871]
p 1098 A93-51457
- A parallel implementation of a multisensor feature-based range-estimation method
p 1099 A93-51967
- Multirate and event-driven Kalman filters for helicopter flight
p 1245 A93-55760

SRIDHAR, J. K.

- Multiple input/multiple output (MIMO) analysis procedures with applications to flight data
p 60 A93-10777

SRIDHARAN, SRINIVASAN

- Mode interaction in stiffened composite shells under combined mechanical and thermal loadings
p 419 A93-16793

SRINATHKUMAR, S.

- Estimation of neutral and maneuver points of aircraft by dynamic maneuvers
[AIAA PAPER 93-3620]
p 1126 A93-48307
- Design, test, and evaluation of three active flutter suppression controllers
[NASA-TM-4338]
p 63 A93-10070
- Active flutter suppression using dipole filters
[NASA-TM-107594]
p 186 A93-13367

SRINIVASA RAO, P.

- Flow studies in ducted twin-rotor contra-rotating axial flow fans
[ASME PAPER 92-GT-380]
p 258 A93-19545

SRINIVASA, K.

- Midhani alloys in aeronautical service
p 70 A93-12368

SRINIVASAN, G. R.

- Flowfield analysis of modern helicopter rotors in hover by Navier-Stokes method
p 481 A93-29435
- URNS - A free-wake Euler/Navier-Stokes numerical method for helicopter rotors
p 692 A93-35634
- Euler calculations of unsteady interaction of advancing rotor with a line vortex
p 1071 A93-49016

SRINIVASAN, G. V.

- Process optimization of Hexoloy SX-SiC towards improved mechanical properties
[DE93-007913]
p 826 A93-28564

SRINIVASAN, GANAPATHI R.

- Numerical simulation of a hovering rotor using embedded grids
p 765 A93-35936

SRINIVASAN, RAM

- Effect of geometry, bleed rates and flow splits on pressure recovery of a canted hybrid vortex-controlled diffuser
[AIAA PAPER 93-1762]
p 1109 A93-49659

SRINIVASAN, SHIVAKUMAR

- Hypersonic leeside delta-wing-flow computations using centered schemes
p 870 A93-42635
- Summary of the GASP code application and evaluation effort for scramjet combustor flowfields
[AIAA PAPER 93-1973]
p 1077 A93-49820

SRIVASTAVA, R.

- APPLE - An aeroelastic analysis system for turbomachines and propfans
[AIAA PAPER 92-4712]
p 358 A93-20320
- On the static stability of forward swept propfans
[AIAA PAPER 93-1634]
p 720 A93-34162
- Efficient hybrid scheme for the analysis of counter-rotating propellers
p 688 A93-34483

SRIVASTAVA, RAKESH

- Simulation of unsteady rotational flow over propfan configuration
[NASA-CR-192234]
p 296 A93-18585

SRIVATSAN, RAGHAVACHARI

- Simulator evaluation of displays for a revised takeoff performance monitoring system
[NASA-TP-3270]
p 189 A93-15366

SRULIJES, J.

- Shock tube validation experiments for the simulation of ram-accelerator-related combustion and gasdynamic problems
p 1016 A93-45499

ST. CLAIR DINGER, ANN

- Effect of jet engine exhaust on SOFIA straitight performance
p 1263 A93-55178

ST. JEAN, MEGAN M.

- Data acquisition and analysis on a Macintosh
p 562 A93-29422

STACK, DANIEL T.

- Turbulence avoidance
p 309 A93-22160

STACK, JOHN P.

- Surface hot-film method for the measurement of transition, separation and reattachment points
[AIAA PAPER 93-2918]
p 1148 A93-48120

STACY, KATHRYN

- Computer-aided light sheet flow visualization
[AIAA PAPER 93-2915]
p 1147 A93-48117

STADLMEIER, P.

- EJ 200 engine monitoring system: On- and off-board data capture, analysis, and management system
p 178 A93-15172

STADNIK, V. N.

- Calculation of the position of aircraft center of gravity on an IBM PC
p 996 A93-45671
- General concepts related to the determination of the individual flight performance characteristics of aircraft for establishing fuel consumption standards and optimal flight regimes
p 996 A93-45673

STAFFORD, D.

- Environmental conditions for certification testing of helicopter advanced composite main rotor components
p 824 A93-36003

STAFFORD, MARK A.

- Experimental investigation of slot injection into supersonic flow with an adverse pressure gradient
[AIAA PAPER 93-2442]
p 1119 A93-50194

STAGG, A. K.

- A performance comparison of massively parallel Parabolized Navier-Stokes solutions
[AIAA PAPER 93-0059]
p 435 A93-20172

STAHL, DAVID

- FAA Technical Center Aeronautical Data Link Research Plan
[DOT/FAA/CT-92/23]
p 417 A93-15698

STAHL, WOLFGANG H.

- Experimental investigations of asymmetric vortex flows behind elliptic cones at incidence
p 757 A93-35637

STALEWSKI, WIENCZYSLAW

- Numerical minimization of the moment coefficient of a supercritical airfoil section
p 1238 A93-56214

STALEY, C. W.

- B-2 flight test update
p 803 A93-38844

STALKER, R. J.

- Experiments on Space Shuttle Orbiter models in a free piston shock tunnel
p 7 A93-11497
- Performance considerations in the operation of free-piston driven hypersonic test facilities
p 1011 A93-45497
- Free piston facilities with air driver gas
p 1011 A93-45528
- Hypervelocity flows of argon produced in a free piston driven expansion tube
p 1012 A93-45530
- Double diaphragm driven free piston expansion tube
p 1016 A93-45533

STALNAKER, R. A.

- Combustion characteristics and passive control of an annular dump combustor
[AIAA PAPER 93-1772]
p 1110 A93-49668

STAMBAUGH, JOHN S.

- System for calibrating a gyro navigator
[AD-D015668]
p 708 A93-26093

STAMMER, ROBERT M.

- A database approach to aircraft carrier airplan production
[AD-A257737]
p 240 A93-17666

STANEK, M. J.

- Investigation of vortex development on a pitching slender body of revolution
p 1095 A93-52445

STANISIC, S.

- A numerical method for solving Navier-Stokes equations for low Mach number compressible flows
p 463 A93-24672

STANKEVICH, I. V.

- Mathematical modeling of the three-dimensional temperature fields of turbine blades
p 1216 A93-53329

STANKOV, B. B.

- Liquid water profiling using remote sensor observations
p 429 A93-22150

STANKOV, BORISLAVA

- Diagnostic studies of clear air turbulence in isentropic coordinates
p 430 A93-22154

STANLEY, KEVIN

- Domain specific software design for decision aiding
p 442 A93-17517

STANNILAND, D. R.

- The use of a deep honeycomb to achieve high flow quality in the ARA 9 ft x 8 ft Transonic Wind Tunnel
p 190 A93-14276

STANSBY, P. K.

- Flow around two circular cylinders by the random-vortex method
p 271 A93-21925

STANTON, LEONARD E.

- Development and fabrication of an autoclave molded PES/Quartz sandwich radome
p 547 A93-28279

STANZIONE, KAYDON A.

- Development of generic helicopter performance methodology for real time mission analyses
p 152 A93-14185

STAPOUNTZIS, H.

- Periodic vortex shedding over delta wings
p 1070 A93-49002

STARIK, A. M.

- Kinetic scheme selection in describing detonation in an H₂-air mixture behind shock waves
p 1253 A93-55032

STARK, MICHAEL E.

- Software Engineering Laboratory Ada performance study: Results and implications
p 441 A93-17172

STARKE, E. A., JR.

- NASA-Uva light aerospace alloy and structure technology program supplement: Aluminum-based materials for high speed aircraft
[NASA-CR-4517]
p 1019 A93-31643

STARZEN, HANS

- Performance of controlled diffusion blades
p 424 A93-18735

STARKEY, VAL

- Process and assembly plans for low cost commercial fuselage structure
p 923 A93-30865

STARKE, DAVID R.

- Fly-by voice, a technology demonstration
p 526 A93-19918

STARNES, JAMES H., JR.

- Response of laminated composite plates to low-speed impact by airgun-propelled and dropped-weight impactors
[AIAA PAPER 93-1402]
p 739 A93-33962

STARODUBTSEVA, O. A.

- Effect of aqueous solutions of water-crystallization inhibiting fluids on Thiokol-based sealants
p 1017 A93-45689

STAROSTIN, F. I.

- Design and investigation of the stand and flying scramjet models - Conceptions and results of experiments
[AIAA PAPER 93-2447]
p 1120 A93-50199

STARRY, STUART J.

- Federal preemption in commercial aviation - Tort litigation under 49 U.S.C. section 1305
p 944 A93-42997

STARTSEV, A. M.

- Three-dimensional flow of viscous gas in the blade passage of a straight compressor cascade
p 5 A93-10187

STARTSEV, A. N.

- 3D/quasi-3D trans- and supersonic flow calculation in advanced centrifugal/axial compressor stages
p 972 A93-46936

STASENKO, A. L.

- Flow density distribution in a two-phase submerged jet
p 836 A93-39144

STASTNY, M.

- Boundary layer effects on the transonic flow in a straight turbine cascade
[ASME PAPER 92-GT-155]
p 249 A93-19382

STAUB, F. W.

- Rotor cavity flow and heat transfer with inlet swirl and radial outflow of cooling air
[ASME PAPER 92-GT-378]
p 406 A93-19536

STAUB, T. A.

- New rotor trim and balance system for helicopter usage monitoring
p 169 A93-15180

STAUFENBIEL, R.

- Low-speed aerodynamics of the hypersonic research configuration ELAC I
p 1237 A93-56035

STAUTER, R. C.

- Measurement of the three-dimensional tip region flowfield in an axial compressor
[ASME PAPER 92-GT-211]
p 252 A93-19434

STAVA, D.

- A study of incipient separation limits for shock-induced boundary layer separation for Mach 6 high Reynolds flow
[AIAA PAPER 93-2481]
p 1084 A93-50222

STEARMAN, RONALD O.

- Aeroelastic system identification of advanced technology aircraft through higher order signal processing
p 525 A93-29297

- STECK, JAMES E.**
Use of neural networks in control of high-alpha maneuvers p 1130 A93-49593
- STECKHAN, P.**
Implementation of an infrared thermal imaging system to measure temperature in a gas turbine engine [AIAA PAPER 93-2469] p 1120 A93-50215
- STECKLEIN, G. O.**
Numerical solution of inviscid hypersonic flow around a conically-derived waverider [AIAA PAPER 93-0320] p 280 A93-23012
- STEELE-PERKINS, A. P.**
Royal Naval helicopter ditching experience p 492 N93-19684
- STEELE, JAMES B.**
A study of blade-vortex interaction sound generation and directionality p 565 A93-29402
- STEELE, ROBERT E.**
Specialty fiber optic systems for mobile platforms and plastic optical fibers; Proceedings of the Meeting, Boston, MA, Sept. 9-11, 1992 [SPIE-1799] p 1105 A93-49462
- STEEVES, EARL C.**
A computational model that couples aerodynamic and structural dynamic behavior of parachutes during the opening process [AD-A264115] p 877 N93-30119
- STEFFEN, CHRISTOPHER J., JR.**
A new flux splitting scheme p 973 A93-47189
- STEFKO, GEORGE L.**
An iterative multidisciplinary analysis for rotor blade shape determination [AIAA PAPER 93-2085] p 1114 A93-49912
- STEGEMAN, JAMES D.**
User's manual for Interactive Data Display System (IDDS) [NASA-TM-105572] p 441 N93-16613
- STEGER, JOSEPH L.**
3D Euler flow solutions using unstructured Cartesian and prismatic grids [AIAA PAPER 93-0331] p 281 A93-23022
- STEHWIEN, WOLFGANG**
Classification of radar clutter in an air traffic control environment p 886 N93-30299
- STEIN, EARL S.**
Air traffic control visual scanning [DOT/FAA/CT-TN92/16] p 35 N93-10459
Prototype stop bar system evaluation at John F. Kennedy International Airport [AD-A258667] p 192 N93-12902
Preliminary studies of planning and flight strip use as air traffic controller memory aids [DOT/FAA/CT-TN92/22] p 503 N93-21759
- STEIN, KEITH R.**
A computational model that couples aerodynamic and structural dynamic behavior of parachutes during the opening process [AD-A264115] p 877 N93-30119
- STEINEBACH, D. A.**
Performance analysis of a turbofan as a part of an airbreathing propulsion system for space shuttles p 1252 A93-56039
- STEINETZ, BRUCE M.**
A hot dynamic seal rig for measuring hypersonic engine seal durability and flow performance [AIAA PAPER 93-1346] p 738 A93-33916
- STEINHILBER, H.**
Loads at the nose landing gears of civil transport aircraft during towbarless towing operations p 45 A93-13629
- STEINHOFF, JOHN**
Free-wake computation of helicopter rotor flowfields in forward flight [AIAA PAPER 93-3079] p 1059 A93-48253
- STEINHOFF, JOHN S.**
Numerical vorticity capturing for vortex-solid body interaction problems [AIAA PAPER 93-3343] p 954 A93-45037
- STEINLE, FRANK W., JR.**
An integrated knowledge system for wind tunnel testing - Project Engineers' Intelligent Assistant [AIAA PAPER 93-0560] p 377 A93-23297
- STENGEL, ROBERT**
Wind shear related research at Princeton University p 145 N93-14854
- STENGEL, ROBERT F.**
Stochastic measures of performance robustness in aircraft control systems p 185 A93-14595
- STENGEL, F. R.**
Calibration of thermal anemometer at very low Reynolds numbers under microgravity p 926 A93-41729
- STENGER, G. J.**
Evaluation of alternatives for increasing A-7D rearward visibility [AD-A255071] p 50 N93-12488
- STENGER, GREGORY J.**
Determination of stresses on laminated aircraft transparencies by the strain gage-hole drilling and sectioning method [AD-A255548] p 164 N93-14571
- STENTOE, W. J.**
Flow control of low heat load turbine airfoils [AD-A260941] p 724 N93-26219
- STEPANENKO, V. N.**
Determination of gas flow rate in a duct from measured static pressures p 520 A93-27625
- STEPANOV, A. N.**
Some aspects of the design of combination landing gear p 891 A93-42374
- STEPHENS, A. T.**
Flight update of aerodynamic math model [AIAA PAPER 93-3596] p 1224 A93-52687
- STEPHENS, JOSEPH R.**
Material requirements for the High Speed Civil Transport [ISABE 93-7067] p 1200 A93-54043
- STEPHENS, M. A.**
Chimera grids in the simulation of three-dimensional flowfields in turbine-blade-coolant passages [AIAA PAPER 93-2559] p 1157 A93-50280
- STEPHENS, V. M.**
Crashworthiness of composite seats for civil aircraft p 703 N93-24773
- STEPNIEWSKI, W. Z.**
Open aircrew VTOL concepts [NASA-CR-177603] p 240 N93-17883
- STERLING, J.**
Combustion noise and combustion instabilities in propulsion systems p 100 N93-10682
- STERNBERG, A.**
Airfoil stability in turbulent flow p 781 N93-27212
- STERR, W.**
Integration of turbo-expander- and turbo-ramjet-engines in hypersonic vehicles [ASME PAPER 92-GT-204] p 353 A93-19428
- STETSON, KENNETH F.**
Unit-Reynolds-number effects on boundary-layer transition p 288 A93-23560
On the breakdown of a hypersonic laminar boundary layer [AIAA PAPER 93-0896] p 472 A93-24956
Developing a data base for the calibration and validation of hypersonic CFD codes - Sharp cones [AIAA PAPER 93-3044] p 1057 A93-48224
- STETTER, H.**
Double mode behaviour of bladed disk assemblies in the resonance frequency range, visualized by means of holographic interferometry [ASME PAPER 92-GT-438] p 357 A93-19580
Prediction of three-dimensional low frequency unsteady transonic flow and forced vibration in axial turbine stages p 971 A93-46934
- STETTNER, MARTIN**
An approach to tiltrotor wing aeroservoelastic optimization through increased productivity [AIAA PAPER 92-4781] p 326 A93-20371
- STEUER, G. D.**
Heat transfer in rotating serpentine passages with trips skewed to the flow [ASME PAPER 92-GT-191] p 403 A93-19416
- STEVENS, DANIEL R.**
Practical considerations in waverider applications [AIAA PAPER 92-4247] p 43 A93-13326
Design of a hypersonic waverider-derived airplane [AIAA PAPER 93-0401] p 384 A93-21108
- STEVENS, J. J.**
Experimental investigations into composite fuselage impact damage resistance and post-impact compression behavior p 159 A93-15812
- STEVENS, JOHN G.**
Employment of radicals and excited state species for supersonic combustion photochemical ignition of premixed hydrogen/oxygen mixtures with ArF laser p 73 N93-11135
- STEVENS, M.**
F/A-18 departure recovery improvement evaluation [AIAA PAPER 93-3671] p 1129 A93-48349
- STEVENS, MARC G.**
F/A-18 controls released departure recovery - Flight test evaluation p 803 A93-38839
F/A-18 controls released departure-recovery flight test evaluation [AD-A256522] p 189 N93-15396
- STEVENS, P. J.**
MIST - A remote briefing system p 437 A93-22132
- STEVENS, PHILIP S.**
An aircraft instrument design for in situ tropospheric OH measurements by laser induced fluorescence at low pressures p 1159 A93-51528
- STEVENSON, LLOYD**
Summary of findings from the PIREP-based analyses conducted during the 1988 to 1990 evaluations of TDWR-based and TDWR/LLWAS-based alert services provided to landing/departing pilots [AD-A253859] p 93 N93-11144
- STEVENSON, RYAN**
Flow visualization and flow field measurements of a 1/12 scale tilt rotor aircraft in hover p 482 A93-29441
- STEVENSON, T. N.**
Modelling of interfacial and thermocline waves [AERO-REPT-9209] p 420 N93-18103
- STEVENSON, WARREN H.**
Turbulence characteristics of an axisymmetric reacting flow [NASA-CR-4110] p 877 N93-30373
- STEWART, CLAYTON**
Detection and classification of acoustic signals from fixed-wing aircraft p 850 A93-37032
- STEWART, DAVID A.**
Convective heat-transfer rate distributions over a 140 deg blunt cone at hypersonic speeds in different gas environments [AIAA PAPER 93-2787] p 1027 A93-46529
- STEWART, DOUG**
Above the sky p 1044 A93-52614
- STEWART, E. C.**
A study of the interaction between a wake vortex and an encountering airplane [AIAA PAPER 93-3642] p 858 A93-40714
- STEWART, ERIC C.**
The role of simulation in determining safe aircraft landing separation criteria p 306 A93-18712
- STEWART, J. F.**
Dual Engine application of the Performance Seeking Control algorithm [AIAA PAPER 93-1822] p 1110 A93-49709
- STEWART, J. H.**
AEDC H2 Facility - New test capabilities for hypersonic air-breathing vehicles [AIAA PAPER 93-2781] p 1012 A93-46525
- STEWART, JAMES F.**
Integrated flight propulsion control research results using the NASA F-15 HIDEC Flight Research Facility [AIAA PAPER 92-4106] p 38 A93-11276
Flight-determined benefits of integrated flight-propulsion control systems p 183 A93-14370
- STEWART, JOHN E.**
A graphically interactive approach to structured and unstructured surface grid quality analysis [AIAA PAPER 93-3351] p 954 A93-45045
- STEWART, R. M.**
Helicopter health monitoring: Current practice and future trends p 169 N93-15179
- STEWART, REGINA M.**
Waterborne polyurethane binder resins for compliant aircraft coatings [AD-A258246] p 199 N93-14573
- STEWART, V. R.**
A study of the effect of a moving ground belt on the vortex created by a jet impinging on the ground in a cross flow [AIAA PAPER 92-4250] p 15 A93-13361
- STEWART, VEARL R.**
Jet-induced ground effects on a parametric flat-plate model in hover [NASA-TM-104001] p 700 N93-26099
- STICHA, PAUL A.**
Development of a concept formulation process aid for analyzing training requirements and developing training devices [AD-A283579] p 912 N93-29972
- STICKLEN, J.**
A domain-specific design architecture for composite material design and aircraft part redesign p 442 N93-17522
- STICKLES, R. W.**
Innovative high temperature aircraft engine fuel nozzle design [ASME PAPER 92-GT-132] p 350 A93-19365
- STIELER, BERNHARD**
Ground- and satellite-derived flight-path measurements as demonstrated in the AFES Avionics Flight Evaluation System (AFES) p 993 N93-31281
On-board derived flight-path measurement as demonstrated by an ILS measurement system p 994 N93-31282
- STILES, LORREN**
Development status of the RAH-66 Comanche p 803 A93-38838
- STILLA, JOACHIM**
Instability of hypersonic flow past blunt cones - Effects of mean flow variations [AIAA PAPER 93-2983] p 1051 A93-48176

STILP, TH.

Measurements of jet aircraft emissions at cruise altitude.
I - The odd-nitrogen gases NO, NO₂, HNO₂ and HNO₃
p 556 A93-24391

STILWELL, P. B.

Fleet fatigue cracking threshold prediction
p 3 A93-13633

STIMAC, L. W.

Sensor alignment Kalman filters for inertial stabilization systems
p 50 A93-11018

STINCHCOMB, W.

Characterization of ceramic composite materials for gas turbine applications
[DE93-009719] p 905 A93-30168

STINTON, D.

Characterization of ceramic composite materials for gas turbine applications
[DE93-009719] p 905 A93-30168

STOB, JOHN

Phoenix: Preliminary design of a high speed civil transport
[NASA-CR-192024] p 334 A93-17976

STOCCO, JOSEPH A.

A High Deflection Diaphragm concept (HDD) for power transmission shafting
p 826 A93-35931

STOCKMAN, N. O.

Low speed test results of subsonic, turbofan scarf inlets
[AIAA PAPER 93-2301] p 1082 A93-50086

High speed test results of subsonic, turbofan scarf inlets
[AIAA PAPER 93-2302] p 1082 A93-50087

STOCKTON, THOMAS E.

Compact high reliability fiber coupled laser diodes for avionics and related applications
p 1152 A93-49470

STOLCIS, LUCA

Compressible flow calculations using a two-equation turbulence model and unstructured grids
p 686 A93-34351

STOLLERY, J. L.

The aerodynamic and structural design of a variable camber wing (VCW)
Experimental studies of vortex flaps and vortex plates
p 121 A93-14406

Plume effects at hypersonic speeds
p 959 A93-45494

The effect of a high thrust pusher propeller on the flow over a straight wing
[AIAA PAPER 93-3436] p 978 A93-47228

Effects of junction modifications on sharp-fin-induced shock wave/boundary layer interaction
[AIAA PAPER 93-2935] p 1046 A93-48133

Plume effects on the flow around a blunt cone at hypersonic speeds
p 787 A93-27460

STOLYAROV, I. F.

Approximation of a flight vehicle trajectory using Walsh functions
p 909 A93-43106

STOLZE, DETLEF

Design and implementation of a Global Positioning System (GPS) supported area navigation system with electronic aircraft
[ILR-MITT-275(1992)] p 889 A93-30671

STONE, A. G.

Rapid prototyping via automatic software code generation from formal specifications - A case study
p 227 A93-14685

STONE, ARTHUR

On definition and use of systems engineering processes, methods and tools
p 1225 A93-53642

STONE, H. W.

Aerodynamic heating environment definition/thermal protection system selection for the HL-20
p 1181 A93-53739

STONE, M. A.

The effects of high-pressure water on the material integrity of selected aircraft coatings and substrates
[SME PAPER AD92-207] p 855 A93-40668

STONE, T. D.

Flow control of low heat load turbine airfoils
[AD-A260941] p 724 A93-26219

STONER, GLENN E.

NASA-UVA Light Aerospace Alloy and Structures Technology Program (LA2ST)
[NASA-CR-193412] p 1019 A93-31739

STOOKESBERRY, D.

An efficient approach to optimal aerodynamic design. I - Analytic geometry and aerodynamic sensitivities
[AIAA PAPER 93-0099] p 264 A93-20204

An efficient approach to optimal aerodynamic design. II - Implementation and evaluation
[AIAA PAPER 93-0100] p 264 A93-20205

Solution of the Euler equations for airfoils using asymptotic methods
[AIAA PAPER 93-2931] p 1045 A93-48130

STORM, R. S.

Process optimization of Hexoloy SX-SiC towards improved mechanical properties
[DE93-007913] p 826 A93-28564

STORMS, BRUCE L.

Lift enhancement of an airfoil using a Gurney flap and vortex generators
[AIAA PAPER 93-0647] p 464 A93-24762

STORTZ, M. W.

Piloted simulation evaluation of pitch control designs for highly augmented STOVL aircraft
[AIAA PAPER 92-4234] p 63 A93-13328

STORTZ, MICHAEL W.

Determination of YAV-8B Reaction Control System bleed flow usage
[AIAA PAPER 92-4232] p 54 A93-13330

Juncture flow improvement for wing/pylon configurations by using CFD methodology
[AIAA PAPER 93-0522] p 283 A93-23264

Navier-Stokes simulation of external/internal transonic flow on the forebody/inlet of the AV-8B Harrier II
[AIAA PAPER 93-3057] p 1058 A93-48234

STOTT, JILLIAN A. K.

The stability of a trailing-line vortex in compressible flow
[NASA-CR-189738] p 298 A93-18771

STOUFFER, S. D.

Evaluation of scramjet nozzle configurations and film cooling for reduction of wall heating
[AIAA PAPER 93-0744] p 358 A93-21118

The effect of entrance radius and film injection on wall heating in scramjet nozzles
p 360 A93-22505

STOUFFER, SCOTT D.

Effects of compression and expansion ramp fuel injector configuration on scramjet combustion and heat transfer
[AIAA PAPER 93-0609] p 358 A93-21114

STOUFFER, VIRGINIA

Public-sector aviation issues: Graduate research award papers, 1990 - 1991
[PB92-222629] p 143 A93-13787

STOUFFLET, B.

Characteristic multigrid method application to solve the Euler equations with unstructured and unstructured grids
p 476 A93-27065

Contribution to Problem 6 using an upwind Euler solver with unstructured meshes
p 869 A93-42627

STOUFFLET, BRUNO

Validation of aerodynamic simulation methods for Hermes spaceplane and future hypersonic vehicles
[AIAA PAPER 92-5065] p 273 A93-22335

The European Data Base - A new CFD validation tool for the design of space vehicles
[AIAA PAPER 93-3045] p 1057 A93-48225

STOUGH, H. PAUL, II

Apparatus and method for improving spin recovery on aircraft
[NASA-CASE-LAR-14747-1] p 526 A93-20039

STOUGH, H. PAUL, III

Stall departure resistance enhancer
[NASA-CASE-LAR-14221-1] p 344 A93-19023

STOVER, JOHN C.

IR window damage measured by reflective scatter
p 851 A93-39544

STOWERS, S. T.

Advanced adaptive computational methods for Navier-Stokes simulations in rotorcraft aerodynamics
[NASA-CR-192282] p 483 A93-20256

STOWERS, STEVEN T.

Numerical analysis of reacting flow using finite rate chemistry models
p 389 A93-21666

STRAGNAC, THOMAS W.

Nonlinear flutter of composite plates with damage evolution
[AIAA PAPER 93-1546] p 829 A93-37441

STRAIN, NATALE A.

Flight evaluation of a stagnation detection hot-film sensor
[AIAA PAPER 92-4085] p 51 A93-13263

STRASH, D. J.

CFD zonal modeling of leading-edge ice effects for a complete aircraft
[AIAA PAPER 93-0167] p 275 A93-22601

A zonal CFD method for three-dimensional wing simulations
[AIAA PAPER 93-3433] p 977 A93-47225

STRATTON, DONALD ALEXANDER

Aircraft guidance for wind shear avoidance: Decision-making under uncertainty
p 889 A93-31005

STRAUB, F. K.

Dynamics of a high speed impeller - Analysis and experimental verification
[AIAA PAPER 93-1362] p 743 A93-34239

STRAUB, HENRIK H.

The Boeing 747-400 upper rudder control system with triple tandem valve
[SAE PAPER 912133] p 327 A93-21843

STRAUSSFOGEL, D.

Validation of engineering methods for predicting hypersonic vehicle control forces and moments
p 906 A93-41897

STRAUSSFOGEL, DENNIS M.

Analysis and design of planar and non-planar wings for induced drag minimization
[NASA-CR-191274] p 131 A93-13463

STRAWA, ANTHONY W.

Aerospace '92 - The year in review
p 455 A93-19976

STRAWN, ROGER

A new procedure for dynamic adaption of three-dimensional unstructured grids
[AIAA PAPER 93-0672] p 560 A93-24780

STRAWN, ROGER C.

A finite-volume Euler solver for computing rotary-wing aerodynamics on unstructured meshes
p 765 A93-35935

A finite-volume Euler solver for computing rotary-wing aerodynamics on unstructured meshes
p 874 A93-43782

STRAZISAR, A. J.

Experimental and computational investigation of the NASA Low-Speed Centrifugal Compressor flow field
[ASME PAPER 92-GT-213] p 252 A93-19436

STREBY, OLIVIER

HHC study in the DNW to reduce BVI noise - An analysis
p 565 A93-29405

STREET, C. L.

Spatial simulation of boundary layer instability - Effects of surface roughness
[AIAA PAPER 93-0075] p 262 A93-20187

STREICHER, JUERGEN

New slant visual range measuring device promises improved airport operations
p 529 A93-27395

STREIFINGER, H.

RB199 engine oil system failure diagnostics by comparison of measured and calculated oil consumption using the OLMOS on-board monitoring system
p 178 A93-15173

STREMEL, PAUL M.

The effect of Reynolds number and turbulence on airfoil aerodynamics at -90 degrees incidence
[AIAA PAPER 93-0206] p 277 A93-22624

STRETCHER, BAXTER R.

Next Generation Weather Radar (NEXRAD) Principal User Processor (PUP) Operational Test and Evaluation (OT&E) operational test plan
[DOT/FAA/CT-TN93/22] p 841 A93-28054

STRGANAC, THOMAS

Calculation of numerical boundary measure for wavelet-Galerkin approximations in aeroelasticity
[AIAA PAPER 93-1539] p 741 A93-34076

STRGANAC, THOMAS W.

Analysis of aeroelastic and resonance responses of a wind tunnel model support system
p 1013 A93-47022

STRIEBICH, RICHARD C.

A condensed phase test cell assembly for the System for Thermal Diagnostic Studies (STDS)
[AD-A258463] p 393 A93-18242

STRIGBERGER, J.

Some special purpose preconditioners for conjugate gradient-like methods applied to CFD
p 772 A93-38638

STRINGER, F. W.

Design features influencing the distribution of fuel within the spray from an air blast fuel injector
[ASME PAPER 92-GT-235] p 353 A93-19448

STRIZ, A. G.

Influence of sweep on structural optimization of a fighter wing
[AIAA PAPER 92-4794] p 323 A93-20290

Application of differential quadrature to the analysis of static aeroelastic phenomena
[AIAA PAPER 93-1505] p 711 A93-34044

STROMBERG, A.

Pressure measurements at supersonic speeds on the research configuration ELAC I
p 1237 A93-56033

STROUB, ROBERT H.

Introduction of the M-85 high-speed rotorcraft concept
p 797 A93-35980

STROUD, W. J.

An accurate nonlinear finite element analysis and test correlation of a stiffened composite wing panel
p 546 A93-27968

STROUD, W. JEFFERSON

Reliability of stiffened structural panels: Two examples
[NASA-TM-107687] p 219 A93-14483

STRUBLE, DAVID G.

Additional developments in embedded computer performance measurement
p 940 A93-42833

STRUCKMEIER, J.

Rarefied gas flow around a 3D-delta-wing
p 870 A93-42639

- STRUINS, R.**
A multidimensional generalization of Roe's flux difference splitter for the Euler equations p 863 A93-42437
Computations of inviscid compressible flows using fluctuation-splitting on triangular meshes [AIAA PAPER 93-3301] p 950 A93-44999
- STRYKOWSKI, P. J.**
The countercurrent mixing layer - Strategies for shear-layer control [AIAA PAPER 93-3260] p 968 A93-46826
Enhancement of mixing in high-speed heated jets using a counterflowing nozzle p 1235 A93-55359
- STUART, THOMAS D.**
Wind-tunnel tests of an inclined cylinder having helical grooves [AIAA PAPER 93-3456] p 979 A93-47239
- STUBBERUD, ALLEN R.**
Neural-network-based catastrophe avoidance control systems p 97 A93-13233
- STUBBS, SANDY M.**
Braking, steering, and wear performance of radial-belted and bias-ply aircraft tires [SAE PAPER 921036] p 158 A93-14656
Method and apparatus for cleaning rubber deposits from airport runways and roadways [NASA-CASE-LAR-14483-1] p 556 N93-22035
- STUCHLIK, D.**
NASA Long Duration Balloon capability development project p 2 A93-11370
- STUCKERT, G. K.**
Effects of free-stream turbulence on boundary-layer transition [AIAA PAPER 93-0488] p 416 A93-23390
- STUCKERT, GREG**
Stability and transition on swept wings [AIAA PAPER 93-0078] p 263 A93-20190
- STUCKERT, GREGORY K.**
Unstable branches of a hypersonic, chemically reacting boundary layer p 128 A93-17262
- STUEVER, ROBERT A.**
The role of simulation in determining safe aircraft landing separation criteria p 306 A93-18712
The challenges of simulating wake vortex encounters and assessing separation criteria [AIAA PAPER 93-3568] p 1096 A93-49518
- STUFFLE, KEVIN**
Preparation and characterization of continuous fiber reinforced zirconium diboride matrix composites for a leading edge material p 1211 A93-53445
- STUMPF, GREGORY J.**
An improved gust front detection algorithm for the TDWR p 432 A93-22191
- STUMPF, WALTER MARTIN**
An integrated finite-state model for rotor deformation, nonlinear airloads, inflow, and trim p 715 N93-25538
- STUREK, WALTER B.**
Navier-Stokes computations for kinetic energy projectiles in steady coning motion: A predictive capability for pitch damping [AD-A264111] p 1033 N93-32028
- STURGESS, G. J.**
Effects of back-pressure in a lean blowout research combustor [ASME PAPER 92-GT-81] p 387 A93-19330
Modification of combustor stoichiometry distribution for reduced NO(x) emission from aircraft engines [ASME PAPER 92-GT-108] p 349 A93-19346
- STURISKY, SELWYN H.**
Development and validation of a comprehensive real time AH-64 Apache simulation model p 799 A93-35992
- STURMAYR, A. M.**
Comparison of ENO and TVD schemes for the parabolized Navier-Stokes equations [AIAA PAPER 93-2970] p 1049 A93-48164
- STURTEVANT, B.**
Performance data of the new free-piston shock tunnel T5 at GALCIT p 1011 A93-45498
- STYLEMANS, C.**
CFD for ramjet and scramjet powered vehicles [ISABE 93-7035] p 1197 A93-54011
- SU, AY**
Effect of an unsteady three-dimensional wake on elastic blade-flapping eigenvalues in hover p 683 A93-34260
Flap-lag damping in hover and forward flight with a three-dimensional wake p 797 A93-35979
- SU, E. Z.**
The employment of artificial intelligence for analyzing air accidents p 226 A93-14375
- SU, J.**
Adaptive clutter suppression for airborne array radars using clutter subspace approximation p 883 A93-43411
- SU, KANG**
Accuracy analysis on image matching guidance systems p 62 A93-12653
- SU, SHEN-JWU**
Improvement of transonic wing buffet by geometric modifications [AIAA PAPER 93-3024] p 1055 A93-48209
- SU, T. Y.**
Navier-Stokes calculations for transport wing-body configurations with nacelles and struts [AIAA PAPER 93-2945] p 1047 A93-48142
Euler analysis of turbofan/superfan integration for a transport aircraft p 214 N93-13206
- SU, WENHAU**
Three-dimensional separated flow over a prolate spheroid p 1235 A93-55379
- SU, YAO-XI**
Design problems of three-dimensional contractions p 1236 A93-55584
- SU, YAOXI**
On the principle of sidewall effects on airfoil testing p 730 A93-33732
- SU, YUHONG**
Viscous shock-layer numerical calculations of three dimensional nonequilibrium flows over hypersonic blunt bodies at high angle of attack p 12 A93-12651
- SUAREZ, CARLOS J.**
Experimental and numerical analysis of the wing rock characteristics of a 'wing-body-tail' configuration [AIAA PAPER 93-0187] p 368 A93-22612
Forebody vortex control with jet and slot blowing on an F/A-18 [AIAA PAPER 93-3449] p 1009 A93-47235
Forebody vortex control on an F/A-18 using small, rotatable 'tip-strakes' [AIAA PAPER 93-3450] p 1009 A93-47236
- SUAREZ, E.**
Pyrometer for turbine applications in the presence of reflection and combustion [AIAA PAPER 93-2374] p 1156 A93-50143
- SUAREZ, J.**
Consolidation of graphite thermoplastic textile preforms for primary aircraft structure p 919 N93-30439
- SWART, THOMAS D.**
Experimental study of the effect of helical grooves on an infinite cylinder [AD-A260890] p 751 N93-25912
- SUBRAMANIAM, N. R.**
An implicit finite difference algorithm for two dimensional Euler equation p 461 A93-24085
- SUBRAMANIAN, C.**
Hetero-redundant architecture with Kalman filter for input processing in flight control system p 182 A93-14293
- SUBRAMANIAN, D. K.**
Hetero-redundant architecture with Kalman filter for input processing in flight control system p 182 A93-14293
- SUBRAMANIAN, S. V.**
A design approach to high Mach number scramjet performance [AIAA PAPER 92-4248] p 55 A93-13360
- SUDANI, NORIKAZU**
Flow visualization studies on sidewall effects in two dimensional transonic airfoil testing [AIAA PAPER 93-0090] p 263 A93-20196
- SUDDHOO, A.**
Time-dependent predictions and analysis of turbine cascade data in the transonic flow region [PNR-90957] p 139 N93-15489
- SUDHAKAR, K.**
Experimental investigation of leading edge vortices using LDA p 861 A93-42254
- SUDHEENDRA, K. S.**
Evolution of helicopters and the status of technology in India p 2 A93-12234
- SUDO, NAOKI**
Digital fly-by-wire system for BK117 FBW research helicopter p 181 A93-14209
- SUEMATSU, KAZUYO**
The operating system for Numerical Wind Tunnel p 383 N93-19290
- SUEMATU, KAZUYO**
The 3D Navier-Stokes calculation of flow about scramjet inlet with strut p 301 N93-19298
- SUEMURA, T.**
Effects of external control circuit on coal-fired supersonic diagonal-type MHD generator p 1173 A93-49619
- SUFFREDINI, BRIAN**
The Edge supersonic transport [NASA-CR-192074] p 335 N93-18055
- SUGAHARA, N.**
Navier-Stokes computation of the three dimensional flow fields through a transonic fan blade [ISABE 93-7030] p 1184 A93-54006
- SUGENO, MICHIO**
Current projects in Fuzzy Control p 1038 N93-31442
- SUGIMORI, M.**
The properties of newly developed highly damage tolerant and easy handleable carbon fiber/modified bismaleimide prepreg system p 1212 A93-53448
- SUGIMOTO, AKIRA**
Effect of wing planforms on induced drag reduction p 127 A93-16932
- SUGIMOTO, KEI**
Analysis of approach paths of a single aircraft p 367 A93-20823
- SUGIYAMA, YOKICHI**
Observation of fluctuation of 2D-nozzle flows [ISABE 93-7110] p 1204 A93-54086
- SUGIYAMA, YUKIO**
The methods of reducing impact loads on occupants in the civil aircraft crash condition p 140 A93-14220
- SUHS, N. E.**
Unsteady flow computations for a three-dimensional cavity with and without an acoustic suppression device [AIAA PAPER 93-3402] p 974 A93-47204
- SULI, ENDRE**
The accuracy of cell vertex finite volume methods on quadrilateral meshes p 227 A93-14526
- SULLINS, G. A.**
Numerical and experimental investigation of mixing enhancement in scramjets [AIAA PAPER 92-5063] p 414 A93-22333
Experimental results of shock trains in rectangular ducts [AIAA PAPER 92-5103] p 274 A93-22373
Demonstration of mode transition in a scramjet combustor p 899 A93-42878
Enhanced fuel-air mixing in hypersonic engines [ISABE 93-7115] p 1221 A93-54090
- SULLIVAN, B. M.**
Subjective response to simulated sonic booms with ground reflections [NASA-TM-107764] p 852 N93-28692
- SULLIVAN, BRENDA M.**
Laboratory study of effects of sonic boom shaping on subjective loudness and acceptability [NASA-TP-3269] p 102 N93-11620
Effect of sonic boom asymmetry on subjective loudness [NASA-TM-107708] p 453 N93-16755
Loudness and annoyance response to simulated outdoor and indoor sonic booms [NASA-TM-107756] p 852 N93-27271
A laboratory study of subjective response to sonic booms measured at White Sands Missile Range [NASA-TM-107746] p 852 N93-27272
- SULLIVAN, CHRISTOPHER C.**
An investigation of a prototype OASYS effectiveness in maneuvering flight [AD-A257901] p 338 N93-18339
- SULLIVAN, J. P.**
Unsteady wing surface pressures in the wake of a propeller p 1095 A93-52436
- SULLIVAN, JOHN P.**
Two-, three-, and four-poster jets in cross flow [AIAA PAPER 93-0023] p 408 A93-20141
- SULLIVAN, P. A.**
Canadian experience with air cushion vehicle skirts p 837 A93-39722
Experimental study of shock wave and hypersonic boundary layer interactions near a convex corner [AIAA PAPER 93-2980] p 1051 A93-48173
On hovercraft overwater heave stability p 1219 A93-53819
Kelvin-Helmholtz wave generation beneath hovercraft skirts p 1219 A93-53820
- SUMI, D.**
Experience with explosive detection systems in airports p 498 N93-21895
- SUMMA, J. M.**
CFD zonal modeling of leading-edge ice effects for a complete aircraft [AIAA PAPER 93-0167] p 275 A93-22601
A zonal CFD method for three-dimensional wing simulations [AIAA PAPER 93-3433] p 977 A93-47225
- SUMMERFIELD, MARTIN**
Power generation source for an electrothermal hypersonic wind tunnel [AIAA PAPER 92-5045] p 376 A93-22317
- SUMMERS, L. G.**
Evaluation of advanced displays for engine monitoring and control [NASA-CR-191418] p 718 N93-24764
- SUMWALT, ROBERT L., III**
The importance of proper aviation weather dissemination to pilots - An airline captain's perspective p 308 A93-22115

SUN, GANG

SUN, GANG

An adaptive region method for computation of vortex sheet behind wing in compressible flow p 116 A93-14262

SUN, JIAN-GUO

A study of surge control by using pulse cut-off for dual spool turbo-jet engine p 1194 A93-53862

SUN, JIANGUO

Adaptive engine stall margin control p 1108 A93-49200

SUN, M.

Flow structures around a constant-rate pitching airfoil and mechanism of dynamic stall p 118 A93-14332

SUN, TIANFENG

Pressure fluctuations on the surface of two circular cylinders in tandem arrangements at high Reynolds numbers p 679 A93-33718

SUN, WAN-FENG

A study of surge control by using pulse cut-off for dual spool turbo-jet engine p 1194 A93-53862

SUN, WEIMIN

Advanced electromagnetic methods for aerospace vehicles [NASA-CR-193468] p 936 N93-31036

SUN, X. D.

Turbulence/gust alleviation using spoiler control p 369 A93-22886

SUN, XIANXUE

Engineering optimization of aeronautical structures p 154 A93-14227

SUN, XIAO-FENG

Calculation of sound field radiated by oscillating cascade p 231 A93-14269

SUN, XIAOFENG

Acoustic experiments of two scaled-model propellers on the ground p 1172 A93-48507

SUN, XIASHENG

Engineering optimization of aeronautical structures p 154 A93-14227

SUN, YEE-WIN

Flutter analysis of stiffened laminated composite plates and shells in supersonic flow p 1216 A93-53224

SUNDARAJAN, V.

Numerical solution of dynamic equations arising in a jet engine simulation p 53 A93-12237
Development of a real time dynamic engine simulation model of a turbo fan engine [ISABE 93-7132] p 1205 A93-54107

SUNDER, R.

Fatigue life under random load history derived from exceedance curves using different algorithms p 1260 A93-56544

SUNDERLAND, CAROLYN

Aero-engine component damping estimation from full-scale aeromechanical test data [AIAA PAPER 93-1873] p 1112 A93-49748

SUNDSRUUD, GERALD J.

Advantages of a one-part resin system for processing aerospace parts by Resin Transfer Molding (RTM) [SME PAPER EM93-112] p 1159 A93-51729

SUNG, B.

Computation of passively controlled transonic wing [AIAA PAPER 93-3474] p 981 A93-47253

SUNG, C. J.

On the structure and response of aerodynamically-strained planar premixed flames [AIAA PAPER 93-0246] p 390 A93-22657

SUNG, CHAO-HO

Incompressible flow computation of forces and moments on bodies of revolution at incidence [AIAA PAPER 93-0787] p 541 A93-24867

SUNG, H. J.

A numerical study of unsteady supersonic compression ramp flows [AIAA PAPER 93-0883] p 470 A93-24943

SUNG, HYUNG JIN

Discrete-vortex simulation of pulsating flow on a turbulent leading-edge separation bubble p 787 N93-27457

SUORSA, R.

Passive range estimation for rotorcraft low-altitude flight p 948 A93-46608

Clustering methods for removing outliers from vision-based range estimates p 1171 A93-51648

Passive range estimation for rotorcraft low-altitude flight p 1190 A93-52881

SUORSA, RAY

Vision based techniques for rotorcraft low altitude flight p 1097 A93-49351

SUORSA, RAYMOND

Validation of vision-based obstacle detection algorithms for low-altitude helicopter flight p 374 A93-19077

SUORSA, RAYMOND E.

A parallel implementation of a multisensor feature-based range-estimation method p 1099 A93-51967

Multirate and event-driven Kalman filters for helicopter flight p 1245 A93-55760

SURACE, CECILIA

Aeroelastic stability characteristics of composite cylindrical shells by the finite element method p 203 A93-14312

Ground vibration test on Piaggio P. 180 aircraft - Comparison between two modal test methods p 509 A93-29246

SURACE, GIUSEPPE

Aeroelastic stability characteristics of composite cylindrical shells by the finite element method p 203 A93-14312

SURD, DAVID J.

High reliability, maintenance-free INS battery development [AD-A264521] p 934 N93-30406

SURGET, J.

Schlieren device and holographic interferometer for hypersonic flow visualization [ONERA, TP NO. 1992-160] p 832 A93-38739

SURIN, V. P.

Optimization of the parameters of the lift-augmentation devices of the wing of a maneuverable aircraft equipped with an active load-reduction system p 804 A93-39189

SURYANARAYAN, S.

Extraction of inherent aerodynamic lag poles for the time domain representation of modal unsteady airloads [AIAA PAPER 93-1591] p 829 A93-37443

SURZHIN, M. K.

An experimental system for studying the vibrations and acoustic emission of cylindrical shells and panels in a field of turbulent pressure pulsations p 1140 A93-51754

SUSSMAN, E. D.

A simulation study of the effects of communication delay on air traffic control [AD-A258593] p 502 N93-19966

SUTHERLAND, LINDA W.

Publications on acoustics research at the Langley Research Center, January 1987 - September 1992 [NASA-TM-107674] p 102 N93-12080

SUTTON, C. W.

Measurement of the dynamic undercarriage response of a Sikorsky S-70B-2 helicopter: Instrumentation and test methods: Flight mechanics technical memorandum [AD-A256319] p 329 N93-16404

SUTTROP, F.

Comment on 'Experimental study on autoignition in a scramjet combustor' p 172 A93-14525

SUWA, SHIGEAKI

On the steady subsonic shear flow past a slender body of revolution p 970 A93-46907

SUZUKI, HARUO

Analysis of wake-induced unsteady flow in axial compressors - Radial variations of wake excitation forces estimated by strip theory p 1086 A93-51123

SUZUKI, HIDETO

Research on combined HOPE navigation technology p 533 N93-20428

SUZUKI, HIROSHI

Augmentation of turbulent heat transfer with a vortex generator attached to a LEBU plate p 411 A93-21729

SUZUKI, K.

The combustion performance of methane-fueled ram combustor [ISABE 93-7079] p 1201 A93-54055

SUZUKI, KAREN E.

Doppler global velocimetry measurements of the vortical flow above an F/A-18 [AIAA PAPER 93-0414] p 415 A93-23333

SUZUKI, KAZUYUKI

Augmentation of turbulent heat transfer with a vortex generator attached to a LEBU plate p 411 A93-21729

SUZUKI, KENJIRO

Augmentation of turbulent heat transfer with a vortex generator attached to a LEBU plate p 411 A93-21729

SUZUKI, KOJIRO

Effects of wall conditions on chemically nonequilibrium shock-layer flow over hypersonic reentry bodies p 970 A93-46908

SUZUKI, M.

Research and development of a turbo-accelerator for super/hypersonic transport [ISABE 93-7066] p 1200 A93-54042

SUZUKI, MANABU

Computer-controlled alignment for a 2000-line color monitor p 886 N93-30324

SUZUKI, OSAMU

A fine structure of the gust front observed with sonic anemometer p 430 A93-22158

Extremely low level jet in the evening in Kanto Plain p 430 A93-22159

SUZUKI, RYUTARO

Propagation results of aeronautical satellite communication experiments using INMARSAT satellite p 533 A93-29607

SUZUKI, SHINJI

Simultaneous structure/control design optimization of a wing structure with a gust load alleviation system p 525 A93-28616

SUZUKI, TAKAHIRO

Guidance and control of HOPE (H-II orbiting plane) [AAS PAPER 91-653] p 1252 A93-55825

SUZUKI, Y.

Effects of wake interaction of two turbine cascades on secondary/tip-leakage flows and losses [ISABE 93-7058] p 1185 A93-54034

SVOBODA, J. V.

Use of microprocessor-based simulator technology and MEG/EEG measurement techniques in pilot emergency-maneuver training p 530 N93-19706

SWADLING, S. J.

Prospects for a second generation supersonic transport p 108 A93-14154

SWANSON, ALEXANDRA A.

Shadowgraph flow visualization of isolated titrator and rotor/wing wakes p 767 A93-35996
Application of the shadowgraph flow visualization technique to a full-scale helicopter rotor in hover and forward flight [AIAA PAPER 93-3411] p 1030 A93-47208

SWANSON, CHARLES

Investigation of advanced counterrotation blade configuration concepts for high speed turboprop systems. Task 5: Unsteady counterrotation ducted propfan analysis. Computer program user's manual [NASA-CR-187125] p 521 N93-20583

SWANSON, GARY

Multi-parameter optimization tool for low-cost commercial fuselage crown designs p 922 N93-30858

SWANSON, GARY D.

Developments in impact damage modeling for laminated composite structures p 922 N93-30857

SWANSON, R. C.

An effective multigrid method for high-speed flows p 6 A93-10533
A multiblock, multigrid solution procedure for multielement airfoils p 967 A93-46812

SWANSON, STEPHEN

Low-speed wind tunnel test results of the Canard Rotor/Wing concept [AIAA PAPER 93-3412] p 975 A93-47209

SWANSON, TED

Flight data for the Cryogenic Heat Pipe (CRYOHP) Experiment [AIAA PAPER 93-2735] p 1027 A93-46488

SWARTWOUT, GREGORY

Three-dimensional flow calculations inside SSME GGGT first stage blade rows p 1017 N93-31585

SWEENEY, CHRISTOPHER

Development and operation of a real-time simulation at the NASA Ames Vertical Motion Simulator [AIAA PAPER 93-3575] p 1208 A93-52671

SWEENEY, DAVID

FAA Technical Center Aeronautical Data Link Research Plan [DOT/FAA/CT-92/23] p 417 N93-15698

SWEET, B.

Engineering a visual system for seeing through fog [SAE PAPER 921130] p 895 A93-41318

SWEET, S. M.

Rapid prototyping via automatic software code generation from formal specifications - A case study p 227 A93-14685

SWEETMAN, BILL

ARPA starts push for joint-service ASTOVL p 856 A93-43625

SWENSON, D. V.

Representation and probability issues in the simulation of multi-site damage p 1026 A93-45785

SWENSON, HARRY N.

Appraisal of digital terrain elevation data for low-altitude flight [NASA-TM-103896] p 35 N93-10745

Flight evaluation of a computer aided low-altitude helicopter flight guidance system p 820 N93-28869

Flight evaluation of a computer aided low-altitude helicopter flight guidance system [NASA-TM-103998] p 994 N93-32225

SWERTFAGER, THOMAS A.

The V-22 for SOF p 800 A93-36026

SWIDER, RAY

Overview of the FAA's differential GPS CAT III technical feasibility demonstration program [AIAA PAPER 93-3836] p 1098 A93-51425

SWIFT, RICHARD ALAN

Structural design using neural networks p 942 N93-31029

- SWIFT, T.**
Repairs to damage tolerant aircraft p 948 A93-45799
- SWIHART, J.**
Keynote address - Advanced Technology demonstrators, prototypes and hypersonic flight [AIAA PAPER 92-4999] p 456 A93-22276
- SWINSICK, SCOTT**
A Taguchi analysis of helicopter maneuverability and agility p 763 A93-35944
- SWITZER, JOHN C.**
A synthetic environment flight simulator: The AFIT virtual cockpit [AD-A259220] p 530 N93-20576
- SWOFFORD, DOYLE P.**
Thermal control of a lidar laser system using a non-conventional ram air heat exchanger p 1028 A93-46821
- SYED, S. A.**
Role of hydrogen/air chemistry in nozzle performance for a hypersonic propulsion system p 359 A93-21668
- SYME, DUNCAN BRIAN**
A transportable luggage examination system based on neutron interrogation p 497 N93-21863
- SYMONDS, COLIN J.**
Towards an integrated approach to proactive monitoring and accident prevention p 495 N93-19700
Accidents and errors: A review of recent UK Army Air Corps accidents p 495 N93-19701
Prediction of success from training p 495 N93-19702
- SYRMOS, V. L.**
Output feedback eigenstructure assignment using two Sylvester equations p 847 A93-38214
- SYRYCZYNSKI, JACEK**
Elementary stall flutter of an aircraft wing p 545 A93-27289
ONERA calculation model of dynamic flow separation on an airfoil section p 1238 A93-56212
- SYVERUD, ELISABET**
Aerodynamic characteristics of a delta wing with a body-hinged leading-edge extension [AIAA PAPER 93-3446] p 978 A93-47233
- SZECZENYI, EDMOND**
The measurement of blade deflections - A new implementation of the strain pattern analysis [ONERA, TP NO. 1992-127] p 831 A93-38601
- SZEMEREY, ISTVAN**
DAR-2: On-board data acquisition system for aircraft engines p 169 N93-15166
- SZENDRO, S.**
Application of flight data for diagnostic purposes p 166 A93-14295
- SZENDRO, SANDOR**
DAR-2: On-board data acquisition system for aircraft engines p 169 N93-15166
- SZNITKO, EWA**
Instability of three-dimensional supersonic boundary layer p 973 A93-46987
- SZODRUCH, JOACHIM**
Laminar-flow instrumentation for wind-tunnel and flight experiments p 479 A93-28605
- SZUMOWSKI, ANDRZEJ P.**
Experimental study of a single strong vortex-airfoil interaction p 481 A93-29432
- SZYMZYK, J. A.**
Experimental investigation of the management of large-sized drops and the onset of Marangoni-convection p 926 A93-41700
- T**
- T HART, W. G. J.**
Flight simulation and constant amplitude fatigue crack growth in aluminum-lithium sheet and plate p 71 A93-13644
- TABAK, R.**
New results in optimal missile avoidance analysis p 369 A93-22937
- TABAKOFF, W.**
Simulation of propulsion system's transient response to planar wave inlet distortion and the effect of compressor wear [AIAA PAPER 93-2384] p 1117 A93-50152
LDV Measurements of unsteady flow fields in radial turbine p 19 N93-10648
LDV measurements of unsteady flow fields in radial turbine [AD-A253592] p 19 N93-10648
LDV measurements of unsteady flow fields in radial turbine [AD-A255728] p 221 N93-15065
- TABATA, AKIRA**
Structure of downbursts associated with heavy rainfall observed in Tokyo p 433 A93-22200
- TABER, A.**
Single event upset in avionics p 1158 A93-50566
- TABIBZADEH, R.**
Investigation of rotor blade roughness effects on turbine performance [ASME PAPER 92-GT-297] p 354 A93-19487
- TACHIBANA, TAKESHI**
Aerodynamic characteristics of a semibuoyant station in the shape of a torus [AIAA PAPER 93-4034] p 1231 A93-54615
- TADA, AKIRA**
Limit cycle in the longitudinal motion of the USB STOL ASKA - Control system functional mockup and actual aircraft [SAE PAPER 921040] p 185 A93-14660
- TADA, H.**
The properties of newly developed highly damage tolerant and easy handleable carbon fiber/modified bismaleimide prepreg system p 1212 A93-53448
- TADGHIGHI, H.**
Effects of a trailing edge flap on the aerodynamics and acoustics of rotor blade-vortex interactions p 244 A93-19144
High-speed helicopter rotor noise - Shock waves as a potent source of sound p 565 A93-29403
- TAFEL, ROBERT W.**
USCG HU-25A/GPS integration p 313 A93-21130
- TAGHAVI, R.**
Computational study of advanced exhaust system transition ducts with experimental validation p 689 A93-34490
- TAGHAVI, RAY**
Aerodynamic characteristics of a delta wing with a body-hinged leading-edge extension [AIAA PAPER 93-3446] p 978 A93-47233
- TAGUCHI, H.**
A study of self-ignition of methane-hydrogen mixture fuel injected into high enthalpy supersonic airstreams [ISABE 93-7049] p 1213 A93-54025
- TAI, ANN T.**
Avionics software performance p 939 A93-42822
- TAI, KOUICHIRO**
Aerodynamic performance of scramjet inlet models with a single strut [AIAA PAPER 93-0741] p 466 A93-24831
- TAI, TSZE C.**
F-14A aircraft low-speed maneuvering aerodynamics [AIAA PAPER 93-0523] p 283 A93-23265
Simulation of DD-963 ship airwake by Navier-Stokes method [AIAA PAPER 93-3002] p 1053 A93-48192
- TAILLEMITTE, JEAN PIERRE**
Helicopter accidents over water in the national navy: Epidemiological study over the period 1980-1991 p 493 N93-19686
- TAJFAR, A. H.**
Design of a nozzle for a hypersonic wind tunnel [AERO-REPT-9113] p 381 N93-16468
- TAKAGI, SHOHEI**
Effect of micron-sized roughness on transition in swept-wing flows [AIAA PAPER 93-0076] p 262 A93-20188
- TAKAGI, SHOUHEI**
Experiments on swept-wing boundary-layer transition p 419 N93-16829
- TAKAHASHI, HITOSHI**
A wind tunnel investigation to determine buffet countermeasures for STOL aircraft alpha-sweep flight testing [NAL-TR-1129] p 65 N93-12362
Wind tunnel investigation of a twin-engine jet transport semi-span model with upper surface blown jet flap [NAL-TR-1134] p 26 N93-12503
- TAKAHASHI, KOJI**
Analytical study on plate edge noise (Noise generation from tandemly situated trailing and leading edges) p 1038 A93-45561
- TAKAHASHI, MARC D.**
Synthesis and evaluation of an H2 control law for a hovering helicopter p 728 A93-34542
H(infinity) helicopter flight control law design with and without rotor state feedback [AIAA PAPER 93-3849] p 1134 A93-51436
- TAKAHASHI, MASAHIRO**
Three-dimensional calculation of a hydrogen jet injection into a supersonic air flow p 950 A93-44374
- TAKAHARA, MIKINARI**
Rarefied gas numerical wind tunnel. Part 7: OREX p 382 N93-19280
- TAKAKI, JUNJI**
The methods of reducing impact loads on occupants in the civil aircraft crash condition p 140 A93-14220
- TAKAKURA, YOKO**
Computations of transonic wind tunnel flows about a fully configured model of aircraft by using multi-domain technique [AIAA PAPER 93-3022] p 1055 A93-48207
- A simple grid generation technique for hypersonic flow around complex configuration p 299 N93-19275
Numerical computations using multi-domain technique p 299 N93-19277
- TAKAMI, HIKARU**
Aerodynamic characteristics of a next generation high-speed civil transport [AIAA PAPER 92-4229] p 15 A93-13356
- TAKAMORI, SUSUMU**
Two-dimensional cascade tests of MCA blades in the high transonic Mach number region. V - Effect of space/chord ratio on the parameters of cascade performance p 267 A93-20930
Air ejector experiments using the two-dimensional supersonic cascade tunnel: Relationship between ejector performance and throat area ratio, part 1 [NAL-TM-642-PT-1] p 25 N93-12352
- TAKAMURA, J.**
Heat transfer in serpentine flow passages with rotation [ASME PAPER 92-GT-190] p 403 A93-19415
- TAKAMURA, MORIYUKI**
Numerical Wind Tunnel hardware p 383 N93-19289
- TAKAMURA, T.**
Influence of blade aerodynamic loading on efficiency of radial-inflow turbines [ASME PAPER 92-GT-91] p 249 A93-19337
- TAKANASHI, SUSUMU**
On the roles of wind tunnel testing and computational fluid dynamics in the aircraft development p 341 N93-19322
- TAKANO, YASUSHI**
Numerical prediction of aerodynamic noise radiated from low Mach number turbulent wake [AIAA PAPER 93-0145] p 452 A93-22589
Numerical computation of aerodynamic noise radiation by the large eddy simulation p 850 A93-38151
- TAKASHIMA, NARUHISA**
Engine/airframe integration for waverider cruise vehicles [AIAA PAPER 93-0507] p 283 A93-23254
- TAKATA, HIROYUKI**
Numerical study on inception of stall cells in rotating stall [ISABE 93-7007] p 1183 A93-53983
- TAKAYAMA, KAZUYOSHI**
Shock waves; Proceedings of the 18th International Symposium, Sendai, Japan, July 21-26, 1991. Vols. 1 & 2 [ISBN 0-387-55686-9] p 1023 A93-45451
- TAKESUE, YUICHI**
Limit cycle in the longitudinal motion of the USB STOL ASKA - Control system functional mockup and actual aircraft [SAE PAPER 921040] p 185 A93-14660
- TAKEUCHI, HISAO**
Numerical simulation of the flow through non-uniform airfoil cascade p 302 N93-19310
- TAKI, M.**
A new cooling system for ultra high temperature turbines [ISABE 93-7073] p 1201 A93-54049
- TAKITA, KEIICHI**
Experimental study on the unsteady aerodynamic response of a three dimensional cascade with oscillating blades p 242 A93-18499
- TAKIZAWA, MINORU**
An optical fiber multi-terminal data bus system for aircraft [NAL-TR-1125] p 52 N93-12370
- TAKIZAWA, N.**
Low-speed wind tunnel study of the direct side-force characteristics of a joined-wing airplane with an upper fin [DE93-767966] p 988 N93-31189
- TAKIZAWA, YOSHISADA**
Guidance and control of HOPE (H-II orbiting plane) [AAS PAPER 91-653] p 1252 A93-55825
- TALBOT, M. D.**
Wind tunnel test techniques for UAV separation investigations [AIAA PAPER 93-0626] p 524 A93-24743
- TALIPOV, R. F.**
Heat transfer on blunt cones in nonuniform supersonic flow in the presence of gas injection from the surface p 972 A93-46975
- TALLAROVIC, JOHN M.**
An experimental investigation of a finite circulation control wing [AD-A259044] p 340 N93-18896
- TALLEY, GREGORY D.**
The T700 ... from salt spray to sand blast p 1205 A93-54292
- TALOTTA, NICHOLAS J.**
Controller evaluation of initial data link terminal air traffic control services: Mini study 2, volume 1 [DOT/FAA/CT-92/2-VOL-1] p 36 N93-11704

- Controller evaluation of initial data link terminal air traffic control services: Mini study 2, volume 2
[DOT/FAA/CT-92/2-VOL-2] p 36 N93-11705
- TALYZINA, V. S.**
Estimation of the change of axial-flow compressor characteristics during long-term service p 1193 A93-52949
- TAM, CHRISTOPHER K. W.**
Dispersion-relation-preserving schemes for computational aeroacoustics p 244 A93-19151
Instability of rectangular jets p 398 A93-19157
Measured acoustic characteristics of ducted supersonic jets at different model scales p 563 A93-24821
[AIAA PAPER 93-0731] p 563 A93-24821
Instability of rectangular jets p 720 A93-34410
- TAM, LUEN T.**
Computation of inviscid flowfield around 3-D aerospace vehicles and comparison with experimental and flight data p 470 A93-24944
Two-layer convective heating prediction procedures and sensitivities for blunt body reentry vehicles p 963 A93-46509
[AIAA PAPER 93-2763] p 963 A93-46509
- TAMANGO, J.**
Mixing and combustion studies using discrete orifice injection at hypervelocity flight conditions p 205 A93-14523
- TAMANOI, YOSHIHIITO**
Air cell [CA-PATENT-APPL-SN-2001346] p 83 N93-10368
- TAMBOUR, Y.**
On the stability of the process of formation of combustion generated particles by coagulation and simultaneous shrinkage due to particle oxidation p 1146 A93-50220
[AIAA PAPER 93-2478] p 1146 A93-50220
- TAMURA, A.**
Navier-Stokes computation of the three dimensional flow fields through a transonic fan blade p 1184 A93-54006
[ISABE 93-7030] p 1184 A93-54006
- TAMURA, ATSUSHIRO**
Numerical simulation of the flow through non-uniform airfoil cascade p 302 N93-19310
- TAMURA, NAOKI**
Numerical simulation of flows in a supersonic air intake p 303 N93-19314
- TAMURA, Y.**
A multi-dimensional upwind scheme for the Euler equations on structured grids p 862 A93-42430
- TAMURA, YOSHIKAKI**
Numerical investigation of supersonic flows around a spiked blunt-body p 471 A93-24947
[AIAA PAPER 93-0887] p 471 A93-24947
- TAN, ALEX C. N.**
Experimental investigation of laminar to turbulent boundary layer transition with separation bubbles at low Reynolds number p 128 A93-17277
- TAN, C. S.**
Aerodynamic design of turbomachinery blading in three-dimensional flow - An application to radial inflow turbines p 248 A93-19324
[ASME PAPER 92-GT-74] p 248 A93-19324
Numerical simulation of compressor endwall and casing treatment flow phenomena p 255 A93-19490
[ASME PAPER 92-GT-300] p 255 A93-19490
Flow phenomena in turbomachines p 930 N93-29141
[AD-A263049] p 930 N93-29141
- TAN, CHOON S.**
Three-dimensional flow in radial turbomachinery and its impact on design p 723 N93-25668
[NASA-CR-192957] p 723 N93-25668
- TAN, CHUNQING**
An experimental study on blade negative curving in a turbine cascade with a large turning angle p 1071 A93-49185
Effect of blade leaning on the development of passage vortices and losses in the passage of turbine cascade with a great turning angle p 1236 A93-55397
- TAN, JIAK-KWANG**
Simulation of vortex bursting p 699 N93-25881
- TAN, P. W.**
Damage detection in smart structures using neural networks and finite-element analyses p 438 A93-22540
- TANABE, SEIICHI**
Turbulent structure in a vortex wake shed from an inclined circular cylinder p 125 A93-15443
- TANAKA, ATSUSHIGE**
Experimental study of mixed compression air-intake for hypersonic airbreathing engines p 355 A93-19519
[ASME PAPER 92-GT-349] p 355 A93-19519
Effects of boundary layer bleed on swept-shock/boundary layer interaction p 1052 A93-48182
[AIAA PAPER 93-2989] p 1052 A93-48182
Wind tunnel tests of the model of intake-airframe integration p 1192 A93-54077
[ISABE 93-7101] p 1192 A93-54077
- A study on Mach 3 two-dimensional mixed compression air-intakes p 1188 A93-54082
[ISABE 93-7106] p 1188 A93-54082
Numerical simulation of the flow through non-uniform airfoil cascade p 302 N93-19310
A numerical investigation for supersonic inlet p 303 N93-19315
Role of wind tunnel tests and CFD analysis for the development of aero-engines in IHI p 365 N93-19326
- TANAKA, F.**
Conceptual design study on combined-cycle engine for hypersonic transport p 1195 A93-53994
[ISABE 93-7018] p 1195 A93-53994
Research and development of a turbo-accelerator for super/hypersonic transport p 1200 A93-54042
[ISABE 93-7066] p 1200 A93-54042
- TANAKA, HIROKI**
Development of a Shape-controlled airfoil by use of SMA p 411 A93-21739
- TANAKA, KAZUHIRO**
Development of a Shape-controlled airfoil by use of SMA p 411 A93-21739
- TANAKA, KEIJI**
A method of wind shear detection for powered-lift STOL aircraft p 1104 A93-48345
[AIAA PAPER 93-3667] p 1104 A93-48345
Wind-shear endurance capability for powered-lift aircraft p 1129 A93-48348
[AIAA PAPER 93-3670] p 1129 A93-48348
- TANAKA, KOHEI**
Wind tunnel tests and CFD in Fuji Heavy Industries p 304 N93-19323
- TANAKA, YASUHIKO**
Development of ultra-hypersonic shock tunnel for aerodynamics test p 376 A93-21900
- TANAKA, YASUYUKI**
Effects of boundary layer bleed on swept-shock/boundary layer interaction p 1052 A93-48182
[AIAA PAPER 93-2989] p 1052 A93-48182
- TANATSUGU, NOBUHIRO**
Test results on air turbo ramjet for a futurespace plane p 359 A93-22325
[AIAA PAPER 92-5054] p 359 A93-22325
Development study on Air Turbo Ramjet engine for a future space plane p 1195 A93-53992
[ISABE 93-7016] p 1195 A93-53992
Test results of the hydrogen fueled model combustor for the air turbo ramjet engine p 1201 A93-54058
[ISABE 93-7082] p 1201 A93-54058
Results of sea-level static tests on air turbo ramjet for a future space plane p 1247 A93-55817
[AAS PAPER 91-640] p 1247 A93-55817
- TANDON, MANOJ**
SR-SCARLET 1: Peregryn p 337 N93-18155
[NASA-CR-192048] p 337 N93-18155
- TANG, CHANGHONG**
Study of aeroservoelastic stability of an aircraft p 182 A93-14259
- TANG, D. M.**
Experimental and theoretical study for nonlinear aeroelastic behavior of a flexible rotor blade p 837 A93-39422
- TANG, DAOMIN**
Acoustical properties of sound absorbing structures at high temperature p 1172 A93-48522
- TANG, DENGBIN**
The numerical calculation and application of compressible boundary layers on laminar-flow-control and natural-laminar-flow wings p 680 A93-33727
Studies of the dynamic stall problem on airfoils p 681 A93-33747
- TANG, DIYI**
A unified model for rotating stall and surge p 259 A93-20119
A blade element method for predicting the off-design performance of compressors p 1107 A93-49187
- TANG, F. C.**
A wind tunnel investigation of the pressure distribution on an F/A-18 wing p 980 A93-47249
[AIAA PAPER 93-3468] p 980 A93-47249
Unsteady pressure and load measurements on an F/A-18 vertical fin p 1095 A93-52451
- TANG, G. C.**
A study of dynamic characteristics of axial compression systems by heat addition p 202 A93-14168
An investigation of post stall transients and recoverability of axial compression systems p 1184 A93-53988
[ISABE 93-7012] p 1184 A93-53988
- TANG, GUO C.**
An investigation of post stall transients and recoverability of axial compression systems. I - A simplified method p 347 A93-19305
[ASME PAPER 92-GT-55] p 347 A93-19305
An investigation of post stall transients and recoverability of axial compression systems. II - Numerical simulations p 347 A93-19306
[ASME PAPER 92-GT-56] p 347 A93-19306
- TANG, GUOCAI**
Numerical research on flows in nonuniform cascades p 253 A93-19469
[ASME PAPER 92-GT-276] p 253 A93-19469
- TANG, JICHENG**
Linear and nonlinear aircraft flight control for the AIAA Controls Design Challenge p 62 A93-13286
[AIAA PAPER 92-4628] p 62 A93-13286
- TANG, MING**
Effects of vitiated air on the results of ground tests of scramjet combustor p 173 A93-16234
- TANG, R. X.**
A new method to study the forming process of complicated sheetmetal aero-parts p 204 A93-14363
- TANG, RUIYUAN**
Experimental study of dynamic stall on an oscillating airfoil p 266 A93-20804
- TANG, SHUO**
Dynamic stability, coupling and active control of elastic vehicles with unsteady aerodynamic forces modeling p 182 A93-14282
Coupling characteristics analysis of elastic vehicle p 1169 A93-51189
- TANG, TIECHENG**
Mechanical testing analyses of new aluminium alloy SPF typical-parts in aircraft p 196 A93-14174
- TANG, WEI**
Numerical analysis of acoustic effect of rotor wakes in rotor-stator interaction p 447 A93-19182
- TANG, YUAN-LIANG**
A model-based approach for detection of objects in low resolution passive millimeter wave images p 808 N93-28418
[NASA-CR-193161] p 808 N93-28418
- TANG, ZHIMING**
Experimental investigation on patterned blades of compressor p 1066 A93-48515
- TANGLER, J.**
A discussion of the results of the rainflow counting of a wide range of dynamics associated with the simultaneous operation of adjacent wind turbines p 434 N93-18705
[DE93-000016] p 434 N93-18705
- TANGONAN, GREGORY L.**
Fiber optics for aircraft entertainment systems p 1172 A93-49478
- TANI, KOICHIRO**
Validation studies of scramjet nozzle performance p 1109 A93-49616
- TANI, KOUICHIRO**
Evaluation of 2D scramjet nozzle performance p 52 A93-11209
Effects of injector geometry on scramjet combustor performance p 359 A93-21670
Starting characteristics of scramjet inlets p 1203 A93-54081
[ISABE 93-7105] p 1203 A93-54081
Mach 4 testing of scramjet inlet models p 26 N93-12369
[NAL-TR-1137] p 26 N93-12369
Analytical and numerical study on steady Mach reflection p 302 N93-19309
- TANIDA, YOSHIMICHI**
Dual transverse injection of H₂ gas into Mach 1.8 flows at University Komaba wind tunnel p 376 A93-21833
- TANIMURA, S.**
Investigation of combustion structure inside low NO(x) combustors for a 1500 C-class gas turbine p 350 A93-19357
[ASME PAPER 92-GT-123] p 350 A93-19357
- TANJU, B.**
Integration of full scale development aircraft GPS user equipment (AN/ARN-151) with Doppler radar systems p 31 A93-11012
- TANNEHILL, JOHN C.**
A new rotated upwind difference scheme for the Euler equations p 261 A93-20179
[AIAA PAPER 93-0066] p 261 A93-20179
- TANNENBAUM, ALLEN**
H(infinity) optimal controllers for a distributed model of an unstable aircraft p 62 A93-13247
Numerical computation and approximations of H(infinity) optimal controllers for a 2-parameter distributed model of an unstable aircraft p 817 A93-37040
- TANNER, R. I.**
Generation of unstructured tetrahedral meshes by advancing front technique p 1021 A93-44206
- TANNOU, MICHIAKI**
Two-dimensional and three-dimensional mixing flow structures with injected through slotted nozzle and circular nozzle into supersonic flows p 1221 A93-54092
[ISABE 93-7117] p 1221 A93-54092
- TANRIKUT, S.**
Comparison of heat transfer measurements with computations for turbulent flow around a 180 deg bend p 201 A93-13980
- TAO, BO**
Three-dimensional separated flow over a prolate spheroid p 1235 A93-55379
- TAO, DEPING**
Numerical simulation of unsteady flow in a transonic cascade p 1066 A93-48502

- TAO, XIANDE**
Optimum balancing of flexible rotor p 205 A93-14489
- TAPOSU, I.**
The aerodynamic loads on aircraft components in violent longitudinal manoeuvres p 476 A93-26898
- TARASENKOV, A. M.**
Problems in the aerodynamics and dynamics of flight vehicles in the light of K.E. Tsiolkovsky's ideas; Lectures Devoted to K.E. Tsiolkovsky's Ideas, 25th, Kaluga, Russia, Sept. 11-14, 1990, Transactions p 237 A93-18376
- TARASOV, A. I.**
Computer-aided study of flight regimes and fuel consumption for helicopter flight operations p 997 A93-45674
- TARASOVA, N. V.**
Hydrodynamics and heat transfer near the stagnation point in an arbitrary axisymmetric nonswirling flow incident on a rotating obstacle p 691 A93-35270
- TARCZYNSKI, T.**
Open aircrew VTOL concepts [NASA-CR-177603] p 240 N93-17883
- TARG, RUSSELL**
Lidar windshear detection for commercial aircraft p 341 A93-17864
- TARPLEY, CHRISTOPHER**
Stability and control of hypersonic waveriders [AIAA PAPER 93-0508] p 370 A93-23255
- TARRANTINI, PAULINE**
High temperature corrosion resistant bearing steel development [AIAA PAPER 93-2000] p 1145 A93-49842
- TARTABINI, PAUL V.**
A systems approach to a DSMC calculation of a control jet interaction experiment [AIAA PAPER 93-2798] p 964 A93-46538
- TASHIMO, MASANORI**
Lift enhancement of ground-effect wing. I - Results of screening tests of various concepts p 271 A93-21737
Lift enhancement of ground-effect wing. II - Experimental investigation of the power augmented ram wing in ground effect through the wind tunnel p 271 A93-21738
Microchannel plate modal gain variations with temperature p 477 A93-27445
- TASHIRO, SHINICHI**
The frequency of incipient vortex-shedding from a circular cylinder in a laminar boundary layer (The effect of the gap ratio on the vortex shedding frequency) p 126 A93-15488
- TASKE, LEO E.**
The characterization and development of materials for advanced textile composites p 1211 A93-53434
- TASKER, FREDERICK A.**
Modified sparse time domain technique for rotor stability testing p 157 A93-14593
- TASSA, A.**
Dynamically adaptive grid and its applications to flow problems p 688 A93-34362
- TASSA, Y.**
Dynamically adaptive grid and its applications to flow problems p 688 A93-34362
- TATARA, A.**
A scoping study for hypersonic transport propulsion systems [ASME PAPER 92-GT-409] p 356 A93-19558
Combustion study on methane-fuel Laboratory Scaled Ram Combustor [ASME PAPER 92-GT-413] p 356 A93-19561
Studies on methane-fuel ram combustor for HST combined cycle engine [ISABE 93-7080] p 1201 A93-54056
- TATEISHI, TOMOHIRO**
Velocity fluctuation based on the difference in the flow pattern in the channels of a centrifugal impeller p 1182 A93-53842
- TATUM, KENNETH E.**
CFD code calibration and inlet-fairing effects on a 3D hypersonic powered-simulation model [AIAA PAPER 93-3041] p 1056 A93-48222
Computational effects of inlet representation on powered hypersonic, airbreathing models p 1094 A93-52427
- TAUBER, WOLFGANG**
Modeling limits of the EMV analysis program CONCEPT by example of the influence of a helicopter structure on a frame antenna [MBB-UD-0614-92-PUB] p 223 N93-15487
- TAUKE, G. J.**
Flight management system on the F-117A p 908 A93-42815
- TAVAFOGHI, M.**
Structure of martensite in titanium alloy Ti-6Al-1.6Zr-3.3Mo-0.3Si p 916 A93-43616
- TAVARES, T. S.**
Aerodynamics of maneuvering slender wings with leading-edge separation p 778 A93-39401
- TAVELLA, DOMINGO**
Computational investigation of a pneumatic forebody flow control concept p 768 A93-37383
- TAVELLA, DOMINGO A.**
A concurrent hybrid Navier-Stokes/Euler approach to fluid dynamic computations [AIAA PAPER 93-0789] p 468 A93-24865
- TAVERNA, MIKE**
Ilyushin takes on the market p 945 A93-43623
- TAYLOR, A. C., III**
An approximately factored incremental strategy for calculating consistent discrete aerodynamic sensitivity derivatives [AIAA PAPER 92-4746] p 265 A93-20344
Observations on computational methodologies for use in large-scale, gradient-based, multidisciplinary design [AIAA PAPER 92-4753] p 436 A93-20351
- TAYLOR, ARTHUR C., III**
Multidisciplinary analysis and sensitivity derivatives for isolated helicopter rotors in hover [AIAA PAPER 92-4696] p 324 A93-20308
Recent advances in steady compressible aerodynamic sensitivity analysis p 1236 A93-55400
Methodology for sensitivity analysis, approximate analysis, and design optimization in CFD for multidisciplinary applications [NASA-CR-192172] p 552 N93-20297
- TAYLOR, C.**
Numerical methods in laminar and turbulent flow; Proceedings of the 7th International Conference, Stanford Univ., CA, July 15-19, 1991. Vol. 7, pts. 1 & 2 [ISBN 0-906674-77-8] p 743 A93-34301
- TAYLOR, DAVID L.**
The Meteorological Data Collection and Reporting System - Status and future directions p 428 A93-22133
- TAYLOR, DEBORAH B.**
A stochastic optimal feedforward and feedback control methodology for superagility [NASA-CR-4471] p 229 N93-13370
- TAYLOR, JEFF C.**
Monte Carlo simulation of radiating reentry flows [AIAA PAPER 93-2809] p 964 A93-46548
Comparisons between DSMC and the Navier-Stokes equations for reentry flows [AIAA PAPER 93-2810] p 964 A93-46549
- TAYLOR, JOHN G.**
Internal performance of Highly Integrated Deployable Exhaust Nozzles [AIAA PAPER 93-2570] p 1084 A93-50288
Supersonic investigation of two dimensional hypersonic exhaust nozzles [NASA-TM-105687] p 179 N93-15342
- TAYLOR, M. V.**
The low frequency aeroacoustics of buried nozzle systems p 1205 A93-54244
- TAYLOR, P. J.**
Landing guidance systems for CAT III operations p 151 A93-17307
- TAYLOR, ROBERT M.**
Aerodynamic surface tip vortex attenuation system [AD-D015606] p 483 N93-20017
- TAYLOR, S. J.**
The development of a prototype aircraft height monitoring unit utilising an SSR-based difference in time of arrival technique p 884 A93-43432
- TAYLOR, V.**
JPL AIRSAR processing activities and developments p 1162 A93-47865
- TCHANG, PATRICK**
Integrated runway meteorological observation system (IRMOS/SIOMA) p 428 A93-22128
- TCHENG, PING**
An improved calibration technique for wind tunnel model attitude sensors p 1253 A93-54356
- TE, ALEXANDER**
Applying and validating the RANS-3D flow-solver for evaluating a subsonic serpentine diffuser geometry [AIAA PAPER 93-2157] p 1079 A93-49973
- TEACHOUT, DUANE A.**
Rewritable optical disk: Application to flight recording p 221 N93-15160
- TEAL, R. S.**
Ladar fiber optic sensor system for aircraft applications p 1105 A93-49467
- TEAL, RICHARD S.**
Desirable characteristics for rotorcraft optical components p 1172 A93-49466
- TEASLEY, STEWART P.**
Description and capabilities of the Navcore-V GPS receiver engine p 312 A93-21127
- TEDLUND, B. E.**
The development of the Boeing Human Model p 561 A93-27150
- TEIMANN, J.**
Sensors with centroid based common sensing scheme and their multiplexing p 1192 A93-52994
- TEIPEL, I.**
Viscous flows in centrifugal compressor diffusers at transonic Mach numbers [ASME PAPER 92-GT-48] p 246 A93-19301
- TEJO, M.**
Nondestructive inspection of in-service aircraft [ETN-93-93059] p 496 N93-20928
- TELEGINA, A. G.**
Characteristics of friction and wear in flight vehicle engine components p 811 A93-39075
- TELESMA, JACK**
External stress-corrosion cracking of a 1.22-m-diameter type 316 stainless steel air valve [NASA-TP-3190] p 737 N93-26201
- TELIONIS, D. P.**
3-D LDV measurements over a delta wing in pitch-up motion [AIAA PAPER 93-0185] p 275 A93-22610
The hemisphere-cylinder in dynamic pitch-up motions [AIAA PAPER 93-2963] p 1048 A93-48157
Periodic vortex shedding over delta wings p 1070 A93-49002
- TELIONIS, DEMETRI P.**
Flow control over delta wings at high angles of attack [AIAA PAPER 93-3494] p 983 A93-47266
- TEN HAVE, J. M.**
European studies to investigate the feasibility of using 1000 ft vertical separation minima above FL(290). III - Further results and overall conclusions p 992 A93-45166
- TENENBAUM, JOEL**
Recent experiment focuses on operational impact of jet stream forecast errors p 487 A93-27394
- TENG, YOUNGQUANG**
Artificial transition - A tool for high Reynolds number simulation? [AIAA PAPER 93-3258] p 967 A93-46799
- TENNING, CARL B.**
Evolution of the Boeing 777 electrical power system p 519 A93-25998
- TENTO, SCOTT W.**
Backward bifurcation for structural divergence of a wing section p 526 A93-29351
- TEPERIN, L. L.**
A comparative analysis of algorithms for solving systems of high-order linear algebraic equations p 96 A93-12977
- TERADA, H.**
Case study and simulation of fatigue damages and DTE of aging aircraft - A review of researches in Japan p 948 A93-45800
- TERAMAE, TETSUO**
An evaluation system for impact damage and erosion of ceramic gas turbine components p 79 A93-12229
- TERAN, A.**
Expedient repair of structural facilities [AD-A260727] p 731 N93-25656
- TEREKHOV, V. I.**
Pressure field and drag of a single cavity with rounded and sharp edges p 1258 A93-55018
- TEREKHOVA, N. M.**
Development of resonance perturbations in a supersonic jet p 1088 A93-51772
- TERENT'eva, L. V.**
Supersonic flow past energy release regions p 1069 A93-48973
Supersonic flow past a cone with heat transfer near its tip p 1089 A93-51780
- TERJESEN, E. J.**
Near-optimal energy transitions for energy-state trajectories of hypersonic aircraft [AIAA PAPER 92-4300] p 69 A93-13276
- TERNOVOL, A. I.**
Experimental simulation of the aerodynamic heating of bodies in a molecular region p 1090 A93-51871
- TERRELL, J. P.**
Heat flux microsensor measurements [AIAA PAPER 92-5038] p 413 A93-22312
- TERRY, T.**
Secondary flow control on slender, sharp-edged configurations [AIAA PAPER 93-3470] p 980 A93-47250
- TERSTEEGEN, J.**
Development and flight testing of a fault-tolerant fly-by-light yaw control system p 1010 N93-31280
- TERUI, YUSHI**
HUD Guidance for the ASKA Experimental STOL Aircraft using Radar Position Information [SAE PAPER 921041] p 150 A93-14661
- TESKE, MILTON E.**
Decay of aircraft vortices near the ground p 961 A93-45751

- Computation of wake/exhaust mixing downstream of advanced transport aircraft
[AIAA PAPER 93-2944] p 1162 A93-48141
- TESSIERAS, B.**
Hypersonic flows over a double or simple ellipse p 868 A93-42614
- TESTUD, JACQUES**
A technique to correct airborne Doppler data for coordinate transformation errors using surface clutter p 807 A93-37699
- TETWSKY, AVRAM K.**
The effects of ionospheric errors on single-frequency GPS users p 313 A93-21141
- TETZLAFF, JUERGEN**
Installations and methods for measurement of aircraft radio components and systems p 1031 N93-31284
- TEWARI, ASHISH**
Nonplanar Doublet-Point method for supersonic unsteady aerodynamics p 682 A93-34120
[AIAA PAPER 93-1588]
Multiple pole rational-function approximations for unsteady aerodynamics p 769 A93-37404
New acceleration potential method for supersonic unsteady aerodynamics of lifting surfaces, further extension of the nonplanar supersonic doublet point method, and nonlinear, nongradient optimized rational function approximations for supersonic, transient response unsteady aerodynamics p 25 N93-12344
- TEZDUYAR, T. E.**
A finite element study of incompressible flows past oscillating cylinders and aerofoils p 241 A93-17750
Finite element computation of compressible flows with the SUPG formulation p 482 A93-29774
- TEZOK, F.**
Further development of the CANAERO computer code to include a time-stepping capability [DREA-CR-91-478] p 562 N93-21820
- TEZUKA, H.**
Active forcing of an axisymmetric leading-edge turbulent separation bubble [AIAA PAPER 93-3245] p 966 A93-46790
- THACKER, MICHAEL D.**
Calculation of transonic longitudinal and lateral-directional characteristics of aircraft by the small disturbance theory [AIAA PAPER 93-3617] p 1125 A93-48304
- THAMBURAJ, RAJ**
In-service considerations affecting component life p 177 N93-14898
- THAME, COLIN**
European environmental studies focus on impact of engine emissions p 92 A93-10730
- THAMES, H. DAVIS, III**
Experimental study of the flow field inside a whirling annular seal p 85 N93-10892
- THAMES, HOWARD D.**
Compressible and incompressible fluid seals: Influence on rotordynamic response and stability [NASA-CR-190746] p 85 N93-10891
- THANGAM, S.**
Computational analysis of nonlinear aeroelastic phenomena during stall flutter of cascaded airfoils [AIAA PAPER 93-2082] p 1079 A93-49909
- THART, W. G. J.**
Flight simulation and constant amplitude fatigue crack growth in aluminum-lithium sheet and plate [NLR-TP-91-104-U] p 331 N93-17562
- THEERTHAMALAI, P.**
Computation of hypersonic flow over a sphere using kinetic flux vector splitting scheme with equilibrium chemistry p 861 A93-42260
- THEIMER, PAUL**
The Eurojet EJ200 engine p 1246 A93-54839
- THEOBALD, B.**
Theoretical and experimental investigations concerning the structural integrity of aeroengine compressor discs p 56 N93-10539
- THEOFILIS, VASSILIOS**
Numerical experiments on the stability of leading edge boundary layer flow - A two-dimensional linear study p 477 A93-27475
- THERET, J. M.**
Control of in-service damage: Application to aircraft engines [DS-2027] p 364 N93-18151
- THERY, CHRISTIAN**
Sonic boom problem for future highspeed aircraft [ONERA-NT-1990-3] p 876 N93-30020
- THEUNISSEN, E.**
A primary flight display for four-dimensional guidance and navigation influence of tunnel size and level of additional information on pilot performance and control behaviour [AIAA PAPER 93-3570] p 1208 A93-52668
- THEVENIN, P.**
Effect of environment on creep-fatigue crack propagation in turbine disc superalloys [ONERA, TP NO. 1993-5] p 916 A93-41023
- THIBERT, J. J.**
Activities of the GARTEUR high lift research program [ONERA, TP NO. 1992-152] p 803 A93-38731
- THIBERT, JEAN-JACQUES**
Toward the second-generation supersonic transport [ONERA, TP NO. 1993-26] p 890 A93-41038
- THIBODEAUX, J. J.**
A PC-based simulation of the National Transonic Facility's safety microprocessor [NASA-TM-109003] p 1038 N93-32224
- THIELE, F.**
An Euler code with new energy equation and new enthalpy damping approach p 686 A93-34352
A Laplace interaction law for the computation of viscous airfoil flow in low and high speed aerodynamics [AIAA PAPER 93-3462] p 979 A93-47244
- THIELE, FRANK**
Stability investigations of airfoil flow by global analysis p 783 N93-27436
- THIENEL, LEE**
Flight data for the Cryogenic Heat Pipe (CRYOHP) Experiment [AIAA PAPER 93-2735] p 1027 A93-46488
- THIES, ANDREW T.**
Instability of rectangular jets p 398 A93-19157
Instability of rectangular jets p 720 A93-34410
- THIRARD, VINCENT**
Experimental results on RIAS digital beamforming radar p 929 A93-43392
- THOLE, KAREN A.**
Hydrodynamic effects on heat transfer for film-cooled turbine blades [AD-A257291] p 361 N93-16080
- THOMANN, HANS**
Flux-vector splitting for compressible low Mach number flow p 1093 A93-52001
- THOMAS, D. R.**
Active control of sound transmission through stiff lightweight composite fuselage constructions p 447 A93-19187
Theoretical studies of the active control of propeller induced cabin noise using secondary force inputs p 995 A93-45124
- THOMAS, HUGH O.**
Pitch control trimming system for canard design aircraft [CA-PATENT-APPL-SN-2013236] p 63 N93-10374
- THOMAS, J.**
MPC75 as the forerunner of a new regional aircraft family p 37 A93-10776
- THOMAS, J. L.**
Reynolds number effects on supersonic asymmetrical flows over a cone p 958 A93-45141
- THOMAS, JACOB**
Transmission error and load distribution analysis of spur and double helical gear pairs used in a split path helicopter transmission design p 549 A93-29426
- THOMAS, JAMES**
Visual approach data collection at St. Louis Lambert Field (STL) [DOT/FAA/CT-TN93/2] p 706 N93-24948
- THOMAS, JAMES L.**
An implicit multigrid scheme for hypersonic strong-interaction flowfields p 6 A93-10534
Multiblock Navier-Stokes solutions about the F/A-18 wing-LEX-fuselage configuration p 767 A93-37378
Computational fluid dynamics for hypersonic airbreathing aircraft p 865 A93-42581
Grid-refinement study of hypersonic laminar flow over a 2-D ramp p 866 A93-42597
- THOMAS, KEVIN W.**
An improved gust front detection algorithm for the TDWR p 432 A93-22191
- THOMAS, MITCHEL E.**
The FAA/NASA flight loads monitoring program - The prototype system and its benefits for the aviation community p 486 A93-25125
- THOMAS, P.**
Theoretical and experimental study of the behavior of particles passing through a shock wave [ONERA, TP NO. 1992-233] p 774 A93-38777
- THOMAS, P. D.**
Evaluation of RNG algebraic turbulence models for boundary layers p 684 A93-34331
- THOMAS, R. H.**
Preliminary experiments on active control of fan noise from a turbofan engine p 759 A93-34957
- THOMAS, RUSSELL H.**
Active control of fan noise from a turbofan engine [AIAA PAPER 93-0597] p 452 A93-23323
- THOMAS, SCOTT D.**
Euler/experiment correlations of sonic boom pressure signatures p 1095 A93-52439
- THOMASON, LEE B.**
Supersonic aeroelastic instability results for a NASP-like wing model [AIAA PAPER 93-1369] p 682 A93-33935
Supersonic aeroelastic instability results for a NASP-like wing model [NASA-TM-107739] p 718 N93-26553
- THOMBS, VICTOR**
V-22 program overview [AIAA PAPER 92-4277] p 457 A93-24299
- THOMPSON, A. E.**
A structural reliability evaluation of fail-safe helicopter dynamic components p 506 A93-27952
- THOMPSON, C. J.**
Subsonic potential flow and the transonic controversy p 479 A93-28544
- THOMPSON, D. E.**
Sound generation by rotating stall in centrifugal turbomachines p 1039 A93-46701
- THOMPSON, D. O.**
Towards quantitative non-destructive evaluation of aging aircraft p 1025 A93-45773
- THOMPSON, D. S.**
Eduction of swirling structure using the velocity gradient tensor p 416 A93-23547
- THOMPSON, DONALD O.**
Review of progress in quantitative nondestructive evaluation. Vol. 11B: Proceedings of the 18th Annual Review, Brunswick, ME, July 28-Aug. 2, 1991 Vol. 11B (ISBN 0-306-44206-X) p 406 A93-19582
- THOMPSON, EDWARD A.**
Optimization of blade arrangement in a randomly mistuned cascade using simulated annealing [AIAA PAPER 93-2254] p 1115 A93-50052
- THOMPSON, H. D.**
Analytical and experimental investigation of annular propulsive nozzles [AD-A262685] p 815 N93-28391
- THOMPSON, H. DOYLE**
Hypervelocity scramjet combustor-nozzle analysis and design [NASA-CR-190965] p 60 N93-12214
Turbulence characteristics of an axisymmetric reacting flow [NASA-CR-4110] p 877 N93-30373
- THOMPSON, J. F.**
Adaptive EAGLE dynamic solution adaptation and grid quality enhancement p 788 N93-27464
- THOMPSON, JOE F.**
Solution-adaptive and quality-enhancing grid generation p 480 A93-28610
- THOMPSON, M. W.**
Issues associated with long-duration high-enthalpy scramjet combustor testing p 721 A93-34497
- THOMPSON, R. A.**
Air/helium ground-test simulation pertinent to the definition of slender body hypersonic aerodynamics [AIAA PAPER 93-0318] p 268 A93-21106
The addition of algebraic turbulence modeling to program LAURA [NASA-TM-107758] p 840 N93-27250
- THOMPSON, RICHARD A.**
Combined LAURA-UPS hypersonic solution procedure [NASA-TM-107682] p 747 N93-25176
- THOMPSON, SCOTT ANDREW**
The unsteady aerodynamics of a delta wing undergoing large-amplitude pitching motions p 134 N93-13929
- THOMPSON, T. E.**
Adapting system engineering principles to the Canadian Airspace System p 887 N93-30338
- THOMPSON, THOMAS L.**
Low-speed wind tunnel test results of the Canard Rotor/Wing concept [AIAA PAPER 93-3412] p 975 A93-47209
- THOMPSON, V. K.**
Zoning of aircraft by electric field modeling p 704 N93-24894
- THOMSON, D. E.**
Foreign object impact assessment of a high-Mach engine inlet [AIAA PAPER 93-1630] p 711 A93-34158
- THORBECK, JUERGEN**
Economical view on composite structures maintenance [SME PAPER EM92-102] p 233 A93-14103
- THORN, R.**
MTR390 - Engine for the future [ASME PAPER 92-GT-250] p 353 A93-19459
- THORNING, ARTHUR G.**
Human factors of aircraft cabin safety p 140 A93-14218

- THORNTON, A. L.**
Ablation problems using a finite control volume technique
[DE93-009861] p 942 N93-29187
- THORNTON, ANTHONY LINN**
Application of a solution adaptive grid to flow over an embedded cavity p 130 N93-13141
- THORNTON, CHARLES H.**
Measuring flight test progress on large scale development programs
[AIAA PAPER 92-4070] p 37 A93-11257
- THORNTON, EARL A.**
NASA-UVA Light Aerospace Alloy and Structures Technology Program (LA2ST)
[NASA-CR-193412] p 1019 N93-31739
- THORNTON, J. T.**
The Foreign Sovereign Immunities Act of 1976 - Misjoinder, nonjoinder, and collusive joinder p 944 A93-42998
- THORNTON, TIM**
Exodus: Prime Mover
[NASA-CR-192051] p 332 N93-17803
- THOURAUD, P.**
Supersonic through flow compressors - A preliminary study: COVAXS p 1001 A93-46930
- THURMAN, DOUGLAS R.**
Measurements and computational analysis of heat transfer and flow in a simulated turbine blade internal cooling passage
[AIAA PAPER 93-1797] p 1218 A93-53585
Measurements and computational analysis of heat transfer and flow in a simulated turbine blade internal cooling passage
[NASA-TM-106189] p 1032 N93-31647
- TIAGUNOV, G. V.**
Resource conservation and improvement of the service characteristics of castings of high-temperature nickel alloys through a high-temperature melt treatment p 824 A93-36718
- TIAN, T. Z.**
The fretting damage and effect of temperature in typical joint of aircraft construction p 203 A93-14196
- TICE, DAVID C.**
Some effects of wing and body geometry on the aerodynamic characteristics of configurations designed for high supersonic Mach numbers
[AIAA PAPER 92-4246] p 463 A93-24493
- TICHY, LORENZ**
Transonic flows on an oscillating airfoil and their effect on the flutter-boundary
[DLR-FB-92-08] p 790 N93-29006
- TIEBENS, G. S.**
Development of the F/A-18 E/F air induction system
[AIAA PAPER 93-2152] p 1101 A93-49969
- TIEDEMANN, R. K.**
Embedded GPS: The Canadian Marconi approach p 886 A93-30330
- TIEDERMAN, WILLIAM G.**
Viscous interaction upstream and downstream of a turbine stator cascade with a periodic wake field
[ASME PAPER 92-GT-162] p 250 A93-19388
- TIEFENAUER, RICHARD L.**
Ultrasonic thickness measurement using the angle technique p 542 A93-25353
- TIEGS, T. N.**
Microwave processing of silicon nitride for advanced gas turbine applications
[DE93-007910] p 917 N93-29767
- TIEMEYER, B.**
Precision navigation with an integrated navigation system p 29 A93-10782
- TIEN, D. C.**
Swirling flows in a contoured-wall combustion chamber
[AIAA PAPER 93-1765] p 1073 A93-49661
- TIEN, J. K.**
Raising the high temperature limit of the nickel-iron-base superalloy p 70 A93-12114
- TIENG, S. M.**
Holographic interferometric investigation of shock wave interaction with a ramp p 271 A93-21921
- TILL, ROBERT D.**
Automatic dependent surveillance (ADS) Pacific engineering trials (PET) p 30 A93-10999
- TILLIAEVA, N. I.**
Variational problem of the profiling of the side walls of the supersonic section of a narrow three-dimensional nozzle p 4 A93-10140
- TILLMAN, T. G.**
Flowfield measurements for a supersonic mixer ejector in forward flight p 399 A93-19217
- TIMMONERI, L.**
Space-time processing for AEW radar p 884 A93-43444
- TIMNAT, Y. M.**
Design and testing methods of high performance combustors for airbreathing engines
[ISABE 93-7024] p 1196 A93-54000
- TIMOSHENKO, V. I.**
Calculation of the irregular interaction of shock waves p 691 A93-35339
- TIMOTEI, DOMINIC**
Visual approach data collection at St. Louis Lambert Field (STL)
[DOT/FAA/CT-TN93/2] p 706 N93-24948
- TINDELL, R. H.**
CFD analysis of the X-29 inlet at high angle of attack p 958 A93-45140
- TING, T.**
An automated mode tracking strategy
[AIAA PAPER 93-1414] p 739 A93-33970
- TIRKAS, PANAYIOTIS A.**
Advanced electromagnetic methods for aerospace vehicles
[NASA-CR-193468] p 936 N93-31036
- TIRRES, LIZET**
Experimental evaluation of a cooled radial-inflow turbine
[AIAA PAPER 93-1795] p 1110 A93-49685
Experimental evaluation of a cooled radial-inflow turbine
[NASA-TM-106230] p 816 N93-28697
- TIRSKII, G. A.**
Influence of second-order boundary layer effects in hypersonic flow past blunt cones of large aspect ratio p 241 A93-18238
- TIRSKIJ, G. A.**
Application of the small parameter method to the problem of three-dimensional flow of a viscous gas past bodies p 1178 A93-53314
- TISCHLER, M. B.**
Investigation of the flight mechanics simulation of a hovering helicopter p 798 A93-35990
- TISCHLER, MARK B.**
Frequency-response techniques for documentation and improvement of rotorcraft simulators p 913 N93-30689
- TISHKOFF, J. M.**
AFOSR Contractors Meeting in Propulsion
[AD-A254484] p 195 N93-12575
- TITARENKO, S. V.**
A study of the effect of surface riblets on the evolution of a solitary wave packet (lambda vortex) in a laminar boundary layer p 1067 A93-48827
- TITOW, O. W.**
Algebraic determination of the shock wave shape in axisymmetric flow over a circular cylinder p 1237 A93-56030
- TIURIKOV, E. V.**
Integrated air separation and propulsion system for aerospace plane with atmospheric oxygen collection
[SAE PAPER 920974] p 195 A93-14633
- TIURIN, V. D.**
A design concept for a flight vehicle computer system with artificial intelligence elements p 757 A93-35663
- TIVANOV, GENADI**
Analysis of the stability characteristics of hypersonic flow of a detonable gas mixture in the stagnation region of a blunt body
[AIAA PAPER 93-1918] p 1076 A93-49784
- TIWARI, S. N.**
Investigation of three-dimensional separation at wing/body junctions in supersonic flows using TVD MacCormack's scheme
[AIAA PAPER 93-0884] p 471 A93-24945
Study of supersonic intersection flowfield at modified wing-body junctions p 692 A93-35621
Grid sensitivity for aerodynamic optimization and flow analysis
[NASA-CR-192980] p 694 N93-25117
- TIWARI, SURENDRA N.**
Grid and design variables sensitivity analyses for NACA four-digit wing-sections
[AIAA PAPER 93-0195] p 276 A93-22616
Grid and aerodynamic sensitivity analyses of airplane components
[AIAA PAPER 93-3475] p 981 A93-47254
Topology and grid adaption for high-speed flow computations
[NASA-CR-4216] p 934 N93-30375
- TJATRA, I. W.**
Structural non-linearity effects on flutter of a swept wing in transonic flows p 410 A93-20714
- TJATRA, I. WAYAN**
Transonic aeroelastic analysis of systems with structural nonlinearities p 217 N93-13769
- TJONNELAND, E.**
Accuracy issues in the prediction of supersonic inlet flows
[ASME PAPER 92-GT-400] p 258 A93-19549
- TJONNELAND, ELLING**
Flow stability issues in supersonic inlet flow analyses
[AIAA PAPER 93-0290] p 279 A93-22690
- TOBAK, MURRAY**
Experimental study of controlled tip disturbance effect on flow asymmetry p 211 A93-17417
Numerical simulation of upstream disturbance on flows around a slender body
[AIAA PAPER 93-2956] p 1047 A93-48150
- TOBE, SHOGO**
Effect of stress level of gust cycles on fatigue crack propagation behavior (Acceleration and retardation of crack propagation under simplified flight simulation loading) p 198 A93-17033
- TOBER, A.**
Measurements of gas composition and temperature inside a can type model combustor p 1123 A93-51644
- TOCKERT, C.**
Concept for an open-neck stratospheric balloon with long-duration flight capability p 40 A93-11371
- TODA, AKIHITO**
Visualization and analysis of supersonic flow in rotating turbine stage. I - Influence of shock wave between stationary and moving blades p 126 A93-15449
Visualization and analysis of supersonic flow in rotating turbine stage. II - Analysis of the flow into the moving blades and their exit flow p 476 A93-27442
- TODD, JOHN R.**
Integrating controls and avionics on commercial aircraft p 892 A93-42778
Direct optical control - A lightweight backup consideration p 907 A93-42808
- TODD, RUSSELL F.**
Setting values for TDWR/LLWAS 3 integration parameters
[AD-A260740] p 755 N93-25645
- TOERNIG, W.**
An implicit finite-difference algorithm for the numerical simulation of supersonic flow over blunt bodies p 770 A93-38325
- TOGNACCINI, R.**
An advanced graphics-interactive system for a multi-block structured grid generation within an industrial environment
[ETN-92-92885] p 440 N93-16288
- TOKARCIC-POLSKY, SUSAN**
Numerical study of the transient flow in the driven tube and the nozzle section of a shock tunnel
[AIAA PAPER 93-2018] p 1078 A93-49856
- TOKARCIC, SUSAN**
Computational flow predictions for hypersonic drag devices p 777 A93-39257
- TOKARZ, ROB**
Exodus: Prime Mover
[NASA-CR-192051] p 332 N93-17803
- TOKUNAGA, TATSURU**
Starting characteristics of scramjet inlets
[ISABE 93-7105] p 1203 A93-54081
- TOKUYAMA, AYANO**
Improving the lift to drag characteristics of low boom configuration
[AIAA PAPER 92-4218] p 16 A93-13380
- TOLER, CARL G.**
Evaluation of CKU-5/A ejection seat catapults under varied acceleration levels
[AD-A248021] p 29 N93-12489
- TOLLE, CHARLES R.**
Vertical guidance for a Lockheed L1011-100 using optimal dynamic interpolation p 369 A93-22884
- TOLUN, S.**
Design of advanced beams considering elasto-plastic behaviour of material p 544 A93-26904
- TOMASHOFSKI, C. A.**
Application of generalized force determination to a full scale low cycle fatigue test of the SH-2G helicopter p 795 A93-35949
An improved method of structural dynamic test design for ground flying and its application to the SH-2F and SH-2G helicopters p 512 N93-19928
- TOMIC, RADOLJUB**
Structural analysis of a nonlinear problem of aeroelasticity for CFC structures p 397 A93-18989
- TOMINAGA, TETSUO**
Performance improvement by forward-skewed blading of axial fan moving blades
[ISABE 93-7055] p 1185 A93-54031
- TOMIO, TAKESHI**
Digital fly-by-wire system for BK117 FBW research helicopter p 181 A93-14209
- TOMIOKA, S.**
A study of self-ignition of methane-hydrogen mixture fuel injected into high enthalpy supersonic airstreams
[ISABE 93-7049] p 1213 A93-54025

- TOMIOKA, YASUHIRO**
Development of ultra-hypersonic shock tunnel for aerodynamics test p 376 A93-21900
- TOMITA, TAKEO**
LIF visualization of 3-dimensional hypersonic mixing [ISABE 93-7114] p 1221 A93-54089
- TONG, DONALD**
Payload vehicle aerodynamic re-entry analysis p 69 A93-12004
- TONG, PIN**
Structural integrity of aging airplanes [ISBN 0-540-53461-X] p 947 A93-45772
Computational schemes for integrity analyses of fuselage panels in aging airplanes p 1025 A93-45774
- TOOSI, MOSTAFA**
The NASA/industry Design Analysis Methods for Vibrations (DAMVIBS) program: McDonnell-Douglas Helicopter Company achievements p 515 N93-21314
- TOPOL, D.**
Active aerodynamic control of wake-airfoil interaction noise - Experiment p 1225 A93-53206
- TOPOL, D. A.**
Active aerodynamic control of wake-airfoil interaction noise - Experiment p 445 A93-19153
Rotor wake/stator interaction noise - Predictions vs data p 1174 A93-52447
- TORCZYNSKI, J. R.**
Reynolds number dependence of the drag coefficient for laminar flow through fine-scale photoetched screens p 1218 A93-53815
- TORECKI, PAWEŁ**
Quantitative Knudsen-number dependences of density disturbances in front of obstructions in supersonic divergent flows p 1239 A93-56220
- TORELLA, G.**
Expert systems for the simulation of gas turbine engines [ASME PAPER 92-GT-408] p 435 A93-19557
- TORELLA, GIOVANNI**
User-friendly codes for the training on gas turbine engines [AIAA PAPER 93-2051] p 1166 A93-49884
Expert Systems for the simulation of turbfan engines [ISABE 93-7133] p 1225 A93-54108
- TORGUE, A.**
Prediction of the performances in combustion of ramjets and stato-rockets by isothermal experiments and modeling p 363 N93-17622
- TORNG, T. Y.**
Computational techniques for probabilistic analysis of turbomachinery [ASME PAPER 92-GT-167] p 351 A93-19393
- TOROK, MICHAEL S.**
Aerodynamic and wake methodology evaluation using model UH-60A experimental data p 767 A93-35997
- TORQUATI, FRANCO**
Scheduling of an aircraft fleet p 443 N93-18665
- TORRES, ABEL O.**
Supersonic/hypersonic aerodynamic methods for aircraft design and analysis p 967 A93-46816
- TORRES, JOSE A.**
Some limitations on the effectiveness of airborne adaptive radar p 501 A93-29596
- TORRES, MANUEL**
Choice of materials for military helicopters p 158 A93-15028
- TORREY, NANCY P.**
NASA advanced design program: Analysis, design, and construction of a solar powered aircraft [NASA-CR-192040] p 332 N93-17802
- TORVIK, PETER J.**
On the maximum range of flying wings [AIAA PAPER 92-4223] p 504 A93-24492
- TOSCANO, WILLIAM B.**
Autogenic-feedback training improves pilot performance during emergency flying conditions [NASA-TM-104005] p 790 N93-27076
- TOSHIMITSU, K.**
Unsteady aerodynamic response of two-dimensional subsonic and supersonic oscillating cascades with chordwise displacement and flexible deformation p 971 A93-46922
- TOSHIMITSU, KAZUHIKO**
Modal analysis of unsteady aerodynamic response of subsonic annular cascade with steady loading under elastic vibration p 126 A93-15495
Experimental study on the unsteady aerodynamic response of a three dimensional cascade with oscillating blades p 242 A93-18499
Study of mixing flow field of a jet in a supersonic cross flow. I - Experimental facilities and preliminary experiments p 857 A93-40430
- TOTAH, JOSEPH**
A critical assessment of UH-60 main rotor blade airfoil data [AIAA PAPER 93-3413] p 975 A93-47210
- TOTLAND, ERNST**
GARTEUR 3D sheer layer experiment [FFA-TN-1992-26] p 987 N93-31052
- TOURJANSKY, NICOLAS**
The measurement of blade deflections - A new implementation of the strain pattern analysis [ONERA, TP NO. 1992-127] p 831 A93-38601
- TOURLIDAKIS, A.**
Adaptation of a 3-D pressure correction Navier-Stokes solver for the accurate modelling of tip clearance flows p 971 A93-46932
Numerical modelling of viscous turbomachinery flows with a pressure correction method p 723 N93-25702
- TOURRETTE, L.**
A two layer k-epsilon computation of transonic viscous flow including separation over the DLR-F5 wing [AIAA PAPER 93-3110] p 1061 A93-48281
- TOUSSAINT, GREGORY J.**
Integrated Blade Inspection System (IBIS) upgrade study [AD-A258912] p 365 N93-19356
- TOWERS, C. E.**
Visualisation and analysis of three dimensional transonic flows by holographic interferometry p 1020 A93-44194
Particle imaging techniques and applications p 1020 A93-44195
- TOWERS, D. P.**
Visualisation and analysis of three dimensional transonic flows by holographic interferometry p 1020 A93-44194
Particle imaging techniques and applications p 1020 A93-44195
- TOWFIGHI, J.**
Instantaneous structure of vortex breakdown on a delta wing via particle image velocimetry p 779 A93-39428
- TOWNE, DOUGLAS M.**
Functional requirements of an advanced instructional design advisor: Simulation authoring, Volume 3 [AD-A256650] p 440 N93-16500
- TOWNSEND, B.**
Analysis of Loran-C performance in the Pemberton area, B.C. p 311 A93-17797
- TOWNSEND, D. P.**
Modal analysis of multistage gear systems coupled with gearbox vibrations p 827 A93-36588
- TOWNSEND, SCOTT E.**
Turbomachinery CFD on parallel computers [NASA-TM-105932] p 228 N93-13154
- TRACY, ANITA L.**
Aeromechanical stability of a bearingless composite rotor in forward flight [AIAA PAPER 93-1305] p 726 A93-33881
- TRACY, MAUREEN B.**
Non-propulsive aerodynamic noise p 99 N93-10673
- TRAINER, WILLIAM T.**
Experimental and analytical investigation of the vibration characteristics of a remotely piloted helicopter [AD-A256131] p 163 N93-14248
- TRAINOR, J. W.**
Circulation control wing model study [AIAA PAPER 93-0094] p 264 A93-20200
- TRAN-CONG, TON**
Introduction of small velocity and pressure variation into a stationary compressible fluid p 473 A93-25060
- TRAN, BOI N.**
Comparison of advanced turboprop interior noise control ground and flight test data p 444 A93-19136
Sound transmission through stiffened double-panel structures lined with elastic porous materials p 444 A93-19139
- TRAN, HUY K.**
Thermal response and ablation characteristics of light weight ceramic ablators [AIAA PAPER 93-2790] p 1018 A93-46532
- TRAN, P.**
Prediction of the ice accretion with viscous effects on aircraft wings [AIAA PAPER 93-0027] p 307 A93-20145
- TRANKLE, THOMAS L.**
Identification of a full subsonic envelope nonlinear aerodynamic model of the F-14 aircraft [AIAA PAPER 93-3634] p 1065 A93-48319
- TRANSUE, AMY E.**
Visual approach data collection at St. Louis Lambert Field (STL) [DOT/FAA/CT-TN93/2] p 706 N93-24948
- TRASHKEEV, S. I.**
Dynamics of the behavior of nematic films in gasdynamic flows p 746 A93-35345
- TRAUB, LANCE W.**
Effects of wing-tip vortex flaps p 959 A93-45153
- TRAYER, MICHAEL L.**
NASA advanced design program: Analysis, design, and construction of a solar powered aircraft [NASA-CR-192040] p 332 N93-17802
- TREFNY, CHARLES JOSEPH**
Experiments and analysis concerning the use of external burning to reduce aerospace vehicle transonic drag p 70 N93-12537
- TREGAY, G. W.**
Flight testing of a fiber optic temperature sensor p 1105 A93-49476
- TREGUB, V. I.**
Inelasticity effect in a unidirectional boron/aluminum composite under uniaxial tension p 825 A93-39024
- TREIBER, DAVID A.**
Modeling supersonic inlet boundary-layer bleed roughness p 872 A93-42891
- TREICHEL, CURT**
Simulators for corporate pilot training and evaluation p 912 N93-30678
- TREILHOU, J. P.**
Resonance frequencies of a gondola submitted to a forced rotation under a stratospheric balloon p 27 A93-11384
- TRENCHARD, MICHAEL E.**
Digital map databases in support of avionic display systems p 544 A93-26888
- TRENT, WILLIAM**
National Airspace System flight planning operational concept NAS-SR-131 [PB93-124659] p 310 N93-18031
National Airspace System: Air traffic control and airspace management operational concept NAS-SR-132 [DOT/FAA/SE-92/5] p 502 N93-20164
- TREPANIER, J. Y.**
Periodic Euler and Navier-Stokes solutions about oscillating airfoils p 241 A93-17799
Euler computations of rotor-stator interaction in turbomachinery cascades using adaptive triangular meshes [AIAA PAPER 93-0386] p 282 A93-23065
- TREPANIER, J.-Y.**
Implicit numerical solution of transonic flows using adaptive triangular grids p 686 A93-34349
- TRETYAKOVA, E. E.**
Resource conservation and improvement of the service characteristics of castings of high-temperature nickel alloys through a high-temperature melt treatment p 824 A93-36718
- TRETYAKOV, P. K.**
Determination of heat transfer to flow in a duct with a pseudodiscontinuity p 1179 A93-53365
- TREUNER, M.**
Experimental investigation of the management of large-sized drops and the onset of Marangoni-convection p 926 A93-41700
- TRIFONOV, A. D.**
An adaptive algorithm for estimation of a state vector in the system of remotely-piloted aircraft control using Kalman filter p 181 A93-14232
- TRIGUB, V. N.**
The asymptotic theory of hypersonic boundary-layer stability p 462 A93-24409
The long-wave limit in the asymptotic theory of hypersonic boundary-layer stability p 462 A93-24410
Flow past three-dimensional irregularities in a hypersonic boundary layer on a cooled body p 775 A93-39119
- TRILLING, TODD W.**
Actuated forebody stroke controls for the F-18 high alpha research vehicle [AIAA PAPER 93-3675] p 1006 A93-44233
Dynamic model testing of the X-31 configuration for high-angle-of-attack flight dynamics research [AIAA PAPER 93-3674] p 1129 A93-48351
- TRIPLETT, WILLIAM**
An industry held hostage p 486 A93-26423
- TRIPP, JOHN S.**
An improved calibration technique for wind tunnel model attitude sensors p 1253 A93-54356
- TRITTLER, G.**
Optimization aspects of an ejector type hypersonic thrust nozzle [ASME PAPER 92-GT-402] p 355 A93-19551
- TRIVEDI, MOHAN M.**
Intelligent robotics: Proceedings of the International Symposium, Bangalore, India, Jan. 2-5, 1991 [SPIE-1571] p 1166 A93-49350
- TROCHET, PATRICK**
Numerical modelling of induced effects of lightning strike on an all composite helicopter p 703 N93-24879
- TROE, J.**
A laser induced fluorescence system for the high enthalpy shock tunnel (HEG) in Goettingen p 1024 A93-45506
- TROFIMOV, V. M.**
Experience with the use of liquid crystals in conjunction with the filament method is studying the structure of supersonic flow downstream of a plane step p 478 A93-27639

- A study of flow structure and heat transfer intensity in the vicinity of an expanding step on a plate p 691 A93-35268
- TROHA, W. T.**
Heat transfer in high turbulence flows: A 2-D planar wall jet p 932 N93-29935
- TROLINGER, JAMES D.**
Optically smart surfaces for aerodynamic measurements [AIAA PAPER 92-3895] p 539 A93-24484
- TROSPER, J. R.**
On dynamics of the juncture vortex [AIAA PAPER 93-3473] p 980 A93-47252
- TROTT, W. M.**
Advanced diagnostics for in situ measurement of particle formation and deposition in thermally stressed jet fuels [AIAA PAPER 93-0363] p 390 A93-23045
- TROTT, WAYNE**
Advanced thermally-stable, coal-derived, jet fuels program: Experiment system and model development [AD-A262747] p 917 N93-29402
- TROUDET, T.**
Design and evaluation of a robust dynamic neurocontroller for a multivariable aircraft control problem p 817 A93-37004
Analysis of fault-tolerant neurocontrol architectures [NASA-TM-105898] p 65 N93-12305
- TROUDET, TERRY**
Neurocontrol design and analysis for a multivariable aircraft control problem p 906 A93-41894
Robustness enhancement of neurocontroller and state estimator [NASA-TM-106028] p 819 N93-26907
- TROUTT, T. R.**
Active control of the shear layer on a static airfoil [AIAA PAPER 93-0442] p 286 A93-23353
- TROVATI, A.**
Cooling geometry optimization using liquid crystal technique p 902 N93-29939
- TROXEL, SETH**
Weather information requirements for Terminal Air Traffic Control Automation. p 429 A93-22146
- TRUCCO, HORACIO A.**
Suggestions for development of three-phase 60 Hz arc heated wind tunnels [AIAA PAPER 93-0795] p 528 A93-24874
- TRUCCO, R.**
Mixing and combustion studies using discrete orifice injection at hypervelocity flight conditions p 205 A93-14523
- TRUE, B.**
Experimental investigation of crossflow jet mixing in a rectangular duct [NASA-TM-106152] p 812 N93-27026
- TRUEBLOOD, MAX B.**
Particulates and aerosols characterized in real time for harsh environments using the UMR mobile aerosol sampling system (MASS) [AIAA PAPER 93-2344] p 1156 A93-50118
- TRUEMAN, C. W.**
RCS of fundamental scatterers in the HF band by wire-grid modeling p 933 N93-30320
- TRUJILLO, EDWARD**
Advanced real time integrated processors p 50 A93-11000
Functionally Integrated Resource Manager for real-time avionics data p 940 A93-42832
- TRUONG, BON**
Hypersonic reconnaissance aircraft [NASA-CR-192049] p 333 N93-17804
- TRUONG, J. P.**
Aerodynamic phenomena in high pulse repetition rate XeCl laser p 1150 A93-48806
- TRUSHIN, O. V.**
Effect of rotation on heat transfer and hydraulic resistance in the radial cooling channels of turbine rotor blades p 1215 A93-52950
- TRUSLOVE, G.**
Cost studies for commercial fuselage crown designs p 920 N93-30440
- TSAI, CHOU-JIU**
Shock oscillation in two-dimensional, inviscid, unsteady channel flow p 288 A93-23563
- TSAI, JEFF F.**
Incompressible flow computation of forces and moments on bodies of revolution at incidence [AIAA PAPER 93-0787] p 541 A93-24867
- TSAI, L.-C.**
Effective sealing of a disk cavity using a double-toothed rim seal [ASME PAPER 92-GT-379] p 406 A93-19537
- TSAI, M.-K.**
Noncoaxial mixing in a rectangular duct p 205 A93-14518
- TSAI, NAN-CHYUAN**
Extended linear quadratic Gaussian control under randomly varying distributed delays p 439 A93-22854
- TSANGARIS, S.**
A multi-zonal local solution methodology for the accelerated solution of the turbulent Navier-Stokes equations p 117 A93-14279
Real gas effects for compressible nozzle flows p 682 A93-33757
On the accuracy and efficiency of CFD methods in real gas hypersonics p 871 A93-42869
Zonal-local solution method for the turbulent Navier-Stokes equations p 1177 A93-53205
- TSAPLIN, M. I.**
Effect of rotation on heat transfer and hydraulic resistance in the radial cooling channels of turbine rotor blades p 1215 A93-52950
- TSCHANZ, J.**
AQUIS: A PC-based air quality and permit information system [DE92-040092] p 434 A93-18587
- TSE, MAN-CHUN**
Overall effects of separation on thin aerofoils [ISBN-0-315-67464-4] p 135 N93-13930
- TSEITLIN, V. Z.**
Using helicopters for transporting large and heavy loads p 306 A93-18350
- TSEKHMISTROVA, N. V.**
Interaction of compression waves with an elastic spherical dome p 550 A93-29718
- TSENG, H. Y.**
The detection and warning of low-level wind shear based on terminal single Doppler radar p 432 A93-22195
- TSENG, STEPHEN P.**
Smart structures stabilized unstable control surfaces [AIAA PAPER 93-1701] p 712 A93-34223
- TSENG, WEI W.**
Numerical simulation of dynamic lift enhancement using oscillatory leading edge flaps [AIAA PAPER 93-0186] p 276 A93-22611
- TSIMBALIUK, V. A.**
Determination of nonstationary aerodynamic loading on cascade blades in the case of dynamic changes of the angle of attack p 544 A93-26817
- TSIRKUNOV, IU. M.**
Hydrodynamics and heat transfer near the stagnation point in an arbitrary axisymmetric nonswirling flow incident on a rotating obstacle p 691 A93-35270
- TSKHOVREBOV, M. M.**
Combined engines for hypersonic flight p 171 A93-14244
The study of experimental turboramjets - Heat state and cooling problems [AIAA PAPER 93-1989] p 1112 A93-49834
- TSO, JIN**
A numerical investigation of a subsonic jet in a crossflow [AIAA PAPER 93-0870] p 469 A93-24931
- TSO, KAM S.**
Complexity metrics for avionics software p 939 A93-42829
- TSUEI, Y. M.**
A numerical study of slit V-gutter flows p 171 A93-14273
- TSUJIMOTO, TAKASHI**
Limit cycle in the longitudinal motion of the USB STOL ASKA - Control system functional mockup and actual aircraft [SAE PAPER 921040] p 185 A93-14660
- TSUJIMOTO, YOSHINOBU**
Velocity fluctuation based on the difference in the flow pattern in the channels of a centrifugal impeller p 1182 A93-53842
- TSUJITA, HOSHIO**
Numerical analysis of flow within cascade with tip clearance p 1176 A93-53192
- TSUKAMOTO, HIROSHI**
Development of a Shape-controlled airfoil by use of SMA p 411 A93-21739
Aerodynamic characteristics of a semibuoyant station in the shape of a torus [AIAA PAPER 93-4034] p 1231 A93-54615
- TSUNG, FU L.**
Numerical simulation of dynamic lift enhancement using oscillatory leading edge flaps [AIAA PAPER 93-0186] p 276 A93-22611
- TSUNG, FU-LIN**
Three-dimensional Navier-Stokes/full-potential coupled analysis for viscous transonic flow p 1178 A93-53218
- TSURUDA, T.**
Coherent anti-Stokes Raman scattering (CARS) thermometry in a model gas turbine can combustor [ASME PAPER 92-GT-134] p 387 A93-19366
CARS thermometry in a liquid fueled model combustor [AIAA PAPER 93-0366] p 390 A93-23047
- TSURUSAKI, HIROMU**
Velocity fluctuation based on the difference in the flow pattern in the channels of a centrifugal impeller p 1182 A93-53842
- TSUYUKI, TARO**
Numerical simulation of flow for a scramjet nozzle p 302 N93-19299
- TSVETKOV, S. I.**
Calculation of a collector-type annular plate heat exchanger p 833 A93-39045
- TSYBAEV, B. G.**
A control algorithm for a navigation-landing system in the case of a priori indeterminacy of failure data p 882 A93-43108
- TSYBALOV, I. G.**
Determination of gas flow rate in a duct from measured static pressures p 520 A93-27625
- TSYGANOV, P. G.**
Effect of the drag of the front body on the restructuring of flow between two bodies in the path of supersonic flow, with one body located in the wake of the other p 14 A93-12973
- TU, EUGENE L.**
Effect of canard position on the longitudinal aerodynamic characteristics of a close-coupled canard-wing-body configuration [AIAA PAPER 92-4632] p 14 A93-13304
Unsteady Navier-Stokes simulation of the canard-wing-body ramp motion [AIAA PAPER 93-3058] p 1058 A93-48235
- TU, HOUJIE**
A new method for resolving transonic nozzle flows using orthogonal stream-lines coordinate system p 1230 A93-54584
- TU, KING-MON**
A model study of the aircraft cabin environment resulting from in-flight fires [DOT/FAA/CT-90/22] p 496 N93-21557
- TU, XING**
Some key problems in the design of the NPU open-circuit low-turbulence wind tunnel p 1139 A93-51188
- TU, Y. K.**
Modal analysis of multistage gear systems coupled with gearbox vibrations p 827 A93-36588
- TUCHMAN, AVI**
Sensors and sensor systems for guidance and navigation; Proceedings of the Meeting, Orlando, FL, Apr. 2, 3, 1991 [SPIE-1478] p 532 A93-27043
- TUCKER, P. K.**
A numerical analysis of supersonic flow over an axisymmetric afterbody [AIAA PAPER 93-2347] p 1083 A93-50121
- TUJIMURA, NAOHISA**
Numerical simulation of flows in a supersonic air intake p 303 N93-19314
- TULAPURKARA, E. G.**
Calculation of laminar and turbulent asymmetric wakes p 684 A93-34318
- TULIAKOV, V. V.**
A method for estimating the survivability of bodies of revolution p 745 A93-35287
- TUNCER, ISMAIL H.**
A viscous-inviscid interaction method for 2-D unsteady, compressible flows [AIAA PAPER 93-3019] p 1055 A93-48206
- TUNG, C.**
Hover performance analysis of advanced rotor blades p 767 A93-35998
- TUNG, C. C.**
Adaptive/conformal wing design for future aircraft p 320 A93-17728
- TUNG, CHAO-HUNG STEVE**
Initial streamwise vorticity formation in a two-stream mixing layer p 698 N93-25752
- TUNG, CHEE**
Characteristics of deformable leading edge for high performance helicopter rotor [AIAA PAPER 93-3526] p 986 A93-47285
Unsteady aerodynamic behavior of an airfoil with and without a slat p 1093 A93-52007
- TUREAUD, THOMAS F.**
Developing numerical techniques for solving low Mach number fluid-acoustic problems p 1235 A93-55353
- TURI, JANOS**
Robust control of an aeroelastic system modeled by a singular integro-differential equation p 97 A93-13197
Finite memory approximations for a singular neutral system arising in aeroelasticity p 97 A93-13246
Robust stabilization of an aero-elastic system p 817 A93-37044
- TURKEL, E.**
An effective multigrid method for high-speed flows p 6 A93-10533

- Pseudo-compressibility methods for the incompressible flow equations [AIAA PAPER 93-3329] p 952 A93-45023
- TURKEL, ELI**
Numerical simulations of a high Mach number jet flow [AIAA PAPER 93-0653] p 540 A93-24766
Numerical simulation of a high Mach number jet flow [NASA-TM-105985] p 551 N93-20057
- TURLEY, STEPHEN E. H.**
Compact high reliability fiber coupled laser diodes for avionics and related applications p 1152 A93-49470
- TURNBULL, A.**
A preliminary sizing method for unmanned aircraft using multi-variate optimisation p 714 N93-25408
- TURNER, A. B.**
Ingestion into the upstream wheel-space of an axial turbine stage [ASME PAPER 92-GT-303] p 354 A93-19493
An externally pressurized air bearing system, journals and thrust, for application to small turbomachinery [ASME PAPER 92-GT-382] p 406 A93-19539
- TURNER, MARK G.**
An investigation of turbulence modelling in transonic fans including a novel implementation of an implicit k-epsilon turbulence model [ASME PAPER 92-GT-308] p 256 A93-19498
Three-dimensional Navier-Stokes computations of transonic fan flow using an explicit flow solver and an implicit k-epsilon solver [ASME PAPER 92-GT-309] p 256 A93-19499
- TURNER, S. R.**
Electromechanical measurement of turbomachinery blade tip-to-casing running clearance [ASME PAPER 92-GT-50] p 400 A93-19303
- TURNOCK, DAVID L.**
Experimental unsteady pressures at flutter on the Supercritical Wing Benchmark Model [AIAA PAPER 93-1592] p 683 A93-34123
- TURNS, S. R.**
Oxides of nitrogen emissions from turbulent hydrocarbon/air jet diffusion flames, phase 2 [PB93-152478] p 756 N93-26533
- TURPEINEN, O. M.**
Aviation safety can benefit from simulation of the dispersion of hazardous material p 487 A93-27393
- TUTIYA, MASAKO**
The operating system for Numerical Wind Tunnel p 383 N93-19290
- TUTTLE, MARK**
Multi-parameter optimization tool for low-cost commercial fuselage crown designs p 922 N93-30858
- TWARDOWSKI, PATRICE**
Design of an optimal single reflective holographic helmet display element p 517 A93-26886
- TWEEDT, D. L.**
Averaging techniques for steady and unsteady calculations of a transonic fan stage [AIAA PAPER 93-3065] p 1059 A93-48241
- TWISS, ROBERT G.**
Characterization of electron beam propagation for hypersonic flight research applications [AIAA PAPER 92-5087] p 452 A93-22357
- TWOMEY, W. J.**
An automated mode tracking strategy [AIAA PAPER 93-1414] p 739 A93-33970
- TWOMEY, WILLIAM**
CST and rotorcraft - Expanding the view p 560 A93-25085
- TWOMEY, WILLIAM J.**
The NASA/industry Design Analysis Methods for Vibrations (DAMVIBS) program: Sikorsky Aircraft: Advances toward interacting with the airframe design process p 515 N93-21315
- TWORZYDLO, W.**
H-P adaptive methods for finite element analysis of aerothermal loads in high-speed flows [NASA-CR-189739] p 420 N93-18093
- TYE, G. W.**
Active control of helicopter transmission noise p 568 A93-29428
- TYLOCK, JAMES**
Optimization-based linear and nonlinear design methodologies for aircraft control. II - Final simulations [AIAA PAPER 92-4627] p 62 A93-13285
Failure-accommodating neural network flight control [AIAA PAPER 92-4394] p 523 A93-24495
- TZENG, C. Y.**
Wind identification along a flight trajectory. III - 2D dynamic approach p 1007 A93-45401
- TZENG, YIH-FENG**
Optimum poststall turning and supersonic turning [AIAA PAPER 93-3659] p 1128 A93-48339
- TZIAVOS, I. N.**
Controlling common mode stabilization errors in airborne gravity gradiometry p 1245 A93-55978

- TZONG, GEORGE T. J.**
Flutter optimization of large transport aircraft [AIAA PAPER 92-4795] p 326 A93-20381
- TZUO, K.-L.**
Optimization of a highly-loaded axial splittler rotor design p 1002 A93-46931

U

- UCER, AHMET S.**
A viscous axisymmetric throughflow prediction method for multi-stage compressors [ASME PAPER 92-GT-293] p 254 A93-19483
- UCHIDA, MASAHIRO**
Development study on Air Turbo Ramjet engine for a future space plane [ISABE 93-7016] p 1195 A93-53992
- UCHIDA, T.**
The conceptual study of supersonic transport structure [AIAA PAPER 92-4219] p 43 A93-13348
- UCHIDA, TADAO**
Limit cycle in the longitudinal motion of the USB STOL ASKA - Control system functional mockup and actual aircraft [SAE PAPER 92-1040] p 185 A93-14660
- UCHIKADO, SHIGERU**
Design of an adaptive flight control system with uncertainties p 95 A93-12322
- UCHIKAWA, ISOROKU**
Limit cycle in the longitudinal motion of the USB STOL ASKA - Control system functional mockup and actual aircraft [SAE PAPER 92-1040] p 185 A93-14660
- UCHIYAMA, ATSUSHI**
Behaviors of the laterally injected jet in film cooling - Measurements of surface temperature and velocity/temperature field within the jet [ASME PAPER 92-GT-180] p 402 A93-19405
- UDD, ERIC**
Embedded fiber optic sensors in large structures p 410 A93-21085
- UEDA, M.**
Diagnostics systems for the TBR-E tokamak [INPE-5428-RPQ/662] p 232 N93-13257
- UEDA, SHUICHI**
Validation studies of scramjet nozzle performance p 1109 A93-49616
Thermal barrier design of gamma-TiAl Functionally Gradient Materials (FGMs) for scramjet engine applications p 1246 A93-54556
- UEDA, SHUICHI**
Off-design performance of scramjet nozzles [ISABE 93-7108] p 1203 A93-54084
- UEDA, SYUICHI**
Application of functionally gradient materials to scramjet engines [ISABE 93-7063] p 1200 A93-54039
- UEDA, SYUICHI**
Evaluation of 2D scramjet nozzle performance p 52 A93-11209
- UEDA, YUKIFUMI**
Numerical simulation of supersonic flows with chemical reactions p 959 A93-45325
- UEMURA, TSUNEHARU**
Digital flight recorded data - A method of estimating down draft from digital flight recorded data p 1241 A93-54559
- UENISHI, K.**
Commercial turbofan engine exhaust nozzle flow analyses p 689 A93-34489
- UGAI, TAKASHI**
The methods of reducing impact loads on occupants in the civil aircraft crash condition p 140 A93-14220
The structure and material testing facility needed for future SST/HST development [AIAA PAPER 92-3887] p 528 A93-24481
- UGRIUMOV, M. L.**
Grid-characteristic method for calculating a three-dimensional boundary layer on the bounding surfaces of the blade passage of a turbomachine p 13 A93-12808
- UHSE, W.**
Technology transfer: Potential of BMFT concept for hypersonics [MBB-LME-202-S-PUB-0505] p 1041 N93-31045
- UHUAD, G. C.**
Study of a circular cross section thrust augmenting ejector [AIAA PAPER 93-2439] p 1118 A93-50191
- UIBEL, RORY H.**
Video luminescent barometry - The induction period [AIAA PAPER 93-0179] p 414 A93-22607

- UJIE, Y.**
A study of self-ignition of methane-hydrogen mixture fuel injected into high enthalpy supersonic airstreams [ISABE 93-7049] p 1213 A93-54025
- UL'YANOV, G. S.**
Experimental studies of supersonic flow past wedges with longitudinal slots on the windward side p 1089 A93-51786
Aerodynamic characteristics of conical triangular-planform wings of low aspect ratio in subsonic stalled flow p 1180 A93-53574
- ULBRICH, ERWIN**
Controls and displays for Douglas Aircraft for the 1990s p 545 A93-27241
- ULBRICH, N.**
Adaptive wall wind tunnel with two measured interfaces - Theory and experiment p 679 A93-33717
A wall interference assessment/correction system [NASA-CR-190617] p 68 N93-11910
A wall interference assessment/correction system [NASA-CR-191889] p 296 N93-18384
- ULM, D. S.**
An Acoustic Emission Pre-failure Warning System for composite structural tests p 1161 A93-52560
- UMOTO, J.**
Effects of external control circuit on coal-fired supersonic diagonal-type MHD generator p 1173 A93-49619
- UNAL, RESIT**
Multidisciplinary design optimization using response surface analysis p 330 N93-16796
- UNDERWOOD, R. C.**
The development of the Boeing Human Model p 561 A93-27150
- UNDREINER, S.**
High lift airfoil flow simulation using a wall-corrected Algebraic Stress Model [AIAA PAPER 93-3109] p 1061 A93-48280
- UNGER, E. R.**
Integrated aerodynamic-structural-control wing design [AIAA PAPER 92-4694] p 324 A93-20307
- UNGER, ERIC ROBERT**
Integrated aerodynamic-structural wing design optimization p 714 N93-25279
- UNGEWITTER, RONALD**
An adaptive grid/Navier-Stokes methodology for the calculation of nozzle afterbody base flows with a supersonic freestream [AIAA PAPER 93-1922] p 1076 A93-49788
- UNNIKRISSNAN, V.**
Structural integrity validation of limited-life engines [ISABE 93-7131] p 1205 A93-54106
- UNO, KAORU**
Visualization and analysis of supersonic flow in rotating turbine stage. I - Influence of shock wave between stationary and moving blades p 126 A93-15449
Visualization and analysis of supersonic flow in rotating turbine stage. II - Analysis of the flow into the moving blades and their exit flow p 476 A93-27442
- UNSWORTH, KELLIE B.**
Advanced composite helicopter MISERS GOLD test/analysis p 508 A93-27974
- UPCHURCH, BILLY T.**
Gas analysis system for the Eight Foot High Temperature Tunnel p 822 A93-37875
- URBACH, A. R.**
Slush hydrogen quantity gaging and mixing for the National Aerospace Plane p 1150 A93-48635
- URBACH, HERMAN B.**
Some implications of a differential turbomachinery equation with viscous correction [AD-A264693] p 935 N93-30571
- USAB, WILLIAM J., JR.**
Development of an unstructured solution adaptive method for the quasi-three-dimensional Euler and Navier-Stokes equations [NASA-CR-193241] p 930 N93-29213
- USUI, H.**
Experimental analysis of turbine rotor flow at design and off-design conditions [ISABE 93-7092] p 1186 A93-54068
- USUKI, K.**
The conceptual study of supersonic transport structure [AIAA PAPER 92-4219] p 43 A93-13348
- UTEZA, O.**
Aerodynamic phenomena in high pulse repetition rate XeCl laser p 1150 A93-48806
- UTHUP, BIJU**
NOZ2D - A two dimensional explicit inviscid upwind code for convergent divergent nozzles p 460 A93-24080
- UTIUZHNIKOV, S. V.**
Influence of second-order boundary layer effects in hypersonic flow past blunt cones of large aspect ratio p 241 A93-18238
A numerical investigation of supersonic flow of a viscous gas over long blunt cones, taking into account equilibrium physicochemical transformations p 775 A93-39124

UTYUZHNIKOV, S. V.

- Application of the small parameter method to the problem of three-dimensional flow of a viscous gas past bodies p 1178 A93-53314
Comparison of gasdynamic models in hypersonic flow p 1179 A93-53315

UTZINGER, ROB

- Advanced hypersonic aircraft design [NASA-CR-192046] p 334 A93-18037

UYEDA, HIROSHI

- Doppler radar observation of tornado and microburst around Chitose Airport p 432 A93-22199

UYTHOVEN, A.

- The Teledyne controls aircraft condition monitoring system p 168 A93-15155

V

VACHTSEVANOS, G.

- An application of fuzzy logic and Dempster-Shafer theory to failure detection and identification p 96 A93-13079

VADDEMPUDI, APPA R.

- Acoustic properties of supersonic helium/air jets at low Reynolds numbers p 446 A93-19160

VAHDATI, M.

- Computation of viscous compressible flows using an upwind algorithm and unstructured meshes p 9 A93-12163

- The application of an adaptive upwind unstructured grid solution algorithm to the simulation of compressible laminar viscous flows over compression corners p 866 A93-42594

VAICAITIS, RIMAS

- Nonlinear response and sonic fatigue of high speed aircraft p 399 A93-19211
Recent advances of time domain approach for nonlinear response and sonic fatigue p 1022 A93-45106

VAIL, CURTIS F.

- Bending-torsion flutter of linear viscoelastic wings including structural damping [AIAA PAPER 93-1475] p 711 A93-34021

VAIRO, D. M.

- Effect of geometry, static stability, and mass distribution on the tumbling characteristics of generic flying-wing models [AIAA PAPER 93-3615] p 1125 A93-48302

VAKULENKO, T. YA.

- Effect of aqueous solutions of water-crystallization inhibiting fluids on Thiocol-based sealants p 1017 A93-45689

VALAREZO, WALTER O.

- Surface hot-film method for the measurement of transition, separation and reattachment points [AIAA PAPER 93-2918] p 1148 A93-48120
Multielement airfoil performance due to Reynolds and Mach number variations p 1095 A93-52442
Reynolds and Mach number effects on multielement airfoils p 785 A93-27446

VALAVANI, L.

- Evaluation of approaches to active compressor surge stabilization [ASME PAPER 92-GT-182] p 352 A93-19407

VALAVANI, LENA

- Active stabilization to prevent surge in centrifugal compression systems [NASA-CR-191625] p 424 A93-18862

VALENTIN, JEAN-CLAUDE

- Satcom Pacific Ocean trials p 501 A93-28198

VALENTINE, GARY W.

- A wideband, embedded/conformal, antenna subsystem concept p 327 A93-22002

VALENTINE, JAMES R.

- Tracking of raindrops in flow over an airfoil [AIAA PAPER 93-0168] p 275 A93-22602

VALERIO, N. R.

- A wind tunnel investigation of the pressure distribution on an F/A-18 wing [AIAA PAPER 93-3468] p 980 A93-47249

VALETT, JON

- Data collection procedures for the Software Engineering Laboratory (SEL) database [NASA-TM-108579] p 230 A93-15579

VALIN, JEAN-YVES

- Airports, air traffic control, and their clients - Reflections on system optimization p 234 A93-15035

VALLET, MICHEL

- Night aircraft noise index and sleep research results p 558 A93-28485

VALLOT, LARRY

- Differential GPS/inertial navigation approach/landing flight test results p 32 A93-11019

VALORANI, M.

- Reactive and inert inviscid flow solutions by quasi-linear formulations and shock fitting p 927 A93-42625

VAN DALEN, A.

- Results of review of Fokker F 28 'Fellowship' maintenance program p 948 A93-45793

VAN DALEN, F.

- Structural optimization in preliminary aircraft design - A finite-element approach p 226 A93-14340

VAN DALSEM, W. R.

- Numerical simulation of STOL operations using thrust-vectoring [AIAA PAPER 92-4254] p 15 A93-13342
Numerical simulation of jet noise p 265 A93-20716
Numerical study of a delta planform with multiple jets in ground effect [SAE PAPER 892283] p 1176 A93-53200

VAN DALSEM, WILLIAM R.

- Flowfield simulation about the stratospheric observatory for infrared astronomy p 1095 A93-52446

VAN DAM, C. P.

- Subsonic high-lift flight research on the NASA Transport System Research Vehicle (TSRV) [AIAA PAPER 92-4103] p 38 A93-11275
Leading-edge transition and relaminarization phenomena on a subsonic high-lift system [AIAA PAPER 93-3140] p 959 A93-45154
Shape optimization for aerodynamic efficiency and low observability [AIAA PAPER 93-3115] p 1062 A93-48285
Two-dimensional computational analysis of a transport high-lift system and a comparison with flight-test results [AIAA PAPER 93-3533] p 1072 A93-49517

VAN DE WALL, ALLAN

- Evaluation and application of the Baldwin-Lomax turbulence model in two-dimensional, unsteady, compressible boundary layers with and without separation in engine inlets [AIAA PAPER 92-3676] p 111 A93-14118
Evaluation and application of the Baldwin-Lomax turbulence model in two-dimensional, unsteady, compressible boundary layers with and without separation in engine inlets [AIAA PAPER 92-3676] p 414 A93-22509

VAN DEN BERG, J. I.

- The application of an Euler method and a Navier Stokes method to the vortical flow about a delta wing [AIAA PAPER 93-3510] p 984 A93-47276

VAN DEN BRAEMBUSSCHE, R.

- Experimental and theoretical analysis of the flow in a centrifugal compressor volute [ASME PAPER 92-GT-30] p 400 A93-19290

VAN DEN BRAEMBUSSCHE, R. A.

- Inverse design of compressor and turbine blades at transonic flow conditions [ASME PAPER 92-GT-430] p 357 A93-19573

VAN DER AUWERAER, H.

- Signal processing and system identification techniques for flutter test data analysis p 529 A93-29282

VAN DER AUWERAER, HERMAN

- Vibro-acoustic analysis of propeller aircraft, integrating advanced experimental modeling with in-flight data analysis p 451 A93-19230
Noise and vibration analysis in propeller aircraft by advanced experimental modeling techniques p 1264 A93-55862

VAN DER MAAREL, H. T. M.

- Adaptive multigrid for the steady Euler equations p 201 A93-13988

VAN DER MERWE, C. A.

- The development of a new air filtration system for the Alouette III helicopter [ISABE 93-7048] p 1199 A93-54024

VAN DER VOOREN, J.

- A fast robust viscous-inviscid interaction solver for transonic flow about wing/body configurations on the basis of full potential theory [AIAA PAPER 93-3026] p 1056 A93-48211

VAN DER WEES, A. J.

- A fast robust viscous-inviscid interaction solver for transonic flow about wing/body configurations on the basis of full potential theory [AIAA PAPER 93-3026] p 1056 A93-48211

VAN DITSCHUIZEN, J. C. A.

- DNW test highlights related to aircraft environment p 190 A93-14274

VAN DRONKELAAR, JAN-HEIN

- Flight simulator research into advanced MLS approach and departure procedures p 149 A93-14234
Development of advanced approach and departure procedures [AIAA PAPER 93-3833] p 1098 A93-51422

VAN DUSSELDORP, DAVID L.

- Performance analysis of a miniaturized airborne GPS receiver p 313 A93-21147

VAN DYKE, KAREN L.

- Receiver Autonomous Integrity Monitoring (RAIM) availability for supplemental GPS navigation p 312 A93-18554

VAN GELDER, P. A.

- In-flight tailload measurements p 155 A93-14285
Acquiring tail load spectra from in-flight measurements [AIAA PAPER 93-1607] p 711 A93-34137

VAN GRAAS, FRANK

- Statistical validation for GPS integrity test p 34 A93-11297
Guidance accuracy considerations for realtime GPS interferometry p 342 A93-21146

VAN HEMEL, J. J. O.

- Estimation of aircraft inertia characteristics from bifilar pendulum test data p 1249 A93-56029

VAN HENGST, J.

- Aerodynamic degradation due to distributed roughness on high lift configuration [AIAA PAPER 93-0028] p 260 A93-20146
Investigation of methods for modeling propeller-induced flow fields [AIAA PAPER 93-0874] p 469 A93-24935

VAN LEER, BRAM

- Grid-refinement study of hypersonic laminar flow over a 2-D ramp p 866 A93-42597
Progress in local preconditioning of the Euler and Navier-Stokes equations [AIAA PAPER 93-3328] p 952 A93-45022
A simulation technique for 2-D unsteady inviscid flows around arbitrarily moving and deforming bodies of arbitrary geometry [AIAA PAPER 93-3391] p 956 A93-45082

VAN MUIJDEN, J.

- A fast robust viscous-inviscid interaction solver for transonic flow about wing/body configurations on the basis of full potential theory [AIAA PAPER 93-3026] p 1056 A93-48211

VAN NEE, RICHARD D. J.

- Multipath effects on GPS code phase measurements p 34 A93-11295

VAN NIEKERK, J. E.

- The design and development of an afterburner [ISABE 93-7041] p 1198 A93-54017

VAN RANSBEECK, P.

- New upwind dissipation models with a multidimensional approach [AIAA PAPER 93-3304] p 950 A93-45002

VAN WIE, D. M.

- Techniques for the measurement of scramjet inlet performance at hypersonic speeds [AIAA PAPER 92-5104] p 274 A93-22374

VAN WILLIGEN, DURK

- MIAS, the integration of MLS with DGPS/DLoran-C p 315 A93-21181

VAN ZYL, L. H.

- Analytic continuation of Pade approximations to the unsteady kernel functions to obtain a better understanding of the analytic continuation of Pade approximations to unsteady parameters in general p 117 A93-14283
Extending the useful frequency of 'rigid' wind tunnel models with active control p 190 A93-14299

VAN ZYL, LOUW H.

- Use of eigenvectors in the solution of the flutter equation p 1022 A93-45151

VANBEEK, C. M.

- Aerodynamic analysis of slipstream/wing/nacelle interference for preliminary design of aircraft configurations p 130 A93-13205

VANBUREN, MARKUS ANTONIUS

- Robust nonlinear feedback guidance for an aerospace plane: A geometric approach p 189 A93-14835

VANDELEIJGRAAF, R.

- The application of phase tracking GPS for flight test trajectory determination [NLR-TP-91349-U] p 994 A93-32337

VANDEMARK, DOUGLAS

- Update on the NASA ER-2 Doppler radar system (EDOP) p 807 A93-37737

VANDEN, K. J.

- Direct and iterative algorithms for the three-dimensional Euler equations [AIAA PAPER 93-3378] p 957 A93-45102
Numerical investigation of subsonic and supersonic asymmetric vortical flow p 961 A93-45727

VANDENBERG, J. I.

- Application of an Euler-equation method to a sharp-edged delta wing configuration with vortex flow [NLR-TP-91306] p 294 A93-17809

VANDENBOSCH, P.

- Category A F-16 accidents in the Belgian Air Force p 492 A93-19675
Combat and training aircraft class A mishaps in the Belgian Air Force 1970-1990 p 492 A93-19677

VANDENKERCKHOVE, J.

- Energy management [ISABE 93-7019] p 1195 A93-53995

- VANDERBEEK, R. D.**
Human factors causes and management strategies in US Air Force F-16 mishaps 1984-present
p 492 N93-19673
- VANDERBURGH, A. H. P.**
On the dynamics of aeroelastic oscillators with one degree of freedom
[REPT-92-96] p 1040 N93-31653
- VANDERVEGT, J. J.**
Bypass transition in compressible boundary layers
p 417 N93-15801
- VANDERVELDEN, ALEXANDER JACOBUS M.**
Aerodynamic design and synthesis of the oblique flying wing supersonic transport
p 713 N93-24768
- VANDERWALL, BEREND**
The influence of the rotor test facilities ROTEST and ROTOS on the rotor inflow
[DLR-MITT-91-16] p 522 N93-21173
Analytic formulation of unsteady profile aerodynamics and its application to simulation of rotors
[ESA-TT-1244] p 485 N93-21659
The influence of variable flow velocity on unsteady airfoil behavior
[DLR-FB-92-22] p 988 N93-31320
- VANDERWERT, TERRY L.**
Case studies - Applications of laser systems for cutting and welding aerospace parts
p 1217 A93-53498
- VANDEWALL, ALLAN**
Evaluation and application of the Baldwin-Lomax turbulence model in two-dimensional, unsteady, compressible boundary layers with and without separation in engine inlets
[NASA-TM-105810] p 82 N93-10087
- VANDIERENDONCK, A. J.**
Proposed revisions to RTCM SC-104 recommended standards for differential NAVSTAR/GPS service for carrier phase applications
[AD-A255276] p 152 N93-15005
- VANDIVER, JAMES L.**
RPH preliminary design, trend analysis and initial analysis of the NPS hummingbird
[AD-A257854] p 338 N93-18304
- VANDONGEN, JOHN**
The effect of TCAS interrogations on the Chicago O'Hare ATRCBS system
[DOT/FAA/CT-92/22] p 318 N93-16498
Results of DATAS investigation of illegal mode S ID's at JFK Airport
[DOT/FAA/CT-92/26] p 318 N93-16841
Results of DATAS investigation of ATRCBS environment at the Los Angeles International Airport
[DOT/FAA/CT-93/6] p 793 N93-28625
- VANDORP, A. L. C.**
NARSIM and EFMS: Tools for research on integrated ATM
[NLR-TP-89336-U] p 319 N93-17954
- VANDROMME, D.**
An implicit treatment of two equations turbulence models for high speed flow computations
p 686 A93-34350
On the numerical simulation of the two-dimensional flow field around a hypersonic air-intake-compressibility effects
[ISABE 93-7100] p 1187 A93-54076
- VANDROMME, DANY**
Computation of supersonic crossflow separation using a new parabolized Navier-Stokes code
p 687 A93-34355
- VANDRONKELAAR, J. H.**
Flight simulation evaluation of the flyability of curved MLS approaches with wide-body aircraft
[NLR-TP-90238-U] p 382 N93-17875
- VANDRONKELAAR, JAN-HEIN**
Evaluation of the flyability of MLS curved approaches for wide-body aircraft
[NLR-TP-91396-U] p 999 N93-32416
- VANENGELLEN, J. A. J.**
A simulator study into low speed longitudinal handling qualities of ACT transport aircraft
[NLR-TP-89387-U] p 527 N93-20743
- VANFOSSSEN, G. J.**
High Reynolds number and turbulence effects on aerodynamics and heat transfer in a turbine cascade
[AIAA PAPER 93-2252] p 1155 A93-50050
Increased heat transfer to elliptical leading edges due to spanwise variations in the freestream momentum: Numerical and experimental results
[NASA-TM-106150] p 838 N93-27020
- VANFOSSSEN, G. JAMES**
High Reynolds number and turbulence effects on aerodynamics and heat transfer in a turbine cascade
[NASA-TM-106187] p 930 N93-29157
- VANGRASS, FRANK**
GPS Interferometry
[NASA-CR-192301] p 319 N93-18873
- VANGSNESS, M. D.**
Effects of back-pressure in a lean blowout research combustor
[ASME PAPER 92-GT-81] p 387 A93-19330
- VANHENGST, J.**
Aerodynamic integration of thrust reversers on the Fokker 100
p 160 N93-13208
- VANIN, A. G.**
Using ultralight flight vehicles for large-scale aerial photography
p 92 A93-10098
- VANLEEUWEN, STORM**
The application of phase tracking GPS for flight test trajectory determination
[NLR-TP-91349-U] p 994 N93-32337
- VANNOSTRAND, W.**
Active rib experiment for shape control of an adaptive wing
[AIAA PAPER 93-1700] p 712 A93-34222
- VANOSDOL, JOHN GARY**
Modeling variable blowing on a slender cone in hypersonic flow
p 138 N93-14836
- VANSTONE, D. A.**
Development and demonstration of a new filter system to control emissions during jet engine testing
[AD-A261203] p 755 N93-26243
- VANTOOREN, M. J. L.**
Stress calculations on the window section of an all-composite aircraft fuselage
[LR-688] p 328 N93-16215
- VARAVVA, V. G.**
Precision increasing and integrity monitoring of navigation data for GPS/inertial hybrid solution
p 149 A93-14157
- VARGAS, MARIO**
Close-up analysis of aircraft ice accretion
[AIAA PAPER 93-0029] p 309 A93-23239
Close-up analysis of aircraft ice accretion
[NASA-TM-105952] p 148 N93-15360
- VARSNEYA, DEEPAK**
Specialty fiber optic systems for mobile platforms and plastic optical fibers; Proceedings of the Meeting, Boston, MA, Sept. 9-11, 1992
[SPIE-1799] p 1105 A93-49462
Implementation of fiber optic technology in flight controls
p 1105 A93-49473
- VASENEV, L. G.**
Three-dimensional flow past an ogival-cylindrical body in combination with a delta wing
p 478 A93-27636
- VASHCHENKO, N. V.**
Selection of a method for protecting aircraft gas turbine engines against damage by foreign objects (Mathematical models)
p 1193 A93-53554
- VASIL'EV, A. V.**
Using spectral analysis for estimating the effect of runway irregularities on the loading of transport aircraft structures
p 996 A93-45669
- VASIL'EV, A. YA.**
Effect of flexural and rotational wing oscillations on the prevention of flow separation
p 1150 A93-48911
- VASIL'EV, IU. B.**
Computational and experimental investigation of a solar energy system for an atmospheric flight vehicle
p 521 A93-29655
- VASIL'EV, S. L.**
High-strength combination fasteners for joint assembly in aircraft structures
p 745 A93-35283
Stress-strain state of the elements of a single-stringer riveted panel
p 746 A93-35288
- VASIL'EV, V. I.**
Intensification of flow mixing behind an oblique shock wave
p 4 A93-10138
Calculation of three-dimensional turbulent jets propagating behind nozzles of rectangular cross section
p 6 A93-10192
- VASILETS, V. M.**
Hybrid complex of the aircraft intellectualized control systems simulation at the stage of their research projecting
[AIAA PAPER 93-3559] p 1222 A93-52660
Semi-full-scale dynamic simulation complex on the basis of centrifuge
[AIAA PAPER 93-3577] p 1208 A93-52673
- VASQUEZ, JUAN R.**
Detection of spoofing, jamming, or failure of a Global Positioning System (GPS)
[AD-A259023] p 319 N93-18951
- VASQUEZ, PETER**
Improved ceramic slip casting technique
[NASA-CASE-LAR-14471-1] p 536 N93-20041
- VASSEL, ALAIN**
Structural stability of 'beta-CEZ' alloy
[ONERA, TP NO. 1992-106] p 824 A93-38586
- VATAZHIN, A. B.**
Turbulent jet flows with condensation and electrophysical effects
p 76 A93-10176
- An electrostatic probe for determining particle characteristics in disperse flow
p 76 A93-10178
A study of a pulsed electrical field near the jet of a turbojet engine
p 52 A93-10179
Experimental study of condensation vapor-air jets
p 76 A93-10180
Atmospheric aerosols due to aircraft and ecological problems
p 1162 A93-48846
- VATSA, V.**
A detailed study of mean-flow solutions for stability analysis of transitional flows
[AIAA PAPER 93-3052] p 1057 A93-48232
- VATSA, V. N.**
Transonic Navier-Stokes flow computations over wing-fuselage geometries
p 1095 A93-52456
- VATSA, VEER N.**
A comparison of the predictive capabilities of several turbulence models using upwind and central-difference computer codes
[AIAA PAPER 93-0192] p 268 A93-21102
Development of a flexible and efficient multigrid-based multiblock flow solver
[AIAA PAPER 93-0677] p 269 A93-21117
- VAUCHERET, X.**
Application of a full potential code to the definition of a transonic test section
[ONERA, TP NO. 1992-84] p 822 A93-38569
- VAUGHN, WALLACE L.**
Current research in oxidation-resistant carbon-carbon composites at NASA Langley Research Center
p 74 N93-12456
- VAUTEY, PHILIPPE**
Thermoplastic and thermosetting matrix composite structures - Comparison of mechanical properties
p 197 A93-15029
- VAVRINCOVA, M.**
Numerical solution of steady and unsteady Euler equations
p 973 A93-46988
- VEALE, J. R.**
Remote sensing of O₂ in a supersonic combustor using diode lasers and fiber optics
[AIAA PAPER 92-5090] p 414 A93-22360
- VEILLETTE, PATRICK R.**
Rudder and elevator effects on the incipient spin characteristics of a typical general aviation training aircraft
[AIAA PAPER 93-0016] p 367 A93-20138
- VEILLETTE, ROBERT J.**
A modified approach to controller partitioning
[NASA-TM-106167] p 848 N93-28051
- VEJTIN, VALERIJ E.**
Fundamentals of flight vehicle design
[ISBN 5-217-01299-4] p 893 A93-43831
- VELAZQUEZ, A.**
Aerodynamics design of convergent-divergent nozzles
[AIAA PAPER 93-2574] p 1085 A93-50290
- VELAZQUEZ, MATTHEW T.**
Ice accretion and performance degradation calculations with LEWICE/NS
[AIAA PAPER 93-0173] p 310 A93-23244
Ice accretion and performance degradation calculations with LEWICE/NS
[NASA-TM-105972] p 148 N93-15354
- VELENSEK, BORIS**
A comparison between numerical models and measurements in a Kaplan turbine guide vanes
p 685 A93-34339
- VELLAICHAMY, SENTHILVEL**
Effect of modeling techniques in the coupled rotor-body vibration analysis
[AIAA PAPER 93-1360] p 710 A93-33928
- VEMAGANTI, GURURAJA R.**
Application of a two-equation turbulence model for high speed compressible flows using unstructured grids
[AIAA PAPER 93-3029] p 1056 A93-48213
- VENEDIKTOV, VLADIMIR D.**
Gas dynamics of cooled turbines
[ISBN 5-217-00809-1] p 721 A93-35685
- VENGADESAN, S.**
Calculation of laminar and turbulent asymmetric wakes
p 684 A93-34318
- VENKATAKRISHNAIAH, T.**
Analytical and experimental investigation of flow through a turbine vane cascade
p 1248 A93-56348
- VENKATAPATHY, ETHIRAJ**
Comparison of continuum and particle simulations of expanding rarefied flows
[AIAA PAPER 93-0728] p 466 A93-24818
Hypersonic single expansion ramp nozzle simulations
p 777 A93-39254
Computational flow predictions for hypersonic drag devices
p 777 A93-39257
Computational results for 2-D and 3-D ramp flows with an upwind Navier-Stokes solver
p 866 A93-42592
Effective treatment of the singular line boundary problem for three-dimensional grids
p 1177 A93-53204

- Development and application of computational aerothermodynamics flowfield computer codes [NASA-CR-192940] p 692 N93-24736
- VENKATESAN, C.**
Development of a structural optimization capability for the aeroelastic tailoring of composite rotor blades with straight and swept tips [AIAA PAPER 92-4779] p 326 A93-20370
A new sensitivity analysis for structural optimization of composite rotor blades [AIAA PAPER 93-1644] p 742 A93-34169
- VENKATESAN, COMANDUR**
Aeroelastic behavior of composite rotor blades with swept tips p 827 A93-35978
- VENKATESWARA RAO, G.**
Post-critical behaviour of a tapered cantilever column subjected to a uniformly distributed tangential follower force p 831 A93-38431
- VENKATRAYULU, N.**
Effect of radial distortion on the performance of a centrifugal compressor p 861 A93-42256
- VENKATRAYULU, N.**
Tip clearance effects on the flow field of an axial turbine rotor blade cascade [ISABE 93-7057] p 1185 A93-54033
- VENNEMANN, D.**
Simulation of hypersonic flight - A concerted European effort p 1136 A93-49301
- VENNERI, SAMUEL L.**
High-performance computing for flight vehicles: Proceedings of the Symposium, Washington, Dec. 7-9, 1992 p 437 A93-20701
- VENTER, S. J.**
The design and development of an afterburner [ISABE 93-7041] p 1198 A93-54017
- VENTRES, C. S.**
New rotor trim and balance system for helicopter usage monitoring p 169 N93-15180
- VERANT, J.-L.**
CFD analysis of hypersonic chemically reacting flowfields around a generic shape [AIAA PAPER 93-0323] p 281 A93-23015
- VERBESTEL, JOHN**
NASTRAN analysis for the Airmass Sunburst model 'C' Ultralight Aircraft p 931 N93-29777
- VERDIER, L.**
Supersonic through flow compressors - A preliminary study: COVAXS p 1001 A93-46930
- VERDON, J. M.**
Analysis of high Reynolds number inviscid/viscid interactions in cascades p 1234 A93-55351
- VERES, J. P.**
Design and test of a small two stage counter-rotating turbine for rocket engine application [AIAA PAPER 93-2136] p 1142 A93-49954
- VERHAAGEN, N. G.**
Boundary layer effects on the flow of a leading edge vortex [AIAA PAPER 93-3463] p 980 A93-47245
- VERHAGGEN, N. G.**
Experimental and numerical investigation of vortex flow over a 76/60-deg double-delta wing [LR-680] p 289 N93-16210
- VERHELST, J. M.**
Boundary layer effects on the flow of a leading edge vortex [AIAA PAPER 93-3463] p 980 A93-47245
- VERHOFF, A.**
An efficient approach to optimal aerodynamic design. I - Analytic geometry and aerodynamic sensitivities [AIAA PAPER 93-0099] p 264 A93-20204
An efficient approach to optimal aerodynamic design. II - Implementation and evaluation [AIAA PAPER 93-0100] p 264 A93-20205
Solution of the Euler equations for airfoils using asymptotic methods [AIAA PAPER 93-2931] p 1045 A93-48130
- VERHOFF, VINCENT G.**
Compound curvature laser window development [AIAA PAPER 93-2177] p 1173 A93-49989
- VERKHOZIN, M. P.**
Helicopters - Handbook [ISBN 5-203-00804-3] p 458 A93-28874
- VERMA, DEVESH**
NO2D - A two dimensional explicit inviscid upwind code for convergent divergent nozzles p 460 A93-24080
- VERMEERSCH, SABINE A.**
Visual grid quality assessment for 3D unstructured meshes [AIAA PAPER 93-3352] p 1036 A93-45046
Experimental and computational investigations of the flowfield around the F117A [AIAA PAPER 93-3508] p 984 A93-47274
- VERMEULEN, J. P.**
Parametric studies of shock wave/boundary layer interactions over 2D compression corners at Mach 6 [VKI-TN-181] p 988 N93-31538
- VERNET, ISABELLE**
Night aircraft noise index and sleep research results p 558 A93-28485
- VERNON, LURA**
In-flight investigation of a rotating cylinder-based structural excitation system for flutter testing [AIAA PAPER 93-1537] p 711 A93-34074
- VERNON, TODD H.**
Flight control system design factors for applying automated testing techniques [NASA-TM-4242] p 910 N93-30764
- VERSTYNEN, HARRY A.**
Design and conduct of a windshear detection flight experiment [AIAA PAPER 92-4092] p 38 A93-11268
- VERTATSCHTSCH, E. J.**
Ladar fiber optic sensor system for aircraft applications p 1105 A93-49467
- VESELOV, V. A.**
A fuel-oil matrix heat exchanger p 833 A93-39052
- VEST, T. A.**
The use of beam-like modal data for stiffness profile estimation by the EBS method. I - Justification and implementation p 1257 A93-54649
- VETTER, A. A.**
Laser Centerline Localizer and Laser Glideslope Indicator for visual guidance on approach to landing p 500 A93-28156
Scanning Laser Aircraft Surveillance System for carrier flight operations p 500 A93-28157
- VETTER, M.**
Experimental studies in the Aachen hypersonic shock tunnel p 1251 A93-56032
- VETTER, THEODORE A.**
Considerations for space and naval aviation applications of ferroelectric memory [AD-A261300] p 759 N93-26294
- VEZINA, L.**
Canadian low-gravity research using parabolic aircraft p 384 A93-21908
- VIALONGA, J.**
Assessment of a 3-D Euler code for subsonic turbine vane flows and study of the non radial blade stacking [ASME PAPER 92-GT-63] p 247 A93-19313
- VICKERS, ROGER S.**
Results from a VHF impulse synthetic-aperture radar p 501 A93-28219
- VICROY, DAN D.**
The challenges of simulating wake vortex encounters and assessing separation criteria [AIAA PAPER 93-3568] p 1096 A93-49518
Airborne Wind Shear Detection and Warning Systems. Fourth Combined Manufacturers' and Technologists' Conference, part 2 [NASA-CP-10105-PT-2] p 144 N93-14844
Airborne Wind Shear Detection and Warning Systems: Fourth Combined Manufacturers' and Technologists' Conference, part 1 [NASA-CP-10105-PT-1] p 488 N93-19590
Vertical wind estimation from horizontal wind measurements p 489 N93-19604
- VICTOR, ALAN S.**
Airship/U.S. naval vessels UHF communications relay demonstration [AIAA PAPER 93-4032] p 1240 A93-54604
- VIDYASAGAR, M.**
Intelligent robotics; Proceedings of the International Symposium, Bangalore, India, Jan. 2-5, 1991 [SPIE-1571] p 1166 A93-49350
- VIEDMA, A.**
Cooling predictions in turbofan engine components p 905 N93-29964
- VEILLARD, ANTOINE**
Monitoring of powerplants in advanced commercial aircraft p 178 N93-15171
- VIGGIANO, F.**
Blade loss dynamics of a magnetically supported rotor p 1257 A93-54653
- VIGNAU, F.**
Recent supersonic transition studies with emphasis on the swept cylinder case p 127 A93-17252
- VIGUIER, J. M.**
Turbomachinery and potential computations [DS-2026] p 363 N93-17740
- VIGUIER, P.**
Aeroelastic computation for a flexible airfoil using the small perturbation method comparison with wind-tunnel results [ONERA, TP NO. 1993-43] p 987 A93-47448
- VIJAYAN, P.**
Adaptive refinement-coarsening scheme for three-dimensional unstructured meshes p 961 A93-45735
- VIJGEN, P. M. H. W.**
Leading-edge transition and relaminarization phenomena on a subsonic high-lift system [AIAA PAPER 93-3140] p 959 A93-45154
Flow prediction over a transport multi-element high-lift system and comparison with flight measurements p 785 N93-27448
- VIJGEN, PAUL M. H. W.**
Subsonic high-lift flight research on the NASA Transport System Research Vehicle (TSRV) [AIAA PAPER 92-4103] p 38 A93-11275
In-flight surface-flow measurements on a subsonic transport high-lift flap system p 166 A93-14327
- VIKTORCHIK, A. G.**
A study of the effect of the shape of a parasail on its lift-drag ratio p 1069 A93-48913
A study of air intake parameters on the aerodynamic characteristics of a parasail p 1092 A93-51908
- VIL'DGRUBE, L. S.**
A method for calculating the aerodynamic and mass characteristics of coaxial rotors with rigid blade fastening (the ABC system) p 1071 A93-49323
- VILSMEIER, JOSEF WALTER**
Aircraft structures in 2000: A technological challenge? [MBB-LME-202-S-PUB-0485] p 998 N93-31058
- VINCENT, A.**
The influence of the fuselage on high alpha vortical flows and the subsequent effect on fin buffeting p 116 A93-14263
- VINER, MELVYN R.**
Acoustic emission monitoring of aging aircraft structures p 407 A93-19697
- VINEY, B.**
Inverse problem using S2-S1 approach for the design of the turbomachine with splitter blades p 971 A93-46929
- VINH, HOANG**
Shape optimization for aerodynamic efficiency and low observability [AIAA PAPER 93-3115] p 1062 A93-48285
- VINH, NGUYEN X.**
Optimum poststall turning and supersonic turning [AIAA PAPER 93-3659] p 1128 A93-48339
- VINOGRADOV, O. V.**
Precision increasing and integrity monitoring of navigation data for GPS/inertial hybrid solution p 149 A93-14157
- VINOGRADOV, R. I.**
Search strategies for a sequence of baseline indices for building sections of a flight-safety automatic control system in the interactive mode p 306 A93-18346
- VINOGRADOV, S. YU.**
Dependence of the service life of a wing on its strength uniformity and landing gear location p 891 A93-42377
- VINOGRADOV, V. A.**
Experimental investigation of hydrogen burning and heat transfer in annular duct at supersonic velocity p 171 A93-14247
Direct measurements of skin friction in a scramjet combustor [AIAA PAPER 93-2443] p 1119 A93-50195
- VIOLAN, P.**
Effect of environment on creep-fatigue crack propagation in turbine disc superalloys [ONERA, TP NO. 1993-5] p 916 A93-41023
- VIRGIN, LAWRENCE N.**
Nonlinear aeroelasticity and chaos p 79 A93-12165
- VISBAL, M. R.**
Initial acceleration effects on the flow field development around rapidly pitching airfoils [AIAA PAPER 93-0438] p 286 A93-23352
Investigation of vortex development on a pitching slender body of revolution p 1095 A93-52445
- VISBAL, MIGUEL**
Computation of a delta-wing roll-and-hold maneuver [AD-A264704] p 909 N93-30498
- VISBAL, MIGUEL R.**
Numerical simulation of delta-wing roll [AIAA PAPER 93-0554] p 285 A93-23293
Structure of vortex breakdown on a pitching delta wing [AIAA PAPER 93-0434] p 474 A93-25528
Computational study of vortex breakdown on a pitching delta wing [AIAA PAPER 93-2974] p 1050 A93-48168
- VISHNEVSKIY, B. L.**
Approximation of a flight vehicle trajectory using Walsh functions p 909 A93-43106
- VISHNIAKOV, V. A.**
Excitation of velocity fluctuations and noise in a wind tunnel p 444 A93-18242

VISHNUHOTLA, V. S.

- Tip clearance effects on the flow field of an axial turbine rotor blade cascade
[ISABE 93-7057] p 1185 A93-54033

VISMARA, G.

- EH 101 ship interface trials p 796 A93-35954

VISSER, H. G.

- Optimal lateral maneuvering for microburst encounters during final approach p 183 A93-14350
Terminal area traffic management [LR-684] p 317 N93-16213

VISSER, K. D.

- Measurements of circulation and vorticity in the leading-edge vortex of a delta wing p 288 A93-23548

VISSER, KENNETH D.

- A computational and experimental investigation of a delta wing with vertical tails
[AIAA PAPER 93-3009] p 1054 A93-48199

VITAGLIANO, P. L.

- An advanced graphics-interactive system for a multi-block structured grid generation within an industrial environment
[ETN-92-92885] p 440 N93-16288

VITIC, A.

- Generation of flow disturbances in transonic wind tunnels p 119 A93-14354

VITKOVSKII, V. V.

- An experimental study of dc discharges in supersonic and subsonic air flows p 14 A93-12980

VITT, P. H.

- Vortex generation and mixing in three-dimensional supersonic combustors
[AIAA PAPER 93-2144] p 1115 A93-49961

VITTAL, B. R.

- Development of an advanced exhaust mixer for a high bypass ratio turbofan engine
[AIAA PAPER 93-2435] p 1118 A93-50188

VITTECOQ, PIERRE

- Harmonic analysis of the aerodynamic forces on a Darrieus rotor p 18 N93-10551

VIVIANI, GARY L.

- Application of parafoils to microwave landing system siting
[AIAA PAPER 93-1213] p 702 A93-35162

VIVIERS, S. S.

- Parameter estimation techniques for flight flutter test analysis p 156 A93-14324

VIZZINI, ANTHONY J.

- Tailoring concepts for improved structural performance of rotorcraft flexbeams p 207 A93-14811
Tapered geometries for improved crashworthiness under side loads p 743 A93-34259

VLADIMIROV, N. I.

- Improvement of aircraft maintenance methods p 395 A93-18326
Improvement of aircraft maintenance methods p 237 A93-18352

VLASOV, E. V.

- Control of coherent structures and aero-acoustic characteristics of subsonic and supersonic turbulent jets p 448 A93-19196
An acoustic suppressor for the jet noise of a turbojet engine p 1003 A93-47510

VLASOV, V. I.

- Development and application of the Monte Carlo method for solving the Boltzmann equation and its models p 1173 A93-51867

VLIETSTRA, ELSO P. M.

- MIAS, the integration of MLS with DGPS/DLoran-C p 315 A93-21181

VO-NGOC, D.

- Experimental investigation of flows behind different Large-Eddy Breakup (LEBU) devices in thick boundary layers p 18 N93-10550

VOELCKERS, U.

- DLR research program overview on airport surface movement guidance and control p 499 A93-27912

VOEVODENKO, N. V.

- Numerical modeling of supersonic flows past wings of different aspect ratios over a wide range of angles of attack within the framework of the plane section law p 5 A93-10141

VOGEL, C. M.

- In-situ bioventing: Two US EPA and Air Force sponsored field studies [PB93-194231] p 1035 N93-32089

VOGEL, D. T.

- Coupling of 3D-Navier-Stokes external flow calculations and internal 3D-heat conduction calculations for cooled turbine blades p 904 N93-29961

VOGEL, SIEGFRIED

- Aeroelastic investigations as applied to Airbus airplanes p 155 A93-14280

VOGELER, K.

- Time-dependent predictions and analysis of turbine cascade data in the transonic flow region [PNR-90957] p 139 N93-15489

VOGT, CARL W.

- The probable cause p 1240 A93-56417

VOJNOV, M. E.

- Synthesis of a data processing and measuring system for flight vehicle control systems p 908 A93-43102

VOLGIN, IU. B.

- Computational and experimental investigation of a solar energy system for an atmospheric flight vehicle p 521 A93-29655

VOLKOV, A. A.

- Characteristics of the detection of overloads in the center of mass of Il-76 and An-12 aircraft due to runway irregularities by a standard on-board recorder p 1008 A93-45666

VOLKOV, I. V.

- Development and application of the Monte Carlo method for solving the Boltzmann equation and its models p 1173 A93-51867

VOLODKO, A. M.

- Helicopters - Handbook [ISBN 5-203-00804-3] p 458 A93-28874

VOLOSHCHENKO, O. V.

- Supersonic combustion and gasdynamic of scramjet p 170 A93-14242

VOLOSHENKO, O. V.

- Gasdynamics of hydrogen-fueled scramjet combustors [AIAA PAPER 93-2145] p 1115 A93-49962

VOLPE, G.

- Performance of compressible flow codes at low Mach numbers p 287 A93-23540

VOLPERT, YEHUDA

- Application of the cyclic J-integral to fatigue crack propagation p 839 N93-27182

VON BACKSTROM, T. W.

- The streamline throughflow method of axial turbomachinery flow analysis [ISABE 93-7031] p 1184 A93-54007

VON ECKROTH, WULF

- Design of a recovery system for a reentry vehicle [AIAA PAPER 93-1224] p 733 A93-35171

VON FLOTOW, ANDREAS H.

- An overview of possible and not-so-possible tasks for active control of sound and vibration p 568 A93-29429

VON GRUENHAGEN, W.

- Inverse simulation: A tool for the validation of simulation programs - First results p 1249 A93-56046

VON GRUENHAGEN, WOLFGANG

- Helicopter in-flight simulator ATTHes - A multipurpose testbed and its utilization [AIAA PAPER 92-4173] p 43 A93-13315
ATTHes - A helicopter in-flight simulator with high bandwidth capability p 821 A93-35988

VON HENKE, FRIEDRICH

- Formal verification of algorithms for critical systems p 846 A93-37623

VONHAGEL, CHRIS

- Ground clutter measurements using the NASA airborne doppler radar: Description of clutter at the Denver and Philadelphia airports p 490 N93-19608

VONSTRYK, O.

- Combining direct and indirect methods in optimal control: Range maximization of a hang glider [REPT-313] p 371 N93-16618

VOOGT, N.

- Investigation of methods for modeling propeller-induced flow fields [AIAA PAPER 93-0874] p 469 A93-24935

VORBRICH, K.

- Integrated DGPS/IMU systems for airborne navigation in Poland p 1241 A93-56049

VOROB'EV, V. F.

- A study of the origin of residual stresses and strains in the transparencies of supersonic aircraft p 801 A93-36784

VORONIN, I. V.

- Evaluation of the efficiency of the direct search method in solving the problem of numerical calculation of the complex hydraulic cooling systems of aviation gas turbine engines p 54 A93-12818

VORONIN, V. I.

- Subsonic separated flow past slender delta wings p 124 A93-15109
Experimental studies of supersonic flow past wedges with longitudinal slots on the windward side p 1089 A93-51786

- Aerodynamic characteristics of conical triangular-planform wings of low aspect ratio in subsonic stalled flow p 1180 A93-53574

VORTAC, O. U.

- En route air traffic controllers use of flight progress strips: A graph-theoretic analysis [AD-A259062] p 319 N93-18927

VOS, JAN B.

- A family of multiblock codes for computational aerothermodynamics - Application to complete vehicle hypersonic flows [AIAA PAPER 93-3042] p 1056 A93-48223

VOSS, RALPH

- TDLM: A Transonic Doublet Lattice Method for 3D potential unsteady transonic flow calculation [DLR-FB-92-25] p 988 N93-31171

VOSTEEN, LOUIS F.

- A unified approach for composite cost reporting and prediction in the ACT program p 920 N93-30441

VOURVOPOULOS, GEORGE

- A pulsed fast-thermal neutron interrogation system p 497 N93-21866

VRADIS, G. C.

- The three-dimensional separated flow structure in a variable aspect ratio sudden expansion duct [AIAA PAPER 93-0213] p 278 A93-22630

VRANOS, A.

- Experimental study of cross flow mixing in cylindrical and rectangular ducts [NASA-CR-187141] p 815 N93-27680

VRATNY, J.

- Profile losses of an annular turbine cascade in unsteady periodic flow [ASME PAPER 92-GT-153] p 249 A93-19380

VTULKIN, S. S.

- An experimental study of a compound supersonic jet p 1069 A93-48914
An experimental study of the dynamic effect of a supersonic underexpanded jet on a plane surface parallel to the nozzle axis p 1092 A93-51913

VU, BRUCE

- A study of CFD algorithms applied to complete aircraft configurations [AIAA PAPER 93-0784] p 468 A93-24864

VU, PHUONG

- A pseudo-loop design strategy for the longitudinal control of hypersonic aircraft [AIAA PAPER 93-3814] p 1132 A93-51405

VUILLOT, A. M.

- 3D viscous flow analysis in axial turbine including tip leakage phenomena p 972 A93-46940
3-D turbomachinery Euler and Navier-Stokes calculations with a multidomain cell-centered approach [AIAA PAPER 93-2576] p 1085 A93-50292

VUKITS, THOMAS J.

- Two-, three-, and four-poster jets in cross flow [AIAA PAPER 93-0023] p 408 A93-20141

VUL, V. M.

- Vibration isolation of aviation power plants taking into account real dynamic characteristics of engine and aircraft p 1244 A93-55863

VULLIERME, J.-J.

- Experimental study of heat transfer close to a plane wall heated in the presence of multiple injections (subsonic flow) p 901 N93-29931

VUTETAKIS, DAVID G.

- High reliability, maintenance-free INS battery development [AD-A264521] p 934 N93-30406

VYSHINSKII, V. V.

- Calculation of separated axisymmetric flow past bodies by solving Euler equations in the inner vortex region p 14 A93-12975

VYSOKOGORETS, M. M.

- Effect of the powerplant configuration on the air flow rate of the jet shield p 54 A93-12820

W

WACHOWICZ, M.

- Model of a map indicator p 341 A93-18532

WACHSPRESS, DANIEL A.

- Rotor design optimization using a free wake analysis [NASA-CR-177612] p 693 N93-25075

WADA, YASUHIRO

- Thermo-chemical models for hypersonic flows p 863 A93-42433

- Computations of transonic wind tunnel flows about a fully configured model of aircraft by using multi-domain technique [AIAA PAPER 93-3022] p 1055 A93-48207

- Numerical computations using multi-domain technique p 299 N93-19277
Numerical simulations of hypersonic rarefied transition regime flows: DSMC method and Navier-Stokes computation p 299 N93-19278

- Computation of re-entry flows with two-temperature model p 301 N93-19295

- The 3D Navier-Stokes calculation of flow about scramjet inlet with strut p 301 N93-19298
- WADE, J. A.**
Stability of the vapour phase in a rotating two-phase fluid system subjected to different gravitational intensities p 926 A93-41714
- WADE, JACK**
Sensors and sensor systems for guidance and navigation; Proceedings of the Meeting, Orlando, FL, Apr. 2, 3, 1991 [SPIE-1478] p 532 A93-27043
- WADE, MICHAEL T.**
Advancing the state of the art hypersonic testing - HYTEST/MTMI [AIAA PAPER 93-2023] p 1113 A93-49860
- WADIA, A. R.**
Low aspect ratio transonic rotors. I - Baseline design and performance [ASME PAPER 92-GT-185] p 352 A93-19410
Low aspect ratio transonic rotors. II - Influence of location of maximum thickness on transonic compressor performance [ASME PAPER 92-GT-186] p 352 A93-19411
- WAGGONER, EDGAR G.**
Assessment of computational issues associated with analysis of high-lift systems p 785 N93-27449
- WAGGOTT, J.**
Effective sealing of a disk cavity using a double-toothed rim seal [ASME PAPER 92-GT-379] p 406 A93-19537
- WAGNER, J. H.**
Heat transfer in rotating serpentine passages with trips skewed to the flow [ASME PAPER 92-GT-191] p 403 A93-19416
- WAGNER, LEE R.**
Human response to helicopter noise - A test of A-weighting p 567 A93-29424
- WAGNER, M.**
Numerical simulation of transition in two- and three-dimensional boundary layers p 973 A93-46980
- WAGNER, MICHAEL J.**
AEW aircraft design [AD-A261800] p 718 N93-26444
- WAGNER, R. D.**
Laminar flow flight experiments - A review p 890 A93-41778
- WAGNER, ROBERT**
Interferometric JFTOT tube deposit measuring device [AD-D015599] p 536 N93-20247
- WAGNER, S.**
Transonic profile design in curvilinear coordinates using an approximate factorization algorithm p 7 A93-10778
- WAGNER, SIEGFRIED**
Experience with boundary element methods to calculate the aerodynamic characteristics of aircraft p 243 A93-19130
- WAHLUND, PER**
Implementation of a multidomain Navier-Stokes code on the Intel iPSC2 hypercube [FFA-TN-1992-37] p 843 N93-28994
- WAILES, W. K.**
Development testing of large ram air inflated wings [AIAA PAPER 93-1204] p 702 A93-35155
- WAINWRIGHT, W. A.**
Advanced technology and the pilot p 45 A93-13412
- WAITES, C.**
Assessment of NDT reliability p 1258 A93-54900
- WAITZ, IAN A.**
Investigation of a contoured wall injector for hypervelocity mixing augmentation p 837 A93-39407
- WAKA, RYOJI**
Turbulent structure in a vortex wake shed from an inclined circular cylinder p 125 A93-15443
- WAKAI, HIROSHI**
A numerical simulations of inner flow of scramjet p 304 N93-19318
- WAKAIRO, KAORU**
Flight simulator evaluation of D-size liquid crystal flat panel displays [NAL-TR-1136] p 52 N93-12367
An optical fiber multi-terminal data bus system for aircraft [NAL-TR-1125] p 52 N93-12370
Liquid crystal flat panel display evaluation tests using a flight simulator [NAL-TR-1122] p 52 N93-12383
- WAKAMATSU, YOSHIO**
Effects of injector geometry on scramjet combustor performance p 359 A93-21670
Effect of film cooling/regenerative cooling on scramjet engine performances [ISABE 93-7036] p 1197 A93-54012
Application of functionally gradient materials to scramjet engines [ISABE 93-7063] p 1200 A93-54039
- Thermal barrier design of gamma-TiAl Functionally Gradient Materials (FGMs) for scramjet engine applications p 1246 A93-54556
Preliminary design of experimental sub-scale scramjet engine [AAS PAPER 91-639] p 1247 A93-55816
Mach 4 testing of scramjet inlet models [NAL-TR-1137] p 26 N93-12369
- WAKASA, MASAYUKI**
Air cell [CA-PATENT-APPL-SN-2001346] p 83 N93-10368
- WAKATSUKI, T.**
Turbine blade vibration monitoring system [ASME PAPER 92-GT-159] p 402 A93-19386
- WALBERG, GERALD D.**
An investigation of aerodynamic heating to spherically blunted cones at angle of attack [AIAA PAPER 93-2764] p 963 A93-46510
- WALCH, STEPHEN P.**
Theoretical characterization of the reaction $\text{NH}_2 + \text{O}$ yields products p 1263 A93-55666
- WALCHLI, LAWRENCE A.**
Results and lessons learned from two Wright Laboratory flight research programs [AIAA PAPER 93-3661] p 1099 A93-48341
- WALDER, A.**
Effect of environment on creep-fatigue crack propagation in turbine disc superalloys [ONERA, TP NO. 1993-5] p 916 A93-41023
- WALDER, RAY**
Control of land use near airports is best means of reducing impact of aircraft noise p 571 A93-29575
- WALDMAN, W.**
Design and implementation of digital filters for analysis of F/A-18 flight test data [AD-A253447] p 17 N93-10342
- WALDMANN, J.**
Merging sparse optical flow and edge connectivity between image features: A representation scheme for 2-D display of scene depth p 845 N93-27179
- WALDRON, WARREN**
Test results of an orifice pulse tube refrigerator p 1149 A93-48612
- WALKER, A. H. C.**
An experimental study of the effects of deformable tip on the performance of fins and finite wings [AIAA PAPER 93-3000] p 1053 A93-48190
- WALKER, D.**
Discrete time $H(\infty)$ control laws for a high performance helicopter p 96 A93-13007
- WALKER, G. J.**
The role of laminar-turbulent transition in gas turbine engines - A discussion [ASME PAPER 92-GT-301] p 255 A93-19491
Stator relative, rotor blade-to-blade near wall flow in a multistage axial compressor with tip clearance variation [AIAA PAPER 93-2389] p 1083 A93-50154
- WALKER, MARY M.**
Application of CFD to a generic hypersonic flight research study [AIAA PAPER 93-0312] p 280 A93-23007
- WALKER, T. H.**
Advanced technology commercial fuselage structure p 918 N93-30432
Cost studies for commercial fuselage crown designs p 920 N93-30440
- WALKER, THOMAS H.**
Advanced technology composite aircraft structures [NASA-CR-190420] p 894 N93-29498
- WALLACE, G.**
Bonded repair of multi-site damage p 947 A93-45786
- WALLACE, N. W.**
Diffraction limited collimating optics for high aspect ratio laser diode arrays p 1172 A93-48411
- WALLACE, TERRY L. A.**
Thermal control/oxidation resistant coatings for titanium-based alloys p 74 N93-12457
- WALLE, G.**
Developments towards versatility in digital engine control units [ISABE 93-7088] p 1202 A93-54064
- WALSH, C.**
Kelvin-Helmholtz wave generation beneath hovercraft skirts p 1219 A93-53820
- WALSH, JOANNE L.**
Aerodynamic performance optimization of a rotor blade using a neural network as the analysis [AIAA PAPER 92-4837] p 324 A93-20295
Recent advances in integrated multidisciplinary optimization of rotorcraft [AIAA PAPER 92-4777] p 325 A93-20369
Recent advances in multidisciplinary optimization of rotorcraft [NASA-TM-107665] p 47 N93-10968
- WALTER, R. F.**
Recent advances in computational analysis of hypersonic vehicles p 1179 A93-53364
- WALTER, RICHARD W., II**
Study of statistical variations of load spectra and material properties on aircraft fatigue life [AD-A257961] p 339 N93-18451
- WALTERS, CURT**
Controls and displays for Douglas Aircraft for the 1990s p 545 A93-27241
- WALTERS, R. W.**
Development and application of GASP 2.0 [AIAA PAPER 92-5067] p 438 A93-22337
- WALTHALL, CHARLES L.**
Assessing spatial and seasonal variations in grasslands with spectral reflectances from a helicopter platform p 426 A93-20621
- WALTHER, R.**
Gasdynamics of hydrogen-fueled scramjet combustors [AIAA PAPER 93-2145] p 1115 A93-49962
- WALTHER, RAINER**
Potential use of alternative fuels in aviation p 1243 A93-54838
- WALTON, ERIC K.**
Effect of wet snow on the null-reference ILS system p 1097 A93-50660
- WALTON, JAMES**
Application of leading-edge vortex manipulations to reduce wing rock amplitudes p 1007 A93-45152
- WALTON, JAMES T.**
Aerothermodynamic flow phenomena of the airframe-integrated supersonic combustion ramjet [NASA-TM-4376] p 196 N93-15528
- WANG, BAOGUO**
Finite-volume-TVD scheme for 3-D Euler transonic flow computations in rotating curvilinear coordinates p 679 A93-33709
- WANG, BO P.**
Optimum design of rotor-bearing systems with eigenvalue constraints [ASME PAPER 92-GT-307] p 405 A93-19497
- WANG, C.**
Linear quadratic tracking problems in Hilbert space - Application to optimal active noise suppression p 1224 A93-52763
- WANG, C. Y.**
The numerical calculation on the flowfields of transverse jet interaction in the base of vehicle at supersonic speeds [AIAA PAPER 93-1931] p 1077 A93-49795
- WANG, CHUN-WEI**
Prediction of turbine cascade flows with a quasi-three-dimensional rotor viscous code and the extension of the algebraic turbulence model [AD-A256831] p 223 N93-15635
- WANG, CLIN M.**
Numerical vorticity capturing for vortex-solid body interaction problems [AIAA PAPER 93-3343] p 954 A93-45037
Unsteady aerodynamic behavior of an airfoil with and without a slat p 1093 A93-52007
- WANG, FRANK Y.**
An exploratory wind tunnel study of supersonic tip vortices [AIAA PAPER 93-2923] p 1045 A93-48124
- WANG, G.**
The prediction of thermal NO(x) in gas turbine exhausts [ISABE 93-7022] p 1195 A93-53998
- WANG, H.**
An approach to the stall monitoring in a single stage axial compressor [AIAA PAPER 93-1872] p 1112 A93-49747
- WANG, H. Y.**
Scaling of the two-phase flow downstream of a gas turbine combustor swirl cup - Mean quantities [ASME PAPER 92-GT-207] p 404 A93-19431
Correlation of droplet behavior with gas-phase structures in a gas turbine combustor [AIAA PAPER 93-1767] p 1152 A93-49663
- WANG, HARRY T. M.**
Fiber optics for aircraft entertainment systems p 1172 A93-49478
- WANG, HONG**
Adaptive array processing for airborne radar p 883 A93-43412
- WANG, J. L.**
Flow structures around a constant-rate pitching airfoil and mechanism of dynamic stall p 118 A93-14332
- WANG, J. P.**
Investigation of precise approach and landing of civil aircraft using integrated system based on GPS p 180 A93-14159

WANG, J.-C.

Face-gear drives: Design, analysis, and testing for helicopter transmission applications
[NASA-TM-106101] p 839 N93-27133

WANG, JIAYUN

The Aircraft/Propulsion Integrated Assessment System p 226 A93-14396
A study of military aircraft and engine tactical/technical performance evaluation p 1242 A93-54596

WANG, JINJUN

An experimental investigation on laminar boundary layer separation over a backward-facing step p 1230 A93-54588

WANG, JOHN T.

An analytically designed subcomponent test to reproduce the failure of a composite wing box beam [AIAA PAPER 93-1344] p 709 A93-33914

WANG, K. C.

Computation of inviscid flowfield around 3-D aerospace vehicles and comparison with experimental and flight data [AIAA PAPER 93-0885] p 470 A93-24944

Two-layer convective heating prediction procedures and sensitivities for blunt body reentry vehicles [AIAA PAPER 93-2763] p 963 A93-46509

WANG, L. C.

An Euler code with new energy equation and new enthalpy damping approach p 686 A93-34352

WANG, L. G.

Remote sensing of O₂ in a supersonic combustor using diode lasers and fiber optics [AIAA PAPER 92-5090] p 414 A93-22360

WANG, LI-JUN

Effects of the pylon pitching stiffness on wing-store flutter p 41 A93-11820

WANG, LI-LI

An impact dynamics investigation on some problems in bird strike on windshields of high speed aircraft p 197 A93-15346

WANG, LI'AN

Effect of steady-state circumferential pressure and temperature distortions on compressor stability p 1106 A93-48503

WANG, LIANGUI

Experimental investigation on patterned blades of compressor p 1066 A93-48515

WANG, LIXING

Worst-case wind modeling and its influence on capturing of aircraft penetration trajectory p 1248 A93-54857

WANG, MINGYING

A preliminary investigation of a method to calibrate strain gauge balances by means of a reference balance p 210 A93-16845

WANG, QIANXI

Analysis of slender bodies of revolution with an angle of attack in extreme ground effect p 679 A93-33716

WANG, QUIN

Designing to aircraft system effectiveness/cost/time with VERT - The system analysis method for aircraft p 153 A93-14204

WANG, S. C.

Surface emitting lasers for avionics applications p 1259 A93-55756

WANG, S. J.

Development and industrial application of the 'all-over-controlled vortex distribution method' for designing radial and mixed flow impellers [ASME PAPER 92-GT-262] p 405 A93-19466

WANG, SHANGJIN

Experimental research for the discharge flow of a centrifugal impeller and the flowfield in the vaneless diffuser p 11 A93-12454

WANG, SHANGWEN

Identification and conversion of foundation parameters for airport pavement p 538 A93-24035

WANG, SHU-HUA

Calculation of sound field radiated by oscillating cascade p 231 A93-14269

WANG, SHUJIE

Adaptive wall wind tunnel with two measured interfaces - Theory and experiment p 679 A93-33717

WANG, SUOFANG

The experimental investigation of combination effect by using injection effect of aeroengine jet exhaust p 898 A93-41742

WANG, T.

Wind identification along a flight trajectory. I - 3D-kinematic approach p 223 A93-16324

Design of multi-stage turbomachinery blading by the circulation method - Actuator duct limit [ASME PAPER 92-GT-286] p 254 A93-19477

Wind identification along a flight trajectory. II - 2D-kinematic approach p 524 A93-28469

Wind identification along a flight trajectory. III - 2D dynamic approach p 1007 A93-45401

WANG, TIECHENG

An experimental study on location of transitional separation bubble on a low Reynolds numbers airfoil p 680 A93-33725

WANG, TONGQING

The numerical calculation for the coupling of multiple propeller discrete noise and its interaction with the fuselage boundary p 231 A93-14268

WANG, W. J.

Time-frequency domain analysis of vibration signals for machinery diagnostics. 3: The present power spectral density [OUEL-1911/92] p 89 N93-11707

WANG, W. L.

A synthesized method in durability analysis p 203 A93-14286

WANG, WEI

Nonlinear multi-point modelling and parameter estimation of the DO 28 research aircraft p 41 A93-12727

WANG, WEN-LIANG

Dynamic analysis of annular cascade structures p 1259 A93-55586

WANG, XING R.

Flight simulator development in China p 191 A93-14410

WANG, XINGFU

An experimental investigation of hydrogen-fueled supersonic combustor p 53 A93-12733

WANG, XUEJUN

The investigation of limit cycle amplitude of nonlinear nose gear p 800 A93-36342

WANG, XUEPING

Study on fracture failure of turbine blades in a series of turbojets p 205 A93-14493

WANG, YI-REN

The effect of wake dynamics on rotor eigenvalues in forward flight p 137 N93-14595

WANG, YIBIN

Numerical simulation of passive control of shock-boundary layer interaction for transonic airfoil p 680 A93-33719

WANG, YONG

A three-dimensional inviscid flow solver in Chimera flow simulation [AIAA PAPER 93-0190] p 276 A93-22614

WANG, YONGMING

A blade element method for predicting the off-design performance of compressors p 1107 A93-49187

WANG, YU

The optimum design of air cycle refrigeration system with high pressure water separation p 202 A93-14180

WANG, YUH-YING

Discontinuous Galerkin finite element method for two dimensional conservation laws [AIAA PAPER 93-0337] p 281 A93-23026

Numerical investigations on airfoil performance subjected to aerodynamic interference from an upstream airfoil [AIAA PAPER 93-0639] p 463 A93-24754

WANG, YURENG

Effects of vitiated air on the results of ground tests of scramjet combustor p 173 A93-16234

WANG, Z. H.

The numerical calculation on the flowfields of transverse jet interaction in the base of vehicle at supersonic speeds [AIAA PAPER 93-1931] p 1077 A93-49795

WANG, Z. Y.

Drag characteristics of extra-thin-fin-riblets in an air flow conduit p 1151 A93-49240

WANG, ZHENYU

A method for aerodynamic calculation by placing linear vari-strength vortex panels on airfoil contour p 1231 A93-54597

WANG, ZHI

The method for developing F-by-F load spectra of fighter aircraft based on manoeuvres p 154 A93-14254

WANG, ZHONGJUN

Improvement in application of eigenstructure assignment to flight control system design p 227 A93-15406

WANG, ZHONGQI

An experimental study on blade negative curving in a turbine cascade with a large turning angle p 1071 A93-49185

Effect of blade leaning on the development of passage vortices and losses in the passage of turbine cascade with a great turning angle p 1236 A93-55397

WANG, ZI-MING

Study of the method for determining residual stress induced by machining in airplane canopies made of PMMA p 534 A93-27366

WANG, ZICAI

The application of optimal robust control in control system design of flying vehicles p 95 A93-11791

WANHILL, R. J. H.

Flight simulation and constant amplitude fatigue crack growth in aluminum-lithium sheet and plate p 71 A93-13644

Damage tolerance behaviour of aluminium-lithium sheet alloys [NLR-TP-91244-U] p 392 N93-17540

Flight simulation and constant amplitude fatigue crack growth in aluminum-lithium sheet and plate [NLR-TP-91104-U] p 331 N93-17562

Fractographic and microstructural analysis of fatigue crack growth in Ti-6Al-4V fan disc forgings p 1004 N93-31742

WANIE, KLAUS MARKUS

Numerical methods for aerothermodynamic design of hypersonic space transport vehicles [MBB-FE-211-S-PUB-0481] p 514 N93-21056

WANJIN, HAN

The blade curving effects in a turbine stator cascade with low aspect ratio [AD-A261063] p 725 N93-26239

WANKE, CRAIG

Hazard assessment and cockpit presentation issues for microburst alerting systems p 308 A93-22112

Experimental evaluation of candidate graphical microburst alert displays p 145 N93-14853

WANNER, JEAN-CLAUDE

Flight safety and human errors p 141 A93-16860

WANNER, NICOLE

Flight safety and human errors p 141 A93-16860

WAPELHORST, LEO

The effect of TCAS interrogations on the Chicago O'Hare ATCRBS system [DOT/FAA/CT-92/22] p 318 N93-16498

Results of DATAS investigation of illegal mode S ID's at JFK Airport [DOT/FAA/CT-92/26] p 318 N93-16841

Results of DATAS investigation of ATCRBS environment at the Los Angeles International Airport [DOT/FAA/CT-93/6] p 793 N93-28625

WARBURTON, FRANK M.

Evaluation of tilt rotor aircraft design utilizing a realtime interactive simulation p 798 A93-35989

WARBURTON, J.

Natural and augmented snowfall growth processes and their interactions with the natural and modified aerosol [PB93-153096] p 755 N93-25874

WARD, B.

Experiments on low aspect ratio hydroplanes to measure lift under static and dynamic conditions [ARE-TM(UHR)-90306] p 21 N93-11365

WARD, C. A.

Stability of the vapour phase in a rotating two-phase fluid system subjected to different gravitational intensities p 926 A93-41714

WARD, DONALD T.

Preliminary design of an intermittent smoke flow visualization system [NASA-CR-186027] p 806 N93-28693

WARD, JOHN R.

Apparatus for reduction of vibration in liquid-injected gas compressor system [AD-D015607] p 554 N93-20772

WARD, PHILLIP W.

The Texas Instruments/Honeywell GPS Guidance Package p 32 A93-11015

WARD, S.

Hybrid prismatic/tetrahedral grid generation for complex 3-D geometries [AIAA PAPER 93-0669] p 465 A93-24778

Prismatic grid generation for three-dimensional complex geometries p 1178 A93-53217

WARDWELL, D. A.

Small scale jet effects and hot gas ingestion investigations at NASA Ames [AIAA PAPER 92-4252] p 67 A93-13339

WARDWELL, DOUGLAS A.

Jet-induced ground effects on a parametric flat-plate model in hover [NASA-TM-104001] p 700 N93-26099

WARE, GEORGE M.

Aerodynamic characteristics of the HL-20 p 1181 A93-53736

WARNATZ, J.

Simulation of nonequilibrium hypersonic flows p 863 A93-42443

WARNER, DAVID N., JR.

Flight test evaluation of precision-code differential GPS for terminal approach and landing p 33 A93-11294

WARREN, GARY P.

Application of multigrid and adaptive grid embedding to the two-dimensional flux-split Euler equations p 202 A93-13990

WARREN, THOMAS J.

A laboratory study of fracture in the presence of lap splice multiple site damage p 1027 A93-45790

WARTIK, STEVE

Domain engineering validation case study: Synthesis for the air traffic display/collision warning monitor domain version 01.00.03
[AD-A259407] p 503 N93-21671

WARWICK, GRAHAM

Unorthodox rising p 1 A93-11250
Counting the cost of composites p 107 A93-14117
Novel nozzle p 1245 A93-54450
Engine for change p 1248 A93-56350

WASCHKA, W.

Heat transfer and leakage in high-speed rotating stepped labyrinth seals p 903 N93-29951

WASHBURN, A. E.

The use of artificial intelligence for buffet environments
[AIAA PAPER 93-1534] p 727 A93-34071

WASHBURN, ANTHONY E.

Experimental investigation of vortex-fin interaction
[AIAA PAPER 93-0050] p 260 A93-20163
A computational and experimental investigation of a delta wing with vertical tails
[AIAA PAPER 93-3009] p 1054 A93-48199

WASHINGTON, WM. D.

Curvature and leading edge sweep back effects on grid fin aerodynamic characteristics
[AIAA PAPER 93-3480] p 981 A93-47258

WASZAK, MARTIN R.

Design, test, and evaluation of three active flutter suppression controllers
[NASA-TM-4338] p 63 N93-10070
Modeling and model simplification of aeroelastic vehicles: An overview
[NASA-TM-107691] p 64 N93-12216
Active flutter suppression using dipole filters
[NASA-TM-107594] p 186 N93-13367

WATANABE, AKIRA

Flight simulator evaluation of D-size liquid crystal flat panel displays
[NAL-TR-1136] p 52 N93-12367
An optical fiber multi-terminal data bus system for aircraft
[NAL-TR-1125] p 52 N93-12370
Liquid crystal flat panel display evaluation tests using a flight simulator
[NAL-TR-1122] p 52 N93-12383

WATANABE, KEIICHIRO

Research and development of ceramic turbine wheels
[ASME PAPER 92-GT-295] p 354 A93-19485

WATANABE, MINORU

Evaluation of acoustic impedance models for a perforated plate
[NAL-TR-1133] p 102 N93-12375

WATANABE, OSAMU

Tip clearance effect on heat transfer and leakage flows on the shroud-wall surface in an axial flow turbine
[ASME PAPER 92-GT-200] p 403 A93-19425

WATANABE, SHIGEYA

Scramjet nozzle experiment with hypersonic external flow
p 899 A93-42879

WATANABE, TAKASHI

A new technique for analysis of unsteady aerodynamic responses of cascade airfoils with blunt leading edge - Unsteady aerodynamic responses of the cascade in incompressible flow p 1086 A93-51122

WATANABE, Y.

Conceptual design of turbo-accelerator for HST combined cycle engine
[ASME PAPER 92-GT-253] p 353 A93-19462
A scoping study for hypersonic transport propulsion systems
[ASME PAPER 92-GT-409] p 356 A93-19558
Conceptual design study on combined-cycle engine for hypersonic transport
[ISABE 93-7018] p 1195 A93-53994
Using fuzzy behaviors for the outdoor navigation of a car with low-resolution sensors
[DE93-002428] p 706 N93-25120

WATANABE, YASUSHI

Study on unsymmetrical supersonic nozzle flows
p 127 A93-16933

WATERS, D.

Synchronous X-ray Sinography for nondestructive imaging of turbine engines under load
[AIAA PAPER 93-1819] p 1153 A93-49707

WATERS, M. H.

Structural and aerodynamic considerations for an oblique all-wing aircraft
[AIAA PAPER 92-4220] p 43 A93-13336

WATERS, MARK

Oblique wing supersonic transport concepts
[AIAA PAPER 92-4230] p 43 A93-13337

WATSON, BRIAN C.

SAPNEW: Parallel finite element code for thin shell structures on the Alliant FX/80
[NASA-CR-190663] p 84 N93-10372

SAPNEW: Parallel finite element code for thin shell structures on the Alliant FX-80
[NASA-CR-189212] p 220 N93-14799

WATSON, CAROLYN B.

Experimental effects of wing location on wing-body pressures at supersonic speeds
[NASA-TM-4434] p 700 N93-26085

WATSON, G. J.

Development and flight testing of a surface pressure measurement installation on the EAP demonstrator aircraft
p 550 N93-19927

WATSON, JAMES C.

F-15 composite engine access door
p 920 N93-30442

WATTLER, A.

Experimental working position simulator to analyse, develop and optimize concepts for computer-aided Air Traffic Management
p 191 A93-14412

WATTS, MICHAEL E.

Data acquisition and analysis on a Macintosh
p 562 A93-29422

WAWNER, FRANKLIN E., JR.

NASA-UVA Light Aerospace Alloy and Structures Technology Program (LA2ST)
[NASA-CR-193412] p 1019 N93-31739

WEATHERILL, N. P.

Adaptive inviscid flow solutions for aerospace geometries on efficiently generated unstructured tetrahedral meshes
[AIAA PAPER 93-3390] p 956 A93-45081
The construction of nearly orthogonal multiblock grids for compressible flow simulation
p 1219 A93-53847

WEATHERILL, NIGEL P.

Techniques for the visual evaluation of computational grids
[AIAA PAPER 93-3353] p 1037 A93-45047
Unstructured grid generation using interactive three-dimensional boundary and efficient three-dimensional volume methods
[AIAA PAPER 93-3452] p 1037 A93-47237

WEAVER, CLARK J.

Implications of three-dimensional tracer studies for two-dimensional assessments of the impact of supersonic aircraft on stratospheric ozone
p 936 A93-41269

WEAVER, KIM

A technique for the measurement of cloud structure on centimeter scales
p 1158 A93-51243

WEAVER, T. L.

Reconfigurable photonic data networks for military aircraft
p 928 A93-42783

WEBB, F. R.

Antennas now and future
p 764 A93-39540

WEBB, JAY C.

Dispersion-relation-preserving schemes for computational aeroacoustics
p 244 A93-19151

WEBB, LANNIE D.

Flight test results from a supercritical mission adaptive wing with smooth variable camber
[AIAA PAPER 92-4101] p 38 A93-11274
Flight-determined engine exhaust characteristics of an F404 engine in an F-18 airplane
[AIAA PAPER 93-2543] p 1121 A93-50267
Flight test results from a supercritical mission adaptive wing with smooth variable camber
[NASA-TM-4415] p 49 N93-11863

WEBB, W. L.

Advancements in aircraft gas turbine engines - Past and future
p 170 A93-14153

WEBB, WILLIAM L.

Mach 5 turboramjet requirements and design approach
[ISABE 93-7015] p 1194 A93-53991

WEBER, DANIEL J.

Correlation of mean velocity measurements downstream of a swept backward-facing step
p 123 A93-14552

WEBER, M.

Establishing two-dimensional flow in a large-scale cascade of controlled-diffusion compressor blades
[AIAA PAPER 93-2383] p 1083 A93-50151

WEBER, MARK

Weather information requirements for Terminal Air Traffic Control Automation
p 429 A93-22146

WEBER, PETER

Classification of radar clutter in an air traffic control environment
p 886 N93-30299

WEBSTER, B. E.

Unsteady compressible airfoil aerodynamics using an adaptive time-discontinuous GLS finite element method
[AIAA PAPER 93-0339] p 281 A93-23027

WEBSTER, G. A.

Development of the neutron diffraction technique for the determination of near surface residual stresses in critical gas turbine components
[PNR-90984] p 58 N93-11112

WEBSTER, P. J.

Development of the neutron diffraction technique for the determination of near surface residual stresses in critical gas turbine components
[PNR-90984] p 58 N93-11112

WEBSTER, P. S.

Development of the neutron diffraction technique for the determination of near surface residual stresses in critical gas turbine components
[PNR-90984] p 58 N93-11112

WECKESSER, LOUIS B.

Thermal shock capabilities of infrared dome materials
p 70 A93-11454

WEEMS, DOUGLAS B.

Evaluation of thermoplastic stiffened panels for application to rotorcraft airframes
p 827 A93-36000

WEERATUNGA, SISIRA

Parallel computation of 3-D Navier-Stokes flowfields for supersonic vehicles
[AIAA PAPER 93-0064] p 261 A93-20177

WEERATUNGA, SISIRA K.

Dynamic overset grid communication on distributed memory parallel processors
[AIAA PAPER 93-3311] p 1036 A93-45007

WEI, JING-BIN

Investigation on bi-flat jet separated flow in a rectangular combustor
p 459 A93-23778

WEI, M.

Maintaining high accuracy GPS positioning 'on the fly'
p 92 A93-11028
Accuracy of GPS-derived acceleration from moving platform tests
p 1240 A93-55973

WEI, SHENGMIN

A multi-functional computer-aided aircraft exterior shape modelling prototype system
p 504 A93-24032

WEI, XINGLU

An aerodynamic design program for contra-rotating turbine cascades
p 1067 A93-48521

WEIBLEN, FRANK

A contribution to noise improvements for aircraft by noise measurement evaluation
p 448 A93-19190

WEIDNER, ELIZABETH H.

Scramjet fuel-air mixing establishment in a pulse facility
p 359 A93-21667

WEIDNER, J. P.

Hypersonic propulsion - Breaking the thermal barrier
p 897 A93-40437

WEIGAND, ALEXANDER

How to enhance safety for future space transportation systems
p 1015 A93-45444

WEIGEL, HENRY S.

Digitization of analog data from in-flight lightning strikes
p 753 N93-24884

WEIH, Y. P.

The detection and warning of low-level wind shear based on terminal single Doppler radar
p 432 A93-22195

WEIHS, D.

Oblique shock formation in impulsively started wedge flows
p 692 A93-35636

WEILAND, C.

A split-matrix Runge-Kutta type space marching procedure
p 8 A93-11921
An extended insight into hypersonic flow phenomena using numerical methods
p 1093 A93-51999

WEILENMANN, MARTIN F.

A test bench for rotorcraft hover control
[AIAA PAPER 93-3853] p 1140 A93-51440

WEILMUNSTER, K. J.

High angle-of-attack inviscid Shuttle Orbiter computation
p 9 A93-12020
Solution strategy for three-dimensional configurations at hypersonic speeds
p 962 A93-46406
Navier-Stokes simulations of the Shuttle Orbiter aerodynamic characteristics with emphasis on pitch trim and bodyflap
[AIAA PAPER 93-2814] p 965 A93-46552
HL-20 computational fluid dynamics analysis
p 1181 A93-53740

WEILMUNSTER, KENNETH J.

Single block three-dimensional volume grids about complex aerodynamic vehicles
p 957 A93-45099

WEINACHT, PAUL

Navier-Stokes computations for kinetic energy projectiles in steady coning motion: A predictive capability for pitch damping
[AD-A264111] p 1033 N93-32028

WEINBERG, H.

Use of microprocessor-based simulator technology and MEG/EEG measurement techniques in pilot emergency-maneuver training
p 530 N93-19706

WEINSTEIN, LEONARD M.

Aerodynamic investigation with focusing schlieren in a cryogenic wind tunnel
[AIAA PAPER 93-3485] p 910 A93-41059
Reflection type skin friction meter
[NASA-CASE-LAR-14520-1-SB] p 296 N93-18275

WEISENBURGER, RICHARD

The NASA/industry Design Analysis Methods for Vibrations (DAMVIBS) program: McDonnell-Douglas Helicopter Company achievements p 515 N93-21314

WEISENSTEIN, DEBRA

Predicted aircraft effects on stratospheric ozone p 93 N93-11096

WEISGERBER, D.

Selection criteria for metallic high temperature structural materials in hypersonic flying equipment [MBB-LME-221-HYPAC-PUB-2-A] p 515 N93-21479

WEISS, S.

System identification for X-31A project support: Lessons learned so far p 512 N93-19914

WEISSHAAR, T. A.

Static aeroelastic control of an adaptive lifting surface p 995 A93-45147

WEISSHAAR, TERRENCE A.

Adaptive aeroelastic composite wings - Control and optimization issues p 185 A93-14818
The design of a long range megatransport aircraft [NASA-CR-192077] p 332 N93-17711

WEITBRECHT, ANDREAS

European merger control in the air transport industry - Comments on the Delta Air Lines/Pan Am decision of the European Commission [ISBN 3-452-22293-4] p 103 A93-11412

WELBURN, M.

The use of non-destructive testing to detect and monitor aircraft corrosion in service p 1258 A93-54896

WELCH, CHRISTOPHER

Method of remotely characterizing thermal properties of a sample [NASA-CASE-LAR-13508-3-CU] p 67 N93-11057

WELCH, GERARD E.

Two-dimensional CFD modeling of wave rotor flow dynamics [AIAA PAPER 93-3318] p 952 A93-45014

WELCH, SHARON S.

Sensors and sensor systems for guidance and navigation II; Proceedings of the Meeting, Orlando, FL, Apr. 22, 23, 1992 [SPIE-1694] p 547 A93-28151

WELCOME, MICHAEL L.

Adaptive Cartesian grid methods for representing geometry in inviscid compressible flow [AIAA PAPER 93-3385] p 955 A93-45076

WELDON, V.

Near-term two-stage-to-orbit, fully reusable, horizontal take-off/landing launch vehicle p 1015 A93-45441

WELGE, H. R.

Civil aircraft challenges in engine/airframe integration [ASME PAPER 92-GT-45] p 322 A93-19299

WELLBORN, STEVEN R.

An experimental investigation of the flow in a diffusing S-duct [NASA-TM-105809] p 60 N93-12077

WELLER, MARTHA H.

A context-based introduction to aircraft radio communications p 570 A93-27164

WELLER, WILLIAM H.

A modal-based procedure for efficiently predicting low vibration rotor designs p 712 A93-34262

WELLMAN, BRENT

Far-field hover acoustic characteristics of the XV-15 tiltrotor aircraft with Advanced Technology Blades p 566 A93-29412

WELLS, EDWARD A.

Advanced Technology Blade testing on the XV-15 Tilt Rotor Research Aircraft p 799 A93-36020
Preliminary flight test results of a fly-by-throttle emergency flight control system on an F-15 airplane [AIAA PAPER 93-1820] p 1100 A93-49708

WELLS, TERRI A.

A thermal/structural analysis process incorporating concurrent engineering [SAE PAPER 92-1185] p 938 A93-41364

WELLS, V.

A numerical study of advanced rotor blades p 481 A93-29436

WELLS, VALANA

An integrated optimum design approach for high speed prop-rotors including acoustic constraints [NASA-CR-193222] p 893 N93-29153

WELLS, VALANA L.

Far field rotor noise [AD-A260703] p 759 N93-25651

WELLS, WILLIAM L.

Hypersonic lateral and directional stability characteristics of aeroassist flight experiment configuration in air and CF4 [NASA-TM-4435] p 875 N93-29166

WELSH, B. L.

A summary of further measurements of steady and oscillatory pressures on a rectangular wing p 1096 A93-52594

WELTERLEN, TRACY J.

Decreasing F-16 nozzle drag using computational fluid dynamics [AIAA PAPER 93-2572] p 1084 A93-50289

WEN, GONGBI

The analysis and computation of viscous-inviscid interactive problem for three dimensional transonic flow p 681 A93-33741

WEN, SHIZHU

Multilevel solution of the elastohydrodynamic lubrication of concentrated contacts in spiroid gears p 1161 A93-52606

WENDLAND, RICHARD A.

Upgrade and extension of the data acquisition system for propulsion and gas dynamic laboratories [AD-A256836] p 235 N93-15637

WENDT, J. F.

An experimental contribution to the flat plate 2D compression ramp, shock/boundary layer interaction problem at Mach 14 - Test case 3.7 p 865 A93-42590

WENDT, JOHN F.

A synthesis of results on the calculation of flow over a 2D ramp and a 3D obstacle - Antibes test cases 3 and 4 p 867 A93-42601

WENIGER, RICHARD J.

Sensor-adaptive control for aircraft paint stripping [SME PAPER AD92-200] p 855 A93-40663

WENNINGER, ED

Out with the mechanical fasteners [AIAA PAPER 92-4210] p 44 A93-13378

WENREN, YONGHU

Numerical vorticity capturing for vortex-solid body interaction problems [AIAA PAPER 93-3343] p 954 A93-45037

WENTZ, K.

Prediction of fluctuating pressure in attached and separated compressible flow [AIAA PAPER 93-0286] p 279 A93-22687

WENTZ, WILLIAM H.

Aviation safety research at the National Institute for Aviation Research Wichita State University: A report to the FAA Technical Center [NIAR-92-2] p 310 N93-16455

WERLEY, NORMAN M.

Performance of higher harmonic control algorithms for helicopter vibration reduction p 890 A93-41904

WERT, JOHN A.

NASA-UVA Light Aerospace Alloy and Structures Technology Program (LA2ST) [NASA-CR-193412] p 1019 N93-31739

WERTHEIMER, JIRI

Aeroelastic challenges for a High Speed Civil Transport [AIAA PAPER 93-1478] p 712 A93-34240

WESFRED, JOSE E.

Coriolis effects on Goertler vortices in the boundary-layer flow on concave wall p 123 A93-14564

WESKE, REID A.

Pseudo Aircraft Systems - A multi-aircraft simulation system for air traffic control research [AIAA PAPER 93-3585] p 1209 A93-52679

WEST, G. S.

Experiments on smooth cantilevered circular cylinders in a low-turbulence uniform flow. Part 2: Fluctuating loads on a cantilever of aspect ratio 30 [PB93-110500] p 555 N93-21382

Experiments on smooth cantilevered circular cylinders in low-turbulence uniform flow. Part 1: Mean loading with aspect ratios in the range 4 to 30 [PB93-111763] p 555 N93-21383

WEST, J. W.

An optical flameout detection system for NASA Langley's 8-Foot High Temperature Tunnel p 1254 A93-54372

WEST, JOHN T.

Scientific visualization using the Flow Analysis Software Toolkit (FAST) p 758 N93-25600

WEST, M. G.

Lateral aerodynamic interference between tanker and receiver in air-to-air refueling p 1136 A93-52444

WEST, PETER R.

NODE-air traffic management systems p 884 A93-43428

WEST, R. L.

Measurement of a one-dimensional mobility using a laser-Doppler velocimeter p 210 A93-16647

WESTERMAN, E. A.

Support of composite fuel cells [SME PAPER EM92-101] p 152 A93-14102

WESTLAND, J.

Clebsch variable model for unsteady inviscid transonic flow with strong shock waves [AIAA PAPER 93-3025] p 1055 A93-48210

WESTMAN, BLAKE

A second-generation high speed civil transport: Stingray [NASA-CR-192022] p 336 N93-18059

WESTON, M. A.

Passive drag reduction of a helicopter airfoil in an unsteady transonic flow p 482 A93-29440

WESTPHAL, W.

Development of advanced carbon-carbon annular flameholders for gas turbines [PNR-90947] p 58 N93-11106

Small particle impact damage in carbon-carbon composites [PNR-90948] p 73 N93-11107

WESTRA, BRYAN W.

Proposal and preliminary design for a high speed civil transport aircraft. Swift: A high speed civil transport for the year 2000 [NASA-CR-192023] p 335 N93-18049

WESTWATER, E. R.

Liquid water profiling using remote sensor observations p 429 A93-22150

The FAA aircraft icing Forecasting Improvement Program - Validation of aircraft icing forecasts in the Denver area [AIAA PAPER 93-0393] p 309 A93-23069

WEY, C.

Comparison of reacting and non-reacting shear layers at a high subsonic Mach number [NASA-TM-106198] p 814 N93-27610

Turbulence measurement in a reacting and non-reacting shear layer at a high subsonic Mach number [NASA-TM-106186] p 989 N93-31839

WHEATON, DUANE L.

Real-time capture, archiving, retrieval, processing, and presentation of large quantities of flight test/research information [AIAA PAPER 92-4073] p 95 A93-11258

WHEELER, BARRY

C-17 - High-tech 'lifter from Long Beach p 713 A93-34519

WHIPPLE, R. D.

Effect of geometry, static stability, and mass distribution on the tumbling characteristics of generic flying-wing models [AIAA PAPER 93-3615] p 1125 A93-48302

WHIPPLE, RAYMOND D.

Dynamic model testing of the X-31 configuration for high-angle-of-attack flight dynamics research [AIAA PAPER 93-3674] p 1129 A93-48351

WHITAKER, DAVID L.

Three-dimensional unstructured grid Euler computations using a fully-implicit, upwind method [AIAA PAPER 93-3337] p 953 A93-45031

WHITAKER, KEVIN W.

Design of exhaust nozzles using GA optimized neural networks [AIAA PAPER 93-0410] p 361 A93-23331

WHITE, G.

Miniature display technologies for integrated helmet systems p 718 A93-34819

V-22 nacelle conversion actuator p 889 A93-40438

WHITE, J. A.

An effective multigrid method for high-speed flows p 6 A93-10533

WHITE, NANCY H.

HL-20 operations and support requirements for the Personnel Launch System mission p 1210 A93-53745

WHITE, R. G.

Grazing angle dependency of SAR imagery p 884 A93-43455

The effect of temperature on the natural frequencies and acoustically induced strains in CFRP plates p 1260 A93-56331

WHITE, ROBERT G.

Nonlinear response of a clamped beam and plate to high levels of excitation p 397 A93-19141

WHITE, ROLAND J.

A wind shear hazard window useful in studying the effect of wind shear on the airplane during the landing approach [AIAA PAPER 93-3643] p 1127 A93-48327

WHITE, T.

Federal Aviation Administration pavement modeling p 379 N93-16315

WHITEFIELD, PHILIP D.

NO(x) scavenging on carbonaceous aerosol surfaces in aircraft exhaust plumes. I [AIAA PAPER 93-2343] p 1164 A93-50117

Particulates and aerosols characterized in real time for harsh environments using the UMR mobile aerosol sampling system (MASS) [AIAA PAPER 93-2344] p 1156 A93-50118

WHITEHEAD, D. S.

Flutter of grouped turbine blades [ASME PAPER 92-GT-227] p 404 A93-19444

- WHITEHEAD, H. R.**
Ground clutter measurements using an aerostat surveillance radar p 929 A93-43381
- WHITEHEAD, JULIA H.**
The FAA/NASA flight loads monitoring program - The prototype system and its benefits for the aviation community p 486 A93-25125
A study of the influence of the data acquisition system sampling rate on the accuracy of measured acceleration loads for transport aircraft p 1000 A93-46808
Research requirements for a real-time flight measurements and data analysis system for subsonic transport high-lift research p 1244 A93-54391
- WHITEHEAD, R. S.**
Lessons learned for composite structures p 920 N93-30444
- WHITEHURST, ROBERT B.**
Experimental supersonic hydrogen combustion employing staged injection behind a rearward-facing step p 744 A93-34496
- WHITELAW, J. H.**
Vaporizer performance p 79 A93-12784
Scalar characteristics in a liquid-fuelled combustor with curved exit nozzle p 1123 A93-51643
- WHITELAW, JAMES H.**
Aerothermodynamics in combustors; IUTAM Symposium, National Taiwan Univ., Taipei, June 3-5, 1991, Selected Papers [ISBN 0-387-55404-1] p 1146 A93-51626
- WHITFIELD, CHARLOTTE E.**
Rotor-rotor interaction for counter-rotating fans. I - Three dimensional flowfield measurements [AIAA PAPER 93-1848] p 1075 A93-49729
- WHITFIELD, D. L.**
Direct and iterative algorithms for the three-dimensional Euler equations [AIAA PAPER 93-3378] p 957 A93-45102
- WHITFIELD, DAVID L.**
Navier-Stokes calculations for the unsteady flowfield of turbomachinery [AIAA PAPER 93-0676] p 465 A93-24786
High resolution numerical simulation of the linearized Euler equations in conservation law form [AIAA PAPER 93-2934] p 1148 A93-48132
Turbofan flowfield simulation using Euler equations with body forces [AIAA PAPER 93-1978] p 1078 A93-49825
- WHITLOW, WOODROW, JR.**
An overview of aeroelasticity studies for the National Aero-Space Plane [AIAA PAPER 93-1313] p 732 A93-33889
Research in unsteady aerodynamics and computational aeroelasticity at the NASA Langley Research Center p 804 A93-39498
Analysis of aeroelastic and resonance responses of a wind tunnel model support system p 1013 A93-47022
- WHITMORE, STEPHEN A.**
Application of a flush airdata sensing system to a wing leading edge (LE-FADS) [AIAA PAPER 93-0634] p 516 A93-24750
Flight and wind-tunnel calibrations of a flush airdata sensor at high angles of attack and sideslip and at supersonic Mach numbers [NASA-TM-104265] p 344 N93-19110
Application of a flush airdata sensing system to a wing leading edge (LE-FADS) [NASA-TM-104267] p 518 N93-20163
- WHITNEY, THOMAS J.**
Determination of stresses on laminated aircraft transparencies by the strain gage-hole drilling and sectioning method [AD-A255548] p 164 N93-14571
- WHITSON, JOHN**
Failure-accommodating neural network flight control [AIAA PAPER 92-4394] p 523 A93-24495
- WHITTAKER, I. C.**
Fleet fatigue cracking threshold prediction p 3 A93-13633
- WHITTAKER, T.**
Near-optimal energy transitions for energy-state trajectories of hypersonic aircraft [AIAA PAPER 92-4300] p 69 A93-13276
- WHITTAKER, THOMAS**
Optimal trajectories for hypersonic launch vehicles p 1251 A93-54563
- WHITTENBERGER, J. D.**
Stress relaxation of low pressure plasma-sprayed NiCrAlY alloys p 1211 A93-52870
- WHITTESEY, R.**
The HYDICE instrument design and its application to planetary instruments p 842 N93-28766
- WHITWORTH, H. A.**
Evaluation of the fatigue behavior of discontinuous and continuous fiber thermoplastic composite laminates p 824 A93-36005
- WICHMAN, KEITH D.**
Real-time in-flight engine performance and health monitoring techniques for flight research application p 169 N93-15169
- WICKARDT, H.**
Aircraft performance in practice p 340 N93-19004
- WICKENS, CHRISTOPHER D.**
A context-based introduction to aircraft radio communications p 570 A93-27164
- WICKS, FRANK E.**
Development of a model to predict electric vehicle performance over a variety of driving conditions p 570 A93-26011
- WICKS, MICHAEL**
Adaptive array processing for airborne radar p 883 A93-43412
- WIDMARK, S.**
A preliminary investigation of a method to calibrate strain gauge balances by means of a reference balance p 210 A93-16845
- WIDNALL, S. E.**
Reform of the aeronautics and astronautics curriculum at MIT [AIAA PAPER 93-0325] p 454 A93-23017
- WIE, Y. S.**
Hybrid laminar flow control applied to advanced turbofan engine nacelles [SAE PAPER 920962] p 123 A93-14628
- WIE, Y.-S.**
Stability theory and transition prediction applied to a general aviation fuselage p 479 A93-28601
- WIE, YONG-SUN**
BLSTA: A boundary layer code for stability analysis [NASA-CR-4481] p 220 N93-14797
- WIEDEMANN, KARL E.**
Thermal control/oxidation resistant coatings for titanium-based alloys p 74 N93-12457
- WIEDERMANN, A.**
Viscous flows in centrifugal compressor diffusers at transonic Mach numbers [ASME PAPER 92-GT-48] p 246 A93-19301
- WIEDMANN, JUERGEN**
Comparison of the damage for various types of fibre reinforced composites due to different lightning test standards (MIL-STD-1757A, German military VG-standard 96903) p 736 N93-24891
- WIEDNER, B.**
Fluid dynamics and convective heat transfer in impinging jets through implementation of a high resolution liquid crystal technique [ISABE 93-7077] p 1220 A93-54053
- WIELER, J. G.**
Reliability considerations for weather hazard warning radar p 431 A93-22187
- WIESEMAN, CAROL D.**
Experimental unsteady pressures at flutter on the Supercritical Wing Benchmark Model [AIAA PAPER 93-1592] p 683 A93-34123
Multiple-function, multi-input/multi-output digital control and on-line analysis [NASA-TM-107697] p 162 N93-13565
- WIESEN, B.**
Rarefied gas flow around a 3D-deltawing p 870 A93-42639
- WIGGENRAAD, J. F. M.**
Structural optimization in preliminary aircraft design - A finite-element approach p 226 A93-14340
Global/local interlaminar stress analysis of a grid-stiffened composite panel p 548 A93-28543
Interlaminar stress analysis at the skin/stiffener interface of a grid-stiffened composite panel [NASA-CR-192177] p 393 N93-17920
- WIGMORE, DAVID B.**
Testing of an energy efficient environmental control system for a patrol-type aircraft [SAE PAPER 921225] p 890 A93-41399
- WILCOX, BRUCE C., JR.**
Inward contaminant leakage tests of the S-Tron Corporation emergency escape breathing device. Phase 1: Tests of the original design. Phase 2: Tests with the redesigned neck seal [DOT/FAA/AM-92/18] p 704 N93-25205
- WILCOX, DAVID C.**
The remarkable ability of turbulence model equations to describe transition p 783 N93-27432
- WILCOX, F.**
Base drag prediction on missile configurations [AIAA PAPER 93-3629] p 1064 A93-48314
- WILD, MARY**
Data collection procedures for the Software Engineering Laboratory (SEL) database [NASA-TM-108579] p 230 N93-15579
- WILDE, G. L.**
ASTOVL model engine simulators for wind tunnel research p 192 N93-13213
- WILDER, M. C.**
Interferometric investigations of compressible dynamic stall over a transiently pitching airfoil [AIAA PAPER 93-0211] p 278 A93-22628
Transition effects on compressible dynamic stall of transiently pitching airfoils [AIAA PAPER 93-2978] p 1050 A93-48171
- WILDER, MICHAEL CURTIS**
Airfoil-vortex interaction and the wake of an oscillating airfoil p 134 N93-13803
- WILEY, JOHN**
Transport resurrection p 41 A93-12434
- WILEY, JOHN L.**
Ongoing and planned R&D efforts in airway facilities maintenance p 458 A93-27134
- WILK, LEONARD S.**
Dynamic attitude measurement system [AIAA PAPER 93-3801] p 1139 A93-51393
- WILKE, W.**
Summaries of the 1991 publications of DLR research reports and DLR communications [ETN-93-92588] p 572 N93-21022
- WILKINS, DANIEL A.**
A high fidelity video delivery system for real-time flight simulation research [AIAA PAPER 93-3558] p 1214 A93-52659
- WILKINSON, CHRIS**
Fractographic investigation of IMI 685 crack propagation specimens for SMP SC33 p 1004 N93-31743
- WILKINSON, STEPHEN P.**
Goertler instability and hypersonic quiet nozzle design p 480 A93-29155
- WILLDEN, K. S.**
Cost studies for commercial fuselage crown designs p 920 N93-30440
- WILLDEN, KURTIS**
Process and assembly plans for low cost commercial fuselage structure p 923 N93-30865
- WILLIAMS, A. G.**
The composite shape and structure of coherent eddies in the convective boundary layer p 93 A93-12643
- WILLIAMS, B. R.**
Comparison of solution of various Euler solvers and one Navier-Stokes solver for the flow about a sharp-edged cropped delta wing [NLR-TP-90340-U] p 418 N93-16411
- WILLIAMS, D. D.**
The role of turbomachinery testing for stability in distorted flow [PNR-90943] p 57 N93-11040
- WILLIAMS, D. L., II**
The use of subscale models to predict self-induced oscillations of flight vehicles [AIAA PAPER 93-0093] p 264 A93-20199
- WILLIAMS, D. R.**
The effect of Reynolds number on vortex asymmetry about slender bodies p 475 A93-26176
- WILLIAMS, DAVID H.**
Piloted simulation of an air-ground profile negotiation process in a time-based Air Traffic Control environment [NASA-TM-107748] p 707 N93-26087
- WILLIAMS, DAVID R.**
The effect of Reynolds number on control of forebody asymmetry by suction and bleed [AIAA PAPER 93-3265] p 968 A93-46831
- WILLIAMS, GLENN W.**
Optically smart surfaces survivability testing at Mach 3 [AD-A261785] p 760 N93-26566
- WILLIAMS, J. E. F.**
Active stabilization of compressor instability and surge in a working engine [ASME PAPER 92-GT-88] p 348 A93-19335
- WILLIAMS, J. S.**
Land subsidence and problems affecting land use at Edwards Air Force Base and vicinity, California, 1990 [PB93-182236] p 1036 N93-32191
- WILLIAMS, JACK**
Improving weather questions on Federal Aviation Administration exams p 308 A93-22110
- WILLIAMS, K. E.**
A numerical investigation of supersonic strut/endwall interactions in annular flow with varying strut thickness [AIAA PAPER 93-2927] p 1045 A93-48128
Experimental and numerical investigation of supersonic turbulent flow in an annular duct [AIAA PAPER 93-3123] p 1063 A93-48291
Investigation of a strut/endwall interaction in supersonic annular flow [AIAA PAPER 93-1925] p 1076 A93-49791
- WILLIAMS, LISA C.**
A nonlinear analysis methodology for the design of skid landing gears p 799 A93-36004
- WILLIAMS, LOUIS J.**
The rebirth of supersonic transport p 457 A93-25325

WILLIAMS, M. R.

- WILLIAMS, M. R.**
Satisfying the customer's requirements
[PNR-90988] p 521 N93-20735
- WILLIAMS, MARC H.**
S-plane aerodynamics of nonplanar lifting surfaces
p 958 A93-45134
Time domain panel method for wings
p 958 A93-45135
Unsteady aerodynamics and flutter based on the potential equation
[AIAA PAPER 93-2086] p 1079 A93-49913
- WILLIAMS, MORGAN**
An adaptive grid/Navier-Stokes methodology for the calculation of nozzle afterbody base flows with a supersonic freestream
[AIAA PAPER 93-1922] p 1076 A93-49788
- WILLIAMS, PATRICK R.**
Aircraft collision avoidance using statistical decision theory
p 500 A93-28155
- WILLIAMS, ROBERT M.**
A primer on polynomial resultants
[AD-A246883] p 98 N93-11463
- WILLIAMS, STEVEN P.**
Trade-offs arising from mixture of color cueing and monocular, binoptic, and stereoscopic cueing information for simulated rotorcraft flight
[NASA-TP-3268] p 338 N93-18333
- WILLIAMS, T. F.**
Studies of jet thermal stability in a flowing system
[ASME PAPER 92-GT-106] p 401 A93-19344
- WILLIAMS, TODD M.**
Initial results of an in-flight investigation of longitudinal flying qualities for augmented, large transports in approach and landing
[AIAA PAPER 93-3816] p 1133 A93-51407
- WILLIAMSON, D. W.**
Helicopter crash survival at sea: United States Navy/Marine Corps experience 1977-1990
p 493 N93-19687
- WILLIAMSON, DANA W.**
Trans-cockpit authority gradient in Navy/Marine aircraft mishaps
p 146 N93-15016
- WILLIAMSON, F. R.**
Ground clutter measurements using an aerostat surveillance radar
p 929 A93-43381
- WILLIAMSON, JAMES S.**
Reusable Ada avionics software packages library system
p 944 A93-42828
- WILLSHIRE, WILLIAM L., JR.**
Non-propulsive aerodynamic noise
p 99 N93-10673
- WILLSON, JAMES G.**
Quantitative-force measurements of pneumatic control on a wing/strake model
[AD-A257343] p 289 N93-16157
- WILMOT, STEPHEN B.**
FDAMS: An extendable and reconfigurable solution for avionics data management systems
p 168 N93-15157
- WILMOTH, R. G.**
Energetics of gas-surface interactions in transitional flows at entry velocities
p 778 A93-39259
- WILMOTH, RICHARD G.**
Shock interference prediction using direct simulation Monte Carlo
p 778 A93-39258
Zonally-decoupled DSMC solutions of hypersonic blunt body wake flows
[AIAA PAPER 93-2808] p 949 A93-44227
A systems approach to a DSMC calculation of a control jet interaction experiment
[AIAA PAPER 93-2798] p 964 A93-46538
Hypersonic blunt body wake computations using DSMC and Navier-Stokes solvers
[AIAA PAPER 93-2807] p 964 A93-46547
- WILSON, C. W.**
The development of a large annular facility for testing gas turbine combustor diffuser systems
[AIAA PAPER 93-2546] p 1139 A93-50269
- WILSON, D.**
A preliminary investigation of the Helmholtz resonator concept for heat flux reduction
[AIAA PAPER 93-2742] p 963 A93-46493
- WILSON, DAVID G.**
Models for predicting the performance of Brayton-cycle engines
[ASME PAPER 92-GT-361] p 355 A93-19525
- WILSON, DAVID J.**
Development of flying qualities and agility evaluation maneuvers
[AIAA PAPER 93-3645] p 1127 A93-48329
- WILSON, DENNIS E.**
The effect of large scale unsteady motion on turbulent reattaching shear layer - Application to the supersonic compression ramp
[AIAA PAPER 93-3100] p 1061 A93-48273
- WILSON, F. W., JR.**
The redesigned Low Level Wind Shear Alert System
p 431 A93-22179

- WILSON, G. C.**
Experimental and computational investigation of flow in catalytic monolith channels
[ASME PAPER 92-GT-118] p 387 A93-19354
- WILSON, J. W.**
Radiation safety in aircraft operations
p 141 A93-14221
- WILSON, JACK**
An improved numerical model for wave rotor design and analysis
[AIAA PAPER 93-0482] p 361 A93-23384
Initial results from the NASA Lewis wave rotor experiment
[AIAA PAPER 93-2521] p 1193 A93-53589
An improved numerical model for wave rotor design and analysis
[NASA-TM-105915] p 60 N93-12418
Initial results from the NASA-Lewis wave rotor experiment
[NASA-TM-106148] p 1005 N93-32368
- WILSON, JAMES W.**
Nowcasts of thunderstorm initiation and evolution
p 752 A93-33773
- WILSON, JOHN C.**
The strake - A simple means for directional control improvement
p 802 A93-37997
Helicopter low-speed yaw control
[NASA-CASE-LAR-14219-1] p 729 N93-25998
- WILSON, K. J.**
Combustion characteristics and passive control of an annular dump combustor
[AIAA PAPER 93-1772] p 1110 A93-49668
Periodic chemical energy release for active combustion control
[ISABE 93-7043] p 1198 A93-54019
- WILSON, M.**
Wall jets created by single and twin high pressure jet impingement
p 744 A93-34847
- WILSON, M. J.**
Unsteady pressures under impinging jets in crossflows
p 399 A93-19220
- WILSON, MARK R.**
Signal processing of jet noise from flyover test data
[AIAA PAPER 93-0736] p 563 A93-24826
De-Dopplerization of aircraft acoustic signals
[AIAA PAPER 93-0737] p 563 A93-24827
- WILSON, R. J.**
Status of the validation of high-angle-of-attack nose-down pitch control margin design guidelines
[AIAA PAPER 93-3623] p 1126 A93-48308
- WILSON, ROBERT F.**
Control design for robust eigenstructure assignment in linear uncertain systems
p 97 A93-13241
- WILSON, ROBERT J.**
Decision making for a public differential GPS service
p 314 A93-21165
- WILT, C. E.**
Development of the F/A-18 E/F air induction system
[AIAA PAPER 93-2152] p 1101 A93-49969
- WILTBERGER, N. L.**
Efficient simulation of incompressible viscous flow over single and multi-element airfoils
p 1095 A93-52448
- WILTBERGER, N. LYN**
Efficient simulation of incompressible viscous flow over multi-element airfoils
p 784 A93-27443
- WIMMERSTROM, PETER**
Studies of fuel-rich magnesium propellants in a small solid fuel ramjet combustor
p 535 A93-27759
- WINCHESKI, B.**
Imaging flaws in thin metal plates using a magneto-optic device
p 397 A93-18670
- WINDIRSCH, P.**
An approach to the stall monitoring in a single stage axial compressor
[AIAA PAPER 93-1872] p 1112 A93-49747
- WINDLEY, PHILLIP J.**
Formal design specification of a Processor Interface Unit
[NASA-CR-189698] p 99 N93-12538
- WINFREE, W. P.**
Assessment of aircraft structural integrity by detecting disbands through ultrasonic scanning
p 406 A93-19587
Automation of disbond detection in aircraft fuselage through thermal image processing
p 407 A93-19598
- WINFREE, WILLIAM P.**
Comparison of heating protocols for detection of disbands in lap joints
p 396 A93-18627
Method of remotely characterizing thermal properties of a sample
[NASA-CASE-LAR-13508-3-CU] p 67 N93-11057
- WING, DAVID J.**
Fluidic scale model multi-plane thrust vector control test results
[AIAA PAPER 93-2433] p 1117 A93-50187

PERSONAL AUTHOR INDEX

- Performance characteristics of two multiaxis thrust-vectoring nozzles at Mach numbers up to 1.28
[NASA-TP-3313] p 874 N93-29160
- WINGROVE, R. C.**
A summary of investigations of severe turbulence incidents using airline flight records
p 308 A93-22153
- WINIECKI, JACEK**
A short range passenger/freighter canard - Some problems of a preliminary aerodynamic concept
[SAE PAPER 921012] p 157 A93-14642
- WINKELMANN, ALLEN E.**
An experimental study of droop leading edge modifications on high and low aspect ratio wings up to 50 deg angle of attack
[AIAA PAPER 93-3496] p 983 A93-47268
- WINKER, J. A.**
The unrealized potential for heavy balloon payloads
p 39 A93-11359
- WINN, ROBERT C.**
Total Quality Management in curriculum development
[AIAA PAPER 93-0326] p 454 A93-23018
- WINN, W. P.**
Aircraft measurement of electric field - Self-calibration
p 753 A93-34694
- WINSTON, MATTHEW M.**
Technology benefits and ground test facilities for high-speed civil transport development
[NASA-TM-107670] p 378 N93-15790
- WINTERFELD, G.**
Correlations between engineering, medical and behavioural aspects in fire-related aircraft accidents
p 494 N93-19693
- WINTERSTEIN, R.**
Euler solutions for blunt bodies using triangular meshes - Artificial viscosity forms and numerical boundary conditions
[AIAA PAPER 93-3333] p 953 A93-45027
- WINTHER, B. A.**
Aeroelastic effects on the B-2 maneuver response
[AIAA PAPER 93-3664] p 1128 A93-48344
- WINZELL, BENGT**
Hypersonic leeward delta-wing-flow computations using centered schemes
p 870 A93-42635
- WIPPICH, HEINZ-GEORG**
Satellite navigation in traffic management
p 914 A93-43549
- WISCHOW, PERRY B.**
Digital map databases in support of avionic display systems
p 544 A93-26888
- WISE, KEVIN A.**
Linear and nonlinear aircraft flight control for the AIAA Controls Design Challenge
[AIAA PAPER 92-4628] p 62 A93-13286
Nonlinear aircraft flight control using dynamic inversion
p 368 A93-22868
TVC control for the AIAA design challenge airplane
[AIAA PAPER 93-3810] p 1122 A93-51402
- WISEMAN, J.**
Theoretical and experimental investigations concerning the structural integrity of aeroengine compressor discs
p 56 N93-10539
- WISHART, D.**
Enhancement of mixing in high-speed heated jets using a counterflowing nozzle
p 1235 A93-55359
- WISHART, D. P.**
Supersonic jet control via point disturbances inside the nozzle
p 861 A93-41930
- WISLER, D. C.**
Unsteady aerodynamics and gust response in compressors and turbines
[ASME PAPER 92-GT-422] p 258 A93-19570
- WISLER, DAVID C.**
Rotor-rotor interaction for counter-rotating fans. I - Three dimensional flowfield measurements
[AIAA PAPER 93-1848] p 1075 A93-49729
- WITCOWSKI, ROBERT D.**
Langley proposed advanced hypervelocity aerophysics facility - A status report
p 1013 A93-47615
- WITHAM, JOHN E.**
Rotorcraft reliability and maintainability - A CAA view of future trends
p 45 A93-13407
- WITHERS, ASHLEY**
Design of the advanced regional aircraft, the DART-75
[NASA-CR-192044] p 333 N93-17972
- WITHERSPOON, F. D.**
High-pressure hypervelocity electrothermal wind-tunnel performance study and subscale tests
p 1137 A93-49617
- WITTIG, S.**
Diffusion controlled evaporation of a multicomponent droplet - Theoretical studies on the importance of variable liquid properties
p 1021 A93-44224
Heat transfer and leakage in high-speed rotating stepped labyrinth seals
p 903 N93-29951

- The aerodynamic effect of coolant ejection in the leading edge region of a film-cooled turbine blade
p 904 N93-29958
- WITTON, J. J.**
Experimental and computational investigation of flow in catalytic monolith channels
[ASME PAPER 92-GT-118] p 387 A93-19354
- WLEZIE, R. W.**
Nozzle installation effects on the noise from supersonic exhaust plumes
p 100 N93-10681
- WLEZIE, RICHARD W.**
Aeroacoustic environment of an advanced short takeoff and vertical landing aircraft in hover
p 231 A93-14539
- WOERNLE, RUDOLF**
Influence of cross section variations on the structural behaviour of composite rotor blades
[MBB-UD-0602-91-PUB] p 332 N93-17569
- WOFSY, STEVE**
Predicted aircraft effects on stratospheric ozone
p 93 N93-11096
- WOHLER, DIANE**
Rotorcraft health and usage monitoring systems: A literature survey
[DOT/FAA/RD-91/6] p 48 N93-11461
- WOHLRATH, WERNER**
Dornier 228 experimental with laminar wing
p 506 A93-27500
- WOJCIC, C. C.**
Niobium alloy heat pipes for use in oxidizing environments
p 200 A93-13791
- WOLBER, DAVE**
Formal representation of the requirements for an Advanced Subsonic Civil Transport (ASCT) flight control system
[NASA-CR-189699] p 98 N93-12346
- WOLF, STEPHEN W. D.**
Development of the NASA-Ames low disturbance supersonic wind tunnel for transition research up to Mach 2.5
[AIAA PAPER 92-3909] p 462 A93-24488
- WOLF, THOMAS**
Flight testing and simulation of an F-15 airplane using throttles for flight control
[AIAA PAPER 92-4109] p 39 A93-11278
- WOLFE, DANIEL**
Methodology development for evaluation of selective-fidelity rotorcraft simulation
p 913 N93-30691
- WOLFE, H. W.**
Prediction of fluctuating pressure in attached and separated compressible flow
[AIAA PAPER 93-0286] p 279 A93-22687
- WOLFE, HOWARD F.**
Nonlinear response of a clamped beam and plate to high levels of excitation
p 397 A93-19141
- WOLFENDEN, A.**
Measurements of dynamic Young's modulus and damping in single crystals of a nickel-based superalloy as a function of temperature
p 1147 A93-52513
- WOLFF, JAMES M.**
Single passage Euler analysis of oscillating cascade unsteady aerodynamics for arbitrary interblade phase angle
[AIAA PAPER 93-0389] p 282 A93-23067
- WOLFSON, MARILYN**
Weather information requirements for Terminal Air Traffic Control Automation
p 429 A93-22146
- WOLFSON, MARILYN W.**
Contributions to the American Meteorological Society's 26th International Conference on Radar Meteorology
[AD-A263385] p 936 N93-29257
- WOLFSON, RONALD I.**
A wideband, embedded/conformal, antenna subsystem concept
p 327 A93-22002
- WOLTERMAN, RICHARD L.**
The effects of crushing surface roughness on the crushing characteristics of composite tubes
p 77 A93-10918
- WOLTERS, W.**
The reduction of skin friction by riblets under the influence of an adverse pressure gradient
p 1218 A93-53810
- WOLVERTON, DAVID A.**
Advanced Transport Operating System (ATOPS) Flight Management/Flight Controls (FM/FC) software description
[NASA-CR-191457] p 808 N93-28621
Advanced Transport Operating System (ATOPS) utility library software description
[NASA-CR-191469] p 1000 N93-32218
- WON, MARK J.**
Applying and validating the RANS-3D flow-solver for evaluating a subsonic serpentine diffuser geometry
[AIAA PAPER 93-2157] p 1079 A93-49973
- WONG, C. C.**
Nuclear thermal rocket entry heating and thermal response preliminary analysis
[AIAA PAPER 93-0378] p 385 A93-23058
- WONG, DOUGLAS T.**
An improved calibration technique for wind tunnel model attitude sensors
p 1253 A93-54356
- WONG, G. S.**
Active control of wing rock of a delta wing at post-stall using tangential leading edge blowing
[AIAA PAPER 93-0056] p 367 A93-20169
- WONG, GRANT SURE-MAN**
Experiments in the control of wing rock at high angle of attack using tangential leading edge blowing
p 1009 N93-31068
- WONG, H.**
Computational aerothermodynamics for 2D and 3D space vehicles
p 1073 A93-49533
- WONG, R. V. C.**
Controlling common mode stabilization errors in airborne gravity gradiometry
p 1245 A93-55978
- WONG, RICHARD**
Sandwich construction in the Starship
p 159 A93-15737
- WONG, TIN-CHEE**
Prediction of asymmetric vortical flows around slender bodies using Navier-Stokes equations
p 478 A93-27925
Passive control of supersonic asymmetric vortical flows around cones
p 220 N93-14692
- WONG, Y. W.**
Applications of laser techniques in fluid mechanics
p 395 A93-17765
- WOO, EDMUND P.**
Development of resins for composites by resin transfer molding
p 921 N93-30853
- WOO, JONG-HO**
Static aeroelastic analysis of a maneuvering aircraft with damaged wing
[AIAA PAPER 92-4765] p 325 A93-20360
Analysis of the static and dynamic response of a T-38 wing and comparison with experimental data
[AD-A262363] p 806 N93-27692
- WOOD, BILL**
Phoenix: Preliminary design of a high speed civil transport
[NASA-CR-192024] p 334 N93-17976
- WOOD, E. R.**
Application of two chaos methods to Higher Harmonic Control data
p 909 A93-43783
- WOOD, J. R.**
Experimental and computational investigation of the NASA Low-Speed Centrifugal Compressor flow field
[ASME PAPER 92-GT-213] p 252 A93-19436
- WOOD, M. E.**
The design and commissioning of an acoustic liner for propeller noise testing in the ARA transonic wind tunnel
[PNR-90880] p 101 N93-11204
- WOOD, N. J.**
The influence of the fuselage on high alpha vortical flows and the subsequent effect on fin buffeting
p 116 A93-14263
Static roll moment characteristics of asymmetric tangential leading edge blowing on a delta wing at high angles of attack
[AIAA PAPER 93-0052] p 261 A93-20165
Active control of wing rock of a delta wing at post-stall using tangential leading edge blowing
[AIAA PAPER 93-0056] p 367 A93-20169
The suppression of single-fin buffeting using tangential leading edge blowing on a delta wing
p 270 A93-21677
Tangential Forebody Blowing-yaw control at high alpha
[AIAA PAPER 93-3406] p 1008 A93-47205
- WOOD, NORMAN J.**
A vortex control technique for the attenuation of fin buffet
p 121 A93-14408
Determination of vortex burst location on delta wings from surface pressure measurements
p 123 A93-14557
An experimental investigation of twin fin buffeting and suppression
[AIAA PAPER 93-0054] p 261 A93-20167
- WOOD, WILLIAM A.**
Combined LAURA-UPS hypersonic solution procedure
[NASA-TM-107682] p 747 N93-25176
- WOODS, W. C.**
Air/helium ground-test simulation pertinent to the definition of slender body hypersonic aerodynamics
[AIAA PAPER 93-0318] p 268 A93-21106
- WOODWARD, D. E.**
The largest freight airship that can fit in Moffett hangar no. 1
[AIAA PAPER 93-4046] p 1242 A93-54613
- WOODWARD, RICHARD P.**
Takeoff/approach noise for a model counterrotation propeller with a forward-swept upstream rotor
[AIAA PAPER 93-0596] p 519 A93-24782
Takeoff/approach noise for a model counterrotation propeller with a forward-swept upstream rotor
[NASA-TM-105979] p 362 N93-16715
In-flight near- and far-field acoustic data measured on the Propfan Test Assessment (PTA) testbed and with an adjacent aircraft
[NASA-TM-103719] p 852 N93-27058
- WOODYATT, BRUCE A.**
Fault signatures obtained from fault implant tests on an F404 engine
[ASME PAPER 92-GT-82] p 348 A93-19331
- WOOLEY, CHRISTINE L.**
Impact of aeroelasticity on propulsion and longitudinal flight dynamics of an air-breathing hypersonic vehicle
[AIAA PAPER 93-1367] p 733 A93-33934
- WORBOYS, M. R.**
Miniature display technologies for integrated helmet systems
p 718 A93-34819
- WORKMAN, GARY L.**
Materials processing in low gravity
[NASA-CR-184421] p 91 N93-12401
FNAS modify matrix and transparent experiments
[NASA-CR-184442] p 198 N93-13311
Fiber pulling apparatus modification
[NASA-CR-184498] p 220 N93-14763
- WORONOWICZ, MICHAEL STANLEY**
Application of a vectorized particle simulation to the study of plates and wedges in high-speed rarefied flow
p 133 N93-13746
- WORSNOP, D. R.**
Stratospheric aircraft exhaust plume and wake chemistry studies
[NASA-CR-189688] p 94 N93-12299
- WORSNOP, DOUGLAS R.**
Icing prevention by ultrasonic nucleation of supercooled water droplets in front of subsonic aircraft
[AD-A258212] p 142 N93-12816
- WORTMANN, J.**
Ceramics for aero-engine applications
[ASME PAPER 92-GT-439] p 388 A93-19581
- WRAY, A. P.**
The development of a large annular facility for testing gas turbine combustor diffuser systems
[AIAA PAPER 93-2546] p 1139 A93-50269
- WRAY, RICHARD B.**
Requirements analysis notebook for the flight data systems definition in the Real-Time Systems Engineering Laboratory (RSEL)
[NASA-CR-185698] p 69 N93-10960
- WRENN, G. A.**
Multidisciplinary design integration system for a supersonic transport aircraft
[AIAA PAPER 92-4841] p 324 A93-20296
- WRIGHT, A. D.**
User's Guide for the NREL Force and Loads Analysis Program
[DE92-010579] p 216 N93-13524
User's Guide for the NREL Teetering Rotor Analysis Program (STRAP)
[DE92-010580] p 216 N93-13525
- WRIGHT, C. W.**
Application of new GPS aircraft control/display system to topographic mapping of the Greenland ice cap
p 499 A93-28152
- WRIGHT, CHESTER A., JR.**
Design recovery for software library population
[AD-A259292] p 572 N93-20611
- WRIGHT, G. A.**
Optical technologies for UV remote sensing instruments
p 853 N93-28788
- WRIGHT, J.**
A multilevel composite grid method for fluid flow computations
[AIAA PAPER 93-0768] p 541 A93-24852
- WRIGHT, J. R.**
Comparison of some direct multi-point force appropriation methods
p 928 A93-43338
Envelope function - A tool for analyzing flutter data
p 1136 A93-52455
- WRIGHT, M. H.**
Issues in large-scale optimization with expensive functions
p 437 A93-20708
- WRIGHT, R. A. S.**
Development of highly loaded root end attachments for composite material high speed flying surfaces
p 539 A93-24122
- WRIGHT, RICHARD D.**
Validation of aviation weather products for the Advanced Traffic Management System
p 430 A93-22161
- WRIGHT, WILLIAM B.**
Advancements in the LEWICE Ice Accretion Model
[AIAA PAPER 93-0171] p 309 A93-23243

WRIGHT, WILLIAM BENJAMIN

Simulation of two-dimensional icing, de-icing and anti-icing phenomena p 142 N93-13364

WRIGLEY, ROBERT C.

The Airborne Ocean Color Imager - System description and image processing p 1157 A93-50369

WRISDALE, IAN EDWARD

Flow prediction for three-dimensional intakes and ducts using viscous-inviscid interaction methods p 218 N93-13953

WROBLEWSKI, WLODZIMIERZ

Modelling of the flow in the blade-ring design process of turbomachinery p 520 A93-27291

WU, C.

Computational study of advanced exhaust system transition ducts with experimental validation p 689 A93-34490

WU, C. A.

Guidelines for NAVSTAR GPS embedded receiver applications p 315 A93-21184

WU, C. C.

Asymptotic methods for the prediction of transonic wind-tunnel wall interference p 730 A93-35625

WU, CHIHUA

Application of model reference adaptive control to speed control system in an aeroengine p 172 A93-14498

WU, CHIVEY

Navier-Stokes calculation of transonic flow past the NTF 65-deg delta wing p 292 N93-16797

WU, DA

An experimental investigation of the effects of swirling flow on the performance of nozzles p 1247 A93-54859

WU, GUANGMAO

Engineering optimization of aeronautical structures p 154 A93-14227

WU, GUOCHUAN

The effects of end-bend regulations of compressor blade on the outlet flow field [ISABE 93-7033] p 1185 A93-54009

WU, GUOHUA

An experimental investigation of endwall flow control in a compressor plane cascade wind tunnel p 1066 A93-48512

WU, H. M.

FUM - An efficient MmB solver for steady inviscid flows p 862 A93-42431

WU, HU

On model for predicting blade force defect in end wall boundary layer inside axial compressor cascade p 862 A93-42271

A new method for predicting the end wall boundary layers and the blade force defects inside the passage of axial compressor cascades p 1236 A93-55589

WU, J. M.

Vortex capture by a two-dimensional airfoil with a small oscillating leading-edge flap [AIAA PAPER 93-3266] p 968 A93-46830

Streaming vorticity flux from oscillating walls with finite amplitude p 1160 A93-52517

WU, J. Z.

Vortex capture by a two-dimensional airfoil with a small oscillating leading-edge flap [AIAA PAPER 93-3266] p 968 A93-46830

Streaming vorticity flux from oscillating walls with finite amplitude p 1160 A93-52517

WU, JIANN-YUARN

A domain decomposition method for parallel transient response calculations p 187 N93-13827

WU, K. C.

Operating experience using venturi flow meters at liquid helium temperature [DE92-014693] p 90 N93-12140

WU, L. Y.

A computational method for inverse design of transonic airfoil and wing [AIAA PAPER 93-3482] p 982 A93-47260

WU, LIYI

An inverse method with regularity condition for transonic airfoil design p 1230 A93-54583

The effects of reaction rate constants and catalytic wall on the hypersonic flow field over blunt bodies p 1230 A93-54586

WU, MEN-ZAN BILL

Velocity and temperature measurements in a non-premixed reacting flow behind a backward facing step p 132 N93-13632

WU, N. E.

Reliability assessment for self-repairing flight control systems p 907 A93-42804

WU, QIFEN

Weighted average method for evaluating the aerodynamic properties of transition flow p 8 A93-11872

WU, S. J.

Adaptive finite volume upwind approach on mixed quadrilateral-triangular meshes p 287 A93-23542

WU, SHUFAN

Analysis and development of a total energy control system for a large transport aircraft p 183 A93-14372

WU, T. W.

Acoustical analysis of gear housing vibration p 567 A93-29420

WU, TIEMIN

Mechanical testing analyses of new aluminium alloy SPF typical-parts in aircraft p 196 A93-14174

WU, TSUNG-HSUN

USCG HU-25A/GPS integration p 313 A93-21130

WU, WANGYI

The analysis and computation of viscous-inviscid interactive problem for three dimensional transonic flow p 681 A93-33741

WU, WENQUAN

Numerical simulation for aeroelasticity in turbomachines with vortex method. I - Theory and method p 53 A93-12452

WU, X. F.

Acoustical analysis of gear housing vibration p 567 A93-29420

WU, X. H.

Streaming vorticity flux from oscillating walls with finite amplitude p 1160 A93-52517

WU, XIAOHUI

An experimental investigation of the effects of swirling flow on the performance of nozzles p 1247 A93-54859

WU, XIAOQING

Superresolution radar imaging with linear prediction data extrapolation p 342 A93-20851

Research on ISAR motion compensation and imaging by modeling electromagnetic data p 342 A93-20852

Studies of superresolution range-Doppler imaging p 928 A93-43344

WU, XINPING

Using a diagonal implicit algorithm to calculate transonic nozzle flow [AIAA PAPER 93-2345] p 1082 A93-50119

WU, Y.-T.

Computational techniques for probabilistic analysis of turbomachinery [ASME PAPER 92-GT-167] p 351 A93-19393

WU, YAOHUA

Comment on 'Equation decoupling - A new approach to the aerodynamic identification of unstable aircraft' p 818 A93-37406

WU, YONG

Integrated fire control simulation systems p 1192 A93-53876

WU, YONGJIAN

Experimental study of dynamic stall on an oscillating airfoil p 266 A93-20804

WUEBBLES, D. J.

Impact of supersonic and subsonic aircraft on ozone: Including heterogeneous chemical reaction mechanisms [DE92-019619] p 224 N93-13655

WUEBBLES, DONALD J.

Predicted aircraft effects on stratospheric ozone p 93 N93-11096

WUETHRICH, CHRISTIAN

Optical blade vibration measurement [ETN-93-93454] p 905 N93-29999

WULFF, G.

Multiple input/multiple output (MIMO) analysis procedures with applications to flight data p 60 A93-10777

WUNG, T. S.

Aerothermodynamics in combustors; IUTAM Symposium, National Taiwan Univ., Taipei, June 3-5, 1991. Selected Papers [ISBN 0-387-55404-1] p 1146 A93-51626

WURSTER, K. E.

Aerodynamic heating environment definition/thermal protection system selection for the HL-20 p 1181 A93-53739

WURTZLER, KENNETH E.

Numerical analysis of a chined forebody with asymmetric strakes [AIAA PAPER 93-0051] p 260 A93-20164

WYGNANSKI, I.

Pilot test of a low Reynolds number DTE-airfoil [AIAA PAPER 93-0643] p 464 A93-24758

Oscillatory blowing, a tool to delay boundary layer separation [AIAA PAPER 93-0440] p 474 A93-25529

The effects of forced oscillations on the performance of airfoils [AIAA PAPER 93-3264] p 968 A93-46829

Oscillatory blowing - A tool to delay boundary-layer separation p 1235 A93-55362

WYSS, M. L.

Averaging techniques for steady and unsteady calculations of a transonic fan stage [AIAA PAPER 93-3065] p 1059 A93-48241

WYZZKOWSKI, J.

Application of FEM model correlation and updating techniques on an aircraft using test data of a ground vibration survey p 509 A93-29267

X

XI, G.

Development and industrial application of the 'all-over-controlled vortex distribution method' for designing radial and mixed flow impellers [ASME PAPER 92-GT-262] p 405 A93-19466

XI, GUANG

Experimental research for the discharge flow of a centrifugal impeller and the flowfield in the vaneless diffuser p 11 A93-12454

XIA, LINXI

A numerical and experimental studies of flow characteristics in centrifugal fans p 695 N93-25339

XIA, SONGBO

A theoretical study on the ETHYLENE system - A fuzzy diagnostic expert system for large rotating machinery p 846 A93-36327

XIA, XUEJIAN

Experimental study on the mechanism of favourable interferences of body strakes p 121 A93-14405

XIA, Z. X.

A computational method for inverse design of transonic airfoil and wing [AIAA PAPER 93-3482] p 982 A93-47260

XIA, ZHIXUN

An inverse method with regularity condition for transonic airfoil design p 1230 A93-54583

XIANLIN, BAN

The application of concentric vortex simulation to calculating the aerodynamic characteristics of bodies of revolution at high angles of attack [AD-A263879] p 876 N93-29919

XIAO, SHUNDA

Nonlinear multi-point modelling and parameter estimation of the DO 28 research aircraft p 41 A93-12727

XIAO, YING-BEN

The investigation on vibration characteristics of all-movable stabilizer of an aircraft p 41 A93-11821

XIAO, Z.

The three-dimensional boundary layer flow due to a rotor-tip vortex [AIAA PAPER 93-3081] p 1060 A93-48255

XIAOQING, ZHENG

Solution of Euler equations for forebody-inlet ensemble of aircraft at high angle of attack [AD-A263905] p 876 N93-29862

XIE, M.

Time-variant analysis of rotorcraft systems dynamics - An exploitation of vector processors p 416 A93-23512

XIE, MINGJUN

Flexible rotorcraft system dynamics with time-variant contact conditions p 340 N93-19034

XIN, JILING

The effects of end-bend regulations of compressor blade on the outlet flow field [ISABE 93-7033] p 1185 A93-54009

XIN, XIAOWEN

On engine parameter estimation with flight test data p 1107 A93-48520

XING, BIN

Improving anti-fatigue optimum design through AI-search strategy p 208 A93-15342

XING, DING-DING

An improved multiple line-vortex method for simulation of separated vortices of slender wings p 1236 A93-55412

XING, HONG-HONG

Development of laser conducting landing system p 150 A93-14320

XING, TU

The application of concentric vortex simulation to calculating the aerodynamic characteristics of bodies of revolution at high angles of attack [AD-A263879] p 876 N93-29919

XING, YUSHAN

The effect of outboard leading-edge bluntness of double-delta wing on its aerodynamic characteristics p 1230 A93-54589

XING, ZONGWEN

Solution of Euler equations for complex forebody-inlet combinations p 680 A93-33730

XIONG, H. L.

A new method to study the forming process of complicated sheetmetal aero-parts p 204 A93-14363

XIONG, JUN-JIANG

The crack initiation approach for durability analysis p 1259 A93-55585

XIONG, YAN

Analysis and correction of ionospheric time delay for differential GPS p 498 A93-24028

XU, C.

Separation control and lift enhancement on airfoil using unsteady excitations p 118 A93-14305

XU, CHENG

Effects of external excitation on the leading-edge separation flowfield p 1071 A93-49198

A preliminary investigation of the control of separated flow by means of excitation p 1182 A93-53859

XU, GENFA

A theoretical study on the ETHYLENE system - A fuzzy diagnostic expert system for large rotating machinery p 846 A93-36327

XU, J. Z.

Three-dimensional flow calculations in turbomachinery using the stream function formulation p 11 A93-12453

An investigation on the artificial viscosity in the transonic stream function formulation [ASME PAPER 92-GT-49] p 246 A93-19302

A three-dimensional numerical method for turbomachinery blading [ASME PAPER 92-GT-291] p 254 A93-19482

XU, LI

Three-dimensional separated flow over a prolate spheroid p 1235 A93-55379

XU, LIJUN

Application of CAD system in geometric modeling for helicopter preliminary design p 153 A93-14203

XU, MIN

On experimental study of 3-D flow in self-correcting wind tunnel p 528 A93-24033

XU, MING

Application of vibration-and-flutter integration analysis system for a trainer p 226 A93-14311

XU, X.

Newton-like methods for fast high resolution simulation of hypersonic viscous flows p 437 A93-20740

XU, YANJI

Numerical computations of turbomachinery cascade turbulent flows with shocks by using multigrid scheme p 112 A93-14167

XU, ZHONG

Experimental investigation on effect of solid particles on blade pressure distribution in compressor cascade flow p 1066 A93-48513

Experimental investigation of effect of particles on blade pressure distribution in impulse cascade flow p 1236 A93-55398

XUE, DAVID Y.

Finite element nonlinear panel flutter with arbitrary temperatures in supersonic flow p 417 A93-23555

Effect of temperature on nonlinear two-dimensional panel flutter using finite elements p 1022 A93-45133

XUE, HONG X.

Stability of fully developed rotating stall [ASME PAPER 92-GT-57] p 348 A93-19307

XUE, Y.

Noise reduction for transonic blade-vortex interactions p 566 A93-29408

Transonic blade-vortex interactions - Noise reduction p 850 A93-37396

XUN, LINGQUING

Application of model reference adaptive control to speed control system in an aeroengine p 172 A93-14498

XUN, XIANXUE

YIDOYU and its application to aircraft design [AD-A259262] p 513 N93-20605

Y**YACAVONE, D. W.**

Helicopter crash survival at sea: United States Navy/Marine Corps experience 1977-1990 p 493 N93-19687

YACAVONE, DAVID W.

Trans-cockpit authority gradient in Navy/Marine aircraft mishaps p 146 N93-15016

YAGER, THOMAS J.

Braking, steering, and wear performance of radial-belted and bias-ply aircraft tires [SAE PAPER 921036] p 158 A93-14656

YAJIMA, N.

The improvement of the static launch method in Japan p 26 A93-11364

Trans-oceanic balloon flight over east China sea p 27 A93-11372

Polar Patrol Balloon Experiment in Antarctica

p 27 A93-11373

YAKALI, HUSEYIN H.

A vision-based method for autonomous landing p 1190 A93-53172

YAKIMENKO, O. A.

Semi-full-scale dynamic simulation complex on the basis of centrifuge [AIAA PAPER 93-3577] p 1208 A93-52673

YAKIMOV, A. N.

Increasing the reliability of an air traffic control radio system p 882 A93-43110

YAKOVENKO, B. V.

General concepts related to the determination of the individual flight performance characteristics of aircraft for establishing fuel consumption standards and optimal flight regimes p 996 A93-45673

YAKOVLEV, A. I.

Hybrid complex of the aircraft intellectualized control systems simulation at the stage of their research projecting [AIAA PAPER 93-3559] p 1222 A93-52660

YAMADA, EITARO

Adaptive grid generation using optimal control theory p 770 A93-38187

YAMAGAMI, T.

The improvement of the static launch method in Japan p 26 A93-11364

Trans-oceanic balloon flight over east China sea p 27 A93-11372

Polar Patrol Balloon Experiment in Antarctica p 27 A93-11373

YAMAGUCHI, MAKOTO

Generalized guidance law for collision courses p 727 A93-34533

YAMAGUCHI, NOBUYUKI

Lift enhancement of ground-effect wing. I - Results of screening tests of various concepts p 271 A93-21737

Lift enhancement of ground-effect wing. II - Experimental investigation of the power augmented ram wing in ground effect through the wind tunnel p 271 A93-21738

Microchannel plate modal gain variations with temperature p 477 A93-27445

Performance improvement by forward-skewed blading of axial fan moving blades [ISABE 93-7055] p 1185 A93-54031

YAMAGUCHI, TAKEHIITO

The coherent structure in a corner turbulent boundary layer p 548 A93-28575

YAMAGUCHI, YUTAKA

Preliminary assessment of tunnel wall interference in the NDA cryogenic wind tunnel [AIAA PAPER 93-0421] p 285 A93-23340

YAMALEEV, N. K.

Application of the small parameter method to the problem of three-dimensional flow of a viscous gas past bodies p 1178 A93-53314

YAMAMOTO, A.

Effects of wake interaction of two turbine cascades on secondary/tip-leakage flows and losses [ISABE 93-7058] p 1185 A93-54034

Experimental analysis of turbine rotor flow at design and off-design conditions [ISABE 93-7092] p 1186 A93-54068

YAMAMOTO, K.

Navier-Stokes computation of the three dimensional flow fields through a transonic fan blade [ISABE 93-7030] p 1184 A93-54006

YAMAMOTO, KAZUOMI

Computation of internal flows using unstructured triangular meshes p 299 N93-19276

A numerical investigation for supersonic inlet p 303 N93-19315

YAMAMOTO, KYOJI

A flat plate wing standing on a wall covered with a thick boundary layer. II - Wing characteristics under the effects of side wall boundary layer and wing tip vortex p 125 A93-15446

YAMAMOTO, MASAHIKO

Evaluation of 2D scramjet nozzle performance p 52 A93-11209

Off-design performance of scramjet nozzles [ISABE 93-7108] p 1203 A93-54084

YAMAMOTO, S.

Higher-order-accurate upwind schemes for solving the compressible Euler and Navier-Stokes equations p 863 A93-42441

YAMAMOTO, SATORU

A fourth-order MUSCL finite-difference scheme for solving the unsteady compressible Euler equations p 1086 A93-51121

Numerical simulations of supersonic flow by a fourth-order compact MUSCL TVD scheme p 302 N93-19308

YAMAMOTO, TETSUYA

Repair materials and processes for the MD-11 Composite Tailcone p 1216 A93-53452

YAMAMOTO, YUKIMITSU

Numerical calculation of hypersonic non-equilibrium flow around OREX p 301 N93-19296

Numerical simulation of hypersonic flow around H-2 Orbiting Plane (HOPE), part 3 p 301 N93-19297

YAMANAKA, KOJI

Adaptive quadratic stabilization control with application to flight controller design [AIAA PAPER 93-3847] p 1133 A93-51434

YAMANAKA, KOJI

Numerical study on the interaction of supersonic flow past a wedge and free jet p 479 A93-28574

YAMANAKA, TATSUO

Overview of Japanese aerospace plane [AIAA PAPER 92-5005] p 384 A93-22282

YAMANE, HIDEAKI

Design of limit-tracking systems incorporating a turbofan engine with constant disturbances [ISABE 93-7090] p 1203 A93-54066

YAMANE, R.

Oscillations of circular shock waves with upstream disturbance p 1023 A93-45463

YAMANE, RYUICHIRO

Oscillation of circular shock waves with upstream nonuniformity p 208 A93-15496

YAMANE, T.

Transonic discharge flows around diffuser vanes from a centrifugal impeller [ISABE 93-7053] p 1185 A93-54029

YAMANE, YOSHIYUKI

Two-dimensional and three-dimensional mixing flow structures with injected through slotted nozzle and circular nozzle into supersonic flows [ISABE 93-7117] p 1221 A93-54092

YAMAOKA, IKUO

Application of functionally gradient materials to scramjet engines [ISABE 93-7063] p 1200 A93-54039

YAMAOKA, YUKIO

Preliminary design of experimental sub-scale scramjet engine [AAS PAPER 91-639] p 1247 A93-55816

YAMASAKI, NOBUHIKO

Experimental study on the unsteady aerodynamic response of a three dimensional cascade with oscillating blades p 242 A93-18499

Study of mixing flow field of a jet in a supersonic cross flow. I - Experimental facilities and preliminary experiments p 857 A93-40430

Numerical simulation of supersonic flows with chemical reactions p 959 A93-45325

YAMASHITA, NORIO

CTS for a low speed wind tunnel p 1251 A93-56278

YAMATO, HIROYUKI

Limit cycle in the longitudinal motion of the USB STOL ASKA - Control system functional mockup and actual aircraft [SAE PAPER 921040] p 185 A93-14660

YAMAUCHI, GLORIA K.

Effects of ingested atmospheric turbulence on measured tail rotor acoustics p 849 A93-35964

YAMAUCHI, MASAFUMI

Numerical investigation of supersonic flows around a spiked blunt-body [AIAA PAPER 93-0887] p 471 A93-24947

YAMAWAKI, S.

Heat transfer in serpentine flow passages with rotation [ASME PAPER 92-GT-190] p 403 A93-19415

A new cooling system for ultra high temperature turbines [ISABE 93-7073] p 1201 A93-54049

YAN, B.

Fluid flows around cascades p 479 A93-28518

YAN, LITANG

Dynamic characteristics of two new vibration modes of the disk-shell shaped gear p 204 A93-14484

The effectiveness of porous squeeze film dampers for suppressing nonsynchronous motions p 545 A93-27316

YAN, MING

A numerical method of unsteady separating flow over delta wings p 681 A93-33746

YAN, W. M.

Numerical study of mixed convection between two corotating symmetrically heated disks p 416 A93-23491

YAN, YUNJU

Vibration characteristics of mistuned bladed disk p 1108 A93-49190

YANAGI, R.

Conceptual design of turbo-accelerator for HST combined cycle engine
[ASME PAPER 92-GT-253] p 353 A93-19462

Conceptual design study on combined-cycle engine for hypersonic transport
[ISABE 93-7018] p 1195 A93-53994

Research and development of a turbo-accelerator for super/hypersonic transport
[ISABE 93-7066] p 1200 A93-54042

YANAGI, RYOJI

Experimental study of mixed compression air-intake for hypersonic airbreathing engines
[ASME PAPER 92-GT-349] p 355 A93-19519

Effects of boundary layer bleed on swept-shock/boundary layer interaction
[AIAA PAPER 93-2989] p 1052 A93-48182

An experimental study of supersonic air-intake with 5-shock system at Mach 3
[AIAA PAPER 93-2305] p 1082 A93-50089

A study on Mach 3 two-dimensional mixed compression air-intakes
[ISABE 93-7106] p 1188 A93-54082

YANAGIHARA, MASAOKI

Simulation analysis of a cable-mount system used for dynamic wind tunnel tests
[NAL-TR-1127] p 68 N93-12359

Accuracy improvement of linear estimated motion using differential type sensors
[NAL-TR-1135] p 91 N93-12365

YANAGIZAWA, MITSUNORI

Calculations of aerodynamic forces on a wing with thrust using BEM
p 300 N93-19286

YANG, CHUN

Sequential smoothing and filtering for maneuvering target tracking
p 440 A93-22978

YANG, D. Y.

Variant bi-conjugate gradient methods for the compressible Navier-Stokes solver with a two-equation model of turbulence
[AIAA PAPER 93-3316] p 951 A93-45012

YANG, DAVID

A formalization and implementation of topological visual navigation in two dimensions
p 435 A93-19101

YANG, ERIC

MM-122: High speed civil transport
[NASA-CR-192011] p 334 N93-17974

YANG, GUO-ZHU

Optimization of oleo-pneumatic shock absorber of aircraft
p 1243 A93-55415

YANG, GUOCAI

The development of swirl five-hole probe
p 987 A93-47341

YANG, H.

BUA inertial terrain-aided navigation (BITAN) algorithm
p 149 A93-14235

YANG, H. Q.

Dynamic stall on a three-dimensional rectangular wing
[AIAA PAPER 93-0637] p 463 A93-24753

Pressure-based high-order TVD methodology for dynamic stall simulation
[AIAA PAPER 93-0680] p 466 A93-24788

Three-dimensional unsteady separating flows around an oscillatory forward-swept wing
[AIAA PAPER 93-2976] p 1050 A93-48170

YANG, HENRY T. Y.

Spatial adaptation procedures on tetrahedral meshes for unsteady aerodynamic flow calculations
[AIAA PAPER 93-0670] p 269 A93-21116

Supersonic flutter analysis of composite plates and shells
p 837 A93-39419

Three-dimensional time-marching aeroelastic analyses using an unstructured-grid Euler method
p 1100 A93-49012

YANG, J.

Physics of forced unsteady flow for a NACA 0015 airfoil undergoing constant-rate pitch-up motion
p 478 A93-27922

YANG, J. Y.

Numerical experiments with nonoscillatory schemes using Eulerian and new Lagrangian formulations
p 862 A93-42432

Computation of shock diffraction in external and internal flows
p 1024 A93-45537

A high-order streamline Godunov scheme for steady hypersonic equilibrium flows
[AIAA PAPER 93-2997] p 1053 A93-48187

YANG, JINGSONG

The experimental investigation of combination effect by using injection effect of aeroengine jet exhaust
p 898 A93-41742

YANG, JOSEPH

Applications of shock-induced mixing to supersonic combustion
p 735 A93-35618

YANG, LIFA

On orthogonal search method of flutter analysis
p 208 A93-15402

YANG, LIXIN

An experimental investigation of hydrogen-fueled supersonic combustor
p 53 A93-12733

YANG, LIXING

Effects of vitiated air on the results of ground tests of scramjet combustor
p 173 A93-16234

YANG, M. L.

FUM - An efficient MmB solver for steady inviscid flows
p 862 A93-42431

YANG, MAOZHAO

One type of automatically adjusted difference scheme with artificial viscosity to calculate ablated exterior shapes
[AD-A254108] p 19 N93-10856

YANG, QING-XIONG

Improving anti-fatigue optimum design through AI-search strategy
p 208 A93-15342

YANG, S. L.

Numerical simulation of a low-emission gas turbine combustor using KIVA-II
p 170 A93-14077

Numerical analysis of the flow fields in a RQL gas turbine combustor
[DE92-017509] p 89 N93-11767

A preliminary study of the effect of equivalence ratio on a low emissions gas turbine combustor using KIVA-2
[DE92-018618] p 215 N93-13321

A three-dimensional algebraic grid generation scheme for gas turbine combustors with inclined slots
[NASA-CR-191095] p 746 N93-24759

YANG, S. Y.

Locally implicit total variation diminishing schemes on mixed quadrilateral-triangular meshes
p 1235 A93-55356

YANG, T. H.

The turbulence and mixing characteristics of the complex flow in a simulated augmentor
p 1123 A93-51642

YANG, VIGOR

Some issues concerning active control of combustion instability in a ramjet
[AIAA PAPER 93-0116] p 360 A93-22566

YANG, W.-J.

Rotating machinery - Transport phenomena; Proceedings of the 3rd International Symposium on Transport Phenomena and Dynamics of Rotating Machinery (ISROMAC-3), Honolulu, HI, Apr. 1-4, 1990
[ISBN 1-56032-147-4] p 1256 A93-54626

Rotating machinery - Dynamics; Proceedings of the 3rd International Symposium on Transport Phenomena and Dynamics of Rotating Machinery (ISROMAC-3), Honolulu, HI, Apr. 1-4, 1990
[ISBN 1-56032-147-4] p 1257 A93-54651

Local heat transfer distribution in a rotating serpentine rib-roughened flow passage
p 1259 A93-55459

YANG, WEI-LI

Numerical simulation of a shock wave/turbulent boundary layer interaction in a duct
[AIAA PAPER 93-3127] p 1063 A93-48293

YANG, WEN-JEI

Heat transfer in serpentine flow passages with rotation
[ASME PAPER 92-GT-190] p 403 A93-19415

YANG, Y. J.

Surface emitting lasers for avionics applications
p 1259 A93-55756

YANG, Y. L.

Aerodynamic design of turbomachinery blading in three-dimensional flow - An application to radial inflow turbines
[ASME PAPER 92-GT-74] p 248 A93-19324

YANG, YAN

Internation aircraft operator information system
[DOT/FAA/CT-93/4] p 949 N93-32232

YANG, YI-REN

Subharmonic bifurcation analysis of wing with store flutter
p 78 A93-12098

YANG, YIREN

Investigation of subharmonic response of limit cycle flutter of wing-store system
p 800 A93-36339

YANG, Z. J.

Lifting forces acting on magnets placed above a superconducting plane
p 79 A93-12332

YANG, ZHENSHEN

Euler solution for wing-body combination at supersonic speeds
p 680 A93-33722

YANG, ZHI-CHUN

Transition of flutter mode of two-dimensional wing with external store
p 41 A93-11818

An investigation of mode shift flutter suppression scheme for empennages
p 182 A93-14268

YANG, ZHICHUN

Effects of pylon yaw and lateral stiffness on the flutter of a delta wing with external store
p 800 A93-36330

YANISHEVSKY, MARKO

Material characterization and fractographic examination of Ti-17 fatigue crack growth specimens for SMP SC33
p 1004 N93-31744

YANSOUNI, B.

Calling the right shots in aircraft maintenance with artificial intelligence
p 238 A93-18763

YAO, CHUNG-SHENG

Reynolds number influences in aeronautics
[NASA-TM-107730] p 889 N93-31732

YAO, HONG

A fuzzy dynamic analysis method for aeromaintenance system
p 225 A93-14177

YAO, HUA

An investigation of real-time diagnostic technique on aeroengine
p 174 A93-16844

Simplified mathematical model and digital simulation of aeroengine
p 1106 A93-48511

YAO, Q. H.

Researches on sonic fatigue of the air-inlet duct of XX aircraft
p 154 A93-14256

YAO, QI-HANG

Investigation of cabin noise reduction in the Y12
p 41 A93-11816

Investigation of cabin noise reduction in the Y12
p 506 A93-27371

YARGER, JILL M.

Pressure distribution for the wing of the YAV-8B airplane; with and without pylons
[NASA-TM-4429] p 136 N93-14451

YASTREBKOV, ANATOLY

Joining carbon composite fins to titanium heat pipes
[AD-A261970] p 825 N93-27667

YASTREBOV, I. L.

A set of IBM PC software for processing helicopter flight tests data to determine the flight performance characteristics
p 1037 A93-45661

YASU, SHOHACHI

Evaluation of 2D scramjet nozzle performance
p 52 A93-11209

YASU, SHOUHACHI

Validation studies of scramjet nozzle performance
p 1109 A93-49616

YASUHARA, MICHIRU

Evaluation of an RNG-based algebraic turbulence model
p 863 A93-42436

Transonic flow calculation around NACA-0012
p 302 N93-19301

YATES, D. E.

Low speed test results of subsonic, turbofan scarf inlets
[AIAA PAPER 93-2301] p 1082 A93-50086

High speed test results of subsonic, turbofan scarf inlets
[AIAA PAPER 93-2302] p 1082 A93-50087

YATES, D. H.

Corrosion resistance of Inconel Alloy 617 in simulated gas turbine environments
[ASME PAPER 92-GT-142] p 388 A93-19374

YATES, LESLIE A.

Nonlinear aerodynamic parameter estimation and model structure identification
[AIAA PAPER 92-4502] p 15 A93-13308

YAVNAI, A.

Information-based criteria of terrain navigability. Part 1: Data-base analysis
p 793 N93-27178

YAZAWA, KENJI

HUD Guidance for the ASKA Experimental STOL Aircraft using Radar Position Information
[SAE PAPER 92-1041] p 150 A93-14661

YAZDI, RENEE ANNA

High-altitude reconnaissance aircraft
p 894 N93-29713

YE, DAJUN

Investigation of the characteristics of 3-dimensional separated flow in an annular compressor blade row with large angles of attack
p 259 A93-20116

YE, TIAN-QI

Contact analysis for riveted and bolted joints of composite laminates
p 204 A93-14384

YE, ZHENRU

Superresolution radar imaging with linear prediction data extrapolation
p 342 A93-20851

Studies of superresolution range-Doppler imaging
p 928 A93-43344

YEDAVALLI, R. K.

Control design for robust eigenstructure assignment in linear uncertain systems
p 97 A93-13241

YEE, D.

Stability of the vapour phase in a rotating two-phase fluid system subjected to different gravitational intensities
p 926 A93-41714

YEH, C. L.

Swirling flows in a contoured-wall combustion chamber
[AIAA PAPER 93-1765] p 1073 A93-49661

- YEH, DUN-YANN**
Transonic flutter suppression using active acoustic excitations
[AIAA PAPER 93-3285] p 969 A93-46841
- YEH, F. C.**
Heat transfer in rotating serpentine passages with trips skewed to the flow
[ASME PAPER 92-GT-191] p 403 A93-19416
- YEH, FREDERICK C.**
High Reynolds number and turbulence effects on aerodynamics and heat transfer in a turbine cascade
[AIAA PAPER 93-2252] p 1155 A93-50050
High Reynolds number and turbulence effects on aerodynamics and heat transfer in a turbine cascade
[NASA-TM-106187] p 930 N93-29157
- YEH, HARRY C.**
Improved silicon nitride for advanced heat engines
[NASA-CR-182193] p 917 N93-29451
- YEH, YEU-PIN**
Numerical study of an axisymmetric turbulent jet-impingement flow
[AIAA PAPER 93-0652] p 543 A93-25545
- YEN, GUAN-WEI**
Kinematic domain decomposition for boundary-motion-induced flow simulations
p 1028 A93-46811
Dynamic-overlapped-grid simulation of aerodynamically determined relative motion
[AIAA PAPER 93-3018] p 1055 A93-48205
- YEN, RUEY-HOR**
Effects of side-inlet angle in a three-dimensional side-dump combustor
p 1109 A93-49610
- YENNI, KENNETH R.**
Design and conduct of a windshear detection flight experiment
[AIAA PAPER 92-4092] p 38 A93-11268
- YEO, URM**
A second-generation high speed civil transport: Stingray
[NASA-CR-192022] p 336 N93-18059
- YEUN, J. J.**
A parametric study of bleed in shock boundary layer interactions
[AIAA PAPER 93-0294] p 280 A93-22694
An investigation of shock wave turbulent boundary layer interaction with bleed through slanted slots
[AIAA PAPER 93-2992] p 1052 A93-48184
An investigation of shock wave turbulent boundary layer interaction with bleed through normal and slanted slots
[AIAA PAPER 93-2155] p 1079 A93-49971
Particle dynamics simulations in inlet separator with an experimentally based bounce model
[AIAA PAPER 93-2156] p 1115 A93-49972
- YEUNG, W. W. H.**
A wake singularity potential flow model for airfoils experiencing trailing-edge stall
p 1067 A93-48544
- YI, J.**
Vibration monitoring and fault diagnosis of inflight aircraft engines
p 170 A93-14176
- YI, JINGHAI**
Experimental investigation on effect of solid particles on blade pressure distribution in compressor cascade flow
p 1066 A93-48513
Experimental investigation of effect of particles on blade pressure distribution in impulse cascade flow
p 1236 A93-55398
- YIDONG, G.**
Review and prospect of Chinese scientific balloon activities
p 1 A93-11368
- YIN, JIANPING**
Cabin noise source-path identification for AD-200 ultralight aircraft
p 444 A93-19138
- YIN, JING**
Slicing model for foreign soft-body objects impacting on blade rows
p 28 A93-12372
Effect of bird impact load types on blade response
p 174 A93-16846
- YIN, JUN**
Studies of superresolution range-Doppler imaging
p 928 A93-43344
- YING, SUSAN X.**
Hybrid grid approach to study dynamic stall
p 122 A93-14548
- YING, WENJIANG**
Study on dynamic characteristics of heat exchanger
p 924 A93-40492
- YIP, B.**
Low-frequency combustion instability mechanisms in a side-dump combustor
p 1247 A93-55220
Combustion instabilities in a side-dump model ramjet combustor
p 362 N93-17613
- YIP, L. P.**
Leading-edge transition and relaminarization phenomena on a subsonic high-lift system
[AIAA PAPER 93-3140] p 959 A93-45154
- Flow prediction over a transport multi-element high-lift system and comparison with flight measurements
p 785 N93-27448
- YIP, LONG P.**
Subsonic high-lift flight research on the NASA Transport System Research Vehicle (TSRV)
[AIAA PAPER 92-4103] p 38 A93-11275
In-flight surface-flow measurements on a subsonic transport high-lift flap system
p 166 A93-14327
Two-dimensional computational analysis of a transport high-lift system and a comparison with flight-test results
[AIAA PAPER 93-3533] p 1072 A93-49517
Stall departure resistance enhancer
[NASA-CASE-LAR-14221-1] p 344 N93-19023
Reynolds number influences in aeronautics
[NASA-TM-107730] p 989 N93-31732
- YOCUM, ADAM M.**
Separated flow in a low speed two-dimensional cascade. I - Flow visualization and time-mean velocity measurements
[ASME PAPER 92-GT-356] p 257 A93-19521
Separated flow in a low speed two-dimensional cascade. II - Cascade performance
[ASME PAPER 92-GT-357] p 257 A93-19522
- YODER, DENNIS A.**
Brush seal leakage performance with gaseous working fluids at static and low rotor speed conditions
[ASME PAPER 92-GT-304] p 405 A93-19494
- YOERKIE, CHARLES M.**
Development and validation of 'quiet tail rotor' technology
p 567 A93-29416
- YOKOTA, KAZUHIKO**
Numerical and experimental study on two- and three-dimensional supersonic flow field with hydrogen injection
[ISABE 93-7118] p 1188 A93-54093
Numerical study on transverse hydrogen injection into a supersonic flowfield
p 302 N93-19311
- YONEZAWA, SATOSHI**
Simultaneous structure/control design optimization of a wing structure with a gust load alleviation system
p 525 A93-28616
- YONG, W.**
Longitudinal closed-loop pilot/vehicle analysis of DFBW aircraft during approach and landing
p 1206 A93-54277
- YOO, KYUNG M.**
An interactive numerical procedure for rotor aeroelastic stability analysis using elastic lifting surface
p 155 A93-14313
Unsteady wake effect on rotor vibratory airloadings
p 509 A93-29439
- YOO, S.**
A zonal CFD method for three-dimensional wing simulations
[AIAA PAPER 93-3433] p 977 A93-47225
- YOON, BOK-HYUN**
Computational analysis of hypersonic flows past elliptic-cone waveriders
[NASA-CR-191304] p 138 N93-14767
- YOON, S.**
Multi-zonal Navier-Stokes code with the LU-SGS scheme
[AIAA PAPER 93-2965] p 1148 A93-48159
- YOON, SEOKKWAN**
Implicit Navier-Stokes solver for three-dimensional compressible flows
p 122 A93-14546
Multigrid convergence of an implicit symmetric relaxation scheme
[AIAA PAPER 93-3357] p 954 A93-45051
Calculation of real-gas effects on airfoil aerodynamic characteristics
p 1229 A93-54477
- YOON, W. S.**
Effects of reacting flows with turbulence and shock waves on efficiency of scramjet combustors
p 69 N93-11133
Turbulence interacting with chemical kinetics in airbreathing combustion of ducted rockets
p 734 N93-26012
- YOROZU, MASAHIRO**
Preliminary assessment of tunnel wall interference in the NDA cryogenic wind tunnel
[AIAA PAPER 93-0421] p 285 A93-23340
- YOSHIDA, HIDENORI**
Three-dimensional viscous flow analysis of compressor cascade channels
p 1181 A93-53837
- YOSHIDA, KENJI**
Improving the lift to drag characteristics of low boom configuration
[AIAA PAPER 92-4218] p 16 A93-13380
- YOSHIDA, MASAHIRO**
The language processor system for the Numerical Wind Tunnel
p 383 N93-19291
- YOSHIDA, T.**
A new cooling system for ultra high temperature turbines
[ISABE 93-7073] p 1201 A93-54049
- YOSHINO, FUMIO**
Turbulent structure in a vortex wake shed from an inclined circular cylinder
p 125 A93-15443
- YOSHIOKA, Y.**
Evaluation of metallurgical degradation on gas turbine components
p 915 A93-40804
Crack simulation and life assessment of gas turbine nozzles
p 915 A93-40805
- YOSHIOKA, YOMEI**
Life assessment of gas turbine bucket coating based on degradation analysis
p 533 A93-24464
- YOSHIOKA, YOSHIRO**
Numerical Wind Tunnel hardware
p 383 N93-19289
- YOSIDUKA, TAKESI**
Design of an adaptive flight control system with uncertainties
p 95 A93-12322
- YOU, LIXIN**
Recent advances in jet simulation techniques for flight vehicles
p 66 A93-12656
Simulation for hot jet by cryogenic wind tunnels
p 730 A93-33750
- YOUNG, DAVID P.**
Using a full potential solver for propulsion system exhaust simulation
p 689 A93-34487
- YOUNG, EVELYN C.**
Sound exposure spectrum levels of sonic booms
p 564 A93-28489
- YOUNG, JIEH-SHAN**
Refined H-infinity controller design for rotorcraft flight control
p 368 A93-22882
- YOUNG, JON**
Modern propeller systems for advanced turboprop aircraft
[AIAA PAPER 93-1846] p 1111 A93-49727
- YOUNG, ROBERT W.**
Sonic boom spectra of Space Shuttle Columbia landing 10 December 1990
p 533 A93-28488
- YOUNG, STEVEN D.**
A performance assessment of a byzantine resilient fault-tolerant computer
[AIAA PAPER 89-3064] p 938 A93-41296
- YOUNG, T. H.**
Stability of fluttered panels subjected to in-plane harmonic forces
p 1151 A93-49017
- YOUNGBERG, J.**
Synchronous X-ray Sinography for nondestructive imaging of turbine engines under load
[AIAA PAPER 93-1819] p 1153 A93-49707
- YOUSSEF, HUSSEIN M.**
Estimation of aerodynamic coefficients using neural networks
[AIAA PAPER 93-3639] p 1165 A93-48324
Multiple radial basis function networks in modeling and control
[AIAA PAPER 93-3731] p 1170 A93-51330
Fault detection, isolation, and reconfiguration for aircraft using neural networks
[AIAA PAPER 93-3870] p 1135 A93-51456
- YOUTSEY, TIMOTHY L.**
Rapid fabrication of flight worthy composite parts
p 209 A93-15792
- YU, C.**
Sonic fatigue analysis of an aircraft wing flap by the matrix difference equation method
p 399 A93-19208
- YU, F. M.**
Holographic interferometric investigation of shock wave interaction with a ramp
p 271 A93-21921
- YU, H. T.**
Development of a unified airport pavement analysis and design system
p 380 N93-16317
- YU, K.**
Periodic chemical energy release for active combustion control
[ISABE 93-7043] p 1198 A93-54019
- YU, KEN**
Passive control of coherent vortices in compressible mixing layers
[AIAA PAPER 93-3262] p 968 A93-46828
- YU, N. J.**
Navier-Stokes calculations for transport wing-body configurations with nacelles and struts
[AIAA PAPER 93-2945] p 1047 A93-48142
- YU, P. J.**
BUAA inertial terrain-aided navigation (BITAN) algorithm
p 149 A93-14235
- YU, QIN-FANG**
Interconversion of two kinds of methods for cabin leakage test
p 1192 A93-53874
- YU, SHENG-TAO**
Convenient method to convert two-dimensional CFD codes into axisymmetric ones
p 689 A93-34499

YU, SHOUZHI

Multiple solutions of the transonic perturbation equation p 987 A93-47331

YU, WENLONG

The analysis of viscous wakes noise in axial flow compressor p 759 A93-33710

YU, X. T.

Separation control and lift enhancement on airfoil using unsteady excitations p 118 A93-14305

YU, YIN

Aeroelastic analysis of composite wing with control surface p 157 A93-14386

YU, YUNG H.

The use of interferometry in the study of rotorcraft aerodynamics p 407 A93-19914
Shock waves and the Ffowcs Williams-Hawkins equation p 480 A93-29411

YUAN, J. P.

Investigation of precise approach and landing of civil aircraft using integrated system based on GPS p 180 A93-14159

YUAN, JIANPING

Analysis and correction of ionospheric time delay for differential GPS p 498 A93-24028

YUAN, K.

Development of a structural optimization capability for the aeroelastic tailoring of composite rotor blades with straight and swept tips [AIAA PAPER 92-4779] p 326 A93-20370

YUAN, KUO-AN

A new sensitivity analysis for structural optimization of composite rotor blades [AIAA PAPER 93-1644] p 742 A93-34169
Aeroelastic behavior of composite rotor blades with swept tips p 827 A93-35978

YUAN, M. J.

Development and industrial application of the 'all-over-controlled vortex distribution method' for designing radial and mixed flow impellers [ASME PAPER 92-GT-262] p 405 A93-19466

YUAN, MINJIAN

Experimental research for the discharge flow of a centrifugal impeller and the flowfield in the vaneless diffuser p 11 A93-12454

YUAN, PIN-JAR

Exact closed-form solution of generalized proportional navigation p 1130 A93-49598

YUAN, XIANGDONG

Dynamic analysis of a gear drive system in aeroengine p 1149 A93-48514

YUAN, XIU-GAN

The optimum design of air cycle refrigeration system with high pressure water separation p 202 A93-14180

YUASA, SABURO

Combustion performance of a hydrogen-fueled small combustor for a micro gas turbine p 389 A93-21731

YUCEIL, B.

A preliminary investigation of the Helmholtz resonator concept for heat flux reduction [AIAA PAPER 93-2742] p 963 A93-46493

YUGE, T.

Active control of vortex breakdown by a spinning wave generator [ISABE 93-7045] p 1219 A93-54021

YUHAS, VINCENT C.

Design and manufacture for producibility of carbon fiber/epoxy composite aircraft skins [SME PAPER EM93-104] p 1043 A93-51732

YUN, QI-LIN

Measurement of turbulent boundary layer in transonic flow p 1236 A93-55411

YUN, RUQUN

Investigation of flows in a controlled diffusion airfoil cascade passage p 1071 A93-49188

YURKANIN, DAVID J.

Micro-physical models for simulating realistic ice accretions [AIAA PAPER 93-0025] p 307 A93-20143

YURKOVICH, RUDY

Aeroelastic system identification of advanced technology aircraft through higher order signal processing p 525 A93-29297

Z

ZABINSKY, ZELDA

Multi-parameter optimization tool for low-cost commercial fuselage crown designs p 922 A93-30858

ZACCARIA, M.

Three-dimensional flow field in a turbine nozzle passage [AIAA PAPER 93-2556] p 1084 A93-50278
Penn State axial flow turbine facility: Performance and nozzle flow field p 1032 A93-31588

ZACHARIAS, GREG L.

Design for tactical situation awareness display [AD-A256194] p 170 A93-15235

ZAEHRING, G.

Axial flow compressors - Mechanical design trends [ISABE 93-7061] p 1199 A93-54037

ZAFFARONI, G.

Fatigue qualification of high thickness composite rotor components p 81 A93-13646

ZAGOLSKI, F.

Preliminary results of the ISM campaign - The Landes, South West France p 1161 A93-47553

ZAGRODNIK, JEFFREY P.

Nickel hydrogen batteries for terrestrial applications p 557 A93-26005

ZAGUZO, I. S.

An experimental study of a method for reducing the jet noise of bypass engines using mechanical flow mixers p 53 A93-12810

Identification of noise sources based on experimental amplitude-frequency noise characteristics of aircraft p 851 A93-39040

An acoustic suppressor for the jet noise of a turbojet engine p 1003 A93-47510

Correction of a method for calculating the noise levels of aircraft at control points during acoustic flight testing p 1102 A93-51758

ZAHNISER, M. S.

Stratospheric aircraft exhaust plume and wake chemistry studies [NASA-CR-189688] p 94 A93-12299

ZAITSEV, E. G.

Underexpanded boundary jet in a wake flow p 775 A93-39123

ZAITSEV, V.

Use of alternative fuels for aviation p 196 A93-14292

ZAITSEVA, A. N.

Protective properties of aviation oils p 735 A93-35299

ZAKALIUKIN, V. M.

Interaction of compression waves with an elastic spherical dome p 550 A93-29718

ZAKALYUKIN, V. M.

Statistical methods in flight vehicle control theory p 1165 A93-49306

ZAKARYAN, G. T.

Selection of the primary aircraft structure at the preliminary design stage p 891 A93-42371

ZAKHARENKO, M. N.

Nonstationary flow of a viscous incompressible fluid past an airfoil p 79 A93-12922

ZAKHAROV, A. G.

A study of the possibility of the parallel execution of a program for calculating the aerodynamic characteristics of flight vehicles using an improved panel method p 95 A93-10045

ZAKHAROV, D. V.

Selection of the turbofan engine size p 899 A93-42379

ZAKHAROV, V. D.

Flight efficiency theory p 812 A93-39202

ZAKHARY, A. S.

Blowout of turbulent disc/pilot stabilized jet diffusion flames [ISABE 93-7026] p 1213 A93-54002

ZAKOTENKO, S. N.

Intensification of flow mixing behind an oblique shock wave p 4 A93-10138

Calculation of three-dimensional turbulent jets propagating behind nozzles of rectangular cross section p 6 A93-10192

ZAKRAJSEK, J. J.

Modal analysis of multistage gear systems coupled with gearbox vibrations p 827 A93-36588

ZAKRZEWSKI, R. R.

Nonlinear time-series-based adaptive control applications p 97 A93-13230

ZALAMEDA, JOSEPH N.

Rapid detection and quantification of impact damage in composite structures p 547 A93-29798

ZALEWSKI, E.

The HYDICE instrument design and its application to planetary instruments p 842 A93-28766

ZAMAN, K. B. M. Q.

Estimation of unsteady lift on a pitching airfoil from wake velocity surveys [AIAA PAPER 93-0437] p 286 A93-23351

Streamwise vorticity generation and mixing enhancement in free jets by 'delta-tabs' [AIAA PAPER 93-3253] p 1180 A93-53592

Estimation of unsteady lift on a pitching airfoil from wake velocity surveys [NASA-TM-105947] p 138 A93-14791

Streamwise vorticity generation and mixing enhancement in free jets by delta-tabs [NASA-TM-106235] p 988 A93-31648

ZAMIAHIN, I. P.

Characteristics of friction and wear in flight vehicle engine components p 811 A93-39075

ZAMIAHIN, L. A.

Characteristics of friction and wear in flight vehicle engine components p 811 A93-39075

ZAMULA, G. N.

Methodology for studying the fracture of aircraft structures in static tests p 801 A93-36785

ZANDIEH, ALI

Boundary layer and pressure measurements on a cylinder with unsteady circulation control p 1177 A93-53207

ZANG, JUN

Dynamic analysis of annular cascade structures p 1259 A93-55586

ZANG, T. A.

Direct numerical simulation of laminar breakdown in high-speed, axisymmetric boundary layers p 8 A93-11527

ZANG, THOMAS A.

Secondary instability mechanisms in compressible axisymmetric boundary layers p 1070 A93-49009

The transition prediction toolkit: LST, SIT, PSE, DNS, and LES p 783 A93-27429

ZANIEWSKI, J.

State of the art of airport pavement analysis and design p 378 A93-16310

ZANIN, B. IU.

Acoustic control of flow separation on a straight and a yawed wing p 125 A93-15256

ZANIN, B. YU.

Calculation of the parameters of instability waves in the preseparation region p 1067 A93-48826

ZANNETTI, LUCA

Design of air intakes and nozzles for transonic rotational flows [ISABE 93-7102] p 1187 A93-54078

ZAREMBA, E. V.

Expanding the operation scope of aircraft through the use of air-cushion landing gear p 321 A93-18354

ZASOLOV, R. A.

Effect of the Reynolds number on the aerodynamic characteristics of a body of revolution over a wide range of angles of attack p 242 A93-18384

ZAVOSH, FRANK

Advanced electromagnetic methods for aerospace vehicles [NASA-CR-193468] p 936 A93-31036

ZBOINSKI, GRZEGORZ

Influence of modelling loading on stress distribution in turbomachinery blade fastening in case of FEM p 520 A93-27296

ZEDAN, M. F.

Unsteady effects of camber on the aerodynamic characteristics of a thin airfoil moving near the ground p 270 A93-21719

Numerical simulation of unsteady flow induced by a flat plate moving near ground p 1094 A93-52432

ZEDAN, MOHAMED

Numerical investigation of flow field in a turbine volute [AIAA PAPER 93-0155] p 542 A93-25505

ZEGHAL, KARIM

A reactive approach for distributed air traffic control [ONERA, TP NO. 1993-83] p 1190 A93-53603

CRAASH - A coordinated collision avoidance system [ONERA, TP NO. 1993-84] p 1191 A93-53604

ZEIGER, MATTHEW

Hermes CX-7: Air transport system design simulation [NASA-CR-192082] p 335 A93-18056

ZEILER, THOMAS A.

Aeroservoelasticity in HiSAIR [AIAA PAPER 92-4719] p 324 A93-20322

Aeroelastic character of a National Aerospace Plane demonstrator concept [AIAA PAPER 93-1314] p 732 A93-33890

Aerothermoelastic analysis of a NASP demonstrator model [AIAA PAPER 93-1366] p 733 A93-33933

A flutter investigation of all-moveable NASP-like wings at hypersonic speeds [AIAA PAPER 93-1315] p 769 A93-37427

ZEITOUN, D.

Reactive and dissipative hypersonic flow in a wind tunnel nozzle p 687 A93-34358

ZELENKA, RICHARD E.

Appraisal of digital terrain elevation data for low-altitude flight [NASA-TM-103896] p 35 A93-10745

Integration of radar altimeter, precision navigation, and digital terrain data for low-altitude flight [NASA-TM-103958] p 36 A93-12320

- ZELINSKII, S. E.**
The problem of avoiding aircraft collisions during group flights p 819 A93-39191
- ZELLNER, B.**
Integration of turbo-expander- and turbo-ramjet-engines in hypersonic vehicles [ASME PAPER 92-GT-204] p 353 A93-19428
- ZEMAN, OTTO**
A new model for super/hypersonic turbulent boundary layers [AIAA PAPER 93-0897] p 472 A93-24957
- ZEMILOV, V. V.**
Unsteady supersonic flow around a blunt body in thermal inhomogeneities in turbulent shock layer flows p 691 A93-35266
- ZEMSKAIA, A. S.**
Optimal conditions for flow turbulence reduction by a set of grids p 836 A93-39122
- ZEN, JUN**
Numerical solution of 3-D turbulent flows inside of new concept nozzles p 114 A93-14211
Digital simulation of transonic flow fields in a planar nozzle p 122 A93-14479
Calculation of pressure ratio at nozzle exit with shock p 122 A93-14480
- ZENG, MING**
Second generation low order panel method and its application for a case of nacelle p 1231 A93-54595
- ZENG, XIAOPING**
An engineering method with artificial intelligence characteristics used for structural layout of wings p 225 A93-14290
- ZENG, YUAN**
Study on aircraft microwave remote sensing of sea-water surface salinity p 92 A93-12407
- ZEROUALI, ANGELA**
Transport processes in hypersonic flows p 7 A93-11302
- ZHA, G.-C.**
Numerical solutions of Euler equations by using a new flux vector splitting scheme p 1087 A93-51740
- ZHADIN, EVGENY A.**
Predicted aircraft effects on stratospheric ozone p 93 A93-11096
- ZHANG, BAOAN**
Elimination of overtemperature in turbojet p 172 A93-14481
- ZHANG, BING-XUAN**
Transonic area rule about lifting configurations p 1183 A93-53868
- ZHANG, BINGXUAN**
Second generation low order panel method and its application for a case of nacelle p 1231 A93-54595
- ZHANG, BODING**
How to consider simulation fidelity and validity for an engineering simulator [AIAA PAPER 93-3598] p 1209 A93-52688
- ZHANG, F. M.**
The employment of artificial intelligence for analyzing air accidents p 226 A93-14375
- ZHANG, GUOQING**
Viscous flow field prediction in axisymmetric passages p 204 A93-14478
- ZHANG, H.**
The hazard and alarm of windshear p 141 A93-14317
Periodic Euler and Navier-Stokes solutions about oscillating airfoils p 241 A93-17799
- ZHANG, H. M.**
An investigation of post stall transients and recoverability of axial compression systems [ISABE 93-7012] p 1184 A93-53988
- ZHANG, HAN-GUO**
Fault tolerant navigation for aircraft landing p 1191 A93-53866
- ZHANG, HONG**
A study on low level windshear hazard index p 1240 A93-55414
- ZHANG, HONG-YUE**
Fault tolerant navigation for aircraft landing p 1191 A93-53866
- ZHANG, HONGCAI**
A U-D factorization-based adaptive extended Kalman filter and its application to flight state estimation p 1169 A93-51198
- ZHANG, HUA**
Improvement of conical similarity rule in swept shock wave/boundary layer interaction [AIAA PAPER 93-2941] p 1046 A93-48139
The experimental evaluation of annular ejector system under concurrent mixing and diffusion p 1250 A93-54593
- ZHANG, HUI M.**
An investigation of post stall transients and recoverability of axial compression systems. I - A simplified method [ASME PAPER 92-GT-55] p 347 A93-19305
- An investigation of post stall transients and recoverability of axial compression systems. II - Numerical simulations [ASME PAPER 92-GT-56] p 347 A93-19306
- ZHANG, JIAN-HUA**
Integrated fire control simulation systems p 1192 A93-53876
- ZHANG, JIN**
The Aircraft/Propulsion Integrated Assessment System p 226 A93-14396
Dynamic analysis of annular cascade structures p 1259 A93-55586
- ZHANG, LIANGLIANG**
Pressure fluctuations on the surface of two circular cylinders in tandem arrangements at high Reynolds numbers p 679 A93-33718
- ZHANG, MINGHENG**
Numerical solution of 3-D turbulent flows inside of new concept nozzles p 114 A93-14211
- ZHANG, N.**
Local heat transfer distribution in a rotating serpentine rib-roughened flow passage p 1259 A93-55459
- ZHANG, NAIPING**
Ground effect on the take-off characteristics of sea-based aircraft p 679 A93-33706
- ZHANG, QI-QIAO**
Bird impact dynamic response analysis for aircraft arc windshield p 41 A93-11815
- ZHANG, QIANG**
Cabin noise source-path identification for AD-200 ultralight aircraft p 444 A93-19138
- ZHANG, QINAN**
A new method for resolving transonic nozzle flows using orthogonal stream-lines coordinate system p 1230 A93-54584
- ZHANG, QIWEI**
Wall-signature methods for high speed wind tunnel wall interference corrections p 375 A93-20803
- ZHANG, S. Y.**
Separation control and lift enhancement on airfoil using unsteady excitations p 118 A93-14305
- ZHANG, SEN-LIN**
Analysis of structural dynamic response for aircraft operating in the environment of nuclear explosion shock waves p 78 A93-11810
- ZHANG, SHI-YING**
A preliminary investigation of the control of separated flow by means of excitation p 1182 A93-53859
- ZHANG, SHIPING**
The effectiveness of porous squeeze film dampers for suppressing nonsynchronous motions p 545 A93-27316
- ZHANG, SHIYING**
Estimation of the maximum values of instantaneous distortion index DC sub theta p 266 A93-20806
Control of separation by dynamic air jets p 1066 A93-48504
Effects of external excitation on the leading-edge separation flowfield p 1071 A93-49198
- ZHANG, SHU-CHENG**
A time dependent method in finite volume for transonic diffuser turbulent flows p 476 A93-27368
- ZHANG, SHU-GUANG**
The influence of fighter agility on air combat effectiveness p 184 A93-14398
- ZHANG, X. Y.**
Researches on sonic fatigue of the air-inlet duct of XX aircraft p 154 A93-14256
- ZHANG, X.-G.**
Design of digital multiple model-following integrated flight/propulsion control systems p 183 A93-14371
- ZHANG, XIAOGU**
The influence of main design parameters on helicopter air resonance and its source of instability p 154 A93-14261
Investigation of the dynamic inflow's influence on rotor control derivatives p 266 A93-20802
Investigation of helicopter air resonance in hover by complex coordinates and mutual excitation analysis p 893 A93-43777
- ZHANG, XIN**
A Laser Doppler Anemometry study of a supersonic jet in a low speed cross-flow p 459 A93-23807
A study of single jet impingement ground effect lift loss [AIAA PAPER 93-0869] p 469 A93-24930
Flow and heat transfer in a turbulent boundary layer through skewed and pitched jets p 1151 A93-49007
- ZHANG, XIN-GUO**
Design of robust digital model-following flight control systems p 907 A93-42810
Design of reconfigurable digital multiple model-following flight control systems p 908 A93-42811
- ZHANG, Y. M.**
Influence of surface heat flux ratio on heat transfer augmentation in square channels with parallel, crossed, and V-shaped angled ribs p 201 A93-13981
- Influence of surface heating condition on local heat transfer in a rotating square channel with smooth walls and radial outward flow [ASME PAPER 92-GT-188] p 402 A93-19413
- ZHANG, YANGJUN**
Numerical simulation of unsteady flow in a transonic cascade p 1066 A93-48502
- ZHANG, YANQI**
A software for optimum design of an aircraft structure p 938 A93-40495
- ZHANG, YOUJIN**
A U-D factorization-based adaptive extended Kalman filter and its application to flight state estimation p 1169 A93-51198
- ZHANG, YUMING**
Heat transfer in a five-pass irregular channel with and without pin-fins p 1256 A93-54633
- ZHANG, ZHENG**
Effects of vitiated air on the results of ground tests of scramjet combustor p 173 A93-16294
- ZHANG, ZHI-LIN**
Bird impact dynamic response analysis for aircraft arc windshield p 41 A93-11815
- ZHANG, ZUGENG**
Vectoring jet effects on the flow and aerodynamic behaviors of fighter model p 1241 A93-54590
- ZHANY, TING**
A study of military aircraft and engine tactical/technical performance evaluation p 1242 A93-54596
- ZHAO, B. C.**
On the configuration buffet of a transport aircraft p 117 A93-14298
- ZHAO, CHANG-AN**
Measurement of turbulent boundary layer in transonic flow p 1236 A93-55411
- ZHAO, CONGZHONG**
The infrared measurement for the reentry-body-translation [AD-A263100] p 914 A93-29134
- ZHAO, JIANXING**
Prediction of the radiation characteristic of a helicopter exhaust jet p 172 A93-14494
A numerical study on the radiation characteristic of an elliptical exhaust jet p 174 A93-16236
- ZHAO, JINGYUN**
Calculation of pressure ratio at nozzle exit with shock p 122 A93-14480
- ZHAO, LING-CHENG**
Transition of flutter mode of two-dimensional wing with external store p 41 A93-11818
Effects of the pylon pitching stiffness on wing-store flutter p 41 A93-11820
Subharmonic bifurcation analysis of wing with store flutter p 78 A93-12098
- ZHAO, LINGCHENG**
Effects of pylon yaw and lateral stiffness on the flutter of a delta wing with external store p 800 A93-36330
Investigation of subharmonic response of limit cycle flutter of wing-store system p 800 A93-36339
- ZHAO, MECHUN**
Effect of blade leaning on the development of passage vortices and losses in the passage of turbine cascade with a great turning angle p 1236 A93-55397
- ZHAO, MEIDE**
A theoretical study on the ETHYLENE system - A fuzzy diagnostic expert system for large rotating machinery p 846 A93-36327
- ZHAO, QING-WEI**
Transonic area rule about lifting configurations p 1183 A93-53868
- ZHAO, XIAOLU**
A CAD computer system for centrifugal compressor impeller with transonic inflow p 259 A93-20118
- ZHAO, XINLI**
Application of SPEED in aviation industry p 225 A93-14178
- ZHAO, ZHENYAN**
Vectoring thrust and two-dimensional nozzle p 1247 A93-54863
- ZHAO, ZIYUAN**
An investigation of real-time diagnostic technique on aeroengine p 174 A93-16844
Simplified mathematical model and digital simulation of aeroengine p 1106 A93-48511
- ZHARKOVA, G. M.**
Dynamics of the behavior of nematic films in gasdynamic flows p 746 A93-35345
- ZHAROV, R. I.**
Monitoring the purity of the working fluids of aircraft hydraulic systems during service p 321 A93-18367
- ZHDANOV, V. L.**
An experimental investigation of base bleed effect on the wake turbulent structure behind a two-dimensional blunt model [MPIS-9/1991] p 139 A93-15131

ZHDANOV, V. P.

Development of a prototype of an expert system for the design of comprehensive scientific-technical development programs for civil aviation p 434 A93-18373

ZHELEZNOV, L. P.

An analytical-experimental method for studying the strength and stability of thin-walled structures p 1029 A93-47084

ZHELEZOV, A. I.

Selection of protective coatings for parts in a computer-aided design system p 746 A93-35290

ZHELTVOODOV, A. A.

Development of separation due to interaction between a shock wave and a turbulent boundary layer perturbed by rarefaction waves p 1233 A93-55019

ZHELTUKHIN, N. A.

Development of resonance perturbations in a supersonic jet p 1088 A93-51772

ZHEN, ZHANG

An experimental investigation of hydrogen-fueled supersonic combustor p 53 A93-12733

ZHENG, D.

Mechanisms and modelling of environment-dependent fatigue crack growth in a nickel based superalloy [AD-A253967] p 71 A93-10717

ZHENG, E.

Investigation of precise approach and landing of civil aircraft using integrated system based on GPS p 180 A93-14159

ZHENG, XIAOQING

Numerical computations of turbomachinery cascade turbulent flows with shocks by using multigrid scheme p 112 A93-14167

Numerical solution of 3-D turbulent flows inside of new concept nozzles p 114 A93-14211

Digital simulation of transonic flow fields in a planar nozzle p 122 A93-14479

Solution of Euler equations for complex forebody-inlet combinations p 680 A93-33730

Numerical solution of Navier-Stokes equations and k-omega turbulence model equations using a staggered upwind method p 1049 A93-48162

A staggered finite volume scheme for solving cascade flow with a two-equation model of turbulence [AIAA PAPER 93-1912] p 1076 A93-49779

ZHIDOV, N. I.

Operation of a cross-flow heat exchanger with partial recirculation of one of the coolants p 833 A93-39051

ZHIKHAREV, C. N.

Separation phenomenon in a hypersonic flow with strong wall cooling - Subcritical regime p 1189 A93-54266

ZHLUKTOV, S. V.

Comparison of gasdynamic models in hypersonic flow p 1179 A93-53315

ZHONG, X.

Hypersonic flutter of a curved shallow panel with aerodynamic heating [AIAA PAPER 93-1318] p 829 A93-37428

ZHONG, XIAOLIN

Application of high-order accurate essentially nonoscillatory schemes to two-dimensional compressible viscous flows p 470 A93-24940

Stabilization of the Burnett equations and application to hypersonic flows p 778 A93-39410

On numerical solutions of Burnett equations for hypersonic flow past 2-D circular blunt leading edges in continuum transition regime [AIAA PAPER 93-3092] p 1060 A93-48266

Development and computation of continuum higher order constitutive relations for high-altitude hypersonic flow p 132 A93-13578

ZHONG, YONGXING

Investigation of flows in a controlled diffusion airfoil cascade passage p 1071 A93-49188

ZHONGQI, WANG

The blade curving effects in a turbine stator cascade with low aspect ratio [AD-A261063] p 725 A93-26239

ZHOU, CHUANRONG

Dynamic analysis of a gear drive system in aeroengine p 1149 A93-48514

ZHOU, DA-QUAN

The investigation on vibration characteristics of all-movable stabilizer of an aircraft p 41 A93-11821

ZHOU, KANGCHENG

Experimental research on a semiwater-gas-fired gas-turbine p 1107 A93-48524

ZHOU, LIXING

Experimental study on turbulent two-phase flow in a dual-inlet side dump combustor p 1106 A93-48506

ZHOU, M. D.

Separation control and lift enhancement on airfoil using unsteady excitations p 118 A93-14305

Vortex capture by a two-dimensional airfoil with a small oscillating leading-edge flap [AIAA PAPER 93-3266] p 968 A93-46830

ZHOU, MING-DE

A preliminary investigation of the control of separated flow by means of excitation p 1182 A93-53859

ZHOU, MINGDE

Effects of external excitation on the leading-edge separation flowfield p 1071 A93-49198

ZHOU, MOCHUN

An experimental study on blade negative curving in a turbine cascade with a large turning angle p 1071 A93-49185

ZHOU, SHENG

The numerical calculation for the coupling of multiple propeller discrete noise and its interaction with the fuselage boundary p 231 A93-14268

Acoustic experiments of two scaled-model propellers on the ground p 1172 A93-48507

ZHOU, TONGLI

Analysis on space shape and tension distribution of towed flexible cables p 1043 A93-48554

ZHOU, WEI

Experimental study on heat transfer of separated impingement jets in short distance p 1149 A93-48518

ZHOU, WEI-BIN

A study on low level windshear hazard index p 1240 A93-55414

ZHOU, WEI-JIANG

Numerical study of supersonic flow over a backward step with transverse injection p 1182 A93-53853

Numerical solution of N-S equations for hypersonic flow over capsule-type vehicles p 1182 A93-53858

ZHOU, XUEHUA

COF2 radiation from an air-tenon wake p 12 A93-12659

Calculation of optical and electric characteristics from hypersonic blunt-body wakes p 680 A93-33729

ZHOU, Y. Q.

Adaptive clutter suppression for airborne array radars using clutter subspace approximation p 883 A93-43411

ZHU, DE-PEI

Wheel shimmy analysis for main landing gear of aircraft p 41 A93-11809

ZHU, DEPEI

Some dynamic problems in design of aircraft landing gear p 155 A93-14321

ZHU, J. X.

Effects of longitudinal vortex generators on heat transfer and flow loss in turbulent channel flows p 1021 A93-44222

ZHU, J. Y.

Coherent anti-Stokes Raman scattering (CARS) thermometry in a model gas turbine can combustor [ASME PAPER 92-GT-134] p 387 A93-19366

CARS thermometry in a liquid fueled model combustor [AIAA PAPER 93-0366] p 390 A93-23047

ZHU, JIANG

A realizable Reynolds stress algebraic equation model [NASA-TM-105993] p 290 A93-16596

ZHU, JIANJIANG

Research on ISAR motion compensation and imaging by modeling electromagnetic data p 342 A93-20852

ZHU, JIUNQIANG

Prediction of the inception of rotating stall for multistage axial flow compressors p 12 A93-12731

ZHU, JUNZHENG

A prediction of the stalling for wings with rear separation p 116 A93-14264

ZHU, KEQIN

Karman vortex street-airfoil interaction p 678 A93-33703

ZHU, PEI-SHEN

Integrated fire control simulation systems p 1192 A93-53876

ZHU, QING

Research of starting test of the small turbojet in simulated altitude condition p 53 A93-11870

Experimental investigation on starting of a turbojet engine in flight p 898 A93-41740

ZHU, REN-BIAO

A study on low level windshear hazard index p 1240 A93-55414

ZHU, SHOUMEI

The numerical model of supersonic air flow field with hydrogen transverse injection p 859 A93-41736

ZHU, XI-XIONG

An impact dynamics investigation on some problems in bird strike on windshields of high speed aircraft p 197 A93-15346

ZHU, XIAOMEI

On dynamic behavior of cracked rotors p 208 A93-15401

ZHU, XIAOPING

Dynamic stability, coupling and active control of elastic vehicles with unsteady aerodynamic forces modeling p 182 A93-14282

ZHU, XINXIONG

Application of SPEED in aviation industry p 225 A93-14178

ZHU, YI-PU

Numerical simulation of hypersonic rarefied gas flow over blunt bodies p 687 A93-34356

ZHU, YIKUN

The Aircraft/Propulsion Integrated Assessment System p 226 A93-14396

A study of military aircraft and engine tactical/technical performance evaluation p 1242 A93-54596

ZHU, Z. Q.

A computational method for inverse design of transonic airfoil and wing [AIAA PAPER 93-3482] p 982 A93-47260

ZHU, ZHAODA

Prospective application of neural networks in superresolution radars p 211 A93-16849

Superresolution radar imaging with linear prediction data extrapolation p 342 A93-20851

Research on ISAR motion compensation and imaging by modeling electromagnetic data p 342 A93-20852

The ISAR image-formation results of Boeing-727 p 342 A93-20857

ISAR motion compensation and superresolution imaging of aircraft p 928 A93-42793

Studies of superresolution range-Doppler imaging p 928 A93-43344

ZHU, ZIQIANG

Numerical simulation of passive control of shock-boundary layer interaction for transonic airfoil p 680 A93-33719

Viscous-inviscid interaction coupled calculation of three-dimensional turbulent separated flow over dents p 681 A93-33748

An inverse method with regularity condition for transonic airfoil design p 1230 A93-54583

Second generation low order panel method and its application for a case of nacelle p 1231 A93-54595

ZHUANG, F. G.

Vortex control technology p 111 A93-14152

ZHUANG, FENG-GAN

An improved multiple line-vortex method for simulation of separated vortices of slender wings p 1236 A93-55412

ZHUK, A. N.

Aerodynamic characteristics of a sweptforward-wing aircraft model in unsteady motion at large angles of attack in subsonic flow p 1068 A93-48902

ZHUK, S. YA.

Adaptive filtering of Doppler velocimeter errors due to the characteristics of the reflecting surface p 992 A93-45650

ZHUK, V. I.

An asymptotic model of a closed separation region in supersonic flow p 4 A93-10139

ZHUKOVSKII, A. E.

Dynamic processes in the powerplants and power-generating equipment of flight vehicles p 832 A93-39027

ZHUKOVSKII, A. I.

Using current numerical methods in a mathematical model of flight vehicle synthesis p 804 A93-39188

ZHURAVLEV, V. V.

3D/quasi-3D trans- and supersonic flow calculation in advanced centrifugal/axial compressor stages p 972 A93-46936

ZHURAVLEVA, G. S.

A study of turbulent flow in a viscous shock layer in the case of gas flow past oblong blunt bodies p 1089 A93-51820

ZIABASHARHAGH, M.

Recess vane passive stall control [ASME PAPER 92-GT-36] p 246 A93-19296

ZIBI, J.

A numerical procedure for aerodynamic optimization of helicopter rotor blades [ONERA, TP NO. 1992-121] p 771 A93-38595

ZIEGENBEIN, PERRY R.

The development of a prediction method for the calculation of blade-vortex interaction noise based on measured airloads p 566 A93-29409

ZIEGLER, CONRAD L.

An observational study of the dryline p 844 A93-36034

ZIEMIANSKI, JOSEPH A.

Propulsion technology challenges for turn-of-the-century commercial aircraft [ISABE 93-7003] p 1194 A93-53980

Propulsion technology challenges for turn-of-the-century commercial aircraft [NASA-TM-106192] p 1005 A93-32351

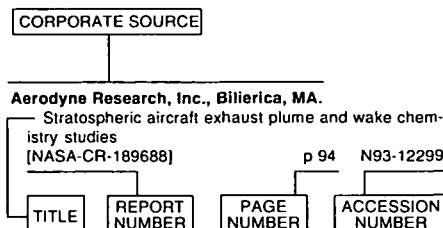
- ZIENKIEWICZ, O. C.**
Adaptivity-fluids-localization. The challenge to computational mechanics p 553 A93-20618
- ZILLIAC, GREG**
A computational study of wingtip vortex flowfield [AIAA PAPER 93-3010] p 1054 A93-48200
- ZILLIAC, GREGORY G.**
Measurements in the near-field of a turbulent wingtip vortex [AIAA PAPER 93-0551] p 285 A93-23290
Turbulent structure of a wingtip vortex in the near field [AIAA PAPER 93-3011] p 1054 A93-48201
- ZIMMERMAN, MARK**
Design of the advanced regional aircraft, the DART-75 [NASA-CR-192044] p 333 A93-17972
- ZIMMERMAN, WILLIAM**
Report on the test set-up for the structural testing of the Airmass Sunburst Ultralight Aircraft p 895 A93-29775
- ZIMMERMANN, H.**
A numerical investigation into the nozzle flow of high by-pass turbofans [ASME PAPER 92-GT-10] p 346 A93-19283
- ZIMMERMANN, HELMUT**
Aeroelastic investigations as applied to Airbus airplanes p 155 A93-14280
- ZINCHENKO, V. I.**
A study of the temperature of bodies in the flow-around regime in the case of surface gas injection p 691 A93-35344
- ZINGALE, CAROLINA**
Preliminary studies of planning and flight strip use as air traffic controller memory aids [DOT/FAA/CT-TN92/22] p 503 A93-21759
- ZINK, M.**
Inflight antenna diagram determination of spaceborne and airborne SAR-systems p 1161 A93-47583
- ZISCHKA, PETER J.**
Tailored composite wings with elastically produced chordwise camber p 923 A93-30876
- ZISHANG, LI**
An analysis of the reliability and maintainability of the Jian 6 and Jian 7 aircraft and ways to improve them [AD-A261060] p 678 A93-26238
- ZLOCKA, MARIA**
Active aircraft recovery from a spin p 524 A93-27295
Investigation of the aircraft spin via sensitivity analysis p 524 A93-27300
- ZOBY, ERNEST V.**
Higher-order viscous shock-layer solutions for high altitude flows [AIAA PAPER 93-2724] p 858 A93-41050
Enhancements to viscous-shock-layer technique p 962 A93-46408
A viscous shock-layer analysis of 2-D and axisymmetric flows [AIAA PAPER 93-2751] p 963 A93-46500
- ZOCCOLI, MICHAEL J.**
An update on the development of the T407/GLC38 modern technology gas turbine engine [ASME PAPER 92-GT-147] p 351 A93-19375
- ZOLTAK, JERZY**
A numerical study of aerodynamic wing design for supercritical conditions of an advanced training and military aircraft p 1238 A93-56213
Determination of the transonic flow field around an airfoil section for a given lift force coefficient p 1239 A93-56215
- ZORI, LAITH A. J.**
Three-dimensional calculations of rotor-airframe interaction in forward flight p 795 A93-35940
- ZORN, GREG**
SR-SCARLET 1: Peregrin [NASA-CR-192048] p 337 A93-18155
- ZOTTO, MARK D.**
Influence of pitch-lag coupling on damping requirements to stabilize 'ground/air resonance' p 158 A93-14784
- ZOU, CONGGING**
The vibration and flutter of composite material laminate p 543 A93-26617
- ZRIBI, MOHAMED**
Dynamical variable structure control of a helicopter in vertical flight p 369 A93-22887
- ZSOLDOS, J. S.**
An experimental investigation of interacting wing-tip vortex pairs [AD-A258471] p 295 A93-18272
- ZUBIN, M. A.**
Regimes of supersonic flow past the windward side of V-shaped wings p 5 A93-10144
Aerodynamic characteristics and static stability margin of conical star-shaped bodies at supersonic velocities p 1067 A93-48848
- ZUBRILOV, ANATOLII P.**
The navigation and flying equipment of the Yak-42 aircraft p 792 A93-39204
- ZUEFLE, ERNST-MICHAEL**
Optical blade vibration measurement [ETN-93-93454] p 905 A93-29999
- ZUEV, V. V.**
Methods and equipment for data processing and acquisition in information management systems p 856 A93-43101
- ZUEVA, E. YU.**
The representation of the aerodynamic torque in simulations of a spacecraft rotary motion p 1141 A93-48835
- ZUK, JOHN**
NASA/FAA helicopter simulator workshop [NASA-CP-3156] p 857 A93-30673
Part 1: Executive summary p 857 A93-30674
- ZUKOSKI, EDWARD E.**
Applications of shock-induced mixing to supersonic combustion p 735 A93-35618
Investigation of a contoured wall injector for hypervelocity mixing augmentation p 837 A93-39407
Shock enhancement and control of hypersonic combustion [AD-A254295] p 72 A93-10843
- ZUMWALT, GLEN W.**
Hysteresis effects on wind tunnel measurements of a two-element airfoil [AIAA PAPER 93-0646] p 464 A93-24761
Flowfield measurements of a two-element airfoil with large separation p 480 A93-29307
- ZUO, PEICHU**
On experimental study of 3-D flow in self-correcting wind tunnel p 528 A93-24033
- ZUPPARDO, JOSEPH C.**
SR-SCARLET 1: Peregrin [NASA-CR-192048] p 337 A93-18155
- ZVEGINTSEV, V. I.**
An experimental study of the thrust and aerodynamic characteristics of an operating ramjet engine in a blowdown wind tunnel p 1107 A93-48828
Experimental studies of aerodynamic performances of hypersonic scramjet in impulse hot-shot tunnel [AIAA PAPER 93-2446] p 1120 A93-50198
- ZVEZDIN, Y. I.**
New corrosion resistant nickel-base super-alloys and technological processes of casting gas turbines parts with directional single crystal and regulable equiaxial minimized microporosity structure p 916 A93-40811

CORPORATE SOURCE INDEX

AERONAUTICAL ENGINEERING / A Continuing Bibliography
1993 Cumulative Index

February 1994

Typical Corporate Source Index Listing



Listings in this index are arranged alphabetically by corporate source. The title of the document is used to provide a brief description of the subject matter. The page number and the accession number are included in each entry to assist the user in locating the abstract in the abstract section. If applicable, a report number is also included as an aid in identifying the document.

A

ABB Kraftwerke A.G., Mannheim (Germany).

Optical blade vibration measurement
[ETN-93-93454] p 905 N93-29999

ABB Power Generation, Inc., Baden (Switzerland).

The aerodynamic effect of coolant ejection in the leading edge region of a film-cooled turbine blade
p 904 N93-29958

Academy of Sciences (USSR), Novosibirsk.

On the disturbances development in the supersonic boundary layer
p 484 N93-20686

Admiralty Research Establishment, Gosport (England).

Experiments on low aspect ratio hydroplanes to measure lift under static and dynamic conditions
[ARE-TM(UHR)-90306] p 21 N93-11365
Lift coefficient of a randomly oscillating hydroplane
[DRA/MAR-TM(MTH)-91320] p 21 N93-11377

Advanced Aviation Concepts, Jupiter, FL.

Workshop on Aeronautical Decision Making (ADM). Volume 2: Plenary Session With Presentations and Proposed Action Plan
[DOT/FAA/RD-92/14-VOL-2] p 146 N93-15013
How expert pilots think p 147 N93-15017
Enhanced Aeronautical Resource Management training alternatives p 147 N93-15019
Proposed action plan to improve ADM effectiveness, part 3: Developing a new ADM paradigm on which to build advanced or expert decision making training p 148 N93-15026

Advisory Group for Aerospace Research and Development, Neuilly-Sur-Seine (France).

AGARD index of publications, 1989-1991
[AGARD-INDEX-89-91] p 104 N93-10610
Directory of factual and numeric databases of relevance to aerospace and defence R and D
[AGARD-R-777] p 104 N93-11710
Aerodynamic Engine/Airframe Integration for High Performance Aircraft and Missiles
[AGARD-CP-498] p 213 N93-13199

Propulsion and Energetics Panel Working Group 20 on Test Cases for Engine Life Assessment Technology
[AGARD-AR-308] p 176 N93-14890

Aircraft Accidents: Trends in Aerospace Medical Investigation Techniques
[AGARD-CP-532] p 490 N93-19653

Flight Testing
[AGARD-CP-519] p 510 N93-19901

Mission planning systems for tactical aircraft (pre-flight and in-flight)
[AGARD-AR-313] p 496 N93-21187

The testing of fixed wing tanker and receiver aircraft to establish their air-to-air refuelling capabilities, volume 11
[AGARD-AG-300-VOL-11] p 514 N93-21305

Heat Transfer and Cooling in Gas Turbines
[AGARD-CP-527] p 901 N93-29926

AGARD Engine Disc Cooperative Test Programme
[AGARD-R-766-ADD] p 1004 N93-31741

Aeritalia S.p.A., Naples (Italy).

The FAIR (Flight Animated and Interactive Reconstruction) tool p 148 N93-15164

Aerodyne Research, Inc., Billerica, MA.

Stratospheric aircraft exhaust plume and wake chemistry studies
[NASA-CR-189688] p 94 N93-12299

Icing prevention by ultrasonic nucleation of supercooled water droplets in front of subsonic aircraft
[AD-A258212] p 142 N93-12816

Aeronautica Macchi S.p.A., Varese (Italy).

Water tunnel studies of inlet/airframe interference phenomena p 215 N93-13216

Aeronautical Research Inst. of Sweden, Bromma.

Implementation of a multidomain Navier-Stokes code on the Intel iPSC2 hypercube
[FFA-TN-1992-37] p 843 N93-28994

Aeronautical Research Inst. of Sweden, Stockholm.

Modal measurements and propeller field excitation on acoustic full scale mockup of SAAB 340 aircraft
[FFA-TN-1992-08] p 1039 N93-31051

GARTUR 3D shear layer experiment
[FFA-TN-1992-26] p 987 N93-31052

Optimal design and imperfection sensitivity of nonlinear shell structures
[FFA-TN-1992-30] p 1030 N93-31123

WBNFLOW: Multi-grid/multi-block potential solver for compressible flow. User's guide
[FFA-TN-1992-43] p 1031 N93-31146

Aeronautical Research Labs., Melbourne (Australia).

Design and implementation of digital filters for analysis of F/A-18 flight test data
[AD-A253447] p 17 N93-10342

Structural fatigue aspects of the P-3 Orion
[ARL-STRUC-TM-558] p 161 N93-13256

Development of a menu driven materials data base for use on personal computers: Aircraft structures technical memorandum
[AD-A256317] p 392 N93-16403

Measurement of the dynamic undercarriage response of a Sikorsky S-70B-2 helicopter: Instrumentation and test methods: Flight mechanics technical memorandum
[AD-A256319] p 329 N93-16404

Damage tolerance assessment of boron/epoxy repairs to fuselage lap joints
[AD-A258383] p 338 N93-18257

Field evaluation of six protective coatings applied to T-56 turbine blades after 2000 hours of engine use
[AD-A261112] p 522 N93-21316

In-flight evaluation of noise levels and assessment of active noise reduction systems in the Seahawk S-70B-2 helicopter
[AD-A260689] p 759 N93-25649

Optimal trajectories for aircraft terrain following and terrain avoidance: A literature review update
[AD-A264075] p 910 N93-30604

Aeronautical Systems Div., Wright-Patterson AFB, OH.

Adverse weather test site selection study
[AD-A259012] p 339 N93-18895

Aerospace Medical Research Labs., Brooks AFB, TX.

Advantages of using a projected head-up display in a flight simulator
[AD-A255332] p 194 N93-14559

Aerospace Medical Research Labs., Wright-Patterson AFB, OH.

Evaluation of three models used for predicting noise propagated long distances overground
[AD-A255963] p 232 N93-14406

Information requirements analyses for transatmospheric vehicles
[AD-A261189] p 718 N93-25949

Aerospatiale, Suresnes (France).

Numerical modelling of induced effects of lightning strike on an all composite helicopter p 703 N93-24879

Aerospatiale, Toulouse (France).

Flight tests of the transport aircraft viewed from the industrial standpoint p 510 N93-19903

Aerospatiale Aquitaine, Saint-Medard en Jalles (France).

Using NDT techniques in the maintenance of aeronautical products
[REPT-921-430-102] p 88 N93-11587

Fiber reinforced composites: A new class of glass and glass ceramic materials for thermomechanical applications
[REPT-921-430-104] p 200 N93-15490

Air Force Environmental Technical Applications Center, Scott AFB, IL.

SAC contrail formation study
[AD-A254410] p 159 N93-12605

Air Force Inspection and Safety Center, Norton AFB, CA.

Does cockpit management training reduce aircrew error? p 146 N93-15014

Cockpit decision making p 146 N93-15015

Air Force Inst. of Tech., Wright-Patterson AFB, OH.

Measurement of aerodynamic shear stress using side chain liquid crystal polymers
[AD-A254312] p 72 N93-10770

One type of automatically adjusted difference scheme with artificial viscosity to calculate ablated exterior shapes
[AD-A254108] p 19 N93-10856

Arguments concerning wind tunnel test studies of the trim characteristics of objects with small asymmetries
[AD-A254111] p 19 N93-10858

Hybrid guidance for maneuvering flight vehicles
[AD-A254110] p 69 N93-11798

Design of an Ada expert system shell for the VHSIC avionics modular flight processor p 98 N93-11947

ACTA Aeronautica et Astronautica Sinica (selected articles)
[AD-A255070] p 110 N93-13946

An examination of wing rock for the F-15
[AD-A256613] p 188 N93-14252

Multiple model adaptive estimation applied to the VISTA F-16 with actuator and sensor failures
[AD-A258444] p 188 N93-14608

Transition induced normal forces and their effects on the aerodynamic characteristics of slender sharp cones
[AD-A256802] p 288 N93-15889

Multiple model adaptive estimation applied to the VISTA F-16 with actuator and sensor failures, volume 2
[AD-A256569] p 371 N93-16165

CFD-based approximation concepts for aerodynamic design optimization with application to a 2-D scramjet vehicle
[AD-A258084] p 333 N93-17893

Applying commercial style acquisition practices to the procurement of commercially available aircraft
[AD-A258143] p 455 N93-18087

An investigation of the influence of advanced aircraft diagnostics on the technological sophistication of maintenance personnel
[AD-A258988] p 240 N93-18887

An experimental investigation of a finite circulation control wing
[AD-A259044] p 340 N93-18896

Detection of spoofing, jamming, or failure of a Global Positioning System (GPS)
[AD-A259023] p 319 N93-18951

Development of an engine/airframe performance matching scheme for jet engine retrofit
[AD-A258822] p 365 N93-18997

- A model of Global Positioning System (GPS) Master Control Station (MCS) operations
[AD-A258846] p 320 N93-19067
- Nozzle/cowl optimization for a hypersonic vehicle on a typical trajectory
[AD-A258827] p 341 N93-19089
- Characterization of stall inception in high-speed single-stage compressors
[AD-A258973] p 365 N93-19093
- Strategies for optimal control design of normal acceleration command following on the F-16
[AD-A258975] p 373 N93-19095
- The effects of viscosity on a conically derived waverider
[AD-A259019] p 424 N93-19101
- Improvements to LOGI/LTR methodology for plants with lightly damped or low frequency poles
[AD-A258841] p 443 N93-19112
- A model for determining task set schedulability in the presence of system effects
[AD-A258915] p 443 N93-19338
- Experimental investigation of the aerodynamics of independently rotating cylindrical shells
[AD-A258917] p 305 N93-19340
- Helicopter flight control system design using the linear quadratic regulator for robust eigenstructure assignment
[AD-A258904] p 373 N93-19351
- Integrated Blade Inspection System (IBIS) upgrade study
[AD-A258912] p 365 N93-19356
- Application of the program profile for the design of low-speed, low-observable configuration airfoils
[AD-A258842] p 305 N93-19364
- A simulation study on take-off and landing dynamics of the aircraft of a fly-by-wire control system
[AD-A259286] p 510 N93-19849
- An investigation of discovery-based learning in the route planning domain
[AD-A259141] p 513 N93-20560
- The influence of structural optimization on the aeroelastic properties of a vertical tail
[AD-A259140] p 513 N93-20575
- A synthetic environment flight simulator: The AFIT virtual cockpit
[AD-A259220] p 530 N93-20576
- Failure identification using multiple model adaptive estimation for the LAMBDA flight vehicle
[AD-A259137] p 527 N93-20596
- YIDOU and its application to aircraft design
[AD-A259262] p 513 N93-20605
- Design recovery for software library population
[AD-A259292] p 572 N93-20611
- An analysis of the reliability and maintainability of the Jian 6 and Jian 7 aircraft and ways to improve them
[AD-A261060] p 678 N93-26238
- The blade curving effects in a turbine stator cascade with low aspect ratio
[AD-A261063] p 725 N93-26239
- Aviation production engineering: Selected articles
[AD-A261231] p 764 N93-27056
- Detection performance of digital polarity sampled phase reversal code pulse compressors
[AD-A262930] p 842 N93-28289
- Rendering the out-the-window view for the AFIT virtual cockpit
[AD-A262599] p 823 N93-28467
- Toward reusable graphics components in Ada
[AD-A262568] p 849 N93-28577
- The infrared measurement for the reentry-body-translation
[AD-A263100] p 914 N93-29134
- Solution of Euler equations for forebody-inlet ensemble of aircraft at high angle of attack
[AD-A263905] p 876 N93-29862
- The application of concentric vortex simulation to calculating the aerodynamic characteristics of bodies of revolution at high angles of attack
[AD-A263879] p 876 N93-29919
- Air Force Occupational Measurement Center, Randolph AFB, TX.**
Aircraft electrical and environmental systems, AFSCs 452x5, 454x5, and 454x6
[AD-A261213] p 717 N93-25733
- Air Force Systems Command, Wright-Patterson AFB, OH.**
Evaluation of CKU-5/A ejection seat catapults under varied acceleration levels
[AD-A248021] p 29 N93-12489
- Computational method in optimal bending-twisting comprehensive design of wings of subsonic and supersonic aircraft
[AD-A262374] p 806 N93-27694
- Effect of canard wing positions on aerodynamic characteristics of swept-forward wing
[AD-A262373] p 789 N93-28493
- International aviation (Selected articles)
[AD-A262566] p 765 N93-28576
- Air Force Wright Aeronautical Labs., Langley AFB, VA.**
Human factors causes and management strategies in US Air Force F-16 mishaps 1984-present
p 492 N93-19673
- Air War Coll., Maxwell AFB, AL.**
Dr. Alexander H. Flax: Technologist of aeronautics
[AD-A258441] p 456 N93-17890
- Airbus Industrie, Blagnac (France).**
Monitoring of powerplants in advanced commercial aircraft
p 178 N93-15171
- Airbus Industrie, Toulouse (France).**
Airbus Industrie TCAS experience
p 152 N93-15186
- Aircraft Research Association Ltd., Bedford (England).**
Test techniques for engine/airframe integration
p 213 N93-13200
- ASTOVL model engine simulators for wind tunnel research
p 192 N93-13213
- Some aspects of intake design, performance and integration with the airframe
p 161 N93-13219
- Alabama Univ., Huntsville.**
Effects of reacting flows with turbulence and shock waves on efficiency of scramjet combustors
p 69 N93-11133
- Materials processing in low gravity
[NASA-CR-184421] p 91 N93-12401
- FNAS modify matrix and transparent experiments
[NASA-CR-184442] p 198 N93-13311
- Fiber pulling apparatus modification
[NASA-CR-184498] p 220 N93-14763
- Turbulence interacting with chemical kinetics in airbreathing combustion of ducted rockets
p 734 N93-26012
- Alabama Univ., Tuscaloosa.**
Comparison of methodologies for describing relaxation in nonequilibrium gaseous systems
p 419 N93-16786
- Alenia, Torino (Italy).**
AM-X high angle of attack flight test experience (single and two seat versions)
p 511 N93-19910
- Alenia Spazio S.p.A., Naples (Italy).**
Review of aeronautical fatigue investigation activities developed in Alenia-GAT during the period May 1990 - March 1991
[ETN-92-92884] p 329 N93-16287
- An advanced graphics-interactive system for a multi-block structured grid generation within an industrial environment
[ETN-92-92885] p 440 N93-16288
- Alenia Spazio S.p.A., Rome (Italy).**
MSC/NASTRAN structure optimization test module version 67 (preliminary)
[REPT-5-191025] p 554 N93-20907
- Alfa Romeo S.p.A., Naples (Italy).**
Aero-thermal design of a cooled transonic NGV and comparison with experimental results
p 904 N93-29957
- Allied-Signal Aerospace Co., Fort Lauderdale, FL.**
RDR-4B doppler weather radar with forward looking wind shear detection capability
p 489 N93-19601
- Allied-Signal Aerospace Co., Torrance, CA.**
Improved silicon nitride for advanced heat engines
[NASA-CR-182193] p 917 N93-29451
- American Airlines Flight Academy, Fort Worth, TX.**
Advanced technology wind shear prediction system evaluation
p 146 N93-14858
- American Gas Association Labs., Cleveland, OH.**
Engine driven chiller and thermal storage integration (Large tonnage engine driven chiller development)
[PB92-227891] p 555 N93-21465
- American Science and Engineering, Inc., Cambridge, MA.**
Automatic detection of explosives using x ray imaging
p 880 N93-30275
- Amtec Engineering, Inc., Bellevue, WA.**
The 3D Navier-Stokes flow analysis for shared and distributed memory MIMD computers
[AD-A256038] p 221 N93-15187
- Analytic Power Corp., Boston, MA.**
Electropneumatic actuator, phase 1
[PB93-174951] p 1033 N93-31876
- Argonne National Lab., IL.**
AQUIS: A PC-based air quality and permit information system
[DE92-040092] p 434 N93-18587
- Poster session: Fifth Users Meeting for the Advanced Photon Source
[DE93-006019] p 732 N93-26498
- Use of local x ray computerized tomography for high-resolution, region-of-interest inspection of large ceramic components for engines
[DE93-005564] p 843 N93-28943
- Forces on a magnet moving past figure-eight coils
[DE93-009965] p 943 N93-29189
- Arizona State Univ., Flagstaff.**
State of the art of airport pavement analysis and design
p 378 N93-16310
- Arizona State Univ., Tempe.**
Optimal output feedback vibration control of rotor-bearing systems
p 86 N93-11220
- Numerical study of advanced rotor blades
p 23 N93-11899
- Optimum Design of High Speed Prop-Rotors
[NASA-CR-190915] p 336 N93-18064
- Design of high speed propellers using multiobjective optimization techniques
p 336 N93-18065
- Optimum design of high speed prop rotors including the coupling of performance, aeroelastic stability and structures
p 337 N93-18066
- Development of a non-linear simulation for generic hypersonic vehicles - ASUHS1
[NASA-CR-192710] p 516 N93-22003
- Generic hypersonic vehicle performance model
[NASA-CR-192953] p 714 N93-25162
- Numerical simulation of leading-edge receptivity to freestream vorticity
p 696 N93-25388
- Far field rotor noise
[AD-A260703] p 759 N93-25651
- Stationary crossflow instability on an infinite swept wing
p 699 N93-25865
- An integrated optimum design approach for high speed prop-rotors including acoustic constraints
[NASA-CR-193222] p 893 N93-29153
- Local heat transfer measurement with liquid crystals on rotating surfaces including non-axisymmetric cases
p 902 N93-29943
- Advanced electromagnetic methods for aerospace vehicles
[NASA-CR-193468] p 936 N93-31036
- Army Aeromedical Research Lab., Fort Rucker, AL.**
Crash experience of the US Army Black Hawk helicopter
p 493 N93-19688
- US Army helicopter inertia reel locking failures
p 493 N93-19689
- US Army's aviation life support equipment retrieval program real world design successes from proactive investigation
p 494 N93-19690
- The effectiveness of airbags in reducing the severity of head injury from gunshot strikes in attack helicopters
p 494 N93-19691
- Army Armament Research, Development and Engineering Center, Picatinny Arsenal, NJ.**
Wind tunnel spin data reduction to obtain aerodynamic spin damping coefficients by using nonlinear equation of motion
[AD-A253880] p 19 N93-10811
- Army Aviation Applied Technology Directorate, Fort Eustis, VA.**
PROAV Cable Warning System (CWS) - U.S. Army aircraft integration assessment and OCONUS field evaluation
[AD-A261233] p 705 N93-26263
- Army Aviation Center, Fort Rucker, AL.**
USA aviation digest index, 1989, volume 11
[AD-A258673] p 571 N93-20388
- Index to USA aviation digest, 1990
[AD-A258678] p 572 N93-20389
- Index to USA aviation digest, 1991
[AD-A258679] p 572 N93-20390
- Army Aviation Research and Development Command, Moffett Field, CA.**
The Application of CFD to rotary wing flow problems
[NASA-TM-102803] p 139 N93-15483
- Army Aviation Systems Command, Cleveland, OH.**
Introduction to test cases for engine life assessment technology
p 176 N93-14891
- Some recent applications of Navier-Stokes codes to rotorcraft
p 786 N93-27452
- Army Aviation Systems Command, Moffett Field, CA.**
Generation of helicopter roll axis bandwidth data through ground-based and in-flight simulation
p 511 N93-19909
- Army Aviation Technical Test Center, Fort Rucker, AL.**
Methodology investigation: Global Positioning System integration (GPS)
[AD-A261054] p 708 N93-26237
- Army Cold Regions Research and Engineering Lab., Hanover, NH.**
State-of-the-art survey of flexible pavement crack sealing procedures in the United States
[AD-A258050] p 382 N93-17708
- Mathematical model of frost heave and thaw settlement in pavements
[CRRLE-REPT-93-2] p 912 N93-30103
- Army Engineer Topographic Labs., Fort Belvoir, VA.**
Automated extraction of aircraft runway patterns from radar imagery
[AD-A254258] p 68 N93-11751

Army Engineer Waterways Experiment Station, Vicksburg, MS.

- In situ material characterization for pavement evaluation by the Spectral-Analysis-of-Surface-Waves (SASW) method
[AD-A255660] p 194 N93-14128
- Reanalysis of multiple-wheel landing gear traffic tests
[AD-A256593] p 194 N93-14238

Army Lab. Command, Watertown, MA.

- Assessment of helicopter component statistical reliability computations
[AD-A258931] p 510 N93-19447

Army Materials Technology Lab., Watertown, MA.

- Hydrogen-induced stress corrosion cracking susceptibility analysis of pitch links from the AH-64 Apache helicopter
[AD-A260692] p 736 N93-25895

Army Natick Labs., MA.

- A computational model that couples aerodynamic and structural dynamic behavior of parachutes during the opening process
[AD-A264115] p 877 N93-30119

Army Natick Research and Development Command, MA.

- The degradation of parachutes: Age and mechanical wear
[AD-A252243] p 24 N93-12179

Army Personnel Research Establishment, Farnborough (England).

- Towards an integrated approach to proactive monitoring and accident prevention p 495 N93-19700
- Accidents and errors: A review of recent UK Army Air Corps accidents p 495 N93-19701

Army Research Inst. for the Behavioral and Social Sciences, Alexandria, VA.

- Simulator motion
[AD-A257683] p 381 N93-17687

Army Research Lab., Aberdeen Proving Ground, MD.

- Helicopter forced response vibration analysis method RTVIB20
[AD-A261809] p 730 N93-26260
- Analysis of the static and dynamic response of a T-38 wing and comparison with experimental data
[AD-A262363] p 806 N93-27692
- Numerical simulation of the flow in a 1:57-scale axisymmetric model of a large blast simulator
[AD-A265551] p 1015 N93-31916
- Navier-Stokes computations for kinetic energy projectiles in steady coning motion: A predictive capability for pitch damping
[AD-A264111] p 1033 N93-32028

Army Research Lab., Adelphi, MD.

- Navier-Stokes simulation of viscous, separated, supersonic flow over a projectile rotating band
[AD-A263073] p 788 N93-27955

Army Safety Center, Fort Rucker, AL.

- Underlying causes of human error in US Army rotary wind accidents p 492 N93-19678

Army Test and Evaluation Command, Aberdeen Proving Ground, MD.

- External acoustical noise measurements for aviation systems
[AD-A263138] p 943 N93-29480

Army Topographic Engineering Center, Fort Belvoir, VA.

- Proposed revisions to RTCM SC-104 recommended standards for differential NAVSTAR/GPS service for carrier phase applications
[AD-A255276] p 152 N93-15005

- Repair, evaluation, maintenance, and rehabilitation research program. Continuous Deformation Monitoring System (CDMS)
[AD-A261833] p 708 N93-26274

Army War Coll., Carlisle Barracks, PA.

- Air piracy and terrorism directed against U.S. Air carriers
[AD-A264120] p 880 N93-30194

Auburn Univ., AL.

- Design of the advanced regional aircraft, the DART-75
[NASA-CR-192044] p 333 N93-17972
- Eagle RTS: A design for a regional transport aircraft
[NASA-CR-192032] p 334 N93-18017

Aurora Flight Sciences Corp., Manassas, VA.

- Development and testing of the Perseus proof-of-concept aircraft
[DE93-010121] p 806 N93-28586

Aviatic Ltd., Budapest (Hungary).

- The SIROM flight data recorder and evaluation system p 168 N93-15165

B**Barna (P. Stephen), Consultant, Norfolk, VA.**

- Investigations of detail design issues for the high speed acoustic wind tunnel using a 60th scale model tunnel. Part 1: Tests with open circuits
[NASA-CR-191671] p 137 N93-14737

- Investigations of detail design issues for the high speed acoustic wind tunnel using a 60th scale model tunnel. Part 2: Tests with the closed circuit
[NASA-CR-191672] p 137 N93-14738

BASF Structural Materials, Inc., Charlotte, NC.

- Advanced fiber/matrix material systems p 921 N93-30854

Bath Univ. (England).

- Flow and heat transfer between gas-turbine discs p 903 N93-29950

Battelle Columbus Labs., OH.

- Federal Aviation Administration pavement modeling p 379 N93-16315
- High reliability, maintenance-free INS battery development
[AD-A264521] p 934 N93-30406

- In-situ bioventing: Two US EPA and Air Force sponsored field studies
[PB93-194231] p 1035 N93-32089

Battelle Pacific Northwest Labs., Richland, WA.

- Ultrahigh temperature assessment study: Ceramic matrix composites
[AD-A262740] p 826 N93-28592
- Construction and testing of simple airfoils to demonstrate structural design, materials choice, and composite concepts p 879 N93-30979

Beidscommissie Remote Sensing, Delft (Netherlands).

- ERS-1 directional wave spectra validation with the airborne SAR PHARS
[BCRS-92-18] p 937 N93-31010

Belgian Air Force, Beauvechain.

- Category A F-16 accidents in the Belgian Air Force p 492 N93-19675

Belgian Air Force, Brussels.

- Combat and training aircraft class A mishaps in the Belgian Air Force 1970-1990 p 492 N93-19677

Bell Helicopter Co., Fort Worth, TX.

- The NASA/industry Design Analysis Methods for Vibrations (DAMVIBS) program: Bell Helicopter Textron accomplishments p 514 N93-21312
- Civil tiltrotor transport point design: Model 940A
[NASA-CR-191446] p 1019 N93-32234

Berry Coll., Mount Berry, GA.

- Multipath effects in a Global Positioning Satellite system receiver p 318 N93-17311

Boeing Co., Seattle, WA.

- Formal representation of the requirements for an Advanced Subsonic Civil Transport (ASCT) flight control system
[NASA-CR-189699] p 98 N93-12346
- Developments in impact damage modeling for laminated composite structures p 922 N93-30857

Boeing Commercial Airplane Co., Seattle, WA.

- Definition of the 2005 flight deck environment
[NASA-CR-4479] p 343 N93-16693
- World jet airplane inventory at year-end 1992
[PB93-174324] p 765 N93-27405
- Quantitative three-dimensional low-speed wake surveys p 785 N93-27447
- Spurious symptom reduction in fault monitoring
[NASA-CR-191453] p 942 N93-29192
- Advanced technology composite aircraft structures
[NASA-CR-190420] p 894 N93-29438
- Composites: A viable option p 918 N93-30429
- Advanced technology commercial fuselage structure p 918 N93-30432
- Cost studies for commercial fuselage crown designs p 920 N93-30440

- Effects of intra- and inter-laminar resin content on the mechanical properties of toughened composite materials p 921 N93-30845
- Process and assembly plans for low cost commercial fuselage structure p 923 N93-30865

Boeing Defense and Space Group, Philadelphia, PA.

- Mechanical and analytical screening of braided composites for transport fuselage applications p 922 N93-30855

Boeing Defense and Space Group, Seattle, WA.

- X-ray computed tomography for casting development
[AD-A261786] p 752 N93-26526
- Three-dimensional water droplet trajectory code validation using an ECS inlet geometry
[NASA-CR-191097] p 791 N93-27267

Boeing Helicopter Co., Philadelphia, PA.

- The NASA/industry Design Analysis Methods for Vibrations (DAMVIBS) program: Boeing Helicopters airframe finite element modeling p 515 N93-21313

California Polytechnic State Univ.

- Fabrication of the V-22 composite AFT fuselage using automated fiber placement p 920 N93-30443

Boeing Military Airplane Development, Seattle, WA.

- Formal design specification of a Processor Interface Unit
[NASA-CR-189698] p 99 N93-12538

Bombardier, Inc., Montreal (Quebec).

- Further development of the CANAERO computer code to include a time-stepping capability
[DREA-CR-91-478] p 562 N93-21820

Boston Univ., MA.

- The onset of vortex turbulence p 788 N93-28251

British Aerospace Defence, Preston (England).

- In-flight structural mode excitation system for flutter testing p 526 N93-19915
- Development and flight testing of a surface pressure measurement installation on the EAP demonstrator aircraft p 550 N93-19927

British Aerospace Public Ltd. Co., Bristol (England).

- A computational approach to predicting the extent of arc root damage in CFC panels p 735 N93-24890

British Broadcasting Corp., Kingswood (England).

- HELITRAK: A helicopter-tracking receiver system for television outside broadcast links
[BBC-RD-1992/5] p 552 N93-20573

Bronx Community Coll., NY.

- Using software metrics and software reliability models to attain acceptable quality software for flight and ground support software for avionics systems p 442 N93-17305

Brookhaven National Lab., Upton, NY.

- Operating experience using venturi flow meters at liquid helium temperature
[DE92-014693] p 90 N93-12140

Brown Univ., Providence, RI.

- Research support for the Laboratory for Lightwave Technology
[AD-A261488] p 760 N93-26343
- Parameter identification for nonlinear aerodynamic systems
[NASA-CR-193072] p 782 N93-27282

Bull HN Italia, Milan.

- Scheduling of an aircraft fleet p 443 N93-18665

Bundesanstalt fuer Flugsicherung, Frankfurt am Main (Germany).

- Activities report of the German Institute for Flight Safety
[ETN-92-92272] p 28 N93-11375

C**California Inst. of Tech., Pasadena.**

- Combustion noise and combustion instabilities in propulsion systems p 100 N93-10682
- Shock enhancement and control of hypersonic combustion
[AD-A254295] p 72 N93-10843
- Mixing and reaction in the subsonic 2-D turbulent free shear layer p 289 N93-16508
- Robust nonlinear control of vectored thrust aircraft
[NASA-CR-192727] p 728 N93-25199
- A theoretical and computational study on active wake control p 878 N93-30892

California Polytechnic State Univ., San Luis Obispo.

- Low bandwidth robust controllers for flight
[NASA-CR-191774] p 372 N93-17800
- MM-122: High speed civil transport
[NASA-CR-192011] p 334 N93-17974
- Phoenix: Preliminary design of a high speed civil transport
[NASA-CR-192024] p 334 N93-17976

- Proposal and preliminary design for a high speed civil transport aircraft. Swift: A high speed civil transport for the year 2000
[NASA-CR-192023] p 335 N93-18049

TBD(exp 3)

- [NASA-CR-192075] p 335 N93-18054

The Edge supersonic transport

- [NASA-CR-192074] p 335 N93-18055

A second-generation high speed civil transport: Stingray

- [NASA-CR-192022] p 336 N93-18059

The Trojan

- [NASA-CR-192013] p 336 N93-18060

Preliminary design of a high speed civil transport: The Opus 0-001

- [NASA-CR-192018] p 336 N93-18061

RTJ-303: Variable geometry, oblique wing supersonic aircraft

- [NASA-CR-192054] p 337 N93-18166

Aerodynamic analysis of hypersonic waverider aircraft

- [NASA-CR-192981] p 780 N93-27093

Low bandwidth robust controllers for flight

- [NASA-CR-193085] p 819 N93-27156

- Robust crossfeed design for hovering rotorcraft
[NASA-CR-193107] p 805 N93-27241
- Helicopter approach capability using the differential global positioning system
[NASA-CR-193183] p 793 N93-28936
- Effects of an aft facing step on the surface of a laminar flow glider wing
[NASA-CR-193302] p 990 N93-31855
- California State Polytechnic Univ., Pomona.**
High speed civil transport
[NASA-CR-192041] p 337 N93-18161
- High-altitude reconnaissance aircraft
p 894 N93-29713
- California State Univ., Long Beach.**
The Fifth Symposium on Numerical and Physical Aspects of Aerodynamic Flows
[NASA-CR-193000] p 783 N93-27427
- A composite structured/unstructured-mesh Euler method for complex airfoil shapes p 784 N93-27439
- Recent progress in the analysis of iced airfoils and wings p 784 N93-27441
- An interactive boundary-layer approach to multielement airfoils at high lift p 785 N93-27445
- California State Univ., Los Angeles.**
Navier-Stokes calculation of transonic flow past the NTF 65-deg delta wing p 292 N93-16797
- California State Univ., Northridge.**
Project ARES 2: High-altitude battery-powered aircraft
p 894 N93-29715
- California State Univ., Sacramento.**
The combustion time lag and its role in ramjet combustion instability p 73 N93-11137
- California Univ., Berkeley.**
Adaptive control of nonlinear nonminimum phase systems p 229 N93-14470
- Robo-line storage: Low latency, high capacity storage systems over geographically distributed networks
[NASA-CR-192910] p 758 N93-25130
- Control of nonlinear systems under input constraints with applications to flight control p 729 N93-25353
- California Univ., Berkeley. Lawrence Berkeley Lab.**
Stratospheric aircraft: Impact on the stratosphere?
[DE92-016997] p 94 N93-12104
- X ray microscopy resource center at the Advanced Light Source
[DE93-010449] p 911 N93-29869
- California Univ., Davis.**
Improved numerical simulation of Euler equations
p 83 N93-10309
- Computational nonlinear control
[AD-A253547] p 98 N93-12258
- A comparison of classical mechanics models and finite element simulation of elastically tailored wing boxes
p 922 N93-30863
- Tailored composite wings with elastically produced chordwise camber p 923 N93-30876
- California Univ., Irvine.**
Fundamental studies of droplet interactions in dense sprays
[AD-A261165] p 737 N93-25948
- California Univ., Los Angeles.**
Fluid flow and heat convection studies for actively cooled airframes
[NASA-CR-190956] p 216 N93-13406
- Turbulence and chaos in classical and quantum systems p 232 N93-14144
- Game theoretic synthesis for robust aerospace controllers p 819 N93-27171
- California Univ., San Diego.**
Studies of hydrogen-air diffusion flames and of compressibility effects related to high-speed propulsion
p 197 N93-29125
- California Univ., San Diego, La Jolla.**
AFOSR Contractors Meeting in Propulsion
[AD-A254484] p 195 N93-12575
- Studies of origin of three-dimensionality in laminar wakes
[AD-A262281] p 841 N93-28242
- Calspan Advanced Technology Center, Buffalo, NY.**
The USAF Advanced Turbine Aerothermal Research Rig (ATARR)
p 911 N93-29945
- Calspan-Buffalo Univ. Research Center, NY.**
A preliminary study associated with the experimental measurement of the aero-optic characteristics of hypersonic configurations
[AD-A253792] p 24 N93-12063
- Calspan Field Services, Inc., Arnold AFS, TN.**
Design philosophy for wind tunnel model positioning systems
[AD-A254958] p 192 N93-12552
- Calspan-State Univ. of New York Joint Venture, Buffalo, NY.**
Theoretical constraints in the design of multivariable control systems
[NASA-CR-191900] p 442 N93-18372
- Cambridge Univ. (England).**
Stall and surge in axial flow compressors p 423 N93-18724
- Active control of stall and surge p 423 N93-18725
- Canadian Forces Headquarters, Ottawa (Ontario).**
The human factor problem in the Canadian Forces aviation p 491 N93-19657
- Canadian Marconi Co. Ltd., Kanata (Ontario).**
Embedded GPS: The Canadian Marconi approach
p 886 N93-30330
- Cape Cod Research, Buzzards Bay, MA.**
Waterborne polyurethane binder resins for compliant aircraft coatings
[AD-A256246] p 199 N93-14573
- Carnegie-Mellon Univ., Pittsburgh, PA.**
CFD analysis on control of secondary losses in STME LOX turbines with endwall fences p 419 N93-17289
- Joint Integrated Avionics Working Group (JIAWG) object-oriented domain analysis method (JODA), version 3.1
[AD-A258468] p 344 N93-18270
- Case Western Reserve Univ., Cleveland, OH.**
Tesseract: Supersonic business transport
[NASA-CR-192072] p 334 N93-17977
- Catholic Univ. of America, Washington, DC.**
Adaptive automation and human performance: Multi-task performance characteristics
[AD-A254596] p 186 N93-12578
- Theory and design of adaptive automation in aviation systems
[AD-A254595] p 160 N93-12613
- Central Research Inst. for Physics, Budapest (Hungary).**
DAR-2: On-board data acquisition system for aircraft engines p 169 N93-15166
- Centre d'Essais Aeronautique Toulouse (France).**
Crack growth prediction models p 1004 N93-31747
- Centre d'Essais en Vol, Bretigny-Air (France).**
Air accidents in the French Air Force
p 492 N93-19676
- Centre d'Etudes de la Navigation Aeronautique, Toulouse (France).**
Evolution of radar data processing in the French air traffic control system p 886 N93-30325
- Centre d'Etudes et de Recherches, Toulouse (France).**
Prediction of the performances in combustion of ramjets and state-rockets by isothermal experiments and modeling
p 363 N93-17622
- Three-dimensional compressible stability-transition calculations using the spatial theory p 783 N93-27431
- Investigations on entropy layer along hypersonic hyperboloids using a defect boundary layer
p 787 N93-27462
- Centre National de la Recherche Scientifique, Ecullly (France).**
Modeling of a turbulent flow in the presence of discrete parietal cooling jets p 904 N93-29960
- Centre National de la Recherche Scientifique, Paris (France).**
Combustion instabilities in a side-dump model ramjet combustor
p 362 N93-17613
- Centro Italiano Ricerche Aerospaziali, Naples.**
Numerical study for the study of medium speed internal noise problems
[DILC-EST-TN-200] p 101 N93-11156
- Artificial intelligence and CFD: Expert systems for the design of airfoils and for grid generation
[DIGE-EST-TN-016] p 48 N93-11161
- Wind tunnel operator aimed comparison between two electronic pressure scanner systems
[DLAS-EST-TR-040] p 67 N93-11225
- Ceskoslovenska Akademie Ved, Prague.**
Czechoslovak development and experience in flight data recorder readout and analysis p 168 N93-15162
- Charles River Analytics, Inc., Cambridge, MA.**
Design for tactical situation awareness display
[AD-A256194] p 170 N93-15235
- Chicago Univ., IL.**
IOPS advisor: Research in progress on knowledge-intensive methods for irregular operations airline scheduling p 443 N93-18686
- Cincinnati Univ., OH.**
LDV Measurements of unsteady flow fields in radial turbine
[AD-A253592] p 19 N93-10648
- Erosion predictions and measurements of high-temperature coatings and superalloys used in turbomachines p 74 N93-12189
- LDV measurements of unsteady flow fields in radial turbine
[AD-A255728] p 221 N93-15065
- Computational gearing mechanics
[NASA-CR-191127] p 751 N93-25884
- Investigation of forced unsteady separated flows using velocity-vorticity form of Navier-Stokes equations
p 840 N93-27451
- Simulation, characterization and control of forced unsteady viscous flows using Navier-Stokes equations
[AD-A264333] p 934 N93-30369
- City of London Polytechnic (England).**
Prediction of success from training p 495 N93-19702
- Civil Aeromedical Inst., Oklahoma City, OK.**
A review of civil aviation propeller-to-person accidents: 1980-1989
[AD-A260695] p 705 N93-25896
- Civil Aviation Authority, London (England).**
UK airmisses involving commercial air transport, May-August 1991
[ETN-92-92260] p 28 N93-11357
- UK airmisses involving commercial air transport, January-April 1991
[ETN-92-92261] p 87 N93-11358
- Reportable accidents to UK registered aircraft, and to foreign registered aircraft in UK airspace, 1990
[CAP-600] p 991 N93-31730
- Reaction to aircraft noise near general aviation airfields
[DORA-8203] p 1040 N93-32377
- UK airmisses involving commercial air transport, September - December 1991
[ETN-93-93930] p 992 N93-32409
- Clarkson Univ., Potsdam, NY.**
An experimental study of flow patterns and endwall heat transfer upstream of a surface-mounted rectangular obstruction in a turbulent boundary layer
p 89 N93-11698
- Lift and drag forces on droplets and particles in wall-bounded shear flows
[DE93-002678] p 419 N93-17761
- An analysis of lift forces on aerosols in a wall bounded turbulent shear flow
[DE93-003362] p 747 N93-24963
- Clemson Univ., SC.**
Signal processing for airborne doppler radar detection of hazardous wind shear as applied to NASA 1991 radar flight experiment data p 490 N93-19612
- Coherent Technologies, Inc., Boulder, CO.**
Solid-state coherent laser radar wind shear measuring systems p 144 N93-14848
- College of William and Mary, Williamsburg, VA.**
The use of multiple models in case-based diagnosis
p 759 N93-25969
- Colorado Univ., Boulder.**
Forced unsteady separated flows on a 45 degree delta wing p 82 N93-10305
- Methodology for studying and training expertise
p 147 N93-15018
- HSCT mission analysis of waverider designs
[NASA-CR-192193] p 515 N93-21646
- Aerodynamic foundations for use of unsteady aerodynamic effects in flight control p 695 N93-25274
- Computation of transonic flow over a porous surface projectile p 696 N93-25409
- Variable-speed generators with flux weakening
p 750 N93-25599
- The HSCT mission analysis of waverider designs
[NASA-CR-193467] p 879 N93-31037
- Columbia Univ., New York, NY.**
Aviation accidents, incidents, and violations: Psychological predictors among US pilots
p 144 N93-14693
- Committee on Appropriations (U.S. Senate).**
National Aeronautics and Space Administration
p 454 N93-17091
- Committee on Commerce, Science, and Transportation (U.S. Senate).**
National Aeronautics and Space Administration
Authorization Act, fiscal year 1993
[S-REPT-102-364] p 234 N93-13798
- NASA's fiscal year 1993 budget
[S-HRG-102-707] p 234 N93-13800
- Committee on Science, Space and Technology (U.S. House).**
NASA authorization, 1993, volume 2
[GPO-56-943-VOL-2] p 234 N93-13799
- Communications Research Centre, Ottawa (Ontario).**
Design issues and initial performance of an adaptive air/ground/air HF communication system
p 934 N93-30342
- CompEngServ Ltd., Ottawa (Ontario).**
Issues of ATC conflict resolution under real-time constraints p 887 N93-30350
- Composite Aircraft Products Ltd. (Canada).**
Pitch control trimming system for canard design aircraft
[CA-PATENT-APPL-SN-2013236] p 63 N93-10374
- Computational Fluid Dynamics Research Corp., Huntsville, AL.**
Influence of supercritical conditions on pre-combustion chemistry and transport behavior of jet fuels
[AD-A261813] p 737 N93-26268

Computational Mechanics Co., Austin, TX.

H-P adaptive methods for finite element analysis of aerothermal loads in high-speed flows
[NASA-CR-189739] p 420 N93-18093

Advanced adaptive computational methods for Navier-Stokes simulations in rotorcraft aerodynamics
[NASA-CR-192282] p 483 N93-20256

Computer Resource Management, Inc., Herndon, VA.

National Airspace System flight planning operational concept NAS-SR-131
[PB93-124659] p 310 N93-18031

Computer Sciences Corp., Hampton, VA.

A comparison using APPL and PVM for a parallel implementation of an unstructured grid generation program
[NASA-CR-191425] p 757 N93-25073

Advanced Transport Operating System (ATOPS) Flight Management/Flight Controls (FM/FC) software description
[NASA-CR-191457] p 808 N93-28621

Advanced Transport Operating System (ATOPS) utility library software description
[NASA-CR-191469] p 1000 N93-32218

Concordia Univ., Montreal (Quebec).

Characteristics of separated flows including cavitation effects
p 84 N93-10874

Use of microprocessor-based simulator technology and MEG/EEG measurement techniques in pilot emergency-maneuver training
p 530 N93-19706

Stochastic finite element analysis for high speed rotors
p 554 N93-20696

Models for performance assessment of HF antennas on the CH-135/Twin Huey helicopter
p 933 N93-30291

Coupling gain computation between antennas on circular cylinders at SHF/EHF frequencies
p 933 N93-30309

RCS of fundamental scatterers in the HF band by wire-grid modelling
p 933 N93-30320

Construcciones Aeronauticas S.A., Madrid (Spain).

Nondestructive inspection of in-service aircraft
[ETN-93-93059] p 496 N93-20928

Continental Airlines, Inc., Los Angeles, CA.

In-service evaluation of wind shear systems
p 146 N93-14857

Continuum Dynamics, Inc., Princeton, NJ.

Rotor design optimization using a free wake analysis
[NASA-CR-177612] p 693 N93-25075

Coordinating Research Council, Inc., Atlanta, GA.

Aircraft and refueler bonding and grounding study
[AD-A262027] p 911 N93-29398

CORE International, Inc., Washington, DC.

Definitive mission for civil aviation master plan for Poland
[PB92-213974] p 459 N93-21713

Cornell Univ., Ithaca, NY.

Tilt rotor hover aeroacoustics
[NASA-CR-177598] p 99 N93-10458

Stall transients including effects of inlet distortion and intake geometry
p 423 N93-18726

Surface shear stress estimates from geostrophic winds for use in sensible and latent heat flux formulations
p 936 N93-30044

Council for National Academic Awards (England).

Design and performance of nozzle-less volute casings for inward flow radial turbines
p 722 N93-25471

Control and optimization of aircraft trajectories
p 729 N93-25543

Simulation of aircraft gas turbine engine
p 723 N93-25751

Cranfield Inst. of Tech., Bedford (England).

DESAID (the development of an expert system for aircraft initial design)
p 163 N93-14448

Rotating stall inception in fans of low hub-tip ratio
p 136 N93-14479

A90 project: Design of a composite fin
[ETN-92-92773] p 329 N93-16562

The aerodynamic characteristics of the Göttingen 797 and Wortmann FX63-137 aerofoil sections at very low Reynolds numbers
[ETN-93-92999] p 295 N93-18128

Experimental investigation of rotating stall in a mismatched three stage axial flow compressor
p 423 N93-18727

Application of recess vane casing treatment to axial flow fans
p 423 N93-18728

A study of stall in a low hub-tip ratio fan
p 423 N93-18729

Review of initial experiments using the Hawk model, dynamic rig facility, and the CED 1401 digital data acquisition equipment
[CRANFIELD-AERO-9017] p 531 N93-21406

Crashworthiness of composite seats for civil aircraft
p 703 N93-24773

A preliminary sizing method for unmanned aircraft using multi-variate optimisation
p 714 N93-25408

An approach to configuration design synthesis of subsonic transport aircraft using artificial intelligence techniques
p 716 N93-25692

Numerical modelling of viscous turbomachinery flows with a pressure correction method
p 723 N93-25702

ASTOVL combat aircraft design synthesis and optimization
p 717 N93-25704

The effects of reaction on axial compressor performance
p 724 N93-25882

Radial inflow turbine study
p 724 N93-25917

Plume effects on the flow around a blunted cone at hypersonic speeds
p 787 N93-27460

Cree Research, Inc., Durham, NC.

High temperature rectifiers and MOS devices in 6H-silicon carbide
[AD-A254725] p 90 N93-12340

D**Dassault Aviation, Istres (France).**

Aid in investigation by figure animation
p 491 N93-19659

Dassault-Breguet Aviation, Saint Cloud (France).

Method for developing the RAFALE flight control system
p 512 N93-19912

David Taylor Research Center, Bethesda, MD.

Simultaneous mapping of the unsteady flow fields by Particle Displacement Velocimetry (PDV)
p 786 N93-27454

Dayton Univ., OH.

Evaluation of alternatives for increasing A-7D rearward visibility
[AD-A255071] p 50 N93-12488

A condensed phase test cell assembly for the System for Thermal Diagnostic Studies (STDS)
[AD-A258463] p 393 N93-18242

An investigation of laser velocimetry measurements within high speed, complex flows
p 748 N93-25237

Dayton Univ. Research Inst., OH.

Determination of stresses on laminated aircraft transparencies by the strain gage-hole drilling and sectioning method
[AD-A255548] p 164 N93-14571

Measurement of modulation transfer functions of simulator displays
[AD-A259401] p 530 N93-21268

DCW Industries, La Canada, CA.

The remarkable ability of turbulence model equations to describe transition
p 783 N93-27432

Defence and Civil Inst. of Environmental Medicine, North York (Ontario).

Canadian Forces helicopter ditchings: 1952-1990
p 493 N93-19685

Defence Research Agency, Farnborough (England).

Heat transfer and aerodynamics of a high rim speed turbine nozzle guide vane with profiled end walls
[AD-A258346] p 295 N93-17991

The experimental study of transition and leading edge contamination of swept wings
[LIB-TRANS-2197] p 782 N93-27274

Heat transfer and aerodynamics of a 3D design nozzle guide vane tested in the Pyestock Isentropic Light Piston Facility
p 901 N93-29928

Fractographic investigation of IMI 685 crack propagation specimens for SMP SC33
p 1004 N93-31743

Department of National Defence, Ottawa (Ontario).

Material characterization and fractographic examination of Ti-17 fatigue crack growth specimens for SMP SC33
p 1004 N93-31744

Department of the Air Force, Washington, DC.

Land subsidence and problems affecting land use at Edwards Air Force Base and vicinity, California, 1990
[PB93-182236] p 1036 N93-32191

Department of the Navy, Washington, DC.

Ribless ram air parachute
[AD-D015351] p 20 N93-11050

Hermetic sealing and EMI shielding gasket
[AD-D015359] p 199 N93-13414

Liquid flow reactor and method of using
[AD-D015392] p 222 N93-15232

Articulated control surface
[AD-D015464] p 371 N93-16463

Mass loaded composite rotor for vibro-acoustic application
[AD-D015604] p 535 N93-20016

Aerodynamic surface tip vortex attenuation system
[AD-D015606] p 483 N93-20017

Interferometric JFTOT tube deposit measuring device
[AD-D015599] p 536 N93-20247

High efficiency, low weight and volume energy absorbent seam
[AD-D015531] p 554 N93-20765

Apparatus for reduction of vibration in liquid-injected gas compressor system
[AD-D015607] p 554 N93-20772

Single screw interrupted thread positive displacement mechanism
[AD-D015596] p 554 N93-20790

System for calibrating a gyro navigator
[AD-D015668] p 708 N93-26093

Articulated fin/wing control system
[AD-D015712] p 909 N93-29278

Department of Transport (England).

737-400 at Kegworth, 8 January 1989: The AAIB investigation
p 491 N93-19661

The UK perspective on aviation security
p 496 N93-21858

Department of Transportation, Cambridge, MA.

Three-dimensional stress analysis of multilayered airport pavements: Integral transform approach
p 381 N93-16319

Detroit Univ., MI.

Aircraft trajectory tracking and prediction
[AD-A259039] p 340 N93-18999

Deutsche Airbus G.m.b.H., Bremen (Germany).

Recent developments in low-speed TPS-testing for engine integration drag and installed thrust reverser simulation
p 160 N93-13207

Deutsche Airbus G.m.b.H., Munich (Germany).

Software flexibility and configuration control for the A340/A330 Aircraft Condition Monitoring System (ACMS)
p 167 N93-15154

Deutsche Forschungs- und Versuchsanstalt fuer Luft- und Raumfahrt, Brunswick (Germany).

GARTUR damage mechanics for composite materials: Analytical/experimental research on delaminations
p 537 N93-21513

Deutsche Forschungs- und Versuchsanstalt fuer Luft- und Raumfahrt, Goettingen (Germany).

Comparative performance tests of a pilot-inlet in several European wind-tunnels at subsonic and supersonic speeds
p 130 N93-13221

Deutsche Forschungsanstalt fuer Luft- und Raumfahrt, Berlin (Germany).

Prediction of jet mixing noise for high subsonic flight speeds
p 100 N93-10685

Correlations between engineering, medical and behavioural aspects in fire-related aircraft accidents
p 494 N93-19693

System identification for X-31A project support: Lessons learned so far
p 512 N93-19914

Deutsche Forschungsanstalt fuer Luft- und Raumfahrt, Brunswick (Germany).

Comparison of flyover noise data from aircraft at high subsonic speeds with prediction
p 100 N93-10674

Investigation of interference phenomena of modern wing-mounted high-bypass-ratio engines by the solution of the Euler-equations
p 213 N93-13204

The jet behaviour of an actual high-bypass engine as determined by LDA-measurements in ground tests
p 175 N93-13218

Investigation of the flowfield around an isolated bypass engine with fan and core jet
p 215 N93-13227

Proceedings of the 16th Symposium on Aircraft Integrated Monitoring Systems
[DLR-MITT-92-01] p 167 N93-15152

A contribution to the dynamic feedforward open loop control of multivariable systems and to the optimal design of command functions
[DLR-FB-92-05] p 441 N93-16515

Development of a realtime DGPS system
[DLR-MITT-92-06] p 503 N93-20749

Fundamentals of adaptive anticipation techniques for the detection of threatening air traffic conflicts: Investigation of the horizontal proximity situation in the case of expected heading changes
[DLR-MITT-91-21] p 503 N93-21004

The influence of the rotor test facilities ROTEST and ROTOS on the rotor inflow
[DLR-MITT-91-16] p 522 N93-21173

Calculation of noise emission caused by jet aircraft during takeoff, approach and horizontal flyover
[DLR-MITT-91-15] p 569 N93-21368

Definition of an airfoil family for the EUROFAR rotor
[DLR-FB-92-04] p 998 N93-31197

The DLR test aircraft in the FZ-BS, -VFW 614/ATTAS, Dornier DO 228-101, MBB BO105 S-3
p 1018 N93-31272

The basic measurement equipment of the DLR test aircraft
p 1000 N93-31273

Ground installations for preparation and evaluation of flight tests
p 1014 N93-31274

Instigation and processing of flight tests in DLR
p 998 N93-31275

ATTAS experimental-cockpit and ATMOS for component and system investigations in flight guidance
p 1014 N93-31276

Testing of an experimental FMS
p 998 N93-31277

- Testing concept of a taxiing control system, summary p 1010 N93-31278
- Pallet for helicopter test instrumentation p 1000 N93-31279
- Development and flight testing of a fault-tolerant fly-by-light yaw control system p 1010 N93-31280
- Ground- and satellite-derived flight-path measurements as demonstrated in the AFES Avionics Flight Evaluation System (AFES) p 993 N93-31281
- On-board derived flight-path measurement as demonstrated by an ILS measurement system p 994 N93-31282
- Installations and methods for measurement of aircraft radio components and systems p 1031 N93-31284
- The influence of variable flow velocity on unsteady airfoil behavior [DLR-FB-92-22] p 988 N93-31320
- Deutsche Forschungsanstalt fuer Luft- und Raumfahrt, Cologne (Germany).**
- Performance of controlled diffusion blades p 424 N93-18735
- Summaries of the 1991 publications of DLR research reports and DLR communications [ETN-93-92588] p 572 N93-21022
- Coupling of 3D-Navier-Stokes external flow calculations and internal 3D-heat conduction calculations for cooled turbine blades p 904 N93-29961
- Deutsche Forschungsanstalt fuer Luft- und Raumfahrt, Goettingen (Germany).**
- On flutter behavior of a 2-D compressor cascade in incompressible flow [DLR-FB-91-26] p 418 N93-16543
- Aerothermodynamic properties of hypersonic flows over radiation-adiabatic surfaces [DLR-FB-91-42] p 485 N93-21761
- Experimental investigations on wing-body combinations and their components at high angles of attack in the subsonic and transonic speed range [DLR-FB-91-43] p 516 N93-21762
- Unsteady Navier-Stokes method for accelerated moving airfoils with separation [DLR-FB-92-03] p 485 N93-21763
- Transonic flows on an oscillating airfoil and their effect on the flutter-boundary [DLR-FB-92-08] p 790 N93-29006
- The ViB-code to simulate 3-D stator/rotor flow in axial turbines [DLR-FB-92-19] p 1003 N93-31170
- TDLM: A Transonic Doublet Lattice Method for 3D potential unsteady transonic flow calculation [DLR-FB-92-25] p 988 N93-31171
- Deutsche Forschungsanstalt fuer Luft- und Raumfahrt, Oberpfaffenhofen (Germany).**
- Motion errors and compensation possibilities p 212 N93-13052
- The real aperture antenna of SAR, a key element for performance p 213 N93-13053
- Identification of icing water clouds by NOAA AVHRR satellite data [DLR-FB-92-11] p 434 N93-16477
- Deutsche Lufthansa A.G., Cologne (Germany).**
- Activities report of Lufthansa [ETN-92-92100] p 28 N93-11319
- Deutsche Lufthansa A.G., Frankfurt am Main (Germany).**
- Software for flight recorder data evaluation developed by Lufthansa p 230 N93-15163
- Deutsche System-Technik G.m.b.H., Bremen (Germany).**
- Testing of an experimental system for image reconnaissance p 1040 N93-31283
- Dornier Luftfahrt G.m.b.H., Friedrichshafen (Germany).**
- Numerical determination of the residual strength of battle damaged composite plates p 537 N93-21533
- Comparison of the damage for various types of fibre reinforced composites due to different lightning test standards (MIL-STD-1757A, German military VG-standard 96903) p 736 N93-24891
- Dornier System G.m.b.H., Friedrichshafen (Germany).**
- Integrated engine control and monitoring with experiences derived from OLMOS p 178 N93-15168
- Dortmund Univ. (Germany).**
- Effects on health of noise disturbances due to air traffic p 1035 N93-31929
- Douglas Aircraft Co., Inc., Long Beach, CA.**
- Composites technology for transport primary structure p 918 N93-30431
- Resin transfer molding for advanced composite primary aircraft structures p 919 N93-30438
- Dow Chemical Co., Midland, MI.**
- Development of resins for composites by resin transfer molding p 921 N93-30853

- Draper (Charles Stark) Lab., Inc., Cambridge, MA.**
- Air-breathing hypersonic vehicle guidance and control studies: An integrated trajectory/control analysis methodology, phase 2 [NASA-CR-189703] p 65 N93-12413
- Aerodynamic forces on maglev vehicles [PB93-154813] p 782 N93-27413
- Duke Univ., Durham, NC.**
- Prediction of unsteady flows in turbomachinery using the linearized Euler equations on deforming grids [NASA-CR-192919] p 747 N93-25109
- Chaos in mechanical systems with especial reference to rotorcraft and missiles [AD-A263703] p 943 N93-29384

E

- Ecole Centrale de Lyon (France).**
- Active control of aeroacoustic couplings by means of adaptive systems [ECL-91-18] p 64 N93-11576
- Ecole Nationale Supérieure de Mécanique et d'Aérotechnique, Poitiers (France).**
- Combustion in supersonic flows p 199 N93-14627
- Damage tolerance of a helicopter rotor high-strength steel p 555 N93-21322
- Ecole Polytechnique, Montreal (Quebec).**
- A comparative study of semi-empirical dynamic stall models p 18 N93-10544
- A field panel method for transonic flows p 18 N93-10547
- Eidgenössische Technische Hochschule, Zurich (Switzerland).**
- Design and application of Active Magnetic Bearings (AMB) for vibration control p 1033 N93-32279
- Electro Magnetic Applications, Inc., Denver, CO.**
- Digitization of analog data from in-flight lightning strikes p 753 N93-24884
- Electro Magnetic Applications, Inc., Lakewood, CO.**
- Development of models for predicting the triggering of lightning by launch vehicles p 734 N93-24899
- Eloret Corp., Palo Alto, CA.**
- Solution of nonlinear flow equations for complex aerodynamic shapes [NASA-CR-190979] p 90 N93-12329
- Eloret Corp., Sunnyvale, CA.**
- Experimental Investigation of Nozzle/Plume Aerodynamics at Hypersonic Speeds [NASA-CR-191368] p 386 N93-18085
- Increase of stagnation pressure and enthalpy in shock tunnels p 295 N93-18086
- Hypersonic flows as related to the national aerospace plane [NASA-CR-191980] p 296 N93-18378
- An experimental investigation of the separating/reattaching flow over a backstep [NASA-CR-192105] p 288 N93-18781
- Development and application of computational aerothermodynamics flowfield computer codes [NASA-CR-192940] p 692 N93-24736
- Engineered Designs, Inc., Cincinnati, OH.**
- Advanced bristle seals for gas turbine engines [AD-A261296] p 752 N93-26564
- Engineering and Economics Research, Inc., Vienna, VA.**
- Poland civil aviation master plan and investment program: Executive summary [PB92-213685] p 459 N93-21342
- Poland civil aviation master plan and investment program [PB92-213693] p 459 N93-21343
- Environmental Science and Engineering, Inc., Gainesville, FL.**
- Physical effects of vegetation on wind-blown sand in the coastal environments of Florida [PB92-188424] p 93 N93-11702
- ERES Consultants, Inc., Savoy, IL.**
- Development of a unified airport pavement analysis and design system p 380 N93-16317
- ESDU International Ltd., London (England).**
- Program for calculation of aileron rolling moment and yawing moment coefficients at subsonic speeds [ESDU-88040] p 136 N93-14514
- Pressure drag and lift contributions for blunted forebodies of fineness ratio 2.0 in transonic flow (M infinity less than or equal to 1.4) [ESDU-89033] p 136 N93-14515
- Direct prediction of a separation boundary for aerofoils using a viscous-coupled calculation method [ESDU-92008] p 136 N93-14516
- Estimation of rate of climb [ESDU-92019] p 164 N93-14541
- Maximum lift of wings with leading-edge devices and trailing-edge flaps deployed [ESDU-92031] p 290 N93-16522

- Drag due to gaps round undeflected trailing-edge controls and flaps at subsonic speeds [ESDU-92039] p 290 N93-16634
- Example of statistical techniques applied to analysis of landing ground roll distance measurements (linear regression, correlation coefficient and F-test) [ESDU-92021] p 330 N93-16635
- Example of statistical techniques applied to analysis of measurements of the landing airborne manoeuvre. (Multiple linear regression with two independent variables and one dependent variable.) [ESDU-92022] p 330 N93-16636
- Fatigue propagation behaviour of short cracks in titanium alloys [ESDU-92023] p 392 N93-16637
- Contribution of ventral fins to sideforce and yawing moment derivatives due to sideslip at low angle of attack [ESDU-92029] p 291 N93-16638
- Fatigue propagation behaviour of short cracks in aluminum alloys [ESDU-92030] p 392 N93-16641
- Pitching moment of low aspect ratio wing-body combinations up to high angles of attack at supersonic speeds [ESDU-92043] p 333 N93-17958
- Energy method for analysis of measured airspeed change in landing airborne manoeuvre [ESDU-92020] p 335 N93-18042
- European Space Agency, Paris (France).**
- Analytic formulation of unsteady profile aerodynamics and its application to simulation of rotors [ESA-TT-1244] p 485 N93-21659
- Flow visualization on helicopter blades using acenaphthen [ESA-TT-1255] p 931 N93-29273
- Flight mechanical model for performance calculations and interactions between flight vehicle and ramjet in regard to the flight orbit [ESA-TT-1267] p 893 N93-29464
- Three-dimensional graphical representation of objects according to movement data in realtime [ESA-TT-1258] p 942 N93-30104
- Flight test of avionic and air-traffic control systems [ESA-TT-1279] p 993 N93-31271
- Exotech, Inc., Fremont, CA.**
- An experimental and analytical study of TIP clearance effects in axial flow compressors [AD-A256434] p 179 N93-15337
- Extrude Hone Corp., Irwin, PA.**
- On machine capacitance dimensional and surface profile measurement system p 750 N93-25579
- Ultrasonic polishing p 750 N93-25580

F

- Fachhochschule, Munich (Germany).**
- Effects of air traffic on nature and environment in the neighborhood of airports by example of the Munich 2 Airport (Germany) p 1035 N93-31932
- Federal Aviation Administration, Atlanta, GA.**
- ILS mathematical modeling study of an ILS glide slope proposed for runway 19L at the Meridian Naval Air Station, Mississippi [DOT/FAA/CT-TN93/8] p 705 N93-24741
- Federal Aviation Administration, Atlantic City, NJ.**
- Air traffic control visual scanning [DOT/FAA/CT-TN92/16] p 35 N93-10459
- High Capacity Voice Recorder (HCVR) Operational Test and Evaluation (OT/E) integration test report [DOT/FAA/CT-TN92/30] p 88 N93-11460
- Upgrade Precision Runway Monitor (PRM) Operational Test and Evaluation (OT/E) test plan [DOT/FAA/CT-TN92/13] p 67 N93-11616
- Controller evaluation of initial data link terminal air traffic control services: Mini study 2, volume 1 [DOT/FAA/CT-92/2-VOL-1] p 36 N93-11704
- Controller evaluation of initial data link terminal air traffic control services: Mini study 2, volume 2 [DOT/FAA/CT-92/2-VOL-2] p 36 N93-11705
- ILS mathematical modeling study of the effects of an ASR-9 structure at the Long Island MacArthur Airport, Islip, NY [DOT/FAA/CT-TN92/25] p 192 N93-12668
- Limited production Precision Runway Monitor (PRM) master test plan [DOT/FAA/CT-TN92/23] p 192 N93-12899
- Prototype stop bar system evaluation at John F. Kennedy International Airport [AD-A258667] p 192 N93-12902
- Terminal Doppler Weather Radar (TDWR) Operational Test and Evaluation (OT/E) integration test plan [DOT/FAA/CT-TN92/6] p 151 N93-13377

A NASPAC-based analysis of the delay and cost effects of the Dallas/Fort Worth metroplex plan
[DOT/FAA/CT-TN92/21] p 193 N93-13447

FAA Technical Center Aeronautical Data Link Research Plan
[DOT/FAA/CT-92/23] p 417 N93-15698

The effect of TCAS interrogations on the Chicago O'Hare ATCRBS system
[DOT/FAA/CT-92/22] p 318 N93-16498

Results of DATAS investigation of illegal mode S ID's at JFK Airport
[DOT/FAA/CT-92/26] p 318 N93-16841

Aircraft wing compartment liner concept to reduce fuel spillage
[DOT/FAA/CT-TN92/34] p 331 N93-17219

Proceedings of the AIAA/FAA Joint Symposium on General Aviation Systems
[AD-A257780] p 240 N93-17732

A simulation study of the effects of communication delay on air traffic control
[AD-A258593] p 502 N93-19966

Data Multiplexing Network (DMN), Phase 3: Equipment Operational Test and Evaluation (OT/E) integration test report
[DOT/FAA/CT-TN92/49] p 503 N93-20612

A model study of the aircraft cabin environment resulting from in-flight fires
[DOT/FAA/CT-90/22] p 496 N93-21557

The effectiveness of hand-held fire extinguishers on cargo container fires
[DOT/FAA/CT-TN92/42] p 496 N93-21821

Proceedings of the First International Symposium on Explosive Detection Technology
[DOT/FAA/CT-92/11] p 496 N93-21856

The 1992 International Aerospace and Ground Conference on Lightning and Static Electricity: Addendum
[DOT/FAA/CT-92/20-ADD-1] p 753 N93-24875

Visual approach data collection at St. Louis Lambert Field (STL)
[DOT/FAA/CT-TN93/2] p 706 N93-24948

The ATC evaluation of the prototype Airport Surveillance Radar Wind Shear Processor (ASR-WSP) at Orlando International Airport
[DOT/FAA/CT-TN92/48] p 748 N93-25210

Narrow-body aircraft water spray optimization study
[DOT/FAA/CT-TN93/3] p 705 N93-25224

Runway Visual Range (RVR) Operational Test and Evaluation (OT&E) integration and OT&E operational test report
[DOT/FAA/CT-TN92/37] p 706 N93-25243

The Data Multiplexing Network (DMN) phase 3 Extended Distance Data Cable (EDDC) test and evaluation
[DOT/FAA/CT-TN93/11] p 752 N93-26160

The ILS mathematical modeling study of the Runway 10 ILS Localizer at Luis Munoz Marin International Airport, San Juan, Puerto Rico
[DOT/FAA/CT-TN93/10] p 792 N93-27017

Next Generation Weather Radar (NEXRAD) Principal User Processor (PUP) Operational Test and Evaluation (OT&E) operational test plan
[DOT/FAA/CT-TN93/22] p 841 N93-28054

Ventilation effects on smoke and temperature in an aircraft cabin quarter-scale model
[DOT/FAA/CT-89/25] p 791 N93-28055

Time delay measurements of current primary FAA air/ground transmitters and receivers
[DOT/FAA/CT-TN93/14] p 842 N93-28555

Results of DATAS investigation of ATCRBS environment at the Los Angeles International Airport
[DOT/FAA/CT-93/6] p 793 N93-28625

Data Multiplexing Network (DMN) equipment Operational Test and Evaluation (OT&E) integration test report
[AD-A263172] p 942 N93-29490

Investigation of advanced technology for airway facilities maintenance training
[DOT/FAA/CT-TN92/24] p 994 N93-32336

Federal Aviation Administration, Cambridge, MA.

Advanced terrain displays to transport category aircraft
[PB92-197136] p 35 N93-10065

Design of instrument approach procedure charts: Comprehension speed of missed approach instructions coded in text or icons
[PB92-205673] p 36 N93-11252

Magneto-optic imaging inspection of selected corrosion specimens
[DOT/FAA/CT-TN92/20] p 88 N93-11617

Proceedings of the Aircraft Wake Vortices conference, volume 1
[PB93-126449] p 485 N93-21796

Proceedings of the Aircraft Wake Vortices conference, volume 2
[PB93-127728] p 559 N93-21799

An analysis of en route controller-pilot voice communications
[AD-A264784] p 935 N93-30611

Federal Aviation Administration, Oklahoma City, OK.

Postmortem alcohol production in fatal aircraft accidents
[AD-A255766] p 143 N93-14026

Comparison of performance on the Shipley Institute of Living Scale, Air Traffic Control Specialist Selection Test, and FAA Academy Screen
[AD-A259249] p 502 N93-20582

Inward contaminant leakage tests of the S-Tron Corporation emergency escape breathing device. Phase 1: Tests of the original design. Phase 2: Tests with the redesigned neck seal
[DOT/FAA/AM-92/18] p 704 N93-25205

Conversion of the CTA, Inc., en route operations concepts database into a formal sentence outline job task taxonomy
[AD-A261410] p 708 N93-26447

Federal Aviation Administration, Washington, DC.

A description of the Mode Select beacon system (Mode S) and its associated benefits to the National Airspace System (NAS)
[DOT/FAA/SE-92/6] p 35 N93-10738

Summary of findings from the PIREP-based analyses conducted during the 1988 to 1990 evaluations of TDWR-based and TDWR/LLWAS-based alert services provided to landing/departing pilots
[AD-A253859] p 93 N93-11144

Future FAA telecommunications plan
[AD-A249133] p 89 N93-11760

Report to Congress: State Block Grant Program
[AD-A254569] p 193 N93-13882

Performance of color-dependent tasks of air traffic control specialists as a function of type and degree of color vision deficiency
[AD-A256614] p 151 N93-14275

Identifying ability requirements for operators of future automated air traffic control systems
[AD-A256615] p 152 N93-14276

Effects of seating configuration and number of type 3 exits on emergency aircraft evacuation
[AD-A256616] p 143 N93-14277

Airborne Wind Shear Detection and Warning Systems. Fourth Combined Manufacturers' and Technologists' Conference, part 2
[NASA-CP-10105-PT-2] p 144 N93-14844

Terminal area forecasts FY 1992 - 2005
[AD-A257977] p 149 N93-15390

Unified Airport Design and Analysis Concepts Workshop
[DOT/FAA/RD-92/17] p 378 N93-16309

Estimating the regional economic significance of airports
[AD-A257658] p 382 N93-17793

Report to Congress: Long-term availability of adequate airport system capacity
[AD-A258209] p 319 N93-18202

Enroute air traffic controllers use of flight progress strips: A graph-theoretic analysis
[AD-A259062] p 319 N93-18927

Criminal acts against civil aviation
[AD-A258760] p 495 N93-19867

National Airspace System: Air traffic control and airspace management operational concept NAS-SR-132
[DOT/FAA/SE-92/5] p 502 N93-20164

FAA international conference on airplane ground deicing
[AD-A263617] p 880 N93-29266

Federal Bureau of Investigation Academy, Quantico, VA.

Insights into US domestic aviation
p 496 N93-21859

Fiat Aviazione S.p.A., Turin (Italy).

Cooling geometry optimization using liquid crystal technique
p 902 N93-29939

Five-College Astronomy Dept., Amherst, MA.

Coherent systems in the terahertz frequency range: Elements, operation, and examples
p 841 N93-27727

Florida Atlantic Univ., Boca Raton.

Dynamic stall effects on hingeless rotor stability with experimental correlation
p 129 N93-13010

Trim analysis by shooting and finite elements and Floquet eigenanalysis by QR and subspace iterations in helicopter dynamics
p 163 N93-13914

Florida Univ., Gainesville.

Physical effects of vegetation on wind-blown sand in the coastal environments of Florida
[PB92-188424] p 93 N93-11702

Management of Automatic Data Processing (ADP) system documentation in the Department of Defense
[AD-A258507] p 571 N93-20048

Fokker B.V., Schiphol-Oost (Netherlands).

Aerodynamic integration of thrust reversers on the Fokker 100
p 160 N93-13208

Foster-Miller Associates, Inc., Waltham, MA.

FAA unified pavement analysis 3-D finite element method
p 379 N93-16314

Analysis of aircraft noise levels in the vicinity of start-of-takeoff roll at Baltimore-Washington International Airport
[PB92-221605] p 559 N93-21501

Framasys A.G., Zurich (Switzerland).

Failure diagnostic with MAINTEx based on AIMS at Swissair
p 110 N93-15181

Fuji Heavy Industries Ltd., Utsunomiya (Japan).

A numerical simulations of inner flow of scramjet
p 304 N93-19318

Wind tunnel tests and CFD in Fuji Heavy Industries
p 304 N93-19323

Fujitsu Ltd., Tokyo (Japan).

A simple grid generation technique for hypersonic flow around complex configuration
p 299 N93-19275

G

Galaxy Scientific Corp., Pleasantville, NJ.

Lightning data acquisition
p 753 N93-24883

Aircraft ice detectors and related technologies for onground and inflight applications
[DOT/FAA/CT-92/27] p 791 N93-27269

Garrett Corp., Phoenix, AZ.

Advanced Turbine Technology Applications Project (ATTAP)
[NASA-CR-189228] p 455 N93-18762

Garrett Turbine Engine Co., Phoenix, AZ.

Compound cycle engine for helicopter application
[NASA-CR-180824] p 55 N93-10348

General Accounting Office, Washington, DC.

National Aero-Space Plane: Key issues facing the program. Testimony before the Subcommittee on Technology and Competitiveness, Committee on Science, Space, and Technology, House of Representatives
[GAO/T-NSIAD-92-26] p 161 N93-13253

National aero-space plane: Restructuring future research and development efforts
[AD-A258799] p 340 N93-18981

Aviation safety: Problems persist in FAA's inspection program. Report to the Chairman, Subcommittee on Aviation, Committee on Public Works and Transportation, House of Representatives
[GAO/RCED-92-14] p 495 N93-19841

Aviation safety: Users differ in views of collision avoidance system and cite problems. Report to the Chairman, Subcommittee on Investigations and Oversight, Committee on Science, Space, and Technology, House of Representatives
[GAO/RCED-92-113] p 502 N93-19843

Report to the Chairman, Legislation, and National Security Subcommittee, Committee on Government Operations, House of Representatives. Unmanned aerial vehicles: More testing needed before production of short-range system
[AD-A259473] p 513 N93-20245

General Dynamics Corp., Fort Worth, TX.

CFD calibration for three-dimensional nozzle/afterbody configurations
p 215 N93-13226

Avionics systems architectures
p 808 N93-27169

General Electric Co., Cincinnati, OH.

Hypersonic inlet efficiency revisited
p 16 N93-10012

CF6-6 high pressure compressor stage 5 locking slot crack propagation spin pit test
p 176 N93-14894

A philosophy for integrated monitoring system design
p 178 N93-15174

General Electric Co., Evendale, OH.

Electro-optic architecture for servicing sensors and actuators in advanced aircraft propulsion systems
[NASA-CR-182269] p 232 N93-13762

General Motors Corp., Indianapolis, IN.

Investigation of advanced counterrotation blade configuration concepts for high speed turboprop systems. Task 4: Advanced fan section aerodynamic analysis
[NASA-CR-187128] p 174 N93-12695

Engine life assessment test case TF41 LP compressor shaft torsional fatigue
p 177 N93-14896

Investigation of advanced counterrotation blade configuration concepts for high speed turboprop systems. Task 4: Advanced fan section aerodynamic analysis computer program user's manual
[NASA-CR-187127] p 364 N93-18702

Investigation of advanced counterrotation blade configuration concepts for high speed turboprop systems. Task 5: Unsteady counterrotation ducted propfan analysis. Computer program user's manual
[NASA-CR-187125] p 521 N93-20583

- Investigation of advanced counterrotation blade configuration concepts for high speed turboprop systems. Task 5: Unsteady counterrotation ducted propfan analysis
[NASA-CR-187126] p 521 N93-20773
- Fuel Injector: Air swirl characterization aerothermal modeling, phase 2, volume 2
[NASA-CR-189193-VOL-2] p 721 N93-25106
- Geological Survey, Sacramento, CA.**
Land subsidence and problems affecting land use at Edwards Air Force Base and vicinity, California, 1990
[PB93-182236] p 1036 N93-32191
- George Washington Univ., Washington, DC.**
Shock-dependent, optimum thrust wings in supersonic flow p 483 N93-20169
Program of research in flight dynamics in the JIAFS at NASA-Langley Research Center p 484 N93-21562
[NASA-CR-191885] p 484 N93-21562
Analysis of fluctuating static pressure measurements in a large high Reynolds number transonic cryogenic wind tunnel p 823 N93-27142
[NASA-TM-108722] p 823 N93-27142
- Georgetown Univ., Washington, DC.**
Assessment of potential aerodynamic benefits from spanwise blowing at the wing tip p 134 N93-13822
- Georgia Inst. of Tech., Atlanta.**
LV software for supersonic flow analysis
[NASA-CR-190911] p 16 N93-10069
SAPNEW: Parallel finite element code for thin shell structures on the Alliant FX/80 p 84 N93-10372
[NASA-CR-190663] p 84 N93-10372
A theory for the analysis of rotorcraft operating in atmospheric turbulence p 48 N93-11725
Application of concurrent engineering methods to the design of an autonomous aerial robot p 212 N93-12555
[AD-A254968] p 212 N93-12555
Velocity and temperature measurements in a non-premixed reacting flow behind a backward facing step p 132 N93-13632
High-speed aerodynamics of upper surface blowing aircraft configurations p 132 N93-13729
A simulation model of atmospheric turbulence for rotorcraft applications p 224 N93-14588
The effect of wake dynamics on rotor eigenvalues in forward flight p 137 N93-14595
SAPNEW: Parallel finite element code for thin shell structures on the Alliant FX-80 p 220 N93-14799
[NASA-CR-189212] p 220 N93-14799
Stability of elastically tailored rotor blades p 164 N93-14828
Finite-state inflow applied to aeroelastic flutter of fixed and rotating wings p 188 N93-14830
Deformation mechanisms of NiAl cyclicly deformed near the brittle-to-ductile transformation temperature p 391 N93-15830
[NASA-CR-191649] p 391 N93-15830
Basic research on design analysis methods for rotorcraft vibrations p 422 N93-18576
[NASA-CR-191917] p 422 N93-18576
Simulation of unsteady rotational flow over propfan configuration p 296 N93-18585
[NASA-CR-192234] p 296 N93-18585
Numerical investigation of performance degradation of wings and rotors due to icing p 339 N93-18783
[NASA-CR-192233] p 339 N93-18783
Guidance and flight control law development for hypersonic vehicles p 526 N93-19960
[NASA-CR-192102] p 526 N93-19960
Research in robust control for hypersonic vehicles p 527 N93-20296
[NASA-CR-192127] p 527 N93-20296
Effect of personal and situational variables on noise annoyance: With special reference to implications for en route noise p 569 N93-21317
[NASA-CR-189676] p 569 N93-21317
An aeroelastic model structure investigation for a manned real-time rotorcraft simulation p 693 N93-24756
Application of finite-state inflow to flap-lag-torsion damping in hover p 714 N93-25486
An integrated finite-state model for rotor deformation, nonlinear airloads, inflow, and trim p 715 N93-25538
An investigation on planar velocimetry by spatial cross-correlation p 697 N93-25664
Image-based ranging and guidance for rotorcraft p 708 N93-26549
[NASA-CR-177608] p 708 N93-26549
- Georgia Tech Research Inst., Atlanta.**
A millimeter-wave radiometer for detecting microbursts p 145 N93-14850
- Gesellschaft fuer Strahlenforschung m.b.H., Munich (Germany).**
Air Traffic and Environment p 1034 N93-31925
[GSF-BAND-8] p 1034 N93-31925
Radiation exposure in aircraft p 1035 N93-31928
- Glasgow Univ. (Scotland).**
The convection speed of the dynamic stall vortex p 21 N93-11464
[AD-A247258] p 21 N93-11464
- Groupement des Industries Françaises Aéronautiques et Spatiales, Paris (France).**
French aerospace equipment p 1041 N93-31734
- Grumman Aerospace Corp., Bethpage, NY.**
Consolidation of graphite thermoplastic textile preforms for primary aircraft structure p 919 N93-30439

H

- Hampton Univ., VA.**
The NASA High-Speed Research Program p 330 N93-16761
Evaluation of candidate working fluid formulations for the electrothermal - chemical wind tunnel p 530 N93-20312
[NASA-CR-192196] p 530 N93-20312
Evaluation of candidate working fluid formulations for the electrothermal-chemical wind tunnel p 1015 N93-31848
[NASA-CR-193366] p 1015 N93-31848
- Hawker Siddeley Canada Ltd., Toronto (Ontario).**
In-service considerations affecting component life p 177 N93-14898
- Hellenic Aerospace Industry, Schimatari (Greece).**
Damage detection by Acousto-Ultrasonic Location (AUL) p 555 N93-21529
- Helsinki Univ. of Technology, Otaniemi (Finland).**
Numerical investigations into the base drag of various wedges using the base flow model developed by Mauri Tanner p 26 N93-12414
[REPT-B-36] p 26 N93-12414
DYNAC: A computer program for analyzing the dynamical stability of aircraft p 66 N93-12415
[REPT-B-31] p 66 N93-12415
- Hercules Aerospace Co., Magna, UT.**
Advanced fiber placement of composite fuselage structures p 923 N93-30864
- High Technology Corp., Hampton, VA.**
BLSTA: A boundary layer code for stability analysis p 220 N93-14797
[NASA-CR-4481] p 220 N93-14797
Modeling the transition region p 298 N93-19015
[NASA-CR-4492] p 298 N93-19015
Roughness-induced generation of crossflow vortices in three-dimensional boundary layers p 780 N93-27096
[NASA-CR-4505] p 780 N93-27096
- Holset Engineering Co., Turnbridge (England).**
Aerodynamic investigation of radial turbines using computational methods p 81 N93-10056
- Honeywell, Inc., Minneapolis, MN.**
Elements of a theory of natural decision making p 147 N93-15021
Taxonomy of flight variables p 147 N93-15022
- Houston Univ., TX.**
Initial streamwise vorticity formation in a two-stream mixing layer p 698 N93-25752
A hybrid multigrid technique for computing steady-state solutions to supersonic flows p 700 N93-26078
- Hughes Aircraft Co., Goleta, CA.**
The Canadian Automated Air Traffic System p 886 N93-30323
- Hughes Danbury Optical Systems, Inc., CT.**
The HYDICE instrument design and its application to planetary instruments p 842 N93-28766
- Human Resources Research Organization, Alexandria, VA.**
Development of a concept formulation process aid for analyzing training requirements and developing training devices p 912 N93-29972
[AD-A263579] p 912 N93-29972
- Hygiene-Inst. des Ruhrgebiets, Gelsenkirchen (Germany).**
Effects of commercial flight pollution on human health p 1035 N93-31931
- Illinois Inst. of Tech., Chicago.**
Nozzle installation effects on the noise from supersonic exhaust plumes p 100 N93-10681
Control of panel flutter at high supersonic speed p 47 N93-10900
- Illinois Univ., Chicago.**
Interferometric reconstruction of three-dimensional high-speed aerodynamic flows p 291 N93-16765
Flexible rotorcraft system dynamics with time-variant contact conditions p 340 N93-19034
- Illinois Univ., Urbana.**
Summary: Experimental validation of real-time fault-tolerant systems p 175 N93-13697
[NASA-CR-190985] p 175 N93-13697
A plume-induced boundary layer separation experiment p 220 N93-14677
[AD-A255397] p 220 N93-14677
Development of user guidelines for a three-dimensional finite element pavement model p 379 N93-16311
- Illinois Univ., Urbana-Champaign.**
A laboratory investigation of raindrop oscillations p 224 N93-13790
Effect of underwing frost on transport aircraft takeoff performance p 791 N93-2752
[DOT/FAA/CT-TN93/9] p 791 N93-2752
Aerodynamics of a finite wing with simulated ice p 784 N93-27437
- Illinois Univ. at Urbana-Champaign, Savoy.**
An experimental study of the relationship between forces and moments and vortex breakdown on a pitching delta wing p 49 N93-12206
Optimal finite-thrust time-bounded direct-ascent interception p 734 N93-25272
- Imperial Coll. of Science and Technology, London (England).**
Performance parameters and assessment p 81 N93-10052
Partial admission and unsteady flow in radial turbines p 81 N93-10059
Structural dynamic characteristics of individual blades p 1005 N93-32272
Structural dynamic characteristics of bladed assemblies p 1005 N93-32273
- Industrial Coll. of the Armed Forces, Washington, DC.**
Standardization of automatic test equipment in the US Air Force p 809 N93-29004
[AD-A262076] p 809 N93-29004
- Industrie Aeronautica e Meccanica Rinaldo Piaggio S.p.A., Genoa (Italy).**
Natural laminar flow test in-flight visualization p 482 N93-19921
- Industry, Science and Technology Canada, Toronto (Ontario).**
Defence electronics industry profile, 1990-1991 p 84 N93-10653
[CTN-92-60515] p 84 N93-10653
- Information and Control Systems, Inc., Hampton, VA.**
A stochastic optimal feedforward and feedback control methodology for superagility p 229 N93-13370
[NASA-CR-4471] p 229 N93-13370
- Institut de Mecanique des Fluides de Lille (France).**
Aeroplane crashes on the runway: Validation and final evaluation of the method of modeling an airframe structure p 165 N93-15126
[IMFL-91-32] p 165 N93-15126
Effect of Reynolds number on the standards of a simplified anemometric probe p 293 N93-17542
[IMFL-91-31] p 293 N93-17542
- Institut de Medicine Navale, Toulon-Naval (France).**
Helicopter accidents over water in the national navy: Epidemiological study over the period 1980-1991 p 493 N93-19686
- Institut fuer Angewandte Geodäsie, Frankfurt am Main (Germany).**
Aerial cartography using SICAD NAV-AIR p 1034 N93-31258
The use of digital road data by a navigation system p 993 N93-31269
- Institut National de Recherche d'Informatique et d'Automatique, Le Chesnay (France).**
Exact-gradient shape optimization of a 2D Euler flow p 422 N93-18623
[INRIA-RR-1540] p 422 N93-18623
A Blotter type numerical model for nonequilibrium viscous hypersonic flows in upwind finite elements p 297 N93-18648
[INRIA-RR-1476] p 297 N93-18648
Influence of the physical modelling of viscous terms on hypersonic flow computations p 297 N93-18652
[INRIA-RR-1493] p 297 N93-18652
- Institut National de Recherche d'Informatique et d'Automatique, Valbonne (France).**
Homothetic-flow approach for hypersonic inviscid non-equilibrium flows p 788 N93-28440
[INRIA-RR-1652] p 788 N93-28440
- Institute for Aerospace Research, Ottawa (Ontario).**
Fatigue crack growth results for Ti-6Al-4V, IMI 685, and Ti-17 p 1004 N93-31746
- Institute for Computer Application Research and Utilization in Science, Inc., Boston, MA.**
Unstructured mesh algorithms for aerodynamic calculations p 785 N93-27444
- Institute for Computer Applications in Science and Engineering, Hampton, VA.**
A general introduction to aeroacoustics and atmospheric sound p 102 N93-12021
[NASA-CR-189717] p 102 N93-12021
Report on the final panel discussion on computational aeroacoustics p 231 N93-12986
[NASA-CR-189718] p 231 N93-12986
Vortex breakdown incipience: Theoretical considerations p 290 N93-16627
[NASA-CR-189734] p 290 N93-16627
The stability of a trailing-line vortex in compressible flow p 298 N93-18771
[NASA-CR-189738] p 298 N93-18771
A contribution to the great Riemann solver debate p 694 N93-25083
[NASA-CR-191409] p 694 N93-25083

Current research activities: Applied and numerical mathematics, fluid mechanics, experiments in transition and turbulence and aerodynamics, and computer science

- [NASA-CR-191408] p 758 N93-25084
Instability of flow in a streamwise corner
[NASA-CR-191410] p 694 N93-25153
Sensitivity calculations for a 2D, inviscid, supersonic forebody problem
[NASA-CR-191444] p 779 N93-27004
Cumulative reports and publications
[NASA-CR-191440] p 847 N93-27063
Godunov-type schemes applied to detonation flows
[NASA-CR-191447] p 780 N93-27090
Some aspects of the aeroacoustics of high-speed jets
[NASA-CR-191458] p 843 N93-28975

Institute of Sound and Vibration Research, Southampton (England).

- The prediction of noise from co-axial jets
[ISVR-TR-215] p 1040 N93-32339
Instituto de Pesquisas Espaciais, Sao Jose dos Campos (Brazil).

- A study upon structural optimization of elastic rotors for mechanical systems
[INPE-5376-TDI/471] p 83 N93-10310
Diagnostics systems for the TBR-E tokamak
[INPE-5428-RPQ/662] p 232 N93-13257
Instituto Nacional de Tecnica Aeroespacial, Madrid (Spain).

- Mechanisms of sound generation in subsonic jets
p 101 N93-10688

Instituto Superior Tecnico, Lisbon (Portugal).

- Experimental analysis of combustion oscillations with reference to ramjet propulsion p 392 N93-17614
On automated analysis of flight test data p 512 N93-19913

International Maritime Satellite Organization, London (England).

- Satellite communications for aeronautical and navigation service p 838 N93-26648

International Technical Associates, Inc., Drexel Hill, PA.

- Open airscrew VTOL concepts
[NASA-CR-177603] p 240 N93-17883

Iowa State Univ. of Science and Technology, Ames.

- Analytical solutions to constrained hypersonic flight trajectories
[NASA-CR-191987] p 297 N93-18602
Investigation of corrosion in aluminum/adhesive lap-splices using pulse-echo ultrasonic techniques
[DE93-008074] p 749 N93-25518

- Trajectory optimization for the National Aerospace plane
[NASA-CR-192954] p 716 N93-25670

Iowa Univ., Iowa City.

- Ship viscous flow: A report on the 1990 SSPA-IIHR Workshop p 840 N93-27466

Ishikawa/Jima-Harima Heavy Industries Co. Ltd., Tokyo (Japan).

- Numerical simulation of flow for a scramjet nozzle p 302 N93-19299
Numerical simulation of the flow through non-uniform airfoil cascade p 302 N93-19310
A numerical investigation for supersonic inlet p 303 N93-19315

- A numerical investigation of 3D transverse injection into the supersonic flow behind rearward facing step p 303 N93-19316

- Role of wind tunnel tests and CFD analysis for the development of aero-engines in IHI p 365 N93-19326

Israel Society of Aeronautics and Astronautics, Tel Aviv.

- Collection of papers of the 31st Israel Annual Conference on Aviation and Astronautics
[ITN-93-85187] p 764 N93-27166

- By-passing of heat exchangers in gas turbines p 814 N93-27189

Israeli Air Force, Zahal.

- Damage tolerance assessment and usage variation analysis for C-130 aircraft in the Israeli Air Force p 839 N93-27210

Istanbul Univ. (Turkey).

- Advances in speech processing p 550 N93-19771

J

Japan Air Lines Co. Ltd., Tokyo.

- Discussion for the ideal AIMS p 167 N93-15153

Jet Propulsion Lab., California Inst. of Tech., Pasadena.

- Dual control vibration tests of flight hardware p 545 A93-27782
JPL AIRSAR processing activities and developments p 1162 A93-47865

Three-stage sorption type cryogenic refrigeration systems and methods employing heat regeneration
[NASA-CASE-NPO-18366-1-CU] p 216 N93-13422

The effect of clock, media, and station location errors on Doppler measurement accuracy p 885 N93-29588
Virtual reality flight control display with six-degree-of-freedom controller and spherical orientation overlay

[NASA-CASE-NPO-18733-1-CU] p 897 N93-30416

Johns Hopkins Univ., Baltimore, MD.

Analytical foundations of gain scheduling
[AD-A264682] p 909 N93-30550

Johns Hopkins Univ., Laurel, MD.

Control of complex dynamic systems by neural networks p 758 N93-25611

Joint Inst. for Advancement of Flight Sciences, Hampton, VA.

Practical input optimization for aircraft parameter estimation experiments
[NASA-CR-191462] p 820 N93-27264

Joint Publications Research Service, Arlington, VA.

JPRS report: Science and technology. Japan. 30th National Aerospace Laboratory Conference
[JPRS-JST-93-009] p 761 N93-25418

JPRS report: Science and technology. Central Eurasia: Engineering and equipment
[JPRS-UEQ-92-003] p 749 N93-25427

JPRS report: Science and technology. Central Eurasia: Engineering and equipment
[JPRS-UEQ-92-007] p 842 N93-28635

JPRS report: Science and technology. Central Eurasia: Engineering and equipment
[JPRS-UEQ-92-006] p 842 N93-28636

JPRS report: Science and technology. Central Eurasia: Engineering and equipment
[JPRS-UEQ-92-010] p 842 N93-28674

JPRS report: Science and technology. Central Eurasia: Engineering and equipment
[JPRS-UEQ-92-008] p 842 N93-28675

JPRS report: Science and technology. Central Eurasia: Engineering and equipment
[JPRS-UEQ-93-003] p 842 N93-28691

JPRS report: Science and technology. Central Eurasia: Engineering and equipment
[JPRS-UEQ-93-004] p 930 N93-29090

Joint Publications Research Service, Washington, DC.

JPRS report: Central Eurasia. Aviation and cosmonautics, no. 9, September 1992
[JPRS-UAC-93-003] p 678 N93-26325

K

Kaman Aerospace Corp., Bloomfield, CT.

An improved method of structural dynamic test design for ground flying and its application to the SH-2F and SH-2G helicopters p 512 N93-19928

Dynamic System Coupler Program (DYSCO 4.1). Volume 1: Theoretical manual
[AD-B131156L] p 848 N93-27531

Dynamic System Coupler Program (DYSCO 4.1). Volume 2: User's manual
[AD-B131157L] p 848 N93-27589

Dynamic System Coupler Program (DYSCO 4.1). Volume 3: User's manual supplement
[AD-B131158L] p 848 N93-27590

Kansas Univ., Lawrence.

Development of nonlinear aerodynamic models for unsteady responses p 19 N93-10845

General aviation aircraft: Normal acceleration data analysis and collection project
[DOT/FAA/CT-91/20] p 713 N93-24739

Design, analysis, and control of large transport aircraft utilizing engine thrust as a backup system for the primary flight controls
[NASA-CR-192938] p 820 N93-27308

Preliminary design studies of an advanced general aviation aircraft p 894 N93-29717

Kansas Univ. Center for Research, Inc., Lawrence.

The Ultra Light Aircraft Testing
[NASA-CR-193043] p 895 N93-29774

Report on the test set-up for the structural testing of the Airmass Sunburst Ultralight Aircraft p 895 N93-29775

Load test set-up for the Airmass Sunburst Ultra-Light Aircraft p 895 N93-29776

NASTRAN analysis for the Airmass Sunburst model 'C' Ultralight Aircraft p 931 N93-29777

Construction, wind tunnel testing and data analysis for a 1/5 scale ultra-light wing model p 876 N93-29778

Selection and static calibration of the Marsh J1678 pressure gauge p 931 N93-29779

Karlsruhe Univ. (Germany).

Heat transfer and leakage in high-speed rotating stepped labyrinth seals p 903 N93-29951

Kawasaki Heavy Industries Ltd., Gifu (Japan).

The role of computational fluid dynamics in aeronautical engineering. 9: Analysis of hypersonic equilibrium air flow p 301 N93-19294

Three dimensional calculation of flow inside supersonic inlet p 303 N93-19313

Wind tunnel test and CFD in Kawasaki Heavy Industries, Gifu p 304 N93-19324

Kayser Threde G.m.b.H., Munich (Germany).

An experimental health monitoring unit for GPS and GLONASS p 706 N93-25018

Klein Associates, Inc., Fairborn, OH.

A cognitive model for training decision making in aircrews p 147 N93-15020

KLM Helicopters B.V., Amsterdam (Netherlands).

Helicopters in action p 340 N93-19005

Koa Oil Co. Ltd. (Japan).

Air cell
[CA-PATENT-APPL-SN-2001346] p 83 N93-10368

Korea Advanced Inst. of Science and Technology, Seoul (Republic of Korea).

Prediction of airfoil stall using Navier-Stokes equations in streamline coordinates p 787 N93-27456

Discrete-vortex simulation of pulsating flow on a turbulent leading-edge separation bubble p 787 N93-27457

Kyushu Univ., Fukuoka (Japan).

Numerical calculations of separating flows around oscillating airfoil p 300 N93-19284

L

Laval Univ. (Quebec).

Dynamic simulation of flexible body systems by the vector solution method p 553 N93-20666

Lawrence Livermore National Lab., CA.

Impact of supersonic and subsonic aircraft on ozone: Including heterogeneous chemical reaction mechanisms
[DE92-019619] p 224 N93-13655

Dual-band infrared imaging applications: Locating buried minefields, mapping sea ice, and inspecting aging aircraft
[DE93-000516] p 453 N93-17225

World commercial aircraft accidents
[DE93-010892] p 791 N93-28571

Leeds Univ. (England).

Impingement/effusion cooling p 932 N93-29954

Liege Univ. (Belgium).

Vibration analysis in turbomachines p 1005 N93-32274

Lightning Location and Protection, Inc., Tucson, AZ.

A single-point warning system for thunderstorms and electric fields p 747 N93-24900

Lightning Technologies, Inc., Pittsfield, MA.

Lightning phenomenology bases for full threat return stroke occurrence following extended leader sweep at flight altitudes p 754 N93-24895

Little (Arthur D.), Inc., Cambridge, MA.

Improved selective catalytic NOx control technology for compressor station reciprocating engines
[PB93-158566] p 755 N93-26529

Lockheed Advanced Development Co., Burbank, CA.

YF-22A prototype advanced tactical fighter demonstration/validation flight test program overview p 805 N93-27173

Lockheed Advanced Development Co., Sunland, CA.

YF-22A prototype advanced tactical fighter demonstration/validation flight test program overview p 511 N93-19906

The development of aircraft in the Lockheed Skunk Works from 1954 to 1991 p 805 N93-27168

Lockheed Aeronautical Systems Co., Burbank, CA.

Advanced composite structural concepts and material technologies for primary aircraft structures p 918 N93-30430

Design, analysis, and fabrication of the technology integration box beam p 919 N93-30433

Lockheed Engineering and Sciences Co., Houston, TX.

Requirements analysis notebook for the flight data systems definition in the Real-Time Systems Engineering Laboratory (RSEL)
[NASA-CR-185698] p 69 N93-10960

Lockheed Missiles and Space Co., Palo Alto, CA.

NASA/LMSC coherent LIDAR airborne shear sensor: System capabilities and flight test plans p 144 N93-14847

Logistics Management Inst., Bethesda, MD.

Making clean gasoline: The effect on jet fuels
[AD-A264302] p 1019 N93-32085

Loral Data Systems, Sarasota, FL.

Solid state flight data recorder with rapid data access p 221 N93-15167

Los Alamos National Lab., NM.

Numerical analysis of the flow fields in a RQL gas turbine combustor
[DE92-017509] p 89 N93-11767

A preliminary study of the effect of equivalence ratio on a low emissions gas turbine combustor using KIVA-2
[DE92-018616] p 215 N93-13321

A computer simulation of the production of an artificially ionized layer using the Arecibo facility
[DE93-010817] p 937 N93-30487

Loughborough Univ. of Technology (England).

An investigation of ground access mode choice for departing passengers
[TT-9201] p 67 N93-11224

Airport stand assignment model
[TT-9104] p 67 N93-11728

Ludwig-Maximilians-Univ., Munich (Germany).

Climatic effects of turbulent emissions in the stratosphere and the higher troposphere p 1035 N93-31927

M**M-DOT, Inc., Phoenix, AZ.**

Thrust augmentation system for low-cost-expendable turbojet engine
[AD-A263727] p 905 N93-30877

MacAulay-Brown, Inc., Dayton, OH.

Inflight evaluation of an acoustic orientation instrument
[AD-A260752] p 719 N93-25909

MacAulay-Brown, Inc., Fairborn, OH.

Development of a flight instrument package
[AD-A260830] p 719 N93-25783

MacDonald, Dettwiler and Associates Ltd., Ottawa (Ontario).

Application and integration of diverse technology in an aviation system: The National Aeronautical Information Processing System p 887 N93-30339

MacDonald, Dettwiler and Associates Ltd., Richmond (British Columbia).

Meteorological information for aviation: A systems approach p 937 N93-30298

MacDonald, Dettwiler Proprietary Ltd., New South Wales (Australia).

Application and integration of diverse technology in an aviation system: The National Aeronautical Information Processing System p 887 N93-30339

Manchester Coll. of Science and Technology (England).

Turbulent flow and heat transfer in idealized blade cooling passages p 902 N93-29938

Manchester Univ. (England).

Lanchester: The man
[AERO-REPT-9111] p 456 N93-16464

The Goldstein Aeronautical Engineering Research Laboratory
[AERO-REPT-9109] p 240 N93-16465

Hypersonic flows including real gas effects
[AERO-REPT-9112] p 289 N93-16467

Design of a nozzle for a hypersonic wind tunnel
[AERO-REPT-9113] p 381 N93-16468

Computational study of real gas effects in high speed high temperature flow, volume 2 p 289 N93-16470

[AERO-REPT-9203-VOL-2] p 289 N93-16470

Aeronautical Engineering Group publications: 1950 - present p 454 N93-16563

Modelling of interfacial and thermocline waves
[AERO-REPT-9209] p 420 N93-18103

Aircraft turns into and down wind
[AERO-REPT-9201] p 337 N93-18131

The aerodynamic performance of laser drilled sheets
[AERO-REPT-9204] p 484 N93-20806

The effect of surface suction near the leading edge of a swept-back wing
[AERO-REPT-9205] p 484 N93-20807

Martin Marietta Aerospace, Washington, DC.

An approach to evaluating reactive airborne wind shear systems p 489 N93-19600

Maryland Univ., College Park.

Contributions to the experimental investigation of rotor/body aerodynamic interactions p 20 N93-10877

The Fourth Workshop on Dynamics and Aeroelastic Stability Modeling of Rotorcraft Systems
[AD-A250665] p 50 N93-12485

Experiments and analysis concerning the use of external burning to reduce aerospace vehicle transonic drag p 70 N93-12537

Performance and control of ascending trajectories to minimize heat load for transatmospheric aero-space planes p 133 N93-13745

Formulation and validation of high-order mathematical models of helicopter flight dynamics p 162 N93-13821

A study of viscous interaction effects on hypersonic waveriders p 135 N93-14160

Optimized scramjet engine integration on a waverider airframe p 722 N93-25480

Aeroelastic response and aeromechanical stability of helicopters with elastically coupled composite rotor blades p 715 N93-25530

Large-eddy simulation of temporally developing boundary layers with embedded streamwise vortices p 750 N93-25753

Techniques for designing rotorcraft control systems
[NASA-CR-192960] p 729 N93-26046

Massachusetts Inst. of Tech., Cambridge.

Advanced terrain displays to transport category aircraft
[PB92-197136] p 35 N93-10065

Nonlinear aeroelasticity of composite structures
[AD-A254285] p 47 N93-10842

Nonlinear stall flutter of wings with bending-torsion coupling
[AD-A254323] p 186 N93-12959

The Orlando TDWR testbed and airborne wind shear date comparison results p 145 N93-14851

Experimental evaluation of candidate graphical microburst alert displays p 145 N93-14853

Systems issues in airborne Doppler radar/LIDAR certification p 145 N93-14855

Active stabilization to prevent surge in centrifugal compression systems
[NASA-CR-191625] p 424 N93-18862

Microburst characteristics determined from 1988-1991 TDWR testbed measurements p 490 N93-19605

Three-dimensional flow in radial turbomachinery and its impact on design
[NASA-CR-192957] p 723 N93-25668

Flow control of low heat load turbine airfoils
[AD-A260941] p 724 N93-26219

Active stabilization of aeromechanical systems
[AD-A261366] p 725 N93-26335

Flow phenomena in turbomachines
[AD-A263049] p 930 N93-29141

A passive infrared ice detection technique for helicopter applications
[NASA-CR-193187] p 880 N93-29152

The influence of non-uniform spanwise inlet temperature on turbine rotor heat transfer p 901 N93-29932

Massachusetts Inst. of Tech., Lexington.

Birds mimicking microbursts on 2 June 1990 in Orlando, Florida
[AD-A255703] p 143 N93-14024

Terminal Doppler weather radar/low-level wind shear alert system integration algorithm specification, version 1.1
[AD-A255319] p 224 N93-14547

Setting values for TDWR/LLWAS 3 integration parameters
[AD-A260740] p 755 N93-25645

Contributions to the American Meteorological Society's 26th International Conference on Radar Meteorology
[AD-A263385] p 936 N93-29257

Two simulation studies of precision runway monitoring of independent approaches to closely spaced parallel runways
[AD-A263433] p 911 N93-29815

Max-Planck-Inst. fuer Stroemungsforschung, Goettingen (Germany).

An experimental investigation of base bleed effect on the wake turbulent structure behind a two-dimensional blunt model
[MPIS-9/1991] p 139 N93-15131

Numerical investigation of swirl-airfoil interactions in transonic area
[MPIS-8/1991] p 297 N93-18627

MCAT Inst., San Jose, CA.

Study of optical techniques for the Ames unitary wind tunnels. Part 4: Model deformation
[NASA-CR-190980] p 68 N93-12349

Study of optical techniques for the Ames unitary wind tunnel. Part 5: Infrared imagery
[NASA-CR-191385] p 194 N93-14809

Study of optical techniques for the Ames unitary wind tunnel, part 7
[NASA-CR-192165] p 382 N93-18520

Study of optical techniques for the Ames unitary wind tunnel: Digital image processing, part 6
[NASA-CR-192164] p 382 N93-18766

Turbulence modeling for hypersonic flight
[NASA-CR-192288] p 483 N93-20235

McDonnell Aircraft Co., Saint Louis, MO.

Multiplexing electro-optic architectures for advanced aircraft integrated flight control systems
[NASA-CR-182268] p 187 N93-13735

Domain specific software design for decision aiding p 442 N93-17517

Prediction of vortex breakdown on a delta wing p 787 N93-27459

Design and manufacturing concepts for thermoplastic structures p 919 N93-30434

McDonnell-Douglas Corp., Long Beach, CA.

The 1990 high-speed civil transport studies
[NASA-CR-189618] p 330 N93-16947

The 1990 high-speed civil transport studies. Summary report
[NASA-CR-189619] p 330 N93-16999

McDonnell-Douglas Electronics Co., Saint Louis, MO.

Analytical and experimental investigation of annular propulsive nozzles
[AD-A262685] p 815 N93-28391

Use of titanium castings without a casting factor
[AD-A264414] p 1018 N93-31192

McDonnell-Douglas Helicopter Co., Mesa, AZ.

The NASA/industry Design Analysis Methods for Vibrations (DAMVIBS) program: McDonnell-Douglas Helicopter Company achievements p 515 N93-21314

McGill Univ., Montreal (Quebec).

Overall effects of separation on thin aerofoils
[ISBN-0-315-67464-4] p 135 N93-13930

McMaster Univ., Hamilton (Ontario).

Classification of radar clutter in an air traffic control environment p 886 N93-30299

Mel Associates, Inc., San Antonio, TX.

Functional requirements of an advanced instructional design advisor: Simulation authoring, Volume 3
[AD-A256650] p 440 N93-16500

Messerschmitt-Boelkow-Blohm G.m.b.H., Munich (Germany).

Surface protection in the aircraft industry
[MBB-Z-0432-92-PUB] p 72 N93-11027

A novel-high-performance system for recording and analysing instantaneous total pressure distortion in air intakes p 214 N93-13215

Integration of turbo-ramjet engines for hypersonic aircraft p 175 N93-13230

Modeling limits of the EMV analysis program CONCEPT by example of the influence of a helicopter structure on a frame antenna
[MBB-UD-0614-92-PUB] p 223 N93-15487

Hot experimental technique: A new requirement of aerothermodynamics
[MBB-FE-202-S-PUB-480] p 293 N93-17543

Test and integration concept for complex helicopter avionic systems
[MBB-UD-0605-91-PUB] p 343 N93-17547

Mathematical optimization: A powerful tool for aircraft design
[MBB-FE-2-S-PUB-478] p 331 N93-17564

Practical architecture of design optimisation software for aircraft structures taking the MBB-LAGRANGE code as an example
[MBB-FE-251-S-PUB-479] p 331 N93-17565

Modern helicopter technologies at MBB and the application in future programmes
[MBB-UD-0599-91-PUB] p 331 N93-17566

Mission oriented investigation of handling qualities through simulation
[MBB-UD-0600-91-PUB] p 332 N93-17567

Current European rotorcraft research activities on development of advanced CFD methods for the design of rotor blades (BRITE/EURAM DACRO project)
[MBB-UD-0601-91-PUB] p 293 N93-17568

Influence of cross section variations on the structural behaviour of composite rotor blades
[MBB-UD-0602-91-PUB] p 332 N93-17569

Integrated helmet system testing for a night-vision helicopter
[MBB-UD-0604-91-PUB] p 343 N93-17570

X-31A high angle of attack and initial post stall flight testing p 511 N93-19911

Development of cure cycles: From laboratory analysis and testing to production of large scale composites
[MBB-Z-0442-92-PUB] p 536 N93-20845

Heat loads as key problem of hypersonic flight
[MBB-FE-202-S-PUB-0486] p 484 N93-21054

Numerical methods for aerothermodynamic design of hypersonic space transport vehicles
[MBB-FE-211-S-PUB-0481] p 514 N93-21056

Application of the Euler method EULFLEX to a fighter-type airplane configuration at transonic speed
[MBB-FE-211-S-PUB-0489-A] p 484 N93-21059

Allowable compression strength for CFRP-components of fighter aircraft determined by CAI-test
[MBB-FE-221-S-PUB-0483] p 537 N93-21462

Selection criteria for metallic high temperature structural materials in hypersonic flying equipment
[MBB-LME-221-HYPAC-PUB-2-A] p 515 N93-21479

Allowable compression strength for CFRP-components of fighter aircraft determined by CAI-test p 537 N93-21531

Advanced aircraft with thrust vector control
[MBB-FE-1-S-PUB-0504] p 998 N93-31043

Consideration of impact damages by dimensioning CFC (Carbon Fiber Reinforced Composites) components
[MBB-FE-221-S-PUB-0501] p 1018 N93-31044

- Technology transfer: Potential of BMFT concept for hypersonics
[MBB-LME-202-S-PUB-0505] p 1041 N93-31045
- Development of nose structure of a reconnaissance container for a supersonic jet aircraft
[MBB-LME-242-S-PUB-0451] p 998 N93-31046
- Aircraft structures in 2000: A technological challenge?
[MBB-LME-202-S-PUB-0485] p 998 N93-31058
- Messerschmitt-Boelkow-Blohm G.m.b.H., Ottobrunn (Germany).**
The integrated design and manufacturing of composite structures for aircraft using an advanced tape layering technology
[MBB-LME-251-S-PUB-0491-A] p 515 N93-21401
- Messerschmitt-Boelkow G.m.b.H., Munich (Germany).**
Reduction of propeller noise by active noise control
p 101 N93-10692
- Michigan State Univ., East Lansing.**
Developing a control system for ARES 2
p 371 N93-16769
- A domain-specific design architecture for composite material design and aircraft part redesign
p 442 N93-17522
- Michigan Technological Univ., Houghton.**
Robust control of intelligent rotor
[AD-A263707] p 909 N93-29985
- Michigan Univ., Ann Arbor.**
A numerical study of hypersonic flow with strong surface blowing
p 129 N93-13128
- Minimum-time flight paths of supersonic aircraft
p 160 N93-13140
- Optimal thrust magnitude on a singular arc in atmospheric flight
p 758 N93-25410
- Axymmetric vortex sheet roll-up
p 788 N93-28078
- MicroNet, Celle (Germany).**
Personal computer based test- and emulation equipment for maintenance and ground support
p 110 N93-15185
- Midwest Research Inst., Golden, CO.**
User's Guide for the NREL Force and Loads Analysis Program
[DE92-010579] p 216 N93-13524
- User's Guide for the NREL Teetering Rotor Analysis Program (STRAP)
[DE92-010580] p 216 N93-13525
- A discussion of the results of the rainflow counting of a wide range of dynamics associated with the simultaneous operation of adjacent wind turbines
[DE93-000018] p 434 N93-18705
- Combined experiment, phase 1
[DE93-000012] p 485 N93-21766
- Millitech Corp., South Deerfield, MA.**
Coherent systems in the terahertz frequency range: Elements, operation, and examples
p 841 N93-27727
- Ministry of Defence, London (England).**
Royal Air Force experience of the Harrier information management system
p 234 N93-15170
- Minnesota Univ., Minneapolis.**
Conceptual design of a Mars transportation system
[NASA-CR-192039] p 420 N93-18047
- A numerical and experimental studies of flow characteristics in centrifugal fans
p 695 N93-25339
- Stabilized space-time finite element formulations for unsteady incompressible flows involving fluid-body interactions
p 843 N93-29040
- Vortex structure and mass transfer near the base of a cylinder and a turbine blade
p 901 N93-29929
- Mississippi State Univ., State College.**
Unsteady three-dimensional thin-layer Navier-Stokes solutions for turbomachinery in transonic flow
p 218 N93-14025
- Solution of compressible Navier-Stokes equations using spectral methods on arbitrary two-dimensional domains
p 218 N93-14041
- Missouri Univ., Rolla.**
New acceleration potential method for supersonic unsteady aerodynamics of lifting surfaces, further extension of the nonplanar supersonic doublet point method, and nonlinear, nongradient optimized rational function approximations for supersonic, transient response unsteady aerodynamics
p 25 N93-12344
- An investigation of the dynamic response of lifting surfaces with concentrated structural nonlinearities
p 162 N93-13807
- Preliminary efforts toward development of data handling and analysis software for unsteady flow measurements: An application for aeroelastic transonic flow configurations
p 291 N93-16768
- Aircraft landing gear shimmy
p 340 N93-19029
- Two-dimensional fin analysis
p 750 N93-25737
- MITech, Inc., Washington, DC.**
Evaluation of category 3 MLS designs
p 888 N93-30358

Mitre Corp., McLean, VA.

The dependent converging instrument approach procedure: An analysis of its safety and applicability
[DOE/FAA/RD-93/6] p 707 N93-25456

Small satellites and RPA's in global-change research
[AD-A260762] p 755 N93-25837

The 1991-1992 aviation system capacity plan
[AD-A263436] p 911 N93-29788

National Airspace System Performance Analysis Capability (NASPAC) simulation model
p 887 N93-30351

Procedural development prototype in Automated En Route Air Traffic Control
p 887 N93-30352

Enhancing availability, performance, and flexibility of air traffic control air-ground services
p 887 N93-30353

Changing role of telecommunications management in air traffic control in the FAA
p 888 N93-30354

Developing automation for terminal air traffic control: Case study of the imaging aid
p 888 N93-30356

Mitsubishi Electric Corp., Kamakura (Japan).

Aerodynamic heating analysis for axisymmetric bodies in supersonic flow
p 303 N93-19312

Mitsubishi Heavy Industries Ltd., Nagoya (Japan).
Wind tunnel testing and CFD simulation in Mitsubishi Heavy Industries
p 305 N93-19325

Mitsubishi Heavy Industries Ltd., Tokyo (Japan).
Computation of internal flows using unstructured triangular meshes
p 299 N93-19276

Numerical calculation of flow field in supersonic combustion chamber
p 304 N93-19317

Moncton Univ., Edmundston (New Brunswick).
Experimental investigation of flows behind different Large-Eddy Breakup (LEBU) devices in thick boundary layers
p 18 N93-10550

Moolj and Associates, Oegstgeest (Netherlands).
Flight simulation leaves the ground
p 194 N93-14616

Motoren- und Turbinen-Union Muenchen G.m.b.H. (Germany).
The influence of intake swirl distortion on the steady-state performance of a low bypass, twin-spool engine
p 214 N93-13211

RB 199 high pressure compressor stage 3 spin pit tests
p 176 N93-14893

Engine technologies for future spaceplanes
[ETN-92-92732] p 177 N93-15143

EJ 200 engine monitoring system: On- and off-board data capture, analysis, and management system
p 178 N93-15172

RB199 engine oil system failure diagnostics by comparison of measured and calculated oil consumption using the OLMOS on-board monitoring system
p 178 N93-15173

Modelling the engine temperature distribution between shut down and restart for life usage monitoring
p 169 N93-15177

Transient thermal behaviour of a compressor rotor with axial cooling air flow and co-rotating or contra-rotating shaft
p 903 N93-29946

N

Nagoya Univ. (Japan).

Analysis of a 2-D airfoil motion flying in-proximity-to a wavy-wall surface: Lifting-surface-method
p 300 N93-19281

Analysis of a 2-D airfoil motion flying in-proximity-to a wavy-wall surface: Finite difference method
p 300 N93-19282

Transonic flow calculation around NACA-0012
p 302 N93-19301

Nangia Associates, Bristol (England).
Application of subsonic first-order panel methods for prediction of inlet and nozzle aerodynamic interactions with airframe
p 130 N93-13223

National Academy of Sciences - National Research Council, Washington, DC.
Aeronautical technologies for the twenty-first century
[NASA-CR-190918] p 4 N93-10647

National Aero-Space Plane Joint Program Office, Wright-Patterson AFB, OH.
A configuration development strategy for the NASP
p 46 N93-10011

The National Aero-Space Plane program: A revolutionary concept
p 511 N93-19908

National Aeronautical Lab., Bangalore (India).
Composites: A catalogue of books and conference proceedings available in the NAL library
[NAL-SP-IC-9201] p 234 N93-13368

Ideal aircraft handling quality models: Longitudinal axis
[NAL-PD-FC-9203] p 187 N93-13566

Indian experience in flight data readout and analysis
p 168 N93-15161

National Aeronautics and Space Administration, Washington, DC.

An effective multigrid method for high-speed flows
p 6 A93-10533

Integrated flight propulsion control research results using the NASA F-15 HIDECC Flight Research Facility
[AIAA PAPER 92-4106] p 38 A93-11276

Flight testing and simulation of an F-15 airplane using throttles for flight control
[AIAA PAPER 92-4109] p 39 A93-11278

The development of an airborne information management system for flight test
[AIAA PAPER 92-4113] p 51 A93-11281

The F-18 High Alpha Research Vehicle - A high-angle-of-attack tested aircraft
[AIAA PAPER 92-4121] p 42 A93-13273

Effects of turbine cooling assumptions on performance and sizing of high-speed civil transport
[AIAA PAPER 92-4217] p 55 A93-13383

Stirling engine - Available tools for long-life assessment
p 195 A93-13824

Systems integration test laboratory - Application and experiences
p 190 A93-13910

Evaluation and application of the Baldwin-Lomax turbulence model in two-dimensional, unsteady, compressible boundary layers with and without separation in engine inlets
[AIAA PAPER 92-3676] p 111 A93-14118

Experimental investigation of an axisymmetric hypersonic scramjet inlet for laser propulsion
p 122 A93-14515

Stochastic measures of performance robustness in aircraft control systems
p 185 A93-14595

Tiltrotor Research Aircraft composite blade repairs - Lessons learned
p 108 A93-14819

Adaptive remeshing for three-dimensional compressible flow computations
p 242 A93-18851

Advances in tilt rotor noise prediction
p 447 A93-19184

A review of crack propagation under unsteady loading
p 399 A93-19207

Heat transfer in rotating serpentine passages with trips skewed to the flow
[ASME PAPER 92-GT-191] p 403 A93-19416

Air-breathing hypersonic cruise - Prospects for Mach 4-7 waverider aircraft
[ASME PAPER 92-GT-437] p 384 A93-19579

Digital avionics systems - Principles and practices (2nd revised and enlarged edition)
[ISBN 0-07-060333-2] p 342 A93-19801

Concurrent optimization of airframe and engine design parameters
[AIAA PAPER 92-4713] p 323 A93-20281

AIAA/USAF/NASA/OAI Symposium on Multidisciplinary Analysis and Optimization, 4th, Cleveland, OH, Sept. 21-23, 1992, Technical Papers. Pts. 1 & 2
p 435 A93-20301

Recent advances in integrated multidisciplinary optimization of rotorcraft
[AIAA PAPER 92-4777] p 325 A93-20369

Spatial and temporal variations of the fluxes of carbon dioxide and sensible and latent heat over the FIFE site
p 425 A93-20586

Assessing spatial and seasonal variations in grasslands with spectral reflectances from a helicopter platform
p 426 A93-20621

Variability of geophysical parameters from aircraft radiance measurements for FIFE
p 426 A93-20622

High-performance computing for flight vehicles; Proceedings of the Symposium, Washington, Dec. 7-9, 1992
p 437 A93-20701

Viscous and inviscid instabilities of a trailing vortex
p 268 A93-21042

Spatial adaptation procedures on tetrahedral meshes for unsteady aerodynamic flow calculations
[AIAA PAPER 93-0670] p 269 A93-21116

Guidance accuracy considerations for realtime GPS interferometry
p 342 A93-21146

Vision-based range estimation using helicopter flight data
p 317 A93-21525

An experimental cockpit display for TDWR wind shear alerts
p 343 A93-22111

Hazard assessment and cockpit presentation issues for microburst alerting systems
p 308 A93-22112

A microcomputer program for estimating low altitude wind and turbulence fields
p 438 A93-22163

A study of hypersonic swept shock wave/turbulent boundary layer interactions using a conical Navier-Stokes code
[AIAA PAPER 92-5050] p 273 A93-22322

Isolator-combustor interaction in a dual-mode scramjet engine
[AIAA PAPER 93-0358] p 360 A93-23041

Simplified jet fuel reaction mechanism for lean burn combustion application
[AIAA PAPER 93-0021] p 390 A93-23238

- Close-up analysis of aircraft ice accretion
[AIAA PAPER 93-0029] p 309 A93-23239
- Surface roughness due to residual ice in the use of low power deicing systems
[AIAA PAPER 93-0031] p 282 A93-23240
- Propagation of high frequency jet noise using geometric acoustics
[AIAA PAPER 93-0147] p 452 A93-23241
- Numerical modeling of anti-icing systems and comparison to test results on a NACA 0012 airfoil
[AIAA PAPER 93-0170] p 327 A93-23242
- Advancements in the LEWICE Ice Accretion Model
[AIAA PAPER 93-0171] p 309 A93-23243
- Ice accretion and performance degradation calculations with LEWICE/NS
[AIAA PAPER 93-0173] p 310 A93-23244
- Ice accretion prediction for a typical commercial transport aircraft
[AIAA PAPER 93-0174] p 310 A93-23245
- Optimization of circular orifice jets mixing into a heated crossflow in a cylindrical duct
[AIAA PAPER 93-0249] p 361 A93-23246
- Acoustic mode measurements in the inlet of a model turbofan using a continuously rotating rake - Data collection/analysis techniques
[AIAA PAPER 93-0599] p 361 A93-23324
- Estimation of unsteady lift on a pitching airfoil from wake velocity surveys
[AIAA PAPER 93-0437] p 286 A93-23351
- An improved numerical model for wave rotor design and analysis
[AIAA PAPER 93-0482] p 361 A93-23384
- Nonlinear relaxation/quasi-Newton algorithm for the compressible Navier-Stokes equations
p 287 A93-23541
- Engineering approach to the prediction of shock patterns in bounded high-speed flows
p 287 A93-23545
- A graphical user-interface for propulsion system analysis
[AIAA PAPER 93-0223] p 440 A93-23699
- Approximation methods for control of structural acoustics models with piezoceramic actuators
p 452 A93-23744
- Interaction strength and model geometry effects on the structure of crossing-shock wave/turbulent boundary-layer interactions
[AIAA PAPER 93-0780] p 467 A93-24862
- Effect of a rotating propeller on the separation angle of attack
[AIAA PAPER 93-0017] p 472 A93-24978
- The rebirth of supersonic transport
p 457 A93-25325
- NASA's hypersonic flight research program
[AIAA PAPER 93-0308] p 457 A93-25516
- Current technologies for waverider aircraft
[AIAA PAPER 93-0400] p 505 A93-25521
- Propulsion/airframe integration issues for waverider aircraft
[AIAA PAPER 93-0506] p 505 A93-25533
- Comparison of all-electric secondary power systems for civil transport
p 519 A93-25997
- Visual field information in Nap-of-the-Earth flight by teleoperated Helmet-Mounted displays
p 517 A93-26884
- Uniform high-order spectral methods for one- and two-dimensional Euler equations
p 476 A93-27068
- A numerical study of mixing in supersonic combustors with hypermixing injectors
[AIAA PAPER 93-0215] p 520 A93-27801
- The NASA/industry design analysis methods for vibrations (DAMVIBS) program - Accomplishments and contributions
p 508 A93-27971
- Experiences at Langley Research Center in the application of optimization techniques to helicopter airframes for vibration reduction
p 508 A93-27972
- Application of new GPS aircraft control/display system to topographic mapping of the Greenland ice cap
p 499 A93-28152
- Schlieren studies of compressibility effects on dynamic stall of transiently pitching airfoils
p 480 A93-28608
- Current status of computational methods for transonic unsteady aerodynamics and aeroelastic applications
p 480 A93-29175
- Laser selection criteria for OH fluorescence measurements in supersonic combustion test facilities
p 549 A93-29315
- Development and validation of 'quiet tail rotor' technology
p 567 A93-29416
- Acoustical analysis of gear housing vibration
p 567 A93-29420
- Euler solutions to nonlinear acoustics of non-lifting rotor blades
p 568 A93-29433
- AIAA/ASME/ASCE/AHS/ASC Structures, Structural Dynamics, and Materials Conference, 34th and AIAA/ASME Adaptive Structures Forum, La Jolla, CA, Apr. 19-22, 1993, Technical Papers, Pts. 1-6
p 738 A93-33876
- Thermomechanical postbuckling analysis of laminated composite shells
[AIAA PAPER 93-1337] p 738 A93-33907
- Dynamics of rotating multicomponent turbomachinery systems
[AIAA PAPER 93-1629] p 742 A93-34157
- Foreign object impact assessment of a high-Mach engine inlet
[AIAA PAPER 93-1630] p 711 A93-34158
- Recent developments in equivalent plate modeling for wing shape optimization
[AIAA PAPER 93-1647] p 742 A93-34172
- Experimental supersonic hydrogen combustion employing staged injection behind a rearward-facing step
p 744 A93-34496
- Issues associated with long-duration high-enthalpy scramjet combustor testing
p 721 A93-34497
- Reaction zone structure for strong, weak overdriven, and weak underdriven oblique detonations
p 746 A93-35492
- Design and evaluation of a robust dynamic neurocontroller for a multivariable aircraft control problem
p 817 A93-37004
- Review of crack propagation under unsteady loading
p 837 A93-39416
- Analysis of hypersonic nozzles including vibrational nonequilibrium and intermolecular force effects
p 861 A93-41916
- Supersonic jet control via point disturbances inside the nozzle
p 861 A93-41930
- Strong vortex/boundary layer interactions. I - Vortices high
p 930 A93-43539
- It's time to go supersonic
p 949 A93-44099
- The NASA Computational Fluid Dynamics (CFD) program - Building technology to solve future challenges
[AIAA PAPER 93-3292] p 1041 A93-44996
- A coarse-grid correction/nonlinear relaxation algorithm for the three-dimensional, compressible Navier-Stokes equations
[AIAA PAPER 93-3317] p 951 A93-45013
- Line relaxation methods for the solution of 2D and 3D compressible flows
[AIAA PAPER 93-3366] p 955 A93-45059
- Development of a skin friction gauge for use in an impulse facility
p 1024 A93-45526
- Hypervelocity flows of argon produced in a free piston driven expansion tube
p 1012 A93-45530
- NASA airframe structural integrity program
p 1026 A93-45782
- Aerodynamic heating in the vicinity of hypersonic, axisymmetric, shock-wave boundary-layer interactions
[AIAA PAPER 93-2766] p 963 A93-46512
- Simulation of ablation in Earth atmospheric entry
[AIAA PAPER 93-2789] p 1027 A93-46531
- Monte Carlo simulation of radiating reentry flows
[AIAA PAPER 93-2809] p 964 A93-46548
- Comparisons between DSMC and the Navier-Stokes equations for reentry flows
[AIAA PAPER 93-2810] p 964 A93-46549
- Passive range estimation for rotorcraft low-altitude flight
p 948 A93-46608
- Strong vortex/boundary layer interactions. II - Vortices low
p 965 A93-46744
- A new flux splitting scheme
p 973 A93-47189
- Flow field measurements in a crossing shockwave turbulent boundary layer interaction at Mach 3
[AIAA PAPER 93-3434] p 977 A93-47226
- On the aerodynamics and performance of active vortex generators
[AIAA PAPER 93-3447] p 979 A93-47234
- Laser holographic interferometric measurements of the flow behind a rearward facing step
[AIAA PAPER 93-3515] p 985 A93-47279
- Absolute intensity measurements of impurity emissions in a shock tunnel and their consequences for laser-induced fluorescence experiments
p 1147 A93-48044
- Hypersonic flow past open cavities
[AIAA PAPER 93-2969] p 1049 A93-48163
- Vortex developments over steady and accelerated airfoils incorporating a trailing edge jet
[AIAA PAPER 93-3008] p 1054 A93-48198
- Aerothermodynamic heating due to shock wave/laminar boundary-layer interactions in high-enthalpy hypersonic flow
[AIAA PAPER 93-3135] p 1064 A93-48299
- Three-dimensional time-marching aeroelastic analyses using an unstructured-grid Euler method
p 1100 A93-49012
- Screening studies of advanced control concepts for airbreathing engines
[AIAA PAPER 92-3320] p 1108 A93-49329
- An experimental study of the effects of bodyside compression on forward swept sidewall compression inlets ingesting a turbulent boundary layer
[AIAA PAPER 93-3125] p 1072 A93-49515
- Investigation of a strut/endwall interaction in supersonic annular flow
[AIAA PAPER 93-1925] p 1076 A93-49791
- Future technology aim of the National Aerospace Plane Program
[AIAA PAPER 93-1988] p 1141 A93-49833
- A k-omega multivariate beta PDF for supersonic turbulent combustion
[AIAA PAPER 93-2197] p 1154 A93-50009
- Modeling of turbulent supersonic H₂-air combustion with a multivariate beta PDF
[AIAA PAPER 93-2198] p 1155 A93-50010
- Experimental and numerical study of swept ramp injection into a supersonic flowfield
[AIAA PAPER 93-2445] p 1119 A93-50197
- WNN 92: Proceedings of the 3rd Workshop on Neural Networks: Academic/Industrial/NASA/Defense, Auburn Univ., AL, Feb. 10-12, 1992 and South Shore Harbour, TX, Nov. 4-6, 1992
[SPIE-1721] p 1167 A93-50726
- A parallel implementation of a multisensor feature-based range-estimation method
p 1099 A93-51967
- A time-accurate high-resolution TVD scheme for solving the Navier-Stokes equations
p 1093 A93-52006
- Passive range estimation for rotorcraft low-altitude flight
p 1190 A93-52881
- International aerospace STI
p 1227 A93-53826
- Propulsion technology challenges for turn-of-the-century commercial aircraft
[ISABE 93-7003] p 1194 A93-53980
- Engine technology challenges for a 21st Century High-Speed Civil Transport
[ISABE 93-7064] p 1200 A93-54040
- A parameter optimization approach to controller partitioning for integrated flight/propulsion control application
p 1206 A93-54268
- Icing Research Tunnel rotating bar calibration measurement system
p 1255 A93-54398
- Development of the wake behind a circular cylinder impulsively started into rotatory and rectilinear motion
p 1236 A93-55736
- International Congress on Recent Developments in Air- and Structure-Borne Sound and Vibration, 2nd, Auburn Univ., AL, Mar. 4-6, 1992, Proceedings, Vols. 1-3
p 1259 A93-55851
- A general introduction to aeroacoustics and atmospheric sound
p 1264 A93-55852
- Index to NASA news releases and speeches, 1991
[NASA-TM-108004] p 104 A93-10815
- Index to NASA news releases and speeches, 1990
[NASA-TM-108003] p 104 A93-10872
- Coordinating Council, Fourth Meeting: NACA Documents Database Project
[NASA-TM-108017] p 234 A93-12671
- Coordinating Council, Sixth Meeting: Who Are Our Key Users?
[NASA-TM-108021] p 234 A93-12672
- Requirements for soldered electrical connections
[NHB-5300.4(3A-2)] p 212 A93-12674
- NASA aeronautics: Research and technology program highlights
[NASA-NP-159] p 109 A93-13110
- NASA SBIR abstracts of 1990 phase 1 projects
[NASA-TM-108145] p 572 A93-21794
- The atmospheric effects of stratospheric aircraft. Report of the 1992 Models and Measurements Workshop, Volume 1: Workshop objectives and summary
[NASA-RP-1292-VOL-1] p 754 A93-25157
- The atmospheric effects of stratospheric aircraft. Report of the 1992 Models and Measurements Workshop, Volume 2: Comparisons with global atmospheric measurements
[NASA-RP-1292-VOL-2] p 754 A93-25158
- The atmospheric effects of stratospheric aircraft. Report of the 1992 Models and Measurements Workshop, Volume 3: Special diagnostic studies
[NASA-RP-1292-VOL-3] p 754 A93-25159
- Aeronautics in NACA and NASA
[NASA-NP-156] p 678 A93-26422
- The NASA SBIR product catalog
[NASA-TM-108242] p 945 A93-29322
- NASA SBIR abstracts of 1991 phase 1 projects
[NASA-TM-108240] p 945 A93-29323
- Research and technology objectives and plans: Summary fiscal year 1991
[NASA-TM-103086] p 946 A93-29452
- European aerospace science and technology, 1992: A bibliography with indexes
[NASA-SP-7105] p 949 A93-32404
- National Aeronautics and Space Administration, Ames Research Center, Moffett Field, CA.
- A robust direct-integration method for rotorcraft maneuver and periodic response
p 61 A93-10919

- Flight test evaluation of precision-code differential GPS for terminal approach and landing p 33 A93-11294
- Near-optimal energy transitions for energy-state trajectories of hypersonic aircraft p 69 A93-13276
- [AIAA PAPER 92-4300] p 69 A93-13276
- Effect of canard position on the longitudinal aerodynamic characteristics of a close-coupled canard-wing-body configuration p 14 A93-13304
- [AIAA PAPER 92-4632] p 14 A93-13304
- The numerical study of 3-D flow past control surfaces [AIAA PAPER 92-4650] p 14 A93-13305
- A comparison of upwind schemes for computation of three-dimensional hypersonic real-gas flows [AIAA PAPER 92-4350] p 15 A93-13306
- Preliminary design features of the RASCAL - A NASA/Army rotorcraft in-flight simulator p 42 A93-13311
- [AIAA PAPER 92-4175] p 42 A93-13311
- Piloted simulation evaluation of pitch control designs for highly augmented STOVL aircraft p 63 A93-13328
- [AIAA PAPER 92-4234] p 63 A93-13328
- Determination of YAV-8B Reaction Control System bleed flow usage p 54 A93-13330
- [AIAA PAPER 92-4232] p 54 A93-13330
- Structural and aerodynamic considerations for an oblique all-wing aircraft p 43 A93-13336
- [AIAA PAPER 92-4220] p 43 A93-13336
- Oblique wing supersonic transport concepts [AIAA PAPER 92-4230] p 43 A93-13337
- Piloted simulation study of two tilt-wing control concepts p 63 A93-13338
- [AIAA PAPER 92-4236] p 63 A93-13338
- Small scale jet effects and hot gas ingestion investigations at NASA Ames p 67 A93-13339
- [AIAA PAPER 92-4252] p 67 A93-13339
- Extracting dimensional geometric parameters from B-spline surface models of aircraft p 43 A93-13340
- [AIAA PAPER 92-4283] p 43 A93-13340
- Numerical simulation of STOL operations using thrust-vectoring p 15 A93-13342
- [AIAA PAPER 92-4254] p 15 A93-13342
- Infrared flow visualization of V/STOL aircraft [AIAA PAPER 92-4253] p 80 A93-13343
- [AIAA PAPER 92-4253] p 80 A93-13343
- Shedding new light on gas dynamics p 80 A93-13435
- Theoretical study of the bond dissociation energies of propyne (C₃H₄) p 230 A93-14099
- Fluid/chemistry modeling for hypersonic flight analysis p 111 A93-14120
- The new challenge of computational aeroscience p 112 A93-14169
- In-flight detection of flow separation, stagnation, and transition p 166 A93-14326
- Navier-Stokes computation of wing/rotor interaction for a tilt rotor in hover p 122 A93-14537
- Implicit Navier-Stokes solver for three-dimensional compressible flows p 122 A93-14546
- Phase II simulation evaluation of the flying qualities of two tilt-wing flap control concepts p 185 A93-14635
- [SAE PAPER 920988] p 185 A93-14635
- HUD Guidance for the ASKA Experimental STOL Aircraft using Radar Position Information p 150 A93-14661
- [SAE PAPER 921041] p 150 A93-14661
- Experimental study of rotor wake/body interactions in hover p 124 A93-14782
- Tiltrotor Research Aircraft composite blade repairs - Lessons learned p 108 A93-14819
- A high-frequency, secondary instability of crossflow vortices that leads to transition p 128 A93-17253
- Representation and presentation of requirements knowledge p 228 A93-17389
- Experimental study of controlled tip disturbance effect on flow asymmetry p 211 A93-17417
- Vision-based range estimation using helicopter flight data p 151 A93-17501
- Validation of vision-based obstacle detection algorithms for low-altitude helicopter flight p 374 A93-19077
- Comparison of advanced turboprop interior noise control ground and flight test data p 444 A93-19136
- The design of test-section inserts for higher speed aeroacoustic testing in the Ames 80-by-120-Foot Wind Tunnel p 374 A93-19149
- Boundary conditions for direct computation of aerodynamic sound generation p 447 A93-19176
- Advances in tilt rotor noise prediction p 447 A93-19184
- On the scaling of small-scale jet noise to large scale p 448 A93-19195
- The use of interferometry in the study of rotorcraft aerodynamics p 407 A93-19914
- A sensitivity study for pneumatic vortex control on a chined forebody p 260 A93-20162
- [AIAA PAPER 93-0049] p 260 A93-20162
- Active control of wing rock of a delta wing at post-stall using tangential leading edge blowing p 367 A93-20169
- [AIAA PAPER 93-0056] p 367 A93-20169
- Parallel computation of 3-D Navier-Stokes flowfields for supersonic vehicles p 261 A93-20177
- [AIAA PAPER 93-0064] p 261 A93-20177
- A solution scheme for the Euler equations based on a multi-dimensional wave model p 261 A93-20178
- [AIAA PAPER 93-0065] p 261 A93-20178
- Stability and transition on swept wings p 263 A93-20190
- [AIAA PAPER 93-0078] p 263 A93-20190
- The use of subscale models to predict self-induced oscillations of flight vehicles p 264 A93-20199
- [AIAA PAPER 93-0093] p 264 A93-20199
- Development of the quasi-procedural method for use in aircraft configuration optimization p 322 A93-20278
- [AIAA PAPER 92-4693] p 322 A93-20278
- Coupled finite-difference/finite-element approach for wing-body aeroelasticity p 409 A93-20302
- [AIAA PAPER 92-4680] p 409 A93-20302
- Survey - Applications of structural optimization methods to fixed wing aircraft and spacecraft p 325 A93-20328
- [AIAA PAPER 92-4726] p 325 A93-20328
- Structural optimization for joined-wing synthesis [AIAA PAPER 92-4761] p 325 A93-20356
- [AIAA PAPER 92-4761] p 325 A93-20356
- Analytical formulation of optimum rotor interdisciplinary design with a three-dimensional wake p 265 A93-20416
- [AIAA PAPER 92-4778] p 265 A93-20416
- Multidisciplinary computational aerosciences p 437 A93-20711
- Numerical simulation of jet noise p 265 A93-20716
- Unsteady two- and three-dimensional Navier-Stokes simulations of multistage turbomachinery flows p 266 A93-20721
- Vision-based range estimation using helicopter flight data p 317 A93-21525
- A summary of investigations of severe turbulence incidents using airline flight records p 308 A93-22153
- Application of space-marching methods to hypersonic forebody flow fields p 272 A93-22305
- [AIAA PAPER 92-5030] p 272 A93-22305
- Arc jet testing in NASA Ames Research Center thermophysics facilities p 385 A93-22315
- [AIAA PAPER 92-5041] p 385 A93-22315
- A study of hypersonic swept shock wave/turbulent boundary layer interactions using a conical Navier-Stokes code p 273 A93-22322
- [AIAA PAPER 92-5050] p 273 A93-22322
- Computation of nonequilibrium radiating shock layers [AIAA PAPER 93-0144] p 414 A93-22588
- [AIAA PAPER 93-0144] p 414 A93-22588
- Video luminescent barometry - The induction period [AIAA PAPER 93-0179] p 414 A93-22607
- [AIAA PAPER 93-0179] p 414 A93-22607
- Two-directional skin friction measurement utilizing a compact internally mounted thin-liquid-film skin friction meter p 414 A93-22608
- [AIAA PAPER 93-0180] p 414 A93-22608
- Experimental and numerical analysis of the wing rock characteristics of a 'wing-body-tail' configuration [AIAA PAPER 93-0187] p 368 A93-22612
- [AIAA PAPER 93-0187] p 368 A93-22612
- Tracking flow features using overset grids p 276 A93-22617
- [AIAA PAPER 93-0197] p 276 A93-22617
- Turbulence modeling for complex hypersonic flows [AIAA PAPER 93-0200] p 277 A93-22620
- [AIAA PAPER 93-0200] p 277 A93-22620
- The effect of Reynolds number and turbulence on airfoil aerodynamics at -90 degrees incidence p 277 A93-22624
- [AIAA PAPER 93-0206] p 277 A93-22624
- The computation of the post-stall behavior of a circulation controlled airfoil p 277 A93-22625
- [AIAA PAPER 93-0207] p 277 A93-22625
- Interferometric investigations of compressible dynamic stall over a transiently pitching airfoil p 278 A93-22628
- [AIAA PAPER 93-0211] p 278 A93-22628
- Vision-based recursive estimation of rotorcraft obstacle locations p 343 A93-22851
- Application of CFD to a generic hypersonic flight research study p 280 A93-23007
- [AIAA PAPER 93-0312] p 280 A93-23007
- Flowfield computations over the Space Shuttle Orbiter with a proposed canard at a Mach number of 5.8 and 50 degrees angle of attack p 281 A93-23014
- [AIAA PAPER 93-0322] p 281 A93-23014
- 3D Euler flow solutions using unstructured Cartesian and prismatic grids p 281 A93-23022
- [AIAA PAPER 93-0331] p 281 A93-23022
- Comparison of predictions with measurements for a quiet supersonic tunnel p 376 A93-23031
- [AIAA PAPER 93-0344] p 376 A93-23031
- Increase in stagnation pressure and enthalpy in shock tunnels p 377 A93-23035
- [AIAA PAPER 93-0350] p 377 A93-23035
- A hybrid structured-unstructured grid method for unsteady turbomachinery flow computations p 282 A93-23066
- [AIAA PAPER 93-0387] p 282 A93-23066
- Engine/airframe integration for waverider cruise vehicles p 283 A93-23254
- [AIAA PAPER 93-0507] p 283 A93-23254
- Stability and control of hypersonic waveriders [AIAA PAPER 93-0508] p 370 A93-23255
- [AIAA PAPER 93-0508] p 370 A93-23255
- Analysis of a hypersonic waverider research vehicle with a hydrocarbon scramjet engine p 386 A93-23256
- [AIAA PAPER 93-0509] p 386 A93-23256
- Juncture flow improvement for wing/pylon configurations by using CFD methodology p 283 A93-23264
- [AIAA PAPER 93-0522] p 283 A93-23264
- Measurements in the near-field of a turbulent wingtip vortex p 285 A93-23290
- [AIAA PAPER 93-0551] p 285 A93-23290
- Streamwise vortex meander in a plane mixing layer [AIAA PAPER 93-0553] p 285 A93-23292
- [AIAA PAPER 93-0553] p 285 A93-23292
- An integrated knowledge system for wind tunnel testing - Project Engineers' Intelligent Assistant p 377 A93-23297
- [AIAA PAPER 93-0560] p 377 A93-23297
- Flight simulator fidelity assessment in a rotorcraft lateral translation maneuver p 378 A93-23510
- Three-dimensional hypersonic shock wave/turbulent boundary-layer interactions p 287 A93-23533
- Direct solution of two-dimensional Navier-Stokes equations for static aeroelasticity problems p 417 A93-23554
- Seed particle response and size characterization in high speed flows p 459 A93-23811
- Development of the NASA-Ames low disturbance supersonic wind tunnel for transition research up to Mach 2.5 p 462 A93-24488
- [AIAA PAPER 92-3909] p 462 A93-24488
- Effect of leading-edge porosity on blade-vortex interaction noise p 563 A93-24727
- [AIAA PAPER 93-0601] p 563 A93-24727
- Corrections to fringe distortion due to flow density gradients in optical interferometry p 539 A93-24748
- [AIAA PAPER 93-0631] p 539 A93-24748
- Unsteady panel method for flows with multiple bodies moving along various paths p 539 A93-24755
- [AIAA PAPER 93-0640] p 539 A93-24755
- Lift enhancement of an airfoil using a Gurney flap and vortex generators p 464 A93-24762
- [AIAA PAPER 93-0647] p 464 A93-24762
- A new procedure for dynamic adaption of three-dimensional unstructured grids p 560 A93-24780
- [AIAA PAPER 93-0672] p 560 A93-24780
- Comparison of continuum and particle simulations of expanding rarefied flows p 466 A93-24818
- [AIAA PAPER 93-0728] p 466 A93-24818
- Fiber-optic interferometric sensors for measurements of pressure fluctuations - Experimental evaluation p 540 A93-24828
- [AIAA PAPER 93-0738] p 540 A93-24828
- Numerical simulation of crossing/turbulent boundary layer interaction at Mach 8.3 comparison of zero and two-equation turbulence models p 467 A93-24861
- [AIAA PAPER 93-0779] p 467 A93-24861
- Hypersonic crossing shock-wave/turbulent-boundary-layer interactions p 467 A93-24863
- [AIAA PAPER 93-0781] p 467 A93-24863
- A concurrent hybrid Navier-Stokes/Euler approach to fluid dynamic computations p 468 A93-24865
- [AIAA PAPER 93-0789] p 468 A93-24865
- A numerical investigation of a subsonic jet in a crossflow p 469 A93-24931
- [AIAA PAPER 93-0870] p 469 A93-24931
- The rebirth of supersonic transport p 457 A93-25325
- Experimental investigations of the time and flow-direction responses of shear-stress-sensitive liquid crystal coatings p 542 A93-25508
- [AIAA PAPER 93-0181] p 542 A93-25508
- Progress in high-lift aerodynamic calculations p 474 A93-25512
- [AIAA PAPER 93-0194] p 474 A93-25512
- Recent developments in high order K-exact reconstruction on unstructured meshes p 475 A93-25546
- [AIAA PAPER 93-0668] p 475 A93-25546
- Passive range sensor refinement using texture and segmentation p 544 A93-27044
- A fast algorithm for image-based ranging p 544 A93-27045
- Performance considerations for high-definition head-mounted displays p 518 A93-27242
- Schlieren studies of compressibility effects on dynamic stall of transiently pitching airfoils p 480 A93-28608
- Conceptual assessment of two high-speed rotorcraft p 508 A93-28612
- Numerical study of the flow establishment time in hypersonic shock tunnels p 480 A93-29153
- Modeling and control design of a wind tunnel model support p 529 A93-29281
- Progress in laser spectroscopic techniques for aerodynamic measurements - An overview p 549 A93-29308
- Noise reduction for transonic blade-vortex interactions p 566 A93-29408
- Shock waves and the Flowcs Williams-Hawkins equation p 480 A93-29411
- Far-field hover acoustic characteristics of the XV-15 tiltrotor aircraft with Advanced Technology Blades p 566 A93-29412

- A comparative analysis of XV-15 tiltrotor hover test data and WOPWOP predictions incorporating the fountain effect p 509 A93-29414
- Data acquisition and analysis on a Macintosh p 562 A93-29422
- Euler solutions to nonlinear acoustics of non-lifting rotor blades p 568 A93-29433
- The development of a CFD potential method for the analysis of tilt-rotors p 481 A93-29434
- Flowfield analysis of modern helicopter rotors in hover by Navier-Stokes method p 481 A93-29435
- Correlation of airloads on a two-bladed helicopter rotor p 481 A93-29438
- Flow visualization and flow field measurements of a 1/12 scale tilt rotor aircraft in hover p 482 A93-29441
- Flutter calculations for fixed and rotating wings with state-space inflow dynamics p 709 A93-33877 [AIAA PAPER 93-1300]
- Sources of helicopter rotor hub inplane shears p 709 A93-33927 [AIAA PAPER 93-1358]
- Full-scale wind tunnel investigation of a helicopter individual blade control system p 726 A93-33929 [AIAA PAPER 93-1361]
- Utilization of CAD/CAE for concurrent design of structural aircraft components p 710 A93-34014 [AIAA PAPER 93-1466]
- Improvements in hover display dynamics for a combat helicopter p 727 A93-34257
- Effect of an unsteady three-dimensional wake on elastic blade-flapping eigenvalues in hover p 683 A93-34260
- Atmospheric turbulence simulation for rotorcraft applications p 757 A93-34264
- Numerical methods in laminar and turbulent flow; Proceedings of the 7th International Conference, Stanford Univ., CA, July 15-19, 1991. Vol. 7, pts. 1 & 2 p 743 A93-34301 [ISBN 0-906674-77-8]
- Multipass three-dimensional Navier-Stokes simulation of turbine rotor-stator interaction p 688 A93-34484
- Gas phase hydrogen permeation in a Ni-Fe-Co superalloy p 735 A93-34510
- Synthesis and evaluation of an H2 control law for a hovering helicopter p 728 A93-34542
- Automatic guidance and control laws for helicopter obstacle avoidance p 728 A93-35518
- URNS - A free-wake Euler/Navier-Stokes numerical method for helicopter rotors p 692 A93-35634
- Visual augmentation for night flight over featureless terrain p 806 A93-35921
- A finite-volume Euler solver for computing rotary-wing aerodynamics on unstructured meshes p 765 A93-35935
- Numerical simulation of a hovering rotor using embedded grids p 765 A93-35936
- Effects of ingested atmospheric turbulence on measured tail rotor acoustics p 849 A93-35964
- Flap-lag damping in hover and forward flight with a three-dimensional wake p 797 A93-35979
- Introduction of the M-85 high-speed rotorcraft concept p 797 A93-35980
- Helicopter response to atmospheric turbulence p 817 A93-35987
- Investigation of the flight mechanics simulation of a hovering helicopter p 798 A93-35990
- Shadowgraph flow visualization of isolated tiltrotor and rotor/wing wakes p 767 A93-35996
- Hover performance analysis of advanced rotor blades p 767 A93-35998
- Advanced Technology Blade testing on the XV-15 Tilt Rotor Research Aircraft p 799 A93-36020
- Piloted simulator investigations of a civil tilt-rotor aircraft on steep instrument approaches p 800 A93-36023
- Computational investigation of a pneumatic forebody flow control concept p 768 A93-37383
- Comparison of two Navier-Stokes codes for simulating high-incidence vortical flow p 768 A93-37387
- Transonic blade-vortex interactions - Noise reduction p 850 A93-37396
- Hypersonic flutter of a curved shallow panel with aerodynamic heating p 829 A93-37428 [AIAA PAPER 93-1318]
- Transonic panel flutter p 829 A93-37438 [AIAA PAPER 93-1476]
- Nonclassical aileron buzz in transonic flow p 829 A93-37439 [AIAA PAPER 93-1479]
- Development update for the NASA Ames 16-Inch Shock Tunnel Facility p 822 A93-37873
- Hypersonic single expansion ramp nozzle simulations p 777 A93-39254
- Computational flow predictions for hypersonic drag devices p 777 A93-39257
- Unsteady transonic two-dimensional Euler solutions using finite elements p 778 A93-39412
- Engineering a visual system for seeing through fog [SAE PAPER 921130] p 895 A93-41318
- Quantitative feedback theory applied to the design of a rotorcraft flight control system p 906 A93-41895
- Implicit multigrid techniques for compressible flows p 862 A93-42429
- Hypersonic cone flow predictions using an implicit upwind space-marching code p 865 A93-42588
- Computational results for 2-D and 3-D ramp flows with an upwind Navier-Stokes solver p 866 A93-42592
- Application of the Galerkin/least-squares formulation to the analysis of hypersonic flows. I - Flow over a two-dimensional ramp p 866 A93-42593
- Application of the Galerkin/least-squares formulation to the analysis of hypersonic flows. II - Flow past a double ellipse p 868 A93-42608
- Computation of thermochemical nonequilibrium flows around a simple and a double ellipse p 869 A93-42629
- The hypersonic double ellipse in rarefied flow p 869 A93-42631
- Pilot-in-the-loop analysis of propulsive-only flight control systems p 908 A93-42812
- Review of chemical-kinetic problems of future NASA missions. I - Earth entries p 872 A93-42899
- Tip vortex geometry of a hovering helicopter rotor in ground effect p 893 A93-43779
- Efficient free wake calculations using analytical/numerical matching p 874 A93-43780
- Direct periodic solutions of rotor free wake calculations p 874 A93-43781
- A finite-volume Euler solver for computing rotary-wing aerodynamics on unstructured meshes p 874 A93-43782
- Technologies for automating rotorcraft nap-of-the-earth flight p 885 A93-43784
- Mesh generation for the computation of flowfields over complex aerodynamic shapes p 995 A93-44888
- The NASA Computational Fluid Dynamics (CFD) program - Building technology to solve future challenges [AIAA PAPER 93-3292] p 1041 A93-44996
- Dynamic overset grid communication on distributed memory parallel processors p 1036 A93-45007 [AIAA PAPER 93-3311]
- Calculation of optimum airfoils using direct solutions of the Navier-Stokes equations p 952 A93-45017 [AIAA PAPER 93-3323]
- Euler solutions for blunt bodies using triangular meshes - Artificial viscosity forms and numerical boundary conditions p 953 A93-45027 [AIAA PAPER 93-3333]
- Numerical vorticity capturing for vortex-solid body interaction problems p 954 A93-45037 [AIAA PAPER 93-3343]
- Moving body overset grid methods for complete aircraft tiltrotor simulations p 954 A93-45044 [AIAA PAPER 93-3350]
- Multigrid convergence of an implicit symmetric relaxation scheme p 954 A93-45051 [AIAA PAPER 93-3357]
- Implicit multigrid Euler solutions with symmetric Total-Variation-Diminishing dissipation p 955 A93-45052 [AIAA PAPER 93-3358]
- Virtual zone Navier-Stokes computations for oscillating control surfaces p 955 A93-45056 [AIAA PAPER 93-3363]
- Effects of spatial order of accuracy on the computation of vortical flowfields p 955 A93-45064 [AIAA PAPER 93-3371]
- 3D automatic Cartesian grid generation for Euler flows p 956 A93-45077 [AIAA PAPER 93-3386]
- Computation of induced drag for elliptical and crescent-shaped wings p 958 A93-45136
- Aerospace plane design challenge - Credible computations p 1015 A93-45145
- Application of leading-edge vortex manipulations to reduce wing rock amplitudes p 1007 A93-45152
- Applications to fixed-wing aircraft and spacecraft p 996 A93-45432
- An overview of Ames experimental aerothermodynamics p 1011 A93-45496
- Initiation of combustion in the thermally choked ram accelerator p 1016 A93-45501
- Computation of crossing shock/turbulent boundary layer interaction at Mach 8.3 p 961 A93-45726
- Viscous hypersonic shock-shock interaction on a blunt body at high altitude p 962 A93-46477 [AIAA PAPER 93-2722]
- Development and operation of new arc heater technology for a large-scale scramjet propulsion test facility p 1016 A93-46528 [AIAA PAPER 93-2786]
- Convective heat-transfer rate distributions over a 140 deg blunt cone at hypersonic speeds in different gas environments p 1027 A93-46529 [AIAA PAPER 93-2787]
- Thermal response and ablation characteristics of light weight ceramic ablators p 1018 A93-46532 [AIAA PAPER 93-2790]
- Measurement and analysis of nitric oxide radiation in an arc-jet flow p 1016 A93-46540 [AIAA PAPER 93-2800]
- Flow resolution and domain of influence in rarefied hypersonic blunt-body flows p 964 A93-46546 [AIAA PAPER 93-2806]
- Comparisons between DSMC and the Navier-Stokes equations for reentry flows p 964 A93-46549 [AIAA PAPER 93-2810]
- Thermal analysis of an arc heater electrode with a rotating arc foot p 1028 A93-46590 [AIAA PAPER 93-2855]
- Passive range estimation for rotorcraft low-altitude flight p 948 A93-46608
- Strong vortex/boundary layer interactions. II - Vortices low p 965 A93-46744
- Effects of bleed-hole geometry and plenum pressure on three-dimensional shock-wave/boundary-layer/bleed interactions p 967 A93-46800 [AIAA PAPER 93-3259]
- Effect of ground and ceiling planes on shape of energized wakes p 974 A93-47207 [AIAA PAPER 93-3410]
- Application of the shadowgraph flow visualization technique to a full-scale helicopter rotor in hover and forward flight p 1030 A93-47208 [AIAA PAPER 93-3411]
- Low-speed wind tunnel test results of the Canard Rotor/Wing concept p 975 A93-47209 [AIAA PAPER 93-3412]
- A critical assessment of UH-60 main rotor blade airfoil data p 975 A93-47210 [AIAA PAPER 93-3413]
- Performance results from a test of an S-76 rotor in the NASA Ames 80- by 120-foot wind tunnel p 975 A93-47211 [AIAA PAPER 93-3414]
- Near-field supersonic flow predictions by an adaptive unstructured tetrahedral grid solver p 977 A93-47223 [AIAA PAPER 93-3430]
- A zonal CFD method for three-dimensional wing simulations p 977 A93-47225 [AIAA PAPER 93-3433]
- Forebody vortex control with jet and slot blowing on an F/A-18 p 1009 A93-47235 [AIAA PAPER 93-3449]
- Forebody vortex control on an F/A-18 using small, rotatable 'tip-strakes' p 1009 A93-47236 [AIAA PAPER 93-3450]
- Navier-Stokes prediction of a delta wing in roll with vortex breakdown p 983 A93-47267 [AIAA PAPER 93-3495]
- Prediction of stall and post-stall behavior of airfoils at low and high Reynolds numbers p 983 A93-47270 [AIAA PAPER 93-3502]
- Measurements in 80- by 120-foot wind tunnel of hazard posed by lift-generated wakes p 1014 A93-47281 [AIAA PAPER 93-3518]
- Characteristics of deformable leading edge for high performance helicopter rotor p 986 A93-47285 [AIAA PAPER 93-3526]
- Investigation of a hypersonic crossing shock wave/turbulent boundary layer interaction p 1044 A93-48043
- Numerical simulation of upstream disturbance on flows around a slender body p 1047 A93-48150 [AIAA PAPER 93-2956]
- Effects of aft geometry on vortex behavior and force production by a tangential jet on a body at high alpha p 1048 A93-48155 [AIAA PAPER 93-2961]
- Effect of forebody tangential slot blowing on flow about a full aircraft geometry p 1048 A93-48156 [AIAA PAPER 93-2962]
- Multi-zonal Navier-Stokes code with the LU-SGS scheme p 1148 A93-48159 [AIAA PAPER 93-2965]
- A numerical study of the effect of geometry variation, turbulence models, and dissipation on the flow past control surfaces p 1048 A93-48161 [AIAA PAPER 93-2967]
- Transition effects on compressible dynamic stall of transiently pitching airfoils p 1050 A93-48171 [AIAA PAPER 93-2978]
- A computational study of wingtip vortex flowfield p 1054 A93-48200 [AIAA PAPER 93-3010]
- Turbulent structure of a wingtip vortex in the near field p 1054 A93-48201 [AIAA PAPER 93-3011]
- Wake-vortex structure from lift and torque induced on a following wing p 1054 A93-48202 [AIAA PAPER 93-3013]
- A solution-adaptive hybrid-grid method for the unsteady analysis of turbomachinery p 1148 A93-48204 [AIAA PAPER 93-3015]

A viscous-inviscid interaction method for 2-D unsteady, compressible flows
[AIAA PAPER 93-3019] p 1055 A93-48206

Navier-Stokes simulation of external/internal transonic flow on the forebody/inlet of the AV-8B Harrier II
[AIAA PAPER 93-3057] p 1058 A93-48234

Unsteady Navier-Stokes simulation of the canard-wing-body ramp motion
[AIAA PAPER 93-3058] p 1058 A93-48235

An initial comparison of CFD with experiment for a geometrically simplified STOVL model
[AIAA PAPER 93-3059] p 1058 A93-48236

Laser Interferometer Skin-Friction measurements of crossing-shock wave/turbulent boundary-layer interactions
[AIAA PAPER 93-3072] p 1148 A93-48247

Free-wake computation of helicopter rotor flowfields in forward flight
[AIAA PAPER 93-3079] p 1059 A93-48253

Fluid-structural interactions using Navier-Stokes flow equations coupled with shell finite element structures
[AIAA PAPER 93-3087] p 1099 A93-48261

Design efficiency evaluation for transonic airfoil optimization - A case for Navier-Stokes design
[AIAA PAPER 93-3112] p 1062 A93-48282

Shape optimization for aerodynamic efficiency and low observability
[AIAA PAPER 93-3115] p 1062 A93-48285

Lateral control at high angles of attack using pneumatic blowing through a chined forebody
[AIAA PAPER 93-3624] p 1126 A93-48309

A method of wind shear detection for powered-lift STOL aircraft
[AIAA PAPER 93-3667] p 1104 A93-48345

Wind-shear endurance capability for powered-lift aircraft
[AIAA PAPER 93-3670] p 1129 A93-48348

Navier-Stokes computations on full-span wing-body configuration with oscillating control surfaces
[AIAA PAPER 93-3687] p 1065 A93-48356

Boundary conditions for direct computation of aerodynamic sound generation
[AIAA PAPER 93-3687] p 1172 A93-49005

Skin friction and velocity profile family for compressible turbulent boundary layers
[AIAA PAPER 93-3687] p 1070 A93-49008

Euler calculations of unsteady interaction of advancing rotor with a line vortex
[AIAA PAPER 93-3687] p 1071 A93-49016

Vision based techniques for rotorcraft low altitude flight
[AIAA PAPER 93-3687] p 1097 A93-49351

Unsteady, three-dimensional, Navier-Stokes simulations of multistage turbomachinery flows
[AIAA PAPER 93-1979] p 1153 A93-49826

Numerical simulations of a pulsed detonation wave augmentation device
[AIAA PAPER 93-1985] p 1112 A93-49832

Numerical study of the transient flow in the driven tube and the nozzle section of a shock tunnel
[AIAA PAPER 93-2018] p 1078 A93-49856

Applying and validating the RANS-3D flow-solver for evaluating a subsonic serpentine diffuser geometry
[AIAA PAPER 93-2157] p 1079 A93-49973

NO(x) reduction additives for aircraft gas turbine engines
[AIAA PAPER 93-2594] p 1122 A93-50306

The Airborne Ocean Color Imager - System description and image processing
[AIAA PAPER 93-2594] p 1157 A93-50369

Electro-optical navigation for aircraft
[AIAA PAPER 93-2594] p 1097 A93-50643

Benefits of variable rotor speed in integrated helicopter/engine control
[AIAA PAPER 93-3851] p 1134 A93-51438

Vision based obstacle detection and grouping for helicopter guidance
[AIAA PAPER 93-3871] p 1098 A93-51457

Clustering methods for removing outliers from vision-based range estimates
[AIAA PAPER 93-3871] p 1171 A93-51648

A parallel implementation of a multisensor feature-based range-estimation method
[AIAA PAPER 93-3871] p 1099 A93-51967

Unsteady aerodynamic behavior of an airfoil with and without a slot
[AIAA PAPER 93-3871] p 1093 A93-52007

Euler/experiment correlations of sonic boom pressure signatures
[AIAA PAPER 93-3871] p 1095 A93-52439

Investigation of vortex development on a pitching slender body of revolution
[AIAA PAPER 93-3871] p 1095 A93-52445

Flowfield simulation about the stratospheric observatory for infrared astronomy
[AIAA PAPER 93-3871] p 1095 A93-52446

Efficient simulation of incompressible viscous flow over single and multiple airfoils
[AIAA PAPER 93-3871] p 1095 A93-52448

A high fidelity video delivery system for real-time flight simulation research
[AIAA PAPER 93-3558] p 1214 A93-52659

Development and operation of a real-time simulation at the NASA Ames Vertical Motion Simulator
[AIAA PAPER 93-3575] p 1208 A93-52671

Simulation motion effect on single axis compensatory tracking
[AIAA PAPER 93-3579] p 1208 A93-52675

Pseudo Aircraft Systems - A multi-aircraft simulation system for air traffic control research
[AIAA PAPER 93-3585] p 1209 A93-52679

A radar altitude and line of sight attachment
[AIAA PAPER 93-3587] p 1223 A93-52680

Enhancing real-time flight simulation execution by intercepting Run-Time Library calls
[AIAA PAPER 93-3591] p 1224 A93-52684

Passive range estimation for rotorcraft low-altitude flight
[AIAA PAPER 93-3591] p 1190 A93-52881

Numerical study of a delta planform with multiple jets in ground effect
[SAE PAPER 892283] p 1176 A93-53200

Low aspect ratio wing code validation experiment
[SAE PAPER 892283] p 1176 A93-53202

Effective treatment of the singular line boundary problem for three-dimensional grids
[SAE PAPER 892283] p 1177 A93-53204

Space marching calculations about hypersonic configurations using a solution-adaptive mesh algorithm
[SAE PAPER 892283] p 1177 A93-53212

Evaluation of 2D ceramic matrix composites in aerodynamic environments
[SAE PAPER 892283] p 1212 A93-53459

Rotor fatigue monitoring data acquisition system
[SAE PAPER 892283] p 1261 A93-54353

Spectral measurements of shock layer radiation in an arc-jet wind tunnel
[SAE PAPER 892283] p 1251 A93-54409

Calculation of real-gas effects on airfoil aerodynamic characteristics
[SAE PAPER 892283] p 1229 A93-54477

Optimal trajectories for hypersonic launch vehicles
[SAE PAPER 892283] p 1251 A93-54563

Research activity at the shock tube facility at NASA Ames
[SAE PAPER 892283] p 1252 A93-54804

Development of separation due to interaction between a shock wave and a turbulent boundary layer perturbed by rarefaction waves
[SAE PAPER 892283] p 1233 A93-55019

Effect of jet engine exhaust on SOFIA stratospheric performance
[SAE PAPER 892283] p 1263 A93-55178

Theoretical characterization of the reaction $\text{NH}_2 + \text{O}$ yields products
[SAE PAPER 892283] p 1263 A93-55666

Multirate and event-driven Kalman filters for helicopter flight
[SAE PAPER 892283] p 1245 A93-55760

Initial piloted simulation study of geared flap control for tilt-wing V/STOL aircraft
[NASA-TM-103872] p 64 A93-10741

Appraisal of digital terrain elevation data for low-altitude flight
[NASA-TM-103896] p 35 A93-10745

Employment of radicals and excited state species for supersonic combustion photochemical ignition of premixed hydrogen/oxygen mixtures with ArF laser
[NASA-TM-103896] p 73 A93-11135

Integration of radar altimeter, precision navigation, and digital terrain data for low-altitude flight
[NASA-TM-103958] p 36 A93-12320

Navier-Stokes simulations of unsteady transonic flow phenomena
[NASA-TM-103962] p 129 A93-12721

Shared mental models and crew decision making
[NASA-TM-103962] p 147 A93-15023

The Application of CFD to rotary wing flow problems
[NASA-TM-102803] p 139 A93-15483

1991 research and technology
[NASA-TM-103924] p 456 A93-16652

An experimental study of a turbulent boundary layer in the trailing edge region of a circulation-control airfoil
[NASA-CR-191262] p 295 A93-17934

Parabolized Navier-Stokes methods for hypersonic flows
[NASA-TM-103962] p 421 A93-18565

Algorithm development with applications to aerodynamics and aeroelasticity
[NASA-TM-103962] p 422 A93-18566

Issues and approach to develop validated analysis tools for hypersonic flows: One perspective
[NASA-TM-103937] p 305 A93-19379

An exploratory investigation of the flight dynamics effects of rotor rpm variations and rotor state feedback in hover
[NASA-TM-103968] p 373 A93-19380

Pre-flight risk assessment in Emergency Medical Service (EMS) helicopters
[NASA-TM-103968] p 494 A93-19692

Lessons learned from an historical look at flight testing
[NASA-TM-103968] p 511 A93-19904

Test techniques for evaluating flight displays
[NASA-TM-103947] p 516 A93-21810

Discrete range clustering using Monte Carlo methods
[NASA-TM-104004] p 706 A93-24914

Applied aerodynamics: Challenges and expectations
[NASA-TM-103963] p 694 A93-25091

Jet-induced ground effects on a parametric flat-plate model in hover
[NASA-TM-104001] p 700 A93-26099

Autogenic-feedback training improves pilot performance during emergency flying conditions
[NASA-TM-104005] p 790 A93-27076

High-lift aerodynamics: Prospects and plans
[NASA-TM-104005] p 784 A93-27442

Efficient simulation of incompressible viscous flow over multi-element airfoils
[NASA-TM-104005] p 784 A93-27443

Some recent applications of Navier-Stokes codes to rotorcraft
[NASA-TM-103981] p 786 A93-27452

Dynamic airfoil stall investigations
[NASA-TM-103981] p 786 A93-27453

Flight evaluation of a computer aided low-altitude helicopter flight guidance system
[NASA-TM-103981] p 820 A93-28869

Neural networks application to divergence-based passive ranging
[NASA-TM-103981] p 885 A93-29653

NASA/FAA helicopter simulator workshop
[NASA-CP-3156] p 857 A93-30673

Part 1: Executive summary
[NASA-CP-3156] p 857 A93-30674

Helicopter simulator standards
[NASA-CP-3156] p 912 A93-30675

Rotorcraft master plan
[NASA-CP-3156] p 857 A93-30677

Simulators for corporate pilot training and evaluation
[NASA-CP-3156] p 912 A93-30678

Helicopter simulator qualification
[NASA-CP-3156] p 912 A93-30681

Helicopter simulation: Making it work
[NASA-CP-3156] p 912 A93-30682

Helicopter training simulators: Key market factors
[NASA-CP-3156] p 912 A93-30683

Determining the transferability of flight simulator data
[NASA-CP-3156] p 913 A93-30685

Progress through precedent: Going where no helicopter simulator has gone before
[NASA-CP-3156] p 913 A93-30686

Transfer of training and simulator qualification or myth and folklore in helicopter simulation
[NASA-CP-3156] p 913 A93-30687

Validation and upgrading of physically based mathematical models
[NASA-CP-3156] p 942 A93-30688

Frequency-response techniques for documentation and improvement of rotorcraft simulators
[NASA-CP-3156] p 913 A93-30689

Bandwidth and SIMDUCE as simulator fidelity criteria
[NASA-CP-3156] p 913 A93-30690

Methodology development for evaluation of selective-fidelity rotorcraft simulation
[NASA-CP-3156] p 913 A93-30691

Applications of structural optimization methods to fixed-wing aircraft and spacecraft in the 1980s
[NASA-TM-103939] p 1033 A93-32212

Flight evaluation of a computer aided low-altitude helicopter flight guidance system
[NASA-TM-103998] p 994 A93-32225

Selected experiments in laminar flow: An annotated bibliography
[NASA-TM-103998] p 990 A93-32226

Expansion-based passive ranging
[NASA-TM-104025] p 994 A93-32348

Analytical and experimental investigations of the oblique detonation wave engine concept
[NASA-TM-102839] p 1006 A93-32374

National Aeronautics and Space Administration. Flight Research Center, Edwards, CA.

The F-18 systems research aircraft facility
[NASA-TM-4433] p 381 A93-16753

National Aeronautics and Space Administration. Goddard Space Flight Center, Greenbelt, MD.

Volume-imaging lidar observations of the convective structure surrounding the flight path of a flux-measuring aircraft
[NASA-TM-102839] p 425 A93-20579

FIFE atmospheric boundary layer budget methods
[NASA-TM-102839] p 426 A93-20591

Assessing spatial and seasonal variations in grasslands with spectral reflectances from a helicopter platform
[NASA-TM-102839] p 426 A93-20621

Errors in long distance kinematic GPS
[NASA-TM-102839] p 314 A93-21154

Turbulence and stall in plane diffusers - Computational study
[NASA-TM-102839] p 744 A93-34311

Update on the NASA ER-2 Doppler radar system (EDOP)
[NASA-TM-102839] p 807 A93-37737

Implications of three-dimensional tracer studies for two-dimensional assessments of the impact of supersonic aircraft on stratospheric ozone
[NASA-TM-102839] p 936 A93-41269

Mapping new and old worlds with laser altimetry
[NASA-TM-102839] p 1034 A93-45699

Flight data for the Cryogenic Heat Pipe (CRYOHP) Experiment
[AIAA PAPER 93-2735] p 1027 A93-46488

Laser Interferometer Skin-Friction measurements of crossing-shock wave/turbulent boundary-layer interactions
[AIAA PAPER 93-3072] p 1148 A93-48247

Magnetic bearings for cryogenic turbomachines
[AIAA PAPER 93-3072] p 1149 A93-48601

Calibration results for NOAA-11 AVHRR channels 1 and 2 from congruent path aircraft observations
[AIAA PAPER 93-3072] p 1143 A93-51237

Airborne gravimetry, altimetry, and GPS navigation errors
[AIAA PAPER 93-3072] p 1240 A93-55975

Requirements for airborne vector gravimetry
[AIAA PAPER 93-3072] p 1241 A93-55976

Predicted aircraft effects on stratospheric ozone
[AIAA PAPER 93-3072] p 93 A93-11096

- Flight dynamics system software development environment (FDS/SDE) tutorial
[NASA-TM-108580] p 230 N93-15502
- Software Management Environment (SME) installation guide
[NASA-TM-108578] p 230 N93-15578
- Data collection procedures for the Software Engineering Laboratory (SEL) database
[NASA-TM-108579] p 230 N93-15579
- Software Engineering Laboratory Ada performance study: Results and implications p 441 N93-17172
- Optical technologies for UV remote sensing instruments p 853 N93-28788
- National Aeronautics and Space Administration. Hugh L. Dryden Flight Research Facility, Edwards, CA.**
- In-flight flow visualization results from the X-29A aircraft at high angles of attack
[AIAA PAPER 92-4102] p 38 A93-11272
- Correlation of forebody pressures and aircraft yawing moments on the X-29A aircraft at high angles of attack
[AIAA PAPER 92-4105] p 38 A93-11273
- Flight test results from a supercritical mission adaptive wing with smooth variable camber
[AIAA PAPER 92-4101] p 38 A93-11274
- Integrated flight propulsion control research results using the NASA F-15 HIDECA Flight Research Facility
[AIAA PAPER 92-4106] p 38 A93-11276
- Flight testing and simulation of an F-15 airplane using throttles for flight control
[AIAA PAPER 92-4109] p 39 A93-11278
- Flight experience with lightweight, low-power miniaturized instrumentation systems
[AIAA PAPER 92-4111] p 39 A93-11280
- The development of an airborne information management system for flight test
[AIAA PAPER 92-4113] p 51 A93-11281
- Measurement of attachment-line location in a wind-tunnel and in supersonic flight
[AIAA PAPER 92-4089] p 39 A93-11285
- Design and utilization of a Flight Test Engineering Database Management System at the NASA Dryden Flight Research Facility
[AIAA PAPER 92-4072] p 97 A93-13264
- Recent flight-test results of optical airdata techniques
[AIAA PAPER 92-4086] p 51 A93-13265
- The F-18 High Alpha Research Vehicle - A high-angle-of-attack testbed aircraft
[AIAA PAPER 92-4121] p 42 A93-13273
- Taking the measure of aerodynamic testing
p 16 A93-13434
- Flight-determined benefits of integrated flight-propulsion control systems p 183 A93-14370
- Development of a hydrogen external burning flight test experiment on the NASA Dryden SR-71A aircraft
[SAE PAPER 920997] p 157 A93-14638
- On some recent advances in multidisciplinary analysis of hypersonic vehicles
[AIAA PAPER 92-5026] p 438 A93-22302
- Stratospheric turbulence measurements and models for aerospace plane design
[AIAA PAPER 92-5072] p 433 A93-22342
- The X-15 airplane - Lessons learned
[AIAA PAPER 93-0309] p 456 A93-23005
- A comparison of hypersonic flight and prediction results
[AIAA PAPER 93-0311] p 280 A93-23006
- Operational and research aspects of a radio-controlled model flight test program
[AIAA PAPER 93-0625] p 504 A93-24742
- Application of a flush airdata sensing system to a wing leading edge (LE-FADS)
[AIAA PAPER 93-0634] p 516 A93-24750
- Thermoelastic vibration test techniques
p 549 A93-29293
- In-flight investigation of a rotating cylinder-based structural excitation system for flutter testing
[AIAA PAPER 93-1537] p 711 A93-34074
- Actuator and aerodynamic modeling for high-angle-of-attack aeroservoelasticity
[AIAA PAPER 93-1419] p 818 A93-37433
- Transonic panel flutter
[AIAA PAPER 93-1476] p 829 A93-37438
- X-29 vortex flow control tests p 804 A93-38846
- Status of the validation of high-angle-of-attack nose-down pitch control margin design guidelines
[AIAA PAPER 93-3623] p 1126 A93-48308
- Flight testing of a fiber optic temperature sensor
p 1105 A93-49476
- Preliminary flight test results of a fly-by-throttle emergency flight control system on an F-15 airplane
[AIAA PAPER 93-1820] p 1100 A93-49708
- Dual Engine application of the Performance Seeking Control algorithm
[AIAA PAPER 93-1822] p 1110 A93-49709
- On the estimation algorithm for adaptive performance optimization of turbofan engines
[AIAA PAPER 93-1823] p 1111 A93-49710
- Flight-determined engine exhaust characteristics of an F404 engine in an F-18 airplane
[AIAA PAPER 93-2543] p 1121 A93-50267
- Identification of integrated airframe-propulsion effects on an F-15 aircraft for application to drag minimization
[AIAA PAPER 93-3764] p 1101 A93-51359
- Performance-seeking control - Program overview and future directions
[AIAA PAPER 93-3765] p 1102 A93-51360
- Flight research simulation takes off
p 1192 A93-53769
- Overview of supersonic laminar flow control research on the F-16XL ships 1 and 2
[NASA-TM-104257] p 20 N93-11221
- Correlation of forebody pressures and aircraft yawing moments on the X-29A aircraft at high angles of attack
[NASA-TM-4417] p 22 N93-11532
- Flight test results from a supercritical mission adaptive wing with smooth variable camber
[NASA-TM-4415] p 49 N93-11863
- A summary of the forebody high-angle-of-attack aerodynamics research on the F-18 and the X-29A aircraft
[NASA-TM-104261] p 25 N93-12353
- Subsonic flight test evaluation of a propulsion system parameter estimation process for the F100 engine
[NASA-TM-4426] p 175 N93-13155
- Stratospheric turbulence measurements and models for aerospace plane design
[NASA-TM-104262] p 223 N93-13288
- In-flight flow visualization results from the X-29A aircraft at high angles of attack
[NASA-TM-4430] p 131 N93-13322
- Pressure distribution for the wing of the YAV-8B airplane; with and without pylons
[NASA-TM-4429] p 136 N93-14451
- Real-time in-flight engine performance and health monitoring techniques for flight research application
p 169 N93-15169
- Operational and research aspects of a radio-controlled model flight test program
[NASA-TM-104266] p 339 N93-18616
- Flight and wind-tunnel calibrations of a flush airdata sensor at high angles of attack and sideslip and at supersonic Mach numbers
[NASA-TM-104265] p 344 N93-19110
- Overview of the NASA Dryden Flight Research Facility aeronautical flight projects testing p 512 N93-19916
- Application of a flush airdata sensing system to a wing leading edge (LE-FADS)
[NASA-TM-104267] p 518 N93-20163
- Flight control system design factors for applying automated testing techniques
[NASA-TM-4242] p 910 N93-30764
- Engine exhaust characteristics evaluation in support of aircraft acoustic testing
[NASA-TM-104263] p 1005 N93-32220
- National Aeronautics and Space Administration. John C. Stennis Space Center, Bay Saint Louis, MS.**
- Liquid hydrogen foil-bearing turbopump
[AIAA PAPER 93-2537] p 1156 A93-50264
- The Airborne Ocean Color Imager - System description and image processing
p 1157 A93-50369
- National Aeronautics and Space Administration. John F. Kennedy Space Center, Cocoa Beach, FL.**
- Joint NASA/USAF Airborne Field Mill Program - Operation and safety considerations during flights of a Lear 28 airplane in adverse weather
[AIAA PAPER 92-4093] p 93 A93-13262
- A review of crack propagation under unsteady loading
p 399 A93-19207
- Design of a recovery system for a reentry vehicle
[AIAA PAPER 93-1224] p 733 A93-35171
- National Aeronautics and Space Administration. Lyndon B. Johnson Space Center, Houston, TX.**
- Numerical dissipation in F3D thin-layer Navier-Stokes solution for flows with wall transpiration
p 9 A93-12010
- A finite element study of incompressible flows past oscillating cylinders and aerofoils p 241 A93-17750
- Results from a GPS Shuttle Training Aircraft flight test
p 384 A93-21148
- Autonomous guidance, navigation and control bridging program plan p 532 A93-27046
- Finite element computation of compressible flows with the SUPG formulation p 482 A93-29774
- Enhanced heat transport in environmental systems using microencapsulated phase change materials
[SAE PAPER 921224] p 926 A93-41398
- Intrusive and nonintrusive measurements of flow properties in arc jets p 943 A93-42584

- A multigrid nonoscillatory method for computing high speed flows
[AIAA PAPER 93-3319] p 958 A93-45103
- Two-layer convective heating prediction procedures and sensitivities for blunt body reentry vehicles
[AIAA PAPER 93-2763] p 963 A93-46509
- DSMC simulation of ionized rarefied flows
[AIAA PAPER 93-3095] p 1061 A93-48269
- Facilities and capabilities catalog for landing and escape systems
[NASA-RP-1282] p 196 N93-14495
- Bearing servicing tool
[NASA-CASE-MSC-21681-1] p 221 N93-14871
- National Aeronautics and Space Administration. Langley Research Center, Hampton, VA.**
- Optimal control of lift/drag ratios on a rotating cylinder
p 76 A93-10275
- An effective multigrid method for high-speed flows
p 6 A93-10533
- An implicit multigrid scheme for hypersonic strong-interaction flowfields p 6 A93-10534
- The effects of crushing surface roughness on the crushing characteristics of composite tubes
p 77 A93-10918
- Differential GPS/inertial navigation approach/landing flight test results p 32 A93-11019
- Design and conduct of a windshear detection flight experiment
[AIAA PAPER 92-4092] p 38 A93-11268
- Subsonic high-lift flight research on the NASA Transport System Research Vehicle (TSRV)
[AIAA PAPER 92-4103] p 38 A93-11275
- Pitch control margin at high angle of attack - Quantitative requirements (flight test correlation with simulation predictions)
[AIAA PAPER 92-4107] p 39 A93-11277
- Measurement of attachment-line location in a wind-tunnel and in supersonic flight
[AIAA PAPER 92-4089] p 39 A93-11285
- Direct numerical simulation of laminar breakdown in high-speed, axisymmetric boundary layers
p 8 A93-11527
- Nonlinear feedback control of highly manoeuvrable aircraft
p 40 A93-11654
- Viscous equilibrium computations using program LAURA p 8 A93-12002
- Numerical simulations of high-speed flows about waveriders with sharp leading edges p 9 A93-12007
- Aerodynamic design of axisymmetric hypersonic wind-tunnel nozzles using a least-squares/parabolized Navier-Stokes procedure p 9 A93-12011
- High angle-of-attack inviscid Shuttle Orbiter computation p 9 A93-12020
- Three-dimensional boundary-layer transition on a cone at Mach 3.5 p 9 A93-12177
- Nonlinear time-series-based adaptive control applications p 97 A93-13230
- Flight test operations using an F-106B research airplane modified with a wing leading-edge vortex flap
[AIAA PAPER 92-4094] p 42 A93-13261
- Joint NASA/USAF Airborne Field Mill Program - Operation and safety considerations during flights of a Lear 28 airplane in adverse weather
[AIAA PAPER 92-4093] p 93 A93-13262
- Flight evaluation of a stagnation detection hot-film sensor
[AIAA PAPER 92-4085] p 51 A93-13263
- Unstructured grid solutions to a wing/pylon/store configuration using VGRID3D/USM3D
[AIAA PAPER 92-4572] p 14 A93-13303
- Pilot/Vehicle display development from simulation to flight
[AIAA PAPER 92-4174] p 51 A93-13310
- Practical considerations in waverider applications
[AIAA PAPER 92-4247] p 43 A93-13326
- Ground vortex formation for uniform and nonuniform jets impinging on a ground plane
[AIAA PAPER 92-4251] p 80 A93-13362
- Aircraft concept optimization using the global sensitivity approach and parametric multiobjective figures of merit
[AIAA PAPER 92-4221] p 45 A93-13381
- Mixed mode stress intensity-factors in transversely loaded plates p 200 A93-13943
- Application of multigrid and adaptive grid embedding to the two-dimensional flux-split Euler equations
p 202 A93-13990
- The new challenge of computational aeroscience
p 112 A93-14169
- Aircraft optimization by a system approach - Achievements and trends p 153 A93-14205
- Radiation safety in aircraft operations
p 141 A93-14221
- Research and applications in structural dynamics and aeroelasticity p 153 A93-14223
- Scramjet combustor and nozzle computations
p 171 A93-14243

- Nonintrusive spectroscopic techniques for supersonic/hypersonic aerodynamics and combustion diagnostics p 203 A93-14245
- In-flight surface-flow measurements on a subsonic transport high-lift flap system p 166 A93-14327
- Prediction and control of slender-wing rock p 182 A93-14331
- Cost - The challenge for advanced materials and structures p 233 A93-14338
- A low-speed wind tunnel study of vortex interaction control techniques on a chine-forebody/delta-wing configuration p 122 A93-14409
- Mixing and combustion studies using discrete orifice injection at hypervelocity flight conditions p 205 A93-14523
- Aeroacoustic environment of an advanced short takeoff and vertical landing aircraft in hover p 231 A93-14539
- Active control of interior noise in model aircraft fuselages using piezoceramic actuators p 231 A93-14540
- Generalized multipoint inverse airfoil design p 122 A93-14541
- Nonlinear vibration and radiation from a panel with transition to chaos p 205 A93-14543
- Comparison of algebraic turbulence models for afterbody flows with jet exhaust p 123 A93-14554
- Hybrid laminar flow control applied to advanced turbofan engine nacelles p 123 A93-14628
- [SAE PAPER 920962] p 123 A93-14628
- Braking, steering, and wear performance of radial-belted and bias-ply aircraft tires p 158 A93-14656
- [SAE PAPER 921036] p 158 A93-14656
- Adaptive aeroelastic composite wings - Control and optimization issues p 185 A93-14818
- Experimental investigations into composite fuselage impact damage resistance and post-impact compression behavior p 159 A93-15812
- A high-frequency, secondary instability of crossflow vortices that leads to transition p 128 A93-17253
- Lidar windshear detection for commercial aircraft p 341 A93-17864
- Longitudinal vortex control - Techniques and applications (The 32nd Lanchester Lecture) p 242 A93-18526
- Comparison of heating protocols for detection of disbond in lap joints p 396 A93-18627
- Imaging flaws in thin metal plates using a magneto-optic device p 397 A93-18670
- The role of simulation in determining safe aircraft landing separation criteria p 306 A93-18712
- Adaptive remeshing for three-dimensional compressible flow computations p 242 A93-18851
- On the coupling between a supersonic boundary layer and a flexible surface p 243 A93-19132
- Acoustic flight test experience with the XV-15 Tiltrotor aircraft with the Advanced Technology Blade (ATB) p 445 A93-19143
- Effects of a trailing edge flap on the aerodynamics and acoustics of rotor blade-vortex interactions p 244 A93-19144
- The noise from supersonic elliptic jets p 445 A93-19156
- Instability of rectangular jets p 398 A93-19157
- The effects of temperature on supersonic jet noise emission p 446 A93-19159
- Acoustic properties of supersonic helium/air jets at low Reynolds numbers p 446 A93-19160
- Assessment and design of low boom configurations for supersonic transport aircraft p 446 A93-19163
- Nonlinear vibration and radiation from a panel with transition to chaos induced by acoustic waves p 398 A93-19173
- A new technique for aerodynamic noise calculation p 447 A93-19177
- Advances in tilt rotor noise prediction p 447 A93-19184
- Evaluation of piezoceramic actuators for control of aircraft interior noise p 447 A93-19186
- Streamline curvature in supersonic shear layers p 244 A93-19194
- Helicopter noise prediction - The current status and future direction p 448 A93-19202
- Radiated noise of ducted fans p 450 A93-19215
- Experimental and analytical investigations of fuselage modal characteristics and structural-acoustic coupling p 451 A93-19229
- The prediction of nonlinear dynamic loads on helicopters from flight variables using artificial neural networks p 322 A93-19231
- Partially exposed polymer dispersed liquid crystals for boundary layer investigations p 399 A93-19250
- Hypersonic flow separation in shock wave boundary layer interactions [ASME PAPER 92-GT-205] p 251 A93-19429
- Assessment of aircraft structural integrity by detecting disbands through ultrasonic scanning p 406 A93-19587
- Automation of disbond detection in aircraft fuselage through thermal image processing p 407 A93-19598
- Aerodynamic optimization of an HSCT configuration using variable-complexity modeling [AIAA PAPER 93-0101] p 322 A93-19806
- Planar imaging of OH density distributions in a supersonic combustion tunnel [AIAA PAPER 93-0042] p 389 A93-20155
- Experimental investigation of vortex-fin interaction [AIAA PAPER 93-0050] p 260 A93-20163
- Spatial simulation of boundary layer instability - Effects of surface roughness [AIAA PAPER 93-0075] p 262 A93-20187
- Effect of micron-sized roughness on transition in swept-wing flows [AIAA PAPER 93-0076] p 262 A93-20188
- Linear stability of three-dimensional boundary layers - Effects of curvature and non-parallelism [AIAA PAPER 93-0079] p 263 A93-20191
- Development of the quasi-procedural method for use in aircraft configuration optimization [AIAA PAPER 92-4693] p 322 A93-20278
- Variable-complexity aerodynamic-structural design of a high-speed civil transport wing [AIAA PAPER 92-4695] p 323 A93-20279
- Aerodynamic performance optimization of a rotor blade using a neural network as the analysis [AIAA PAPER 92-4837] p 324 A93-20295
- Multidisciplinary design integration system for a supersonic transport aircraft [AIAA PAPER 92-4841] p 324 A93-20296
- Analysis, modelling and simulation of the large-angle magnetic suspension test fixture p 375 A93-20297
- Fiber optic-based laser vapor screen flow visualization systems for aerodynamic research in large-scale subsonic and transonic wind tunnels p 408 A93-20298
- Calculations of separated vortex flows at low speed for low-aspect-ratio wings p 264 A93-20300
- Integrated aerodynamic-structural-control wing design [AIAA PAPER 92-4694] p 324 A93-20307
- Multidisciplinary analysis and sensitivity derivatives for isolated helicopter rotors in hover [AIAA PAPER 92-4696] p 324 A93-20308
- Improving the efficiency of aerodynamic shape optimization procedures [AIAA PAPER 92-4697] p 264 A93-20309
- Aerodynamic shape optimization via sensitivity analysis on decomposed computational domains [AIAA PAPER 92-4698] p 265 A93-20310
- Aeroservoelasticity in HiSAIR [AIAA PAPER 92-4719] p 324 A93-20322
- An approximately factored incremental strategy for calculating consistent discrete aerodynamic sensitivity derivatives [AIAA PAPER 92-4746] p 265 A93-20344
- Observations on computational methodologies for use in large-scale, gradient-based, multidisciplinary design [AIAA PAPER 92-4753] p 436 A93-20351
- Geometric requirements for multidisciplinary analysis of aerospace-vehicle design [AIAA PAPER 92-4773] p 436 A93-20366
- Recent advances in integrated multidisciplinary optimization of rotorcraft [AIAA PAPER 92-4777] p 325 A93-20369
- Development of a structural optimization capability for the aeroelastic tailoring of composite rotor blades with straight and swept tips [AIAA PAPER 92-4779] p 326 A93-20370
- Analytical formulation of optimum rotor interdisciplinary design with a three-dimensional wake [AIAA PAPER 92-4778] p 265 A93-20416
- High-performance computing for flight vehicles; Proceedings of the Symposium, Washington, Dec. 7-9, 1992 p 437 A93-20701
- Design of a wing shape for study of hypersonic crossflow transition in flight p 265 A93-20713
- Numerical simulation of shock-induced combustion/detonation p 410 A93-20719
- A comparison of the predictive capabilities of several turbulence models using upwind and central-difference computer codes [AIAA PAPER 93-0192] p 268 A93-21102
- Near wake structure for a generic ASTV configuration [AIAA PAPER 93-0271] p 268 A93-21103
- Unsteady loads measurements in a generic high speed engine model by means of recessed transducers [AIAA PAPER 93-0287] p 342 A93-21104
- Air/helium ground-test simulation pertinent to the definition of slender body hypersonic aerodynamics [AIAA PAPER 93-0318] p 268 A93-21106
- A gridless Euler/Navier-Stokes solution algorithm for complex-aircraft applications [AIAA PAPER 93-0333] p 268 A93-21107
- Design of a hypersonic waverider-derived airplane [AIAA PAPER 93-0401] p 384 A93-21108
- Subsonic static and dynamic stability characteristics of the test technique demonstrator NASP configuration [AIAA PAPER 93-0519] p 268 A93-21111
- Computational analysis of hypersonic shock wave/wall jet interaction [AIAA PAPER 93-0604] p 269 A93-21113
- Effects of compression and expansion ramp fuel injector configuration on scramjet combustion and heat transfer [AIAA PAPER 93-0609] p 358 A93-21114
- Spatial adaptation procedures on tetrahedral meshes for unsteady aerodynamic flow calculations [AIAA PAPER 93-0670] p 269 A93-21116
- Development of a flexible and efficient multiblock-based multiblock flow solver [AIAA PAPER 93-0677] p 269 A93-21117
- Evaluation of scramjet nozzle configurations and film cooling for reduction of wall heating [AIAA PAPER 93-0744] p 358 A93-21118
- Transonic shock oscillations calculated with a new interactive boundary layer coupling method [AIAA PAPER 93-0777] p 269 A93-21119
- Dynamic analysis of pretwisted elastically-coupled rotor blades p 326 A93-21125
- Analysis of DGPS/INS and MLS/INS final approach navigation errors and control performance data p 315 A93-21183
- Workshop report - A validation study of Navier-Stokes codes for transverse injection into a Mach 2 flow p 270 A93-21330
- Sensing a change in the wind p 307 A93-21627
- Scramjet fuel-air mixing establishment in a pulse facility p 359 A93-21667
- Supersonic dynamic stability characteristics of the test technique demonstrator NASP configuration [AIAA PAPER 92-5009] p 367 A93-22285
- Evaluation of some significant issues affecting trajectory and control management for air-breathing hypersonic vehicles [AIAA PAPER 92-5011] p 384 A93-22287
- Closed form solutions of constrained trajectories - Application in optimal ascent of aerospace plane [AIAA PAPER 92-5012] p 385 A93-22288
- A historical perspective on hypersonic research at the NASA/NASA Langley Research Center (1944-1984) [AIAA PAPER 92-5034] p 456 A93-22308
- Heat flux microsensor measurements [AIAA PAPER 92-5038] p 413 A93-22312
- CFD comparisons with wind tunnel and flight data for the X-15 [AIAA PAPER 92-5047] p 273 A93-22319
- Instability and transition in three-dimensional supersonic boundary layers [AIAA PAPER 92-5049] p 273 A93-22321
- Aero-space plane figures of merit [AIAA PAPER 92-5058] p 365 A93-22328
- Development and application of GASP 2.0 [AIAA PAPER 92-5067] p 438 A93-22337
- Hypersonic turbulent expansion-corner flow with shock impingement [AIAA PAPER 92-5101] p 274 A93-22371
- The effect of entrance radius and film injection on wall heating in scramjet nozzles p 360 A93-22505
- Tracking of raindrops in flow over an airfoil [AIAA PAPER 93-0168] p 275 A93-22602
- Turbulence model evaluation for the prediction of flows over a supercritical airfoil with deflected aileron at high Reynolds number [AIAA PAPER 93-0191] p 276 A93-22615
- Grid and design variables sensitivity analyses for NACA four-digit wing-sections [AIAA PAPER 93-0195] p 276 A93-22616
- Development of an engineering level prediction method for high angle of attack aerodynamics [AIAA PAPER 93-0208] p 278 A93-22626
- Application of CFD to a generic hypersonic flight research study [AIAA PAPER 93-0312] p 280 A93-23007
- Shock-dependent, thrust wings for supersonic flow [AIAA PAPER 93-0321] p 280 A93-23013
- Transition on a sharp cone at high enthalpy - New measurements in the shock tunnel T5 at GALCIT [AIAA PAPER 93-0343] p 281 A93-23030
- Wall pressure fluctuations beneath swept shock wave/boundary layer interactions [AIAA PAPER 93-0384] p 282 A93-23063
- Control of pressure fluctuations in the reattachment region of a supersonic free shear layer [AIAA PAPER 93-0385] p 282 A93-23064
- Engine/airframe integration for waverider cruise vehicles [AIAA PAPER 93-0507] p 283 A93-23254
- Three-dimensional supersonic vortex breakdown [AIAA PAPER 93-0526] p 284 A93-23267
- An installed nacelle design method using multiblock Euler solver [AIAA PAPER 93-0528] p 284 A93-23269

Application of a Navier-Stokes aeroelastic method to improve fighter wing performance at maneuver flight conditions
[AIAA PAPER 93-0529] p 284 A93-23270

Active control of fan noise from a turbofan engine
[AIAA PAPER 93-0597] p 452 A93-23323

An application of artificial neural networks to experimental data approximation
[AIAA PAPER 93-0408] p 440 A93-23330

Doppler global velocimetry measurements of the vortical flow above an F/A-18
[AIAA PAPER 93-0414] p 415 A93-23333

Estimation of unsteady lift on a pitching airfoil from wake velocity surveys
[AIAA PAPER 93-0437] p 286 A93-23351

Analytical comparison of convective heat transfer correlations in supercritical hydrogen
p 416 A93-23477

Effect of sidewall suction on flow in two-dimensional wind tunnels
p 287 A93-23538

Measurements of circulation and vorticity in the leading-edge vortex of a delta wing
p 288 A93-23548

Finite element nonlinear panel flutter with arbitrary temperatures in supersonic flow
p 417 A93-23555

Flexure-torsion behavior of prismatic beams. I - Section properties via power series
p 417 A93-23557

Approximation methods for control of structural acoustics models with piezoceramic actuators
p 452 A93-23744

Doppler global velocimetry - The next generation?
[AIAA PAPER 92-3897] p 539 A93-24486

Some effects of wing and body geometry on the aerodynamic characteristics of configurations designed for high supersonic Mach numbers
[AIAA PAPER 92-4246] p 463 A93-24493

Comprehensive analysis of bearingless rotors - Model development and experimental correlation of modes, response, trim and stability
[AIAA PAPER 93-0624] p 504 A93-24741

Navier-Stokes computations and experimental comparisons for multielement airfoil configurations
[AIAA PAPER 93-0645] p 464 A93-24760

Fundamental issues in subsonic/transonic expansion corner aerodynamics
[AIAA PAPER 93-0649] p 465 A93-24764

Signal processing of jet noise from flyover test data
[AIAA PAPER 93-0736] p 563 A93-24826

De-Dopplerization of aircraft acoustic signals
[AIAA PAPER 93-0737] p 563 A93-24827

An experimental parametric study of geometric, Reynolds number, and ratio of specific heats effects in three-dimensional sidewall compression scramjet inlets at Mach 6
[AIAA PAPER 93-0740] p 466 A93-24830

Waverider design for generalized shock geometries
[AIAA PAPER 93-0774] p 467 A93-24858

Vortex/surface interaction
[AIAA PAPER 93-0863] p 468 A93-24925

Investigation of three-dimensional separation at wing/body junctions in supersonic flows using TVD McCormack's scheme
[AIAA PAPER 93-0884] p 471 A93-24945

An upwind, kinetic flux-vector splitting method for flows in chemical and thermal non-equilibrium
[AIAA PAPER 93-0894] p 472 A93-24954

The FAA/NASA flight loads monitoring program - The prototype system and its benefits for the aviation community
p 486 A93-25125

Boundary-layer transition extent measurements on a cone and flat plate at Mach 3.5
[AIAA PAPER 93-0342] p 474 A93-25517

Computational analysis of methods for reduction of induced drag
[AIAA PAPER 93-0524] p 474 A93-25536

Experimental measurement of structural intensity on an aircraft fuselage
p 544 A93-26999

Uniform high-order spectral methods for one- and two-dimensional Euler equations
p 476 A93-27068

On the accurate prediction of the wall-normal velocity in compressible boundary-layer flow
p 477 A93-27474

Investigation of vortex breakdown on delta wings using Navier-Stokes equations
p 478 A93-27924

Prediction of asymmetric vortical flows around slender bodies using Navier-Stokes equations
p 478 A93-27925

Application of a two-point exponential approximation method in optimizing rotorcraft airframe structures
p 507 A93-27956

An accurate nonlinear finite element analysis and test correlation of a stiffened composite wing panel
p 546 A93-27968

The NASA/industry design analysis methods for vibrations (DAMVIBS) program - Accomplishments and contributions
p 508 A93-27971

Experiences at Langley Research Center in the application of optimization techniques to helicopter airframes for vibration reduction
p 508 A93-27972

An experimental and analytical investigation on the response of GR/EP composite I-frames
p 546 A93-27975

Rapid detection and quantification of impact damage in composite structures
p 547 A93-27978

Sensors and sensor systems for guidance and navigation II; Proceedings of the Meeting, Orlando, FL, Apr. 22, 23, 1992
[SPIE-1694] p 547 A93-28151

Global/local interlaminar stress analysis of a grid-stiffened composite panel
p 548 A93-28543

Stability theory and transition prediction applied to a general aviation fuselage
p 479 A93-28601

Euler study on porous transonic airfoils with a view toward multipoint design
p 479 A93-28604

Sensitivity-based scaling for approximating structural response
p 548 A93-28618

Goertler instability and hypersonic quiet nozzle design
p 480 A93-29155

Current status of computational methods for transonic unsteady aerodynamics and aeroelastic applications
p 480 A93-29175

Aero-optical phase measurements using Fourier transform holographic interferometry
p 549 A93-29302

A study of blade-vortex interaction sound generation and directivity
p 565 A93-29402

High-speed helicopter rotor noise - Shock waves as a potent source of sound
p 565 A93-29403

Sensitivity of acoustic predictions to variation of input parameters
p 565 A93-29404

HHC study in the DNW to reduce BVI noise - An analysis
p 565 A93-29405

The influence of quadrupole sources in the boundary layer and wake of a blade on helicopter rotor noise
p 566 A93-29410

Far-field hover acoustic characteristics of the XV-15 tiltrotor aircraft with Advanced Technology Blades
p 566 A93-29412

A comparative analysis of XV-15 tiltrotor hover test data and WOPWOP predictions incorporating the fountain effect
p 509 A93-29414

Tiltrotor ground noise reduction from rotor parametric changes as predicted by ROTONET
p 567 A93-29415

Development and validation of 'quiet tail rotor' technology
p 567 A93-29416

ADDRAS - An integrated systems approach
p 562 A93-29423

Active control of interior noise in a large scale cylinder using piezoelectric actuators
p 568 A93-29425

The development of a CFD potential method for the analysis of tilt-rotors
p 481 A93-29434

Recent developments in rotor wake modeling for helicopter noise prediction
p 481 A93-29437

Airfoil shape optimization using sensitivity analysis on viscous flow equations
p 682 A93-33755

A new parallel-vector finite element analysis software on distributed-memory computers
[AIAA PAPER 93-1307] p 756 A93-33883

An overview of aeroelasticity studies for the National Aero-Space Plane
[AIAA PAPER 93-1313] p 732 A93-33889

Aeroelastic character of a National Aerospace Plane demonstrator concept
[AIAA PAPER 93-1314] p 732 A93-33890

An experimental and analytical study of a lifting-body wind-tunnel model exhibiting body-freedom flutter
[AIAA PAPER 93-1316] p 732 A93-33891

Thermomechanical postbuckling analysis of laminated composite shells
[AIAA PAPER 93-1337] p 738 A93-33907

Energy-absorbing-beam design for composite aircraft subfloors
[AIAA PAPER 93-1339] p 709 A93-33909

An analytically designed subcomponent test to reproduce the failure of a composite wing box beam
[AIAA PAPER 93-1344] p 709 A93-33914

A method of predicting quasi-steady aerodynamics for flutter analysis of high speed vehicles using steady CFD calculations
[AIAA PAPER 93-1364] p 682 A93-33931

Further studies using matched filter theory and stochastic simulation for gust loads prediction
[AIAA PAPER 93-1365] p 726 A93-33932

Aerothermoelastic analysis of a NASP demonstrator model
[AIAA PAPER 93-1366] p 733 A93-33933

Impact of aeroelasticity on propulsion and longitudinal flight dynamics of an air-breathing hypersonic vehicle
[AIAA PAPER 93-1367] p 733 A93-33934

Supersonic aeroelastic instability results for a NASP-like wing model
[AIAA PAPER 93-1369] p 682 A93-33935

Response of laminated composite plates to low-speed impact by airgun-propelled and dropped-weight impactors
[AIAA PAPER 93-1402] p 739 A93-33962

ISAC - A tool for aeroservoelastic modeling and analysis
[AIAA PAPER 93-1421] p 726 A93-33974

Wing flutter boundary prediction using unsteady Euler aerodynamic method
[AIAA PAPER 93-1422] p 739 A93-33975

An inverse method for computation of structural stiffness distributions of aeroelastically optimized wings
[AIAA PAPER 93-1540] p 741 A93-34077

Stiffness, thermal expansion, and thermal bending formulation of stiffened, fiber-reinforced composite panels
[AIAA PAPER 93-1569] p 741 A93-34102

Extension of a nonlinear systems theory to general-frequency unsteady transonic aerodynamic responses
[AIAA PAPER 93-1590] p 683 A93-34122

Experimental unsteady pressures at flutter on the Supercritical Wing Benchmark Model
[AIAA PAPER 93-1592] p 683 A93-34123

Unsteady transonic potential flow over a flexible fuselage
[AIAA PAPER 93-1593] p 683 A93-34124

A new sensitivity analysis for structural optimization of composite rotor blades
[AIAA PAPER 93-1644] p 742 A93-34169

Sensitivity analysis of aeroelastic response of a wing using piecewise pressure representation
[AIAA PAPER 93-1645] p 742 A93-34170

Sensitivity analysis of flutter response of a typical section and a wing in transonic flow
[AIAA PAPER 93-1646] p 742 A93-34171

Instability of rectangular jets
p 720 A93-34410

Commercial turbofan engine exhaust nozzle flow analyses
p 689 A93-34489

Experimental supersonic hydrogen combustion employing staged injection behind a rearward-facing step
p 744 A93-34496

Optimal discrete-time dynamic output-feedback design - A w-domain approach
p 757 A93-34536

Optimal open multistep discretization formulas for real-time simulation
p 757 A93-34539

Preliminary experiments on active control of fan noise from a turbofan engine
p 759 A93-34957

Temperature and suction effects on the instability of an infinite swept attachment line
p 691 A93-35486

Implicit upwind solution algorithms for three-dimensional unstructured meshes
p 691 A93-35607

Results from a conical Euler methodology developed for unsteady vortical flows
p 692 A93-35612

Calculation of compressible boundary layers by a hybrid finite element method
p 692 A93-35613

Study of supersonic intersection flowfield at modified wing-body junctions
p 692 A93-35621

Aeromechanical stability of helicopters with composite rotor blades in forward flight
p 794 A93-35904

Three-dimensional calculations of rotor-airframe interaction in forward flight
p 795 A93-35940

A study of the rotor wake of a small-scale rotor model in forward flight using laser light sheet flow visualization with comparisons to analytical models
p 766 A93-35957

Prediction of BVI noise patterns and correlation with wake interaction locations
p 849 A93-35966

Aeroelastic behavior of composite rotor blades with swept tips
p 827 A93-35978

Multiblock Navier-Stokes solutions about the F/A-18 wing-LEX-fuselage configuration
p 767 A93-37378

Limitations of linear theory for sonic boom calculations
p 850 A93-37380

Effects of blowing on delta wing vortices during dynamic pitching
p 768 A93-37384

A flutter investigation of all-moveable NASP-like wings at hypersonic speeds
[AIAA PAPER 93-1315] p 769 A93-37427

Formal verification of algorithms for critical systems
p 846 A93-37623

Recent experiences with implementing a video based six degree of freedom measurement system for airplane models in a 20 foot diameter vertical spin tunnel
p 821 A93-37763

Radii effect on the translation spring constant of force transducer beams
p 829 A93-37867

Gas analysis system for the Eight Foot High Temperature Tunnel
p 822 A93-37875

Digital resolver for helicopter model blade motion analysis
p 830 A93-37878

The stroke - A simple means for directional control improvement
p 802 A93-37997

- Shock interference prediction using direct simulation Monte Carlo p 778 A93-39258
- Energetics of gas-surface interactions in transitional flows at entry velocities p 778 A93-39259
- Investigation of a contoured wall injector for hypervelocity mixing augmentation p 837 A93-39407
- Large-amplitude finite element flutter analysis of composite panels in hypersonic flow p 837 A93-39417
- Research in unsteady aerodynamics and computational aeroelasticity at the NASA Langley Research Center p 804 A93-39498
- Hypersonic propulsion - Breaking the thermal barrier p 897 A93-40437
- A study of the interaction between a wake vortex and an encountering airplane p 858 A93-40714
[AIAA PAPER 93-3642]
- Experimental investigation of spherical-convergent-flap thrust-vectoring two-dimensional plug nozzles p 898 A93-41045
[AIAA PAPER 93-2431]
- Internal performance characteristics of vectored axisymmetric ejector nozzles p 898 A93-41046
[AIAA PAPER 93-2432]
- Prediction of static performance for single expansion ramp nozzles p 898 A93-41047
[AIAA PAPER 93-2571]
- Application of the multigrid solution technique to hypersonic entry vehicles p 858 A93-41049
[AIAA PAPER 93-2721]
- Higher-order viscous shock-layer solutions for high altitude flows p 858 A93-41050
[AIAA PAPER 93-2724]
- Comparison of coordinate-invariant and coordinate-aligned upwinding for the Euler equations p 858 A93-41053
[AIAA PAPER 93-3306]
- Symmetry breaking in vortical flows over cones - Theory and numerical experiments p 859 A93-41056
[AIAA PAPER 93-3408]
- Rarefied-flow shuttle aerodynamics flight model p 859 A93-41057
[AIAA PAPER 93-3441]
- Vortex features of F-106B aircraft at subsonic speeds p 859 A93-41058
[AIAA PAPER 93-3471]
- Aerodynamic investigation with focusing schlieren in a cryogenic wind tunnel p 910 A93-41059
[AIAA PAPER 93-3485]
- A performance assessment of a byzantine resilient fault-tolerant computer p 938 A93-41296
[AIAA PAPER 89-3064]
- Thermal analysis of a shower-head burner p 898 A93-41400
[SAE PAPER 921226]
- Natural laminar flow and laminar flow control p 859 A93-41776
[ISBN 0-387-97773-6]
- Laminar flow control - Introduction and overview p 859 A93-41777
- Laminar flow flight experiments - A review p 890 A93-41778
- Flight research on natural laminar flow applications p 890 A93-41779
- Subsonic natural-laminar-flow airfoils p 860 A93-41780
- Wave interaction theory and LFC p 860 A93-41781
- Supersonic laminar flow control p 860 A93-41782
- The Langley 8-ft transonic pressure tunnel laminar-flow-control experiment p 910 A93-41783
- Constrained control allocation p 938 A93-41891
- Validation of engineering methods for predicting hypersonic vehicle control forces and moments p 906 A93-41897
- Damping of surface pressure fluctuations in hypersonic turbulent flow past expansion corners p 860 A93-41914
- Spectral solution of the viscous blunt-body problem p 860 A93-41915
- Aeroelastic response, loads, and stability of a composite rotor in forward flight p 906 A93-41919
- Computational fluid dynamics for hypersonic airbreathing aircraft p 865 A93-42581
- Application of the Galerkin/least-squares formulation to the analysis of hypersonic flows. I - Flow over a two-dimensional ramp p 866 A93-42593
- Grid-refinement study of hypersonic laminar flow over a 2-D ramp p 866 A93-42597
- Application of the Galerkin/least-squares formulation to the analysis of hypersonic flows. II - Flow past a double ellipse p 868 A93-42608
- Application of program LAURA to thermochemical nonequilibrium flow through a nozzle p 871 A93-42644
- Strong vortex/boundary layer interactions. I - Vortices high p 930 A93-43539
- A numerical study of wave propagation in a confined mixing layer by eigenfunction expansions p 873 A93-43629
- Zonally-decoupled DSMC solutions of hypersonic blunt body wake flows p 949 A93-44227
[AIAA PAPER 93-2808]
- An approximate method for calculating heating rates on three-dimensional vehicles p 949 A93-44228
[AIAA PAPER 93-2881]
- Unstructured grids for sonic-boom analysis p 949 A93-44229
[AIAA PAPER 93-2929]
- A computational investigation of fuel mixing in a hypersonic scramjet p 1001 A93-44230
[AIAA PAPER 93-2994]
- A convective and radiative heat transfer analysis for the FIRE II forebody p 1021 A93-44231
[AIAA PAPER 93-3194]
- Actuated forebody strake controls for the F-18 high alpha research vehicle p 1006 A93-44233
[AIAA PAPER 93-3675]
- Microburst avoidance crew procedures for forward-look sensor equipped aircraft p 1007 A93-44234
[AIAA PAPER 93-3942]
- Cryogenic wind tunnels p 1010 A93-44886
- Langley 8-foot high-temperature tunnel oxygen measurement system p 1010 A93-44892
- The NASA Computational Fluid Dynamics (CFD) program - Building technology to solve future challenges p 1041 A93-44996
[AIAA PAPER 93-3292]
- A multi-dimensional kinetic-based upwind solver for the Euler equations p 950 A93-45001
[AIAA PAPER 93-3303]
- Aerodynamic shape optimization using preconditioned conjugate gradient methods p 952 A93-45016
[AIAA PAPER 93-3322]
- Surface boundary conditions for the numerical solution of the Euler equations p 953 A93-45028
[AIAA PAPER 93-3334]
- Three-dimensional unstructured grid Euler computations using a fully-implicit, upwind method p 953 A93-45031
[AIAA PAPER 93-3337]
- Line relaxation methods for the solution of 2D and 3D compressible flows p 955 A93-45059
[AIAA PAPER 93-3366]
- Time-accurate simulation of a self-excited oscillatory supersonic external flow with a multi-block solution-adaptive mesh algorithm p 956 A93-45078
[AIAA PAPER 93-3387]
- An upwind multigrid algorithm for calculating flows on unstructured grids p 957 A93-45088
- Preconditioned domain decomposition scheme for three-dimensional aerodynamic sensitivity analysis p 957 A93-45096
- Single block three-dimensional volume grids about complex aerodynamic vehicles p 957 A93-45099
- Advancing-layers method for generation of unstructured viscous grids p 957 A93-45101
- Effect of temperature on nonlinear two-dimensional panel flutter using finite elements p 1022 A93-45133
- Active control of aerothermoelastic effects for a conceptual hypersonic aircraft p 1007 A93-45137
- Plume and wake dynamics, mixing, and chemistry behind a high speed civil transport aircraft p 1034 A93-45139
- Reynolds number effects on supersonic asymmetrical flows over a cone p 958 A93-45141
- Sensitivity analysis of a wing aeroelastic response p 958 A93-45142
- Static aeroelastic control of an adaptive lifting surface p 995 A93-45147
- Effect of stiffness characteristics on the response of composite grid-stiffened structures p 1022 A93-45148
- Leading-edge transition and relaminarization phenomena on a subsonic high-lift system p 959 A93-45154
[AIAA PAPER 93-3140]
- Elements of NASA's high-speed research program p 947 A93-45155
[AIAA PAPER 93-2842]
- Vortex flap flight test operations, a safe approach p 995 A93-45168
- Performance data of the new free-piston shock tunnel T5 at GALCIT p 1011 A93-45498
- An evaluation of the pressure proof test concept for 2024-T3 aluminum alloy sheet p 1026 A93-45780
- Optical methods of stress analysis applied to cracked components p 1027 A93-45798
- Solution strategy for three-dimensional configurations at hypersonic speeds p 962 A93-46406
- Enhancements to viscous-shock-layer technique p 962 A93-46408
- PNS predictions of axisymmetric hypersonic blunt-body and afterbody flowfields p 962 A93-46479
[AIAA PAPER 93-2725]
- A viscous shock-layer analysis of 2-D and axisymmetric flows p 963 A93-46500
[AIAA PAPER 93-2751]
- Simulation of ablation in Earth atmospheric entry p 1027 A93-46531
[AIAA PAPER 93-2789]
- Application of an engineering inviscid-boundary layer method to slender three-dimensional vehicle forebodies p 963 A93-46534
[AIAA PAPER 93-2793]
- A systems approach to a DSMC calculation of a control jet interaction experiment p 964 A93-46538
[AIAA PAPER 93-2798]
- Hypersonic blunt body wake computations using DSMC and Navier-Stokes solvers p 964 A93-46547
[AIAA PAPER 93-2807]
- Monte Carlo simulation of radiating reentry flows p 964 A93-46548
[AIAA PAPER 93-2809]
- Navier-Stokes simulations of the Shuttle Orbiter aerodynamic characteristics with emphasis on pitch trim and bodyflap p 965 A93-46552
[AIAA PAPER 93-2814]
- Aerodynamics of Shuttle Orbiter at high altitudes p 965 A93-46553
[AIAA PAPER 93-2815]
- Survey of nonequilibrium re-entry heating for entry flight conditions p 1039 A93-46682
[AIAA PAPER 93-3230]
- Strong vortex/boundary layer interactions. II - Vortices low p 965 A93-46744
- Remote sensing cloud properties from high spectral resolution infrared observations p 1034 A93-46780
- Control of a supersonic reattaching shear layer p 966 A93-46793
[AIAA PAPER 93-3248]
- High speed propeller acoustics and aerodynamics - A boundary element approach p 967 A93-46804
- On the possibility of singularities in the acoustic field of supersonic sources when BEM is applied to a wave equation p 1039 A93-46805
- Use of Convex supercomputers for flight simulation at NASA Langley p 1013 A93-46806
- Two leading-edge droop modifications for tailoring stall characteristics of a general aviation trainer configuration p 1008 A93-46807
- A study of the influence of the data acquisition system sampling rate on the accuracy of measured acceleration loads for transport aircraft p 1000 A93-46808
- Effects of floor location on response of composite fuselage frames p 997 A93-46809
- Kinematic domain decomposition for boundary-motion-induced flow simulations p 1028 A93-46811
- A multiblock, multigrid solution procedure for multielement airfoils p 967 A93-46812
- Supersonic/hypersonic aerodynamic methods for aircraft design and analysis p 967 A93-46816
- Transition in supersonic flow past axisymmetric bodies p 967 A93-46817
- Thermal control of a lidar laser system using a non-conventional ram air heat exchanger p 1028 A93-46821
- A three dimensional view of velocity using lasers p 1028 A93-46822
- The all-electric aircraft - In your future? p 997 A93-46824
- The adaptive wall test section for the NASA Langley 0.3-m Transonic Cryogenic Tunnel p 1013 A93-46825
- Control of unsteady shock-induced turbulent boundary layer separation upstream of blunt fins p 969 A93-46839
[AIAA PAPER 93-3281]
- Langley proposed advanced hypervelocity aerophysics facility - A status report p 1013 A93-47015
- Testing experience with unheated stain-gage balances in the NTF p 1013 A93-47021
- Analysis of aeroelastic and resonance responses of a wind tunnel model support system p 1013 A93-47022
- Advanced cargo aircraft may offer a potential renaissance in freight transportation p 991 A93-47023
- Requirements for facilities and measurement techniques to support CFD development for hypersonic aircraft p 1014 A93-47024
- A method for the prediction of induced drag for planar and nonplanar wings p 976 A93-47216
[AIAA PAPER 93-3420]
- Unstructured viscous grid generation by advancing-layers method p 979 A93-47238
[AIAA PAPER 93-3453]
- Development of a system for transition characterization p 1030 A93-47246
[AIAA PAPER 93-3465]
- Application of natural laminar flow to a supersonic transport concept p 997 A93-47248
[AIAA PAPER 93-3467]
- Supersonic vortex breakdown over a delta wing in transonic flow p 980 A93-47251
[AIAA PAPER 93-3472]
- Grid and aerodynamic sensitivity analyses of airplane components p 981 A93-47254
[AIAA PAPER 93-3475]
- Calculation of AGARD Wing 445.6 flutter using Navier-Stokes aerodynamics p 981 A93-47255
[AIAA PAPER 93-3476]
- Computational analysis of off-design waveriders p 982 A93-47262
[AIAA PAPER 93-3488]
- Computational study of a conical wing having unit aspect ratio at supersonic speeds p 984 A93-47272
[AIAA PAPER 93-3505]
- Flow visualization of mast-mounted-sight/main rotor aerodynamic interactions p 1009 A93-47280
[AIAA PAPER 93-3517]

Semi-discrete Galerkin solution of the compressible boundary-layer equations with viscous-inviscid interaction
[AIAA PAPER 93-3520] p 985 A93-47282

Computer-aided light sheet flow visualization
[AIAA PAPER 93-2915] p 1147 A93-48117

Surface hot-film method for the measurement of transition, separation and reattachment points
[AIAA PAPER 93-2918] p 1148 A93-48120

Interpretation of waverider performance data using computational fluid dynamics
[AIAA PAPER 93-2921] p 1044 A93-48122

Interaction of the sonic boom with atmospheric turbulence
[AIAA PAPER 93-2943] p 1171 A93-48140

Computation of wake/exhaust mixing downstream of advanced transport aircraft
[AIAA PAPER 93-2944] p 1162 A93-48141

Active control of asymmetric conical flow using spinning and rotary oscillations
[AIAA PAPER 93-2958] p 1048 A93-48152

The hemisphere-cylinder in dynamic pitch-up motions
[AIAA PAPER 93-2963] p 1048 A93-48157

Shock-vortex interaction over a 65-degree delta wing in transonic flow
[AIAA PAPER 93-2973] p 1049 A93-48167

An overview of recent subsonic laminar flow control flight experiments
[AIAA PAPER 93-2987] p 1052 A93-48180

A computational and experimental investigation of a delta wing with vertical tails
[AIAA PAPER 93-3009] p 1054 A93-48199

Dynamic-overlapped-grid simulation of aerodynamically determined relative motion
[AIAA PAPER 93-3018] p 1055 A93-48205

Application of a two-equation turbulence model for high speed compressible flows using unstructured grids
[AIAA PAPER 93-3029] p 1056 A93-48213

CFD code calibration and inlet-fairing effects on a 3D hypersonic powered-simulation model
[AIAA PAPER 93-3041] p 1056 A93-48222

A detailed study of mean-flow solutions for stability analysis of transitional flows
[AIAA PAPER 93-3052] p 1057 A93-48232

Demonstration of multipoint design procedures for transonic airfoils
[AIAA PAPER 93-3114] p 1062 A93-48284

Exploratory study of shock reflection near an expansion corner
[AIAA PAPER 93-3132] p 1063 A93-48297

Aerothermodynamic heating due to shock wave/laminar boundary-layer interactions in high-enthalpy hypersonic flow
[AIAA PAPER 93-3135] p 1064 A93-48299

Flowfield measurements about a multi-element airfoil at high Reynolds numbers
[AIAA PAPER 93-3137] p 1064 A93-48300

Effect of geometry, static stability, and mass distribution on the tumbling characteristics of generic flying-wing models
[AIAA PAPER 93-3615] p 1125 A93-48302

Status of the validation of high-angle-of-attack nose-down pitch control margin design guidelines
[AIAA PAPER 93-3623] p 1126 A93-48308

Kinematics and aerodynamics of the velocity vector roll
[AIAA PAPER 93-3625] p 1126 A93-48310

Unsteady aerodynamic models for maneuvering aircraft
[AIAA PAPER 93-3626] p 1126 A93-48311

Base drag prediction on missile configurations
[AIAA PAPER 93-3629] p 1064 A93-48314

Nonlinear aerodynamic modeling using multivariate orthogonal functions
[AIAA PAPER 93-3636] p 1065 A93-48321

Development of lateral-directional departure criteria
[AIAA PAPER 93-3650] p 1128 A93-48333

Nonsmooth trajectory optimization - An approach using continuous simulated annealing
[AIAA PAPER 93-3657] p 1099 A93-48337

Dynamic model testing of the X-31 configuration for high-angle-of-attack flight dynamics research
[AIAA PAPER 93-3674] p 1129 A93-48351

Simulation of tail buffet using delta wing-vertical tail configuration
[AIAA PAPER 93-3688] p 1065 A93-48357

Secondary instability mechanisms in compressible axisymmetric boundary layers
p 1070 A93-49009

Effect of curvature on stationary crossflow instability of a three-dimensional boundary layer
p 1070 A93-49010

Three-dimensional time-marching aeroelastic analyses using an unstructured-grid Euler method
p 1100 A93-49012

An experimental study of the effects of bodyside compression on forward swept sidewall compression inlets ingesting a turbulent boundary layer
[AIAA PAPER 93-3125] p 1072 A93-49515

Hypersonic aerodynamic characteristics for Langley Test Technique Demonstrator
[AIAA PAPER 93-3443] p 1072 A93-49516

Two-dimensional computational analysis of a transport high-lift system and a comparison with flight-test results
[AIAA PAPER 93-3533] p 1072 A93-49517

The challenges of simulating wake vortex encounters and assessing separation criteria
[AIAA PAPER 93-3568] p 1096 A93-49518

Investigation of high-alpha lateral-directional control power requirements for high-performance aircraft
[AIAA PAPER 93-3647] p 1130 A93-49519

Flow analysis and design optimization methods for nozzle-afterbody of a hypersonic vehicle
p 1073 A93-49531

Analytical solutions to constrained hypersonic flight trajectories
p 1141 A93-49596

High-pressure hypervelocity electrothermal wind-tunnel performance study and subscale tests
p 1137 A93-49617

Numerical study of the performance of swept, curved compression surface scramjet inlets
[AIAA PAPER 93-1837] p 1074 A93-49721

Summary of the GASP code application and evaluation effort for scramjet combustor flowfields
[AIAA PAPER 93-1973] p 1077 A93-49820

Turbulent flowfield simulation using Euler equations with body forces
[AIAA PAPER 93-1978] p 1078 A93-49825

Unsteady, three-dimensional, Navier-Stokes simulations of multistage turbomachinery flows
[AIAA PAPER 93-1979] p 1153 A93-49826

Structural design and analysis of a Mach zero to five turbo-ramjet system
[AIAA PAPER 93-1983] p 1112 A93-49830

Vortex generation and mixing in three-dimensional supersonic combustors
[AIAA PAPER 93-2144] p 1115 A93-49961

Analysis and demonstration of a Scramaccelerator system
[AIAA PAPER 93-2183] p 1142 A93-49995

A k-omega multivariate beta PDF for supersonic turbulent combustion
[AIAA PAPER 93-2197] p 1154 A93-50009

Modeling of turbulent supersonic H₂-air combustion with a multivariate beta PDF
[AIAA PAPER 93-2198] p 1155 A93-50010

Review of NASA's Hypersonic Research Engine Project
[AIAA PAPER 93-2323] p 1116 A93-50103

Fluidic scale model multi-plane thrust vector control test results
[AIAA PAPER 93-2433] p 1117 A93-50187

Hypersonic ignition and thrust production in a scramjet
[AIAA PAPER 93-2444] p 1119 A93-50196

Experimental and numerical study of swept ramp injection into a supersonic flowfield
[AIAA PAPER 93-2445] p 1119 A93-50197

A numerical study of the unsteady processes associated with the type IV shock interaction
[AIAA PAPER 93-2479] p 1083 A93-50221

Internal performance of Highly Integrated Deployable Exhaust Nozzles
[AIAA PAPER 93-2570] p 1084 A93-50288

Three-dimensional simulation of the Denver 11 July 1988 microburst-producing storm
p 1164 A93-50373

A magnetic suspension system with a large angular range
p 1139 A93-51295

Hodograph analysis in aircraft trajectory optimization
[AIAA PAPER 93-3742] p 1101 A93-51338

The Generalized Legendre-Clebsch Condition on state/control constrained arcs
[AIAA PAPER 93-3746] p 1170 A93-51342

Near-optimal, asymptotic tracking in control problems involving state-variable inequality constraints
[AIAA PAPER 93-3748] p 1170 A93-51344

Matched asymptotic expansion of the Hamilton-Jacobi-Bellman equation for aeroassisted plane-change maneuvers
[AIAA PAPER 93-3752] p 1143 A93-51348

An investigation of the fuel-optimal periodic trajectories of a hypersonic vehicle
[AIAA PAPER 93-3753] p 1101 A93-51349

Robust control of hypersonic vehicles considering propulsive and aeroelastic effects
[AIAA PAPER 93-3762] p 1131 A93-51357

Dynamics of hypersonic flight vehicles exhibiting significant aeroelastic and aeropropulsive interactions
[AIAA PAPER 93-3763] p 1131 A93-51358

Cancellation control law for lateral-directional dynamics of a supermaneuverable aircraft
[AIAA PAPER 93-3775] p 1131 A93-51370

Design of a flight control system for a highly maneuverable aircraft using mu synthesis
[AIAA PAPER 93-3776] p 1132 A93-51371

An aircraft instrument design for in situ tropospheric OH measurements by laser induced fluorescence at low pressures
p 1159 A93-51528

Numerical simulation and physical aspects of supersonic vortex breakdown
p 1093 A93-52011

Development of a microcomputer-based magnetic heading sensor
p 1160 A93-52152

Computational effects of inlet representation on powered hypersonic, airbreathing models
p 1094 A93-52427

Euler analysis of forebody-strake vortex flows at supersonic speeds
p 1094 A93-52429

Application of nonlinear systems theory to transonic unsteady aerodynamic responses
p 1095 A93-52438

Experimental study of pylon cross sections for a subsonic transport airplane
p 1103 A93-52440

Multielement airfoil performance due to Reynolds and Mach number variations
p 1095 A93-52442

Vector unsymmetric eigenequation solver for nonlinear flutter analysis on high-performance computers
p 1160 A93-52449

Computation of maximized gust loads for nonlinear aircraft using matched-filter-based schemes
p 1136 A93-52452

Finite state aeroelastic model for use in rotor design optimization
p 1104 A93-52454

Transonic Navier-Stokes flow computations over wing-fuselage geometries
p 1095 A93-52456

Streaming vorticity flux from oscillating walls with finite amplitude
p 1160 A93-52517

An evaluation of software tools for the design and development of cockpit displays
[AIAA PAPER 93-3593] p 1224 A93-52685

Instrumentation and telemetry systems for free-flight drop model testing
p 1209 A93-52754

Characterization of the faulted behavior of digital computers and fault tolerant systems
p 1224 A93-52762

Linear quadratic tracking problems in Hilbert space - Application to optimal active noise suppression
p 1224 A93-52763

Upwind-biased, point-implicit relaxation strategies for hypersonic flowfield simulations on supercomputers
p 1175 A93-52770

Analysis of a turning point problem in flight trajectory optimization
p 1210 A93-52885

Case study of a low-reflectivity pulsating microburst - Numerical simulation of the Denver, 8 July 1989, storm
p 1222 A93-52898

Observations of liquid jets injected into a highly accelerated supersonic boundary layer
p 1177 A93-53214

Transition correlation in subsonic flow over a flat plate
p 1178 A93-53231

Aerodynamic characteristics of the HL-20
p 1181 A93-53736

Six-degree-of-freedom guidance and control-entry analysis of the HL-20
p 1210 A93-53737

Effect of lift-to-drag ratio in pilot rating of the HL-20 landing task
p 1210 A93-53738

Aerodynamic heating environment definition/thermal protection system selection for the HL-20
p 1181 A93-53739

HL-20 computational fluid dynamics analysis
p 1181 A93-53740

HL-20 operations and support requirements for the Personnel Launch System mission
p 1210 A93-53745

An improved calibration technique for wind tunnel model attitude sensors
p 1253 A93-54356

Development of a tethered satellite force transducer
p 1251 A93-54368

An improved method for determining force balance calibration accuracy
p 1254 A93-54369

An optical flameout detection system for NASA Langley's 8-Foot High Temperature Tunnel
p 1254 A93-54372

Research requirements for a real-time flight measurements and data analysis system for subsonic transport high-lift research
p 1244 A93-54391

Data acquisition for aeroelastic testing at the NASA Langley Transonic Dynamics Facility
p 1250 A93-54397

Instrumentation and data acquisition for full-scale aircraft crash testing
p 1250 A93-54399

NASA Langley's Aircraft Landing Dynamics Facility
p 1250 A93-54400

Spectral analysis of unsteady surface pressure on a pusher propeller
p 1232 A93-54646

Recent advances in steady compressible aerodynamic sensitivity analysis
p 1236 A93-55400

Effect of boundary conditions and panel geometry on the response of laminated panels subjected to transverse pressure loads
p 1259 A93-55674

- Development of the wake behind a circular cylinder impulsively started into rotatory and rectilinear motion p 1236 N93-55736
- A general introduction to aeroacoustics and atmospheric sound p 1264 N93-55852
- Structural-acoustic coupling in aircraft fuselage structures p 1243 N93-55856
- Design, test, and evaluation of three active flutter suppression controllers p 63 N93-10070
- [NASA-TM-4338] p 63 N93-10070
- Interactive grid generation program for CAP-TSD [NASA-TM-102705] p 17 N93-10349
- Non-propulsive aerodynamic noise p 99 N93-10673
- Effect of planform and body on supersonic aerodynamics of multibody configurations p 19 N93-10824
- [NASA-TP-3212] p 19 N93-10824
- Recent advances in multidisciplinary optimization of rotorcraft [NASA-TM-107665] p 47 N93-10968
- Method of remotely characterizing thermal properties of a sample p 67 N93-11057
- [NASA-CASE-LAR-13508-3-CU] p 67 N93-11057
- Winds of change: Expanding the frontiers of flight. Langley Research Center's 75 years of accomplishment, 1917-1992 p 104 N93-11100
- [NASA-NP-130] p 104 N93-11100
- A problem formulation for glideslope tracking in wind shear using advanced robust control techniques [NASA-TM-104164] p 64 N93-11176
- Rigid body mode identification of the PAH-2 helicopter using the eigensystem realization algorithm [NASA-TM-107690] p 88 N93-11544
- Further buffeting tests in a cryogenic wind tunnel [NASA-TM-107621] p 22 N93-11610
- Laboratory study of effects of sonic boom shaping on subjective loudness and acceptability [NASA-TP-3269] p 102 N93-11620
- Low-speed longitudinal and lateral-directional aerodynamic characteristics of the X-31 configuration [NASA-TM-4351] p 22 N93-11622
- Boundary layer relaminarization device [NASA-CASE-LAR-14470-1] p 23 N93-11876
- Publications on acoustics research at the Langley Research Center, January 1987 - September 1992 [NASA-TM-107674] p 102 N93-12080
- Modeling and model simplification of aeroelastic vehicles: An overview p 64 N93-12216
- [NASA-TM-107691] p 64 N93-12216
- A monitor for the laboratory evaluation of control integrity in digital control systems operating in harsh electromagnetic environments p 65 N93-12304
- [NASA-TM-4402] p 65 N93-12304
- An approach to constrained aerodynamic design with application to airfoils p 24 N93-12321
- [NASA-TP-3260] p 24 N93-12321
- Current Technology for Thermal Protection Systems [NASA-CP-3157] p 69 N93-12447
- Current research in oxidation-resistant carbon-carbon composites at NASA Langley Research Center p 74 N93-12456
- Thermal control/oxidation resistant coatings for titanium-based alloys p 74 N93-12457
- Active cooling from the sixties to NASP p 49 N93-12458
- Thermostructural applications of heat pipes for cooling leading edges of high-speed aerospace vehicles p 91 N93-12460
- A brief overview of NASA Langley's research program in formal methods p 228 N93-12958
- Future regional transport aircraft market, constraints, and technology stimuli p 109 N93-13025
- [NASA-TM-107669] p 109 N93-13025
- Effects of forebody strakes and Mach number on overall aerodynamic characteristics of configuration with 55 deg cropped delta wing p 131 N93-13353
- [NASA-TP-3253] p 131 N93-13353
- Active flutter suppression using dipole filters [NASA-TM-107594] p 186 N93-13367
- [NASA-TM-107594] p 186 N93-13367
- Multiple-function multi-input/multi-output digital control and on-line analysis p 162 N93-13565
- [NASA-TM-107697] p 162 N93-13565
- Reliability of stiffened structural panels: Two examples [NASA-TM-107687] p 219 N93-14483
- Passive control of supersonic asymmetric vortical flows around cones p 220 N93-14692
- Airborne Wind Shear Detection and Warning Systems. Fourth Combined Manufacturers' and Technologists' Conference, part 2 [NASA-CP-10105-PT-2] p 144 N93-14844
- Simulator evaluation of displays for a revised takeoff performance monitoring system p 189 N93-15366
- [NASA-TP-3270] p 189 N93-15366
- Finite-difference solution for laminar or turbulent boundary layer flow over axisymmetric bodies with ideal gas, CF₄, or equilibrium air chemistry p 222 N93-15434
- [NASA-TP-3271] p 222 N93-15434
- Technology benefits and ground test facilities for high-speed civil transport development [NASA-TM-107670] p 378 N93-15790
- Relationship between mechanical-property and energy-absorption trends for composite tubes [NASA-TP-3284] p 392 N93-16537
- Effect of sonic boom asymmetry on subjective loudness p 453 N93-16755
- [NASA-TM-107708] p 453 N93-16755
- Transient/structural analysis of a combustor under explosive loads [NASA-TM-107660] p 420 N93-17779
- [NASA-TM-107660] p 420 N93-17779
- Reflection type skin friction meter [NASA-CASE-LAR-14520-1-SB] p 296 N93-18275
- Application of a neural network as a potential aid in predicting NTF pump failure [NASA-TM-107667] p 442 N93-18332
- Trade-offs arising from mixture of color cueing and monocular, binocular, and stereoscopic cueing information for simulated rotorcraft flight [NASA-TP-3268] p 338 N93-18333
- Manual flying of curved precision approaches to landing with electromechanical instrumentation. A piloted simulation study [NASA-TP-3255] p 344 N93-18408
- [NASA-TP-3255] p 344 N93-18408
- Stall departure resistance enhancer [NASA-CASE-LAR-14221-1] p 344 N93-19023
- Longitudinal-control design approach for high-angle-of-attack aircraft [NASA-TP-3302] p 373 N93-19108
- Lumped mass modelling for the dynamic analysis of aircraft structures p 510 N93-19460
- Airborne Wind Shear Detection and Warning Systems: Fourth Combined Manufacturers' and Technologists' Conference, part 1 [NASA-CP-10105-PT-1] p 488 N93-19590
- Program overview: 1991 flight test objectives p 488 N93-19591
- Flight test operations p 488 N93-19592
- NASA wind shear flight test in situ results p 488 N93-19593
- Air/ground wind shear information integration: Flight test results p 488 N93-19594
- Doppler radar results p 488 N93-19595
- Wind shear hazard determination p 488 N93-19597
- Three-dimensional numerical simulation of the 20 June 1991, Orlando microburst p 488 N93-19598
- Vertical wind estimation from horizontal wind measurements p 489 N93-19604
- Ground clutter measurements using the NASA airborne doppler radar: Description of clutter at the Denver and Philadelphia airports p 490 N93-19608
- NASA airborne radar wind shear detection algorithm and the detection of wet microbursts in the vicinity of Orlando, Florida p 490 N93-19611
- Rarefied-flow Shuttle aerodynamics model [NASA-TM-107698] p 458 N93-19976
- Apparatus and method for improving spin recovery on aircraft [NASA-CASE-LAR-14747-1] p 526 N93-20039
- Improved ceramic slip casting technique [NASA-CASE-LAR-14471-1] p 536 N93-20041
- Computational parametric study of sidewall-compression scramjet inlet performance at Mach 10 [NASA-TM-4411] p 552 N93-20299
- Analytical and experimental investigation of flutter suppression by piezoelectric actuation [NASA-TP-3241] p 513 N93-20584
- Experimental and analytical investigation of dynamic characteristics of extension-twist-coupled composite tubular spars p 553 N93-20585
- [NASA-TP-3225] p 553 N93-20585
- A Government/Industry Summary of the Design Analysis Methods for Vibrations (DAMVIBS) Program [NASA-CP-10114] p 514 N93-21310
- The NASA/Industry Design Analysis Methods for Vibrations (DAMVIBS) program: A government overview p 514 N93-21311
- Swept wing attachment line contamination fence [NASA-CASE-LAR-13400-1] p 485 N93-22015
- Method and apparatus for cleaning rubber deposits from airport runways and roadways [NASA-CASE-LAR-14483-1] p 556 N93-22035
- Evaluation of advanced displays for engine monitoring and control [NASA-CR-191418] p 718 N93-24764
- High-order cyclo-difference techniques: An alternative to finite differences [NASA-TM-107745] p 693 N93-25074
- Combined LAURA-UPS hypersonic solution procedure [NASA-TM-107682] p 747 N93-25176
- Use of high performance networks and supercomputers for real-time flight simulation p 731 N93-25574
- Nozzle diffuser for use with an open test section of a wind tunnel [NASA-CASE-LAR-14424-1-SB] p 731 N93-25996
- Helicopter low-speed yaw control [NASA-CASE-LAR-14219-1] p 729 N93-25998
- Method of measuring cross-flow vortices by use of an array of hot-film sensors [NASA-CASE-LAR-14824-1-SB] p 751 N93-26000
- Visualization of a Mach 2 reacting flow using Planar Laser-Induced Fluorescence (PLIF) p 731 N93-26006
- Workshop Report: A validation study of Navier-Stokes codes for transverse injection into a Mach 2 flow p 751 N93-26008
- Experimental effects of wing location on wing-body pressures at supersonic speeds [NASA-TM-4434] p 700 N93-26085
- Piloted simulation of an air-ground profile negotiation process in a time-based Air Traffic Control environment [NASA-TM-107748] p 707 N93-26087
- Conical Euler analysis and active roll suppression for unsteady vortical flows about rolling delta wings [NASA-TP-3259] p 701 N93-26134
- Supersonic aeroelastic instability results for a NASP-like wing model [NASA-TM-107739] p 718 N93-26553
- Development of a large-scale, outdoor, ground-based test capability for evaluating the effect of rain on airfoil lift [NASA-TM-4420] p 779 N93-26899
- Assessment of a flow-through balance for hypersonic wind tunnel models with scramjet exhaust flow simulation [NASA-TM-4441] p 779 N93-27005
- Transition aerodynamics for 20-percent-scale VTOL unmanned aerial vehicle [NASA-TM-4419] p 779 N93-27032
- The addition of algebraic turbulence modeling to program LAURA [NASA-TM-107758] p 840 N93-27250
- Multidisciplinary design optimization: An emerging new engineering discipline [NASA-TM-107761] p 806 N93-27258
- Loudness and annoyance response to simulated outdoor and indoor sonic booms [NASA-TM-107756] p 852 N93-27271
- A laboratory study of subjective response to sonic booms measured at White Sands Missile Range [NASA-TM-107746] p 852 N93-27272
- The transition prediction toolkit: LST, SIT, PSE, DNS, and LES p 783 N93-27429
- Reynolds and Mach number effects on multielement airfoils p 785 N93-27446
- Flow prediction over a transport multi-element high-lift system and comparison with flight measurements p 785 N93-27448
- Assessment of computational issues associated with analysis of high-lift systems p 785 N93-27449
- Effect of pylon cross-sectional geometries on propulsion integration for a low-wing transport [NASA-TP-3333] p 788 N93-28070
- Subjective response to simulated sonic booms with ground reflections [NASA-TM-107764] p 852 N93-28692
- Performance characteristics of two multiaxis thrust-vectoring nozzles at Mach numbers up to 1.28 [NASA-TP-3313] p 874 N93-29160
- Evaluation of four advanced nozzle concepts for short takeoff and landing performance [NASA-TP-3314] p 875 N93-29165
- Hypersonic lateral and directional stability characteristics of aerassist flight experiment configuration in air and CF₄ [NASA-TM-4435] p 875 N93-29166
- High-Reynolds-number test of a 5-percent-thick low-aspect-ratio semispan wing in the Langley 0.3-meter transonic cryogenic tunnel: Wing pressure distributions [NASA-TM-4227] p 875 N93-29449
- Aerodynamic characteristics of a rotorcraft airfoil designed for the tip region of a main rotor blade [NASA-TM-4264] p 876 N93-29450
- Structural evaluation of curved stiffened composite panels fabricated using a THERM-Xsm process p 919 N93-30435
- Noise transmission properties and control strategies for composite structures p 919 N93-30436
- A unified approach for composite cost reporting and prediction in the ACT program p 920 N93-30441
- First NASA Advanced Composites Technology Conference, part 2 [NASA-CP-3104-PT-2] p 921 N93-30841
- Development of stitching reinforcement for transport wing panels p 921 N93-30852
- Design and analysis of grid stiffened concepts for aircraft composite primary structural applications p 922 N93-30861

- Optimization of composite sandwich cover panels subjected to compressive loadings p 922 A93-30862
- Multiple methods integration for structural mechanics analysis and design p 923 A93-30867
- Structural response of bead-stiffened thermoplastic shear webs p 923 A93-30873
- An overview of the crash dynamics failure behavior of metal and composite aircraft structures p 923 A93-30875
- Reynolds number influences in aeronautics [NASA-TM-107730] p 989 A93-31732
- Supersonic aerodynamic characteristics of an advanced F-16 derivative aircraft configuration [NASA-TP-3355] p 989 A93-31733
- Airborne derivation of microburst alerts from ground-based Terminal Doppler Weather Radar information: A flight evaluation [NASA-TM-108990] p 1000 A93-32223
- A PC-based simulation of the National Transonic Facility's safety microprocessor [NASA-TM-109003] p 1038 A93-32224
- The X-15/HL-20 operations support comparison [NASA-TM-4453] p 1017 A93-32379
- A high-fidelity, six-degree-of-freedom batch simulation environment for tactical guidance research and evaluation [NASA-TM-4440] p 1010 A93-32380
- National Aeronautics and Space Administration, Lewis Research Center, Cleveland, OH.**
- Dynamic analysis of a pre-and-post ice impacted blade [AIAA PAPER 92-4273] p 54 A93-13333
- The multi-heat addition turbine engine [AIAA PAPER 92-4272] p 54 A93-13334
- Effects of turbine cooling assumptions on performance and sizing of high-speed civil transport [AIAA PAPER 92-4217] p 55 A93-13383
- Stirling engine - Available tools for long-life assessment p 195 A93-13824
- Numerical simulation of a low-emission gas turbine combustor using KIVA-II p 170 A93-14077
- Evaluation and application of the Baldwin-Lomax turbulence model in two-dimensional, unsteady, compressible boundary layers with and without separation in engine inlets [AIAA PAPER 92-3676] p 111 A93-14118
- The new challenge of computational aeroscience p 112 A93-14169
- Study on vortex flow control of inlet distortion p 122 A93-14520
- Analysis of airframe and engine control interactions and integrated flight/propulsion control p 185 A93-14596
- Concurrent processing adaptation of aerodynamic analysis of propfans p 173 A93-14624
- Technical note - Plasma-sprayed ceramic thermal barrier coatings for smooth intermetallic alloys p 209 A93-15702
- Heat transfer performance comparisons of five different rectangular channels with parallel angled ribs p 397 A93-18752
- Dispersion-relation-preserving schemes for computational aeroacoustics p 244 A93-19151
- Forward rotor vortex effects on counter rotating propeller noise p 245 A93-19221
- Coupled multi-disciplinary simulation of composite engine structures in propulsion environment [ASME PAPER 92-GT-6] p 346 A93-19279
- Stability of fully developed rotating stall [ASME PAPER 92-GT-57] p 348 A93-19307
- Aeroloids and secondary flows in a transonic mixed flow turbine stage [ASME PAPER 92-GT-72] p 248 A93-19322
- Aerodynamic design of turbomachinery blading in three-dimensional flow - An application to radial inflow turbines p 248 A93-19324
- Three-dimensional flow phenomena in a transonic, high-through-flow, axial-flow compressor stage [ASME PAPER 92-GT-169] p 250 A93-19395
- Numerical solutions for unsteady subsonic vortical flows around loaded cascades [ASME PAPER 92-GT-173] p 250 A93-19399
- Forcing function effects on unsteady aerodynamic gust response. I - Forcing functions [ASME PAPER 92-GT-174] p 251 A93-19400
- Forcing function effects on unsteady aerodynamic gust response. II - Low solidity airfoil row response [ASME PAPER 92-GT-175] p 251 A93-19401
- Heat transfer in rotating serpentine passages with trips skewed to the flow [ASME PAPER 92-GT-191] p 403 A93-19416
- Experimental and computational investigation of the NASA Low-Speed Centrifugal Compressor flow field [ASME PAPER 92-GT-213] p 252 A93-19436
- Numerical simulation of compressor endwall and casing treatment flow phenomena [ASME PAPER 92-GT-300] p 255 A93-19490
- Brush seal leakage performance with gaseous working fluids at static and low rotor speed conditions [ASME PAPER 92-GT-304] p 405 A93-19494
- Ceramic matrix composites for rocket engine turbine applications [ASME PAPER 92-GT-394] p 388 A93-19547
- Accuracy considerations in the computational analysis of jet noise [AIAA PAPER 93-0146] p 451 A93-19804
- Two-, three-, and four-poster jets in cross flow [AIAA PAPER 93-0023] p 408 A93-20141
- Effects of icing on the aerodynamic performance of high lift airfoils [AIAA PAPER 93-0026] p 259 A93-20144
- An efficient constraint to account for mistuning effects in the optimal design of engine rotors [AIAA PAPER 92-4711] p 358 A93-20280
- Concurrent optimization of airframe and engine design parameters [AIAA PAPER 92-4713] p 323 A93-20281
- Multidisciplinary propulsion simulation using NPSS [AIAA PAPER 92-4709] p 435 A93-20318
- Structural tailoring of aircraft engine blade subject to ice impact constraints [AIAA PAPER 92-4710] p 358 A93-20319
- APPLE - An aeroelastic analysis system for turbomachines and propfans [AIAA PAPER 92-4712] p 358 A93-20320
- Structural Tailoring/Analysis for Hypersonic Components - A computational simulation [AIAA PAPER 92-4722] p 325 A93-20324
- Design of a hypersonic waverider-derived airplane [AIAA PAPER 93-0401] p 384 A93-21108
- Evaluation and application of the Baldwin-Lomax turbulence model in two-dimensional, unsteady, compressible boundary layers with and without separation in engine inlets [AIAA PAPER 92-3676] p 111 A93-14118
- Results of Low Power Deicer tests on a swept inlet component in the NASA Lewis Icing Research Tunnel [AIAA PAPER 93-0032] p 327 A93-22551
- An algebraic turbulence model for three-dimensional viscous flows [AIAA PAPER 93-0083] p 274 A93-22552
- Prediction of active control of subsonic centrifugal compressor rotating stall [AIAA PAPER 93-0153] p 274 A93-22591
- CFD zonal modeling of leading-edge ice effects for a complete aircraft [AIAA PAPER 93-0167] p 275 A93-22601
- LEWICE droplet trajectory calculations on a parallel computer [AIAA PAPER 93-0172] p 438 A93-22604
- Two and three-dimensional prediffuser combustor studies with air-water mixture [AIAA PAPER 93-0240] p 390 A93-22652
- A parametric study of bleed in shock boundary layer interactions [AIAA PAPER 93-0294] p 280 A93-22694
- Modeling and strain gauging of eddy current repulsion deicing systems [AIAA PAPER 93-0296] p 327 A93-22696
- LDV flowfield measurements on a straight and swept wing with a simulated ice accretion [AIAA PAPER 93-0300] p 280 A93-23001
- Icing effects on aircraft stability and control determined from flight data - Preliminary results [AIAA PAPER 93-0398] p 370 A93-23073
- Simplified jet fuel reaction mechanism for lean burn combustion application [AIAA PAPER 93-0021] p 390 A93-23238
- Close-up analysis of aircraft ice accretion [AIAA PAPER 93-0029] p 309 A93-23239
- Surface roughness due to residual ice in the use of low power deicing systems [AIAA PAPER 93-0031] p 282 A93-23240
- Propagation of high frequency jet noise using geometric acoustics [AIAA PAPER 93-0147] p 452 A93-23241
- Numerical modeling of anti-icing systems and comparison to test results on a NACA 0012 airfoil [AIAA PAPER 93-0170] p 327 A93-23242
- Advancements in the LEWICE Ice Accretion Model [AIAA PAPER 93-0171] p 309 A93-23243
- Ice accretion and performance degradation calculations with LEWICE/NS [AIAA PAPER 93-0173] p 310 A93-23244
- Ice accretion prediction for a typical commercial transport aircraft [AIAA PAPER 93-0174] p 310 A93-23245
- Optimization of circular orifice jets mixing into a heated crossflow in a cylindrical duct [AIAA PAPER 93-0249] p 361 A93-23246
- An overview of shed ice impact studies in the NASA Lewis Icing Research Tunnel [AIAA PAPER 93-0301] p 283 A93-23247
- Acoustic mode measurements in the inlet of a model turbofan using a continuously rotating rake - Data collection/analysis techniques [AIAA PAPER 93-0599] p 361 A93-23324
- Estimation of unsteady lift on a pitching airfoil from wake velocity surveys [AIAA PAPER 93-0437] p 286 A93-23351
- Pdf prediction of supersonic hydrogen flames [AIAA PAPER 93-0448] p 391 A93-23358
- An improved numerical model for wave rotor design and analysis [AIAA PAPER 93-0482] p 361 A93-23384
- High accuracy computation of fluid-structure interaction in transonic cascades [AIAA PAPER 93-0485] p 287 A93-23387
- Effects of free-stream turbulence on boundary-layer transition [AIAA PAPER 93-0488] p 416 A93-23390
- Time-variant analysis of rotorcraft systems dynamics - An exploitation of vector processors p 416 A93-23512
- Liquid water content measurements using the Phase Doppler Particle Analyzer in the NASA Lewis Icing Research Tunnel [AIAA PAPER 93-0298] p 378 A93-23698
- A graphical user-interface for propulsion system analysis [AIAA PAPER 93-0223] p 440 A93-23699
- A coupled multi-block solution procedure for spray combustion in complex geometries [AIAA PAPER 93-0108] p 539 A93-24230
- Three-dimensional unstructured grid Euler method applied to turbine blades [AIAA PAPER 93-0196] p 461 A93-24233
- Driven cavity simulation of turbomachine blade flows with vortex control [AIAA PAPER 93-0390] p 461 A93-24238
- Aircraft icing problems - After 50 years [AIAA PAPER 93-0392] p 486 A93-24239
- Three-dimensional Navier-Stokes calculations using solution-adapted grids [AIAA PAPER 93-0431] p 462 A93-24240
- Numerical simulations of a high Mach number jet flow [AIAA PAPER 93-0653] p 540 A93-24766
- Unstructured 3D Delaunay mesh generation applied to planes, trains and automobiles [AIAA PAPER 93-0673] p 560 A93-24781
- Takeoff/approach noise for a model counterrotation propeller with a forward-swept upstream rotor [AIAA PAPER 93-0596] p 519 A93-24782
- Acoustic mode measurements in the inlet of a model turbofan using a continuously rotating rake [AIAA PAPER 93-0598] p 563 A93-24783
- Navier-Stokes calculations for the unsteady flowfield of turbomachinery [AIAA PAPER 93-0676] p 465 A93-24786
- Measured acoustic characteristics of ducted supersonic jets at different model scales [AIAA PAPER 93-0731] p 563 A93-24821
- Computation of supersonic jet noise under imperfectly expanded conditions [AIAA PAPER 93-0735] p 563 A93-24825
- Computing 3-D steady supersonic flow via a new Lagrangian approach [AIAA PAPER 93-0891] p 471 A93-24951
- Effect of a rotating propeller on the separation angle of attack [AIAA PAPER 93-0017] p 472 A93-24978
- Nonreflecting boundary conditions for linearized unsteady aerodynamic calculations [AIAA PAPER 93-0882] p 475 A93-25553
- BIPS Turboalternator-Compressor characteristics and application to the NASA Solar Dynamic Ground Demonstration Program p 532 A93-25965
- Comparison of all-electric secondary power systems for civil transport p 519 A93-25997
- Robust integrated flight/propulsion control design for a STOVL aircraft using H-infinity control design techniques p 524 A93-26432
- A numerical study of mixing in supersonic combustors with hypermixing injectors [AIAA PAPER 93-0215] p 520 A93-27801
- Cruise noise of an advanced propeller with swirl recovery vanes p 564 A93-28609
- Linearized Euler predictions of unsteady aerodynamic loads in cascades p 480 A93-29318
- Acoustical analysis of gear housing vibration p 567 A93-29420
- Active control of helicopter transmission noise p 568 A93-29428
- Damage progression in stiffened composite panels [AIAA PAPER 93-1345] p 738 A93-33915

- A hot dynamic seal rig for measuring hypersonic engine seal durability and flow performance
[AIAA PAPER 93-1346] p 738 A93-33916
- Quantification of uncertainties in composites
[AIAA PAPER 93-1440] p 734 A93-33989
- Dynamics of rotating multicomponent turbomachinery systems
[AIAA PAPER 93-1629] p 742 A93-34157
- An efficient procedure for cascade aeroelastic stability determination using nonlinear, time-marching aerodynamic solvers
[AIAA PAPER 93-1631] p 719 A93-34159
- Experimental investigation of counter-rotating propfan flutter at cruise conditions
[AIAA PAPER 93-1632] p 720 A93-34160
- Unsteady aerodynamics and flutter of propfans using a three-dimensional Full-Potential Solver
[AIAA PAPER 93-1633] p 720 A93-34161
- On the static stability of forward swept propfans
[AIAA PAPER 93-1634] p 720 A93-34162
- BLASIM - A computational tool to assess ice impact damage on engine blades
[AIAA PAPER 93-1638] p 720 A93-34165
- Probabilistically configured adaptive composite structures
[AIAA PAPER 93-1679] p 743 A93-34191
- Efficient hybrid scheme for the analysis of counter-rotating propellers
p 688 A93-34483
- Study on vortex generator flow control for the management of inlet distortion
p 689 A93-34488
- Computational study of advanced exhaust system transition ducts with experimental validation
p 689 A93-34490
- Reaction zone structure for strong, weak overdriven, and weak underdriven oblique detonations
p 746 A93-35492
- Results of a low power ice protection system test and a new method of imaging data analysis
p 795 A93-35932
- Identification of the open loop dynamics of the T700 turboshaft engine
p 809 A93-35934
- Modal analysis of multistage gear systems coupled with gearbox vibrations
p 827 A93-36588
- Design and evaluation of a robust dynamic neurocontroller for a multivariable aircraft control problem
p 817 A93-37004
- Modeling of linear isentropic flow systems
p 828 A93-37046
- Unsteady blade pressures on a propfan at takeoff - Euler analysis and flight data
p 810 A93-37389
- Aeroelastic dynamics of mistuned blade assemblies with closely spaced blade modes
[AIAA PAPER 93-1628] p 810 A93-37446
- Characteristics of three-dimensional turbulent jets in crossflow
p 772 A93-38695
- Flip-flop jet nozzle extended to supersonic flows
p 778 A93-39409
- Unsteady transonic two-dimensional Euler solutions using finite elements
p 778 A93-39412
- Neurocontrol design and analysis for a multivariable aircraft control problem
p 906 A93-41894
- Hypersonic stability and transition
p 864 A93-42579
- CFD for hypersonic propulsion
p 865 A93-42585
- Multigrid calculation of three-dimensional viscous cascade flows
p 872 A93-42889
- The NASA Computational Fluid Dynamics (CFD) program - Building technology to solve future challenges
[AIAA PAPER 93-3292] p 1041 A93-44996
- Field by field hybrid upwind splitting methods
[AIAA PAPER 93-3302] p 950 A93-45000
- An extended Lagrangian method
[AIAA PAPER 93-3305] p 951 A93-45003
- Two-dimensional CFD modeling of wave rotor flow dynamics
[AIAA PAPER 93-3318] p 952 A93-45014
- An accuracy assessment of Cartesian-mesh approaches for the Euler equations
[AIAA PAPER 93-3335] p 953 A93-45029
- Navier-Stokes analysis of three-dimensional S-ducts
p 959 A93-45146
- Low-to-high altitude predictions of three-dimensional ablative re-entry flowfields
p 1027 A93-46407
- Comparative wind tunnel tests at high Reynolds numbers of NACA 64 621 airfoils with two airfoil configurations
p 967 A93-46823
- A new flux splitting scheme
p 973 A93-47189
- Adaptive computations of flow around a delta wing with vortex breakdown
[AIAA PAPER 93-3400] p 974 A93-47202
- An improved far field drag calculation method for nonlinear CFD codes
[AIAA PAPER 93-3417] p 975 A93-47213
- A numerical investigation of supersonic strut/endwall interactions in annular flow with varying strut thickness
[AIAA PAPER 93-2927] p 1045 A93-48128
- High resolution numerical simulation of the linearized Euler equations in conservation law form
[AIAA PAPER 93-2934] p 1148 A93-48132
- Intake flow modeling in a four stroke diesel using KIVA3
[AIAA PAPER 93-2952] p 1148 A93-48146
- Some practical turbulence modeling options for Reynolds-averaged full Navier-Stokes calculations of three-dimensional flows
[AIAA PAPER 93-2964] p 1048 A93-48158
- A lag model for turbulent boundary layers developing over rough bleed surfaces
[AIAA PAPER 93-2988] p 1052 A93-48181
- An investigation of shock wave turbulent boundary layer interaction with bleed through slanted slots
[AIAA PAPER 93-2992] p 1052 A93-48184
- A three-dimensional pressure flux-split RNS application to sub/supersonic flow in inlets and ducts
[AIAA PAPER 93-3063] p 1058 A93-48239
- Averaging techniques for steady and unsteady calculations of a transonic fan stage
[AIAA PAPER 93-3065] p 1059 A93-48241
- Experimental and numerical investigation of supersonic turbulent flow in an annular duct
[AIAA PAPER 93-3123] p 1063 A93-48291
- Numerical simulation of a shock wave/turbulent boundary layer interaction in a duct
[AIAA PAPER 93-3127] p 1063 A93-48293
- Flowfield dynamics in blunt fin-induced shock wave/turbulent boundary layer interactions
[AIAA PAPER 93-3133] p 1063 A93-48298
- Screening studies of advanced control concepts for airbreathing engines
[AIAA PAPER 93-3320] p 1108 A93-49329
- Flight testing of a fiber optic temperature sensor
p 1105 A93-49476
- A review of chemically reactive turbulent flow mixing mechanisms and a new design for a low NO(x) combustor
p 1109 A93-49508
- Mixing in the dome region of a staged gas turbine combustor
p 1109 A93-49612
- An efficient liner cooling scheme for advanced small gas turbine combustors
[AIAA PAPER 93-1763] p 1109 A93-49660
- Experimental evaluation of a cooled radial-inflow turbine
[AIAA PAPER 93-1795] p 1110 A93-49685
- Installed F/A-18 inlet flow calculations at 60 deg angle-of-attack and 10 deg side slip
[AIAA PAPER 93-1806] p 1074 A93-49695
- Calculation of scramjet inlet with thick boundary-layer ingestion
[AIAA PAPER 93-1836] p 1074 A93-49720
- 3-D viscous flow CFD analysis of the propeller effect on an advanced ducted propeller subsonic inlet
[AIAA PAPER 93-1847] p 1075 A93-49728
- Unsteady aerodynamic flow phenomena in a transonic compressor stage
[AIAA PAPER 93-1868] p 1075 A93-49743
- Investigation of a strut/endwall interaction in supersonic annular flow
[AIAA PAPER 93-1925] p 1076 A93-49791
- Nonintrusive, multipoint velocity measurements in high-pressure combustion flows
[AIAA PAPER 93-2032] p 1145 A93-49867
- An analytical study of dilution jet mixing in a cylindrical duct
[AIAA PAPER 93-2043] p 1113 A93-49876
- Computations of spray, fuel-air mixing, and combustion in a lean-premixed-prevaporized combustor
[AIAA PAPER 93-2069] p 1153 A93-49901
- Computation of the flow field in an annular gas turbine combustor
[AIAA PAPER 93-2074] p 1113 A93-49903
- Advanced instrumentation for next-generation aerospace propulsion control systems
[AIAA PAPER 93-2079] p 1154 A93-49906
- Blade row interaction effects on flutter and forced response
[AIAA PAPER 93-2084] p 1114 A93-49911
- An iterative multidisciplinary analysis for rotor blade shape determination
[AIAA PAPER 93-2085] p 1114 A93-49912
- Unsteady aerodynamics and flutter based on the potential equation
[AIAA PAPER 93-2086] p 1079 A93-49913
- Design and test of a small two stage counter-rotating turbine for rocket engine application
[AIAA PAPER 93-2136] p 1142 A93-49954
- Low-noise, high-strength, spiral-bevel gears for helicopter transmissions
[AIAA PAPER 93-2149] p 1154 A93-49966
- A comparative study of Full Navier-Stokes and Reduced Navier-Stokes analyses for separating flows within a diffusing inlet S-duct
[AIAA PAPER 93-2154] p 1079 A93-49970
- Development and use of hydrogen-air torches in an altitude facility
[AIAA PAPER 93-2176] p 1137 A93-49988
- Compound curvature laser window development
[AIAA PAPER 93-2177] p 1173 A93-49989
- Integrated CFD modeling of gas turbine combustors
[AIAA PAPER 93-2196] p 1115 A93-50008
- A model for the selective amplification of spatially coherent waves in a centrifugal compressor on the verge of rotating stall
[AIAA PAPER 93-2236] p 1080 A93-50039
- High Reynolds number and turbulence effects on aerodynamics and heat transfer in a turbine cascade
[AIAA PAPER 93-2252] p 1155 A93-50050
- Optimization of blade arrangement in a randomly mistuned cascade using simulated annealing
[AIAA PAPER 93-2254] p 1115 A93-50052
- Engineering science research issues in high power density transmission dynamics for aerospace applications
[AIAA PAPER 93-2299] p 1155 A93-50084
- In-stream measurements of combustion during Mach 5 to 7 tests of the Hypersonic Research Engine (HRE)
[AIAA PAPER 93-2324] p 1116 A93-50104
- Gravity sensitivity of a resistojet water vaporizer
[AIAA PAPER 93-2402] p 1156 A93-50167
- Performance characteristics of a variable-area vane nozzle for vectoring an ASTOVL exhaust jet up to 45 deg
[AIAA PAPER 93-2437] p 1118 A93-50189
- Effects of flow-path variations on internal reversing flow in a tailpipe offtake configuration for ASTOVL aircraft
[AIAA PAPER 93-2438] p 1118 A93-50190
- Initial development of the two-dimensional ejector shear layer - Experimental results
[AIAA PAPER 93-2440] p 1118 A93-50192
- Comparison of the initial development of shear layers in two-dimensional and axisymmetric ejector configurations
[AIAA PAPER 93-2441] p 1119 A93-50193
- A comparison between numerically modelled and experimentally measured loss mechanisms in wave rotors
[AIAA PAPER 93-2522] p 1120 A93-50252
- Analytic methods for design of wave cycles for wave rotor core engines
[AIAA PAPER 93-2523] p 1121 A93-50253
- Three-dimensional numerical simulation of gradual opening in a wave rotor passage
[AIAA PAPER 93-2526] p 1156 A93-50254
- Brush seal low surface speed hard-rub characteristics
[AIAA PAPER 93-2534] p 1156 A93-50261
- Navier-Stokes analysis of radial turbine rotor performance
[AIAA PAPER 93-2555] p 1121 A93-50277
- Three-dimensional flow field in a turbine nozzle passage
[AIAA PAPER 93-2556] p 1084 A93-50278
- Chimera grids in the simulation of three-dimensional flowfields in turbine-blade-coolant passages
[AIAA PAPER 93-2559] p 1157 A93-50280
- Nonlinear dynamic simulation of single- and multi-spool core engines
[AIAA PAPER 93-2580] p 1122 A93-50294
- Application of controller partitioning optimization procedure to integrated flight/propulsion control design for a STOLV aircraft
[AIAA PAPER 93-3766] p 1131 A93-51361
- Integrated flight/propulsion control - Subsystem specifications for performance
[AIAA PAPER 93-3808] p 1132 A93-51400
- A comparative study of multivariable robustness analysis methods as applied to integrated flight and propulsion control
[AIAA PAPER 93-3809] p 1102 A93-51401
- Antiwindup analysis and design approaches for MIMO systems
[AIAA PAPER 93-3811] p 1123 A93-51403
- A time-accurate high-resolution TVD scheme for solving the Navier-Stokes equations
p 1093 A93-52006
- Unsteady wing surface pressures in the wake of a propeller
p 1095 A93-52436
- Efficient finite element method for aircraft deicing problems
p 1103 A93-52443
- Chemical stability of titanium diboride reinforcement in nickel aluminide matrices
p 1147 A93-52473
- Progress towards understanding and predicting heat transfer in the turbine gas path
p 1215 A93-52751
- Stress relaxation of low pressure plasma-sprayed NiCrAlY alloys
p 1211 A93-52870
- Low-Reynolds-number k-epsilon model for unsteady turbulent boundary-layer flows
p 1177 A93-53208
- Design for cyclic loading endurance of composites
p 1216 A93-53395
- Overview of NASA's advanced high temperature engine materials technology program
p 1212 A93-53453

- The chemistry of Saudi Arabian sand - A deposition problem on helicopter turbine airfoils
p 1216 A93-53468
- Measurements and computational analysis of heat transfer and flow in a simulated turbine blade internal cooling passage
[AIAA PAPER 93-1797] p 1218 A93-53585
- Initial results from the NASA Lewis wave rotor experiment
[AIAA PAPER 93-2521] p 1193 A93-53589
- Laser velocimeter measurements of the flow field generated by a forward-swept propfan during flutter
[AIAA PAPER 93-2919] p 1180 A93-53591
- Streamwise vorticity generation and mixing enhancement in free jets by 'delta-tabs'
[AIAA PAPER 93-3253] p 1180 A93-53592
- Propulsion technology challenges for turn-of-the-century commercial aircraft
[ISABE 93-7003] p 1194 A93-53980
- Emission characteristics of a model gas turbine combustor at practical conditions
[ISABE 93-7023] p 1196 A93-53999
- Forcing function modeling for flow induced vibration
[ISABE 93-7027] p 1196 A93-54003
- Engine technology challenges for a 21st Century High-Speed Civil Transport
[ISABE 93-7064] p 1200 A93-54040
- Material requirements for the High Speed Civil Transport
[ISABE 93-7067] p 1200 A93-54043
- Fluid dynamics and convective heat transfer in impinging jets through implementation of a high resolution liquid crystal technique
[ISABE 93-7077] p 1220 A93-54053
- Aerodynamic inverse design and analysis for a full engine
[ISABE 93-7086] p 1186 A93-54062
- Three-dimensional flow analysis inside turbomachinery stages with steady and unsteady Navier-Stokes method
[ISABE 93-7095] p 1186 A93-54071
- A parameter optimization approach to controller partitioning for integrated flight/propulsion control application
p 1206 A93-54268
- Mixing of multiple jets with a confined subsonic crossflow
p 1189 A93-54324
- Icing Research Tunnel rotating bar calibration measurement system
p 1255 A93-54398
- Analysis of high Reynolds number inviscid/viscid interactions in cascades
p 1234 A93-55351
- Comparison of radiated noise from shrouded and unshrouded propellers
p 1264 A93-55861
- Radial turbine cooling
p 82 A93-10061
- Evaluation and application of the Baldwin-Lomax turbulence model in two-dimensional, unsteady, compressible boundary layers with and without separation in engine inlets
[NASA-TM-105810] p 82 A93-10087
- Comparison of all-electric secondary power systems for civil subsonic transports
[NASA-TM-105852] p 55 A93-10456
- Nondestructive evaluation of ceramic and metal matrix composites for NASA's HITEMP and enabling propulsion materials programs
[NASA-TM-105807] p 85 A93-10963
- An interactive preprocessor for the NASA engine performance program
[NASA-TM-105786] p 56 A93-10983
- System and method for cancelling expansion waves in a wave rotor
[NASA-CASE-LEW-15218-1] p 86 A93-11172
- The engine design engine. A clustered computer platform for the aerodynamic inverse design and analysis of a full engine
[NASA-TM-105838] p 21 A93-11223
- A concept for a counterrotating fan with reduced tone noise
[NASA-TM-105736] p 101 A93-11370
- Overview of high performance aircraft propulsion research
[NASA-TM-105839] p 59 A93-11530
- Design of a high-temperature experiment for evaluating advanced structural materials
[NASA-TM-105833] p 88 A93-11624
- An experimental investigation of the flow in a diffusing S-duct
[NASA-TM-105809] p 60 A93-12077
- Dynamic analysis of a pre-and-post ice impacted blade
[NASA-TM-105829] p 90 A93-12197
- Stochastic sensitivity measure for mistuned high-performance turbines
[NASA-TM-105821] p 90 A93-12277
- Analysis of fault-tolerant neurocontrol architectures
[NASA-TM-105898] p 65 A93-12305
- Concurrent optimization of airframe and engine design parameters
[NASA-TM-105908] p 60 A93-12402
- An improved numerical model for wave rotor design and analysis
[NASA-TM-105915] p 60 A93-12418
- Probabilistic evaluation of fuselage-type composite structures
[NASA-TM-105881] p 212 A93-12735
- Split torque transmission load sharing
[NASA-TM-105884] p 212 A93-12736
- Computer program for calculating and fitting thermodynamic functions
[NASA-RP-1271] p 231 A93-12967
- Turbomachinery CFD on parallel computers
[NASA-TM-105932] p 228 A93-13154
- AGARD WG13 aerodynamics of high speed air intakes: Assessment of CFD results
p 215 A93-13220
- Radial turbine cooling
[NASA-TM-105658] p 130 A93-13292
- An algebraic turbulence model for three-dimensional viscous flows
[NASA-TM-105931] p 110 A93-14102
- Estimation of unsteady lift on a pitching airfoil from wake velocity surveys
[NASA-TM-105947] p 138 A93-14791
- Icing effects on aircraft stability and control determined from flight data: Preliminary results
[NASA-TM-105977] p 188 A93-14831
- Results of low power deicer tests on a swept inlet component in the NASA Lewis icing research tunnel
[NASA-TM-105968] p 138 A93-14911
- Surface roughness due to residual ice in the use of low power deicing systems
[NASA-TM-105971] p 139 A93-15338
- Supersonic investigation of two dimensional hypersonic exhaust nozzles
[NASA-TM-105687] p 179 A93-15342
- Root damage analysis of aircraft engine blade subject to ice impact
[NASA-TM-105779] p 222 A93-15343
- Numerical modeling of anti-icing systems and comparison to test results on a NASA 0012 airfoil
[NASA-TM-105975] p 148 A93-15345
- Ice accretion and performance degradation calculations with LEWICE/NS
[NASA-TM-105972] p 148 A93-15354
- Optimization of circular orifice jets mixing into a heated cross flow in a cylindrical duct
[NASA-TM-105984] p 179 A93-15359
- Close-up analysis of aircraft ice accretion
[NASA-TM-105952] p 148 A93-15360
- Acoustic mode measurements in the inlet of a model turbofan using a continuously rotating rake: Data collection/analysis techniques
[NASA-TM-105936] p 179 A93-15403
- An overview of shed ice impact in the NASA Lewis Icing Research Tunnel
[NASA-TM-105969] p 139 A93-15404
- Computation of supersonic jet noise under imperfectly expanded conditions
[NASA-TM-105961] p 233 A93-15430
- User manual for NASA Lewis 10 by 10 foot supersonic wind tunnel
[NASA-TM-105626] p 194 A93-15498
- Simplified jet-A kinetic mechanism for combustor application
[NASA-TM-105940] p 200 A93-15504
- An integral equation solution for multistage turbomachinery design calculations
[NASA-TM-105970] p 179 A93-15521
- Ice accretion prediction for a typical commercial transport aircraft
[NASA-TM-105976] p 149 A93-15522
- Propulsion system performance resulting from an integrated flight/propulsion control design
[NASA-TM-105874] p 180 A93-15525
- Aerothermodynamic flow phenomena of the airframe-integrated supersonic combustion ramjet
[NASA-TM-4376] p 196 A93-15528
- Vibration isolation technology: An executive summary of systems development and demonstration
[NASA-TM-105937] p 110 A93-15573
- Propagation of high frequency jet noise using geometric acoustics
[NASA-TM-106013] p 233 A93-15575
- Bypass transition in compressible boundary layers
p 417 A93-15801
- A realizable Reynolds stress algebraic equation model
[NASA-TM-105993] p 290 A93-16596
- User's manual for Interactive Data Display System (IDDS)
[NASA-TM-105572] p 441 A93-16613
- Effect of a rotating propeller on the separation angle of attack and distortion in ducted propeller inlets
[NASA-TM-105935] p 290 A93-16625
- Experimental investigation of an ejector-powered free-jet facility
[NASA-TM-105868] p 291 A93-16704
- Acoustic mode measurements in the inlet of a model turbofan using a continuously rotating rake
[NASA-TM-105989] p 362 A93-16705
- Takeoff/approach noise for a model counterrotation propeller with a forward-swept upstream rotor
[NASA-TM-105979] p 362 A93-16715
- A critical analysis of the accuracy of several numerical techniques for combustion kinetic rate equations
[NASA-TP-3315] p 362 A93-16941
- Consecutive plate acoustic suppressor apparatus and methods
[NASA-CASE-LEW-15430-1] p 453 A93-17051
- Brush seal bristle flexure and hard-rub characteristics
[NASA-TM-105864] p 421 A93-18321
- Integrity testing of brush seal in shroud ring of T-700 engine
[NASA-TM-105863] p 421 A93-18380
- Dynamics of rotating multi-component turbomachinery systems
[NASA-TM-105997] p 421 A93-18426
- Numerical simulation of a high Mach number jet flow
[NASA-TM-105985] p 551 A93-20057
- Structural dynamics branch research and accomplishments to FY 1992
[NASA-TM-105824] p 552 A93-20368
- The 1992 Research/Technology report
[NASA-TM-105924] p 459 A93-20902
- Controller partitioning for integrated flight/propulsion control implementation
[NASA-TM-105804] p 527 A93-21197
- Application of artificial neural networks to the design optimization of aerospace structural components
[NASA-TM-4389] p 555 A93-21831
- Multi-heat addition turbine engine
[NASA-CASE-LEW-15094-1] p 522 A93-22034
- Fuel injector: Air swirl characterization aerothermal modeling, phase 2, volume 1
[NASA-CR-189193-VOL-1] p 721 A93-24754
- A three-dimensional algebraic grid generation scheme for gas turbine combustors with inclined slots
[NASA-CR-191095] p 746 A93-24759
- Surface and flow field measurements in a symmetric crossing shock wave/turbulent boundary-layer interaction
[NASA-TM-106086] p 693 A93-24911
- Screening studies of advanced control concepts for airbreathing engines
[NASA-TM-106042] p 721 A93-25079
- NASA Lewis 8- by 6-foot supersonic wind tunnel user manual
[NASA-TM-105771] p 730 A93-25080
- Experimental performance of a ventral nozzle with pitch and yaw vectoring capability for SSTOVL aircraft
[NASA-TM-106054] p 722 A93-25129
- Gas turbine system simulation: An object-oriented approach
[NASA-TM-106044] p 723 A93-25673
- Bibliography on propulsion airframe integration technologies for high-speed civil transport applications, 1980-1991
[NASA-TM-105602] p 678 A93-26136
- Rotating rake design for unique measurement of fan-generated spinning acoustic modes
[NASA-TM-105946] p 724 A93-26161
- External stress-corrosion cracking of a 1.22-m-diameter type 316 stainless steel air valve
[NASA-TP-3190] p 737 A93-26201
- Fabrication of composite propfan blades for a cruise missile wind tunnel model
[NASA-TM-105270] p 752 A93-26202
- A large hemi-anechoic enclosure for community-compatible aeroacoustic testing of aircraft propulsion systems
[NASA-TM-106015] p 760 A93-26551
- An overview of elevated temperature damage mechanisms and fatigue behavior of a unidirectional SCS-6/Ti-15-3 composite
[NASA-TM-106131] p 825 A93-26702
- Robustness enhancement of neurocontroller and state estimator
[NASA-TM-106028] p 819 A93-26907
- Structural tailoring of aircraft engine blade subject to ice impact constraints
[NASA-TM-106033] p 838 A93-26999
- Nitric oxide formation in a lean, premixed-prevaporized jet A/air flame tube: An experimental and analytical study
[NASA-TM-105722] p 844 A93-27012
- Increased heat transfer to elliptical leading edges due to spanwise variations in the freestream momentum: Numerical and experimental results
[NASA-TM-106150] p 838 A93-27020

- Experimental investigation of crossflow jet mixing in a rectangular duct
[NASA-TM-106152] p 812 N93-27026
- In-flight near- and far-field acoustic data measured on the Propan Test Assessment (PTA) testbed and with an adjacent aircraft
[NASA-TM-103719] p 852 N93-27058
- Fault detection of helicopter gearboxes using the multi-valued influence matrix method
[NASA-TM-106100] p 838 N93-27069
- A transfer matrix approach to vibration localization in mistuned blade assemblies
[NASA-TM-106112] p 838 N93-27088
- Probabilistic assessment of composite structures
[NASA-TM-106024] p 825 N93-27092
- CFD mixing analysis of axially opposed rows of jets injected into confined crossflow
[NASA-TM-106179] p 813 N93-27128
- Velocity and drop size measurements in a swirl-stabilized, combustor spray
[NASA-TM-106130] p 813 N93-27130
- Performance characteristics of a variable-area vane nozzle for vectoring an ASTOVL exhaust jet up to 45 deg
[NASA-TM-106114] p 813 N93-27131
- Brush seal low surface speed hard-rub characteristics
[NASA-TM-106169] p 838 N93-27132
- Face-gear drives: Design, analysis, and testing for helicopter transmission applications
[NASA-TM-106101] p 839 N93-27133
- An analytical study of dilution jet mixing in a cylindrical duct
[NASA-TM-106181] p 814 N93-27160
- Numerical modeling of runback water on ice protected aircraft surfaces
[NASA-TM-106169] p 840 N93-27438
- Experimental and computational ice shapes and resulting drag increase for a NACA 0012 airfoil
p 784 N93-27440
- Comparison of reacting and non-reacting shear layers at a high subsonic Mach number
[NASA-TM-106198] p 814 N93-27610
- NDE of PWA 1480 single crystal turbine blade material
[NASA-TM-106140] p 815 N93-27640
- A modified approach to controller partitioning
[NASA-TM-106167] p 848 N93-28051
- Status of the Fiber Optic Control System Integration (FOCSI) program
[NASA-TM-106151] p 841 N93-28053
- Experimental evaluation of a cooled radial-inflow turbine
[NASA-TM-106230] p 816 N93-28697
- Jet mixer noise suppressor using acoustic feedback
[NASA-CASE-LEW-15170-1] p 853 N93-28953
- Effects of flow-path variations on internal reversing flow in a tailpipe offtake configuration for ASTOVL aircraft
[NASA-TM-106149] p 900 N93-29065
- High Reynolds number and turbulence effects on aerodynamics and heat transfer in a turbine cascade
[NASA-TM-106187] p 930 N93-29157
- The 3-D viscous flow CFD analysis of the propeller effect on an advanced ducted propeller subsonic inlet
[NASA-TM-106240] p 900 N93-29162
- Gravity sensitivity of a resistojet water vaporizer
[NASA-TM-106220] p 914 N93-29194
- Navier-Stokes analysis of three-dimensional flow and heat transfer inside turbine blade rows
p 905 N93-29963
- Blasim: A computational tool to assess ice impact damage on engine blades
[NASA-TM-106225] p 1031 N93-31193
- Overview of aerothermodynamic loads definition study
p 1016 N93-31583
- Three-dimensional analysis of the Pratt and Whitney alternate design SSME fuel turbine
p 1031 N93-31584
- Three-dimensional flow calculations inside SSME GGGT first stage blade rows
p 1017 N93-31585
- Localization of aeroelastic modes in mistuned high-energy turbines
p 1032 N93-31586
- Measurements and computational analysis of heat transfer and flow in a simulated turbine blade internal cooling passage
[NASA-TM-106189] p 1032 N93-31647
- Streamwise vorticity generation and mixing enhancement in free jets by delta-tabs
[NASA-TM-106235] p 988 N93-31648
- Engine technology challenges for a 21st Century High-Speed Civil Transport
[NASA-TM-106216] p 1004 N93-31671
- Enhanced mixing of a rectangular supersonic jet by natural and induced screech
[NASA-TM-106245] p 989 N93-31672
- Turbulence measurement in a reacting and non-reacting shear layer at a high subsonic Mach number
[NASA-TM-106186] p 989 N93-31839
- Efficient fault diagnosis of helicopter gearboxes
[NASA-TM-106253] p 1032 N93-31846
- Hypersonic engine component experiments in high heat flux, supersonic flow environment
[NASA-TM-106273] p 1032 N93-31860
- Propulsion technology challenges for turn-of-the-century commercial aircraft
[NASA-TM-106192] p 1005 N93-32351
- Initial results from the NASA-Lewis wave rotor experiment
[NASA-TM-106148] p 1005 N93-32368
- National Aeronautics and Space Administration.**
Marshall Space Flight Center, Huntsville, AL.
- Hot streaks and phantom cooling in a turbine rotor passage. I - Separate effects
[ASME PAPER 92-GT-75] p 401 A93-19325
- Hot streaks and phantom cooling in a turbine rotor passage. II - Combined effects and analytical modelling
[ASME PAPER 92-GT-76] p 401 A93-19326
- An experimental study of heat transfer in a large-scale turbine rotor passage
[ASME PAPER 92-GT-195] p 403 A93-19420
- Investigation of rotor blade roughness effects on turbine performance
[ASME PAPER 92-GT-297] p 354 A93-19487
- Variability of geophysical parameters from aircraft radiance measurements for FIFE
p 426 A93-20622
- Some unsteady fluid forces on pump impellers
p 413 A93-22265
- The Burnett shock structures in low density hypersonic flows
[AIAA PAPER 92-5048] p 273 A93-22320
- A study of CFD algorithms applied to complete aircraft configurations
[AIAA PAPER 93-0784] p 468 A93-24864
- Natural environment application for NASP-X-30 design and mission planning
[AIAA PAPER 93-0851] p 531 A93-24915
- Solution-adaptive and quality-enhancing grid generation
p 480 A93-28610
- The microstrip proportional counter
p 549 A93-29485
- Aircraft measurement of electric field - Self-calibration
p 753 A93-34694
- Enhanced heat transport in environmental systems using microencapsulated phase change materials
[SAE PAPER 92-1224] p 926 A93-41398
- Hypersonic stagnation line merged layer flow on blunt axisymmetric bodies of arbitrary shape
[AIAA PAPER 93-2723] p 962 A93-46478
- Burnett solutions along the stagnation line of a cooled cylinder in low-density hypersonic flows
[AIAA PAPER 93-2726] p 962 A93-46480
- Subscale hot-fire testing of a formed platelet liner
[AIAA PAPER 93-1827] p 1141 A93-49713
- An adaptive grid/Navier-Stokes methodology for the calculation of nozzle afterbody base flows with a supersonic freestream
[AIAA PAPER 93-1922] p 1076 A93-49788
- A numerical analysis of supersonic flow over an axisymmetric afterbody
[AIAA PAPER 93-2347] p 1083 A93-50121
- Liquid hydrogen foil-bearing turbopump
[AIAA PAPER 93-2537] p 1156 A93-50264
- Computation of optimal low- and medium-thrust orbit transfers
[AIAA PAPER 93-3855] p 1144 A93-51442
- Navier-Stokes analysis of turbine flowfield and external heat transfer
[ISABE 93-7075] p 1186 A93-54051
- National Aeronautics and Space Administration.**
Pasadena Office, CA.
- Three-stage sorption type cryogenic refrigeration systems and methods employing heat regeneration
[NASA-CASE-NPO-18366-1-CU] p 216 N93-13422
- Virtual reality flight control display with six-degree-of-freedom controller and spherical orientation overlay
[NASA-CASE-NPO-18733-1-CU] p 897 N93-30416
- National Aeronautics and Space Administration.**
Wallops Flight Facility, Wallops Island, VA.
- Recent refinements and increased capabilities in balloon vertical performance analysis
p 40 A93-11361
- Determination of balloon gas mass and revised estimates of drag and virtual mass coefficients
p 7 A93-11362
- NASA balloon design and flight - Philosophy and criteria
p 40 A93-11363
- Status of the NASA Balloon Program
p 1 A93-11365
- NASA Long Duration Balloon capability development project
p 2 A93-11370
- Scientific ballooning payload termination loads
p 27 A93-11383
- Application of new GPS aircraft control/display system to topographic mapping of the Greenland ice cap
p 499 A93-28152
- Update on the NASA ER-2 Doppler radar system (EDOP)
p 807 A93-37737
- National Aerospace Lab., Amsterdam (Netherlands).**
- Aerodynamic analysis of slipstream/wing/nacelle interference for preliminary design of aircraft configurations
p 130 N93-13205
- DME-derived positions compared with MLS- and ILS-derived positions
[NLR-TP-90119-U] p 318 N93-16343
- Comparison of solution of various Euler solvers and one Navier-Stokes solver for the flow about a sharp-edged cropped delta wing
[NLR-TP-90340-U] p 418 N93-16411
- Review of aeronautical fatigue investigations in the Netherlands during the period March 1989 - March 1991
[NLR-TP-91092-U] p 331 N93-17535
- Damage tolerance behaviour of aluminium-lithium sheet alloys
[NLR-TP-91244-U] p 392 N93-17540
- Navstar global positioning system: Introduction and status
[NLR-TP-91008-U] p 318 N93-17559
- Flight simulation and constant amplitude fatigue crack growth in aluminum-lithium sheet and plate
[NLR-TP-91104-U] p 331 N93-17562
- Application of an Euler-equation method to a sharp-edged delta wing configuration with vortex flow
[NLR-TP-91306] p 294 N93-17809
- Flight simulation evaluation of the flyability of curved MLS approaches with wide-body aircraft
[NLR-TP-90238-U] p 382 N93-17875
- Interlaminar stress analysis at the skin/stiffener interface of a grid-stiffened composite panel
[NASA-CR-192177] p 393 N93-17920
- Beyond the frequency limits of time-linearized methods
[NLR-TP-91216-U] p 295 N93-17929
- NARSIM and EFMS: Tools for research on integrated ATM
[NLR-TP-89336-U] p 319 N93-17954
- Load experience variability of fighter aircraft
[NLR-TP-89172-U] p 514 N93-20742
- A simulator study into low speed longitudinal handling qualities of ACT transport aircraft
[NLR-TP-89387-U] p 527 N93-20743
- A break-down of sting interference effects
[NLR-TP-91220-U] p 1014 N93-31042
- Performance of gas turbine compressor cleaners
[NLR-TP-91237-U] p 1003 N93-31111
- Experiences with two GPS receivers in northern Europe
[NLR-TP-91168-U] p 993 N93-31120
- Computational methods for aerodynamic design of aircraft components
[NLR-TP-92072-4] p 987 N93-31148
- Fractographic and microstructural analysis of fatigue crack growth in TI-6Al-4V fan disc forgings
p 1004 N93-31742
- Low cycle fatigue behaviour of titanium disc alloys
p 1004 N93-31745
- Review of aerodynamic design in the Netherlands
[NLR-TP-91260-U] p 999 N93-31840
- Ageing aircraft research in the Netherlands
[NLR-TP-91443-U] p 999 N93-32203
- Damage severity of monitored fatigue load spectra
[NLR-TP-92009-U] p 999 N93-32205
- Instrumentation for in-flight acoustic measurements in an engine inlet duct of a Fokker 100 aircraft
[NLR-TP-91200-U] p 1001 N93-32332
- The application of phase tracking GPS for flight test trajectory determination
[NLR-TP-91349-U] p 994 N93-32337
- Development of a method to predict transonic limit cycle oscillation characteristics of fighter aircraft
[NLR-TP-91359-U] p 999 N93-32338
- Panel methods for aerodynamic analysis and design
[NLR-TP-91404-U] p 990 N93-32357
- NLR inviscid transonic unsteady loads prediction methods in aeroelasticity
[NLR-TP-91410-U] p 990 N93-32358
- Low cycle fatigue behaviour of titanium disc alloys
[NLR-TP-91346-U] p 1006 N93-32372
- Accelerated and real-time corrosion testing of aluminum-lithium alloys
[NLR-TP-91203-U] p 1020 N93-32385
- Transmission of sound through a rotor
[NLR-TP-92014-U] p 1006 N93-32386
- Evaluation of the flyability of MLS curved approaches for wide-body aircraft
[NLR-TP-91396-U] p 999 N93-32416
- National Aerospace Lab., Kakuda (Japan).**
- Mach 4 testing of scramjet inlet models
[NAL-TR-1137] p 26 N93-12369

- Analytical and numerical study on steady Mach reflection p 302 N93-19309
- National Aerospace Lab., Tokyo (Japan).**
Air ejector experiments using the two-dimensional supersonic cascade tunnel: Relationship between ejector performance and throat area ratio, part 1 [NAL-TM-642-PT-1] p 25 N93-12352
Flight test progress of the STOL research aircraft ASKA [NAL-TM-643] p 49 N93-12354
Simulation analysis of a cable-mount system used for dynamic wind tunnel tests [NAL-TR-1127] p 68 N93-12359
On stability and control of SSTO spaceplane in super- and hypersonic ascending phase [NAL-TR-1128T] p 65 N93-12361
A wind tunnel investigation to determine buffet countermeasures for STOL aircraft alpha-sweep flight testing [NAL-TR-1129] p 65 N93-12362
Accuracy improvement of linear estimated motion using differential type sensors [NAL-TR-1135] p 91 N93-12365
Flight simulator evaluation of D-size liquid crystal flat panel displays [NAL-TR-1136] p 52 N93-12367
An optical fiber multi-terminal data bus system for aircraft [NAL-TR-1125] p 52 N93-12370
Evaluation of acoustic impedance models for a perforated plate [NAL-TR-1133] p 102 N93-12375
Liquid crystal flat panel display evaluation tests using a flight simulator [NAL-TR-1122] p 52 N93-12383
Wind tunnel investigation of a twin-engine jet transport semi-span model with upper surface blown jet flap [NAL-TR-1134] p 26 N93-12503
Special publication of National Aerospace Laboratory [DE93-716176] p 239 N93-15946
Special publication of National Aerospace Laboratory [DE93-716195] p 239 N93-15949
Experiments on swept-wing boundary-layer transition p 419 N93-16829
Proceedings of the Ninth NAL Symposium on Aircraft Computational Aerodynamics [NAL-SP-16] p 299 N93-19273
Numerical computations using multi-domain technique p 299 N93-19277
Monte Carlo simulation of normal shock wave. Part 1: Lennard-Jones potential p 300 N93-19279
Rarefied gas numerical wind tunnel. Part 7: OREX p 382 N93-19280
Numerical simulation of unsteady large scale separated flow around oscillating airfoil p 300 N93-19285
Numerical Wind Tunnel: Requirements and the outline p 383 N93-19288
Numerical Wind Tunnel hardware p 383 N93-19289
The operating system for Numerical Wind Tunnel p 383 N93-19290
The language processor system for the Numerical Wind Tunnel p 383 N93-19291
Generation of longitudinal vortices in supersonic flow p 301 N93-19292
Computation of re-entry flows with two-temperature model p 301 N93-19295
Numerical calculation of hypersonic non-equilibrium flow around OREX p 301 N93-19296
Numerical simulation of hypersonic flow around H-2 Orbiting Plane (HOPE), part 3 p 301 N93-19297
The 3D Navier-Stokes calculation of flow about scramjet inlet with strut p 301 N93-19298
Wind tunnel wall interference correction at subsonic speeds p 304 N93-19320
Two problems reducing the data accuracy in Transonic Wind Tunnel testing p 304 N93-19321
On the roles of wind tunnel testing and computational fluid dynamics in the aircraft development p 341 N93-19322
Low-speed wind tunnel study of the direct side-force characteristics of a joined-wing airplane with an upper fin [DE93-767966] p 988 N93-31189
- National Center for Atmospheric Research, Boulder, CO.**
Meeting review: Third NCAR Research Aircraft Fleet Workshop [PB92-222710] p 223 N93-12818
TDWR 1991 Program Review p 145 N93-14852
A statistical characterization of Denver-area microbursts [AD-A262127] p 845 N93-27675
- National Inst. for Fusion Science, Nagoya (Japan).**
Beta-limiting phenomena in high-aspect-ratio toroidal helical plasmas [NIFS-188] p 569 N93-20546
- National Oceanic and Atmospheric Administration, Boulder, CO.**
Preliminary evaluation of aviation-impact variables derived from numerical models [PB93-190197] p 1034 N93-31202
- National Oceanic and Atmospheric Administration, Silver Spring, MD.**
Vortex wake characteristics of B757-200 and B767-200 aircraft using the tower fly-by technique [PB93-180255] p 878 N93-30387
Vortex wake characteristics of B757-200 and B767-200 aircraft using the tower fly-by technique [PB93-180263] p 878 N93-30388
- National Parachute Technology Council, Albuquerque, NM.**
Facilities and capabilities catalog for landing and escape systems [NASA-RP-1282] p 196 N93-14495
- National Physical Lab., Teddington (England).**
The technical background to standards for shackles [NPL-DMM(A)-51] p 86 N93-11325
A study of the effects of tolerances on rigging screws, turnbuckles, and associated components in BS4429: 1987 [NPL-DMM(A)-53] p 86 N93-11326
The technical background to standards for eyebolts [NPL-DMM(A)-52] p 87 N93-11327
A prediction model for noise from low-altitude military aircraft [AD-A262494] p 852 N93-27662
- National Research Council of Canada, Ottawa (Ontario).**
Noise studies for environmental impact assessment of an outdoor engine test facility p 99 N93-10672
Fly-by voice, a technology demonstration p 526 N93-19918
The flight test and data analysis program for the development of a Boeing/De Havilland Dash 8 simulator model p 512 N93-19930
Fluid/structures interactions. Aircraft considerations p 527 N93-20628
Effect of vortex behavior on loads acting on a 65 deg delta wing oscillating in roll at high incidence p 782 N93-27220
- National Science Foundation, Washington, DC.**
Scientific and engineering research facilities at universities and colleges: 1992 [NSF-92-325] p 192 N93-13407
NSF Science and Technology Centers [NSF-92-104] p 193 N93-13712
- National Space Development Agency, Ibaraki (Japan).**
Research on combined HOPE navigation technology p 533 N93-20428
- National Transportation Safety Board, Washington, DC.**
Aircraft accident report: Atlantic Southeast Airlines, Inc. Flight 2311, uncontrolled collision with terrain, an Embraer EMB-120, N270AS, Brunswick, Georgia, 5 April 1991 [PB92-910403] p 28 N93-11471
Aircraft accident report: Explosive decompression-loss of cargo door in flight, United Airlines Flight 811, Boeing 747-122, N4713U, Honolulu, HI, 24 February 1989 [PB92-910402] p 28 N93-12193
Aircraft accident report: Britt Airways, Inc., d/b/a Continental Express Flight 2574, in-flight structural breakup, EMB-120RT, N33701, Eagle Lake, Texas, September 11, 1991 [PB92-910405] p 143 N93-13426
Aircraft accident/incident summary report: Controlled flight into terrain, Bruno's Inc., Beechjet, N25BR, Rome, Georgia, December 11, 1991 [PB92-910404] p 143 N93-13470
Special investigation report: Piper Aircraft Corporation PA-46 Malibu/Mirage Accidents/Incident, 31 May 1989 - 17 March 1991 [PB92-917007] p 149 N93-15577
Special investigation report: Flight attendant training and performance during emergency situations [PB92-917006] p 310 N93-16834
Aircraft accident report: Tomy International, Inc., d/b/a Scenic Air Tours flight 22, Beech Model E18S, N342E in-flight collision with terrain, Mount Haleakala, Maui, Hawaii, 22 April 1992 [PB93-910401] p 705 N93-25827
Annual review of aircraft accident data: US general aviation calendar year 1989 [PB93-160687] p 790 N93-27033
Aircraft accident report: Takeoff stall in icing conditions. USAIR Flight 405 FOKKER F-28, N485US, LaGuardia Airport, Flushing, New York, 22 March 1992 [PB93-910402] p 790 N93-27034
Aircraft accident report: Controlled collision with terrain GP Express Airlines, Inc., Flight 861, A Beechcraft C99, N118GP, Anniston, Alabama, 8 June 1992 [PB93-910403] p 790 N93-27035
- National Weather Service, Kansas City, MO.**
Proceedings of the National Weather Service Aviation Workshop: Postprint volume [PB92-176148] p 94 N93-11803
- Naval Academy, Annapolis, MD.**
The unified method of aeroelasticity p 372 N93-18143
- Naval Aerospace Medical Research Lab., Pensacola, FL.**
Performance-based testing and success in Naval advanced flight training [AD-A260838] p 717 N93-25933
- Naval Air Development Center, Warminster, PA.**
A primer on polynomial resultants [AD-A246883] p 98 N93-11463
Fatigue crack growth in AerMet 100 steel [AD-A249068] p 74 N93-12248
- Naval Air Rework Facility, North Island, CA.**
Particulate emissions from gas turbine engines [AD-A261374] p 725 N93-26339
- Naval Air Station, Norfolk, VA.**
Helicopter crash survival at sea: United States Navy/Marine Corps experience 1977-1990 p 493 N93-19687
- Naval Air Warfare Center, Patuxent River, MD.**
Standardization of precipitation static test methods and equipment for the Navy [AD-A257025] p 165 N93-15361
F/A-18 controls released departure recovery flight test evaluation [AD-A256522] p 189 N93-15396
Software design document for the generic avionics data bus tool kit [AD-A259329] p 519 N93-21259
Applications of stress envelope concepts to aircraft EMP and lightning survivability p 704 N93-24898
- Naval Air Warfare Center, Trenton, NJ.**
Determination of surface heat transfer and film cooling effectiveness in unsteady wake flow conditions p 902 N93-29933
- Naval Air Warfare Center, Warminster, PA.**
HIP consolidation of aluminum-rich intermetallic alloys and their composites [NAWCADWAR-92003-60] p 199 N93-14726
A neural network prototype for predicting F-14B strains at the B.L. 10 longeron [AD-A255272] p 165 N93-15004
Stress corrosion susceptibility of ultra-high strength steels for Naval aircraft applications [AD-A256126] p 199 N93-15189
- Naval Aviation HQ, Yeovil (England).**
Royal Naval helicopter ditching experience p 492 N93-19684
- Naval Civil Engineering Lab., Port Hueneme, CA.**
An experimental examination of the thermal and acoustic environments on runway joint seals [AD-A257965] p 382 N93-17734
- Naval Command, Control and Ocean Surveillance Center, San Diego, CA.**
Advanced Unmanned Search System (AUSS) supervisory command, control and navigation [AD-A263171] p 793 N93-28990
Uplink laser propagation measurements through the sea surface, haze and clouds [AD-A264687] p 935 N93-30553
- Naval Oceanographic and Atmospheric Research Lab., Bay Saint Louis, MS.**
Embedded training capabilities for the LAMPS MK 3 system [AD-A250697] p 49 N93-11838
- Naval Oceanographic Office, Bay Saint Louis, MS.**
Adaptive EAGLE dynamic solution adaptation and grid quality enhancement p 788 N93-27464
- Naval Postgraduate School, Monterey, CA.**
A method of testing two-dimensional airfoils [AD-A253210] p 17 N93-10375
Experimental and analytical investigation of the vibration characteristics of a remotely piloted helicopter [AD-A256131] p 163 N93-14248
Extended surface heat sinks for electronic components: A computer optimization [AD-A256134] p 218 N93-14254
The V-22 Osprey: A case analysis [AD-A256445] p 164 N93-14601
Modeling and control of a trailing wire antenna towed by an orbiting aircraft [AD-A256450] p 219 N93-14610
Analysis of in-flight structural failures of P-3C wing leading edge segments [AD-A256212] p 165 N93-15238
Flowfield study of a close-coupled canard configuration [AD-A256311] p 139 N93-15245

- Prediction of turbine cascade flows with a quasi-three-dimensional rotor viscous code and the extension of the algebraic turbulence model
[AD-A256831] p 223 N93-15635
- Upgrade and extension of the data acquisition system for propulsion and gas dynamic laboratories
[AD-A256836] p 235 N93-15637
- Atomization of JP-10/B4C gelled sury fuel
[AD-A256827] p 391 N93-15686
- Computational investigations of a NACA 0012 airfoil in low Reynolds number flows
[AD-A257300] p 288 N93-15920
- Static pressure measurements of the shock-boundary layer interaction in a simulated fan passage
[AD-A256724] p 361 N93-15979
- Optimization of an internally finned rotating heat pipe
[AD-A256725] p 453 N93-15980
- Correction of inertial measurements using GPS updates for underwater navigation
[AD-A257329] p 317 N93-15988
- Quantitative-force measurements of pneumatic control on a wing/stroke model
[AD-A257343] p 289 N93-16157
- Statistical fatigue analysis of the SH-60B servo beam rail component
[AD-A257474] p 332 N93-17660
- A database approach to aircraft carrier airplan production
[AD-A257737] p 240 N93-17666
- Design of robust suboptimal controllers for a generalized quadratic criterion
[AD-A257746] p 372 N93-17670
- X-ray diffraction and electron microscope studies of Yttria Stabilized Zirconia (YSZ) ceramic coatings exposed to vanadia
[AD-A258055] p 392 N93-17676
- A multi-faceted engineering study of aerodynamic errors of the Service Aircraft Instrumentation Package (SAIP)
[AD-A258059] p 293 N93-17677
- Preliminary analysis of the J-52 aircraft engine component improvement program
[AD-A257640] p 363 N93-17686
- IR imaging for combustion characteristics and optical properties of boron/boron oxide
[AD-A257747] p 393 N93-17693
- An investigation of two-propeller tilt wing V/STOL aircraft flight characteristics
[AD-A257751] p 332 N93-17694
- Analysis of consolidation of intermediate level maintenance for Atlantic Fleet T700-GE-401 engines
[AD-A257754] p 363 N93-17695
- Flowfield computations over the Space Shuttle orbiter with a proposed canard at a Mach number of 5.8 and 50 deg angle of attack
[AD-A258058] p 293 N93-17756
- A computational and experimental investigation of the propulsive and lifting characteristics of oscillating airfoils and airfoil combinations in incompressible flow
[AD-A258019] p 294 N93-17819
- Identification and control of non-linear time-varying dynamical systems using artificial neural networks
[AD-A257595] p 372 N93-18193
- RPH preliminary design, trend analysis and initial analysis of the NPS hummingbird
[AD-A257854] p 338 N93-18304
- Numerical analysis of the flow in a turbulent rectangular duct simulating the cooling passages in a turbine blade
[AD-A257855] p 420 N93-18305
- Automatic pulse shaping with the AN/FPN-42 and AN/FPN-44A Loran-C transmitters
[AD-A257860] p 319 N93-18309
- Lift enhancement using a close-coupled oscillating canard
[AD-A257877] p 296 N93-18336
- An investigation of a prototype OASYS effectiveness in maneuvering flight
[AD-A257901] p 338 N93-18339
- Study of statistical variations of load spectra and material properties on aircraft fatigue life
[AD-A257961] p 339 N93-18451
- Experimental study of the effect of helical grooves on an infinite cylinder
[AD-A260890] p 751 N93-25912
- Model fan passage flow simulation
[AD-A261613] p 752 N93-26167
- Special tooling disposition for aircraft entering post production support
[AD-A261614] p 678 N93-26168
- Trailing vortex/tree-surface interaction
[AD-A261654] p 701 N93-26195
- Development and testing of the digital control system for the Archytas unmanned air vehicle
[AD-A261656] p 729 N93-26196
- Unsteady airfoil flow solutions on moving zonal grids
[AD-A261925] p 701 N93-26198
- Considerations for space and naval aviation applications of ferroelectric memory
[AD-A261300] p 759 N93-26294
- Thermally induced stresses in a composite exposed to fire
[AD-A261714] p 737 N93-26371
- AEW aircraft design
[AD-A261800] p 718 N93-26444
- The design of a robust autopilot for the Archytas prototype via linear quadratic synthesis
[AD-A262151] p 820 N93-27546
- Testing a wheeled landing gear system for the TH-57 helicopter
[AD-A262152] p 806 N93-27547
- Estimating characteristic life and reliability of an aircraft engine component improvement in the early stages of the implementation process
[AD-A262118] p 815 N93-28184
- Modification and calibration of the Naval Postgraduate School Academic Wind Tunnel
[AD-A262092] p 823 N93-28189
- An analysis of the correlation between the J52 engine component improvement program and improved maintenance parameters
[AD-A262062] p 816 N93-28984
- Mathematical modeling and control law development for the atmospheric monitoring and control system of the Controlled Environment Research Chamber (CERC) at NASA Ames Research Center
[AD-A261978] p 911 N93-29436
- Three-dimensional fiber-optic LDV measurements in the endwall region of a linear cascade of controlled-diffusion stator blades
[AD-A263513] p 933 N93-29968
- Preliminary development of a VTOL unmanned air vehicle for the close-range mission
[AD-A263514] p 933 N93-29969
- A concluding study of the altitude determination deficiencies of the Service Aircraft Instrumentation Package (SAIP)
[AD-A263515] p 897 N93-29971
- Naval Research Lab., Washington, DC.**
Software requirements for the A-7E aircraft
[AD-A255746] p 229 N93-15052
- A parallel implicit incompressible flow solver using unstructured meshes
[AD-A263395] p 931 N93-29851
- Naval Safety Center, Norfolk, VA.**
Trans-cockpit authority gradient in Navy/Marine aircraft mishaps
p 146 N93-15016
- Naval Surface Warfare Center, Bethesda, MD.**
Unsteady vortex loop/dipole theory applied to the work and acoustics of an ideal low speed propeller
[AD-A264057] p 876 N93-29891
- Some implications of a differential turbomachinery equation with viscous correction
[AD-A264693] p 935 N93-30571
- Naval Surface Warfare Center, Dahlgren, VA.**
Detailed near surface flow about yawed, stranded cables
[AD-A257382] p 418 N93-15857
- Nevada Univ. System, Reno.**
Natural and augmented snowfall growth processes and their interactions with the natural and modified aerosol
[PB93-153096] p 755 N93-25874
- Nissan Motor Co. Ltd., Tokyo (Japan).**
Numerical simulations of hypersonic rarefied transition regime flows: DSMC method and Navier-Stokes computation
p 299 N93-19278
- Numerical simulation of flows in a supersonic air intake
p 303 N93-19314
- North Carolina Agricultural and Technical State Univ., Greensboro.**
Flight simulator for hypersonic vehicle and a study of NASP handling qualities
p 530 N93-19456
- Uniform roughness studies
[WL-TR-92-3041] p 751 N93-25951
- North Carolina State Univ., Raleigh.**
Experimental investigation of the effects of aft blowing with various nozzle exit geometries on a 3.0 caliber tangent ogive at high angles of attack: Forebody pressure distributions
[NASA-CR-190935] p 22 N93-11605
- An investigation of the effects of aft blowing on a 3.0 caliber tangent ogive body at high angles of attack
[NASA-CR-190934] p 24 N93-12004
- Modeling of turbulent supersonic H₂-air combustion with an improved joint beta PDF
[NASA-CR-191929] p 391 N93-16389
- Mean flow interactions of a counter-rotating propeller
p 552 N93-20289
- A k-omega-multivariate beta PDF for supersonic combustion
[NASA-CR-191930] p 537 N93-21749
- A new LU-SGS flow solver for calculating reentry flows
p 698 N93-25759
- Northern Research and Engineering Corp., Woburn, MA.**
Alternative systems for fuel gas boosters for small gas turbine engines
[PB92-223049] p 212 N93-12977
- Northrop Corp., Hawthorne, CA.**
F-15 composite engine access door
p 920 N93-30442
- Lessons learned for composite structures
p 920 N93-30444
- A Rayleigh-Ritz analysis methodology for cutouts in composite structures
p 923 N93-30869
- Northrop Corp., Pico Rivera, CA.**
A procedure for defining lightning risk to air vehicles
p 703 N93-24885
- Northwest Airlines, Inc., Saint Paul, MN.**
Results of in-service evaluation of wind shear systems
p 146 N93-14856
- Norton AFB Ballistic Missile Office, CA.**
A method for investigating human factor aspects of military aircraft accidents
p 491 N93-19656
- Notre Dame Univ., IN.**
An experimental and computational investigation of slender wings undergoing wing rock
p 187 N93-13915
- The unsteady aerodynamics of a delta wing undergoing large-amplitude pitching motions
p 134 N93-13929
- Wake similarity and vortex formation for two-dimensional bluff bodies
p 138 N93-15101
- Exodus: Prime Mover
[NASA-CR-192051] p 332 N93-17803
- Hermes CX-7: Air transport system design simulation
[NASA-CR-192082] p 335 N93-18056
- Arrow 227: Air transport system design simulation
[NASA-CR-192053] p 336 N93-18063
- The S.T.o.R.M. (tm): Air transport system design simulation
[NASA-CR-192070] p 338 N93-18349
- JEFF: Air transport system design simulation
[NASA-CR-192069] p 338 N93-18350
- The F-92 RELIANT: Air transport system design simulation
[NASA-CR-192050] p 339 N93-18386
- Design study to simulate the development of a commercial transportation system
p 894 N93-29718
- Structural design using neural networks
p 942 N93-31029
- Oak Ridge National Lab., TN.**
Ceramic Technology Project
[DE92-018748] p 73 N93-11442
- Variable speed rotary compressor and adjustable speed drive efficiencies measured in the laboratory
[DE92-040026] p 222 N93-15278
- Materials development program, ceramic technology project addendum to program plan: Cost effective ceramics for heat engines
[DE93-003663] p 394 N93-18537
- Using fuzzy behaviors for the outdoor navigation of a car with low-resolution sensors
[DE93-002428] p 706 N93-25120
- Process optimization of Hexoloy SX-SiC towards improved mechanical properties
[DE93-007813] p 826 N93-28564
- Microwave processing of silicon nitride for advanced gas turbine applications
[DE93-007910] p 917 N93-29767
- Characterization of ceramic composite materials for gas turbine applications
[DE93-009719] p 905 N93-30168
- Office National d'Etudes et de Recherches Aérospatiales, Bagnoux (France).**
Aerothermic calculations of flows in interdisc cavities of turbines
p 903 N93-29947
- Office National d'Etudes et de Recherches Aérospatiales, Paris (France).**
Tests of models equipped with TPS in low speed ONERA F1 pressurized wind tunnel
p 213 N93-13201
- Detailed analysis of wing-nacelle interaction for commercial transport aircraft
p 213 N93-13203
- Photoluminescent thermography in hypersonic blowdown wind tunnel: Feasibility study with pinpoint measurement
[ONERA-NT-1992-8] p 297 N93-18617
- Electron beam probing of blow-down hypersonic flows
[ONERA-NT-1992-7] p 298 N93-18701
- RAMSES: Multi-spectral experimental radar station installed on board the Transall
p 550 N93-19925
- Topological approach for the study of electromagnetic coupling
[ONERA-P-1992-2] p 551 N93-20230
- Modelisation and computation of composite materials
p 537 N93-21518

- Calculation of fully three-dimensional separated flow with an unsteady viscous-inviscid interaction method
p 786 N93-27455
- Sonic boom problem for future highspeed aircraft
[ONERA-NT-1990-3] p 876 N93-30020
- Computation of far-field helicopter rotor tone noise
[ONERA-P-1990-5] p 943 N93-30110
- Contribution to the study of the interaction between acoustic waves and coherent structures induced by a prismatic cylinder in a rectangular cavity
[ONERA-NT-1990-10] p 918 N93-30203
- Office of the White House Press Secretary, Washington, DC.**
- Aeronautics and space report of the President: Fiscal year 1992 activities
p 854 N93-27041
- Ohio Aerospace Inst., Brook Park.**
- Navier-Stokes analysis of radial turbine rotor performance
[NASA-CR-191153] p 815 N93-28609
- Analysis of unsteady wave processes in a rotating channel
[NASA-CR-191154] p 816 N93-28617
- Three-dimensional numerical simulation of gradual opening in a wave rotor passage
[NASA-CR-191157] p 900 N93-29072
- Ohio State Univ., Cleveland.**
- Hypersonic reconnaissance aircraft
[NASA-CR-192049] p 333 N93-17804
- Advanced hypersonic aircraft design
[NASA-CR-192046] p 334 N93-18037
- Compatibility of potential reinforcing ceramics with Ni and Fe aluminides
[NASA-CR-192232] p 394 N93-18784
- Ohio State Univ., Columbus.**
- Time dependent heat transfer rates in high Reynolds number hypersonic flowfields
p 216 N93-13664
- An investigation of jet engine test cell aerodynamics by means of scale model test studies with comparisons to full-scale test results
p 193 N93-14060
- A manned hypersonic reconnaissance vehicle which does not require airborne fueling
p 333 N93-17888
- SR-SCARLET 1: Peregrin
[NASA-CR-192048] p 337 N93-18155
- Design concepts for the development of cooperative problem-solving systems
[NASA-CR-192708] p 707 N93-25261
- Design of a cooperative problem-solving system for enroute flight planning: An empirical study of its use by airline dispatchers
[NASA-CR-192709] p 707 N93-25330
- Operation of the helicopter antenna radiation prediction code
[NASA-CR-193259] p 1030 N93-31110
- Ohio Univ., Athens.**
- GPS Interferometry
[NASA-CR-192301] p 319 N93-18873
- Okayama Univ. of Science (Japan).**
- Development of a boundary element method program for numerical analysis of supersonic unsteady flow
p 300 N93-19283
- Oklahoma State Univ., Stillwater.**
- Chaotic vortical motion in the near region of a plane jet
p 131 N93-13493
- Oklahoma Univ., Norman.**
- Computational analysis of hypersonic flows past elliptic-cone waveriders
[NASA-CR-191304] p 138 N93-14767
- Computational analysis of hypersonic flows past generalized cone-derived waveriders
p 483 N93-20288
- Old Dominion Univ., Norfolk, VA.**
- Navier-Stokes dynamics and aeroelastic computations for vortical flows, buffet and aeroelastic applications
[NASA-CR-190692] p 17 N93-10098
- Effect of passive flow-control devices on turbulent low-speed base flow
p 82 N93-10304
- A finite element method for nonlinear panel flutter
p 84 N93-10472
- Control of low-speed turbulent separated flow over a backward-facing ramp
p 219 N93-14475
- Polymer infiltration studies
[NASA-CR-191652] p 200 N93-15431
- Volume 2: Explicit, multistage upwind schemes for Euler and Navier-Stokes equations
[NASA-CR-191647] p 418 N93-16558
- Approaches to control of the large angle magnetic suspension test fixture
[NASA-CR-191890] p 381 N93-16695
- Boundary-layer measurements on a high Reynolds number three-element airfoil
p 292 N93-16787
- Multidisciplinary design optimization using response surface analysis
p 330 N93-16796
- Methodology for sensitivity analysis, approximate analysis, and design optimization in CFD for multidisciplinary applications
[NASA-CR-192172] p 552 N93-20297

- Grid sensitivity for aerodynamic optimization and flow analysis
[NASA-CR-192980] p 694 N93-25117
- A computational aerodynamic design optimization method using sensitivity analysis
p 716 N93-25552
- Nonlinear analyses of composite aerospace structures in sonic fatigue
[NASA-CR-193124] p 930 N93-29154
- Topology and grid adaption for high-speed flow computations
[NASA-CR-4216] p 934 N93-30375
- Design and implementation of fuzzy logic controllers
[NASA-CR-193268] p 1038 N93-31649
- Large angle magnetic suspension test fixture
[NASA-CR-193123] p 1015 N93-31836
- Operational Test and Evaluation Force, Norfolk, VA.**
- Follow-on operational test and evaluation of the NAVSTAR global positioning system air integration/installation program
[AD-A263067] p 793 N93-27925
- Orincon Corp., La Jolla, CA.**
- Conditioned based machinery maintenance (helicopter fault detection)
[AD-A255796] p 329 N93-16396
- Oxford Univ. (England).**
- Time-frequency domain analysis of vibration signals for machinery diagnostics. 3: The present power spectral density
[OUEL-1911/92] p 69 N93-11707
- Mathematical problems in inviscid hypersonic flow
p 131 N93-13451
- An experimental study of under-expanded jets
p 696 N93-25467
- Measurement of turbulent spots and intermittency modelling at gas-turbine conditions
p 902 N93-29934

P

- Pacific Northwest Lab., Richland, WA.**
- Ultra wide band 3-D cross section (RCS) holography
[DE92-019133] p 89 N93-11802
- An evaluation of thermal energy storage options for precooled gas turbine inlet air
[DE93-005980] p 754 N93-24975
- A demonstration of simple airfoils: Structural design and materials choices
[DE93-007882] p 789 N93-28662
- Paderborn Univ. (Germany).**
- Neural network based condition monitoring
p 230 N93-15183
- Paris VI Univ. (France).**
- Modellisation and computation of composite materials
p 537 N93-21518
- Pennsylvania State Univ., University Park.**
- Explicit Navier-Stokes computation of turbomachinery flows
p 83 N93-10370
- The prediction of noise radiation from supersonic elliptic jets
p 100 N93-10684
- Analysis and design of planar and non-planar wings for induced drag minimization
[NASA-CR-191274] p 131 N93-13463
- Multi-point inverse design of isolated airfoils and airfoils in cascade in incompressible flow
p 163 N93-14462
- Thermoviscoelastic analysis of pavements
p 379 N93-16313
- Experimental analysis of the aeroacoustics of cascaded airfoils
[AD-A257945] p 420 N93-18121
- Prediction of forces and moments for hypersonic flight vehicle control effectors
[NASA-CR-193033] p 728 N93-24762
- Supersonic shock wave/vortex interaction
[NASA-CR-192917] p 695 N93-25249
- An experimental study of the sources of fluctuating pressure loads beneath swept shock/boundary-layer interactions
[NASA-CR-192918] p 749 N93-25266
- Heat transfer measurements in swept shock wave/turbulent boundary-layer interactions
p 750 N93-25705
- Reduction in size and unsteadiness of a VTOL ground vortex by ground fences
[NASA-CR-192997] p 700 N93-26049
- Oxides of nitrogen emissions from turbulent hydrocarbon/air jet diffusion flames, phase 2
[PB93-152478] p 756 N93-26533
- A model-based approach for detection of objects in low resolution passive millimeter wave images
[NASA-CR-193161] p 808 N93-28418
- Penn State axial flow turbine facility: Performance and nozzle flow field
p 1032 N93-31588
- Pennsylvania Univ., Philadelphia.**
- Action composition for the animation of natural language instructions
[AD-A254963] p 228 N93-12554
- Phillips Lab., Kirtland AFB, NM.**
- Vortex shedding by blunt/bluff bodies at high Reynolds numbers. Volume 4: Rectangles
[AD-A264154] p 877 N93-30151
- Vortex shedding by blunt/bluff bodies at high Reynolds numbers. Volume 1: Data analysis
[AD-A264151] p 877 N93-30171
- Vortex shedding by Blunt/Bluff bodies at high Reynolds numbers. Volume 2: Cylinders, octagon, hexagon
[AD-A264152] p 877 N93-30172
- Vortex shedding by blunt/bluff bodies at high Reynolds numbers. Volume 3: Cubes
[AD-A264153] p 877 N93-30173
- Physics and Electronics Lab. TNO, The Hague (Netherlands).**
- Definition study PHARUS
[AD-A256560] p 221 N93-14805
- Pittsburgh State Univ., KS.**
- Industry survey of space system cost benefits from New Ways Of Doing Business
p 454 N93-17325
- Pittsburgh Univ., PA.**
- Platinum-modified diffusion aluminide coatings on nickel-base superalloys
[AD-A263597] p 917 N93-29981
- Poitiers Univ. (France).**
- Experimental study of heat transfer close to a plane wall heated in the presence of multiple injections (subsonic flow)
p 901 N93-29931
- Politecnico di Milano (Italy).**
- A Navier-Stokes solver with different turbulence models applied to film-cooled turbine cascades
p 904 N93-29962
- PPG Industries, Inc., Huntsville, AL.**
- T-38 forward windshield development and performance demonstration report
[AD-A259240] p 513 N93-20579
- Pratt and Whitney Aircraft, East Hartford, CT.**
- Thermal barrier coating life prediction model development, phase 2
[NASA-CR-189111] p 198 N93-12589
- Creep fatigue life prediction for engine hot section materials (isotropic)
[NASA-CR-189221] p 364 N93-18578
- Pratt and Whitney Aircraft, West Palm Beach, FL.**
- Fatigue in single crystal nickel superalloys
[AD-A254603] p 74 N93-12237
- Fatigue in single crystal nickel superalloys
[AD-A254704] p 198 N93-12746
- F100 second stage fan disk bolt hole crack propagation ferris wheel test
p 177 N93-14897
- Fatigue in single crystal nickel superalloys
[AD-A258038] p 393 N93-17704
- Fatigue in single crystal nickel superalloys
[AD-A259191] p 536 N93-20275
- Fatigue in single crystal nickel superalloys
[AD-A260709] p 736 N93-25843
- Fatigue in single crystal nickel superalloys
[AD-A265451] p 1019 N93-31795
- Pratt and Whitney Aircraft of Canada Ltd., Longueuil (Quebec).**
- Prediction of jet impingement cooling scheme characteristics (airfoil leading edge application)
p 932 N93-29941
- PRC Systems Services Co., Edwards, CA.**
- High-temperature strain measurement techniques: Current developments and challenges
p 217 N93-13669
- Princeton Economic Research, Inc., NJ.**
- Preliminary studies of planning and flight strip use as air traffic controller memory aids
[DOT/FAA/CT-TN92/22] p 503 N93-21759
- Princeton Univ., NJ.**
- Studies of a flat wake rotor theory
[NASA-CR-190936] p 25 N93-12343
- Robust nonlinear feedback guidance for an aerospace plane: A geometric approach
p 189 N93-14835
- Wind shear related research at Princeton University
p 145 N93-14854
- Chemical kinetic and aerodynamic structures of flames
[AD-A256015] p 391 N93-15931
- Hypersonics revisited
p 781 N93-27167
- Aircraft guidance for wind shear avoidance: Decision-making under uncertainty
p 889 N93-31005
- Purcell (Anthony) Consultants, Luenburg (Nova Scotia).**
- Acoustic noise generation at the air/ocean boundary
[DREA-CR-90-445] p 99 N93-10642
- Purdue Univ., Elkhart, IN.**
- Performance of thermal adhesives in forced convection
p 924 N93-30974
- Purdue Univ., Indianapolis, IN.**
- Applications of active adaptive noise control to jet engines
[NASA-CR-192277] p 522 N93-21210

Purdue Univ., West Lafayette, IN.

- Unsteady propeller/wing aerodynamic interactions
p 24 N93-12190
- Hypervelocity scramjet combustor-nozzle analysis and design
[NASA-CR-190965] p 60 N93-12214
- Application of a solution adaptive grid to flow over an embedded cavity
p 130 N93-13141
- The design of a long range megatransport aircraft
[NASA-CR-192077] p 332 N93-17711
- Hot film wall shear instrumentation for compressible boundary layer transition research
[NASA-CR-191360] p 294 N93-17855
- The WINCOF-I code: Detailed description
[NASA-CR-190779] p 677 N93-24760
- Transient performance of fan engine with water ingestion
[NASA-CR-190778] p 677 N93-25134
- Simulation of vortex bursting
p 699 N93-25881
- Development of an unstructured solution adaptive method for the quasi-three-dimensional Euler and Navier-Stokes equations
[NASA-CR-193241] p 930 N93-29213
- Design of a turbofan powered regional transport aircraft
p 894 N93-29721
- Heat transfer with moderate free stream turbulence
p 932 N93-29936
- Turbulence characteristics of an axisymmetric reacting flow
[NASA-CR-4110] p 877 N93-30373

Q**Queensland Univ., Brisbane (Australia).**

- Experiments on smooth cantilevered circular cylinders in a low-turbulence uniform flow. Part 2: Fluctuating loads on a cantilever of aspect ratio 30
[PB93-110500] p 555 N93-21382
- Experiments on smooth cantilevered circular cylinders in low-turbulence uniform flow. Part 1: Mean loading with aspect ratios in the range 4 to 30
[PB93-111763] p 555 N93-21383

Quest Integrated, Inc., Kent, WA.

- Active control of combustion instability in a ramjet using large-eddy simulations
[AD-A255226] p 175 N93-14111

R**Rafael Armament Development Authority, Haifa (Israel).**

- Information-based criteria of terrain navigability. Part 1: Data-base analysis
p 793 N93-27178
- Airfoil stability in turbulent flow
p 781 N93-27212

Rahikone Oy (Finland).

- Steering system of a vehicle, such as a snow removing machine for airfields
[CA-PATENT-APPL-SN-1293201] p 83 N93-10367

RAND Corp., Santa Monica, CA.

- Numerical simulation of hypersonic aerodynamics and the computational needs for the design of an aerospace plane
[AD-A260681] p 699 N93-25894
- Aerospace-plane flights and stratospheric ozone: Review and preliminary assessment of the National Aerospace Plane (NASP) operations
[RAND/N-3464-AF] p 755 N93-26327

Regional Engineering Coll., Kerala (India).

- New adaptive controllers for aircraft
p 847 N93-27180

Rensselaer Polytechnic Inst., Troy, NY.

- An investigation of dynamic stress reduction of multi-body aircraft using active gust control
p 187 N93-13916
- Design and analysis of curved composite components for rotorcraft fuselage frames
p 716 N93-25701
- Structural dynamic analysis of bearingless rotor blade
p 717 N93-25719
- Keynote address: Unsteady, multimode transition in gas turbine engines
p 901 N93-29927

Research and Development Labs., Culver City, CA.

- Summer research program (1992). High School Apprenticeship Program (HSAP) reports. Volume 16: Arnold Engineering Development Center Civil Engineering Laboratory
[AD-A262024] p 945 N93-29396

Research Triangle Inst., Hampton, VA.

- Comparison of simulated and actual wind shear radar data products
p 490 N93-19610

Resource International, Inc., Columbus, OH.

- State of the art review of rutting and cracking in pavements
p 380 N93-16316

Rhode Island Univ., Kingston.

- Mechanisms and modelling of environment-dependent fatigue crack growth in a nickel based superalloy
[AD-A253967] p 71 N93-10717

Rice Univ., Houston, TX.

- The semi-discrete Galerkin finite element modelling of compressible viscous flow past an airfoil
[NASA-CR-192161] p 483 N93-20018
- Numerical study of cavity natural convection flow with augmenting and counteracting effects by projection finite element method
p 749 N93-25540

Rockwell International Corp., Cedar Rapids, IA.

- Airborne doppler radar research at Rockwell International
p 489 N93-19602

Rockwell International Corp., Downey, CA.

- Zoning of aircraft: A review of the definitions
p 703 N93-24880
- Strategic avionics technology definition studies. Subtask 3-1A: Electrical Actuation (ELA) systems
[NASA-CR-193237] p 914 N93-29215

Rolls-Royce, Inc., Atlanta, GA.

- Advanced materials in gas turbine engines: An assessment
[PNR-90946] p 58 N93-11105
- Development of advanced carbon-carbon annular flameholders for gas turbines
[PNR-90947] p 58 N93-11106
- Small particle impact damage in carbon-carbon composites
[PNR-90948] p 73 N93-11107

Rolls-Royce Ltd., Bristol (England).

- RB211-524B disc and drive cones hot cyclic spinning test
p 177 N93-14895

Rolls-Royce Ltd., Derby (England).

- Neutron diffraction residual stress studies for aero-engine component applications
[PNR-90908] p 85 N93-11014

- Materials: Toward the non-metallic engine
[PNR-90915] p 56 N93-11019

- Application of laminar flow to aero engine nacelles
[PNR-90916] p 20 N93-11020

- An experimental evaluation of prediction methods for contrafans
[PNR-90924] p 56 N93-11023

- Testing for integrity
[PNR-90927] p 56 N93-11024

- The prediction of convective heat transfer in rotating square ducts
[PNR-90929] p 85 N93-11025

- Short fatigue crack growth in a nickel-base superalloy at room and elevated temperature
[PNR-90892] p 72 N93-11031

- A test facility for the thermofluid-dynamics of gas bearing lubrication films
[PNR-90897] p 72 N93-11032

- On the basis of experience: Built in product reliability
[PNR-90932] p 85 N93-11034

- Rotational CARS measurements in a rotating cavity with axial throughflow of cooling air: Oxygen concentration measurements
[PNR-90935] p 72 N93-11035

- Rolls-Royce civil engine technology
[PNR-90936] p 56 N93-11036

- The Trent: Towards greater thrust
[PNR-90937] p 56 N93-11037

- From RB211 to Trent: An ongoing development strategy
[PNR-90938] p 56 N93-11038

- Introduction to the Rolls-Royce design process
[PNR-90939] p 57 N93-11039

- The role of turbomachinery testing for stability in distorted flow
[PNR-90943] p 57 N93-11040

- The application of manufacturing systems engineering for aero engine gears
[PNR-90944] p 86 N93-11054

- Experimental heat transfer results in turbine stators and rotors and a comparison with theory
[PNR-90945] p 57 N93-11055

- Concorde propulsion: Did we get it right? The Rolls-Royce/SNECMA Olympus 593 engine reviewed
[PNR-90970] p 57 N93-11061

- Simultaneous engineering in the design of aero engines
[PNR-90973] p 57 N93-11062

- The Trent family of engines
[PNR-90974] p 58 N93-11063

- Aero engine ceramics: The vision, the reality, and the progress
[PNR-90983] p 72 N93-11066

- Advanced three-shaft engines: Configured for reliability, efficiency, and growth
[PNR-90986] p 58 N93-11068

- Maintainability of large gas turbine aero engines
[PNR-90987] p 58 N93-11069

- A combined experimental and theoretical study of laminar flow control with particular relevance to aero engine nacelles
[PNR-90991] p 20 N93-11070

- Civil aircraft engines: The next generation
[PNR-90962] p 58 N93-11085

- The development of the Rolls-Royce Trent aero gas turbine
[PNR-90949] p 58 N93-11108

- Development of the neutron diffraction technique for the determination of near surface residual stresses in critical gas turbine components
[PNR-90984] p 58 N93-11112

- A European collaborative NLF nacelle flight demonstrator
[PNR-90992] p 20 N93-11113

- A knowledge-based blackboard system to interpret graphical data from vibration tests of gas turbines
[PNR-90993] p 59 N93-11114

- The design and commissioning of an acoustic liner for propeller noise testing in the ARA transonic wind tunnel
[PNR-90880] p 101 N93-11204

- The use of simultaneous engineering for the design and manufacture of the low pressure turbine for the Rolls-Royce Trent engine
[PNR-90887] p 59 N93-11206

- Innovation in engineering
[PNR-90889] p 59 N93-11207

- Simultaneous engineering in aero gas turbine design and manufacture
[PNR-90890] p 59 N93-11208

- The changing nature of design
[PNR-91011] p 48 N93-11334

- Time-dependent predictions and analysis of turbine cascade data in the transonic flow region
[PNR-90957] p 139 N93-15489

- The effect of aircraft inlets on the behaviour of aero engine axial flow compressors
p 422 N93-18722

- Stall in axial flow aero engine compressors
p 422 N93-18723

- Endwall flows and blading design for axial flow compressors
p 423 N93-18730

- Handling and using information systems with new technology
[PNR-90910] p 572 N93-20734

- Satisfying the customer's requirements
[PNR-90988] p 521 N93-20735

- Modelling thermal behaviour of turbomachinery discs and casings
p 903 N93-29949

- Royal Aerospace Establishment, Bedford (England).**

- Introduction of electronic pressure scanning at the Royal Aerospace Establishment
[RAE-TM-AERO-2222] p 23 N93-11882

- The 13 ft by 9 ft low speed wind tunnel facility at DRA (Aerospace Division) Bedford (England)
[RAE-TM-AERO-2228] p 23 N93-11883

- Strain-gauge balance performance and internal temperature gradients measured in a cryogenic environment
[RAE-TM-AERO-2232] p 68 N93-11906

- Royal Aerospace Establishment, Farnborough (England).**

- The measurement of the velocity field induced by a gust generator in a closed-circuit subsonic wind-tunnel
[RAE-TM-MAT/STR-1102] p 67 N93-11435

- Developments in icing test techniques for aerospace applications in the RAE Pyestock (England) altitude test facility
[RAE-TM-P-1214] p 48 N93-11485

- Royal Aircraft Establishment, Farnborough (England).**

- An evaluation of a method of reconstituting fatigue loading from Rainflow counting
[RAE-TR-89057] p 82 N93-10198

- Flight test and analysis procedures for new handling criteria
[RAE-TM-FM-26] p 47 N93-10803

- Further noise measurements in a slotted cryogenic wind tunnel
[RAE-TM-AERO-2201] p 101 N93-10805

- Measurements and computations of external heat transfer and film cooling in turbines
[RAE-TM-P-1223] p 722 N93-25455

- Royal Inst. of Tech., Stockholm (Sweden).**

- The numerical solution of low Mach number flow in confined regions by Richardson extrapolation
[TRITA-NA-9207] p 789 N93-29005

- Royal Netherlands Air Force, The Hague.**

- Underlying causes of accidents: Casual networks
p 491 N93-19658

- Royal Norwegian Air Force, Blindern.**

- F-16 accidents: The Norwegian experience
p 492 N93-19674

Royal Signals and Radar Establishment, Malvern (England).

- The development of the speaker independent ARM continuous speech recognition system [RSRE-MEMO-4473] p 87 N93-11383
- Preliminary results on the use of linear discriminant analysis in the ARM continuous speech recognition system [RSRE-MEMO-4511] p 87 N93-11384
- The use of linear discriminant analysis in the ARM continuous speech recognition system [RSRE-MEMO-4512] p 87 N93-11385
- Rutgers - The State Univ., Newark, NJ.**
- F-14 wing lug coating investigation [AD-A257384] p 328 N93-15858

S

Salford Univ. (England).

- Flow prediction for three-dimensional intakes and ducts using viscous-inviscid interaction methods p 218 N93-13953

Samtech S.A., Liege (Belgium).

- Vibration analysis in turbomachines p 1005 N93-32274

San Diego State Univ., CA.

- Cockpit resource management proficiency as a factor of primary flight training [AD-A256995] p 328 N93-16262

San Jose State Univ., CA.

- On the typography of flight-deck documentation [NASA-CR-177605] p 571 N93-19970

Sandia National Labs., Albuquerque, NM.

- Measured data for the Sandia 34-meter vertical axis wind turbine [DE92-019807] p 94 N93-12075
- Wind load design methods for ground-based heliostats and parabolic dish collectors [DE93-002737] p 433 N93-15839
- Stress calculation for the Sandia 34-meter wind turbine using the local circulation method and turbulent wind [DE93-004480] p 560 N93-22045
- Reliability assessment at airline inspection facilities. Volume 1: A generic protocol for inspection reliability experiments [DOT/FAA/CT-92/12-VOL-1] p 704 N93-25110
- A simple, approximate model of parachute inflation [DE93-002465] p 694 N93-25121
- The natural excitation technique (NEX) for modal parameter extraction from operating wind turbines [DE93-010611] p 845 N93-28603
- Reliability assessment at airline inspection facilities. Volume 2: Protocol for an eddy current inspection reliability experiment [DOT/FAA/CT-92/12-VOL-2] p 842 N93-28685
- The development of a parachute system for aerial delivery from high speed cargo aircraft [DE93-008339] p 790 N93-29035
- Ablation problems using a finite control volume technique [DE93-009861] p 942 N93-29187
- Scandinavian Airlines System, Stockholm (Sweden).**
- Flight data and flight safety in SAS p 168 N93-15156

Science Applications International Corp., Santa Clara, CA.

- Principles of nuclear-based explosive detection systems p 497 N93-21861
- PFNA technique for the detection of explosives p 497 N93-21865
- Explosive detection system based on Electronic Neutron Generator (ENG) p 497 N93-21870
- Experience with explosive detection systems in airports p 498 N93-21895

Science Applications International Corp., Torrance, CA.

- Effects of buoyancy on gas jet diffusion flames [NASA-CR-191109] p 935 N93-31031

Science Univ. of Tokyo (Japan).

- Calculations of aerodynamic forces on a wing with thrust using BEM p 300 N93-19286

Scientific-Atlantic, Inc., San Diego, CA.

- Onboard System Evaluation of Rotors Vibration, Engines (OBSERVE) monitoring system [AD-A255366] p 165 N93-15227

Scientific Research Associates, Inc., Glastonbury, CT.

- Two- and three-dimensional blade vortex interactions [NASA-CR-177567] p 293 N93-16942
- Projectile base bleed technology. Part 2: User's guide CMINT computer code, version 5.04-BRL [AD-A258630] p 551 N93-19999

Scintrex Ltd., Concord (Ontario).

- Explosives detection systems for airport security gas chromatographic based devices p 881 N93-30276

Search Technology, Inc., Norcross, GA.

- Specification of adaptive aiding systems [AD-A254537] p 159 N93-12602

Sener Ingenieria y Sistemas S.A., Madrid (Spain).

- Cooling predictions in turbofan engine components p 905 N93-29964

Sensstar Corp., Kanata (Ontario).

- Future directions in aviation security p 880 N93-30274

Sextant Avionique, Saint Medard en Jalles (France).

- Liquid crystal displays replacing the CRT and CLE of future cockpits p 518 N93-19783

Sheffield Univ. (England).

- Identification of system dynamics of a high incidence research model [RR-407] p 339 N93-18507

Sherbrooke Univ. (Quebec).

- Harmonic analysis of the aerodynamic forces on a Darnius rotor p 18 N93-10551

Sikorsky Aircraft, Stratford, CT.

- The NASA/industry Design Analysis Methods for Vibrations (DAMVIBS) program: Sikorsky Aircraft: Advances toward interacting with the airframe design process p 515 N93-21315

Societe Francaise d'Instruments de Mesure, Massy.

- Ground Support Equipment (GSE) for Aircraft Condition Monitoring System (ACMS) p 110 N93-15158

Societe Nationale d'Etude et de Construction de Moteurs d'Aviation, Evry (France).

- Fatigue of turboengine discs [DS-2136] p 364 N93-18149

- Control of in-service damage: Application to aircraft engines [DS-2027] p 364 N93-18151

- Supersonic transport: Which material for the engine [DS-2023] p 522 N93-21459

Societe Nationale d'Etude et de Construction de Moteurs d'Aviation, Moissy-Cramayel (France).

- Turbomachinery and potential computations [DS-2026] p 363 N93-17740

- Direct numerical simulation of combustion in turbulent supersonic flow [DS-2138] p 393 N93-17746

- Improving military transport aircraft through highly integrated engine-wing design [DS-1607] p 333 N93-17850

- Turbine engine combustor design at SNECMA [DS-2129] p 363 N93-17851

- The beta-CEZ, a new high performance titanium alloy for aerospace engines [DS-2022] p 393 N93-17852

- Aerodynamic design and analysis of fans using 3D computational codes [DS-2140] p 294 N93-17880

- The technological evolution of high thrust turbine engines [DS-1881] p 364 N93-17882

- Optimization and sensitivity computations for the conception of internal ventilation system in the aircraft engine [ETN-93-93375] p 521 N93-20913

Societe Nationale d'Etude et de Construction de Moteurs d'Aviation, Paris (France).

- SNECMA M88 engine development status [ASME-90-GT-118] p 363 N93-17849

Societe Nationale d'Etudes et de Construction de Moteurs Aeronautiques, Moissy-Cramayel (France).

- Flight analysis of air intake/engine compatibility p 161 N93-13212

- LARZAC HP turbine disk crack initiation and propagation spin pit test p 176 N93-14892

Software Productivity Consortium, Herndon, VA.

- Domain engineering validation case study: Synthesis for the air traffic display/collision warning monitor domain version 01.00.03 [AD-A259407] p 503 N93-21671

Sony Corp. of America, San Diego, CA.

- Computer-controlled alignment for a 2000-line color monitor p 886 N93-30324

Sorbent Technologies Corp., Twinsburg, OH.

- Development and demonstration of a new filter system to control emissions during jet engine testing [AD-A261203] p 755 N93-26243

Southampton Univ. (England).

- An experimental and a theoretical investigation of rotor pitch damping using a model rotor p 47 N93-10322

- Application of eigenstructure assignment to the control of powered lift combat aircraft p 64 N93-11871

Southeastern Center for Electrical Engineering Education, Inc., Saint Cloud, FL.

- Inflight evaluation of an acoustic orientation instrument [AD-A260752] p 719 N93-25909

- Design, fabrication, and testing of a three-dimensional acoustic orientation instrument (3-D AOI): Drawings, engineering and associated lists (conceptual and development design) [AD-A260934] p 760 N93-25915

Southwest Research Inst., San Antonio, TX.

- Development of a method to determine the autoxidation of turbine fuels [AD-A260578] p 736 N93-25902

- Effect of a metal deactivator fuel additive on fuel deposition in fuel atomizers at high temperature [AD-A260915] p 736 N93-25914

Space Exploration Association, Cedarville, OH.

- Joining carbon composite fins to titanium heat pipes [AD-A261970] p 825 N93-27667

SRI International Corp., Menlo Park, CA.

- Unified airport pavement design procedure p 380 N93-16318

- Comparison of the electrical charging and discharging environments of multiple aircraft-borne electric-field measurement systems p 704 N93-24887

- Kinetics and energy transfer in nonequilibrium fluid flows [AD-A263612] p 875 N93-29284

Stanford Univ., CA.

- Development and computation of continuum higher order constitutive relations for high-altitude hypersonic flow p 132 N93-13578

- Application of a vectorized particle simulation to the study of plates and wedges in high-speed rarefied flow p 133 N93-13746

- Aeronomy coexperiments on drag-free satellites with proportional thrusters: GP-B and STEP p 195 N93-13922

- Robust controller and estimator design using minimax methods p 229 N93-13925

- Hypersonic panel flutter in a rarefied atmosphere p 188 N93-13928

- Navier-Stokes flowfield computation of wing/rotor interaction for a tilt rotor aircraft in hover p 135 N93-14035

- Aerodynamic design and synthesis of the oblique flying wing supersonic transport p 713 N93-24768

- Computational study of the aerodynamics and control by blowing of asymmetric vortical flows over delta wings p 693 N93-24772

- Direct solutions of the Navier-Stokes equations with application to static aeroelasticity p 748 N93-25259

- Structural and aerodynamic optimization of joined-wing aircraft p 715 N93-25526

- Navier-Stokes simulations of unsteady transonic flow phenomena p 697 N93-25542

- Tangential fuselage blowing on an ogive cylinder p 697 N93-25545

- Analysis of wing wake roll-up using a vortex-in-cell method p 697 N93-25706

- An investigation of photothermal velocimetry for application to transient, high-speed gas flows p 698 N93-25720

- Hypersonic panel flutter in a rarefied atmosphere [NASA-CR-4514] p 780 N93-27084

- An aerodynamic model for one and two degree of freedom wing rock of slender delta wings [NASA-CR-193130] p 781 N93-27150

- The generation of side force by distributed suction [NASA-CR-193129] p 839 N93-27151

- Center for Aeronautics and Space Information Sciences [NASA-CR-193140] p 848 N93-27289

- Turbulence: The chief outstanding difficulty of our subject p 783 N93-27428

- Attitude determination using GPS: Development of an all solid-state guidance, navigation, and control sensor for air and space vehicles based on the global positioning system p 888 N93-30605

- Turbulent drag reduction: Studies of feedback control and flow over riblets p 878 N93-30645

- The numerical simulation of circulation controlled airfoil flowfields p 879 N93-30947

- Strong parallel blade-vortex interaction and noise propagation in helicopter flight p 944 N93-30980

- Experiments in the control of wing rock at high angle of attack using tangential leading edge blowing p 1009 N93-31068

State Univ. of New York, Buffalo.

- Methods and principles for determining task dependent interface content [NASA-CR-190837] p 36 N93-10961

- Modeling variable blowing on a slender cone in hypersonic flow p 138 N93-14836

Sterling Software, Inc., Moffett Field, CA.

- Scientific visualization using the Flow Analysis Software Toolkit (FAST) p 758 N93-25600

Stewart Hughes Ltd., Eastleigh (England).

- Helicopter health monitoring: Current practice and future trends p 169 N93-15179

Strathclyde Univ., Glasgow (Scotland).

Online vibration control of a flexible rotor/bearing system p 219 N93-14468

Sundstrand Data Control, Inc., Redmond, WA.

FDAMS: An extendable and reconfigurable solution for avionics data management systems p 168 N93-15157
Rewritable optical disk: Application to flight recording p 221 N93-15160

Sverdrup Technology, Inc., Brook Park, OH.

A numerical study of mixing in supersonic combustors with hypermixing injectors p 294 N93-17884
[NASA-CR-191027]
Multidisciplinary tailoring of hot composite structures [NASA-TM-106027] p 550 N93-19971
Computation of H₂/air reacting flowfields in drag-reduction external combustion p 536 N93-20237
[NASA-CR-191071]

Sverdrup Technology, Inc., Cleveland, OH.

Numerical simulation of free shear flows: Towards a predictive computational aeroacoustics capability [NASA-CR-191015] p 781 N93-27097

Swedish Air Force, Stockholm.

How do we investigate the human factor in aircraft accidents? p 491 N93-19655

Swissair, Zurich (Switzerland).

The ecological balance of Swissair: An example of waste management p 1035 N93-31930

Systems Control Technology, Inc., Arlington, VA.

Rotorcraft en route ATC route standards [AD-A249129] p 35 N93-10323
Rotorcraft health and usage monitoring systems: A literature survey [DOT/FAA/RD-91/6] p 48 N93-11461
Tiltrotor aircraft noise: A summary of the presentations and discussions at the 1991 FAA/Georgia Tech Workshop [DOT/FAA/RD-91/23] p 232 N93-14912

Systems Control Technology, Inc., Palo Alto, CA.

Intelligent diagnostics systems p 98 N93-11931

Systems Technology, Inc., Hawthorne, CA.

Ground based simulation evaluation of the effects of time delays and motion on rotorcraft handling qualities [AD-A256921] p 328 N93-16186

T**Tana-Jyry, Ky (Finland).**

Transmission system for a transfer device gripping a double wheel [CA-PATENT-APPL-SN-2024585] p 731 N93-25178

Technical Research Centre of Finland, Espoo.

Motion simulation of underwater vehicles [VTT-PUBS-97] p 443 N93-18698
Interaction between ice and propeller [VTT-TIED-1281] p 841 N93-27832

Technical Univ. of Budapest (Hungary).

Detection of technical states with aircraft p 168 N93-15159

Technion - Israel Inst. of Tech., Haifa.

Merging sparse optical flow and edge connectivity between image features: A representation scheme for 2-D display of scene depth p 845 N93-27179
Regression rate mechanism in a solid fuel ramjet p 814 N93-27185

Development of a pulse ramjet based on twin valveless pulse combustors coupled to operate in antiphase p 814 N93-27186

Analysis of thrust modulation of ram-rockets by a vortex valve p 814 N93-27187

Leading edge vortices in a chordwise periodic flow p 782 N93-27218

Analysis of wind-tunnel data for elliptic cross-sectioned forebodies at Mach numbers 0.4 to 5.0 p 782 N93-27221

Technion Research and Development Foundation Ltd., Haifa (Israel).

Multi-disciplinary optimization of aeroservoelastic systems [NASA-CR-191255] p 220 N93-14766

Technische Hogeschool, Delft (Netherlands).

On-line aircraft state and parameter estimation p 512 N93-19929

Technische Univ., Berlin (Germany).

Stability investigations of airfoil flow by global analysis p 783 N93-27436

Design and implementation of a Global Positioning System (GPS) supported area navigation system with electronic aircraft [ILR-MITT-275(1992)] p 889 N93-30671

Technische Univ., Brunswick (Germany).

Sensor fault detection using nonlinear observer and polynomial classifier p 170 N93-15182
Realization of real time graphics in vehicles with high dynamic motion p 443 N93-18630

Protection of taxiing traffic in airports through mode S secondary radar technology [ETN-93-93455] p 791 N93-28206

Technische Univ., Darmstadt (Germany).

The effect of main stream flow angle on flame tube film cooling p 932 N93-29953

Technische Univ., Delft (Netherlands).

Flight testing: Past, present, and future p 164 N93-14615

Experimental and numerical investigation of vortex flow over a 76/60-deg double-delta wing [LR-680] p 289 N93-16210

Terminal area traffic management [LR-684] p 317 N93-16213

Stress calculations on the window section of an all-composite aircraft fuselage [LR-688] p 328 N93-16215

The Airbus floor beam: Towards a cost-effective composite design and manufacture research project sponsored by Airbus industry [LR-677] p 329 N93-16283

Helicopter installations: From motor to rotor [LR-675] p 329 N93-16345

Development of a computer assisted toolbox for aerodynamic design of aircraft at subcritical conditions with application to three-surface and canard aircraft [ISBN-90-6275-768-5] p 441 N93-16567

Carrier wave signals interfering with Loran-C [ETN-92-92528] p 318 N93-17584

Professor Wittenberg: His speciality and versatility [ISBN-90-6275-670-0] p 240 N93-19002

Propelling force and resistance p 298 N93-19003

Aircraft performance in practice p 340 N93-19004

What is the progress in propulsion? p 298 N93-19006

On the dynamics of aeroelastic oscillators with one degree of freedom [REPT-92-96] p 1040 N93-31653

Technische Univ., Eindhoven (Netherlands).

Quiet by design: Numerical acousto-elastic analysis of aircraft structures [ISBN-90-386-0042-9] p 893 N93-29268

On the verification of a theory for sculling propulsion [ETN-93-94040] p 1031 N93-31519

Technische Univ., Hanover (Germany).

Determination of the zone of the stall cell by means of the baroclinic wave theory p 424 N93-18733

Rotating stall cell and Von Karman vortex street: A meteorological theory p 424 N93-18734

Technische Univ., Munich (Germany).

Experimental analysis of steady-state and dynamic monitoring of power shaft turbines p 178 N93-15176

Combining direct and indirect methods in optimal control: Range maximization of a hang glider [REPT-313] p 371 N93-16618

Tel-Aviv Univ. (Israel).

Spurious frequencies as a result of numerical boundary treatments p 839 N93-27170

Application of the cyclic J-integral to fatigue crack propagation p 839 N93-27182

Towards an analytical treatment of the aerolastic problem of a circular wing p 781 N93-27214

Teledyne Controls, Los Angeles, CA.

The Teledyne controls aircraft condition monitoring system p 168 N93-15155

Helicopter flight data recorder and health and usage monitoring system p 169 N93-15178

Tennessee Univ., Knoxville.

Dynamics of vortex rings in cross-flow p 134 N93-13917

Tennessee Univ. Space Inst., Tullahoma.

A wall interference assessment/correction system [NASA-CR-190617] p 68 N93-11910

A wall interference assessment/correction system [NASA-CR-191889] p 296 N93-18384

Test Wing (6510th), Edwards AFB, CA.

Testing of an automatic, low altitude, all terrain ground collision avoidance system p 502 N93-19924

Texas A&M Univ., College Station.

Analysis of wing-body junction flowfields using the incompressible Navier-Stokes equations, volumes 1 and 2 p 17 N93-10320

Compressible and incompressible fluid seals: Influence on rotordynamic response and stability [NASA-CR-190746] p 85 N93-10891

Experimental study of the flow field inside a whirling annular seal p 85 N93-10892

Leading edge film cooling heat transfer including the effect of mainstream turbulence p 23 N93-11886

Parametric study of air sampling cyclones p 135 N93-14173

A finite element model for analysis of thermoviscoplastic behavior of hypersonic leading edge structures subject to intense aerothermal heating p 137 N93-14631

Micro mechanical behavior of pavements p 379 N93-16312

Transportation Research Center of Ohio

Digital data acquisition and preliminary instrumentation study for the F-16 laminar flow control vehicle p 292 N93-16784

Preliminary design of an intermittent smoke flow visualization system [NASA-CR-186027] p 806 N93-28693

Multiparticle imaging technique for two-phase fluid flows using pulsed laser speckle velocimetry [DE93-011734] p 935 N93-30489

Texas Univ., Arlington.

Optimum design of aircraft structures with manufacturing and buckling constraints p 162 N93-13815

Texas Univ., Austin.

Effects of sweep on the physics of unsteady shock-induced turbulent separated flows [AD-A247035] p 22 N93-11742

An experimental/computational study of heat transfer in sharp fin induced shock wave/turbulent boundary layer interactions at low hypersonic Mach numbers p 217 N93-13826

A domain decomposition method for parallel transient response calculations p 187 N93-13827

Hydrodynamic effects on heat transfer for film-cooled turbine blades [AD-A257291] p 361 N93-16080

Expedient repair of structural facilities [AD-A260727] p 731 N93-25656

The Center of Excellence for Hypersonics Training and Research at the University of Texas at Austin [NASA-CR-193070] p 781 N93-27126

Textron Bell Helicopter, Fort Worth, TX.

Embedded ADM reduces helicopter human error accidents p 147 N93-15024

Measuring risk in single-engine and twin-engine helicopters p 148 N93-15025

Thompson-Hickling Aviation, Inc., Ottawa (Ontario). Engineering management consideration for an integrated aeronautical mobile satellite service p 933 N93-30337

Tohoku Univ., Sendai (Japan).

Three dimensional boundary-layer transition on a swept wing p 419 N93-16818

Numerical simulations of supersonic flow by a fourth-order compact MUSCL TVD scheme p 302 N93-19308

Tokyo Inst. of Tech. (Japan).

Current projects in Fuzzy Control p 1038 N93-31442

Tokyo Univ. (Japan).

Effect of the flow non-uniformity on the mixing layer at the interface of parallel supersonic flows [ISAS-RN-646] p 128 N93-12716

LES turbulence modeling using DNS data base p 299 N93-19274

Numerical study on transverse hydrogen injection into a supersonic flowfield p 302 N93-19311

Toledo Univ., OH.

Simulation of two-dimensional icing, de-icing and anti-icing phenomena p 142 N93-13364

Aeroelastic stability and response of rotating structures [NASA-CR-191803] p 371 N93-16560

Analysis and evaluation of an integrated laminar flow control propulsion system [NASA-CR-192162] p 551 N93-20268

Estimating turbine limit load [NASA-CR-191105] p 699 N93-25883

Toronto Univ. (Ontario).

Theoretical and experimental investigations concerning the structural integrity of aeroengine compressor discs p 56 N93-10539

The modelling of turbulence and downbursts for flight simulators p 193 N93-13542

Smart materials p 536 N93-20624

An experimental investigation of a round turbulent jet in a cross-flow p 553 N93-20689

Transport Canada, Ottawa (Ontario).

Adapting system engineering principles to the Canadian Airspace System p 887 N93-30338

Airspace Design Expert System (ADES), a 2D/3D mapping and modelling tool incorporating an expert system for use in instrument approach design p 888 N93-30357

Transportation Research Board, Washington, DC.

Public-sector aviation issues: Graduate research award papers, 1990 - 1991 [PB92-222629] p 143 N93-13787

Airport landside planning and operations [PB93-167880] p 822 N93-26636

Transportation Research Center of Ohio, East Liberty.

Longitudinal acceleration test of overhead luggage bins in a transport airframe section [DOT/FAA/CT-92/9] p 991 N93-31652

Trimble Navigation, Sunnyvale, CA.

System analysis for a kinematic positioning system based on the global positioning system
[AD-A262830] p 885 N93-29468

TRW, Inc., Houston, TX.

Reference equations of motion for automatic rendezvous and capture
[NASA-CR-185676] p 914 N93-29652

TRW-Warner Robins, GA.

Technical operating report on the Data Integration and Collection Environment (DICE) instrumentation system design
[AD-A258444] p 455 N93-17891

Turbulence Prediction Systems, Boulder, CO.

Development of the Advance Warning Airborne System(AWAS) p 144 N93-14849

U**Ulstein Turbine A/S, Kongsberg (Norway).**

The integration of geometric modeling into an inverse design method and application of a PC-based inverse design method and comparison with test results
p 81 N93-10058

United Kingdom Atomic Energy Authority, Abingdon (England).

Parameters influencing the hot-spot ignition of aviation fuel/air and ethylene/air mixtures p 704 N93-24886
Zoning of aircraft by electric field modelling p 704 N93-24894

Alternative equipment test procedures for simultaneous current injection on multiple cable bundles
p 747 N93-24903

United Kingdom Atomic Energy Authority, Harwell (England).

A transportable luggage examination system based on neutron interrogation p 497 N93-21863

United Technologies Corp., East Hartford, CT.

Advanced turbine design for coal-fueled engines
[DE93-000224] p 554 N93-21254

Structural Tailoring of Advanced Turboprops (STAT).
Theoretical manual
[NASA-CR-191017] p 556 N93-22005

United Technologies Corp., Stratford, CT.

Sikorsky Aircraft Advanced Rotorcraft Transmission (ART) program
[NASA-CR-191079] p 840 N93-27268

United Technologies Corp., West Palm Beach, FL.

Fatigue in single crystal nickel superalloys
[AD-A261742] p 737 N93-26282

United Technologies Corp., Windsor Locks, CT.

User's manual for UCAP: Unified Counter-Rotation Aero-Acoustics Program
[NASA-CR-191034] p 852 N93-27148

United Technologies Research Center, East Hartford, CT.

Investigation of hot streak migration and film cooling effects on heat transfer in rotor/stator interacting flows, report 1
[AD-A250688] p 102 N93-12490

Electro-optic architecture (EOA) for sensors and actuators in aircraft propulsion systems
[NASA-CR-182270] p 233 N93-15116

Experimental investigation of turbine disk cavity aerodynamics and heat transfer
[NASA-CR-193831] p 812 N93-27115

Unsteady transition measurements on a pitching three-dimensional wing p 820 N93-27450

Experimental study of cross flow mixing in cylindrical and rectangular ducts
[NASA-CR-187141] p 815 N93-27680

Universal Energy Systems, Inc., Dayton, OH.

Calculations on unsteady type 4 interaction at Mach 8
[AD-A265214] p 990 N93-32004

Universität der Bundeswehr, Hamburg (Germany).

Some experiments and ideas on GPA before reaching steady state of engine p 178 N93-15175

Universität der Bundeswehr Muenchen, Neubiberg (Germany).

Overview on test cases for computation of internal flows in turbomachines p 214 N93-13209

Experimental and numerical examinations of the influence of inlet distortion perturbations on the working behavior of turbofan compressors
[ETN-93-92733] p 364 N93-18628

University Coll. of Swansea (Wales).

Adaptivity-fluids-localization. The challenge to computational mechanics p 553 N93-20618

The effect of orthogonal-mode rotation on forced convection in a circular-sectioned tube fitted with full circumferential transverse ribs p 932 N93-29937

University of Central Florida, Orlando.

Design of an air traffic computer simulation system to support investigation of civil tiltrotor aircraft operations
[NASA-CR-190811] p 36 N93-11139

Implementing system simulation of C3 systems using autonomous objects
[NASA-CR-190845] p 89 N93-11716

Design of an air traffic computer simulation system to support investigation of civil tiltrotor aircraft operations
[NASA-CR-192920] p 707 N93-26052

University of South Florida, Tampa.

The role of under-determined approximations in engineering and science application p 441 N93-16763

Effect of design selection on response surface performance
[NASA-CR-4520] p 895 N93-29885

University of Southern California, Los Angeles.

Control of lift and drag in unsteady flows
[AD-A253146] p 17 N93-10340

Dynamical effects of suction/heating on turbulent boundary layers
[AD-A248459] p 87 N93-11416

Control of asymmetric jet
[AD-A255967] p 219 N93-14400

Functional requirements of an advanced instructional design advisor: Simulation authoring, Volume 3
[AD-A256650] p 440 N93-16500

Control of jet noise
[NASA-CR-193552] p 1040 N93-32221

University of Technology, Leicester (England).

Information systems for airport operations
[TT-9202] p 152 N93-14729

University of Western Kentucky, Bowling Green.

A pulsed fast-thermal neutron interrogation system
p 497 N93-21866

University of Western Ontario, London.

Flow over a leading edge with distributed roughness
p 18 N93-10549

Utah State Univ., Logan.

Functional requirements of an advanced instructional design advisor: Simulation authoring, Volume 3
[AD-A256650] p 440 N93-16500

V**Vibro-Meter S.A., Fribourg (Switzerland).**

New rotor trim and balance system for helicopter usage monitoring p 169 N93-15180

Vigyan Research Associates, Inc., Hampton, VA.

Euler analysis of turbofan/superfan integration for a transport aircraft p 214 N93-13206

Modeling and control study of the NASA 0.3-meter transonic cryogenic tunnel for use with sulfur hexafluoride medium
[NASA-CR-189737] p 418 N93-16379

Pilot weather advisor
[NASA-CR-189723] p 318 N93-16692

Modifications to Langley 0.3-m TCT adaptive wall software for heavy gas test medium, phase 1 studies
[NASA-CR-189736] p 291 N93-16710

Design optimization of natural laminar flow bodies in compressible flow
[NASA-CR-44778] p 292 N93-16940

A feasibility study of using Langley 0.3-m transonic cryogenic tunnel sidewall boundary-layer removal system for heavy gas testing
[NASA-CR-191438] p 747 N93-25087

Unstructured viscous grid generation by advancing-front method
[NASA-CR-191449] p 780 N93-27067

Virginia Polytechnic Inst. and State Univ., Blacksburg.
The hemisphere-cylinder at an angle of attack p 21 N93-11250

Laminar boundary-layer breakdown
[AD-A254489] p 90 N93-12162

Verification of rain-flow reconstructions of a variable amplitude load history
[NASA-CR-189670] p 91 N93-12411

Transonic aeroelastic analysis of systems with structural nonlinearities p 217 N93-13769

Airfoil-vortex interaction and the wake of an oscillating airfoil p 134 N93-13803

An experimental investigation of interacting wing-tip vortex pairs
[AD-A258471] p 295 N93-18272

Formulation of a structural model for flutter analysis of low aspect ratio composite aircraft wings p 372 N93-19019

Crossflow stability and transition experiments in a swept-wing flow
[NASA-TM-108650] p 555 N93-21819

Flow visualizations of perpendicular blade vortex interactions
[NASA-CR-192725] p 748 N93-25208

The transient development of vortices over delta wings p 695 N93-25269

Integrated aerodynamic-structural wing design optimization p 714 N93-25279

Experimental and computational investigation of helium injection into air at supersonic and hypersonic speeds p 696 N93-25487

Adjoint methods for aerodynamic wing design
[NASA-CR-193086] p 805 N93-27089

Active magnetic bearings applied to industrial compressors p 841 N93-27570

Direct measurements of skin friction in supersonic combustion flow fields
[AD-A262878] p 825 N93-28226

An experimental study of flow over a 6 to 1 prolate spheroid at incidence p 874 N93-29124

Generation of carbon monoxide in compartment fires
[PB93-146702] p 880 N93-29211

Static and dynamic large deflection flexural response of graphite-epoxy beams
[NASA-CR-4118] p 934 N93-30374

Compressible turbulence in a high-speed high Reynolds number mixing layer p 878 N93-30583

Integrated structural design, vibration control, and aeroelastic tailoring by multiobjective optimization p 1030 N93-31137

Virginia Univ., Charlottesville.

Planar measurement of flow field parameters in nonreacting supersonic flows with laser-induced iodine fluorescence p 133 N93-13801

Technical needs and research opportunities provided by projected aeronautical and space systems
[NASA-CR-192124] p 386 N93-16629

NASA-UVA light aerospace alloy and structure technology program supplement: Aluminum-based materials for high speed aircraft
[NASA-CR-4517] p 1019 N93-31643

NASA-UVA Light Aerospace Alloy and Structures Technology Program (LA2ST)
[NASA-CR-193412] p 1019 N93-31739

Von Karman Inst. for Fluid Dynamics,

Rhode-Saint-Genese (Belgium).
Introduction to Flutter of Winged Aircraft, volume 1
[VKI-LS-1992-01] p 372 N93-18142

Computational Fluid Dynamics, volume 2
[VKI-LS-1992-04-VOL-2] p 421 N93-18563

Validation of central and upwind 3D compressible flow solvers p 421 N93-18564

Axial Flow Compressors, volume 1
[VKI-LS-1992-02-VOL-1] p 422 N93-18721

Axial Flow Compressors, volume 2
[VKI-LS-1992-02-VOL-2] p 423 N93-18731

Rotating stall: Modeling-measurement techniques; unsteady loss-unsteady flow field p 424 N93-18732

Thermal effects of a coolant film along the suction side of a high pressure turbine nozzle guide vane p 901 N93-29930

Parametric studies of shock wave/boundary layer interactions over 2D compression corners at Mach 6
[VKI-TN-181] p 988 N93-31538

Vrije Univ., Brussels (Belgium).

The PEP Symposium on CFD Techniques for Propulsion Applications p 214 N93-13210

W**Washington Univ., Saint Louis, MO.**

Mode interaction in stiffened composite shells under combined mechanical and thermal loadings p 419 N93-16793

Artificial intelligence methodologies in flight related differential game, control and optimization problems
[AD-A262405] p 848 N93-28498

Washington Univ., Seattle.

Numerical simulation of the acoustic instability in the spatially developing, confined, supersonic mixing layer p 132 N93-13521

Investigation of the aerothermodynamics of hypervelocity reacting flows in the ram accelerator
[NASA-CR-191715] p 140 N93-15588

Multi-parameter optimization tool for low-cost commercial fuselage crown designs p 922 N93-30858

West Virginia Univ., Morgantown.

Determination of the stability and control derivatives of the F/A-18 HARV from flight data using the maximum likelihood method
[NASA-CR-191216] p 186 N93-12903

The ground vortex flow field associated with a jet in a cross flow impinging on a ground plane for uniform and annular turbulent axisymmetric jets
[NASA-CR-4513] p 789 N93-28449

Westinghouse Electric Corp., Baltimore, MD.

Acquisition and use of Orlando, Florida and Continental Airbus radar flight test data p 489 N93-19603

Westinghouse Science and Technology Center,

Pittsburgh, PA.
A review of the development of a luggage explosive detection system p 497 N93-21862

Wichita State Univ., KS.

A simplified numerical procedure to compute the optimal trajectory of an aircraft p 48 N93-11719

Aviation safety research at the National Institute for Aviation Research Wichita State University: A report to the FAA Technical Center [NIAR-92-2] p 310 N93-16455

The airline quality report, 1992 [NIAR-92-11] p 310 N93-18036

Consumer interest in the air safety data of the airline quality rating. Testimony to the US House of Representatives, Committee on Government Operations, Government Activities and Transportation Subcommittee [NIAR-92-4] p 495 N93-19941

General aviation aircraft: Normal acceleration data analysis and collection project [DOT/FAA/CT-91/20] p 713 N93-24739

International aircraft operator information system [DOT/FAA/CT-93/4] p 949 N93-32232

Wilkes Coll., Wilkes-Barre, PA.

Wind tunnel seeding particles for laser velocimeter p 292 N93-16770

Windsor Univ. (Ontario).

Resonant response analysis of a high speed gear p 553 N93-20662

Wisconsin Univ., Madison.

Undulator Spectromicroscopy Facility at the Advanced Light Source [DE93-007964] p 823 N93-28490

Wisconsin Univ. Hospital, Madison.

Modeling the effects of drop drag and breakup on fuel sprays [AD-A263650] p 931 N93-29388

Worcester Polytechnic Inst., MA.

NASA advanced design program: Analysis, design, and construction of a solar powered aircraft [NASA-CR-192040] p 332 N93-17802

Solar powered multipurpose remotely powered aircraft p 895 N93-29722

Wright Lab., Wright-Patterson AFB, OH.

X-29 linear aerodynamic perturbation model [AD-A254810] p 160 N93-12752

Survey on techniques used in aerodynamic nozzle/airframe integration p 161 N93-13224

Propulsion integration results of the STOL and Maneuver Technology Demonstrator p 161 N93-13228

Hypersonic propulsion system force accounting p 175 N93-13229

Symposium proceedings on Quantitative Feedback Theory [AD-A255527] p 187 N93-13872

A compilation of the mathematics leading to the doublet lattice method [AD-A256304] p 136 N93-14441

Proceedings of the USAF Structural Integrity Program [AD-A255379] p 110 N93-14549

Subsonic aerodynamic research laboratory [AD-A256060] p 137 N93-14661

Add-on damping treatment for the F-15 upper-outer wing skin [AD-A258470] p 337 N93-18248

Wright Laboratory research and development facilities handbook [AD-A258746] p 572 N93-20403

URV flight test of an Ada implemented self-repairing flight control system [AD-A259205] p 527 N93-20551

Studies in air/air supersonic mixing layers p 700 N93-26007

Optically smart surfaces survivability testing at Mach 3 [AD-A261785] p 760 N93-26566

An assessment of inlet total-pressure distortion requirements for the Compressor Research Facility (CFR) [AD-A262299] p 815 N93-27679

Advanced thermally-stable, coal-derived, jet fuels program: Experiment system and model development [AD-A262747] p 917 N93-29402

A real-time, hardware-in-the-loop simulation of an unmanned aerial research vehicle [AD-A262477] p 893 N93-29409

Modal survey of a full-scale F-18 wind tunnel model [AD-A262482] p 875 N93-29410

Heat transfer in high turbulence flows: A 2-D planar wall jet p 932 N93-29935

Computation of a delta-wing roll-and-hold maneuver [AD-A264704] p 909 N93-30498

Wyle Labs., Inc., El Segundo, CA.

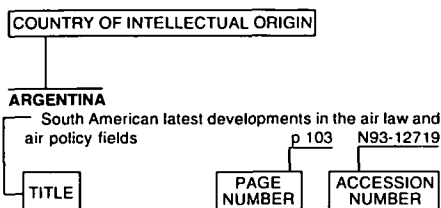
Air Force procedure for predicting noise around airbases: Noise exposure model (Noisemap) [AD-A255769] p 224 N93-14655

FOREIGN TECHNOLOGY INDEX

AERONAUTICAL ENGINEERING / A Continuing Bibliography
1993 Cumulative Index

February 1994

Typical Foreign Technology Index Listing



Listings in this index are arranged alphabetically by country of intellectual origin. The title of the document is used to provide a brief description of the subject matter. The page number and accession number are included in each entry to assist the user in locating the abstract in the abstract section. If applicable, a report number is also included as an aid in identifying the document.

A

ARGENTINA

South American latest developments in the air law and air policy fields p 103 A93-12719

AUSTRALIA

Experiments on Space Shuttle Orbiter models in a free piston shock tunnel p 7 A93-11497
Free piston shock tunnels - Developments and capabilities p 66 A93-12316
Drag and drag partition on rough surfaces p 79 A93-12460
The composite shape and structure of coherent eddies in the convective boundary layer p 93 A93-12643
Output feedback control for output tracking of nonlinear uncertain systems p 96 A93-13177
New lamps for old - Safety regulation through structural airworthiness standards p 28 A93-13630
Jet streams and associated turbulence and their effects on air transport flight operations p 154 A93-14231
Accuracy of a simple hole damage analysis method in composite structures p 197 A93-15748
Experimental investigation of laminar to turbulent boundary layer transition with separation bubbles at low Reynolds number p 128 A93-17277
Elastic constants for unidirectional boron-epoxy composites p 387 A93-18636
Fault signatures obtained from fault implant tests on an F404 engine [ASME PAPER 92-GT-82] p 348 A93-19331
The effect of compressor rotor tip crops on turboshaft engine performance [ASME PAPER 92-GT-83] p 348 A93-19332
The role of laminar-turbulent transition in gas turbine engines - A discussion [ASME PAPER 92-GT-301] p 255 A93-19491
Aeronautical engineering education for the armed forces p 453 A93-21681
A study of the flexural properties of carbon-epoxy composites in certain environments p 390 A93-21999

Microburst observations in tropical Australia p 432 A93-22198
Quasi-one-dimensional modelling of free-piston shock tunnels [AIAA PAPER 93-0352] p 377 A93-23037
Introduction of small velocity and pressure variation into a stationary compressible fluid p 473 A93-25060
A history of visual approach guidance indicator systems in Australia p 498 A93-25171
Crack growth and repair of multi-site damage of fuselage lap joints p 547 A93-28291
Inter-noise '91: Proceedings of the 20th International Conference on Noise Control Engineering, Sydney, Australia, Dec. 2-4, 1991. Vols. 1 & 2 [ISBN 0-909882-12-6] p 557 A93-28476
Advances in the design of jet engine test facilities for military aircraft in Australia p 529 A93-28491
Noise-induced reaction in a work community adjacent to aircraft runways - The Royal Australian Airforce p 559 A93-28496
Subsonic potential flow and the transonic controversy p 479 A93-28544
Numerical simulation of two-dimensional compressible flows p 687 A93-34357
Life analysis of a gas turbine fan disc p 897 A93-40803
Life prediction - Thermal fatigue from isothermal data p 916 A93-40807
Design verification of ground run-up noise suppressors for afterburning engines p 910 A93-42892
Generation of unstructured tetrahedral meshes by advancing front technique p 1021 A93-44206
Performance considerations in the operation of free-piston driven hypersonic test facilities p 1011 A93-45497
Development of a skin friction gauge for use in an impulse facility p 1024 A93-45526
Free piston facilities with air driver gas p 1011 A93-45528
Hypervelocity flows of argon produced in a free piston driven expansion tube p 1012 A93-45530
Double diaphragm driven free piston expansion tube p 1016 A93-45533
Computational fluid dynamics code validation using a free piston hypervelocity shock tunnel p 960 A93-45545
Numerical simulation of two-dimensional and axisymmetric compressible flows p 960 A93-45546
Bonded repair of multi-site damage p 947 A93-45786
Absolute intensity measurements of impurity emissions in a shock tunnel and their consequences for laser-induced fluorescence experiments p 1147 A93-48044
Drag measurements on blunted cones and a scramjet vehicle in hypervelocity flow p 1050 A93-48172
Hypersonic ignition and thrust production in a scramjet [AIAA PAPER 93-2979] p 1119 A93-50196
Aspects of fatigue affecting the design and maintenance of modern military aircraft p 1043 A93-52548
The prediction of thermal NO(x) in gas turbine exhausts [ISABE 93-7022] p 1195 A93-53998
Neural network fault diagnosis of a turbofan engine [ISABE 93-7091] p 1203 A93-54067
Measurement and prediction of flow in a gas turbine engine exhaust plume [ISABE 93-7113] p 1204 A93-54088
Reinforcement of the F-111 wing pivot fitting with a boron/epoxy doubler system - Materials engineering aspects p 1214 A93-54241
The effect of temperature on the natural frequencies and acoustically induced strains in CFRP plates p 1260 A93-56331
Design and implementation of digital filters for analysis of F/A-18 flight test data [AD-A253447] p 17 N93-10342
Structural fatigue aspects of the P-3 Orion [ARL-STRUC-TM-558] p 161 N93-13256

Development of a menu driven materials data base for use on personal computers: Aircraft structures technical memorandum [AD-A256317] p 392 N93-16403
Measurement of the dynamic undercarriage response of a Sikorsky S-70B-2 helicopter: Instrumentation and test methods: Flight mechanics technical memorandum [AD-A256319] p 329 N93-16404
Damage tolerance assessment of boron/epoxy repairs to fuselage lap joints [AD-A258383] p 338 N93-18257
Field evaluation of six protective coatings applied to T-56 turbine blades after 2000 hours of engine use [AD-A261112] p 522 N93-21316
Experiments on smooth cantilevered circular cylinders in a low-turbulence uniform flow. Part 2: Fluctuating loads on a cantilever of aspect ratio 30 [PB93-110500] p 555 N93-21382
Experiments on smooth cantilevered circular cylinders in low-turbulence uniform flow. Part 1: Mean loading with aspect ratios in the range 4 to 30 [PB93-111763] p 555 N93-21383
In-flight evaluation of noise levels and assessment of active noise reduction systems in the Seahawk S-70B-2 helicopter [AD-A260689] p 759 N93-25649
Optimal trajectories for aircraft terrain following and terrain avoidance: A literature review update [AD-A264075] p 910 N93-30604
AUSTRIA
An aerodynamic model for the longitudinal motion of flight training devices p 1207 A93-54278

B

BELGIUM

A flux-difference finite volume method for steady Euler equations on adaptive unstructured grids p 116 A93-14277
Vibro-acoustic analysis of propeller aircraft, integrating advanced experimental modeling with in-flight data analysis p 451 A93-19230
Experimental and theoretical analysis of the flow in a centrifugal compressor volute [ASME PAPER 92-GT-30] p 400 A93-19290
Inverse design of compressor and turbine blades at transonic flow conditions [ASME PAPER 92-GT-430] p 357 A93-19573
Experimental study on the three dimensional flow within a compressor cascade with tip clearance. I - Velocity and pressure fields [ASME PAPER 92-GT-215] p 258 A93-19574
Experimental study on the three dimensional flow within a compressor cascade with tip clearance. II - The tip leakage vortex [ASME PAPER 92-GT-432] p 258 A93-19575
Europe adapts CST to its needs p 560 A93-25088
Application of FEM model correlation and updating techniques on an aircraft using test data of a ground vibration survey p 509 A93-29267
Signal processing and system identification techniques for flutter test data analysis p 529 A93-29282
New upwind dissipation models with a multidimensional approach [AIAA PAPER 93-3304] p 950 A93-45002
The three dimensional flow in a compressor cascade at design and off-design conditions p 971 A93-46927
Energy management [ISABE 93-7019] p 1195 A93-53995
Noise and vibration analysis in propeller aircraft by advanced experimental modeling techniques p 1264 A93-55862
The PEP Symposium on CFD Techniques for Propulsion Applications p 214 N93-13210
Introduction to Flutter of Winged Aircraft, volume 1 [VKI-LS-1992-01] p 372 N93-18142
Computational Fluid Dynamics, volume 2 [VKI-LS-1992-04-VOL-2] p 421 N93-18563
Validation of central and upwind 3D compressible flow solvers p 421 N93-18564

- Axial Flow Compressors, volume 1
[VKI-LS-1992-02-VOL-1] p 422 N93-18721
- Axial Flow Compressors, volume 2
[VKI-LS-1992-02-VOL-2] p 423 N93-18731
- Rotating stall: Modeling-measurement techniques;
unsteady loss-unsteady flow field p 424 N93-18732
- Thermal effects of a coolant film along the suction side
of a high pressure turbine nozzle guide vane
p 901 N93-29930
- Parametric studies of shock wave/boundary layer
interactions over 2D compression corners at Mach 6
[VKI-TN-181] p 988 N93-31538
- Vibration analysis in turbomachines
p 1005 N93-32274

BOSNIA AND HERCEGOVINA

- A collocated finite volume method for predicting flows
at all speeds p 1087 A93-51736

BRAZIL

- Nozzle flow computations using the Euler equations
p 112 A93-14170
- Generalized vortex lattice method for oscillating lifting
surfaces in subsonic flow p 123 A93-14555
- Investigation of a two-dimensional scramjet inlet,
freestream $M = 8-18$ and $T_{sub} 0 = 4100$ K
p 270 A93-21669
- Numerical prediction of flap losses in a transonic wind
tunnel p 288 A93-23552
- Controller design using fuzzy logic - A case study
p 756 A93-33793
- Supersonic panel flutter analysis of shallow shells
p 927 A93-41935
- An implicit time-marching procedure for high speed
flow
[AIAA PAPER 93-3315] p 951 A93-45011
- Computation of wake roll-up for complete aircraft
configurations p 984 A93-47275
- Code validation for high speed flow simulation over the
VLS launcher fairing
[AIAA PAPER 93-3046] p 1057 A93-48226
- An investigation on the use of a heavy gas to improve
the performance of the equilibrium interface technique in
shock tube flows
[AIAA PAPER 93-2017] p 1078 A93-49855
- Optimal performance of airplanes flying through
wind shear
[AIAA PAPER 93-3846] p 1102 A93-51480
- Initial development of a research flight simulator
software
[AIAA PAPER 93-3590] p 1223 A93-52683
- A study upon structural optimization of elastic rotors for
mechanical systems
[INPE-5376-TDI/471] p 83 N93-10310
- Diagnostics systems for the TBR-E tokamak
[INPE-5428-RPC/662] p 232 N93-13257

BULGARIA

- A joint Soviet-Bulgarian scientific program for free-flight
and tethered aerostat observations p 2 A93-11374

C**CANADA**

- Maintaining high accuracy GPS positioning 'on the fly'
p 92 A93-11028
- Aircraft model for multicriterial analysis in decision
making
[AIAA PAPER 92-4192] p 44 A93-13370
- Effects of prior fatigue damage on crack propagation
rates in 2024-T351 aluminum alloy p 71 A93-13640
- Numerical solution of transonic full-potential-equivalent
equations in von Mises co-ordinates
p 111 A93-14080
- Starch media blasting for aerospace finishing
applications
[SAE PAPER 920948] p 107 A93-14091
- Lockheed adopts media blast dry stripping for the
C-130
[SAE PAPER 920949] p 107 A93-14092
- Generation of flow disturbances in transonic wind
tunnels p 119 A93-14354
- A design study on the effect of support and system
parameters on the natural frequencies of rotor systems
p 210 A93-16374
- Analysis of Loran-C performance in the Pemberton area,
B.C.
p 311 A93-17797
- Performance degradation due to hoar frost on lifting
surfaces p 305 A93-17798
- Periodic Euler and Navier-Stokes solutions about
oscillating airfoils p 241 A93-17799
- Effective 406-MHz ELT demonstrates the potential to
save more lives p 311 A93-18543
- Calling the right shots in aircraft maintenance with
artificial intelligence p 238 A93-18763

- A new Lagrangian method for steady supersonic flow
computation. II - Slip-line resolution. III - Strong shocks
p 243 A93-18855

- Flow field measurements in a turbulent free jet issuing
from a sharp-edged square slot p 244 A93-19158
- Aerodynamic performance of a transonic low aspect ratio
turbine nozzle
[ASME PAPER 92-GT-31] p 245 A93-19291
- Experimental and computational investigation of flow in
catalytic monolith channels
[ASME PAPER 92-GT-118] p 387 A93-19354
- The combustion of droplets within gas turbine
combustors - Some recent observations on combustor
efficiency
[ASME PAPER 92-GT-135] p 388 A93-19367
- An experimental investigation of convective heat transfer
at the leading edge of a gas turbine airfoil
[ASME PAPER 92-GT-248] p 405 A93-19457
- Powder metallurgy repair of turbine components
[ASME PAPER 92-GT-312] p 354 A93-19500
- Measurement of unsteady flow and heat transfer in a
linear turbine cascade
[ASME PAPER 92-GT-323] p 256 A93-19507
- Effect of manufacturing deviations on performance of
axial flow compressor blading
[ASME PAPER 92-GT-326] p 257 A93-19510
- Erosion resistant titanium nitride coating for turbine
compressor applications
[ASME PAPER 92-GT-417] p 388 A93-19565
- Acoustic emission monitoring of aging aircraft
structures p 407 A93-19697
- Prediction of the ice accretion with viscous effects on
aircraft wings
[AIAA PAPER 93-0027] p 307 A93-20145
- Spatial and temporal variations of the fluxes of carbon
dioxide and sensible and latent heat over the FIFE site
p 425 A93-20586
- Application issues of fiber optic sensors in aircraft
structures p 410 A93-21094
- A new algorithm of Receiver Autonomous Integrity
Monitoring (RAIM) for GPS navigation
p 314 A93-21161
- Statistical quality control for kinematic GPS positioning
p 314 A93-21162
- High Mach number dynamic stability of blunt slender
cones at angle of attack p 271 A93-21721
- Analysis of a high-performance C/A-code GPS receiver
in kinematic mode p 317 A93-21822
- Canadian low-gravity research using parabolic aircraft
p 384 A93-21908
- Weather-related accidents in the Canadian aviation
industry - An analysis of the chief contributory factors
p 307 A93-22106
- Weather forecasts for aviation in Canada (FACN and
FTCN) - The way they are taught and how they can be
made more suitable to the needs of pilots
p 454 A93-22108
- Terminal forecast amendments - A 'cloudy' issue
p 431 A93-22167
- An aerospace plane as a detonation wave
ramjet/airframe integrated waverider
[AIAA PAPER 92-5022] p 272 A93-22298
- Euler computations of rotor-stator interaction in
turbomachinery cascades using adaptive triangular
meshes
[AIAA PAPER 93-0386] p 282 A93-23065
- Multi-block grid generation for complete aircraft
configurations p 460 A93-23838
- Analysis of flight flutter test data p 523 A93-23839
- Aircraft take-off laboratory simulation for de/anti-icing
study p 528 A93-23840
- Repair of delaminations and impact damage in
composite aircraft structures p 457 A93-24107
- Further analysis of high-rate rolling experiments of a
65 deg delta wing
[AIAA PAPER 93-0620] p 523 A93-24737
- Aviation safety can benefit from simulation of the
dispersion of hazardous material p 487 A93-27393
- Nonsteady, one-dimensional, internal, compressible
flows - Theory and applications
[ISBN 0-19-507358-4] p 548 A93-28749
- Modal analysis in the certification of a commercial
aircraft p 509 A93-29241
- Bearings-only and Doppler-bearing tracking using
instrumental variables p 501 A93-29600
- An analysis of the post-instability behaviour of a
two-dimensional airfoil with a structural nonlinearity
[AIAA PAPER 93-1474] p 726 A93-34020
- The role of Kutta waves on oscillatory shock motion
on an airfoil experiencing heavy buffeting
[AIAA PAPER 93-1589] p 682 A93-34121
- Implicit numerical solution of transonic flows using
adaptive triangular grids p 686 A93-34349
- Machinery arrangements for small VTOL transport
aircraft p 713 A93-34848

- Measurements of wear and acoustic emission from
fuel-wetted surfaces p 744 A93-34925
- Neural network controllers for the X29 aircraft
p 817 A93-37005
- A self-steering array for the SHARP microwave-powered
aircraft p 792 A93-37090
- Evaluation and extension of the flutter-margin method
for flight flutter prediction p 828 A93-37393
- Some special purpose preconditioners for conjugate
gradient-like methods applied to CFD
p 772 A93-38638
- Development of a transonic Euler method for complete
aircraft configurations p 779 A93-39721
- Canadian experience with air cushion vehicle skirts
p 837 A93-39722
- An aerodynamic model for flapping-wing flight
p 858 A93-40470
- Tobacco smoking in aircraft - A fog of legal rhetoric?
p 944 A93-40474
- Materials development for light design - A suppliers
view p 915 A93-40777
- Stability of the vapour phase in a rotating two-phase
fluid system subjected to different gravitational
intensities p 926 A93-41714
- The development of an efficient ornithopter wing
p 873 A93-43685
- An adaptive finite element method for turbulent free
shear flow past a propeller
[AIAA PAPER 93-3388] p 956 A93-45079
- A simple multigrid procedure for explicit time-marching
on unstructured grids p 956 A93-45087
- Fast design of circular-harmonic filters using simulated
annealing p 1038 A93-45556
- A viscous shock-layer analysis of 2-D and axisymmetric
flows
[AIAA PAPER 93-2751] p 963 A93-46500
- Finite element solution of the 3D compressible
Navier-Stokes equations by a velocity-vorticity method
p 974 A93-47196
- A wind tunnel investigation of the pressure distribution
on an F/A-18 wing
[AIAA PAPER 93-3468] p 980 A93-47249
- Experimental study of shock wave and hypersonic
boundary layer interactions near a convex corner
[AIAA PAPER 93-2980] p 1051 A93-48173
- Transition for three-dimensional boundary layers on
wings in the transonic regime
[AIAA PAPER 93-3049] p 1057 A93-48229
- Use of full flight simulator technology enhances
classroom training sessions p 1136 A93-49277
- Optical actuators for fly-by-light applications
p 1172 A93-49475
- Reduced order proportional integral observer with
application p 1166 A93-49605
- Implementation of an infrared thermal imaging system
to measure temperature in a gas turbine engine
[AIAA PAPER 93-2469] p 1120 A93-50215
- A new approach to robust fault detection and
identification p 1166 A93-50631
- Numerical solutions of Euler equations by using a new
flux vector splitting scheme p 1087 A93-51740
- Ground facility interference on aircraft configurations
with separated flow p 1140 A93-52441
- Unsteady pressure and load measurements on an
F/A-18 vertical fin p 1095 A93-52451
- Navier-Stokes investigation of blunt trailing-edge airfoils
using O grids p 1095 A93-52459
- Nonlinear aspects of transonic aeroelasticity
p 1096 A93-52642
- Experimental evaluation of flat plate boundary layer
growth over an anti-icing fluid film p 1140 A93-52645
- Evolution of flight simulation
[AIAA PAPER 93-3545] p 1207 A93-52652
- Internally coherent system of innovation - The case of
flight simulation
[AIAA PAPER 93-3548] p 1226 A93-52653
- Pilot evaluations of augmented flight simulator motion
[AIAA PAPER 93-3580] p 1208 A93-52676
- Implementation of expert systems within an interactive
tactical environment
[AIAA PAPER 93-3583] p 1223 A93-52678
- Thrust imparted to an airfoil by passage through a
sinusoidal upwash field p 1178 A93-53219
- Some acoustic features of perforated test section walls
with splitter plates p 1226 A93-53222
- Clean melting and the removal of defects from
aero-engine materials p 1217 A93-53503
- On hovercraft overwater heave stability
p 1219 A93-53819
- Kelvin-Helmholtz wave generation beneath hovercraft
skirts p 1219 A93-53820
- Hypersonic shock-induced combustion ramjet
performance analysis
[ISABE 93-7037] p 1197 A93-54013

- Thermodynamic and neural network computer modelling of implanted component faults in a gas turbine engine
[ISABE 93-7089] p 1202 A93-54065
- Effect of nozzle design on the performance of a highly loaded turbine stage
[ISABE 93-7096] p 1203 A93-54072
- Aerodynamics of turbine blades with trailing-edge damage - Measurements and computations
[ISABE 93-7130] p 1189 A93-54105
- Static and dynamic errors in heat flux measurements
p 1254 A93-54366
- Uncertainty assessments for engine thrust derived from two methods
p 1254 A93-54392
- Accuracy of GPS-derived acceleration from moving platform tests
p 1240 A93-55973
- Requirements for airborne vector gravimetry
p 1241 A93-55976
- Pitch control trimming system for canard design aircraft
[CA-PATENT-APPL-SN-2013236] p 63 A93-10374
- Theoretical and experimental investigations concerning the structural integrity of aeroengine compressor discs
p 56 A93-10539
- A comparative study of semi-empirical dynamic stall models
p 18 A93-10544
- A field panel method for transonic flows
p 18 A93-10547
- Flow over a leading edge with distributed roughness
p 18 A93-10549
- Experimental investigation of flows behind different Large-Eddy Breakup (LEBU) devices in thick boundary layers
p 18 A93-10550
- Harmonic analysis of the aerodynamic forces on a Darrieus rotor
p 18 A93-10551
- Acoustic noise generation at the air/ocean boundary
[DREA-CR-90-445] p 99 A93-10642
- Defence electronics industry profile, 1990-1991
[CTN-92-60515] p 84 A93-10653
- Noise studies for environmental impact assessment of an outdoor engine test facility
p 99 A93-10672
- Characteristics of separated flows including cavitation effects
p 84 A93-10874
- The modelling of turbulence and downbursts for flight simulators
p 193 A93-13542
- Overall effects of separation on thin aerofoils
[ISBN-0-315-67464-4] p 135 A93-13930
- In-service considerations affecting component life
p 177 A93-14898
- The human factor problem in the Canadian Forces aviation
p 491 A93-19657
- Canadian Forces helicopter ditchings: 1952-1990
p 493 A93-19685
- Use of microprocessor-based simulator technology and MEG/EEG measurement techniques in pilot emergency-maneuver training
p 530 A93-19706
- Fly-by voice, a technology demonstration
p 526 A93-19918
- The flight test and data analysis program for the development of a Boeing/De Havilland Dash 8 simulator model
p 512 A93-19930
- Smart materials
p 536 A93-20624
- Fluid/structures interactions. Aircraft considerations
p 527 A93-20628
- Resonant response analysis of a high speed gear
p 553 A93-20662
- Dynamic simulation of flexible body systems by the vector solution method
p 553 A93-20666
- An experimental investigation of a round turbulent jet in a cross-flow
p 553 A93-20689
- Stochastic finite element analysis for high speed rotors
p 554 A93-20696
- Further development of the CANAERO computer code to include a time-stepping capability
[DREA-CR-91-478] p 562 A93-21820
- Transmission system for a transfer device gripping a double wheel
[CA-PATENT-APPL-SN-2024585] p 731 A93-25178
- Effect of vortex behavior on loads acting on a 65 deg delta wing oscillating in roll at high incidence
p 782 A93-27220
- Prediction of jet impingement cooling scheme characteristics (airfoil leading edge application)
p 932 A93-29941
- Future directions in aviation security
p 880 A93-30274
- Explosives detection systems for airport security gas chromatographic based devices
p 881 A93-30276
- Models for performance assessment of HF antennas on the CH-135/Twin Huey helicopter
p 933 A93-30291
- Meteorological information for aviation: A systems approach
p 937 A93-30298
- Classification of radar clutter in an air traffic control environment
p 886 A93-30299
- Coupling gain computation between antennas on circular cylinders at SHF/EHF frequencies
p 933 A93-30309
- RCS of fundamental scatterers in the HF band by wire-grid modelling
p 933 A93-30320
- Embedded GPS: The Canadian Marconi approach
p 886 A93-30330
- Engineering management consideration for an integrated aeronautical mobile satellite service
p 933 A93-30337
- Adapting system engineering principles to the Canadian Airspace System
p 887 A93-30338
- Application and integration of diverse technology in an aviation system: The National Aeronautical Information Processing System
p 887 A93-30339
- Design issues and initial performance of an adaptive air/ground/air HF communication system
p 934 A93-30342
- Issues of ATC conflict resolution under real-time constraints
p 887 A93-30350
- Airspace Design Expert System (ADES), a 2D/3D mapping and modelling tool incorporating an expert system for use in instrument approach design
p 888 A93-30357
- Material characterization and fractographic examination of Ti-17 fatigue crack growth specimens for SMP SC33
p 1004 A93-31744
- Fatigue crack growth results for Ti-6Al-4V, IMI 685, and Ti-17
p 1004 A93-31746
- CHINA**
- Review and prospect of Chinese scientific balloon activities
p 1 A93-11368
- The application of optimal robust control in control system design of flying vehicles
p 95 A93-11791
- Wheel shimmy analysis for main landing gear of aircraft
p 41 A93-11809
- Analysis of structural dynamic response for aircraft operating in the environment of nuclear explosion shock waves
p 78 A93-11810
- Bird impact dynamic response analysis for aircraft arc windshield
p 41 A93-11815
- Investigation of cabin noise reduction in the Y12
p 41 A93-11816
- Transition of flutter mode of two-dimensional wing with external store
p 41 A93-11818
- Effects of the pylon pitching stiffness on wing-store flutter
p 41 A93-11820
- The investigation on vibration characteristics of all-movable stabilizer of an aircraft
p 41 A93-11821
- Research of starting test of the small turbojet in simulated altitude condition
p 53 A93-11870
- Weighted average method for evaluating the aerodynamic properties of transition flow
p 8 A93-11872
- A method of calculating elastic curve of semiflexible plate
p 66 A93-12097
- Subharmonic bifurcation analysis of wing with store
p 78 A93-12098
- Slicing model for foreign soft-body objects impacting on blade rows
p 28 A93-12372
- Study on aircraft microwave remote sensing of sea-water surface salinity
p 92 A93-12407
- Numerical simulation for aeroelasticity in turbomachines with vortex method. I - Theory and method
p 53 A93-12452
- Three-dimensional flow calculations in turbomachinery using the stream function formulation
p 11 A93-12453
- Experimental research for the discharge flow of a centrifugal impeller and the flowfield in the vaneless diffuser
p 11 A93-12454
- Viscous shock-layer numerical calculations of three dimensional nonequilibrium flows over hypersonic blunt bodies at high angle of attack
p 12 A93-12651
- Accuracy analysis on image matching guidance systems
p 62 A93-12653
- Recent advances in jet simulation techniques for flight vehicles
p 66 A93-12656
- COF2 radiation from an air-teflon wake
p 12 A93-12659
- Aerospace - Collected translations of selected papers, 1992
p 2 A93-12726
- Nonlinear multi-point modelling and parameter estimation of the DO 28 research aircraft
p 41 A93-12727
- Analytical method for subsonic cascade profile
p 12 A93-12730
- Prediction of the inception of rotating stall for multistage axial flow compressors
p 12 A93-12731
- A maximum likelihood method for flight test data compatibility check
p 95 A93-12732
- An experimental investigation of hydrogen-fueled supersonic combustor
p 53 A93-12733
- Compressible laminar and turbulent boundary layer computation for the three-dimensional wing
p 12 A93-12735
- Effect of hub treatment on performance of an axial flow compressor
p 53 A93-12736
- Vortex control technology
p 111 A93-14152
- Investigation of precise approach and landing of civil aircraft using integrated system based on GPS
p 180 A93-14159
- Numerical computations of turbomachinery cascade turbulent flows with shocks by using multigrad scheme
p 112 A93-14167
- A study of dynamic characteristics of axial compression systems by heat addition
p 202 A93-14168
- Mechanical testing analyses of new aluminum alloy SPF typical-parts in aircraft
p 196 A93-14174
- Vibration monitoring and fault diagnosis of inflight aircraft engines
p 170 A93-14176
- A fuzzy dynamic analysis method for aeromaintenance system
p 225 A93-14177
- Application of SPEED in aviation industry
p 225 A93-14178
- The optimum design of air cycle refrigeration system with high pressure water separation
p 202 A93-14180
- The fretting damage and effect of temperature in typical joint of aircraft construction
p 203 A93-14196
- A proposal concerning the dynamic analysis method of continuous gust design rules
p 181 A93-14197
- A parametric approach to preliminary design for aircraft and spacecraft configuration
p 225 A93-14201
- Application of CAD system in geometric modelling for helicopter preliminary design
p 153 A93-14203
- Designing to aircraft system effectiveness/cost/time with VERT - The system analysis method for aircraft
p 153 A93-14204
- Numerical solution of 3-D turbulent flows inside of new concept nozzles
p 114 A93-14211
- Flow characteristics of an S-shaped inlet at high incidence
p 114 A93-14213
- Engineering optimization of aeronautical structures
p 154 A93-14227
- Variable structure controller design and its real-time analysis for microprocessor-based flight control systems
p 181 A93-14229
- BUAA inertial terrain-aided navigation (BITAN) algorithm
p 149 A93-14235
- A new aircraft integrated positioning and communication system based on satellite
p 150 A93-14236
- An algebraic turbulence model with memory for the computation of three dimensional turbulent boundary layers
p 115 A93-14248
- Numerical analysis of the 3-D turbulent flow in an S-shaped diffuser
p 116 A93-14252
- The method for developing F-by-F load spectra of fighter aircraft based on manoeuvres
p 154 A93-14254
- Researches on sonic fatigue of the air-inlet duct of XX aircraft
p 154 A93-14256
- Study of aeroservoelastic stability of an aircraft
p 182 A93-14259
- The influence of main design parameters on helicopter air resonance and its source of instability
p 154 A93-14261
- An adaptive region method for computation of vortex sheet behind wing in compressible flow
p 116 A93-14262
- A prediction of the stalling for wings with rear separation
p 116 A93-14264
- Calculation of transonic flow over bodies of varying complexity using Singular Perturbation Method
p 116 A93-14265
- The numerical calculation for the coupling of multiple propeller discrete noise and its interaction with the fuselage boundary
p 231 A93-14268
- Calculation of sound field radiated by oscillating cascade
p 231 A93-14269
- Dynamic stability, coupling and active control of elastic vehicles with unsteady aerodynamic forces modeling
p 182 A93-14282
- A synthesized method in durability analysis
p 203 A93-14286
- An investigation of mode shift flutter suppression scheme for empennages
p 182 A93-14288
- An engineering method with artificial intelligence characteristics used for structural layout of wings
p 225 A93-14290
- Separation control and lift enhancement on airfoil using unsteady excitations
p 118 A93-14305
- Application of vibration-and-flutter integration analysis system for a trainer
p 226 A93-14311
- Investigation on air refueling scheduling
p 108 A93-14315
- The hazard and alarm of windshear
p 141 A93-14317
- Development of laser conducting landing system
p 150 A93-14320
- Some dynamic problems in design of aircraft landing gear
p 155 A93-14321
- Flow structures around a constant-rate pitching airfoil and mechanism of dynamic stall
p 118 A93-14332
- New model of bird impact response analysis and its engineering solution
p 156 A93-14336

- A method for optimizing the meridional passage of the rotor in centrifugal compressors p 119 A93-14344
- Experimental investigations of the separation behavior in 3D shock wave/turbulent boundary-layer interactions p 119 A93-14345
- Analysis and feedback control of aircraft flight in wind shear p 183 A93-14349
- An experimental study for interaction flow between shock wave and turbulent boundary layer p 120 A93-14355
- Numerical solution of radiative flowfield on the nose region of blunt bodies p 120 A93-14359
- A new method to study the forming process of complicated sheetmetal aero-parts p 204 A93-14363
- A digital simulation and its experimental investigation for the response of gas-turbine engines to intake flow distortion p 120 A93-14366
- Analysis and development of a total energy control system for a large transport aircraft p 183 A93-14372
- The employment of artificial intelligence for analyzing air accidents p 226 A93-14375
- Contact analysis for riveted and bolted joints of composite laminates p 204 A93-14384
- Aeroelastic analysis of composite wing with control surface p 157 A93-14386
- Euler solutions simulating strong shock waves and vortex phenomena over 3D wings p 121 A93-14392
- The Aircraft/Propulsion Integrated Assessment System p 226 A93-14396
- The influence of fighter agility on air combat effectiveness p 184 A93-14398
- A new method for calculation of helicopter maneuvering flight p 184 A93-14401
- Experimental study on the mechanism of favourable interferences of body strakes p 121 A93-14405
- Flight simulator development in China p 191 A93-14410
- A control technology of integrated system of engineering supported by software engineering environments p 226 A93-14415
- Stochastic modeling and adaptive control algorithm of brake bending p 227 A93-14417
- Viscous flow field prediction in axisymmetric passages p 204 A93-14478
- Digital simulation of transonic flow fields in a planar nozzle p 122 A93-14479
- Calculation of pressure ratio at nozzle exit with shock p 122 A93-14480
- Elimination of overtemperature in turbojet p 172 A93-14481
- A simple spanwise mixing model for turbulent diffusion and secondary flows in multistage axial-flow compressors p 204 A93-14482
- A method for optimizing the meridional passage in a centrifugal compressor p 204 A93-14483
- Dynamic characteristics of two new vibration modes of the disk-shell shaped gear p 204 A93-14484
- Optimum balancing of flexible rotor p 205 A93-14489
- Study on fracture failure of turbine blades in a series of turbojets p 205 A93-14493
- Prediction of the radiation characteristic of a helicopter exhaust jet p 172 A93-14494
- Estimation of maximal local temperature at exit of annular combustor p 172 A93-14496
- Hybrid real-time simulation of a two-rotor engine p 172 A93-14497
- Application of model reference adaptive control to speed control system in an aeroengine p 172 A93-14498
- A minimum-time acceleration control strategy for a two-rotor aeroengine p 172 A93-14499
- An AF3 algorithm for the calculation of transonic nonconservative full potential flows over wings or wing/body combinations p 125 A93-15341
- Improving anti-fatigue optimum design through AI-search strategy p 208 A93-15342
- Fewest-fault integral optimization algorithm for engine fault diagnosis p 173 A93-15343
- An impact dynamics investigation on some problems in bird strike on windshields of high speed aircraft p 197 A93-15346
- On dynamic behavior of cracked rotors p 208 A93-15401
- On orthogonal search method of flutter analysis p 208 A93-15402
- Improvement in application of eigenstructure assignment to flight control system design p 227 A93-15406
- Unsteady transonic aerodynamic loadings on the airfoil caused by heaving, pitching oscillations and control surface p 126 A93-15627
- Effects of vitiated air on the results of ground tests of scramjet combustor p 173 A93-16234
- An experimental investigation on the combustor with bypass flow in integral liquid fuel ramjet p 174 A93-16235
- A numerical study on the radiation characteristic of an elliptical exhaust jet p 174 A93-16236
- The numerical calculation of aircraft propeller noise p 174 A93-16239
- An investigation of real-time diagnostic technique on aeroengine p 174 A93-16844
- A preliminary investigation of a method to calibrate strain gauge balances by means of a reference balance p 210 A93-16845
- Effect of bird impact load types on blade response p 174 A93-16846
- Prospective application of neural networks in superresolution radars p 211 A93-16849
- Cabin noise source-path identification for AD-200 ultralight aircraft p 444 A93-19138
- Influence of a thermal barrier coating on the performance of a turboprop engine p 347 A93-19297
- [ASME PAPER 92-GT-38] An investigation on the artificial viscosity in the transonic stream function formulation p 246 A93-19302
- [ASME PAPER 92-GT-49] An investigation of post stall transients and recoverability of axial compression systems. I - A simplified method [ASME PAPER 92-GT-55] p 347 A93-19305
- An investigation of post stall transients and recoverability of axial compression systems. II - Numerical simulations [ASME PAPER 92-GT-56] p 347 A93-19306
- An investigation of spanwise mixing in multistage axial flow compressors p 247 A93-19314
- [ASME PAPER 92-GT-64] Development and industrial application of the 'all-over-controlled vortex distribution method' for designing radial and mixed flow impellers p 405 A93-19466
- [ASME PAPER 92-GT-262] Numerical research on flows in nonuniform cascades [ASME PAPER 92-GT-276] p 253 A93-19469
- A three-dimensional numerical method for turbomachinery blading p 254 A93-19482
- [ASME PAPER 92-GT-291] Investigation of the characteristics of 3-dimensional separated flow in an annular compressor blade row with large angles of attack p 259 A93-20116
- A fool-proof aerodynamic design code for turbine cascades p 259 A93-20117
- A CAD computer system for centrifugal compressor impeller with transonic inflow p 259 A93-20118
- A unified model for rotating stall and surge p 259 A93-20119
- The computation of internal flow fields in centrifugal compressor impellers p 259 A93-20120
- Investigation of the dynamic inflow's influence on rotor control derivatives p 266 A93-20802
- Wall-signature methods for high speed wind tunnel wall interference corrections p 375 A93-20803
- Experimental study of dynamic stall on an oscillating airfoil p 266 A93-20804
- Estimation of the maximum values of instantaneous distortion index DC sub theta p 266 A93-20806
- Fine control of Mach number in subsonic wind tunnel p 375 A93-20808
- A method of finite element dynamic model optimization p 367 A93-20812
- Superresolution radar imaging with linear prediction data extrapolation p 342 A93-20851
- Research on ISAR motion compensation and imaging by modeling electromagnetic data p 342 A93-20852
- The ISAR image-formation results of Boeing-727 p 342 A93-20857
- Investigation on bi-fall jet separated flow in a rectangular combustor p 459 A93-23778
- On closed-loop identification of a certain aeroengine under flight conditions p 519 A93-24026
- Analysis and correction of ionospheric time delay for differential GPS p 498 A93-24028
- Fully automatic FEM data pre-processing for aeronautical electrical machine p 538 A93-24030
- A multi-functional computer-aided aircraft exterior shape modelling prototype system p 504 A93-24032
- On experimental study of 3-D flow in self-correcting wind tunnel p 528 A93-24033
- Identification and conversion of foundation parameters for airport pavement p 538 A93-24035
- The vibration and flutter of composite material laminate p 543 A93-26617
- The effectiveness of porous squeeze film dampers for suppressing nonsynchronous motions p 545 A93-27316
- Study of the method for determining residual stress induced by machining in airplane canopies made of PMMA p 534 A93-27366
- A time dependent method in finite volume for transonic diffuser turbulent flows p 476 A93-27368
- A study on the marginal analysis method for the airline yield management p 487 A93-27370
- Investigation of cabin noise reduction in the Y12 p 506 A93-27371
- A method and a software for constructing F-by-F random load spectrum p 506 A93-27375
- Karman vortex street-airfoil interaction p 678 A93-33703
- Two important improvements upon wall pressure signature correction method of low-speed wind tunnel p 730 A93-33704
- Ground effect on the take-off characteristics of sea-based aircraft p 679 A93-33706
- Finite-volume-TVD scheme for 3-D Euler transonic flow computations in rotating curvilinear coordinates p 679 A93-33709
- The analysis of viscous wakes noise in axial flow compressor p 759 A93-33710
- On the favorable interference in the supersonic flow p 679 A93-33713
- Numerical solution of non-isentropic transonic cascade flow by time-marching method p 679 A93-33715
- Analysis of slender bodies of revolution with an angle of attack in extreme ground effect p 679 A93-33716
- Pressure fluctuations on the surface of two circular cylinders in tandem arrangements at high Reynolds numbers p 679 A93-33718
- Numerical simulation of passive control of shock-boundary layer interaction for transonic airfoil p 680 A93-33719
- Euler solution for wing-body combination at supersonic speeds p 680 A93-33722
- The influence of wall friction on sidewall interference p 680 A93-33723
- An experimental study on location of transitional separation bubble on a low Reynolds numbers airfoil p 680 A93-33725
- The numerical calculation and application of compressible boundary layers on laminar-flow-control and natural-laminar-flow wings p 680 A93-33727
- Calculation of optical and electric characteristics from hypersonic blunt-body wakes p 680 A93-33729
- Solution of Euler equations for complex forebody-inlet combinations p 680 A93-33730
- On the principle of sidewall effects on airfoil testing p 730 A93-33732
- The stagnation line solution of the equilibrium flow with radiation and mass injection p 680 A93-33733
- Numerical simulation of the turbulent drag reduction by plate manipulators p 681 A93-33736
- A kind of improved flux-split method for solving the Euler equations p 681 A93-33739
- The analysis and computation of viscous-inviscid interactive problem for three dimensional transonic flow p 681 A93-33741
- A numerical method of unsteady separating flow over delta wings p 681 A93-33746
- Studies of the dynamic stall problem on airfoils p 681 A93-33747
- Viscous-inviscid interaction coupled calculation of three-dimensional turbulent separated flow over dents p 681 A93-33748
- Simulation for hot jet by cryogenic wind tunnels p 730 A93-33750
- An Euler code with new energy equation and new enthalpy damping approach p 686 A93-34352
- Numerical simulation of hypersonic rarefied gas flow over blunt bodies p 687 A93-34356
- Correlation of conical interactions induced by sharp fins and serrations p 692 A93-35635
- A theoretical study on the ETHYLENE system - A fuzzy diagnostic expert system for large rotating machinery p 846 A93-36327
- Effects of pylon yaw and lateral stiffness on the flutter of a delta wing with external store p 800 A93-36330
- Investigation of subharmonic response of limit cycle flutter of wing-store system p 800 A93-36339
- The investigation of limit cycle amplitude of nonlinear nose gear p 800 A93-36342
- Comment on 'Equation decoupling - A new approach to the aerodynamic identification of unstable aircraft' p 818 A93-37406
- Study on dynamic characteristics of heat exchanger p 924 A93-40492
- Parameter selection of electro-impulse de-icing systems p 889 A93-40493
- A software for optimum design of an aircraft structure p 938 A93-40495
- The numerical model of supersonic air flow field with hydrogen transverse injection p 859 A93-41736
- Experimental investigation on starting of a turbojet engine in flight p 898 A93-41740
- The experimental investigation of combination effect by using injection effect of aeroengine jet exhaust p 898 A93-41742
- Processing integral impeller 4-coordinate numerically controlled milling machine p 926 A93-41749
- On model for predicting blade force defect in end wall boundary layer inside axial compressor cascade p 862 A93-42271

- FUM - An efficient MmB solver for steady inviscid flows p 862 A93-42431
- ISAR motion compensation and superresolution imaging of aircraft p 928 A93-42793
- Studies of superresolution range-Doppler imaging p 928 A93-43344
- Adaptive clutter suppression for airborne array radars using clutter subspace approximation p 883 A93-43411
- Investigation of helicopter air resonance in hover by complex coordinates and mutual excitation analysis p 893 A93-43777
- Passive control of shock wave/boundary layer interaction at hypersonic speed [AIAA PAPER 93-3249] p 966 A93-46794
- Artificial transition - A tool for high Reynolds number simulation? [AIAA PAPER 93-3258] p 967 A93-46799
- A computational method for inverse design of transonic airfoil and wing [AIAA PAPER 93-3482] p 982 A93-47260
- Multiple solutions of the transonic perturbation equation p 987 A93-47331
- The development of swirl five-hole probe p 987 A93-47341
- Improvement of conical similarity rule in swept shock wave/boundary layer interaction [AIAA PAPER 93-2941] p 1046 A93-48139
- 2-D theoretical analysis of circumferential grooved casing treatment p 1066 A93-48501
- Numerical simulation of unsteady flow in a transonic cascade p 1066 A93-48502
- Effect of steady-state circumferential pressure and temperature distortions on compressor stability p 1106 A93-48503
- Control of separation by dynamic air jets p 1066 A93-48504
- Experimental study on turbulent two-phase flow in a dual-inlet side dump combustor p 1106 A93-48506
- Acoustic experiments of two scaled-model propellers on the ground p 1172 A93-48507
- A calculation of secondary flows and deviation angles in multistage axial-flow compressors p 1066 A93-48509
- Simplified mathematical model and digital simulation of aeroengine p 1106 A93-48511
- An experimental investigation of endwall flow control in a compressor plane cascade wind tunnel p 1066 A93-48512
- Experimental investigation on effect of solid particles on blade pressure distribution in compressor cascade flow p 1066 A93-48513
- Dynamic analysis of a gear drive system in aeroengine p 1149 A93-48514
- Experimental investigation on patterned blades of compressor p 1066 A93-48515
- Numerical analysis of aerodynamic losses in film-cooled vane cascade p 1066 A93-48517
- Experimental study on heat transfer of separated impingement jets in short distance p 1149 A93-48518
- On engine parameter estimation with flight test data p 1107 A93-48520
- An aerodynamic design program for contra-rotating turbine cascades p 1067 A93-48521
- Acoustical properties of sound absorbing structures at high temperature p 1172 A93-48522
- Performance improvement of gas turbine with steam injection p 1107 A93-48523
- Experimental research on a semiwater-gas-fired gas-turbine p 1107 A93-48524
- Exhaust system model test and research p 1107 A93-48525
- Analysis on space shape and tension distribution of towed flexible cables p 1043 A93-48554
- Improving the design of the main fuel pump of Turbo-Jet 7 p 1107 A93-48555
- An experimental study on blade negative curving in a turbine cascade with a large turning angle p 1071 A93-49185
- A computer program for meridional flows in multistage axial flow compressors with turbulence and multi-effects of 3-D flows p 1165 A93-49186
- A blade element method for predicting the off-design performance of compressors p 1107 A93-49187
- Investigation of flows in a controlled diffusion airfoil cascade passage p 1071 A93-49188
- Vibration characteristics of mistuned bladed disk p 1108 A93-49190
- An optimization method for statistical ascertainment of the most probable peak temperature at combustor exit p 1108 A93-49195
- Effects of external excitation on the leading-edge separation flowfield p 1071 A93-49198
- Adaptive engine stall margin control p 1108 A93-49200
- Frontally tapered squared trench casing treatment for improvement of compressor performance p 1108 A93-49202
- A new type of fuel control model p 1108 A93-49204
- Drag characteristics of extra-thin-fin-riblets in an air flow conduit p 1151 A93-49240
- The numerical calculation on the flowfields of transverse jet interaction in the base of vehicle at supersonic speeds [AIAA PAPER 93-1931] p 1077 A93-49795
- Using a diagonal implicit algorithm to calculate transonic nozzle flow [AIAA PAPER 93-2345] p 1082 A93-50119
- Some key problems in the design of the NPU open-circuit low-turbulence wind tunnel p 1139 A93-51188
- Coupling characteristics analysis of elastic vehicle p 1169 A93-51189
- New derivation of relationship between Mach angle and Mach number p 1086 A93-51190
- Verification of the TOTLOS method for calculating aerodynamic loss in film-cooled turbine cascade p 1087 A93-51191
- A transfer matrix method for calculation of support stiffness of aeroengine stator p 1122 A93-51193
- A U-D factorization-based adaptive extended Kalman filter and its application to flight state estimation p 1169 A93-51198
- Multilevel solution of the elastohydrodynamic lubrication of concentrated contacts in spiroid gears p 1161 A93-52606
- A dual-Euler method for solving all-attitude angles of the aircraft [AIAA PAPER 93-3589] p 1223 A93-52682
- How to consider simulation fidelity and validity for an engineering simulator [AIAA PAPER 93-3598] p 1209 A93-52688
- An implicit difference scheme of Euler equation for unsteady transonic flow p 1182 A93-53852
- Numerical study of supersonic flow over a backward step with transverse injection p 1182 A93-53853
- Numerical solution of N-S equations for hypersonic flow over capsule-type vehicles p 1182 A93-53858
- A preliminary investigation of the control of separated flow by means of excitation p 1182 A93-53859
- Analytical expression of dissipation integral for kinetic energy integral equation p 1183 A93-53860
- A study of surge control by using pulse cut-off for dual spool turbo-jet engine p 1194 A93-53862
- Fault tolerant navigation for aircraft landing p 1191 A93-53866
- Transonic area rule about lifting configurations p 1183 A93-53868
- A study of aircraft global dynamic stability in rapid rolling maneuver p 1206 A93-53869
- Interconversion of two kinds of methods for cabin leakage test p 1192 A93-53874
- Integrated fire control simulation systems p 1192 A93-53876
- Harmonic oscillation in FBW system p 1206 A93-53877
- A study of damage tolerance of the landing gear structure p 1219 A93-53881
- An investigation of post stall transients and recoverability of axial compression systems [ISABE 93-7012] p 1184 A93-53988
- The effects of end-bend regulations of compressor blade on the outlet flow field [ISABE 93-7033] p 1185 A93-54009
- Impingement cooling with film coolant extraction in the airfoil leading edge regions [ISABE 93-7078] p 1220 A93-54054
- Longitudinal closed-loop pilot/vehicle analysis of DFBW aircraft during approach and landing p 1206 A93-54277
- Development of computational solid mechanics and its application in aerospace engineering p 1255 A93-54419
- Future development and application of general structural analysis softwares in the aviation industry in China p 1262 A93-54420
- Correlative behaviours of shock/boundary layer interaction induced by sharp fin and semicone p 1230 A93-54581
- An inverse method with regularity condition for transonic airfoil design p 1230 A93-54583
- A new method for resolving transonic nozzle flows using orthogonal stream-lines coordinate system p 1230 A93-54584
- The effects of reaction rate constants and catalytic wall on the hypersonic flow field over blunt bodies p 1230 A93-54586
- Design of shockless supersonic region in the axisymmetric transonic flow p 1230 A93-54587
- An experimental investigation on laminar boundary layer separation over a backward-facing step p 1230 A93-54588
- The effect of outboard leading-edge bluntness of double-delta wing on its aerodynamic characteristics p 1230 A93-54589
- Vectoring jet effects on the flow and aerodynamic behaviors of fighter model p 1241 A93-54590
- The experimental evaluation of annular ejector system under concurrent mixing and diffusion p 1250 A93-54593
- The forms of unsteady concentrated vortex-breakdown and its reactions to disturbance p 1231 A93-54594
- Second generation low order panel method and its application for a case of nacelle p 1231 A93-54595
- A study of military aircraft and engine tactical/technical performance evaluation p 1242 A93-54596
- A method for aerodynamic calculation by placing linear vari-strength vortex panels on airfoil contour p 1231 A93-54597
- The body-fitted coordinates generation for multi-element airfoils p 1231 A93-54598
- Two problems applied to the rheographical transformation of axisymmetric flow p 1231 A93-54599
- Heat transfer in a five-pass irregular channel with and without pin-fins p 1256 A93-54633
- Three-dimensional flow analysis of a four-stage transonic axial compressor with inlet guide vanes p 1232 A93-54643
- The economic effectiveness analysis of technological progress in aviation industry p 1265 A93-54854
- Worst-case wind modeling and its influence on capturing of aircraft penetration trajectory p 1248 A93-54857
- An experimental investigation of the effects of swirling flow on the performance of nozzles p 1247 A93-54859
- Vectoring thrust and two-dimensional nozzle p 1247 A93-54863
- Three-dimensional separated flow over a prolate spheroid p 1235 A93-55379
- Effect of blade leaning on the development of passage vortices and losses in the passage of turbine cascade with a great turning angle p 1236 A93-55397
- Experimental investigation of effect of particles on blade pressure distribution in impulse cascade flow p 1236 A93-55398
- Measurement of turbulent boundary layer in transonic flow p 1236 A93-55411
- An improved multiple line-vortex method for simulation of separated vortices of slender wings p 1236 A93-55412
- A study on low level windshear hazard index p 1240 A93-55414
- Optimization of oleo-pneumatic shock absorber of aircraft p 1243 A93-55415
- Design problems of three-dimensional contractions p 1236 A93-55584
- The crack initiation approach for durability analysis p 1259 A93-55585
- Dynamic analysis of annular cascade structures p 1259 A93-55586
- A new method for predicting the end wall boundary layers and the blade force defects inside the passage of axial compressor cascades p 1236 A93-55589
- A simulation study on take-off and landing dynamics of fly-by-wire control system aircraft p 1249 A93-55590
- One type of automatically adjusted difference scheme with artificial viscosity to calculate ablated exterior shapes [AD-A254108] p 19 A93-10855
- Arguments concerning wind tunnel test studies of the trim characteristics of objects with small asymmetries [AD-A254111] p 19 A93-10858
- Hybrid guidance for maneuvering flight vehicles [AD-A254110] p 69 A93-11798
- ACTA Aeronautica et Astronautica Sinica (selected articles) [AD-A255070] p 110 A93-13946
- Transition induced normal forces and their effects on the aerodynamic characteristics of slender sharp cones [AD-A256802] p 288 A93-15889
- A simulation study on take-off and landing dynamics of the aircraft of a fly-by-wire control system [AD-A259286] p 510 A93-19849
- YIDOUYU and its application to aircraft design [AD-A259262] p 513 A93-20605
- Stress calculation for the Sandia 34-meter wind turbine using the local circulation method and turbulent wind [DE93-004480] p 560 A93-22045
- An analysis of the reliability and maintainability of the Jian 6 and Jian 7 aircraft and ways to improve them [AD-A261060] p 678 A93-26238

- The blade curving effects in a turbine stator cascade with low aspect ratio
[AD-A261063] p 725 N93-26239
- Aviation production engineering: Selected articles
[AD-A261231] p 764 N93-27056
- Computational method in optimal bending-twisting comprehensive design of wings of subsonic and supersonic aircraft
[AD-A262374] p 806 N93-27694
- Detection performance of digital polarity sampled phase reversal code pulse compressors
[AD-A262930] p 842 N93-28289
- Effect of canard wing positions on aerodynamic characteristics of swept-forward wing
[AD-A262373] p 789 N93-28493
- International aviation (Selected articles)
[AD-A262566] p 765 N93-28576
- The infrared measurement for the reentry-body-translation
[AD-A263100] p 914 N93-29134
- Solution of Euler equations for forebody-inlet ensemble of aircraft at high angle of attack
[AD-A263905] p 876 N93-29862
- The application of concentric vortex simulation to calculating the aerodynamic characteristics of bodies of revolution at high angles of attack
[AD-A263879] p 876 N93-29919

CZECHOSLOVAKIA

- Modified surge in an axial flow compressor
[ASME PAPER 92-GT-59] p 247 A93-19309
- Profile losses of an annular turbine cascade in unsteady periodic flow
[ASME PAPER 92-GT-153] p 249 A93-19380
- Boundary layer effects on the transonic flow in a straight turbine cascade
[ASME PAPER 92-GT-155] p 249 A93-19382
- On aerodynamic loading of linear compressor cascades
[ASME PAPER 92-GT-275] p 253 A93-19468
- Prediction of secondary losses in axial compressors
[ASME PAPER 92-GT-288] p 254 A93-19479
- Velocity vector LDA measurement inside a pitched blade impeller
p 924 A93-40390
- Numerical solution of steady and unsteady Euler equations
p 973 A93-46988
- Czechoslovak development and experience in flight data recorder readout and analysis
p 168 N93-15162

D

DENMARK

- Noise evaluation of light propeller-driven aircraft
p 398 A93-19189
- Control measures used to reduce community noise from civil aviation in Denmark
p 425 A93-19191
- Prediction of rotor dynamic destabilizing forces in axial flow compressors
p 272 A93-22263

E

EGYPT

- Further study of high speed single free jets
p 873 A93-43687
- Blowout of turbulent disc/pilot stabilized jet diffusion flames
[ISABE 93-7026] p 1213 A93-54002

F

FINLAND

- Calculation of transonic viscous flow around a delta wing
p 113 A93-14191
- Ice prediction systems for runways
p 376 A93-22174
- CWAS - Clean wing advisory system: A new approach to ice detection
[AIAA PAPER 93-0747] p 516 A93-24835
- Effects of equipment calibration, test flight procedures and analysing methods on the accuracy of ILS glide path measurements
p 881 A93-41600
- Steering system of a vehicle, such as a snow removing machine for airfields
[CA-PATENT-APPL-SN-1293201] p 83 N93-10367
- Numerical investigations into the base drag of various wedges using the base flow model developed by Mauri Tanner
[REPT-B-36] p 26 N93-12414
- DYNAC: A computer program for analyzing the dynamical stability of aircraft
[REPT-B-31] p 66 N93-12415
- Motion simulation of underwater vehicles
[VTT-PUBS-97] p 443 N93-18698
- Interaction between ice and propeller
[VTT-TIED-1281] p 841 N93-27832

FRANCE

- Long-duration balloon flights in the middle stratosphere
p 40 A93-11369
- Concept for an open-neck stratospheric balloon with long-duration flight capability
p 40 A93-11371
- Resonance frequencies of a gondola submitted to a forced rotation under a stratospheric balloon
p 27 A93-11384
- ONERA makes progress in rotor aerodynamics, aeroelasticity, and acoustics
p 2 A93-11621
- Numerical solution of a free-boundary problem in hypersonic flow theory - Nonequilibrium viscous shock layers
p 8 A93-11920
- Numerical simulation of compressible mixing zones
p 10 A93-12427
- Experimental analysis of turbulence within supersonic mixing layers
p 11 A93-12428
- Effect of wall heating on a supersonic turbulent boundary layer
p 11 A93-12429
- Flow problems posed by reentry in planetary atmospheres
p 11 A93-12432
- Rotation and cavitation of a marginal vortex
p 11 A93-12433
- Design of propulsion systems for low operating costs
p 55 A93-13405
- Aircraft tracking optimization of parameters selection
p 3 A93-13628
- Super Puma MK II - Rotor and gearbox fatigue
p 46 A93-13636
- Aircraft lightning initiation and interception from in situ electric measurements and fast video observations
p 140 A93-14064
- Integration of flight control and carrier landing aid system
[ONERA, TP NO. 1993-6] p 181 A93-14187
- Computational methods applied to the aerodynamics of spaceplanes and launchers
[ONERA, TP NO. 1992-140] p 114 A93-14216
- Experimental study of the acoustic spinning modes generated by a helicopter turboshaft engine
[ONERA, TP NO. 1992-141] p 230 A93-14266
- Experimental and theoretical studies of helicopter rotor-fuselage interaction
[ONERA, TP NO. 1992-142] p 120 A93-14356
- Progress and taboos in air safety orientations of research in human factors in air transport
p 141 A93-14374
- Aircrew integrated management
p 141 A93-14376
- Analytical solutions for hypersonic flow past slender power-law bodies at small angle of attack
p 122 A93-14550
- Coriolis effects on Goertler vortices in the boundary-layer flow on concave wall
p 123 A93-14564
- Choice of materials for military helicopters
p 158 A93-15028
- Thermoplastic and thermosetting matrix composite structures - Comparison of mechanical properties
p 197 A93-15029
- The modeling of forging and precision-casting forming processes
p 207 A93-15030
- Introduction to regulatory problems for supersonic transports
p 234 A93-15032
- Study of a Mach 2 supersonic transport aircraft
p 124 A93-15034
- Airports, air traffic control, and their clients - Reflections on system optimization
p 234 A93-15035
- LOCSTAR - A satellite radiodetermination system for Europe
p 150 A93-15037
- Control of the pilot-system interface
p 166 A93-15040
- Methodology in the development of avionics
p 166 A93-15043
- Cost control of the A320 software - The aircraft manufacturer's point of view
p 227 A93-15044
- A longitudinal control law integrating flight controls and engine controls
p 186 A93-15046
- Onboard maintenance monitoring systems in modern aircraft
p 167 A93-15047
- The static-memory crash recorders
p 167 A93-15048
- The United States in the conquest of the hypersonic
p 109 A93-15056
- Tomorrow's security
p 141 A93-15058
- The Concorde wing - A useful model
p 126 A93-16400
- Identification of weakly nonlinear dynamic systems by means of random excitations
p 227 A93-16472
- Strong coupling between inviscid fluid and boundary layer for airfoils with a sharp edge. II - 2D unsteady case for isolated airfoil and straight blade cascade
p 126 A93-16473
- Propulsion of a supersonic transport: What are the challenges? II - Achievements
p 174 A93-16852
- The ramjet engine in high speed propulsion
p 174 A93-16853
- The pioneers of thermopulsive nozzles
p 235 A93-16854

Toulouse - Flight tests of the Airbus A340

- p 159 A93-16859
- Flight safety and human errors
p 141 A93-16860
- Photoluminescent thermography - Feasibility study with pointwise measurements
p 211 A93-16861
- Zvezda - The Russian pioneer in the field of life-support and escape systems for aeronautics and space
p 195 A93-16878
- Recent supersonic transition studies with emphasis on the swept cylinder case
p 127 A93-17252
- The SSR mode-S data-link
p 312 A93-18553
- Airborne MLS equipment
p 312 A93-18555
- Assessment of a 3-D Euler code for subsonic turbine vane flows and study of the non radial blade stacking
[ASME PAPER 92-GT-63] p 247 A93-19313
- Advances in the numerical integration of the 3-D Euler equations in vibrating cascades
[ASME PAPER 92-GT-170] p 351 A93-19396
- Coupled 3-D aeroelastic stability analysis of bladed disks
[ASME PAPER 92-GT-171] p 351 A93-19397
- Numerical simulation of the flow field around supersonic air-intakes
[ASME PAPER 92-GT-206] p 251 A93-19430
- Navier-Stokes computation on a pivoting doors thrust reverser and comparison with tests
[ASME PAPER 92-GT-254] p 353 A93-19463
- Ramjet NOx emission - Use of a 3D CFD method for the combustor design of a super/hyper-sonic transport propulsion system
[ASME PAPER 92-GT-255] p 353 A93-19464
- Direct numerical simulation of nitric oxide evolution in underexpanded jets
[ASME PAPER 92-GT-372] p 355 A93-19534
- Analysis of three-dimensional viscous flow in a supersonic axial flow compressor rotor with emphasis on tip leakage flow
[ASME PAPER 92-GT-388] p 257 A93-19543
- Aircraft engine integration for the M88-Rafale couple
[ASME PAPER 92-GT-403] p 322 A93-19552
- Applications of space techniques to civil aviation operations
p 312 A93-20007
- The GPS system - Satellite radio-navigation
p 312 A93-20008
- Numerical prediction of instabilities in transonic internal flows using an Euler TVD code
[AIAA PAPER 93-0072] p 262 A93-20184
- GPS continuity - Initial findings
p 314 A93-21167
- INS/DGPS integration for trajectory determination of a test vehicle
p 315 A93-21178
- Simulation in aeronautics
p 437 A93-21868
- International Conference on Aviation Weather Systems, 4th, Paris, France, June 24-28, 1991, Preprints
p 426 A93-22101
- Integrated runway meteorological observation system (IRMOS/SIOMA)
p 428 A93-22128
- Maximum hail concentration that can be met by an aircraft in stormy precipitations
p 430 A93-22152
- Microbursts detection with airborne Doppler lidar
p 433 A93-22201
- Evaluation of clear-air radar PROUST and Doppler radar RONSARD for airport low level-wind shear detection
p 433 A93-22202
- Some aspects of the aerodynamic methodology in hypersonic vehicle concept studies
[AIAA PAPER 92-5027] p 272 A93-22303
- Validation of aerodynamic simulation methods for Hermes spaceplane and future hypersonic vehicles
[AIAA PAPER 92-5065] p 273 A93-22335
- Improvement of the ONERA 3D icing code, comparison with 3D experimental shapes
[AIAA PAPER 93-0169] p 275 A93-22603
- Experimental studies of the turbulent structure of supersonic mixing layers
[AIAA PAPER 93-0217] p 278 A93-22633
- Validation of a Navier-Stokes code using a (k,epsilon) turbulence model applied to a three-dimensional transonic channel
[AIAA PAPER 93-0293] p 279 A93-22693
- Numerical simulation of three-dimensional supersonic flows using Euler and boundary layer solvers
[AIAA PAPER 93-0531] p 284 A93-23272
- Exact-gradient shape optimization of a 2-D Euler flow
p 462 A93-24308
- A numerical method for solving Navier-Stokes equations for low Mach number compressible flows
p 463 A93-24672
- TGV tunnel entry simulations using a finite element code with automatic remeshing
[AIAA PAPER 93-0890] p 471 A93-24950
- Hypersonic inviscid and viscous flow computations with a new optimized thermodynamic equilibrium model
[AIAA PAPER 93-0893] p 471 A93-24953
- Validation of electromagnetic-topology concepts on a complex structure
[ONERA, TP NO. 1992-63] p 542 A93-25327

- MESH3D - A tool for the construction of three-dimensional meshes
[ONERA, TP NO. 1992-164] p 561 A93-25339
- High temperature thin film strain gauges
[ONERA, TP NO. 1992-171] p 542 A93-25346
- Experimental study of three-dimensional separation on a large-size model
[ONERA, TP NO. 1992-174] p 473 A93-25348
- Design of an advanced nacelle for a very high bypass ratio engine
p 505 A93-25362
- Future supersonic transport studies at Aerospatiale
p 505 A93-25491
- Recent developments in international laminar flow research programs for transport aircraft
[ONERA, TP NO. 1992-163] p 457 A93-26878
- Eurostar rotor aerodynamic tests
[ONERA, TP NO. 1992-173] p 475 A93-26880
- Design of an optimal single reflective holographic helmet display element
p 517 A93-26886
- Characteristic multigrid method application to solve the Euler equations with unstructured and unnested grids
p 476 A93-27065
- Numerical simulation of homogeneous non-Gaussian random vector fields
p 561 A93-27584
- Ignition and spread of combustion within a supersonic boundary layer
p 535 A93-27732
- The high accuracy applications of the GPS system to static positioning
p 500 A93-28193
- GNSS - A global system of satellite-aided navigation
p 500 A93-28194
- Differential GPS and its applications in the aeronautical realm
p 500 A93-28195
- Volcanic clouds
p 487 A93-28196
- Can one do without the magnetic reference?
p 501 A93-28197
- Satcom Pacific Ocean trials
p 501 A93-28198
- Night aircraft noise index and sleep research results
p 558 A93-28485
- An overview on practical application of helicopter noise certification rules
p 487 A93-29442
- Numerical analysis of the three-dimensional boundary layer on a turbomachinery rotor blade
p 685 A93-34341
- Calculation of the flow around a high-lift airfoil using an explicit code and an algebraic Reynolds stress model
p 685 A93-34344
- An implicit treatment of two equations turbulence models for high speed flow computations
p 686 A93-34350
- Taking into account surface roughness in computing hypersonic re-entry body
p 686 A93-34354
- Computation of supersonic crossflow separation using a new parabolized Navier-Stokes code
p 687 A93-34355
- Reactive and dissipative hypersonic flow in a wind tunnel nozzle
p 687 A93-34358
- Computation of turbulent compressible flows on a DLR wing and a blade to blade passage using an upwind scheme
p 687 A93-34359
- Zero-gravity atmospheric flight by robust nonlinear inverse dynamics
p 728 A93-34550
- Rotor blade airfoil design by numerical optimization and unsteady calculations
[ONERA, TP NO. 1992-65] p 766 A93-35993
- Influence of coupling incidence and velocity variations on the airfoil dynamic stall
p 767 A93-35999
- The development of a crashworthy composite fuselage and landing gear
p 799 A93-36001
- The Cabri two-seat helicopter - Design and first flights
p 799 A93-36019
- A technique to correct airborne Doppler data for coordinate transformation errors using surface clutter
p 807 A93-37699
- Electrostatic discharges
[ONERA, TP NO. 1992-82] p 844 A93-38567
- Nonlinear analysis and flight dynamics
[ONERA, TP NO. 1992-83] p 818 A93-38568
- Application of a full potential code to the definition of a transonic test section
[ONERA, TP NO. 1992-84] p 822 A93-38569
- Modal identification of aircraft structures - ONERA methods
[ONERA, TP NO. 1992-86] p 802 A93-38570
- Thin gradient heat fluxmeters developed at ONERA
[ONERA, TP NO. 1992-87] p 831 A93-38571
- Viscous nonequilibrium flow calculations
[ONERA, TP NO. 1992-89] p 771 A93-38573
- Calculations of viscous nonequilibrium flows in nozzles
[ONERA, TP NO. 1992-91] p 771 A93-38574
- Contribution of visualization to the study of unsteady aspects of vortex breakdown
[ONERA, TP NO. 1992-93] p 771 A93-38576
- Potential and prospects of intermetallic materials for applications in the aerospace industry
[ONERA, TP NO. 1992-99] p 824 A93-38580
- Experiments on shock wave-boundary layer interaction at high Mach number with entropy layer effect
[ONERA, TP NO. 1992-101] p 771 A93-38581
- Infrared thermography for hot-shot wind tunnel
[ONERA, TP NO. 1992-103] p 831 A93-38583
- Structural stability of 'beta-CEZ' alloy
[ONERA, TP NO. 1992-106] p 824 A93-38586
- Supersonic vortical flows around an ogive-cylinder - Laminar and turbulent computations
[ONERA, TP NO. 1992-111] p 771 A93-38588
- Structured grid variational adaption - Reaching the limit?
[ONERA, TP NO. 1992-114] p 771 A93-38590
- A new adaptive test section at ONERA
Chalais-Meudon
[ONERA, TP NO. 1992-117] p 822 A93-38592
- Digital image processing applied to heat transfer measurement in hypersonic wind tunnel
[ONERA, TP NO. 1992-118] p 831 A93-38593
- A numerical procedure for aerodynamic optimization of helicopter rotor blades
[ONERA, TP NO. 1992-121] p 771 A93-38595
- Aerodynamic rotor loads prediction method with free wake for low speed descent flights
[ONERA, TP NO. 1992-122] p 772 A93-38596
- Validation of R85/METAR on the Puma RAE flight tests
[ONERA, TP NO. 1992-123] p 802 A93-38597
- Study of soft-in-torsion blades - ROSOH operation
[ONERA, TP NO. 1992-124] p 803 A93-38598
- Application of European CFD methods for helicopter rotors in forward flight
[ONERA, TP NO. 1992-125] p 772 A93-38599
- Blade-vortex interaction noise - Prediction and comparison with flight and wind tunnel tests
[ONERA, TP NO. 1992-126] p 851 A93-38600
- The measurement of blade deflections - A new implementation of the strain pattern analysis
[ONERA, TP NO. 1992-127] p 831 A93-38601
- Numerical calculation of helicopter rotor equations and comparison with experiment
[ONERA, TP NO. 1992-128] p 772 A93-38602
- Designing new multi-phase intermetallic materials based on phase compatibility considerations
[ONERA, TP NO. 1992-131] p 772 A93-38605
- Transonic and supersonic flow calculations around aircrafts using a multidomain Euler code
[ONERA, TP NO. 1992-137] p 772 A93-38610
- Laser velocimetry around helicopter blades in the DNW wind tunnel of the NLR
[ONERA, TP NO. 1992-143] p 831 A93-38613
- Two-dimensional laser velocimetry for the study of dual-flow jets with flight effect in the CEPRA 19 anechoic wind tunnel
[ONERA, TP NO. 1992-144] p 831 A93-38614
- Laser-velocimeter study of vortex breakdown on a 70-deg swept delta wing in incompressible flow
[ONERA, TP NO. 1992-147] p 773 A93-38728
- Analysis of turbulence in supersonic flows by means of laser velocimetry
[ONERA, TP NO. 1992-148] p 773 A93-38729
- Activities of the GARTEUR high lift research program
[ONERA, TP NO. 1992-152] p 803 A93-38731
- Testing techniques for straight transonic and supersonic cascades
[ONERA, TP NO. 1992-155] p 773 A93-38734
- Materials problems connected with the propulsion of supersonic air carriers
[ONERA, TP NO. 1992-157] p 824 A93-38736
- Schlieren device and holographic interferometer for hypersonic flow visualization
[ONERA, TP NO. 1992-160] p 832 A93-38739
- Definition and evaluation of new helicopter rotor blade tips
[ONERA, TP NO. 1992-179] p 773 A93-38741
- Shock/boundary layer interaction in a hypersonic flow in the presence of an entropy layer
[ONERA, TP NO. 1992-181] p 773 A93-38743
- Shock wave/boundary layer interaction in a two-dimensional laminar hypersonic flow
[ONERA, TP NO. 1992-182] p 773 A93-38744
- A viscous-inviscid solver for high-lift incompressible flows over multi-element airfoils at deep separation conditions
[ONERA, TP NO. 1992-183] p 774 A93-38745
- Viscous-inviscid calculation of high-lift separated compressible flows over airfoils and wings
[ONERA, TP NO. 1992-184] p 774 A93-38746
- Phenomenology and simplified modeling of a vortex wake generated by a transverse jet
[ONERA, TP NO. 1992-194] p 774 A93-38755
- A French look at the future supersonic transport
[ONERA, TP NO. 1992-209] p 803 A93-38763
- The limit model of a thin strip exhibiting two delaminations
[ONERA, TP NO. 1992-212] p 832 A93-38764
- Toward the silent helicopter
[ONERA, TP NO. 1992-229] p 851 A93-38774
- Theoretical and experimental study of the behavior of particles passing through a shock wave
[ONERA, TP NO. 1992-233] p 774 A93-38777
- The role of the radiologist in the medicolegal procedure after an aviation accident
p 853 A93-39701
- An existence theorem for a free boundary problem of hypersonic flow theory
p 857 A93-40405
- Passive control of a shock wave/turbulent boundary layer interaction in a transonic flow
p 858 A93-40444
- Effect of structural uncertainties on flutter analysis
p 924 A93-40445
- Effect of environment on creep-fatigue crack propagation in turbine disc superalloys
[ONERA, TP NO. 1993-5] p 916 A93-41023
- Infrared thermography characterization of Goertler vortex type patterns in hypersonic flows
[ONERA, TP NO. 1993-13] p 925 A93-41029
- Infrared thermography of plastic instabilities in a single crystal superalloy
[ONERA, TP NO. 1993-18] p 916 A93-41031
- Toward the second-generation supersonic transport
[ONERA, TP NO. 1993-26] p 890 A93-41038
- Analysis of implicit treatments for a centred Euler solver
p 864 A93-42449
- Helicopter control law based on sliding mode with model following
p 907 A93-42559
- Hypersonic flows for reentry problems. Vols. 1 & 2
[ISBN 0-387-54428-3] p 864 A93-42576
- Experiments on shock-wave/boundary-layer interactions produced by two-dimensional ramps and three-dimensional obstacles
p 865 A93-42589
- Experimental study of the flow around a double ellipsoid configuration
p 867 A93-42603
- Solution of the Euler equations around a double ellipsoidal shape using unstructured meshes and including real gas effects
p 867 A93-42604
- Navier-Stokes calculations over a double ellipse and a double ellipsoid by an implicit non-centered method
p 867 A93-42607
- Hypersonic flows over a double or simple ellipse
p 868 A93-42614
- Contribution to Problem 6 using an upwind Euler solver with unstructured meshes
p 869 A93-42627
- Evaluation of contributions for test case 7.1.1 and 7.1.2
p 870 A93-42636
- Experimental density flowfields over a delta wing located in rarefied hypersonic flows
p 870 A93-42637
- Quasi monodimensional inviscid non equilibrium nozzle flow computation
p 927 A93-42646
- Progress and taboos in flight safety - Human-factors research in air transportation
p 879 A93-42654
- Reduction of aerodynamic skin-friction drag
p 871 A93-42656
- The ring laser gyro and its applications
p 927 A93-42657
- The impact of air traffic on the atmospheric environment
p 936 A93-42659
- Evolution of European air space toward precision navigation (P/RNAV)
p 882 A93-43369
- The Airborne Collision Avoidance System (ACAS)
p 883 A93-43370
- Experimental results on RIAS digital beamforming radar
p 929 A93-43392
- A Mode S implementation - Experiments about data-link and interconnected Mode S sensors
p 883 A93-43409
- Digital pulse compression with low range sidelobes
p 929 A93-43463
- Field by field hybrid upwind splitting methods
[AIAA PAPER 93-3302] p 950 A93-45000
- Behavior of precipitating water drops under the influence of electrical and aerodynamical forces
p 1034 A93-45176
- Hypersonic flow calculations using a multidomain MUSCL Euler solver
p 960 A93-45547
- Comment on 'Flow near the trailing edge of an airfoil'
p 961 A93-45754
- On the legitimacy and accuracy of downwash computations by panel methods on 3D wings
p 970 A93-46885
- Method of characteristics for computing three-dimensional boundary layers
p 970 A93-46886
- Experiments on shock wave/boundary layer interaction in hypersonic flow
p 970 A93-46888
- Societe Francaise des Mecaniciens, SNECMA, and ONERA, Symposium on Recent Advances in Compressor and Turbine Aerothermodynamics, Courbevoie, France, Nov. 24, 25, 1992, Reports
p 1001 A93-46926
- Turbine blade forces due to partial admission
p 1029 A93-46928
- Inverse problem using S2-S1 approach for the design of the turbomachine with splitter blades
p 971 A93-46929

- Supersonic through flow compressors - A preliminary study: COVAXS p 1001 A93-46930
- 3D viscous flow analysis in axial turbine including tip leakage phenomena p 972 A93-46940
- Navier-Stokes flow simulation in a 2D high pressure turbine cascade with a cooled slot trailing edge p 972 A93-46941
- Intensive industrial use of 3D Euler numerical methods for axial flow turbine analysis and design p 1002 A93-46943
- On the shock-fitting scheme of Hall-Crawley for time-linearized time-harmonic flows using Euler equations p 972 A93-46946
- Three-dimensional analysis of turbine rotor flow including tip clearance [ASME PAPER 93-GT-111] p 987 A93-47446
- Aeroelastic computation for a flexible airfoil using the small perturbation method comparison with wind-tunnel results [ONERA, TP NO. 1993-43] p 987 A93-47448
- Helicopter external noise prediction and reduction [ONERA, TP NO. 1993-48] p 1039 A93-47450
- Preliminary results of the ISM campaign - The Landes, South West France p 1161 A93-47553
- On the compression process in a free-piston shock-tunnel p 1136 A93-48041
- Comparison of ENO and TVD schemes for the parabolized Navier-Stokes equations [AIAA PAPER 93-2970] p 1049 A93-48164
- Experimental study of 3-D separation on a large scale model [AIAA PAPER 93-3007] p 1053 A93-48197
- The European Data Base - A new CFD validation tool for the design of space vehicles [AIAA PAPER 93-3045] p 1057 A93-48225
- CARS studies in hypersonic flows [AIAA PAPER 93-3047] p 1144 A93-48227
- DSMC numerical investigation of rarefied compression corner flow [AIAA PAPER 93-3096] p 1061 A93-48270
- High lift airfoil flow simulation using a wall-corrected Algebraic Stress Model [AIAA PAPER 93-3109] p 1061 A93-48280
- A two layer k-epsilon computation of transonic viscous flow including separation over the DLR-F5 wing [AIAA PAPER 93-3110] p 1061 A93-48281
- Experimental study of transitional axisymmetric shock-boundary layer interactions at Mach 5 [AIAA PAPER 93-3131] p 1063 A93-48296
- Aerodynamic phenomena in high pulse repetition rate XeCl laser p 1150 A93-48806
- STANAG 3910 - The data bus for the next generation of European avionics systems [SAE PAPER 931595] p 1104 A93-49344
- Position sensor with two wavelength time domain multiplexing for civil aircraft application p 1104 A93-49432
- New concepts for fiber optic position sensors p 1106 A93-49477
- Second-order effects in hypersonic laminar boundary layers p 1073 A93-49529
- Real gas effects in two- and three-dimensional hypersonic, laminar boundary layers p 1073 A93-49530
- The computation over unstructured grids of inviscid hypersonic reactive flow by upwind finite-volume schemes p 1073 A93-49532
- Viscous analysis of high pressure turbine inlet guide vane flow including cooling injections [AIAA PAPER 93-1798] p 1074 A93-49687
- Methodology for commercial engine/aircraft optimization [AIAA PAPER 93-1807] p 1166 A93-49696
- Advanced SST auxiliary air intakes design and analysis [AIAA PAPER 93-2304] p 1082 A93-50088
- A comparison between centered and upwind schemes for two-phase compressible flows [AIAA PAPER 93-2346] p 1083 A93-50120
- 3-D turbomachinery Euler and Navier-Stokes calculations with a multidomain cell-centered approach [AIAA PAPER 93-2576] p 1085 A93-50292
- A two-dimensional analysis of multiple matrix cracking in a laminated composite close to its characteristic damage state p 1157 A93-50405
- Investigation of a combustion zone behind a wedge p 1146 A93-51631
- Thermometry inside a swirling turbulent flame - CARS advantages and limitations p 1146 A93-51634
- Microstructure of yttria stabilized zirconia-hafnia plasma sprayed thermal barrier coatings [ONERA, TP NO. 1993-54] p 1146 A93-51936
- High-frequency acoustic radiation from a curved duct of circular cross section [ONERA, TP NO. 1993-55] p 1173 A93-51937
- New calculation methods contribution on turbomachinery design and development [ONERA, TP NO. 1993-60] p 1092 A93-51940
- Implicit schemes for unsteady Euler equations on unstructured meshes [ONERA, TP NO. 1993-64] p 1171 A93-51944
- Aerodynamic calculation of complex three-dimensional configurations p 1094 A93-52426
- High temperature heat exchangers for gas turbines and future hypersonic air breathing propulsion [ONERA, TP NO. 1993-75] p 1218 A93-53596
- Origin of the carbon rich sliding interface in alkali containing matrix-SiC nicalon fibre composites [ONERA, TP NO. 1993-77] p 1212 A93-53598
- CARS temperature measurements in combustion [ONERA, TP NO. 1993-78] p 1212 A93-53599
- Corrosion of ceramic matrix composites [ONERA, TP NO. 1993-82] p 1213 A93-53602
- A reactive approach for distributed air traffic control [ONERA, TP NO. 1993-83] p 1190 A93-53603
- CRAASH - A coordinated collision avoidance system [ONERA, TP NO. 1993-84] p 1191 A93-53604
- The acoustics of axial compressors [ONERA, TP NO. 1993-102] p 1226 A93-53615
- Acoustic-wave propagation in ducts and free-field radiation [ONERA, TP NO. 1993-103] p 1226 A93-53616
- 3D laminar and 2D turbulent computations with the Navier-Stokes solver FLU3M [ONERA, TP NO. 1993-105] p 1180 A93-53618
- Stability analysis through bifurcation theory. I, II [ONERA, TP NO. 1993-108] p 1225 A93-53620
- Non-linear flight dynamics [ONERA, TP NO. 1993-109] p 1206 A93-53621
- Investigation of the flow field through a variable pitch fan rotor with an inlet total pressure distortion [ISABE 93-7029] p 1184 A93-54005
- CFD for ramjet and scramjet powered vehicles [ISABE 93-7035] p 1197 A93-54011
- 3D and 2.5D viscous flow computations for axial flow turbine blades [ISABE 93-7093] p 1186 A93-54069
- Recent developments performed at ONERA for the simulation of 3D inviscid and viscous flows in turbomachinery by the solution of Euler and Navier-Stokes equations [ISABE 93-7094] p 1186 A93-54070
- Optimization of afterbodies and engine nozzle by using CFD methods [ISABE 93-7098] p 1187 A93-54074
- On the numerical simulation of the two-dimensional flow field around a hypersonic air-intake-compressibility effects [ISABE 93-7100] p 1187 A93-54076
- Compact heat exchanger fitted to engines of the inverted type [ISABE 93-7120] p 1221 A93-54095
- A Eulerian/Lagrangian modelling to calculate the evolution of a water droplets spray [ISABE 93-7121] p 1221 A93-54096
- A new methodology for helicopter internal noise reduction application to the AS332 L2 p 1243 A93-54723
- Low-frequency combustion instability mechanisms in a side-dump combustor p 1247 A93-55220
- AGARD index of publications, 1989-1991 [AGARD-INDEX-89-91] p 104 A93-10610
- Active control of aeroacoustic couplings by means of adaptive systems [ECL-91-18] p 64 A93-11576
- Using NDT techniques in the maintenance of aeronautical products [REPT-921-430-102] p 88 A93-11587
- Directory of factual and numeric databases of relevance to aerospace and defence R and D [AGARD-R-777] p 104 A93-11710
- Aerodynamic Engine/Airframe Integration for High Performance Aircraft and Missiles [AGARD-CP-498] p 213 A93-13199
- Tests of models equipped with TPS in low speed ONERA F1 pressurized wind tunnel p 213 A93-13201
- Detailed analysis of wing-nacelle interaction for commercial transport aircraft p 213 A93-13203
- Flight analysis of air intake/engine compatibility p 161 A93-13212
- Combustion in supersonic flows p 199 A93-14627
- Propulsion and Energetics Panel Working Group 20 on Test Cases for Engine Life Assessment Technology [AGARD-AR-308] p 176 A93-14890
- LARZAC HP turbine disk crack initiation and propagation spin pit test p 176 A93-14892
- Aeroplane crashes on the runway: Validation and final evaluation of the method of modeling an airframe structure [IMFL-91-32] p 165 A93-15126
- Ground Support Equipment (GSE) for Aircraft Condition Monitoring System (ACMS) p 110 A93-15158
- Monitoring of powerplants in advanced commercial aircraft p 178 A93-15171
- Airbus Industrie TCAS experience p 152 A93-15186
- Fiber reinforced composites: A new class of glass and glass ceramic materials for thermomechanical applications [REPT-921-430-104] p 200 A93-15490
- Effect of Reynolds number on the standards of a simplified anemometric probe [IMFL-91-31] p 293 A93-17542
- Combustion instabilities in a side-dump model ramjet combustor p 362 A93-17613
- Prediction of the performances in combustion of ramjets and stato-rockets by isothermal experiments and modeling p 363 A93-17622
- Turbomachinery and potential computations [DS-2026] p 363 A93-17740
- Direct numerical simulation of combustion in turbulent supersonic flow [DS-2138] p 393 A93-17746
- SNECMA M88 engine development status [ASME-90-GT-118] p 363 A93-17849
- Improving military transport aircraft through highly integrated engine-wing design [DS-1607] p 333 A93-17850
- Turbine engine combustor design at SNECMA [DS-2129] p 363 A93-17851
- The beta-CEZ, a new high performance titanium alloy for aerospace engines [DS-2022] p 393 A93-17852
- Aerodynamic design and analysis of fans using 3D computational codes [DS-2140] p 294 A93-17880
- The technological evolution of high thrust turbine engines [DS-1881] p 364 A93-17882
- Fatigue of turboengine discs [DS-2136] p 364 A93-18149
- Control of in-service damage: Application to aircraft engines [DS-2027] p 364 A93-18151
- Photoluminescent thermography in hypersonic blowdown wind tunnel: Feasibility study with pinpoint measurement [ONERA-NT-1992-8] p 297 A93-18617
- Exact-gradient shape optimization of a 2D Euler flow [INRIA-RR-1540] p 422 A93-18623
- A Blottner type numerical model for nonequilibrium viscous hypersonic flows in upwind finite elements [INRIA-RR-1476] p 297 A93-18648
- Influence of the physical modelling of viscous terms on hypersonic flow computations [INRIA-RR-1493] p 297 A93-18652
- Electron beam probing of blow-down hypersonic flows [ONERA-NT-1992-7] p 298 A93-18701
- Aircraft Accidents: Trends in Aerospace Medical Investigation Techniques [AGARD-CP-532] p 490 A93-19653
- Aid in investigation by figure animation p 491 A93-19659
- Air accidents in the French Air Force p 492 A93-19676
- Helicopter accidents over water in the national navy: Epidemiological study over the period 1980-1991 p 493 A93-19686
- Liquid crystal displays replacing the CRT and CLE of future cockpits p 518 A93-19783
- Flight Testing [AGARD-CP-519] p 510 A93-19901
- Flight tests of the transport aircraft viewed from the industrial standpoint p 510 A93-19903
- Method for developing the RAFALE flight control system p 512 A93-19912
- RAMSES: Multi-spectral experimental radar station installed on board the Transall p 550 A93-19925
- Topological approach for the study of electromagnetic coupling [ONERA-P-1992-2] p 551 A93-20230
- Optimization and sensitivity computations for the conception of internal ventilation system in the aircraft engine [ETN-93-93375] p 521 A93-20913
- Mission planning systems for tactical aircraft (pre-flight and in-flight) [AGARD-AR-313] p 496 A93-21187
- The testing of fixed wing tanker and receiver aircraft to establish their air-to-air refuelling capabilities, volume 11 [AGARD-AG-300-VOL-11] p 514 A93-21305
- Damage tolerance of a helicopter rotor high-strength steel p 555 A93-21322
- Supersonic transport: Which material for the engine [DS-2023] p 522 A93-21459

- Modelisation and computation of composite materials
p 537 A93-21518
- Numerical modelling of induced effects of lightning strike on an all composite helicopter p 703 A93-24879
- Three-dimensional compressible stability-transition calculations using the spatial theory p 783 A93-27431
- Calculation of fully three-dimensional separated flow with an unsteady viscous-inviscid interaction method
p 786 A93-27455
- Investigations on entropy layer along hypersonic hyperboloids using a defect boundary layer
p 787 A93-27462
- Homenthalpic-flow approach for hypersonic inviscid non-equilibrium flows
[INRIA-RR-1652] p 788 A93-28440
- Heat Transfer and Cooling in Gas Turbines
[AGARD-CP-527] p 901 A93-29926
- Experimental study of heat transfer close to a plane wall heated in the presence of multiple injections (subsonic flow)
p 901 A93-29931
- Aerothermic calculations of flows in interdisc cavities of turbines p 903 A93-29947
- Modeling of a turbulent flow in the presence of discrete parietal cooling jets p 904 A93-29960
- Sonic boom problem for future highspeed aircraft
[ONERA-NT-1990-3] p 876 A93-30020
- Computation of far-field helicopter rotor tone noise
[ONERA-P-1990-5] p 943 A93-30110
- Contribution to the study of the interaction between acoustic waves and coherent structures induced by a prismatic cylinder in a rectangular cavity
[ONERA-NT-1990-10] p 918 A93-30203
- Evolution of radar data processing in the French air traffic control system p 886 A93-30325
- French aerospace equipment p 1041 A93-31734
- AGARD Engine Disc Cooperative Test Programme
[AGARD-R-766-ADD] p 1004 A93-31741
- Crack growth prediction models p 1004 A93-31747

G

GERMANY

- Multidisciplinary design of composite aircraft structures by Lagrange p 76 A93-10273
- MPC75 as the forerunner of a new regional aircraft family p 37 A93-10776
- Transonic profile design in curvilinear coordinates using an approximate factorization algorithm p 7 A93-10778
- Current developments in structural technology
p 77 A93-10780
- Precision navigation with an integrated navigation system p 29 A93-10782
- Real time DGPS service for precise positioning - Activities in the Federal Republic of Germany
p 1 A93-11027
- Transport processes in hypersonic flows
p 7 A93-11302
- A split-matrix Runge-Kutta type space marching procedure p 8 A93-11921
- Critical considerations on European air transport politics p 103 A93-12718
- Helicopter in-flight simulator ATTHes - A multipurpose testbed and its utilization
[AIAA PAPER 92-4173] p 43 A93-13315
- Air transport within the European single market - How will it look after 1992? A suggested view on the future
p 104 A93-13424
- Loads at the nose landing gears of civil transport aircraft during towbarless towing operations p 45 A93-13629
- Analysis of multiple crack propagation in stiffened sheet p 81 A93-13638
- Condensation of nitrogen in hypersonic flows - Measurements confirm a theoretical model
p 111 A93-13945
- Economical view on composite structures maintenance
[SME PAPER EM92-102] p 233 A93-14103
- Numerical investigation of the unsteady flow through a counter-rotating fan p 112 A93-14166
- A very efficient tool for the structural analysis of hypersonic vehicles under high temperature aspects
p 203 A93-14194
- MELINA - A multi-block, multi-grid 3D Euler code with sub block technique for local mesh refinement
p 115 A93-14217
- Aeroelastic investigations as applied to Airbus airplanes p 155 A93-14280
- MPC75 - The evolution of a new regional airliner for the late nineties p 155 A93-14289
- Design and fabrication of a composite transmission housing for a helicopter tail rotor p 156 A93-14339
- The Hermes Carrier Aircraft (HCA)
p 195 A93-14347
- The influence of rotor and fuselage wakes on rotorcraft stability and control p 183 A93-14373

- High capacity aircraft p 157 A93-14395
- Experimental working position simulator to analyse, develop and optimize concepts for computer-aided Air Traffic Management p 191 A93-14412
- Comment on "Experimental study on autoignition in a scramjet combustor" p 172 A93-14525
- The opportunities and risks of the supersonic transport market - The Lufthansa point of view
p 234 A93-15033
- The design development of the monolithic CFRP centre fuselage skin of the European fighter aircraft
p 159 A93-15782
- Composite wing results of Deutsche Airbus technology program p 109 A93-15808
- The production of a monolithic CFRP fuselage skin for the European Fighter Aircraft p 109 A93-15810
- Numerical simulation of a three-dimensional wave packet in a growing flat plate boundary layer
p 128 A93-17265
- Technological challenges with smart structures in German aircraft industry p 320 A93-17714
- The smart structures technology in the vibration control of helicopter blades in forward flight p 366 A93-17721
- Motion and decay of trailing vortices within the atmospheric surface layer p 425 A93-18548
- DLR, Annual report 1991/92 p 383 A93-18717
- DGLR/AIAA Aerodynamics Conference, 14th, Aachen, Germany, May 11-14, 1992, Proceedings, Vols. 1 & 2
[DGLR BERICHT 92-03] p 444 A93-19126
- Experience with boundary element methods to calculate the aerodynamic characteristics of aircraft
p 243 A93-19130
- Helicopter main rotor/tail rotor noise radiation characteristics from scaled model rotor experiments in the DNW p 445 A93-19142
- New design concepts for silencing aeroacoustic wind tunnels p 445 A93-19147
- Experimental investigation of tip clearance noise in axial flow machines p 445 A93-19155
- On sound attenuation in boundary layers
p 446 A93-19164
- A contribution to noise improvements for aircraft by noise measurement evaluation p 448 A93-19190
- Acoustic performance of low pressure axial fan rotors with different blade chord length and radial load distribution p 449 A93-19212
- Aeroacoustic wind tunnel testing of a counterrotating shrouded propfan-model p 449 A93-19213
- Experimental determination of the main noise sources in a propfan model by analysis of the acoustic spinning modes in the exit plane p 449 A93-19214
- Prediction of jet mixing noise in high-speed flight
p 450 A93-19216
- The noise of jet aircraft flying with high speeds at low altitudes p 450 A93-19218
- Experimental results on propeller noise attenuation using an 'active noise control' technique p 450 A93-19223
- Reduction of propeller noise by active noise control
p 450 A93-19224
- A numerical investigation into the nozzle flow of high by-pass turbofans
[ASME PAPER 92-GT-10] p 346 A93-19283
- Viscous flows in centrifugal compressor diffusers at transonic Mach numbers
[ASME PAPER 92-GT-48] p 246 A93-19301
- Three dimensional transonic flow measurements in an axial turbine with conical walls
[ASME PAPER 92-GT-61] p 247 A93-19311
- Simulation of the secondary air system of aero engines
[ASME PAPER 92-GT-68] p 348 A93-19318
- Design and rotor performance of a 5:1 mixed-flow supersonic compressor
[ASME PAPER 92-GT-73] p 348 A93-19323
- Experimental analysis of transonic flow through the variable nozzle of a radial inflow turbine
[ASME PAPER 92-GT-90] p 248 A93-19336
- Aerodynamic design of pivotable nozzle vanes for radial-inflow turbines
[ASME PAPER 92-GT-94] p 349 A93-19340
- Experimental and theoretical investigation of a research atomizer/combustion chamber configuration
[ASME PAPER 92-GT-137] p 401 A93-19369
- Blade excitation by circumferentially asymmetric rotating stall in centrifugal compressors
[ASME PAPER 92-GT-148] p 351 A93-19376
- Excitation of blade vibration due to surge of centrifugal compressors
[ASME PAPER 92-GT-149] p 351 A93-19377
- Unsteady pressure measurements in a rotating centrifugal impeller
[ASME PAPER 92-GT-152] p 402 A93-19379
- Transonic flow through turbine cascades with nonuniform pitch
[ASME PAPER 92-GT-158] p 250 A93-19385

- Integration of turbo-expander- and turbo-ramjet-engines in hypersonic vehicles
[ASME PAPER 92-GT-204] p 353 A93-19428
- Investigations on a radial compressor tandem-rotor stage with adjustable geometry
[ASME PAPER 92-GT-218] p 404 A93-19440
- Advanced Ducted Engines - Impact of unsteady aerodynamics on fan vibration properties
[ASME PAPER 92-GT-228] p 252 A93-19445
- MTR390 - Engine for the future
[ASME PAPER 92-GT-250] p 353 A93-19459
- Balance of moments for hypersonic vehicles
[ASME PAPER 92-GT-251] p 253 A93-19460
- Prediction of 2D viscous transonic flow in compressor cascades using a semi-empirical shock/boundary-layer interaction method
[ASME PAPER 92-GT-277] p 253 A93-19470
- Unsteady boundary-layer transition in flow periodically disturbed by wakes
[ASME PAPER 92-GT-283] p 254 A93-19475
- Calculation of wake-induced unsteady flow in a turbine cascade
[ASME PAPER 92-GT-306] p 255 A93-19496
- The effects of incident turbulence and moving wakes on laminar heat transfer in gas turbines
[ASME PAPER 92-GT-377] p 406 A93-19535
- Optimization aspects of an ejector type hypersonic thrust nozzle
[ASME PAPER 92-GT-402] p 355 A93-19551
- Double mode behaviour of bladed disk assemblies in the resonance frequency range, visualized by means of holographic interferometry
[ASME PAPER 92-GT-438] p 357 A93-19580
- Ceramics for aero-engine applications
[ASME PAPER 92-GT-439] p 388 A93-19581
- Accurate solution of the 2D Euler equations with an efficient cell-vertex upwind scheme
[AIAA PAPER 93-0071] p 262 A93-20183
- A theoretical approach for describing secondary instability features in three-dimensional boundary-layer flows
[AIAA PAPER 93-0080] p 263 A93-20192
- Optimization of anisotropic structures considering strength, stiffness and aeroelastic constraints
[AIAA PAPER 92-4796] p 408 A93-20291
- The legal status of ekranoplanes p 453 A93-20900
- Water instead of chemical corrosives against aircraft paint - Environment-friendly paint-stripping methods could mean drastic cost reductions for the aircraft industry
p 239 A93-21850
- Robust control of the separation of hypersonic lifting vehicles
[AIAA PAPER 92-5013] p 385 A93-22289
- Study of flow phenomena in high speed intakes
[AIAA PAPER 92-5029] p 272 A93-22304
- German university research in hypersonics
[AIAA PAPER 92-5033] p 239 A93-22307
- CFD analysis of hypersonic chemically reacting flowfields around a generic shape
[AIAA PAPER 93-0323] p 281 A93-23015
- Time-dependent 3-component laser-Doppler-anemometer and simultaneous position measurements in the flow of an aircraft engine
p 538 A93-23809
- Terrorism and air-specific perils and the liability of air freight carriers under Article 17 of the Warsaw Agreement p 570 A93-24252
- Responsibility and assignment of roles on overlong flights p 570 A93-24253
- Measurements of jet aircraft emissions at cruise altitude, I - The odd-nitrogen gases NO, NO₂, HNO₂ and HNO₃
p 556 A93-24391
- Helmet Mounted Sight and display testing
p 517 A93-26883
- New slant visual range measuring device promises improved airport operations p 529 A93-27395
- Integration of high bypass ratio engines on modern transonic wings for regional aircraft p 506 A93-27479
- Increased safety through knowledge-based pilot assistance p 518 A93-27499
- Dornier 228 experimental with laminar wing
p 506 A93-27500
- Combustion and reaction kinetics: Proceedings of the 22nd International Annual Conference of ICT, Karlsruhe, Germany, July 2-5, 1991 p 535 A93-27726
- Data communication for airborne differential GPS/GLONASS application p 499 A93-27910
- Integration of a course and position reference system with GPS p 499 A93-27911
- DLR research program overview on airport surface movement guidance and control p 499 A93-27912
- Ground Movement and Control System (GMCS)
p 499 A93-27913
- SIPORT DEPCOS and SIPORT ARRCOS - More than an electronic airstrip replacement p 499 A93-27914

- Hypersonic viscous flow simulations p 478 A93-27926
- Loudness versus level of aircraft noise p 557 A93-28477
- The costs of noise at the new Munich airport p 558 A93-28493
- Laminar-flow instrumentation for wind-tunnel and flight experiments p 479 A93-28605
- Short-term atmospheric effects of high-altitude aircraft emissions p 559 A93-28865
- Modal sensors and actuators for individual blade control [AIAA PAPER 93-1703] p 712 A93-34225
- Frequency-domain identification of BO 105 derivative models with rotor degrees of freedom p 712 A93-34263
- An integrated flow simulation system on a parallel computer. I - Basic concept. II - The flow solver p 688 A93-34370
- Optimization of endurance performance p 713 A93-34400
- Enhancement of endurance performance by periodic optimal camber control p 727 A93-34541
- Taking to the skies under hydrogen power - Deutsche Aerospace Airbus studies the use of alternative fuels for civil aviation p 677 A93-34947
- Stable cross type parachute with inflation aid [AIAA PAPER 93-1201] p 702 A93-35152
- Overview of Tiger dynamics validation program p 794 A93-35907
- A closed loop controller for BVI impulsive noise reduction by Higher Harmonic Control p 849 A93-35963
- ATHeS - A helicopter in-flight simulator with high bandwidth capability p 821 A93-35988
- Evaluation of tilt rotor aircraft design utilizing a realtime interactive simulation p 798 A93-35989
- High temperature fracture mechanism of gas-pressure sintered silicon nitride p 825 A93-38893
- A novel aircraft-based tandem mass spectrometer for atmospheric ion and trace gas measurements p 825 A93-40672
- Experimental investigation of the management of large-sized drops and the onset of Marangoni-convection p 926 A93-41700
- Calibration of thermal anemometer at very low Reynolds numbers under microgravity p 926 A93-41729
- Periodic maximum range cruise with singular control p 890 A93-41903
- Transonic aerodynamics including strong effects from heat addition p 862 A93-42428
- Simulation of nonequilibrium hypersonic flows p 863 A93-42443
- Enhanced numerical inviscid and viscous fluxes for cell centered finite volume schemes p 864 A93-42444
- Workshop on hypersonic flows for reentry problems January 22-25th 1990 (Antibes) - Inaugural address p 856 A93-42577
- Gas-kinetic and Navier-Stokes simulations of reentry flows p 865 A93-42582
- Computation of flows over 2D ramps p 866 A93-42595
- Computational results for flows over compression ramps p 866 A93-42599
- Implicit upwind finite-difference simulation of laminar hypersonic flow over a 2D ramp p 867 A93-42600
- Experimental study of the longitudinal hypersonic corner flow field - HERMES-R&D research program, problem no. 5 p 867 A93-42602
- An upwind relaxation method for hypersonic viscous flows over a double-ellipsoidal body p 867 A93-42606
- Computation of the hypersonic flow over a double ellipsoid p 868 A93-42610
- Numerical simulation of laminar hypersonic flow past a double-ellipsoid p 868 A93-42612
- Viscous and inviscid hypersonic flow about a double ellipsoid p 868 A93-42616
- Hypersonic viscous flow past double ellipse and past double ellipsoid - Numerical results p 868 A93-42618
- Attempt to evaluate the computations for test case 6.1 - Cold hypersonic flow past ellipsoidal shapes p 869 A93-42620
- Inviscid hypersonic flow over a delta wing p 870 A93-42634
- Experiments on the heat transfer and on the aerodynamic coefficients of a delta wing in rarefied hypersonic flows p 870 A93-42638
- Rarefied gas flow around a 3D-deltawing p 870 A93-42639
- Non-equilibrium flow in an arc heated wind tunnel p 910 A93-42642
- On the accuracy and efficiency of CFD methods in real gas hypersonics p 871 A93-42869
- Antenna design for adaptive airborne MTI p 884 A93-43440
- Real time PRF control system for SAR p 884 A93-43464
- Satellite navigation in traffic management p 914 A93-43549
- Increasing airport safety and capacity using automated maneuvering area control p 885 A93-43550
- Effects of longitudinal vortex generators on heat transfer and flow loss in turbulent channel flows p 1021 A93-44222
- Diffusion controlled evaporation of a multicomponent droplet - Theoretical studies on the importance of variable liquid properties p 1021 A93-44224
- DeAs - A programming system for data processing and system control: New software developments for wind tunnel operation p 1036 A93-44452
- Visualization and view simulation based on transputers p 1037 A93-45150
- How to enhance safety for future space transportation systems p 1015 A93-45444
- Shock tube application - High enthalpy European wind tunnels p 1011 A93-45452
- Formation of the shock reflection on a wedge p 1023 A93-45476
- Applications of infrared measurement technique in hypersonic facilities p 1024 A93-45505
- A laser induced fluorescence system for the high enthalpy shock tunnel (HEG) in Goettingen p 1024 A93-45506
- Evaluation methodologies applied for pressurized fuselages of Airbus A/C p 948 A93-45796
- Propeller noise reduction by means of unsymmetrical blade-spacing p 1039 A93-46706
- Prediction of three-dimensional low frequency unsteady transonic flow and forced vibration in axial turbine stages p 971 A93-46934
- The determination of hybrid analytical-numerical solutions for the three-dimensional compressible boundary layer p 1029 A93-46979
- Numerical simulation of transition in two- and three-dimensional boundary layers p 973 A93-46980
- Multigrid methods for calculating 3D flows in complex geometries p 973 A93-46984
- The three-dimensional representation of the pressure distribution on wedged delta wings with supersonic leading edges in supersonic-hypersonic flow p 973 A93-46989
- The three-dimensional representation of the lift and pitching moment coefficients on wedged rectangular wings in supersonic flow p 973 A93-46990
- Numerical simulation of linear interference wave development in three-dimensional boundary layers p 1029 A93-46993
- A Laplace interaction law for the computation of viscous airflow flow in low and high speed aerodynamics [AIAA PAPER 93-3462] p 979 A93-47244
- Inflight antenna diagram determination of spaceborne and airborne SAR-systems p 1161 A93-47583
- A refined procedure to generate calibrated imagery from airborne synthetic aperture radar data p 1162 A93-47657
- Nonlocal vs. local instability of compressible flows including body metric, flow divergence and 3D-wave propagation [AIAA PAPER 93-2982] p 1051 A93-48175
- Instability of hypersonic flow past blunt cones - Effects of mean flow variations [AIAA PAPER 93-2983] p 1051 A93-48176
- Investigation of the flowfield over parallel-arranged launch vehicles [AIAA PAPER 93-3060] p 1058 A93-48237
- Hypersonic configuration optimization with an Euler/boundary layer coupling technique [AIAA PAPER 93-3116] p 1062 A93-48286
- A new flying qualities criterion for flying wings [AIAA PAPER 93-3668] p 1128 A93-48346
- Computational methods for viscous hypersonic flows p 1152 A93-49523
- Increase in mortality rates due to aircraft noise p 1163 A93-49551
- A comparison between the impact of noise from aircraft, road traffic and trains on long-term recall and recognition of a text in children aged 12-14 years p 1163 A93-49552
- The influence of nocturnal aircraft noise on sleep and on catecholamine secretion p 1163 A93-49554
- Results of a low-altitude flight noise study in Germany - Acute extraural effects p 1163 A93-49557
- Specific features of military low-altitude flight noise - Criteria for risk of damage and physiological effects p 1164 A93-49558
- Review - Extraural health effects of aircraft noise p 1164 A93-49559
- Trajectory control for a low-lift re-entry vehicle p 1141 A93-49592
- Numerical analysis of high aspect ratio cooling passage flow and heat transfer [AIAA PAPER 93-1829] p 1153 A93-49714
- An approach to the stall monitoring in a single stage axial compressor [AIAA PAPER 93-1872] p 1112 A93-49747
- Real gas simulation of air Blow-Down Facilities [AIAA PAPER 93-2022] p 1137 A93-49859
- A new and working automatic calibration machine for wind tunnel internal force balances [AIAA PAPER 93-2467] p 1138 A93-50214
- Neutron-induced single event upsets in static RAMs observed at 10 KM flight altitude p 1158 A93-50561
- Reentry control to a drag vs. energy profile [AIAA PAPER 93-3790] p 1143 A93-51385
- The influence of swirl generator characteristics on flow and combustion in turbulent diffusion flames p 1159 A93-51632
- An extended insight into hypersonic flow phenomena using numerical methods p 1093 A93-51999
- Numerical simulation of shock/shock and shock-wave/boundary-layer interactions in hypersonic flows p 1093 A93-52000
- Computation of subsonic viscous and transonic viscous-inviscid unsteady flow p 1094 A93-52012
- Identification of actuation system and aerodynamic effects of direct-lift-control flaps p 1103 A93-52435
- Stringer peeling effects at stiffened composite panels in the postbuckling range p 1160 A93-52453
- Identification of nonlinear mechanical systems using combined state and parameter evaluation p 1224 A93-52732
- Flight safety in Europe p 1227 A93-53726
- Stumbling blocks for airport construction in the new German federal states p 1227 A93-53727
- Axial flow compressors - Mechanical design trends [ISABE 93-7061] p 1199 A93-54037
- Heat transfer and material temperature conditions in the leading edge area of impingement-cooled turbine vanes [ISABE 93-7076] p 1220 A93-54052
- Developments towards versatility in digital engine control units [ISABE 93-7088] p 1202 A93-54064
- Numerical simulation of a two-dimensional supersonic mixed-compression inlet [ISABE 93-7107] p 1188 A93-54083
- Numerical study of nitric oxide formation in a hypersonic ramjet engine [ISABE 93-7125] p 1204 A93-54100
- Heat loads as key problem of hypersonic flight p 1222 A93-54276
- New digital capacitive measurement system for blade clearances p 1254 A93-54376
- Optimization of sandwich structures with respect to local instabilities with MBB-LAGRANGE p 1255 A93-54540
- Optimization of large scale systems in elasticity p 1255 A93-54544
- Zeppelin NT - A new concept in airship technology, based on rigid airship principles [AIAA PAPER 93-4045] p 1242 A93-54612
- Performance simulation of a combustion engine charged by a variable geometry turbocharger. I - Prerequisites, boundary conditions and model development. II - Simulation algorithm, computed results p 1256 A93-54648
- Review of helicopter noise research in Europe p 1263 A93-54725
- Results about the structure of the shock wave reflection process for strong incoming shock waves p 1233 A93-54810
- Future aero engine design trade offs p 1246 A93-54836
- All-composite fan blade for advanced ducted engines p 1246 A93-54837
- Potential use of alternative fuels in aviation p 1243 A93-54838
- Presence and future of the electro-chemical processes in aero-engine production p 1257 A93-54840
- Combustor development for advanced helicopter engines p 1246 A93-54841
- ADP - Engine concept of the future p 1246 A93-54842
- Laser and skill enhance results p 1257 A93-54843
- Integration of an integrated helmet system for PAH 2 p 1244 A93-55298
- Vibration excitation in laminar hypersonic boundary layers p 1237 A93-56028
- Algebraic determination of the shock wave shape in axisymmetric flow over a circular cylinder p 1237 A93-56030
- Predevelopment of a flight control system for a small civil aircraft p 1249 A93-56031
- Experimental studies in the Aachen hypersonic shock tunnel p 1251 A93-56032
- Pressure measurements at supersonic speeds on the research configuration ELAC I p 1237 A93-56033
- Supersonic and hypersonic flow computations for the research configuration ELAC I and comparison to experimental data p 1237 A93-56034

Low-speed aerodynamics of the hypersonic research configuration ELAC I p 1237 A93-56035
Flow computation for the hypersonic configuration ELAC I at low speeds and large incidence p 1238 A93-56036

Experimental investigations of hypersonic shock-boundary layer interaction p 1238 A93-56037
Computation of viscous hypersonic non-equilibrium blunt body flow p 1238 A93-56038
Performance analysis of a turbofan as a part of an airbreathing propulsion system for space shuttles p 1252 A93-56039

Computation of hypersonic high-temperature nozzle flow p 1238 A93-56040
Inverse simulation: A tool for the validation of simulation programs - First results p 1249 A93-56046
Comparison of flyover noise data from aircraft at high subsonic speeds with prediction p 100 A93-10674
Prediction of jet mixing noise for high subsonic flight speeds p 100 A93-10685
Reduction of propeller noise by active noise control p 101 A93-10692

Surface protection in the aircraft industry [MBB-Z-0432-92-PUB] p 72 A93-11027
Activities report of Lufthansa [ETN-92-92100] p 28 A93-11319
Activities report of the German Institute for Flight Safety [ETN-92-92272] p 28 A93-11375
Motion errors and compensation possibilities p 212 A93-13052

The real aperture antenna of SAR, a key element for performance p 213 A93-13053
Investigation of interference phenomena of modern wing-mounted high-bypass-ratio engines by the solution of the Euler-equations p 213 A93-13204
Recent developments in low-speed TPS-testing for engine integration drag and installed thrust reversal simulation p 160 A93-13207

Overview on test cases for computation of internal flows in turbomachines p 214 A93-13209
The influence of intake swirl distortion on the steady-state performance of a low bypass, twin-spool engine p 214 A93-13211

A novel-high-performance system for recording and analysing instantaneous total pressure distortion in air intakes p 214 A93-13215
The jet behaviour of an actual high-bypass engine as determined by LDA-measurements in ground tests p 175 A93-13218

Comparative performance tests of a pitot-inlet in several European wind-tunnels at subsonic and supersonic speeds p 130 A93-13221
Investigation of the flowfield around an isolated bypass engine with fan and core jet p 215 A93-13227
Integration of turbo-ramjet engines for hypersonic aircraft p 175 A93-13230
RB 199 high pressure compressor stage 3 spin pit tests p 176 A93-14893

An experimental investigation of base bleed effect on the wake turbulent structure behind a two-dimensional blunt model [MPIS-9/1991] p 139 A93-15131

Engine technologies for future spaceplanes [ETN-92-92732] p 177 A93-15143
Proceedings of the 16th Symposium on Aircraft Integrated Monitoring Systems [DLR-MITT-92-01] p 167 A93-15152

Software flexibility and configuration control for the A340/A330 Aircraft Condition Monitoring System (ACMS) p 167 A93-15154
Software for flight recorder data evaluation developed by Lufthansa p 230 A93-15163
Integrated engine control and monitoring with experiences derived from OLMOS p 178 A93-15168
EJ 200 engine monitoring system: On- and off-board data capture, analysis, and management system p 178 A93-15172

RB199 engine oil system failure diagnostics by comparison of measured and calculated oil consumption using the OLMOS on-board monitoring system p 178 A93-15173

Some experiments and ideas on GPA before reaching steady state of engine p 178 A93-15175
Experimental analysis of steady-state and dynamic monitoring of power shaft turbines p 178 A93-15176
Modelling the engine temperature distribution between shut down and restart for life usage monitoring p 169 A93-15177

Sensor fault detection using nonlinear observer and polynomial classifier p 170 A93-15182
Neural network based condition monitoring p 230 A93-15183

Personal computer based test- and emulation equipment for maintenance and ground support p 110 A93-15185

Modeling limits of the EMV analysis program CONCEPT by example of the influence of a helicopter structure on a frame antenna [MBB-UD-0614-92-PUB] p 223 A93-15487

Identification of icing water clouds by NOAA AVHRR satellite data [DLR-FB-92-11] p 434 A93-16477

Contribution to the dynamic feedforward control of multivariable systems and to the optimal design of command functions [DLR-FB-92-05] p 441 A93-16515

On flutter behavior of a 2-D compressor cascade in incompressible flow [DLR-FB-91-26] p 418 A93-16543

Combining direct and indirect methods in optimal control: Range maximization of a hang glider [REPT-313] p 371 A93-16618

Hot experimental technique: A new requirement of aerothermodynamics [MBB-FE-202-S-PUB-480] p 293 A93-17543

Test and integration concept for complex helicopter avionic systems [MBB-UD-0605-91-PUB] p 343 A93-17547

Mathematical optimization: A powerful tool for aircraft design [MBB-FE-2-S-PUB-478] p 331 A93-17564

Practical architecture of design optimisation software for aircraft structures taking the MBB-LAGRANGE code as an example [MBB-FE-251-S-PUB-479] p 331 A93-17565

Modern helicopter technologies at MBB and the application in future programmes [MBB-UD-0599-91-PUB] p 331 A93-17566

Mission oriented investigation of handling qualities through simulation [MBB-UD-0600-91-PUB] p 332 A93-17567

Current European rotorcraft research activities on development of advanced CFD methods for the design of rotor blades (BRITE/EURAM DACRO project) [MBB-UD-0601-91-PUB] p 293 A93-17568

Influence of cross section variations on the structural behaviour of composite rotor blades [MBB-UD-0602-91-PUB] p 332 A93-17569

Integrated helmet system testing for a nightflying helicopter [MBB-UD-0604-91-PUB] p 343 A93-17570

Numerical investigation of swirl-airfoil interactions in transonic area [MPIS-8/1991] p 297 A93-18627

Experimental and numerical examinations of the influence of inlet distortion perturbations on the working behavior of turbofan compressors [ETN-93-92733] p 364 A93-18628

Realization of real time graphics in vehicles with high dynamic motion [ETN-93-92739] p 443 A93-18630

Determination of the zone of the stall cell by means of the baroclinic wave theory p 424 A93-18733

Rotating stall cell and Von Karman vortex street: A meteorological theory p 424 A93-18734

Performance of controlled diffusion blades p 424 A93-18735

Correlations between engineering, medical and behavioural aspects in fire-related aircraft accidents p 494 A93-19693

X-31A high angle of attack and initial post stall flight testing p 511 A93-19911

System identification for X-31A project support: Lessons learned so far p 512 A93-19914

Development of a realtime DGPS system [DLR-MITT-92-06] p 503 A93-20749

Development of cure cycles: From laboratory analysis and testing to production of large scale composites [MBB-Z-0442-92-PUB] p 536 A93-20845

Fundamentals of adaptive anticipation techniques for the detection of threatening air traffic conflicts: Investigation of the horizontal proximity situation in the case of expected heading changes [DLR-MITT-91-21] p 503 A93-21004

Summaries of the 1991 publications of DLR research reports and DLR communications [ETN-93-92588] p 572 A93-21022

Heat loads as key problem of hypersonic flight [MBB-FE-202-S-PUB-0486] p 484 A93-21054

Numerical methods for aerothermodynamic design of hypersonic space transport vehicles [MBB-FE-211-S-PUB-0481] p 514 A93-21056

Application of the Euler method EUFLEX to a fighter-type airplane configuration at transonic speed [MBB-FE-211-S-PUB-0489-A] p 484 A93-21059

The influence of the rotor test facilities ROTEST and ROTOS on the rotor inflow [DLR-MITT-91-16] p 522 A93-21173

Calculation of noise emission caused by jet aircraft during takeoff, approach and horizontal flyover [DLR-MITT-91-15] p 569 A93-21368

The integrated design and manufacturing of composite structures for aircraft using an advanced tape layering technology [MBB-LME-251-S-PUB-0491-A] p 515 A93-21401

Allowable compression strength for CFRP-components of fighter aircraft determined by CAI-test [MBB-FE-221-S-PUB-0483] p 537 A93-21462

Selection criteria for metallic high temperature structural materials in hypersonic flying equipment [MBB-LME-221-HYPAC-PUB-2-A] p 515 A93-21479

GARTEUR damage mechanics for composite materials: Analytical/experimental research on delaminations p 537 A93-21513

Allowable compression strength for CFRP-components of fighter aircraft determined by CAI-test p 537 A93-21531

Numerical determination of the residual strength of battle damaged composite plates p 537 A93-21533

Analytic formulation of unsteady profile aerodynamics and its application to simulation of rotors [ESA-TT-1244] p 485 A93-21659

Aerothermodynamic properties of hypersonic flows over radiation-adiabatic surfaces [DLR-FB-91-42] p 485 A93-21761

Experimental investigations on wing-body combinations and their components at high angles of attack in the subsonic and transonic speed range [DLR-FB-91-43] p 516 A93-21762

Unsteady Navier-Stokes method for accelerated moving airfoils with separation [DLR-FB-92-03] p 485 A93-21763

Comparison of the damage for various types of fibre reinforced composites due to different lightning test standards (MIL-STD-1757A, German military VG-standard 96903) p 736 A93-24891

An experimental health monitoring unit for GPS and GLONASS p 706 A93-25018

Stability investigations of airfoil flow by global analysis p 783 A93-27436

Protection of taxiing traffic in airports through mode S secondary radar technology [ETN-93-93455] p 791 A93-28206

Transonic flows on an oscillating airfoil and their effect on the flutter-boundary [DLR-FB-92-08] p 790 A93-29006

Flow visualization on helicopter blades using acenaphthen [ESA-TT-1255] p 931 A93-29273

Flight mechanical model for performance calculations and interactions between flight vehicle and ramjet in regard to the flight orbit [ESA-TT-1267] p 893 A93-29464

Transient thermal behaviour of a compressor rotor with axial cooling air flow and co-rotating or contra-rotating shaft p 903 A93-29946

Heat transfer and leakage in high-speed rotating stepped labyrinth seals p 903 A93-29951

The effect of main stream flow angle on flame tube film cooling p 932 A93-29953

Coupling of 3D-Navier-Stokes external flow calculations and internal 3D-heat conduction calculations for cooled turbine blades p 904 A93-29961

Optical blade vibration measurement [ETN-93-93454] p 905 A93-29999

Three-dimensional graphical representation of objects according to movement data in realtime [ESA-TT-1258] p 942 A93-30104

Design and implementation of a Global Positioning System (GPS) supported area navigation system with electronic aircraft [ILR-MITT-275(1992)] p 889 A93-30671

Advanced aircraft with thrust vector control [MBB-FE-1-S-PUB-0504] p 998 A93-31043

Consideration of impact damages by dimensioning CFC (Carbon Fiber Reinforced Composites) components [MBB-FE-221-S-PUB-0501] p 1018 A93-31044

Technology transfer: Potential of BMFT concept for hypersonics [MBB-LME-202-S-PUB-0505] p 1041 A93-31045

Development of nose structure of a reconnaissance container for a supersonic jet aircraft [MBB-LME-242-S-PUB-0451] p 998 A93-31046

Aircraft structures in 2000: A technological challenge? [MBB-LME-202-S-PUB-0485] p 998 A93-31058

The ViB-code to simulate 3-D stator/rotor flow in axial turbines [DLR-FB-92-19] p 1003 A93-31170

TDLM: A Transonic Doublet Lattice Method for 3D potential unsteady transonic flow calculation [DLR-FB-92-25] p 988 A93-31171

Definition of an airfoil family for the EUROFAIR rotor [DLR-FB-92-04] p 998 A93-31197

Aerial cartography using SICAD NAV-AIR p 1034 A93-31258
The use of digital road data by a navigation system p 993 A93-31269

GREECE

- Flight test of avionic and air-traffic control systems [ESA-TT-1279] p 993 N93-31271
- The DLR test aircraft in the FZ-BS, -VFW 614/ATTAS, Dornier DO 228-101, MBB BO105 S-3 p 1018 N93-31272
- The basic measurement equipment of the DLR test aircraft p 1000 N93-31273
- Ground installations for preparation and evaluation of flight tests p 1014 N93-31274
- Instigation and processing of flight tests in DLR p 998 N93-31275
- ATTAS experimental-cockpit and ATMOS for component and system investigations in flight guidance p 1014 N93-31276
- Testing of an experimental FMS p 998 N93-31277
- Testing concept of a taxiing control system, summary p 1010 N93-31278
- Pallet for helicopter test instrumentation p 1000 N93-31279
- Development and flight testing of a fault-tolerant fly-by-light yaw control system p 1010 N93-31280
- Ground- and satellite-derived flight-path measurements as demonstrated in the AFES Avionics Flight Evaluation System (AFES) p 993 N93-31281
- On-board derived flight-path measurement as demonstrated by an ILS measurement system p 994 N93-31282
- Testing of an experimental system for image reconnaissance p 1040 N93-31283
- Installations and methods for measurement of aircraft radio components and systems p 1031 N93-31284
- The influence of variable flow velocity on unsteady airfoil behavior [DLR-FB-92-22] p 988 N93-31320
- Air Traffic and Environment [GSF-BAND-8] p 1034 N93-31925
- Climatic effects of turbofan emissions in the stratosphere and the higher troposphere p 1035 N93-31927
- Radiation exposure in aircraft p 1035 N93-31928
- Effects on health of noise disturbances due to air traffic p 1035 N93-31929
- Effects of commercial flight pollution on human health p 1035 N93-31931
- Effects of air traffic on nature and environment in the neighborhood of airports by example of the Munich 2 Airport (Germany) p 1035 N93-31932
- ## GREECE
- A multi-zonal local solution methodology for the accelerated solution of the turbulent Navier-Stokes equations p 117 N93-14279
- Transition prediction in attached and separated shear layers using an integral method [ASME PAPER 92-GT-281] p 253 A93-19473
- Meridional flow calculation using advanced CFD techniques [ASME PAPER 92-GT-325] p 256 A93-19509
- Parametrical investigation of the interaction between turbulent wall shear layers and normal shock waves, including separation p 681 A93-33752
- Real gas effects for compressible nozzle flows p 682 A93-33757
- Recent advances in the numerical analysis of ram air wings - The three dimensional simulation code 'PARA3D' p 702 A93-35154
- [AIAA PAPER 93-1203] p 702 A93-35154
- Adaptation of a 3-D pressure correction Navier-Stokes solver for the accurate modelling of tip clearance flows p 971 A93-46932
- Design of axisymmetric channels with rotational flow [AIAA PAPER 93-3117] p 1062 A93-48287
- Zonal-local solution method for the turbulent Navier-Stokes equations p 1177 A93-53205
- Controlling common mode stabilization errors in airborne gravity gradiometry p 1245 A93-55978
- Damage detection by Acousto-Ultrasonic Location (AUL) p 555 N93-21529

H

HUNGARY

- Solid state flight data recorders and their application in the flight operation analysis p 166 A93-14200
- Application of flight data for diagnostic purposes p 166 A93-14295
- Detection of technical states with aircraft p 168 N93-15159
- The SIROM flight data recorder and evaluation system p 168 N93-15165
- DAR-2: On-board data acquisition system for aircraft engines p 169 N93-15166

ICELAND

- A review of aging aircraft technology - An I.A.I. perspective p 3 A93-13634

INDIA

- Multiple input/multiple output (MIMO) analysis procedures with applications to flight data p 60 A93-10777
- A low-speed aerodynamic model for harmonically oscillating aircraft configurations p 8 A93-11500
- Steady and quasisteady resonant lock-in of finned projectiles p 61 A93-12012
- A civil aircraft industry for India p 2 A93-12233
- Evolution of helicopters and the status of technology in India p 2 A93-12234
- Numerical solution of dynamic equations arising in a jet engine simulation p 53 A93-12237
- A mathematical model to determine the health of components based on SOAP data p 53 A93-12238
- Turbine blade cascade flows p 10 A93-12361
- Use of NASA LS (1) general aviation airfoil for a small wind turbine - An experience in Denmark p 92 A93-12364
- An aerodynamic model of multiple lifting surfaces including wake deformation and tip effect p 10 A93-12366
- Review of human error accidents in civil aviation p 27 A93-12367
- Midhani alloys in aeronautical service p 70 A93-12368
- Computer aided aerodynamic design of high pressure axial flow fan blade element p 16 A93-13649
- Hetero-redundant architecture with Kalman filter for input processing in flight control system p 182 A93-14293
- Modelling for aileron induced unsteady aerodynamic effects for parameter estimation p 118 A93-14323
- Stability considerations for enhanced manoeuvrability - An overview p 184 A93-14397
- Philosophical approach to the basic understanding of the mechanics of jet propulsion [SAE PAPER 920960] p 173 A93-14626
- Prediction of engine casing temperature of fighter aircraft for infrared signature studies [SAE PAPER 920961] p 206 A93-14627
- Photoelastic stress analysis of skewed cutout in a sandwich skew plate subjected to inplane and transverse eccentric load p 210 A93-16604
- Turbomachine blade vibration [ISBN 0-470-21764-2] p 344 A93-17899
- Flow studies in ducted twin-rotor contra-rotating axial flow fans [ASME PAPER 92-GT-390] p 258 A93-19545
- The role of noise in two-dimensional vortex merging p 408 A93-19967
- National Conference on Aerodynamics, 6th, Bangalore, India, Sept. 1992, Proceedings p 480 A93-24076
- Acoustic flux vector splitting scheme for Euler equations p 460 A93-24078
- Numerical modeling of leading edge separated flow at incompressible speeds p 460 A93-24079
- NOZ2D - A two dimensional explicit inviscid upwind code for convergent divergent nozzles p 460 A93-24080
- Aerodynamically efficient wing design with structural considerations p 460 A93-24081
- Numerical computation of viscous hypersonic flow around spherically blunted cones at angle of attack p 460 A93-24082
- A two-dimensional elliptic grid generator for a wing-body section involving grid control functions p 460 A93-24083
- A Navier-Stokes simulation of vortex shedding from square cylinder in unconfined domain p 538 A93-24084
- An implicit finite difference algorithm for two dimensional Euler equation p 461 A93-24085
- An upwind formulation for the solution of thin-layer Navier-Stokes equations p 461 A93-24088
- Incompressible potential flow calculation about harmonically oscillating three-dimensional configurations p 461 A93-24089
- Three-dimensional flow simulation over axisymmetric bodies using Navier-Stokes equations at hypersonic Mach numbers p 461 A93-24090
- Experiments on rarefied supersonic free jets using impact probes p 461 A93-24091
- A study of aerodynamic performance of a contra-rotating axial compressor stage p 463 A93-24524
- Delaminations of barely visible impact damage in CFRP laminates p 737 A93-33798
- Nonplanar Doublet-Point method for supersonic unsteady aerodynamics [AIAA PAPER 93-1588] p 682 A93-34120
- Calculation of laminar and turbulent asymmetric wakes p 684 A93-34318

FOREIGN TECHNOLOGY INDEX

- A technique for accelerated convergence in transonic flow p 685 A93-34347
- New analytical solutions for proportional navigation p 728 A93-34545
- Flap-lag damping in hover and forward flight with a three-dimensional wake p 797 A93-35979
- Multiple pole rational-function approximations for unsteady aerodynamics p 769 A93-37404
- Post-critical behaviour of a tapered cantilever column subjected to a uniformly distributed tangential follower force p 831 A93-38431
- Optimisation of constant altitude-constant airspeed flight for piston-prop aircraft p 889 A93-40473
- Mach disk of dual coaxial axisymmetric jets p 861 A93-41932
- Experimental investigation of leading edge vortices using LDA p 861 A93-42254
- Effect of radial distortion on the performance of a centrifugal compressor p 861 A93-42256
- Lift and pitching moment measurements in vertical gusts p 906 A93-42259
- Computation of hypersonic flow over a sphere using kinetic flux vector splitting scheme with equilibrium chemistry p 861 A93-42260
- Structure of martensite in titanium alloy Ti-6Al-1.5Zr-3.3Mo-0.3Si p 916 A93-43616
- Aileron and sideslip-induced unsteady aerodynamic modeling for lateral parameter estimation p 1007 A93-45144
- Estimation of neutral and maneuver points of aircraft by dynamic maneuvers [AIAA PAPER 93-3620] p 1126 A93-48307
- Parameter estimates of an aeroelastic aircraft as affected by model simplifications [AIAA PAPER 93-3640] p 1127 A93-48325
- The onset of disintegration and corona in water drops falling at terminal velocity in horizontal electric fields p 1163 A93-49130
- Intelligent robotics; Proceedings of the International Symposium, Bangalore, India, Jan. 2-5, 1991 [SPIE-1571] p 1166 A93-49350
- Computer aided design of turbo-machinery components p 1166 A93-50489
- Some measurements of stall in an axial impeller [ISABE 93-7008] p 1183 A93-53984
- A study on 3-D velocity distribution of isothermal flows behind an afterburner flame stabilizer [ISABE 93-7039] p 1197 A93-54015
- Correlations for flow property variation at outlet of a centrifugal impeller [ISABE 93-7054] p 1185 A93-54030
- Tip clearance effects on the flow field of an axial turbine rotor blade cascade [ISABE 93-7057] p 1185 A93-54033
- Characterisation of conventional and controlled diffusion stator blades in a transonic compressor stage [ISABE 93-7124] p 1189 A93-54099
- Structural integrity validation of limited-life engines [ISABE 93-7131] p 1205 A93-54106
- Development of a real time dynamic engine simulation model of a turbo fan engine [ISABE 93-7132] p 1205 A93-54107
- Analytical and experimental investigation of flow through a turbine vane cascade p 1248 A93-56348
- Fatigue life under random load history derived from exceedance curves using different algorithms p 1260 A93-56544
- Composites: A catalogue of books and conference proceedings available in the NAL library [NAL-SP-IC-9201] p 234 A93-13368
- Ideal aircraft handling quality models: Longitudinal axis [NAL-PD-FC-9203] p 187 A93-13566
- Indian experience in flight data readout and analysis p 168 N93-15161
- New adaptive controllers for aircraft p 847 N93-27180
- ## INDONESIA
- Spanish-Indonesian cooperation in the development, production, certification and marketing of CN-235 commuter aircraft p 108 A93-14156
- Calculation of 3-D unsteady subsonic flow with separation bubble using singularity method p 115 A93-14251
- Five years operational experiences with Indonesian Low Speed Tunnel (ILST) p 191 A93-14403
- ## INTERNATIONAL ORGANIZATION
- ICAO analyses trends in fuel consumption by world's airlines p 1 A93-10733
- Advanced technology and the pilot p 45 A93-13412
- Future systems for air traffic control p 150 A93-15052
- In the pursuit of a single European air traffic control system p 150 A93-15053
- Advanced technology constant challenge and evolutionary process p 109 A93-15054

The VKI compression tube annular cascade facility
CT3
[ASME PAPER 92-GT-336] p 375 A93-19511
Experimental investigation of a 2D parallel vortex/airfoil
interaction p 538 A93-23808
Flying qualities of the Hermes spaceplane and the shape
definition process p 532 A93-28437
Control of land use near airports is best means of
reducing impact of aircraft noise p 571 A93-29575
Millisecond aerodynamic force measurement with
side-jet model in the ISL shock tunnel
p 822 A93-39414
On-board maintenance aids p 764 A93-39538
A multidimensional generalization of Roe's flux
difference splitter for the Euler equations
p 863 A93-42437
An experimental contribution to the flat plate 2D
compression ramp, shock/boundary layer interaction
problem at Mach 14 - Test case 3.7
p 865 A93-42590
Viscous, 2-D, laminar hypersonic flows over
compression ramps p 866 A93-42591
A synthesis of results on the calculation of flow over a
2D ramp and a 3D obstacle - Antibes test cases 3 and 4
p 867 A93-42601
Airbus or the revival of European civil aviation
p 856 A93-42655
Progress in industrial holography in France
p 1020 A93-44197
Computations of inviscid compressible flows using
fluctuation-splitting on triangular meshes
[AIAA PAPER 93-3301] p 950 A93-44999
Shock tube validation experiments for the simulation of
ram-accelerator-related combustion and gasdynamic
problems p 1016 A93-45499
Shock tunnel studies of external combustion in high
supersonic air flows p 1017 A93-45517
Three dimensional aero-thermal characteristics of a high
pressure turbine nozzle guide vane
p 1002 A93-46942
Asymmetric vortical solutions in supersonic corners -
Steady 3D space-marching versus time-dependent conical
results
[AIAA PAPER 93-2957] p 1047 A93-48151
Efforts to reduce CFIT accidents should address failures
of the aviation system itself p 1096 A93-49280
Simulation of hypersonic flight - A concerted European
effort p 1136 A93-49301
Introduction to the physical aspects of hypersonic
aerodynamics p 1072 A93-49522
Computational aerothermodynamics for 2D and 3D
space vehicles p 1073 A93-49533
Shock tunnel experiments and approximate methods
on hypervelocity side-jet control effectiveness
[AIAA PAPER 93-1929] p 1077 A93-49794
The leading edge vortex of a rotating stall cell
[ISABE 93-7009] p 1183 A93-53985
The energy dissipation in a rotating stall cell
[ISABE 93-7010] p 1183 A93-53986
The Eurojet EJ200 engine p 1246 A93-54839

ISRAEL
Navier-Stokes calculations of the flow about wing-flap
combinations p 112 A93-14171
Integrated utilities management system for aircraft
p 153 A93-14208
Feasibility study of an active aeroelastic control system
for the F-16 aircraft p 181 A93-14224
Nonlinear rotor-fuselage coupled response to generic
periodic control modes using advanced computation
techniques p 153 A93-14226
Lateral aerodynamics characteristics of forebodies at
high angle of attack in subsonic and transonic flows
p 118 A93-14302
Drag/thrust estimation via aircraft performance flight
testing p 156 A93-14322
Leading edge vortices in a chordwise periodic flow
p 119 A93-14333
Post buckling of laminated composite stiffened curved
panels subjected to cyclic shear and compression
p 204 A93-14334
Numerical study of jet interaction at super- and
hypersonic speeds for flight vehicle control
p 184 A93-14379
Experimental study of controlled tip disturbance effect
on flow asymmetry p 211 A93-17417
Thrust vectoring - Theory, laboratory, and flight tests
p 367 A93-21657
A rapid procedure for obtaining time-average
interferograms of vibrating bodies p 412 A93-21857
Stability of the vertical autorotation of a single-winged
samara p 274 A93-22443
New results in optimal missile avoidance analysis
p 369 A93-22937
Application of the receding horizon strategy to singularly
perturbed pursuit-evasion problems p 369 A93-22980

Pilot test of a low Reynolds number DTE-airfoil
[AIAA PAPER 93-0643] p 464 A93-24758
Oscillatory blowing, a tool to delay boundary layer
separation
[AIAA PAPER 93-0440] p 474 A93-25529
Visual field information in Nap-of-the-Earth flight by
teleoperated Helmet-Mounted displays
p 517 A93-26884
A generic harmonic rotor model for helicopter flight
simulation p 506 A93-27480
Experimental and nonlinear vortex lattice method results
for various wing-canard configurations
p 479 A93-28607
Mathematical phenomenology for
thrust-vectoring-induced agility comparisons
p 525 A93-28613
Observability analysis of piece-wise constant systems.
I - Theory p 501 A93-29599
On the order reduction of LQG designed controllers
[AIAA PAPER 93-1420] p 756 A93-33973
Experimental validation of a discrete vortex method for
inviscid axisymmetric flow around parachute canopies
[AIAA PAPER 93-1216] p 689 A93-35165
Oblique shock formation in impulsively started wedge
flows p 692 A93-35636
Investigation of the flight mechanics simulation of a
hovering helicopter p 798 A93-35990
Nonlinear analysis of composite thin-walled helicopter
blades p 827 A93-36006
Pseudo-compressibility methods for the incompressible
flow equations
[AIAA PAPER 93-3329] p 952 A93-45023
A singularities tracking conservation law scheme for
compressible duct flows p 960 A93-45542
The effects of forced oscillations on the performance
of airfoils
[AIAA PAPER 93-3264] p 968 A93-46829
Numerical simulation of upstream disturbance on flows
around a slender body
[AIAA PAPER 93-2956] p 1047 A93-48150
Aircraft with single axis aerodynamically deployed
wings
[AIAA PAPER 93-3673] p 1129 A93-48350
Analysis of the stability characteristics of hypersonic flow
of a detonable gas mixture in the stagnation region of a
blunt body
[AIAA PAPER 93-1918] p 1076 A93-49784
Ignition of boron particles coated by a thin titanium
film
[AIAA PAPER 93-2201] p 1145 A93-50013
Boron particle ignition in high-speed flow
[AIAA PAPER 93-2202] p 1145 A93-50014
On the stability of the process of formation of combustion
generated particles by coagulation and simultaneous
shrinkage due to particle oxidation
[AIAA PAPER 93-2478] p 1146 A93-50220
Decentralized autonomous attitude determination using
an inertially stabilized payload
[AIAA PAPER 93-3857] p 1134 A93-51444
Design and testing methods of high performance
combustors for airbreathing engines
[ISABE 93-7024] p 1196 A93-54000
Study of a pulse ramjet based on twin valveless
combustors coupled to operate in antiphase
[ISABE 93-7038] p 1197 A93-54014
Oscillatory blowing - A tool to delay boundary-layer
separation p 1235 A93-55362
Multi-disciplinary optimization of aeroservoelastic
systems
[NASA-CR-191255] p 220 A93-14766
Collection of papers of the 31st NAE Annual
Conference on Aviation and Astronautics
[ITN-93-85187] p 764 A93-27166
Spurious frequencies as a result of numerical boundary
treatments p 839 A93-27170
Information-based criteria of terrain navigability. Part 1:
Data-base analysis p 793 A93-27178
Merging sparse optical flow and edge connectivity
between image features: A representation scheme for 2-D
display of scene depth p 845 A93-27179
Application of the cyclic J-integral to fatigue crack
propagation p 839 A93-27182
Regression rate mechanism in a solid fuel ramjet
p 814 A93-27185
Development of a pulse ramjet based on twin valveless
pulse combustors coupled to operate in antiphase
p 814 A93-27186
Analysis of thrust modulation of ram-rockets by a vortex
valve p 814 A93-27187
By-passing of heat exchangers in gas turbines
p 814 A93-27189
Damage tolerance assessment and usage variation
analysis for C-130 aircraft in the Israeli Air Force
p 839 A93-27210
Airfoil stability in turbulent flow
p 781 A93-27212

Towards an analytical treatment of the aerostatic
problem of a circular wing p 781 A93-27214
Leading edge vortices in a chordwise periodic flow
p 782 A93-27218
Analysis of wind-tunnel data for elliptic cross-sectioned
forebodies at Mach numbers 0.4 to 5.0
p 782 A93-27221

ITALY
Breakdown analysis on delta wing vortices
p 7 A93-10779
GPS integrity monitoring and system improvement with
ground station and multistationary satellite support
p 33 A93-11044
Wing pressure loads in canard configurations - A
comparison between numerical results and experimental
data p 7 A93-11499
Boundary integral equation methods for aerodynamics
p 9 A93-12158
The role of fatigue testing in the design, development
and certification of the ATR 42/72 p 46 A93-13637
Fatigue qualification of high thickness composite rotor
components p 81 A93-13646
Numerical simulations of high speed inlet flows
p 115 A93-14246
Further studies on the asymmetrical flow past yawed
cylinders p 118 A93-14304
Aeroelastic stability characteristics of composite
cylindrical shells by the finite element method
p 203 A93-14312
On the measurements of the skin friction in 3-D flows
- Application to a complete 3-D shear layer flow
p 118 A93-14329
Parametric aeroelastic analysis of composite wing-boxes
with active strain-energy tuning p 156 A93-14361
Detection of Goertler vortices in hypersonic flow
p 120 A93-14382
A sensitivity analysis of the stability of a
tug-rope-sailplane system p 184 A93-14400
Vortex breakdown study on a 65-deg delta wing tested
in static and dynamic conditions p 121 A93-14407
Toward an integration of aerodynamics and
aeroacoustics of rotors p 243 A93-19127
A numerical method for the prediction of quadrupole
shock wave noise p 448 A93-19201
Secondary flows in a transonic cascade - Validation of
a 3-D Navier-Stokes code
[ASME PAPER 92-GT-62] p 247 A93-19312
AerodeSIGN and performance analysis of a radial
transonic impeller for a 9:1 pressure ratio compressor
[ASME PAPER 92-GT-183] p 352 A93-19408
Incidence angle and pitch-chord effects on secondary
flows downstream of a turbine cascade
[ASME PAPER 92-GT-184] p 251 A93-19409
Expert systems for the simulation of gas turbine
engines
[ASME PAPER 92-GT-408] p 435 A93-19557
SAAW - Italy's answer to the windshear challenge
p 431 A93-22175
Low area ratio aircraft fuel jet-pump performances with
and without cavitation p 272 A93-22264
Vortical solutions in supersonic corner flows
[AIAA PAPER 93-0760] p 466 A93-24845
Multigrid techniques for hypersonic viscous flows
[AIAA PAPER 93-0771] p 487 A93-24855
On high speed turbulence modeling of shock-wave
boundary-layer interaction
[AIAA PAPER 93-0778] p 541 A93-24860
Ground vibration test on Piaggio P. 180 aircraft -
Comparison between two modal test methods
p 509 A93-29246
Compressible flow in a hovercraft air cushion
p 480 A93-29316
Reacting gas and surface coupling in high temperature
air flows p 686 A93-34353
EH 101 ship interface trials p 796 A93-35954
Design and manufacturing concepts of Eurofar Model
No. 2 blades p 798 A93-35983
Dynamic stability derivatives evaluation in a low-speed
wind tunnel p 821 A93-37402
Wind tunnel operator aimed comparison between two
electronic pressure scanner systems
p 830 A93-37876
Experimental investigation on aircraft dynamic stability
parameters p 905 A93-40326
High-speed turbulence modeling of
shock-wave/boundary-layer interaction
p 927 A93-41910
Equilibrium and nonequilibrium modeling of hypersonic
inviscid flows p 864 A93-42448
Scattering kernels for gas-surface interaction
p 943 A93-42580
Adaptive mesh embedding for reentry flow problems
p 869 A93-42619
A contribution to the prediction of hypersonic
non-equilibrium flows p 869 A93-42624

- Reactive and inert inviscid flow solutions by quasi-linear formulations and shock fitting p 927 A93-42625
- Inviscid calculations by an upwind finite element method of hypersonic flows over a double (single) ellipse p 869 A93-42626
- Inviscid finite-volume lambda formulation p 872 A93-42888
- Improvements in code validation algorithms for secondary surveillance radar p 883 A93-43408
- An integrated weather channel designed for an up-to-date ATC radar system p 929 A93-43434
- Space-time processing for AEW radar p 884 A93-43444
- Radar signals analysis oriented to target characterization applied to civilian ATC radar p 885 A93-43475
- Evaluation by holographic interferometry of impact damage in composite aeronautical structures p 1020 A93-44193
- Surface boundary conditions for the numerical solution of the Euler equations p 953 A93-45028
- [AIAA PAPER 93-3334] On the possibility of singularities in the acoustic field of supersonic sources when BEM is applied to a wave equation p 1039 A93-46805
- Numerical analysis of airfoil cascades subjected to unsteady flow p 972 A93-46944
- On the modelling of separated flows about airfoils [AIAA PAPER 93-3479] p 981 A93-47257
- Experimental analysis of rotary derivatives on a modern aircraft configuration [AIAA PAPER 93-3514] p 985 A93-47278
- Analysis of stability characteristics of a high performance aircraft [AIAA PAPER 93-3616] p 1125 A93-48303
- Vortical solutions in supersonic corner flows p 1071 A93-49015
- Multigrid techniques for hypersonic viscous flows p 1071 A93-49027
- Longitudinal dynamics of a towed sailplane p 1130 A93-49577
- Secondary flow computation by means of an inviscid multigrid Finite Volume Lambda Formulation [AIAA PAPER 93-1974] p 1077 A93-49821
- An analysis of air-turborocket performance [AIAA PAPER 93-1982] p 1141 A93-49829
- User-friendly codes for the training on gas turbine engines [AIAA PAPER 93-2051] p 1166 A93-49884
- Numerical model for predictions of reverse flow combustor aerothermal characteristics p 1123 A93-51645
- Experimental study on the aerodynamic effects of a forward-sweep angle p 1094 A93-52434
- Nozzle effects on linear stability behaviour of combustors [ISABE 93-7044] p 1198 A93-54020
- Studies on coolant problems in aeronautical turbine cascades [ISABE 93-7074] p 1220 A93-54050
- Finite-rate H₂/air combustion effects in CRJ for hypersonic launchers [ISABE 93-7084] p 1202 A93-54060
- Performance and configuration analysis of jet-engine off-design behavior [ISABE 93-7087] p 1202 A93-54063
- Design of air intakes and nozzles for transonic rotational flows [ISABE 93-7102] p 1187 A93-54078
- A study of the stability of vortical structures in supersonic inlets [ISABE 93-7103] p 1187 A93-54079
- Influence of chemical kinetics effects in nozzles shape design [ISABE 93-7112] p 1188 A93-54087
- A finite element code for gas turbine combustor flow with Stretched Laminar Flamelet modelling [ISABE 93-7127] p 1204 A93-54102
- Numerical simulation of gas turbine combustors with complex geometries [ISABE 93-7128] p 1204 A93-54103
- Expert Systems for the simulation of turbfan engines [ISABE 93-7133] p 1225 A93-54108
- Instrumentation and data acquisition system for the C.I.R.A. Transonic Pilot Tunnel p 1250 A93-54395
- Helicopter noise reduction programme - AGUSTA achievements p 1262 A93-54721
- Damping in aerospace composite materials p 1260 A93-55869
- Free streamline-boundary layer analysis for separated flow over an airfoil p 1239 A93-56327
- Numerical study for the study of medium speed internal noise problems [DILC-EST-TN-200] p 101 A93-11156
- Artificial intelligence and CFD: Expert systems for the design of airfoils and for grid generation [DIGE-EST-TN-016] p 48 A93-11161

- Wind tunnel operator aimed comparison between two electronic pressure scanner systems [DLAS-EST-TR-040] p 67 N93-11225
- Water tunnel studies of inlet/airframe interference phenomena p 215 N93-13216
- The FAIR (Flight Animated and Interactive Reconstruction) tool p 148 N93-15164
- Review of aeronautical fatigue investigation activities developed in Alenia-GAT during the period May 1990 - March 1991 p 329 N93-16287
- An advanced graphics-interactive system for a multi-block structured grid generation within an industrial environment [ETN-92-92885] p 440 N93-16288
- AM-X high angle of attack flight test experience (single and two seat versions) p 511 N93-19910
- Natural laminar flow test in-flight visualization p 482 N93-19921
- MSC/NASTRAN structure optimization test module version 67 (preliminary) p 554 N93-20907
- [REPT-5-191025] Cooling geometry optimization using liquid crystal technique p 902 N93-29939
- Aero-thermal design of a cooled transonic NGV and comparison with experimental results p 904 N93-29957
- A Navier-Stokes solver with different turbulence models applied to film-cooled turbine cascades p 904 N93-29962

J

JAPAN

- Iterative temperature calculation method for rectangular sandwich panel fins p 76 A93-10667
- Measurement technique for Loran-C pulse wave distortion measures and performance in an environment of noise p 29 A93-10988
- Trends of the airborne cockpit display format p 50 A93-11203
- Digital map display technology p 77 A93-11206
- Limit of sampling periods for nonlinear flight trajectory controller of aircraft p 61 A93-11207
- Evaluation of 2D scramjet nozzle performance p 52 A93-11209
- The improvement of the static launch method in Japan p 26 A93-11364
- Trans-oceanic, polar patrol balloons and future prospects p 26 A93-11366
- Trans-oceanic balloon flight over east China sea p 27 A93-11372
- Polar Patrol Balloon Experiment in Antarctica p 27 A93-11373
- An evaluation system for impact damage and erosion of ceramic gas turbine components p 79 A93-12229
- Transonic flutter/divergence characteristics of aeroelastically tailored and non-tailored high-aspect-ratio forward-swept wings p 10 A93-12273
- Design of an adaptive flight control system with uncertainties p 95 A93-12322
- Dynamic characteristics of an airfoil at high speed change of pitch angle p 10 A93-12324
- Lifting forces acting on magnets placed above a superconducting plane p 79 A93-12332
- The conceptual study of supersonic transport structure [AIAA PAPER 92-4219] p 43 A93-13348
- Aerodynamic characteristics of a next generation high-speed civil transport [AIAA PAPER 92-4229] p 15 A93-13356
- Feasibility study on single bypass variable cycle engine with ejector [AIAA PAPER 92-4268] p 55 A93-13366
- Improving the lift to drag characteristics of low boom configuration [AIAA PAPER 92-4218] p 16 A93-13380
- Aeronautical fatigue: Key to safety and structural integrity; Proceedings of the 16th ICAF Symposium, Tokyo, Japan, May 22-24, 1991 [ISBN 4-9900181-1-7] p 80 A93-13626
- Aging review of the YS-11 aircraft p 46 A93-13635
- Damage tolerance assessment on the multisite cracks for the YS-11 aircraft p 46 A93-13642
- Numerical analysis of three-dimensional viscous flows around an advanced counterrotating propeller p 112 A93-14165
- Digital fly-by-wire system for BK117 FBW research helicopter p 181 A93-14209
- The methods of reducing impact loads on occupants in the civil aircraft crash condition p 140 A93-14220
- Integrated control law synthesis of gust load alleviation and flutter margin augmentation for a transport aircraft p 182 A93-14281
- The cryogenic approach to simulating hot jet in transonic wind-tunnel testing p 117 A93-14297

- Compression after impact (CAI) properties of CF/PEEK (APC-2) and conventional CF/epoxy stiffened panels p 196 A93-14307
- Experimental investigation of aerothermal problems associated with hypersonic flight of HST p 120 A93-14380
- Stiffness design method of symmetric laminates using lamination parameters p 206 A93-14569
- Limit cycle in the longitudinal motion of the USB STOL ASKA - Control system functional mockup and actual aircraft [SAE PAPER 921040] p 185 A93-14660
- HUD Guidance for the ASKA Experimental STOL Aircraft using Radar Position Information [SAE PAPER 921041] p 150 A93-14661
- Turbulent structure in a vortex wake shed from an inclined circular cylinder p 125 A93-15443
- A flat plate wing standing on a wall covered with a thick boundary layer. II - Wing characteristics under the effects of side wall boundary layer and wing tip vortex p 125 A93-15446
- Visualization and analysis of supersonic flow in rotating turbine stage. I - Influence of shock wave between stationary and moving blades p 126 A93-15449
- Experimental and numerical study on the basic performance of a two-dimensional right-angled intake flow p 208 A93-15486
- The frequency of incipient vortex-shedding from a circular cylinder in a laminar boundary layer (The effect of the gap ratio on the vortex shedding frequency) p 126 A93-15488
- Numerical analysis of two-dimensional turbulent flows through an oscillating cascade p 126 A93-15494
- Modal analysis of unsteady aerodynamic response of subsonic annular cascade with steady loading under elastic vibration p 126 A93-15495
- Oscillation of circular shock waves with upstream nonuniformity p 208 A93-15496
- Experimental study of dynamic fluid forces and moments for a long annular seal p 209 A93-15684
- Aircraft fatigue failures and tasks of structural reliability analysis p 210 A93-16246
- Structural optimization of a cantilevered rotating beam p 210 A93-16248
- Effect of wing planforms on induced drag reduction p 127 A93-16932
- Study on unsymmetrical supersonic nozzle flows p 127 A93-16933
- Estimation of aerodynamic characteristics from flight test data. II - Analysis methods under in-flight wind tunnel test concept p 191 A93-16934
- Marching grid generation for external viscous flow problems p 228 A93-16979
- Effect of stress level of gust cycles on fatigue crack propagation behavior (Acceleration and retardation of crack propagation under simplified flight simulation loading) p 198 A93-17033
- A high-frequency, secondary instability of crossflow vortices that leads to transition p 128 A93-17253
- Experimental study on the unsteady aerodynamic response of a three dimensional cascade with oscillating blades p 242 A93-18499
- Lifting surface theory for steady aerodynamic analysis of ducted counter rotation propfan [ASME PAPER 92-GT-14] p 347 A93-19286
- Pressure fluctuation on casing wall of isolated axial compressor rotors at low flow rate [ASME PAPER 92-GT-33] p 246 A93-19293
- Blade loading and shock wave in a transonic circular cascade diffuser [ASME PAPER 92-GT-34] p 246 A93-19294
- Influence of blade aerodynamic loading on efficiency of radial-inflow turbines [ASME PAPER 92-GT-91] p 249 A93-19337
- Ignition and exhaust emission characteristics of spray combustion in a pre-chamber type vortex combustor [ASME PAPER 92-GT-119] p 350 A93-19355
- Investigation of combustion structure inside low NO(x) combustors for a 1500 C-class gas turbine [ASME PAPER 92-GT-123] p 350 A93-19357
- Turbine blade vibration monitoring system [ASME PAPER 92-GT-159] p 402 A93-19386
- Rim seal experiments and analysis of a rotor-stator system with nonaxisymmetric main flow [ASME PAPER 92-GT-160] p 402 A93-19387
- Behaviors of the laterally injected jet in film cooling - Measurements of surface temperature and velocity/temperature field within the jet [ASME PAPER 92-GT-180] p 402 A93-19405
- Heat transfer in serpentine flow passages with rotation [ASME PAPER 92-GT-190] p 403 A93-19415
- Tip clearance effect on heat transfer and leakage flows on the shroud-wall surface in an axial flow turbine [ASME PAPER 92-GT-200] p 403 A93-19425

- Overview of the Japanese National Project for Super/Hyper-Sonic Transport propulsion system [ASME PAPER 92-GT-252] p 239 A93-19461
- Conceptual design of turbo-accelerator for HST combined cycle engine [ASME PAPER 92-GT-253] p 353 A93-19462
- Some topics of research on hypersonic airbreathing engines at National Aerospace Laboratory [ASME PAPER 92-GT-256] p 353 A93-19465
- Research and development of ceramic turbine wheels [ASME PAPER 92-GT-295] p 354 A93-19485
- Experimental study of mixed compression air-intake for hypersonic airbreathing engines [ASME PAPER 92-GT-349] p 355 A93-19519
- Combustion study on methane-fuel Laboratory Scaled Ram Combustor [ASME PAPER 92-GT-413] p 356 A93-19561
- Some asymptotic aspects of the nonstationary aerofoil theory p 259 A93-19966
- Flow measurements behind V-gutter under non-combusting condition [AIAA PAPER 93-0020] p 408 A93-20139
- Flow visualization studies on sidewall effects in two dimensional transonic airfoil testing [AIAA PAPER 93-0090] p 263 A93-20196
- Air flow dynamics around an aerofoil by the stabilized finite difference method p 266 A93-20741
- Recent aircraft accidents p 307 A93-20819
- Analysis of approach paths of a single aircraft p 367 A93-20823
- A new technique for analysis of unsteady aerodynamic responses of cascade airfoils with blunt leading edge. I - Theory p 267 A93-20909
- Blade loading of transonic circular cascade diffuser p 267 A93-20919
- Aircraft experiments on microgravity pool boiling - Vapor-liquid behaviour and heat transfer characteristics in boiling of n-pentane, CFC-113 and water p 410 A93-20920
- Transitional characteristics of vortices issued from a body which creates asymmetric flow field - In a case of thin symmetrical airfoil with angle of attack under rotational oscillation of small amplitude p 267 A93-20923
- Numerical analysis of two-dimensional flows around elliptic wings above a flat plate p 267 A93-20924
- Performance analysis of supersonic through-flow fan by the lifting surface theory. I - Disturbance flow field and determination of blade loadings p 267 A93-20929
- Two-dimensional cascade tests of MCA blades in the high transonic Mach number region. V - Effect of space/chord ratio on the parameters of cascade performance p 267 A93-20930
- Streamwise variation of mean velocity field for the turbulent boundary layer interacting with controlled longitudinal vortex arrays p 267 A93-20933
- Study on the numerical problem of the boundary element method in analysis of flow around a three-dimensional wing-body p 268 A93-20934
- Effects of injector geometry on scramjet combustor performance p 359 A93-21670
- Experimental study on the characteristics of the near wake of a rotating flat plate. III - Influence of the shape near the trailing edge on periodic-velocity-fluctuation phenomena p 451 A93-21727
- Augmentation of turbulent heat transfer with a vortex generator attached to a LEBU plate p 411 A93-21729
- Combustion performance of a hydrogen-fueled small combustor for a micro gas turbine p 389 A93-21731
- Lift enhancement of ground-effect wing. I - Results of screening tests of various concepts p 271 A93-21737
- Lift enhancement of ground-effect wing. II - Experimental investigation of the power augmented ram wing in ground effect through the wind tunnel p 271 A93-21738
- Development of a Shape-controlled airfoil by use of SMA p 411 A93-21739
- Characteristics of liquid jet atomization across a high-speed airstream. I - Experiment on shape of spray, spatial distribution of injected liquid and Sauter mean diameter p 411 A93-21743
- Characteristics of liquid jet atomization across a high-speed airstream. II - Calculation of spatial distribution of liquid, variation of drop diameter and drop trajectory p 412 A93-21744
- Dual transverse injection of H₂ gas into Mach 1.8 flows at University Komaba wind tunnel p 376 A93-21833
- Radiation mechanism for the aerodynamic sound of gears - An explanation for the radiation process by air flow observation p 451 A93-21859
- Development of ultra-hypersonic shock tunnel for aerodynamics test p 376 A93-21900
- A fine structure of the gust front observed with sonic anemometer p 430 A93-22158
- Extremely low level jet in the evening in Kanto Plain p 430 A93-22159
- Doppler radar observation of tornado and microburst around Chitose Airport p 432 A93-22199
- Structure of downbursts associated with heavy rainfall observed in Tokyo p 433 A93-22200
- Overview of Japanese aerospace plane [AIAA PAPER 92-5005] p 384 A93-22282
- Atmospheric reentry flight test of winged space vehicle [AIAA PAPER 92-5053] p 385 A93-22324
- Test results on air turbo ramjet for a futurespace plane [AIAA PAPER 92-5054] p 359 A93-22325
- Penetration and mixing of bubbling liquid jets from multiple injectors normal to a supersonic air stream [AIAA PAPER 92-5060] p 413 A93-22330
- Study on steady and unsteady unstart phenomena due to compound choking and/or fluctuations in combustor of scramjet engines [AIAA PAPER 92-5102] p 359 A93-22372
- Numerical prediction of aerodynamic noise radiated from low Mach number turbulent wake [AIAA PAPER 93-0145] p 452 A93-22589
- Experimental and numerical investigation of Mach 2.5 supersonic mixed compression inlet [AIAA PAPER 93-0289] p 279 A93-22689
- Preliminary assessment of tunnel wall interference in the NDA cryogenic wind tunnel [AIAA PAPER 93-0421] p 285 A93-23340
- Application of feedback linearization method in a digital restructurable flight control system p 370 A93-23514
- Life assessment of gas turbine bucket coating based on degradation analysis p 533 A93-24464
- The structure and material testing facility needed for future SST/HST development [AIAA PAPER 92-3887] p 528 A93-24481
- The analysis of unsteady, three-dimensional flow separation [AIAA PAPER 93-0642] p 540 A93-24757
- Two-dimensional Navier-Stokes analysis of high-lift multi-element airfoils using the q-omega turbulence model [AIAA PAPER 93-0679] p 466 A93-24787
- Analytical investigation of a regeneratively cooled scramjet engine [AIAA PAPER 93-0739] p 519 A93-24829
- Aerodynamic performance of scramjet inlet models with a single strut [AIAA PAPER 93-0741] p 466 A93-24831
- Numerical simulation of supersonic flow around space plane for airframe-engine integration [AIAA PAPER 93-0886] p 471 A93-24946
- Numerical investigation of supersonic flows around a spiked blunt-body [AIAA PAPER 93-0887] p 471 A93-24947
- Visualization and analysis of supersonic flow in rotating turbine stage. II - Analysis of the flow into the moving blades and their exit flow p 476 A93-27442
- Surging limits of multistage axial-flow compressors p 476 A93-27443
- Microchannel plate modal gain variations with temperature p 477 A93-27445
- Continuous judgment of helicopter noise - On the validity of Leq and Zwicker's method (ISO 532B) p 558 A93-28478
- Numerical study on the interaction of supersonic flow past a wedge and free jet p 479 A93-28574
- The coherent structure in a corner turbulent boundary layer p 548 A93-28575
- Optimal takeoff of a helicopter for category A V/STOL operations p 525 A93-28611
- Simultaneous structure/control design optimization of a wing structure with a gust load alleviation system p 525 A93-28616
- Propagation results of aeronautical satellite communication experiments using INMARSAT satellite p 533 A93-29607
- A study on two-dimensional and three-dimensional secondary jet interactions with a supersonic flow p 683 A93-34273
- A study on three-dimensional shock wave/turbulent boundary layer interaction induced by sweptback sharp fins at supersonic flow p 684 A93-34274
- Numerical simulation of starting process in a hypersonic nozzle p 684 A93-34275
- Nonreflecting boundary conditions of three-dimensional Euler equation calculations for strut cascades p 689 A93-34491
- Ignition analysis of unpremixed reactants with chain mechanism in a supersonic mixing layer p 735 A93-35619
- Optimal takeoff procedures for a transport category tiltrotor p 802 A93-37377
- Numerical Fluid Dynamics Symposium, 5th, Tokyo, Japan, Dec. 19-21, 1991, Proceedings p 830 A93-38126
- CFD development and a future high speed computer p 847 A93-38128
- The application of CFD to turbomachine design - Past and future p 769 A93-38130
- Domain splitting explicit time marching scheme for simulation of unsteady high Reynolds number flow p 830 A93-38140
- VSL analysis of nonequilibrium flows around a hypersonic body p 769 A93-38146
- Hypersonic chemically reacting flow of a reentry body p 769 A93-38147
- Numerical analysis for chemically non-equilibrium flow p 770 A93-38148
- Numerical prediction of aerodynamic sound using large eddy simulation p 850 A93-38150
- Numerical computation of aerodynamic noise radiation by the large eddy simulation p 850 A93-38151
- Turbulent flow simulation around the aerofoil with pseudo-compressibility p 830 A93-38155
- Numerical calculation of separated flows around wing section in unsteady motion by using incompressible Navier-Stokes equations p 770 A93-38158
- Numerical solution of viscous compressible flows using algebraic turbulence models p 770 A93-38162
- A numerical simulation of a scram jet combustor flow p 810 A93-38181
- Adaptive grid generation using optimal control theory p 770 A93-38187
- Unsteady analysis of helicopter rotor p 770 A93-38193
- Numerical study on atom-molecule radiation flowfield around a hypersonic blunt body p 770 A93-38434
- Study of mixing flow field of a jet in a supersonic cross flow. I - Experimental facilities and preliminary experiments p 857 A93-40430
- The experimental study of the effect of sweptback angles and the front shape of the fin on reduction of shock wave/turbulent boundary layer interaction region p 858 A93-40431
- Evaluation of metallurgical degradation on gas turbine components p 915 A93-40804
- Crack simulation and life assessment of gas turbine nozzles p 915 A93-40805
- Creep crack growth and tail part behavior of low alloy steels and Ni based super alloy p 916 A93-40808
- A multi-dimensional upwind scheme for the Euler equations on structured grids p 862 A93-42430
- Thermo-chemical models for hypersonic flows p 863 A93-42433
- Evaluation of an RNG-based algebraic turbulence model p 863 A93-42436
- Higher-order-accurate upwind schemes for solving the compressible Euler and Navier-Stokes equations p 863 A93-42441
- Problem 6.4.1 - Rarefied flow around a double ellipse p 869 A93-42630
- Scramjet nozzle experiment with hypersonic external flow p 899 A93-42879
- Three-dimensional calculation of a hydrogen jet injection into a supersonic air flow p 950 A93-44374
- Adaptive-prismatic-grid method for external viscous flow computations [AIAA PAPER 93-3314] p 951 A93-45010
- Numerical experiment of the flight trajectory simulation by fluid dynamics and flight dynamics coupling [AIAA PAPER 93-3324] p 952 A93-45018
- Numerical simulation of supersonic flows with chemical reactions p 959 A93-45325
- Shock waves; Proceedings of the 18th International Symposium, Sendai, Japan, July 21-26, 1991. Vols. 1 & 2 [ISBN 0-387-55686-9] p 1023 A93-45451
- Formation of shock waves in transient base flow p 1023 A93-45460
- Oscillations of circular shock waves with upstream disturbance p 1023 A93-45463
- Aerodynamic heating phenomenon in three dimensional shock wave/turbulent boundary layer interaction induced by sweptback fins in hypersonic flows p 960 A93-45507
- Radiative heat transfer from non-equilibrium high-enthalpy shock layers p 1024 A93-45515
- A combined facility of ballistic range and shock tunnel using a fast action valve p 1012 A93-45532
- Analytical study on plate edge noise (Noise generation from tandemly situated trailing and leading edges) p 1038 A93-45561
- Effects of nozzle contour on the aerodynamic characteristics of underexpanded annular impinging jets p 1024 A93-45563
- Case study and simulation of fatigue damages and DTE of aging aircraft - A review of researches in Japan p 948 A93-45800
- Active forcing of an axisymmetric leading-edge turbulent separation bubble [AIAA PAPER 93-3245] p 966 A93-46790
- On the steady subsonic shear flow past a slender body of revolution p 970 A93-46907

- Effects of wall conditions on chemically nonequilibrium shock-layer flow over hypersonic reentry bodies
p 970 A93-46908
- Unsteady aerodynamic response of two-dimensional subsonic and supersonic oscillating cascades with chordwise displacement and flexible deformation
p 971 A93-46922
- A visualizing method of streamlines around hypersonic vehicles
[AIAA PAPER 93-3440] p 1014 A93-47230
- Mechanical anisotropy in directionally solidified turbine blade
p 1018 A93-47356
- Normal shock wave oscillations in supersonic diffusers
p 1044 A93-48042
- Surface hot-film method for the measurement of transition, separation and reattachment points
[AIAA PAPER 93-2918] p 1148 A93-48120
- Intense studies on unsteady secondary separations and oscillating shock waves in three-dimensional shock waves/turbulent boundary layer interaction regions induced by sharp and blunt fins
[AIAA PAPER 93-2939] p 1046 A93-48137
- Aerodynamic heating with boundary layer transition and heat protection with mass addition on blunt body in hypersonic flows
[AIAA PAPER 93-2984] p 1051 A93-48177
- Effects of boundary layer bleed on swept-shock/boundary layer interaction
[AIAA PAPER 93-2989] p 1052 A93-48182
- Computations of transonic wind tunnel flows about a fully configured model of aircraft by using multi-domain technique
[AIAA PAPER 93-3022] p 1055 A93-48207
- A study on aerodynamic sound generated by interaction of jet and plate
[AIAA PAPER 93-3118] p 1171 A93-48288
- A method of wind shear detection for powered-lift STOL aircraft
[AIAA PAPER 93-3667] p 1104 A93-48345
- Pilots' control behavior including feedback structures identified by an improved method
[AIAA PAPER 93-3669] p 1129 A93-48347
- Wind-shear endurance capability for powered-lift aircraft
[AIAA PAPER 93-3670] p 1129 A93-48348
- Validation studies of scramjet nozzle performance
p 1109 A93-49616
- Effects of external control circuit on coal-fired supersonic diagonal-type MHD generator
p 1173 A93-49619
- An experimental study of supersonic air-intake with 5-shock system at Mach 3
[AIAA PAPER 93-2305] p 1082 A93-50089
- Two-dimensional numerical simulation for Mach-3 multishock air-intake with bleed systems
[AIAA PAPER 93-2306] p 1082 A93-50090
- A study of a direct-injection stratified-charge rotary engine for motor vehicle application
[SAE PAPER 93-0677] p 1158 A93-50524
- A fourth-order MUSCL finite-difference scheme for solving the unsteady compressible Euler equations
p 1086 A93-51121
- A new technique for analysis of unsteady aerodynamic responses of cascade airfoils with blunt leading edge - Unsteady aerodynamic responses of the cascade in incompressible flow
p 1086 A93-51122
- Analysis of wake-induced unsteady flow in axial compressors - Radial variations of wake excitation forces estimated by strip theory
p 1086 A93-51123
- Guidance and control law for automatic landing flight experiment of reentry space vehicle
[AIAA PAPER 93-3818] p 1143 A93-51409
- A new way of pole placement in LQR and its application to flight control
[AIAA PAPER 93-3845] p 1133 A93-51433
- Adaptive quadratic stabilization control with application to flight controller design
[AIAA PAPER 93-3847] p 1133 A93-51434
- Effect of rounding side corners on vortices shedding and downwash from square cylinder of finite length placed on a ground plane
p 1160 A93-51893
- Numerical analysis of flow within cascade with tip clearance
p 1176 A93-53192
- Pressure distribution measurement around hypersonic delta winged semicone - Measurement by means of magnet tape
p 1176 A93-53193
- Experimental investigation into the mechanism of discrete frequency noise (DFN) generation from a NACA 0012 blade
p 1225 A93-53194
- The properties of newly developed highly damage tolerant and easy handleable carbon fiber/modified bismaleimide prepreg system
p 1212 A93-53448
- Repair materials and processes for the MD-11 Composite Tailcone
p 1216 A93-53452
- Numerical analysis of a flat plate in a pitching motion.
II - Effect on the flow of the position of the pivot, etc
p 1181 A93-53798
- Study on surge and rotating stall in axial compressors.
III - Numerical model for multiblade-row compressors
p 1181 A93-53799
- Three-dimensional viscous flow analysis of compressor cascade channels
p 1181 A93-53837
- Shock shapes around slender diamond cones traveling at hypersonic speed
p 1181 A93-53840
- Analysis of unstarted supersonic flow in cascade by semiactuator disk theory
p 1181 A93-53841
- Velocity fluctuation based on the difference in the flow pattern in the channels of a centrifugal impeller
p 1182 A93-53842
- Numerical analysis of the flow through a centrifugal impeller by vortex distribution model of a boundary layer.
I - Theoretical analysis
p 1182 A93-53843
- Research and development of aircraft engine in Japan - Historical review
[ISABE 93-7000] p 1227 A93-53977
- Japan's research and development program for airbreathing engine technologies
[ISABE 93-7005] p 1194 A93-53981
- A 2-D compressible N-S simulation of starting- and stalling-flows in a compressor cascade system
[ISABE 93-7006] p 1183 A93-53982
- Numerical study on inception of stall cells in rotating stall
[ISABE 93-7007] p 1183 A93-53983
- Development study on Air Turbo Ramjet engine for a future space plane
[ISABE 93-7016] p 1195 A93-53992
- Conceptual design study on combined-cycle engine for hypersonic transport
[ISABE 93-7018] p 1195 A93-53994
- Navier-Stokes computation of the three dimensional flow fields through a transonic fan blade
[ISABE 93-7030] p 1184 A93-54006
- Effect of film cooling/regenerative cooling on scramjet engine performances
[ISABE 93-7036] p 1197 A93-54012
- Isothermal flow characteristics behind V-shape gutter with and without injection
[ISABE 93-7040] p 1198 A93-54016
- Active control of vortex breakdown by a spinning wave generator
[ISABE 93-7045] p 1219 A93-54021
- Noise reduction of supersonic heated jet with jet mixing enhancement by tabs
[ISABE 93-7046] p 1198 A93-54022
- A study of self-ignition of methane-hydrogen mixture fuel injected into high enthalpy supersonic airstreams
[ISABE 93-7049] p 1213 A93-54025
- Ignition and combustion performance of a scramjet combustor with a fuel injection strut
[ISABE 93-7050] p 1199 A93-54026
- Study on unstart and its propagation along modules due to compound choking and/or fluctuations in combustor of scramjet engines
[ISABE 93-7052] p 1199 A93-54028
- Transonic discharge flows around diffuser vanes from a centrifugal impeller
[ISABE 93-7053] p 1185 A93-54029
- Performance improvement by forward-skewed blading of axial fan moving blades
[ISABE 93-7055] p 1185 A93-54031
- Effects of wake interaction of two turbine cascades on secondary/tip-leakage flows and losses
[ISABE 93-7058] p 1185 A93-54034
- New approximate method of stress analysis for bladed rotating discs
[ISABE 93-7059] p 1219 A93-54035
- Application of functionally gradient materials to scramjet engines
[ISABE 93-7063] p 1200 A93-54039
- Research and development of a turbo-accelerator for super/hypersonic transport
[ISABE 93-7066] p 1200 A93-54042
- Research and development of high pressure compressor for SST and HST engine
[ISABE 93-7068] p 1186 A93-54044
- Tandem transverse hydrogen gas injection into a supersonic airflow
[ISABE 93-7069] p 1201 A93-54045
- Direct simulation of reacting fuel gas flows in a supersonic mixing layer
[ISABE 93-7072] p 1201 A93-54048
- A new cooling system for ultra high temperature turbines
[ISABE 93-7073] p 1201 A93-54049
- The combustion performance of methane-fueled ram combustor
[ISABE 93-7079] p 1201 A93-54055
- Studies on methane-fuel ram combustor for HST combined cycle engine
[ISABE 93-7080] p 1201 A93-54056
- Test results of the hydrogen fueled model combustor for the air turbo ramjet engine
[ISABE 93-7082] p 1201 A93-54058
- Design of limit-tracking systems incorporating a turbopfan engine with constant disturbances
[ISABE 93-7090] p 1203 A93-54066
- Experimental analysis of turbine rotor flow at design and off-design conditions
[ISABE 93-7092] p 1186 A93-54068
- Wind tunnel tests of the model of intake-airframe integration
[ISABE 93-7101] p 1192 A93-54077
- Starting characteristics of scramjet inlets
[ISABE 93-7105] p 1203 A93-54081
- A study on Mach 3 two-dimensional mixed compression air-intakes
[ISABE 93-7106] p 1188 A93-54082
- Off-design performance of scramjet nozzles
[ISABE 93-7108] p 1203 A93-54084
- Observation of fluctuation of 2D-nozzle flows
[ISABE 93-7110] p 1204 A93-54086
- LIF visualization of 3-dimensional hypersonic mixing
[ISABE 93-7114] p 1221 A93-54089
- Two-dimensional and three-dimensional mixing flow structures with injected through slotted nozzle and circular nozzle into supersonic flows
[ISABE 93-7117] p 1221 A93-54092
- Numerical and experimental study on two- and three-dimensional supersonic flow field with hydrogen injection
[ISABE 93-7118] p 1188 A93-54093
- Characteristics of heat exchanger in supersonic/subsonic flows
[ISABE 93-7119] p 1221 A93-54094
- Various applications of robots in aircraft engine overhaul
[ISABE 93-7129] p 1175 A93-54104
- Study on flow field around slender diamond cone traveling at hypersonic speed
p 1189 A93-54314
- Estimation of aerodynamic characteristics from flight-test data. IV - Principal component analysis and perpendicular error method
p 1241 A93-54551
- Minimum time turn of a helicopter
p 1248 A93-54554
- Thermal barrier design of gamma-TiAl Functionally Gradient Materials (FGMs) for scramjet engine applications
p 1246 A93-54556
- Digital flight recorded data - A method of estimating down draft from digital flight recorded data
p 1241 A93-54559
- Estimation of aerodynamic characteristics from flight-test data. V - Effects of gust and its time lag
p 1230 A93-54560
- Aerodynamic characteristics of a semibuoyant station in the shape of a torus
[AIAA PAPER 93-4034] p 1231 A93-54615
- International Symposium on Ultra-High Temperature Materials, Tajimi, Japan, Dec. 5, 6, 1991, Proceedings
p 1252 A93-54708
- HOPE and its thermal protection systems
p 1252 A93-54711
- Ultra-high temperature materials in the research and development of super/hypersonic transport propulsion system
p 1252 A93-54712
- Status of R&D of high-performance materials for severe environments (Composite materials)
p 1253 A93-54728
- Numerical studies of Mach reflection with air chemistry
p 1233 A93-54815
- Preliminary design of experimental sub-scale scramjet engine
[AAS PAPER 91-639] p 1247 A93-55816
- Results of sea-level static tests on air turbo ramjet for a future space plane
[AAS PAPER 91-640] p 1247 A93-55817
- Guidance and control of HOPE (H-II orbiting plane)
[AAS PAPER 91-653] p 1252 A93-55825
- Hypersonic vehicle research by using a large shock tunnel
[AAS PAPER 91-607] p 1250 A93-55841
- Analytical study on the separation dynamics of LUNAR-A/penetrator
p 1265 A93-56272
- CTS for a low speed wind tunnel
p 1251 A93-56278
- Air cell
[CA-PATENT-APPL-SN-2001346] p 83 N93-10368
- Air ejector experiments using the two-dimensional supersonic cascade tunnel: Relationship between ejector performance and throat area ratio, part 1
[NAL-TM-642-PT-1] p 25 N93-12352
- Flight test progress of the STOL research aircraft ASKA
[NAL-TM-643] p 49 N93-12354
- Simulation analysis of a cable-mount system used for dynamic wind tunnel tests
[NAL-TR-1127] p 68 N93-12359

L

On stability and control of SSTD spaceplane in super- and hypersonic ascending phase
[NAL-TR-11287] p 65 N93-12361

A wind tunnel investigation to determine buffet countermeasures for STOL aircraft alpha-sweep flight testing
[NAL-TR-1129] p 65 N93-12362

Accuracy improvement of linear estimated motion using differential type sensors
[NAL-TR-1135] p 91 N93-12365

Flight simulator evaluation of D-size liquid crystal flat panel displays
[NAL-TR-1136] p 52 N93-12367

Mach 4 testing of scramjet inlet models
[NAL-TR-1137] p 26 N93-12369

An optical fiber multi-terminal data bus system for aircraft
[NAL-TR-1125] p 52 N93-12370

Evaluation of acoustic impedance models for a perforated plate
[NAL-TR-1133] p 102 N93-12375

Liquid crystal flat panel display evaluation tests using a flight simulator
[NAL-TR-1122] p 52 N93-12383

Wind tunnel investigation of a twin-engine jet transport semi-span model with upper surface blown jet flap
[NAL-TR-1134] p 26 N93-12503

Effect of the flow non-uniformity on the mixing layer at the interface of parallel supersonic flows
[ISAS-RN-646] p 128 N93-12716

Discussion for the ideal AIMS
p 167 N93-15153

Special publication of National Aerospace Laboratory [DE93-716176] p 239 N93-15946

Special publication of National Aerospace Laboratory [DE93-716195] p 239 N93-15949

Three dimensional boundary-layer transition on a swept wing
p 419 N93-16818

Experiments on swept-wing boundary-layer transition
p 419 N93-16829

Proceedings of the Ninth NAL Symposium on Aircraft Computational Aerodynamics
[NAL-SP-16] p 299 N93-19273

LES turbulence modeling using DNS data base
p 299 N93-19274

A simple grid generation technique for hypersonic flow around complex configuration
p 299 N93-19275

Computation of internal flows using unstructured triangular meshes
p 299 N93-19276

Numerical computations using multi-domain technique
p 299 N93-19277

Numerical simulations of hypersonic rarefied transition regime flows: DSMC method and Navier-Stokes computation
p 299 N93-19278

Monte Carlo simulation of normal shock wave. Part 1: Lennard-Jones potential
p 300 N93-19279

Rarefied gas numerical wind tunnel. Part 7: OREX
p 382 N93-19280

Analysis of a 2-D airfoil motion flying in-proximity-to a wavy-wall surface: Lifting-surface-method
p 300 N93-19281

Analysis of a 2-D airfoil motion flying in-proximity-to a wavy-wall surface: Finite difference method
p 300 N93-19282

Development of a boundary element method program for numerical analysis of supersonic unsteady flow
p 300 N93-19283

Numerical calculations of separating flows around oscillating airfoil
p 300 N93-19284

Numerical simulation of unsteady large scale separated flow around oscillating airfoil
p 300 N93-19285

Calculations of aerodynamic forces on a wing with thrust using BEM
p 300 N93-19286

Numerical Wind Tunnel: Requirements and the outline
p 383 N93-19288

Numerical Wind Tunnel hardware
p 383 N93-19289

The operating system for Numerical Wind Tunnel
p 383 N93-19290

The language processor system for the Numerical Wind Tunnel
p 383 N93-19291

Generation of longitudinal vortices in supersonic flow
p 301 N93-19292

The role of computational fluid dynamics in aeronautical engineering. 9: Analysis of hypersonic equilibrium air flow
p 301 N93-19294

Computation of re-entry flows with two-temperature model
p 301 N93-19295

Numerical calculation of hypersonic non-equilibrium flow around OREX
p 301 N93-19296

Numerical simulation of hypersonic flow around H-2 Orbiting Plane (HOPE), part 3
p 301 N93-19297

The 3D Navier-Stokes calculation of flow about scramjet inlet with strut
p 301 N93-19298

Numerical simulation of flow for a scramjet nozzle
p 302 N93-19299

Transonic flow calculation around NACA-0012
p 302 N93-19301

Numerical simulations of supersonic flow by a fourth-order compact MUSCL TVD scheme
p 302 N93-19308

Analytical and numerical study on steady Mach reflection
p 302 N93-19309

Numerical simulation of the flow through non-uniform airfoil cascade
p 302 N93-19310

Numerical study on transverse hydrogen injection into a supersonic flowfield
p 302 N93-19311

Aerodynamic heating analysis for axisymmetric bodies in supersonic flow
p 303 N93-19312

Three dimensional calculation of flow inside supersonic inlet
p 303 N93-19313

Numerical simulation of flows in a supersonic air intake
p 303 N93-19314

A numerical investigation for supersonic inlet
p 303 N93-19315

A numerical investigation of 3D transverse injection into the supersonic flow behind rearward facing step
p 303 N93-19316

Numerical calculation of flow field in supersonic combustion chamber
p 304 N93-19317

A numerical simulations of inner flow of scramjet
p 304 N93-19318

Wind tunnel wall interference correction at subsonic speeds
p 304 N93-19320

Two problems reducing the data accuracy in Transonic Wind Tunnel testing
p 304 N93-19321

On the roles of wind tunnel testing and computational fluid dynamics in the aircraft development
p 341 N93-19322

Wind tunnel tests and CFD in Fuji Heavy Industries
p 304 N93-19323

Wind tunnel test and CFD in Kawasaki Heavy Industries, Gifu
p 304 N93-19324

Wind tunnel testing and CFD simulation in Mitsubishi Heavy Industries
p 305 N93-19325

Role of wind tunnel tests and CFD analysis for the development of aero-engines in IHI
p 365 N93-19326

Research on combined HOPE navigation technology
p 533 N93-20428

Beta-limiting phenomena in high-aspect-ratio toroidal helical plasmas
[NIFS-188] p 569 N93-20546

JPRS report: Science and technology. Japan. 30th National Aerospace Laboratory Conference
[JPRS-JST-93-009] p 761 N93-25418

Low-speed wind tunnel study of the direct side-force characteristics of a joined-wing airplane with an upper fin
[DE93-767966] p 988 N93-31189

K

KENYA

Some aspects of variable geometry gas turbine operation
[ASME PAPER 92-GT-407] p 356 A93-19556

KOREA, REPUBLIC OF

Influence of trailing-edge grid structure on Navier-Stokes computation of turbomachinery cascade flow
p 111 A93-14078

An interactive numerical procedure for rotor aeroelastic stability analysis using elastic lifting surface
p 155 A93-14313

A numerical study of unsteady supersonic compression ramp flows
[AIAA PAPER 93-0883] p 470 A93-24943

Unsteady wake effect on rotor vibratory airloadings
p 509 A93-29439

An analysis on high speed impulsive noise of transonic helicopter rotor
p 849 A93-35965

An efficient method to calculate rotor flow in hover and forward flight
[AIAA PAPER 93-3336] p 953 A93-45030

S-plane aerodynamics of nonplanar lifting surfaces
p 958 A93-45134

Vibration analysis of composite wing with tip mass using finite elements
p 1023 A93-45175

Computation of passively controlled transonic wing
[AIAA PAPER 93-3474] p 981 A93-47253

Navier-Stokes calculations of rotating BERP planform blade flowfields
[AIAA PAPER 93-3527] p 986 A93-47286

Two-dimensional transonic flow around VKI turbine cascade
p 1232 A93-54640

Reynolds stress profiles in the near wake of an oscillating airfoil
p 1236 A93-55380

A prediction model for the vortex shedding noise from the wake of an airfoil or axial flow fan blades
p 1265 A93-55995

Prediction of airfoil stall using Navier-Stokes equations in streamline coordinates
p 787 N93-27456

Discrete-vortex simulation of pulsating flow on a turbulent leading-edge separation bubble
p 787 N93-27457

LATVIA

Improvement of aircraft maintenance methods
p 395 A93-18326

A model of the maintenance of a fleet of TU-204 aircraft at a maintenance and repair center
p 237 A93-18327

Selection of methods and equipment for monitoring the technical condition of booster system components
p 395 A93-18329

Refinement of algorithms for calculating the remaining life from magnetic recording instrument data
p 320 A93-18330

Justification for the linear recording of fatigue damage summation for aircraft structures under operating conditions
p 320 A93-18331

A method for evaluating the technical condition of hydraulic control boosters without their disassembly
p 395 A93-18335

Probability analysis of a method for diagnosing gas turbine engines on the basis of thermodynamic parameters
p 345 A93-18337

Characteristics of fatigue crack growth under the service-spectrum loading of the tail boom of a helicopter
p 321 A93-18339

Effect of design and service-related factors on the formation of combustion residues in the fuel nozzles of gas turbine engines
p 345 A93-18342

Accuracy of nonparametric reliability estimates under varying operation conditions
p 396 A93-18343

Analysis of random components during measurements in the computerized diagnostic system Analiz-86
p 321 A93-18344

Automation of aircraft service testing tasks using the automatic control system Bezopasnost'-3
p 306 A93-18345

Search strategies for a sequence of baseline indices for building sections of a flight-safety automatic control system in the interactive mode
p 306 A93-18346

A methodological approach to the development of service and technical specifications for an actively controlled multistrut landing gear
p 321 A93-18349

Using helicopters for transporting large and heavy loads
p 306 A93-18350

Optimizing the cruising fuel efficiency of commercial aircraft on the basis of flight manual data
p 321 A93-18351

Aerodynamic questions related to the safety and cost-effective utilization of airships
p 818 A93-39125

A practical course in aircraft maintenance. I - The powerplant
p 811 A93-39175

Maintenance of the liquid and gas systems of the IL-76 aircraft
p 804 A93-39203

The navigation and flying equipment of the Yak-42 aircraft
p 792 A93-39204

LEBANON

Design and implementation of a flight simulation system
p 66 A93-12216

M

MALTA

Airport technology international 1993
p 532 A93-26920

MOLDOVA

Canonical correlation relationships among spectral and phytometric variables for twenty winter wheat fields
p 433 A93-22992

N

NETHERLANDS

Development of a TRN/INS/GPS integrated navigation system
p 30 A93-11004

Multipath effects on GPS code phase measurements
p 34 A93-11295

On the use of the method of matched asymptotic expansions in propeller aerodynamics and acoustics
p 8 A93-11553

Bulging of fatigue cracks in a pressurized aircraft fuselage
p 81 A93-13639

Flight simulation and constant amplitude fatigue crack growth in aluminum-lithium sheet and plate
p 71 A93-13644

Adaptive multigrid for the steady Euler equations
p 201 A93-13988

The development of an efficient take-off performance monitor (TOPM)
p 180 A93-14186

Flight simulator research into advanced MLS approach and departure procedures
p 149 A93-14234

Damage severity of monitored fatigue load spectra
p 154 A93-14253

In-flight tailload measurements
p 155 A93-14285

Structural optimization in preliminary aircraft design - A finite-element approach p 226 A93-14340

Optimal lateral maneuvering for microburst encounters during final approach p 183 A93-14350

Design philosophies of the Basic Research Simulator p 191 A93-14414

A 'low-cost' full flight simulator for basic IFR training p 374 A93-18776

Transmission of sound through a rotor p 447 A93-19183

Performance of gas turbine compressor cleaners [ASME PAPER 92-GT-360] p 355 A93-19524

Aerodynamic degradation due to distributed roughness on high lift configuration [AIAA PAPER 93-0028] p 260 A93-20146

MIAS, the integration of MLS with DGPS/DLoran-C p 315 A93-21181

Investigation of methods for modeling propeller-induced flow fields [AIAA PAPER 93-0874] p 469 A93-24935

Numerical experiments on the stability of leading edge boundary layer flow - A two-dimensional linear study p 477 A93-27475

Polyethylene pyrolysis model for combustion calculations in solid fuel ramjets p 520 A93-27739

Technical solutions to reduce and to control the noise load in the Netherlands p 564 A93-28492

Global/local interlaminar stress analysis of a grid-stiffened composite panel p 548 A93-28543

Acquiring tail load spectra from in-flight measurements [AIAA PAPER 93-1607] p 711 A93-34137

Theodorsen's ideal propeller performance with ambient pressure in the slipstream p 768 A93-37400

A dual polarised active phased array antenna with low cross polarisation for a polarimetric airborne SAR p 883 A93-43401

The PHARUS project, first results of the realization phase p 884 A93-43454

Motion compensation in a time domain SAR processor p 885 A93-43466

Adaptive waveform selection with a neural network p 942 A93-43470

Simplified finite element representation of fuselage frames with flexible castellations p 992 A93-43570

European studies to investigate the feasibility of using 1000 ft vertical separation minima above FL(290). III - Further results and overall conclusions p 992 A93-45166

Results of review of Fokker F 28 'Fellowship' maintenance program p 948 A93-45793

An optimal detection algorithm for harmonic interference signals in Loran-C p 993 A93-46889

Boundary layer effects on the flow of a leading edge vortex [AIAA PAPER 93-3463] p 980 A93-47245

The application of an Euler method and a Navier Stokes method to the vortical flow about a delta wing [AIAA PAPER 93-3510] p 984 A93-47276

The realization phase of the PHARUS project p 1162 A93-47658

Clebsch variable model for unsteady inviscid transonic flow with strong shock waves [AIAA PAPER 93-3025] p 1055 A93-48210

A fast robust viscous-inviscid interaction solver for transonic flow about wing/body configurations on the basis of full potential theory p 1056 A93-48211

Efficient multigrid computation of steady hypersonic flows p 1152 A93-49527

Numerical aspects of a block structured compressible flow solver p 1169 A93-51279

Development of advanced approach and departure procedures [AIAA PAPER 93-3833] p 1098 A93-51422

Monitoring load experience of individual aircraft p 1103 A93-52450

A primary flight display for four-dimensional guidance and navigation influence of tunnel size and level of additional information on pilot performance and control behaviour [AIAA PAPER 93-3570] p 1208 A93-52668

The development of SIMONA - A simulator facility for advanced research into simulation techniques, motion system control and navigation systems technologies [AIAA PAPER 93-3574] p 1208 A93-52670

The reduction of skin friction by riblets under the influence of an adverse pressure gradient p 1218 A93-53810

Estimation of aircraft inertia characteristics from bifilar pendulum test data p 1249 A93-56029

Flight testing: Past, present, and future p 164 A93-14615

Flight simulation leaves the ground p 194 A93-14616

Definition study PHARUS [AD-A256560] p 221 A93-14805

Experimental and numerical investigation of vortex flow over a 76/60-deg double-delta wing p 289 A93-16210

Terminal area traffic management [LR-680] p 317 A93-16213

Stress calculations on the window section of an all-composite aircraft fuselage [LR-688] p 328 A93-16215

The Airbus floor beam: Towards a cost-effective composite design and manufacture research project sponsored by Airbus industry [LR-677] p 329 A93-16283

DME-derived positions compared with MLS- and ILS-derived positions [NLR-TP-90119-U] p 318 A93-16343

Helicopter installations: From motor to rotor [LR-675] p 329 A93-16345

Comparison of solution of various Euler solvers and one Navier-Stokes solver for the flow about a sharp-edged cropped delta wing [NLR-TP-90340-U] p 418 A93-16411

Development of a computer assisted toolbox for aerodynamic design of aircraft at subcritical conditions with application to three-surface and canard aircraft [ISBN-90-6275-768-5] p 441 A93-16567

Review of aeronautical fatigue investigations in the Netherlands during the period March 1989 - March 1991 [NLR-TP-91092-U] p 331 A93-17535

Damage tolerance behaviour of aluminium-lithium sheet alloys [NLR-TP-91244-U] p 392 A93-17540

Navstar global positioning system: Introduction and status [NLR-TP-91008-U] p 318 A93-17559

Flight simulation and constant amplitude fatigue crack growth in aluminum-lithium sheet and plate [NLR-TP-91104-U] p 331 A93-17562

Carrier wave signals interfering with Loran-C [ETN-92-92528] p 318 A93-17584

Application of an Euler-equation method to a sharp-edged delta wing configuration with vortex flow [NLR-TP-91306] p 294 A93-17809

Flight simulation evaluation of the flyability of curved MLS approaches with wide-body aircraft [NLR-TP-90238-U] p 382 A93-17875

Beyond the frequency limits of time-linearized methods [NLR-TP-91216-U] p 295 A93-17929

NARSIM and EFMS: Tools for research on integrated ATM [NLR-TP-89336-U] p 319 A93-17954

Professor Wittenberg: His speciality and versatility [ISBN-90-6275-670-0] p 240 A93-19002

Propelling force and resistance p 298 A93-19003

Aircraft performance in practice p 340 A93-19004

Helicopters in action p 340 A93-19005

What is the progress in propulsion? p 298 A93-19006

On-line aircraft state and parameter estimation p 512 A93-19929

Load experience variability of fighter aircraft [NLR-TP-89172-U] p 514 A93-20742

A simulator study into low speed longitudinal handling qualities of ACT transport aircraft [NLR-TP-89387-U] p 527 A93-20743

Quiet by design: Numerical acousto-elastic analysis of aircraft structures [ISBN-90-386-0042-9] p 893 A93-29268

ERS-1 directional wave spectra validation with the airborne SAR PHARS [BCRS-92-18] p 937 A93-31010

A break-down of sting interference effects [NLR-TP-91220-U] p 1014 A93-31042

Performance of gas turbine compressor cleaners [NLR-TP-91237-U] p 1003 A93-31111

Experiences with two GPS receivers in northern Europe [NLR-TP-91168-U] p 993 A93-31120

Computational methods for aerodynamic design of aircraft components [NLR-TP-92072-4] p 987 A93-31148

On the verification of a theory for sculling propulsion [ETN-93-94040] p 1031 A93-31519

On the dynamics of aeroelastic oscillators with one degree of freedom [REPT-92-96] p 1040 A93-31653

Fractographic and microstructural analysis of fatigue crack growth in Ti-6Al-4V fan disc forgings p 1004 A93-31742

Low cycle fatigue behaviour of titanium disc alloys p 1004 A93-31745

Review of aerodynamic design in the Netherlands [NLR-TP-91260-U] p 999 A93-31840

Ageing aircraft research in the Netherlands [NLR-TP-91443-U] p 999 A93-32203

Damage severity of monitored fatigue load spectra [NLR-TP-92009-U] p 999 A93-32205

Instrumentation for in-flight acoustic measurements in an engine inlet duct of a Fokker 100 aircraft [NLR-TP-91200-U] p 1001 A93-32332

The application of phase tracking GPS for flight test trajectory determination [NLR-TP-91349-U] p 994 A93-32337

Development of a method to predict transonic limit cycle oscillation characteristics of fighter aircraft [NLR-TP-91359-U] p 999 A93-32338

Panel methods for aerodynamic analysis and design [NLR-TP-91404-U] p 990 A93-32357

NLR inviscid transonic unsteady loads prediction methods in aeroelasticity [NLR-TP-91410-U] p 990 A93-32358

Low cycle fatigue behaviour of titanium disc alloys [NLR-TP-91346-U] p 1006 A93-32372

Accelerated and real-time corrosion testing of aluminum-lithium alloys [NLR-TP-91203-U] p 1020 A93-32385

Transmission of sound through a rotor [NLR-TP-92014-U] p 1006 A93-32386

Evaluation of the flyability of MLS curved approaches for wide-body aircraft [NLR-TP-91396-U] p 999 A93-32416

NEW ZEALAND

The role of national meteorological services in aviation servicing under the final phase of the World Area Forecast System p 431 A93-22162

The airborne boundary concept for airport noise management p 564 A93-28482

Computer-based modelling of aircraft noise impact p 559 A93-28497

ELF, VLF and LF radiation from a very large loop antenna with a mountain core p 924 A93-40334

NIGER

Aerodynamic analysis of slipstream/wing/nacelle interference for preliminary design of aircraft configurations p 130 A93-13205

Aerodynamic integration of thrust reversers on the Fokker 100 p 160 A93-13208

Interlaminar stress analysis at the skin/stiffener interface of a grid-stiffened composite panel [NASA-CR-192177] p 393 A93-17920

NORWAY

Final results from a study of community response to aircraft noise around Oslo Airport Fornebu p 425 A93-19192

Comparison of airport noise calculation models p 564 A93-28480

Alternative approach routes to runway 24 at Oslo Airport, Fornebu p 487 A93-28481

Influence of aircraft noise on speech intelligibility p 558 A93-28483

Preliminary results from a study of community response to noise from military aircraft exercise p 558 A93-28484

Final results from a study of community response to aircraft noise around Oslo Airport Fornebu p 558 A93-28486

Arctic environment - Helicopter operations in cold climates p 1189 A93-54288

The integration of geometric modeling into an inverse design method and application of a PC-based inverse design method and comparison with test results p 81 A93-10058

O

OMAN

An implicit finite-difference algorithm for the numerical simulation of supersonic flow over blunt bodies p 770 A93-38325

P

POLAND

Vibration control algorithms for flexible rotors p 95 A93-10741

A short range passenger/freighter canard - Some problems of a preliminary aerodynamic concept [SAE PAPER 921012] p 157 A93-14642

Results of testing of models of joint-wing utility class aircraft [SAE PAPER 921013] p 157 A93-14643

Geometrically nonlinear local flutter analysis of supersonic airplane skin plates in the potential supersonic flow [ISBN 83-01-10939-4] p 394 A93-17569

Laboratory for modelling of prospective board equipment systems for aircraft p 374 A93-18529

Model of a map indicator p 341 A93-18532

- The optimum value of the nozzle outlet angle of turbine stages
[ASME PAPER 92-GT-224] p 404 A93-19442
- The comparison of different simplified mathematical models of the gas turbine combustion chamber as an object of temperature and pressure control
[ASME PAPER 92-GT-347] p 354 A93-19518
- Flutter calculations for a system with interacting nonlinearities
[AIAA PAPER 92-4682] p 409 A93-20304
- Elementary stall flutter of an aircraft wing
p 545 A93-27289
- Modelling of the flow in the blade-ring design process of turbomachinery
p 520 A93-27291
- Problems in the modeling of helicopter flight
p 506 A93-27293
- Modeling and analysis of the winch launch of a glider
p 528 A93-27294
- Active aircraft recovery from a spin
p 524 A93-27295
- Influence of modelling loading on stress distribution in turbomachinery blade fastening in case of FEM
p 520 A93-27296
- Investigation of the aircraft spin via sensitivity analysis
p 524 A93-27300
- Experimental study of a single strong vortex-airfoil interaction
p 481 A93-29432
- Instability of three-dimensional supersonic boundary layer
p 973 A93-46987
- Two dimensional incompressible flow through a vibrating bladed disc - Theoretical model
p 973 A93-46991
- Analysis of spatial motion dynamics of a helicopter for various models of the induced velocity field
p 1191 A93-53721
- Finite element analysis of natural vibrations of an aeroplane with asymmetric variable wing geometry
p 1218 A93-53776
- Integrated DGPS/IMU systems for airborne navigation in Poland
p 1241 A93-56049
- ONERA calculation model of dynamic flow separation on an airfoil section
p 1238 A93-56212
- A numerical study of aerodynamic wing design for supercritical conditions of an advanced training and military aircraft
p 1238 A93-56213
- Numerical minimization of the moment coefficient of a supercritical airfoil section
p 1238 A93-56214
- Determination of the transonic flow field around an airfoil section for a given lift force coefficient
p 1239 A93-56215
- Numerical study of slightly compressible Navier-Stokes simulation of blade-vortex interaction
p 1239 A93-56216
- Consideration of mass elements of the control system in a flutter analysis
p 1249 A93-56217
- The whirl-flutter problem in aircraft construction
p 1249 A93-56218
- Interaction of compressible vortices with a rigid plate
p 1239 A93-56219
- Quantitative Knudsen-number dependences of density disturbances in front of obstructions in supersonic divergent flows
p 1239 A93-56220
- Thermodynamic aspects of model testing in cryogenic wind tunnels
p 1251 A93-56222

PORTUGAL

- Misalignments of airborne laser beams due to mechanical vibrations
p 394 A93-17762
- Propagation of transverse anti-plane waves in orthotropic layers
p 412 A93-21878
- Air traffic noise monitoring in and around Lisbon Airport
p 564 A93-28494
- Comparison of several convection discretization schemes for all Mach number arbitrary 2D flows
p 685 A93-34345
- On the analysis of an impinging jet on ground effects
p 1260 A93-56339
- Experimental analysis of combustion oscillations with reference to ramjet propulsion
p 392 A93-17614
- On automated analysis of flight test data
p 512 A93-19913

R

ROMANIA

- The aerodynamic loads on aircraft components in violent longitudinal manoeuvres
p 476 A93-26898
- Aerodynamic forces and moments on a dihedral swept wing in a translation with attack and side-slip angle
p 476 A93-26903
- The numerical simulation of the hydrodynamic field from the pump impellers zone by means of the finite element method
p 476 A93-26905
- Permeable airfoils in incompressible flow
p 768 A93-37401
- Lifting line theory for supersonic flow applications
p 778 A93-39402

- A novel development of the Ludwig tube, for extended test duration
p 1011 A93-45529
- Optimal symmetric trajectories over a fixed-time domain
[AIAA PAPER 93-3848] p 1133 A93-51435

RUSSIA

- Dynamics of a high-rpm compressor
p 75 A93-10009
- Collection of works on measuring and computing systems for research on the aerodynamics, dynamics, and strength of flight vehicles
p 75 A93-10026
- A pressure distribution measuring system with pneumatic switches and automatic band selection
p 75 A93-10029
- Measurement of aerodynamic forces at high temperatures
p 75 A93-10030
- A data processing and measuring system with a traversing probe for studying flow in the rotating impeller of an axial-flow fan
p 75 A93-10032
- Software for the control of measurement data acquisition, processing, and monitoring during strength testings
p 94 A93-10042
- Hemispherical and spherical flow parameter detectors
p 75 A93-10044
- A study of the possibility of the parallel execution of a program for calculating the aerodynamic characteristics of flight vehicles using an improved panel method
p 95 A93-10045
- Determination of the membrane and flexural shell deformations from the readings of a two-sided rosette-type strain gage
p 75 A93-10047
- A transfer standard of an air flow rate unit VET 150-2-87
p 66 A93-10049
- Extreme value heat transfer problems for three-dimensional bodies moving at hypersonic velocities
p 4 A93-10079
- Approximate methods for heat flows toward the surface of three-dimensional bodies
p 4 A93-10080
- Using ultralight flight vehicles for large-scale aerial photography
p 92 A93-10098
- Viscous instability of hypersonic flow past a wedge
p 4 A93-10137
- Intensification of flow mixing behind an oblique shock wave
p 4 A93-10138
- An asymptotic model of a closed separation region in supersonic flow
p 4 A93-10139
- Variational problem of the profiling of the side walls of the supersonic section of a narrow three-dimensional nozzle
p 4 A93-10140
- Numerical modeling of supersonic flows past wings of different aspect ratios over a wide range of angles of attack within the framework of the plane section law
p 5 A93-10141
- A method for determining the aerodynamic coefficients of asymmetric bodies with allowance for nonlinear influence factors of the body shape
p 5 A93-10142
- Calculation of a three-dimensional boundary layer at the lee side of a finite-span delta wing in the case of viscous interaction with hypersonic flow
p 5 A93-10143
- Regimes of supersonic flow past the windward side of V-shaped wings
p 5 A93-10144
- Effect of longitudinal microribbing on the drag of a body of revolution
p 5 A93-10147
- Calculation of a gas-dispersion laminar boundary layer on a plate with allowance for liquid film formation
p 76 A93-10148
- A study of the effect of nonstationary perturbations on flow in the front separation region
p 5 A93-10150
- Turbulent jet flows with condensation and electrophysical effects
p 76 A93-10176
- An electrostatic probe for determining particle characteristics in disperse flow
p 76 A93-10173
- A study of a pulsed electrical field near the jet of a turbojet engine
p 52 A93-10179
- Experimental study of condensation vapor-air jets
p 76 A93-10180
- Three-dimensional flow of viscous gas in the blade passage of a straight compressor cascade
p 5 A93-10187
- Boundary layer separation in a corner formed by two planes
p 6 A93-10188
- Effect of a large-scale inhomogeneity of the incoming flow on flow in a plane turbine cascade
p 6 A93-10189
- Calculation of three-dimensional turbulent jets propagating behind nozzles of rectangular cross section
p 6 A93-10192
- Self-excited oscillations at supersonic off-design jet outflow
p 6 A93-10402
- On improving adequacy of modeling in wind tunnel problems
p 6 A93-10404
- Effect of heat supply on the gasdynamic parameters of gas flow in Laval nozzles
p 12 A93-12760
- A flow calculation and aerodynamic design method for turbomachine cascades
p 12 A93-12764

- Calculation of the three-dimensional interaction of a shock wave with a boundary layer on a cylinder
p 12 A93-12766
- Numerical solution of the integral equations of the aerodynamics of porous surfaces
p 13 A93-12768
- Nonlinear deformation mechanics of multilayer transparency elements - General theory relations
p 79 A93-12800
- Stabilization of the dynamic characteristics of the automatic control systems of a flight vehicle
p 62 A93-12802
- Computational studies of the characteristics of axial compressor cascades and stages in unsteady incoming flow
p 13 A93-12805
- A method for calculating flow past an arbitrary airfoil profile in the presence of flow separation
p 13 A93-12807
- Grid-characteristic method for calculating a three-dimensional boundary layer on the bounding surfaces of the blade passage of a turbomachine
p 13 A93-12808
- Effect of the proximity of the machined surface on the discharge coefficients of laser cutter nozzles
p 79 A93-12809
- An experimental study of a method for reducing the jet noise of bypass engines using mechanical flow mixers
p 53 A93-12810
- Allowing for the effect of flow nonisothermality on total pressure losses in the afterburner diffusers of augmented turbofan engines
p 53 A93-12811
- A study of heat transfer from a disk in a rotating cavity with axial and radial-axial flow of a liquid
p 54 A93-12812
- Parametric diagnostics of the steady states of gas turbine engines
p 54 A93-12815
- Evaluation of the efficiency of the direct search method in solving the problem of numerical calculation of the complex hydraulic cooling systems of aviation gas turbine engines
p 54 A93-12818
- Effect of the powerplant configuration on the air flow rate of the jet shield
p 54 A93-12820
- A nomographic model for multicriterial optimization during the design of a flight vehicle powerplant
p 95 A93-12821
- A method for estimating the technico-economic efficiency of measures increasing the reliability of gas turbine engines in service
p 54 A93-12822
- Evaporation and specific heats of motor fuels
p 71 A93-12823
- Viscosity of aviation fuel components (n-alkanes)
p 71 A93-12824
- Shock wave interference on a wing with a partition at hypersonic velocities
p 13 A93-12839
- Maximizing the critical Mach number for lifting wing profiles
p 13 A93-12841
- Nonstationary flow of a viscous incompressible fluid past an airfoil
p 79 A93-12922
- Monotonicity characteristics of some plane vortex flows of incompressible fluids and subsonic gas flows
p 13 A93-12932
- Increasing the lift-drag ratio of wings of small aspect ratio at hypersonic velocities
p 13 A93-12933
- Effect of the drag of the front body on the restructuring of flow between two bodies in the path of supersonic flow, with one body located in the wake of the other
p 14 A93-12973
- A study of the laminar-turbulent transition in a boundary layer and separation on cones at supersonic velocities
p 14 A93-12974
- Calculation of separated axisymmetric flow past bodies by solving Euler equations in the inner vortex region
p 14 A93-12975
- A comparative analysis of algorithms for solving systems of high-order linear algebraic equations
p 96 A93-12977
- Effect of flight conditions on the sound insulation of the aircraft passenger compartment
p 42 A93-12978
- An experimental study of dc discharges in supersonic and subsonic air flows
p 14 A93-12980
- Precision increasing and integrity monitoring of navigation data for GPS/inertial hybrid solution
p 149 A93-14157
- Flight path optimization and suboptimal control laws synthesis for transport mission of maneuverable aircraft
p 180 A93-14160
- A new production technology for complex-shaped structural elements 'creep forming'
p 202 A93-14175
- Accelerated method of the Euler equation solution in transonic airfoil flow problem
p 113 A93-14193
- An adaptive algorithm for estimation of a state vector in the system of remotely-piloted aircraft control using Kalman filter
p 181 A93-14232
- Supersonic combustion and gasdynamic of scramjet
p 170 A93-14242
- Combined engines for hypersonic flight
p 171 A93-14244

- Experimental investigation of hydrogen burning and heat transfer in annular duct at supersonic velocity p 171 A93-14247
- Experimental study of crossflow instability and laminar-turbulent transition on a swept wing p 115 A93-14250
- Use of alternative fuels for aviation p 196 A93-14292
- Wing rock of lifting systems p 118 A93-14330
- RISK - Interactive multidisciplinary system for designing airframes p 226 A93-14337
- Simulation of a hypersonic flow over vehicles at low Reynolds numbers p 120 A93-14381
- Air transportation system for shipping outsized cargoes p 141 A93-14394
- Estimation of the probability of large flight parameters deviations p 184 A93-14399
- Integrated air separation and propulsion system for aerospace plane with atmospheric oxygen collection [SAE PAPER 920974] p 195 A93-14633
- Steady state model for the thermal regimes of shells of airships and hot air balloons p 207 A93-15072
- Wind lifting of aerosol particles p 223 A93-15079
- Subsonic separated flow past slender delta wings p 124 A93-15109
- Calculation of flow of a rarefied gas past a sphere for an arbitrary Knudsen number p 124 A93-15146
- Oblique wave evolution in a plane subsonic boundary layer p 124 A93-15178
- Instability of the periodic deflection of a panel surface in a turbulent boundary layer p 208 A93-15188
- Modeling of interfaces in problems of flow of a ponderable fluid past a wing profile p 124 A93-15189
- Calculation of radiant energy transfer in hypersonic flow past blunt bodies using the P1 and P2 approximations of the spherical harmonic method p 124 A93-15209
- A fast method for calculating three-dimensional transonic potential flows in turbomachine blade rows p 125 A93-15215
- A method for calculating supersonic three-dimensional flows in pyramidal nozzles p 125 A93-15216
- A conformal-integral method for solving the direct problem in turbomachine cascade aerodynamics p 125 A93-15217
- Principles of the design of automated meteorological support systems for aviation [ISBN 5-286-00342-7] p 151 A93-15224
- Instability of local separated flows with respect to small-amplitude perturbations p 125 A93-15254
- Acoustic control of flow separation on a straight and a yawed wing p 125 A93-15256
- Flow past a finite-span wing in the presence of external acoustic loading p 127 A93-16707
- Effect of the body shape on head shock attenuation at a large distance from the axis p 127 A93-16708
- Synthesis of robust motion stabilization laws for flight vehicles p 227 A93-16777
- Solution of the terminal guidance problem for a flight vehicle using analytical mechanics methods p 228 A93-16778
- Modeling of human operator actions in the stochastic trajectory tracking problem for a dynamic plant p 228 A93-16783
- Autonomous mobile laser complex p 395 A93-17767
- Detection and parameter estimation of atmospheric turbulence by ground-based and airborne CO2 Doppler lidars p 395 A93-17862
- Effect of airfoil porosity on the shock wave position and intensity at transonic velocities p 241 A93-18222
- Breakdown of steady state axisymmetric flow in a shock layer formed as a result of the impingement of a supersonic underexpanded jet on a perpendicular plane obstacle p 241 A93-18230
- Two-phase injection from the front surface of a blunt body in hypersonic flow p 241 A93-18233
- Influence of second-order boundary layer effects in hypersonic flow past blunt cones of large aspect ratio p 241 A93-18238
- Effect of real air properties on integral aerodynamic characteristics p 242 A93-18241
- Excitation of velocity fluctuations and noise in a wind tunnel p 444 A93-18242
- Integral equations in the problem of flow past an airfoil p 395 A93-18243
- A new method for determining the number of flight vehicle prototypes subject to full-scale testing p 434 A93-18316
- Improvement of aircraft maintenance methods p 237 A93-18352
- Expanding the operation scope of aircraft through the use of air-cushion landing gear p 321 A93-18354
- Calculation of fuel economy for the Tu-154 aircraft in relation to the washing of the NK-8-2U engine at civil aviation maintenance facilities p 345 A93-18356
- A system for washing the combustion chamber nozzles and flow path components of the NK-8-2U engine during service p 373 A93-18357
- Diagnostics of the hydraulic system of Tu-204 aircraft p 396 A93-18360
- Characteristics of the diagnostics of booster system components p 321 A93-18361
- Vibrational monitoring and diagnostics of the technical condition of gas turbine engines at civil aviation repair facilities p 374 A93-18362
- Improving the service characteristics of an aircraft through the gyroscopic damping of its structure p 366 A93-18363
- Assessment of flight data in real time p 341 A93-18364
- Graph-theory studies of the possibility of occurrence of flight accidents and incidents during the take-off under special operating conditions p 306 A93-18365
- Monitoring the purity of the working fluids of aircraft hydraulic systems during service p 321 A93-18367
- Crack growth under conditions of service loading p 396 A93-18370
- Improvement of rotating brushes for surface cleaning p 396 A93-18371
- A unified approach to the construction of the throttle characteristics of postrepair turbojet engines, with the NK-8-2U engine used as an example p 345 A93-18372
- Development of a prototype of an expert system for the design of comprehensive scientific-technical development programs for civil aviation p 434 A93-18373
- Analysis of the pump station of an aircraft hydraulic system as a subject of diagnosis p 321 A93-18374
- Selection of the time scale for preventive measures under service conditions p 237 A93-18375
- Problems in the aerodynamics and dynamics of flight vehicles in the light of K.E. Tsiolkovsky's ideas; Lectures Devoted to K.E. Tsiolkovsky's Ideas, 25th, Kaluga, Russia, Sept. 11-14, 1990, Transactions p 237 A93-18376
- Method and results of studies of flow past supersonic flight vehicles at moderate and large angles of attack p 242 A93-18377
- Solution of trajectory optimization methods using the Pontryagin maximum principle p 366 A93-18378
- The use of the Polhamus and discrete vortex methods for calculating the nonlinear characteristics of delta wings and wings with a strake p 242 A93-18379
- Calculation of the parameters of a crane helicopter with one disabled engine p 366 A93-18381
- Estimation of the external loading of airships in flight p 366 A93-18383
- Effect of the Reynolds number on the aerodynamic characteristics of a body of revolution over a wide range of angles of attack p 242 A93-18384
- Astronautics and society p 383 A93-18391
- On space correlation of pressure pulsations on the streamlined surface before a step p 244 A93-19135
- On the acoustic radiation nature of a turbulent vortex ring p 446 A93-19167
- Control of coherent structures and aero-acoustic characteristics of subsonic and supersonic turbulent jets p 448 A93-19196
- Experimental investigations and efficiency prediction of jet noise reduction techniques p 449 A93-19206
- Optimization of a multistage axial compressor stochastic approach [ASME PAPER 92-GT-163] p 351 A93-19389
- Using contra-rotating rotors for decreasing sizes and component number in small GTE [ASME PAPER 92-GT-414] p 356 A93-19562
- Optimization of a multistage axial compressor in a gas turbine engine system [ASME PAPER 92-GT-424] p 357 A93-19572
- Nonequilibrium excitation of internal molecular degrees of freedom in the shock layer during hypersonic flight p 412 A93-21922
- The asymptotic theory of hypersonic boundary-layer stability p 462 A93-24409
- The long-wave limit in the asymptotic theory of hypersonic boundary-layer stability p 462 A93-24410
- Control synthesis with incomplete, complete, and supercomplete measurements p 561 A93-27603
- A data processing and control system for counteracting wind shear p 524 A93-27604
- Shock wave ahead of a liquid jet in supersonic cross flow p 477 A93-27605
- Calculation of three-dimensional supersonic flow past lifting surfaces p 477 A93-27607
- Problems in the optimum design of a wing profile for nonseparated flow over a range of angles of attack p 477 A93-27614
- A method for calculating the characteristics of plane compressor cascades for different values of the Reynolds criterion p 545 A93-27616
- Estimation of the life of aircraft structures under stochastic steady state loading p 545 A93-27620
- Wave resistance of swept wings with superersonic edges p 478 A93-27624
- Determination of gas flow rate in a duct from measured static pressures p 520 A93-27625
- Consideration of the completeness of combustion and dissociation and recombination processes in mathematical models of jet engines for high supersonic flight velocities p 520 A93-27627
- Calculating the cutting depth during the milling of large gas turbine engine blades p 545 A93-27628
- A set of application programs for the smoothing of curves and surfaces by the method of monoidal transformations in the geometric module of a CAD system for the design of flight vehicles p 561 A93-27629
- Three-dimensional flow past an ogival-cylindrical body in combination with a delta wing p 478 A93-27636
- Interaction of Tollmien-Schlichting waves with localized disturbances p 545 A93-27637
- Experience with the use of liquid crystals in conjunction with the filament method in studying the structure of supersonic flow downstream of a plane step p 478 A93-27639
- Effect of combustion on the interaction of an underexpanded wall hydrogen jet with supersonic flow in a plane duct p 534 A93-27658
- A study of the problem of developing a weakly invariant flight vehicle control system p 561 A93-27688
- An identification method for dynamic systems with delay p 562 A93-27689
- Helicopters - Handbook [ISBN 5-203-00804-3] p 458 A93-28874
- Flight safety in a perturbed atmosphere [ISBN 5-277-00815-2] p 487 A93-29431
- Computational and experimental investigation of a solar energy system for an atmospheric flight vehicle p 521 A93-29655
- Choice of the heating system for high-temperature generators using chemical fuel p 559 A93-29660
- Algorithms and automated techniques for the design of control systems for moving objects p 562 A93-29690
- Selection of transducer measuring ranges in flight vehicle control systems p 526 A93-29691
- Interaction of compression waves with an elastic spherical dome p 550 A93-29718
- Methods and results of theoretical investigations for high-speed parachute systems [AIAA PAPER 93-1227] p 690 A93-35173
- Computation of aeroelastic characteristics and stress-strained state of parachutes [AIAA PAPER 93-1237] p 744 A93-35178
- Unsteady supersonic flow around a blunt body in thermal inhomogeneities in turbulent shock layer flows p 691 A93-35266
- A study of flow structure and heat transfer intensity in the vicinity of an expanding step on a plate p 691 A93-35268
- Hydrodynamics and heat transfer near the stagnation point in an arbitrary axisymmetric nonswirling flow incident on a rotating obstacle p 691 A93-35270
- Ensuring the reliability and service life of flight vehicle structures by engineering methods p 745 A93-35276
- Single-impact calibrated electromagnetic tightening of long-life bolted joints in aviation structures p 745 A93-35277
- Effect of a combination of design and process-related factors on the fatigue strength of bolted joints in acoustically loaded aircraft structures p 745 A93-35278
- Ways of increasing the service life and reliability of bolted joints p 745 A93-35281
- High-strength combination fasteners for joint assembly in aircraft structures p 745 A93-35283
- Mathematical statement of the problem of optimizing the design of an airframe for ease of manufacture p 745 A93-35286
- A method for estimating the survivability of bodies of revolution p 745 A93-35287
- Stress-strain state of the elements of a single-stringer riveted panel p 746 A93-35288
- Effect of overloads on the service life of the structural elements of aircraft p 746 A93-35289
- Selection of protective coatings for parts in a computer-aided design system p 746 A93-35290
- Selecting a method for sealing riveted joints in fuel compartments p 746 A93-35295
- Protective properties of aviation oils p 735 A93-35299
- An algorithm with prediction in a control problem with functional constraints p 757 A93-35307
- Calculation of the irregular interaction of shock waves p 691 A93-35339
- A study of the temperature of bodies in the flow-around regime in the case of surface gas injection p 691 A93-35344

- Dynamics of the behavior of nematic films in gasdynamic flows p 746 A93-35345
- Intermode exchange in a supersonic boundary layer p 691 A93-35346
- A design concept for a flight vehicle computer system with artificial intelligence elements p 757 A93-35663
- Flight-vehicle drives (2nd revised and enlarged edition) [ISBN 5-217-00802-4] p 713 A93-35676
- Modeling and optimization of aircraft assembly [ISBN 5-217-00808-3] p 677 A93-35677
- Instrument systems of flight vehicles and their design [ISBN 5-217-00793-1] p 718 A93-35678
- Gas dynamics of cooled turbines [ISBN 5-217-00809-1] p 721 A93-35685
- Studies of atmospheric eddy dynamics and energetics and climate problems [ISBN 5-286-00610-8] p 753 A93-35689
- Improved static and dynamic performance of helicopter powerplant p 809 A93-35928
- Helicopter aerodynamics research techniques and rotor-fuselage interaction analysis p 765 A93-35938
- MI-26 autorotational landings p 816 A93-35955
- Some considerations on indication means for helicopter pilot vision systems p 807 A93-36018
- Resource conservation and improvement of the service characteristics of castings of high-temperature nickel alloys through a high-temperature melt treatment p 824 A93-36718
- Stress-strain analysis and optimal design of aircraft structures p 827 A93-36782
- A study of the origin of residual stresses and strains in the transparencies of supersonic aircraft p 801 A93-36784
- Methodology for studying the fracture of aircraft structures in static tests p 801 A93-36785
- Optimization of the stiffness and mass characteristics of lifting surface structures modeled by an elastic beam p 827 A93-36789
- Problems of the organization of the mass testing of large structural elements of aircraft using testing machines p 821 A93-36791
- A study of the strength of a closed system of wings p 828 A93-36792
- A method for the optimum design of a large-aspect-ratio wing p 828 A93-36793
- Load-bearing capacity of an aircraft wing based on the condition of compressed surface fracture p 801 A93-36794
- Efficiency of using longitudinal and circumferential bands in the structures of an aircraft fuselage p 801 A93-36795
- Numerical modeling of the impact of a bird against aircraft transparencies p 801 A93-36797
- A study of the effect of the static aeroelasticity of a swept wing on its weight response p 801 A93-36798
- A plate loaded by a transverse impulse force and in-plane forces p 828 A93-36799
- Optimal design of honeycomb sandwich shell aircraft structures of composite materials p 828 A93-36800
- Inelasticity effect in a unidirectional boron/aluminum composite under uniaxial tension p 825 A93-39024
- Dynamic processes in the powerplants and power-generating equipment of flight vehicles p 832 A93-39027
- A study of the stability of the acceleration circuit of the hydromechanical automatic control system of an aviation gas turbine engine p 810 A93-39028
- Control of the quality of dynamic processes in the valves of power-generating equipment p 832 A93-39030
- Computational models of dampers for computer-aided design p 832 A93-39032
- Absolute stability of an automatic control system for gas turbine engines p 810 A93-39033
- The required damping and control process quality in a fuel pressure regulator p 810 A93-39034
- Correction of the frequency characteristic of the waveguide circuit of an acoustic-jet temperature transducer p 832 A93-39036
- A study of the effect of the working medium on the start-up characteristic of an aviation gas turbine engine p 811 A93-39037
- Identification of noise sources based on experimental amplitude-frequency noise characteristics of aircraft p 851 A93-39040
- Algorithms for constructing models of the interaction of diagnostic systems with reserved aviation equipment p 847 A93-39043
- Heat exchangers of gas turbine engines p 833 A93-39044
- Calculation of a collector-type annular plate heat exchanger p 833 A93-39045
- A model for calculating the element of a high-temperature heat exchanger with spiral-wire fins p 833 A93-39046
- A heat transfer element of a high-temperature heat exchanger p 833 A93-39047
- The use of aviation gas-liquid heat exchangers employing heat pipes p 833 A93-39050
- Operation of a cross-flow heat exchanger with partial recirculation of one of the coolants p 833 A93-39051
- A fuel-oil matrix heat exchanger p 833 A93-39052
- Development of a process for fabricating a plate heat exchanger for the heat recovery system of gas turbine engines p 834 A93-39053
- Determination of the dynamic characteristics of heat exchangers for the heat recovery system of gas turbine engines p 834 A93-39054
- Solution of the problem of determining the dynamic characteristics of the cross-flow heat exchanger of the heat recovery system of gas turbine engines p 834 A93-39055
- A method for calculating the dynamic characteristics of heat exchangers with single-phase cryogenic coolants p 851 A93-39057
- An experimental study of the air drying process in air coolers p 834 A93-39059
- Quality of the surface layer and operating properties of aircraft engine components p 834 A93-39061
- Prediction and control of the service-related properties of parts at the technological preparation stage and during the manufacture process p 834 A93-39062
- Enhancing the performance of aircraft engine blades by surface hardening p 811 A93-39072
- Effect of ion treatments on the fatigue strength of blades p 811 A93-39073
- Characteristics of friction and wear in flight vehicle engine components p 811 A93-39075
- Automated measurement of residual stresses in the surface layer of parts p 834 A93-39081
- High-efficiency machining methods for aviation materials [ISBN 5-230-16902-8] p 835 A93-39084
- Theory of the machining of polyhedral holes by plunge cutting p 835 A93-39091
- Some characteristics of the design of heads for the cutting of bevel gears with negative curvature of the circular-arc tooth line p 835 A93-39093
- Effect of a deformed electric field on the precision of the electrochemical machining of gas turbine engine components p 835 A93-39094
- Increasing the efficiency of the electrochemical dimensional machining of gas turbine engine blades of EP718VD alloy p 835 A93-39095
- Increasing the durability of gas turbine engine compressor blades by using a combined hardening/finishing treatment to control the stressed state of the surface layer p 835 A93-39099
- Hardening/finishing treatment of compressor blades using a machine with planetary container motion p 835 A93-39102
- Effect of the technological process structure on residual stress distribution in the blade foil of gas turbine engines p 836 A93-39106
- Modeling of the multiparameter assembly of engineering products for a specified priority of output geometrical parameters p 836 A93-39109
- Aerodynamic resistance of three-dimensional bodies with a starlike cross section at supersonic velocities, and problems of its calculation p 774 A93-39116
- Supersonic flow of a gas over a semiinfinite plate with small-scale harmonic spanwise oscillations p 775 A93-39118
- Flow past three-dimensional irregularities in a hypersonic boundary layer on a cooled body p 775 A93-39119
- Interference of an oblique shock with a shock layer on a blunt edge for small Reynolds numbers p 775 A93-39120
- Optimal conditions for flow turbulence reduction by a set of grids p 836 A93-39122
- Underexpanded boundary jet in a wake flow p 775 A93-39123
- A numerical investigation of supersonic flow of a viscous gas over long blunt cones, taking into account equilibrium physicochemical transformations p 775 A93-39124
- Problems in physical gas dynamics p 775 A93-39126
- Kinetic theory of nonequilibrium flows of gas and disperse media with internal degrees of freedom and chemical reactions p 851 A93-39127
- Kinetic theory of hypersonic flows of a viscous gas p 775 A93-39130
- Asymptotic structure of a limiting hypersonic flow in a shock wave p 776 A93-39131
- The problem of two Coulomb centers and its applications in physical aerodynamics p 776 A93-39132
- Nonequilibrium limiting hypersonic flow of a gas past three-dimensional tapered bodies with a separated shock p 776 A93-39133
- An approximate method for calculating nonequilibrium flows near blunt bodies p 776 A93-39134
- Hypersonic limiting flows of a relaxing gas with pressure changes in the main approximation p 776 A93-39135
- Effect of the thermodynamic air model on the aerodynamic characteristics of profiles with bends p 776 A93-39136
- Numerical modeling of ionization in nonequilibrium nitrogen flows in hypersonic nozzles p 836 A93-39137
- Calculation of the effect of the shock wave of a delta wing on a second wing at supersonic velocities p 776 A93-39141
- Calculation of the effect of flow concavity in a hypersonic nozzle on the aerodynamics of a flight vehicle model p 776 A93-39142
- Numerical study of spontaneous nitrogen condensation in the axisymmetric hypersonic nozzles of wind tunnels p 777 A93-39143
- Flow density distribution in a two-phase submerged jet p 836 A93-39144
- Nonequilibrium heat transfer near the critical point of blunt bodies p 777 A93-39145
- Modeling of the physicochemical processes of nonequilibrium heat transfer in the subsonic jets of an induction plasmatron p 836 A93-39147
- An experimental study of the three-dimensional interaction of a transverse jet with hypersonic flow p 777 A93-39150
- Modeling of flow in a pulsed shock tunnel p 777 A93-39152
- The minimal multiplier method in calculations of the stability, limiting vibration cycles, and limiting states of nonlinearly deformed structures p 836 A93-39176
- Estimation of wing stability in flow from the characteristics of the transient process p 836 A93-39177
- Effect of the aerodynamic interference of the rotor and the fuselage on the power requirements for the horizontal flight of a helicopter p 819 A93-39179
- Selection of the scheme and optimal parameters of the turbine of a high-temperature bypass engine with a low bypass ratio p 811 A93-39180
- A mathematical model of the vibrational impact hardening of parts p 837 A93-39185
- Expert evaluation of the technological level of aviation gas turbine engine designs p 811 A93-39187
- Using current numerical methods in a mathematical model of flight vehicle synthesis p 804 A93-39188
- Optimization of the parameters of the lift-augmentation devices of the wing of a maneuverable aircraft equipped with an active load-reduction system p 804 A93-39189
- Spanwise aileron oscillations p 819 A93-39190
- The problem of avoiding aircraft collisions during group flights p 819 A93-39191
- Kinematics of aeroinertial aircraft rotation p 819 A93-39192
- Fuel film formation in the fuel-air premixer of the combustion chamber p 812 A93-39193
- An experimental study of thrust reverser models p 812 A93-39195
- Experience in the design of supercritical cascades for the flow straightener of a transonic fan p 777 A93-39196
- Selection of the principal initial parameters for an axial-flow birotary turbine p 837 A93-39198
- Some recommendations concerning the prevention of fuel boiling in the igniters of the combustion chambers of gas turbine engines p 812 A93-39200
- The possibility of reducing the emission of benzo(a)pyrene with the exhaust gases of aviation gas turbine engines by water injection into the combustion chamber p 812 A93-39201
- Flight efficiency theory p 812 A93-39202
- New corrosion resistant nickel-base super-alloys and technological processes of casting gas turbines parts with directional single crystal and regulable equiaxed minimized microporosity structure p 916 A93-40811
- Current methods of selecting the configurations and parameters of flight vehicles p 891 A93-42369
- Optimization of equipment layout in the fuselage of maneuverable aircraft p 891 A93-42370
- Selection of the primary aircraft structure at the preliminary design stage p 891 A93-42371
- Effect of gasdynamic parameters on the specific weight of gas-turbine aircraft engines p 899 A93-42372
- Structure of a knowledge base used in the computerized synthesis of aircraft layout p 891 A93-42373
- Some aspects of the design of combination landing gear p 891 A93-42374
- Formalization of the problem of preliminary aircraft design p 891 A93-42375
- Computerized synthesis of three-dimensional kinematic landing gear schemes with a single turning axis p 891 A93-42376
- Dependence of the service life of a wing on its strength uniformity and landing gear location p 891 A93-42377

Determination of the takeoff characteristics of jet engines during the preliminary design of aircraft

p 892 A93-42378

Selection of the turbofan engine size

p 899 A93-42379

Selection of the powerplant for a thermoplane

p 899 A93-42380

Characteristics of data processing during the development of a data base for a CAD system for aircraft design

p 892 A93-42381

A numerical study of the flutter of conical shells

p 927 A93-42405

Evolution of a three-dimensional nonequilibrium boundary layer in a dihedral angle behind a perturbation source

p 872 A93-43013

Stability conditions for a transonic decelerating flow in a duct

p 872 A93-43027

Active algorithms for controlling the rotational motion of flight vehicles

p 908 A93-43079

Methods and equipment for data processing and acquisition in information management systems

p 856 A93-43101

Synthesis of a data processing and measuring system for flight vehicle control systems

p 908 A93-43102

Experimental and algorithmic means of identifying mathematical models of flight vehicle

p 909 A93-43103

Approximation of a flight vehicle trajectory using Walsh functions

p 909 A93-43106

A control algorithm for a navigation-landing system in the case of a priori indeterminacy of failure data

p 882 A93-43108

Estimation of the service periods for complex systems in the case of a priori indeterminacy of system reliability data

p 856 A93-43109

Increasing the reliability of an air traffic control radio system

p 882 A93-43110

Calculation of the passive noise power for onboard single-pulse automatic direction tracking systems

p 882 A93-43111

Half-scale modeling experience in the testing of radio navigation and landing systems

p 882 A93-43112

Using numerical control algorithms in stabilization systems with digital correction

p 941 A93-43113

Software support for a computerized air situation documentation system

p 941 A93-43115

Fundamentals of flight vehicle design

[ISBN 5-217-01299-4] p 893 A93-43831

Airport radar systems (2nd revised and enlarged edition)

[ISBN 5-277-00610-9] p 992 A93-44505

Design of aircraft, helicopters, and aviation engines

[ISBN 5-277-01192-7] p 947 A93-44508

Air dissociation effects on aerodynamic characteristics of an aerospace plane

p 959 A93-45149

Problems in the aerodynamics, strength, and flight operations of aircraft

p 947 A93-45659

Classification of the principal fuel saving methods in flight operations

p 996 A93-45660

A set of IBM PC software for processing helicopter flight tests data to determine the flight performance characteristics

p 1037 A93-45661

Determination of the takeoff and landing characteristics of aircraft by using a conditional polar

p 1007 A93-45662

Optimization of the blade angle of the AV-2 propeller for improving the flight performance characteristics of An-2 aircraft

p 996 A93-45663

Determination of the vertical velocity component of aircraft landing on an airfield with a longitudinally sloping runway

p 1007 A93-45664

Results of operational testing of a system for computing optimal flight regimes

p 996 A93-45665

Characteristics of the detection of overloads in the center of mass of Il-76 and An-12 aircraft due to runway irregularities by a standard on-board recorder

p 1008 A93-45666

Operating an aircraft during the landing on an airfield with a substantial longitudinal macroslope of the runway

p 1008 A93-45667

Aircraft monitoring of the planeness of the existing and new runways

p 991 A93-45668

Using spectral analysis for estimating the effect of runway irregularities on the loading of transport aircraft structures

p 996 A93-45669

Prediction of fatigue crack growth kinetics in the plane structural elements of aircraft in the biaxial stress state

p 1025 A93-45670

Calculation of the position of aircraft center of gravity on an IBM PC

p 996 A93-45671

The fuel/timing problem in a computer-aided flight preparation system for civil aircraft

p 996 A93-45672

General concepts related to the determination of the individual flight performance characteristics of aircraft for establishing fuel consumption standards and optimal flight regimes

p 996 A93-45673

Computer-aided study of flight regimes and fuel consumption for helicopter flight operations

p 997 A93-45674

Calculation of safe altitudes

p 991 A93-45675

Algorithmic method for optimizing the precision characteristics of a fuel metering system

p 999 A93-45681

Damping of a gyro horizon-compass with arbitrary displacement of the suspension point

p 1025 A93-45684

Effect of aqueous solutions of water-crystallization inhibiting fluids on Thiokol-based sealants

p 1017 A93-45689

Experience in specifying/prolonging the airframe time limits

p 948 A93-45797

A report on the status of MHD hypersonic ground test technology in Russia

[AIAA PAPER 93-3193] p 1012 A93-46656

A numerical solution of the asymptotic problem of boundary layer separation in an incompressible liquid upstream of the corner point of a body

p 965 A93-46699

Propulsion system simulator with propan for tests on a large scale model of IL-114 airplane in a full-size wind tunnel of TsAGI

p 1013 A93-46933

3D/quasi-3D trans- and supersonic flow calculation in advanced centrifugal/axial compressor stages

p 972 A93-46936

Direct and inverse problems of calculating the axisymmetric and 3D flow in axial compressor blade rows

p 972 A93-46938

Numerical simulation of aerothermodynamics processes in gas turbine engine components

p 1002 A93-46939

Heat transfer on blunt cones in nonuniform supersonic flow in the presence of gas injection from the surface

p 972 A93-46975

Problems of the strength and fatigue of the elements of aircraft structures

p 1029 A93-47076

Coupling conditions for substructures with varying idealization

p 1029 A93-47078

A study of the effect of the support fastening compliance on the stress-strain state of aircraft transparencies

p 997 A93-47079

An analytical-experimental method for studying the strength and stability of thin-walled structures

p 1029 A93-47084

Optimization of an aeroelastic system using the dynamic stability condition

p 1029 A93-47085

Dynamic analysis of a compound elastic surface

p 1030 A93-47086

Load rating for a delta wing box based on a reliability criterion

p 1030 A93-47093

Mathematical model for the effect of turbulent velocity pulsations on the stability of a powerplant

p 1003 A93-47508

Localization of noise sources in the exhaust jet of a turbofan engine

p 1003 A93-47509

An acoustic suppressor for the jet noise of a turbojet engine

p 1003 A93-47510

Chemical-kinetics characteristics of combustion in a supersonic turbulent flow

p 1018 A93-47512

Investigation of flame stabilizers in the form of perforated grids

p 1003 A93-47513

Experimental study of the effect of external turbulence and the shape of the surface on the characteristics of laminar and transition boundary layers

p 987 A93-47522

Abnormal peaks of increased heat-transfer on the blunted delta wing in the hypersonic flow

[AIAA PAPER 93-3129] p 1063 A93-48294

Reliability and durability problems

p 1150 A93-48825

Calculation of the parameters of instability waves in the preseparation region

p 1067 A93-48826

A study of the effect of surface riblets on the evolution of a solitary wave packet (lambda vortex) in a laminar boundary layer

p 1067 A93-48827

An experimental study of the thrust and aerodynamic characteristics of an operating ramjet engine in a blowdown wind tunnel

p 1107 A93-48828

The representation of the aerodynamic torque in simulations of a spacecraft rotary motion

p 1141 A93-48835

Optimal impulsive interorbital transfers with aerodynamic maneuvers

p 1141 A93-48838

Determination of the shape of a wing profile in boundary layer flow with a given velocity diagram

p 1067 A93-48844

Atmospheric aerosols due to aircraft and ecological problems

p 1162 A93-48846

Aerodynamic characteristics and static stability margin of conical star-shaped bodies at supersonic velocities

p 1067 A93-48848

Effect of the size of a plane obstacle on self-oscillations generated in an underexpanded supersonic jet

p 1068 A93-48849

Problems in the aerodynamics of flight vehicles and their parts

p 1068 A93-48901

Aerodynamic characteristics of a sweptforward-wing aircraft model in unsteady motion at large angles of attack in subsonic flow

p 1068 A93-48902

Determination of the aerodynamic balance efficiency of aircraft

p 1130 A93-48903

The use of triangular elements in panel methods for calculating flow past flight vehicles

p 1068 A93-48904

Numerical calculation of polars and heat transfer for supersonic three-dimensional flow past wings with allowance for radiation

p 1068 A93-48905

Calculation of subsonic flow of a gas past an airfoil

p 1068 A93-48908

Effect of the wing planform on the optimal deformation of the middle surface

p 1150 A93-48909

Minimization of the induced drag of nonplanar lifting systems

p 1068 A93-48910

Effect of flexural and rotational wing oscillations on the prevention of flow separation

p 1150 A93-48911

Pressure pulsations on a delta wing in incompressible flow

p 1069 A93-48912

A study of the effect of the shape of a parasail on its lift-drag ratio

p 1069 A93-48913

An experimental study of a compound supersonic jet

p 1069 A93-48914

Effect of anomalous aerodynamic heating during the descent of a parachute along a trajectory

p 1069 A93-48924

Approximate method for the aerodynamic design of flight vehicles for high supersonic flight speeds

p 1069 A93-48966

Some Fuchs-type equations in fluid mechanics

p 1165 A93-48967

Three-dimensional hypersonic flow of a gas past wings

p 1069 A93-48971

Supersonic flow past energy release regions

p 1069 A93-48973

Hypersonic flow past a low-aspect-ratio triangular plate at large angles of attack

p 1069 A93-48974

Automated design and fabrication of radio-electronic circuits

p 1151 A93-49000

Statistical methods in flight vehicle control theory

p 1165 A93-49306

Problems in the optimization of complex engineering systems

p 1165 A93-49307

A method for calculating the aerodynamic and mass characteristics of coaxial rotors with rigid blade fastening (the ABC system)

p 1071 A93-49323

Formulas for determining the induced velocity in the direct and inverse rotor problems

p 1071 A93-49324

Real-time simulation of maneuverable aircraft flight conditions on altitude test cell

[AIAA PAPER 93-1845] p 1137 A93-49726

Propan engines

[AIAA PAPER 93-1981] p 1112 A93-49828

The study of experimental turbofanjets - Heat state and cooling problems

[AIAA PAPER 93-1989] p 1112 A93-49834

Harnessing nitrous oxide for elevation of temperature and pressure in piston facilities

[AIAA PAPER 93-2016] p 1137 A93-49854

Gasdynamics of hydrogen-fueled scramjet combustors

[AIAA PAPER 93-2145] p 1115 A93-49962

Experimental studies of aerodynamic performances of hypersonic scramjet in impulse hot-shot tunnel

[AIAA PAPER 93-2446] p 1120 A93-50198

Design and investigation of the stand and flying scramjet models - Conceptions and results of experiments

[AIAA PAPER 93-2447] p 1120 A93-50199

Intelligent systems of flight-vehicle control

p 1167 A93-50951

Behavior of the particular quality characteristics of an intelligent flight vehicle control system in a multicriterial formulation

p 1168 A93-50952

Definition of the structure of expert preferences for the multicriterial analysis of control systems

p 1168 A93-50953

Multilevel control systems and optimization of their structures

p 1168 A93-50954

Multilevel intelligent control systems for flight vehicles

p 1168 A93-50955

Generation of a plant description dictionary based on expert survey data

p 1168 A93-50956

An information-search system in cybernetics

p 1168 A93-50957

Architecture of multiprocessor data processing machines and dispatching of the knowledge acquisition process in flight control

p 1168 A93-50958

Control problem for a plant with artificial intelligence

p 1168 A93-50960

Prediction and planning of a flight vehicle route in the presence of motion inhibiting factors

p 1130 A93-50961

Nontraditional methods of controlling the stability of a laminar subsonic boundary layer

p 1085 A93-50962

- Minimizing the wall effects in wind tunnels with a sectional pressure chamber p 1085 A93-50965
- Substitution of oriented differences for central differences in a program for calculating smooth supersonic flows p 1085 A93-50966
- Numerical modeling of flow in a hypersonic laminar boundary layer p 1086 A93-50967
- Calculation of perturbation propagation upstream in a hypersonic laminar boundary layer p 1086 A93-50968
- The problem of viscous hypersonic flow past blunt bodies in the spreading plane p 1086 A93-50969
- Supersonic flow past a rectangular wing of finite thickness p 1086 A93-50972
- Optimization of algorithms for information processing and control p 1169 A93-51062
- Synthesis of the optimal control of flight vehicle braking with allowance for the discrete nature of control action generation p 1169 A93-51063
- Optimal structure of discrete algorithms of finite-dimensional continuous-discrete filtering in the presence of Markov noise p 1169 A93-51065
- Main directions of improving the quality of aluminum-lithium alloys for welded aircraft structures p 1146 A93-51104
- Determination of the natural vibrations of an acoustic medium in the cabin of a passenger aircraft by the finite element method p 1102 A93-51752
- An experimental system for studying the vibrations and acoustic emission of cylindrical shells and panels in a field of turbulent pressure pulsations p 1140 A93-51754
- Spectra of pressure pulsations on the surface of a cone in the transition region at supersonic flow velocities p 1088 A93-51755
- Scale-up of the spectra of aerodynamic pressure pulsations with narrowband maxima p 1088 A93-51756
- Correction of a method for calculating the noise levels of aircraft at control points during acoustic flight testing p 1102 A93-51758
- Acoustic intensity of nonisothermal coaxial jets with an inverted velocity profile p 1124 A93-51759
- An approach to the calculation of the far acoustic field of a propeller p 1124 A93-51760
- Determination of fan noise in a lined duct with flow using the Green function method p 1124 A93-51761
- An aeroacoustic stand for evaluating the efficiency of sound-absorbing structures under conditions of acoustic wave propagation in a moving medium p 1140 A93-51762
- Steady transonic weakly perturbed flows in vibrationally relaxing gas p 1088 A93-51768
- Optimal wing shapes in a hypersonic nonequilibrium flow p 1088 A93-51770
- Numerical optimization methods for variational inverse boundary value problems of aerodynamics p 1088 A93-51771
- Development of resonance perturbations in a supersonic jet p 1088 A93-51772
- Heat transfer on tip fins in hypersonic flow p 1088 A93-51775
- Laminarization of the boundary layer on a vibrating wing p 1089 A93-51776
- Nonplanar wings with a minimum induced drag p 1089 A93-51779
- Supersonic flow past a cone with heat transfer near its tip p 1089 A93-51780
- Aerothermodynamics of the high-altitude flight p 1089 A93-51783
- Experimental studies of supersonic flow past wedges with longitudinal slots on the windward side p 1089 A93-51786
- Steady state supersonic flows of a vibrationally excited gas past thin bodies p 1089 A93-51818
- A study of turbulent flow in a viscous shock layer in the case of gas flow past oblong blunt bodies p 1089 A93-51820
- Atmospheric disturbances over mountains and the flight safety p 1164 A93-51856
- Development and application of the Monte Carlo method for solving the Boltzmann equation and its models p 1173 A93-51867
- Modeling the flow around a body via the solution of the relaxation kinetic equation p 1089 A93-51868
- Approximate calculation of the aerodynamic characteristics of simple bodies in hypersonic rarefied-gas flow p 1090 A93-51869
- Calculation of the aerodynamic characteristics of bodies with meshlike surfaces in hypersonic rarefied-gas flow p 1090 A93-51870
- Experimental simulation of the aerodynamic heating of bodies in a molecular region p 1090 A93-51871
- Certain improved algorithms for calculating the aerodynamic characteristics of flight vehicles in free-molecular flow p 1090 A93-51872
- Investigation of the effect of physical processes on heat transfer to blunt bodies at low Reynolds numbers p 1090 A93-51877
- Effect of Reynolds number on the aerodynamic characteristics of a semicone with a wing in the case of hypersonic flow velocities p 1090 A93-51878
- Investigation of the structure of a multicomponent viscous shock layer p 1090 A93-51879
- An economical difference factorization algorithm for the numerical calculation of the system of equations for a thin viscous shock layer p 1091 A93-51880
- Investigation of supersonic shaped nozzles in a low-pressure wind tunnel p 1091 A93-51881
- A study of pressure fluctuations on the surface of a delta wing near the sharp leading edge p 1091 A93-51882
- Self-excitation of intense oscillations in flow inside a wind tunnel with an open test section p 1091 A93-51883
- Characteristics of the flame air heater of a hypersonic wind tunnel p 1140 A93-51884
- Problems in the aerodynamics of flight vehicles and their components p 1091 A93-51901
- Calculation of compressible gas flow on optimal difference grids p 1091 A93-51902
- A finite difference study of the aerodynamic characteristics of wing profiles at transonic velocities p 1091 A93-51903
- Spline-collocation solution of a Fredholm equation of the second kind in the problem of flow past an airfoil p 1092 A93-51904
- Calculation of aerodynamic loads on the wing of rigid and elastic aircraft with allowance for load correction from experimental data p 1103 A93-51905
- Interference between a high-lift sweptforward wing and the horizontal nose plane at subsonic velocities p 1135 A93-51906
- A study of the aerodynamics of a wing with end slots p 1092 A93-51907
- A study of air intake parameters on the aerodynamic characteristics of a parasail p 1092 A93-51908
- Aerodynamic characteristics of airship models of different shapes p 1092 A93-51909
- Calculation of supersonic flow past a body of revolution with a piecewise linear distribution of singularities at its axis p 1092 A93-51910
- Determination of the aerodynamic characteristics of thin bodies of revolution with an arbitrary number of cantilever surfaces in inhomogeneous flow p 1092 A93-51911
- Calculation of a plane supersonic jet simulating the exhaust jet of a hypersonic flight vehicle engine p 1103 A93-51912
- An experimental study of the dynamic effect of a supersonic underexpanded jet on a plane surface parallel to the nozzle axis p 1092 A93-51913
- Hybrid complex of the aircraft intellectualized control systems simulation at the stage of their research projecting [AIAA PAPER 93-3559] p 1222 A93-52660
- Semi-full-scale dynamic simulation complex on the basis of centrifuge [AIAA PAPER 93-3577] p 1208 A93-52673
- Nonlinear deformation mechanics of multilayer transparency elements - Some calculation results p 1191 A93-52937
- A nonlinear finite element of an arbitrary beam p 1215 A93-52939
- Stabilization of the dynamic characteristics of the two-channel automatic control system of aircraft p 1205 A93-52941
- A method for the spectral-time identification of the longitudinal and lateral motions of an aircraft p 1205 A93-52942
- Identification of the phase characteristics and wind-induced perturbations of an aircraft from flight test results p 1206 A93-52943
- Solution of the boundary value problem in flight dynamics by the opposite motion method p 1206 A93-52944
- A study of optical distortions arising in radiation transmission through cavities with gas flow around them p 1225 A93-52945
- Non-self-similarity of a boundary layer flow of a high-temperature gas in a Laval nozzle p 1176 A93-52946
- Estimation of the change of axial-flow compressor characteristics during long-term service p 1193 A93-52949
- Effect of rotation on heat transfer and hydraulic resistance in the radial cooling channels of turbine rotor blades p 1215 A93-52950
- Estimation of the effect of the longitudinal moment due to the engine thrust on the mass of a subsonic passenger aircraft p 1191 A93-52954
- Calculation of the position of the flow separation line in an analog model of flow past a body p 1176 A93-52958
- Effect of boundary layer suction on the thrust and aerodynamic efficiency of a hypersonic flight vehicle p 1176 A93-52959
- Viscosity of aviation fuel components - Aromatic hydrocarbons (alkyl benzenes) p 1211 A93-52961
- The combined effect of clearances and peripheral overlaps on the efficiency of microturbines with shroudless rotors p 1193 A93-52963
- Estimation of the parameters of the electrodynamic system engine-exhaust jet p 1193 A93-52965
- Calculation of sandwich plates with polymer composite skins under conditions of high humidity p 1215 A93-52968
- Design and fabrication of panels with cutouts p 1215 A93-52973
- An experimental study of reinforced panels of composite materials p 1215 A93-52975
- A procedure for the thermal and strength testing of radiotransparent shells p 1209 A93-52976
- A finite element for modeling skins of composite materials p 1215 A93-52979
- Application of the small parameter method to the problem of three-dimensional flow of a viscous gas past bodies p 1178 A93-53314
- Comparison of gasdynamic models in hypersonic flow p 1179 A93-53315
- Mathematical modeling of the three-dimensional temperature fields of turbine blades p 1216 A93-53329
- Construction of wakes in the discrete vortex method p 1179 A93-53333
- Determination of heat transfer to flow in a duct with a pseudodiscontinuity p 1179 A93-53365
- Calculation of a compressible three-dimensional boundary layer on a swept wing p 1179 A93-53551
- Calculation of flow fields near a lifting wing p 1179 A93-53552
- Selection of a method for protecting aircraft gas turbine engines against damage by foreign objects (Mathematical models) p 1193 A93-53554
- The flow lag angle in the rotor of a centrifugal compressor with allowance for viscosity effects p 1179 A93-53555
- Moving wall effects in transverse subsonic flow past a rotating cylinder p 1179 A93-53573
- Aerodynamic characteristics of conical triangular-planform wings of low aspect ratio in subsonic stalled flow p 1180 A93-53574
- Unsteady aerodynamic characteristics of three rectangular wings of different aspect ratios p 1180 A93-53575
- Design of high-load aviation turbomachines using modern 3D computational methods [ISABE 93-7032] p 1196 A93-54008
- Separation phenomenon in a hypersonic flow with strong wall cooling - Subcritical regime p 1189 A93-54266
- Study of artificial and natural turbulence in atmospheric boundary layer with a CW Doppler CO₂ lidar p 1257 A93-54799
- Equations of the steady motion of aircraft in spin and spiral dive p 1248 A93-54969
- Optimal control of the rocking and damping of swings p 1263 A93-54998
- Steady-state supersonic flow of a vibrationally excited gas past a slender body of revolution at a small angle of attack p 1233 A93-55014
- An airfoil in transonic flow in the presence of wind gusts and weak shock waves p 1233 A93-55015
- Pressure field and drag of a single cavity with rounded and sharp edges p 1258 A93-55018
- Development of separation due to interaction between a shock wave and a turbulent boundary layer perturbed by rarefaction waves p 1233 A93-55019
- Determination of the N₂(+)+e recombination rate constant from ballistic experiments p 1234 A93-55026
- Hypersonic flow of a gas past wing with heat transfer p 1234 A93-55030
- Kinetic scheme selection in describing detonation in an H₂-air mixture behind shock waves p 1253 A93-55032
- Effect of the atmosphere density gradient on aerodynamic stabilization p 1252 A93-55034
- Vibration isolation of aviation power plants taking into account real dynamic characteristics of engine and aircraft p 1244 A93-55863
- On the disturbances development in the supersonic boundary layer p 484 A93-20686
- JPRS report: Science and technology. Central Eurasia: Engineering and equipment [JPRS-UEQ-92-003] p 749 A93-25427
- JPRS report: Science and technology. Central Eurasia: Engineering and equipment [JPRS-UEQ-92-007] p 842 A93-28635

- JPRS report: Science and technology. Central Eurasia: Engineering and equipment
[JPRS-UEQ-92-006] p 842 N93-28636
- JPRS report: Science and technology. Central Eurasia: Engineering and equipment
[JPRS-UEQ-92-010] p 842 N93-28674
- JPRS report: Science and technology. Central Eurasia: Engineering and equipment
[JPRS-UEQ-92-008] p 842 N93-28675
- JPRS report: Science and technology. Central Eurasia: Engineering and equipment
[JPRS-UEQ-93-003] p 842 N93-28691
- JPRS report: Science and technology. Central Eurasia: Engineering and equipment
[JPRS-UEQ-93-004] p 930 N93-29090

S

SAUDI ARABIA

- Some physico-chemical characteristics of lubricating oil used in gas turbines p 70 A93-12202
- Unsteady effects of camber on the aerodynamic characteristics of a thin aerofoil moving near the ground p 270 A93-21719
- Robust digital control of a high-performance engine p 359 A93-21792
- Experimental investigations of asymmetric vortex flows behind elliptic cones at incidence p 757 A93-35637
- Newtonian and hypersonic flows over oscillating bodies of revolution. I - Circular cones p 857 A93-39942
- Newtonian and hypersonic flows over oscillating bodies of revolution. II - Parabolic bodies p 872 A93-42931
- Unsteady ground effects on aerodynamic coefficients of finite wings with camber p 976 A93-47218
- [AIAA PAPER 93-3423] p 976 A93-47218
- Wind tunnel investigation of wind shear effect on turning flight p 1127 A93-48326
- [AIAA PAPER 93-3641] p 1127 A93-48326
- Effect of rotary atmospheric gusts on fighter airplane p 1127 A93-48328
- [AIAA PAPER 93-3644] p 1127 A93-48328
- Numerical simulation of unsteady flow induced by a flat plate moving near ground p 1094 A93-52432

SINGAPORE

- Analysis of complicated plates by a nine-node spline plate element p 206 A93-14616
- Applications of laser techniques in fluid mechanics p 395 A93-17765
- Aircraft grid generation using interactive environment p 438 A93-22639
- [AIAA PAPER 93-0224] p 438 A93-22639
- A wake singularity potential flow model for airfoils experiencing trailing-edge stall p 1067 A93-48544

SOUTH AFRICA

- Analytic continuation of Pade approximations to the unsteady kernel functions to obtain a better understanding of the analytic continuation of Pade approximations to unsteady parameters in general p 117 A93-14283
- Extending the useful frequency of 'rigid' wind tunnel models with active control p 190 A93-14299
- Parameter estimation techniques for flight flutter test analysis p 156 A93-14324
- Case studies in composite material structural design, manufacture and testing p 157 A93-14385
- Life cycle assessment of an impingement-cooled gas turbine blade p 358 A93-20321
- [AIAA PAPER 92-4716] p 358 A93-20321
- Effects of grain size and carbides on the creep resistance and rupture properties of a conventionally cast nickel-base superalloy p 389 A93-21699
- Development of highly loaded root end attachments for composite material high speed flying surfaces p 539 A93-24122
- Numerical simulation of inviscid transonic flow over two-dimensional slender bodies p 686 A93-34348
- Use of eigenvectors in the solution of the flutter equation p 1022 A93-45151
- Effects of wing-tip vortex flaps p 959 A93-45153
- The streamline throughflow method of axial turbomachinery flow analysis p 1184 A93-54007
- [ISABE 93-7031] p 1184 A93-54007
- The design and development of an afterburner p 1198 A93-54017
- [ISABE 93-7041] p 1198 A93-54017
- The development of a new air filtration system for the Alouette III helicopter p 1199 A93-54024
- [ISABE 93-7048] p 1199 A93-54024
- Thermal fatigue life assessment of a convection-cooled gas turbine blade p 1199 A93-54038
- [ISABE 93-7062] p 1199 A93-54038
- A comparative assessment of two present generation turbine analysis codes p 1203 A93-54073
- [ISABE 93-7097] p 1203 A93-54073
- SPAIN**
- Dynamic stability of bodies of revolution in compressible flow p 12 A93-12558
- The Tenth Conference on Air Navigation - A landmark in the history of civil aviation p 34 A93-12559

- Specific educational aspects of airport engineering in Spain and the Hispanic world p 103 A93-12560
- Aerodynamic characteristics of transport airplanes in low speed configuration p 113 A93-14172
- Aeronautical technologies and communications - Toward advanced technology passenger terminals p 529 A93-27477
- Control of contaminants in gas turbines with variable-flow combustion chambers and hydrogen addition p 520 A93-27478
- Prandtl theory applied to paraglider aerodynamics [AIAA PAPER 93-1220] p 690 A93-35169
- Extended range operations of two and three turbofan engines p 802 A93-37391
- The finite element method in the 1990's p 925 A93-40823
- [ISBN 0-387-54930-7] p 925 A93-40823
- Numerical simulation of hypersonic flow over a double ellipse using a Taylor-Galerkin finite element formulation with adaptive grids p 868 A93-42617
- Comparison of some direct multi-point force appropriation methods p 928 A93-43338
- Aerodynamics design of convergent-divergent nozzles [AIAA PAPER 93-2574] p 1085 A93-50290
- The community response to aircraft noise around six Spanish airports p 1264 A93-55845
- Mechanisms of sound generation in subsonic jets p 101 N93-10688
- Nondestructive inspection of in-service aircraft [ETN-93-93059] p 496 N93-20928
- Cooling predictions in turbofan engine components p 905 N93-29964

SWEDEN

- Numerical simulation of turbulent reacting flows in combustion chambers p 171 A93-14271
- A low speed wind-tunnel with extreme flow quality - Design and tests p 190 A93-14352
- Calculation of three-dimensional boundary layers on rotor blades using integral methods p 252 A93-19433
- [ASME PAPER 92-GT-210] p 252 A93-19433
- Studies of fuel-rich magnesium propellants in a small solid fuel ramjet combustor p 535 A93-27759
- Fatigue effects of noise among airplane mechanics p 558 A93-28495
- Damage tolerance assessment of the fighter aircraft 37 Viggen main wing attachment p 802 A93-37390
- The SAAB 2000 initial flight test - Status report p 804 A93-38847
- Navier-Stokes stall predictions using an algebraic Reynolds-stress model p 778 A93-39260
- Characterization of delamination and fiber fractures in carbon fiber reinforced plastics induced from impact p 915 A93-40787
- Leeside flow over delta wing at $M = 7.15$ - Experimental results for test case 7.1.2 p 870 A93-42632
- Hypersonic leeside delta-wing-flow computations using centered schemes p 870 A93-42635
- Numerical simulation of vortex shedding past triangular cylinders at high Reynolds number using a k-epsilon turbulence model p 871 A93-42873
- Reynolds stress transport modelling of shock/boundary-layer interaction p 1046 A93-48134
- [AIAA PAPER 93-2936] p 1046 A93-48134
- Some stability characteristics of the boundary layer on a yawed cone p 1057 A93-48228
- [AIAA PAPER 93-3048] p 1057 A93-48228
- Ongoing GPS experiments demonstrate potential of satellite navigation technology p 1097 A93-49278
- CFD analysis and testing on a twin inlet ramjet p 1075 A93-49723
- [AIAA PAPER 93-1839] p 1075 A93-49723
- Aeroelastic stability of supersonic nozzles with separated flow p 1142 A93-50300
- [AIAA PAPER 93-2588] p 1142 A93-50300
- On design methods for bolted joints in composite aircraft structures p 1158 A93-50430
- Effects of blade geometry and mode shape on fan flutter p 1196 A93-54004
- [ISABE 93-7028] p 1196 A93-54004
- Large eddy simulation of turbulent combustion behind flame holders p 1198 A93-54018
- [ISABE 93-7042] p 1198 A93-54018
- Flight data and flight safety in SAS p 168 N93-15156
- Implementation of a multidomain Navier-Stokes code on the Intel iPSC2 hypercube p 843 N93-28994
- [FFA-TN-1992-37] p 843 N93-28994
- The numerical solution of low Mach number flow in confined regions by Richardson extrapolation p 789 N93-29005
- [TRITA-NA-9207] p 789 N93-29005
- Modal measurements and propeller field excitation on acoustic full scale mockup of SAAB 340 aircraft p 1039 N93-31051
- [FFA-TN-1992-08] p 1039 N93-31051
- GARTEUR 3D shear layer experiment p 987 N93-31052
- [FFA-TN-1992-26] p 987 N93-31052
- Optimal design and imperfection sensitivity of nonlinear shell structures p 1030 N93-31123
- [FFA-TN-1992-30] p 1030 N93-31123

- WBNFLOW: Multi-grid/multi-block potential solver for compressible flow. User's guide (FFA-TN-1992-43) p 1031 N93-31146
- SWITZERLAND**
- Development of a system for aerodynamic fast-response probe measurements p 203 A93-14325
- The vortex behaviour of the rotating-stall cell of a centrifugal compressor with vane diffuser [ASME PAPER 92-GT-66] p 400 A93-19316
- Use of advanced CFD codes in the turbomachinery design process p 256 A93-19508
- [ASME PAPER 92-GT-324] p 256 A93-19508
- Impact of weather on aviation - A global view p 308 A93-22143
- 2D hypersonic viscous flow past a double ellipse geometry p 868 A93-42613
- Ilyushin takes on the market p 945 A93-43623
- First moves towards an 'intelligent' GPWS p 896 A93-43624
- ARPA starts push for joint-service ASTOVL p 856 A93-43625
- Visualisation and analysis of three dimensional transonic flows by holographic interferometry p 1020 A93-44194
- Particle imaging techniques and applications p 1020 A93-44195
- Shock-wave/boundary layer interactions at hypersonic speeds by an implicit Navier-Stokes solver [AIAA PAPER 93-2938] p 1046 A93-48136
- Precise pitching airfoil computations by use of dynamic unstructured meshes p 1049 A93-48165
- [AIAA PAPER 93-2971] p 1049 A93-48165
- A family of multiblock codes for computational aerothermodynamics - Application to complete vehicle hypersonic flows p 1056 A93-48223
- [AIAA PAPER 93-3042] p 1056 A93-48223
- A test bench for rotorcraft hover control p 1140 A93-51440
- [AIAA PAPER 93-3853] p 1140 A93-51440
- Flux-vector splitting for compressible low Mach number flow p 1093 A93-52001
- Stagnation point computations of nonequilibrium inviscid blunt body flow p 1093 A93-52005
- Operating helicopters in a demanding environment - Mountain flying/high evaluations p 1190 A93-54289
- Blade loss dynamics of a magnetically supported rotor p 1257 A93-54653
- New rotor trim and balance system for helicopter usage monitoring p 169 N93-15180
- Failure diagnostic with MAINTEx based on AIMS at Swissair p 110 N93-15181
- The aerodynamic effect of coolant ejection in the leading edge region of a film-cooled turbine blade p 904 N93-29958
- The ecological balance of Swissair: An example of waste management p 1035 N93-31930
- Design and application of Active Magnetic Bearings (AMB) for vibration control p 1033 N93-32279

T

TAIWAN, PROVINCE OF CHINA

- Two modified versions of Hsu-Lee's elliptic solver of grid generation p 95 A93-11085
- Optimal vibration control for a flexible rotor with gyroscopic effects p 98 A93-13420
- Multizone Navier-Stokes computations for a transonic projectile using MacCormack finite difference method p 113 A93-14192
- A numerical study of slit V-gutter flows p 171 A93-14273
- Noncoaxial mixing in a rectangular duct p 205 A93-14518
- Theoretical investigation of combustion characteristics in ram-jet dump combustor with side-inlet p 346 A93-19121
- Improvement of high-AOA airfoil stalling performance by internal acoustic excitation p 243 A93-19134
- A study on stability and response analysis of a nonlinear rotor system with mass unbalance and side load [ASME PAPER 92-GT-7] p 400 A93-19280
- Analysis of steady and unsteady turbine cascade flows by a locally implicit hybrid algorithm p 249 A93-19361
- [ASME PAPER 92-GT-127] p 249 A93-19361
- Optimum design of rotor-bearing systems with eigenvalue constraints p 405 A93-19497
- [ASME PAPER 92-GT-307] p 405 A93-19497
- Holographic interferometric investigation of shock wave interaction with a ramp p 271 A93-21921
- The detection and warning of low-level wind shear based on terminal single Doppler radar p 432 A93-22195
- Computations of a twin-jet impingement on a flat surface p 271 A93-22227
- Numerical simulation of unsteady transonic nozzle flows p 272 A93-22230

- Refined H-infinity controller design for rotorcraft flight control p 368 A93-22882
- A new flight control design scheme using optimal dynamic output feedback p 368 A93-22883
- Output tracking control of nonlinear systems with weakly non-minimum phase p 439 A93-22968
- Discontinuous Galerkin finite element method for two dimensional conservation laws [AIAA PAPER 93-0337] p 281 A93-23026
- Numerical study of mixed convection between two corotating symmetrically heated disks p 416 A93-23491
- Optimal control law synthesis for flutter suppression using active acoustic excitations p 370 A93-23516
- Adaptive finite volume upwind approach on mixed quadrilateral-triangular meshes p 287 A93-23542
- Shock oscillation in two-dimensional, inviscid, unsteady channel flow p 288 A93-23563
- Numerical investigations on airfoil performance subjected to aerodynamic interference from an upstream airfoil [AIAA PAPER 93-0639] p 463 A93-24754
- Ignition process of fuel droplet arrays in a supersonic flowfield p 535 A93-27766
- Analysis of the friction and wear mechanisms of multilayered plasma-sprayed ceramic coatings p 548 A93-28567
- Method for assessing the electric power system reliability of multiple-engine aircraft p 810 A93-27398
- Numerical experiments with nonoscillatory schemes using Eulerian and new Lagrangian formulations p 862 A93-42432
- A constrained flight route monitor system in terminal control area for air traffic control p 882 A93-42816
- Variant bi-conjugate gradient methods for the compressible Navier-Stokes solver with a two-equation model of turbulence p 951 A93-45012
- Flutter analysis of composite panels on many supports p 1022 A93-45119
- Computation of shock diffraction in external and internal flows p 1024 A93-45537
- Transonic flutter suppression using active acoustic excitations [AIAA PAPER 93-3285] p 969 A93-46841
- Computations of aerodynamic drag for turbulent transonic projectiles with and without spin [AIAA PAPER 93-3416] p 975 A93-47212
- A high-order streamline Godunov scheme for steady hypersonic equilibrium flows [AIAA PAPER 93-2997] p 1053 A93-48187
- Improvement of transonic wing buffet by geometric modifications [AIAA PAPER 93-3024] p 1055 A93-48209
- Modelling three-dimensional gas-turbine-combustor model flow using second-moment closure [AIAA PAPER 93-3104] p 1149 A93-48277
- Upwind finite-volume Navier-Stokes computations on unstructured triangular meshes p 1070 A93-49011
- Stability of fluttered panels subjected to in-plane harmonic forces p 1151 A93-49017
- Exact closed-form solution of generalized proportional navigation p 1130 A93-49598
- Effects of side-inlet angle in a three-dimensional side-dump combustor p 1109 A93-49610
- Swirling flows in a contoured-wall combustion chamber [AIAA PAPER 93-1765] p 1073 A93-49661
- The turbulence and mixing characteristics of the complex flow in a simulated augmentor p 1123 A93-51642
- A second-order upwind finite-volume method for the Euler solution on unstructured triangular meshes p 1087 A93-51738
- Flutter analysis of stiffened laminated composite plates and shells in supersonic flow p 1216 A93-53224
- Instability of a supersonic vortex sheet inside a circular duct p 1234 A93-55142
- Locally implicit total variation diminishing schemes on mixed quadrilateral-triangular meshes p 1235 A93-55356
- Discontinuous Galerkin finite element method for Euler and Navier-Stokes equations p 1235 A93-55357
- Sweeping algorithm for unstructured-grid generation on two-dimensional non-convex domains p 1262 A93-56413

TURKEY

- A viscous axisymmetric throughflow prediction method for multi-stage compressors [ASME PAPER 92-GT-293] p 254 A93-19483
- Design of advanced beams considering elasto-plastic behaviour of material p 544 A93-26904
- Nonequilibrium turbulence modeling study on light dynamic stall of a NACA0012 airfoil p 768 A93-37379

- Numerical simulation of ramjet and scramjet combustion using two-dimensional Euler equations with finite rate chemistry [ISABE 93-7083] p 1202 A93-54059
- Advances in speech processing p 550 A93-19771

U

UKRAINE

- Design characteristics of the functional systems of aircraft and prediction of their technical condition p 320 A93-18334
- Design features of the GTD 8000 and GTD 15000 marine gas turbine engines [ASME PAPER 92-GT-15] p 400 A93-19287
- Determination of nonstationary aerodynamic loading on cascade blades in the case of dynamic changes of the angle of attack p 544 A93-26817
- A nonsearch adaptive control system with a reference model and derivative measurement p 561 A93-26838
- A one-dimensional theory for supersonic gas jets above the critical pressure p 774 A93-39115
- Adaptive filtering of Doppler velocimeter errors due to the characteristics of the reflecting surface p 992 A93-45650
- A study of the interaction of a nonstationary shock wave with a boundary layer on a plate in the transition regime p 1150 A93-48850
- Effect of the formation of excited oxygen molecules on the kinetics of exchange reactions and the heat flux during braking in the upper layers of the atmosphere p 1070 A93-48975

UNITED ARAB EMIRATES

- Axial length influence on the performance of centrifugal impellers p 205 A93-14517
- Advanced direct-design procedure for centrifugal impellers p 411 A93-21659

UNITED KINGDOM

- European environmental studies focus on impact of engine emissions p 92 A93-10730
- Evolving noise issue could persist into the next century p 99 A93-10731
- Aspects of multivariable flight control law design for helicopters using eigenstructure assignment p 60 A93-10916
- Progress towards joint civil use of GPS and GLONASS p 29 A93-10977
- Effect of skywave interference on the coverage of Loran-C p 33 A93-11095
- Unorthodoxy rising p 1 A93-11250
- Handling the legal consequences of aviation disasters - Passenger compensation [ISBN 3-452-22293-4] p 103 A93-11411
- European merger control in the air transport industry - Comments on the Delta Air Lines/Pan Am decision of the European Commission [ISBN 3-452-22293-4] p 103 A93-11412
- A330 - Completing the family p 40 A93-11418
- Potent Trent p 53 A93-11419
- The smart truck p 40 A93-11420
- Breaking through the 10 exp 6 barrier p 27 A93-11498
- The 21st century navigation station p 34 A93-12123
- Options for control and navigation of unmanned aircraft p 34 A93-12124
- Optimization of time saving in navigation through an area of variable flow p 34 A93-12125
- Computation of viscous compressible flows using an upwind algorithm and unstructured meshes p 9 A93-12163
- The approach to airworthiness clearance with the introduction of advanced materials and manufacturing technologies into the design of aerospace structures p 2 A93-12235
- Advanced three-shaft engines - Configured for reliability, efficiency and growth p 53 A93-12236
- Review of the normal force fluctuations of aerofoils with separated flow p 10 A93-12317
- Transport resurrection p 41 A93-12434
- Microstructural study of aluminide surface coatings on single crystal nickel base superalloy substrates p 70 A93-12771
- Vaporizer performance p 79 A93-12784
- Discrete time H(infinity) control laws for a high performance helicopter p 96 A93-13007
- Rotorcraft reliability and maintainability: Future design requirements; Proceedings of the Conference, London, United Kingdom, Mar. 20, 1991 [ISBN 0-903409-88-7] p 45 A93-13401
- The military operator's experience of reliability and maintainability characteristics p 80 A93-13403
- Aircraft designer's viewpoint of reliability and maintainability p 45 A93-13404
- Reliability testing of the EH101 p 45 A93-13406

- Rotorcraft reliability and maintainability - A CAA view of future trends p 45 A93-13407
- Civil spin-off from military aircraft cockpit research p 45 A93-13415
- Hovering decisions p 46 A93-13700
- Maintainable A330 p 107 A93-13957
- Hot end cleaning - Corrosion pitting of turbine discs [SAE PAPER 920930] p 202 A93-14081
- Counting the cost of composites p 107 A93-14117
- Prospects for a second generation supersonic transport p 108 A93-14154
- Automatic guidance and control for recovery of remotely piloted vehicles p 181 A93-14188
- Over wing propeller aerodynamics p 113 A93-14189
- A study of propeller/wing interaction including the effect of ground proximity p 113 A93-14190
- Integration of aircraft design and manufacture using artificial intelligence paradigms p 225 A93-14202
- Passive boundary-layer bleed for supersonic intakes p 114 A93-14212
- Human factors of aircraft cabin safety p 140 A93-14218
- Turbulence modelling requirements for the prediction of viscous transonic aerofoil flows p 115 A93-14249
- Aeroservoelastic analysis of an aircraft model incorporating the minimum state method for approximating unsteady aerodynamics p 154 A93-14258
- The influence of the fuselage on high alpha vortical flows and the subsequent effect on fin buffeting p 116 A93-14263
- The use of a deep honeycomb to achieve high flow quality in the ARA 9 ft x 8 ft Transonic Wind Tunnel p 190 A93-14276
- Parallel implementation of the feature associated mesh embedding method for the 2D-Euler equations (FAME2D) p 225 A93-14278
- The aerodynamic and structural design of a variable camber wing (VCW) p 117 A93-14291
- On the configuration buffet of a transport aircraft p 117 A93-14298
- The effect of wind tunnel constraint on unsteady aerodynamics experiments p 190 A93-14300
- Design of manoeuvrable simple and complex planform transonic wings with attained thrust-, panel- and Euler-methods p 117 A93-14301
- The simulation of aircraft landing gear dynamics p 155 A93-14318
- A semi-empirical theory of the noise in slotted tunnels caused by diffuser suction p 231 A93-14353
- Rapid wind tunnel prototype using stereolithography and equivalent technologies p 191 A93-14365
- Design of digital multiple model-following integrated flight/p propulsion control systems p 183 A93-14371
- Supersonic wing/body interference p 121 A93-14391
- Experimental studies of vortex flaps and vortex plates p 121 A93-14406
- A vortex control technique for the attenuation of fin buffet p 121 A93-14408
- The accuracy of cell vertex finite volume methods on quadrilateral meshes p 227 A93-14526
- Method of simulating unsteady turbomachinery flows with multiple perturbations p 123 A93-14556
- Determination of vortex burst location on delta wings from surface pressure measurements p 123 A93-14557
- Robust fault detection of jet engine sensor systems using eigenstructure assignment p 173 A93-14608
- The development of titanium alloys for gas turbines p 197 A93-15031
- Unsteady transonic flow past a quarter-plane p 127 A93-16664
- Managing mistakes p 109 A93-17100
- Optical design of a wide-angle simulator probe p 211 A93-17140
- Boundary layer transition and control; Proceedings of the Conference, Univ. of Cambridge, United Kingdom, Apr. 8-12, 1991 [ISBN 0-903409-86-0] p 211 A93-17251
- Application of laminar flow to aero engine nacelles p 128 A93-17256
- Laminar flow research in the 1940-1950s - A personal recollection p 235 A93-17271
- Engineering aspects of laminar flow research at Handley Page p 235 A93-17275
- Fixed and rotary wing all weather operations; Proceedings of the Conference, London, United Kingdom, Apr. 23, 24, 1991 [ISBN 0-903409-90-9] p 142 A93-17301
- Autoland, the developing need p 142 A93-17302
- Fixed and rotary wing all weather operations system requirements p 142 A93-17303
- The certification of head up displays for category 3 operation p 142 A93-17304

- A review of alternative philosophies p 142 A93-17305
- Landing guidance systems for CAT III operations p 151 A93-17307
- Air Traffic Control ground movement control in low visibility p 151 A93-17308
- Helicopter approaches in low visibility using RGPS and EFIS p 142 A93-17309
- Helicopter automatic flight control systems for all weather operations - EH101 and beyond p 186 A93-17310
- Ground visual aids - Recent research at RAE Bedford p 191 A93-17311
- Breaking the stall barrier p 159 A93-17502
- European navigation into the 21st century; Proceedings of the Conference, London, United Kingdom, Feb. 12, 1991 p 311 A93-17751
- [ISBN 0-903409-82-8] p 311 A93-17751
- The future of area navigation in Western Europe p 311 A93-17752
- European navigation into the 21st century - Frequency considerations p 311 A93-17754
- Airborne trials of Loran-C p 311 A93-17756
- Flight management systems p 311 A93-17757
- ARINC 629 DATABUS; Proceedings of the Conference, London, United Kingdom, Sept. 24, 1991 p 311 A93-17835
- [ISBN 0-903409-95-X] p 311 A93-17835
- Concept of closed-circuit TV system for transport aircraft under examination p 306 A93-18542
- Key trends in human factors of aircraft maintenance; Proceedings of the Conference, London, United Kingdom, Oct. 31, 1991 p 237 A93-18754
- [ISBN 1-85768-0057] p 237 A93-18754
- The designs for safety p 321 A93-18755
- The human factors aspects of aircraft ground handling p 237 A93-18756
- The benefits of ground maintenance simulators p 238 A93-18757
- Looking and seeing - A practical problem p 238 A93-18758
- Integrating the maintenance requirement maintenance ground based data systems - The missing link? p 238 A93-18760
- Artificial intelligence techniques for improving aircraft maintenance efficiency; Proceedings of the Conference, London, United Kingdom, Feb. 21, 1991 p 238 A93-18761
- [ISBN 0-903409-84-4] p 238 A93-18761
- Expert systems for maintenance engineering p 434 A93-18762
- The Royal Air Force experience of artificial intelligence aircraft maintenance p 435 A93-18764
- Knowledge based systems and avionics equipment failure diagnosis p 238 A93-18765
- Advanced expert systems increase aircraft maintenance efficiency - An overview p 238 A93-18767
- Progress towards common standards for flight simulator qualification p 374 A93-18774
- Developing control strategies for ASTOVL aircraft p 366 A93-18777
- Aero engine reliability, integrity and safety; Proceedings of the Conference, Bristol, United Kingdom, Oct. 17, 18, 1991 p 345 A93-18778
- [ISBN 0-903409-70-4] p 345 A93-18778
- Safety through integrity and reliability p 239 A93-18779
- ETOPS across the Atlantic p 306 A93-18780
- Lifting philosophies for aero engine fracture critical parts p 345 A93-18783
- Aspects of turbine blade design for integrity p 345 A93-18784
- Testing for integrity p 346 A93-18785
- Reliability and safety considerations in engine management systems design p 346 A93-18786
- Engine Health Monitoring p 346 A93-18787
- Engine reliability from an independent overhaul shops perspective p 239 A93-18788
- Very high reliability - Cost and consequences p 397 A93-18789
- Adaptive remeshing for three-dimensional compressible flow computations p 242 A93-18851
- Experiments on the active control of boundary layer transition p 243 A93-19133
- Boundary-layer induced noise in aircraft p 444 A93-19137
- Active control of sound transmission through stiff lightweight composite fuselage constructions p 447 A93-19187
- Combined noise and flow control of supersonic jets using swirl p 398 A93-19204
- Unsteady pressures under impinging jets in crossflows p 399 A93-19220
- Wing vortex refraction effects from BAC 1-11 flight tests p 450 A93-19226
- Analysis of high speed multistage compressor throughflow using spanwise mixing [ASME PAPER 92-GT-13] p 347 A93-19285
- Recess vane passive stall control [ASME PAPER 92-GT-36] p 246 A93-19296
- Electromechanical measurement of turbomachinery blade tip-to-casing running clearance [ASME PAPER 92-GT-50] p 400 A93-19303
- Turbulence evaluation within the secondary flow region of a turbine cascade [ASME PAPER 92-GT-60] p 247 A93-19310
- Calculation of turbulent flow for an enclosed rotating cone [ASME PAPER 92-GT-70] p 400 A93-19320
- Compressible flow pressure losses in wye-junctions [ASME PAPER 92-GT-71] p 248 A93-19321
- A study of stall in a low hub/tip ratio fan [ASME PAPER 92-GT-85] p 248 A93-19334
- Active stabilization of compressor instability and surge in a working engine [ASME PAPER 92-GT-88] p 348 A93-19335
- The effects of blade loading in radial and mixed flow turbines [ASME PAPER 92-GT-92] p 349 A93-19338
- The design and evaluation of a high pressure ratio radial turbine [ASME PAPER 92-GT-93] p 349 A93-19339
- Unsteady pressure measurements on the rotor of a model turbine stage in a transient flow facility [ASME PAPER 92-GT-156] p 250 A93-19383
- Techniques for aerodynamic loss measurement of transonic turbine cascades with trailing-edge region coolant ejection [ASME PAPER 92-GT-157] p 250 A93-19384
- The dynamic characteristics of a high pressure turbine stage in a transient wind tunnel [ASME PAPER 92-GT-166] p 375 A93-19392
- Discharge coefficients of holes angled to the flow direction [ASME PAPER 92-GT-192] p 403 A93-19417
- The measurement and prediction of the tip clearance flow in linear turbine cascades [ASME PAPER 92-GT-214] p 252 A93-19437
- Design features influencing the distribution of fuel within the spray from an air blast fuel injector [ASME PAPER 92-GT-235] p 353 A93-19448
- Heat transfer and aerodynamics of a high rim speed turbine nozzle guide vane with profiled end walls [ASME PAPER 92-GT-243] p 253 A93-19452
- Measurements of the effect of free-stream turbulence length scale on heat transfer [ASME PAPER 92-GT-244] p 405 A93-19453
- A simple method for estimating secondary losses in turbines at the preliminary design stage [ASME PAPER 92-GT-294] p 254 A93-19484
- Viscous throughflow modelling for multi-stage compressor design [ASME PAPER 92-GT-302] p 255 A93-19492
- Ingestion into the upstream wheel space of an axial turbine stage [ASME PAPER 92-GT-303] p 354 A93-19493
- The extension of a solution-adaptive 3D Navier-Stokes solver towards geometries of arbitrary complexity [ASME PAPER 92-GT-363] p 257 A93-19527
- An externally pressurized air bearing system, journals and thrust, for application to small turbomachinery [ASME PAPER 92-GT-382] p 406 A93-19539
- Improving dynamic response of a single-spool gas turbine engine using a nonlinear controller [ASME PAPER 92-GT-392] p 355 A93-19546
- An optimisation-matching procedure for variable cycle jet engines [ASME PAPER 92-GT-406] p 356 A93-19555
- A novel approach to high resolution compressible cascade flow analysis using the Navier-Stokes equations [ASME PAPER 92-GT-419] p 258 A93-19567
- Static roll moment characteristics of asymmetric tangential leading edge blowing on a delta wing at high angles of attack [AIAA PAPER 93-0052] p 261 A93-20165
- An experimental investigation of twin fin buffeting and suppression [AIAA PAPER 93-0054] p 261 A93-20167
- Vibration reduction for helicopter airframes - An application of the general-purpose structural optimization program STARS [AIAA PAPER 92-4782] p 326 A93-20372
- Newton-like methods for fast high resolution simulation of hypersonic viscous flows p 437 A93-20740
- Work performed in the United Kingdom to establish the feasibility of RAIM in a GPS receiver in flight p 314 A93-21157
- The modelling of aerodynamic flows by solution of the Euler equations on mixed polyhedral grids p 269 A93-21218
- The suppression of single-fin buffeting using tangential leading edge blowing on a delta wing p 270 A93-21677
- Potential aerospace applications for metal matrix composites p 389 A93-21678
- The user friendly airliner (The 37th Roy Chadwick Lecture) p 307 A93-21718
- The prediction of riblet behaviour with a low-Reynolds number k-epsilon model p 270 A93-21720
- Advancing helicopters p 327 A93-21836
- Flow around two circular cylinders by the random-vortex method p 271 A93-21925
- MIST - A remote briefing system p 437 A93-22132
- Numerical forecasting of liquid water content to assess airframe icing risk p 429 A93-22147
- Short range forecasts for air traffic control using high resolution aircraft data p 431 A93-22164
- Passive control of pre-entry shock in supersonic intakes [AIAA PAPER 93-0291] p 279 A93-22691
- Battle damage repairs p 239 A93-22698
- Turbulence/gust alleviation using spoiler control p 369 A93-22886
- Flow quality improvement in a high speed blowdown wind tunnel [AIAA PAPER 93-0353] p 377 A93-23038
- Design of insensitive multirate aircraft control using optimized eigenstructure assignment p 370 A93-23515
- Measurement of shed vorticity and circulation from rotating aerofoil by particle image velocimetry p 538 A93-23804
- A Laser Doppler Anemometry study of a supersonic jet in a low speed cross-flow p 459 A93-23807
- A moving mesh system for the calculation of unsteady flows [AIAA PAPER 93-0641] p 464 A93-24756
- The effect of shock motion on entropy production [AIAA PAPER 93-0665] p 465 A93-24777
- A physically guided zonal approach for two-dimensional aerofoil flows [AIAA PAPER 93-0790] p 468 A93-24869
- A study of single jet impingement ground effect lift loss [AIAA PAPER 93-0869] p 469 A93-24930
- Maps and charts for visual air navigation p 498 A93-25170
- NASP - Waveriders in a hypersonic sky. I p 532 A93-25355
- Saab 2000 - An exercise in growth and commonality p 505 A93-25357
- NASP - Waveriders in a hypersonic sky. II p 532 A93-25359
- An examination of vortex convection effects during blade-vortex interaction p 473 A93-25360
- The application and analysis of liquid crystal thermographs in short duration hypersonic flow [AIAA PAPER 93-0182] p 542 A93-25509
- Designed for work p 506 A93-27276
- Experiments on a 60 deg delta wing with vortex flaps and vortex plates p 477 A93-27482
- Recent developments in compressor-based Joule-Thomson cooling p 547 A93-28244
- Fluid flows around cascades p 479 A93-28518
- Regional fanjet aircraft optimization studies p 508 A93-28602
- Measurements of aerodynamic rotary stability derivatives using a whirling arm facility p 525 A93-28603
- Enhancements to modal testing using finite elements p 548 A93-29258
- Theoretical modelling of rotor noise radiation p 566 A93-29407
- Validation of high frequency airload calculations using full scale flight test acoustic data p 567 A93-29417
- Competition in a single European air transport market; Proceedings of the Conference, London, United Kingdom, Dec. 1, 1992 p 458 A93-29473
- [ISBN 1-85768-080-4] p 458 A93-29473
- Datalinks - Civil aircraft; Proceedings of the Conference, London, United Kingdom, Nov. 24, 1992 p 501 A93-29474
- [ISBN 1-85768-075-8] p 501 A93-29474
- Air transport growth - How will airports manage?; Proceedings of the Conference, London, United Kingdom, Oct. 21, 1992 p 458 A93-29475
- [ISBN 1-85768-065-0] p 458 A93-29475
- Spaceplanes - Back to the future p 733 A93-34265
- MAKS - Eastern promise? p 733 A93-34266
- An optical fiber based position sensor with immunity to temperature variation p 743 A93-34287
- Numerical methods in laminar and turbulent flow; Proceedings of the 7th International Conference, Stanford Univ., CA, July 15-19, 1991. Vol. 7, pts. 1 & 2 p 743 A93-34301
- [ISBN 0-906674-77-8] p 743 A93-34301
- A cell-vortex TVD scheme for transonic viscous flow p 685 A93-34346
- Compressible flow calculations using a two-equation turbulence model and unstructured grids p 686 A93-34351

- Computation of viscous transonic aerofoil flows using eddy-viscosity based turbulence models p 687 A93-34360
- The interaction between a steady jet flow and a supersonic blade tip p 688 A93-34415
- C-17 - High-tech 'lifter' from Long Beach p 713 A93-34519
- New European regulations for rotorcraft; Proceedings of the Conference, London, United Kingdom, Mar. 16, 1993 [ISBN 1-85768-085-5] p 701 A93-34616
- Miniature display technologies for integrated helmet systems p 718 A93-34819
- Wall jets created by single and twin high pressure jet impingement p 744 A93-34847
- Some contributions to propulsion theory - Fuel consumption formulae and general range equation p 713 A93-34850
- The stability and aerodynamic performances of clusters of small cruciform parachutes [AIAA PAPER 93-1242] p 690 A93-35181
- Influence of the canopy-payload coupling on the dynamic stability in pitch of a parachute system [AIAA PAPER 93-1248] p 690 A93-35185
- Potential impact of combined NO(x) and SO(x) emissions from future High Speed Civil Transport aircraft on stratospheric aerosols and ozone p 753 A93-35372
- The development of the coupled rotor-fuselage model (CRFM) p 794 A93-35903
- Coupled rotor fuselage mode shapes - A tool in understanding helicopter response p 797 A93-35977
- Relative sensitivity of Loran-C phase tracking and cycle selection to CWI p 792 A93-36502
- Comment on 'In-flight measurement of static pressures' p 807 A93-37407
- Hydrometeor identification using cross polar radar measurements and aircraft verification p 844 A93-37719
- Advanced Tupolev twinjet combines Russian and Western technologies p 802 A93-38565
- Avionic systems/design and maintenance; Proceedings of the Conference, Hounslow, United Kingdom, Apr. 22, 1993 [ISBN 1-85768-095-2] p 764 A93-39535
- Installation of electrical cable looms p 764 A93-39536
- Software - Design for maintenance p 847 A93-39537
- HIRF and lightning p 764 A93-39539
- Antennas now and future p 764 A93-39540
- Critical dispatch - A pilot's view p 790 A93-39541
- New cabin electronics p 804 A93-39542
- Corroboration of a moment-method calculation of the maximum mutual coupling between two HF antennas mounted on a helicopter p 881 A93-40332
- New algorithms for hyperbolic radionavigation p 881 A93-40359
- Mechanical damage to aircraft structures from lightning strikes p 879 A93-40432
- Surge recovery and compressor working line control using compressor exit Mach number measurement p 897 A93-40435
- The use of satellites for aeronautical communications, navigation and surveillance p 881 A93-40436
- Some contributions to propulsion theory - The Stream Force Theorem and applications to propulsion p 924 A93-40472
- Crack analysis using discontinuous boundary elements p 925 A93-40775
- Recent evolution of gas turbine materials and the development of models for life prediction p 915 A93-40802
- Wave interaction theory and LFC p 860 A93-41781
- Linear quadratic Gaussian/loop transfer recovery design for a helicopter in low-speed flight p 906 A93-41896
- A nonlinear control strategy for robust sliding mode performance in the presence of unmatched uncertainty p 938 A93-42556
- Computation of hypersonic turbulent flow over a rearward facing step p 865 A93-42587
- The application of an adaptive upwind unstructured grid solution algorithm to the simulation of compressible laminar viscous flows over compression corners p 866 A93-42594
- Hypersonic viscous flow over two-dimensional ramps p 866 A93-42596
- The application of an adaptive unstructured grid method to the solution of hypersonic flows past double ellipse and double ellipsoid configurations p 868 A93-42609
- Finite volume 3DNS and PNS solutions of hypersonic viscous flow around a delta wing using Osher's flux difference splitting p 870 A93-42633
- Appraisal of the rarefied flow computations (problems 6.4.1 and 7.2.1) p 871 A93-42640
- Design of robust digital model-following flight control systems p 907 A93-42810
- Design of reconfigurable digital multiple model-following flight control systems p 908 A93-42811
- Big time doorstep delivery p 892 A93-42995
- Radar 92; Proceedings of the International Conference, Brighton, United Kingdom, Oct. 12, 13, 1992 [ISBN 0-85296-533-2] p 929 A93-43376
- An SSR/IFF Environment Model p 883 A93-43406
- Measurements of SSR bearing errors due to site obstructions p 883 A93-43407
- NODE-air traffic management systems p 884 A93-43428
- The development of a prototype aircraft height monitoring unit utilising an SSR-based difference in time of arrival technique p 884 A93-43432
- Bistatic radar using satellite-borne illuminators of opportunity p 914 A93-43437
- Grazing angle dependency of SAR imagery p 884 A93-43455
- Analysis of the effects of blade pitch on the radar return signal from rotating aircraft blades p 885 A93-43476
- Results from a set of low speed blade-vortex interaction experiments p 872 A93-43540
- Transonic shockwave/turbulent boundary layer interactions on a porous surface p 873 A93-43686
- Some contributions to propulsion theory - Non-isentropic duct flow and the general drag wake traverse p 874 A93-43688
- Being an engineer - A risky occupation? Proceedings of the Conference, London, United Kingdom, June 8, 1993 [ISBN 1-85768-120-7] p 945 A93-43869
- Line relaxation methods for the solution of 2D and 3D compressible flows [AIAA PAPER 93-3366] p 955 A93-45059
- Adaptive inviscid flow solutions for aerospace geometries on efficiently generated unstructured tetrahedral meshes [AIAA PAPER 93-3390] p 956 A93-45081
- The free vibration of cylindrically-curved rectangular panels p 1022 A93-45113
- Theoretical studies of the active control of propeller induced cabin noise using secondary force inputs p 995 A93-45124
- British Airways ETOPs flight planning system p 990 A93-45164
- The use of digital map data to provide enhanced navigation and displays for poor weather penetration and recovery p 992 A93-45165
- Plume effects at hypersonic speeds p 959 A93-45494
- Applications of liquid crystal surface thermography to hypersonic flow p 1023 A93-45504
- Computation of unsteady nozzle flows p 960 A93-45543
- Aspects of aging aircraft - A transatlantic view p 1026 A93-45776
- The effect of exfoliation corrosion on the fatigue behavior of structural aluminium alloys p 1017 A93-45778
- Backfire unveiled p 997 A93-46024
- Non-equilibrium thermal radiation from air shock layers modelled with the Direct Simulation Monte Carlo method [AIAA PAPER 93-2805] p 1028 A93-46544
- Active boundary-layer control in diffusers [AIAA PAPER 93-3255] p 966 A93-46798
- The cryogenic wind tunnel p 1013 A93-46915
- The practical application of solution-adaptation to the numerical simulation of complex turbomachinery problems p 970 A93-46916
- The prediction and the active control of surge in multi-stage axial-flow compressors p 1002 A93-46945
- Tangential Forebody Blowing-yaw control at high alpha [AIAA PAPER 93-3406] p 1008 A93-47205
- Computational analysis of drag reduction and buffet alleviation in viscous transonic flow over porous airfoils [AIAA PAPER 93-3419] p 976 A93-47215
- Scaling of incipient separation in high speed laminar flows [AIAA PAPER 93-3435] p 978 A93-47227
- The effect of a high thrust pusher propeller on the flow over a straight wing [AIAA PAPER 93-3436] p 978 A93-47228
- Effects of junction modifications on sharp-fin-induced shock wave/boundary layer interaction [AIAA PAPER 93-2935] p 1046 A93-48133
- An experimental study of the effects of deformable tip on the performance of fins and finite wings [AIAA PAPER 93-3000] p 1053 A93-48190
- Behaviour of the Johnson-King turbulence model in axisymmetric supersonic flows [AIAA PAPER 93-3032] p 1056 A93-48214
- Flow and heat transfer in a turbulent boundary layer through skewed and pitched jets p 1151 A93-49007
- High speed database evaluation - Further work [SAE PAPER 931597] p 1151 A93-49346
- Compact high reliability fiber coupled laser diodes for avionics and related applications p 1152 A93-49470
- Computational methods in hypersonic aerodynamics [ISBN 0-7923-1673-8] p 1072 A93-49521
- A laminar flow rotor for a radial inflow turbine [AIAA PAPER 93-1796] p 1074 A93-49686
- Smoke measurements inside a gas turbine combustor [AIAA PAPER 93-2070] p 1113 A93-49902
- Studies into the hail ingestion characteristics of turbofan engines [AIAA PAPER 93-2174] p 1115 A93-49987
- Numerical and experimental investigation of turbine tip gap flow [AIAA PAPER 93-2253] p 1081 A93-50051
- 3-dimensional interactions in the rotor of an axial turbine [AIAA PAPER 93-2255] p 1081 A93-50053
- The development of a large annular facility for testing gas turbine combustor diffuser systems [AIAA PAPER 93-2546] p 1139 A93-50269
- The 'Rolls-Royce' way of validating fan integrity [AIAA PAPER 93-2602] p 1122 A93-50311
- The well made engine p 1122 A93-50352
- Implications of European legislation post 1992; Proceedings of the Conference, London, United Kingdom, Mar. 12, 1992 [ISBN 1-85768-015-4] p 1043 A93-50353
- Carbon composite repairs of helicopter metallic primary structures p 1101 A93-50429
- On boundary-layer transition in transonic flow p 1087 A93-51280
- Design of a controller for a high performance fighter aircraft using Robust Inverse Dynamics Estimation (RIDE) [AIAA PAPER 93-3779] p 1132 A93-51374
- Design of a low sensitivity and norm multivariable controller using eigenstructure assignment and the method of inequalities [AIAA PAPER 93-3802] p 1170 A93-51394
- Genetic design of digital model-following flight-control systems [AIAA PAPER 93-3883] p 1135 A93-51468
- Scalar characteristics in a liquid-fuelled combustor with curved exit nozzle p 1123 A93-51643
- Measurements of gas composition and temperature inside a can type model combustor p 1123 A93-51644
- International standards for the qualification of airplane flight simulators; Conference, London, United Kingdom, Jan. 16, 17, 1992, Document Approved [ISBN 1-85768-040-5] p 1140 A93-51934
- The application of scheduled H-infinity controllers to a VSTOL aircraft p 1135 A93-52249
- Induced drag of a crescent wing planform p 1094 A93-52430
- Lateral aerodynamic interference between tanker and receiver in air-to-air refueling p 1136 A93-52444
- Envelope function - A tool for analyzing flutter data p 1136 A93-52455
- Automatic navigation in the air and at sea p 1099 A93-52593
- A summary of further measurements of steady and oscillatory pressures on a rectangular wing p 1096 A93-52594
- Air carriers' liability for passenger injury or death - The Japanese Initiative and Response to the recent EC Consultation Paper p 1226 A93-52930
- Air transport and the environment - Regulating aircraft noise p 1226 A93-52931
- Friction surfacing and linear friction welding p 1217 A93-53499
- The application of diffusion bonding in the manufacture of aeroengine components p 1217 A93-53514
- Wind of change p 1209 A93-53625
- Low-frequency combustion oscillations in a model afterburner p 1193 A93-53702
- Production of oscillatory flow in wind tunnels p 1218 A93-53812
- A dynamic stiffness/boundary element method for the prediction of interior noise levels p 1226 A93-53817
- The construction of nearly orthogonal multiblock grids for compressible flow simulation p 1219 A93-53847
- Design and technology for engine manufacture [ISABE 93-7002] p 1194 A93-53979
- Review of stall, surge and active control in axial compressors [ISABE 93-7011] p 1184 A93-53987
- An ultra low NO(x) pilot combustor for staged low NO(x) combustion [ISABE 93-7020] p 1195 A93-53996
- The unsteady flow past a supersonic splitter plate [ISABE 93-7047] p 1185 A93-54023
- Thermal design and analysis of an exhaust diffuser unit in a ceramic composite p 1220 A93-54036

- Experimental investigation of boundary layer transition on a flat plate with C4 leading edge
[ISABE 93-7123] p 1222 A93-54098
- The low frequency aeroacoustics of buried nozzle systems
p 1205 A93-54244
- Europe's new windtunnel
p 1210 A93-54275
- Helicopter operations in severe environments; Proceedings of the Conference, London, United Kingdom, June 4, 1992
[ISBN 1-85768-045-6] p 1175 A93-54287
- Royal Navy helicopter operations in the maritime environment
p 1190 A93-54290
- Royal Air Force support helicopters - Night operations
p 1190 A93-54293
- Avionic systems in support of covert helicopter operations
p 1193 A93-54294
- Development of a tethered satellite force transducer
p 1251 A93-54368
- An improved method for determining force balance calibration accuracy
p 1254 A93-54369
- Novel nozzle
p 1245 A93-54450
- Airship insurance in London
[AIAA PAPER 93-4043] p 1265 A93-54611
- Prediction of rotating disc flow and heat transfer in gas turbine engines
p 1256 A93-54634
- Fighting for air
p 1243 A93-54650
- The quiet helicopter; Proceedings of the Conference, London, United Kingdom, Mar. 17, 1992
[ISBN 1-85768-020-0] p 1262 A93-54718
- Helicopter noise - Public perspective
p 1261 A93-54719
- Helicopter noise certification
p 1262 A93-54720
- European research into helicopter internal noise
p 1243 A93-54724
- Desert store
p 1229 A93-54866
- Russian survivor
p 1243 A93-54867
- NDT for corrosion in aerospace structures; Proceedings of the Conference, London, United Kingdom, Feb. 12, 1992
[ISBN 0-903409-99-2] p 1257 A93-54894
- The civil scene - The authorities re-appraisal of ageing aircraft
p 1229 A93-54895
- The use of non-destructive testing to detect and monitor aircraft corrosion in service
p 1258 A93-54896
- NDT for corrosion in aerospace structures - A review of NDT techniques
p 1258 A93-54897
- Enhancement of conventional NDT methods for corrosion detection in layered skins
p 1258 A93-54898
- The inspection of aeronautical structures using transient thermography
p 1258 A93-54899
- Assessment of NDT reliability
p 1258 A93-54900
- Bear facts
p 1229 A93-55175
- IR sensors; Proceedings of the Conference, London, United Kingdom, Feb. 18, 1992
[ISBN 1-85768-010-3] p 1244 A93-55294
- Future trends in IR sensors
p 1258 A93-55295
- Displaying the night
p 1244 A93-55297
- Passive IR surveillance for helicopter systems - The Sea Owl equipment
p 1244 A93-55299
- A general introduction to aeroacoustics and atmospheric sound
p 1264 A93-55852
- West powers East
p 1244 A93-56349
- Engine for change
p 1248 A93-56350
- Three-dimensional mesh embedding for the Navier-Stokes equations using upwind control volumes
p 1239 A93-56402
- Performance parameters and assessment
p 81 N93-10052
- Aerodynamic investigation of radial turbines using computational methods
p 81 N93-10056
- Partial admission and unsteady flow in radial turbines
p 81 N93-10059
- An evaluation of a method of reconstituting fatigue loading from Rainflow counting
[RAE-TR-89057] p 82 N93-10198
- An experimental and a theoretical investigation of rotor pitch damping using a model rotor
p 47 N93-10322
- Flight test and analysis procedures for new handling criteria
[RAE-TM-FM-26] p 47 N93-10803
- Further noise measurements in a slotted cryogenic wind tunnel
[RAE-TM-AERO-2201] p 101 N93-10805
- Neutron diffraction residual stress studies for aero-engine component applications
[PNR-90908] p 85 N93-11014
- Materials: Toward the non-metallic engine
[PNR-90915] p 56 N93-11019
- Application of laminar flow to aero engine nacelles
[PNR-90916] p 20 N93-11020
- An experimental evaluation of prediction methods for contrails
[PNR-90924] p 56 N93-11023
- Testing for integrity
[PNR-90927] p 56 N93-11024
- The prediction of convective heat transfer in rotating square ducts
[PNR-90929] p 85 N93-11025
- Short fatigue crack growth in a nickel-base superalloy at room and elevated temperature
[PNR-90982] p 72 N93-11031
- A test facility for the thermofluid-dynamics of gas bearing lubrication films
[PNR-90987] p 72 N93-11032
- On the basis of experience: Built in product reliability
[PNR-90932] p 85 N93-11034
- Rotational CARS measurements in a rotating cavity with axial throughflow of cooling air: Oxygen concentration measurements
[PNR-90935] p 72 N93-11035
- Rolls-Royce civil engine technology
[PNR-90936] p 56 N93-11036
- The Trent: Towards greater thrust
[PNR-90937] p 56 N93-11037
- From RB211 to Trent: An ongoing development strategy
[PNR-90938] p 56 N93-11038
- Introduction to the Rolls-Royce design process
[PNR-90939] p 57 N93-11039
- The role of turbomachinery testing for stability in distorted flow
[PNR-90943] p 57 N93-11040
- The application of manufacturing systems engineering for aero engine gears
[PNR-90944] p 86 N93-11054
- Experimental heat transfer results in turbine stators and rotors and a comparison with theory
[PNR-90945] p 57 N93-11055
- Concorde propulsion: Did we get it right? The Rolls-Royce/SNECMA Olympus 593 engine reviewed
[PNR-90970] p 57 N93-11061
- Simultaneous engineering in the design of aero engines
[PNR-90973] p 57 N93-11062
- The Trent family of engines
[PNR-90974] p 58 N93-11063
- Aero engine ceramics: The vision, the reality, and the progress
[PNR-90983] p 72 N93-11066
- Advanced three-shaft engines: Configured for reliability, efficiency, and growth
[PNR-90986] p 58 N93-11068
- Maintainability of large gas turbine aero engines
[PNR-90987] p 58 N93-11069
- A combined experimental and theoretical study of laminar flow control with particular relevance to aero engine nacelles
[PNR-90991] p 20 N93-11070
- Civil aircraft engines: The next generation
[PNR-90962] p 58 N93-11085
- The development of the Rolls-Royce Trent aero gas turbine
[PNR-90949] p 58 N93-11108
- Development of the neutron diffraction technique for the determination of near surface residual stresses in critical gas turbine components
[PNR-90984] p 58 N93-11112
- A European collaborative NLF nacelle flight demonstrator
[PNR-90992] p 20 N93-11113
- A knowledge-based blackboard system to interpret graphical data from vibration tests of gas turbines
[PNR-90993] p 59 N93-11114
- The design and commissioning of an acoustic liner for propeller noise testing in the ARA transonic wind tunnel
[PNR-90880] p 101 N93-11204
- The use of simultaneous engineering for the design and manufacture of the low pressure turbine for the Rolls-Royce Trent engine
[PNR-90887] p 59 N93-11206
- Innovation in engineering
[PNR-90889] p 59 N93-11207
- Simultaneous engineering in aero gas turbine design and manufacture
[PNR-90890] p 59 N93-11208
- An investigation of ground access mode choice for departing passengers
[TT-9201] p 67 N93-11224
- The technical background to standards for shackles
[NPL-DMM(A)-51] p 86 N93-11325
- A study of the effects of tolerances on rigging screws, turnbuckles, and associated components in BS4429: 1987
[NPL-DMM(A)-53] p 86 N93-11326
- The technical background to standards for eyebolts
[NPL-DMM(A)-52] p 87 N93-11327
- The changing nature of design
[PNR-91011] p 48 N93-11334
- UK airmisses involving commercial air transport, May-August 1991
[ETN-92-92260] p 28 N93-11357
- UK airmisses involving commercial air transport, January-April 1991
[ETN-92-92261] p 87 N93-11358
- Experiments on low aspect ratio hydroplanes to measure lift under static and dynamic conditions
[ARE-TM(UHR)-90306] p 21 N93-11365
- Lift coefficient of a randomly oscillating hydroplane
[DRA/MAR-TM(MTH)-91320] p 21 N93-11377
- The development of the speaker independent ARM continuous speech recognition system
[RSRE-MEMO-4473] p 87 N93-11383
- Preliminary results on the use of linear discriminant analysis in the ARM continuous speech recognition system
[RSRE-MEMO-4511] p 87 N93-11384
- The use of linear discriminant analysis in the ARM continuous speech recognition system
[RSRE-MEMO-4512] p 87 N93-11385
- The measurement of the velocity field induced by a gust generator in a closed-circuit subsonic wind-tunnel
[RAE-TM-MAT/STR-1102] p 67 N93-11435
- The convection speed of the dynamic stall vortex
[AD-A247258] p 21 N93-11464
- Developments in icing test techniques for aerospace applications in the RAE Pyestock (England) altitude test facility
[RAE-TM-P-1214] p 48 N93-11485
- Time-frequency domain analysis of vibration signals for machinery diagnostics. 3: The present power spectral density
[OUEL-1911/92] p 89 N93-11707
- Airport stand assignment model
[TT-9104] p 67 N93-11728
- Application of eigenstructure assignment to the control of powered lift combat aircraft
p 64 N93-11871
- Introduction of electronic pressure scanning at the Royal Aerospace Establishment
[RAE-TM-AERO-2222] p 23 N93-11882
- The 13 ft by 9 ft low speed wind tunnel facility at DRA (Aerospace Division) Bedford (England)
[RAE-TM-AERO-2228] p 23 N93-11883
- Strain-gauge balance performance and internal temperature gradients measured in a cryogenic environment
[RAE-TM-AERO-2232] p 68 N93-11906
- Test techniques for engine/airframe integration
p 213 N93-13200
- ASTOVL model engine simulators for wind tunnel research
p 192 N93-13213
- Some aspects of intake design, performance and integration with the airframe
p 161 N93-13219
- Application of subsonic first-order panel methods for prediction of inlet and nozzle aerodynamic interactions with airframe
p 130 N93-13223
- Mathematical problems in inviscid hypersonic flow
p 131 N93-13451
- Flow prediction for three-dimensional intakes and ducts using viscous-inviscid interaction methods
p 218 N93-13953
- DESAID (the development of an expert system for aircraft initial design)
p 163 N93-14448
- Online vibration control of a flexible rotor/bearing system
p 219 N93-14468
- Rotating stall inception in fans of low hub-tip ratio
p 136 N93-14479
- Program for calculation of aileron rolling moment and yawing moment coefficients at subsonic speeds
[ESDU-88040] p 136 N93-14514
- Pressure drag and lift contributions for blunted forebodies of fineness ratio 2.0 in transonic flow (M infinity less than or equal to 1.4)
[ESDU-89033] p 136 N93-14515
- Direct prediction of a separation boundary for aerofoils using a viscous-coupled calculation method
[ESDU-92008] p 136 N93-14516
- Estimation of rate of climb
[ESDU-92019] p 164 N93-14541
- Information systems for airport operations
[TT-9202] p 152 N93-14729
- RB211-524B disc and drive cones hot cyclic spinning test
p 177 N93-14895
- Royal Air Force experience of the Harrier information management system
p 234 N93-15170
- Helicopter health monitoring: Current practice and future trends
p 169 N93-15179
- Time-dependent predictions and analysis of turbine cascade data in the transonic flow region
[PNR-90957] p 139 N93-15489
- Lanchester: The man
[AERO-REPT-9111] p 456 N93-16464
- The Goldstein Aeronautical Engineering Research Laboratory
[AERO-REPT-9109] p 240 N93-16465
- Hypersonic flows including real gas effects
[AERO-REPT-9112] p 289 N93-16467

V

VENEZUELA

- Dynamical variable structure control of a helicopter in vertical flight p 369 A93-22887
Dynamic compensator design in nonlinear aerospace systems p 1036 A93-44150

Y

YUGOSLAVIA

- Structural analysis of a nonlinear problem of aeroelasticity for CFC structures p 397 A93-18989
A comparison between numerical models and measurements in a Kaplan turbine guide vanes p 685 A93-34339

Z

ZAMBIA

- Seasonal weather hazards p 431 A93-22180

Design of a nozzle for a hypersonic wind tunnel [AERO-REPT-9113] p 381 N93-16468
Computational study of real gas effects in high speed high temperature flow, volume 2 [AERO-REPT-9203-VOL-2] p 289 N93-16470
Maximum lift of wings with leading-edge devices and trailing-edge flaps deployed [ESDU-92031] p 290 N93-16522
A90 project: Design of a composite fin [ETN-92-92773] p 329 N93-16562
Aeronautical Engineering Group publications: 1950 - present [AERO-REPT-9108] p 454 N93-16563
Drag due to gaps round undeflected trailing-edge controls and flaps at subsonic speeds [ESDU-92039] p 290 N93-16634
Example of statistical techniques applied to analysis of landing ground roll distance measurements (linear regression, correlation coefficient and F-test) [ESDU-92021] p 330 N93-16635
Example of statistical techniques applied to analysis of measurements of the landing airborne manoeuvre. (Multiple linear regression with two independent variables and one dependent variable.) [ESDU-92022] p 330 N93-16636
Fatigue propagation behaviour of short cracks in titanium alloys [ESDU-92023] p 392 N93-16637
Contribution of ventral fins to sideforce and yawing moment derivatives due to sideslip at low angle of attack [ESDU-92029] p 291 N93-16638
Fatigue propagation behaviour of short cracks in aluminum alloys [ESDU-92030] p 392 N93-16641
Pitching moment of low aspect ratio wing-body combinations up to high angles of attack at supersonic speeds [ESDU-92043] p 333 N93-17958
Heat transfer and aerodynamics of a high rim speed turbine nozzle guide vane with profiled end walls [AD-A258346] p 295 N93-17991
Energy method for analysis of measured airspeed change in landing airborne manoeuvre [ESDU-92020] p 335 N93-18042
Modelling of interfacial and thermocline waves [AERO-REPT-9209] p 420 N93-18103
The aerodynamic characteristics of the Gottingen 797 and Wortmann FX63-137 aerofoil sections at very low Reynolds numbers [ETN-93-92999] p 295 N93-18128
Aircraft turns into and down wind [AERO-REPT-9201] p 337 N93-18131
Identification of system dynamics of a high incidence research model [RR-407] p 339 N93-18507
The effect of aircraft inlets on the behaviour of aero engine axial flow compressors p 422 N93-18722
Stall in axial flow aero engine compressors p 422 N93-18723
Stall and surge in axial flow compressors p 423 N93-18724
Active control of stall and surge p 423 N93-18725
Experimental investigation of rotating stall in a mismatched three stage axial flow compressor p 423 N93-18727
Application of recess vane casing treatment to axial flow fans p 423 N93-18728
A study of stall in a low hub/tip ratio fan p 423 N93-18729
Endwall flows and blading design for axial flow compressors p 423 N93-18730
737-400 at Kegworth, 8 January 1989: The AAIB investigation p 491 N93-19661
Royal Naval helicopter ditching experience p 492 N93-19684
Towards an integrated approach to proactive monitoring and accident prevention p 495 N93-19700
Accidents and errors: A review of recent UK Army Air Corps accidents p 495 N93-19701
Prediction of success from training p 495 N93-19702
In-flight structural mode excitation system for flutter testing p 526 N93-19915
Development and flight testing of a surface pressure measurement installation on the EAP demonstrator aircraft p 550 N93-19927
HELITRAK: A helicopter-tracking receiver system for television outside broadcast links [BBC-RD-1992/5] p 552 N93-20573
Adaptivity-fluids-localization. The challenge to computational mechanics p 553 N93-20618
Handling and using information systems with new technology [PNR-90910] p 572 N93-20734

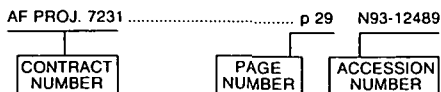
Satisfying the customer's requirements [PNR-90988] p 521 N93-20735
The aerodynamic performance of laser drilled sheets [AERO-REPT-9204] p 484 N93-20806
The effect of surface suction near the leading edge of a swept-back wing [AERO-REPT-9205] p 484 N93-20807
Review of initial experiments using the Hawk model, dynamic rig facility, and the CED 1401 digital data acquisition equipment [CRANFIELD-AERO-9017] p 531 N93-21406
The UK perspective on aviation security p 496 N93-21858
A transportable luggage examination system based on neutron interrogation p 497 N93-21863
Crashworthiness of composite seats for civil aircraft p 703 N93-24773
Parameters influencing the hot-spot ignition of aviation fuel/air and ethylene/air mixtures p 704 N93-24886
A computational approach to predicting the extent of arc root damage in CFC panels p 735 N93-24890
Zoning of aircraft by electric field modelling p 704 N93-24894
Alternative equipment test procedures for simultaneous current injection on multiple cable bundles p 747 N93-24903
A preliminary sizing method for unmanned aircraft using multi-variate optimisation p 714 N93-25408
Measurements and computations of external heat transfer and film cooling in turbines [RAE-TM-P-1223] p 722 N93-25455
An experimental study of under-expanded jets p 696 N93-25467
Design and performance of nozzle-less volute casings for inward flow radial turbines p 722 N93-25471
Control and optimization of aircraft trajectories p 729 N93-25543
An approach to configuration design synthesis of subsonic transport aircraft using artificial intelligence techniques p 716 N93-25692
Numerical modelling of viscous turbomachinery flows with a pressure correction method p 723 N93-25702
ASTOVL combat aircraft design synthesis and optimization p 717 N93-25704
Simulation of aircraft gas turbine engine p 723 N93-25751
The effects of reaction on axial compressor performance p 724 N93-25882
Radial inflow turbine study [AD-A260767] p 724 N93-25917
Satellite communications for aeronautical and navigation service p 838 N93-26648
The experimental study of transition and leading edge contamination of swept wings [LIB-TRANS-2197] p 782 N93-27274
Plume effects on the flow around a blunted cone at hypersonic speeds p 787 N93-27460
A prediction model for noise from low-altitude military aircraft [AD-A262494] p 852 N93-27662
Heat transfer and aerodynamics of a 3D design nozzle guide vane tested in the Pyestock Isentropic Light Piston Facility p 901 N93-29928
Measurement of turbulent spots and intermittency modelling at gas-turbine conditions p 902 N93-29934
The effect of orthogonal-mode rotation on forced convection in a circular-sectioned tube fitted with full circumferential transverse ribs p 932 N93-29937
Turbulent flow and heat transfer in idealized blade cooling passages p 902 N93-29938
Modelling thermal behaviour of turbomachinery discs and casings p 903 N93-29949
Flow and heat transfer between gas-turbine discs p 903 N93-29950
Impingement/effusion cooling p 932 N93-29954
Reportable accidents to UK registered aircraft, and to foreign registered aircraft in UK airspace, 1990 [CAP-600] p 991 N93-31730
Fractographic investigation of IMI 685 crack propagation specimens for SMP SC33 p 1004 N93-31743
Structural dynamic characteristics of individual blades p 1005 N93-32272
Structural dynamic characteristics of bladed assemblies p 1005 N93-32273
The prediction of noise from co-axial jets [ISVR-TR-215] p 1040 N93-32339
Reaction to aircraft noise near general aviation airfields [DORA-8203] p 1040 N93-32377
UK airmisses involving commercial air transport, September - December 1991 [ETN-93-93930] p 992 N93-32409

CONTRACT NUMBER INDEX

AERONAUTICAL ENGINEERING / A Continuing Bibliography
1993 Cumulative Index

February 1994

Typical Contract Number Index Listing



Listings in this index are arranged alphanumerically by contract number. Under each contract number the accession numbers denoting documents that have been produced as a result of research done under the contract are shown. The accession number denotes the number by which the citation is identified in the abstract section. Preceding the accession number is the page number on which the citation may be found.

AE12A/159 p 234 N93-15170
AF PROJ. 1123 p 194 N93-14559
AF PROJ. 2104 p 731 N93-25656
AF PROJ. 2308 p 195 N93-12575
AF PROJ. 2401 p 136 N93-14441
AF PROJ. 2403 p 337 N93-18248
AF PROJ. 2403 p 187 N93-13872
AF PROJ. 2403 p 527 N93-20551
AF PROJ. 2404 p 893 N93-29409
AF PROJ. 2418 p 137 N93-14661
AF PROJ. 2418 p 110 N93-14549
AF PROJ. 2420 p 1018 N93-31192
AF PROJ. 3048 p 826 N93-28592
AF PROJ. 3066 p 917 N93-29402
AF PROJ. 3153 p 815 N93-27679
AF PROJ. 622-02-F-7231 p 752 N93-26526
AF PROJ. 7231 p 224 N93-14655
AF PROJ. 7231 p 29 N93-12489
AF PROJ. 7321 p 232 N93-14406
AF-AFOSR-0035-90 p 930 N93-29141
AF-AFOSR-0059-90 p 725 N93-26335
AF-AFOSR-0062-90 p 760 N93-26343
AF-AFOSR-0064-90 p 737 N93-25948
AF-AFOSR-0112-86 p 22 N93-11742
AF-AFOSR-0138-90 p 909 N93-30550
AF-AFOSR-0159-91 p 186 N93-12959
AF-AFOSR-0179-90 p 779 N93-27004
AF-AFOSR-0228-91 p 98 N93-12258
AF-AFOSR-0249-90 p 934 N93-30369
AF-AFOSR-0285-89 p 71 N93-10717
AF-AFOSR-0293-89 p 391 N93-15931
AF-AFOSR-0301-90 p 219 N93-14400
AF-AFOSR-0397-89 p 21 N93-11464
AF-AFOSR-0427-89 p 902 N93-29934
AF-AFOSR-0518-89 p 848 N93-28498
AF-AFOSR-0804-92 p 72 N93-10843
AF-AFOSR-81-0282 p 206 A93-14545
AF-AFOSR-86-0157 p 778 A93-39401
AF-AFOSR-86-0266 p 465 A93-24774
AF-AFOSR-86-0266 p 467 A93-24861
AF-AFOSR-86-0266 p 961 A93-45726
AF-AFOSR-86-0266 p 1044 A93-48043
AF-AFOSR-87-0029 p 480 A93-28608
AF-AFOSR-87-0158 p 184 A93-14587
AF-AFOSR-88-0037 p 688 A93-34405
AF-AFOSR-88-0037 p 969 A93-46857
AF-AFOSR-88-0074 p 97 A93-13246
AF-AFOSR-88-0120 p 271 A93-21863
AF-AFOSR-88-0121 p 844 A93-37719
AF-AFOSR-89-0001 p 76 A93-10275
AF-AFOSR-89-0001 p 97 A93-13246

AF-AFOSR-89-0033 p 465 A93-24774
AF-AFOSR-89-0079 p 76 A93-10275
AF-AFOSR-89-0130 p 1236 A93-55736
AF-AFOSR-89-0130 p 961 A93-45750
AF-AFOSR-89-0283 p 1070 A93-49002
AF-AFOSR-89-0315 p 467 A93-24862
AF-AFOSR-89-0323 p 1148 A93-48247
AF-AFOSR-89-0395A p 1239 A93-56327
AF-AFOSR-89-0395 p 974 A93-47202
AF-AFOSR-89-0417 p 957 A93-45092
AF-AFOSR-89-0417 p 984 A93-47274
AF-AFOSR-89-0417 p 286 A93-23352
AF-AFOSR-89-0417 p 961 A93-45750
AF-AFOSR-89-0445 p 525 A93-28613
AF-AFOSR-89-0475 p 1087 A93-51280
AF-AFOSR-89-0508 p 1147 A93-52473
AF-AFOSR-89-5500 p 472 A93-24986
AF-AFOSR-90-0024 p 62 A93-13247
AF-AFOSR-90-0064 p 817 A93-37040
AF-AFOSR-90-0091 p 539 A93-24412
AF-AFOSR-90-0093 p 452 A93-23744
AF-AFOSR-90-0131 p 476 A93-27068
AF-AFOSR-90-0156 p 473 A93-25510
AF-AFOSR-90-0173 p 1236 A93-55736
AF-AFOSR-90-0188 p 969 A93-46832
AF-AFOSR-90-0217 p 735 A93-35618
AF-AFOSR-90-0217 p 282 A93-23064
AF-AFOSR-90-0217 p 966 A93-46793
AF-AFOSR-90-0249 p 478 A93-27922
AF-AFOSR-90-0262 p 249 A93-19362
AF-AFOSR-91-0005 p 778 A93-39410
AF-AFOSR-91-0022 p 962 A93-46477
AF-AFOSR-91-0042 p 465 A93-24778
AF-AFOSR-91-0055 p 961 A93-45735
AF-AFOSR-91-0063 p 1178 A93-53217
AF-AFOSR-91-0101 p 864 A93-42446
AF-AFOSR-91-0180 p 285 A93-23289
AF-AFOSR-91-0242 p 956 A93-45077
AF-AFOSR-91-0250 p 280 A93-22694
AF-AFOSR-91-0251 p 1079 A93-49971
AF-AFOSR-91-0262 p 475 A93-26183
AF-AFOSR-91-0262 p 691 A93-35486
AF-AFOSR-91-0310 p 439 A93-22899
AF-AFOSR-91-0351 p 475 A93-26183
AF-AFOSR-91-0374 p 282 A93-23067
AF-AFOSR-91-0412 p 1079 A93-49914
AF-AFOSR-91-0412 p 416 A93-23390
AF-AFOSR-91-0412 p 1037 A93-46834
AF-AFOSR-91-0412 p 472 A93-24972
AF-AFOSR-91-0412 p 983 A93-47266
AF-AFOSR-91-0412 p 740 A93-34073
AF-AFOSR-91-0412 p 757 A93-34219
AF-AFOSR-91-0412 p 769 A93-37941
AF-AFOSR-91-0412 p 1052 A93-48183
ARPA ORDER 6685 p 221 N93-15187
BMFT-0326501-D p 256 A93-19507
BMFT-0326800D p 905 N93-29999
BMFT-0326801G p 255 A93-19496
BRITE/EURAM-1082 p 422 N93-18623
CEC-AERO-0003-C p 863 A93-42437
CEC-AERO-0003-P p 950 A93-45002
CEC-AERO-2037-P p 950 A93-45002
CEC-AER2-CT92-0040/PL-2037 p 950 A93-44999
CEC-SC1/900369 p 686 A93-34351
CNR-CTB-90,01960,11 p 1260 A93-55869
CNR-91,02814,11 p 272 A93-22264
CNR-92,00539,CT,01 p 1239 A93-56327
DA PROJ. 1L1-61102-AH-45 p 55 N93-10348
DA PROJ. 1L1-61102-AH-45 p 392 N93-16537
DA PROJ. 1L1-61102-AH-45 p 338 N93-18333
DA PROJ. 1L1-61102-AH-45 p 848 N93-27531
DA PROJ. 1L1-61102-AH-45 p 848 N93-27589
DA PROJ. 1L1-61102-AH-45 p 848 N93-27590
DA PROJ. 1L1-61102-AH-45 p 876 N93-29450
DA PROJ. 1L1-62209-AH-76 p 553 N93-20585
DA PROJ. 1L1-62211-A-47-AA p 47 N93-10968
DA PROJ. 1L1-62211-A-47-AB p 212 N93-12736
DA PROJ. 1L1-62211-A-47-A p 751 N93-25884
DA PROJ. 1L1-62211-A-47-A p 838 N93-27069
DA PROJ. 1L1-62211-A-47-A p 839 N93-27133
DA PROJ. 1L1-62211-A-47-A p 840 N93-27268
DA PROJ. 1L1-62211-A-47-A p 1032 N93-31846
DA PROJ. 1L1-62618-AH-80 p 730 N93-26260

DA PROJ. 1L1-62786-D-283 p 806 N93-27692
DA PROJ. 2Q2-63007-A-795 p 788 N93-27955
DAAA15-90-C-0019 p 24 N93-12179
DAA21-91-C-0085 p 381 N93-17687
DAA29-83-K-0002 p 912 N93-29972
DAA46-85-K-0008 p 170 N93-15235
DAAH01-90-C-0373 p 340 N93-18999
DAAH01-90-C-0813 p 207 A93-14811
DAAH01-92-C-R359 p 917 N93-29981
DAAH04-93-G-0001 p 221 N93-15187
DAAH04-93-G-0001 p 205 A93-14542
DAAH04-93-G-0001 p 905 A93-30877
DAAH04-93-G-0001 p 725 N93-33880
DAAH04-93-G-0001 p 726 A93-33881
DAAH04-93-G-0001 p 710 A93-33928
DAAJ02-85-C-0033 p 1059 A93-48254
DAAJ02-85-C-0049 p 848 N93-27531
DAAJ02-85-C-0049 p 848 N93-27589
DAAJ02-85-C-0049 p 848 N93-27590
DAAJ02-90-C-0013 p 37 A93-10917
DAAJ02-91-C-0022 p 507 A93-27953
DAAJ02-91-C-0030 p 828 A93-37350
DAAJ02-92-C-0008 p 165 N93-15227
DAAJ02-92-C-0010 p 752 N93-26564
DAAK70-87-C-0043 p 1116 A93-50113
DAAK70-87-C-0043 p 736 N93-25914
DAAK70-87-C-0043 p 736 N93-25914
DAAK70-87-C-0043 p 255 A93-19489
DAAK70-87-C-0043 p 270 A93-21658
DAAK70-87-C-0043 p 425 A93-20579
DAAK70-87-C-0043 p 370 A93-23509
DAAK70-87-C-0043 p 778 A93-39410
DAAK70-87-C-0043 p 1148 A93-48146
DAAK70-87-C-0043 p 931 N93-29388
DAAK70-87-C-0043 p 837 A93-39422
DAAK70-87-C-0043 p 943 N93-29384
DAAK70-87-C-0043 p 713 A93-35630
DAAK70-87-C-0043 p 794 A93-35902
DAAK70-87-C-0043 p 124 A93-14782
DAAK70-87-C-0043 p 323 A93-20287
DAAK70-87-C-0043 p 469 A93-24932
DAAK70-87-C-0043 p 469 A93-24933
DAAK70-87-C-0043 p 726 A93-33930
DAAK70-87-C-0043 p 711 A93-34173
DAAK70-87-C-0043 p 743 A93-34259
DAAK70-87-C-0043 p 794 A93-35904
DAAK70-87-C-0043 p 766 A93-35941
DAAK70-87-C-0043 p 906 A93-41919
DAAK70-87-C-0043 p 1059 A93-48254
DAAK70-87-C-0043 p 1060 A93-48258
DAAK70-87-C-0043 p 281 A93-23027
DAAK70-87-C-0043 p 826 A93-35953
DAAK70-87-C-0043 p 892 A93-43776
DAAK70-87-C-0043 p 1071 A93-49016
DAAK70-87-C-0043 p 546 A93-27970
DAAK70-87-C-0043 p 157 A93-14593
DAAK70-87-C-0043 p 768 A93-37385
DAAK70-87-C-0043 p 158 A93-14784
DAAK70-87-C-0043 p 1178 A93-53233
DAAK70-87-C-0043 p 766 A93-35995
DAAK70-87-C-0043 p 1049 A93-48166
DAAK70-87-C-0043 p 820 N93-27450
DAAK70-87-C-0043 p 1059 A93-48253
DAAK70-87-C-0043 p 783 N93-27432
DAAK70-87-C-0043 p 241 A93-17750
DAAK70-87-C-0043 p 185 A93-14595
DAAK70-87-C-0043 p 481 A93-29435
DAAK70-87-C-0043 p 692 A93-35634
DAAK70-87-C-0043 p 1071 A93-49016
DAAK70-87-C-0043 p 1045 A93-48125
DAAK70-87-C-0043 p 1056 A93-48221
DAAK70-87-C-0043 p 220 N93-14677
DAAK70-87-C-0043 p 778 A93-39410
DAAK70-87-C-0043 p 19 N93-10648
DAAK70-87-C-0043 p 221 N93-15065
DAAK70-87-C-0043 p 481 A93-29436
DAAK70-87-C-0043 p 759 N93-25651
DAAK70-87-C-0043 p 875 N93-29284
DAAK70-87-C-0043 p 1060 A93-48255
DAAK70-87-C-0043 p 90 A93-12340
DAAK70-87-C-0043 p 794 A93-35902
DAAK70-87-C-0043 p 797 A93-35979
DAAK70-87-C-0043 p 62 A93-13247

CONTRACT

DAAL03-91-G-0096

DAAL03-91-G-0096 p 470 A93-24936
DAAL03-91-G-0159 p 50 N93-12485
DAAL03-91-G-0215 p 1052 A93-48179
DAAL03-92-G-0120 p 1155 A93-50084
DAAL03-92-G-0240 p 1064 A93-48313
DAAL03-92-G-0303 p 909 N93-29985
DAA15-88-C-0040 p 551 N93-19999
DACA76-86-C-0024 p 435 A93-19101
DACW72-89-C-0025 p 885 N93-29468
DAHC35-89-D-0046 p 912 N93-29972
DAJA45-89-C-0006 p 724 N93-25917
DASG60-92-C-0137 p 825 N93-27667
DE-AC01-87ER-80477 p 1149 A93-48601
DE-AC02-76CH-00016 p 90 N93-12140
DE-AC02-83CH-10093 p 216 N93-13524
DE-AC03-76SF-00098 p 216 N93-13525
DE-AC03-76SF-00098 p 434 N93-18705
DE-AC03-76SF-00098 p 485 N93-21766
DE-AC03-76SF-00098 p 94 N93-12104
DE-AC03-76SF-00098 p 911 N93-29869
DE-AC04-76DP-00789 p 437 A93-20739
DE-AC04-76DP-00789 p 390 A93-23045
DE-AC04-76DP-00789 p 385 A93-23058
DE-AC04-76DP-00789 p 702 A93-35157
DE-AC04-76DP-00789 p 703 A93-35174
DE-AC04-76DP-00789 p 928 A93-42909
DE-AC04-76DP-00789 p 1059 A93-48245
DE-AC04-76DP-00789 p 1061 A93-48269
DE-AC04-76DP-00789 p 1218 A93-53815
DE-AC04-76DP-00789 p 1255 A93-54402
DE-AC04-76DP-00789 p 94 N93-12075
DE-AC04-76DP-00789 p 393 N93-15839
DE-AC04-76DP-00789 p 560 N93-22045
DE-AC04-76DP-00789 p 694 N93-25121
DE-AC04-76DP-00789 p 845 N93-28603
DE-AC04-76DP-00789 p 900 N93-29035
DE-AC04-76DP-00789 p 942 N93-29187
DE-AC04-76DP-00789 p 73 N93-11442
DE-AC04-76DP-00789 p 222 N93-15278
DE-AC04-76DP-00789 p 394 N93-18537
DE-AC04-76DP-00789 p 497 N93-21866
DE-AC04-76DP-00789 p 706 N93-25120
DE-AC04-76DP-00789 p 826 N93-28564
DE-AC04-76DP-00789 p 917 N93-29767
DE-AC04-76DP-00789 p 905 N93-30168
DE-AC06-76RL-01830 p 89 N93-11802
DE-AC06-76RL-01830 p 754 N93-24975
DE-AC06-76RL-01830 p 789 N93-28662
DE-AC21-89MC-26052 p 554 N93-21254
DE-BI79-90BO-08243 p 97 A93-13230
DE-FC03-90ER-61010 p 806 N93-28586
DE-FC05-85ER-25000 p 122 A93-14548
DE-FC05-85ER-25000 p 860 A93-41915
DE-FG02-86ER-13636 p 557 A93-24566
DE-FG02-86ER-12813 p 935 N93-30489
DE-FG02-86ER-13919 p 419 N93-17761
DE-FG02-86ER-13919 p 747 N93-24963
DE-FG02-86ER-25053 p 956 A93-45077
DE-FG02-90GR-61057 p 1034 A93-46780
DE-FG02-92ER-45468 p 823 N93-28490
DE-FG03-92ER-25140 p 955 A93-45076
DE-FG05-91ER-81207 p 1178 A93-53233
DEN3-335 p 455 N93-18762
DFG-FA-117/2-1 p 128 A93-17265
DFG-FA-117/2-3 p 128 A93-17265
DFG-SFB-167 p 1021 A93-44224
DFG-SFB-204 p 557 A93-28477
DFG-SFB-212 p 712 A93-34263
DFG-SFB-241 p 1103 A93-52435
DFG-SFB-253 p 1112 A93-49747
DFG-SFB-253 p 272 A93-22304
DFG-SFB-253 p 1024 A93-45505
DFG-SFB-253 p 1251 A93-56032
DFG-SFB-253 p 1237 A93-56033
DFG-SFB-253 p 1237 A93-56035
DFG-SFB-253 p 1238 A93-56037
DFG-SFB-253 p 1238 A93-56038
DFG-SFB-257 p 203 A93-14194
DFG-ZI-18/31 p 862 A93-42428
DND-FA-220788 p 405 A93-19457
DREA-W7707-9-0036-01-OSC p 99 N93-10642
DRET-88-003-01 p 165 N93-15126
DRET-88-150 p 10 A93-12427
DRET-88-214 p 538 A93-23808
DRET-89-003-17 p 293 N93-17542
DRET-89-174 p 10 A93-12427
DRET-89-2045 p 10 A93-12427
DRET-90-068 p 11 A93-12428
DTAF01-90-Z-02005 p 278 A93-22633
DTAF01-90-Z-02005 p 429 A93-22150
DTAF01-90-Z-02005 p 791 N93-27252
DTAF01-91-Z-02036 p 936 N93-29257
DTFA-92-G-002 p 1120 A93-50217
DTFA-92-G-002 p 1213 A93-54001
DTFA01-80-Y-10524 p 427 A93-22118
DTFA01-82-Y-10513 p 845 N93-27675

DTFA01-84-Z-02038 p 912 N93-30103
DTFA01-87-C-00014 p 35 N93-10323
DTFA01-87-C-00014 p 48 N93-11461
DTFA01-87-C-00019 p 232 N93-14912
DTFA01-87-C-00019 p 308 A93-22121
DTFA01-88-Z-02015 p 857 N93-30673
DTFA01-89-C-00001 p 31 A93-11008
DTFA01-89-C-00001 p 1098 A93-51423
DTFA01-89-C-00001 p 707 N93-25456
DTFA01-89-C-00002 p 151 N93-13377
DTFA01-89-Z-02030 p 993 A93-46891
DTFA01-89-Z-02033 p 821 A93-37069
DTFA01-89-Z-02033 p 143 N93-14024
DTFA01-89-Z-02033 p 224 N93-14547
DTFA01-89-Z-02033 p 755 N93-25645
DTFA01-89-Z-02033 p 911 N93-29815
DTFA01-90-A-02005 p 309 A93-23069
DTFA01-90-C-00042 p 146 N93-15013
DTFA01-90-C-00046 p 486 A93-24048
DTFA01-90-Z-00049 p 432 A93-22188
DTFA01-90-Z-02005 p 429 A93-22149
DTFA01-90-Z-02049 p 427 A93-22114
DTFA01-90-Z-02049 p 428 A93-22125
DTFA01-90-Z-02049 p 752 A93-33773
DTFA01-91-C-00040 p 147 N93-15022
DTFA01-91-Y-01004 p 310 N93-18031
DTFA01-91-Y-01004 p 502 N93-20164
DTFA02-91-C-9108 p 319 N93-18927
DTFA03-83-A-00038 p 390 A93-22652
DTFA03-83-A-00038 p 677 N93-24760
DTFA03-83-A-00038 p 677 N93-25134
DTFA03-86-C-00042 p 753 N93-24884
DTFA03-86-C-00042 p 753 N93-24884
DTFA03-87-C-00043 p 497 N93-21865
DTFA03-88-C-00066 p 991 N93-31652
DTFA03-89-C-00043 p 791 N93-27269
DTFA03-89-C-00050 p 503 N93-21759
DTFA03-90-C-00010 p 994 N93-32336
DTFA03-91-C-00038 p 142 N93-12816
DTFA05-89-C-79042 p 413 A93-22178
DTFR53-91-C-00072 p 782 N93-27413
DTRS-57-87-C-00006 p 342 A93-21146
DTRS-57-88-C-00078 p 35 N93-10065
DTRS-57-89-00009 p 559 N93-21501
DTRS56-83-C-0009 p 1026 A93-45788
DTRS57-88-C-00019 p 1027 A93-45790
DTRS57-90-P-80689 p 1026 A93-45787
DTRS57-92-C-00012 p 1153 A93-49707
DTRS67-92-C-00011 p 1110 A93-49706
EPA-68-CO-0003 p 1035 N93-32089
ESA-9281/91/F/RD(SC) p 706 N93-25018
FAA PROJ. AM-B-93-PHY-152 p 704 N93-25205
FAA-F2003-C p 35 N93-10459
FAA-F2006-E p 193 N93-13447
FAA-F2006-G p 706 N93-24948
FAA-F2205-A p 417 N93-15698
FAA-T0603-S p 192 N93-12668
FAA-T1101-F p 705 N93-24741
FAA-T2001-B p 792 N93-27017
FAA-T2001-B p 793 N93-28625
F07624-91-C-0019 p 36 N93-11704
F04606-89-D-0039 p 36 N93-11705
F04606-89-D-0040 p 228 N93-12554
F04701-88-C-0110 p 407 A93-19693
F08630-91-C-0030 p 455 N93-17891
F08635-89-C-0208 p 928 A93-42782
F08635-89-C-0209 p 440 A93-22978
F08635-89-C-0211 p 1053 A93-48189
F08635-90-C-0053 p 480 A93-28610
F08635-90-C-0100 p 788 N93-27464
F08635-90-C-0100 p 1262 A93-56413
F08635-90-C-0100 p 755 N93-26243
F08635-90-C-0100 p 390 A93-23047
F08635-90-G-0100 p 1196 A93-53999
F19628-89-C-0001 p 387 A93-19366
F19628-90-C-0002 p 501 A93-29596
F19628-90-C-0002 p 343 A93-22111
F19628-90-C-0002 p 432 A93-22190
F19628-90-C-0003 p 224 N93-14547
F19628-90-C-0003 p 755 N93-25645
F19628-90-C-0003 p 936 N93-29257
F19628-90-C-0003 p 911 N93-29815
F19628-90-C-0003 p 344 N93-18270
F29601-85-C-0038 p 684 A93-34335
F30602-85-C-0221 p 228 A93-17389
F30602-85-C-0221 p 228 A93-17389
F33601-89-D-0045 p 1124 A93-48153
F33615-80-C-2059 p 352 A93-19411
F33615-81-C-2078 p 815 N93-28391
F33615-81-C-3403 p 513 N93-20579
F33615-83-C-3011 p 1100 A93-49796
F33615-84-C-3404 p 50 N93-12488
F33615-85-C-2515 p 164 N93-14571
F33615-85-C-3420 p 411 A93-21653
F33615-86-C-5044 p 926 A93-41398
F33615-86-C-5044 p 855 A93-40663

F33615-86-D-0540 p 516 A93-25922
F33615-87-C-0534 p 719 N93-25783
F33615-87-C-0534 p 719 N93-25909
F33615-87-C-1550 p 408 A93-20293
F33615-87-C-2729 p 914 A93-42927
F33615-87-C-2746 p 724 A93-26219
F33615-87-C-2767 p 926 A93-41398
F33615-87-C-2767 p 387 A93-19330
F33615-87-C-2806 p 401 A93-19344
F33615-87-C-2806 p 389 A93-21651
F33615-87-C-2822 p 809 A93-36268
F33615-87-C-2839 p 387 A93-19330
F33615-87-C-3022 p 1144 A93-49658
F33615-87-C-3022 p 1109 A93-49659
F33615-87-C-3215 p 751 N93-25951
F33615-87-C-3227 p 1025 A93-45775
F33615-87-C-3402 p 279 A93-22687
F33615-87-C-3607 p 777 A93-39255
F33615-87-C-5242 p 182 A93-14306
F33615-87-D-0609 p 1070 A93-49003
F33615-88-C-0003 p 920 N93-30442
F33615-88-C-2517 p 719 N93-25783
F33615-88-C-2817 p 719 N93-25909
F33615-88-C-2829 p 760 N93-25915
F33615-88-C-2830 p 440 N93-16500
F33615-88-C-2836 p 77 A93-11341
F33615-88-C-2889 p 735 A93-34561
F33615-88-C-2907 p 401 A93-19325
F33615-88-C-3612 p 401 A93-19326
F33615-88-C-5404 p 361 N93-16080
F33615-89-C-0532 p 411 A93-21665
F33615-89-C-1110 p 965 A93-46750
F33615-89-C-3003 p 730 A93-34498
F33615-90-C-0005 p 159 N93-12602
F33615-90-C-1464 p 396 A93-18619
F33615-90-C-1468 p 832 A93-38975
F33615-90-C-2001 p 752 N93-26526
F33615-90-C-2028 p 516 A93-25922
F33615-90-C-2033 p 718 N93-25948
F33615-90-C-2047 p 941 A93-42856
F33615-90-C-2052 p 982 A93-47263
F33615-90-C-2089 p 530 N93-21268
F33615-90-C-3001 p 938 A93-42785
F33615-90-C-3004 p 939 A93-42822
F33615-90-C-3600 p 1153 A93-49839
F33615-91-C-1753 p 1081 A93-50054
F33615-91-C-2204 p 387 A93-19356
F33615-91-C-3205 p 1245 A93-54467
F33615-91-C-5708 p 393 N93-18242
F33615-92-C-3605 p 173 A93-14629
F33657-84-D-0165 p 990 N93-32004
F33657-88-D-2188 p 15 A93-13309
F33657-90-C-2269 p 276 A93-22614
F33657-90-D-2190 p 1127 A93-48329
F40600-82-C-0005 p 939 A93-42829
F40600-84-C-0010 p 377 A93-23040
F40600-84-C-0002 p 740 A93-33978
F42650-86-C-3276 p 855 A93-40668
F4606-89-D-0039 p 1133 A93-51408
F49610-92-J-0110 p 725 N93-26239
F49620-79-C-0226 p 678 N93-26238
F49620-86-C-0066 p 273 A93-22320
F49620-86-C-0111 p 962 A93-46480
F49620-86-C-0113 p 934 N93-30406
F49620-86-C-0127 p 730 A93-35625
F49620-86-C-033 p 730 A93-35625
F49620-87-C-0016 p 192 N93-12552
F49620-87-K-0008 p 855 A93-40665
F49620-88-C-0022 p 925 A93-40666
F49620-88-C-0041 p 281 A93-20300
F49620-88-C-0053 p 206 A93-14545
F49620-88-C-0061 p 47 N93-10842
F49620-88-C-0076 p 1224 A93-52763
F49620-88-C-0087 p 735 A93-35618
F49620-90-C-0038 p 286 A93-23352
F49620-90-C-0076 p 908 A93-42813
F49620-91-C-0003 p 475 A93-26176
F49620-91-C-0010 p 968 A93-46831
F49620-91-C-0014 p 97 A93-13246
F49620-91-C-0026 p 818 A93-37392
F49620-91-C-0037 p 932 N93-29936
F49620-91-C-0037 p 275 A93-22594
F49620-91-C-0037 p 475 A93-26897
F49620-91-C-0037 p 837 A93-39427
F49620-91-C-0037 p 906 A93-41889
F49620-91-C-0037 p 285 A93-23294
F49620-91-C-0037 p 128 A93-17262
F49620-91-C-0037 p 531 A93-24478
F49620-91-C-0037 p 17 N93-10340
F49620-91-C-0037 p 945 N93-29396
F49620-91-C-0037 p 699 N93-25894
F49620-91-C-0037 p 755 N93-26327
F49620-91-C-0037 p 1061 A93-48271
F49620-91-C-0037 p 263 A93-20189
F49620-91-C-0037 p 24 N93-12063
F49620-91-C-0037 p 465 A93-24772

CONTRACT NUMBER INDEX

CONTRACT NUMBER INDEX

NAG3-1124

F49620-91-C-0042	p 463 A93-24753	NAG1-1139	p 1143 A93-51348	p 1065 A93-48357
	p 466 A93-24788	NAG1-1145	p 476 A93-27068	p 17 N93-10098
F49620-92-C-0030	p 737 N93-26268	NAG1-1150	p 1028 A93-46811	p 265 A93-20416
F49620-92-J-0065	p 285 A93-23289		p 1055 A93-48205	p 1104 A93-52454
F49620-92-J-0078	p 779 N93-27004	NAG1-1151	p 417 A93-23557	p 1019 N93-31643
F49620-92-J-0079	p 902 N93-29934	NAG1-1156	p 288 A93-23548	p 1019 N93-31739
F49620-92-J-0090	p 470 A93-24940	NAG1-1160	p 322 A93-19806	p 504 A93-24741
	p 1060 A93-48266		p 323 A93-20279	p 322 A93-19231
F49620-92-J-0105	p 469 A93-24928	NAG1-1161	p 262 A93-20187	p 530 N93-20312
F49620-92-J-0146	p 473 A93-25510	NAG1-1177	p 1034 A93-46780	p 1015 N93-31848
F49620-92-J-0189	p 1081 A93-50041	NAG1-1188	p 264 A93-20309	p 472 A93-24954
F49620-92-J-0271	p 263 A93-20190		p 265 A93-20310	p 950 A93-45001
F49620-92-J-0339	p 1037 A93-46834		p 682 A93-33755	p 953 A93-45028
F49620-92-J-0418	p 277 A93-22619		p 952 A93-45016	p 389 A93-20155
F49620-92-J-0426	p 968 A93-46826		p 957 A93-45096	p 744 A93-34496
F49620-92-J-0450	p 741 A93-34076		p 1073 A93-49531	p 1119 A93-50197
	p 829 A93-37441	NAG1-1192	p 283 A93-23254	p 40 A93-11654
F49620-92-J-0462	p 534 A93-25532	NAG1-1196	p 692 A93-35613	NAG1-822
F49620-92-J-150	p 1020 A93-44168		p 985 A93-47282	NAG1-833
F49620-93-J-0135	p 1037 A93-46834		p 483 N93-20018	p 326 A93-20370
F49620-93-J-0186	p 1080 A93-50036	NAG1-1198	p 976 A93-47216	p 742 A93-34169
F49620-91-C-0042	p 1050 A93-48170		p 131 N93-13463	p 827 A93-35978
GRI-5086-233-1436	p 212 N93-12977	NAG1-1201	p 294 N93-17855	p 837 A93-39407
GRI-5086-260-1308	p 756 N93-26533	NAG1-1209	p 281 A93-23030	p 1160 A93-52517
GRI-5088-293-1716	p 555 N93-21465		p 1011 A93-45498	p 906 A93-41897
GRI-5091-254-2235	p 755 N93-26529	NAG1-1210	p 757 A93-34536	p 728 N93-24762
GWA 89-TA	p 378 N93-16309	NAG1-1232	p 275 A93-22602	p 60 N93-12214
HSE-1533	p 86 N93-11325	NAG1-1244	p 1101 A93-51338	p 756 A93-33883
	p 86 N93-11326	NAG1-1245	p 80 A93-13362	p 1160 A93-52449
	p 87 N93-11327		p 789 N93-28449	p 860 A93-41915
MDA903-90-C-0006	p 1019 N93-32085	NAG1-1253	p 794 A93-35904	p 1232 A93-54646
MDA972-92-J-1018	p 503 N93-21671		p 906 A93-41919	p 9 A93-12007
MIPR-FY1455-90-N0658	p 825 N93-28226	NAG1-1255	p 385 A93-22288	p 982 A93-47262
MIPR-FY1455-91-N0638	p 917 N93-29402		p 1099 A93-48337	p 138 N93-14767
MIPR-FY1457-88-N5052	p 826 N93-28592		p 1141 A93-49596	p 274 A93-22371
MOD-AT/2037/331	p 1028 A93-46544		p 297 N93-18602	p 860 A93-41914
MOESC-B02452089	p 376 A93-21833	NAG1-1256	p 716 N93-25670	p 1063 A93-48297
MOESC-01550151	p 246 A93-19294	NAG1-1257	p 1101 A93-51349	p 128 A93-17253
MOESC-01550171	p 403 A93-19425		p 1170 A93-51344	p 262 A93-20188
MOESC-63460086	p 209 A93-15684	NAG1-1265	p 526 N93-19960	p 284 A93-23267
NAGW-1072	p 287 A93-23541		p 1236 A93-55400	p 478 A93-27925
	p 951 A93-45013		p 552 N93-20297	p 980 A93-47251
	p 977 A93-47226	NAG1-1267	p 795 A93-35940	p 1048 A93-48152
NAGW-1128	p 517 A93-26884	NAG1-1271	p 474 A93-25536	p 1049 A93-48167
NAGW-1331	p 861 A93-41916	NAG1-1295	p 467 A93-24858	p 1093 A93-52011
	p 1027 A93-46531		p 515 N93-21646	p 265 A93-20416
	p 964 A93-46548		p 879 N93-31037	p 709 A93-33877
	p 964 A93-46549	NAG1-1333-S1	p 1083 A93-50221	p 683 A93-34260
	p 985 A93-47279	NAG1-1339	p 1056 A93-48213	p 797 A93-35979
	p 1049 A93-48163	NAG1-1340	p 956 A93-45078	p 378 A93-23510
	p 1154 A93-50009	NAG1-1341	p 1131 A93-51358	p 700 N93-26049
	p 1155 A93-50010		p 516 N93-22003	p 447 A93-19184
	p 391 N93-16389		p 714 N93-25162	p 509 A93-29414
	p 537 N93-21749	NAG1-1342	p 36 N93-10961	p 482 A93-29441
NAGW-1467	p 1147 A93-48044	NAG1-1358	p 930 N93-29154	p 99 N93-10458
NAGW-1708	p 220 N93-14766	NAG1-1361	p 442 N93-18372	p 695 N93-25249
NAGW-1809	p 242 A93-18851	NAG1-1362	p 1171 A93-48140	p 758 N93-25130
	p 955 A93-45059	NAG1-1371	p 808 N93-28418	p 124 A93-14782
NAGW-2266	p 386 N93-16629	NAG1-1373	p 265 A93-20416	p 414 A93-22608
NAGW-419	p 848 N93-27289	NAG1-1378	p 895 N93-29885	p 36 N93-11139
NAGW-478	p 242 A93-18851	NAG1-1380	p 1132 A93-51371	p 89 N93-11716
NAGW-581	p 930 A93-43539	NAG1-1396	p 468 A93-24925	p 707 N93-26052
	p 965 A93-46744	NAG1-1411	p 742 A93-34170	p 322 A93-20278
	p 1024 A93-45526		p 742 A93-34171	p 566 A93-29408
	p 1012 A93-45530	NAG1-1423	p 319 N93-18873	p 850 A93-37396
NAGW-964	p 781 N93-27126	NAG1-1433	p 440 A93-23330	p 806 N93-28693
NAGW-966	p 287 A93-23545	NAG1-1451	p 1131 A93-51357	p 862 A93-42429
NAG1-1003	p 1039 A93-46682		p 527 N93-20296	p 955 A93-45052
NAG1-1005	p 969 A93-46839	NAG1-1466	p 805 N93-27089	p 783 N93-27427
NAG1-1007	p 422 N93-18576	NAG1-189	p 1115 A93-49961	p 265 A93-20416
NAG1-1038	p 25 N93-12343	NAG1-224	p 45 A93-13381	p 68 N93-11910
NAG1-1047	p 445 A93-19156		p 324 A93-20307	p 296 N93-18384
	p 446 A93-19160		p 548 A93-28618	p 995 A93-44888
	p 100 N93-10684	NAG1-226	p 1078 A93-49825	p 780 N93-27093
NAG1-1052	p 322 A93-20278	NAG1-244	p 1154 A93-50009	p 336 N93-18064
NAG1-1056	p 375 A93-20297		p 1155 A93-50010	p 336 N93-18065
	p 1139 A93-51295		p 391 N93-16389	p 337 N93-18066
	p 381 N93-16695		p 537 N93-21749	p 820 N93-27308
	p 1015 N93-31836	NAG1-321	p 1131 A93-51370	p 728 N93-25199
NAG1-1057	p 1159 A93-51528	NAG1-343	p 546 A93-27975	p 729 N93-26046
NAG1-1058	p 1030 N93-31110		p 934 N93-30374	p 1153 A93-49901
NAG1-1063	p 547 A93-27978	NAG1-345	p 895 N93-29774	p 1063 A93-48298
NAG1-1065	p 782 N93-27282		p 895 N93-29775	p 451 A93-19804
NAG1-1067	p 200 N93-15431		p 895 N93-29776	p 140 N93-15588
NAG1-1070	p 282 A93-23063		p 931 N93-29777	p 719 A93-34159
	p 749 N93-25266		p 876 N93-29778	p 1114 A93-49912
NAG1-1072	p 282 A93-23064		p 931 N93-29779	p 1148 A93-48146
	p 966 A93-46793	NAG1-361	p 866 A93-42593	p 416 A93-23512
	p 97 A93-13230		p 868 A93-42608	p 738 A93-33915
NAG1-1081	p 936 N93-31036	NAG1-421	p 398 A93-19157	p 170 A93-14077
NAG1-1082	p 1126 A93-48311		p 720 A93-34410	p 746 N93-24759
NAG1-1087	p 1040 N93-32221	NAG1-530	p 471 A93-24945	p 361 A93-23246
NAG1-1096	p 465 A93-24764		p 692 A93-35621	p 179 N93-15359
NAG1-1098	p 262 A93-20188	NAG1-602	p 175 N93-13697	p 170 A93-14077
NAG1-1111	p 452 A93-23744	NAG1-633	p 418 N93-16558	p 1113 A93-49903
NAG1-1116	p 748 N93-25208	NAG1-648	p 182 A93-14331	p 1109 A93-49612
NAG1-1119				p 1196 A93-53999

NAG3-1127

NAG3-1127 p 930 N93-29213
 NAG3-1134 p 280 A93-23001
 NAG3-1137 p 358 A93-20320
 NAG3-1146 p 1206 A93-54268
 NAG3-1163 p 810 A93-37446
 p 90 N93-12277
 NAG3-1165 p 699 N93-25883
 NAG3-1168 p 1177 A93-53208
 NAG3-1173 p 1115 A93-50052
 NAG3-1177 p 1132 A93-51400
 NAG3-1178 p 1058 A93-48239
 NAG3-1179 p 348 A93-19307
 NAG3-1187 p 1118 A93-50192
 p 1119 A93-50193
 NAG3-1192 p 475 A93-25553
 p 480 A93-29318
 p 747 N93-25109
 p 809 A93-35934
 NAG3-1198 p 280 A93-22694
 NAG3-1213 p 16 N93-10069
 NAG3-1215 p 358 A93-20320
 NAG3-1230 p 1123 A93-51403
 NAG3-1232 p 358 A93-20320
 NAG3-1234 p 719 A93-34159
 p 720 A93-34161
 p 1079 A93-49913
 NAG3-1267 p 244 A93-19151
 NAG3-1272 p 522 N93-21210
 NAG3-181 p 85 N93-10892
 NAG3-311 p 397 A93-18752
 NAG3-330 p 967 A93-46823
 NAG3-376 p 1045 A93-48128
 p 1063 A93-48291
 p 1076 A93-49791
 NAG3-481 p 390 A93-22652
 p 677 N93-24760
 p 677 N93-25134
 NAG3-502 p 877 N93-30373
 NAG3-555 p 1032 N93-31588
 NAG3-666 p 309 A93-23239
 p 148 N93-15360
 NAG3-724 p 719 A93-34159
 NAG3-725 p 1063 A93-48293
 NAG3-730 p 688 A93-34483
 p 296 N93-18585
 NAG3-732 p 250 A93-19399
 NAG3-742 p 90 N93-12277
 NAG3-767 p 1148 A93-48132
 NAG3-768 p 259 A93-20144
 p 339 N93-18783
 NAG3-770 p 424 N93-18862
 NAG3-772 p 248 A93-19324
 p 723 N93-25668
 NAG3-773 p 1155 A93-50084
 NAG3-836 p 391 A93-23358
 NAG3-841 p 689 A93-34490
 NAG3-855 p 245 A93-19221
 NAG3-869 p 465 A93-24786
 NAG3-895 p 84 N93-10372
 p 220 N93-14799
 NAG3-904 p 828 A93-37046
 NAG3-927 p 880 N93-29152
 NAG3-929 p 1157 A93-50280
 NAG3-937 p 551 N93-20268
 NAG3-942 p 394 N93-18784
 NAG3-943 p 408 A93-20141
 NAG3-989 p 1220 A93-54053
 NAG3-998 p 185 A93-14596
 p 1102 A93-51401
 NAG5-245 p 314 A93-21154
 p 1240 A93-55975
 NAG5-902 p 425 A93-20579
 NAG8-751 p 753 A93-34694
 NAG9-449 p 241 A93-17750
 p 482 A93-29774
 NAL PROJ. FC-8-121 p 187 N93-13566
 NAL PROJ. ST-1-166 p 234 N93-13368
 NANB-1-D1176 p 880 N93-29211
 NASA ORDER C-30050-R p 170 A93-14077
 p 1113 A93-49903
 NASA ORDER C-99066-G p 744 A93-34311
 p 772 A93-38695
 p 290 N93-16596
 NASA ORDER L-20278-D p 1038 N93-31649
 NASW-4003 p 4 N93-10647
 NASW-4435 p 332 N93-17711
 p 332 N93-17802
 p 333 N93-17972
 p 334 N93-17974
 p 334 N93-17976
 p 334 N93-17977
 p 334 N93-18017
 p 420 N93-18047
 p 335 N93-18049
 p 335 N93-18054
 p 335 N93-18055

NAS1-13169

NAS1-14101

NAS1-14472

NAS1-15830

NAS1-16394

NAS1-16460

NAS1-17067

NAS1-17070

NAS1-17130

NAS1-17146

NAS1-17497

NAS1-17699

NAS1-17919

NAS1-17925

NAS1-18027

NAS1-18028

NAS1-18037

NAS1-18107

NAS1-18240

NAS1-18378

NAS1-18450

NAS1-18458

NAS1-18471

NAS1-18565

NAS1-18584

NAS1-18585

NAS1-18586

NAS1-18599

NAS1-18605

p 335 N93-18056
 p 336 N93-18059
 p 336 N93-18060
 p 336 N93-18061
 p 336 N93-18063
 p 337 N93-18155
 p 337 N93-18161
 p 337 N93-18166
 p 338 N93-18349
 p 338 N93-18350
 p 339 N93-18386
 p 244 A93-19144
 p 847 N93-27063
 p 847 N93-27063
 p 847 N93-27063
 p 515 N93-21313
 p 846 A93-37623
 p 847 N93-27063
 p 847 N93-27063
 p 567 A93-29416
 p 515 N93-21313
 p 919 N93-30433
 p 1103 A93-52440
 p 548 A93-28543
 p 393 N93-17920
 p 343 N93-16693
 p 942 N93-29192
 p 718 N93-24764
 p 444 A93-19136
 p 451 A93-19229
 p 1243 A93-55856
 p 243 A93-19132
 p 452 A93-23744
 p 1224 A93-52763
 p 847 N93-27063
 p 38 A93-11275
 p 166 A93-14327
 p 479 A93-28601
 p 298 N93-19015
 p 783 N93-27429
 p 330 N93-16947
 p 330 N93-16999
 p 205 A93-14523
 p 1137 A93-49617
 p 251 A93-19429
 p 507 A93-27956
 p 930 A93-43539
 p 965 A93-46744
 p 742 A93-34170
 p 759 A93-34957
 p 958 A93-45142
 p 1048 A93-48157
 p 384 A93-22287
 p 65 N93-12413
 p 399 A93-19250
 p 417 A93-23555
 p 910 A93-41059
 p 1022 A93-45133
 p 1160 A93-52449
 p 220 N93-14692
 p 14 A93-13303
 p 260 A93-20163
 p 264 A93-20300
 p 276 A93-22615
 p 478 A93-27924
 p 479 A93-28604
 p 767 A93-37378
 p 858 A93-41053
 p 859 A93-41056
 p 418 N93-16379
 p 291 N93-16710
 p 292 N93-16940
 p 747 N93-25087
 p 989 N93-31733
 p 98 N93-12346
 p 99 N93-12538
 p 406 A93-19587
 p 407 A93-19598
 p 477 A93-27474
 p 1070 A93-49009
 p 783 N93-27429
 p 76 A93-10275
 p 6 A93-10533
 p 243 A93-19132
 p 476 A93-27068
 p 691 A93-35486
 p 1236 A93-55736
 p 1264 A93-55852
 p 102 N93-12021
 p 231 N93-12986
 p 290 N93-16627
 p 298 N93-18771
 p 694 N93-25083
 p 758 N93-25084
 p 847 N93-27063

NAS1-18703
 NAS1-18745
 NAS1-18746
 NAS1-18754
 NAS1-18796
 NAS1-18799
 NAS1-18834
 NAS1-18841
 NAS1-18842
 NAS1-18856
 NAS1-18888
 NAS1-18889
 NAS1-18935
 NAS1-19000
 NAS1-19038
 NAS1-19060
 NAS1-19061
 NAS1-19091
 NAS1-19145
 NAS1-19161
 NAS1-19236
 NAS1-19237
 NAS1-19250
 NAS1-19299
 NAS1-19317
 NAS1-19320
 NAS1-19480
 NAS1-19529
 NAS1-19551
 NAS1-19672
 NAS1-19864
 NAS1-811
 NAS2-12340
 NAS2-12635
 NAS2-12819
 NAS2-12961
 NAS2-12965
 NAS2-12989
 NAS2-12996
 NAS2-13070

p 284 A93-23269
 p 231 A93-14539
 p 420 N93-18093
 p 923 N93-30876
 p 1019 N93-32234
 p 919 N93-30435
 p 921 N93-30854
 p 921 N93-30853
 p 923 N93-30869
 p 122 A93-14409
 p 919 N93-30433
 p 159 A93-15812
 p 894 N93-29498
 p 918 N93-30432
 p 920 N93-30440
 p 921 N93-30845
 p 922 N93-30855
 p 922 N93-30857
 p 1101 A93-51338
 p 38 A93-11275
 p 205 A93-14543
 p 398 A93-19173
 p 447 A93-19184
 p 324 A93-20322
 p 284 A93-23270
 p 563 A93-24826
 p 563 A93-24827
 p 741 A93-34077
 p 741 A93-34102
 p 683 A93-34124
 p 949 A93-44229
 p 1056 A93-48213
 p 1065 A93-48321
 p 1112 A93-49830
 p 1101 A93-51338
 p 757 N93-25073
 p 808 N93-28621
 p 1000 N93-32218
 p 244 A93-19184
 p 569 N93-21317
 p 229 N93-13370
 p 447 A93-19184
 p 468 A93-24925
 p 565 A93-29402
 p 1034 A93-45139
 p 94 N93-12299
 p 406 A93-19587
 p 268 A93-21103
 p 1021 A93-44231
 p 318 N93-16692
 p 38 A93-11275
 p 166 A93-14327
 p 263 A93-20191
 p 265 A93-20713
 p 273 A93-22321
 p 959 A93-45154
 p 1178 A93-53231
 p 220 N93-14797
 p 780 N93-27096
 p 205 A93-14543
 p 243 A93-19132
 p 398 A93-19173
 p 546 A93-27975
 p 269 A93-21113
 p 270 A93-21330
 p 273 A93-22319
 p 767 A93-37378
 p 953 A93-45031
 p 1057 A93-48232
 p 873 A93-43629
 p 290 N93-16627
 p 298 N93-18771
 p 694 N93-25083
 p 758 N93-25084
 p 694 N93-25153
 p 779 N93-27004
 p 847 N93-27063
 p 780 N93-27090
 p 843 N93-28975
 p 278 A93-22626
 p 962 A93-46479
 p 957 A93-45101
 p 979 A93-47238
 p 1054 A93-48199
 p 780 N93-27067
 p 1077 A93-49820
 p 1073 A93-49531
 p 61 A93-10919
 p 293 N93-16942
 p 240 N93-17883
 p 261 A93-20177
 p 977 A93-47225
 p 377 A93-23297
 p 368 A93-22612
 p 1212 A93-53459
 p 508 A93-28612

CONTRACT NUMBER INDEX

CONTRACT NUMBER INDEX

NSF DMS-89-22805

NAS2-13092	p 693	N93-25075	NCA2-568	p 1062	A93-48285	NCC2-751	p 805	N93-27241
NAS2-13187	p 73	N93-11135	NCA2-578	p 211	A93-17417	NCC2-759	p 186	N93-12903
NAS2-13194	p 977	A93-47225		p 1047	A93-48150	NCC2-762	p 1251	A93-54409
NAS2-13203	p 377	A93-23297	NCA2-581	p 1062	A93-48285	NCC2-775	p 793	N93-28936
NAS2-13252	p 166	A93-14326	NCA2-594	p 1134	A93-51438	NCC2-795	p 893	N93-29153
NAS2-13285	p 483	N93-20256	NCA2-611	p 283	A93-23254	NCC3-116	p 391	N93-15830
NAS2-13286	p 459	A93-23811		p 370	A93-23255	NCC3-124	p 864	A93-42579
NAS2-13300	p 459	A93-23811	NCA2-621	p 1126	A93-48309	NCC3-208	p 815	N93-28609
NAS2-13383	p 1009	A93-47235	NCA2-644	p 953	A93-45027		p 816	N93-28617
	p 1009	A93-47236	NCA2-663	p 953	A93-45027		p 900	N93-29072
NAS2-13513	p 263	A93-20190	NCA2-742	p 1062	A93-48282	NCC3-233	p 838	N93-27088
NAS3-22822	p 935	N93-31031	NCC1-112	p 964	A93-46548	NERC-GR/3/5896	p 844	A93-37719
NAS3-23288	p 364	N93-18578		p 964	A93-46549	NGL-05-020-243	p 780	N93-27084
NAS3-23691	p 403	A93-19416	NCC1-140	p 1027	A93-46531	NGL-22-0069-640	p 148	N93-15360
NAS3-23941	p 556	N93-22005	NCC1-158	p 938	A93-41891	NGL-22-009-640	p 308	A93-22112
NAS3-23944	p 198	N93-12589		p 1126	A93-48310	NGL-22-069-640	p 309	A93-23239
NAS3-24105	p 1074	A93-49720		p 1128	A93-48333	NGL-31-001-252	p 185	A93-14595
NAS3-24222	p 852	N93-27148	NCC1-159	p 759	N93-25969	NGR-36-009-017	p 342	A93-21146
NAS3-24227	p 397	A93-18752	NCC1-163	p 38	A93-11275	NGT-44-001-800	p 700	N93-26078
NAS3-24346	p 55	N93-10348		p 959	A93-45154	NGT-50142	p 744	A93-34496
NAS3-24350	p 721	N93-24754	NCC1-24	p 930	A93-43539	NGT-50172	p 273	A93-22322
	p 721	N93-25106		p 965	A93-46744	NGT-50341	p 122	A93-14541
NAS3-24385	p 917	N93-29451	NCC1-29	p 484	N93-21562	NGT-50404	p 738	A93-33907
NAS3-25266	p 248	A93-19322		p 820	N93-27264	NGT-50406	p 269	A93-21116
	p 325	A93-20324	NCC1-46	p 22	N93-11605		p 1100	A93-49012
	p 309	A93-23243		p 24	N93-12004	NGT-50545	p 268	A93-21042
	p 520	A93-27801	NCC1-68	p 276	A93-22616	NGT-50714	p 549	A93-29315
	p 810	A93-37389		p 981	A93-47254	NGT-50897	p 1119	A93-50197
	p 959	A93-45146		p 694	N93-25117	NGT-50952	p 467	A93-24862
	p 975	A93-47213		p 934	N93-30375		p 1148	A93-48247
	p 1045	A93-48128	NCC2-172	p 480	A93-29411	NIVR-01904-N	p 990	N93-32358
	p 1063	A93-48291	NCC2-315	p 308	A93-22153	NIVR-07801-N	p 999	N93-32338
	p 1074	A93-49695	NCC2-327	p 571	N93-19970	NR PROJ. M00-96	p 717	N93-25933
	p 1074	A93-49720	NCC2-374	p 829	A93-37428	NR PROJ. RN1-5-W-33	p 418	N93-15857
	p 1076	A93-49791		p 829	A93-37438	NR PROJ. S03-97	p 793	N93-28990
	p 231	N93-12967		p 829	A93-37439	NR PROJ. Y13-16	p 382	N93-17734
	p 781	N93-27097		p 778	A93-39412	NSC-CS79-0210-D006-21	p 882	A93-42816
NAS3-25270	p 174	N93-12695		p 216	N93-13406	NSC-CS81-0210-D006-02	p 882	A93-42816
	p 364	N93-18702	NCC2-420	p 414	A93-22588	NSC-78-0210-D006-19	p 1022	A93-45119
	p 521	N93-20583		p 777	A93-39254	NSC-79-0210-D006-03	p 243	A93-19134
	p 521	N93-20773		p 777	A93-39257	NSC-79-0210-D006-15	p 1087	A93-51738
NAS3-25343	p 233	N93-15116		p 866	A93-42592	NSC-79-0401-E002-34	p 1024	A93-45537
NAS3-25344	p 232	N93-13762		p 869	A93-42629	NSC-79-0404-E002-03	p 439	A93-22968
NAS3-25345	p 187	N93-13735		p 1018	A93-46540	NSC-80-0210-D006-04	p 535	A93-27766
NAS3-25421	p 568	A93-29428		p 1078	A93-49856	NSC-80-0401-E006-39	p 288	A93-23563
NAS3-25423	p 840	N93-27268		p 682	N93-24736	NSC-80-0401-E011-07	p 1151	A93-49017
NAS3-25425	p 1234	A93-55351	NCC2-452	p 287	A93-23533	NSC-81-0210-E002-34	p 1053	A93-48187
NAS3-25450	p 1027	A93-46407		p 467	A93-24863	NSC-81-0401-E002-584	p 1109	A93-49610
NAS3-25653	p 378	A93-23698		p 296	N93-18378	NSC-81-0401-E007-537	p 1149	A93-48277
NAS3-25785	p 560	A93-24781	NCC2-458	p 1007	A93-45152	NSC-82-0210-D006-008	p 1070	A93-49011
NAS3-25820	p 791	N93-27267	NCC2-465	p 298	N93-18781	NSC-82-0401-D006-001	p 1073	A93-49661
NAS3-25950	p 1113	A93-49876	NCC2-478	p 1263	A93-55666	NSCRC-80-0401-E009-04	p 98	A93-13420
NAS3-25952	p 815	N93-27680	NCC2-487	p 377	A93-23035	NSERC-A-1080	p 1133	A93-51434
NAS3-25963	p 1052	A93-48181		p 1078	A93-49856	NSERC-A-5625	p 1133	A93-51434
NAS3-26064	p 287	A93-23387		p 386	N93-18085	NSERC-G-1613	p 974	A93-47196
	p 778	A93-39412		p 295	N93-18086	NSERC-OGPIN-013	p 974	A93-47196
NAS3-26252	p 327	A93-22696	NCC2-498	p 386	A93-23256	NSERC-STREQ-040	p 974	A93-47196
NAS3-26310	p 275	A93-22601	NCC2-505	p 261	A93-20177	NSF ACS-89-58522	p 955	A93-45076
NAS3-26321	p 438	A93-22604		p 1148	A93-48159	NSF ASC-88-58101	p 956	A93-45077
NAS3-26602	p 416	A93-23390	NCC2-520	p 228	A93-17389	NSF ASC-90-05874	p 476	A93-27068
NAS3-26616	p 1115	A93-50008	NCC2-540	p 129	N93-12721	NSF ASC-91-13895	p 476	A93-27068
NAS3-30524	p 426	A93-20591	NCC2-545	p 295	N93-17934	NSF ATM-88-20708	p 1156	A93-50118
NAS3-30854	p 1149	A93-48601	NCC2-553	p 777	A93-39254	NSF ATM-89-05901	p 1261	A93-56236
NAS7-918	p 897	N93-30416	NCC2-555	p 122	A93-14537	NSF ATM-89-09155	p 1159	A93-51528
NAS8-33108	p 413	A93-22265		p 285	A93-23292	NSF ATM-89-14546	p 309	A93-22172
NAS8-35840	p 926	A93-41398	NCC2-573	p 343	A93-22851	NSF ATM-89-19697	p 753	A93-34694
NAS8-36801	p 401	A93-19325	NCC2-575	p 544	A93-27045	NSF ATM-90-01960	p 426	A93-20591
	p 401	A93-19326		p 1097	A93-50643	NSF ATM-90-19969	p 1163	A93-49069
NAS8-36949	p 480	A93-28610		p 708	N93-26549	NSF CBT-87-13833	p 352	A93-18404
	p 788	N93-27464	NCC2-582	p 964	A93-46546	NSF CBT-88-14364	p 928	A93-42920
NAS8-36955	p 91	N93-12401	NCC2-585	p 483	N93-20235	NSF CBT-90-015P	p 270	A93-21658
	p 198	N93-13311	NCC2-605	p 955	A93-45056	NSF CBT-91-0018P	p 1235	A93-55353
NAS8-37351	p 403	A93-19420	NCC2-615	p 707	N93-25261	NSF CDR-88-03012	p 711	A93-34173
NAS8-37400	p 962	A93-46478		p 707	N93-25330		p 816	A93-35959
NAS8-37462	p 812	N93-27115	NCC2-616	p 955	A93-45056		p 1080	A93-50036
NAS8-38609	p 220	N93-14763		p 1148	A93-48159	NSF CTS-87-96352	p 241	A93-17750
NAS8-38867	p 1186	A93-54051	NCC2-624	p 906	A93-41895	NSF CTS-89-06452	p 1220	A93-54053
NAS8-38870	p 403	A93-19420	NCC2-630	p 283	A93-23264	NSF CTS-90-12309	p 1115	A93-49972
NAS9-17885	p 532	A93-27046	NCC2-633	p 735	A93-34510	NSF CTS-90-17181	p 1236	A93-55736
NAS9-17900	p 9	A93-12010	NCC2-653	p 1251	A93-54409	NSF CTS-91-16532	p 968	A93-46826
	p 69	N93-10960	NCC2-657	p 1048	A93-48156	NSF CTS-92-10436	p 1057	A93-48230
	p 914	N93-29652	NCC2-659	p 128	A93-17253	NSF CTS-92-15487	p 1059	A93-48250
NAS9-17952	p 926	A93-41398	NCC2-676	p 539	A93-24755	NSF DDM-90-08451	p 45	A93-13381
NAS9-18880	p 914	N93-29215	NCC2-677	p 129	N93-12721		p 322	A93-18066
NATO-0441/87	p 1070	A93-49002	NCC2-689	p 90	N93-12329		p 323	A93-20279
NAB9RA-H-09087	p 755	N93-25874	NCC2-701	p 990	N93-31855	NSF DDM-90-09597	p 266	A93-20729
NCA2-259	p 277	A93-22625	NCC2-711	p 908	A93-42812	NSF DDM-91-14678	p 266	A93-20729
NCA2-326	p 1177	A93-53212		p 372	N93-17800	NSF DMC-86-15336	p 324	A93-20307
NCA2-485	p 414	A93-22607		p 819	N93-27156	NSF DMR-91-20007	p 409	A93-20644
NCA2-500	p 414	A93-22607	NCC2-716	p 68	N93-12349	NSF DMS-88-10150	p 476	A93-27068
NCA2-512	p 757	A93-34264		p 194	N93-14809	NSF DMS-88-11084	p 62	A93-13247
	p 817	A93-35987		p 382	N93-18520		p 817	A93-37040
NCA2-513	p 264	A93-20199		p 382	N93-18766	NSF DMS-89-07019	p 97	A93-13197
NCA2-522	p 1177	A93-53212	NCC2-729	p 1048	A93-48155		p 817	A93-37044
NCA2-541	p 282	A93-23066	NCC2-746	p 386	A93-23256	NSF DMS-89-19074	p 955	A93-45076
	p 1148	A93-48204	NCC2-747	p 954	A93-45044	NSF DMS-89-22805	p 864	A93-42446

NSF DMS-90-0024P

NSF DMS-90-0024P p 864 A93-42446
NSF DMS-90-07642 p 475 A93-26183
..... p 691 A93-35486
..... p 969 A93-46857
NSF DMS-91-57546 p 27 A93-11367
NSF DPP-87-15809 p 1245 A93-55972
NSF DPP-91-00155 p 556 A93-24213
NSF EAR-89-16323 p 817 A93-37040
NSF ECS-87-04047 p 97 A93-13230
NSF ECS-89-13773 p 96 A93-13078
NSF ECS-90-08947 p 439 A93-22926
NSF ECS-91-09962 p 1167 A93-50638
..... p 1167 A93-50744
NSF ESC-90-15159 p 953 A93-45028
NSF INT-88-14895 p 779 A93-27004
NSF INT-89-22490 p 1033 A93-31876
NSF ISI-88-60898 p 1224 A93-52763
NSF MCS-85-04316 p 1236 A93-55736
NSF MSM-84-51157 p 270 A93-21658
NSF MSM-86-0009P p 482 A93-29774
NSF MSM-87-96352 p 206 A93-14561
NSF MSM-90-08953 p 710 A93-33987
..... p 943 A93-41929
..... p 407 A93-19699
NSF STI-89-02064 p 185 A93-14818
NSG-1157 p 995 A93-45147
..... p 371 A93-16560
NSG-3139 p 751 A93-25884
NSG-3188 p 1084 A93-50278
NSG-3555 p 789 A93-29005
NUTEK-726-91-01071 p 843 A93-28994
NUTEK-90-02278P p 1031 A93-31146
NUTEK-92-01540P p 409 A93-20644
N00014-56-J-0011 p 127 A93-16666
N00014-82-C-0451 p 118 A93-15857
N00014-83-K-0239 p 128 A93-15857
N00014-83-K-0422 p 789 A93-29005
N00014-84-K-0232 p 540 A93-24757
N00014-84-K-0232 p 540 A93-24757
N00014-86-K-0066 p 127 A93-16666
N00014-86-K-0759 p 270 A93-21662
..... p 1177 A93-53209
..... p 27 A93-11367
N00014-87-G-1259 p 1234 A93-55352
N00014-87-K-0174 p 1039 A93-46701
N00014-87-K-0837 p 736 A93-25902
N00014-87-K-2057 p 744 A93-34476
N00014-88-C-0677 p 1178 A93-53216
N00014-88-K-0001 p 1172 A93-49005
N00014-88-K-0592 p 961 A93-45730
N00014-89-J-1221 p 873 A93-43541
N00014-89-J-1275 p 1026 A93-45788
N00014-89-J-1276 p 984 A93-47271
N00014-89-J-1319 p 1178 A93-53216
N00014-89-J-1342 p 270 A93-21662
N00014-89-J-1366 p 1177 A93-53209
..... p 768 A93-37381
N00014-89-J-1400 p 840 A93-27466
N00014-89-J-1670 p 244 A93-19151
N00014-89-J-1836 p 96 A93-13079
N00014-89-K-3113 p 979 A93-47242
N00014-90-C-0047 p 175 A93-14111
N00014-90-C-0089 p 278 A93-22627
N00014-90-J-1169 p 1011 A93-45498
N00014-90-J-1305 p 841 A93-28242
N00014-90-J-1314 p 439 A93-22854
N00014-90-J-1513 p 439 A93-22855
..... p 416 A93-23390
N00014-90-J-1520 p 873 A93-43541
N00014-90-J-1909 p 295 A93-18272
..... p 74 A93-12237
..... p 198 A93-12746
..... p 393 A93-17704
..... p 536 A93-20275
..... p 736 A93-25843
..... p 737 A93-26282
..... p 1019 A93-31795
N00014-91-C-2177 p 1158 A93-50566
N00014-91-J-1072 p 97 A93-13233
N00014-91-J-1086 p 262 A93-20187
..... p 277 A93-22618
..... p 1178 A93-53216
N00014-91-J-1204 p 90 A93-12162
N00014-91-J-1309 p 295 A93-18272
N00014-91-J-1773 p 439 A93-22899
N00014-91-J-1950 p 439 A93-22926
..... p 1020 A93-44168
..... p 1167 A93-50638
..... p 329 A93-16396
N00014-92-C-0059 p 87 A93-11416
N00014-92-J-1062 p 965 A93-46787
N00014-92-J-1148 p 968 A93-46826
N00014-92-J-1406 p 1235 A93-55359
..... p 965 A93-46787
N00014-92-J-1731 p 360 A93-22566
N00014-92-J-4030 p 414 A93-22333
N00039-91-C-0001 p 758 A93-25611

N00123-89-G-0549 p 571 N93-20048
N00123-89-G-0591 p 328 N93-16262
N00140-87-C-6321 p 350 A93-19365
N00140-88-C-0677 p 201 A93-13978
..... p 102 N93-12490
..... p 1065 A93-48319
N00421-88-D-0227 p 799 A93-35991
N00421-91-C-0045 p 1211 A93-53445
N60921-90-C-0033 p 369 A93-22885
N61339-89-C-0045 p 160 N93-12613
N62269-90-0022-5931 p 199 N93-14573
N62269-91-C-0249 p 557 A93-24916
N62271-90-M-3421 p 531 A93-24478
N66001-88-D-0088 p 10 A93-12427
ONERA-21336-SAT-2-CDC p 486 A93-24048
PHS-R49-CCR-302486-06 p 843 N93-28994
PROJ. AU-4093 p 85 N93-10891
RF PROJ. 4502 p 790 N93-27076
RTOP 199-70-12-14 p 885 N93-29588
RTOP 310-10-63-84-02 p 815 N93-27640
RTOP 323-51-60 p 318 N93-16692
RTOP 324-01-00 p 229 N93-13370
RTOP 324-02-01-01 p 499 A93-28152
RTOP 461-6103 p 843 N93-28975
RTOP 50-90-52-01 p 472 A93-24978
RTOP 505-03-10 p 290 N93-16625
..... p 900 N93-29162
..... p 362 N93-16941
RTOP 505-31-42 p 420 N93-17779
RTOP 505-43-31-05 p 286 A93-23351
RTOP 505-52-62 p 138 N93-14791
..... p 129 N93-12721
RTOP 505-59-00 p 292 N93-16940
RTOP 505-59-10-02 p 24 N93-12321
RTOP 505-59-10-03 p 220 N93-14797
RTOP 505-59-10 p 990 N93-32226
..... p 19 N93-10824
RTOP 505-59-30-01 p 22 N93-11610
..... p 700 N93-26085
..... p 989 N93-31733
..... p 779 N93-27032
RTOP 505-59-30-02 p 789 N93-28449
..... p 875 N93-29165
RTOP 505-59-36 p 373 N93-19380
..... p 693 N93-25075
..... p 779 N93-27005
RTOP 505-59-40-03 p 298 N93-19015
RTOP 505-59-50-01 p 780 N93-27067
RTOP 505-59-50-05 p 136 N93-14451
RTOP 505-59-53 p 1038 N93-32224
RTOP 505-59-85-01 p 418 N93-16379
RTOP 505-59-86-02 p 291 N93-16710
..... p 747 N93-25087
..... p 989 N93-31732
RTOP 505-60-01-02 p 875 N93-29449
RTOP 505-61-01-01 p 108 A93-14819
RTOP 505-61-51 p 568 A93-29433
..... p 64 A93-10741
..... p 139 N93-15483
RTOP 505-61-52 p 973 A93-47189
RTOP 505-61-59-76 p 876 N93-29450
RTOP 505-62-OK p 222 N93-15343
..... p 838 N93-26999
RTOP 505-62-00 p 791 N93-27267
RTOP 505-62-10 p 361 A93-23384
..... p 1194 A93-53980
..... p 60 N93-12418
..... p 751 N93-25884
..... p 840 N93-27268
..... p 815 N93-28609
..... p 816 N93-28617
..... p 900 N93-29072
..... p 1032 N93-31846
..... p 1005 N93-32351
..... p 1005 N93-32368
RTOP 505-62-20 p 111 A93-14118
..... p 82 N93-10087
RTOP 505-62-21 p 90 N93-12277
..... p 290 N93-16596
..... p 551 N93-20057
..... p 677 N93-24760
..... p 677 N93-25134
..... p 838 N93-27088
..... p 874 N93-29160
RTOP 505-62-30-01 p 520 A93-27801
RTOP 505-62-40 p 294 N93-17884
..... p 817 A93-37004
..... p 1108 A93-49329
..... p 1206 A93-54268
..... p 65 N93-12305
..... p 180 N93-15525
..... p 527 N93-21197
..... p 721 N93-25079
..... p 819 N93-26907
..... p 848 N93-28051
..... p 841 N93-28053

CONTRACT NUMBER INDEX

RTOP 505-62-51 p 723 N93-25673
RTOP 505-62-52 p 403 A93-19416
..... p 1093 A93-52006
..... p 21 N93-11223
..... p 60 N93-12077
..... p 231 N93-12967
..... p 228 N93-13154
..... p 179 N93-15521
..... p 441 N93-16613
..... p 721 N93-24754
..... p 693 N93-24911
..... p 721 N93-25106
..... p 838 N93-27020
..... p 781 N93-27097
..... p 813 N93-27130
..... p 814 N93-27610
..... p 930 N93-29157
..... p 1032 N93-31647
..... p 988 N93-31648
..... p 989 N93-31672
..... p 989 N93-31839
..... p 1032 N93-31860
RTOP 505-62-53 p 550 N93-19971
RTOP 505-62-84 p 194 N93-15498
..... p 730 N93-25080
..... p 737 N93-26201
..... p 834 N93-30374
RTOP 505-63-01-11 p 220 N93-14799
RTOP 505-63-1B p 17 N93-10349
RTOP 505-63-21-01 p 508 A93-27971
RTOP 505-63-36-01 p 508 A93-27972
..... p 553 N93-20585
..... p 514 N93-21310
RTOP 505-63-36-06 p 325 A93-20369
..... p 47 N93-10968
RTOP 505-63-36 p 212 N93-12736
..... p 838 N93-27069
..... p 839 N93-27133
..... p 555 N93-21831
RTOP 505-63-5B p 91 N93-12411
RTOP 505-63-50-04 p 442 N93-18332
RTOP 505-63-50-06 p 392 N93-16537
RTOP 505-63-50-08 p 480 A93-29175
RTOP 505-63-50-12 p 701 N93-26134
..... p 162 N93-13565
RTOP 505-63-50-15 p 513 N93-20584
RTOP 505-63-50 p 780 N93-27084
..... p 806 N93-27258
..... p 895 N93-29885
RTOP 505-63-513 p 552 N93-20368
RTOP 505-63-51 p 567 A93-29420
RTOP 505-63-53-01 p 219 N93-14483
RTOP 505-63-53 p 742 A93-34157
..... p 421 N93-18426
..... p 98 N93-12346
RTOP 505-64-10-07 p 99 N93-12538
..... p 65 N93-12304
RTOP 505-64-10-10 p 144 N93-14844
RTOP 505-64-12-01 p 488 N93-19590
..... p 1000 N93-32223
RTOP 505-64-13-01 p 344 N93-18408
..... p 707 N93-26087
RTOP 505-64-13-12 p 718 N93-24764
RTOP 505-64-13-22 p 942 N93-29192
RTOP 505-64-13-23 p 343 N93-16693
RTOP 505-64-13-32 p 338 N93-18333
RTOP 505-64-13 p 1099 A93-51967
..... p 36 N93-12320
..... p 808 N93-28621
..... p 1000 N93-32218
RTOP 505-64-20-01 p 63 N93-10070
RTOP 505-64-30-01 p 373 N93-19108
..... p 1010 N93-32380
RTOP 505-64-36 p 317 A93-21525
..... p 35 N93-10745
..... p 516 N93-21810
..... p 706 N93-24914
..... p 994 N93-32225
..... p 994 N93-32348
RTOP 505-64-52-01 p 64 N93-11176
..... p 820 N93-27264
RTOP 505-64-52-03 p 64 N93-12216
..... p 186 N93-13367
..... p 885 N93-29653
RTOP 505-64-52 p 189 N93-15366
RTOP 505-66-01-02 p 948 A93-46608
RTOP 505-66-11 p 1190 A93-52881
..... p 779 N93-26899
RTOP 505-68-01-02 p 90 N93-12197
RTOP 505-68-1C p 309 A93-23239
RTOP 505-68-10 p 282 A93-23240
..... p 327 A93-23242
..... p 309 A93-23243
..... p 310 A93-23244
..... p 310 A93-23245
..... p 361 A93-23246

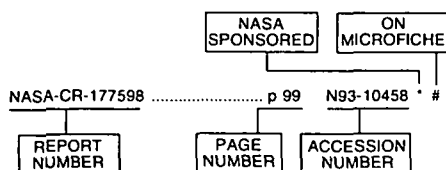
	p 188	N93-14831		p 200	N93-15504
	p 138	N93-14911		p 844	N93-27012
	p 139	N93-15338	RTOP 537-01-20-01	p 94	N93-12299
	p 148	N93-15345	RTOP 537-01-22-01	p 330	N93-16947
	p 148	N93-15354		p 330	N93-16999
	p 148	N93-15360	RTOP 537-01-22	p 55	A93-13383
	p 149	N93-15522	RTOP 537-02-00	p 1200	A93-54040
RTOP 505-68-30-03	p 131	N93-13353		p 1004	N93-31671
RTOP 505-68-30-04	p 22	N93-11622	RTOP 537-02-20	p 179	N93-15359
RTOP 505-68-30	p 344	N93-19110		p 746	N93-24759
RTOP 505-68-32	p 59	N93-11530		p 815	N93-27680
	p 722	N93-25129	RTOP 537-02-21	p 812	N93-27026
	p 700	N93-26099		p 813	N93-27128
	p 813	N93-27131		p 814	N93-27160
	p 900	N93-29065	RTOP 537-02-22	p 760	N93-26551
RTOP 505-68-40	p 339	N93-18616	RTOP 537-02-23	p 452	A93-23241
	p 518	N93-20163		p 233	N93-15430
RTOP 505-68-50	p 51	A93-11281		p 233	N93-15575
RTOP 505-68-52	p 381	N93-16753		p 291	N93-16704
RTOP 505-68-71	p 25	N93-12353		p 678	N93-26136
RTOP 505-68-84	p 1255	A93-54398	RTOP 537-03-20	p 1005	N93-32220
RTOP 505-69-20-01	p 109	N93-13025	RTOP 537-03-21-03	p 102	N93-11620
	p 378	N93-15790		p 453	N93-16755
RTOP 505-69-50	p 323	A93-20281		p 852	N93-27271
	p 440	A93-23699		p 852	N93-27272
	p 56	N93-10983		p 852	N93-28692
	p 60	N93-12402	RTOP 537-03-23-03	p 780	N93-27096
	p 699	N93-25883	RTOP 538-01-10	p 519	A93-25997
	p 1033	N93-32212		p 55	N93-10456
RTOP 505-70-62-06	p 693	N93-25074	RTOP 553-13-00	p 212	N93-12735
RTOP 505-70-64-01	p 65	N93-12413	RTOP 584-03-11	p 838	N93-27132
RTOP 505-90-00	p 694	N93-25091	RTOP 590-13-11	p 195	A93-13824
RTOP 505-90-11	p 877	N93-30373	RTOP 590-14-61-01	p 88	N93-11544
RTOP 505-90-21-02	p 934	N93-30375	RTOP 590-21-11	p 421	N93-18321
RTOP 505-90-51-01	p 1264	A93-55852		p 421	N93-18380
RTOP 505-90-52-01	p 6	A93-10533		p 364	N93-18578
	p 452	A93-23744	RTOP 677-21-36	p 426	A93-20621
	p 476	A93-27068	RTOP 677-21-40	p 426	A93-20621
	p 1236	A93-55736	RTOP 694-03-0A	p 935	N93-31031
	p 102	N93-12021	RTOP 694-03-0C	p 110	N93-15573
	p 231	N93-12986	RTOP 763-01-21	p 179	N93-15342
	p 290	N93-16627	RTOP 763-21-51	p 223	N93-13288
	p 298	N93-18771	RTOP 763-23-41	p 718	N93-26553
	p 694	N93-25083	RTOP 763-23-45-86	p 1019	N93-31643
	p 758	N93-25084	RTOP 906-11-00	p 196	N93-14495
	p 694	N93-25153	RTOP 906-11-01-01	p 1017	N93-32379
	p 847	N93-27063	SERC-GR/D/21189	p 375	A93-19392
RTOP 505-90-53-02	p 780	N93-27090	SERC-GR/E/28062	p 375	A93-19392
RTOP 506-40-21	p 757	N93-25073	SERC-GR/E/77039	p 270	A93-21720
RTOP 506-40-41-01	p 420	N93-18093	SERC-GR/E/89056	p 437	A93-20740
RTOP 506-40-41	p 875	N93-29166		p 870	A93-42633
RTOP 506-40-41	p 305	N93-19379	SERC-GR/F/58288	p 33	A93-11095
RTOP 506-40-71-04	p 552	N93-20299	SERC-GR/G/2586/3	p 173	A93-14608
RTOP 506-40-91-01	p 222	N93-15434	SERC-GR/H/23368	p 938	A93-42556
	p 747	N93-25176	SERC-GR/H/26390	p 978	A93-47227
	p 840	N93-27250	SLS42B/590	p 787	N93-27460
RTOP 506-42-31	p 914	N93-29194	SMD097865	p 289	N93-16470
RTOP 506-43-31-04	p 69	N93-12447	SRC-GR/D/53029	p 932	N93-29954
RTOP 506-48-11-04	p 458	N93-19976	STW-GWI27.0277	p 1031	N93-31519
RTOP 506-62-31	p 1006	N93-32374	SWRI PROJ. 12-2301	p 719	N93-25909
RTOP 509-10-11	p 1031	N93-31193	TFR-91-402	p 789	N93-29005
RTOP 510-01-50	p 85	N93-10963	UF PROJ. 4910451123312	p 93	N93-11702
	p 88	N93-11624	W-31-109-ENG-38	p 434	N93-18587
RTOP 510-02-11	p 921	N93-30841		p 732	N93-26498
RTOP 510-02-12	p 825	N93-27092		p 843	N93-28943
RTOP 510-06-50	p 825	N93-26702		p 943	N93-29189
RTOP 532-06-37-03	p 1019	N93-32234	W-7405-ENG-36	p 89	N93-11767
RTOP 533-02-11	p 49	N93-11863		p 215	N93-13321
RTOP 533-02-35	p 806	N93-28693	W-7405-ENG-48	p 937	N93-30487
RTOP 533-02-36	p 38	A93-11276		p 955	A93-45076
	p 39	A93-11278		p 224	N93-13655
	p 175	N93-13155		p 453	N93-17225
RTOP 533-02-38	p 22	N93-11532	W-7405-ENG-82	p 791	N93-28571
	p 25	N93-12353		p 396	A93-18611
	p 131	N93-13322		p 407	A93-19595
RTOP 533-02-39	p 20	N93-11221		p 749	N93-25518
RTOP 533-02-51	p 910	N93-30764			
RTOP 533-05-01	p 917	N93-29451			
RTOP 535-03-01	p 724	N93-26161			
RTOP 535-03-10-01	p 788	N93-28070			
RTOP 535-03-10	p 361	A93-23324			
	p 101	N93-11370			
	p 174	N93-12695			
	p 179	N93-15403			
	p 362	N93-16705			
	p 362	N93-16715			
	p 521	N93-20583			
	p 521	N93-20773			
	p 752	N93-26202			
	p 852	N93-27058			
	p 852	N93-27148			
RTOP 535-03-11-03	p 102	N93-12080			
RTOP 535-05-10	p 130	N93-13292			
	p 110	N93-14102			
	p 816	N93-28697			
RTOP 537-01-11	p 390	A93-23238			

REPORT NUMBER INDEX

AERONAUTICAL ENGINEERING / A Continuing Bibliography
1993 Cumulative Index

February 1994

Typical Report Number Index Listing



Listings in this index are arranged alphanumerically by report number. The page number indicates the page on which the citation is located. The accession number denotes the number by which the citation is identified. An asterisk (*) indicates that the item is a NASA report. A pound sign (#) indicates that the item is available on microfiche.

A-90110 p 139 N93-15483 * #
A-90195 p 1006 N93-32374 * #
A-90275 p 293 N93-16942 * #
A-91175 p 64 N93-10741 * #
A-91241 p 35 N93-10745 * #
A-92020 p 857 N93-30673 * #
A-92063 p 456 N93-16652 * #
A-92094 p 305 N93-19379 * #
A-92099 p 1033 N93-32212 * #
A-92139 p 516 N93-21810 * #
A-92143 p 99 N93-10458 * #
A-92158 p 36 N93-12320 * #
A-92159 p 129 N93-12721 * #
A-92160 p 694 N93-25091 * #
A-92173 p 373 N93-19380 * #
A-92198 p 885 N93-29653 * #
A-93012 p 990 N93-32226 * #
A-93020 p 240 N93-17883 * #
A-93033 p 994 N93-32225 * #
A-93040 p 700 N93-26099 * #
A-93044 p 706 N93-24914 * #
A-93046 p 790 N93-27076 * #
A-93049 p 571 N93-19970 * #
A-93050 p 693 N93-25075 * #
A-93061 p 708 N93-26549 * #
A-93087 p 994 N93-32348 * #

AAS PAPER 91-607 p 1250 A93-55841
AAS PAPER 91-639 p 1247 A93-55816
AAS PAPER 91-640 p 1247 A93-55817
AAS PAPER 91-653 p 1252 A93-55825

AD-A246883 p 98 N93-11463 #
AD-A247035 p 22 N93-11742 #
AD-A247258 p 21 N93-11464 #
AD-A248021 p 29 N93-12489 #
AD-A248459 p 87 N93-11416 #
AD-A249068 p 74 N93-12248 #
AD-A249129 p 35 N93-10323 #
AD-A249133 p 89 N93-11760 #
AD-A250688 p 102 N93-12490 #
AD-A250697 p 49 N93-11838 #
AD-A252243 p 24 N93-12179 #
AD-A252495 p 35 N93-10065 #
AD-A253146 p 17 N93-10340 #
AD-A253210 p 17 N93-10375 #
AD-A253447 p 17 N93-10342 #
AD-A253547 p 98 N93-12258 #
AD-A253592 p 19 N93-10648 #
AD-A253792 p 24 N93-12063 #
AD-A253859 p 93 N93-11144 #
AD-A253880 p 19 N93-10811 #
AD-A253967 p 71 N93-10717 #
AD-A254108 p 19 N93-10856 #
AD-A254110 p 69 N93-11798 #

AD-A254111 p 19 N93-10858 #
AD-A254258 p 68 N93-11751 #
AD-A254285 p 47 N93-10842 #
AD-A254295 p 72 N93-10843 #
AD-A254312 p 72 N93-10770 #
AD-A254323 p 186 N93-12959 #
AD-A254410 p 159 N93-12605 #
AD-A254484 p 195 N93-12575 #
AD-A254489 p 90 N93-12162 #
AD-A254537 p 159 N93-12602 #
AD-A254569 p 193 N93-13882 #
AD-A254595 p 160 N93-12613 #
AD-A254596 p 186 N93-12578 #
AD-A254603 p 74 N93-12237 #
AD-A254704 p 198 N93-12746 #
AD-A254725 p 90 N93-12340 #
AD-A254810 p 160 N93-12752 #
AD-A254958 p 192 N93-12552 #
AD-A254963 p 228 N93-12554 #
AD-A254968 p 212 N93-12555 #
AD-A255065 p 50 N93-12485 #
AD-A255070 p 110 N93-13946 #
AD-A255071 p 50 N93-12488 #
AD-A255226 p 175 N93-14111 #
AD-A255272 p 165 N93-15004 #
AD-A255276 p 152 N93-15005 #
AD-A255319 p 224 N93-14547 #
AD-A255332 p 194 N93-14559 #
AD-A255366 p 165 N93-15227 #
AD-A255379 p 110 N93-14549 #
AD-A255397 p 220 N93-14677 #
AD-A255527 p 187 N93-13872 #
AD-A255548 p 164 N93-14571 #
AD-A255622 p 104 N93-11710 #
AD-A255629 p 104 N93-10610 #
AD-A255660 p 194 N93-14128 #
AD-A255703 p 143 N93-14024 #
AD-A255728 p 221 N93-15065 #
AD-A255746 p 229 N93-15052 #
AD-A255766 p 143 N93-14026 #
AD-A255769 p 224 N93-14655 #
AD-A255796 p 329 N93-16396 #
AD-A255797 p 149 N93-15390 #
AD-A255963 p 232 N93-14406 #
AD-A255967 p 219 N93-14400 #
AD-A256015 p 391 N93-15931 #
AD-A256038 p 221 N93-15187 #
AD-A256060 p 137 N93-14661 #
AD-A256126 p 199 N93-15189 #
AD-A256131 p 163 N93-14248 #
AD-A256134 p 218 N93-14254 #
AD-A256194 p 170 N93-15235 #
AD-A256212 p 165 N93-15238 #
AD-A256246 p 199 N93-14573 #
AD-A256304 p 136 N93-14441 #
AD-A256311 p 139 N93-15245 #
AD-A256317 p 392 N93-16403 #
AD-A256319 p 329 N93-16404 #
AD-A256374 p 35 N93-10459 #
AD-A256434 p 179 N93-15337 #
AD-A256444 p 188 N93-14608 #
AD-A256445 p 164 N93-14601 #
AD-A256450 p 219 N93-14610 #
AD-A256503 p 36 N93-11704 #
AD-A256522 p 189 N93-15396 #
AD-A256560 p 221 N93-14805 #
AD-A256569 p 371 N93-16165 #
AD-A256593 p 194 N93-14238 #
AD-A256613 p 188 N93-14252 #
AD-A256614 p 151 N93-14275 #
AD-A256615 p 152 N93-14276 #
AD-A256616 p 143 N93-14277 #
AD-A256650 p 440 N93-16500 #
AD-A256724 p 361 N93-15979 #
AD-A256725 p 453 N93-15980 #
AD-A256802 p 288 N93-15889 #
AD-A256827 p 391 N93-15686 #
AD-A256831 p 223 N93-15635 #
AD-A256836 p 235 N93-15637 #
AD-A256921 p 328 N93-16186 #
AD-A256995 p 328 N93-16262 #
AD-A257025 p 165 N93-15361 #
AD-A257028 p 36 N93-11705 #

AD-A257106 p 231 N93-12986 * #
AD-A257291 p 361 N93-16080 #
AD-A257300 p 288 N93-15920 #
AD-A257329 p 317 N93-15988 #
AD-A257343 p 289 N93-16157 #
AD-A257382 p 418 N93-15857 #
AD-A257384 p 328 N93-15858 #
AD-A257474 p 332 N93-17660 #
AD-A257595 p 372 N93-18193 #
AD-A257640 p 363 N93-17686 #
AD-A257658 p 382 N93-17793 #
AD-A257683 p 381 N93-17687 #
AD-A257737 p 240 N93-17666 #
AD-A257746 p 372 N93-17670 #
AD-A257747 p 393 N93-17693 #
AD-A257751 p 332 N93-17694 #
AD-A257754 p 363 N93-17695 #
AD-A257780 p 240 N93-17732 #
AD-A257854 p 338 N93-18304 #
AD-A257855 p 420 N93-18305 #
AD-A257860 p 319 N93-18309 #
AD-A257877 p 296 N93-18336 #
AD-A257901 p 338 N93-18339 #
AD-A257945 p 420 N93-18121 #
AD-A257961 p 339 N93-18451 #
AD-A257965 p 382 N93-17734 #
AD-A257974 p 213 N93-13199 #
AD-A258019 p 294 N93-17819 #
AD-A258038 p 393 N93-17704 #
AD-A258050 p 382 N93-17708 #
AD-A258055 p 392 N93-17676 #
AD-A258058 p 293 N93-17756 #
AD-A258059 p 293 N93-17677 #
AD-A258084 p 333 N93-17893 #
AD-A258143 p 455 N93-18087 #
AD-A258209 p 319 N93-18202 #
AD-A258212 p 142 N93-12816 #
AD-A258346 p 295 N93-17991 #
AD-A258383 p 338 N93-18257 #
AD-A258441 p 456 N93-17890 #
AD-A258444 p 455 N93-17891 #
AD-A258463 p 393 N93-18242 #
AD-A258468 p 344 N93-18270 #
AD-A258470 p 337 N93-18248 #
AD-A258471 p 295 N93-18272 #
AD-A258507 p 571 N93-20048 #
AD-A258593 p 502 N93-19966 #
AD-A258630 p 551 N93-19999 #
AD-A258667 p 192 N93-12902 #
AD-A258673 p 571 N93-20388 #
AD-A258678 p 572 N93-20389 #
AD-A258679 p 572 N93-20390 #
AD-A258746 p 572 N93-20403 #
AD-A258760 p 495 N93-19867 #
AD-A258799 p 340 N93-18981 #
AD-A258822 p 365 N93-18997 #
AD-A258827 p 341 N93-19089 #
AD-A258841 p 443 N93-19112 #
AD-A258842 p 305 N93-19364 #
AD-A258846 p 320 N93-19067 #
AD-A258904 p 373 N93-19351 #
AD-A258912 p 365 N93-19356 #
AD-A258915 p 443 N93-19338 #
AD-A258917 p 305 N93-19340 #
AD-A258931 p 510 N93-19447 #
AD-A258973 p 365 N93-19093 #
AD-A258975 p 373 N93-19095 #
AD-A258988 p 240 N93-18867 #
AD-A259012 p 339 N93-18895 #
AD-A259019 p 424 N93-19101 #
AD-A259023 p 319 N93-18951 #
AD-A259039 p 340 N93-18999 #
AD-A259044 p 340 N93-18896 #
AD-A259062 p 319 N93-18927 #
AD-A259137 p 527 N93-20596 #
AD-A259140 p 513 N93-20575 #
AD-A259141 p 513 N93-20560 #
AD-A259191 p 536 N93-20275 #
AD-A259205 p 527 N93-20551 #
AD-A259220 p 530 N93-20576 #
AD-A259240 p 513 N93-20579 #
AD-A259249 p 502 N93-20582 #
AD-A259262 p 513 N93-20605 #

REPORT

AD-A259286

REPORT NUMBER INDEX

AD-A259286	p 510	N93-19849	#	AD-A262740	p 826	N93-28592	#	AD-D015606	p 483	N93-20017
AD-A259292	p 572	N93-20611	#	AD-A262747	p 917	N93-29402	#	AD-D015607	p 554	N93-20772
AD-A259329	p 519	N93-21259	#	AD-A262830	p 885	N93-29468	#	AD-D015668	p 708	N93-26093
AD-A259401	p 530	N93-21268	#	AD-A262878	p 825	N93-28226	#	AD-D015712	p 909	N93-29278
AD-A259407	p 503	N93-21671	#	AD-A262930	p 842	N93-28289	#	AERO-REPT-9108	p 454	N93-16563
AD-A259473	p 513	N93-20245	#	AD-A263049	p 930	N93-29141	#	AERO-REPT-9109	p 240	N93-16465
AD-A259594	p 502	N93-20582	#	AD-A263067	p 793	N93-27925	#	AERO-REPT-9111	p 456	N93-16464
AD-A259605	p 290	N93-16627	#	AD-A263073	p 788	N93-27955	#	AERO-REPT-9112	p 289	N93-16467
AD-A259931	p 212	N93-12736	#	AD-A263100	p 914	N93-29134	#	AERO-REPT-9113	p 381	N93-16468
AD-A259994	p 694	N93-25083	#	AD-A263135	p 707	N93-25456	#	AERO-REPT-9201	p 337	N93-18131
AD-A260010	p 417	N93-15698	#	AD-A263138	p 943	N93-29480	#	AERO-REPT-9203-VOL-2	p 289	N93-16470
AD-A260011	p 192	N93-12668	#	AD-A263171	p 793	N93-28990	#	AERO-REPT-9204	p 484	N93-20806
AD-A260041	p 569	N93-21317	#	AD-A263172	p 942	N93-29490	#	AERO-REPT-9205	p 484	N93-20807
AD-A260221	p 318	N93-16841	#	AD-A263385	p 936	N93-29257	#	AERO-REPT-9209	p 420	N93-18103
AD-A260295	p 516	N93-21810	#	AD-A263395	p 931	N93-29851	#	AESO-2-90-REV	p 725	N93-26339
AD-A260529	p 232	N93-14912	#	AD-A263433	p 911	N93-29815	#	AFESC/ESL-TR-88-79	p 731	N93-25656
AD-A260578	p 736	N93-25902	#	AD-A263436	p 911	N93-29788	#	AFIT/CI/CIA-92-019D	p 333	N93-17893
AD-A260681	p 699	N93-25894	#	AD-A263481	p 705	N93-25224	#	AFIT/CI/CIA-92-067	p 72	N93-10770
AD-A260689	p 759	N93-25649	#	AD-A263513	p 933	N93-29968	#	AFIT/ENY/GAE/92D-09	p 305	N93-19364
AD-A260692	p 736	N93-25895	#	AD-A263514	p 933	N93-29969	#	AFIT/GA/ENG/92J-01-VOL-2	p 371	N93-16165
AD-A260695	p 705	N93-25896	#	AD-A263515	p 897	N93-29971	#	AFIT/GA/ENG/92J-01	p 188	N93-14608
AD-A260703	p 759	N93-25651	#	AD-A263579	p 912	N93-29972	#	AFIT/GAE/ENY/92D-08	p 373	N93-19095
AD-A260709	p 736	N93-25843	#	AD-A263597	p 917	N93-29981	#	AFIT/GAE/ENY/92D-10	p 341	N93-19089
AD-A260727	p 731	N93-25656	#	AD-A263612	p 875	N93-29284	#	AFIT/GAE/ENY/92D-11	p 305	N93-19340
AD-A260740	p 755	N93-25645	#	AD-A263617	p 880	N93-29286	#	AFIT/GAE/ENY/92D-14	p 443	N93-19112
AD-A260752	p 719	N93-25909	#	AD-A263650	p 931	N93-29388	#	AFIT/GAE/ENY/92D-17	p 373	N93-19351
AD-A260762	p 755	N93-25837	#	AD-A263665	p 706	N93-25243	#	AFIT/GAE/ENY/92D-19	p 365	N93-18997
AD-A260763	p 298	N93-18771	#	AD-A263703	p 943	N93-29384	#	AFIT/GAE/ENY/92D-21	p 365	N93-19093
AD-A260767	p 724	N93-25917	#	AD-A263707	p 909	N93-29985	#	AFIT/GAE/ENY/92D-22	p 340	N93-18896
AD-A260830	p 719	N93-25783	#	AD-A263727	p 905	N93-30877	#	AFIT/GAE/ENY/92D-23	p 424	N93-19101
AD-A260838	p 717	N93-25933	#	AD-A263879	p 876	N93-29919	#	AFIT/GAE/ENY/92D-24	p 513	N93-20575
AD-A260890	p 751	N93-25912	#	AD-A263905	p 876	N93-29862	#	AFIT/GAE/ENY/92M-01	p 188	N93-14252
AD-A260915	p 736	N93-25914	#	AD-A264057	p 876	N93-29891	#	AFIT/GCE/ENG/92D-07	p 513	N93-20560
AD-A260934	p 760	N93-25915	#	AD-A264075	p 910	N93-30604	#	AFIT/GCM/LSY/92-6	p 455	N93-18087
AD-A260941	p 724	N93-26219	#	AD-A264111	p 1033	N93-32028	#	AFIT/GCS/ENG/92D-02	p 443	N93-19338
AD-A261054	p 708	N93-26237	#	AD-A264115	p 877	N93-30119	#	AFIT/GCS/ENG/92D-17	p 530	N93-20576
AD-A261060	p 678	N93-26238	#	AD-A264120	p 880	N93-30194	#	AFIT/GCS/ENG/92D-23	p 572	N93-20611
AD-A261063	p 725	N93-26239	#	AD-A264151	p 877	N93-30171	#	AFIT/GCS/ENG/93M-03	p 849	N93-28577
AD-A261112	p 522	N93-21316	#	AD-A264152	p 877	N93-30172	#	AFIT/GCS/ENG/93M-04	p 823	N93-28467
AD-A261165	p 737	N93-25948	#	AD-A264153	p 877	N93-30173	#	AFIT/GE/ENG/92D-19	p 527	N93-20596
AD-A261189	p 718	N93-25949	#	AD-A264154	p 877	N93-30151	#	AFIT/GE/ENG/92D-37	p 319	N93-18951
AD-A261203	p 755	N93-26243	#	AD-A264302	p 1019	N93-32085	#	AFIT/GLM/LSM/92S-9	p 240	N93-18887
AD-A261213	p 717	N93-25733	#	AD-A264333	p 934	N93-30369	#	AFIT/GSE/ENY/92D-03	p 365	N93-19356
AD-A261231	p 764	N93-27056	#	AD-A264414	p 1018	N93-31192	#	AFIT/GSO/ENS/92D-9	p 320	N93-19067
AD-A261233	p 705	N93-26263	#	AD-A264521	p 934	N93-30406	#	AFL-RN-92-11-78	p 934	N93-30369
AD-A261253	p 496	N93-21856	#	AD-A264682	p 909	N93-30550	#	AFOSS-TR-93-0073	p 737	N93-25948
AD-A261270	p 496	N93-21557	#	AD-A264687	p 935	N93-30553	#	AFOSS-92-0154TR	p 22	N93-11742
AD-A261296	p 752	N93-26564	#	AD-A264693	p 935	N93-30571	#	AFOSS-92-0675TR	p 17	N93-10340
AD-A261300	p 759	N93-26294	#	AD-A264704	p 909	N93-30498	#	AFOSS-92-0692TR	p 24	N93-12063
AD-A261366	p 725	N93-26335	#	AD-A264784	p 935	N93-30611	#	AFOSS-92-0728TR	p 98	N93-12258
AD-A261374	p 725	N93-26339	#	AD-A264938	p 677	N93-24760	#	AFOSS-92-0740TR	p 195	N93-12575
AD-A261376	p 485	N93-21796	#	AD-A265028	p 704	N93-25110	#	AFOSS-92-0783TR	p 186	N93-12959
AD-A261377	p 559	N93-21799	#	AD-A265066	p 779	N93-27004	#	AFOSS-92-0787TR	p 71	N93-10717
AD-A261410	p 708	N93-26447	#	AD-A265068	p 752	N93-26160	#	AFOSS-92-0804TR	p 72	N93-10843
AD-A261488	p 760	N93-26343	#	AD-A265214	p 990	N93-32004	#	AFOSS-92-0807TR	p 47	N93-10842
AD-A261613	p 752	N93-26167	#	AD-A265290	p 677	N93-25134	#	AFOSS-92-0864TR	p 219	N93-14400
AD-A261614	p 678	N93-26168	#	AD-A265451	p 1019	N93-31795	#	AFOSS-92-0894TR	p 391	N93-15931
AD-A261654	p 701	N93-26195	#	AD-A265551	p 1015	N93-31916	#	AFOSS-93-0102TR	p 760	N93-26343
AD-A261656	p 729	N93-26196	#	AD-A266070	p 791	N93-28055	#	AFOSS-93-0126TR-VOL-16	p 945	N93-29396
AD-A261714	p 737	N93-26371	#	AD-A266273	p 791	N93-27269	#	AFOSS-93-0137TR	p 737	N93-26268
AD-A261742	p 737	N93-26282	#	AD-A266302	p 842	N93-28555	#	AFOSS-93-0142TR	p 725	N93-26335
AD-A261785	p 760	N93-26566	#	AD-A266375	p 751	N93-25884	#	AFOSS-93-0187TR	p 848	N93-28498
AD-A261786	p 752	N93-26526	#	AD-A266406	p 840	N93-27268	#	AFOSS-93-0194TR	p 930	N93-29141
AD-A261800	p 718	N93-26444	#	AD-A266538	p 839	N93-27133	#	AFOSS-93-0207TR	p 934	N93-30369
AD-A261809	p 730	N93-26260	#	AD-A266817	p 1004	N93-31741	#	AFOSS-93-0325TR	p 909	N93-30550
AD-A261813	p 737	N93-26268	#	AD-A267027	p 843	N93-28975	#	AGARD-AG-300-VOL-11	p 514	N93-21305
AD-A261833	p 708	N93-26274	#	AD-A267175	p 841	N93-28054	#	AGARD-AR-308	p 176	N93-14890
AD-A261925	p 701	N93-26198	#	AD-A267676	p 793	N93-28625	#	AGARD-AR-313	p 496	N93-21187
AD-A261964	p 503	N93-21759	#	AD-B131156L	p 848	N93-27531	#	AGARD-CP-498	p 213	N93-13199
AD-A261970	p 825	N93-27667	#	AD-B131157L	p 848	N93-27589	#	AGARD-CP-519	p 510	N93-19901
AD-A261978	p 911	N93-29436	#	AD-B131158L	p 848	N93-27590	#	AGARD-CP-527	p 901	N93-29926
AD-A262024	p 945	N93-29396	#	AD-B156202L	p 876	N93-29450	#	AGARD-CP-532	p 490	N93-19653
AD-A262027	p 502	N93-20164	#	AD-B168787L	p 999	N93-32205	#	AGARD-INDEX-89-91	p 104	N93-10610
AD-A262050	p 816	N93-28984	#	AD-B168788L	p 994	N93-32337	#	AGARD-R-766-ADD	p 1004	N93-31741
AD-A262062	p 809	N93-29004	#	AD-B168789L	p 1020	N93-32385	#			
AD-A262076	p 823	N93-28189	#	AD-B168790L	p 1006	N93-32372	#			
AD-A262092	p 815	N93-28184	#	AD-B168791L	p 1003	N93-31111	#			
AD-A262118	p 845	N93-27675	#	AD-B168792L	p 990	N93-32357	#			
AD-A262127	p 753	N93-24875	#	AD-B169113L	p 990	N93-32358	#			
AD-A262138	p 820	N93-27546	#	AD-B169203L	p 999	N93-32203	#			
AD-A262151	p 806	N93-27547	#	AD-B169204L	p 1001	N93-32332	#			
AD-A262152	p 559	N93-21501	#	AD-B169205L	p 999	N93-32416	#			
AD-A262236	p 841	N93-28242	#	AD-B169208L	p 999	N93-31840	#			
AD-A262281	p 815	N93-27679	#	AD-B169597L	p 999	N93-32338	#			
AD-A262299	p 806	N93-27692	#	AD-B169664L	p 1006	N93-32386	#			
AD-A262363	p 789	N93-28493	#	AD-B169726L	p 569	N93-20546	#			
AD-A262373	p 806	N93-27694	#	AD-D015351	p 20	N93-11050	#			
AD-A262374	p 848	N93-28498	#	AD-D015359	p 199	N93-13414	#			
AD-A262405	p 893	N93-29409	#	AD-D015392	p 222	N93-15232	#			
AD-A262477	p 875	N93-29410	#	AD-D015464	p 371	N93-16463	#			
AD-A262482	p 852	N93-27662	#	AD-D015531	p 554	N93-20765	#			
AD-A262494	p 765	N93-28576	#	AD-D015596	p 554	N93-20790	#			
AD-A262566	p 849	N93-28577	#	AD-D015599	p 536	N93-20247	#			
AD-A262568	p 823	N93-28467	#	AD-D015604	p 535	N93-20016	#			
AD-A262599	p 815	N93-28391	#							
AD-A262685										

REPORT NUMBER INDEX

AIAA PAPER 93-0173

AGARD-R-777	p 104	N93-11710	#	AIAA PAPER 92-4253	p 80	A93-13343	#	AIAA PAPER 92-5054	p 359	A93-22325	#
AIAA PAPER 89-3064	p 938	A93-41296	#	AIAA PAPER 92-4254	p 15	A93-13342	#	AIAA PAPER 92-5058	p 385	A93-22328	#
AIAA PAPER 92-0089	p 541	A93-24979	#	AIAA PAPER 92-4256	p 570	A93-24296	#	AIAA PAPER 92-5060	p 413	A93-22330	#
AIAA PAPER 92-2634	p 693	N93-24911	#	AIAA PAPER 92-4257	p 103	A93-13363	#	AIAA PAPER 92-5063	p 414	A93-22333	#
AIAA PAPER 92-2657	p 472	A93-24986	#	AIAA PAPER 92-4261	p 63	A93-13365	#	AIAA PAPER 92-5065	p 273	A93-22335	#
AIAA PAPER 92-2664	p 473	A93-24988	#	AIAA PAPER 92-4268	p 55	A93-13366	#	AIAA PAPER 92-5067	p 438	A93-22337	#
AIAA PAPER 92-2713	p 473	A93-24990	#	AIAA PAPER 92-4272	p 54	A93-13334	#	AIAA PAPER 92-5072	p 433	A93-22342	#
AIAA PAPER 92-3070	p 838	N93-27020	#	AIAA PAPER 92-4273	p 54	A93-13333	#	AIAA PAPER 92-5087	p 452	A93-22357	#
AIAA PAPER 92-3168	p 531	A93-24478	#	AIAA PAPER 92-4277	p 457	A93-24299	#	AIAA PAPER 92-5090	p 414	A93-22360	#
AIAA PAPER 92-3320	p 1108	A93-49329	#	AIAA PAPER 92-4279	p 55	A93-13352	#	AIAA PAPER 92-5091	p 273	A93-22361	#
AIAA PAPER 92-3569	p 291	N93-16704	#	AIAA PAPER 92-4280	p 44	A93-13353	#	AIAA PAPER 92-5098	p 359	A93-22368	#
AIAA PAPER 92-3622	p 60	N93-12077	#	AIAA PAPER 92-4283	p 43	A93-13340	#	AIAA PAPER 92-5101	p 274	A93-22371	#
AIAA PAPER 92-3672	p 536	N93-20237	#	AIAA PAPER 92-4285	p 570	A93-24300	#	AIAA PAPER 92-5102	p 359	A93-22372	#
AIAA PAPER 92-3676	p 111	A93-14118	#	AIAA PAPER 92-4300	p 69	A93-13276	#	AIAA PAPER 92-5103	p 274	A93-22373	#
AIAA PAPER 92-3676	p 414	A93-22509	#	AIAA PAPER 92-4350	p 15	A93-13306	#	AIAA PAPER 92-5104	p 274	A93-22374	#
AIAA PAPER 92-3686	p 531	A93-24479	#	AIAA PAPER 92-4394	p 523	A93-24495	#	AIAA PAPER 93-0006	p 389	A93-20129	#
AIAA PAPER 92-3745	p 175	N93-13155	#	AIAA PAPER 92-4421	p 523	A93-24497	#	AIAA PAPER 93-0007	p 306	A93-20130	#
AIAA PAPER 92-3887	p 528	A93-24481	#	AIAA PAPER 92-4468	p 62	A93-13280	#	AIAA PAPER 93-0010	p 366	A93-20132	#
AIAA PAPER 92-3895	p 539	A93-24484	#	AIAA PAPER 92-4502	p 15	A93-13308	#	AIAA PAPER 93-0016	p 367	A93-20138	#
AIAA PAPER 92-3897	p 539	A93-24486	#	AIAA PAPER 92-4572	p 14	A93-13303	#	AIAA PAPER 93-0017	p 472	A93-24978	#
AIAA PAPER 92-3909	p 462	A93-24488	#	AIAA PAPER 92-4575	p 15	A93-13309	#	AIAA PAPER 93-0017	p 290	N93-16625	#
AIAA PAPER 92-3920	p 462	A93-24294	#	AIAA PAPER 92-4604	p 42	A93-13284	#	AIAA PAPER 93-0020	p 408	A93-20139	#
AIAA PAPER 92-4040	p 463	A93-24489	#	AIAA PAPER 92-4627	p 62	A93-13285	#	AIAA PAPER 93-0021	p 390	A93-23238	#
AIAA PAPER 92-4070	p 37	A93-11257	#	AIAA PAPER 92-4628	p 62	A93-13286	#	AIAA PAPER 93-0021	p 200	N93-15504	#
AIAA PAPER 92-4072	p 97	A93-13264	#	AIAA PAPER 92-4632	p 14	A93-13304	#	AIAA PAPER 93-0022	p 357	A93-20140	#
AIAA PAPER 92-4073	p 95	A93-11258	#	AIAA PAPER 92-4650	p 14	A93-13305	#	AIAA PAPER 93-0023	p 408	A93-20141	#
AIAA PAPER 92-4075	p 37	A93-11260	#	AIAA PAPER 92-4680	p 409	A93-20302	#	AIAA PAPER 93-0025	p 307	A93-20143	#
AIAA PAPER 92-4076	p 95	A93-11261	#	AIAA PAPER 92-4681	p 264	A93-20303	#	AIAA PAPER 93-0026	p 259	A93-20144	#
AIAA PAPER 92-4077	p 37	A93-11262	#	AIAA PAPER 92-4682	p 409	A93-20304	#	AIAA PAPER 93-0027	p 307	A93-20145	#
AIAA PAPER 92-4078	p 42	A93-13269	#	AIAA PAPER 92-4693	p 322	A93-20278	#	AIAA PAPER 93-0028	p 260	A93-20146	#
AIAA PAPER 92-4081	p 61	A93-11264	#	AIAA PAPER 92-4694	p 324	A93-20307	#	AIAA PAPER 93-0029	p 309	A93-23239	#
AIAA PAPER 92-4082	p 61	A93-11265	#	AIAA PAPER 92-4695	p 323	A93-20279	#	AIAA PAPER 93-0029	p 148	N93-15360	#
AIAA PAPER 92-4083	p 61	A93-11266	#	AIAA PAPER 92-4696	p 324	A93-20308	#	AIAA PAPER 93-0030	p 307	A93-20147	#
AIAA PAPER 92-4085	p 51	A93-13263	#	AIAA PAPER 92-4697	p 264	A93-20309	#	AIAA PAPER 93-0031	p 282	A93-23240	#
AIAA PAPER 92-4086	p 51	A93-13265	#	AIAA PAPER 92-4698	p 265	A93-20310	#	AIAA PAPER 93-0031	p 139	N93-15338	#
AIAA PAPER 92-4088	p 7	A93-11267	#	AIAA PAPER 92-4708	p 451	A93-20316	#	AIAA PAPER 93-0032	p 327	A93-22551	#
AIAA PAPER 92-4089	p 39	A93-11285	#	AIAA PAPER 92-4709	p 435	A93-20318	#	AIAA PAPER 93-0032	p 138	N93-14911	#
AIAA PAPER 92-4090	p 51	A93-13272	#	AIAA PAPER 92-4710	p 358	A93-20319	#	AIAA PAPER 93-0034	p 260	A93-20148	#
AIAA PAPER 92-4092	p 38	A93-11268	#	AIAA PAPER 92-4711	p 358	A93-20280	#	AIAA PAPER 93-0036	p 322	A93-20150	#
AIAA PAPER 92-4093	p 93	A93-13262	#	AIAA PAPER 92-4712	p 358	A93-20320	#	AIAA PAPER 93-0039	p 260	A93-20152	#
AIAA PAPER 92-4094	p 42	A93-13261	#	AIAA PAPER 92-4713	p 323	A93-20281	#	AIAA PAPER 93-0042	p 389	A93-20155	#
AIAA PAPER 92-4098	p 34	A93-13267	#	AIAA PAPER 92-4716	p 60	N93-12402	#	AIAA PAPER 93-0049	p 260	A93-20162	#
AIAA PAPER 92-4099	p 38	A93-11271	#	AIAA PAPER 92-4717	p 358	A93-20321	#	AIAA PAPER 93-0050	p 260	A93-20163	#
AIAA PAPER 92-4101	p 38	A93-11274	#	AIAA PAPER 92-4719	p 324	A93-20322	#	AIAA PAPER 93-0051	p 260	A93-20164	#
AIAA PAPER 92-4101	p 49	N93-11863	#	AIAA PAPER 92-4721	p 325	A93-20323	#	AIAA PAPER 93-0052	p 261	A93-20165	#
AIAA PAPER 92-4102	p 38	A93-11272	#	AIAA PAPER 92-4722	p 325	A93-20324	#	AIAA PAPER 93-0053	p 261	A93-20166	#
AIAA PAPER 92-4102	p 131	N93-13322	#	AIAA PAPER 92-4724	p 409	A93-20326	#	AIAA PAPER 93-0054	p 261	A93-20167	#
AIAA PAPER 92-4103	p 38	A93-11275	#	AIAA PAPER 92-4726	p 325	A93-20328	#	AIAA PAPER 93-0056	p 367	A93-20169	#
AIAA PAPER 92-4105	p 38	A93-11273	#	AIAA PAPER 92-4730	p 409	A93-20329	#	AIAA PAPER 93-0059	p 435	A93-20172	#
AIAA PAPER 92-4105	p 22	N93-11532	#	AIAA PAPER 92-4745	p 436	A93-20343	#	AIAA PAPER 93-0063	p 261	A93-20176	#
AIAA PAPER 92-4106	p 38	A93-11276	#	AIAA PAPER 92-4746	p 265	A93-20344	#	AIAA PAPER 93-0064	p 261	A93-20177	#
AIAA PAPER 92-4107	p 39	A93-11277	#	AIAA PAPER 92-4752	p 436	A93-20350	#	AIAA PAPER 93-0065	p 261	A93-20178	#
AIAA PAPER 92-4109	p 39	A93-11278	#	AIAA PAPER 92-4753	p 436	A93-20351	#	AIAA PAPER 93-0066	p 261	A93-20179	#
AIAA PAPER 92-4111	p 39	A93-11280	#	AIAA PAPER 92-4756	p 409	A93-20352	#	AIAA PAPER 93-0067	p 262	A93-20180	#
AIAA PAPER 92-4113	p 51	A93-11281	#	AIAA PAPER 92-4761	p 325	A93-20356	#	AIAA PAPER 93-0068	p 262	A93-20181	#
AIAA PAPER 92-4118	p 42	A93-13266	#	AIAA PAPER 92-4765	p 325	A93-20360	#	AIAA PAPER 93-0071	p 262	A93-20183	#
AIAA PAPER 92-4121	p 42	A93-13273	#	AIAA PAPER 92-4773	p 436	A93-20366	#	AIAA PAPER 93-0072	p 262	A93-20184	#
AIAA PAPER 92-4122	p 61	A93-11284	#	AIAA PAPER 92-4777	p 325	A93-20369	#	AIAA PAPER 93-0074	p 262	A93-20186	#
AIAA PAPER 92-4123	p 102	A93-11256	#	AIAA PAPER 92-4778	p 47	N93-10968	#	AIAA PAPER 93-0075	p 262	A93-20187	#
AIAA PAPER 92-4148	p 43	A93-13314	#	AIAA PAPER 92-4779	p 265	A93-20416	#	AIAA PAPER 93-0076	p 262	A93-20188	#
AIAA PAPER 92-4161	p 66	A93-13312	#	AIAA PAPER 92-4780	p 326	A93-20370	#	AIAA PAPER 93-0077	p 263	A93-20189	#
AIAA PAPER 92-4173	p 43	A93-13315	#	AIAA PAPER 92-4781	p 323	A93-20287	#	AIAA PAPER 93-0078	p 263	A93-20190	#
AIAA PAPER 92-4174	p 51	A93-13310	#	AIAA PAPER 92-4782	p 326	A93-20371	#	AIAA PAPER 93-0079	p 263	A93-20191	#
AIAA PAPER 92-4175	p 42	A93-13311	#	AIAA PAPER 92-4783	p 326	A93-20372	#	AIAA PAPER 93-0080	p 263	A93-20192	#
AIAA PAPER 92-4190	p 2	A93-13368	#	AIAA PAPER 92-4794	p 323	A93-20289	#	AIAA PAPER 93-0083	p 274	A93-22552	#
AIAA PAPER 92-4191	p 103	A93-13369	#	AIAA PAPER 92-4795	p 323	A93-20290	#	AIAA PAPER 93-0089	p 263	A93-20195	#
AIAA PAPER 92-4192	p 44	A93-13370	#	AIAA PAPER 92-4796	p 326	A93-20381	#	AIAA PAPER 93-0090	p 263	A93-20196	#
AIAA PAPER 92-4193	p 63	A93-13345	#	AIAA PAPER 92-4813	p 408	A93-20291	#	AIAA PAPER 93-0091	p 264	A93-20197	#
AIAA PAPER 92-4194	p 44	A93-13371	#	AIAA PAPER 92-4814	p 408	A93-20293	#	AIAA PAPER 93-0093	p 264	A93-20199	#
AIAA PAPER 92-4195	p 44	A93-13372	#	AIAA PAPER 92-4834	p 436	A93-20394	#	AIAA PAPER 93-0094	p 264	A93-20200	#
AIAA PAPER 92-4196	p 51	A93-13373	#	AIAA PAPER 92-4837	p 436	A93-20411	#	AIAA PAPER 93-0099	p 264	A93-20204	#
AIAA PAPER 92-4209	p 15	A93-13377	#	AIAA PAPER 92-4841	p 324	A93-20295	#	AIAA PAPER 93-0100	p 264	A93-20205	#
AIAA PAPER 92-4210	p 44	A93-13378	#	AIAA PAPER 92-4999	p 324	A93-20296	#	AIAA PAPER 93-0101	p 322	A93-19806	#
AIAA PAPER 92-4217	p 55	A93-13383	#	AIAA PAPER 92-5005	p 456	A93-22276	#	AIAA PAPER 93-0108	p 539	A93-24230	#
AIAA PAPER 92-4218	p 16	A93-13380	#	AIAA PAPER 92-5009	p 384	A93-22282	#	AIAA PAPER 93-0116	p 360	A93-22566	#
AIAA PAPER 92-4219	p 43	A93-13348	#	AIAA PAPER 92-5011	p 367	A93-22285	#	AIAA PAPER 93-0118	p 360	A93-22568	#
AIAA PAPER 92-4220	p 43	A93-13336	#	AIAA PAPER 92-5012	p 384	A93-22287	#	AIAA PAPER 93-0131	p 390	A93-22578	#
AIAA PAPER 92-4221	p 45	A93-13381	#	AIAA PAPER 92-5013	p 385	A93-22288	#	AIAA PAPER 93-0133	p 274	A93-22580	#
AIAA PAPER 92-4223	p 504	A93-24492	#	AIAA PAPER 92-5018	p 385	A93-22289	#	AIAA PAPER 93-0144	p 414	A93-22588	#
AIAA PAPER 92-4225	p 16	A93-13382	#	AIAA PAPER 92-5022	p 413	A93-22294	#	AIAA PAPER 93-0145	p 452	A93-22589	#
AIAA PAPER 92-4226	p 97	A93-13354	#	AIAA PAPER 92-5026	p 272	A93-22298	#	AIAA PAPER 93-0146	p 451	A93-19804	#
AIAA PAPER 92-4228	p 44	A93-13355	#	AIAA PAPER 92-5027	p 438	A93-22302	#	AIAA PAPER 93-0147	p 452	A93-23241	#
AIAA PAPER 92-4229	p 15	A93-13356	#	AIAA PAPER 92-5029	p 272	A93-22303	#	AIAA PAPER 93-0147	p 233	N93-15575	#
AIAA PAPER 92-4230	p 43	A93-13337	#	AIAA PAPER 92-5030	p 272	A93-22304	#	AIAA PAPER 93-0149	p 564	A93-25504	#
AIAA PAPER 92-4232	p 54	A93-13330	#	AIAA PAPER 92-5033	p 272	A93-22305	#	AIAA PAPER 93-0153	p 274	A93-22591	#
AIAA PAPER 92-4234	p 63	A93-13328	#	AIAA PAPER 92-5034	p 239	A93-22307	#	AIAA PAPER 93-0154	p 275	A93-22592	#
AIAA PAPER 92-4236	p 63	A93-13338	#	AIAA PAPER 92-5037	p 456	A93-22308	#	AIAA PAPER 93-0155	p 542	A93-25505	#
AIAA PAPER 92-4237	p 44	A93-13359	#	AIAA PAPER 92-5038	p 376	A93-22311	#	AIAA PAPER 93-0157	p 275	A93-22594	#
AIAA PAPER 92-4242	p 51	A93-13351	#	AIAA PAPER 92-5041	p 413	A93-22312	#	AIAA PAPER 93-0167	p 275	A93-22601	#
AIAA PAPER 92-4246	p 463	A93-24493	#	AIAA PAPER 92-5045	p 385	A93-22315	#	AIAA PAPER 93-0168	p 275	A93-22602	#
AIAA PAPER 92-4247	p 43	A93-13326	#	AIAA PAPER 92-5047	p 273	A93-22319	#	AIAA PAPER 93-0169	p 275	A93-22603	#

AIAA PAPER 93-0173	p 148	N93-15354 *	#	AIAA PAPER 93-0386	p 282	A93-23065 #	AIAA PAPER 93-0647	p 464	A93-24762 *	#
AIAA PAPER 93-0174	p 310	A93-23245 #		AIAA PAPER 93-0387	p 282	A93-23066 *	AIAA PAPER 93-0648	p 464	A93-24763 #	
AIAA PAPER 93-0174	p 149	N93-15522 *	#	AIAA PAPER 93-0389	p 282	A93-23067 #	AIAA PAPER 93-0649	p 465	A93-24764 *	#
AIAA PAPER 93-0176	p 414	A93-22605 #		AIAA PAPER 93-0390	p 461	A93-24238 *	AIAA PAPER 93-0652	p 543	A93-25545 #	
AIAA PAPER 93-0179	p 414	A93-22607 *	#	AIAA PAPER 93-0391	p 282	A93-23068 #	AIAA PAPER 93-0653	p 540	A93-24766 *	#
AIAA PAPER 93-0180	p 414	A93-22608 *	#	AIAA PAPER 93-0392	p 486	A93-24239 *	AIAA PAPER 93-0653	p 551	N93-20057 *	#
AIAA PAPER 93-0181	p 542	A93-25508 *	#	AIAA PAPER 93-0393	p 309	A93-23069 #	AIAA PAPER 93-0656	p 540	A93-24769 #	
AIAA PAPER 93-0182	p 542	A93-25509 #		AIAA PAPER 93-0397	p 327	A93-23072 #	AIAA PAPER 93-0659	p 465	A93-24772 #	
AIAA PAPER 93-0183	p 367	A93-22609 #		AIAA PAPER 93-0398	p 370	A93-23073 *	AIAA PAPER 93-0660	p 465	A93-24773 #	
AIAA PAPER 93-0184	p 473	A93-25510 #		AIAA PAPER 93-0398	p 188	N93-14831 *	AIAA PAPER 93-0661	p 465	A93-24774 #	
AIAA PAPER 93-0185	p 275	A93-22610 #		AIAA PAPER 93-0399	p 474	A93-25520 #	AIAA PAPER 93-0665	p 465	A93-24777 #	
AIAA PAPER 93-0186	p 276	A93-22611 #		AIAA PAPER 93-0400	p 505	A93-25521 *	AIAA PAPER 93-0668	p 475	A93-25546 *	#
AIAA PAPER 93-0187	p 368	A93-22612 *	#	AIAA PAPER 93-0401	p 384	A93-21108 #	AIAA PAPER 93-0669	p 465	A93-24778 #	
AIAA PAPER 93-0188	p 276	A93-22613 #		AIAA PAPER 93-0402	p 505	A93-25522 #	AIAA PAPER 93-0670	p 269	A93-21116 #	
AIAA PAPER 93-0190	p 276	A93-22614 #		AIAA PAPER 93-0404	p 440	A93-23326 #	AIAA PAPER 93-0672	p 560	A93-24780 *	#
AIAA PAPER 93-0191	p 276	A93-22615 *	#	AIAA PAPER 93-0408	p 440	A93-23330 *	AIAA PAPER 93-0673	p 560	A93-24781 *	#
AIAA PAPER 93-0192	p 268	A93-21102 *	#	AIAA PAPER 93-0410	p 361	A93-23331 *	AIAA PAPER 93-0676	p 465	A93-24786 *	#
AIAA PAPER 93-0193	p 473	A93-25511 #		AIAA PAPER 93-0414	p 415	A93-23333 *	AIAA PAPER 93-0677	p 269	A93-21117 #	
AIAA PAPER 93-0194	p 474	A93-25512 *	#	AIAA PAPER 93-0421	p 285	A93-23340 #	AIAA PAPER 93-0679	p 466	A93-24787 #	
AIAA PAPER 93-0195	p 276	A93-22616 *	#	AIAA PAPER 93-0426	p 454	A93-23344 *	AIAA PAPER 93-0680	p 466	A93-24788 #	
AIAA PAPER 93-0196	p 461	A93-24233 *	#	AIAA PAPER 93-0427	p 386	A93-23345 *	AIAA PAPER 93-0728	p 466	A93-24818 *	#
AIAA PAPER 93-0197	p 276	A93-22617 *	#	AIAA PAPER 93-0431	p 462	A93-24240 *	AIAA PAPER 93-0731	p 563	A93-24821 *	#
AIAA PAPER 93-0198	p 277	A93-22618 #		AIAA PAPER 93-0434	p 474	A93-25528 #	AIAA PAPER 93-0735	p 563	A93-24825 *	#
AIAA PAPER 93-0199	p 277	A93-22619 #		AIAA PAPER 93-0435	p 286	A93-23349 #	AIAA PAPER 93-0735	p 233	N93-15430 #	
AIAA PAPER 93-0200	p 277	A93-22620 *	#	AIAA PAPER 93-0436	p 286	A93-23350 #	AIAA PAPER 93-0736	p 563	A93-24826 *	#
AIAA PAPER 93-0206	p 277	A93-22624 *	#	AIAA PAPER 93-0437	p 286	A93-23351 #	AIAA PAPER 93-0737	p 563	A93-24827 *	#
AIAA PAPER 93-0207	p 277	A93-22625 *	#	AIAA PAPER 93-0438	p 286	A93-23352 #	AIAA PAPER 93-0738	p 540	A93-24828 *	#
AIAA PAPER 93-0208	p 278	A93-22626 *	#	AIAA PAPER 93-0440	p 474	A93-25529 #	AIAA PAPER 93-0739	p 519	A93-24829 #	
AIAA PAPER 93-0209	p 278	A93-22627 #		AIAA PAPER 93-0442	p 286	A93-23353 #	AIAA PAPER 93-0740	p 466	A93-24830 *	#
AIAA PAPER 93-0211	p 278	A93-22628 *	#	AIAA PAPER 93-0448	p 391	A93-23358 *	AIAA PAPER 93-0741	p 466	A93-24831 #	
AIAA PAPER 93-0213	p 278	A93-22630 #		AIAA PAPER 93-0455	p 534	A93-25532 #	AIAA PAPER 93-0744	p 358	A93-21118 #	
AIAA PAPER 93-0215	p 520	A93-27801 #		AIAA PAPER 93-0482	p 361	A93-23384 #	AIAA PAPER 93-0745	p 540	A93-24833 #	
AIAA PAPER 93-0215	p 294	N93-17884 *	#	AIAA PAPER 93-0482	p 60	N93-12418 *	AIAA PAPER 93-0747	p 516	A93-24835 #	
AIAA PAPER 93-0216	p 278	A93-22632 #		AIAA PAPER 93-0483	p 415	A93-23385 #	AIAA PAPER 93-0748	p 540	A93-24836 #	
AIAA PAPER 93-0217	p 278	A93-22633 #		AIAA PAPER 93-0484	p 286	A93-23386 #	AIAA PAPER 93-0749	p 486	A93-24837 #	
AIAA PAPER 93-0219	p 415	A93-22635 #		AIAA PAPER 93-0485	p 287	A93-23387 *	AIAA PAPER 93-0751	p 504	A93-24838 #	
AIAA PAPER 93-0222	p 415	A93-22638 #		AIAA PAPER 93-0488	p 416	A93-23390 *	AIAA PAPER 93-0760	p 466	A93-24845 #	
AIAA PAPER 93-0223	p 440	A93-23699 #		AIAA PAPER 93-0505	p 283	A93-23253 #	AIAA PAPER 93-0761	p 467	A93-24846 #	
AIAA PAPER 93-0224	p 438	A93-22639 #		AIAA PAPER 93-0506	p 505	A93-25533 *	AIAA PAPER 93-0767	p 540	A93-24851 #	
AIAA PAPER 93-0240	p 390	A93-22652 *	#	AIAA PAPER 93-0507	p 283	A93-23254 #	AIAA PAPER 93-0768	p 541	A93-24852 #	
AIAA PAPER 93-0246	p 390	A93-22657 #		AIAA PAPER 93-0508	p 370	A93-23255 *	AIAA PAPER 93-0771	p 467	A93-24855 #	
AIAA PAPER 93-0249	p 361	A93-23246 #		AIAA PAPER 93-0509	p 386	A93-23256 *	AIAA PAPER 93-0774	p 467	A93-24858 *	#
AIAA PAPER 93-0251	p 179	N93-15359 *	#	AIAA PAPER 93-0510	p 328	A93-23257 #	AIAA PAPER 93-0776	p 475	A93-25550 #	
AIAA PAPER 93-0251	p 360	A93-22660 #		AIAA PAPER 93-0511	p 386	A93-23258 #	AIAA PAPER 93-0777	p 269	A93-21119 #	
AIAA PAPER 93-0271	p 268	A93-21103 *	#	AIAA PAPER 93-0519	p 268	A93-21111 #	AIAA PAPER 93-0778	p 541	A93-24860 #	
AIAA PAPER 93-0286	p 279	A93-22687 #		AIAA PAPER 93-0522	p 283	A93-23264 *	AIAA PAPER 93-0779	p 467	A93-24861 *	#
AIAA PAPER 93-0287	p 342	A93-21104 *	#	AIAA PAPER 93-0523	p 283	A93-23265 #	AIAA PAPER 93-0780	p 467	A93-24862 *	#
AIAA PAPER 93-0289	p 279	A93-22689 #		AIAA PAPER 93-0524	p 474	A93-25536 *	AIAA PAPER 93-0781	p 467	A93-24863 *	#
AIAA PAPER 93-0290	p 279	A93-22690 #		AIAA PAPER 93-0525	p 284	A93-23266 #	AIAA PAPER 93-0784	p 468	A93-24864 *	#
AIAA PAPER 93-0291	p 279	A93-22691 #		AIAA PAPER 93-0526	p 284	A93-23267 #	AIAA PAPER 93-0786	p 541	A93-24868 #	
AIAA PAPER 93-0292	p 279	A93-22692 #		AIAA PAPER 93-0527	p 284	A93-23268 #	AIAA PAPER 93-0787	p 541	A93-24867 #	
AIAA PAPER 93-0293	p 279	A93-22693 #		AIAA PAPER 93-0528	p 284	A93-23269 #	AIAA PAPER 93-0789	p 468	A93-24865 *	#
AIAA PAPER 93-0294	p 280	A93-22694 *	#	AIAA PAPER 93-0529	p 284	A93-23270 *	AIAA PAPER 93-0790	p 468	A93-24869 #	
AIAA PAPER 93-0295	p 376	A93-22695 #		AIAA PAPER 93-0531	p 284	A93-23272 #	AIAA PAPER 93-0791	p 541	A93-24870 #	
AIAA PAPER 93-0296	p 327	A93-22696 *	#	AIAA PAPER 93-0532	p 285	A93-23273 #	AIAA PAPER 93-0793	p 541	A93-24872 #	
AIAA PAPER 93-0298	p 378	A93-23698 #		AIAA PAPER 93-0543	p 415	A93-23283 #	AIAA PAPER 93-0795	p 528	A93-24874 #	
AIAA PAPER 93-0299	p 376	A93-22697 #		AIAA PAPER 93-0550	p 285	A93-23289 #	AIAA PAPER 93-0798	p 528	A93-24876 #	
AIAA PAPER 93-0300	p 280	A93-23001 *	#	AIAA PAPER 93-0551	p 285	A93-23290 #	AIAA PAPER 93-0806	p 533	A93-24882 #	
AIAA PAPER 93-0301	p 283	A93-23247 *	#	AIAA PAPER 93-0553	p 285	A93-23292 *	AIAA PAPER 93-0807	p 533	A93-24883 #	
AIAA PAPER 93-0301	p 139	N93-15404 *	#	AIAA PAPER 93-0554	p 285	A93-23293 #	AIAA PAPER 93-0809	p 534	A93-24884 #	
AIAA PAPER 93-0308	p 457	A93-25516 *	#	AIAA PAPER 93-0555	p 285	A93-23294 #	AIAA PAPER 93-0847	p 557	A93-24914 #	
AIAA PAPER 93-0309	p 456	A93-23005 *	#	AIAA PAPER 93-0556	p 543	A93-25539 #	AIAA PAPER 93-0851	p 531	A93-24915 *	#
AIAA PAPER 93-0311	p 280	A93-23006 *	#	AIAA PAPER 93-0560	p 377	A93-23297 *	AIAA PAPER 93-0852	p 557	A93-24916 #	
AIAA PAPER 93-0312	p 280	A93-23007 #		AIAA PAPER 93-0596	p 519	A93-24782 *	AIAA PAPER 93-0863	p 468	A93-24925 *	#
AIAA PAPER 93-0318	p 268	A93-21106 *	#	AIAA PAPER 93-0596	p 362	N93-16715 #	AIAA PAPER 93-0864	p 468	A93-24926 #	
AIAA PAPER 93-0319	p 280	A93-23011 #		AIAA PAPER 93-0597	p 452	A93-23323 *	AIAA PAPER 93-0865	p 468	A93-24927 #	
AIAA PAPER 93-0320	p 280	A93-23012 #		AIAA PAPER 93-0598	p 563	A93-24783 #	AIAA PAPER 93-0866	p 469	A93-24928 #	
AIAA PAPER 93-0321	p 280	A93-23013 *	#	AIAA PAPER 93-0598	p 362	N93-16705 *	AIAA PAPER 93-0869	p 469	A93-24930 #	
AIAA PAPER 93-0322	p 281	A93-23014 *	#	AIAA PAPER 93-0599	p 361	A93-23324 #	AIAA PAPER 93-0870	p 469	A93-24931 *	#
AIAA PAPER 93-0323	p 281	A93-23015 #		AIAA PAPER 93-0599	p 179	N93-15403 *	AIAA PAPER 93-0871	p 469	A93-24932 #	
AIAA PAPER 93-0324	p 454	A93-23016 #		AIAA PAPER 93-0600	p 562	A93-24726 #	AIAA PAPER 93-0872	p 469	A93-24933 #	
AIAA PAPER 93-0325	p 454	A93-23017 #		AIAA PAPER 93-0601	p 563	A93-24727 *	AIAA PAPER 93-0873	p 469	A93-24934 #	
AIAA PAPER 93-0326	p 454	A93-23018 #		AIAA PAPER 93-0604	p 269	A93-21113 *	AIAA PAPER 93-0874	p 469	A93-24935 #	
AIAA PAPER 93-0330	p 415	A93-23021 #		AIAA PAPER 93-0609	p 358	A93-21114 *	AIAA PAPER 93-0875	p 470	A93-24936 #	
AIAA PAPER 93-0331	p 281	A93-23022 *	#	AIAA PAPER 93-0620	p 523	A93-24737 #	AIAA PAPER 93-0876	p 470	A93-24937 #	
AIAA PAPER 93-0333	p 268	A93-21107 *	#	AIAA PAPER 93-0621	p 523	A93-24738 #	AIAA PAPER 93-0878	p 470	A93-24939 #	
AIAA PAPER 93-0337	p 281	A93-23026 #		AIAA PAPER 93-0622	p 523	A93-24739 #	AIAA PAPER 93-0879	p 470	A93-24940 #	
AIAA PAPER 93-0339	p 281	A93-23027 #		AIAA PAPER 93-0623	p 524	A93-24740 #	AIAA PAPER 93-0882	p 475	A93-25553 *	#
AIAA PAPER 93-0342	p 474	A93-25517 *	#	AIAA PAPER 93-0624	p 504	A93-24741 *	AIAA PAPER 93-0883	p 470	A93-24943 #	
AIAA PAPER 93-0343	p 281	A93-23030 *	#	AIAA PAPER 93-0625	p 504	A93-24742 *	AIAA PAPER 93-0884	p 471	A93-24945 *	#
AIAA PAPER 93-0344	p 376	A93-23031 *	#	AIAA PAPER 93-0625	p 339	N93-18616 #	AIAA PAPER 93-0885	p 470	A93-24944 #	
AIAA PAPER 93-0348	p 528	A93-25518 #		AIAA PAPER 93-0626	p 524	A93-24743 #	AIAA PAPER 93-0886	p 471	A93-24946 #	
AIAA PAPER 93-0349	p 377	A93-23034 *	#	AIAA PAPER 93-0627	p 531	A93-24744 #	AIAA PAPER 93-0887	p 471	A93-24947 #	
AIAA PAPER 93-0350	p 377	A93-23035 *	#	AIAA PAPER 93-0631	p 539	A93-24748 #	AIAA PAPER 93-0890	p 471	A93-24950 #	
AIAA PAPER 93-0351	p 377	A93-23036 #		AIAA PAPER 93-0634	p 516	A93-24750 #	AIAA PAPER 93-0891	p 471	A93-24951 *	#
AIAA PAPER 93-0352	p 377	A93-23037 #		AIAA PAPER 93-0634	p 518	N93-20163 *	AIAA PAPER 93-0893	p 471	A93-24953 #	
AIAA PAPER 93-0353	p 377	A93-23038 #		AIAA PAPER 93-0636	p 463	A93-24752 #	AIAA PAPER 93-0894	p 472	A93-24954 *	#
AIAA PAPER 93-0357	p 377	A93-23040 #		AIAA PAPER 93-0637	p 463	A93-24753 #	AIAA PAPER 93-0896	p 472	A93-24956 #	
AIAA PAPER 93-0358	p 360	A93-23041 *	#	AIAA PAPER 93-0639	p 463	A93-24754 #	AIAA PAPER 93-0897	p 472	A93-24957 #	
AIAA PAPER 93-0359	p 385	A93-23042 #		AIAA PAPER 93-0640	p 539	A93-24755 *	AIAA PAPER 93-0902	p 560	A93-24960 #	
AIAA PAPER 93-0363	p 390	A93-23045 #		AIAA PAPER 93-0641	p 464	A93-24756 #	AIAA PAPER 93-0918	p 472	A93-24972 #	
AIAA PAPER 93-0366	p 390	A93-23047 #		AIAA PAPER 93-0642	p 540	A93-24757 #	AIAA PAPER 93-1017	p 344	N93-19110	

REPORT NUMBER INDEX

AIAA PAPER 93-2438

AIAA PAPER 93-1207	p 702	A93-35158	#	AIAA PAPER 93-1633	p 720	A93-34161	#	AIAA PAPER 93-2043	p 814	N93-27160	#
AIAA PAPER 93-1209	p 702	A93-35159	#	AIAA PAPER 93-1634	p 720	A93-34162	#	AIAA PAPER 93-2044	p 813	N93-27128	#
AIAA PAPER 93-1210	p 689	A93-35160	#	AIAA PAPER 93-1638	p 720	A93-34165	#	AIAA PAPER 93-2049	p 1113	A93-49882	#
AIAA PAPER 93-1213	p 702	A93-35162	#	AIAA PAPER 93-1644	p 742	A93-34169	#	AIAA PAPER 93-2051	p 1166	A93-49884	#
AIAA PAPER 93-1216	p 689	A93-35165	#	AIAA PAPER 93-1645	p 742	A93-34170	#	AIAA PAPER 93-2069	p 1153	A93-49901	#
AIAA PAPER 93-1220	p 690	A93-35169	#	AIAA PAPER 93-1646	p 742	A93-34171	#	AIAA PAPER 93-2070	p 1113	A93-49902	#
AIAA PAPER 93-1224	p 733	A93-35171	#	AIAA PAPER 93-1647	p 742	A93-34172	#	AIAA PAPER 93-2074	p 1113	A93-49903	#
AIAA PAPER 93-1227	p 690	A93-35173	#	AIAA PAPER 93-1648	p 711	A93-34173	#	AIAA PAPER 93-2077	p 1114	A93-49904	#
AIAA PAPER 93-1232	p 703	A93-35174	#	AIAA PAPER 93-1679	p 743	A93-34191	#	AIAA PAPER 93-2079	p 1154	A93-49906	#
AIAA PAPER 93-1234	p 690	A93-35175	#	AIAA PAPER 93-1697	p 757	A93-34219	#	AIAA PAPER 93-2082	p 1079	A93-49909	#
AIAA PAPER 93-1236	p 690	A93-35177	#	AIAA PAPER 93-1700	p 712	A93-34222	#	AIAA PAPER 93-2084	p 1114	A93-49911	#
AIAA PAPER 93-1237	p 744	A93-35178	#	AIAA PAPER 93-1701	p 712	A93-34223	#	AIAA PAPER 93-2085	p 1114	A93-49912	#
AIAA PAPER 93-1241	p 728	A93-35180	#	AIAA PAPER 93-1702	p 743	A93-34224	#	AIAA PAPER 93-2086	p 1079	A93-49913	#
AIAA PAPER 93-1242	p 690	A93-35181	#	AIAA PAPER 93-1703	p 712	A93-34225	#	AIAA PAPER 93-2087	p 1079	A93-49914	#
AIAA PAPER 93-1247	p 677	A93-35184	#	AIAA PAPER 93-1761	p 1144	A93-49658	#	AIAA PAPER 93-2136	p 1142	A93-49954	#
AIAA PAPER 93-1248	p 690	A93-35185	#	AIAA PAPER 93-1762	p 1109	A93-49659	#	AIAA PAPER 93-2139	p 1114	A93-49957	#
AIAA PAPER 93-1255	p 703	A93-35188	#	AIAA PAPER 93-1763	p 1109	A93-49660	#	AIAA PAPER 93-2140	p 1114	A93-49958	#
AIAA PAPER 93-1300	p 709	A93-33877	#	AIAA PAPER 93-1765	p 1073	A93-49661	#	AIAA PAPER 93-2143	p 1114	A93-49960	#
AIAA PAPER 93-1301	p 756	A93-33878	#	AIAA PAPER 93-1767	p 1152	A93-49663	#	AIAA PAPER 93-2144	p 1115	A93-49961	#
AIAA PAPER 93-1302	p 725	A93-33879	#	AIAA PAPER 93-1772	p 1110	A93-49668	#	AIAA PAPER 93-2145	p 1115	A93-49962	#
AIAA PAPER 93-1304	p 725	A93-33880	#	AIAA PAPER 93-1795	p 1110	A93-49685	#	AIAA PAPER 93-2146	p 1154	A93-49963	#
AIAA PAPER 93-1305	p 726	A93-33881	#	AIAA PAPER 93-1795	p 816	N93-28697	#	AIAA PAPER 93-2149	p 1154	A93-49966	#
AIAA PAPER 93-1307	p 756	A93-33883	#	AIAA PAPER 93-1796	p 1074	A93-49686	#	AIAA PAPER 93-2151	p 1154	A93-49968	#
AIAA PAPER 93-1313	p 732	A93-33889	#	AIAA PAPER 93-1797	p 1218	A93-53585	#	AIAA PAPER 93-2152	p 1101	A93-49969	#
AIAA PAPER 93-1314	p 732	A93-33890	#	AIAA PAPER 93-1797	p 1032	N93-31647	#	AIAA PAPER 93-2154	p 1079	A93-49970	#
AIAA PAPER 93-1315	p 769	A93-37427	#	AIAA PAPER 93-1798	p 1074	A93-49687	#	AIAA PAPER 93-2155	p 1079	A93-49971	#
AIAA PAPER 93-1316	p 732	A93-33891	#	AIAA PAPER 93-1799	p 1074	A93-49688	#	AIAA PAPER 93-2156	p 1115	A93-49972	#
AIAA PAPER 93-1317	p 738	A93-33892	#	AIAA PAPER 93-1805	p 1173	A93-49694	#	AIAA PAPER 93-2157	p 1079	A93-49973	#
AIAA PAPER 93-1318	p 829	A93-37428	#	AIAA PAPER 93-1806	p 1074	A93-49695	#	AIAA PAPER 93-2173	p 1137	A93-49986	#
AIAA PAPER 93-1337	p 738	A93-33907	#	AIAA PAPER 93-1807	p 1166	A93-49696	#	AIAA PAPER 93-2174	p 1115	A93-49987	#
AIAA PAPER 93-1339	p 709	A93-33909	#	AIAA PAPER 93-1808	p 1100	A93-49697	#	AIAA PAPER 93-2176	p 1137	A93-49988	#
AIAA PAPER 93-1341	p 709	A93-33911	#	AIAA PAPER 93-1809	p 1100	A93-49698	#	AIAA PAPER 93-2177	p 1173	A93-49989	#
AIAA PAPER 93-1343	p 709	A93-33913	#	AIAA PAPER 93-1815	p 1110	A93-49703	#	AIAA PAPER 93-2178	p 1137	A93-49990	#
AIAA PAPER 93-1344	p 709	A93-33914	#	AIAA PAPER 93-1816	p 1110	A93-49704	#	AIAA PAPER 93-2179	p 1138	A93-49991	#
AIAA PAPER 93-1345	p 738	A93-33915	#	AIAA PAPER 93-1817	p 1110	A93-49705	#	AIAA PAPER 93-2180	p 1138	A93-49992	#
AIAA PAPER 93-1346	p 738	A93-33916	#	AIAA PAPER 93-1818	p 1110	A93-49706	#	AIAA PAPER 93-2183	p 1142	A93-49995	#
AIAA PAPER 93-1358	p 709	A93-33927	#	AIAA PAPER 93-1819	p 1153	A93-49707	#	AIAA PAPER 93-2196	p 1115	A93-50008	#
AIAA PAPER 93-1360	p 710	A93-33928	#	AIAA PAPER 93-1820	p 1100	A93-49708	#	AIAA PAPER 93-2197	p 1154	A93-50009	#
AIAA PAPER 93-1361	p 726	A93-33929	#	AIAA PAPER 93-1822	p 1110	A93-49709	#	AIAA PAPER 93-2198	p 1155	A93-50010	#
AIAA PAPER 93-1362	p 743	A93-34239	#	AIAA PAPER 93-1823	p 1111	A93-49710	#	AIAA PAPER 93-2201	p 1145	A93-50013	#
AIAA PAPER 93-1363	p 726	A93-33930	#	AIAA PAPER 93-1827	p 1141	A93-49713	#	AIAA PAPER 93-2202	p 1145	A93-50014	#
AIAA PAPER 93-1364	p 682	A93-33931	#	AIAA PAPER 93-1829	p 1153	A93-49714	#	AIAA PAPER 93-2203	p 1155	A93-50015	#
AIAA PAPER 93-1365	p 726	A93-33932	#	AIAA PAPER 93-1836	p 1074	A93-49720	#	AIAA PAPER 93-2229	p 1080	A93-50035	#
AIAA PAPER 93-1366	p 733	A93-33933	#	AIAA PAPER 93-1837	p 1074	A93-49721	#	AIAA PAPER 93-2230	p 1080	A93-50036	#
AIAA PAPER 93-1367	p 733	A93-33934	#	AIAA PAPER 93-1839	p 1075	A93-49723	#	AIAA PAPER 93-2231	p 1080	A93-50037	#
AIAA PAPER 93-1369	p 682	A93-33935	#	AIAA PAPER 93-1840	p 1111	A93-49724	#	AIAA PAPER 93-2234	p 1080	A93-50038	#
AIAA PAPER 93-1371	p 739	A93-33937	#	AIAA PAPER 93-1845	p 1137	A93-49726	#	AIAA PAPER 93-2236	p 1080	A93-50039	#
AIAA PAPER 93-1383	p 719	A93-33946	#	AIAA PAPER 93-1846	p 1111	A93-49727	#	AIAA PAPER 93-2238	p 1081	A93-50040	#
AIAA PAPER 93-1391	p 710	A93-33954	#	AIAA PAPER 93-1847	p 1075	A93-49728	#	AIAA PAPER 93-2239	p 1081	A93-50041	#
AIAA PAPER 93-1400	p 739	A93-33960	#	AIAA PAPER 93-1847	p 900	N93-29162	#	AIAA PAPER 93-2240	p 1155	A93-50042	#
AIAA PAPER 93-1402	p 739	A93-33962	#	AIAA PAPER 93-1848	p 1075	A93-49729	#	AIAA PAPER 93-2246	p 1155	A93-50047	#
AIAA PAPER 93-1403	p 734	A93-33963	#	AIAA PAPER 93-1856	p 1144	A93-49734	#	AIAA PAPER 93-2252	p 1155	A93-50050	#
AIAA PAPER 93-1413	p 739	A93-33969	#	AIAA PAPER 93-1857	p 1145	A93-49735	#	AIAA PAPER 93-2252	p 930	N93-29157	#
AIAA PAPER 93-1414	p 739	A93-33970	#	AIAA PAPER 93-1867	p 1111	A93-49742	#	AIAA PAPER 93-2253	p 1081	A93-50051	#
AIAA PAPER 93-1419	p 818	A93-37433	#	AIAA PAPER 93-1868	p 1075	A93-49743	#	AIAA PAPER 93-2254	p 1115	A93-50052	#
AIAA PAPER 93-1420	p 756	A93-33973	#	AIAA PAPER 93-1869	p 1075	A93-49744	#	AIAA PAPER 93-2255	p 1081	A93-50053	#
AIAA PAPER 93-1421	p 726	A93-33974	#	AIAA PAPER 93-1870	p 1076	A93-49745	#	AIAA PAPER 93-2256	p 1081	A93-50054	#
AIAA PAPER 93-1422	p 739	A93-33975	#	AIAA PAPER 93-1871	p 1111	A93-49746	#	AIAA PAPER 93-2257	p 1081	A93-50055	#
AIAA PAPER 93-1427	p 740	A93-33978	#	AIAA PAPER 93-1872	p 1112	A93-49747	#	AIAA PAPER 93-2259	p 1155	A93-50084	#
AIAA PAPER 93-1431	p 710	A93-33981	#	AIAA PAPER 93-1873	p 1112	A93-49748	#	AIAA PAPER 93-2301	p 1082	A93-50086	#
AIAA PAPER 93-1438	p 710	A93-33987	#	AIAA PAPER 93-1912	p 1076	A93-49779	#	AIAA PAPER 93-2302	p 1082	A93-50087	#
AIAA PAPER 93-1440	p 734	A93-33989	#	AIAA PAPER 93-1913	p 1076	A93-49780	#	AIAA PAPER 93-2304	p 1082	A93-50088	#
AIAA PAPER 93-1450	p 740	A93-33999	#	AIAA PAPER 93-1918	p 1076	A93-49784	#	AIAA PAPER 93-2305	p 1082	A93-50089	#
AIAA PAPER 93-1466	p 710	A93-34014	#	AIAA PAPER 93-1922	p 1076	A93-49788	#	AIAA PAPER 93-2306	p 1082	A93-50090	#
AIAA PAPER 93-1474	p 726	A93-34020	#	AIAA PAPER 93-1924	p 1112	A93-49790	#	AIAA PAPER 93-2323	p 1116	A93-50103	#
AIAA PAPER 93-1475	p 711	A93-34021	#	AIAA PAPER 93-1925	p 1076	A93-49791	#	AIAA PAPER 93-2324	p 1116	A93-50104	#
AIAA PAPER 93-1476	p 829	A93-37438	#	AIAA PAPER 93-1929	p 1077	A93-49794	#	AIAA PAPER 93-2325	p 1116	A93-50105	#
AIAA PAPER 93-1477	p 740	A93-34022	#	AIAA PAPER 93-1931	p 1077	A93-49795	#	AIAA PAPER 93-2326	p 1116	A93-50106	#
AIAA PAPER 93-1478	p 712	A93-34240	#	AIAA PAPER 93-1933	p 1100	A93-49796	#	AIAA PAPER 93-2327	p 1145	A93-50107	#
AIAA PAPER 93-1479	p 829	A93-37439	#	AIAA PAPER 93-1971	p 1077	A93-49819	#	AIAA PAPER 93-2328	p 1116	A93-50108	#
AIAA PAPER 93-1505	p 711	A93-34044	#	AIAA PAPER 93-1973	p 1077	A93-49820	#	AIAA PAPER 93-2336	p 1116	A93-50113	#
AIAA PAPER 93-1511	p 740	A93-34050	#	AIAA PAPER 93-1974	p 1077	A93-49821	#	AIAA PAPER 93-2338	p 1117	A93-50115	#
AIAA PAPER 93-1534	p 727	A93-34071	#	AIAA PAPER 93-1975	p 1077	A93-49822	#	AIAA PAPER 93-2343	p 1164	A93-50117	#
AIAA PAPER 93-1535	p 727	A93-34072	#	AIAA PAPER 93-1976	p 1078	A93-49823	#	AIAA PAPER 93-2344	p 1156	A93-50118	#
AIAA PAPER 93-1536	p 740	A93-34073	#	AIAA PAPER 93-1978	p 1078	A93-49825	#	AIAA PAPER 93-2345	p 1082	A93-50119	#
AIAA PAPER 93-1537	p 711	A93-34074	#	AIAA PAPER 93-1979	p 1153	A93-49826	#	AIAA PAPER 93-2346	p 1083	A93-50120	#
AIAA PAPER 93-1538	p 727	A93-34075	#	AIAA PAPER 93-1980	p 1078	A93-49827	#	AIAA PAPER 93-2347	p 1083	A93-50121	#
AIAA PAPER 93-1539	p 741	A93-34076	#	AIAA PAPER 93-1981	p 1112	A93-49828	#	AIAA PAPER 93-2374	p 1156	A93-50143	#
AIAA PAPER 93-1540	p 741	A93-34077	#	AIAA PAPER 93-1982	p 1141	A93-49829	#	AIAA PAPER 93-2381	p 814	N93-27610	#
AIAA PAPER 93-1546	p 829	A93-37441	#	AIAA PAPER 93-1983	p 1112	A93-49830	#	AIAA PAPER 93-2382	p 1083	A93-50150	#
AIAA PAPER 93-1569	p 741	A93-34102	#	AIAA PAPER 93-1985	p 1112	A93-49832	#	AIAA PAPER 93-2383	p 1083	A93-50151	#
AIAA PAPER 93-1581	p 741	A93-34113	#	AIAA PAPER 93-1988	p 1141	A93-49833	#	AIAA PAPER 93-2384	p 1117	A93-50152	#
AIAA PAPER 93-1583	p 719	A93-34115	#	AIAA PAPER 93-1989	p 1112	A93-49834	#	AIAA PAPER 93-2386	p 1117	A93-50153	#
AIAA PAPER 93-1588	p 682	A93-34120	#	AIAA PAPER 93-1996	p 1153	A93-49839	#	AIAA PAPER 93-2389	p 1083	A93-50154	#
AIAA PAPER 93-1589	p 682	A93-34121	#	AIAA PAPER 93-1997	p 1153	A93-49840	#	AIAA PAPER 93-2402	p 1156	A93-50167	#
AIAA PAPER 93-1590	p 683	A93-34122	#	AIAA PAPER 93-2000	p 1145	A93-49842	#	AIAA PAPER 93-2402	p 914	N93-29194	#
AIAA PAPER 93-1591	p 829	A93-37443	#	AIAA PAPER 93-2016	p 1137	A93-49854	#	AIAA PAPER 93-2429	p 1117	A93-50185	#
AIAA PAPER 93-1592	p 683	A93-34123	#	AIAA PAPER 93-2017	p 1078	A93-49855	#	AIAA PAPER 93-2430	p 1117	A9	

AIAA PAPER 93-2439

REPORT NUMBER INDEX

AIAA PAPER 93-2439	p 1118 A93-50191 #	AIAA PAPER 93-2924	p 1045 A93-48125 #	AIAA PAPER 93-3070	p 1059 A93-48245 #
AIAA PAPER 93-2440	p 1118 A93-50192 *	AIAA PAPER 93-2926	p 1045 A93-48127 #	AIAA PAPER 93-3072	p 1148 A93-48247 #
AIAA PAPER 93-2441	p 1119 A93-50193 #	AIAA PAPER 93-2927	p 1045 A93-48128 *	AIAA PAPER 93-3075	p 1059 A93-48250 #
AIAA PAPER 93-2442	p 1119 A93-50194 #	AIAA PAPER 93-2929	p 949 A93-44229 #	AIAA PAPER 93-3079	p 1059 A93-48253 *
AIAA PAPER 93-2443	p 1119 A93-50195 #	AIAA PAPER 93-2931	p 1045 A93-48130 #	AIAA PAPER 93-3080	p 1059 A93-48254 #
AIAA PAPER 93-2444	p 1119 A93-50196 #	AIAA PAPER 93-2933	p 1046 A93-48131 #	AIAA PAPER 93-3081	p 1060 A93-48255 #
AIAA PAPER 93-2445	p 1119 A93-50197 #	AIAA PAPER 93-2934	p 1148 A93-48132 *	AIAA PAPER 93-3082	p 1060 A93-48256 #
AIAA PAPER 93-2446	p 1120 A93-50198 #	AIAA PAPER 93-2935	p 1046 A93-48133 #	AIAA PAPER 93-3083	p 1060 A93-48257 #
AIAA PAPER 93-2447	p 1120 A93-50199 #	AIAA PAPER 93-2936	p 1046 A93-48134 #	AIAA PAPER 93-3084	p 1060 A93-48258 #
AIAA PAPER 93-2450	p 1138 A93-50200 #	AIAA PAPER 93-2938	p 1046 A93-48136 #	AIAA PAPER 93-3087	p 1099 A93-48261 *
AIAA PAPER 93-2452	p 1120 A93-50201 #	AIAA PAPER 93-2939	p 1046 A93-48137 #	AIAA PAPER 93-3091	p 1099 A93-48265 #
AIAA PAPER 93-2466	p 1138 A93-50213 #	AIAA PAPER 93-2941	p 1046 A93-48139 #	AIAA PAPER 93-3092	p 1060 A93-48266 #
AIAA PAPER 93-2467	p 1138 A93-50214 #	AIAA PAPER 93-2942	p 947 A93-45155 *	AIAA PAPER 93-3095	p 1061 A93-48269 *
AIAA PAPER 93-2469	p 1120 A93-50215 #	AIAA PAPER 93-2943	p 1171 A93-48140 *	AIAA PAPER 93-3096	p 1061 A93-48270 #
AIAA PAPER 93-2471	p 1138 A93-50216 #	AIAA PAPER 93-2944	p 1162 A93-48141 *	AIAA PAPER 93-3097	p 1061 A93-48271 #
AIAA PAPER 93-2474	p 1120 A93-50217 #	AIAA PAPER 93-2945	p 1047 A93-48142 #	AIAA PAPER 93-3100	p 1061 A93-48273 #
AIAA PAPER 93-2478	p 1146 A93-50220 #	AIAA PAPER 93-2946	p 1047 A93-48143 #	AIAA PAPER 93-3104	p 1149 A93-48277 #
AIAA PAPER 93-2479	p 1083 A93-50221 *	AIAA PAPER 93-2948	p 1047 A93-48144 #	AIAA PAPER 93-3109	p 1061 A93-48280 #
AIAA PAPER 93-2481	p 1084 A93-50222 #	AIAA PAPER 93-2949	p 1174 A93-48145 #	AIAA PAPER 93-3110	p 1061 A93-48281 #
AIAA PAPER 93-2521	p 1193 A93-53589 #	AIAA PAPER 93-2952	p 1148 A93-48146 *	AIAA PAPER 93-3112	p 1062 A93-48282 *
AIAA PAPER 93-2521	p 1005 N93-32368 #	AIAA PAPER 93-2955	p 1047 A93-48149 #	AIAA PAPER 93-3113	p 1062 A93-48283 #
AIAA PAPER 93-2522	p 1120 A93-50252 *	AIAA PAPER 93-2956	p 1047 A93-48150 #	AIAA PAPER 93-3114	p 1062 A93-48284 *
AIAA PAPER 93-2523	p 1121 A93-50253 *	AIAA PAPER 93-2957	p 1047 A93-48151 #	AIAA PAPER 93-3115	p 1062 A93-48285 *
AIAA PAPER 93-2526	p 1156 A93-50254 *	AIAA PAPER 93-2958	p 1048 A93-48152 *	AIAA PAPER 93-3116	p 1062 A93-48286 #
AIAA PAPER 93-2526	p 900 N93-29072 #	AIAA PAPER 93-2959	p 1124 A93-48153 #	AIAA PAPER 93-3117	p 1062 A93-48287 #
AIAA PAPER 93-2527	p 816 N93-28617 *	AIAA PAPER 93-2960	p 1124 A93-48154 #	AIAA PAPER 93-3118	p 1171 A93-48288 #
AIAA PAPER 93-2534	p 1156 A93-50261 #	AIAA PAPER 93-2961	p 1048 A93-48155 *	AIAA PAPER 93-3123	p 1063 A93-48291 *
AIAA PAPER 93-2534	p 838 N93-27132 #	AIAA PAPER 93-2962	p 1048 A93-48156 #	AIAA PAPER 93-3125	p 1072 A93-49515 #
AIAA PAPER 93-2537	p 1156 A93-50264 #	AIAA PAPER 93-2963	p 1048 A93-48157 *	AIAA PAPER 93-3127	p 1063 A93-48293 #
AIAA PAPER 93-2542	p 1139 A93-50266 #	AIAA PAPER 93-2964	p 1048 A93-48158 *	AIAA PAPER 93-3129	p 1063 A93-48294 #
AIAA PAPER 93-2543	p 1121 A93-50267 *	AIAA PAPER 93-2965	p 1148 A93-48159 *	AIAA PAPER 93-3131	p 1063 A93-48296 #
AIAA PAPER 93-2544	p 1121 A93-50268 #	AIAA PAPER 93-2967	p 1048 A93-48161 *	AIAA PAPER 93-3132	p 1063 A93-48297 *
AIAA PAPER 93-2546	p 1139 A93-50269 #	AIAA PAPER 93-2968	p 1049 A93-48162 #	AIAA PAPER 93-3133	p 1063 A93-48298 *
AIAA PAPER 93-2555	p 1121 A93-50277 *	AIAA PAPER 93-2969	p 1049 A93-48163 #	AIAA PAPER 93-3135	p 1064 A93-48299 #
AIAA PAPER 93-2555	p 815 N93-28609 #	AIAA PAPER 93-2970	p 1049 A93-48164 #	AIAA PAPER 93-3137	p 1064 A93-48300 *
AIAA PAPER 93-2556	p 1084 A93-50278 *	AIAA PAPER 93-2971	p 1049 A93-48165 #	AIAA PAPER 93-3140	p 959 A93-45154 *
AIAA PAPER 93-2559	p 1157 A93-50280 *	AIAA PAPER 93-2972	p 1049 A93-48166 #	AIAA PAPER 93-3193	p 1012 A93-46656 #
AIAA PAPER 93-2564	p 1142 A93-50284 #	AIAA PAPER 93-2973	p 1049 A93-48167 *	AIAA PAPER 93-3194	p 1021 A93-44231 *
AIAA PAPER 93-2567	p 1121 A93-50285 #	AIAA PAPER 93-2974	p 1050 A93-48168 #	AIAA PAPER 93-3230	p 1039 A93-46682 *
AIAA PAPER 93-2568	p 1084 A93-50286 #	AIAA PAPER 93-2975	p 1050 A93-48169 #	AIAA PAPER 93-3242	p 965 A93-46787 #
AIAA PAPER 93-2569	p 1121 A93-50287 #	AIAA PAPER 93-2976	p 1050 A93-48170 #	AIAA PAPER 93-3244	p 966 A93-46789 #
AIAA PAPER 93-2570	p 1084 A93-50288 *	AIAA PAPER 93-2978	p 1050 A93-48171 *	AIAA PAPER 93-3245	p 966 A93-46790 #
AIAA PAPER 93-2571	p 898 A93-41047 *	AIAA PAPER 93-2979	p 1050 A93-48172 #	AIAA PAPER 93-3246	p 966 A93-46791 #
AIAA PAPER 93-2572	p 1084 A93-50289 #	AIAA PAPER 93-2980	p 1051 A93-48173 #	AIAA PAPER 93-3247	p 966 A93-46792 #
AIAA PAPER 93-2574	p 1085 A93-50290 #	AIAA PAPER 93-2981	p 1051 A93-48174 #	AIAA PAPER 93-3248	p 966 A93-46793 *
AIAA PAPER 93-2576	p 1085 A93-50292 #	AIAA PAPER 93-2982	p 1051 A93-48175 #	AIAA PAPER 93-3249	p 966 A93-46794 #
AIAA PAPER 93-2578	p 1085 A93-50293 #	AIAA PAPER 93-2983	p 1051 A93-48176 #	AIAA PAPER 93-3251	p 1028 A93-46796 #
AIAA PAPER 93-2580	p 1122 A93-50294 #	AIAA PAPER 93-2984	p 1051 A93-48177 #	AIAA PAPER 93-3253	p 1180 A93-53592 *
AIAA PAPER 93-2581	p 1157 A93-50295 #	AIAA PAPER 93-2985	p 1051 A93-48178 #	AIAA PAPER 93-3253	p 988 N93-31648 *
AIAA PAPER 93-2588	p 1142 A93-50300 #	AIAA PAPER 93-2986	p 1052 A93-48179 #	AIAA PAPER 93-3255	p 966 A93-46798 #
AIAA PAPER 93-2589	p 1142 A93-50301 #	AIAA PAPER 93-2987	p 1052 A93-48180 *	AIAA PAPER 93-3258	p 967 A93-46799 #
AIAA PAPER 93-2594	p 1122 A93-50306 *	AIAA PAPER 93-2988	p 1052 A93-48181 *	AIAA PAPER 93-3259	p 967 A93-46800 *
AIAA PAPER 93-2602	p 1122 A93-50311 #	AIAA PAPER 93-2989	p 1052 A93-48182 #	AIAA PAPER 93-3260	p 968 A93-46826 #
AIAA PAPER 93-2609	p 1122 A93-50316 #	AIAA PAPER 93-2991	p 1052 A93-48183 #	AIAA PAPER 93-3261	p 968 A93-46827 #
AIAA PAPER 93-2611	p 1142 A93-50318 #	AIAA PAPER 93-2992	p 1052 A93-48184 *	AIAA PAPER 93-3262	p 968 A93-46828 #
AIAA PAPER 93-2677	p 913 A93-42234 #	AIAA PAPER 93-2994	p 1001 A93-44230 *	AIAA PAPER 93-3263	p 989 N93-31672 *
AIAA PAPER 93-2720	p 962 A93-46476 #	AIAA PAPER 93-2995	p 1053 A93-48185 #	AIAA PAPER 93-3264	p 968 A93-46829 #
AIAA PAPER 93-2721	p 858 A93-41049 #	AIAA PAPER 93-2997	p 1053 A93-48187 #	AIAA PAPER 93-3265	p 968 A93-46831 #
AIAA PAPER 93-2722	p 962 A93-46477 *	AIAA PAPER 93-2998	p 1053 A93-48188 #	AIAA PAPER 93-3266	p 968 A93-46830 #
AIAA PAPER 93-2723	p 962 A93-46478 *	AIAA PAPER 93-2999	p 1053 A93-48189 #	AIAA PAPER 93-3267	p 969 A93-46832 #
AIAA PAPER 93-2724	p 858 A93-41050 #	AIAA PAPER 93-3000	p 1053 A93-48190 #	AIAA PAPER 93-3273	p 1037 A93-46834 #
AIAA PAPER 93-2725	p 962 A93-46479 #	AIAA PAPER 93-3002	p 1053 A93-48192 #	AIAA PAPER 93-3274	p 969 A93-46835 #
AIAA PAPER 93-2726	p 962 A93-46480 #	AIAA PAPER 93-3007	p 1053 A93-48197 #	AIAA PAPER 93-3281	p 969 A93-46839 *
AIAA PAPER 93-2728	p 1039 A93-46482 #	AIAA PAPER 93-3008	p 1054 A93-48198 *	AIAA PAPER 93-3285	p 969 A93-46841 #
AIAA PAPER 93-2735	p 1027 A93-46488 *	AIAA PAPER 93-3009	p 1054 A93-48199 *	AIAA PAPER 93-3286	p 969 A93-46842 #
AIAA PAPER 93-2742	p 963 A93-46493 #	AIAA PAPER 93-3010	p 1054 A93-48200 *	AIAA PAPER 93-3291	p 1021 A93-44995 #
AIAA PAPER 93-2751	p 963 A93-46500 #	AIAA PAPER 93-3011	p 1054 A93-48201 #	AIAA PAPER 93-3292	p 1041 A93-44996 #
AIAA PAPER 93-2763	p 963 A93-46509 #	AIAA PAPER 93-3013	p 1054 A93-48202 *	AIAA PAPER 93-3293	p 1021 A93-44997 #
AIAA PAPER 93-2764	p 963 A93-46510 #	AIAA PAPER 93-3015	p 1148 A93-48204 *	AIAA PAPER 93-3301	p 950 A93-44999 #
AIAA PAPER 93-2766	p 963 A93-46512 *	AIAA PAPER 93-3018	p 1055 A93-48205 *	AIAA PAPER 93-3302	p 950 A93-45000 *
AIAA PAPER 93-2781	p 1012 A93-46525 #	AIAA PAPER 93-3019	p 1055 A93-48206 #	AIAA PAPER 93-3303	p 950 A93-45001 *
AIAA PAPER 93-2782	p 1012 A93-46526 #	AIAA PAPER 93-3022	p 1055 A93-48207 #	AIAA PAPER 93-3304	p 950 A93-45002 #
AIAA PAPER 93-2786	p 1016 A93-46528 #	AIAA PAPER 93-3023	p 1055 A93-48208 #	AIAA PAPER 93-3305	p 951 A93-45003 *
AIAA PAPER 93-2787	p 1027 A93-46529 #	AIAA PAPER 93-3024	p 1055 A93-48209 #	AIAA PAPER 93-3306	p 858 A93-41053 *
AIAA PAPER 93-2789	p 1027 A93-46531 #	AIAA PAPER 93-3025	p 1055 A93-48210 #	AIAA PAPER 93-3310	p 1036 A93-45006 #
AIAA PAPER 93-2790	p 1018 A93-46532 *	AIAA PAPER 93-3026	p 1056 A93-48211 #	AIAA PAPER 93-3311	p 1036 A93-45007 *
AIAA PAPER 93-2793	p 963 A93-46534 #	AIAA PAPER 93-3029	p 1056 A93-48213 *	AIAA PAPER 93-3314	p 951 A93-45010 #
AIAA PAPER 93-2798	p 964 A93-46538 #	AIAA PAPER 93-3032	p 1056 A93-48214 #	AIAA PAPER 93-3315	p 951 A93-45011 #
AIAA PAPER 93-2800	p 1016 A93-46540 #	AIAA PAPER 93-3040	p 1056 A93-48221 #	AIAA PAPER 93-3316	p 951 A93-45012 #
AIAA PAPER 93-2805	p 1028 A93-46544 *	AIAA PAPER 93-3041	p 1056 A93-48222 *	AIAA PAPER 93-3317	p 951 A93-45013 *
AIAA PAPER 93-2806	p 964 A93-46546 #	AIAA PAPER 93-3042	p 1056 A93-48223 #	AIAA PAPER 93-3318	p 952 A93-45014 *
AIAA PAPER 93-2807	p 964 A93-46547 #	AIAA PAPER 93-3044	p 1057 A93-48224 *	AIAA PAPER 93-3319	p 958 A93-45103 *
AIAA PAPER 93-2808	p 949 A93-44227 #	AIAA PAPER 93-3045	p 1057 A93-48225 #	AIAA PAPER 93-3322	p 952 A93-45016 *
AIAA PAPER 93-2809	p 964 A93-46548 #	AIAA PAPER 93-3046	p 1057 A93-48226 #	AIAA PAPER 93-3323	p 952 A93-45017 *
AIAA PAPER 93-2810	p 964 A93-46549 #	AIAA PAPER 93-3047	p 1144 A93-48227 #	AIAA PAPER 93-3324	p 952 A93-45018 #
AIAA PAPER 93-2814	p 965 A93-46552 #	AIAA PAPER 93-3048	p 1057 A93-48228 #	AIAA PAPER 93-3325	p 1022 A93-45019 #
AIAA PAPER 93-2815	p 965 A93-46553 #	AIAA PAPER 93-3049	p 1057 A93-48229 #	AIAA PAPER 93-3328	p 952 A93-45022 #
AIAA PAPER 93-2855	p 1028 A93-46590 #	AIAA PAPER 93-3050	p 1057 A93-48230 #	AIAA PAPER 93-3329	p 952 A93-45023 #
AIAA PAPER 93-2881	p 949 A93-44228 *	AIAA PAPER 93-3052	p 1057 A93-48232 *	AIAA PAPER 93-3331	p 953 A93-45025 #
AIAA PAPER 93-2902	p 1147 A93-48111 #	AIAA PAPER 93-3057	p 1058 A93-48234 *	AIAA PAPER 93-3333	p 953 A93-45027 *
AIAA PAPER 93-2914	p 1044 A93-48116 #	AIAA PAPER 93-3058	p 1058 A93-48235 *	AIAA PAPER 93-3334	p 953 A93-45028 *
AIAA PAPER 93-2915	p 1147 A93-48117 #	AIAA PAPER 93-3059	p 1058 A93-48236 #	AIAA PAPER 93-3335	p 953 A93-45029 *
AIAA PAPER 93-2918	p 1148 A93-48120 #	AIAA PAPER 93-3060	p 1058 A93-48237 #	AIAA PAPER 93-3336	p 953 A93-45030 #
AIAA PAPER 93-2919	p 1180 A93-53591 #	AIAA PAPER 93-3063	p 1058 A93-48239 #	AIAA PAPER 93-3337	p 953 A93-45031 *
AIAA PAPER 93-2921	p 1044 A93-48122 #	AIAA PAPER 93-3064	p 1059 A93-48240 #	AIAA PAPER 93-3339	p 954 A93-45033 #
AIAA PAPER 93-2923	p 1045 A93-48124 #	AIAA PAPER 93-3065	p 1059 A93-48241 *	AIAA PAPER 93-3343	p 954 A93-45037 *

REPORT NUMBER INDEX

AR-007-113

AIAA PAPER 93-3349	p 954	A93-45043	#	AIAA PAPER 93-3511	p 984	A93-47277	#	AIAA PAPER 93-3742	p 1101	A93-51338	#
AIAA PAPER 93-3350	p 954	A93-45044	#	AIAA PAPER 93-3514	p 985	A93-47278	#	AIAA PAPER 93-3746	p 1170	A93-51342	#
AIAA PAPER 93-3351	p 954	A93-45045	#	AIAA PAPER 93-3515	p 985	A93-47279	#	AIAA PAPER 93-3748	p 1170	A93-51344	#
AIAA PAPER 93-3352	p 1036	A93-45046	#	AIAA PAPER 93-3517	p 1009	A93-47280	#	AIAA PAPER 93-3752	p 1143	A93-51348	#
AIAA PAPER 93-3353	p 1037	A93-45047	#	AIAA PAPER 93-3518	p 1014	A93-47281	#	AIAA PAPER 93-3753	p 1101	A93-51349	#
AIAA PAPER 93-3357	p 954	A93-45051	#	AIAA PAPER 93-3520	p 985	A93-47282	#	AIAA PAPER 93-3762	p 1131	A93-51357	#
AIAA PAPER 93-3358	p 955	A93-45052	#	AIAA PAPER 93-3521	p 985	A93-47283	#	AIAA PAPER 93-3763	p 1131	A93-51358	#
AIAA PAPER 93-3363	p 955	A93-45056	#	AIAA PAPER 93-3523	p 985	A93-47284	#	AIAA PAPER 93-3764	p 1101	A93-51359	#
AIAA PAPER 93-3366	p 955	A93-45059	#	AIAA PAPER 93-3526	p 986	A93-47285	#	AIAA PAPER 93-3765	p 1102	A93-51360	#
AIAA PAPER 93-3371	p 955	A93-45064	#	AIAA PAPER 93-3527	p 986	A93-47286	#	AIAA PAPER 93-3766	p 1131	A93-51361	#
AIAA PAPER 93-3378	p 957	A93-45102	#	AIAA PAPER 93-3530	p 986	A93-47287	#	AIAA PAPER 93-3774	p 1131	A93-51369	#
AIAA PAPER 93-3385	p 955	A93-45076	#	AIAA PAPER 93-3533	p 1072	A93-49517	#	AIAA PAPER 93-3775	p 1131	A93-51370	#
AIAA PAPER 93-3386	p 956	A93-45077	#	AIAA PAPER 93-3537	p 986	A93-47288	#	AIAA PAPER 93-3776	p 1132	A93-51371	#
AIAA PAPER 93-3387	p 956	A93-45078	#	AIAA PAPER 93-3538	p 986	A93-47289	#	AIAA PAPER 93-3777	p 1132	A93-51372	#
AIAA PAPER 93-3388	p 956	A93-45079	#	AIAA PAPER 93-3540	p 986	A93-47292	#	AIAA PAPER 93-3778	p 1132	A93-51373	#
AIAA PAPER 93-3390	p 956	A93-45081	#	AIAA PAPER 93-3545	p 1207	A93-52652	#	AIAA PAPER 93-3779	p 1132	A93-51374	#
AIAA PAPER 93-3391	p 956	A93-45082	#	AIAA PAPER 93-3548	p 1226	A93-52653	#	AIAA PAPER 93-3790	p 1143	A93-51385	#
AIAA PAPER 93-3400	p 974	A93-47202	#	AIAA PAPER 93-3550	p 1222	A93-52654	#	AIAA PAPER 93-3791	p 1143	A93-51386	#
AIAA PAPER 93-3401	p 974	A93-47203	#	AIAA PAPER 93-3551	p 1207	A93-52655	#	AIAA PAPER 93-3795	p 1159	A93-51388	#
AIAA PAPER 93-3402	p 974	A93-47204	#	AIAA PAPER 93-3552	p 1222	A93-52656	#	AIAA PAPER 93-3798	p 1106	A93-51391	#
AIAA PAPER 93-3406	p 1008	A93-47205	#	AIAA PAPER 93-3558	p 1214	A93-52659	#	AIAA PAPER 93-3801	p 1139	A93-51393	#
AIAA PAPER 93-3407	p 1008	A93-47206	#	AIAA PAPER 93-3559	p 1222	A93-52660	#	AIAA PAPER 93-3802	p 1170	A93-51394	#
AIAA PAPER 93-3408	p 859	A93-41056	#	AIAA PAPER 93-3560	p 1214	A93-52695	#	AIAA PAPER 93-3808	p 1132	A93-51400	#
AIAA PAPER 93-3410	p 974	A93-47207	#	AIAA PAPER 93-3563	p 1223	A93-52663	#	AIAA PAPER 93-3809	p 1102	A93-51401	#
AIAA PAPER 93-3411	p 1030	A93-47208	#	AIAA PAPER 93-3566	p 1207	A93-52665	#	AIAA PAPER 93-3810	p 1122	A93-51402	#
AIAA PAPER 93-3412	p 975	A93-47209	#	AIAA PAPER 93-3568	p 1096	A93-49518	#	AIAA PAPER 93-3811	p 1123	A93-51403	#
AIAA PAPER 93-3413	p 975	A93-47210	#	AIAA PAPER 93-3570	p 1208	A93-52668	#	AIAA PAPER 93-3812	p 1123	A93-51404	#
AIAA PAPER 93-3414	p 975	A93-47211	#	AIAA PAPER 93-3574	p 1208	A93-52670	#	AIAA PAPER 93-3814	p 1132	A93-51405	#
AIAA PAPER 93-3416	p 975	A93-47212	#	AIAA PAPER 93-3575	p 1208	A93-52671	#	AIAA PAPER 93-3815	p 1133	A93-51406	#
AIAA PAPER 93-3417	p 975	A93-47213	#	AIAA PAPER 93-3577	p 1208	A93-52673	#	AIAA PAPER 93-3816	p 1133	A93-51407	#
AIAA PAPER 93-3418	p 976	A93-47214	#	AIAA PAPER 93-3579	p 1208	A93-52675	#	AIAA PAPER 93-3817	p 1133	A93-51408	#
AIAA PAPER 93-3419	p 976	A93-47215	#	AIAA PAPER 93-3580	p 1208	A93-52676	#	AIAA PAPER 93-3818	p 1143	A93-51409	#
AIAA PAPER 93-3420	p 976	A93-47216	#	AIAA PAPER 93-3582	p 1214	A93-52677	#	AIAA PAPER 93-3832	p 1097	A93-51421	#
AIAA PAPER 93-3422	p 976	A93-47217	#	AIAA PAPER 93-3583	p 1223	A93-52678	#	AIAA PAPER 93-3833	p 1098	A93-51422	#
AIAA PAPER 93-3423	p 976	A93-47218	#	AIAA PAPER 93-3585	p 1209	A93-52679	#	AIAA PAPER 93-3834	p 1098	A93-51423	#
AIAA PAPER 93-3424	p 1008	A93-47219	#	AIAA PAPER 93-3587	p 1223	A93-52680	#	AIAA PAPER 93-3835	p 1098	A93-51424	#
AIAA PAPER 93-3425	p 976	A93-47220	#	AIAA PAPER 93-3588	p 1223	A93-52681	#	AIAA PAPER 93-3836	p 1098	A93-51425	#
AIAA PAPER 93-3426	p 977	A93-47221	#	AIAA PAPER 93-3589	p 1223	A93-52682	#	AIAA PAPER 93-3842	p 1170	A93-51431	#
AIAA PAPER 93-3427	p 1008	A93-47222	#	AIAA PAPER 93-3590	p 1223	A93-52683	#	AIAA PAPER 93-3845	p 1133	A93-51433	#
AIAA PAPER 93-3430	p 977	A93-47223	#	AIAA PAPER 93-3591	p 1224	A93-52684	#	AIAA PAPER 93-3846	p 1102	A93-51480	#
AIAA PAPER 93-3432	p 977	A93-47224	#	AIAA PAPER 93-3593	p 1224	A93-52685	#	AIAA PAPER 93-3847	p 1133	A93-51434	#
AIAA PAPER 93-3433	p 977	A93-47225	#	AIAA PAPER 93-3594	p 1224	A93-52686	#	AIAA PAPER 93-3848	p 1133	A93-51435	#
AIAA PAPER 93-3434	p 977	A93-47226	#	AIAA PAPER 93-3596	p 1224	A93-52687	#	AIAA PAPER 93-3849	p 1134	A93-51436	#
AIAA PAPER 93-3435	p 978	A93-47227	#	AIAA PAPER 93-3598	p 1209	A93-52688	#	AIAA PAPER 93-3850	p 1134	A93-51437	#
AIAA PAPER 93-3436	p 978	A93-47228	#	AIAA PAPER 93-3604	p 1175	A93-52690	#	AIAA PAPER 93-3851	p 1134	A93-51438	#
AIAA PAPER 93-3437	p 978	A93-47229	#	AIAA PAPER 93-3606	p 1191	A93-52691	#	AIAA PAPER 93-3852	p 1134	A93-51439	#
AIAA PAPER 93-3440	p 1014	A93-47230	#	AIAA PAPER 93-3607	p 1214	A93-52697	#	AIAA PAPER 93-3853	p 1140	A93-51440	#
AIAA PAPER 93-3441	p 859	A93-41057	#	AIAA PAPER 93-3615	p 1125	A93-48302	#	AIAA PAPER 93-3855	p 1144	A93-51442	#
AIAA PAPER 93-3442	p 978	A93-47231	#	AIAA PAPER 93-3616	p 1125	A93-48303	#	AIAA PAPER 93-3857	p 1134	A93-51444	#
AIAA PAPER 93-3443	p 1072	A93-49516	#	AIAA PAPER 93-3617	p 1125	A93-48304	#	AIAA PAPER 93-3868	p 1171	A93-51454	#
AIAA PAPER 93-3444	p 978	A93-47232	#	AIAA PAPER 93-3618	p 1125	A93-48305	#	AIAA PAPER 93-3869	p 1171	A93-51455	#
AIAA PAPER 93-3446	p 978	A93-47233	#	AIAA PAPER 93-3619	p 1125	A93-48306	#	AIAA PAPER 93-3870	p 1135	A93-51456	#
AIAA PAPER 93-3447	p 979	A93-47234	#	AIAA PAPER 93-3620	p 1126	A93-48307	#	AIAA PAPER 93-3871	p 1098	A93-51457	#
AIAA PAPER 93-3449	p 1009	A93-47235	#	AIAA PAPER 93-3623	p 1126	A93-48308	#	AIAA PAPER 93-3880	p 1135	A93-51465	#
AIAA PAPER 93-3450	p 1009	A93-47236	#	AIAA PAPER 93-3624	p 1126	A93-48309	#	AIAA PAPER 93-3881	p 1135	A93-51466	#
AIAA PAPER 93-3452	p 1037	A93-47237	#	AIAA PAPER 93-3625	p 1126	A93-48310	#	AIAA PAPER 93-3883	p 1135	A93-51468	#
AIAA PAPER 93-3453	p 979	A93-47238	#	AIAA PAPER 93-3626	p 1126	A93-48311	#	AIAA PAPER 93-3888	p 1144	A93-51472	#
AIAA PAPER 93-3454	p 949	A93-44232	#	AIAA PAPER 93-3627	p 1127	A93-48312	#	AIAA PAPER 93-3942	p 1007	A93-44234	#
AIAA PAPER 93-3456	p 979	A93-47239	#	AIAA PAPER 93-3628	p 1064	A93-48313	#	AIAA PAPER 93-4031	p 1242	A93-54603	#
AIAA PAPER 93-3457	p 1014	A93-47240	#	AIAA PAPER 93-3629	p 1064	A93-48314	#	AIAA PAPER 93-4032	p 1240	A93-54604	#
AIAA PAPER 93-3459	p 979	A93-47242	#	AIAA PAPER 93-3631	p 1064	A93-48316	#	AIAA PAPER 93-4033	p 1229	A93-54605	#
AIAA PAPER 93-3462	p 979	A93-47244	#	AIAA PAPER 93-3633	p 1065	A93-48318	#	AIAA PAPER 93-4034	p 1231	A93-54615	#
AIAA PAPER 93-3463	p 980	A93-47245	#	AIAA PAPER 93-3634	p 1065	A93-48319	#	AIAA PAPER 93-4035	p 1242	A93-54606	#
AIAA PAPER 93-3463	p 1030	A93-47246	#	AIAA PAPER 93-3636	p 1065	A93-48321	#	AIAA PAPER 93-4036	p 1231	A93-54607	#
AIAA PAPER 93-3466	p 980	A93-47247	#	AIAA PAPER 93-3638	p 1165	A93-48323	#	AIAA PAPER 93-4037	p 1255	A93-54608	#
AIAA PAPER 93-3467	p 997	A93-47248	#	AIAA PAPER 93-3639	p 1165	A93-48324	#	AIAA PAPER 93-4038	p 1246	A93-54609	#
AIAA PAPER 93-3468	p 980	A93-47249	#	AIAA PAPER 93-3640	p 1127	A93-48325	#	AIAA PAPER 93-4040	p 1242	A93-54610	#
AIAA PAPER 93-3470	p 980	A93-47250	#	AIAA PAPER 93-3641	p 1127	A93-48326	#	AIAA PAPER 93-4043	p 1265	A93-54611	#
AIAA PAPER 93-3471	p 859	A93-41058	#	AIAA PAPER 93-3642	p 858	A93-40714	#	AIAA PAPER 93-4045	p 1242	A93-54612	#
AIAA PAPER 93-3472	p 980	A93-47251	#	AIAA PAPER 93-3643	p 1127	A93-48327	#	AIAA PAPER 93-4046	p 1242	A93-54613	#
AIAA PAPER 93-3473	p 980	A93-47252	#	AIAA PAPER 93-3644	p 1127	A93-48328	#	AIAA PAPER 93-4047	p 1243	A93-54614	#
AIAA PAPER 93-3474	p 981	A93-47253	#	AIAA PAPER 93-3645	p 1127	A93-48329	#				
AIAA PAPER 93-3475	p 981	A93-47254	#	AIAA PAPER 93-3647	p 1130	A93-49519	#	AL-TP-1992-0020	p 228	N93-12554	#
AIAA PAPER 93-3476	p 981	A93-47255	#	AIAA PAPER 93-3648	p 1128	A93-48331	#	AL-TP-1992-0035-VOL-3	p 440	N93-16500	#
AIAA PAPER 93-3478	p 981	A93-47256	#	AIAA PAPER 93-3649	p 1128	A93-48332	#	AL-TP-1992-0056	p 530	N93-21268	#
AIAA PAPER 93-3479	p 981	A93-47257	#	AIAA PAPER 93-3650	p 1128	A93-48333	#				
AIAA PAPER 93-3480	p 981	A93-47258	#	AIAA PAPER 93-3657	p 1099	A93-48337	#	AL-TR-1991-0111	p 29	N93-12489	#
AIAA PAPER 93-3481	p 982	A93-47259	#	AIAA PAPER 93-3659	p 1128	A93-48339	#	AL-TR-1991-0126	p 232	N93-14406	#
AIAA PAPER 93-3482	p 982	A93-47260	#	AIAA PAPER 93-3661	p 1099	A93-48341	#	AL-TR-1992-0042	p 194	N93-14559	#
AIAA PAPER 93-3484	p 1003	A93-47291	#	AIAA PAPER 93-3662	p 1128	A93-48342	#	AL-TR-1992-0059	p 224	N93-14655	#
AIAA PAPER 93-3485	p 910	A93-41059	#	AIAA PAPER 93-3664	p 1128	A93-48344	#	AL-TR-1992-0082	p 718	N93-25949	#
AIAA PAPER 93-3487	p 982	A93-47261	#	AIAA PAPER 93-3667	p 1104	A93-48345	#	AL-TR-1992-0151	p 852	N93-27662	#
AIAA PAPER 93-3488	p 982	A93-47262	#	AIAA PAPER 93-3668	p 1128	A93-48346	#	AL-TR-1992-0154	p 760	N93-25915	#
AIAA PAPER 93-3491	p 982	A93-47263	#	AIAA PAPER 93-3669	p 1129	A93-48347	#	AL-TR-1992-0160	p 719	N93-25909	#
AIAA PAPER 93-3492	p 982	A93-47264	#	AIAA PAPER 93-3670	p 1129	A93-48348	#				
AIAA PAPER 93-3493	p 982	A93-47265	#	AIAA PAPER 93-3671	p 1129	A93-48349	#	AL/BROOKS-TR-1992-0155	p 719	N93-25783	#
AIAA PAPER 93-3494	p 983	A93-47266	#	AIAA PAPER 93-3673	p 1129	A93-48350	#				
AIAA PAPER 93-3495	p 983	A93-47267	#	AIAA PAPER 93-3674	p 1129	A93-48351	#	ANL/APS/TM-11	p 732	N93-26498	#
AIAA PAPER 93-3496	p 983	A93-47268	#	AIAA PAPER 93-3675	p 1006	A93					

AR-9301

REPORT NUMBER INDEX

AR-9301	p 806	N93-28586	#	ASME PAPER 92-GT-167	p 351	A93-19393	ASME PAPER 92-GT-363	p 257	A93-19527
ARAED-TR-92011	p 19	N93-10811	#	ASME PAPER 92-GT-169	p 250	A93-19395 *	ASME PAPER 92-GT-364	p 257	A93-19528
				ASME PAPER 92-GT-170	p 351	A93-19396	ASME PAPER 92-GT-366	p 257	A93-19530
ARC-93-1	p 516	N93-22003 *	#	ASME PAPER 92-GT-171	p 351	A93-19397	ASME PAPER 92-GT-367	p 375	A93-19531
ARC-93-3	p 714	N93-25162 *	#	ASME PAPER 92-GT-172	p 352	A93-19398	ASME PAPER 92-GT-369	p 388	A93-19532
				ASME PAPER 92-GT-173	p 250	A93-19399 *	ASME PAPER 92-GT-36	p 246	A93-19296
ARE-TM(UHR)-90306	p 21	N93-11365	#	ASME PAPER 92-GT-174	p 251	A93-19400 *	ASME PAPER 92-GT-372	p 355	A93-19534
				ASME PAPER 92-GT-175	p 251	A93-19401 *	ASME PAPER 92-GT-377	p 406	A93-19535
				ASME PAPER 92-GT-178	p 352	A93-19404	ASME PAPER 92-GT-378	p 406	A93-19536
ARI-RR-1637	p 912	N93-29972	#	ASME PAPER 92-GT-180	p 402	A93-19405	ASME PAPER 92-GT-379	p 406	A93-19537
ARI-RR-902	p 94	N93-12299 *	#	ASME PAPER 92-GT-182	p 352	A93-19407	ASME PAPER 92-GT-382	p 406	A93-19539
				ASME PAPER 92-GT-183	p 352	A93-19408	ASME PAPER 92-GT-388	p 257	A93-19543
ARI-TR-961	p 381	N93-17687	#	ASME PAPER 92-GT-184	p 251	A93-19409	ASME PAPER 92-GT-38	p 347	A93-19297
				ASME PAPER 92-GT-185	p 352	A93-19410	ASME PAPER 92-GT-390	p 258	A93-19545
ARL-CR-3-PT-2	p 551	N93-19999	#	ASME PAPER 92-GT-186	p 352	A93-19411	ASME PAPER 92-GT-392	p 355	A93-19546
ARL-CR-43	p 751	N93-25884 *	#	ASME PAPER 92-GT-187	p 402	A93-19412	ASME PAPER 92-GT-394	p 388	A93-19547 *
ARL-CR-49	p 840	N93-27268 *	#	ASME PAPER 92-GT-188	p 402	A93-19413	ASME PAPER 92-GT-400	p 258	A93-19549
ARL-CR-50	p 917	N93-29981	#	ASME PAPER 92-GT-190	p 403	A93-19415	ASME PAPER 92-GT-401	p 355	A93-19550
				ASME PAPER 92-GT-191	p 403	A93-19416	ASME PAPER 92-GT-402	p 355	A93-19551
ARL-FLIGHT-MECH-TM-462	p 329	N93-16404	#	ASME PAPER 92-GT-192	p 403	A93-19417	ASME PAPER 92-GT-403	p 322	A93-19552
				ASME PAPER 92-GT-195	p 403	A93-19420 *	ASME PAPER 92-GT-404	p 356	A93-19553
ARL-MR-91	p 1032	N93-31647 *	#	ASME PAPER 92-GT-1	p 245	A93-19276	ASME PAPER 92-GT-405	p 356	A93-19554
				ASME PAPER 92-GT-200	p 403	A93-19425	ASME PAPER 92-GT-406	p 356	A93-19555
ARL-STRUC-R-449	p 338	N93-18257	#	ASME PAPER 92-GT-203	p 388	A93-19427	ASME PAPER 92-GT-407	p 356	A93-19556
				ASME PAPER 92-GT-204	p 353	A93-19428	ASME PAPER 92-GT-408	p 435	A93-19557
ARL-STRUC-TM-555	p 17	N93-10342	#	ASME PAPER 92-GT-205	p 251	A93-19429 *	ASME PAPER 92-GT-409	p 356	A93-19558
ARL-STRUC-TM-558	p 161	N93-13256	#	ASME PAPER 92-GT-206	p 251	A93-19430	ASME PAPER 92-GT-413	p 356	A93-19561
ARL-STRUC-TM-584	p 392	N93-16403	#	ASME PAPER 92-GT-207	p 404	A93-19431	ASME PAPER 92-GT-414	p 356	A93-19562
				ASME PAPER 92-GT-209	p 251	A93-19432	ASME PAPER 92-GT-415	p 357	A93-19563
ARL-TR-102	p 788	N93-27955	#	ASME PAPER 92-GT-210	p 252	A93-19433	ASME PAPER 92-GT-416	p 357	A93-19564
ARL-TR-111	p 1015	N93-31916	#	ASME PAPER 92-GT-211	p 252	A93-19434	ASME PAPER 92-GT-417	p 388	A93-19565
ARL-TR-112	p 1033	N93-32028	#	ASME PAPER 92-GT-213	p 252	A93-19436 *	ASME PAPER 92-GT-418	p 258	A93-19566
ARL-TR-29	p 392	N93-16537 *	#	ASME PAPER 92-GT-214	p 252	A93-19437	ASME PAPER 92-GT-419	p 258	A93-19567
ARL-TR-2	p 522	N93-21316	#	ASME PAPER 92-GT-215	p 258	A93-19574	ASME PAPER 92-GT-422	p 258	A93-19570
ARL-TR-30	p 553	N93-20585 *	#	ASME PAPER 92-GT-217	p 252	A93-19439	ASME PAPER 92-GT-423	p 406	A93-19571
ARL-TR-5	p 910	N93-30604	#	ASME PAPER 92-GT-218	p 404	A93-19440	ASME PAPER 92-GT-424	p 357	A93-19572
ARL-TR-75	p 730	N93-26260	#	ASME PAPER 92-GT-224	p 404	A93-19442	ASME PAPER 92-GT-430	p 357	A93-19573
ARL-TR-99	p 806	N93-27692	#	ASME PAPER 92-GT-227	p 404	A93-19444	ASME PAPER 92-GT-432	p 258	A93-19575
ARL-TR-9	p 759	N93-25649	#	ASME PAPER 92-GT-228	p 252	A93-19445	ASME PAPER 92-GT-433	p 435	A93-19576
				ASME PAPER 92-GT-229	p 404	A93-19446	ASME PAPER 92-GT-437	p 384	A93-19579 *
ARO-23555.12-EG	p 943	N93-29384	#	ASME PAPER 92-GT-235	p 353	A93-19448	ASME PAPER 92-GT-438	p 357	A93-19580
ARO-24623.126-EG-UIR	p 931	N93-29388	#	ASME PAPER 92-GT-241	p 404	A93-19450	ASME PAPER 92-GT-439	p 388	A93-19581
ARO-27558.9-EG	p 220	N93-14677	#	ASME PAPER 92-GT-243	p 253	A93-19452	ASME PAPER 92-GT-45	p 322	A93-19299
ARO-27864.3-EG-SDI	p 875	N93-29284	#	ASME PAPER 92-GT-244	p 405	A93-19453	ASME PAPER 92-GT-47	p 347	A93-19300
ARO-28002.1-EG	p 759	N93-25651	#	ASME PAPER 92-GT-248	p 405	A93-19457	ASME PAPER 92-GT-48	p 246	A93-19301
ARO-28860.1-EG-CF	p 50	N93-12485	#	ASME PAPER 92-GT-250	p 353	A93-19459	ASME PAPER 92-GT-49	p 246	A93-19302
ARO-30299.1-EG-II	p 909	N93-29985	#	ASME PAPER 92-GT-251	p 253	A93-19460	ASME PAPER 92-GT-4	p 245	A93-19277
				ASME PAPER 92-GT-252	p 239	A93-19461	ASME PAPER 92-GT-50	p 400	A93-19303
ASC-TR-92-5012	p 339	N93-18895	#	ASME PAPER 92-GT-253	p 353	A93-19462	ASME PAPER 92-GT-51	p 347	A93-19304
				ASME PAPER 92-GT-254	p 353	A93-19463	ASME PAPER 92-GT-55	p 347	A93-19305
ASE/EM-92-105	p 19	N93-10648	#	ASME PAPER 92-GT-255	p 353	A93-19464	ASME PAPER 92-GT-56	p 347	A93-19306
				ASME PAPER 92-GT-256	p 353	A93-19465	ASME PAPER 92-GT-57	p 348	A93-19307 *
ASL-91-4	p 880	N93-29152 *	#	ASME PAPER 92-GT-262	p 405	A93-19466	ASME PAPER 92-GT-58	p 348	A93-19308
				ASME PAPER 92-GT-275	p 253	A93-19468	ASME PAPER 92-GT-59	p 247	A93-19309
ASME PAPER 91-GT-129	p 475	A93-26897		ASME PAPER 92-GT-276	p 253	A93-19469	ASME PAPER 92-GT-5	p 245	A93-19278
ASME PAPER 92-GT-106	p 401	A93-19344		ASME PAPER 92-GT-277	p 253	A93-19470	ASME PAPER 92-GT-60	p 247	A93-19310
ASME PAPER 92-GT-108	p 349	A93-19346		ASME PAPER 92-GT-281	p 253	A93-19473	ASME PAPER 92-GT-61	p 247	A93-19311
ASME PAPER 92-GT-10	p 346	A93-19283		ASME PAPER 92-GT-282	p 253	A93-19474	ASME PAPER 92-GT-62	p 247	A93-19312
ASME PAPER 92-GT-110	p 349	A93-19347		ASME PAPER 92-GT-283	p 254	A93-19475	ASME PAPER 92-GT-63	p 247	A93-19313
ASME PAPER 92-GT-115	p 349	A93-19351		ASME PAPER 92-GT-286	p 254	A93-19477	ASME PAPER 92-GT-64	p 247	A93-19314
ASME PAPER 92-GT-116	p 401	A93-19352		ASME PAPER 92-GT-288	p 254	A93-19479	ASME PAPER 92-GT-66	p 400	A93-19316
ASME PAPER 92-GT-118	p 387	A93-19354		ASME PAPER 92-GT-291	p 254	A93-19482	ASME PAPER 92-GT-68	p 348	A93-19318
ASME PAPER 92-GT-119	p 350	A93-19355		ASME PAPER 92-GT-293	p 254	A93-19483	ASME PAPER 92-GT-6	p 346	A93-19279 *
ASME PAPER 92-GT-122	p 387	A93-19356		ASME PAPER 92-GT-294	p 254	A93-19484	ASME PAPER 92-GT-70	p 400	A93-19320
ASME PAPER 92-GT-123	p 350	A93-19357		ASME PAPER 92-GT-295	p 354	A93-19485	ASME PAPER 92-GT-71	p 248	A93-19321
ASME PAPER 92-GT-125	p 350	A93-19359		ASME PAPER 92-GT-297	p 354	A93-19487 *	ASME PAPER 92-GT-72	p 248	A93-19322 *
ASME PAPER 92-GT-127	p 249	A93-19361		ASME PAPER 92-GT-298	p 254	A93-19488	ASME PAPER 92-GT-73	p 348	A93-19323
ASME PAPER 92-GT-128	p 249	A93-19362		ASME PAPER 92-GT-299	p 255	A93-19489	ASME PAPER 92-GT-74	p 248	A93-19324 *
ASME PAPER 92-GT-129	p 350	A93-19363		ASME PAPER 92-GT-300	p 255	A93-19490	ASME PAPER 92-GT-75	p 401	A93-19325 *
ASME PAPER 92-GT-132	p 350	A93-19365		ASME PAPER 92-GT-301	p 255	A93-19491	ASME PAPER 92-GT-76	p 401	A93-19326 *
ASME PAPER 92-GT-134	p 387	A93-19366		ASME PAPER 92-GT-302	p 255	A93-19492	ASME PAPER 92-GT-77	p 401	A93-19327
ASME PAPER 92-GT-135	p 388	A93-19367		ASME PAPER 92-GT-303	p 354	A93-19493	ASME PAPER 92-GT-7	p 400	A93-19280
ASME PAPER 92-GT-136	p 249	A93-19368		ASME PAPER 92-GT-304	p 405	A93-19494 *	ASME PAPER 92-GT-81	p 387	A93-19330
ASME PAPER 92-GT-137	p 401	A93-19369		ASME PAPER 92-GT-306	p 255	A93-19496	ASME PAPER 92-GT-82	p 348	A93-19331
ASME PAPER 92-GT-138	p 350	A93-19370		ASME PAPER 92-GT-307	p 405	A93-19497	ASME PAPER 92-GT-83	p 348	A93-19332
ASME PAPER 92-GT-139	p 401	A93-19371		ASME PAPER 92-GT-308	p 256	A93-19498	ASME PAPER 92-GT-84	p 248	A93-19333
ASME PAPER 92-GT-13	p 347	A93-19285		ASME PAPER 92-GT-309	p 256	A93-19499	ASME PAPER 92-GT-85	p 248	A93-19334
ASME PAPER 92-GT-140	p 388	A93-19372		ASME PAPER 92-GT-30	p 400	A93-19290	ASME PAPER 92-GT-88	p 348	A93-19335
ASME PAPER 92-GT-141	p 402	A93-19373		ASME PAPER 92-GT-312	p 354	A93-19500	ASME PAPER 92-GT-90	p 248	A93-19336
ASME PAPER 92-GT-142	p 388	A93-19374		ASME PAPER 92-GT-315	p 354	A93-19501	ASME PAPER 92-GT-91	p 249	A93-19337
ASME PAPER 92-GT-147	p 351	A93-19375		ASME PAPER 92-GT-31	p 245	A93-19291	ASME PAPER 92-GT-92	p 349	A93-19338
ASME PAPER 92-GT-148	p 351	A93-19376		ASME PAPER 92-GT-320	p 405	A93-19506	ASME PAPER 92-GT-93	p 349	A93-19339
ASME PAPER 92-GT-149	p 351	A93-19377		ASME PAPER 92-GT-323	p 256	A93-19507	ASME PAPER 92-GT-94	p 349	A93-19340
ASME PAPER 92-GT-14	p 347	A93-19286		ASME PAPER 92-GT-324	p 256	A93-19508	ASME PAPER 92-GT-95	p 387	A93-19341
ASME PAPER 92-GT-152	p 402	A93-19379		ASME PAPER 92-GT-325	p 256	A93-19509	ASME PAPER 93-GT-111	p 987	A93-47446
ASME PAPER 92-GT-									

REPORT NUMBER INDEX

DOT/FAA/NR-92/9

AVSCOM-TR-91-A-010	p 328	N93-16186	#	CTN-92-60362	p 63	N93-10374	DODA-AR-007-082	p 329	N93-16404	#
AVSCOM-TR-91-B-003	p 876	N93-29450	* #	CTN-92-60365	p 83	N93-10367	DODA-AR-007-103	p 338	N93-18257	#
AVSCOM-TR-92-B-012	p 47	N93-10968	* #	CTN-92-60388	p 99	N93-10642				
AVSCOM-TR-92-C-009	p 839	N93-27133	* #	CTN-92-60390	p 83	N93-10368	DOE/ER-12813/1	p 935	N93-30489	#
AVSCOM-TR-92-C-015	p 838	N93-27069	* #	CTN-92-60515	p 84	N93-10653	DOE/ER-13919/5	p 419	N93-17761	#
AVSCOM-TR-92-C-030	p 212	N93-12736	* #	CTN-93-60683	p 731	N93-25178	DOE/ER-45468/1	p 823	N93-28490	#
AVSCOM-TR-92-C-034	p 1032	N93-31846	* #	CTN-93-60715	p 562	N93-21820	DOE/ER-61010/002	p 806	N93-28586	#
				DE92-010579	p 216	N93-13524				
B-245206	p 495	N93-19841	#	DE92-010580	p 216	N93-13525	DOE/FAA/RD-93/6	p 707	N93-25456	#
B-247195	p 502	N93-19843	#	DE92-014693	p 90	N93-12140				
				DE92-016997	p 94	N93-12104	DOE/MC-26052/3140	p 554	N93-21254	#
BBC-RD-1992/5	p 552	N93-20573		DE92-017509	p 89	N93-11767				
				DE92-018616	p 215	N93-13321	DOE/NASA/0335-4	p 455	N93-18762	* #
BCRS-92-18	p 937	N93-31010	#	DE92-018748	p 73	N93-11442				
				DE92-019133	p 89	N93-11802	DORA-8203	p 1040	N93-32377	
BFLRF-280	p 736	N93-25902	#	DE92-019619	p 224	N93-13655				
BFLRF-281	p 736	N93-25914	#	DE92-019807	p 94	N93-12075	DOT-VNTSC-FAA-90-5	p 502	N93-19966	#
				DE92-040026	p 222	N93-15278	DOT-VNTSC-FAA-91-15	p 93	N93-11144	#
BNL-47507	p 90	N93-12140	#	DE92-040092	p 434	N93-18587	DOT-VNTSC-FAA-92-3	p 36	N93-11252	#
				DE93-000012	p 485	N93-21766	DOT-VNTSC-FAA-92-4	p 35	N93-10065	#
BR106727	p 67	N93-11435	#	DE93-000016	p 434	N93-18705	DOT-VNTSC-FAA-92-5	p 559	N93-21501	#
BR111319	p 47	N93-10803	#	DE93-000516	p 554	N93-21254	DOT-VNTSC-FAA-93-2	p 935	N93-30611	#
BR113381	p 82	N93-10198	#	DE93-002428	p 453	N93-17225				
BR114028	p 21	N93-11365	#	DE93-002465	p 706	N93-25120	DOT-VNTSC-FA1H2-92	p 88	N93-11617	#
BR116372	p 101	N93-10805	#	DE93-002678	p 694	N93-25121				
BR305563	p 21	N93-11377	#	DE93-002737	p 419	N93-17761	DOT/FAA/ACS-91-1	p 911	N93-29788	#
BR305818	p 23	N93-11882	#	DE93-003362	p 433	N93-15839				
BR308890	p 87	N93-11383	#	DE93-003663	p 747	N93-24963	DOT/FAA/AM-92/18	p 704	N93-25205	#
BR308896	p 23	N93-11883	#	DE93-004480	p 394	N93-18537	DOT/FAA/AM-92/24	p 143	N93-14026	#
BR308899	p 87	N93-11384	#	DE93-005564	p 560	N93-22045	DOT/FAA/AM-92/26	p 152	N93-14276	#
BR308900	p 87	N93-11385	#	DE93-005580	p 843	N93-28943	DOT/FAA/AM-92/27	p 143	N93-14277	#
BR30937	p 68	N93-11906	#	DE93-006019	p 754	N93-24975	DOT/FAA/AM-92/28	p 151	N93-14275	#
BR310269	p 722	N93-25455	#	DE93-007882	p 732	N93-26498	DOT/FAA/AM-92/30	p 502	N93-20582	#
				DE93-007910	p 789	N93-28662	DOT/FAA/AM-92/31	p 319	N93-18927	#
CA-PATENT-APPL-SN-1293201	p 83	N93-10367		DE93-007913	p 917	N93-29767	DOT/FAA/AM-93/1	p 708	N93-26447	#
CA-PATENT-APPL-SN-2001346	p 83	N93-10368		DE93-007964	p 826	N93-28564	DOT/FAA/AM-93/2	p 705	N93-25896	#
CA-PATENT-APPL-SN-2013236	p 63	N93-10374		DE93-008074	p 823	N93-28490				
CA-PATENT-APPL-SN-2024585	p 731	N93-25178		DE93-008339	p 749	N93-25518	DOT/FAA/AOR-100-93/007	p 193	N93-13447	#
				DE93-008719	p 790	N93-29035				
CAP-600	p 991	N93-31730		DE93-009861	p 905	N93-30168	DOT/FAA/CT-TN92/10	p 677	N93-24760	* #
				DE93-009865	p 942	N93-29187	DOT/FAA/CT-TN92/11	p 677	N93-25134	* #
CDNSWC-MRD-80-93-10	p 935	N93-30571	#	DE93-010121	p 943	N93-29189	DOT/FAA/CT-TN92/13	p 67	N93-11616	#
				DE93-010449	p 806	N93-28586	DOT/FAA/CT-TN92/16	p 35	N93-10459	#
CDNSWC/PAS-92/52	p 876	N93-29891	#	DE93-010611	p 911	N93-29869	DOT/FAA/CT-TN92/20	p 88	N93-11617	#
				DE93-010817	p 845	N93-28603	DOT/FAA/CT-TN92/21	p 193	N93-13447	#
CECOM-TR-92-B-014	p 338	N93-18333	* #	DE93-010892	p 937	N93-30487	DOT/FAA/CT-TN92/22	p 503	N93-21759	#
				DE93-011734	p 791	N93-28571	DOT/FAA/CT-TN92/23	p 192	N93-12899	#
CEL-TR-92-49	p 755	N93-26243	#	DE93-016176	p 935	N93-30489	DOT/FAA/CT-TN92/24	p 994	N93-32336	#
				DE93-016195	p 239	N93-15946	DOT/FAA/CT-TN92/25	p 192	N93-12668	#
CFDRC-4240/2	p 737	N93-26268	#	DE93-016248	p 239	N93-15949	DOT/FAA/CT-TN92/30	p 88	N93-11460	#
				DE93-017966	p 25	N93-12352	DOT/FAA/CT-TN92/34	p 331	N93-17219	#
CIT/REF-06-769(E)	p 724	N93-25917	#	DE93-018622	p 988	N93-31189	DOT/FAA/CT-TN92/37	p 706	N93-25243	#
				DE93-018623	p 569	N93-20546	DOT/FAA/CT-TN92/38	p 142	N93-12816	#
CMOTT-92-14	p 290	N93-16596	* #		p 569	N93-20546	DOT/FAA/CT-TN92/42	p 496	N93-21821	#
				DGLR BERICHT 92-03	p 444	A93-19126	DOT/FAA/CT-TN92/48	p 748	N93-25210	#
CMU/SEI-92-SR-3	p 344	N93-18270	#				DOT/FAA/CT-TN92/49	p 503	N93-20612	#
				DGLR-91-27	p 1018	N93-31044	DOT/FAA/CT-TN92/6	p 151	N93-13377	#
CONF-911212-2	p 94	N93-12104	#	DGLR-92-03-087	p 1041	N93-31045	DOT/FAA/CT-TN93/10	p 792	N93-27017	#
CONF-9206262-1	p 224	N93-13655	#				DOT/FAA/CT-TN93/11	p 752	N93-26160	#
CONF-9207155-1	p 453	N93-17225	#	DIGE-EST-TN-016	p 48	N93-11161	DOT/FAA/CT-TN93/14	p 842	N93-28555	#
CONF-920747-7	p 89	N93-11767	#				DOT/FAA/CT-TN93/22	p 841	N93-28054	#
CONF-920792-51	p 911	N93-29869	#	DILC-EST-TN-200	p 101	N93-11156	DOT/FAA/CT-TN93/2	p 706	N93-24948	#
CONF-920799-1	p 89	N93-11802	#				DOT/FAA/CT-TN93/3	p 705	N93-25224	#
CONF-920799-5	p 749	N93-25518	#	DLAS-EST-TR-040	p 67	N93-11225	DOT/FAA/CT-TN93/8	p 705	N93-24741	#
CONF-9209160-20	p 434	N93-18587	#				DOT/FAA/CT-TN93/9	p 791	N93-27252	#
CONF-9209273-1	p 747	N93-24963	#	DLR-FB-90-28	p 485	N93-21659	DOT/FAA/CT-TN9	p 942	N93-29490	#
CONF-9210290-SUMM	p 732	N93-26498	#	DLR-FB-90-37	p 931	N93-29273				
CONF-921049-2	p 434	N93-18705	#	DLR-FB-90-51	p 942	N93-30104	DOT/FAA/CT-89/25	p 791	N93-28055	#
CONF-921055-2	p 90	N93-12140	#	DLR-FB-91-03	p 893	N93-29464	DOT/FAA/CT-90/22	p 496	N93-21557	#
CONF-921110-14	p 215	N93-13321	#	DLR-FB-91-26	p 418	N93-16543	DOT/FAA/CT-90/6	p 502	N93-19966	#
CONF-921110-26	p 222	N93-15278	#	DLR-FB-91-42	p 485	N93-21761	DOT/FAA/CT-91/20	p 713	N93-24739	#
CONF-9211178-3	p 789	N93-28662	#	DLR-FB-91-43	p 516	N93-21762	DOT/FAA/CT-92/11	p 496	N93-21856	#
CONF-930416-1	p 943	N93-29189	#	DLR-FB-92-03	p 485	N93-21763	DOT/FAA/CT-92/12-VOL-1	p 704	N93-25110	#
CONF-930502-2	p 843	N93-28943	#	DLR-FB-92-04	p 988	N93-31197	DOT/FAA/CT-92/12-VOL-2	p 842	N93-28685	#
CONF-930502-3	p 826	N93-28564	#	DLR-FB-92-05	p 441	N93-16515	DOT/FAA/CT-92/17	p 240	N93-17732	#
CONF-930502-4	p 917	N93-29767	#	DLR-FB-92-08	p 790	N93-29006	DOT/FAA/CT-92/2-VOL-1	p 36	N93-11704	#
CONF-930502-6	p 905	N93-30168	#	DLR-FB-92-11	p 434	N93-16477	DOT/FAA/CT-92/2-VOL-2	p 36	N93-11705	#
CONF-930519-5	p 706	N93-25120	#	DLR-FB-92-19	p 1003	N93-31170	DOT/FAA/CT-92/20-ADD-1	p 753	N93-24875	#
CONF-930580-1	p 694	N93-25121	#	DLR-FB-92-22	p 988	N93-31320	DOT/FAA/CT-92/22	p 318	N93-16498	#
CONF-930580-2	p 790	N93-29035	#	DLR-FB-92-25	p 988	N93-31171	DOT/FAA/CT-92/23	p 417	N93-15698	#
CONF-9306128-1	p 942	N93-29187	#				DOT/FAA/CT-92/24	p 192	N93-12902	#
							DOT/FAA/CT-92/26	p 318	N93-16841	#
							DOT/FAA/CT-92/27	p 791	N93-27269	#
CRAFELD-AERO-9017	p 531	N93-21406	#	DLR-MITT-91-11	p 993	N93-31271	DOT/FAA/CT-92/9	p 991	N93-31652	#
				DLR-MITT-91-15	p 569	N93-21368	DOT/FAA/CT-93/4	p 949	N93-32232	#
CRC-583	p 911	N93-29398	#	DLR-MITT-91-16	p 522	N93-21173	DOT/FAA/CT-93/6	p 793	N93-28625	#
				DLR-MITT-91-21	p 503	N93-21004				
CRREL-REPT-93-2	p 912	N93-30103	#	DLR-MITT-92-01	p 167	N93-15152	DOT/FAA/EE-92/01	p 559	N93-21501	#
				DLR-MITT-92-06	p 503	N93-20749	DOT/FAA/EE-92/03	p 569	N93-21317	* #
CRREL-92-18	p 382	N93-17708	#							
				DODA-AR-006-630	p 910	N93-30604	DOT/FAA/NR-92/12	p 755	N93-25645	#
CSDL-R-2463	p 782	N93-27413	#	DODA-AR-006-678	p 17	N93-10342	DOT/FAA/NR-92/13-REV	p 845	N93-27675	#
				DODA-AR-007-074	p 392	N93-16403	DOT/FAA/NR-92/3	p 224	N93-14547	#
CSL-N91-1	p 186	N93-12578	#	DODA-AR-007-077	p 759	N93-25649	DOT/FAA/NR-92/6	p 93	N93-11144	#
							DOT/FAA/NR-92/9	p 911	N93-29815	#
CSS-CR-1210-92-1	p 418	N93-15857	#							

DOT/FAA/PP-92-1	p 193	N93-13882	#	E-7465	p 138	N93-14791	#	ESDU-92043	p 333	N93-17958
DOT/FAA/PP-92-4	p 319	N93-18202	#	E-7471	p 233	N93-15575	#	ETN-92-92063	p 89	N93-11707
DOT/FAA/PP-92-6	p 382	N93-17793	#	E-7473	p 148	N93-15360	#	ETN-92-92100	p 28	N93-11319
DOT/FAA/RD-90/19	p 35	N93-10323	#	E-7476	p 362	N93-16705	#	ETN-92-92109	p 223	N93-15487
DOT/FAA/RD-91/23	p 232	N93-14912	#	E-7479	p 362	N93-16715	#	ETN-92-92126	p 72	N93-11027
DOT/FAA/RD-91/6	p 48	N93-11461	#	E-7481	p 233	N93-15430	#	ETN-92-92162	p 167	N93-15152
DOT/FAA/RD-92/14-VOL-2	p 146	N93-15013	#	E-7492	p 139	N93-15404	#	ETN-92-92164	p 422	N93-18721
DOT/FAA/RD-92/17	p 378	N93-16309	#	E-7493	p 179	N93-15521	#	ETN-92-92165	p 423	N93-18731
DOT/FAA/RD-92/19-1-PT-1	p 488	N93-19590	#	E-7494	p 139	N93-15338	#	ETN-92-92169	p 240	N93-19002
DOT/FAA/RD-92/19-1-PT-2	p 144	N93-14844	#	E-7495	p 138	N93-14911	#	ETN-92-92188	p 101	N93-11204
DOT/FAA/RD-92/2	p 857	N93-30673	#	E-7497	p 148	N93-15354	#	ETN-92-92191	p 59	N93-11206
DOT/FAA/RD-92/3	p 36	N93-11252	#	E-7498	p 148	N93-15345	#	ETN-92-92192	p 59	N93-11207
DOT/FAA/RD-92/4	p 35	N93-10065	#	E-7499	p 149	N93-15522	#	ETN-92-92193	p 59	N93-11208
DOT/FAA/RD-93/11	p 935	N93-30611	#	E-7500	p 188	N93-14831	#	ETN-92-92194	p 72	N93-11031
DOT/FAA/RD-93/14	p 936	N93-29257	#	E-7504	p 294	N93-17884	#	ETN-92-92196	p 72	N93-11032
DOT/FAA/RD-93/15	p 912	N93-30103	#	E-7508	p 179	N93-15359	#	ETN-92-92198	p 85	N93-11014
DOT/FAA/SD-92/1-VOL-2	p 559	N93-21799	#	E-7509	p 551	N93-20057	#	ETN-92-92204	p 56	N93-11019
DOT/FAA/SE-92/4	p 310	N93-18031	#	E-7525	p 290	N93-16596	#	ETN-92-92205	p 20	N93-11020
DOT/FAA/SE-92/5	p 502	N93-20164	#	E-7527	p 421	N93-18426	#	ETN-92-92209	p 56	N93-11023
DOT/FAA/SE-92/6	p 35	N93-10738	#	E-7572-1	p 760	N93-26551	#	ETN-92-92210	p 56	N93-11024
DOT/FRA/NMI-92/21	p 782	N93-27413	#	E-7587	p 825	N93-27092	#	ETN-92-92211	p 85	N93-11025
DOT/VNTSC-FAA-92-7-VOL-1	p 485	N93-21796	#	E-7589	p 550	N93-19971	#	ETN-92-92212	p 85	N93-11034
DOT/VNTSC-FAA-92-7-VOL-2	p 559	N93-21799	#	E-7590	p 819	N93-26907	#	ETN-92-92215	p 72	N93-11035
DRA-TM-AERO/PROP-8	p 295	N93-17991	#	E-7593-VOL-1	p 721	N93-24754	#	ETN-92-92216	p 56	N93-11036
DRA/MAR-TM(MTH)-91320	p 21	N93-11377	#	E-7593-VOL-2	p 721	N93-25106	#	ETN-92-92217	p 56	N93-11037
DREA-CR-90-445	p 99	N93-10642	#	E-7599	p 838	N93-26999	#	ETN-92-92218	p 56	N93-11038
DREA-CR-91-478	p 562	N93-21820	#	E-7620	p 721	N93-25079	#	ETN-92-92219	p 57	N93-11039
DRIC-BR-312886	p 295	N93-17991	#	E-7624	p 536	N93-20237	#	ETN-92-92220	p 57	N93-11040
DS-1607	p 333	N93-17850	#	E-7632	p 723	N93-25673	#	ETN-92-92221	p 86	N93-11054
DS-1881	p 364	N93-17882	#	E-7643	p 900	N93-29065	#	ETN-92-92222	p 57	N93-11055
DS-2022	p 393	N93-17852	#	E-7648	p 722	N93-25129	#	ETN-92-92223	p 58	N93-11105
DS-2023	p 522	N93-21459	#	E-7674	p 746	N93-24759	#	ETN-92-92224	p 58	N93-11106
DS-2026	p 363	N93-17740	#	E-7705	p 699	N93-25883	#	ETN-92-92225	p 73	N93-11107
DS-2027	p 364	N93-18151	#	E-7708	p 815	N93-27680	#	ETN-92-92226	p 58	N93-11108
DS-2129	p 363	N93-17851	#	E-7709	p 677	N93-25134	#	ETN-92-92230	p 139	N93-15489
DS-2136	p 364	N93-18149	#	E-7716	p 693	N93-24911	#	ETN-92-92235	p 58	N93-11085
DS-2138	p 393	N93-17746	#	E-7719	p 677	N93-24760	#	ETN-92-92237	p 57	N93-11061
DS-2140	p 294	N93-17880	#	E-7720	p 935	N93-31031	#	ETN-92-92238	p 57	N93-11062
E-3813	p 877	N93-30373	#	E-7729	p 825	N93-26702	#	ETN-92-92239	p 58	N93-11063
E-5861	p 362	N93-16941	#	E-7742	p 838	N93-27069	#	ETN-92-92242	p 72	N93-11066
E-5894	p 231	N93-12967	#	E-7743	p 839	N93-27133	#	ETN-92-92243	p 58	N93-11112
E-6287	p 88	N93-11624	#	E-7764	p 838	N93-27088	#	ETN-92-92245	p 58	N93-11068
E-6402	p 852	N93-27058	#	E-7768	p 813	N93-27131	#	ETN-92-92246	p 58	N93-11069
E-6751	p 196	N93-15528	#	E-7791	p 930	N93-29157	#	ETN-92-92247	p 20	N93-11070
E-6810	p 737	N93-26201	#	E-7799	p 813	N93-27130	#	ETN-92-92248	p 20	N93-11113
E-6897	p 441	N93-16613	#	E-7799	p 751	N93-25884	#	ETN-92-92249	p 59	N93-11114
E-6938	p 678	N93-26136	#	E-7808	p 724	N93-26161	#	ETN-92-92253	p 48	N93-11334
E-6967	p 194	N93-15498	#	E-7814	p 781	N93-27097	#	ETN-92-92256	p 86	N93-11325
E-6994-1	p 555	N93-21831	#	E-7821	p 1005	N93-32368	#	ETN-92-92257	p 86	N93-11326
E-7022	p 130	N93-13292	#	E-7831	p 841	N93-28053	#	ETN-92-92258	p 87	N93-11327
E-7067	p 179	N93-15342	#	E-7832	p 812	N93-27026	#	ETN-92-92260	p 28	N93-11357
E-7121	p 844	N93-27012	#	E-7834	p 838	N93-27020	#	ETN-92-92261	p 87	N93-11358
E-7138	p 101	N93-11370	#	E-7835	p 791	N93-27267	#	ETN-92-92272	p 28	N93-11375
E-7196	p 730	N93-25080	#	E-7853	p 848	N93-28051	#	ETN-92-92294	p 21	N93-11377
E-7206	p 222	N93-15343	#	E-7861	p 838	N93-27132	#	ETN-92-92296	p 21	N93-11365
E-7210	p 56	N93-10983	#	E-7868	p 814	N93-29194	#	ETN-92-92299	p 67	N93-11435
E-7216	p 527	N93-21197	#	E-7870	p 813	N93-27128	#	ETN-92-92300	p 48	N93-11485
E-7234	p 552	N93-20368	#	E-7884	p 814	N93-27160	#	ETN-92-92303	p 23	N93-11882
E-7237	p 85	N93-10963	#	E-7887	p 989	N93-31839	#	ETN-92-92305	p 23	N93-11883
E-7238	p 60	N93-12077	#	E-7891	p 1032	N93-31647	#	ETN-92-92306	p 68	N93-11906
E-7240	p 82	N93-10087	#	E-7894	p 1005	N93-32351	#	ETN-92-92316	p 87	N93-11383
E-7241	p 90	N93-12277	#	E-7898	p 814	N93-27610	#	ETN-92-92318	p 87	N93-11384
E-7252	p 90	N93-12197	#	E-7905	p 815	N93-28609	#	ETN-92-92319	p 87	N93-11385
E-7264	p 21	N93-11223	#	E-7925	p 816	N93-28617	#	ETN-92-92337	p 64	N93-11576
E-7278	p 59	N93-11530	#	E-7937	p 1031	N93-31193	#	ETN-92-92350	p 88	N93-11587
E-7280	p 421	N93-18321	#	E-7939	p 816	N93-28697	#	ETN-92-92352	p 200	N93-15490
E-7281	p 421	N93-18380	#	E-7944	p 988	N93-31648	#	ETN-92-92356	p 421	N93-18563
E-7282	p 55	N93-10456	#	E-7948	p 900	N93-29072	#	ETN-92-92378	p 67	N93-11728
E-7300	p 752	N93-26202	#	E-7955	p 900	N93-29162	#	ETN-92-92379	p 67	N93-11224
E-7327	p 291	N93-16704	#	E-7957	p 989	N93-31672	#	ETN-92-92409	p 101	N93-11156
E-7331	p 180	N93-15525	#	E-7958	p 1032	N93-31846	#	ETN-92-92413	p 48	N93-11161
E-7339	p 212	N93-12735	#	E-7964	p 1032	N93-31860	#	ETN-92-92414	p 67	N93-11225
E-7348	p 212	N93-12736	#	E-7975	E-8002			ETN-92-92511	p 318	N93-17559
E-7350	p 815	N93-27640	#	E-7984	ECL-91-18	p 64	N93-11576	ETN-92-92512	p 393	N93-17920
E-7351	p 60	N93-12402	#	E-7987	EPA/600/A-93/116	p 1035	N93-32089	ETN-92-92516	p 331	N93-17535
E-7382	p 60	N93-12418	#	E-7995	ESA-TT-1244	p 485	N93-21659	ETN-92-92519	p 331	N93-17562
E-7398	p 220	N93-14799	#	E-7998	ESA-TT-1255	p 931	N93-29273	ETN-92-92522	p 392	N93-17540
E-7422	p 459	N93-20902	#	E-7999	ESA-TT-1258	p 942	N93-30104	ETN-92-92528	p 318	N93-17584
E-7425	p 110	N93-14102	#	E-8002	ESA-TT-1267	p 893	N93-29464	ETN-92-92556	p 293	N93-17542
E-7442	p 228	N93-13154	#	ESDU-88040	ESA-TT-1279	p 993	N93-31271	ETN-92-92572	p 331	N93-17564
E-7443	p 290	N93-16625	#	ESDU-89033				ETN-92-92574	p 293	N93-17543
E-7451	p 179	N93-15403	#	ESDU-92008				ETN-92-92575	p 331	N93-17565
E-7452	p 110	N93-15573	#	ESDU-92019				ETN-92-92576	p 331	N93-17566
E-7454	p 200	N93-15504	#	ESDU-92020				ETN-92-92577	p 332	N93-17567
E-7457				ESDU-92021				ETN-92-92578	p 293	N93-17568
				ESDU-92022				ETN-92-92579	p 332	N93-17569
				ESDU-92023				ETN-92-92580	p 343	N93-17570
				ESDU-92029				ETN-92-92581	p 343	N93-17547
				ESDU-92030				ETN-92-92721	p 165	N93-15126
				ESDU-92031				ETN-92-92731	p 139	N93-15131
				ESDU-92039				ETN-92-92732	p 177	N93-15143
								ETN-92-92757	p 536	N93-20845
								ETN-92-92760	p 572	N93-20734
								ETN-92-92761	p 521	N93-20735
								ETN-92-92766	p 339	N93-18507

REPORT NUMBER INDEX

ISABE 93-7035

ETN-92-92773	p 329	N93-16562	#	ETN-93-94061	p 1020	N93-32385	#	H-1858	p 20	N93-11221	* #
ETN-92-92775	p 454	N93-16563	#	ETN-93-94063	p 1014	N93-31042	#	H-1862	p 25	N93-12353	* #
ETN-92-92776	p 456	N93-16464	#	ETN-93-94064	p 1003	N93-31111	#	H-1865	p 223	N93-13288	* #
ETN-92-92777	p 240	N93-16465	#	ETN-93-94065	p 999	N93-31840	#	H-1873	p 1005	N93-32220	* #
ETN-92-92778	p 289	N93-16467	#	ETN-93-94069	p 1006	N93-32372	#	H-1875	p 344	N93-19110	* #
ETN-92-92779	p 381	N93-16468	#	ETN-93-94070	p 994	N93-32337	#	H-1881	p 339	N93-18616	* #
ETN-92-92780	p 289	N93-16470	#	ETN-93-94071	p 999	N93-32338	#	H-1886	p 518	N93-20163	* #
ETN-92-92795	p 441	N93-16567	#	ETN-93-94073	p 999	N93-32416	#	H-1917	p 806	N93-28693	* #
ETN-92-92854	p 514	N93-20742	#	ETN-93-94074	p 990	N93-32357	#				
ETN-92-92856	p 527	N93-20743	#	ETN-93-94075	p 990	N93-32358	#	HTC-9204	p 220	N93-14797	* #
ETN-92-92872	p 329	N93-16283	#	ETN-93-94076	p 999	N93-32203	#	ICASE-92-52	p 102	N93-12021	* #
ETN-92-92875	p 289	N93-16210	#	ETN-93-94078	p 999	N93-32205	#	ICASE-92-53	p 231	N93-12986	* #
ETN-92-92878	p 317	N93-16213	#	ETN-93-94079	p 1006	N93-32386	#	ICASE-92-63	p 290	N93-16627	* #
ETN-92-92880	p 328	N93-16215	#	ETN-93-94081	p 987	N93-31148	#	ICASE-92-64	p 694	N93-25083	* #
ETN-92-92884	p 329	N93-16287	#	ETN-93-94090	p 937	N93-31010	#	ICASE-92-65	p 298	N93-18771	* #
ETN-92-92885	p 440	N93-16288	#	ETN-93-94175	p 889	N93-30671	#	ICASE-92-70	p 694	N93-25153	* #
ETN-93-91916	p 569	N93-21368	#	ETN-93-94192	p 888	N93-31043	#	ICASE-93-13	p 779	N93-27004	* #
ETN-93-91917	p 522	N93-21173	#	ETN-93-94193	p 1018	N93-31044	#	ICASE-93-15	p 780	N93-27090	* #
ETN-93-91921	p 503	N93-21004	#	ETN-93-94194	p 998	N93-31058	#	ICASE-93-20	p 843	N93-28975	* #
ETN-93-91931	p 485	N93-21761	#	ETN-93-94195	p 1041	N93-31045	#	ICOMP-92-13	p 90	N93-12277	* #
ETN-93-91932	p 516	N93-21762	#	ETN-93-94197	p 998	N93-31046	#	ICOMP-92-26	p 551	N93-20057	* #
ETN-93-91933	p 485	N93-21763	#	ETN-93-94213	p 1039	N93-31051	#	ICOMP-92-27	p 290	N93-16596	* #
ETN-93-92007	p 294	N93-17809	#	ETN-93-94214	p 987	N93-31052	#	ICOMP-93-10	p 838	N93-27088	* #
ETN-93-92397	p 418	N93-16543	#	ETN-93-94216	p 1030	N93-31123	#	ILR-MITT-275(1992)	p 889	N93-30671	#
ETN-93-92401	p 441	N93-16515	#	ETN-93-94220	p 1031	N93-31146	#	IMFL-91-31	p 293	N93-17542	#
ETN-93-92403	p 434	N93-16477	#	ETN-93-94223	p 988	N93-31538	#	IMFL-91-32	p 165	N93-15126	#
ETN-93-92408	p 503	N93-20749	#	ETN-93-94285	p 1040	N93-31653	#	INPE-5376-TDI/471	p 83	N93-10310	#
ETN-93-92588	p 572	N93-21022	#	FASTC-ID(RS)T-0309-92	p 842	N93-28289	#	INPE-5428-RPO/662	p 232	N93-13257	#
ETN-93-92618	p 372	N93-18142	#	FASTC-ID(RS)T-0311-92	p 914	N93-29134	#	INRIA-RR-1476	p 297	N93-18648	#
ETN-93-92651	p 297	N93-18648	#	FASTC-ID(RS)T-0312-92	p 725	N93-26239	#	INRIA-RR-1493	p 297	N93-18652	#
ETN-93-92658	p 297	N93-18652	#	FASTC-ID(RS)T-0313-92	p 510	N93-19849	#	INRIA-RR-1540	p 422	N93-18623	#
ETN-93-92662	p 422	N93-18623	#	FASTC-ID(RS)T-0316-92	p 513	N93-20605	#	INRIA-RR-1652	p 788	N93-28440	#
ETN-93-92730	p 297	N93-18627	#	FASTC-ID(RS)T-0608-91	p 110	N93-13946	#	INT-PATENT-CLASS-A47L-11/282	p 556	N93-22035	*
ETN-93-92733	p 364	N93-18628	#	FASTC-ID(RS)T-0625-92	p 765	N93-28576	#	INT-PATENT-CLASS-B23P-19/00	p 221	N93-14871	*
ETN-93-92739	p 443	N93-18630	#	FASTC-ID(RS)T-0626-92	p 764	N93-27056	#	INT-PATENT-CLASS-B29C-41/18	p 83	N93-10368	*
ETN-93-92859	p 318	N93-16343	#	FASTC-ID(RS)T-0628-92	p 678	N93-26238	#	INT-PATENT-CLASS-B62D-5/12	p 83	N93-10367	*
ETN-93-92863	p 418	N93-16411	#	FASTC-ID(RS)T-0786-91	p 19	N93-10856	#	INT-PATENT-CLASS-B64C-13/00	p 63	N93-10374	*
ETN-93-92870	p 329	N93-16345	#	FASTC-ID(RS)T-0787-91	p 19	N93-11798	#	INT-PATENT-CLASS-B64C-17/00	p 63	N93-10374	*
ETN-93-92886	p 554	N93-20907	#	FASTC-ID(RS)T-0788-91	p 19	N93-10858	#	INT-PATENT-CLASS-B64C-27/00	p 729	N93-25998	* #
ETN-93-92999	p 295	N93-18128	#	FASTC-ID(RS)T-0790-91	p 288	N93-15889	#	INT-PATENT-CLASS-B64D-27/08	p 63	N93-10374	*
ETN-93-93002	p 337	N93-18131	#	FASTC-ID(RS)T-0825-92	p 789	N93-28493	#	INT-PATENT-CLASS-B64F-1/10	p 731	N93-25178	*
ETN-93-93004	p 484	N93-20806	#	FASTC-ID(RS)T-0826-92	p 806	N93-27694	#	INT-PATENT-CLASS-F02K-3/04	p 522	N93-22034	*
ETN-93-93005	p 484	N93-20807	#	FASTC-ID(RS)T-0869-92	p 876	N93-29919	#	INT-PATENT-CLASS-F02K-3/08	p 522	N93-22034	*
ETN-93-93009	p 420	N93-18103	#	FASTC-ID(RS)T-0870-92	p 876	N93-29919	#	INT-PATENT-CLASS-F25B-1/00	p 216	N93-13422	*
ETN-93-93044	p 551	N93-20230	#	FEL-91-A375	p 221	N93-14805	#	INT-PATENT-CLASS-G01M-9/00	p 296	N93-18275	*
ETN-93-93059	p 496	N93-20928	#	FEL-92-C282	p 937	N93-31010	#	INT-PATENT-CLASS-G01M-9/00	p 731	N93-25998	*
ETN-93-93073	p 443	N93-18698	#	FFA-TN-1992-08	p 1039	N93-31051	#	INT-PATENT-CLASS-G01M-9/00	p 751	N93-26000	*
ETN-93-93078	p 298	N93-18701	#	FFA-TN-1992-26	p 987	N93-31052	#	INT-PATENT-CLASS-G01N-25/72	p 67	N93-11057	*
ETN-93-93079	p 297	N93-18617	#	FFA-TN-1992-30	p 1030	N93-31123	#	INT-PATENT-CLASS-H01M-12/00	p 83	N93-10368	*
ETN-93-93080	p 485	N93-21659	#	FFA-TN-1992-37	p 843	N93-28994	#	INT-PATENT-CLASS-H01M-4/04	p 83	N93-10368	*
ETN-93-93318	p 319	N93-17954	#	FFA-TN-1992-43	p 1031	N93-31146	#	IS-M-740	p 749	N93-25518	#
ETN-93-93319	p 382	N93-17875	#	FR-692101	p 229	N93-13370	* #	ISABE 93-7000	p 1227	A93-53977	
ETN-93-93322	p 295	N93-17929	#	FR21998-16	p 737	N93-26282	#	ISABE 93-7001	p 1194	A93-53978	
ETN-93-93372	p 363	N93-17740	#	FR9201-01	p 752	N93-26564	#	ISABE 93-7002	p 1194	A93-53979	
ETN-93-93375	p 521	N93-20913	#	GAO/NSIAD-92-311	p 513	N93-20245	#	ISABE 93-7003	p 1194	A93-53980	
ETN-93-93377	p 363	N93-17849	#	GAO/NSIAD-93-71	p 340	N93-18981	#	ISABE 93-7005	p 1194	A93-53981	
ETN-93-93380	p 294	N93-17880	#	GAO/RCED-92-113	p 502	N93-19843	#	ISABE 93-7006	p 1183	A93-53982	
ETN-93-93383	p 364	N93-17882	#	GAO/RCED-92-14	p 495	N93-19841	#	ISABE 93-7007	p 1183	A93-53983	
ETN-93-93385	p 393	N93-17746	#	GAO/T-NSIAD-92-26	p 161	N93-13253	#	ISABE 93-7008	p 1183	A93-53984	
ETN-93-93386	p 333	N93-17850	#	GARTUR-AD(AG07)TP069	p 987	N93-31052	#	ISABE 93-7009	p 1183	A93-53985	
ETN-93-93387	p 364	N93-18149	#	GARTUR/TP-055	p 527	N93-20743	#	ISABE 93-7010	p 1183	A93-53986	
ETN-93-93389	p 363	N93-17851	#	GE-R89AEB208	p 232	N93-13762	* #	ISABE 93-7011	p 1184	A93-53987	
ETN-93-93391	p 364	N93-18151	#	GPO-56-943-VOL-2	p 234	N93-13799	#	ISABE 93-7012	p 1184	A93-53988	
ETN-93-93392	p 393	N93-17852	#	GPO-57-099	p 234	N93-13800	#	ISABE 93-7015	p 1194	A93-53991	
ETN-93-93393	p 522	N93-21459	#	GPO-59-010	p 234	N93-13798	#	ISABE 93-7016	p 1195	A93-53992	
ETN-93-93425	p 484	N93-21054	#	GRI-91/0258	p 555	N93-21465	#	ISABE 93-7018	p 1195	A93-53994	
ETN-93-93427	p 514	N93-21056	#	GRI-92/0239	p 212	N93-12977	#	ISABE 93-7019	p 1195	A93-53995	
ETN-93-93430	p 484	N93-21059	#	GRI-92/0364	p 755	N93-26529	#	ISABE 93-7020	p 1195	A93-53996	
ETN-93-93431	p 537	N93-21462	#	GRI-92/0470-PHASE-2	p 756	N93-26533	#	ISABE 93-7021	p 1195	A93-53997	
ETN-93-93432	p 515	N93-21479	#	GSF-BAND-8	p 1034	N93-31925	#	ISABE 93-7022	p 1195	A93-53998	
ETN-93-93433	p 515	N93-21401	#	GTEC-21-5854-1	p 55	N93-10348	* #	ISABE 93-7023	p 1196	A93-53999	*
ETN-93-93434	p 905	N93-29999	#	GU-AERO-9202	p 21	N93-11464	#	ISABE 93-7024	p 1196	A93-54000	
ETN-93-93454	p 791	N93-28206	#	H-1631	p 910	N93-30764	* #	ISABE 93-7025	p 1213	A93-54001	
ETN-93-93455	p 1034	N93-31925	#	H-1708	p 136	N93-14451	* #	ISABE 93-7026	p 1213	A93-54002	
ETN-93-93532	p 531	N93-21406	#	H-1809	p 175	N93-13155	* #	ISABE 93-7027	p 1196	A93-54003	*
ETN-93-93578	p 893	N93-29268	#	H-1825	p 131	N93-13322	* #	ISABE 93-7028	p 1196	A93-54004	
ETN-93-93712	p 931	N93-29273	#	H-1844	p 381	N93-16753	* #	ISABE 93-7029	p 1184	A93-54005	
ETN-93-93713	p 942	N93-30104	#	H-1851	p 22	N93-11532	* #	ISABE 93-7030	p 1184	A93-54006	
ETN-93-93714	p 893	N93-29464	#	H-1855	p 49	N93-11863	* #	ISABE 93-7031	p 1184	A93-54007	
ETN-93-93722	p 943	N93-30110	#					ISABE 93-7032	p 1196	A93-54008	
ETN-93-93723	p 876	N93-30020	#					ISABE 93-7033	p 1185	A93-54009	
ETN-93-93728	p 918	N93-30203	#					ISABE 93-7034	p 1197	A93-54010	
ETN-93-93733	p 790	N93-29006	#					ISABE 93-7035	p 1197	A93-54011	
ETN-93-93739	p 988	N93-31320	#								
ETN-93-93776	p 841	N93-27832	#								
ETN-93-93899	p 788	N93-28440	#								
ETN-93-93917	p 993	N93-31271	#								
ETN-93-93930	p 992	N93-32409	#								
ETN-93-93932	p 991	N93-31730	#								
ETN-93-93933	p 1040	N93-32377	#								
ETN-93-93953	p 998	N93-31197	#								
ETN-93-93955	p 1003	N93-31170	#								
ETN-93-93956	p 988	N93-31171	#								
ETN-93-94040	p 1031	N93-31519	#								
ETN-93-94059	p 993	N93-31120	#								
ETN-93-94060	p 1001	N93-32332	#								

ISABE 93-7036

REPORT NUMBER INDEX

ISABE 93-7036	p 1197 A93-54012	ISBN 0-387-53859-3	p 864 A93-42576	ISBN-9-05-411061-9	p 937 N93-31010 #
ISABE 93-7037	p 1197 A93-54013	ISBN 0-387-54428-3	p 864 A93-42576	ISBN-90-386-0042-9	p 893 N93-29268 #
ISABE 93-7038	p 1197 A93-54014	ISBN 0-387-54930-7	p 925 A93-40823	ISBN-90-6275-670-0	p 240 N93-19002 #
ISABE 93-7039	p 1197 A93-54015	ISBN 0-387-55404-1	p 1146 A93-51626	ISBN-90-6275-768-5	p 441 N93-16567 #
ISABE 93-7040	p 1198 A93-54016	ISBN 0-387-55686-9	p 1023 A93-45451	ISBN-92-835-0672-3	p 213 N93-13199 #
ISABE 93-7041	p 1198 A93-54017	ISBN 0-387-97737-6	p 859 A93-41776 *	ISBN-92-835-0680-4	p 104 N93-11710 #
ISABE 93-7042	p 1198 A93-54018	ISBN 0-470-21764-2	p 344 A93-17899	ISBN-92-835-0682-0	p 104 N93-10610 #
ISABE 93-7043	p 1198 A93-54019	ISBN 0-540-53461-X	p 947 A93-45772	ISBN-92-835-0686-3	p 176 N93-14890 #
ISABE 93-7044	p 1198 A93-54020	ISBN 0-7803-0469-1	p 29 A93-10976	ISBN-92-835-0687-1	p 490 N93-19653 #
ISABE 93-7045	p 1219 A93-54021	ISBN 0-7923-1673-8	p 1072 A93-49521	ISBN-92-835-0688-X	p 510 N93-19901 #
ISABE 93-7046	p 1198 A93-54022	ISBN 0-8138-0398-5	p 240 A93-17526	ISBN-92-835-0697-9	p 496 N93-21187 #
ISABE 93-7047	p 1185 A93-54023	ISBN 0-8138-0749-2	p 341 A93-17574	ISBN-92-835-0698-7	p 514 N93-21305 #
ISABE 93-7048	p 1199 A93-54024	ISBN 0-8194-0587-6	p 532 A93-27043	ISBN-92-835-0701-0	p 901 N93-29926 #
ISABE 93-7049	p 1213 A93-54025	ISBN 0-8194-0701-1	p 1166 A93-49350	ISBN-92-835-0709-6	p 1004 N93-31741 #
ISABE 93-7050	p 1199 A93-54026	ISBN 0-8194-0713-5	p 1158 A93-51250	ISBN-951-22-0519-X	p 66 N93-12415 #
ISABE 93-7052	p 1199 A93-54028	ISBN 0-8194-0818-2	p 544 A93-27237	ISBN-951-22-1042-8	p 26 N93-12414 #
ISABE 93-7053	p 1185 A93-54029	ISBN 0-8194-0859-X	p 547 A93-28151 *	ISBN-951-38-4014-X	p 841 N93-27832 #
ISABE 93-7054	p 1185 A93-54030	ISBN 0-8194-0926-X	p 1263 A93-55176	ISBN-951-38-4075-1	p 443 N93-18698 #
ISABE 93-7055	p 1185 A93-54031	ISBN 0-8194-0967-7	p 1151 A93-49455		
ISABE 93-7057	p 1185 A93-54033	ISBN 0-8194-0978-2	p 1105 A93-49462	ISVR-TR-215	p 1040 N93-32339
ISABE 93-7058	p 1185 A93-54034	ISBN 0-85296-533-2	p 929 A93-43376	ITN-93-85187	p 764 N93-27166
ISABE 93-7059	p 1219 A93-54035	ISBN 0-903409-70-4	p 345 A93-18778	JIAA-TR-108	p 839 N93-27151 *
ISABE 93-7060	p 1220 A93-54036	ISBN 0-903409-82-8	p 311 A93-17751	JIAA-TR-109	p 781 N93-27150 *
ISABE 93-7061	p 1199 A93-54037	ISBN 0-903409-84-4	p 238 A93-18761	JPRS-JST-93-009	p 761 N93-25418 #
ISABE 93-7062	p 1199 A93-54038	ISBN 0-903409-86-0	p 211 A93-17251	JPRS-UAC-93-003	p 678 N93-26325 #
ISABE 93-7063	p 1200 A93-54039	ISBN 0-903409-88-7	p 45 A93-13401	JPRS-UEQ-92-003	p 749 N93-25427 #
ISABE 93-7064	p 1200 A93-54040	ISBN 0-903409-90-9	p 142 A93-17301	JPRS-UEQ-92-006	p 842 N93-28636 #
ISABE 93-7065	p 1200 A93-54041	ISBN 0-903409-95-X	p 311 A93-17835	JPRS-UEQ-92-007	p 842 N93-28635 #
ISABE 93-7066	p 1200 A93-54042	ISBN 0-903409-99-2	p 1257 A93-54894	JPRS-UEQ-92-008	p 842 N93-28675 #
ISABE 93-7067	p 1200 A93-54043 *	ISBN 0-906674-77-8	p 743 A93-34301 *	JPRS-UEQ-92-010	p 842 N93-28674 #
ISABE 93-7068	p 1186 A93-54044	ISBN 0-909882-12-6	p 557 A93-28476	JPRS-UEQ-93-003	p 842 N93-28691 #
ISABE 93-7069	p 1201 A93-54045	ISBN 0-933283-05-9	p 482 A93-29780	JPRS-UEQ-93-004	p 930 N93-29090 #
ISABE 93-7072	p 1201 A93-54048	ISBN 1-56032-147-4	p 1256 A93-54626		
ISABE 93-7073	p 1201 A93-54049	ISBN 1-56032-147-4	p 1257 A93-54651		
ISABE 93-7074	p 1220 A93-54050	ISBN 1-56091-179-4	p 412 A93-21840		
ISABE 93-7075	p 1186 A93-54051 *	ISBN 1-56347-044-6	p 78 A93-12151		
ISABE 93-7076	p 1220 A93-54052	ISBN 1-56347-046-2	p 107 A93-14151		
ISABE 93-7077	p 1220 A93-54053 *	ISBN 1-56347-071-3	p 1194 A93-53976		
ISABE 93-7078	p 1220 A93-54054	ISBN 1-56555-007-2	p 1167 A93-50726 *	JSR-91-330	p 755 N93-25837 #
ISABE 93-7079	p 1201 A93-54055	ISBN 1-85768-0057	p 237 A93-18754	JTN-92-80390	p 299 N93-19273 #
ISABE 93-7080	p 1201 A93-54056	ISBN 1-85768-010-3	p 1244 A93-55294	JTN-92-80393	p 52 N93-12370 #
ISABE 93-7081	p 1213 A93-54057	ISBN 1-85768-015-4	p 1043 A93-50353	JTN-92-80395	p 68 N93-12359 #
ISABE 93-7082	p 1201 A93-54058	ISBN 1-85768-020-0	p 1262 A93-54718	JTN-92-80396	p 65 N93-12361 #
ISABE 93-7083	p 1202 A93-54059	ISBN 1-85768-040-5	p 1140 A93-51934	JTN-92-80397	p 65 N93-12362 #
ISABE 93-7084	p 1202 A93-54060	ISBN 1-85768-045-6	p 1175 A93-54287	JTN-92-80401	p 102 N93-12375 #
ISABE 93-7085	p 1202 A93-54061	ISBN 1-85768-065-0	p 458 A93-29475	JTN-92-80402	p 26 N93-12503 #
ISABE 93-7086	p 1186 A93-54062 *	ISBN 1-85768-075-8	p 501 A93-29474	JTN-92-80403	p 91 N93-12365 #
ISABE 93-7087	p 1202 A93-54063	ISBN 1-85768-080-4	p 458 A93-29473	JTN-92-80404	p 52 N93-12367 #
ISABE 93-7088	p 1202 A93-54064	ISBN 1-85768-085-5	p 701 A93-34616	JTN-92-80405	p 26 N93-12369 #
ISABE 93-7089	p 1202 A93-54065	ISBN 1-85768-095-2	p 764 A93-39535	JTN-92-80409	p 52 N93-12383 #
ISABE 93-7090	p 1203 A93-54066	ISBN 1-85768-120-7	p 945 A93-43869	JTN-92-80411	p 25 N93-12352 #
ISABE 93-7091	p 1203 A93-54067	ISBN 3-452-22293-4	p 103 A93-11411	JTN-92-80412	p 49 N93-12354 #
ISABE 93-7092	p 1186 A93-54068	ISBN 3-452-22293-4	p 103 A93-11412		
ISABE 93-7093	p 1186 A93-54069	ISBN 3-922010-68-7	p 444 A93-19126		
ISABE 93-7094	p 1186 A93-54070	ISBN 4-9900181-1-7	p 80 A93-13626	KU-FRL-926-1	p 713 N93-24739 #
ISABE 93-7095	p 1186 A93-54071 *	ISBN 5-203-00804-3	p 458 A93-28874	L-16704	p 875 N93-29449 *
ISABE 93-7096	p 1203 A93-54072	ISBN 5-217-00793-1	p 718 A93-35678	L-16761	p 189 N93-15366 *
ISABE 93-7097	p 1203 A93-54073	ISBN 5-217-00802-4	p 713 A93-35676	L-16855	p 876 N93-29450 *
ISABE 93-7098	p 1187 A93-54074	ISBN 5-217-00808-3	p 677 A93-35677	L-16889-PT-2	p 921 N93-30841 *
ISABE 93-7099	p 1187 A93-54075	ISBN 5-217-00809-1	p 721 A93-35685	L-16921	p 22 N93-11622 *
ISABE 93-7100	p 1187 A93-54076	ISBN 5-217-01299-4	p 893 A93-43831	L-16950	p 553 N93-20585 *
ISABE 93-7101	p 1192 A93-54077	ISBN 5-230-16902-8	p 835 A93-39084	L-16964	p 344 N93-18408 *
ISABE 93-7102	p 1187 A93-54078	ISBN 5-277-00610-9	p 992 A93-44505	L-16976	p 19 N93-10824 *
ISABE 93-7103	p 1187 A93-54079	ISBN 5-277-00815-2	p 487 A93-29431	L-16998	p 875 N93-29165 *
ISABE 93-7104	p 1187 A93-54080	ISBN 5-277-01192-7	p 947 A93-44508	L-17004	p 779 N93-26899 *
ISABE 93-7105	p 1203 A93-54081	ISBN 5-286-00342-7	p 151 A93-15224	L-17024	p 513 N93-20584 *
ISABE 93-7106	p 1188 A93-54082	ISBN 5-286-00610-8	p 753 A93-35689	L-17041	p 63 N93-10070 *
ISABE 93-7107	p 1188 A93-54083	ISBN 83-01-10939-9	p 394 A93-17569	L-17050	p 102 N93-11620 *
ISABE 93-7108	p 1203 A93-54084	ISBN 962-7128-06-6	p 1100 A93-49105	L-17057	p 65 N93-12304 *
ISABE 93-7109	p 1204 A93-54085			L-17059	p 701 N93-26134 *
ISABE 93-7110	p 1204 A93-54086	ISBN 0-16-037924-5	p 104 N93-11100 *	L-17060	p 131 N93-13353 *
ISABE 93-7112	p 1188 A93-54087	ISBN 0-16-038961-5	p 234 N93-13800 #	L-17085	p 338 N93-18333 *
ISABE 93-7113	p 1204 A93-54088	ISBN 0-16-038977-1	p 234 N93-13799 #	L-17087	p 392 N93-16537 *
ISABE 93-7114	p 1221 A93-54089	ISBN 0-309-04732-3	p 4 N93-10647 *	L-17088	p 779 N93-27005 *
ISABE 93-7115	p 1221 A93-54090	ISBN 0-309-05171-1	p 143 N93-13787	L-17096	p 1010 N93-32380 *
ISABE 93-7117	p 1221 A93-54092	ISBN 0-315-67464-4	p 135 N93-13930	L-17102	p 222 N93-15434 *
ISABE 93-7118	p 1188 A93-54093	ISBN 0-85679-813-4	p 136 N93-14516	L-17108	p 24 N93-12321 *
ISABE 93-7119	p 1221 A93-54094	ISBN 0-85679-824-X	p 164 N93-14541	L-17112	p 779 N93-27032 *
ISABE 93-7120	p 1221 A93-54095	ISBN 0-85679-825-8	p 335 N93-18042	L-17118	p 69 N93-12447 *
ISABE 93-7121	p 1221 A93-54096	ISBN 0-85679-826-6	p 330 N93-16635	L-17123	p 373 N93-19108 *
ISABE 93-7123	p 1222 A93-54098	ISBN 0-85679-827-4	p 330 N93-16636	L-17134	p 552 N93-20299 *
ISABE 93-7124	p 1189 A93-54099	ISBN 0-85679-828-2	p 392 N93-16637	L-17143	p 989 N93-31733 *
ISABE 93-7125	p 1204 A93-54100	ISBN 0-85679-832-0	p 136 N93-14514	L-17148	p 700 N93-26085 *
ISABE 93-7127	p 1204 A93-54102	ISBN 0-85679-835-5	p 291 N93-16638	L-17149	p 788 N93-28070 *
ISABE 93-7128	p 1204 A93-54103	ISBN 0-85679-836-3	p 392 N93-16641	L-17151	p 874 N93-29160 *
ISABE 93-7129	p 1175 A93-54104	ISBN 0-85679-837-1	p 290 N93-16522	L-17154	p 875 N93-29166 *
ISABE 93-7130	p 1189 A93-54105	ISBN 0-85679-847-9	p 290 N93-16634	L-17190	p 1017 N93-32379 *
ISABE 93-7131	p 1205 A93-54106	ISBN 0-85679-850-9	p 136 N93-14515		
ISABE 93-7132	p 1205 A93-54107	ISBN 0-85679-853-3	p 333 N93-17958		
ISABE 93-7133	p 1225 A93-54108	ISBN 0-86-039500-6	p 991 N93-31730	LA-SUB-93-152	p 937 N93-30487 #
		ISBN 0-86776-461-9	p 555 N93-21383 #	LA-UR-92-1964	p 89 N93-11767 #
ISAS-RN-646	p 128 N93-12716 #	ISBN 0-86776-464-3	p 555 N93-21382 #	LA-UR-92-2391	p 215 N93-13321 #
		ISBN 0-904747-36-X	p 67 N93-11224 #		
ISBN 0-07-060333-2	p 342 A93-19801 *	ISBN 0-904747-37-8	p 152 N93-14729 #	LBL-31884	p 94 N93-12104 #
ISBN 0-19-507358-4	p 548 A93-28749	ISBN 0-904947-31-9	p 67 N93-11728 #	LBL-32323	p 911 N93-29869 #
ISBN 0-306-44206-X	p 406 A93-19582	ISBN 1-871564-41-7	p 531 N93-21406 #		

REPORT NUMBER INDEX

NAS 1.26:177612

LC-92-15610	p 143	N93-13787	#	NAS 1.15:102839	p 1006	N93-32374	#	NAS 1.15:106112	p 838	N93-27088	#
LC-92-64197	p 4	N93-10647	#	NAS 1.15:103086	p 946	N93-29452	#	NAS 1.15:106114	p 813	N93-27131	#
LESC-29702	p 69	N93-10960	#	NAS 1.15:103719	p 852	N93-27058	#	NAS 1.15:106130	p 813	N93-27130	#
LIB-TRANS-2197	p 782	N93-27274	#	NAS 1.15:103872	p 64	N93-10741	#	NAS 1.15:106131	p 825	N93-26702	#
LMI-PL015R1	p 1019	N93-32085	#	NAS 1.15:103896	p 35	N93-10745	#	NAS 1.15:106140	p 815	N93-27640	#
LR-675	p 329	N93-16345	#	NAS 1.15:103924	p 456	N93-16652	#	NAS 1.15:106148	p 1005	N93-32368	#
LR-677	p 329	N93-16283	#	NAS 1.15:103937	p 305	N93-19379	#	NAS 1.15:106149	p 900	N93-29065	#
LR-680	p 289	N93-16210	#	NAS 1.15:103939	p 1033	N93-32212	#	NAS 1.15:106150	p 838	N93-27020	#
LR-684	p 317	N93-16213	#	NAS 1.15:103947	p 516	N93-21810	#	NAS 1.15:106151	p 841	N93-28053	#
LR-688	p 328	N93-16215	#	NAS 1.15:103958	p 36	N93-12320	#	NAS 1.15:106152	p 812	N93-27026	#
MAE-T1960	p 25	N93-12343	#	NAS 1.15:103962	p 129	N93-12721	#	NAS 1.15:106167	p 848	N93-28051	#
MBB-FE-1-S-PUB-0504	p 998	N93-31043	#	NAS 1.15:103963	p 694	N93-25091	#	NAS 1.15:106169	p 838	N93-27132	#
MBB-FE-2-S-PUB-478	p 331	N93-17564	#	NAS 1.15:103968	p 373	N93-19380	#	NAS 1.15:106179	p 813	N93-27128	#
MBB-FE-202-S-PUB-0486	p 484	N93-21054	#	NAS 1.15:103981	p 885	N93-29653	#	NAS 1.15:106181	p 814	N93-27160	#
MBB-FE-202-S-PUB-480	p 293	N93-17543	#	NAS 1.15:103989	p 990	N93-32226	#	NAS 1.15:106186	p 989	N93-31839	#
MBB-FE-211-S-PUB-0481	p 514	N93-21056	#	NAS 1.15:103998	p 994	N93-32225	#	NAS 1.15:106187	p 930	N93-29157	#
MBB-FE-211-S-PUB-0489-A	p 484	N93-21059	#	NAS 1.15:104001	p 700	N93-26099	#	NAS 1.15:106189	p 1032	N93-31647	#
MBB-FE-221-S-PUB-0483	p 537	N93-21462	#	NAS 1.15:104004	p 706	N93-24914	#	NAS 1.15:106192	p 1005	N93-32351	#
MBB-FE-221-S-PUB-0501	p 1018	N93-31044	#	NAS 1.15:104005	p 790	N93-27076	#	NAS 1.15:106198	p 814	N93-27610	#
MBB-FE-251-S-PUB-479	p 331	N93-17565	#	NAS 1.15:104025	p 994	N93-32348	#	NAS 1.15:106216	p 1004	N93-31671	#
MBB-LME-202-S-PUB-0485	p 998	N93-31058	#	NAS 1.15:104164	p 64	N93-11176	#	NAS 1.15:106220	p 914	N93-29194	#
MBB-LME-202-S-PUB-0505	p 1041	N93-31045	#	NAS 1.15:104257	p 20	N93-11221	#	NAS 1.15:106225	p 1031	N93-31193	#
MBB-LME-221-HYPAC-PUB-2-A	p 515	N93-21479	#	NAS 1.15:104261	p 25	N93-12353	#	NAS 1.15:106230	p 816	N93-28697	#
MBB-LME-242-S-PUB-0451	p 998	N93-31046	#	NAS 1.15:104262	p 223	N93-13288	#	NAS 1.15:106235	p 988	N93-31648	#
MBB-LME-251-S-PUB-0491-A	p 515	N93-21401	#	NAS 1.15:104263	p 1005	N93-32220	#	NAS 1.15:106240	p 900	N93-29162	#
MBB-UD-0599-91-PUB	p 331	N93-17566	#	NAS 1.15:104265	p 344	N93-19110	#	NAS 1.15:106245	p 989	N93-31672	#
MBB-UD-0600-91-PUB	p 332	N93-17567	#	NAS 1.15:104266	p 339	N93-18616	#	NAS 1.15:106253	p 1032	N93-31846	#
MBB-UD-0601-91-PUB	p 293	N93-17568	#	NAS 1.15:104267	p 518	N93-20163	#	NAS 1.15:106273	p 1032	N93-31860	#
MBB-UD-0602-91-PUB	p 332	N93-17569	#	NAS 1.15:105272	p 752	N93-26202	#	NAS 1.15:107594	p 186	N93-13367	#
MBB-UD-0604-91-PUB	p 343	N93-17570	#	NAS 1.15:105572	p 441	N93-16613	#	NAS 1.15:107621	p 22	N93-11610	#
MBB-UD-0605-91-PUB	p 343	N93-17547	#	NAS 1.15:105573	p 678	N93-26136	#	NAS 1.15:107665	p 47	N93-10968	#
MBB-UD-0614-92-PUB	p 223	N93-15487	#	NAS 1.15:105577	p 194	N93-15498	#	NAS 1.15:107667	p 442	N93-18332	#
MBB-Z-0432-92-PUB	p 72	N93-11027	#	NAS 1.15:105579	p 130	N93-13292	#	NAS 1.15:107669	p 109	N93-13025	#
MBB-Z-0442-92-PUB	p 536	N93-20845	#	NAS 1.15:105786	p 179	N93-15342	#	NAS 1.15:107670	p 378	N93-15790	#
MCAT-92-016	p 68	N93-12349	#	NAS 1.15:105804	p 844	N93-27012	#	NAS 1.15:107674	p 102	N93-12080	#
MCAT-92-020	p 194	N93-14809	#	NAS 1.15:105807	p 101	N93-11370	#	NAS 1.15:107682	p 747	N93-25176	#
MCAT-92-021	p 382	N93-18766	#	NAS 1.15:105809	p 730	N93-25080	#	NAS 1.15:107687	p 219	N93-14483	#
MCAT-92-022	p 382	N93-18520	#	NAS 1.15:105810	p 222	N93-15343	#	NAS 1.15:107690	p 88	N93-11544	#
MCAT-93-07	p 483	N93-20235	#	NAS 1.15:105821	p 56	N93-10983	#	NAS 1.15:107691	p 64	N93-12216	#
MDC-K0395-2	p 330	N93-16947	#	NAS 1.15:105824	p 527	N93-21197	#	NAS 1.15:107697	p 162	N93-13565	#
MDC-K0395-3	p 330	N93-16999	#	NAS 1.15:105829	p 85	N93-10963	#	NAS 1.15:107698	p 458	N93-19976	#
MDC-92K0374	p 718	N93-24764	#	NAS 1.15:105833	p 60	N93-12077	#	NAS 1.15:107708	p 453	N93-16755	#
MIT-ATC-187	p 224	N93-14547	#	NAS 1.15:105838	p 82	N93-10087	#	NAS 1.15:107730	p 989	N93-31732	#
MPIS-8/1991	p 297	N93-18627	#	NAS 1.15:105839	p 90	N93-12277	#	NAS 1.15:107739	p 718	N93-26553	#
MPIS-9/1991	p 139	N93-15131	#	NAS 1.15:105852	p 552	N93-20368	#	NAS 1.15:107745	p 693	N93-25074	#
MS-CIS-91-28	p 228	N93-12554	#	NAS 1.15:105853	p 90	N93-12197	#	NAS 1.15:107746	p 852	N93-27272	#
MTL-TR-92-71	p 510	N93-19447	#	NAS 1.15:105858	p 88	N93-11624	#	NAS 1.15:107748	p 707	N93-26087	#
MTL/TR-92-69	p 736	N93-25895	#	NAS 1.15:105863	p 21	N93-11223	#	NAS 1.15:107756	p 852	N93-27271	#
MTR-92W00228	p 707	N93-25456	#	NAS 1.15:105868	p 59	N93-11530	#	NAS 1.15:107758	p 840	N93-27250	#
NADC-911111-60	p 74	N93-12248	#	NAS 1.15:105874	p 55	N93-10456	#	NAS 1.15:107761	p 806	N93-27258	#
NADC-91112-50	p 98	N93-11463	#	NAS 1.15:105881	p 421	N93-18380	#	NAS 1.15:107764	p 852	N93-28692	#
NAL-PD-FC-9203	p 187	N93-13566	#	NAS 1.15:105884	p 421	N93-18321	#	NAS 1.15:107766	p 104	N93-10872	#
NAL-SP-IC-9201	p 234	N93-13368	#	NAS 1.15:105898	p 291	N93-16704	#	NAS 1.15:107769	p 104	N93-10815	#
NAL-SP-16	p 299	N93-19273	#	NAS 1.15:105908	p 180	N93-15525	#	NAS 1.15:107770	p 234	N93-12671	#
NAL-TM-642-PT-1	p 25	N93-12352	#	NAS 1.15:105915	p 212	N93-12735	#	NAS 1.15:107774	p 234	N93-12672	#
NAL-TM-643	p 49	N93-12354	#	NAS 1.15:105924	p 65	N93-12305	#	NAS 1.15:107776	p 572	N93-21794	#
NAL-TM-645	p 988	N93-31189	#	NAS 1.15:105932	p 60	N93-12402	#	NAS 1.15:107778	p 945	N93-29323	#
NAL-TR-1122	p 52	N93-12383	#	NAS 1.15:105936	p 459	N93-20902	#	NAS 1.15:107781	p 945	N93-29322	#
NAL-TR-1125	p 52	N93-12370	#	NAS 1.15:105937	p 110	N93-14102	#	NAS 1.15:107782	p 230	N93-15578	#
NAL-TR-1127	p 68	N93-12359	#	NAS 1.15:105940	p 228	N93-13154	#	NAS 1.15:107783	p 230	N93-15579	#
NAL-TR-1128T	p 65	N93-12361	#	NAS 1.15:105946	p 290	N93-16625	#	NAS 1.15:107785	p 230	N93-15502	#
NAL-TR-1129	p 65	N93-12362	#	NAS 1.15:105952	p 179	N93-15403	#	NAS 1.15:107786	p 555	N93-21819	#
NAL-TR-1133	p 102	N93-12375	#	NAS 1.15:105959	p 110	N93-15573	#	NAS 1.15:107787	p 823	N93-27142	#
NAL-TR-1134	p 26	N93-12503	#	NAS 1.15:105968	p 200	N93-15504	#	NAS 1.15:107789	p 1000	N93-32223	#
NAL-TR-1135	p 91	N93-12365	#	NAS 1.15:105969	p 724	N93-26161	#	NAS 1.15:107790	p 1038	N93-32224	#
NAL-TR-1136	p 52	N93-12367	#	NAS 1.15:105970	p 138	N93-14791	#	NAS 1.15:107791	p 875	N93-29449	#
NAL-TR-1137	p 26	N93-12369	#	NAS 1.15:105971	p 148	N93-15360	#	NAS 1.15:107792	p 910	N93-30764	#
NAMRL-1378	p 717	N93-25933	#	NAS 1.15:105972	p 233	N93-15430	#	NAS 1.15:107793	p 876	N93-29450	#
NAS 1.15:102705	p 17	N93-10349	#	NAS 1.15:105976	p 138	N93-14911	#	NAS 1.15:107794	p 63	N93-10070	#
NAS 1.15:102803	p 139	N93-15483	#	NAS 1.15:105977	p 139	N93-15404	#	NAS 1.15:107795	p 22	N93-11622	#
				NAS 1.15:105978	p 179	N93-15521	#	NAS 1.15:107796	p 196	N93-15528	#
				NAS 1.15:105985	p 139	N93-15338	#	NAS 1.15:107797	p 555	N93-21831	#
				NAS 1.15:105989	p 148	N93-15354	#	NAS 1.15:107798	p 65	N93-12304	#
				NAS 1.15:105993	p 148	N93-15345	#	NAS 1.15:107799	p 552	N93-20299	#
				NAS 1.15:105997	p 148	N93-15522	#	NAS 1.15:107800	p 49	N93-11863	#
				NAS 1.15:106013	p 149	N93-15522	#	NAS 1.15:107801	p 22	N93-11532	#
				NAS 1.15:106015	p 188	N93-14831	#	NAS 1.15:107802	p 779	N93-27032	#
				NAS 1.15:106020	p 362	N93-16715	#	NAS 1.15:107803	p 779	N93-26899	#
				NAS 1.15:106027	p 179	N93-15359	#	NAS 1.15:107804	p 175	N93-13155	#
				NAS 1.15:106028	p 551	N93-20057	#	NAS 1.15:107805	p 136	N93-14451	#
				NAS 1.15:106033	p 360	N93-16705	#	NAS 1.15:107806	p 131	N93-13322	#
				NAS 1.15:106042	p 290	N93-16596	#	NAS 1.15:107807	p 381	N93-16753	#
				NAS 1.15:106044	p 421	N93-18426	#	NAS 1.15:107808	p 700	N93-26085	#
				NAS 1.15:106054	p 233	N93-15575	#	NAS 1.15:107809	p 875	N93-29166	#
				NAS 1.15:106086	p 760	N93-26551	#	NAS 1.15:107810	p 1010	N93-32380	#
				NAS 1.15:106100	p 825	N93-27092	#	NAS 1.15:107811	p 779	N93-27005	#
					p 550	N93-19971	#	NAS 1.15:107812	p 1017	N93-32379	#
					p 819	N93-26907	#	NAS 1.15:107813	p 212	N93-12674	#
					p 838	N93-26999	#	NAS 1.15:107814	p 949	N93-32404	#
					p 721	N93-25079	#	NAS 1.15:107815	p 420	N93-17779	#
					p 723	N93-25673	#	NAS 1.15:107816	p 293	N93-16942	#
					p 722	N93-25129	#	NAS 1.15:107817	p 99	N93-10458	#
					p 693	N93-24911	#	NAS 1.15:107818	p 240	N93-17883	#
					p 838	N93-27069	#	NAS 1.15:107819	p 571	N93-19970	#
					p 839	N93-271					

NAS 1.26:180824	p 55	N93-10348 *	#	NAS 1.26:191469	p 1000	N93-32216 *	#	NAS 1.26:193183	p 793	N93-28936 *	#
NAS 1.26:182193	p 917	N93-29451 *	#	NAS 1.26:191625	p 424	N93-18862 *	#	NAS 1.26:193187	p 880	N93-29152 *	#
NAS 1.26:182268	p 187	N93-13735 *	#	NAS 1.26:191647	p 418	N93-16558 *	#	NAS 1.26:193222	p 893	N93-29153 *	#
NAS 1.26:182269	p 232	N93-13762 *	#	NAS 1.26:191649	p 391	N93-15830 *	#	NAS 1.26:193237	p 914	N93-29215 *	#
NAS 1.26:182270	p 233	N93-15116 *	#	NAS 1.26:191652	p 200	N93-15431 *	#	NAS 1.26:193241	p 930	N93-29213 *	#
NAS 1.26:184421	p 91	N93-12401 *	#	NAS 1.26:191671	p 137	N93-14737 *	#	NAS 1.26:193259	p 1030	N93-31110 *	#
NAS 1.26:184442	p 198	N93-13311 *	#	NAS 1.26:191672	p 137	N93-14738 *	#	NAS 1.26:193268	p 1038	N93-31649 *	#
NAS 1.26:184498	p 220	N93-14763 *	#	NAS 1.26:191715	p 140	N93-15588 *	#	NAS 1.26:193302	p 990	N93-31855 *	#
NAS 1.26:185676	p 914	N93-29652 *	#	NAS 1.26:191774	p 372	N93-17800 *	#	NAS 1.26:193366	p 1015	N93-31848 *	#
NAS 1.26:185698	p 69	N93-10960 *	#	NAS 1.26:191803	p 371	N93-16560 *	#	NAS 1.26:193412	p 1019	N93-31739 *	#
NAS 1.26:186027	p 806	N93-28693 *	#	NAS 1.26:191885	p 484	N93-21562 *	#	NAS 1.26:193467	p 879	N93-31037 *	#
NAS 1.26:187125	p 521	N93-20583 *	#	NAS 1.26:191889	p 296	N93-18384 *	#	NAS 1.26:193468	p 936	N93-31036 *	#
NAS 1.26:187126	p 521	N93-20773 *	#	NAS 1.26:191890	p 381	N93-16695 *	#	NAS 1.26:193552	p 1040	N93-32221 *	#
NAS 1.26:187127	p 364	N93-18702 *	#	NAS 1.26:191900	p 442	N93-18372 *	#	NAS 1.26:193831	p 812	N93-27115 *	#
NAS 1.26:187128	p 174	N93-12695 *	#	NAS 1.26:191917	p 422	N93-18576 *	#	NAS 1.26:4110	p 877	N93-30373 *	#
NAS 1.26:187141	p 815	N93-27680 *	#	NAS 1.26:191929	p 391	N93-16389 *	#	NAS 1.26:4118	p 934	N93-30374 *	#
NAS 1.26:189111	p 198	N93-12589 *	#	NAS 1.26:191930	p 537	N93-21749 *	#	NAS 1.26:4216	p 934	N93-30375 *	#
NAS 1.26:189193-VOL-1	p 721	N93-24754 *	#	NAS 1.26:191980	p 296	N93-18378 *	#	NAS 1.26:4471	p 229	N93-13370 *	#
NAS 1.26:189193-VOL-2	p 721	N93-25106 *	#	NAS 1.26:191987	p 297	N93-18602 *	#	NAS 1.26:4478	p 292	N93-16940 *	#
NAS 1.26:189212	p 220	N93-14799 *	#	NAS 1.26:192011	p 334	N93-17974 *	#	NAS 1.26:4479	p 343	N93-16693 *	#
NAS 1.26:189221	p 364	N93-18578 *	#	NAS 1.26:192013	p 336	N93-18060 *	#	NAS 1.26:4481	p 220	N93-14797 *	#
NAS 1.26:189228	p 455	N93-18762 *	#	NAS 1.26:192018	p 336	N93-18061 *	#	NAS 1.26:4492	p 298	N93-19015 *	#
NAS 1.26:189618	p 330	N93-16947 *	#	NAS 1.26:192022	p 336	N93-18059 *	#	NAS 1.26:4505	p 780	N93-27096 *	#
NAS 1.26:189619	p 330	N93-16999 *	#	NAS 1.26:192023	p 335	N93-18049 *	#	NAS 1.26:4513	p 789	N93-28449 *	#
NAS 1.26:189670	p 91	N93-12411 *	#	NAS 1.26:192024	p 334	N93-17976 *	#	NAS 1.26:4514	p 780	N93-27084 *	#
NAS 1.26:189676	p 569	N93-21317 *	#	NAS 1.26:192032	p 334	N93-18017 *	#	NAS 1.26:4517	p 1019	N93-31643 *	#
NAS 1.26:189688	p 94	N93-12299 *	#	NAS 1.26:192039	p 420	N93-18047 *	#	NAS 1.26:4520	p 895	N93-29885 *	#
NAS 1.26:189698	p 99	N93-12538 *	#	NAS 1.26:192040	p 332	N93-17802 *	#	NAS 1.55:10105-PT-1	p 488	N93-19590 *	#
NAS 1.26:189699	p 98	N93-12346 *	#	NAS 1.26:192041	p 337	N93-18161 *	#	NAS 1.55:10105-PT-2	p 144	N93-14844 *	#
NAS 1.26:189703	p 65	N93-12413 *	#	NAS 1.26:192044	p 333	N93-17972 *	#	NAS 1.55:10114	p 514	N93-21310 *	#
NAS 1.26:189717	p 102	N93-12021 *	#	NAS 1.26:192046	p 334	N93-18037 *	#	NAS 1.55:3104-PT-2	p 921	N93-30841 *	#
NAS 1.26:189718	p 231	N93-12986 *	#	NAS 1.26:192048	p 337	N93-18155 *	#	NAS 1.55:3156	p 857	N93-30673 *	#
NAS 1.26:189723	p 318	N93-16692 *	#	NAS 1.26:192049	p 333	N93-17804 *	#	NAS 1.55:3157	p 69	N93-12447 *	#
NAS 1.26:189734	p 290	N93-16627 *	#	NAS 1.26:192050	p 339	N93-18386 *	#	NAS 1.60:3190	p 737	N93-26201 *	#
NAS 1.26:189736	p 291	N93-16710 *	#	NAS 1.26:192051	p 332	N93-17803 *	#	NAS 1.60:3212	p 19	N93-10824 *	#
NAS 1.26:189737	p 418	N93-16379 *	#	NAS 1.26:192053	p 336	N93-18063 *	#	NAS 1.60:3225	p 553	N93-20585 *	#
NAS 1.26:189738	p 298	N93-18771 *	#	NAS 1.26:192054	p 337	N93-18166 *	#	NAS 1.60:3241	p 513	N93-20584 *	#
NAS 1.26:189739	p 420	N93-18093 *	#	NAS 1.26:192069	p 338	N93-18350 *	#	NAS 1.60:3253	p 131	N93-13353 *	#
NAS 1.26:190420	p 894	N93-29498 *	#	NAS 1.26:192070	p 338	N93-18349 *	#	NAS 1.60:3255	p 344	N93-18408 *	#
NAS 1.26:190617	p 68	N93-11910 *	#	NAS 1.26:192072	p 334	N93-17977 *	#	NAS 1.60:3259	p 701	N93-26134 *	#
NAS 1.26:190663	p 84	N93-10372 *	#	NAS 1.26:192074	p 335	N93-18055 *	#	NAS 1.60:3260	p 24	N93-12321 *	#
NAS 1.26:190692	p 17	N93-10098 *	#	NAS 1.26:192075	p 335	N93-18054 *	#	NAS 1.60:3268	p 338	N93-18333 *	#
NAS 1.26:190746	p 85	N93-10891 *	#	NAS 1.26:192077	p 332	N93-17711 *	#	NAS 1.60:3269	p 102	N93-11620 *	#
NAS 1.26:190778	p 677	N93-25134 *	#	NAS 1.26:192082	p 335	N93-18056 *	#	NAS 1.60:3270	p 189	N93-15366 *	#
NAS 1.26:190779	p 677	N93-24760 *	#	NAS 1.26:192102	p 526	N93-19960 *	#	NAS 1.60:3271	p 222	N93-15434 *	#
NAS 1.26:190811	p 36	N93-11139 *	#	NAS 1.26:192105	p 298	N93-18781 *	#	NAS 1.60:3284	p 392	N93-16537 *	#
NAS 1.26:190837	p 36	N93-10961 *	#	NAS 1.26:192124	p 386	N93-16629 *	#	NAS 1.60:3302	p 373	N93-19108 *	#
NAS 1.26:190845	p 89	N93-11716 *	#	NAS 1.26:192127	p 527	N93-20296 *	#	NAS 1.60:3313	p 874	N93-29160 *	#
NAS 1.26:190911	p 16	N93-10069 *	#	NAS 1.26:192161	p 483	N93-20018 *	#	NAS 1.60:3314	p 875	N93-29165 *	#
NAS 1.26:190915	p 336	N93-18064 *	#	NAS 1.26:192162	p 551	N93-20268 *	#	NAS 1.60:3315	p 362	N93-16941 *	#
NAS 1.26:190918	p 4	N93-10647 *	#	NAS 1.26:192164	p 382	N93-18766 *	#	NAS 1.60:3333	p 788	N93-28070 *	#
NAS 1.26:190934	p 24	N93-12004 *	#	NAS 1.26:192165	p 382	N93-18520 *	#	NAS 1.60:3355	p 989	N93-31733 *	#
NAS 1.26:190935	p 22	N93-11605 *	#	NAS 1.26:192172	p 552	N93-20297 *	#	NAS 1.61:1271	p 231	N93-12967 *	#
NAS 1.26:190936	p 25	N93-12343 *	#	NAS 1.26:192177	p 393	N93-17920 *	#	NAS 1.61:1282	p 196	N93-14495 *	#
NAS 1.26:190956	p 216	N93-13406 *	#	NAS 1.26:192193	p 515	N93-21646 *	#	NAS 1.61:1292-VOL-1	p 754	N93-25157 *	#
NAS 1.26:190965	p 60	N93-12214 *	#	NAS 1.26:192196	p 530	N93-20312 *	#	NAS 1.61:1292-VOL-2	p 754	N93-25158 *	#
NAS 1.26:190979	p 90	N93-12329 *	#	NAS 1.26:192232	p 394	N93-18784 *	#	NAS 1.61:1292-VOL-3	p 754	N93-25159 *	#
NAS 1.26:190980	p 68	N93-12349 *	#	NAS 1.26:192233	p 339	N93-18783 *	#	NAS 1.71:1AR-13400-1	p 485	N93-22015 *	#
NAS 1.26:190985	p 175	N93-13697 *	#	NAS 1.26:192234	p 296	N93-18585 *	#	NAS 1.71:1AR-14221-1	p 344	N93-19023 *	#
NAS 1.26:191015	p 781	N93-27097 *	#	NAS 1.26:192277	p 522	N93-21210 *	#	NAS 1.71:1AR-14470-1	p 23	N93-11876 *	#
NAS 1.26:191017	p 556	N93-22005 *	#	NAS 1.26:192282	p 483	N93-20256 *	#	NAS 1.71:1AR-14471-1	p 536	N93-20041 *	#
NAS 1.26:191027	p 294	N93-17884 *	#	NAS 1.26:192288	p 483	N93-20235 *	#	NAS 1.71:1AR-14747-1	p 526	N93-20039 *	#
NAS 1.26:191034	p 852	N93-27148 *	#	NAS 1.26:192301	p 319	N93-18873 *	#	NAS 1.71:LEW-15170-1	p 853	N93-28953 *	#
NAS 1.26:191071	p 536	N93-20237 *	#	NAS 1.26:192708	p 707	N93-25261 *	#	NAS 1.71:LEW-15218-1	p 86	N93-11172 *	#
NAS 1.26:191079	p 840	N93-27268 *	#	NAS 1.26:192709	p 707	N93-25330 *	#	NAS 1.71:LEW-15430-1	p 453	N93-17051 *	#
NAS 1.26:191095	p 746	N93-24759 *	#	NAS 1.26:192710	p 516	N93-22003 *	#	NAS 1.71:NPO-18733-1-CU	p 897	N93-30416 *	#
NAS 1.26:191097	p 791	N93-27267 *	#	NAS 1.26:192725	p 748	N93-25208 *	#	NAS 1.83:156	p 104	N93-11100 *	#
NAS 1.26:191105	p 699	N93-25883 *	#	NAS 1.26:192727	p 728	N93-25199 *	#	NAS 1.83:159	p 678	N93-26422 *	#
NAS 1.26:191109	p 935	N93-31031 *	#	NAS 1.26:192910	p 758	N93-25130 *	#		p 109	N93-13110 *	#
NAS 1.26:191127	p 751	N93-25884 *	#	NAS 1.26:192917	p 695	N93-25249 *	#	NASA-CASE-LAR-13400-1	p 485	N93-22015 *	#
NAS 1.26:191153	p 815	N93-28609 *	#	NAS 1.26:192918	p 749	N93-25266 *	#	NASA-CASE-LAR-13508-3-CU	p 67	N93-11057 *	#
NAS 1.26:191154	p 816	N93-28617 *	#	NAS 1.26:192919	p 747	N93-25109 *	#	NASA-CASE-LAR-14219-1	p 729	N93-25998 *	#
NAS 1.26:191157	p 900	N93-29072 *	#	NAS 1.26:192920	p 707	N93-26052 *	#	NASA-CASE-LAR-14221-1	p 344	N93-19023 *	#
NAS 1.26:191216	p 186	N93-12903 *	#	NAS 1.26:192938	p 820	N93-27308 *	#	NASA-CASE-LAR-14424-1-SB	p 731	N93-25996 *	#
NAS 1.26:191255	p 220	N93-14766 *	#	NAS 1.26:192940	p 692	N93-24736 *	#	NASA-CASE-LAR-14470-1	p 23	N93-11876 *	#
NAS 1.26:191262	p 295	N93-17934 *	#	NAS 1.26:192953	p 714	N93-25162 *	#	NASA-CASE-LAR-14471-1	p 536	N93-20041 *	#
NAS 1.26:191274	p 131	N93-13463 *	#	NAS 1.26:192954	p 716	N93-25670 *	#	NASA-CASE-LAR-14483-1	p 556	N93-22035 *	#
NAS 1.26:191304	p 138	N93-14767 *	#	NAS 1.26:192957	p 723	N93-25668 *	#	NASA-CASE-LAR-14520-1-SB	p 296	N93-18275 *	#
NAS 1.26:191360	p 294	N93-17855 *	#	NAS 1.26:192960	p 729	N93-26046 *	#	NASA-CASE-LAR-14747-1	p 526	N93-20039 *	#
NAS 1.26:191368	p 386	N93-18085 *	#	NAS 1.26:192980	p 694	N93-25117 *	#	NASA-CASE-LAR-14824-1-SB	p 751	N93-26000 *	#
NAS 1.26:191385	p 194	N93-14809 *	#	NAS 1.26:192981	p 780	N93-27093 *	#				
NAS 1.26:191408	p 758	N93-25084 *	#	NAS 1.26:192997	p 700	N93-26049 *	#	NASA-CASE-LEW-15094-1	p 522	N93-22034 *	#
NAS 1.26:191409	p 694	N93-25083 *	#	NAS 1.26:193000	p 783	N93-27427 *	#	NASA-CASE-LEW-15170-1	p 853	N93-28953 *	#
NAS 1.26:191410	p 694	N93-25153 *	#	NAS 1.26:193003	p 728	N93-24762 *	#	NASA-CASE-LEW-15218-1	p 86	N93-11172 *	#
NAS 1.26:191418	p 718	N93-24764 *	#	NAS 1.26:193043	p 895	N93-29774 *	#	NASA-CASE-LEW-15430-1	p 453	N93-17051 *	#
NAS 1.26:191425	p 757	N93-25073 *	#	NAS 1.26:193070	p 781	N93-27126 *	#				
NAS 1.26:191438	p 747	N93-25087 *	#	NAS 1.26:193072	p 782	N93-27282 *	#	NASA-CASE-MSC-21881-1	p 221	N93-14871 *	#
NAS 1.26:191440	p 847	N93-27063 *	#	NAS 1.26:193085	p 819	N93-27156 *	#				
NAS											

REPORT NUMBER INDEX

NASA-TM-105810

NASA-CP-3156	p 857	N93-30673 *	#	NASA-CR-191440	p 847	N93-27063 *	#	NASA-CR-193085	p 819	N93-27156 *	#
NASA-CP-3157	p 69	N93-12447 *	#	NASA-CR-191444	p 779	N93-27004 *	#	NASA-CR-193086	p 805	N93-27089 *	#
				NASA-CR-191446	p 1019	N93-32234 *	#	NASA-CR-193107	p 805	N93-27241 *	#
NASA-CR-177567	p 293	N93-16942 *	#	NASA-CR-191447	p 780	N93-27090 *	#	NASA-CR-193123	p 1015	N93-31836 *	#
NASA-CR-177598	p 99	N93-10458 *	#	NASA-CR-191449	p 780	N93-27067 *	#	NASA-CR-193124	p 930	N93-29154 *	#
NASA-CR-177603	p 240	N93-17883 *	#	NASA-CR-191453	p 942	N93-29192 *	#	NASA-CR-193129	p 839	N93-27151 *	#
NASA-CR-177605	p 571	N93-19970 *	#	NASA-CR-191457	p 808	N93-28621 *	#	NASA-CR-193130	p 781	N93-27150 *	#
NASA-CR-177608	p 708	N93-26549 *	#	NASA-CR-191458	p 843	N93-28975 *	#	NASA-CR-193140	p 848	N93-27289 *	#
NASA-CR-177612	p 693	N93-25075 *	#	NASA-CR-191462	p 820	N93-27264 *	#	NASA-CR-193161	p 808	N93-28418 *	#
NASA-CR-180824	p 55	N93-10348 *	#	NASA-CR-191469	p 1000	N93-32218 *	#	NASA-CR-193183	p 793	N93-28936 *	#
NASA-CR-182193	p 917	N93-29451 *	#	NASA-CR-191625	p 424	N93-18862 *	#	NASA-CR-193187	p 880	N93-29152 *	#
NASA-CR-182268	p 187	N93-13735 *	#	NASA-CR-191647	p 418	N93-16558 *	#	NASA-CR-193222	p 893	N93-29153 *	#
NASA-CR-182269	p 232	N93-13762 *	#	NASA-CR-191649	p 391	N93-15830 *	#	NASA-CR-193237	p 914	N93-29215 *	#
NASA-CR-182270	p 233	N93-15116 *	#	NASA-CR-191652	p 200	N93-15431 *	#	NASA-CR-193241	p 930	N93-29213 *	#
NASA-CR-184421	p 91	N93-12401 *	#	NASA-CR-191671	p 137	N93-14737 *	#	NASA-CR-193259	p 1030	N93-31110 *	#
NASA-CR-184442	p 198	N93-13311 *	#	NASA-CR-191712	p 137	N93-14738 *	#	NASA-CR-193268	p 1038	N93-31649 *	#
NASA-CR-184498	p 220	N93-14763 *	#	NASA-CR-191715	p 140	N93-15588 *	#	NASA-CR-193302	p 990	N93-31855 *	#
NASA-CR-185676	p 914	N93-29652 *	#	NASA-CR-191774	p 372	N93-17800 *	#	NASA-CR-193366	p 1015	N93-31848 *	#
NASA-CR-185698	p 69	N93-10960 *	#	NASA-CR-191803	p 371	N93-18560 *	#	NASA-CR-193412	p 1019	N93-31739 *	#
NASA-CR-186027	p 806	N93-28693 *	#	NASA-CR-191885	p 484	N93-21562 *	#	NASA-CR-193467	p 879	N93-31037 *	#
NASA-CR-187125	p 521	N93-20583 *	#	NASA-CR-191889	p 296	N93-18384 *	#	NASA-CR-193468	p 936	N93-31036 *	#
NASA-CR-187126	p 521	N93-20773 *	#	NASA-CR-191890	p 381	N93-16695 *	#	NASA-CR-193552	p 1040	N93-32221 *	#
NASA-CR-187127	p 364	N93-18702 *	#	NASA-CR-191900	p 442	N93-18372 *	#	NASA-CR-193831	p 812	N93-27115 *	#
NASA-CR-187128	p 174	N93-12695 *	#	NASA-CR-191917	p 422	N93-18576 *	#	NASA-CR-4110	p 877	N93-30373 *	#
NASA-CR-187141	p 815	N93-27680 *	#	NASA-CR-191929	p 391	N93-16389 *	#	NASA-CR-4118	p 934	N93-30374 *	#
NASA-CR-189111	p 198	N93-12589 *	#	NASA-CR-191930	p 537	N93-21749 *	#	NASA-CR-4216	p 934	N93-30375 *	#
NASA-CR-189193-VOL-1	p 721	N93-24754 *	#	NASA-CR-191980	p 296	N93-18378 *	#	NASA-CR-4471	p 229	N93-13370 *	#
NASA-CR-189193-VOL-2	p 721	N93-25106 *	#	NASA-CR-191987	p 297	N93-18602 *	#	NASA-CR-4478	p 292	N93-16940 *	#
NASA-CR-189212	p 220	N93-14799 *	#	NASA-CR-192011	p 334	N93-17974 *	#	NASA-CR-4479	p 343	N93-16693 *	#
NASA-CR-189221	p 364	N93-18578 *	#	NASA-CR-192013	p 336	N93-18060 *	#	NASA-CR-4481	p 220	N93-14797 *	#
NASA-CR-189228	p 455	N93-18762 *	#	NASA-CR-192018	p 336	N93-18061 *	#	NASA-CR-4492	p 298	N93-19015 *	#
NASA-CR-189618	p 330	N93-16947 *	#	NASA-CR-192022	p 336	N93-18059 *	#	NASA-CR-4505	p 780	N93-27098 *	#
NASA-CR-189619	p 330	N93-16999 *	#	NASA-CR-192023	p 335	N93-18049 *	#	NASA-CR-4513	p 789	N93-28449 *	#
NASA-CR-189670	p 91	N93-12411 *	#	NASA-CR-192024	p 334	N93-17976 *	#	NASA-CR-4514	p 780	N93-27084 *	#
NASA-CR-189676	p 569	N93-21317 *	#	NASA-CR-192032	p 334	N93-18017 *	#	NASA-CR-4517	p 1019	N93-31643 *	#
NASA-CR-189688	p 94	N93-12299 *	#	NASA-CR-192039	p 420	N93-18047 *	#	NASA-CR-4520	p 895	N93-29885 *	#
NASA-CR-189698	p 99	N93-12538 *	#	NASA-CR-192040	p 332	N93-17802 *	#				
NASA-CR-189699	p 98	N93-12346 *	#	NASA-CR-192041	p 337	N93-18161 *	#	NASA-NP-130	p 104	N93-11100 *	
NASA-CR-189703	p 65	N93-12413 *	#	NASA-CR-192044	p 333	N93-17972 *	#	NASA-NP-156	p 678	N93-26422 *	#
NASA-CR-189717	p 102	N93-12021 *	#	NASA-CR-192046	p 334	N93-18037 *	#	NASA-NP-159	p 109	N93-13110 *	#
NASA-CR-189718	p 231	N93-12986 *	#	NASA-CR-192048	p 337	N93-18155 *	#				
NASA-CR-189723	p 318	N93-16692 *	#	NASA-CR-192049	p 333	N93-17804 *	#	NASA-RP-1271	p 231	N93-12967 *	#
NASA-CR-189734	p 290	N93-16627 *	#	NASA-CR-192050	p 339	N93-18386 *	#	NASA-RP-1282	p 196	N93-14495 *	#
NASA-CR-189736	p 291	N93-16710 *	#	NASA-CR-192051	p 332	N93-17803 *	#	NASA-RP-1292-VOL-1	p 754	N93-25157 *	#
NASA-CR-189737	p 418	N93-16379 *	#	NASA-CR-192053	p 336	N93-18063 *	#	NASA-RP-1292-VOL-2	p 754	N93-25158 *	#
NASA-CR-189738	p 298	N93-18771 *	#	NASA-CR-192054	p 337	N93-18166 *	#	NASA-RP-1292-VOL-3	p 754	N93-25159 *	#
NASA-CR-189739	p 420	N93-18093 *	#	NASA-CR-192059	p 338	N93-18350 *	#				
NASA-CR-190420	p 894	N93-29498 *	#	NASA-CR-192070	p 338	N93-18349 *	#	NASA-SBIR-PC-90	p 572	N93-21794 *	#
NASA-CR-190617	p 68	N93-11910 *	#	NASA-CR-192072	p 334	N93-17977 *	#				
NASA-CR-190663	p 84	N93-10372 *	#	NASA-CR-192074	p 335	N93-18055 *	#	NASA-SP-7105	p 949	N93-32240 *	#
NASA-CR-190692	p 17	N93-10098 *	#	NASA-CR-192075	p 335	N93-18054 *	#				
NASA-CR-190746	p 85	N93-10891 *	#	NASA-CR-192077	p 332	N93-17711 *	#	NASA-TM-102705	p 17	N93-10349 *	#
NASA-CR-190778	p 677	N93-25134 *	#	NASA-CR-192082	p 335	N93-18056 *	#	NASA-TM-102803	p 139	N93-15483 *	#
NASA-CR-190779	p 677	N93-24760 *	#	NASA-CR-192102	p 526	N93-19980 *	#	NASA-TM-102839	p 1006	N93-32374 *	#
NASA-CR-190811	p 36	N93-11139 *	#	NASA-CR-192105	p 298	N93-18781 *	#	NASA-TM-103086	p 946	N93-29452 *	#
NASA-CR-190837	p 36	N93-10961 *	#	NASA-CR-192124	p 386	N93-16629 *	#	NASA-TM-103719	p 852	N93-27058 *	#
NASA-CR-190845	p 89	N93-11716 *	#	NASA-CR-192127	p 527	N93-20296 *	#	NASA-TM-103872	p 64	N93-10741 *	#
NASA-CR-190911	p 16	N93-10069 *	#	NASA-CR-192161	p 483	N93-20018 *	#	NASA-TM-103896	p 65	N93-10745 *	#
NASA-CR-190915	p 336	N93-18064 *	#	NASA-CR-192162	p 551	N93-20268 *	#	NASA-TM-103924	p 456	N93-16652 *	#
NASA-CR-190918	p 4	N93-10647 *	#	NASA-CR-192164	p 382	N93-18766 *	#	NASA-TM-103937	p 305	N93-19379 *	#
NASA-CR-190934	p 24	N93-12004 *	#	NASA-CR-192165	p 382	N93-18520 *	#	NASA-TM-103939	p 1033	N93-32212 *	#
NASA-CR-190935	p 22	N93-11605 *	#	NASA-CR-192172	p 552	N93-20297 *	#	NASA-TM-103947	p 516	N93-21810 *	#
NASA-CR-190936	p 25	N93-12343 *	#	NASA-CR-192177	p 393	N93-17920 *	#	NASA-TM-103958	p 36	N93-12320 *	#
NASA-CR-190956	p 216	N93-13406 *	#	NASA-CR-192193	p 515	N93-21646 *	#	NASA-TM-103962	p 129	N93-12721 *	#
NASA-CR-190965	p 60	N93-12214 *	#	NASA-CR-192196	p 530	N93-20312 *	#	NASA-TM-103963	p 694	N93-25091 *	#
NASA-CR-190979	p 90	N93-12329 *	#	NASA-CR-192232	p 394	N93-18784 *	#	NASA-TM-103968	p 373	N93-19380 *	#
NASA-CR-190980	p 68	N93-12349 *	#	NASA-CR-192233	p 339	N93-18783 *	#	NASA-TM-103981	p 885	N93-29653 *	#
NASA-CR-190985	p 175	N93-13697 *	#	NASA-CR-192234	p 296	N93-18585 *	#	NASA-TM-103989	p 990	N93-32226 *	#
NASA-CR-191015	p 781	N93-27097 *	#	NASA-CR-192277	p 522	N93-21210 *	#	NASA-TM-103998	p 994	N93-32225 *	#
NASA-CR-191017	p 556	N93-22005 *	#	NASA-CR-192282	p 483	N93-20256 *	#	NASA-TM-104001	p 700	N93-26099 *	#
NASA-CR-191027	p 294	N93-17884 *	#	NASA-CR-192288	p 483	N93-20235 *	#	NASA-TM-104004	p 706	N93-24914 *	#
NASA-CR-191034	p 852	N93-27148 *	#	NASA-CR-192301	p 319	N93-18873 *	#	NASA-TM-104005	p 790	N93-27076 *	#
NASA-CR-191071	p 536	N93-20237 *	#	NASA-CR-192708	p 707	N93-25261 *	#	NASA-TM-104025	p 994	N93-32348 *	#
NASA-CR-191079	p 840	N93-27268 *	#	NASA-CR-192709	p 707	N93-25330 *	#	NASA-TM-104164	p 64	N93-11176 *	#
NASA-CR-191095	p 746	N93-24759 *	#	NASA-CR-192710	p 516	N93-22003 *	#	NASA-TM-104257	p 20	N93-11221 *	#
NASA-CR-191097	p 791	N93-27267 *	#	NASA-CR-192725	p 748	N93-25208 *	#	NASA-TM-104261	p 25	N93-12353 *	#
NASA-CR-191105	p 699	N93-25883 *	#	NASA-CR-192727	p 728	N93-25199 *	#	NASA-TM-104262	p 223	N93-13288 *	#
NASA-CR-191109	p 935	N93-31031 *	#	NASA-CR-192910	p 758	N93-25130 *	#	NASA-TM-104263	p 1005	N93-32220 *	#
NASA-CR-191127	p 751	N93-25884 *	#	NASA-CR-192917	p 695	N93-25249 *	#	NASA-TM-104265	p 344	N93-19110 *	#
NASA-CR-191153	p 815	N93-28609 *	#	NASA-CR-192918	p 749	N93-25266 *	#	NASA-TM-104266	p 339	N93-18616 *	#
NASA-CR-191154	p 816	N93-28617 *	#	NASA-CR-192919	p 747	N93-25109 *	#	NASA-TM-104267	p 518	N93-20163 *	#
NASA-CR-191157	p 900	N93-29072 *	#	NASA-CR-192920	p 707	N93-26052 *	#	NASA-TM-105270	p 752	N93-26202 *	#
NASA-CR-191216	p 186	N93-12903 *	#	NASA-CR-192938	p 820	N93-27308 *	#	NASA-TM-105572	p 441	N93-16613 *	#
NASA-CR-191255	p 220	N93-14766 *	#	NASA-CR-192940	p 692	N93-24736 *	#	NASA-TM-105602	p 678	N93-26136 *	#
NASA-CR-191262	p 295	N93-17934 *	#	NASA-CR-192953	p 714	N93-25162 *	#	NASA-TM-105626	p 194	N93-15498 *	#
NASA-CR-191274	p 131	N93-13463 *	#	NASA-CR-192954	p 716	N93-25670 *	#	NASA-TM-105658	p 130	N93-13292 *	#
NASA-CR-191304	p 138	N93-14767 *	#	NASA-CR-192957	p 723	N93-25668 *	#	NASA-TM-105687	p 179	N93-15342 *	#
NASA-CR-191360	p 294	N93-17855 *	#	NASA-CR-192960	p 729	N93-26046 *	#	NASA-TM-105722	p 844	N93-27012 *	#
NASA-CR-191368	p 386	N93-18085 *	#	NASA-CR-192980	p 694	N93-25117 *	#	NASA-TM-105736	p 101	N93-11370 *	#
NASA-CR-191385	p 194	N93-14809 *	#	NASA-CR-192981	p 780	N93-27093 *	#	NASA-TM-105771	p 730	N93-25080 *	#
NASA-CR-191408	p 758	N93-25084 *	#	NASA-CR-192997	p 700	N93-26049 *	#	NASA-TM-105779	p 222	N93-15343 *	#
NASA-CR-191409	p 694	N93-25083 *	#	NASA-CR-193000	p 783	N93-27427 *	#	NASA-TM-105786	p 56	N93-10983 *	#
NASA-CR-191410	p 694	N93-25153 *	#	NASA-CR-193033	p 728	N93-24762 *	#	NASA-TM-105804	p 527	N93-21197 *	#
NASA-CR-191418	p 718	N93-24764 *	#	NASA-CR-193043	p 895	N93-29774 *	#	NASA-TM-105807	p 85	N93-10963 *	#
NASA-CR-191425	p 757	N93-25073 *	#	NASA-CR-193070	p 781	N93-27126 *	#	NASA			

NASA-TM-105821	p 90	N93-12277	#	NASA-TM-107730	p 989	N93-31732	#	NIST/GCR-92/619	p 880	N93-29211	
NASA-TM-105824	p 552	N93-20368	#	NASA-TM-107739	p 718	N93-26553	#				
NASA-TM-105829	p 90	N93-12197	#	NASA-TM-107745	p 693	N93-25074	#	NLPN92-737	p 805	N93-27089	#
NASA-TM-105833	p 88	N93-11624	#	NASA-TM-107746	p 852	N93-27272	#				
NASA-TM-105838	p 21	N93-11223	#	NASA-TM-107748	p 707	N93-26087	#	NLR-TP-89172-U	p 514	N93-20742	#
NASA-TM-105839	p 59	N93-11530	#	NASA-TM-107756	p 852	N93-27271	#	NLR-TP-89336-U	p 319	N93-17954	#
NASA-TM-105852	p 55	N93-10456	#	NASA-TM-107758	p 840	N93-27250	#	NLR-TP-89387-U	p 527	N93-20743	#
NASA-TM-105863	p 421	N93-18380	#	NASA-TM-107761	p 806	N93-27258	#	NLR-TP-90119-U	p 318	N93-16343	#
NASA-TM-105864	p 291	N93-16704	#	NASA-TM-107764	p 852	N93-28692	#	NLR-TP-90238-U	p 382	N93-17875	#
NASA-TM-105868	p 180	N93-15525	#	NASA-TM-108003	p 104	N93-10872	#	NLR-TP-90340-U	p 418	N93-16411	#
NASA-TM-105874	p 212	N93-12735	#	NASA-TM-108004	p 104	N93-10815	#	NLR-TP-91008-U	p 318	N93-17559	#
NASA-TM-105881	p 212	N93-12736	#	NASA-TM-108017	p 234	N93-12671	#	NLR-TP-91011-U	p 393	N93-17920	#
NASA-TM-105884	p 65	N93-12305	#	NASA-TM-108021	p 234	N93-12672	#	NLR-TP-91092-U	p 331	N93-17535	#
NASA-TM-105898	p 60	N93-12402	#	NASA-TM-108145	p 572	N93-21794	#	NLR-TP-91104-U	p 331	N93-17562	#
NASA-TM-105908	p 60	N93-12418	#	NASA-TM-108240	p 945	N93-29323	#	NLR-TP-91168-U	p 993	N93-31120	#
NASA-TM-105915	p 459	N93-20902	#	NASA-TM-108242	p 945	N93-29322	#	NLR-TP-91200-U	p 1001	N93-32332	#
NASA-TM-105924	p 110	N93-14102	#	NASA-TM-108578	p 230	N93-15578	#	NLR-TP-91203-U	p 1020	N93-32385	#
NASA-TM-105931	p 228	N93-13154	#	NASA-TM-108579	p 230	N93-15579	#	NLR-TP-91216-U	p 295	N93-17929	#
NASA-TM-105932	p 290	N93-16625	#	NASA-TM-108580	p 230	N93-15502	#	NLR-TP-91220-U	p 1014	N93-31042	#
NASA-TM-105935	p 179	N93-15403	#	NASA-TM-108650	p 555	N93-21819	#	NLR-TP-91237-U	p 1003	N93-31111	#
NASA-TM-105936	p 110	N93-15573	#	NASA-TM-108722	p 823	N93-27142	#	NLR-TP-91244-U	p 392	N93-17540	#
NASA-TM-105937	p 200	N93-15504	#	NASA-TM-108890	p 1000	N93-32223	#	NLR-TP-91260-U	p 999	N93-31840	#
NASA-TM-105940	p 724	N93-26161	#	NASA-TM-109003	p 1038	N93-32224	#	NLR-TP-91306	p 294	N93-17809	#
NASA-TM-105946	p 138	N93-14791	#	NASA-TM-109227	p 875	N93-29449	#	NLR-TP-91346-U	p 1006	N93-32372	#
NASA-TM-105947	p 148	N93-15360	#	NASA-TM-109442	p 910	N93-30764	#	NLR-TP-91349-U	p 994	N93-32337	#
NASA-TM-105952	p 233	N93-15430	#	NASA-TM-109443	p 876	N93-29450	#	NLR-TP-91359-U	p 999	N93-32338	#
NASA-TM-105961	p 138	N93-14911	#	NASA-TM-109444	p 63	N93-10070	#	NLR-TP-91396-U	p 999	N93-32416	#
NASA-TM-105968	p 139	N93-15404	#	NASA-TM-109445	p 22	N93-11622	#	NLR-TP-91404-U	p 990	N93-32357	#
NASA-TM-105969	p 179	N93-15521	#	NASA-TM-109446	p 196	N93-15528	#	NLR-TP-91410-U	p 990	N93-32358	#
NASA-TM-105970	p 139	N93-15338	#	NASA-TM-109447	p 555	N93-21831	#	NLR-TP-91443-U	p 999	N93-32203	#
NASA-TM-105971	p 148	N93-15354	#	NASA-TM-109448	p 65	N93-12304	#	NLR-TP-92009-U	p 999	N93-32205	#
NASA-TM-105972	p 148	N93-15345	#	NASA-TM-109449	p 552	N93-20299	#	NLR-TP-92014-U	p 1006	N93-32386	#
NASA-TM-105975	p 149	N93-15522	#	NASA-TM-109450	p 49	N93-11863	#	NLR-TP-92072-U	p 987	N93-31148	#
NASA-TM-105976	p 188	N93-14831	#	NASA-TM-109451	p 22	N93-11532	#	NOAA-TM-ERL-ARL-199-VOL-1	p 878	N93-30387	#
NASA-TM-105977	p 362	N93-16715	#	NASA-TM-109452	p 779	N93-27032	#	NOAA-TM-ERL-ARL-199-VOL-2	p 878	N93-30388	#
NASA-TM-105979	p 179	N93-15359	#	NASA-TM-109453	p 779	N93-26899	#				
NASA-TM-105984	p 551	N93-20057	#	NASA-TM-109454	p 175	N93-13155	#	NOAA-TM-ERL-FSL-5	p 1034	N93-31202	#
NASA-TM-105985	p 362	N93-16705	#	NASA-TM-109455	p 136	N93-14451	#				
NASA-TM-105989	p 290	N93-16596	#	NASA-TM-109456	p 131	N93-13322	#	NOAA-TM-NWS-CR-102	p 94	N93-11803	#
NASA-TM-105993	p 421	N93-18426	#	NASA-TM-109457	p 381	N93-16753	#				
NASA-TM-105997	p 233	N93-15575	#	NASA-TM-109458	p 700	N93-26085	#	NOARL-PR-92-020-252	p 49	N93-11838	#
NASA-TM-106013	p 760	N93-26551	#	NASA-TM-109459	p 875	N93-29166	#				
NASA-TM-106015	p 825	N93-27092	#	NASA-TM-109460	p 1010	N93-32380	#	NPL-DMM(A)-51	p 86	N93-11325	#
NASA-TM-106024	p 550	N93-19971	#	NASA-TM-109461	p 779	N93-27005	#	NPL-DMM(A)-52	p 87	N93-11327	#
NASA-TM-106027	p 819	N93-26907	#	NASA-TM-109462	p 1017	N93-32379	#	NPL-DMM(A)-53	p 86	N93-11326	#
NASA-TM-106028	p 838	N93-26999	#								
NASA-TM-106033	p 721	N93-25079	#	NASA-TP-3190	p 737	N93-26201	#	NPS-AA-92-001CR	p 179	N93-15337	#
NASA-TM-106042	p 723	N93-25673	#	NASA-TP-3212	p 19	N93-10824	#				
NASA-TM-106044	p 722	N93-25129	#	NASA-TP-3225	p 553	N93-20585	#	NRAD-TR-1533	p 793	N93-28990	#
NASA-TM-106054	p 693	N93-24911	#	NASA-TP-3241	p 513	N93-20584	#				
NASA-TM-106086	p 838	N93-27069	#	NASA-TP-3253	p 131	N93-13533	#	NREC-1626-3	p 212	N93-12977	#
NASA-TM-106100	p 839	N93-27133	#	NASA-TP-3255	p 344	N93-18408	#				
NASA-TM-106101	p 838	N93-27088	#	NASA-TP-3259	p 701	N93-26134	#	NREL/TP-257-4655-PHASE-1	p 485	N93-21766	#
NASA-TM-106112	p 813	N93-27131	#	NASA-TP-3260	p 24	N93-12321	#	NREL/TP-257-4671	p 216	N93-13525	#
NASA-TM-106114	p 813	N93-27130	#	NASA-TP-3268	p 338	N93-18333	#	NREL/TP-257-4674	p 216	N93-13524	#
NASA-TM-106130	p 825	N93-26702	#	NASA-TP-3269	p 102	N93-11620	#	NREL/TP-442-5159	p 434	N93-18705	#
NASA-TM-106131	p 815	N93-27640	#	NASA-TP-3270	p 189	N93-15366	#				
NASA-TM-106140	p 1005	N93-32368	#	NASA-TP-3271	p 222	N93-15434	#	NRL/FR/5530-92-9194	p 229	N93-15052	#
NASA-TM-106148	p 900	N93-29065	#	NASA-TP-3284	p 392	N93-16537	#				
NASA-TM-106149	p 838	N93-27020	#	NASA-TP-3302	p 373	N93-19108	#	NRL/MR/6410-93-7178	p 931	N93-29851	#
NASA-TM-106150	p 841	N93-28053	#	NASA-TP-3313	p 874	N93-29160	#				
NASA-TM-106151	p 812	N93-27026	#	NASA-TP-3314	p 875	N93-29165	#	NSF-92-104	p 193	N93-13712	#
NASA-TM-106152	p 848	N93-28051	#	NASA-TP-3315	p 362	N93-16941	#	NSF-92-325	p 192	N93-13407	#
NASA-TM-106167	p 838	N93-27132	#	NASA-TP-3333	p 788	N93-28070	#				
NASA-TM-106169	p 813	N93-27128	#	NASA-TP-3355	p 989	N93-31733	#	NSF/ISI-89032	p 1033	N93-31876	#
NASA-TM-106179	p 814	N93-27160	#								
NASA-TM-106181	p 989	N93-31839	#	NATICK/TR-92/035	p 24	N93-12179	#	NTSB/AAR-92/01/SUM	p 143	N93-13470	#
NASA-TM-106186	p 930	N93-29157	#	NATICK/TR-93/029	p 877	N93-30119	#	NTSB/AAR-92/02	p 28	N93-12193	#
NASA-TM-106187	p 1032	N93-31647	#					NTSB/AAR-92/03	p 28	N93-11471	#
NASA-TM-106189	p 1005	N93-32351	#	NAVY-CASE-70723	p 199	N93-13414	#	NTSB/AAR-92/04	p 143	N93-13426	#
NASA-TM-106192	p 814	N93-27610	#	NAVY-CASE-73567	p 536	N93-20247	#	NTSB/AAR-93/01	p 705	N93-25827	#
NASA-TM-106198	p 1004	N93-31671	#					NTSB/AAR-93/02	p 790	N93-27034	#
NASA-TM-106216	p 914	N93-29194	#	NAWCADWAR-92003-60	p 199	N93-14726	#	NTSB/AAR-93/03	p 790	N93-27035	#
NASA-TM-106220	p 1031	N93-31193	#	NAWCADWAR-92018-60	p 199	N93-15189	#				
NASA-TM-106225	p 816	N93-28697	#	NAWCADWAR-92033-60	p 160	N93-12613	#	NTSB/ARG-93/01	p 790	N93-27033	#
NASA-TM-106230	p 988	N93-31648	#	NAWCADWAR-92034-60	p 159	N93-12602	#				
NASA-TM-106235	p 900	N93-29162	#	NAWCADWAR-92035-60	p 186	N93-12578	#	NTSB/SIR-92/02	p 310	N93-16834	#
NASA-TM-106240	p 989	N93-31672	#	NAWCADWAR-92042-60	p 165	N93-15004	#	NTSB/SIR-92/03	p 149	N93-15577	#
NASA-TM-106245	p 1032	N93-31846	#	NAWCADWAR-92045-60	p 328	N93-15858	#				
NASA-TM-106253	p 1032	N93-31860	#	NAWCADWAR-92060-60	p 199	N93-14573	#	OC-R-92-U-0349	p 329	N93-16396	#
NASA-TM-106273	p 186	N93-13367	#								
NASA-TM-107594	p 22	N93-11610	#	NCAR/TN-374+PROC	p 223	N93-12818	#				
NASA-TM-107621	p 420	N93-17779	#					OMB-3145-0058	p 193	N93-13712	#
NASA-TM-107660	p 47	N93-10968	#	NCEL-N-1846	p 382	N93-17734	#				
NASA-TM-107665	p 442	N93-18332	#					ONERA-NT-1990-10	p 918	N93-30203	#
NASA-TM-107667	p 109	N93-13025	#	NDU-ICAF-92-S79	p 809	N93-29004	#	ONERA-NT-1990-3	p 876	N93-30020	#
NASA-TM-107669	p 378	N93-15790	#					ONERA-NT-1992-7	p 298	N93-18701	#
NASA-TM-107670	p 102	N93-12080	#	NHB-5300.4(3A-2)	p 212	N93-12674	#	ONERA-NT-1992-8	p 297	N93-18617	#
NASA-TM-107674	p 747	N93-25176	#								
NASA-TM-107682	p 219	N93-14483	#	NIAR-92-11	p 310	N93-18036	#	ONERA-P-1990-5	p 943	N93-30110	#
NASA-TM-107687	p 88	N93-11544	#	NIAR-92-2	p 310	N93-16455	#	ONERA-P-1992-2	p 551	N93-20230	#
NASA-TM-107690	p 64	N93-12216	#	NIAR-92-4	p 495	N93-19941	#				
NASA-TM-107691	p 162	N93-13565	#	NIAR-93-12	p 949	N93-32232	#	ONERA, TP NO. 1992-101	p 771	A93-38581	#
NASA-TM-107697	p 458	N93-19976	#					ONERA, TP NO. 1992-103	p 831	A93-38583	#
NASA-TM-107698	p 458	N93-19976	#	NIFS-188	p 569	N93-20546	#	ONERA, TP NO. 1992-106	p 824	A93-38586	#
NASA-TM-107708	p 453	N93-16755	#					ONERA, TP NO. 1992-111	p 771	A93-38588	#

REPORT NUMBER INDEX

SAE PAPER 920947

ONERA, TP NO. 1992-114	p 771	A93-38590	PB92-205673	p 36	N93-11252	#	PW-FR21998-10	p 74	N93-12237	#
ONERA, TP NO. 1992-117	p 822	A93-38592	PB92-213685	p 459	N93-21342	#	PW-FR21998-12	p 393	N93-17704	#
ONERA, TP NO. 1992-118	p 831	A93-38593	PB92-213693	p 459	N93-21343	#	PW-FR21998-14	p 536	N93-20275	#
ONERA, TP NO. 1992-121	p 771	A93-38595	PB92-213974	p 459	N93-21713	#				
ONERA, TP NO. 1992-122	p 772	A93-38596	PB92-221605	p 559	N93-21501	#	PW/GESP-FR-21988-15	p 736	N93-25843	#
ONERA, TP NO. 1992-123	p 802	A93-38597	PB92-222629	p 143	N93-13787	#	PW/GESP-FR-21998-09	p 198	N93-12746	#
ONERA, TP NO. 1992-124	p 803	A93-38598	PB92-222710	p 223	N93-12818	#				
ONERA, TP NO. 1992-125	p 772	A93-38599	PB92-223049	p 212	N93-12977	#	PW/GESP-FR21998-19	p 1019	N93-31795	#
ONERA, TP NO. 1992-126	p 851	A93-38600	PB92-227891	p 555	N93-21465	#				
ONERA, TP NO. 1992-127	p 831	A93-38601	PB92-910402	p 28	N93-12193	#	PWA-5767-109	p 556	N93-22005	#
ONERA, TP NO. 1992-128	p 772	A93-38602	PB92-910403	p 28	N93-11471	#	PWA-5894	p 364	N93-18578	#
ONERA, TP NO. 1992-131	p 772	A93-38605	PB92-910404	p 143	N93-13470	#				
ONERA, TP NO. 1992-137	p 772	A93-38610	PB92-910405	p 143	N93-13426	#	P305695-04	p 48	N93-11485	#
ONERA, TP NO. 1992-140	p 114	A93-14216	PB92-917006	p 310	N93-16834	#				
ONERA, TP NO. 1992-141	p 230	A93-14266	PB92-917007	p 149	N93-15577	#	QUEST-TR-575	p 175	N93-14111	#
ONERA, TP NO. 1992-142	p 120	A93-14356	PB93-111763	p 555	N93-21382	#				
ONERA, TP NO. 1992-143	p 831	A93-38613	PB93-111763	p 555	N93-21383	#	R-1790-14A-VOL-1	p 848	N93-27531	#
ONERA, TP NO. 1992-144	p 831	A93-38614	PB93-124659	p 310	N93-18031	#	R-1790-14B-VOL-2	p 848	N93-27589	#
ONERA, TP NO. 1992-147	p 773	A93-38728	PB93-126423	p 502	N93-19966	#	R-1790-14C-VOL-3	p 848	N93-27590	#
ONERA, TP NO. 1992-148	p 773	A93-38729	PB93-126449	p 485	N93-21796	#				
ONERA, TP NO. 1992-152	p 803	A93-38731	PB93-127728	p 559	N93-21799	#	RAE-TM-AERO-2201	p 101	N93-10805	#
ONERA, TP NO. 1992-155	p 773	A93-38734	PB93-146702	p 880	N93-29211	#	RAE-TM-AERO-2222	p 23	N93-11882	#
ONERA, TP NO. 1992-157	p 824	A93-38736	PB93-152478	p 756	N93-26533	#	RAE-TM-AERO-2228	p 23	N93-11883	#
ONERA, TP NO. 1992-160	p 832	A93-38739	PB93-153096	p 755	N93-25874	#	RAE-TM-AERO-2231	p 22	N93-11610	#
ONERA, TP NO. 1992-163	p 457	A93-26878	PB93-154813	p 782	N93-27413	#	RAE-TM-AERO-2232	p 68	N93-11906	#
ONERA, TP NO. 1992-164	p 561	A93-25339	PB93-158566	p 755	N93-26529	#				
ONERA, TP NO. 1992-171	p 542	A93-25346	PB93-160687	p 790	N93-27033	#	RAE-TM-FM-26	p 47	N93-10803	#
ONERA, TP NO. 1992-173	p 475	A93-26880	PB93-162782	p 502	N93-20164	#				
ONERA, TP NO. 1992-174	p 473	A93-25348	PB93-167886	p 822	N93-26636	#	RAE-TM-MAT/STR-1102	p 67	N93-11435	#
ONERA, TP NO. 1992-179	p 773	A93-38741	PB93-174324	p 765	N93-27405	#				
ONERA, TP NO. 1992-181	p 773	A93-38743	PB93-174951	p 1033	N93-31876	#	RAE-TM-P-1214	p 48	N93-11485	#
ONERA, TP NO. 1992-182	p 773	A93-38744	PB93-180255	p 878	N93-30387	#	RAE-TM-P-1223	p 722	N93-25455	#
ONERA, TP NO. 1992-183	p 774	A93-38745	PB93-180263	p 878	N93-30388	#				
ONERA, TP NO. 1992-184	p 774	A93-38746	PB93-182236	p 1036	N93-32191	#	RAE-TR-89057	p 82	N93-10198	#
ONERA, TP NO. 1992-194	p 774	A93-38755	PB93-190197	p 1034	N93-31202	#				
ONERA, TP NO. 1992-209	p 803	A93-38763	PB93-194231	p 1035	N93-32089	#	RAND/N-3253-AF	p 699	N93-25894	#
ONERA, TP NO. 1992-212	p 832	A93-38764	PB93-910401	p 705	N93-25827	#	RAND/N-3464-AF	p 755	N93-26327	#
ONERA, TP NO. 1992-229	p 851	A93-38774	PB93-910402	p 790	N93-27034	#				
ONERA, TP NO. 1992-233	p 774	A93-38777	PB93-910403	p 790	N93-27035	#	RAZ-000-563	p 562	N93-21820	#
ONERA, TP NO. 1992-63	p 542	A93-25327								
ONERA, TP NO. 1992-65	p 766	A93-35993	PL-TR-92-1053-VOL-1	p 877	N93-30171	#	REPT-B-31	p 66	N93-12415	#
ONERA, TP NO. 1992-82	p 844	A93-38567	PL-TR-92-1053-VOL-2	p 877	N93-30172	#	REPT-B-36	p 26	N93-12414	#
ONERA, TP NO. 1992-83	p 818	A93-38568	PL-TR-92-1053-VOL-3	p 877	N93-30173	#				
ONERA, TP NO. 1992-84	p 822	A93-38569	PL-TR-92-1053-VOL-4	p 877	N93-30151	#	REPT-1281-10-1	p 328	N93-16186	#
ONERA, TP NO. 1992-86	p 802	A93-38570					REPT-153-6442	p 515	N93-21646	#
ONERA, TP NO. 1992-87	p 831	A93-38571	PNL-SA-20954	p 89	N93-11802	#	REPT-160-573	p 220	N93-14766	#
ONERA, TP NO. 1992-89	p 771	A93-38573	PNL-SA-21578	p 789	N93-28662	#	REPT-3-448724-22529	p 98	N93-12258	#
ONERA, TP NO. 1992-91	p 771	A93-38574					REPT-31-8071(04)	p 455	N93-18762	#
ONERA, TP NO. 1992-93	p 771	A93-38576	PNL-8427	p 754	N93-24975	#	REPT-313	p 371	N93-16618	#
ONERA, TP NO. 1992-99	p 824	A93-38580					REPT-5-191025	p 554	N93-20907	#
ONERA, TP NO. 1993-101	p 1144	A93-48227	PNR-90880	p 101	N93-11204	#	REPT-699-099-352	p 1019	N93-32234	#
ONERA, TP NO. 1993-102	p 1226	A93-53615	PNR-90887	p 59	N93-11206	#	REPT-722792-4	p 1030	N93-31110	#
ONERA, TP NO. 1993-103	p 1226	A93-53616	PNR-90889	p 59	N93-11207	#	REPT-88-61608	p 917	N93-29451	#
ONERA, TP NO. 1993-105	p 1180	A93-53618	PNR-90890	p 59	N93-11208	#	REPT-92-105	p 221	N93-15065	#
ONERA, TP NO. 1993-106	p 1085	A93-50292	PNR-90892	p 72	N93-11031	#	REPT-92-96	p 1040	N93-31653	#
ONERA, TP NO. 1993-108	p 1225	A93-53620	PNR-90897	p 72	N93-11032	#	REPT-921-430-102	p 88	N93-11587	#
ONERA, TP NO. 1993-109	p 1206	A93-53621	PNR-90908	p 85	N93-11014	#	REPT-921-430-104	p 200	N93-15490	#
ONERA, TP NO. 1993-12	p 471	A93-24953	PNR-90910	p 572	N93-20734	#				
ONERA, TP NO. 1993-132	p 1221	A93-54095	PNR-90915	p 56	N93-11019	#	RIACS-TR-93-01	p 560	A93-24780	#
ONERA, TP NO. 1993-13	p 925	A93-41029	PNR-90916	p 20	N93-11020	#				
ONERA, TP NO. 1993-15	p 281	A93-23015	PNR-90924	p 56	N93-11023	#	RR-CE130	p 555	N93-21383	#
ONERA, TP NO. 1993-18	p 916	A93-41031	PNR-90927	p 56	N93-11024	#	RR-CE131	p 555	N93-21382	#
ONERA, TP NO. 1993-26	p 890	A93-41038	PNR-90929	p 85	N93-11025	#				
ONERA, TP NO. 1993-3	p 279	A93-22693	PNR-90932	p 85	N93-11034	#	RR-407	p 339	N93-18507	#
ONERA, TP NO. 1993-41	p 987	A93-47446	PNR-90935	p 72	N93-11035	#				
ONERA, TP NO. 1993-43	p 987	A93-47448	PNR-90936	p 56	N93-11036	#	RSRE-MEMO-4473	p 87	N93-11383	#
ONERA, TP NO. 1993-48	p 1039	A93-47450	PNR-90937	p 56	N93-11037	#	RSRE-MEMO-4511	p 87	N93-11384	#
ONERA, TP NO. 1993-4	p 275	A93-22603	PNR-90938	p 56	N93-11038	#	RSRE-MEMO-4512	p 87	N93-11385	#
ONERA, TP NO. 1993-54	p 1146	A93-51936	PNR-90939	p 57	N93-11039	#				
ONERA, TP NO. 1993-55	p 1173	A93-51937	PNR-90943	p 57	N93-11040	#	RTD-5824-AN-01	p 724	N93-25917	#
ONERA, TP NO. 1993-5	p 916	A93-41023	PNR-90944	p 86	N93-11054	#				
ONERA, TP NO. 1993-60	p 1092	A93-51940	PNR-90945	p 57	N93-11055	#	R89351	p 170	N93-15235	#
ONERA, TP NO. 1993-64	p 1171	A93-51944	PNR-90946	p 58	N93-11105	#	R91-930020-F-PT-2	p 551	N93-19999	#
ONERA, TP NO. 1993-6	p 181	A93-14187	PNR-90947	p 58	N93-11106	#				
ONERA, TP NO. 1993-75	p 1218	A93-53596	PNR-90948	p 73	N93-11107	#	S-HRG-102-707	p 234	N93-13800	#
ONERA, TP NO. 1993-77	p 1212	A93-53598	PNR-90949	p 58	N93-11108	#				
ONERA, TP NO. 1993-78	p 1212	A93-53599	PNR-90957	p 139	N93-15489	#	S-REPT-102-364	p 234	N93-13798	#
ONERA, TP NO. 1993-82	p 1213	A93-53602	PNR-90962	p 58	N93-11085	#				
ONERA, TP NO. 1993-83	p 1190	A93-53603	PNR-90970	p 57	N93-11061	#	S-682	p 196	N93-14495	#
ONERA, TP NO. 1993-84	p 1191	A93-53604	PNR-90973	p 57	N93-11062	#				
ONERA, TP NO. 1993-88	p 1074	A93-49687	PNR-90974	p 58	N93-11063	#	SAE AIR 4566	p 1103	A93-52175	#
ONERA, TP NO. 1993-97	p 1053	A93-48197	PNR-90983	p 72	N93-11066	#				
			PNR-90984	p 58	N93-11112	#	SAE ARP 1493	p 1103	A93-52165	#
OPNAV-3960-12	p 793	N93-27925	PNR-90986	p 58	N93-11068	#	SAE ARP 4387	p 1103	A93-52166	#
			PNR-90987	p 58	N93-11069	#	SAE ARP 4402	p 1160	A93-52167	#
ORNL/M-2309	p 394	N93-18537	PNR-90988	p 521	N93-20735	#	SAE ARP 4712	p 1096	A93-52168	#
			PNR-90991	p 20	N93-11070	#	SAE ARP 4729	p 1160	A93-52170	#
ORNL/TM-11984	p 73	N93-11442	PNR-90992	p 20	N93-11113	#				
			PNR-90993	p 59	N93-11114	#	SAE AS 1606	p 1124	A93-52171	#
OU-AME-91-2	p 138	N93-14767	PNR-91011	p 48	N93-11334	#				
							SAE PAPER 892283	p 1176	A93-53200	#
QUEL-1911/92	p 89	N93-11707					SAE PAPER 912119	p 412	A93-21842	#
			PSGDL-R-92/93-0002	p 749	N93-25266	#	SAE PAPER 912133	p 327	A93-21843	#
PB92-176148	p 94	N93-11803					SAE PAPER 92-1994	p 20	N93-11221	#
PB92-188424	p 93	N93-11702	PSU-ME-R-90/91-0005-PHASE-2	p 756	N93-26533	#	SAE PAPER 920930	p 202	A93-14081	#
PB92-197136	p 35	N93-10065	PSU/ARL-TR-92-08	p 420	N93-18121	#	SAE PAPER 920947	p 202	A93-14090	#

SAE PAPER 920948

REPORT NUMBER INDEX

SAE PAPER 920948	p 107	A93-14091	SPIE-1721	p 1167	A93-50726 *	US-PATENT-CLASS-244-145	p 20	N93-11050
SAE PAPER 920949	p 107	A93-14092	SPIE-1753	p 1263	A93-55176	US-PATENT-CLASS-244-17.11	p 729	N93-25998 *
SAE PAPER 920960	p 173	A93-14626	SPIE-1788	p 1151	A93-49455	US-PATENT-CLASS-244-17.19	p 729	N93-25998 *
SAE PAPER 920961	p 206	A93-14627	SPIE-1799	p 1105	A93-49462	US-PATENT-CLASS-244-219	p 371	N93-16463
SAE PAPER 920962	p 123	A93-14628 *				US-PATENT-CLASS-244-219	p 909	N93-29278
SAE PAPER 920967	p 173	A93-14629	SSD93D0354	p 914	N93-29215 *	US-PATENT-CLASS-244-75R	p 729	N93-25998 *
SAE PAPER 920968	p 185	A93-14630				US-PATENT-CLASS-29-263	p 221	N93-14871 *
SAE PAPER 920974	p 195	A93-14633	SUDAAR-614	p 780	N93-27084 *	US-PATENT-CLASS-29-426.5	p 221	N93-14871 *
SAE PAPER 920984	p 191	A93-14634				US-PATENT-CLASS-29-898.01	p 221	N93-14871 *
SAE PAPER 920988	p 185	A93-14635 *	SWRI-PN-12-3384	p 760	N93-25915 #	US-PATENT-CLASS-29-898.07	p 221	N93-14871 *
SAE PAPER 920989	p 157	A93-14636				US-PATENT-CLASS-29-898.08	p 221	N93-14871 *
SAE PAPER 920997	p 157	A93-14638 *	TAO-60322	p 757	N93-25073 *	US-PATENT-CLASS-364-453	p 708	N93-26093
SAE PAPER 921006	p 206	A93-14639				US-PATENT-CLASS-374-4	p 67	N93-11057 *
SAE PAPER 921009	p 157	A93-14641	TDCK-91-3982	p 221	N93-14805 #	US-PATENT-CLASS-374-57	p 67	N93-11057 *
SAE PAPER 921012	p 157	A93-14642				US-PATENT-CLASS-374-5	p 67	N93-11057 *
SAE PAPER 921013	p 157	A93-14643	TEC-DRP-92-8	p 885	N93-29468 #	US-PATENT-CLASS-60-226.1	p 522	N93-22034
SAE PAPER 921016	p 185	A93-14645				US-PATENT-CLASS-60-39.17	p 522	N93-22034
SAE PAPER 921022	p 158	A93-14649	TEC-R-168	p 68	N93-11751 #	US-PATENT-CLASS-62-335	p 216	N93-13422 *
SAE PAPER 921023	p 158	A93-14650	TEC-R-191	p 152	N93-15005 #	US-PATENT-CLASS-62-434	p 216	N93-13422 *
SAE PAPER 921036	p 158	A93-14656 *				US-PATENT-CLASS-62-467	p 216	N93-13422 *
SAE PAPER 921037	p 158	A93-14657	TEES-AERO-TR-91-1	p 806	N93-28693 *	US-PATENT-CLASS-73-147	p 67	N93-11057 *
SAE PAPER 921038	p 197	A93-14658				US-PATENT-CLASS-73-147	p 296	N93-18275 *
SAE PAPER 921039	p 108	A93-14659	TELAC-91-16A	p 186	N93-12959 #	US-PATENT-CLASS-73-147	p 731	N93-25996 *
SAE PAPER 921040	p 185	A93-14660				US-PATENT-CLASS-73-147	p 751	N93-26000 *
SAE PAPER 921041	p 150	A93-14661 *	TOP-7-3-526	p 943	N93-29480 #	US-PATENT-CLASS-73-178R	p 751	N93-26000 *
SAE PAPER 921130	p 895	A93-41318 *	TP-930072	p 931	N93-29388 #	US-PATENT-CLASS-73-204.11	p 751	N93-26000 *
SAE PAPER 921182	p 890	A93-41361				US-PATENT-CLASS-73-9	p 296	N93-18275 *
SAE PAPER 921183	p 855	A93-41362						
SAE PAPER 921185	p 938	A93-41364	TR-92-12	p 420	N93-18093 *	US-PATENT-5,078,344	p 20	N93-11050
SAE PAPER 921223	p 926	A93-41397	TR-93-02	p 483	N93-20256 *	US-PATENT-5,114,104	p 371	N93-16463
SAE PAPER 921224	p 926	A93-41398				US-PATENT-5,123,616	p 554	N93-20765
SAE PAPER 921225	p 890	A93-41399	TRB/TRR-1332	p 143	N93-13787 #	US-PATENT-5,129,800	p 554	N93-20790
SAE PAPER 921226	p 898	A93-41400 *	TRB/TRR-1373	p 822	N93-26636 #	US-PATENT-5,131,758	p 67	N93-11057 *
SAE PAPER 930677	p 1158	A93-50524				US-PATENT-5,157,938	p 216	N93-13422 *
SAE PAPER 931591	p 1104	A93-49340	TRC-EM-CAB-9306	p 936	N93-31036 *	US-PATENT-5,158,251	p 483	N93-20017
SAE PAPER 931595	p 1104	A93-49344				US-PATENT-5,165,169	p 221	N93-14871 *
SAE PAPER 931596	p 1104	A93-49345	TRITA-NA-9207	p 789	N93-29005 #	US-PATENT-5,166,882	p 708	N93-26093
SAE PAPER 931597	p 1151	A93-49346				US-PATENT-5,178,004	p 296	N93-18275 *
SAE PAPER 931598	p 1165	A93-49347	TRW-91J431.1-182	p 914	N93-29652 *	US-PATENT-5,184,460	p 522	N93-22034 *
						US-PATENT-5,186,420	p 909	N93-29278
SAE SP-885	p 412	A93-21840	TT-9104	p 67	N93-11728 #	US-PATENT-5,199,128	p 556	N93-22035 *
			TT-9201	p 67	N93-11224 #	US-PATENT-5,209,111	p 751	N93-26000 *
SAE-92-1996	p 25	N93-12353 *	TT-9202	p 152	N93-14729 #	US-PATENT-5,209,430	p 729	N93-25998 *
						US-PATENT-5,211,057	p 731	N93-25998 *
SAND-91-2228	p 94	N93-12075 #	UCB/CSD-91/651	p 758	N93-25130 *	USAATCOM-TR-93-D-1	p 705	N93-26263 #
SAND-91-7012	p 560	N93-22045 #						
SAND-92-1666	p 845	N93-28603 #	UCRL-ID-112905	p 791	N93-28571 #			
SAND-92-1889C	p 790	N93-29035 #				USAAVSCOM-TR-88-D-14A-VOL-1	p 848	N93-27531 #
SAND-92-2282C	p 694	N93-25121 #	UCRL-JC-108951	p 224	N93-13655 #	USAAVSCOM-TR-88-D-14B-VOL-2	p 848	N93-27589 #
SAND-92-7009	p 433	N93-15839 #	UCRL-JC-111214	p 453	N93-17225 #	USAAVSCOM-TR-88-D-14C-VOL-3	p 848	N93-27590 #
SAND-93-0284C	p 942	N93-29187 #				USAAVSCOM-TR-92-A-004	p 139	N93-15483 *
			UDR-TR-90-106	p 164	N93-14571 #	USAFETAC/PR-92/003	p 159	N93-12605 #
SBIR-91-2	p 945	N93-29323 *	UDR-TR-90-121	p 50	N93-12488 #			
SCR-91RR-5	p 48	N93-11461 #	UM-AERO-91-46	p 988	N93-31320 #	USGS/WRI-92-4035	p 1036	N93-32191
SCT-A8924-1	p 232	N93-14912 #	UPN-90100411	p 93	N93-11702 #	UTRC-R89-927889	p 233	N93-15116 *
SCT-90-RR67	p 35	N93-10323 #	URI-MSL-921	p 71	N93-10717 #	UTRC-91-29-REPT-1	p 102	N93-12490 #
						UTRC-93-957878-27	p 812	N93-27115 *
SEL-86-003	p 230	N93-15502 *	US-PATENT-APPL-SN-000064	p 344	N93-19023 *	UVA/528266/MS94/113	p 1019	N93-31739 *
SEL-92-001	p 230	N93-15578 *	US-PATENT-APPL-SN-046256	p 853	N93-28953 #	UVA/528366/CE92/101	p 386	N93-16629 *
SEL-92-002	p 230	N93-15579 *	US-PATENT-APPL-SN-056503	p 897	N93-30416 #			
			US-PATENT-APPL-SN-146939	p 67	N93-11057 *	VKI-LS-1992-01	p 372	N93-18142 #
SME PAPER AD92-196	p 855	A93-40661	US-PATENT-APPL-SN-349381	p 708	N93-26093	VKI-LS-1992-02-VOL-1	p 422	N93-18721 #
SME PAPER AD92-198	p 855	A93-40662	US-PATENT-APPL-SN-519626	p 20	N93-11050	VKI-LS-1992-02-VOL-2	p 423	N93-18731 #
SME PAPER AD92-200	p 855	A93-40663	US-PATENT-APPL-SN-524108	p 67	N93-11057 *	VKI-LS-1992-04-VOL-2	p 421	N93-18563 #
SME PAPER AD92-203	p 855	A93-40665	US-PATENT-APPL-SN-573769	p 535	N93-20016			
SME PAPER AD92-205	p 925	A93-40666	US-PATENT-APPL-SN-591532	p 371	N93-16463	VKI-TN-181	p 988	N93-31538 #
SME PAPER AD92-206	p 855	A93-40667	US-PATENT-APPL-SN-614411	p 483	N93-20017			
SME PAPER AD92-207	p 855	A93-40668	US-PATENT-APPL-SN-647902	p 522	N93-22034 *	VPI-AOE-191	p 295	N93-18272 #
			US-PATENT-APPL-SN-682153	p 556	N93-22035 *			
SME PAPER EM92-100	p 196	A93-14101	US-PATENT-APPL-SN-718322	p 554	N93-20772	VPI-E-87-7	p 934	N93-30374 *
SME PAPER EM92-101	p 152	A93-14102	US-PATENT-APPL-SN-731233	p 554	N93-20790	VTT-PUBS-97	p 443	N93-18698 #
SME PAPER EM92-102	p 233	A93-14103	US-PATENT-APPL-SN-742238	p 296	N93-18275 *	VTT-TIED-1281	p 841	N93-27832 #
SME PAPER EM92-111	p 202	A93-14114	US-PATENT-APPL-SN-743468	p 731	N93-25996 *			
SME PAPER EM92-115	p 107	A93-14112	US-PATENT-APPL-SN-758919	p 554	N93-20765	WES/MP/GL-92-32	p 194	N93-14238 #
SME PAPER EM92-124	p 107	A93-14116	US-PATENT-APPL-SN-768094	p 67	N93-11057 *	WES/TR/GL-92-10	p 194	N93-14128 #
SME PAPER EM92-215	p 925	A93-40654	US-PATENT-APPL-SN-781520	p 216	N93-13422 *	WES/TR/SL-REMR-CS-39	p 708	N93-26274 #
SME PAPER EM92-252	p 925	A93-40656	US-PATENT-APPL-SN-785637	p 221	N93-14871 *			
SME PAPER EM93-100	p 1043	A93-51727	US-PATENT-APPL-SN-788908	p 729	N93-25998 *	WL-TM-92-338-FIGC	p 160	N93-12752 #
SME PAPER EM93-103	p 1159	A93-51733	US-PATENT-APPL-SN-790607	p 909	N93-29278	WL-TM-92-350-FIBG	p 875	N93-29410 #
SME PAPER EM93-104	p 1043	A93-51732	US-PATENT-APPL-SN-806066	p 485	N93-22015 *	WL-TM-93-300	p 760	N93-26566 #
SME PAPER EM93-106	p 1159	A93-51728	US-PATENT-APPL-SN-823805	p 751	N93-26000 *			
SME PAPER EM93-112	p 1159	A93-51729	US-PATENT-APPL-SN-823809	p 23	N93-11876 *	WL-TR-91-2079	p 724	N93-26219 #
			US-PATENT-APPL-SN-864812	p 199	N93-13414	WL-TR-91-3112	p 513	N93-20579 #
SP-15	p 239	N93-15946 #	US-PATENT-APPL-SN-875955	p 222	N93-15232 #	WL-TR-91-4061	p 826	N93-28592 #
SP-16	p 239	N93-15949 #	US-PATENT-APPL-SN-889003	p 86	N93-11172 #	WL-TR-92-0004	p 572	N93-20403 #
			US-PATENT-APPL-SN-906903	p 536	N93-20247 #	WL-TR-92-1068	p 455	N93-17891 #
SPC-92050-CMC	p 503	N93-21671 #	US-PATENT-APPL-SN-948057	p 526	N93-20039 *	WL-TR-92-2035	p 361	N93-16080 #
			US-PATENT-APPL-SN-950580	p 536	N93-20041 *	WL-TR-92-2040	p 393	N93-18242 #
			US-PATENT-APPL-SN-961943	p 453	N93-17051 *			
SPIE-1478	p 532	A93-27043						
SPIE-1571	p 1166	A93-49350	US-PATENT-CLASS-15-52	p 556	N93-22035 *			
SPIE-1582	p 1158	A93-51250	US-PATENT-CLASS-15-80	p 556	N93-22035 *			
SPIE-1664	p 544	A93-27237	US-PATENT-CLASS-15-87	p 556	N93-22035 *			
SPIE-1694	p 547	A93-28151 *						

REPORT NUMBER INDEX

XH-DOT/FAA/NR

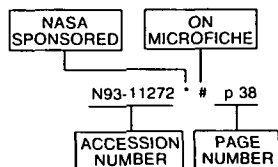
WL-TR-92-2066	p 815	N93-27679	#
WL-TR-92-2082	p 934	N93-30406	#
WL-TR-92-2105	p 917	N93-29402	#
WL-TR-92-3009	p 50	N93-12488	#
WL-TR-92-3025	p 164	N93-14571	#
WL-TR-92-3028	p 136	N93-14441	#
WL-TR-92-3041	p 751	N93-25951	#
WL-TR-92-3053	p 137	N93-14661	#
WL-TR-92-3063	p 187	N93-13872	#
WL-TR-92-3069	p 337	N93-18248	#
WL-TR-92-3101	p 527	N93-20551	#
WL-TR-92-4032	p 752	N93-26526	#
WL-TR-92-4045	p 110	N93-14549	#
WL-TR-92-4090	p 1018	N93-31192	#
WL-TR-93-2048	p 815	N93-28391	#
WL-TR-93-2051	p 825	N93-28226	#
WL-TR-93-3002	p 990	N93-32004	#
WL-TR-93-3005	p 893	N93-29409	#
WL-TR-93-3016	p 909	N93-30498	#
WRDC-TR-90-0001	p 572	N93-20403	#
XH-DOT/FAA/NR	p 845	N93-27675	#

ACCESSION NUMBER INDEX

AERONAUTICAL ENGINEERING / A Continuing Bibliography
1993 Cumulative Index

February 1994

Typical Accession Number Index Listing



Listings in this index are arranged alphanumerically by accession number. The page number indicates the page on which the citation is located. The accession number denotes the number by which the citation is identified. An asterisk (*) indicates that the item is a NASA report. A pound sign (#) indicates that the item is available on microfiche.

A93-10009	p 75	A93-10960	p 77
A93-10026	p 75	A93-10963	p 77
A93-10029	p 75	A93-10971	p 77
A93-10030	p 75	A93-10976	p 29
A93-10032	p 75	A93-10977	p 29
A93-10042	p 94	A93-10981	p 29
A93-10044	p 75	A93-10982	p 50
A93-10045	p 95	A93-10987	p 29
A93-10047	p 75	A93-10988	p 29
A93-10049	p 66	A93-10996	p 77
A93-10079	p 4	A93-10998	p 30
A93-10080	p 4	A93-10999	p 30
A93-10098	p 92	A93-11000	p 50
A93-10137	p 4	A93-11004	p 30
A93-10138	p 4	A93-11005	p 30
A93-10139	p 4	A93-11006	p 30
A93-10140	p 4	A93-11007	p 30
A93-10141	p 5	A93-11008	p 31
A93-10142	p 5	A93-11009	p 31
A93-10143	p 5	A93-11010	p 31
A93-10144	p 5	A93-11012	p 31
A93-10147	p 5	A93-11013	p 31
A93-10148	p 76	A93-11014	p 32
A93-10150	p 5	A93-11015	p 32
A93-10176	p 76	A93-11018	p 50
A93-10178	p 76	A93-11019	p 32
A93-10179	p 52	A93-11020	p 1
A93-10180	p 76	A93-11021	p 32
A93-10187	p 5	A93-11022	p 32
A93-10188	p 6	A93-11023	p 32
A93-10189	p 6	A93-11024	p 32
A93-10192	p 6	A93-11027	p 1
A93-10273	p 76	A93-11028	p 92
A93-10275	p 76	A93-11032	p 33
A93-10328	p 26	A93-11035	p 33
A93-10402	p 6	A93-11044	p 33
A93-10404	p 6	A93-11085	p 95
A93-10533	p 6	A93-11095	p 33
A93-10534	p 6	A93-11203	p 50
A93-10667	p 76	A93-11206	p 77
A93-10730	p 92	A93-11207	p 61
A93-10731	p 99	A93-11209	p 52
A93-10732	p 52	A93-11250	p 1
A93-10733	p 1	A93-11251	p 37
A93-10741	p 95	A93-11256	# p 102
A93-10776	p 37	A93-11257	# p 37
A93-10777	p 60	A93-11258	# p 95
A93-10778	p 7	A93-11260	# p 37
A93-10779	p 7	A93-11261	# p 95
A93-10780	p 77	A93-11262	# p 37
A93-10782	p 29	A93-11264	# p 61
A93-10916	p 60	A93-11265	# p 61
A93-10917	p 37	A93-11266	# p 61
A93-10918	p 77	A93-11267	# p 7
A93-10919	p 61	A93-11268	* # p 38

A93-11271	# p 38
A93-11272	* # p 38
A93-11273	* # p 38
A93-11274	* # p 38
A93-11275	* # p 38
A93-11276	# p 38
A93-11277	* # p 39
A93-11278	# p 39
A93-11280	* # p 39
A93-11281	# p 51
A93-11284	# p 61
A93-11285	# p 39
A93-11294	# p 33
A93-11295	# p 34
A93-11297	# p 34
A93-11298	# p 34
A93-11300	p 104
A93-11302	p 7
A93-11341	p 77
A93-11346	p 78
A93-11357	p 39
A93-11359	p 39
A93-11361	* p 40
A93-11362	* p 7
A93-11363	* p 40
A93-11364	* p 26
A93-11365	* p 1
A93-11366	* p 26
A93-11367	* p 27
A93-11368	* p 1
A93-11369	* p 40
A93-11370	* p 2
A93-11371	* p 40
A93-11372	* p 27
A93-11373	* p 27
A93-11374	* p 2
A93-11383	* p 27
A93-11384	* p 27
A93-11404	* p 92
A93-11411	* p 103
A93-11412	* p 103
A93-11418	* p 40
A93-11419	* p 53
A93-11420	* p 40
A93-11454	* p 70
A93-11497	* p 7
A93-11498	* p 27
A93-11499	* p 7
A93-11500	* p 8
A93-11527	* p 8
A93-11553	* p 8
A93-11621	* p 2
A93-11654	* p 40
A93-11682	* p 78
A93-11791	* p 95
A93-11809	* p 41
A93-11810	* p 78
A93-11815	* p 41
A93-11816	* p 41
A93-11818	* p 41
A93-11820	* p 41
A93-11821	* p 41
A93-11870	* p 53
A93-11872	* p 8
A93-11920	* p 8
A93-11921	* p 8
A93-12002	* p 8
A93-12004	* p 69
A93-12007	* p 9
A93-12010	* p 9
A93-12011	* p 9
A93-12012	* p 61
A93-12020	* p 9
A93-12097	* p 66
A93-12098	* p 78
A93-12114	* p 70
A93-12123	* p 34
A93-12124	* p 34
A93-12125	* p 34
A93-12151	* p 78
A93-12153	* p 78
A93-12156	* p 9
A93-12157	* p 78

A93-12158	p 9
A93-12163	p 9
A93-12165	p 79
A93-12177	p 9
A93-12202	p 70
A93-12216	p 66
A93-12224	p 66
A93-12229	p 79
A93-12233	p 2
A93-12234	p 2
A93-12235	p 2
A93-12236	p 53
A93-12237	p 53
A93-12238	p 53
A93-12273	p 10
A93-12316	p 66
A93-12317	p 10
A93-12322	p 95
A93-12324	p 10
A93-12332	p 79
A93-12361	p 10
A93-12364	p 92
A93-12366	p 10
A93-12367	p 27
A93-12368	p 70
A93-12372	p 28
A93-12407	p 92
A93-12427	p 10
A93-12428	p 11
A93-12429	p 11
A93-12432	p 11
A93-12433	p 11
A93-12434	p 41
A93-12452	p 53
A93-12453	p 11
A93-12454	p 11
A93-12460	p 79
A93-12558	p 12
A93-12559	p 34
A93-12560	p 103
A93-12643	p 93
A93-12651	p 12
A93-12653	p 62
A93-12656	p 66
A93-12659	p 12
A93-12718	p 103
A93-12719	p 103
A93-12726	p 2
A93-12727	p 41
A93-12730	p 12
A93-12731	p 12
A93-12732	p 95
A93-12733	p 53
A93-12735	p 12
A93-12736	p 53
A93-12760	p 12
A93-12764	p 12
A93-12766	p 12
A93-12768	p 13
A93-12771	p 70
A93-12781	p 71
A93-12784	p 79
A93-12800	p 79
A93-12802	p 62
A93-12805	p 13
A93-12807	p 13
A93-12808	p 13
A93-12809	p 79
A93-12810	p 53
A93-12811	p 53
A93-12812	p 54
A93-12815	p 54
A93-12818	p 54
A93-12820	p 54
A93-12821	p 95
A93-12822	p 54
A93-12823	p 71
A93-12824	p 71
A93-12839	p 13
A93-12841	p 13
A93-12922	p 79
A93-12932	p 13
A93-12933	p 13

A93-12973	p 14
A93-12974	p 14
A93-12975	p 14
A93-12977	p 96
A93-12978	p 42
A93-12980	p 14
A93-13007	p 96
A93-13011	p 96
A93-13078	p 96
A93-13079	p 96
A93-13126	p 62
A93-13177	p 96
A93-13197	p 97
A93-13230	* p 97
A93-13233	p 97
A93-13241	p 97
A93-13246	p 97
A93-13247	p 62
A93-13261	* # p 42
A93-13262	* # p 93
A93-13263	* # p 51
A93-13264	* # p 97
A93-13265	* # p 51
A93-13266	* # p 42
A93-13267	* # p 34
A93-13269	* # p 42
A93-13272	* # p 51
A93-13273	* # p 42
A93-13276	* # p 69
A93-13280	* # p 62
A93-13284	* # p 42
A93-13285	* # p 62
A93-13286	* # p 62
A93-13303	* # p 14
A93-13304	* # p 14
A93-13305	* # p 14
A93-13306	* # p 15
A93-13308	* # p 15
A93-13309	* # p 15
A93-13310	* # p 51
A93-13311	* # p 42
A93-13312	* # p 66
A93-13314	* # p 43
A93-13315	* # p 43
A93-13326	* # p 43
A93-13328	* # p 63
A93-13330	* # p 54
A93-13333	* # p 54
A93-13334	* # p 54
A93-13336	* # p 43
A93-13337	* # p 43
A93-13338	* # p 63
A93-13339	* # p 67
A93-13340	* # p 43
A93-13342	* # p 15
A93-13343	* # p 80
A93-13345	* # p 63
A93-13348	* # p 43
A93-13351	* # p 51
A93-13352	* # p 55
A93-13353	* # p 44
A93-13354	* # p 97
A93-13355	* # p 44
A93-13356	* # p 15
A93-13359	* # p 44
A93-13360	* # p 55
A93-13361	* # p 15
A93-13362	* # p 80
A93-13363	* # p 103
A93-13365	* # p 63
A93-13366	* # p 55
A93-13368	* # p 2
A93-13369	* # p 103
A93-13370	* # p 44
A93-13371	* # p 44
A93-13372	* # p 44
A93-13373	* # p 51
A93-13377	* # p 15
A93-13378	* # p 44
A93-13380	* # p 16
A93-13381	* # p 45
A93-13382	* # p 16
A93-13383	* # p 55

ACCESSION

A93-13401

A93-13401 p 45
 A93-13403 p 80
 A93-13404 p 45
 A93-13405 p 55
 A93-13406 p 45
 A93-13407 p 45
 A93-13409 p 2
 A93-13412 p 45
 A93-13415 p 45
 A93-13420 p 98
 A93-13423 p 104
 A93-13424 p 104
 A93-13434 p 16
 A93-13435 p 80
 A93-13437 p 80
 A93-13447 p 80
 A93-13448 p 3
 A93-13626 p 80
 A93-13627 p 3
 A93-13628 p 3
 A93-13629 p 45
 A93-13630 p 28
 A93-13631 p 46
 A93-13632 p 3
 A93-13633 p 3
 A93-13634 p 3
 A93-13635 p 46
 A93-13636 p 46
 A93-13637 p 46
 A93-13638 p 81
 A93-13639 p 81
 A93-13640 p 71
 A93-13642 p 46
 A93-13644 p 71
 A93-13646 p 81
 A93-13648 p 71
 A93-13649 p 16
 A93-13700 p 46
 A93-13791 p 200
 A93-13824 p 195
 A93-13910 p 190
 A93-13943 p 200
 A93-13945 p 111
 A93-13957 p 107
 A93-13976 p 201
 A93-13978 p 201
 A93-13980 p 201
 A93-13981 p 201
 A93-13982 p 201
 A93-13988 p 201
 A93-13990 p 202
 A93-14064 p 140
 A93-14067 p 107
 A93-14077 p 170
 A93-14078 p 111
 A93-14080 p 111
 A93-14081 p 202
 A93-14090 p 202
 A93-14091 p 107
 A93-14092 p 107
 A93-14099 p 230
 A93-14101 p 196
 A93-14102 p 152
 A93-14103 p 233
 A93-14112 p 107
 A93-14114 p 202
 A93-14116 p 107
 A93-14117 p 107
 A93-14118 # p 111
 A93-14120 p 111
 A93-14151 p 107
 A93-14152 p 111
 A93-14153 p 170
 A93-14154 p 108
 A93-14156 p 108
 A93-14157 p 149
 A93-14158 p 165
 A93-14159 p 180
 A93-14160 p 180
 A93-14161 p 180
 A93-14165 p 112
 A93-14166 p 112
 A93-14167 p 112
 A93-14168 p 202
 A93-14169 p 112
 A93-14170 p 112
 A93-14171 p 112
 A93-14172 p 113
 A93-14174 p 196
 A93-14175 p 202
 A93-14176 p 170
 A93-14177 p 225
 A93-14178 p 225
 A93-14180 p 202
 A93-14183 p 108
 A93-14185 p 152

A93-14186 p 180
 A93-14187 p 181
 A93-14188 p 181
 A93-14189 p 113
 A93-14190 p 113
 A93-14191 p 113
 A93-14192 p 113
 A93-14193 p 113
 A93-14194 p 203
 A93-14196 p 203
 A93-14197 p 181
 A93-14200 p 166
 A93-14201 p 225
 A93-14202 p 225
 A93-14203 p 153
 A93-14204 p 153
 A93-14205 p 153
 A93-14208 p 153
 A93-14209 p 181
 A93-14210 p 114
 A93-14211 p 114
 A93-14212 p 114
 A93-14213 p 114
 A93-14215 p 114
 A93-14216 p 114
 A93-14217 p 115
 A93-14218 p 140
 A93-14219 p 153
 A93-14220 p 140
 A93-14221 p 141
 A93-14223 p 153
 A93-14224 p 181
 A93-14226 p 153
 A93-14227 p 154
 A93-14229 p 181
 A93-14231 p 154
 A93-14232 p 181
 A93-14234 p 149
 A93-14235 p 149
 A93-14236 p 150
 A93-14242 p 170
 A93-14243 p 171
 A93-14244 p 171
 A93-14245 p 203
 A93-14246 p 115
 A93-14247 p 171
 A93-14248 p 115
 A93-14249 p 115
 A93-14250 p 115
 A93-14251 p 115
 A93-14252 p 116
 A93-14253 p 154
 A93-14254 p 154
 A93-14256 p 154
 A93-14258 p 154
 A93-14259 p 182
 A93-14261 p 154
 A93-14262 p 116
 A93-14263 p 116
 A93-14264 p 116
 A93-14265 p 116
 A93-14266 p 230
 A93-14268 p 231
 A93-14269 p 231
 A93-14271 p 171
 A93-14272 p 171
 A93-14273 p 171
 A93-14274 p 190
 A93-14275 p 116
 A93-14276 p 190
 A93-14277 p 116
 A93-14278 p 225
 A93-14279 p 117
 A93-14280 p 155
 A93-14281 p 182
 A93-14282 p 182
 A93-14283 p 117
 A93-14285 p 155
 A93-14286 p 203
 A93-14288 p 182
 A93-14289 p 155
 A93-14290 p 225
 A93-14291 p 117
 A93-14292 p 196
 A93-14293 p 182
 A93-14295 p 166
 A93-14297 p 117
 A93-14298 p 117
 A93-14299 p 190
 A93-14300 p 190
 A93-14301 p 117
 A93-14302 p 118
 A93-14304 p 118
 A93-14305 p 118
 A93-14306 p 182
 A93-14307 p 196

A93-14311 p 226
 A93-14312 p 203
 A93-14313 p 155
 A93-14315 p 108
 A93-14317 p 141
 A93-14318 p 155
 A93-14320 p 150
 A93-14321 p 155
 A93-14322 p 156
 A93-14323 p 118
 A93-14324 p 156
 A93-14325 p 203
 A93-14326 p 166
 A93-14327 p 166
 A93-14329 p 118
 A93-14330 p 118
 A93-14331 p 182
 A93-14332 p 118
 A93-14333 p 119
 A93-14334 p 204
 A93-14336 p 156
 A93-14337 p 226
 A93-14338 p 233
 A93-14339 p 156
 A93-14340 p 226
 A93-14344 p 119
 A93-14345 p 119
 A93-14346 p 156
 A93-14347 p 195
 A93-14348 p 119
 A93-14349 p 183
 A93-14350 p 183
 A93-14351 p 183
 A93-14352 p 190
 A93-14353 p 231
 A93-14354 p 119
 A93-14355 p 120
 A93-14356 p 120
 A93-14359 p 120
 A93-14361 p 156
 A93-14363 p 204
 A93-14365 p 191
 A93-14366 p 120
 A93-14370 p 183
 A93-14371 p 183
 A93-14372 p 183
 A93-14373 p 183
 A93-14374 p 141
 A93-14375 p 226
 A93-14376 p 141
 A93-14379 p 184
 A93-14380 p 120
 A93-14381 p 120
 A93-14382 p 120
 A93-14384 p 204
 A93-14385 p 157
 A93-14386 p 157
 A93-14391 p 121
 A93-14392 p 121
 A93-14394 p 141
 A93-14395 p 157
 A93-14396 p 226
 A93-14397 p 184
 A93-14398 p 184
 A93-14399 p 184
 A93-14400 p 184
 A93-14401 p 184
 A93-14403 p 191
 A93-14405 p 121
 A93-14406 p 121
 A93-14407 p 121
 A93-14408 p 121
 A93-14409 p 122
 A93-14410 p 191
 A93-14412 p 191
 A93-14414 p 191
 A93-14415 p 226
 A93-14417 p 227
 A93-14478 p 204
 A93-14479 p 122
 A93-14480 p 122
 A93-14481 p 172
 A93-14482 p 204
 A93-14483 p 204
 A93-14484 p 204
 A93-14489 p 205
 A93-14493 p 205
 A93-14494 p 172
 A93-14496 p 172
 A93-14497 p 172
 A93-14498 p 172
 A93-14499 p 172
 A93-14503 p 197
 A93-14504 p 197
 A93-14515 p 122
 A93-14516 p 172

A93-14517 p 205
 A93-14518 p 205
 A93-14519 p 172
 A93-14520 p 122
 A93-14523 p 205
 A93-14525 p 172
 A93-14526 p 227
 A93-14537 p 122
 A93-14539 p 231
 A93-14540 p 231
 A93-14541 p 122
 A93-14542 p 205
 A93-14543 p 205
 A93-14545 p 206
 A93-14546 p 122
 A93-14548 p 122
 A93-14550 p 122
 A93-14552 p 123
 A93-14554 p 123
 A93-14555 p 123
 A93-14556 p 123
 A93-14557 p 123
 A93-14561 p 206
 A93-14564 p 123
 A93-14569 p 206
 A93-14571 p 206
 A93-14587 p 184
 A93-14593 p 157
 A93-14594 p 185
 A93-14595 p 185
 A93-14596 p 185
 A93-14608 p 173
 A93-14616 p 206
 A93-14624 p 173
 A93-14626 p 173
 A93-14627 p 206
 A93-14628 p 123
 A93-14629 p 173
 A93-14630 p 185
 A93-14633 p 195
 A93-14634 p 191
 A93-14635 p 185
 A93-14636 p 157
 A93-14638 p 157
 A93-14639 p 206
 A93-14641 p 157
 A93-14642 p 157
 A93-14643 p 157
 A93-14645 p 185
 A93-14649 p 158
 A93-14650 p 158
 A93-14656 p 158
 A93-14657 p 158
 A93-14658 p 197
 A93-14659 p 108
 A93-14660 p 185
 A93-14661 p 150
 A93-14678 p 206
 A93-14685 p 227
 A93-14782 p 124
 A93-14783 p 158
 A93-14784 p 158
 A93-14811 p 207
 A93-14812 p 207
 A93-14818 p 185
 A93-14819 p 108
 A93-14820 p 158
 A93-15028 p 158
 A93-15029 p 197
 A93-15030 p 207
 A93-15031 p 197
 A93-15032 p 234
 A93-15033 p 234
 A93-15034 p 124
 A93-15035 p 234
 A93-15037 p 150
 A93-15040 p 166
 A93-15042 p 173
 A93-15043 p 166
 A93-15044 p 227
 A93-15046 p 186
 A93-15047 p 167
 A93-15048 p 167
 A93-15049 p 159
 A93-15052 p 150
 A93-15053 p 150
 A93-15054 p 109
 A93-15056 p 109
 A93-15058 p 141
 A93-15068 p 207
 A93-15070 p 207
 A93-15072 p 207
 A93-15079 p 223
 A93-15109 p 124
 A93-15146 p 124
 A93-15178 p 124

A93-15188 p 208
 A93-15189 p 124
 A93-15209 p 124
 A93-15215 p 125
 A93-15216 p 125
 A93-15217 p 125
 A93-15224 p 151
 A93-15254 p 125
 A93-15256 p 125
 A93-15341 p 125
 A93-15342 p 208
 A93-15343 p 173
 A93-15346 p 197
 A93-15375 p 208
 A93-15401 p 208
 A93-15402 p 208
 A93-15406 p 227
 A93-15409 p 208
 A93-15443 p 125
 A93-15446 p 125
 A93-15449 p 126
 A93-15486 p 208
 A93-15488 p 126
 A93-15494 p 126
 A93-15495 p 126
 A93-15496 p 208
 A93-15525 p 209
 A93-15627 p 126
 A93-15684 p 209
 A93-15702 p 209
 A93-15737 p 159
 A93-15738 p 209
 A93-15748 p 197
 A93-15757 p 198
 A93-15782 p 159
 A93-15789 p 209
 A93-15792 p 209
 A93-15801 p 141
 A93-15804 p 209
 A93-15808 p 109
 A93-15810 p 109
 A93-15812 p 159
 A93-16163 p 209
 A93-16234 p 173
 A93-16235 p 174
 A93-16236 p 174
 A93-16239 p 174
 A93-16246 p 210
 A93-16248 p 210
 A93-16324 p 223
 A93-16374 p 210
 A93-16400 p 126
 A93-16412 p 195
 A93-16472 p 227
 A93-16473 p 126
 A93-16604 p 210
 A93-16611 p 210
 A93-16623 p 198
 A93-16647 p 210
 A93-16664 p 127
 A93-16666 p 127
 A93-16707 p 127
 A93-16708 p 127
 A93-16777 p 227
 A93-16778 p 228
 A93-16783 p 228
 A93-16844 p 174
 A93-16845 p 210
 A93-16846 p 174
 A93-16849 p 211
 A93-16852 p 174
 A93-16853 p 174
 A93-16854 p 235
 A93-16859 p 159
 A93-16860 p 141
 A93-16861 p 211
 A93-16878 p 195
 A93-16932 p 127
 A93-16933 p 127
 A93-16934 p 191
 A93-16979 p 228
 A93-17033 p 198
 A93-17095 p 167
 A93-17100 p 109
 A93-17140 p 211
 A93-17251 p 211
 A93-17252 p 127
 A93-17253 p 128
 A93-17256 p 128
 A93-17264 p 128
 A93-17265 p 128
 A93-17271 p 235
 A93-17275 p 235
 A93-17277 p 128
 A93-17301 p 142

ACCESSION NUMBER INDEX

ACCESSION NUMBER INDEX

A93-20148

A93-17302	p 142	A93-18543	p 311	A93-19192	p 425	A93-19361	p 249	A93-19493	p 354
A93-17303	p 142	A93-18548	p 425	A93-19193	p 398	A93-19362	p 249	A93-19494 *	p 405
A93-17304	p 142	A93-18553	p 312	A93-19194 *	p 244	A93-19363	p 350	A93-19496	p 255
A93-17305	p 142	A93-18554	p 312	A93-19195 *	p 448	A93-19365	p 350	A93-19497	p 405
A93-17306	p 151	A93-18555	p 312	A93-19196	p 448	A93-19366	p 387	A93-19498	p 256
A93-17307	p 151	A93-18611	p 396	A93-19201	p 448	A93-19367	p 388	A93-19499	p 256
A93-17308	p 151	A93-18618	p 396	A93-19202 *	p 448	A93-19368	p 249	A93-19500	p 354
A93-17309	p 142	A93-18619	p 396	A93-19203	p 448	A93-19369	p 401	A93-19501	p 354
A93-17310	p 186	A93-18627 *	p 396	A93-19204	p 398	A93-19370	p 350	A93-19506	p 405
A93-17311	p 191	A93-18636	p 387	A93-19206	p 449	A93-19371	p 401	A93-19507	p 256
A93-17326	p 235	A93-18652	p 397	A93-19207	p 399	A93-19372	p 388	A93-19508	p 256
A93-17389 *	p 228	A93-18670 *	p 397	A93-19208	p 399	A93-19373	p 402	A93-19509	p 256
A93-17392	p 211	A93-18712 *	p 306	A93-19209	p 449	A93-19374	p 388	A93-19510	p 257
A93-17408	p 211	A93-18717	p 383	A93-19211	p 399	A93-19375	p 351	A93-19511	p 375
A93-17417 *	p 211	A93-18752 *	p 397	A93-19212	p 449	A93-19376	p 351	A93-19518	p 354
A93-17501 *	p 151	A93-18754	p 237	A93-19213	p 449	A93-19377	p 351	A93-19519	p 355
A93-17502	p 159	A93-18755	p 321	A93-19214	p 449	A93-19379	p 402	A93-19521	p 257
A93-17526	p 240	A93-18756	p 237	A93-19215 *	p 450	A93-19380	p 249	A93-19522	p 257
A93-17569	p 394	A93-18757	p 238	A93-19216	p 450	A93-19382	p 249	A93-19524	p 355
A93-17574	p 341	A93-18758	p 238	A93-19217	p 399	A93-19383	p 250	A93-19525	p 355
A93-17714	p 320	A93-18759	p 238	A93-19218	p 450	A93-19384	p 250	A93-19527	p 257
A93-17721	p 366	A93-18760	p 238	A93-19219	p 244	A93-19385	p 250	A93-19528	p 257
A93-17727	p 394	A93-18761	p 238	A93-19220	p 399	A93-19386	p 402	A93-19530	p 257
A93-17728	p 320	A93-18762	p 434	A93-19221 *	p 245	A93-19387	p 402	A93-19531	p 375
A93-17750 *	p 241	A93-18763	p 238	A93-19222	p 245	A93-19388	p 250	A93-19532	p 388
A93-17751	p 311	A93-18764	p 435	A93-19223	p 450	A93-19389	p 351	A93-19534	p 355
A93-17752	p 311	A93-18765	p 238	A93-19224	p 450	A93-19392	p 375	A93-19535	p 406
A93-17754	p 311	A93-18767	p 238	A93-19226	p 450	A93-19393	p 351	A93-19536	p 406
A93-17756	p 311	A93-18774	p 374	A93-19229 *	p 451	A93-19395 *	p 250	A93-19537	p 406
A93-17757	p 311	A93-18776	p 374	A93-19230	p 451	A93-19396	p 351	A93-19539	p 406
A93-17762	p 394	A93-18777	p 366	A93-19231 *	p 322	A93-19397	p 351	A93-19543	p 257
A93-17765	p 395	A93-18778	p 345	A93-19250 *	p 399	A93-19398	p 352	A93-19545	p 258
A93-17767	p 395	A93-18779	p 239	A93-19276	p 245	A93-19399 *	p 250	A93-19546	p 355
A93-17797	p 311	A93-18780	p 306	A93-19277	p 245	A93-19400 *	p 251	A93-19547 *	p 388
A93-17798	p 305	A93-18782	p 345	A93-19278	p 245	A93-19401 *	p 251	A93-19549	p 258
A93-17799	p 241	A93-18783	p 345	A93-19279 *	p 346	A93-19404	p 352	A93-19550	p 355
A93-17835	p 311	A93-18784	p 345	A93-19280	p 400	A93-19405	p 402	A93-19551	p 355
A93-17862	p 395	A93-18785	p 346	A93-19283	p 346	A93-19407	p 352	A93-19552	p 322
A93-17864 *	p 341	A93-18786	p 346	A93-19285	p 347	A93-19408	p 352	A93-19553	p 356
A93-17899	p 344	A93-18787	p 346	A93-19286	p 347	A93-19409	p 251	A93-19554	p 356
A93-18054	p 395	A93-18788	p 239	A93-19287	p 400	A93-19410	p 352	A93-19555	p 356
A93-18222	p 241	A93-18789	p 397	A93-19289	p 400	A93-19411	p 352	A93-19556	p 356
A93-18230	p 241	A93-18790	p 346	A93-19290	p 400	A93-19412	p 402	A93-19557	p 435
A93-18233	p 241	A93-18851	p 242	A93-19291	p 245	A93-19413	p 402	A93-19558	p 356
A93-18238	p 241	A93-18855	p 243	A93-19292	p 246	A93-19415	p 403	A93-19561	p 356
A93-18241	p 242	A93-18932	p 312	A93-19293	p 246	A93-19416	p 403	A93-19562	p 356
A93-18242	p 444	A93-18978	p 397	A93-19294	p 246	A93-19417	p 403	A93-19563	p 357
A93-18243	p 395	A93-18989	p 397	A93-19296	p 246	A93-19420 *	p 403	A93-19564	p 357
A93-18316	p 434	A93-19077 *	p 374	A93-19297	p 347	A93-19425	p 403	A93-19565	p 388
A93-18326	p 395	A93-19080	p 435	A93-19299	p 322	A93-19427	p 388	A93-19566	p 258
A93-18327	p 237	A93-19101	p 435	A93-19300	p 347	A93-19428	p 353	A93-19567	p 258
A93-18329	p 395	A93-19121	p 346	A93-19301	p 246	A93-19429 *	p 251	A93-19570	p 258
A93-18330	p 320	A93-19126	p 444	A93-19302	p 246	A93-19430	p 251	A93-19571	p 406
A93-18331	p 320	A93-19127	p 243	A93-19303	p 400	A93-19431	p 404	A93-19572	p 357
A93-18334	p 320	A93-19130	p 243	A93-19304	p 347	A93-19432	p 251	A93-19573	p 357
A93-18335	p 395	A93-19132 *	p 243	A93-19305	p 347	A93-19433	p 252	A93-19574	p 258
A93-18337	p 345	A93-19133	p 243	A93-19306	p 347	A93-19434	p 252	A93-19575	p 258
A93-18339	p 321	A93-19134	p 243	A93-19307 *	p 348	A93-19436 *	p 252	A93-19576	p 435
A93-18342	p 345	A93-19135	p 244	A93-19308	p 348	A93-19437	p 252	A93-19579 *	p 384
A93-18343	p 396	A93-19136 *	p 444	A93-19309	p 247	A93-19439	p 252	A93-19580	p 357
A93-18344	p 321	A93-19137	p 444	A93-19310	p 247	A93-19440	p 404	A93-19581	p 388
A93-18345	p 306	A93-19138	p 444	A93-19311	p 247	A93-19442	p 404	A93-19582	p 406
A93-18346	p 306	A93-19139	p 444	A93-19312	p 247	A93-19444	p 404	A93-19587 *	p 406
A93-18349	p 321	A93-19141	p 397	A93-19313	p 247	A93-19445	p 252	A93-19595	p 407
A93-18350	p 306	A93-19142	p 445	A93-19314	p 247	A93-19446	p 404	A93-19598 *	p 407
A93-18351	p 321	A93-19143 *	p 445	A93-19316	p 400	A93-19448	p 353	A93-19659	p 375
A93-18352	p 237	A93-19144 *	p 244	A93-19318	p 348	A93-19450	p 404	A93-19693	p 407
A93-18354	p 321	A93-19147	p 445	A93-19320	p 400	A93-19452	p 253	A93-19697	p 407
A93-18356	p 345	A93-19148	p 374	A93-19321	p 248	A93-19453	p 405	A93-19699	p 407
A93-18357	p 373	A93-19149 *	p 374	A93-19322 *	p 248	A93-19457	p 405	A93-19801 *	p 342
A93-18360	p 396	A93-19150	p 244	A93-19323	p 348	A93-19459	p 353	A93-19804 *	p 451
A93-18361	p 321	A93-19151 *	p 244	A93-19324 *	p 248	A93-19460	p 253	A93-19806 *	p 322
A93-18362	p 374	A93-19153	p 445	A93-19325 *	p 401	A93-19461	p 239	A93-19914 *	p 407
A93-18363	p 366	A93-19154	p 445	A93-19326 *	p 401	A93-19462	p 353	A93-19966	p 259
A93-18364	p 341	A93-19155	p 445	A93-19327	p 401	A93-19463	p 353	A93-19967	p 408
A93-18365	p 306	A93-19156 *	p 445	A93-19330	p 387	A93-19464	p 353	A93-19976	p 455
A93-18367	p 321	A93-19157 *	p 398	A93-19331	p 348	A93-19465	p 353	A93-20007	p 312
A93-18370	p 396	A93-19158	p 244	A93-19332	p 348	A93-19466	p 405	A93-20008	p 312
A93-18371	p 396	A93-19159 *	p 446	A93-19333	p 248	A93-19468	p 253	A93-20116	p 259
A93-18372	p 345	A93-19160 *	p 446	A93-19334	p 248	A93-19469	p 253	A93-20117	p 259
A93-18373	p 434	A93-19163 *	p 446	A93-19335	p 348	A93-19470	p 253	A93-20118	p 259
A93-18374	p 321	A93-19164	p 446	A93-19336	p 248	A93-19473	p 253	A93-20119	p 259
A93-18375	p 237	A93-19167	p 446	A93-19337	p 249	A93-19474	p 253	A93-20120	p 259
A93-18376	p 237	A93-19172	p 446	A93-19338	p 349	A93-19475	p 254	A93-20129 #	p 389
A93-18377	p 242	A93-19173 *	p 398	A93-19339	p 349	A93-19477	p 254	A93-20130 #	p 306
A93-18378	p 366	A93-19176 *	p 447	A93-19340	p 349	A93-19479	p 254	A93-20132 #	p 366
A93-18379	p 242	A93-19177 *	p 447	A93-19341	p 387	A93-19482	p 254	A93-20138 #	p 367
A93-18381	p 366	A93-19182	p 447	A93-19344	p 401	A93-19483	p 254	A93-20139 #	p 408
A93-18383	p 366	A93-19183	p 447	A93-19346	p 349	A93-19485	p 254	A93-20140 #	p 357
A93-18384	p 242	A93-19184	p 447	A93-19347	p 349	A93-19487 *	p 354	A93-20141 *	p 408
A93-18391	p 383	A93-19185	p 322	A93-19351	p 349	A93-19488	p 254	A93-20143 #	p 307
A93-18499	p 242	A93-19186 *	p 447	A93-19352	p 401	A93-19489	p 255	A93-20144 *	p 259
A93-18526 *	p 242	A93-19187	p 447	A93-19355	p 350	A93-19490 *	p 255	A93-20145 #	p 307
A93-18529	p 374	A93-19189	p 398	A93-19356	p 387	A93-19491	p 255	A93-20146 #	p 260
A93-18532	p 341	A93-19190	p 448	A93-19357	p 350	A93-19492	p 255	A93-20147 #	p 307
A93-18542	p 306	A93-19191	p 425	A93-19359	p 350			A93-20148 #	p 260

A93-20150

ACCESSION NUMBER INDEX

A93-20150	#	p 322	A93-20721	*	p 266	A93-21667	*	p 359	A93-22172	p 309	A93-22618	#	p 277
A93-20152	#	p 260	A93-20729		p 266	A93-21668		p 359	A93-22173	p 412	A93-22619	#	p 277
A93-20155	*	p 389	A93-20738		p 266	A93-21669		p 270	A93-22174	p 376	A93-22620	*	p 277
A93-20162	*	p 260	A93-20739		p 437	A93-21670		p 359	A93-22175	p 431	A93-22624	*	p 277
A93-20163	*	p 260	A93-20740		p 437	A93-21671		p 359	A93-22176	p 413	A93-22625	*	p 277
A93-20164	#	p 260	A93-20741		p 266	A93-21677		p 270	A93-22178	p 413	A93-22626	#	p 278
A93-20165	#	p 261	A93-20802		p 266	A93-21678		p 389	A93-22179	p 431	A93-22627	#	p 278
A93-20166	#	p 261	A93-20803		p 375	A93-21681		p 453	A93-22180	p 431	A93-22628	#	p 278
A93-20167	#	p 261	A93-20804		p 266	A93-21688		p 411	A93-22181	p 309	A93-22630	#	p 278
A93-20169	*	p 367	A93-20806		p 266	A93-21699		p 389	A93-22184	p 431	A93-22632	#	p 278
A93-20172	#	p 435	A93-20808		p 375	A93-21718		p 307	A93-22187	p 431	A93-22633	#	p 278
A93-20176	#	p 261	A93-20812		p 367	A93-21719		p 270	A93-22188	p 432	A93-22635	#	p 415
A93-20177	#	p 261	A93-20819		p 307	A93-21720		p 270	A93-22190	p 432	A93-22638	#	p 415
A93-20178	*	p 261	A93-20823		p 367	A93-21721		p 271	A93-22191	p 432	A93-22639	#	p 438
A93-20179	#	p 261	A93-20823		p 367	A93-21727		p 451	A93-22195	p 432	A93-22652	#	p 390
A93-20180	#	p 262	A93-20851		p 342	A93-21729		p 411	A93-22196	p 432	A93-22657	#	p 390
A93-20181	#	p 262	A93-20852		p 342	A93-21731		p 389	A93-22198	p 432	A93-22660	#	p 360
A93-20183	#	p 262	A93-20857		p 342	A93-21737		p 271	A93-22199	p 432	A93-22667	#	p 279
A93-20184	#	p 262	A93-20900		p 453	A93-21738		p 271	A93-22200	p 433	A93-22668	#	p 279
A93-20186	#	p 262	A93-20909		p 267	A93-21739		p 411	A93-22201	p 433	A93-22690	#	p 279
A93-20187	*	p 262	A93-20919		p 267	A93-21743		p 411	A93-22202	p 433	A93-22691	#	p 279
A93-20188	*	p 262	A93-20923		p 267	A93-21744		p 412	A93-22207	p 271	A93-22692	#	p 279
A93-20189	#	p 263	A93-20924		p 267	A93-21765		p 384	A93-22230	p 272	A93-22693	#	p 279
A93-20190	*	p 263	A93-20929		p 267	A93-21792		p 359	A93-22263	p 272	A93-22694	*	p 280
A93-20191	#	p 263	A93-20930		p 267	A93-21822		p 317	A93-22264	p 272	A93-22695	#	p 376
A93-20192	#	p 263	A93-20933		p 267	A93-21823		p 317	A93-22265	p 413	A93-22696	#	p 327
A93-20195	#	p 263	A93-20934		p 268	A93-21824		p 317	A93-22275	p 317	A93-22697	#	p 376
A93-20196	#	p 263	A93-21042	*	p 268	A93-21833		p 376	A93-22276	#	A93-22698		p 239
A93-20197	#	p 264	A93-21085		p 410	A93-21836		p 327	A93-22282	#	A93-22830		p 438
A93-20199	#	p 264	A93-21094		p 410	A93-21840		p 412	A93-22285	*	A93-22851	*	p 343
A93-20200	#	p 264	A93-21102	*	p 268	A93-21842		p 412	A93-22287	*	A93-22854		p 439
A93-20204	#	p 264	A93-21103	*	p 268	A93-21843		p 327	A93-22288	*	A93-22855		p 439
A93-20205	#	p 264	A93-21104	*	p 342	A93-21850		p 239	A93-22289	#	A93-22856		p 368
A93-20278	#	p 322	A93-21106	*	p 268	A93-21857		p 412	A93-22294	#	A93-22868		p 368
A93-20279	#	p 323	A93-21107	*	p 268	A93-21859		p 451	A93-22298	#	A93-22869		p 368
A93-20280	*	p 358	A93-21108	#	p 384	A93-21863		p 271	A93-22302	#	A93-22870		p 385
A93-20281	#	p 323	A93-21111	*	p 268	A93-21868		p 437	A93-22303	#	A93-22882		p 368
A93-20287	#	p 323	A93-21113	*	p 269	A93-21878		p 412	A93-22304	#	A93-22883		p 368
A93-20289	#	p 323	A93-21114	*	p 358	A93-21900		p 376	A93-22305	#	A93-22884		p 369
A93-20290	#	p 323	A93-21116	#	p 269	A93-21908		p 384	A93-22307	#	A93-22885		p 369
A93-20291	#	p 408	A93-21117	#	p 269	A93-21921		p 271	A93-22308	#	A93-22886		p 369
A93-20293	#	p 408	A93-21118	#	p 358	A93-21922		p 412	A93-22311	#	A93-22887		p 369
A93-20295	#	p 324	A93-21119	#	p 269	A93-21925		p 271	A93-22312	#	A93-22889		p 439
A93-20296	#	p 324	A93-21125	*	p 326	A93-21934		p 412	A93-22315	#	A93-22905		p 369
A93-20297	*	p 375	A93-21127	*	p 312	A93-21966		p 343	A93-22317	#	A93-22926		p 439
A93-20298	*	p 408	A93-21128	*	p 312	A93-21999		p 390	A93-22319	#	A93-22937		p 369
A93-20300	*	p 264	A93-21130		p 313	A93-22002		p 327	A93-22320	#	A93-22968		p 439
A93-20301	*	p 435	A93-21141		p 313	A93-22101		p 426	A93-22321	#	A93-22971		p 439
A93-20302	#	p 409	A93-21142		p 313	A93-22104		p 426	A93-22322	#	A93-22978		p 440
A93-20303	#	p 264	A93-21143		p 313	A93-22105		p 453	A93-22324	#	A93-22980		p 369
A93-20304	#	p 409	A93-21144		p 313	A93-22108		p 307	A93-22325	#	A93-22992		p 433
A93-20307	#	p 324	A93-21145		p 313	A93-22110		p 454	A93-22328	#	A93-23001	*	p 280
A93-20308	#	p 324	A93-21146	*	p 342	A93-22119	*	p 308	A93-22330	#	A93-23005	#	p 456
A93-20309	#	p 264	A93-21147	*	p 313	A93-22111	*	p 343	A93-22333	#	A93-23006	#	p 280
A93-20310	#	p 265	A93-21148	*	p 384	A93-22112	*	p 308	A93-22335	#	A93-23007	#	p 280
A93-20316	#	p 451	A93-21152	*	p 314	A93-22113	*	p 426	A93-22337	#	A93-23011	#	p 280
A93-20318	#	p 435	A93-21154	*	p 314	A93-22115	*	p 427	A93-22342	#	A93-23012	#	p 280
A93-20319	#	p 358	A93-21155	*	p 314	A93-22116	*	p 308	A93-22347	#	A93-23013	#	p 280
A93-20320	#	p 358	A93-21157	*	p 314	A93-22118	*	p 427	A93-22357	#	A93-23014	#	p 281
A93-20321	#	p 358	A93-21160	*	p 384	A93-22119	*	p 427	A93-22360	#	A93-23015	#	p 281
A93-20322	#	p 324	A93-21161	*	p 314	A93-22120	*	p 427	A93-22361	#	A93-23016	#	p 454
A93-20323	#	p 325	A93-21162	*	p 314	A93-22121	*	p 308	A93-22368	#	A93-23017	#	p 454
A93-20324	#	p 325	A93-21165	*	p 314	A93-22123	*	p 427	A93-22371	#	A93-23018	#	p 415
A93-20326	#	p 409	A93-21167	*	p 314	A93-22125	*	p 427	A93-22372	#	A93-23021	#	p 281
A93-20328	#	p 325	A93-21176	*	p 315	A93-22128	*	p 428	A93-22373	#	A93-23022	#	p 281
A93-20329	#	p 409	A93-21178	*	p 315	A93-22129	*	p 428	A93-22374	#	A93-23026	#	p 281
A93-20343	#	p 436	A93-21180	*	p 315	A93-22130	*	p 428	A93-22443	#	A93-23027	#	p 281
A93-20344	*	p 265	A93-21181	*	p 315	A93-22131	*	p 428	A93-22505	*	A93-23030	#	p 281
A93-20350	*	p 436	A93-21182	*	p 315	A93-22133	*	p 428	A93-22509	#	A93-23031	#	p 376
A93-20351	#	p 436	A93-21183	*	p 315	A93-22134	*	p 428	A93-22551	#	A93-23034	#	p 377
A93-20352	#	p 409	A93-21184	*	p 315	A93-22136	*	p 428	A93-22552	#	A93-23035	#	p 377
A93-20356	#	p 325	A93-21186	*	p 316	A93-22137	*	p 428	A93-22556	#	A93-23036	#	p 377
A93-20360	#	p 325	A93-21188	*	p 316	A93-22139	*	p 428	A93-22568	#	A93-23037	#	p 377
A93-20366	#	p 436	A93-21190	*	p 316	A93-22140	*	p 428	A93-22578	#	A93-23038	#	p 377
A93-20369	#	p 325	A93-21192	*	p 316	A93-22141	*	p 429	A93-22580	#	A93-23040	#	p 377
A93-20370	*	p 326	A93-21193	*	p 342	A93-22143	*	p 429	A93-22588	#	A93-23041	#	p 360
A93-20371	#	p 326	A93-21197	*	p 316	A93-22144	*	p 308	A93-22591	#	A93-23042	#	p 385
A93-20372	#	p 326	A93-21198	*	p 316	A93-22145	*	p 308	A93-22592	#	A93-23045	#	p 390
A93-20381	#	p 326	A93-21199	*	p 316	A93-22146	*	p 429	A93-22594	#	A93-23047	#	p 390
A93-20394	#	p 436	A93-21201	*	p 317	A93-22147	*	p 429	A93-22599	#	A93-23058	#	p 385
A93-20411	#	p 436	A93-21218	*	p 269	A93-22149	*	p 429	A93-22601	#	A93-23059	#	p 386
A93-20416	#	p 265	A93-21330	*	p 270	A93-22150	*	p 429	A93-22602	#	A93-23063	#	p 282
A93-20420	#	p 409	A93-21525	*	p 317	A93-22151	*	p 430	A93-22603	#	A93-23064	#	p 282
A93-20579	*	p 425	A93-21627	*	p 307	A93-22152	*	p 430	A93-22604	#	A93-23065	#	p 282
A93-20586	*	p 425	A93-21629	*	p 410	A93-22153	*	p 308	A93-22605	#	A93-23066	#	p 282
A93-20591	*	p 426	A93-21630	*	p 317	A93-22154	*	p 308	A93-22607	#	A93-23067	#	p 282
A93-20621	#	p 426	A93-21651	*	p 389	A93-22155	*	p 309	A93-22608	#	A93-23068	#	p 282
A93-20622	#	p 426	A93-21653	*	p 411	A93-22156	*	p 309	A93-22609	#	A93-23069	#	p 309
A93-20644	#	p 409	A93-21656	*	p 270	A93-22159	*	p 430	A93-22610	#	A93-23072	#	p 327
A93-20701	#	p 437	A93-21657	*	p 367	A93-22160	*	p 430	A93-22611	#	A93-23073	#	p 370
A93-20708	#	p 437	A93-21658	*	p 270	A93-22161	*	p 430	A93-22612	#	A93-23238	#	p 390
A93-20711	#	p 437	A93-21659	*	p 411	A93-22162	*	p 431	A93-22613	#	A93-23239	#	p 309
A93-20713	*	p 265	A93-21660	*	p 411	A93-22163	*	p 438	A93-22614	#	A93-23240	#	p 282
A93-20714	#	p 410	A93-21662	*	p 270	A93-22164	*	p 438	A93-22615	#	A93-23241	#	p 452
A93-20716	*	p 265	A93-21665	*	p 411	A93-22165	*	p 431	A93-22616	#			

ACCESSION NUMBER INDEX

A93-28476

A93-23244	#	p 310	A93-24078	p 460	A93-24833	#	p 540	A93-25511	#	p 473	A93-27445	p 477
A93-23245	#	p 310	A93-24079	p 460	A93-24835	#	p 516	A93-25512	* #	p 474	A93-27474	p 477
A93-23246	#	p 361	A93-24080	p 460	A93-24836	#	p 540	A93-25516	* #	p 457	A93-27475	p 477
A93-23247	* #	p 283	A93-24081	p 460	A93-24837	#	p 486	A93-25517	* #	p 474	A93-27477	p 529
A93-23253	#	p 283	A93-24082	p 460	A93-24838	#	p 504	A93-25518	#	p 528	A93-27478	p 520
A93-23254	#	p 283	A93-24083	p 460	A93-24845	#	p 466	A93-25520	#	p 474	A93-27479	p 506
A93-23255	* #	p 370	A93-24084	p 538	A93-24846	#	p 467	A93-25521	* #	p 505	A93-27480	p 506
A93-23256	* #	p 386	A93-24085	p 461	A93-24851	#	p 540	A93-25522	#	p 505	A93-27482	p 477
A93-23257	#	p 328	A93-24088	p 461	A93-24852	#	p 541	A93-25528	#	p 474	A93-27499	p 518
A93-23258	#	p 386	A93-24089	p 461	A93-24855	#	p 467	A93-25532	#	p 534	A93-27500	p 506
A93-23264	* #	p 283	A93-24090	p 461	A93-24858	* #	p 467	A93-25533	* #	p 505	A93-27584	p 561
A93-23265	#	p 283	A93-24091	p 461	A93-24860	#	p 541	A93-25536	* #	p 474	A93-27603	p 561
A93-23266	#	p 284	A93-24107	p 457	A93-24861	* #	p 467	A93-25539	#	p 543	A93-27604	p 524
A93-23267	* #	p 284	A93-24122	p 539	A93-24862	* #	p 467	A93-25545	#	p 543	A93-27605	p 477
A93-23268	#	p 284	A93-24173	p 556	A93-24863	* #	p 467	A93-25546	* #	p 475	A93-27607	p 477
A93-23269	* #	p 284	A93-24213	p 556	A93-24864	* #	p 468	A93-25550	#	p 475	A93-27614	p 477
A93-23270	#	p 284	A93-24230	* #	A93-24865	* #	p 468	A93-25553	* #	p 475	A93-27616	p 545
A93-23272	#	p 284	A93-24233	* #	A93-24867	#	p 541	A93-25553	* #	p 475	A93-27620	p 545
A93-23273	#	p 285	A93-24238	* #	A93-24868	#	p 541	A93-25568	#	p 534	A93-27624	p 478
A93-23283	#	p 415	A93-24239	* #	A93-24869	#	p 468	A93-25911	#	p 534	A93-27625	p 520
A93-23289	#	p 285	A93-24240	* #	A93-24870	#	p 541	A93-25922	#	p 516	A93-27627	p 520
A93-23290	* #	p 285	A93-24252	p 570	A93-24872	#	p 541	A93-25962	#	p 543	A93-27628	p 545
A93-23292	* #	p 285	A93-24253	p 570	A93-24874	#	p 528	A93-25965	#	p 532	A93-27629	p 561
A93-23293	#	p 285	A93-24294	#	A93-24876	#	p 528	A93-25979	#	p 543	A93-27636	p 478
A93-23294	#	p 285	A93-24296	#	A93-24882	#	p 533	A93-25993	#	p 532	A93-27637	p 545
A93-23297	* #	p 377	A93-24299	#	A93-24883	#	p 533	A93-25997	#	p 519	A93-27639	p 478
A93-23323	* #	p 452	A93-24300	#	A93-24884	#	p 534	A93-25998	#	p 519	A93-27658	p 534
A93-23324	#	p 361	A93-24308	p 462	A93-24914	#	p 557	A93-26005	#	p 557	A93-27688	p 561
A93-23326	#	p 440	A93-24391	p 556	A93-24915	* #	p 531	A93-26011	#	p 570	A93-27689	p 562
A93-23330	* #	p 440	A93-24409	p 462	A93-24916	#	p 557	A93-26062	#	p 543	A93-27726	p 535
A93-23331	#	p 361	A93-24410	p 462	A93-24925	* #	p 468	A93-26064	#	p 543	A93-27732	p 535
A93-23333	* #	p 415	A93-24412	p 539	A93-24926	#	p 468	A93-26114	#	p 519	A93-27739	p 520
A93-23340	#	p 285	A93-24464	p 533	A93-24927	#	p 468	A93-26176	#	p 475	A93-27759	p 535
A93-23344	#	p 454	A93-24478	#	A93-24928	#	p 469	A93-26183	#	p 475	A93-27766	p 535
A93-23345	#	p 386	A93-24479	#	A93-24930	#	p 469	A93-26423	#	p 486	A93-27782	* #
A93-23349	#	p 286	A93-24481	#	A93-24931	* #	p 469	A93-26432	#	p 524	A93-27801	p 520
A93-23350	#	p 286	A93-24484	#	A93-24932	#	p 469	A93-26617	#	p 543	A93-27903	p 506
A93-23351	#	p 286	A93-24486	#	A93-24933	#	p 469	A93-26817	#	p 544	A93-27904	p 529
A93-23352	#	p 286	A93-24488	* #	A93-24934	#	p 469	A93-26838	#	p 561	A93-27909	p 499
A93-23353	#	p 286	A93-24489	#	A93-24935	#	p 469	A93-26878	#	p 457	A93-27910	p 499
A93-23358	* #	p 391	A93-24492	#	A93-24936	#	p 470	A93-26880	#	p 475	A93-27911	p 499
A93-23384	#	p 361	A93-24493	* #	A93-24937	#	p 470	A93-26882	#	p 517	A93-27912	p 499
A93-23385	#	p 415	A93-24495	#	A93-24939	#	p 470	A93-26883	#	p 517	A93-27913	p 499
A93-23386	#	p 286	A93-24497	#	A93-24940	#	p 470	A93-26884	#	p 517	A93-27914	p 499
A93-23387	* #	p 287	A93-24509	p 533	A93-24943	#	p 470	A93-26886	#	p 517	A93-27922	p 478
A93-23390	* #	p 416	A93-24524	p 463	A93-24944	#	p 470	A93-26888	#	p 544	A93-27924	* #
A93-23477	* #	p 416	A93-24566	p 557	A93-24945	* #	p 471	A93-26897	#	p 475	A93-27925	* #
A93-23491	#	p 416	A93-24672	p 463	A93-24946	#	p 471	A93-26898	#	p 476	A93-27926	p 478
A93-23509	#	p 370	A93-24726	#	A93-24947	#	p 471	A93-26903	#	p 476	A93-27951	p 506
A93-23510	* #	p 378	A93-24727	* #	A93-24950	#	p 471	A93-26904	#	p 544	A93-27952	p 506
A93-23511	#	p 370	A93-24737	#	A93-24951	* #	p 471	A93-26905	#	p 476	A93-27953	p 507
A93-23512	* #	p 416	A93-24738	#	A93-24953	#	p 471	A93-26920	#	p 532	A93-27954	p 507
A93-23514	#	p 370	A93-24739	#	A93-24954	* #	p 472	A93-26946	#	p 524	A93-27956	* #
A93-23515	#	p 370	A93-24740	#	A93-24955	#	p 472	A93-26948	#	p 524	A93-27959	p 507
A93-23516	#	p 370	A93-24741	* #	A93-24956	#	p 472	A93-26999	#	p 544	A93-27962	p 507
A93-23517	#	p 416	A93-24742	* #	A93-24957	#	p 472	A93-27043	#	p 532	A93-27963	p 507
A93-23533	#	p 287	A93-24743	#	A93-24960	#	p 560	A93-27044	#	p 544	A93-27964	p 507
A93-23538	#	p 287	A93-24744	#	A93-24972	#	p 472	A93-27045	#	p 544	A93-27965	p 546
A93-23540	#	p 287	A93-24748	* #	A93-24978	#	p 472	A93-27065	#	p 476	A93-27966	p 508
A93-23541	* #	p 287	A93-24750	* #	A93-24979	#	p 541	A93-27068	#	p 476	A93-27967	p 508
A93-23542	#	p 287	A93-24752	#	A93-24986	#	p 472	A93-27132	#	p 457	A93-27968	* #
A93-23545	* #	p 287	A93-24753	#	A93-24988	#	p 473	A93-27133	#	p 570	A93-27969	p 546
A93-23546	#	p 287	A93-24754	#	A93-24990	#	p 473	A93-27134	#	p 570	A93-27970	p 546
A93-23547	#	p 416	A93-24755	* #	A93-25060	#	p 473	A93-27136	#	p 486	A93-27971	p 508
A93-23548	* #	p 288	A93-24756	#	A93-25085	#	p 560	A93-27150	#	p 561	A93-27972	p 508
A93-23549	#	p 288	A93-24757	#	A93-25088	#	p 560	A93-27164	#	p 570	A93-27973	p 546
A93-23552	#	p 288	A93-24758	#	A93-25125	#	p 486	A93-27165	#	p 570	A93-27974	p 508
A93-23553	#	p 416	A93-24759	#	A93-25170	#	p 498	A93-27166	#	p 571	A93-27975	* #
A93-23554	* #	p 417	A93-24760	* #	A93-25171	#	p 498	A93-27168	#	p 487	A93-27978	* #
A93-23555	* #	p 417	A93-24761	#	A93-25172	#	p 498	A93-27189	#	p 571	A93-28151	* #
A93-23557	* #	p 417	A93-24762	* #	A93-25173	#	p 498	A93-27237	#	p 544	A93-28152	p 499
A93-23560	#	p 288	A93-24763	#	A93-25174	#	p 504	A93-27238	#	p 505	A93-28153	p 500
A93-23563	#	p 288	A93-24764	* #	A93-25198	#	p 542	A93-27239	#	p 517	A93-28155	p 500
A93-23565	#	p 288	A93-24766	* #	A93-25249	#	p 486	A93-27241	#	p 545	A93-28156	p 500
A93-23698	* #	p 378	A93-24769	#	A93-25250	#	p 504	A93-27242	#	p 518	A93-28157	p 500
A93-23699	#	p 440	A93-24772	#	A93-25252	#	p 534	A93-27276	#	p 506	A93-28175	p 547
A93-23744	#	p 452	A93-24773	#	A93-25325	#	p 457	A93-27289	#	p 545	A93-28176	p 518
A93-23778	#	p 459	A93-24774	#	A93-25327	#	p 542	A93-27291	#	p 520	A93-28179	p 518
A93-23804	#	p 538	A93-24777	#	A93-25339	#	p 561	A93-27293	#	p 506	A93-28180	p 564
A93-23807	#	p 459	A93-24778	#	A93-25346	#	p 542	A93-27294	#	p 528	A93-28193	p 500
A93-23808	#	p 538	A93-24780	* #	A93-25348	#	p 473	A93-27295	#	p 524	A93-28194	p 500
A93-23809	#	p 538	A93-24781	#	A93-25353	#	p 542	A93-27296	#	p 520	A93-28195	p 500
A93-23811	* #	p 459	A93-24782	* #	A93-25355	#	p 532	A93-27300	#	p 524	A93-28196	p 487
A93-23838	#	p 460	A93-24783	* #	A93-25357	#	p 505	A93-27316	#	p 545	A93-28197	p 501
A93-23839	#	p 523	A93-24786	* #	A93-25359	#	p 532	A93-27366	#	p 534	A93-28198	p 501
A93-23840	#	p 528	A93-24787	#	A93-25360	#	p 473	A93-27368	#	p 476	A93-28219	p 501
A93-23870	#	p 569	A93-24788	#	A93-25362	#	p 505	A93-27370	#	p 487	A93-28244	p 547
A93-23872	#	p 569	A93-24818	#	A93-25480	#	p 498	A93-27371	#	p 506	A93-28279	p 547
A93-24026	#	p 519	A93-24821	* #	A93-25493	#	p 505	A93-27375	#	p 506	A93-28290	p 547
A93-24028	#	p 498	A93-24825	* #	A93-25495	#	p 505	A93-27393	#	p 487	A93-28291	p 547
A93-24030	#	p 538	A93-24826	* #	A93-25504	#	p 564	A93-27394	#	p 487	A93-28392	p 501
A93-24032	#	p 504	A93-24827	* #	A93-25505	#	p 542	A93-27395	#	p 529	A93-28393	p 535
A93-24033	#	p 528	A93-24828	* #	A93-25508	* #	p 542	A93-27396	#	p 529	A93-28396	p 458
A93-24035	#	p 538	A93-24829	#	A93-25509	#	p 542	A93-27442	#	p 476	A93-28437	p 532
A93-24048	#	p 486	A93-24830	* #	A93-25510	#	p 473	A93-27443	#	p 476	A93-28469	p 524
A93-24076	#	p 460	A93-24831	#							A93-28476	p 557

A93-28477

A93-28477 p 557
 A93-28478 p 558
 A93-28479 p 521
 A93-28480 p 564
 A93-28481 p 487
 A93-28482 p 564
 A93-28483 p 558
 A93-28484 p 558
 A93-28485 p 558
 A93-28486 p 558
 A93-28488 p 533
 A93-28489 p 564
 A93-28491 p 529
 A93-28492 p 564
 A93-28493 p 558
 A93-28494 p 564
 A93-28495 p 558
 A93-28496 p 559
 A93-28497 p 559
 A93-28518 p 479
 A93-28543 p 548
 A93-28544 p 479
 A93-28567 p 548
 A93-28574 p 479
 A93-28575 p 548
 A93-28601 p 479
 A93-28602 p 508
 A93-28603 p 525
 A93-28604 p 479
 A93-28605 p 479
 A93-28606 p 479
 A93-28607 p 479
 A93-28608 p 480
 A93-28609 p 564
 A93-28610 p 480
 A93-28611 p 525
 A93-28612 p 508
 A93-28613 p 525
 A93-28614 p 565
 A93-28615 p 548
 A93-28616 p 525
 A93-28618 p 548
 A93-28749 p 548
 A93-28865 p 559
 A93-28874 p 458
 A93-29130 p 458
 A93-29153 p 480
 A93-29155 p 480
 A93-29175 p 480
 A93-29241 p 509
 A93-29246 p 509
 A93-29258 p 548
 A93-29264 p 549
 A93-29267 p 509
 A93-29281 p 529
 A93-29282 p 529
 A93-29293 p 549
 A93-29297 p 525
 A93-29301 p 549
 A93-29302 p 549
 A93-29304 p 549
 A93-29307 p 480
 A93-29308 p 549
 A93-29315 p 549
 A93-29316 p 480
 A93-29318 p 480
 A93-29326 p 480
 A93-29351 p 526
 A93-29401 p 565
 A93-29402 p 565
 A93-29403 p 565
 A93-29404 p 565
 A93-29405 p 565
 A93-29406 p 566
 A93-29407 p 566
 A93-29408 p 566
 A93-29409 p 566
 A93-29410 p 566
 A93-29411 p 480
 A93-29412 p 566
 A93-29414 p 509
 A93-29415 p 567
 A93-29416 p 567
 A93-29417 p 567
 A93-29418 p 567
 A93-29419 p 567
 A93-29420 p 567
 A93-29421 p 509
 A93-29422 p 562
 A93-29423 p 562
 A93-29424 p 567
 A93-29425 p 568
 A93-29426 p 549
 A93-29428 p 568
 A93-29429 p 568
 A93-29430 p 568

A93-29431 p 487
 A93-29432 p 481
 A93-29433 p 568
 A93-29434 p 481
 A93-29435 p 481
 A93-29436 p 481
 A93-29437 p 481
 A93-29438 p 481
 A93-29439 p 509
 A93-29440 p 482
 A93-29441 p 482
 A93-29442 p 487
 A93-29443 p 569
 A93-29473 p 458
 A93-29474 p 501
 A93-29475 p 458
 A93-29485 p 549
 A93-29563 p 535
 A93-29575 p 571
 A93-29596 p 501
 A93-29599 p 501
 A93-29600 p 501
 A93-29607 p 533
 A93-29639 p 502
 A93-29655 p 521
 A93-29660 p 559
 A93-29690 p 562
 A93-29691 p 526
 A93-29718 p 550
 A93-29774 p 482
 A93-29780 p 482
 A93-33700 p 708
 A93-33703 p 678
 A93-33704 p 730
 A93-33706 p 679
 A93-33709 p 679
 A93-33710 p 759
 A93-33713 p 679
 A93-33715 p 679
 A93-33716 p 679
 A93-33717 p 679
 A93-33718 p 679
 A93-33719 p 680
 A93-33722 p 680
 A93-33723 p 680
 A93-33725 p 680
 A93-33727 p 680
 A93-33729 p 680
 A93-33730 p 680
 A93-33732 p 730
 A93-33733 p 680
 A93-33736 p 681
 A93-33739 p 681
 A93-33741 p 681
 A93-33746 p 681
 A93-33747 p 681
 A93-33748 p 681
 A93-33750 p 730
 A93-33752 p 681
 A93-33755 p 682
 A93-33757 p 682
 A93-33773 p 752
 A93-33793 p 756
 A93-33798 p 737
 A93-33876 p 738
 A93-33877 p 709
 A93-33878 p 756
 A93-33879 p 725
 A93-33880 p 725
 A93-33881 p 726
 A93-33883 p 756
 A93-33889 p 732
 A93-33890 p 732
 A93-33891 p 732
 A93-33892 p 738
 A93-33907 p 738
 A93-33909 p 709
 A93-33911 p 709
 A93-33913 p 709
 A93-33914 p 709
 A93-33915 p 738
 A93-33916 p 738
 A93-33927 p 709
 A93-33928 p 710
 A93-33929 p 726
 A93-33930 p 726
 A93-33931 p 682
 A93-33932 p 726
 A93-33933 p 733
 A93-33934 p 733
 A93-33935 p 682
 A93-33937 p 739
 A93-33946 p 719
 A93-33954 p 710
 A93-33960 p 739
 A93-33962 p 739

A93-33963 # p 734
 A93-33969 # p 739
 A93-33970 # p 739
 A93-33973 # p 756
 A93-33974 # p 726
 A93-33975 # p 739
 A93-33978 # p 740
 A93-33981 # p 710
 A93-33987 # p 710
 A93-33989 # p 734
 A93-33999 # p 740
 A93-34014 # p 710
 A93-34020 # p 726
 A93-34021 # p 711
 A93-34022 # p 740
 A93-34044 # p 711
 A93-34050 # p 740
 A93-34071 # p 727
 A93-34072 # p 727
 A93-34073 # p 740
 A93-34074 # p 711
 A93-34075 # p 727
 A93-34076 # p 741
 A93-34077 # p 741
 A93-34102 # p 741
 A93-34113 # p 741
 A93-34115 # p 719
 A93-34120 # p 682
 A93-34121 # p 682
 A93-34122 # p 683
 A93-34123 # p 683
 A93-34124 # p 683
 A93-34130 # p 741
 A93-34137 # p 711
 A93-34157 # p 742
 A93-34158 # p 711
 A93-34159 # p 719
 A93-34160 # p 720
 A93-34161 # p 720
 A93-34162 # p 720
 A93-34165 # p 720
 A93-34169 # p 742
 A93-34170 # p 742
 A93-34171 # p 742
 A93-34172 # p 742
 A93-34173 # p 711
 A93-34191 # p 743
 A93-34219 # p 757
 A93-34222 # p 712
 A93-34223 # p 712
 A93-34224 # p 743
 A93-34225 # p 712
 A93-34239 # p 743
 A93-34240 # p 712
 A93-34256 # p 712
 A93-34257 # p 727
 A93-34259 # p 743
 A93-34260 # p 683
 A93-34261 # p 743
 A93-34262 # p 712
 A93-34263 # p 712
 A93-34264 # p 757
 A93-34265 # p 733
 A93-34266 # p 733
 A93-34273 # p 683
 A93-34274 # p 684
 A93-34275 # p 684
 A93-34287 # p 743
 A93-34301 # p 743
 A93-34308 # p 684
 A93-34311 # p 744
 A93-34318 # p 684
 A93-34331 # p 684
 A93-34335 # p 684
 A93-34339 # p 685
 A93-34341 # p 685
 A93-34344 # p 685
 A93-34345 # p 685
 A93-34346 # p 685
 A93-34347 # p 685
 A93-34348 # p 686
 A93-34349 # p 686
 A93-34350 # p 686
 A93-34351 # p 686
 A93-34352 # p 686
 A93-34353 # p 686
 A93-34354 # p 686
 A93-34355 # p 687
 A93-34356 # p 687
 A93-34357 # p 687
 A93-34358 # p 687
 A93-34359 # p 687
 A93-34360 # p 687
 A93-34362 # p 688
 A93-34370 # p 688
 A93-34375 # p 720

A93-34400 p 713
 A93-34405 p 688
 A93-34410 p 720
 A93-34415 p 688
 A93-34469 p 744
 A93-34472 p 744
 A93-34476 p 744
 A93-34483 p 688
 A93-34484 p 688
 A93-34485 p 688
 A93-34486 p 688
 A93-34487 p 689
 A93-34488 p 689
 A93-34489 p 689
 A93-34490 p 689
 A93-34491 p 689
 A93-34495 p 721
 A93-34496 p 744
 A93-34497 p 721
 A93-34498 p 730
 A93-34499 p 689
 A93-34510 p 735
 A93-34519 p 713
 A93-34533 p 727
 A93-34536 p 757
 A93-34539 p 757
 A93-34540 p 727
 A93-34541 p 727
 A93-34542 p 728
 A93-34545 p 728
 A93-34550 p 728
 A93-34561 p 735
 A93-34587 p 677
 A93-34616 p 701
 A93-34694 p 753
 A93-34819 p 718
 A93-34821 p 760
 A93-34847 p 744
 A93-34848 p 713
 A93-34850 p 713
 A93-34925 p 744
 A93-34944 p 760
 A93-34947 p 677
 A93-34957 p 759
 A93-35152 # p 702
 A93-35154 # p 702
 A93-35155 # p 702
 A93-35157 # p 702
 A93-35158 # p 702
 A93-35159 # p 702
 A93-35160 # p 689
 A93-35162 # p 702
 A93-35165 # p 689
 A93-35169 # p 690
 A93-35171 # p 733
 A93-35173 # p 690
 A93-35174 # p 703
 A93-35175 # p 690
 A93-35177 # p 690
 A93-35178 # p 744
 A93-35180 # p 728
 A93-35181 # p 690
 A93-35184 # p 677
 A93-35185 # p 690
 A93-35188 # p 703
 A93-35266 # p 691
 A93-35268 # p 691
 A93-35270 # p 691
 A93-35276 # p 745
 A93-35277 # p 745
 A93-35278 # p 745
 A93-35281 # p 745
 A93-35283 # p 745
 A93-35286 # p 745
 A93-35287 # p 745
 A93-35288 # p 746
 A93-35289 # p 746
 A93-35290 # p 746
 A93-35295 # p 746
 A93-35299 # p 735
 A93-35307 # p 757
 A93-35339 # p 691
 A93-35344 # p 691
 A93-35345 # p 746
 A93-35346 # p 691
 A93-35372 # p 753
 A93-35482 # p 691
 A93-35492 # p 746
 A93-35518 # p 728
 A93-35607 # p 691
 A93-35609 # p 692
 A93-35612 # p 692
 A93-35613 # p 692
 A93-35618 # p 735
 A93-35619 # p 735
 A93-35621 # p 692

A93-35623 p 692
 A93-35625 p 730
 A93-35630 p 713
 A93-35634 p 692
 A93-35635 p 692
 A93-35636 p 692
 A93-35637 p 757
 A93-35663 p 757
 A93-35676 p 713
 A93-35677 p 677
 A93-35678 p 718
 A93-35685 p 721
 A93-35689 p 753
 A93-35901 p 763
 A93-35902 p 794
 A93-35903 p 794
 A93-35904 p 794
 A93-35906 p 794
 A93-35907 p 794
 A93-35908 p 794
 A93-35909 p 795
 A93-35912 p 795
 A93-35915 p 845
 A93-35916 p 795
 A93-35920 p 845
 A93-35921 p 806
 A93-35922 p 853
 A93-35923 p 763
 A93-35924 p 763
 A93-35926 p 853
 A93-35927 p 763
 A93-35928 p 809
 A93-35929 p 809
 A93-35930 p 826
 A93-35931 p 826
 A93-35932 p 795
 A93-35933 p 809
 A93-35934 p 809
 A93-35935 p 765
 A93-35936 p 765
 A93-35937 p 765
 A93-35938 p 765
 A93-35939 p 765
 A93-35940 p 795
 A93-35941 p 766
 A93-35944 p 763
 A93-35948 p 795
 A93-35949 p 795
 A93-35951 p 796
 A93-35952 p 796
 A93-35953 p 826
 A93-35954 p 796
 A93-35955 p 816
 A93-35956 p 796
 A93-35957 p 766
 A93-35959 p 816
 A93-35960 p 816
 A93-35961 p 817
 A93-35963 p 849
 A93-35964 p 849
 A93-35965 p 849
 A93-35966 p 849
 A93-35967 p 850
 A93-35968 p 850
 A93-35971 p 763
 A93-35973 p 764
 A93-35975 p 796
 A93-35976 p 796
 A93-35977 p 797
 A93-35978 p 827
 A93-35979 p 797
 A93-35980 p 797
 A93-35981 p 797
 A93-35982 p 797
 A93-35983 p 798
 A93-35984 p 798
 A93-35985 p 798
 A93-35986 p 798
 A93-35987 p 817
 A93-35988 p 821
 A93-35989 p 798
 A93-35990 p 798
 A93-35991 p 799
 A93-35992 p 799
 A93-35993 p 766
 A93-35994 p 766
 A93-35995 p 766
 A93-35996 p 767
 A93-35997 p 767
 A93-35998 p 767
 A93-35999 p 767
 A93-36000 p 827
 A93-36001 p 799
 A93-36003 p 824
 A93-36004 p 799
 A93-36005 p 824

ACCESSION NUMBER INDEX

ACCESSION NUMBER INDEX

A93-42585

A93-36006	p 827	A93-37867 *	p 829	A93-39024	p 825	A93-39407 *	p 837	A93-41362	p 855
A93-36007	p 845	A93-37872	p 821	A93-39027	p 832	A93-39409 *	p 778	A93-41364	p 938
A93-36010	p 846	A93-37873 *	p 822	A93-39028	p 810	A93-39410	p 778	A93-41397	p 926
A93-36018	p 807	A93-37875 *	p 822	A93-39030	p 832	A93-39412	p 778	A93-41398	p 926
A93-36019	p 799	A93-37876	p 830	A93-39032	p 832	A93-39414	p 822	A93-41399	p 890
A93-36020 *	p 799	A93-37877	p 822	A93-39033	p 810	A93-39416 *	p 837	A93-41400 *	p 898
A93-36021	p 800	A93-37878 *	p 830	A93-39034	p 810	A93-39417 *	p 837	A93-41575	p 926
A93-36023 *	p 800	A93-37882	p 808	A93-39036	p 832	A93-39418	p 819	A93-41600	p 881
A93-36025	p 800	A93-37885	p 808	A93-39037	p 811	A93-39419	p 837	A93-41700	p 926
A93-36026	p 800	A93-37890	p 830	A93-39040	p 851	A93-39422	p 837	A93-41714	p 926
A93-36034	p 844	A93-37933	p 769	A93-39043	p 847	A93-39427	p 837	A93-41729	p 926
A93-36268	p 809	A93-37941	p 769	A93-39044	p 833	A93-39428	p 779	A93-41736	p 859
A93-36327	p 846	A93-37997 *	p 802	A93-39045	p 833	A93-39498 *	p 804	A93-41740	p 898
A93-36330	p 800	A93-38126	p 830	A93-39046	p 833	A93-39535	p 764	A93-41742	p 898
A93-36339	p 800	A93-38128	p 847	A93-39047	p 833	A93-39536	p 764	A93-41749	p 926
A93-36342	p 800	A93-38130	p 769	A93-39050	p 833	A93-39537	p 847	A93-41751	p 927
A93-36502	p 792	A93-38140	p 830	A93-39051	p 833	A93-39538	p 764	A93-41776 *	p 859
A93-36588 *	p 827	A93-38146	p 769	A93-39052	p 833	A93-39539	p 764	A93-41777 *	p 859
A93-36718	p 824	A93-38147	p 769	A93-39053	p 834	A93-39540	p 764	A93-41778 *	p 890
A93-36782	p 827	A93-38148	p 770	A93-39054	p 834	A93-39542	p 804	A93-41779 *	p 890
A93-36784	p 801	A93-38150	p 850	A93-39055	p 834	A93-39544	p 851	A93-41780 *	p 860
A93-36785	p 801	A93-38151	p 850	A93-39057	p 851	A93-39599	p 805	A93-41781 *	p 860
A93-36789	p 827	A93-38155	p 830	A93-39059	p 834	A93-39600	p 805	A93-41782 *	p 860
A93-36791	p 821	A93-38158	p 770	A93-39061	p 834	A93-39701	p 853	A93-41783 *	p 910
A93-36792	p 828	A93-38162	p 770	A93-39062	p 834	A93-39721	p 779	A93-41889	p 906
A93-36793	p 828	A93-38181	p 810	A93-39072	p 811	A93-39722	p 837	A93-41890	p 906
A93-36794	p 801	A93-38187	p 770	A93-39073	p 811	A93-39762	p 844	A93-41891 *	p 938
A93-36795	p 801	A93-38193	p 770	A93-39075	p 811	A93-39942	p 857	A93-41893	p 906
A93-36797	p 801	A93-38200	p 824	A93-39081	p 834	A93-39949	p 924	A93-41894 *	p 906
A93-36798	p 801	A93-38203	p 792	A93-39084	p 835	A93-39963	p 915	A93-41895 *	p 906
A93-36799	p 828	A93-38214	p 847	A93-39091	p 835	A93-40328	p 905	A93-41896	p 906
A93-36800	p 828	A93-38325	p 770	A93-39093	p 835	A93-40332	p 881	A93-41897 *	p 906
A93-37004	p 817	A93-38431	p 831	A93-39094	p 835	A93-40334	p 924	A93-41903	p 890
A93-37005	p 817	A93-38434	p 770	A93-39095	p 835	A93-40359	p 881	A93-41904	p 890
A93-37032	p 850	A93-38535	p 853	A93-39099	p 835	A93-40362	p 915	A93-41906	p 860
A93-37034	p 846	A93-38564	p 792	A93-39102	p 835	A93-40390	p 924	A93-41910	p 927
A93-37040	p 817	A93-38565	p 802	A93-39106	p 836	A93-40405	p 857	A93-41911	p 927
A93-37041	p 846	A93-38567	p 844	A93-39109	p 836	A93-40430	p 857	A93-41912	p 860
A93-37044	p 817	A93-38568	p 818	A93-39115	p 774	A93-40431	p 858	A93-41914 *	p 860
A93-37046 *	p 828	A93-38569	p 822	A93-39116	p 774	A93-40432	p 879	A93-41915 *	p 860
A93-37068	p 792	A93-38570	p 802	A93-39118	p 775	A93-40435	p 897	A93-41916 *	p 861
A93-37069	p 821	A93-38571	p 831	A93-39119	p 775	A93-40436	p 881	A93-41918	p 899
A93-37071	p 807	A93-38573	p 771	A93-39120	p 775	A93-40437 *	p 897	A93-41919 *	p 906
A93-37072	p 828	A93-38574	p 771	A93-39122	p 836	A93-40438	p 889	A93-41929	p 943
A93-37074	p 807	A93-38576	p 771	A93-39123	p 775	A93-40444	p 858	A93-41930 *	p 861
A93-37075	p 818	A93-38580	p 824	A93-39124	p 775	A93-40445	p 924	A93-41932	p 861
A93-37090	p 792	A93-38581	p 771	A93-39125	p 818	A93-40470	p 858	A93-41934	p 861
A93-37174	p 801	A93-38583	p 831	A93-39126	p 775	A93-40472	p 924	A93-41935	p 927
A93-37175	p 801	A93-38586	p 824	A93-39127	p 851	A93-40473	p 889	A93-42234	# p 913
A93-37350	p 828	A93-38588	p 771	A93-39130	p 775	A93-40474	p 944	A93-42254	p 861
A93-37376	p 802	A93-38590	p 771	A93-39131	p 776	A93-40475	p 897	A93-42256	p 861
A93-37377	p 802	A93-38592	p 822	A93-39132	p 776	A93-40492	p 924	A93-42259	p 906
A93-37378 *	p 767	A93-38593	p 831	A93-39133	p 776	A93-40493	p 889	A93-42260	p 861
A93-37379	p 768	A93-38595	p 771	A93-39134	p 776	A93-40495	p 938	A93-42271	p 862
A93-37379 *	p 768	A93-38596	p 772	A93-39135	p 776	A93-40654	p 925	A93-42369	p 891
A93-37380 *	p 850	A93-38597	p 802	A93-39136	p 776	A93-40656	p 925	A93-42370	p 891
A93-37381 *	p 768	A93-38598	p 803	A93-39137	p 836	A93-40661	p 855	A93-42371	p 891
A93-37383 *	p 768	A93-38599	p 772	A93-39141	p 776	A93-40662	p 855	A93-42372	p 899
A93-37384 *	p 768	A93-38600	p 851	A93-39142	p 776	A93-40663	p 855	A93-42373	p 891
A93-37385	p 768	A93-38601	p 831	A93-39143	p 777	A93-40665	p 855	A93-42374	p 891
A93-37386	p 768	A93-38602	p 772	A93-39144	p 836	A93-40666	p 925	A93-42375	p 891
A93-37387 *	p 768	A93-38605	p 772	A93-39145	p 777	A93-40667	p 855	A93-42376	p 891
A93-37389 *	p 810	A93-38610	p 772	A93-39147	p 836	A93-40668	p 855	A93-42377	p 891
A93-37390	p 802	A93-38613	p 831	A93-39150	p 777	A93-40672	p 925	A93-42378	p 892
A93-37391	p 802	A93-38614	p 831	A93-39152	p 777	A93-40714 *	# p 858	A93-42379	p 899
A93-37392	p 818	A93-38629	p 831	A93-39175	p 811	A93-40775	p 925	A93-42380	p 899
A93-37393	p 828	A93-38638	p 772	A93-39176	p 836	A93-40777	p 915	A93-42381	p 892
A93-37394	p 802	A93-38639 *	p 772	A93-39177	p 836	A93-40787	p 915	A93-42405	p 927
A93-37396 *	p 850	A93-38701	p 810	A93-39179	p 819	A93-40802	p 915	A93-42426	p 862
A93-37398	p 810	A93-38728	p 773	A93-39180	p 811	A93-40803	p 897	A93-42428	p 862
A93-37399	p 768	A93-38729	p 773	A93-39185	p 837	A93-40804	p 915	A93-42429 *	p 862
A93-37400	p 768	A93-38731	p 803	A93-39187	p 811	A93-40805	p 915	A93-42430	p 862
A93-37401	p 768	A93-38734	p 773	A93-39188	p 804	A93-40807	p 916	A93-42431	p 862
A93-37402	p 821	A93-38736	p 824	A93-39189	p 804	A93-40808	p 916	A93-42432	p 862
A93-37403	p 829	A93-38739	p 832	A93-39190	p 819	A93-40811	p 916	A93-42433	p 863
A93-37404	p 769	A93-38741	p 773	A93-39191	p 819	A93-40814	p 916	A93-42436	p 863
A93-37406	p 818	A93-38743	p 773	A93-39192	p 819	A93-40823	p 925	A93-42437	p 863
A93-37407	p 807	A93-38744	p 773	A93-39193	p 812	A93-41023	p 916	A93-42441	p 863
A93-37427 *	# p 769	A93-38745	p 774	A93-39195	p 812	A93-41029	p 925	A93-42442	p 863
A93-37428 *	# p 829	A93-38746	p 774	A93-39198	p 837	A93-41031	p 916	A93-42443	p 863
A93-37433 *	# p 818	A93-38755	p 774	A93-39200	p 812	A93-41038	p 890	A93-42444	p 864
A93-37438 *	# p 829	A93-38763	p 803	A93-39201	p 812	A93-41045 *	# p 898	A93-42446	p 864
A93-37439 *	# p 829	A93-38764	p 832	A93-39202	p 812	A93-41046 *	# p 898	A93-42448	p 864
A93-37441 *	# p 829	A93-38774	p 851	A93-39203	p 804	A93-41047 *	# p 898	A93-42449	p 864
A93-37443 *	# p 829	A93-38777	p 774	A93-39204	p 792	A93-41049 *	# p 858	A93-42556	p 938
A93-37446 *	# p 810	A93-38837	p 803	A93-39255	p 777	A93-41050 *	# p 858	A93-42559	p 907
A93-37482	p 823	A93-38838	p 803	A93-39257 *	p 777	A93-41053 *	# p 859	A93-42576	p 864
A93-37623 *	p 846	A93-38839	p 803	A93-39258	p 778	A93-41056 *	# p 859	A93-42577	p 856
A93-37691	p 844	A93-38840	p 803	A93-39259 *	p 778	A93-41058 *	# p 859	A93-42578	p 927
A93-37694	p 844	A93-38841	p 808	A93-39260	p 778	A93-41059 *	# p 910	A93-42579 *	p 864
A93-37699	p 807	A93-38843	p 818	A93-39271	p 812	A93-41269 *	p 936	A93-42580	p 943
A93-37719	p 844	A93-38844	p 803	A93-39401	p 778	A93-41296 *	# p 938	A93-42581 *	p 865
A93-37737	p 807	A93-38846 *	p 804	A93-39402	p 778	A93-41318	p 895	A93-42582 *	p 865
A93-37763 *	p 821	A93-38847	p 804	A93-39403	p 778	A93-41361	p 890	A93-42584 *	p 943
A93-37853	p 808	A93-38893	p 825					A93-42585 *	p 865
A93-37856	p 846	A93-38975	p 832						
A93-37866	p 847								

A93-42587

A93-42587 p 865
 A93-42588 p 865
 A93-42589 p 865
 A93-42590 p 865
 A93-42591 p 866
 A93-42592 p 866
 A93-42593 p 866
 A93-42594 p 866
 A93-42595 p 866
 A93-42596 p 866
 A93-42597 p 866
 A93-42599 p 866
 A93-42600 p 867
 A93-42601 p 867
 A93-42602 p 867
 A93-42603 p 867
 A93-42604 p 867
 A93-42606 p 867
 A93-42607 p 867
 A93-42608 p 868
 A93-42609 p 868
 A93-42610 p 868
 A93-42612 p 868
 A93-42613 p 868
 A93-42614 p 868
 A93-42616 p 868
 A93-42617 p 868
 A93-42618 p 868
 A93-42619 p 869
 A93-42620 p 869
 A93-42624 p 869
 A93-42625 p 927
 A93-42626 p 869
 A93-42627 p 869
 A93-42629 p 869
 A93-42630 p 869
 A93-42631 p 869
 A93-42632 p 870
 A93-42633 p 870
 A93-42634 p 870
 A93-42635 p 870
 A93-42636 p 870
 A93-42637 p 870
 A93-42638 p 870
 A93-42639 p 870
 A93-42640 p 871
 A93-42642 p 910
 A93-42644 p 871
 A93-42646 p 927
 A93-42654 p 879
 A93-42655 p 856
 A93-42656 p 871
 A93-42657 p 927
 A93-42659 p 936
 A93-42777 p 896
 A93-42778 p 892
 A93-42780 p 896
 A93-42781 p 927
 A93-42782 p 928
 A93-42783 p 928
 A93-42784 p 896
 A93-42785 p 938
 A93-42786 p 896
 A93-42793 p 928
 A93-42794 p 892
 A93-42797 p 939
 A93-42798 p 881
 A93-42804 p 907
 A93-42806 p 907
 A93-42807 p 907
 A93-42808 p 907
 A93-42810 p 907
 A93-42811 p 908
 A93-42812 p 908
 A93-42813 p 908
 A93-42815 p 908
 A93-42816 p 882
 A93-42822 p 939
 A93-42824 p 939
 A93-42828 p 944
 A93-42829 p 939
 A93-42830 p 939
 A93-42831 p 939
 A93-42832 p 940
 A93-42833 p 940
 A93-42846 p 940
 A93-42851 p 940
 A93-42852 p 940
 A93-42853 p 856
 A93-42855 p 896
 A93-42856 p 941
 A93-42862 p 941
 A93-42863 p 941
 A93-42865 p 941
 A93-42869 p 871
 A93-42870 p 871

A93-42873 p 871
 A93-42874 p 872
 A93-42877 p 899
 A93-42878 p 899
 A93-42879 p 899
 A93-42884 p 899
 A93-42885 p 900
 A93-42888 p 872
 A93-42889 p 872
 A93-42891 p 872
 A93-42892 p 910
 A93-42899 p 872
 A93-42909 p 928
 A93-42920 p 928
 A93-42927 p 914
 A93-42931 p 872
 A93-42995 p 892
 A93-42997 p 944
 A93-42998 p 944
 A93-42999 p 945
 A93-43013 p 872
 A93-43027 p 872
 A93-43079 p 908
 A93-43101 p 856
 A93-43102 p 908
 A93-43103 p 909
 A93-43106 p 909
 A93-43108 p 882
 A93-43109 p 856
 A93-43110 p 882
 A93-43111 p 882
 A93-43112 p 882
 A93-43113 p 941
 A93-43115 p 941
 A93-43338 p 928
 A93-43344 p 928
 A93-43369 p 882
 A93-43370 p 883
 A93-43376 p 929
 A93-43381 p 929
 A93-43392 p 929
 A93-43401 p 883
 A93-43405 p 929
 A93-43406 p 883
 A93-43407 p 883
 A93-43408 p 883
 A93-43409 p 883
 A93-43410 p 883
 A93-43411 p 883
 A93-43412 p 883
 A93-43428 p 884
 A93-43432 p 884
 A93-43434 p 929
 A93-43437 p 914
 A93-43440 p 884
 A93-43444 p 884
 A93-43454 p 884
 A93-43455 p 884
 A93-43463 p 929
 A93-43464 p 884
 A93-43466 p 885
 A93-43470 p 942
 A93-43475 p 885
 A93-43476 p 885
 A93-43502 p 929
 A93-43539 p 930
 A93-43540 p 872
 A93-43541 p 873
 A93-43549 p 914
 A93-43550 p 885
 A93-43570 p 892
 A93-43616 p 916
 A93-43623 p 945
 A93-43624 p 896
 A93-43625 p 856
 A93-43628 p 873
 A93-43629 p 873
 A93-43650 p 856
 A93-43677 p 945
 A93-43685 p 873
 A93-43686 p 873
 A93-43687 p 873
 A93-43688 p 874
 A93-43776 p 892
 A93-43777 p 893
 A93-43778 p 930
 A93-43779 p 893
 A93-43780 p 874
 A93-43781 p 874
 A93-43782 p 874
 A93-43783 p 909
 A93-43784 p 885
 A93-43831 p 893
 A93-43869 p 945
 A93-44099 p 949
 A93-44142 p 1006

A93-44143 p 992
 A93-44150 p 1036
 A93-44151 p 1006
 A93-44168 p 1020
 A93-44193 p 1020
 A93-44194 p 1020
 A93-44195 p 1020
 A93-44197 p 1020
 A93-44206 p 1021
 A93-44222 p 1021
 A93-44224 p 1021
 A93-44227 * # p 949
 A93-44228 * # p 949
 A93-44229 * # p 949
 A93-44230 * # p 1001
 A93-44231 * # p 1021
 A93-44232 * # p 949
 A93-44233 * # p 1006
 A93-44234 * # p 1007
 A93-44374 p 950
 A93-44375 p 950
 A93-44380 p 1015
 A93-44452 p 1036
 A93-44458 p 1038
 A93-44505 p 992
 A93-44508 p 947
 A93-44850 p 995
 A93-44851 p 1021
 A93-44852 p 995
 A93-44862 p 1033
 A93-44886 p 1010
 A93-44888 p 995
 A93-44892 p 1010
 A93-44995 # p 1021
 A93-44996 # p 1041
 A93-44997 # p 1021
 A93-44999 # p 950
 A93-45000 * # p 950
 A93-45001 * # p 950
 A93-45002 * # p 950
 A93-45003 * # p 951
 A93-45006 # p 1036
 A93-45007 * # p 1036
 A93-45010 # p 951
 A93-45011 # p 951
 A93-45012 # p 951
 A93-45013 * # p 951
 A93-45014 * # p 952
 A93-45016 * # p 952
 A93-45017 * # p 952
 A93-45018 # p 952
 A93-45019 # p 1022
 A93-45022 # p 952
 A93-45023 # p 952
 A93-45025 # p 953
 A93-45027 * # p 953
 A93-45028 * # p 953
 A93-45029 * # p 953
 A93-45030 # p 953
 A93-45031 * # p 953
 A93-45033 # p 954
 A93-45037 * # p 954
 A93-45043 # p 954
 A93-45044 * # p 954
 A93-45045 # p 954
 A93-45046 # p 1036
 A93-45047 # p 1037
 A93-45051 * # p 954
 A93-45052 * # p 955
 A93-45056 * # p 955
 A93-45059 # p 955
 A93-45064 * # p 955
 A93-45076 # p 955
 A93-45077 * # p 956
 A93-45078 * # p 956
 A93-45079 # p 956
 A93-45081 # p 956
 A93-45082 # p 956
 A93-45083 # p 956
 A93-45087 # p 956
 A93-45088 * # p 957
 A93-45089 # p 1022
 A93-45092 # p 957
 A93-45093 # p 957
 A93-45095 # p 957
 A93-45096 * # p 957
 A93-45099 * # p 957
 A93-45101 * # p 957
 A93-45102 # p 957
 A93-45103 * # p 958
 A93-45106 # p 1022
 A93-45113 p 1022
 A93-45119 p 1022
 A93-45124 p 995
 A93-45133 * p 1022
 A93-45134 p 958

A93-45135 p 958
 A93-45136 p 958
 A93-45137 p 1007
 A93-45138 p 958
 A93-45139 p 1034
 A93-45140 p 958
 A93-45141 p 958
 A93-45142 p 958
 A93-45143 p 995
 A93-45144 p 1007
 A93-45145 p 1015
 A93-45146 p 959
 A93-45147 p 995
 A93-45148 p 1022
 A93-45149 p 959
 A93-45150 p 1037
 A93-45151 p 1022
 A93-45152 p 1007
 A93-45153 p 959
 A93-45154 * # p 959
 A93-45155 * # p 947
 A93-45164 p 990
 A93-45165 p 992
 A93-45166 p 992
 A93-45167 p 1011
 A93-45168 p 995
 A93-45175 p 1023
 A93-45176 p 1034
 A93-45325 p 959
 A93-45401 p 1007
 A93-45431 p 1037
 A93-45432 p 996
 A93-45441 p 1015
 A93-45444 p 1015
 A93-45451 p 1023
 A93-45452 p 1011
 A93-45460 p 1023
 A93-45463 p 1023
 A93-45476 p 1023
 A93-45494 p 959
 A93-45496 p 1011
 A93-45497 p 1011
 A93-45498 p 1011
 A93-45499 p 1016
 A93-45500 p 1023
 A93-45504 p 1023
 A93-45505 p 1024
 A93-45506 p 1024
 A93-45507 p 960
 A93-45515 p 1024
 A93-45517 p 1017
 A93-45526 p 1024
 A93-45528 p 1011
 A93-45529 p 1011
 A93-45530 p 1012
 A93-45532 p 1012
 A93-45533 p 1016
 A93-45537 p 1024
 A93-45542 p 960
 A93-45543 p 960
 A93-45545 p 960
 A93-45546 p 960
 A93-45547 p 960
 A93-45550 p 1001
 A93-45556 p 1038
 A93-45561 p 1038
 A93-45563 p 1024
 A93-45565 p 992
 A93-45569 p 947
 A93-45560 p 996
 A93-45561 p 1037
 A93-45562 p 1007
 A93-45563 p 996
 A93-45564 p 1007
 A93-45565 p 996
 A93-45566 p 1008
 A93-45567 p 1008
 A93-45568 p 991
 A93-45569 p 996
 A93-45570 p 1025
 A93-45571 p 996
 A93-45572 p 996
 A93-45573 p 996
 A93-45574 p 997
 A93-45575 p 991
 A93-45581 p 999
 A93-45584 p 1025
 A93-45589 p 1017
 A93-45599 p 1034
 A93-45726 p 961
 A93-45727 p 961
 A93-45728 p 961
 A93-45730 p 961
 A93-45735 p 961
 A93-45740 p 1025

A93-45741 p 997
 A93-45745 p 1025
 A93-45750 p 961
 A93-45751 p 961
 A93-45754 p 961
 A93-45772 p 947
 A93-45773 p 1025
 A93-45774 p 1025
 A93-45775 p 1025
 A93-45776 p 1026
 A93-45777 p 1026
 A93-45778 p 1017
 A93-45779 p 1001
 A93-45780 p 1026
 A93-45781 p 947
 A93-45782 p 1026
 A93-45783 p 991
 A93-45784 p 997
 A93-45785 p 1026
 A93-45786 p 947
 A93-45787 p 1026
 A93-45788 p 1026
 A93-45789 p 948
 A93-45790 p 1027
 A93-45791 p 1027
 A93-45793 p 948
 A93-45794 p 1012
 A93-45795 p 948
 A93-45796 p 948
 A93-45797 p 948
 A93-45798 p 1027
 A93-45799 p 948
 A93-45800 p 948
 A93-45807 p 1018
 A93-46024 p 997
 A93-46406 p 962
 A93-46407 p 1027
 A93-46408 p 962
 A93-46476 # p 962
 A93-46477 * # p 962
 A93-46478 * # p 962
 A93-46479 * # p 962
 A93-46480 # p 962
 A93-46482 # p 1039
 A93-46488 * # p 1027
 A93-46493 # p 963
 A93-46500 # p 963
 A93-46509 * # p 963
 A93-46510 # p 963
 A93-46512 # p 963
 A93-46525 # p 1012
 A93-46526 # p 1012
 A93-46528 * # p 1016
 A93-46529 * # p 1027
 A93-46531 # p 1027
 A93-46532 * # p 1018
 A93-46534 # p 963
 A93-46538 * # p 964
 A93-46540 # p 1016
 A93-46544 # p 1028
 A93-46546 # p 964
 A93-46547 * # p 964
 A93-46548 # p 964
 A93-46549 # p 964
 A93-46552 * # p 965
 A93-46553 * # p 965
 A93-46590 * # p 1028
 A93-46608 p 948
 A93-46656 # p 1012
 A93-46682 # p 1039
 A93-46699 p 965
 A93-46701 p 1039
 A93-46706 p 1039
 A93-46744 p 965
 A93-46748 p 965
 A93-46750 p 965
 A93-46780 p 1034
 A93-46787 # p 965
 A93-46789 # p 966
 A93-46790 # p 966
 A93-46791 # p 966
 A93-46792 # p 966
 A93-46793 # p 966
 A93-46794 # p 966
 A93-46796 # p 1028
 A93-46798 # p 966
 A93-46799 # p 967
 A93-46800 * # p 967
 A93-46802 p 1028
 A93-46804 p 967
 A93-46805 * p 1039
 A93-46806 p 1013
 A93-46807 p 1008
 A93-46808 p 1000
 A93-46809 p 997
 A93-46811 p 1028

ACCESSION NUMBER INDEX

ACCESSION NUMBER INDEX

A93-49470

A93-46812	#	p 967	A93-47223	#	p 977	A93-48125	#	p 1045	A93-48253	#	p 1059	A93-48544	p 1067
A93-46816	#	p 967	A93-47224	#	p 977	A93-48127	#	p 1045	A93-48254	#	p 1059	A93-48554	p 1043
A93-46817	#	p 967	A93-47225	#	p 977	A93-48128	#	p 1045	A93-48255	#	p 1060	A93-48555	p 1107
A93-46821	#	p 1028	A93-47226	#	p 977	A93-48130	#	p 1045	A93-48256	#	p 1060	A93-48601	p 1149
A93-46822	#	p 1028	A93-47227	#	p 978	A93-48131	#	p 1046	A93-48257	#	p 1060	A93-48612	p 1149
A93-46823	#	p 967	A93-47228	#	p 978	A93-48132	#	p 1148	A93-48258	#	p 1060	A93-48616	p 1149
A93-46824	#	p 997	A93-47229	#	p 978	A93-48133	#	p 1046	A93-48261	#	p 1099	A93-48635	p 1150
A93-46825	#	p 1013	A93-47230	#	p 1014	A93-48134	#	p 1046	A93-48265	#	p 1099	A93-48606	p 1150
A93-46826	#	p 968	A93-47231	#	p 978	A93-48136	#	p 1046	A93-48266	#	p 1060	A93-48825	p 1150
A93-46827	#	p 968	A93-47232	#	p 978	A93-48137	#	p 1046	A93-48269	#	p 1061	A93-48826	p 1067
A93-46828	#	p 968	A93-47233	#	p 978	A93-48139	#	p 1046	A93-48270	#	p 1061	A93-48827	p 1067
A93-46829	#	p 968	A93-47234	#	p 979	A93-48140	#	p 1171	A93-48271	#	p 1061	A93-48828	p 1107
A93-46830	#	p 968	A93-47235	#	p 1009	A93-48141	#	p 1162	A93-48273	#	p 1061	A93-48835	p 1141
A93-46831	#	p 968	A93-47236	#	p 1009	A93-48142	#	p 1047	A93-48277	#	p 1149	A93-48838	p 1141
A93-46832	#	p 969	A93-47237	#	p 1037	A93-48143	#	p 1047	A93-48280	#	p 1061	A93-48844	p 1067
A93-46833	#	p 1037	A93-47238	#	p 979	A93-48144	#	p 1047	A93-48281	#	p 1061	A93-48846	p 1162
A93-46834	#	p 969	A93-47239	#	p 979	A93-48145	#	p 1174	A93-48282	#	p 1062	A93-48848	p 1067
A93-46835	#	p 969	A93-47240	#	p 1014	A93-48146	#	p 1148	A93-48283	#	p 1062	A93-48849	p 1068
A93-46839	#	p 969	A93-47242	#	p 979	A93-48149	#	p 1047	A93-48284	#	p 1062	A93-48850	p 1150
A93-46841	#	p 969	A93-47244	#	p 979	A93-48150	#	p 1047	A93-48285	#	p 1062	A93-48901	p 1068
A93-46842	#	p 969	A93-47245	#	p 980	A93-48151	#	p 1047	A93-48286	#	p 1062	A93-48902	p 1068
A93-46857	#	p 969	A93-47246	#	p 1030	A93-48152	#	p 1048	A93-48287	#	p 1062	A93-48903	p 1130
A93-46885	#	p 970	A93-47247	#	p 980	A93-48153	#	p 1124	A93-48288	#	p 1171	A93-48904	p 1068
A93-46886	#	p 970	A93-47248	#	p 997	A93-48154	#	p 1124	A93-48291	#	p 1063	A93-48905	p 1068
A93-46888	#	p 993	A93-47249	#	p 980	A93-48155	#	p 1048	A93-48293	#	p 1063	A93-48908	p 1068
A93-46889	#	p 993	A93-47250	#	p 980	A93-48156	#	p 1048	A93-48294	#	p 1063	A93-48909	p 1150
A93-46891	#	p 993	A93-47251	#	p 980	A93-48157	#	p 1048	A93-48296	#	p 1063	A93-48910	p 1068
A93-46907	#	p 970	A93-47252	#	p 980	A93-48158	#	p 1048	A93-48297	#	p 1063	A93-48911	p 1150
A93-46908	#	p 970	A93-47253	#	p 981	A93-48159	#	p 1148	A93-48298	#	p 1063	A93-48912	p 1069
A93-46915	#	p 1013	A93-47254	#	p 981	A93-48161	#	p 1048	A93-48299	#	p 1064	A93-48913	p 1069
A93-46916	#	p 970	A93-47255	#	p 981	A93-48162	#	p 1049	A93-48300	#	p 1064	A93-48914	p 1069
A93-46922	#	p 971	A93-47256	#	p 981	A93-48163	#	p 1049	A93-48301	#	p 1125	A93-48924	p 1069
A93-46926	#	p 1001	A93-47257	#	p 981	A93-48164	#	p 1049	A93-48302	#	p 1125	A93-48966	p 1069
A93-46927	#	p 971	A93-47258	#	p 981	A93-48165	#	p 1049	A93-48303	#	p 1125	A93-48967	p 1165
A93-46928	#	p 1029	A93-47259	#	p 982	A93-48166	#	p 1049	A93-48304	#	p 1125	A93-48971	p 1069
A93-46929	#	p 971	A93-47260	#	p 982	A93-48167	#	p 1049	A93-48305	#	p 1125	A93-48973	p 1069
A93-46930	#	p 1001	A93-47261	#	p 982	A93-48168	#	p 1050	A93-48306	#	p 1125	A93-48974	p 1069
A93-46931	#	p 1002	A93-47262	#	p 982	A93-48169	#	p 1050	A93-48307	#	p 1126	A93-48975	p 1070
A93-46932	#	p 971	A93-47263	#	p 982	A93-48170	#	p 1050	A93-48308	#	p 1126	A93-49000	p 1151
A93-46933	#	p 1013	A93-47264	#	p 982	A93-48171	#	p 1050	A93-48309	#	p 1126	A93-49002	p 1070
A93-46934	#	p 971	A93-47265	#	p 982	A93-48172	#	p 1050	A93-48310	#	p 1126	A93-49003	p 1070
A93-46936	#	p 972	A93-47266	#	p 983	A93-48173	#	p 1051	A93-48311	#	p 1126	A93-49005	p 1172
A93-46938	#	p 972	A93-47267	#	p 983	A93-48174	#	p 1051	A93-48312	#	p 1127	A93-49007	p 1151
A93-46939	#	p 1002	A93-47268	#	p 983	A93-48175	#	p 1051	A93-48313	#	p 1064	A93-49008	p 1070
A93-46940	#	p 972	A93-47269	#	p 983	A93-48176	#	p 1051	A93-48314	#	p 1064	A93-49009	p 1070
A93-46941	#	p 972	A93-47270	#	p 983	A93-48177	#	p 1051	A93-48316	#	p 1064	A93-49010	p 1070
A93-46942	#	p 1002	A93-47271	#	p 984	A93-48178	#	p 1051	A93-48318	#	p 1065	A93-49011	p 1070
A93-46943	#	p 1002	A93-47272	#	p 984	A93-48179	#	p 1052	A93-48319	#	p 1065	A93-49012	p 1100
A93-46944	#	p 972	A93-47274	#	p 984	A93-48180	#	p 1052	A93-48321	#	p 1065	A93-49014	p 1071
A93-46945	#	p 1002	A93-47275	#	p 984	A93-48181	#	p 1052	A93-48323	#	p 1165	A93-49015	p 1071
A93-46946	#	p 972	A93-47276	#	p 984	A93-48182	#	p 1052	A93-48324	#	p 1165	A93-49016	p 1071
A93-46975	#	p 972	A93-47277	#	p 984	A93-48183	#	p 1052	A93-48325	#	p 1127	A93-49017	p 1151
A93-46979	#	p 1029	A93-47278	#	p 985	A93-48184	#	p 1052	A93-48326	#	p 1127	A93-49026	p 1151
A93-46980	#	p 973	A93-47279	#	p 985	A93-48185	#	p 1053	A93-48327	#	p 1127	A93-49027	p 1071
A93-46984	#	p 973	A93-47280	#	p 1009	A93-48187	#	p 1053	A93-48328	#	p 1127	A93-49069	p 1163
A93-46987	#	p 973	A93-47281	#	p 1014	A93-48188	#	p 1053	A93-48329	#	p 1127	A93-49105	p 1100
A93-46988	#	p 973	A93-47282	#	p 985	A93-48189	#	p 1053	A93-48331	#	p 1128	A93-49130	p 1163
A93-46989	#	p 973	A93-47283	#	p 985	A93-48190	#	p 1053	A93-48332	#	p 1128	A93-49185	p 1071
A93-46990	#	p 973	A93-47284	#	p 985	A93-48192	#	p 1053	A93-48333	#	p 1128	A93-49186	p 1165
A93-46991	#	p 973	A93-47285	#	p 986	A93-48197	#	p 1053	A93-48337	#	p 1099	A93-49187	p 1107
A93-46993	#	p 1029	A93-47286	#	p 986	A93-48198	#	p 1054	A93-48339	#	p 1128	A93-49188	p 1071
A93-47015	#	p 1013	A93-47287	#	p 986	A93-48199	#	p 1054	A93-48341	#	p 1099	A93-49190	p 1108
A93-47021	#	p 1013	A93-47288	#	p 986	A93-48200	#	p 1054	A93-48342	#	p 1128	A93-49195	p 1108
A93-47022	#	p 1013	A93-47289	#	p 986	A93-48201	#	p 1054	A93-48344	#	p 1128	A93-49198	p 1071
A93-47023	#	p 991	A93-47291	#	p 1003	A93-48202	#	p 1054	A93-48345	#	p 1104	A93-49200	p 1108
A93-47024	#	p 1014	A93-47292	#	p 986	A93-48204	#	p 1148	A93-48346	#	p 1128	A93-49202	p 1108
A93-47076	#	p 1029	A93-47293	#	p 987	A93-48205	#	p 1055	A93-48347	#	p 1129	A93-49204	p 1108
A93-47078	#	p 1029	A93-47331	#	p 987	A93-48206	#	p 1055	A93-48348	#	p 1129	A93-49240	p 1151
A93-47079	#	p 997	A93-47341	#	p 987	A93-48207	#	p 1055	A93-48349	#	p 1129	A93-49277	p 1136
A93-47084	#	p 1029	A93-47356	#	p 1018	A93-48209	#	p 1055	A93-48350	#	p 1129	A93-49278	p 1097
A93-47085	#	p 1029	A93-47446	#	p 987	A93-48210	#	p 1055	A93-48351	#	p 1129	A93-49279	p 1174
A93-47086	#	p 1030	A93-47448	#	p 987	A93-48211	#	p 1055	A93-48355	#	p 1129	A93-49280	p 1096
A93-47093	#	p 1030	A93-47450	#	p 1039	A93-48212	#	p 1056	A93-48356	#	p 1065	A93-49301	p 1135
A93-47189	#	p 973	A93-47508	#	p 1003	A93-48213	#	p 1056	A93-48357	#	p 1065	A93-49306	p 1165
A93-47196	#	p 974	A93-47509	#	p 1003	A93-48214	#	p 1056	A93-48411	#	p 1172	A93-49307	p 1165
A93-47201	#	p 974	A93-47510	#	p 1003	A93-48221	#	p 1056	A93-48501	#	p 1066	A93-49323	p 1071
A93-47202	#	p 974	A93-47512	#	p 1018	A93-48222	#	p 1056	A93-48502	#	p 1066	A93-49324	p 1071
A93-47203	#	p 974	A93-47513	#	p 1003	A93-48223	#	p 1056	A93-48503	#	p 1106	A93-49329	#
A93-47204	#	p 974	A93-47522	#	p 987	A93-48224	#	p 1057	A93-48504	#	p 1066	A93-49331	p 1043
A93-47205	#	p 1008	A93-47553	#	p 1161	A93-48225	#	p 1057	A93-48506	#	p 1106	A93-49336	p 1144
A93-47206	#	p 1008	A93-47583	#	p 1161	A93-48226	#	p 1057	A93-48507	#	p 1172	A93-49337	p 1100
A93-47207	#	p 974	A93-47650	#	p 1147	A93-48227	#	p 1144	A93-48509	#	p 1066	A93-49340	p 1104
A93-47208	#	p 1030	A93-47657	#	p 1162	A93-48228	#	p 1057	A93-48511	#	p 1106	A93-49344	p 1104
A93-47209	#	p 975	A93-47658	#	p 1162	A93-48229	#	p 1057	A93-48512	#	p 1066	A93-49345	p 1104
A93-47210	#	p 975	A93-47676	#	p 1162	A93-48230	#	p 1057	A93-48513	#	p 1066	A93-49346	p 1151
A93-47211	#	p 975	A93-47865	#	p 1162	A93-48232	#	p 1057	A93-48514	#	p 1149	A93-49347	p 1165
A93-47212	#	p 975	A93-48041	#	p 1136	A93-48234	#	p 1058	A93-48515	#	p 1066	A93-49350	p 1166
A93-47213	#	p 975	A93-48042	#	p 1044	A93-48235	#	p 1058	A93-48517	#	p 1066	A93-49351	p 1097
A93-47214	#	p 976	A93-48043	#	p 1044	A93-48236	#	p 1058	A93-48				

A93-49471

A93-49471 p 1105
 A93-49473 p 1105
 A93-49474 p 1105
 A93-49475 p 1172
 A93-49476 p 1105
 A93-49477 p 1106
 A93-49478 p 1172
 A93-49479 p 1097
 A93-49480 p 1166
 A93-49481 p 1166
 A93-49505 p 1152
 A93-49507 p 1072
 A93-49508 * p 1109
 A93-49515 # p 1072
 A93-49516 * # p 1072
 A93-49517 * # p 1072
 A93-49518 * # p 1096
 A93-49519 * # p 1130
 A93-49521 p 1072
 A93-49522 p 1072
 A93-49523 p 1152
 A93-49527 p 1152
 A93-49529 p 1073
 A93-49530 p 1073
 A93-49531 * p 1073
 A93-49532 p 1073
 A93-49533 p 1073
 A93-49551 p 1163
 A93-49552 p 1163
 A93-49554 p 1163
 A93-49557 p 1163
 A93-49558 p 1164
 A93-49559 p 1164
 A93-49577 p 1130
 A93-49590 p 1097
 A93-49592 p 1141
 A93-49593 p 1130
 A93-49594 p 1130
 A93-49595 p 1130
 A93-49596 * p 1141
 A93-49598 p 1130
 A93-49605 p 1166
 A93-49610 p 1109
 A93-49612 * p 1109
 A93-49616 p 1109
 A93-49617 * p 1137
 A93-49619 p 1173
 A93-49658 # p 1144
 A93-49659 # p 1109
 A93-49660 * # p 1109
 A93-49661 # p 1073
 A93-49663 # p 1152
 A93-49668 # p 1110
 A93-49685 * # p 1110
 A93-49686 # p 1074
 A93-49687 # p 1074
 A93-49688 # p 1074
 A93-49694 # p 1173
 A93-49695 * # p 1074
 A93-49696 # p 1166
 A93-49697 # p 1100
 A93-49698 # p 1100
 A93-49703 # p 1110
 A93-49704 # p 1110
 A93-49706 # p 1110
 A93-49707 # p 1153
 A93-49708 * # p 1100
 A93-49709 * # p 1110
 A93-49710 # p 1111
 A93-49713 * # p 1141
 A93-49714 # p 1153
 A93-49720 * # p 1074
 A93-49721 * # p 1074
 A93-49723 # p 1075
 A93-49724 # p 1111
 A93-49726 # p 1137
 A93-49727 # p 1111
 A93-49728 * # p 1075
 A93-49729 # p 1075
 A93-49734 # p 1144
 A93-49735 # p 1145
 A93-49742 # p 1111
 A93-49743 # p 1075
 A93-49744 # p 1075
 A93-49745 # p 1076
 A93-49746 # p 1111
 A93-49747 # p 1112
 A93-49748 # p 1112
 A93-49779 # p 1076
 A93-49780 # p 1076
 A93-49784 # p 1076
 A93-49788 * # p 1076
 A93-49790 # p 1112
 A93-49791 # p 1076
 A93-49794 # p 1077

A93-49795 # p 1077
 A93-49796 # p 1100
 A93-49819 # p 1077
 A93-49820 * # p 1077
 A93-49821 # p 1077
 A93-49822 # p 1077
 A93-49823 # p 1078
 A93-49825 * # p 1078
 A93-49826 # p 1153
 A93-49827 # p 1078
 A93-49828 # p 1112
 A93-49829 # p 1141
 A93-49830 * # p 1112
 A93-49832 * # p 1112
 A93-49833 * # p 1141
 A93-49834 # p 1112
 A93-49839 # p 1153
 A93-49840 # p 1153
 A93-49842 # p 1145
 A93-49854 # p 1137
 A93-49855 # p 1078
 A93-49856 * # p 1078
 A93-49858 # p 1078
 A93-49859 # p 1137
 A93-49860 # p 1113
 A93-49867 * # p 1145
 A93-49870 # p 1113
 A93-49876 * # p 1113
 A93-49882 # p 1113
 A93-49884 # p 1166
 A93-49901 * # p 1153
 A93-49902 # p 1113
 A93-49903 * # p 1113
 A93-49904 # p 1114
 A93-49906 * # p 1154
 A93-49909 # p 1079
 A93-49911 * # p 1114
 A93-49912 * # p 1114
 A93-49913 * # p 1079
 A93-49914 # p 1079
 A93-49954 * # p 1142
 A93-49957 # p 1114
 A93-49958 # p 1114
 A93-49960 # p 1114
 A93-49961 * # p 1115
 A93-49962 # p 1115
 A93-49963 # p 1154
 A93-49966 * # p 1154
 A93-49968 # p 1154
 A93-49969 # p 1101
 A93-49970 * # p 1079
 A93-49971 # p 1079
 A93-49972 # p 1115
 A93-49973 * # p 1079
 A93-49986 # p 1137
 A93-49987 # p 1115
 A93-49988 * # p 1137
 A93-49989 * # p 1173
 A93-49990 # p 1137
 A93-49991 # p 1138
 A93-49992 # p 1138
 A93-49995 * # p 1142
 A93-50008 * # p 1115
 A93-50009 # p 1154
 A93-50010 # p 1155
 A93-50013 # p 1145
 A93-50014 # p 1145
 A93-50015 # p 1155
 A93-50035 # p 1080
 A93-50036 # p 1080
 A93-50037 # p 1080
 A93-50038 # p 1080
 A93-50039 * # p 1080
 A93-50040 # p 1081
 A93-50041 # p 1081
 A93-50042 # p 1155
 A93-50047 # p 1155
 A93-50050 * # p 1155
 A93-50051 # p 1081
 A93-50052 * # p 1115
 A93-50053 # p 1081
 A93-50054 # p 1081
 A93-50055 # p 1081
 A93-50084 * # p 1155
 A93-50086 # p 1082
 A93-50087 # p 1082
 A93-50088 # p 1082
 A93-50089 # p 1082
 A93-50090 # p 1082
 A93-50103 * # p 1116
 A93-50104 * # p 1116
 A93-50105 # p 1116
 A93-50106 # p 1116
 A93-50107 # p 1145
 A93-50108 # p 1116
 A93-50113 # p 1116

A93-50115 # p 1117
 A93-50117 # p 1164
 A93-50118 # p 1156
 A93-50119 # p 1082
 A93-50120 # p 1083
 A93-50121 * # p 1083
 A93-50143 # p 1156
 A93-50150 # p 1083
 A93-50151 # p 1083
 A93-50152 # p 1117
 A93-50153 # p 1117
 A93-50154 # p 1083
 A93-50167 * # p 1156
 A93-50185 # p 1117
 A93-50186 # p 1117
 A93-50187 * # p 1117
 A93-50188 # p 1118
 A93-50189 * # p 1118
 A93-50190 * # p 1118
 A93-50191 # p 1118
 A93-50192 * # p 1118
 A93-50193 * # p 1119
 A93-50194 # p 1119
 A93-50195 # p 1119
 A93-50196 * # p 1119
 A93-50197 # p 1119
 A93-50198 # p 1120
 A93-50199 # p 1120
 A93-50200 # p 1138
 A93-50201 # p 1120
 A93-50213 # p 1138
 A93-50214 # p 1138
 A93-50215 # p 1120
 A93-50216 # p 1138
 A93-50217 # p 1120
 A93-50220 # p 1146
 A93-50221 * # p 1083
 A93-50222 * # p 1084
 A93-50252 * # p 1120
 A93-50253 * # p 1121
 A93-50254 * # p 1156
 A93-50261 * # p 1156
 A93-50264 # p 1156
 A93-50266 # p 1139
 A93-50267 * # p 1121
 A93-50268 # p 1121
 A93-50269 # p 1139
 A93-50277 * # p 1121
 A93-50278 * # p 1084
 A93-50280 * # p 1157
 A93-50284 # p 1142
 A93-50285 # p 1121
 A93-50286 # p 1084
 A93-50287 # p 1121
 A93-50288 * # p 1084
 A93-50289 # p 1084
 A93-50290 # p 1085
 A93-50292 # p 1085
 A93-50293 # p 1085
 A93-50294 * # p 1122
 A93-50295 # p 1157
 A93-50300 # p 1142
 A93-50301 # p 1142
 A93-50306 * # p 1122
 A93-50311 # p 1122
 A93-50316 # p 1122
 A93-50318 # p 1142
 A93-50330 # p 1174
 A93-50333 # p 1174
 A93-50352 # p 1122
 A93-50353 # p 1043
 A93-50369 # p 1157
 A93-50373 * # p 1164
 A93-50405 # p 1157
 A93-50420 # p 1157
 A93-50429 # p 1101
 A93-50430 # p 1158
 A93-50486 # p 1043
 A93-50487 # p 1101
 A93-50488 # p 1173
 A93-50489 # p 1166
 A93-50524 # p 1158
 A93-50543 # p 1158
 A93-50561 # p 1158
 A93-50566 # p 1158
 A93-50631 # p 1166
 A93-50636 # p 1097
 A93-50638 # p 1167
 A93-50643 * # p 1097
 A93-50660 # p 1097
 A93-50726 * # p 1167
 A93-50744 # p 1167
 A93-50779 # p 1167
 A93-50950 # p 1164
 A93-50951 # p 1167
 A93-50952 # p 1168

A93-50953 p 1168
 A93-50954 p 1168
 A93-50955 p 1168
 A93-50956 p 1168
 A93-50957 p 1168
 A93-50958 p 1168
 A93-50960 p 1168
 A93-50961 p 1130
 A93-50962 p 1085
 A93-50965 p 1085
 A93-50966 p 1085
 A93-50967 p 1086
 A93-50968 p 1086
 A93-50969 p 1086
 A93-50972 p 1086
 A93-51062 p 1169
 A93-51063 p 1169
 A93-51065 p 1169
 A93-51104 p 1146
 A93-51121 p 1086
 A93-51122 p 1086
 A93-51123 p 1086
 A93-51188 p 1139
 A93-51189 p 1169
 A93-51190 p 1086
 A93-51191 p 1087
 A93-51193 p 1122
 A93-51198 p 1169
 A93-51237 # p 1143
 A93-51243 # p 1158
 A93-51250 # p 1158
 A93-51279 # p 1169
 A93-51280 # p 1087
 A93-51295 * # p 1139
 A93-51328 # p 1170
 A93-51329 # p 1130
 A93-51330 # p 1170
 A93-51331 # p 1143
 A93-51338 * # p 1101
 A93-51342 * # p 1170
 A93-51344 * # p 1170
 A93-51348 * # p 1143
 A93-51349 # p 1101
 A93-51357 * # p 1131
 A93-51358 * # p 1131
 A93-51359 * # p 1101
 A93-51360 * # p 1102
 A93-51361 * # p 1131
 A93-51369 # p 1131
 A93-51370 * # p 1131
 A93-51371 * # p 1132
 A93-51372 # p 1132
 A93-51373 # p 1132
 A93-51374 # p 1132
 A93-51385 # p 1143
 A93-51386 # p 1143
 A93-51388 # p 1159
 A93-51391 # p 1106
 A93-51393 # p 1139
 A93-51394 # p 1170
 A93-51400 * # p 1132
 A93-51401 * # p 1102
 A93-51402 # p 1122
 A93-51403 # p 1123
 A93-51404 # p 1123
 A93-51405 # p 1132
 A93-51406 # p 1133
 A93-51407 # p 1133
 A93-51408 # p 1133
 A93-51409 # p 1143
 A93-51421 # p 1097
 A93-51422 # p 1098
 A93-51423 # p 1098
 A93-51424 # p 1098
 A93-51425 # p 1098
 A93-51431 # p 1170
 A93-51433 # p 1133
 A93-51434 # p 1133
 A93-51435 # p 1133
 A93-51436 # p 1134
 A93-51437 # p 1134
 A93-51438 # p 1134
 A93-51439 # p 1134
 A93-51440 # p 1140
 A93-51442 * # p 1144
 A93-51444 # p 1134
 A93-51454 # p 1171
 A93-51455 # p 1171
 A93-51456 # p 1135
 A93-51457 * # p 1098
 A93-51465 # p 1135
 A93-51466 # p 1135
 A93-51468 # p 1135
 A93-51472 # p 1144
 A93-51480 # p 1102
 A93-51497 # p 1174

A93-51528 * p 1159
 A93-51626 p 1146
 A93-51631 p 1146
 A93-51632 p 1159
 A93-51634 p 1146
 A93-51642 p 1123
 A93-51643 p 1123
 A93-51644 p 1123
 A93-51645 p 1123
 A93-51648 * p 1171
 A93-51727 p 1043
 A93-51728 p 1159
 A93-51729 p 1159
 A93-51732 p 1043
 A93-51733 p 1159
 A93-51736 p 1087
 A93-51738 p 1087
 A93-51740 p 1087
 A93-51752 p 1102
 A93-51754 p 1140
 A93-51755 p 1088
 A93-51756 p 1088
 A93-51758 p 1102
 A93-51759 p 1124
 A93-51760 p 1124
 A93-51761 p 1124
 A93-51762 p 1140
 A93-51768 p 1088
 A93-51770 p 1088
 A93-51771 p 1088
 A93-51772 p 1088
 A93-51775 p 1088
 A93-51776 p 1089
 A93-51779 p 1089
 A93-51780 p 1089
 A93-51783 p 1089
 A93-51786 p 1089
 A93-51818 p 1089
 A93-51820 p 1089
 A93-51856 p 1164
 A93-51867 p 1173
 A93-51868 p 1089
 A93-51869 p 1090
 A93-51870 p 1090
 A93-51871 p 1090
 A93-51872 p 1090
 A93-51877 p 1090
 A93-51878 p 1090
 A93-51879 p 1090
 A93-51880 p 1091
 A93-51881 p 1091
 A93-51882 p 1091
 A93-51883 p 1091
 A93-51884 p 1140
 A93-51893 p 1160
 A93-51901 p 1091
 A93-51902 p 1091
 A93-51903 p 1091
 A93-51904 p 1092
 A93-51905 p 1103
 A93-51906 p 1135
 A93-51907 p 1092
 A93-51908 p 1092
 A93-51909 p 1092
 A93-51910 p 1092
 A93-51911 p 1092
 A93-51912 p 1103
 A93-51913 p 1092
 A93-51934 p 1140
 A93-51936 p 1146
 A93-51937 p 1173
 A93-51940 p 1092
 A93-51944 p 1171
 A93-51967 p 1099
 A93-51999 p 1093
 A93-52000 p 1093
 A93-52001 p 1093
 A93-52005 p 1093
 A93-52006 p 1093
 A93-52007 * p 1093
 A93-52011 * p 1093
 A93-52012 p 1094
 A93-52152 * p 1160
 A93-52165 p 1103
 A93-52166 p 1103
 A93-52167 p 1160
 A93-52168 p 1096
 A93-52170 p 1160
 A93-52171 p 1124
 A93-52175 p 1103
 A93-52249 p 1135
 A93-52419 p 1160
 A93-52426 p 1094
 A93-52427 * p 1094
 A93-52429 * p 1094
 A93-52430 p 1094

ACCESSION NUMBER INDEX

ACCESSION NUMBER INDEX

A93-54894

A93-52432	p 1094	A93-52961	p 1211	A93-53772	p 1192	A93-54048	p 1201	A93-54399	p 1250
A93-52434	p 1094	A93-52963	p 1193	A93-53774	p 1209	A93-54049	p 1201	A93-54400	p 1250
A93-52435	p 1103	A93-52965	p 1193	A93-53776	p 1218	A93-54050	p 1220	A93-54402	p 1251
A93-52436	p 1095	A93-52968	p 1215	A93-53798	p 1181	A93-54051	p 1186	A93-54409	p 1255
A93-52437	p 1135	A93-52973	p 1215	A93-53799	p 1181	A93-54052	p 1220	A93-54411	p 1255
A93-52438	p 1095	A93-52975	p 1215	A93-53810	p 1218	A93-54053	p 1220	A93-54420	p 1262
A93-52439	p 1095	A93-52976	p 1209	A93-53812	p 1218	A93-54054	p 1220	A93-54450	p 1245
A93-52440	p 1103	A93-52979	p 1215	A93-53815	p 1218	A93-54055	p 1201	A93-54467	p 1245
A93-52441	p 1140	A93-52994	p 1192	A93-53817	p 1226	A93-54056	p 1201	A93-54469	p 1229
A93-52442	p 1095	A93-53172	p 1190	A93-53819	p 1219	A93-54057	p 1213	A93-54477	p 1229
A93-52443	p 1103	A93-53192	p 1176	A93-53820	p 1219	A93-54058	p 1201	A93-54540	p 1255
A93-52444	p 1136	A93-53193	p 1176	A93-53826	p 1227	A93-54059	p 1202	A93-54544	p 1255
A93-52445	p 1095	A93-53194	p 1225	A93-53837	p 1181	A93-54060	p 1202	A93-54549	p 1239
A93-52446	p 1095	A93-53200	p 1176	A93-53840	p 1181	A93-54061	p 1202	A93-54550	p 1240
A93-52447	p 1174	A93-53202	p 1176	A93-53841	p 1181	A93-54062	p 1186	A93-54551	p 1241
A93-52448	p 1095	A93-53204	p 1177	A93-53842	p 1182	A93-54063	p 1202	A93-54554	p 1248
A93-52449	p 1160	A93-53205	p 1177	A93-53843	p 1182	A93-54064	p 1202	A93-54556	p 1246
A93-52450	p 1103	A93-53206	p 1225	A93-53847	p 1219	A93-54065	p 1202	A93-54559	p 1241
A93-52451	p 1095	A93-53207	p 1177	A93-53852	p 1182	A93-54066	p 1203	A93-54560	p 1230
A93-52452	p 1136	A93-53208	p 1177	A93-53853	p 1182	A93-54067	p 1203	A93-54563	p 1251
A93-52453	p 1160	A93-53209	p 1177	A93-53858	p 1182	A93-54068	p 1186	A93-54581	p 1230
A93-52454	p 1104	A93-53212	p 1177	A93-53859	p 1182	A93-54069	p 1186	A93-54584	p 1230
A93-52455	p 1136	A93-53214	p 1177	A93-53860	p 1183	A93-54070	p 1186	A93-54586	p 1230
A93-52456	p 1095	A93-53216	p 1178	A93-53862	p 1194	A93-54071	p 1203	A93-54587	p 1230
A93-52457	p 1095	A93-53217	p 1178	A93-53866	p 1191	A93-54072	p 1203	A93-54588	p 1230
A93-52458	p 1136	A93-53218	p 1178	A93-53868	p 1183	A93-54073	p 1203	A93-54589	p 1230
A93-52459	p 1095	A93-53219	p 1178	A93-53869	p 1206	A93-54074	p 1187	A93-54590	p 1241
A93-52473	p 1147	A93-53222	p 1226	A93-53874	p 1192	A93-54075	p 1187	A93-54593	p 1250
A93-52513	p 1147	A93-53224	p 1216	A93-53876	p 1192	A93-54076	p 1187	A93-54594	p 1231
A93-52517	p 1160	A93-53231	p 1178	A93-53877	p 1206	A93-54077	p 1192	A93-54595	p 1231
A93-52548	p 1043	A93-53233	p 1178	A93-53881	p 1219	A93-54078	p 1187	A93-54596	p 1242
A93-52560	p 1161	A93-53314	p 1178	A93-53976	p 1194	A93-54079	p 1187	A93-54597	p 1231
A93-52593	p 1099	A93-53315	p 1179	A93-53977	p 1227	A93-54080	p 1187	A93-54598	p 1231
A93-52594	p 1096	A93-53329	p 1216	A93-53978	p 1194	A93-54081	p 1203	A93-54599	p 1231
A93-52601	p 1161	A93-53333	p 1179	A93-53979	p 1194	A93-54082	p 1188	A93-54601	p 1229
A93-52606	p 1161	A93-53364	p 1179	A93-53980	p 1194	A93-54083	p 1188	A93-54603	# 1242
A93-52614	p 1044	A93-53365	p 1179	A93-53981	p 1194	A93-54084	p 1203	A93-54604	# 1240
A93-52642	p 1096	A93-53395	p 1216	A93-53982	p 1183	A93-54085	p 1204	A93-54605	# 1229
A93-52645	p 1140	A93-53405	p 1191	A93-53983	p 1183	A93-54086	p 1188	A93-54606	# 1242
A93-52651	p 1207	A93-53419	p 1211	A93-53984	p 1183	A93-54087	p 1204	A93-54607	# 1231
A93-52652	# 1207	A93-53420	p 1211	A93-53985	p 1183	A93-54088	p 1204	A93-54608	# 1255
A93-52653	# 1226	A93-53423	p 1226	A93-53986	p 1183	A93-54089	p 1221	A93-54609	# 1246
A93-52654	# 1222	A93-53429	p 1216	A93-53987	p 1184	A93-54090	p 1221	A93-54610	# 1242
A93-52655	# 1207	A93-53434	p 1211	A93-53988	p 1184	A93-54092	p 1221	A93-54611	# 1265
A93-52656	# 1222	A93-53445	p 1211	A93-53989	p 1194	A93-54093	p 1188	A93-54612	# 1242
A93-52659	# 1214	A93-53448	p 1212	A93-53992	p 1195	A93-54094	p 1221	A93-54613	# 1242
A93-52660	# 1222	A93-53451	p 1212	A93-53993	p 1195	A93-54095	p 1221	A93-54614	# 1243
A93-52663	# 1223	A93-53452	p 1216	A93-53994	p 1195	A93-54096	p 1221	A93-54615	# 1231
A93-52665	# 1207	A93-53453	p 1212	A93-53995	p 1195	A93-54098	p 1222	A93-54626	p 1256
A93-52667	# 1214	A93-53459	p 1212	A93-53996	p 1195	A93-54099	p 1189	A93-54633	p 1256
A93-52668	# 1208	A93-53468	p 1216	A93-53997	p 1195	A93-54100	p 1204	A93-54634	p 1256
A93-52670	# 1208	A93-53493	p 1217	A93-53998	p 1195	A93-54102	p 1204	A93-54636	p 1256
A93-52671	# 1208	A93-53498	p 1217	A93-53999	p 1196	A93-54103	p 1204	A93-54639	p 1232
A93-52673	# 1208	A93-53499	p 1217	A93-54000	p 1196	A93-54104	p 1175	A93-54640	p 1232
A93-52675	# 1208	A93-53503	p 1217	A93-54001	p 1213	A93-54105	p 1189	A93-54646	p 1232
A93-52676	# 1208	A93-53506	p 1212	A93-54002	p 1213	A93-54106	p 1205	A93-54647	p 1232
A93-52677	# 1214	A93-53514	p 1217	A93-54003	p 1196	A93-54107	p 1205	A93-54648	p 1256
A93-52678	# 1223	A93-53515	p 1217	A93-54004	p 1196	A93-54108	p 1225	A93-54649	p 1257
A93-52679	# 1209	A93-53551	p 1179	A93-54005	p 1184	A93-54241	p 1214	A93-54650	p 1243
A93-52680	# 1223	A93-53552	p 1179	A93-54006	p 1184	A93-54244	p 1205	A93-54651	p 1257
A93-52681	# 1223	A93-53554	p 1193	A93-54007	p 1184	A93-54250	p 1214	A93-54653	p 1257
A93-52682	# 1223	A93-53555	p 1179	A93-54008	p 1196	A93-54266	p 1189	A93-54708	p 1252
A93-52683	# 1223	A93-53556	p 1179	A93-54009	p 1185	A93-54268	p 1206	A93-54711	p 1252
A93-52684	# 1224	A93-53573	p 1179	A93-54010	p 1197	A93-54275	p 1210	A93-54712	p 1252
A93-52685	# 1224	A93-53574	p 1180	A93-54011	p 1197	A93-54276	p 1222	A93-54718	p 1262
A93-52686	# 1224	A93-53575	p 1180	A93-54012	p 1197	A93-54277	p 1206	A93-54719	p 1261
A93-52687	# 1224	A93-53585	# 1218	A93-54013	p 1197	A93-54278	p 1207	A93-54720	p 1262
A93-52688	# 1209	A93-53589	# 1193	A93-54014	p 1197	A93-54279	p 1175	A93-54722	p 1262
A93-52690	# 1175	A93-53591	# 1180	A93-54015	p 1197	A93-54287	p 1189	A93-54723	p 1243
A93-52691	# 1191	A93-53592	# 1180	A93-54016	p 1198	A93-54288	p 1190	A93-54724	p 1243
A93-52695	# 1214	A93-53596	p 1218	A93-54017	p 1198	A93-54289	p 1190	A93-54725	p 1263
A93-52732	p 1224	A93-53598	p 1212	A93-54018	p 1198	A93-54290	p 1205	A93-54728	p 1253
A93-52751	p 1215	A93-53599	p 1212	A93-54019	p 1198	A93-54291	p 1190	A93-54799	p 1257
A93-52754	p 1209	A93-53602	p 1213	A93-54020	p 1198	A93-54292	p 1175	A93-54800	p 1252
A93-52762	p 1224	A93-53603	p 1190	A93-54021	p 1198	A93-54293	p 1189	A93-54805	p 1233
A93-52763	p 1224	A93-53604	p 1191	A93-54022	p 1198	A93-54294	p 1189	A93-54810	p 1233
A93-52770	p 1175	A93-53615	p 1226	A93-54023	p 1185	A93-54314	p 1254	A93-54815	p 1233
A93-52870	p 1211	A93-53616	p 1226	A93-54024	p 1199	A93-54324	p 1254	A93-54816	p 1246
A93-52881	p 1190	A93-53618	p 1180	A93-54025	p 1213	A93-54347	p 1254	A93-54837	p 1246
A93-52885	p 1210	A93-53621	p 1225	A93-54026	p 1199	A93-54353	p 1261	A93-54838	p 1243
A93-52898	p 1222	A93-53625	p 1206	A93-54028	p 1199	A93-54356	p 1253	A93-54840	p 1246
A93-52930	p 1226	A93-53626	p 1209	A93-54029	p 1185	A93-54362	p 1254	A93-54843	p 1257
A93-52931	p 1226	A93-53642	p 1225	A93-54030	p 1185	A93-54366	p 1254	A93-54854	p 1265
A93-52937	p 1191	A93-53702	p 1193	A93-54031	p 1185	A93-54368	p 1254	A93-54857	p 1248
A93-52939	p 1215	A93-53721	p 1191	A93-54033	p 1185	A93-54369	p 1254	A93-54859	p 1247
A93-52941	p 1205	A93-53726	p 1227	A93-54034	p 1185	A93-54372	p 1254	A93-54863	p 1247
A93-52942	p 1205	A93-53727	p 1227	A93-54035	p 1219	A93-54376	p 1254	A93-54866	p 1229
A93-52943	p 1206	A93-53736	p 1181	A93-54036	p 1220	A93-54377	p 1254	A93-54867	p 1243
A93-52944	p 1206	A93-53737	p 1210	A93-54037	p 1199	A93-54378	p 1254	A93-54894	p 1257
A93-52945	p 1225	A93-53738	p 1210	A93-54038	p 1199	A93-54381	p 1261		
A93-52946	p 1176	A93-53739	p 1181	A93-54039	p 1200	A93-54382	p 1250		
A93-52949	p 1193	A93-53740	p 1181	A93-54040	p 1200	A93-54389	p 1244		
A93-52950	p 1215	A93-53745	p 1210	A93-54042	p 1200	A93-54391	p 1254		
A93-52954	p 1191	A93-53768	p 1209	A93-54043	p 1200	A93-54392	p 1254		
A93-52958	p 1176	A93-53769	p 1192	A93-54044	p 1200	A93-54393	p 1250		
A93-52959	p 1176	A93-53770	p 1225	A93-54045	p 1186	A93-54394	p 1250		
		A93-53771	p 1192			A93-54398	p 1255		

A93-54895

A93-54895 p 1229
 A93-54896 p 1258
 A93-54897 p 1258
 A93-54898 p 1258
 A93-54899 p 1258
 A93-54900 p 1258
 A93-54969 p 1248
 A93-54998 p 1263
 A93-55014 p 1233
 A93-55015 p 1233
 A93-55018 p 1258
 A93-55019 p 1233
 A93-55026 p 1234
 A93-55030 p 1234
 A93-55032 p 1253
 A93-55034 p 1252
 A93-55142 p 1234
 A93-55146 p 1234
 A93-55175 p 1229
 A93-55176 p 1263
 A93-55178 p 1263
 A93-55220 p 1247
 A93-55294 p 1244
 A93-55295 p 1258
 A93-55297 p 1244
 A93-55298 p 1244
 A93-55299 p 1244
 A93-55331 p 1263
 A93-55351 p 1234
 A93-55352 p 1234
 A93-55353 p 1235
 A93-55356 p 1235
 A93-55357 p 1235
 A93-55359 p 1235
 A93-55360 p 1235
 A93-55362 p 1235
 A93-55364 p 1235
 A93-55369 p 1258
 A93-55379 p 1235
 A93-55380 p 1236
 A93-55397 p 1236
 A93-55398 p 1236
 A93-55400 p 1236
 A93-55411 p 1236
 A93-55412 p 1236
 A93-55414 p 1240
 A93-55415 p 1243
 A93-55459 p 1259
 A93-55465 p 1259
 A93-55493 p 1247
 A93-55494 p 1247
 A93-55584 p 1236
 A93-55585 p 1259
 A93-55586 p 1259
 A93-55589 p 1236
 A93-55590 p 1249
 A93-55666 p 1263
 A93-55674 p 1259
 A93-55697 p 1253
 A93-55736 p 1236
 A93-55753 p 1249
 A93-55756 p 1259
 A93-55760 p 1245
 A93-55816 p 1247
 A93-55817 p 1247
 A93-55825 p 1252
 A93-55841 p 1250
 A93-55845 p 1264
 A93-55851 p 1259
 A93-55852 p 1264
 A93-55856 p 1243
 A93-55857 p 1264
 A93-55859 p 1264
 A93-55860 p 1248
 A93-55861 p 1264
 A93-55862 p 1264
 A93-55863 p 1244
 A93-55866 p 1259
 A93-55869 p 1260
 A93-55871 p 1253
 A93-55874 p 1260
 A93-55972 p 1245
 A93-55973 p 1240
 A93-55974 p 1240
 A93-55975 p 1240
 A93-55976 p 1241
 A93-55977 p 1241
 A93-55978 p 1245
 A93-55995 p 1265
 A93-55996 p 1260
 A93-56028 p 1237
 A93-56029 p 1249
 A93-56030 p 1237
 A93-56031 p 1249
 A93-56032 p 1251
 A93-56033 p 1237

A93-56034 p 1237
 A93-56035 p 1237
 A93-56036 p 1238
 A93-56037 p 1238
 A93-56038 p 1238
 A93-56039 p 1252
 A93-56040 p 1238
 A93-56046 p 1249
 A93-56049 p 1241
 A93-56212 p 1238
 A93-56213 p 1238
 A93-56214 p 1238
 A93-56215 p 1239
 A93-56216 p 1239
 A93-56217 p 1249
 A93-56218 p 1249
 A93-56219 p 1239
 A93-56220 p 1239
 A93-56222 p 1251
 A93-56236 p 1261
 A93-56272 p 1265
 A93-56278 p 1251
 A93-56327 p 1239
 A93-56331 p 1260
 A93-56339 p 1260
 A93-56348 p 1248
 A93-56349 p 1244
 A93-56350 p 1248
 A93-56402 p 1239
 A93-56403 p 1262
 A93-56413 p 1262
 A93-56417 p 1240
 A93-56537 p 1265
 A93-56540 p 1265
 A93-56544 p 1260
 N93-10011 p 46
 N93-10012 p 16
 N93-10052 # p 81
 N93-10056 # p 81
 N93-10058 # p 81
 N93-10059 # p 81
 N93-10061 # p 82
 N93-10065 # p 35
 N93-10069 # p 16
 N93-10070 # p 63
 N93-10087 # p 82
 N93-10098 # p 17
 N93-10198 # p 82
 N93-10304 p 82
 N93-10305 p 82
 N93-10309 p 83
 N93-10310 # p 83
 N93-10320 p 17
 N93-10322 p 47
 N93-10323 # p 35
 N93-10340 # p 17
 N93-10342 # p 17
 N93-10348 # p 55
 N93-10349 # p 17
 N93-10367 p 83
 N93-10368 p 83
 N93-10370 p 83
 N93-10372 # p 84
 N93-10374 p 63
 N93-10375 # p 17
 N93-10456 # p 55
 N93-10458 # p 99
 N93-10459 # p 35
 N93-10472 p 84
 N93-10539 p 56
 N93-10544 p 18
 N93-10547 p 18
 N93-10549 p 18
 N93-10550 p 18
 N93-10551 p 18
 N93-10610 # p 104
 N93-10642 # p 99
 N93-10647 # p 4
 N93-10648 # p 19
 N93-10653 # p 84
 N93-10672 # p 99
 N93-10673 # p 99
 N93-10674 # p 100
 N93-10681 # p 100
 N93-10682 # p 100
 N93-10684 # p 100
 N93-10685 # p 100
 N93-10688 # p 101
 N93-10692 # p 101
 N93-10717 # p 71
 N93-10738 # p 35
 N93-10741 # p 64
 N93-10745 # p 35
 N93-10770 # p 72
 N93-10803 # p 47

N93-10805 # p 101
 N93-10811 # p 19
 N93-10815 # p 104
 N93-10824 # p 19
 N93-10842 # p 47
 N93-10843 # p 72
 N93-10845 # p 19
 N93-10856 # p 19
 N93-10858 # p 19
 N93-10872 # p 104
 N93-10874 p 84
 N93-10877 p 20
 N93-10891 # p 85
 N93-10892 # p 85
 N93-10900 p 47
 N93-10960 # p 69
 N93-10961 # p 36
 N93-10963 # p 85
 N93-10968 # p 47
 N93-10983 # p 56
 N93-11014 # p 85
 N93-11019 # p 56
 N93-11020 # p 20
 N93-11023 # p 56
 N93-11024 # p 56
 N93-11025 # p 85
 N93-11027 # p 72
 N93-11031 # p 72
 N93-11032 # p 72
 N93-11034 # p 85
 N93-11035 # p 72
 N93-11036 # p 56
 N93-11037 # p 56
 N93-11038 # p 56
 N93-11039 # p 57
 N93-11040 # p 57
 N93-11050 p 20
 N93-11054 # p 86
 N93-11055 # p 57
 N93-11057 # p 67
 N93-11061 # p 57
 N93-11062 # p 57
 N93-11063 # p 58
 N93-11066 # p 72
 N93-11068 # p 58
 N93-11069 # p 58
 N93-11070 # p 20
 N93-11085 # p 58
 N93-11096 # p 93
 N93-11100 # p 104
 N93-11105 # p 58
 N93-11106 # p 58
 N93-11107 # p 73
 N93-11108 # p 58
 N93-11112 # p 58
 N93-11113 # p 20
 N93-11114 # p 59
 N93-11133 # p 69
 N93-11135 # p 73
 N93-11137 # p 73
 N93-11139 # p 36
 N93-11144 # p 93
 N93-11156 # p 101
 N93-11161 # p 48
 N93-11172 # p 86
 N93-11176 # p 64
 N93-11204 # p 101
 N93-11206 # p 59
 N93-11207 # p 59
 N93-11208 # p 59
 N93-11220 # p 86
 N93-11221 # p 20
 N93-11223 # p 21
 N93-11224 # p 67
 N93-11225 # p 67
 N93-11250 # p 21
 N93-11252 # p 36
 N93-11319 # p 28
 N93-11325 # p 86
 N93-11326 # p 86
 N93-11327 # p 87
 N93-11334 # p 48
 N93-11357 # p 28
 N93-11358 # p 87
 N93-11365 # p 21
 N93-11370 # p 101
 N93-11375 # p 28
 N93-11377 # p 21
 N93-11383 # p 87
 N93-11384 # p 87
 N93-11385 # p 87
 N93-11416 # p 87
 N93-11435 # p 67
 N93-11442 # p 73
 N93-11460 # p 88
 N93-11461 # p 48

N93-11463 # p 98
 N93-11464 # p 21
 N93-11471 # p 28
 N93-11485 # p 48
 N93-11530 # p 59
 N93-11532 # p 22
 N93-11544 # p 88
 N93-11576 # p 64
 N93-11587 # p 88
 N93-11605 # p 22
 N93-11610 # p 22
 N93-11616 # p 67
 N93-11617 # p 88
 N93-11620 # p 102
 N93-11622 # p 22
 N93-11624 # p 88
 N93-11698 # p 89
 N93-11702 # p 93
 N93-11704 # p 36
 N93-11705 # p 36
 N93-11707 # p 89
 N93-11710 # p 104
 N93-11716 # p 89
 N93-11719 p 48
 N93-11725 p 48
 N93-11728 # p 67
 N93-11742 # p 22
 N93-11751 # p 68
 N93-11760 # p 89
 N93-11767 # p 89
 N93-11798 # p 69
 N93-11802 # p 89
 N93-11803 # p 94
 N93-11838 # p 49
 N93-11863 # p 49
 N93-11871 p 64
 N93-11876 # p 23
 N93-11882 # p 23
 N93-11883 # p 23
 N93-11886 # p 23
 N93-11899 # p 23
 N93-11906 # p 68
 N93-11910 # p 68
 N93-11931 # p 98
 N93-11947 # p 98
 N93-12004 # p 24
 N93-12021 # p 102
 N93-12063 # p 24
 N93-12075 # p 94
 N93-12077 # p 60
 N93-12080 # p 102
 N93-12104 # p 94
 N93-12140 # p 90
 N93-12162 # p 90
 N93-12179 # p 24
 N93-12189 # p 74
 N93-12190 # p 24
 N93-12193 # p 28
 N93-12197 # p 90
 N93-12206 # p 49
 N93-12214 # p 60
 N93-12216 # p 64
 N93-12237 # p 74
 N93-12248 # p 74
 N93-12258 # p 98
 N93-12277 # p 90
 N93-12299 # p 94
 N93-12304 # p 65
 N93-12305 # p 65
 N93-12320 # p 36
 N93-12321 # p 24
 N93-12329 # p 90
 N93-12340 # p 90
 N93-12343 # p 25
 N93-12344 # p 25
 N93-12346 # p 98
 N93-12349 # p 68
 N93-12352 # p 25
 N93-12353 # p 25
 N93-12354 # p 49
 N93-12359 # p 68
 N93-12361 # p 65
 N93-12362 # p 65
 N93-12365 # p 91
 N93-12367 # p 52
 N93-12369 # p 26
 N93-12370 # p 52
 N93-12375 # p 102
 N93-12383 # p 52
 N93-12401 # p 91
 N93-12402 # p 60
 N93-12411 # p 91
 N93-12413 # p 65
 N93-12414 # p 26
 N93-12415 # p 66
 N93-12418 # p 60

N93-12447 # p 69
 N93-12456 # p 74
 N93-12457 # p 74
 N93-12458 # p 49
 N93-12460 # p 91
 N93-12485 # p 50
 N93-12488 # p 50
 N93-12489 # p 29
 N93-12490 # p 102
 N93-12503 # p 26
 N93-12537 p 70
 N93-12538 # p 99
 N93-12552 # p 192
 N93-12554 # p 228
 N93-12555 # p 212
 N93-12575 # p 195
 N93-12578 # p 186
 N93-12589 # p 198
 N93-12602 # p 159
 N93-12605 # p 159
 N93-12613 # p 160
 N93-12668 # p 192
 N93-12671 # p 234
 N93-12672 # p 234
 N93-12674 # p 212
 N93-12695 # p 174
 N93-12716 # p 128
 N93-12721 # p 129
 N93-12735 # p 212
 N93-12736 # p 212
 N93-12746 # p 198
 N93-12752 # p 160
 N93-12816 # p 142
 N93-12818 # p 223
 N93-12899 # p 192
 N93-12902 # p 192
 N93-12903 # p 186
 N93-12958 # p 228
 N93-12959 # p 186
 N93-12967 # p 231
 N93-12977 # p 212
 N93-12986 # p 231
 N93-13010 p 129
 N93-13025 # p 109
 N93-13052 # p 212
 N93-13053 # p 213
 N93-13110 # p 109
 N93-13128 p 129
 N93-13140 p 160
 N93-13141 p 130
 N93-13154 # p 228
 N93-13155 # p 175
 N93-13199 # p 213
 N93-13200 # p 213
 N93-13201 # p 213
 N93-13203 # p 213
 N93-13204 # p 213
 N93-13205 # p 130
 N93-13206 # p 214
 N93-13207 # p 160
 N93-13208 # p 160
 N93-13209 # p 214
 N93-13210 # p 214
 N93-13211 # p 214
 N93-13212 # p 161
 N93-13213 # p 192
 N93-13215 # p 214
 N93-13216 # p 215
 N93-13218 # p 175
 N93-13219 # p 161
 N93-13220 # p 215
 N93-13221 # p 130
 N93-13223 # p 130
 N93-13224 # p 161
 N93-13226 # p 215
 N93-13227 # p 215
 N93-13228 # p 161
 N93-13229 # p 175
 N93-13230 # p 175
 N93-13253 # p 161
 N93-13256 # p 161
 N93-13257 # p 232
 N93-13288 # p 223
 N93-13292 # p 130
 N93-13311 # p 198
 N93-13321 # p 215
 N93-13322 # p 131
 N93-13353 # p 131
 N93-13364 # p 142
 N93-13367 # p 186
 N93-13368 # p 234
 N93-13370 # p 229
 N93-13377 # p 151
 N93-13406 # p 216
 N93-13407 # p 192
 N93-13414 # p 199

ACCESSION NUMBER INDEX

ACCESSION NUMBER INDEX

N93-18305

N93-13422	#	p 216	N93-14610	#	p 219	N93-15173	#	p 178	N93-16345	#	p 329	N93-17613	#	p 362
N93-13426	#	p 143	N93-14615	#	p 164	N93-15174	#	p 178	N93-16379	#	p 418	N93-17614	#	p 392
N93-13447	#	p 193	N93-14616	#	p 194	N93-15175	#	p 178	N93-16389	#	p 391	N93-17622	#	p 363
N93-13451	#	p 131	N93-14627	#	p 199	N93-15176	#	p 178	N93-16396	#	p 329	N93-17660	#	p 332
N93-13463	#	p 131	N93-14631	#	p 137	N93-15177	#	p 169	N93-16403	#	p 392	N93-17666	#	p 240
N93-13470	#	p 143	N93-14655	#	p 224	N93-15178	#	p 169	N93-16404	#	p 329	N93-17670	#	p 372
N93-13493	#	p 131	N93-14661	#	p 137	N93-15179	#	p 169	N93-16411	#	p 418	N93-17676	#	p 292
N93-13521	#	p 132	N93-14677	#	p 220	N93-15180	#	p 169	N93-16455	#	p 310	N93-17677	#	p 293
N93-13524	#	p 216	N93-14692	#	p 220	N93-15181	#	p 110	N93-16463	#	p 371	N93-17686	#	p 363
N93-13525	#	p 216	N93-14693	#	p 144	N93-15182	#	p 170	N93-16464	#	p 456	N93-17687	#	p 381
N93-13542	#	p 193	N93-14726	#	p 199	N93-15183	#	p 230	N93-16465	#	p 240	N93-17693	#	p 393
N93-13565	#	p 162	N93-14729	#	p 152	N93-15185	#	p 110	N93-16467	#	p 289	N93-17694	#	p 332
N93-13566	#	p 187	N93-14737	#	p 137	N93-15186	#	p 152	N93-16468	#	p 381	N93-17695	#	p 363
N93-13578	#	p 132	N93-14738	#	p 137	N93-15187	#	p 221	N93-16470	#	p 289	N93-17704	#	p 393
N93-13632	#	p 132	N93-14763	#	p 220	N93-15189	#	p 199	N93-16477	#	p 434	N93-17708	#	p 382
N93-13655	#	p 224	N93-14766	#	p 220	N93-15227	#	p 165	N93-16498	#	p 318	N93-17711	#	p 332
N93-13664	#	p 216	N93-14767	#	p 138	N93-15232	#	p 222	N93-16500	#	p 440	N93-17732	#	p 240
N93-13669	#	p 217	N93-14791	#	p 138	N93-15235	#	p 170	N93-16508	#	p 289	N93-17734	#	p 382
N93-13697	#	p 175	N93-14797	#	p 220	N93-15238	#	p 165	N93-16515	#	p 441	N93-17740	#	p 363
N93-13712	#	p 193	N93-14799	#	p 220	N93-15245	#	p 139	N93-16522	#	p 290	N93-17746	#	p 393
N93-13729	#	p 132	N93-14805	#	p 221	N93-15278	#	p 222	N93-16537	#	p 392	N93-17756	#	p 293
N93-13735	#	p 187	N93-14809	#	p 194	N93-15337	#	p 179	N93-16543	#	p 418	N93-17761	#	p 419
N93-13745	#	p 133	N93-14828	#	p 164	N93-15338	#	p 139	N93-16558	#	p 418	N93-17779	#	p 420
N93-13746	#	p 133	N93-14830	#	p 188	N93-15342	#	p 179	N93-16560	#	p 371	N93-17793	#	p 382
N93-13762	#	p 232	N93-14831	#	p 188	N93-15343	#	p 222	N93-16562	#	p 329	N93-17800	#	p 372
N93-13769	#	p 217	N93-14835	#	p 189	N93-15345	#	p 148	N93-16563	#	p 454	N93-17802	#	p 332
N93-13787	#	p 143	N93-14836	#	p 138	N93-15354	#	p 148	N93-16567	#	p 441	N93-17803	#	p 332
N93-13790	#	p 224	N93-14844	#	p 144	N93-15359	#	p 179	N93-16596	#	p 290	N93-17804	#	p 333
N93-13798	#	p 234	N93-14847	#	p 144	N93-15360	#	p 148	N93-16613	#	p 441	N93-17809	#	p 294
N93-13799	#	p 234	N93-14848	#	p 144	N93-15361	#	p 165	N93-16618	#	p 371	N93-17819	#	p 294
N93-13800	#	p 234	N93-14849	#	p 144	N93-15366	#	p 189	N93-16625	#	p 290	N93-17849	#	p 363
N93-13801	#	p 133	N93-14850	#	p 145	N93-15390	#	p 149	N93-16627	#	p 290	N93-17850	#	p 333
N93-13803	#	p 134	N93-14851	#	p 145	N93-15396	#	p 189	N93-16629	#	p 386	N93-17851	#	p 363
N93-13807	#	p 162	N93-14852	#	p 145	N93-15403	#	p 179	N93-16634	#	p 290	N93-17852	#	p 393
N93-13815	#	p 162	N93-14853	#	p 145	N93-15404	#	p 139	N93-16635	#	p 330	N93-17855	#	p 294
N93-13821	#	p 162	N93-14854	#	p 145	N93-15430	#	p 233	N93-16636	#	p 330	N93-17875	#	p 382
N93-13822	#	p 134	N93-14855	#	p 145	N93-15431	#	p 200	N93-16637	#	p 392	N93-17880	#	p 284
N93-13826	#	p 217	N93-14856	#	p 146	N93-15434	#	p 222	N93-16638	#	p 291	N93-17882	#	p 364
N93-13827	#	p 187	N93-14857	#	p 146	N93-15483	#	p 139	N93-16641	#	p 392	N93-17883	#	p 240
N93-13872	#	p 187	N93-14858	#	p 146	N93-15487	#	p 223	N93-16652	#	p 456	N93-17884	#	p 294
N93-13882	#	p 193	N93-14871	#	p 221	N93-15489	#	p 139	N93-16692	#	p 318	N93-17888	#	p 333
N93-13914	#	p 163	N93-14890	#	p 176	N93-15490	#	p 200	N93-16693	#	p 343	N93-17890	#	p 456
N93-13915	#	p 187	N93-14891	#	p 176	N93-15498	#	p 194	N93-16695	#	p 381	N93-17891	#	p 455
N93-13916	#	p 187	N93-14892	#	p 176	N93-15502	#	p 230	N93-16704	#	p 291	N93-17893	#	p 333
N93-13917	#	p 134	N93-14893	#	p 176	N93-15504	#	p 200	N93-16705	#	p 362	N93-17920	#	p 393
N93-13922	#	p 195	N93-14894	#	p 176	N93-15521	#	p 179	N93-16710	#	p 291	N93-17929	#	p 295
N93-13925	#	p 229	N93-14895	#	p 177	N93-15522	#	p 149	N93-16715	#	p 362	N93-17934	#	p 295
N93-13928	#	p 188	N93-14896	#	p 177	N93-15525	#	p 180	N93-16753	#	p 381	N93-17954	#	p 319
N93-13929	#	p 134	N93-14897	#	p 177	N93-15528	#	p 196	N93-16755	#	p 453	N93-17958	#	p 333
N93-13930	#	p 135	N93-14898	#	p 177	N93-15573	#	p 110	N93-16761	#	p 330	N93-17972	#	p 333
N93-13946	#	p 110	N93-14911	#	p 138	N93-15575	#	p 233	N93-16763	#	p 441	N93-17974	#	p 334
N93-13953	#	p 218	N93-14912	#	p 232	N93-15577	#	p 149	N93-16765	#	p 291	N93-17976	#	p 334
N93-14024	#	p 143	N93-15004	#	p 165	N93-15578	#	p 230	N93-16768	#	p 291	N93-17977	#	p 334
N93-14025	#	p 218	N93-15005	#	p 152	N93-15579	#	p 230	N93-16769	#	p 371	N93-17991	#	p 295
N93-14026	#	p 143	N93-15013	#	p 146	N93-15588	#	p 140	N93-16770	#	p 292	N93-18017	#	p 334
N93-14035	#	p 135	N93-15014	#	p 146	N93-15589	#	p 223	N93-16784	#	p 292	N93-18031	#	p 310
N93-14041	#	p 218	N93-15015	#	p 146	N93-15635	#	p 235	N93-16786	#	p 419	N93-18036	#	p 310
N93-14060	#	p 193	N93-15016	#	p 146	N93-15637	#	p 235	N93-16787	#	p 292	N93-18037	#	p 334
N93-14102	#	p 110	N93-15017	#	p 147	N93-15686	#	p 391	N93-16793	#	p 419	N93-18042	#	p 335
N93-14111	#	p 175	N93-15018	#	p 147	N93-15698	#	p 417	N93-16796	#	p 330	N93-18047	#	p 420
N93-14128	#	p 194	N93-15019	#	p 147	N93-15790	#	p 378	N93-16797	#	p 292	N93-18049	#	p 335
N93-14144	#	p 232	N93-15020	#	p 147	N93-15801	#	p 417	N93-16818	#	p 419	N93-18054	#	p 335
N93-14160	#	p 135	N93-15021	#	p 147	N93-15830	#	p 391	N93-16829	#	p 419	N93-18055	#	p 335
N93-14173	#	p 135	N93-15022	#	p 147	N93-15839	#	p 433	N93-16834	#	p 310	N93-18056	#	p 335
N93-14238	#	p 194	N93-15023	#	p 147	N93-15857	#	p 418	N93-16841	#	p 318	N93-18059	#	p 336
N93-14248	#	p 163	N93-15024	#	p 147	N93-15858	#	p 328	N93-16940	#	p 292	N93-18060	#	p 336
N93-14252	#	p 188	N93-15025	#	p 148	N93-15889	#	p 288	N93-16941	#	p 362	N93-18061	#	p 336
N93-14254	#	p 218	N93-15026	#	p 148	N93-15920	#	p 288	N93-16942	#	p 293	N93-18063	#	p 336
N93-14275	#	p 151	N93-15052	#	p 229	N93-15931	#	p 391	N93-16947	#	p 330	N93-18064	#	p 336
N93-14276	#	p 152	N93-15065	#	p 221	N93-15946	#	p 239	N93-16999	#	p 330	N93-18065	#	p 336
N93-14277	#	p 143	N93-15101	#	p 138	N93-15949	#	p 239	N93-17051	#	p 453	N93-18066	#	p 337
N93-14400	#	p 219	N93-15116	#	p 233	N93-15979	#	p 361	N93-17091	#	p 454	N93-18085	#	p 386
N93-14406	#	p 232	N93-15126	#	p 165	N93-15980	#	p 453	N93-17172	#	p 441	N93-18086	#	p 295
N93-14441	#	p 136	N93-15131	#	p 139	N93-15988	#	p 317	N93-17219	#	p 331	N93-18087	#	p 455
N93-14448	#	p 163	N93-15143	#	p 177	N93-16080	#	p 361	N93-17225	#	p 453	N93-18093	#	p 420
N93-14451	#	p 136	N93-15152	#	p 167	N93-16157	#	p 289	N93-17289	#	p 419	N93-18103	#	p 420
N93-14462	#	p 163	N93-15153	#	p 167	N93-16165	#	p 371	N93-17305	#	p 442	N93-18121	#	p 420
N93-14468	#	p 219	N93-15154	#	p 167	N93-16186	#	p 328	N93-17311	#	p 318	N93-18128	#	p 295
N93-14470	#	p 229	N93-15155	#	p 168	N93-16210	#	p 289	N93-17325	#	p 454	N93-18131	#	p 337
N93-14475	#	p 219	N93-15156	#	p 168	N93-16213	#	p 317	N93-17517	#	p 442	N93-18142	#	p 372
N93-14479	#	p 136	N93-15157	#	p 168	N93-16215	#	p 328	N93-17522	#	p 442	N93-18143	#	p 372
N93-14483	#	p 219	N93-15158	#	p 110	N93-16262	#	p 328	N93-17535	#	p 331	N93-18149	#	p 364
N93-14495	#	p 196	N93-15159	#	p 168	N93-16283	#	p 329	N93-17540	#	p 392	N93-18151	#	p 364
N93-14514	#	p 136	N93-15160	#	p 221	N93-16287	#	p 329	N93-17542	#	p 293	N93-18155	#	p 337
N93-14515	#	p 136	N93-15161	#	p 168	N93-16288	#	p 440	N93-17543	#	p 293	N93-18161	#	p 337
N93-14516	#	p 136	N93-15162	#	p 168	N93-16309	#	p 378	N93-17547	#	p 343	N93-18166	#	p 337
N93-14541	#	p 164	N93-15163	#	p 230	N93-16310	#	p 378	N93-17559	#	p 318	N93-18193	#	p 372
N93-14547	#	p 224	N93-15164	#	p 148	N93-16311	#	p 379	N93-17562	#	p 331	N93-18202	#	p 319
N93-14549	#	p 110	N93-15165	#	p 168									

N93-18309

N93-18309 # p 319
 N93-18321 # p 421
 N93-18332 # p 442
 N93-18333 # p 338
 N93-18336 # p 296
 N93-18339 # p 338
 N93-18349 # p 338
 N93-18350 # p 338
 N93-18372 # p 442
 N93-18378 # p 296
 N93-18380 # p 421
 N93-18384 # p 296
 N93-18386 # p 339
 N93-18408 # p 344
 N93-18426 # p 421
 N93-18451 # p 339
 N93-18507 # p 339
 N93-18520 # p 382
 N93-18537 # p 394
 N93-18563 # p 421
 N93-18564 # p 421
 N93-18565 # p 421
 N93-18566 # p 422
 N93-18576 # p 422
 N93-18578 # p 364
 N93-18585 # p 296
 N93-18587 # p 434
 N93-18602 # p 297
 N93-18616 # p 339
 N93-18617 # p 297
 N93-18623 # p 422
 N93-18627 # p 297
 N93-18628 # p 364
 N93-18630 # p 443
 N93-18648 # p 297
 N93-18652 # p 297
 N93-18665 # p 443
 N93-18666 # p 443
 N93-18668 # p 443
 N93-18698 # p 298
 N93-18701 # p 364
 N93-18702 # p 434
 N93-18705 # p 422
 N93-18721 # p 422
 N93-18722 # p 422
 N93-18723 # p 422
 N93-18724 # p 423
 N93-18725 # p 423
 N93-18726 # p 423
 N93-18727 # p 423
 N93-18728 # p 423
 N93-18729 # p 423
 N93-18730 # p 423
 N93-18731 # p 423
 N93-18732 # p 424
 N93-18733 # p 424
 N93-18734 # p 424
 N93-18735 # p 424
 N93-18762 # p 455
 N93-18766 # p 382
 N93-18771 # p 298
 N93-18781 # p 298
 N93-18783 # p 339
 N93-18784 # p 394
 N93-18862 # p 424
 N93-18873 # p 319
 N93-18887 # p 240
 N93-18895 # p 339
 N93-18896 # p 340
 N93-18927 # p 319
 N93-18951 # p 319
 N93-18981 # p 340
 N93-18997 # p 365
 N93-18999 # p 340
 N93-19002 # p 240
 N93-19003 # p 298
 N93-19004 # p 340
 N93-19005 # p 340
 N93-19006 # p 298
 N93-19015 # p 298
 N93-19019 # p 372
 N93-19023 # p 344
 N93-19029 # p 340
 N93-19034 # p 340
 N93-19067 # p 320
 N93-19089 # p 341
 N93-19093 # p 365
 N93-19095 # p 373
 N93-19101 # p 424
 N93-19108 # p 373
 N93-19110 # p 344
 N93-19112 # p 443
 N93-19273 # p 299
 N93-19274 # p 299
 N93-19275 # p 299
 N93-19276 # p 299
 N93-19277 # p 299

N93-19278 # p 299
 N93-19279 # p 300
 N93-19280 # p 382
 N93-19281 # p 300
 N93-19282 # p 300
 N93-19283 # p 300
 N93-19284 # p 300
 N93-19285 # p 300
 N93-19286 # p 300
 N93-19288 # p 383
 N93-19289 # p 383
 N93-19290 # p 383
 N93-19291 # p 383
 N93-19292 # p 301
 N93-19294 # p 301
 N93-19295 # p 301
 N93-19296 # p 301
 N93-19297 # p 301
 N93-19298 # p 301
 N93-19299 # p 302
 N93-19301 # p 302
 N93-19308 # p 302
 N93-19309 # p 302
 N93-19310 # p 302
 N93-19311 # p 302
 N93-19312 # p 303
 N93-19313 # p 303
 N93-19314 # p 303
 N93-19315 # p 303
 N93-19316 # p 303
 N93-19317 # p 304
 N93-19318 # p 304
 N93-19320 # p 304
 N93-19321 # p 304
 N93-19322 # p 341
 N93-19323 # p 304
 N93-19324 # p 304
 N93-19325 # p 305
 N93-19326 # p 365
 N93-19338 # p 443
 N93-19340 # p 305
 N93-19351 # p 373
 N93-19356 # p 365
 N93-19364 # p 305
 N93-19379 # p 305
 N93-19380 # p 373
 N93-19447 # p 510
 N93-19456 # p 530
 N93-19460 # p 510
 N93-19590 # p 488
 N93-19591 # p 488
 N93-19592 # p 488
 N93-19593 # p 488
 N93-19594 # p 488
 N93-19595 # p 488
 N93-19597 # p 488
 N93-19598 # p 488
 N93-19600 # p 489
 N93-19601 # p 489
 N93-19602 # p 489
 N93-19603 # p 489
 N93-19604 # p 489
 N93-19605 # p 490
 N93-19608 # p 490
 N93-19610 # p 490
 N93-19611 # p 490
 N93-19612 # p 490
 N93-19653 # p 490
 N93-19655 # p 491
 N93-19656 # p 491
 N93-19657 # p 491
 N93-19658 # p 491
 N93-19659 # p 491
 N93-19661 # p 491
 N93-19673 # p 492
 N93-19674 # p 492
 N93-19675 # p 492
 N93-19676 # p 492
 N93-19677 # p 492
 N93-19678 # p 492
 N93-19684 # p 492
 N93-19685 # p 493
 N93-19686 # p 493
 N93-19687 # p 493
 N93-19688 # p 493
 N93-19689 # p 493
 N93-19690 # p 494
 N93-19691 # p 494
 N93-19692 # p 494
 N93-19693 # p 494
 N93-19700 # p 495
 N93-19701 # p 495
 N93-19702 # p 495
 N93-19706 # p 530
 N93-19771 # p 550
 N93-19783 # p 518

N93-19841 # p 495
 N93-19843 # p 502
 N93-19849 # p 510
 N93-19867 # p 495
 N93-19901 # p 510
 N93-19903 # p 510
 N93-19904 # p 511
 N93-19906 # p 511
 N93-19908 # p 511
 N93-19909 # p 511
 N93-19910 # p 511
 N93-19911 # p 511
 N93-19912 # p 512
 N93-19913 # p 512
 N93-19914 # p 512
 N93-19915 # p 526
 N93-19916 # p 512
 N93-19918 # p 526
 N93-19921 # p 482
 N93-19924 # p 502
 N93-19925 # p 550
 N93-19927 # p 550
 N93-19928 # p 512
 N93-19929 # p 512
 N93-19930 # p 512
 N93-19941 # p 495
 N93-19960 # p 526
 N93-19966 # p 502
 N93-19970 # p 571
 N93-19971 # p 550
 N93-19976 # p 458
 N93-19999 # p 551
 N93-20016 # p 535
 N93-20017 # p 483
 N93-20018 # p 483
 N93-20039 # p 526
 N93-20041 # p 536
 N93-20048 # p 571
 N93-20057 # p 551
 N93-20163 # p 518
 N93-20164 # p 502
 N93-20169 # p 483
 N93-20230 # p 551
 N93-20235 # p 483
 N93-20237 # p 536
 N93-20245 # p 513
 N93-20247 # p 536
 N93-20256 # p 483
 N93-20268 # p 551
 N93-20275 # p 536
 N93-20288 # p 483
 N93-20289 # p 552
 N93-20296 # p 527
 N93-20297 # p 552
 N93-20299 # p 552
 N93-20312 # p 530
 N93-20368 # p 552
 N93-20388 # p 571
 N93-20389 # p 572
 N93-20390 # p 572
 N93-20403 # p 572
 N93-20428 # p 533
 N93-20546 # p 569
 N93-20551 # p 527
 N93-20560 # p 513
 N93-20573 # p 552
 N93-20575 # p 513
 N93-20579 # p 513
 N93-20582 # p 502
 N93-20583 # p 521
 N93-20584 # p 513
 N93-20585 # p 553
 N93-20596 # p 527
 N93-20605 # p 513
 N93-20611 # p 572
 N93-20612 # p 503
 N93-20618 # p 553
 N93-20624 # p 536
 N93-20628 # p 527
 N93-20662 # p 553
 N93-20666 # p 553
 N93-20686 # p 554
 N93-20689 # p 553
 N93-20734 # p 572
 N93-20735 # p 521
 N93-20742 # p 514
 N93-20743 # p 527
 N93-20749 # p 503
 N93-20765 # p 554
 N93-20772 # p 554
 N93-20773 # p 521
 N93-20790 # p 554
 N93-20806 # p 484
 N93-20807 # p 484

N93-20845 # p 536
 N93-20902 # p 459
 N93-20907 # p 554
 N93-20913 # p 521
 N93-20928 # p 496
 N93-21004 # p 503
 N93-21022 # p 572
 N93-21054 # p 484
 N93-21056 # p 514
 N93-21059 # p 484
 N93-21173 # p 522
 N93-21187 # p 496
 N93-21197 # p 527
 N93-21210 # p 522
 N93-21254 # p 554
 N93-21259 # p 519
 N93-21268 # p 530
 N93-21305 # p 514
 N93-21310 # p 514
 N93-21311 # p 514
 N93-21312 # p 514
 N93-21313 # p 515
 N93-21314 # p 515
 N93-21315 # p 515
 N93-21316 # p 522
 N93-21317 # p 569
 N93-21322 # p 555
 N93-21342 # p 459
 N93-21343 # p 459
 N93-21368 # p 569
 N93-21382 # p 555
 N93-21383 # p 555
 N93-21401 # p 515
 N93-21406 # p 531
 N93-21459 # p 522
 N93-21462 # p 537
 N93-21465 # p 555
 N93-21479 # p 515
 N93-21501 # p 559
 N93-21513 # p 537
 N93-21518 # p 537
 N93-21529 # p 555
 N93-21531 # p 537
 N93-21533 # p 537
 N93-21557 # p 496
 N93-21562 # p 484
 N93-21646 # p 515
 N93-21659 # p 485
 N93-21671 # p 503
 N93-21713 # p 459
 N93-21749 # p 537
 N93-21759 # p 503
 N93-21761 # p 485
 N93-21762 # p 516
 N93-21763 # p 485
 N93-21766 # p 485
 N93-21794 # p 572
 N93-21796 # p 485
 N93-21799 # p 559
 N93-21810 # p 516
 N93-21819 # p 555
 N93-21820 # p 562
 N93-21821 # p 496
 N93-21831 # p 555
 N93-21856 # p 496
 N93-21858 # p 496
 N93-21859 # p 496
 N93-21861 # p 497
 N93-21862 # p 497
 N93-21863 # p 497
 N93-21865 # p 497
 N93-21866 # p 497
 N93-21870 # p 497
 N93-21895 # p 498
 N93-22003 # p 516
 N93-22005 # p 556
 N93-22015 # p 485
 N93-22034 # p 522
 N93-22035 # p 556
 N93-22045 # p 560
 N93-24736 # p 692
 N93-24739 # p 713
 N93-24741 # p 705
 N93-24754 # p 721
 N93-24756 # p 693
 N93-24759 # p 746
 N93-24760 # p 677
 N93-24762 # p 728
 N93-24764 # p 718
 N93-24768 # p 713
 N93-24772 # p 693
 N93-24773 # p 703
 N93-24875 # p 753
 N93-24879 # p 703
 N93-24880 # p 703
 N93-24883 # p 753

N93-24884 # p 753
 N93-24885 # p 703
 N93-24886 # p 704
 N93-24887 # p 704
 N93-24890 # p 735
 N93-24891 # p 736
 N93-24894 # p 704
 N93-24895 # p 754
 N93-24898 # p 704
 N93-24899 # p 734
 N93-24900 # p 747
 N93-24903 # p 747
 N93-24911 # p 693
 N93-24914 # p 706
 N93-24948 # p 706
 N93-24963 # p 747
 N93-24975 # p 754
 N93-25018 # p 706
 N93-25073 # p 757
 N93-25074 # p 693
 N93-25075 # p 693
 N93-25079 # p 721
 N93-25080 # p 730
 N93-25083 # p 694
 N93-25084 # p 758
 N93-25087 # p 747
 N93-25091 # p 694
 N93-25106 # p 721
 N93-25109 # p 747
 N93-25110 # p 704
 N93-25117 # p 694
 N93-25120 # p 706
 N93-25121 # p 694
 N93-25129 # p 722
 N93-25130 # p 758
 N93-25134 # p 677
 N93-25153 # p 694
 N93-25157 # p 754
 N93-25158 # p 754
 N93-25159 # p 754
 N93-25162 # p 714
 N93-25176 # p 747
 N93-25178 # p 731
 N93-25199 # p 728
 N93-25205 # p 704
 N93-25208 # p 748
 N93-25210 # p 748
 N93-25224 # p 705
 N93-25237 # p 748
 N93-25243 # p 706
 N93-25249 # p 695
 N93-25259 # p 748
 N93-25261 # p 707
 N93-25266 # p 749
 N93-25269 # p 695
 N93-25272 # p 734
 N93-25274 # p 695
 N93-25279 # p 714
 N93-25330 # p 707
 N93-25339 # p 695
 N93-25353 # p 729
 N93-25388 # p 696
 N93-25408 # p 714
 N93-25409 # p 696
 N93-25410 # p 758
 N93-25418 # p 761
 N93-25427 # p 749
 N93-25455 # p 722
 N93-25456 # p 707
 N93-25467 # p 696
 N93-25471 # p 722
 N93-25480 # p 722
 N93-25486 # p 714
 N93-25487 # p 696
 N93-25518 # p 749
 N93-25526 # p 715
 N93-25530 # p 715
 N93-25538 # p 715
 N93-25540 # p 749
 N93-25542 # p 697
 N93-25543 # p 729
 N93-25545 # p 697
 N93-25552 # p 716
 N93-25574 # p 731
 N93-25579 # p 750
 N93-25580 # p 750
 N93-25599 # p 750
 N93-25600 # p 758
 N93-25611 # p 758
 N93-25645 # p 755
 N93-25649 # p 759
 N93-25651 # p 759
 N93-25656 # p 731
 N93-25664 # p 697
 N93-25668 # p 723
 N93-25670 # p 716

ACCESSION NUMBER INDEX

ACCESSION NUMBER INDEX

N93-30691

N93-25673 * #	p 723	N93-26702 * #	p 825	N93-27448 * #	p 785	N93-29125	p 917	N93-29963 * #	p 905
N93-25692	p 716	N93-26899 * #	p 779	N93-27449 * #	p 785	N93-29134	#	N93-29964	#
N93-25701	p 716	N93-26907 * #	p 819	N93-27450 * #	p 820	N93-29141	#	N93-29968	#
N93-25702	p 723	N93-26999 * #	p 838	N93-27451 * #	p 840	N93-29152 * #	p 880	N93-29969	#
N93-25704	p 717	N93-27004 * #	p 779	N93-27452 * #	p 786	N93-29153 * #	p 893	N93-29971	#
N93-25705	p 750	N93-27005 * #	p 779	N93-27453 * #	p 786	N93-29154 * #	p 930	N93-29972	#
N93-25706	p 697	N93-27012 * #	p 844	N93-27454 * #	p 786	N93-29157 * #	p 930	N93-29981	#
N93-25719	p 717	N93-27017	#	N93-27455 * #	p 786	N93-29160	#	N93-29985	#
N93-25720	p 698	N93-27020 * #	p 838	N93-27456 * #	p 787	N93-29162 * #	p 874	N93-29999	#
N93-25733	#	N93-27026 * #	p 812	N93-27457 * #	p 787	N93-29165 * #	p 900	N93-30020	#
N93-25737	#	N93-27032 * #	p 779	N93-27459 * #	p 787	N93-29166 * #	p 875	N93-30044	#
N93-25751	p 723	N93-27033	#	N93-27460	#	N93-29187	#	N93-30103	#
N93-25752	p 698	N93-27034	#	N93-27462 * #	p 787	N93-29189	#	N93-30104	#
N93-25753	p 750	N93-27035	#	N93-27464 * #	p 788	N93-29192 * #	p 942	N93-30110	#
N93-25759	p 698	N93-27041	#	N93-27466 * #	p 840	N93-29194 * #	p 914	N93-30119	#
N93-25783	#	N93-27056	#	N93-27531	#	N93-29211	p 880	N93-30151	#
N93-25827	#	N93-27058	#	N93-27546	#	N93-29213	#	N93-30168	#
N93-25837	#	N93-27063 * #	p 852	N93-27547	#	N93-29215	#	N93-30171	#
N93-25843	#	N93-27067 * #	p 847	N93-27549	#	N93-29257	#	N93-30172	#
N93-25865	p 699	N93-27069 * #	p 838	N93-27570	#	N93-29258	#	N93-30173	#
N93-25874	#	N93-27076 * #	p 790	N93-27579	#	N93-29273	#	N93-30184	#
N93-25881	p 755	N93-27084 * #	p 780	N93-27590	#	N93-29278	p 909	N93-30203	#
N93-25882	p 699	N93-27088	#	N93-27610	#	N93-29284	#	N93-30274	#
N93-25883	#	N93-27089	#	N93-27640	#	N93-29286	#	N93-30275	p 880
N93-25884	#	N93-27090	#	N93-27662	#	N93-29288	#	N93-30276	p 881
N93-25894	#	N93-27092 * #	p 825	N93-27667	#	N93-29322	#	N93-30291	p 933
N93-25895	#	N93-27093 * #	p 780	N93-27675	#	N93-29323	#	N93-30298	p 937
N93-25896	#	N93-27096 * #	p 780	N93-27679	#	N93-29384	#	N93-30299	p 886
N93-25902	#	N93-27097 * #	p 781	N93-27680	#	N93-29388	#	N93-30309	p 933
N93-25909	#	N93-27115	#	N93-27692	#	N93-29396	#	N93-30320	p 933
N93-25912	#	N93-27126 * #	p 812	N93-27694	#	N93-29398	#	N93-30324	p 886
N93-25914	#	N93-27128 * #	p 781	N93-27727 * #	p 841	N93-29402	#	N93-30325	p 886
N93-25915	#	N93-27130 * #	p 813	N93-27832	#	N93-29409	#	N93-30330	p 886
N93-25917	#	N93-27131 * #	p 813	N93-27925	#	N93-29410	#	N93-30337	p 933
N93-25933	#	N93-27132 * #	p 838	N93-27955	#	N93-29436	#	N93-30338	p 887
N93-25948	#	N93-27133 * #	p 839	N93-28051	#	N93-29449	#	N93-30339	p 887
N93-25949	#	N93-27142 * #	p 823	N93-28053 * #	p 841	N93-29450	#	N93-30342	p 934
N93-25951	#	N93-27148 * #	p 852	N93-28054	#	N93-29451	#	N93-30350	p 887
N93-25969	#	N93-27150 * #	p 781	N93-28055	#	N93-29452 * #	p 917	N93-30351	p 887
N93-25996	#	N93-27151 * #	p 839	N93-28070	#	N93-29464	#	N93-30352	p 887
N93-25998 * #	p 731	N93-27156 * #	p 819	N93-28078	#	N93-29468	#	N93-30353	p 888
N93-26000	#	N93-27160 * #	p 814	N93-28184	#	N93-29480	#	N93-30354	p 888
N93-26006	#	N93-27166	p 764	N93-28189	#	N93-29498	#	N93-30355	p 888
N93-26007	#	N93-27167	p 781	N93-28206	#	N93-29588	#	N93-30358	p 888
N93-26008	#	N93-27168	p 805	N93-28226	#	N93-29652 * #	p 914	N93-30369	#
N93-26012	#	N93-27169	p 808	N93-28242	#	N93-29653 * #	p 885	N93-30373 * #	p 877
N93-26046 * #	p 729	N93-27170	p 839	N93-28251	#	N93-29713	#	N93-30374	#
N93-26049	#	N93-27171	p 819	N93-28289	#	N93-29715	#	N93-30375	#
N93-26052	#	N93-27173	p 805	N93-28391	#	N93-29717	#	N93-30387	#
N93-26078	#	N93-27178	p 793	N93-28418	#	N93-29718	#	N93-30388	#
N93-26085	#	N93-27179	p 845	N93-28440	#	N93-29721	#	N93-30406	#
N93-26087	#	N93-27180	p 847	N93-28449	#	N93-29722	#	N93-30416	#
N93-26093	#	N93-27182	p 839	N93-28467	#	N93-29774	#	N93-30429	#
N93-26099	#	N93-27185	p 814	N93-28490	#	N93-29775	#	N93-30430	#
N93-26134	#	N93-27186	p 814	N93-28498	#	N93-29776	#	N93-30431	#
N93-26136	#	N93-27187	p 814	N93-28555	#	N93-29777	#	N93-30432	#
N93-26160	#	N93-27189	p 814	N93-28564	#	N93-29778	#	N93-30433	#
N93-26161	#	N93-27210	p 839	N93-28571	#	N93-29779	#	N93-30434	#
N93-26167	#	N93-27212	p 781	N93-28576	#	N93-29788	#	N93-30435	#
N93-26168	#	N93-27214	p 782	N93-28577	#	N93-29815	#	N93-30436	#
N93-26195	#	N93-27218	p 782	N93-28586	#	N93-29851	#	N93-30438	#
N93-26196	#	N93-27220	p 782	N93-28592	#	N93-29852	#	N93-30439	#
N93-26198	#	N93-27221	p 782	N93-28603	#	N93-29869	#	N93-30440	#
N93-26201	#	N93-27221 * #	p 805	N93-28609	#	N93-29891	#	N93-30441	#
N93-26202	#	N93-27250	#	N93-28617	#	N93-29899	#	N93-30442	#
N93-26219	#	N93-27252	#	N93-28621	#	N93-29919	#	N93-30443	#
N93-26237	#	N93-27258	#	N93-28625	#	N93-29926	#	N93-30444	#
N93-26238	#	N93-27264	#	N93-28635	#	N93-29927	#	N93-30487	#
N93-26239	#	N93-27267	#	N93-28636	#	N93-29928	#	N93-30489	#
N93-26243	#	N93-27268	#	N93-28662	#	N93-29929	#	N93-30498	#
N93-26260	#	N93-27269	#	N93-28674	#	N93-29930	#	N93-30500	#
N93-26263	#	N93-27271	#	N93-28675	#	N93-29931	#	N93-30553	#
N93-26268	#	N93-27272	#	N93-28685	#	N93-29933	#	N93-30571	#
N93-26274	#	N93-27274	#	N93-28691	#	N93-29934	#	N93-30583	#
N93-26282	#	N93-27282	#	N93-28692	#	N93-29936	#	N93-30604	#
N93-26294	#	N93-27289	#	N93-28697	#	N93-29937	#	N93-30611	#
N93-26325	#	N93-27308	#	N93-28766	#	N93-29938	#	N93-30645	#
N93-26327	#	N93-27405	#	N93-28788	#	N93-29941	#	N93-30671	#
N93-26335	#	N93-27413	#	N93-28869	#	N93-29943	#	N93-30673	#
N93-26339	#	N93-27427	#	N93-28936	#	N93-29946	#	N93-30674	#
N93-26343	#	N93-27428	#	N93-28943	#	N93-29947	#	N93-30675	#
N93-26371	#	N93-27429	#	N93-28953	#	N93-29949	#	N93-30677	#
N93-26422	#	N93-27431	#	N93-28975	#	N93-29950	#	N93-30678	#
N93-26444	#	N93-27432	#	N93-28984	#	N93-29951	#	N93-30681	#
N93-26447	#	N93-27436	#	N93-28990	#	N93-29953	#	N93-30682	#
N93-26498	#	N93-27437	#	N93-28994	#	N93-29954	#	N93-30683	#
N93-26526	#	N93-27438	#	N93-29004	#	N93-29957	#	N93-30685	#
N93-26529	#	N93-27439	#	N93-29005	#	N93-29958	#	N93-30687	#
N93-26533	#	N93-27440	#	N93-29006	#	N93-29961	#	N93-30688	#
N93-26549	#	N93-27441	#	N93-29035	#	N93-29962	#	N93-30689	#
N93-26551	#	N93-27442	#	N93-29040	#			N93-30690	#
N93-26553	#	N93-27443	#	N93-29065	#			N93-30691	#
N93-26564	#	N93-27444	#	N93-29072	#				
N93-26566	#	N93-27445	#	N93-29090	#				
N93-26636	#	N93-27446	#	N93-29124	#				
N93-26648	#	N93-27447	#						

N93-30764

ACCESSION NUMBER INDEX

N93-30764	#	p 910	N93-31745	#	p 1004
N93-30841	#	p 921	N93-31746	#	p 1004
N93-30845	#	p 921	N93-31747	#	p 1004
N93-30852	#	p 921	N93-31795	#	p 1019
N93-30853	#	p 921	N93-31836	#	p 1015
N93-30854	#	p 921	N93-31839	#	p 989
N93-30855	#	p 922	N93-31840	#	p 999
N93-30857	#	p 922	N93-31846	#	p 1032
N93-30858	#	p 922	N93-31848	#	p 1015
N93-30861	#	p 922	N93-31855	#	p 990
N93-30862	#	p 922	N93-31860	#	p 1032
N93-30863	#	p 922	N93-31876	#	p 1033
N93-30864	#	p 923	N93-31916	#	p 1015
N93-30865	#	p 923	N93-31925	#	p 1034
N93-30867	#	p 923	N93-31927	#	p 1035
N93-30869	#	p 923	N93-31928	#	p 1035
N93-30873	#	p 923	N93-31929	#	p 1035
N93-30875	#	p 923	N93-31930	#	p 1035
N93-30876	#	p 923	N93-31931	#	p 1035
N93-30877	#	p 905	N93-31932	#	p 1035
N93-30892	#	p 878	N93-32004	#	p 990
N93-30947	#	p 879	N93-32028	#	p 1033
N93-30974	#	p 924	N93-32085	#	p 1019
N93-30979	#	p 879	N93-32089	#	p 1035
N93-30980	#	p 944	N93-32191	#	p 1036
N93-31005	#	p 889	N93-32203	#	p 999
N93-31010	#	p 937	N93-32205	#	p 999
N93-31029	#	p 942	N93-32212	#	p 1033
N93-31031	#	p 935	N93-32218	#	p 1000
N93-31036	#	p 936	N93-32220	#	p 1005
N93-31037	#	p 879	N93-32221	#	p 1040
N93-31042	#	p 1014	N93-32223	#	p 1000
N93-31043	#	p 998	N93-32224	#	p 1038
N93-31044	#	p 1018	N93-32225	#	p 994
N93-31045	#	p 1041	N93-32226	#	p 990
N93-31046	#	p 998	N93-32232	#	p 949
N93-31051	#	p 1039	N93-32234	#	p 1019
N93-31052	#	p 987	N93-32272	#	p 1005
N93-31058	#	p 998	N93-32273	#	p 1005
N93-31068	#	p 1009	N93-32274	#	p 1005
N93-31110	#	p 1030	N93-32279	#	p 1033
N93-31111	#	p 1003	N93-32332	#	p 1001
N93-31120	#	p 993	N93-32336	#	p 994
N93-31123	#	p 1030	N93-32337	#	p 994
N93-31137	#	p 1030	N93-32338	#	p 999
N93-31146	#	p 1031	N93-32339	#	p 1040
N93-31148	#	p 987	N93-32348	#	p 994
N93-31170	#	p 1003	N93-32351	#	p 1005
N93-31171	#	p 988	N93-32357	#	p 990
N93-31189	#	p 988	N93-32358	#	p 990
N93-31192	#	p 1018	N93-32368	#	p 1005
N93-31193	#	p 1031	N93-32372	#	p 1006
N93-31197	#	p 998	N93-32374	#	p 1006
N93-31202	#	p 1034	N93-32377	#	p 1040
N93-31258	#	p 1034	N93-32379	#	p 1017
N93-31269	#	p 993	N93-32380	#	p 1010
N93-31271	#	p 993	N93-32385	#	p 1020
N93-31272	#	p 1018	N93-32386	#	p 1006
N93-31273	#	p 1000	N93-32404	#	p 949
N93-31274	#	p 1014	N93-32409	#	p 992
N93-31275	#	p 998	N93-32416	#	p 999
N93-31276	#	p 1014			
N93-31277	#	p 998			
N93-31278	#	p 1010			
N93-31279	#	p 1000			
N93-31280	#	p 1010			
N93-31281	#	p 993			
N93-31282	#	p 994			
N93-31283	#	p 1040			
N93-31284	#	p 1031			
N93-31320	#	p 988			
N93-31442	#	p 1038			
N93-31519	#	p 1031			
N93-31538	#	p 988			
N93-31583	#	p 1016			
N93-31584	#	p 1031			
N93-31585	#	p 1017			
N93-31586	#	p 1032			
N93-31588	#	p 1032			
N93-31643	#	p 1019			
N93-31647	#	p 1032			
N93-31648	#	p 988			
N93-31649	#	p 1038			
N93-31652	#	p 991			
N93-31653	#	p 1040			
N93-31671	#	p 1004			
N93-31672	#	p 989			
N93-31730	#	p 991			
N93-31732	#	p 989			
N93-31733	#	p 989			
N93-31734	#	p 1041			
N93-31739	#	p 1019			
N93-31741	#	p 1004			
N93-31742	#	p 1004			
N93-31743	#	p 1004			
N93-31744	#	p 1004			

SPECIAL NOTICE

The abstract sections of the monthly supplements of *Aeronautical Engineering* can be bound separately. Individual abstracts can be located readily by means of the page numbers given at each entry, e.g., p 723 N93-25673. To assist the user in binding Supplements SP-7037 (288) through SP-7037 (299), a title page is included in this Cumulative Index.

AERONAUTICAL ENGINEERING

A CONTINUING BIBLIOGRAPHY

Abstracts

January – December 1993

TABLE OF CONTENTS

<i>SP-7037 Supplement</i>	<i>Page</i>
288	1
289	107
290	237
291	457
292	573
293	677
294	763
295	855
296	947
297	1043
298	1175
299	1229

REPORT DOCUMENT PAGE

1. Report No. NASA SP-7037 (300)	2. Government Accession No.	3. Recipient's Catalog No.	
4. Title and Subtitle Aeronautical Engineering A Cumulative Index to the 1993 Issues		5. Report Date February 1994	
		6. Performing Organization Code JTT	
7. Author(s)		8. Performing Organization Report No.	
		10. Work Unit No.	
9. Performing Organization Name and Address NASA Scientific and Technical Information Program		11. Contract or Grant No.	
		13. Type of Report and Period Covered Special Publication	
12. Sponsoring Agency Name and Address National Aeronautics and Space Administration Washington, DC 20546-0001		14. Sponsoring Agency Code	
		15. Supplementary Notes	
16. Abstract This is a cumulative index to the abstracts contained in NASA SP-7037 (288) through NASA SP-7037 (299) of <i>Aeronautical Engineering: A Continuing Bibliography</i> . NASA SP-7037 and its supplements have been compiled by the Center for AeroSpace Information of the National Aeronautics and Space Administration (NASA). This cumulative index includes subject, personal author, corporate source, foreign technology, contract number, report number, and accession number indexes.			
17. Key Words (Suggested by Author(s)) Aerodynamics Aeronautical Engineering Aeronautics Bibliographies		18. Distribution Statement Unclassified - Unlimited Subject Category - 01	
19. Security Classif. (of this report) Unclassified		20. Security Classif. (of this page) Unclassified	21. No. of Pages 680
		22. Price A99/HC	

FEDERAL REGIONAL DEPOSITORY LIBRARIES

ALABAMA

AUBURN UNIV. AT MONTGOMERY LIBRARY

Documents Dept.
7300 University Dr.
Montgomery, AL 36117-3596
(205) 244-3650 Fax: (205) 244-0678

UNIV. OF ALABAMA

Amelia Gayle Gorgas Library
Govt. Documents
Box 870266
Tuscaloosa, AL 35487-0266
(205) 348-6046 Fax: (205) 348-8833

ARIZONA

DEPT. OF LIBRARY, ARCHIVES, AND PUBLIC RECORDS

Federal Documents
Third Floor State Capitol
1700 West Washington
Phoenix, AZ 85007
(602) 542-4121 Fax: (602) 542-4400,
542-4500

ARKANSAS

ARKANSAS STATE LIBRARY

State Library Services
One Capitol Mall
Little Rock, AR 72201
(501) 682-2869

CALIFORNIA

CALIFORNIA STATE LIBRARY

Govt. Publications Section
914 Capitol Mall - P.O. Box 942837
Sacramento, CA 94237-0001
(916) 322-4572 Fax: (916) 324-8120

COLORADO

UNIV. OF COLORADO - BOULDER

Norlin Library
Govt. Publications
Campus Box 184
Boulder, CO 83309-0184
(303) 492-8834 Fax: (303) 492-2185

DENVER PUBLIC LIBRARY

Govt. Publications Dept. BS/GPD
1357 Broadway
Denver, CO 80203
(303) 571-2135

CONNECTICUT

CONNECTICUT STATE LIBRARY

231 Capitol Avenue
Hartford, CT 06106
(203) 566-4971 Fax: (203) 566-3322

FLORIDA

UNIV. OF FLORIDA LIBRARIES

Documents Dept.
Library West
Gainesville, FL 32611-2048
(904) 392-0366 Fax: (904) 392-7251

GEORGIA

UNIV. OF GEORGIA LIBRARIES

Govt. Documents Dept.
Jackson Street
Athens, GA 30602
(404) 542-8949 Fax: (404) 542-6522

HAWAII

UNIV. OF HAWAII

Hamilton Library
Govt. Documents Collection
2550 The Mall
Honolulu, HI 96822
(808) 948-8230 Fax: (808) 956-5968

IDAHO

UNIV. OF IDAHO LIBRARY

Documents Section
Moscow, ID 83843
(208) 885-6344 Fax: (208) 885-6817

ILLINOIS

ILLINOIS STATE LIBRARY

Reference Dept.
300 South Second
Springfield, IL 62701-1796
(217) 782-7596 Fax: (217) 524-0041

INDIANA

INDIANA STATE LIBRARY

Serials/Documents Section
140 North Senate Avenue
Indianapolis, IN 46204
(317) 232-3678 Fax: (317) 232-3728

IOWA

UNIV. OF IOWA LIBRARIES

Govt. Publications Dept.
Washington & Madison Streets
Iowa City, IA 52242
(319) 335-5926 Fax: (319) 335-5830

KANSAS

UNIV. OF KANSAS

Govt. Documents & Map Library
6001 Malatt Hall
Lawrence, KS 66045-2800
(913) 864-4660 Fax: (913) 864-5380

KENTUCKY

UNIV. OF KENTUCKY LIBRARIES

Govt. Publications/Maps Dept.
Lexington, KY 40506-0039
(606) 257-3139 Fax: (606) 257-1563,
257-8379

LOUISIANA

LOUISIANA STATE UNIV.

Middleton Library
Govt. Documents Dept.
Baton Rouge, LA 70803
(504) 388-2570 Fax: (504) 388-6992

LOUISIANA TECHNICAL UNIV.

Prescott Memorial Library
Govt. Documents Dept.
305 Wisteria Street
Ruston, LA 71270-9985
(318) 257-4962 Fax: (318) 257-2447

MAINE

TRI-STATE DOCUMENTS DEPOS.

Raymond H. Fogler Library
Govt. Documents & Microforms Dept.
Univ. of Maine
Orono, ME 04469
(207) 581-1680

MARYLAND

UNIV. OF MARYLAND

Hornbake Library
Govt. Documents/Maps Unit
College Park, MD 20742
(301) 454-3034 Fax: (301) 454-4985

MASSACHUSETTS

BOSTON PUBLIC LIBRARY

Govt. Documents Dept.
666 Boylston Street
Boston, MA 02117
(617) 536-5400 ext. 226
Fax: (617) 267-8273, 267-8248

MICHIGAN

DETROIT PUBLIC LIBRARY

5201 Woodward Avenue
Detroit, MI 48202-4093
(313) 833-1440, 833-1409
Fax: (313) 833-5039

LIBRARY OF MICHIGAN

Govt. Documents Unit
P.O. Box 30007
Lansing, MI 48909
(517) 373-0640 Fax: (517) 373-3381

MINNESOTA

UNIV. OF MINNESOTA

Wilson Library
Govt. Publications Library
309 19th Avenue South
Minneapolis, MN 55455
(612) 624-5073 Fax: (612) 626-9353

MISSISSIPPI

UNIV. OF MISSISSIPPI

J.D. Williams Library
Federal Documents Dept.
106 Old Gym Bldg.
University, MS 38677
(601) 232-5857 Fax: (601) 232-5453

MISSOURI

UNIV. OF MISSOURI - COLUMBIA

Ellis Library
Govt. Documents
Columbia, MO 65201
(314) 882-6733 Fax: (314) 882-8044

MONTANA

UNIV. OF MONTANA

Maureen & Mike Mansfield Library
Documents Div.
Missoula, MT 59812-1195
(406) 243-6700 Fax: (406) 243-2060

NEBRASKA

UNIV. OF NEBRASKA - LINCOLN

D.L. Love Memorial Library
Documents Dept.
Lincoln, NE 68588
(402) 472-2562

NEVADA

UNIV. OF NEVADA

Reno Library
Govt. Publications Dept.
Reno, NV 89557
(702) 784-6579 Fax: (702) 784-1751

NEW JERSEY

NEWARK PUBLIC LIBRARY

U.S. Documents Div.
5 Washington Street -
P.O. Box 630
Newark, NJ 07101-0630
(201) 733-7812 Fax: (201) 733-5648

NEW MEXICO

UNIV. OF NEW MEXICO

General Library
Govt. Publications Dept.
Albuquerque, NM 87131-1466
(505) 277-5441 Fax: (505) 277-6019

NEW MEXICO STATE LIBRARY

325 Don Gaspar Avenue
Santa Fe, NM 87503
(505) 827-3826 Fax: (505) 827-3820

NEW YORK

NEW YORK STATE LIBRARY

Documents/Gift & Exchange Section
Federal Depository Program
Cultural Education Center
Albany, NY 12230
(518) 474-5563 Fax: (518) 474-5786

NORTH CAROLINA

UNIV. OF NORTH CAROLINA -

CHAPEL HILL

CB#3912, Davis Library
BA/SS Dept. - Documents
Chapel Hill, NC 27599
(919) 962-1151 Fax: (919) 962-0484

NORTH DAKOTA

NORTH DAKOTA STATE UNIV. LIB.

Documents Office
Fargo, ND 58105
(701) 237-8886 Fax: (701) 237-7138
In cooperation with Univ. of North
Dakota, Chester Fritz Library
Grand Forks

OHIO

STATE LIBRARY OF OHIO

Documents Dept.
65 South Front Street
Columbus, OH 43266
(614) 644-7051 Fax: (614) 752-9178

OKLAHOMA

OKLAHOMA DEPT. OF LIBRARIES

U.S. Govt. Information Div.
200 NE 18th Street
Oklahoma City, OK 73105-3298
(405) 521-2502, ext. 252, 253
Fax: (405) 525-7804

OKLAHOMA STATE UNIV.

Edmon Low Library
Documents Dept.
Stillwater, OK 74078
(405) 744-6546 Fax: (405) 744-5183

OREGON

PORTLAND STATE UNIV.

Millar Library
934 SW Harrison - P.O. Box 1151
Portland, OR 97207
(503) 725-3673 Fax: (503) 725-4527

PENNSYLVANIA

STATE LIBRARY OF PENN.

Govt. Publications Section
Walnut St. & Commonwealth Ave. -
P.O. Box 1601
Harrisburg, PA 17105
(717) 787-3752

SOUTH CAROLINA

CLEMSON UNIV.

Cooper Library
Public Documents Unit
Clemson, SC 29634-3001
(803) 656-5174 Fax: (803) 656-3025
In cooperation with Univ. of South
Carolina, Thomas Cooper Library,
Columbia

TENNESSEE

MEMPHIS STATE UNIV. LIBRARIES

Govt. Documents
Memphis, TN 38152
(901) 678-2586 Fax: (901) 678-2511

TEXAS

TEXAS STATE LIBRARY

United States Documents
P.O. Box 12927 - 1201 Brazos
Austin, TX 78711
(512) 463-5455 Fax: (512) 463-5436

TEXAS TECH. UNIV. LIBRARY

Documents Dept.
Lubbock, TX 79409
(806) 742-2268 Fax: (806) 742-1920

UTAH

UTAH STATE UNIV.

Merrill Library & Learning Resources
Center, UMC-3000
Documents Dept.
Logan, UT 84322-3000
(801) 750-2684 Fax: (801) 750-2677

VIRGINIA

UNIV. OF VIRGINIA

Alderman Library
Govt. Documents
Charlottesville, VA 22903-2498
(804) 824-3133 Fax: (804) 924-4337

WASHINGTON

WASHINGTON STATE LIBRARY

Document Section
MS AJ-11
Olympia, WA 98504-0111
(206) 753-4027 Fax: (206) 753-3546

WEST VIRGINIA

WEST VIRGINIA UNIV. LIBRARY

Govt. Documents Section
P.O. Box 6069
Morgantown, WV 26506
(304) 293-3640

WISCONSIN

ST. HIST. SOC. OF WISCONSIN LIBRARY

Govt. Publications Section
816 State Street
Madison, WI 53706
(608) 262-2781 Fax: (608) 262-4711
In cooperation with Univ. of Wisconsin -
Madison, Memorial Library

MILWAUKEE PUBLIC LIBRARY

Documents Div.
814 West Wisconsin Avenue
Milwaukee, WI 53233
(414) 278-2167 Fax: (414) 278-2137

POSTMASTER
Address Correction Requested
(Sections 137 and 159 Post Manual)

National Aeronautics and
Space Administration
Code JTT
Washington, DC 20546-0001

Official Business
Penalty for Private Use, \$300

BULK RATE
POSTAGE & FEES PAID
NASA
PERMIT No. G-27